Scientific and Technical Aerospace Reports

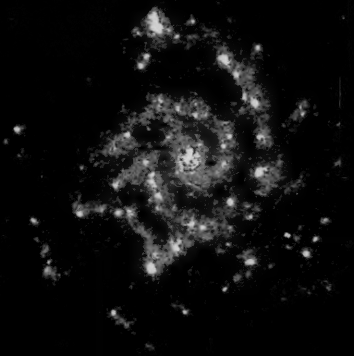

An Abstract Journal

Volume 32, Number 7
July 1994
N94-25544 to N94-28398

The NASA STI Program ... in Profile

Since its founding, NASA has been dedicated to the advancement of aeronautics and space science. The NASA Scientific and Technical Information (STI) Program plays a key part in helping NASA maintain this important role.

The NASA STI Program provides access to the NASA STI Database, the largest collection of aeronautical and space science STI in the world. The Program is also NASA's institutional mechanism for disseminating the results of its research and development activities.

Specialized services that help round out the Program's diverse offerings include creating custom thesauri, translating material to or from 34 foreign languages, building customized databases, organizing and publishing research results ... even providing videos.

For more information about the NASA STI Program, you can:

- **Phone** the NASA Access Help Desk at (301) 621-0390
- **Fax** your question to the NASA Access Help Desk at (301) 621-0134
- **E-mail** your question via the **Internet** to help@sti.nasa.gov
- **Write** to:

NASA Access Help Desk
NASA Center for AeroSpace Information
800 Elkridge Landing Road
Linthicum Heights, MD 21090-2934

Scientific and Technical Aerospace Reports

STAR

Scientific and Technical Aerospace Reports (STAR), is published each month as a major product of the NASA Scientific and Technical Information (STI) Program.

Inside this issue you will find:

- **Front Matter** containing a typical citation and abstract sample explaining the standard format, including codes for ordering reports
- **An Abstract Section** containing citations and abstracts of reports and publications that provide comprehensive coverage of worldwide aerospace-related topics including aeronautics and space science technology. *STAR* lists published and publicly available reports entered into the NASA STI Database during the four weeks preceding publication of this issue. These citations and abstracts are listed by subject categories.
- **An Index Section**
  - Subject
  - Personal author
  - Corporate source
  - Contract number
  - Report number
- **An Appendix** containing a guide for ordering cited reports, registering with the NASA STI Program, and using the available products and services. Additionally, price schedules, phone numbers, and addresses are included in this information packed section.

NASA also sponsors the companion journal, *NASA Open Volumes on Aerospace (NOVA)*, which lists abstracts of the open literature on aerospace subjects available worldwide. *NOVA* is for internal NASA use only, available from the NASA Center for AeroSpace Information (CASI).

Entries found in *STAR* are available through the NASA online retrieval service, RECON, and through DIALOG as the Aerospace Database.

The NASA STI Program gathers information through national and international agreements and exchanges and makes this information available to the NASA community and to the public in many forms through various outlets.

For additional information on the NASA STI Program, call the NASA Access Help Desk at (301) 621-0390, or write to:

NASA Center for AeroSpace Information
800 Elkridge Landing Road
Linthicum Heights, Maryland 21090-2934

US ISSN 0036-8741

This publication was prepared by the NASA Center for AeroSpace Information,
800 Elkridge Landing Road, Linthicum Heights, MD 21090-2934, (301) 621-0390.

Volume 32 Number 7 / July 1994

TABLE OF CONTENTS

AERONAUTICS For related information see also *Astronautics.*

01 AERONAUTICS (GENERAL) 2641

02 AERODYNAMICS 2643
Includes aerodynamics of bodies, combinations, wings, rotors, and control surfaces; and internal flow in ducts and turbomachinery. For related information see also *34 Fluid Mechanics and Heat Transfer.*

03 AIR TRANSPORTATION AND SAFETY 2659
Includes passenger and cargo air transport operations; and aircraft accidents. For related information see also *16 Space Transportation* and *85 Urban Technology and Transportation.*

04 AIRCRAFT COMMUNICATIONS AND NAVIGATION 2664
Includes digital and voice communication with aircraft; air navigation systems (satellite and ground based); and air traffic control. For related information see also *17 Space Communications, Spacecraft Communications, Command and Tracking* and *32 Communications and Radar.*

05 AIRCRAFT DESIGN, TESTING AND PERFORMANCE 2666
Includes aircraft simulation technology. For related information see also *18 Spacecraft Design, Testing and Performance* and *39 Structural Mechanics.* For land transportation vehicles see *85 Urban Technology and Transportation.*

06 AIRCRAFT INSTRUMENTATION 2672
Includes cockpit and cabin display devices; and flight instruments. For related information see also *19 Spacecraft Instrumentation* and *35 Instrumentation and Photography.*

07 AIRCRAFT PROPULSION AND POWER 2673
Includes prime propulsion systems and systems components, e.g., gas turbine engines and compressors; and onboard auxiliary power plants for aircraft. For related information see also *20 Spacecraft Propulsion and Power, 28 Propellants and Fuels,* and *44 Energy Production and Conversion.*

08 AIRCRAFT STABILITY AND CONTROL 2676
Includes aircraft handling qualities; piloting; flight controls; and autopilots. For related information see also *05 Aircraft Design, Testing and Performance.*

09 RESEARCH AND SUPPORT FACILITIES (AIR) 2679
Includes airports, hangars and runways; aircraft repair and overhaul facilities; wind tunnels; shock tubes; and aircraft engine test stands. For related information see also *14 Ground Support Systems and Facilities (Space).*

ASTRONAUTICS For related information see also *Aeronautics.*

12 ASTRONAUTICS (GENERAL) 2682
For extraterrestrial exploration see *91 Lunar and Planetary Exploration.*

13 ASTRODYNAMICS 2690
Includes powered and free-flight trajectories; and orbital and launching dynamics.

14 GROUND SUPPORT SYSTEMS AND FACILITIES (SPACE) 2690
Includes launch complexes, research and production facilities; ground support equipment, e.g., mobile transporters; and simulators. For related information see also *09 Research and Support Facilities (Air).*

15 LAUNCH VEHICLES AND SPACE VEHICLES 2691
Includes boosters; operating problems of launch/space vehicle systems; and reusable vehicles. For related information see also *20 Spacecraft Propulsion and Power.*

16 SPACE TRANSPORTATION 2691
Includes passenger and cargo space transportation, e.g., shuttle operations; and space rescue techniques. For related information see also *03 Air Transportation and Safety* and *18 Spacecraft Design, Testing and Performance.* For space suits see *54 Man/System Technology and Life Support.*

17 SPACE COMMUNICATIONS, SPACECRAFT COMMUNICATIONS, COMMAND AND TRACKING .. 2693
Includes telemetry; space communications networks; astronavigation and guidance; and radio blackout. For related information see also *04 Aircraft Communications and Navigation* and *32 Communications and Radar.*

N.A.—No abstracts were assigned to this category for this issue.

18 SPACECRAFT DESIGN, TESTING AND PERFORMANCE 2693
Includes satellites; space platforms; space stations; spacecraft systems and components such as thermal and environmental controls; and attitude controls. For life support systems see *54 Man/System Technology and Life Support.* For related information see also *05 Aircraft Design, Testing and Performance, 39 Structural Mechanics,* and *16 Space Transportation.*

19 SPACECRAFT INSTRUMENTATION 2698
For related information see also *06 Aircraft Instrumentation* and *35 Instrumentation and Photography.*

20 SPACECRAFT PROPULSION AND POWER 2699
Includes main propulsion systems and components, e.g., rocket engines; and spacecraft auxiliary power sources. For related information see also *07 Aircraft Propulsion and Power, 28 Propellants and Fuels, 44 Energy Production and Conversion,* and *15 Launch Vehicles and Space Vehicles.*

CHEMISTRY AND MATERIALS

23 CHEMISTRY AND MATERIALS (GENERAL) 2704

24 COMPOSITE MATERIALS 2704
Includes physical, chemical, and mechanical properties of laminates and other composite materials. For ceramic materials see *27 Nonmetallic Materials.*

25 INORGANIC AND PHYSICAL CHEMISTRY 2712
Includes chemical analysis, e.g., chromatography; combustion theory; electrochemistry; and photochemistry. For related information see also *77 Thermodynamics and Statistical Physics.*

26 METALLIC MATERIALS 2722
Includes physical, chemical, and mechanical properties of metals, e.g., corrosion; and metallurgy.

27 NONMETALLIC MATERIALS 2747
Includes physical, chemical, and mechanical properties of plastics, elastomers, lubricants, polymers, textiles, adhesives, and ceramic materials. For composite materials see *24 Composite Materials.*

28 PROPELLANTS AND FUELS 2758
Includes rocket propellants, igniters and oxidizers; their storage and handling procedures; and aircraft fuels. For related information see also *07 Aircraft Propulsion and Power, 20 Spacecraft Propulsion and Power,* and *44 Energy Production and Conversion.*

29 MATERIALS PROCESSING 2760
Includes space-based development of products and processes for commercial application. For biological materials see *55 Space Biology:*

ENGINEERING For related information see also *Physics.*

31 ENGINEERING (GENERAL) 2762
Includes vacuum technology; control engineering; display engineering; cryogenics; and fire prevention.

32 COMMUNICATIONS AND RADAR 2765
Includes radar; land and global communications; communications theory; and optical communications. For related information see also *04 Aircraft Communications and Navigation* and *17 Space Communications, Spacecraft Communications, Command and Tracking.* For search and rescue see *03 Air Transportation and Safety,* and *16 Space Transportation.*

33 ELECTRONICS AND ELECTRICAL ENGINEERING 2779
Includes test equipment and maintainability; components, e.g., tunnel diodes and transistors; microminiaturization; and integrated circuitry. For related information see also *60 Computer Operations and Hardware* and *76 Solid-State Physics.*

34 FLUID MECHANICS AND HEAT TRANSFER 2789
Includes boundary layers; hydrodynamics; fluidics; mass transfer and ablation cooling. For related information see also *02 Aerodynamics* and *77 Thermodynamics and Statistical Physics.*

35 INSTRUMENTATION AND PHOTOGRAPHY 2809
Includes remote sensors; measuring instruments and gauges; detectors; cameras and photographic supplies; and holography. For aerial photography see *43 Earth Resources and Remote Sensing.* For related information see also *06 Aircraft Instrumentation* and *19 Spacecraft Instrumentation.*

36 LASERS AND MASERS 2815
Includes parametric amplifiers. For related information see also *76 Solid-State Physics.*

37 MECHANICAL ENGINEERING 2821
Includes auxiliary systems (nonpower); machine elements and processes; and mechanical equipment.

38 QUALITY ASSURANCE AND RELIABILITY 2834
Includes product sampling procedures and techniques; and quality control.

39 STRUCTURAL MECHANICS 2836
Includes structural element design and weight analysis; fatigue; and thermal stress. For applications see *05 Aircraft Design, Testing and Performance* and *18 Spacecraft Design, Testing and Performance.*

GEOSCIENCES For related information see also *Space Sciences.*

42 GEOSCIENCES (GENERAL) .... N.A.

43 EARTH RESOURCES AND REMOTE SENSING 2847
Includes remote sensing of earth resources by aircraft and spacecraft; photogrammetry; and aerial photography. For instrumentation see *35 Instrumentation and Photography.*

44 ENERGY PRODUCTION AND CONVERSION 2853
Includes specific energy conversion systems, e.g., fuel cells; global sources of energy; geophysical conversion; and windpower. For related information see also *07 Aircraft Propulsion and Power, 20 Spacecraft Propulsion and Power,* and *28 Propellants and Fuels.*

45 ENVIRONMENT POLLUTION 2865
Includes atmospheric, noise, thermal, and water pollution.

46 GEOPHYSICS 2876
Includes aeronomy; upper and lower atmosphere studies; ionospheric and magnetospheric physics; and geomagnetism. For space radiation see *93 Space Radiation.*

47 METEOROLOGY AND CLIMATOLOGY 2891
Includes weather forecasting and modification.

48 OCEANOGRAPHY 2898
Includes biological, dynamic, and physical oceanography; and marine resources. For related information see also *43 Earth Resources and Remote Sensing.*

LIFE SCIENCES

51 LIFE SCIENCES (GENERAL) 2900

52 AEROSPACE MEDICINE 2908
Includes physiological factors; biological effects of radiation; and effects of weightlessness on man and animals.

53 BEHAVIORAL SCIENCES 2937
Includes psychological factors; individual and group behavior; crew training and evaluation; and psychiatric research.

54 MAN/SYSTEM TECHNOLOGY AND LIFE SUPPORT 2940
Includes human engineering; biotechnology; and space suits and protective clothing. For related information see also *16 Space Transportation.*

55 SPACE BIOLOGY 2944
Includes exobiology; planetary biology; and extraterrestrial life.

MATHEMATICAL AND COMPUTER SCIENCES

59 MATHEMATICAL AND COMPUTER SCIENCES (GENERAL) 2945

60 COMPUTER OPERATIONS AND HARDWARE 2947
Includes hardware for computer graphics, firmware, and data processing. For components see *33 Electronics and Electrical Engineering.*

61 COMPUTER PROGRAMMING AND SOFTWARE 2956
Includes computer programs, routines, algorithms, and specific applications, e.g., CAD/CAM.

62 COMPUTER SYSTEMS 2979
Includes computer networks and special application computer systems.

63 CYBERNETICS 2984
Includes feedback and control theory, artificial intelligence, robotics and expert systems. For related information see also *54 Man/System Technology and Life Support.*

64 NUMERICAL ANALYSIS 2990
Includes iteration, difference equations, and numerical approximation.

65 STATISTICS AND PROBABILITY 3001
Includes data sampling and smoothing; Monte Carlo method; and stochastic processes.

66 SYSTEMS ANALYSIS 3005
Includes mathematical modeling; network analysis; and operations research.

67 THEORETICAL MATHEMATICS 3005
Includes topology and number theory.

PHYSICS For related information see also *Engineering.*

70 PHYSICS (GENERAL) 3007
For precision time and time interval (PTTI) see *35 Instrumentation and Photography*; for geophysics, astrophysics or solar physics see *46 Geophysics, 90 Astrophysics*, or *92 Solar Physics.*

71 ACOUSTICS 3009
Includes sound generation, transmission, and attenuation. For noise pollution see *45 Environment Pollution.*

72 ATOMIC AND MOLECULAR PHYSICS 3011
Includes atomic structure, electron properties, and molecular spectra.

73 NUCLEAR AND HIGH-ENERGY PHYSICS 3031
Includes elementary and nuclear particles; and reactor theory. For space radiation see *93 Space Radiation.*

74 OPTICS 3033
Includes light phenomena and optical devices. For lasers see *36 Lasers and Masers.*

75 PLASMA PHYSICS 3041
Includes magnetohydrodynamics and plasma fusion. For ionospheric plasmas see *46 Geophysics.* For space plasmas see *90 Astrophysics.*

76 SOLID-STATE PHYSICS 3049
Includes superconductivity. For related information see also *33 Electronics and Electrical Engineering* and *36 Lasers and Masers.*

77 THERMODYNAMICS AND STATISTICAL PHYSICS 3071
Includes quantum mechanics; theoretical physics; and Bose and Fermi statistics. For related information see also *25 Inorganic and Physical Chemistry* and 34 *Fluid Mechanics and Heat Transfer.*

SOCIAL SCIENCES

80 SOCIAL SCIENCES (GENERAL) 3075
Includes educational matters.

81 ADMINISTRATION AND MANAGEMENT 3093
Includes management planning and research.

82 DOCUMENTATION AND INFORMATION SCIENCE 3095
Includes information management; information storage and retrieval technology; technical writing; graphic arts; and micrography. For computer documentation see *61 Computer Programming and Software.*

83 ECONOMICS AND COST ANALYSIS 3101
Includes cost effectiveness studies.

84 LAW, POLITICAL SCIENCE AND SPACE POLICY 3101
Includes NASA appropriation hearings; aviation law; space law and policy; international law; international cooperation; and patent policy.

85 URBAN TECHNOLOGY AND TRANSPORTATION 3102
Includes applications of space technology to urban problems; technology transfer; technology assessment; and surface and mass transportation. For related information see *03 Air Transportation and Safety, 16 Space Transportation,* and *44 Energy Production and Conversion.*

SPACE SCIENCES For related information see also *Geosciences.*

88 SPACE SCIENCES (GENERAL) .... **N.A.**

89 ASTRONOMY **3102**
Includes radio, gamma-ray, and infrared astronomy; and astrometry.

90 ASTROPHYSICS **3103**
Includes cosmology; celestial mechanics; space plasmas; and interstellar and interplanetary gases and dust. For related information see also *75 Plasma Physics.*

91 LUNAR AND PLANETARY EXPLORATION **3106**
Includes planetology; and manned and unmanned flights. For spacecraft design or space stations see *18 Spacecraft Design, Testing and Performance.*

92 SOLAR PHYSICS **3110**
Includes solar activity, solar flares, solar radiation and sunspots. For related information see also *93 Space Radiation.*

93 SPACE RADIATION **3112**
Includes cosmic radiation; and inner and outer earth's radiation belts. For biological effects of radiation see *52 Aerospace Medicine.* For theory see *73 Nuclear and High-Energy Physics.*

GENERAL

Includes aeronautical, astronautical, and space science related histories, biographies, and pertinent reports too broad for categorization; histories or broad overviews of NASA programs.

99 GENERAL **3117**

SUBJECT INDEX **I-1**

PERSONAL AUTHOR INDEX **I-187**

CORPORATE SOURCE INDEX **I-211**

CONTRACT NUMBER INDEX **I-243**

REPORT NUMBER INDEX **I-249**

APPENDIX **A-1**

TYPICAL CITATION AND ABSTRACT

NASA SPONSORED
ON MICROFICHE
↓↓

ACCESSION NUMBER → **N94-12270*#** United Technologies Corp., West Palm Beach, FL. Pratt and Whitney. ← CORPORATE SOURCE

TITLE → **ADVANCED CONTROL FOR AIRBREATHING ENGINES, VOLUME 1: PRATT AND WHITNEY**

AUTHOR → J. A. Ralph Jul. 1993 83 p ← PUBLICATION DATE

CONTRACT OR GRANT → (Contract NAS3-25952; RTOP 505-62-61)

REPORT NUMBERS → (NASA-CR-189203; E-8006; NAS 1.26:189203) Avail: CASI HC A05/MF A01 ← AVAILABILITY SOURCE AND PRICE CODE

The application of advanced control concepts to air breathing engines may yield significant improvements in aircraft/engine performance and operability. Screening studies of advanced control concepts for air breathing engines were conducted by three major domestic aircraft engine manufacturers to determine the potential impact of concepts on turbine engine performance and operability. The purpose of the studies was to identify concepts which offered high potential yet may incur high research and development risk. A target suite of proposed advanced control concepts was formulated and evaluated in a two phase study to quantify each concept's impact on desired engine characteristics. To aid in the evaluation specific aircraft/engine combinations were considered: a Military High Performance Fighter mission, a High Speed Civil Transport mission, and a Civil Tiltrotor mission. Each of the advanced control concepts considered in the study are defined and described. The concept potential impact on engine performance was determined. Relevant figures of merit on which to evaluate the concepts are determined. Finally, the concepts are ranked with respect to the target aircraft/engine missions. A final report describing the screening studies was prepared by each engine manufacturer. Volume 1 of these reports describes the studies performed by Pratt & Whitney. Author (revised)

VOLUME 32 NUMBER 7 / July 1994

Scientific and Technical Aerospace Reports

A Monthly Publication of the National Aeronautics and Space Administration

01 AERONAUTICS (GENERAL)

N94-26212# National Aerospace Lab., Amsterdam (Netherlands).
TECHNICAL AND SCIENTIFIC RESEARCH FOR AERONAUTICS AND ASTRONAUTICS [TECHNISCH-WETENSCHAPPELIJK ONDERZOEK VOOR LUCHT- EN RUIMTEVAART]
Dec. 1992 18 p In DUTCH
(ETN-94-95392) Avail: CASI HC A03/MF A01

The activities of the National Aerospace Laboratory (NLR) are surveyed. In the field of aerodynamics research, activities are conducted in the low speed, high speed, supersonic, and Dutch-German wind tunnels, and in the laboratory for propulsion aerodynamics and aeroacoustics. In the domain of aircraft and helicopters, flight tests are performed, and research is conducted on two laboratory aircraft, a flight simulator, and an air traffic simulator. In the construction and materials division loading and fatigue of aircraft structures, as well as new materials, are investigated. In the field of astronautics, satellite positioning; microgravity; automation and robotics; temperature control; and Earth observation are studied. Information systems for aerospace applications are developed. Aerospace pollution and environmental control by aircrafts and satellites are investigated. ESA

N94-26596*# National Aeronautics and Space Administration. Ames Research Center, Moffett Field, CA.
SHAKE TEST RESULTS OF THE MDHC TEST STAND IN THE 40- BY 80-FOOT WIND TUNNEL
Benton H. Lau and Randall Peterson Jan. 1994 40 p
(RTOP 505-59-36)
(NASA-TM-108801; A-94029; NAS 1.15:108801) Avail: CASI HC A03/MF A01

A shake test was conducted to determine the modal properties of the MDHC (McDonnell Douglas Helicopter Company) test stand installed in the 40- by 80- Foot Wind Tunnel at Ames Research Center. The shake test was conducted for three wind-tunnel balance configurations with and without balance dampers, and with the snubber engagement to lock the balance frame. A hydraulic shaker was used to apply random excitation at the rotor hub in the longitudinal and lateral directions. A GenRad 2515 computer-aided test system computed the frequency response functions at the rotor hub and support struts. From these response functions, the modal properties, including the natural frequency, damping ratio, and mode shape were calculated. The critical modes with low damping ratios are identified as the test-stand second longitudinal mode for the dampers-off configuration, the test-stand yaw mode for the dampers-on configuration, and the test stand first longitudinal mode for the balance-frame locked configuration. Author

N94-27284*# National Aeronautics and Space Administration. Langley Research Center, Hampton, VA.
FAA/NASA JOINT UNIVERSITY PROGRAM FOR AIR TRANSPORTATION RESEARCH, 1992-1993
Frederick R. Morrell, Comp. Feb. 1994 161 p Conference held in Athens, OH, 17-18 Jun. 1993; sponsored in part by FAA
(Grants NGL-22-009-640; NGL-31-001-252; NGR-36-009-017)
(NASA-CP-3246; NAS 1.55:3246; DOT/FAA/CT-94/03) Avail: CASI HC A08/MF A02

The research conducted during the academic year 1992-1993 under the FAA/NASA sponsored Joint University Program for Air Transportation Research is summarized. The year end review was held at Ohio University, Athens, Ohio, 17-18 June 1993. The Joint University Program is a coordinated set of three grants sponsored by the Federal Aviation Administration and NASA Langley Research Center, one each with the Massachusetts Institute of Technology, Ohio University, and Princeton University. Completed works, status reports, and annotated bibliographies are presented for research topics, which include navigation, guidance, and control theory and practice, aircraft performance, human factors and air traffic management. An overview of the year's activities for each university is also presented. For individual titles, see N94-27285 through N94-27298.

N94-27285*# Massachusetts Inst. of Tech., Cambridge. Flight Transportation Lab.
AN INVESTIGATION OF AIR TRANSPORTATION TECHNOLOGY AT THE MASSACHUSETTS INSTITUTE OF TECHNOLOGY, 1992-1993 c03
Robert W. Simpson *In* NASA. Langley Research Center, FAA/NASA Joint University Program for Air Transportation Research, 1992-1993 Feb. 1994 p 3-8 (For primary document see N94-27284 07-01)
Avail: CASI HC A02/MF A02

An investigation of air transportation technology at MIT during 1992 - 1993 is presented. One completed project and two continuing research activities are under the sponsorship of the FAA/NASA Joint University Program. The completed project was on tracking aircraft around a turn with wind effects. Active research projects are on ASLOTS - an interactive adaptive system of automated approach spacing of aircraft and alerting in automated and datalink capable cockpits. Author (revised)

N94-27286*# Massachusetts Inst. of Tech., Cambridge. Dept. of Aeronautics and Astronautics.
A GRAPHICAL WORKSTATION BASED PART-TASK FLIGHT SIMULATOR FOR PRELIMINARY RAPID EVALUATION OF ADVANCED DISPLAYS c06
Craig Wanke, James Kuchar, Edward Hahn, A. Pritchett, and R. John Hansman *In* NASA. Langley Research Center, FAA/NASA Joint University Program for Air Transportation Research, 1992-1993 Feb. 1994 p 9-15 See also A94-11991 Submitted for publication (For primary document see N94-27284 07-01)
(Contract NAG2-12; NAG2-716; NAG1-690; NGL-22-009-640; DTRS57-88-C-0078TD39; NSF MSS-85-52702; BARR-10-119)
Avail: CASI HC A02/MF A02

Advances in avionics and display technology are significantly changing the cockpit environment in current transport aircraft. The MIT Aeronautical Systems Lab (ASL) developed a part-task flight simulator specifically to study the effects of these new technologies on flight crew situational awareness and performance. The simulator is based on a commercially-available graphics workstation, and can be rapidly reconfigured to meet the varying demands of experimental studies. The simulator was successfully used to evaluate graphical microbursts alerting displays, electronic instrument approach plates, terrain awareness and alerting displays, and ATC routing amendment delivery through digital datalinks. Author (revised)

N94-27287*# Massachusetts Inst. of Tech., Cambridge. Dept. of Aeronautics and Astronautics.
A DATA FUSION ALGORITHM FOR MULTI-SENSOR MICROBURST HAZARD ASSESSMENT c03
Craig R. Wanke and R. John Hansman *In* NASA. Langley Research Center, FAA/NASA Joint University Program for Air Transportation Research, 1992-1993 Feb. 1994 p 17-28 See also A92-55328 Submitted for

publication Sponsored in part by FAA (For primary document see N94-27284 07-01)
(Contract NGL-22-009-640; F19628-90-C-0002)
Avail: CASI HC A03/MF A02

A recursive model-based data fusion algorithm for multi-sensor microburst hazard assessment is described. An analytical microburst model is used to approximate the actual windfield, and a set of 'best' model parameters are estimated from measured winds. The winds corresponding to the best parameter set can then be used to compute alerting factors such as microburst position, extent, and intensity. The estimation algorithm is based on an iterated extended Kalman filter which uses the microburst model parameters as state variables. Microburst state dynamic and process noise parameters are chosen based on measured microburst statistics. The estimation method is applied to data from a time-varying computational simulation of a historical microburst event to demonstrate its capabilities and limitations. Selection of filter parameters and initial conditions is discussed. Computational requirements and datalink bandwidth considerations are also addressed. Author

N94-27288*# Ohio Univ., Athens. Dept. of Electrical and Computer Engineering.
INVESTIGATION OF AIR TRANSPORTATION TECHNOLOGY AT OHIO UNIVERSITY, 1992-1993 c03
Robert W. Lilley *In* NASA. Langley Research Center, FAA/NASA Joint University Program for Air Transportation Research, 1992-1993 Feb. 1994 p 31-33 (For primary document see N94-27284 07-01)
Avail: CASI HC A01/MF A02

The Joint University Program in Air Transportation Systems provides opportunities for progress by students, staff and faculty at the Avionics Engineering Center, Ohio University. During the 1992-93 year, four conference papers and two M.S. theses were produced; these are summarized in the bibliography. The conference papers are included in their entirety, for reference. Author

N94-27289*# Ohio Univ., Athens.
FAULT DETECTION AND ISOLATION c38
Greg Bernath *In* NASA. Langley Research Center, FAA/NASA Joint University Program for Air Transportation Research, 1992-1993 Feb. 1994 p 35-43 Sponsored in part by FAA (For primary document see N94-27284 07-01)
(Grant NGR-36-009-17)
Avail: CASI HC A02/MF A02

In order for a current satellite-based navigation system (such as the Global Positioning System, GPS) to meet integrity requirements, there must be a way of detecting erroneous measurements, without help from outside the system. This process is called Fault Detection and Isolation (FDI). Fault detection requires at least one redundant measurement, and can be done with a parity space algorithm. The best way around the fault isolation problem is not necessarily isolating the bad measurement, but finding a new combination of measurements which excludes it. Author

N94-27290*# Ohio Univ., Athens. Avionics Engineering Center.
IMPROVED MODELING OF GPS SELECTIVE AVAILABILITY c04
Michael S. Braasch, AnnMarie Fink, and Keith Duffus *In* NASA. Langley Research Center, FAA/NASA Joint University Program for Air Transportation Research, 1992-1993 Feb. 1994 p 45-54 Presented at the Institute of Navigation 1993 National Technical Meeting, San Francisco, CA, 20-22 Jan. 1993 (For primary document see N94-27284 07-01)
(Grant NGR-36-009-017)
Avail: CASI HC A02/MF A02

Selective Availability (SA) represents the dominant error source for stand-alone users of the Global Positioning System (GPS). Even for DGPS, SA mandates the update rate required for a desired level of accuracy in realtime applications. As was witnessed in the recent literature, the ability to model this error source is crucial to the proper evaluation of GPS-based systems. A variety of SA models were proposed to date; however, each has its own shortcomings. Most of these models were based on limited data sets or data which were corrupted by additional error sources. A comprehensive treatment of the problem is presented. The phenomenon of SA is discussed and a technique is presented whereby both clock and orbit components of SA are identifiable. Extensive SA data sets collected from Block 2 satellites are presented. System Identification theory then is used to derive a robust model of SA from the data. This theory also allows for the statistical analysis of SA. The stationarity of SA over time and across different satellites is analyzed and its impact on the modeling problem is discussed. Author

N94-27291*# Ohio Univ., Athens. Avionics Engineering Center.
REALTIME MITIGATION OF GPS SA ERRORS USING LORAN-C c04
Soo Y. Braasch *In* NASA. Langley Research Center, FAA/NASA Joint University Program for Air Transportation Research, 1992-1993 Feb. 1994 p 55-61 Presented at the Wild Goose Association, Annual Convention and Technical Symposium, Birmingham, England, 24-27 Aug. 1992 Sponsored in part by FAA (For primary document see N94-27284 07-01)
(Grant NGR-36-009-17)
Avail: CASI HC A02/MF A02

The hybrid use of Loran-C with the Global Positioning System (GPS) was shown capable of providing a sole-means of enroute air radionavigation. By allowing pilots to fly direct to their destinations, use of this system is resulting in significant time savings and therefore fuel savings as well. However, a major error source limiting the accuracy of GPS is the intentional degradation of the GPS signal known as Selective Availability (SA). SA-induced position errors are highly correlated and far exceed all other error sources (horizontal position error: 100 meters, 95 percent). Realtime mitigation of SA errors from the position solution is highly desirable. How that can be achieved is discussed. The stability of Loran-C signals is exploited to reduce SA errors. The theory behind this technique is discussed and results using bench and flight data are given. Author (revised)

N94-27292*# Ohio Univ., Athens. Avionics Engineering Center.
A GPS COVERAGE MODEL c04
Trent A. Skidmore *In* NASA. Langley Research Center, FAA/NASA Joint University Program for Air Transportation Research, 1992-1993 Feb. 1994 p 63-72 Presented at the Institute of Navigation 1992 National Technical Meeting, Washington, DC, 29 Jun. - 1 Jul. 1992 See also A94-12567 (For primary document see N94-27284 07-01)
(Contract NGR-36-009-017; DTRS57-87-C-00006)
Avail: CASI HC A02/MF A02

The results of several case studies using the Global Positioning System coverage model developed at Ohio University are summarized. Presented are results pertaining to outage area, outage dynamics, and availability. Input parameters to the model include the satellite orbit data, service area of interest, geometry requirements, and horizon and antenna mask angles. It is shown for precision-landing Category 1 requirements that the planned GPS 21 Primary Satellite Constellation produces significant outage area and unavailability. It is also shown that a decrease in the user equivalent range error dramatically decreases outage area and improves the service availability. Author (revised)

N94-27293*# Ohio Univ., Athens.
GROUND STATION SITING CONSIDERATIONS FOR DGPS c04
James D. Waid *In* NASA. Langley Research Center, FAA/NASA Joint University Program for Air Transportation Research, 1992-1993 Feb. 1994 p 73-83 Presented at the Institute of Navigation 1993 National Technical Meeting, San Francisco, CA, 20-22 Jan. 1993 Sponsored in part by FAA (For primary document see N94-27284 07-01)
(Grants NAG1-1423; NGR-36-009-017)
Avail: CASI HC A03/MF A02

Aircraft guidance and positioning in the final approach and landing phases of flight requires a high degree of accuracy. The Global Positioning System operating in differential mode (DGPS) is being considered for this application. Prior to implementation, all sources of error must be considered. Multipath was shown to be the dominant source of error for DGPS and theoretical studies verified that multipath is particularly severe within the final approach and landing regions. Because of aircraft dynamics, the ground station segment of DGPS is the part of the system where multipath can most effectively be reduced. Ground station siting will be a key element in reducing multipath errors for DGPS system. This situation can also be improved by using P-code or narrow correlator C/A-code receivers along with a multipath rejecting antenna. A study of GPS multipath errors for a stationary DGPS ground station is presented. A discussion of GPS multipath error characteristics are presented along with some actual multipath data.

The data was collected for different ground station siting configurations using P-code, standard C/A-code, and narrow correlator C/A-code receiver architectures and two separate antenna constructions. Author (revised)

N94-27294*# Princeton Univ., NJ. Dept. of Mechanical and Aerospace Engineering.
INVESTIGATION OF AIR TRANSPORTATION TECHNOLOGY AT PRINCETON UNIVERSITY, 1992-1993 **c03**
Robert F. Stengel *In* NASA. Langley Research Center, FAA/NASA Joint University Program for Air Transportation Research, 1992-1993 Feb. 1994 p 87-97 (For primary document see N94-27284 07-01)
Avail: CASI HC A03/MF A02

The Air Transportation Research Program at Princeton University proceeded along five avenues during the past year: (1) Flight Control System Robustness; (2) Microburst Hazards to Aircraft; (3) Wind Rotor Hazards to Aircraft; (4) Intelligent Aircraft/Airspace Systems; and (5) Aerospace Optical Communications. This research resulted in a number of publications, including theses, archival papers, and conference papers. An annotated bibliography of publications that appeared between June 1992 and June 1993 is included. The research that these papers describe was supported in whole or in part by the Joint University Program, including work that was completed prior to the reporting period. Author (revised)

N94-27295*# Princeton Univ., NJ. Lab. for Control and Automation.
DESIGNING ROBUST CONTROL LAWS USING GENETIC ALGORITHMS **c61**
Chris Marrison *In* NASA. Langley Research Center, FAA/NASA Joint University Program for Air Transportation Research, 1992-1993 Feb. 1994 p 99-109 (For primary document see N94-27284 07-01)
Avail: CASI HC A03/MF A02

The purpose of this research is to create a method of finding practical, robust control laws. The robustness of a controller is judged by Stochastic Robustness metrics and the level of robustness is optimized by searching for design parameters that minimize a robustness cost function. Author

N94-27296*# Princeton Univ., NJ. Dept. of Mechanical and Aerospace Engineering.
OPTIMAL NONLINEAR ESTIMATION FOR AIRCRAFT FLIGHT CONTROL IN WIND SHEAR **c03**
Sandeep S. Mulgund *In* NASA. Langley Research Center, FAA/NASA Joint University Program for Air Transportation Research, 1992-1993 Feb. 1994 p 111-130 (For primary document see N94-27284 07-01)
Avail: CASI HC A03/MF A02

The most recent results in an ongoing research effort at Princeton in the area of flight dynamics in wind shear are described. The first undertaking in this project was a trajectory optimization study. The flight path of a medium-haul twin-jet transport aircraft was optimized during microburst encounters on final approach. The assumed goal was to track a reference climb rate during an aborted landing, subject to a minimum airspeed constraint. The results demonstrated that the energy loss through the microburst significantly affected the qualitative nature of the optimal flight path. In microbursts of light to moderate strength, the aircraft was able to track the reference climb rate successfully. In severe microbursts, the minimum airspeed constraint in the optimization forced the aircraft to settle on a climb rate smaller than the target. A tradeoff was forced between the objectives of flight path tracking and stall prevention. Author (revised)

N94-27297*# Princeton Univ., NJ. Dept. of Mechanical and Aerospace Engineering.
AIR TRAFFIC MANAGEMENT AS PRINCIPLED NEGOTIATION BETWEEN INTELLIGENT AGENTS **c04**
J. P. Wangermann *In* NASA. Langley Research Center, FAA/NASA Joint University Program for Air Transportation Research, 1992-1993 Feb. 1994 p 131-140 (For primary document see N94-27284 07-01)
Avail: CASI HC A02/MF A02

The major challenge facing the world's aircraft/airspace system (AAS) today is the need to provide increased capacity, while reducing delays, increasing the efficiency of flight operations, and improving safety. Technologies are emerging that should improve the performance of the system, but which could also introduce uncertainty, disputes, and inefficiency if not properly implemented. The aim of our research is to apply techniques from intelligent control theory and decision-making theory to define an Intelligent Aircraft/Airspace System (IAAS) for the year 2025. The IAAS would make effective use of the technical capabilities of all parts of the system to meet the demand for increased capacity with improved performance. Author

N94-27298*# Princeton Univ., NJ. Dept. of Mechanical and Aerospace Engineering.
OPTICAL COMMUNICATIONS FOR TRANSPORT AIRCRAFT **c32**
Robert Stengel *In* NASA. Langley Research Center, FAA/NASA Joint University Program for Air Transportation Research , 1992-1993 Feb. 1994 p 141-145 (For primary document see N94-27284 07-01)
Avail: CASI HC A01/MF A02

Optical communications for transport aircraft are discussed. The problem involves: increasing demand for radio-frequency bands from an enlarging pool of users (aircraft, ground and sea vehicles, fleet operators, traffic control centers, and commercial radio and television); desirability of providing high-bandwidth dedicated communications to and from every aircraft in the National Airspace System; need to support communications, navigation, and surveillance for a growing number of aircraft; and improved meteorological observations by use of probe aircraft. The solution involves: optical signal transmission support very high data rates; optical transmission of signals between aircraft, orbiting satellites, and ground stations, where unobstructed line-of-sight is available; conventional radio transmissions of signals between aircraft and ground stations, where optical line-of-sight is unavailable; and radio priority given to aircraft in weather. CASI

N94-27960# Federal Aviation Administration, Washington, DC.
THE 1993 FEDERAL AVIATION ADMINISTRATION PLAN FOR RESEARCH, ENGINEERING AND DEVELOPMENT
Feb. 1994 198 p
Avail: CASI HC A09/MF A03

The FAA manages and operates the National Airspace System (NAS), a significant national resource. However, the demands on this system are continuously growing, and changing technologies provide the opportunity to dramatically improve system effectiveness and efficiency. To this end, the FAA's Research, Engineering, and Development (RE&D) Program is an investment in the future that will sustain the United States' preeminence in aviation throughout the world. Without this investment, the United States leadership would erode. Thus, the importance of aviation to the Nation mandates a comprehensive RE&D program to ensure both the safety of public air transportation and the fulfillment of national priorities and policy goals. Various aspects of the RE&D Program plan are discussed. Derived from text

N94-28203* National Aeronautics and Space Administration, Washington, DC.
AERONAUTICAL ENGINEERING: A CONTINUING BIBLIOGRAPHY WITH INDEXES (SUPPLEMENT 301)
Feb. 1994 367 p
(NASA-SP-7037(301); NAS 1.21:7037(301)) Avail: CASI HC A16

This bibliography lists 1291 reports, articles, and other documents introduced into the NASA scientific and technical information system in Feb. 1994. Subject coverage includes: design, construction and testing of aircraft and aircraft engines; aircraft components, equipment, and systems; ground support systems; and theoretical and applied aspects of aerodynamics and general fluid dynamics. Author

02 AERODYNAMICS

Includes aerodynamics of bodies, combinations, wings, rotors, and control surfaces; and internal flow in ducts and turbomachinery.

For related information see also *34 Fluid Mechanics and Heat Transfer.*

N94-25592# Air Force Inst. of Tech., Wright-Patterson AFB, OH. School of Engineering.
EVALUATION OF A CONCENTRATION PROBE FOR APPLICATION IN A SUPERSONIC FLOW FIELD M.S. Thesis
John S. Alsup Dec. 1993 67 p
(AD-A273915; AFIT/GAE/ENY/93D-3) Avail: CASI HC A04/MF A01

Aspirating, concentration probes are used to measure binary gas concentrations in a supersonic flow. In the past, a tank discharge method has been used to calibrate concentration probes. An alternate calibration method has been developed and tested on a probe in a steady, subsonic/sonic flow. This study evaluated the calibration and performance of a concentration probe in a steady, supersonic flow over a range of mixture ratios of air and helium. The results of this study and a comparison of the two calibration methods are presented. DTIC

N94-26104# Aeronautical Research Inst. of Sweden, Stockholm. Aerodynamics Dept.

CALCULATION OF VISCOUS DRAG OF TWO LOW ANGLE OF ATTACK SUPERCRITICAL PROFILES [BERAEKNING AV VISKOESA MOTSTAANDET FOER TVAA SUPERKRISTISKA PROFILER VID LAAGA ANFALLSVINKLAR]

S. Paaso 3 May 1984 40 p In SWEDISH Sponsored by Foersvarets Materialverk, Stockholm, Sweden
(FFA-TN-1984-22; ETN-94-93902) Avail: CASI HC A03/MF A01

Two supercritical profile calculations were carried out to determine which profile is better at subcritical Mach numbers. The tests were carried out on natural scale Reynolds numbers and on prototype Reynolds numbers. The NACA 64A010 profile was included in the test to check control the results obtained by the programs and the formulas used and to compare the supercritical profiles with a NACA type profile. The supercritical profiles appeared to have similar drag curves, and the NACA 64A010 showed lower drag at low angle of attack. The prototype drag profiles differ a little in relation to the natural profile. ESA

N94-26131*# Sverdrup Technology, Inc., Brook Park, OH.

PERFORMANCE OF RENORMALIZATION GROUP ALGEBRAIC TURBULENCE MODEL ON BOUNDARY LAYER TRANSITION SIMULATION Final Report

Kyung H. Ahn Feb. 1994 19 p
(Contract NAS3-25266; RTOP 535-03-10)
(NASA-CR-194466; E-8521; NAS 1.26:194466) Avail: CASI HC A03/MF A01

The RNG-based algebraic turbulence model, with a new method of solving the cubic equation and applying new length scales, is introduced. An analysis is made of the RNG length scale which was previously reported and the resulting eddy viscosity is compared with those from other algebraic turbulence models. Subsequently, a new length scale is introduced which actually uses the two previous RNG length scales in a systematic way to improve the model performance. The performance of the present RNG model is demonstrated by simulating the boundary layer flow over a flat plate and the flow over an airfoil. Author (revised)

N94-26143*# National Aeronautics and Space Administration. Ames Research Center, Moffett Field, CA.

CORRELATION OF AIRLOADS ON A TWO-BLADED HELICOPTER ROTOR

Francisco J. Fernandez and Wayne Johnson (Johnson Aeronautics, Palo Alto, CA.) Apr. 1993 26 p
(RTOP 505-59-36)
(NASA-TM-103982; A-93001; NAS 1.15:103982) Avail: CASI HC A03/MF A01

Airloads measured on a two-bladed helicopter rotor in flight during the Ames' Tip Aerodynamic and Acoustic Test are compared with calculations from a comprehensive helicopter analysis (CAMRAD/JA), and the pressures compared with calculations from a full-potential rotor code (FPR). The flight-test results cover an advance ratio range of 0.19 to 0.38. The lowest-speed case is characterized by the presence of significant blade-vortex interactions. Good correlation of peak-to-peak vortex-induced loads and the corresponding pressures is obtained. Results of the correlation for this two-bladed rotor are substantially similar to those for three- and four-bladed rotors, including the tip-vortex core size for best correlation, calculation of the peak-to-peak loads on the retreating side, and calculation of vortex iduced loads on inboard radial stations. The higher-speed cases are characterized by the presence of transonic flow on the outboard sections of the blade. Comparison of calculated and measured airloads on the advancing side is not considered appropriate because the presence of shocks makes chordwise integration of the measured data difficult. However, good correlation of the corresponding pressures is obtained. Author

N94-26154*# National Aeronautics and Space Administration. Langley Research Center, Hampton, VA.

COMMENTS REGARDING TWO UPWIND METHODS FOR SOLVING TWO-DIMENSIONAL EXTERNAL FLOWS USING UNSTRUCTURED GRIDS

W. L. Kleb Feb. 1994 29 p
(RTOP 232-01-04-04)
(NASA-TM-109078; NAS 1.15:109078) Avail: CASI HC A03/MF A01

Steady flow over the leading portion of a multicomponent airfoil section is studied using computational fluid dynamics (CFD) employing an unstructured grid. To simplify the problem, only the inviscid terms are retained from the Reynolds-averaged Navier-Stokes equations - leaving the Euler equations. The algorithm is derived using the finite-volume approach, incorporating explicit time-marching of the unsteady Euler equations to a time-asymptotic, steady-state solution. The inviscid fluxes are obtained through either of two approximate Riemann solvers: Roe's flux difference splitting or van Leer's flux vector splitting. Results are presented which contrast the solutions given by the two flux functions as a function of Mach number and grid resolution. Additional information is presented concerning code verification techniques, flow recirculation regions, convergence histories, and computational resources. Author (revised)

N94-26191# Naval Postgraduate School, Monterey, CA.

COMPUTATIONAL INVESTIGATION OF THE COMPRESSIBLE DYNAMIC STALL CHARACTERISTICS OF THE SIKORSKY SSC-A09 AIRFOIL M.S. Thesis

Thomas A. Johnston Sep. 1993 260 p
(AD-A274867) Avail: CASI HC A12/MF A03

Steady and unsteady two dimensional flowfield analysis was conducted for a Sikorsky SSC-A09 airfoil in compressible, high Reynolds number flows. Limited verification with experimental measurement was achieved. Computational methods included a steady, linear panel method with compressibility corrections; a laminar and turbulent boundary layer method; an unsteady, linear panel method; and a numerical solution method of the thin layer, compressible Navier-Stokes equations using a body-fitted C-type computational grid. The Baldwin-Lomax, two-layer, zero-equation turbulence model was used. Wind tunnel wall interference effects were ignored. Steady and unsteady airloads and instantaneous flow pictures are presented. In steady flow with little or no separation, computed lift, drag, pitching moment, and skin friction coefficients, as well as displacement thickness and boundary layer velocity profiles at several angles of attack, were generally found to be in good agreement with experimental data. DTIC

N94-26248# Imperial Coll. of Science and Technology, London (England). Dept. of Aeronautics.

MODELLING OF IONISATION REACTIONS AND OF THE RESULTING ELECTRIC FIELDS IN ONE-DIMENSIONAL HYPERSONIC SHOCK WAVES WITH THE DIRECT SIMULATION MONTE CARLO METHOD

M. A. Gallis and J. K. Harvey Jul. 1992 13 p
(Contract AT/2037/331) (ISSN 0308-7247)
(IC-Aero-92-01; ETN-94-95226) Avail: CASI HC A03/MF A01

The direct simulation Monte Carlo method is applied to ionized hypersonic rarefied flows. Calculations of the reaction rates are made with the method proposed by G.A. Bird and with the maximum entropy approach, which is extended to include reactions between monatomic and ionized particles. The assumptions made for the simulation of plasmas are discussed. A method for the treatment of electrons and the calculation of the electric field is described. The new approach for modeling plasmas is compared with the current modeling technique and both methods are compared with experimental data. Calculations for two normal shock wave test cases were performed: a real air test case at Mach 29 and an atomic hydrogen test case at Mach 60. The approach is in good agreement with the experimental data and offers a better explanation of the effects of nonequilibrium phenomena in the flow. ESA

N94-26342# Aeronautical Research Labs., Melbourne (Australia).

LOW-SPEED PRESSURE DISTRIBUTION MEASUREMENTS OVER THE AFT-FUSELAGE, FINS, AND STABILATORS OF A 1/9TH SCALE F/A-18 WIND-TUNNEL MODEL

L. D. MacLaren and H. A. Quick Oct. 1993 93 p
(AD-A274870; ARL-RR-9; DODA-AR-008-367) Avail: CASI HC A05/MF A01

The steady-state aerodynamic pressure distribution over the aft fuselage, fin and stabilator of a 1/9th scale F/A-18 model has been measured for varying conditions at low speeds. Pressure distributions are presented in the form of a parametric study and the integration of the pressures to obtain total loads is included to indicate the overall effects of angle of attack, sideslip, stabilator deflection and the LEX fence. The results from these wind tunnel tests have illustrated the degree to which vortical flow dominates the conditions over the aft end of the aircraft, due to the presence of the primary LEX vortex and to local separations from sharp edged surfaces. DTIC

N94-26483*# National Aeronautics and Space Administration. Langley Research Center, Hampton, VA.

INVESTIGATION OF THE AERODYNAMIC ENVIRONMENT FOR AN ADVANCED LIGHTWEIGHT ROTOR IN FORWARD FLIGHT. VOLUME 4: LASER VELOCIMETER WAKE DATA, ADVANCE RATIO OF 0.037 (Diskette Supplement)

W. Derry Mace (Lockheed Engineering and Sciences Co., Hampton, VA.), Joe W. Elliott, Martin A. Peryea (Bell Helicopter Co., Fort Worth, TX.), Albert G. Brand (Bell Helicopter Co., Fort Worth, TX.), and Tom L. Wood (Bell Helicopter Co., Fort Worth, TX.) Nov. 1993 423 p Sponsored by Army Aviation and Troop Command, St. Louis, MO Diskette supplement: IBM compatible 1.4 Mbyte 3.5-inch diskette in MS-DOS format
(RTOP 505-59-87-85; DA Proj. 1L1-61102-AH-45)
(NASA-TM-109040-Vol-4; NAS 1.15:109040-Vol-4;
ATCOM-TR-93-A-012-Vol-4; NONP-Suppl-DK-94-205048) Avail: CASI SET A22 (HC,DK)

An Advanced Lightweight Rotor (ALR) model was tested in high-speed forward flight, mu = 0.37, at the 14- by 22-Foot Subsonic Tunnel at LaRC. A two-component laser velocimeter was used to obtain azimuthally dependent velocities in the inflow region and in the wake of the rotor. Data are presented without analysis. Author (revised)

N94-26489*# National Aeronautics and Space Administration. Langley Research Center, Hampton, VA.

INVESTIGATION OF THE AERODYNAMIC ENVIRONMENT FOR AN ADVANCED LIGHTWEIGHT ROTOR IN FORWARD FLIGHT. VOLUME 1: LASER VELOCIMETER INFLOW DATA, ADVANCE RATIO OF 0.37, THRUST COEFFICIENT OF 0.0081 AND HOVER TIP SPEED OF 603 FEET/SECOND (Diskette Supplement)

W. Derry Mace (Lockheed Engineering and Sciences Co., Hampton, VA.), Joe W. Elliott (Army Aviation Systems Command, Hampton, VA.), Martin A. Peryea (Textron Bell Helicopter, Fort Worth, TX.), Albert G. Brand (Textron Bell Helicopter, Fort Worth, TX.), and Tom L. Wood (Textron Bell Helicopter, Fort Worth, TX.) Nov. 1993 383 p Diskette supplement: IBM compatible 1.4 Mbyte 3.5-inch diskette in MS-DOS format
(RTOP 505-59-87-85; DA Proj. 1L1-61102-AH-45)
(NASA-TM-109040-Vol-1; NAS 1.15:109040-Vol-1;
ATCOM-TR-93-A-012-Vol-1; NONP-Suppl-DK-94-205049) Avail: CASI SET A22 (HC,DK)

An Advanced Lightweight Rotor (ALR) model was tested in high-speed forward flight, mu = 0.37, at the 14- by 22-Foot Subsonic Tunnel at LaRC. A two-component laser velocimeter was used to obtain azimuthally dependent velocities in the inflow region and in the wake of the rotor. Data are presented without analysis. Author (revised)

N94-26492*# National Aeronautics and Space Administration. Langley Research Center, Hampton, VA.

INVESTIGATION OF THE AERODYNAMIC ENVIRONMENT FOR AN ADVANCED LIGHTWEIGHT ROTOR IN FORWARD FLIGHT. VOLUME 2: LASER VELOCIMETER INFLOW DATA, ADVANCE RATIO OF 0.37, THRUST COEFFICIENT OF 0.0064 AND HOVER TIP SPEED OF 710 FEET/SECOND (Diskette Supplement)

W. Derry Mace (Lockheed Engineering and Sciences Co., Hampton, VA.), Joe W. Elliott (Army Aviation Systems Command, Fort Eustis, VA.), Martin A. Peryea (Textron Bell Helicopter, Fort Worth, TX.), Albert G. Brand (Textron Bell Helicopter, Fort Worth, TX.), and Tom L. Wood (Textron Bell Helicopter, Fort Worth, TX.) Nov. 1993 381 p Diskette supplement: IBM compatible 1.4 Mbyte 3.5-inch diskette in MS-DOS format
(RTOP 505-59-87-85; DA Proj. 1L1-61102-AH-45)
(NASA-TM-109040-Vol-2; NAS 1.15:109040-Vol-2;
ATCOM-TR-93-A-012-Vol-2; NONP-Suppl-DK-94-205050) Avail: CASI SET A22 (HC,DK)

An Advanced Lightweight Rotor (ALR) model was tested in high-speed forward flight, mu = 0.37, at the 14- by 22-Foot Subsonic Tunnel at LaRC. A two-component laser velocimeter was used to obtain azimuthally dependent velocities in the inflow region and in the wake of the rotor. Data are presented without analysis. Author (revised)

N94-26497*# National Aeronautics and Space Administration. Langley Research Center, Hampton, VA.

INVESTIGATION OF THE AERODYNAMIC ENVIRONMENT FOR AN ADVANCED LIGHTWEIGHT ROTOR IN FORWARD FLIGHT. VOLUME 3: LASER VELOCIMETER INFLOW DATA, ADVANCE RATIO OF 0.37, THRUST COEFFICIENT OF 0.0064 AND HOVER TIP SPEED OF 603 FEET/SECOND (Diskette Supplement)

W. Derry Mace (Lockheed Engineering and Sciences Co., Hampton, VA.), Joe W. Elliott (Army Aviation Systems Command, Hampton, VA.), Martin A. Peryea (Textron Bell Helicopter, Fort Worth, TX.), Albert G. Brand (Textron Bell Helicopter, Fort Worth, TX.), and Tom L. Wood (Textron Bell Helicopter, Fort Worth, TX.) Nov. 1993 384 p Diskette supplement: IBM compatible 1.4 Mbyte 3.5-inch diskette in MS-DOS format
(RTOP 505-59-87-85; DA Proj. 1L1-61102-AH-45)
(NASA-TM-109040-Vol-3; NAS 1.15:109040-Vol-3;
ATCOM-TR-93-A-012-Vol-3; NONP-Suppl-DK-94-209487) Avail: CASI SET A22 (HC,DK)

An Advanced Lightweight Rotor (ALR) model was tested in high-speed forward flight, mu = 0.37, at the 14- by 22-Foot Subsonic Tunnel at LaRC. A two-component laser velocimeter was used to obtain azimuthally dependent velocities in the inflow region and in the wake of the rotor. Data are presented without analysis. Author (revised)

N94-26535# Naval Postgraduate School, Monterey, CA.

A FINITE WAKE THEORY FOR TWO-DIMENSIONAL ROTARY WING UNSTEADY AERODYNAMICS M.S. Thesis

Mark A. Couch 23 Sep. 1993 69 p
(AD-A274921) Avail: CASI HC A04/MF A01

The unsteady aerodynamic forces and moments of an oscillating airfoil for the fixed wing case were determined by Theodorsen along with the development of a lift deficiency function. Loewy subsequently developed an analogous lift deficiency function for the rotary wing case in which there are an infinite number of layers of shed vorticity, or wakes, below the reference airfoil. With the advent of computer panel codes that calculate the time histories of the wakes generated by oscillating airfoils, a theory is developed for the rotary wing case in which there are a finite number of layers of shed vorticity below the reference airfoil. This theory includes a lift deficiency function that is completely analogous to Loewy and Theodorsen. It has long been recognized that an airfoil oscillating in pure plunge produces a propulsive force (Katzmayr effect). Garrick used Theodorsen's work to develop equations for the propulsive force that include the lift deficiency function as a parameter. When either Loewy's lift deficiency function or the finite wake lift deficiency function is used, the effect of the propulsive force is greatly enhanced with the proper phase relationship of the wakes. The finite wake theory along with Garrick's work is used to describe the performance characteristics of Higher Harmonic Control. Specifically for the OH-6A, coupled pitch-plunge motion results in a propulsive force that significantly reduces the rotor drag force. DTIC

N94-26538*# National Aeronautics and Space Administration. Ames Research Center, Moffett Field, CA.

A COMPARATIVE STUDY OF SERIAL AND PARALLEL AEROELASTIC COMPUTATIONS OF WINGS

Chansup Byun (MCAT Inst., Moffett Field, CA.) and Guru P. Guruswamy Jan. 1994 24 p
(RTOP 505-10-11)
(NASA-TM-108805; A-94039; NAS 1.15:108805) Avail: CASI HC A03/MF A01

A procedure for computing the aeroelasticity of wings on parallel multiple-instruction, multiple-data (MIMD) computers is presented. In this procedure, fluids are modeled using Euler equations, and structures are modeled using modal or finite element equations. The procedure is designed in such a way that each discipline can be developed and maintained independently by using a domain decomposition approach. In the present

parallel procedure, each computational domain is scalable. A parallel integration scheme is used to compute aeroelastic responses by solving fluid and structural equations concurrently. The computational efficiency issues of parallel integration of both fluid and structural equations are investigated in detail. This approach, which reduces the total computational time by a factor of almost 2, is demonstrated for a typical aeroelastic wing by using various numbers of processors on the Intel iPSC/860.
Author (revised)

N94-26547*# National Aeronautics and Space Administration. Langley Research Center, Hampton, VA.
COMPUTATIONAL PREDICTION OF ISOLATED PERFORMANCE OF AN AXISYMMETRIC NOZZLE AT MACH NUMBER 0.90
John R. Carlson Feb. 1994 26 p
(RTOP 505-62-30-01)
(NASA-TM-4506; L-17248; NAS 1.15:4506) Avail: CASI HC A03/MF A01

An improved ability to predict external propulsive performance was incorporated into the three-dimensional Navier-Stokes code PAB3D. The improvements are the ability to account for skin friction and external pressure forces. Performance parameters for two axisymmetric supersonic cruise nozzle configurations were calculated to test the improved methodology. Internal and external flow-field regions were computed using a two-equation kappa-epsilon turbulent viscous-stress model. The computed thrust-minus-drag ratios were within 1 percent of the absolute level of experimental data and the trends of data were predicted accurately. The predicted trend of integrated nozzle pressure drag matched the trend of the integrated experimental pressure drag over a range of nozzle pressure ratios, but absolute drag levels were not accurately predicted.
Author (revised)

N94-26548*# Analytical Services and Materials, Inc., Hampton, VA.
THE MEASUREMENT OF DISTURBANCE LEVELS IN THE LANGLEY RESEARCH CENTER 20-INCH MACH 6 TUNNEL Final Report
P. C. Stainback and L. R. Kubendran Mar. 1994 23 p
(Contract NAS1-19320; RTOP 505-70-59-03)
(NASA-CR-4571; NAS 1.26:4571) Avail: CASI HC A03/MF A01

Constant-temperature anemometry was used to measure the disturbance levels in the Langley Research Center 20-inch Mach 6 Tunnel over a limited range of total pressures. The measurements were made using a dual wire probe where each wire was operated at a high but different overheat. The fluctuating voltages were digitized and a system of two equations was solved to obtain the instantaneous mass flow and total temperature fluctuations as a function of time. Statistical techniques were used to obtain statistical quantities of interest.
Author

N94-26552*# National Aeronautics and Space Administration. Langley Research Center, Hampton, VA.
PRESSURE DISTRIBUTIONS ON A 0.02-SCALE SPACE SHUTTLE ORBITER NOSE AT MACH 21.5 IN HELIUM
George C. Ashby, Jr., Peter T. Bernot, and William C. Woods Jan. 1994 75 p
(RTOP 506-40-41-01)
(NASA-TM-4495; L-17038; NAS 1.15:4495) Avail: CASI HC A04/MF A01

Pressure distributions on a 0.02-scale model of the Space Shuttle orbiter forward fuselage were obtained in the 22-inch aerodynamic leg of the Langley Hypersonic Helium Tunnel Facility at a nominal free-stream Mach number of 21.5 and a ratio of specific heats of 1.67 for inclusion in the database of the Shuttle entry air data system (SEADS). The data were measured at model angles of attack of 0 deg to 50 deg in 5 deg increments for zero sideslip angle and at model sideslip angles of -5 deg to 5 deg for angles of attack equal to 5, 20, 35, and 40 deg. These data displayed trends similar to those observed in other wind tunnels at Mach 6 and 10 in air. Specifically noted is a shift in the location of the stagnation point at angles of attack above 15 deg; this effect did not, however, occur in flight. By comparison, the data obtained at Mach 6 in the Langley Hypersonic CF4 Tunnel, corresponding to a lower ratio of specific heats in the postshock region than those in helium and air, showed some reduction of the stagnation point shift at the higher angles of attack. The differences between flight and wind tunnel pressure distributions are believed due primarily to high-temperature gas chemistry effects in flight, which include lower effective specific heat ratios but which were not completely duplicated in the wind tunnels.
Author (revised)

N94-26602*# National Aeronautics and Space Administration. Langley Research Center, Hampton, VA.
PILOTED SIMULATION STUDY OF AN ILS APPROACH OF A TWIN-PUSHER BUSINESS/COMMUTER TURBOPROP AIRCRAFT CONFIGURATION
Donald R. Riley, Jay M. Brandon, and Louis J. Glaab (Lockheed Engineering and Sciences Co., Hampton, VA.) Jan. 1994 120 p
(RTOP 535-03-01-03)
(NASA-TM-4516; L-17215; NAS 1.15:4516) Avail: CASI HC A06/MF A02

A six-degree-of-freedom nonlinear simulation of a twin-pusher, turboprop business/commuter aircraft configuration representative of the Cessna ATPTB (Advanced turboprop test bed) was developed for use in piloted studies with the Langley General Aviation Simulator. The math models developed are provided, simulation predictions are compared with with Cessna flight-test data for validation purposes, and results of a handling quality study during simulated ILS (instrument landing system) approaches and missed approaches are presented. Simulated flight trajectories, task performance measures, and pilot evaluations are presented for the ILS approach and missed-approach tasks conducted with the vehicle in the presence of moderate turbulence, varying horizontal winds and engine-out conditions. Six test subjects consisting of two research pilots, a Cessna test pilot, and three general aviation pilots participated in the study. This effort was undertaken in cooperation with the Cessna Aircraft Company.
Author (revised)

N94-26672 Carleton Univ., Ottawa (Ontario). Dept. of Mechanical and Aerospace Engineering.
AN INVESTIGATION INTO THE AERODYNAMIC EFFECTS OF WING PATCHES M.S. Thesis
Cameron Lindsay Carnegie 5 Oct. 1992 121 p
(ISBN-0-315-84121-4; CTN-94-61058) Copyright Avail: Micromedia Ltd., Technical Information Centre, 240 Catherine Street, Suite 305, Ottawa, Ontario, K2P 2G8, Canada HC/MF

Many of the aircraft battle damage repair methods involve application of a patch as thick as 12.7 mm over the damaged area to compensate for loss of structural and skin strength. The effect of such patches on the aerodynamics of the CF-18 aircraft wing is investigated. Boundary layer information was obtained by a series of wind tunnel tests on chamfered and unchamfered plates of various thicknesses at Reynolds numbers of 2,100 to 33,650. The results were expressed as polynomial curve fits with Delta H (the difference in shape factor across the patch edge) and (Delta Theta)/h (the ratio between the difference in momentum thickness across the patch edge and the step height or patch thickness) as functions of h divided by the initial momentum thickness. These plate correlation curves were then encoded into the Stalled Airfoil Modelling Package, which was used to analyze the effect of the patches on the flow over the CF-18 wing profile. The results revealed that even for the thickest patch (12.7 mm), the influence on lift is limited at low angles of attack but increases for angles of attack over 3 deg. The influence of the patches on drag is generally much greater and can double the drag coefficient with the thickest patches. A computer code listing is included.
Author (CISTI)

N94-26693*# National Aeronautics and Space Administration. Langley Research Center, Hampton, VA.
EXPERIMENTAL AND THEORETICAL STUDY OF AERODYNAMIC CHARACTERISTICS OF SOME LIFTING BODIES AT ANGLES OF ATTACK FROM -10 DEGREES TO 53 DEGREES AT MACH NUMBERS FROM 2.30 TO 4.62
M. Leroy Spearman and Abel O. Torres Mar. 1994 25 p
(RTOP 505-69-20-01)
(NASA-TM-4528; L-17269; NAS 1.15:4528) Avail: CASI HC A03/MF A01

Lifting bodies are of interest for possible use as space transportation vehicles because they have the volume required for significant payloads and the aerodynamic capability to negotiate the transition from high angles of attack to lower angles of attack (for cruise flight) and thus safely reenter the atmosphere and perform conventional horizontal landings.

Results are presented for an experimental and theoretical study of the aerodynamic characteristics at supersonic speeds for a series of lifting bodies with 75 deg delta planforms, rounded noses, and various upper and lower surface cambers. The camber shapes varied in thickness and in maximum thickness location, and hence in body volume. The experimental results were obtained in the Langley Unitary Plan Wind Tunnel for both the longitudinal and the lateral aerodynamic characteristics. Selected experimental results are compared with calculated results obtained through the use of the Hypersonic Arbitrary-Body Aerodynamic Computer Program.
Author (revised)

N94-26702# Institute for Aerospace Research, Ottawa (Ontario).

INFLUENCE OF THE TRANSONIC DOUBLET IN THE FARFIELD OF A LIFTING AIRFOIL

M. Mokry Oct. 1993 19 p
(IAR-AN-78; NRC-32161; CTN-94-61016) Avail: CASI HC A03/MF A01

In consideration of a need to extend the range of applicability of a linear method of correction for subsonic wind tunnel wall interference on airfoils to cases where the local supersonic pockets are extensive yet do not reach the upper and lower test section walls, a computational fluid dynamics based method for calculating the strength of the transonic doublet for a lifting, supercritical airfoil is presented. Experimentation with the finite volume, time-stepping solver of the Euler equation demonstrates that the computational domain used with the vortex boundary condition in farfield can be substantially reduced if the doublet term is also included. The increase of doublet strength due to nonlinear compressibility effects is a function of the far-upstream Mach number and lift coefficient, and is of an order of magnitude of the doublet strength based on the cross sectional area of the airfoil. The open-jet formula was shown to provide a sufficiently accurate incremental velocity correction to the previously corrected wind tunnel data by the linear subsonic method of Mokry and Ohman (1980).
Author (CISTI)

N94-26706*# National Aeronautics and Space Administration. Langley Research Center, Hampton, VA.

FIBER-OPTIC-BASED LASER VAPOR SCREEN FLOW VISUALIZATION SYSTEM FOR AERODYNAMIC RESEARCH IN LARGER SCALE SUBSONIC AND TRANSONIC WIND TUNNELS

Gary E. Erickson and Andrew S. Inenaga (Aerometrics, Inc., Sunnyvale, CA.) Jan. 1994 69 p
(RTOP 505-68-30-03)
(NASA-TM-4514; L-17198; NAS 1.15:4514) Avail: CASI HC A04/MF A01

Laser vapor screen (LVS) flow visualization systems that are fiber-optic based were developed and installed for aerodynamic research in the Langley 8-Foot Transonic Pressure Tunnel and the Langley 7- by 10-Foot High Speed Tunnel. Fiber optics are used to deliver the laser beam through the plenum shell that surrounds the test section of each facility and to the light-sheet-generating optics positioned in the ceiling window of the test section. Water is injected into the wind tunnel diffuser section to increase the relative humidity and promote condensation of the water vapor in the flow field about the model. The condensed water vapor is then illuminated with an intense sheet of laser light to reveal features of the flow field. The plenum shells are optically sealed; therefore, video-based systems are used to observe and document the flow field. Operational experience shows that the fiber-optic-based systems provide safe, reliable, and high-quality off-surface flow visualization in smaller and larger scale subsonic and transonic wind tunnels. The design, the installation, and the application of the Langley Research Center (LaRC) LVS flow visualization systems in larger scale wind tunnels are highlighted. The efficiency of the fiber optic LVS systems and their insensitivity to wind tunnel vibration, the tunnel operating temperature and pressure variations, and the airborne contaminants are discussed.
Author (revised)

N94-27161*# National Aeronautics and Space Administration. Langley Research Center, Hampton, VA.

LEADING-EDGE VORTEX-SYSTEM DETAILS OBTAINED ON F-106B AIRCRAFT USING A ROTATING VAPOR SCREEN AND SURFACE TECHNIQUES (Videotape Supplement)

John E. Lamar, Jay Brandon, Kathryn Stacy, Thomas D. Johnson, Jr. (Lockheed Engineering and Sciences Co., Hampton, VA.), Kurt Severance, and Brooks A. Childers Nov. 1993 See also N94-23512 Videotape supplement: 14 min., color, sound, VHS
(RTOP 505-59-30-03)
(NASA-TP-3374-Video-Suppl; L-0793-127; NAS 1.60:3374-Video-Suppl; NONP-Suppl-VT-94-209775) Avail: CASI VHS A01/BETA A22

In this video the following sequences are presented: flight-test operational procedures; animation of post-processing key elements; digitization process of flight video tape; extractor procedure demonstration; reconstructor procedure demonstration; reconstructor used to compare flight results from 1985 with those in 1991; enhancer procedure demonstration; and mapping of oil-flow photograph onto surface geometry for comparison with vapor-screen-determined vortex characteristics.
Author

N94-27235# National Aerospace Lab., Tokyo (Japan). Advanced Aircraft Research Group.

WIND TUNNEL INVESTIGATION OF AN STOL AIRCRAFT MODEL: AN EFFECT OF ENGINE NACELLE SHAPE [STOL ZENKI MOKEI FUDO SHIKEN: ENJIN NASERU KEIJO KOKA]

Hitoshi Takahashi Jan. 1993 27 p In JAPANESE Prepared in cooperation with STOL Research Aircraft Group
(ISSN 0452-2982)
(NAL-TM-653; JTN-94-80621) Avail: CASI HC A03/MF A01

In initial wind tunnel tests on STOL experimental aircraft developed and researched by the National Aerospace Laboratory, a simulator engine nacelle which is longer and larger than that of 8 percent scales of FJR engines used in actual aircraft, was installed and tested on a model. To estimate ASKA's aerodynamics force data from wind tunnel data, the data was modified to take into account the different shapes of engine nacelle used in the simulated engine and that used in an 8 percent scale FJR (Fan Jet Research) engine. To confirm the adequacy of the modification, wind tunnel tests were conducted on a model with 8 percent scales FJR engine. From the comparison of the present test data with the initial test data and modified data, it was found that the correction of forces was overestimated and the correction of moments was fairly good.
Author (NASDA)

N94-27554 National Aerospace Lab., Amsterdam (Netherlands). Aerodynamics Div.

HIGH-LIFT SYSTEM ANALYSIS METHOD USING UNSTRUCTURED MESHES

K. M. J. deCock 15 Sep. 1992 30 p Presented at the AGARD FDP Meeting and Symposium on High-Lift System Aerodynamics, Banff, Canada, 5-8 Oct. 1992 Limited Reproducibility: More than 20% of this document may be affected by microfiche quality
(NLR-TP-92351-U; ETN-94-95452; AD-B175579) Avail: CASI HC A03

A two dimensional high lift configuration analysis method is described. The flow model used is based on the Euler equations, discretized on unstructured meshes. The generation of the unstructured meshes is based on the principle of successive grid adaption with respect to the geometry. This approach makes later extension towards fully integrated grid adaption with respect to the solution straightforward. The main characteristics of the Euler solver are upwind flux difference splitting of the convective part of the Euler equations (second order accurate discretization in space) and four stage Runge-Kutta local time stepping. Results obtained with this analysis method are shown for the NACA0012 airfoil and three element airfoils.
ESA

N94-27592# Deutsche Forschungsanstalt fuer Luft- und Raumfahrt, Goettingen (Germany). Abt. Grenzschichten und Unterschallstroemungen.

CONTROL OF LEADING-EDGE SEPARATION ON AN AIRFOIL BY LOCALIZED EXCITATION [STEUERUNG DER VORDERKANTENABLOSUNG AN EINEM FLUGELPROFIL DURCH LOKALE ANREGUNG]

Alexander Dovgal (Academy of Sciences, USSR, Novosibirsk.) May 1993 56 p Sponsored by Alexander von Humbolt Foundation
(ISSN 0939-2963)
(DLR-FB-93-16; ETN-94-95494) Avail: CASI HC A04/MF A01

The experimental investigation on the control of the separated flow over a low Reynolds number airfoil placed at high angles of attack was carried out. To reduce the separated flow and improve the airfoil's performance, some kind of periodic forcing can be used. A version of this control method consists in excitation of the flow through a narrow slot at the surface of the model near its leading edge. Such a technique was examined with emphasis on its operational principles. The study continues others concerning the use of a localized excitation for the separation control and makes clear some details about mechanisms responsible for the effect of the excitation on a separating flow. ESA

N94-27741# Deutsche Forschungsanstalt fuer Luft- und Raumfahrt, Goettingen (Germany). Abt. Hochgeschwindigkeits-Aerodynamik.
METHODS IN UNSTEADY AERODYNAMICS [VERFAHREN IN DER INSTATIONAEREN AERODYNAMIK]
Wolfgang Geissler Jun. 1993 515 p In GERMAN
(ISSN 0939-2963)
(DLR-FB-93-21; ETN-94-95498) Avail: CASI HC A22/MF A04

Methods in unsteady aerodynamics used for the solution of aeroelastic and partly also for aeroacoustic problems are described. After a discussion of the necessary fundamental fluid mechanic inputs, the development and application of integral equation methods are described in two and three space dimensions for subsonic and supersonic flows. Unsteady airfoil flows as well as flows about wings, bodies, engine cowls, and aerodynamic interference problems between accelerated moving (oscillating) aircraft components are investigated. To handle nonlinear problems of unsteady flows with shock waves and/or with separation, corresponding numerical methods were discussed. In all cases comparisons with experimental data were performed. ESA

N94-27955 ESDU International Ltd., London (England).
NORMAL FORCE OF LOW ASPECT RATIO CROPPED-DELTA WINGS AT PRE-STALL ANGLES OF ATTACK AND SUBSONIC SPEEDS
Dec. 1993 17 p
(ISSN 0141-397X)
(ESDU-93034; ISBN-0-85679-887-8) Avail: ESDU

ESDU 93034 presents graphical data at taper ratios of 0, 0.5, and 1, applying at Mach numbers of 0.5 and below, at at Mach numbers of 0.8 and 0.95. They were obtained by correlating experimental data drawn from the literature for delta, cropped delta, and rectangular thin, uncambered and untwisted, sharp-edge wings of aspect ratio from 0.2 to 4 and apply up to angles of attack of 35 degrees, that is up to the stall. Below an angle of attack of 5 degrees, the normal force is obtained from the normal-force curve slop at zero angle of attack, and a graph is provided for that based on the method of ESDU 70011. The accuracy of the method is within 5%. ESDU

N94-28057 ESDU International Ltd., London (England).
CONTRIBUTION OF BODY-MOUNTED FINS AND TAILPLANES TO LATERAL DERIVATIVES DUE TO SIDESLIP AT SUBSONIC SPEEDS FOR GENERAL BODY WIDTH TO HEIGHT RATIO
Apr. 1993 35 p
(ISSN 0141-397X)
(ESDU-93007; ISBN-0-85679-859-2) Avail: ESDU

ESDU 93007 applies to single or twin fins on aircraft at angles of attack up to 6 degrees and angles of sideslip up to 4 degrees. It treats a wider range of body height/width ratios than ESDU 82010 which deals with the single body mounted fin for geometries typical of transport aircraft where body height/width ratio is close to one. The fin sideforce is calculated by applying a semi-empirical interference factor to a basic lift-curve slope estimated from ESDU 70011 for the wing obtained when the fin is reflected about its root chord. The interference factor takes account of body, wing and tailplane interference, and three factors are provided depending on the relative positions of all lifting surfaces. For twin fins a further empirical factor is applied. Yawing and rolling moments follow once the point of action of the sideforce is known; the point empirically determined in ESDU 82010 based on an assumed elliptical loading along the fin quarter-chord line was found to be satisfactory here as well. Methods are also given for estimating the small contributions to the yawing and rolling moments from a body-mounted tailplane. Plots of predicted results against experimental data extracted from 24 sources in the literature (together with some unpublished results) show the sideforce, yawing moment and rolling moment derivatives to be estimated within 0.08, 0.04 and 0.02 respectively. The ranges of geometry covered by the test data are tabulated, and two fully worked examples illustrate the use of the methods. ESDU

N94-28063 ESDU International Ltd., London (England).
LIFT-CURVE SLOPE FOR STRUCTURAL RESPONSE CALCULATIONS
Dec. 1993 20 p
(ISSN 0143-2702)
(ESDU-93013; ISBN-0-85679-865-7) Avail: ESDU

ESDU 93013 provides data for the rate of change with wind direction of the force components in the directions of the principal axes of the structure. The values are an essential input to the calculation methods of ESDU 89049 and 91010 for calculating the response of structures to buffeting by across-wind turbulence and the response in galloping, respectively. For building shapes, essentially prismatic blocks with only small edge rounding, tables give values for the two components for a range of cross-section aspect ratios and three levels of along-wind turbulence intensity; the values were obtained from the force correlations in ESDU 80003. For beam sections, values for both components are given for angle, channel, I-, H-, T- and X-sections and for two channel sections back-to-back; the data were obtained from the correlations in ESDU 82007. For bridge decks, data extracted from the literature are given for the across-wind component (that is, the rate of change of lift with wind direction) for over 30 different types of bridge. Where available, data are included on the solidity and aspect ratio of the barrier and on the turbulence levels in the original wind-tunnel tests. ESDU

N94-28071*# Texas A&M Univ., College Station. Dept. of Aerospace Engineering.
NONEQUILIBRIUM RADIATION AND CHEMISTRY MODELS FOR AEROCAPTURE VEHICLE FLOWFIELDS Final Report
Leland A. Carlson Mar. 1994 189 p
(Grant NAG1-1003)
(NASA-CR-195706; NAS 1.26:195706; TAMRF-6382-94-01) Avail: CASI HC A09/MF A02

The primary accomplishments of the project were as follows: (1) From an overall standpoint, the primary accomplishment of this research was the development of a complete gasdynamic-radiatively coupled nonequilibrium viscous shock layer solution method for axisymmetric blunt bodies. This method can be used for rapid engineering modeling of nonequilibrium re-entry flowfields over a wide range of conditions. (2) Another significant accomplishment was the development of an air radiation model that included local thermodynamic nonequilibrium (LTNE) phenomena. (3) As part of this research, three electron-electronic energy models were developed. The first was a quasi-equilibrium electron (QEE) model which determined an effective free electron temperature and assumed that the electronic states were in equilibrium with the free electrons. The second was a quasi-equilibrium electron-electronic (QEEE) model which computed an effective electron-electronic temperature. The third model was a full electron-electronic (FEE) differential equation model which included convective, collisional, viscous, conductive, vibrational coupling, and chemical effects on electron-electronic energy. (4) Since vibration-dissociation coupling phenomena as well as vibrational thermal nonequilibrium phenomena are important in the nonequilibrium zone behind a shock front, a vibrational energy and vibration-dissociation coupling model was developed and included in the flowfield model. This model was a modified coupled vibrational dissociation vibrational (MCVDV) model and also included electron-vibrational coupling. (5) Another accomplishment of the project was the usage of the developed models to investigate radiative heating. (6) A multi-component diffusion model which properly models the multi-component nature of diffusion in complex gas mixtures such as air, was developed and incorporated into the blunt body model. (7) A model was developed to predict the magnitude and characteristics of the shock wave precursor ahead of vehicles entering the Earth's atmosphere. (8) Since considerable data exists for radiating nonequilibrium flow behind normal shock waves, a normal shock wave version of the blunt body code was developed. (9) By comparing predictions from the models and codes with available normal shock data and the flight data of Fire II, it is believed that the developed flowfield and nonequilibrium radiation models have been essentially validated for engineering applications. Derived from text

N94-28072*# Texas A&M Univ., College Station. Dept. of Aerospace Engineering.
AN INITIAL INVESTIGATION INTO METHODS OF COMPUTING TRANSONIC AERODYNAMIC SENSITIVITY COEFFICIENTS Final Report
Leland A. Carlson Mar. 1994 118 p
(Grant NAG1-793)

(NASA-CR-195705; NAS 1.26:195705; TAMRF-5802-94-01) Avail: CASI HC A06/MF A02

The primary accomplishments of the project are as follows: (1) Using the transonic small perturbation equation as a flowfield model, the project demonstrated that the quasi-analytical method could be used to obtain aerodynamic sensitivity coefficients for airfoils at subsonic, transonic, and supersonic conditions for design variables such as Mach number, airfoil thickness, maximum camber, angle of attack, and location of maximum camber. It was established that the quasi-analytical approach was an accurate method for obtaining aerodynamic sensitivity derivatives for airfoils at transonic conditions and usually more efficient than the finite difference approach. (2) The usage of symbolic manipulation software to determine the appropriate expressions and computer coding associated with the quasi-analytical method for sensitivity derivatives was investigated. Using the three dimensional fully conservative full potential flowfield model, it was determined that symbolic manipulation along with a chain rule approach was extremely useful in developing a combined flowfield and quasi-analytical sensitivity derivative code capable of considering a large number of realistic design variables. (3) Using the three dimensional fully conservative full potential flowfield model, the quasi-analytical method was applied to swept wings (i.e. three dimensional) at transonic flow conditions. (4) The incremental iterative technique has been applied to the three dimensional transonic nonlinear small perturbation flowfield formulation, an equivalent plate deflection model, and the associated aerodynamic and structural discipline sensitivity equations; and coupled aeroelastic results for an aspect ratio three wing in transonic flow have been obtained. Derived from text

N94-28076 ESDU International Ltd., London (England).

PROGRAM FOR CALCULATION OF MAXIMUM LIFT COEFFICIENT OF PLAIN AEROFOILS AND WINGS AT SUBSONIC SPEEDS

Aug. 1993 27 p
(ISSN 0141-397X)
(ESDU-93015; ISBN-0-85679-867-3) Avail: ESDU

ESDU 93015 introduces a Fortran program for aerofoils and wings without high-lift devices. For aerofoils the method of ESDU 84026 is used, which itself relies on the prediction of lift-curve slope from ESDU Aero W.01.01.05. Sections can have a rough leading-edge (such as would result from ice formation) or a smooth leading-edge. The program applies a test to the section geometry data to determine whether the section has rear loading and trailing-edge thickness; such modern aerofoils have a higher maximum lift. If the user has not specified the section is modern, and the test shows that it is, the program will compute on that basis and print a warning. For wings the method of ESDU 89034 is used and assumes smooth leading-edges. The program first finds the spanwise location of peak loading for the given planform at each Mach number. The section geometry at each of those locations is then input, together with a camber and twist distribution which may be linear or non-linear. In the latter case, aerofoil data are also required at the wing root and at 2/3 of span to calculate the zero lift incidence at those two sections. The input and output formats are fully explained and illustrated with worked examples. The program is provided on disc (uncompiled) in the software volume as ESDUpac A9315. ESDU

N94-28091 ESDU International Ltd., London (England).

COMPUTATION OF STATIC PRESSURE DOWNSTREAM OF A NORMAL SHOCK FOR HYPERSONIC FLIGHT (AMBIENT TEMPERATURE KNOWN)

Aug. 1993 16 p
(ISSN 0141-4054)
(ESDU-93020; ISBN-0-85679-873-8) Avail: ESDU

ESDU 93020 is ancillary to and is for use in conjunction with ESDU 88025, which provides a definitive method for deriving primary air-data parameters in hypersonic flight with excellent precision, provided an accurate value of static pressure is available. ESDU 93020 provides an accurate means of deriving this static pressure without relying on a static pressure system. It is not possible to evaluate the relationship between the sensed static pressure and the real ambient pressure when the air is calorically and thermally imperfect as it is behind the shock in hypersonic flight. The static pressure is then used in the method of ESDU 88025. ESDU 93020 uses the ratio of static to total pressures behind a normal (detached) shock which is given in terms of quantities tabulated in ESDU 88025 and requires a knowledge of total temperature and pressure. However, it also requires a knowledge of the ambient temperature and the lapse rate, either from meteorological balloons or satellite observation, although an accuracy of 4 or 5 K for ambient temperature will be satisfactory. A worked example illustrates the use of the method for the same flight conditions used in the example in ESDU 88025. ESDU

N94-28140 ESDU International Ltd., London (England).

WING LIFT INCREMENT AT ZERO ANGLE OF ATTACK DUE TO DEPLOYMENT OF SINGLE-SLOTTED FLAPS AT LOW SPEEDS

Dec. 1993 17 p Supersedes Aero-F.01.01.08
(ISSN 0141-397X)
(ESDU-93019; Aero-F.01.01.08; ISBN-0-85679-872-X) Avail: ESDU

ESDU 93019 presents an empirical method that depends on determining the increment for an aerofoil representative of the wing and applying factors to allow for three-dimensional and part-span effects. ESDU 86033 is used to predict the increment for the aerofoil, depending on the extended deployed chord, and the section included trailing-edge angle. That increment is factored by the ratio of the wing to aerofoil lift curve slopes obtained respectively from ESDU 70011 and Aero W.01.01.05, thereby, accounting for aspect ratio, taper, and sweep effects. Finally, part-span factors are applied that depend on the spanwise center of pressure of the loading due to incidence obtained from ESDU 83040. The range of parameters for which the method was validated are tabulated and include aspect ratios of 3.7 to 9, taper ratios from 0.2 to 1, leading-edge sweep up to 48 degrees, Mach numbers up to 0.26, and flap deflections of 10 to 45 degrees. Sketches show the correlation between experimental results drawn from the literature and predicted results; for all results, 90 percent were correlated within 15 percent while for part-span cases alone 80 percent of the data were correlated to within 5 percent. A worked example illustrates the use of the method. ESDU

N94-28144 ESDU International Ltd., London (England).

EXAMPLES OF EXCRESCENCE DRAG PREDICTION FOR TYPICAL WING COMPONENTS OF A SUBSONIC TRANSPORT AIRCRAFT AT THE CRUISE CONDITION

Dec. 1993 88 p
(ISSN 0141-397X)
(ESDU-93032; ISBN-0-85679-885-1) Avail: ESDU

ESDU 93032 illustrates the application to a real situation of the ESDU data on drag due to cavities, grooves, steps, ridges, and control gaps, and the drag magnification factor applied to them to account for the effects of a nonuniform pressure distribution. An aileron, a leading-edge slat, a spoiler, a trailing-edge flap, a typical fuel tank access door, and a main undercarriage unit door are considered. For each component the necessary information is provided: graphs of flow data (Mach number, velocity, temperature, and density) and a detailed sketch showing all dimensions and sealing arrangement. Two cases are treated for each component: an ideal state with airtight seals and no avoidable surface mismatches, and a situation with poor sealing or surface mismatches. The comparison between results for the two cases illustrates the penalties from poor sealing or fits, and the possible effects of in-service deterioration. Detailed calculations are given for one feature of each excrescence, and the complete drag calculation is summarized in tabular form. The major contributions to the drag of each component are discussed and methods of reducing them are considered. The results from all the examples are finally reviewed to indicate the basic principles in design for low excrescence drag, and, to show their relative importance, the contribution of each component is expressed as a fraction of a plausible total excrescence drag for the wing. ESDU

N94-28188*# National Aeronautics and Space Administration. Ames Research Center, Moffett Field, CA.

HIGH-SPEED RESEARCH: SONIC BOOM, VOLUME 1

Thomas A. Edwards, ed. Feb. 1994 231 p Conference held in Moffett Field, CA, 12-14 May 1993; sponsored by NASA
(RTOP 537-03-21)
(NASA-CP-10132; A-94045; NAS 1.55:10132) Avail: CASI HC A11/MF A03

The second High-Speed Research Program Sonic Boom Workshop was held at NASA Ames Research Center May 12-14, 1993. The workshop was organized into three sessions dealing with atmospheric propagation, acceptability, and configuration design. Volume 1 includes papers on atmospheric propagation and acceptability studies. Significant progress is noted in these areas in the time since the previous workshop a year earlier. In particular, several papers demonstrate an improved capability to model the effect of atmospheric turbulence on sonic booms. This is a key issue in determining the stability and acceptability of shaped sonic booms. In the area of acceptability, the PLdB metric has withstood considerable scrutiny and is validated as a loudness metric for a wide variety of sonic boom shapes. The differential loudness of asymmetric sonic booms is better understood, too. For individual titles, see N94-28189 through N94-28198.

N94-28189*# Pennsylvania State Univ., University Park. Graduate Program in Acoustics.

PROGRESS IN MODELING ATMOSPHERIC PROPAGATION OF SONIC BOOMS

Allan D. Pierce *In* NASA. Ames Research Center, High-Speed Research: Sonic Boom, Volume 1 Feb. 1994 p 1-18 (For primary document see N94-28188 07-02)

Avail: CASI HC A03/MF A03

The improved simulation of sonic boom propagation through the real atmosphere requires greater understanding of how the transient acoustic pulses popularly termed sonic booms are affected by humidity and turbulence. A realistic atmosphere is invariably somewhat turbulent, and may be characterized by an ambient fluid velocity v and sound speed c that vary from point to point. The absolute humidity will also vary from point to point, although possibly not as irregularly. What is ideally desired is a relatively simple scheme for predicting the probable spreads in key sonic boom signature parameters. Such parameters could be peak amplitudes, rise times, or gross quantities obtainable by signal processing that correlate well with annoyance or damage potential. The practical desire for the prediction scheme is that it require a relatively small amount of knowledge, possibly of a statistical nature, concerning the atmosphere along, the propagation path from the aircraft to the ground. The impact of such a scheme, if developed, implemented, and verified, would be that it would give the persons who make planning decisions a tool for assessing the magnitude of environmental problems that might result from any given overflight or sequence of overflights. The technical approach that has been followed by the author and some of his colleagues is to formulate a hierarchy of simple approximate models based on fundamental physical principles and then to test these models against existing data. For propagation of sonic booms and of other types of acoustic pulses in nonturbulent model atmospheres, there exists a basic overall theoretical model that has evolved as an outgrowth of geometrical acoustics. This theoretical model depicts the sound as propagating within ray tubes in a manner analogous to sound in a waveguide of slowly varying cross-section. Propagation along the ray tube is quasi-one-dimensional, and a wave equation for unidirectional wave propagation is used. A nonlinear term is added to this equation to account for nonlinear steepening, and the formulation has been carried through to allow for spatially varying sound speed, ambient density, and ambient wind velocities. The model intrinsically neglects diffraction, so it cannot take into account what has previously been mentioned in the literature as possibly important mechanisms for turbulence-related distortion. The model as originally developed could predict an idealized N-waveform which often agrees with data in terms of peak amplitude and overall positive phase duration. It is possible, moreover, to develop simple methods based on the physics of relaxation processes for incorporating molecular relaxation into the quasi-one-dimensional model of nonlinear propagation along ray tubes. Derived from text

N94-28190*# Pennsylvania State Univ., University Park. Graduate Program in Acoustics.

IMPLICATIONS FOR HIGH SPEED RESEARCH: THE RELATIONSHIP BETWEEN SONIC BOOM SIGNATURE DISTORTION AND ATMOSPHERIC TURBULENCE

Victor W. Sparrow and Thomas A. Gionfriddo *In* NASA. Ames Research Center, High-Speed Research: Sonic Boom, Volume 1 Feb. 1994 p 19-64 (For primary document see N94-28188 07-02)

Avail: CASI HC A03/MF A03

In this study there were two primary tasks. The first was to develop an algorithm for quantifying the distortion in a sonic boom. Such an algorithm should be somewhat automatic, with minimal human intervention. Once the algorithm was developed, it was used to test the hypothesis that the cause of a sonic boom distortion was due to atmospheric turbulence. This hypothesis testing was the second task. Using readily available sonic boom data, we statistically tested whether there was a correlation between the sonic boom distortion and the distance a boom traveled through atmospheric turbulence. Derived from text

N94-28191*# Rensselaer Polytechnic Inst., Troy, NY. Dept. of Mechanical Engineering.

INTERACTION OF THE SONIC BOOM WITH ATMOSPHERIC TURBULENCE

Zvi Rusak and Julian D. Cole *In* NASA. Ames Research Center, High-Speed Research: Sonic Boom, Volume 1 Feb. 1994 p 65-91 (For primary document see N94-28188 07-02)

Avail: CASI HC A03/MF A03

Theoretical research was carried out to study the effect of free-stream turbulence on sonic boom pressure fields. A new transonic small-disturbance model to analyze the interactions of random disturbances with a weak shock was developed. The model equation has an extended form of the classic small-disturbance equation for unsteady transonic aerodynamics. An alternative approach shows that the pressure field may be described by an equation that has an extended form of the classic nonlinear acoustics equation that describes the propagation of sound beams with narrow angular spectrum. The model shows that diffraction effects, nonlinear steepening effects, focusing and caustic effects and random induced vorticity fluctuations interact simultaneously to determine the development of the shock wave in space and time and the pressure field behind it. A finite-difference algorithm to solve the mixed type elliptic-hyperbolic flows around the shock wave was also developed. Numerical calculations of shock wave interactions with various deterministic and random fluctuations will be presented in a future report. Author (revised)

N94-28192*# Texas Univ., Austin. Applied Research Labs.

SONIC BOOM PROPAGATION THROUGH TURBULENCE: A RAY THEORY APPROACH

Leick D. Robinson *In* NASA. Ames Research Center, High-Speed Research: Sonic Boom, Volume 1 Feb. 1994 p 93-107 (For primary document see N94-28188 07-02)

Avail: CASI HC A03/MF A03

A ray theory approach is used to examine the propagation of sonic booms through a turbulent ground layer, and to make predictions about the received waveform. The rays are not propagated one at a time, as is typical in ray theory; instead, sufficient rays to represent a continuous wave front are propagated together. New rays are interpolated as needed to maintain the continuity of the wave front. In order to predict the received boom signature, the wave front is searched for eigenrays after it has propagated to the receiver. The Comte-Bellot turbulence model is used to generate an instantaneous 'snapshot' of the turbulent field. The transient acoustic wave is assumed to be sufficiently short in duration such that the time-dependacde of the turbulent field may be neglected. Author (revised)

N94-28193*# Texas Univ., Austin. Applied Research Labs.

THE PROPAGATION OF SPARK-PRODUCED N WAVES THROUGH TURBULENCE

Bart Lipkens *In* NASA. Ames Research Center, High-Speed Research: Sonic Boom, Volume 1 Feb. 1994 p 109-132 (For primary document see N94-28188 07-02)

Avail: CASI HC A03/MF A03

A model experiment was designed and built to simulate the propagation of sonic booms through atmospheric turbulence. The setup of the model experiment is described briefly. Measurements of the N waves after they propagated across the turbulent velocity field reveal the same waveform distortion and change in rise time as for sonic booms. The data from the model experiment is used to test sonic boom models. Some models yield predictions for the waveform distortion, while others give estimates of the rise time of the sonic booms. A new theoretical model for the propagation of plane N waves through a turbulent medium is described.
Derived from text

N94-28194*# Wyle Labs., Inc., Arlington, VA.

ON THE AGING OF SONIC BOOMS

Kenneth J. Plotkin *In* NASA. Ames Research Center, High-Speed Research: Sonic Boom, Volume 1 Feb. 1994 p 133-151 (For primary document

see N94-28188 07-02)
Avail: CASI HC A03/MF A03

This paper presents view-graphs and notes on sonic boom aging. Topic covered include sonic boom propagation, George's minimized F-function, final minimum shock boom, amplitude and age parameters, off-track aging, scaling flight test experiments, the potential for thin shocks, and results of a Boomfile flight test that showed significant waveform distortion. CASI

N94-28195*# National Aeronautics and Space Administration. Langley Research Center, Hampton, VA.
EXPERIMENTAL STUDIES OF LOUDNESS AND ANNOYANCE RESPONSE TO SONIC BOOMS c71
Brenda M. Sullivan (Lockheed Engineering and Sciences Co., Hampton, VA.) and Jack D. Leatherwood *In* NASA. Ames Research Center, High-Speed Research: Sonic Boom, Volume 1 Feb. 1994 p 153-175 (For primary document see N94-28188 07-02)
Avail: CASI HC A03/MF A03

The purpose of this paper is to summarize the most recent sonic boom laboratory studies performed at NASA-LaRC using the Sonic Boom Simulator. The first used synthesized idealized outdoor boom shapes which were filtered to represent booms heard inside a house. The test explored the efficacy of various metrics in assessing both loudness and annoyance responses to these booms. The second test investigated the effects of adding single reflections to idealized boom signatures, and the third compared booms recorded from real aircraft with idealized boom signatures to determine if subjects rated the real booms differently. In these studies, as in previous studies performed at NASA-LaRC, there was a continuing effort to evaluate metrics for predicting the subjective effects of sonic booms. Author (revised)

N94-28196*# Bolt, Beranek, and Newman, Inc., Canoga Park, CA. BBV Systems and Technologies.
COMPARISON OF METHODS OF PREDICTING COMMUNITY RESPONSE TO IMPULSIVE AND NONIMPULSIVE NOISE c71
Sanford Fidell and Karl S. Pearsons *In* NASA. Ames Research Center, High-Speed Research: Sonic Boom, Volume 1 Feb. 1994 p 177-189 (For primary document see N94-28188 07-02)
Avail: CASI HC A03/MF A03

Several scientific, regulatory, and policy-coordinating bodies have developed methods for predicting community response to sonic booms. The best known of these is the dosage-response relationship of Working Group 84 of the National Academy of Science's Committee on Hearing, Bioacoustics and Biomechanics. This dosage-response relationship between C-weighted DayNight Average Sound Level and the prevalence of annoyance with high energy impulsive sounds was derived from limited amounts of information about community response to regular, prolonged, and expected exposure to artillery and sonic booms. U.S. Army Regulation 201 adapts this approach to predictions of the acceptability of impulsive noise exposure in communities. This regulation infers equivalent degrees of effect with respect to a well known dosage-response relationship for general (nonimpulsive) transportation noise. Differences in prevalence of annoyance predicted by various relationships lead to different predictions of the compatibility of land uses with sonic boom exposure. An examination of these differences makes apparent several unresolved issues in current practice for predicting and interpreting the prevalence of annoyance due to sonic boom exposure. Author (revised)

N94-28197*# McDonnell-Douglas Aerospace, Long Beach, CA. Transport Aircraft.
VARIABILITY OF MEASURED SONIC BOOM SIGNATURES c71
K. R. Elmer and M. C. Joshi *In* NASA. Ames Research Center, High-Speed Research: Sonic Boom, Volume 1 Feb. 1994 p 191-218 (For primary document see N94-28188 07-02)
(Contract NAS1-19060)
Avail: CASI HC A03/MF A03

The topics discussed include the following: atmospheric turbulence; BOOMFILE Database description; BOOMFILE flight conditions; XB-70 Database descriptions; analysis progression; extended database; prediction method; overpressure variability dependence on flight conditions; loudness variability on flight conditions; sonic boom variability in repeat flights; and statistical distributions. CASI

N94-28198*# Oceanographic Consultants.
SONIC BOOMS AND MARINE MAMMALS: INFORMATIONAL STATUS AND RECOMMENDATIONS c51
William C. Cummings *In* NASA. Ames Research Center, High-Speed Research: Sonic Boom, Volume 1 Feb. 1994 p 219-231 (For primary document see N94-28188 07-02)
Avail: CASI HC A03/MF A03

The topics discussed include the following: introduction to marine mammals; marine mammal hearing; noise effects; sonic booms; sonic boom effects on marine mammals; predictions; and recommendations. CASI

N94-28315 Canadian Aeronautics and Space Inst., Ottawa (Ontario).
ABSTRACTS OF PAPERS PRESENTED AT THE 4TH CASI AERODYNAMICS SYMPOSIUM
1993 153 p Symposium held in Toronto, Ontario, 3-4 May 1993 Prepared in cooperation with National Research Council of Canada, Ottawa, Ontario Original contains color illustrations
(ISBN-0-920203-01-9; CTN-94-61078) Avail: Issuing Activity (Canadian Aeronautics and Space Inst., 130 Slater Street, Suite 818, Ottawa, ON K1P 6E2 Canada)

A symposium on aerodynamics was held to provide opportunities to exchange views on current technical topics. Papers were presented on wind tunnel tests, aerodynamic interactions, cabin noise suppression, propeller loads, turbine cascades, T-tail configurations, wind tunnel models, aircraft configurations, laminar / turbulent transitions, boundary layer prediction, shock wave interaction, Euler and Navier-Stokes flow computations, aerodynamic loads, ducted tip wings, airfoil stall modelling, flow modelling, drag prediction, nacelle design, computational grid generation, flow measurement, flow around airfoils, ice accretion on wings, and wind tunnel sidewall interference. Separate abstracts have been prepared for 37 papers from this symposium. For individual titles, see N94-28316 through N94-28352.

N94-28316 Institute for Aerospace Research, Ottawa (Ontario).
WIND TUNNEL INVESTIGATION OF PROPFAN SLIPSTREAM/WING INTERACTIONS ON A DE HAVILLAND AIR MOTOR POWERED SEMISPAN MODEL AT MACH NUMBERS 0.6 AND 0.7
V. D. Nguyen, L. H. Ohman (De Havilland Aircraft Co. of Canada Ltd., Downsview, Ontario.), and R. J. D. Poole (De Havilland Aircraft Co. of Canada Ltd., Downsview, Ontario.) *In* Canadian Aeronautics and Space Inst., Abstracts of Papers Presented at the 4th CASI Aerodynamics Symposium 1993 p 1-4 (For primary document see N94-28315 07-02)
Avail: Issuing Activity (Canadian Aeronautics and Space Inst., 130 Slater Street, Suite 818, Ottawa, ON K1P 6E2 Canada)

A wind tunnel investigation was carried out to assess the aerodynamic interactions of the propeller slipstream on a three dimensional wing of supercritical design, and to determine the flow characteristics immediately behind the propeller plane. A semispan model comprising a fuselage, zero sweep wing, and a powered nacelle was tested, to be representative of a generic model suitable for the design and performance analysis of a possible future transport aircraft. The wing was instrumented with 288 surface pressure orifices and the wing pressure distributions were measured and integrated to yield lift, drag, and pitching moment coefficients. Corrections for wall interference were made using the software package of Mokry et al (1987). Flow characteristics behind the propeller plane were determined using special five-hole probe rakes. The balance data indicated that the model force and moment coefficients were significantly affected by the propeller action. The slipstream was found to have at least an equally large effect as the propeller thrust negating the thrust component on the pitching moment. An increase in section lift coefficient was indicated for the propeller upwash zone and a decrease in the downwash zone. The propeller and its slipstream had little effect on the shock locations on the upper wing when the flow became supercritical. Author (CISTI)

N94-28317 De Havilland Aircraft Co. of Canada Ltd., Downsview (Ontario).
FLOW FIELD INVESTIGATION IN THE NEAR SLIPSTREAM OF AN 8-BLADED PROPFAN ON THE DE HAVILLAND WTEJ HALF-MODEL AT MACH NUMBERS 0.6 AND 0.7
L. H. Ohman, R. J. D. Poole, V. D. Nguyen (Institute for Aerospace Research, Ottawa, Ontario.), and J. Beenen (Institute for Aerospace Research, Ottawa,

Ontario.) *In* Canadian Aeronautics and Space Inst., Abstracts of Papers Presented at the 4th CASI Aerodynamics Symposium 1993 p 5-8 (For primary document see N94-28315 07-02)
Avail: Issuing Activity (Canadian Aeronautics and Space Inst., 130 Slater Street, Suite 818, Ottawa, ON K1P 6E2 Canada)

Flow field data were acquired in the near slipstream of an 8-bladed 15-in. diameter propfan, nacelle mounted on a half-model wing configuration in a wind tunnel. The generally accepted five-hole probe technique was employed for the flow field measurements, with the probe heads located behind the propeller plane. Data were acquired at Mach numbers 0.6 and 0.7 at a Reynolds number of about 7.5 million. The propeller rpm and model angle of attack were varied moderately at each Mach number. It is shown that the radial flow angle was dominated by the nacelle geometry and virtually unaffected by the propeller action. The distribution of the circumferential flow angle and the propeller induced swirl angle was very non-uniform, mainly due to the effect of wing-lift induced upwash. The total pressure distribution was similar in character to that of the swirl angle. The Mach number losses or gains due to the action of the propeller were small. The value of the power coefficient derived from the motor power, with the survey rakes mounted, was found to be sensitive to rake orientation. A single-probe measurement investigation revealed that for the blade loading conditions used, probe arrangement indeed had a significant interference effect on the circumferential flow angle. For higher blade loadings, the probe interference effects became negligible. Author (CISTI)

N94-28318 De Havilland Aircraft Co. of Canada Ltd., Downsview (Ontario). Structures Research and Development.
ASSESSING THE EFFECTS OF TUNED VIBRATION ABSORBERS (TVAs) ON INTERIOR CABIN NOISE LEVELS: A CORRELATION BETWEEN ANALYTICAL ACOUSTIC PREDICTIONS AND FLIGHT TEST MEASUREMENTS **c71**
Ralph Garcea *In* Canadian Aeronautics and Space Inst., Abstracts of Papers Presented at the 4th CASI Aerodynamics Symposium 1993 p 9-12 (For primary document see N94-28315 07-02)
Avail: Issuing Activity (Canadian Aeronautics and Space Inst., 130 Slater Street, Suite 818, Ottawa, ON K1P 6E2 Canada)

Analytical predictions of interior noise levels were correlated with actual flight test data obtained during a program undertaken to develop the proper design and optimal distribution of tuned vibration absorbers for the Dash-8 Series 300 aircraft. The measured operational deflection shape data of the fuselage structure were used as boundary conditions for the interior noise predictions using a boundary element method model and finite element method modal analysis. The analytical modelling procedures used to represent the interior cavity, the underlying assumptions on which the predictions were based, and the correlations obtained are reported. The main assumptions were that the fuselage model was closed with rigid end caps (simulating cabin bulkheads) and that the interior acoustic field was solely due to the vibration of the fuselage skin. In addition, a panel acoustic power contribution analysis was performed to identify the most heavily radiating panels. For example, the skin panels between frames 271 and 290 contributed 62 percent of the total radiated output power at 60 Hz. The flight data and noise predictions correlated well, showing decreased sound pressure levels within the cabin interior due to the effects of the tuned vibration absorbers. Author (CISTI)

N94-28319 De Havilland Aircraft Co. of Canada Ltd., Downsview (Ontario).
PROPELLER OFF-AXIS LOADS DUE TO THRUST AXIS INCIDENCE AND NACELLE MAGNUS FORCE **c07**
P. Vyriotes, J. Petzke, and D. Barber *In* Canadian Aeronautics and Space Inst., Abstracts of Papers Presented at the 4th CASI Aerodynamics Symposium 1993 p 13-16 (For primary document see N94-28315 07-02)
Avail: Issuing Activity (Canadian Aeronautics and Space Inst., 130 Slater Street, Suite 818, Ottawa, ON K1P 6E2 Canada)

Propeller and nacelle loads for various configurations were measured in a series of wind tunnel tests. Wind tunnel data for four- and six-blade research propellers demonstrated the influence of blade angle, advance ratio, and model incidence on propeller shaft loads and nacelle force. Complementary theoretical estimates of the off-axis hub loads were performed using panel and lifting line theories. Favorable correlation between experimental and theoretical data was demonstrated. The test data showed that when the propeller was yawed, the swirl induced nacelle force was comparable in magnitude, but perpendicular to, the propeller shaft side force. The effect of an inlet on the propeller shaft loads was also examined. For an axisymmetric nacelle, the normal force and yawing moment acting on the propeller shaft remained approximately zero. The presence of a pitot inlet nacelle immediately behind the propeller induced an additional normal force and yawing moment on the propeller shaft which was independent of the nacelle yaw angle. If the propeller and nacelle were then pitched, the intake induced loads would contribute to the shaft loads. If the propeller and nacelle were yawed, the intake induced force would act in the same sense as the nacelle force. Author (CISTI)

N94-28320 Carleton Univ., Ottawa (Ontario).
EFFECT OF SURFACE FINISH ON TURBINE AIRFOIL CASCADE LOSSES **c07**
Rama Radmard, Peter J. Turyk (Pratt and Whitney Aircraft of Canada Ltd., Mississauga, Ontario.), and William E. Carscallen (National Research Council of Canada, Ottawa, Ontario.) *In* Canadian Aeronautics and Space Inst., Abstracts of Papers Presented at the 4th CASI Aerodynamics Symposium 1993 p 17-20 (For primary document see N94-28315 07-02)
Avail: Issuing Activity (Canadian Aeronautics and Space Inst., 130 Slater Street, Suite 818, Ottawa, ON K1P 6E2 Canada)

The importance of surface finish on airfoil pressure loss measurement was investigated in a four-passage transonic cascade at nominal exit Mach numbers of 0.7, 0.9, and 1.1. Stagnation pressure and flow angles were measured one quarter chord downstream of the airfoil row using a yawing wedge probe. Three airfoil profiles were used: a baseline airfoil typical of a midsection of a high pressure turbine first vane, plus two thicker airfoils of 27 percent and 48 percent maximum thickness to true chord ratio. The thicker airfoils exhibit lower total pressure loss than the baseline at all three exit conditions. Flow visualization runs showed separation was consistently occurring at the locations of what seemed to be surface defects on each of the airfoil profiles. The airfoils were manually refinished to remove the surface discontinuities and reinstalled. Tests were performed at Mach number 0.7 and results show that the full span pressure losses were reduced with the refinished airfoils. The reduction in total losses decreased as the airfoil thickness increased. The trend of loss with airfoil thickness remained the same as in the original tests. Author (CISTI)

N94-28321 Atomic Energy of Canada Ltd., Pinawa (Manitoba). Containment Analysis Branch.
THE EFFECT OF AXIAL VELOCITY RATIO, TURBULENCE INTENSITY, INCIDENCE, AND LEADING EDGE GEOMETRY ON THE MIDSPAN PERFORMANCE OF A TURBINE CASCADE **c07**
D. R. Whitehouse, S. H. Moustapha (Pratt and Whitney Aircraft of Canada Ltd., Longueuil, Quebec.), and S. A. Sjolander (Carleton Univ., Ottawa, Ontario.) *In* Canadian Aeronautics and Space Inst., Abstracts of Papers Presented at the 4th CASI Aerodynamics Symposium 1993 p 21-24 (For primary document see N94-28315 07-02)
Avail: Issuing Activity (Canadian Aeronautics and Space Inst., 130 Slater Street, Suite 818, Ottawa, ON K1P 6E2 Canada)

Tests were carried out in a low-speed large-scale planar cascade test section to investigate the effect of axial velocity ratio (AVR), incidence, and turbulence intensity (TI) on the midspan performance of a turbine blade. The effect of leading edge geometry was investigated by comparing the results with those of Rodger (1992). Flow measurements were made with three-hole pressure probes mounted in planes upstream and downstream of the cascade. Measurements included midspan total pressure loss and flow performance. As the positive incidence increases, the overspeed increases, creating a strong adverse pressure gradient near the blade leading edge. Flow visualization confirmed the presence of boundary layer separation at +20 deg incidence. The strong adverse pressure gradient caused by the endplates (used to establish two-dimensional flow) appears to be the dominating influence on the boundary layer. An observed sensitivity of blade losses to AVR at high positive incidence highlights the importance of comparing loss measurements at AVR=1.0. Losses rose very quickly as AVR was reduced below 1.0. Turbulence intensity and changes in leading edge geometry had little or no effect on blade off-design losses for the AVR range studied. Author (CISTI)

N94-28322 De Havilland Aircraft Co. of Canada Ltd., Downsview (Ontario). Aerodynanics Technology.

EXPERIMENTAL AND THEORETICAL STUDIES OF T-TAIL CONFIGURATIONS FOR COMMUTER AIRCRAFT APPLICATIONS c05

J. B. Coll, S. W. Cosby, and A. B. Paige *In* Canadian Aeronautics and Space Inst., Abstracts of Papers Presented at the 4th CASI Aerodynamics Symposium 1993 p 25-28 (For primary document see N94-28315 07-02)

Avail: Issuing Activity (Canadian Aeronautics and Space Inst., 130 Slater Street, Suite 818, Ottawa, ON K1P 6E2 Canada)

The design of a horizontal tail leading edge for a commuter aircraft is discussed relative to the existing production standard and an experimental comparison is made between them. Three fin cap fairing definitions are shown and an assessment of their respective performance in light of wind tunnel test results is offered. Three objectives were set for the modification of the existing production standard horizontal tail section: reduction of high speed buffet due to shock waves near the leading edge; retention of the existing low speed characteristics of the airfoil section; and minimization of structural modifications to the existing aircraft layout. Analysis of the standard and modified tails was restricted to two-dimensional sections and was performed using the potential method of Bauer et al (1977) with viscous corrections and a Boeing Euler code with coupled boundary layer (Choupani and Om, 1987). The modified leading edge was shown to have similar lift characteristics to the standard leading edge but a significantly reduced buffet level. The two modified fin cap fairings produced significantly lower drag than the production standard version. The extended fore and aft fairing had an impressive reduction in buffet level at high Mach and Reynolds numbers. Author (CISTI)

N94-28323 Institute for Aerospace Research, Ottawa (Ontario).

MEASUREMENTS OF STEADY AND DYNAMIC PRESSURE ON AN F/A-18 WIND TUNNEL MODEL AT HIGH ANGLES OF ATTACK

F. C. Tang and B. H. K. Lee *In* Canadian Aeronautics and Space Inst., Abstracts of Papers Presented at the 4th CASI Aerodynamics Symposium 1993 p 29-32 (For primary document see N94-28315 07-02)

Avail: Issuing Activity (Canadian Aeronautics and Space Inst., 130 Slater Street, Suite 818, Ottawa, ON K1P 6E2 Canada)

A wind tunnel investigation was conducted to expand the knowledge of high angle of attack aerodynamics and the structure of vortical flows. Measurements were made in the transonic test section of a 1.5 by 1.5-m wind tunnel using a six percent scale model of a F/A-18 aircraft in the Mach number regime of 0.25 to 0.9. Pressures on the upper and lower starboard leading edge extension and wing surfaces were measured and oil dots flow visualization experiments were carried out. The surface skin friction lines show presence of wing-tip and leading-edge vortices. Three dimensional pressure distribution plots of the wing surface show low pressure regions typical of those detected in the presence of vortical flow. The results are in good correlation with those obtained from flow visualization. Spectral analyses of the wing surface pressure signals indicate that the unsteady pressures can be represented by a Gaussian distribution. The deduced wing normal force has statistical properties resembling that of a Gaussian random process. At Mach number 0.6, the wing normal force coefficient varies with angles of attack monotonically. The fluctuating normal force coefficient rises rapidly at angles of attack around 25 degrees. The increase of unsteadiness is due to the bursting of vortex ahead of the wing at higher angles of attack. Author (CISTI)

N94-28324 Bombardier, Inc., Montreal (Quebec). Canadair Group.

APPLICATION OF THE MBTEC EULER CODE TO THE CHALLENGER AND THE CF-18 COMPLETE AIRCRAFT CONFIGURATIONS c05

F. Kafyeke and P. Piperni *In* Canadian Aeronautics and Space Inst., Abstracts of Papers Presented at the 4th CASI Aerodynamics Symposium 1993 p 33-36 (For primary document see N94-28315 07-02)

Avail: Issuing Activity (Canadian Aeronautics and Space Inst., 130 Slater Street, Suite 818, Ottawa, ON K1P 6E2 Canada)

The Canadair Multiblock Transonic Euler Code (MBTEC) has been extended to handle the geometry of complete aircraft configurations. Application of MBTEC to the Canadair CL-601 and CF-18 aircraft configurations is illustrated. MBTEC uses a system of Euler equations written in conservative form and is discretized on a structured body-fitted grid, using a finite volume technique. The scheme employs central differencing for the spatial operators. The resulting ordinary differential equations are integrated in time using a five-stage Runge-Kutta method. Artificial viscosity is added to stabilize the scheme and various convergence acceleration techniques are used including residual averaging and enthalpy damping. The code also has modified boundary condition formulations including additional boundary conditions for turbofan inlets and exhausts. The CL-601 grids use 30-600 blocks. Results have been used to indicate the effects of the winglet and of the interference between the nacelle and the wing. The CF-18 grids use 108 blocks and results have been obtained for a cruise condition at Mach 0.95 and a high angle of incidence condition at Mach 0.6, in comparison with wind tunnel data. Author (CISTI)

N94-28325 De Havilland Aircraft Co. of Canada Ltd., Downsview (Ontario). Research and Development Methods Group.

INFRARED IMAGING FOR TRANSITION DETECTION IN A TRANSONIC BLOWDOWN WIND TUNNEL c74

I. Fejtek, G. D. Jones, and R. Panza-Giosa *In* Canadian Aeronautics and Space Inst., Abstracts of Papers Presented at the 4th CASI Aerodynamics Symposium 1993 p 37-40 (For primary document see N94-28315 07-02)

Avail: Issuing Activity (Canadian Aeronautics and Space Inst., 130 Slater Street, Suite 818, Ottawa, ON K1P 6E2 Canada)

Detection of boundary layer transition from laminar to turbulent flow is an important capability in wind tunnel testing. Infrared imaging offers a technique for detecting such transitions that is nonintrusive, available continuously in real time, easy to use, and affordable. Experiences with this new technology are reported, with reference to wind tunnel tests of a supercritical airfoil. It is shown by a simple expression that if there is a temperature difference across a boundary layer, the heat transfer in a laminar boundary layer is low and the heat transfer in a turbulent boundary layer is high, up to ten times greater. If the flowing fluid is cooler than the model being tested, the surface temperature of that part of the model experiencing laminar flow will remain nearly unchanged while that where the flow is turbulent will drop. In the wind tunnel tests described, the thermal imaging system comprised an infrared scanner and a personal computer based system controller. High intensity infrared heat lamps were found to be the best way of heating the model surface, which was coated with thermally insulating nonreflective paint. It is seen that infrared imaging is not only useful for detecting the boundary layer transition but also for detecting large regions of separated flow. Author (CISTI)

N94-28326 Ecole Polytechnique, Montreal (Quebec). Dept. of Mechanical Engineering.

UNIFIED APPROACH FOR DIRECT AND INVERSE BOUNDARY LAYER PREDICTION USING CUBIC SPLINE COLLOCATION c34

A. Ilinca, B. C. Basu, and J. Godin *In* Canadian Aeronautics and Space Inst., Abstracts of Papers Presented at the 4th CASI Aerodynamics Symposium 1993 p 41-44 (For primary document see N94-28315 07-02)

Avail: Issuing Activity (Canadian Aeronautics and Space Inst., 130 Slater Street, Suite 818, Ottawa, ON K1P 6E2 Canada)

A method proposed to improve the accuracy of the velocity profile together with its first and second derivatives in the normal direction for incompressible boundary layers has been extended to the compressible case. The method, which uses spline collocation in the direction normal to the wall and finite difference discretization in the direction parallel to the wall, has also been applied to inverse problems in incompressible boundary layers. The direct problem consists in predicting the velocity and temperature profiles inside the compressible boundary layer while the temperature and the velocity or pressure distribution at the edge of the boundary layer are known. An inverse problem is one in which the streamwise distribution of wall shear or displacement thickness is given, while the external pressure or velocity is unknown. The numerical procedure is presented for the incompressible case both for direct and inverse problems. The computation is performed on a structured, rectangular, nonuniform grid. Results are shown for direct computation of a compressible boundary layer and inverse computation of an incompressible boundary layer. Author (CISTI)

N94-28327 Ecole Polytechnique, Montreal (Quebec). Dept. of Mechnical Engineering.

TRANSITION FOR THREE-DIMENSIONAL, COMPRESSIBLE BOUNDARY LAYERS c34

R. Martinuzzi, F. Lamarre, and I. Paraschivoiu *In* Canadian Aeronautics

and Space Inst., Abstracts of Papers Presented at the 4th CASI Aerodynamics Symposium 1993 p 45-48 (For primary document see N94-28315 07-02)
Avail: Issuing Activity (Canadian Aeronautics and Space Inst., 130 Slater Street, Suite 818, Ottawa, ON K1P 6E2 Canada)

The SCOLIC computer code was developed for three dimensional compressible boundary layers on airfoils operating in the transonic regime. The problem of estimating the location of the laminar to turbulent transition is solved using temporal stability theory, and the point of transition is estimated according to an amplification or N-factor criterion. The methodology used in the computer code is described and some results using SCOLIC are presented. Transition predictions obtained with SCOLIC were compared to experimental data for seven different airfoils and it was found that the results were generally satisfactory. Test results for the NAE airfoil series are typically represented by the NAE-80-060. The calculated N-values suggest that the profile design is very effective at suppressing instabilities. Eventually, an instability of frequency 11,456 Hz, with point of inception at about 10 percent chord, does lead to transition around 64 percent chord which agrees remarkably well with experimental observations. For the E-580 NLF airfoil, computed results indicate that instabilities at 162 Hz and 143 Hz lead to transition at about 60 percent chord, while the transition is experimentally observed to occur at 62.6 to 65 percent chord. SCOLIC reproduces the suppression of leading edge instabilities observed with this airfoil. Author (CISTI)

N94-28328 Toronto Univ. (Ontario). Inst. for Aerospace Studies.
EXPERIMENTAL STUDY ON THE SHOCK WAVE INTERACTION WITH A HYPERSONIC BOUNDARY LAYER NEAR A CONVEX CORNER
R. J. Hawboldt, P. A. Sullivan, and J. J. Gottlieb *In* Canadian Aeronautics and Space Inst., Abstracts of Papers Presented at the 4th CASI Aerodynamics Symposium 1993 p 49-52 (For primary document see N94-28315 07-02)
Avail: Issuing Activity (Canadian Aeronautics and Space Inst., 130 Slater Street, Suite 818, Ottawa, ON K1P 6E2 Canada)

For many proposed scramjet engine inlet geometries, a thick boundary layer can develop on a long external compression surface before the flow is turned around a convex corner into the engine by an oblique shock wave. Separation at the corner is possible, thereby reducing the performance of the inlet. Experiments were conducted in a hypersonic gun tunnel to compare the onset and extent of separation of a laminar boundary layer caused by a shock wave impinging near a convex corner to the case of a shock reflecting from a flat plate. Some data were also provided for the validation of computational fluid dynamics codes. Surface static pressure was measured on a planar model that comprised a flat shock generator plate and an instrumented plate configured as either a flat plate or as a convex corner. The surface static pressure distribution was measured through four shock wave and flat plate boundary layer interactions and over two different convex corners. The interactions fell into three categories depending on the location of the separation and reattachment points with respect to the convex corner. The extent of flow separation is minimized when the separation point is located at the convex corner. For laminar flow, the ideal of perfect shock cancellation at the convex corner is unattainable. Author (CISTI)

N94-28329 De Havilland Aircraft Co. of Canada Ltd., Downsview (Ontario). Research and Development Methods Group.
EULER AND NAVIER-STOKES WING/FUSELAGE COMPUTATIONS OF THE DE HAVILLAND DASH 8 AIRCRAFT
I. Fejtek and G. D. Jones *In* Canadian Aeronautics and Space Inst., Abstracts of Papers Presented at the 4th CASI Aerodynamics Symposium 1993 p 53-56 (For primary document see N94-28315 07-02)
Avail: Issuing Activity (Canadian Aeronautics and Space Inst., 130 Slater Street, Suite 818, Ottawa, ON K1P 6E2 Canada)

Computational techniques have been developed for the accurate calculation of the flow field in the wing/fuselage junction area of aircraft. Solving the Euler equations coupled with an integral boundary layer analysis for the wing/fuselage problem presents difficulties in modelling confluent boundary layers. Solution of the Navier-Stokes equations offers the potential for far greater accuracy for this type of calculation. The thin-layer approximation is made both normal to the wing and to the fuselage to compute the boundary layers. The equations are transformed into a generalized, body-fitted, curvilinear coordinate system and nondimensionalized with respect to freestream flow values. The system of equations is closed by relating the pressure to the conservative flow variables through the equation of state for a perfect gas. The numerical algorithm used to solve the three dimensional compressible thin-layer Navier-Stokes equations is an implicit, time accurate scheme called LU-ADI factorization. The computational grid is single-block and structured, with the wing and wake lying on one boundary of the computational domain. Results are presented for a preliminary solution obtained for the Dash-8 aircraft at zero angle of incidence and Mach number 0.6, showing rapid deceleration of flow ahead of the leading edge of the wing root. Author (CISTI)

N94-28330 Institute for Aerospace Research, Ottawa (Ontario). High Speed Aerodynamics Lab.
APPLICATION OF THE INFLUENCE FUNCTION METHOD USING THE INTERFERENCE DISTRIBUTED LOADS CODE TO PREDICTION OF STORE AERODYNAMIC LOAD DURING SEPARATION FROM THE CF-18 FIGHTER AIRCRAFT
Ahmed Malek *In* Canadian Aeronautics and Space Inst., Abstracts of Papers Presented at the 4th CASI Aerodynamics Symposium 1993 p 57-60 (For primary document see N94-28315 07-02)
Avail: Issuing Activity (Canadian Aeronautics and Space Inst., 130 Slater Street, Suite 818, Ottawa, ON K1P 6E2 Canada)

A hybrid numerical and experimental technique was used to predict aerodynamic loads for a series of external stores for the CF-18 aircraft. The method recognizes that every store has a unique response to the local flow angularities, both the upwash and sidewash, in the proximity of the parent aircraft. The numerical technique, based on the influence function method (IFM), requires that the store of interest be calibrated in a known nonuniform flow field and that the parent aircraft flowfield angularities are known at the store flight regimes of interest. In recognition of the costly wind tunnel test data required by the method's calibration process, a numerical tool, the Interference Distributed Loads (IDL) code, was used in conjunction with the IFM to calculate the influence coefficients of the store of interest. Upwash and sidewash distributions in the under-wing flow field of a CF-18 model were obtained from wind tunnel measurements and the IFM/IDL method was used to predict the aerodynamic loads for a particular CF-18 external store. The predictions were compared with previous calculations in which stores calibration was performed in a flow field generated by an ogive-cylinder body. The IFM/IDL method provided better prediction of store moment coefficients, while the previous method gives better prediction of the store force coefficients. Author (CISTI)

N94-28331 British Columbia Univ., Vancouver. Dept. of Mechanical Engineering.
AERODYNAMIC PERFORMANCE OF NOVEL DUCTED-TIP WINGS
S. Z. Duan and S. I. Green *In* Canadian Aeronautics and Space Inst., Abstracts of Papers Presented at the 4th CASI Aerodynamics Symposium 1993 p 61-64 (For primary document see N94-28315 07-02)
Avail: Issuing Activity (Canadian Aeronautics and Space Inst., 130 Slater Street, Suite 818, Ottawa, ON K1P 6E2 Canada)

Experiments were conducted in a low speed wind tunnel to study the impact of a ducted-tip wing on lift/drag performance. The wing tested was a rectangular planform NACA 66-209 airfoil fitted with 92 surface pressure taps and fitted with a variety of wing tips. The first type of tip was a nearly circular section duct attached to the wing, ranging from the full chord to 65 percent of chord length. The second kind of tip was a pair of NACA 0006 short airfoils joined at both span ends, resulting in a rectangular box assembly. A simple tip extension forming a square cut wing was used for baseline performance measurements. The partial chord ducted wing tip had superior performance to all the other tip geometries, and results are presented showing lift coefficient, drag coefficient and lift/drag ratio, and pressure distribution. At modest angles of attack, the ducted tip is significantly less efficient than a conventional tip, while at angles of attack of about 8 deg or more, the ducted tip has up to 6 percent better lift/drag performance than a square cut wing tip of equal span. The main cause of this performance improvement is the greatly reduced induced drag at high lift coefficients. It is suggested that there is a significant role for the ducted tip design in both military and civilian propeller applications. Author (CISTI)

N94-28332 Nanyang Technological Inst. (Singapore).
POTENTIAL FLOW MODELLING OF AIRFOIL STALL
W. W. H. Yeung and G. V. Parkinson (British Columbia Univ., Vancouver.)

In Canadian Aeronautics and Space Inst., Abstracts of Papers Presented at the 4th CASI Aerodynamics Symposium 1993 p 65-68 (For primary document see N94-28315 07-02)
Avail: Issuing Activity (Canadian Aeronautics and Space Inst., 130 Slater Street, Suite 818, Ottawa, ON K1P 6E2 Canada)

Examples are presented of recent work using classical analytical methods to model airfoil stall. Where separated flow is involved as with airfoils near stall, it is realistic to assume that the airfoil surface exposed to the wake is at constant pressure, and that the shear layers bounding the wake can be simulated by free streamlines. The airfoil pressure loading and the flow pattern outside the wake can then be determined using the powerful properties of singularities in creating the flow models and conformal mapping in solving the resulting boundary value problems. The method is first applied to single and two-element airfoils experiencing trailing edge stall. For a single airfoil, a simple series of conformal transformations is used to map a Joukowsky airfoil, with part of its upper surface removed, onto a circle for which the flow problem is solved. The simplicity of this method permits its extension to airfoil-flap configurations in which trailing edge stall occurs on the flap. The pressure distribution calculated by the theory for a single Joukowsky airfoil closely matching a NACA 23012 profile was compared to wind tunnel measurements and showed good agreement. Author (CISTI)

N94-28333 British Columbia Univ., Vancouver. Dept. of Mechanical Engineering.

NON-ISOENERGETIC INVISCID SLOT FLOW

D. M. Stropky, I. S. Gartshore, and M. Salcudean *In* Canadian Aeronautics and Space Inst., Abstracts of Papers Presented at the 4th CASI Aerodynamics Symposium 1993 p 69-72 (For primary document see N94-28315 07-02)
Avail: Issuing Activity (Canadian Aeronautics and Space Inst., 130 Slater Street, Suite 818, Ottawa, ON K1P 6E2 Canada)

A new method was developed for predicting the flow from an arbitrarily inclined slot into a uniform free stream of arbitrarily different density and total pressure. With inviscid flow, the streamline separating the injectant and main stream can be considered as a solid boundary. The flowfield is divided into two zones, an internal region containing the slot fluid and an external region composed of the free stream fluid. Each region is solved independently, while the dividing streamline shape that provides continuity of static pressure is determined via an iterative procedure. Selected results are presented, showing that inviscid theory, when carefully applied, can describe the essential features of the flow provided some allowance is made for separation from the downstream lip at higher mass flow ratios and higher slot angles, and provided that the mainstream boundary layer is thin relative to the slot width. For application to secondary injection devices such as film-cooled turbine blades, the method shows that diffusive effects in most cases are not important for predicting the mass flow ratio.
Author (CISTI)

N94-28334 Canadair Ltd., Montreal (Quebec).

CALCULATION OF UNSTEADY INCOMPRESSIBLE INVISCID FLOW ABOUT WINGS AND BODIES USING CANAERO-T PANEL MODEL

F. I. Tezok and J. T. Conway (Agder Coll. of Engineering, Gromstad, Norway.) *In* Canadian Aeronautics and Space Inst., Abstracts of Papers Presented at the 4th CASI Aerodynamics Symposium 1993 p 73-77 (For primary document see N94-28315 07-02)
Avail: Issuing Activity (Canadian Aeronautics and Space Inst., 130 Slater Street, Suite 818, Ottawa, ON K1P 6E2 Canada)

CANAERO-T is a low order, time-stepping panel method modeling the unsteady potential flow around a configuration using linear source panels on the surface and bi-linearly varying doublet panel distribution along the span and camber surface. The implementation and testing of the CANAERO-T unsteady code is described, along with a description of the mathematical formulation of the method, some features of which appear to be unique. Results and discussions are presented for the case of an impulsively started wing, an impulsively started oscillating wing, and a submarine performing a slow oscillation of drift angle. Pressure distributions and wake structures calculated for the wings are illustrated. The oscillating wing solution clearly shows an oscillatory shape of the wake and a wake self interaction causing a mushrooming effect in the wake geometry downstream. Author (CISTI)

N94-28335 De Havilland Aircraft Co. of Canada Ltd., Downsview (Ontario). Research and Development Methods Group.

DRAG PREDICTION BY WAKE INTEGRALS USING 3-D MULTI-GRID EULER METHOD (MGAERO)

G. C. Waller *In* Canadian Aeronautics and Space Inst., Abstracts of Papers Presented at the 4th CASI Aerodynamics Symposium 1993 p 78-81 (For primary document see N94-28315 07-02)
Avail: Issuing Activity (Canadian Aeronautics and Space Inst., 130 Slater Street, Suite 818, Ottawa, ON K1P 6E2 Canada)

A method of drag prediction for Euler methods by integration of flow properties across the model wake developed by van Dam was applied to the MGAERO three dimensional multi-grid program used in aircraft aerodynamic design. Van Dam derived integral expressions for lift and drag based on the equations of motion for steady, inviscid three dimensional flow about a lifting wing. In MGAERO, the van Dam method is applied by placing a survey plane normal to freestream downstream of the model, and the cross-flow velocity components are calculated over a rectangular mesh. The derivative of the velocities gives local vorticity, which in turn is integrated to give local stream function. These variables give the lift and induced drag terms; wave drag is derived from the integral of entropy over the survey plane. The MGAERO wave drag estimate value compares sensibly with van Dam's estimates for a NACA-0012 airfoil, and the MGAERO wake integral drag value is greatly improved over the surface pressure integration value. In applying wake integral drag estimation to the design of a high-wing turboprop configuration, good agreement in lift curve and induced drag was obtained with a vortex lattice panel program. The MGAERO program represents a more detailed model of the aircraft and its flowfield, so that more subtle design changes can be evaluated against drag.
Author (CISTI)

N94-28336 Waterloo Univ. (Ontario). Dept. of Mechanical Engineering.

A NEW APPROACH TO TURBOPROP FORWARD NACELLE DESIGN
c07

I. Adare, I. Fejtek (De Havilland Aircraft Co. of Canada Ltd., Downsview, Ontario.), S. Bedi, and J. Coll (De Havilland Aircraft Co. of Canada Ltd., Downsview, Ontario.) *In* Canadian Aeronautics and Space Inst., Abstracts of Papers Presented at the 4th CASI Aerodynamics Symposium 1993 p 82-85 (For primary document see N94-28315 07-02)
Avail: Issuing Activity (Canadian Aeronautics and Space Inst., 130 Slater Street, Suite 818, Ottawa, ON K1P 6E2 Canada)

An innovative nacelle design capability was developed that significantly reduces the time for turboprop forward nacelle design and simplifies the effort required to generate nacelle shapes. The approach is an extension of the surface modeling methodologies developed by Bedi et al, in which the forward nacelle is viewed as being a blended surface joining, at the front end, a circular shape representing the spinner opening and another elongated shape representing the inlet opening, and at the aft end, a near-rectangular shape. By providing control over the manner in which the blending is performed, a variety of nacelle shapes can be generated which are smooth and which meet various geometric constraints imposed by engine and gearbox locations. The blending technique used in the modeling is based on the Bernstein basis functions. Once the surface is created using the above blending method, it is automatically divided into a network of quadrilateral panels. The output is in a surface panel format suitable for input to the aerodynamics computer program VSAERO. The interactive computer algebra package MAPLE is an integral part of the method. The entire design process comprising nacelle surface blending, surface grid generation, and VSAERO analysis can take under an hour of elapsed time on a workstation. Further refinements of the method are planned.
Author (CISTI)

N94-28337 Toronto Univ. (Ontario). Inst. for Aerospace Studies.

VISCOUS AIRFOIL COMPUTATIONS USING ADAPTIVE STRUCTURED GRIDS

D. J. Hall and D. W. Zingg *In* Canadian Aeronautics and Space Inst., Abstracts of Papers Presented at the 4th CASI Aerodynamics Symposium 1993 p 86-89 (For primary document see N94-28315 07-02)
Avail: Issuing Activity (Canadian Aeronautics and Space Inst., 130 Slater Street, Suite 818, Ottawa, ON K1P 6E2 Canada)

A solution adaptive grid generator can reduce the numerical errors in fluid flow computations by clustering grid points in regions of high error. A study of adaptive redistribution applied to viscous airfoil flows is presented

which uses the adaptive method of Eiseman. An elliptic system of partial differential equations is formulated with control functions which adaptively cluster points to specified regions in each coordinate direction. The adaptive grid generation scheme is applied to C-grid configurations about airfoil sections. Results are presented for unadapted hypberbolic and elliptic grids as well as for adapted elliptic grids. Parametric studies were conducted to determine a suitable set of input parameters for both boundary layer and streamwise pressure adaptation. Several forms of the weight function were investigated and it was found that a Mach number gradient formulation with a clustering parameter dependent on the grid geometry gives good results. The results show that grid adaptation effectively reduces the lift and overall drag errors for all cases and all grids studied. The magnitude of the error reduction depends on both the flow characteristics and the initial grid. In particular, errors in friction drag are substantially reduced.
Author (CISTI)

N94-28338 Institute for Aerospace Research, Ottawa (Ontario). High Speed Aerodynamics Lab.

SOLUTION OF THE EULER EQUATIONS USING UNSTRUCTURED GRIDS

D. J. Jones and B. MacLeod *In* Canadian Aeronautics and Space Inst., Abstracts of Papers Presented at the 4th CASI Aerodynamics Symposium 1993 p 90-93 (For primary document see N94-28315 07-02)
Avail: Issuing Activity (Canadian Aeronautics and Space Inst., 130 Slater Street, Suite 818, Ottawa, ON K1P 6E2 Canada)

Unstructured grids have many advantages over structured grids in solving computational problems of aerodynamic interest. A technique for generating unstructured grids has been developed, based on Voronoi regions and Delaunay triangulation, which can produce grids with nearly equilateral triangles in two dimensions. In an application of the technique, the Delaunay grid was obtained and then the method of Stolcis and Johnston (1990), based largely on Jameson's method, was used to obtain solutions to the Euler equations. Emphasis was first placed on supersonic flow situations including a rare application to symmetric blunt body flows. The development was recently extended to subsonic free stream situations for airfoils as part of a validation exercise. Results from four cases are illustrated: flow around a cylinder at Mach 3, Mach 1.2 flow around a NACA 0012 airfoil at 7 deg angle of attack, flow around a sphere at Mach 1.08, and Mach 0.75 flow around a RAE2822 airfoil at 3 deg angle of attack.
Author (CISTI)

N94-28339 Toronto Univ. (Ontario). Inst. for Aerospace Studies.

ATTACHED AND SEPARATED TRAILING EDGE FLOW MEASUREMENTS WITH A TRIPLE-SPLIT HOT-FILM PROBE

M. D. Doiron, D. W. Zingg, and P. Godin *In* Canadian Aeronautics and Space Inst., Abstracts of Papers Presented at the 4th CASI Aerodynamics Symposium 1993 p 94-97 (For primary document see N94-28315 07-02)
Avail: Issuing Activity (Canadian Aeronautics and Space Inst., 130 Slater Street, Suite 818, Ottawa, ON K1P 6E2 Canada)

Attached and separated trailing-edge flow measurements with a triple-split hot-film probe are presented. The probe, consisting of three nickel films deposited on a quartz cylinder and operating on the basis of variations in local convective heat transfer coefficient, has the potential to provide inexpensive measurements of separated flows. Measurements of mean-flow and turbulent stresses near the trailing edge of a 17 percent thick airfoil with moderate aft-loading were obtained at zero and 9.2 deg angles of attack at a Mach number of 0.15. Computations were also performed using the Baldwin-Lomax algebraic model and the Baldwin-Barth one-equation model (1990). Computed and measured force and moment coefficients, surface pressure distributions, and mean velocity and turbulent shear stress profiles are compared. The computations show reasonable agreement with the experimental measurements for the attached flow case but differ substantially when the flow is separated. Author (CISTI)

N94-28340 Institute for Aerospace Research, Ottawa (Ontario).

A STUDY OF BLUNT TRAILING EDGE AIRFOILS USING THE NAVIER STOKES CODE: ARC2D

M. Khalid and D. J. Jones *In* Canadian Aeronautics and Space Inst., Abstracts of Papers Presented at the 4th CASI Aerodynamics Symposium 1993 p 98-101 (For primary document see N94-28315 07-02)
Avail: Issuing Activity (Canadian Aeronautics and Space Inst., 130 Slater Street, Suite 818, Ottawa, ON K1P 6E2 Canada)

The performance of a number of turbulence models is compared in terms of their ability to predict viscous flow in the boundary layer and near-wake region of airfoil profiles with blunt trailing edges. The Baldwin-Lomax model (1978) uses different expressions for tubulent viscosity in the inner and outer viscous region, with a blending formula in the overlap region. This approach was also adapted in the current Johnson-King model (1985), which relates the nonequilibrium eddy viscosity to the maximum shear stress distribution in the chordwise direction, which in turn is obtained from the kinetic energy equation. The other two models evaluated were the Baldwin-Barth and the mixing length models. For velocity profiles, the Johnson-King model provided the closest approximation to experimental data. The computations, and to some extent the velocity profile measurements, demonstrated the existence of a complex vortical flow system behind the trailing edge of an airfoil. This system influences the flow field in a global sense and has some bearing on airfoil aerodynamic performance. Author (CISTI)

N94-28341 Toronto Univ. (Ontario). Inst. for Aerospace Studies.

THIN-LAYER NAVIER-STOKES COMPUTATIONS FOR MULTI-ELEMENT AIRFOILS

A. R. Wilkinson, T. E. Nelson, D. W. Zingg, and G. W. Johnston *In* Canadian Aeronautics and Space Inst., Abstracts of Papers Presented at the 4th CASI Aerodynamics Symposium 1993 p 102-105 (For primary document see N94-28315 07-02)
Avail: Issuing Activity (Canadian Aeronautics and Space Inst., 130 Slater Street, Suite 818, Ottawa, ON K1P 6E2 Canada)

Recent work on grid generation and Navier-Stokes computations for multi-element airfoils is presented. Decomposition of the flow domain into topologically rectangular blocks is accomplished using an automated procedure. The compressible thin-layer Navier-Stokes equations are solved using the diagonal form of the implicit approximate factorization algorithm of Beam and Warming (1986) extended for multiblock grids. Turbulence is modelled using the one-equation model of Baldwin and Barth (1990). The accuracy of the flow solver was investigated by detailed comparisons with experiment for several high-lift geometries with varying amounts of separation. Accurate results are generally obtained for attached and mildly separated flows. When the region of separated flow is larger, its thickness tends to be underestimated, and as a consequence, maximum lift and post-stall behavior are not predicted accurately. Although the turbulence model is a major source of error, other sources of error such as the thin-layer approximation and the treatment of the turbulent normal stresses cannot be ignored. Author (CISTI)

N94-28342 Ecole Polytechnique, Montreal (Quebec). Dept. of Mechanical Engineering.

TECHNIQUES FOR ACCURATELY SOLVING UNSTEADY SHOCK WAVES AND CONTACT DISCONTINUITIES **c34**

M. Paraschivoiu, J. Y. Trepanier, and R. Camarero *In* Canadian Aeronautics and Space Inst., Abstracts of Papers Presented at the 4th CASI Aerodynamics Symposium 1993 p 106-109 (For primary document see N94-28315 07-02)
Avail: Issuing Activity (Canadian Aeronautics and Space Inst., 130 Slater Street, Suite 818, Ottawa, ON K1P 6E2 Canada)

The upwind difference scheme of Roe (1986) is able to solve discontinuities exactly when a grid line is oriented and located along the discontinuity. Based on this property, a technique is suggested for managing the grid in order to exactly capture the shock waves and contact discontinuities appearing in inviscid, incompressible, unsteady flows. The shock wave discontinuities are first located. The neighboring mesh is then moved on the shocks for steady cases and with the shock for unsteady discontinuities. The movement takes into account the actual direction in which information is propagated. The solver used was developed by Trepanier et al (1991) and is based on a finite volume methodology applied to the solution of two-dimensional Euler equations on a general moving grid with moving boundaries. The mass, momentum, and energy flux are evaluated by solving an approximated Riemann problem. In the algorithms for grid management, triangulation is optimized so that cell boundaries are set normal to wave motion and each element is moved so that the shock itself forms part of the mesh line. The algorithms are tested for shock tube flow, oblique shock reflection, and parallel streams. Grid management was able to refine and coarse the grid until the discontinuity is captured exactly. Author (CISTI)

N94-28343 Ecole Polytechnique, Montreal (Quebec). Dept. of Mechanical Engineering.

A NEW FLUX VECTOR SPLITTING SCHEME c34

G.-C. Zha and E. Bilgen *In* Canadian Aeronautics and Space Inst., Abstracts of Papers Presented at the 4th CASI Aerodynamics Symposium 1993 p 110-113 (For primary document see N94-28315 07-02)

Avail: Issuing Activity (Canadian Aeronautics and Space Inst., 130 Slater Street, Suite 818, Ottawa, ON K1P 6E2 Canada)

A new flux vector splitting scheme is suggested which uses the velocity component normal to the volume interface as the characteristic speed and yields the vanishing individual mass flux at the stagnation, which may achieve accuracy for viscous flows. The scheme is very simple and easy to implement. The scheme has been applied to solve the one-dimensional and multi-dimensional Euler equations for shock tube flow. The solutions are monotone, and the normal shock wave profiles are crisp. For a one-dimensional shock tube problem with shock and contact discontinuities, the present scheme and Roe's flux difference splitting scheme give the best results compared to those from Van Leer's flux vector splitting scheme (1991) and Liou-Steffen's AUSM scheme (1991). For multi-dimensional transonic flows, sharp monotone normal shock wave profiles with mostly one transition zone are obtained. The results agree well with those from Van Leer's scheme and the AUSM scheme. Author (CISTI)

N94-28344 National Research Council of Canada, Ottawa (Ontario).

SOLUTION-ADAPTIVE SIMULATION OF TRANSONIC CASCADE FLOWS

T. C. Currie *In* Canadian Aeronautics and Space Inst., Abstracts of Papers Presented at the 4th CASI Aerodynamics Symposium 1993 p 114-117 (For primary document see N94-28315 07-02)

Avail: Issuing Activity (Canadian Aeronautics and Space Inst., 130 Slater Street, Suite 818, Ottawa, ON K1P 6E2 Canada)

A solution adaptive, two-dimensional code has been developed to solve the Euler or Navier-Stokes equations on triangular grids. The Euler fluxes of mass, momentum, and energy are integrated over the faces of non-overlapping polygonal cells formed from the median dual of a triangular mesh. Interfacial fluxes are evaluated using Roe's flux difference splitting scheme (1981). A Galerkin discretization of the viscous terms is used, assuming piecewise linear variation of the primitive variables within the triangular cells. The discretized equations are solved with either a multigrid accelerated Runge-Kutta time-marching scheme or a fully implicit Newton-Raphson procedure. The multigrid algorithm is a particularly simple one adapted from a scheme originally developed by Denton (1984) and later by Wang et. al. (1991) for structured grids. The code described has been validated against several benchmarks including inviscid flow in a supersonic compressor cascade and laminar flow over a flat plate. Author (CISTI)

N94-28345 Ecole Polytechnique, Montreal (Quebec). Dept. of Mechanical Engineering.

ICE ACCRETION ON AIRCRAFT WINGS c03

P. Tran, M. T. Brahimi, and I. Paraschivoiu *In* Canadian Aeronautics and Space Inst., Abstracts of Papers Presented at the 4th CASI Aerodynamics Symposium 1993 p 118-121 (For primary document see N94-28315 07-02)

Avail: Issuing Activity (Canadian Aeronautics and Space Inst., 130 Slater Street, Suite 818, Ottawa, ON K1P 6E2 Canada)

A three dimensional inviscid code for ice accretion on wings (Tran et al, 1992) was modified to account for viscous effects by matching the flow field to solutions obtained with a boundary layer calculation code. The flow field calculation uses a viscous inviscid interaction technique involving a panel method based on the integral singularity method, a boundary layer correction, and a suitable matching procedure using the transpiration velocity model. The numerical solution for analyzing the ice accretion consists in computing the flow characteristics around the wing and then calculating the impingement of droplets on the wing. The laminar boundary layer calculation is based on the method of Thwaites (1960) and the transition to turbulent flow is calculated using Michel's (1951) criterion. Droplet trajectories are calculated by assuming that the volume and density of the droplet remain constant and the initial droplet velocity equals the freestream velocity. The velocity field is used to compute the trajectory of a given droplet to determine whether it impinges on the wing. The droplet impact point calculation is two-dime nsional. Comparison of ice accretion obtained with INTERICE for a NACA 0012 airfoil are presented, showing good agreement with experimental results. The importance of viscous effects near the leading edge is noted. Author (CISTI)

N94-28346 Carleton Univ., Ottawa (Ontario). Dept. of Mechanical and Aerospace Engineering.

PRELIMINARY ASSESSMENT OF AERODYNAMIC EFFECTS OF WING REPAIR PATCHES

R. J. Kind and C. Carnegie *In* Canadian Aeronautics and Space Inst., Abstracts of Papers Presented at the 4th CASI Aerodynamics Symposium 1993 p 122-125 (For primary document see N94-28315 07-02)

Avail: Issuing Activity (Canadian Aeronautics and Space Inst., 130 Slater Street, Suite 818, Ottawa, ON K1P 6E2 Canada)

A preliminary assessment was obtained of the possible negative effects of aircraft damage repair patches on the aerodynamic performance of a CF-18 aircraft wing. Wind tunnel tests were conducted to measure the effects of patches of various thickness on two-dimensional boundary layers. The wind tunnel data were used to develop a set of correlation curves for describing the main effects of patches on boundary layers. These correlations are incorporated into computations for analysis of two-dimensional viscous incompressible flow, including stall effects, over airfoils. An inviscid potential flow (panel method) program is coupled with a boundary layer program into which the correlations are incorporated. Boundary layer displacement and separation effects modify the potential flow solution, and the predicted drag and lift on the airfoil. The results suggest that half-inch thick patches on a CF-18 wing would cause large reductions in lift at angles of attack near that for section stall, but that only moderate lift reductions would occur at lower angles of attack, provided that most of the pressure recovery aft of the suction peak has occurred before the flow reaches the patch. Patches cause substantial drag increases at all angles of attack below stall. Author (CISTI)

N94-28347 Ecole Polytechnique, Montreal (Quebec). Dept. of Mechanical Engineering.

UNSTEADY THREE DIMENSIONAL EULER SOLUTIONS ON MOVING GRIDS c34

A. Ilinca, J. Y. Trepanier, M. Reggio, and R. Camarero *In* Canadian Aeronautics and Space Inst., Abstracts of Papers Presented at the 4th CASI Aerodynamics Symposium 1993 p 126-129 (For primary document see N94-28315 07-02)

Avail: Issuing Activity (Canadian Aeronautics and Space Inst., 130 Slater Street, Suite 818, Ottawa, ON K1P 6E2 Canada)

A method for predicting unsteady, three dimensional compressible flows governed by the Euler system of equations is presented. The approach uses the Euler-Lagrange formulation, a finite volume scheme based on Roe's approximate Riemann solver (1981) and unstructured moving grids. To achieve flexibility in the aspects related to the geometric representation as well as grid management, tetrahedra have been used as the elementary discretization cells. An algorithm for the management and coupling of moving tetrahedra with the flow solver has been devised. The method has been tested on static and moving meshes and the results show the correct behavior of different flow fields. Some preliminary results for simple geometries are presented. These address the oblique shock wave in the flow past a dihedron, flow in a three dimensional channel, and flow inside a cube with a moving face. Author (CISTI)

N94-28348 George Washington Univ., Washington, DC. Dept. of Civil, Mechanical and Environmental Engineering.

RECENT ADVANCES IN THE SPECTRAL ELEMENT METHOD c34

Catherine Mavriplis *In* Canadian Aeronautics and Space Inst., Abstracts of Papers Presented at the 4th CASI Aerodynamics Symposium 1993 p 130-133 (For primary document see N94-28315 07-02)

Avail: Issuing Activity (Canadian Aeronautics and Space Inst., 130 Slater Street, Suite 818, Ottawa, ON K1P 6E2 Canada)

The spectral element method is used for direct simulation of incompressible fluid flow in two and three dimensions. The full unsteady viscous Navier-Stokes equations are solved. To increase this method's flexibility in handling complex geometry flows found in real engineering problems, an adaptive grid generation method is being developed. Once a grid is constructed and the solution to the Navier-Stokes equations has started, the grid can be adapted as the flow develops in time to optimally reallocate resolutions to regions of flow where it is most needed. Further increase in flexibility can be achieved by loosening restrictions on the elements to be used. Certain aspects of the adaptive grid generation method and formulation using triangular elements are discussed. Components of the grid system are illustrated with a one-dimensional solution to the Burgers equation, a good model for the Navier-Stokes equation. Triangular elements have been developed which employ fast tensor products to calculate elemental residuals. The success of the triangular element implementation is illustrated by a convergence plot for the solution of Poisson's equation on a two triangle grid with Dirichlet boundary conditions. The Poisson equation serves as the kernel of the Navier-Stokes solver. Author (CISTI)

N94-28349 Canadair Ltd., Montreal (Quebec).

MULTIGRID SOLUTIONS OF THE 2D EULER/NAVIER-STOKES EQUATIONS ON UNSTRUCTURED MESHES **c34**

Farzad Mokhtarian *In* Canadian Aeronautics and Space Inst., Abstracts of Papers Presented at the 4th CASI Aerodynamics Symposium 1993 p 134-135 (For primary document see N94-28315 07-02)

Avail: Issuing Activity (Canadian Aeronautics and Space Inst., 130 Slater Street, Suite 818, Ottawa, ON K1P 6E2 Canada)

In solutions of the two-dimensional Euler Navier-Stokes equations on unstructured triangular meshes, discretization of the governing equations is achieved using a finite element Galerkin approximation. Integration to steady state is performed using a multistage time stepping scheme, and convergence is accelerated using implicit residual smoothing and an unstructured multigrid algorithm. An algebraic turbulence model based on the Baldwin-Lomax model is implemented, based on the use of local background structured turbulence meshes. The local structured meshes are constructed using a hyperbolic mesh generator, which uses the boundary point distribution of the unstructured mesh as its initial condition. The local structured turbulence meshes are triangulated to carry out the interpolation procedure required for the execution of the turbulence model. The code is validated by comparing turbulent flow solutions about RAE2822 and NACA0012 airfoils with experimental data. The efficiency of the code is also evaluated with regard to calculations in Euler as well as both laminar and turbulent Navier-Stokes modes, with special attention to the grid and thus, to the processing requirements of the code. Author (CISTI)

N94-28350 Institute for Aerospace Research, Ottawa (Ontario).

EXPERIMENTAL INVESTIGATIONS INTO THE WALL INTERFERENCE AND SIDEWALL BOUNDARY LAYER EFFECTS IN THE NATIONAL RESEARCH COUNCIL/INST. FOR AEROSPACE RESEARCH HIGH REYNOLDS NUMBER 2-D TEST FACILITY **c34**

Y. Nishimura and K. A. Schippers *In* Canadian Aeronautics and Space Inst., Abstracts of Papers Presented at the 4th CASI Aerodynamics Symposium 1993 p 136-139 (For primary document see N94-28315 07-02)

Avail: Issuing Activity (Canadian Aeronautics and Space Inst., 130 Slater Street, Suite 818, Ottawa, ON K1P 6E2 Canada)

A wind tunnel was used to investigate the aerodynamic characteristics of a supercritical airfoil section. Tests were conducted in two different sized test sections. Comparisons of results from the two test sections are used to show the effects of the sidewall boundary layer. The investigations supported the present method of making the Mach number and incidence corrections for the ceiling/floor wall interference effects based on the classical concept of representing the model with a system of vortex, doublet, and source. The influence of the sidewall boundary layer effects result in not only a decrease in local freestream Mach number but also in an inducement of a spanwise Mach number gradient, which affects the spanwise distribution of the airfoil aerodynamic characteristics. Investigations on short-span models in the smaller of the two test sections show that the sidewall boundary layer effect in disturbing the two dimensionality of the test section flow leads to a spanwise nonuniformity of the drag distribution, especially near the flow conditions for the airfoil drag divergence where the drag levels are sensitive to even small Mach number differences across the span. Author (CISTI)

N94-28351 Institute for Aerospace Research, Ottawa (Ontario).

COMPUTATION OF WIND-TUNNEL SIDE-WALL INTERFERENCE USING 3D NAVIER-STOKES CODE **c34**

D. F. Hawken *In* Canadian Aeronautics and Space Inst., Abstracts of Papers Presented at the 4th CASI Aerodynamics Symposium 1993 p 140-143 (For primary document see N94-28315 07-02)

Avail: Issuing Activity (Canadian Aeronautics and Space Inst., 130 Slater Street, Suite 818, Ottawa, ON K1P 6E2 Canada)

Progress is reported in the numerical modeling of wind tunnel sidewall interference using the ARC3D code. This code was originally configured to compute flows through a duct containing a center body, and was altered to compute flows about wings of constant cross section. ARC3D solves the Euler equations or the thin-layer Navier-Stokes equations transformed into the numerical cordinate system and converted into a conservative second order accurate central difference equation for flow evolution at each internal cell vertex. The residual at each internal cell vertex is updated by adding the fluxes through the walls of an equivalent cell surrounding each internal cell vertex. Second- and fourth-order artificial dissipation terms are added to the fluxes to prevent instability of the solution. The system of equations is iterated towards the steady state using an implicit approximate factorization time-stepping algorithm. Pressure profiles across the airfoils obtained using preliminary ARC3D calculations are illustrated. Various methods used to eliminate pressure spikes generated by the code are discussed. Author (CISTI)

N94-28352 Institute for Aerospace Research, Ottawa (Ontario). High Speed Aerodynamics Lab.

EVALUATION OF THE BUOYANCY DRAG ON AUTOMOBILE MODELS IN LOW SPEED WIND TUNNELS **c34**

Miroslav Mokry *In* Canadian Aeronautics and Space Inst., Abstracts of Papers Presented at the 4th CASI Aerodynamics Symposium 1993 p 144-147 (For primary document see N94-28315 07-02)

Avail: Issuing Activity (Canadian Aeronautics and Space Inst., 130 Slater Street, Suite 818, Ottawa, ON K1P 6E2 Canada)

Of the several sources of inaccuracy in interpreting wind tunnel data for automobile models, the most prominent is the blockage interference. Streamwise variation of the wall induced pressure gives, in addition, rise to buoyancy drag. Buoyancy drag is analyzed in closed, 3/4 open, and slotted wind tunnels. The disturbance velocity potential is represented by a simple layer distribution. A numerical solution is obtained by a first-order panel method, approximating the surface by an assembly of flat panels, with a piecewise constant source density. The increment of the pressure coefficient due to wall interference considers only the contributions of the wall panels. Examples of the calculated buoyancy drag are given for the generic car model of the Motor Industry Research Association. Judged by the magnitude of the buoyancy drag, experiments at high blockage ratios would be highly distorted if performed in a closed-wall test section. However, with 30 percent open area ratio slotted walls, the buoyancy drag is reduced to about the same magnitude as that for test sections with low blockage ratios. Author (CISTI)

N94-27902*# Texas A&M Univ., College Station. Dept. of Aerospace Engineering.

INVESTIGATION OF AERODYNAMIC DESIGN ISSUES WITH REGIONS OF SEPARATED FLOW

Tom Gally *In* Old Dominion Univ., The 1993 NASA-ODU American Society for Engineering Education (ASEE) Summer Faculty Fellowship Program Dec. 1993 p 89-90 (For primary document see N94-27893 07-80)

Avail: CASI HC A01/MF A03

N94-27919*# Virginia State Univ., Petersburg. Dept. of Engineering Technology.

AERODYNAMIC HEATING IN HYPERSONIC FLOWS

C. Subba Reddy *In* Old Dominion Univ., The 1993 NASA-ODU American Society for Engineering Education (ASEE) Summer Faculty Fellowship Program Dec. 1993 p 154-155 (For primary document see N94-27893 07-80)

Avail: CASI HC A01/MF A03

N94-27929*# California Univ., Davis. Dept. of Mechanical and Aeronautical Engineering.
PREDICTION OF LEADING-EDGE TRANSITION AND RELAMINARIZATION PHENOMENA ON A SUBSONIC MULTI-ELEMENT HIGH-LIFT SYSTEM
C. P. vanDam *In* Old Dominion Univ., The 1993 NASA-ODU American Society for Engineering Education (ASEE) Summer Faculty Fellowship Program Dec. 1993 p 194-195 (For primary document see N94-27893 07-80)
Avail: CASI HC A01/MF A03

N94-27930*# California State Univ., Los Angeles. Dept. of Mechanical Engineering.
COMPUTATION OF TRANSONIC VISCOUS FLOW PAST THE NTF 65-DEGREE DELTA WING
Chivey Wu *In* Old Dominion Univ., The 1993 NASA-ODU American Society for Engineering Education (ASEE) Summer Faculty Fellowship Program Dec. 1993 p 196-199 (For primary document see N94-27893 07-80)
Avail: CASI HC A01/MF A03

N94-28021# Southampton Univ. (England). Dept. of Aeronautics and Astronautics.
COMPARISON OF THE INTERACTIONS OF TWO AND THREE DIMENSIONAL TRANSVERSE JETS WITH A HYPERSONIC FREE STREAM
H. E. G. Powrie, G. J. Ball, and R. A. East *In* AGARD, Computational and Experimental Assessment of Jets in Cross Flow Nov. 1993 8 p Sponsored by Defence Research Agency (For primary document see N94-28003 07-34)
Copyright Avail: CASI HC A02/MF A04

N94-28022# Institut Franco-Allemand de Recherches, Saint-Louis (France).
EXPERIMENTS ON INTERACTION FORCE OF JETS IN HYPERVELOCITY CROSS-FLOW IN A SHOCK TUNNEL
K. W. Naumann, H. Ende, G. Mathieu, and A. George *In* AGARD, Computational and Experimental Assessment of Jets in Cross Flow Nov. 1993 12 p (For primary document see N94-28003 07-34)
Copyright Avail: CASI HC A03/MF A04

N94-28027# Deutsche Aerospace A.G., Munich (Germany). Military Aircraft Div.
EFFECTS, LIMITS, AND LIMITATIONS OF SPANWISE BLOWING
W. H. Staudacher *In* AGARD, Computational and Experimental Assessment of Jets in Cross Flow Nov. 1993 10 p (For primary document see N94-28003 07-34)
Copyright Avail: CASI HC A02/MF A04

N94-28029# Stanford Univ., CA.
THEORETICAL AND EXPERIMENTAL INVESTIGATION OF A DELTA WING WITH TURBULENT LEADING-EDGE JETS
K. J. Craig, L. Roberts, D. I. Greenwell (Bath Univ., England.), and N. J. Wood (Bath Univ., England.) *In* AGARD, Computational and Experimental Assessment of Jets in Cross Flow Nov. 1993 13 p (For primary document see N94-28003 07-34)
Copyright Avail: CASI HC A03/MF A04

N94-28031# Aerospatiale, Verrieres-L-Buisson (France).
NUMERICAL ASSESSMENT OF AERODYNAMIC INTERACTIONS ON MISSILES WITH TRANSVERSE JETS CONTROL
M. Dormieux and R. Marsaa-Poey *In* AGARD, Computational and Experimental Assessment of Jets in Cross Flow Nov. 1993 11 p Sponsored in part by Ministry of Defence (For primary document see N94-28003 07-34)
Copyright Avail: CASI HC A03/MF A04

N94-28039# Office National d'Etudes et de Recherches Aerospatiales, Paris (France). Direction de l'Aerodynamique.
EXPERIMENTAL STUDY ON THE INTERACTIONS BETWEEN A TRANSVERSE HEATED SUPERSONIC JET AND AN EXTERNAL SUPERSONIC FLOW [ETUDE EXPERIMENTALE SUR LES INTERACTIONS ENTRE UN JET SUPERSONIQUE CHAUFFE TRANSVERSAL ET UN ECOULEMENT SUPERSONIQUE EXTERNE]
R. Gaillard, P. Geffroy, L. Jacquin, and G. Losfeld *In* AGARD, Computational and Experimental Assessment of Jets in Cross Flow Nov. 1993 12 p In FRENCH (For primary document see N94-28003 07-34)
Copyright Avail: CASI HC A03/MF A04

N94-28040# City Univ., London (England). Dept. of Mechanical Engineering and Aeronautics.
INCLINED AIR-JETS USED AS VORTEX GENERATORS TO SUPPRESS SHOCK-INDUCED SEPARATION
H. H. Pearcey, K. Rao, and D. M. Sykes *In* AGARD, Computational and Experimental Assessment of Jets in Cross Flow Nov. 1993 10 p Sponsored by British Aerospace Defence Ltd. (For primary document see N94-28003 07-34)
Copyright Avail: CASI HC A02/MF A04

03 AIR TRANSPORTATION AND SAFETY

Includes passenger and cargo air transport operations; and aircraft accidents.

For related information see also *16 Space Transportation* and *85 Urban Technology and Transportation.*

N94-25780# Organisatie voor Toegepast Natuurwetenschappelijk Onderzoek, The Hague (Netherlands). Physics and Electronics Lab.
A FEASIBILITY STUDY ON BIRD CLASSIFICATION WITH NEURAL NETWORK Final Report
P. P. Meiler Jun. 1992 61 p
(AD-A273753; FEL-91-A301; TDCK-TD-91-4352) Avail: CASI HC A04/MF A01

This study shows that it is feasible to classify flying birds using radar and neural network technology. The Royal Dutch Airforce is interested in the capability to classify birds because this capability can be used to avoid collisions between birds and airplanes. The Automatic Gain Control (AGC) signal which is generated by the Flycatcher tracking radar has a relationship with the wing stroke pattern of a bird. An automatic system to classify birds using the AGC signal could be used in a bird collision warning system. Such a system does not yet exist. A prototype of a bird classification system has been implemented and evaluated. Test results based on simulated AGC data show that the prototype is able to classify birds. The prototype uses simulated AGC data because there is not yet enough real AGC data available to use neural network technology. Acquisition of real AGC data is too expensive to be done in the framework of a feasibility study. According to the test results it is recommended to acquire real AGC data. DTIC

N94-26293 Aerospatiale, Toulouse (France).
SYSTEM FOR GENERATING, ABOARD AN AIRCRAFT, DURING TAKEOFF, OF A SIGNAL CAPABLE OF PRODUCING AN ALERT OR AN ALARM, IN CASE OF MALFUNCTION Patent [SYSTEME POUR L'ELABORATION A BORD D'UN AERONUF D'UN SIGNAL D'INFORMATION PENDANT LE DECOLLAGE AVEC ALERTE OU ALARM EN CAS D'ANOMALIE]
Jean-Louis Bonafe, inventor (to Aerospatiale) 13 Dec. 1991 15 p In FRENCH Filed 13 Jun. 1990
(CA-Patent-Appl-SN-2,018,940; Int-Patent-Class-G01C2300; CA-Patent-Class-354-25; CTN-92-60366) Copyright Avail: Micromedia Ltd., Technical Information Centre, 165 Hotel de Ville, Place du Portage, Phase 2, Hull, Quebec J8X 3X2, Canada HC

A system is disclosed for generating an alarm signal on an aircraft in case of takeoff malfunctions. According to the invention, means are provided for delivering signals representative of the theoretical and real accelerations of the aircraft, at a given instant. Other means are provided for calculating the predicted real distance travelled by the aircraft at a theoretical aircraft velocity corresponding to the real aircraft velocity, and for calculating the ratio of the above calculated distance to the theoretical distance travelled by the aircraft. The above ratio is compared to a predetermined level guaranteeing a minimum safe distance for braking and stopping the aircraft. An information signal is supplied to alarm means which are capable of emitting an alarm signal if the above ratio is greater than or equal to the predetermined level. According to another characteristic of the invention, the system includes means for determining the variation in the longitudinal component of the wind and for providing alarm signals when this variation is greater than or equal to a predetermined level. CISTI

N94-27081# Federal Aviation Administration, Atlantic City, NJ.
IMPACT OF IMPROVED MATERIALS AND CABIN WATER SPRAY ON COMMUTER AIRCRAFT POSTCRASH FIRE SURVIVABILITY
Timothy R. Marker Nov. 1993 35 p
(AD-A274421; DOT/FAA/CT-TN93/40) Avail: CASI HC A03/MF A01

Twelve full-scale tests were conducted in a modified Metro-liner fuselage to study the impact of using improved fire retardant materials and a cabin water spray system on postcrash fire survivability. Currently, commuter category aircraft as defined in Part 23 are exempt from meeting the stringent Federal Aviation Regulations (FAR's) requiring seat cushion fire blocking layers and low heat/smoke release panels in large transport aircraft. A zoned cabin water spray system which allowed for the individual activation of spray zones depending on cabin temperature was designed and installed in the fuselage. The system consisted of four 100 inch long zones, each containing 6 nozzles. Of the twelve tests, five were run with the water spray system and a different combination of cabin materials. These five tests were repeated without the water spray system in order to establish baseline data for each material combination. Two additional tests were conducted to investigate the impact of a partially obstructed forward test and also to evaluate the effect that the channel-type floor geometry used in the Metro-liner aircraft has on flame propagation during a cabin fire. Temperature, smoke levels, and gas concentrations were continuously monitored at a forward cabin location and each test was recorded on video. DTIC

N94-27746# Deutsche Forschungsanstalt fuer Luft- und Raumfahrt, Cologne (Germany). Transport Research Div.
METHODOLOGY DEVELOPMENT OF FORECASTING INTER-REGIONAL AIR TRANSPORT DEMAND IN CHINA [ENTWICKLUNG VON PROGNOSEMETHODEN FUER DIE INTERREGIONALE LUFTVERKEHRSNACHFRAGE IN CHINA]
Ming Zhang (Chinese Aeronautical Establishment, Beijing.), Mingming Feng (Chinese Aeronautical Establishment, Beijing.), Hans-Gustav Nuesser, and Dieter Wilken Jul. 1993 84 p
(ISSN 0939-2963)
(DLR-FB-93-24; ETN-94-95500) Avail: CASI HC A05/MF A01

The selection and calibration of three types of mode specific models to be used to forecast air transport demand in China are described. These mode specific models are the growth factor method, a direct demand travel flow, and a trip generation model. For a forecast application with data available in China, a combined flow and trip generation model is recommended, which was calibrated on the basis of cross sectional data as well as time series data. For improving the forecast method, it is suggested to collect multimodal data of travel flows in the domestic air transport network of China. ESA

N94-27766# National Transportation Safety Board, Washington, DC.
AIRCRAFT ACCIDENT REPORT: RUNWAY DEPARTURE FOLLOWING LANDING AMERICAN AIRLINES FLIGHT 102, MCDONNELL DOUGLAS DC-10-30, N139AA, DALLAS/FORT WORTH INTERNATIONAL AIRPORT, TEXAS, APRIL 14, 1993
14 Feb. 1994 173 p
(PB94-910402; NTSB/AAR-94/01; Rept-6109B) Avail: CASI HC A08/MF A02

This report explains the runway departure of American Airlines flight 102, a DC-10-30, after landing at Dallas/Fort Worth International Airport, Texas, on April 14, 1993. The safety issues discussed in the report include weather conditions affecting the flight, flight crew and air traffic control training and procedures, airplane emergency evacuation lighting, and runway maintenance. Recommendations concerning these issues were made to the Federal Aviation Administration, Dallas/Fort Worth International Airport, and American Airlines, Inc. Author

N94-27881# National Transportation Safety Board, Washington, DC.
SPECIAL INVESTIGATION REPORT: SAFETY ISSUES RELATED TO WAKE VORTEX ENCOUNTERS DURING VISUAL APPROACH TO LANDING
Feb. 1994 98 p
(PB94-917002; NTSB/SIR-94/01; Rept-6264) Avail: CASI HC A05/MF A02

Since December 1992, there have been five accidents and incidents in which an airplane on approach to landing encountered the wake vortex of a preceding Boeing 767 (B-767). Thirteen occupants died in two of the accidents. The encounters, which occurred during visual conditions, were severe enough to create an unrecoverable loss of control for a Cessna Citation, a Cessna 182, and an Israel Aircraft Industries Westwind. Additionally, there were significant but recoverable losses of control for a McDonnell Douglas MD-88 and a B-737 (both required immediate and aggressive flight control deflections by their flight crews). Safety Board data show that between 1983 and 1993, there were at least 61 accidents and incidents in the United States, including the 5 mentioned above, that resulted from probable encounters with wake vortices. In these 61 encounters, 27 occupants were killed, 8 were seriously injured, and 40 airplanes were substantially damaged or destroyed. The Safety Board conducted a special investigation to examine in detail the circumstances surrounding the five recent accidents and incidents to determine what improvements may be needed in existing procedures to reduce the likelihood of wake vortex encounters. The Safety Board's investigation initially focused on why the B-757 appeared to be involved in a disproportionate number of wake vortex encounters. Several reports indicated that the B-757 generated wake vortices that were more severe than would be expected for an airplane of its weight. However, as a result of a thorough study and analysis of the issue, the Safety Board found little technical evidence to support the notion that the wake vortex of a B-757 is significantly stronger than indicated by its weight. Derived from text

N94-28230# Deutsche Lufthansa A.G., Frankfurt am Main (Germany).
LUFTHANSA YEARBOOK 1992 [LUFTHANSA JAHRBUCH 1992]
Elisabeth Heidan, Dirk Hoefinghoff, and Dierk Wuensche Oct. 1992 301 p In GERMAN
(ISSN 0176-5086)
(DSK-9734-H-92; ETN-94-95278) Copyright Avail: CASI HC A14/MF A03

In the perspective of the single European market, the following aspects of air traffic are investigated from the Lufthansa point of view: flight safety, European community environment policy, and development of harmonization among air traffic authorities in Europe. Other topics are included, such as the new Munich airport, A-340 test program, influence of economical recession on air traffic, effect of deregulation in the U.S., and integrators in air freight market. For individual titles, see N94-28231 through N94-28250.

N94-28231# Deutsche Lufthansa A.G., Frankfurt am Main (Germany).
THE SINGLE EUROPEAN MARKET AND AIR TRAFFIC CHANCES AND RISKS [BINNENMARKT UND LUFTVERKEHR: CHANCEN UND RISIKEN]
Manfred Momberger *In its* Lufthansa Yearbook 1992 Oct. 1992 p 32-43 In GERMAN (For primary document see N94-28230 07-03)
Copyright Avail: CASI HC A03/MF A03

The new competition conditions in air business, due to the single European market, are examined. The Brussels commission proposed a liberalization law, which guarantees price freedom and allows any service to be offered by any airline in any country of the European community; former capacity restrictions were suppressed. Freight and charter activities were submitted to the same conditions. In order to avoid the excesses of American deregulation, which causes a concentration of traffic on big, dominating companies, a liberalization through elimination of unnecessary rules was desired by European bureaucracy. The future development of air traffic is found to be currently restricted by the lack of runway capacity in European airports. Prices are assumed to be increased since the government aids are suppressed. The problem of airline mergers and cooperations, which could cause the overwhelming supremacy of United Airlines, British Airways and Japan Airlines, was examined. ESA

N94-28232# Deutsche Lufthansa A.G., Frankfurt am Main (Germany).
DEREGULATION OF AIR TRAFFIC IN AMERICA: A MODEL TO BE INITIATED? [DEREGULIERUNG DES LUFTVERKEHRS IN AMERIKA: NACHAHMENSWERTES MODELL?]
Henry A. Schrader *In its* Lufthansa Yearbook 1992 Oct. 1992 p 44-53 In GERMAN (For primary document see N94-28230 07-03)
Copyright Avail: CASI HC A02/MF A03

The consequences of deregulation in the U.S. are reviewed and their transposition to the European case are examined. After fifteen years of deregulation three airlines are dominating the commercial aviation market and the other ones are facing overcapacity problems. Oil crisis, economic recession, and deregulation of the American financial system from 1984 to 1990 played an important role in the sluggishness of the current aviation market. Some advantages were offered to the consumer by deregulation: price drop, increased choice of proposed flights such as regional lines and development of a so called social tourism, enhanced by low prices. On the other hand, some point to point connections disappeared so that passengers had to be in transit in overcrowded hubs and service quality dropped. If a similar liberalization occurs in Europe the influence of national administrations might avoid such excesses and allow profitability and travel easiness to be combined. ESA

N94-28233# Deutsche Lufthansa A.G., Frankfurt am Main (Germany).
AIR TRAFFIC OF THE EUROPEAN COMMUNITY WITH EUROPEAN NEIGHBORS [DER LUFTVERKEHR DER EG MIT DEN EUROPAEISCHEN NACHBARN]
Stefan Beyhoff *In its* Lufthansa Yearbook 1992 Oct. 1992 p 54-59 In GERMAN (For primary document see N94-28230 07-03)
Copyright Avail: CASI HC A02/MF A03

The European air transportation market is examined considering the changes due to the single European market and the political and economical evolutions in Eastern Europe. For EFTA (European Free Trade Association) countries (Finland, Iceland, Norway, Austria, Sweden, and Switzerland) a solution was found: the treaty on European economic space applies the liberalization rules to the EFTA countries which asked for European Community membership. As regards countries from Eastern Europe, bilateral agreements currently exist between individual states; with the countries from the former Soviet Union, the situation is even more confused. It is noticed that, in the case of integration of Eastern Europe states in the European Community, flight safety and infrastructure problems make a differentiated utilization of liberalization measures necessary. ESA

N94-28234# Deutsche Lufthansa A.G., Frankfurt am Main (Germany).
A SKY ABOVE EUROPE [EIN HIMMEL UEBER EUROPA]
Helga L. Hillebrand *In its* Lufthansa Yearbook 1992 Oct. 1992 p 60-69 In GERMAN (For primary document see N94-28230 07-03)
Copyright Avail: CASI HC A02/MF A03

The necessary integration of European flight safety is examined in the framework of the single European market. Members of ECAC (European Civil Aviation Conference) decided in 1990 to develop the four phases EATCHIP (European Air Traffic Control Harmonization and Integration Program) and to buy and operate the needed equipments for harmonization measures. First phase of EATCHIP will allow air space to be structured and some new routes to be opened. The second phase will supply a detailed planning of middle term harmonization; third phase will be devoted to the structure of a European radar system; with the fourth phase an improved onboard/ground communication system will be introduced. EATMS (European Air Traffic Management System) was developed in cooperation with ICAO (International Civil Aviation Organization), European Community Commission and European industry. APATSI (Airport/Air Traffic System Interface) was created for determining requirements and equipments for a new airport management strategy. A central flow management unit will allow a modern data base to be available. It is concluded that a European, well organized flight security system allows air traffic to be increased by 80%. ESA

N94-28235# Deutsche Lufthansa A.G., Frankfurt am Main (Germany).
THE SINGLE EUROPEAN MARKET: ECONOMICAL ADVANCE, ECOLOGICAL PROBLEM? [DER EG-BINNENMARKT: OEKONOMISCHER FORTSCHRITT OEKOLOGISCHES PROBLEM?]
Horst Busacker *In its* Lufthansa Yearbook 1992 Oct. 1992 p 70-79 In GERMAN (For primary document see N94-28230 07-03)
Copyright Avail: CASI HC A02/MF A03

The impact on the environment of air traffic increase due to the single European market is addressed and the chances of the European Community for a successful protection of environment are evaluated. The evolution of the European environmental policy was explained, since the 1972 Paris summit, where chiefs of states and governments decided to work for a better quality of life, until the creation of European Environment Agency and the writing of the single European act, which outlines the responsibility of member states in environment protection. Environmental damages due to air traffic were recalled: aircraft noise, harmful emissions such as carbon, sulfur and nitrogen oxides, waste treatment and ground water protection. Current activities for international standardization of aircraft nuisances are reported: the Committee on Aviation Environmental Protection of ICAO (International Civil Aviation Organization), the abatement of nuisances caused by air transport group of ECAC (European Civil Aviation Conference) decided the nitrogen oxide emissions have to be dropped from 40%; the European Commission edited a green book titled 'A common strategy for a sustainable mobility'. ESA

N94-28236# Deutsche Lufthansa A.G., Frankfurt am Main (Germany).
THE ADVANTAGES OF THE LOCATION GERMANY MUST NOT BE JEOPARDIZED IN AIR TRAFFIC [VORTEILE DES STANDORTS DEUTSCHLAND IN LUFTVERKEHR NICHT GEFAEHRDEN]
Wolf-Ruediger Ussler *In its* Lufthansa Yearbook 1992 Oct. 1992 p 80-89 In GERMAN (For primary document see N94-28230 07-03)
Copyright Avail: CASI HC A02/MF A03

The relationships between air traffic and industry in Germany are studied. It is noted that good air transportation capabilities are necessary for the installation of foreign companies in German cities and that Germany is the biggest air traffic market in Europe. Considering the expected increase in air traffic, airport capacities and infrastructures and air space control are shown to be insufficient and ineffective, and the need for political measures and important investments is ascertained. The high level of financial charges weighing on German companies is shown to be an important disadvantage regarding competitiveness, nevertheless high wages are the condition for social and political stability and high productivity, which are symbols of German quality. It is concluded that the harmonization process due to the single European market, which is a necessary condition for fair economical competition, will enhance the advantages of Germany as a geographic node and a door towards Eastern Europe. ESA

N94-28237# Deutsche Lufthansa A.G., Frankfurt am Main (Germany).
LUFTHANSA FACING THE SINGLE EUROPEAN MARKET [LUFTHANSA VOR DEM BINNENMARKT]
Axel C. Pfeil *In its* Lufthansa Yearbook 1992 Oct. 1992 p 90-104 In GERMAN (For primary document see N94-28230 07-03)
Copyright Avail: CASI HC A03/MF A03

Lufthansa's situation in the context of a single European market and the changes in the global air transportation industry is described. Lufthansa must compete with European airlines, American carriers, and Asiatic air companies whose cost structures are extremely favorable. Business and private travelers have become more and more sensitive to prices, customer faithfulness is disappearing, infrastructure capacities are too limited and expensive, and high speed trains are gaining market shares. The growth strategy of Lufthansa is based on the following: its well known strength; strategic alliances with Scandinavian Airlines, Swissair, and Austrian Airlines; and selective participation in key markets. The introduction of a profit center organization and the splitting of the global company into more flexible structures are assumed to make Lufthansa a competitive airline. ESA

N94-28238# Deutsche Lufthansa A.G., Frankfurt am Main (Germany).
AIR TRAFFIC ADMINISTRATION ENROUTE TO EUROPE [LUFTFAHRTVERWALTUNG AUF DEM WEG NACH EUROPA]
Jochen Pieper *In its* Lufthansa Yearbook 1992 Oct. 1992 p 105-108 In GERMAN (For primary document see N94-28230 07-03)
Copyright Avail: CASI HC A01/MF A03

Joint Aviation Authorities in the framework of the single European market and based on the recommendations of ICAO (International Civil Aviation Organization) are presented. Twelve joint aviation regulations were edited in 1992. The regulations address definitions, technical rules, turbofans, propfans, auxiliary power turbines, maintenance and time since overall, sailplanes, and all weather operations. ECAC (European Civil Aviation Conference) was in charge of air transportation personnel; the member states must accept the qualification of any pilot from another member state. Nevertheless training rules were compared in all states and discrepancies found could lead to pilot technical and theoretical testing. A common training program for pilots was written. The program will be mandatory for flight crew licensing. ESA

N94-28239# Deutsche Lufthansa A.G., Frankfurt am Main (Germany).
MUNICH AIRPORT: THE NEW LUFTHANSA HUB [FLUGHAFEN MUENCHEN: DIE NEUE LUFTHANSA-DREHSCHEIBE]
Horst Waehner *In its* Lufthansa Yearbook 1992 Oct. 1992 p 112-121 In GERMAN (For primary document see N94-28230 07-03)
Copyright Avail: CASI HC A02/MF A03

The new Munich airport (Germany), which is regarded as an example of functionality and successful integration in the landscape, is described. The airport offers to passengers central check-in in the main building with suburban railway connection and decentral checking in the four areas of the terminal. A personal transport system was developed for comfortable connections. Lufthansa was involved in the airport planning and supplied its knowhow for fashioning passenger areas. Daily, nonstop flights to 47 European cities and to New York, Miami, and Tokyo are proposed. Three hall modules compose a functional entity for import, export, and transit freight with a payload capacity of 250,000 tons. A new maintenance hall was built. Forty-three aircraft can be checked out each day. It can be concluded that Munich airport is user friendly, environmentally safe, and technically advanced. ESA

N94-28240# Deutsche Lufthansa A.G., Frankfurt am Main (Germany).
AIR TRAFFIC IN RECESSION [LUFTVERKEHR IN DER REZESSION]
Erich Meier *In its* Lufthansa Yearbook 1992 Oct. 1992 p 122-129 In GERMAN (For primary document see N94-28230 07-03)
Copyright Avail: CASI HC A02/MF A03

The air transportation market is analyzed in the framework of the current economic crisis. It is noticed that recession hurt air traffic in 1974/1975 and from 1980 to 1982; nevertheless the current situation seems to be the most difficult in the history of air transportation. It is recalled that signs of economic recession were visible before the Gulf War, but airlines were too optimistic in considering the eight previous years of prosperity. Air transportation is shown to be an early indicator of crisis; however, most airlines were not prepared for the recession and consistently overestimated the necessary capacity. The most recent studies conclude that the current crisis is only an episodic phenomenon. An annual growth rate of world air traffic of 5.5 percent is predicted until the year 2000. ESA

N94-28241# Deutsche Lufthansa A.G., Frankfurt am Main (Germany).
GERMAN-AMERICAN RELATIONS IN AIR TRAFFIC ARE TO BE CRITICIZED [DEUTSCHE-AMERIKANISCHE LUFTVERKEHRSBEZIEHUNGEN UN DER KRITIK]
Georg W. Rehm *In its* Lufthansa Yearbook 1992 Oct. 1992 p 130-135 In GERMAN (For primary document see N94-28230 07-03)
Copyright Avail: CASI HC A02/MF A03

The consequences of the arrival of numerous American airlines on the North Atlantic market are examined. The equilibrium in European/American air transportation is found to be disturbed; American companies can build hubs with their shuttle flights in Europe while Europeans do not have equivalent opportunities in the U.S. After the German reunification, Lufthansa thinks that the validity area of 1978 traffic agreement must be extended. Price war caused high losses and some airlines were suspected of dumping and 'predatory pricing'. ESA

N94-28242# Deutsche Lufthansa A.G., Frankfurt am Main (Germany).
A340 TESTING [AIRBUS A340 IM TEST]
Udo Guenzel *In its* Lufthansa Yearbook 1992 Oct. 1992 p 136-141 In GERMAN (For primary document see N94-28230 07-03)
Copyright Avail: CASI HC A02/MF A03

The quadrijet, long range A340 aircraft is described. After the first testing flights, reliability, security, aerodynamic quality, and starting power are proved to be totally satisfying, and landing powers are even surpassed. The 2000 flight test hours were planned so that Joint Aviations Authorities simultaneously give airworthiness certificate to both versions of the aircraft, A340-200 and A340-300. Test aircraft were equipped with a telemetry facility for direct online data transfer from test flight operations to a special control center, which could supply information to the test crew. Turbofan thrust was measured at several flight altitudes; external and internal noise and aircraft stability were evaluated. The fly by wire technology was particularly examined, in order for aerodynamic controls, flaps and redundancy systems to be tested. The CFM56 turbofan is depicted as an environmentally safe, low consumption and low noise gas turbine engine. ESA

N94-28243# Deutsche Lufthansa A.G., Frankfurt am Main (Germany).
FIRST CANADAIR JET FLIES FOR LUFTHANSA CITY LINE [ERSTER CANADAIR JET FLIEGT FUER LUFTHANSA CITYLINE]
Klaus Mueller *In its* Lufthansa Yearbook 1992 Oct. 1992 p 142-145 In GERMAN (For primary document see N94-28230 07-03)
Copyright Avail: CASI HC A01/MF A03

The new Canadair jet, which is a 50 seat, short range aircraft, derived from the Challenger CL-601 business travel aircraft, is described. The aircraft was developed for takeoff and landing on small airports without modern runways. It is equipped with two General Electric CF34-3A1 turbofan engines with thrust inverters, which are environmentally safe: low fuel consumption, nitrogen oxide emissions and noise levels. Hot air is used for deicing of lift wings and turbine inlets. The cockpit is equipped with headup guidance system, electronic flight information system, EICAS (Engine Indication and Crew Alerting System), and dual flight management system. The Canadair Jet is the first aircraft of its category to be certificated for all weather operations and is equipped with collision and shear wind warning systems. ESA

N94-28244# Deutsche Lufthansa A.G., Frankfurt am Main (Germany).
INTEGRATORS: A CHALLENGE FOR AIR CARGO [INTEGRATORS: HERAUSFORDERUNG FUER DIE LUFTFRACHT]
Erwin Maruhn *In its* Lufthansa Yearbook 1992 Oct. 1992 p 146-152 In GERMAN (For primary document see N94-28230 07-03)
Copyright Avail: CASI HC A02/MF A03

Activities of integrators, which have deeply modified the freight market, whose annual growth is predicted to be of 6.5% until the year 2000, are described. New logistics and distribution concepts allowed a large development of just in time delivery; integrators appeared in the U.S. after the air cargo deregulation act in 1977. Their advantages are quickness, reliability and service quality, enhanced by a uniform organization, use of modern telecommunication technologies and sending handling, based on the hub and spoke system, in a harmonized network. In order to react to this concurrence, Lufthansa created a 'collect and deliver' company, which supplies house to house carriage with combined ground and air transportation, and cooperates in Traxon, a global information system, with other companies involved in air cargo, such as Air France, Japan Airlines and Cathay Pacific. In 1990, Lufthansa took a financial stake in DHL integrator. It is concluded that only customers can jeopardize the place of the integrators on freight market. ESA

N94-28245# Deutsche Lufthansa A.G., Frankfurt am Main (Germany).
POWERFUL SELLING AND SALES STRATEGY [SCHLAGKRAEFTIGE VERKAUFS- UND VERTRIEBSSTRATEGIE]
Adrian vonDoernberg *In its* Lufthansa Yearbook 1992 Oct. 1992 p 156-165 In GERMAN (For primary document see N94-28230 07-03)
Copyright Avail: CASI HC A02/MF A03

The commercial strategy of Lufthansa for reacting to air traffic changes is described. A stricter organization structure was developed for marketing and selling. An offensive marketing communication program was developed for defining the Lufthansa product on the market and for dismantling selling barriers by customers and dispatch clerks. The partnership concept was used to enhance cooperation with middle class travel agencies; regional offices created customer advisory boards in order to maintain narrow contacts with users. The passenger service was improved with a new customer system: bonus program, accelerated check-in, self service facilities and better lounges are now proposed. Lufthansa decided these modifications in order to assess its leadership on quality, considering the increasing concurrence of the strongly growing private travel market. ESA

N94-28246# Deutsche Lufthansa A.G., Frankfurt am Main (Germany).
LUFTHANSA LONG RANGE SERVICES: MORE SIMPLICITY [EINFACH EIN BISSCHEN MEHR: LUFTHANSA-LANGSTRECKENSERVICE]
Dierk Wuensche *In its* Lufthansa Yearbook 1992 Oct. 1992 p 166-171 In GERMAN (For primary document see N94-28230 07-03)
Copyright Avail: CASI HC A02/MF A03

The long range service strategy of Lufthansa is described. It was decided to fullfil the individual wishes of international travelers, with larger comfort and improved meals. The complete B747 fleet was provided with new equipments. First and Business classes were supplied with greater spacing of seats, and an entertainment facility with an in-seat video system. All improvements were examined during test flights and a survey was made among passengers to obtain their opinion. ESA

N94-28247# Deutsche Lufthansa A.G., Frankfurt am Main (Germany).
LUFTHANSA AND EUROPE [LUFTHANSA UND OSTEUROPA]
Dirk Hoefinghoff *In its* Lufthansa Yearbook 1992 Oct. 1992 p 172-175 In GERMAN (For primary document see N94-28230 07-03)
Copyright Avail: CASI HC A01/MF A03

The air transportation market towards countries from East Europe is investigated. Germany is geographically the biggest turntable in Europe for West to East air traffic. Lufthansa is a leader on this market with 220 flights per week to 14 East European towns and offers its technology and knowhow to former communist countries in order for infrastructure problems, such as communication, maintenance and safety deficiencies, to be solved. The concurrence is strong in East European transportation, since air companies can offer low price products and are buying modern, western aircraft; Lufthansa decided to open offices in all capitals in order to protect its leadership. ESA

N94-28248# Deutsche Lufthansa A.G., Frankfurt am Main (Germany).
KNOW-HOW EXPORT: LUFTHANSA TECHNOLOGY AT SHANNON [KNOW-HOW-EXPORT: LUFTHANSA-TECHNIK IN SHANNON]
Herbert A. Groeger *In its* Lufthansa Yearbook 1992 Oct. 1992 p 176-179 In GERMAN (For primary document see N94-28230 07-03)
Copyright Avail: CASI HC A01/MF A03

Lufthansa created in 1989 Shannon Aerospace, in cooperation with the GPA leasing firm and Swissair. Shannon Aerospace is an overhaul center in Ireland, which is particularly dedicated to airframe maintenance. The three companies made heavy investments for personnel training. The enterprise philosophy and culture for Shannon Aerospace are focused on quality, customer information and environment protection. ESA

N94-28249# Deutsche Lufthansa A.G., Frankfurt am Main (Germany).
AFTER THIRTY YEARS: FAREWELL OF EUROPA JET [NACH FAST DREISSIG JAHREN: ABSCHIED VON EUROPA JET]
Heinrich Grossbongardt *In its* Lufthansa Yearbook 1992 Oct. 1992 p 180-185 In GERMAN (For primary document see N94-28230 07-03)
Copyright Avail: CASI HC A02/MF A03

The role of Boeing 727 in Lufthansa operations is explained. Lufthansa ordered the first Boeing 727 in 1961, which had a cruise velocity of 900 kph and could land on short runways. During thirty years, 61 Europa Jets from several generations flew for Lufthansa and showed high safety and reliability performances; nine quick change versions were bought so that the transformation in 25 minutes from a passenger aircraft to a cargo aircraft was possible. From the beginning, Boeing 727 was regarded by the passengers as the most comfortable civil aircraft. In 1992 Autumn the last Boeing 727 are replaced by A-320 aircraft, whose specific consumption and loading on environment are lower. It is noticed that Lufthansa Boeing 727 carried 60 million passengers 500 million km. ESA

N94-28250# Deutsche Lufthansa A.G., Frankfurt am Main (Germany).
A SYMBOL OF RELIABILITY: Ju 52 [SYMBOL DER ZUVERLAESSIGKEIT: DIE JU 52] **c05**
Ralf Nolting *In its* Lufthansa Yearbook 1992 Oct. 1992 p 186-191 In GERMAN (For primary document see N94-28230 07-03)
Copyright Avail: CASI HC A02/MF A03

The story of Junker 52 (Ju 52) aircraft is presented. Lufthansa possessed 78 machines of this type in 1940 and in 1985 wished to find at least one JU 52 as a symbol of aviation tradition, German knowhow as pioneer aircraft. A Ju 52 was found in Florida and sent to Germany. The old aircraft was restored during sixteen months and its structure and turbines were totally overhauled; the cabin was equipped with new seats and the cockpit with modern navigation instruments. The renewed aircraft flew for eight months over the U.S. and ended its trip by a formation flight with a Boeing 737 aircraft above Seattle. The turbine engines were modified for noise reduction. ESA

N94-27285*# Massachusetts Inst. of Tech., Cambridge. Flight Transportation Lab.
AN INVESTIGATION OF AIR TRANSPORTATION TECHNOLOGY AT THE MASSACHUSETTS INSTITUTE OF TECHNOLOGY, 1992-1993
Robert W. Simpson *In* NASA. Langley Research Center, FAA/NASA Joint University Program for Air Transportation Research, 1992-1993 Feb. 1994 p 3-8 (For primary document see N94-27284 07-01)
Avail: CASI HC A02/MF A02

N94-27287*# Massachusetts Inst. of Tech., Cambridge. Dept. of Aeronautics and Astronautics.
A DATA FUSION ALGORITHM FOR MULTI-SENSOR MICROBURST HAZARD ASSESSMENT
Craig R. Wanke and R. John Hansman *In* NASA. Langley Research Center, FAA/NASA Joint University Program for Air Transportation Research, 1992-1993 Feb. 1994 p 17-28 See also A92-55328 Submitted for publication Sponsored in part by FAA (For primary document see N94-27284 07-01)
(Contract NGL-22-009-640; F19628-90-C-0002)
Avail: CASI HC A03/MF A02

N94-27288*# Ohio Univ., Athens. Dept. of Electrical and Computer Engineering.
INVESTIGATION OF AIR TRANSPORTATION TECHNOLOGY AT OHIO UNIVERSITY, 1992-1993
Robert W. Lilley *In* NASA. Langley Research Center, FAA/NASA Joint University Program for Air Transportation Research, 1992-1993 Feb. 1994 p 31-33 (For primary document see N94-27284 07-01)
Avail: CASI HC A01/MF A02

N94-27294*# Princeton Univ., NJ. Dept. of Mechanical and Aerospace Engineering.
INVESTIGATION OF AIR TRANSPORTATION TECHNOLOGY AT PRINCETON UNIVERSITY, 1992-1993
Robert F. Stengel *In* NASA. Langley Research Center, FAA/NASA Joint University Program for Air Transportation Research, 1992-1993 Feb. 1994 p 87-97 (For primary document see N94-27284 07-01)
Avail: CASI HC A03/MF A02

N94-27296*# Princeton Univ., NJ. Dept. of Mechanical and Aerospace Engineering.
OPTIMAL NONLINEAR ESTIMATION FOR AIRCRAFT FLIGHT CONTROL IN WIND SHEAR
Sandeep S. Mulgund *In* NASA. Langley Research Center, FAA/NASA Joint University Program for Air Transportation Research, 1992-1993 Feb. 1994 p 111-130 (For primary document see N94-27284 07-01)
Avail: CASI HC A03/MF A02

N94-28345 Ecole Polytechnique, Montreal (Quebec). Dept. of Mechanical Engineering.
ICE ACCRETION ON AIRCRAFT WINGS
P. Tran, M. T. Brahimi, and I. Paraschivoiu *In* Canadian Aeronautics and Space Inst., Abstracts of Papers Presented at the 4th CASI Aerodynamics Symposium 1993 p 118-121 (For primary document see N94-28315 07-02)
Avail: Issuing Activity (Canadian Aeronautics and Space Inst., 130 Slater Street, Suite 818, Ottawa, ON K1P 6E2 Canada)

04 AIRCRAFT COMMUNICATIONS AND NAVIGATION

Includes digital and voice communication with aircraft; air navigation systems (satellite and ground based); and air traffic control.

For related information see also *17 Space Communications, Spacecraft Communications, Command and Tracking* and *Communications and Radar.*

N94-25788# Federal Aviation Administration, Atlantic City, NJ.
AIRBORNE DATA LINK OPERATIONAL EVALUATION TEST PLAN
Albert J. Rehmann and R. H. Mogford (Computer Technology Associates, Inc., Pleasantville, NJ.) Aug. 1993 47 p
(AD-A274096; DOT/FAA/CT-TN93/30) Avail: CASI HC A03/MF A01

This plan describes an end-to-end study of operational concepts and procedures associated with the introduction of electronic data communications between flight crews and air traffic controllers. Full performance controllers from terminal facilities will interact with type-related line pilots in four cockpit simulators networked into the Federal Aviation Administration Technical Center's Air Traffic Control Laboratory. Measures of human performance will gain insight into flight crew alerting, display, placement, and the utility of voice annunciation of data link messages. Direct measures of workload, communications efficiency, data link attention time (measured by head position), and aircraft state will be gathered and translated into recommendations for the cockpit display configuration. DTIC

N94-25808# Technical Research Centre of Finland, Espoo. Machine Automation Lab.
DEAD RECKONING NAVIGATION
Hannu Hakala Sep. 1992 88 p Sponsored by Technology Development Center, Finland
(ISSN 1235-0605)
(VTT-TIED-1402; ISBN-951-38-4216-9; ETN-94-95249) Copyright Avail: CASI HC A05/MF A01

Navigation systems for automotive navigation are considered. Basic in-car navigation is based on dead reckoning, which is enhanced with methods like map matching, proximity beacons, or satellite navigation systems. The method of dead reckoning in vehicle navigation applications is described. The terminology used in this area is explained. The basic theory of dead reckoning is given. The principles of common types of odometers and differential odometer are described. Examples of odometer realizations and distance measurement devices are presented. The other component of dead reckoning calculations, heading, can be measured with magnetic compasses, gyroscopes, optical gyros, and other means. These methods are explained and component realizations are shown. Inertial navigation systems are described. Dead reckoning and inertial navigation methods are compared. ESA

N94-25810# Air Force Inst. of Tech., Wright-Patterson AFB, OH.
ANALYSIS AND SIMULATION OF A GPS RECEIVER DESIGN USING COMBINED DELAY-LOCK AND MODIFIED TANLOCK LOOPS M.S. Thesis
George D. Harris Dec. 1993 93 p
(AD-A274037; AFIT/GE/ENG/93D-13) Avail: CASI HC A05/MF A01

The purpose of this thesis was to investigate the performance of two types of tracking loops used in global positioning system (GPS) receivers. The first loop, the delay-lock loop (DLL), is responsible for maintaining synchronization with the received PN sequence. The second loop, the modified tanlock loop (MTLL), is responsible for maintaining synchronization with the carrier signal. The performance of the two loops is investigated first separately then their performance is evaluated when operated together. This thesis is an investigation on the ability of these two loops to overcome corruption of the input signal due to noise. Expanding the dynamic operating range of these loops can significantly improve GPS receiver operation. Results indicate the performance of the loops was better than theoretical predictions by maintaining lock across a wide range of loop gains and SNR's. However, when the loops were combined, the loops did not perform as predicted by theory. All simulations display phenomena which was not present in the theoretical predictions. DTIC

N94-26197 Federal Aviation Administration, Atlantic City, NJ. Technical Center.
AIR TRAFFIC CONTROLLER WORKING MEMORY: CONSIDERATIONS IN AIR TRAFFIC CONTROL TACTICAL OPERATIONS Technical Report, Oct. 1992 - Sep. 1993
Earl S. Stein and Daniel Garland Sep. 1993 71 p Limited Reproducibility: More than 20% of this document may be affected by microfiche quality
(AD-A273722; DOT/FAA/CT-TN-93/37) Avail: CASI HC A04

The Air Traffic Control (ATC) environment is characterized by a continuous sequence of ever-changing, transient information, such as a series of aircraft being handled by an air traffic controller which must be encoded and retained, primarily, for tactical use (3 to 5 minutes) and secondarily, for strategic planning. This information is complicated by the limitations and constraints of human memory, in particular, working memory. Working memory can potentially degrade performance. The primary objective of this report is to raise an awareness of the memory requirements of ATC tactical operations by presenting information on working memory processes that are relevant to ATC tasks, and the vulnerability of these processes to disruption. This report focuses on developing an understanding of the role working memory plays in air traffic controller performance by emphasizing the constraints, and the factors that may overcome or minimize memory loss of critical ATC information. Two hundred twenty-nine references are cited in this report. DTIC

N94-26309# Pacific Northwest Lab., Richland, WA.
DIFFERENTIAL GLOBAL POSITIONING SYSTEM FOR THE SURFACE-TOWED ORDNANCE LOCATING SYSTEM: TESTING, RESULTS, AND USER'S GUIDE
T. L. Stewart and C. W. Hubbard Oct. 1993 64 p
(Contract DE-AC06-76RL-01830)
(DE94-002980; PNL-8921) Avail: CASI HC A04/MF A01

Researchers at the Pacific Northwest Laboratory integrated and tested a Global Positioning System (GPS) for use with the Naval Explosive Ordnance Disposal Technology Center's (NEODTC) Surface-Towed Ordnance Locating System (STOLS). The GPS automatically and continuously provides latitude, longitude, and elevation information at the mobile GPS unit. The results of testing the GPS are shown in this report. The results reveal accuracies in the submeter range in real time and within a few centimeters using post-processing software. A description of hardware and software components is also included, along with system drawings and parts lists. DOE

N94-26493# Naval Postgraduate School, Monterey, CA. Dept. of Electrical and Computer Engineering.
MIMO RECURSIVE LEAST SQUARES CONTROL ALGORITHM FOR THE AN/FPN-44A LORAN-C TRANSMITTER M.S. Thesis
John D. Wood Sep. 1993 107 p
(AD-A274820) Avail: CASI HC A06/MF A02

A multiple-input, multiple-output (MIMO) recursive least squares (RLS) algorithm is developed to shape and control the Loran-C RF pulse of the AN/FPN-44A tube type transmitter. The control algorithm is incorporated into a transmitter simulation program, where it seeks to produce an optimal transmitter drive waveform (TDW). An optimal TDW produces a near ideal RF pulse. The control algorithm uses a MIMO reference model of the transmitter; parameters of the model are obtained using recursive least squares multichannel time series techniques. The MIMO reference model has the ability to adapt to the non-LTI characteristics of the simulated transmitter. The MIMO RLS control algorithm is implemented in both an ideal and a realistic noisy environment. In the ideal environment, when representing the RF pulse with parameters of its half-cycle peak amplitudes and zero-crossings, the MIMO RLS controller is able to shape the RF pulse and control its zero-crossings. Quantization and system noise in the non-ideal environment results in performance deterioration of the control algorithm. The performance of the MIMO RLS algorithm is compared against another method of control, the steepest descent algorithm. DTIC

N94-26539# Technische Univ., Delft (Netherlands). Mathematische Geodesie en Puntsbepaling.
HIGH-PRODUCTION GLOBAL POSITIONING SYSTEM METHODS FOR SURVEY APPLICATIONS: THE PSEUDO-KINEMATIC METHOD WITH THE TRIMVEC PROGRAMMING SYSTEM Thesis [HOGE-PRODUKTIE GPS TEN BEHOEVE VAN LANDMEETKUNDIGE TOEPASSIGEN: DE PSEUDO-KINEMATISCHE METHODE METDE TRIMVEC-PROGRAMMATUUR]
M. W. Schram Aug. 1992 140 p In DUTCH
(ETN-94-95035) Avail: CASI HC A07/MF A02

Four productive GPS (Global Positioning System) methods were developed to overcome the long observation period of the static method. The semi kinematic, pseudo kinematic, 'rapid static', and continuous kinematic methods are presented. The applicability of the pseudo kinematic method was investigated, using the Trimvec programming system. The pseudo kinematic method provides a 30% higher production than the static method. The highest production is obtained for baselines of about 10 km. ESA

N94-26826# Systems Control Technology, Inc., Arlington, VA.
ROTORCRAFT LOW ALTITUDE IFR BENEFIT/COST ANALYSIS: CONCLUSIONS AND RECOMMENDATIONS Final Report
Robert K. Anoll, Robert B. Newman, and Edwin D. McConkey Oct. 1993 153 p
(Contract DTFA01-87-C-00014)
(AD-A274241; SCT-92RR-8; DOT/FAA/RD-93/22) Avail: CASI HC A08/MF A02

The Rotorcraft Master Plan advocates the establishment of additional communications, navigation, and surveillance (CNS) facilities, as well as the analysis and development of systems to satisfy the increasing demand for widespread instrument flight rules (IFR) rotorcraft operations within the National Airspace System (NAS). The objective of this study is to determine if there is an economic basis for improvement of these low altitude IFR services within the NAS in order to better support rotorcraft IFR operations. The findings of this study will aid FAA decision making in that regard. In view of prior implementation decisions on LORAN-C and GPS, the emphasis in this effort is on communications, surveillance, procedural changes, and avionics. This report is the last of a series of three reports that address rotorcraft low altitude benefit/cost analysis. This final report reviews the operational requirements and constraints for specific rotorcraft missions identified in the previous reports in this series. It also reviews all of the alternatives identified for improving rotorcraft operations. The alternatives considered include additional communications and surveillance equipment, both existing equipment and future systems identified in the Aviation Systems Capital Investment Plan (CIP), and the air traffic control (ATC) procedural changes. A benefit/cost (B/C) analysis is conducted for each communication, surveillance, and procedural improvement identified. DTIC

N94-27071# Air Force Inst. of Tech., Wright-Patterson AFB, OH. School of Engineering.
DEVELOPMENT OF A PERFORMANCE EVALUATION TOOL (MMSOFE) FOR DETECTION OF FAILURES WITH MULTIPLE MODEL ADAPTIVE ESTIMATION (MMAE) M.S. Thesis
Robert L. Nielsen Dec. 1993 180 p
(AD-A274218; AFIT/GE/Eng/93S-37) Avail: CASI HC A09/MF A02

Multiple model Kalman Filter (KF) techniques are used extensively for Multiple Model Adaptive Estimation (MMAE), Multiple Model Adaptive Control (MMAC), and Distributed Kalman Filter (DKF) applications to determine Bayesian-blended optimal estimates of states, uncertain parameters, and optimal control signals. Multiple model methods are used for sensor management, Failure Detection and Isolation (FDI), and other Guidance and Control (G and C) applications. A simulation tool called the Multiple Model Simulation for Optimal Filter Evaluation (MMSOFE) has been in this research. MMSOFE is based on the well-benchmarked single Kalman filter tool called Multimode Simulation for Optimal Filter Evaluation (MSOFE). MMSOFE is a highly portable and versatile multiple and single Kalman filter evaluation tool. It is capable of performing simulations with one filter or up to 98 elemental filters in a multiple model adaptive filter structure. It can be adapted easily for other multiple model applications. MMSOFE was applied to failure detection and isolation of measurement jamming and spoofing-type failures, similar to jamming and spoofing of a Global Positioning System (GPS). A satellite orbit estimation test case was used. DTIC

N94-27210 National Defence Research Establishment, Stockholm (Sweden). Dept. of Weapon Systems, Effects and Protection.
SATELLITE NAVIGATION SYSTEM GPS: A REVIEW OF PRINCIPLES AND PERFORMANCE AND DEVELOPMENTS IN GENERAL [SATELLITNAVIGERINGSSYSTEMET GPS: OEVERSIKT OEVER FUNKTION OCH PRESTANDA SAMT UTVECKLINGSTENDENSER I STORT]
S. Arnzen Jun. 1993 65 p In SWAHILI
(PB94-124534; FOA-C-20931-2.1) Avail: Issuing Activity (National Technical Information Service (NTIS))

The report gives a summary of principles and performance, obtained accuracy, and developments in general for the US DoD owned GPS-system. Additionally, the Russian Glonass and other interesting civilian systems are shortly described. The main part of the docment was prepared as an appendix to a study at the military staff level called 'Satellite navigation systems.' The study was prepared in 1991/92 with the aim of supporting the supreme commander in the decision of how to handle the use of GPS in the armed forces in the near future. NTIS

N94-27275 Hazeltine Corp., Braintree, MA.
AUTOMATIC, REAL-TIME FAULT MONITOR VERIFYING NETWORK IN A MICROWAVE LANDING SYSTEM Patent
Darrell D. Roelofs, inventor (to Hazeltine), Alfred R. Lopez, inventor (to Hazeltine), and Kenneth R. Doris, inventor (to Hazeltine) 14 Dec. 1993 20 p
(CA-Patent-1325261; Int-Patent-Class-G01S-007/40; CTN-94-61096)
Copyright Avail: Micromedia Ltd., Technical Information Centre, 240 Catherine Street, Suite 305, Ottawa, Ontario, K2P 2G8, Canada HC/MF

A system for automatic real-time verification of the fault monitoring of an executive monitor of a microwave landing system (MLS) is disclosed. When an internally generated out-of-tolerance or erroneous signal is detected by the monitor, the system generates an alarm and declares it valid. The system also includes a station control board connected on line with the executive monitor which provides a signal to the monitor representative of erroneous or out-of-tolerance data in order to initiate an alarm in the executive monitor. The actual data obtained by the executive monitor is stored until proper fault monitoring verification occurs. A filter counting means is employed to record a history of the out-of-tolerance data received by the executive monitor so that the filter counting means can be preconditioned during the verification process to receive one additional out-of-tolerance sample to thereby generate an alarm within the executive monitor. A switch is used to permit an internally generated out-of-tolerance sample to be analyzed instead of the sampled information generated by the antenna system. Author (CISTI)

N94-27423*# National Aeronautics and Space Administration. Langley Research Center, Hampton, VA.
PACKET RADIO DATA LINK APPLICATIONS IN THE NASA LANGLEY RESEARCH CENTER TRANSPORT SYSTEMS RESEARCH VEHICLE
Wesley C. Easley, Donald Carter, and David G. McLuer (Lockheed Engineering and Sciences Co., Hampton, VA.) Jan. 1994 30 p
(RTOP 505-64-13-11)
(NASA-TM-109071; NAS 1.15:109071) Avail: CASI HC A03/MF A01

An amateur packet radio system operating in the very high frequency (VHF) range has been implemented in the Transport Systems Research Vehicle at the NASA Langley Research Center to provide an economical, bidirectional, real-time, ground-to-air data link. The packet system has been used to support flight research involving air traffic control (ATC), differential global positioning systems (DGPS), and windshear terminal doppler weather radar (TDWR). A data maximum rate of 2400 baud was used. Operational reliability of the packet system has been very good. Also, its versatility permits numerous specific configurations. These features, plus its low cost, have rendered it very satisfactory for support of data link flight experiments that do not require high data transfer rates. Author (revised)

N94-27667 Defence Research Establishment Pacific, Victoria (British Columbia). Research and Development Branch.
DIFFERENTIAL GPS METHODS AND PERFORMANCE FOR MARINE APPLICATIONS Final Report
Gerard Lachapelle Jan. 1993 58 p
(Contract DREP-W7708-2-0529/01-XSA)

(DREP-93-09; DSIS-94-00049; CTN-94-61119) Avail: CASI HC A04/MF A01

A survey is provided of current and emerging technology in differential dynamic global positioning systems (GPS), particularly in the marine environment. Measures of accuracy for GPS positions are defined. Error sources in GPS include receiver noise, multipath reflection, combined receiver noise and multipath, orbital errors, loss of phase lock, cycle slip detection and recovery, ionospheric group delay and carrier phase advance, ionospheric scintillation, tropospheric refractivity, and selective availability. The concepts of differential GPS are outlined along with a description of algorithms and procedures. Differential GPS reduces or eliminates orbital, ionospheric, tropospheric, selective availability, and clock errors and provides better quality control, but amplifies the remaining errors. Measured performance of differential GPS systems are summarized, with emphasis on new technology and algorithms. These algorithms and technologies include single and double difference methods, carrier phase smoothing, and carrier phase ambiguity resolution. Results are presented for a case study examining the performance of P code receivers and high performance C/A code receivers in a survey launch environment. Future issues and trends in differential GPS are addressed in the areas of equipment, methodologies, and infrastructure. Author (CISTI)

N94-27768*# Cornell Univ., Ithaca, NY. Dept. of Computer Science.
REFINEMENT FOR FAULT-TOLERANCE: AN AIRCRAFT HAND-OFF PROTOCOL
Keith Marzullo, Fred B. Schneider, and Jon Dehn Apr. 1994 20 p
(Contracts NAG2-593; N00140-87-C-8904; N00014-91-J-1219; NSF CCR-87-01103; NSF CCR-90-14363)
(NASA-CR-195697; NAS 1.26:195697; TR-94-1417) Avail: CASI HC A03/MF A01

Part of the Advanced Automation System (AAS) for air-traffic control is a protocol to permit flight hand-off from one air-traffic controller to another. The protocol must be fault-tolerant and, therefore, is subtle -- an ideal candidate for the application of formal methods. This paper describes a formal method for deriving fault-tolerant protocols that is based on refinement and proof outlines. The AAS hand-off protocol was actually derived using this method; that derivation is given. Author

N94-27831 National Aerospace Lab., Amsterdam (Netherlands). Informatics Div.
FLIGHT TESTING OF GPS AND GPS-AIDED SYSTEMS
O. B. M. Pietersen, M. A. G. Peters, and N. vanDriel 16 Mar. 1992 17 p Presented at the 80th AGARD Flight Mechanics Panel on Flight Testing Symposium, Chania, Crete, 11-14 May 1992 Limited Reproducibility: More than 20% of this document may be affected by microfiche quality
(NLR-TP-92151-U; ETN-94-95444) Avail: CASI HC A03

Flight test programs carried out are described: trials to investigate the suitability of differential global positioning system (GPS) for precision approaches; trials to determine the advantages of aiding a GPS receiver by inertial navigation system (INS) and of the use of null steering antennas; and trials to evaluate an in house developed navigation filter in which three navigation sensors, GPS, INS, and terrain referenced navigation (TRN), were integrated. An integrated navigation system is concluded to offer a greater robustness and a higher accuracy of the navigation solution, taking into account the weaknesses the individual sensors have. Differential GPS can eliminate a number of systematic errors, improving the attainable accuracy. ESA

N94-27290*# Ohio Univ., Athens. Avionics Engineering Center.
IMPROVED MODELING OF GPS SELECTIVE AVAILABILITY
Michael S. Braasch, AnnMarie Fink, and Keith Duffus *In* NASA. Langley Research Center, FAA/NASA Joint University Program for Air Transportation Research, 1992-1993 Feb. 1994 p 45-54 Presented at the Institute of Navigation 1993 National Technical Meeting, San Francisco, CA, 20-22 Jan. 1993 (For primary document see N94-27284 07-01)
(Grant NGR-36-009-017)
Avail: CASI HC A02/MF A02

N94-27291*# Ohio Univ., Athens. Avionics Engineering Center.
REALTIME MITIGATION OF GPS SA ERRORS USING LORAN-C
Soo Y. Braasch *In* NASA. Langley Research Center, FAA/NASA Joint University Program for Air Transportation Research, 1992-1993 Feb. 1994 p 55-61 Presented at the Wild Goose Association, Annual Convention and Technical Symposium, Birmingham, England, 24-27 Aug. 1992 Sponsored in part by FAA (For primary document see N94-27284 07-01)
(Grant NGR-36-009-17)
Avail: CASI HC A02/MF A02

N94-27292*# Ohio Univ., Athens. Avionics Engineering Center.
A GPS COVERAGE MODEL
Trent A. Skidmore *In* NASA. Langley Research Center, FAA/NASA Joint University Program for Air Transportation Research, 1992-1993 Feb. 1994 p 63-72 Presented at the Institute of Navigation 1992 National Technical Meeting, Washington, DC, 29 Jun. - 1 Jul. 1992 See also A94-12567 (For primary document see N94-27284 07-01)
(Contract NGR-36-009-017; DTRS57-87-C-00006)
Avail: CASI HC A02/MF A02

N94-27293*# Ohio Univ., Athens.
GROUND STATION SITING CONSIDERATIONS FOR DGPS
James D. Waid *In* NASA. Langley Research Center, FAA/NASA Joint University Program for Air Transportation Research, 1992-1993 Feb. 1994 p 73-83 Presented at the Institute of Navigation 1993 National Technical Meeting, San Francisco, CA, 20-22 Jan. 1993 Sponsored in part by FAA (For primary document see N94-27284 07-01)
(Grants NAG1-1423; NGR-36-009-017)
Avail: CASI HC A03/MF A02

N94-27297*# Princeton Univ., NJ. Dept. of Mechanical and Aerospace Engineering.
AIR TRAFFIC MANAGEMENT AS PRINCIPLED NEGOTIATION BETWEEN INTELLIGENT AGENTS
J. P. Wangermann *In* NASA. Langley Research Center, FAA/NASA Joint University Program for Air Transportation Research, 1992-1993 Feb. 1994 p 131-140 (For primary document see N94-27284 07-01)
Avail: CASI HC A02/MF A02

N94-27918*# Saint Cloud State Coll., MN. Dept. of Electrical Engineering.
A SIMULATION OF GPS AND DIFFERENTIAL GPS SENSORS
James M. Rankin *In* Old Dominion Univ., The 1993 NASA-ODU American Society for Engineering Education (ASEE) Summer Faculty Fellowship Program Dec. 1993 p 149-153 (For primary document see N94-27893 07-80)
Avail: CASI HC A01/MF A03

05 AIRCRAFT DESIGN, TESTING AND PERFORMANCE

Includes aircraft simulation technology.
For related information see also *18 Spacecraft Design, Testing and Performance* and *39 Structural Mechanics.*For land transportation vehicles see *85 Urban Technology and Transportation.*

N94-25590# McDonnell-Douglas Astronautics Co., Saint Louis, MO.
AIRCRAFT MANEUVERS FOR THE EVALUATION OF FLYING QUALITIES AND AGILITY. VOLUME 1: MANEUVER DEVELOPMENT PROCESS AND INITIAL MANEUVER SET Final Report, 1 Sep. 1990 - 1 Jun. 1993
David J. Wilson, David R. Riley, and Kevin D. Citurs Aug. 1993 165 p
(Contract F33615-90-C-3600)
(AD-A273913; WL-TR-93-3081) Avail: CASI HC A08/MF A02

A set of aircraft maneuvers has been developed to augment evaluation maneuvers used currently by the flying qualities and flight test communities. These maneuvers extend evaluation to full aircraft dynamics throughout the aircraft flight envelope. As a result, a tie has been established between operational use and design parameters without losing control of the aircraft evaluation process. Twenty maneuvers are described as an initial set to examine primarily high angle of attack conditions. Perhaps as important as the maneuvers themselves is the method used to select them. These maneuvers will allow direct measurement of flying qualities throughout the flight envelope instead of merely comparing parameters to specification values. DTIC

N94-25772# Air Force Inst. of Tech., Wright-Patterson AFB, OH.
WEAPON SYSTEM INTEGRATION FOR THE AFIT VIRTUAL COCKPIT M.S. Thesis
William E. Gerhard, Jr. 1993 67 p
(AD-A274058; AFIT/GCS/Eng/93D-10) Avail: CASI HC A04/MF A01

The Air Force Institute of Technology is continuing research in the Virtual Cockpit. The Virtual Cockpit makes use of high performance graphics workstations, Virtual Environment technology, and Distributed Interactive Simulation network protocols to create a flight simulator based on the capabilities of the McDonnell Douglas F-15E Strike Eagle. The work presented in this thesis focuses on the design and implementation issues for integrating a weapons delivery capability. Weapons simulated include the following: RADAR and IR guided air-to-air missiles, gravity and precision guided bombs, and a 20mm cannon. Virtual Environment displays used include the following: color NTSC and monochrome high resolution helmet mounted displays employing a Polhemus Fastrack sensor, and a display using five separate BARCO projectors simultaneously. The Target graphics system was a four processor, SGI Onyx workstation with a Reality Engine graphics pipeline. Graphics rendering was accomplished with an AFIT developed object oriented simulation software package based on the SGI Performer 1.2 application development environment. DTIC

N94-25905# Air Force Inst. of Tech., Wright-Patterson AFB, OH. School of Engineering.
EVALUATION OF MODERATE ANGLE OF ATTACK ROLL OF A DUAL ENGINE, THRUST VECTORING AIRCRAFT USING QUANTITATIVE FEEDBACK THEORY M.S. Thesis
Kevin E. Boyum Dec. 1993 207 p
(AD-A274118; AFIT/GE/ENG/93D-01) Avail: CASI HC A10/MF A03

This thesis develops an innovative approach to the design of a flight control system for performing the large-amplitude velocity vector roll maneuver at high angles of attack (AOA's). A six degree of freedom aircraft model is developed from the fundamental nine-state equations of motion using a modified linearization technique. The MIMO (multiple-input multiple-output) Quantitative Feedback Theory (QFT) robust control design technique is then used to jointly address the system nonlinearities present in this maneuver and the changes in the system parameters due to changes in flight condition, treating them as structured uncertainty in the design of a three-axis rate-commanded control system. The development of a weighting matrix, based on the fundamentals of the aileron-rudder interconnect, aids in this design process. Nonlinear six degree-of-freedom closed-loop control system simulations demonstrate the accuracy of the developed models, the validity of the QFT designed compensator and prefilter, and the successful initiation and arrest of the velocity vector roll maneuver. DTIC

N94-25961# McDonnell-Douglas Aerospace Information Services Co., Saint Louis, MO.
AIRCRAFT MANEUVERS FOR THE EVALUATION OF FLYING QUALITIES AND AGILITY. VOLUME 3: SIMULATION DATA Final Report, Sep. 1990 - Jun. 1993
David J. Wilson, David R. Riley, and Kevin D. Citurs Aug. 1993 536 p
(Contract F33615-90-C-3600)
(AD-A273814; WL-TR-93-3083-Vol-3) Avail: CASI HC A23/MF A04

A set of aircraft maneuvers was developed to augment evaluation maneuvers used currently by the flying qualities and flight test communities. These maneuvers extend evaluation to full aircraft dynamics throughout the aircraft flight envelope. As a result, a tie was established between operational use and design parameters without losing control of the aircraft evaluation process. Twenty maneuvers are described as an initial set to examine primarily high-angle-of attack conditions. Perhaps as important as the maneuvers themselves is the method used to select them. These maneuvers will allow direct measurement of flying qualities throughout the flight envelope instead of merely comparing parameters to specification values. DTIC

N94-26091*# National Aeronautics and Space Administration. Ames Research Center, Moffett Field, CA.
EGADS: A MICROCOMPUTER PROGRAM FOR ESTIMATING THE AERODYNAMIC PERFORMANCE OF GENERAL AVIATION AIRCRAFT
John E. Melton Jan. 1994 57 p
(RTOP 505-59-53)
(NASA-TM-104013; A-93066; NAS 1.15:104013) Avail: CASI HC A04/MF A01

EGADS is a comprehensive preliminary design tool for estimating the performance of light, single-engine general aviation aircraft. The software runs on the Apple Macintosh series of personal computers and assists amateur designers and aeronautical engineering students in performing the many repetitive calculations required in the aircraft design process. The program makes full use of the mouse and standard Macintosh interface techniques to simplify the input of various design parameters. Extensive graphics, plotting, and text output capabilities are also included. Author (revised)

N94-26151*# National Aeronautics and Space Administration. Ames Research Center, Moffett Field, CA.
DESIGN OPTIMIZATION OF HIGH-SPEED PROPROTOR AIRCRAFT
David R. Schleicher, James D. Phillips, and Kevin B. Carbajal Apr. 1993 40 p
(RTOP 505-69-36)
(NASA-TM-103988; A-93010; NAS 1.15:103988) Avail: CASI HC A03/MF A01

NASA's high-speed rotorcraft (HSRC) studies have the objective of investigating technology for vehicles that have both low downwash velocities and forward flight speed capability of up to 450 knots. This paper investigates a tilt rotor, a tilt wing, and a folding tilt rotor designed for a civil transport mission. Baseline aircraft models using current technology are developed for each configuration using a vertical/short takeoff and landing (V/STOL) aircraft design synthesis computer program to generate converged vehicle designs. Sensitivity studies and numerical optimization are used to illustrate each configuration's key design tradeoffs and constraints. Minimization of the gross takeoff weight is used as the optimization objective function. Several advanced technologies are chosen, and their relative impact on future configurational development is discussed. Finally, the impact of maximum cruise speed on vehicle figures of merit (gross weight, productivity, and direct operating cost) is analyzed. The three most important conclusions from the study are payload ratios for these aircraft will be commensurate with current fixed-wing commuter aircraft; future tilt rotors and tilt wings will be significantly lighter, more productive, and cheaper than competing folding tilt rotors; and the most promising technologies are an advanced-technology proprotor for both tilt rotor and tilt wing and advanced structural materials for the folding tilt rotor. Author (revised)

N94-26182# Naval Postgraduate School, Monterey, CA.
AN ANALYSIS OF MULTIPLE SENSOR SYSTEM PAYLOADS FOR UNMANNED AERIAL VEHICLES M.S. Thesis
John F. Keane Sep. 1993 101 p
(AD-A274905) Avail: CASI HC A06/MF A02

Unmanned aerial vehicles (UAV's) presently under consideration by the Program Executive Officer for Cruise Missile Projects and Unmanned Aerial Vehicles (PEOCNPUAV) will be equipped solely with electrooptical (EO) sensors. This thesis provides a comparative analysis of the mission effectiveness between UAV's equipped with EO sensors and those equipped with a multiple sensor system payload. A historical review of UAV development and employment is provided so that the reader may gain some insight into past UAV shortcomings in the hopes that they might be prevented in future systems. A typical reconnaissance, surveillance, and target acquisition (RSTA) mission scenario is defined and a comparison made between UAV's equipped with EO sensors and those equipped with multiple sensor system payloads. The measure of effectiveness used for this comparison is the time required by the UAV to search 100 percent of an assigned area. The physical and operating characteristics of available sensor systems are discussed in detail. An optimization model is developed for selecting multiple sensor payloads from those sensor systems described. The model considers the sensor's physical characteristics, unit cost, identification capability, and false alarm rate when determining the optimum payload. The optimum sensor system payloads are selected and the best alternatives to EO sensors for performing RSTA missions in a hostile environment are recommended under a range of budgets. DTIC

N94-26235*# California Polytechnic State Univ., San Luis Obispo. Aeronautical Engineering.

ANALYSIS AND OPTIMIZATION OF PRELIMINARY AIRCRAFT CONFIGURATIONS IN RELATIONSHIP TO EMERGING AGILITY METRICS Final Report, 15 Sep. 1991 - 14 Sep. 1993

Doral R. Sandlin and Brent Alan Bauer Dec. 1993 133 p
(Grant NAG2-743)
(NASA-CR-195228; NAS 1.26:195228) Avail: CASI HC A07/MF A02

This paper discusses the development of a FORTRAN computer code to perform agility analysis on aircraft configurations. This code is to be part of the NASA-Ames ACSYNT (AirCraft SYNThesis) design code. This paper begins with a discussion of contemporary agility research in the aircraft industry and a survey of a few agility metrics. The methodology, techniques and models developed for the code are then presented. Finally, example trade studies using the agility module along with ACSYNT are illustrated. These trade studies were conducted using a Northrop F-20 Tigershark aircraft model. The studies show that the agility module is effective in analyzing the influence of common parameters such as thrust-to-weight ratio and wing loading on agility criteria. The module can compare the agility potential between different configurations. In addition one study illustrates the module's ability to optimize a configuration's agility performance. Author

N94-26488# Galaxy Scientific Corp., Pleasantville, NJ.

EFFECTS OF PLASTIC MEDIA BLASTING ON AIRCRAFT SKIN Final Report

Charles C. Chen, Mark Muller, and John W. Reinhardt Nov. 1993 113 p
(Contract DTFA03-89-C-00043)
(AD-A274817; DOT/FAA/CT-91/27) Avail: CASI HC A06/MF A02

The use of methylene chloride chemical solvents in aviation paint removal is becoming increasingly unacceptable in view of restrictive Environmental Protection Agency (EPA) regulations. A readily available alternative, plastic media blasting (PMB), must be examined for its effects on the thin aluminum used as skin material in civilian aircraft. This study examines the effects of plastic media blasting or the crack propagation rates of 2024-T3 aluminum in alclad of 0.032, 0.040, 0.050 inch thickness, and in anodized of 0.032, 0.040, and 0.050 inch thickness. A technical search was performed for the following topics: (1) fatigue crack growth (FCG) rate comparison between PMB and chemical stripping, (2) effects of heavy particulate contamination on the fatigue life of aircraft skin, (3) acceptable level of contamination in the plastic media, (4) effects of multiple strippings on FCG, (5) maximum number of strippings allowed, and (6) specifications of controlled parameters to safely operate a PMB system. Fatigue crack propagation tests, Almen strip tests, Scanning Electron Microscope (SEM) photography, and surface toughness measurements were conducted. The results of the technical search and the tests performed are presented, as well as supplementary Almen strip arc height data. This study also presents an overview of nine alternative aviation paint stripping methods in terms of paint stripping effectiveness, substrate damage, environmental impact, health impact, and cost. DTIC

N94-26531# Naval Postgraduate School, Monterey, CA.

COMPUTER CODE FOR INTERACTIVE ROTORCRAFT PRELIMINARY DESIGN USING A HARMONIC BALANCE METHOD FOR ROTOR TRIM M.S. Thesis

Robert K. Nicholson, Jr. 23 Sep. 1993 91 p
(AD-A274924) Avail: CASI HC A05/MF A01

The Joint Army/Navy Rotorcraft Analysis and Design (JANRAD) computer program was developed to aid in the analysis of helicopter rotor performance, stability and control, and rotor dynamics. JANRAD is an interactive, user friendly program, capable of accurately and quickly solving helicopter design problems at the preliminary design level. The program was written as a collection of MATLAB script and function files (M-files) using the 386-MATLAB version 3.5 programming language. The M-file janrad.in invokes the user interface routines and calls various analysis modules (M-files) which contain the appropriate analysis and output routines. Each of these modules use a common routine, trim.m, which employs blade element theory and a harmonic balance method for rotor trim. The program is limited to conditions of steady flight with no winds and is accurate at a hover and for forward airspeeds greater than or equal to 50 knots. DTIC

N94-26604*# National Aeronautics and Space Administration. Ames Research Center, Moffett Field, CA.

EXPERIMENTAL INVESTIGATION OF ADVANCED HUB AND PYLON FAIRING CONFIGURATIONS TO REDUCE HELICOPTER DRAG

D. M. Martin (Sterling Software, Inc., Palo Alto, CA.), R. W. Mort (Bell Helicopter Co., Fort Worth, TX.), L. A. Young, and P. K. Squires (Bell Helicopter Co., Fort Worth, TX.) Sep. 1993 93 p
(RTOP 505-59-36)
(NASA-TM-4540; A-93079; NAS 1.15:4540) Avail: CASI HC A05/MF A01

New hub and pylon fairing designs were tested on a one-fifth scale Bell Helicopter Textron Model 222 helicopter with a bearingless main rotor hub. The blades were not installed for this test. The fairings were designed by NASA and Bell Helicopter Textron under a joint program and tested in the Ames Research Center 7-by 10-Foot Wind Tunnel. All six aircraft forces and moments were measured using the tunnel scales system. Previous research has identified the integrated hub and pylon fairing approach as the most efficient in reducing helicopter drag. Three hub fairings and three pylon fairings were tested (in various combinations) resulting in a total of 16 different configurations, including the baseline helicopter model without fairings. The geometry of the new fairings is described in detail. Test results are presented in the form of plots of the six model forces and moments. The data show that model drag can be reduced by as much as 20 percent by combining a small hub fairing (that has a circular arc upper surface and a flat lower surface) integrated with a nontapered pylon fairing. To minimize drag, the gap between the lower surface of the hub and upper surface of the pylon fairing must be kept to a minimum. Results show that the aerodynamic effects of the fairings on static longitudinal and directional stability can also be important. Author (revised)

N94-26606*# Lockheed Engineering and Sciences Co., Hampton, VA.

A TECHNIQUE FOR INTEGRATING ENGINE CYCLE AND AIRCRAFT CONFIGURATION OPTIMIZATION Final Report

Karl A. Geiselhart Feb. 1994 77 p
(Contract NAS1-19000; RTOP 505-69-50-01)
(NASA-CR-191602; NAS 1.26:191602) Avail: CASI HC A05/MF A01

A method for conceptual aircraft design that incorporates the optimization of major engine design variables for a variety of cycle types was developed. The methodology should improve the lengthy screening process currently involved in selecting an appropriate engine cycle for a given application or mission. The new capability will allow environmental concerns such as airport noise and emissions to be addressed early in the design process. The ability to rapidly perform optimization and parametric variations using both engine cycle and aircraft design variables, and to see the impact on the aircraft, should provide insight and guidance for more detailed studies. A brief description of the aircraft performance and mission analysis program and the engine cycle analysis program that were used is given. A new method of predicting propulsion system weight and dimensions using thermodynamic cycle data, preliminary design, and semi-empirical techniques is introduced. Propulsion system performance and weights data generated by the program are compared with industry data and data generated using well established codes. The ability of the optimization techniques to locate an optimum is demonstrated and some of the problems that had to be solved to accomplish this are illustrated. Results from the application of the program to the analysis of three supersonic transport concepts installed with mixed flow turbofans are presented. The results from the application to a Mach 2.4, 5000 n.mi. transport indicate that the optimum bypass ratio is near 0.45 with less than 1 percent variation in minimum gross weight for bypass ratios ranging from 0.3 to 0.6. In the final application of the program, a low sonic boom fix a takeoff gross weight concept that would fly at Mach 2.0 overwater and at Mach 1.6 overland is compared with a baseline concept of the same takeoff gross weight that would fly Mach 2.4 overwater and subsonically overland. The results indicate that for the design mission, the low boom concept has a 5 percent total range penalty relative to the baseline. Additional cycles were optimized for various design overland distances and the effect of flying off-design overland distances is illustrated. Author (revised)

N94-26608*# National Aeronautics and Space Administration. Langley Research Center, Hampton, VA.
TESTS OF HIGHLY LOADED SKIDS ON A CONCRETE RUNWAY
Sandy M. Stubbs and Robert H. Daugherty Mar. 1994 19 p
(RTOP 505-63-10-02)
(NASA-TP-3435; L-17324; NAS 1.60:3435) Avail: CASI HC A03/MF A01

Skids have been used at various times for aircraft landing gear ever since the Wright Flyer appeared in the early 1900's. Typically, skids have been employed as aircraft landing gear either at low speeds or at low bearing pressures. Tests were conducted to examine the friction and wear characteristics of various metals sliding on a rough, grooved concrete runway. The metals represented potential materials for an overload protection skid for the Space Shuttle orbiter. Data from tests of six skid specimens conducted at higher speeds and bearing pressures than those of previous tests in the open literature are presented. Skids constructed of tungsten with embedded carbide chips exhibited the lowest wear, whereas a skid constructed of Inconel 718 exhibited high wear rates. Friction coefficients for all the skid specimens were moderate and would provide adequate stopping performance on a long runway. Because of its low wear rate, a skid constructed of tungsten with embedded carbide chips is considered to be a likely candidate for an aircraft skid or overload protection skid. Author (revised)

N94-26835# Defense Science Board, Washington, DC.
REPORT OF THE DEFENSE SCIENCE BOARD TASK FORCE ON AIRCRAFT ASSESSMENT Final Report
Feb. 1993 31 p
(AD-A274531) Avail: CASI HC A03/MF A01

The Defense Science Board Task Force on Aircraft Assessment was convened to respond to the direction received from Congress in the National Defense Authorization Act for Fiscal Year 1993, (Public Law 102-484). The Authorization Act requested the Defense Science Board address two issues that are related to the DoD Tactical Aviation Modernization Program. The two issues pertain to (1) potential common aircraft/avionics for use by the Navy and Air Force for parallel missions, and (2) technical risk assessments for the F-22, F/A-18E/F, and A/F-X aircraft DTIC

N94-26864 Materials Research Labs., Ascot Vale (Australia).
DEVELOPMENT AND EVALUATION OF A NEAR INFRARED REFLECTING AND LOW VISIBILITY PAINT SCHEME FOR RAAF P-3C ORION AIRCRAFT
L. V. Wake Oct. 1993 18 p Limited Reproducibility: More than 20% of this document may be affected by microfiche quality
(AD-A274881; MRL-TR-93-35; DODA-AR-008-565) Avail: CASI HC A03

In this report, the development and trialling of a tactical, low visibility paint scheme (LVPS) for RAAF P-3C Orion aircraft is discussed. The LVPS was formulated in grey colors using solar heat reflecting pigments to reduce overheating problems which had resulted in the abandonment of an earlier camouflage trial. The paint scheme, which is one of several schemes under consideration by RAAF, employs strict countershading principles with pale grey underneath the aircraft, light grey on the fuselage sides and vertical flight control surfaces and mid-grey on top of the fuselage and upper flight control surfaces. Evaluation of the paint scheme was carried out at RAAF Edinburgh under summertime conditions and showed that the increase in heat load by use of the solar heat reflecting paint scheme (SHR)-LVPS on the Environmental Control System (ECS) of the aircraft was 0.53 kW compared with the existing paint scheme. This compares favorably with the reported heat load increase of 1.7 kW for counter-shaded aircraft using conventionally formulated grey paints. It is concluded that the use of the SHR-LVPS would have essentially no effect on P-3C operational temperatures except under severe environmental conditions where an increase in temperatures of 0.3 C in the cabin and 1.3 C at the flight stations could be expected. DTIC

N94-26906 National Academy of Engineering, Washington, DC.
FUTURE OF AEROSPACE
1993 89 p Conference held in Honor of Alexander H. Flax on February 28, 1992 Sponsored by National Academy of Sciences, Washington, DC Limited Reproducibility: More than 20% of this document may be affected by microfiche quality
(PB94-120185; ISBN-0-309-04881-8) Copyright Avail: CASI HC A05

Contents: Alexander H. Flax: Highlights of an Engineering Career; Defense Aerospace and the New World Order; The Future of Manned Spaceflight; Aviation--The Timeless Industry; Higher-Order Technology--Applying Technical Excellence to New Airplane Development; and The Future of Rotary-Wing Aircraft. NTIS

N94-26954 Technische Univ., Delft (Netherlands). Faculty of Aerospace Engineering.
EXPERIMENTAL STUDY OF THE ANGLED CRACK IN GLARE 3
K. J. J. M. Zaal 1994 66 p Limited Reproducibility: More than 20% of this document may be affected by microfiche quality
(PB94-126554; M-667) Avail: Issuing Activity (National Technical Information Service (NTIS))

The aim of the present investigation is to perform both an experimental and a theoretical study of the behavior of cracks in GLARE loaded under a combined mode I and mode II loading, using the angled crack problem. Cracks originating from impact damage in aircraft fuselages can experience a mixed mode I and II load at the start of their life. For GLARE, the more fibrous nature of GLARE compared to aluminum may change the propagation. The experiments were performed on specimens made of GLARE-3, with the main material directions aligned with the specimen axis. As reference materials, both aluminum 2024-T3 and 7075-T6 are used. For angled cracks, the propagation direction has been predicted by Erdogan and Sih, Williams and Ewing and Theocaris et al. NTIS

N94-26969# Technische Univ., Delft (Netherlands). Faculty of Aerospace Engineering.
DEVELOPMENT OF FIBRE-METAL LAMINATES, ARALL AND GLARE, NEW FATIGUE RESISTANT MATERIALS
J. Schijve Jan. 1993 25 p Presented at the 1993 FATIGUE, Montreal, Ontario, 3-7 May 1993 See also N90-26368 and PB92-133412
(PB94-126471; LR-715) Avail: CASI HC A03/MF A01

Research on adhesive-bonded sheet metal laminates (such as ARALL and GLARE) is described as a predecessor of a new class of materials, the fiber-metal laminates. It is explained why fiber-metal laminates have such a high fatigue resistance, especially against fatigue crack growth. Additional advantages of the barrier function of the fiber layers are indicated. Applications are discussed. Comments are made on developing a material for practical applications. NTIS

N94-27105# Naval Air Warfare Center, Warminster, PA. Aircraft Div.
METHODS FOR EXPERIMENTALLY DETERMINING COMMERCIAL JET AIRCRAFT LANDING PARAMETERS FROM VIDEO IMAGE DATA Final Report
Richard P. Micklos and Thomas DeFiore Aug. 1993 60 p
(Contract DTFA03-92-Z-0029)
(AD-A274207; DOT/FAA/CT-93/7) Avail: CASI HC A04/MF A01

As part of its Aging Aircraft Research Program, the Federal Aviation Administration is establishing a passive system of measuring aircraft landing contact parameters at commercial airports. This research involves the broader application of recent US NAVY technology used to measure landing contact conditions of Navy carrier aircraft and develop/assess Navy landing loads design criteria. This technique is based on digitizing and analyzing high resolution video images recorded by cameras strategically stationed along the runway apron, and it does not require the installation of any instrumentation on the aircraft or changes to normal aircraft operating procedures. This report describes the application of the Navy's latest procedures for precisely determining the kinematics of typical commercial aircraft landings and provides the results of a demonstration survey conducted at the Federal Aviation Administration (FAA) Technical Center in June 1992. In addition, the proposed runway camera configuration for a production landing survey at a high volume airport is presented. DTIC

N94-27273 Boeing Commercial Airplane Co., Seattle, WA.
COMPOSITE LEADING EDGE/SPAR MEMBER FOR AN AIRCRAFT CONTROL SURFACE Patent
Rudolf Braun, inventor (to Boeing) and Richard Jensen, inventor (to Boeing) 4 Jan. 1994 24 p
(CA-Patent-1-325-765; Int-Patent-Class-B32B-031/24; CTN-94-61094)
Copyright Avail: Micromedia Ltd., Technical Information Centre, 240 Catherine Street, Suite 305, Ottawa, Ontario, K2P 2G8, Canada HC/MF

A one-piece composite leading edge/spar member for an aircraft control

surface is provided which is of a lighter and stronger construction offering dimensional stability. An efficient method for manufacturing the member is also disclosed. The member of the invention includes a forward leading edge portion and an aft spar portion, which are connected together as a continuous one-piece tubular member of composite material. The forward leading edge portion may be rounded, and the aft spar portion may include an aft web portion and first and second rebate portions. The rebate portions connect the web portion to the rounded forward leading edge portion, and provide surfaces for the attachment of skin surface members. In a preferred mode of fabricating the member, a composite material is applied or wrapped around a mandrel, with the material perimetrically surrounding and covering the rounded leading edge and the spar forming portions of the mandrel. A forming pressure may then be applied to the composite material to shape and mold the material into the same shape as the rounded leading edge and spar forming portions. This method permits the composite material to be filament wound around the mandrel instead of being wrapped on a layer by layer basis. Filament winding would be particularly well suited for mass production of leading edge/spar members of the invention.
Author (CISTI)

N94-27439*# National Aeronautics and Space Administration. Langley Research Center, Hampton, VA.
PROCEEDINGS OF THE NON-LINEAR AERO PREDICTION REQUIREMENTS WORKSHOP
Michael J. Logan, ed. Mar. 1994 163 p Workshop held in Hampton, VA, 8-9 Dec. 1993 Sponsored by NASA, Washington
(RTOP 505-68-70-09)
(NASA-CP-10138; NAS 1.55:10138) Avail: CASI HC A08/MF A02

The purpose of the Non-Linear Aero Prediction Requirements Workshop, held at NASA Langley Research Center on 8-9 Dec. 1993, was to identify and articulate requirements for non-linear aero prediction capabilities during conceptual/preliminary design. The attendees included engineers from industry, government, and academia in a variety of aerospace disciplines, such as advanced design, aerodynamic performance analysis, aero methods development, flight controls, and experimental and theoretical aerodynamics. Presentations by industry and government organizations were followed by panel discussions. This report contains copies of the presentations and the results of the panel discussions. Author (revised)

N94-27666 Defence Research Establishment Pacific, Victoria (British Columbia). Research and Development Branch.
THE DEVELOPMENT OF AN IN-MOTION RADIOGRAPHY SYSTEM FOR LARGE AREA AIRCRAFT SCANNING
Richard D. Finlayson, John K. Cornes, Dan S. Liesch, and William R. Sturrock Jul. 1993 22 p
(DREP-TM-93-53; DSIS-94-00099; CTN-94-61118) Avail: CASI HC A03/MF A01

An in-motion radiography system (IMRS) includes a portable x-ray unit, adapted for the requirements of in-motion radiography, and an x-y scanning arrangement to allow large area scanning. Two separate IMRS experiments were performed, each with a different slit length set on a focusing collimator. A long slit length allowed a fast scan that exposed the film in one pass of the x-ray tube, creating a low resolution radiograph. A shorter slit length was set to allow for exposure of the film in several strips, thus eliminating the parallax error caused by the cone-shaped radiation field and creating a higher resolution radiograph. The results show that an IMRS is a fast and reliable means for inspecting large aircraft surfaces. Inspection of helicopter rotor blades for water ingress in honeycomb is seen as one possible use for the IMRS, expecially for very large blades. In-motion radiography is simple and based on standard radiographic procedures, with some slight modifications in exposure settings. Almost any radiography system could be adapted to use in-motion radiography if the tube or the part is able to move in the desired scanning motion. In-house testing of the IMRS is complete and ready for an on-aircraft trial. Author (CISTI)

N94-27796 National Aerospace Lab., Amsterdam (Netherlands). Structures and Materials Div.
INVESTIGATION OF THE BOND STRENGTH OF A DISCRETE SKIN-STIFFENER INTERFACE
H. G. S. J. Thuis and J. F. M. Wiggenraad 24 Apr. 1992 14 p Presented at the AGARD/SMP Specialists Meeting on Debonding/Delamination of Composites, Patras, Greece, 25-27 May 1992 Limited Reproducibility: More than 20% of this document may be affected by microfiche quality
(NLR-TP-92183-U; ETN-94-95446) Avail: CASI HC A03

The results of an experimental study on the effects of several design parameters on the strength of a skin-stiffener interface are presented. Design parameters considered are skin and stiffener laminate properties and the width of the bond layer. Test specimens consisting of a blade type stiffener secondarily bonded to skin laminate were fabricated. The specimens were tested by lateral tension tests, four point bending tests, and pull-off tests. Calculations were made with the numerical program BONDST. The test results are compared with each other and with the calculated results. Conclusions are drawn and design guidelines are provided. ESA

N94-28092 ESDU International Ltd., London (England).
EXAMPLES OF FLIGHT PATH OPTIMISATION USING A MULTIVARIATE GRADIENT-SEARCH METHOD
Dec. 1993 24 p
(ISSN 0141-4054)
(ESDU-93021; ISBN-0-85679-874-6) Avail: ESDU

ESDU 93021 deals with one method of optimization of a complete sortie, applied as an example to a subsonic transport and used to demonstrate the penalties incurred by constraints imposed by design and operational considerations. It requires an appropriate numerical optimization technique able to solve constrained multivariate problems. That used here is RQPMIN developed at the then Royal Aircraft Establishment. The examples were to minimize block fuel for given range, maximize range for given ramp mass, minimize time for given range, and minimize direct operating costs (in this case a linear combination of time and block fuel) for given range. Each case is initially run with no constraints other than those to ensure flight is possible (for example, thrust at the appropriate rating must exceed drag). Progressive constraints are then introduced relating speed to minimum drag speed, providing a given margin to buffet onset, limiting rates of climb and descent by rates of cabin pressure change and by a maximum cabin differential pressure, and limiting cabin attitude for passenger comfort. The results are discussed. A comparison is also made of results for optimum climb paths of a transport aircraft with results obtained for the same cases in ESDU 90012 using energy height methods. ESDU

N94-28094 ESDU International Ltd., London (England).
EXAMPLE OF STATISTICAL TECHNIQUES APPLIED TO ANALYSIS OF EFFECTS OF SMALL CHANGES
Nov. 1993 6 p
(ISSN 0141-4054)
(ESDU-93023; ISBN-0-85679-876-2) Avail: ESDU

ESDU 93023 uses second segment climb measurements to provide simple examples of statistical significance testing and confidence levels. Certification trials of a twin turbo-prop aircraft established that second segment climb gradient exceeded scheduled by a mean margin of 0.09 percent with a standard deviation of 0.35 percent. The comprehensive nature of the tests allowed the values to be taken as applying to the population. Two sets of ten points were then obtained, each set with a variant of the aircraft differing from the basic design by small aerodynamic changes. Use of Fisher's Variance Ratio F test established that the standard deviations (variances) of both sets did not differ significantly from that of the population. The means of both samples were then compared with that of the population using the normal cumulative distribution function to establish the confidence that the differences arose by chance. In one case the difference is seen to be significant and the performance had to be rescheduled. The necessary changes are calculated, and the probability that any single test point might fall below the new scheduled level is established. ESDU

N94-25695*# Rensselaer Polytechnic Inst., Troy, NY. Dept. of Mechanical Engineering, Aerospace Engineering, and Mechanics.
THE LIGHTCRAFT PROJECT: FLIGHT TECHNOLOGY FOR A HYPERSONIC MASS TRANSIT SYSTEM Abstract Only
Leik Myrabo and Kenneth Bouchard *In* USRA, Proceedings of the 8th Annual Summer Conference: NASA/USRA Advanced Design Program 1992 p 250 (For primary document see N94-25665 07-80)
Avail: CASI HC A01/MF A04

N94-25708*# Auburn Univ., AL. Dept. of Aerospace Engineering.
DESIGN OF THE ADVANCED REGIONAL AIRCRAFT, THE DART-75
Steve Elliot, Jason Gislason, Mark Huffstetler, Jon Mann, Ashley Withers, and Mark Zimmerman *In* USRA, Proceedings of the 8th Annual Summer Conference: NASA/USRA Advanced Design Program 1992 p 367-373 (For primary document see N94-25665 07-80)
Avail: CASI HC A02/MF A04

N94-25709*# Auburn Univ., AL. Dept. of Aerospace Engineering.
EAGLE RTS: A DESIGN OF A REGIONAL TRANSPORT
Paul Bryer, Jon Buckles, Paul Lemke, and Kirk Peake *In* USRA, Proceedings of the 8th Annual Summer Conference: NASA/USRA Advanced Design Program 1992 p 373-378 (For primary document see N94-25665 07-80)
Avail: CASI HC A02/MF A04

N94-25710*# California Polytechnic State Univ., San Luis Obispo. Dept. of Aeronautical Engineering.
PRELIMINARY DESIGN OF NINE HIGH SPEED CIVIL TRANSPORTS
Doral Sandlin, Robert vantRiet, Dani Soban, and Ty Hoang *In* USRA, Proceedings of the 8th Annual Summer Conference: NASA/USRA Advanced Design Program 1992 p 379-390 (For primary document see N94-25665 07-80)
Avail: CASI HC A03/MF A04

N94-25711*# California State Polytechnic Univ., Pomona. Dept. of Aerospace Engineering.
SUPERCRUISER ARROW HS-8
Paul Lord, Edward Kao, Joey B. Abobo, Todd A. Collins, Leong Ma, Adnan Murad, Hitesh Naran, Thuan P. Nguyen, Timithy I. Nuon, and Dimitri D. Thomas *In* USRA, Proceedings of the 8th Annual Summer Conference: NASA/USRA Advanced Design Program 1992 p 391-405 (For primary document see N94-25665 07-80)
Avail: CASI HC A03/MF A04

N94-25712*# California State Univ., Northridge. Dept. of Mechanical Engineering.
PROJECT ARES 3
Dan Raymer, Phyllis Russell, Tim Fox, Doug Meyers, Steven Lovric, Robert Grabow, Manfred Epp, Warren Wynn, Jr., Zoltan Mako, and Gunther Linzner et al *In* USRA, Proceedings of the 8th Annual Summer Conference: NASA/USRA Advanced Design Program 1992 p 406-412 (For primary document see N94-25665 07-80)
Avail: CASI HC A02/MF A04

N94-25713*# Case Western Reserve Univ., Cleveland, OH. Dept. of Mechanical and Aerospace Engineering.
TESSERACT SUPERSONIC BUSINESS TRANSPORT
Eli Reshotko, Gary Garbinski, James Fellenstein, Mary Botting, Joan Hooper, Michael Ryan, Peter Struk, Ben Taggart, Maggie Taillon, and Gary Warzynski *In* USRA, Proceedings of the 8th Annual Summer Conference: NASA/USRA Advanced Design Program 1992 p 413-424 (For primary document see N94-25665 07-80)
Avail: CASI HC A03/MF A04

N94-25714*# Kansas Univ., Lawrence. Dept. of Aerospace Engineering.
A REVOLUTIONARY APPROACH TO COMPOSITE CONSTRUCTION AND FLIGHT MANAGEMENT SYSTEMS FOR SMALL, GENERAL AVIATION AIRPLANES
Jan Roskam and Ed Wenninger *In* USRA, Proceedings of the 8th Annual Summer Conference: NASA/USRA Advanced Design Program 1992 p 425-436 (For primary document see N94-25665 07-80)
Avail: CASI HC A03/MF A04

N94-25715*# Notre Dame Univ., IN. Dept. of Aerospace and Mechanical Engineering.
DESIGN STUDY TO SIMULATE THE DEVELOPMENT OF A COMMERCIAL FREIGHT TRANSPORTATION SYSTEM
Stephen M. Batill, Kevin Costello, and Jim Pinkelman *In* USRA, Proceedings of the 8th Annual Summer Conference: NASA/USRA Advanced Design Program 1992 p 437-452 (For primary document see N94-25665 07-80)
Avail: CASI HC A03/MF A04

N94-25716*# Ohio State Univ., Columbus. Dept. of Aeronautical and Astronautical Engineering.
THE DESIGN OF FOUR HYPERSONIC RECONNAISSANCE AIRCRAFT
G. M. Gregorek and D. T. Detwiler *In* USRA, Proceedings of the 8th Annual Summer Conference: NASA/USRA Advanced Design Program 1992 p 453-462 (For primary document see N94-25665 07-80)
Avail: CASI HC A02/MF A04

N94-25717*# Ecole Polytechnique Feminine, Sceaux (France).
DESIGN OF A REFUELING TANKER DELIVERING LIQUID HYDROGEN
Daniel Lourme, Caroline Barnier, Sabine Faure, Marie-Helene Pompei, and Karine Pruniaux *In* USRA, Proceedings of the 8th Annual Summer Conference: NASA/USRA Advanced Design Program 1992 p 463-466 (For primary document see N94-25665 07-80)
Avail: CASI HC A01/MF A04

N94-25718*# Purdue Univ., West Lafayette, IN. School of Aeronautics and Astronautics.
THE DESIGN OF A LONG-RANGE MEGATRANSPORT AIRCRAFT
Terrence A. Weisshaar and Carl L. Allen *In* USRA, Proceedings of the 8th Annual Summer Conference: NASA/USRA Advanced Design Program 1992 p 467-476 (For primary document see N94-25665 07-80)
Avail: CASI HC A02/MF A04

N94-25719*# Worcester Polytechnic Inst., MA. Dept. of Mechanical Engineering.
SOLAR POWERED MULTIPURPOSE REMOTELY POWERED AIRCRAFT
A. N. Alexandrou, W. W. Durgin, R. F. Cohn, D. J. Olinger, Charlotte K. Cody, Agnes Chan, Kwok-Hung Cheung, Kristin Conley, Paul M. Crivelli, and Christian T. Javorski et al *In* USRA, Proceedings of the 8th Annual Summer Conference: NASA/USRA Advanced Design Program 1992 p 477-489 (For primary document see N94-25665 07-80)
Avail: CASI HC A03/MF A04

N94-27917*# Mississippi State Univ., Mississippi State. Dept. of Aerospace Engineering.
WING DESIGN FOR A CIVIL TILTROTOR TRANSPORT AIRCRAFT: A PRELIMINARY STUDY
Masoud Rais-Rohani *In* Old Dominion Univ., The 1993 NASA-ODU American Society for Engineering Education (ASEE) Summer Faculty Fellowship Program Dec. 1993 p 147-148 (For primary document see N94-27893 07-80)
Avail: CASI HC A01/MF A03

N94-28017# British Aerospace Defense Ltd., Farnborough (England).
EXPERIMENTS INTO THE SCALING PARAMETERS REQUIRED FOR EXHAUST GAS INGESTION TESTING OF VERTICAL LANDING AIRCRAFT
P. Curtis and P. J. Bradley *In* AGARD, Computational and Experimental Assessment of Jets in Cross Flow Nov. 1993 9 p (For primary document see N94-28003 07-34)
Copyright Avail: CASI HC A02/MF A04

N94-28033*# National Aeronautics and Space Administration. Ames Research Center, Moffett Field, CA.
NUMERICAL SIMULATION OF A POWERED-LIFT LANDING
Kalpana Chawla (MCAT Inst., Moffett Field, CA.) and William R. VanDalsem *In* AGARD, Computational and Experimental Assessment of Jets in Cross Flow Nov. 1993 10 p (For primary document see N94-28003 07-34)
Copyright Avail: CASI HC A02/MF A04

N94-28034# Wright Lab., Wright-Patterson AFB, OH.
A STUDY OF JET EFFECT AND GROUND EFFECT INTERFERENCE ON A STOL FIGHTER
David J. Moorhouse, James G. Reinsberg (McDonnell-Douglas Aerospace Information Services Co., Saint Louis, MO.), and Frank J. Shirk (McDonnell-Douglas Aerospace Information Services Co., Saint Louis, MO.) *In* AGARD, Computational and Experimental Assessment of Jets in Cross

Flow Nov. 1993 10 p (For primary document see N94-28003 07-34)
Copyright Avail: CASI HC A02/MF A04

N94-28035*# National Aeronautics and Space Administration. Ames Research Center, Moffett Field, CA.
TRANSITIONAL FLIGHT CHARACTERISTICS OF A GEOMETRICALLY SIMPLIFIED STOVL MODEL
Karlin R. Roth *In* AGARD, Computational and Experimental Assessment of Jets in Cross Flow Nov. 1993 10 p (For primary document see N94-28003 07-34)
Copyright Avail: CASI HC A02/MF A04

N94-28250# Deutsche Lufthansa A.G., Frankfurt am Main (Germany).
A SYMBOL OF RELIABILITY: Ju 52 [SYMBOL DER ZUVERLAESSIGKEIT: DIE JU 52]
Ralf Nolting *In its* Lufthansa Yearbook 1992 Oct. 1992 p 186-191 In GERMAN (For primary document see N94-28230 07-03)
Copyright Avail: CASI HC A02/MF A03

N94-28322 De Havilland Aircraft Co. of Canada Ltd., Downsview (Ontario). Aerodynamics Technology.
EXPERIMENTAL AND THEORETICAL STUDIES OF T-TAIL CONFIGURATIONS FOR COMMUTER AIRCRAFT APPLICATIONS
J. B. Coll, S. W. Cosby, and A. B. Paige *In* Canadian Aeronautics and Space Inst., Abstracts of Papers Presented at the 4th CASI Aerodynamics Symposium 1993 p 25-28 (For primary document see N94-28315 07-02)
Avail: Issuing Activity (Canadian Aeronautics and Space Inst., 130 Slater Street, Suite 818, Ottawa, ON K1P 6E2 Canada)

N94-28324 Bombardier, Inc., Montreal (Quebec). Canadair Group.
APPLICATION OF THE MBTEC EULER CODE TO THE CHALLENGER AND THE CF-18 COMPLETE AIRCRAFT CONFIGURATIONS
F. Kafyeke and P. Piperni *In* Canadian Aeronautics and Space Inst., Abstracts of Papers Presented at the 4th CASI Aerodynamics Symposium 1993 p 33-36 (For primary document see N94-28315 07-02)
Avail: Issuing Activity (Canadian Aeronautics and Space Inst., 130 Slater Street, Suite 818, Ottawa, ON K1P 6E2 Canada)

06 AIRCRAFT INSTRUMENTATION

Includes cockpit and cabin display devices; and flight instruments.

For related information see also *19 Spacecraft Instrumentation* and *35 Instrumentation and Photography.*

N94-26021# Air Force Inst. of Tech., Wright-Patterson AFB, OH. School of Engineering.
WEAPON SYSTEM SENSOR INTEGRATION FOR A DIS-COMPATIBLE VIRTUAL COCKPIT M.S. Thesis
Matthew N. Erichsen Dec. 1993 153 p
(AD-A274088; AFIT/GCS/Eng/93-07) Avail: CASI HC A08/MF A02

This thesis continues the virtual cockpit (VC) research which investigates distributed interactive virtual flying environments. The VC v1.0 used the SIMNET protocols to only communicate position and orientation over a common network. A simple cockpit instrumentation configuration and limited head-up display (HUD) showed aircraft state. With VC v1.0, weapons or sensors could not interact in the simulation environment. The VC v2.0 transitions from the SIMNET protocol to a partial implementation of the Distributed Interactive Simulation (DIS) v2.0.3 protocol. Simulated radar and forward looking infrared (FLIR) sensors were developed to aid operator detection and designation when employing various munition types. Simulated munition types include: radar or IR missiles; free-fall, laser guided, or electro-optic (EO) guided bombs; and a 20mm cannon. Virtual environments were created with CRT out-the-window presentations, color NTSC and monochrome high-resolution helmet mounted displays employing Polhemus head tracking sensors, and simultaneously five-channels on BARCO projectors. Target graphics systems included SGI workstations with Onyx processors using Reality Engines. Graphics rendering was accomplished with an AFIT developed object oriented simulation software package based on the SGI Performer 1.2 application development environment. DTIC

N94-26028# Galaxy Scientific Corp., Pleasantville, NJ.
DIGITAL SYSTEMS VALIDATION BOOK PLAN. VOLUME 3: HANDBOOK Final Report
Joan Janowitz Jul. 1993 17 p
(Contract DTFA03-89-C-00043)
(AD-A274099; DOT/FAA/CT-93/16-Vol-3) Avail: CASI HC A03/MF A01

The Digital Systems Validation Handbook is a tutorial series designed to provide certification engineers information on current topics related to digital avionics. The book plan lays the foundation for volume three of this series. The purpose of the handbook book plan is to identify technology and related issues that certification engineers are likely to encounter. Volume three of the handbook series will consist of approximately 20 chapters. Sixteen chapters are described in the book plan. Four were reserved for technologies or issues that might emerge during the course of the volume three life cycle. A list of potential handbook topics was derived from a survey of the literature, conference and seminar attendance, results of an informal questionnaire, and interviews with Federal Aviation Administration (FAA) National Resource Specialists, experts in the field of certification and digital avionics, National Aeronautics and Space Administration (NASA) officials, and persons in private industry. From this input, the list of potential topics was developed and refined into handbook chapters. In addition to the chapter list and descriptions, the handbook purpose, scope, and use is discussed. The unabridged list of topics is included in the book plan appendix. DTIC

N94-26030# Federal Aviation Administration, Atlantic City, NJ.
DIGITAL ALTIMETER SETTING INDICATOR (DASI) OPERATIONAL TEST AND EVALUATION (OT/E) OPERATIONAL TEST PROCEDURES
Michael Greco, Paul Biagi, and Eric Hoover Dec. 1993 35 p
(AD-A274100; DOT/FAA/CT-TN93/44) Avail: CASI HC A03/MF A01

The Digital Altimeter Setting Indicator (DASI) is a system which measures the atmospheric pressure and converts the measured pressure value into the actual sea level pressure based on the United States (U.S.) Standard Atmospheric Table. The value then computed is known as the altimeter setting indicator (ASI) value and is presented to an air traffic controller, in a digital format, e.g., 29.50 inches of mercury. The ASI value is then transmitted by the air traffic controller to an aircraft pilot for use in setting the altimeter in the aircraft. If a perfectly calibrated altimeter is set to the ASI value existing at any given station whose elevation is designated as Hp, the pointer of the altimeter instrument will indicate an altitude of Hp when the instrument is at the altitude of the sensor in the DASI system. Hp is an elevation in geopotential meters above mean sea level of the altimeter setting indicator pressure sensor. The purpose of this operational test and evaluation (OT&E) test procedure is to describe the test and evaluation activities which will ensure the DASI system meets all the requirements of the DASI Specification, FAA-E-2569B, and integrates properly into the National Airspace System (NAS). The OT&E procedure includes the test cases, responsibilities, test support hardware and software, and test conduct associated with the testing of the DASI. The DASI test is developed and executed in accordance with the current FAA Test and Evaluation Policy Order, FAA Order 1810.4B. DTIC

N94-26340# David Sarnoff Research Center, Princeton, NJ.
COLOR HEAD DOWN DISPLAY PROGRAM Final Report, 1 Sep. 1988 - 1 Mar. 1993
D. L. Jose, A. C. Ipri, and R. G. Stewart Apr. 1993 66 p
(Contract F33615-88-C-1825)
(AD-A274807; WL-TR-93-1103) Avail: CASI HC A04/MF A01

The purpose of the CHDD program was to develop a large-area AMLCD for cockpit applications. A 4- x 8-in. polysilicon AMLCD with 320,000 display cells was designed with integrated scanners and fabricated. A support electronics system was constructed that accepted multisource RGB video. This system reformatted the video information to drive the display at 180 fields/second and synchronized the display to a color sequential backlight. Moving the color information into the temporal domain, maintained the color pixel density identical to the cell density. A 192 x 192 pixel active matrix circuit with integrated drive and scan functions was fabricated in thin-film single-crystal silicon, using standard IC processing, and subsequently placed on glass to form a transmissive AMLCD. The first assembled 2.5- x 2.5-in. monochrome display shows greater than 85 percent pixel functionality. The speed, low leakage current, and high drive capability of single-crystal silicon devices should allow the fabrication of displays with integrated system-level peripheral circuitry, high pixel density, and improved contrast and optical aperture ratios. DTIC

N94-26989# Krug Life Sciences, Inc., San Antonio, TX. San Antonio Div.
STANDARDIZATION OF AIRCRAFT CONTROL AND PERFORMANCE SYMBOLOGY ON THE USAF HEAD-UP DISPLAY Final Report, Jan. 1990 - 1993
Lisa F. Weinstein, William R. Ercoline, Ian McKenzie, D. F. Bitton, and Kent K. Gillingham Nov. 1993 81 p
(Contract F33615-92-C-0018)
(AD-A274283; AL/CF-TR-1993-0088) Avail: CASI HC A05/MF A01

Researchers and pilots throughout the world continue to examine and debate the utility of the head-up display (HUD) for presenting instrument flight information. Although initially intended for the presentation of landing and weapons delivery information, the HUD has evolved into a flight instrument that researchers and pilots claim is successfully replacing many of the traditional panel instruments. Since the Attitude Awareness Workshop of 1985, the United States Air Force (USAF) has conducted numerous research projects to determine the most effective way to integrate the HUD with the other mission-essential instrument displays. The requirement to use the HUD for instrument flight, as well as a need to determine the optimal configuration of the HUD symbols, prompted a significant portion of that research. The research efforts conducted by scientists in the Visual Orientation Laboratory (VOL) and the Flight Motion Effects Branch of the Armstrong Laboratory (AL/CFTF) are summarized. Suggested standardization guidelines based on empirical findings are discussed, including the use of: counter-pointers for airspeed and altitude indicators, vertical and horizontal asymmetry for pitch-ladder configurations, a ghost horizon, analog information for vertical velocity, energy management symbology, and quickening for climb/dive markers. DTIC

N94-27864*# National Aeronautics and Space Administration. Langley Research Center, Hampton, VA.
EFFECTS OF HISTORICAL AND PREDICTIVE INFORMATION ON ABILITY OF TRANSPORT PILOT TO PREDICT AN ALERT
Anna C. Trujillo Mar. 1994 25 p
(RTOP 505-64-13)
(NASA-TM-4547; L-17305; NAS 1.15:4547) Avail: CASI HC A03/MF A01

In the aviation community, the early detection of the development of a possible subsystem problem during a flight is potentially useful for increasing the safety of the flight. Commercial airlines are currently using twin-engine aircraft for extended transport operations over water, and the early detection of a possible problem might increase the flight crew's options for safely landing the aircraft. One method for decreasing the severity of a developing problem is to predict the behavior of the problem so that appropriate corrective actions can be taken. To investigate the pilots' ability to predict long-term events, a computer workstation experiment was conducted in which 18 airline pilots predicted the alert time (the time to an alert) using 3 different dial displays and 3 different parameter behavior complexity levels. The three dial displays were as follows: standard (resembling current aircraft round dial presentations); history (indicating the current value plus the value of the parameter 5 sec in the past); and predictive (indicating the current value plus the value of the parameter 5 sec into the future). The time profiles describing the behavior of the parameter consisted of constant rate-of-change profiles, decelerating profiles, and accelerating-then-decelerating profiles. Although the pilots indicated that they preferred the near term predictive dial, the objective data did not support its use. The objective data did show that the time profiles had the most significant effect on performance in estimating the time to an alert. Author (revised)

N94-27882*# National Aeronautics and Space Administration. Langley Research Center, Hampton, VA.
EFFECTS OF EXPECTED-VALUE INFORMATION AND DISPLAY FORMAT ON RECOGNITION OF AIRCRAFT SUBSYSTEM ABNORMALITIES
Michael T. Palmer and Kathy H. Abbott Mar. 1994 76 p
(RTOP 505-64-13-22)
(NASA-TP-3395; L-17262; NAS 1.60:3395) Avail: CASI HC A05/MF A01

This study identifies improved methods to present system parameter information for detecting abnormal conditions and to identify system status. Two workstation experiments were conducted. The first experiment determined if including expected-value-range information in traditional parameter display formats affected subject performance. The second experiment determined if using a nontraditional parameter display format, which presented relative deviation from expected value, was better than traditional formats with expected-value ranges included. The inclusion of expected-value-range information onto traditional parameter formats was found to have essentially no effect. However, subjective results indicated support for including this information. The nontraditional column deviation parameter display format resulted in significantly fewer errors compared with traditional formats with expected-value-ranges included. In addition, error rates for the column deviation parameter display format remained stable as the scenario complexity increased, whereas error rates for the traditional parameter display formats with expected-value ranges increased. Subjective results also indicated that the subjects preferred this new format and thought that their performance was better with it. The column deviation parameter display format is recommended for display applications that require rapid recognition of out-of-tolerance conditions, especially for a large number of parameters. Author

N94-27286*# Massachusetts Inst. of Tech., Cambridge. Dept. of Aeronautics and Astronautics.
A GRAPHICAL WORKSTATION BASED PART-TASK FLIGHT SIMULATOR FOR PRELIMINARY RAPID EVALUATION OF ADVANCED DISPLAYS
Craig Wanke, James Kuchar, Edward Hahn, A. Pritchett, and R. John Hansman *In* NASA. Langley Research Center, FAA/NASA Joint University Program for Air Transportation Research, 1992-1993 Feb. 1994 p 9-15 See also A94-11991 Submitted for publication (For primary document see N94-27284 07-01)
(Contract NAG2-12; NAG2-716; NAG1-690; NGL-22-009-640; DTRS57-88-C-0078TD39; NSF MSS-85-52702; BARR-10-119)
Avail: CASI HC A02/MF A02

07 AIRCRAFT PROPULSION AND POWER

Includes prime propulsion systems and systems components, e.g., gas turbine engines and compressors; and onboard auxilliary power plants for aircraft.

For related information see also *20 Spacecraft Propulsion and Power, 28 Propellants and Fuels,* and *44 Energy Production and Conversion.*

N94-25617# Air Force Inst. of Tech., Wright-Patterson AFB, OH.
DEVELOPMENT AND IMPLEMENTATION OF A SCRAMJET CYCLE ANALYSIS CODE WITH A FINITE-RATE-CHEMISTRY COMBUSTION MODEL FOR USE ON A PERSONAL COMPUTER M.S. Thesis
Clarence F. Chenault Dec. 1993 254 p
(AD-A273834; AFIT/GAE/ENY/93D-7) Avail: CASI HC A12/MF A03

This study compared the performance of an equilibrium combustion model to a finite-rate-chemistry combustion model for a fixed geometry scramjet flying at the flight conditions of Mach 12, 15, and 18 with a constant dynamic pressure of 50,000 Pa. An integrated PC-based code, developed specifically for this study, models the combustor as an equilibrium combustion process or as finite-rate-chemistry combustion process. This integrated program is based on two existing programs, Ramjet Performance Analysis (RJPA) and 3 STREAM. The effects of mixing schedule, combustor length, and combustor exit area were investigated. The results of this study indicate that inefficient mixing is the primary cause of Scramjet performance loss regardless of the flight speed. Combustor length and combustor exit area also had a strong impact on performance. DTIC

N94-26176# Science Applications International Corp., San Antonio, TX. Logistics Technology Div.
AIRCRAFT TURBINE ENGINE RELIABILITY AND INSPECTION INVESTIGATIONS Final Report

Bruce A. Richter, Margaret Ridenour-Bender, and Mike Tsao Oct. 1993 120 p Sponsored by FAA
(AD-A274860; SAIC-67-6733; DOT/FAA/CT-92/29) Avail: CASI HC A06/MF A02

This study of JT9D, CF6, and PT6 aircraft engine reliability represents a follow-on effort to the JT8D engine study which was published in the Federal Aviation Administration (FAA) Technical Center Final Report DOT/FAA/CT-91/10. As with the JT8D engine study, this study trended in-flight shutdowns and unscheduled removal rates of JT9D, CF6, and PT6 turbine aircraft engines for a thirty-six-month period covering February 1988 through January 1991. As in the previous report, the methodology was to review which air carriers consistently exceeded the standard deviation norm for in-flight shutdowns and unscheduled engine removals on a monthly basis and then examine the engine component failures reported by those carriers. Engine component failures were grouped as follows: bearings, airfoils, cases, controls and accessories, fuel/oil systems, and others (not trended). For this study of the JT9D, CF6, and PT6 engines, controls and accessories typically produced the largest number of in-flight flameouts, compressor stalls, and engine shutdowns. In addition to the actuarial analysis and component failure mode trending performed on the JT9D, CF6, and PT6 engines, application of an inspection procedure developed for the JT8D engine was made on the JT9D and CF6 engine cases. DTIC

N94-26345# Wright Lab., Wright-Patterson AFB, OH.
AN INVESTIGATION OF THE SURGE BEHAVIOR OF A HIGH-SPEED TEN-STAGE AXIAL FLOW COMPRESSOR Final Report, Aug. 1990 - Aug. 1992
Patrick Russler May 1993 162 p
(AF Proj. 3066)
(AD-A274910; WL-TR-93-2076) Avail: CASI HC A08/MF A02

During a ten-stage compressor rig test conducted at Wright-Patterson AFB, several instances of compressor surge were observed. While surge is known to occur in high-speed multi-stage compressors, very little transient data pertaining to such events exists in the open literature, exclusive of engine data. In an attempt to make more data of this type available to researchers, surge data from this test are presented in this report. The predictions of a computer-based transient compressor model are compared to the data for study. Furthermore, an unexplained instability phenomenon is investigated: a constant surge/rotating stall boundary. During the test, it was found that the speed boundary between surge and rotating stall occurred between 80% and 81% rotor speed. This boundary did not change when the compressor discharge volume was changed. This seemed to contradict accepted theory, which predicts a shift in the surge/rotating stall boundary. An investigation into the possible causes of this phenomenon is conducted as part of this report. Several theories are explored, including the possibility of excess volume communicating with the compressor during instability. Although the excess volume theory is not proven, it remains the most likely cause of the unusual surge/rotating stall boundary behavior. DTIC

N94-26573*# National Aeronautics and Space Administration. Lewis Research Center, Cleveland, OH.
FOCUSED SCHLIEREN FLOW VISUALIZATION STUDIES OF MULTIPLE VENTURI FUEL INJECTORS IN A HIGH PRESSURE COMBUSTOR
K. S. Chun, R. J. Locke (Sverdrup Technology, Inc., Brook Park, OH.), C. M. Lee, and W. J. Ratvasky Jan. 1994 19 p Presented at the 32nd Aerospace Sciences Meeting and Exhibit, Reno, NV, 10-13 Jan. 1994; sponsored by AIAA Original contains color illustrations
(Contract NAS3-25266; RTOP 537-02-20)
(NASA-TM-106479; E-8409; NAS 1.15:106479; AIAA Paper 94-0280)
Avail: CASI HC A03/MF A01; 4 functional color pages

Multiple venturi fuel injectors were used to obtain uniform fuel distributions, better atomization and vaporization in the premixing/prevaporizing section of a lean premixed/prevaporized flame tube combustor. A focused Schlieren system was used to investigate the fuel/air mixing effectiveness of various fuel injection configurations. The Schlieren system was focused to a plane within the flow field of a test section equipped with optical windows. The focused image plane was parallel to the axial direction of the flow and normal to the optical axis. Images from that focused plane, formed by refracted light due to density gradients within the flow field, were filmed with a high-speed movie camera at framing rates of 8,000 frames per second (fps). Three fuel injection concepts were investigated by taking high-speed movies of the mixture flows at various operating conditions. The inlet air temperature was varied from 600 F to 1000 F, and inlet pressures from 80 psia to 150 psia. Jet-A fuel was used typically at an equivalence ratio of 0.5. The intensity variations of the digitized Schlieren images were analytically correlated to spatial density gradients of the mixture flows. Qualitative measurements for degree of mixedness, intensity of mixing, and mixing completion time are shown. Various mixing performance patterns are presented with different configurations of fuel injection points and operating conditions. Author (revised)

N94-26588*# Pratt and Whitney Aircraft, East Hartford, CT.
PROGRAM TO DEVELOP A PERFORMANCE AND HEAT LOAD PREDICTION SYSTEM FOR MULTISTAGE TURBINES Technical Progress Report No. 44, 1-31 Jan. 1994
Om Sharma 28 Feb. 1994 6 p
(Contract NAS3-25804)
(NASA-CR-195223; NAS 1.26:195223; PWA-6228-47) Avail: CASI HC A02/MF A01

Flows in low-aspect ratio turbines, such as the SSME fuel turbine, are three dimensional and highly unsteady due to the relative motion of adjacent airfoil rows and the circumferential and spanwise gradients in total pressure and temperature, The systems used to design these machines, however, are based on the assumption that the flow is steady. The codes utilized in these design systems are calibrated against turbine rig and engine data through the use of empirical correlations and experience factors. For high aspect ratio turbines, these codes yield reasonably accurate estimates of flow and temperature distributions. However, future design trends will see lower aspect ratio (reduced number of parts) and higher inlet temperature which will result in increased three dimensionality and flow unsteadiness in turbines. Analysis of recently acquired data indicate that temperature streaks and secondary flows generated in combustors and up-stream airfoils can have a large impact on the time-averaged temperature and angle distributions in downstream airfoil rows. Derived from text

N94-26673 Carleton Univ., Ottawa (Ontario). Dept. of Mechanical and Aerospace Engineering.
SIMULATING INDIRECT THRUST MEASUREMENT METHODS AS USED ON MODERN HIGH-BYPASS TURBOFANS M.S. Thesis
Jonathan David Stevenson Dec. 1992 143 p
(ISBN-0-315-84123-0; CTN-94-61059) Copyright Avail: Micromedia Ltd., Technical Information Centre, 240 Catherine Street, Suite 305, Ottawa, Ontario, K2P 2G8, Canada HC/MF

As yet, there is no known reliable method for directly measuring the thrust of a turbofan in flight. Manufacturers of civil turbofans use various indirect thrust measurements to indicate performance of an engine to the flight deck. Included among these are engine pressure ratio (EPR), integrated engine pressure ratio (IEPR), fan mechanical speed as a percentage of its design speed (N1), and various turbine gas temperatures. Of key concern is whether these thrust indicators give an accurate account of the actual engine thrust. A study was undertaken to determine the effect of advanced engine cycles on typical values of the most popular thrust setting parameters, using a generic computer model of a twin-spool high bypass ratio turbofan. A preliminary investigation was conducted to determine the effects of various kinds of engine deterioration on the engine performance and the indirect thrust indicators. The results show very little difference between the most popular thrust indicator methods used. EPR and IEPR have the unique advantage of being self-correcting to a wide range of ambient takeoff temperatures, but are affected by changes in altitude, forward speed, and engine cycle. N1 appears to exhibit different behavior at takeoff and cruise operation, but has the advantage of being intuitive to pilots. Author (CISTI)

N94-27432*# McDonnell-Douglas Aerospace Information Services Co., Saint Louis, MO. New Aircraft and Missile Products Div.
DESIGN AND FLIGHT TEST OF THE PROPULSION CONTROLLED AIRCRAFT (PCA) FLIGHT CONTROL SYSTEM ON THE NASA F-15 TEST AIRCRAFT
Edward A. Wells and James M. Urnes, Sr. Feb. 1994 42 p
(Contract NAS2-13312; RTOP 533-02-36)
(NASA-CR-186028; H-1965; NAS 1.26:186028; Rept-94B0005) Avail: CASI HC A03/MF A01

This report describes the design, development and flight testing of the

Propulsion Controlled Aircraft (PCA) flight control system performed at McDonnell Douglas Aerospace (MDA), St. Louis, Missouri and at the NASA Dryden Flight Research Facility, Edwards Air Force Base, California. This research and development program was conducted by MDA and directed by NASA through the Dryden Flight Research Facility for the period beginning January 1991 and ending December 1993. A propulsion steering backup to the aircraft conventional flight control system has been developed and flight demonstrated on a NASA F-15 test aircraft. The Propulsion Controlled Aircraft (PCA) flight system utilizes collective and differential thrust changes to steer an aircraft that experiences partial or complete failure of the hydraulically actuated control surfaces. The PCA flight control research has shown that propulsion steering is a viable backup flight control mode and can assist the pilot in safe landing recovery of a fighter aircraft that has damage to or loss of the flight control surfaces. NASA, USAF and Navy evaluation test pilots stated that the F-15 PCA design provided the control necessary to land the aircraft. Moreover, the feasibility study showed that PCA technology can be directly applied to transport aircraft and provide a major improvement in the survivability of passengers and crew of controls damaged aircraft. Author

N94-27593# Deutsche Forschungsanstalt fuer Luft- und Raumfahrt, Brunswick (Germany). Abt. Antriebsintegration.

EXPERIMENTAL AND THEORETICAL INVESTIGATIONS OF THE INFLUENCE OF THE JET ON THE FLOW AROUND A BYPASS-ENGINE [EXPERIMENTELLE UND THEORETISCHE UNTERSUCHUNGEN UEBER DEN STRAHLEINFLUSS BEI DER UMSTROEMUNG EINES BYPASS-TRIEBWERKES]

Andreas Korus Dec. 1992 130 p In GERMAN
(ISSN 0939-2963)
(DLR-FB-93-17; ETN-94-95495) Avail: CASI HC A07/MF A02

The characteristics of jet flows and their interference with boat tails are described, and experimental investigations with a 'hot jet simulator' of the bypass engine CF6-50 on the 'jet simulation tunnel' are described. The influences of the nozzle pressure ratios and the free stream Mach number on the pressure distributions of the engine contours and the jet behavior, as well as the mutual effects on the fan and core jet are investigated, due to measurements with a cold core jet. Subsequently, the results of the jets on the flow around the bypass engine carried out theoretically using the coupled STC (Stream Tube Curvature)-GENMIX code. An Euler code was used to examine the influence of the shape of the jet profile on the pressure distribution of the core cowl contour. The results received from the measurements and the calculations were compared. ESA

N94-27608# National Aerospace Lab., Kakuda (Japan).

A STUDY ON HEAT TRANSFER IN A SCRAMJET LEADING EDGE MODEL

Shuichi Ueda, Noboru Sakuranaka, Toshihito Saito, Katsuhiro Ito, Yoshio Wakamatsu, and Kiwamu Imai Dec. 1992 15 p Original contains color illustrations
(ISSN 0389-4010)
(NAL-TR-1187T; JTN-94-80615) Avail: CASI HC A03/MF A01

Heating tests and analysis of a cooling panel that simulates the leading edge of a scramjet engine inlet or strut were performed using a crossflow type water-cooled panel with a circular leading edge. The cooling panel was fabricated by nickel electroforming and heated by supersonic hot gas. An NTO (Nitrogen TetraOxide) and MMH (MonoMethyl Hydrazine) rectangular chamber was used as the gas generator. The free stream Mach number at the nozzle exit was about 2.67. Water was used as the coolant, and heat flux distribution was measured based on the temperature increase. Thermal analyses were performed using a two-dimensional CFD (Computational Fluid Dynamics) code and a finite element code. The results of the analysis were compared with the experimental data. Author (NASDA)

N94-27654*# Duke Univ., Durham, NC. Dept. of Mechanical Engineering and Materials Science.

PREDICTION OF UNDSTEADY FLOWS IN TURBOMACHINERY USING THE LINEARIZED EULER EQUATIONS ON DEFORMING GRIDS Final Report

William S. Clark and Kenneth C. Hall Mar. 1994 111 p
(Grant NAG3-1192; RTOP 505-62-10)
(NASA-CR-195285; E-8630; NAS 1.26:195285) Avail: CASI HC A06/MF A02

A linearized Euler solver for calculating unsteady flows in turbomachinery blade rows due to both incident gusts and blade motion is presented. The model accounts for blade loading, blade geometry, shock motion, and wake motion. Assuming that the unsteadiness in the flow is small relative to the nonlinear mean solution, the unsteady Euler equations can be linearized about the mean flow. This yields a set of linear variable coefficient equations that describe the small amplitude harmonic motion of the fluid. These linear equations are then discretized on a computational grid and solved using standard numerical techniques. For transonic flows, however, one must use a linear discretization which is a conservative linearization of the non-linear discretized Euler equations to ensure that shock impulse loads are accurately captured. Other important features of this analysis include a continuously deforming grid which eliminates extrapolation errors and hence, increases accuracy, and a new numerically exact, nonreflecting far-field boundary condition treatment based on an eigenanalysis of the discretized equations. Computational results are presented which demonstrate the computational accuracy and efficiency of the method and demonstrate the effectiveness of the deforming grid, far-field nonreflecting boundary conditions, and shock capturing techniques. A comparison of the present unsteady flow predictions to other numerical, semi-analytical, and experimental methods shows excellent agreement. In addition, the linearized Euler method presented requires one or two orders-of-magnitude less computational time than traditional time marching techniques making the present method a viable design tool for aeroelastic analyses. Author

N94-27739# Deutsche Forschungsanstalt fuer Luft- und Raumfahrt, Brunswick (Germany). Abt. Antriebsintegration.

THE DESIGN OF A COUNTER ROTATING ULTRA-HIGH-BYPASS FAN SIMULATOR FOR WINDTUNNEL INVESTIGATION [AUSLEGUNG EINES COUNTER ROTATING ULTRA-HIGH-BYPASS FAN SIMULATORS FUER WINDKANALUNTERSUCHUNGEN]

Heinz Hoheisel Mar. 1993 84 p Original contains color illustrations
(ISSN 0939-2963)
(DLR-FB-93-20; ETN-94-95497) Avail: CASI HC A05/MF A01

The procedure and special aspects that had to be taken into account during the design of an engine simulator to be used for simulating the integration of airframes and engines with ultra high bypass ratios are described. The simulator should be able to simulate the aerodynamics and acoustics of the real engine. For this reason, the simulator was designed with a counter rotating fan. The counter rotation of the fan was generated by a reverse gearbox, similar to the real engine where a gearbox is necessary to maintain a good LP turbine efficiency. ESA

N94-27778*# United Technologies Corp., East Hartford, CT. Pratt and Whitney Div.

COUPLED 2-DIMENSIONAL CASCADE THEORY FOR NOISE AN D UNSTEADY AERODYNAMICS OF BLADE ROW INTERACTION IN TURBOFANS. VOLUME 2: DOCUMENTATION FOR COMPUTER CODE CUP2D

Donald B. Hanson Washington Jan. 1994 42 p
(Contract NAS3-25952; RTOP 535-03-10)
(NASA-CR-4506-Vol-2; E-7766; NAS 1.26:4506-Vol-2) Avail: CASI HC A03/MF A01

A two dimensional linear aeroacoustic theory for rotor/stator interaction with unsteady coupling was derived and explored in Volume 1 of this report. Computer program CUP2D has been written in FORTRAN embodying the theoretical equations. This volume (Volume 2) describes the structure of the code, installation and running, preparation of the input file, and interpretation of the output. A sample case is provided with printouts of the input and output. The source code is included with comments linking it closely to the theoretical equations in Volume 1. Author (revised)

N94-28018# Rolls-Royce Ltd., Bristol (England). Powerplant Technology.

INFLUENCE OF HEADWIND ON HOT GAS REINGESTION AND CONSIDERATION OF PRESSURE RATIO SCALING

C. J. Penrose *In* AGARD, Computational and Experimental Assessment of Jets in Cross Flow Nov. 1993 9 p (For primary document see N94-28003 07-34)
Copyright Avail: CASI HC A02/MF A04

N94-28019# Rolls-Royce Ltd., Bristol (England). Powerplant Technology.
UNSTEADY ASPECTS OF HOT GAS REINGESTION AND STATISTICAL ANALYSIS
R. Beasley *In* AGARD, Computational and Experimental Assessment of Jets in Cross Flow Nov. 1993 6 p (For primary document see N94-28003 07-34)
Copyright Avail: CASI HC A02/MF A04

N94-28037# Karlsruhe Univ. (Germany).
ANALYSIS OF COOLING JETS NEAR THE LEADING EDGE OF TURBINE BLADES
E. Benz, S. Wittig, A. Beeck (ABB Power Generation, Inc., Baden, Switzerland.), and L. Fottner (Universitaet der Bundeswehr Muenchen, Neubiberg, Germany.) *In* AGARD, Computational and Experimental Assessment of Jets in Cross Flow Nov. 1993 12 p (For primary document see N94-28003 07-34)
Copyright Avail: CASI HC A03/MF A04

N94-28319 De Havilland Aircraft Co. of Canada Ltd., Downsview (Ontario).
PROPELLER OFF-AXIS LOADS DUE TO THRUST AXIS INCIDENCE AND NACELLE MAGNUS FORCE
P. Vyriotes, J. Petzke, and D. Barber *In* Canadian Aeronautics and Space Inst., Abstracts of Papers Presented at the 4th CASI Aerodynamics Symposium 1993 p 13-16 (For primary document see N94-28315 07-02)
Avail: Issuing Activity (Canadian Aeronautics and Space Inst., 130 Slater Street, Suite 818, Ottawa, ON K1P 6E2 Canada)

N94-28320 Carleton Univ., Ottawa (Ontario).
EFFECT OF SURFACE FINISH ON TURBINE AIRFOIL CASCADE LOSSES
Rama Radmard, Peter J. Turyk (Pratt and Whitney Aircraft of Canada Ltd., Mississauga, Ontario.), and William E. Carscallen (National Research Council of Canada, Ottawa, Ontario.) *In* Canadian Aeronautics and Space Inst., Abstracts of Papers Presented at the 4th CASI Aerodynamics Symposium 1993 p 17-20 (For primary document see N94-28315 07-02)
Avail: Issuing Activity (Canadian Aeronautics and Space Inst., 130 Slater Street, Suite 818, Ottawa, ON K1P 6E2 Canada)

N94-28321 Atomic Energy of Canada Ltd., Pinawa (Manitoba). Containment Analysis Branch.
THE EFFECT OF AXIAL VELOCITY RATIO, TURBULENCE INTENSITY, INCIDENCE, AND LEADING EDGE GEOMETRY ON THE MIDSPAN PERFORMANCE OF A TURBINE CASCADE
D. R. Whitehouse, S. H. Moustapha (Pratt and Whitney Aircraft of Canada Ltd., Longueuil, Quebec.), and S. A. Sjolander (Carleton Univ., Ottawa, Ontario.) *In* Canadian Aeronautics and Space Inst., Abstracts of Papers Presented at the 4th CASI Aerodynamics Symposium 1993 p 21-24 (For primary document see N94-28315 07-02)
Avail: Issuing Activity (Canadian Aeronautics and Space Inst., 130 Slater Street, Suite 818, Ottawa, ON K1P 6E2 Canada)

N94-28336 Waterloo Univ. (Ontario). Dept. of Mechanical Engineering.
A NEW APPROACH TO TURBOPROP FORWARD NACELLE DESIGN
I. Adare, I. Fejtek (De Havilland Aircraft Co. of Canada Ltd., Downsview, Ontario.), S. Bedi, and J. Coll (De Havilland Aircraft Co. of Canada Ltd., Downsview, Ontario.) *In* Canadian Aeronautics and Space Inst., Abstracts of Papers Presented at the 4th CASI Aerodynamics Symposium 1993 p 82-85 (For primary document see N94-28315 07-02)
Avail: Issuing Activity (Canadian Aeronautics and Space Inst., 130 Slater Street, Suite 818, Ottawa, ON K1P 6E2 Canada)

08 AIRCRAFT STABILITY AND CONTROL

Includes aircraft handling qualities; piloting; flight controls; and autopilots.

For related information see also *05 Aircraft Design, Testing and Performance.*

N94-25640# Cranfield Inst. of Tech., Bedford (England). Flight Dynamics Group.
THE APPLICATION OF A C(STAR) FLIGHT CONTROL LAW TO LARGE CIVIL TRANSPORT AIRCRAFT Ph.D. Thesis
Edmund Field Mar. 1993 45 p Sponsored by United Kingdom Science and Engineering Research Council
(Cranfield-Aero-9303; ISBN-1-871564-58-1; ETN-94-95222) Avail: CASI HC A03/MF A01

The aim of the program is to design flight control laws to give fly by wire civil transport aircraft excellent flying qualities at all flight conditions. The most critical flight phase of a civil transport is the landing approach. An analysis of the C(star) parameter is presented. The C(star) criterion was one of the first handling qualities criteria designed to take account of advanced aerodynamic designs of modern aircraft and higher order systems introduced by flight control systems. Several aircraft have since employed control laws based around the C(star) parameter. A proportional feedback C(star) controller was applied to a Boeing 747-100 in landing approach configuration, and assessed against the C(star) criterion. ESA

N94-25653# Cranfield Inst. of Tech., Bedford (England). College of Aeronautics.
REPORT ON A VISIT TO THE ARVIN/CALSPAN CORPORATION, BUFFALO, NEW YORK, USA, SEPTEMBER 1992
Edmund Field Apr. 1993 61 p Sponsored by Eric Beverley Memorial Trust
(Cranfield-Aero-9305; NFP-9202; ISBN-1-871564-59-X; ETN-94-95277)
Avail: CASI HC A04/MF A01

A literature search of reports related to flying and handling qualities of advanced fly by wire aircraft was performed. An engineering test flight in a variable stability Learjet in-flight simulator was carried out to demonstrate features of modern flight control systems designs. Recent developments in the field were discussed with the personnel. Contact was also made with the stability, control, simulation, and flight qualities group which was conducting total in flight simulation (TIFS). ESA

N94-25771# Air Force Inst. of Tech., Wright-Patterson AFB, OH. School of Engineering.
DESIGN OF A SUBSONIC ENVELOPE FLIGHT CONTROL SYSTEM FOR THE VISTA F-16 USING QUANTITATIVE FEEDBACK THEORY M.S. Thesis
Odell R. Reynolds Dec. 1993 180 p
(AD-A274057; AFIT/GE/Eng/93D-34) Avail: CASI HC A09/MF A02

A controlled plant's characteristics can vary widely throughout its operational envelope. This is a major problem in nominal plant-based control system design. Hence, gain scheduling is often used for full envelop design. In this paper, it is proposed to address the plant's variability using robust control design concepts. In particular, the frequency domain based Quantitative Feedback Theory Multiple-Input Multiple-Output robust control design method is employed for the synthesis of a full envelop flight control system for an F-16 derivative. Compensators for the aircraft's pitch and lateral directional channels are designed, and the designs are validated using linear simulations. DTIC

N94-25785# Air Force Inst. of Tech., Wright-Patterson AFB, OH. School of Engineering.
NEURAL NETWORKS FOR DYNAMIC FLIGHT CONTROL M.S. Thesis
Ronald E. Setzer Dec. 1993 140 p
(AD-A274089; AFIT/GE/Eng/93D-36) Avail: CASI HC A07/MF A02

This thesis examines the application of artificial neural networks (NN's) to the problem of dynamic flight control. The specific application is the control of a flying model helicopter. The control interface is provided through a hardware and software test bed called the Fast Adaptive Maneuvering Experiment (FAME). The NN design approach uses two NN's: one trained as an emulator of the plant and the other trained to control the emulator. The emulator neural network is designed to reproduce the flight dynamics of the experimental plant. The controller is then designed to produce the appropriate control inputs to drive the emulator to a desired final state. Previous research in the area of NN's for controls has almost exclusively been applied to simulations. To develop a controller for a real plant, a neural network must be created which will accurately recreate the dynamics of the plant. This thesis demonstrates the ability of a neural network to emulate a real, dynamic, nonlinear plant. DTIC

N94-25833# Air Force Inst. of Tech., Wright-Patterson AFB, OH. School of Engineering.

DESIGN OF A FLIGHT CONTROLLER FOR AN UNMANNED RESEARCH VEHICLE WITH CONTROL SURFACE FAILURES USING QUANTITATIVE FEEDBACK THEORY M.S. Thesis

Mark S. Keating Dec. 1993 163 p

(AD-A274049; AFIT/GE/Eng/93D-18) Avail: CASI HC A08/MF A02

This thesis describes the application of the multiple-input multiple-output (MIMO) Quantitative Feedback Theory (QFT) design technique to the design of a digital flight control system for the Lambda Unmanned Research Vehicle (URV). The QFT technique allows the synthesis of a control system which is robust in the presence of structured plant uncertainties. Uncertainties considered in this design are the aircraft's plant variation within the flight envelope and the effects of damage to aircraft control surfaces. Mathematical models of control surface failure effects on aircraft dynamics are derived and used to modify an existing small perturbation model of the Lambda. The QFT technique is applied to design a control system utilizing aircraft pitch rate, roll rate and sideslip angle as feedback variables. The inherent cross-coupling rejection qualities of QFT and an aileron-rudder interconnect are utilized to design a control system which results in a coordinated flight. An outer-loop autopilot is then designed around the QFT controller to further assist turn coordination. Sensor noise effects on aircraft states are also analyzed. DTIC

N94-25998# Air Force Inst. of Tech., Wright-Patterson AFB, OH. School of Engineering.

DISCOVERY LEARNING IN AUTONOMOUS AGENTS USING GENETIC ALGORITHMS M.S. Thesis

Edward O. Gordon Dec. 1993 209 p

(AD-A274083; AFIT/GE-93D-10) Avail: CASI HC A10/MF A03

As the new Distributed Interactive Simulation (DIS) draft standard evolves into a useful document and distributed simulations begin to emerge that implement parts of the standard, there is renewed interest in available methods to effectively control autonomous aircraft agents in such a simulated environment. This investigation examines the use of a genetics-based classifier system for agent control. These are robust learning systems that use the adaptive search mechanisms of genetic algorithms to guide the learning system in forming new concepts (decision rules) about its environment. By allowing the rule base to evolve, it adapts agent behavior to environmental changes. Addressed are the learning needs of autonomous aircraft agents, showing how multiple learning strategies are possible and that the best approach is a coherent combination of these. A design is described for a control system using a distributed filtering architecture and a genetics-based classifier system modified to support a phasing-rule niching system based on phase tags. Finally, a prototype system called the Phased Pilot Learning System (PPLS) is implemented based on this design and tested within a limited simulation environment. Results from empirical tests show that this approach is a viable alternative to other control methods. DTIC

N94-26192# Naval Postgraduate School, Monterey, CA.

LINEAR MODELING OF ROTORCRAFT FOR STABILITY ANALYSIS AND PRELIMINARY DESIGN M.S. Thesis

Walter M. Wirth, Jr. Sep. 1993 188 p

(AD-A274869) Avail: CASI HC A09/MF A02

This thesis investigates linear state space modeling of single main rotor helicopters culminating in a computer program that can be used for stability and control analysis for any single main rotor helicopter or preliminary design of a helicopter. The trim solution for a flight condition is found, the aircraft is perturbed about the nominal point, and the stability and control derivatives are determined. State space models and analysis tools are provided by the program. A notional attack helicopter designed for the 1993 American Helicopter Society Design Competition and a notional utility helicopter are used as examples. DTIC

N94-26593*# National Aeronautics and Space Administration. Langley Research Center, Hampton, VA.

THE RELATIONSHIP OF AN INTEGRAL WIND SHEAR HAZARD TO AIRCRAFT PERFORMANCE LIMITATIONS

M. S. Lewis, P. A. Robinson, D. A. Hinton, and R. L. Bowles Feb. 1994 18 p

(RTOP 505-64-12-01)

(NASA-TM-109080; NAS 1.15:109080) Avail: CASI HC A03/MF A01

The development and certification of airborne forward-looking wind shear detection systems has required a hazard definition stated in terms of sensor observable wind field characteristics. This paper outlines the definition of the F-factor wind shear hazard index and an average F-factor quantity, calculated over a specified averaging interval, which may be used to judge an aircraft's potential performance loss due to a given wind shear field. A technique for estimating airplane energy changes during a wind shear encounter is presented and used to determine the wind shear intensity, as a function of the averaging interval, that presents significant hazard to transport category airplanes. The wind shear hazard levels are compared to averaged F-factor values at various averaging intervals for four actual wind shear encounters. Results indicate that averaging intervals of about one kilometer could be used in a simple method to discern hazardous shears. Author (revised)

N94-26636 Carleton Univ., Ottawa (Ontario). Dept. of Mechanical and Aerospace Engineering.

AN ADAPTIVE KALMAN FILTER FOR TACTICAL MISSILES GUIDANCE SYSTEMS M.S. Thesis

Jingming Li 15 Jan. 1993 142 p

(ISBN-0-315-84115-X; CTN-94-61055) Copyright Avail: Micromedia Ltd., Technical Information Centre, 240 Catherine Street, Suite 305, Ottawa, Ontario, K2P 2G8, Canada HC/MF

The Kalman filter can be used to upgrade inertial navigation systems (INS's) without costly upgrading of the hardware. Current methods of integrating Kalman filters into INS's are investigated. A standard Kalman filter algorithm is implemented in the INS for a glide weapon system in order to assess the performance of the filter. An adaptive Kalman filter is then implemented to illustrate the performance improvement. The Kalman filter estimates the navigation error in real time with the aid of other external signal sources. The INS receives these signals and makes appropriate compensations. The estimation results from the standard Kalman filter may diverge from the actual error signal either because of the changing dynamics or inaccurate parameters. The adaptive Kalman filter could tune itself to work within the new environment. A Kalman filter convergent criterion and an on-line noise covariance estimation algorithm are described. An approach that combines the S Kalman filter and on-line variable indentifications is suggested. Simulation results for the standard and adaptive Kalman filters are discussed and compared. Author (CISTI)

N94-26710# Institute for Aerospace Research, Ottawa (Ontario).

THE EFFECTS OF TAILWINDS AND CONTROL CROSS COUPLING ON ROTORCRAFT HANDLING QUALITIES FOR STEEP, DECELERATING INSTRUMENT APPROACHES AND MISSED APPROACHES

S. W. Baillie, S. Kereliuk, and J. M. Morgan Sep. 1993 72 p

(IAR-AN-77; NRC-32159; CTN-94-61007) Avail: CASI HC A04/MF A01

The expansion of the rotorcraft instrument flight envelope to allow steep, decelerating approaches to low speeds and altitudes will profoundly improve the utility of those vehicles. As a supplement to previously published investigations, a research program was conducted using the Bell 205 Airborne Simulator, whose results provide a data base on which rotorcraft instrument flight certification standards can be formulated for rotorcraft operations equivalent to Category III A. The research was conducted to document the effect of conducting steep, decelerating approaches in the presence of tailwinds. The handling qualities factors of terminating the approach with one of three missed approach procedures were investigated, and the height loss at the initiation of a missed approach procedure was documented. The handling qualities degradation induced by inter-axis control cross coupling was also assessed. The handling qualities and performance were found to be acceptable at speeds down to 10 knots when approaches were performed with a tailwind present. The initiation of missed approach procedures resulted in minimum altitudes that approached 20 feet in some cases. Increased levels of inter-axis control cross coupling had little effect on handling qualities on approach. CISTI

N94-26821*# Georgia Inst. of Tech., Atlanta. School of Aerospace Engineering.

RESEARCH IN ROBUST CONTROL FOR HYPERSONIC AIRCRAFT Progress Report No. 3, 1 Sep. 1993 - 28 Feb. 1994

A. J. Calise Mar. 1994 27 p
(Grant NAG1-1451)
(NASA-CR-195250; NAS 1.26:195250) Avail: CASI HC A03/MF A01

The research during the third reporting period focused on fixed order robust control design for hypersonic vehicles. A new technique was developed to synthesize fixed order H(sub infinity) controllers. A controller canonical form is imposed on the compensator structure and a homotopy algorithm is employed to perform the controller design. Various reduced order controllers are designed for a simplified version of the hypersonic vehicle model used in our previous studies to demonstrate the capabilities of the code. However, further work is needed to investigate the issue of numerical ill-conditioning for large order systems and to make the numerical approach more reliable. Author (revised)

N94-27112# Department of the Navy, Washington, DC.

FLUID DYNAMIC LINEAR ACCELEROMETER Patent Application

David E. Keyser, inventor (to Navy) 17 May 1993 16 p
(AD-D016042; US-Patent-Appl-SN-063844) Avail: CASI HC A03/MF A01

A linear acceleration sensing device operates through a fluid medium. A fluid signal output represents a differential pressure from the elastic deformation of a fluid-filled diaphragm or bellows assembly. A pair of fluid proximity sensors operate differentially in a fluid control network and detect the elastic deformation of the diaphragm assembly caused by increased hydrostatic pressure resulting from a change in acceleration, or g-force. DTIC

N94-27132# Air Force Inst. of Tech., Wright-Patterson AFB, OH. School of Engineering.

AUTOMATION OF FORMATION FLIGHT CONTROL M.S. Thesis

Vincent P. Reyna 1994 193 p
(AD-A274137; AFIT/GE/Eng/94M-01) Avail: CASI HC A09/MF A03

The research contained in this thesis explores the concepts of Automated Formation Flight Control documented in three previous AFIT theses. The generic formation analyzed consists of a Leader and Wingman, with the Wingman referencing its maneuvers off of Leader maneuvers. Specifically, planar formation flight control concerning only heading and velocity changes is considered. Next, the vertical separation constraint is relaxed to allow wing maneuvers outside of the flight plane of the lead in order to minimize the energy expended by the wing in a maneuver. Analysis of the two forms of formation flight control investigated in this thesis reveals the close relationship between formation geometry, aircraft time constants, controller gains, formation performance, and control system stability. Integral control action is determined to be necessary for formation flight control. Nonlinear simulations are accomplished on a digital computer to validate the analysis of the automated formation flight control system. Comparisons are made between the two forms of formation flight control considered, and a third, energy conserving maneuvers, in order to determine which is best for each phase of flight. DTIC

N94-27206# National Aerospace Lab., Tokyo (Japan). Flight Research Div.

OPTIMAL CONTROL OF HELICOPTERS FOLLOWING POWER FAILURE [HERIKOPUTA NO ENJIN KOSHOJI NO SAITEKI HIKO SEIGYO]

Yoshinori Okuno Jan. 1993 49 p In JAPANESE
(ISSN 0389-4010)
(NAL-TR-1190; JTN-94-80617) Avail: CASI HC A03/MF A01

Helicopter control procedures following power failure were theoretically investigated by applying nonlinear optimal control theory to the following four optimization problems: (1) Minimization of the touchdown speed following power failure. Comparisons between the calculated optimal solutions and the empirical flight test results showed that the pilots used nonoptimal controls, especially in the timing and amplitude of the collective flare before touchdown; (2) Prediction of the Height-Velocity (H-V) boundaries. The optimization problems were formulated to minimize the unsafe region under the condition that the touchdown speed is within the landing gear capacity. The calculated H-V boundaries showed good correlation with the flight test results. In addition, parameters such as the flight-path angle at the moment of power failure, collective control delay, collective setting during descent, landing site location and its available field length, and wind speed were found to have significant effects on the success of the emergency landing; (3) Optimization of the takeoff procedure for Category A STOL operation. The results show that the required takeoff distance using the normal takeoff procedure can be significantly reduced if the takeoff path and the critical decision point are specifically optimized for a given set of operating conditions, e.g., gross weight, ambient conditions, and heliport configuration; (4) Evaluation of the take-off performance for Category A VTOL operation. The calculated maximum weight when assuming the normal takeoff procedure showed good agreement with the certificated takeoff weight. Additionally, optimization of the takeoff path was shown to allow the payload to be increased. Author (NASDA)

N94-27395 National Aerospace Lab., Amsterdam (Netherlands). Structures and Materials Div.

THE DETERMINISTIC POWER-SPECTRAL-DENSITY METHOD

R. Noback 17 Mar. 1992 63 p Presented at Gust Specialists Meeting, Dallas, TX, 15 Apr. 1992 Limited Reproducibility: More than 20% of this document may be affected by microfiche quality
(Contract OV/RLD-132)
(AD-B175894; ETN-94-95443; NLR-TP-92114-U) Avail: CASI HC A04

The Deterministic Power Spectral Density (DPSD) method was derived directly from the continuous PSD method. It can be regarded as a 'translation' from the frequency domain to the space or time domain. The critical gust profile, giving maximum response, is obtained directly. The method was compared with the matched filter theory and with simulation. The DPSD method gives the same results as the continuous PSD method, for linear systems. The DPSD method was applied to a nonlinear system, using equivalent gain to obtain the critical gust profile. Results were compared with those obtained with simulation. ESA

N94-27414*# Akron Univ., OH.

COMPUTER CODE FOR CONTROLLER PARTITIONING WITH IFPC APPLICATION: A USER'S MANUAL Final Report

Phillip H. Schmidt and Asim Yarkhan Mar. 1994 76 p
(Grant NAG3-11467; RTOP 505-62-50)
(NASA-CR-195291; E-8654; NAS 1.26:195291) Avail: CASI HC A05/MF A01

A user's manual for the computer code for partitioning a centralized controller into decentralized subcontrollers with applicability to Integrated Flight/Propulsion Control (IFPC) is presented. Partitioning of a centralized controller into two subcontrollers is described and the algorithm on which the code is based is discussed. The algorithm uses parameter optimization of a cost function which is described. The major data structures and functions are described. Specific instructions are given. The user is led through an example of an IFCP application. Author (revised)

N94-27648 Carleton Univ., Ottawa (Ontario). Dept. of Mechanical and Aerospace Engineering.

CONTROLLED OSCILLATION OF FOREBODY VORTICES BY NOZZLE JET BLOWING M.S. Thesis

Karim Alexan Dec. 1992 166 p
(ISBN-0-315-84134-6; CTN-94-61064) Copyright Avail: Micromedia Ltd., Technical Information Centre, 240 Catherine Street, Suite 305, Ottawa, Ontario, K2P 2G8, Canada HC/MF

The flowfield surrounding an ogive-cylinder type model immersed in a free stream fluid as its angle of attack is increased is discussed and the most promising methods of forebody vortex manipulation are reviewed. A scheme for controlling the behavior of forebody vortices at high angles of attack is experimentally investigated in a water tunnel at low speed. A detailed log of the repair work and modifications done to the water tunnel, a summary of operating procedures, and recommendations for its continued operation are provided. The use of port and starboard positioned, forward blowing nozzles located near the forebody apex is investigated. The ability of blowing to alter the orientation of asymmetrically positioned streamwise vortices is assessed and the possibility of using relatively rapid port-starboard oscillatory blowing to obtain a desired time-averaged side force and yaw moment is explored. The dynamic response of an F-18 aircraft to rapid oscillatory blowing at high angles of attack is approximated. The resulting amplitudes of oscillation indicate that this motion would likely be felt by the pilot but suggestions are made for improved performance of this oscillatory blowing system and for future research into oscillatory blowing for forebody vortex manipulation. Author (CISTI)

N94-27660*# National Aeronautics and Space Administration. Langley Research Center, Hampton, VA.
TECHNIQUES TO IMPROVE MANEUVER STABILITY CHARACTERISTICS OF A NONLINEAR WIDE-BODY TRANSPORT AIRPLANE IN CRUISE FLIGHT
William D. Grantham, Lee H. Person, Jr., Melvin L. Bailey (Lockheed Engineering and Sciences Co., Hampton, VA.), and Stephen A. Tingas (Lockheed Aeronautical Systems Co., Marietta, GA.) Mar. 1994 66 p
(RTOP 505-64-52-01)
(NASA-TM-4521; L-17205; NAS 1.15:4521) Avail: CASI HC A04/MF A01

The maneuver control stability characteristics of an aircraft are a flying qualities parameter of critical importance, to ensure structural protection as well as adequate predictability to the pilot. Currently, however, maneuver stability characteristics are not uniquely addressed in the Federal Aviation Regulations (FAR) Part 25, for transport aircraft. In past transport category certification programs, the Federal Aviation Administration (FAA) has used a combination of requirements (longitudinal control, vibration and buffeting, high-speed characteristics, and out-of-trim characteristics) to ensure safe and controllable maneuver stability characteristics over a range of flight conditions and airplane configurations. Controversies exist regarding each of these regulations, however, and considerable expenditures in terms of design studies and testing time have resulted from the requirements. It is also recognized that additional engineering guidance is needed for identifying acceptable nonlinear maneuver stability characteristics, particularly as they relate to relaxed stability, highly augmented transport configurations. The current trend in large aircraft design is toward relaxed, or even negative, static margins for improved fuel efficiency. The advanced flight control systems developed for these aircraft, in many instances, have rendered current aforementioned maneuver stability criteria either too stringent or of little practical use. Current design requirements do not account for these advanced designs. The objective was to evaluate a broad spectrum of linear and nonlinear longitudinal stability characteristics to generate data for defining satisfactory and unacceptable maneuver characteristics, as defined by pilot opinion. Primary emphasis was placed on two techniques of varying column force per normal acceleration. This study was a joint venture with four pilots participating; one from NASA, one from the FAA, and two from industry. Author (revised)

N94-27798 National Aerospace Lab., Amsterdam (Netherlands). Fluid Dynamics Div.
UNDERSTANDING AND DEVELOPMENT OF A PREDICTION METHOD OF TRANSONIC LIMIT CYCLE OSCILLATION CHARACTERISTICS OF FIGHTER AIRCRAFT
Jos J. Meijer and Atlee M. Cunningham, Jr. 31 May 1992 17 p Presented at the 18th ICAS Congress, Beijing, China, 21-25 Sep. 1992; and AIAA Atmospheric Flight Mechanics Conference, Hilton Head, SC, 10-12 Aug. 1992 Sponsored by AF, General Dynamics Fort Worth, TX; Ministry of Defence, The Hague, Netherlands; and National Aerospace Lab., Amsterdam, Netherlands Limited Reproducibility: More than 20% of this document may be affected by microfiche quality
(Contract NIVR-07801N)
(NLR-TP-92210-U; ETN-94-95448) Avail: CASI HC A03

An analysis of steady wind tunnel data, obtained for a fighter type aircraft, has indicated that shock induced and trailing edge separation play a dominant role in the development of limit cycle oscillations (LCO) at transonic speeds. On the basis of these data, a semiempirical LCO prediction method is being developed. Its preliminary version was applied to several configurations and correctly identified those which have encountered LCO. It has already shown the potential for application early in the design process of new aircraft to determine and understand the nonlinear aeroelastic characteristics. An upgraded form is described and results of the latest predictions are used to further assess various parametric effects. The ultimate refinements are expected from unsteady wind tunnel force and pressure measurements for which preliminary results are presented. ESA

N94-28028# McDonnell-Douglas Aerospace Information Services Co., Saint Louis, MO.
PNEUMATIC MANAGEMENT OF BLUNTED-FOREBODY FLOW ASYMMETRY FOR HIGH-ANGLE-OF-ATTACK DIRECTIONAL CONTROL
Frederick W. Roos, Charles L. Magness, and Daniel V. Brown *In* AGARD, Computational and Experimental Assessment of Jets in Cross Flow Nov. 1993 6 p (For primary document see N94-28003 07-34)
Copyright Avail: CASI HC A02/MF A04

09 RESEARCH AND SUPPORT FACILITIES (AIR)

Includes airports, hangars and runways; aircraft repair and overhaul facilities; wind tunnels; shock tubes; and aircraft engine test stands.

For related information see also *14 Ground Support Systems and Facilities (Space).*

N94-25652# Technical Research Centre of Finland, Espoo. Metals Lab.
MEASUREMENT OF LABORATORY QUALITY [LABORATORION LAADUNMITTAUS]
Juha Sillanpaeae Mar. 1992 43 p In FINNISH
(ISSN 1235-0605)
(VTT-TIED-1427; ISBN-951-38-4321-1; ETN-94-95276) Copyright Avail: CASI HC A03/MF A01

Principles of assessing quality and developing assessment systems are described and examples and information on quality indicators generally used are given. The evaluation of customer satisfaction is addressed as an important quality indicator for laboratory work. ESA

N94-25740# Air Force Inst. of Tech., Wright-Patterson AFB, OH.
DYNAMIC RESPONSE OF A COMPRESSOR RESEARCH FACILITY M.S. Thesis
Janet W. Grondin Dec. 1993 226 p
(AD-A273836; AFIT/GAE/ENY/93D-16) Avail: CASI HC A11/MF A03

The response of the Wright Laboratory Compressor Research Facility to a small amplitude, acoustic, sinusoidal disturbance was investigated. The fluid transmission line equations for laminar, one-dimensional flow in a circular duct were solved and verified through a laboratory experiment using a scale model of the facility. The resonant frequencies of the facility were determined for a variety of flow conditions. Techniques for analytically modeling end impedance and flow straightening elements were also studied. The fundamental frequency of the facility was determined to be between 5.5 and 6.5 Hz depending on the flow conditions and geometry configurations specified. DTIC

N94-25773# Dayton Univ. Research Inst., OH.
IMAGE QUALITY AND THE DISPLAY MODULATION TRANSFER FUNCTION: EXPERIMENTAL FINDINGS Final Report, Jan. 1991 - Mar. 1992
Ronald J. Evans Sep. 1993 89 p
(Contract F33615-90-C-0005)
(AD-A274061; AL/HR-TR-1993-0131) Avail: CASI HC A05/MF A01

Image quality metrics represent an attempt to quantify differences in the quality of the transmission and display of visual information. This report focuses on the components in the image transfer process which contribute to image quality as well as tasks through which image quality may be empirically defined. The components consist of the content of the original image, display device characteristics, and observer characteristics. Special attention within these three components is given to the display Modulation Transfer Function (MTF) which has traditionally been the major contributor to image quality metrics. Ambiguities exist in the definition and measurement of display MTF's and these problems are discussed as they pertain to image quality. Additional discussion includes the use of threshold versus suprathreshold tasks as empirical measures of image quality and the use of the Contract Sensitivity Function (CSF) versus the MTF of the eye in image quality metrics. An argument is presented which questions the use of either the CSF or MTF for suprathreshold tasks. In order to test the use of display MTF's in metrics, a methodology is described for digitally filtering images with filter representing hypothetical display MTF's. Although this method permits a subset of display MTF's to be compared, further efforts are requiredto compare MTF's which exhibit a crossover effect in the spatial frequency domain. Finally, empirical observations suggest that other display parameters (e.g., luminance) must be weighted more heavily in image quality metrics. DTIC

N94-26141*# Sverdrup Technology, Inc., Brook Park, OH.
NASA LEWIS RESEARCH CENTER LEAN-, RICH-BURN MATERIALS TEST BURNER RIG Final Report
C. A. Stearns and R. C. Robinson Feb. 1994 58 p
(Contract NAS3-25266; RTOP 537-04-20)
(NASA-CR-194437; E-8285; NAS 1.26:194437) Avail: CASI HC A04/MF A01

The lean-, rich-burn materials test burner rig at NASA LeRC is used to evaluate the high temperature environmental durability of aerospace materials. The rig burns jet fuel and pressurized air, and sample materials can be subjected to both lean-burn and rich-burn environments. As part of NASA's Enabling Propulsion Materials (EPM) program, an existing rig was adapted to simulate the rich-burn quick-quench lean-burn (RQL) combustor concept which is being considered for the HSCT (high speed civil transport) aircraft. RQL materials requirements exceed that of current superalloys, thus ceramic matrix composites (CMC's) emerged as the leading candidate materials. The performance of these materials in the quasi reducing environment of the rich-burn section of the RQL is of fundamental importance to materials development. This rig was developed to conduct such studies, and its operation and capabilities are described. Author (revised)

N94-26196 Massachusetts Inst. of Tech., Lexington.
MACHINE INTELLIGENT GUST FRONT ALGORITHM
Richard L. Delanoy and Seth W. Troxel 4 Nov. 1993 95 p Sponsored in part by AF Limited Reproducibility: More than 20% of this document may be affected by microfiche quality
(Contracts DTFA01-93-Z-02012; F19628-90-C-0002)
(AD-A273695; ATC-196; DOT/FAA/RD-93/1) Avail: CASI HC A05

The Federal Aviation Administration has sponsored research and development of algorithms for automatic gust front detection as part of a suite of hazardous weather detection capabilities for airports. These algorithms are intended for use with Doppler radar systems, specifically the Terminal Doppler Weather Radar (TDWR) and the Airport Surveillance Radar enhanced with a Wind Shear Processor (ASR-9 WSP). Although gust fronts are observable with fairly reliable signatures in TDWR data existing gust front detection algorithms have achieved only modest levels of detection performance. For smaller airports not slated to receive a dedicated TDWR, the ASR-9 WSP will provide a less expensive wind shear detection capability. Gust front detection in ASR-9 SP data is an even more difficult problem, given the reduced sensitivity and less reliable Doppler measurements of this radar. A Machine Intelligent Gust Front Algorithm (MIGFA) has been constructed at Lincoln Laboratory. MIGFA is a radical departure from previous design strategies. Incorporating knowledge-based, signal-processing techniques initially developed at Lincoln Laboratory for automatic target recognition, MIGFA uses meteorological knowledge, spatial and temporal context, conditional data fusion, delayed thresholding, and pixel-level fusion of evidence to improve gust front detection performance significantly. In tests comparing MIGFA with an existing state-of-the-art algorithm applied to ASR-9 WSP data, MIGFA has substantially outperformed the older algorithm. DTIC

N94-26200# Wichita State Univ., KS. National Inst. for Aviation Research.
THE DEVELOPMENT OF A HORIZONTAL IMPACT SLED FACILITY AND SUBSEQUENT CRASHWORTHINESS EXPERIMENTS Final Report
Walter D. Bernhart, Joseph A. Mitchell, Karl W. Petzold, and Juan C. Rodriguez Jun. 1993 208 p
(NIAR-93-15; DOT/FAA/TN93/42) Avail: CASI HC A10/MF A03

The goal of this program was to develop a horizontal impact sled test laboratory for the National Institute for Aviation Research (NIAR) at Wichita State University to effectively serve the aviation industry relative to seat performance as well as other aircraft components. The fundamental goal was achieved in the fall of 1992 and the ensuing period has been spent in testing programs with at least five commercial clients, three of which were FAA observed certification tests. Author

N94-26202# Federal Aviation Administration, Atlantic City, NJ. Technical Center.
SOFT GROUND ARRESTING SYSTEM FOR AIRPORTS Final Report
James C. White, Satish K. Agrawal, and Robert E. Cook (Comrise Technologies, Inc.) Dec. 1993 75 p
(DOT/FAA/CT-93/80) Avail: CASI HC A04/MF A01

Aircraft can and do overrun the ends of runways, sometimes with disastrous consequences. Safety overrun areas are designed to provide an additional 1,000 feet of length for stopping overrunning aircraft. At many airports, however, the additional 1,000-foot safety area is not available. At these locations, soft ground arresting systems can be employed to decelerate or stop an overrunning aircraft. A mathematical model representing the interface between the aircraft and the soft ground was developed. This model was used to predict aircraft gear loads, deceleration, and stopping distance within the soft ground system. The validity of the mathematical model was confirmed by eight tests with the use of an instrumented Boeing 727 aircraft. A phenolic foam bed 680 feet long by 48 feet wide and 18 inches deep was used to demonstrate the effectiveness of safely stopping a Boeing 727 aircraft entering the bed at 50 knots and 60 knots: at 50 knots the aircraft came to a complete stop in 420 feet and at 60 knots in 540 feet. The aircraft was successfully extracted from the bed, the foam was successfully repaired, and airport rescue and fire fighting equipment and personnel were able to maneuver without difficulty on the foam. Author

N94-26305 Norwegian Defence Research Establishment, Kjeller.
SAFETY STANDARDS FOR AIRCRAFT SHELTER [SIKRINGSAVSTAND FOR FLYBUNKER]
Jens Brandstorp 27 Mar. 1992 69 p In NORWEGIAN Limited Reproducibility: More than 20% of this document may be affected by microfiche quality
(FFI-92/4003; ETN-94-94957) Avail: CASI HC A04

A reexamination of papers concerning Hardened Aircraft Shelter (HAS) explosion tests is presented. Of special interest is the physical background of all the phenomena which occur during or after the internal blast loading on the concrete walls. It is believed that a better physical understanding will benefit the analysis of practical explosion tests. A simulation model which systemizes the physical correlations and thereby predicts the Quantity-Distance (QD) for the debris from aircraft shelters was developed. When the test program of the U.S./Norwegian aircraft shelters in New Mexico (U.S.) are finished during 1992, these results will be compared with those of the simulation model. During the analysis of the earlier tests, a substantial difference in the break up mechanism was proved. This effect causes the size of the model debris to become greater than the full scale debris. A theory concerning this matter is developed. A major difference is also seen between frontside debris and rearside debris QD results. ESA

N94-26603*# Lockheed Engineering and Sciences Co., Hampton, VA.
PROPAGATION OF EXPERIMENTAL UNCERTAINTIES FROM THE TUNNEL TO THE BODY COORDINATE SYSTEM IN 3-D LDV FLOW FIELD STUDIES
Dan H. Neuhart Mar. 1994 46 p
(Contract NAS1-19000; RTOP 505-59-30-04)
(NASA-CR-191607; NAS 1.26:191607) Avail: CASI HC A03/MF A01

An analysis of experimental laser Doppler velocimetry (LDV) data uncertainties that propagate from measurements in the tunnel coordinate system to results in the model system are provided. Calculations of uncertainties as functions of the variables that comprise the final result requires assessment of the contribution each variable makes. Such an analysis enables and necessitates the experimentalists to identify and address the contributing error sources in the experimental measurement system. This provides an opportunity to improve the quality of data derived from experimental systems. This is especially important in experiments where small changes in test conditions are expected to produce small, detectable changes in results. In addition, the need for high-quality experimental data for CFD method validation demands a thorough assessment of experimental uncertainty. Transforming from one Cartesian coordinate system to another by three sequential rotations, equations were developed to transform the variables initially obtained in the original coordinates into variables in the final coordinate system. Based on the transformation equations, propagation equations for errors in the experimentally-derived flow quantities were derived for a model at angle of attack. Experimental uncertainties were then propagated from the tunnel coordinate system into the model system. Author (revised)

N94-26684*# National Aeronautics and Space Administration. Langley Research Center, Hampton, VA.
RESEARCH AND TEST FACILITIES
1993 102 p
(NASA-TM-109685; NAS 1.15:109685) Avail: CASI HC A06/MF A02

A description is given of each of the following Langley research and test facilities: 0.3-Meter Transonic Cryogenic Tunnel, 7-by 10-Foot High Speed Tunnel, 8-Foot Transonic Pressure Tunnel, 13-Inch Magnetic Suspension & Balance System, 14-by 22-Foot Subsonic Tunnel, 16-Foot Transonic Tunnel, 16-by 24-Inch Water Tunnel, 20-Foot Vertical Spin Tunnel, 30-by 60-Foot Wind Tunnel, Advanced Civil Transport Simulator (ACTS), Advanced Technology Research Laboratory, Aerospace Controls Research Laboratory (ACRL), Aerothermal Loads Complex, Aircraft Landing Dynamics Facility (ALDF), Avionics Integration Research Laboratory, Basic Aerodynamics Research Tunnel (BART), Compact Range Test Facility, Differential Maneuvering Simulator (DMS), Enhanced/Synthetic Vision & Spatial Displays Laboratory, Experimental Test Range (ETR) Flight Research Facility, General Aviation Simulator (GAS), High Intensity Radiated Fields Facility, Human Engineering Methods Laboratory, Hypersonic Facilities Complex, Impact Dynamics Research Facility, Jet Noise Laboratory & Anechoic Jet Facility, Light Alloy Laboratory, Low Frequency Antenna Test Facility, Low Turbulence Pressure Tunnel, Mechanics of Metals Laboratory, National Transonic Facility (NTF), NDE Research Laboratory, Polymers & Composites Laboratory, Pyrotechnic Test Facility, Quiet Flow Facility, Robotics Facilities, Scientific Visualization System, Scramjet Test Complex, Space Materials Research Laboratory, Space Simulation & Environmental Test Complex, Structural Dynamics Research Laboratory, Structural Dynamics Test Beds, Structures & Materials Research Laboratory, Supersonic Low Disturbance Pilot Tunnel, Thermal Acoustic Fatigue Apparatus (TAFA), Transonic Dynamics Tunnel (TDT), Transport Systems Research Vehicle, Unitary Plan Wind Tunnel, and the Visual Motion Simulator (VMS). CASI

N94-26815# Technische Univ., Delft (Netherlands). Faculty of Aerospace Engineering.
EXPERIMENTAL INVESTIGATION OF THE FLOW QUALITY IN THE GLT20 SUBSONIC-TRANSONIC BOUNDARY LAYER WIND TUNNEL
F. Motallebi Apr. 1993 136 p
(PB94-126539; LR-720) Avail: CASI HC A07/MF A02

The design of modern subsonic civil aircrafts requires a detailed knowledge of boundary layer behavior over the aircraft. Wind tunnel experiments are needed to obtain the necessary design information and to provide test data for numerical validations. The primary purpose of the present work was to gather experimental data over the quality of the boundary layer flow developing on the bottom wall of a newly built wind tunnel in order to assess its suitability as an experimental tool for fundamental research on the structure of turbulent boundary layer flows in both subsonic and transonic flow regimes. NTIS

N94-27113# Department of the Navy, Washington, DC.
RECONFIGURABLE AIRCRAFT STICK CONTROL Patent Application
Thomas M. Kelso, inventor (to Navy), John K. Kotch, inventor (to Navy), Damon Boyle, inventor (to Navy), David H. Meiser, inventor (to Navy), and William Flaherty, inventor (to Navy) 29 Sep. 1993 19 p
(AD-D016043; US-Patent-Appl-SN-129729) Avail: CASI HC A03/MF A01

A reconfigurable aircraft stick control for an aircraft simulator that enables pitch and roll to be simulated is presented. It includes a generic base that has mounting means that are adapted to be connected to a stick control of the type having a standard production grip as well as a stick control that uses a yoke. The control sticks include linkages that are easily connected to the mounting means on the base so that control sticks can be exchanged with minimum expenditure of time and effort to thereby simulate the control sticks on aircraft that are being simulated. Torque motors can be connected to the simulator to detect the speed and displacement of the control stick and to provide resistance to movement of the control sticks so as to simulate actual flying conditions. DTIC

N94-27247# National Aerospace Lab., Tokyo (Japan). Aircraft Aerodynamics Div.
THE RENEWING OF THE TEST SECTION OF THE NAL TRANSONIC WIND TUNNEL. PART 1: RECONSTRUCTION OF THE 1ST CORNER TURNING VANES AND AERODYNAMIC STRESS MEASUREMENT [KOGIKEN SENONSOKU FUDO SOKUTEI DO KAISHU. SONO 1: DAIICHI KUKKYOKUBU HENRYUYOKU KAISHU TO ORYOKU SOKUTEI]
Akira Koike, Nobuyuki Hosoe, Yasuo Oguni, Koichi Suzuki, and Hitoshi Miwa Dec. 1992 27 p In JAPANESE
(ISSN 0452-29822)
(NAL-TM-651; JTN-94-80619) Avail: CASI HC A03/MF A01

National Aerospace Laboratory (NAL) transonic wind tunnel was constructed in 1960, and in-depth repairs of its superannuated parts was begun in 1985. The newly reconstructed turning vanes are described. The thickness of the turning vanes was 6 mm at first and it was increased to 9 mm in 1968 to prevent cracks caused by fatigue from developing. Despite this increase in thickness, cracks were observed again. With the present reconstruction, the thickness was increased to 12 mm. Tests designed to measure the stresses within the vanes by aerodynamic force and pressure fluctuations of incoming flow were conducted before and after reconstruction. Results from the measurements are presented including a correlation analysis between the stress and the pressure fluctuation. Author (NASDA)

N94-27425*# National Aeronautics and Space Administration. Langley Research Center, Hampton, VA.
DESCRIPTION OF THE EXPERIMENTAL AVIONICS SYSTEMS INTEGRATION LABORATORY (EASILY)
Bruce K. E. Outlaw Jan. 1994 17 p
(RTOP 505-64-13-11)
(NASA-TM-109072; NAS 1.15:109072) Avail: CASI HC A03/MF A01

The Experimental Avionics Systems Integration Laboratory (EASILY) is a comprehensive facility used for development, integration, and preflight validation of hardware and software systems for the Terminal Area Productivity (TAP) Program's Transport Systems Research Vehicle (TSRV) experimental transport aircraft. This report describes the history, capabilities, and subsystems of EASILY. A functional description of the many subsystems is provided to give potential users the necessary knowledge of the capabilities of this facility. Author

N94-27587# Deutsche Forschungsanstalt fuer Luft- und Raumfahrt, Cologne (Germany). Abt. Kryo-Kanal Koeln.
THE CRYOGENIC TUNNEL COLOGNE AT DLR Progress Report, 1992 [DER KRYO-KANAL KOELN (KKK) DER DLR (STAND 1992)]
Guenter Viehweger, Ruediger Rebstock, Bernhard Stahl, Karl Wichmann, Wilhelm Becker, Rolf Kronen, and Dieter Distelrath Mar. 1992 78 p In GERMAN
(ISSN 0939-298X)
(DLR-Mitt-93-10; ETN-94-95489) Avail: CASI HC A05/MF A01

Information for users of the cryogenic wind tunnel is provided. This wind tunnel is a facility with a closed circuit test section. The cross section is 2.4 by 2.4 m. With a drive power of 1 MW, a maximum speed of 115 m/s can be achieved. Dry, gaseous nitrogen is used as the test gas. The test gas can be cooled down to 100 K by injecting liquid nitrogen. By cooling down the test gas, the maximum Reynolds number can be increased by a factor of 5.5 to 9.5 Mio. The independent variation of the test parameters allows the separation of the influence of Mach and Reynolds numbers and dynamic pressure (deformation) on the results. This report provides customers with the information required for the preliminary planning of test programs and for the preliminary layout of models for intended tests. ESA

N94-27594 Institute for Aerospace Research, Ottawa (Ontario).
INSTALLATION OF MODELS IN THE 2 m X 3 m LOW SPEED WIND TUNNEL
K. Hansen Mar. 1991 57 p
(LTR-LA-286; CTN-94-61011) Avail: CASI HC A04/MF A01

Details are provided for installing models in the 2 by 3 meter low speed wind tunnel located in the Building M-2 aeronautical research facilities in the Applied Aerodynamics Laboratory of the Canadian Institute for Aerospace Research. Drawings are included which provide enough information to permit wind tunnel users to prepare models and

instrumentation for attachment in the facility. Only the components which interface between models or instrumentation and permanent wind tunnel hardware are detailed, and usually, only the relevant attachment interface details of the component are presented. A hardware selection guide assists wind tunnel users in selecting appropriate model attachment components. A pictorial review of model installations illustrates the variety of tests performed and demonstrates the adaptability of the wind tunnel facility.
Author (CISTI)

N94-27879 Toronto Univ. (Ontario). Inst. for Aerospace Studies.
A SIMULATOR INVESTIGATION OF HELICOPTER FLIGHT CONTROL SYSTEM MODE TRANSITIONS
L. D. Reid, P. Rajagopal, and W. O. Graf Jan. 1994 141 p
(Contract W2207-0-AF10) (ISSN 0082-5255)
(UTIAS-348) Copyright Avail: Issuing Activity

The UTIAS Flight Research Simulator was modified to represent a fly-by-wire helicopter with a digital flight control system (FCS) and a side-arm controller. A smooth FCS mode selection algorithm was developed and successfully tested. The pilot/helicopter response to mode transitions was studied for formation flying and precision hover. Both normal and failure-induced transitions were investigated by a group of 9 evaluation pilots. The results were obtained in the form of Cooper/Harper handling qualities ratings (HQR) and station-keeping performance measurements. It was found that for the present mode selection algorithm, the type of mode transition did not significantly influence the experimental results. However, the mode pair (initial mode combined with final mode) was found to influence both HQR's and performance. The mode with the poorest handling qualities was involved in most of the significant effects. In some instances the mode in place before transition influenced the HQR's and performance after transition. Tests were also carried out to study the influence of simulator configuration on the experimental results. In addition to the standard configuration, one with no motion and one using a stereoscopic visual display system were employed. In general no significant effects were found except in one instance when there was a significant difference between the no-motion and stereoscopic configurations. Author

N94-27997# Sandia National Labs., Albuquerque, NM.
SIMULATING HIGH-FREQUENCY WIND FOR LONG DURATIONS
Andrew McFarlane (Cherry Creek High School, Englewood, CO.), Paul Veers, and Larry Schluter 1993 11 p Presented at the 13th Energy-Sources Technology Conference and Exhibition (ETCE) on Wind Energy, New Orleans, LA, 23-26 Jan. 1994
(Contract DE-AC04-94AL-85000)
(DE94-002739; SAND-93-1584C; CONF-940113-4) Avail: CASI HC A03/MF A01 (US Sales Only)

A wind simulator that can provide high-frequency synthetic wind data indefinitely was developed to numerically test various aspects of wind turbine control systems. The wind simulator builds synthetic wind data in two basic steps. First, using an auto-regressive method, the simulator creates low-frequency wind speeds at a small number of time steps for each one-hour interval. This low-frequency part of the wind has a Weibull distribution and an exponential auto correlation. Second, it creates high-frequency data and superimposes it on top of the low-frequency wind speed data. The high-frequency part has zero mean, Gaussian distribution and frequency content selected from a library of turbulence pads. The low- and high-frequency parts are summed to produce the final result. This process repeats itself for as many one-hour intervals as the user desires and lends itself to the eventual addition of diurnal and seasonal effects.
DOE

N94-25586# National Research Inst. for Metals, Tokyo (Japan).
STUDY ON UTILIZATION OF SUPER CLEAN, HIGH VACUUM SPACE [CHOSEIJO SHINKU KUKAN NO RIYO NI KANSURU CHOSA KENKYU]
Kazuhiro Yoshihara, Yoshio Sakka, Haruki Shiraishi, Tetsuji Noda, Josei Nagakawa, Ryosuke Hasegawa, Toshiyuki Hirano, Tsuyoshi Ozaki, Keikichi Nakamura, and Kazuo Saito et al *In its* Bulletin of National Research Institute for Metals in Fiscal Year 1993, no. 14 29 Jan. 1993 p 393-401 In JAPANESE (For primary document see N94-25544 07-26)
Avail: CASI HC A02/MF A04

N94-27903*# Wilkes Coll., Wilkes-Barre, PA. Dept. of Mechanical and Material Engineering.
MICROSPHERES FOR LASER VELOCIMETRY IN HIGH TEMPERATURE WIND TUNNEL
Anthony Ghorieshi *In* Old Dominion Univ., The 1993 NASA-ODU American Society for Engineering Education (ASEE) Summer Faculty Fellowship Program Dec. 1993 p 91-99 (For primary document see N94-27893 07-80)
Avail: CASI HC A02/MF A03

N94-27905*# Drexel Univ., Philadelphia, PA. Dept. of Electrical and Computer Engineering.
NEURAL CONTROL OF MAGNETIC SUSPENSION SYSTEMS
W. Steven Gray *In* Old Dominion Univ., The 1993 NASA-ODU American Society for Engineering Education (ASEE) Summer Faculty Fellowship Program Dec. 1993 p 102-103 (For primary document see N94-27893 07-80)
Avail: CASI HC A01/MF A03

N94-27908*# Old Dominion Univ., Norfolk, VA. Dept. of Mechanical Engineering.
SYSTEM IDENTIFICATION OF THE LARGE-ANGLE MAGNETIC SUSPENSION TEST FACILITY (LAMSTF)
Jen-Kuang Huang *In its* The 1993 NASA-ODU American Society for Engineering Education (ASEE) Summer Faculty Fellowship Program Dec. 1993 p 114-115 (For primary document see N94-27893 07-80)
Avail: CASI HC A01/MF A03

N94-27912*# Old Dominion Univ., Norfolk, VA. Dept. of Engineering Technology.
EXPERIMENTAL APPARATUS FOR OPTIMIZATION OF FLAP POSITION FOR A THREE-ELEMENT AIRFOIL MODEL
Drew Landman *In its* The 1993 NASA-ODU American Society for Engineering Education (ASEE) Summer Faculty Fellowship Program Dec. 1993 p 126-128 (For primary document see N94-27893 07-80)
Avail: CASI HC A01/MF A03

12 ASTRONAUTICS (GENERAL)

For extraterrestrial exploration see *91 Lunar and Planetary Exploration.*

N94-26249# Technical Research Centre of Finland, Espoo. Instrument Lab.
TECHNOLOGY DEVELOPMENT IN SPACE PROJECTS [AVARUUSTOIMINNAN TEKNOLOGIAMAHDOLLISUUDET]
Vaeinoe Kelhae and Jouko Kurki Jan. 1993 29 p In FINNISH
(ISSN 1235-0605)
(VTT-TIED-1438; ISBN-951-38-4332-7; ETN-94-95264) Copyright Avail: CASI HC A03/MF A01

Space activities have existed for 34 years around the world. Demanding technology operating in extreme conditions has been developed for space projects, instruments, satellites and shuttles. The nature of space technology is basic development and it also serves well the purposes of conventional, industrial and commercial applications. ESA's industrial return makes it possible for the industry and research organizations to participate in space projects. In that way, Finland has a possibility to widen its technological know-how base, get technology knowledge for developing new commercial products, and get a base for controlling quality. Many of the space instrument and Earth observation projects (for example, GOMOS ozone analyzer) are also socially important. ESA

N94-26278*# National Aeronautics and Space Administration. Langley Research Center, Hampton, VA.
SELECTED TOPICS IN ROBOTICS FOR SPACE EXPLORATION
Raymond C. Montgomery, ed. and Howard Kaufman, ed. (Rensselaer Polytechnic Inst., Troy, NY.) Dec. 1993 276 p Workshop held in Hampton, VA, 17-18 Mar. 1993; sponsored in part by Rensselaer Polytechnic Institute
(RTOP 233-03-01-01)
(NASA-CP-10131; NAS 1.55:10131) Avail: CASI HC A13/MF A03

Papers and abstracts included represent both formal presentations and experimental demonstrations at the Workshop on Selected Topics in Robotics for Space Exploration which took place at NASA Langley Research Center, 17-18 March 1993. The workshop was cosponsored by the Guidance, Navigation, and Control Technical Committee of the NASA Langley Research Center and the Center for Intelligent Robotic Systems for Space Exploration (CIRSSE) at RPI, Troy, NY. Participation was from industry, government, and other universities with close ties to either Langley Research Center or to CIRSSE. The presentations were very broad in scope with attention given to space assembly, space exploration, flexible structure control, and telerobotics. For individual titles, see N94-26279 through N94-26292.

N94-26279*# Rensselaer Polytechnic Inst., Troy, NY. Dept. of Electrical, Computer and Systems Engineering.

A GLOBAL APPROACH TO KINEMATIC PATH PLANNING TO ROBOTS WITH HOLONOMIC AND NONHOLONOMIC CONSTRAINTS

Adam Divelbiss, Sanjeev Seereeram, and John T. Wen *In* NASA. Langley Research Center, Selected Topics in Robotics for Space Exploration Dec. 1993 p 3-25 (For primary document see N94-26278 07-12)

Avail: CASI HC A03/MF A03

Robots in applications may be subject to holonomic or nonholonomic constraints. Examples of holonomic constraints include a manipulator constrained through the contact with the environment, e.g., inserting a part, turning a crank, etc., and multiple manipulators constrained through a common payload. Examples of nonholonomic constraints include no-slip constraints on mobile robot wheels, local normal rotation constraints for soft finger and rolling contacts in grasping, and conservation of angular momentum of in-orbit space robots. The above examples all involve equality constraints; in applications, there are usually additional inequality constraints such as robot joint limits, self collision and environment collision avoidance constraints, steering angle constraints in mobile robots, etc. The problem of finding a kinematically feasible path that satisfies a given set of holonomic and nonholonomic constraints, of both equality and inequality types is addressed. The path planning problem is first posed as a finite time nonlinear control problem. This problem is subsequently transformed to a static root finding problem in an augmented space which can then be iteratively solved. The algorithm has shown promising results in planning feasible paths for redundant arms satisfying Cartesian path following and goal endpoint specifications, and mobile vehicles with multiple trailers. In contrast to local approaches, this algorithm is less prone to problems such as singularities and local minima. Author (revised)

N94-26280*# Rensselaer Polytechnic Inst., Troy, NY. Dept. of Mechanical Engineering, Aeronautical Engineering, and Mechanics.

APPLICATION OF THE CIRSSE COOPERATING ROBOT PATH PLANNER TO THE NASA LANGLEY TRUSS ASSEMBLY PROBLEM **c63**

Jonathan M. Weaver and Stephen J. Derby *In* NASA. Langley Research Center, Selected Topics in Robotics for Space Exploration Dec. 1993 p 28-35 Sponsored by NASA, Washington (For primary document see N94-26278 07-12)

(Grant NAGw-1333)

Avail: CASI HC A02/MF A03

A method for autonomously planning collision free paths for two cooperating robots in a static environment was developed at the Center for Intelligent Robotic Systems for Space Exploration (CIRSSE). The method utilizes a divide-and-conquer type of heuristic and involves non-exhaustive mapping of configuration space. While there is no guarantee of finding a solution, the planner was successfully applied to a variety of problems including two cooperating 9 degrees of freedom (dof) robots. Although developed primarily for cooperating robots the method is also applicable to single robot path planning problems. A single 6 dof version of the planner was implemented for the truss assembly east, at NASA Langley's Automated Structural Assembly Lab (ASAL). The results indicate that the planner could be very useful in addressing the ASAL path planning problem and that further work along these lines is warranted. Author (revised)

N94-26281*# Rensselaer Polytechnic Inst., Troy, NY. Dept. of Electrical, Computer, and Systems Engineering.

INERTIAL-SPACE DISTURBANCE REJECTION FOR SPACE-BASED MANIPULATORS **c37**

Kevin Holt and Alan A. Desrochers *In* NASA. Langley Research Center, Selected Topics in Robotics for Space Exploration Dec. 1993 p 37-43 (For primary document see N94-26278 07-12)

Avail: CASI HC A02/MF A03

The implementation of a disturbance rejection controller for a 6-DOF PUMA manipulator mounted on a 3-DOF platform was described. A control algorithm is designed to track the desired position and attitude of the end-effector in inertial space, subject to unknown disturbances in the platform axes. Experimental results are presented for step, sinusoidal, and random disturbances in the platform rotational axis and in the neighborhood of kinematic singularities. Robotic manipulators were proposed as a means of reducing the amount of extra vehicular activity time required for space station assembly and maintenance. The proposed scenario involves a robotic manipulator attached to some mobile platform, such as a spacecraft, satellite, or the space station itself. Disturbances in the platform position and attitude may prevent the manipulator from successfully completing the task. The possibility of using the manipulator to compensate for platform disturbances was explored. The problem of controlling a robotic manipulator on a mobile platform has received considerable attention in the past few years. Joshi and Desrochers designed a nonlinear feedback control law to carry out tasks (with respect to the robot base frame) in the presence of roll, pitch and yaw disturbances in the platform axes. Dubowsky, Vance, and Torres proposed a time-optimal planning algorithm for a robotic manipulator mounted on a spacecraft, subject to saturation limits in the attitude control reaction jets. Papadopoulos and Dubowsky developed a general framework for analyzing the control of free-floating space manipulator systems. Most recently, Torres and Dubowsky have presented a technique called the enhanced disturbance map to find manipulator trajectories that reduce the effect of disturbances in the spacecraft position and attitude. One common assumption in the literature is that the disturbance signal is exactly known. If this is the case, then the end-effector location can be calculated without relying on direct end-point sensing. However, this assumption is invalid if there is a significant delay in the platform position and attitude measurements, or if the kinematics of the platform are not well known, or if the platform is a non-rigid structure. In the more likely case that only the nominal platform location and upper bound on the disturbance signal are known, direct end-point sensing is needed to measure the end-effector location. Author (revised)

N94-26282*# Rensselaer Polytechnic Inst., Troy, NY. Dept. of Electrical, Computer and Systems Engineering.

DIRECT MODEL REFERENCE ADAPTIVE CONTROL OF ROBOTIC ARMS **c37**

Howard Kaufman, David C. Swift, Steven T. Cummings, and Jeffrey R. Shankey *In* NASA. Langley Research Center, Selected Topics in Robotics for Space Exploration Dec. 1993 p 45-71 (For primary document see N94-26278 07-12)

Avail: CASI HC A03/MF A03

The results of controlling A PUMA 560 Robotic Manipulator and the NASA shuttle Remote Manipulator System (RMS) using a Command Generator Tracker (CGT) based Model Reference Adaptive Controller (DMRAC) are presented. Initially, the DMRAC algorithm was run in simulation using a detailed dynamic model of the PUMA 560. The algorithm was tuned on the simulation and then used to control the manipulator using minimum jerk trajectories as the desired reference inputs. The ability to track a trajectory in the presence of load changes was also investigated in the simulation. Satisfactory performance was achieved in both simulation and on the actual robot. The obtained responses showed that the algorithm was robust in the presence of sudden load changes. Because these results indicate that the DMRAC algorithm can indeed be successfully applied to the control of robotic manipulators, additional testing was performed to validate the applicability of DMRAC to simulated dynamics of the shuttle RMS. Author (revised)

N94-26283*# National Aeronautics and Space Administration. Goddard Space Flight Center, Greenbelt, MD.

PERFORMANCE MEASURES FROM THE EXPLORER PLATFORM BERTHING EXPERIMENT **c18**

Stephen Leake *In* NASA. Langley Research Center, Selected Topics in Robotics for Space Exploration Dec. 1993 p 73-94 (For primary document see N94-26278 07-12)

Avail: CASI HC A03/MF A03

The Explorer Platform is a Modular Mission Spacecraft: it has several subunits that are designed to be replaced on orbit. The Goddard Space Flight Center Robotics Lab undertook an experiment to evaluate various robotic approaches to replacing one of the units; a large (approximately 1 meter by 1 meter by 0.5 meter) power box. The hardware consists of a Robotics Research Corporation K-1607 (RRC) manipulator mounted on a large gantry robot, a Kraft handcontroller for teleoperation of RRC, a Lightweight Servicing Tool (LST) mounted on the RRC, and an Explorer Platform mockup (EP) with a removable box (MMS) that has fixtures that mate with the LST. Sensors include a wrist wrench sensor on the RRC and Capaciflectors mounted on the LST and the MMS. There are also several cameras, but no machine vision is used. The control system for the RRC is entirely written by Goddard; it consists of Ada code on three Multibus I 386/387 CPU boards doing the real-time robot control, and C on a 386 PC processing Capaciflector data. The gantry is not moved during this experiment. The task is the exchange of the MMS; it is removed and replaced. This involves four basic steps: mating the LST to the MMS, demating the MMS from the EP, mating the MMS to the EP, and demating the LST form the MMS. Each of the mating steps must be preceeded by an alignment to bring the mechanical fixtures within their capture range. Two basic approaches to alignment are explored: teleoperation with the operator viewing thru cameras, and Capaciflector based autonomy. To evaluate the two alignment approaches, several runs were run with each approach and the final pose was recorded. Comparing this to the ideal alignment pose gives accuracy and repeatability data. In addition the wrenches exerted during the mating tasks were recorded; this gives information on how the alignment step affects the mating step. There are also two approaches to mating; teleoperation, and impedance based autonomy. The wrench data taken during mating using these two approaches is used to evaluate them. Section 2 describes the alignment results, section 3 describes the mating results, and finally Section 4 gives some conclusions. Author (revised)

N94-26284*# National Aeronautics and Space Administration. Langley Research Center, Hampton, VA.
BERTHING OF SPACE STATION FREEDOM USING THE SHUTTLE REMOTE MANIPULATOR SYSTEM **c18**
Paul Cooper and Martha E. Demeo (Vigyan Research Associates, Inc., Hampton, VA.) *In its* Selected Topics in Robotics for Space Exploration Dec. 1993 p 95-123 (For primary document see N94-26278 07-12)
Avail: CASI HC A03/MF A03

A large-angle, flexible, multi-body, dynamic modeling capability was developed to help validate analytical simulations of the dynamic motion and control forces which occur while berthing of Space Station Freedom to the Shuttle Orbiter during early assembly flights. The dynamics and control of the station, the attached Shuttle Remote Manipulator System, and the Orbiter during a berthing maneuver are described. Emphasis is placed on the modeling of the Shuttle Remote Manipulator System in the multi-body simulation. The influence of the elastic behavior of the station and of the Remote Manipulator System on the attitude control of the station/Orbiter system during the maneuver is investigated. Author (revised)

N94-26285*# National Aeronautics and Space Administration. Langley Research Center, Hampton, VA.
STATUS REPORT OF RMS ACTIVE DAMPING AUGMENTATION **c39**
Mike Gilbert and Martha E. Demeo (Vigyan Research Associates, Inc., Hampton, VA.) *In its* Selected Topics in Robotics for Space Exploration Dec. 1993 p 149-172 (For primary document see N94-26278 07-12)
Avail: CASI HC A03/MF A03

A status report of Remote Manipulator System (RMS) active damping augmentation is presented. Topics covered include: active damping augmentation; benefits of RMS ADA; simulated payload definition; sensor and actuator definition; ADA control law design; Shuttle Engineering Simulator (SES) real-time simulation; and astronaut evaluation. CASI

N94-26286*# National Aeronautics and Space Administration. Langley Research Center, Hampton, VA.
AUTONOMOUS RENDEZVOUS AND DOCKING FOR SPACE STATION FREEDOM **c18**
James L. Garrison, Jr. and Stephen J. Katzberg *In its* Selected Topics in Robotics for Space Exploration Dec. 1993 p 173-191 (For primary document see N94-26278 07-12)
Avail: CASI HC A03/MF A03

Viewgraphs on autonomous rendezvous and docking (AR&D) for Space Station Freedom are presented. Topics covered include: requirements for AR&D experience; Comet spacecraft performance; AR&D mission profile; analytical models for approach trajectory, loosely coupled configuration, and contact dynamics; and application to space infrastructure. CASI

N94-26287*# Prairie View Agricultural and Mechanical Coll., TX.
MODELING AND EXPERIMENTAL VERIFICATION OF SINGLE EVENT UPSETS **c60**
T. N. Fogarty, J. O. Attia, A. A. Kumar, T. S. Tang (Texas A&I Univ., Kingsville.), and J. S. Lindner (Texas A&I Univ., Kingsville.) *In* NASA. Langley Research Center, Selected Topics in Robotics for Space Exploration Dec. 1993 p 193-211 Sponsored in part by NASA. Johnson Space Center (For primary document see N94-26278 07-12)
(Grants NAG9-659; NAG9-331)
Avail: CASI HC A03/MF A03

The research performed and the results obtained at the Laboratory for Radiation Studies, Prairie View A&M University and Texas A&I University, on the problem of Single Events Upsets, the various schemes employed to limit them and the effects they have on the reliability and fault tolerance at the systems level, such as robotic systems are reviewed. Author (revised)

N94-26288*# National Aeronautics and Space Administration. Ames Research Center, Moffett Field, CA.
SIMULATION MODELING FOR LONG DURATION SPACECRAFT CONTROL SYSTEMS **c18**
Mark A. Boyd and Salvatore J. Bavuso (National Aeronautics and Space Administration. Langley Research Center, Hampton, VA.) *In* NASA. Langley Research Center, Selected Topics in Robotics for Space Exploration Dec. 1993 p 213-221 (For primary document see N94-26278 07-12)
Avail: CASI HC A02/MF A03

The use of simulation is described and it is contrasted to analytical solution techniques for evaluation of analytical reliability models. The role importance sampling plays in simulation of models of this type was also discussed. The simulator tool used for our analysis is described. Finally, the use of the simulator tool was demonstrated by applying it to evaluate the reliability of a fault tolerant hypercube multiprocessor intended for spacecraft designed for long duration missions. The reliability analysis was used to highlight the advantages and disadvantages offered by simulation over analytical solution of Markovian and non-Markovian reliability models. Author (revised)

N94-26289*# SET Group, Denver, CO.
TECHNOLOGY DRIVERS FOR FLIGHT TELEROBOTIC SYSTEM SOFTWARE **c61**
Robert Labaugh *In* NASA. Langley Research Center, Selected Topics in Robotics for Space Exploration Dec. 1993 p 223-232 (For primary document see N94-26278 07-12)
Avail: CASI HC A02/MF A03

Viewgraphs on technology drivers for flight telerobotic system software are included. Topics covered include: flight software lines of code; flight computer architecture; system safety; safety critical parameters; system safety - software functions. Author (revised)

N94-26290*# National Aeronautics and Space Administration. Langley Research Center, Hampton, VA.
EARLY LUNAR ROVER MISSION STUDIES **c91**
V. P. Gillespie *In its* Selected Topics in Robotics for Space Exploration Dec. 1993 p 233-246 (For primary document see N94-26278 07-12)
Avail: CASI HC A03/MF A03

Viewgraphs on Early Lunar Rover Mission studies are included. The chronology of events and study project description are addressed. Issues identified for analysis and basic questions to be addressed are listed. LaRC Early Lunar Mission study results are included. CASI

N94-26291*# Sandia National Labs., Albuquerque, NM.

THE ROBOTIC ALL-TERRAIN LUNAR EXPLORATION ROVER (RATLER): INCREASED MOBILITY THROUGH SIMPLICITY **c91**

J. Bryan Pletta *In* NASA. Langley Research Center, Selected Topics in Robotics for Space Exploration Dec. 1993 p 247-267 (For primary document see N94-26278 07-12)

Avail: CASI HC A03/MF A03

A new concept mobility chassis for a robotic rover is described which is inherently simple with few moving parts or complex linkages. The RATLER design utilizes a four-wheel drive, skid steered propulsion system in conjunction with passive articulation of the dual body vehicle. This uniquely simple method of chassis articulation allows all four wheels to remain in contact with the ground even while climbing obstacles as large as 1.3 wheel diameters. A prototype mobility platform was built which is approximately 1 m(sup 2) with 0.5 m diameter wheels and all-wheel electric drive. The theoretical mobility limitations are discussed and compared with the results of field trials of the prototype platform. The theoretical model contrasted with measured performance is then used to predict the expected mobility of the RATLER design on the Lunar surface. Author (revised)

N94-26292*# Sandia National Labs., Albuquerque, NM. Advanced Vehicle Development Dept.

A MULTITASKING BEHAVIORAL CONTROL SYSTEM FOR THE ROBOTIC ALL-TERRAIN LUNAR EXPLORATION ROVER (RATLER) **c37**

Paul Klarer *In* NASA. Langley Research Center, Selected Topics in Robotics for Space Exploration Dec. 1993 p 269-278 (For primary document see N94-26278 07-12)

Avail: CASI HC A02/MF A03

An approach for a robotic control system which implements so called 'behavioral' control within a realtime multitasking architecture is proposed. The proposed system would attempt to ameliorate some of the problems noted by some researchers when implementing subsumptive or behavioral control systems, particularly with regard to multiple processor systems and realtime operations. The architecture is designed to allow synchronous operations between various behavior modules by taking advantage of a realtime multitasking system's intertask communications channels, and by implementing each behavior module and each interconnection node as a stand-alone task. The potential advantages of this approach over those previously described in the field are discussed. An implementation of the architecture is planned for a prototype Robotic All Terrain Lunar Exploration Rover (RATLER) currently under development and is briefly described. Author (revised)

N94-27151*# National Aeronautics and Space Administration, Washington, DC.

ACCESS TO SPACE STUDY Summary Report

Jan. 1994 78 p

(NASA-TM-109693; NAS 1.15:109693) Avail: CASI HC A05/MF A01

This report summarizes the results of a comprehensive NASA in-house study to identify and assess alternate approaches to access to space through the year 2030, and to select and recommend a preferred cause of action. The goals of the study were to identify the best vehicles and transportation architectures to make major reductions in the cost of space transportation (at least 50%), while at the same time increasing safety for flight crews by at least an order of magnitude. In addition, vehicle reliability was to exceed 0.98 percent, and, as important, the robustness, pad time, turnaround time, and other aspects of operability were to be vastly improved. This study examined three major optional architectures: (1) retain and upgrade the Space Shuttle and expendable launch vehicles; (2) develop new expendable vehicles using conventional technologies and transition from current vehicles beginning in 2005; and (3) develop new reusable vehicles using advanced technology, and transition from current vehicles beginning in 2008. The launch-needs, mission model utilized for for the study was based upon today's projection of civil, defense, and commercial mission payload requirements. Derived from text

N94-27358*# National Aeronautics and Space Administration. Lewis Research Center, Cleveland, OH.

VISION 21: INTERDISCIPLINARY SCIENCE AND ENGINEERING IN THE ERA OF CYBERSPACE

Dec. 1993 274 p Symposium held in Westlake, OH, 30-31 Mar. 1993; cosponsored by Ohio Aerospace Inst.

(Contract NAS3-25266; RTOP 506-41-11)

(NASA-CP-10129; E-8238; NAS 1.55:10129) Avail: CASI HC A12/MF A03

The symposium Vision-21: Interdisciplinary Science and Engineering in the Era of Cyberspace was held at the NASA Lewis Research Center on March 30-31, 1993. The purpose of the symposium was to simulate interdisciplinary thinking in the sciences and technologies which will be required for exploration and development of space over the next thousand years. The keynote speakers were Hans Moravec, Vernor Vinge, Carol Stoker, and Myron Krueger. The proceedings consist of transcripts of the invited talks and the panel discussion by the invited speakers, summaries of workshop sessions, and contributed papers by the attendees. For individual titles, see N94-27359 through N94-27376.

N94-27359*# San Diego State Univ., CA. Dept. of Mathematical Sciences.

THE COMING TECHNOLOGICAL SINGULARITY: HOW TO SURVIVE IN THE POST-HUMAN ERA

Vernor Vinge *In* NASA. Lewis Research Center, Vision 21: Interdisciplinary Science and Engineering in the Era of Cyberspace Dec. 1993 p 11-22 (For primary document see N94-27358 07-12)

Avail: CASI HC A03/MF A03

The acceleration of technological progress has been the central feature of this century. I argue in this paper that we are on the edge of change comparable to the rise of human life on Earth. The precise cause of this change is the imminent creation by technology of entities with greater than human intelligence. There are several means by which science may achieve this breakthrough (and this is another reason for having confidence that the event will occur): (1) the development of computers that are 'awake' and superhumanly intelligent (to date, most controversy in the area of AI relates to whether we can create human equivalence in a machine. But if the answer is 'yes, we can', then there is little doubt that beings more intelligent can be constructed shortly thereafter); (2) large computer networks (and their associated users) may 'wake up' as a superhumanly intelligent entity; (3) computer/human interfaces may become so intimate that users may reasonably be considered superhumanly intelligent; and (4) biological science may find ways to improve upon the natural human intellect. The first three possibilities depend in large part on improvements in computer hardware. Progress in computer hardware has followed an amazingly steady curve in the last few decades. Based largely on this trend, I believe that the creation of greater than human intelligence will occur during the next thirty years. Derived from text

N94-27360*# National Aeronautics and Space Administration. Ames Research Center, Moffett Field, CA.

TELEPRESENCE IN THE HUMAN EXPLORATION OF MARS: FIELD STUDIES IN ANALOG ENVIRONMENTS **c91**

Carol R. Stoker *In* NASA. Lewis Research Center, Vision 21: Interdisciplinary Science and Engineering in the Era of Cyberspace Dec. 1993 p 23-34 (For primary document see N94-27358 07-12)

Avail: CASI HC A03/MF A03

This paper describes the role of telepresence in performing exploration of Mars. As part of an effort to develop telepresence to support Mars exploration, NASA is developing telepresence technology and using it to perform exploration in space analog environments. This paper describes experiments to demonstrate telepresence control of an underwater remotely operated vehicle (TROV) to perform scientific field work in isolated and hostile environments. Toward this end, we have developed a telepresence control system and interfaced it to an underwater remotely operated vehicle. This vehicle was used during 1992 to study aquatic ecosystems in Antarctica including a study of the physical and biological environment of permanently ice-covered lake. We also performed a preliminary analysis of the potential for using the TROV to study the benthic ecology under the sea ice in McMurdo sound. These expeditions are opening up new areas of research by using telepresence control of remote vehicles to explore isolated and extreme environments on Earth while also providing an impetus to develop technology which will play a major role in the human exploration of Mars. Antarctic field operations, in particular, provide an excellent analog experience for telepresence operation in space. Author

N94-27361*# Carnegie-Mellon Univ., Pittsburgh, PA. Robotics Inst.
THE UNIVERSAL ROBOT c37
Hans Moravec *In* NASA. Lewis Research Center, Vision 21: Interdisciplinary Science and Engineering in the Era of Cyberspace Dec. 1993 p 35-41 (For primary document see N94-27358 07-12)
Avail: CASI HC A02/MF A03

Our artifacts are getting smarter, and a loose parallel with the evolution of animal intelligence suggests one future course for them. Computerless industrial machinery exhibits the behavioral flexibility of single-celled organisms. Today's best computer-controlled robots are like the simpler invertebrates. A thousand-fold increase in computer power in the next decade should make possible machines with reptile-like sensory and motor competence. Properly configured, such robots could do in the physical world what personal computers now do in the world of data - act on our behalf as literal-minded slaves. Growing computer power over the next half-century will allow this reptile stage to be surpassed, in stages producing robots that learn like mammals, model their world like primates, and eventually reason like humans. Depending on your point of view, humanity will then have produced a worthy successor, or transcended some of its inherited limitations and so transformed itself into something quite new. Author

N94-27362*# National Aeronautics and Space Administration. Lewis Research Center, Cleveland, OH.
VENI, VIDEO, VICI: THE MERGING OF COMPUTER AND VIDEO TECHNOLOGIES c60
Jay G. Horowitz *In its* Vision 21: Interdisciplinary Science and Engineering in the Era of Cyberspace Dec. 1993 p 43-50 (For primary document see N94-27358 07-12)
Avail: CASI HC A02/MF A03

The topics covered include the following: High Definition Television (HDTV) milestones; visual information bandwidth; television frequency allocation and bandwidth; horizontal scanning; workstation RGB color domain; NTSC color domain; American HDTV time-table; HDTV image size; digital HDTV hierarchy; task force on digital image architecture; open architecture model; future displays; and the ULTIMATE imaging system. CASI

N94-27363*# National Aeronautics and Space Administration. Lewis Research Center, Cleveland, OH.
INTERDISCIPLINARY TECHNOLOGY c20
Lester D. Nichols *In its* Vision 21: Interdisciplinary Science and Engineering in the Era of Cyberspace Dec. 1993 p 51-60 (For primary document see N94-27358 07-12)
Avail: CASI HC A02/MF A03

The 'computational test-cell' will enable the incorporation of new methodologies, such as concurrent engineering and probabilistic methods, into the propulsion design process. This will provide the capability to conduct credible, interdisciplinary analyses of new propulsion concepts and designs. Probabilistic methods can be used as the basis for reliability-based design. Recently methods have been devised that provide the capability of simulating the performance of propulsion systems at several levels of resolution. These methods make it possible to quantify uncertainty and to establish confidence bounds for the calculated values. The introduction of reliability-based design methodology along with probabilistic analyses will provide a tool to reduce the design space for new systems and to reduce our dependence on hardware testing for proof-of-concept and system integration demonstrations. The resulting simulations will reduce the need for testing and identify potential operational problems early in the design process. This capability will make it possible to compute the expected performance, stability, reliability, and life of propulsion components, subsystems, and systems at design and off-design conditions, to bring life cycle cost trade-offs early into the design process and to determine optimum designs to satisfy specified mission requirements. Author

N94-27364*# Bradford Univ. (England).
PARALLEL ALGORITHM FOR DOMINANT POINTS CORRESPONDENCES IN ROBOT BINOCULAR STEREO VISION c61
A. Al-Tammami and B. Singh *In* NASA. Lewis Research Center, Vision 21: Interdisciplinary Science and Engineering in the Era of Cyberspace Dec. 1993 p 71-81 (For primary document see N94-27358 07-12)
Avail: CASI HC A03/MF A03

This paper presents an algorithm to find the correspondences of points representing dominant feature in robot stereo vision. The algorithm consists of two main steps: dominant point extraction and dominant point matching. In the feature extraction phase, the algorithm utilizes the widely used Moravec Interest Operator and two other operators: the Prewitt Operator and a new operator called Gradient Angle Variance Operator. The Interest Operator in the Moravec algorithm was used to exclude featureless areas and simple edges which are oriented in the vertical, horizontal, and two diagonals. It was incorrectly detecting points on edges which are not on the four main directions (vertical, horizontal, and two diagonals). The new algorithm uses the Prewitt operator to exclude featureless areas, so that the Interest Operator is applied only on the edges to exclude simple edges and to leave interesting points. This modification speeds-up the extraction process by approximately 5 times. The Gradient Angle Variance (GAV), an operator which calculates the variance of the gradient angle in a window around the point under concern, is then applied on the interesting points to exclude the redundant ones and leave the actual dominant ones. The matching phase is performed after the extraction of the dominant points in both stereo images. The matching starts with dominant points in the left image and does a local search, looking for corresponding dominant points in the right image. The search is geometrically constrained the epipolar line of the parallel-axes stereo geometry and the maximum disparity of the application environment. If one dominant point in the right image lies in the search areas, then it is the corresponding point of the reference dominant point in the left image. A parameter provided by the GAV is thresholded and used as a rough similarity measure to select the corresponding dominant point if there is more than one point the search area. The correlation is used as a final decision tool when there is still more than one point in the search area. If there is no dominant point in the search area of if the points in the search area are below a correlation threshold, then the dominant point in the reference image is occluded and can not be corresponded. The algorithm has been modeled, implemented and shown to be fast, robust and parallel. The parallelism is created from three main features: locality of the operators; a memory optimization scheme; and the ability to fully parallelize the extraction phase which is the most computational intensive task in the algorithm. The last feature is achieved by performing the extraction phase on the two images simultaneously. Author

N94-27365*# Carnegie-Mellon Univ., Pittsburgh, PA. Studio for Creative Inquiry.
SCULPTING IN CYBERSPACE: PARALLEL PROCESSING THE DEVELOPMENT OF NEW SOFTWARE c62
Rob Fisher *In* NASA. Lewis Research Center, Vision 21: Interdisciplinary Science and Engineering in the Era of Cyberspace Dec. 1993 p 83-99 (For primary document see N94-27358 07-12)
Avail: CASI HC A03/MF A03

Stimulating creativity in problem solving, particularly where software development is involved, is applicable to many disciplines. Metaphorical thinking keeps the problem in focus but in a different light, jarring people out of their mental ruts and sparking fresh insights. It forces the mind to stretch to find patterns between dissimilar concepts, in the hope of discovering unusual ideas in odd associations (Technology Review January 1993, p. 37). With a background in Engineering and Visual Design from MIT, I have for the past 30 years pursued a career as a sculptor of interdisciplinary monumental artworks that bridge the fields of science, engineering and art. Since 1979, I have pioneered the application of computer simulation to solve the complex problems associated with these projects. A recent project for the roof of the Carnegie Science Center in Pittsburgh made particular use of the metaphoric creativity technique described above. The problem-solving process led to the creation of hybrid software combining scientific, architectural and engineering visualization techniques. David Steich, a Doctoral Candidate in Electrical Engineering at Penn State, was commissioned to develop special software that enabled me to create innovative free-form sculpture. This paper explores the process of inventing the software through a detailed analysis of the interaction between an artist and a computer programmer. Author

N94-27366*# Scotter Research and Development Ltd., Thunder Bay (Ontario).
SPIRAL SURVEY EXPEDITION: A PROPOSAL TO ORGANIZE FOR THE SURVEY, EXPLORATION AND EVENTUAL COLONIZATION OF THE MILKY WAY GALAXY c91

Scott Galloway *In* NASA. Lewis Research Center, Vision 21: Interdisciplinary Science and Engineering in the Era of Cyberspace Dec. 1993 p 101-114 (For primary document see N94-27358 07-12)
Avail: CASI HC A03/MF A03

This paper details a plan to explore the galaxy. Areas of interest to an era of cyberspace include the Tech-Index information system for the expedition and the role cyberspace has in increasing expedition productivity and increasing the capabilities of cyberspace by expanding the goals and data set. The paper offers lists of projects for the cybermarket pool. The expedition is described also as a developers tool for cyberspace to acknowledge the scope of the human mind far surpasses present engineering yet guides our direction of energies and materials. Maintaining the biological capability to reproduce the Terran biosphere via Evolution park conservation areas is discussed. The ecological repair of Spaceship Earth and the build up of an interstellar industrial base from simple recyling and educational programs is meshed with a proposed 'reverse engineering cyberspace' plan. A set of constructive contests are proposed with 3 new currencies offered as prizes. The Planet, The Solar System, The Galaxy are 3 areas of focus. Each of these areas are considered in a cyberspectrum of (1) Sentience; (2) Biological diversity; and (3) Energy/Matter resources. Author

N94-27367*# Rutgers Univ., New Brunswick, NJ. Dept. of Computer Science.

UTILITY FOG: A UNIVERSAL PHYSICAL SUBSTANCE c76

J. Storrs Hall *In* NASA. Lewis Research Center, Vision 21: Interdisciplinary Science and Engineering in the Era of Cyberspace Dec. 1993 p 115-126 (For primary document see N94-27358 07-12)
Avail: CASI HC A03/MF A03

Active, polymorphic material ('Utility Fog') can be designed as a conglomeration of 100-micron robotic cells ('foglets'). Such robots could be built with the techniques of molecular nanotechnology. Controllers with processing capabilities of 1000 MIPS per cubic micron, and electric motors with power densities of one milliwatt per cubic micron are assumed. Utility Fog should be capable of simulating most everyday materials, dynamically changing its form and properties, and forms a substrate for an integrated virtual reality and telerobotics. Author

N94-27368*# National Aeronautics and Space Administration, Washington, DC.

SPACE STATION TECHNOLOGY TESTBED: 2010 DEEP SPACE TRANSPORT c18

Alan C. Holt *In* NASA. Lewis Research Center, Vision 21: Interdisciplinary Science and Engineering in the Era of Cyberspace Dec. 1993 p 127-151 (For primary document see N94-27358 07-12)
Avail: CASI HC A03/MF A03

A space station in a crew-tended or permanently crewed configuration will provide major R&D opportunities for innovative, technology and materials development and advanced space systems testing. A space station should be designed with the basic infrastructure elements required to grow into a major systems technology testbed. This space-based technology testbed can and should be used to support the development of technologies required to expand our utilization of near-Earth space, the Moon and the Earth-to-Jupiter region of the Solar System. Space station support of advanced technology and materials development will result in new techniques for high priority scientific research and the knowledge and R&D base needed for the development of major, new commercial product thrusts. To illustrate the technology testbed potential of a space station and to point the way to a bold, innovative approach to advanced space systems' development, a hypothetical deep space transport development and test plan is described. Key deep space transport R&D activities are described would lead to the readiness certification of an advanced, reusable interplanetary transport capable of supporting eight crewmembers or more. With the support of a focused and highly motivated, multi-agency ground R&D program, a deep space transport of this type could be assembled and tested by 2010. Key R&D activities on a space station would include: (1) experimental research investigating the microgravity assisted, restructuring of micro-engineered, materials (to develop and verify the in-space and in-situ 'tuning' of materials for use in debris and radiation shielding and other protective systems), (2) exposure of microengineered materials to the space environment for passive and operational performance tests (to develop in-situ maintenance and repair techniques and to support the development, enhancement, and implementation of protective systems, data and bio-processing systems, and virtual reality and telepresence/kinetic processes), (3) subsystem tests of advanced nuclear power, nuclear propulsion and communication systems (using boom extensions, remote station-keeping platforms and mobile EVA crew and robots), and (4) logistics support (crew and equipment) and command and control of deep space transport assembly, maintenance, and refueling (using a station-keeping platform). Author

N94-27369*# Massachusetts Univ., Lowell. Center for Productivity Enhancement.

AN ARTIFICIAL REALITY ENVIRONMENT FOR REMOTE FACTORY CONTROL AND MONITORING c31

Charles Paul Kosta and Patrick D. Krolak *In* NASA. Lewis Research Center, Vision 21: Interdisciplinary Science and Engineering in the Era of Cyberspace Dec. 1993 p 153-162 (For primary document see N94-27358 07-12)
Avail: CASI HC A02/MF A03

Work has begun on the merger of two well known systems, VEOS (HITLab) and CLIPS (NASA). In the recent past, the University of Massachusetts Lowell developed a parallel version of NASA CLIPS, called P-CLIPS. This modification allows users to create smaller expert systems which are able to communicate with each other to jointly solve problems. With the merger of a VEOS message system, PCLIPS-V can now act as a group of entities working within VEOS. To display the 3D virtual world we have been using a graphics package called HOOPS, from Ithaca Software. The artificial reality environment we have set up contains actors and objects as found in our Lincoln Logs Factory of the Future project. The environment allows us to view and control the objects within the virtual world. All communication between the separate CLIPS expert systems is done through VEOS. A graphical renderer generates camera views on X-Windows devices; Head Mounted Devices are not required. This allows more people to make use of this technology. We are experimenting with different types of virtual vehicles to give the user a sense that he or she is actually moving around inside the factory looking ahead through windows and virtual monitors. Author

N94-27370*# Sverdrup Technology, Inc., Cleveland, OH.

THE FERMI PARADOX: AN APPROACH BASED ON PERCOLATION THEORY c55

Geoffrey A. Landis *In* NASA. Lewis Research Center, Vision 21: Interdisciplinary Science and Engineering in the Era of Cyberspace Dec. 1993 p 163-167 (For primary document see N94-27358 07-12)
Avail: CASI HC A01/MF A03

If even a very small fraction of the hundred billion stars in the galaxy are home to technological civilizations which colonize over interstellar distances, the entire galaxy could be completely colonized in a few million years. The absence of such extraterrestrial civilizations visiting Earth is the Fermi paradox. A model for interstellar colonization is proposed using the assumption that there is a maximum distance over which direct interstellar colonization is feasible. Due to the time lag involved in interstellar communications, it is assumed that an interstellar colony will rapidly develop a culture independent of the civilization that originally settled it. Any given colony will have a probability P of developing a colonizing civilization, and a probability (1-P) that it will develop a non-colonizing civilization. These assumptions lead to the colonization of the galaxy occuring as a percolation problem. In a percolation problem, there will be a critical value of percolation probability, P(sub c). For P less than P(sub c), colonization will always terminate after a finite number of colonies. Growth will occur in 'clusters', with the outside of each cluster consisting of non-colonizing civilizations. For P greater than P(sub c), small uncolonized voids will exist, bounded by non-colonizing civilizations. For P approximately = to P(sub c), arbitrarily large filled regions exist, and also arbitrarily large empty regions. Author

N94-27371*# National Aeronautics and Space Administration. Lewis Research Center, Cleveland, OH.

A DIRECT CURRENT RECTIFICATION SCHEME FOR MICROWAVE SPACE POWER CONVERSION USING TRAVELING WAVE ELECTRON ACCELERATION c20

Robert M. Manning *In its* Vision 21: Interdisciplinary Science and Engineering in the Era of Cyberspace Dec. 1993 p 169-178 (For

primary document see N94-27358 07-12)
Avail: CASI HC A02/MF A03

The formation of the Vision-21 conference held three years ago allowed the present author to reflect and speculate on the problem of converting electromagnetic energy to a direct current by essentially reversing the process used in traveling wave tubes that converts energy in the form of a direct current to electromagnetic energy. The idea was to use the electric field of the electromagnetic wave to produce electrons through the field emission process and accelerate these electrons by the same field to produce an electric current across a large potential difference. The acceleration process was that of cyclotron auto-resonance. Since that time, this rather speculative ideas has been developed into a method that shows great promise and for which a patent is pending and a prototype design will be demonstrated in a potential laser power beaming application. From the point of view of the author, a forum such as Vision-21 is becoming an essential component in the rather conservative climate in which our initiatives for space exploration are presently formed. Exchanges such as Vision-21 not only allows us to deviate from the 'by-the-book' approach and rediscover the ability and power in imagination, but provides for the discussion of ideas hitherto considered 'crazy' so that they may be given the change to transcend from the level of eccentricity to applicability. Author

N94-27372*# Sverdrup Technology, Inc., Brook Park, OH.
EMERGING COMPUTER TECHNOLOGIES AND THE NEWS MEDIA OF THE FUTURE **c60**
Debra A. Vrabel *In* NASA. Lewis Research Center, Vision 21: Interdisciplinary Science and Engineering in the Era of Cyberspace Dec. 1993 p 181-183 (For primary document see N94-27358 07-12)
Avail: CASI HC A01/MF A03

The media environment of the future may be dramatically different from what exists today. As new computing and communications technologies evolve and synthesize to form a global, integrated communications system of networks, public domain hardware and software, and consumer products, it will be possible for citizens to fulfill most information needs at any time and from any place, to obtain desired information easily and quickly, to obtain information in a variety of forms, and to experience and interact with information in a variety of ways. This system will transform almost every institution, every profession, and every aspect of human life--including the creation, packaging, and distribution of news and information by media organizations. This paper presents one vision of a 21st century global information system and how it might be used by citizens. It surveys some of the technologies now on the market that are paving the way for new media environment. Author

N94-27373*# National Aeronautics and Space Administration, Washington, DC.
INERTIAL ELECTROSTATIC CONFINEMENT AS A POWER SOURCE FOR ELECTRIC PROPULSION **c20**
George H. Miley (Illinois Univ., Urbana.), R. Burton (Illinois Univ., Urbana.), J. Javedani (Illinois Univ., Urbana.), Y. Yamamoto (Illinois Univ., Urbana.), A. Satsangi (Illinois Univ., Urbana.), Y. Gu (Illinois Univ., Urbana.), P. Heck (Illinois Univ., Urbana.), R. Nebel (Los Alamos National Lab., NM.), N. Schulze (Illinois Univ., Urbana.), and J. Christensen (Illinois Univ., Urbana.) et al *In* NASA. Lewis Research Center, Vision 21: Interdisciplinary Science and Engineering in the Era of Cyberspace Dec. 1993 p 185-229 (For primary document see N94-27358 07-12)
Avail: CASI HC A03/MF A03

The potential use of an Inertial Electrostatic Confinement (IEC) power source for space propulsion has previously been suggested by the authors and others. In the past, these discussions have generally followed the charged-particle electric-discharge engine (QED) concept proposed by Bussard, in which the IEC is used to generate an electron beam which vaporizes liquid hydrogen for use as a propellant. However, in the present study, we consider an alternate approach, using the IEC to drive a conventional electric thruster unit. This has the advantage of building on the rapidly developing technology for such thrusters, which operate at higher specific impulse. Key issues related to this approach include the continued successful development of the physics and engineering of the IEC unit, as well as the development of efficient step-down dc voltage transformers. The IEC operates by radial injection of energetic ions into a spherical vessel. A very high ion density is created in a small core region at the center of the vessel, resulting in extremely high fusion power density in the core. Present experiments at the U. of Illinois in small IEC devices (less than 60-cm. dia.) have demonstrated much of the basic physics underlying this concept, e.g. producing approximately 10(exp 6) D-D neutrons/sec steady-state with deuterium gas flow injection. The ultimate goal is to increase the power densities by several orders of magnitude and to convert to D-He-3 injection. If successful, such an experiment would represent a milestone proof-of-principle device for eventual space power use. Further discussion of IEC physics and status will be presented with a description of the overall propulsion system and estimated performance. Author

N94-27374*# Brubaker Group, Los Angeles, CA.
A WIDELY ADAPTABLE HABITAT CONSTRUCTION SYSTEM UTILIZING SPACE RESOURCES **c54**
Harry B. Wykes *In* NASA. Lewis Research Center, Vision 21: Interdisciplinary Science and Engineering in the Era of Cyberspace Dec. 1993 p 231-240 (For primary document see N94-27358 07-12)
Avail: CASI HC A02/MF A03

This study suggests that the cost of providing accommodations for various manned activities in space may be reduced by the extensive use of resources that are commonly found throughout the solar system. Several concepts are proposed for converting these resources into simple products with many uses. Concrete is already being considered as a possible moonbase material. Manufacturing equipment should be as small and simple as possible, which leads to the idea of molding it into miniature modules that can be produced and assembled in large numbers to create any conceivable shape. Automated equipment could build up complex structures by laying down layer after layer in a process resembling stereolithography. These tiny concrete blocks handle compression loads and provide a barrier to harmful radiation. They are joined by a web of tension members that could be made of wire or fiber-reinforced plastic. The finished structure becomes air-tight with the addition of a flexible liner. Wire can be made from the iron modules found in lunar soil. In addition to its structural role, a relatively simple apparatus can bend and weld it into countless products like chairs and shelving that would otherwise need to be supplied from Earth. Wire woven into a loose blanket could be an effective micrometeoroid shield, tiny wire compression beams could be assembled into larger beams which in turn form larger beams to create very large space-frame structures. A technology developed with lunar materials could be applied to the moons of Mars or the asteroids. To illustrate its usefulness several designs for free-flying habitats are presented. They begin with a minimal self-contained living unit called the Cubicle. It may be multiplied into clusters called Condos. These are shown in a rotating tether configuration that provides a substitute for gravity. The miniature block proposal is compared with an alternate design based on larger triangular components and a tetrahedral geometry. The overall concept may be expanded to envision city-sized self-sufficient environments where humans could confortably live their entire lives. One such proposal is the Hive. It is configured around a unique sunlight collection system that could provide all its energy needs and that could be scaled up to compensate for the reduced solar intensity at greater distances from the sun. Its outer perimeter consists of a cylindrical section mated to two conical end walls that taper inwards toward a small aperture at the center of rotation. Light collected by two huge mirrors of unusual design enters the aperture and is redirected to the inside of the cylinder. The conical end walls are shielded from direct sunlight and are designed to radiate heat into space. They are lined with air ducts that passively recirculate the atmosphere while extracting moisture by condensation. Although there is no immediate demand for spacecraft on this scale, their consideration can influence even the earliest stages of the development process. Author

N94-27375*# National Aeronautics and Space Administration. Lewis Research Center, Cleveland, OH.
ROCKET ENGINE NUMERICAL SIMULATION **c20**
Ken Davidian *In its* Vision 21: Interdisciplinary Science and Engineering in the Era of Cyberspace Dec. 1993 p 241-245 (For primary document see N94-27358 07-12)
Avail: CASI HC A01/MF A03

The topics are presented in view graph form and include the following: a definition of the rocket engine numerical simulator (RENS); objectives; justification; approach; potential applications; potential users; RENS work flowchart; RENS prototype; and conclusions. CASI

N94-27376*# Carnegie-Mellon Univ., Pittsburgh, PA. Robotics Inst.
PIGS IN CYBERSPACE c54
Hans Moravec *In* NASA. Lewis Research Center, Vision 21: Interdisciplinary Science and Engineering in the Era of Cyberspace Dec. 1993 p 259-264 (For primary document see N94-27358 07-12)
Avail: CASI HC A02/MF A03

Exploration and colonization of the universe awaits, but Earth-adapted biological humans are ill-equipped to respond to the challenge. Machines have gone farther and seen more, limited though they presently are by insect-like behavior inflexibility. As they become smarter over the coming decades, space will be theirs. Organizations of robots of ever increasing intelligence and sensory and motor ability will expand and transform what they occupy, working with matter, space and time. As they grow, a smaller and smaller fraction of their territory will be undeveloped frontier. Competitive success will depend more and more on using already available matter and space in ever more refined and useful forms. The process, analogous to the miniaturization that makes today's computers a trillion times more powerful than the mechanical calculators of the past, will gradually transform all activity from grossly physical homesteading of raw nature, to minimum-energy quantum transactions of computation. The final frontier will be urbanized, ultimately into an arena where every bit of activity is a meaningful computation: the inhabited portion of the universe will be transformed into a cyberspace. Because it will use resources more efficiently, a mature cyberspace of the distant future will be effectively much bigger than the present physical universe. While only an infinitesimal fraction of existing matter and space is doing interesting work, in a well developed cyberspace every bit will be part of a relevant computation or storing a useful datum. Over time, more compact and faster ways of using space and matter will be invented, and used to restructure the cyberspace, effectively increasing the amount of computational spacetime per unit of physical spacetime. Computational speed-ups will affect the subjective experience of entities in the cyberspace in a paradoxical way. At first glimpse, there is no subjective effect, because everything, inside and outside the individual, speeds up equally. But, more subtly, speed-up produces an expansion of the cyber universe, because, as thought accelerates, more subjective time passes during the fixed (probably lightspeed) physical transit time of a message between a given pair of locations - so those fixed locations seem to grow farther apart. Also, as information storage is made continually more efficient through both denser utilization of matter and more efficient encodings, there will be increasingly more cyber-stuff between any two points. The effect may somewhat resemble the continuous-creation process in the old steady-state theory of the physical universe of Hoyle, Bondi and Gold, where hydrogen atoms appear just fast enough throughout the expanding cosmos to maintain a constant density. Author

N94-28207# European Space Research Organization, Noordwikj (Netherlands). Publications Div.
SCIENCE BEYOND THE ATMOSPHERE: THE HISTORY OF SPACE RESEARCH IN EUROPE
Arturo Russo, ed. Noordwijk, The Netherlands Jul. 1993 220 p Symposium held in Palermo, Italy, 5-7 Nov. 1992
(ESA-HSR-SPECIAL) Avail: CASI HC A10/MF A03

The papers included were prepared for a symposium held in Palermo in early November 1992. The aim of the symposium, organized in the framework of the ESA History Project, was to discuss critically the development of the scientific programs of ESRO and ESA by bringing together some of the main protagonists of the history of space research in Europe and a few historians working in the field. The symposium was sponsored by the University of Palermo, the Italian National Research Council and the European Space Agency. Topics covered include: Space science in ESRO and ESA; how space scientists and governments saw ESRO in the early 1960's; solar research in the early days of COPERS and ESRO; ionospheric research by rockets and satellites in Europe in the 1960's; the start of the space research in Sweden during the COPERS and early ESRO years; and from sounding rocket to small satellites, a way of complementing ESRO/ESA flight opportunities. Author (revised)

N94-28358# Helsinki Univ. of Technology, Espoo (Finland). Lab. of Space Technology.
LABORATORY OF SPACE TECHNOLOGY Annual Report, 1992
M. Hallikainen May 1993 45 p See also PB93-111904
(PB94-133204; ISBN-951-22-1353-2) Avail: CASI HC A03/MF A01

The activities of the Laboratory of Space Technology in 1992 are described. The Laboratory is responsible for teaching space technology at the university. The main area in research is airborne and spaceborne remote sensing, including instrumentation, measurements, and development of geophysical inversion algorithms. Data from the ESA ERS-1 SAR was used in several projects, including remote sensing of sea ice, snow, and forests. In satellite technology, design and construction of our own satellite HUTSAT (Helsinki University of Technology Satellite) was started. In connection with the 22nd European Microwave Conference, the Laboratory of Space Technology organized a one-day Workshop on Microwaves in Environmental Monitoring. NTIS

N94-25670*# California Univ., Los Angeles. Dept. of Mechanical, Aerospace and Nuclear Engineering.
MANNED MISSION TO MARS WITH PERIODIC REFUELING FROM ELECTRICALLY PROPELLED TANKERS
Laura Gogan, Joseph Melko, Fritz Wang, Daniel Lourme, Sophie Ben Moha, Christele Lardon, and Muriel Richard *In* USRA, Proceedings of the 8th Annual Summer Conference: NASA/USRA Advanced Design Program 1992 p 22-30 Prepared in cooperation with Ecole Polytechnique Feminine, Sceaux, France (For primary document see N94-25665 07-80)
Avail: CASI HC A02/MF A04

N94-25674*# Florida Agricultural and Mechanical Univ., Tallahassee. Dept. of Mechanical Engineering.
THE EXTENDED MISSION ROVER (EMR)
W. Shields, Anthony Halecki, Manh Chung, Ken Clarke, Kevin Frankle, Fariba Kassemkhani, John Kuhlhoff, Josh Lenzini, David Lobdell, and Sam Morgan et al *In* USRA, Proceedings of the 8th Annual Summer Conference: NASA/USRA Advanced Design Program 1992 p 67-73 Prepared in cooperation with Florida State Univ., Tallahassee (For primary document see N94-25665 07-80)
Avail: CASI HC A02/MF A04

N94-25682*# Houston Univ., TX. International Center for Space Architecture.
LOWEST COST, NEAREST TERM OPTIONS FOR A MANNED MARS MISSION
Bob Sauls, Michael Mortensen, Renee Myers, Giovanni Guacci, and Fred Montes *In* USRA, Proceedings of the 8th Annual Summer Conference: NASA/USRA Advanced Design Program 1992 p 114-123 (For primary document see N94-25665 07-80)
Avail: CASI HC A02/MF A04

N94-25687*# Massachusetts Inst. of Tech., Cambridge. Dept. of Aeronautics and Astronautics.
PROJECT COLUMBIAD: REESTABLISHMENT OF HUMAN PRESENCE ON THE MOON
Joseph Shea, Stanley Weiss, Harold Alexander, Peter Belobaba, Greg Loboda, Maresi Berry, Mark Bower, Charles Bruen, Patrick Cazeau, and Michael Clarke et al *In* USRA, Proceedings of the 8th Annual Summer Conference: NASA/USRA Advanced Design Program 1992 p 170-177 (For primary document see N94-25665 07-80)
Avail: CASI HC A02/MF A04

N94-25692*# Pennsylvania State Univ., University Park. Dept. of Aerospace Engineering.
COMET NUCLEUS AND ASTEROID SAMPLE RETURN MISSIONS
Robert G. Melton, Roger C. Thompson, Thomas F. Starchville, Jr., C. Adams, A. Aldo, K. Dobson, C. Flotta, J. Gagliardino, M. Lear, and C. McMillan et al *In* USRA, Proceedings of the 8th Annual Summer Conference: NASA/USRA Advanced Design Program 1992 p 216-227 (For primary document see N94-25665 07-80)
Avail: CASI HC A03/MF A04

13 ASTRODYNAMICS

Includes powered and free-flight trajectories; and orbital and launching dynamics.

N94-25787 Technische Univ., Delft (Netherlands). Sectie Fysische, Meetkundige en Ruimtegeodesie.

HILL EQUATIONS FOR SATELLITE ORBIT DETERMINATION Thesis [DE VERGELIJKINGEN VAN HILL VOOR DE BEPALING VAN EEN SATELLIETBAAN]

R. G. vanCoevorden Nov. 1992 92 p In DUTCH Limited Reproducibility: More than 20% of this document may be affected by microfiche quality
(ETN-94-95374) Avail: CASI HC A05

Equations of motion using a periodical circular orbit are addressed. The orbital perturbations are given with respect to this moving triad. This set of equations, called the Hill equations, exists of three second order linear differential equations. They describe the problem in a first order approximation. Depending on the type of the disturbing forces, there exist different solutions of these equations. When there are no disturbing forces, the equations are called the homogeneous Hill equations, and only the initial values of the state vector can change the shape of the orbit. Disturbing forces which are more complex, can be transformed into Fourier series and then used in the equations to get an exact analytical solution of the approximated problem. By looking at the complete solution of the Hill equations, it can be seen that there are a few cases in which the solutions are not valid. The so called critical frequencies give a resonant effect on the orbital perturbations. These frequencies are the zero frequency and the once per revolution frequency. Resonant sources are for instance: drag, solar pressure, etc. A simple rendezvous problem, which describes the use of the homogeneous equations of motion, is discussed, some resonant sources are explained, and two examples of some relativistic effects are given. The cases in which the disturbing frequency is almost equal to a critical frequency are described. The amplitudes of the perturbations can grow very big in these so called near resonance cases. As a result of this work, the Hill equations can be said to be very good for educative purposes, because they give a very good view on the effects of disturbing forces on the orbit of a satellite. It should always be kept in mind that many simplifications are made when deriving the Hill equations. ESA

N94-26001# Air Force Inst. of Tech., Wright-Patterson AFB, OH. School of Engineering.

THE MODAL SOLUTION TO THE MOON'S ORBIT USING CANONICAL FLOQUET PERTURBATION THEORY M.S. Thesis

Kurt A. Vogel Dec. 1993 100 p
(AD-A273732; AFIT/GA/ENY/93D-9) Avail: CASI HC A05/MF A02

Using the restricted three body problem, the equations of motion (EOM) and Hamiltonian are computed for the moon's orbit in physical variables. A periodic orbit is found in the vicinity of the moon's orbit, and classical Floquet theory is applied to the periodic orbit to give stability information and the complete solution to the equations of variation. Floquet theory also supplies a transformation from physical variables to modal variables. This transformation to modal variables is made canonical by constraining the initial transformation matrix to be symplectic. Actual lunar data is used to calculate the modes for the real moon's orbit. Once satisfied that the moon's real-world modes are in (or near) the linear regime of the periodic orbit, the modal EOM are found by doing a perturbation expansion on the new modal Hamiltonian. The modal results from the real lunar orbit are compared with the modal EOM/expansion results. The modal expansion proves to be an accurate solution to the moon's orbit given enough expansion terms. DTIC

N94-27771*# National Aeronautics and Space Administration. Langley Research Center, Hampton, VA.

LIFETIMES OF LUNAR SATELLITE ORBITS

Kurt W. Meyer (George Washington Univ., Hampton, VA.), James J. Buglia (Flight Mechanics and Control, Inc., Hampton, VA.), and Prasun N. Desai Mar. 1994 37 p
(RTOP 506-49-11-01)
(NASA-TP-3394; L-17264; NAS 1.60:3394) Avail: CASI HC A03/MF A01

The Space Exploration Initiative has generated a renewed interest in lunar mission planning. The lunar missions currently under study, unlike the Apollo missions, involve long stay times. Several lunar gravity models have been formulated, but mission planners do not have enough confidence in the proposed models to conduct detailed studies of missions with long stay times. In this report, a particular lunar gravitational model, the Ferrari 5 x 5 model, was chosen to determine the lifetimes for 100-km and 300-km perilune altitude, near-circular parking orbits. The need to analyze orbital lifetimes for a large number of initial orbital parameters was the motivation for the formulation of a simplified gravitational model from the original model. Using this model, orbital lifetimes were found to be heavily dependent on the initial conditions of the nearly circular orbits, particularly the initial inclination and argument of perilune. This selected model yielded lifetime predictions of less than 40 days for some orbits, and other orbits had lifetimes exceeding a year. Although inconsistencies and limitations are inherent in all existing lunar gravity models, primarily because of a lack of information about the far side of the moon, the methods presented in this analysis are suitable for incorporating the moon's nonspherical gravitational effects on the preliminary design level for future lunar mission planning. Author (revised)

14 GROUND SUPPORT SYSTEMS AND FACILITIES (SPACE)

Includes launch complexes, research and production facilities; ground support equipment, e.g., mobile transporters; and simulators.

For related information see also *09 Research and Support Facilities (Air).*

N94-25769# Air Force Inst. of Tech., Wright-Patterson AFB, OH.

SYSTEM DESIGN ANALYSIS OF A LIGHTWEIGHT LASER SATELLITE TERMINAL M.S. Thesis

Brian C. Page Dec. 1993 81 p
(AD-A274033; AFIT/GSO/ENG/93D-03) Avail: CASI HC A05/MF A01

This study investigated the technological feasibility of a man-portable satellite laser communications system. Areas of interest were: an end-to-end system analysis on the communications link; evaluation of atmospheric effects; and evaluation of semiconductor lasers as the laser source. A literature search revealed that satellite laser communication research is primarily directed at intersatellite links. There have been some proposed systems for space-to-ground laser communications systems, but they all utilize large fixed ground stations. The focus of this research effort is directed at a small man-portable ground station capitalizing on recent advances in semiconductor laser devices. Baseline satellite communication systems were analyzed for both conventional radio frequency systems and a laser communication system. Modifications to the laser communications system were explored, and found to be feasible for some applications. Atmospheric effects were explored and are a major contributor to system degradation. Semiconductor laser sources were evaluated and are currently useful for some satellite laser communication applications. DTIC

N94-26142*# National Aeronautics and Space Administration. Lewis Research Center, Cleveland, OH.

A LARGE HIGH VACUUM, HIGH PUMPING SPEED SPACE SIMULATION CHAMBER FOR ELECTRIC PROPULSION

Stanley P. Grisnik and James E. Parkes (Sverdrup Technology, Inc., Brook Park, OH.) Jan. 1994 10 p Presented at the 23rd International Electric Propulsion Conference, Seattle, WA, 13-16 Sep. 1993; sponsored by AIAA, AIDAA, DGLR, and JSASS
(Contract NAS3-25266; RTOP 506-42-31)
(NASA-TM-106453; E-8080; NAS 1.15:106453; IEPC-93-151) Avail: CASI HC A02/MF A01

Testing high power electric propulsion devices poses unique requirements on space simulation facilities. Very high pumping speeds are required to maintain high vacuum levels while handling large volumes of exhaust products. These pumping speeds are significantly higher than those available in most existing vacuum facilities. There is also a requirement for relatively large vacuum chamber dimensions to minimize facility wall/thruster plume interactions and to accommodate far field plume diagnostic measurements. A 4.57 m (15 ft) diameter by 19.2 m (63 ft) long vacuum chamber at

NASA Lewis Research Center is described. The chamber utilizes oil diffusion pumps in combination with cryopanels to achieve high vacuum pumping speeds at high vacuum levels. The facility is computer controlled for all phases of operation from start-up, through testing, to shutdown. The computer control system increases the utilization of the facility and reduces the manpower requirements needed for facility operations.

Author (revised)

N94-27424*# National Aeronautics and Space Administration. Lewis Research Center, Cleveland, OH.

HYDROGEN-OXYGEN TORCH IGNITOR

George A. Repas Mar. 1994 17 p
(RTOP 584-03-21)
(NASA-TM-106493; E-8480; NAS 1.15:106493) Avail: CASI HC A03/MF A01

The hydrogen-oxygen torch igniter described herein has been successfully used for many years at various NASA Lewis Research Center rocket test facilities to provide ignition for rocket engine research hardware. This igniter is inexpensive, simple to operate, and has demonstrated very good reliability. It has been used as an ignition source for rocket engines that utilized a variety of propellant combinations; some of these engines developed up to 40,000 lb of thrust.

Author (revised)

N94-25696*# Texas Univ., Austin. Dept. of Aerospace Engineering and Engineering Mechanics.

SPACE HABITAT, ASSEMBLY AND REPAIR FACILITY

Todd A. Colangelo, Debora C. Hoetger, Addison C. Kuo, Michael C. Lo, Leland R. Marcus, Phillip P. Tran, Chris J. Tutt, Chad M. Wassmuth, and Gregory M. Wildgrube *In* USRA, Proceedings of the 8th Annual Summer Conference: NASA/USRA Advanced Design Program 1992 p 251-263
(For primary document see N94-25665 07-80)
Avail: CASI HC A03/MF A04

15 LAUNCH VEHICLES AND SPACE VEHICLES

Includes boosters; operating problems of launch/space vehicle systems; and reusable vehicles.

For related information see also *20 Spacecraft Propulsion and Power.*

N94-27868*# National Aeronautics and Space Administration. Hugh L. Dryden Flight Research Facility, Edwards, CA.

MULTIDISCIPLINARY AEROELASTIC ANALYSIS OF A GENERIC HYPERSONIC VEHICLE

K. K. Gupta and K. L. Petersen Washington Oct. 1993 13 p
Presented at the AIAA 5th International Aerospace Planes Conference, Munich, Germany, 30 Nov. - 3 Dec. 1993
(RTOP 505-70-00)
(NASA-TM-4544; H-1956; NAS 1.15:4544; AIAA Paper 93-5028) Avail: CASI HC A03/MF A01

This paper presents details of a flutter and stability analysis of aerospace structures such as hypersonic vehicles. Both structural and aerodynamic domains are discretized by the common finite element technique. A vibration analysis is first performed by the STARS code employing a block Lanczos solution scheme. This is followed by the generation of a linear aerodynamic grid for subsequent linear flutter analysis within subsonic and supersonic regimes of the flight envelope; the doublet lattice and constant pressure techniques are employed to generate the unsteady aerodynamic forces. Flutter analysis is then performed for several representative flight points. The nonlinear flutter solution is effected by first implementing a CFD solution of the entire vehicle. Thus, a 3-D unstructured grid for the entire flow domain is generated by a moving front technique. A finite element Euler solution is then implemented employing a quasi-implicit as well as an explicit solution scheme. A novel multidisciplinary analysis is next effected that employs modal and aerodynamic data to yield aerodynamic damping characteristics. Such analyses are performed for a number of flight points to yield a large set of pertinent data that define flight flutter characteristics of the vehicle. This paper outlines the finite-element-based integrated analysis procedures in detail, which is followed by the results of numerical analyses of flight flutter simulation.

Author

16 SPACE TRANSPORTATION

Includes passenger and cargo space transportation, e.g., shuttle operations; and space rescue techniques.

For related information see also *03 Air Transportation and Safety* and *18 Spacecraft Design, Testing and Performance.* For space suits see *54 Man/System Technology and Life Support.*

N94-26017# Air Force Inst. of Tech., Wright-Patterson AFB, OH.

A COMPARISON OF USERS' AND PROVIDERS' PERCEPTIONS OF CRITICAL SPACELIFT VEHICLE CHARACTERISTICS AND CAPABILITIES M.S. Thesis

Dawson S. Oslund and Mark M. Shafer Sep. 1993 134 p
(AD-A273907; AFIT/GLM/LAR/93S-32) Avail: CASI HC A07/MF A02

This study compares spacelift vehicle users' and providers' perceptions of critical spacelift vehicle characteristics and capabilities. The researchers conducted a mail survey of military, commercial, and civil spacelift vehicle users and providers to determine a criticality rating for each of the 22 characteristics and capabilities identified through a literature review. Primary results of the study indicate: the three most critical characteristics and capabilities are reliability, launch cost, and resilience; the three least critical characteristics and capabilities are man-rateable, reusability, and gross lift-off weight; only launch cost has a significantly different mean criticality rating among spacelift vehicle users and providers; and 13 of the 22 characteristics and capabilities have significantly different mean criticality ratings between military and commercial respondents. The researchers conclude that differences between users' and providers' perceptions are inconsequential, but further study of military and commercial perceptions is necessary.

DTIC

N94-26135*# Thiokol Corp., Brigham City, UT. Space Operations.

STS-56, RSRM-031, 360L031 KSC PROCESSING CONFIGURATION AND DATA REPORT Final Report

8 Dec. 1993 89 p
(Contract NAS8-38100)
(NASA-CR-193922; NAS 1.26:193922; TWR-63641) Avail: CASI HC A05/MF A01

KSC Processing Configuration and Data Report is being provided as a historical document and as an enhancement to future RSRM manufacturing and processing operations. The following sections provide information on segment receipt, aft booster build-up, booster assembly, and closeout for STS-56, RSRM flight set 36OL031. Section 2.0 contains a summary of RSRM-031 processing. Section 3.0 discusses any significant problems or special issues that require special attention. Sections 4.0 through 6.0 contain narrative descriptions of all key events, including any related processing problems. Appendix A provides engineering specifications and changes. A list and matrix of all problem reports (PR's) pertinent to this flight set is provided in Appendix B. The matrix was provided by the Thiokol LSS Quality Engineering office. Copies of the PR's generated during the processing of RSRM-031 will be provided upon request. Appendix C contains the motor set status matrix, which provides milestone dates for the RSRM-031 flow. Section 7.0 provides recommendations, if any, for the improvement of flight hardware processing. Section 8.0 contains data sheets that provide flight hardware parts and consumables information installed during the booster build-up and stacking operations by location, lot/serial number, expiration and cure dates/times, and installation dates.

Derived from text

N94-26153*# Thiokol Corp., Brigham City, UT. Space Operations.

STS-51, RSRM-033, 360T033 KSC PROCESSING CONFIGURATION AND DATA REPORT Final Report

Robert C. Hillard 9 Dec. 1993 104 p
(Contract NAS8-38100)
(NASA-CR-193923; NAS 1.26:193923; TWR-64563) Avail: CASI HC A06/MF A02

KSC Processing Configuration and Data Report is being provided as a historical document and as an enhancement to future RSRM manufacturing and processing operations. The following sections provide information on segment receipt, aft booster build up, motor assembly, and closeout for STS-51, RSRM flight set 360T033. Section 2.0 contains a summary of RSRM-033 processing. Section 3.0 discusses any significant problems or special issues that require special attention. Sections 4.0 through 6.0 contain narrative descriptions of all key events, including any related processing problems. Appendix A provides engineering specifications and changes. A list and matrix of all problem reports (PR's) pertinent to this flight set is provided in Appendix B. The matrix was provided by the Thiokol LSS Quality Engineering office. Copies of the PR's generated during the processing of RSRM-033 will be provided upon request. Appendix C contains the motor set status matrix, which provides milestone dates for the RSRM-033 flow. Section 7.0 provides recommendations for the improvement of flight hardware processing. Section 8.0 contains data sheets that provide flight hardware parts and consumable information installed during the booster build-up and stacking operations by location, lot/serial number, expiration and cure dates/times, and installation dates. Derived from text

N94-26529# Naval Postgraduate School, Monterey, CA.
APPLICATION OF SPACE SHUTTLE PROJECT HERCULES IMAGERY IN THE INVESTIGATION OF SHIP CLOUD TRACKS M.S. Thesis
Larry E. Whitmeyer Sep. 1993 141 p
(AD-A274923) Avail: CASI HC A07/MF A02

An assessment is made as to the utility obtained via the Project HERCULES electronic still camera system, utilized onboard the Space Shuttle, toward the MAST Space Test Program investigation of ship-induced cloud tracks. Project HERCULES and MAST concepts are described. A detailed discussion is presented of the integration requirements, mission conduct, and payload support procedures involved in using the HERCULES system during the STS-56 mission to image potential shiptrack areas and Naval-related sites. Five HERCULES imagery cases are analyze with feature measurements. Alternate camera systems are described, and then compared with the HERCULES system. Recommendations are made for the MAST payload. Although utility is seen in the geolocation and digital format offered by HERCULES images, the present configuration permits only limited use in the shiptrack and Naval-related application. However, a firm procedural knowledge-base has been established for the MAST experiment. DTIC

N94-27436*# National Aeronautics and Space Administration. Lewis Research Center, Cleveland, OH.
RISKS AND ISSUES IN FIRE SAFETY ON THE SPACE STATION
Robert Friedman Dec. 1993 8 p Presented at the Probabilistic Safety and Management Conference, San Diego, CA, 21-25 Mar. 1994; sponsored by the Society for Risk Analysis
(RTOP 323-44-03)
(NASA-TM-106430; E-8272; NAS 1.15:106430) Avail: CASI HC A02/MF A01

A fire in the inhabited portion of a spacecraft is a greatly feared hazard, but fire protection in space operations is complicated by two factors. First, the spacecraft cabin is an enclosed volume, which limits the resources for fire fighting and the options for crew escape. Second, an orbiting spacecraft experiences a balance of forces, creating a near-zero-gravity (microgravity) environment that profoundly affects the characteristics of fire initiation, spread, and suppression. The current Shuttle Orbiter is protected by a fire-detection and suppression system whose requirements are derived of necessity from accepted terrestrial and aircraft standards. While experience has shown that Shuttle fire safety is adequate, designers recognize that improved systems to respond specifically to microgravity fire characteristics are highly desirable. Innovative technology is particularly advisable for the Space Station, a forthcoming space community with a complex configuration and long-duration orbital missions, in which the effectiveness of current fire-protection systems is unpredictable. The development of risk assessments to evaluate the probabilities and consequences of fire incidents in spacecraft are briefly reviewed. It further discusses the important unresolved issues and needs for improved fire safety in the Space Station, including those of material selection, spacecraft atmospheres, fire detection, fire suppression, and post-fire restoration. Author (revised)

N94-27774*# National Aeronautics and Space Administration. Langley Research Center, Hampton, VA.
MINIMUM ACCOMMODATION FOR AEROBRAKE ASSEMBLY, PHASE 2 Final Report
Stephen J. Katzberg, Davy A. Haynes, Robin D. Tutterow, Judith J. Watson, and James W. Russell (Lockheed Engineering and Sciences Co., Hampton, VA.) Apr. 1994 23 p
(RTOP 594-81-21-05)
(NASA-TM-107608; NAS 1.15:107608) Avail: CASI HC A03/MF A01

A multi-element study was done to assess the practicality of a Space Station Freedom-based aerobrake system for the Space Exploration Initiative. The study was organized into six parts related to structure, aerodynamics, robotics and assembly, thermal protection system, inspection, and verification, all tied together by an integration study. The integration activity managed the broad issues related to meeting mission requirements. This report is a summary of the issues addressed by the integration team. Author

N94-27956*# National Aeronautics and Space Administration. John F. Kennedy Space Center, Cocoa Beach, FL.
DEBRIS/ICE/TPS ASSESSMENT AND INTEGRATED PHOTOGRAPHIC ANALYSIS FOR SHUTTLE MISSION STS-60 Final Report, 1-14 Feb. 1994
Gregory N. Katnik, Barry C. Bowen, J. Bradley Davis, Jorge E. Rivera, and Robert F. Speece Mar. 1994 110 p Original contains color illustrations
(NASA-TM-109193; NAS 1.15:109193) Avail: CASI HC A06/MF A02; 44 functional color pages

A debris/ice/thermal protection system (TPS) assessment and integrated photographic analysis was conducted for Shuttle mission STS-60. Debris inspections of the flight elements and launch pad were performed before and after launch. Icing conditions on the External Tank were assessed by the use of computer programs, nomographs, and infrared scanner data during cryogenic loading of the vehicle followed by on-pad visual inspection. High speed photography of the launch was analyzed to identify ice/debris sources and evaluate potential vehicle damage and/or in-flight anomalies. This report documents the ice/debris/TPS conditions and integrated photographic analysis of Shuttle mission STS-60, and the resulting effect on the Space Shuttle Program. Author

N94-28178*# National Aeronautics and Space Administration. John F. Kennedy Space Center, Cocoa Beach, FL.
REPORT OF THE SHUTTLE PROCESSING REVIEW TEAM
30 Jun. 1993 43 p
(NASA-TM-109728; NAS 1.15:109728) Avail: CASI HC A03/MF A01

The intent of this report is to summarize the assessment of the shuttle processing operations at the Kennedy Space Center (KSC) as requested by the NASA Administrator. He requested a team reaffirmation that safety is the number one priority and review operations to ensure confidence in the shuttle processing procedures at KSC. Derived from text

N94-28199*# Lockheed Engineering and Sciences Co., Houston, TX.
STS-55 SPACE SHUTTLE MISSION REPORT
Robert W. Fricke, Jr. Jul. 1993 51 p Sponsored by NASA. Johnson Space Center
(NASA-CR-195741; NAS 1.26:195741; JSC-08284; NSTS-08284) Avail: CASI HC A04/MF A01

A summary of the Space Shuttle Payloads, Orbiter, External Tank, Solid Rocket Booster, Redesigned Solid Rocket Motor, and the Main Engine subsystems performance during the 55th flight of the Space Shuttle Program and the 14th flight of Columbia is presented. Derived from text

N94-28205*# National Aeronautics and Space Administration. Lyndon B. Johnson Space Center, Houston, TX.
ARTEMIS COMMON LUNAR LANDER. PHASE 2: STUDY RESULTS FOR EXTERNAL REVIEW
10 Mar. 1992 131 p
(NASA-TM-109699; NAS 1.15:109699) Avail: CASI HC A07/MF A02

The purpose of the Artemis Program is to gather vital reconnaissance data by conducting robotic exploration missions to the lunar surface both prior to and concurrent with human exploration missions. The Artemis Program includes rapid, near-term development of a variety of small experimental and operational payloads, provides a low-cost capability to deliver these payloads to any location on the lunar surface, and supports the analysis of the data returned. The Artemis Program will improve the understanding of lunar geosciences, demonstrate the Moon's unique capability as an astronomical platform to study the universe, and to conduct scientific and technology development experiments, and will prepare for,

enhance, and complement human mission The Artemis Common Lunar Lander Phase 2 Study results for external review are included.
Author (revised)

N94-28220*# Lockheed Engineering and Sciences Co., Houston, TX.
STS-57 SPACE SHUTTLE MISSION REPORT
Robert W. Fricke, Jr. Aug. 1993 52 p Sponsored by NASA. Johnson Space Center
(NASA-CR-195739; NAS 1.26:195739; JSC-08285; NSTS-08285) Avail: CASI HC A04/MF A01

The STS-57 Space Shuttle Program Mission Report provides a summary of the Payloads, as well as the Orbiter, External Tank (ET), Solid Rocket Booster (SRB), Redesigned Solid Rocket Motor (RSRM), and the Space Shuttle main engine (SSME) systems performance during the fifty-sixth flight of the Space Shuttle Program and fourth flight of the Orbiter vehicle Endeavour (OV-105). In addition to the Orbiter, the flight vehicle consisted of an ET (ET-58); three SSME's which were designated as serial numbers 2019, 2034, and 2017 in positions 1, 2, and 3, respectively; and two SRB's which were designated BI-059. The lightweight RSRM's that were installed in each SRB were designated as 360L032A for the left SRB and 360W032B for the right SRB. The STS-57 Space Shuttle Program Mission Report fulfills the Space Shuttle Program requirement, as documented in NSTS 07700, Volume 8, Appendix E. That document states that each major organizational element supporting the Program will report the results of their hardware evaluation and mission performance plus identify all related in-flight anomalies. Author (revised)

N94-28221*# Lockheed Engineering and Sciences Co., Houston, TX.
STS-56 SPACE SHUTTLE MISSION REPORT
Robert W. Fricke, Jr. Jul. 1993 52 p Sponsored by NASA. Johnson Space Center
(NASA-CR-195740; NAS 1.26:195740; NSTS-08283) Avail: CASI HC A04/MF A01

The STS-56 Space Shuttle Program Mission Report provides a summary of the Payloads, as well as the Orbiter, External Tank (ET), Solid Rocket Booster (SRB), Redesigned Solid Rocket Motor (RSRM), and the Space Shuttle main engine (SSME) systems performance during the fifty-fourth flight of the Space Shuttle Program and sixteenth flight of the Orbiter vehicle Discovery (OV-103). In addition to the Orbiter, the flight vehicle consisted of an ET (ET-54); three SSME's, which were designated as serial numbers 2024, 2033, and 2018 in positions 1, 2, and 3, respectively; and two SRB's which were designated BI-058. The lightweight RSRM's that were installed in each SRB were designated as 360L031A for the left SRB and 360L031B for the right SRB. Author

N94-27928*# Old Dominion Univ., Norfolk, VA.
SPACE TRANSPORTATION VEHICLE DESIGN EVALUATION USING SATURATED DESIGNS
Resit Unal *In its* The 1993 NASA-ODU American Society for Engineering Education (ASEE) Summer Faculty Fellowship Program Dec. 1993 p 192-193 (For primary document see N94-27893 07-80)
Avail: CASI HC A01/MF A03

17 SPACE COMM., SPACECRAFT COMM., COMMAND & TRACKING

Includes telemetry; space communications networks; astronavigation and guidance; and radio blackout.

For related information see also *04 Aircraft Communications and Navigation* and *32 Communications and Radar.*

N94-27427*# National Aeronautics and Space Administration. Lewis Research Center, Cleveland, OH.
THE TELEMEDICINE SPACEBRIDGE PROJECT: A JOINT US/RUSSIAN VENTURE IN LONG DISTANCE MEDICINE VIA SATELLITE
John E. Zuzek, Michael A. Cauley, and James E. Hollansworth Mar. 1994 12 p Presented at the 15th International Communications Satellite Systems Conference, San Diego, CA, 28 Feb. - 3 Mar. 1994; sponsored by AIAA
(RTOP 106-70-00)
(NASA-TM-106523; E-8646; NAS 1.15:106523; AIAA Paper 94-1119)
Avail: CASI HC A03/MF A01

The Telemedicine Spacebridge Demonstration Project is a joint U.S./Russian program whose purpose is to further the application of telemedicine both internationally, domestically, and in space. The system has been set up to use a Russian satellite over the Atlantic Ocean and a U.S. domestic satellite to allow physicians a two-way video and audio link between various sites of medical centers in the United States and the Central Hospital in Moscow, Russia. This paper contains a description of the project background, the Spacebridge system, the individual pieces of the system, and the operational experience gained thus far in the project.
Author (revised)

N94-27583# European Space Agency. European Space Research and Technology Center, ESTEC, Noordwijk (Netherlands). Standards Approval Board for Space Data Communications.
TELECOMMAND DECODER SPECIFICATION
Sep. 1993 115 p
(ISSN 0379-4059)
(ESA-PSS-04-151-Issue-1; ETN-94-95457) Copyright Avail: CASI HC A06/MF A02

The purpose of the specification is to establish uniform requirements for the implementation of spacecraft telecommand systems to be flown onboard ESA spacecraft. The ESA telecommand concept embraces multiple layers of data communication protocols which are specified in two documents: the radio frequency and modulation standard; and the packet telecommand standard. The telecommand subsystem requirements, which apply to free flying spacecraft, are overviewed. The physical layer document provides the information required for a broader view of the overall telecommand system. Particular attention is given to the interference between the physical and the coding layers at the receiving end and the actions at the receiving end. Specifications concerning the coding, the functions of the transfer, the authentication, and the command pulse distribution unit are included. The requirements on telemetry reporting are summarized. Interface functional design specifications are given. ESA

18 SPACECRAFT DESIGN, TESTING AND PERFORMANCE

Includes satellites; space platforms; space stations; spacecraft systems and components such as thermal and environmental controls; and attitude controls.

For life support systems see *54 Man/System Technology and Life Support.* For related information see also *05 Aircraft Design, Testing and Performance, 39 Structural Mechanics,* and *16 Space Transportation.*

N94-25595# Air Force Inst. of Tech., Wright-Patterson AFB, OH. School of Engineering.
HUMAN VISUAL SYSTEM ENHANCEMENT OF RECONSTRUCTED SATELLITE IMAGES M.S. Thesis
James E. Treleaven 15 Dec. 1993 72 p
(AD-A273867; AFIT/GEO/ENP/93D-04) Avail: CASI HC A04/MF A01

The enhancement of satellite images was investigated. The goal was to develop and test a suite of image enhancement software routines to improve the quality of reconstructed images for the human visual system. The primary focus was to enhance satellite features. Enhancement was accomplished in both the spatial domain and the frequency domain. In the spatial domain, routines were developed to enhance image contrast and edges. In the frequency domain, a routine was developed using research into the human visual system. The transfer function of the human visual system was used to develop a filter for frequency domain enhancement. A data set of images was developed using software to simulate the image degradation caused by atmospheric turbulence and the randomness of the image measurement process. The parameters varied in the simulation were atmospheric coherence diameter and total photon count. The routines were applied to this data set and the results were evaluated by various image fidelity criteria. All enhancement routines provided enhancement dependent upon the parameters of the data set simulation. Contrast enhancement worked well when photon count was low. Edge enhancement worked well when photon count was high. The frequency domain filter worked well always. DTIC

N94-25615 Air Force Inst. of Tech., Wright-Patterson AFB, OH.
A COMPARISON OF THREE APPROXIMATE MATHEMATICAL MODELS FOR THE GRAVITY GRADIENT STABILIZED SATELLITE M.S. Thesis
R. K. Adams Dec. 1993 138 p Limited Reproducibility: More than 20% of this document may be affected by microfiche quality
(AD-A273832; AFIT/GA/ENY/93D-1) Avail: CASI HC A07

This study compared an exact nonlinear model for the gravity gradient satellite to the two classical approximate models: the linearized model; and the truncated nonlinear model. These two models are typically used for analysis of the motion and stability of gravity gradient satellites. Rigid body dynamics using molecular mass models and circular orbits were assumed to isolate the comparison to the different models. The complete equations of motion of the exact nonlinear model resulted in more complex motions about the classical points of relative equilibria. DTIC

N94-25659# Air Force Inst. of Tech., Wright-Patterson AFB, OH. School of Engineering.
PROTOTYPE SPACE FABRICATION PLATFORM M.S. Thesis
James A. Bessel, James M. Ceney, David M. Crean, Edward A. Ingham, and David J. Pabst Dec. 1993 497 p
(AD-A273904; AFIT/GSE/ENY/93D-1) Avail: CASI HC A21/MF A04

Current plans for constructing large structures in space entail fabricating the primary components, such as truss segments, on the ground and assembling them in space. This process requires an exorbitant number of support missions, and methods to minimize the number must be considered. Whenever the space shuttle is launched, its external tank is jettisoned and destroyed prior to reaching orbit. This aerospace grade aluminum structure can be carried into orbit and utilized extrusively. The Prototype Space Fabrication Platform (SFP) fabricates aluminum materials, reduced from external tanks, into functional trusses. The trusses are strong and can be used as the primary components for future structures in space. The fabrication process produces a continuous truss allowing the end user to determine the length. The SFP can fabricate the same amount of truss from one external tank as four dedicated shuttle missions can deliver in the cargo bay. The SFP utilizes electrodynamic propulsion, via shielded coils, for maneuvering. The novel propulsion system facilitates a versatile payload transportation and delivery capability. The SFP can continuously track a target from all directions. The tracking system is ideal for docking since plume impingement is not a concern. With the assistance of remote manipulators, the SFP can deliver a payload in a wide variety of orientations. Under most conditions, the remote manipulator and maneuvering commands originate from ground workstations. Required manned presence is greatly reduced, and the time when the space shuttle is off station is effectively utilized. The logistical complications, currently inhibiting advancement in space, can be eliminated. DTIC

N94-25738# Air Force Inst. of Tech., Wright-Patterson AFB, OH.
AUTOMATING SATELLITE RANGE SCHEDULING M.S. Thesis
S. M. Schalck Dec. 1993 167 p
(AD-A273829; AFIT/GSO/ENS/93D-14) Avail: CASI HC A08/MF A02

The objective was to develop a computer based satellite range scheduling (SRS) algorithm to create a 24 hour satellite support schedule. The algorithm's goal was to schedule as many satellite support requests as possible. An iterative heuristic approach was used to schedule satellite support requests in three successive subproblems. The first subproblem involves scheduling low altitude satellite support requests using a mixed integer programming approach. The next two subproblems each involve scheduling 12 hour blocks of medium and high altitude satellite support requests, again using a mixed integer programming approach. Fourteen 24 hour schedules were generated using actual data with encouraging results. At least 95 percent of the satellite support requests were scheduled for each day. These results are in-line with results obtained by range schedulers and previous studies. Because of the promising results, this algorithm may be used to automate a portion of the satellite range scheduling problem. DTIC

N94-25776# Air Force Inst. of Tech., Wright-Patterson AFB, OH. School of Engineering.
MODAL CONTROL OF A SATELLITE IN AN UNSTABLE PERIODIC ORBIT ABOUT THE EARTH-SUN INTERIOR LAGRANGE POINT M.S. Thesis
Douglas J. Hopper Dec. 1993 95 p
(AD-A273707; AFIT/GA/ENY/93D-3) Avail: CASI HC A05/MF A01

A periodic 'halo' orbit which exists about the interior Lagrange point for the Earth-sun system was decomposed using Floquet theory into modal variables, which are dynamically decoupled subspaces for the six degree of freedom system. Modal control consisted of evaluating the diverging mode and maneuvering to counteract its divergence. In the unperturbed system, this was successful. Control costs were low, and the significance is that the controller did nothing to suppress modes that were oscillatory or converging. The effect of the moon's motion allowed the scheme to operate with reasonable control costs, but the effect of eccentricity caused divergence in spite of the controller. DTIC

N94-25832# Air Force Inst. of Tech., Wright-Patterson AFB, OH.
DESIGN ANALYSIS OF A COMBINED OPTICAL/LADAR DEEP-SPACE SURVEILLANCE SATELLITE M.S. Thesis
Bradley K. Fournier Dec. 1993 95 p
(AD-A274040; AFIT/GSO/Eng/93D-1) Avail: CASI HC A05/MF A01

This research determines the performance requirements of a combined optical/LADAR space-based system in order to detect and track deep-space satellites from a near-earth orbit satellite. The research derives the necessary equations to compare both direct and heterodyne detection techniques. The selection of the candidate laser systems is based on current space developed LADAR technology. The selection of the detector, detector size, and optic size are determined in order to maximize the signal-to-noise ratio. The analysis includes the effects of beam truncation, obscuration, pixel geometry, and background radiance. The results indicate that the direct detection technique with a GaA1As semiconductor laser and a charge-couple device detector provided the best signal-to-noise ratio for the range selected. In addition, the visible detection capability of the smallest entrance pupil system is compared with that of GEODSS. For the parameters chosen, the results indicate that this system should, on average, be able to detect objects of smaller size than GEODSS. DTIC

N94-25904# Air Force Inst. of Tech., Wright-Patterson AFB, OH. School of Engineering.
A VIRTUAL ENVIRONMENT FOR SATELLITE MODELING AND ORBITAL ANALYSIS IN A DISTRIBUTED INTERACTIVE SIMULATION M.S. Thesis
Andrea A. Kunz Dec. 1993 98 p
(AD-A274114; AFIT/GCS/ENG/93D-14) Avail: CASI HC A05/MF A02

In response to the need for a more realistic, interactive, and immersive space simulation system, the Joint National Intelligence Defense Staff (JNIDS) has sponsored the development of the Satellite Modeler at the Air Force Institute of Technology (AFIT). The Satellite Modeler (SM) is a virtual environment (VE) application that allows analyst-users to enter a virtual near-Earth space environment and visualize realistic satellite models performing accurate orbital motion. The Satellite Modeler provides manipulation functions that allow a user to interact with multiple satellite models and satellite constellations. The system affords the user multiple vantage points within the environment to view satellites in orbit. It also functions as a network actor in a distributed simulation environment. The Satellite Modeler achieves accurate physical modeling of satellite motion by using the North American Air Defense (NORAD) Command SGP4 orbital model and associated orbital elements for satellites currently in orbit. System functionality is realized within an object-oriented framework and accessible through a graphical user interface (GUI). This thesis is the second of a three-year effort to create a three dimensional virtual environment for modeling and manipulating satellite objects. DTIC

N94-25996# Air Force Inst. of Tech., Wright-Patterson AFB, OH. School of Engineering.
SATELLITE ATTITUDE DETERMINATION USING LINEAR COMBINATION OF MODELS M.S. Thesis
Martin S. Chin Dec. 1993 96 p
(AD-A274082; AFIT/GE-93D-05) Avail: CASI HC A05/MF A01

In satellite analysis, it is often necessary to determine the attitude of

a satellite from a two dimensional image of the satellite. This thesis describes work performed to determine the attitude of a satellite relative to a reference position. The attitude is described in terms of the scaling, rotation, and translation of the reference that will result in a pose that can be projected to form the image of interest. The techniques used are based on finding coefficients for the linear combination of basis images and decomposition of a composite transformation matrix. The methods were initially modeled in Mathematica and applied to simple objects, then implemented on a Silicon Graphics Workstation and applied to a model of an actual satellite. An accurate estimate of the pose of a satellite in a 2D image can be estimated based on the information contained in the image and a 3D model of the satellite or a set of images of the satellite at known orientations. Results of a performance analysis of the SGI implementation, a user's guide, source code in Mathematica and a software reference are included.
DTIC

N94-26103*# Lockheed Engineering and Sciences Co., Hampton, VA.
USER'S GUIDE FOR THE THERMAL ANALYST'S HELP DESK EXPERT SYSTEM
Rachel A. Ormsby Jan. 1994 63 p
(Contract NAS1-19000; RTOP 477-50-00-01)
(NASA-CR-194885; NAS 1.26:194885) Avail: CASI HC A04/MF A01

A guide for users of the Thermal Analyst's Help Desk is provided. Help Desk is an expert system that runs on a DOS based personal computer and operates within the EXSYS expert system shell. Help Desk is an analysis tool designed to provide users having various degrees of experience with the capability to determine first approximations of thermal capacity for spacecraft and instruments. The five analyses supported in Help Desk are: surface area required for a radiating surface, equilibrium temperature of a surface, enclosure temperature and heat loads for a defined position in orbit, enclosure temperature and heat loads over a complete orbit, and selection of appropriate surface properties. The two geometries supported by Help Desk are a single flat plate and a rectangular box enclosure.
Author (revised)

N94-26250# Technical Research Centre of Finland, Espoo. Instrument Lab.
MOUNTING OF SSM'S [SSM-PEILIEN KIINNITYS]
Juha Pohjonen Jan. 1993 25 p In FINNISH
(ISSN 1235-0605)
(VTT-TIED-1442; ISBN-951-38-4335-1; ETN-94-95265) Copyright Avail: CASI HC A03/MF A01

A step by step description of how to mount SSM's (Second Surface Mirrors) on the space instruments is presented. Experiences of the first SSM implementation are described. The Soho satellite has in its payload, an instrument ERNE, which has a radiation wing covered with SSM. SSM's are easy to use and reliable for thermal control design to space instruments. SSM's have a very small alpha(sub s) compared to the epsilon(sub n). The radiation from the Sun is reflected and at the same time the heat generated by the instrument is emitted to the space. This gives a good opportunity to tune the thermal control design according to the temperature.
ESA

N94-26532# Naval Postgraduate School, Monterey, CA.
A STUDY ON PIEZOELECTRIC ACTUATORS AND SENSORS FOR VIBRATION CONTROL OF FLEXIBLE SPACE STRUCTURES M.S. Thesis
Franklin D. Hixenbaugh 23 Sep. 1993 45 p
(AD-A274925) Avail: CASI HC A03/MF A01

The procedure for applying piezoelectric ceramic material to the Naval Postgraduate School's Flexible Spacecraft Simulator (FSS) for the purpose of active damping control is detailed. A step by step procedure to properly mount and test piezoelectric ceramic actuators and sensors is developed followed by performance demonstration by two control laws: Positive Position Feedback (PPF), and Proportional Derivative (PD). A digital controller for PD control is also developed.
DTIC

N94-26609*# National Aeronautics and Space Administration. Langley Research Center, Hampton, VA.
STRUCTURAL EVALUATION OF CONCEPTS FOR A SOLAR ENERGY CONCENTRATOR FOR SPACE STATION ADVANCED DEVELOPMENT PROGRAM
Winfred S. Kenner and Marvin D. Rhodes Feb. 1994 32 p
(RTOP 506-43-41-02)
(NASA-TP-3375; L-17239; NAS 1.60:3375) Avail: CASI HC A03/MF A01

Solar dynamic power systems have a higher thermodynamic efficiency than conventional photovoltaic systems; therefore they are attractive for long-term space missions with high electrical power demands. In an investigation conducted in support of a preliminary concept for Space Station Freedom, an approach for a solar dynamic power system was developed and a number of the components for the solar concentrator were fabricated for experimental evaluation. The concentrator consists of hexagonal panels comprised of triangular reflective facets which are supported by a truss. Structural analyses of the solar concentrator and the support truss were conducted using finite-element models. A number of potential component failure scenarios were postulated and the resulting structural performance was assessed. The solar concentrator and support truss were found to be adequate to meet a 1.0-Hz structural dynamics design requirement in pristine condition. However, for some of the simulated component failure conditions, the fundamental frequency dropped below the 1.0-Hz design requirement. As a result, two alternative concepts were developed and assessed. One concept incorporated a tetrahedral ring truss support for the hexagonal panels: the second incorporated a full tetrahedral truss support for the panels. The results indicate that significant improvements in stiffness can be obtained by attaching the panels to a tetrahedral truss, and that this concentrator and support truss will meet the 1.0-Hz design requirement with any of the simulated failure conditions.
Author (revised)

N94-26712# Toronto Univ., Downsview (Ontario). Inst. for Aerospace Studies.
SUBSTRUCTURE SYNTHESIS METHODS FOR VISCOELASTIC STRUCTURES
Duan Qian Sep. 1993 199 p
(ISSN 0082-5255)
(UTIAS-349; CTN-94-61012) Copyright Avail: CASI HC A09/MF A03

Viscoelastic damping models are necessary for accurate dynamic analysis of flexible aerospace structures. The method of substructure synthesis is extended to systems with general linear viscoelastic damping. The stationary variational principles for discrete symmetric and nonsymmetric viscoelastic systems are first developed in parallel for the time, Laplace, and frequency domain. The corresponding substructure synthesis methods are then formulated. On the basis of the Rayleigh-Ritz method, each substructure is represented by a set of admissible trial vectors. Real trial vectors, such as eigenvectors and Lanczos vectors of the corresponding undamped substructure as well as Ritz vectors obtained by spatial discretization of simple functions, are recommended. The geometric compatibility between substructures can be approximated by a weighted residual method, and the traditional state space formulation is avoided. The effort involved in the reduction process is almost independent of the complexity of viscoelastic models. Beam and plate examples are presented to illustrate the effectiveness of the substructure synthesis method in terms of reducing the size of final equations to obtain accurate solutions of eigenvalues, frequency responses, and transient responses for viscoelastic symmetric systems.
Author (CISTI)

N94-26750 Naval Postgraduate School, Monterey, CA.
A SURVEY OF UNCONTROLLED SATELLITE REENTRY AND IMPACT PREDICTION M.S. Thesis
Brian D. Neuenfeldt and William K. Henderson 23 Sep. 1993 268 p
Limited Reproducibility: More than 20% of this document may be affected by microfiche quality
(AD-A274903) Avail: CASI HC A12

The primary goal of this thesis is to identify the 'state of the art' in orbit decay induced uncontrolled reentry/impact prediction methods, with an emphasis on the physics of the final few revolutions to impact. This was accomplished through a comprehensive literature survey from the 1950's to the present of unclassified military and civil databases. The results of the survey show that the current U.S. and international reentry/impact prediction methodologies are based on analysis which is over 30 years old. Of the various 'extensions' to the current reentry theory, of which the NORAD method is recognized as the international standard, there does not appear to be any one method which is singularly superior to the others. It has also been shown that numerous reentry investigations made simplifying assumptions due to insufficient data needed to accurately model reentry and also because of computing limitations of their day. Also, current deterministic dynamic models appear to inadequately describe the actual uncontrolled reentry process, due to a lack of observational data, uncertainty in determining aerodynamic coefficients, atmospheric density, and point mass modeling where changes in vehicle configuration, attitude, and lift are neglected. Stochastic and statistical methods could be applied to the current methodology to better analyze the various uncertainties, which could help to improve the overall predicted impact time and location; however, further research into these methods along with the physics of uncontrolled reentry is necessary. DTIC

N94-26791*# Auburn Univ., AL.
PHYSICS OF DEBRIS CLOUDS FROM HYPERVELOCITY IMPACTS Final Report, 10 Apr. 1992 - 9 Oct. 1993
Ralph Zee 1993 70 p
(Contract NAS8-39131)
(NASA-CR-193932; NAS 1.26:193932) Avail: CASI HC A04/MF A01

The protection scheme developed for long duration space platforms relies primarily upon placing thin metal plates or 'bumpers' around flight critical components. The effectiveness of this system is highly dependent upon its ability to break up and redistribute the momentum of any particle which might otherwise strike the outer surface of the spacecraft. Therefore it is of critical importance to design the bumpers such that maximum dispersion of momentum is achieved. This report is devoted to an in-depth study into the design and development of a laboratory instrument which would permit the in-situ monitoring of the momentum distribution as the impact event occurs. A series of four designs were developed, constructed and tested culminating with the working instrument which is currently in use. Each design was individually tested using the Space Environmental Effects Facility (SEEF) at the Marshall Space Flight Center in Huntsville, Alabama. Along with the development of the device, an experimental procedure was developed to assist in the investigation of various bumper materials and designs at the SEEF. Preliminary results were used to compute data which otherwise were not experimentally obtainable. These results were shown to be in relative agreement with previously obtained values derived through other methods. The results of this investigation indicated that momentum distribution could in fact be measured in-situ as the impact event occurred thus giving a more accurate determination of the effects of experimental parameters on the momentum spread. Data produced by the instrument indicated a Gaussian-type momentum distribution. A second apparatus was developed and it was placed before the shield in the line of travel utilized a plate to collect impact debris scattered backwards. This plate had a passage hole in the center to allow the particle to travel through it and impact the proposed shield material. Applying the law of conservation of angular momentum a backward momentum vector was determined from the angular velocity of the plate. The forward scattered and backward scattered momentum values were then analyzed to judge the distribution of debris. Loss of momentum was attributed to the inaccuracies of the means of measurement. Assumptions of symmetrical debris for the forward and backward scattered directions also contributed to this loss. Author

N94-26808# Los Alamos National Lab., NM.
A SPACE FIBER-OPTIC X RAY BURST DETECTOR
C. E. Moss, D. E. Casperson, M. A. Echave, B. C. Edwards, J. R. Miller, W. W. Saylor, M. R. Sweet, and J. E. Valencia Oct. 1993 6 p
Presented at the Nuclear Science Symposium, San Francisco, CA, 2-5 Nov. 1993
(Contract W-7405-eng-36)
(DE94-002722; LA-UR-93-3807; CONF-931107-7) Avail: CASI HC A02/MF A01

We describe a novel, lightweight x-ray burst detector that can be embedded in a satellite structure, thus forming a 'smart skin,' which has minimal impact on the host satellite. The design is based on two types of optical fibers coupled to photodiodes. The first is a scintillating fiber, which gives a fast signal for timing. The second is a germanium-doped silica fiber, which darkens for a few milliseconds when irradiated with a burst of x rays. The resulting slow signal is used to discriminate against electrostatic discharges. The coincidence of a fast signal from the scintillating fiber with a slow signal from the darkening fiber is the signature of an x-ray burst. The response is linear at low doses and becomes nonlinear at high doses. We have two techniques to test the instrument in a space experiment scheduled for 1994. First, a small, space-qualified flash x-ray unit can illuminate the fibers. Second, we can detect space background radiation. The cumulative dose will be monitored by RADFET dosimeters. Future work on embedding the fibers and the electronics as Application Specific Integrated Circuits (ASIC's) in the spacecraft skin could lead to use of these detectors on many satellites. DOE

N94-27357# Instituto de Pesquisas Espaciais, Sao Jose dos Campos (Brazil).
DYNAMICS AND ROBUST CONTROL FOR UNCERTAIN FLEXIBLE SPACE SYSTEMS
L. C. Gadelha DeSouza (Cranfield Inst. of Tech., Bedford, England.) Sep. 1992 261 p
(INPE-5510-TAE/020) Avail: CASI HC A12/MF A03

The uncertain nature of the dynamics of flexible space structures makes sensitivity and robustness questions of great importance when designing control systems, mainly, because nominal performance and robust stability are conflicting objectives in control systems design. A coupled rigid body/flexible structural dynamics model of the MB-1 Space Station configuration is developed and employed to investigate such important issues arising in robust control design. Selection of a reduced order model plays an important role in flexible spacecraft control leading to expected errors between the design model and the actual system. On the other hand, the inability of ground testing of large flexible structure for model verification leads to structural parameters which can possess appreciable errors. An asymptotic Linear Quadratic Gaussian (LQG) design procedure based on a modified version of the Parameter Robust Linear Quadratic Gaussian (PRLQG) approach is developed for designing a robust controller that accounts for unmodelled dynamics and parameter uncertainty for multi-input multi-output systems. The unmodelled dynamics are assumed to be characterized as a single block dynamic uncertainty at a point in the closed-loop system. Plant parameter variations are represented as an internal feedback loop via the input-output decomposition. A direct structural relationship between parameter uncertainties and the weighting matrices in the design of the LQG controller is exploited. This robust control design procedure is then applied to design a robust controller for attitude control and vibration suppression of the MB-1 Space Station model taking into account this mixed uncertainty model. This yields considerable improvement in robustness with respect to parameter variation without affecting the level of nominal performance and robustness with respect to unmodelled dynamics achieved. Extensive control simulations have shown that even under severe dynamic initial conditions the controller was able to impose quick convergence properties to the system. Author

N94-27382# General Accounting Office, Washington, DC.
SPACE PROJECTS: ASTROPHYSICS FACILITY PROGRAM CONTAINS COST AND TECHNICAL RISKS. REPORT TO CONGRESSIONAL REQUESTERS
David R. Warren 28 Jan. 1994 16 p
(GAO/NSIAD-94-80; B-255776) Avail: CASI HC A03/MF A01; GAO, P.O. Box 6015, Gaithersburg, MD 20877 HC

NASA is developing the Advanced X-ray Astrophysics Facility (AXAF) to be one of the mainstays of this nation's space science program during the next decade. It is to be used to investigate important questions such as the age and origin of the universe. The status of the 1992 redesigned AXAF program is reviewed to assess the reasonableness of NASA's estimate of program costs and to determine the extent to which the redesign will provide scientific returns comparable to the original program. It is recognized that a recent congressional direction may affect a portion of this program, but the cost and technical impacts of that decision are uncertain at this time. However, the results of the work in other segments of the program are still relevant. Derived from text

N94-27397# European Space Agency. European Space Research and Technology Center, ESTEC, Noordwijk (Netherlands). Product Assurance and Safety Dept./Automation and Informatics.
THE RADIATION DESIGN HANDBOOK
May 1993 444 p
(ISSN 0379-4059)

(ESA-PSS-01-609-Issue-1; ETN-94-95286) Copyright Avail: CASI HC A19/MF A04

A handbook which provides general engineering guidelines suitable for project groups engaged in the design of spacecraft required to operate in regions of space where they will be exposed to significant doses of radiation is presented. The charged particle environment in geomagnetospheric space, and the physics of radiation effects on solid state devices and materials (including ionization effects, single event upsets and bulk displacement damage) in all the designs of devices likely to be used in spacecraft are discussed. Methods of assessing the impact of these effects are given, including procedures for calculating the orbital radiation environment, dose depth curves within electronic enclosures, and the end of life degradation of devices and circuits. While no rigid procedures for handling these problems can be set out, special attention is given to methods of alleviating the problems presented. These methods cover tradeoff studies of orbit versus shield weight, layout rules for spacecraft, the use of redundancy and housekeeping dosimetry, device selection, device verification, and the design of radiation tolerant circuits. ESA

N94-27421*# AC, Inc., Huntsville, AL.

DEVELOPMENT AND APPLICATION OF CONTAMINATION TECHNOLOGY FOR MSFC MANAGED SPACE SYSTEMS Annual Progress Report, 10 Dec. 1992 - 10 Dec. 1993

1993 93 p Prepared in cooperation with Science Applications International Corp., Huntsville, AL
(Contract NAS8-39244)
(NASA-CR-193934; NAS 1.26:193934) Avail: CASI HC A05/MF A01

The second annual report on the development and application of contamination technology for MSFC managed space systems covering the period from 10 Dec. 1992 to 10 Dec. 1993 is presented. During this time period, studies were concluded which proved that in-process corrosion protection is not required during Redesigned Solid Rocket Motor (RSRM) case processing. Also completed were a series of tests evaluating the effects of environmental exposure and contamination on 2219-T87 aluminum (Space Shuttle External Tank) OSEE response and bonding properties. Correlations were developed between OSEE response, contamination type/level, and primer adhesion. The results showed that the wet tape and water break free tests currently employed during ET processing may not detect bond affecting levels of some potential contaminants; however, the contaminants were detected with OSEE analysis. Finally, exposure/contamination studies were initiated with HP9-4-30 steel. HP9-4-30 was selected for evaluation because it represents a class of metals commom to MSFC managed space flight systems which are less prone to oxidation than D6AC steel or aluminum. Author (revised)

N94-27775*# National Aeronautics and Space Administration. Lyndon B. Johnson Space Center, Houston, TX.

THE TMIS LIFE-CYCLE PROCESS DOCUMENT, REVISION A

Nov. 1991 42 p
(NASA-TM-109698; NAS 1.15:109698; SSP-30542-Rev-A) Avail: CASI HC A03/MF A01

The Technical and Management Information System (TMIS) Life-Cycle Process Document describes the processes that shall be followed in the definition, design, development, test, deployment, and operation of all TMIS products and data base applications. This document is a roll out of TMIS Standards Document (SSP 30546). The purpose of this document is to define the life cycle methodology that the developers of all products and data base applications and any subsequent modifications shall follow. Included in this methodology are descriptions of the tasks, deliverables, reviews, and approvals that are required before a product or data base application is accepted in the TMIS environment. Derived from text

N94-27789*# Maryland Univ., College Park. Dept. of Aerospace Engineering.

A PARAMETRIC SENSITIVITY STUDY FOR SINGLE-STAGE-TO-ORBIT HYPERSONIC VEHICLES USING TRAJECTORY OPTIMIZATION

T. Alan Lovell and D. K. Schmidt 21 Mar. 1994 38 p
(Grant NAG1-1540)
(NASA-CR-195703; NAS 1.26:195703) Avail: CASI HC A03/MF A01

The class of hypersonic vehicle configurations with single stage-to-orbit (SSTO) capability reflect highly integrated airframe and propulsion systems. These designs are also known to exhibit a large degree of interaction between the airframe and engine dynamics. Consequently, even simplified hypersonic models are characterized by tightly coupled nonlinear equations of motion. In addition, hypersonic SSTO vehicles present a major system design challenge; the vehicle's overall mission performance is a function of its subsystem efficiencies including structural, aerodynamic, propulsive, and operational. Further, all subsystem efficiencies are interrelated, hence, independent optimization of the subsystems is not likely to lead to an optimum design. Thus, it is desired to know the effect of various subsystem efficiencies on overall mission performance. For the purposes of this analysis, mission performance will be measured in terms of the payload weight inserted into orbit. In this report, a trajectory optimization problem is formulated for a generic hypersonic lifting body for a specified orbit-injection mission. A solution method is outlined, and results are detailed for the generic vehicle, referred to as the baseline model. After evaluating the performance of the baseline model, a sensitivity study is presented to determine the effect of various subsystem efficiencies on mission performance. This consists of performing a parametric analysis of the basic design parameters, generating a matrix of configurations, and determining the mission performance of each configuration. Also, the performance loss due to constraining the total head load experienced by the vehicle is evaluated. The key results from this analysis include the formulation of the sizing problem for this vehicle class using trajectory optimization, characteristics of the optimal trajectories, and the subsystem design sensitivities. Author (revised)

N94-28183*# National Aeronautics and Space Administration. Lyndon B. Johnson Space Center, Houston, TX.

AN ANALYSIS OF THE LOADS APPLIED TO A HEAVY SPACE STATION RACK DURING TRANSLATION AND ROTATION TASKS

Lara E. Stoycos (Lockheed Engineering and Sciences Co., Houston, TX.) and Glenn K. Klute Feb. 1994 29 p
(NASA-TM-104790; S-760; NAS 1.15:104790) Avail: CASI HC A03/MF A01

To prepare for Space Station Alpha's on-orbit assembly, maintenance, and resupply, NASA requires information about the crew members' ability to move heavy masses on orbit. Ease of movement in microgravity and orbiter stay time constraints may change the Space Station equipment and outfitting design requirements. Therefore, the time and effort required to perform a particular task and how and where the forces and torque should be applied become critical in evaluating the design effort. Thus, the three main objectives of this investigation were to: (1) quantify variables such as force and torque as they relate to heavy mass handling techniques; (2) predict the time required to perform heavy mass handling tasks; and (3) note any differences between males and females in their ability to manipulate a heavy mass. Author

N94-25667*# Arizona Univ., Tucson. Dept. of Aerospace and Mechanical Engineering.

AUTONOMOUS SPACE PROCESSOR FOR ORBITAL DEBRIS ADVANCED DESIGN PROJECT IN SUPPORT OF SOLAR SYSTEM EXPLORATION

Kumar Ramohalli, Dominique Mitchell, Brett Taft, Paul Chinnock, and Bjoern Kutz *In* USRA, Proceedings of the 8th Annual Summer Conference: NASA/USRA Advanced Design Program 1992 p 6-17 (For primary document see N94-25665 07-80)
Avail: CASI HC A03/MF A04

N94-25671*# University of Central Florida, Orlando. Dept. of Mechanical and Aerospace Engineering.

ASSURED CREW RETURN VEHICLE POST LANDING CONFIGURATION DESIGN AND TEST

Loren A. Anderson and Pamela Kay Armitage *In* USRA, Proceedings of the 8th Annual Summer Conference: NASA/USRA Advanced Design Program 1992 p 31-39 (For primary document see N94-25665 07-80)
Avail: CASI HC A02/MF A04

N94-25699*# Naval Academy, Annapolis, MD. Dept. of Aerospace Engineering.

LOW-COST UNMANNED LUNAR LANDER

Walter K. Daniel *In* USRA, Proceedings of the 8th Annual Summer

Conference: NASA/USRA Advanced Design Program 1992 p 271-273 (For primary document see N94-25665 07-80)
Avail: CASI HC A01/MF A04

N94-25700*# Naval Postgraduate School, Monterey, CA. Space Systems Academic Group.
HIGH TEMPERATURE SUPERCONDUCTING INFRARED IMAGING SATELLITE
B. Angus, J. Covelli, N. Davinic, J. Hailey, E. Jones, V. Ortiz, J. Racine, D. Satterwhite, T. Spriesterbach, and D. Sorensen et al *In* USRA, Proceedings of the 8th Annual Summer Conference: NASA/USRA Advanced Design Program 1992 p 274-286 (For primary document see N94-25665 07-80)
Avail: CASI HC A03/MF A04

N94-25701*# Naval Postgraduate School, Monterey, CA. Space Systems Academic Group.
LOW EARTH ORBIT COMMUNICATIONS SATELLITE
D. Moroney, D. Lashbrook, B. McKibben, N. Gardener, T. Rivers, G. Nottingham, B. Golden, B. Barfield, J. Bruening, and D. Wood et al *In* USRA, Proceedings of the 8th Annual Summer Conference: NASA/USRA Advanced Design Program 1992 p 287-297 (For primary document see N94-25665 07-80)
Avail: CASI HC A03/MF A04

N94-26283*# National Aeronautics and Space Administration. Goddard Space Flight Center, Greenbelt, MD.
PERFORMANCE MEASURES FROM THE EXPLORER PLATFORM BERTHING EXPERIMENT
Stephen Leake *In* NASA. Langley Research Center, Selected Topics in Robotics for Space Exploration Dec. 1993 p 73-94 (For primary document see N94-26278 07-12)
Avail: CASI HC A03/MF A03

N94-26284*# National Aeronautics and Space Administration. Langley Research Center, Hampton, VA.
BERTHING OF SPACE STATION FREEDOM USING THE SHUTTLE REMOTE MANIPULATOR SYSTEM
Paul Cooper and Martha E. Demeo (Vigyan Research Associates, Inc., Hampton, VA.) *In its* Selected Topics in Robotics for Space Exploration Dec. 1993 p 95-123 (For primary document see N94-26278 07-12)
Avail: CASI HC A03/MF A03

N94-26286*# National Aeronautics and Space Administration. Langley Research Center, Hampton, VA.
AUTONOMOUS RENDEZVOUS AND DOCKING FOR SPACE STATION FREEDOM
James L. Garrison, Jr. and Stephen J. Katzberg *In its* Selected Topics in Robotics for Space Exploration Dec. 1993 p 173-191 (For primary document see N94-26278 07-12)
Avail: CASI HC A03/MF A03

N94-26288*# National Aeronautics and Space Administration. Ames Research Center, Moffett Field, CA.
SIMULATION MODELING FOR LONG DURATION SPACECRAFT CONTROL SYSTEMS
Mark A. Boyd and Salvatore J. Bavuso (National Aeronautics and Space Administration. Langley Research Center, Hampton, VA.) *In* NASA. Langley Research Center, Selected Topics in Robotics for Space Exploration Dec. 1993 p 213-221 (For primary document see N94-26278 07-12)
Avail: CASI HC A02/MF A03

N94-27368*# National Aeronautics and Space Administration, Washington, DC.
SPACE STATION TECHNOLOGY TESTBED: 2010 DEEP SPACE TRANSPORT
Alan C. Holt *In* NASA. Lewis Research Center, Vision 21: Interdisciplinary Science and Engineering in the Era of Cyberspace Dec. 1993 p 127-151 (For primary document see N94-27358 07-12)
Avail: CASI HC A03/MF A03

N94-28020# Laboratoire d'Aerothermique du CNRS, Meudon (France).
CONTROL JETS IN INTERACTION WITH HYPERSONIC RAREFIED FLOW [JETS TRANSVERSAUX EN INTERACTION AVEC DES ECOULEMENTS HYPERSONIQUES RAREFIES]
J. Allegre and M. Raffin *In* AGARD, Computational and Experimental Assessment of Jets in Cross Flow Nov. 1993 9 p In FRENCH Sponsored by ESA (For primary document see N94-28003 07-34)
Copyright Avail: CASI HC A02/MF A04

19 SPACECRAFT INSTRUMENTATION

For related information see also *06 Aircraft Instrumentation* and *35 Instrumentation and Photography.*

N94-26223 Air Force Inst. of Tech., Wright-Patterson AFB, OH. School of Engineering.
AN APPROXIMATE SOLUTION FOR THE SPINUP DYNAMICS OF NEAR AXISYMMETRIC AXIAL GYROSTATS USING THE METHOD OF MULTIPLE SCALES M.S. Thesis
Stewart J. Kowall Dec. 1993 125 p Limited Reproducibility: More than 20% of this document may be affected by microfiche quality
(AD-A273723; AFIT/GA/ENY/93D-5) Avail: CASI HC A06

Approximate solutions for the spinup of a near axisymmetric gyrostat are derived using the straightforward expansion method and the method of multiple scales. Two method of multiple scale solutions are presented. The first is derived using cartesian coordinates while the second is derived using cylindrical coordinates. The multiple scales solutions are compared to numerically integrated results for oblate and prolate configurations. A comparison for flat spin recovery is also accomplished. Excellent results are obtained for oblate configurations. Trajectory separatrix crossings hindered the results for prolate configurations and flat spin recoveries.
DTIC

N94-28200# RADEX, Inc., Bedford, MA.
MODELING THE DMSP AND CRRES DOSIMETERS USING THE PATH LENGTH DISTRIBUTION METHOD Report No. 3
C. A. Hein and J. N. Bass 14 May 1993 106 p
(Contract F19628-90-C-0090)
(RXR-93051; PL-TR-93-2120) Avail: CASI HC A06/MF A02

The Path Length Distribution method is used to model the performance of the dosimeter instruments used aboard the DMSP and CRRES satellites. The Monte Carlo methods used to compute the path length distributions for the isotropic, mirror plan, and sin exp N alpha pitch angle proton angular distributions are used to compute the instrument proton flux and dose count response functions and geometric factors for power law and Maxwellian proton energy spectra. Comparisons of the geometric factor computations using the path length method with the infinite slab approximation and the truncated infinite slab path length distribution are also made. Tables and graphs of modeled instrument performance are provided. Author (revised)

N94-28210# Panametrics, Inc., Waltham, MA.
DEVELOP AND FABRICATE A RADIATION DOSE MEASUREMENT SYSTEM FOR SATELLITES Report No. 3
Paul R. Morel, Frederick Hanser, Jeff Belue, and Ram Cohen Jul. 1993 44 p
(Contract F19628-90-C-0147)
(PL-TR-93-2161) Avail: CASI HC A03/MF A01

A second generation dosimeter has been designed to fulfill the need for accurate radiation dose measurements. Two identical dosimeters, a flight unit and a backup unit, are being fabricated, tested, and calibrated. The flight dosimeter is to be integrated into the payload of the Advanced Photovoltaic and Electronic Experiments (APEX) satellite, as part of the Photovoltaic Array Space Power Plus Diagnostics (PASP Plus) experiment.
Author (revised)

N94-28217# Panametrics, Inc., Waltham, MA.
DEVELOP AND FABRICATE A RADIATION DOSE MEASUREMENT SYSTEM FOR SATELLITES Report No. 2
Paul R. Morel, Frederick Hanser, Jeff Belue, and Ram Cohen Apr. 1993

41 p
(Contract F19628-90-C-0147)
(PL-TR-93-2099) Avail: CASI HC A03/MF A01

A second-generation dosimeter has been designed to fulfill the need for accurate radiation dose measurements. Two identical dosimeters, a flight unit and a backup unit, are being fabricated, tested and calibrated. The flight dosimeter is to be integrated into the payload of the Advanced Photovoltaic Electronic Experiment (APEX) satellite, as part of the Photovoltaic Array Space Power Plus Diagnostics (PASP Plus) experiment. Author

20 SPACECRAFT PROPULSION AND POWER

Includes main propulsion systems and components, e.g., rocket engines; and spacecraft auxilliary power sources.

For related information see also *07 Aircraft Propulsion and Power, 28 Propellants and Fuels, 44 Energy Production and Conversion,* and *15 Launch Vehicles and Space Vehicles.*

N94-25600# Sandia National Labs., Albuquerque, NM.
CHARACTERISTICS AND CONTROL RESPONSE OF THE TOPAZ 2 REACTOR SYSTEM REAL-TIME DYNAMIC SIMULATOR
K. S. Kwok 12 Nov. 1993 7 p Presented at the 11th Symposium on Space Nuclear Power Systems, Albuquerque, NM, 9-13 Jan. 1994
(Contract DE-AC04-94AL-85000)
(DE94-003788; SAND-93-2695C; CONF-940101-25) Avail: CASI HC A02/MF A01

A dynamic simulator of the TOPAZ 2 reactor system has been developed for the Nuclear Electric Propulsion Space Test Program. The simulator combines first-principle modeling and empirical correlations in its algorithm to attain the modeling accuracy and computational through-put that are required for real-time execution. The overall execution time of the simulator for each time step is 15 ms when no data is written to the disk and 18 ms when nine double precision data points are written to the disk once in every time step. The simulation program has been tested, and it is able to handle a step decrease of 8 dollars worth of reactivity. It also provides simulations of fuel, emitter, collector, stainless steel, and ZrH moderator failures. Presented in this paper are the models used in the calculations, a sample simulation session, and a discussion of the performance and limitations of the simulator. The simulator has been found to provide realistic real-time dynamic response of the TOPAZ 2 reactor system under both normal and casualty conditions. DOE

N94-25613# Los Alamos National Lab., NM.
A REVIEW OF CARBIDE FUEL CORROSION FOR NUCLEAR THERMAL PROPULSION APPLICATIONS
Dennis G. Pelaccio (New Mexico Univ., Albuquerque.), Mohamed S. El-Genk (New Mexico Univ., Albuquerque.), and Darryl P. Butt 1993 14 p Presented at the 11th Symposium on Space Nuclear Power Systems, Albuquerque, NM, 9-13 Jan. 1994
(Contract W-7405-eng-36)
(DE94-003938; LA-UR-93-4136; CONF-940101-26) Avail: CASI HC A03/MF A01

At the operation conditions of interest in nuclear thermal propulsion reactors, carbide materials have been known to exhibit a number of life limiting phenomena. These include the formation of liquid, loss by vaporization, creep and corresponding gas flow restrictions, and local corrosion and fuel structure degradation due to excessive mechanical and/or thermal loading. In addition, the radiation environment in the reactor core can produce a substantial change in its local physical properties, which can produce high thermal stresses and corresponding stress fractures (cracking). Time-temperature history and cyclic operation of the nuclear reactor can also accelerate some of these processes. The University of New Mexico's Institute for Space Nuclear Power Studies, under NASA sponsorship has recently initiated a study to model the complicated hydrogen corrosion process. In support of this effort, an extensive review of the open literature was performed, and a technical expert workshop was conducted. This paper summarizes the results of this review. DOE

N94-25638# European Space Agency, Paris (France).
ABLATION OF SOLID-PROPELLANT ROCKET-MOTOR NOZZLE MATERIALS
V. Borie (Office National d'Etudes et de Recherches Aerospatiales, Paris, France.) May 1993 306 p Transl. into ENGLISH of Ablation des Materiaux de Tuyeres de Propulseurs a Propergol Solide (Paris, France, ONERA) 1990 p 1-247 Original language document announced as N92-28780
(ESA-TT-1289; ONERA-NT-1990-13; ETN-94-95197) Avail: CASI HC A14/MF A03

An aerothermochemical analysis of the ablation of carbon-carbon materials located at the nozzle throats of large rocket motors was developed. This analysis includes the calculation of the equilibrium characteristics of the combustion products in the chamber, the calculation of the characteristics in the inviscid part of the flow in the nozzle, the determination of the convective transfer coefficients along the walls of the nozzle, the acquisition of experimental data concerning the ablation rates and the surface roughness of the carbon-carbon materials constituting the nozzle throats, a description of the chemical attack of these materials by the aggressive species present in the combustion products of the solid propellants, and the computer evaluation of the heat transfer and of the ablation of large rocket motor nozzle throats. The experimental results obtained are compared with the experimental data of the same type provided in the literature concerning the ablation of carbon materials. The computed results are in good agreement with the measured ablations on large scale rocket motors when the hypothesis of a transition between a laminar boundary layer flow existing on a virgin material and a turbulent boundary layer flow existing on very rough material during ablation is made in the modeling. ESA

N94-25798# Brookhaven National Lab., Upton, NY.
SMALL LOW MASS ADVANCED PBR'S FOR BI-MODAL OPERATION
H. Ludewig, M. Todosow, and J. R. Powell 1 Oct. 1993 6 p Presented at the 11th Symposium on Space Nuclear Power Systems, Albuquerque, NM, 9-13 Jan. 1994
(Contract DE-AC02-76CH-00016)
(DE94-003201; BNL-49663; CONF-940101-23) Avail: CASI HC A02/MF A01

A preliminary assessment is made of a low mass bimodal reactor for use as a propulsion unit and as a heat source for generating electricity. This reactor is based on the particle bed reactor (PBR) concept. It will be able to generate both thrust and electricity simultaneously. This assessment indicates that the reactor can generate approximately 6.8 (4) N of thrust using hydrogen as a coolant and 100 KWe using a closed Brayton cycle (CBC) power conversion system. Two cooling paths pass through the reactor allowing a simultaneous operation of both modes. The development of all the components for this reactor are within the experience base of the NTP project. DOE

N94-25926# Johns Hopkins Univ., Laurel, MD. Applied Physics Lab.
PRELIMINARY REENTRY SAFETY ASSESSMENT OF THE GENERAL PURPOSE HEAT SOURCE MODULE FOR THE CASSINI MISSION: AEROSPACE NUCLEAR SAFETY PROGRAM
D. W. Conn and P. T. Brenza Apr. 1993 57 p
(Contract DE-AI01-93NE-32170)
(DE94-001646; DOE/NE-32170/23; ANSP-M-23) Avail: CASI HC A04/MF A01

As asked by the U.S. Department of Energy/Office of Special Applications, and in support of the Environmental Impact Statement for the Cassini mission, The Johns Hopkins University/Applied Physics Laboratory (JHU/APL) has conducted preliminary one dimensional ablation and thermal analyses of the General Purpose Heat Source (GPHS). The predicted earth entry conditions provided by the Jet Propulsion Laboratory (JPL) for a Cassini Venus - Venus - Earth - Jupiter gravity assist (VVEJGA) trajectory were used as initial conditions. The results of this study, which constitute the initial reentry analysis assessment leading to the Cassini Updated Safety Analysis Report (USAR), are discussed in this document. DOE

N94-25929# Space Power, Inc., San Jose, CA.
SPACE-R THERMIONIC SPACE NUCLEAR POWER SYSTEM: DESIGN AND TECHNOLOGY DEMONSTRATION
Oct. 1993 13 p

(Contract DE-AC03-92SF-19441)
(DE94-001890; DOE/SF-19441/T5) Avail: CASI HC A03/MF A01 (US Sales Only)

The preferred moderator being considered for SPACE-R is yttrium hydride encased in beryllium tubes. The baseline beryllium performs a dual function as it acts as a moderator and provides containment for hydrogen. The permeation rate of hydrogen from the hydride through the beryllium shell at the operating temperature is an important factor for the functionality and reliability of the Be-YHx moderator. Hydrogen containment capability of beryllium is comparable to enamel which was used in SNAP and Topaz 2 reactors. However, limited experimental data base exists for the hydrogen permeation through fabricated beryllium enclosures at high temperature. Permeation of hydrogen in beryllium is strongly affected by surface conditions, thickness of surface oxide, surface and bulk traps, impurity content, and microstructure. The objective of this experiment is to determine the permeation rate of hydrogen from yttrium hydride and zirconium hydride through beryllium in the temperature range of 773 to 973 K. In addition, Topaz 2 type zirconium hydride specimens with and without the proprietary oxide coating canned in stainless steel will be tested to measure the hydrogen permeation rate. The thermionic system evaluation test (TSET) stainless steel canned ZrHx samples currently at Phillips Laboratory will be used for the latter test with Phillips Laboratory participation at the Space Power, Incorporated, hydrogen leak test stand. A key technology demonstration of the effectiveness of transferred arc plasma spraying of a 1 mil molybdenum coating on the Be cladding will be performed. The effectiveness of the molybdenum coating in preventing any interaction of Be with stainless steel in NaK will be assessed and demonstrated. DOE

N94-25930# Space Power, Inc., San Jose, CA.
SPACE-R THERMIONIC SPACE NUCLEAR POWER SYSTEM DESIGN AND TECHNOLOGY DEMONSTRATION
Oct. 1993 66 p
(Contract DE-AC03-92SF-19441)
(DE94-002017; DOE/SF-19441/T6) Avail: CASI HC A04/MF A01 (US Sales Only)

This document provides the INERTEK experimental test plans for the SPACE-R thermionic space nuclear power system. These plans are: monocrystal alloy one dimensional creep test, monocrystal alloy two dimensional creep test, fuel specimen in-pile test, moderator irradiation test, demonstration of high performance single cell thermionic fuel element (TFE) without fuel, and long cell fuel element irradiation demonstration. DOE

N94-25956# Sandia National Labs., Albuquerque, NM.
RISK PERSPECTIVES FOR TOPAZ 2 FLIGHT MISSION
A. C. Payne, Jr. and F. E. Haskin (New Mexico Univ., Albuquerque.) 1993 6 p Presented at the 11th Symposium on Space Nuclear Power Systems, Albuquerque, NM, 9-13 Jan. 1994
(Contract DE-AC04-94AL-85000)
(DE94-003229; SAND-93-2297C; CONF-940101-20) Avail: CASI HC A02/MF A01

The purpose of this paper is to present a preliminary estimate of the nuclear-related public health risk presented by launching and operating the Russian Topaz 2 space reactor as part of the Nuclear Electric Propulsion Space Test Program (NEPSTP). This risk is then compared to the risks from the operation of commercial nuclear power reactors and previously planned and/or launched space nuclear power missions. For the current mission profile, the initial estimate of the risk posed by launching and operating Topaz 2 is significantly less (at least two orders of magnitude) than that estimated for prior space nuclear missions. Even allowing for the large uncertainties in this estimate, it does not appear that the NEPSTP mission will present a significant health risk to the public. DOE

N94-25969# Jet Propulsion Lab., California Inst. of Tech., Pasadena.
NUCLEAR ELECTRIC PROPULSION FOR FUTURE NASA SPACE SCIENCE MISSIONS
Chen-wan L. Yen 20 Jul. 1993 65 p
(Contract DE-AI03-91SF-19043)
(DE93-019086; DOE/SF-19043/T4; JPL-PUB-D-10689) Avail: CASI HC A04/MF A01

This study was made to assess the needs, potential benefits and the applicability of early (circa year 2000) Nuclear Electric Propulsion (NEP) technology in conducting NASA science missions. The study goals are: to obtain the performance characteristics of near term NEP technologies; to measure the performance potential of NEP for important OSSA missions; to compare NEP performance with that of conventional chemical propulsion; to identify key NEP system requirements; to clarify and depict the degree of importance NEP might have in advancing NASA space science goals; and to disseminate the results in a format useful to both NEP users and technology developers. This is a mission performance study and precludes investigations of multitudes of new mission operation and systems design issues attendant in a NEP flight. DOE

N94-26090*# National Aeronautics and Space Administration. Lewis Research Center, Cleveland, OH.
AN INVESTIGATION OF MAGNETIC FIELD EFFECTS ON PLUME DENSITY AND TEMPERATURE PROFILES OF AN APPLIED-FIELD MPD THRUSTER
S. Ray Bullock and R. M. Myers (Sverdrup Technology, Inc., Brook Park, OH.) Jan. 1994 14 p Presented at the 23rd International Electric Propulsion Conference, Seattle, WA, 13-16 Sep. 1993; sponsored by AIAA
(Contract NAS3-25266; RTOP 506-42-31)
(NASA-TM-106416; E-8253; NAS 1.15:106416; IEPC-93-140) Avail: CASI HC A03/MF A01

Applied-field magnetoplasmadynamic (MPD) thruster performance is below levels required for primary propulsion missions. While MPD thruster performance has been found to increase with the magnitude of the applied-field strength, there is currently little understanding of the impact of applied-field shape on thruster performance. The results of a study in which a single applied-field thruster was operated using three solenoidal magnets with diameters of 12.7, 15.2, and 30.4-cm are presented. Thruster voltage and anode power deposition were measured for each applied field shape over a range of field strengths. Plume electron number density and temperature distributions were measured using a Langmuir probe in an effort to determine the effect of field shape on plume confinement by the diverging magnetic-field for each of the three magnetic field shapes. Results show that the dependence of the measured thruster characteristics on field shape were non-monotonic and that the field shape had a significant effect on the plume density and temperature profiles. Author

N94-26156*# Rockwell International Corp., Canoga Park, CA. Rocketdyne Div.
ORBIT TRANSFER ROCKET ENGINE TECHNOLOGY PROGRAM ENHANCED HEAT TRANSFER COMBUSTOR TECHNOLOGY Final Report, Jan. 1986 - Dec. 1991
William S. Brown Dec. 1991 143 p
(Contract NAS3-23773)
(NASA-CR-189236; NAS 1.26:189236; RI/RD91-235) Avail: CASI HC A07/MF A02

In order to increase the performance of a high performance, advanced expander-cycle engine combustor, higher chamber pressures are required. In order to increase chamber pressure, more heat energy is required to be transferred to the combustor coolant circuit fluid which drives the turbomachinery. This requirement was fulfilled by increasing the area exposed to the hot-gas by using combustor ribs. A previous technology task conducted 2-d hot air and cold flow tests to determine an optimum rib height and configuration. In task C.5 a combustor calorimeter was fabricated with the optimum rib configuration, 0.040 in. high ribs, in order to determine their enhancing capability. A secondary objective was to determine the effects of mixture ratio changers on the enhancement during hot-fire testing. The program used the Rocketdyne Integrated Component Evaluator (ICE) reconfigured into a thrust chamber only mode. The test results were extrapolated to give a projected enhancement from the ribs for a 16 in. long cylindrical combustor at 15 Klb nominal thrust level. The hot-gas wall ribs resulted in a 58 percent increase in heat transfer. When projected to a full size 15K combustor, it becomes a 46 percent increase. The results of those tests, a comparison with previous 2-d results, the effects of mixture ratio and combustion gas flow on the ribs and the potential ramifications for expander cycle combustors are detailed. Author

N94-26166 Gosudarstvennyi Komitet po Ispolzovaniyu Atomnoi Energii, Obninsk (USSR). Fiziko-Ehnergeticheskij Inst.
PARAMETRIC ANALYSIS OF THE SPACE POWER PLANTS ON THE BASE OF CRITERION OF SPECIFIC MASS IN GENERALIZED DESIGN VARIANTS [PARAMETRICHESKIJ ANALIZ KOSMICHESKIKH EHNERGETICHESKIKH USTANOVOK PO KRITERIYUUDEL'NOJ MASSY V OBOBSHCHENNYKH PROEKTNYKH PEREMENNYKH]
A. G. Yuferov and V. A. Linnik 1992 27 p In RUSSIAN Limited Reproducibility: More than 20% of this document may be affected by microfiche quality
(DE93-634153; FEI-2272) Avail: CASI HC A03 (US Sales Only)

Influence of efficiency and medium-entropy temperatures on specific mass of the space power plant and specific square of refrigerator-radiator with account for heat losses and mass coefficients of subsystems is considered. The sensitivity functions for specific characteristics with regard to variations of design variants are deduced. DOE

N94-26208*# Sverdrup Technology, Inc., Brook Park, OH.
GASEOUS HYDROGEN/OXYGEN INJECTOR PERFORMANCE CHARACTERIZATION Final Report
W. A. deGroot and H. H. Tsuei (Pennsylvania State Univ., University Park.) Feb. 1994 11 p Presented at the 32nd Aerospace Sciences Meeting and Exhibit, Reno, NV, 10-13 Jan. 1994; sponsored by AIAA
(Contract NAS3-25266; RTOP 506-42-31)
(NASA-CR-194464; E-8513; NAS 1.26:194464; AIAA Paper 94-0220) Avail: CASI HC A03/MF A01

Results are presented of spontaneous Raman scattering measurements in the combustion chamber of a 110 N thrust class gaseous hydrogen/oxygen rocket. Temperature, oxygen number density, and water number density profiles at the injector exit plane are presented. These measurements are used as input profiles to a full Navier-Stokes computational fluid dynamics (CFD) code. Predictions of this code while using the measured profiles are compared with predictions while using assumed uniform injector profiles. Axial and radial velocity profiles derived from both sets of predictions are compared with Rayleigh scattering measurements in the exit plane of a 33:1 area ratio nozzle. Temperature and number density Raman scattering measurements at the exit plane of a test rocket with a 1:1.36 area ratio nozzle are also compared with results from both sets of predictions.
Author (revised)

N94-26209*# Sverdrup Technology, Inc., Brook Park, OH.
STATIONARY PLASMA THRUSTER PLUME EMISSIONS Final Report
David H. Manzella Mar. 1994 13 p Presented at the 23rd International Electric Propulsion Conference, Seattle, WA, 13-16 Sep. 1993; sponsored by AIAA
(Contract NAS3-25266; RTOP 506-42-31)
(NASA-CR-194471; E-8612; NAS 1.26:194471; IEPC-93-097) Avail: CASI HC A03/MF A01

The emission spectrum from a xenon plasma produced by a Stationary Plasma Thruster provided by the Ballistic Missile Defense Organization (BMDO) was measured. Approximately 270 individual Xe I, Xe II, and XE III transitions were identified. A total of 250 mW of radiated optical emission was estimated from measurements taken at the thruster exit plane. There was no evidence of erosion products in the emission signature. Ingestion and ionization of background gas at elevated background pressure was detected. The distribution of excited states could be described by temperatures ranging from fractions of 1 eV to 4 eV with a high degree of uncertainty due to the nonequilibrium nature of this plasma. The plasma was over 95 percent ionized at the thruster exit plane. Between 10 and 20 percent of the ions were doubly charged. Two modes of operation were identified. The intensity of plasma emission increased by a factor of two during operation in an oscillatory mode. The transfer between the two modes of operation was likely related to unidentified phenomena occurring on a time scale of minutes. Author (revised)

N94-26230*# Rockwell International Corp., Canoga Park, CA. Rocketdyne Div.
STS-51 PAD ABORT. OV103-ENGINE 2033 (ME-2) FUEL FLOWMETER SENSOR OPEN CIRCUIT
12 Aug. 1993 168 p
(Contract NAS8-40000)
(NASA-CR-193924; NAS 1.26:193924; RSS-8912) Avail: CASI HC A08/MF A02

The STS-51 initial launch attempt of Discovery (OV-103) was terminated on KSC launch pad 39B on 12 Aug. 1993 at 9:12 AM E.S.T. due to a sensor redundancy failure in the liquid hydrogen system of ME-2 (Engine 2033). The event description and time line are summarized. Propellant loading was initiated on 12 Aug. 1993 at 12:00 AM EST. All space shuttle main engine (SSME) chill parameters and Launch Commit Criteria (LCC) were nominal. At engine start plus 1.34 seconds a Failure Identification (FID) was posted against Engine 2033 for exceeding the 1800 spin intra-channel (A1-A2) Fuel Flowrate sensor channel qualification limit. The engine was shut down at 1.50 seconds followed by Engines 2032 and 2030. All shut down sequences were nominal and the mission was safely aborted. SSME Avionics hardware and software performed nominally during the incident. A review of vehicle data table (VDT) data and controller software logic revealed no failure indications other than the single FID 111-101, Fuel Flowrate Intra-Channel Test Channel A disqualification. Software logic was executed according to requirements and there was no anomalous controller software operation. Immediately following the abort, a Rocketdyne/NASA failure investigation team was assembled. The team successfully isolated the failure cause to an open circuit in a Fuel Flowrate Sensor. This type of failure has occurred eight previous times in ground testing. The sensor had performed acceptably on three previous flights of the engine and SSME flight history shows 684 combined fuel flow rate sensor channel flights without failure. The disqualification of an Engine 2 (SSME No. 2033) Fuel Flowrate sensor channel was a result of an instrumentation failure and not engine performance. All other engine operations were nominal. This disqualification resulted in an engine shutdown and safe sequential shutdown of all three engines prior to ignition of the solid boosters. Author (revised)

N94-26231*# Rockwell International Corp., Canoga Park, CA. Rocketdyne Div.
TEST RESULTS OF THE RS-44 INTEGRATED COMPONENT EVALUATOR LIQUID OXYGEN/HYDROGEN ROCKET ENGINE Final Report, Apr. 1986 - Apr. 1987
R. F. Sutton and B. W. Lariviere 12 Oct. 1993 381 p
(Contract NAS3-23773)
(NASA-CR-194443; NAS 1.26:194443; RI/RD92-127) Avail: CASI HC A17/MF A03

An advanced LOX/LH2 expander cycle rocket engine, producing 15,000 lbf thrust for Orbital Transfer Vehicle missions, was tested to determine ignition, transition, and main stage characteristics. Detail design and fabrication of the pump fed RS44 integrated component evaluator (ICE) was accomplished using company discretionary resources and was tested under this contracted effort. Successful demonstrations were completed to about the 50 percent fuel turbopump power level (87,000 RPM), but during this last test, a high pressure fuel turbopump (HPFTP) bearing failed curtailing the test program. No other hardware were affected by the HPFTP premature shutdown. The ICE operations matched well with the predicted start transient simulations. The tests demonstrated the feasibility of a high performance advanced expander cycle engine. All engine components operated nominally, except for the HPFTP, during the engine hot-fire tests. A failure investigation was completed using company discretionary resources. Author

N94-26537# Illinois Univ., Urbana. Fusion Studies Lab.
FLOWING DPF DESIGN FOR PROPULSION EXPERIMENTS Final Report, 3 May 1990 - 30 Aug. 1992
G. H. Miley, J. B. Javedani, B. A. Temple, H. Kislev, and R. T. Nachtrieb Aug. 1993 66 p
(Contract F29601-90-K-0048)
(AD-A274973; PL-TR-93-3053) Avail: CASI HC A04/MF A01

Recent studies show the Dense Plasma Focus (DPF) to be a viable candidate for use as a long-range space propulsion system with a high power-to-weight ratio. This Air Force contract provided support for study and modification of the University of Illinois (UI) DPF to develop a basic thrust experiment. A key aspect of such a system is to employ gas injection into the DPF electrode region, as opposed to the static fill technique commonly employed in present experimental devices. The design and initial operation of a prototype gas-puff injection facility is described, preliminary results are reviewed, and plans for future use are detailed. The projected performance of a future propulsion system using this technique is also examined. A list of the publications and conference presentations based on research done under this contract is included. DTIC

N94-26542*# Rockwell International Corp., Canoga Park, CA. Rocketdyne Div.

ORBIT TRANSFER ROCKET ENGINE TECHNOLOGY PROGRAM Final Report, Jun. 1983 - May 1992

N. B. Gustafson and T. J. Harmon 15 Oct. 1993 127 p
(Contract NAS3-23773)
(NASA-CR-189229; NAS 1.26:189229; RI/RD92-139) Avail: CASI HC A07/MF A02

An advanced near term (1990's) space-based Orbit Transfer Vehicle Engine (OTVE) system was designed, and the technologies applicable to its construction, maintenance, and operations were developed under Tasks A through F of the Orbit Transfer Rocket Engine Technology Program. Task A was a reporting task. In Task B, promising OTV turbomachinery technologies were explored: two stage partial admission turbines, high velocity ratio diffusing crossovers, soft wear ring seals, advanced bearing concepts, and a rotordynamic analysis. In Task C, a ribbed combustor design was developed. Possible rib and channel geometries were chosen analytically. Rib candidates were hot air tested and laser velocimeter boundary layer analyses were conducted. A channel geometry was also chosen on the basis of laser velocimeter data. To verify the predicted heat enhancement effects, a ribbed calorimeter spool was hot fire tested. Under Task D, the optimum expander cycle engine thrust, performance and envelope were established for a set of OTV missions. Optimal nozzle contours and quick disconnects for modularity were developed. Failure Modes and Effects Analyses, maintenance and reliability studies and component study results were incorporated into the engine system. Parametric trades on engine thrust, mixture ratio, and area ratio were also generated. A control system and the health monitoring and maintenance operations necessary for a space-based engine were outlined in Task E. In addition, combustor wall thickness measuring devices and a fiberoptic shaft monitor were developed. These monitoring devices were incorporated into preflight engine readiness checkout procedures. In Task F, the Integrated Component Evaluator (I.C.E.) was used to demonstrate performance and operational characteristics of an advanced expander cycle engine system and its component technologies. Sub-system checkouts and a system blowdown were performed. Short transitions were then made into main combustor ignition and main stage operation. Author (revised)

N94-26560# Sandia National Labs., Albuquerque, NM.

AN ASSESSMENT OF TESTING REQUIREMENT IMPACTS ON NUCLEAR THERMAL PROPULSION GROUND TEST FACILITY DESIGN

L. R. Shipers, C. A. Ottinger, and L. C. Sanchez 25 Oct. 1993 13 p Presented at the 11th Symposium on Space Nuclear Power Systems, Albuquerque, NM, 9-13 Jan. 1994
(Contract DE-AC04-94AL-85000)
(DE94-002933; SAND-93-2296C; CONF-940101-18) Avail: CASI HC A03/MF A01

Programs to develop solid core nuclear thermal propulsion (NTP) systems were under way at the Department of Defense (DoD), the National Aeronautics and Space Administration (NASA), and the Department of Energy (DOE). These programs recognized the need for a new ground test facility to support development of NTP systems. However, the different military and civilian applications have led to different ground test facility requirements. The Department of Energy (DOE) in its role as landlord and operator of the proposed research reactor test facilities initiated an effort to explore opportunities for a common ground test facility to meet both DoD and NASA needs. The baseline design and operating limits of the proposed DoD NTP ground test facility are described. The NASA ground test facility requirements are reviewed and their potential impact on the DoD facility baseline is discussed. DOE

N94-26613*# National Aeronautics and Space Administration. Goddard Space Flight Center, Greenbelt, MD.

HANDBOOK FOR HANDLING AND STORAGE OF NICKEL-CADMIUM BATTERIES: LESSONS LEARNED

Floyd E. Ford (Swales and Associates, Beltsville, MD.), Gopalakrishna M. Rao, and Thomas Y. Yi Feb. 1994 77 p
(Contract NAS5-30375)
(NASA-RP-1326; NAS 1.61:1326; Rept-94B00027) Avail: CASI HC A05/MF A01

The handbook provides guidelines for the handling and storage of conventional NiCd flight batteries. The guidelines are based on many years of experience with ground and in-flight handling of batteries. The overall goal is to minimize the deterioration and irreversible effects of improper handling of NiCd flight batteries on flight performance. A secondary goal is to provide the reader with an understanding, in nonanalytical terms, of the degradation mechanisms of NiCd cells and how these mechanisms are affected by improper ground handling of flight hardware. Section 2 provides the reader with a brief introduction to NiCd cells. The effects of the environment on NiCd batteries are discussed in Section 3, and Section 4 contains 12 guidelines for battery handling and storage with supporting rationale for each guideline. The appendix provides a synopsis of NiCd cell design and evolution over 30 years of space flight on Goddard Space Flight Center (GSFC) satellites, along with a chronological review of key events that influenced the design of NiCd cells being flown today. Author

N94-27150*# Alabama Univ., Huntsville. Dept. of Mechanical Engineering.

VERIFICATION OF THERMAL ANALYSIS CODES FOR MODELING SOLID ROCKET NOZZLES Final Report

M. Keyhani (Tennessee Univ., Knoxville.) May 1993 22 p
(Grant NAG8-212)
(NASA-CR-195248; NAS 1.26:195248; UTK-R01-1372-59) Avail: CASI HC A03/MF A01

One of the objectives of the Solid Propulsion Integrity Program (SPIP) at Marshall Space Flight Center (MSFC) is development of thermal analysis codes capable of accurately predicting the temperature field, pore pressure field and the surface recession experienced by decomposing polymers which are used as thermal barriers in solid rocket nozzles. The objective of this study is to provide means for verifications of thermal analysis codes developed for modeling of flow and heat transfer in solid rocket nozzles. In order to meet the stated objective, a test facility was designed and constructed for measurement of the transient temperature field in a sample composite subjected to a constant heat flux boundary condition. The heating was provided via a steel thin-foil with a thickness of 0.025 mm. The designed electrical circuit can provide a heating rate of 1800 W. The heater was sandwiched between two identical samples, and thus ensure equal power distribution between them. The samples were fitted with Type K thermocouples, and the exact location of the thermocouples were determined via X-rays. The experiments were modeled via a one-dimensional code (UT1D) as a conduction and phase change heat transfer process. Since the pyrolysis gas flow was in the direction normal to the heat flow, the numerical model could not account for the convection cooling effect of the pyrolysis gas flow. Therefore, the predicted values in the decomposition zone are considered to be an upper estimate of the temperature. From the analysis of the experimental and the numerical results the following are concluded: (1) The virgin and char specific heat data for FM 5055 as reported by SoRI can not be used to obtain any reasonable agreement between the measured temperatures and the predictions. However, use of virgin and char specific heat data given in Acurex report produced good agreement for most of the measured temperatures. (2) Constant heat flux heating process can produce a much higher heating rate than the radiative heating process. The results show that heating rates of 125 C/s (225 F/s) can be achieved. (3) The electrical resistance of the FM 5055 samples were about 150 Omega in the virgin state, and decreased to about 35 Omega when charred. A reliable scheme must be developed to electrically insulate the composite from the heater foil in order to prevent any current leakage into the sample which can result in volumetric heating of the char zone of the composite.
Derived from text

N94-27166*# Christian Brothers Coll., Memphis, TN. Dept. of Mechanical Engineering.

INTEGRATED MODEL DEVELOPMENT FOR LIQUID FUELED ROCKET PROPULSION SYSTEMS Final Report

L. Michael Santi Jun. 1993 63 p
(Grant NAG8-212)
(NASA-CR-195253; NAS 1.26:195253) Avail: CASI HC A04/MF A01

As detailed in the original statement of work, the objective of phase two of this research effort was to develop a general framework for rocket engine performance prediction that integrates physical principles, a rigorous mathematical formalism, component level test data, system level test data, and theory-observation reconciliation. Specific phase two development tasks are defined. Derived from text

N94-27212*# Rockwell International Corp., Bay Saint Louis, MS. Rocketdyne Div.
ORBITAL TRANSFER VEHICLE ENGINE TECHNOLOGY HIGH VELOCITY RATIO DIFFUSING CROSSOVER Final Report, Dec. 1983 - 1989
Brian W. Lariviere Dec. 1992 155 p
(Contract NAS3-23773)
(NASA-CR-194447; NAS 1.26:194447; RI/RD89-111) Avail: CASI HC A08/MF A02

High speed, high efficiency head rise multistage pumps require continuous passage diffusing crossovers to effectively convey the pumped fluid from the exit of one impeller to the inlet of the next impeller. On Rocketdyne's Orbital Transfer Vehicle (OTV), the MK49-F, a three stage high pressure liquid hydrogen turbopump, utilizes a 6.23 velocity ratio diffusing crossover. This velocity ratio approaches the diffusion limits for stable and efficient flow over the operating conditions required by the OTV system. The design of the high velocity ratio diffusing crossover was based on advanced analytical techniques anchored by previous tests of stationary two-dimensional diffusers with steady flow. To secure the design and the analytical techniques, tests were required with the unsteady whirling characteristics produced by an impeller. A tester was designed and fabricated using a 2.85 times scale model of the MK49-F turbopumps first stage, including the inducer, impeller, and the diffusing crossover. Water and air tests were completed to evaluate the large scale turbulence, non-uniform velocity, and non-steady velocity on the pump and crossover head and efficiency. Suction performance tests from 80 percent to 124 percent of design flow were completed in water to assess these pump characteristics. Pump and diffuser performance from the water and air tests were compared with the actual MK49-F test data in liquid hydrogen. Author

N94-27213*# Rockwell International Corp., Canoga Park, CA. Rocketdyne Div.
ORBITAL TRANSFER ROCKET ENGINE TECHNOLOGY 7.5K-LB THRUST ROCKET ENGINE PRELIMINARY DESIGN Final Report, Dec. 1987 - Oct. 1988
T. J. Harmon and E. Roschak 15 Oct. 1993 233 p
(Contract NAS3-23773)
(NASA-CR-190754; NAS 1.26:190754; RI/RD88-291) Avail: CASI HC A11/MF A03

A preliminary design of an advanced LOX/LH2 expander cycle rocket engine producing 7,500 lbf thrust for Orbital Transfer vehicle missions was completed. Engine system, component and turbomachinery analysis at both on design and off design conditions were completed. The preliminary design analysis results showed engine requirements and performance goals were met. Computer models are described and model outputs are presented. Engine system assembly layouts, component layouts and valve and control system analysis are presented. Major design technologies were identified and remaining issues and concerns were listed. Author

N94-27662*# Toledo Univ., OH.
A STUDY OF DC-DC CONVERTERS WITH MCT'S FOR ARCJET POWER SUPPLIES Final Report
Thomas A. Stuart Jan. 1994 76 p
(Grant NAG3-1102; RTOP 506-42-31)
(NASA-CR-191204; E-8386; NAS 1.26:191204) Avail: CASI HC A05/MF A01

Many arcjet DC power supplies use PWM full bridge converters with large arrays of parallel FET's. This report investigates an alternative supply using a variable frequency series resonant converter with small arrays of parallel MCT's (metal oxide semiconductor controlled thyristors). The reasons for this approach are to: increase reliability by reducing the number of switching devices; and decrease the surface mounting area of the switching arrays. The variable frequency series resonant approach is used because the relatively slow switching speed of the MCT precludes the use of PWM. The 10 kW converter operated satisfactorily with an efficiency of over 91 percent. Test results indicate this efficiency could be increased further by additional optimization of the series resonant inductor. Author

N94-25685*# Maryland Univ., College Park. Dept. of Aerospace Engineering.
MINOTAUR (MARYLAND'S INNOVATIVE ORBITAL TECHNOLOGICALLY ADVANCED UNIVERSITY ROCKET)
Mark J. Lewis, Dave Akin, Charles Lind, T. Rice, ed., and W. Vincent, ed. *In* USRA, Proceedings of the 8th Annual Summer Conference: NASA/USRA Advanced Design Program 1992 p 146-158 (For primary document see N94-25665 07-80)
Avail: CASI HC A03/MF A04

N94-25690*# Ohio State Univ., Columbus. Dept. of Aeronautical and Astronautical Engineering.
PROJECT WISH: THE EMERALD CITY
Hayrani Oz, Jim Dunne, Stan Butchar, Tommy George, Rob Hellstrom, Tricia Kringen, George Owens, Mike Perrea, Paul Semeraro, and Phil Thorndike *In* USRA, Proceedings of the 8th Annual Summer Conference: NASA/USRA Advanced Design Program 1992 p 196-208 (For primary document see N94-25665 07-80)
Avail: CASI HC A03/MF A04

N94-27363*# National Aeronautics and Space Administration. Lewis Research Center, Cleveland, OH.
INTERDISCIPLINARY TECHNOLOGY
Lester D. Nichols *In its* Vision 21: Interdisciplinary Science and Engineering in the Era of Cyberspace Dec. 1993 p 51-60 (For primary document see N94-27358 07-12)
Avail: CASI HC A02/MF A03

N94-27371*# National Aeronautics and Space Administration. Lewis Research Center, Cleveland, OH.
A DIRECT CURRENT RECTIFICATION SCHEME FOR MICROWAVE SPACE POWER CONVERSION USING TRAVELING WAVE ELECTRON ACCELERATION
Robert M. Manning *In its* Vision 21: Interdisciplinary Science and Engineering in the Era of Cyberspace Dec. 1993 p 169-178 (For primary document see N94-27358 07-12)
Avail: CASI HC A02/MF A03

N94-27373*# National Aeronautics and Space Administration, Washington, DC.
INERTIAL ELECTROSTATIC CONFINEMENT AS A POWER SOURCE FOR ELECTRIC PROPULSION
George H. Miley (Illinois Univ., Urbana.), R. Burton (Illinois Univ., Urbana.), J. Javedani (Illinois Univ., Urbana.), Y. Yamamoto (Illinois Univ., Urbana.), A. Satsangi (Illinois Univ., Urbana.), Y. Gu (Illinois Univ., Urbana.), P. Heck (Illinois Univ., Urbana.), R. Nebel (Los Alamos National Lab., NM.), N. Schulze (Illinois Univ., Urbana.), and J. Christensen (Illinois Univ., Urbana.) et al *In* NASA. Lewis Research Center, Vision 21: Interdisciplinary Science and Engineering in the Era of Cyberspace Dec. 1993 p 185-229 (For primary document see N94-27358 07-12)
Avail: CASI HC A03/MF A03

N94-27375*# National Aeronautics and Space Administration. Lewis Research Center, Cleveland, OH.
ROCKET ENGINE NUMERICAL SIMULATION
Ken Davidian *In its* Vision 21: Interdisciplinary Science and Engineering in the Era of Cyberspace Dec. 1993 p 241-245 (For primary document see N94-27358 07-12)
Avail: CASI HC A01/MF A03

N94-28032# Deutsche Forschungs- und Versuchsanstalt fuer Luft- und Raumfahrt, Goettingen (Germany). Inst. for Experimental Fluid Mechanics.
FIRST EXPERIMENTAL ASSESSMENT OF RCS PLUME-FLOW FIELD INTERACTION ON HERMES LEADING EDGE THRUSTER CONFIGURATION
T. Poertner *In* AGARD, Computational and Experimental Assessment of Jets in Cross Flow Nov. 1993 13 p (For primary document see N94-28003 07-34)
Copyright Avail: CASI HC A03/MF A04

23 CHEMISTRY AND MATERIALS (GENERAL)

N94-26353# New Orleans Univ., LA. Dept. of Chemistry.
COMPUTATIONAL ANALYSIS OF SOME ASPECTS OF A SYNTHETIC ROUTE TO AMMONIUM DINITRAMIDE Technical Report
Tore Brinck and Peter Politzer 27 Dec. 1993 6 p
(Contract N00014-91-J-4057)
(AD-A274648) Avail: CASI HC A02/MF A01

The optimized geometry of 1, C2H5-0-C(double bonds oxygen)N(NO2)2, a precursor to ammonium dinitramide, has been computed at the ab initio HF/6-31G* level. We find no structural evidence that 1 exists in the ionic form, C2H5-O-C(triple bonds)O + N(NO2)2(-). The reaction of 1 with NH3 passes through a transition state that is consistent with a concerted substitution (Ingold mechanism) in which N(NO2)2(-) is the leaving group. DTIC

N94-26779# Ames Lab., IA.
THE COORDINATION AND ATOM TRANSFER CHEMISTRY OF TITANIUM PORPHYRIN COMPLEXES Ph.D. Thesis
J. A. Hays Nov. 1993 101 p
(Contract W-7405-eng-82)
(DE94-003091; IS-T-1637) Avail: CASI HC A06/MF A02

Preparation, characterization, and reactivity of ((eta)(sup 2) alkyne)(meso tetratolylpoprphrinato) titanium(II) complexes are described, along with intermetal oxygen atom transfer reactions involving Ti(IV) and Ti(III) porphyrin complexes. The (eta)(sup 2)- alkyne complexes are prepared by reaction of (TTP)TiCl2 with LiAlH4 in presence of alkyne. Structure of (OEP)Ti((eta)(sup 2)-Ph-C(triple bond)C-Ph) (OEP=octaethylporphryin) was determined by XRD. The compounds undergo simple substitution to displace the alkyne and produce doubly substituted complexes. Structure of (TTP)Ti(4-picoline)(sub 2) was also determined by XRD. Reaction of (TTP)Ti(double bond)O with (OEP)Ti-Cl yields intermetal O/Cl exchange, which is a one-electron redox process mediated by O atom transfer. Also a zero-electron redox process mediated by atom transfer is observed when (TTP)TiCl2 is reacted with (OEP)Ti(double bond)O. DOE

N94-27708# Sandia National Labs., Albuquerque, NM.
TRACE ORGANIC CHEMICAL DETECTION USING AN ULTRAVIOLET EXCITATION MOLECULAR BEAM FLUOROMETER
B. L. Preppernau and P. J. Hargis 1993 5 p Presented at the 4th Laser Applications to Chemical Analysis Meeting, Jackson Hole, WY, 8-11 Mar. 1994
(Contract DE-AC04-94AL-85000)
(DE94-002649; SAND-93-2599C; CONF-940341-1) Avail: CASI HC A01/MF A01

Detection of airborne environmental contaminants, such as organic solvents, requires unambiguous compound identification and sensitivity to concentrations below those permitted by regulating agencies. One promising detection approach uses a pulsed supersonic molecular beam vacuum expansion in combination with fluorescence signal spectral analysis to identify species in a chemical mixture. This report describes the use and performance of the ultraviolet excitation molecular beam fluorometer. DOE

N94-27745# Los Alamos National Lab., NM. Polymers and Coatings Group.
STABILIZATION OF POLYANILINE SOLUTIONS
Debra A. Wrobleski and Brian C. Benicewicz 1993 3 p Presented at the 207th Spring National Meeting of the American Chemical Society, San Diego, CA, 13-18 Mar. 1994
(Contract W-7405-eng-36)
(DE94-003958; LA-UR-93-3967; CONF-940301-2) Avail: CASI HC A01/MF A01

Adding hindered amine light stabilizers (HALS) to N-methyl- pyrrolidinone (NMP) solutions of polyaniline delays gelation. It is hypothesized that HALS act in some manner other than as traditional antioxidants in preventing gelation; the secondary amine functional group appears to play a critical role, perhaps by disrupting the physical crystallization network that may contribute to gelation. Pyrrolidine, a secondary amine, or ammonia is an effective cosolvent with NMP in dissolving PAn-EB (emeraldine base). DOE

N94-27387# Tohoku Univ., Sendai (Japan). Inst. for Chemical Reaction Science.
REACTIVITY OF NITRATE RADICAL (NO3) TOWARD ORGANIC COMPOUNDS [NAITORETO RAJIKARU (NO3) NO YUKIBUTSU NI TAISURU HANNOSEI]
Osamu Ito *In its* Bulletin of the Institute for Chemical Reaction Science, Tohoku University, Volume 2 30 Sep. 1992 p 15-31 In JAPANESE
(For primary document see N94-27385 07-25)
Avail: CASI HC A03/MF A02

24 COMPOSITE MATERIALS

Includes physical, chemical, and mechanical properties of laminates and other composite materials.

For ceramic materials see *27 Nonmetallic Materials.*

N94-25608# Fairfax Materials Research, Inc., Alexandria, VA.
COMPUTER MODELLING OF CYCLIC DEFORMATION OF HIGH-TEMPERATURE MATERIALS Technical Progress Report, 1 Feb. - 31 May 1993
M. S. Duesbery 14 Jun. 1993 34 p
(Contract N00014-91-C-0067)
(AD-A273852) Avail: CASI HC A03/MF A01

This program aims at improving current methods of lifetime assessment by building in the characteristics of the micro-mechanisms known to be responsible for damage and failure. The broad approach entails the integration, where necessary, augmentation of the micro-scale research results currently available in the literature into a macro-scale model with predictive capability. In more detail, the program will develop a set of hierarchically structured models at different length scales, from atomic to macroscopic, at each level taking as parametric input the results of the model at the next smaller scale. In this way the known microscopic properties can be transported by systematic procedures to the unknown macro-scale region. It may not be possible to eliminate empiricism completely, because some of the quantities involved cannot yet be estimated to the required degree of precision. In this case the aim will be at least to eliminate functional empiricism. DTIC

N94-25651# Technical Research Centre of Finland, Espoo. Textile Lab.
CONTINUOUS FIBER REINFORCED THERMOPLASTIC COMPOSITES: LITERATURE SURVEY [JATKUVAKUITUKUJITTEISET KESTOMUOVIKOMPOSSIITIT: KIRJALLISUUSTUKIMUS]
Juha Sarlin and Marja-Terttu Tuomisto Nov. 1992 58 p In FINNISH
Sponsored by Technology Development Centre, Finland
(ISSN 1235-0605)
(VTT-TIED-1422; ISBN-951-38-4316-5; ETN-94-95275) Copyright Avail: CASI HC A04/MF A01

Continuous reinforced thermoplastic composites are addressed. Thermoplastic materials represent only a fraction of the total market for polymer matrix structural composites. However, there are numerous reasons for increased use of thermoplastic materials as load bearing structures. One of the foremost is that they are environmentally friendly due to their nonreactive solvent free processing and recycling. Thermoplastic matrix systems also have some technical advantages in service. For example, toughness, chemical resistance, and short production cycle times are some of the finest properties of thermoplastic composites. The main limitations on the use of continuous fiber reinforced thermoplastic composites are their molding properties. The high viscosity of polymer melts somewhat limits their production methods. Production is usually of quite simple parts, such as plates and continuous profiles. Furthermore, the required high molding pressures increase production costs in short series. One stage in the production of continuous fiber reinforced thermoplastic composites is the impregration process. A number of different methods and variations of them have been developed. Focus is given to the hybrid yarn method. Another essential fact is the factor controlling the moldability of these kinds of materials. Different viscosity properties of polymer melts, including very long or continuous fibers, are described. ESA

N94-25734# Technical Research Centre of Finland, Espoo. Metals Lab.
EFFECT OF IMPACT FACE DAMAGE ON STRENGTH OF SANDWICH COMPOSITES

Pertti Auerkari Jan. 1993 23 p
(ISSN 1235-0621)
(VTT-PUBS-128; ISBN-951-38-4246-0; ETN-94-95247) Copyright Avail: CASI HC A03/MF A01

The effect of accidental impacts during manufacturing, maintenance or servicing of marine and aerospace sandwich structures is discussed. In particular, the effect of low energy impact damage on residual strength is considered. Methods for evaluating the service performance of accidentally impact loaded sandwich structures are proposed. A low energy impact face defect decreases the face load of a sandwich composite. The expression describing the critical lateral face load in compression is discussed. Experimental studies suggest that the diameter of the impact delamination defect is approximately equal to the impact energy multiplied by the square root of the number of equal impacts, which corresponds to the critical energy criterion for fatigue. ESA

N94-25739# Air Force Inst. of Tech., Wright-Patterson AFB, OH.
INVESTIGATION OF COMPRESSIVE BEHAVIOR FOR METAL MATRIX COMPOSITES WITH A CIRCULAR HOLE M.S. Thesis
Janet L. Gooder Dec. 1993 135 p
(AD-A273835; AFIT/GAE/ENY/93D-15) Avail: CASI HC A07/MF A02

The notched and unnotched macromechanical response due to micromechanical behavior of (O/+ or -45/90)(sub s) SCS-6/Beta 21S and (0/90)(sub 2S), Sigma/Beta 21S subjected to static compressive loads at room temperature was investigated. The stress-strain behavior and mechanical response in the presence of a circular hole was examined. A clear description of the progressive nature of damage, which ultimately resulted in failure, was provided. The effect of elevated temperature was shown for SCS-6/Beta 21S. The ultimate compressive strength and elastic modulus were reported for both MMC's. Sigma/Beta 21S and SCS-6/Beta 21S were mildly notch sensitive at room temperature. Notch sensitivity of SCS-6/Beta 21S was slightly reduced at 650 C. Internal failure mechanisms of fiber debonding, matrix cracking, matrix yielding, fiber failure, and fiber microbuckling were observed in various combinations during the loading. Damage mechanisms were observed similarly in notched and unnotched specimens. Damage initiation in the notched specimens was concentrated in the region adjacent to the hole. Sigma/Beta 21S and unnotched SCS-6/Beta 21S at room temperature failed in an extensional mode, while notched SCS-6/Beta 21S and unnotched SCS-6/Beta 21S at 650 C failed in a shear mode. The ultimate compressive failure of each depended on the ultimate strength of the fibers. DTIC

N94-25779# Boeing Defense and Space Group, Seattle, WA.
X RAY COMPUTED TOMOGRAPHY FOR EMERGING AEROSPACE MATERIALS AND PROCESSES DEVELOPMENT Interim Report, Sep. 1991 - May 1993
Richard H. Bossi, Gary E. Georgeson, and Raymond D. Rempt 1 May 1993 68 p
(Contract F33615-88-C-5404)
(AD-A273721; WL-TR-93-4054) Avail: CASI HC A04/MF A01

The development and qualification of new materials and processes requires characterization of the product as a function of manufacturing and operational parameters. X ray computed tomography (CT) provides quantitative measurements of material characteristics in terms of the dimensions, density, and composition. The results of studies involving CT testing of various materials demonstrate the ability of CT to provide valuable information for material process understanding and characterization. The cost benefit of CT is found in the reduction of risk and schedule savings by reducing cycle time in process development steps. CT is a tool which increases new design options by allowing internal measurement and evaluation at previously inaccessible locations in complex structures. X ray CT will be a critical tool for organizations competing in emerging materials and processes development. DTIC

N94-25805# Pacific Northwest Lab., Richland, WA.
STRUCTURE AND PROPERTIES OF INTERMETALLIC COMPOSITES SYNTHESIZED IN SITU USING SOLID STATE DISPLACEMENT REACTIONS
C. H. Henager, Jr., J. L. Brimhall, and J. P. Hirth (Washington State Univ., Pullman.) Sep. 1993 29 p Presented at the 1st International Symposium on Structural Intermetallics, Champion, PA, 26-30 Sep. 1993
(Contract DE-AC06-76RL-01830)
(DE94-004312; PNL-SA-22561; CONF-930997-7) Avail: CASI HC A03/MF A01

Solid state displacement reactions can produce in situ intermetallic matrix composites in a process where an intermetallic phase(s) and a potential reinforcing phase(s) are grown together during a solid state reaction. Interwoven and dispersed microstructures, important for desirable composite properties, have been produced by means of displacement reaction processing techniques. Two such composites have been synthesized: MoSi2 reinforced with SiC particles, and NiAl/Ni3Al reinforced with Al2O3. Strength in bending and chevron-notch fracture toughness have been determined as a function of temperature and measured properties compare favorably with composites produced by other means. The measured properties are discussed with regard to the observed microstructures. The potential for displacement reaction processing is assessed and appears to be a cost-effective synthesis method compared to others. DOE

N94-25857# Air Force Inst. of Tech., Wright-Patterson AFB, OH. School of Engineering.
A NONLINEAR THREE-DIMENSIONAL MICROMECHANICS MODEL FOR FIBER-REINFORCED LAMINATED COMPOSITES Ph.D. Thesis
David D. Robertson Nov. 1993 256 p
(AD-A273772; AFIT/DS/AA/93-3) Avail: CASI HC A12/MF A03

In this study, a three dimensional micromechanics model is developed. The present capabilities of the model include both unidirectional and laminated composite layups with various types of nonlinear analysis such as a thermoelastic-plastic analysis employing the Prandtl-Reuss flow relations, a thermoviscoplastic analysis using Bodner-Partom unified constitutive theory, and an interfacial damage progression scheme based on a statistical interfacial failure criteria. Such nonlinearities are critical factors during thermomechanical fatigue (TMF) loading of high temperature composites. Solutions were obtained and extensive comparisons performed with existing micromechanics models, finite element analysis, and experiment with excellent results. In addition, the analysis was developed to require minimal computer resources. For instance, the majority of problems may be accomplished on a personal computer in a matter of seconds. DTIC

N94-25859# Air Force Inst. of Tech., Wright-Patterson AFB, OH. School of Engineering.
INFLUENCE OF EMBEDDED OPTICAL FIBERS ON COMPRESSIVE STRENGTH OF ADVANCED COMPOSITES M.S. Thesis
Stefan B. Dosedel Dec. 1993 131 p
(AD-A273775; AFIT/GAE/ENY/93D-12) Avail: CASI HC A07/MF A02

This study investigated the effects of embedding optical fibers into advanced composite materials. This combination was meant to simulate 'smart structures' that have been shown to sense several different variables in the composite including strain, temperature, and damage. A laminate orientation taken from an existing aircraft structure was used to fabricate sixteen groups of specimens which were subjected to compression testing in an IITRI fixture to determine the ultimate compressive strength and modulus of elasticity. Ten of these groups were fabricated with optical fibers while the other six were control groups and contained no optical fibers. This study showed that varying the number of embedded optical fibers, optical fiber size, optical fiber orientation, and optical fiber location in the composite structure can reduce the compressive strength of the structure by up to 27%. This maximum degradation occurred when multiple optical fibers were placed perpendicular to the composite structural fibers. No deleterious effects were seen when the optical fiber was placed parallel to the composite structural fibers. No change in modulus of elasticity was seen for any of the groups tested. DTIC

N94-25863# Air Force Inst. of Tech., Wright-Patterson AFB, OH. School of Engineering.
A STUDY OF GRAPHITE PEEK COMPOSITE WITH CENTRAL ELLIPTICAL HOLES UNDER TENSION M.S. Thesis
Bill J. Lau Dec. 1993 123 p
(AD-A273779; AFIT/GAE/ENY/93D-20) Avail: CASI HC A06/MF A02

This study investigated the stress-strain response and failure modes of graphite / polyether etherketone (Gr/PEEK) tension specimens containing a central elliptical hole. Both experiments and finite element numerical analyses were conducted. Test specimens included seven layups and three hole geometries; three of each combination were tested. The holes consisted of an ellipse with major axis aligned with the load axis, an ellipse with major axis transverse to the load axis, and a circle. Strain gages were located adjacent to the hole and midway between the hole and tab on all specimens. Strain data was used to plot stress-strain response. The analysis utilized a nonlinear finite element program, assuming plane stress. Linear stress-strain relationships are applied incrementally; piecewise cubic spline interpolation functions represent the material data provided to the program, accounting for the material nonlinearity. A strain energy failure criterion determines element failures. Analytical stress-strain results correlated well with experiment, with some divergence noted. Damage progression of the finite element models agreed with observed failure surfaces, except for unidirectional and crossply layups. These failed more suddenly, and the program is unable to capture this phenomenon. Interlaminar stresses developing in the actual tests and coarse regions of the finite element meshes were identified as probable sources of error. DTIC

N94-25876# Air Force Inst. of Tech., Wright-Patterson AFB, CH. School of Engineering.

CHARACTERIZATION OF FATIGUE DAMAGE IN A METAL MATRIX COMPOSITE (SCS-6/Ti-15-3) AT ELEVATED TEMPERATURE Ph.D. Thesis

Brian P. Sanders Dec. 1993 324 p
(AD-A273797; AFIT/DS/AA/93-4) Avail: CASI HC A14/MF A03

The fatigue characteristics of a unidirectional titanium based metal matrix composite site (MMC) were investigated at elevated temperature (427 C). A hybrid strain controlled loading made was used to subject the 0 deg and 90 deg laminas to fatigue. Along with the fatigue tests, microscopy and analytical modeling were also conducted. This combination of activities led to defining the initiation and progression of damage and deformation in the MMC. When loading was parallel to the fiber direction, the fatigue behavior was initially dominated by creep deformation of the matrix. Then, depending on the maximum strain, specimen failure was the result either fiber fractures or matrix cracking. In contrast, when loading was perpendicular to the fiber direction, the fatigue response was first dominated by the initiation of fiber-matrix interface damage. Then, if the maximum strain was above .35%, the dominant damage mechanism was matrix cracking. Below this strain level, the damage was a mixture of matrix microcracks and the progression of fiber-matrix interface damage. The analysis for this fiber orientation included unique methods to model the interface damage. This hybrid approach involving experiments, microscopy, and analytical modeling provided better understanding of the fatigue behavior of the MCC. DTIC

N94-25938# Lawrence Livermore National Lab., CA.

NUMERICAL SIMULATIONS OF INTERFACIAL DEBONDING IN DUCTILE-PHASE REINFORCED INTERMETALLIC MATRIX COMPOSITES

G. A. Henshall, E. Zywicz, and M. J. Strum 10 Aug. 1993 18 p
Presented at the Mechanism and Mechanics of Composite Fracture Meeting, Pittsburgh, PA, 17-21 Oct. 1993
(Contract W-7405-eng-48)
(DE94-003639; UCRL-JC-114725; CONF-931078-2) Avail: CASI HC A03/MF A01

The fracture toughness of brittle intermetallic compounds can be improved by ductile-phase reinforcements. The effectiveness of the ductile phase in bridging cracks, and therefore increasing the composite toughness, is known qualitatively to depend upon the extent of debonding between the two phases. Numerical crack-growth simulations are used here to provide semi-quantitative predictions of the influence of interfacial debonding on the macroscopic stress-displacement behavior and, hence, the fracture toughness of an idealized Pb/glass composite. The interfacial toughness required to cause debonding, characterized by a constant critical energy release rate, is varied parametrically. As expected, higher interfacial toughness results in less interphase debonding, higher composite strength, and greater ductile-phase constraint. Consequently, the increase in ductile-phase triaxiality can potentially accelerate internal void formation and growth or facilitate cleavage fracture, either of which would likely decrease the toughness of the composite. DOE

N94-25982# Pacific Northwest Lab., Richland, WA.

GENERAL MOTORS CORPORATION AND PACIFIC NORTHWEST LABORATORY STAFF EXCHANGE: INSPECTION OF CASE HARDENED STEELS AND METAL-MATRIX COMPOSITES

M. S. Good and D. D. Rogers (General Motors Corp., Saginaw, MI.) Oct. 1993 19 p
(Contract DE-AC06-76RL-01830)
(DE94-003470; PNL-8926) Avail: CASI HC A03/MF A01

Staff exchanges, such as the one described in this report, are intended to facilitate communication and collaboration among scientists and engineers at Department of Energy (DOE) laboratories, in US industry, and academia. Funding support for these exchanges is provided by the DOE, Office of Energy Research, Laboratory Technology Transfer Program. The exchanges offer the opportunity for the laboratories to transfer technology and expertise to industry, gain a perspective on industry's problems, and develop the basis for further cooperative efforts through Cooperative Research and Development Agreements (CRADA's) or other mechanisms. The objectives of this report were as follows: for Pacific Northwest Laboratory (PNL) staff to present technology to General Motors (GM) staff on nondestructive measurement of hardened steel components and uniformity of particle dispersion in metal-matrix composites for evaluation for possible application in GM's manufacturing processes; for GM staff to discuss with PNL staff common manufacturing processes, metallurgy, and flaw criteria for hardening of various components and manufacturing of metal-matrix composites; and to provide an initial step in building a long-term collaborative relationship between PNL and GM. Information in this report on the staff exchange of PNL staff with GM Corporation includes the purpose and objectives, a summary of activities, significant accomplishments, significant problems, industry benefits realized, recommended follow-on work and potential benefits from that work, and three appendixes. Appendix A is a description of ultrasonic backscatter technology and its applications to the two nondestructive inspection interests defined by GM. Appendix B is a list of key contacts and the schedule of activities pertaining to the staff exchange. Appendix C is an article from American Society for Metals News relating to sensor needs. DOE

N94-25999# Air Force Inst. of Tech., Wright-Patterson AFB, OH. School of Engineering.

INVESTIGATION OF TENSION-COMPRESSION FATIGUE BEHAVIOR OF A CROSS-PLY METAL MATRIX COMPOSITE AT ROOM AND ELEVATED TEMPERATURES M.S. Thesis

Elizabeth A. Boyum Dec. 1993 165 p
(AD-A273731; AFIT/GAE/ENY/93D-6) Avail: CASI HC A08/MF A02

This research, the first load-controlled tension-compression fatigue testing to be performed on a MMC, extends the existing knowledge of MMC fatigue damage mechanisms to include the tension compression loading condition. To accomplish this, a (0/90) (sub 2s), SCS-6/Ti-15-3 laminate was subjected to tension-tension fatigue at room temperature, and tension-compression fatigue at both room temperature and 427 C. Stress and strain data was taken to evaluate the macro-mechanic behavior of the material. Microscopy and fractography were performed to characterize the damage on a micro-mechanic level. On a maximum applied stress basis, the room temperature tension-tension specimens had longer fatigue lives than the room temperature tension-compression specimens. The room and high temperature tension-compression fatigue lives were nearly identical in the fiber-dominated high stress region of the SN curve. However, the increased ductility and diffused plasticity of the titanium matrix at 427 C delayed the onset and severity of matrix cracking, and thus increased the elevated temperature fatigue lives in the matrix dominated region of the SN curve. In all cases, matrix damage initiated at reaction zone cracks which nucleated both matrix plasticity and matrix cracking. DTIC

N94-26019# Ames Lab., IA.

FRACTURE BEHAVIOR OF 20% Nb PARTICULATE REINFORCED ALUMINA COMPOSITE

S. Lane, S. B. Biner, and O. Buck 1993 11 p Presented at the High Performance Metal and Ceramic Matrix Composites, San Francisco, CA, 27 Feb. - 3 Mar. 1994
(Contract W-7405-eng-82)
(DE94-002830; IS-M-775; CONF-940229-1) Avail: CASI HC A03/MF A01

The composites consist of alumina matrix with 0.05 wt % MgO and 20 Vol % Nb with an average particle size of 30 to 100 microns produced by dry mixing and sintering to near their theoretical densities. Fracture toughness tests were carried out in three point bending on chevron notched samples. Results indicate that R-curve of the composites exhibited more than 300%

increase in crack growth resistance compared to crack growth resistance of alumina produced with the identical procedures. Crack growth resistance curve of the composites increased with increasing Nb particle size. Metallorgraph indicated that failure of Nb particles in crack path ranges from full interface separation without any significant deformation of Nb particles to cleavage failure without any evidence of interface separation. DOE

N94-26099# Lawrence Livermore National Lab., CA.
DESIGN STUDY OF FIBER-COMPOSITE PENETRATOR CASES
R. W. Logan, S. E. Groves, and R. E. Lyon 22 Oct. 1993 15 p
Presented at the Annual Winter Meeting of the American Society of Mechanical Engineers, New Orleans, LA, 28 Nov. - 3 Dec. 1993
(Contract W-7405-eng-48)
(DE94-003203; UCRL-JC-114833; CONF-931121-33) Avail: CASI HC A03/MF A01

A design study was conducted to demonstrate the viability of carbon-fiber reinforced epoxy composites as structural case materials for penetrating warheads. The objective was to conduct well-instrumented experimental studies of composite-body penetrators perforating mild steel plates and quantitatively model these plate penetrations using two and three dimensional finite element codes over a wide range of velocities and impact conditions in order to develop predictive capability for composite design and for use in tradeoff studies with existing case materials. Understanding of the failure of composite-body penetrators would be demonstrated by a rational design iteration which significantly improved performance. Initial studies utilized existing one-degree tapered cylindrical carbon fiber/epoxy composite cases fabricated by wet-filament winding. These sharp-tipped, steel-nose, composite penetrators were strain-gaged, piggy-backed with 57 kilograms, and impacted into steel plates in a velocity-boosted droptower at impact velocities ranging from 3 to 18 meters per second. Load, time, and position data were recorded during the impact event as well as the axial and hoop strains in the composite case. Monolithic 4340 hardened steel penetrators with both sharp- and flat-tip three-caliber ogive noses were also impacted into mild steel plates. Data from the composite-case and steel penetrators were used to calibrate a multiaxial, rate-dependent, flow and failure model for the mild steel plates in NIKE2D. The authors were then able to successfully predict survival and failure of the composite-case penetrators in normal-incidence droptower tests for different target thickness and velocity combinations. DOE

N94-26127*# National Aeronautics and Space Administration. Marshall Space Flight Center, Huntsville, AL.
THE EFFECTS OF EMBEDDED INTERNAL DELAMINATIONS ON COMPOSITE LAMINATE COMPRESSION STRENGTH; AN EXPERIMENTAL REVIEW
Alan T. Nettles Mar. 1994 23 p Sponsored by NASA, Washington
(NASA-TM-108440; NAS 1.15:108440) Avail: CASI HC A03/MF A01

Delaminations in laminated composite materials can degrade the compressive strength of these materials. Delaminations can form as a result of impact damage or processing flaws. In order to better understand the effects of these delaminations on the compressive behavior of laminated composite plates, programs have been conducted to assess the criticality of prescribed delaminations of known size, shape, and location on the compression strength of laminated composites. A review of these programs is presented along with highlights of pertinent findings from each. Author

N94-26190# Naval Postgraduate School, Monterey, CA.
EFFECTS OF POST-FABRICATION PROCESSING ON THE TENSILE PROPERTIES OF CENTRIFUGALLY CAST SiC PARTICULATE REINFORCED ALUMINUM COMPOSITES M.S. Thesis
Kurt A. Muller Sep. 1993 39 p
(AD-A274865) Avail: CASI HC A03/MF A01

A centrifugally cast A356 aluminum-matrix composite reinforced with silicon carbide (SiC) particles was thermomechanically processed by rolling and the resulting properties were studied. Tensile testing, hardness testing, and optical microscopy were conducted. This study included evaluations of the mechanical properties of the composite following rolling at varying strains, temperature, strain per pass, and aging treatments. The effects of both single and multistep rolling processes were evaluated, and the composites were tested following solution treatment. Testing revealed that the ductility was associated with progressive homogenization of the particulate distribution at increasing strain levels. It was found that rolling just under the solvus temperature produced poorer mechanical properties for the composite than for those rolled at a temperature significantly above or below the solvus temperature. Strain per pass was found to have insignificant effect on the final properties, with total strain being the controlling factor. For equal strength conditions, the underaged composite was more ductile than the overaged composite. DTIC

N94-26260# Technical Research Centre of Finland, Espoo. Metals Lab.
DESIGN AND LIFE-TIME OF POLYMER MATRIX COMPOSITE STRUCTURES: SUMMARY [MUOVIKOMPOSIITTIRAKENTEEN SUUNNITTELU JA ELINIKAE: YHTEENVETO]
Pekka H. Pankakoski, Pertti Auerkari, Pentti Kauppinen, Matti Sarkimo, and Tero Uuttu Nov. 1992 42 p In ENGLISH and FINNISH Sponsored by Technology Development Center, Finland; Technical Research Centre of Finland, Espoo; Oy Muotenko Ab, Finland; Neste Oy, Finland; and Hollming Oy, Rauma, Finland Original contains color illustrations
(ISSN 1235-0605)
(VTT-TIED-1415; ISBN-951-38-4309-2; ETN-94-95272) Copyright Avail: CASI HC A03/MF A01

The following cases were studied experimentally: impact resistance and residual bending strength of a sandwich panel made of a PVC foam core between carbon fiber reinforced epoxy skins; fatigue life of a thick glass fiber reinforced epoxy laminate beam; and resistance to cyclic overheating and impact damage of glass fiber reinforced VE pressure vessels and pressure piping. The impact resistance of a sandwich composite with carbon fiber reinforced epoxy skin and PVC foam core was investigated by measuring the surface and intermediate layer damage after controlled and repeated impacts by a 20 mm spherical indenter. High resolution ultrasonic mapping was used for characterizing the internal delamination defects. The effect of non penetrating impacts on the residual bending strength was reasonably well predicted from both the incident impact energy and number of impacts as well as from the size of the ultrasonically determined impact damage. The bending strength of the laminate beams in cyclic loading was measured and the results were compared to the actual service conditions. The results show that the life time was mostly influenced by strongly localized damage at the point of peak stresses. Non insulated GFRP (Glass Fiber Reinforced Plastic) pipes were experimentally investigated, with particular consideration to the effects of short term thermal overloads and impact damage. It appears possible to significantly extend the service temperature range for this material in noninsulated pressure vessels and pipes, with consequent savings in optimizing material costs and process efficiency at the time of design. Impact testing and subsequent static pressure testing showed that for a given type of material, the leakage pressure of the vessel can be relatively easily predicted from the incident impact energy or from the ultrasonically determined size of the impact defect. ESA

N94-26447# California Univ., Santa Barbara.
BIMATERIAL INTERFACES AND THEIR ROLE IN THE MECHANICAL PERFORMANCE OF THE IN-SITU COMPOSITES Final Report, 1 Jan. - 31 Dec. 1993
Anthony G. Evans 31 Dec. 1993 348 p
(Contract N00014-93-I-0213)
(AD-A274688) Avail: CASI HC A15/MF A03

This is the annual report of the Office of Naval Research grant at UCSB on Strength and Fracture Energy of Bimaterials. Bimaterials Interfaces includes three sections: Mechanics of Interfaces, Coating Design for Composite Systems, and Mechanics of Brittle Matrix Composites. For more details see the Executive Summary. DTIC

N94-26450# Carborundum Co., Niagara Falls, NY. Research and Development Div.
HIGH PERFORMANCE FIBERS Final Report
J. Economy 1994 3 p
(Contract N00014-97-J-4108)
(AD-A274693) Avail: CASI HC A01/MF A01

A two and a half year ONR/ARPA funded program to develop a low cost process for manufacture of a high strength/high modulus sigma/E boron nitride (BN) fiber was initiated on 7/1/90 and ended on 12/31/92. The preparation of high sigma/E BN fibers had been demonstrated in the late 1960's by the PI using a batch nitriding of B2O3 fiber with NH3 followed by stress graphitization at approximately 2000 deg C. Such fibers displayed values comparable to PAN based carbon fibers but the mechanicals were variable most likely because of redeposition of volatiles at 2000 deg C. In addition, the cost of the fibers was very high due to the need for many hours of nitriding necessary to convert the BsO3 fibers. the use of batch nitriding negated two possible cost advantages of this concept, namely, the ease of drawing very fine, multi-filament yarn of B2O3 and more importantly the very low cost of the starting materials. DTIC

N94-26544# Technical Research Centre of Finland, Espoo. Building Materials Lab.

COMPOSITE RAW MATERIALS FOR THE BUILDING INDUSTRY [RAKENNUSTEOLLISUUDEN KOMPOSIITTIEN OSAMATERIAALIT]

Leena Sarvaranta, ed. Dec. 1992 93 p In FINNISH
(ISSN 1235-0605)
(VTT-TIED-1433; ISBN-951-38-4327-0; ETN-94-95260) Copyright Avail: CASI HC A05/MF A01

A composite material is obtained by combining two or more different components. Thus an interface exists between these components. Interfaces are often mechanically the weakest and chemically the most unstable spots within the composite material. The choice and use of building materials is related to their availability, price and reliability in design. However, designers do not always have the relevant data concerning new composite materials. In research and development of new composites, simple rules of thumb are needed for the preliminary design. For a heavier calculation and the analysis of test results, models are needed for evaluating the dimensioning value of a given quantity. Systems including fiber and matrix, particle and matrix, and laminate and core are discussed from a mechanistic point of view. A general outline is given of the fire properties of materials and some special properties of composites are discussed. Fire regulations and the applicability of calculation methods are discussed. An approach to the prediction of durability of building materials and products is presented. The influence of building materials on the environment is discussed with regard to mineral materials, metals, synthetic polymers and timber. Concrete, ceramic materials, metals, timber and polymers are reviewed as potential matrix materials for composites in the building industry. Carbon, ceramic, glass, metal, aramide, polyester, polyacrylonitrile, polyolefine and wood fibers are reviewed as potential reinforcement for different matrices. ESA

N94-26557# North Carolina Agricultural and Technical State Univ., Greensboro.

INVESTIGATION OF FORCED AND ISOTHERMAL CHEMICAL VAPOR INFILTRATED SiC/SiC CERAMIC MATRIX COMPOSITES

J. Sankar, A. D. Kelkar, and R. Vaidyanathan Sep. 1993 216 p
Prepared for Oak Ridge National Lab., TN
(Contract DE-AC05-84OR-21400)
(DE94-004544; ORNL/Sub-88-SC423/01) Avail: CASI HC A10/MF A03

Mechanical properties of two different layups for each of the forced chemical vapor infiltration (FCVI) (41 specimens) and isothermal chemical vapor infiltration (CVI) (36 specimens) materials were investigated in air at room temperature (RT), 1000 C, and at room temperature after thermal shock (RT/TS) and exposure to oxidation (RT/OX). The FCVI specimens had a nominal interfacial coating thickness of 0.3 microns of pyrolytic carbon, while CVI specimens had a coating thickness of 0.1 microns. Effect of reinforcement and interfacial bond on mechanical properties of composite were investigated. Scanning electron microscopy (SEM) and transmission electron microscopy (TEM) were employed to analyze the fiber-matrix interface and the toughening mechanisms in this ceramic composite system. DOE

N94-26711# Sherbrooke Univ. (Quebec).

FATIGUE RESISTANCE UNDER TENSION-COMPRESSION OF LAMINATES IM6/5245C AND AS4/3501-6 [RESISTANCE EN FATIGUE TENSION-COMPRESSION DES STRATIFIES IM6/5245C ET AS4/3501-6]

Dominique Lefebvre, Catherine Randon, Patrick Larose, and Clermont Roy Jun. 1993 164 p In FRENCH
(IAR-CR-25; NRC-32160; CTN-94-61008) Avail: CASI HC A08/MF A02

Results are presented from a study of two laminate layups (S2 and S12) made with the AS4/3501-6 graphite/epoxy system. The performance of these layups was observed under static and cyclic loading and compared with the performance obtained with IM6/5245C laminates. Quasi three dimensional finite element analysis was used to calculate the edge stresses. The tests were conducted with specimens 150 mm long and stabilized with anti-buckling guides for compression loading. The damage development was monitored and documented using ultrasonic C-scan, photoelastic coatings, and edge replication. A comparison of experimental fatigue results was made with those obtained with MRLife and residual strength prediction code. The static compression resistance of the AS4/3501-6 composites was found to be superior to that of the IM6/5245C laminates, and the resistance of the S2 layups was superior to that of the S12 layups. The fatigue life of the S12 layups in both the IM6 and AS4 composites was equivalent for the same cyclic loading in compression. The fatigue life of the S2 layups in the AS4 composites was lower than in the IM6 composites. The MRLife program did not satisfactorily predict the fatigue life of the composites studied under compression loading. Author (CISTI)

N94-26796# Sandia National Labs., Albuquerque, NM.

A CONSTITUTIVE MODEL FOR LAYERED WIRE MESH AND ARAMID CLOTH FABRIC

M. K. Neilsen, J. D. Pierce, and R. D. Krieg (Tennessee Univ., Knoxville.) Sep. 1993 65 p
(Contract DE-AC04-94AL-85000)
(DE94-003275; SAND-91-2850; TTC-1251) Avail: CASI HC A04/MF A01

A new package for the air transport of hazardous materials is currently being developed in the Transportation Systems Department at Sandia National Laboratories. The baseline design has a unique impact limiter which uses layers of aluminum screen wire and aramid cloth fabric. A primary motivation for selecting this unusual combination of materials is the need for the impact limiter to not only limit the amount of load transmitted to the primary container but also to remain in place during impact events so that it provides a thermal barrier during a subsequent fire. A series of uniaxial and confined compression tests indicated that the layered material does not behave like other well characterized materials. No existing constitutive models were able to satisfactorily capture the behavior of the layered material; thus, a new plasticity model was developed. The new material model was then used to characterize the response of air transport packages with layered impact limiters to hypothetical accidental impact events. Responses predicted by these analyses compared favorably with experiments at Sandia's rocket sled test facility in which a one-fourth scale package was subjected to side and end impacts at velocities of 428 and 650 fps, respectively. DOE

N94-26895# Electromagnetic Sciences, Inc., Norcross, GA.

FERRITE PHASE SHIFTERS USING STRESS INSENSITIVE MATERIALS Final Report, Jul. 1991 - Jul. 1993

Todd Vaughn, Paul Cox, Gordon Harrison, and Pete Rodrigue Oct. 1993 205 p
(Contract N00014-91-C-2202)
(AD-A274639) Avail: CASI HC A10/MF A03

This R&D program sponsored by the Naval Research Laboratory and being conducted by EMS Technologies, Inc., Norcross, Georgia, is focused toward achieving improved performance in microwave switching components via use of 'stress insensitive' microwave ferrite materials for applications where stable hysteresis characteristics of the materials are critical to the RF performance. The program, therefore, primarily addresses how to relieve or improve the magnetostrictive characteristics of the materials with emphasis on the specific application and demonstration of these materials in microwave switching components, particularly ferrite toroidal phase shifters. Material investigations were focused on Mn(+3) substitutions in yttrium-gadolinium iron garnet. These compounds were evaluated in dual toroid waveguide phase shifter structures with temperature, pressure & Rf power as variables manganese substitution per formula unit for Fe+3 of 0.11 to 0.13 (2.2 to 2.6%) produced compounds which exhibited stable performance from magnetostrictive stresses in phaser structures. DTIC

N94-26930# Lawrence Livermore National Lab., CA.

PROCESSING AND MECHANICAL PROPERTIES OF LAMINATED METAL COMPOSITES OF Al 6090-25 VOLUME PERCENT SiC(SUB p) AND Al 5182

C. K. Syn, D. R. Lesuer, and O. D. Sherby (Stanford Univ., CA.) 19 Mar. 1993 11 p Presented at the International Symposium on Light Materials for Transportation Systems, Kyongju, Republic of Korea, 20-23 Jun. 1993

(Contract W-7405-eng-48)
(DE94-001070; UCRL-JC-113468; CONF-9306274-1) Avail: CASI HC A03/MF A01

Multilayer laminate metal composites (LMC's) containing equal volume percent of Al 5182 and Al 6090-25 volume percent SiC(sub p) were made. The laminates were prepared by hot pressing alternate layers to a fourth of initial height at 450 C in an argon gas atmosphere. Some laminates were warm rolled by repeatedly heating to 450 C and rolling. The large plastic deformation ensured good bonding between layers. Tensile properties, fracture toughness, and damping capacity of these deformation-bonded laminates were measured. Surface descaling prior to lamination enhanced the tensile properties and toughness substantially. Post-lamination T6 heat treatment increased tensile yield and flow stress and reduced the ductility. Interfaces and dissimilar properties of the component materials enhanced the damping capacity. Yield and tensile strengths were slightly lower than values calculated from the rule of averages based on the component materials. Toughness and damping capacity were, on the other hand, far superior to those of component materials. Ductility of the laminates was increased as the layer thickness was reduced. DOE

N94-26978# Dynamet Technology, Inc., Burlington, MA.
MATERIAL OPTIMIZATION AND MANUFACTURING DEVELOPMENT OF REDUCED COST POWDER METAL TITANIUM ALLOY COMPONENTS FOR GAS TURBINE ENGINE APPLICATION, PHASE 2 Final Report, Oct. 1991 - May 1993
Stanley Abkowitz, Robert Djingheuzian, Susan M. Abkowitz, Harold Heussi, and Paul Weihrauch Nov. 1993 114 p
(Contract DAAL04-91-C-0046)
(AD-A274410; ARL-CR-110) Avail: CASI HC A06/MF A02

This Small Business Innovation Research (SBIR) program has demonstrated the economic benefits of cold-hot isostatic pressing (CHIP) powder metallurgy (P/M) materials and manufacturing technology to produce lightweight titanium alloy components. The tooling was developed, and a turbine engine bearing housing preform and a tank track pin were produced. The study also established a data base of the static and dynamic mechanical properties as a function of the chloride impurity level of the commercially available elemental titanium powders and their associated costs. DTIC

N94-27076# Department of the Navy, Washington, DC.
METHOD FOR IMPROVING ELECTROMAGNETIC SHIELDING PERFORMANCE OF COMPOSITE MATERIALS BY ELECTROPULSING Patent Application
David S. Dixon, inventor (to Navy) and Michael Obara, inventor (to Navy) 30 Jul. 1993 16 p
(AD-D016050; US-Patent-Appl-SN-105818) Avail: CASI HC A03/MF A01

A method of improving the electromagnetic (EM) shielding performance of a composite material is provided. The composite has conductive and semi-conductive filler particles suspended in a non-conductive resin. The filler particles make up 0-40 weight percent of the composite. The composite is subjected to an exponentially decaying pulse from an energy source such that the energy of the pulse is less than that required to cause localized melting of the composite. DTIC

N94-27091# Department of the Navy, Washington, DC.
METHOD FOR IMPROVING ELECTROMAGNETIC SHIELDING PERFORMANCE OF COMPOSITE MATERIALS BY ELECTROPLATING Patent Application
David S. Dixon, inventor (to Navy), Michael Obara, inventor (to Navy), James Masi, inventor (to Navy), and William Bradley, inventor (to Navy) 30 Jul. 1993 16 p
(AD-D016038; US-Patent-Appl-SN-105316) Avail: CASI HC A03/MF A01

A method of improving the electromagnetic (EM) shielding performance of a composite material is provided. The composite material has conductive and semi-conductive filler particles suspended in a non-conductive resin. The filler particles make up 0-40 weight percent of the composite material. The composite material is electroplated with a conductive material onto a portion of its surface to improve the electrical connection between the conductive material and a portion of the filler particles. DTIC

N94-27107# Massachusetts Univ., Lowell. Dept. of Chemistry.
POLYIMIDE/INORGANIC COMPOSITE-INTERPENETRATING POLYMER NETWORK FOR STABLE SECOND-ORDER NONLINEAR OPTICS Technical Report
Sutiyao Marturunkakul, Jeng-I Chen, Lian Li, Xin L. Jiang, and Ru J. Jeng 10 Dec. 1993 8 p
(Contract N00014-90-J-1148)
(AD-A274646; Rept-1148-94-03) Avail: CASI HC A02/MF A01

A new class of IPN system has been prepared and investigated. This IPN system combines the polybismaleinimide network and the NLO-active phenoxysilicon network. The second-order NLO coefficients, d33, values of the samples range from 2.5 to 6.7 pm/V depending on the composition and the processing conditions. The temporal stability of the second-order nonlinearities for these samples at 110 C varies from 47 to 88% retention after 274 h. DTIC

N94-27125# Cornell Univ., Ithaca, NY. Dept. of Materials Science and Engineering.
INTERFACE PHENOMENA IN METAL-CERAMIC COMPOSITES Final Report, 1 May 1990 - 30 Apr. 1993
Rishi Raj 27 Sep. 1993 52 p
(Grant AF-AFOSR-0279-90)
(AD-A274167; AFOSR-93-0885TR) Avail: CASI HC A04/MF A01

This report describes theoretical and experimental results that link the properties of the heterointerface to the macroscopic mechanical behavior of metallic composites where the continuous phase is a metal and the hard phase is a ceramic (MMC's) or an intermetallic (IMC's). The results emphasize that the properties of the composites depend on the interaction between cohesive strength of the M/C or M/I interface and the physical microstructural scale of the metal. This result is general and is expected to apply from room temperature properties, such as toughness, to creep resistance at very high temperatures. At room temperature, the effect of scale is based on the dislocation pile-up model for delamination at the interface. At high temperatures, the climb rate of dislocations in the metal layer depends on its width and on the pinning efficiency of lattice dislocations at the interface. DTIC

N94-27135# Army Topographic Engineering Center, Fort Belvoir, VA.
MULTIVARIATE SPECTRAL ANALYSIS TO EXTRACT MATERIALS FROM MULTISPECTRAL DATA Final Report, Sep. 1990 - Sep. 1992
Robert S. Rand and Donald A. Davis Sep. 1993 121 p
(AD-A274142; TEC-0039) Avail: CASI HC A06/MF A02

This effort investigates various multivariate analysis techniques for classification/identification to extract natural and manmade features reliably from broad-band spectral imaging data/multispectral imagery. An enhanced Bayesian method is proposed and is demonstrated to exhibit increased accuracy over three conventional supervised classifiers. Broad-band spectral properties of various materials are examined, and the perturbations on spectra of pure materials introduced by mixtures are shown. A mixing model that uses multiple linear regression constrained by two physical properties is tested. DTIC

N94-27142# Georgia Inst. of Tech., Atlanta.
DEFORMATION, CONSTITUTIVE BEHAVIOR, AND DAMAGE OF ADVANCED STRUCTURAL MATERIALS UNDER MULTIAXIAL LOADING Final Report, 1 May 1990 - 30 Apr. 1993
Stephen D. Antolovich, David L. McDowell, and Ritesh P. Shah 30 Apr. 1993 23 p
(Grant AF-AFOSR-0162-90)
(AD-A274165; AFOSR-93-0895TR) Avail: CASI HC A03/MF A01

In the grant period just completed, the metallurgical variables identified in the previous period have been addressed. Room temperature multiaxial testing of polycrystalline NiAl has been completed and high temperature experiments are being planned. In addition, compression testing of polycrystalline NiAl at room temperature has also been done. These experiments were included in the program to further investigate the results of the multiaxial experiments. The prime objective of these experiments is to differentiate damage and plasticity observed in this material under compression. Finite element analysis based on micromechanics will be done to study the stress distribution at the grain boundaries. Together, these experiments will form the basis for development of a constitutive model which takes into consideration crystal plasticity and damage. DTIC

N94-27201# Technische Univ., Delft (Netherlands). Faculty of Aerospace Engineering.
IMPACT TESTS ON FIBRE METAL LAMINATES UNDER A TENSILE LOAD
A. Vlot Mar. 1993 34 p
(PB94-126570; LR-714) Avail: CASI HC A03/MF A01

The well-known sensitivity of conventional composites to incidental damage, such as impact, has slowed their widespread application to thin, damage tolerance-critical primary structures such as fuselage pressure cabin skins. Therefore, impact tests were performed to determine the impact characteristics of fiber metal laminates (GLARE and ARALL). Comparative low and high velocity impact tests were performed on monolithic aluminum, fiber metal laminates, and carbon thermoplastic composites. Additional impact tests were performed on monolithic aluminum and ARALL specimens under tensile loading. NTIS

N94-27253 National Defence Research Establishment, Stockholm (Sweden). Dept. of Weapon Systems, Effects and Protection.
THERMOPLASTIC OR THERMOSETTING COMPOSITES IN AIRCRAFTS [TERMOPLAST-ELLER HAERDPLASTKOMPOSITER I FLYGPLANSTILLAEMPNINGAR]
O. Dickman and F. Larsson Sep. 1993 64 p In SWAHILI
(PB94-123809; FOA-A-20055-2.5) Avail: Issuing Activity (National Technical Information Service (NTIS))

This report discusses the differences in production processing and performance between thermosetting and thermoplastic fiber reinforced composites, and contains the results of a survey of the opinions of the aerospace industry, research institutes and material suppliers regarding the use of thermosets and thermoplastics. The materials considered are intended for applications as loadbearing structures and for radar camouflage in aircraft. In comparison with thermosetting resins, thermoplastics possess the advantages of high damage tolerance and low moisture absorption at high temperatures, but modified thermosetting resins have been developed with almost equal performance in these respects. Some thermoplastics have the disadvantage of being sensitive to organic solvents. Manufacture of composite components with thermoplastic matrices shows great potential for using cheap and rapid production processes, although at the present time such methods are not available for continuous fiber composites. The advantage with thermosetting resins is in the main the extensive experience and knowledge concerning production processing and performance. Anticipated new regulations for improved working environments, reduced environmentally damaging waste and increased recycling favor thermoplastics. NTIS

N94-27255# National Aerospace Lab., Tokyo (Japan). Aeroengine Div.
HIGH TEMPERATURE TENSION TEST EQUIPMENT OF HEAT RESISTANT COMPOSITE MATERIALS [TAINETSU FUKUGO ZAIRYU YO KOON HIPPARI SHIKEN SOCHI NO SHISAKU]
Yasushi Sofue and Akinori Ogawa Jan. 1993 11 p In JAPANESE
(ISSN 0452-2982)
(NAL-TM-652; JTN-94-80620) Avail: CASI HC A03/MF A01

In the application of heat resistant composites to structural members in the high temperature atmosphere, it is very important to evaluate their mechanical behavior in high temperature atmospheres. This paper described a high temperature test system to evaluate high temperature elongation and tensile strength of heat resistant composites in the air. The preliminary strength tests of two composite materials, SiC (Silicon Carbide)/LAS (Lithium Alumino Silicate) and SiC/SiC were conducted from room temperature to 1300 C in the air using a displacement measuring system with two pairs of simple laser sensors. Author (NASDA)

N94-27279# National Aerospace Lab., Tokyo (Japan).
SP/MSP TESTS FOR THE EVALUATION OF FGM [FGM KAIHATSU NO TAMENO SP/MSP SHIKENHOU]
Masayuki Niino, Yoshio Wakamatsu, Akinaga Kumakawa, Toshihito Saito, Hideaki Takahashi, Toshiyuki Hashida, and Masahiro Saito Jun. 1992 81 p In JAPANESE
(ISSN 0289-260X)
(NAL-SP-17; JTN-94-80611) Avail: CASI HC A05/MF A01

Two related papers are included. The first one is a specification on the newly developed modified small punch (MSP) method and the second one is a research paper on the evaluation of the MSP method using ceramic materials. The first defines testing apparatus, preparation method and dimensions of test pieces, and testing procedures. In the second paper, fracture characteristics of ceramics/metal composite materials are evaluated using the MSP method and the results are compared with those obtained by using the conventional SP method. Microscopic fracture processes are observed by the acoustic emission method. The testing temperature was varied to 1873 K. For individual titles, see N94-27280 through N94-27281.

N94-27280# National Aerospace Lab., Tokyo (Japan).
SP/MSP TESTS FOR THE EVALUATION OF FGM [FGM KAIHATSU NO TAMENO SP/MSP SHIKENHOU]
Masayuki Niino, Yoshio Wakamatsu, Akinaga Kumagawa, Toshihito Saito, Hideaki Takahashi, Toshiyuki Hashida, and Masahiro Saito *In its* SP/MSP Tests for the Evaluation of FGM Jun. 1992 p 1-11 In JAPANESE
(For primary document see N94-27279 07-24)
Avail: CASI HC A03/MF A01

The development of functionally gradient materials (FGM's) as next-generation super heat resisting materials, which can be continuously subjected to extreme environments, has been a national project in Japan since 1987. To perform computer design calculations able to determine the minimum thermal stress condition of FGM's, all the known material properties of each applied microstructure, e.g., non-FGM's, such as ceramic/metal composites, must be included in the design data base. Standard testing methods must also be developed for evaluation of mechanical properties of miniaturized samples. To evaluate the fracture strength of ceramics and ceramic/metal composites (non-FGM's), small punch (SP) tests, and for brittle materials, modified small punch (MSP) tests, have been developed to improve both specimen clamping procedures and deflection measurements. These tests enable accurate and well reproducible results to be obtained for brittle and ductile materials from room to very high temperatures, thereby enabling suitable evaluation of material properties such as Young's modulus, fracture strength, yield strength, fracture strain, and fracture energy. In addition, by utilizing SP/MSP test data from miniaturized specimens, fracture toughness values can be estimated from the correlation between fracture toughness and fracture stress. Described here are experiments carried out to standardize the SP/MSP test procedures study in order to develop a data base from which to study deflection and fracture characteristics of FGM's. Author (NASDA)

N94-27281# Tohoku Univ., Sendai (Japan). Mechanical Engineering.
RESEARCH ON THE DEVELOPMENT OF FRACTURE CHARACTERISTICS EVALUATION SYSTEM FOR CERAMICS AND METAL COMPOSITE MATERIALS [SERAMIKKUSU/KINZOKU FUKUGO ZAIRYO NO TAMENO HAKAI TOKUSEI HYOKA SHISUTEMU NO KAIHATSU NI KANSURU KENKYU]
Masahiro Saito *In* NAL, SP/MSP Tests for the Evaluation of FGM Jun. 1992 p 13-79 In JAPANESE Sponsored by Science and Technology Agency, Tokyo, Japan (For primary document see N94-27279 07-24)
Avail: CASI HC A04/MF A01

Modified small punch (MSP) method is developed for fracture characteristics evaluation of brittle materials and test results are reported. The MSP method is developed by the modification of the small punch (SP) method, which was developed to evaluate the ductility and brittleness transition temperature of ductile metal materials. Testing procedures and test results of SP method and MSP method are compared using zirconium and stainless steel composite materials. Reproducibility of test results and bending and yield strength test results from both methods are correlated. Fracture mechanisms for ceramic materials, zirconium and stainless steel composite material, and zirconium and stainless steel fiber reinforced composite material are studied by using yield strength method and MSP method together with acoustic emission test. Microscopic fracture mechanisms for these materials are also studied by the use of electronic scanning microscopic observations. Several ceramic materials and ceramic/metal composite materials at a high temperature of 1873 K are studied and test results from SP method and MSP method are compared. Author (NASDA)

N94-27314 Concordia Univ., Montreal (Quebec). Dept. of Mechanical Engineering.

HOT DEFORMATION BEHAVIOUR OF Si(p)/Al COMPOSITES AND THEIR MATRICES AND AN Al-Mg-Si ALLOY M.S. Thesis

Peter Sakaris Apr. 1993 143 p
(ISBN-0-315-84699-2; CTN-94-61089) Copyright Avail: Micromedia Ltd., Technical Information Centre, 240 Catherine Street, Suite 305, Ottawa, Ontario, K2P 2G8, Canada HC/MF

Research was conducted to determine the hot working behavior of an Al-Mg-Si alloy (6201), a cast Al-Si alloy (A356), and two SiC Al-matrix composites (using A356 and 6061) under continuous deformation conditions. A torsion testing method was employed since it enables a large strain to be applied to a specimen at a relatively constant rate. Stress-strain curves, fracture strains, and strain rates were determined at typical hot working temperatures. Flow stress (FS) and strain to failure (STF) data were compared to published results. The flow stresses decrease monotonically with increasing deformation temperature T. At very high temperatures, FS is similar for all materials, but as T falls to 300 C, the A356 rises more rapidly than 6061. FS for the composites rises more rapidly than the matrix alloys. The ductility of all materials increases as T increases. STF rises more rapidly for SiC/A356 than for SiC/6061 indicating that the SiC particles have much less effect as additional crack initiators in A356. Single activation energies could be computed for each material. The 6061 Al is somewhat stronger than Al because of the particles at low temperatures and the increased level of solute at high temperatures. The solutioned specimens had high peak stresses and considerable work softening at 300 C due to dynamic formation and coalescence of precipitates.
Author (CISTI)

N94-27352*# California Univ., San Diego, La Jolla. Dept. of Applied Mechanics and Engineering Sciences.

THE EXPERIMENTAL BEHAVIOR OF SPINNING PRETWISTED LAMINATED COMPOSITE PLATES Final Technical Report, 1 May 1990 - 30 Sep. 1993

John B. Kosmatka and Alex J. Lapid 1993 219 p
(Contract NCC3-173)
(NASA-CR-195220; NAS 1.26:195220; SSRP-93/10) Avail: CASI HC A10/MF A03

The purpose of the research is to gain an understanding of the material and geometric couplings present in advanced composite turbo-propellers. Twelve pre-twisted laminated composite plates are tested. Three different ply lay-ups (2 symmetric and 1 asymmetric) and four different geometries (flat and 30x pre-twist about the mid-chord, quarter-chord, and leading edge) distinguish each plate from one another. Four rotating and non-rotating tests are employed to isolate the material and geometric couplings of an advanced turbo propeller. The first series of tests consist of non-rotating static displacement, strain, and vibrations. These tests examine the effects of ply lay-up and geometry. The second series of tests consist of rotating displacement, strain, and vibrations with various pitch and sweep settings. These tests utilize the Dynamic Spin Rig Facility at the NASA Lewis Research Center. The rig allows the spin testing of the plates in a near vacuum environment. The tests examine how the material and plate geometry interact with the pitch and sweep geometry of an advanced turbo-propeller. Author (revised)

N94-27433*# Lockheed Engineering and Sciences Co., Hampton, VA.

FATIGUE RESISTANCE OF UNNOTCHED AND POST IMPACT(+/- 30 DEG/0 DEG) 3-D BRAIDED COMPOSITES Final Report

Marc A. Portanova Jan. 1994 33 p
(Contract NAS1-19000; RTOP 510-02-12-09)
(NASA-CR-191590; NAS 1.26:191590) Avail: CASI HC A03/MF A01

The fatigue resistance of a multiaxial braided (3-D) graphite/expoxy composite in both unnotched and post impacted conditions has been evaluated. The material tested is a (+/- 30/0 deg) multiaxial braid constructed from AS4/12K tow graphite fibers and British Petroleum E905L epoxy resin. These materials were braided as dry preforms and the epoxy was added using a resin transfer molding process (RTM). The unnotched and post-impact specimens were tested in compression-compression fatigue at 10 Hz with a stress ratio of R=10. The unnotched tension-tension fatigue specimens were tested at S Hz with a stress ration of R=0.1. Damage initiation and growth was documented through the application of radiography and ultrasonic through transmission (C-scans). Visible inspection of surface and edge damage was also noted to describe the initiation and progression of damage in these materials. The mechanisms leading to damage initiation were established and failure modes were determined. Stiffness and strength degradation were measured as a function of applied cycles. These 3-D braided composite results were compared to strain levels currently used to design primary structure in commercial aircraft composite components made from prepreg tape and autoclave cured.
Author

N94-27586# Aerospatiale Aquitaine, Saint-Medard en Jalles (France).

TESTING PROCEDURE FOR TOUGHNESS CHARACTERISATION OF CERAMIC MATRIX COMPOSITES

S. Yotte, J. M. Quenisset, M. Bouquet, and C. Lambert 1993 12 p
Presented at EACM, Amsterdam, Netherlands, 1992 Sponsored by Aerospatiale, France, and SEP, France
(Rept-932-430-101; ETN-94-95459) Avail: CASI HC A03/MF A01

A methodological approach of the toughness characterization of Ceramic Matrix Composites (CMC's) is proposed. The testing procedure is based on the determination of damage zone propagation curves from which an energy release rate can be derived, if a steady state propagation can be achieved. Also a parameter representative of the composite's ability to develop a damage zone can be defined during the first period of propagation. Prior to any testing, an experimental setup satisfying various procedure requirements can be defined through a three step approach: a critical examination of the testing methods commonly used for the toughness characterization of homogeneous isotropic materials; a two dimensional (2D) linear elastic analysis of the stress distribution in front of a notch tip; and a 3D numerical simulation of a toughness test while taking into account the damagable behavior of the related CMC's. ESA

N94-27640*# National Aeronautics and Space Administration. Lewis Research Center, Cleveland, OH.

A HYDROSTATIC STRESS-DEPENDENT ANISOTROPIC MODEL OF VISCOPLASTICITY

D. N. Robinson (Akron Univ., OH.), Q. Tao (Akron Univ., OH.), and M. J. Verrilli Mar. 1994 16 p
(RTOP 505-63-12)
(NASA-TM-106525; E-8651; NAS 1.15:106525) Avail: CASI HC A03/MF A01

A hydrostatic stress-dependent, anisotropic model of viscoplasticity is formulated as an extension of Bodner's model. This represents a further extension of the isotropic Bodner model over that made to anisotropy by Robinson and MitiKavuma. Account is made of the inelastic deformation that can occur in metallic composites under hydrostatic stress. A procedure for determining the material parameters is identified that is virtually identical to the established characterization procedure for the original Bodner model. Characterization can be achieved using longitudinal/transverse tensile and shear tests and hydrostatic stress tests; alternatively, four off-axis tensile tests can be used. Conditions for a yield stress minimum under off-axis tension are discussed. The model is applied to a W/Cu composite; characterization is made using off-axis tensile data generated at NASA Lewis Research Center (LeRC). Author (revised)

N94-27658*# National Aeronautics and Space Administration. Langley Research Center, Hampton, VA.

IMPLEMENTATION OF THERMAL RESIDUAL STRESSES IN THE ANALYSIS OF FIBER BRIDGED MATRIX CRACK GROWTH IN TITANIUM MATRIX COMPOSITES

John G. Bakuckas, Jr. (Galaxy Scientific Corp., Pleasantville, NJ.) and W. Steven Johnson Feb. 1994 44 p
(RTOP 505-63-50-04)
(NASA-TM-109082; NAS 1.15:109082) Avail: CASI HC A03/MF A01

In this research, thermal residual stresses were incorporated in an analysis of fiber-bridged matrix cracks in unidirectional and cross-ply titanium matrix composites (TMC) containing center holes or center notches. Two TMC were investigated, namely, SCS-6/Timelal-21S laminates. Experimentally, matrix crack initiation and growth were monitored during tension-tension fatigue tests conducted at room temperature and at an elevated temperature of 200 C. Analytically, thermal residual stresses were included in a fiber bridging (FB) model. The local R-ratio and stress-intensity factor in the matrix due to thermal and mechanical loadings were calculated and used to evaluate the matrix crack growth behavior in the two materials studied. The frictional shear stress term, tau, assumed in this model was used as a curve-fitting parameter to matrix crack growth data. The scatter band in the values of tau used to fit the matrix crack growth data was significantly reduced when thermal residual stresses were included in the fiber bridging analysis. For a given material system, lay-up and temperature, a single value of tau was sufficient to analyze the crack growth data. It was revealed in this study that thermal residual stresses are an important factor overlooked in the original FB models. Author

N94-27688 McMaster Univ., Hamilton (Ontario). School of Graduate Studies.

THE DEFORMATION OF COPPER-TUNGSTEN COMPOSITES Ph.D. Thesis

James Warren Poole Apr. 1993 239 p
(ISBN-0-315-84939-8; CTN-94-61111) Copyright Avail: Micromedia Ltd., Technical Information Centre, 240 Catherine Street, Suite 305, Ottawa, Ontario, K2P 2G8, Canada HC/MF

A series of plane strain compression experiments and finite element method (FEM) calculations was performed on continuous copper-tungsten fiber composites to examine the role of volume fraction and fiber arrangement on the mechanical behavior when the fiber axis was perpendicular to the loading direction. The flow pattern in the matrix was quantified by measuring the shape change of a fine gold grid which had been fabricated on the surface of the sample prior to deformation. It was determined that the pattern of deformation in the matrix was controlled by the spacing and geometric arrangement of the fibers. The damage process by fiber cracking or interfacial decohesion can be understood by the local distribution of stresses (as calculated by FEM) in the fibers and at the fiber matrix interface. The development of the deformation texture in the matrix and the observations of the pattern of subsequent recrystallization events can be related to the flow pattern in the matrix. The combination of careful experiments with FEM calculations was demonstrated to represent a powerful approach in studying problems involving composite materials. Author (CISTI)

N94-27710# Sandia National Labs., Albuquerque, NM.

SOL-GEL DERIVED SILICA/SILOXANE COMPOSITE MATERIALS: THE EFFECT OF LOADING LEVEL AND CATALYST ACTIVITY ON SILICA DOMAIN FORMATION

E. P. Black, T. A. Ulibarri, G. Beaucage, D. W. Schaefer, R. A. Assink, D. F. Bergstrom (Dow Corning Corp., Midland, MI.), P. A. Giwa-Agbomeirele (Dow Corning Corp., Midland, MI.), and G. T. Burns (Dow Corning Corp., Midland, MI.) 1993 5 p Presented at the 207th Spring National Meeting of the American Chemical Society, San Diego, CA, 13-18 Mar. 1994
(Contract DE-AC04-94AL-85000)
(DE94-002734; SAND-93-2542C; CONF-940301-1) Avail: CASI HC A01/MF A01

Currently, the production of in situ reinforcement in polymeric systems by sol-gel methods is undergoing rapid development. However, understanding of synthesis/structure/property relationships is still lacking. In order to produce sol-gel derived composite materials with sufficient mechanical properties for commercial applications, this deficit of information must be addressed. We have completed a detailed investigation of in situ silica growth in polydimethylsiloxane (PDMS)/tetraethylorthosilicate (TEOS) systems. Factors which affect the domain growth, such as catalyst activity and silica loading, have been examined by solid state Si-29 NMR, SEM, mechanical testing, and small angle neutron scattering. DOE

N94-27813# Ames Lab., IA.

CHARACTERIZATION OF ZnS-GaP NAON-COMPOSITES Ph.D. Thesis

V. Todd Dec. 1993 72 p
(Contract W-7405-eng-82)
(DE94-004888; IS-T-1669) Avail: CASI HC A04/MF A01

It proved possible to produce consistent, high-quality nanocrystalline ZnS powders with grain sizes as small as 8 nm. These powders are nano-porous and are readily impregnated with GaP precursor, although inconsistently. Both crystal structure and small grain size of the ZnS can be maintained through the use of GaP. Heat treatment of the impregnated powders results in a ZnS-GaP composite structure where the grain sizes of the phases are on the order of 10-20 nm. Conventional powder processing should be able to produce optically dense ceramic compacts with improved mechanical properties and suitable IR transmission characteristics. DOE

N94-28376# Technical Research Centre of Finland, Espoo. Lab. of Production Engineering.

JOINING OF FIBRE REINFORCED METAL MATRIX COMPOSITE MATERIALS

Kazutoshi Nishimoto (Osaka Univ., Japan.) and Risto Karppi 1993 24 p
(ISSN 1235-0605)
(PB94-132453; VTT/RN-1463; ISBN-951-38-4357-2) Copyright Avail: CASI HC A03/MF A01

The joining processes of metal matrix composite materials (MMC), especially those reinforced with fibers and the problems involved in each process are briefly reviewed in the literature survey. The report focuses on the fiber reinforced aluminum matrix composites. The joining processes described include diffusion bonding, resistance welding, brazing, soldering and fusion welding. These joining processes require heating and/or pressure which tend to cause the degradation of MMC joint properties. The strength of the joint produced by any of these processes therefore remains markedly inferior to the base materials. NTIS

N94-27897*# Northwestern Univ., Evanston, IL. Dept. of Mechanical Engineering.

EFFECTS OF PHYSICAL AGING ON LONG-TERM BEHAVIOR OF COMPOSITES

L. Catherine Brinson *In* Old Dominion Univ., The 1993 NASA-ODU American Society for Engineering Education (ASEE) Summer Faculty Fellowship Program Dec. 1993 p 74-77 (For primary document see N94-27893 07-80)
Avail: CASI HC A01/MF A03

N94-27914*# Arizona Univ., Tucson. Dept. of Aerospace and Mechanical Engineering.

MECHANICALLY FASTENED COMPOSITE LAMINATES SUBJECTED TO COMBINED BEARING-BYPASS AND SHEAR LOADING

Erdogan Madenci *In* Old Dominion Univ., The 1993 NASA-ODU American Society for Engineering Education (ASEE) Summer Faculty Fellowship Program Dec. 1993 p 130-136 (For primary document see N94-27893 07-80)
Avail: CASI HC A02/MF A03

25 INORGANIC AND PHYSICAL CHEMISTRY

Includes chemical analysis, e.g., chromatography; combustion theory; electrochemistry; and photochemistry.

For related information see also *77 Thermodynamics and Statistical Physics..*

N94-25745# Norwegian Defence Research Establishment, Kjeller.

THE CHEMICAL DETECTOR PAPER AS A POTENTIAL ALARM

Per B. Storeboe 18 May 1993 37 p
(FFI-93/6007; ETN-94-95209) Avail: CASI HC A03/MF A01

The coloring of chemical detector paper was examined by numerical simulation. The computer program 'GAS-RISK', which is designed to compute aerosol evolution in a realistic way, was the tool used. In an operational analysis all the soldiers in a platoon were supplied with detector papers, and both on target and slightly off target chemical attacks were simulated. Rocket bursts released a fine aerosol. The performance of the paper was excellent under these conditions. The first colored paper in the position showed up before a single NAIAD, positioned in the front, gave alarm. ESA

N94-25747# Groningen Rijksuniv. (Netherlands).

POLYMER-BOUND RHODIUM HYDROFORMYLATION CATALYSTS Ph.D. Thesis

Tjeerd Jongsma 1992 118 p
(ETN-94-95388) Avail: CASI HC A06/MF A02

A survey of the applicability of bulky phosphite modified rhodium hydroformylation catalysts in polymer bound catalyst systems is presented. To get more insight into the catalytic cycle of this class of catalysts, a mechanistic study was carried out on the low molecular weight homogeneous tri (2-t-butylphenyl) phosphite rhodium hydroformylation catalyst. Using the information gained by this study a bulky phosphite was designed and attached to a polymer chain. The copolymer chain used to bind the ligands of the catalyst appeared to be formed by an ideally azeotropic copolymerization. This means that the ligands are perfectly randomly distributed along and among the polymer chains. This facilitates the study of the polymer bound catalyst, for the mean inter ligand distance can directly be related to the polymer chain loading. The bulky phosphite ligand used yielded active catalysts and no decrease of activity was observed when the catalyst was attached to the polymer chain, but the coordination constant of the ligand for rhodium was too low for application of this system in continuous flow reactors. A slightly smaller phosphite, which forms bis-phosphite rhodium complexes, was used in the proceeding studies. A closer examination of the influence of the polymer chain in the complex formation and activity of the copolymer bound catalyst was performed. Especially the dependency of the complex formation on the chain loading alpha (phosphite comonomer fraction) is studied. An X-ray study of the low molecular weight bis-phosphite rhodium complex was performed and proved to be of great help in understanding the sterical conformation of low molecular weight as well as polymer bound rhodium phosphite complexes. The polymer bound catalyst was grafted on an inert silica sphere. The so formed silica grafted polymer bound catalyst system was successfully used in a continuous flow reactor for the hydroformylation of styrene. ESA

N94-25913 International Centre for Theoretical Physics, Trieste (Italy).
ON THE THERMAL IGNITION WITH VARIABLE PRE-EXPONENTIAL FACTOR
S. S. Okoya Oct. 1992 9 p Limited Reproducibility: More than 20% of this document may be affected by microfiche quality
(DE93-616009; IC-92/337) Avail: CASI HC A02 (US Sales Only)

This work is concerned with the exothermic chemical reaction, taking the diffusion of the reactant into account and assuming an Arrhenius temperature dependence with variable pre-exponential factor. Of particular interest is the Frank-Kamenetskii parameter delta which we explicitly obtained in terms of the dimensionless activation number epsilon and the peak temperature excess theta(sub m) under physically reasonable assumptions. DOE

N94-25934# Air-Conditioning and Refrigeration Technology Inst., Inc., Arlington, VA.
MEASUREMENT OF VISCOSITY, DENSITY, AND GAS SOLUBILITY OF REFRIGERANT BLENDS IN SELECTED SYNTHETIC LUBRICANTS
Richard C. Cavestri (Imagination Resources, Inc., Dublin, OH.) Oct. 1993 57 p
(Contract DE-FG02-91CE-23810)
(DE94-003609; DOE/CE-23810/22C) Avail: CASI HC A04/MF A01

Liquid/liquid miscibilities of four different 32 ISO VG polyolesters and one alkylbenzene at three concentrations was determined with five refrigerant blends, including HC-290. A vapor lubricant equilibrium (VLE) viscosity reduction of 32 ISO VG mineral oil with HCFC-22 has been completed. Composite viscosity reduction information by the fractionate components from R-502 in 32 ISO VG mineral oil has been obtained from -10 C (14 F) to 125 C (257 F) isotherms. Vapor lubricant equilibrium (VLE) viscosity reduction for 32 ISO VG mixed acid polyolester with HFC-134a has also been completed. DOE

N94-25964# Arnold Engineering Development Center, Arnold AFS, TN.
UV ABSORPTION TECHNIQUE FOR MONITORING MOBILE SOURCE NO EMISSIONS Final Report, 1 Oct. 1992 - 30 Sep. 1993
R. P. Howard and W. J. Phillips Nov. 1993 20 p
(AD-A273858; AEDC-TR-93-18) Avail: CASI HC A03/MF A01

Ultraviolet (UV) absorption techniques developed and used by the Arnold Engineering Development Center (AEDC) for measurements of nitric oxide (NO) in exhaust flows of turbine and liquid-propellant rocket engines were adapted for measurements of NO in the exhausts of automobiles. Measurements were performed across a roadway with a 10-percent mixture of NO being released into the exhaust stream of a small truck traveling at speeds ranging from 6 to 30 mph. Emission factors for these simulated exhausts ranged from 0.92 to 23.05 gm/mi. Nitric oxide was detected in measurements using NO-resonance lamp radiation passed twice across the roadway for emission factors as low as 1.78 gm/mi. Nitric oxide absorption was not detected on exhaust measurements of automobiles traveling (coasting) at constant speeds. Nitric oxide was detected at measurable levels on automobiles forced to stop and then accelerate through the measurement station. DTIC

N94-25978# Sandia National Labs., Albuquerque, NM.
OPTIMIZATION OF EXPERIMENTAL CONDITIONS IN IR REFLECTANCE DETERMINATION OF BPSG PROPERTIES
L. Zhang (New Mexico Univ., Albuquerque.), J. E. Franke (New Mexico Univ., Albuquerque.), T. M. Niemczyk (New Mexico Univ., Albuquerque.), and D. M. Haaland 1993 4 p Presented at the Techcon Conference on Semiconductor Research Corporation, Atlanta, GA, 28-30 Sep. 1993
(Contract DE-AC04-94AL-85000)
(DE94-002742; SAND-93-2118C; CONF-9309208-4) Avail: CASI HC A01/MF A01

Experiments were performed to examine sensitivity of thin-film property determinations to several experimental variables when applying multivariate calibration methods to infrared reflection spectroscopic data. Results indicate that low angles of incidence are best for robust quantitative determination of boron, phosphorus, and film thickness in borophosphosilicate glass (BPSG) dielectric films. However, the polarization state of the incidence beam does not affect the quantitative prediction ability. DOE

N94-26014# Oak Ridge Y-12 Plant, TN.
PLASMA SURFACE CLEANING USING MICROWAVE PLASMAS
C. C. Tsai (Oak Ridge National Lab., TN.), H. H. Haselton (Oak Ridge National Lab., TN.), W. D. Nelson (Oak Ridge National Lab., TN.), D. E. Schechter (Oak Ridge National Lab., TN.), L. M. Thompson, V. B. Campbell, A. L. Glover, and J. M. Googin 1993 15 p Presented at the Annual Vacuum Society Science Symposium, Triangle Park, NC, 15-19 Nov. 1993
(Contract DE-AC05-84OS-21400)
(DE94-002754; Y/DV-1298; CONF-9311110-1) Avail: CASI HC A03/MF A01

In a microwave electron cyclotron resonance (ECR) plasma source, reactive plasmas of oxygen and its mixture with argon are used for plasma-cleaning experiments. Aluminum test samples (0.95 x 1.9 cm) were coated with thin films (less than or equal to 20 (mu)m in thickness) of Shell Vitrea oil and cleaned by using such reactive plasmas. The plasma cleaning was done in various discharge conditions with fixed microwave power, RF power, biased potential, gas pressures (0.5 and 5 mtorr), and operating time up to 35 min. The status of plasma cleaning has been monitored by using mass spectroscopy. Mass loss of the samples after plasma cleaning was measured to estimate cleaning rates. Measured clean rates of low pressure (0.5 mtorr) argon/oxygen plasmas were as high as 2.7 (mu)/min. X-ray photoelectron spectroscopy was used to determine cleanliness of the sample surfaces and confirm the effectiveness of plasma cleaning in achieving atomic levels of surface cleanliness. In this paper, significant results are reported and discussed. DOE

N94-26075# Bettis Atomic Power Lab., Pittsburgh, PA.
THE USE OF ON-LINE ION CHROMATOGRAPHY FOR HIGH TEMPERATURE AND HIGH PRESSURE REACTION STUDIES
Garry J. Lynch Oct. 1993 26 p Presented at the Pittsburgh Conference on Analytical Chemistry and Applied Spectroscopy, Chicago, IL, 28 Feb. - 4 Mar. 1994
(Contract DE-AC11-93PN-38195)
(DE94-002525; WAPD-T-3009; CONF-940209-1) Avail: CASI HC A03/MF A01

This paper describes the use of on-line ion chromatography as a tool for chemistry reaction studies in small volume systems. The technique was used to study chemistry behavior in a high temperature and high pressure autoclave system. A dual analyzer, multi-channel on-line ion chromatograph (IC) was configured to automate the sampling and analysis. Analytical channels were set up for analysis of inorganic anions, monovalent cations, conductivity, and pH. Conductivity and pH were measured using the IC as a flow injection analyzer. Use of the IC system provides significant advantages over conventional sampling and analysis techniques: Reduction in sample volume, a closed sampling system that protects air or light sensitive analytes from breakdown, around-the-clock test performance combined with automatic calibration and quality control checking, and detection and tracking of reaction products or unexpected contaminants. Methods used to correct measured concentrations for the effects of sampling and for calculation of control chemical loss half-lives are presented. A limited evaluation of the flow injection analysis methods for conductivity and pH is provided. DOE

N94-26122# California Univ., Berkeley. Lawrence Berkeley Lab.
CHARACTERIZATION OF ACOUSTIC EFFECTS ON FLAME STRUCTURES BY BEAM DEFLECTION TECHNIQUE
B. Bedat, L. W. Kostiuk, and R. K. Cheng Oct. 1993 12 p Presented at the Fall Meeting of the Western States Section of the Combustion Institute, Menlo Park, CA, 18-19 Oct. 1993
(Contract DE-AC03-76SF-00098)
(DE94-003240; LBL-34700; CONF-931076-3) Avail: CASI HC A03/MF A01

This work shows that acoustic effects are the cause of the small amplitude flame wrinkling and movements seen in all the different gravitational conditions. The comparison between the acoustic velocity and beam deflection spectra for the two conditions studied (glass beads and fiber glass) demonstrates clearly this flame/acoustic coupling. This acoustic study shows that the burner behaves like a Helmholtz resonator. The estimated resonance frequency corresponds well to the experimental measurements. The fiber glass damps the level of the resonance frequency and the flame motion. The changes shown in normalized beam deflection spectra give further support of this damping. This work demonstrates that the acoustics has a direct influence on flame structure in the laminar case, and the preliminary results for the turbulent case also show a strong coupling. The nature of this flame/acoustic coupling are still not well understood. Further investigation should include determining the frequency limits and the sensitivity of the flame to acoustic perturbations. DOE

N94-26158 Korean Atomic Energy Research Inst., Daeduk (Republic of Korea).
DEVELOPMENT OF LASER SPECTROSCOPIC TECHNOLOGY IN NUCLEAR INDUSTRY
Jong Min Lee, Byung Heon Cha, Seong Ho Kim, Hyung Ki Cha, Chang Hwan Lim, Kye Seok Song, Jung Bok Kim, Si Pyo Rho, Jae Min Han, and Do Yung Jeong et al May 1992 184 p In KOREAN Limited Reproducibility: More than 20% of this document may be affected by microfiche quality
(DE93-633327; KAERI/RR-1117/92) Avail: CASI HC A09 (US Sales Only)

The goal of this project is to carry out the fundamental researches for the selective photoionization process of heavy atoms as well as the development of experimentally related instruments. Main research results carried out in this year are (1) multi-step photoionization spectroscopy of Hg atom by 3-color 3-step ionization scheme, (2) selective photoionization using polarization spectroscopy, (3) design and construction of ion separator chamber, and (4) theoretical study for spectroscopic parameters of mercury. This technology can be applied to several area of nuclear industry such as the utilization of radioactive waste, the development of new materials, and high sensitive analysis of heavy atomic elements. DOE

N94-26169 International Centre for Theoretical Physics, Trieste (Italy).
FERMI-LIQUID TO NON-FERMI-LIQUID TRANSITION IN A DYNAMICAL GENERALIZATION OF THE CPA IN A DISORDERED HUBBARD MODEL
I. Dasgupta and A. Mookerjee Jul. 1993 13 p Limited Reproducibility: More than 20% of this document may be affected by microfiche quality
(DE94-601875; IC-93/213) Avail: CASI HC A03 (US Sales Only)

Based on the augmented space formalism and a generalization of the alloy analogy, including the effect of the dynamics of the exchange bath, it is shown that a half-filled Hubbard model shows Fermi-liquid behavior at low values of the interaction parameter U. This gives way to non-Fermi liquid behavior at a critical U, where the system is still metallic. It is also shown that quenched disorder tends to lower this critical value of U. DOE

N94-26170 Melbourne Univ., Parkville (Australia). School of Physics.
NEUTRON REFLECTION INTERFEROMETRY
V. P. Gudkov, G. I. Opat, and A. G. Klein 12 May 1993 20 p Limited Reproducibility: More than 20% of this document may be affected by microfiche quality
(DE94-601876; UM-P-93/19) Avail: CASI HC A03 (US Sales Only)

It is shown that the analysis of stratified surface layers by neutron reflection interferometry is considerably enhanced by performing the reflectometry with phase information. Two methods of providing such information are presented. One is the Lloyd's mirror configuration, in which a directly propagating ray that interferes with the reflected ray supplies the phase information. The method has much in common with holography. The other is by the physical addition of an extra reference layer, whose amplitude and phase are known theoretically. It is concluded that in addition to the large intensity of the reflected neutron beam, the total reflection gives an analytical relation between phase of the reflection coefficient and the density distribution. This gives rise the possibility of obtaining density distributions near surfaces in a model independent way. Moreover, a comparison is possible of reflective coefficients from original and artificially layered surfaces, provided that the thickness of the layer is small enough. DOE

N94-26205*# Eloret Corp., Palo Alto, CA.
THEORETICAL DETERMINATION OF CHEMICAL RATE CONSTANTS USING NOVEL TIME-DEPENDENT METHODS Final Technical Report, 1 Jan. 1991 - 31 Jan. 1994
Christopher E. Dateo 12 Mar. 1994 7 p
(Contract NCC2-737)
(NASA-CR-195221; NAS 1.26:195221) Avail: CASI HC A02/MF A01

The work completed within the grant period 10/1/91 through 12/31/93 falls primarily in the area of reaction dynamics using both quantum and classical mechanical methodologies. Essentially four projects have been completed and have been or are in preparation of being published. The majority of time was spent in the determination of reaction rate coefficients in the area of hydrocarbon fuel combustion reactions which are relevant to NASA's High Speed Research Program (HSRP). These reaction coefficients are important in the design of novel jet engines with low NOx emissions, which through a series of catalytic reactions contribute to the deterioration of the earth's ozone layer. A second area of research studied concerned the control of chemical reactivity using ultrashort (femtosecond) laser pulses. Recent advances in pulsed-laser technologies have opened up a vast new field to be investigated both experimentally and theoretically. The photodissociation of molecules adsorbed on surfaces using novel time-independent quantum mechanical methods was a third project. And finally, using state-of-the-art, high level ab initio electronic structure methods in conjunction with accurate quantum dynamical methods, the rovibrational energy levels of a triatomic molecule with two nonhydrogen atoms (HCN) were calculated to unprecedented levels of agreement between theory and experiment. Author

N94-26251# Technical Research Centre of Finland, Espoo. Chemical Lab.
USE OF OXYGEN-17 ISOTOPE IN THE CHARACTERIZATION OF ZEOLITES AND RELATED STRUCTURES BY NUCLEAR MAGNETIC RESONANCE SPECTROSCOPY
Aila Maijanen, Arto Annila, Pia Qvintus-Leino, and Anneli Hase Apr. 1993 29 p Sponsored by Neste Foundation, Finland
(ISSN 1235-0605)
(VTT-TIED-1448; ISBN-951-38-4350-5; ETN-94-95266) Copyright Avail: CASI HC A03/MF A01

Solid state Nuclear Magnetic Resonance (NMR) spectroscopy is a powerful tool in the structure determination of zeolites. The current status of the use of O-17 NMR in the characterization of zeolites and related structures is surveyed. All the major components of zeolites contain an NMR active isotope: Si-29, Al-27 and O-17. The natural abundance of O-17 is low (0.037%), and thus, it requires enrichment of the sample with O-17 isotope. O-17 is a quadrupolar nucleus and the qadrupolar interaction broadens and shifts the NMR signal. Thus, in order to get higher resolution, a high static magnetic field and magic angle spinning technique with high spinning frequency should be used. Dynamic angle spinning and double rotation techniques were shown to improve the resolution of O-17 NMR spectra. Lineshape simulations are necessary to determine the O-17 NMR parameters of quadrupolar interaction. ESA

N94-26296# Hawaii Natural Energy Inst., Honolulu.
MOLTEN SALT TECHNIQUES FOR REPRODUCIBLE EXCESS HEAT Final Report
Bor Y. Liaw 5 Jan. 1994 4 p

(Contract N00014-92-J-1673)
(AD-A274935) Avail: CASI HC A01/MF A01

Major accomplishments were electrochemical characterization of Ni electrode system in the hydride-containing molten salts and calorimetry measurements of anomalous temperature excursion in the electrolysis of the Ni-H-based molten salt systems. The excess heat generation in molten salt systems is progressing well through the increasing understanding of electrochemical behavior of the cell and the availability of a variety of electrode materials used in the cell. Several issues are still open for improvements: the control of the cell behavior, the integrity of anode materials, the role of impurities in excess heat generation, and the threshold loading at elevated temperatures - just to name a few. DTIC

N94-26320# General Electric Co., Schenectady, NY.
ZINC(2) OXIDE STABILITY IN ALKALINE SODIUM PHOSPHATE SOLUTIONS AT ELEVATED TEMPERATURES
S. E. Ziemniak and E. P. Opalka Apr. 1993 29 p
(Contract DE-AC12-76SN-00052)
(DE94-003316; KAPL-4762) Avail: CASI HC A03/MF A01

Zinc oxide (ZnO) is shown to transform into either of two phosphate-containing compounds in relatively dilute alkaline sodium phosphate solutions at elevated temperatures via ZnO(s) + Na(+) + H2PO4(-)) (r reversible) NaZnPO4(s) + H2O or 2 ZnO(s) + H3PO4(aq) (r reversible) Zn2(OH)PO4(s) + H2O. X-ray diffraction analyses indicate that NaZnPO4 possesses an orthorhombic unit cell having lattice parameters a = 8.710 (+/-) 0.013, b = 15.175 (+/-) 0.010, and c = 8.027 (+/-) 0.004 A. The thermodynamic equilibria for these reactions were defined in the system ZnO-Na2O-P2O5-H2O for Na/P molar ratios between 2.1 and 3. Based on observed reaction threshold values for sodium phosphate concentration and temperature, the standard entropy (S deg) and free energy of formation ((Delta)G(sub f)(sup deg)) for NaZnPO4 were calculated to be 169.0 J/mol-K and -1510.6 kJ/mol, respectively; similar values for Zn2(OH)PO4 (tarbuttite) were 235.9 J/mol-K and -1604.6 kJ/mol. Additions of sodium sulfite and sulfate did not alter the above reactions. DOE

N94-26369# Rochester Univ., NY.
TRANSITION METAL ACTIVATION AND FUNCTIONALIZATION OF CARBON-HYDROGEN BONDS
1993 3 p
(Contract DE-FG02-86ER-13569)
(DE94-003650; DOE/ER-13569/8) Avail: CASI HC A01/MF A01

A method was developed for synthesizing a new complex for studying C-H activation, (HBPz*(sub 3))Rh(CNCH2CMe(sub 3))(PhN=C=NCH2)CMe(sub 3). This complex loses the carbodiimide ligand, thereby serving as a precursor for a 16-electron Rh(I) fragment which activates (via oxidative addition) a wide range of aromatic and aliphatic C-H bonds. The mechanism of activation of benzene by this fragment was studied. Reaction of (Tp'Rh(CNR)) fragment with aliphatic hydrocarbons was also studied. A study of C-H bond activation by the complex MnH3(dmpe)(sub 2) was completed. Reactions of (Ru(dmpe)(sub 2)) with several small molecules were also investigated. Effects of fluorine substituents on aromatic ring on C-H activation were looked at. Studies of (eta)(sup 2)-arene coordination with ((C5Me(sub 5))Rh(PMe(sub 3))) were completed; studies of reaction of this complex with 1,3-disubstituted benzenes are in progress. DOE

N94-26391# International Centre for Theoretical Physics, Trieste (Italy).
STRUCTURE OF IONIC FLUIDS IN EQUILIBRIUM WITH A MICROPOROUS IONIC MATRIX
H. Tatlipinar, G. Pastore (Trieste Univ., Italy.), and M. P. Tosi (Scuola Normale Superiore, Pisa, Italy.) Jul. 1993 10 p
(DE94-600563; IC-93/205) Avail: CASI HC A02/MF A01 (US Sales Only)

The Ornstein-Zernike equations for the structure of a fluid of positive ions in equilibrium with a disordered matrix formed by chlorine ions are solved numerically in the hypernetted-chain approximation, and the results are compared with those obtained for the corresponding molten salt at complete equilibrium. Quenching of the halogen frame in a model appropriate to CuCl enhances the delocalization of the Cu ions. A similar, though less striking, reduction in the short range order of the metal-ion components is accompanied by an enhancement of its state of intermediate-range order in models appropriate to trivalent metal halides with octahedral or tetrahedral-type coordination. DOE

N94-26392# Bhabha Atomic Research Centre, Bombay (India).
RADIOCHEMISTRY DIVISION ANNUAL PROGRESS REPORT : 1991
V. Natarajan, comp., ed., S. V. Godbole, comp., ed., and R. H. Iyer, comp., ed. 1993 192 p
(DE94-600652; BARC-1993/P/001) Avail: CASI HC A09/MF A02 (US Sales Only)

The research and development activities of the Radiochemistry Division during 1991 are briefly described under the headings: (1) Nuclear chemistry, (2) Actinide chemistry, and (3) Spectroscopy. In the field of nuclear chemistry, the main emphasis has been on the studies of fission process induced by reactor neutrons and light and heavy ions on actinides and low Z (Z less than 80) elements. Actinide chemistry research work deals mostly with studies on the solvent extraction behaviour of actinide and lanthanide ions from aqueous media using different organic reagents including CMPO and macrocyclic ligands. The spectroscopic studies include development of methods for the estimation of trace metallic impurities and rare earths in nuclear fuel materials and EPR investigations of high T(sub c) superconductors. A list of publications by the scientific staff of the Division is given at the end. DOE

N94-26406# Academy of Sciences (USSR), Leningrad. Inst. Yadernoj Fiziki.
AUTOMATED SYSTEM FOR GAS DETECTORS PROVIDING WITH BINARY MIXTURES [AVTOMATIZOVANNAYA SISTEMA OBESPECHENIYA BINARNMI SMESYAMI GAZOVYKH DETEKOROV]
L. M. Kochenda, A. G. Krivshich, S. M. Kozlov, E. A. Lobachev, A. A. Markov, V. I. Medvedev, V. A. Trofimov, and L. A. Shchipunov 1992 55 p In RUSSIAN
(DE93-634192; LIYaF-1768) Avail: CASI HC A04/MF A01 (US Sales Only)

The design peculiarities of an automated system providing gas detectors with binary mixtures are described. Operational characteristics and preliminary experimental data of the system utilization are given. Functional capabilities of the system use as a monitoring set when calibrating new created detectors and during a prolonged exploitation are considered. DOE

N94-26444# Colorado State Univ., Fort Collins.
TEMPLATE SYNTHESIS OF METAL MICROTUBULE ENSEMBLES UTILIZING CHEMICAL, ELECTROCHEMICAL, AND VACUUM DEPOSITION TECHNIQUES Interim Report
Charles J. Brumlik, Charles R. Martin, and Vinod P. Menon 3 Jan. 1994 37 p
(Contract N00014-82-K-0612)
(AD-A274676; TR-90-ONR) Avail: CASI HC A03/MF A01

Microtubules are an interesting type of microstructure that resemble miniature drinking straws. Such tubular microstructures are found in nature. In addition, we and others have been investigating strategies for making synthetic analogs. We are especially interested in the idea of making metal microtubules. Four procedures for preparing metal microtubules are described in this paper. The general approach, called template-synthesis, entails using the pores in a microporous membrane as templates for forming the tubules. Microporous anodic aluminum oxide membranes and nuclear track-etch membranes are used as the template membranes. Gold and silver microtubules are made with outer diameters as small as 200 nm. These microstructures are characterized by scanning electron microscopy. DTIC

N94-26476# Tokyo Univ. (Japan). Inst. for Solid State Physics.
A MIMIC MODEL OF Pt-Rh CATALYST PREPARED BY ELECTROCHEMICAL DEPOSITION OF Rh ON Pt (100) SURFACE
Masahiro Taniguchi, Erik K. Uzembaev, and Kenichi Tanaka Mar. 1993 22 p Sponsored by Ministry of Education, Science and Culture, Tokyo, Japan
(ISSN 0082-4798)
(Rept-A-2664; JTN-94-80535) Avail: CASI HC A03/MF A01

Electrochemical deposition of Rh ions on a (5 x 20) Pt (100) surface gave the (1 x 1) LEED (Low-Energy Electron Diffraction) pattern with high back ground intensity. By exposing the (1 x 1) Rh/Pt (100) surface to O2 or NO, a characteristic p (3 x 1) Rh-O overlayer is built up at about 400

K, which is the same structure observed on the Pt(0.25) Rh(0.75) (100) surface exposed to NO or O2. Once the p(3 x 1) Rh-O overlayer is formed, a reversible structural change, p(3 x 1) = (1 x 1), can be caused at room temperature by adding H2 and O2. The p(3 x 1) Rh-O overlayer on Pt (100) surface may represent a highly efficient catalyst for NO(x) reduction. Author (NASDA)

N94-26487# Naval Postgraduate School, Monterey, CA.
AN APPARATUS FOR MEASUREMENT OF IGNITION AND BURNING CHARACTERISTICS OF METALLIC PARTICLES M.S. Thesis
Stephen Gulakowski 17 Sep. 1993 36 p
(AD-A274815) Avail: CASI HC A03/MF A01

An apparatus was designed for use in determining ignition and combustion characteristics of metallic fuel particles and liquid fuel droplets. The design was tailored around the available data acquisition systems and diagnostic instruments. The apparatus consisted of a small windowed combustion bomb, a CO2 laser for particle ignition, a thermal imaging camera for recording the ignition process, a helium-neon laser and a 1024 element linear diode array sampled at 1Mhz for measuring forward scattered light and determining particle size (Fraunhofer diffraction). All major components were individually utilized. However, equipment limitations prevented actual use of the system for measurement of the burning rates of particles. Recommendations are made which would permit the original objectives to be met. DTIC

N94-26518# Secretariat d'Etat a la Recherche, Algiers (Algeria). Centre de Developpement des Materiaux.
QUALITATIVE ANALYSIS OF RARE EARTH ELEMENTS CONTAINED IN THE PHOSPHOGYPSUM [ANALYSE QUALITATIVE DES ELEMENTS DES TERRES RARES CONTENUS DANS LE PHOSPHOGYPSE]
S. Chegrouche and A. Mellah Oct. 1992 14 p In FRENCH
(DE93-614153; SER/CDM-LA-31) Avail: CASI HC A03/MF A01 (US Sales Only)

In this study, we have characterized the phosphogypsum from the industrial phosphoric acid of Annaba chemical plant (Algeria). This procedure was achieved by x-ray diffraction in order to know different forms of sulphates contained in the phosphogypsum before its treatment. After chemical treatment, we have identified qualitatively the rare earth by x-ray fluorescence spectrometry. DOE

N94-26519# Weizmann Inst. of Science, Rehovoth (Israel).
THE 27TH ANNUAL MEETING OF THE ISRAEL SOCIETY FOR MICROSCOPY AND THE 12TH ANNUAL MEETING OF THE ISRAEL SOCIETY FOR HISTOCHEMISTRY AND CYTOCHEMISTRY
May 1993 123 p Meetings held in Rehovot, Israel, 23-24 May 1993
(DE93-632416; INIS-MF-13600; CONF-9305247) Avail: CASI HC A06/MF A02 (US Sales Only)

Investigations in life science and material science by the use of electron and scanning electron microscopy methods, are presented. Works on life processes, cell metabolism, physiological and pathological of human body systems are discussed. Crystal structure, corrosion, corrosion cracking, welds quality, phase studies and chemical reactions kinetics of metals, alloys, ceramics, composites and semiconductor materials are included. DOE

N94-26643*# California Univ., Santa Barbara. Quantum Inst.
AN INVESTIGATION OF THE EFFECT OF SURFACE IMPURITIES ON THE ADSORPTION KINETICS OF HYDROGEN CHEMISORBED ONTO IRON Annual Status Report, 1 Jan. - 31 Dec. 1993
Mickey R. Shanabarger 1993 7 p
(Contract NCC2-63)
(NASA-CR-195213; NAS 1.26:195213) Avail: CASI HC A02/MF A01

The goal of this program was to develop an understanding of heterogeneous kinetic processes for those molecular species which produce gaseous hydrogen degradation of the mechanical properties of metallic structural materials. Although hydrogen degradation of metallic materials is believed to result from dissolved protonic hydrogen, the heterogeneous hydrogen interface transport processes often dominate the kinetics of degradation. The initial step in the interface transport process is the dissociative chemisorption of the molecular species at the metal surface followed by hydrogen absorption into and transport through the bulk. The interaction of hydrogen with the surfaces of alpha-2(Ti3Al) titanium aluminide, gamma(TiAl) titanium aluminide, and beryllium were studied. Author (revised)

N94-26781# Michigan Univ., Ann Arbor.
HIGH DEFINITION RAMAN MICROSCOPIC IMAGING
M. D. Morris 1993 4 p
(Contract DE-FG02-89ER-13996)
(DE94-003158; DOE/ER-13996/4) Avail: CASI HC A01/MF A01

Confocal Raman microscopy was developed and used to study molecular sulfur inclusions in glass pellets. The Raman spectrum of water was used as a noninvasive temperature probe in operating electrophoresis capillaries. A macro-scale imager was used to image water Raman scattering using 30 mW 532 nm. The imager can be used to map boundaries, impurity distributions, and morphological changes in polymers and ceramics. A holographic beam splitter was obtained. Surface-enhanced Raman spectra was obtained from inside zebra fish embryos as a model system. Future research plans are given. DOE

N94-26794# Sandia National Labs., Albuquerque, NM.
MULTIVARIATE CALIBRATION APPLIED TO NEAR-INFRARED SPECTROSCOPY FOR THE QUANTITATIVE ANALYSIS OF DILUTE AQUEOUS SOLUTIONS
D. M. Haaland and H. D. T. Jones 1993 7 p Presented at the 9th International Conference on Fourier Transform Spectroscopy, Calgary, 23-27 Aug. 1993
(Contract DE-AC04-76DP-00789)
(DE94-003231; SAND-93-0997C; CONF-930826-3) Avail: CASI HC A02/MF A01

The penetration depths possible with near-infrared spectroscopy make it well suited for reagentless monitoring of analytes in body fluids or noninvasive monitoring of human tissue. As an initial step in achieving these goals, we have conducted near-infrared in-vitro experiments of dilute aqueous solutions containing analytes of physiological importance. By combining partial least squares (PLS) multivariate calibration methods with Latin Hypercube statistical design, we have obtained precise near-infrared spectral determinations of urea, creatinine, and NaCl in dilute aqueous solutions. Cross-validated PLS calibrations for the three analytes and temperature were very precise and resulted in R(exp 2) values greater than 0.997. DOE

N94-26823# Polish Academy of Sciences, Warsaw. Inst. Podstawowych Problemow Techniki.
MODERN PHOTOACOUSTIC SPECTROSCOPY PROBLEMS. THEORY AND EXPERIMENT (A REVIEW)
G. S. Mityurich (Gomel Polytechnic Inst., USSR.), J. Motylewski, and J. Ranachowski 1993 164 p
(ISSN 0208-5658)
(IFTR-41/1993) Avail: CASI HC A08/MF A02

The review presents investigation of photoacoustic transformation in condensed media, including naturally gyrotropic and magnetoactive substances. The analysis is performed on numerous theoretical models of linear as well as nonlinear sound generation mechanism. Sound wave excitation is assumed to be amplitude or polarization-modulated light beam. The potentiality of linear and circular dichroism parameters determination by means of photoacoustic and photodeflectional spectroscopy is evaluated. The experimental stands for subsequent gyrotropic media investigation in IFTR are described. Author

N94-26893# National Inst. of Standards and Technology, Gaithersburg, MD.
GORDON RESEARCH CONFERENCE ON THE PHYSICS AND CHEMISTRY OF LASER DIAGNOSTICS IN COMBUSTION Final Report
Kermit C. Smyth 16 Jul. 1993 24 p Conference held in Plymouth, NH, 12-16 Jul. 1993
(AD-A274609) Avail: CASI HC A03/MF A01

The 1993 Gordon Research Conference on the Physics and Chemistry of Laser Diagnostics in Combustion was held at Plymouth State College (South) in Plymouth, New Hampshire, July 12-16, 1993. This conference is primarily concerned with the fundamental physics and chemistry underlying the wide variety of laser-based optical spectroscopic diagnostic techniques which are used for studying combustion processes. The focus is on in-situ and nonperturbing optical methods for one-, two-, and three-dimensional measurements of species concentrations, temperature, and velocity. The development of such quantitative methods using linear and nonlinear optical interactions encompasses a broad scope of interdisciplinary research including basic and applied physics and chemistry. DTIC

N94-26907# National Inst. of Standards and Technology, Gaithersburg, MD. Fire Safety Engineering Div.
ANNUAL CONFERENCE ON FIRE RESEARCH, 1993: BOOK OF ABSTRACTS
Wanda J. Duffin, ed. Oct. 1993 212 p Conference held in Rockville, MD, Oct. 1993 See also PB83-155887 and PB93-188845
(PB94-121324; NISTIR-5280) Avail: CASI HC A10/MF A03

The NIST Annual Conference on Fire Research has long been a prime forum for presentation and discussion of the latest advances in fire science and engineering. The conference includes mostly fire research performed within Federal laboratories, or sponsored by Federal agencies. However, some private sector and foreign fire research is also included. This year's conference focuses on the development, verification of fire safety engineering tools, and their application to building fires, transportation fires, underground fires, and large fires. This will enable scientists and engineers to describe recent work on fire models and measurement methods and users to describe experiences and limitations in the use of these tools. NTIS

N94-26951# Brookhaven National Lab., Upton, NY.
VOLTAMMETRIC STUDIES OF POLY(CARBON DISULFIDE)
L. Geng (Moltech Corp., Stony Brook, NY.), J. Xu (Moltech Corp., Stony Brook, NY.), S. Prasad (Moltech Corp., Stony Brook, NY.), T. A. Skotheim (Moltech Corp., Stony Brook, NY.), H. S. Lee, and J. McBreen 1992 7 p Presented at the 16th Materials Research Society (MRS) Fall Meeting, Boston, MA, 30 Nov. - 5 Dec. 1992
(Contracts DE-AC02-76CH-00016; DE-FG01-90ER-81050)
(DE94-001385; BNL-49457; CONF-921101-139) Avail: CASI HC A02/MF A01

Poly(carbon disulfide) was studied by cyclic voltammetry using glassy carbon and platinum macro- and microdisk electrodes. The electron transfer kinetics is significantly faster at glassy carbon electrodes than at Pt electrodes. It is chemically reversible with moderate electron transfer rates. Voltammetric results of poly(carbon disulfide) are in good agreement with battery testing data. The k(sup 0) value measured at a Pt microdisk electrode is 7 x 10(exp 3) cm/sec. Electrochemical data suggest that PCS can be a potential cathode material for low current density lithium batteries. DOE

N94-26988 Bhabha Atomic Research Centre, Bombay (India).
SPECTROSCOPY DIVISION Progress Report, Jan. 1991 - Jun. 1992
S. A. Ahmad, ed. and V. B. Kartha, ed. 1993 135 p Limited Reproducibility: More than 20% of this document may be affected by microfiche quality
(DE94-604074; BARC-1993/P/003) Avail: CASI HC A07 (US Sales Only)

The research and development activities of the Spectroscopy Division during the calendar years 1990-1992 are reported in the form of individual summaries. These are arranged under the headings: (1) analytical spectroscopy, (2) infrared and Raman spectroscopy, (3) atomic spectra, (4) molecular and electronic spectra, (5) laser spectroscopy, (6) synchrotron, beam foil and plasma spectroscopy, (7) optics, (8) design, fabrication and workshop etc. The list of publications and papers presented at the various conferences, symposia etc. by the staff members of the Division during the report period is given at the end. DOE

N94-27226 SRI International Corp., Menlo Park, CA.
LASER PROBES OF NATURAL GAS IGNITION CHEMISTRY Final Report, Jan. 1987 - Dec. 1992
David R. Crosley, Gregory P. Smith, and David M. Golden Oct. 1993 48 p See also the 1991 Annual Report, PB92-227776
(Contract GRI-5087-260-1444; Proj. SRI-PYH-3092)
(PB94-128345; SRI-MP-93-087R; GRI-93/0271) Avail: Issuing Activity (National Technical Information (NTIS)

The goal of the research program is the development and use of laser-induced fluorescence (LIF) of various hydrocarbon species as a probe of natural gas combustion chemistry, to further an understanding of the chemical kinetics mechanisms of ignition and gas phase and catalytically stabilized natural gas combustion. Spectroscopic and collisional diagnostics experiments were performed, low pressure flame profiles were taken and compared with flame model calculations, and radial structure of these flames were investigated to develop an optimized natural gas combustion mechanism. NTIS

N94-27246# Electrotechnical Lab., Tsukuba (Japan).
RESEARCHES OF THE ELECTROTECHNICAL LABORATORY. NO. 53: SPECTRAL EMISSION FROM COMBUSTION GAS CONTAINING SCATTERING MEDIA [DENSHI GIJITSU SOGO KENKYUSHO KENKYU HOKOKU, DAI 53 GO: SANRANTAI O FUKUMU NENSHO GASU KARA NO SUPEKUTORU HOSHA NI KANSURU KENKYU]
Kazuo Onda 1 Sep. 1993 94 p In JAPANESE
(ISSN 0366-9106)
(JTN-94-80603) Avail: CASI HC A05/MF A01

The spherical harmonics (P(sub N)) approximation of radiative transfer equation, which is mathematically rigorous and can take into account of anisotropical scattering, is extended to a case where radiative properties are variable in a three-dimensional enclosure. Next the monochromatic optical properties of ash polydispersions in coal combustion gas are estimated intending to realize actual conditions. As an example of numerical analyses light scattering and absorbing effects by ash polydispersions in the coal-fired Magnetohydrodynamics (MHD) combustion gas are predicted and compared with the experimental results obtained in a laboratory-scale test duct. Also spectral emissions particular to the coal-fired MHD combustion gas are clarified and the wing reversal method to minimize the self-resonance absorption error in measurement of main-stream gas temperature and potassium number density is studied analytically and experimentally in the far-wing wavelength region. Author (NASDA)

N94-27256 Pennsylvania State Univ., University Park.
BASIC RESEARCH ON NATURAL GAS COMBUSTION PHENOMENA Final Report, Sep. 1989 - Dec. 1992
Michael Frenklach and William C. Gardiner (Texas Univ., Austin.) 15 Jan. 1993 81 p See also PB92-149681
(Contract GRI-5086-260-1307)
(PB94-129046; GRI-93/0351) Avail: Issuing Activity (National Technical Information (NTIS)

Experimental and theoretical contributions were made to advance our understanding of the chemical reaction mechanism of natural gas combustion. A radically different technology of mechanism development was shown to be needed in order to progress toward parameterizations of the detailed reaction mechanism that will be suitable for calibrating the reduced-variable mechanisms required for fluid dynamics computer codes. Experimental support of the mechanism development was provided by shock tube investigations of the profiles of OH, CO, CH3 and CH3O intermediates that play key roles in the combustion process. NTIS

N94-27385# Tohoku Univ., Sendai (Japan). Inst. for Chemical Reaction Science.
BULLETIN OF THE INSTITUTE FOR CHEMICAL REACTION SCIENCE, TOHOKU UNIVERSITY, VOLUME 2 [TOHOKU DAIGAKU HANNO KAGAKU KENKYUSHO HOKOKU DAI 2 KAN]
30 Sep. 1992 182 p In JAPANESE
(ISSN 0916-7471)
(JTN-94-80602) Avail: CASI HC A09/MF A02

The following topics were included: emulsion liquid membrane, diaphragms (mechanics), liquid separation, purification, refining, gallium, indium, nitrate radical, reactivity, toluene, alcohol, ether, sulfur compounds, alkene, methyl derivatives, benzyl derivatives, flash photolysis, Electron Paramagnetic Resonance (EPR), microwave pulse generator, phase compensation, microwave spectra, optical microscope, microscope stage, cooling system, temperature control, methanol, flow calorimeter, specific heat, heat of reaction, aqueous ammonia, high temperature, high pressure, electrolytic cell, glass filter, porous glass, vycor grass, borosilicate glass, and joining. This material also contains bibliographies which lists 103 abstracts. For individual titles, see N94-27386 through N94-27392.

N94-27386# Tohoku Univ., Sendai (Japan). Inst. for Chemical Reaction Science.
DEVELOPMENT OF LIQUID MEMBRANE SEPARATION PROCESSES [EKIMAKU BUNRI PUROSESU NO KAIHATSU]
Mitsunori Hozawa *In its* Bulletin of the Institute for Chemical Reaction

Science, Tohoku University, Volume 2 30 Sep. 1992 p 1-14 In JAPANESE (For primary document see N94-27385 07-25)
Avail: CASI HC A03/MF A02

Liquid membrane with carrier is expected as an economical and high selective separation technique which follows an action of bio-membrane. This review surveys the recent works on development of practical liquid membrane processes, placing the focus on the three themes: (1) optimum operating conditions of liquid surfactant membrane; (2) development of a long-life supported liquid membrane; and (3) application of liquid membranes to a hydrometallurgical process of gallium and indium from a black ore.
Author (NASDA)

N94-27387# Tohoku Univ., Sendai (Japan). Inst. for Chemical Reaction Science.
REACTIVITY OF NITRATE RADICAL (NO3) TOWARD ORGANIC COMPOUNDS [NAITORETO RAJIKARU (NO3) NO YUKIBUTSU NI TAISURU HANNOSEI] **c23**
Osamu Ito *In its* Bulletin of the Institute for Chemical Reaction Science, Tohoku University, Volume 2 30 Sep. 1992 p 15-31 In JAPANESE (For primary document see N94-27385 07-25)
Avail: CASI HC A03/MF A02

A method to evaluate the reaction rate constants for the reactions of the nitrate radical with various organic compounds in organic solution by applying the flash photolysis method is outlined. For many organic compounds, the reaction rate constants in the solution are greater than those in the gas phase by factors of 50 to 100. This finding indicates that the electronic structure of the nitrate radical in solution is quite different from that in the gas phase. By the comparison of the absolute rate constants, it is clearly indicated that the reaction modes of the nitrate radical are dependent on the reactants. For the compounds with hydrogen having high ionization potentials, the hydrogen atom abstraction is the main route; for compound with double bonds, the addition mode becomes predominant. For organic compounds with low ionization potentials, the electron transfer reaction occurs even though they have considerably active hydrogen. The reaction modes are also clearly shown by transient absorption bands which are secondly produced by the reaction of the nitrate radical with substrates. The sulfur compounds exhibit a variety of the reaction mechanism depending on the oxidation state of the sulfur, which affords a good example for the interchange of the reaction routes.
Author (NASDA)

N94-27388# Tohoku Univ., Sendai (Japan). Inst. for Chemical Reaction Science.
FOUR PHASE MICROWAVE PULSE GENERATOR FOR PULSED EPR SPECTROMETER [PARUSU EPR YO 4 ISO MAIKUROHA PARUSU HASSEIKI NO SHISAKU] **c33**
Yasunori Ohba, Rie Satoh, and Masamoto Iwaizumi *In its* Bulletin of the Institute for Chemical Reaction Science, Tohoku University, Volume 2 30 Sep. 1992 p 33-37 In JAPANESE (For primary document see N94-27385 07-25)
Avail: CASI HC A01/MF A02

In NMR (Nuclear Magnetic Resonance), pulsed-FT (Fourier Transformation) is superior to CW (Continuous Wave) method in respect to sensitivity and multidimensional spectrum. When pulsed-FT is applied to EPR (Electron Paramagnetic Resonance) high resolution can be achieved in addition to the advantages in NMR, so that it is useful to study intermediates of chemical reaction. Pulsed-FT enables to excite entire spectrum by one pulse, however, it is difficult to cover the whole EPR spectrum zone. Therefore, QD (Quadrature Detection) which detect EPR signal at the phase of 0 and 90 degrees to the reference signal is applied in EPR. This enables us to double the observation spectrum zone, and improve S/N (Signal to Noise) ratio and pulse power efficiency, because QD can distinguish frequency of EPR signal from that of excitation microwave. In order to apply QD in ESR (Electron Spin Resonance), it is important to balance the two phases (0 and 0 degrees), although it is difficult in frequency range used in X band region of EPR. The CYCLOPS (Cyclically Ordered Phase Sequence) which can correct EPR signals by FID (Free Induction Decay) measured by four phase (0, 90, 180, 270 deg) microwave pulses is useful to obtain well-balanced phases. In this study, a four phase microwave pulse generator for X band region was manufactured, and the performance of it was discussed.
Author (NASDA)

N94-27389# Tohoku Univ., Sendai (Japan). Inst. for Chemical Reaction Science.
VARIABLE TEMPERATURE COLD STAGE FOR MICROSCOPE OBSERVATION [ONDO KAHEN KENBIKYO TEION SUTEJI NO SHISAKU] **c35**
Hirosi Yamada, Minoru Hanaya (Tokyo Inst. of Tech., Japan.), Youichi Kanno, Takemitu Kikuchi, and Shinji Onodera *In its* Bulletin of the Institute for Chemical Reaction Science, Tohoku University, Volume 2 30 Sep. 1992 p 39-40 In JAPANESE (For primary document see N94-27385 07-25)
Avail: CASI HC A01/MF A02

It is considerably important to measure crystallization velocity in vitreous state for understanding of crystallization mechanism and quantitative analysis of crystallization process. For this measurement, a microscope equipped with a variable temperature cold stage is useful to regulate temperature to be constant for a long period because some crystallization takes a long time around glass transition point. However, since conventional cold stages are cooled by liquid nitrogen gas flow, it is difficult to cool continuously for a long time and to regulate the temperature accurately. This report presents a cold stage cooled by methanol flow which can control the temperature of samples accurately. The device consists of the microscopic stage cooled by cold methanol flow equipped with a thermocouple to regulate the temperature. As a result, this device makes it possible to observe a specimen within the range of 200 to 260 K with deviation of 0.05 K for one month. Therefore, very slow crystallization in low temperature can be measured by this device.
Author (NASDA)

N94-27390# Tohoku Univ., Sendai (Japan). Inst. for Chemical Reaction Science.
HIGH-TEMPERATURE AND HIGH-PRESSURE FLOW CALORIMETER [KOON KOATSU RYUTSUSHIKI NETSURYOKEI] **c35**
Yoshio Abe, Yoichi Kanno, Minoru Takahashi, and Chiaki Yokoyama *In its* Bulletin of the Institute for Chemical Reaction Science, Tohoku University, Volume 2 30 Sep. 1992 p 41-45 In JAPANESE (For primary document see N94-27385 07-25)
Avail: CASI HC A01/MF A02

Flow calorimetry is a useful method for measuring the specific heat of fluids. Flow calorimeter also can be used as a flowing style chemical reactor and so that the heat of reaction will be measured using it. In this study, the flow calorimeter used for the specific heat measurement of aqueous ammonia and the reaction heat measurement is manufactured and tested. The specific heat of water and 10 and 20 weight percent of aqueous ammonia were measured successfully.
Author (NASDA)

N94-27391# Tohoku Univ., Sendai (Japan). Inst. for Chemical Reaction Science.
GLASS CYLINDRICAL FILTER FOR ELECTROLYSIS CELL [DENKAISOYO GARASU ENTO FIRUTA NO SEISAKU] **c35**
Shinichi Abe and Fuminori Akiyama *In its* Bulletin of the Institute for Chemical Reaction Science, Tohoku University, Volume 2 30 Sep. 1992 p 47-48 In JAPANESE (For primary document see N94-27385 07-25)
Avail: CASI HC A01/MF A02

Some electrolysis requires separation of electrolytic solution by a filter between two electrodes in order to prevent products from reacting secondarily at another electrode. These filters are usually made of a glass filter or ion exchanger membrane, and they are fixed at the electrolysis cell or cover one electrode. This report presents a detachable glass cylindrical filter for electrolytic reaction. The glass cylindrical filter was made from glass filter powder placed in a mold and heated at 800 C for 18 minutes. Using this filter, electrolytic reduction of carbon dioxide was performed in 0 C hot water with benzoin. This reaction produces aqueous oil from carbon dioxide and water. The products were compared with and without the filter and, although the yield did not differ between the two reaction systems, products without the filter contained highly polymerized oil compared to those with the filter. This suggests that the aqueous oil was produced at the cathode and polymerized at the anode.
Author (NASDA)

N94-27392# Tohoku Univ., Sendai (Japan). Inst. for Chemical Reaction Science.
POROUS VYCOR GLASS TUBE JOINED TO BOROSILICATE GLASS [TAKOSHITSU BAIKORU GARASUKAN NO YOSETSU] **c35**

Shinichi Abe, Takemitsu Kikuchi, and Shinji Onodera *In its* Bulletin of the Institute for Chemical Reaction Science, Tohoku University, Volume 2 30 Sep. 1992 p 49-50 In JAPANESE (For primary document see N94-27385 07-25)
Avail: CASI HC A01/MF A02

Porous glass can absorb various size of molecules with large surface area even in high temperature. However, it is difficult to use porous glass tubes at high-temperature, for example as a separation membrane for hydrogen condensation, because adhesives at joining sites could be damaged. In this study, welding of a porous glass tube and a glass tube was attempted to develop a gas separation membrane used at 500 C. Since forms present in porous glass may cause crack at high temperature, it is necessary to remove such forms by heat processing. Such porous glass is called to be porous vycor glass, which contains quartz 6 percents, and can be joined with a quartz tube. As a result, a gas separator with porous glass membrane which is joined by this process could endure high temperature up to 600 C and could maintain high vacuum. Author (NASDA)

N94-27567# National Inst. of Standards and Technology, Boulder, CO. Thermophysics Div.
THERMOPHYSICAL PROPERTIES OF HFC-143a AND HFC-152a
W. M. Haynes Oct. 1993 27 p
(Contract DE-FG02-91CE-23810)
(DE94-004236; DOE/CE-23810/22A) Avail: CASI HC A03/MF A01

Numerous fluids have been identified as promising alternative refrigerants, but much of the information needed to predict their behavior as pure fluids and as components in mixtures does not exist. In particular, reliable thermophysical properties data and models are needed to predict the performance of the new refrigerants in heating and cooling equipment and to design and optimize equipment to be reliable and energy efficient. The objective of this project is to provide highly accurate, selected thermophysical properties data for refrigerants HFC-143a, CH_3CF_3, and HFC-152a, CH_3CHF_2, and to use these data to fit complex equations of state and detailed transport property models. The new data will fill gaps in the existing data sets and resolve problems and uncertainties that exist in and between the data sets. DOE

N94-27687 Tel-Aviv Univ. (Israel).
NOVEL OXIDIZING REAGENTS DERIVED FROM ELEMENTAL FLUORINE Ph.D. Thesis
Moshe Kol Aug. 1991 165 p In HEBREW
(ITN-94-85231) Copyright Avail: Issuing Activity (Tel-Aviv Univ., Exact Sciences Library, Ramat Aviv 69978, Israel)

Two novel fluorine-derived oxidizing systems were studied: hypofluorous acid in acetonitrile, and methyl hypofluorite. This research is part of a program aimed at introducing fluorine into organic synthesis methodology. Nuclear magnetic resonance (NMR) and mass spectrometer measurements of an oxidizer formed by passing nitrogen-diluted fluorine through a solution of water in acetonitrile proved the oxidizer to be a complex of hypofluorous acid and acetonitrile. A wide-range study of the reactions of the above oxidizer with electron-rich systems was performed. Both of the hypofluorite systems studied were found to be powerful oxidants which made possible a variety of transformations under mild conditions. ISA

N94-27712# Department of Energy, Morgantown, WV. Technology Center.
PRESSURE-GAIN COMBUSTION
G. A. Richards, J. Yip, R. S. Gemmen, M. C. Janus, T. Norton, and W. A. Rogers 1993 9 p Presented at the Joint Contractors Meeting on Advanced Turbine Systems, Fuel Cells and Coal-Fired Heat, Morgantown, WV, 3-5 Aug. 1993
(DE94-002975; DOE/METC-C/94/7106; CONF-930893-39) Avail: CASI HC A02/MF A01

Pulse combustion has been proposed for gas turbine applications in many early articles and more recently has been demonstrated to produce so-called 'pressure-gain' in a small gas turbine. The basic concept is that the oscillatory combustion occurs as a constant-volume process, which produces a gain in the stagnation pressure of air flowing through the combustor, rather than the pressure loss associated with conventional, steady combustion. If properly utilized, this pressure-gain could enhance simple-cycle gas turbine efficiency several percent depending on the operating conditions. In addition, pulse combustors have demonstrated relatively low NO(x) pollutant levels in some applications. The combined potential for higher cycle efficiency and lower pollutant levels is the basis for the present investigation. Tests in progress at the Morgantown Energy Technology Center (METC) have considered a baseline pulse combustor configuration that has shown good oscillating performance, low NO(x) emissions, but disappointing results in terms of pressure-gain. However, a combination of numeric simulations and test data suggest that pressure-gain can be produced by a select combination of operating conditions and combustor geometry, but is especially sensitive to the combustor inlet geometry. Tests in progress will evaluate the effect of inlet geometry and operating pressure on both pollutant emissions and pressure-gain. DOE

N94-27728# Los Alamos National Lab., NM. Chemical Science and Technology Div.
ZEEMAN LASER INTERFEROMETRY FOR DETECTION AND CHEMICAL ANALYSIS
Roger G. Johnston 1993 6 p Presented at the 4th Laser Applications to Chemical Analysis Meeting, Jackson Hole, WY, 8-11 Mar. 1994
(Contract W-7405-eng-36)
(DE94-003963; LA-UR-93-3930; CONF-940341-3) Avail: CASI HC A02/MF A01

Zeeman interferometry has a number of applications for ultrasensitive detection and chemical analysis, including refractive index detection, micro-thermometry, thermooptic spectroscopy, and light scattering. DOE

N94-27822# National Lab. for High Energy Physics, Tsukuba (Japan).
HYDROGEN PHYSICS
Susumu Ikeda, ed. Feb. 1993 114 p Presented at the Hydrogen Physics, Tsukuba, Japan, 29-30 Sep. 1992
(DE94-701317; KEK-PROC-92-20; CONF-9209397) Avail: CASI HC A06/MF A02

The workshop on hydrogen bond was restarted changing its name to 'Hydrogen Physics' for grasping hydrogen bond from a wider viewpoint and expecting the new development in this field hereafter. As the basic attitude, the phenomena related to hydrogen bond are reviewed from two different systems: hydrogen-lattice system and hydrogen-electron system. The Hydrogen Physics meeting was held on September 29 and 30, 1992, at National Laboratory for High Energy Physics, and 19 lectures were given. The themes were proton dynamics of hydrogen bond, water science and water with good taste, collective movement and fluctuation of water, neutron diffraction of water, hydrogen bond in water as seen from Raman scattering, electron and proton movements in organic crystals, new deuterium substitution effect of proton transfer in hydrogen bond in solids, infrared spectroscopy for one-dimensional hydrogen bond crystals, MSR in solid hydrogen, hydrogen in alkali metal-graphite intercalation compounds, lattice anomalies and Grueneisen parameters in high Tc superconducting salts, bio-substances and hydrogen, hydrogen bond net in nucleotide and control of crystalline structure change by hydrogen vapor pressure, ATP and structural change and crystal water of guanosine, spread of protons and electrons in hydrogen bond, anisotropy of loose scattering according to ice rule, high pressure effect and isotope mixed crystal effect of KHS crystals without hydrogen crystal network, state of motion and phase transformation of hydrogen in KDP, and development of hydrogen bond research by neutron scattering. This publication contains the papers and the transparencies presented at the meeting. DOE

N94-27854*# Pratt and Whitney Aircraft, East Hartford, CT. Commercial Engine Business.
BROAD SPECIFICATION FUELS COMBUSTION TECHNOLOGY PROGRAM, PHASE 2 Final Report
R. P. Lohmann, R. A. Jeroszko, and J. B. Kennedy Oct. 1990 235 p
(Contract NAS3-23269)
(NASA-CR-191066; NAS 1.26:191066) Avail: CASI HC A11/MF A03

An experimental evaluation of two advanced technology combustor concepts was conducted to evolve and assess their capability for operation on broadened properties fuels. The concepts were based on the results of Phase 1 of the Broad Specification Fuel Combustor Technology Program which indicated that combustors with variable geometry or staged combustion zones had a flexibility of operation that could facilitate operation on these fuels. Emphasis in defining these concepts included the use of single pipe as opposed to duplex or staged fuels systems to avoid the risk of coking associated with the reduction in thermal stability expected in broadened properties fuels. The first concept was a variable geometry combustor in which the airflow into the primary zone could be altered through valves on the front while the second was an outgrowth of the staged Vorbix combustor, evolved under the NASA/P&W ECCP and EEE programs incorporating simplified fuel and air introduction. The results of the investigation, which involved the use of Experimental Referee Broad Specification (ERBS) fuel, indicated that in the form initially conceived, both of these combustor concepts were deficient in performance relative to many of the program goals for performance emissions. However, variations of both combustors were evaluated that incorporated features to simulate conceptual enhancement to demonstrate the long range potential of the combustor. In both cases, significant improvements relative to the program goals were observed. Author (revised)

N94-27959 ESDU International Ltd., London (England).
THERMOPHYSICAL PROPERTIES OF REFRIGERANT R-134a (1,1,1,2-TETRAFLUOROETHANE)
Mar. 1993 17 p
(ISSN 0141-4062)
(ESDU-93001; ISBN-0-85679-855-X) Avail: ESDU

ESDU 93003 gives equations obtained from a critical evaluation of experimental data in the literature for the variation along the saturation line with temperature, for both the liquid and the vapor, of density, ehthalpy, heat capacity at constant pressure, dynamic viscosity, and thermal conductivity. Results on the saturation line evaluated in SI units using the equations are tabulated at 5K intervals and at 5 C intervals from the melting point to the critical point, or as close to it as possible for some properties. Results for the ideal gas evaluated also in SI units using the equations are tabulated at 5 K and at 5 C intervals from the melting point to 1000 K. In the absence of experimental values, some of these results involve extrapolation and they are indicated in the tables. Conversion factors to facilitate use of the data in British units are included. ESDU

N94-27998 Morelos Univ., Cuernavaca (Mexico).
APPLICATION OF THE POSITRON ANNIHILATION TECHNIQUE TO THE STUDY OF VAPOR ABSORPTION PROCESS IN POLYETHYLENE (LDPE) AND IN IMIDE POLYMER (6FDA-TMPD PI) Ph.D. Thesis
V. Sanchez Mendieta 1992 92 p Limited Reproducibility: More than 20% of this document may be affected by microfiche quality
(DE94-602737; INIS-mf-13615) Avail: CASI HC A05 (US Sales Only)

It is well known that positron annihilation lifetime (PAL) spectra in polymers have a long-lived component that can be ascribed to ortho-positronium (o-Ps). The lifetime, (tau)(sub 3), is considered to be a measure of the size of the micro-vacancies in which o-Ps is trapped and is annihilated through pick-off annihilation with the rate which depends on the size of the vacancy. Positron lifetime measurements were performed for two different kinds of polymers (low density polyethylene and a polyimide) (6FDA-TMPD) during sorption of various vapors (hexane, cyclohexane, benzene, acrylic acid, methyl acrylate, water, and oxygen). The vapor sorption affected the long-lived component (ortho-positronium component) in a systematic way regardless of the kind of the vapor molecules, i.e. for the polyethylene both the lifetime and the intensity of the long-lived component were enhanced, while for the polyimide they were decreased significantly. These different effects are interpreted in terms of different states of sorbed molecules in rubbery (the polyethylene) and in glassy (the polyimide) polymers. DOE

N94-28058 ESDU International Ltd., London (England).
THERMAL CONDUCTIVITY OF LIQUID ALIPHATIC ALCOHOLS
Mar. 1993 82 p Supersedes ESDU-75024
(ISSN 0141-4062)
(ESDU-93008; ESDU-75024; ISBN-0-85679-860-6) Avail: ESDU

ESDU 93008 gives data for all isomers up to C6, for 6C7 isomers, 4C8 isomers, 2C9 isomers, and for the normal alcohols from C10 to C20. Experimental results drawn from the literature for each compound were fitted with a four term polynomial equation in reduced temperature. The coefficients were also faired with changing molecular structure to ensure the best correlation not only for the individual compounds but also as members of their chemical series. The coefficient correlations also allowed values to be predicted for compounds for which no measured data exist. For these compounds, it was found only one coefficient varied across the families, while the other three remained constant. The equations were used to tabulate thermal conductivity values from the melting point to about 0.9 critical temperature in SI units at 10 K and 10 degree C intervals. The critical point, coefficients and sources of the data are given for each compound. Conversion factors are provided for common British units, the effect of pressure is briefly considered and the likely accuracy of the tabulated values is discussed. ESDU

N94-28059 ESDU International Ltd., London (England).
VAPOUR PRESSURES AND CRITICAL POINTS OF LIQUIDS: ALIPHATIC AND CYCLIC KETONES
Mar. 1993 94 p
(ISSN 0141-4062)
(ESDU-93009; ISBN-0-85679-861-4) Avail: ESDU

ESDU 93009 presents vapor pressure data for all isomers (26 compounds) of aliphatic ketones up to C7, 13 aliphatic ketones between C8 and C15, mesityl and isomesityl oxides, and cyclo-butanone, -pentanone, -hexanone, -heptanone and -octanone. The data were obtained by a critical evaluation of experimental results in the literature correlated by a method that allows the extrapolation of results in the higher pressure ranges into the low pressure region. The method also enabled correlations to be developed for compounds for which only restricted results were available using correlations for compounds for which a wide range of data existed. The Wagner equation was used over the full liquid range from the melting point to the critical point. The coefficients of the equation are given for each compound and three tables of vapor pressure values calculated using them are included: in SI units at 5 K intervals, in mm of mercury or atmospheres at 10 degree C intervals, in lbf/sq in at 20 degree F intervals. A table also gives the saturation temperature at various specified pressures, and indicates the possible uncertainty in the calculated values. The sources of the data for each compound are included. ESDU

N94-28060 ESDU International Ltd., London (England).
ORTHOBARIC DENSITIES AND MOLAR VOLUMES OF LIQUIDS: ALIPHATIC AND CYCLIC KETONES
Mar. 1993 102 p
(ISSN 0141-4062)
(ESDU-93010; ISBN-0-85679-862-2) Avail: ESDU

ESDU 93010 tabulates density and molar volumes for all isomers (26 compounds) of aliphatic ketones up to C7, 13 aliphatic ketones between C8 and Cl5, mesityl and isomesityl oxides, and cyclo-butanone, -pentanone, -hexanone, -heptanone and -octanone. The tables are in units of kg/cu m and cu cm/mol respectively from near the melting point to within a few degrees of the critical point. The temperature interval chosen is varied from 10 K to 1 K to keep the increments in density reasonably small. Although the Rackett equation does not represent the variation of density over the full temperature range so well as the equation used in ESDU 93010 (log reduced density as a polynomial function of reduced temperature), it was used to estimate the critical density. The estimated values were slightly adjusted to give a smooth variation between compounds. The log/polynomial equation was then fitted to the experimental data for density for each compound taken from a wide range of sources in the literature; values established for the coefficients in the equation for each compound are also tabulated. Estimates of the accuracy of the predictions are included, as is a list of the sources of data actually used for each compound. Values at the critical point are provided together with normal boiling and melting points. ESDU

N94-28062 ESDU International Ltd., London (England).
VISCOSITY OF LIQUIDS: HALOGENATED ETHANES
Nov. 1993 65 p
(ISSN 0141-4062)
(ESDU-93012; ISBN-0-85679-864-9) Avail: ESDU

ESDU 93012 tabulates the viscosity of 49 halogenated ethanes at saturation pressure for temperatures from just above the melting point to approximately 0.9 of the critical temperature. Experimental data extracted from the literature were fitted by an equation for the logarithm of dynamic viscosity as a function of reduced temperature. The equation contains four constants and the values determined for them from the correlation are tabulated for each compound. Viscosities are given at 10 K and 10 degree Celsius intervals, together with an assessment of the uncertainty in each value. The sources of the data for each compound are listed, and the critical temperature is given. It is noted that viscosity increases by 1 percent for a pressure increase of 10 bar, and an equation is suggested for calculating the effect of pressure up to 500 bar. ESDU

N94-28069# Spauschus Associates, Inc., Stockbridge, GA.
SOLUBILITY, VISCOSITY, AND DENSITY OF REFRIGERANT/LUBRICANT MIXTURES
D. R. Henderson Oct. 1993 65 p
(Contract DE-FG02-91CE-23810)
(DE94-004237; DOE/CE-23810/22B) Avail: CASI HC A04/MF A01

This report presents results of measurements on low refrigerant concentration mixtures (0, 10, 20, and 30 weight percent) of CFC-12; HCFC's 22, 123, and 124; and HFC's 134a, 32, and 125 with mineral oil, alkylbenzene, and polyolester lubricants. Viscosity, solubility (vapor pressure), and density data are reported for 23 working fluids composed of combinations of these refrigerants and companion lubricants. These data, reduced to engineering form, are presented in form of a Daniel chart and a plot of density versus temperature and composition. Extensive numerical analysis has been performed in order to derive equations which allow two independent variables, temperature and composition, and to provide for corrections in composition due to vapor space volume in the test apparatus; details of these calculations are provided. DOE

N94-28097 ESDU International Ltd., London (England).
ORTHOBARIC DENSITIES AND MOLAR VOLUMES OF LIQUIDS: FUSED RING COMPOUNDS
Sep. 1993 66 p
(ISSN 0141-4062)
(ESDU-93029; ISBN-0-85679-882-7) Avail: ESDU

ESDU 93029 tabulates density and molar volume for 30 compounds in units of kg/cu m and cu cm/mol respectively from near the melting point to the critical point (although for some compounds the tables are terminated at about 0.8 of critical temperature). The temperature interval is varied from 10 K to 1 K to keep the increments in density reasonably small. The critical density was calculated using the Rackett and Riedel equations and values of critical pressure and temperature adjusted until the predictions of critical density from the two equations were in good agreement. Experimental data for density for each compound were taken from a wide range of sources in the literature and fitted by an equation for log reduced density as a polynomial function of reduced temperature. Values for the coefficients in the equation are tabulated for each compound together with estimates of the accuracy of the predictions using them and a list of the sources of data used. Values at the critical point are also given together with normal boiling and melting points. Vapor pressure data for all the compounds are given in ESDU 93028. ESDU

N94-28138 ESDU International Ltd., London (England).
THERMAL CONDUCTIVITY OF LIQUID CARBOXYLIC ACIDS
Jun. 1993 44 p Supersedes ESDU-79029
(ISSN 0141-4062)
(ESDU-93017; ESDU-79029; ISBN-0-85679-869-X) Avail: ESDU

ESDU 93017 gives data for 22 n-alkanoic acids, 3 iso-alkanoic acids, and 11 alkenoic acids. Experimental results drawn from the literature for each compound were fitted with a four-term polynomial equation in reduced temperature. The coefficients were also faired with changing molecular structure to ensure the best correlation not only for the individual compounds but also as members of their chemical series. The coefficient correlations also allowed values to be predicted for compounds for which no measured data exist. The equations were used to tabulate thermal conductivity values from the melting point to about 0.9 critical temperature in SI units at 10 K and 10 C intervals. The critical point, coefficients, and sources of the data are given for each compound. Conversion factors are provided for common British units, the effect of pressure is briefly considered and the likely accuracy of the tabulated values is discussed. ESDU

N94-28142 ESDU International Ltd., London (England).
VAPOUR PRESSURES AND CRITICAL POINTS OF LIQUIDS: FUSED RING COMPOUNDS
Sep. 1993 80 p
(ISSN 0141-4062)
(ESDU-93028; ISBN-0-85679-881-9) Avail: ESDU

ESDU 93028 presents vapor pressure data for 37 compounds. The data were obtained by a critical evaluation of experimental results in the literature. Where the data were less extensive or reliable, it was found possible to develop a correlation using a method that relates the second differential of the Wagner vapor pressure equation to the difference between the ideal gas and the liquid heat capacities. The Wagner equation was used over a temperature range usually from close to the melting point to the critical point, although for some compounds the correlation was stopped at about 0.8 of the critical temperature. The coefficients of the equation are given for each compound and two tables of vapor pressure values calculated using them are included: in SI units at 5 K intervals and in mm of mercury or atmospheres (for the higher values) at 5 C intervals. A table also gives the saturation temperature at various specified pressures and indicates the possible uncertainty in the calculated values. An Antoine equation is given fitting the Wagner equation values between 2 and 200 kPa with an rms deviation of between 0.05 and 0.1 percent. The sources of data for each compound are also listed. Density data for the majority of the compounds are given in ESDU 93029. ESDU

N94-28215# Air Force Logistics Command, Edwards AFB, CA. Propulsion Directorate.
FREON RECOVERY FROM NITROGEN TETROXIDE AND FREON SOLUTIONS Final Report
Robert O. Bucsh Apr. 1993 34 p
(PL-TR-92-3051) Avail: CASI HC A03/MF A01

A reactor was designed, built, and tested to extract N2O4 from a N2O4 in Freon solution. A two step chemistry process was developed, the N2O4 is extracted from the Freon as KNO2 and KNO3 with aqueous KOH. The KNO2 is converted to N2 aud K2SO4 by sulfamic acid. The excess KOH is neutralized with nitric acid to produce an innocuous KNO3 solution. The concentration of N2O4 left in the treated Freon is below the detection limit of the analytical method used. It was discovered that N2O4 reacts with Freon over time to produce halogenated nitroethanes. The reactor has been delivered to the Western Space and Missile Center (WSMC). Author

N94-25561# National Research Inst. for Metals, Tokyo (Japan).
COMBUSTION SYNTHESIS METHOD [NENSHO GOSEIHO NI KANSURU KENKYU]
Yoshinari Kaieda, Minoru Otaguchi, Nobutaka Oguro, and Z. A. Munir *In its* Bulletin of National Research Institute for Metals in Fiscal Year 1993, No. 14 29 Jan. 1993 p 149-151 In JAPANESE Prepared in cooperation with California Univ., Davis (For primary document see N94-25544 07-26)
Avail: CASI HC A01/MF A04

N94-25569# National Research Inst. for Metals, Tokyo (Japan). Chemical Processing Div.
FUNDAMENTAL STUDY ON NEW SYNTHETIC TECHNOLOGY BY PHTHALOCYANINE COMPLEXES [FUTAROSHIANIN SAKUTAI NI YORU SHINGOSEI GIJUTSU NI KANSURU KISO KENKYU]
Hiroaki Isago, Yutaka Kagaya, and Ryosuke Hasegawa *In its* Bulletin of National Research Institute for Metals in Fiscal Year 1993, No. 14 29 Jan. 1993 p 231-240 In JAPANESE (For primary document see N94-25544 07-26)
Avail: CASI HC A02/MF A04

N94-27909*# College of William and Mary, Williamsburg, VA. Dept. of Chemistry.
KINETIC PARAMETERS FROM THERMOGRAVIMETRIC ANALYSIS
Richard L. Kiefer *In* Old Dominion Univ., The 1993 NASA-ODU American Society for Engineering Education (ASEE) Summer Faculty Fellowship Program Dec. 1993 p 116-119 (For primary document see N94-27893 07-80)
Avail: CASI HC A01/MF A03

N94-28159# Tohoku Univ., Sendai (Japan). Inst. for Advanced Materials Processing.
ENERGY DISPERSIVE X RAY DIFFRACTION (EDXD) APPARATUS FOR LIQUIDS AT HIGH TEMPERATURE
Kazumasa Sugiyama, Valery G. Petkov (Research Development Corp. of Japan, Tokyo.), Susumu Takeda (Research Development Corp. of Japan, Tokyo.), and Yoshio Waseda *In its* The Science Reports of the Research

Institutes, Tohoku University. Series A: Physics, Chemistry, and Metallurgy. Volume 38, No. 1: Amorphous Materials 14 29 Mar. 1993 p 1-13 (For primary document see N94-28158 07-26)
Avail: CASI HC A03/MF A02

N94-28165# Tohoku Univ., Sendai (Japan). Inst. for Materials Research.
THE ELECTROCATALYTIC OXIDATION OF ETHYLENE AND METHANE, AND REDUCTION OF OXYGEN ON GAS-DIFFUSION ELECTRODES MADE OF AMORPHOUS NICKEL-VALVE METAL-PLATINUM GROUP METAL ALLOYS
Toshiaki Shimada (Nippon Mining Co. Ltd., Kitaibaraki, Japan.), Asahi Kawashima, Hiroki Habazaki, Katsuhiko Asami, and Koji Hashimoto *In its* The Science Reports of the Research Institutes, Tohoku University. Series A: Physics, Chemistry, and Metallurgy. Volume 38, No. 1: Amorphous Materials 14 29 Mar. 1993 p 63-75 (For primary document see N94-28158 07-26)
Avail: CASI HC A03/MF A02

26 METALLIC MATERIALS

Includes physical, chemical, and mechanical properties of metals, e.g., corrosion; and metallurgy.

N94-25544# National Research Inst. for Metals, Tokyo (Japan).
BULLETIN OF NATIONAL RESEARCH INSTITUTE FOR METALS IN FISCAL YEAR 1993, NO. 14 [KENKYU HOKOKUSHU 14: HEISEI 5 NEN BAN]
Norio Nagata, ed., Masae Sumida, ed., Takayuki Yoshioka, ed., Shigeo Yamamoto, ed., Yoshio Sakka, ed., Shinobu Matsushima, ed., Shozo Ikeda, ed., Kazuo Kadowaki, ed., and Yoshihisa Izuka, ed. et al 29 Jan. 1993 387 p In JAPANESE
(ISSN 0285-7030)
(Rept-14; JTN-94-80543) Avail: CASI HC A17/MF A04

The following topics were discussed: metal matrix composites, intermetallic compounds, alloys, steels, ceramics, amorphous compounds, titanium alloys, phtalocyanin complex compound, thin films, superconductors, semiconductors, fatigue, corrosion, corrosion propagation, stress propagation, crack propagation, damage process, creep, stress corrosion cracking, high temperature environments, cryogenic environments, hydrogen embrittlement, solid-liquid interface, magnetic floated crucibles, high field magnets, gas sensors, surface properties, grain boundaries, plasmas, emission spectroscopy, electron beam lithography, stirring technology, ultra high vacuum, vacuum apparatus, x ray spectroscopy, auger spectroscopy, scanning tunneling microscopy, and mass spectroscopy. For individual titles, see N94-25545 through N94-25586.

N94-25545# National Research Inst. for Metals, Tokyo (Japan). Surface and Interface Div.
DEVELOPMENT OF INTERMETALLIC COMPOUNDS FOR HIGH PERFORMANCE LUMINESCENCE ELEMENTS [KOSEINO HAKKO SOSHIYO KINZOKUKAN KAGOBUTSU ZAIRYO NO KAIHATSU NI KANSURU KENKYU]
Nobuyuki Koguchi, Akio Kiyosawa, Satoshi Takahashi, Toyohiro Chikyo, Shinya Hashimoto, Jun Fujiwara, Kazuhiro Yoshihara, Kazuhiro Nii, and Shigeyuki Akiba *In its* Bulletin of National Research Institute for Metals in Fiscal Year 1993, No. 14 29 Jan. 1993 p 1-15 In JAPANESE Sponsored by Science and Technology Agency, Tokyo, Japan (For primary document see N94-25544 07-26)
Avail: CASI HC A03/MF A04

Materials capable of laser emission in the mid-infrared wavelength range are studied for 3-5 and 4-6 group semiconductors. This study was intended to establish the ways of making thin films out of these materials, construct double heterojunction or multi-quantum well structure to lasers, and to raise the laser operational temperature in this wavelength range. The study found that, in 3-5 group semiconductors, heterojunction joining with flat surfaces can be generated by inserting In(1-y)Al(y)Sb component tapered layers between the InSb substrate and the confinement layers in order to prepare the In(1-x)Ga(x) Sb/In(1-y)Al(y)Sb laser. Ga molecular beams were ionized by two photon excitation, utilizing light resonance absorption. In 4-6 group semiconductors, a new material Pb(1-x-y)Cd(x)Sr(y)S proved to be suitable for lasers. By MBE (Molecular Beam Epitaxy), the technique to control this film thickness in an atom's precision was established, and Pb(1-x-y)Cd(x)Sr(y)S/PbS double heterojunction and multi-quantum well lasers were produced. By employing the Pb(1-x-y)Cd(x)Sr(y)S/PbS double heterojunction, laser emission succeeded at 240 K, the highest operational temperature in this wavelength range. Author (NASDA)

N94-25546# National Research Inst. for Metals, Tokyo (Japan). Advanced Materials Processing Div.
CORROSION RESISTANCE AT WELDED ZONES OF NUCLEAR FUEL REPROCESSING SYSTEM [KAKU NENRYO SAISHORI SOCHI YOSETSUBU NO TAISHOKUSEI NI KANSURU KENKYU]
Harukata Nakamura, Hirosada Irie, Takehiko Watanabe, Kazuo Ei, Susumu Tsukamoto, Yoshiki Muramatsu, Seiji Kuroda, Tetsuo Fujii, and Haruo Baba *In its* Bulletin of National Research Institute for Metals in Fiscal Year 1993, No. 14 29 Jan. 1993 p 17-28 In JAPANESE (For primary document see N94-25544 07-26)
Avail: CASI HC A03/MF A04

Research was conducted to improve the corrosion resistance at welded zones of nuclear fuel recycling system made of austenitic stainless steel. The following results were obtained. Crystal granules as fine as those of the basic material were obtained at welded zones by employing the pulse TIG (Tungsten Gas Welding) welding method specially developed to reduce the granule size. The TIG welded zones of austenitic stainless steel with finer crystal granules have far more corrosion resistance than those which did not undergo this process. Welded zones with electron beam treatment proved to have extremely high corrosion resistance. In research on the surface treatment with laser, surface fusion solidification by CO2 laser did not effectively reduce the size of crystal granules, but high speed solidification fusion treatment by laser utilizing the segregation effect contributed much to improve corrosion resistance. However, this high speed treatment caused some cracks in the stainless steel. To obtain some basic knowledge about fusion and solidification, cladding experiments were made on Ti and Ta. Corrosion resistance of valve metals such as Ti and Zr in nitric acid solution with oxidizing ions was evaluated by the AC (Alternation Current) impedance method. Complete corrosion resistance was seen when oxidizing ions were present. In boiling nitric acid, a correlation was noticed between DC (Direct Current) polarization resistance values and corrosion rates calculated by the decrease in weight. Author (NASDA)

N94-25547# National Research Inst. for Metals, Tokyo (Japan).
INTERACTIONS BETWEEN CORROSION FATIGUE AND STRESS CORROSION CRACK ON STEEL FOR LIGHT WATER REACTORS [KEISUIROYO KINZOKU ZAIRYO NO FUSHOKU HIRO-ORYOKU FUSHHOKUWARE SOGO SAYO NI KANSURU KENKYU]
Norio Nagata, Tadao Ishihara, Shinobu Matsushima, Yasuyuki Katada, Shunji Sato, and Shigeo Ohashi *In its* Bulletin of National Research Institute for Metals in Fiscal Year 1993, No. 14 29 Jan. 1993 p 29-42 In JAPANESE (For primary document see N94-25544 07-26)
Avail: CASI HC A03/MF A04

In order to evaluate material safety in the coolant environment, investigation is conducted concerning the interactions between corrosion fatigue and stress corrosion crack as well as environment factors which influence the incidence and crack growth in hot, high pressure water. Rolling alloy steel JIS (Japanese Industrial Standards) SQV2A used for pressure vessels and forging material SFVQ1A served as test samples. In the compound load experiment of fatigue and tension at low strain rate, no notable interactions were recognized which may affect the crack growth rate. It was found that the crack growth rate is proportional to the density of dissolved oxygen, and inversely proportional to the flow rate. The faster the crack growth rate was, the lower the corrosion electric potential was, especially in materials including more sulfur. No distinct correlation was found between the corrosion electric potential and dissolved oxygen. In dissolution study of MnS between cracked fractures, dissolution occurred more easily (at lower temperature) in crevices than on free surfaces. In the fatigue test in hot, high pressure water fatigue life of SQV2A material found more dependency on the strain rate (slower strain rate shortened the fatigue life) than that of SFVQ1A material. Author (NASDA)

N94-25548# National Research Inst. for Metals, Tokyo (Japan). Environmental Performance Div.

PREPARATION OF CREEP DATA SHEET: MATERIAL STRENGTH DATA SHEET Report No. 3 [KURIPU DETA SHITO NO SAKUSEI: ZAIRYO KYODO DETA SHITO] **c39**

Chiaki Tanaka, Koichi Yagi, Sadao Ikeda, Hiroshi Ito, Eiji Baba, Masaru Shimizu, Hideo Tanaka, Kenji Yokokawa, Hideo Nagai, and Osamu Kanamaru et al *In its* Bulletin of National Research Institute for Metals in Fiscal Year 1993, No. 14 29 Jan. 1993 p 43-63 In JAPANESE (For primary document see N94-25544 07-26)
Avail: CASI HC A03/MF A04

Continuing from the first and the second term, creep rupture data sheet on metals for high temperatures was continued targeting for 100,000 hours. Creep strain data sheet for elastic analysis, conceived in the second term was carried out this term. Additionally, research was planned into the Cr group steel, which is increasingly in demand for high temperature equipment, and material sampling and testing commenced accordingly. In 1986, the creep data sheet (B Version) was published for the first time, including the creep rupture data exceeding final target of 100,000 hours. Since then, B versions were published on 12 different materials this term. There has been much research using the data from creep data sheets and test samples, including creep strain characteristics, stress relaxation characteristics, creep rupture characteristics and life estimate, with substantial results. In the creep test technology aiming for highly reliable data, deterioration factors of thermocouples were investigated. The results from creep data sheets and related research contributed to improvement in strength reliability of metals at high temperatures. Author (NASDA)

N94-25549# National Research Inst. for Metals, Tokyo (Japan).

R AND D FOR CREATION, MEASUREMENT, APPLICATION OF ULTRA-HIGH VACUUM [GOKUKOSHINKU NO HASSEI, KEISOKU, RIYO GIJUTSU NO KAIHATSU NI KANSURU KENKYU] **c31**

Kazuhiro Yoshihara, Masahiro Tosa, and Michiko Yoshitake *In its* Bulletin of National Research Institute for Metals in Fiscal Year 1993, No. 14 29 Jan. 1993 p 65-74 In JAPANESE (For primary document see N94-25544 07-26)
Avail: CASI HC A02/MF A04

Stainless steel has widely been used as material for vacuum vessels. Attempts were made, utilizing surface deposition phenomenon, to make the stainless steel surface absorbent of gas. First, BN and SUS304 steel were mixed and put on a steel board. This BN/SUS304 steel mixture proved to be effective as coating material for the surfaces of super high vacuum vessels, because low gas absorbing BN can easily be coated at low temperature. In the next experiment of BN treatment with magnetron spatter electrodes, BN/SUS304 steel mixture films were uniformly evaporated and coated inside a compact vacuum vessel. Measurement by the throughput method revealed that the gas release rate in this compact vacuum vessel was smaller by one digit than that in a vessel without BN coating. Thus, a vacuum chamber was easily made into a super high vacuum chamber with high performance. In the third experiment, Ti separation films with getter functions for O2 and CO2 were obtained by evaporating Nb films on Ti and heating it in vacuum at approximately 800 K. These films function as getters at 473 K and do not require as high a temperature as sublimation pumps. It was thus proved that it is possible to use the material separation Ti film/Nb film/ Ti in getter pumps for released gas caused by filaments or heat from the filaments. Author (NASDA)

N94-25550# National Research Inst. for Metals, Tokyo (Japan). Materials Design Div.

KNOWLEDGE BASE SYSTEMS FOR CHEMICAL COMPOUNDS DESIGNING SUPPORT [KAGAKU BUSSHITSU SEKKEI TO SHIEN NO TAME NO CHIHSIKI BESU SHISUTEMU NI KANSURU KENKYU] **c82**

Michio Yamazaki, Kenichi Hoshimoto, Toshihiro Yamagata, Katsumi Ono, Hidehiro Onodera, Hiroshi Harada, and Tadaharu Yokokawa *In its* Bulletin of National Research Institute for Metals in Fiscal Year 1993, No. 14 29 Jan. 1993 p 75-86 In JAPANESE (For primary document see N94-25544 07-26)
Avail: CASI HC A03/MF A04

An attempt was made to construct a dialog type alloy design system and conception support knowledge base system utilizing treatises as sources of knowledge. This was intended to investigate intelligence base systems that would contribute to the development in steel material. The alloy design program presently in use is incorporated with a procedure type program, and it is unlikely that intelligence base be practically applied in our development because creating variations will be a totally different research requiring tremendous amount of work. Meanwhile, conception support systems which provide information wanted by researchers will be very useful because the present world is full of research informations. Under these circumstances, a dialog type knowledge search system with natural language was prepared. It revealed that a system incorporating a personal computer could not be put into practical use due to memory and processing speed restrictions, however, some basic functions were confirmed. More practical search system and intelligence compiling tools were developed employing an engineering work station and the expert shell. Although these systems are still prototypes, they are expected to serve as effective development support tools by enriching the knowledge contents. Author (NASDA)

N94-25551# National Research Inst. for Metals, Tokyo (Japan). Physical Properties Div.

HYDROGEN TRAPPING WITH Pd COATED ALLOY FILMS [PD HIFUKU SHITA GOKINMAKU NO SUISO NO TORAPPINGU GENSHO NI KANSURU KENKYU]

Muneyuki Amano, Chikashi Nishimura, and Masao Komaki *In its* Bulletin of National Research Institute for Metals in Fiscal Year 1993, No. 14 29 Jan. 1993 p 87-92 In JAPANESE (For primary document see N94-25544 07-26)
Avail: CASI HC A02/MF A04

Alloy films subject to oxidization must be coated with a material, such as Pd, which is not easily oxidized and has high permeability before they can be used as hydrogen separation films. Research into hydrogen trapping with Pd-coated V-15 at percent Ni alloy films at 373-673 K was conducted. The research focused on film surfaces before Pd coating and impure objects affecting hydrogen permeability, and measures to eliminate this phenomenon are investigated. The following results are obtained: (1) surface layers generated by machine polishing cause notable H2 trapping at approximately 473 K or less; (2) oxidized films remained between Pd films and alloy films, and caused hydrogen trapping at low temperatures; (3) impurities, especially oxygen atoms, which intruded into alloy films reduce hydrogen permeability significantly at 673 K, but this can be prevented by adding an adequate amount of deoxidizer such as Y, Ti and Zr; (4) deoxidation was not effective in repressing hydrogen trapping on V-15 at percent Ni alloy at approximately 473 K or less. This was considered to be influenced by their surfaces; (5) it was concluded that a solid solution O effectively reduces the valid area for hydrogen permeation; and (6) the hydrogen diffusion coefficient in V-15 at percent Ni alloy was bigger than that in Pd, but was much smaller than that in V. Author (NASDA)

N94-25552# National Research Inst. for Metals, Tokyo (Japan). Chemical Processing Div.

BASIC RESEARCH ON LEVITATION FUSING/SOLIDIFICATION TECHNOLOGY [FUYO YOKAI GYOKO GIJUTSU NI KANSURU KISOTEKI KENKYU]

Kazuyuki Sakuraya, Akira Fukuzawa, Toshiaki Watanabe, Sadao Furuyama, Satoshi Iwasaki, and Tatsuro Mitsui *In its* Bulletin of National Research Institute for Metals in Fiscal Year 1993, No. 14 29 Jan. 1993 p 93-96 In JAPANESE (For primary document see N94-25544 07-26)
Avail: CASI HC A01/MF A04

Research was made on levitation force toward metal balls in cold crucibles to obtain basic data for the most suitable levitation fuse conditions. Cold crucibles with different slit width and number of slits were prepared. The number of slits on the crucibles varied from one to 24. Different power frequencies varying from 3 to 10 kHz were applied. In two cases with coil positions allowing maximum levitation force, levitation force increased as the number of slits did, although it was not proportional. In these two cases, levitation force increased as the slit width increased as well. However, in the third case where the coil position did not allow the maximum levitation force, the results were opposite from the above cases. It was thus concluded that the coil positions and shapes (windings and height) are important factors to be considered for levitation force as well as the number of slits, slit width, and power frequencies.

Author (NASDA)

N94-25553# National Research Inst. for Metals, Tokyo (Japan). Failure Physics Div.

INNER FIBER OBSERVATION FOR METAL MATRIX COMPOSITES UNDER THE STRESS LOAD CONDITION UTILIZING SYNCHROTRON ORBITAL RADIATION (SR) BY X-RAY CT [SHINKUROTORON HOSHAKO (SR) O RIYO SHITA X SEN CT BU YORU ORYOKU FUKA JOTAI NI OKERU FUKUGO ZAIRYO NO NA!BU KANSATSY]

Chitoshi Masuda, Yoshihisa Tanaka, P. Mahajan, Katsuhisa Usami (Hitachi Ltd., Tokyo, Japan.), and Tatsumi Hirano (Hitachi Ltd., Tokyo, Japan.) *In its* Bulletin of National Research Institute for Metals in Fiscal Year 1993, No. 14 29 Jan. 1993 p 97-106 In JAPANESE (For primary document see N94-25544 07-26)

Avail: CASI HC A02/MF A04

Observations were made of inner fiber damage in metal matrix composites (MMC) by using stress load equipment in concert with X-ray CT (Computer Tomography) equipment. A layer of test samples was prepared from long fiber strengthened MMC's, and a stress load was applied to observe the breaking process. The X-ray images of SiC (C)/C/A6N01 material and B (W)/A6N01 material after the stress load process showed different break structures. Inner fiber ruptures and strengthened fiber slippings that were observed should contribute useful information to clarify the relationship between the surface and dynamic characteristics. By observing particle dispersion strengthened MCC's by means of X-ray CT, it was found that the accompanying void generation, up to the maximum tension force, remained almost unchanged, like that with no load; although, the void size increased as the load increased. Voids were also generated just before the sample failed. In conclusion, it is possible to measure and analyze the damage in MMC's due to strain load tension processes. It is also possible to gather data on broken fiber length as it relates to rupture characteristics. It was also confirmed that the equipment developed in this research was effective. Author (NASDA)

N94-25554# National Research Inst. for Metals, Tokyo (Japan). Environmental Performance Div.

OBSERVATION ON METAL SURFACE IN AQUEOUS SOLUTION USING AN ELECTROCHEMICAL SCANNING TUNNELING MICROSCOPE (STM) [SOSAGATA TONNERU KENBIKYO NI YORU KINZOKU/SUIYOEKI KAIMEN NO SOKUTEI NI KANSURU KENKYU]

Saburo Matsuoka, Hiroyuki Masuda, and Nobuo Nagashima *In its* Bulletin of National Research Institute for Metals in Fiscal Year 1993, No. 14 29 Jan. 1993 p 107-114 In JAPANESE (For primary document see N94-25544 07-26)

Avail: CASI HC A02/MF A04

A Scanning Tunneling Microscope (STM) which can function in an aqueous solution was constructed to observe damage at high magnification including corrosion, corrosion fatigue, and stress corrosion generated in aqueous solution. The surfaces of gold, pure iron thin film, low alloy SNCM439, and austenitic stainless steel SUS304 were observed in the anode and cathode areas in an aqueous solution of NaCl (1 percent) and HNO3 (0.1 percent). By using a coated probe and a bipotentiostat, which allows the electric potentials of the probe and test samples to be set separately, the STM observed large areas ranging from the cathode to the anode in high magnification mode. The maximum possible magnification was 70 nm in X-Y scan areas, equivalent to 200 metal atoms. Transitional surface changes by corrosive dissolution could be observed, and thus, corrosion could be measured quantitatively by subtracting an STM image from another. Author (NASDA)

N94-25555# National Research Inst. for Metals, Tokyo (Japan).

FUNDAMENTAL STUDY ON MONITORING TECHNOLOGY ON LOCAL SURFACE DAMAGES [HYOMEN KYOKUBU SONSHO NO MONITARINGU GIJUTSU NI KANSURU KISOTEKI KENNYU]

Yasuyuki Katada and Shunji Sato *In its* Bulletin of National Research Institute for Metals in Fiscal Year 1993, No. 14 29 Jan. 1993 p 115-122 In JAPANESE (For primary document see N94-25544 07-26)

Avail: CASI HC A02/MF A04

Research was conducted to evaluate the surface corrosion/damage of steel used for pressure vessels in hot, high pressure water environments. The research simulated the environment of light water reactor coolants. The research was intended to establish electrochemical measurement technology in the above environment and to clarify/resolve the cracking mechanism in this environment by applying the AC (Alternating Current) impedance method to local damage and checking the possibility of this method in the future. Mn-Mo-Ni alloy steel and Wedge Opening Loading (WOL) type test samples were used as test samples, and polarization and AC impedance were measured. The following results were obtained: (1) electrochemical measurement systems were established including the AC impedance method in the environment of hot, high pressure water; and (2) the AC impedance method proved to be applicable for local damage evaluation. This was concluded by the clear characteristic differences seen between the WOL type test samples with cracks and those without cracks after impedance measurement. Author (NASDA)

N94-25556# National Research Inst. for Metals, Tokyo (Japan).

STUDY ON PHASE TRANSFORMATION DUE TO DEFORMATION IN FERROMAGNETIC FIELDS AT CRYOGENIC CONDITION [GOKUTEION, KYOJIBAKA HENKEI NI YOUR SOHENTAI NI KANSURU KEKNKYU]

Kotobu Nagai, Toshio Ogata, Toshimi Yuri, Osamu Umezawa, and Keisuke Ishikawa *In its* Bulletin of National Research Institute for Metals in Fiscal Year 1993, No. 14 29 Jan. 1993 p 123-129 In JAPANESE Prepared in cooperation with Tokyo Univ., Japan; and Toshiba Corp., Kanagawa, Japan Sponsored by Science and Technology Agency, Tokyo, Japan (For primary document see N94-25544 07-26)

Avail: CASI HC A02/MF A04

Deformation restoration tools and phase transformation quantization methods were studied to establish the relationship between deformation and phase transformation. The purpose of this study was the quantitative evaluation of effects on the phase transformation of metastable austenitic stainless steel caused by deformation and ferromagnetic fields. Deformation load equipment was constructed to apply a load of two tons in maximum to a small deformation tensile bar. This was intended to simulate magnets with rather large gauges of 50 mm inside diameter. By utilizing the paramagnetism of the austenitic phase and the ferromagnetism of the bcc (body centered cubic) martensitic phase formed with the phase transformation, a quantization method with high precision was developed by magnetization curves in the liquid helium temperature. Next, the relationship between deformation and phase transformation amount was investigated on 300 system austenitic stainless steel. The bcc martensitic phase was not formed on 304L or 316LN steel by refrigeration down to 4 K. The formed 316LN steel remained stable in shape until its tension fracture at room temperature, while some bcc martensitic phase was formed on 304L steel. At 77 K or less, both samples transformed due to deformation, and it was aggravated by the effect of magnetic fields. Author (NASDA)

N94-25557# National Research Inst. for Metals, Tokyo (Japan). Materials Physics Div.

STUDY ON CHARACTERISTICS AND ELECTRONIC STRUCTURES OF MATERIALS WITH STRONG ELECTRONIC CORRELATIONS BY FERROMAGNETIC FIELDS [KYOJIBA NI YORU TSUYOI DENSHI SOKAN O YUSURU BUSS HITSU NO BUSSEI TO DENSHI KOZO NI KANSURU KENKYU]

Haruyoshi Aoki, Shinya Uji, Tadashi Shimizu, Kiyoshi Inoue, Toshihisa Asano, and Yoshikazu Sakai *In its* Bulletin of National Research Institute for Metals in Fiscal Year 1993, No. 14 29 Jan. 1993 p 131-136 In JAPANESE (For primary document see N94-25544 07-26)

Avail: CASI HC A02/MF A04

Joint research was carried out with research institutes in France on the development and application of ferromagnetic field technologies. In order to clarify how the specific magnetic characteristics such as Cu spinning and Gd moment contribute to conductivity, Gd(2-x)Ce(x)CuO4 was used for a systematic study of electrical and magnetic field resistance against Ce concentration. Magnetism was precisely measured to obtain magnetic characteristics including magnetic transition and its relationship with conduction phenomena. The Gd group is quite suitable for the study of correlation between the two dimensional conduction and magnetism because its magnetic characteristics systematically change against Ce concentration. Current-magnetic effects of InSb were investigated in ferromagnetic fields at extremely low temperatures. At the quantum limit, it was clarified that the diagonal component becomes zero while the electroconductivity tensor stays constant. Author (NASDA)

N94-25558# National Research Inst. for Metals, Tokyo (Japan). Chemical Processing Div.

STUDY ON REACTIONS BETWEEN MOLTEN METAL AND OXIDE BY MAGNETIC FLOTATION DISSOLUTION METHOD [JIKI FUJO YOKAIHO NI YORU YOYU KINZOKU-SANKABUTSU KAN HANNO NI KANSURU KENKYU]

Akira Fukuzawa, Kazuyuki Sakuraya, Toshiaki Watanabe, and Yasumitsu Fukuzawa *In its* Bulletin of National Research Institute for Metals in Fiscal Year 1993, No. 14 29 Jan. 1993 p 137-139 In JAPANESE Sponsored by Science and Technology Agency, Tokyo, Japan (For primary document see N94-25544 07-26)

Avail: CASI HC A01/MF A04

The cold crucible type non-contacting dissolution method was investigated as a means to dissolve active metals or metals with high melting points and to prepare materials with high purity. The non-contacting electroslag refining method was investigated. This was intended to provide reaction and purifying functions to the cold crucible type non-contacting dissolution equipment which is now under development. While it is difficult to process slags with low surface tension without a vessel, it was assumed that a thin slag coating on metal surfacesmight be achieved. To investigate this assumption, experiments were made on Si containing iron in a cold crucible reactor with power frequency of 200 kHz. SiO2 films were successfully formed on the surfaces. An investigation was also made into oxide solubility with power in 4 MHz. Author (NASDA)

N94-25559# National Research Inst. for Metals, Tokyo (Japan).

STUDY ON FERROMAGNETIC FIELD MAGNET USING STRONG AND HIGHLY CONDUCTIVE MATERIAL [KOKYODO, KODODEN ZAIRYO O MOCHIITA KYOJIKAI MAGUNETTO NI KANSURU KENKYU]

Hiroshi Maeda, Kiyoshi Inoue, Hitoshi Wada, Yoshiaki Tanaka, Kikuo Ito, Takao Takeuchi, Toshihisa Asano, Yoshikazu Sakai, Tsukasa Kiyoshi, and Yukikazu Iwasa *In its* Bulletin of National Research Institute for Metals in Fiscal Year 1993, No. 14 29 Jan. 1993 p 141-143 In JAPANESE Prepared in cooperation with MIT, Cambridge Sponsored by Science and Technology Agency, Tokyo, Japan (For primary document see N94-25544 07-26)

Avail: CASI HC A01/MF A04

Strong, highly conductive materials which can be used for ferromagenetic fields were developed and evaluated jointly with the Francis Bitter National Magnet Laboratory in the United States. The design and preparation of such materials were also studied. In this research, Cu-Nb and Cu-Ag alloy filaments were developed, and the pulse magnet was considered as a constant conductive magnet with ferromagnetic fields. Several problems were found with Cu-Nb alloy. On the other hand, Cu-Ag showed some outstanding results. The conductivity and strength of the Cu-Ag alloy were improved during the annealing process. Additionally, high mechanical strength was obtained with intermediate annealing. However, measurement showed that the increase in the resistance of Cu-Ag alloy in ferromagnetic fields resembled that of other Cu group alloys; that is, resistance increase did not reach saturation in ferromagnetic fields. This fact requires some investigation into magnet design. It was also found that the resistance at extremely low temperatures decreased to approximately 30 percent of that at room temperature. Author (NASDA)

N94-25560# National Research Inst. for Metals, Tokyo (Japan).

STUDY ON MEASUREMENT AND EVALUATION METHODS FOR SUPERCONDUCTIVE CHARACTERISTICS [CHODENDO TOKUSEI NO SOKUTEI HYOKAHO NI KANSURU KENKYU] **c33**

Hitoshi Wada, Kikuo Ito, Tsuneo Kuroda, Michiya Yuyama, L. F. Goodrich, S. Bray, J. W. Ekin, and R. Goldfarb *In its* Bulletin of National Research Institute for Metals in Fiscal Year 1993, No. 14 29 Jan. 1993 p 145-148 In JAPANESE Prepared in cooperation with National Inst. of Standards and Technology, Gaithersburg, MD Sponsored by Science and Technology Agency, Tokyo, Japan (For primary document see N94-25544 07-26)

Avail: CASI HC A01/MF A04

Research was conducted jointly with the National Institute of Standards and Technology (USA) regarding test and evaluation methods for superconductors. The main themes were as follows: (1) measurement of the critical current of oxidized superconductors; (2) measurement of alternating current loss in advanced metal superconductors; and (3) development of software programs for measurement automation. For the measurement of the critical current of oxidized superconductors, the pulse current method was improved in order to have the accuracy necessary to deal with the problem of heat generation at electrodes. As a result of the technique developed, highly accurate measurement of critical current was attained even at silver pasted electrodes. In the next experiments, the transverse stress of Nb3Al wires was measured. Attention was paid because it is expected to be the next superconductor to be used in the future after Nb3Sn. It was clarified that the critical current degradation due to axial and transverse stress in Nb3Al wires is extremely smaller than that in Nb3Sn wires. Also, the values obtained in the experiment suggested that there was little difference between axial and transverse stress dependency in the critical current of Nb3Al superconductive filaments. Author (NASDA)

N94-25561# National Research Inst. for Metals, Tokyo (Japan).

COMBUSTION SYNTHESIS METHOD [NENSHO GOSEIHO NI KANSURU KENKYU] **c25**

Yoshinari Kaieda, Minoru Otaguchi, Nobutaka Oguro, and Z. A. Munir *In its* Bulletin of National Research Institute for Metals in Fiscal Year 1993, No. 14 29 Jan. 1993 p 149-151 In JAPANESE Prepared in cooperation with California Univ., Davis (For primary document see N94-25544 07-26)

Avail: CASI HC A01/MF A04

Joint research was performed regarding the creation of chemical compound material by combustion synthesis as well as evaluation of the chemical compound material created. The basic mechanism of combustion synthesis was clarified using TiN and rarefied nitrogen gas. In this research, heat generation was reduced and the temperature lowered preventing overall dissolution and promoting nitrogen gas intrusion. Thus, improving the TiN conversion rate was investigated. When rarefied gas was used for nitrogen material at combustion synthesis, the slower the reaction spread speed was the more TiN was generated. This reverse dependency between TiN conversion rate and the reaction spread speed is relevant to the fact that violent reactions spread avoiding powder clusters. This prevents nitrogen gas from intruding inside. Mild reactions spread slowly, supplying sufficient nitrogen gas to the areas of reaction, thus increasing the TiN conversion rate. This rate improves in materials which contain the end product, TiN, from the beginning. However, if the TiN percentage in a material exceeds 50 percent, combustion synthesis stops. Author (NASDA)

N94-25562# National Research Inst. for Metals, Tokyo (Japan). Chemical Processing Div.

DEVELOPMENT OF SO(x) AND NO(x) SOLID ELECTROLYTE SENSORS [SO(X), NO(X) KOTAI DENKAISHITSU SENSA NO KAIHATSU NI KANSURU KENKYU] **c35**

Hiroaki Nakamura, Mikihiko Kobayashi, Akira Kasahara, Yoichi Ogawa, Hiroaki Isago, and Isao Morinaka *In its* Bulletin of National Research Institute for Metals in Fiscal Year 1993, No. 14 29 Jan. 1993 p 153-164 In JAPANESE (For primary document see N94-25544 07-26)

Avail: CASI HC A03/MF A04

Compounds suitable for solid electrolyte sensors were sought, and the composing methods were investigated in order to improve measurement of SO(x) and NO(x). Various compounds were dissolved, and test samples were made amorphous by quick cooling to compose each group of M2O-B2O3-M2SO4 (M = Li, K, Na) as solid electrolytes for SO(x). The samples composed by this method showed electric conductivity of 10(exp -3) S/cm or more, which meant that the samples could be solid electrolytes. Polarization measurement indicated that the samples were ion conductors. K2O-B2O3-K2SO4 was used as a solid electrolyte for a low density sensor to measure electromotive force. The actual electromotive force values and theoretical values were almost the same at 0.5 ppm or more. When the electromotive force was measured using Li2O-B2O3-Li2SO4 for a high density sensor, the actual values and theoretical values coincided at 10-1000 ppm. The electromotive force responsiveness of solid electrolyte sensors to the changes in gas density was approximately 1 minute, proving that Li2O-B2O3-Li2SO4 is available as a solid electrolyte for sensors. Electric conductivity rose in the composed sample of Ca(NO3)2-NaNO3 and CsNO3-NaNO3 composed by pressurized baking. Both samples showed high electric conductivity, revealing possible applications in sensors. Author (NASDA)

N94-25563# National Research Inst. for Metals, Tokyo (Japan). Materials Physics Div.

STUDY ON SYNTHESIS AND CHARACTERISTICS OF INTERMETALLIC COMPOUND WITH STRONG ELECTRON CORRELATION [TSUYOI DENSHI SOKAN O YUSURU KINZOKUKAN KAGOBUTSU NO GOSEI TO BUSSEI NI KANSURU KENKYU]

Haruyoshi Aoki, Shinya Uji, Masanori Yata, and Keikichi Nakamura *In its* Bulletin of National Research Institute for Metals in Fiscal Year 1993, No. 14 29 Jan. 1993 p 165-172 In JAPANESE (For primary document see N94-25544 07-26)

Avail: CASI HC A02/MF A04

Research was made on electronic structures of intermetallic compounds containing Ce and U with strong electron correlation. At the same time, thin films were prepared from such compounds to investigate the characteristic changes and new phenomena deriving from pseudo-binary structures. Epitaxy thin films of CeSi2 and CeSb were synthesized by MBE (Molecular Beam Epitaxy). CeSi2 (001) single crystal thin films were composed by evaporating Ce on Si (001) surfaces kept at 1000 C. The galvanomagnetic characteristics observed in thick films of 10 nm or more were the same as those of bulk single crystals. The thinner the films were, the more they were affected by magnetic diffusion for electrical conductivity. CeSb (100) single crystal films were composed by simultaneous evaporation of Ce and Sb on sapphire (0001) surfaces. The same electric conductivity characteristics as those in bulk single crystals were obtained on thick films. The films, however, were quite unstable in the air, and measurement of galvanomagnetic characteristics was not possible. Electronic structures of CeSb and UGe2 were studied by de Haas-Van Alphem (dHvA) effects, and a new high frequency dHvA branch was found for CeSb, which was closely related to important issues on electron structures.
Author (NASDA)

N94-25564# National Research Inst. for Metals, Tokyo (Japan). Materials Physics Div.

STUDY ON COMPUTERIZED EXPERIMENT OF AMORPHOUS TRANSFORMATION PROCESS BY SOLID PHASE REACTION [KOSO HANNO NI YORU AMORUFASU SEISEI KATEI NO KEISANKI JIKKEN NI KANSURU KENKYU] c76

Katsuyuki Kusunoki, Masato Enomoto, and Tamio Oguchi *In its* Bulletin of National Research Institute for Metals in Fiscal Year 1993, No. 14 29 Jan. 1993 p 173-185 In JAPANESE (For primary document see N94-25544 07-26)

Avail: CASI HC A03/MF A04

Recently, attention has been shifted from the traditional liquid quick cooling to amorphous alloy composition by solid phase reaction. Computer simulation at the atomic level was conducted to clarify the transformation of stable crystal phase to metastable amorphous phase. Molecular dynamics of Leonard-Jones type interatomic potential was employed to simulate the annealing of single crystals and diffusion couples as well as tension of single crystals, and changes in structure were studied. Crystals do not become amorphous in groups containing only simple substances and atomic holes. It requires alloy groups or processes which generate a large amount of negative excess volume to make crystal amorphous by solid phase reaction regardless of the amount of mixed enthalpy. For crystals to become amorphous, atomic couples in different sizes must occur at random to break the crystal regularity.
Author (NASDA)

N94-25565# National Research Inst. for Metals, Tokyo (Japan). Physical Properties Div.

STUDY ON ALLOY FILMS FOR HYDROGEN SEPARATION [SUISO BUNRIYO GOKINMAKU NI KANSURU KENKYU]

Muneyuki Amano, Chikashi Nishimura, and Masao Komaki *In its* Bulletin of National Research Institute for Metals in Fiscal Year 1993, No. 14 29 Jan. 1993 p 187-193 In JAPANESE (For primary document see N94-25544 07-26)

Avail: CASI HC A02/MF A04

Hydrogen permeability was studied on Pd coated V-Ni alloy films and V-Mo alloy films at 373-673 K. This revealed that an appropriate composition of Ni and Mo will provide potential materials for hydrogen permeation films at temperatures as low as 473 K. The appropriate percentages of Ni or Mo with little hydrogen embrittlement was approximately 15 at percentage and 30 at percentage. With these percentages, both alloy films showed better hydrogen permeability than Pd, and no cracks were formed. Hydrogen permeation of V-Ni and V-Mo alloy films showed a small correlation to temperature. This was because the hydrogen solid solution ratio increases in the same proportion as the hydrogen diffusion coefficient falls with the decrease in temperature. Ductility deteriorates if diffraction phases are present in V-Ni radical alloys. In the tension test of V-15 at percentage Ni alloys, diffracted test samples which went through the melting process did not show much flexibility, whereas the flexibility of the one without diffraction was greater by a significant percentage. Twin deformation and slipping deformation were detected on those samples. The hydrogen solid solution rate was faster at V-Mo alloy film surfaces than at V-Ni alloy film surfaces.
Author (NASDA)

N94-25566# National Research Inst. for Metals, Tokyo (Japan). Mechanical Properties Div.

STUDY ON THE MECHANISM OF TITANIUM ALLOY TOUGHNESS AND THE IMPROVEMENT OF PROPERTIES [CHITAN GOKIN NO KYOJINKA KIKO TO TOKUSEI KOJO NI KANSURU KENKYU]

Norio Kainuma, Masuo Hagiwara, Fumio Morito, Seiichi Muneki, Junji Takahashi, Yoshikuni Kawabe, Mitsutane Fujita, Yoshinari Kaieda, Hirosada Irie, and Osamu Ohashi *In its* Bulletin of National Research Institute for Metals in Fiscal Year 1993, No. 14 29 Jan. 1993 p 195-205 In JAPANESE (For primary document see N94-25544 07-26)

Avail: CASI HC A03/MF A04

The mechanisms of high strength and toughness of titanium alloys were investigated to further improve these properties. The research details were: (1) enhancement of precipitation hardening titanium alloys; (2) enhancement of titanium alloys by rapid solidification powder metallurgy; and (3) quality improvement of joint parts. Micro-dispersion proved to mitigate degradation in fatigue characteristics. Ductility of age hardening materials showed dependency on grain diameters, although strength of these materials did not. Toughness did not depend on crystal grains, but it depended only on strength. Fine two phase texture was obtained with high fatigue strength when PREP (Plasma Rotating Electrode Process) was applied to regular alpha-beta type titanium alloys. The HIP (Hot Isotactic Pressing) process on electron beam welded zones improved the fatigue strength of welded zones. Diffusion welding was studied on Ti-15V-3Cr-3Sn-3A1 (15-3) alloys and Ti-6A1-4V (6-4) alloys. Diffusion junction was easy with 6-4 alloys, but was difficult with 15-3 alloys.
Author (NASDA)

N94-25567# National Research Inst. for Metals, Tokyo (Japan). Mechanical Properties Div.

STUDY ON IMPROVEMENTS IN FRETTING FATIGUE CHARACTERISTICS OF HIGH STRENGTH STRUCTURAL MEMBER [KOKYODO KOZO ZAIRYO NO FURETTINGU HIRO TOKUSEI NOJO NI KANSURU KANKYU]

Masae Sumida, Kozo Nakazawa, Ryuichi Hamano, Norio Maruyama, Yoshikuni Kawabe, Satoshi Nishijima, Tetsuo Fujii, and Kazuo Saito *In its* Bulletin of National Research Institute for Metals in Fiscal Year 1993, No. 14 29 Jan. 1993 p 207-218 In JAPANESE (For primary document see N94-25544 07-26)

Avail: CASI HC A03/MF A04

Pad-pressure effects on the fretting fatigue lives of high tension steel and Ti-6A1-4V alloy were investigated. It was clarified that fairly small pressure would minimize the fatigue lives. This is considered to be caused by the centralization of friction and pressure to small contact surfaces. Research was made regarding how cathode anti-corrosion modification affects on fretting fatigue behavior of high tension steel in sea water. Fretting fatigue strength under natural corrosion in sea water deteriorated remarkably compared with that in the air. However, the cathode anti-corrosion modification improved the fretting fatigue strength in sea water and made it higher than that in the air. Environmental influence on fretting fatigue behavior of Ti-6A1-4A alloy was also investigated. The fretting fatigue strength in artificial sea water is generally lower than that in the air. The fretting fatigue strength in LiCl-CH3OH was approximately twice as strong as regular fretting fatigue strength. The corrosion fatigue behavior of high strength steel in sea water was researched. Thin films were coated on the steel surfaces by magnetron spattering and ion mixing. The cohesion of the films effectively improved by the two methods together, preventing the fatigue life from deteriorating due to hydrogen embrittlement.
Author (NASDA)

N94-25568# National Research Inst. for Metals, Tokyo (Japan). Materials Design Div.
STUDY ON KNOWLEDGE EXTRACTION AND SYSTEMATIZATION FOR MATERIAL DESIGN [ZAIRYO SEKKEI NO TAME NO CHISHIKI NO CHUSHUTSU TO TAIKEIKA NI KANSURU KENKYU] c82
Kenichi Hoshimoto, Yutaka Kurihara, Akimitsu Miyazaki, Ryuichi Kaneko, Tadaharu Yokokawa, Shuichi Iwata, and Mitsutane Fujita *In its* Bulletin of National Research Institute for Metals in Fiscal Year 1993, No. 14 29 Jan. 1993 p 219-230 In JAPANESE (For primary document see N94-25544 07-26)
Avail: CASI HC A03/MF A04

Investigation was conducted on knowledge extraction from published data as well as from visual information which is difficult to computerize, and filing of comprehensive material information which includes images and graphics. Functional inspection was studied for image data processing. Similarities in microscopic photographs of alloy texture were studied by both professionals and non-professionals, and their results were analyzed statistically by multi-dimensional scaling. Alloy texture was expressed roughly in three factors: crystal shapes, anisotropy, and fineness. Quantization of texture characteristics expresses the relationship between texture characteristics and characteristic values regressively and clearly. Next, data collection and data base development regarding binary alloy phase were researched, and software programs were developed accordingly. The image was quantized with an image scanner, and was classified into nodes, lines, and domains to be expressed in a graphic table. Search function was facilitated by search user interface which did not require specific languages for data search on the data base. Author (NASDA)

N94-25569# National Research Inst. for Metals, Tokyo (Japan). Chemical Processing Div.
FUNDAMENTAL STUDY ON NEW SYNTHETIC TECHNOLOGY BY PHTHALOCYANINE COMPLEXES [FUTAROSHIANIN SAKUTAI NI YORU SHINGOSEI GIJUTSU NI KANSURU KISO KENKYU] c25
Hiroaki Isago, Yutaka Kagaya, and Ryosuke Hasegawa *In its* Bulletin of National Research Institute for Metals in Fiscal Year 1993, No. 14 29 Jan. 1993 p 231-240 In JAPANESE (For primary document see N94-25544 07-26)
Avail: CASI HC A02/MF A04

Bis(tetra t-butylphthalocyaninato) praseodymium (3) and Pr(sup t)Pc2 (Pr = praseodymium, Pc = phthalocianine) were composed as a mixture of multiple isomers by heating a mixture of 4-t-butyl phthalonitrile and praseodymium acetate at 300 C. Bis(tetra t-butylphthalocyaninato) praseodymium (3) has a bulky t-butyl group as a side chain group. Compared to LnPc2 (Ln = lanthanidic ion) which does not have substituents, Pr(sup t)Pc2 proved to have 100-1000 times higher solvency for organic solvents. Pr(sup t)Pc2 showed ESR (Electron Spin Resonance) signals specific to unpaired pi electrons and was radical in toluene solution. The similarity in the electron absorption spectra between Pr(sup t)Pc2 and PrPc2 suggested that PrPc2 was also radical. The electron absorption spectra of LnPc2 were blue in solvents with large donors and green in solvents with small donors, indicating clear solvent dependency. This solvent dependency of Pr(sup t)Pc2 electron absorption spectra is similar to that shown in Ln complexes with large atomic numbers rather than that in LnPc2 complexes with small atomic numbers. Thus, t-butyl radicals are considered to contribute to the stabilization of unpaired pi electrons. Pr(sup t)Pc2 evaporation thin films dipped in electrolytic solution showed different cyclic voltamogram depending on the types and density of electrolytes. Oxidation waves control the diffusion rate of electrolytes in solution, and their potential is linearly dependent to the logarithm of the density of electrolytes. These oxidation waves are also influenced by factors other than electron transfer reactions. Author (NASDA)

N94-25570# National Research Inst. for Metals, Tokyo (Japan). Surface and Interface Div.
STUDY ON SUBSTANCE DIFFUSION IN THIN FILMS WITH CONTROLLED STRUCTURES [KOZO SEIGYO SARETA HAKUMAKUCHU NI OKERU BUSSHITSU NO KAKUSAN GENSHO NI KANSURU KENKYU] c27
Kazuhiro Yoshihara, Yuji Ikeda, Masahiro Tosa, and Michiko Yoshitake *In its* Bulletin of National Research Institute for Metals in Fiscal Year 1993, No. 14 29 Jan. 1993 p 241-252 In JAPANESE (For primary document see N94-25544 07-26)
Avail: CASI HC A03/MF A04

Research was conducted into different combinations of film coating (both metal and ceramics) on metals. The purpose was to obtain basic knowledge for technology to develop new materials by investigating the surface properties and structures. For ceramic thin films, various types of stainless steel were heated and the surface segregation rate of sulfur was measured. Next, Al2O3 was coated onto the same types of steel and adherence was studied after repeated heating. The result showed that materials containing sulfur which segregated fast had less adherence. Sulfur segregation and Al2O3 exfoliation were both retarded on steels containing Rare Earth Metals (REM). In short, sulfur segregates at surfaces, retarding adherence and promoting exfoliation, whereas REM suppresses surface segregation and exfoliation by trapping sulfur in steels as sulfate. Yttria dispersion was also effective for segregation/exfoliation retarding. For metallic thin films, diffusion of substrate elements on film surfaces was observed by applying low temperature heat so that bulk diffusion could be ignored. Combinations of two elements out of niobium, titanium, and copper were studied. On both samples with titanium as substrates, titanium diffused and condensed on film surfaces. These condensed layers of substrate elements were reproduced even after they were removed by spattering. Author (NASDA)

N94-25571# National Research Inst. for Metals, Tokyo (Japan). Surface and Interface Div.
STUDY ON MICROSCOPIC STRUCTURAL CONTROLS AND ELECTRONIC PROPERTIES AT MATERIAL SURFACES BY ION BEAMS [BIMUHO NI YORU HYOMEN KAIMEN NO BISHITEKI KOZO SEIGYO TO DENSHI BUSSEI NI KANSURU KISOTEKI KENKYU] c76
Kazuo Saito, Masatsugu Kaise, Tadahisa Matsushima, Mitsuru Uehara, Shozo Ikeda, and Kazunori Hayashi *In its* Bulletin of National Research Institute for Metals in Fiscal Year 1993, No. 14 29 Jan. 1993 p 253-257 In JAPANESE (For primary document see N94-25544 07-26)
Avail: CASI HC A01/MF A04

This research was intended to clarify the mechanism of improving material properties, superconductivity, magnetic characteristics, and atom coupling relevant to electron structures through structural and composition controls by ion beams. Nitrogen ions were implanted to orientation (001) steel thin films at low (10 to 30 K) and room (300 K) temperatures to synthesize nonequilibrium nitride Fe16N2. Different alpha solid solutions or alpha' martensite with different lattice constants were composed at different temperatures. That is, with implantation at room temperature, mainly thermodynamically stable alpha' martensite was obtained. At low temperature implantation, however, nitrogen solid solution of alpha Fe seemed to have been composed as a nonequilibrium phase. Fe16N2 phase was generated after the nitrogen implanted sample was annealed at 423 K for an hour. The diffraction positions of Fe16N2 (002) and (004) were nearly of ideal values at low temperature implantation, and half values were also smaller. At room temperature implantation, alpha' martensite was generated with its c axis vertical to the film surface. Because this phase was stable at high temperature, it was considered to have little driving force for transformation to Fe16N2. Author (NASDA)

N94-25572# National Research Inst. for Metals, Tokyo (Japan). Advanced Materials Processing Div.
STUDY ON PRODUCTION OF MATERIALS WITH ONE DIRECTION SOLIDIFICATION TEXTURE [ICHIHOKO GYOKO SOSHIKI ZAIRYO NO SOSEI NI KANSURU KENKYU] c76
Akira Sato, Toru Namai, Yoshiaki Osawa, and Goro Aragane *In its* Bulletin of National Research Institute for Metals in Fiscal Year 1993, No. 14 29 Jan. 1993 p 259-268 In JAPANESE (For primary document see N94-25544 07-26)
Avail: CASI HC A02/MF A04

By utilizing the solidification process of metal alloys, investigation was made focusing on the following four items with the purposes of producing materials with one directional solidification texture and developing new structured materials. Moldless upward continuous casting: Al-Cu and Al-Si alloy rods with a wide range of freezing points were produced. The crystals of these rods were completely in one direction lengthwise. It was also clarified that pure aluminum rods with various surface shapes could be produced by refractory molding tools. Composite material production by centrifugal casting: Research was conducted to improve wear resistance

and heat dilatation at specific areas of materials by controlling the distribution of the primary Si crystals resulting from centrifugal segregation. The primary Si crystals tend to segregate around the outer circumference of test samples due to centrifugal force. This segregated distribution changes the material properties. Supersonic oscillation application to melting metals: Two methods were investigated to apply supersonic oscillation to melting metals. One was to transmit oscillation by melting metals, and the other to use Al coated film steel horns. Both methods were effective in preventing steel loss from melting steels and grain refinement of solidified texture. Fundamental studies of materials with one direction solidification: It was confirmed that the dendrite became coarse when the solidification rate and solute density were lowered while the temperature was kept constant.
Author (NASDA)

N94-25573# National Research Inst. for Metals, Tokyo (Japan). Advanced Materials Processing Div.

STUDY ON SOLIDIFICATION OF NON-HOMOGENEOUS MELTING/SOLIDIFICATION MATERIALS [FUKINSHITSU YOKAI GYOKOZAI NO GYOKO NI KANSURU KENKYU]

Goro Omori, Osamu Nakano, Tatsuro Mitsui, Hiroo Suge, Nobuo Sakuma, and Kazumasa Togano *In its* Bulletin of National Research Institute for Metals in Fiscal Year 1993, No. 14 29 Jan. 1993 p 269-273 In JAPANESE (For primary document see N94-25544 07-26)
Avail: CASI HC A01/MF A04

An attempt was made to produce homogeneous cast lumpby quick solidification from a uniform liquid state. Al-Pb alloys were used for this experiment, and fundamental data were obtained along with property evaluation. The purpose is the production of homogeneous cast lumps of monotectic alloys with big differences in melting points, specific gravities, and little solubility limits with each other. First, Al-Pb alloys up to 30 mass percent on the excess monotectic side were prepared as an amount for Pb in order to obtain fundamental data for alloy production. The factor influencing the texture homogenization was considered to be the cooling rate at two liquid phase separation areas, and Pb diffusion conditions in Al base were studied with the correlation between the cooling rate and textures. At rapid solidification, the cooling rate at two liquid phase separation areas became slower as the alloy mass and Pb density increased. The cooling rate much influenced the solidified textures, and faster cooling rates caused fine, uniform Pb grain diffusion. ZnCl2 and SnCl2 were effective as fusing agents for hot Pb galvanizing. Among various plating methods, excellent wetness and coherency are obtained with the method in which a fusing agent is applied to Al-Pb alloy base and it is solidified by cooling, and then melting Pb is dripped. Author (NASDA)

N94-25574# National Research Inst. for Metals, Tokyo (Japan). Advanced Materials Processing Div.

STUDY ON INTERFACIAL REACTION ANALYSIS AT INTERFACIAL JOINING [KAIMEN SETSUGO NI OKERU KAIMENSO HANNO NO KAISEKI NI KANSURU KENKYU]

Ken Sasabe and Sadao Fukushima *In its* Bulletin of National Research Institute for Metals in Fiscal Year 1993, No. 14 29 Jan. 1993 p 275-285 In JAPANESE (For primary document see N94-25544 07-26)
Avail: CASI HC A03/MF A04

Two items were investigated in this research: (1) interfacial coherency by reactions between the solid phase and liquid phase; and (2) interfacial reactions at interfacial coherency by reactions between the solid phase and liquid phase. Compositions of the interface between the solid Cu and the liquid Sn-Pb alloy were studied, and the interface structures of wet ends were assessed. Then, the extended wet work of the Sn-Pb alloy on the Cu board was roughly estimated based on the earlier assessment. The estimated extended wet work was quite similar to the wet behaviors which had been known traditionally. Several types of amorphous alloy coatings were joined with the purpose of developing a welding method without depriving characteristics of amorphous metals obtained by rapid cooling. The resistance spot welding revealed that Co base alloy coating produces joints with good quality, and that it has a potential for practical application. It was assumed that spot welding by laser beams could also be performed on Co base alloy coatings. There remains some joining problems such as contact heat resistance between electrodes and parent metals, quantization of the effects for welding by the overheat of melting metals, and rough coating surfaces. Author (NASDA)

N94-25575# National Research Inst. for Metals, Tokyo (Japan). Advanced Materials Processing Div.

STUDY ON FILM GENERATION PHENOMENA BY PARTICLE DEPOSITION [RYUSHI DEPOJISHON NI YORU HIMAKU KEISEI GENSHO NI KANSURU KANSYU]

Seiji Kuroda, Takeshi Fukushima, Shigeru Kitahara, and Dai Maruo *In its* Bulletin of National Research Institute for Metals in Fiscal Year 1993, No. 14 29 Jan. 1993 p 287-298 In JAPANESE (For primary document see N94-25544 07-26)
Avail: CASI HC A03/MF A04

Film generation phenomena were investigated focusing on the plasma spray method, one of the particle deposition methods in which films are created by depositing powdery particles. In the plasma spray method, powders of various materials fused by hot and high speed plasma jets become high speed flying powders and hit main substrates. Research was performed on the cooling speed of fusing particles which hit solid surfaces and spread. Heat transfer coefficients between stacked particles were assessed by the heat conduction rate in the direction of film thickness. The cooling rates calculated from those values show that they could be 10(exp 6) K/s or more. Next, quick cooling stresses of various materials were determined by measuring the curvature of the main board during film generation in order to conduct systematic investigation on the dependency of stresses on the temperature of the main board. The quick cooling stress is a very important factor because it affects the cohesiveness of the films and it can also cause deformation. The cooling stresses of Al and Ni are between 30 and 80 MPa at 373 K, and the stresses deteriorate as the temperature rises. Mo shows similar cooling stress values. In other words, the quick cooling stresses of high strength alloys at high temperature are around 100 MPa, whereas those of ceramics are only about 10 MPa. It is considered that quick cooling stresses are determined by stress mitigating mechanisms such as creeps, plastic deformation, and microcracks. Author (NASDA)

N94-25576# National Research Inst. for Metals, Tokyo (Japan). Materials Characterization Div.

STUDY ON DEVELOPMENT OF CHEMICAL MEASUREMENT METHOD UTILIZING PLASMAS [PURAZUMA O RIYO SHITA KAGAKU KEISOKUHO NO KAIHATSU NI KANSURU KENKYU] c75

Morimasa Saito and Fumio Hirose *In its* Bulletin of National Research Institute for Metals in Fiscal Year 1993, No. 14 29 Jan. 1993 p 299-307 In JAPANESE (For primary document see N94-25544 07-26)
Avail: CASI HC A02/MF A04

Research was performed on the influence of parameters on the ion intensity, quantization of small amount impurities in highly pure Mo, sample solution analysis, and ionization mechanisms by glow discharge. The ion intensity was affected by the sample location for discharge, discharge current, and discharge voltage, but not by the sample shape. The maximum ion intensity was obtained when the sample was located 8 mm from the ion slit. After confirming that other conditions had to be set constant, these results were applied to quantization of impurities in highly pure Mo. Relative sensitivity coefficients were determined by the spark ion source mass spectrometry, and satisfactory results were obtained. A solution sampling method was investigated for lesser segregation influences by matrices and elements. Quantization of solution samples was made by dipping a highly pure graphite bar in the solution and doping. The Penning ionization ratio was determined by investigating the elements' ion intensities obtained by using Ar, Kr, and Xe gases. It is determined that there is no difference in the relative sensitivity coefficients between these discharge gases. The Penning ionization ratio is 75 to 85 percent. Author (NASDA)

N94-25577# National Research Inst. for Metals, Tokyo (Japan). Materials Characterization Div.

STUDY ON IMPROVEMENT IN PHYSICAL ANALYSIS METHOD OF METALLIC MATERIALS [KINZOKU ZAIRYO NO BUTSURI BUNSEKI SHUHO NO KODOKA NI KANSURU KENKYU]

Yoshio Tamura, Tsuneo Okoshi, Kazuhiro Honma, Takashi Kimura, Kazuyuki Ogawa, Haruo Doi, and Yukihiro Isoda *In its* Bulletin of National Research Institute for Metals in Fiscal Year 1993, No. 14 29 Jan. 1993 p 309-321 In JAPANESE (For primary document see N94-25544 07-26)
Avail: CASI HC A03/MF A04

Refinement of technology for crystal structures was investigated with the purpose of improvement in physical analysis. The research had two themes. One is an analysis by x ray diffraction. The x ray diffraction determining the long periodical structures of binary alloys was extended in order to determine site locations and the mutual substitution amount between Ti and Al elements of ternary TiAl-X alloys. These alloys were produced by adding V, Mn, Zr, or Nb to binary TiAl alloys. It was found that V and Mn atoms were chiefly solid solutionized to Al sites, and Zr and Nb atoms to Ti sites. The mutual substitution amount between Al and Ti atoms decreased as the density of V and Mn increased. The other theme is an analysis by high resolution electron microscopy. Fe 30 mol percent FeO, composed by sintering carbonyl and FeO powders, was observed at Fe/FeO interfaces by a high resolution electron microscope. The results were compared with the composition analysis results of oxidized crystals obtained by Auger electron spectroscopy. Migration areas of distorted FeO cubes with decreased oxygen were generated at (111) Fe/(110) FeO interfaces. Excess oxygen was diffused from FeO in the areas with decreased oxygen, and those areas played a significant role to the joint of Fe/FeO phases.
Author (NASDA)

N94-25578# National Research Inst. for Metals, Tokyo (Japan). Materials Characterization Div.

STUDY ON ANALYZING METHOD ESTABLISHMENT FOR METALLIC MATERIAL DEVELOPMENT [KINZOKUKEI ZAIRYO KAIHATSU NI TOMONAU BUNSEKIHO NO KAKURITSU NI KANSURU KENKYU]

Haruno Okouchi, Osamu Kujirai, Fumio Hirose, Muneyuki Kori, Shunichi Suzuki, Katsuyuki Takahashi, Masayoshi Kiyokawa, Takayuki Yoshioka, Koichi Sato, and Tsuyoshi Kobayashi et al *In its* Bulletin of National Research Institute for Metals in Fiscal Year 1993, No. 14 29 Jan. 1993 p 323-335 In JAPANESE (For primary document see N94-25544 07-26)

Avail: CASI HC A03/MF A04

Research was conducted on the inductively coupled plasma (ICP) emission spectrometry and the graphite furnace atomic absorption spectrometry as means for atomic spectrometry. For the ICP emission spectrometry, simultaneous determination of hydride components (As, Bi, Sb, Se, and Te) in Mo as well as non-hydride components (Co, Cr, Cu, Fe, Mn, Ni, Ti, V, Zn, and Zr) in MoO3 were studied. Direct determination was investigated on Ni base super heat resisting alloys (Al, B, Co, Cr, Cu, Fe, Mn, Mo, Nb, P, S, Si, Ti, and Ta) by spark abrasion/ICP emission spectrometry. For the graphite furnace atomic absorption spectrometry, a series of platform techniques were studied. Determination of acid solubilized and insolubilized Al in steel was also researched. In and Cd in Ni base super heat resisting alloys were studied for direct determination of sample solution. A potential method for direct determination was found after systematic investigation into Pb, Mn, and Co with different melting point. Acid decomposition glass bead/X-ray fluorescence analyses were performed on various superconductors (Bi-, Y-, La-, Nd-, and Ti-groups) as well as seven main elements in Ti alloys. The theoretical acid alpha coefficient method and the fundamental parameter method were compared for matrix correction. Accurate, precise results were obtained. The glow discharge mass analysis method was established for impure rare earth elements in rare earth metals. Si separation by distillation in dystetic metals (Nb, Ta, V, and Zr) and absorptiometric method were established.
Author (NASDA)

N94-25579# National Research Inst. for Metals, Tokyo (Japan). Failure Physics Div.

STUDY ON VARIATION OF DAMAGE GENERATION MECHANISM BY FATIGUE ON TIAl COMPOUNDS DUE TO DIFFERENT SLIP SYSTEMS [SUBERIKEI NO SA NI MOTOZUKU TIAL NO HIRO SONSHO HASSEI KIKO NO HENKA NI KANSURU KENKYU]

Koji Yamaguchi, Masuo Shimodaira, Kazuo Kobayashi, Minoru Nobuki, and Kenki Hahsimoto *In its* Bulletin of National Research Institute for Metals in Fiscal Year 1993, No. 14 29 Jan. 1993 p 337-343 In JAPANESE (For primary document see N94-25544 07-26)

Avail: CASI HC A02/MF A04

TiAl intermetallic compounds are expected as new, light materials with heat resistance. They also have rare properties, and break by brittleness at 700 C or less, while they break by ductility accompanied by slip distortion at above 700 C. Axial strain control fatigue tests were conducted on such a compound at 800 C and room temperature to study repeated distortion and fatigue strength properties as well as fatigue damage generation mechanisms at different temperatures. The test sample used was Ti(34.7)Al(1.74)V (weight percent) which was uniformly annealed. The fatigue strength of the test sample did not deteriorate as the temperature rose. On the contrary, it showed higher fatigue strength. As for fatigue strength at room temperature, cracks were observed at grain boundaries hitting coarse slip lines at separated slip planes parallel to coarse slip lines and around the intersection of duplex slip lines. The fatigue fracture generated at 800 C was almost the same as that generated at room temperature. However, at 800 C, twin distortion across grain boundaries was noted in addition to slip distortion. This twin distortion caused a intergranular crack at the intersection of grain boundaries and the twin distortion, and the facet was patterned with stripes.
Author (NASDA)

N94-25580# National Research Inst. for Metals, Tokyo (Japan). Failure Physics Div.

STUDY ON HIGH TEMPERATURE DAMAGE CONTROL AND LIFE IMPROVEMENT [KOON SONSHO SEIGYO TO JUMYO ENCHOKA NI KANSURU KENKYU]

Norio Shinya, Seiichi Ikeda, Junro Kyono, Ryo Horiuchi, Hideo Tanaka, Masaharu Murata, Hideaki Kushima, and Koichi Yagi *In its* Bulletin of National Research Institute for Metals in Fiscal Year 1993, No. 14 29 Jan. 1993 p 345-353 In JAPANESE (For primary document see N94-25544 07-26)

Avail: CASI HC A02/MF A04

Fundamental research was conducted with the purpose of improving the life of heat resisting steel by reducing the occurrence of high temperature damage as well as by recovering from the caused damage. Intergranular creep cavities and surface cracks were studied. The research themes were to: (1) extinguish creep cavities by sintering process; (2) coat creep cavity surfaces with stable deposited materials to freeze the cavity growth; (3) refine the grain of only the surface layers to retard the generation of surface cracks; and (4) propose some concrete ideas on processing to improve the life of heat resisting steel. The sintering rates of creep cavities by simple heating and hydrostatic heating were slow, and both heating methods were effective for minute cavities at early stages of generation, but not for big, grown cracks. On the other hand, compressive stress heating accelerated sintering in creep cavities, extinguishing big crack-like creep cavities. Heat resisting steel of high temperature strength improved by the addition of Ti and V broke in low ductility due to cracks grown from surfaces to grain boundaries. These surface cracks easily occur with large crystals, and accordingly, a method was developed to refine the grains of only surface layers. VN deposition and fine recrystallized grains were obtained to prevent grains from growing. Thus, only the granules at surface layers could be refined, and materials with these surface layers showed excellent mechanical characteristics.
Author (NASDA)

N94-25581# National Research Inst. for Metals, Tokyo (Japan). Failure Physics Div.

STUDY ON ELUCIDATION OF DAMAGE GENERATION PROCESS BY ELECTRON BEAM LITHOGRAPHY [DENSHISEN RISOGURAFI NI YORU SONSHO KATEI NO KAIMEI NI KANSURU KENKYU] c39

Norio Shinya, Satoshi Kishimoto, Mitsuru Egashira, Junro Kyono, and R. A. Carolan *In its* Bulletin of National Research Institute for Metals in Fiscal Year 1993, No. 14 29 Jan. 1993 p 355-361 In JAPANESE (For primary document see N94-25544 07-26)

Avail: CASI HC A02/MF A04

Two micro-deformation measurement methods were developed to assess local micro-deformations that lead to damages in materials as well as to analyze the damage generation process. The two methods, both utilizing electron beam lithography, were the microgrid method (direct measurement of microgrids) and the electron moire method (electron beam scanning). With these methods, creep micro-deformations were observed and measured on metallic materials. The slip amount and creep strains were different at each grain boundary or crystal grain. Creep strains were not uniform even in the same grain boundary: high tension strained areas and low strained areas alternate and formed stripe patterns. This ununiformity in distribution was related to the grain boundary slip and cracking. High strains were observed around the areas with grain boundary slip, whereas the strains around the areas with no grain boundary slip were low. Simulation of creep deformation was made on a computer by the polycrystal limited factor model which was developed considering the different grain boundary slips. The results were quite similar to those from the experiments with electron beam lithography, and it was confirmed that uneven strains in creep grains of polycrystal metals were closely related to the grain boundary slip. Author (NASDA)

N94-25582# National Research Inst. for Metals, Tokyo (Japan). Environmental Performance Div.

STUDY ON PERFORMANCE EVALUATION OF PRESSURE VESSEL STEEL IN CORROSION ENVIRONMENTS WITH SULFIDE [RYUKABUTSU KANKYO NI OKERU ATSURYOKU YOKIKO NO SEINO HYOKA NI KANSURU KENKYU]

Takao Aoki and Keiji Nakano *In its* Bulletin of National Research Institute for Metals in Fiscal Year 1993, No. 14 29 Jan. 1993 p 363-367 In JAPANESE (For primary document see N94-25544 07-26)

Avail: CASI HC A01/MF A04

Research was conducted on the stress corrosion fracture behaviors of sulfide in high tensile steel by performing a low strain rate test and studying the effects caused by environmental factors. The purpose of the research is to check if chloride solution containing S2O3(2-) was suitable for moist hydrogen sulfide environments. This was considered to be a better method to replace the hydrogen sulfide addition method which is currently adopted but is quite dangerous. The maximum ductility deterioration by hydrogen absorption in high tensile steel was detected when the Na2S2O3 density was 10(exp -3) mol/l during the low strain rate test. The corrosion environment in the test solution was as severe as that in NACE (National Association of Corrosion Engineers) TM0284-86 solution, but slightly milder than that in NACE TM0177-86 solution (standard NACE solution). More hydrogen was absorbed in steel as the amount of Na2S2O3 increased. However, once the absorbance reached saturation (10(exp -2) mol/l or more), sulfide scales were generated on metal surfaces, and absorption declined. Author (NASDA)

N94-25583# National Research Inst. for Metals, Tokyo (Japan). Environmental Performance Div.

STUDY ON EVALUATION OF CRACK GENERATION AND CRACK GROWTH BEHAVIORS UNDER STATIC LOADING AT HIGH TEMPERATURE AND UNDER COMBINED LOADING [KOON SEIKAJU OYOBI KURIKAESHI KAJUKA NO KIRETSU HASSEI OYOBI SEICHO KYODO NO HYOKA NI KANSURU KENKYU] **c39**

Koichi Yagi, Masaaki Tabuchi, Kenji Yokokawa, Osamu Kanamaru, Kiyoshi Kubo, Toshio Oba, and Fusayuki Suzuki (Yokohama National Univ., Japan.) *In its* Bulletin of National Research Institute for Metals in Fiscal Year 1993, No. 14 29 Jan. 1993 p 369-377 In JAPANESE (For primary document see N94-25544 07-26)

Avail: CASI HC A02/MF A04

Creep, crack generation under creep fatigue, and creep crack growth were investigated in correlation with microscopical observation with the purpose of improving the evaluation level of creep crack growth behaviors and rupture lives under creep-fatigue loading. A creep crack growth test was conducted on 316 stainless steels and NCF800H alloys to find the correlation between the creep crack growth rate (da/dt) and the breaking style parameter C. The results showed that the da/dt-C correlation was closely related to the breaking style, and it could be classified into two groups based on the breaking style. However, this correlation was not true if a creep damage ranged over a large area around the crack end. A creep fatigue test was conducted under combined loading on coarse grained and fine grained 321 stainless steels. Determination of the creep damage amount and fatigue damage amount by linear life damage rules revealed that the correlation between these two amounts was related to the breaking style, and furthermore, to the breaking process as well. Author (NASDA)

N94-25584# National Research Inst. for Metals, Tokyo (Japan). Environmental Performance Div.

STUDY ON FATIGUE CRACK PROPAGATION CHARACTERISTICS AROUND WELDED JOINT INTERFACE IN COMPLEXED CONDITIONS [KANKYOKA NI OKERU SETSUGO KAIMEN KINBO NO HIRO KIRETSU DENPA TOKUSEI HYOKA NI KANSURU KENKYU] **c39**

Akihiko Ota, Naoyuki Suzuki, Yoshio Maeda, Toshio Mawari, Saburo Matsuoka, and Satoshi Nishijima *In its* Bulletin of National Research Institute for Metals in Fiscal Year 1993, No. 14 29 Jan. 1993 p 379-386 In JAPANESE (For primary document see N94-25544 07-26)

Avail: CASI HC A02/MF A04

Marine structures are often constructed by welding, and they are subject to repeated loading such as waves and mechanical vibrations which can create fatigue cracks and consequently break the structures. Fatigue crack propagation properties of welded joints are studied under random loading in the air, synthetic sea water, and compressive cycling. It was found that the most crucial factor that controls fatigue crack propagation was high tensile residual stress fields of welded joints. This stress constantly kept the cracks open, simplifying fatigue crack propagation, and therefore, the rate of crack propagation could be assessed with high accuracy. In the transverse matching welded joints with cracks in the center, crack closure did not occur due to the tensile residual stress constantly induced at the crack ends in the center of the test samples. Fatigue crack propagation was accelerated both in artificial sea water and in compressive cycling compared to that in the air, and the fatigue lowest values were about half. Serious crack closures occurred in compressive cycling in which dry hours exceeded 45 minutes, and the fatigue crack propagation rate deteriorated remarkably. Mean fatigue crack propagation rate under the random loading is estimated precisely using equivalent stress intensity factor limit. Author (NASDA)

N94-25585# National Research Inst. for Metals, Tokyo (Japan). Advanced Materials Processing Div.

STUDY ON MELTED SOLUTION STIRRING UNDER MICROGRAVITY [BISHO JURYOKU KANKYO NI OKERU YUEKI NO KAKUHAN NI KANSURU CHOSA KENKYU] **c29**

Akira Sato, Ken Sasabe, Isao Nakatani, Kiyoshi Ozawa, Akira Fukuzawa, Kazuyuki Sakuraya, Kazumasa Togano, Hiroaki Kumakura, Daniel Robert Dietdrich, and Masao Takeyama et al *In its* Bulletin of National Research Institute for Metals in Fiscal Year 1993, No. 14 29 Jan. 1993 p 387-392 In JAPANESE (For primary document see N94-25544 07-26)

Avail: CASI HC A02/MF A04

The techniques of stirring and stopping the melted solution are studied for experiments to create materials to be used for Japanese Experiment Module (JEM) in space stations. The following results were obtained: (1) since the required material has to be solid and then melted and solidified again, mixing fins must be either put in/out in the melted solution or they must be solidified with alloys (if this issue is solved, fins will be effective under microgravity, and also convenient for experiments on a large scale); (2) there has not been many examples of sound wave or ultrasonic wave vibrations having been applied to material processing except for experiments on crystal refinement at solidification (mixing effects under normal gravity must be investigated first); (3) material processing by induction generates heat (there is more potential for utilizing electromagnetism under microgravity than under normal gravity, because little electric power is required to control melted materials under microgravity); (4) material property values must be assessed first before utilizing convection in mixing; and (5) under microgravity, it is possible to mix/stop mixing melted solution by generating artificial gravity. However, this seems to be more effective for removing bubbles and inclusions than for mixing. Author (NASDA)

N94-25586# National Research Inst. for Metals, Tokyo (Japan).

STUDY ON UTILIZATION OF SUPER CLEAN, HIGH VACUUM SPACE [CHOSEIJO SHINKU KUKAN NO RIYO NI KANSURU CHOSA KENKYU] **c09**

Kazuhiro Yoshihara, Yoshio Sakka, Haruki Shiraishi, Tetsuji Noda, Josei Nagakawa, Ryosuke Hasegawa, Toshiyuki Hirano, Tsuyoshi Ozaki, Keikichi Nakamura, and Kazuo Saito et al *In its* Bulletin of National Research Institute for Metals in Fiscal Year 1993, no. 14 29 Jan. 1993 p 393-401 In JAPANESE (For primary document see N94-25544 07-26)

Avail: CASI HC A02/MF A04

Creation of new materials is entering a new phase with recent development in control and analysis technologies. Nowadays, it is becoming possible to freely control individual atoms, ions, electrons, and photons. However, technologies in metallic materials are not yet ready for super high vacuum environment unlike those in semiconductors. A new field in metallurgy will start with the creation of new materials by dealing with super pure material atoms individually on clean surfaces and interfaces in special research institutions. Such institutions should provide super clean, high vacuum environment to allow a series of processes from refinement, synthesis, and processing to evaluation. For this purpose, it is important to establish a transportation system where equipment relevant to material creation is all connected in super clean, high vacuum so that samples can be transported between equipment to minimize changes in material quality. These institutions are likely to be used for joint researches, and the first issue to arise will be management and administration of this transportation system in high vacuum. Secondly, there is an issue of the parties to be responsible for administration/management of main equipment on each line. Researchers that may utilize these institutions must be considered as well. Author (NASDA)

N94-25623# Technical Research Centre of Finland, Espoo. Production Engineering Lab.

WELDABILITY OF DIRECT-QUENCHED AND TEMPERED (DQT) HIGH STRENGTH STEEL HT80

Pekka Nevasmaa, Mark Cederberg, and Martti Vilpas Oct. 1992 42 p
Sponsored by Nordisk Industrifond; Technology Development Center, Finland; and Technical Research Centre of Finland, Espoo
(ISSN 1235-0621)
(VTT-TIED-1406; ISBN-951-38-4300-9; ETN-94-95251) Copyright Avail: CASI HC A03/MF A01

The test results obtained in welding and weldability tests of a Direct Quenched and Tempered steel DQT HT80 are discussed. The tests comprised mechanical testing of joints welded with arc energies of 20 and 45 kJ/cm using Submerged Arc Welding (SAW) and Flux Cored Arc Welding (FCAW) processes. The results of weld thermal simulation and implant weldability tests for the steel are reported. The results demonstrate the improved weldability of the DQT HT80 steel, as compared to quenched and tempered steels of similar strength level. The need for preheat was found 70 to 90 C lower for the DQT steel. Cracking of weld metal suggested that increasing preheat and interpass temperatures become necessary with heavier plate thicknesses of 40 mm and above. SAW yielded higher weld metal toughness than FCAW. The maximal hardness properties of DQT HT80 steel were found to deteriorate as the arc energy increased from 20 to 45 kJ/cm. The Charpy 5 tests confirmed the tendency of decreasing toughness with prolonged cooling times. ESA

N94-25643# Technical Research Centre of Finland, Espoo. Metallurgy Lab.

COMPUTER AIDED SIMULATION OF HEAT TREATMENT

Raimo Arola, Hannu Martikainen, and Jouko Virta Jan. 1993 50 p
Sponsored by Nordic Industrial Fund; Technology Development Center of Finland; and Technical Research Centre of Finland, Espoo Original contains color illustrations
(ISSN 1235-0621)
(VTT-PUBS-131; ISBN-951-38-4249-5; ETN-94-95238) Copyright Avail: CASI HC A03/MF A01

Computer aided simulation of the heat treatment of components and charges is examined. Programs for the simulation of heat treatment are reviewed. Test simulations including calculation of temperature, phase composition, and stresses and strains during heating and cooling are performed. The results of the simulations and the results of heat treating experiments are compared. Heat transfer during heating up varies between different treatments, components of the charge, and surfaces of the component. Heat transfer data defined on the basis of the measurements instead of literature data were used. Plastic straining and residual stresses after heating can be formed in an AISI 316 bar heated up at the edge of the charge in a pit furnace. Permanent bending of these bars as a result of heating is not observed. In the oil quenching of a 42CrMo4 cylinder, where martensite and bainite are formed in austenite decomposition, the simulation results depend on the TTT (Time Temperature Transformation) diagram. Several TTT diagrams for the steel grade are found. ESA

N94-25784# Technical Research Centre of Finland, Espoo. Production Engineering Lab.

WELDABILITY OF ACCELERATED-COOLED (AcC) HIGH STRENGTH TMCP STEEL HT50

Pekka Nevasmaa, Mark Cederberg, and Martti Vilpas Oct. 1992 40 p
Sponsored by Nordisk Industrifond; Technology Development Center, Finland; and Technical Research Centre of Finland, Espoo
(ISSN 1235-0621)
(VTT-TIED-1410; ISBN-951-38-4304-1; ETN-94-95252) Copyright Avail: CASI HC A03/MF A01

The test results obtained in welding and weldability tests of two Accelerated Cooled AcC Thermomechanically Processed (TMCP) HT50 class steels are discussed. The tests comprised mechanical testing of joints welded with arc energies ranging from 10 to 100 kJ/cm using Submerged Arc Welding (SAW) and Flux Cored Arc Welding (FCAW) processes. The results of weld thermal simulation and implant weldability tests are reported. The results demonstrate the excellent weldability of AcC HT50 steels, as compared to normalized or quenched and tempered steels of similar strength level. Welding without preheat was possible up to 50 and 60 mm plate thickness using low arc energies of 10 and 22 kJ/cm, respectively, provided that redried electrodes are used. For the arc energy range used with SAW and FCAW, weld metal toughness properties were found to be adequate. Excellent maximal hardness low temperature toughness properties were demonstrated in Charpy 5 tests. All AcC YS 420 steel weldments fulfilled the impact energy requirement in the arc energy range of 10 to 50 kJ/cm. Charpy 5 tests of simulated hardness measurements confirmed that there were no significant changes in the toughness level with the weld cooling time t(sub 8/5) between 12 and 52 seconds. ESA

N94-25803# Pacific Northwest Lab., Richland, WA.

MICROSTRUCTURAL DEVELOPMENT IN LOW ACTIVATION FERRITIC ALLOYS IRRADIATED TO 200 dpa AT 420 C

D. S. Gelles 1993 11 p Presented at the 6th International Conference on Fusion Reactor Materials, Stresa, Italy, 27 Sep. - 1 Oct. 1993
(Contract DE-AC06-76RL-01830)
(DE94-004269; PNL-SA-22526; CONF-930928-21) Avail: CASI HC A03/MF A01

Density change and microstructural development are reported for nine low activation ferritic steels covering the range 2.3 to 12 Cr with varying additions of V and/or W for hardening and up to 6.5 Mn for austenite stability. Specimens were examined following irradiation in FFTF/MOTA at 4200 C to a dose exceeding 200 dpa. Void swelling was found, but the swelling remained at 5% or below, with the worst case in an alloy of 9Cr-2Mn-1WV. The carbide structure pinning Martensite lath boundaries remains in place. DOE

N94-25804# Pacific Northwest Lab., Richland, WA.

RADIATION HARDENING EFFECTS ON LOCALIZED DEFORMATION AND STRESS CORROSION CRACKING OF STAINLESS STEELS

S. M. Bruemmer, J. I. Cole, J. L. Brimhall, R. D. Carter (Michigan Univ., Ann Arbor.), and G. S. Was (Michigan Univ., Ann Arbor.) Aug. 1993 9 p Presented at the 6th International Symposium on Environmental Degradation of Materials in Nuclear Power Systems: Water Reactors, San Diego, CA, 3-5 Aug. 1993
(Contracts DE-AC06-76RL-01830; DE-FG02-93ER-12130)
(DE94-004308; PNL-SA-21725; CONF-930825-14) Avail: CASI HC A02/MF A01

Radiation hardening in austenitic stainless steels modifies deformation characteristics and correlate well with increased susceptibility to intergranular stress corrosion cracking (IGSCC). Available data on neutron-irradiated materials have been analyzed and correlations developed between fluence, yield strength, and cracking susceptibility in high-temperature water environments. Large heat-to-heat differences in critical fluence (0.2 to 2.5 x 10(exp 21) n/cm(exp 2)) for IGSCC are documented. In many cases, this variability is consistent with yield strength differences among irradiated materials. IGSCC correlates better to yield strength than to fluence for most heats suggesting a possible role of radiation-induced hardening (and microstructure) on cracking. Microstructural evolution during proton and heavy-ion irradiation has been characterized in low-carbon 302SSs. Hardening results from dislocation loops. SEM and TEM are used to examine dose, strain, and temperature effects on deformation. This hardened microstructure produces inhomogeneous planar deformation within the matrix. Regularly spaced steps are created at the surface during deformation which increase in number with increasing macroscopic strain. Twinning is the dominant deformation mechanism at low temperature, while dislocation channeling is observed at 288 C. Deformation characteristics are discussed in terms of potential impact on IGSCC. DOE

N94-25819# Sandia National Labs., Albuquerque, NM.

ISSUES FOR CONVERSION COATING OF ALUMINUM ALLOYS WITH HYDROTALCITE

C. A. Drewien and R. G. Buchheit 1993 10 p Presented at the Corrosion 1994: National Association of Corrosion Engineers International Annual Conference, Baltimore, MD, 28 Feb. - 4 Mar. 1994
(Contract DE-AC04-94AL-85000)
(DE94-003804; SAND-93-2205C; CONF-940222-6) Avail: CASI HC A02/MF A01

Hydrotalcite coatings on aluminum alloys are being developed for corrosion protection of aluminum in aggressive saline environments. Coating bath composition, surface pretreatment, and alloying elements in aluminum all influence the performance of these coatings during salt spray testing. The coating bath, comprised of lithium carbonate, requires aging by dissolution of aluminum into the bath in order to grow corrosion resistant coatings. Coatings formed in non-aged baths do not perform well in salt spray testing. The alloying elements in aluminum alloys, especially copper, influence the coating growth and formation leading to thin coatings. The effect of the alloy elements is to limit the supply of aluminum to the coating/electrolyte interface and hinder growth of hydrotalcite upon aluminum alloys. DOE

N94-25822# Westinghouse Savannah River Co., Aiken, SC.

EFFECT OF NITROCARBURIZING ON SHAPE OF TITANIUM ALLOY PARTS

E. A. Clark 27 Sep. 1993 20 p
(Contract DE-AC09-89SR-18035)
(DE94-004040; WSRC-TR-93-474) Avail: CASI HC A03/MF A01

Components are being developed for plutonium casting in support of Lawrence Livermore National Laboratory. A vendor used a proprietary process to grow a nitrocarburized surface layer on a titanium alloy shot sleeve to be used in a prototype die casting machine. The shot sleeve was significantly out-of-round upon return from the vendor and could not be used. Purpose of this study was to determine whether the shape change could have been caused by this surface treatment. Visual observation of disk and ring samples exposed first to surface treatment alone temperature and then the actual nitrocarburizing environment revealed no gross warping in either case. Dimension measurements of each sample before and after both the thermal treatment and the nitrocarburizing revealed no significant changes. Visual examination of the shot sleeve revealed a surface flaw likely made during handling after machining at SRS and before the part was nitrocarburized. The out-of-roundness of the shot sleeve could be related to the damage observed on the surface, but the possibility of warping during the nitrocarburizing cannot be excluded. Nitrocarburization should remain a candidate method to protect titanium alloys from molten metals. DOE

N94-25906 Selskapet for Industriell og Teknisk Forskning, Trondheim (Norway). Div. of Metallurgy.

DISSOLUTION OF SECONDARY PHASES DURING EXTRUSION

U. H. Tundal 3 May 1993 7 p Sponsored by Hydro Aluminum A/S
(PB94-124583; STF34-A93094) Avail: Issuing Activity (National Technical Information Service (NTIS))

The report is a summary of the presentation made by U. Tundal at the seminar on the EXPOMAT EXTRUSION PROJECT at Karmoy, Norway, May 4, 1993. The title of the presentation was 'Growth and dissolution of Magnesium Silicide-particles'. First, some results from the Doctoral Thesis on 'Dissolution of Particles in Binary Alloys' were presented. Then a brief introduction to the project on modeling growth and dissolution of particles in connection to the extrusion process was made. NTIS

N94-25954# Michigan Univ., Ann Arbor. Dept. of Nuclear Engineering.

THE ROLE OF GRAIN BOUNDARY CHEMISTRY AND STRUCTURE IN THE ENVIRONMENTALLY-ASSISTED INTERGRANULAR CRACKING OF NICKEL-BASE ALLOYS

G. S. Was 1993 19 p
(Contract DE-FG02-85ER-45184)
(DE94-003159; DOE/ER-45184/9) Avail: CASI HC A03/MF A01

Progress focused on determination of the role of C and Cr on deformation and IG cracking behavior of Ni(5-30)Cr9Fe, determination of the effect of grain boundary misorientation on IG cracking behavior, construction of an electron backscattering pattern (EBSP) imaging system, determination of effect of the environment on creep and cracking, and characterization of the surface film. Results showed that both C and Cr are potent solid solution strengtheners which can reduce the steady state creep rate at 360 C by several orders of magnitude. Intergranular cracking of 100 micron grain samples of high purity Ni16Cr9Fe at 360 C occurs by formation of grain boundary voids and interlinkage, driven by dislocation creep in the matrix. Creep experiments in primary water at 360 C and an applied cathodic potential show that the creep rate is increased by an order of magnitude over that in Ar and the percent IG fracture increases as well. Oxide film composition and thickness is a sensitive function of the C content, increasing in thickness and Ni(OH)2 content with increase in C or decrease in Cr to 5 wt%. Thermomechanical treatments along with electron channeling pattern (ECP) analysis were used to create and index samples with enhanced fractions of coincident site lattice boundaries (CSLB's). Constant extension rate tensile (CERT) experiments on samples with a high percentage of CSLB's showed IG cracking compared with general high angle boundaries. However, these experiments were conducted on grain sizes of 300 microns, while commercial material is an order of magnitude smaller. An electron backscattering pattern imaging system has been constructed for an environmental scanning electron microscope which can image grains below five micron. The system has been successfully benchmarked against results from ECP analysis. DOE

N94-25974# Los Alamos National Lab., NM.

NEW EQUATION OF STATE FOR STAINLESS STEEL 347

J. C. Boettger Dec. 1993 9 p
(Contract W-7405-eng-36)
(DE94-004189; LA-12685-MS) Avail: CASI HC A02/MF A01

A new SESAME equation of state (EOS) for stainless steel 347 was generated using the computer program GRIZZLY, and was added to the SESAME EOS library as material number 4271. This new EOS is superior to its predecesser (material number 4270) in several respects. DOE

N94-25987# Pacific Northwest Lab., Richland, WA.

EFFECT OF LOADING MODE ON THE FRACTURE TOUGHNESS OF A REDUCED ACTIVATION FERRITIC/MARTENSITIC STAINLESS STEEL

H. Li (Washington State Univ., Pullman.), J. P. Hirth (Washington State Univ., Pullman.), R. H. Jones, and D. S. Gelles Sep. 1993 20 p Presented at the 6th International Conference on Fusion Reactor Materials, Stresa, Italy, 27 Sep. - 1 Oct. 1993
(Contract DE-AC06-76RL-01830)
(DE94-004290; PNL-SA-22545; CONF-930928-16) Avail: CASI HC A03/MF A01

The critical J integrals of mode 1 (J(sub 1C)), mixed-mode 1/3 (J(sub MC)), and mode 3 (J(sub 3C)) were examined for a ferritic stainless steel (F-82H) at ambient temperature. A determination of J(sub MC) was made using modified compact-tension specimens. Different ratios of tension/shear stress were achieved by varying the principal axis of the crack plane between 0 and 55 deg from the load line. The results showed that J(sub MC)s and tearing moduli (T(sub M)) varied with the crack angles and were lower than their mode 1 and mode 3 counterparts. Both the minimum J(sub MC) and T(sub M) occurred at a crack angle between 40 and 50 deg, where (sigma)(sub i)/(sigma)(sub iii) was 1.2 to 0.84. The J(sub min) was 240 kJ/sq m, and ratios of J(sub 1C)/J(sub min) and J(sub 3C)/J(sub min) were about 2.1 and 1.9, respectively. Morphology of fracture surfaces was consistent with the change of J(sub MC) and T(sub M) values. While the upper shelf-fracture toughness of F-82H depends on loading mode, the J(sub min) remains very high. Other important considerations include the effect of mixed-mode loading on the DBT temperature, and effects of hydrogen and irradiation on J(sub min). DOE

N94-26004# Brookhaven National Lab., Upton, NY.

STRUCTURE AND PHASE TRANSFORMATIONS IN URANIUM METAL

J. D. Axe, G. Gruebel (European Synchrotron Radiation Facility, Grenoble, France.), and G. H. Lander (Karlsruhe Univ., Germany.) 1993 15 p Presented at the Actinides 1993, Santa Fe, NM, 19-24 Sep. 1993
(Contract DE-AC05-84OR-21400)
(DE94-003892; BNL-49620; CONF-930905-22) Avail: CASI HC A03/MF A01

In common with other elemental actinides, metallic uranium exists in several allotropic forms, differing from one another by complex but subtle atomic rearrangements. This article reviews progress in understanding the successive phase transformations from the perspective of soft-mode instabilities. DOE

N94-26022# Los Alamos National Lab., NM.
DEVIATORIC STRESSES AND PLASTIC STRAIN RATES IN STRONG SHOCK WAVES FOR SIX METALS
D. L. Tonks Nov. 1993 32 p
(Contract W-7405-eng-36)
(DE94-002964; LA-12641) Avail: CASI HC A03/MF A01

The strong shock theory of D. C. Wallace (Phys. Rev. B24, 5597 (1981) and Phys. Rev. B24, 5607 (1981)) is used to calculate the shock structure for 1100 Al, 2024 Al, Cu, Fe, Ta, and U. Emphasis is given to the behavior of plasticity, i.e., average deviatoric stresses, plastic and total strains, and strain rates, which are given in figures for a number of shock strengths. This information will be useful for modeling plasticity in metals under extreme conditions. It was used for part of the PTW model for mechanical behavior. DOE

N94-26069# Los Alamos National Lab., NM.
DEBYE-WALLER FACTORS OF THE LIGHT ACTINIDE METALS
A. C. Lawson, J. A. Goldstone, B. Cort, R. I. Sheldon, and E. M. Foltyn 1993 15 p Presented at the Actinides 1993; 1994 TMS Annual Meeting on Actinides, Santa Fe, NM; San Francisco, CA, 19-24 Sep. 1993; 27 Feb. - 3 Mar. 1994
(Contracts W-7405-eng-36; W-31-109-eng-38)
(DE94-000685; LA-UR-93-3463; CONF-930905-9; CONF-940221-1) Avail: CASI HC A03/MF A01

Time-of-flight neutron powder diffraction was used to determine the Debye-Waller factors of light actinide metals. The Debye-Waller factor is a measure of the mean-square atomic displacement that arises from the thermal motion of the atoms in any solid. Its temperature dependence determines a Debye-Waller temperature, Theta(sub DW), that is characteristic of the elastic properties of the solid. The data are obtained by Rietveld analysis of neutron diffraction powder patterns obtained at several temperatures. Results are presented for alpha-U, alpha-Np, alpha-Pu and delta-Pu(0.95)Al(0.05). The Theta(sub DW)'s are temperature dependent, and anharmonic interatomic forces seem to be required to explain the results. DOE

N94-26070# Rhode Island Univ., Kingston.
SURFACE PHYSICS WITH COLD AND THERMAL NEUTRON REFLECTOMETRY
A. Steyerl Sep. 1993 23 p
(Contract DE-FG02-91ER-45445)
(DE94-001447; DOE/ER-45445/9) Avail: CASI HC A03/MF A01

Within the past two and one half years of the project 'Surface Physics With Cold and Thermal Neutron Reflectometry' a new thermal neutron reflectometer was constructed at the Rhode Island Nuclear Science Center (RINSC). It was used to study various liquid and solid surfaces. Furthermore, neutron reflection experiments were begun at different laboratories in collaboration with Dr. G.P. Fetcher (at Argonne National Laboratory), Dr. T. Russell (IBM Almaden), and Drs. S.K. Satija and A. Karim (at the National Institute for Standards and Technology). The available resources allowed partial construction of an imaging system for ultracold neutrons. It is expected to provide an extremely high resolution in momentum and energy transfer in surface studies using neutron reflectometry. Much of the work reported here was motivated by the possibility of later implementation at the planned Advanced Neutron Source at Oak Ridge. In a separate project, the first concrete plans for an intense source of ultracold neutrons for the Advanced Neutron Source were developed. DOE

N94-26073# Tokyo Univ. (Japan). Inst. for Solid State Physics.
ALUMINUM-ION SPUTTERING FROM Al SURFACES WITH VERY-LOW-ENERGY IONS
Michio Okada and Yoshitada Murata Apr. 1993 35 p Sponsored by Ministry of Education, Science and Culture, Tokyo, Japan and Japanese Society for the Promotion of Science, Tokyo, Japan
(ISSN 0082-4798)
(Rept-A-2668; JTN-94-80539) Avail: CASI HC A03/MF A01

Sputtering of Al(+) for N2(+), N(+), and Ne(+) incidence was observed at the threshold energy of approximately 20 eV. The polar-angle distribution of the sputtered Al(+) ions gives almost the same lobe position at different angles of incidence. In N(+) and Ne(+) incidence on the Al (111) surface, a sharp structure which correlates with the crystal structure, was observed in the angular distribution of the sputtered Al(+) ions. In ion incidence on the open surface of Al (110), chemical interaction between a projectile and the target material plays an important role in the sputtering process. The mechanisms of ion sputtering induced by very low-energy ions (less than or equal to 200 eV) are discussed. Author (NASDA)

N94-26087# California Univ., Berkeley. Lawrence Berkeley Lab.
INFLUENCE OF GRAIN STRUCTURE AND SOLUTE COMPOSITION ON THE WORK HARDENING BEHAVIOR OF ALUMINIUM AT CRYOGENIC TEMPERATURES
D. Chu and J. W. Morris, Jr. Jul. 1993 10 p Presented at the International Cryogenic Engineering Conference and International Cryogenic Materials Conference, Albuquerque, NM, 12-16 Jul. 1993
(Contract DE-AC03-76SF-00098)
(DE94-003415; LBL-34019; CONF-930703-38) Avail: CASI HC A02/MF A01

An unrecrystallized structure is found to significantly improve work hardening characteristics by lowering the work hardening rate during the early stages of deformation. This is in contrast to a recrystallized structure, which requires a higher work hardening rate to accommodate the greater degree of multiple slip necessary to maintain strain compatibility between the more randomly oriented grains. The stronger texture associated with the unrecrystallized structure allows deformation to occur more efficiently. Addition of magnesium also improves work hardening by increasing overall level of the work hardening rate. The improved characteristics of the work hardening behavior result in a parallel increase in both the strength and ductility at cryogenic temperatures. These findings are positive since they suggest a method by which improvements in the work hardening behavior and subsequent mechanical properties may be obtained through practical modifications of the microstructure and composition. DOE

N94-26092# Oak Ridge National Lab., TN.
STRUCTURE OF THE MODULATED MAGNETIC PHASE OF Mn3Sn
J. W. Cable, N. Wakabayashi (Keio Univ., Yokahama, Japan.), and P. Radhakrishna (Indian Inst. of Science, Bangalore.) 1993 14 p Presented at the 38th Annual Conference on Magnetism and Magnetic Materials, Minneapolis, MN, 15-18 Nov. 1993
(Contract DE-AC05-84OR-21400)
(DE94-002788; CONF-931133-6) Avail: CASI HC A03/MF A01

The triangular antiferromagnetic order that occurs in hexagonal Mn3Sn below 420 K becomes modulated below 270 K in what is generally described as a helical modulation propagating along the c axis with a period of about 10 or 12 c(sub 0). However, such a modulation is inconsistent with a recently observed energy gap in the magnetic excitation spectra for this phase. The magnetic structure of this modulated phase was reexamined by neutron diffraction and two distinct modulations were found, both propagating along the c axis and both with periods that are commensurate with the lattice below about 120 K. The satellite reflections associated with these two modulations have quite different intensities and temperature dependences suggesting coexistent modulated phases. For the dominant 11 c(sub 0) phase, a third harmonic is observed with an intensity that is four percent of the first harmonic but no fifth or seventh harmonic is found to a sensitivity of about 10(exp -4). The presence of this third harmonic shows a significant distortion of the helical modulation wave. The observed harmonic intensity distribution was compared with magnetic structure factor calculations for configurational models with moment directions bunched around the easy axes in the basal plane. The results of this comparison are given in this paper. DOE

N94-26160 Comision Nacional de Energia Atomica, Buenos Aires (Argentina). Dept. de Materiales.
DIFFUSION OF SUBSTITUTIONAL ELEMENTS IN Ti IN ITS hcp PHASE [DIFUSION DE ELEMENTOS SUSTITUCIONALES EN TI EN SU FASE HCP]
R. A. Perez and F. Dyment 1993 6 p In SPANISH Presented at the SAM 1993: 17th Metallurgical Sessions of the Argentine Metals Association; 2nd Argentine Meeting on Ceramics and Refractories, San Carlos de Bariloche, Argentina, 13-16 Apr. 1993 Limited Reproducibility:

More than 20% of this document may be affected by microfiche quality
(DE93-633762; INIS-AR-017; CONF-9304174) Avail: CASI HC A02 (US Sales Only)

Heavy Ions Rutherford Backscattering Spectrometry (HIRBS) was used to analyze diffusion profiles. Penetrations of about a micron were measured; in this form it was possible to complete the range of temperature of diffusion studies in the hop phase of Ti extending it until the overlap with even lower temperatures measured previously with RBS. The ion-material interaction along the trajectory of the heavy ion beam was considered in the method developed to convert HIRBS spectra in diffusion profiles. The results obtained for Zr and Hf diffusion in Ti in the range 1133 - 823 K for Zr and 1145 - 823 K for Hf are discussed in this paper. DOE

N94-26161 Comision Nacional de Energia Atomica, Buenos Aires (Argentina). Dept. de Materiales.

Zr-RICH CORNER OF THE Zr-Sn-O DIAGRAM [ESQUINA RICA EN COMPOSICION DE CIRCONIO DEL DIAGRAMA ZR-SN-O]

L. A. Roberti, D. E. Arias, and L. Gribaudo (Consejo Nacional de Investigaciones Cientificas y Tecnicas, Buenos Aires, Argentina.) 1993 6 p In SPANISH Presented at the SAM 1993: 17th Metallurgical Sessions of the Argentine Metals Association; 2nd Argentine Meeting on Ceramics and Refractories, San Carlos de Bariloche, Argentina, 13-16 Apr. 1993 Limited Reproducibility: More than 20% of this document may be affected by microfiche quality
(DE93-633764; INIS-AR-021; CONF-9304174) Avail: CASI HC A02 (US Sales Only)

The understanding of the effect of light elements (in particular, oxygen, nitrogen, and hydrogen) on the behavior of alloys for nuclear use is necessary because of its technological importance. The Zr-Sn-O system is perhaps the most representative of all possible ternary systems which can be used to simulate a simplified Zircaloy-type alloy in which the effect of O can be studied. However, in the specialized literature, experimental data on phase equilibria and thermophysical properties of this system are not easily found. In the present work, the equilibrium compositions of the alpha and beta phases of the Zr-Sn-O system at temperatures between 1150 and 1323 K are calculated, using the scarce available information. First results of the calculations show satisfactory coincidences with experimental data. Future work will be oriented towards the proposal of isothermal cross-sections calculated by a modelling of phases with wider Sn and O composition ranges, and involving equilibria with the phases Zr4Sn, Zr5Sn3, ZrO2, ZrSnO4. DOE

N94-26162 Comision Nacional de Energia Atomica, Buenos Aires (Argentina). Dept. de Materiales.

GRAIN BY GRAIN STUDY OF THE MECHANISMS OF CRACK PROPAGATION DURING IODINE SCC OF Zry-4 [ANALISIS DE TENSIONES DURANTE LA PROPAGACION TRANSGRANULAR DE FISURAS POR CORROSION BAJO TENSIONES DE VAINAS DE ZIRCALOY]

R. E. HaddadAndalag and A. O. Dorado (Consejo Nacional de Investigaciones Cientificas y Tecnicas, Buenos Aires, Argentina.) 1993 6 p In SPANISH Presented at the SAM 1993: 17th Metallurgical Sessions of the Argentine Metals Association; 2nd Argentine Meeting on Ceramics and Refractories, San Carlos de Bariloche, Argentina, 13-16 Apr. 1993 Limited Reproducibility: More than 20% of this document may be affected by microfiche quality
(DE93-633765; INIS-AR-022; CONF-9304174) Avail: CASI HC A02 (US Sales Only)

This paper describes the tests conducted to determine the conditions leading to cracking of a specified grain of metal, focusing on the crystallographic orientation of crack paths, the critical stress conditions and the significance of the fractographic features encountered. In order to get orientable cracking, a technique was developed to produce iodine SCC, by means of pressurizing tubes of a specially heat treated Zry-4 having very large grains, shaped as discs of a few millimeters in diameter and grown up to the wall thickness. Careful orientation of fractured grains, performed by means of a back-reflection Laue technique with a precision better than one degree, has proved that transgranular cracking occurs only along basal planes. The effect of anisotropy, plasticity, triaxiality and residual stresses originated in thermal contraction has to be considered to account for the influence of the stress state. A grain by grain calculation led to the conclusion that transgranular cracking always occurs on those bearing the maximum resolved tensile stress on basal planes. There are clear indications of the need of a triaxial stress state for the process to occur. Fracture modes other than pseudo-cleavage have been encountered, including intergranular separation, ductile tearing produced by prismatic slip, and propagation along twin boundaries. In each case, the fractographic features have been identified, and associations have been made with fractographs obtained in normal fuel cladding. DOE

N94-26263# Comision Nacional de Energia Atomica, Buenos Aires (Argentina). Dept. de Materiales.

Zr-Sn-Nb ALLOYS: PRELIMINARY STUDIES [ALEACION ZR-SN-NB. TRABAJOS PRELIMINARES]

C. A. Danon and D. E. Arias 1993 5 p In SPANISH Presented at the SAM 1993: 17th Metallurgical Sessions of the Argentine Metals Association; 2nd Argentine Meeting on Ceramics and Refractories, San Carlos de Bariloche, Argentina, 13-16 Apr. 1993
(DE93-633767; INIS-AR-024; CONF-9304174) Avail: CASI HC A01/MF A01 (US Sales Only)

Studies of the Zr-Sn-Nb diagram have been started, focussing on the Zr-rich corner, near the composition of Zirlo commercial alloy, Zr-1Sn-1Nb, and with Fe and O contents usual in nuclear grade materials. Three alloys were melted, namely Zr-4Sn-2.4Nb (A), Zr-1Sn-3Nb (B) and Zr-2.1Sn-1Nb (C). Alpha/beta transformation temperatures were measured through the variation of electrical resistivity(p) vs temperature (T). Values of 560 deg C, 670 deg C and 750 deg C were measured for the alpha yields alpha+beta reaction and 980 deg C, 910 deg C and 1000 deg C for the alpha+beta yields beta reaction, for the A, B and C alloys, respectively in that order. Some samples were submitted to heat treatments (62 and 216 hours at 825 deg C, 120 hours at 875 deg C). Optical and scanning electronic microscopy of those samples confirmed our resistivity results. DOE

N94-26264# Comision Nacional de Energia Atomica, Buenos Aires (Argentina). Dept. de Materiales.

STRESS CORROSION CRACKING AND DEALLOYING OF COPPER-GOLD ALLOY IN IODINE VAPOR [CORROSION BAJO TENSION Y DEALEADO DEL COBRE-ORO EN ATMOSFERA DE IODO]

M. F. Galvez, G. L. Bianchi, and J. R. Galvele 1993 6 p In SPANISH Presented at the SAM 1993: 17th Metallurgical Sessions of the Argentine Metals Association; 2nd Argentine Meeting on Ceramics and Refractories, San Carlos de Bariloche, Argentina, 13-16 Apr. 1993
(DE93-633790; INIS-AR-026; CONF-9304174) Avail: CASI HC A02/MF A01 (US Sales Only)

The susceptibility to stress corrosion cracking of copper-gold alloy in iodine vapor was studied and the results were analyzed under the scope of the surface mobility stress corrosion cracking mechanism. The copper-gold alloy undergoes stress corrosion cracking in iodine. Copper iodide was responsible of that behavior. The copper-gold alloy shows two processes in parallel: stress corrosion cracking and dealloying. As was predicted by the surface mobility stress corrosion cracking mechanism, the increase in strain rate induces an increase in the crack propagation rate. DOE

N94-26272# Oak Ridge National Lab., TN.

AN ATOM PROBE INVESTIGATION OF THE INFLUENCE OF TRACE IMPURITIES ON THE MECHANICAL BEHAVIOR OF NiAl

R. Jayaram, C. T. Liu, and M. K. Miller 1993 10 p Presented at the Fall Meeting of the Minerals, Metals and Materials Society: Physical Metallurgy and Materials, Pittsburgh, PA, 17-21 Oct. 1993
(Contract DE-AC05-84OR-21400)
(DE94-002797; CONF-931009-11) Avail: CASI HC A02/MF A01

Atom probe field ion microscopy (APFIM) and transmission electron microscopy (TEM) have been used to investigate the influence of trace metallic impurities on the enormous increase in the yield stress of boron-doped NiAl. Previous atom probe studies of NiAl containing 0.12 at. % boron had demonstrated that 0.026 at. % of the boron was in solid solution. The remainder reacted with trace metallic impurities, presumably present in high purity Ni, to form ultrafine MB2 precipitates ranging in size from less than 2 nm to 20 nm. Atom probe measurements had shown that their number densities were significant enough to make the dominant contribution to the observed increase in yield stress. An attempt was made in the present work to minimize the effect of these precipitates by an additional aging treatment. Field ion microscope (FIM) and TEM micrographs revealed that 2 nm precipitates coarsened significantly during aging. Microstructure of aged NiAl was consistent with observed mechanical behavior showing a significantly smaller increase in the yield stress. An approximate value of the Orowan stress, based on TEM estimates of the size and number density of the precipitates, is in reasonable agreement with the measured value. This APFIM/TEM investigation has indicated a practical approach to minimize the detrimental role of trace impurities in NiAl. DOE

N94-26273# Ames Lab., IA.
LIQUID AND SOLID SOLUBILITY OF Ag IN Bi2Sr2CaCu2O8
R. W. McCallum, K. W. Dennis, L. Margulies, and M. J. Kramer 1993
11 p Presented at the Fall Meeting of the Minerals, Metals and Materials Society: Physical Metallurgy and Materials, Pittsburgh, PA, 17-21 Oct. 1993
(Contract W-7405-eng-82)
(DE94-002829; IS-M-776; CONF-931009-13) Avail: CASI HC A03/MF A01

Currently, leading candidates for usable high temperature superconducting wires are Bi-Sr-Ca-Cu-O tapes produced by modifying the powder in tube process. In order to obtain crystallographic texture, these tapes are processed by partial melting then slow cooling through the peritectic. While it is well known that Ag suppresses the lowest liquidus temperature of the Bi based materials, no serious investigation of the Bi-Sr-Ca-CuO-Ag phase diagram has been undertaken. Solubilities of Ag in Bi2212 melt was determined by ICP-AES and TEM/EDS on samples of Bi2212 and 20 wt % Ag which were melt-spun in air at temperatures of 900 to 1200 C. The most prominent feature of the phase diagram was found to be liquid immiscibility at all temperatures. There exists a eutectic on each side of this gap. For the Ag rich side the eutectic is at 98 at. % Ag and depresses the melting by 15 C over that for pure silver for the same oxygen partial pressure. The oxide rich eutectic contains no more than 4 at % Ag and depresses the solidus by 30 C. The solid solubility of Ag in Bi-Sr-Ca-Cu-O glass (oxide glass) is found to be less than the detection limits of TEM/EDS and Ag is systematically excluded from the oxide glass. DOE

N94-26294# Comision Nacional de Energia Atomica, Buenos Aires (Argentina). Dept. of Materiales.
ANALYSIS OF THE EFFECT ON GROWTH KINETICS OF GAMMA PRIMA PHASE IN INCONEL 713C ALLOYS [ANALISIS DE LA CINETICA DE CRECIMIENTO DE LA FASE GAMMA PRIMA EN LA ALEACION INCONEL 713C]
S. I. Thorp (Buenos Aires Univ., Argentina.), R. A. Versaci, A. Ges (Universidad Nacional del Centro de la Provincia de Buenos Aires, Tandil, Argentina.), and H. A. Palacio (Universidad Nacional del Centro de la Provincia de Buenos Aires, Tandil, Argentina.) 1993 6 p In SPANISH Presented at the SAM 1993: 17th Metallurgical Sessions of the Argentine Metals Association; 2nd Argentine Meeting on Ceramics and Refractories, San Carlos de Bariloche, Argentina, 13-16 Apr. 1993
(DE93-633763; INIS-AR-019; CONF-9304174) Avail: CASI HC A02/MF A01 (US Sales Only)

This work shows the analysis of the effect on growth kinetics of gamma prima phase in Inconel 713C alloy of two thermic treatments. In this study, SEM are used and the results are analyzed by means of the theory developed by Lifshitz, Slyozov and Wagner (LSW theory). The findings have revealed that with such theory it is not possible to determine if the process of growth is controlled either through diffusion or through diffusion in the interface as to the time employed in the experiment (2600 hours); the time required is approximately 10,000 hours. DOE

N94-26295# Comision Nacional de Energia Atomica, Buenos Aires (Argentina). Dept. de Materiales.
EUTECTIC TRANSFORMATION L IN EQUILIBRIUM TO Zr6Fe23 + Fe(TAU) IN THE Fe-Zr SYSTEM [TRANSFORMACION EUTECTICA L IN EQUILIBRIUM TO ZR6FE23 + FE(TAU) EN EL SISTEMA FE-ZR]
M. S. Granovsky and D. E. Arias 1993 6 p In SPANISH Presented at the SAM 1993: 17th Metallurgical Sessions of the Argentine Metals Association; 2nd Argentine Meeting on Ceramics and Refractories, San Carlos de Bariloche, Argentina
(DE93-633766; INIS-AR-023; CONF-9304174) Avail: CASI HC A02/MF A01 (US Sales Only)

The knowledge of the phase diagram of the Fe-Zr system is important because Fe is always present as an impurity in commercial Zr-base nuclear grade alloys. This diagram has four intermetallic compounds, namely Zr3Fe, Zr2Fe, ZrFe2 and Zr6Fe23. ZrFe2 with a cubic Laves C15 structure melts congruently at 1673 deg C and Zr6Fe23 with a cubic Th6Mn23-type structure is a product of the peritectic ZrFe2 + L(r reversible)Zr6Fe23 reaction at 1482 deg C. As a part of the work on the Fe-rich portion of the system, the eutectic transformation L(r reversible)Zr6Fe23 + Fe(tau), its temperature and its composition have been studied. In order to find the eutectic temperature, sample of Zr15Fe65 and Zr4Fe96 were thermally treated at the temperature higher and lower than 1337 deg C, which was reported in the last revision of the diagram (1988). It was observed that samples treated at 1345 deg C, 1340 deg C, 1335 deg C and 1325 deg C partially melted while those treated at 1320 deg C did not. An eutectic temperature of (1325 +/- 5) deg C could be determined from the results of metallographic, X-ray and microanalysis experiments. The composition of the eutectic was determined to be (90 +/- 1) at % Fe, with the electron microprobe, by automatically averaging results on regions 10(mu)m long. DOE

N94-26322# Lawrence Livermore National Lab., CA.
IRON: WHAT IS MELT?
A. G. Duba Jun. 1993 4 p Presented at the 14th International Conference of the International Association for the Advancement of High Pressure Science and Technology, Colorado Springs, CO, 27 Jun. - 2 Jul. 1993
(Contract W-7405-eng-48)
(DE94-003373; UCRL-JC-114723; CONF-930676-64) Avail: CASI HC A01/MF A01

The melting point of iron reported from a variety of phenomena observed in the laser-heated diamond-anvil-cell (DAC) and in shock wave studies differs widely. Although the three groups of investigators observing the same phenomena in the DAC are in good agreement to about 40 GPa, they disagree significantly with other measurements of melting point based on observation of different phenomena in the DAC. These latter data are in substantial agreement with some of the reported melting temperatures from two groups of investigators who measured temperature along the Hugoniot. However, a third group of investigators observe a sound velocity discontinuity along the Hugoniot and calculate a significantly lower temperature for melting. Melting point determination in iron is subject to the interpretation of physical phenomena, experimental errors which are probably larger than estimated, and perhaps undetected chemical reactions. DOE

N94-26337# Minerals, Metals and Materials Society, Warrendale, PA.
TITANIUM 1992: VOLUME 3: SCIENCE AND TECHNOLOGY
1993 1037 p
(AD-A274800) Avail: CASI HC A99/MF A10

Partial contents include: (1) Surfaces, Environmental Effects, Protection; (2) Raw Materials, Melting, Recycling and Primary Processing; (3) Metal Matrix Composites; (4) Non-Aerospace Applications; (5) Inspection, NDE, Quality Assurance, Defects; and (6) Aerospace Applications. DTIC

N94-26349# Sandia National Labs., Albuquerque, NM.
EXPERIMENTAL DETERMINATION OF THE CU-IN-PB TERNARY PHASE DIAGRAM
A. Bolcavage (Wisconsin Univ., Madison.), C. R. Kao (Wisconsin Univ., Madison.), Y. A. Chang (Wisconsin Univ., Madison.), and A. D. Romig, Jr. 1993 10 p Presented at the Materials Week 1993, Pittsburgh, PA, 17-21 Oct. 1993
(Contract DE-AC04-94AL-85000)
(DE94-003765; SAND-93-2736C; CONF-9310224-1) Avail: CASI HC A02/MF A01

Use of lead-indium solders in microelectronics packaging has increased over the last decade. Increased usage is due to improved properties, such as greater thermo-mechanical fatigue resistance, lower intermetallic formation rates with base metallizations (such as copper), and lower reflow temperatures. However, search of the literature reveals no comprehensive studies on phase equilibrium relations between copper metal and lead-indium solder. Our effort involves a combination of experimental data acquisition and computer modeling to obtain the Cu-In-Pb ternary phase diagram. Isotherms and isopleths of interest at low temperatures are achieved by means of differential scanning calorimetry and electron probe microanalysis.

Thermodynamic models of these sections served as a guide for efficient experimentation. DOE

N94-26351# Lawrence Livermore National Lab., CA.
THE ORIGINS OF ORDERING IN CuPt
J. F. Clark (Cincinnati Univ., OH.), F. J. Pinski (Cincinnati Univ., OH.), P. A. Sterne (California Univ., Davis.), D. D. Johnson, J. B. Staunton (Warwick Univ., Coventry, England.), and B. Ginatempo (Messina Univ., Italy.) Aug. 1993 9 p Presented at the NATO Advanced Study Workshop on Metallic Alloys: Experimental and Theoretical Perspectives, Boca Raton, FL, 16-21 Jul. 1993
(Contract W-7405-eng-48)
(DE94-003864; UCRL-JC-114721; CONF-930759-5) Avail: CASI HC A02/MF A01

The alloy CuPt is one of the few that order into a L1(sub 1) crystal structure, i.e. planes of copper and planes of planes of platinum perpendicular to the group of zone axes (111) direction. For disordered CuPt, the calculated Warren-Cowley short-range order parameter indicates an instability to concentration fluctuations with a wave-vector of ((1/2), (1/2), (1/2)), consistent with L1(sub 1) ordering. We show that this rare tendency is due to this ordering vector arising from the large joint density of states associated with L point and X point van-Hove singularities which lie near the Fermi energy. DOE

N94-26362# Minerals, Metals and Materials Society, Warrendale, PA. Structural Metals Div.
TITANIUM 1992: SCIENCE AND TECHNOLOGY, VOLUME 2 RENCE (7TH) IN SAN DIEGO, CALIFORNIA ON JUNE 29-JULY 2, 1992. VOLUME 2
F. H. Froes, ed. and I. L. Caplan, ed. 1993 1021 p Symposium held at the Seventh World Titanium Conference, San Diego, CA, 29 Jun. - 2 Jul. 1992; sponsored by the Titanium Committee of the Minerals, Metals and Materials
(AD-A274799) Avail: CASI HC A99/MF A10

Partial contents include the following: (1) Intermetallics; (2) Forging, Forming, Joining, and Casting; and Physical and Mechanical Properties. DTIC

N94-26452# Pennsylvania Univ., Philadelphia. Dept. of Chemistry.
TRANSITION METALS IN HIGHLY CORRELATED DISCOTIC PHASES: DESIGNING METALLOMESOGENS WITH SELECTED INTERMOLECULAR ORGANIZATIONS Technical Report
Hanxing Zheng, Chung K. Lai, and Timothy M. Swager 8 Jan. 1994 3 p
(Contract N00014-92-J-1416)
(AD-A274695; TR-4-ONR) Avail: CASI HC A01/MF A01

The diketonate Schiff-base complexes shown below were investigated, and the square planar derivatives (M=Ni, Cu, Pd) were found to display discotic hexagonal disordered phases (Dhd). The M=VO analogs are not liquid crystalline. None of the complexes can exhibit a disc-shape independently, and in the mesophase they must organize into a superstructure which on time average leads to antiparallel alignment of nearest neighbors. These discotic antiphases exhibit a number of important properties including low melting points, low viscosity, and close intermolecular contacts of 3.6A. Additionally when put between two untreated slides, these mesophases were found to readily align with the column axes perpendicular to the surfaces. The Cu and Ni complexes exhibited very similar mesophases and lattice constants whereas the Pd complexes displayed larger intercolumnar distances and higher clearing temperatures. The differences are ascribed to greater intermolecular associations displayed by the Pd complexes. X-ray diffraction studies revealed the Ni and the Cu complexes to have an additional halo centered at approximately 7.2A which may be the result of a doubling of the period along the column axes resulting from the antiparallel arrangement of the antiphase superstructure. DTIC

N94-26477# Tokyo Univ. (Japan). Inst. for Solid State Physics.
TOWARD INSULATING QUASICRYSTALLINE ALLOY IN Al-Pd-Re ICOSAHEDRAL PHASE
Hirofumi Akiyama, Yuko Honda, Tatsuo Hashimoto, Keiichi Edagawa, and Shin Takeuchi Apr. 1993 13 p
(ISSN 0082-4798)
(Rept-A-2666; JTN-94-80537) Avail: CASI HC A03/MF A01

The resistivities in Al70Pd20Re10 alloy of the icosahedral phase are quite sample-dependent, possibly due to slight variation of the alloy composition. In some samples, the resistivity at room temperature is approximately 0.01 omega cm and that at 4.2 K is as high as approximately 0.1 omega cm; these values are much higher than any reported values so far for quasi-crystals. The temperature dependence of the conductivity is almost linear above 4.2 K and the magnetoconductivity is negative. These dependencies are interpreted by the theory of weak localization which takes into account the spin-orbit scattering. Author (NASDA)

N94-26481# Midwest Research Inst., Golden, CO.
RECOMBINATION AND METASTABILITY IN AMORPHOUS SILICON AND SILICON GERMANIUM ALLOYS
M. Silver (North Carolina Univ., Chapel Hill.) Nov. 1993 15 p
(Contract DE-AC02-83CH-10093)
(DE94-000237; NREL/TP-451-5834) Avail: CASI HC A03/MF A01

This report describes work during the second year of a continuing research study. The work is designed to help us understand how recombination, trapping, and band-mobility modification affecting the electronic properties of amorphous semiconductors can be measured, characterized, and described by an appropriate spectrum of defect states. We also worked to determine how light-induced defects in a Si:H and native defects in a-Si:H and native defects in a-Si:H and native defects in a SiGe:H affect transport properties in these materials. During this second year, we continued our experiments on electroluminescence (EL) and transient forward bias current, as well as photocurrent before and after light soaking. We started a program to study thin (0.4 micron) p-i-n solar cells, and we studied the effect of optical bias on charge transport in a Si:H films. We performed analytical calculations on a model that predicts an exponential energy region for band tails from dilute random charges. We developed a model for the carrier-recombination-lifetime distribution. We solved the equations for H-diffusion including deep trap levels. Lastly, we analyzed simulation data under forward bias in p-i-n devices. The most interesting and important results were obtained on the EL spectra in thin solar cell devices. We found that, at elevated temperatures, thin p-i-n devices displayed primarily defect luminescence (0.8-0.9 eV), while in thick (greater than 2 micron) devices the luminescence observed was the main band (l.l-1.2 eV). We also found that, in thin cells with buffered layers, p-b-i-n's the main band luminescence was more pronounced than that in simple p-i-n's. For the first time, we have distinguished between bulk and junction-controlled recombination. DOE

N94-26522# Westinghouse Hanford Co., Richland, WA.
NONSWELLING BEHAVIOR OF HT9 ALLOY IRRADIATED TO HIGH EXPOSURE
A. L. Pitner, S. L. Hecht, and R. G. Trenchard Oct. 1993 18 p Presented at the American Nuclear Society (ANS) Winter Meeting, San Francisco, CA, 14-18 Nov. 1993
(Contract DE-AC06-87RL-10930)
(DE94-003502; WHC-SA-1967; CONF-931160-32) Avail: CASI HC A03/MF A01

In-reactor monitoring of assembly axial growths in the Fast Flux Test Facility (FFTF) showed the ferritic/martensitic alloy HT9 to be essentially swelling free out to a fast neutron fluence of at least 37 x 10(exp 22) n/sq cm. This superior performance directly contributes to the ability to achieve high fuel burnup levels necessary for the ultimate viability of an economical Liquid Metal Reactor (LMR) fuel system. DOE

N94-26533# Naval Postgraduate School, Monterey, CA.
STUDY OF PRECIPITATION AND RECRYSTALLIZATION IN Al ALLOY 2519 BY BACKSCATTERED ELECTRON IMAGING METHODS M.S. Thesis
Peter J. Zohorsky Sep. 1993 64 p
(AD-A274919) Avail: CASI HC A04/MF A01

This study examines the effects of pre-strain deformation temperature, overaging temperature, and other variations in thermomechanical processing (TMP) on the mean size and size distribution of q-phase precipitate particles in Al alloy 2519. Examination was performed using the scanning electron microscope in the backscattered imaging mode, and quantitative image analysis methods were employed. The goal was to find a combination of

TMP parameters which produces q-phase particles exceeding a critical diameter for particle stimulated nucleation (PSN) of recrystallization. A necessary prerequisite for superplasticity is a uniformly fine, equiaxed grain size, and PSN is theorized to be capable of such grain refinement. Such a microstructure has been developed in aluminum alloys containing large second phase particles when the alloys are subjected to cold work and recrystallization treatments. DTIC

N94-26556# Pacific Northwest Lab., Richland, WA.

MICROSTRUCTURAL DEVELOPMENT IN IRRADIATED VANADIUM ALLOYS

D. S. Gelles and J. F. Stubbins (Illinois Univ., Urbana.) Sep. 1993 12 p Presented at the 6th International Conference on Fusion Reactor Materials, Stresa, Italy, 27 Sep. - 1 Oct. 1993
(Contract DE-AC06-76RL-01830)
(DE94-004307; PNL-SA-22470; CONF-930928-15) Avail: CASI HC A03/MF A01

Three simple vanadium alloys, V-5Al, V-1Ni, and V-2Ti-1Ni were examined to determine the effects of fast neutron irradiation on microstructural evolution. Specimens were irradiated in EBR II at temperatures in the range 425 to 600 C to doses of 15 and 31 dpa. Each alloy responded very differently to irradiation. All V-5Al specimens were generally void-free and contained high densities of coherent precipitates, and moderate densities of network dislocations. Swelling was much higher in V-1Ni. Voids were uniformly distributed, but with widely varying shape and size. Precipitation of two types also developed. The response in V-2Ti-1Ni was intermediate to that of the other two alloys. Irradiation produced extensive precipitation of thin rods and a moderate density of large voids often associated with much larger precipitate particles. The dislocation structure strongly interacted with the rod precipitate particles. DOE

N94-26575# Pacific Northwest Lab., Richland, WA.

INFLUENCE OF HELIUM GENERATION RATE AND TEMPERATURE HISTORY ON MECHANICAL PROPERTIES OF MODEL Fe-Cr-Ni ALLOYS IRRADIATED IN FFTF AT RELATIVELY LOW DISPLACEMENT RATES

M. L. Hamilton, F. A. Garner, and D. J. Edwards 1993 9 p Presented at the 6th International Conference on Fusion Reactor Materials, Stresa, Italy 1 Oct. 1993 Prepared in cooperation with Associated Western Universities, Inc., Salt Lake City, UT
(Contracts DE-AC06-76RL-01830; DE-FG06-89ER-75522)
(DE94-004264; PNL-SA-22444; CONF-930928-20) Avail: CASI HC A02/MF A01

In agreement with earlier studies conducted at higher displacement rates, evolution of mechanical properties of model Fe-Cr-Ni alloys irradiated at lower displacement rates in the Ni-59 isotopic doping experiment does not appear to be strongly affected by large differences in helium generation rate. This insensitivity to helium/dpa ratio is exhibited during both isothermal and non-isothermal irradiation. The overall behavior of the model alloys used in this study is dominated by the tendency to converge to a saturation strength level that is independent of thermomechanical starting state and helium/dpa ratio, but which is dependent on irradiation temperature and alloy composition. DOE

N94-26582# Bettis Atomic Power Lab., West Mifflin, PA.

AN EXPERIMENTAL STUDY ON THE EFFECTS OF COMPRESSIVE STRESS ON THE FATIGUE CRACK GROWTH OF LOW-ALLOY STEEL

D. P. Jones, R. G. Hoppe, J. L. Hechmer (Babcock and Wilcox Co., Barberton, OH.), and B. A. James (Colorado School of Mines, Golden.) 1993 23 p Presented at the 1993 American Society of Mechanical Engineers (ASME) Pressure Vessel and Piping Conference, New Orleans, LA, 21-25 Jun. 1993
(Contract DE-AC11-93PN-38195)
(DE94-004447; WAPD-T-2973; CONF-9306289-1) Avail: CASI HC A03/MF A01

A series of fatigue crack growth rate tests was conducted in order to study effects of negative stress ratio on fatigue crack growth rate of low-alloy steel in air. Four-point bend specimens were used to simulate linear stress distributions typical of pressure vessel applications. This type of testing adds to knowledge on negative stress ratio effects for low-alloy steels obtained in the past from uniform tension-compression tests. Applied bending stress range was varied over twice the yield strength. Load control was used for tests for which the stress range was less than twice the yield strength and deflection control was used for the higher stress range tests. Crack geometries were both short and long fatigue cracks started at notches and tight fatigue cracks for which crack closure could occur over the full crack face. Results are presented in terms of the stress intensity factor ratio R = K(sub MIN)/K(sub MAX). The negative R-ratio test results were correlated to an equation of the form da/dN = C(Delta K/(A-R))(exp n), where A, C, and n are curve fitting parameters. It was found that effects of negative R-ratio on fatigue crack growth rates for even the high stress range tests could be bounded by correlating the above equation to only positive R-ratio test results and extending the resulting equation into the negative R-ratio regime. DOE

N94-26585# Pacific Northwest Lab., Richland, WA.

STRUCTURE AND PROPERTIES OF COMPOSITES SYNTHESIZED IN SITU USING SOLID STATE DISPLACEMENT REACTIONS

C. H. Henager, Jr. and J. L. Brimhall Oct. 1993 21 p Presented at the Fall Meeting of the Minerals, Metals and Materials Society: Physical Metallurgy and Materials, Pittsburgh, PA, 17-21 Oct. 1993
(Contract DE-AC06-76RL-01830)
(DE94-004589; PNL-SA-21630; CONF-931009-16) Avail: CASI HC A03/MF A01

Solid state displacement reactions can produce in situ intermetallic and ceramic matrix composites in a process where an intermetallic or ceramic phase(s) and a potential reinforcing phase(s) are grown together during a solid state reaction. Interpenetrating and dispersed microstructures, important for desirable composite properties, have been produced by means of displacement reaction processing techniques. Two such composites have been synthesized which exhibit two distinct microstructures: MoSi2 reinforced with SiC particles, which exhibits a dispersed-phase structure, and NiAl/Ni3Al reinforced with Al2O3, which exhibits an interpenetrating-phase structure. Strength in bending and chevron-notch fracture toughness have been determined as a function of temperature, and measured properties compare favorably with composites produced by other means. The measured properties are discussed with regard to the observed microstructures. The potential for displacement reaction processing is assessed, and it appears to be a cost-effective synthesis method compared to others. DOE

N94-26587# Argonne National Lab., IL. Materials Science Div.

SUPPRESSION OF THERMAL GRAIN GROWTH IN NICKEL BY PRIOR ELECTRON IRRADIATION

Yuzun Gao,, Charles W. Allen, and R. C. Birtcher Nov. 1993 7 p Presented at the Fall Meeting of the Materials Research Society, Boston, MA, 29 Nov. - 3 Dec. 1993
(Contract W-31-109-eng-38)
(DE94-004602; ANL/MSD/CP-80133; CONF-931108-14) Avail: CASI HC A02/MF A01

An anomalous effect of electron irradiation on thermal grain growth in Ni has been observed using in situ TEM. Grain growth during thermal annealing was suppressed in areas irradiated with electrons. Grain growth suppression required a minimum electron energy between 100 and 200 keV. This alteration of thermal grain growth is attributed to electron beam injection of a surface contaminant such as carbon. This work points out that care must be exercised in the execution and evaluation of in situ TEM or ion beam experiments that deal with microstructural changes which are highly compositionally sensitive. DOE

N94-26607# Los Alamos National Lab., NM.

A TRI-JUNCTION DIFFUSION COUPLE ANALYSIS OF THE Nb-Cr-Ti SYSTEM AT 950 C

D. J. Thoma and J. H. Perepezko (Wisconsin Univ., Madison.) 1993 12 p Presented at the Fall Meeting of the Minerals, Metals and Materials Society: Physical Metallurgy and Materials, Pittsburgh, PA, 17-21 Oct. 1993
(Contract W-7405-eng-36)
(DE94-002637; LA-UR-93-3586; CONF-931009-10) Avail: CASI HC A03/MF A01

With a three-way diffusion couple consisting of a tri-junction between three elements, a whole spectrum of phase development and ternary equilibria is available within a single isothermal sample. Binary equilibria (for the three binary systems) are also available in single sample by analyzing diffusion zones at composition limits outside the field of ternary interaction. The tri-junction approach was employed to evaluate ternary phase formation, ternary solubility limits of binary phases, and diffusion paths in a candidate high-temperature structural system (Nb-Cr-Ti). Ternary phase equilibria and tie lines have been defined at 950 C and results confirmed with isothermal anneals of two-phase ternary alloys. The continuous solubility in TiCr2-NbCr2 region is broadened by at least 5 at. % from binary intermetallic phase fields. No new ternary phases were detected in the Nb-CrTi system at 950 C. By examining the relative shifts in the diffusion interfaces, a qualitative ranking of interdiffusion suggests that addition of Nb restricts diffusion of Cr into Ti compared to binary (Cr/Ti) behavior. DOE

N94-26610# Sandia National Labs., Albuquerque, NM.

CHEMICAL VAPOR DEPOSITION AND CHARACTERIZATION OF TUNGSTEN BORON ALLOY FILMS

P. M. Smith, J. G. Fleming, R. D. Lujan, E. Roherty-Osmun, J. S. Reid (California Inst. of Tech., Pasadena.), A. K. Hochberg, and D. A. Roberts 1993 8 p Presented at the Advanced Metalization for Ultralarge Scale Integration Applications in 1993, San Diego, CA, 5-10 Oct. 1993
(Contract DE-AC04-94AL-85000)
(DE94-002648; SAND-93-2445C; CONF-9310218-1) Avail: CASI HC A02/MF A01

A low pressure chemical vapor deposition (LPCVD) process for depositing W(X)B(1-X) films from WF6 and B2H6 is described. The depositions were performed in a cold wall reactor on 6 in. Si wafers at 400 C. During deposition, pressure was maintained at a fixed level in the range of 200 to 260 mTorr. Ratio of WF6/B2H6 was varied from 0.05 to 1.07. Carrier gas was either 100 sccm of Ar with a gas flow of 308 to 591 sccm, or 2000 sccm of Ar and 2000 sccm of H2 with the overall gas flow from 4213 to 4452 sccm. Two stable deposition regions were found separated by an unstable region that produced non-uniform films. The B-rich films produced in one of the stable deposition regions had W concentrations of 30 at.% and resistivities between 200 and 300 micro-ohm cm. The W-rich films produced in the other stable deposition region had W concentrations of 80 at.% and resistivities of 100 micro-ohm cm. As-deposited films had densities similar to bulk material of similar stoichiometry. Barrier properties of the films against diffusion of Cu to 700 C in vacuum were measured by four-point probe. Also, annealing was carried out to 900 C in order to determine phases formed as the films crystallize. These studies indicate that W(X)B(1-X) films may be useful barriers in ULSI metallization applications. DOE

N94-26621# Los Alamos National Lab., NM.

DEFORMATION TWINNING: INFLUENCE OF STRAIN RATE

G. T. Gray, III 1993 14 p Presented at the Fall Meeting of the Minerals, Metals and Materials Society: Physical Metallurgy and Materials, Pittsburgh, PA, 17-21 Oct. 1993
(Contract W-7405-eng-36)
(DE94-002693; LA-UR-93-3720; CONF-931009-9) Avail: CASI HC A03/MF A01

Twins in most crystal structures, including advanced materials such as intermetallics, form more readily as the temperature of deformation is decreased or the rate of deformation is increased. Both parameters lead to the suppression of thermally-activated dislocation processes which can result in stresses high enough to nucleate and grow deformation twins. Under high strain rate or shock-loading/impact conditions, deformation twinning is observed to be promoted even in high stacking fault energy FCC metals and alloys, composites, and ordered intermetallics which normally do not readily deform via twinning. Under such conditions and in particular under the extreme loading rates typical of shock wave deformation, the competition between slip and deformation twinning can be examined in detail. In this paper, examples of deformation twinning in the intermetallics TiAl, Ti-48Al-IV, and Ni3A as well as in the cermet Al-B4C as a function of strain rate will be presented. Discussion includes: the microstructural and experimental variables influencing twin formation in these systems and twinning topics related to high strain rate loading; the high velocity of twin formation; and the influence of deformation twinning on the constitutive response of advanced materials. DOE

N94-26633 Carleton Univ., Ottawa (Ontario). Dept. of Mechanical and Aerospace Engineering.

THE PROCESSING OF POWDER METALLURGICALLY PRODUCED NEAR GAMMA-TITANIUM ALUMINIDE Ph.D. Thesis

Jonathan Carl Beddoes Jan. 1993 267 p
(ISBN-0-315-84018-8; CTN-94-61049) Copyright Avail: Micromedia Ltd., Technical Information Centre, 240 Catherine Street, Suite 305, Ottawa, Ontario, K2P 2G8, Canada HC/MF

The technology of Ti-Al intermetallics for aerospace applications is reviewed, and inherent structural and deformation characteristics are described. The relationship between microstructure and processing is examined with a focus on powder metallurgical, hot isostatic pressing (HIP), and hot deformation processes. Mechanical properties attainable with near gamma-TiAl alloys are presented and the effect of ternary elements examined. The microstructural characteristics of Ti-54 percent Al and Ti-48 percent Al-2 percent W were investigated to elucidate the microstructural evolution occurring during powder manufacture. HIP compacts exhibited a nonuniform grain size associated with a varying volume fraction of dendrite regions in the powder. Tensile ductility is related to the homogeneity of deformation between prior dendrites and interdendritic regions. The hot workability of Ti-48 percent Al-2 percent W was determined by isothermal constant strain rate forging simulations. Deformation and forgeability maps are presented for HIP material, showing the temperature strain domain at which sound forgings are produced. Combining the deformation and forgeability maps indicates that crack-free forgings are only produced by temperature/strain rate combinations at which superplastic flow contributes to the accommodation of strain. Author (CISTI)

N94-26653 National Physical Lab., Teddington (England). Materials Metrology Div.

STABILITY OF REFERENCE MASSES 2: THE EFFECT OF ENVIRONMENT AND CLEANING METHODS ON THE SURFACES OF STAINLESS STEEL AND ALLIED MATERIALS

M. P. Seah, J. H. Qiu (Surrey Univ., Guildford, England.), P. J. Cumpson, and J. E. Castle (Surrey Univ., Guildford, England.) Apr. 1993 42 p Sponsored by Dept. of Trade and Industry, London, England
(ISSN 0959-2423)
(NPL-DMM(A)-95; ETN-94-95224) Copyright Avail: Issuing Activity (National Physical Lab., Teddington, Middlesex, TW11 OLW, England)

The surfaces of Immaculate 5, En58AM, and Nimonic 105 materials were studied. X ray photoelectron spectroscopy analysis was performed after cleaning using simple washing methods, and after contamination in the laboratory environment for periods of up to 156 days, using filtered and unfiltered laboratory air. The surfaces are covered by a thin oxide and this is further covered by a thin layer of carbonaceous contamination of atmospheric origin. Some of the contamination is removed by surfactants contained in various proprietary cleaners or by boiling water. The first exposure to boiling water increases the chromium content of the oxide. Exposure to the environment causes the carbonaceous contamination thickness to grow at a rate described by either the simple diffusion theory of 'logarithmic' theory such that the increase in mass of a kilogram artefact is around 15 micro-g/year after five years. If the laboratory air is filtered and moving at a low rate the carbonaceous contamination growth is low. If the filter is removed and the flow rate raised, the carbonaceous contamination rate increases. It is recommended that masses made from these materials are initially subjected to a boiling water wash for five minutes to develop a stable oxide thickness, stored in static filtered air to reduce the carbonaceous contamination, and cleaned using a dilute aqueous solution of gentle surfactant cleaners or by a steam cleaning method. ESA

N94-26679# Colorado School of Mines, Golden. Center for Welding and Joining Research.

THE INFLUENCE OF WELD METAL ALLOYING ADDITIONS TO EXTEND THE HEAT INPUT RANGE FOR THE SUBMERGED ARC WELDING OF HIGH STRENGTH STEELS Final Report

S. Liu, D. L. Olson, and J. E. Ramirez 16 Dec. 1993 46 p
(Contract N00014-90-J-1889)
(AD-A274284; CSM-CWR-093-015) Avail: CASI HC A03/MF A01

Weld metal microstructural development for high strength steels when welded with submerged arc welding process was investigated as a function of consumable composition and thermal experience. Of specific interest is the effect of systematic variations of microalloying additions on broadening of applicable heat input range. Controlled weld metal oxygen content, particularly in the range of 300 to 400 ppm, has been found to improve HY-130 steel weld metal toughness. Molybdenum additions was found to increase the strength of the HY-130 steel weld deposits. Copper additions up to 3.5 wt.pct. were found to strengthen the high strength steel weld metals, in particular, those of higher heat input, 3.6 kJ/mm. Niobium additions alone did not provide as powerful strengthening effect in the high heat input weld metals as the copper additions. In the case of copper-enriched welds, multi-pass welding induced both the precipitation and overaging of epsilon copper precipitates in the reheated weld metal which resulted in non-uniform mechanical properties. When added together, copper and niobium produced the synergistic effect of dual precipitation (Epsilon copper and niobium carbides) which provided the needed strength and thermal stability to the reheated weld metal even at high heat inputs. With this novel approach, the applicable heat input range to produce both adequate weld metal strength and toughness in high strength steels (Sigma y greater than 690 MPa) can be extended significantly. The optimal additions for copper and niobium were found to be 3.3 and up to 0.1 wt. pct. DTIC

N94-26799 Minerals, Metals and Materials Society, Warrendale, PA.

TITANIUM 1992: SCIENCE AND TECHNOLOGY, VOLUME 1

F. H. Froes, ed. and I. L. Caplan, ed. 1993 1037 p Symposium held in San Diego, CA, 29 Jun. - 2 Jul. 1992; sponsored by the Titanium Committee of the Minerals, Metals and Materials Structural Metals Div. Limited Reproducibility: More than 20% of this document may be affected by microfiche quality

(AD-A274798-Vol-1) Avail: CASI HC A99

The partial contents of this document include the following: (1) Titanium process modelling; (2) Alloy theory and phase transformations in titanium alloys; (3) Microstructure-property relationships in titanium alloys; (4) Fatigue and fracture toughness properties of Ti-6Al-4V with Acicular Alpha Microstructures; (5) The effect of thermal treatment on the cryogenic mechanical properties of cast 5Al-2.5Sn ELI titanium; (6) Oxygen effects on the mechanical properties of Timetal-21S; (7) Effect of cold work and heat treatment in alpha region on mechanical properties of Ti-15-3 alloy; (8) Role of composition and microstructure in dynamic and static fracture of alpha-beta titanium alloys; (9) Void nucleation, void growth and tensile behavior of Ti-10V-2Fe-3Al; (10) The influence of silicon and silicides on the properties of near-alpha titanium alloys; and (11) The effect of deformation and heat treatment conditions on structure and mechanical properties of gamma alloys. DTIC

N94-26824# Polish Academy of Sciences, Warsaw. Inst. Podstawowych Problemow Techniki.

ON EXPERIMENTAL STUDIES OF YIELD SURFACES OF METALS: A MORE GENERAL APPROACH

Wojciech Szczepinski and Jozef Miastkowski 1993 29 p

(ISSN 0208-5658)

(IFTR-42/1993) Avail: CASI HC A03/MF A01

In all existing experimental studies of the effect of plastic deformation on yield condition the results of tests are represented by assuming a certain standard coordinate system. When thin-walled tubular specimens are used the coordinate axes x,y are assumed to coincide with the axial and circumferential directions on the tube. When specimens are cut out from a prestressed metal sheet the coordinate axes are so chosen that they are parallel to the edges of the sheet. It is shown that the interpretation of experimental results may be more instructive if for the same test variously oriented coordinate systems x,y are used. Numerous experimental results are recalculated for variously oriented coordinate systems and then represented in the respective stress space corresponding to the assumed orientation of the reference axes. Various representations of the deformation-induced changes of the yield surface will constitute the experimental basis for a more sound analysis of the theory of deformation-induced anisotropy of metals. If the plastic properties of the tested material in its initial state are isotropic we can always choose arbitrarily a reference system in which the deformation-induced anisotropy will later be described. Author (revised)

N94-26912# Sandia National Labs., Albuquerque, NM.

THE ELECTROCHEMICAL BEHAVIOR OF THE Al3Fe INTERMETALLIC COMPOUND AND LOCALIZED CORROSION OF IMPURE 1100 Al

R. G. Buchheit, L. M. Maestas, and N. R. Sorensen 1993 13 p Presented at the 183rd Electrochemical Society Meeting, Honolulu, HI, 16-21 May 1993

(Contract DE-AC04-94AL-85000)

(DE94-002037; SAND-93-1649C; CONF-930571-29) Avail: CASI HC A03/MF A01

Pitting of 1100 Al(Al-1.0(Fe,Cu,Si)) due to Al3Fe constituent particles has been studied by examining a variety of intrinsic, extrinsic, and environmental factors that contribute to localized corrosion. Consistent with results from other studies, Al3Fe is noble with respect to its microstructural surroundings and pitting is localized to the particle periphery. Polarization curves indicate that cathodic electron transfer reactions are supported on Al3Fe at high rates; however, anodic electron transfer reactions are not. Interparticle spacing appears to play a strong role in determining where pitting will occur, while Al3Fe particle area plays a lesser role. Solution pH, applied potential, and exposure time each have measurable effects on the electrochemical behavior of Al3Fe and the alpha-Al matrix phase which can impact either the galvanic potential of the Al3Fe/alpha-Al couple, or charge transfer processes on Al3Fe particles. DOE

N94-26931# Oak Ridge National Lab., TN.

THE ROLE OF POINT DEFECT CLUSTERS IN REACTOR PRESSURE VESSEL EMBRITTLEMENT

R. E. Stoller 1993 8 p Presented at the 6th International Symposium on Environmental Degradation of Materials in Nuclear Power Systems: Water Reactors, San Diego, CA, 3-5 Aug. 1993

(Contract DE-AC05-84OR-21400)

(DE94-001122; CONF-930825-13) Avail: CASI HC A02/MF A01

Radiation-induced point defect clusters (PDC) are a plausible source of matrix hardening in reactor pressure vessel (RPV) steels in addition to copper-rich precipitates. These PDC's can be of either interstitial or vacancy type, and could exist in either two or three dimensional shapes, e.g. small loops, voids, or stacking fault tetrahedra. Formation and evolution of PDC's are primarily determined by displacement damage rate and irradiation temperature. There is experimental evidence that size distributions of these clusters are also influenced by impurities such as copper. A theoretical model has been developed to investigate potential role of PDC's in RPV embrittlement. The model includes a detailed description of interstitial cluster population; vacancy clusters are treated in a more approximate fashion. The model has been used to examine a broad range of irradiation and material parameters. Results indicate that magnitude of hardening increment due to these clusters can be comparable to that attributed to copper precipitates. Both interstitial and vacancy type defects contribute to this hardening, with their relative importance determined by the specific irradiation conditions. DOE

N94-26935# Argonne National Lab., IL.

SOLIDIFICATION MODELING OF A SPIRAL CASTING TO DETERMINE MATERIAL FLUIDITY

S. Ahuja, H. M. Domanus, R. C. Schmitt, L. Chuzhoy (Caterpillar Tractor Co., Peoria, IL.), and J. V. Grabel (Caterpillar Tractor Co., Peoria, IL.) 1993 11 p Presented at the Fall Meeting of the Minerals, Metals and Materials Society: Physical Metallurgy and Materials, Pittsburgh, PA, 17-21 Oct. 1993

(Contract W-31-109-eng-38)

(DE94-002212; ANL/ET/CP-79010; CONF-931009-7) Avail: CASI HC A03/MF A01

In casting, fluidity is the measure of the distance a metal can flow in a channel before being stopped by solidification. During mold filling, the metal loses heat to the surrounding mold, thereby cooling and becoming more viscous until the leading portion solidifies and no further flow is possible. A coupled heat-transfer and fluid-flow modeling of a spiral, involving the use of thermophysical properties to determine material fluidity, has been conducted. Fluidity experiments were performed by Caterpillar; several spiral test castings were poured. Simulations of these experiments utilized the Casting Process Simulator (CAPS) software developed at Argonne National Laboratory. Two types of two dimensional spiral geometries with different assumptions were considered: a two dimensional laterally stretched spiral and a three dimensional lateral spiral. Computed mold filling is in good agreement with the experiment. Time required by metal/gas interface to attain specific positions in the spiral arm also compares favorably with the experiment. Influence of process variables, especially pour time, is discussed. CAPS software was used to investigate validity of dimensionality assumptions and to evaluate ability of CAPS to model fluidity adequately. DOE

N94-26957# Argonne National Lab., IL.
POWDER SYNTHESIS, FABRICATION, AND TRANSPORT PROPERTIES OF LONG-LENGTH Ag CLAD Bi-2223 CONDUCTORS
A. N. Iyer, U. Balachandran, P. Haldar (Intermagnetics General Corp., Guilderland, NY.), J. G. Hoehn, Jr. (Intermagnetics General Corp., Guilderland, NY.), and L. R. Motowidlo (IGC/Advanced Supercomputers, Inc., Waterbury, CT.) Oct. 1993 19 p Presented at the Fall Meeting of the Minerals, Metals and Materials Society: Physical Metallurgy and Materials, Pittsburgh, PA, 17-21 Oct. 1993
(Contract W-31-109-eng-38)
(DE94-002376; ANL/ET/CP-79400; CONF-931009-12) Avail: CASI HC A03/MF A01

Prereacted, polyphase powders of Pb-doped Bi-Sr-Ca-Cu-O (2223) were prepared by the solid-state reaction of appropriate amounts of Bi2O3, PbO, SrCO3, CaCO3, and CuO. The calcined powders were characterized by thermal analysis, x-ray diffraction, and scanning electron microscopy. The powders were then used to fabricate long lengths of flexible Ag-clad 2223 superconductor tapes, via the powder-in-tube technique. Growth of the 2223 phase in the tapes at each heat-treatment step has been studied. At 4.2 and 27 K improved process conditions yielded transport critical current density (J(sub c)) values greater than 10(exp 5) A/sq cm at zero field; at 77 K, J(sub c) exceeded 4 x 10(exp 4) A/sq cm. Long tapes (up to 70 m in length) have been fabricated and cowound into superconducting pancake coils and their transport properties have been characterized at 4.2, 27, 64, and 77 K. DOE

N94-27006# Oak Ridge Y-12 Plant, TN.
VAPOR DEPOSITION OF COPPER ON STAINLESS STEEL 304L
R. W. Vasofsky 17 Aug. 1993 9 p Presented at the Environmentally Conscious Manufacturing Congress 1993, Arlington, VA, 30 Aug. - 1 Sep. 1993
(Contract DE-AC05-84OS-21400)
(DE94-001945; Y/DZ-1032; CONF-9308150-9) Avail: CASI HC A02/MF A01

The Oak Ridge Y-12 Plant is seeking to minimize the generation of hazardous wastes in its operations. The standard procedure for electroplating a thin layer of copper on type 304L stainless steel requires several aqueous pretreatment steps which generate Resource Conservation and Recovery Act (RCRA) hazardous wastes. A more environmentally acceptable procedure was evaluated. Copper was vacuum deposited onto 304L coupons under differing deposition conditions and properties of coatings produced, including microstructure and adhesive strength, were examined. Results indicated that a noncolumnar, fine grain copper coating with high adhesion can be produced using this environmentally more acceptable approach. DOE

N94-27009# Naval Postgraduate School, Monterey, CA. Dept. of Mechanical Engineering.
THE INFLUENCE OF TIG WELDING THERMAL CYCLES ON HSLA-100 STEEL PLATE Technical Report
Alan G. Fox and Sanjiwan D. Bhole Nov. 1993 22 p
(AD-A274248; NPS-ME-93-008) Avail: CASI HC A03/MF A01

A series of five bead on plate autogenous tungsten-inert-gas (TIG) welds were performed on U.S. Navy HSLA-100 steel. Power variations in these welds was achieved by altering the welding speed, voltage and current and were as follows (in kJ/mm); 0.7, 1.1, 1.2, 1.6, and 2.2. No evidence was found of either weld metal or underbead heat affected zone (HAZ) cracking in any of the welds illustrating the advantage of low carbon steel for both weld wire and base plate. Microhardness traverses across both the weld metals and HAZ's gave a maximum. Vickers diamond pyramid hardness of 345 HV in the coarse grain HAZ next to the fusion line in the lowest power weld; for the highest power weld this was somewhat lower at 328 HV. These are well below 375 which is usually considered to be the lowest Vickers Hardness value for which severe hydrogen induced cold cracking is observed in this type of steel. Optical, scanning and transmission electron microscopy studies of the coarse grain HAZ microstructure in the regions of maximum hardness was correlated with the continuous cooling transformation diagram for this steel and good agreement between observed and predicted microstructures was obtained. DTIC

N94-27304 Waterloo Univ. (Ontario). Dept. of Electrical Engineering.
MODELLING AND STABILITY OF A SHAPE MEMORY ALLOY POSITION CONTROL SYSTEM M.S. Thesis
Daniel Richard Madill 1993 142 p
(ISBN-0-315-84467-1; CTN-94-61070) Copyright Avail: Micromedia Ltd., Technical Information Centre, 240 Catherine Street, Suite 305, Ottawa, Ontario, K2P 2G8, Canada HC/MF

Shape memory alloys are a class of materials capable of producing a significant force or displacement in response to a thermal control input. Combined with their light weight, the large strains and forces available make shape memory alloys attractive for robotic applications where thermally activated devices are practical. Unfortunately, shape memory alloys are highly nonlinear, exhibiting a significant and complex hysteresis in their strain versus temperature characteristics. While models of this nonlinear characteristic have been developed, no attempt has been made to analyze the stability of a closed-loop feedback control system involving a shape memory actuator. Accordingly, the physical phenomena inherent in shape memory alloys are investigated along with their dynamic behavior. A new model for the nonlinear shape memory behavior is developed that overcomes some of the shortcomings of earlier models. Using this new model, the L2-stability of a simple position control system is proven. Experimental results are provided to confirm the model. The performance of other actuator configurations and control strategies is also examined. Author (CISTI)

N94-27305 Waterloo Univ. (Ontario). Dept. of Mechanical Engineering.
THE HIGH STRAIN RATE BEHAVIOUR OF TANTALUM M.S. Thesis
Daryl G. Beckenhauer 1993 172 p
(ISBN-0-315-84472-8; CTN-94-61071) Copyright Avail: Micromedia Ltd., Technical Information Centre, 240 Catherine Street, Suite 305, Ottawa, Ontario, K2P 2G8, Canada HC/MF

Using a miniature direct impact Hopkinson bar, the high strain rate deformation behavior of tantalum was determined. The effects of strain rate, grain size, cold working, pre-shocking, and alloying on the flow stress of tantalum were examined. A novel method of non-contact heating was developed for the Hopkinson bar specimens. The high strain rate flow stress behavior was then determined for tantalum and Ta-10W alloy at high temperatures. True stress-strain curves from these tests were compared to results from the literature and to constitutive equations developed. These comparisons support the validity of the test results but indicate that for tantalum and tantalum alloys, variations in the degree of previous cold working and material purity are extremely important considerations when using miniature specimens. Author (CISTI)

N94-27306 Waterloo Univ. (Ontario). Dept. of Mechanical Engineering.
MICROSTRUCTURE AND MECHANICAL BEHAVIOUR OF L1(2) TITANIUM TRIALUMINIDES Ph.D. Thesis
Maria Bozena Winnicka 1993 119 p
(ISBN-0-315-84488-4; CTN-94-61072) Copyright Avail: Micromedia Ltd., Technical Information Centre, 240 Catherine Street, Suite 305, Ottawa, Ontario, K2P 2G8, Canada HC/MF

Several intermetallic compounds Al-X-Ti (x = Cu, Fe, Mn, Cr) with the L1(2) crystal structure based on Al3Ti were studied to elucidate their mechanical behavior based on various microstructural parameters. The alloys were produced by double induction melting and subsequently homogenized in vacuum. The microstructure was determined using optical and electron microscopy and x-ray diffraction. Excellent agreement was found regarding alloy composition studied with the published ternary phase diagrams. The long range order parameter S was determined for the alloys studied based on the x-ray diffraction results. Mechanical tests included harness tests, compression tests at atmospheric pressure and various temperatures (liquid N2 to 900 C) and compression tests at room temperature and hydrostatic pressures ranging from 170 to 1,000 MPa. It was found that mechanical properties depend in a systematic way on the alloy Ti content and do not depend on the atomic number of the modifying element. The S parameter inversely depends on the amount of Ti in the alloys. Ashby's ductile to brittle transition theory was applied to explain the alloy behavior. No anomaly of yield strength with temperature was found, except for Cu-modified Al3Ti. A modified Stroh's model was proposed to describe the nucleation stage of microcracks. Author (CISTI)

N94-27325 Selskapet for Industriell og Teknisk Forskning, Trondheim (Norway). Div. of Metallurgy.
PROCESS MODELLING OF ALUMINIUM ALLOYS. MODELLING OF THE QUENCH SENSITIVITY OF ALLOY AA6082 Progress Report No. 2
D. H. Bratland, F. Tondel, and O. Grong 17 Jun. 1993 52 p See also PB93-170777 Sponsored by Hydro Aluminum A/S, Oslo, Norway
(PB94-124567; STF34-A93129) Avail: Issuing Activity (National Technical Information Service (NTIS))

In the present investigation a process model has been developed to describe the quench sensitivity of AA6082 extrusions. The model is based on well-established principles of thermodynamics, kinetic theory and simple dislocation mechanics, and allows calculation of the peak hardness following artificial aging for a wide range of cooling conditions. The results show that the peak hardness is both a function of the cooling rate through the critical temperature range for Beta'-Mg2Si precipitation and the intrinsic dispersoid density in the material, in agreement with general experience. NTIS

N94-27326 Selskapet for Industriell og Teknisk Forskning, Trondheim (Norway). Div. of Metallurgy.
SQUEEZE CASTING: A LITERATURE REVIEW
T. Rolland 3 Feb. 1993 58 p Sponsored by Norsk Hydro, Oslo, Norway
(PB94-124575; STF34-A93005) Avail: Issuing Activity (National Technical Information Service (NTIS))

The report gives a review of the process description, advantages of squeeze casting, process parameters, the effect of pressure, microstructure, mechanical properties, and structural defects in squeeze cast aluminum and magnesium alloys. NTIS

N94-27328 Selskapet for Industriell og Teknisk Forskning, Trondheim (Norway). Div. of Metallurgy.
COMPETENCE 2000: STUDY ON TRAINING REQUIREMENTS OF THE NORWEGIAN METALLURGICAL INDUSTRY
L. Kolbeinsen 21 Jun. 1993 24 p
(PB94-124609; STF34-A93134) Avail: Issuing Activity (National Technical Information Service (NTIS))

The report was presented at a seminar on training requirements in the metallurgical industries of Europe. The Norwegian metallurgical industry is atypical compared to most European countries, due to the abundant supply of hydroelectric power in the country, but also due to the fact that the industry is totally dependent on its ability to export its products. The study is based on a survey of the present state of the industry in combination with an unsophisticated analysis of future trends. NTIS

N94-27426*# National Aeronautics and Space Administration. Lewis Research Center, Cleveland, OH.
THERMOGRAVIMETRIC STUDY OF OXIDATION OF A PdCr ALLOY USED FOR HIGH-TEMPERATURE SENSORS
Darwin L. Boyd (Kent State Univ., OH.) and Mary V. Zeller Mar. 1994 10 p
(RTOP 505-62-50)
(NASA-TM-106473; E-8342; NAS 1.15:106473) Avail: CASI HC A02/MF A01

In this study, the oxidation of Pd-13 weight percent Cr, a candidate alloy for high-temperature strain gages, was investigated by thermogravimetry. Although the bulk alloy exhibits linear electrical resistivity versus temperature and stable resistivity at elevated temperatures, problems attributed to oxidation occur when this material is fabricated into strain gages. In this work, isothermal thermogravimetry (TG) was used to study the oxidation kinetics. Results indicate that the oxidation of Pd-13 weight percent Cr was approximately parabolic in time at 600 C but exhibited greater passivation from 700 to 900 C. At 1100 C, the oxidation rate again increased. Author (revised)

N94-27570# Pacific Northwest Lab., Richland, WA.
GRAIN BOUNDARY CHROMIUM CONCENTRATION EFFECTS ON THE IGSCC AND IASCC OF AUSTENITIC STAINLESS STEELS
S. M. Bruemmer, B. W. Arey, and L. A. Charlot Aug. 1993 17 p Presented at the 6th International Symposium on Environmental Degradation of Materials in Nuclear Power Systems: Water Reactors, San Diego, CA, 3-5 Aug. 1993
(Contract DE-AC06-76RL-01830)
(DE94-004268; PNL-SA-22941; CONF-930825-15) Avail: CASI HC A03/MF A01

Comparisons are made between grain boundary composition and intergranular stress corrosion cracking (IGSCC) of 304 and 309 austenitic stainless steels in high-temperature water environments. Chromium depletion had the dominant effect on cracking resistance with the extent of IG cracking controlled by the interfacial chromium concentration. The minimum chromium concentration required to promote cracking was a function of the applied strain rate during slow-strain-rate tensile tests in 288 C air-saturated water. Depletion from bulk levels of 18 weight percent to approximately 13.5 weight percent Cr at grain boundaries prompted 100 percent IG cracking at a strain rate of 1 x 10(exp -6)/s, while embrittlement was observed with only a slight depletion to approximately 17 weight percent at 2 x 10(exp -7)/s. Insights into critical interfacial compositions promoting IGSCC are discussed in reference to cracking of irradiated stainless steel nuclear reactor core components. DOE

N94-27616# Oak Ridge National Lab., TN.
CURRENT STATUS OF RESEARCH AND DEVELOPMENT ON NICKEL AND IRON ALUMINIDES
C. T. Liu, E. P. George, and C. G. McKamey 1993 13 p Presented at the 3rd International SAMPE Symposium on Intermetallics, Chiba, Japan, 7-10 Dec. 1993
(Contract DE-AC05-84OR-21400)
(DE94-004247; CONF-931239-1) Avail: CASI HC A03/MF A01

This paper provides a comprehensive review of current status of research and development on nickel and iron aluminides based on Ni3Al, NiAl, Fe3Al and FeAl. These aluminides possess attractive properties for elevated-temperature structural use; however, brittle fracture and poor fracture resistance have limited their use as engineering materials in many cases. In recent years, considerable effort has been devoted to the study of the brittle fracture behavior of these aluminides; as a result, both intrinsic and extrinsic factors governing brittle fracture have been identified. Surprisingly, moisture-induced hydrogen embrittlement has been recognized as one of the major causes of low ductility and brittle fracture in Ni3Al, Fe3Al and FeAl at ambient temperatures. These efforts have led to the development of ductile and strong aluminide alloys for structural applications. Industrial interest in these aluminide alloys is high, and several examples of industrial involvement are mentioned. DOE

N94-27619# California Univ., Berkeley. Lawrence Berkeley Lab.
RESEARCH INTO THE MICROSTRUCTURE AND MECHANICAL BEHAVIOR OF EUTECTIC Bi-Sn AND In-Sn
J. L. F. Goldstein, Z. Mei, and J. W. Morris, Jr. Aug. 1993 11 p Presented at the 8th International Electronic Materials and Processes Congress, San Jose, CA, 30 Aug. - 2 Sep. 1993
(Contract DE-AC03-76SF-00098)
(DE94-004558; LBL-34793; CONF-9308103-1) Avail: CASI HC A03/MF A01

This manuscript reports on research into two low-melting, lead-free solder alloys: eutectic Bi-Sn and eutectic In-Sn. The microstructures were found to depend on both cooling rate and substrate, with the greatest variability in the In-Sn alloy. The nature of the intermetallic layer formed at the solder-substrate interface depends on both the solder and the substrate (Cu versus Ni). Also, the microstructure of the Bi-Sn can recrystallize during deformation, which is not the case with In-Sn. Data from creep and constant strain rate tests are given for slowly cooled samples. The creep behavior of In-Sn is constant with temperature, but the creep seems to be controlled by the In-rich phase in In-Sn on Cu and by the Sn-rich phase in In-Sn on Ni. Bi-Sn exhibits different creep behavior at temperatures above 40 C than at 20 C or lower. Stress-strain curves of Bi-Sn on Cu and In-Sn on Cu are similar, while In-Sn on Ni behaves differently. This is explained in terms of the deformation patterns in the alloys. DOE

N94-27622# Pacific Northwest Lab., Richland, WA.
EFFECT OF PRECIPITATE STRUCTURE ON HOT DEFORMATION OF Al-Mg-Mn ALLOYS
J. S. Vetrano, C. A. Lavender, M. T. Smith, and S. M. Bruemmer Oct. 1993 13 p Presented at the Materials Week 1993, Pittsburgh, PA, 17-21 Oct. 1993

(Contract DE-AC06-76RL-01830)
(DE94-004596; PNL-SA-23016; CONF-9310224-2) Avail: CASI HC A03/MF A01

The size and nature of precipitates have strong effects on microstructural evolution from the cold-worked state through the course of deformation at high temperatures. Through selected heat treatments and minor alloying alterations, the precipitate structure of AA5083 has been manipulated. Minor additions of Zr have been used to create fine (50 to 100 nm) precipitates. The number and size distribution of medium-sized (less than 1 micron) Mn-rich precipitates were modified by increasing the Mn concentration in conjunction with several heat treatment paths. Effects of these precipitates on the dislocation structure, recrystallization behavior, and grain growth during high-temperature deformation have been elucidated. DOE

N94-27694# California Univ., Berkeley. Lawrence Berkeley Lab.
CRYOGENIC FRACTURE BEHAVIOR OF 316LN IN MAGNETIC FIELDS UP TO 14.6 T
J. W. Chan (California Univ., Berkeley.), D. Chu (California Univ., Berkeley.), C. Tseng (California Univ., Berkeley.), and J. W. Morris, Jr. (California Univ., Berkeley.) Jul. 1993 8 p Presented at the International Cryogenic Engineering Conference and International Cryogenic Materials Conference, Albuquerque, NM, 12-16 Jul. 1993
(Contract DE-AC03-76SF-00098)
(DE94-005215; LBL-34017; CONF-930703-40) Avail: CASI HC A02/MF A01

Some of the proposed magnet case alloys for the International Thermonuclear Experimental Reactor (ITER) are metastable austenitic stainless steels. The case will be subjected to high loads and can be as much as 100 mm thick. Case assembly will probably require thick section welding with its attendant chemical inhomogeneity. Even alloys that are thermally stable with respect to martensitic transformation can, under these conditions of high stresses, cryogenic temperature, and high magnetic fields, undergo transformation. Previous work at 8 T has shown a measurable magnetic field effect on the 4.2 K tensile and fracture toughness properties of AISI300 series metastable austenitic stainless steels. Thus, it is important to understand how these alloys will behave under conditions of high magnetic fields and cryogenic temperature, particularly at the higher magnetic fields that will be used in ITER. Data at 4.2 K for 316LN indicates that the change in fracture toughness is not monotonic. It initially decreases and then later increases with applied field. DOE

N94-27730# China Nuclear Information Centre, Beijing.
EXPERIMENT OF NEUTRON MULTIPLICATION IN BERYLLIUM
Jiang Wenmian (Southwestern Inst. of Physics, Sichuan, China.), Chen Yuan (Southwestern Inst. of Physics, Sichuan, China.), Chen Gang (Southwestern Inst. of Physics, Sichuan, China.), Liu Rong (Southwestern Inst. of Physics, Sichuan, China.), Guo Haiping (Southwestern Inst. of Physics, Sichuan, China.), Chen Wenjiang (Southwestern Inst. of Physics, Sichuan, China.), and Chen Jian (Southwestern Inst. of Physics, Sichuan, China.) Sep. 1992 15 p
(DE94-604605; CNIC-00687; SINPC-0002) Avail: CASI HC A03/MF A01 (US Sales Only)

Using the Total Absorption Method, the neutron multiplications in beryllium have been measured. A deionized water sphere with the radius of 75 cm and a polyethylene sphere with the radius of 69 cm were used as the total neutron absorbers. Neutron distributions in the spheres were measured using U-235 fission chambers. The relative and the efficiency-determined methods were compared. Important sources of experimental errors were analyzed in detail. Four groups of neutron multiplications in beryllium up to 14.85 cm thick for two total absorbers and two methods of measurement have been obtained and the agreement among them is satisfactory. Measured results have been compared with ANISN calculations. It is shown that the measured results are 3% to 14% and 1% to 7% lower than the calculations using ENDF/B-IV and ENDF/B-VI respectively. DOE

N94-27755# Sandia National Labs., Albuquerque, NM.
ISOTHERMAL CORROSION TESTING OF STEELS IN MOLTEN NITRATE SALTS
M. R. Prairie, S. R. Dunkin, J. M. Chavez, R. W. Bradshaw (Sandia National Labs., Livermore, CA.), and S. H. Goods (Sandia National Labs., Livermore, CA.) 1993 8 p Presented at the American Society of Mechanical Engineers (ASME) International Solar Energy Conference, San Francisco, CA, 27-30 Mar. 1994
(Contract DE-AC04-94AL-85000)
(DE94-004695; SAND-93-2334C; CONF-940326-5) Avail: CASI HC A02/MF A01

Tests were performed to evaluate the corrosivity of several nitrate salt mixtures on the containment materials likely to be used in a molten-salt solar central receiver power plant. The objective was to determine if common salt impurities (e.g., chloride) aggravate corrosion. The test was conducted for 7008 hours on A36 carbon steel at 320 C and 304 and 316 stainless steels at 570 C. Seven salt mixtures containing a variety of impurity concentrations were used. Corrosion rates were determined by descaled weight loss for coupons removed periodically from the melts. The nitrate mixtures were analyzed for changes in impurity levels and accumulation of soluble corrosion products. Test results indicate generally that corrosion is slow and that impurities do not contribute dramatically to corrosion rates of carbon and stainless steels. DOE

N94-27786# Pacific Northwest Lab., Richland, WA.
BENCH-SCALE SYNTHESIS OF NANOSCALE MATERIALS
M. F. Buehler, J. G. Darab, D. W. Matson, and J. C. Linehan Dec. 1993 10 p Presented at the NASA 2003 Conference, Anaheim, CA, 7 Dec. 1993
(Contract DE-AC06-76RL-01830)
(DE94-004787; PNL-SA-23284; CONF-931235-4) Avail: CASI HC A02/MF A01

A flow-through hydrothermal method used to synthesize nanoscale powders is introduced by Pacific Northwest Laboratory. The process, Rapid Thermal Decomposition of precursors in Solution (RTDS), combines high-pressure and high-temperature conditions to rapidly form nanoscale particles. The RTDS process was demonstrated on a laboratory scale and scaled up to accommodate production rates attractive to industry. The process is able to produce a wide variety of metal oxides and oxyhydroxides. The powders are characterized by scanning and transmission electron microscopic methods, surface-area measurements, and x-ray diffraction. Typical crystallite sizes are less than 20 nanometers, with BET surface areas ranging from 100 to 400 m(sup 2)/g. A description of the RTDS process is presented along with powder characterization results. In addition, data on the sintering of nanoscale ZrO2 produced by RTDS are included. DOE

N94-27788# Sandia National Labs., Albuquerque, NM.
AN ANODIC DISSOLUTION-BASED MECHANISM FOR THE RAPID CRACKING, PRE-EXPOSURE PHENOMENON DEMONSTRATED BY Al-Li-Cu ALLOYS
R. G. Buchheit, F. D. Wall (Virginia Univ., Charlottesville.), G. E. Stoner (Virginia Univ., Charlottesville.), and J. P. Moran (Aluminum Co. of America, Alcoa Center, PA.) 1993 17 p Presented at the Corrosion 1994: National Association of Corrosion Engineers (NACE) International Annual Conference, Baltimore, MD, 28 Feb. - 4 Mar. 1994
(Contract DE-AC04-94AL-85000)
(DE94-004798; SAND-93-1099C; CONF-940222-9) Avail: CASI HC A03/MF A01

Al-Li-Cu alloys were observed to fail in less than 24 hours after removal from a one week immersion in aerated 3.5 w/o NaCl solution. Anodic dissolution-based mechanisms proposed previously for this phenomenon were amended based on further experiment and characterization of the rapid cracking process. Amendments are based on studies of the relative electrochemical behavior of the microstructural elements in the subgrain boundary region, time to failure SCC testing in a simulated crack solution, evolution of crack potential and pH with time, fractographic examination of failed samples, and x ray diffraction of films passivating crack walls. Results suggest that an active path exists along subgrain boundaries that are comprised of the highly reactive T(sub 1) (Al2CuLi) precipitate phase and a solute depleted zone that does not readily passivate when exposed to the crack environment. The matrix phase does appear to passivate in the crack environment thereby confining the crack to the subgrain boundary region. This active path is enabled when cracks are isolated from a bulk environment, but is disabled otherwise. Potential and pH conditions required for cracking are discussed as is the formation of a hydrotalcite Li2(Al2(OH)6)2(center dot)CO3(center dot)3H2O film that appears to be responsible for passivating crack walls. DOE

N94-27792# Sandia National Labs., Livermore, CA.
PHASE STABILITY IN THE Cd-Mg SYSTEM
M. Asta, R. McCormack (California Univ., Berkeley. Lawrence Berkeley Lab.), and D. deFontaine (California Univ., Berkeley. Lawrence Berkeley Lab.) 1993 6 p Presented at the Fall Meeting of the Minerals, Metals and Materials Society: Physical Metallurgy and Materials, Pittsburgh, PA, 17-21 Oct. 1993
(Contracts DE-AC04-76DR-00789; DE-AC03-76SF-00098)
(DE94-004976; SAND-94-8475C; CONF-931009-17) Avail: CASI HC A02/MF A01

Results of a theoretical study of solid-state phase equilibria and short-range order in Cd-Mg alloys are reported. Results of first-principles linear muffin-tin orbital method total-energy calculations for seven hcp-based superstructures were combined with cluster-variation-method calculations of thermodynamic properties in order to compute the Cd-Mg phase diagram. Effect on the calculated phase diagram of contributions to the alloy free energy arising from atomic vibrations and structural relaxations are assessed using available experimental information for ordered and disordered alloys in the Cd-Mg system. DOE

N94-27795 National Aerospace Lab., Amsterdam (Netherlands). Structures and Materials Div.
FRACTURE TOUGHNESS AND CRACK RESISTANCE OF DAMAGE TOLERANT AND HIGH STRENGTH Al-Li ALLOYS
R. J. H. Wanhill, L. Schra, and W. G. J. tHart 4 Jul. 1991 11 p Presented at the 6th Aluminium-Lithium Conference, Garmisch-Partenkirchen, Germany, Oct. 1991 Limited Reproducibility: More than 20% of this document may be affected by microfiche quality
(NLR-TP-91249-U; ETN-94-95442) Avail: CASI HC A03

Aluminum lithium (Al-Li) alloy development is motivated by prospective weight savings owing to decreased density and increased stiffness compared with conventional alloys. From an engineering viewpoint, Al-Li alloy development may be considered successful if other properties are simply maintained. Fracture toughnesses and crack resistances of several damage tolerant and high strength Al-Li sheet alloys are compared with those of the conventional 2024-T3 and 7075-T6 alloys. The practical significance for aircraft structures is discussed. ESA

N94-27797 National Aerospace Lab., Amsterdam (Netherlands). Structures and Materials Div.
STATUS AND PROSPECTS FOR ALUMINIUM-LITHIUM ALLOYS IN AIRCRAFT STRUCTURES
R. J. H. Wanhill 6 May 1992 70 p Presented at the Specialists' Conference on Fatigue of Aircraft Materials, Oct. 1992 Sponsored by Netherlands Agency for Aerospace Programs, Delft Limited Reproducibility: More than 20% of this document may be affected by microfiche quality
(NLR-TP-92193-U; ETN-94-95447) Avail: CASI HC A04

The status and prospects for widespread application of Al-Li alloys in aircraft structures are examined. Particular attention is paid to the damage tolerance engineering properties of fatigue crack growth and fracture. At present the application of Al-Li alloys is very limited, because they are not direct replacements for conventional alloys and the basic material costs are usually too high. Widespread application of Al-Li alloys may well require a new generation of alloys, especially for primary structures. In the meantime, experience will be gained by selective application of the current generation of Al-Li alloys in secondary structures. ESA

N94-27803 Toronto Univ. (Ontario). Dept. of Metallurgy and Materials Science.
A TRANSMISSION ELECTRON MICROSCOPE STUDY OF Ni4W PRECIPITATES IN A Ni-37 WT. PERCENT W ALLOY Ph.D. Thesis
Haixiong Zhao Jul. 1990 199 p
(ISBN-0-315-59932-4; CTN-94-60995) Copyright Avail: Micromedia Ltd., Technical Information Centre, 240 Catherine Street, Suite 305, Ottawa, Ontario, K2P 2G8, Canada HC/MF

The morphology and interfacial structure of the Ni4W body-centered phase in a Ni-W alloy were studied by transmission electron microscopy. A lath-shaped Ni4W precipitate and a multivariant domain (MVD) composite particle composed of laths of perpendicular structural variants of the Ni4W phase were observed in the Ni face centered cubic matrix. In a lath-shaped particle, a single set of shear loops was found at the (100) side plane. Sets of interfacial ledges, lying parallel to the lath axis and with different 011-type Burgers vectors, were identified at the habit plane. At the MVD/matrix interface, which corresponded to the (100) plane of the laths, screw dislocations as well as strong diffraction contrast oscillation were observed. Two sets of shear loops lying in the (0,-1,1) perpendicular twin boundaries of the MVD with alternating anti-parallel Burgers vectors in the 011 direction were observed. These accommodate the alternating shear strain resulting from the alternating arrangement of perpendicular twins in the MVD. The displacement field associated with such screw dislocation arrays was evaluated. The results indicate that the minimization and accommodation of the transformation strain determined both the morphology and related interface structure of the Ni4W phase. Author (CISTI)

N94-27807 Japan Atomic Energy Research Inst., Tokyo.
CREEP RUPTURE PROPERTIES OF A NICKEL-BASE HEAT-RESISTANT ALLOY HASTELLOY XR UNDER VARYING TEMPERATURE/STRESS CONDITION
Hirokazu Tsuji (Japan Atomic Energy Research Inst., Tokai.), Hajime Nakajima (Japan Atomic Energy Research Inst., Tokai.), Tatsuhiko Tanabe, and Yuji Nakasone May 1993 29 p In JAPANESE Limited Reproducibility: More than 20% of this document may be affected by microfiche quality
(DE94-701175; JAERI-M-93-105) Avail: CASI HC A03 (US Sales Only)

A series of constant temperature and load creep rupture tests and varying temperature and/or load creep rupture tests was carried out on a nickel-base heat-resistant alloy Hastelloy XR, which was developed for applications in the High-Temperature Engineering Test Reactor, at 850 to 1000 C in the simulated HTGR helium gas. This report describes the applicability of the conventional creep damage rules, i.e., the life fraction, the strain fraction and their mixed rules, to the alloy. The applicability was examined using the data under varying both temperature and load conditions as well as those, which were obtained in the previous work, under constant temperature and varying load conditions. The life fraction rule showed the best applicability of these three criteria. The good applicability of the rule was considered to show that the change of the chemical composition and/or the microstructure during exposure to the high-temperature simulated HTGR helium environment was not appreciable to affect the creep strength of Hastelloy XR. Though the life fraction rule under varying both temperature and load conditions is slightly less applicable than that under constant temperature and varying load conditions, it has been concluded that the rule is applicable in engineering design of high-temperature components made of Hastelloy XR. DOE

N94-27829# Comision Nacional de Energia Atomica, Buenos Aires (Argentina).
HYDROTHERMAL GROWTH AND CHARACTERIZATION OF OXIDES IN ZIRCONIUM ALLOYS
M. Villegas, A. M. Olmedo, R. A. A. Bordoni, M. A. Blesa, G. Rigotti, and A. J. G. Maroto 1993 2 p Presented at the 8th Argentine Congress on Physico-Chemistry, Mar del Plata, Argentina, 19-22 Apr. 1993
(DE94-602981; INIS-AR-039; CONF-9304214) Avail: CASI HC A01/MF A01 (US Sales Only)

The morphological and microstructural characterization of hydrothermally grown oxides is required to predict long term alloy corrosion behavior. Gere, two Zirconium alloys are compared: Zry-4 and Zr-2.5% Nb, both used for fuel elements and in-core structural components in water cooled nuclear reactors. Long term experiments were performed in autoclaves without recirculation, with high pressure steam at 435 C, and in on-line autoclaves in Embalse Nuclear Power Plant, under primary circuit chemistry. The oxides were characterized at different growth stages. The possible growth mechanisms are discussed. Derived from text

N94-27832# Comision Nacional de Energia Atomica, Buenos Aires (Argentina).
EFFECT OF DIFFERENT IONS ON THE ANODIC BEHAVIOUR OF ALLOY 800 IN CHLORIDE SOLUTIONS AT HIGH TEMPERATURE
C. J. Lafont and M. G. Alvarez 1993 3 p Presented at the SAM 1993: 17th Metallurgical Sessions of the Argentine Metals Association; 2nd Argentine Meeting on Ceramics and Refractories, San Carlos de Bariloche, Argentina, 13-16 Apr. 1993
(DE94-602982; INIS-AR-042; CONF-9304174) Avail: CASI HC A01/MF A01 (US Sales Only)

The anodic behavior and passivity breakdown of alloy 800 in sodium bicarbonate and sodium phosphate aqueous solutions was studied in the temperature range from 100 C to 280 C by means of electrochemical techniques. The effect of phosphate or bicarbonate additions on the pitting susceptibility and pitting morphology of the alloy in chloride solutions was also examined. The composition of the tested material was: 19.55% Cr; 30.80% Ni; 0.064% C; 0.75% Mn; 0.37% Si; 0.29% Ti; 0.09% Cu; 0.002% S; 0.013% P; 0.27% Al; 0.07% Co; bal. Fe. The results showed that the presence of bicarbonate or phosphate ions increases the pitting potential of alloy 800 in chloride solutions. Changes in pitting morphology were found in phosphate containing solutions, while the pits found in bicarbonate containing solutions were similar to those formed in pure chloride solutions. DOE

N94-27876# Japan Atomic Energy Research Inst., Tokyo.
ION-DRIVEN PERMEATION OF DEUTERIUM IN METALS
Wei-Min Shu (Kyushu Univ., Fukuoka, Japan.), Yasunori Hayashi (Kyushu Univ., Fukuoka, Japan.), and Kenji Okuno (Japan Atomic Energy Research Inst., Naka.) Mar. 1993 68 p
(DE94-701104; JAERI-M-93-043) Avail: CASI HC A04/MF A01

A general model of ion-driven permeation of hydrogen isotopes at steady state is presented. In this model, new transport parameters, which not only have clear physical meanings but also contain the implanted range, are developed to distinguish the regime of ion-driven permeation at steady state. The model shows that the transport regime of ion-driven permeation depends on the incident ion flux, the thickness of membrane, the implanted range, diffusion coefficients, and recombination coefficients on both sides of the membrane. The permeation behavior of deuterium implanted into pure iron, Fe-Ti alloys, and pure molybdenum are investigated. The permeation spike, permeation regime, and the effect of the incident ion energy on permeation rate are discussed. DOE

N94-27950 British Columbia Univ., Vancouver. Dept. of Metals and Materials Engineering.
THE TRANSITION FROM STRESS CORROSION CRACKING TO CORROSION FATIGUE IN AA-7075 AND AA-8090 Ph.D. Thesis
Johann Rechberger Sep. 1989 214 p
(ISBN-0-315-59526-4; CTN-94-61005) Copyright Avail: Micromedia Ltd., Technical Information Centre, 240 Catherine Street, Suite 305, Ottawa, Ontario, K2P 2G8, Canada HC/MF

The transition between stress corrosion cracking (SCC) and corrosion fatigue (CF) was investigated in two high-strength aluminum alloys, the well established Al-Zn-Mg-Cu alloy AA-7075 and the new generation Al-Li-Cu-Mg alloy 8090. The effect of crack tip strain rate (CTSR) on environmentally assisted cracking was studied in the artificially aged condition using fatigue precracked double cantilever beam specimens, with the crack plane parallel to the rolling plane, under monotonic and cyclic loading. At low K-rates (average change in stress intensity over time), real-time crack velocities under monotonic slow or constant load conditions were comparable to crack velocities obtained with cyclic loading experiments. As K-rate increased, real-time crack velocities decreased due to plasticity induced crack growth retardation effects and decrease in crack tip film rupture. With alloy 7075, a crack tunnelling mechanism was found to overcome this crack growth retardation. Alloy 8090 exhibited high resistance to SCC. It is concluded that transition from intergranular SCC to intergranular CF occurs at a critical K-rate. Below this rate, crack velocities are not increased by cyclic loading; instead, crack growth retardation effects can result in lower real-time crack velocities than those typical for constant load tests at comparable stress intensities but much lower K-rates. Author (CISTI)

N94-27961 McMaster Univ., Hamilton (Ontario). School of Graduate Studies.
LOW STRAIN BEHAVIOUR OF A PARTICULATE REINFORCED ALUMINUM ALLOY Ph.D. Thesis
Stephen Corbin 1992 292 p
(ISBN-0-315-84906-1; CTN-94-61107) Copyright Avail: Micromedia Ltd., Technical Information Centre, 240 Catherine Street, Suite 305, Ottawa, Ontario, K2P 2G8, Canada HC/MF

An investigation was conducted on the strengthening that arises when an Al alloy is reinforced with approximately equiaxial SiC particles. The results indicate that most of the strengthening derived from the particles develops at low strains, mainly due to the high strain hardening rate during onset of plastic flow. Examination of the Bauschinger effect in the composites indicates that an internal stress develops rapidly in the low strain regime. Microstructural observations suggest that the nature of this flow is influenced by the SiC particle distribution. Initial plasticity appears to be associated with relatively particle-free regions of the microstructure. A self consistent model is developed for calculating the stress partitioning that occurs between the Al matrix and the SiC particles during the elastic/plastic transition and beyond. Excellent quantitative agreement between the experimentally measured elastic modulus and the model prediction was achieved. The influence of particle distribution was examined by representing the composite microstructure as a bimodal mixture consisting of a particle-rich and a particle-free phase. Like the self consistent model, this model also predicts an increase in the initial strain hardening rate. Unlike in the other model, the magnitude of that rate is comparable to experimental measurements. Author (CISTI)

N94-28158# Tohoku Univ., Sendai (Japan). Inst. for Materials Research.
THE SCIENCE REPORTS OF THE RESEARCH INSTITUTES, TOHOKU UNIVERSITY. SERIES A: PHYSICS, CHEMISTRY, AND METALLURGY. VOLUME 38, NO. 1: AMORPHOUS MATERIALS 14
29 Mar. 1993 167 p
(JTN-94-80610) Avail: CASI HC A08/MF A02

The following topics were discussed: energy dispersive x ray diffraction apparatus, liquid phases, differential scanning calorimeter, multilayered thin films, Nuclear Magnetic Resonance (NMR), spectral analysis, quasi-crystal structure, amorphous alloys, crystallization, amorphization, corrosion resistance, magnetron sputtering, oxidation, oxygen reduction, hydrogenation, electrocatalytic oxidation, electrodes, methane formation, stress relaxation, embrittlement, glassy structure, glass transition, phase transformation, flaking, atomization, metallic mold casting, mechanical properties, nanoscale icosahedral particle, crystal growth, crystal lattices, bismuth germanate, and alloys. For individual titles, see N94-28159 through N94-28171.

N94-28159# Tohoku Univ., Sendai (Japan). Inst. for Advanced Materials Processing.
ENERGY DISPERSIVE X RAY DIFFRACTION (EDXD) APPARATUS FOR LIQUIDS AT HIGH TEMPERATURE c25
Kazumasa Sugiyama, Valery G. Petkov (Research Development Corp. of Japan, Tokyo.), Susumu Takeda (Research Development Corp. of Japan, Tokyo.), and Yoshio Waseda *In its* The Science Reports of the Research Institutes, Tohoku University. Series A: Physics, Chemistry, and Metallurgy. Volume 38, No. 1: Amorphous Materials 14 29 Mar. 1993 p 1-13
(For primary document see N94-28158 07-26)
Avail: CASI HC A03/MF A02

A high temperature Energy Dispersive X-ray Diffraction (EDXD) apparatus was built using a vertical type goniometer, which makes it possible to measure the diffraction profiles of liquids up to 1,873 K. The fundamentals of this apparatus were tested by obtaining the interference function of a SiO2 glass over Q = 200 nm(exp -1) at room temperature. The feasibility of this EDXD apparatus for high temperature liquids was confirmed by structural study of liquid bismuth germanate (Bi4Ge3O12) at 1,373 K. Author (NASDA)

N94-28160# Tohoku Univ., Sendai (Japan). Inst. for Advanced Materials Processing.
STRUCTURAL STUDY OF Cu/Co MULTILAYER BY ANOMALOUS SMALL-ANGLE X RAY SCATTERING c76
Eiichiro Matsubara and Yoshio Waseda *In its* The Science Reports of the Research Institutes, Tohoku University. Series A: Physics, Chemistry, and Metallurgy. Volume 38, No. 1: Amorphous Materials 14 29 Mar. 1993 p 14-23 (For primary document see N94-28158 07-26)
Avail: CASI HC A02/MF A02

The diffraction peaks in the small-angle region due to a long period of a Cu/Co multilayer were observed with the anomalous small-angle X-ray scattering in reflection geometry. These peaks appear to be enhanced because of a large negative value of the real part of the anomalous dispersion term of Co just below the Co K-absorption edge. By comparing the relative integrated intensities of these peaks with the theoretical values calculated from a trapezoidal concentration model, the concentration profile along the surface normal in this multilayer has been determined. Author (NASDA)

N94-28161# Tohoku Univ., Sendai (Japan). Inst. for Materials Research.
DIFFERENTIAL SCANNING CALORIMETRIC STUDY OF SOLID STATE AMORPHIZATION AND CRYSTALLIZATION IN Zr/Co AND Zr/Ni MULTILAYERS **c76**
Tomoyasu Aihara, Jr., Kiyoshi Aoki, and Tsuyoshi Masumoto *In its* The Science Reports of the Research Institutes, Tohoku University. Series A: Physics, Chemistry, and Metallurgy. Volume 38, No. 1: Amorphous Materials 14 29 Mar. 1993 p 24-33 (For primary document see N94-28158 07-26)
Avail: CASI HC A02/MF A02

The processes of Solid State Amorphization (SSA) and subsequent crystallization in Zr/Co and Zr/Ni multilayered thin films have been studied by Differential Scanning Calorimetry (DSC). The thermodynamic values, i.e., the enthalpy change delta H(sub a) and the activation energy E(sub a) for amorphization as well as the enthalpy change delta H(sub x) and the activation energy E(sub x) for crystallization, were evaluated from the DSC experiments. These values were compared with those of the corresponding rapidly quenched amorphous alloys. The activation energies E(sub a), calculated by the modified Ozawa method, are 150 and 132 kJmol(exp -1) for Zr/Co and Zr/Ni multilayers respectively. These values are equivalent to the previously reported activation energy of diffusion of Co or Ni in the rapidly quenched amorphous Zr-Co or Zr-Ni alloys. Author (NASDA)

N94-28162# Tohoku Univ., Sendai (Japan). Inst. for Materials Research.
NMR STUDY OF QUASICRYSTAL Al(70)Pd(20)T(M10) ALLOY (T(M):Cr, Mn, Fe, AND Co) **c76**
Takeshi Shinohara and Takashi Sato *In its* The Science Reports of the Research Institutes, Tohoku University. Series A: Physics, Chemistry, and Metallurgy. Volume 38, No. 1: Amorphous Materials 14 29 Mar. 1993 p 34-42 (For primary document see N94-28158 07-26)
Avail: CASI HC A02/MF A02

Nuclear Magnetic Resonance (Al-27, Mn-55, and Co-59) measurements have been made on quasicrystalline phases of the Al70Pd20T(sub M)10 alloy (T(sub M): Cr, Mn, Fe and Co) in the temperature range between 5 K and room temperature. There is no marked temperature dependence in peak shift and line width of either the Al-27 or Co-59 NMR spectra, except for the Al-27 and Mn-55 spectra in the Al70Pd20Mn10. However, the peak shift of these spectra depends upon the constituent transition element. For the Al70Pd20Mn10, the negative Al-27 Knight shift and line broadening at low temperatures indicate that there exist two classes of Mn atoms, magnetic and nonmagnetic ones. Author (NASDA)

N94-28163# Tohoku Univ., Sendai (Japan). Inst. for Materials Research.
FORMATION AND CRYSTALLIZATION OF HYDROGEN-INDUCED AMORPHOUS Ti3InH(4.5) ALLOY **c76**
Katsuhiko Mori, Kiyoshi Aoki, and Tsuyoshi Masumoto *In its* The Science Reports of the Research Institutes, Tohoku University. Series A: Physics, Chemistry, and Metallurgy. Volume 38, No. 1: Amorphous Materials 14 29 Mar. 1993 p 43-52 (For primary document see N94-28158 07-26)
Avail: CASI HC A02/MF A02

Structural changes of a titanium compound Ti3In with the D0(19) structure caused by hydrogenation have been investigated by X-Ray Diffraction (XRD) and transmission electron microscopy. Crystallization and hydrogen desorption behavior of the hydrogen-induced amorphous alloy have been studied by differential scanning calorimetry, XRD, and hydrogen analysis. On hydrogenation of the Ti3In compound, an amorphous single phase a-Ti3InH(4.5) is formed below about 350 K where the c-Ti3InHx phase having the bcc (body centered cubic) structure is formed. Hydrogen absorption of Ti3In occurs between 32 and 36 ks drastically which gives rise to non-solid solution type amorphization at 300 K. The a-Ti3InH(4.5) crystallizes to fcc (face centered cubic) type c-Ti3InH(4.5) above 484 K. Hydrogen is desorbed from the crystalline phase above the crystallization temperature. Author (NASDA)

N94-28164# Tohoku Univ., Sendai (Japan). Inst. for Materials Research.
THE CORROSION BEHAVIOR OF SPUTTER-DEPOSITED MAGNESIUM-VALVE METAL ALLOYS
Eiichi Hirota, Hiroki Habazaki, Asahi Kawashima, Katsuhiko Asami, and Koji Hashimoto *In its* The Science Reports of the Research Institutes, Tohoku University. Series A: Physics, Chemistry, and Metallurgy. Volume 38, No. 1: Amorphous Materials 14 29 Mar. 1993 p 53-62 (For primary document see N94-28158 07-26)
Avail: CASI HC A02/MF A02

An attempt was made for preparation of magnesium alloys with valve metals, such as titanium, zirconium, niobium, and tantalum whose melting point far exceed the boiling point of magnesium. These alloys became single phase solid solutions in wide composition ranges but were crystalline in contrast to the fact that other alloys with valve metals such as nickel-, copper-, and aluminum-base alloys were amorphous in wide composition ranges. The alloys containing sufficient amounts of valve metals showed high corrosion resistance due to spontaneous passivation in 1 M HCl at 30 C. The high corrosion resistance was attributed to the formation of passive oxyhydroxide films in which valve metal cations were remarkably concentrated. However, because of crystalline alloys and because of the presence of active magnesium, their corrosion resistance is lower than that of valve metals. Author (NASDA)

N94-28165# Tohoku Univ., Sendai (Japan). Inst. for Materials Research.
THE ELECTROCATALYTIC OXIDATION OF ETHYLENE AND METHANE, AND REDUCTION OF OXYGEN ON GAS-DIFFUSION ELECTRODES MADE OF AMORPHOUS NICKEL-VALVE METAL-PLATINUM GROUP METAL ALLOYS **c25**
Toshiaki Shimada (Nippon Mining Co. Ltd., Kitaibaraki, Japan.), Asahi Kawashima, Hiroki Habazaki, Katsuhiko Asami, and Koji Hashimoto *In its* The Science Reports of the Research Institutes, Tohoku University. Series A: Physics, Chemistry, and Metallurgy. Volume 38, No. 1: Amorphous Materials 14 29 Mar. 1993 p 63-75 (For primary document see N94-28158 07-26)
Avail: CASI HC A03/MF A02

Exploratory work has been done on the performance of electrocatalytic reduction of oxygen and anodic oxidation of ethylene and methane on the gas-diffusion electrodes prepared from amorphous alloys containing one atomic percent platinum group elements. Gas-diffusion electrodes were made by coating the mixture of catalysts prepared by immersion in 46 percent HF from melt-spun ribbon shaped amorphous alloys, carbon black, poly tetra fluoro ethylene and sugar, and subsequent baking in nitrogen gas. The electrode made of catalyst prepared from amorphous nickel-niobium alloy containing platinum and ruthenium was the most active for electrocatalytic reduction of oxygen. For electro-oxidation of ethylene and methane, amorphous nickel-valve metal alloy containing only platinum possesses higher activity in comparison to the electrode made of platinum black powder. Author (NASDA)

N94-28166# Tohoku Univ., Sendai (Japan). Inst. for Materials Research.
CO2 METHANATION CATALYSTS PREPARED FROM AMORPHOUS NI-VALVE METAL ALLOYS CONTAINING PLATINUM GROUP ELEMENTS
Kenichiro Wakuda, Hiroki Habazaki, Asahi Kawashima, Katsuhiko Asami, and Koji Hashimoto *In its* The Science Reports of the Research Institutes, Tohoku University. Series A: Physics, Chemistry, and Metallurgy. Volume 38, No. 1: Amorphous Materials 14 29 Mar. 1993 p 76-87 (For primary document see N94-28158 07-26)
Avail: CASI HC A03/MF A02

The amorphous Ni-valve metal (Ti, Zr, Nb, and Ta) alloys containing a few at percent of platinum group elements were activated by immersion into hydrofluoric acid and used for hydrogenation of carbon dioxide at 100 to 300 C. This surface activation led to formation of nanocrystalline surface alloys with high surface area, and to surface enrichment of platinum group elements on the titanium, niobium, and tantalum-containing alloys, but not on the zirconium-containing alloys. The surface of the latter alloys was mainly composed of nickel. The activity and selectivity for methane formation on the titanium, niobium, and tantalum-containing alloys were significantly affected by the difference in the platinum group elements; the ruthenium and rhodium-containing alloys showed higher activity and selectivity for methane formation while the platinum-containing alloys exhibited the lowest activity for methane formation and produced mainly carbon monoxide. The zirconium-containing alloys showed the one order of magnitude higher activity for methanation of carbon dioxide in comparison with the titanium, niobium, and tantalum-containing alloys and produced exclusively methane independent of platinum group elements contained. The alloying with zirconium seems very important to prepare the alloy catalysts having the extremely high activity. Author (NASDA)

N94-28167# Tohoku Univ., Sendai (Japan). Inst. for Materials Research.
MECHANICAL BEHAVIOR OF AMORPHOUS ALLOYS AT ELEVATED TEMPERATURES
Hiroshi Okumura, Akihisa Inoue, and Tsuyoshi Masumoto *In its* The Science Reports of the Research Institutes, Tohoku University. Series A: Physics, Chemistry, and Metallurgy. Volume 38, No. 1: Amorphous Materials 14 29 Mar. 1993 p 88-98 (For primary document see N94-28158 07-26)
Avail: CASI HC A03/MF A02

Mechanical behavior of amorphous alloys has been investigated through the static and dynamic mechanical measurements. Two stress relaxation systems are observed in the dynamic measurements; the sub-T(sub g) relaxation and the T(sub g) relaxation. These relaxations seem to cause the change in the deformation mode from inhomogeneous to homogeneous deformation which is seen in the static stress-strain curves. The stress relaxation systems also correlate to the ductility of amorphous alloys. The decrease in the stress relaxation resulting from the lack of the sub-T(sub g) relaxation causes embrittlement. Author (NASDA)

N94-28168# Tohoku Univ., Sendai (Japan). Inst. for Materials Research.
FORMATION OF GLASSY Pd-Ni-P ALLOYS BY MECHANICAL ALLOYING AND THEIR STRUCTURE AND THERMAL STABILITY
Akihisa Inoue, Kensuke Matsuki, and Tsuyoshi Masumoto *In its* The Science Reports of the Research Institutes, Tohoku University. Series A: Physics, Chemistry, and Metallurgy. Volume 38, No. 1: Amorphous Materials 14 29 Mar. 1993 p 99-111 (For primary document see N94-28158 07-26)
Avail: CASI HC A03/MF A02

This report reviews the recent research on whether or not the application of mechanical alloying to metallic alloys causes a glassy structure defined by the distinct appearance of glass transition and supercooled liquid region before crystallization. The amorphous phase in Pd48Ni32P20 alloy produced by mechanical alloying of a pre-alloyed ingot consisting of Pd5P2 and Ni3P phases was found to exhibit distinct glass transition, followed by the appearance of a wide supercooled liquid region and then crystallization. Based on these data, it has been concluded that the mechanical alloying method is useful for the formation of glassy metallic materials, in addition to the preparation of amorphous materials without glass transition and nonequilibrium crystalline phases. Author (NASDA)

N94-28169# Tohoku Univ., Sendai (Japan). Inst. for Materials Research.
STUDY ON THE PRODUCTION OF FLAKY AMORPHOUS ALLOY POWDERS BY IMPACT FLATTENING OF ATOMIZED LIQUID DROPLETS ON A RAPIDLY ROTATING WHEEL
Akihisa Inoue, Masahiro Oguchi (Teikoku Piston Ring Co. Ltd., Okaya, Japan.), and Tsuyoshi Masumoto *In its* The Science Reports of the Research Institutes, Tohoku University. Series A: Physics, Chemistry, and Metallurgy. Volume 38, No. 1: Amorphous Materials 14 29 Mar. 1993 p 112-128 (For primary document see N94-28158 07-26)
Avail: CASI HC A03/MF A02

A two-stage quenching technique consisting of impact flattening of atomized supercooled liquid droplets caused the production of flaky amorphous powders with a thickness of 1 to 3 micrometers and an aspect ratio of 20 to 300 in Co-, Fe-, and Al-based systems. The flaky powders consist of an amorphous phase over the entire particle size range even in the alloy systems where no amorphous phase is formed in the particle size below 25 micrometers by high-pressure gas atomization. The improvement of the production ratio of the amorphous powders is due to the following three factors: the second-stage cooling of supercooled liquid droplets, the reduction of powder thickness to 1 to 3 micrometers, and the high thermal conductive stage between rotator and powder resulting from the high-energy collision. The flaky powders also have a smooth surface and edge combined with a uniform thickness, leading to good luster, high reflection ratio against light, high corrosion resistance, high mechanical strength, and anisotropic magnetic properties. Furthermore, the unique morphology causes a high laminating tendency in a resin. By utilizing these advantages, the flaky amorphous powders are expected to be used as magnetic filler and corrosion-resistant coating materials. Author (NASDA)

N94-28170# Tohoku Univ., Sendai (Japan). Inst. for Materials Research.
PRODUCTION OF AN AMORPHOUS Fe(75)Si(10)B(15) SHEET BY A METALLIC MOLD CASTING METHOD AND ITS PROPERTIES
Akihisa Inoue, Hirokazu Yamamoto (Unikita Ltd., Uji, japan.), Takanobu Saito (Daido Steel Co. Ltd., Nagoya, Japan.), and Tsuyoshi Masumoto *In its* The Science Reports of the Research Institutes, Tohoku University. Series A: Physics, Chemistry, and Metallurgy. Volume 38, No. 1: Amorphous Materials 14 29 Mar. 1993 p 129-137 (For primary document see N94-28158 07-26)
Avail: CASI HC A02/MF A02

The application of a metallic mold casting method to an Fe75Si10B15 alloy with the largest glass-forming ability in (Fe, Co, Ni) -Si-B system was found to cause the formation of a mostly single amorphous phase in a sheet form with a thickness of 0.1 mm. No distinct difference in thermal stability (crystallization temperature and heat of crystallization), hardness, Curie temperature, and magnetization is detected between the as-cast sheet and the melt-spun amorphous ribbon with a thickness of 0.02 mm. On the other hand, bending ductility, heat of relaxation, delta H(sub r), and coercivity, H(sub c), which can be regarded as structure sensitive properties, are significantly different from those for the amorphous ribbon. That is, the sheet sample fractures during bending deformation and has a smaller delta H(sub r) and a larger H(sub c). The difference is induced presumably because the sheet sample has a more relaxed atomic configuration on a short-range scale as compared with that for the amorphous ribbon sample. Author (NASDA)

N94-28171# Tohoku Univ., Sendai (Japan). Inst. for Materials Research.
FORMATION AND HIGH MECHANICAL STRENGTH OF Al-BASED ALLOYS CONTAINING A NANOSCALE ICOSAHEDRAL PHASE AS A MAIN CONSTITUENT
Akihisa Inoue, Mitsuru Watanabe (Akita Univ., Japan.), Hisamichi Kimura, and Tsuyoshi Masumoto *In its* The Science Reports of the Research Institutes, Tohoku University. Series A: Physics, Chemistry, and Metallurgy. Volume 38, No. 1: Amorphous Materials 14 29 Mar. 1993 p 138-160 (For primary document see N94-28158 07-26)
Avail: CASI HC A03/MF A02

This report reviews recent results on the achievement of high tensile strength and good ductility for rapidly solidified Al-Mn-Ln and Al-Cr-Ln (Ln = lanthanide metal) alloys containing an icosahedral phase as a main constituent phase. The good mechanical properties are attributed to the simultaneous achievement of the following three structural effects resulting from rapid solidification and appropriate alloy design: the formation of a mixed structure consisting of nanoscale icosahedral particles surrounded by Al phase; the formation of the icosahedral phase at low solute concentrations; and the achievement of an ultra-fine mixed state of icosahedral and approximant regions caused by the phase strain-induced approximant transition in the nanoscale icosahedral particles. The utilization of the structural effects is expected to cause high mechanical strengths combined with good ductility for other quasicrystalline alloys. Author (NASDA)

N94-28185# Aerospace Corp., El Segundo, CA. Engineering and Technology Group.
PHOTOELECTRON SPECTROSCOPIC STUDIES OF THE ELECTRONIC STRUCTURE AND BONDING IN TiC AND TiN
S. V. Didziulis, J. R. Lince, T. B. Stewart, and E. Eklund (International Business Machines Corp., Armonk, NY.) 30 Sep. 1993 41 p
(Contract F04701-88-C-0089)
(ATR-93(8361)-2) Avail: CASI HC A03/MF A01

Titanium carbide (TiC) and nitride (TiN) possess remarkable physical properties, such as extremely high hardness and melting point, that promote their use as anti-wear materials under harsh tribological conditions. These physical properties must arise from chemical bonding phenomena that result from the inclusion of the non-metal atom within the metallic matrix, and these bonding phenomena should be apparent in measurements of the valence-band electronic structures TiC and TiN. The surface electronic structure and bonding in TiC(100) and TiN (110) with core and valence level photoelectron spectroscopies (PES) using x rays (1486.6 eV) and synchrotron radiation in the range of 28 to 180 eV were explored. Intensity changes in the valence-band features are followed as a function of incident photon energy; these changes are then compared to theoretical atomic photoionization cross sections to determine the atomic origins of these features. Resonant PES at the Ti 3p absorption edge is used to determine titanium 3d contributions to the valence band and to show differences in the electronic structures in TiC and TiN. A new resonance phenomenon near the Ti 3s edge in TiC was observed, and its possible assignment is discussed. The electronic structure and bonding in these materials is well described by molecular orbital theory, where the Ti and non-metal ions in their formal oxidation states (e.g., Ti(4+) and C(4-) in TiC) undergo covalent bonding interactions. Overall, the PES results indicate greater covalent mixing for TiC as compared to TiN, consistent with the differences in the electronegativities of the atoms. Specifically, stronger covalent interactions between the C 2s, 2p and the Ti 3d, 4s, and 4p levels must occur to explain the spectroscopic differences between TiC and TiN. In addition, there is no evidence for an occupied TiC valence level having predominantly Ti character (unlike TiN), precluding the existence of direct Ti-Ti bonding in TiC. Any such orbital overlap is significantly affected by the carbon atoms in the lattice. Author (revised)

N94-28187 Department of the Navy, Washington, DC.
METHOD OF BONDING MOLYBDENUM TO STEEL Patent
William A. Ferrando, inventor (to Navy), Subhash D. Karmarkar, inventor (to Navy), Scott M. Hoover, inventor (to Navy), and Amarnath P. Divecha, inventor (to Navy) 19 Oct. 1993 4 p Filed 21 Jul. 1992 Supersedes AD-D015410
(AD-D016079; US-Patent-5,253,797; US-Patent-Appl-SN-916428; US-Patent-Class-228-194) Avail: US Patent and Trademark Office

A thin layer of silver metal is formed between a molybdenum surface and a steel surface. The silver metal layer is diffusion bonded to the molybdenum surface and diffusion bonded to the steel surface, thus bonding the molybdenum and steel surfaces together. DTIC

N94-28212# Army Research Lab., Watertown, MA.
MECHANICAL PROPERTIES AND MICROSTRUCTURE OF THERMOMECHANICALLY PROCESSED, HIGH MANGANESE STEEL Final Report
J. F. Chinella Aug. 1993 16 p Repr. from High Manganese, High Nitrogen Austenitic Steels (Metals Park, OH, ASM International) 1993 p 143-153
(ARL-TR-146) Avail: CASI HC A03/MF A01

Thermomechanical treatments (TMT's) were performed on an austenitic Fe-12.5Mn-2.0Mo-1.15C Hadfield steel to achieve a material with high strength and resistance to plastic instability. Mechanical properties were evaluated by tensile deformation; microstructures and deformation modes were evaluated by optical or electron microscopy. Solution treated 16-18 Rockwell C hardness (HRC) material was warm rolled to a hardness of 39-53 HRC. During tensile deformation, strain hardening occurred with increasing loads and high uniform elongations to ultimate strengths equivalent to 56-57 HRC. Microstructures and deformation modes resemble those attributed to austenitic steels and other face centered cubic alloys with low to moderate stacking fault energy. Deformation was localized within grains in a orientation dependent crystallographic manner, often concentrated within bands consisting of slip and twinning. Substructures and microcracks were often restrained to grain size scale. Author (revised)

N94-28359# Helsinki Univ. of Technology, Espoo (Finland). Lab. of Foundry Engineering.
HIGH QUALITY ALUMINIUM CASTINGS CONFERENCE
J. Poranen, ed. and J. J. Vuorinen, ed. 1993 225 p Conference held in Otaniemi, Finland on May 13-14, 1993
(PB94-133592; ISBN-951-22-1638-8) Avail: CASI HC A10/MF A03

The importance of the theme of the conference, high quality aluminum castings, is quite obvious. Firstly, aluminum is the most common metal in the world. Its crustal abundance is eight percent. Secondly, the pressure to reduce the mass of machine parts is becoming higher and higher. Aluminum, owing to its specific density of only one third of that of steel, is self-evidently one of the most interesting materials in aiming at mass reductions. Thirdly, there are severe quality problems in aluminum castings, especially in those made of secondary aluminum. Finland is a country with no primary aluminum production, and therefore secondary aluminum is a more important raw material than primary aluminum in Finland. NTIS

N94-27900*# Norfolk State Univ., VA. Dept. of Chemistry and Physics.
AN EXPERIMENTAL INVESTIGATION OF FATIGUE DAMAGE IN ALUMINUM 2024-T3 ALLOYS
Milton W. Ferguson *In* Old Dominion Univ., The 1993 NASA-ODU American Society for Engineering Education (ASEE) Summer Faculty Fellowship Program Dec. 1993 p 83-84 (For primary document see N94-27893 07-80)
Avail: CASI HC A01/MF A03

27 NONMETALLIC MATERIALS

Includes physical, chemical, and mechanical properties of plastics, elastomers, lubricants, polymers, textiles, adhesives, and ceramic materials.

For composite materials see *24 Composite Materials.*

N94-25596# Army Research Lab., Watertown, MA. Materials Directorate.
DYNAMIC RESPONSE OF S-2 GLASS REINFORCED PLASTIC STRUCTURAL ARMOR
Shun-Chin Chou and Eugenio DeLuca Dec. 1993 120 p
(AD-A273868; ARL-SR-5) Avail: CASI HC A06/MF A02

A progress report on work conducted in FY93 to define the dynamic response of S-2 glass reinforced plastic laminate under ballistic loading is presented. The work is divided into three parts, a description of ballistic impact damage in monolithic laminates produced by fragment simulators and measurement of target residual compressive strength, determination of material dynamic properties, and measurement and analysis of stress levels in glass reinforced plastic laminates under ballistic impact. Enlargement and extension of the data base constructed is planned for FY94. The overall objectives of this effort are to provide design guidelines for application of S-2 glass reinforced plastic in vehicular structures and to define the dynamic behavior of this material for general applications in armor technology. DTIC

N94-25748# Groningen Rijksuniv. (Netherlands).
HIGH IMPACT STRENGTH POLY(LACTIDE) TOUGH BIODEGRADABLE MATERIALS Ph.D. Thesis
Dirk Wybe Grijpma 1993 179 p Sponsored by Stichting Biomat, Netherlands Prepared in cooperation with DSM/NV Nederlandse Staatsmijnen, Geelen, Netherlands, and Ministere van Economische Zaken, s'Gravenhage, Netherlands
(ETN-94-95389) Avail: CASI HC A09/MF A02

Research on poly(lactide) aimed at gaining more insight into the factors which determine the physical properties and the applicability of these degradable polymers in biomedical devices is described. An important aspect is the preparation of strong and tough amorphous materials, which are able to degrade in the human body by hydrolysis to harmless compounds. These materials are primarily designed for use as bone plates and screws in maxillofacial surgery, but many other uses in medicine and in other fields are conceivable. Materials based on L-lactide were prepared by copolymerization with several other cyclic esters, by blending amorphous poly(lactide) polymers with degradable rubbers and by synthesizing (star)block copolymers containing poly(lactide) sequences. Fundamental problems relating the poly(lactide) chain stiffness and configuration in the melt to the observed fracture behavior are addressed, as well as more practical problems such as the influence of processing variables on the properties of poly(lactide). ESA

N94-25749 Groningen Rijksuniv. (Netherlands).
LANGMUIR-BLODGETT FILM OF AMYLOSE-ESTERS AND CHIRAL AZO-DYES (STRUCTURE AND SECOND ORDER NONLINEAR OPTICAL BEHAVIOUR) Ph.D. Thesis
Monique Annette Schoondorp 1992 145 p Sponsored by Akzo Corporate Research, Netherlands Limited Reproducibility: More than 20% of this document may be affected by microfiche quality
(ETN-94-95390) Avail: CASI HC A07

The structure and second order nonlinear optical behavior of several Langmuir-Blodgett films, which are ultrathin films produced by the Langmuir-Blodgett technique, are described. The behavior and structure of mono and multilayers of a series of amylose-esters with various alkyl side chains is studied. The structure of mono and multilayer mixtures and amylose-acetate and a chiral p nitro azobenzene dye are studied. Second Harmonic Generation (SHG) from thin films of mixtures of an aggregated chiral p nitro azobenzene dye and amylose-acetate is used as an indication of nonlinear optical efficiency. The structure and SHG of Langmuir-Blodgett films of two chiral amphiphilic azo dyes are described. ESA

N94-25844# Melbourne Univ., Parkville (Australia). School of Physics.
NNN-ISING MODEL SIMULATION OF NANODOMAIN TEXTURES IN RELAXOR-TYPE LEAD SCANDIUM TANTALATE
H. Qian, J. L. Peng, and L. A. Bursill 1993 21 p
(DE94-601884; UM-P-93/23) Avail: CASI HC A03/MF A01 (US Sales Only)

Chemical domain textures for lead scandium tantalate (PST) are modelled using Monte Carlo (MCS) and next-nearest-neighbour Ising (NNNI) models. A wide range of degrees of short- and long-range ordering of the (Ta,Sc) atoms occur in ceramic specimens, depending on processing routes. The simulations help to understand and quantify the chemical domain textures, chemical domain wall configurations and other chemical defects which may occur in certain relaxor-type perovskite-type oxides. The results are compared to dark-field transmission electron microscopic observations. Some new types of small defects were discovered. These are described and classified. The results provide a first step towards the development of a microscopic statistical physics framework for analytical theories of the dielectric response of relaxor-type ceramics, where the frequency and temperature variation of the permittivity are due essentially to dipolar-type fluctuations on nanometer scales. DOE

N94-25854# Colorado School of Mines, Golden. Dept. of Metallurgical Engineering.
CRYSTALLIZATION AND MICROSTRUCTURAL CONTROL OF FERROELECTRIC THIN-FILMS AND GLASS-CERAMICS Interim Report, 1 Mar. 1992 - 30 Sep. 1993
Michael J. Haun 30 Sep. 1993 111 p
(Contract N00014-92-J-1390)
(AD-A273767) Avail: CASI HC A06/MF A02

Research on solution-derived ferroelectric thin films and melt derived ferroelectric glass ceramics is being conducted in parallel with considerable overlap in the compositions studied and the evaluations of the crystallization behavior, microstructural development, and resulting properties. By establishing the similarities and differences between the two systems, techniques developed for one technology can then be applied to advance the other. The investigation is focusing on the Pb(Zr(x)Ti(1-x))O3-Pb5Ge3O11 (PZTPG) system. Compositions from this system combine the glass forming ability and low processing temperatures of PG with the excellent electrical properties of PZT. These compositions crystallize into multiple ferroelectric phases, and thus by controlling the ratios of these phases unique combinations of properties may be possible. The high PG compositions are being investigated for pyroelectric applications, while the high PZT compositions are of interest for piezoelectric applications. This program investigates melt-derived PG-PZT compositions, the crystallization of multiple ferroelectric phases, and the crystallization of PZT from a glass. This research demonstrates the feasibility of developing piezoelectric glass-ceramics with low processing temperatures that utilize powder processing techniques, such as pressing, screen printing, or tape casting, and indicates the potential of incorporation of these materials into low-fired multilayer packages as a sensors or actuators. DTIC

N94-25892 National Physical Lab., Teddington (England). Div. of Materials Metrology.
TECHNIQUE TO PREDICT THE CURING BEHAVIOUR OF UNSATURATED POLYESTER MATERIALS
P. A. J. Gibbs and M. Rides 1993 22 p See also PB94-124864
(PB94-124856; DMM(A)-120) Copyright Avail: Issuing Activity (National Technical Information Service (NTIS))

The curing behavior of a thermosetting unsaturated polyester dough molding compound (DMC) has been investigated using differential scanning calorimetry (DSC). The cure reaction was found to have two separate distinct regions: an inhibition period where the material was prevented from curing by the action added inhibitors with little or no change occurring in the rheological behavior of the material, and a cure region where the DMC hardens to produce the final cured article. A kinetic model has been developed for polyester DMC's using a kinetic model containing two rate constants derived from DSC measurements. The model obtained has been used to estimate fill times and in-mold hardening times during processing. Good agreement has been obtained between molding practice and the kinetic model indicating that a good model has been obtained. NTIS

N94-25893 National Physical Lab., Teddington (England). Div. of Materials Metrology.
MODELLING THE INHIBITION CURE BEHAVIOUR OF UNSATURATED POLYESTER MOULDING MATERIALS
P. A. J. Gibbs and N. Rides 1993 22 p See also PB94-124856
(PB94-124864; DMM(A)-107) Copyright Avail: Issuing Activity (National Technical Information Service (NTIS))

Much work has been carried out on measuring the curing behavior of unsaturated polyester molding compounds. However, previous modeling work has usually ignored the effect that cure-preventing inhibitors have of the curing behavior of the material. An analysis method has been developed for determining the inhibition behavior of an unsaturated polyester dough molding compound (DMC) using dynamic mechanical thermal analysis (DMTA) and differential scanning calorimetry (DSC) techniques. Results obtained from the analysis have shown that the inhibition reaction is significant at molding temperatures, and a surprising correlation between surface finish and inhibition has been identified. NTIS

N94-25894 National Physical Lab., Teddington (England). Div. of Materials Metrology.
STRESS RELAXATION IN DOUGH MOULDING COMPOUNDS
A. Cook, D. Dawson, and B. C. Duncan 1993 36 p
(PB94-124872; NPL-DMM(A)-110) Copyright Avail: Issuing Activity (National Technical Information Service (NTIS))

The stress relaxation of dough molding compounds (DMC's) has been investigated using the stress relaxation test developed at the National Physical Laboratory. Polyester and phenolic DMC's show acceptable load retention at room temperature. However, at 100 C, which is a more realistic operating temperature for the thermostat housing components, both materials show very rapid rates of stress relaxation. The degree of isothermal shrinkage experienced by these materials is relatively low, suggesting that viscoelastic stress relaxation is responsible for the poor load retention properties of these DMC's. None of the materials tested here has an acceptable service life and all perform worse than post-cured granular phenolic components. NTIS

N94-25932# Sandia National Labs., Albuquerque, NM.
ADVANCES IN PREPARING AND CHARACTERIZING LOW DENSITY PAN-CARBON MICROCELLULAR FOAM
R. R. Lagasse, P. K. Leslie, K. R. Thompson, and R. J. Weagley Sep. 1993 20 p
(Contract DE-AC04-94AL-85000)
(DE94-002278; SAND-93-0172) Avail: CASI HC A03/MF A01

This report documents an improved preparation of low density microcellular carbon as well as characterization of spatial homogeneity. The report also documents the process for preparing the microcellular carbon from polyacrylonitrile raw material. A microcellular polymer precursor (0.025 g/cc) is first prepared via a solution-based process and then pyrolyzed to produce the microcellular carbon in a monolithic form (0.05 g/cc). The process improvement developed in this study permits the pore structure of the microcellular polymer precursor and the microcellular carbon to be reproduced consistently in different laboratories. Pore structure is affected by the completeness of dissolution of the polymer raw material, which can be adjusted via dissolution temperature or particle size of the raw material. The second topic in this report involves determining the spatial fluctuation in mass density caused by periodic, millimeter-scale bands, known as 'tree rings,' visible on machined surfaces of the carbon monoliths. To measure the fluctuations, a high precision, spatially resolved x ray transmission technique was developed. The periodic bands caused less than +/- 2% variation of mass density in a microcellular carbon having average density 0.041 g/cc. DOE

N94-25959# Lawrence Livermore National Lab., CA.
AN INVESTIGATION OF CAVITATION IN A MECHANICALLY ALLOYED 15 VOLUME PERCENT SiCp/IN9021 ALUMINUM COMPOSITE
K. Higashi (Osaka Prefecture Univ., Sakai, Japan.), T. Okada (Osaka

Prefecture Univ., Sakai, Japan.), T. Mukai (Osaka Prefecture Univ., Sakai, Japan.), S. Tanimura (Osaka Prefecture Univ., Sakai, Japan.), T. G. Nieh, and J. Wadsworth Jul. 1993 8 p Presented at the International Union of Materials Research Societies on Advanced Materials, Tokyo, Japan, 31 Aug. - 4 Sep. 1993
(Contract W-7405-eng-48)
(DE94-003371; UCRL-JC-114736; CONF-9308122-16) Avail: CASI HC A02/MF A01

A mechanically alloyed 15 vol % SiC(sub p)/IN9021 aluminum composite exhibited a maximum elongation of 610 % at a very high strain of 5 s(exp -1) at 823 K. Nonetheless, the maximum elongation was obtained at a lower strain rate than that where the maximum m value (about 0.5) was obtained. This discrepancy between the optimum superplastic strain rate for the largest elongation and the strain rate for the maximum m value was believed to be associated with the cavitation behavior. Cavitation behavior of the SiC(sub p)/IN9021 aluminum composite was, therefore, carried out. It was found that cavities initiated at the ends of particulate reinforcements and parallel to the applied stress direction within initial small strains, and their subsequent growth and coalescence, invariably lead to premature failure. Experimental results indicate that cavity growth is plasticity controlled and can be described by a model proposed by Stowell. DOE

N94-25973# Massachusetts Inst. of Tech., Cambridge.
CONTROLLED SYNTHESIS OF POLYENES BY CATALYTIC METHODS
R. R. Schrock 1993 5 p
(Contract DE-FG02-86ER-13564)
(DE94-004168; DOE/ER-13564/12) Avail: CASI HC A01/MF A01

Four studies are reported: living cyclopolymerization of diethyl dipropargylmalonate by Mo(CH-t-Bu)(NAr)(OCMe(CF3)2)2 in dimethoxyethane; effect of chain length on conductivity of polyacetylene; nonlinear optical analysis of a series of triblock copolymers containing model polyenes; and synthesis of bifunctional hexafluoro-t-butoxide Mo species and their use as initiators in ROMP reactions. DOE

N94-25985# Lawrence Livermore National Lab., CA.
CHARACTERIZATION OF PHYSICALLY VAPOR DEPOSITED AF2400 THIN FILMS
R. Chow, M. K. Spragge, G. E. Loomis, F. Rainer, R. Ward, I. M. Thomas, and M. R. Kozlowski Nov. 1993 8 p Presented at the Fall Meeting of the Materials Research Society (MRS), Boston, MA, 29 Nov. - 3 Dec. 1993
(Contract W-7405-eng-48)
(DE94-004019; UCRL-JC-114506; CONF-931108-13) Avail: CASI HC A02/MF A01

Anti-reflective coatings made with Teflon AF2400 had the highest damage thresholds recorded for physical vapor deposited coatings at the Lawrence Livermore National Laboratory damage facility. Physical vapor deposited layers of Teflon AF2400, a perfluorinated amorphous polymer, maintained the bulk optical properties of a high transmittance from 200 nm to 1600 nm, and a low refractive index. In addition, the refractive index can be intentionally reduced by control of two common deposition parameters, deposition rate, and substrate temperature. Scanning electron microscopy and nuclear magnetic resonance observations indicated that morphological changes caused the variations in the refractive index rather than compositional changes. The coatings adhered to fused silica and silicon wafers under normal laboratory handling conditions. DOE

N94-26005# Wisconsin Univ., Madison.
MORPHOLOGICAL ANALYSIS OF IONOMERS
1993 6 p
(Contract DE-FG02-88ER-45370)
(DE94-003660; DOE/ER-45370/T1) Avail: CASI HC A02/MF A01

This paper reports work on the study of ion containing polymers. X-ray absorption fine structure studies have been carried out on lightly sulfonated polystyrenes and polyurethane cationomers. In the polystyrenes, nickel, zinc, and cadmium-neutralized ionomers were studied. A simulation package, FEFF5, was available to model the polystyrenes, and the experimental data was input into the simulation to arrive at an atomic arrangement which fit the experimental data. The cationomers structure is still unresolved, and the question of water absorption is a problem for this system. NMR of Na-23 is also being used to study the local environment of the cation in sodium-neutralized lightly sulfonated polystyrene. Small angle neutron scattering experiments were also performed to explore the role of temperature in solution of sodium-neutralized carboxy-telechelic polystyrene ionomers in toluene. By adjusting the labelling levels and the angular range, the neutron scattering experiments probe either the aggregate structure or the single chain structure. DOE

N94-26007# Dayton Univ., OH. Research Inst.
ACCELERATED SCREENING METHODS FOR DETERMINING CHEMICAL AND THERMAL STABILITY OF REFRIGERANT-LUBRICANT MIXTURES. PART 2: EXPERIMENTAL COMPARISON AND VERIFICATION OF METHODS
R. Kauffman Oct. 1993 18 p
(Contract DE-FG02-91CE-23810)
(DE94-003664; DOE/CE-23810/20D-Pt-2) Avail: CASI HC A03/MF A01

Initial research focused on conductivity measurements to perform in heated situ degradation measurements of CFC-12/mineral oil and HCFC-22/mineral oil mixtures at 175 C in sealed glass tubes. Tungsten rods were sealed into round bottoms of the sealed tubes to provide electrical connections for in situ conductivity measurements. Steel, Cu, and W were used as catalysts as well as conductivity probes. Conductivity measurements have been made with both ac and dc voltage inputs. Preliminary results indicate that in situ conductivity measurements correlate with refrigerant/lubricant degradation as determined by other analytical techniques (color, gas chromatography). Some of the continuous conductivity measurement tests appear to accelerate as well as monitor the refrigerant/lubricant degradation. W posts with a valve steel catalyst appear optimum combination for conductivity measurements. Ferric fluoride catalysts and differential thermal analysis were also investigated. Initial tests indicate that the ferric fluoride catalyst has potential for testing lubricant stability at temperatures lower than 175 C. Differential thermal analysis have minimal potential for in situ measurements of long-term refrigerant/lubricant degradation processes. DOE

N94-26074# Oregon Univ., Eugene. Depts. of Chemistry and Physics.
THE FORMATION OF CONDUCTING GOLD FILMS BY THERMAL DECOMPOSITION AND DIRECT PATTERNING USING ELECTRON BEAM LITHOGRAPHY OF THE GOLD CLUSTER Au55P(C6H5)312C16 Technical Report, Mar. 1992 - Dec. 1993
Ceceli A. Duchi, M. Kanskar, J. C. Wu, M. N. Wybourne, and Sui X. Cai 6 Dec. 1993 20 p
(Contract N00014-92-J-1412)
(AD-A273720; UO-JFWK-MNW-13) Avail: CASI HC A03/MF A01

The fabrication and electrical conductivities of conducting gold cluster films are presented. The films are deposited onto a Si3N4 substrate from a gold cluster solution by spin coating. After thermal decomposition and annealing at 180 C, a granular gold film with a resistivity of about 10(exp -6) ohms-m is formed. Resistivity measurements as a function of temperature show a low residual resistivity ratio. The low temperature resistivity indicates an electron mean-free-path close to the cluster diameter, and the temperature dependent resistivity is found to be in agreement with the Block-Gruneisen model. The spin coated gold cluster film also acts as a negative electron beam resist. Fine structures as small as 0.1 microns can be patterned directly by electron beam exposure. The electron beam exposed structures were found not to be conducting even after chemical extraction and firing. DTIC

N94-26080# Oak Ridge National Lab., TN.
COLLABORATIVE RESEARCH ON ION IMPLANTATION OF CERAMICS
C. J. McHargue 29 Jul. 1993 11 p
(Contract DE-AC05-84OR-21400)
(DE93-019177; ORNL/FTR-4702) Avail: CASI HC A03/MF A01 (US Sales Only)

Discussions were held with members of The Royal Institution of Great Britain on theoretical calculations in ceramic crystals relating to our ion-implantation results. Experiments were conducted by the staff of the National Institute for Engineering and Industrial Research (MTI) on sapphire crystals ion implanted at Oak Ridge National Laboratory (ORNL). Results of each experiment were analyzed in order to determine conditions for the next one. The results of recent experiments in France that are part of an ORNL University Claude Bernard collaboration in ion implantation of ceramics are discussed. Rain erosion and thermal shock tests on ORNL-supplied specimens of surface-modified sapphire and diamond have been completed at the Cavendish Laboratory. An invited paper, 'Ion Implantation-Induced Amorphization of Sapphire,' was presented at the International Conference on Mechanisms of Formation of Metastable Microstructures. Experiment details were discussed with Prof. T.F. Page for continuation. DOE

N94-26085# California Univ., Berkeley. Lawrence Berkeley Lab.
CRACKING OF TEXTURED ZINC COATING DURING FORMING PROCESS
Z. Mei and J. W. Morris, Jr. Sep. 1993 10 p Presented at the International Symposium on the Physical Metallurgy of Zinc Coated Steels: Processing, Structure and Properties, San Francisco, CA, 28 Feb. - 3 Mar. 1994
(Contract DE-AC03-76SF-00098)
(DE94-003414; LBL-34795; CONF-940235-1) Avail: CASI HC A02/MF A01

A model is presented to relate cracking of a zinc coating on steel during the forming process of its crystallographic texture. There are three deformation modes that can accommodate strains in a zinc coating caused by external loadings: basal slip, twinning, and cleavage cracking. Twinning of a zinc hexagonal crystal induces a contraction along its c-axis while cleavage relaxes tensile strain along its c-axis. Because of this, when basal slip in grains of a textured zinc coating is difficult under a given loading, either twinning or cleavage occurs depending on whether the basal plane is parallel or normal to the loading axis and whether the loading is tensile or compressive. The loadings during formability or surface friction tests cause twinning in the basal-textured coating and cleavage cracking in the prism-textured coating. The prism-textured coating contains in extraordinarily high hardness since none of the three deformation modes may be operative under compression. These results derived from the model are confirmed with recent studies on electrogalvanized steels. DOE

N94-26088# Ecole Centrale de Lyon (France). Dept. de Technologie des Surfaces.
MICROPYROLYSIS OF POLYMER THIN FILMS FOR CERAMICS Ph.D. Thesis [MICRO-PYROLYSE DE COUCHES MINCES DE POLYMERS PRECURSEURS DE CERAMIQUES]
Sandrine Bec 1992 160 p In FRENCH Sponsored by Societe Rhone-Poulenc Chimie, France
(ECL-92-62; ETN-94-95280) Avail: CASI HC A08/MF A02

Polymer pyrolysis is one method to make ceramic coatings. With this technique, uncracked and adhering coatings thicker than 0.5 micrometers cannot be obtained. The aim is to understand spontaneous cracking phenomena during the transformation by pyrolysis of a thin polysilazane film into 'SiCN' ceramic. The analysis of the behavior of coatings pyrolyzed under various atmospheres is performed using a micropyrolysis apparatus. It allows in situ observation of the surface by optical microscopy during pyrolysis heat treatment. The changes during heating are demonstrated. It is shown that cracking during heating occurs at around 580 C under nitrogen or argon atmosphere. Chemical characterization shows that the coatings are SiCNO ceramic with an oxydized layer at their surface. Mechanical modeling and the construction of a one dimensional model allow the cracking and decohesion phenomena quantitatively to be described. Parameters which control these cracking phenomena are studied. Mechanical characterization of coatings at different stages of the pyrolysis treatment is done by nanoindentation. It is shown that the cracking occurs simultaneously with a large increase of the material's mechanical properties between 550 C and 650 C, coupled with a shrinkage at these temperatures. This shows that the cracking is due to the polymer/ceramic transition. ESA

N94-26124# Los Alamos National Lab., NM.
THE FRACTURE BEHAVIOR OF A CVD CRYSTALLINE Si3N4/AMORPHOUS Si3N4 COMPOSITE
I. E. Reimanis, J. J. Petrovic, H. Suematsu, and T. E. Mitchell 1993 8 p Presented at the 1st Meeting of the Pacific Rim Ceramic Societies, Honolulu, HI, 7-10 Nov. 1993
(Contract W-7405-eng-36)
(DE94-002646; LA-UR-93-3614; CONF-931142-2) Avail: CASI HC A02/MF A01

The mechanical properties of a chemically vapor deposited alpha-Si3N4/amorphous Si3N4 composite were examined at 25 C and up to 1400 C using a microhardness tester. The composite consists of an amorphous matrix containing elongated alpha-Si3N4 particles (5-50 microns in diameter) which in some cases are radially microcracked. The conditions for spontaneous microcracking due to thermal residual stress are derived for a cylinder embedded in a matrix. Heat treatment of the composite at 1200 C results in a microstructure where the matrix consists of nanometer-sized particles separated by thin (50 A) layer of carbon. The indentation fracture toughness of the heat treated material improves remarkably due to extended microcracking through the carbon layer. DOE

N94-26167# Physical Sciences, Inc., Andover, MA.
THE IMPORTANCE OF VIBRATIONALLY EXCITED NITROGEN IN SILICON NITRIDE DEPOSITION SYSTEMS Final Report, 3 May 1991 - 2 May 1993
Lawrence G. Piper Aug. 1993 52 p
(Contract F33615-91-C-2112)
(AD-A274874; PSI-1126/TR-1257; WL-TR-93-2097) Avail: CASI HC A04/MF A01

The kinetics of N2(X,v) quenching by silane was studied. These studies were a first step in understanding the kinetic processes important in silicon nitride coating systems using the remote plasma enhanced chemical vapor deposition technique. The experiments were carried out in a discharge-flow reactor and used metastable energy transfer diagnostics to detect N2(X,v) in vibrational levels from zero up to at least 13. Author (DTIC)

N94-26211# Groningen Rijksuniv. (Netherlands).
BIOMEDICAL POLYURETHANE NETWORKS Ph.D. Thesis
Peter Bruin 1992 119 p
(ETN-94-95391) Avail: CASI HC A06/MF A02

The possibilities of using polyurethanes, especially cross linked ones, as biomaterials are investigated. The preparation, properties, and medical applications of some polyurethane networks are discussed. The design and synthesis of biodegradable lysine diisocyanate based elastomeric polyurethane networks are discussed. Its use as a material for the construction of a macroporous bottom layer (dermal analog) in two layer artificial skin is evaluated. The preparation and evaluation of a microporous polyetherurethane wound covering having a high water vapor permeability is considered. A two ply biodegradable microporous small caliber vascular prosthesis composed of polyurethane and poly(L-lactide) is described. The synthesis and properties of densely cross linked polyurethane networks, and their potential user in ophthalmology (intraocular lens, keratoprosthesis) are described. ESA

N94-26247# Sandia National Labs., Albuquerque, NM.
INERT STRENGTH OF PRISTINE SILICA GLASS FIBERS
W. L. Smith and T. A. Michalske Nov. 1993 5 p
(Contract DE-AC04-94AL-85000)
(DE94-004685; SAND-92-1107) Avail: CASI HC A01/MF A01

Silica glass fibers have been produced and tested under ultra high vacuum (UHV) conditions to investigate the inert strength of pristine fibers in absence of reactive agents. Analysis of the coefficient of variation in diameter, upsilon(sub d), versus the coefficient of variation of breaking strength, upsilon(sub sigma), does not adequately explain the variation of breaking stress. Distribution of fiber tensile strength data suggests that the inert strength of such fibers is not single valued and that the intrinsic strength is controlled by defects in the glass. Furthermore, comparison of room temperature UHV data with LN2 data indicates that these intrinsic strengths are not temperature dependent. DOE

N94-26332# Oak Ridge National Lab., TN.
CERAMIC TECHNOLOGY PROJECT Semiannual Progress Report, Oct. 1992 - Mar. 1993
D. R. Johnson Sep. 1993 452 p
(Contract DE-AC05-84OR-21400)
(DE94-003782; ORNL/TM-12428) Avail: CASI HC A20/MF A04

This project was developed to meet the ceramic technology requirements of the OTS's automotive technology programs. Although progress has been made in developing reliable structural ceramics, further work is needed to reduce cost. The work described in this report is organized according to the following work breakdown structure project elements: materials and processing - monolithics (silicon nitride and silicon carbide), ceramic composites, thermal and wear coatings, joining, and ceramic-ceramic joints; materials design methodology - contact interfaces and new concepts; data base and life prediction - structural qualification, time-dependent behavior, environmental effects, fracture mechanics, and nondestructive evaluation development; and technology transfer. DOE

N94-26422# Argonne National Lab., IL.
CRYSTAL CHEMISTRY AND SELF-LUBRICATING PROPERTIES OF MONOCHALCOGENIDES GALLIUM SELENIDE AND TIN SELENIDE
A. Erdemir Feb. 1993 25 p Presented at the American Society of Mechanical Engineers/Society of Tribologists and Lubrication Engineers (ASME/STLE) Joint Tribology Cconference, New Orleans, LA, 24-27 Oct. 1993
(Contract W-31-109-eng-38)
(DE93-041177; ANL/MCT/CP-79124; CONF-9310170-1) Avail: CASI HC A03/MF A01

This paper describes the fundamentals of the crystal chemistry and self-lubricating mechanisms of two monochalcogenides; tin selenide and gallium selenide. Specifically, it enumerates their inter-atomic array and bond structure in crystalline states, and correlates this fundamental knowledge with their self-lubricating capacity. Friction tests assessing the self-lubricating performance of gallium and tin selenides were carried out on a pin-on-disk machine. Specifically, large crystalline pieces of gallium selenide and tin selenide were cut and cleaved into flat squares and subsequently rubbed against the sapphire balls. In another case, the fine powders (particle size approximately 50-100 microns) of gallium selenide and tin selenide were manually fed into the sliding interfaces of 440C pins and 440C disks. For the specific test conditions explored, it was found that the friction coefficients of the sapphire/gallium selenide and sapphire/tin selenide pairs were approximately 0.23 and approximately 0.35, respectively. The friction coefficients of 440C pin/440C disk test pairs with gallium selenide and tin selenide powders were on the orders of approximately 0.22 and approximately 0.38, respectively. For comparison, a number of parallel friction tests were performed with MoS2 powders and compacts, and the results of these tests were also reported. The friction data together with the crystal-chemical knowledge and the electron microscopic evidence supported the conclusion that the lubricity and self-lubricating mechanisms of these solids are closely related to their crystal chemistry and the nature of interlayer bonding. DOE

N94-26434# Army Armament Research, Development and Engineering Center, Picatinny Arsenal, NJ.
DESIGN OF A COMPUTER EXPERT SYSTEM FOR ADHESIVE SELECTION USING ARTIFICIAL INTELLIGENCE TECHNIQUES Technical Report
Karen L. Meyler and Joseph A. Brescia Nov. 1993 32 p
(AD-A274715; ARAED-TR-93021) Avail: CASI HC A03/MF A01

The Adhesives Section, Materials Technology Branch of the U.S. Army Armament Research, Development and Engineering Center was funded to design and build an expert system prototype capable of using artificial intelligence (AI) techniques to aid in the selection of a proper adhesive or sealant for Army material. The adhesives expert system prototype is designed to operate on an IBM-PC compatible 80486 computer having a minimum of four MB RAM and eight MB hard disc space. The system will operate using MS-DOS 5.0 Windows 3.1. Kappa PC version 2.1, a C-based application development and delivery environment for PC's by IntelliCorp, Inc. was identified as a suitable expert system shell program. The adhesives selector expert system (ASES) is currently being developed with this system using object-oriented programming techniques and rulebased reasoning. DTIC

N94-26554# Lawrence Livermore National Lab., CA.
NANOSCALE PLASTICITY IN SILICA GLASS
J. N. Glosli, D. B. Boercker, A. Tesar, and J. Belak Oct. 1993 6 p Presented at the American Society for Precision Engineering (ASPE) Conference, Seattle, WA, 7-12 Nov. 1993
(Contract W-7405-eng-48)
(DE94-004212; UCRL-JC-113769; CONF-9311102-5) Avail: CASI HC A02/MF A01

Mechanisms of nano-scale plasticity and damage initiation in silica glass are examined using molecular dynamics simulation. Computer experiments are carried out by indenting a sharp diamond-like tool, containing 4496 atoms, into a silica slab consisting of 12,288 atoms. Both elastic and plastic deformation of silica is observed during nanoindentation simulation; this transition occurs at an indentation of 1.25 nm, and the calculated hardness (15GPa for 1.5 nm indentation) agrees with experiment. DOE

N94-26564# Sandia National Labs., Albuquerque, NM.
THE DEPOSITION OF BORON NITRIDE AND CARBON FILMS ON SILICA GLASS FIBERS
W. L. Smith, T. A. Michalske, and R. R. Rye Nov. 1993 5 p
(Contract DE-AC04-94AL-85000)
(DE94-004684; SAND-92-1108) Avail: CASI HC A01/MF A01

A chemical vapor deposition technique is used to produce amorphous boron nitride and carbon thin films on high strength silica glass fibers. In this method, the fiber is drawn under ultra high vacuum conditions and low pressure process gases, in the presence of a hot tungsten filament, are used to grow films at low substrate temperatures. Films deposited with this technique do not degrade the intrinsic pristine strength of the silica fibers under dry conditions and, when stressed in chemically aggressive environments, act as effective barrier coatings. DOE

N94-26580# Oak Ridge National Lab., TN. Chemical and Analytical Sciences Div.
DEPOSITION OF a-SiC:H USING ORGANOSILANES IN AN ARGON/HYDROGEN PLASMA
Leon Maya 1993 7 p Presented at the Fall Meeting of the Materials Research Society, Boston, MA, 29 Nov. - 3 Dec. 1993
(Contract DE-AC05-84OR-21400)
(DE94-004428; CONF-931108-18) Avail: CASI HC A02/MF A01

Selected organosilanes were examined as precursors for the deposition of amorphous hydrogenated silicon carbide in an argon/hydrogen plasma. Effect of process variables on the quality of the films was established by means of FTIR, Auger spectroscopy, XPS, XRD, chemical analysis, and weight losses upon pyrolysis. For a given power level there is a limiting feeding rate of the precursor under which operation of the system is dominated by thermodynamics and leads to high quality silicon carbide films that are nearly stoichiometric and low in hydrogen. Beyond that limit, carbosilane polymer formation and excessive hydrogen incorporation takes place. The hydrogen content of the plasma affects the deposition rate and the hydrogen content of the film. In the thermodynamically dominated regime the nature of the precursor has no effect on the quality of the film, it affects only the relative utilization efficiency. DOE

N94-26594# Argonne National Lab., IL.
MECHANICAL PROPERTIES OF NANOPHASE MATERIALS
R. W. Siegel and G. E. Fougere Nov. 1993 29 p Presented at the North Atlantic Treaty Organization Advanced Study Meeting of Institute on Nanophase Materials, Corfu, Greece, 20 Jun. - 2 Jul. 1993
(Contracts W-31-109-eng-38; DE-FG02-86ER-45229)
(DE94-004625; ANL/MSD/CP-79851; CONF-9306223-3) Avail: CASI HC A03/MF A01

It has become possible in recent years to synthesize new materials under controlled conditions with constituent structures on a nanometer size scale (below 100 nm). These novel nanophase materials have grain-size dependent mechanical properties significantly different than those of their coarser-grained counterparts. For example, nanophase metals are much stronger and apparently less ductile than conventional metals, while nanophase ceramics are more ductile and more easily formed than conventional ceramics. The observed mechanical property changes are related to grain size limitations and/or the large percentage of atoms in grain boundary environments; they can also be affected by such features as flaw populations, strains and impurity levels that can result from differing synthesis and processing methods. An overview of what is presently known about the mechanical properties of nanophase materials, including both metals and ceramics, is presented. Some possible atomic mechanisms responsible for the observed behavior in these materials are considered in light of their unique structures. DOE

N94-26641*# Southwest Texas State Univ., San Marcos. Dept. of Chemistry.
TRIFLUOROMETHYL-SUBSTITUTED POLYMERS Semiannual Status Report, 1 Jul. - 31 Dec. 1993
1993 9 p
(Grant NAG1-631)
(NASA-CR-195217; NAS 1.26:195217) Avail: CASI HC A02/MF A01

Current work sponsored by the grant at Southwest Texas State University is directed toward the synthesis and characterization of: (1) N-alkylated polyamides derived from o-fluorinated diacids; (2) highly fluorinated polyethers; (3) polyesters derived from 2-hydroxy-2-propyl substituted arenes and/or 2,5-difluoroterephthalic acid; and (4) silicon-containing fluoropolymers. Work during the period from 1 July to 31 Dec. 1993 focused primarily on items 3 and 4 and on the development of a phosphorus containing modification of '12F-PEK.' CASI

N94-26645 Technische Univ., Eindhoven (Netherlands).
MODELLING AND PREDICTING PROPERTIES OF POLYMERS IN THE AMORPHOUS GLASSY STATE Ph.D. Thesis
Servatius Maria Vleeshouwer 1993 163 p Limited Reproducibility: More than 20% of this document may be affected by microfiche quality
(ETN-94-95345) Avail: CASI HC A08

The purpose of the work is the theoretical analysis of the glass transition and the glassy state of polymers, starting from equilibrium. The properties of the glassy state are related to the melt with the formation history as an important factor determining the nature of the glass. The description of the equation of state of polymer melts with the Holey-Huggins (HH) theory is reviewed. The free volume and free volume fluctuations defined in this theory are input parameter for the glass formation theory. A quasi equilibrium approach of the polymer glass with the HH theory is presented. Theories that describe and predict the glass transition and relaxation phenomena in glasses are given. The relation between mobility and free volume, temperature and pressure is examined and a new relation covering data sets is presented. The development of the glass formation theory from the RSC (Robertson, Simha and Curro) theory is presented. Six results, obtained with the glass simulation theory are discussed. The presence of molecular voids and their size distribution is approached from two opposite sides: theoretically, based on the HH theory, and experimentally, using positron lifetime spectroscopy. ESA

N94-26652 National Physical Lab., Teddington (England). Materials Metrology Div.
PIEZOELECTRIC MEASUREMENTS ON IMPACT LOADED PZT CERAMICS
J. A. Close, R. Stevens, and M. G. Gee Jan. 1993 22 p Sponsored by Dept. of Trade and Industry, London, England Limited Reproducibility: More than 20% of this document may be affected by microfiche quality
(ISSN 0959-2423)
(NPL-DMM(A)-88; ETN-94-95223; PB93-219202) Copyright Avail: Issuing Activity (National Physical Lab., Teddington, Middlesex, TW11 OLW, England)

Samples of commercially produced, Poled lead Zirconate Titanate (PZT) piezoceramics were subject to longitudinal, compressive impact loading by a free falling striker providing a single, clean stress pulse. Values of the piezoelectric charge coefficient, d(sub 33) were derived and compared with those obtained via the conventional low frequency, low stress resonance method. The electrochemical coupling factor was also derived. The results obtained from the impact rig gave values for the d(sub 33) coefficient that are up to twice those gained from the resonance rig. Aging of the piezoelectric device under stress was studied by means of plotting d(sub 33) as a function of the number of impacts suffered. Samples of all the compositions displayed a drop in the values of d(sub 33) of between 18 and 49 when subject to 5000 impacts of approximately 40 MPa in magnitude. A sample of X-cut alpha quartz was subjected to the same tests as the PZT compositions. The quartz showed potential as a reference material for measurements of the piezoelectric response of impact loaded PZT ceramics. ESA

N94-26654 National Physical Lab., Teddington (England). Materials Metrology Div.
CEN-VAMAS ROUND ROBIN ON GRAIN SIZE MEASUREMENT FOR ADVANCED TECHNICAL CERAMICS Final Report
L. Dortmans (Centre for Technical Ceramics, Einhoven, Netherlands.), R. Morrell, and G. deWith (Centre for Technical Ceramics, Einhoven, Netherlands.) Dec. 1992 88 p
(ISSN 1016-2186)
(VAMAS-TR-12; ETN-94-95281) Copyright Avail: Issuing Activity (National Physical Lab., Teddington, Middlesex, TW11 OLW, England)

The results of a joint CEN/VAMAS (CEN/Versailles project on Advanced Materials and Standards) round robin on grain size measurement for advanced technical ceramics are analyzed. The round robin was established to verify the equivalence of line and circle methods for manual determination of mean linear intercept length proposed in a new CEN standard ENV 623-3, but also examined the possibilities of standardizing measurements of porosity and grain size distribution using overlaid grid intersection counting methods. Two alumina ceramics with very different microstructures and a computer drawn 'ideal' microstructure were used. The results show that scatter levels of 20% are obtained for measurement of the mean linear intercept length and the grain size distribution. They are primarily due to: quality of specimen preparation, selection of area for analysis, interpretation of features observed and, also random positioning of lines, circles, and grids on the micrograph. These levels of scatter are considered to be acceptable. The 30% scatter for the grid method porosity measurement is mainly due to the low level of very fine porosity in the nominally dense ceramic used and to the interpretation of a micrograph. The grid methods for grain size distribution measurement seem suitable for implementation in future standards. In all cases, the quality of micrograph preparation and interpretation needs further attention. ESA

N94-26661 Toronto Univ. (Ontario).
STRESS-INDUCED PHASE TRANSFORMATION IN ZrO2 MATERIALS M.S. Thesis
Jianfeng Han 29 Jan. 1993 101 p
(ISBN-0-315-83373-4; CTN-94-61043) Copyright Avail: Micromedia Ltd., Technical Information Centre, 240 Catherine Street, Suite 305, Ottawa, Ontario, K2P 2G8, Canada HC/MF

It is well known that the tetragonal to monoclinic transformation in zirconia ceramics is martensitic in nature and can be induced by applied stress. Transformation which results in enhanced toughness is particularly important. A study was conducted to develop a basic understanding of this driving stress through both experimentation and theoretical modeling. To characterize the stress which induces the transformation, an in-situ observation system was employed to examine the transformation event in a suitable localized stress field on a single edge-notched beam bar (SENB) whose stress distribution is modeled by finite element calculation. The real-time initiation of dendrite-like transformation bands was observed at the notch of SENB bars during in-situ loading experiments. The transformation was confirmed by Raman spectroscopy, and an important feature of the martensitic transformation was observed by laser microscopy. Based on a model developed from thermodynamics, the critical stress which induces transformation can be described by a combination of hydrostatic and deviatoric stress components. This stress was found to obey the Mohr-Coulomb criterion suggested by Chen and Morel, and its magnitude was observed to vary with grain size. The developed dendrite-like bands are discussed based on the concept of the autocatalytic effect. Author (CISTI)

N94-26676# Los Alamos National Lab., NM.
ION BEAM MIXING OF MARKER LAYERS INTO AMORPHOUS ALUMINUM OXIDE
E. A. Cooper and M. Nastasi 1993 15 p Presented at the Nuclear Instruments and Methods in Physics Research on Radiation Effects in Insulators, Nagoya, Japan, Sep. 1993
(Contract W-7405-eng-36)
(DE94-000901; LA-UR-93-3278; CONF-9309259-1) Avail: CASI HC A03/MF A01

Thin layers of various marker species embedded in amorphous Al_2O_3 were ion beam mixed with 210 keV Ar in a temperature range of -166 to 790 C. All of the metal markers (Ag, Fe, and Zr) were found to mix only to a ballistic level. The oxide markers studied were Fe_2O_3, Cr_2O_3, Y_2O_3, and ZrO_2. Thermally assisted ion mixing was seen, in decreasing amounts, in Fe_2O_3, Y_2O_3, and Cr_2O_3. No thermally assisted ion beam mixing was observed for ZrO_2 or the metal markers. DOE

N94-26708*# Thiokol Corp., Brigham City, UT. Space Operations.
NEW RUBBER QUALIFICATION FOR THE IGNITER ADAPTER Final Report
Mark A. Humpherys 13 Jan. 1994 8 p
(Contract NAS8-38100)
(NASA-CR-193936; NAS 1.26:193936; TWR-65405) Avail: CASI HC A02/MF A01

Kirkhill Rubber Company (KRC) has informed Thiokol Corporation that two raw materials used in the asbestos and silica filled acrylonitrile butadience rubber (NBR) formulation per STW 2621 are no longer available from their vendors. Agerite White (Di-beta-naphthyl-paraphenylene diamine), manufactured by B. F. Goodrich, is an antioxidant used in NBR. This raw material makes up roughly 1-2 percent of the finished product. KRC proposed that this raw material be replaced by Agerite Stalite S (mixture of octylated diphenylamines) distributed by R. T. Vanderbilt Co. Protox-166 zinc oxide, manufactured by Zinc Corporation of America, is an activator currently used in NBR. This material also makes up about 1-2 percent of the finished material. Protox-166 is an American process grade zinc oxide. It is proposed by KRC to replace Protox-166 with Kadox-930C, a French process grade zinc oxide. American process grades have an ASTM minimum purity of 99.0 percent; the French process grades have a minimum purity of 99.5 percent. Previous testing per WTP-0270 has demonstrated that the mechanical and thermal properties of the rubber with the new ingredients are comparable to the 'old' rubber. The test results are reported in TWR-61790. One igniter adapter, Part no. 7U77562-02 serial no. 2 was insulated per ETP-1206 using the new rubber formulation and a modified lay up and cure method to demonstrate that there is no impact on this process. The results of this demonstration are reported. Author (revised)

N94-26770# Brookhaven National Lab., Upton, NY.
X RAY ABSORPTION STUDIES OF Ti/POLYMER AND Cr/POLYMER INTERFACES
R. L. Opila (Bell Telephone Labs., Inc., Murray Hill, NJ.), K. Konstadinidis (Bell Telephone Labs., Inc., Murray Hill, NJ.), A. O Ibidunni (Bell Telephone Labs., Inc., North Andover, MA.), A. J. Davenport, and H. S. Isaacs 1993 6 p Presented at the Spring Meeting of the Materials Research Society, San Francisco, CA, 12-16 Apr. 1993
(Contract DE-AC02-76CH-00016)
(DE94-003008; BNL-48489; CONF-930405-49) Avail: CASI HC A02/MF A01

The interface formed between metals (Ti and Cr) and polymers (epoxy and triazine) have been studied, non-destructively, using x-ray absorption spectroscopy. The metals were sputtered onto the polymer surfaces. Titanium reacts extensively, up to Ti thickness of 100 A while Cr remains primarily metallic. In situ heating at 200 C increases the extent of reaction for both metals. Heating has a greater effect on metal/epoxy interfaces than metal/triazine. Titanium and Cr were ion implanted into the polymer in order to determine the interactions of isolated metal atoms with the polymer. Titanium and Cr appear to form oxides as the final reaction product, and the Ti is tetrahedrally coordinated. DOE

N94-26783# Rensselaer Polytechnic Inst., Troy, NY. Dept. of Materials Engineering.
MECHANISM OF MECHANICAL FATIGUE OF SILICA GLASS
M. Tomozawa 1993 9 p
(Contract DE-FG02-85ER-45217)
(DE94-003165; DOE/ER-45217/8) Avail: CASI HC A02/MF A01

Results are summarized for the following topics: blunt crack tip existence, mechanical behavior of glasses with blunt cracks, water entry into glass under stress, water diffusion into SiO2 glass at low temperature, mechanical properties of glasses with high water content, cyclic fatigue, fatigue resistance improvement by coating, IR peaks of silica-water, water diffusion and structural changes in silica glasses, water diffusion and time dependent mechanical properties, and the effects of N and C implantation on devitrification of silica glasses. DOE

N94-26822# Lawrence Associates, Inc., Dayton, OH.
AN X RAY ABSORPTION FINE STRUCTURE STUDY OF ORDERING IN POLYTHIOPHENE THIN FILMS Interim Report, 1 Jan. - 1 Sep. 1993
Guy A. DeRose, H. Jiang, P. D. Haaland, W. W. Adams, T. J. Bunning, R. W. Hoffman (Case Western Reserve Univ., Cleveland, OH.), and C. A. Zorman (Case Western Reserve Univ., Cleveland, OH.) Sep. 1993 76 p
(AF Proj. 2422)
(AD-A274235; WL-TR-93-4107) Avail: CASI HC A05/MF A01

Thin film organic nonlinear optical (NLO) materials are being investigated for laser hardening applications due to their enhanced processability. Plasma-polymerized thiophene films formed by the flowing afterglow synthesis of polyaromatic heterocycles allow one to modulate the refractive index profile in real-time, thus allowing an organic analog of a rugate to be realized. Since the relationships between the molecular structure, NLO response, and processing conditions are poorly understood, the feasibility of using x ray absorption fine structure (XAFS) spectroscopy was examined. This method allows the local environment of x ray absorbing atoms in polythiophene and plasma-polymerized 2,5 dichlorothiophene and 2,5 dibromothiophene thin films at the sulfur K-edge and, as appropriate, the chlorine and bromine K-edges to be probed. Argon absorption was found to limit the data range of the S and Cl edge data. The Br K-edge data indicated that the local Br environment was maintained in the plasma-polymerized films of 2,5 dibromothiophene within experimental error. As a result, XAFS spectroscopy has been shown to be a useful technique for investigating the molecular structure of an important category of nonlinear optical materials. DTIC

N94-26842# Aerospace Corp., El Segundo, CA. Technology Operations.
AN ULTRASONIC TESTING TECHNIQUE FOR MONITORING THE CURE AND MECHANICAL PROPERTIES OF POLYMERIC MATERIALS
Eric C. Johnson, Jessica D. Pollchik, and Sherrie L. Zacharius 22 Aug. 1993 18 p
(Contract F04701-88-C-0089)
(AD-A274536; TR-93(3935)-12; SMC-TR-93-64) Avail: CASI HC A03/MF A01

Thin specimens (approx. 10 mils) can be tested using an ultrasonic technique to determine their moduli and Poisson's ratio. For this report, the thin specimen's ultrasonic response is FFT analyzed in an attempt to extend the technique for cure monitoring of polymeric systems. Two such systems are examined and the ultrasonic results compared with differential scanning calorimetry and dynamic mechanical measurements. Two parameters were measured as a function of time: the ultrasonic peak frequency and amplitude. The results suggest that it may be possible to monitor the cure through observation of these two parameters. DTIC

N94-26925# Florida State Univ., Gainesville. Dept. of Chemistry.
MECHANICAL PROPERTIES OF POLYANILINE PREPARED BY POLYMERIZATION IN AN ORGANIZED MONOLAYER Technical Report No. 2
Raj Bodalia and Randolph Duran 9 Dec. 1993 5 p
(Contract N00014-91-J-1655)
(AD-A274350) Avail: CASI HC A01/MF A01

Poly (2-penta decyl aniline) was prepared at the air-aqueous acid interface using the Langmuir film balance technique. Compressional modulus of polymers prepared at different conditions were measured from surface - pressure - area isotherms. Mechanical properties of polymers prepared at different applied surface pressures were found to remain unchanged while those of polymers prepared at different temperatures changed significantly. A lower compressional modulus obtained at higher temperature can be related to its lower molecular weight. These results fit very well with the theoretical model. This study indicates that polymers with better mechanical properties can be obtained by carrying out the reaction at a lower temperature. DTIC

N94-26933# Lawrence Livermore National Lab., CA.
EQUIVALENT PERFORMANCE IN DIFFERENT HELICAL RESONATOR PLASMA POLYMERIZATION COATER PLATFORMS
R. M. Brusasco Nov. 1993 19 p Presented at the 40th National Symposium of the American Vacuum Society (AVS), Orlando, FL, 15-19 Nov. 1993
(Contract W-7405-eng-48)
(DE94-001517; UCRL-JC-113724; CONF-9311104-4) Avail: CASI HC A03/MF A01

Plasma polymerization is used in fabricating target mandrels for implosion experiments on the NOVA laser. As part of effort to translate the theoretical aspects of plasma polymerization fundamentals into practical improvements in a production oriented environment, a study was done to determine the cause of differences in polymer deposition characteristics between two similar plasma polymerization devices. Full characterization of the coating system parameters revealed differences in the flow rate, RF power dissipation and system pressure which were subsequently changed to make the coaters equivalent in this sense; this was found insufficient to ensure equivalent performance. An experiment designed to test effect of changing operating conditions of helical resonator plasma applicator indicated that the cause of performance discrepancy did not lie with the plasma generation equipment. Substrate positioning was found to be a critical factor in determining the deposition rate of plasma polymer but played no significant role in the development of rough surfaces. Surface texture was dependent upon gas flow rates and RF power dissipation. DOE

N94-26974# North Carolina State Univ., Raleigh.
LOW TEMPERATURE DEPOSITION AND CHARACTERIZATION OF N- AND P-TYPE SILICON CARBIDE THIN FILMS AND ASSOCIATED OHMIC AND SCHOTTKY CONTACTS Semiannual Technical Report, 1 Jul. - 31 Dec. 1993
R. F. Davis, R. J. Nemanich, M. C. Benjamin, S. Kern, and L. M. Porter Dec. 1993 50 p
(Contract N00014-92-J-1500)
(AD-A274345) Avail: CASI HC A03/MF A01

The cleaning and etching of the vicinal alpha (6H)-SiC(0001) surface has been emphasized in this reporting period because of its recently demonstrated importance in the MBE of SiC and AlN films on SiC wafers and layers. Etching with a solution of 1:1:10HF:H2: ethanol and a hydrogen plasma sharply reduced both the oxide and the C surface concentrations as determined by AES and XPS spectra. Controlled growth of both Beta-SiC and alpha (6H)-SiC films have been achieved on SiC wafers and films. Flow ratios of C2H4 and Si2H6 of 1:1 result in 6H-SiC while C-rich ratios give 3C-SiC. Surface reconstruction as a function of surface treatment have also been related to the deposited SiC polytype. The initial stages of AlN film growth has also been investigated in terms of defects via TEM. Two types of defects were found in the AlN film: one caused by lattice mismatch; the other by the presence of steps in the SiC surface. The interfacial chemistry and microstructure, electrical properties and the Schottky barrier heights of thin films on Alpha (6H)-SiC(0001) surfaces were investigated after annealing to 700 deg C and a maximum time of 60 min. The reaction zone contained Ti5Si3 and TiC. The electrical properties changed little as a function of heat treatment. DTIC

N94-26977# Florida Univ., Gainesville. Dept. of Chemistry.
LB-DEPOSITED, SIDE-CHAIN SUBSTITUTED POLYANILINE, POLYPYRROLE AND THE CORRESPONDING MONOMERS, STUDIED BY STM Technical Report No. 22
P. Quint, T. Bailey, W. Sigmund, and R. S. Duran 9 Dec. 1993 5 p
(Contract N00014-91-J-1655)
(AD-A274405) Avail: CASI HC A01/MF A01

STM investigations were carried out on monolayers of two conducting polymers and the corresponding monomers. The substances in question--2-pentadecyl aniline, poly-2-pentadecyl aniline, 3-hexadecyl pyrrole, and poly-3-hexadecyl pyrrole--were transferred from the liquid/air interface on a MoS2 substrate by the Langmuir-Blodgett technique. The polymers were polymerized at the liquid/air interface with ammonium persulfate in the sub phase as the oxidizing agent. All compounds showed high orientational and positional order on the substrate surface. Two different structures were observable, rows and rod like structures. The distance between the rods was found, for all compounds, to be equal to 4.3 A. The row distances were found to be different for every substance. We think that the rods are the alkyl side chains, and the rows represent the polymer chain or molecular monomer aggregates. DTIC

N94-27021# Pacific Northwest Lab., Richland, WA.
ENGINEERING LIMITATIONS OF CERAMIC COMPOSITES FOR HIGH PERFORMANCE AND HIGH TEMPERATURE APPLICATIONS
E. L. Courtright Aug. 1993 12 p Presented at the Conference on Processing, Fabricating and Application of Advanced Composites: Putting MMCs, CMCs and PMCs To Work, Long Beach, CA, 9-11 Aug. 1993
(Contract DE-AC06-76RL-01830)
(DE94-001676; PNL-SA-22816; CONF-930858-1) Avail: CASI HC A03/MF A01

Some of the engineering limitations of ceramic matrix composites in high-temperature applications are reviewed in terms of fundamental properties. The issues associated with toughness control in the regimes where fiber pullout is not extensive are discussed. Toughening will decrease with increasing temperature because fiber strength decreases and interfacial sliding resistance increases. The temperatures regime where reinforcement fibers become creep limited, as opposed to strength limited, will influence design considerations. Matrix cracking becomes an important high temperature design limiting parameter, particularly where oxygen can rapidly gain access to bridging fibers. Even the direct permeation of oxygen through uncracked matrices may be sufficient to internally degrade fibers and limit performance in some systems. DOE

N94-27033# Florida Univ., Gainesville. Dept. of Chemistry.
FERROELECTRICITY IN A LANGMUIR-BLODGETT MULTILAYER FILM OF A LIQUID CRYSTALLINE SIDE-CHAIN POLYMER
S. Pfeiffer, R. Shashidar, T. L. Fare, J. Naciri, and J. Adams 12 Sep. 1993 13 p
(Contract N00014-91-J-1655)
(AD-A274477; TR-17) Avail: CASI HC A03/MF A01

The first observation of ferroelectric behavior in a Langmuir-Blodgett (LB) film of a liquid crystalline polymer is reported. It is established that a 30-layer film exhibits spontaneous polarization and electro-optic switching. The magnitude as well as temperature dependence of the polarization of the LB film is found to be similar to that of the bulk material. The polarization current in the LB film follows the applied triangular wave field to higher frequencies as compared to the same material in a surface stabilized sandwich cell. DTIC

N94-27036# Oklahoma State Univ., Stillwater. Dept. of Chemistry.
LIQUID CRYSTALLINE SIDE-CHAIN POLYSILOXANES WITH 4-AMINO-4'-STILBENE-CARBOXYLIC ESTER MESOGENS
Marietta O. Bautista, Warren T. Ford, R. S. Duran, and Matthias Naumann 9 Dec. 1993 5 p
(Contract N00014-91-J-1655)
(AD-A274510; TR-19) Avail: CASI HC A01/MF A01

The liquid crystalline phases of polysiloxanes have been characterized by DSC, optical microscopy, and powder x ray diffraction. The polysiloxanes form monolayers at the air/water interface with molecular areas of 30 - 35 A(exp 2), and the films do not collapse at pressures of about 40 mN/m. The monolayers of CPS-1 and -2 showed good stability on water compared to those of HPS-1 and -2 as measured by isobaric surface area changes as a function of time. Moreover, there was little hysteresis between isotherms obtained by compression and subsequent decompression below 40 mN/m for CPS-1 and -2. DTIC

N94-27080# Florida Univ., Gainesville. Dept. of Chemistry.
KINETICS OF 2-PENTADECYLANILINE POLYMERIZATIONS IN MONOLAYERS: RELATIONSHIPS BETWEEN EXPERIMENTAL DATA AND A NEW THEORETICAL MODEL
Raj Bodalia, Randolph S. Duran, Jose Manzanares (Valencia Univ., Spain.), and Howard Reiss (California Univ., Los Angeles.) 12 Sep. 1993 38 p
(Contract N00014-91-J-1655)
(AD-A274419; TR-20) Avail: CASI HC A03/MF A01

A simple theoretical model that provides a detailed understanding of aniline polymerization kinetics in a monolayer is presented. Even though the model is primitive, it agrees very well with our experimentally measured data. The rate constant and activation energy obtained in our previous study from the modified Gee and Rideal-equation were found as geometric and arithmetic means, respectively, of values which correspond to the initiation and propagation steps. This model allows us to predict an average degree of polymerization and thus an average molecular weight and the fraction of reacted monomer at any stage during the polymerization reaction. Also, some predictions regarding the temperature dependence of molecular weight can be made from this model. DTIC

N94-27086 Massachusetts Univ., Amherst. Dept. of Polymer Science and Engineering.
ULTRASTRUCTURE PROCESSING OF MACROMOLECULAR MATERIALS Final Technical Report
Frank E. Karasz 11 Feb. 1993 23 p Limited Reproducibility: More than 20% of this document may be affected by microfiche quality
(Grant AF-AFOSR-90-C-0019)
(AD-A274460) Avail: CASI HC A03

The research has concurrently involved several areas of investigation in the physical chemistry of macromolecules. A major theme was the study of the properties of polymer blends. Experimentally the effects of microstructure on miscibility in a number of model systems was investigated by thermal, mechanical, and varied spectroscopic techniques, and a wide understanding of the fundamental basis of the metastable miscibility found in an unexpectedly large number of high temperature systems, i.e. these typically involving polyimides or related materials with high Tg's was gained. In complementary investigations, computer simulation studies of the equilibrium behavior of various blends and under several relevant constraints were performed. The work also investigated dynamic aspects, particularly phase separation at differing effective quench depths. Another line of investigation concerned itself with electro-optically active conjugated polymers, principally poly(p-phenylene vinylene) and its derivatives, modifications and blends. Certain solution properties of polymer systems were also studied. Measurements were taken to investigate translational diffusion of solvated polymers in porous media and other properties of polar and non-polar macromolecules. DTIC

N94-27087# Florida Univ., Gainesville. Center for Macromolecular Science.

LANGMUIR-BLODGETT AND STM INVESTIGATIONS OF CONDUCTING POLYMER THIN FILMS

R. S. Duran, W. Sigmund, T. Bailey, and M. Hara 16 Dec. 1993 5 p
(Contract N00014-91-J-1655)
(AD-A274512; TR-23) Avail: CASI HC A01/MF A01

The monomer 3-hexadecyl pyrrole was spread and polymerized at air/aqueous interfaces using a Langmuir trough. During polymerization under isobaric conditions, a monotonic decrease in surface area was observed; however, upon expansion and recompression of the monolayer, the surface area for the polymer was found to be larger than that of the monomer. Monomer and polymer monolayers were also transferred to solid supports and studied by scanning tunneling microscopy. DTIC

N94-27111# Department of the Navy, Washington, DC.

POLYURETHANE SELF-PRIMING TOPCOATS Patent Application

Charles R. Hedgedus, inventor (to Navy), Donald J. Hirst, inventor (to Navy), and Anthony T. Eng, inventor (to Navy) 16 Apr. 1993 23 p
(AD-D016041; US-Patent-Appl-SN-054497) Avail: CASI HC A03/MF A01

A corrosion-resistant coating which can be applied directly to a surface as a self-priming topcoat comprising a polyurethane resin binder and a combination of pigments consisting essentially of an alkaline earth metal metaborate, zinc salts of benzoic acids, and an alkaline earth metal phosphate such as zinc-barium phosphate. In addition, the coating contains from 5 - 40 parts by weight of a titanium dioxide pigment, up to about 3.0 parts by weight of an oil soluble dispersant and up to about 50 parts by weight of at least one organic solvent. DTIC

N94-27147 Department of the Navy, Washington, DC.

PHOSPHAZENE-CONTAINING AMINE AS CURING AGENT FOR PHTHALONITRILE-BASE POLYMER Patent

Teddy M. Keller, inventor (to Navy) 4 May 1993 6 p Filed 15 Mar. 91
(AD-D016029; US-Patent-5,208,318; US-Patent-Appl-SN-670; US-Patent-Class-528-168) Avail: US Patent and Trademark Office

Phosphazene-containing amines having at least one amine or substituted amine moiety reactive with nitrite groups of the phthalonitrile monomers or oligomeric resins are useful curing agents for phthalonitriles. Typically, the phosphazene-containing amines useful as curing agents in the present invention have the formula: wherein each of X(1-6) is a hydrogen, an unsubstituted amine group, or an amine group substituted with C1-C12 alkyl groups or aromatic groups, at least one of X(1-6) includes an amine group, and each of R'(1-6) is an alkyl, aromatic, or alkyl-substituted aromatic moiety, or a linear polymer of the phosphazene-based amine monomer. The curing agents enhance the speed of cure and also add flame retardancy to the cured polymers. DTIC

N94-27148 Department of the Navy, Washington, DC.

ACCORDION-LIKE POLYMERS FOR NONLINEAR APPLICATIONS Patent

John D. Stenger-Smith, inventor (to Navy), Ronald Henry, inventor (to Navy), James Hoover, inventor (to Navy), Geoffrey Lindsay, inventor (to Navy), and John Fischer, inventor (to Navy) 21 Sep. 1993 18 p Filed 20 Mar. 92
(AD-D016031; US-Patent-5,247,055; US-Patent-Appl-SN-856437; US-Patent-Class-528-310) Avail: US Patent and Trademark Office

The present invention discloses new polymers which can assume an accordion-like conformation of the backbone. These polymers are prepared by the copolymerization of two difunctional, chemically precoupled precursors to chromophoric units. The resulting polymers have a head-to-head, tail-to-tail topology (a syndioregic arrangement of rigid units along the polymer backbone), and the molecular units are designed to fold into an accordion conformation. This useful microstructure (a three-dimensional conformation) forms spontaneously (self-assembles); or, it can be brought about by field-assisted processing. Films and fibers of these polymers have useful second-order nonlinear optical properties, and may be used for the modulation and switching of optical communications signals. DTIC

N94-27158 National Defence Research Establishment, Stockholm (Sweden). Dept. of Weapon Systems, Effects and Protection.

EXAMINATION OF HARDNESS, FRACTURE TOUGHNESS AND MICROSTRUCTURE IN Al2O3-B4C BINARY CERAMICS [UNDERSOEKNING AV AL2O3-B4C-KERAMKOMPOSITERS HARDHET, BROTTSEGHET OCH MIKROSTRUKTUR]

H. Carleson and P. O. Olsson Jun. 1993 19 p In SWEDISH
(PB94-124237; FOA-C-20928-2.4) Avail: Issuing Activity (National Technical Information Service (NTIS))

This report presents the results of an investigation into various properties of hot-pressed and pressureless sintered alumina/boron carbide composites. The composition is varied from pure Al2O3 to pure B4C. The properties investigated include hardness, fracture toughness, and microstructure. Phase analysis showed that for the major samples only two phases, Al2O3 and B4C were formed. NTIS

N94-27163# Florida Univ., Gainesville. Dept. of Chemistry.

CHEMICAL POLYMERIZATION AND LANGMUIR-BLODGETT TECHNIQUES. 2: THE POLYMERIZATION OF MONOLAYERS OF 3-SUBSTITUTED PYRROLES

W. M. Sigmund, C. Marestin, S. Keil, H. Zhou, Randolph S. Duran, M. Z. Elsabee (Cairo Univ., Egypt.), J. Ruehe (Max-Planck-Inst. fuer Polymerforschung, Mainz, Germany.), and G. Wegner (Max-Planck-Inst. fuer Polymerforschung, Mainz, Germany.) 12 Sep. 1993 34 p
(Contract N00014-91-J-1655)
(AD-A274478; TR-24) Avail: CASI HC A03/MF A01

Derivatives of 3-substituted pyrroles were spread at the air-water interface. Stable films could be obtained for pyrroles with side chains containing more than 10 carbons. 3-Hexdecanoyl pyrrole could not be polymerized as a monolayer whereas the alkyl derivatives could be polymerized successfully without having additional monomer in the subphase. It was possible to yield a true two-dimensional polymer monolayer film, without chain overlapping. The monolayers could be transferred onto hydrophobized substrates with transfer ratios being about unity. The polymers formed were soluble in chloroform and THF. Molecular weight averages obtained by GPC ranged from 3,500 to 6,000 when polymerized on ammonium peroxodisulfate and 5,000 to 15,000 when polymerized on ferric chloride subphase solutions. H-1 NMR indicates that the polymerization is highly regular, leading to a constitutionally ordered 2,5 poly(3-alkyl pyrrole). DTIC

N94-27203 Department of the Navy, Washington, DC.

THERMOPLASTIC ELASTOMERS HAVING ALTERNATE CRYSTALLINE STRUCTURE FOR US AS HIGH ENERGY BINDERS Patent

Gerald E. Manser, inventor (to Navy) and Richard S. Miller, inventor (to Navy) 11 May 1993 8 p Filed 6 Jan. 92
(AD-D016035; US-Patent-5,210,153; US-Patent-Appl-SN-815878; US-Patent-Class-525-410) Avail: US Patent and Trademark Office

Block polymers which are thermoplastic elastomers are provided for use as binders in high-energy compositions such as propellants, explosives, gasifiers or the like. The block polymers have an ABA structure wherein the A blocks are crystalline at temperatures below 60 C and the B blocks are amorphous at temperatures above -20 C. Both the A and B blocks are polyethers formed from monomers of oxetanes and/or tetrahydrofuran. The block polymers melt in the range of 60 C to 120 C and have low viscosities above their melting points due to mutual miscibility of the A and B blocks. DTIC

N94-27215 National Defence Research Establishment, Stockholm (Sweden). Dept. of Weapon Systems, Effects and Protection.
INTELLIGENT MATERIAL SYSTEMS AND STRUCTURES. PART 6: MEASUREMENTS OF ADHESION BETWEEN OPTICAL FIBRES AND COMPOSITE MATERIALS [INTELLIGENTA MATERIALSYSTEM OCH STRUKTURER. DEL 6: METODER FOER ATT BESTAEMMA VIDHAEFTNING MELLAN OPTISKA FIBRER OCH MATRISMATERIAL]
J. Schoeld Jun. 1993 36 p In SWAHILI; Text in SWEDISH; summary in ENGLISH See also PB93-195923 and PB93-204600
(PB94-123577; FOA-C-20934-8.4-Pt-6) Avail: Issuing Activity (National Technical Information Service (NTIS))

The concept 'Intelligent Material Systems and Structures' (IMSS) includes structurally embedded sensors and actuators. The adhesion between sensors and matrix is essential for the performance of the system. The adhesion between two types of optical fibers and the matrix (two types of epoxy resin) was investigated, since optical fibers may potentially be used as sensors in polymer fiber composites. There is a lack of knowledge concerning measurements of adhesion between optical fibers and composite materials. Several methods were however developed for measurements of adhesion between reinforcing fibers and matrix materials. A literature survey of these techniques is included. NTIS

N94-27217 National Physical Lab., Teddington (England). Div. of Materials Metrology.
ULTRASONIC MEASUREMENT TECHNIQUE TO DETERMINE THE STATE OF CURE IN THERMOSETTING MATERIALS
P. A. J. Gibbs, M. Rides, and P. Williamson 1993 21 p
(PB94-124328; NPL-DMM(A)-114) Copyright Avail: Issuing Activity (National Technical Information Service (NTIS))

The possibility of using ultrasonics as a non-destructive test method for determining the state of cure in thermosetting materials is investigated. Four variations of an unsaturated polyester molding material were used to evaluate ultrasonics for cure monitoring. The test materials were each cured at a series of test temperatures up to 100 C. During cure the changes in velocity and attenuation of a transmitted ultrasonic pulse were measured at regular intervals. The ultrasonic velocity and attenuation measurements were then related to the test material's state of cure. NTIS

N94-27230*# Alabama Univ., Huntsville.
MATERIALS CHARACTERIZATION ON EFFORTS FOR ABLATIVE MATERIALS Final Report
Thomas P. Tytula, Kristin C. Schad, and Myles H. Swann Sep. 1992 53 p
(Contract NAS8-38609)
(NASA-CR-193929; NAS 1.26:193929; UAH-QERL-92-1) Avail: CASI HC A04/MF A01

Experimental efforts to develop a new procedure to measure char depth in carbon phenolic nozzle material are described. Using a Shor Type D Durometer, hardness profiles were mapped across post fired sample blocks and specimens from a fired rocket nozzle. Linear regression was used to estimate the char depth. Results are compared to those obtained from computed tomography in a comparative experiment. There was no significant difference in the depth estimates obtained by the two methods. Author

N94-27241# Tokyo Univ. (Japan). Inst. for Solid State Physics.
TECHNICAL REPORT OF ISSP. SER. A, NO. 2673: TWO SUCCESSIVE SPIN GLASS TRANSITIONS IN NON-DILUTED HEISENBERG-LIKE SPIN GLASS Ni(0.42)Mn(0.58) TiO3
Hazuki Kawano, Hideki Yoshizawa, Atsuko Ito, and Kiyoichiro Motoya Apr. 1993 14 p
(ISSN 0082-4798)
(JTN-94-80559) Avail: CASI HC A03/MF A01

Two successive Spin Glass (SG) transitions were observed in a non-diluted Heisenberg-like SG system with a weak planar single-ion anisotropy, Ni(0.42)Mn(0.58)TiO3. The moment lying in the easy plane freezes at T(sub SG)(sup parallel) = 9.5 +/- 1.0 K, while the remaining component perpendicular to the easy plane freezes at a lower temperature T(sub SG)(sup perpendicular) = 6.0 +/- 0.5 K, being consistent with theory on the Heisenberg-like SG system with a weak single-ion anisotropy. The diffuse scattering profile is well described by a Lorentzian in an intermediate phase T(sub SG)(sup parallel) greater than or equal to T greater than T(sub SG)(sup perpendicular) as well as in a paramagnetic phase T greater than T(sub SG)(sup parallel), whereas it strongly deviates from the Lorentzian below T(sub SG)(sup perpendicular). Author (NASDA)

N94-27429*# Stuckey (James M.), Decatur, AL.
CRYOGENIC INSULATION STUDIES Final Report, 15 Sep. 1993 - 9 Mar. 1994
James M. Stuckey 9 Mar. 1994 10 p
(NASA Order H-70979-D)
(NASA-CR-195266; NAS 1.26:195266; Rept-A-5) Avail: CASI HC A02/MF A01

The following are discussed: CPR-488/141-B problem (CPR XUS); CPR XUS foam popcorning (wind tunnel test); BX-250/141-B spray problem; NCFI 24-57 (NCFI-141B); PDL 4034/141B pour foam; primer for ET; and potential TMCPP toxic problem. CASI

N94-27611# Minnesota Mining and Mfg. Co., Saint Paul. Corporate Research Labs.
DUAL CURE LOW-VOC COATING PROCESS Semiannual Report, 1 Apr. - 30 Sep. 1992
K. E. Kinzer Oct. 1993 38 p
(Contract DE-AC04-88ID-12692)
(DE94-000365; DOE/ID-12692/4) Avail: CASI HC A03/MF A01

The objective of Phase 3 of 3M's contract with the U.S. Department of Energy is to complete proof-of-principle testing in full-scale systems of the dual cure photocatalyst technology developed in earlier Phases of the program. The Phase 3 commercial applications to be demonstrated are aerospace topcoats, aerospace primers, and solventless manufacture of tape backings. This report details activities of Phase 3 during this reporting period. In the second six months of Phase 3, work has continued in all three applications. Significant progress has been made in improving the performance of the urethane/acrylate formulation being used for the aerospace topcoat application. Key improvements have been made in obtaining increased reverse impact, initial gloss and gloss retention during accelerated weathering. Technical challenges have continued with the aerospace primer formulation. Efforts in this six months have continued to focus on establishing a good baseline epoxy/acrylate formulation with reliable cure conditions. Work on the third demonstration application, development of solventless backing saturants for electrical tape backings, has essentially been completed. Optimal dual cure resin formulations have been identified and utilized in preparing complete tape constructions. These tapes have been evaluated and characterized in terms of benchmark UL and internal 3M specifications for electrical tape performance. DOE

N94-27675# Department of the Navy, Washington, DC.
DISCRETE VACUUM ULTRA VIOLET REFLECTIVE INTERFERENCE FILTER Patent Application
William R. Hunter, inventor (to Navy) and James P. Long, inventor (to Navy) 27 Jun. 1993 22 p
(AD-D016059; US-Patent-Appl-SN-099489; Navy-Case-74607) Avail: CASI HC A03/MF A01

A thin film reflecting interference filter (RIF) is designed to suppress unwanted harmonics thereby improving the monochromaticity of the radiation. An interference layer of material which has a well-defined plasma oscillation is deposited on a substrate and a mismatch layer is formed thereon. This interference layer exploits the interference between wavefronts reflected from the layer-substrate and the vacuum-layer interfaces to suppress higher order harmonics, while allowing good reflectance at the fundamental wavelength. This is achieved by positioning the RIF in the radiation at an angle of incidence which is greater than the critical angle of the desired fundamental wavelength, but less than critical angles of the harmonics to be suppressed. The mismatch layer increases the reflectance of the unwanted harmonics at the vacuum-layer interface, thus allowing more complete destructive interference of the unwanted harmonics. The RIF can be tuned by altering the thickness of the layer, the composition of the layer, and/or the angle of incidence of the radiation. Author (DTIC)

N94-27692# Imagination Resources, Inc., Dublin, OH.
COMPATIBILITY OF REFRIGERANTS AND LUBRICANTS WITH ENGINEERING PLASTICS
R. C. Cavestri Dec. 1993 167 p

(Contract DE-FG02-91CE-23810)
(DE94-004959; DOE/CE-23810/15) Avail: CASI HC A08/MF A02

Twenty-three plastics have been subjected to immersion studies using seven different lubricants at 60 C and 100 C, and 10 different refrigerants at ambient and 60 C. In the first part of the study, 22 hermetic stress crack-creep rupture test chambers were used to determine dynamic effects of a constant dead weight load on plastic test bars immersed at 20 C in a 40% refrigerant 32 ISOVG branched acid polyolester lubricant. The creep modulus data of the 10 refrigerants, using a dead weight load of 25% of ultimate tensile, are compared to values for air and HCFC-22. In the second part, the plastic test bars were aged for 14 days at constant refrigerant pressure 300 psia with 17 refrigerant lubricant combinations at 150 C. Additional evaluations were conducted to elucidate the effects of temperature, refrigerant, and lubricant on the plastics. At 150 C, high acid formation (high TAN) was further examined with dehydrated plastics. These evaluations indicate that dehydrating the plastics reduced, but did not eliminate, high TAN values and that heat alone caused the lost physicals. Alternative HFC refrigerants had little impact on plastics; some polyolester lubricants caused identifiable changes. DOE

N94-27695# Ames Lab., IA.
SYNTHESIS, RHEOLOGY, AND FORMING OF Y-Ba-Cu-O CERAMICS Ph.D. Thesis
T. M. Green Jul. 1993 145 p
(Contract W-7405-eng-82)
(DE94-005558; IS-T-1642) Avail: CASI HC A07/MF A02

A chemical synthesis route is discussed which results in a low temperature precursor to YBaCuO ceramics; it is based on use of molten Ba(OH)2 8H2O flux. Two different chemical systems have been examined; the first one, based on nitrate salts, has been demonstrated to be a viable precursor material for tape casting and extrusion; the second, made from acetate salts, has been used for powder synthesis and extrusion. Rheology of pastes shows that their flow may be fit to either Bingham plastic or Hershel-Bulkley models. Yield stress is controlled in both pastes by volume fraction solids. Viscosity also follows solids loading in the paste. Shear thinning is controlled by colloidal nature of precursor. The paste has colloidal microstructure. Comparison of concentric cylinder rheometry and piston extrusion rheometry shows order of magnitude differences in yield stress, resulting from the test method and paste dilation. DOE

N94-27716# Argonne National Lab., IL.
ELECTRO-OPTIC MATERIALS BY SOLID SOURCE MOCVD
R. Hiskes (Hewlett-Packard Labs., Palo Alto, CA.), S. A. Dicarolis (Hewlett-Packard Labs., Palo Alto, CA.), J. Fouquet (Hewlett-Packard Labs., Palo Alto, CA.), Z. Lu (Stanford Univ., CA.), R. S. Feigelson (Stanford Univ., CA.), and R. K. Route (Stanford Univ., CA.) Dec. 1993 12 p Presented at the Fall Meeting of the Materials Research Society (MRS), Boston, MA, 29 Nov. - 3 Dec. 1993
(Contract W-31-109-eng-38)
(DE94-005120; ANL/MSD/CP-81580; CONF-931108-36) Avail: CASI HC A03/MF A01

The solid source MOCVD technique, employing a single powder vaporization source composed of mixed beta-diketonate metalorganic compounds, has been used to grow thin films of a variety of electro-optic materials including lithium niobate, strontium barium niobate, and potassium niobate. Preliminary results for potassium niobate films indicate that a volatile potassium organometallic source can be useful for growing potassium niobate by MOCVD. High single phase (001) oriented strontium barium niobate films have been deposited which exhibit waveguiding behavior. The most extensive work has been done on lithium niobate deposited epitaxially on a variety of substrates. Oriented z-axis (001) films have been grown on c-axis sapphire with and without a (111) oriented platinum base electrode and on a bulk grown lithium niobate substrate. Films grown directly on c-axis sapphire at 700 C exhibit x-ray rocking curve linewidths as low as .044 degrees, nearly perfect in-plane orientation as determined by x-ray phi scans, and a peak-to-peak surface roughness of less than 40 A. Optical waveguiding has been demonstrated by single prism coupling technique on similar films 1175 - 2000 A thick grown at 500 C, with optical losses of approximately 2 db/cm at 632.8 nm measured over 3.5 cm long films. Polarization vs. electric field measurements on 1100 A thick films grown on platinum show a hysteresis loop indicating ferroelectric behavior. DOE

N94-27726# Sandia National Labs., Albuquerque, NM.
ION IMPLANTATION IN SILICATE GLASSES
G. W. Arnold 1993 31 p Presented at the 3rd Pacific Rim Forum on Composite Materials: Low-Cost High-Volume Composite Materials, Honolulu, HI, 7-10 Nov. 1993
(Contract DE-AC04-94AL-85000)
(DE94-003785; SAND-93-0574C; CONF-931168-2) Avail: CASI HC A03/MF A01

This review examines the effects of ion implantation on the physical properties of silicate glasses, the compositional modifications that can be brought about, and the use of metal implants to form colloidal nanosize particles for increasing the nonlinear refractive index. DOE

N94-27747# Los Alamos National Lab., NM.
CORROSION RESISTANT COATINGS FROM CONDUCTING POLYMERS
Debra A. Wrobleski, Brian C. Benicewicz, Karen G. Thompson (National Aeronautics and Space Administration. John F. Kennedy Space Center, Cocoa Beach, FL.), and Coleman J. Bryan (National Aeronautics and Space Administration. John F. Kennedy Space Center, Cocoa Beach, FL.) 1993 3 p Presented at the 207th Spring National Meeting of the American Chemical Society, San Diego, CA, 13-18 Mar. 1994
(Contract W-7405-eng-48)
(DE94-003959; LA-UR-93-3966; CONF-940301-3) Avail: CASI HC A01/MF A01

Cr-based corrosion resistant undercoatings will have to be replaced because of environmental and health concerns. A coating system of a conducting polyaniline primer layer topcoated with epoxy or polyurethane, is being evaluated for corrosion resistance on mild steel in 0.1 M HCl or in a marine setting. Results of both laboratory and Beach Site testing indicate that this coating is very effective; even when the coatings are scratched to expose bare metal, the coated samples show very little signs of corrosion in the exposed area. DOE

N94-27801 University of Western Ontario, London. Faculty of Engineering Science.
ELECTROCHEMICAL PROPERTIES OF PASSIVE FILMS ON 440C STAINLESS STEEL Ph.D. Thesis
Timothy Lawrence Walzak Oct. 1990 384 p
(ISBN-0-315-64248-3; CTN-94-60994) Copyright Avail: Micromedia Ltd., Technical Information Centre, 240 Catherine Street, Suite 305, Ottawa, Ontario, K2P 2G8, Canada HC/MF

Type 440C stainless steel is a high-C, high-Cr martensitic steel used in applications requiring high hardness and wear resistance in combination with moderate corrosion resistance. Typical applications include precision aerospace bearings and critical components in computer disk drives. The properties of passive films formed on 440C steel were investigated using advanced electrochemical techniques with a view to establishing a method to measure film stability directly in the passivation baths. Electrochemical measurements were sensitive to the passive film properties and were able to quantify the effect of cooling rate on passive film stability. The techniques used included linear polarization, AC impedance, small amplitude cyclic voltammetry, and coulostatic transient measurements. These provided results that exhibited excellent agreement with the AC impedance technique providing the most information about the interfacial reactions. It was found that the full electrochemical characterization of the passive film stability required evaluation of both the polarization resistance and the interfacial capacitance, thus precluding use of DC measurements. The coulostatic technique demonstrates the most promise as a monitoring tool as it provides a rapid, simple measurement of both the polarization resistance and capacitance. Author (CISTI)

N94-27812# Japan Atomic Energy Research Inst., Tokyo.
OUTGAS AND VACUUM SEAL CHARACTERISTICS OF IRRADIATED POLYIMIDE O-RING
Takuya Terakado (Japan Atomic Energy Research Inst., Naka.), Kiyoshi Shibanuma (Japan Atomic Energy Research Inst., Naka.), Yoshinao Ohkawa (Japan Atomic Energy Research Inst., Naka.), and Tadao Seguchi (Japan Atomic Energy Research Inst., Takasaki.) Mar. 1993 49 p
(DE94-701200; JAERI-M-93-067) Avail: CASI HC A03/MF A01

In application of polymeric materials to the fusion experimental reactor, outgas and vacuum seal characteristics of irradiated polyimide were studied. Crystalline polyimide is used as a test specimen, which is cut into the equivalent of O-ring V40 for JIS vacuum flange 25A. Irradiation conditions of the test specimen are three, i.e., absorbed dose 0, 5 and 10 MGy corresponding to 0, 50 and 100 hours of irradiation, respectively, under the induced dose rate of 10(exp 5) Sv/h in the vacuum vessel after shutdown of the experimental reactor, and temperature conditions of the test specimen are room temperature, 180 C, baking temperature of the vacuum vessel, and 350 C, baking temperature of plasma facing components, such as the divertor and the first wall. In outgas characteristic, outgassing rate and outgas mass spectra were measured, and in vacuum seal characteristic, the relation between helium leak rate and compression ratio of the test specimen was evaluated. By comparing the test results, outgassing and vacuum seal characteristics of irradiated polyimide O-ring were clarified. DOE

N94-27837 International Centre for Theoretical Physics, Trieste (Italy).
FRAGMENTATION OF Ge(1-x) Sn(x) Se2 GLASSES
G. Saffarini Aug. 1993 16 p Limited Reproducibility: More than 20% of this document may be affected by microfiche quality
(DE94-603009; IC-93/246) Avail: CASI HC A03 (US Sales Only)

Density, differential scanning calorimetry (DSC), X-ray diffraction (XRD), and X-ray photoelectron spectroscopy (XPS) measurements of Ge(1-x)Sn(x)Se2 within 0.0 less than or equal to x less than or equal to 0.6 have been obtained. Upon increasing the Sn content, the density measurements show a non-monotonic decrease, while the differential scanning calorimetry measurements show a monotonic decrease of the glass transition temperature. The X-ray diffraction measurements on these glasses give interference functions which have first sharp diffraction peaks (FSDP) indicating the presence of intermediate range order (IRO). The X-ray photoelectron spectroscopy measurements were used to determine the plasmon energies from the L(sub 3)M(sub 4,5)M(sub 4,5) selenium Auger peaks which may be looked upon as being determined by the local electron density about the selenium atoms. It is found that the plasmon energies deduced from the Auger peaks change markedly with the Sn content in these glasses. These results are consistent with the fragmentation of the molecular cluster network model proposed by Mikrut and McNeil. DOE

N94-27845 China Nuclear Information Centre, Beijing.
EXPERIMENT AND RESEARCH ON MATERIALS IRRADIATED BY PLASMA RADIATION
Hong Wenyu (Southwestern Inst. of Physics, Sichuan, China.), Yao Lianghua (Southwestern Inst. of Physics, Sichuan, China.), Tang Sujun (Southwestern Inst. of Physics, Sichuan, China.), Chang Shufen (Southwestern Inst. of Physics, Sichuan, China.), and Li Guodong (Southwestern Inst. of Physics, Sichuan, China.) Aug. 1992 11 p Limited Reproducibility: More than 20% of this document may be affected by microfiche quality
(DE94-605011; CNIC-00660; SIP-0052) Avail: CASI HC A03 (US Sales Only)

The TiC and SiC coating on the graphite substrate and wall carbonization were studied by plasma radiation in HL-1 tokamak. Samples were analyzed with auger electron spectroscopy (AES), scanning electron microscopy (SEM), x ray photoelectron spectroscopy (XPS), and x ray diffraction spectroscopy (XDS). The results show that the TiC and SiC materials coated on limiter and wall and wall carbonization can reduce the metal and oxygen impurities and improve the plasma merit. DOE

N94-27857 China Nuclear Information Centre, Beijing.
THE ZnO THIN FILMS WITH C-AXIS ORIENTATION PREPARED ON THE ROOM TEMPERATURE SUBSTRATE BY THE ECR MULTIPOLAR PLASMA SPUTTERING METHOD
Zhaoyuan Ning (Academia Sinica, Hefei, China.), Yanling Zhang (Academia Sinica, Hefei, China.), Zhaoxing Ren (Academia Sinica, Hefei, China.), Yujin Xiao (Academia Sinica, Hefei, China.), and Xiangqun Li (Academia Sinica, Hefei, China.) Aug. 1992 11 p Limited Reproducibility: More than 20% of this document may be affected by microfiche quality
(DE94-605039; CNIC-00653; ASIPP-0035) Avail: CASI HC A03 (US Sales Only)

Zinc oxide (ZnO) films with c-axis orientation have been prepared on room temperature substrates by a reactive sputtering deposition utilizing electron cyclotron resonance multipolar (ECRM) plasma apparatus built with Nd-Fe-B magnets and 2.45 GHz, TE(sub 10) mode microwave. The plasma distributions in the axial direction were found to be sensitive to the magnetic field configurations in the plasma cavity. The XRD, TEM, and SEM analyses indicated that the deposited ZnO films were of nanometer size, smooth, and dense with high c-axis orientation. DOE

N94-25570# National Research Inst. for Metals, Tokyo (Japan). Surface and Interface Div.
STUDY ON SUBSTANCE DIFFUSION IN THIN FILMS WITH CONTROLLED STRUCTURES [KOZO SEIGYO SARETA HAKUMAKUCHU NI OKERU BUSSHITSU NO KAKUSAN GENSHO NI KANSURU KENKYU]
Kazuhiro Yoshihara, Yuji Ikeda, Masahiro Tosa, and Michiko Yoshitake *In its* Bulletin of National Research Institute for Metals in Fiscal Year 1993, No. 14 29 Jan. 1993 p 241-252 In JAPANESE (For primary document see N94-25544 07-26)
Avail: CASI HC A03/MF A04

N94-27904*# Mary Washington Coll., Fredricksburg, VA. Dept. of Chemistry.
NEW MONOMERS FOR HIGH PERFORMANCE POLYMERS
Roy F. Gratz *In* Old Dominion Univ., The 1993 NASA-ODU American Society for Engineering Education (ASEE) Summer Faculty Fellowship Program Dec. 1993 p 100-101 (For primary document see N94-27893 07-80)
Avail: CASI HC A01/MF A03

N94-27926*# College of William and Mary, Williamsburg, VA. Dept. of Chemistry.
PROPERTY ENCHANCEMENT OF POLYIMIDE FILMS BY WAY OF THE INCORPORATION OF LANTHANIDE METAL IONS Abstract Only
David W. Thompson *In* Old Dominion Univ., The 1993 NASA-ODU American Society for Engineering Education (ASEE) Summer Faculty Fellowship Program Dec. 1993 p 189 (For primary document see N94-27893 07-80)
Avail: CASI HC A01/MF A03

28 PROPELLANTS AND FUELS

Includes rocket propellants, igniters, and oxidizers; their storage and handling procedures; and aircraft fuels.

For related information see also *07 Aircraft Propulsion and Power, 20 Spacecraft Propulsion and Power,* and *44 Energy Production and Conversion.*

N94-25901# Coordinating Research Council, Inc., Atlanta, GA. Octane Technology and Test Procedures Group.
CRC CUSTOMER VERSUS RATER OCTANE NUMBER REQUIREMENT PROGRAM (1990)
Oct. 1993 127 p
(AD-A273997; CRC-586) Avail: CASI HC A07/MF A02

A CRC cooperative program was conducted to determine the difference in octane requirements between technical raters and 'customers' (the general driving public). The tests were conducted in two phases, with the second being a repeat of the first to verify the results obtained. The trained raters used the CRC E-15 procedure to determine the octane requirement of the vehicles while the customers' perception and objection to knock were determined through the use of a questionnaire. The customers' responses (perception and objection level) were based upon audible knock, acceleration performance, and after-run on a series of full-boiling-range customer/rater unleaded (FBRCU) reference-fuels. Data were analyzed from 168 1988-1991 model-year vehicles, with 126 of these tested in Phase 2. The results showed that the customers, objections, and perceptions were overwhelmingly based on knock, rather than acceleration performance or after-run. Two general methods, a population comparison and a delta analysis, were used to estimate the difference between customer and rater octane requirements. In the first method, the data were analyzed by comparing satisfaction curves for the technical and customer octane requirements (population comparison). DTIC

N94-25907 Swedish Inst. for Materials Testing, Boras.
ANALYTICAL METHOD FOR ESTIMATION OF THE TOTAL AMOUNT OF AROMATIC AND POLY AROMATIC COMPOUNDS IN DIESEL FUEL [ANALYSMETOD FOER BESTAEMNING AV HALTEN AROMATER OCH POLY-AROMATER I DIESELOLJA]
L. Cedheim, B. Lundgren, and P. Marstorp 1993 38 p In SWEDISH
(PB94-123692; SP-RAPP-1993:14) Avail: Issuing Activity (National Technical Information Service (NTIS))

The total amounts of PAH and of aromatic compounds have been estimated with a HPLC method. The type of the compounds in the PAH fraction was elucidated with a GCMS method. The HPLC method is based on a modified version of IP 391/1990. The main difference between the old and the modified method is that the flow direction through the columns will be reversed after the dicyclic aromatic fraction has elucidated. The time when the reversion of the flow direction should occur is determined with aid of an additive, azulene. NTIS

N94-26198# Sandia National Labs., Livermore, CA.
A MATERIALS COMPATIBILITY STUDY IN FM-1, A LIQUID COMPONENT OF A PASTE EXTRUDABLE EXPLOSIVE
S. H. Goods, T. J. Shepodd, B. E. Mills, and P. Foster (Mason and Hanger-Silas Mason Co., Inc., Amarillo, TX.) Sep. 1993 27 p
(Contract DE-AC04-76DR-00789)
(DE94-001166; SAND-93-8237) Avail: CASI HC A03/MF A01

The chemical compatibility of various metallic and organic containment materials with a constituent of a paste extrudable explosive (PEX) has been examined through a series of long-term exposures. Corrosion coupons and mechanical test specimens (polymers only) were exposed to FM-1, a principal liquid component of PEX, at 74 C. The LLNL designator for this formulation is RX-08-FK. Compatibility was determined in the following manner: by measuring changes in weight, physical dimensions, and mechanical properties; by examining the coupons for discoloration, surface attack, and corrosion products; and by analyzing for dissolved metals in the FM-1. Of the metals and alloys examined, none of the 300 series stainless steels exhibited adequate corrosion resistance after 74 days of exposure. Copper showed evidence of severe uniform surface attack. Monel 400 also exhibited signs of chemical attack. Nickel and tantalum showed less evidence of attack, although neither was immune to the liquid. Gold coupons developed a 'tarnish' film. The gold along with an aluminum alloy, 6061 (in the T6 condition) performed the most satisfactorily. A wide range of polymers were tested for 61 days at 74 C. The materials that exhibited the most favorable response in terms of weight change, dimensional stability, and mechanical properties were Kalrez, PTFE Teflon, and polyethylene. DOE

N94-26437# Army Armament Research, Development and Engineering Center, Picatinny Arsenal, NJ.
THERMAL CONDUCTIVITY OF PAX 2A EXPLOSIVE BY DSC Final Report
Joel Harris Dec. 1993 11 p
(AD-A274721; ARAED-TR-93020) Avail: CASI HC A03/MF A01

A technique to determine the coefficient of thermal conductivity by Differential Thermal Calorimetry (DSC) was developed. The thermal conductivity for teflon (polytetrafluoroethylene), high melt explosive (HMX), and PAX-2A explosive were determined. The thermal conductivity values determined for teflon and HMX agree with those found in literature; whereas, the value for PAX-2A was determined to be 14.26 + or - 0.26 x 10(exp -4) calories/cm-s-deg C. DTIC

N94-26486# Eagle-Picher Industries, Inc., Joplin, MO.
EFFECTS OF REPEATING RESISTANCE TESTING ON FIRING ABILITY OF IGNITER EP360-3 Interim Report, Mar. - Sep. 1993
Gary ODay Oct. 1993 54 p
(Contract F33601-93-P-7648)
(AD-A274814; SPP-9309052; WL-TR-93-2104) Avail: CASI HC A04/MF A01

This report summarizes work completed under U.S. Air Force Contract F3360193P7648 Item Number 02 completed 8 September 1993. The objective of this test was to determine if repeated resistance checks of an igniter will degrade the igniters ability to fire. An Eagle-Picher Industries, Inc. EP 360-3 igniter (part number 31-32-026-0) was used for this test. A control group was tested for firing sensitivity. A second group had 10,001 resistance checks taken at 1 milliamp. The second group was then tested for firing sensitivity. No significant difference was found between the two groups. DTIC

N94-26753# Little (Arthur D.), Inc., Cambridge, MA.
NATURAL GAS APPLICATIONS FOR HYBRID VEHICLES. Final Report, Oct. 1992 - Jul. 1993
Jeffrey M. Bentley Aug. 1993 68 p Sponsored by Gas Research Inst., Chicago, IL
(PB94-117108; Rept-41377; GRI-93/0266) Avail: CASI HC A04/MF A01

Hybrid vehicle technology holds the potential for improved efficiency and emissions compared with internal combustion (IC) engines and improved range and refueling convenience over electric vehicles. This study evaluated the potential for using natural gas as a hybrid vehicle fuel. Potential regulatory and market drivers were evaluated for hybrids generally and natural gas hybrids in specific. Heat engine options and other configuration issues were investigated to determine efficiency, emissions, or other benefits of light- and heavy-duty hybrids. Several hybrid vehicle configurations were evaluated to determine the specific packaging attributes of natural gas in a hybrid configuration. Generally, conventional IC engines appear adequate for most emissions-sensitive hybrid applications with no great advantage being gained from using turbines or other more advanced heat engines. The largest technology barrier to a near-term hybrid is the weight of available or near-term batteries. Smaller, light-duty hybrid vehicles will be more sensitive to this weight handicap than larger vehicles such as the urban transit bus. NTIS

N94-26800 General Atomics Technologies Corp., San Diego, CA.
CRYOGENIC SIZE REDUCTION OF SOLID PROPELLANT Final Report
Will P. Creedon and Michael H. Spritzer Mar. 1993 115 p Limited Reproducibility: More than 20% of this document may be affected by microfiche quality
(AD-A274844; ESL-TR-92-30) Avail: CASI HC A06

A growing need exists to develop improved methods for the disposal and/or recovery of solid rocket propellants. Laboratory, bench-scale, and prototype tests were performed to develop the dry washout concept for size reduction and removal of solid propellants using cryogenic media. Three propellant types were investigated: Hazard Class 1.1 composite modified double base (CMDB), Hazard Class 1.1 cross-linked double base (XLDB), and Hazard Class 1.3 hydroxl terminated polybutadiene (HTPB). No propellant initiations were detected. The laboratory tests established that essentially no change in the sensitivity of the test propellants occurs between ambient and cryogenic temperature. Impact, friction, low-level shock, and electrostatic discharge sensitivity tests were conducted. Over 2000 trials were conducted. The bench-scale tests demonstrated the safety of liquid nitrogen washout and established parameter ranges for effective propellant removal. Removal rates of greater than 60 pounds per hour were achieved for all propellant types. The prototype tests demonstrated cryogenic washout of several reduced scale motors in a semiautomated process. Two motors were processed, one containing 40 pounds of XLDB propellant, the other containing 60 pounds of HTPB propellant. Propellant removal rates ranged from 8.3 pounds per hour to 156 pounds per hour with liquid nitrogen flow of less than 4 gpm. DTIC

N94-26905 New Energy and Industrial Technology Development Organization, Tokyo (Japan).
FEASIBILITY STUDY ON INTRODUCTION OF TRANSPORTATION-USE PETROLEUM SUBSTITUTION ENERGY
Mar. 1993 112 p In JAPANESE Limited Reproducibility: More than 20% of this document may be affected by microfiche quality
(DE94-725205; NEDO-P-9225) Avail: CASI HC A06

As a part of the development of petroleum substitution energy, development of vehicles using petroleum substitution fuel has been promoted to meet a need for abating pollution caused by automobile exhaust gas in cities. This investigation is first made on the trends of making the existing cars low-pollutant, of policies for wide use/promotion of substitution fuel cars, and of possession of vehicles. It is then made on assumption of future performance and cost of electric vehicles, methanol cars and CNG cars through hearing on expert opinions from makers, promotion organizations, etc. Based on the assumption, shares of existing cars and petroleum substitution cars in newly registered cars are set up in time sequence, and a built simulation model for wide spread estimates the number of vehicles which can be spread by 2010. The result shows the number of vehicles to be spread is 380,000, and it is lower than those targeted and predicted by industry-associated organizations. For wide spread, it is important to select suitable markets for substitution fuel cars as promotion targets. DOE

N94-26914 New Energy and Industrial Technology Development Organization, Tokyo (Japan).
PRESENT SITUATION OF THE DEVELOPMENT OF PETROLEUM SUBSTITUTION ENERGY (FRANCE)
Mar. 1993 47 p In JAPANESE Limited Reproducibility: More than 20% of this document may be affected by microfiche quality
(DE94-725201; NEDO-P-9206) Avail: CASI HC A03

Survey is made to grasp the developmental trend of petroleum substitution energy in France. Since EC's market integration in 1993, France has been forced to change its energy policy to EC rules and has attempted opening the domestic market and strengthening the international competitiveness, taking measures such as adoption of the act on the internationalization of open tenders for public works. The petroleum industry requires a capital investment which is 5 billion francs annually or 45 billion francs in total through 2000 to cope with regulations related to petroleum industry wastes. The industry circle is against the carbon tax proposed by the EC commission, and companies in the petroleum industry are going ahead with their own environmental measures. The government is expected to make an increase in tax on petroleum products which amounts to 1.5 billion francs in fiscal 1993. However, the petroleum industry is in bad shape. The move toward promotion of the use of substitutional fuels using agricultural products as raw materials has been intensifying. Reduced dependence on nuclear power and introduction of substitutional fuels are proposed; however, Electricite de France makes an upward revision of nuclear power plant construction projects. The conventional nuclear power generation promotion line will be maintained together with diversification of energy sources, energy conservation, and environmental policies. DOE

N94-27719# Lawrence Livermore National Lab., CA.
UNCERTAINTIES IN THE CHARACTERIZATION OF THE THERMAL ENVIRONMENT OF A SOLID ROCKET PROPELLANT FIRE
J. C. Diaz Oct. 1993 6 p Presented at the 2nd Probabilistic Safety Assessment and Management Conference, San Diego, CA, 20-24 Mar. 1994
(Contract W-7405-eng-48)
(DE94-002023; UCRL-JC-113809; CONF-940312-25) Avail: CASI HC A02/MF A01

There has been an interest in developing models capable of predicting the response of systems to Minuteman (MM) 3 third-stage solid propellant fires. Input parameters for such an effort include the boundary conditions that describe the fire temperature, heat flux, emissivity, and propellant burn rate. In this study, scanning spectroscopy and pyrometry were used to infer plume temperatures. Each diagnostic system possessed strengths and weaknesses. The intention was to use various supportive methods to infer plume temperature and emissivity because no one diagnostic had proven capabilities for determining temperature under these conditions. Furthermore, these diagnostics were being used near the limit of their applicability. All these points created some uncertainty in the data collected. DOE

N94-27725# Lawrence Livermore National Lab., CA.
THE ADDITION OF MOLECULAR OXYGEN TO HYDROPEROXY-PROPYL RADICALS
Joseph W. Bozzelli (New Jersey Inst. of Tech., Newark.) and William J. Pitz Oct. 1993 25 p Presented at the Fall Meeting of the Western States Section of the Combustion Institute, Menlo Park, CA, 18-19 Oct. 1993
(Contract W-7405-eng-48)
(DE94-003662; UCRL-JC-115320; CONF-931076-4) Avail: CASI HC A03/MF A01

The addition of hydroperoxy-alkyl radicals to molecular oxygen is an important process leading to chain branching in the low temperature oxidation of paraffins and at conditions related to autoignition and engine knock. The product channels for the addition of hydroperoxy-propyl radicals to molecular oxygen were estimated using bimolecular QRRK analysis and transition state theory. Thermochemistry of all the relevant species was estimated using group additivity. The main products at 1 - 15 atm are stabilization, alkyl carbonyl + OH, and in some cases an olefinic hydroperoxide + HO2. Product channels for each of the three hydroperoxy-alkyl isomers were analyzed, and rate expressions for each channel were calculated for a series of pressures over a temperature range of 600 - 1600 K. DOE

N94-28222# California Univ., Livermore. Lawrence Livermore Lab.
PROPELLANTS AND EXPLOSIVES IN BALLISTIC MISSILES
Edward James 15 Jul. 1993 33 p
(Contract W-7405-eng-48)
(UCRL-LR-113578) Avail: CASI HC A03/MF A01

The driving purpose of this document is to clarify technical facts that have been brought up by the findings and recommendations of the Drell report. Some of the findings and recommendations have been seriously challenged. The technical matters discussed in this report are intended to clarify some issues and misunderstandings. They are as follows: (1) detonation threshold (SDT or DDT) of Insensitive High Explosive (IHE) vs. conventional PBX nuclear warhead explosive (2) relative ignitability of Class 1.1 vs. Class 1.3 propellants; (3) magnitude of near- and far-field damage by accidental explosion or detonation; and (4) operational range penalties incurred with missile modifications. Neither the safety of the fusing and firing of the nuclear weapon nor the propellant igniter system are dealt with here. Primarily our attention is centered on handling accidents pertinent to SLBM's; however, related hazards in some other systems that have relevance are addressed. Author (revised)

N94-28226 Department of the Navy, Washington, DC.
LIQUID MONOPROPELLANTS Patent
Edward E. Baroody, inventor (to Navy), Horst G. Adolph, inventor (to Navy), Mortimer J. Kamlet, inventor (to Navy), Robert C. Gill, inventor (to Navy), and Herman S. Haiss, inventor (to Navy) 26 Oct. 1993 5 p Filed 3 Dec. 1979
(AD-D016074; US-Patent-5,256,220; US-Patent-Appl-SN-101402; US-Patent-Class-149-88) Avail: US Patent and Trademark Office

A novel formulation of liquid monopropellants is presented. The formulation is a mixture of high energy ingredients consisting of bis (2-fluoro-2,2-dinitroethyl) amine, bis (2-fluoro-2,2-dinitroethyl) formal, and bis (2,2,2-trinitroethyl) formal together with conventional liquid fuels and propellants to create a synergistic formulation having new and unexpected physical and chemical properties. DTIC

N94-25705*# Washington Univ., Seattle. Dept. of Aeronautics and Astronautics.
PROJECT MINERVA: A LOW-COST MANNED MARS MISSION BASED ON INDIGENOUS PROPELLANT PRODUCTION
Adam P. Bruckner, Hobie Anderson, Kelly Caviezel, Todd Daggert, Mike Folkers, Mark Fornia, Steven Hamling, Bryan Johnson, Martin Kalberer, and Mike Machula et al *In* USRA, Proceedings of the 8th Annual Summer Conference: NASA/USRA Advanced Design Program 1992 p 325-342 (For primary document see N94-25665 07-80)
Avail: CASI HC A03/MF A04

29 MATERIALS PROCESSING

Includes space-based development of products and processes for commercial applications.
For biological materials see *55 Space Biology.*

N94-25849*# California Univ., Berkeley. Lawrence Berkeley Lab.
INTERFACE CONFIGURATION EXPERIMENT: PRELIMINARY RESULTS
Paul Concus, Robert Finn (Stanford Univ., CA.), and Mark Weislogel (National Aeronautics and Space Administration. Lewis Research Center, Cleveland, OH.) Sep. 1993 16 p Presented at the Joint L+1 Science Review for USML-1 and USMP-1, Huntsville, AL, 22-24 Sep. 1993 Sponsored by NASA. Lewis Research Center
(Contract DE-AC03-76SF-00098)
(NASA-TM-109684; NAS 1.15:109684; DE94-003413; LBL-34819; CONF-9309279-1) Avail: CASI HC A03/MF A01

The Interface Configuration Experiment (ICE) was carried out on USML-1 to investigate liquid-gas interfaces in certain rotationally-symmetric containers having prescribed, mathematically derived shapes. These containers have the property that they admit an entire continuum of distinct equilibrium rotationally-symmetric interfaces for a given liquid volume and contact angle. Furthermore, it can be shown that none of these interfaces can be stable. It was found, after the containers were filled in orbit, that an initial equilibrium interface from the symmetric continuum reoriented, when perturbed, to a stable interface that was not rotationally symmetric, in accordance with the mathematical theory. DOE

N94-27220*# Alabama Univ., Huntsville. Center for Microgravity and Materials Research.
MODELLING OF THE MEA FLOAT ZONE USING ACCELEROMETER DATA Final Report, 24 Jun. 1991 - 4 Sep. 1993
J. Iwan D. Alexander 4 Sep. 1993 33 p
(Contract NAS8-36955)
(NASA-CR-193933; NAS 1.26:193933) Avail: CASI HC A03/MF A01

During a floating zone experiment involving the growth of indium on a recent orbiter mission, (STS 32) oscillation of the zone shapes were observed to occur in response to the background acceleration. An understanding of the nature of the response of the zone shape to forced (g-jitter) oscillations and predictions of its impact on future experiments is of great interest not only to the PI's but to other commercial and academic investigators who plan to fly similar experiments in the orbiter and on space station. Motivated by this, a 15 month study was undertaken to analyze the nature of the g-sensitivity of the STS 32 floating zone crystal growth experiment. Numerical models were used to describe the time-dependent free surface motion of the zone as it responds to the spacecraft residual acceleration. Relevant experimental data concerning the acceleration environment was obtained from the Honeywell in Space Accelerometer (HISA) investigators through MSFC's ACAP program and processed and analyzed. For the indium floating zone experiment, a series of calculations were made using time-dependent axial accelerations g(t). The form of g(t) included simple sinusoidal disturbances as well as actual data (subject to appropriate filtering) measured on the STS 32 mission. Focus was on the calculation of the response of the free surface of the zone as well as the internal flows and internal heat transfer. The influence of solidification on the response of the zone shape was also examined but found to be negligible. Author (revised)

N94-27341# Ishikawajima-Harima Heavy Industries Co. Ltd., Tokyo (Japan).
REPORT OF THREE MICROGRAVITY EXPERIMENTS BY THE DROP SHAFT [HEISEI 4 NENDO BISHO JURYOKU JIKKEN NI YORU SHIKEN KENKYU SEIKA HOKOKUSHO]
Shoichiro Kaibara, Koji Nezaki, Ryoji Imai, Toshikazu Yano, Isao Tanaka, Katsuhide Kitamura, Ichiro Tanasawa, Ikuya Haze, Keiichi Kuwahara, and Nobuya Suguri et al Tokyo, Japan Japan Space Utilization Promotion Center Mar. 1993 52 p In JAPANESE Prepared in cooperation with Kawasaki Heavy Industry, Hyogo, Japan and Inst. of Industrial Science, Tokyo Univ., Tokyo, Japan Sponsored by Japan Motorcycle Racing Organization, Tokyo, Japan
(JTN-94-80579) Avail: CASI HC A04/MF A01

The following were studied in microgravity: (1) welding phenomena; (2) fluid behaviors; and (3) truss structure attenuation properties. The following results were obtained: (1) welding experiments turned out to be possible to conduct in precipitation tower facilities; (2) in the basic studies utilizing differences in surface tensions by temperature slopes, data identical to theoretical formulae were obtained, proving the effectiveness of forecast by the formulae. In the experiment of specific periods for sloshing, it was found that basic dimensional sloshing was instantly generated but it did not sustain, and that high-dimensional sloshing waves were also generated on free surfaces but they attenuated pretty soon. Considerably large sloshing waves generated were important for calculation of dynamic pressure applied to vessels. And (3) data obtained on vibration/amplitude ratio in drop tests in microgravity were quite similar to those obtained under simulated non-gravity environment. The amount of play affected vibration behaviors in simulated non-gravity, but it had no effects in normal gravity. Subtle differences in supporting points affect vibration behaviors in both normal and simulated non-gravity environments. Author (NASDA)

N94-27664*# Nichols Research Corp., Arlington, VA.
SPACE EXPERIMENTS WITH PARTICLE ACCELERATORS (SEPAC) Final Report, 29 Sep. 1992 - 31 Dec. 1993
William W. L. Taylor 9 Feb. 1994 102 p
(Contract NAS8-39569)
(NASA-CR-193935; NAS 1.26:193935) Avail: CASI HC A06/MF A02

The scientific emphasis of this contract has been on the physics of beam ionosphere interactions, in particular, what are the plasma wave levels stimulated by the Space Experiments with Particle Accelerators (SEPAC) electron beam as it is ejected from the Electron Beam Accelerator (EBA) and passes into and through the ionosphere. There were two different phenomena expected. The first was generation of plasma waves by the interaction of the DC component of the beam with the plasma of the ionosphere, by wave particle interactions. The second was the generation of waves at the pulsing frequency of the beam (AC component). This is referred to as using the beam as a virtual antenna, because the beam of electrons is a coherent electrical current confined to move along the earth's magnetic field. As in a physical antenna, a conductor at a radio or TV station, the beam virtual antenna radiates electromagnetic waves at the frequency of the current variations. These two phenomena were investigated during the period of this contract. Derived from text

N94-28002# Japan Space Utilization Promotion Center, Tokyo.
PROMETHEUS IN SPACE: RESEARCH COMMITTEE ON FUNCTIONAL NEW MATERIAL Survey Report
Yoshihiro Hamakawa (Osaka Univ., Japan.), Yoshinobu Nakada (Mitsubishi Electric Corp., Tokyo, Japan.), Yoji Ishikawa (Obayashi Corp., Tokyo, Japan.), Osamu Okawa (Chiyoda Corp., Japan.), Keiichi Shibata (Toyo Engineering Corp., Chiba, Japan.), Shin-Ichi Kamei (Mitsubishi Research Inst., Inc., Tokyo, Japan.), Naoto Motegi (Toshiba Corp., Tokyo, Japan.), Joji Shinohara (Ishikawajima-Harima Heavy Industries Co. Ltd., Tokyo, Japan.), Misao Hashimoto (Nippon Steel Corp., Tokyo, Japan.), and Tadashi Sugihara (Mitsubishi Electric Corp., Tokyo, Japan.) et al Mar. 1993 163 p Sponsored by Japan Motorcycle Racing Organization Original contains color illustrations
(JTN-94-80580) Avail: CASI HC A08/MF A02

Development of new functional materials is vitally important in science and technology in the next century. Space can be utilized for investigating or fabricating new functional materials from the following three viewpoints: investigation of the materials that can be practically used in space, including those for space rockets, space satellites, and space stations; utilization of space as a material research laboratory where advanced technologies for fabricating materials can be learned under precise control on an atomic scale; and production of materials and devices of high utility in terms of performance, quantity, and size by taking advantage of the features of space such as microgravity, high vacuum, vast space, and plenty of solar energy. The effectiveness of expensive research in space could be justified from the following standpoints: to fabricate materials in space and use them in space; to fabricate materials in space and transport them to the earth; and to just forget about a direct economic payback with an expectation of a dramatic progress in material science in the future, resulting from fundamental research in space. Author (NASDA)

N94-25585# National Research Inst. for Metals, Tokyo (Japan). Advanced Materials Processing Div.
STUDY ON MELTED SOLUTION STIRRING UNDER MICROGRAVITY [BISHO JURYOKU KANKYO NI OKERU YUEKI NO KAKUHAN NI KANSURU CHOSA KENKYU]
Akira Sato, Ken Sasabe, Isao Nakatani, Kiyoshi Ozawa, Akira Fukuzawa, Kazuyuki Sakuraya, Kazumasa Togano, Hiroaki Kumakura, Daniel Robert Dietdrich, and Masao Takeyama et al *In its* Bulletin of National Research Institute for Metals in Fiscal Year 1993, No. 14 29 Jan. 1993 p 387-392 In JAPANESE (For primary document see N94-25544 07-26)
Avail: CASI HC A02/MF A04

N94-25707*# Worcester Polytechnic Inst., MA. Dept. of Mechanical Engineering.
MICROGRAVITY IGNITION EXPERIMENT
Vahid Motevalli, William Elliott, Keith Garrant, and Ryan Marcotte *In* USRA, Proceedings of the 8th Annual Summer Conference: NASA/USRA

Advanced Design Program 1992 p 358-364 (For primary document see N94-25665 07-80)
Avail: CASI HC A02/MF A04

31 ENGINEERING (GENERAL)

Includes vacuum technology; control engineering; display engineering; cryogenics; and fire prevention.

N94-25622# Technical Research Centre of Finland, Espoo. Structural Engineering Lab.
DESIGN OF COLD-FORMED HSS CHANNELS FOR BENDING AND ECCENTRIC COMPRESSION: BENDING IN THE PLANE OF SYMMETRY
Asko Talja Oct. 1992 96 p Sponsored by Technology Development Center of Finland; Rautaruukki Oy, Finland; Ministry of Environment, Finland; TE-EM Oy, Finland; Aaro Kohonen Oy, Finland; Magnus Malmberg Oy, Finland; and Juva Engineering Ltd., Finland
(VTT-TIED-1403; ISBN-951-38-4217-7; ETN-94-95250) Copyright Avail: CASI HC A05/MF A01

Open channel sections manufactured from High Strength Steels (HSS) were tested. The sections were bent in the plane of symmetry of the cross sections. The roll formed test profiles, one double U, two C and two hat profiles with yield stress of 560 to 670 N/sq mm and material thickness of 4 to 6 mm were taken from normal production. The buckling of plates or edge stiffeners was observed in some profiles. Tests for bending, eccentric compression and concentrated load were made. The test results together with other tests results from literature are compared with the design resistances determined according to the proposed design method. The method is satisfactory for normal design, but in some cases it was found to be too conservative. Comparisons with the other test results confirmed that the accuracy of the design rules do not depend on the yield strength or wall thickness. ESA

N94-25641# Technical Research Centre of Finland, Espoo. Safety Engineering Lab.
SAFETY ANALYSIS IN CONCEPTUAL DESIGN OF PROCESS CONTROL Ph.D. Thesis - Tampere Univ.
Arja Toola Oct. 1992 101 p Sponsored by Finnish Work Environmental Fund, and City of Tampere Scientific Foundation, Finland
(ISSN 1235-0621)
(VTT-PUBS-117; ISBN-951-38-4235-5; ETN-94-95233) Copyright Avail: CASI HC A06/MF A02

The conceptual design of process control systems, and the problem of safety requirements determination are investigated. Safety analysis methods of process design are applied. A two phase method Safe Control Requirements Analysis Method (SCRAM) was applied for analyzing the safety aspects of large processes within reasonable time. The first phase studies potential accidents on the basis of materials handled in the process circumstances. The second phase studies ways in which the process is led to unsafe states and how accidents may subsequently develop. The basic idea is to find the hazardous states of the process, the critical process parameters, and the accident chains. The desired operating conditions and parameters to be controlled are determined. The results show that the method identifies safety critical parameters and control actions and can be used for control system designers' purposes. ESA

N94-25775# Cranfield Inst. of Tech., Bedford (England). School of Industrial Manufacturing Science.
THE EFFECTIVENESS OF AMT INVESTMENT IN UK METAL COMPONENT MANUFACTURE
David Hamblin and Edward Nugent Nov. 1991 54 p Sponsored by Dept. of Trade and Industry, London, England
(Ind-Manu-Sci-Tech-Rept-3; ISBN-1-871564-484; ETN-94-95214) Copyright Avail: CASI HC A04/MF A01

The aim of the research was to investigate the effectiveness of capital investment, particularly investment in Advanced Manufacturing Technology (AMT). AMT encompasses not only production, but also design and administration areas. The intention was to make recommendations for the future direction of investment in the industry. The structure of the industry which comprises 54 companies is outlined. In order to obtain sufficiently detailed and accurate data, each company was visited. Discussions were held with managers covering the areas of production, engineering, finance, design, sales and marketing, quality and other strategic issues affecting investment decision making. The study conclusions and recommendations are presented. An overview of the industry and the survey sample are given. Company performance, practice relationships which link practice, and performance are discussed. ESA

N94-26027# Sandia National Labs., Albuquerque, NM.
PRIMARY STANDARDS LABORATORY REPORT 1ST HALF 1993
W. G. T. Levy, comp. Nov. 1993 30 p
(Contract DE-AC04-94AL-85000)
(DE94-003138; SAND-93-2246) Avail: CASI HC A03/MF A01

Sandia National Laboratories operates the Primary Standards Laboratory for the Department of Energy, Albuquerque Operations Office (DOE/AL). This report summarizes metrology activities that received emphasis in the first half of 1993 and provides information pertinent to the operation of the DOE/AL system-wide Standards and Calibration Program. DOE

N94-26084# Air Force Civil Engineering Center, Tyndall AFB, FL. Support Agency.
ENGINEERING TECHNICAL LETTER (ETL) 93-5: FIRE PROTECTION ENGINEERING CRITERIA, ELECTRONIC EQUIPMENT INSTALLATIONS
22 Dec. 1993 15 p
(AD-A274835) Avail: CASI HC A03/MF A01

This Engineering Technical Letter (ETL) provides criteria for protection of electronic equipment from smoke and fire. This ETL applies to all commands with electronic equipment installations. It also applies to new construction. To the extent that it is possible, renovation, modernization, and rehabilitation work shall also comply with the requirements of this ETL. DTIC

N94-26259# Technical Research Centre of Finland, Espoo. Nuclear Engineering Lab.
FIRE SIMULATION BASED ON CONVECTION CALCULATION [VIRTAUSLASKENTAAN PERUSTUVA TULIPALOJEN SIMULOINTI]
Risto Huhtanen and Tommy Jacobson Oct. 1992 51 p In FINNISH
(ISSN 1235-0605)
(VTT-TIED-1411; ISBN-951-38-4305-X; ETN-94-95271) Copyright Avail: CASI HC A04/MF A01

Fire simulation based on the convection calculation is described, and the result is compared to results obtained from a fire test carried out in an abandoned nuclear station. In the simulation, the convection field of the whole building is described, as well as the structures and extreme conditions affecting it. The fire is described as a data source whose value varies with time. The heat transmission in the structures is described using a separate heat transfer program. The result correctly describes the convection and temperature field caused by the fire. A 'discrete-transfer' method for calculating the heat radiation, progressing obliquely in relation to the calculation network, is given. ESA

N94-26261# Technical Research Centre of Finland, Espoo. Safety Engineering Lab.
EVALUATION AND IMPROVEMENT OF THE INQUEST SYSTEM ON WORK ACCIDENTS (TOT) [TYOEPAIKKAONNETTOMMUUKSIEN TUTKINTAJAERJESTELMAEN (TOT) ARVIOINTI JA KEHITTAEMINEN]
Jukka Lepistoe Nov. 1992 100 p In FINNISH
(ISSN 1235-0605)
(VTT-TIED-1418; ISBN-951-38-4312-2; ETN-94-95273) Copyright Avail: CASI HC A05/MF A02

A project to evaluate and improve the work accident inquest system TOT (Finnish acronym) is reported. The study began with visits to workplaces where mortal accidents had occurred. Inquest reports, accident information dissemination, and the use of inquest reports, were examined. The study showed that work-related accidental deaths had a warning value, due to the gravity of the event, that could be exploited in the prevention field. The inquest system was shown to operate stably, all elements operating at least satisfactorily, and no improvement objective could be distinguished as more urgent than another. Improvement possibilities in the general system operation and in the capacity of workplaces to use inquest reports were shown. ESA

N94-26341# Phillips Lab., Kirtland AFB, NM.
THE MICROSTRUCTURAL RESPONSE OF GRANULAR SOIL UNDER UNIAXIAL STRAIN Final Report, Sep. 1990 - Nov. 1992
John J. Gill Oct. 1993 112 p
(AD-A274808; PL-TR-92-1064) Avail: CASI HC A06/MF A02

Soil mechanical behavior is described and phenomenological (macroscopic) and microstructural (particulate) theories, developed to predict the constitutive response of granular media, are discussed. Special emphasis is given to the concept of fabric in granular media and how the concept relates to observed mechanical behavior. This report describes an experimental effort to quantify changes which occur in a cuboid specimen of granular silica material under uniaxial strains of up to 10 percent. The material tested was a poorly graded ottowa sand with specimens consisting of either 0.5- or 0.75-mm-diam. granules. The displacement fields perpendicular to the loading axis are generally not directly proportional to applied macroscopic strain as typically predicted by a local theory. Rather, the three 'zones' existing in a specimen under uniaxial strain are (1) a zone in which relatively high local displacements (and strain) occur (near the loading cap), (2) a zone behind this 'front' wherein the grains move directly in relation to the advance of the loading cap, and (3) a zone which has not yet responded to the advancing cap. Sidewall friction, although not negligible, appears not to play an overriding role in the grain micromotions. DTIC

N94-26429# Argonne National Lab., IL.
ELEVENTH SYMPOSIUM ON ENERGY ENGINEERING SCIENCES: PROCEEDINGS
1993 300 p Symposium held in Argonne, IL, 3-5 May 1993
(Contract W-31-109-eng-38)
(DE93-019930; CONF-9305134) Avail: CASI HC A13/MF A03

The Eleventh Symposium on Energy Engineering Sciences was held on 3-5 May 1993, at the Argonne National Laboratory, Argonne, Illinois. These proceedings include the program, list of participants, and the papers that were presented during the eight technical sessions held at this meeting. This symposium was organized into eight technical sessions: Surfaces and interfaces; thermophysical properties and processes; inelastic behavior; nondestructive characterization; multiphase flow and thermal processes; optical and other measurement systems; stochastic processes; and large systems and control. Individual projects were processed separately for the databases. DOE

N94-26634 Carleton Univ., Ottawa (Ontario). Norman Paterson School of International Affairs.
THE PROLIFERATION OF AEROSPACE WEAPONS TECHNOLOGY: BALLISTIC MISSILES AND THE CASE OF BRAZIL M.A. Thesis
Terrence John Vossen 13 Apr. 1993 147 p
(ISBN-0-315-84082-X; CTN-94-61050) Copyright Avail: Micromedia Ltd., Technical Information Centre, 240 Catherine Street, Suite 305, Ottawa, Ontario, K2P 2G8, Canada HC/MF

The rationale behind the development of ballistic missile production in Brazil is examined by exploring the political, military, and economic determinants of ballistic missile demand in that country. To ascertain how Brazil developed missile production capabilities, the contributions of aerospace industries in industrialized states, the Brazilian space program, trade between less-developed countries, and illicit trade in missile technology are assessed. It is argued that missile development increasingly became a function of economic as opposed to security considerations, and that technologies transferred from developed country aerospace firms and Brazil's space program were primarily responsible for the creation of production capabilities. It is also contended that the proliferation of missile technology to Brazil was consistent with the workings of a system evident in the aerospace weapons technology market that sustains the horizontal spread of weapons production capabilities. Author (CISTI)

N94-26756 National Inst. of Standards and Technology, Gaithersburg, MD. Building and Fire Research Lab.
SUMMARIES OF BFRL FIRE RESEARCH IN-HOUSE PROJECTS AND GRANTS, 1993
Nora H. Jason Sep. 1993 230 p See also PB93-116390, 1992 Limited Reproducibility: More than 20% of this document may be affected by microfiche quality
(PB94-121050; NISTIR-5263) Avail: CASI HC A11

The report describes the fire research projects performed in the Building and Fire Research Laboratory (BFRL) and under its extramural grants program during fiscal year 1993. The BFRL Fire Research Program has directed its efforts under three program thrusts. The in-house priority projects, grants, and externally-funded efforts thus form an integrated, focussed ensemble. The publication is organized along those lines: fire risk and hazard prediction - carbon monoxide prediction, turbulent combustion, soot, engineering analysis, fire hazard assessment, and large fires; fire safety of products and materials - materials combustion, furniture flammability, and wall and ceiling fires; and advanced technologies for fire sensing and control - fire detection and fire suppression. For the convenience of the reader, an alphabetical listing of all grants is contained in Part 2.0. NTIS

N94-26778# Lawrence Livermore National Lab., CA.
FABRICATION TECHNOLOGY
K. L. Blaedel Mar. 1993 9 p
(Contract W-7405-eng-48)
(DE94-003017; UCRL-ID-112774) Avail: CASI HC A02/MF A01

The mission of the Fabrication Technology thrust area is to have an adequate base of manufacturing technology, not necessarily resident at Lawrence Livermore National Laboratory (LLNL), to conduct the future business of LLNL. The specific goals continue to be to do the following: (1) develop an understanding of fundamental fabrication processes; (2) construct general purpose process models that will have wide applicability; (3) document findings and models in journals; (4) transfer technology to LLNL programs, industry, and colleagues; and (5) develop continuing relationships with the industrial and academic communities to advance the collective understanding of fabrication processes. The strategy to ensure success is changing. For technologies in which they are expert and which will continue to be of future importance to LLNL, they can often attract outside resources both to maintain their expertise by applying it to a specific problem and to help fund further development. A popular vehicle to fund such work is the Cooperative Research and Development Agreement with industry. For technologies needing development because of their future critical importance and in which they are not expert, they use internal funding sources. These latter are the topics of the thrust area. Three FY-92 funded projects are discussed in this section. Each project clearly moves the Fabrication Technology thrust area towards the goals outlined above. They have also continued their membership in the North Carolina State University Precision Engineering Center, a multidisciplinary research and graduate program established to provide the new technologies needed by high-technology institutions in the U.S. As members, they have access to and use of the results of their research projects, many of which parallel the precision engineering efforts at LLNL. DOE

N94-26804# Lawrence Livermore National Lab., CA.
CALCULATIONS OF MATERIAL REMOVAL, REMOVAL RATE, AND PRESTON COEFFICIENT IN CONTINUOUS LAPPING/POLISHING MACHINES
P. P. Hed 18 Oct. 1993 9 p
(Contract W-7405-eng-48)
(DE94-002619; UCRL-ID-115321) Avail: CASI HC A02/MF A01

Lapping and polishing machines usually do not have deterministic model to pre-determine removal rate and total material to be removed. The removal process is mainly affected by relative motion between the lap and the substrates, by load applied, and by mechano-chemical characteristics of the substrate material, as well as the abrasive and lap materials. Therefore, frequent measurements of the removal is necessary. This paper, written for optical technicians, includes formulas to calculate material removal from mass loss and removal rate from mass loss during operation. Establishing the removal rate helps by reducing the frequency of intermediate thickness measurements. The paper also includes the calculation of Preston coefficient, which is a measure of lapping process efficiency. DOE

N94-26819 Technische Univ., Delft (Netherlands).
PHYSICAL MODELLING AND ADAPTIVE PREDICTIVE CONTROL OF DIFFUSION/LPCVD REACTORS Ph.D. Thesis
H. deWaard 22 Dec. 1992 285 p Limited Reproducibility: More than 20% of this document may be affected by microfiche quality
(PB94-126398) Avail: CASI HC A13

The aim of this study is to design a temperature controller for batch electric diffusion/low pressure chemical vapor deposition (LPCVD) furnaces, that complies with the increasingly more stringent requirements of VLSI processing. A mathematical model has been developed for batch electric diffusion/LPCVD reactors that are currently used in the semiconductor industry for the fabrication of micro-electronic devices. The model has been formulated in terms of partial integro-differential equations, which are derived from the basic energy conservation law of physics. The model takes into account the effects of radiation and conduction. Chapter 2 gives a detailed description of the furnace system and provides some insight into the processes that take place. In chapter 3, the model of the diffusion/LPPCVD furnace is derived. Chapter 4 deals with the design of a temperature control system for the diffusion/LPCVD reactor, that makes use of the model as developed in chapter 3. Chapter 5 gives the results of the control designs, both of simulation and of application on a real furnace. Results of the linear quadratic Gaussian controller, the (non-adaptive) reduced order controller, and the adaptive predictive controller are presented. Finally, in chapter 6, some conclusions are drawn and suggestions for further research are given. NTIS

N94-27144# RedZone Robotics, Inc., Pittsburgh, PA.

AUTOMATED IN-SITU INSPECTION SYSTEMS FOR UNDERGROUND STORAGE TANKS Final Technical Report, 16 Aug. - 29 Dec. 1993

Chris C. Fromme and Warren C. Whittaker 29 Dec. 1993 35 p
(Contract DACA88-93-C-0008)
(AD-A274644; Rept-9224-RPT-004.1) Avail: CASI HC A03/MF A01

The Army-has 20,000 underground fuel storage tanks (UST's) that must be brought into compliance with the new federal regulations by 1998. To be compliant, a tank must be closed, upgraded or replaced. This report covers the investigative research for the development of a robotic system capable of performing an in situ ultrasonic thickness inspection on the interior of a fueled UST. The robotic system is designed to meet the criteria outlined in the Draft Standard for the Robotic inspection of Underground Storage Tanks developed for the EPA. This robotic inspection will allow the Army to make an informed decision on the appropriate action to be taken for a given tank. The robotic system offers a cost effective way to monitor a tank when compared with the existing manual technology that produces the same results. The robotic technology also moves the human out of the UST which eliminates the human liability factor in the hazardous environment. DTIC

N94-27976# Ministry of Agriculture, Forestry, and Fisheries, Ibaraki (Japan). National Research Inst. of Fisheries Engineering.

TECHNICAL REPORT OF NATIONAL RESEARCH INSTITUTE OF FISHERIES ENGINEERING: FISHING BOAT AND INSTRUMENT, NO. 12 [SUISAN KOGAKU KENKYUJO GIHO: GYOSEN KOGAKU DAI 12 GO]

Toshibumi Noma, Yasuo Morita, Hiroshi Masuda, Masaaki Yamamoto, Ryutaro Yamamoto, Toshihiko Kawashima, Katsuo Hasegawa, Yoshinari Tsuruta, and Tomonari Akamatsu et al 25 Mar. 1992 62 p In JAPANESE
(ISSN 0388-970X)
(JTN-94-80595) Avail: CASI HC A04/MF A01

The following topics were discussed: ships, fishing boats, high speed boats, marine safety, intact stability, righting, regulation, standards, law, IMO (International Maritime Organization), EHP (Effective Horse Power), horse power prediction, regression analysis, friction drag, ship configuration, calculus, ship engines, diesel engines, engine tests, combustion stability, combustion analysis, vibration analysis, test facilities, data acquisition, data processing, data analysis, personal computers, NO(sub x), exhaust emission, exhaust gases, and cetane index. For individual titles, see N94-27977 through N94-27980.

N94-27977# Ministry of Agriculture, Forestry, and Fisheries, Ibaraki (Japan). Ship Performance Section.

RECENT TREND OF DOMESTIC AND INTERNATIONAL REGULATIONS ON INTACT STABILITY OF SHIPS FOR SAFETY [SENPAKU NO ANZENSEI TO HI SONSHOJI FUKUGENSEI KISOKU NO SAIKIN NO DOKO]

Yasuyuki Yamakoshi *In its* Technical Report of National Research Institute of Fisheries Engineering: Fishing Boat and Instrument, No. 12 25 Mar. 1992 p 1-32 In JAPANESE (For primary document see N94-27976 07-31)
Avail: CASI HC A03/MF A01

It is important to develop an adequate regulation or standard for ships from a viewpoint of safety of life and ship at sea. The present report deals with recent trend of domestic and international regulations or standards on intact stability of ships with special attention to the activity of IMO (International Maritime Organization) and domestic standards of intact stability of ships established after 1986. Recently the importance of development of the rational regulations on intact stability of ships based on physical grounds has been recognized. Therefore, an advanced research for safety of life and ship at sea should be required. Author (NASDA)

N94-27978# Ministry of Agriculture, Forestry, and Fisheries, Ibaraki (Japan). Ship Performance Section.

E. H. P. ESTIMATION OF HIGH SPEED FISHING BOATS BY SOME EXISTING METHODS [KOSOKU ENGAN GYOSEN NI TAISURU BARIKI SUITEIHO NO TEKIYO NI TSUITE]

Toshikazu Masuya *In its* Technical Report of National Research Institute of Fisheries Engineering: Fishing Boat and Instrument, No. 12 25 Mar. 1992 p 33-42 In JAPANESE (For primary document see N94-27976 07-31)
Avail: CASI HC A02/MF A01

In recent years, the speed of coastal fishing boats are increasing up to 1.0 or more in Froude number. So the designers of fishing boats require the development of the estimation methods of EHP (Effective Horse Power) in high Froude number. Therefore, in this report, some existing methods are examined for the estimation of EHP on such high speed fishing boats by comparison with the results of the model experiments. Consequently, two methods show fairly good results. One is a formula by Radojcic and the other is a chart by Osumi-Kihara. Author (NASDA)

N94-27979# National Research Inst. of Fisheries Engineering, Tokyo (Japan). Engine and Machinery Section.

COMPUTER AIDED DATA RECORDING AND ANALYZING SYSTEM FOR THE ENGINE TEST [SHIKEN KIKAN NI OKERU DETA SHUROKU/KAISEKI SHISUTEMU]

Kenichi Oda and Katsuo Hasegawa *In its* Technical Report of National Research Institute of Fisheries Engineering: Fishing Boat and Instrument, No. 12 25 Mar. 1992 p 43-48 In JAPANESE (For primary document see N94-27976 07-31)
Avail: CASI HC A02/MF A01

This report describes computer aided data recording and analyzing system for the test engines in a laboratory. The system was developed for the purpose of recording and analyzing the engine data speedy and correctly. It is composed of two personal computers, A/D (Analogue to Digital)-converters and some measuring instruments. One of the computers functions as the analyzer of the low speed data, such as flow rate of fuel oil and several temperatures of the test engines; and another one functions as the analyzer of the high speed data, such as combustion pressure or vibration. These computers are connected with RS-232C interface, so researchers can control the system only to give the start command to the computer which treats low speed data. Author (NASDA)

N94-27980# National Research Inst. of Fisheries Engineering, Tokyo (Japan). Engine and Machinery Section.

THE EMISSION CHARACTERISTICS OF A HIGH SPEED DIESEL ENGINE [KOGATA DIZERU KIKAN NO NOKKUSU HAISHUTSU TOKUSEI]

Katsuo Hasegawa, Kenichi Oda, and Toshio Yamada *In its* Technical Report of National Research Institute of Fisheries Engineering: Fishing Boat and Instrument, No. 12 25 Mar. 1992 p 49-58 In JAPANESE (For primary document see N94-27976 07-31)
Avail: CASI HC A02/MF A01

The engine performances and the emission characteristics of a high speed diesel engine were experimentally investigated. The results indicate that NO(x) emission increases with a decrease in RPM (Revolution Per Minute) and increase of the inlet air temperature under the constant brake-mean effective pressures. It is very effective to delay the fuel injection timing for NO(x) emission reduction especially within the low speed range. NO(x) emission is influenced by temperature and pressure at the pre-mixed combustion. It also strongly depends on the cetane index of fuel. The NO(x) emission rate is closely related with the maximum pressure under specific operational conditions. Author (NASDA)

N94-25549# National Research Inst. for Metals, Tokyo (Japan).
R AND D FOR CREATION, MEASUREMENT, APPLICATION OF ULTRA-HIGH VACUUM [GOKUKOSHINKU NO HASSEI, KEISOKU, RIYO GIJUTSU NO KAIHATSU NI KANSURU KENKYU]
Kazuhiro Yoshihara, Masahiro Tosa, and Michiko Yoshitake *In its* Bulletin of National Research Institute for Metals in Fiscal Year 1993, No. 14 29 Jan. 1993 p 65-74 In JAPANESE (For primary document see N94-25544 07-26)
Avail: CASI HC A02/MF A04

N94-25676*# Georgia Inst. of Tech., Atlanta. School of Textile and Fiber Engineering.
DESIGN FOR PRODUCING FIBERGLASS FABRIC IN A LUNAR ENVIRONMENT
Rafer M. Benson, Dana R. Causby, Michael C. Johnson, Mark A. Storey, Dal T. Tran, and Thomas A. Zahr *In* USRA, Proceedings of the 8th Annual Summer Conference: NASA/USRA Advanced Design Program 1992 p 80-85 (For primary document see N94-25665 07-80)
Avail: CASI HC A02/MF A04

N94-25677*# Georgia Inst. of Tech., Atlanta. School of Textile and Fiber Engineering.
LUNAR PREFORM MANUFACTURING
Gregory N. Leong, Sandra Nease, Vicky Lager, Raffy Yaghjian, and Chris Waller *In* USRA, Proceedings of the 8th Annual Summer Conference: NASA/USRA Advanced Design Program 1992 p 86-90 (For primary document see N94-25665 07-80)
Avail: CASI HC A01/MF A04

N94-27369*# Massachusetts Univ., Lowell. Center for Productivity Enhancement.
AN ARTIFICIAL REALITY ENVIRONMENT FOR REMOTE FACTORY CONTROL AND MONITORING
Charles Paul Kosta and Patrick D. Krolak *In* NASA. Lewis Research Center, Vision 21: Interdisciplinary Science and Engineering in the Era of Cyberspace Dec. 1993 p 153-162 (For primary document see N94-27358 07-12)
Avail: CASI HC A02/MF A03

32 COMMUNICATIONS AND RADAR

Includes radar; land and global communications; communications theory; and optical communications.

For related information see also *04 Aircraft Communications and Navigation* and *17 Space Communications, Spacecraft Communications, Command and Tracking.* For search and rescue see *03 Air Transportation and Safety,* and *16 Space Transportation.*

N94-25639# Cranfield Inst. of Tech., Bedford (England). College of Aeronautics.
DEVELOPMENT OF SATELLITE TELECOMMUNICATIONS DURING THE PERIOD 1990 - 2005
D. Kumar Jan. 1993 60 p
(Cranfield-Aero-9301; ISBN-1-871564-56-5; ETN-94-95221) Avail: CASI HC A04/MF A01

The evolution of the global telecommunications market is reviewed. The changes that take place are a result of advances in technology as well as three powerful and interconnected forces: privatization, globalization, and liberalization. The introduction of new technologies in the form of Integrated Services Digital Networks (ISDN's) and integrated terminal equipment resulted in the transformation of the telecommunications services market from a single service industry limited by technology constraints into a multiservice industry limited by applications. As a result of privatization and globalization, the former national telecommunications carriers are beginning to expand overseas in order to grow. The changes indicate a shift in traffic structure as well as in the global satellite market structure. The analysis shows that satellite telecommunications will grow over the next fifteen years. ESA

N94-25647# Air Force Inst. of Tech., Wright-Patterson AFB, OH. School of Engineering.
EVALUATION OF AN ACOUSTIC CHARGE TRANSPORT (ACT) DEVICE FOR ADAPTIVE INTERFERENCE SUPPRESSION IN SPREAD SPECTRUM COMMUNICATIONS SYSTEMS M.S. Thesis
Michael S. Mills Dec. 1993 106 p
(AD-A274073; AFIT/GE/Eng/93D-27) Avail: CASI HC A06/MF A02

Analytical results have shown that adaptive filtering can be a powerful tool for the rejection of narrowband interference in a direct sequence spread spectrum receiver. However, the complexity of adaptive filtering hardware has hindered the experimental validation of these results. This thesis describes a unique adaptive filter architecture for implementing the Widrow-Hoff least mean square (LMS) algorithm using two state of the art acoustic charge transport (ACT) programmable transversal filters (PTF's). Signal to noise ratio improvement measurements demonstrate the effectiveness of the adaptive filter for suppressing single- and dual-tone jammers at jammer to signal ratios (JSR's) of up to 30 dB. It is shown that the ACT adaptive interference rejection system can consistently produce 55 dB notch depths with 3-dB bandwidths as low as 300 kHz with minimal degradation to the spread spectrum signal. It is also shown that the adaptive system can eliminate single tone jammers at any frequency within the spread spectrum bandwidth at any of 10, 20, or 30 dB JSRs within 10 to 15 iterations of the adaptive algorithm. The only drawback with the adaptive system as tested is the amount of time taken to perform an iteration because of the requirement to update the PTF tap weights sequentially. Suggestions are given as to how this particular parameter of the adaptive interference system could be optimized. DTIC

N94-25660# Rome Lab., Griffiss AFB, NY.
COMPONENT CHARACTERIZATION AND DEVELOPMENT 2 Technical Report, Oct. 1991 - Dec. 1992
Jacqueline D. Smith Sep. 1993 45 p
(AF Proj. 4600)
(AD-A274002; RL-TR-93-165) Avail: CASI HC A03/MF A01

The effort entitled, 'Component Characterization and Development II' was established in the Rome Lab Photonics Center Analog & Lightwave Photonics Branch as part of the overall in-house program plan to advanced the state-of-the-art in optics and electrooptics. The objective of the effort is to specify, acquire, and/or develop components for Air Force Command, Control, Communications, and Intelligence (C3I) applications. The source of prototype devices was designated to include academia, industry, and government organizations. Actual performance data was measured for both electro-optic and fiber-optic based devices that were of interest to communications, spatial laser control, and optical beamforming applications. Additionally, several novel approaches to device fabrication were investigated through a BAA contract with Syracuse University. DTIC

N94-25725# Carnegie-Mellon Univ., Pittsburgh, PA. Robotics Inst.
THE QUESTION OF STANDARDS FOR DIGITAL INTERACTIVE TELEVISION
Robert Thibadeau Nov. 1993 18 p
(Contract MDA972-92-J-1010; ARPA Order 6873)
(AD-A273872; CMU-RI-TR-93-23) Avail: CASI HC A03/MF A01

Pervasive change is near. Among the central elements of this change will be digital interactive television. It is generally thought that interactive television can have a profound beneficial impact on every element of the economy from average homeowner, to small and large business, and government agency. We have the opportunity now to engage public debate on what form interactive television should take. Should it come about as a series of private, mutually incompatible, insular systems, or should it be like television has traditionally been treated, subject to FCC standards akin to existing NTSC and the recently agreed HDTV standards. This article attempts to provide a framework for a broad discussion of such standards. DTIC

N94-25728# Air Force Inst. of Tech., Wright-Patterson AFB, OH. School of Engineering.
HYPERSPECTRAL ANALYSIS OF SPACE OBJECTS: SIGNAL TO NOISE EVALUATION M.S. Thesis
Daniel Hrovat Dec. 1993 154 p
(AD-A273882; AFIT/GSO/ENP/93D-02) Avail: CASI HC A08/MF A02

Hyperspectral analysis of space objects is being considered as a means of enhancing Space Object Identification (SOI) capabilities. This study develops a mathematical simulation based on fundamental radiometry principles to evaluate the feasibility of hyperspectral analysis of space objects. The study uses Signal to Noise Ratio (SNR) as the basis for the feasibility evaluation, and addresses the question: Is there enough target signal in narrow wavelength bandwidths to conduct hyperspectral measurements of space objects? The analysis characterizes the target signal and noise sources using fundamental radiometry, and develops a flexible radiometry model which calculates the target signal count rate, and SNR for a specified target-sensor configuration. The model was applied to four case studies, and revealed: (1) Enough target signal is present in narrow wavelength bandwidths for hyperspectral measurements; (2) Differences exist in signal strength as a function of wavelength and bandwidth which may serve as a basis for Space Object Identification applications. Hyperspectral analysis of space objects warrants further investigation. DTIC

N94-25736# Calspan-Buffalo Univ. Research Center, NY.
MODELING ELECTROMAGNETIC EFFECTS IN MMICs FOR T/R MODULES Final Report, Dec. 1991 - Nov. 1992
Daniel J. Kenneally Jul. 1993 162 p
(Contract F30602-88-D-0026)
(AD-A273808; RL-TR-93-156) Avail: CASI HC A08/MF A02

An investigation of circuit modeling of electromagnetic environment effects (E3) in the microwave monolithic integrated circuits contained in T/R models is documented. The work was performed at Rome Laboratory under an Expert Science and Engineering contract with Calspan/University of Buffalo Research Center. Topics include multi-port vector characterizations, data acquisition, CAD testing and validations of models for selected MMIC's (and models), and recommendations and plans for further assessments of E3 in advanced MMIC's, T/R modules and multi-chip (MCM) nodules. An extensive bibliography on contemporary MMIC design and GaAsFET modeling is also included. DTIC

N94-25757# Northwestern Univ., Evanston, IL. Dept. of Electrical Engineering and Computer Science.
EXTENSION OF ON-SURFACE RADIATION CONDITION (OSRC) THEORY TO FULL-VECTOR ELECTROMAGNETIC WAVE SCATTERING BY THREE-DIMENSIONAL CONDUCTING, DIELECTRIC, AND COATED TARGETS Final Report, 1 Jul. 1988 - 27 Aug. 1993
Allen Taflove and Korada R. Umashankar 27 Aug. 1993 253 p
(Contract N00014-88-K-0475)
(AD-A274023) Avail: CASI HC A12/MF A03

This project introduced radiation boundary condition (RBC) and absorbing boundary condition (ABC) theory to the engineering electromagnetics community. An approximate method for obtaining the scattering of 2-D and 3-D bodies, the on-surface radiation condition (OSRC) method, was formulated and validated. RBC's and ABC's were shown to work well at points closer to scatterers than anyone had expected. Finite-difference time domain (FD-TD) methods exploiting these ABC's were pursued for applications in scattering, radiation, penetration, biomedical studies, and nonlinear optics. Multiprocessing supercomputer software was developed for FD-TD, leading to the largest scale detailed electromagnetic wave interaction models ever conducted, including entire jet fighter aircraft modeled for radar cross section (RCS) at UHF frequencies up to 500 MHz. DTIC

N94-25766# Air Force Inst. of Tech., Wright-Patterson AFB, OH.
ANALYZING ADAPTIVE BEAMFORMER PERFORMANCE IN A STABLE MULTIPATH ENVIRONMENT M.S. Thesis
Mark Godino Dec. 1993 91 p
(AD-A274029; AFIT/GE/ENG/93D-09) Avail: CASI HC A05/MF A01

Fighter aircraft equipped with X-Band radars having an adaptive beamforming capability exhibit degraded performance due to radome multipath reflection (RMR). The reflections from the radome into the antenna array degrade the pattern and cause the formation of large sidelobes. This phenomenon makes detection of LO targets difficult when jamming enters the high RMR sidelobes. Actual radomes are curved and cause reflected wavefronts to be nonplanar. Analyzing beamformer performance under these conditions is difficult, since the beamformer response is defined as the amplitude and phase change experienced by a complex plane wave as a function of frequency and location. To work with planar wavefronts and for the sake of simplicity, we model the radome as two flat plates parallel to array broadside, one at each end of the array. This radome model demonstrates degraded beamformer performance by causing large sidelobes to form. This approximates the characteristics of the multipath environment caused by a real radome. The ability of a linearly constrained, minimum variance beamformer to cancel interference arriving in the sidelobes is evaluated. The cancellation performance depends on how many taps are employed and the source frequency bandwidth. Results are provided for a linear, equally spaced sixteen element array. DTIC

N94-25797# Air Force Inst. of Tech., Wright-Patterson AFB, OH.
A METHOD FOR POPULATING THE KNOWLEDGE BASE OF APTAS, A DOMAIN-ORIENTED APPLICATION COMPOSITION SYSTEM M.S. Thesis
Raleigh A. Sandy, III Dec. 1993 130 p
(AD-A274034; AFIT/GCE/ENG/93D-13) Avail: CASI HC A07/MF A02

A formal process is described for populating the knowledge base of the Automatic Programming Technologies for Avionics Software (APTAS) system. This process was developed using a general knowledge base population process that applies to many knowledge-based software engineering systems. This general process is also described. The formal process for APTAS was demonstrated by storing new information from the radar tracking domain into the knowledge base of APTAS. Several procedures, some automatic and some manual, were implemented to support the formal process. DTIC

N94-25824# Air Force Inst. of Tech., Wright-Patterson AFB, OH. School of Engineering.
A STUDY OF TWO DIMENSIONAL TAPERED PERIODIC EDGE TREATMENTS TO REDUCE WIDEBAND EDGE DIFFRACTION M.S. Thesis
Russell A. Burleson Dec. 1993 226 p
(AD-A274054; AFIT/GE/Eng/93D-02) Avail: CASI HC A11/MF A03

This is a brief summary of a study to reduce diffraction from an infinite two dimensional edge using tapered periodic surfaces. The concept is to use the impedance characteristics of a periodic surface to create a tapered impedance; much like a tapered resistance commonly used for diffraction reduction. This approach has several advantages over tapered resistive treatments to include ease of fabrication, better engineering control of the impedance and negligible loss absorbed by the taper. In this study, four periodic tapers were design, built and tested. These tapers were also modeled using a variety of numerical techniques. The results from this study were quite promising. DTIC

N94-25866 Joint Inst. for Nuclear Research, Dubna (USSR). Lab. of Theoretical Physics.
ELECTROMAGNETIC PROPERTIES OF A TOROIDAL SOLENOID
G. N. Afanasev and V. M. Dubovik 1991 39 p Limited Reproducibility: More than 20% of this document may be affected by microfiche quality
(DE93-613032; JINR-E-4-91-425) Avail: CASI HC A03 (US Sales Only)

The electromagnetic properties of the toroidal solenoid with an alternate current are discussed. The multipole expansion for the electromagnetic field of the toroidal solenoid is obtained and the explicit expressions for the toroidal form factors and moments are given. Concrete realization of the current flowing in the solenoid's winding is presented. It is shown that the uniform rotation of the toroidal solenoid with a constant current in its winding leads to the appearance of the magnetic field outside the solenoid. DOE

N94-25915 Joint Inst. for Nuclear Research, Dubna (USSR).
FOCUSING PROPERTIES OF A THREE-ELEMENT QUADRUPOLE LENS SYSTEM AND ITS STIGMATIC FOCUSING BEHAVIOUR
Yu. Zafar 1991 15 p Limited Reproducibility: More than 20% of this document may be affected by microfiche quality
(DE93-616534; JINR-R-6-91-557) Avail: CASI HC A03 (US Sales Only)

The focusing properties of a three-element quadrupole lens system (triplet) have been studied in its general thick-lens form, and analytical expressions of corresponding matrix elements have been obtained. A graphical method has been utilized to determine the stigmatic focusing region of the triplet system generally, and in the special case of electrostatic triplet system installed in 'on-line SPIN-3 facility' in YASNAPP-2, JINR. DOE

N94-25924# Oak Ridge National Lab., TN.

DESIGN OF FOLDED WAVEGUIDE ANTENNA FOR ALCATOR C-MOD

C. H. Fogelman, T. S. Bigelow, M. D. Carter, D. J. Hoffman, B. W. Riemer, J. J. Yugo, S. N. Golovato (Massachusetts Inst. of Tech., Cambridge.), and P. Bonoli (Massachusetts Inst. of Tech., Cambridge.) 1993 4 p Presented at the Symposium on Fusion Engineering, Hyannis, MA, 11-15 Oct. 1993
(Contract DE-AC05-84OR-21400)
(DE94-003584; CONF-931018-65) Avail: CASI HC A01/MF A01

The Oak Ridge National Laboratory (ORNL) ion cyclotron range of frequencies (ICRF) antenna for Alcator C-Mod is a folded waveguide (FWG) antenna designed to determine whether the FWG can serve as a high power density, ceramic-free antenna for both present heating and fast wave current drive (FWCD) applications and for future tokamaks such as the International Thermonuclear Experimental Reactor (ITER) and the Tokamak Physics Experiment (TPX). The FWG is particularly attractive because it has a low internal electric field per unit power coupled to the Plasma. This results in more power capability and has been demonstrated by 1-MW (unloaded) tests on the Radio Frequency Test Facility (RFTF). The experiment will characterize the impact of an FWG on impurity control in the presence of high power density and on central beating. The antenna is designed to withstand the tokamak environment, including high heat fluxes, high-temperature bakeout, and major disruptions, without vacuum leaks. The front face is curved to fit the plasma outline. Two front plates are fabricated for the antenna one with full-width slits at every other location between vanes and the other with alternating right and left half-width slits at every location between vanes for pi-phasing. DOE

N94-25937# Lawrence Livermore National Lab., CA. Plasma Physics Research Inst. and M Div.

TWO DIMENSIONAL SELF-CONSISTENT FLUID SIMULATION OF RF INDUCTIVE SOURCES

G. DiPeso, V. Vahedi, D. W. Hewett, and T. D. Rognlien 17 Nov. 1993 19 p Presented at the 40th National Symposium of the American Vacuum Society, Orlando, FL, 15-19 Nov. 1993
(Contract W-7405-eng-48)
(DE94-003635; UCRL-JC-115684; CONF-9311104-13) Avail: CASI HC A03/MF A01

The two-dimensional (R-Z) electromagnetic code FMRZ was written tc model inductive sources self-consistently in time. The code models an argon plasma with momentum-transfer, excitation, and ionization as electron-neutral reactions and scattering and charge-exchange for the ion-neutral reactions. The electrons and ions are treated as Maxwellian fluid species and a reduced set of Maxwell's equations is used to advance the electromagnetic fields. The set of equations used in FMRZ is not subject to typical numerical constraints present in many time dynamic codes allowing one to choose appropriate time and space scales to resolve only the frequencies and scale lengths of interest. The model retains nonlinear driving terms which give rise to a pondermotive force that distorts the density profile. Density and power profiles will be used to illustrate the physical effects of various terms in the equations. Trends in average density and temperature compare well with an analytic model. DOE

N94-25950# Atmospheric and Environmental Research, Inc., Cambridge, MA.

A RESEARCH PROGRAM ON RADIATIVE TRANSFER MODEL DEVELOPMENT IN SUPPORT OF THE ARM PROGRAM

S. A. Clough 1 Oct. 1993 15 p
(Contract DE-FG02-90ER-61064)
(DE94-001146; DOE/ER-61064/3) Avail: CASI HC A03/MF A01

The objective of this research effort is to develop radiative transfer models that are consistent with ARM spectral radiance measurements for clear and cloudy atmospheres. Our approach is to develop the model physics and related databases with a line-by-line model in the context of available spectral radiance measurements. The line-by-line model then functions as an intermediate standard to both develop and validate rapid radiative transfer models appropriate to GCM applications. A preprint of an extended abstract for the 1994 AMS volume describing a Quality Measurement Experiment using the ARM spectral data is included as an attachment. DOE

N94-25960# Rome Lab., Griffiss AFB, NY.

LOW NOISE MEASUREMENTS IN AN RF ENVIRONMENT

Daniel E. Warren Aug. 1993 17 p
(AD-A273813; RL-TR-93-151) Avail: CASI HC A03/MF A01

A problem that is often ignored when making radiated noise measurements is described. The measurements are secondary to the cleaning up of the total spectrum before any measurements can be made of a selected bandwidth. DTIC

N94-25990# Westinghouse Electric Corp., Baltimore, MD. Electronic Systems Group.

METEOR BURST COMMUNICATIONS (MBC) THROUGHPUT IMPROVEMENT TESTS Final Report

May 1993 69 p
(Contract MDA972-91-C-0051; ARPA Order 7777)
(AD-A273941) Avail: CASI HC A04/MF A01

This report summarizes the initial work done with the analog adaptive and a high data rate non-adaptive meteor burst communications (MBC) system leading to the digital adaptive processor. Performance of the digital adaptive system is given. DTIC

N94-26011# Organisatie voor Toegepast Natuurwetenschappelijk Onderzoek, The Hague (Netherlands). Physics and Electronics Lab.

ZERNIKE MOMENTS AND ROTATION INVARIANT OBJECT RECOGNITION. A NEURAL NETWORK ORIENTED CASE STUDY Final Report

P. F. Krekel Dec. 1992 88 p
(AD-A273749; FEL-92-A394; TDCK-TD-92-3840) Avail: CASI HC A05/MF A01

This report presents the results of the feasibility study investigating the characteristics of complex Zernike moments and their application in translation-, scale-, and rotation-invariant object recognition problems. The complex Zernike moments are used as characterizing features in a neural network based target recognition approach for the classification of objects in images recorded by sensors mounted on an airborne platform. The complex Zernike moments are a transformation of the image by the projection of the image onto an extended set of orthogonal polynomials. The emphasis of this study is laid on the evaluation of the performances of Zernike moments in relation with the application of neural networks. Therefore, three types of classifiers are evaluated: a multi-layer perceptron (MLP) neural network, a Bayes statistical classifier and a nearest-neighbor classifier. Experiments are based on a set of binary images simulating military vehicles extracted from the natural background. From these experiments the conclusion can be drawn that complex Zernike moments are efficient and effective object characterizing features that are robust under rotation of the object in the image and to a certain extent under varying affine projections of the object onto the image plane. DTIC

N94-26105 Norwegian Defence Research Establishment, Kjeller.

TECHNICAL DESCRIPTION OF THE VULCANO SOFTWARE LIBRARY [TEKNISK BESKRIVELSE AV BIBLIOTEKSRUTINER I VULCANO]

Asta Storeboe Villanger and Walther Aasen 16 Apr. 1993 34 p In NORWEGIAN Limited Reproducibility: More than 20% of this document may be affected by microfiche quality
(ISSN 0802-2437)
(FFI-93/7024; ETN-94-94891) Avail: CASI HC A03

A computer model for VHF, UHF and SHF radiowave propagation (approximately 30 MHz to 20 GHz) is described. Fundamental features of the propagation models are outlined, and specific calls to the VULCANO library are defined. ESA

N94-26177# Naval Research Lab., Washington, DC.

THEORETICAL ASPECTS OF THE AGILE MIRROR Interim Report

Wallace M. Manheimer and Richard Fernsler 5 Jan. 1994 40 p
(AD-A274890; NRL/MR/6707-93-7425) Avail: CASI HC A03/MF A01

A planar plasma mirror which can be oriented electronically could have the capability of providing electronic steering of a microwave beam in a radar or electronic warfare system. This system is denoted the agile mirror. A recent experiment has demonstrated such a planar plasma and the associated microwave reflection. This plasma was produced by a hollow cathode glow discharge, where the hollow cathode was a grooved metallic trench in a Lucite plate. Various theoretical aspects of this configuration of an agile mirror are examined here. DTIC

N94-26189# Naval Research Lab., Washington, DC.
DIRECT-CONVERSION-TO-BASEBAND FOR A NONLINEAR FM SIGNAL Memorandum Report
Ching-Tai Lin and Ben H. Cantrell 3 Jan. 1994 27 p
(AD-A274861; NRL/MR/5333-93-7437) Avail: CASI HC A03/MF A01

This report examines both nonlinear FM signals and a 'direct conversion to baseband' process in a radar application system. A phase predistortion function was generated which modifies the transmitted linear FM signal and synthesizes the desirable effect of a sidelobe weighting function. To avoid a mismatch in obtaining the in-phase and quadrature signal components at two separate processing channels, a low IF signal was directly converted to its baseband by a combination of sampling, filtering, and decimation. A band-limited nonlinear FM signal with a low pulse compression ratio is considered and processed. The compressed signal is also obtained through a pulse compression filter matched to the transmitted signal. DTIC

N94-26232# Norwegian Defence Research Establishment, Kjeller.
DETECTION OF TRANSIENT VECTOR-FIELDS IN ADDITIVE NOISE [DETEKSJON AV TRANSIENTE 3-DIMENSJONALE VEKTORSIGNALER MED ADDITIV STOEY]
Bent Groenvold 10 May 1993 80 p In NORWEGIAN
(FFI-93/7028; ETN-94-95212) Avail: CASI HC A05/MF A01

A method for detection of a passing ship using a single three axial magnetometer is proposed. The ship is approximated as a magnetic dipole, that makes a perturbation of the geomagnetic field at the sensor point during the passage. An analysis of the magnetic signals was carried out. A description of the ambient magnetic noise is given, and a model for the noise spectrum was chosen. The detection is done by a bank of matched filters, and a projection of the measures field vectors on to an expected field vector. The size of the filter bank is discussed, and computations are done to determine this. Simulations of the method were made to determine the gain in signal to noise ratio. ESA

N94-26310# Lawrence Livermore National Lab., CA.
ELECTRICAL ANALYSIS OF WIDEBAND AND DISTRIBUTED WINDOWS USING TIME-DEPENDENT FIELD CODES
C. C. Shang, M. Caplan, H. U. Nickel, and M. Thumm 16 Sep. 1993 4 p Presented at the 18th International Conference on Infrared and Millimeter Waves, Essex, England, 6-10 Sep. 1993
(Contract W-7405-eng-48)
(DE94-002987; UCRL-JC-114504; CONF-9309266-1) Avail: CASI HC A01/MF A01

Windows, which provide the barrier to maintain the vacuum envelope in a microwave tube, are critical components in high-average-power microwave sources, especially at millimeter wavelengths. As RF power levels approach the 100's of kWs to 1 MW range (CW), the window assembly experiences severe thermal and mechanical stresses. Depending on the source, the bandwidth of the window may be less than 1 GHz for gyrotron oscillators or up to approximately 20 GHz for the FOM Institute's fast-tunable, free-electron-maser. The bandwidth requirements give rise to a number of window configurations where the common goal is locally distributed heat dissipation. In order to better understand the transmission and RF properties of these microwave structures, the authors use detailed time-dependent field solvers. DOE

N94-26315# European Space Agency, Paris (France).
NUMERIC SOLUTION OF THE ELECTRIC FIELD INTEGRAL EQUATION USING GALERKIN'S METHOD FOR AXIALLY SYMMETRIC CASES Ph.D. Thesis - Tech. Univ. Graz
Klemens Lileg (Deutsche Forschungsanstalt fuer Luft- und Raumfahrt, Oberpfaffenhofen, Germany.) Aug. 1993 139 p Transl. into ENGLISH of Numerische Loesung der elektrischen Feldintegralgleichung mittels Galerkin verfahren fuer axialsymmetrische Faelle (Oberpfaffenhofen, Germany, DLR) Dec. 1990 p 1-133 Original language document was announced as N91-30394
(ESA-TT-1264; DLR-FB-90-58; ETN-94-95287) Avail: CASI HC A07/MF A02

The electric field integral equation is solved for a cylindrical antenna with flat end caps using the method of moments. Trigonometric subdomain functions are used as basis functions; the weighting functions have the same shape as the basis functions (Galerkin's method). For the end caps, the approximation of the Numerical Electromagnetics Code (NEC) program is used; the excitation is due to a homogeneous field in a gap in the center of the antenna. The integrals to be calculated are evaluated precisely, numerically. The admittance thus calculated converges better than that calculated using NEC but in many cases it is not completely satisfactory. Therefore the approximate solution for the end caps is replaced with a more accurate calculation. Hemispherical end caps are introduced and trigonometric subdomain functions analogous to those used on the cylinder are used as basis functions. All additional calculations are evaluated without approximations again. Now the results for the admittance converge in all cases even for the small number of segments. The impedance was measured for a number of monopoles of various thicknesses; good agreement with the calculations is obtained for all frequencies. ESA

N94-26317# European Space Agency, Paris (France).
POLARIMETRIC INVESTIGATION OF EDGE SCATTERING BY MONO- AND BISTATIC MICROWAVE IMAGING
Wolfgang Herdeg (Deutsche Forschungsanstalt fuer Luft- und Raumfahrt, Oberpfaffenhofen, Germany.) Aug. 1993 166 p Transl. into ENGLISH of Polarimetrische Untersuchung der Kantenstreuung in der mono- und bistatischen Mikrowellenabbildung (Oberpfaffenhoffen, Germany, DLR) Jul. 1991 p 1-153 Original language document was announced as N93-22656
(ESA-TT-1284; DLR-FB-91-32; ETN-94-95289) Avail: CASI HC A08/MF A02

The scattering of electromagnetic waves from edges in dependence on frequency, aspect angle, polarization, and bistatic angle is investigated. The edges of simple metal objects, namely cubes, plates, and wedges, are resolved in range and cross range using a high resolution microwave imaging process and are investigated as canonical structures. The Geometrical Theory of Diffraction (GTD) serves as the theoretical model. The scattering coefficients of the GTD are compared with experiment. The polarimetric results are presented using the Huynen parameters. In order to carry through bistatic measurements on a monostatic radar range, microwave mirrors are introduced. These are large metal plates which reflect the bistatic scatter contribution to the monostatic radar. Experimental results verify the proposed concepts. ESA

N94-26335# Naval Command, Control and Ocean Surveillance Center, San Diego, CA.
RADAR DETECTION OF LOW-ALTITUDE TARGETS IN A MARITIME ENVIRONMENT. VOLUME 2: METEOROLOGICAL AND RADAR DATA Final Report, Sep. 1989 - Sep. 1993
Kenneth D. Anderson Nov. 1993 172 p
(AD-A274658; NCCOSC/RDT/E-1630-Vol-2) Avail: CASI HC A08/MF A02

Results from a unique analytical and measurement effort to assess low-altitude short-range radar detection in an evaporation ducting environment validate propagation model predictions of reduced radar detection ranges within the radio horizon. Discrepancies between measured and predicted radar data demand a close examination of both meteorological data and surface layer theory. At ranges near and beyond the horizon, radar detection crucially depends both on the surface layer refractivity profile and on the adjacent mixed layer refractivity profile. An empirical model is described that merges the surface layer with the mixed layer forming a unified boundary layer. Other discrepancies, which are thought to be caused either by inadequate surface layer modeling (perhaps the moisture stability function) or by inadequate boundary layer meteorological measurements, suggest the need for improvements in surface layer modeling and new techniques to measure the refractivity structure. The combination of direct boundary layer (surface and mixed layer) meteorological measurements, remotely sensed radar measurements, and advanced numerical modeling capability provides valuable insight for a better understanding of the atmospheric boundary layer and its effects on the radar detection of low-altitude short-range targets. DTIC

N94-26347# Naval Postgraduate School, Monterey, CA.
METHODS FOR IMPROVING LOW-ANGLE, LOW-ALTITUDE RADAR TRACKING ACCURACY M.S. Thesis
Ali Ozkara 23 Sep. 1993 69 p
(AD-A274914) Avail: CASI HC A04/MF A01

This thesis studies the problem of low-angle, low-altitude target tracking where the presence of multipath causes large angle errors. The problem is examined for a low sidelobe monopulse radar over a flat earth. A detailed multipath model is used to simulate the reflecting surface and the reflected signal is included in the monopulse processing simulation. Using this model the tracking error is obtained, and two multipath error reduction techniques are evaluated. The first method uses frequency agility to measure the angle over a wide frequency range. By averaging the results of many frequencies, the angle estimate can be significantly improved over that of a single frequency. The second method is referred to is difference beam phase toggling. By flipping the difference beam phase by 180 deg for two subsequent pulses, the return from a reflected path can be inside to cancel. DTIC

N94-26359# Naval Postgraduate School, Monterey, CA.
NEW BINARY INTEGRATION STRATEGIES AND CORRESPONDING R90 CALCULATIONS M.S. Thesis
Doo J. Kim 23 Sep. 1993 139 p
(AD-A274786) Avail: CASI HC A07/MF A02

Often to increase the probability of having a track that will not later be deleted by a radar some simple logic criterion is used. This thesis evaluates the performance of a new binary integration technique. This technique requires M hits out of N looks with x less than M hits being consecutive. Closed form expressions for the cumulative probability of detection are derived and Monte Carlo methods are used to verify the results. A significant increase in the cumulative probability of detection is shown to occur when this type of logic is imposed. Also derived are the corresponding confidence calculations on R60-R95 (a measure of radar performance defined as the range such that the cumulative probability of detecting an approaching target is 0.60-0.95) for each set of detections. DTIC

N94-26482# Oak Ridge National Lab., TN.
AN EFFICIENT COMMUNICATION SCHEME FOR SOLVING THE S(SUB n) EQUATIONS ON MESSAGE-PASSING MULTIPROCESSORS
Y. Y. Azmy 1993 7 p Presented at the ANS Winter Meeting, San Francisco, CA, 14-18 Nov. 1993
(Contract DE-AC05-84OR-21400)
(DE94-000378; CONF-931160-19) Avail: CASI HC A02/MF A01

Early models of Intel's hypercube multiprocessors, e.g. the IPSC/1 and iPSC/2, were characterized by the high latency of message-passing. This relatively weak dependence of the communication penalty on the size of messages, in contrast to its strong dependence on the number of messages, justified using the Fan-in Fan-out algorithm to perform global operations, such as global sums, etc. Recent models of message passing computers, such as the iPSC/860 and the Paragon, have been found to possess much smaller latency, thus forcing a re-examination of the issue of performance optimization with respect to communication schemes. Essentially, the Fan-in Fan-out scheme minimizes the number of nonsimultaneous messages sent but not the volume of data traffic across the network. Furthermore, if a global operation is performed in conjunction with the message-passing, a large fraction of the attached nodes remains idle as the number of utilized processors is halved in each step of the process. On the other hand, the Recursive Halving scheme offers the smallest communication cost for global operations, but has some drawbacks. First, it requires the simultaneous exchange of messages between adjacent nodes, which while permissible on many message-passing computers, requires additional programming on the iPSC/860, the target platform in this work. Second, full utilization of the processors requires that the message length be a multiple of two, resulting in significant idleness of the processors if this is not the case. In this paper, we present an alternative scheme that eliminates the first drawback by communicating along a monodirectional ring, and reduces the impact of the second drawback by requiring only that the number of nodes divides the message length, a standard requirement for retaining load balance. DOE

N94-26611*# National Aeronautics and Space Administration. Langley Research Center, Hampton, VA.
DESIGN AND EVALUATION OF AN ELECTROMAGNETIC BEAM WAVEGUIDE FOR MEASURING ELECTRICAL PROPERTIES OF MATERIALS
M. C. Bailey Feb. 1994 32 p
(RTOP 505-64-52-04)
(NASA-TP-3418; L-17298; NAS 1.60:3418) Avail: CASI HC A03/MF A01

A beam waveguide was designed that is based upon the propagation characteristics of the fundamental Gaussian beam and the focusing properties of spherical dielectric lenses. The 20-GHz, two-horn, four-lens system was constructed and experimentally evaluated by probing the field in a plane perpendicular to the beam axis at the center of the beam waveguide system. The critical parameters were determined by numerical sensitivity studies, and the lens-horn critical spacing was adjusted to better focus the beam at the probe plane. The measured performance was analyzed by consideration of higher order Gaussian-Laguerre beam modes. The beam waveguide system was successfully used in the measurements of the electromagnetic transmission properties of Shuttle thermal-protection tiles while the tile surface was being heated to reentry-level temperatures with a high-power laser. Author

N94-26618 Regina Univ. (Saskatchewan). Dept. of Electrical Engineering.
THE APPLICATION OF FD-TD METHOD TO ANTENNA RADIATION PATTERNS M.S. Thesis
Qi Zhang Apr. 1992 105 p
(ISBN-0-315-83893-0; CTN-94-61036) Copyright Avail: Micromedia Ltd., Technical Information Centre, 240 Catherine Street, Suite 305, Ottawa, Ontario, K2P 2G8, Canada HC/MF

The finite difference time domain (FD-TD) method is applied to study antenna radiation patterns, especially those of array antennas, linear antennas, aperture antennas, and horn antennas. Several absorbing algorithms are reviewed and Reynolds' absorbing boundary is chosen for the FD-TD method due to its flexibility and simplicity for the numerical analysis. The accuracy of the FD-TD method in obtaining far-field patterns of various antennas is assessed. The numerical error caused by the finite mesh size of the FD-TD algorithm in the far field radiation pattern study is reduced. It has been recognized that the directional angle of the numerical wavefront is different from that of the physical wavefront. In the numerical simulation of the aperture and horn antennas, the amount of this shift can be predicted and is confirmed by the numerical results. A simple algorithm is developed to offset this shift and consequently the accuracy of the numerical results is improved. This algorithm will be very useful for future application of the FD-TD method in the far field antenna pattern study. In order to illustrate the capability of the FD-TD algorithm, several different types of antenna are analyzed. Wherever possible, most results are compared with the theoretical results and good agreements are found. Author (CISTI)

N94-26619 Regina Univ. (Saskatchewan). Dept. of Computer Science.
A ROUGH SET APPROACH TO SPEECH RECOGNITION M.S. Thesis
Zhigang Zhao Sep. 1992 93 p
(ISBN-0-315-83894-9; CTN-94-61037) Copyright Avail: Micromedia Ltd., Technical Information Centre, 240 Catherine Street, Suite 305, Ottawa, Ontario, K2P 2G8, Canada HC/MF

Speech recognition is a very difficult classification problem due to the variations in loudness, speed, and tone of voice. In the last 40 years, many methodologies have been developed to solve this problem, but most lack learning ability and depend fully on the knowledge of human experts. Systems of this kind are hard to develop and difficult to maintain and upgrade. A study was conducted to investigate the feasibility of using a machine learning approach in solving speech recognition problems. The system is based on rough set theory. It first generates a set of decision rules using a set of reference words called training samples, and then uses the decision rules to recognize new words. The main feature of this system is that, under the supervision of human experts, the machine learns and applies knowledge on its own to the designated tasks. The main advantages of this system over a traditional system are its simplicity and adaptiveness, which suggest that it may have significant potential in practical applications of computer speech recognition. Furthermore, the studies presented demonstrate the potential application of rough-set based learning systems in solving other important pattern classification problems, such as character recognition, system fault detection, and trainable robotic control. Author (CISTI)

N94-26624 Carleton Univ., Ottawa (Ontario). Dept. of Electronics.
ANALYSIS OF LINEAR COMBINING AND ITS APPLICATION TO FREQUENCY-HOPPED SIGNALS Ph.D. Thesis
Rolands Eriks Ezers 3 May 1993 123 p
(ISBN-0-315-84007-2; CTN-94-61046) Copyright Avail: Micromedia Ltd., Technical Information Centre, 240 Catherine Street, Suite 305, Ottawa, Ontario, K2P 2G8, Canada HC/MF

A novel analytical method has been developed for obtaining performance for fast frequency hopped (FFH) noncoherent frequency shift keyed (NCFSK) communication systems employing linear diversity combining (LDC). The method combines circularly symmetric function theory, Fourier-Bessel series, and Fourier series. Performance measures are obtained for demodulation of FFH NCFSK systems with time diversity (TD) and LDC, and for the time synchronization of a FFH NCFSK satellite communication system with TD and LDC in broad-band noise and multiple tone jamming. Results using this method compare well to other reported results. A novel analytical result was also derived for computing the bit error probability for demodulation of FFH NCFSK systems with TD and 4-2- or 2-1-moment method diversity combining in independent Rayleigh fading with a diversity level of two. In a complete review of diversity combining techniques, the advantages and drawbacks of LDC under various noise, fading, and jamming conditions are discussed. For uplink coarse-time synchronization, TD and LDC could be used to improve performance. A binary NCFSK modulator and demodulator with TD and LDC was implemented in a hardware experiment, showing the viability and practicality of LDC. Author (CISTI)

N94-26625 Victoria Univ. (British Columbia). Dept. of Electrical and Computer Engineering.
IMPROVED PERFORMANCE OF HYBRID ERROR CONTROL TECHNIQUES FOR REAL-TIME DIGITAL COMMUNICATIONS OVER NOISY CHANNELS Ph.D. Thesis
Charlie Qing Yang 1993 196 p
(ISBN-0-315-84281-4; CTN-94-61019) Copyright Avail: Micromedia Ltd., Technical Information Centre, 240 Catherine Street, Suite 305, Ottawa, Ontario, K2P 2G8, Canada HC/MF

Delay-related performance characteristics are investigated for asynchronous time division multiplexing links. Two methods based on an imbedded Markov chain model are developed and applied to the system with a noisy feedback channel yielding analytical expressions for the buffer occupancy and the block delay. A recursive expression for packet loss probability for systems with a finite transmitter buffer is obtained. The concept of delay limited error control coding is introduced for real-time communications. Performance improvement by truncation of a type-2 hybrid automatic repeat-request (ARQ) protocol with one retransmission is examined showing that the truncated protocol has a bounded delay and bounded queue length under typical conditions. The error performance of the truncated protocol is further analyzed for various mobile fading channels. Matched rate hybrid error control coding for both adaptive and non-adaptive cases is also studied. A new adaptive error control protocol using Reed-Solomon codes is proposed using novel feedback transmissions to achieve faster estimation of channel states. Numerical optimization is carried out by introducing overall and modified throughput as efficiency criteria. Based on channel bit error rate measurement, optimum overall throughput is obtained with minimum implementation complexity. Author (CISTI)

N94-26626 Victoria Univ. (British Columbia). Dept. of Electrical and Computer Engineering.
ON THE PERFORMANCE OF TRELLIS CODED 8PSK WITH REED SOLOMON CODES M.S. Thesis
Yasuo Harada 1993 191 p
(ISBN-0-315-84289-X; CTN-94-61020) Copyright Avail: Micromedia Ltd., Technical Information Centre, 240 Catherine Street, Suite 305, Ottawa, Ontario, K2P 2G8, Canada HC/MF

Concatenated trellis-coded 8-ary phase shift keying (8PSK) with Reed Solomon (RS) codes is studied over additive white Gaussian noise and Rayleigh fading channels. Trellis coded modulation (TCM) achieves high coding gain without any bandwidth expansion. The basic analysis of its performance is reviewed and confirmed by simulation using a truncated Viterbi decoder. Trellis-coded 8PSK, which has an asymptotic coding gain of 3.6 dB, can be further improved by concatenation with RS codes. By concatenating TCM with an RS code, the bandwidth of the overall system is expanded by the reciprocal of the RS coding rate. Improvement in bit error rate performance is studied for this coding system with various combinations of RS codes. A code with a rate of 0.9 and a good bit error rate performance is chosen for further study for erasure and error decoding. Results suggest the performance can be improved with sufficient reliability of decoded symbols. The reliability of the input symbols to the RS decoder is obtained by a modified Viterbi decoder. Such a decoder is studied and the performance of the bit error rate is shown. To improve performance, a new, modified Viterbi decoder with averaged reliability information is proposed, and the bit error rate improvement is confirmed by computer simulation. Author (CISTI)

N94-26630 Carleton Univ., Ottawa (Ontario). Dept. of Systems and Computer Engineering.
SPEECH CODING AT LOW TO MEDIUM BIT RATES Ph.D. Thesis
Wilfred Paul Leblanc 1 Sep. 1992 135 p
(ISBN-0-315-84012-9; CTN-94-61048) Copyright Avail: Micromedia Ltd., Technical Information Centre, 240 Catherine Street, Suite 305, Ottawa, Ontario, K2P 2G8, Canada HC/MF

Improved search techniques coupled with improved codebook design methodologies are proposed to improve the performance of conventional code-excited linear predictive coders for speech. Improved methods for quantizing the short term filter are developed by employing a tree search algorithm and joint codebook design to multistage vector quantization. Joint codebook design procedures are developed to design locally optimal multistage codebooks. Weighting during centroid computation is introduced to improve the outlier performance of the multistage vector quantizer. Multistage vector quantization is shown to be both robust against input characteristics and in the presence of channel errors. Spectral distortions of about 1 dB are obtained at rates of 22-28 bits/frame. Structured codebook design procedures for excitation in code-excited linear predictive coders are compared to general codebook design procedures. Little is lost using significant structure in the excitation codebooks while greatly reducing the search complexity. Sparse multistage configurations are proposed for reducing computational complexity and memory size. Improved search procedures are applied to code-excited linear prediction which attempt joint optimization of the short term filter, the adaptive codebook, and the excitation. Improvements in signal to noise ratio of 1-2 dB are realized in practice. Author (CISTI)

N94-26650 Physics and Electronics Lab. TNO, The Hague (Netherlands).
ANNEX REPORT FEL-92-A163: DESCRIPTION OF THE LInk AND BER TEST ANALYSIS SYSTEM (LIBERTAS) FOR THE FREQUENCY BAND V (14.5 - 15.3 GHz) [BIJLAGE RAPPORT FEL-92-A163; BESCHRIJVING VAN HET LINK EN BER TEST ANALYSE SYSTEEM (LIBERTAS) VOOR FREQUENTIEBAND V (14.5 - 15.3 GHZ)]
J. Niemantsverdriet and J. vandenOever Feb. 1993 41 p In DUTCH
Sponsored by Ministry of Defence, The Hague, Netherlands
(Contract A92/KL/643)
(FEL-92-A442; FEL-92-A163; TD92-3681; ETN-94-94947) Copyright
Avail: Issuing Activity (TNO Physics and Electronic Lab, P. O. Box 96864, 2509 JG The Hague, Netherlands)

The changes of the band 4 measurement system LIBERTAS to make it suitable for measurements in the frequency band 5 (14.5 to 15.3 GHz) are described. This measurement system was developed for propagation measurements carried out in frequency band 5 for interduster radio relay connections. The measurement system is completely automated. Path losses, cross polarization, and bit error rates can be measured. The operation, construction, and specifications of the system are described. The requirements for the measurement system are given. ESA

N94-26751 Naval Postgraduate School, Monterey, CA.
COMBATTING INHERENT VULNERABILITIES OF CFAR ALGORITHMS AND A NEW ROBUST CFAR DESIGN M.S. Thesis
Patrick J. Bowman Sep. 1993 158 p Limited Reproducibility: More than 20% of this document may be affected by microfiche quality
(AD-A274918) Avail: CASI HC A08

A current trend in radar technology is automatic detection and tracking systems. An integral part of these automatic systems is the constant false alarm rate (CFAR) detector. A CFAR detector is the signal process algorithm that controls the rate at which target detections are falsely declared. Given the current state of radar technology, CFAR algorithms are necessary elements of any automatic radar system. Unfortunately, CFAR systems are inherently vulnerable to degradation caused by large clutter edges, multiple targets, and jamming environments. This thesis presents eight popular and studied CFAR architectures. A comprehensive review of each system's structure, analysis, and performance is detailed. Also the performances of each CFAR processor are compared numerically for two different in-phase (I) and quadrature (Q) detectors: envelope approximation detector and the square law detector. In addition, each system is comprehensively compared to one another in the troublesome environments mention above. This thesis continues with the development of an original CFAR architecture, the excision greatest-of (EXGO). Although more complex, this processor is shown to be more robust than the other established techniques particularly in the presence of clutter edges, multiple targets, and electronic countermeasures (ECM) environments. DTIC

N94-26803# Lawrence Livermore National Lab., CA.

USING THE TSAR ELECTROMAGNETIC MODELING SYSTEM

S. T. Pennock and G. W. Laguna Sep. 1993 41 p
(Contract W-7405-eng-48)
(DE94-002617; UCRL-ID-115227) Avail: CASI HC A03/MF A01

A new user, upon receipt of the TSAR EM modeling system, may be overwhelmed by the number of software packages to learn and the number of manuals associated with those packages. This is a document to describe the creation of a simple TSAR model, beginning with an MGED solid and continuing the process through final results from TSAR. It is not intended to be a complete description of all the parts of the TSAR package. Rather, it is intended simply to touch on all the steps in the modeling process and to take a new user through the system from start to finish. There are six basic parts to the TSAR package. The first, MGED, is part of the BRL-CAD package and is used to create a solid model. The second part, ANASTASIA, is the program used to sample the solid model and create a finite-difference mesh. The third program, IMAGE, lets the user view the mesh itself and verify its accuracy. If everything about the mesh is correct, the process continues to the fourth step, SETUP-TSAR, which creates the parameter files for compiling TSAR and the input file for running a particular simulation. The fifth step is actually running TSAR, the field modeling program. Finally, the output from TSAR is placed into SIG, B2RAS or another program for post-processing and plotting. Each of these steps will be described below. The best way to learn to use the TSAR software is to actually create and run a simple test problem. As an example of how to use the TSAR package, let's create a sphere with a rectangular internal cavity, with conical and cylindrical penetrations connecting the outside to the inside, and find the electric field inside the cavity when the object is exposed to a Gaussian plane wave. We will begin with the solid modeling software, MGED, a part of the BRL-CAD modeling release. DOE

N94-26836# Scientech, Inc., Idaho Falls, ID.

S-76 HIGH INTENSITY RADIATED FIELDS, VOLUME 2 Final Report

Jerry Blair Oct. 1993 169 p
(AD-A274572; DOT/FAA/CT-93/5-Vol-2) Avail: CASI HC A08/MF A02

The Federal Aviation Administration (FAA) Technical Center sponsored a series of High Intensity Radiated Fields (HIRF) test on a Sikorsky S-76 rotorcraft. The project was conducted to evaluate the practically of performing aircraft level HIRF tests, determine the effects of HIRF on a specific rotorcraft with the potential to obtain information on rotorcraft in general, and evaluate the effects of exposure to real world HIRF emitters. HIRF ground and flight tests were conducted to achieve the objective of the project. Site calibration (SCAL) measurements were made in the test area to determine the levels at which the S-76 would be irradiated when placed in the test area. Ground tests consisted of Low Level Swept Coupling (LLSC) and Low Level Swept Fields (LLSF) tests. The flight tests were flown directly into the main beam of a variety of pulsed and continuous wave (CW) transmitters including the Over the Horizon Back Scatter (OTHB), PAVE PAWS, ASR-9, FPS-65, and FPS-16 radars. Results of the S-76 tests added credibility to the existence of HIRF as a flight safety hazard. In the evaluation of the emitters, the flight tests showed repeatable instances where exposure resulted in instrumentation disruptions. It should be noted that all the observed disruptions were of a non-critical nature. DTIC

N94-26844# Syracuse Univ., NY. Dept. of Electrical and Computer Engineering.

COMPUTER PROGRAM FOR NUMERICAL EVALUATION OF THE PERFORMANCE OF AN OVERMODED TM01 CIRCULAR TO TE10 RECTANGULAR WAVEGUIDE MODE CONVERTER Final Report, Aug. 1991 - Aug. 1993

Joseph R. Mautz and Roger F. Harrington Dec. 1993 145 p
(Contract DAAL02-90-K-0027)
(AD-A274548; TR-93-1; ARL-CR-129) Avail: CASI HC A07/MF A02

Two identical rectangular waveguides are fed by means of two symmetrically placed apertures in a circular waveguide. Several modes can propagate in the circular waveguide but only the TE10 mode can propagate in the rectangular waveguides. The rectangular waveguides have identical dimensions but may be terminated with different loads. Power is transmitted from the propagating modes in the circular waveguide to the TE10 mode in each rectangular waveguide. A computer program was written to evaluate this power and the magnitude of each orthogonal component of the tangential electric field in the apertures. This program is obtained by modifying an existing program. The modifications are described and listed. Sample input and output data are provided. DTIC

N94-26854# Scientech, Inc., Idaho Falls, ID.

S-76 HIGH INTENSITY RADIATED FIELDS, VOLUME 1 Final Report

Jerry Blair Oct. 1993 88 p
(AD-A274571; DOT/FAA/CT-93/5-Vol-1) Avail: CASI HC A05/MF A01

The Federal Aviation Administration (FAA) Technical Center sponsored a series of High Intensity Radiated Fields (HIRF) test on a Sikorsky S-76 rotorcraft. The project was conducted to evaluate the practicality of performing aircraft level HIRF tests, determine the effects of HIRF on a specific rotorcraft with the potential to obtain information on rotorcraft in general, and evaluate the effects of exposure to real world HIRF emitters. HIRF ground and flight tests were conducted to achieve the objective of the project. Site calibration (SCAL) measurements were made in the test area to determine the levels at which the S-76 would be irradiated when placed in the test area. Ground tests consisted of Low Level Swept Coupling (LLSC) and Low Level Swept Fields (LLSF) tests. The flight tests were flown directly into the main beam of a variety of pulsed and continuous wave (CW) transmitters including the Over the Horizon Back Scatter (OTHB), PAVE PAWS, ASR-9, FPS-65, and FPS-16 radars. Results of the S-76 tests added credibility to the existence of HIRF as a flight safety hazard. In the evaluation of the emitters, the flight tests showed repeatable instances where exposure resulted in instrumentation disruptions. It should be noted that all the observed disruptions were of a non-critical nature. DTIC

N94-26872 Technische Univ., Twente (Netherlands). Tele-Informatics and Open Systems Group.

EXAMPLE OF THE EXPANSE SIGNALLING PROTOCOL

J. T. VanderVeen 1993 18 p Limited Reproducibility: More than 20% of this document may be affected by microfiche quality
(ISSN 0924-3755)
(PB94-125283; TIOS-93/15) Copyright Avail: Issuing Activity (National Technical Information Service (NTIS))

Requirements from new applications, from mobility and from ATM have a significant impact on the development of signalling protocols for B-ISDN. One of the signalling protocols taking most of these requirements into account is EXPANSE. The EXPANSE protocol follows an object-oriented approach and separates calls from services (connections) and services form channels. This report gives a comprehensive example of using the EXPANSE protocol. NTIS

N94-26877 Technische Univ., Delft (Netherlands). Lab. of Electromagnetic Research.

ELECTROMAGNETIC FIELDS AND INTERFERENCE

Dirk Quak and Adrianus T. deHoop 1993 33 p Limited Reproducibility: More than 20% of this document may be affected by microfiche quality
(PB94-126489; ET/EM-1993-18) Copyright Avail: Issuing Activity (National Technical Information Service (NTIS))

The presence of electromagnetic fields is in essence the cause of many interference problems in electric and electronic circuits. To analyze an interference problem, it is therefore essential to consider the electromagnetic field concept with its vectorial nature. Simple illustrations are: the emission of radiation by (short) wire segments (electric dipoles) and (small) loops (magnetic dipoles) and the susceptibility to radiation of such wire segments or loops in the near- or far-field regions and in the dependence on their orientation. NTIS

N94-26884# Lockheed Sanders, Inc., Nashua, NH.
RAPID PROTOTYPING OF APPLICATION SPECIFIC SIGNAL PROCESSORS (RASSP)
23 Dec. 1993 102 p
(Contract N00014-93-C-2172)
(AD-A274324; NRL-93-2172/93ACSD-02) Avail: CASI HC A06/MF A02

This document provides, for each of the computer-aided design (CAD) tools in the initial baseline RASSP design environment, a description of its role in the environment, an assessment of strengths and weaknesses, and manufacturer's contact information. This RASSP initial design environment is summarized in Table 1 which specifies the tool name, the manufacturer, and a short description of each tool. The detailed description and assessment of each tool comprises the remainder of this document following the introduction. DTIC

N94-26909 Technische Univ., Delft (Netherlands). Lab. of Electromagnetic Research.
INTERFERENCE ANALYSIS OF MULTICHANNEL TRANSMISSION LINES: A SYSTEM'S ANALYSIS
Adrianus T. deHoop and Dirk Quak 1993 19 p Limited Reproducibility: More than 20% of this document may be affected by microfiche quality
(PB94-126505; ET/EM-1993-17) Copyright Avail: Issuing Activity (National Technical Information Service (NTIS))

In this chapter a system's description is presented of the interference analysis of multichannel transmission lines. A multichannel transmission line consists of a cylindrical configuration that is capable of guiding electromagnetic waves along its axial or longitudinal direction. The guiding structure may be composed of electrically conducting wires, electrically conducting strips, a conducting ground plane, and/or a number of optical communication fibers. It is assumed that the system's performance of the transmission line can be characterized by a finite number of discrete modes for which equivalent cross-sectional voltages and equivalent axial electric currents can be defined. In terms of these voltages and currents, the crosstalk and the influence of interfering external electromagnetic fields along the line can be analyzed. The associated array and matrix manipulations can be carried out with standard commercially available software. NTIS

N94-26924# Air Force Inst. of Tech., Wright-Patterson AFB, OH. School of Engineering.
AN ANALYSIS OF FM JAMMING AND NOISE QUALITY MEASURES M.S. Thesis
Timothy N. Taylor Dec. 1993 182 p
(AD-A274349; AFIT/GE/ENG/93D-38) Avail: CASI HC A09/MF A02

This thesis provides a description of FM-by-noise jamming, both at RF and at the output of the radar receiver, in terms of spectra, time-domain waveforms, and univariate probability density of amplitude. Particular emphasis is given to the case where the peak frequency deviation of the FM modulator is sufficiently small that Woodward's Theorem does not provide a good approximation of the RF spectrum. Additionally, noise quality measures which have been used to measure noise quality of radar jammers are considered theoretically and experimentally, and it is concluded that a noise measure which incorporates both a spectral measure and a probability density measure should be adopted. One such measure is proposed here. Lastly, a technique for measuring the noise quality of an operational jammer is demonstrated and the programs necessary to measure noise quality of an operational jammer are included here. DTIC

N94-26963 Massachusetts Inst. of Tech., Lexington.
ENCODING APPROACHES FOR DATA LINK TRANSMISSION OF WEATHER GRAPHICS
Jeffrey L. Gertz and Robert D. Grappel 10 Dec. 1993 21 p Limited Reproducibility: More than 20% of this document may be affected by microfiche quality
(Contracts DTFA01-93-Z-02012; F19628-90-C-0002)
(AD-A274497; ATC-205; DOT/FAA/RD-93/33) Avail: CASI HC A03

To provide pilots with necessary information to make informed decisions on the avoidance of hazardous weather and to maintain situational awareness of the weather conditions, the FAA is actively developing the capability to provide real-time graphical weather information to aircraft through the use of bandwidth-limited data links such as Mode S. The information content of weather images and the restricted bandwidth of the transmission channel require that the images be extensively compressed. This paper provides the results of a study concerning the applicability of various data compression algorithms to the weather image problem. Its conclusion is that the Polygon-Ellipse Algorithm developed at Lincoln Laboratory provides the best combination of compression, computational efficiency, and image quality for the encoding of weather images over the Mode S data link or other similarly bit-limited data links. DTIC

N94-26975# Polytechnic Univ., Brooklyn, NY. Dept. of Electrical Engineering.
EXPERIMENTS AND NUMERICAL SIMULATIONS OF ELECTROMAGNETIC WAVE PROPAGATION IN PLASMA VARYING RAPIDLY IN SPACE AND TIME Final Report, 1 Oct. 1992 - 30 Sep. 1993
S. P. Kuo 30 Sep. 1993 87 p
(Grant AF-AFOSR-0002-91)
(AD-A274376; AFOSR-93-0884TR) Avail: CASI HC A05/MF A01

In this work, the electromagnetic wave propagating in a fast growing plasma is studied experimentally and numerically. Theoretical models are developed to assist the numerical simulations. The plasma media involved in the study is classified into two categories: (1) the plasma density varies both temporally and spatially; (2) the plasma density is a function of time only. It is shown that the results of the numerical simulations based on the theoretical models agree well with those of the experiments. The agreement validates the developed theoretical models which can be used to guide and understand the future experiments on high power microwave pulse propagation and the future experiments for developing practical plasma devices. This study shows that the spectrum of a microwave will be modified while propagating through a fast growing plasma. DTIC

N94-26980# Scientech, Inc., Idaho Falls, ID.
S-76 HIGH INTENSITY RADIATED FIELDS, VOLUME 3 Final Report
Jerry Blair Oct. 1993 211 p Sponsored by FAA
(AD-A274416; DOT/FAA/CT-93/5-Vol-3) Avail: CASI HC A10/MF A03

The Federal Aviation Administration (FAA) Technical Center sponsored a series of High Intensity Radiated Fields (HIRF) tests on a Sikorsky S-76 rotorcraft. The project was conducted to evaluate the practically of performing aircraft level HIRF tests, determine the effects of HIRF on a specific rotorcraft with the potential to obtain information on rotorcraft in general, and evaluate the effects of exposure to 'real world' HIRF emitters. HIRF ground and flight tests were conducted to achieve the objective of the project. Site calibration (SCAL) measurements were made in the test area to determine the levels at which the S-76 would be irradiated when placed in the test area. Ground tests consisted of Low Level Swept Coupling (LLSC) and Low Level Swept Fields (LLSF) tests. The flight tests were flown directly into the main beam of a variety of pulsed and continuous wave (CW) transmitters including the Over the Horizon Back Scatter (OTHB), PAVE PAWS, ASR-9, FPS-65, and FPS-16 radars. Results of the S-76 tests added credibility to the existence of HIRF as a flight safety hazard. In the evaluation of the emitters, the flight tests showed repeatable instances where exposure resulted in instrumentation disruptions. It should however be noted that all the observed disruptions were of a non-critical nature. DTIC

N94-27041# Foerenade Fabriksverken, Linkoeping (Sweden). Huvudavdelning foer Informationsteknologi.
MICROWAVE COUPLING INTO A SLOTTED CAVITY
Mats Baeckstroem and Jorgen Loren May 1993 40 p
(PB94-123742; FOA-C-30712-8.3,3.2) Avail: CASI HC A03/MF A01

Simple formulas for shielding effectiveness and for absorption cross-section of a wire inside a shielded structure, intended to be used in analysis and practical design work of shielded compartments, are evaluated with respect to measured data. The outcome is encouraging and motivates further work. NTIS

N94-27068# Rhode Island Univ., Kingston. Dept. of Electrical Engineering.

PARAMETRIC TIME-SCALE METHODS IN SIGNAL ANALYSIS Final Report, 1 Jul. 1992 - 30 Jun. 1993

R. Kumaresan 30 Jun. 1993 9 p
(Contract F49620-92-J-0378)
(AD-A274212; AFOSR-93-0902TR) Avail: CASI HC A02/MF A01

The researchers have separated the Kaiser-Teager algorithm for separating the contributions of the amplitude modulation and frequency modulation of a signal consisting of multiple components. To achieve this separation, they use an instantaneous non-linear operator, which turns out to be the determinant of a Toeplitz matrix formed with the signal samples. Because of its instantaneously adaptive nature, they can use this algorithm to track parameter variations that are not too rapid. The researchers demonstrate this using a synthetic signal containing two AM-FI4 signal components and a speech signal. They also point out the methods relationship to Prony's method. The researchers proposed a demodulator-filter approach for tracking harmonic signals and applied it to speech processing. DTIC

N94-27073# Air Force Inst. of Tech., Wright-Patterson AFB, OH. School of Engineering.

PROCESSING OF WIDE-ANGLE SYNTHETIC APERTURE RADAR SIGNALS FOR TARGET DETECTION M.S. Thesis

Kurt W. Knurr Dec. 1993 115 p
(AD-A274225; AFIT/GE/Eng/93D-22) Avail: CASI HC A06/MF A02

This study investigated methods of targets detection using Wide-Angle Synthetic Aperture Radar (WASAR). WASAR uses multiple aspect angle Synthetic Aperture Radar (SAR) images of the same scene. The SAR images were generated using a pre-release software package from package from Loral Corporation. The software was able to generate 512 by 512 pixel SAR images that contained various vegetation return which for our purposes we classified as clutter. Within this clutter, targets (M35 trucks) could be placed at random location and orientations. The software also had the capability of generating fully-polarimetic WASAR images with multiple depression angles. This data was then processed and various detection algorithms tested to exploit the amount and diversity of information available from the multiple images. SAR images are generally known to contain large amounts of data, and WASAR images contain even more due to the multiple images. Various pre-processing filters were analyzed for detection optimization. These filters included: polarimetric averaging, polarimetric span, polarimetric optimal weighting, and polarimetric whitening filters. Simple classical detection (thresholding) algorithms were evaluated using these preprocessed data sets. The use of WASAR imagery improved detection by allowing thresholds to be set higher than for simple SAR thereby avoiding false alarms yet still allowing detection of the known targets. DTIC

N94-27085# Phillips Lab., Hanscom AFB, MA.

PERFORMANCE STATISTICS BULLETIN: HIGH ALTITUDE METEOR SCATTER PROPAGATION, AUGUST, SEPTEMBER, OCTOBER 1989 Interim Report

Alan D. Bailey, Jens C. Ostergaard, Regina M. Burton, Carlton H. Curtis, and Wayne I. Klemetti 7 Sep. 1993 218 p
(AF Proj. 4643)
(AD-A274455; PL-TR-93-2196; ERP-1129) Avail: CASI HC A10/MF A03

A representative sampling of meteor scatter propagation performance statistics is presented from the PL/GP High Latitude Meteor Scatter Test Bed. The data address questions of meteor scatter propagation under disturbed ionospheric conditions, as well as normal meteor scatter propagation in the polar region. The time and frequency variations of the propagation transfer function are characterized over the 35 to 147 MHz range, including the availability of useful meteor trails, the potential communication capacity associated with those trails, the occurrence and persistence of ionospheric scatter and sporadic E-layers, variations in the signal-to-noise ratios of each scatter return, and the effects of auroral and polar cap absorption (PCA) events on meteor scatter propagation and communications. Statistics covering Arrival Rate, Duration, Duty Cycle, and Noise Temperature are presented. This bulletin is one of a series of polar meteor scatter data bulletins. DTIC

N94-27127 Air Force Inst. of Tech., Wright-Patterson AFB, OH. School of Engineering.

RADAR CROSS SECTION VISUALIZATION USING SAMPLE BUFFER PROGRESSIVE REFINEMENT VOLUME RENDERING M.S. Thesis

Alain L. Jones Dec. 1993 66 p Limited Reproducibility: More than 20% of this document may be affected by microfiche quality
(AD-A274179; AFIT/GCS/ENG/93D-13) Avail: CASI HC A04

This thesis explores how to interactively examine the radar cross section characteristics of an object. As such, this research encompasses two rapidly burgeoning fields: scientific visualization and low-observables technology. DTIC

N94-27136 Physics and Electronics Lab. TNO, The Hague (Netherlands).

OVER-THE-HORIZON PROPAGATION MEASUREMENTS AT SIX RADAR-FREQUENCY BANDS AT THE ATLANTIC OCEAN COAST

R. B. Boekema Jul. 1993 70 p Limited Reproducibility: More than 20% of this document may be affected by microfiche quality
(AD-A274151; FEL-92-B438; TDCK-93-0303) Avail: Issuing Activity (Defense Technical Information Center (DTIC))

In the autumn of 1989, the propagation subgroup of NATO AC/243 has conducted a propagation experiment near Lorient France, at the Atlantic Ocean. The purpose of this experiment was to gain an insight into the influence of the evaporation duct above the sea on the propagation of radar signals of different frequencies in an over-the-horizon situation and into the applicability of model predictions. The geometry of the experiment has been chosen to represent a typical ship defence situation. The measurements have shown that for the present case the nearly always present evaporation duct results in a signal enhancement with the strongest effects at the 10.5 and 16 GHz frequencies. An extended study of the quality of the model predictions, possible by the unique set of measurement results, shows some interesting matters. If the process of prediction is divided into two parts, the calculation of the duct height from the meteorological data and the path loss calculation from this duct height, the conclusion is made that the first part is responsible for the largest inaccuracies. The used duct height calculation method showed systematic deviations for different meteorological conditions. The inaccuracy of the duct height calculation makes useful path loss predictions at the millimeter-wave frequencies (35 and 94 GHz) impossible for this over-the-horizon situation. The predictions at the lower frequencies are much better, but not always satisfactory. The deviation analyses in this report can be useful to improve propagation models. DTIC

N94-27146 Department of the Navy, Washington, DC.

METHOD OF CORRECTING ROTATIONAL MOTION ERROR IN SAR AND ISAR IMAGERY Patent

Duane Roth, inventor (to Navy) 5 Oct. 1993 14 p Filed 1 Jul. 91
(AD-D016033; US-Patent-5,250,952; US-Patent-Appl-SN-727257) Avail: US Patent and Trademark Office

A method of correcting rotational motion error in SAR and ISAR imagery includes shifting the center of the image to zero doppler and thus to the center of rotation of the target being imaged, selecting a dominant scatterer at an off-center range cell to provide a phase reference, calculating the rotational motion error function from the phase of the selected scatterer, using the rotational motion error function to interpolate raw radar return image data between the original unequal angular samples to obtain equal angular samples of the target reflectivity function, and performing an image quality check and producing a value which is a relative measure of focus of the image. Also, the method includes repeating the steps starting with selecting a new dominant scatterer as a phase reference. Further, the performing step of the method includes storing and comparing the relative measures of focus provided by repeating of the steps to arrive at the corrected image which is the most focused and then saving the corrected image determined to be the the most focused. DTIC

N94-27159 National Defence Research Establishment, Linkoeping (Sweden).

FOA 39 [EKONOMI- OCH PRODUKTIONSRAPPORT 1992. INSTITUTIONEN FOER SIGNALSPANINGS- OCH MOTMEDELSSYSTEM]

E. S. Johansson and B. Heelge Feb. 1993 31 p In SWEDISH; Text in SWEDISH; summary in ENGLISH
(PB94-124252; FOA-C-30705-3.6) Avail: Issuing Activity (National Technical Information Service (NTIS))

This report gives an overview of activities of the Division of Electronic Support Measures and Electronic Countermeasures during the year 1992.
NTIS

N94-27170 Adroit Systems, Inc., Fairborn, OH.
IMAGE QUALITY ANALYSIS OF COMPRESSED SYNTHETIC APERTURE RADAR IMAGERY Final Report, Sep. 1991 - Dec. 1992
Gilbert G. Kuperman and Todd D. Penrod Jan. 1993 56 p Limited Reproducibility: More than 20% of this document may be affected by microfiche quality
(Contract F33615-89-C-0532)
(AD-A273399; AL/CF-TR-1993-0156) Avail: Issuing Activity (Defense Technical Information Center (DTIC))

The study investigated the effects of image compression processing on synthetic aperture radar imagery. Image quality measurements were performed before and after compression. Image fidelity measurements were made comparing the compressed and original versions of each image. Operator performance was assessed using an interpretability rating scale. Possible effects of an interaction between compression and automatic target recognizer performance were explored using a generic constant false alarm rate automatic target cuer algorithm. DTIC

N94-27202 Department of the Navy, Washington, DC.
FOCAL PLANE ANTENNA ARRAY FOR MILLIMETER WAVES Patent
William M. Waters, inventor (to Navy) 17 Aug. 1993 10 p Filed 28 Apr. 92
(AD-D016034; US-Patent-5,237,334; US-Patent-Appl-SN-876696) Avail: US Patent and Trademark Office

A millimeter wave imaging system receives millimeter wave radiation and provides video imaging signals based thereon. The system comprises an imaging lens for receiving incoming radiation; a focal plane antenna array disposed at the focal plane of the lens on which radiation received by the lens is focused; and signal processing and display circuitry for processing the output of the antenna array and for producing and displaying corresponding video imaging signals. The focal plane antenna array comprises a planar array of a plurality of conical horns and circular waveguides which, in use, are disposed at the focal plane of the lens; and a microstrip detector assembly coupled to the waveguides for detecting the radiation received thereby. The microstrip detector assembly comprises a dielectric substrate having a plurality of microstrip conductors embedded therein, each microstrip conductor being coupled to a respective one of the waveguides, and a diode detector being connected to each microstrip conductor. DTIC

N94-27219 National Defence Research Establishment, Linkoeping (Sweden). Huvudavdelning foer Informationsteknologi.
MILCOM 92 AND STANDARDIZATION FOR HF-COMMUNICATION. A STUDY TOUR TO THE USA IN OCTOBER 1992 [MILCOM 92 OCH STANDARDISERING PA HF-OMRADET. EN STUDIERESA TILL USA OKTOBER 1992]
L. Ahlin, G. Andersson, and B. Johansson Jun. 1993 29 p In SWAHILI
(PB94-124427; FOA-C-30714-3.5) Avail: Issuing Activity (National Technical Information Service (NTIS))

A study tour to the USA with the main purpose of increasing the knowledge of ongoing developments of standards for HF-communication was performed. The journey also included a visit at the annual MILCOM conference. Besides the conference we also visited the Institute for Telecommunication Sciences (ITS) and the Defense Information Systems Agency (DISA) for discussions about system standards for HF-nets. The report relates an overview of some interesting papers presented at the MILCOM conference. NTIS

N94-27233 Tel-Aviv Univ. (Israel).
SPECTRAL AND TEMPORAL CORRELATIONS OF MULTIFREQUENCY WAVES IN THE TURBULENT ATMOSPHERE Ph.D. Thesis
Zion Azar Jun. 1990 158 p In HEBREW
(ITN-94-85229) Copyright Avail: Issuing Activity (Tel-Aviv Univ., Exact Sciences Library, Ramat Aviv 69978, Israel)

When an optical beam propagates through a randomly inhomogeneous medium it acquires both phase and intensity fluctuations which are the result of random scattering and diffraction by the refractive index inhomogeneities in the random medium. While these fluctuations severely limit the performance of surveillance, communication and lidar systems that use the random medium as their transmission channel, the study of the statistical properties of the received fluctuation may also reveal useful information about the nature and structure of the random medium and the optical source (the inverse problem). In order to extract the information contained in the scattered field it is necessary to observe the scattered radiation field as completely as possible. In recent years, considerable effort has been dedicated, both theoretically and experimentally, to determine the intensity correlation function of two collinear initially overlapping optical beams, propagating in a random medium, and having different frequencies. Spectral diversity (simultaneous measurements of the received radiation at several different frequencies at the same point) not only adds important data to ease the solution of the inverse problem, but its incorporation into practical devices also significantly improves the signal to noise ratio in electro-optical systems. The experimental results can be explained in terms of in-system turbulence. Moreover, we have developed a novel optical method to measure the inner scale of turbulence from the bichromatic correlation coefficient by using this theoretical study. Author (ISA)

N94-27234 Tel-Aviv Univ. (Israel). School of Physics and Astronomy.
THEORETICAL AND EXPERIMENTAL ANALYSIS OF THE SPATIAL AND TEMPORAL BEHAVIOUR OF THE INTENSITY OF AN ELECTRO-MAGNETIC WAVE REFLECTED FROM A DIFFUSE TARGET AFTER PASSING THROUGH A TURBULENT ATMOSPHERE M.S. Thesis
Sagie Tsadka Jun. 1991 105 p In HEBREW
(ITN-94-85230) Copyright Avail: Issuing Activity (Tel-Aviv Univ., Exact Sciences Library, Ramat Aviv 69978, Israel)

New methods are presented for the remote sensing, along a selected optical path, of atmospheric parameters such as the average wind speed and the turbulence-strength parameter. The theoretical basis of the method is presented. Turbulence-induced irregularities in the earth's atmospheric refractive index result from the existence of fluctuations in air temperature and velocity in eddies. Passage through such eddies causes distortion of optical wavefronts, leading to focusing or defocusing and local deviations in the direction of propagation and, through interference, irradiation fluctuations at a receiver. Although these random effects are complicated, statistical averaging enables the turbulence effects to be described quantitatively. Use of the wave equation for electromagnetic (EM) waves, with a random refractive index enables a formal integral solution to be found for the random EM field propagating through the turbulent medium. It is usual to use the statistical moments of this EM field to describe the spatial and temporal behavior of the intensity during the passage of the field through the atmosphere. The statistics of the turbulence structure and the nature of the interaction between the wave front and the turbulence eddies are embedded in these moments. The behavior is analyzed of a laser beam which propagates through a turbulent atmosphere and is reflected back to a receiver by a diffuse target on which a speckle type of field is being generated. The extended Huygens-Fresnel principle is used to obtain first- and second-order statistics of the received intensity of the reflected beam after propagation through weak turbulent media. ISA

N94-27242 Tel-Aviv Univ. (Israel).
CODED COMMUNICATIONS WITH NONIDEAL INTERLEAVING Ph.D. Thesis
Shaul Laufer Feb. 1991 185 p
(ITN-94-85235) Copyright Avail: Issuing Activity (Tel-Aviv Univ., Exact Sciences Library, Ramat Aviv 69978, Israel)

Burst error channels - a type of block interference channels - feature increasing capacity but decreasing cutoff rate as the memory rate increases. Despite the large capacity, there is degradation in the performance of practical coding schemes when the memory length is excessive. A short-coding error parameter (SCEP) was introduced, which expresses a bound on the average decoding-error probability for codes shorter than the block interference length. The performance of a coded slow frequency-hopping communication channel is analyzed for worst-case partial band jamming and nonideal interleaving, by deriving expressions for the capacity and cutoff rate. The capacity and cutoff rate, respectively, are shown to approach and depart from those of a memoryless channel corresponding to the transmission of a single code letter per hop. For multiaccess communications over a slot-synchronized collision channel without feedback, the channel was considered as a block interference channel with memory length equal to the number of letters transmitted in each slot. The effects of an asymmetrical background noise and a reduced collision error rate were studied, as aspects of real communications. The performance of specific convolutional and Reed-Solomon codes was examined for slow frequency-hopping systems with nonideal interleaving. An upper bound is presented for the performance of a Viterbi decoder for a convolutional code with nonideal interleaving, and a soft decision diversity combining technique is introduced. Author (ISA)

N94-27244 Tel-Aviv Univ. (Israel). Dept. of Geophysics and Planetary Sciences.
DYNAMIC AND KINEMATIC P WAVE TRACING FOR A THREE-DIMENSIONAL ELASTIC INHOMOGENEOUS MEDIA BY THE ASYMPTOTIC RAY THEORY AND APPLICATION M.S. Thesis
Philippe Pascal Artsztein Jul. 1990 153 p In HEBREW
(ITN-94-85239) Copyright Avail: Issuign Activity (Tel-Aviv Univ., Exact Sciences Library, Ramat Aviv 69978, Israel)

This work deals with calculation of ray trajectories and P wave amplitudes in a three-dimensional medium characterized by variable velocity. The first chapter deals with the construction of a three-dimensional structure generator. A new method for creating complicated structures, such as those containing lenses or pinchouts is presented. The material interfaces are calculated by the pseudo polynomial spline interpolation method. The second chapter contains a review of the asymptotic ray theory. Simple algorithms for calculating the P wave trajectories in an inhomogeneous elastic medium, based on the solution of a system of six differential equations, are proposed. A method for calculating the directions of the reflected/transmitted rays is described. The third chapter deals with dynamic ray tracing. The propagating wave amplitudes are calculated by solving a system of 14 differential equations. This chapter also deals with the changes in amplitudes of the wave fronts upon crossing material dicontinuities. In the fourth chapter a scanning method for solving the two point ray tracing problem is presented. According to this method, a kinematic and dynamic ray tracing for common shot or normal incidence ray tracing is performed. At the end of the chapter, time-to-depth mappings are described by two methods: (A) ray tracing migration and (B) ray tracing inversion. Author (ISA)

N94-27249# Electrotechnical Lab., Tsukuba (Japan).
RESEARCHES OF THE ELECTROTECHNICAL LABORATORY. NO. 955: SPEECH RECOGNITION BY DESCRIPTION OF ACOUSTIC CHARACTERISTIC VARIATIONS [DENSHI GIJITSU SOGO KENKYUSHO KENKYU HOKOKU, DAI 955 GO: ONKYOTEKI TOKUSEI NO HENDU NO KIJITSU O MOCHIITA ONSEI NINSHIKI NI KANSURU KENKYU]
Satoru Hayamizu 10 Sep. 1993 120 p In JAPANESE
(ISSN 0366-9106)
(JTN-94-80604) Avail: CASI HC A06/MF A02

A new speech recognition technique is proposed. This technique systematically describes acoustic characteristic variations using a large scale speech database, thereby, obtaining high recognition accuracy. Rules are extracted to represent knowledge concerning acoustic characteristic variations by observing the actual speech database. A general framework based on maps of the sets of variation factors to the acoustic feature spaces is proposed. A single recognition model is not used for each element of descriptive units regardless of the states of the variation factors. Large-scaled and systematic different recognition models are used for different states. A technique to structurize the representation of acoustic characteristic variations by clustering recognition models depending on variation factors is proposed. To investigate acoustic characteristic variations for phonetic contexts efficiently, word sets for reading texts of speech database are selected so that the maximum number of three phoneme sequences are covered in small number of words as possible. A selection algorithm, in which the first criterion is to maximize the number of different three phoneme sequences in the word set and the second criterion is to maximize the entropy of the three phonemes, is proposed. Read speed data of the word sets are collected and labelled as acoustic-phonetic segments. Experiments of speaker-independent word recognition using this speech database were conducted to show the description effectiveness of the acoustic characteristic variations using networks of acoustic-phonetic segments. The experiment shows the recognition errors are reduced. Basic framework for estimating the acoustic characteristics in unknown phonetic contexts using decision trees is proposed. Author (NASDA)

N94-27270 Hazeltine Corp., Braintree, MA.
BEAMFORMING/NULL-STEERING ADAPTIVE ARRAY Patent
Raymond J. Masak, inventor (to Hazletine) 14 Dec. 1993 23 p
(CA-Patent-1325260; Int-Patent-Class-G01S-003/42; CTN-94-61095)
Copyright Avail: Micromedia Ltd., Technical Information Centre, 240 Catherine Street, Suite 305, Ottawa, Ontario, K2P 2G8, Canada HC/MF

Phase-coded spread spectrum communication signals may be acquired and synchronized in the presence of interference with the aid of an adaptive array antenna under control of a least mean square algorithm performing power minimization. Although the signal to interference ratio at the adaptive array output port of such a system is adequate for acquisition and synchronization, it provides unacceptable message quality. Accordingly, an adaptive processor is provided which simultaneously performs beamforming and null steering to cancel interference affecting a desired signal. The null steering means cancels at least a portion of the undesired signal and is operative to reduce the gain of the radiation pattern of an array antenna in the direction of the source of the interference. The beamforming means enhances at least a portion of the desired signal and is operative to increase the gain of the radiation pattern of an array antenna in the direction of the source of the desired signal. Second means are provided for coordinating the null steering and beamforming means. The null steering and beamforming loops employ on and off epoch processors. Author (CISTI)

N94-27274 Queens Univ., Kingston (Ontario). Dept. of Electrical Engineering.
EQUALIZATION AND CANCELLATION OF NONLINEAR INTERSYMBOL INTERFERENCE IN A DISPERSIVE SATELLITE COMMUNICATION CHANNEL M.S. Thesis
Jeffrey Chan Aug. 1993 141 p
(ISBN-0-315-85147-3; CTN-94-61098) Copyright Avail: Micromedia Ltd., Technical Information Centre, 240 Catherine Street, Suite 305, Ottawa, Ontario, K2P 2G8, Canada HC/MF

Methods for compensating for nonlinear intersymbol interference (ISI) in satellite communication channels are examined, using a model of the satellite channel consisting of a dynamic linear filter followed by a static nonlinearity and then by another dynamic linear filter. Noise is added after the nonlinearity to represent the noise in the downlink to the ground receiver. Two general methods to compensate for the nonlinear ISI are equalization and cancellation. Six specific techniques for nonlinear ISI compensation were studied in detail. It is concluded that the best four techniques in terms of bit error probability are, in order from best to worst: fast orthogonal search equalization; fast orthogonal search cancellation; parallel cascades without the trailing extra linear filter, in a cancellation configuration; and parallel cascades with the trailing extra linear filter, in a cancellation configuration. Of these four, the last technique requires the least memory and processing time whereas the first requires the most memory and processing time. When these four methods are compared with the linear fractionally spaced equalizer, it is found that the bit error probability is greatest for the fractionally spaced equalizer, but the equalizer also requires the least memory and processing time. Author (CISTI)

N94-27301 Queens Univ., Kingston (Ontario). Dept. of Electrical Engineering.
THE PERFORMANCE OF NONORTHOGONAL NONCOHERENT FREQUENCY HOPPED M-ARY FSK IN ADDITIVE WHITE GAUSSIAN NOISE, FADING AND JAMMING M.S. Thesis
Robert Allan Brett May 1993 235 p
(ISBN-0-315-85243-7; CTN-94-61102) Copyright Avail: Micromedia Ltd., Technical Information Centre, 240 Catherine Street, Suite 305, Ottawa, Ontario, K2P 2G8, Canada HC/MF

A tight upper bound approximation of the performance of noncoherent nonorthogonal M-ary frequency shift keying (MFSK) on fading channels is derived and verified by simulation. The performance of forward error correction coded nonorthogonal MFSK is compared to that of uncoded orthogonal MFSK occupying the same bandwidth and requiring the same energy per information bit. An analytical technique for finding the bit error probabilities of frequency hopped (FH) orthogonal MFSK in arbitrary combinations of jamming, fading, and noise is derived for an arbitrary number of signalling dimensions and an arbitrary level of diversity. No results previously existed for this problem. A versatile simulator is developed for computing the performance of FH nonorthogonal MFSK in the same environments. Comparisons are made between coded nonorthogonal FH/MFSK and uncoded orthogonal FH/MFSK in fading, additive white Gaussian noise, and multitone jamming. Author (CISTI)

N94-27308 Concordia Univ., Montreal (Quebec). Dept. of Electrical and Computer Engineering.
DEVELOPMENTS IN THE APPLICATION OF THE GEOMETRICAL THEORY OF DIFFRACTION AND COMPUTER GRAPHICS TO AIRCRAFT INTER-ANTENNA COUPLING ANALYSIS M.S. Thesis
Michael Bogusz Jan. 1993 189 p
(ISBN-0-315-84643-7; CTN-94-61083) Copyright Avail: Micromedia Ltd., Technical Information Centre, 240 Catherine Street, Suite 305, Ottawa, Ontario, K2P 2G8, Canada HC/MF

The need for a systematic methodology for the analysis of aircraft electromagnetic compatibility (EMC) problems is examined. The available computer aids used in aircraft EMC analysis are assessed and a theoretical basis is established for the complex algorithms which identify and quantify electromagnetic interactions. An overview is presented of one particularly well established aircraft antenna to antenna EMC analysis code, the Aircraft Inter-Antenna Propagation with Graphics (AAPG) Version 07 software. The specific new algorithms created to compute cone geodesics and their associated path losses and to graph the physical coupling path are discussed. These algorithms are validated against basic principles. Loss computations apply the uniform geometrical theory of diffraction and are subsequently compared to measurement data. The increased modelling and analysis capabilities of the newly developed AAPG Version 09 are compared to those of Version 07. Several models of real aircraft, namely the Electronic Systems Trainer Challenger, are generated and provided as a basis for this preliminary comparative assessment. Issues such as software reliability, algorithm stability, and quality of hardcopy output are also discussed. Author (CISTI)

N94-27335# Instituto de Pesquisas Espaciais, Sao Jose dos Campos (Brazil).
NON-ADAPTIVE ROBUST FILTERS FOR SPECKLE NOISE REDUCTION
Alejandro C. Frery and Sidnei J. S. SantAnna 1993 11 p
(INPE-5519-PRE/1794) Avail: CASI HC A03/MF A01

After briefly reviewing some classical filters for speckle removal, five filters with characteristics of robustness, suitable for speckle noise reduction, are derived and implemented. These filters are the ones based on the trimmed maximum likelihood and moments estimators, the ones based on the median, on the inter-quartile range, and on the median absolute deviation. Assuming that observations within a synthetic aperture radar image are outcomes of independent Rayleigh random variables, these filters exhibit a good performance from both the signal-to-noise reduction and from the edge preserving criteria. The problem of filtering in an image is posed as an estimation problem. Author

N94-27340# Toshiba Research and Development Center, Kawasaki (Japan). Energy and Mechanical Research Lab.
A COMPACT 150 GHz SIS RECEIVER COOLED BY 4 K GM REFRIGERATOR
Masahiko Takahashi, Hideo Hatakeyama, Toru Kuriyama, Hideki Nakagome, Ryohei Kawabe, Hiroyuki Iwashita, Gerrard McCulloch, Katsunori Shibata, and Nobuharu Ukita 1993 13 p
(Rept-36; JTN-94-80577) Avail: CASI HC A03/MF A01

An SIS (Superconductor Insulator Superconductor) mixer is used for the astronomical millimeter radio observation because of its high sensitivity. The SIS mixer, however, must be cooled at the 4 K level, and either liquid helium or a GM (Gifford-McMahon) + JT refrigerator has been used for a long time. This paper describes the construction and experimental results of a compact SIS receiver, 720 mm in height, 260 mm in length, 260 mm in width, and 35 kg in weight. The technical point of the receiver was to adopt a 4 K GM refrigerator which used Er3Ni as a regenerator material to cool the SIS mixer. The cooling temperature of 3.4 K was achieved for the SIS mixer and the cool down time from the room temperature to the 4 K level was 4.5 hours. The power consumption for the compressor unit was 3.3 kW. This SIS receiver has been installed on the 45 meter antenna at Nobeyama Radio Observatory and used for astronomical observation for more than 3,000 hours. Author (NASDA)

N94-27345 Concordia Univ., Montreal (Quebec). Dept. of Electrical and Computer Engineering.
ANALYSIS OF A MULTIACCESS/SWITCHING TECHNIQUE FOR MULTIBEAM SATELLITES IN A PRIORITIZED ISDN ENVIRONMENT M.S. Thesis
Mohamed Hachicha Aug. 1992 148 p
(ISBN-0-315-84632-1; CTN-94-61081) Copyright Avail: Micromedia Ltd., Technical Information Centre, 240 Catherine Street, Suite 305, Ottawa, Ontario, K2P 2G8, Canada HC/MF

An integrated multibeam satellite system with a new multiple access technique and an on-board baseband switch with priority rule is analyzed. The performance analysis includes the computation of the various packet loss, call blocking, and packet delays of a typical user in an integrated satellite internetworking environment. The uplink technique employed is a hybrid packet/circuit switched approach of the demand assignment type, while the downlink is a time division multiplexing technique. On board the satellite, a baseband nonblocking switch is used to route packets from input to output ports. Various amounts of input and output buffering as well as priority rules and a head-of-line blocking resolution algorithm are employed to improve the performance of the data services without affecting other services' performance. The delay and throughput characteristics of the services are determined by examining the relationships between the head-of-line resolution, buffer sizes, and internal speedup ratio of the baseband switch. Author (CISTI)

N94-27546# Center for Mathematics and Computer Science, Amsterdam (Netherlands). Dept. of Computer Science/Dept. of Algorithmics and Architecture.
SINGLE TERM OFF-LINE COINS
Niels T. Ferguson Mar. 1993 16 p
(ISSN 0169-118X)
(CWI-CS-R9318; ETN-94-95431) Copyright Avail: CASI HC A03/MF A01

A construction for offline electronic coins that is both far more efficient and much simpler than previous systems is presented. Instead of using many terms, each for a single bit of the challenge, the system uses a single term for a large number of possible challenges. The withdrawal protocol does not use a cut and choose methodology as with earlier systems, but uses a direct construction. ESA

N94-27551# Center for Mathematics and Computer Science, Amsterdam (Netherlands). Dept. of Computer Science/Dept. of Algorithmics and Architecture.
AN EFFICIENT OFF-LINE ELECTRONIC CASH SYSTEM BASED ON THE REPRESENTATION PROBLEM
Stefan A. Brands Mar. 1993 80 p
(ISSN 0169-118X)
(CWI-CS-R9323; ETN-94-95436) Copyright Avail: CASI HC A05/MF A01

An offline electronic cash system based entirely on discrete logarithms is presented. Using the representation problem as a basic concept, some techniques are introduced that enable the construction of protocols for withdrawal and payment that do not use the cut and choose methodology of earlier systems. As a consequence, the cash system is much more efficient in both computation and communication complexity. The correctness of the system can be proven to a very great extent. The construction of an efficient cash system with security related to factoring or computation of RSA roots, in an analogous way to the discrete log based system, is discussed. The decision variant of the Diffie-Hellmann problem, that is strongly related to undeniable signatures, is discussed. ESA

N94-27669*# Rockwell International Corp., Anaheim, CA. Tactical Systems Div.
NASA SATELLITE COMMUNICATIONS APPLICATION RESEARCH. PHASE 2: EFFICIENT HIGH POWER, SOLID STATE AMPLIFIER FOR EFH COMMUNICATIONS Final Report, 9 Jun. 1992 - 31 Jul. 1993
James Benet 31 Jul. 1993 42 p
(Contract NASw-4513)
(NASA-CR-195713; NAS 1.26:195713) Avail: CASI HC A03/MF A01

The final report describes the work performed from 9 Jun. 1992 to 31 Jul. 1993 on the NASA Satellite Communications Application Research (SCAR) Phase 2 program, Efficient High Power, Solid State Amplifier for

EHF Communications. The purpose of the program was to demonstrate the feasibility of high-efficiency, high-power, EHF solid state amplifiers that are smaller, lighter, more efficient, and less costly than existing traveling wave tube (TWT) amplifiers by combining the output power from up to several hundred solid state amplifiers using a unique orthomode spatial power combiner (OSPC). Derived from text

N94-27734# Department of the Navy, Washington, DC.
FIBER OPTIC TRUE TIME-DELAY ARRAY ANTENNA FEED SYSTEM Patent Application
Ronald D. Esman, inventor (to Navy) and Lew Goldberg, inventor (to Navy) 17 Sep. 1993 39 p
(AD-D016063; US-Patent-Appl-SN-122671; Navy-Case-74788) Avail: CASI HC A03/MF A01

The fiber-optic true time-delay array antenna feed is a device for dynamically generating a plurality of identical electromagnetic radiation (EMR) signals with continuously variable time-delay separations. The EMR signal to be transmitted modulates a continuous-wave optical signal from a laser source which is applied to a plurality of high dispersion single-mode optical fibers acting as synchronized true time-delay modulators forming an array antennas feed system. Each fiber is chosen to have the same nominal time delay but a different net dispersion. Photodetectors convert the optical intensity back into an EMR electrical signal to feed each of the elements of the array antenna. DTIC

N94-27738# Deutsche Forschungsanstalt fuer Luft- und Raumfahrt, Oberpfaffenhofen (Germany). Abt. HF-Systeme.
CALIBRATION OF SAR SYSTEMS Ph.D. Thesis - Stuttgart Univ. [KALIBRATION VON SAR-SYSTEMEN]
Manfred Zink May 1993 164 p In GERMAN
(ISSN 0939-2963)
(DLR-FB-93-18; ETN-94-95496) Avail: CASI HC A08/MF A02

A comprehensive description of necessary procedures for radiometric calibration of SAR (Synthetic Aperture Radar) systems is presented. Relative calibration allows successive measurements to be compared. Absolute calibration relates the SAR image intensity to radar backscattering coefficients and provides information about the accuracy of this relationship. Estimation and removal of all system related influences results in pure object signatures. The goal for the microwave remote sensing activities is to model the relationship between geophysical parameters, like soil moisture or leaf area index, and measured backscattering coefficients. Such quantitative analyses and the development and interpretation of models in different geophysical applications require calibrated data. With calibrated data the list of applications and geophysical parameters which can be monitored will extend considerably. ESA

N94-27806 Carleton Univ., Ottawa (Ontario). Dept. of Systems and Computer Engineering.
SHORT-BLOCK DATA DETECTION TECHNIQUES EMPLOYING CHANNEL ESTIMATION FOR FADING TIME-DISPERSIVE CHANNELS Ph.D. Thesis
Stewart N. Crozier 26 Mar. 1990 236 p
(ISBN-0-315-58970-1; CTN-94-60997) Copyright Avail: Micromedia Ltd., Technical Information Centre, 240 Catherine Street, Suite 305, Ottawa, Ontario, K2P 2G8, Canada HC/MF

Three short-block data detection techniques based on linear, nonlinear decision directed, and maximum likelihood estimation principles are investigated, using short alternating blocks of data and training symbols. The training blocks are useful for both channel tracking and data block detection; each data block is detected as a unit. Previous restrictions imposed on short-block detection schemes were removed, resulting in reduced complexity algorithms (useful at higher signaling rates) and higher throughput efficiency. The higher the signaling rate, the more inherent diversity a time-dispersive fading channel can provide, and the better the error rate performance. Performance is evaluated for phase shift keying using a Rayleigh fading channel model with severe time dispersion. The performance is compared to that of conventional linear and decision feedback equalizers. The block detection schemes examined all require an estimate of the channel impulse response. A channel estimation algorithm is presented and optimum training sequences are determined and tabulated. A simple formula for the expected degradation in performance caused by channel estimation errors is also derived. Simulation results confirm the accuracy of this approximation for high signal to noise ratios. Author (CISTI)

N94-27838# Institute of Plasma Physics, Prague (Czechoslovakia).
ON RADIO FREQUENCY WAVE INDUCED RADIAL TRANSPORT AND WAVE HELICITY
V. Petrzilka Sep. 1992 9 p
(IPPCZ-326) Avail: CASI HC A02/MF A01

Expressions for wave induced radial transport are derived allowing simple estimates. The transport is enhanced due to the presence of poloidal magnetostatic field and in the vicinity of the ion cyclotron resonance. The direction of the wave induced transport depends also on the wave polarization. Author

N94-27871 Ottawa Univ. (Ontario). Dept. of Electrical Engineering.
RECEIVING ANTENNAS FOR ELECTROMAGNETIC PULSES AND TRANSIENTS Ph.D. Thesis
Karunanayake P. A. P Esselle 1990 261 p
(ISBN-0-315-62312-8; CTN-94-60991) Copyright Avail: Micromedia Ltd., Technical Information Centre, 240 Catherine Street, Suite 305, Ottawa, Ontario, K2P 2G8, Canada HC/MF

The pulse receiving characteristics of several thin-wire antennas were investigated. A loop antenna with uniformly distributed impedance was analyzed using an equivalent circuit, and the frequency- and time-domain receiving characteristics of a resistively loaded loop antenna were obtained. The antenna was found to be dispersive and not suitable for receiving electromagnetic pulses or transients. Resistively loaded straight dipole antennas were then considered. The Wu-King resistively loaded dipole was found to have the maximally flat frequency response close to the upper roll-off frequency, when terminated with a high impedance load. Thirdly, a time-domain stepping in time procedure was developed for analyzing V-antennas. After identifying limitations of these antennas in receiving fast pulses and transient, a new V-antenna consisting of a resistively loaded thin-wire V-dipole or monopole was developed. This antenna has 3 dB bandwidth from 110 MHz to 10 GHz and higher sensitivity than the Wu-King antenna. An experimental V-antenna and Wu-King monopole antenna were fabricated using thin film deposition and tested. The V-antenna is capable of receiving a 520-ps near-Gaussian pulse without significant distortion and has a flat receiving response from 35 MHz to 3 GHz. The Wu-King antenna had an upper roll-off frequency of about 300 MHz. Author (CISTI)

N94-27946*# Rockwell International Corp., Anaheim, CA. Tactical Systems Div.
NASA SATELLITE COMMUNICATIONS APPLICATION RESEARCH, PHASE 2 ADDENDUM. EFFICIENT HIGH POWER, SOLID STATE AMPLIFIER FOR EHF COMMUNICATIONS Final Report, 1 Aug. 1993 - 31 Mar. 1994
James Benet 28 Mar. 1994 38 p
(Contract NASw-4513)
(NASA-CR-195712; NAS 1.26:195712; C92-432.4/034) Avail: CASI HC A03/MF A01

This document is an addendum to the NASA Satellite Communications Application Research (SCAR) Phase 2 Final Report, 'Efficient High Power, Solid State Amplifier for EHF Communications.' This report describes the work performed from 1 August 1993 to 11 March 1994, under contract number NASW-4513. During this reporting period an array of transistor amplifiers was repaired by replacing all MMIC amplifier chips. The amplifier array was then tested using three different feedhorn configurations. Descriptions, procedures, and results of this testing are presented in this report, and conclusions are drawn based on the test results obtained. Derived from text

N94-28211# Massachusetts Univ., Lowell. Center for Atmospheric Research.
VHF-UHF NOISE SURVEYS AT GULKANA, ELMENSDORF AFB, GALENA AFB, KOTZEBUE AND CAPE LISBURNE, ALASKA AND NRL, POMONKEY, MARYLAND Report No. 4
Jens C. Ostergaard Feb. 1993 105 p
(Contract F19628-90-K-0039)
(PL-TR-93-2136) Avail: CASI HC A06/MF A02

This report presents results of a series of site and noise surveys performed in Alaska. Surveys were performed at the former OTH-B site at Gulkana with the aim of determining the spectrum occupancy and background noise level at nominally 38 MHz, 420 MHz, and 440 MHz. Three site surveys were performed at Elmendorf AFB near Anchorage, aimed at determining the spectrum occupancy and background noise levels at 40 to 50 MHz. Noise surveys were also performed at three existing radar sites, Galena, Kotzebue, and Cape Lisburne, at 40 to 50 MHz. This report contains a presentation of the survey and measurement methodology, including antenna patterns, absolute noise level calibrations, and noise level predictions. The features of the individual sites are presented with a discussion of the data collected. Author

N94-28355 Helsinki Univ. of Technology, Espoo (Finland). Electromagnetics Lab.

POLARIZABILITY MATRIX OF LAYERED CHIRAL SPHERE

M. E. Ermutlu and A. H. Sihvola Jun. 1993 15 p Sponsored by Suomen Akatemja Limited Reproducibility: More than 20% of this document may be affected by microfiche quality

(PB94-132834; ISBN-951-22-1667-1) Avail: CASI HC A03

Using quasi-static analysis, this article solves the dipole moments that are induced by electromagnetic field in a layered chiral sphere, consisting of a spherical core and a spherical shell. The result is the low-frequency polarizability of the sphere, and can be used to calculate the Rayleigh scattering of this object. Due to the chirality, the polarizability matrix has four components, electric and magnetic co- and cross-polarizabilities, that are functions of the permittivity, permeability, and chirality parameters of the core and shell materials and the ratio of their radii. The analysis is based on straightforward expansions of the field solutions in each region, and on making use of the boundary conditions, which leads to the inversion of a 8 x 8 matrix. The result can be shown to satisfy all the checks of earlier known special cases of homogeneous chiral sphere and layered dielectric-magnetic sphere. NTIS

N94-28379# Helsinki Univ. of Technology, Espoo (Finland). Electromagnetics Lab.

FIELDS AND POTENTIALS IN GENERAL UNIAXIAL BIANISOTROPIC MEDIA I. AXIAL SOURCES Report No. 147

Werner S. Weiglhofer (Glasgow Univ., Scotland.) and Ismo V. Lindell May 1993 16 p

(ISSN 0784-848X)

(PB94-132875; ISBN-951-22-1582-9) Avail: CASI HC A03/MF A01

An electromagnetic field representation in terms of two scalar Hertz potentials is derived pertaining to source-free regions and fields radiated from axial sources in general uniaxial bianisotropic media. The corresponding scalar Green's functions are obtained as single integral representations. Provided that the eight medium parameters of the uniaxial bianisotropic medium fulfill one algebraic relation, complete analytic solutions become available. Because of the general nature of the medium, the theoretical formalism is applicable to a wide variety of materials and substances which--through impressive advances in the materials and macromolecular sciences--are playing an ever more important role in the fabrication of optical and electronic devices. NTIS

N94-28380# Helsinki Univ. of Technology, Espoo (Finland). Electromagnetics Lab.

PLANE WAVE PROPAGATION AND POLARIZATION PROPERTIES IN TRANSVERSELY BIANISOTROPIC UNIAXIAL MEDIUM Report No. 146

Paivi K. Koivisto May 1993 18 p See also PB93-187219

(ISSN 0784-848X)

(PB94-132883; ISBN-951-22-1581-0) Avail: CASI HC A03/MF A01

A transversely bianisotropic uniaxial medium can be constructed by mixing metal helices into an isotropic host medium in such a way that the axes of the helices are perpendicular to a fixed direction in space but randomly oriented in the transverse plane. In general, the host medium can be either reciprocal or nonreciprocal. Eigenwaves, expressions for the plane wave fields, and polarization behavior are derived for the plane wave propagating perpendicular to the symmetry axis. The polarization properties of chiral and reciprocal transversely bianisotropic uniaxial media are studied in order to find a suitable parameter combination for a polarization transformer. Several numerical examples are given to illustrate the propagation properties of the transversely bianisotropic uniaxial medium. NTIS

N94-28381# Helsinki Univ. of Technology, Espoo (Finland). Electromagnetics Lab.

EIGENWAVES IN THE GENERAL UNIAXIAL BIANISOTROPIC MEDIUM WITH SYMMETRIC PARAMETER DYADICS Report No. 148

Ismo V. Lindell and Ari J. Viitanen May 1993 19 p

(ISSN 0784-848X)

(PB94-132891; ISBN-951-22-1583-7) Avail: CASI HC A03/MF A01

The uniaxial bianisotropic medium is a generalization of the well-studied bi-isotropic and chiral media. Special cases of uniaxial media with axial or transverse chirality were previously studied by these authors, and they were seen to have interesting and practical polarization transformation properties and, moreover, to be more easily fabricable than truly isotropic (bi-isotropic) chiral media. The present problem considers plane-wave propagation in the most general uniaxial bianisotropic medium, with symmetric parameter dyadics. The dispersion equation for such a dyadic is solved together with the eigenpolarizations of the two eigenwaves. Numerical examples for the wavenumbers corresponding to the two eigenwaves of the medium are given. Applications as a polarization transformer are discussed. NTIS

N94-28382# Helsinki Univ. of Technology, Espoo (Finland). Electromagnetics Lab.

ELECTROMAGNETIC MODELING OF BI-ISOTROPIC MEDIA

A. Sihvola May 1993 41 p

(PB94-132909; ISBN-951-22-1584-5) Avail: CASI HC A03/MF A01

The topic of this article is the characterization of heterogeneous bi-isotropic media. The chiral and nonreciprocal materials are treated as special cases. First the polarizability matrices are presented for spherical and ellipsoidal bi-isotropic inclusions. With these, the mixing problem is attacked, where the full effective bi-isotropic material parameters are calculated for a mixture containing bi-isotropic inclusions. Special emphasis is on the physical interpretation of the results, i.e., the ways to see and understand the manner in which the individual nonreciprocity and chirality parameters affect the macroscopic properties of the medium. The focus is also on the duality and symmetry properties of the magnetoelectric parameter expressions. Also, time dispersion is studied; the effect of the mixing process on the dispersion in the chirality of the mixture is analyzed. Finally, it is shown that there exist deep analogies between the polarizabilities of bi-isotropic media on one hand and those of anisotropic media on the other. NTIS

N94-28384# Helsinki Univ. of Technology, Espoo (Finland). Electromagnetics Lab.

PLANE WAVE PROPAGATION IN AN ANISOTROPIC CHIRAL MEDIUM WITH ISOTROPIC PERMITTIVITY AND PERMEABILITY

A. J. Viitanen and I. V. Lindell Jun. 1993 13 p

(PB94-133097; ISBN-951-22-1651-5) Avail: CASI HC A03/MF A01

Plane wave propagation in an anisotropic chiral medium with isotropic permittivity and permeability, and with symmetric chirality dyadic, is considered. The eigenvalue equation is formed, and the wave numbers and the corresponding eigenpolarizations are given. The results indicate that it is possible to construct a polarization transformer in which one can also choose the handedness. NTIS

N94-28387# Helsinki Univ. of Technology, Espoo (Finland). Electromagnetics Lab.

ELECTROSTATIC IMAGE SOLUTION FOR THE CONDUCTING PROLATE SPHEROID

J. C. E. Sten and I. V. Lindell Mar. 1993 16 p See also PB92-142199

(PB94-133154; ISBN-951-22-1648-5) Avail: CASI HC A03/MF A01

Electrostatic image theory for a point charge on the axis of a perfectly conducting prolate spheroid is formulated. The exact image expression is found using the Havelock identity, according to which the external harmonics of the potential solution emanate from a system of continuous image sources distributed along the focal line. Many tests for the theory are performed and graphical examples given. In the case of a slightly prolate sphere, the first correction to the image solution for the conducting sphere by Lord Kelvin is developed. An expression for the image polarization density function is derived for the dipolar source. NTIS

N94-28388# Helsinki Univ. of Technology, Espoo (Finland). Electromagnetics Lab.
ANALYTIC SOLUTION FOR THE DYADIC GREEN'S FUNCTION OF A NONRECIPROCAL UNIAXIAL BIANISOTROPIC MEDIUM
W. S. Weiglhofer and I. V. Lindell Jun. 1993 11 p
(PB94-133162; ISBN-951-22-1642-6) Avail: CASI HC A03/MF A01

The dyadic Green's function for an unbounded nonreciprocal uniaxial bianisotropic medium is derived in explicit form. Such uniaxial bianisotropic media can be realized by randomly dispersing uniaxial metallic inclusions with parallel orientations into an isotropic host medium. The availability of an analytic solution for the dyadic Green's function marks therefore an important step towards an understanding of radiation from sources and propagation of waves in composite materials. NTIS

N94-28390# Helsinki Univ. of Technology, Espoo (Finland). Electromagnetics Lab.
IMAGE THEORY FOR DC PROBLEMS INVOLVING A CONDUCTING HALF SPACE BOUNDED BY THE GENERAL ANISOTROPIC IMPEDANCE SURFACE
I. V. Lindell and M. J. Flykt May 1993 19 p See also PB93-224996
(PB94-132917; ISBN-951-22-1592-6) Avail: CASI HC A03/MF A01

A novel image theory is introduced. The theory is applicable to DC problems involving current sources in an isotropic conducting half space bounded by a planar, reciprocal, anisotropic impedance surface. The theory is a generalization involving an isotropic impedance surface and that involving a perfect anisotropic impedance surface with zero and infinite resistivities in two orthogonal directions on the plane. The image for a point current source is a combination of an electric line current source and a transverse quadrupole magnetic line current source. The magnetic current component vanishes for vanishing anisotropy while the electric current component vanishes for perfect anisotropy. NTIS

N94-28391# Helsinki Univ. of Technology, Espoo (Finland). Electromagnetics Lab.
GREEN DYADIC AND DIPOLE FIELDS FOR A MEDIUM WITH ANISOTROPIC CHIRALITY
I. V. Lindell and W. S. Weighlhofer Jun. 1993 15 p See also PB93-224764
(PB94-132933; ISBN-951-22-1637-X) Avail: CASI HC A03/MF A01

A closed-form expression is derived for the Green dyadic corresponding to a reciprocal bianisotropic medium with isotropic permittivity and permeability and arbitrary anisotropic chirality. Such a medium can be approximated, for example, by inserting in an isotropic host medium an equal number of similar right- and left-handed metal helices with suitable orientations. The solution is applied to determine the electric field of an electric dipole embedded in such a medium. Evaluation of its far-field shows that the wave is split into two plane waves with different wave-normal directions. NTIS

N94-28397# Helsinki Univ. of Technology, Espoo (Finland). Electromagnetics Lab.
DIELECTRIC POLARIZABILITY OF SPHERE WITH ARBITRARY ANISOTROPY
A. H. Sihvola Jun. 1993 12 p
(PB94-133113; ISBN-951-22-1668-X) Avail: CASI HC A03/MF A01

The polarizability of a dielectrically anisotropic sphere is studied. The anisotropy is general, consisting of a symmetric and antisymmetric part of the permittivity dyadic. The polarizability is also dyadic with its components depending on the relations of the permittivity components of the material. In certain special cases, the components of the polarizability matrix decouple and become only functions of the corresponding permittivity components, but in general, all nine polarizabilities depend on all nine permittivities. NTIS

N94-27298*# Princeton Univ., NJ. Dept. of Mechanical and Aerospace Engineering.
OPTICAL COMMUNICATIONS FOR TRANSPORT AIRCRAFT
Robert Stengel *In* NASA. Langley Research Center, FAA/NASA Joint University Program for Air Transportation Research , 1992-1993 Feb. 1994 p 141-145 (For primary document see N94-27284 07-01)
Avail: CASI HC A01/MF A02

N94-27894*# Arizona State Univ., Tempe. Dept. of Electrical Engineering.
HYBRID TECHNIQUES FOR COMPLEX AEROSPACE ELECTROMAGNETICS PROBLEMS
Jim Aberle *In* Old Dominion Univ., The 1993 NASA-ODU American Society for Engineering Education (ASEE) Summer Faculty Fellowship Program Dec. 1993 p 65-67 (For primary document see N94-27893 07-80)
Avail: CASI HC A01/MF A03

N94-27964# National Inst. of Polar Research, Tokyo (Japan).
ENERGY PARAMETERS OF THE INCIDENT AURORAL ELECTRONS DERIVED BY THE INTENSITY RATIO OF AURORAL EMISSIONS [TAHACHO FOTO META KANSOKU NI YORU KOKA DENSHI ENERUGI PARAMETA NO SUITEI]
Takayuki Ono, Ryusuke Satake (University of Electro-Communications, Chofu, Japan.), Takeo Yoshino (University of Electro-Communications, Chofu, Japan.), and Takeo Hirasawa *In its* Antarctic Record, Vol. 36, No. 2 30 Jul. 1992 p 163-180 In JAPANESE (For primary document see N94-27963 07-46)
Avail: CASI HC A03/MF A02

33 ELECTRONICS AND ELECTRICAL ENGINEERING

Includes test equipment and maintainability; components, e.g., tunnel diodes and transistors; microminiaturization; and integrated circuitry.

For related information see also *60 Computer Operations and Hardware* and *76 Solid-State Physics.*

N94-25618# Nationaal Inst. voor Kernfysica en Hoge Energiefysica, Amsterdam (Netherlands).
RF-STATION CONTROL CRATE
M. G. vanBeuzekom and J. T. vanEs 1992 21 p In DUTCH
(DIGEL-1992-9; ETN-94-94902) Avail: CASI HC A03/MF A01

The control electronics for the RF station of the storage ring AmPS (Amsterdam Pulse Stretcher) is described. The electronics connects the computer system and the hardware of the RF station. The central part of the controller crate is the bitbus controller. The attenuators and phase shifters of the RF station are controlled by servomotors. ESA

N94-25620# Nationaal Inst. voor Kernfysica en Hoge Energiefysica, Amsterdam (Netherlands).
DIGITAL INPUT MODULE
P. P. M. Jansweijer, J. L. Visschers, A. N. M. Zwart, and A. T. H. vanReen 1993 102 p In DUTCH
(DIGEL-1993-6; ETN-94-94956) Avail: CASI HC A06/MF A02

A digital input module (DIM) was developed to read the 96 wires of a wire chamber. The DIM is a nine unit VME module. Together with a DART readout module, the DIM allows 96 digital input signals (balanced ECL) to be read. The 96 inputs are divided over six front connectors, each of which has a single output signal to control a possible threshold of a wire chamber. ESA

N94-25644# Technical Research Centre of Finland, Espoo. Instrument Lab.
ASPECTS OF THE CIRCUIT BOARD THERMAL DESIGN
Matti Karjalainen Jan. 1993 30 p
(ISSN 1235-0621)
(VTT-PUBS-132; ISBN-951-38-4250-9; ETN-94-95239) Copyright Avail: CASI HC A03/MF A01

The thermal design of electronics in the space environment is investigated. The effects of environmental and design parameters on the thermal behavior of printed circuit boards are discussed. The tools that can be used to achieve more solid designs, to increase reliability, and decrease failure rate of printed circuit boards are presented. A thermal design procedure for spaceborne electronics and guidelines to follow in designing electronics to be operated in space are given. The procedure is a three step iterative cycle where first, circuit board blueprints are scanned with digital scanner to determine the copper density distribution for the board. The second phase is to determine the thermal resistance for radiative process for preset node size in a given temperature range using a program made for this purpose. These values are used to make a model of the board. ESA

N94-25664# Sandia National Labs., Albuquerque, NM.
ELECTRIC-FIELD DEPENDENCE OF ELECTROREFLECTANCE AND PHOTOCURRENT SPECTRA AT VISIBLE WAVELENGTHS IN MOVPE-GROWN InAlGaP MULTIPLE STRAINED QUANTUM-WELL STRUCTURES
I. J. Fritz, O. Blum, R. P. Schneider, Jr., A. J. Howard, and D. M. Follstaedt 1993 6 p Presented at the Fall Meeting of the Materials Research Society, Boston, MA, 29 Nov. - 3 Dec. 1993
(Contract DE-AC04-94AL-85000)
(DE94-004692; SAND-93-1529C; CONF-931108-20) Avail: CASI HC A02/MF A01

The authors present electric-field dependent electroreflectance and photocurrent spectra of visible-bandgap In(x)(Al(y)Ga(1 - y))(sub 1 - x)P/In(x')(Al(y'))Ga(1 - y')(sub 1 - x')P multiple-quantum-well (MQW) structures. These structures, grown by metal-organic vapor phase epitaxy on 6 deg-misoriented (100) GaAs substrates, have undoped MQW's sandwiched between doped In(0.5)Al(0.5)P layers, forming p-i-n diodes. Quantum-well compositions in the range 0.46 less than or equal to x less than or equal to 0.52 and 0 less than or equal to y less than or equal to 0.4, corresponding to bandgaps in the red to yellow-green range, were used. The Stark shifts in these various samples were measured and found to depend on the details of the Mg p-type doping profile, confirming important diffusion effects, in agreement with secondary ion mass spectrometry and capacitance-voltage data. The results show that these new materials are promising for visible-wavelength optical modulator applications. DOE

N94-25770# Air Force Inst. of Tech., Wright-Patterson AFB, OH.
FILTERING, CODING, AND COMPRESSION WITH MALVAR WAVELETS M.S. Thesis
Stephen R. Hall Dec. 1993 156 p
(AD-A274055; AFIT/GSO/Eng/93D-02) Avail: CASI HC A08/MF A02

This thesis develops and evaluates a number of new concepts and tools for the analysis of signals using Malvar wavelets (lapped orthogonal transforms). Windowing, often employed as a spectral estimation technique, can result in irreparable distortions in the transformed signal. By utilizing the Malvar wavelet, any signal distortion resulting from the transformation can be eliminated or cancelled during reconstruction. This is accomplished by placing conditions on the window and the basis function and then incorporating the window into the orthonormal representation. Paradigms for both a complex-valued and a real-valued Malvar wavelet are summarized. I-lie algorithms for the wavelets were implemented in the DOD standard language, Ada. The code was verified to ensure perfect reconstruction could be obtained, and experiments were performed using the wavelet programs. Various compression techniques were investigated and evaluated using the Malvar wavelet in both homomorphic and non-homomorphic systems. The Malvar wavelet has the unique ability to overlap adjacent windows without increasing the number of transform coefficients. Various amounts of window overlap were investigated to determine if there is an optimal amount which should be used. In addition, the real-valued basis function was used to attempt real-valued deconvolution. DTIC

N94-25806# Argonne National Lab., IL.
REFERENCE ELECTRODES FOR SOLID POLYMER ELECTROLYTES
C. S. Johnson and D. W. Dees 1993 13 p Presented at the 184th Meeting of the Electrochemical Society, New Orleans, LA, 10-15 Oct. 1993
(Contract W-31-109-eng-38)
(DE94-004583; ANL/CMT/CP-79723; CONF-931024-1) Avail: CASI HC A03/MF A01

Electrochemical experiments were conducted on a binary metallic lithium-tin alloy that may be suitable as a reference electrode of the first kind in studies of lithium-polymer batteries. Two types of tin electrodes were tested: bulk tin foil and tin thin films deposited on a stainless steel substrate. Electrochemical test cells were fabricated, with tin, metallic lithium, poly(ethylene oxide), and lithium trifluoromethanesulfonate as electrodes and polymer electrolyte material. To form the alloy, the tin electrodes were galvanostatically loaded in situ with lithium. Each cell reached one or more steady-state voltage plateaus during the electrochemical reduction of lithium cations at the tin electrode surface. The lithiated tin foil electrode (1 C/cm(exp 2) of charge passed; area approximately 5 cm(exp 2); thickness = 1.0 mm) demonstrated good voltage stability over months under open-circuit conditions. This electrode maintained an average open circuit voltage of 0.7336 V with only +/- 0.17 mV variance. Composition of phases in the thin film electrodes (x in Li(x)Sn) was coulometrically varied via reversible lithium loading and unloading reactions. Results show that three different, two-phase compositions may be formed that maintain flat voltage regions at approximately 0.53, 0.63, and 0.73 V vs lithium metal. DOE

N94-25812# Sandia National Labs., Albuquerque, NM.
ADVANCED QUALIFICATION TECHNIQUES
P. S. Winokur, M. R. Shaneyfelt, T. L. Meisenheimer, and D. M. Fleetwood 1993 11 p Presented at the 2nd European Conference on Radiations and Their Effects on Devices and Systems, Saint Malo, France, 13-16 Sep. 1993
(Contract DE-AC04-94AL-85000)
(DE94-003709; SAND-93-1323C; CONF-930953-2) Avail: CASI HC A03/MF A01

This paper demonstrates use of the Qualified Manufacturers List (QML) methodology to qualify commercial and military microelectronics for use in space applications. QML 'builds in' the hardness of product through statistical process control (SPC) of technology parameters relevant to the radiation response, test structure to integrated circuit (IC) correlations, and techniques for extrapolating laboratory test results to low-dose-rate space scenarios. Each of these elements is demonstrated and shown to be a cost-effective alternative to expensive end-of-line IC testing. Several examples of test structured-IC correlations are provided and recent work on complications arising from transistor scaling and geometry is discussed. The use of a 10-keV x-ray wafer-level test system to support SPC and establish 'process capability' is illustrated and a comparison of 10-keV x-ray and Co-60 gamma irradiations is provided for a wide range of CMOS technologies. The x-ray tester is shown to be cost-effective and its use in lot acceptance/qualification is recommended. Finally, a comparison is provided between MIL-STD-883D, Test Method 1019.4, which governs the testing of packaged semiconductor microcircuits in the DoD, and ESA/SSC Basic Specification No. 22900, Europe's Total Dose Steady-State Irradiation Test Method. Test Method 1019.4 focuses on conservative estimates of MOS hardness for space and tactical applications, while Basic Specification 22900 focuses on improved simulation of low-dose-rate space environments. DOE

N94-25845# Air Force Inst. of Tech., Wright-Patterson AFB, OH.
OBJECT IMAGING ACCOMPLISHED WITH AN INTEGRATED CIRCUIT ROBOTIC TACTILE SENSOR INCORPORATING A PIEZOELECTRIC POLYVINYLIDENE FLUORIDE THIN FILM M.S. Thesis
John M. Emmert Dec. 1993 259 p
(AD-A274038; AFIT/GE/Eng/93D-06) Avail: CASI HC A12/MF A03

The purpose of this research effort was to investigate the performance of a piezoelectric tactile sensor design and appropriately refine it. The sensor was fabricated from an 8 x 8 electrode array MOS integrated circuit. Each taxel in the array was 400 microns x 400 microns. A 6 mm x 6 mm piece of piezoelectric polyvinylidene fluoride was adhered to the electrode array using a urethane dielectric adhesive to form the active sensing area of the sensor. An amplifier was investigated to enhance the range of the tactile sensor's output signal. The amplifier is a high input impedance differential amplifier with a linear range from 1 to 17 V. The unique feature of the differential amplifier was that it used a power supply of only 12 V. The spatial resolution of the sensor is 0.7 mm. The lower force limit of the sensor is 1 g while the upper limit, limited by a previous amplifier design with a range from 2.5 to 7 V, is 130 g. The dynamic range of the sensor is 130:1. The sensor's force sensitivity is 7.35 g. The pyroelectric bandwidth of the sensor is 0.083 Hz, and the temperature sensitivity of the sensor is 0.39 C. DTIC

N94-25975# Sandia National Labs., Albuquerque, NM.
DOUBLE LAYER CAPACITANCE OF CARBON FOAM ELECTRODES
F. M. Delnick, D. Ingersoll, and D. Firsich (EG and G Mound Applied Technologies, Miamisburg, OH.) 1993 10 p Presented at the 3rd International Seminar on Double Layer Capacitors and Similar Energy Storage

Systems, Deerfield Beach, FL, 6-8 Dec. 1993
(Contract DE-AC04-94AL-85000)
(DE94-002651; SAND-93-2681C; CONF-931204-1) Avail: CASI HC A02/MF A01

We have evaluated a wide variety of microcellular carbon foams prepared by the controlled pyrolysis and carbonization of several polymers including: polyacrylonitrile (PAN), polymethacrylonitrile (PMAN), resorcinol/formaldehyde (RF), divinylbenzene/methacrylonitrile (DVB), phenolics (furfuryl/alcohol), and cellulose polymers such as Rayon. The porosity may be established by several processes including: gelation (1-5), phase separation (1-3,5-8), emulsion (1,9,10), aerogel/xerogel formation (1,11,12,13), replication (14), and activation. In this report we present the complex impedance analysis and double layer charging characteristics of electrodes prepared from one of these materials for double layer capacitor applications, namely activated cellulose derived microcellular carbon foam. DOE

N94-25977# Sandia National Labs., Albuquerque, NM.
A GENERAL PURPOSE I(SUB DDQ) MEASUREMENT CIRCUIT
K. M. Wallquist (New Mexico Univ., Albuquerque.), C. F. Hawkins (New Mexico Univ., Albuquerque.), and A. W. Righter 1993 32 p Presented at the International Test Conference, Baltimore, MD, 18-21 Oct. 1993
(Contract DE-AC04-94AL-85000)
(DE94-002733; SAND-93-2356C; CONF-9310223-1) Avail: CASI HC A03/MF A01

A relatively high-speed I(sub DDQ) measurement circuit called QuiC-Mon is described. Depending upon IC settling times, upper measurement rates range from 50 kHz to 250 kHz at 100 nA resolution. It provides an inexpensive solution for fast, sensitive I(sub DDQ) measurements in CMOS IC wafer probe or packaged part production testing. DOE

N94-25995# Air Force Inst. of Tech., Wright-Patterson AFB, OH. School of Engineering.
A PHYSICS-BASED HETEROJUNCTION BIPOLAR TRANSISTOR MODEL FOR INTEGRATED CIRCUIT SIMULATION M.S. Thesis
James A. Fellows Dec. 1993 250 p
(AD-A274081; AFIT/GE/Eng/93D-07) Avail: CASI HC A11/MF A03

The purpose of this research effort was to derive a physics-based dc model for a Heterojunction Bipolar Transistor (HBT). The dc model was then linearized to arrive at a small-signal model that accurately predicts the device's electrical behavior at microwave frequencies. This new model offers features not found in previous analytical or physics-based HBT models such as consideration of a cylindrical emitter-base geometry and is direct implementation into SPICE (Simulation Program with Integrated Circuit Emphasis). The device model parameters were determined from a knowledge of the device material, geometry, and fabrication process. The model was then developed by using semiconductor physics to calculate modified parameters for the existing SPICE bipolar junction transistor (BJT) model. DTIC

N94-26047# California Univ., Berkeley. Lawrence Berkeley Lab.
EXPLORATORY TECHNOLOGY RESEARCH PROGRAM FOR ELECTROCHEMICAL ENERGY STORAGE
K. Kinoshita, ed. Oct. 1993 34 p
(Contract DE-AC03-76SF-00098)
(DE94-003479; LBL-34081) Avail: CASI HC A03/MF A01

This report summarizes the progress made by the Exploratory Technology Research (ETR) Program for Electrochemical Energy Storage during calendar year 1992. The primary objective of the ETR Program, which is sponsored by the US Department of Energy (DOE) and managed by Lawrence Berkeley Laboratory (LBL), is to identify electrochemical technologies that can satisfy stringent performance, durability, and economic requirements for electric vehicles (EV's). The ultimate goal is to transfer the most-promising electrochemical technologies to the private sector or to another DOE program (e.g., SNL's Electric Vehicle Advanced Battery Systems Development Program, EVABS) for further development and scale-up. Besides LBL, which has overall responsibility for the ETR Program, LANL and BNL have participated in the ETR Program by providing key research support in several of the program elements. The ETR Program consists of three major elements: Exploratory Research; Applied Science Research; and Air Systems Research. The objectives and the specific battery and electrochemical systems addressed by each program element are discussed in the following sections, which also include technical summaries that relate to the individual programs. Financial information that relates to the various programs and a description of the management activities for the ETR Program are described in the Executive Summary. DOE

N94-26102 Department of the Navy, Washington, DC.
METHOD OF OPTIMIZING THE CHARGING OF A BATTERY OF STORAGE CELLS, AND APPARATUS FOR PERFORMING THE METHOD Patent
Guy Busson, inventor (to Navy) 12 Oct. 1993 10 p Filed 7 Feb. 1992
(AD-D016066; US-Patent-5,252,906; US-Patent-Appl-SN-832586) Avail: CASI HC A02/MF A01

The invention relates to a method enabling a battery of storage cells to be charged in a charging mode for compensating for discharging to an external circuit, or in a maintenance mode for compensating for self-discharging of the battery. The method consists in: determine the charging capacity of the battery, as a function of the temperature (Tb) of the battery, the charging capacity decreasing and becoming less than the reference capacity when the temperature increases during a charging period; calculating the electricity balance between the quantity of electricity received by the battery and the quantity of electricity supplied by the battery to an external circuit; and deciding to switch from maintenance mode to charging mode each time that the electricity balance is less than the charging capacity. Author (DTIC)

N94-26144# Argonne National Lab., IL.
A SHUTTLE MECHANISM FOR MOLTEN-ELECTROLYTE LITHIUM BATTERIES
T. D. Kaun and P. A. Nelson 1993 12 p Presented at the 184th Meeting of the Electrochemical Society, New Orleans, LA, 10-15 Oct. 1993
(Contract W-31-109-eng-38)
(DE94-002914; ANL/CMT/CP-79729; CONF-931024-5) Avail: CASI HC A03/MF A01

The lithium-transport rates arising from a lithium shuttle mechanism (LSM) were examined by potentiometric control of a lithium-alloy electrode in a temperature range of 400 to 515 C in three electrolytes: LiCl-KCl, LiCl-LiBr-KBr, and LiF-LiCl-LiBr. Lithium transport in Li/FeS(x) cells by LSM was found to occur by diffusion of reduced lithium species across the separator layer, which was controlled by the Li-activity of the Li-alloy electrode. Solubility of lithium was strongly affected by electrolyte composition, especially K(+) content, which in turn regulated the lithium transport rate. As evidenced by LSM rates, the solubilized lithium would appear to form dimers (e.g. Li2(+) or LiK(+)). The half-cell self-discharge rates, which were measured, correlate well with self-discharge rates in developmental cells ranging from 0.1 to 10 mA/sq cm. Innovative application of the LSM has led to the development of overcharge tolerant Li/FeS(x) cells. A bimodal self-discharge characteristic (a 20-fold increase toward the end of charge) results from a 150-250 mV step increase in lithium activity of a two-phase Li-alloy electrode (Li-Al plus Li-Al 5Fe2). Three versions of the battery cell (100 sq cm separator area) have been demonstrated: LiAl+Li5Al5Fe2 (10% of capacity) /LiCl-LiBr-KBr(MgO)/FeS2, as well as a FeS-type, (both operated at 400 C) and LiAl+Li5Al5Fe2 (10% of capacity) /LiF-LiCl-LiBr(MgO)/FeS (operated at 475C). These cells exhibit a unique combination of overcharge capacity and extended trickle-charge tolerance at 2-5 mA/sq cm. Additionally, Li/FeS2 cells having overcharge tolerance have operated with stable performance for greater than 500 cycles. The overcharge tolerance rates are sufficient for battery cells to exhibit built-in charge/equalization capability by way of full-battery trickle charging. DOE

N94-26175# Naval Postgraduate School, Monterey, CA.
TEST METHODS AND CUSTOM HARDWARE FOR FUNCTIONAL TESTING OF A HIGH SPEED GaAs DRAM M.S. Thesis
Michael P. Butler Sep. 1993 78 p
(AD-A274859) Avail: CASI HC A05/MF A01

The goal of this project is to produce a digital circuit operating near a frequency of 250 MHz to test a new experimental gallium arsenide (GaAs) dynamic random access memory (DRAM). This thesis presents the design of the digital circuit using 'off-the-shelf' emitter coupled logic (ECL) and the design of a six layer printed circuit test fixture. The use of ECL is illustrated including general design rules, high speed design considerations, and basic transmission line theory. Finally, the design is laid out and simulated using commercially available computer aided design (CAD) and computer aided manufacturing (CAM) tools. Examples and shortcomings of schematic capture, logic simulation, PCB design, and auto-routing are discussed as applicable to fabrication of the final product. DTIC

N94-26301# Naval Postgraduate School, Monterey, CA.
HYBRID POWER SYSTEM FOR REMOTE COMMUNICATIONS STATIONS M.S. Thesis
Christopher R. Pietras Sep. 1993 186 p
(AD-A274963) Avail: CASI HC A09/MF A02

The U.S. Coast Guard is upgrading communications equipment at remote sites in Alaska in support of the Coastal Voice Distress Network. The VHF-FM Search and Rescue sites are powered by a primary power system consisting of a thermoelectric generator. Thermoelectric generators are very inefficient devices which consume vast quantities of propane to create electricity. The upgrade necessitates added power requirements on the power supply system at the remote sites. These requirements compel the redesign and/or upgrade of the power system. If thermoelectric generators continue to be utilized as the primary power system, additional helicopter visits to the sites to deliver propane will be required. These helicopter flights are costly and sometimes hazardous due to severe weather. This thesis investigates a variety of power system options capable of providing electrical power to the communications sites. Specifically, this thesis addresses three objectives. The first is a discussion of current alternative energy source technology available to supply the required power. The second is an analysis of the specific power system requirements and constraints. The third objective and major thrust of the research is the design of a reliable hybrid power system for this application, capable of utilizing the inexhaustible natural energy available at the remote sites. The engineering parameters for a hybrid power system were studied and calculations made based on commercially available components. The difficulties in the design due to extreme weather conditions and unavailability of natural power resource information at specific sites are addressed. This thesis presents the groundwork associated with hybrid power system designs for use at remote communications sites. DTIC

N94-26312# Lawrence Livermore National Lab., CA.
MICROWAVE AND PULSED POWER
E. K. Freytag Mar. 1993 30 p
(Contract W-7405-eng-48)
(DE94-003019; UCRL-ID-112776) Avail: CASI HC A03/MF A01

The goals of the Microwave and Pulsed Power thrust area are to identify realizable research and development efforts and to conduct high-quality research in those pulse power and microwave technologies that support existing and emerging programmatic requirements at Lawrence Livermore National Laboratory (LLNL). Our main objective is to work on nationally important problems while enhancing our basic understanding of enabling technologies such as component design and testing, compact systems packaging, exploratory physics experiments, and advanced systems integration and performance. During FY-92, we concentrated our research efforts on the six project areas described in this report. We are investigating the superior electronic and thermal properties of diamond that may make it an ideal material for a high-power, solid-state switch. We are studying the feasibility of using advanced Ground Penetrating Imaging Radar technology for reliable non-destructive evaluation of bridges and other high-value concrete structures. These studies include conceptual designs, modeling, experimental verifications, and image reconstruction of simulated radar data. We are exploring the efficiency of pulsed plasma processing techniques used for the removal of NO(x) from various effluent sources. We have finished the investigation of the properties of a magnetically delayed low-pressure gas switch, which was designed here at LLNL. We are applying statistical electromagnetic theory techniques to help assess microwave effects on electronic subsystems, by using a mode stirred chamber as our measurement tool. We are investigating the generation of perfluoroisobutylene (PFIB) in proposed CFC replacement fluids when they are subjected to high electrical stresses and breakdown environments. DOE

N94-26328# Case Western Reserve Univ., Cleveland, OH. Dept. of Chemistry.
IN SITU SPECTROSCOPIC APPLICATIONS TO THE STUDY OF RECHARGEABLE LITHIUM BATTERIES Final Report
Rachael Barbour, Sunghyun Kim, Donald Tryk, and Daniel A. Scherson Aug. 1993 20 p Prepared in cooperation with California Univ., Berkeley. Lawrence Berkeley Lab.
(Contract DE-AC03-76SF-00098)
(DE94-003478; LBL-34514) Avail: CASI HC A03/MF A01

In situ attenuated total reflection Fourier transform infrared spectroscopy (ATR/FTIR) has been employed to examine the reactivity of lithium towards polyethylene oxide (PEO) at ca. 60 C. Uncertainties regarding the cleanliness of the Li surfaces were minimized by electrodepositing a film of metallic Li directly onto a thin layer of gold (ca. 60 Angstrom) vapor deposited on a Ge ATR optical element during the spectroscopic measurements. The ATR/FTIR features observed upon stripping the Li layer were consistent with the formation of alkoxide-type moieties resulting from the Li-induced cleavage of the ether-type functionalities. Electronic and structural aspects of the electrochemical insertion of lithium from nonaqueous electrolytes into FeS2 have been investigated using in situ Fe K-edge x ray absorption fine structure (XAFS). The results obtained indicate that the incorporation of Li(sup +) in the pyrite lattice brings about a marked decrease in the amplitude of the extended XAFS (EXAFS) oscillations, particularly for shells associated with distant atoms and a rounding of the x ray absorption near edge structure (XANES) region. An analysis of the EXAFS spectra yielded a value for the FeS distance of 2.29 +/- 0.02 Angstrom. On this basis and additional in situ room temperature Fe-57 Mossbauer effect spectroscopy data for the same system, it has been proposed that the electrically formed material involves a highly disordered, possibly amorphous, form of Fe(1-x)S, with Li+ counterbalancing the charge. DOE

N94-26343# Columbia Univ., New York, NY. Dept. of Electrical Engineering.
MULTICHIP MODULE HIGH SPEED TESTING Quarterly Progress Report, 1 Oct. - 31 Dec. 1993
Robert J. Davis and David H. Auston 31 Dec. 1993 4 p
(Contract N00014-91-J-4045)
(AD-A274873) Avail: CASI HC A01/MF A01

Last quarter, we reported Al/SiO2/Al capacitor structures formed on an optical fiber, as the first step toward an electrooptic test probe. We have now fabricated an amorphous hydrogenated silicon (a-Si:H) photodetector directly on an optical fiber. We have been investigating the use of electrooptically active polymers for the purpose of electrooptic testing. Important problems remaining to be solved are low electrooptic efficiency and geometry; detection system speed, efficiency, and noise; and optical alignment. DTIC

N94-26344# Honeywell, Inc., Minneapolis, MN. Systems and Research Center.
OPTOELECTRONIC TECHNOLOGY CONSORTIUM Quarterly Technical Report No. 6, 1 Oct. - 31 Dec. 1993
Mary Hibbs-Brenner 4 Jan. 1994 10 p
(Contract MDA972-92-C-0071; ARPA Order 8351C)
(AD-A274909) Avail: CASI HC A02/MF A01

The Optoelectronic Technology Consortium has been established to position U.S. industry as the world leader in optical interconnect technology by developing, fabricating, integrating and demonstrating the producibility of optoelectronic components for high-density/high-data-rate processors and accelerating the insertion of this technology into military and commercial applications. This objective will be accomplished by a program focused in three areas. OETC will demonstrate an aggregate data transfer rate of 16 Gb/s between single transmitter and receiver packages, as well as the expandability of this technology by combining four links in parallel to achieve a 64 Gb/s link. By collaborating during the precompetitive technology development stage, OETC will advance the development of optical components and produce links for a multiboard processor testbed demonstration. Under the OETC program Honeywell will develop packaged AlGaAs arrays of waveguide modulators and polymer based, high density, parallel optical backplane technology compatible with low-cost manufacturability. DTIC

N94-26372# Sandia National Labs., Albuquerque, NM.
CHARACTERISTICS AND DEVELOPMENT REPORT FOR THE T1576 POWER SUPPLY AND THE MC3935 BATTERY
P. C. Butler and C. E. Robinson Oct. 1993 95 p
(Contract DE-AC04-94AL-85000)
(DE94-003675; SAND-91-2845) Avail: CASI HC A05/MF A01

This report describes the requirements, designs, performance, and development histories for the T1576 power supply and the MC3935 rechargeable battery. These devices are used to power Permissive Action Link (PAL) ground controllers. The T1576 consists of a stainless steel container, one SA3553 connector, and one MC3935 battery. The MC3935 is a vented nickel/cadmium battery with 24 cells connected in series. It was designed to deliver 5.5 Amp-hours at 25 C and the one-hour rate, with a nominal voltage of 28 V. The battery was designed to operate for 5 years or 500 full charge/discharge cycles. The power supply is expected to last indefinitely with replacement batteries and hardware. DOE

N94-26380 Gosudarstvennyi Komitet po Ispolzovaniyu Atomnoi Energii, Serpukhov (USSR). Inst. Fiziki Vysokikh Ehnergij.
THE 12-CHANNEL FLASH-ADC FASTBUS MODULE [12-KANAL'NYJ MODUL' PARALLEL'NYKH ATSP V FASTBUS]
A. A. Kuznetsov, V. I. Rychenkov, V. A. Senko, and A. V. Sidorov 1992 8 p In RUSSIAN Limited Reproducibility: More than 20% of this document may be affected by microfiche quality
(DE93-634229; IFVE-OEA-92-4) Avail: CASI HC A02 (US Sales Only)

The slave module intended for digitizing the shape of single signals in 12-channels at once is described. The module is designed on the base of FADC integrated circuits KR1107PV5A and memory chips K1500RU073. Resolution is 6 bit with up to 90 MHz sampling frequency. DOE

N94-26438 Gosudarstvennyi Komitet po Ispolzovaniyu Atomnoi Energii, Serpukhov (USSR). Inst. Fiziki Vysokikh Ehnergij.
SIGNAL AMPLIFIER-SHAPERS FOR MULTIWIRE DETECTORS [USILITELI-FORMIROVATELI SIGNALOV DIYA MNOGOPROVOLOCHNYKH DETEKTOROV]
Yu. B. Bushnin and A. K. Konoplyannikov 1992 4 p In RUSSIAN Limited Reproducibility: More than 20% of this document may be affected by microfiche quality
(DE93-634171; IFVE-OEA-92-105) Avail: CASI HC A01 (US Sales Only)

Circuit diagram and specification of 8 and 16 channel modules of amplifier-shapers are described for multiwire detectors. The modules have input impedance 200 Ohm sensitivity threshold 1.5 micro-A, output pulse width 80 nsec. DOE

N94-26443 International Centre for Theoretical Physics, Trieste (Italy).
THE ELECTRIC FIELD BETWEEN NON CONDUCTIVE RECTANGULAR CHARGED SURFACES PLACED NEAR A SMALL SPHERICAL CONDUCTIVE EARTHED SURFACE AND DETERMINATION OF CRITICAL DENSITY OF CHARGE
F. Vila Oct. 1992 24 p Limited Reproducibility: More than 20% of this document may be affected by microfiche quality
(DE93-634324; IC-92/371) Avail: CASI HC A03 (US Sales Only)

In this work, we give a full theoretical treatment of the problem of how to determine the electric fields between nonconductive rectangular charged surface placed near a small spherical conductive earthed surface, and of critical density of charge. DOE

N94-26449# Ohio State Univ., Columbus.
JOINT SERVICES ELECTRONICS PROGRAM Annual Report
Leon Peters, Jr. Oct. 1993 141 p
(Contract N00014-89-J-1007)
(AD-A274692; Rept-721563-6-APP) Avail: CASI HC A07/MF A02

This Appendix contains the reprints published under JSEP in the time September 1992 to September 1993. In addition to the 10 reprints contained herein, there are 6 papers already accepted for publication during the next contract period, 11 papers submitted and 16 papers in preparation. DTIC

N94-26491# Maine Univ., Orono.
ADC TEST SUPPORT PROGRAM Technical Report, 1 Aug. - 30 Oct. 1993
Fred H. Irons and Donald M. Hummels 30 Oct. 1993 16 p
(Contract N00014-93-1-1007)
(AD-A274819) Avail: CASI HC A03/MF A01

This report summarizes accomplishments made under Grant No.: N00014-93-1-1007 for providing ADC Test Support to the ARPA HBT/ADC technology development program during the period of 1 Aug. through 30 Oct. 1993. The following were accomplishments for this period: (1) Attended and participated in a planning meeting at the Mayo Foundation on 19 Jul. 1993 to discuss testing issues and develop an agenda for the September Workshop; (2) Attended and participated in the ADC testing workshop on 1 Sep. 1993 at Lincoln Laboratory. Information and example test results were presented for newly developed tests; (3) Started training a graduate research assistant on a program devoted to subject ADC architectures and relation to dynamic errors; (4) Performed initial tests to illustrate interaction of ADC error table models to generic ADC performance and interactions with input circuit VSWR and matching. DTIC

N94-26536# Physical Optics Corp., Torrance, CA.
LOW THRESHOLD ALL-OPTICAL CROSSBAR SWITCH ON GaAs-GaAlAs CHANNEL WAVEGUIDE ARRAYS Annual Report, 14 Aug. 1992 - 14 Aug. 1993
Tomasz Jannson 14 Aug. 1993 31 p
(Contract F49620-92-C-0047)
(AD-A274971; AFOSR-94-0033TR) Avail: CASI HC A03/MF A01

POC proposed a 10 x 10 all-optical crossbar switch based on an optically activated modulator. A laser beam with an energy higher than the bandgap of the GaAs switches the propagation direction of the guided beam. Strong index modulation (greater than 2%) can be induced by this method, which is not dependent on polarization for the EO effect. Both TE and TM guided waves have the same induced index change. Because there are no electrical contacts, this all-optical switch has no RC time limits. The switching speed is limited only by the generated carrier lifetime, which is in the picosecond range. Being the basic building block for high-speed optoelectronic computing and signal processing, this generic concept is applicable to a broad variety of photonic components, including optical logic gates, EO modulators, variable delay lines, and crossbar reconfigurable interconnects. To optimize the switching efficiency, several optical switch designs were studied, including cross switches and directional coupler switches. To realize the multichannel optical switches, a compact self-aligned packaging technique was developed. An all-optical switch using a 0.8 micrometer pumping laser beam and a 1.3 micrometer probe beam was demonstrated, and efficiency as a function of pumping power and wavelength was studied. DTIC

N94-26546 Korean Atomic Energy Research Inst., Daeduk (Republic of Korea).
A STUDY ON THE DEVELOPMENT OF HIGH-T(c) SUPERCONDUCTING WIRE
Dong Yeon Won, In Soon Chang, Jong Min Lee, Tae Yoon Um, Kyae Won Hong, Ho Jin Lee, Hee Kwun Lee, Chan Joong Kim, Soon Dong Park, and Woo Gon Kim et al Oct. 1992 113 p In KOREAN Limited Reproducibility: More than 20% of this document may be affected by microfiche quality
(DE93-632438; KAERI/RR-1138/92) Avail: CASI HC A06 (US Sales Only)

In this study, Y-Ba-Cu-O was prepared by partial melt process and superconducting wire was fabricated by powder-in-tube method. First, mechanical properties, electrical properties, microstructure and oxygen diffusion behavior were observed. Second, through fabricated superconducting wire, conceptual design, composition, and plasticity of filament superconducting wire were investigated. DOE

N94-26589# Argonne National Lab., IL. Energy Technology Div.
PROCESSING AND PROPERTIES OF Ag-CLAD BI-2223 TAPES
U. Balachandran, A. N. Iyer, P. Haldar (Intermagnetics General Corp., Guilderland, NY.), and L. R. Motowidlo (IGC/Advanced Supercomputers, Inc., Waterbury, CT.) Nov. 1993 14 p Presented at the 6th US-Japan Workshop on Superconductivity, Houston, TX, 6-7 Dec. 1993
(Contract W-31-109-eng-38)
(DE94-004603; ANL/ET/CP-81211; CONF-931238-1) Avail: CASI HC A03/MF A01

We prepared partially reacted, polyphase, Pb-doped Bi-Sr-Ca-Cu-O (2223) powders by solid-state and wet-chemical routes. The calcined powders were characterized by thermal analysis, x-ray diffraction, and scanning electron microscopy. We then fabricated long lengths of flexible Ag-clad 2223 tapes by the powder-in-tube technique. Multifilamentary conductors have been prepared by stacking circular single-core Ag-sheathed superconductor rods into larger Ag tube and then drawing and rolling the tube to final size. The tapes were given appropriate heat treatment and the growth of the 2223 phase at each step of the heat treatment was studied. At 4.2 and 27 K, improved process conditions yielded transport critical current density (J(sub c)) values greater than 10(exp 5) A/sq cm at zero field; at 77 K, J(sub c) exceeded 4 x 10(exp 4) A/sq cm. Using a two-step rolling with an intermediate heat treatment, we have fabricated conductors approximately 70 m long. The J(sub c) value of these long conductors is approximately 2 x 10(exp 4) A/sq cm at 77 K in self field. Superconducting pancake coils were fabricated from the long-length tapes by the wind-and-react technique. DOE

N94-26627 Carleton Univ., Ottawa (Ontario). Dept. of Systems and Computer Engineering.
KALMAN FILTERING OF NARROWBAND INTERFERENCE FROM DIRECT SEQUENCE SPREAD SPECTRUM COMMUNICATIONS SYSTEMS Ph.D. Thesis
Brian William Kozminchuk Aug. 1992 259 p
(ISBN-0-315-84011-0; CTN-94-61047) Copyright Avail: Micromedia Ltd., Technical Information Centre, 240 Catherine Street, Suite 305, Ottawa, Ontario, K2P 2G8, Canada HC/MF

A novel and viable interference excisor based on a Kalman filtering technique is presented. The behavior and performance of block and recursive least squares algorithms is examined for the case of single- and swept-tone interferers. An extended Kalman filtering technique is suggested for the latter case. The Kalman technique is compared to the lattice recursive least squares algorithm from the perspective of bit error rate performance, showing the 1-2 dB superiority of the Kalman approach. A theoretical bit error rate formula is developed for frequency modulation interference generated by a state space model. It is shown that phase noise at the Kalman filter output will set the limiting performance level along with signal distortion, and that the Kalman filter has more problems with narrowband Gaussian noise. In considering means of counteracting these effects, the most important is the addition of phase smoothing, which can result in performance improvements of up to 4-5 dB. An adaptive filtering scheme using the Kalman filter approach is also presented, in which one of its parameters is varied over time while monitoring a mean-squared error function in order to locate the optimum setting for the filter. Its performance for narrowband Gaussian noise is shown to be similar to that of the optimized nonadaptive case. Author (CISTI)

N94-26631 Toronto Univ. (Ontario). Dept. of Electrical and Computer Engineering.
AN INTEGRATED DELTA-SIGMA BASED IIR FILTER M.S. Thesis
Dennis Kin-Wah Au 1993 103 p
(ISBN-0-315-83593-1; CTN-94-61038) Copyright Avail: Micromedia Ltd., Technical Information Centre, 240 Catherine Street, Suite 305, Ottawa, Ontario, K2P 2G8, Canada HC/MF

Delta-sigma based infinite impulse response (IIR) filters are a recently developed circuit technique for efficiently realizing IIR filters operating directly on oversampled delta-sigma modulated signals. The design and single-chip implementation of a fifth-order delta-sigma based IIR filter are described. The filter coefficients are fully programmable and with the use of a structure that is inherently scaled for dynamic range, good filter performance is maintained over a wide variety of transfer functions. To eliminate multi-bit multiplications, five second-order digital delta-sigma modulators were used and dynamic range improvement was obtained through the use of multi-bit quantizers in these modulators. The filter was implemented as a very large scale integration chip using 1.2 micron complementary metal oxide semiconductor technology, occupying an area of 4,355 by 5,962 square microns. Simulations indicate that the clock range should operate up to 45 MHz. Author (CISTI)

N94-26646 Prins Maurits Lab. TNO, Rijswijk (Netherlands). Pulse Physics Lab.
PULSE TRANSFORMER CHARACTERIZATION Final Report [KARAKTERISERING VAN DE PULSTRANSFORMATOR]
W. H. P. Mosterdijk Dec. 1992 31 p In DUTCH Sponsored by DWOO, The Hague, Netherlands, and TNO Defence Research, Delft, Netherlands Original contains color illustrations
(Contract A87/K/045)
(PML-1992-73; TD92-2408; ETN-94-94936) Copyright Avail: Issuing Activity (TNO-Prins Maurits Lab., P. O. Box 45, 2280 AA Rijswijk, Netherlands)

The pulse transformer at TNO PML-Pulse Physics, Delft, is characterized. It constitutes the final step of an energy compression system (Kapitza facility) which can amplify the current up to 24 times, and consists of a primary single layer winding of 24 turns enclosed in a secondary winding. There is a sine wave current source with adjustable frequencies for the characterization. The measurements show that the main inductances decrease and the ohmic resistances increase with increasing frequency, due to differential currents, skin and proximity effect, and parasitic currents induced in the aluminum secondary winding. From the measurements a coupling factor of 0.94 is calculated for 200 Hz, which is slightly below the design specification of 0.98. ESA

N94-26675 Carleton Univ., Ottawa (Ontario). Dept. of Electronics.
ULTRALINEAR WIDEBAND INTEGRATED CIRCUIT DESIGN M.S. Thesis
John Nisbet Jan. 1993 209 p
(ISBN-0-315-84130-3; CTN-94-61061) Copyright Avail: Micromedia Ltd., Technical Information Centre, 240 Catherine Street, Suite 305, Ottawa, Ontario, K2P 2G8, Canada HC/MF

The design of ultralinear wideband integrated circuits (IC's) is treated from three perspectives: system design concerns, modeling and simulation techniques, and circuit design considerations. The system design phase uses concurrent treatment of noise and distortion to produce an appropriate block-and-level description of hardware partitioning. Conventional SPICE models and analysis can be used for design, but accurate simulations must include modeling refinements such as component mismatches and thermal distortion. The ultralinear design techniques include the use of local feedback and feedforward, current-mode and translinear topologies, and a variety of layout techniques which reduce electrical and thermal mismatches. The design techniques are applied to produce a surface acoustic wave driver amplifier IC with 1/10 the cost, 1/5 the area, and 1/4 the power consumption of an equivalent discrete implementation. These techniques can easily be applied to faster bipolar processes to achieve wide bandwidth, superb linearity, and low power consumption. Author (CISTI)

N94-26704 Carleton Univ., Ottawa (Ontario). Dept. of Electronics.
ALL-OPTICAL GAIN SWITCHING OF ERBIUM-DOPED FIBRE AMPLIFIERS M.S. Thesis
Glenn Peter Cheney 17 Dec. 1992 140 p
(ISBN-0-315-84120-6; CTN-94-61057) Copyright Avail: Micromedia Ltd., Technical Information Centre, 240 Catherine Street, Suite 305, Ottawa, Ontario, K2P 2G8, Canada HC/MF

The gain switching characteristics of erbium-doped fiber amplifiers with signal wavelengths in the 1525-1550 nm range are examined. Short duration, high energy pulses at wavelengths within the signal bandwidth are used for rapid switching of the amplifier gain at the signal wavelength. Experimental results indicate that the switching time is governed by the pulse duration and pulse energy for switching pulses generated by a Q-switched erbium-doped fibre laser. Switchoff times on the order of 10 ns were observed. This is many orders of magnitude lower than the fluorescence lifetime of erbium ions in a glass host, which limits the switching speed of amplifiers controlled by pump power modulation alone. The dynamic range of switching, defined as the difference in the amplifier gain before and after switching, is determined by the amplifier gain and the peak power of the short-duration switching pulse. Author (CISTI)

N94-26777# Lawrence Livermore National Lab., CA.
DIAGNOSTICS AND MICROELECTRONICS
J. W. Balch Mar. 1993 23 p
(Contract W-7405-eng-48)
(DE94-003016; UCRL-ID-112773) Avail: CASI HC A03/MF A01

This report discusses activities of the Diagnostics and Microelectronics thrust area which conducts activities in semiconductor devices and semiconductor fabrication technology for programs at Lawrence Livermore National Laboratory. Our multidisciplinary engineering and scientific staff use modern computational tools and semi-conductor microfabrication equipment to develop high-performance devices. Our work concentrates on three broad technologies of semiconductor microdevices: (1) silicon on 3-5 semiconductor microelectronics, (2) lithium niobate-based and 3-5 semiconductor-based photonics, and (3) silicon-based micromachining for application to microstructures and microinstruments. In FY-92, we worked on projects in seven areas. The projects are described in this report: novel photonic detectors; a wideband phase modulator; an optoelectronic terahertz beam system; the fabrication of microelectrode electrochemical sensors; diamond heatsinks; advanced micromachining technologies; and electrophoresis using silicon microchannels. DOE

N94-26797 Naval Command, Control and Ocean Surveillance Center, San Diego, CA.
GENERALIZED EMULATION MICROCIRCUIT PROGRAM Viewgraphs
H. Hanson and J. Christensen Oct. 1993 20 p Limited Reproducibility: More than 20% of this document may be affected by microfiche quality
(AD-A274749) Avail: CASI HC A03

This was a viewgraph presentation at the Government and Industry DMS Solutions Workshop. It explained the form, fit, function, and validation of the Generalized Emulation Microcircuit Program. DTIC

N94-26830# Air Force Inst. of Tech., Wright-Patterson AFB, OH. School of Engineering.
PARTITIONING STRUCTURAL VHDL CIRCUITS FOR PARALLEL EXECUTION ON HYPERCUBES M.S. Thesis
Kevin L. Kapp Dec. 1993 212 p
(AD-A274390; AFIT/GCE/ENG/93D-07) Avail: CASI HC A10/MF A03

Distributing simulations among multiple processors is one approach to reducing VHDL simulation time for large VLSI circuit designs. However, parallel simulation introduces the problem of how to partition the logic gates and system behaviors among the available processors in order to obtain maximum speedup. This research investigates deliberate partitioning algorithms that account for the complex inter-dependency structure of the circuit behaviors. Once an initial partition has been obtained, a border annealing algorithm is used to iteratively improve the partition. In addition, methods of measuring the cost of a partition and relating it to the resulting simulation performance are investigated. Structural circuits ranging from one thousand to over four thousand behaviors are simulated. The deliberate partitions consistently provided superior speedup to a random distribution of the circuit behaviors. DTIC

N94-26845# Aerospace Corp., El Segundo, CA. Technology Operations.
INVESTIGATION OF ACC/CCI TUNNEL DIODES
Gary W. Stupian and Gerald P. Chotkevys 1 Nov. 1993 33 p
(Contract F04701-88-C-0089)
(AD-A274549; TR-93(3478)-1; SMC-TR-93-57) Avail: CASI HC A03/MF A01

A tunnel-diode RF detector failed in DMSP system-level testing. An investigation was initiated by the prime contractor (Aerojet) with the assistance of The Aerospace Corporation. Destructive physical analyses carried out by Aerospace's Electronics Technology Center and by a commercial laboratory at the direction of Aerojet revealed a number of problems in the manufacturing process. Aerojet and Aerospace personnel visited the manufacturers of the detector module and the diodes and made recommendations that reduced or eliminated many of these difficulties. A search of the literature indicated that mechanical stress in the mesa region of the tunnel diodes was known to cause degradation and further suggested that elevated-temperature exposure would effectively screen out defective devices. Aerospace recommended such a screen. The implementation of this screen and the measures taken to clean up the manufacturer's process have greatly improved the reliability of the tunnel-diode detectors. The efficacy of the steps taken has been demonstrated clearly by comparison of electrical test results on the old and the improved components. Some time after our evaluation of the DMSP diodes, Aerospace was asked by NASA to examine diodes from the same vendor used for detectors on the AMSU/A mission. DTIC

N94-26890# Westinghouse Science and Technology Center, Pittsburgh, PA.
PROCESSING, FABRICATION, AND DEMONSTRATION OF HTS INTEGRATED MICROWAVE CIRCUITS, APPENDIX A
1993 27 p
(AD-A274600) Avail: CASI HC A03/MF A01

Electronics based on high transition temperature superconductive thin film materials is presently viable in some important niches, particularly in passive microwave circuits. Applications requiring Josephson junctions are impeded by the lack of reproducible junctions, but the junctions that can be produced are good candidates for the new Rapid Single Flux Quantum class of extremely fast digital circuits. Other devices that take advantage of the weak fluxoid pinning of some films are also promising, particularly the flux flow transistor. The availability of both Josephson and flux flow devices at 77 K invites exploration of hybrid technologies using HTS multi-chip modules supporting silicon CMOS chips and superconductive chips at the same time. The superconductive contribution to the emerging applications can result in significant performance advantages, particularly in remote sensing and communications. DTIC

N94-27027# Ohio State Univ., Columbus. Electroscience Lab.
JOINT SERVICES ELECTRONICS PROGRAM Annual Report No. 16
Leon Peters, Jr. Nov. 1993 72 p
(Contract N00014-89-J-1007)
(AD-A274643; ESL-721563-6) Avail: CASI HC A04/MF A01

The transfer of the compact range and target identification technology initiated under JSEP support for time domain studies continues to make large advances. The installation of a large compact reflector and a modern radar of our design has been completed for ASD at Wright Patterson Air Force Base. This system will have all of the sensitivity of the Mini Range reported last year and yet has a 14 ft quiet (or target) zone. The reflector includes all the most updated features of the ESL design. Dr. Brian Kent of ASD has expressed complete satisfaction with its performance. It is the range we would like to have, but can never afford. A large even more advanced compact range is currently being designed for NASA, Langley which is specifically being focused for measurements as low as 300 MHz. This new range will fit in a room 40 ft x 40 ft x 80 ft instead of the previously required 120 ft x 120 ft x 360 ft. The cost savings in this care are enormous. Our JSEP research continues to focus on electromagnetic related topics. DTIC

N94-27038# Foerenade Fabriksverken, Linkoeping (Sweden). Huvudavdelning foer Informationsteknologi.
HPm-TUBES: LITERATURE SURVEY COMPRISING 1992
Lennart Lundgren Jun. 1993 35 p See also PB93-117802
(PB94-123643; FOA-C-30715-8.3) Avail: CASI HC A03/MF A01

The present issue is the third in a new series of annual reports covering pulsed high power microwave (HPM) tubes and related technology. The literature survey is a continuation of the earlier annual report series: Microwave Tubes - Literature survey, the last issue comprising year 1986. The report gives a survey of the progress in the field, an evaluation of the state of the art, and trends of future developments. NTIS

N94-27057# Westinghouse Electric Corp., Baltimore, MD.
FERROELECTRIC FLUORIDE MEMORY FET DEVELOPMENT Interim Technical Report, Aug. 1990 - Jun. 1992
Donald R. Lampe Oct. 1993 111 p
(Contract N00014-90-C-0159)
(AD-A274341) Avail: CASI HC A06/MF A02

This Interim Technical Report covers the development and integration of Barium Magnesium Fluoride (BMF) ferroelectric thin films for incorporation into the gate dielectric of a metal-insulator-silicon field effect transistor, capable of functioning in a non-volatile, nondestructive-readout (NDRO) ferroelectric random access memory (FERRAM). Also provided is a detailed description of the test vehicles implemented for the study of fabrication process integration and optimization and the resultant properties of ferroelectric/(semiconductor) memory FET (FEMFET) and related structures. The BMF films were deposited by co-evaporation in ultra high vacuum from barium fluoride and magnesium fluoride effusion sources. A substrate temperature of 200 C during deposition followed by an anneal in hydrogen at 480 C resulted in polarization orientation closest to the preferred. Film samples exhibited polarization, Ps, as high as 4.55 micro-C/sq cm. The permittivity varied from a value of 9 at 5 kHz to 8.4 at 500 kHz. This compares closely with the average value of 10 reported for bulk single crystals. The ferroelectric switching speed of the thin film was approximately 45 nanoseconds. DTIC

N94-27061# Carnegie-Mellon Univ., Pittsburgh, PA. Dept. of Computer Science.

SYMBOLIC MODEL CHECKING FOR SEQUENTIAL CIRCUIT VERIFICATION

J. R. Burch, E. M. Clarke, D. E. Long, K. L. McMillan, and D. L. Dill 15 Jul. 1993 49 p
(Contract F33615-90-C-1465; ARPA Order 4976)
(AD-A274375; CMU-CS-93-211) Avail: CASI HC A03/MF A01

The temporal logic model checking algorithm of Clarke, Emerson, and Sistla is modified to represent state graphs using binary decision diagrams (BDD's) and partitioned transition relations. Because this representation captures some of the regularity in the state space of circuits with data path logic, the authors are able to verify circuits with an extremely large number of states. This new technique is demonstrated on a synchronous pipelined design with approximately 5 x 10(exp 120) states. The model checking algorithm handles full CTL with fairness constraints. Consequently, the authors are able to express a number of important liveliness and fairness properties, which would otherwise not be expressible in CTL. Empirical results are given on the performance of the algorithm applied to both synchronous and asynchronous circuits with data path logic. DTIC

N94-27079# Florida Univ., Gainesville. Dept. of Materials Science and Engineering.

VISIBLE LIGHT EMITTING MATERIALS AND INJECTION DEVICES Quarterly Progress Report, 1 Sep. - 30 Nov. 1993

Paul H. Holloway 30 Nov. 1993 25 p
(Contract N00014-92-J-1895)
(AD-A274418) Avail: CASI HC A03/MF A01

Progress report on visible light emitting materials and injection devices is presented. Topics covered include: molecular beam epitaxy growth of II-VI and III-Nitrides; ohmic contact formation; strain in II-VI; electrical and optical characterization; MOCVD growth; development of diode lasers; theoretical calculations of dopants in ZnSe; GaN part of DARPA-URI project on wide band-gap semiconductors for short wavelength emitters; and gain modeling in II-VI strained-layer QW structures. CASI

N94-27109# Department of the Navy, Washington, DC.

ENHANCED ADAPTIVE STATISTICAL FILTER PROVIDING IMPROVED PERFORMANCE FOR TARGET MOTION ANALYSIS NOISE DISCRIMINATION STATEMENT OF GOVERNMENT INTEREST Patent Application

Francis J. OBrien, inventor (to Navy), Marcus L. Graham, inventor (to Navy), and Kai F. Gong, inventor (to Navy) 22 Sep. 1993 18 p
(AD-D016039; US-Patent-Appl-SN-127145) Avail: CASI HC A03/MF A01

An adaptive statistical filter system for receiving a data stream comprising a series of data values from a sensor associated with successive points in time. Each data value includes a data component representative of the motion of a target and a noise component, with the noise components of data values associated with proximate points in time being correlated. The adaptive statistical filter system includes a prewhitener module, a plurality of statistical filters of different orders and a selection module. The prewhitener module receives the data stream from the sensor and generates a corrected data stream comprising a series of corrected data values each associated with a data value of the data stream, each including a data component and a noise component with the noise components of data values associated with proximate points in time being decorrelated. The plural statistical filters are coupled to receive the corrected data stream in parallel from the prewhitener. DTIC

N94-27145 Department of the Navy, Washington, DC.

AC TO DC POWER CONVERTER WITH REGULATED BI-POLAR OUTPUTS Patent

George A. Banura, inventor (to Navy) 12 Oct. 1993 12 p Filed 22 Jul. 91
(AD-D016032; US-Patent-5,252,911; US-Patent-Appl-SN-733488) Avail: US Patent and Trademark Office

An AC to DC power converter unit includes an AC/DC converter section operable to convert an AC input into a plurality of unregulated internal DC outputs and a pair of positive and negative switching DC/DC converter sections connected to said AC/DC converter section and receiving a pair of positive and negative unregulated internal DC outputs therefrom being of a first voltage level and generating a pair of dual positive and negative regulated external DC outputs being or a second voltage level different from said first voltage level. DTIC

N94-27303 Queens Univ., Kingston (Ontario). Dept. of Electrical Engineering.

DESIGN AND TEST OF A REGENERATIVE SATELLITE TRANSMULTIPLEXER M.S. Thesis

Kenny King-Ming Hung May 1993 194 p
(ISBN-0-315-85280-1; CTN-94-61104) Copyright Avail: Micromedia Ltd., Technical Information Centre, 240 Catherine Street, Suite 305, Ottawa, Ontario, K2P 2G8, Canada HC/MF

In a multiple access scheme for regenerative satellite communications, the bulk frequency division multiple access (FDMA) uplink signal is demodulated on board the satellite and then remodulated for time division multiplexing (TDM) downlink transmission. Conversion from frequency to time division multiplex format requires that the uplink signal be frequency demultiplexed and each individual carrier be subsequently demodulated. For thin-route application which consists of a large number of channels with fixed data rate, multicarrier demodulation can be accomplished efficiently by a digital transmultiplexer (TMUX) using a fast Fourier transform processor followed by a bank of per-channel processors. A time domain description of the TMUX algorithm is derived which elucidates how the TMUX functions. The per-channel processor performs timing and carrier recovery for optimum and coherent data detection. Timing recovery is necessarily achieved asynchronously by a filter coefficient interpolation. Carrier recovery is performed using an all-digital phase-locked loop. The combination of both timing and carrier loops is investigated for a multi-user system. The performance of the overall system is assessed over a multi-user, additive white Gaussian noise channel for a bit energy to noise power spectral density ratio down to zero dB. Author (CISTI)

N94-27327 Selskapet for Industriell og Teknisk Forskning, Trondheim (Norway). Div. of Metallurgy.

CHANNEL MODEL FOR AC ELECTRIC ARC

H. L. Larsen 2 Jun. 1993 48 p
(PB94-124591; STF34-A93113) Avail: Issuing Activity (National Technical Information Service (NTIS))

This report contains the results from calculations of free-burning AC electric arcs in argon. In order to calculate the arc current and arc voltage, the external electric circuit must be taken into consideration. The external circuit is modeled by an equivalent circuit consisting of an ideal AC voltage source, a loss resistance, and an inductance. The qualitative behavior of the current-voltage characteristic is in agreement with observed characteristics, but experimental data are necessary in order to check whether the calculated power loss is reasonable. Non-symmetry was modeled by introducing different anode and cathode falls in the two half periods. An attempt at taking into account different cathode current densities in the two half periods, depending on whether the electrode or silicon melt is cathode, did not give satisfactory results. Thermionic emission was assumed in both half periods, but this may not be the right mechanism when the silicon melt is cathode. The time delay of the AC arc compared to the DC case is modeled by a time constant. It was shown that this preset time constant must be in agreement with the mean 'mechanical' relaxation time in the arc in order to fulfill the energy balance. By updating the time constant until this is achieved, the time constant is eliminated as a parameter that must be chosen a priori. NTIS

N94-27574*# Jet Propulsion Lab., California Inst. of Tech., Pasadena.

CENTER FOR SPACE MICROELECTRONICS TECHNOLOGY Technical Report, 1992

1 Nov. 1993 118 p
(Contract NAS7-918; RTOP 582-03-11-21-00)
(NASA-CR-195282; JPL-Publ-93-27; NAS 1.26:195282) Avail: CASI HC A06/MF A02

The 1992 Technical Report of the Jet Propulsion Laboratory Center for Space Microelectronics Technology summarizes the technical accomplishments, publications, presentations, and patents of the center during the past year. The report lists 187 publications, 253 presentations, and 111 new technology reports and patents in the areas of solid-state devices, photonics, advanced computing, and custom microcircuits. Author (revised)

N94-27606# Tokyo Univ. (Japan). Synchrotron Radiation Lab.
TECHNICAL REPORT OF ISSP. SER. A, NO. 2688: SUPPRESSION OF HIGHER-ORDER MODES IN AN RF CAVITY BY RESISTIVE MATERIAL
Tadashi Koseki, Yukihide Kamiya, and Masaaki Izawa Jun. 1993 10 p
(ISSN 0082-4798)
(JTN-94-80574) Avail: CASI HC A02/MF A01

A new RF (Radio Frequency, 500 MHz) cavity which has a simple damped structure for the 1.5 GeV VUV (Vacuum Ultraviolet Rays) ring will be presented in this paper. The feature of the cavity design is that HOM's (Higher-Order Modes) propagate out from the cavity through the beam-duct with a large diameter and are absorbed in resistive parts in the duct. A low power measurement on a prototype model of the cavity has been carried out, and the Q-values of HOM's are confirmed to drastically reduce. Thus the coupled-bunch instabilities due to HOM's are expected to be sufficiently suppressed. Author (NASDA)

N94-27618# California Univ., Berkeley. Lawrence Berkeley Lab.
A FULLY INTEGRATED 16 CHANNEL DIGITALLY TRIMMED PULSE SHAPING AMPLIFIER
W. E. Hearn and M. E. Wright Nov. 1993 6 p Presented at the Nuclear Science Symposium; Institute of Electrical and Electronic Engineers (IEEE) Medical Imaging Conference, San Francisco, CA; San Francisco, CA, 2-5 Nov. 1993; 4-6 Nov. 1993
(Contract DE-AC03-76SF-00098)
(DE94-004555; LBL-33594; CONF-931107-25; CONF-9311114-8) Avail: CASI HC A02/MF A01

A fully integrated CMOS pulse shaping amplifier has been developed at LBL. All frequency dependent networks are included on the chip. A provision is made for tuning to compensate for process variations. The overall architecture and details of the circuitry are discussed. Test results are presented. DOE

N94-27628 International Centre for Theoretical Physics, Trieste (Italy).
TRANSMITTANCE FLUCTUATIONS AND NON-LINEARITY IN RANDOM CHAINS IN THE PRESENCE OF APPLIED ELECTRIC FIELDS
Susil K. Manna, Prabhat K. Thakur (Bose Research Inst., Calcutta, India.), and Abhijit Mookerjee Jul. 1993 16 p Limited Reproducibility: More than 20% of this document may be affected by microfiche quality
(DE94-603665; IC-93/222) Avail: CASI HC A03 (US Sales Only)

Numerical investigations of transmittance fluctuations in disordered chains in the presence of external electric fields have been conducted. An almost constant fluctuation was obtained in a length scale smaller than the localization length. However, the value of the fluctuation in the plateau region is dependent on the external electric field and strength of disorder. The transmittance autocorrelation was also studied as a function of external electric field to probe nonlinearity in transmittance. DOE

N94-27642 Waterloo Univ. (Ontario).
THE ANALYSIS OF THERMAL AND 1/F NOISE IN MOS DEVICES, CIRCUITS AND SYSTEMS Ph.D. Thesis
Paul Arthur Layman 1989 252 p
(ISBN-0-315-57811-4; CTN-94-60983) Copyright Avail: Micromedia Ltd., Technical Information Centre, 240 Catherine Street, Suite 305, Ottawa, Ontario, K2P 2G8, Canada HC/MF

The deterministic and stochastic limits to decreasing the size of metal oxide semiconductor (MOS) devices are reviewed, focusing on thermal and 1/f noise. An existing compact circuit model is modified to include a new thermal noise model that includes channel length modulation and carrier heating. A 1/f noise model is also incorporated. These models show improvements over existing space models. Noise measurements are described and compared to the new models. Thermal and 1/f noise calculations are incorporated into a new two-dimensional device simulator which handles arbitrary structures and includes external bias resistors. Noise calculations are performed by characterizing thermal and 1/f noise on an elemental basis, then solving the transpose system to determine the total noise in the desired terminal current. A new damping method is proposed for use with Newton's method to solve the partial differential equations in the simulator, which uses a new triangular grid structure that allows direct refinement. A new refinement algorithm is presented along with an interactive grid generation program. The impact of noise at circuit level is examined analytically and numerically using a dynamic random access memory storage cell as a test vehicle. Several design considerations and tradeoffs are discussed and possible limits are introduced. Author (CISTI)

N94-27650 Waterloo Univ. (Ontario). Dept. of Electrical Engineering.
AN ELECTRONIC SWITCH BASED ON QUANTUM INTERFERENCE M.S. Thesis
Andrew M. Sarangan 1993 159 p
(ISBN-0-315-84609-7; CTN-94-61066) Copyright Avail: Micromedia Ltd., Technical Information Centre, 240 Catherine Street, Suite 305, Ottawa, Ontario, K2P 2G8, Canada HC/MF

As semiconductor devices shrink towards dimensions comparable to the mean free path of electrons, their electrical characteristics become more and more dominated by the wavelike nature of electrons. Since electron waves in semiconductors and optical waves in dielectrics are similar in many respects, the theoretical models used for studying optical devices can be modified and applied to electron wave devices. A quantum directional coupler switch is studied as the electronic analogy of the optical directional coupler. Since the quantum directional coupler switch is believed to be capable of switching at very high speeds at extremely low power levels, it has potential application in many areas of electronics. In studying the electrical characteristics of this device, two different approaches were taken. First, an electron wave coupled mode theory was developed and applied to study the switching behavior of the device. This theory is formal and physically insightful, but its accuracy extends only as far as the number of modes used in the wave function expression. The second approach was an electron wave beam propagation method which is less insightful but numerically more accurate and rigorous. By using a combination of these methods, a good appreciation of the operation of the device can be obtained. CISTI

N94-27653 Waterloo Univ. (Ontario). Dept. of Electrical Engineering.
AN EFFICIENT AND ACCURATE GREEN'S FUNCTION ANALYSIS OF PACKAGED MICROWAVE INTEGRATED CIRCUITS Ph.D. Thesis
Reza Faraji-Dana 1993 137 p
(ISBN-0-315-84425-6; CTN-94-61069) Copyright Avail: Micromedia Ltd., Technical Information Centre, 240 Catherine Street, Suite 305, Ottawa, Ontario, K2P 2G8, Canada HC/MF

A field theoretical approach is developed for the analysis of monolithic microwave integrated circuits (MMIC's). The usual mixed potential integral equation with Galerkin's moment method is used, as well as the characteristic Green's function technique. The original structure is separated into three layered media surrounding the source from the three directions, and the spectral domain technique is then applied to each layer to find the respective characteristic Green's function. Combining these one-dimensional Green's functions in an integral form gives the spatial Green's function (SGF) for the original packaged structure. The integral form of the SGF is exact for variable separable structures. Prony's approximation can be used to evaluate the integral. Surrounding wall effects can be isolated from the original open microstrip structure, and this creates an efficient computer-aided design tool for predicting circuit performance. Experiments were also performed on a number of packaged microstrip circuits to verify the numerical results of the moment method. The validity of the Green's function was examined for non-separable structures. As a special case, the Green's function of a line current over a truncated slab was analyzed and a close agreement was found between the approximate Green's function method and a formally exact moment method. Author (CISTI)

N94-27672# Department of the Navy, Washington, DC.
MICRO-ELECTRON DEFLECTOR Patent Application
Cha-Mei Tang, inventor (to Navy), Antonio C. Ting, inventor (to Navy), and Thomas A. Swyden, inventor (to Navy) 15 Nov. 1993 47 p
(AD-D016055; US-Patent-Appl-SN-151678; Navy-Case-74713) Avail: CASI HC A03/MF A01

The present invention relates to electron beam deflection devices, and more particularly to medium power vacuum deflection amplifiers and to cathodes for production of chopped electron ribbons for power amplifiers in the microwave and millimeter-wave range. DTIC

N94-27673# Department of the Navy, Washington, DC.
CONTROL SYSTEM FOR TRACKING NONLINEAR SYSTEMS Patent Application
Ira B. Schwartz, inventor (to Navy), Ioana Triandaf, inventor (to Navy),

Thomas Carroll, inventor (to Navy), and Lou Pecora, inventor (to Navy) 23 Jun. 1993 65 p
(AD-D016057; US-Patent-Appl-SN-080155; Navy-Case-74854) Avail: CASI HC A04/MF A01

The present invention relates to control of nonlinear systems, and more particularly to a control system for tracking the operation of a nonlinear system, such as a laser or electronic system, over a range of operating conditions. DTIC

N94-27770*# Virginia Polytechnic Inst. and State Univ., Blacksburg. Dept. of Electrical Engineering.
EFFECTIVE CONDUCTIVITY OF WIRE MESH REFLECTORS FOR SPACE DEPLOYABLE ANTENNA SYSTEMS
William A. Davis Mar. 1994 86 p
(Contract NAS1-18471; RTOP 233-01-03-22)
(NASA-CR-191605; NAS 1.26:191605) Avail: CASI HC A05/MF A01

This report summarizes efforts to characterize the measurement of conductive mesh and smooth surfaces using proximity measurements for a dielectric resonator. The resonator operates in the HEM11 mode and is shown to have an evanescent field behavior in the vicinity of the sample surface, raising some question to the validity of measurements requiring near normal incidence on the material. In addition, the slow radial field decay outside of the dielectric resonator validates the sensitivity to the planar supporting structure and potential radiation effects. Though these concerns become apparent along with the sensitivity to the gap between the dielectric and the material surface, the basic concept of the material measurement using dielectric resonators has been verified for useful comparison of material surface properties. The properties, particularly loss, may be obtained by monitoring the resonant frequency along with the resonator quality factor (Q), 3 dB bandwidth, or the midband transmission amplitude. Comparison must be made to known materials to extract the desired data. Author

N94-27817 Japan Atomic Energy Research Inst., Tokyo.
THE EFFECT OF Ti CONDUIT ON THE CRITICAL CURRENT IN (Nb, Ti)3Sn CABLE-IN-CONDUIT CONDUCTORS
Yoshihide Wadayama (Japan Atomic Energy Research Inst., Naka.), Toshinari Ando (Japan Atomic Energy Research Inst., Naka.), Hideo Nakajima (Japan Atomic Energy Research Inst., Naka.), Masataka Nishi (Japan Atomic Energy Research Inst., Naka.), Yukio Yasukawa (Japan Atomic Energy Research Inst., Naka.), Hiroshi Tsuji (Japan Atomic Energy Research Inst., Naka.), and Hisaaki Hiue Mar. 1993 20 p In JAPANESE Limited Reproducibility: More than 20% of this document may be affected by microfiche quality
(DE94-701204; JAERI-M-93-065) Avail: CASI HC A03/MF A01

The effect of titanium conduit on the critical current in (Nb,Ti)3Sn cable-in-conduit conductors was investigated to obtain a high performance conductor which would be applied to large superconducting magnets such as those for fusion machines. Titanium has equivalent thermal contraction coefficient to that of (Nb,Ti)3Sn filaments, and it is expected by using titanium as the conduit to suppress degradation of critical current due to excess thermal prestrain on (Nb,Ti)3Sn filaments. Some titanium conduit sample conductors were made, and their critical current performance were measured together with some stainless steel (SUS316) and copper-nickel alloy (Cu-10Ni) conduit conductors. The experimental results indicated that the titanium conduit conductors had no critical current degradation due to thermal strain, whereas the stainless steel and copper-nickel alloy conduit conductors showed remarkable degradation on their critical current performance and greater degradation was observed with smaller void conductor. In conclusion, titanium is verified to be excellent conduit material for (Nb,Ti)3Sn cable-in-conduit conductors. DOE

N94-27821# Japan Atomic Energy Research Inst., Tokyo.
EXPERIMENTAL RESULTS OF 40-kA Nb3Al CONDUCTOR
Yoshikazu Takahashi (Japan Atomic Energy Research Inst., Naka.), Makoto Sugimoto (Japan Atomic Energy Research Inst., Naka.), Takaaki Isono (Japan Atomic Energy Research Inst., Naka.), Masayuki Oshikiri (Japan Atomic Energy Research Inst., Naka.), Fumikazu Hosono (Japan Atomic Energy Research Inst., Naka.), Yoshihide Wadayama (Japan Atomic Energy Research Inst., Naka.), Tomoyuki Sasaki (Japan Atomic Energy Research Inst., Naka.), Hiromi Hanawa (Japan Atomic Energy Research Inst., Naka.), Shuichi Seki (Japan Atomic Energy Research Inst., Naka.), and Hiroshi Wakabayashi (Japan Atomic Energy Research Inst., Naka.) et al Mar. 1993 61 p In JAPANESE
(DE94-701207; JAERI-M-93-072) Avail: CASI HC A04/MF A01

A 40-kA Nb3Al conductor was developed for the toroidal field (TF) coils of the experimental fusion reactors. Presently, Nb3Sn is mainly used for high-field superconductor (more than 12 T) and is commercially available in a various type. On the other hand, the critical current (Ic) degradation of the Nb3Al was only 5% under an intrinsic axial strain of 0.4%, according to the experimental results. In case of Nb3Sn, the degradation was 30%. Therefore, it is shown that Nb3Al has excellent mechanical performance and it very useful for the toroidal field coil which is operated under large electromagnetic force. However, Nb3Al is not practical to use at present due to the difficulty of its fabrication. This conductor could be operated up to the current of 46 kA at an external field of 11.2 T, which was the required field of the TF coils in the International Thermonuclear Experimental Reactor (ITER). According to this development, Nb3Al will become a useful superconductor for large-scale, high-field application, such as the fusion machine. DOE

N94-28186 Department of the Navy, Washington, DC.
MICROPROCESSOR CHIP INCORPORATING OPTICAL SIGNAL COUPLING TRANSCEIVER Patent
David H. Nhu, inventor (to Navy) 17 Aug. 1993 5 p Filed 23 Feb. 1990 Supersedes AD-D014547
(AD-D016077; US-Patent-5,237,441; US-Patent-Appl-SN-483686; US-Patent-Class-359-152) Avail: US Patent and Trademark Office

Microprocessor and transceiver circuitry are incorporated into a single chip for enhanced, high speed operation of an electronic circuit board by use of optical fiber connections between two or more of such single chips and external peripherals. The transceiver circuitry includes transmitter and receiver sections through which the optical signals are respectively generated and received by a light emitting diode and a photodiode. DTIC

N94-28357# Helsinki Univ. of Technology, Espoo (Finland). Electron Physics Lab.
DRY ETCHING PROCESS DEVELOPMENT FOR SUBMICRON AND NANOMETER SEMICONDUCTOR DEVICES
V. Stepanov Jun. 1993 27 p
(PB94-133196; ISBN-951-22-1673-6) Avail: CASI HC A03/MF A01

The reactive ion etching of GaAs, AlGaAs, and Si was investigated for submicron and nanometer scale semiconductor structure processing. Different parameters were varied and studied to achieve the desired controllability and reproducibility of fabrication process. That included the estimation of the influence of power density, pressure, gas flow rate, and relative composition, as well as etching time on controllable etch rates and profiles, damage and roughness, and anisotropy and selectivity. The investigations of dry etching allowed the fabrication of GaAs and Si pillar structures with diameter less than 30 nm. NTIS

N94-25560# National Research Inst. for Metals, Tokyo (Japan).
STUDY ON MEASUREMENT AND EVALUATION METHODS FOR SUPERCONDUCTIVE CHARACTERISTICS [CHODENDO TOKUSEI NO SOKUTEI HYOKAHO NI KANSURU KENKYU]
Hitoshi Wada, Kikuo Ito, Tsuneo Kuroda, Michiya Yuyama, L. F. Goodrich, S. Bray, J. W. Ekin, and R. Goldfarb *In its* Bulletin of National Research Institute for Metals in Fiscal Year 1993, No. 14 29 Jan. 1993 p 145-148 In JAPANESE Prepared in cooperation with National Inst. of Standards and Technology, Gaithersburg, MD Sponsored by Science and Technology Agency, Tokyo, Japan (For primary document see N94-25544 07-26)
Avail: CASI HC A01/MF A04

N94-27388# Tohoku Univ., Sendai (Japan). Inst. for Chemical Reaction Science.
FOUR PHASE MICROWAVE PULSE GENERATOR FOR PULSED EPR SPECTROMETER [PARUSU EPR YO 4 ISO MAIKUROHA PARUSU HASSEIKI NO SHISAKU]
Yasunori Ohba, Rie Satoh, and Masamoto Iwaizumi *In its* Bulletin of the Institute for Chemical Reaction Science, Tohoku University, Volume 2 30 Sep. 1992 p 33-37 In JAPANESE (For primary document see N94-27385 07-25)
Avail: CASI HC A01/MF A02

N94-27922*# Hampton Univ., VA. Dept. of Mathematics.
A TRI-STATE OPTICAL SWITCH FOR LOCAL AREA NETWORK COMMUNICATIONS
Garfield Simms *In* Old Dominion Univ., The 1993 NASA-ODU American Society for Engineering Education (ASEE) Summer Faculty Fellowship Program Dec. 1993 p 170-176 (For primary document see N94-27893 07-80)
Avail: CASI HC A02/MF A03

N94-28078# Moore (M. J.) (England).
INTRODUCTION TO COMBINED CYCLES
M. J. Moore *In* VKI, Combined Cycles for Power Plants 1993 49 p
(For primary document see N94-28077 07-37)
Copyright Avail: CASI HC A03/MF A04

34 FLUID MECHANICS AND HEAT TRANSFER

Includes boundary layers; hydrodynamics; fluidics; mass transfer; and ablation cooling.

For related information see also *02 Aerodynamics* and *77 Thermodynamics and Statistical Physics.*

N94-25587 Air Force Inst. of Tech., Wright-Patterson AFB, OH. School of Engineering.
NUMERICAL SIMULATION OF TOMOGRAPHIC RECONSTRUCTION FOR THE STUDY OF TURBULENCE USING OPTICAL WAVEFRONT SENSOR MEASUREMENTS M.S. Thesis
Robert L. Johnson Dec. 1993 82 p Limited Reproducibility: More than 20% of this document may be affected by microfiche quality
(AD-A273851; AFIT/GAP/ENP/93D-04) Avail: Issuing Activity (Defense Technical Information Center (DTIC))

The optical quality of a coherent beam passing through a turbulent flow layer can be severely degraded by phase errors. The principle goal of this research is to model the use of wavefront sensor measurements and computed tomography to reconstruct refractive index distributions of transparent objects for the study of turbulent flows. Tomography is the processing of measurements of one-dimensional line integrals through a two-dimensional function to reconstruct a two-dimensional estimate of the function. A least-squares wavefront phase reconstructor is modeled using Zernike polynomials and triangle functions as elementary functions for the reconstructor. Two tomographic reconstruction algorithms are implemented: (1) iterative reconstruction; and (2) filtered back-projection. Through numerical simulation, the effects of undersampling and limited wavefront sensor resolution are studied. Distorted wavefront data are generated by performing line integrals through known objects with different numbers and ranges of view angle. Wavefront reconstruction is applied using varying resolution. Two tomographic reconstruction methods are employed and comparisons are made with the original known objects. Results show that a least-squares wavefront reconstructor using triangle functions provides better results. Increasing the number and range of view angles generally improves the quality of the tomographic reconstruction. Furthermore, iterative tomographic reconstruction techniques prove superior when limited data are available. DTIC

N94-25597# California Univ., Berkeley. Lawrence Berkeley Lab.
VORTEX METHODS
A. J. Chorin Jun. 1993 65 p Presented at the Les Houches Summer School of Theoretical Physics, Les Houches, France, 28 Jun. - 30 Jul. 1993 Revised
(Contract DE-AC03-76SF-00098)
(DE94-003245; LBL-34124; CONF-9306196-1) Avail: CASI HC A04/MF A01

Vortex methods originated from the observation that, in incompressible inviscid flow, vorticity (or, more accurately, circulation) is a conserved quantity, as can be readily deduced from the absence of tangential stresses. Thus, if the vorticity is known at time $t = 0$, one can find the flow at a later time by simply following the vorticity. In this narrow context, a vortex method is a numerical method that follows vorticity. The author restricts himself in these lectures to a special class of numerical vortex methods, those that are based on a Lagrangian transport of vorticity in hydrodynamics by smoothed particles (blobs) and those whose analysis contributes to the understanding of blob methods. Blob methods started in the 1930's. DOE

N94-25604# Pennsylvania State Univ., University Park. Applied Research Lab.
THE HIGH REYNOLDS NUMBER FLOW THROUGH AN AXIAL-FLOW PUMP
W. C. Zierke, W. A. Straka, and P. D. Taylor Nov. 1993 267 p
(Contract N00039-92-C-0100)
(AD-A273844; ARL/PSU-TR-93-12) Avail: CASI HC A12/MF A03

The high Reynolds number pump (HIREP) facility at ARL Penn State has been used to perform a low-speed, large-scale experiment of the incompressible flow of water through a two-blade-row turbomachine. HIREP can involve blade chord Reynolds numbers as high as 6,000,000 and can accommodate a variety of instrumentation in both a stationary and a rotating frame of reference. The objectives of this experiment were as follows: to provide a database for comparison with three-dimensional, viscous (turbulent) flow computations; to evaluate the engineering models; and to improve our physical understanding of many of the phenomena involved in this complex flow field. The experimental results include a large quantity of data acquired throughout HIREP. A five-hole probe survey of the inlet flow 37.0 percent chord upstream of the inlet guide vane (IGV) leading edge is sufficient to give information for the inflow boundary conditions, while some static-pressure information is available to help establish an outflow boundary condition. DTIC

N94-25605# California Inst. of Tech., Pasadena. Div. of Engineering and Applied Science.
HYDRODYNAMICS, ACOUSTICS AND SCALING OF TRAVELING BUBBLE CAVITATION M.S. Thesis
Yan P. KuhndeChizelle 24 Sep. 1993 193 p
(Contracts N00014-91-J-1295; N00014-91-J-1426)
(AD-A273846; ENG-200-30) Avail: CASI HC A09/MF A03

Recent observations of the geometries of growing and collapsing bubbles over axisymmetric headforms have revealed the complexity of the 'microfluidmechanics' associated with these flows. Among the complex features observed were bubble to bubble interaction, cavitation noise generation and bubble interaction with the boundary layer which leads to the shearing of the underside of the bubble and alters the collapsing process. All of these previous tests were performed on small headform sizes. The focus of this research is to determine the dynamics governing the growth and collapse of traveling bubbles and to analyze the scaling effects due to variations in geometry size, Reynolds number, and cavitation number. For this effect, cavitating flows over Schiebe headforms of different sizes (5.08 cm, 25.4 cm, and 50.8 cm in diameter) were studied in the David Taylor Large Cavitation Channel (LCC). The scaling effects captured on high-speed film and electrode sensors as well as the noise signals generated during the collapse of the cavities are presented. DTIC

N94-25654# Ecole Centrale de Lyon (France). Lab. de Mecanique des Fluides.
EXPERIMENTAL CONTRIBUTION TO THE STUDY OF SECONDARY FLOWS IN CENTRIFUGAL TURBOPUMP STATOR COMPONENTS Ph.D. Thesis [CONTRIBUTION EXPERIMENTALE A L'ETUDE DES ECOULEMENTS SECONDAIRES DANS LES ORGANES STATORIQUES DES TURBOPOMPES CENTRIFUGES]
Sahraoui Bouziane 1992 232 p In FRENCH Sponsored by SEP, France, and CNES Original contains color illustrations
(ECL-92-35; ETN-94-95279) Avail: CASI HC A11/MF A03

The flow characteristics in centrifugal turbomachines is investigated. Particular attention is given to the turbomachine stator components. The purposes of the study were: to validate the flow model for centrifugal turbopumps; to perform flow measurements on a test bed model in order to acquire accurate stator and U-bend pipe flow data; and to acquire local flow data for future numerical flow characterizations. The validity of the quasi three dimensional hypothesis is investigated. The characteristics of the low energy fluid accumulation zone are discussed. The effect of the stability of the blade root on the accumulation zone vortices is studied. The stator configuration choice is explained. The method applied for simulating the inducer's flow is described. The results of the flow visualization measurements showed that the outlet flow can be improved. ESA

N94-25657# Air Force Inst. of Tech., Wright-Patterson AFB, OH. School of Engineering.
EXPERIMENTAL ANALYSIS OF HEAT TRANSFER CHARACTERISTICS AND PRESSURE DROP THROUGH SCREEN REGENERATIVE HEAT EXCHANGERS M.S. Thesis
Jeffrey L. Wiese Dec. 1993 120 p
(AD-A273902; AFIT/GAE/ENY/93D-30) Avail: CASI HC A06/MF A02

This study investigated the effect on heat transfer and friction characteristics for screen regenerative heat exchangers with the screen thickness reduced by rolling. The experiments were performed on 250 and 325 mesh, 304 stainless steel screen using helium gas. Reynolds numbers, based on hydraulic radius, Re, were between 10 and 100. Both the Colburn factor, StPr(2/3), and friction factor, f, decreased as the screen thickness was reduced. A correlation was found for predicting friction factor, f. The drag coefficient per screen remained nearly unchanged for thicknesses reduced not more than 30 percent. The decrease in Colburn factor was significant for Re less than 40. For Re between 40 and 100 the decrease in Colburn factor was less than the experimental uncertainty. DTIC

N94-25763# Technische Univ., Delft (Netherlands). Faculty of Technical Mathematics and Informatics.
ABSTRACTION IN, SPECIFICATION AND PROOF OF SOFTWARE FOR A 1D HEAT-TRANSFER PROBLEM
H. H. tenCate 1993 22 p
(ISSN 0922-5641)
(Rept-93-45; ETN-94-95400) Copyright Avail: CASI HC A03/MF A01

Abstraction is shown to be an important concept to reduce complexity in parallel computing. The influence of abstraction on numerical software is demonstrated. It is shown that separating 'what, how, when, where', in other words separating a specification, its realization, and its implementation, has a lot of advantages. One advantage is that the obtained software has a clear and simple structure. Another advantage concerns portability, especially important in the field of parallel computing where no universal parallel computer model exists. In this area, software ought to be ported to other computer models easily. The investigation shows that a formal specification is a natural sequel to abstraction by discussing software development for a 1D (one dimensional) heat transfer problem. Aspects concerning formal verification are discussed. ESA

N94-25778# Cranfield Inst. of Tech., Bedford (England). Dept. of Aerospace Science.
RIEMANN SOLVERS FOR SOLVING THE INCOMPRESSIBLE NAVIER-STOKES EQUATIONS USING THE ARTIFICIAL COMPRESSIBILITY METHOD
D. T. Elsworth and E. F. Toro Jun. 1992 25 p
(Cranfield-Aero-9208; ISBN-1-871564-549; ETN-94-95215) Avail: CASI HC A03/MF A01

Five Riemann solvers for the artificial compressibility equations are presented. The mathematical character of the artificial compressibility equations is introduced. The exact and the two rarefaction Riemann solvers are presented. The local linearization solver, the Roe solver, and the HLLC (Harten-Leer-Lax Riemann where the C stands for contact) solver are included. Riemann solvers for the split two dimensional artificial compressibility equations are presented. The results of numerical tests performed on the various Riemann solvers and conclusions are given. These solvers give accurate results when used to produce global solutions to the test problem. The rarefaction solvers are computationally expensive, and offer no special advantage over the other solvers. The linear solver is the cheapest computationally, is simple and accurate to use in a program to find the solution to the Navier-Stokes equations. The HLLC solver is also relatively cheap, and very robust. Under certain conditions it may be better to select this solver above the linear one. ESA

N94-25858# Air Force Inst. of Tech., Wright-Patterson AFB, OH. School of Engineering.
SHOCK WAVE INTERACTION WITH L-SHAPED STRUCTURES M.S. Thesis
Richard C. Miller Dec. 1993 104 p
(AD-A273774; AFIT/GAP/ENP/93D-07) Avail: CASI HC A06/MF A02

This study investigated the interaction of shock waves with L-shaped structures using the CTH hydrodynamics code developed by Sandia National Laboratories. Computer models of shock waves traveling through air were developed using techniques similar to shock tube experiments. Models of L-shaped buildings were used to determine overpressures achieved by the reflecting shock versus angle of incidence of the shock front. An L-shaped building model rotated 45 degrees to the planar shock front produced the highest reflected overpressure of 9.73 atmospheres in the corner joining the two wings, a value 9.5 times the incident overpressure of 1.02 atmospheres. The same L-shaped building was modeled with the two wings separated by 4.24 meters to simulate an open courtyard. This open area provided a relief path for the incident shock wave, creating a peak overpressure of only 4.86 atmospheres on the building's wall surfaces from the same 1.02 atmosphere overpressure incident shock wave. DTIC

N94-25862# Air Force Inst. of Tech., Wright-Patterson AFB, OH. School of Engineering.
EFFECTS OF CRENULATIONS ON THREE DIMENSIONAL LOSSES IN A LINEAR COMPRESSOR CASCADE M.S. Thesis
William L. Spacy, II Dec. 1993 196 p
(AD-A273778; AFIT/GAE/ENY/93D-26) Avail: CASI HC A09/MF A03

An experimental investigation into the effect of compressor blade trailing edge geometry on three dimensional flows in a linear cascade was conducted at the AFIT linear cascade test facility. Hot-wire/hot-film anemometry along with total pressure instrumentation was used to analyze crenulation generated vortices and their interaction with the three dimensional flows in the cascade. The effects of this interaction on the performance parameters associated with the cascade were quantified. The results indicate that wake mixing is better for crenulated trailing edges and that the precise geometry of the crenulations is critical to performance. One crenulation geometry was found to increase wake mixing while slightly reducing the total pressure losses. DTIC

N94-25872# California Inst. of Tech., Pasadena. Graduate Aeronautical Labs.
FLOW PAST A CIRCULAR CYLINDER WITH A PERMEABLE WAKE SPLITTER PLATE Annual Report, 1 Oct. 1992 - 30 Sep. 1993
Gregory S. Cardell 1 Aug. 1993 228 p
(Contract N00014-90-J-1589)
(AD-A273765) Avail: CASI HC A11/MF A03

Measurements in the near wake region of a circular cylinder in a uniform flow in the Reynolds number range 2.5 x 10(exp 3) is approximately less than Re is approximately less than 1.8 x 10(exp 4) with permeable splitter plates spanning the wake center plane are presented. Permeability is defined by the pressure drop across the plates, and the relationship between permeability and plate solidity is determined for a set of plates constructed from woven wire mesh permitting unambiguous characterization of the splitter plates by the solidity. The effects of different solidities on the flow in the near wake are investigated using smoke wire flow visualization, hot-wire anemometry, and measurements of the mean pressure at the cylinder surface, and the results are related to cylinder flow without a splitter plate. Flow visualization results demonstrate that the introduction of low solidity splitter plates does not change the basic near wake structure, and that sufficiently high solidity uncouples the large-scale wake instability from the body, with the primary vortex formation occurring downstream of the separation bubble due to instability of the wake profile. Hot-wire and surface pressure measurements confirm and quantify the flow visualization results, showing that the permeable splitter plates reduce the drag and modify the primary wake frequency. When the solidity is high enough that the wake is convectively unstable, the base pressure is independent of the Reynolds number and solidity. For a wide range of solidities, the same asymptotic value of the Strouhal number is reached at high Reynolds numbers. The relationship between the Strouhal number and the base pressure is discussed. DTIC

N94-25874# Air Force Inst. of Tech., Wright-Patterson AFB, OH. School of Engineering.
WAKE PASSAGE EFFECTS ON THE LOSSES IN A LINEAR TURBINE CASCADE M.S. Thesis
James A. Braunschneider Dec. 1993 121 p
(AD-A273794; AFIT/GAE/ENY/93D-6) Avail: CASI HC A06/MF A02

A linear turbine cascade was used to investigate the effects of wake passage due to stator-rotor interaction. The wakes were modeled by passing 1.98 mm (0.078 in) diameter bars upstream of a linear cascade blade row. Total pressure loss coefficients, mass averaged total pressure loss coefficients, and velocities were used to characterize the effects of wake passage. Bar passing frequencies of 80, 160, 320 bars/sec were tested. These frequencies were tested, with the bars at 6.35 mm (0.25 in) intervals and at two Reynolds numbers, 341,000 and 455,000. Bar spacings of 12.7 mm (0.5 in), and 89 mm (3.5 in) were also examined. For a bar spacing of 12.7 mm these tests were made at a Reynolds number of 455,000 and bar passing frequencies of 80 bars/sec, 160 bars/sec, and with the bars stopped. The varying Reynolds numbers did not affect the results nor was there appreciable differences for the range of wake passing frequencies. However, for the same bar passing frequency, losses were effectively halved by doubling the spacing. The lack of influence of frequency and the effect of spacing was consistent with the time scale used. The maximum time scale reached was 0.95 so any influence due to changes in frequency were not felt in the blade passage. Whereas, for the same frequency, with half the bars, there were half the losses in the passage at any given time. DTIC

N94-25991# Air Force Inst. of Tech., Wright-Patterson AFB, OH. School of Engineering.

A NUMERICAL DETERMINATION OF BIFURCATION POINTS FOR LOW REYNOLDS NUMBER CONICAL FLOWS M.S. Thesis

Larry K. Waters Dec. 1993 78 p

(AD-A273984; AFIT/GAE/ENY/93D-29) Avail: CASI HC A05/MF A01

It has long been established that supersonic flow over axisymmetric conical bodies at high angles of attack tend to develop a side force due to vortical asymmetry. One of the proposed reasons for the asymmetry is a bifurcation point in the solution of the Navier-Stokes equations. This study investigated the possible existence of a bifurcation point in the Navier-Stokes equations for subsonic flow. Newton's method, with gauss elimination, was used-to solve the steady-state, viscous, compressible Navier-Stokes equations in spherical coordinates assuming conical similarity. DTIC

N94-26096# Texas Univ., Austin. Inst. for Fusion Studies.

SHEAR FLOW GENERATION FROM THE INTERACTION OF NEOCLASSICAL AND DRIFT WAVE TRANSPORT PROCESSES

X. N. Su, P. N. Yushmanov, J. Q. Dong, and W. Horton Oct. 1993 49 p

(Contract DE-FG05-80ET-53088)

(DE94-003135; DOE/ET-53088/T4) Avail: CASI HC A03/MF A01

Self-consistent shear flow generation from the interaction of neoclassical and drift wave turbulence effects is investigated. The neoclassical poloidal flow damping is shown to compete with the flow generation driven by the divergence of the Reynolds stress. When there is no external driving force except for the free energy released from toroidal shear flow, the turbulent fluctuations occur as a transient pulse which takes the system along an equilibrium path to a relaxed state. External torques, such as parallel neutral beam injection, are needed to maintain significant fluctuation levels. For a system driven by a fixed ion temperature gradient, although linearly the poloidal shear flow generated substantially reduces the growth rate, the simulation results show that a sequence of nonlinear pulses occurs that eventually build the fluctuations up to a level that is not significantly affected by the poloidal flow. In this new, highly nonlinear state the transport is intermittent occurring through a sequence of pulses of duration 100 L(sub n)/c(sub s) for typical parameters. DOE

N94-26117# Midwest Research Inst., Golden, CO.

THE IDENTIFICATION OF INFLOW FLUID DYNAMICS PARAMETERS THAT CAN BE USED TO SCALE FATIGUE LOADING SPECTRA OF WIND TURBINE STRUCTURAL COMPONENTS

N. D. Kelley Nov. 1993 8 p Presented at the 13th Energy-sources Technology Conference and Exhibition (ETCE) on Wind Energy, New Orleans, LA, 23-26 Jan. 1994

(Contract DE-AC02-83CH-10093)

(DE94-000231; NREL/TP-442-6008; CONF-940113-5) Avail: CASI HC A02/MF A01

We have recently shown that the alternating load fatigue distributions measured at several locations on a wind turbine operating in a turbulent flow can be described by a mixture of at least three parametric statistical models. The rainflow cycle counting of the horizontal and vertical inflow components results in a similar mixture describing the cyclic content of the wind. We believe such a description highlights the degree of non-Gaussian characteristics of the flow. We present evidence that the severity of the low-cycle, high-amplitude alternating stress loads seen by wind turbine components are a direct consequence of the degree of departure from normality in the inflow. We have examined the details of the turbulent inflow associated with series large loading events that took place on two adjacent wind turbines installed in a large wind park in San Gorgonio Pass, California. In this paper, we describe what we believe to be the agents in the flow that induced such events. We also discuss the atmospheric mechanisms that influence the low-cycle, high-amplitude range loading seen by a number of critical wind turbine components. We further present results that can be used to scale the specific distribution shape as functions of measured inflow fluid dynamics parameters. DOE

N94-26121# Oak Ridge Associated Universities, Inc., TN.

EXPERIMENTAL AND NUMERICAL INVESTIGATION OF SHOCK WAVE PROPAGATION THROUGH COMPLEX GEOMETRY, GAS CONTINUOUS, TWO-PHASE MEDIA Ph.D. Thesis

J. Chien-Chih Liu (California Univ., Berkeley.) 1993 294 p

(Contract DE-AC05-76OR-00033)

(DE94-001408; DOE/OR-00033/T565) Avail: CASI HC A13/MF A03

The work presented here investigates the phenomenon of shock wave propagation in gas continuous, two-phase media. The motivation for this work stems from the need to understand blast venting consequences in the HYLIFE inertial confinement fusion (ICF) reactor. The HYLIFE concept utilizes lasers or heavy ion beams to rapidly heat and compress D-T targets injected into the center of a reactor chamber. A segmented blanket of failing molten lithium or Li2BeF4 (Flibe) jets encircles the reactors central cavity, shielding the reactor structure from radiation damage, absorbing the fusion energy, and breeding more tritium fuel. DOE

N94-26187# Notre Dame Univ., IN. Dept. of Aerospace and Mechanical Engineering.

THE EFFECTS OF THREE-DIMENSIONAL IMPOSED 3-D DISTURBANCES ON BLUFF-BODY NEAR WAKE FLOWS Annual Report

Albin A. Szewczyk 29 Oct. 1993 7 p

(Contract N00014-90-J-4083)

(AD-A274845) Avail: CASI HC A02/MF A01

This experimental research effort focuses on the underlying three-dimensional flow structure in the near wake of a bluff body when subjected to imposed geometrical disturbances. We want to understand the effects of three dimensionality that are characterized by vortex splitting and looping and how they are related to other wake parameters such as base pressure shedding frequency, wake width, and wake formation length. DTIC

N94-26316# European Space Agency, Paris (France).

CHEMICAL AND VIBRATIONAL NONEQUILIBRIUM VISCOUS FLOWS: MODELLING, INTERNAL AND EXTERNAL FLOW APPLICATIONS

Cyril Flament (Office National d'Etudes et de Recherches Aerospatiales, Paris, France.) Aug. 1993 336 p Transl. into ENGLISH of Ecoulements de fluide visqueux en desequilibre chimique et vibrationnel: Modelisation, applications internes et externes (Paris, France, ONERA) 1991 p 1-276 Original language document was announced as N92-19221

(ESA-TT-1274; ONERA-NT-1991-2; ETN-94-95288) Avail: CASI HC A15/MF A03

A study aimed at the elaboration of a numerical code for solving chemical and vibrational nonequilibrium viscous flows is reported. This work includes the analysis and the use of several physical models (transport properties, thermodynamic functions, chemical kinetics, vibrational relaxation, and dissociation vibration coupling), the numerical analysis of equations with source terms (rendering implicit, Total Variation Diminishing (TVD) scheme), and applications to hypersonic flows for various nozzle and reentry body configurations. Quasimonodimensional Euler results are presented for the test nozzles R6 and F4, whose reservoir conditions are respectively, 50 bars, 4800K and 2000 bars, 8500K. Axisymmetric Navier-Stokes results for the flow around a sphere cylinder (Mach number M = 15.3) and around a hyperboloid (Mach number = 15.4) are detailed. The effects of each physical phenomenon (nonequilibrium, thermal conductivity, diffusion, vibration dissociation coupling) and numerical aspect (computational grid, averages) are studied. The results are in good agreement with those obtained by other calculations for both internal and external flows. ESA

N94-26319# Carnegie-Mellon Univ., Pittsburgh, PA. Dept. of Chemical Engineering.

PREDICTIVE MODELING OF PARTICLE-LADEN, TURBULENT FLOWS

Jennifer L. Sinclair, E. J. Bolio, and C. Hrenya 1993 29 p
(Contract DE-FG22-92PC-92540)
(DE94-003298; DOE/PC-92540/T3) Avail: CASI HC A03/MF A01

An Eulerian two-fluid mathematical model is considered for the flow prediction of gas-particle systems. The model expands on the Sinclair and Jackson model by recognizing a turbulent continuous phase. Both the gas- and the particle-phase velocity fields are composed of by a mean and a fluctuating component, and the important physical phenomena arising from the interaction of these components are included in the model. The gas turbulence is modeled by a single-phase closure, namely the k-(var epsilon) low Reynolds model by Myong and Kasagi, and modified to account for the presence of a dilute particle phase. The solid phase is considered as a rapid granular flow; hence, a closure based on the kinetic-theory analogy is used for the description of the stresses associated with this phase. Along with the relation between the fluxes of both phases and the pressure drop, the model is capable of predicting features related to the local flow structure, such as the mean and fluctuating velocity components and the concentration of both phases. In this report, the model is applied to the case of steady, fully developed flow in a vertical cylindrical pipe. An extensive comparison of the model predictions with experimental data is included. The sensitivity of the model predictions to the properties describing the particle collisions is also explored. DOE

N94-26331# Argonne National Lab., IL.

POTENTIAL CAPABILITIES OF REYNOLDS STRESS TURBULENCE MODEL IN THE COMMIX-RSM CODE

F. C. Chang and M. Bottoni 1993 11 p Presented at the NASA 2003 Conference, Anaheim, CA, 7 Dec. 1993
(Contract W-31-109-eng-38)
(DE94-003716; ANL/ET/CP-79607; CONF-931235-3) Avail: CASI HC A03/MF A01

A Reynolds stress turbulence model has been implemented in the COMMIX code, together with transport equations describing turbulent heat fluxes, variance of temperature fluctuations, and dissipation of turbulence kinetic energy. The model has been verified partially by simulating homogeneous turbulent shear flow, and stable and unstable stratified shear flows with strong buoyancy-suppressing or enhancing turbulence. This article outlines the model, explains the verifications performed thus far, and discusses potential applications of the COMMIX-RSM code in several domains, including, but not limited to, analysis of thermal striping in engineering systems, simulation of turbulence in combustors, and predictions of bubbly and particulate flows. DOE

N94-26401 Laboratorio de Computacao Cientifica, Rio de Janeiro (Brazil).

A THERMODYNAMICALLY CONSISTENT CONSTITUTIVE THEORY FOR A RIGID SOLID-STOKESIAN FLUID MIXTURE

H. C. Mattos (Pontificia Univ. Catolica, Rio de Janeiro, Brazil.), M. L. M. Costa (Pontificia Univ. Catolica, Rio de Janeiro, Brazil.), R. Sampaio (Pontificia Univ. Catolica, Rio de Janeiro, Brazil.), and R. M. S. daGama 1992 13 p Limited Reproducibility: More than 20% of this document may be affected by microfiche quality
(DE93-633202; LNCC-027/92) Avail: CASI HC A03 (US Sales Only)

This work is concerned with the modelling for the flow of a stokesian fluid through a rigid porous medium, using a theory of mixtures viewpoint. A systematic procedure to obtain constitutive relations that verify automatically the principle of objectivity and a local version of the second law of thermodynamics is proposed. The prescription of two thermodynamic potentials for each constituent is sufficient to define a complete set of constitutive relations. DOE

N94-26427# Lawrence Livermore National Lab., CA.

MIX INDUCED BY SINGLE SHOCK PASSAGE THROUGH A MATERIAL INTERFACE

V. C. Rupert, W. P. Crowley, and G. D. Kramer Jul. 1993 8 p Presented at the 19th International Sympsium on Shcok Waves, Marseille, France, 26-30 Jul. 1993
(Contract W-7405-eng-48)
(DE93-019505; UCRL-JC-114800; CONF-930788-4) Avail: CASI HC A02/MF A01

The question of perturbation growth at a shocked interface between materials with different densities has been studied in earnest in the last few years. The authors have been interested in the case of single-shock crossing the interface as a counterpart to the work done with one or several reflected waves. Using the LAM code the authors are systematically studying the interaction of a single shock with a wavy interface. During this first phase, they concentrated on the effect of the initial interface shape and on the Mach number dependence of the mixing process. Their simulations addressed a shock incident from a high-density gas into a low-density gas interface, and from a low-density gas onto a high-density gas interface. DOE

N94-26467*# High Technology Corp., Hampton, VA.

ON PREDICTION OF EQUILIBRIUM STATES IN HOMOGENEOUS COMPRESSIBLE TURBULENCE

Ridha Abid Mar. 1994 29 p
(Contract NAS1-19299; RTOP 505-70-62-15)
(NASA-CR-4570; NAS 1.26:4570) Avail: CASI HC A03/MF A01

Direct numerical simulations of compressible, homogeneous, turbulent shear flows are used to evaluate Reynolds stress models. Three pressure-strain models, which are either linear, quadratic, or cubic in the anisotropy tensor are considered. Dilatational dissipation and pressure-strain correlation models do not correctly capture the compressibility effects seen in the direct simulations. In particular, the increase in the anisotropy of normal stresses and the reduction in the shear stress are not reproduced by any of the models. Also, the use of the incompressible form of the dissipation-rate equation to determine the solenoidal part of the dissipation is found to be questionable. Author

N94-26468# Purdue Univ., West Lafayette, IN.

INTERFACIAL AREA AND INTERFACIAL TRANSFER IN TWO-PHASE FLOW

M. Ishii 1993 48 p
(Contract DE-FG02-90ER-14147)
(DE93-041226; DOE/ER-14147/3) Avail: CASI HC A03/MF A01

A joint research program funded by the DOE/BES at Purdue University and the University of Wisconsin-Milwaukee has been underway. The main efforts of the Purdue program were concentrated on the following tasks: Development of Four Sensor Measurement Method; Experimental Study of Axial Changes of Transverse Void and Interfacial Area Profiles in Bubbly Flow; Modeling of the Probe-Particle Interaction Using Monte Carlo Numerical Simulation; and Experimental Study of the Stability of Interface of Very Large Bubbles. Highlights of these research results are reported. DOE

N94-26479# Technische Univ., Eindhoven (Netherlands). Low Temperature Physics Group.

A NUMERICAL STUDY OF QUANTIZED VORTICES IN HeII Ph.D. Thesis

Ronald Godfried Kari Aarts 1993 125 p Sponsored by Netherlands Organization for the Advancement of Scientific Research
(ISBN-9-03-860232-4; ETN-94-95340) Avail: CASI HC A06/MF A02

The numerical simulation of the motion of quantized vortices in a superfluid is discussed. These vortices play an important role in the flow properties of pure superfluid He-4 (He-II) and of (He-3)-(He-4) mixtures at low temperatures. The hydrodynamic properties of He II are described by the two fluid model in which the liquid is treated as a mixture of a normal component and a superfluid component. In flow experiments critical velocities are observed. The Schwarz reconnection vortex tangle model is applied. Numerical considerations involving the stability of the algorithm, and the choice of an accurate algorithm to solve the equation of motion of the vortices are included. Results of vortex tangle simulations are presented. ESA

N94-26499*# Institute for Computer Applications in Science and Engineering, Hampton, VA.

THE NONLINEAR GALERKIN METHOD: A MULTI-SCALE METHOD APPLIED TO THE SIMULATION OF HOMOGENEOUS TURBULENT FLOWS Final Report

A. Debussche (Paris XI Univ., Orsay, France.), T. Dubois (Paris XI Univ., Orsay, France.), and R. Temam (Paris XI Univ., Orsay, France.) Dec.

1993 87 p Submitted for publication
(Contract NAS1-19480; RTOP 505-90-52-01)
(NASA-CR-191581; NAS 1.26:191581; ICASE-93-93) Avail: CASI HC A05/MF A01

Using results of Direct Numerical Simulation (DNS) in the case of two-dimensional homogeneous isotropic flows, the behavior of the small and large scales of Kolmogorov like flows at moderate Reynolds numbers are first analyzed in detail. Several estimates on the time variations of the small eddies and the nonlinear interaction terms were derived; those terms play the role of the Reynolds stress tensor in the case of LES. Since the time step of a numerical scheme is determined as a function of the energy-containing eddies of the flow, the variations of the small scales and of the nonlinear interaction terms over one iteration can become negligible by comparison with the accuracy of the computation. Based on this remark, a multilevel scheme which treats differently the small and the large eddies was proposed. Using mathematical developments, estimates of all the parameters involved in the algorithm, which then becomes a completely self-adaptive procedure were derived. Finally, realistic simulations of (Kolmorov like) flows over several eddy-turnover times were performed. The results are analyzed in detail and a parametric study of the nonlinear Galerkin method is performed. Author (revised)

N94-26534# Michigan Univ., Ann Arbor.

HIGH RESOLUTION MEASUREMENTS OF MIXING AND REACTION PROCESSES IN TURBULENT FLOWS Annual Report, 1 Oct. 1992 - 31 Sep. 1993

W. J. Dahm 30 Nov. 1993 41 p
(Grant AF-AFOSR-0541-89)
(AD-A274970; AFOSR-94-0031TR) Avail: CASI HC A03/MF A01

Fully-resolved, two-, three-, and four-dimensional, spatio-temporal imaging measurements of the fine structure of conserved scalar mixing in turbulent flows are being used to identify new insights into molecular mixing and develop practical models for turbulent combustion. During the past year, the high wavenumber part of the scalar mixing spectrum was measured and appears to confirm the Batchelor model. However, the cutoff wavenumber is found to lie significantly lower than classical theory suggests. The first measurements of the distribution of dissipation layer separations in turbulent flows were also obtained. These results show a surprisingly simple and potentially insightful -3 power law scaling for scalar mixing that has not yet been explained. A new strained dissipation and reaction layer (SDRL) model was developed that relates the chemical state of nonequilibrium reaction chemistry to the mixing state of one or more conserved scalar fields. This model was coupled with our high resolution Rayleigh imaging measurements to predict combustion species concentration and reaction rate fields in turbulent reacting flows. Results from this model show striking agreement with direct species imaging measurements in turbulent combustion, and allow access to species that cannot be measured directly. This new physically-based formulation appears to unify the previous flamelet and distributed reaction models within a single model capable of treating even deep nonequilibrium combustion. DTIC

N94-26558# Wisconsin Univ., Madison. Plasma Physics Research.

THE DYNAMICS OF INTERACTING NONLINEARITIES GOVERNING LONG WAVELENGTH DRIFTWAVE TURBULENCE Ph.D. Thesis

D. E. Newman Sep. 1993 107 p
(Contract DE-FG02-89ER-53291)
(DE94-001785; DOE/ER-53291/225) Avail: CASI HC A06/MF A02

Because of the ubiquitous nature of turbulence and the vast array of different systems which have turbulent solutions, the study of turbulence is an area of active research. Much present day understanding of turbulence is rooted in the well established properties of homogeneous Navier-Stokes turbulence, which, due to its relative simplicity, allows for approximate analytic solutions. This work examines a group of turbulent systems with marked differences from Navier-Stokes turbulence, and attempts to quantify some of their properties. This group of systems represents a variety of drift wave fluctuations believed to be of fundamental importance in laboratory fusion devices. From extensive simulation of simple local fluid models of long wavelength drift wave turbulence in tokamaks, a reasonably complete picture of the basic properties of spectral transfer and saturation has emerged. These studies indicate that many conventional notions concerning directions of cascades, locality and isotropy of transfer, frequencies of fluctuations, and stationarity of saturation are not valid for moderate to long wavelengths. In particular, spectral energy transfer at long wavelengths is dominated by the E x B nonlinearity, which carries energy to short scale in a manner that is highly nonlocal and anisotropic. In marked contrast to the canonical self-similar cascade dynamics of Kolmogorov, energy is efficiently passed between modes separated by the entire spectrum range in a correlation time. At short wavelengths, transfer is dominated by the polarization drift nonlinearity. While the standard dual cascade applies in this subrange, it is found that finite spectrum size can produce cascades that are reverse directed and are nonconservative in enstrophy and energy similarity ranges. In regions where both nonlinearities are important, cross-coupling between the nolinearities gives rise to large no frequency shifts as well as changes in the spectral dynamics. DOE

N94-26595*# Georgia Inst. of Tech., Atlanta. School of Aerospace Engineering.

COMPUTATIONAL STRATEGIES FOR THREE-DIMENSIONAL FLOW SIMULATIONS ON DISTRIBUTED COMPUTER SYSTEMS Ph.D. Thesis Semiannual Status Report, 15 Aug. 1993 - 15 Feb. 1994

Richard Allen Weed and L. N. Sankar Mar. 1994 58 p
(Grant NAG2-869)
(NASA-CR-195249; NAS 1.26:195249) Avail: CASI HC A04/MF A01

An increasing amount of research activity in computational fluid dynamics has been devoted to the development of efficient algorithms for parallel computing systems. The increasing performance to price ratio of engineering workstations has led to research to development procedures for implementing a parallel computing system composed of distributed workstations. This thesis proposal outlines an ongoing research program to develop efficient strategies for performing three-dimensional flow analysis on distributed computing systems. The PVM parallel programming interface was used to modify an existing three-dimensional flow solver, the TEAM code developed by Lockheed for the Air Force, to function as a parallel flow solver on clusters of workstations. Steady flow solutions were generated for three different wing and body geometries to validate the code and evaluate code performance. The proposed research will extend the parallel code development to determine the most efficient strategies for unsteady flow simulations. Author (revised)

N94-26637 Carleton Univ., Ottawa (Ontario). Dept. of Mechanical and Aerospace Engineering.

BEHAVIOUR OF SEPARATION BUBBLES IN SHARP-EDGED GAPS OF FINITE DIMENSIONS M.S. Thesis

Nathalie Hetu Apr. 1993 177 p
(ISBN-0-315-84113-3; CTN-94-61054) Copyright Avail: Micromedia Ltd., Technical Information Centre, 240 Catherine Street, Suite 305, Ottawa, Ontario, K2P 2G8, Canada HC/MF

Measurements are presented for the nominally two-dimensional flow in a sharp-edged gap with finite length and height, and complemented with extensive flow visualization. The gap geometry is seen to have a significant influence on both the streamwise and transverse dimensions of the two-dimensional separation bubble present at the gap inlet. The height and length of the bubble remain a constant proportion of the gap height for various values of the height/length ratio. However, in a slightly diffusing clearance gap, the flow remains separated throughout. The Reynolds number, varied from 150,000 to 325,000, was found to have no influence on the flow in the gap. The discharge coefficient was calculated at four clearances, showing a correlation between its value and the gap height/length ratio. An existing model of the flow through a two-dimensional gap with a leading edge separation bubble is examined in light of the presented data and expanded to evaluate the discharge coefficient at various clearances. A second expression is suggested which improves the prediction, and the discharge coefficients evaluated in this manner are compared to those calculated from measurements made in the tip gap of a planar cascade of turbine blades. Results suggest that the prediction model developed can provide reasonable estimates of the discharge coefficient in actual tip gaps. Author (CISTI)

N94-26671 Carleton Univ., Ottawa (Ontario). Dept. of Mechanical and Aerospace Engineering.

AN INVESTIGATION OF THE EFFECTS OF THE HIGH MAXIMUM-THICKNESS-TO-CHORD RATIO ON THE PERFORMANCE OF NOZZLE GUIDE VANES IN A TRANSONIC PLANAR CASCADE M.S. Thesis

Rama Radmard Mar. 1993 209 p
(ISBN-0-315-84107-9; CTN-94-61053) Copyright Avail: Micromedia Ltd., Technical Information Centre, 240 Catherine Street, Suite 305, Ottawa, Ontario, K2P 2G8, Canada HC/MF

The performance of turbine airfoils is usually predicted by empirical correlations, which however are inadequate for the case of airfoils with maximum thickness to chord ratio (MTCR) higher than 25 percent. Studies were conducted to create a data base from which the performance of turbine airfoils with a MTCR higher than 25 percent could be predicted. A planar cascade consisting of four airfoils was constructed to allow the investigation of the effect of the MTCR on the airfoil performance. Three airfoil sets with MTCR of 15.2 percent (baseline), 26.6 percent, and 48.2 percent were used. Measurements included surface Mach number distributions for the baseline airfoil, total pressure loss coefficients, and deviation angles for isentropic exit Mach numbers of 0.7 (design), 0.9, and 1.1. The effect of varying the inlet boundary layer thickness and free-stream turbulence level was also examined. The results showed that the 26.6 percent airfoil produced lower losses as predicted by the Kacker and Okapuu (1982) correlation. The introduction of turbulence produced a significant redistribution of losses in the exit plane. The secondary loss decreased as the leading edge diameter was increased. Except for the baseline blade where high under-turning in exit flow angle was observed, the airfoils showed a decrease in over-turning with increasing exit Mach number, as predicted by Ainley and Mathieson (1951). Author (CISTI)

N94-26763# Argonne National Lab., IL.

VALIDATED HEAT-TRANSFER AND PRESSURE-DROP PREDICTION METHODS BASED ON THE DISCRETE-ELEMENT METHOD. PHASE 2: TWO-DIMENSIONAL RIB ROUGHNESS

C. A. James (Mississippi State Univ., Mississippi State.), B. K. Hodge (Mississippi State Univ., Mississippi State.), and R. P. Taylor (Mississippi State Univ., Mississippi State.) May 1993 98 p
(Contract W-31-109-eng-38)
(DE94-002379; ANL/ESD/TM-55) Avail: CASI HC A05/MF A02

Surface roughness is a commonly used approach for enhancing the rate of heat transfer of surfaces, such as in heat-exchanger tubes. Because the improved thermal performance of roughened surfaces is at the expense of increased flow resistance (increased pressure drop or friction factor), accurate prediction techniques for determining the friction factors and Nusselt numbers for roughened surfaces are required if such features are to be considered as design options. This report presents the results of the second phase of a research program sponsored by Argonne National Laboratory to validate models for the prediction of friction factors and Nusselt numbers for fully developed turbulent flow in enhanced heat-exchanger tubes. The first phase was concerned with validating a roughness model for turbulent flow in tubes internally roughened with three-dimensional distributed roughness elements, such as sandgrains, spheres, hemispheres, and cones. The second phase is concerned with devising and validating methods for the prediction of friction factors and Nusselt numbers for turbulent flow in tubes internally roughened with repeated, two-dimensional ribs aligned perpendicular to the flow. The ribs are spaced sufficiently far apart that the leeward-side separated flow reattaches to the wall before again separating in order to negotiate the next rib. This heat-transfer enhancement mechanism is called the separation and reattachment mechanism, after Rabas (1989). This work is limited to rectangular rib shapes. DOE

N94-26801 Aeronautical Research Labs., Melbourne (Australia).

COMPUTATION OF NON-ISENTROPIC INTERNAL FLOWS WITH VARIABLE DENSITY

E. Brizuela Nov. 1993 53 p Limited Reproducibility: More than 20% of this document may be affected by microfiche quality
(AD-A274848; ARL-TR-10; DODA-AR-007-102) Avail: CASI HC A04

A computational fluid dynamics code named MULTIFLOW-2D has been acquired and is being put into service for the numerical simulation of gas turbine-type combustors. Certain areas of the code were found to be in need of improvement for this application. The areas marked for improvement are as follows: (1) the grid generation algorithm; (2) the manner of discretization of the continuity and momentum equations; and (3) the treatment of the inlet boundary conditions. Improvements to these areas were developed and incorporated to the code, and the code functioning in non-reactive flows was tested by means of numerical experiments. Verification against physical experiments is planned. DTIC

N94-26832# University of Southern California, Los Angeles. Dept. of Aerospace Engineering.

NUMERICAL STUDIES ON THE DYNAMICS OF BUBBLE, TURBULENT, FREE SHEAR FLOWS: EFFECT OF THE INTER-PHASE COUPLING ON THE GLOBAL FLOW EVOLUTION Final Report, 1 Nov. 1990 - 31 Oct. 1993

Eckart Meiburg 23 Dec. 1993 42 p
(AD-A274521) Avail: CASI HC A03/MF A01

We use direct numerical simulations to analyze the evolution of a temporally growing two-dimensional free shear layer seeded with a dilute suspension of bubbles under gravity. The bubble concentrations are dilute enough so that bubble bubble interactions are negligible, but cumulative effects of bubbles alter the flow field. The evolution of the bubbles can then be determined by tracking many individual bubbles, and the flow field is advanced using the Navier-Stokes equations with a coupling term in the momentum equation representing the effect of the bubbles on the flow. We interpret the results in terms of the difference in the vorticity, bubble concentration, and pressure fields relative to the passive or one way coupled case. Due to the nature of the vorticity production mechanism, the net circulation is not affected by the bubbles, but local variations do occur, especially near the vortex center. In addition to the effect of the bubbles on the flow, the bubble field is also altered as a result of the two-way coupling. The location of bubble accumulation is shifted away from the vortex center and the magnitude of this accumulation is reduced relative to the passive case. DTIC

N94-26979# Rensselaer Polytechnic Inst., Troy, NY. Center for Multiphase Research.

AN EXPERIMENTAL STUDY OF PLUNGING LIQUID JET INDUCED AIR CARRYUNDER AND DISPERSION Final Report

R. T. Lahey, Jr. and D. A. Drew 17 Dec. 1993 71 p
(Contract N00014-91-J-1271)
(AD-A274414) Avail: CASI HC A04/MF A01

This report is divided into four parts. Part-1 provides an introduction to plunging jet phenomena and summarizes the major findings of our previous research. Part-2 presents a summary of the major experimental findings obtained during at Rensselaer. Part-3 describes two proposed mechanisms responsible for air entrainment. Part-4 presents the results of two different numerical calculations, one using a Euler-Lagrangian approach and the other based on solving a full two-fluid model with a CFD code. Finally, Part-5 presents our conclusions and recommendations for future research. DTIC

N94-27026# California Inst. of Tech., Pasadena. Graduate Aeronautical Labs.

NOMINALLY 2-DIMENSIONAL FLOW ABOUT A NORMAL FLAT PLATE Annual Report, 1 Oct. 1992 - 30 Sep. 1993

Derek Lisoski 1 Aug. 1993 104 p
(Contract N00014-90-J-1589)
(AD-A274472) Avail: CASI HC A06/MF A02

Towing tank and water channel experiments and a two-dimensional vortex element numerical model were used to study the forces experienced by a bluff flat plate set normal to a nominally two-dimensional flow. Intrinsic (small scale) and extrinsic (large scale) three-dimensional motions in the experimental flow were isolated and their separate and combined effects on forces and overall wake development were studied. Transient flow development starting from rest, as well as steady flow conditions, were investigated. A force balance was used to measure the unsteady lift and drag of vertically oriented models projecting through a free surface with various lower end conditions; simultaneous LIF flow visualizations imaged the structure of the vortices in the wake. Plate aspect ratio, lower end condition, and angle of attack were varied to effect changes in large scale three-dimensional motions, while changes in Reynolds number and Richardson number (flow stratification) modified the small scale three dimensionality intrinsic to the flow. DTIC

N94-27059# Texas Univ., Austin. Dept. of Mechanical Engineering.

TURBULENT BOUNDARY LAYER INNER-OUTER INTERACTIONS Final Report, 1 Aug. 1989 - 31 Dec. 1992

David Guy Bogard, Choon Lim Gan, and Atul Kohli 6 Dec. 1993 123 p
(Contract N00014-89-J-1701)
(AD-A274357) Avail: CASI HC A06/MF A02

A summary of work performed to study the interactions between the inner and outer regions of a turbulent boundary layer is presented. The interactions were studied by observing the response of the boundary layer to different perturbations. The inner region was modified by adding surface roughness, and the outer region suppressed using large eddy breakup (LEBU) devices. Velocity measurements were made with a three component LDV, a scanning LDV, and an X-type hot-film probe. The scanning LDV was developed to obtain continuous time history measurements of instantaneous velocity profiles down to $y+ = 10$. Details of the structure of bursts, sweeps, and shear layers over smooth and rough walls were determined using conditional sampling with simultaneous measurements from a detector probe and a mapping probe. This allowed the mapping of the complete three-dimensional structure of the three-component velocity field for these structures. Both single point detection, using quadrant and VITA techniques, and a unique spatially coherent structure detection technique were used. The spatial detection technique developed in this project takes advantage of the two-dimensional velocity field information obtained from the scanning LDV. DTIC

N94-27119# Air Force Inst. of Tech., Wright-Patterson AFB, OH. School of Engineering.

A PARALLEL COMPUTATIONAL FLUID DYNAMICS UNSTRUCTURED GRID GENERATOR M.S. Thesis

Deborah E. Davis Dec. 1993 86 p
(AD-A274129; AFIT/GCS/Eng/93D-05) Avail: CASI HC A05/MF A01

This research addressed the development of a parallel computational fluid dynamics unstructured grid generator using Delaunay triangulation. The generator is applied to simple elliptical and cylindrical two-dimensional bodies. The methodologies used included Watson's point insertion algorithm, Holmes and Snyder's point creation algorithm, a discretized surface definition, Anderson's clustering function, and a Laplacian smoother. The first version of the software involved a processor boundary exchange at the end of each iteration with no inter-processor communications during the iterations. The second version used inter-processor communication during each iteration instead of the boundary exchange. Version 1 demonstrated a speedup of 1.8 for some portions of the code, but proved to be unscalable for more than two nodes due to the interdependency of the triangular elements. The results of Version 2 were similar. Two distribution methodologies, a simple 360-degree distribution and recursive spectral bisection (RSB), were examined. For the initial grid distribution, the distribution generated by the RSB code would be similar to the distribution generated by the 360-degree methodology and would require significantly more time to execute. DTIC

N94-27129# Air Force Inst. of Tech., Wright-Patterson AFB, OH. School of Engineering.

EXPERIMENTAL VERIFICATION OF TOMOGRAPHIC RECONSTRUCTION OF TURBULENT AIR FLOW STRUCTURE USING OPTICAL WAVEFRONT MEASUREMENTS M.S. Thesis

Bryon L. Pedersen Dec. 1993 65 p
(AD-A274392; AFIT/GEO/Eng/93D-01) Avail: CASI HC A04/MF A01

The performance of an aircraft based optical system is degraded by aero-optic turbulence. The varying index of refraction within the turbulent field causes phase perturbation in an optical wave. In order to compensate for aero-optic turbulence effects, the nature of the turbulence must be understood. Large scale, organized structure within the turbulence has been found to contribute significantly to the overall phase perturbation caused by a turbulent field. A unique approach was devised to determine the turbulence structure using tomographic reconstruction techniques. Tomography provides an excellent means to determine the underlying structure within a turbulent field. The tomographic reconstruction produces a three-dimensional index of refraction plot of the turbulent field, revealing the structure within the turbulent field. An experiment was designed to determine the feasibility of the tomographic technique for reconstructing the turbulence structure. An optical wave was propagated through a turbulent field. A shearing interferometer was used to measure the wave front of the perturbed optical wave. The wave front phase map provided the projection data for a tomographic reconstruction of the index of refraction of the turbulent field. The experimental results verified the feasibility of the tomographic technique. DTIC

N94-27205# National Aerospace Lab., Tokyo (Japan). Computational Sciences Div.

APPROXIMATE RIEMANN SOLVERS: IMPROVEMENT OF THE HLLEM SCHEME AND ITS GENERALIZATION FOR CHEMICALLY REACTING FLOWS [KONJI RIMAN KAIHO NITSUITE: HLLEM SUKIMU NO KAIRYO TO HANNORYU ENO KAKUCHO]

Yasuhiro Wada Dec. 1992 24 p In JAPANESE
(ISSN 0389-4010)
(NAL-TR-1189; JTN-94-80616) Avail: CASI HC A03/MF A01

The characteristics of approximate Riemann solvers were investigated such as those of Osher and Roe, which are used as a 'building block' for construction of modern shock-capturing schemes. Also a new approximate Riemann solver is proposed which is the result of an improved HLLEM (Harten Lax van Leer Einfeldt Modified) scheme, satisfying the positivity and entropy condition. The data obtained indicate that this new Riemann solver can be generalized for non-equilibrium flows such as a chemically reacting high temperature one. Author (NASDA)

N94-27252 Materials Research Labs., Ascot Vale (Australia).

NUMERICAL SIMULATION OF THE REIGNITION OF DETONATION BY REFLECTED SHOCKS

D. A. Jones, E. S. Oran, and M. Sichel Dec. 1992 12 p Limited Reproducibility: More than 20% of this document may be affected by microfiche quality
(AD-A274755) Avail: CASI HC A03

We study the diffraction and decay of a detonation wave which occurs when the detonation propagates past an increase in cross-sectional area in a rectangular detonation tube. The computations solve the time-dependent two-dimensional Euler equations using an operator split Flux-Corrected Transport algorithm in an Ar diluted stoichiometric H_2/O_2 mixture. Previous studies have shown that the initial effect is the decoupling of the reaction front from the shock and the formation of a decaying blast wave or bubble in the larger tube. The detonation may then continue to decay, or be reignited by reflection of the bubble off confining surfaces. In this paper, we focus on reignition by shock reflection. DTIC

N94-27307 Waterloo Univ. (Ontario). Dept. of Mathematics.

A SECOND-ORDER SHOCK-ADAPTIVE GODUNOV SCHEME BASED ON THE GENERALIZED LAGRANGIAN FORMULATION M.S. Thesis

Claude Lepage 1993 140 p
(ISBN-0-315-84549-X; CTN-94-61073) Copyright Avail: Micromedia Ltd., Technical Information Centre, 240 Catherine Street, Suite 305, Ottawa, Ontario, K2P 2G8, Canada HC/MF

Application of the Godunov scheme to the Euler equations of gas dynamics, based on the Eulerian formulation of flow, smears discontinuities (especially sliplines) over several computational cells, while the accuracy in the smooth flow regions is of the order of a function of the cell width. Based on the generalized Lagrangian formulation (GLF), the Godunov scheme yields far superior results. By the use of coordinate streamlines in the GLF, the slipline (itself a streamline) is resolved crisply. Infinite shock resolution is achieved through the splitting of shock cells, while the accuracy in the smooth flow regions is improved using a nonconservative formulation of the governing equations coupled to a second order extension of the Godunov scheme. Furthermore, GLF requires no grid generation for boundary value problems and the simple structure of the solution to the Riemann problem in the GLF is exploited in the numerical implementation of the shock adaptive scheme. Numerical experiments reveal high efficiency and unprecedented resolution of shock and slipline discontinuities. CISTI

N94-27313 Concordia Univ., Montreal (Quebec). Dept. of Mechanical Engineering.

THEORETICAL AND EXPERIMENTAL INVESTIGATION OF CONVERGING CYLINDRICAL SHOCK WAVES PROPAGATING IN NARROW CYLINDRICAL CHAMBERS M.S. Thesis

Gley Zitouni Sep. 1992 125 p
(ISBN-0-315-84694-1; CTN-94-61088) Copyright Avail: Micromedia Ltd., Technical Information Centre, 240 Catherine Street, Suite 305, Ottawa, Ontario, K2P 2G8, Canada HC/MF

The propagation and stability of converging cylindrical shocks produced in an annular shock tube equipped with a three increment area contraction were investigated for various cylindrical chamber widths and two annular shock Mach numbers of 1.26 and 1.44. The method of characteristics, integrated using the Hartree scheme, was employed to determine the shock Mach number and pressure-time variations in the cylindrical chamber. These numerical values were verified experimentally by employing a set of piezoelectric pressure transducers placed at five different locations. In narrow cylindrical chambers, a new test section was used to determine the boundary layer effect on the shock strength. For a cylindrical chamber width of 2.5 mm, experimental results were found to be in excellent agreement with the inviscid numerical solution. For smaller widths, an empirical equation of the shock Mach number variation was developed. Stability of the converging shocks was examined from the series of spark shadowgraphs taken near the geometric center. Author (CISTI)

N94-27319# California Inst. of Tech., Pasadena. Graduate Aeronautical Labs.
RESEARCH ON BLUFF BODY VORTEX WAKES
Anatol Roshko, Anthony Leonar, and Morteza Gharib 1993 13 p
(Contract N00014-90-J-1589)
(AD-A273780) Avail: CASI HC A03/MF A01

The long-term objective is to enhance fundamental understanding of the near-wake dynamics of vortex-shedding bluff bodies and the resulting forces. It is desired to better understand the role of Reynolds number, the role of three dimensional effects, the effects of forcing and force history, and the role of body geometry. The report first summarizes the combined experimental, computational, and theoretical investigations. Results on the effects of both a steady and a periodic axial component of flow on a circular cylinder wake are then given. Derived from text

N94-27377*# Texas A&M Univ., College Station. Turbomachinery Lab.
BULK-FLOW ANALYSIS, PART A Final Report
Dara W. Childs 10 Dec. 1993 120 p
(Contract NAS8-37821)
(NASA-CR-193911-Pt-A; NAS 1.26:193911-Pt-A) Avail: CASI HC A06/MF A02

The bulk-flow analysis results for this contract are incorporated in the following publications: 'Fluid-Structure Interaction Forces at Pump-Impeller Shroud Surfaces for Axial Vibration Analysis'; 'Centrifugal Acceleration Modes for Incompressible Fluid in the Leakage Annulus Between a Shrouded Pump Impeller and Its Housing'; 'Influence of Impeller Shroud Forces on Pump Rotordynamics'; 'Pressure Oscillation in the Leakage Annulus Between a Shrouded Impeller and Its Housing Due to Impeller-Discharge-Pressure Disturbances'; and 'Compressibility Effects on Rotor Forces in the Leakage Path Between a Shrouded Pump Impeller and Its Housing'. These publications are summarized and included in this final report. Computational Fluid Mechanics (CFD) results developed by Dr. Erian Baskharone are reported separately. For individual titles, see N94-27378 through N94-27379.

N94-27378*# Texas A&M Univ., College Station. Dept. of Mechanical Engineering.
INFLUENCE OF IMPELLER SHROUD FORCES ON TURBOPUMP ROTOR DYNAMICS
J. P. Williams (Rockwell Space Operations Co., Houston, TX.) and Dara W. Childs *In its* Bulk-Flow Analysis, Part A 10 Dec. 1993 8 p Submitted for publication (For primary document see N94-27377 07-34)
Avail: CASI HC A02/MF A02

The shrouded-impeller leakage path forces calculated by Childs have been analyzed to answer two questions. First, because of certain characteristics or the results of Childs, the forces could not be modeled with traditional approaches. Therefore, an approach has been devised to include the forces in conventional rotordynamic analyses. The forces were found to be well-modeled with this approach. Finally, the effect these forces had on a simple rotor-bearing system was analyzed, and, therefore, they, in addition to seal forces, were applied to a Jeffcott rotor. The traditional methods of dynamic system analysis were modified to incorporate the impeller forces and yielded results for the eigenproblem, frequency response, critical speed, transient response, and an iterative technique for finding the frequency of free vibration as well as system stability. All results lead to the conclusion that the forces have little influence on natural frequency but can have appreciable effects on system stability. Specifically, at higher values of fluid swirl at the leakage path entrance, relative stability is reduced. The only unexpected response characteristics that occurred are attributed to the nonlinearity of the model. Author

N94-27379*# Texas A&M Univ., College Station.
COMPRESSIBILITY EFFECTS ON ROTOR FORCES IN THE LEAKAGE PATH BETWEEN A SHROUDED PUMP IMPELLER AND ITS HOUSING
Nhai The Cao *In its* Bulk-Flow Analysis, Part A 10 Dec. 1993 76 p
(For primary document see N94-27377 07-34)
Avail: CASI HC A05/MF A02

A modified approach to Childs' previous work on fluid-structure interaction forces in the leakage path between an impeller shroud and its housing is presented in this paper. Three governing equations consisting of continuity, path-momentum, and circumferential-momentum equations were developed to describe the leakage path inside a pump impeller. Radial displacement perturbations were used to solve for radial and circumferential force coefficients. In addition, impeller-discharge pressure disturbances were used to obtain pressure oscillation responses due to precessing impeller pressure wave pattern. Childs' model was modified from an incompressible model to a compressible barotropic-fluid model (the density of the working fluid is a function of the pressure and a constant temperature only). Results obtained from this model yielded interaction forces for radial and circumferential force coefficients. Radial and circumferential forces define reaction forces within the impeller leakage path. An acoustic model for the same leakage path was also developed. The convective, Coriolis, and centrifugal acceleration terms are removed from the compressible model to obtain the acoustics model. A solution due to impeller discharge pressure disturbances model was also developed for the compressible and acoustics models. The results from these modifications are used to determine what effects additional perturbation terms in the compressible model have on the acoustic model. The results show that the additional fluid mechanics terms in the compressible model cause resonances (peaks) in the force coefficient response curves. However, these peaks only occurred at high values of inlet circumferential velocity ratios greater than 0.7. The peak pressure oscillation was shown to occur at the wearing ring seal. Introduction of impeller discharge disturbances with $n = 11$ diametral nodes showed that maximum peak pressure oscillations occurred at nondimensional precession frequencies of $f = 6.4$ and $f = 7.8$ for this particular pump. Bolleter's results suggest that for peak pressure oscillations to occur at the wearing ring seal, the nondimensional excitation frequency should be on the order of $f = 2.182$ for $n = 11$. The resonances found in this research do not match the excitation frequencies predicted by Bolleter. At the predicted peak excitation frequencies given by Bolleter, the compressible model shows an attenuation of the pressure oscillations at the seal exit. The compressibility of the fluid does not have a significant influence on the model at low values of nondimensional excitation frequency. At high values of nondimensional frequency, the effects of compressibility become more significant. For the acoustic analysis, the convective, Coriolis, and centrifugal acceleration terms do affect the results to a limited extent for precession excitation and to a large extent for a pressure excitation when the fluid operates at relatively high Mach numbers. Author

N94-27435*# Institute for Computer Applications in Science and Engineering, Hampton, VA.
A RAPID-PRESSURE CORRELATION REPRESENTATION CONSISTENT WITH THE TAYLOR-PROUDMAN THEOREM MATERIALLY-FRAME-INDIFFERENT IN THE 2D LIMIT Final Report
J. R. Ristorcelli, J. L. Lumley (Cornell Univ., Ithaca, NY.), and R. Abid (High Technology Corp., Hampton, VA.) Jan. 1994 51 p Submitted for publication
(Contract NAS1-19480; RTOP 505-90-52-01)
(NASA-CR-191591; NAS 1.26:191591; ICASE-94-1) Avail: CASI HC A04/MF A01

A nonlinear representation for the rapid-pressure correlation appearing in the Reynolds stress equations, consistent with the Taylor-Proudman theorem, is presented. The representation insures that the modeled second-order equations are frame-invariant with respect to rotation when the flow is two-dimensional in planes perpendicular to the axis of rotation. The representation satisfies realizability in a new way: a special ansatz is used to obtain analytically, the values of coefficients valid away from the realizability limit: the model coefficients are functions of the state of the turbulence that are valid for all states of the mechanical turbulence attaining their constant limiting values only when the limit state is achieved. Utilization of all the mathematical constraints are not enough to specify all the coefficients in the model. The unspecified coefficients appear as free parameters which are used to insure that the representation is asymptotically consistent with the known equilibrium states of a homogeneous sheared turbulence. This is done by insuring that the modeled evolution equations have the same fixed points as those obtained from computer and laboratory experiments for the homogeneous shear. Results of computations of the homogeneous shear, with and without rotation, and with stabilizing and destabilizing curvature, are shown. Results are consistently better, in a wide class of flows which the model not been calibrated, than those obtained with other nonlinear models. Author

N94-27562# Houston Univ., TX. Dept. of Mechanical Engineering.
TRANSVERSE VORTICITY MEASUREMENTS IN THE UNIVERSITY OF HOUSTON TWO STREAM SHEAR LAYER FACILITY Final Technical Report
P. Purtell 7 Dec. 1993 2 p
(Contract N00014-93-1-0170)
(AD-A273910) Avail: CASI HC A01/MF A01

This brief report describes the goals and results from the University of Houston part of a joint investigation into transverse vorticity measurements. A yaw calibration facility was designed, built, and installed; the tunnel wall positions were adjusted to obtain a nominal zero streamwise pressure gradient condition for the mixing layer; detailed velocity traverses were conducted at the exit plane to document the initial conditions for the mixing layer at each of the flow conditions; hot-wire surveys of the time mean flow field were obtained for the fixed velocity ratio to determine the evolution of momentum thickness of the mixing layer; and software modifications were performed to obtain the voltage time series record from the vorticity probe and other related signals. Derived from text

N94-27588# Deutsche Forschungsanstalt fuer Luft- und Raumfahrt, Goettingen (Germany). Abt. Numerische Stroemungsmechanik.
DIRECT SIMULATION MONTE-CARLO OF NEAR CONTINUUM HYPERSONIC FLOW WITH CHEMICAL REACTIONS Ph.D. Thesis - Stuttgart Univ. [DIREKTES MONTE-CARLO-SIMULATIONSVERFAHREN FUER KONTINUUMSNAHE HYPERSCHALLSTROEMUNGEN MIT CHEMISCHEN REAKTIONEN]
Stefan Dietrich Jan. 1993 73 p In GERMAN Original contains color illustrations
(ISSN 0939-2963)
(DLR-FB-93-01; ETN-94-95490) Avail: CASI HC A04/MF A01

Phenomenological models for use in the 'direct simulation Monte Carlo' method are studied. Emphasis is given to the modeling of chemical reactions. The use of these models is enhanced due to new computational techniques allowing, for example, a more efficient movement of particles in structured and unstructured grids. The drag of a cylinder in the transitional regime of cold hypersonic flows is calculated, and detailed comparisons to an experiment are made. The hypersonic flow with chemical reactions past a cylinder is simulated. Available nonequilibrium Navier-Stokes results for the same flow are used for comparison. The influence of chemical reactions on the wake structure behind the cylinder is also investigated. ESA

N94-27617# Bettis Atomic Power Lab., West Mifflin, PA.
AN IMPROVEMENT IN THE MODIFIED FINITE ELEMENT PROCEDURE FOR UNDERWATER SHOCK ANALYSIS
S. K. Chan 1992 12 p Presented at the 63rd Shock and Vibration Symposium, Las Cruces, NM, 27 Oct. 1992
(Contract DE-AC11-93PN-38195)
(DE94-004451; WAPD-T-2956; CONF-9210176-6) Avail: CASI HC A03/MF A01

The modified finite element procedure for underwater shock analysis decomposes the total pressure field into the incident, reflected, and radiated pressure. The incident pressure is calculated by using a closed form solution. The reflected and radiated pressure are calculated in two separate finite element analyses. Artificial damping is added in the finite element analyses. Since these two pressures are generated from the fluid-structure interface and mostly propagate away from the interface, the artificial damping has no significant effect on the result. The modified finite element procedure was developed using a displacement formulated finite element to model the fluid region. In the paper, a pressure formulated finite element is used to model the fluid region which has a potential of saving 90 percent of the computer time. In doing so, the reflected and radiated pressure are calculated in one analysis which greatly simplifies the analysis procedure and saves more computer time. Two verification examples are given. DOE

N94-27639*# National Aeronautics and Space Administration. Marshall Space Flight Center, Huntsville, AL.
THERMOCAPILLARY FLOW WITH EVAPORATION AND CONDENSATION AND ITS EFFECT ON LIQUID RETENTION IN LOW-G FLUID ACQUISITION DEVICES Final Report
George R. Schmidt Washington Feb. 1994 268 p Sponsored by NASA, Washington
(Proj. 91-15)
(NASA-TP-3463; M-743; NAS 1.60:3463) Avail: CASI HC A12/MF A03

The steady motion, thermal and free surface behavior of a volatile, wetting liquid in microgravity are studied using scaling and numerical techniques. The objective is to determine whether the thermocapillary and two-phase convection arising from thermodynamic nonequilibrium along the porous surfaces of spacecraft liquid acquisition devices could cause the retention failures observed with liquid hydrogen and heated vapor pressurant. Why these devices seem immune to retention loss when pressurized with heated helium or heated directly through the porous structure was also examined. Results show that highly wetting fluids exhibit large negative and positive dynamic pressure gradients towards the meniscus interline when superheated and subcooled, respectively. With superheating, the pressure variation and recoil force arising from liquid/vapor phase change exert the same influence on surface morphology and promote retention. With subcooling, however, the pressure distribution produces a suction that degrades mechanical equilibrium of the surface. This result indicates that thermocapillary-induced deformation arising from subcooling and condensation is the likely cause for retention loss. In addition, increasing the level of nonequilibrium by reducing accommodation coefficient suppresses deformation and explains why this failure mode does not occur in instances of direct screen heating or pressurization with a heated inert gas. Author (revised)

N94-27705# Los Alamos National Lab., NM.
MACH REFLECTION OF SPHERICAL DETONATION WAVES
L. M. Hull 1993 9 p Presented at the 2nd Probabilistic Safety Assessment and Management Conference (PSAM), San Diego, CA, 20-24 Mar. 1994
(Contract W-7405-eng-36)
(DE93-016604; LA-UR-93-2080; CONF-940312-4) Avail: CASI HC A02/MF A01

When two detonation waves collide, the shape of the wave front at their intersection can be used to categorize the flow as regular or irregular reflection. In the case of regular reflection, the intersection of the waves forms a cusp. In the case of irregular reflection, the cusp is replaced by a leading shock locus that bridges the incident waves. Many workers have studied irregular or Mach reflection of detonation waves, but most of the their experimental work has focused on the interaction of plane detonation waves. Reflection of spherical detonation waves has received less attention. This study also differs from previous work in that the focus is to measure the relationship between the detonation velocity and the local wave curvature for irregular reflection of spherical detonation waves. Two explosives with different detonation properties, PBX 9501 and PBX 9502, are compared. DOE

N94-27709# Los Alamos National Lab., NM.
MODELLING THE MASS MIGRATION PHENOMENA IN PARTIALLY FROZEN HEAT PIPES
Michael D. Keddy, Michael A. Merrigan, and Eric Critchley (Phillips Lab., Kirtland AFB, NM.) 1993 6 p Presented at the 11th Symposium on Space Nuclear Power Systems, Albuquerque, NM, 9-13 Jan. 1994
(Contract W-7405-eng-36)
(DE94-002716; LA-UR-93-3651; CONF-940101-16) Avail: CASI HC A02/MF A01

Liquid metal heat pipes operated at power throughputs well below their design point and with sink temperatures below the freezing temperature of the working fluid may fail as a result of the working fluid migrating to a cold region within the pipe, freezing there, and not returning to the evaporator section. Eventually, sufficient working fluid inventory may be lost to the cold region to cause a local dry-out condition in the evaporator. A joint

experimental and analytical effort by the Air Force Phillips Laboratory and Los Alamos National Laboratory is underway to investigate this phenomena. This paper presents an analytical model developed to describe this phenomena. The model provides for analytic determination of heat pipe temperature profiles, freeze-front locations and mass migration rates.
DOE

N94-27782*# Arizona Univ., Tucson. Dept. of Aerospace and Mechanical Engineering.

NUMERICAL SIMULATION OF RECEPTIVITY AND TRANSITION IN A BOUNDARY LAYER ON A FLAT PLATE WITH A SUCTION HOLE Final Report

Hermann F. Fasel Mar. 1994 22 p
(Contract NCC1-1422; NAG1-1433)
(NASA-CR-195708; NAS 1.26:195708) Avail: CASI HC A03/MF A01

A Navier-Stokes solver has been modified to allow for unsteady boundary conditions to be imposed at the inflow boundary. Because the streamwise derivatives are discretized with three-point compact differences, there is no need for special treatment of the points adjacent to the inflow boundary, provided that all necessary derivatives are properly specified at the boundary points. The unsteady boundary conditions can be obtained from a previous computation, from a solution of the parabolized stability equations (PSE), or from an analytical exact or approximate solution of the Navier-Stokes equations, e.g. an asymptotic expansion solution to model a sound wave interacting with the boundary layer. Derived from text

N94-27799 National Aerospace Lab., Amsterdam (Netherlands). Informatics. Div.

TIME-STEP ENLARGEMENT AND OPTIMAL SMOOTHING IN RUNGE-KUTTA TIME-INTEGRATION ALGORITHMS BY IMPLICIT AND EXPLICIT SMOOTHING

R. C. A. Linders 26 Jun. 1992 85 p Limited Reproducibility: More than 20% of this document may be affected by microfiche quality
(NLR-TP-92221-U; ETN-94-95449; AD-B176008) Avail: CASI HC A05

Runge-Kutta (RK) time integration schemes are used in many industrial codes for the computation of steady flows, using the Euler and Navier-Stokes equations. For equations with diffusion, the maximum time step in a RK scheme is of O(h squared). A technique to enlarge the maximum time step to O(h) for diffusion convection equations is presented. This is achieved by applying an implicit smoothing operator to the residues in the RK scheme. An explicit smoothing operator, tuned to the implicit smoothing operator, is also needed, to obtain optimal high frequency damping. A four stage RK scheme is used to illustrate the technique. The ability to represent shock waves, with a four stage RK scheme with implicit and explicit smoothing, is demonstrated using the Burgers' equation. ESA

N94-27802*# Texas Univ., Austin. Dept. of Aerospace Engineering and Engineering Mechanics.

FLOWFIELD DYNAMICS IN BLUNT FIN-INDUCED SHOCK WAVE/TURBULENT BOUNDARY LAYER INTERACTIONS Final Report, 13 Mar. 1989 - 9 Nov. 1993

David S. Dolling and Leon Brusniak Jan. 1994 83 p
(Grant NAG3-1023)
(NASA-CR-195170; NAS 1.26:195170) Avail: CASI HC A05/MF A01

Fluctuating wall pressure measurements have been made on centerline upstream of a blunt fin in a Mach 5 turbulent boundary layer. By examining the ensemble averaged wall pressure distributions for different separation shock foot positions, it has been shown that local fluctuating wall pressure measurements are due to a distinct pressure distribution, Rho(sub i), which undergoes a stretching and flattening effect as its upstream boundary translates aperiodically between the upstream influence and separation lines. The locations of the maxima and minima in the wall pressure standard deviation can be accurately predicted using this distribution, providing quantitative confirmation of the model. This model also explains the observed cross-correlations and ensemble average measurements within the interaction. Using the Rho(sub i) model, wall pressure signals from under the separated flow region were used to reproduce the position-time history of the separation shock foot. Further, the negative time delay peak in the cross-correlation between the predicted and actual shock foot histories suggests that the separated region fluctuations precede shock foot motion. The unsteady behavior of the primary horseshoe vortex and its relation to the unsteady separation shock are described. Author (revised)

N94-27853 National Aerospace Lab., Amsterdam (Netherlands). Space Div.

GRAVITY DEPENDENCE OR PRESSURE DROP AND HEAT TRANSFER IN STRAIGHT TWO-PHASE HEAT TRANSPORT SYSTEM CONDENSER DUCTS

A. A. M. Delil 21 Apr. 1992 16 p Presented at the 22nd International Conference on Environmental Systems Thermal Control Technology 1 Session, Seattle, WA, 13-16 Jul. 1992 Limited Reproducibility: More than 20% of this document may be affected by microfiche quality
(NLR-TP-92167-U; ETN-94-95445) Avail: CASI HC A03

Condensers are crucial components of two phase heat transport systems envisaged for future large spacecraft. To properly design such condensers, experimental data, obtained from ground testing and reduced gravity aircraft and rocket flight testing, plus results of thermal modeling and scaling calculations, are used. A frequently reported result of such activities is that condensation lengths required in low gravity environment exceed the corresponding lengths on earth, in horizontal ducts, up to one order of magnitude and more, while the accompanying pressure drops are almost the same. Since the flow patterns are different in the two situations, it is better to theoretically, and experimentally, investigate the impact of gravity on condensation pressure drops and heat transfer for an identical flow pattern, namely annual-wavy-mist, observed along almost the entire condensation length for vapor qualities ranging from close to 1 down to values below 0.1, both in low gravity environment and in vertical downflow in a gravity field. Within the validity range of the model used the impact of gravitation on condenser pressure drop and full condensation length is shown to be manifest for two different working fluids, ammonia and R114, and various duct diameters and thermal loading conditions (the power transported, the operating and sink temperatures). ESA

N94-27867*# National Aeronautics and Space Administration. Langley Research Center, Hampton, VA.

NEW CONSTITUTIVE EQUATION FOR THE VOLUME VISCOSITY IN FLUIDS

Allan J. Zuckerwar and Robert L. Ash (Old Dominion Univ., Norfolk, VA.) Mar. 1994 21 p Prepared for presentation at the 127th Meeting of the Acoustical Society of America, Cambridge, MA, 6-10 Jun. 1994
(RTOP 505-59-54-02)
(NASA-TM-109104; NAS 1.15:109104) Avail: CASI HC A03/MF A01

The traditional volume viscosity, Stokes' hypothesis, and acoustical relaxation are reviewed. The lossy Navier-Stokes Equation is applied to periodic (acoustic) flow, and it is shown that the traditional volume viscosity leads to a result which contradicts that describing acoustical relaxation. It is demonstrated that the addition of a second volume viscosity term to the constitutive equation, to account for pressure relaxation, resolves the conflict, and leads to a direct correspondence between the volume viscosity parameters and the acoustical relaxation parameters. The representation of volume viscosity is formulated for the case of multiple relaxations, as occur in air. Finally, an application of the new constitutive equation to a simple convective compressible flow, namely a linearly accelerating flow, demonstrates the impact of volume viscosity upon the flow and the physical conditions for which it is important. Author

N94-27873 University of Western Ontario, London. Dept. of Applied Mathematics.

CIRCULAR CYLINDER IN AXIAL FLOW Ph.D. Thesis

Stephen P. Sawchuk Aug. 1990 280 p
(ISBN-0-315-59114-5; CTN-94-60993) Copyright Avail: Micromedia Ltd., Technical Information Centre, 240 Catherine Street, Suite 305, Ottawa, Ontario, K2P 2G8, Canada HC/MF

The boundary layer formed on the outer surface of a semi-infinite cylinder in steady axial incompressible flow is studied. Governing equations are solved using local similarity techniques and a nonsimilar numerical approach. Two similarity transformations can be used to obtain solutions. In the extreme case when the cylinder radius is much larger than the boundary layer thickness, only one of the transformations leads to the correct solution, the Blasius solution. The other transformation yields an axial velocity profile deceptively close to the Blasius. Solutions obtained by either transformation merge at downstream locations. An overall numerical solution is obtained by applying Keller's box method with primitive variables and similarity coordinates. Similarity coordinates scale the axial and radial coordinates such that the boundary layer growth does not appear explicitly as one moves downstream. Thus, the numerical mesh does not need to be enlarged and this leads to increased computational efficiency. Results are obtained in the range that starts with the Blasius solution and proceed far downstream. A local similarity method is also applied to obtain solutions valid over a wide range of flow. Results obtained by these methods compare well with previously obtained solutions but extend the range of solution considerably. Author (CISTI)

N94-27880 Toronto Univ. (Ontario). Inst. for Aerospace Studies.
TVD FLUX-DIFFERENCE SPLIT METHODS FOR HIGH-SPEED THERMOCHEMICAL NONEQUILIBRIUM FLOWS WITH STRONG SHOCKS
Clinton P. T. Groth Dec. 1993 250 p
(ISSN 0082-5255)
(UTIAS-350) Copyright Avail: Issuing Activity

This study is concerned with the numerical solution of high-speed nonequilibrium gaseous flows with strong shocks. The extension of modern total-variation-diminishing (TVD) shock-capturing schemes to include thermochemical nonequilibrium high-temperature effects is of primary interest. Partially decoupled upwind-based TVD flux-difference split schemes for the solution of the conservation laws governing two-dimensional nonequilibrium vibrationally relaxing and chemically reacting flows of thermally-perfect gaseous mixtures are presented. Both time-split semi-implicit and factored implicit flux-limited TVD upwind schemes are described. The semi-implicit formulation is more appropriate for unsteady applications whereas the factored implicit form is useful for obtaining steady-state solutions. As well, a multigrid version of the fully implicit TVD scheme is also proposed for the more efficient computation of time-invariant solutions. The multigrid algorithm is based on the full approximation storage (FAS) and full multigrid (FMG) concepts and employs the partially-decoupled factored implicit scheme as the smoothing operator in conjunction with a four-level V-cycle coarsegrid-correction procedure. In the proposed methods, a novel partially-decoupled flux-difference splitting approach is adopted. The fluid conservation laws and the finite-rate species concentration and vibrational energy equations are decoupled by means of a frozen flow approximation. The resulting partially-decoupled gas dynamic and thermodynamic subsystems are then integrated alternately in lagged manner within a two-stage time marching procedure, thereby providing explicit coupling between the two equations sets. Extensions of Roe's approximate Riemann solvers, giving the eigenvalues and eigenvectors of the fully coupled systems, are used to evaluate the numerical flux functions. Additional modifications to the Riemann solutions are also described which ensure that the approximate solutions are not aphysical. Moreover, concerns associated with the satisfaction of monotonicity, positivity, and maximum principles are addressed. The proposed partially-decoupled methods are shown to have some computational advantages over chemistry-split and fully coupled techniques in coping with large systems of equations with stiff source terms. The predictive capabilities of the shock-capturing methods are demonstrated and their usefulness appraised, by solving a number of different flows with both complicated shock structure and complex nonlinear wave interactions. The problems considered include nonstationary oblique shock-wave reflections and diffractions and steady high-speed nozzle, compression ramp, and blunt-body flows. The numerical results are compared to available experimental data in many cases. Author

N94-27931*# Alabama Univ., Huntsville. Mechanical and Aerospace Engineering.
SUPERFLUID HELIUM SLOSHING DYNAMICS INDUCED OSCILLATIONS AND FLUCTUATIONS OF ANGULAR MOMENTUM, FORCE AND MOMENT ACTUATED ON SPACECRAFT DRIVEN BY GRAVITY GRADIENT OR JITTER ACCELERATION ASSOCIATED WITH SLEW MOTION Final Report
R. J. Hung Feb. 1994 106 p
(Contract NAS8-38609)
(NASA-CR-193928; NAS 1.26:193928) Avail: CASI HC A06/MF A02

The generalized mathematical formulation of sloshing dynamics for partially filled liquid of cryogenic superfluid helium II in dewar containers driven by the gravity gradient and jitter accelerations associated with slew motion for the purpose to perform scientific observation during the normal spacecraft operation are investigated. An example is given with the Advanced X-Ray Astrophysics Facility-Spectroscopy (AXAF-S) for slew motion which is responsible for the sloshing dynamics. The jitter accelerations include slew motion, spinning motion, atmospheric drag on the spacecraft, spacecraft attitude motions arising from machinery vibrations, thruster firing, pointing control of spacecraft, crew motion, etc. Explicit mathematical expressions to cover these forces acting on the spacecraft fluid systems are derived. The numerical computation of sloshing dynamics is based on the non-inertia frame spacecraft bound coordinate, and solve time-dependent, three-dimensional formulations of partial differential equations subject to initial and boundary conditions. The explicit mathematical expressions of boundary conditions to cover capillary force effect on the liquid-vapor interface in microgravity environments are also derived. The formulations of fluid moment and angular moment fluctuations in fluid profiles induced by the sloshing dynamics, together with fluid stress and moment fluctuations exerted on the spacecraft dewar containers have also been derived. Examples are also given for cases applicable to the AXAF-S spacecraft sloshing dynamics associated with slew motion. Author

N94-27947 Queens Univ., Kingston (Ontario). Dept. of Mechanical Engineering.
THE NUMERICAL CALCULATION OF LAMINAR AND TURBULENT FLOWS USING PENALTY FUNCTION FINITE VOLUME METHODS Ph.D. Thesis
Jacques Simoneau Oct. 1990 279 p
(ISBN-0-315-61377-7; CTN-94-61001) Copyright Avail: Micromedia Ltd., Technical Information Centre, 240 Catherine Street, Suite 305, Ottawa, Ontario, K2P 2G8, Canada HC/MF

Two new algorithms are presented for calculating both laminar and turbulent flows. These algorithms are developed using finite volume methods but achieve pressure velocity coupling via penalty function methods. First, a sequential approach is introduced, where the penalized momentum equations are solved in a segregated manner. Various formulations for the coefficient and source terms are tested and the best one is identified. Second, a coupled approach is derived in which all momentum equations are solved simultaneously. Various solvers are tested and an efficient algorithm is identified. Preliminary tests reveal that the penalty approach is robust and requires no under relaxation of the momentum equations. The velocity and pressure fields do not suffer from modification of the continuity equation, and results are as accurate as those obtained using SIMPLE type algorithms. The sequential method is found to be slow but, when an appropriate solver is used, the coupled approach is faster than SIMPLE type algorithms. The coupled algorithm is fully tested, and its performance is compared with the SIMPLEC algorithm for four two-dimensional laminar and turbulent flows. The coupled method is, on average, about twice as fast as SIMPLEC. Author (CISTI)

N94-28003# Advisory Group for Aerospace Research and Development, Neuilly-Sur-Seine (France). Fluid Dynamics Panel.
COMPUTATIONAL AND EXPERIMENTAL ASSESSMENT OF JETS IN CROSS FLOW [EVALUATION NUMERIQUE ET EXPERIMENTALE DES JETS DANS DES COURANTS TRANSVERSAUX]
Nov. 1993 479 p In ENGLISH and FRENCH Symposium held in Winchester, England, 19-22 Apr. 1993 Original contains color illustrations
(AGARD-CP-534; ISBN-92-835-0720-7) Copyright Avail: CASI HC A21/MF A04

The 37 papers prepared for the AGARD Fluid Dynamics Panel (FDP) Symposium on Computational and Experimental Assessment of Jets in Cross Flow are included. The primary objective of the Symposium was to provide a forum for assessing advances made in the technology and application of jets in cross flow which have occurred since the last meeting on this subject. Major topics covered included enhanced descriptions of the fundamental flow structure of jets in cross flow, experimental methods, thrust vectoring, jet impingement and exhaust gas reingestion, hypersonic crossflow, and numerics and turbulence modeling. For individual titles, see N94-28004 through N94-28040.

N94-28004*# National Aeronautics and Space Administration. Ames Research Center, Moffett Field, CA.
FIFTY YEARS OF JET IN CROSS FLOW RESEARCH
Richard J. Margason *In* AGARD, Computational and Experimental Assessment of Jets in Cross Flow Nov. 1993 41 p (For primary document see N94-28003 07-34)
Copyright Avail: CASI HC A03/MF A04

The jet in cross flow (JICF) is a basic flowfield which is relevant to a wide variety of applications which are described to provide context for JICF investigations. Material consistent with the scope of topics presented at the 72nd AGARD Fluid Dynamics Panel Meeting and Symposium on Computational and Experimental Assessment of Jets in Cross Flow on 19-22 April 1993 in Winchester, U.K. is summarized. The JICF research was divided into three time periods: (1) early research - up to 1970, (2) research during the 1970's, and (3) research since 1980. The following areas of experimental activity are discussed; the definition of an effective correlation parameter; the jet flowfield including the jet trajectories, cross-section shape, and jet induced pressures; the effects of jet deflection angle, nozzle shape, pressure ratio, velocity decay, and temperature; and the effect of confined flowfield, ground effects, multiple jets, and adjacent surface geometry. In addition, computational methods are discussed including both potential flow based methods, some with empirical and semi-analytical extensions, and Navier-Stokes based computational fluid dynamics (CFD) investigations. Currently modern CFD methods have been able to compute many of the mean flow characteristics of the JICF. Existing CFD methods have not resolved the separated flow region in the near wake of the jet exit. There is also a need for high quality, extensive experimental data which will enable the verification of current and future CFD results and to define unsteady flow characteristics. Author (revised)

N94-28005# Southampton Univ. (England). Dept. of Aeronautics and Astronautics.

TRANSIENT FLOW FEATURES OF A SUPERSONIC JET IN A LOW SPEED CROSS FLOW

X. Zhang (City Univ., London, England.), D. W. Hurst, and G. M. Lilley *In* AGARD, Computational and Experimental Assessment of Jets in Cross Flow Nov. 1993 16 p (For primary document see N94-28003 07-34)

(Contract D/ERI/9/4/2040/4)

Copyright Avail: CASI HC A03/MF A04

The transient features of a supersonic jet exhausting into a low speed cross flow were studied experimentally. The experiments were conducted in the Southampton University's 3.5 m x 2.6 m low speed wind tunnel. Three supersonic jets at ambient temperatures were used, one being a convergent nozzle and the other two being convergent-divergent nozzles having respectively design Mach numbers, M(sub d) = 1.4 and 1.7. Each jet issued in the normal direction to a flat plate mounted at zero incidence in the center of the wind tunnel. The jet pressure ratio varied between 1.2 and 5.0 and the cross flow velocity between 14m/s and 38m/s. Both over-expanded and under-expanded jets were used. The low speed cross flow was found to introduce complex multiple narrow band tones. Changes in the transient flow modes and the levels of the tones were observed from time resolved pressure measurements at various positions on the flat plate. Author (revised)

N94-28006# Commonwealth Scientific and Industrial Research Organization, Highett (Australia). Div. of Building, Construction and Engineering.

UNSTEADY WAKE STRUCTURES IN TRANSVERSE JETS

R. M. Kelso, C. Delo (Princeton Univ., NJ.), and A. J. Smits (Princeton Univ., NJ.) *In* AGARD, Computational and Experimental Assessment of Jets in Cross Flow Nov. 1993 8 p Sponsored in part by Fannie and John Hertz Foundation and NSF (For primary document see N94-28003 07-34)

Copyright Avail: CASI HC A02/MF A04

The unsteady vortex structures in the wake of a transverse jet were studied using a new laser scanning apparatus to obtain three-dimensional images of fluorescent dyes in a water channel flow. By scanning the laser at high repetition rates and by using a high-speed video camera to record the images, the three-dimensional, time-evolving concentration field in the wake can be obtained and later reconstructed. Using this system, the separation and roll-up of the flat plate boundary layer and the subsequent convection of that vorticity away from the wall can be visualized. The relationship between the separation and roll-up on the other side of the wake can also be studied. On the basis of the reconstructed concentration fields, an attempt is made to describe the mechanisms of wake vortex formation and explain the results of some previous authors. Author

N94-28007*# Florida Agricultural and Mechanical Univ., Tallahassee. Dept. of Mechanical Engineering.

SEPARATED FLOW GENERATED BY A VECTORED JET IN A CROSSFLOW

A. Krothapalli and C. Shih *In* AGARD, Computational and Experimental Assessment of Jets in Cross Flow Nov. 1993 7 p Sponsored by NASA. Ames Research Center Prepared in cooperation with Florida State Univ., Tallahassee (For primary document see N94-28003 07-34)

Copyright Avail: CASI HC A02/MF A04

Results of an experimental investigation to determine the characteristics of the separated flow region generated by a subsonic vectored rectangular jet in a subsonic crossflow is presented. Using surface visualization techniques, it was found that the upstream separated flow consist of horseshoe vortices that are formed periodically with a frequency corresponding to that of the vortex shedding behind the jet. The size of the recirculation region around the jet is found to decrease with increasing jet vector angle. The variation of the mean primary separation distance upstream of the jet, with velocity ratio revealed the existence of two different flow regimes. The change from one to the other depends on the velocity ratio and the jet vector angle. It is shown that the Strouhal number, based on the vortex shedding frequency and a combination of jet exit and freestream velocities, varies uniquely with velocity ratio. Author

N94-28008# Stanford Univ., CA. High Temperature Gasdynamics Lab.

SCALAR MIXING IN THE SUBSONIC JET IN CROSSFLOW

S. H. Smith, A. Lozano, M. G. Mungal, and R. K. Hanson *In* AGARD, Computational and Experimental Assessment of Jets in Cross Flow Nov. 1993 13 p Sponsored by AFOSR (For primary document see N94-28003 07-34)

Copyright Avail: CASI HC A03/MF A04

Results are presented on the structure and mixing of subsonic jets in crossflow. These results are obtained by using planar laser-induced fluorescence of acetone vapor which is carried as a marker of the jet fluid. In addition to providing instantaneous realizations of the jet structure, the data is quantitative in providing instantaneous measures of the jet mixture fraction. Jet to crossflow velocity ratios ranging from 6 to 14, corresponding to momentum ratios of 36 to 196 were examined. It is found that the instantaneous structure is quite complex, dominated by large-scale motions, and bear little resemblance to ensemble-averaged field. Jet fluid is seen in the wake structure in the curved portion of the jet, even though the amounts are small. Mean and rms concentration fluctuations are presented for select cases. Author (revised)

N94-28009# Surrey Univ., Guildford (England). Fluid Mechanics Research Group.

THE INTERACTION REGION ASSOCIATED WITH TWIN JETS AND A NORMAL CROSSFLOW

N. Toy, E. Savory, S. McCusker, and P. J. Disimile (Cincinnati Univ., OH.) *In* AGARD, Computational and Experimental Assessment of Jets in Cross Flow Nov. 1993 11 p (For primary document see N94-28003 07-34)

Copyright Avail: CASI HC A03/MF A04

An experimental investigation of the interaction between twin jets and a normal crossflow using real-time, quantitative, video image analysis of smoke-seeded jets to yield information concerning overall jet growth rates, the widths of the interface regions, intermittencies, p.d.f.s, and spectra of the interface fluctuations is presented. The cases covered are side-by-side and in-line jets, with a nozzle spacing of 5 nozzle exit diameters and a jet velocity/crossflow velocity ratio of 8, together with the single jet cases. Additional data, in the form of velocity vector distributions from five-hole pressure probe measurements, were obtained for comparison with the intermittency profiles in planes across the jets for the case of side-by-side jets with a nozzle spacing of 5 diameters and a ratio of 6. Finally, a parametric study of the effect on the overall jet penetration of velocity ratio (from 4 to 10), nozzle spacing (from 1 to 5 diameters) and nozzle orientation to the crossflow (from in-line to side-by-side, but with normal injection angle) was carried out using a new digital image processing system. The velocity data for the side-by-side case shows that the deflected jets are dominated by one single vortex pair such that the inner vortex of each jet pair are not evident. The video analysis of the three main configurations, side-by-side, in-line and single jet, shows that in all cases the width of the mixing region at any downstream location is similar in

magnitude to the jet half-width (as defined by the mean interface location). The interface widths are similar for the side-by-side and in-line jets but these are greater than the single jet for the intermittency distributions across the interface regions which will enable correlation between the different jet configurations. The parametric study shows that, for a given jet ratio, the in-line jets (0 deg angle) penetrate further than those set at other angles to the crossflow and that changes of angle between 30 deg and 60 deg have less effect upon the overall penetration. For the in-line case it is the second jet, issuing into the lower static pressure region downstream of the first jet, that penetrates furthest into the crossflow.
Author

N94-28010# Loughborough Univ. of Technology (England). Dept. of Transport Technology.

EXPERIMENTAL DATA FOR CFD VALIDATION OF IMPINGING JETS IN CROSSFLOW WITH APPLICATION TO ASTOVL FLOW PROBLEMS

P. Behrouzi and J. J. McGuirk *In* AGARD, Computational and Experimental Assessment of Jets in Cross Flow Nov. 1993 11 p Sponsored by British Aerospace Public Ltd. Co. (For primary document see N94-28003 07-34)

Copyright Avail: CASI HC A03/MF A04

An experimental facility, used to gather validation data suitable for testing CFD model predictions of multijet ground impingement flows, is described. Water is used as the working medium and LDV measurements of twin impinging jets are reported, both with and without a cross-flowing stream. Emphasis is placed on the presentation of mean and rms velocity contours in the foundation formation region between the jets. The effect of jet splay angle has also been studied. For zero splay or 10 deg of splay-out, the fountain is observed to develop as an upwash flow spatially separated from the two jet flows (jet spacing at six jet diameters); for 10 deg splay-in, a noticeable fountain/jet interaction is observed. Splay-out reduces the strength of the fountain by around 50 percent whereas splay-in has an opposite, strengthening effect for the seven jet diameter impingement height studied here. The effect of a cross-flow (jet/cross-flow velocity ratio of 10) leads to a clear downwind shift of the fountain origin and inclination of the fountain rise. The results presented offer a sufficiently comprehensive mapping of the mean velocity and turbulence fields to form suitable test cases for the validation of CFD models for ground effect flows.
Author (revised)

N94-28011# Von Karman Inst. for Fluid Dynamics, Rhode-Saint-Genese (Belgium).

EXPERIMENTAL INVESTIGATION OF THE INTERACTION OF A THRUST REVERSER JET WITH AN EXTERNAL SUBSONIC FLOW

J.-M. Charbonnier, K. Deckers, and G. Wens *In* AGARD, Computational and Experimental Assessment of Jets in Cross Flow Nov. 1993 10 p (For primary document see N94-28003 07-34)

Copyright Avail: CASI HC A02/MF A04

An experimental modelization of a door-type thrust reverser is conducted in a subsonic wind tunnel. The geometry of the model is defined in order to simulate both the internal and external flow of a real thrust reverser. Different door configurations are studied for a selected value of the mass flux injection ratio of three. Visualizations illustrate qualitatively the jet interaction, and extensive mean velocity and pressure measurements are conducted in sections perpendicular to the upstream flow direction with a five hole probe. The total pressure losses and the drag force produced by the thrust reverser are deduced from the measurements. As a result, it shows that the smaller opening angle of the door (56 deg), with a becquet deflection of 15 deg gives the larger drag force. In addition to the classical pair of counter rotating vortices observed in jet in cross flow interactions, a second pair of counter rotating vortices below the main pair is found. The vorticity field is described with good agreement by a simple vortex model simulating the two pairs of vortices. Author (revised)

N94-28012# Nangia Associates, Bristol (England).

VECTORED JETS-INDUCED INTERFERENCE ON AIRCRAFT, PREDICTION AND VERIFICATION

R. K. Nangia *In* AGARD, Computational and Experimental Assessment of Jets in Cross Flow Nov. 1993 14 p Sponsored by Defence Research Agency (For primary document see N94-28003 07-34)

Copyright Avail: CASI HC A03/MF A04

The prediction of vectored jet-induced effects on V/STOL configurations during transition phase and maneuvers constitutes an important aspect in the understanding, design, control, and operation of such aircraft. In this paper, a semiempirical modelling of the jet is used within the framework of subsonic singularity methods. Comparisons with experimental data on a wing-body configuration have been presented. In general, acceptable agreement has been demonstrated. Overall, the emphasis has been on predicting jet interference effects on practical configurations with multijet effects and forward and aft nozzles. Configuration effects include tails which operate in a much stronger jet downwash than the wing. Optimization studies can be enabled prior to experimental programs. This process will allow the design cycle to commence with a good idea of the relative effectiveness of the various controls and the changes needed in the flight control system to cope with partially jet-borne phases of flight. Therefore there is a significant potential for encouraging cost and time savings. Areas for further work and improvements of the model have been proposed. It is believed that these aspects will have a constructive impact on current and future practical VSTOL and ASTOVL developments. Author (revised)

N94-28013# Deutsche Aerospace A.G., Munich (Germany). Military Aircraft.

NUMERICAL INVESTIGATION OF THRUST VECTORING BY INJECTION OF SECONDARY AIR INTO NOZZLE FLOWS

T. Berens *In* AGARD, Computational and Experimental Assessment of Jets in Cross Flow Nov. 1993 15 p Sponsored by DGLR (For primary document see N94-28003 07-34)

Copyright Avail: CASI HC A03/MF A04

Injection of secondary air into nozzle flows is an efficient method to control the thrust vector angle of an aircraft. A numerical investigation of thrust vectoring has been carried out for hypersonic aircraft in the transonic flight regime. In this speed range, single duct asymmetrical single expansion ramp nozzles operate far off design due to large nozzle exit areas required for optimal thrust coefficients at hypersonic cruise Mach numbers, thus producing large thrust components in the downward direction. Injecting secondary air into the nozzle flow in the critical transonic flight Mach number regime can lead to favorable gross thrust vector angles and thus improved thrust efficiency in flight direction. For a hypersonic aircraft's rectangular convergent-divergent nozzle configuration with a single expansion ramp, two dimensional Euler calculations of the complete afterbody flow field were carried out in the transonic flight regime, investigating subsonic as well as supersonic injection of the aircraft's forebody boundary layer air into the nozzle flow. Subsonic flow of the injected air along the expansion ramp produces a favorable pressure distribution on the ramp and results in advantageous thrust vectors with small force components normal to the flight direction and in best thrust efficiency. The interaction between the external flow, the jet plume flow, and the secondary air flow, as well as the behavior of the thrust vector, due to pressure and temperature variations of the injected forebody boundary layer air, are discussed. Also investigated was the impact of the aircraft's angle of attack on the complete nozzle flow field.
Author (revised)

N94-28014# Melbourne Univ., Parkville (Australia). Dept. of Mechanical and Manufacturing Engineering.

TOPOLOGICAL STRUCTURE OF A JET IN A CROSS FLOW

A. E. Perry, R. M. Kelso, and T. T. Lim *In* AGARD, Computational and Experimental Assessment of Jets in Cross Flow Nov. 1993 8 p Sponsored by Australian Research Council Original contains color illustrations (For primary document see N94-28003 07-34)

Copyright Avail: CASI HC A02/MF A04

Experimental studies of round jets in cross flow have been made using flying hot-wire and flow visualization techniques. The velocity ratio of the flow ranged from about two to six with the Reynolds number up to 6200. The flying hot wire enables time- and phase-averaged measurements to be made in regions of the flow which cannot be measured accurately using stationary wires. These quantitative results together with the complementary flow visualization studies have allowed the mean topological features of the jet in cross flow to be identified using critical point theory. An understanding of these flow features may provide insight into the large-scale mixing processes which occur in the shear layer of the jet.
Author (revised)

N94-28015# Stanford Univ., CA. Environmental Fluid Mechanics Lab.
AN EXPERIMENTAL STUDY OF SIPHONAL JETS IN A TURBULENT BOUNDARY LAYER CROSSFLOW
C. A. ORiordan, S. G. Monismith, and J. R. Koseff *In* AGARD, Computational and Experimental Assessment of Jets in Cross Flow Nov. 1993 11 p Sponsored by NSF and Charles Lee Powell Foundation (For primary document see N94-28003 07-34)
Copyright Avail: CASI HC A03/MF A04

Experiments were conducted in a laboratory flume to study the interaction of bivalve siphonal jets with the turbulent boundary layer which forms in the benthic region of shallow estuaries. Beds of siphonate bivalves (clams) 1.8 meters long were simulated to study the formation of a phytoplankton-depleted layer (concentration boundary layer) over bivalves. Refiltration of excurrent fluid through incurrent siphons, which represents a decrease in aggregate feeding efficiency, was measured for two test beds with S/d(sub o) = 6 and 16 and siphon pairs oriented perpendicular to the cross flow direction. Results are expressed as a function of the nondimensional distance downstream, x/d(sub o), the velocity ratio, VR=u(sub j)/U(sub infinity), and the nondimensional animal spacing, S/d(sub o). Laser induced fluorescence was used to obtain quantitative concentration profiles in order to describe the evolution of the flow and to identify parameters that describe the jet/boundary layer interaction.
Author (revised)

N94-28016*# Wright Lab., Wright-Patterson AFB, OH.
EXPERIMENTS ON THE GROUND VORTEX FORMED BY AN IMPINGING JET IN CROSS FLOW
William B. Blake and Vearl R. Stewart (KSA Technology, Columbus, OH.) *In* AGARD, Computational and Experimental Assessment of Jets in Cross Flow Nov. 1993 13 p Sponsored by NASA. Langley Research Center and KSA Technology (For primary document see N94-28003 07-34)
(Contract F33615-89-C-3611)
Copyright Avail: CASI HC A03/MF A04

An inclined jet impinging on the ground creates a wall flow that spreads radially from the point of impingement. If a cross-flow is introduced, the upstream component of the wall flow will separate from the ground and create what has been termed the 'ground vortex.' The ground vortex has been shown to have a significant impact on aircraft aerodynamics and is one of the major contributors to hot gas ingestion. The paper discusses a recent study which included a generic wing-body configuration for assessing the impact of the ground vortex on configuration aerodynamics. Wind tunnel tests using fixed ground boards, moving ground belts, and moving model tests are discussed. The emphasis of the data is macroscopic, i.e. forward location of the vortex, effects of ground height, etc. Author (revised)

N94-28017# British Aerospace Defense Ltd., Farnborough (England).
EXPERIMENTS INTO THE SCALING PARAMETERS REQUIRED FOR EXHAUST GAS INGESTION TESTING OF VERTICAL LANDING AIRCRAFT c05
P. Curtis and P. J. Bradley *In* AGARD, Computational and Experimental Assessment of Jets in Cross Flow Nov. 1993 9 p (For primary document see N94-28003 07-34)
Copyright Avail: CASI HC A02/MF A04

The phenomenon of Hot Gas Recirculation for vertical landing jet aircraft and the effect of exhaust gas ingestion on aircraft performance is described. Additionally, our experience with experimental modelling of HGR for aircraft configurations and the scaling of the important parameters is presented. The conflict between scaling the buoyancy of the flowfield and correct modelling of the pressure field is explored, and a number of fundamental experiments addressing this problem are related. It is shown that in the region close to the jets and when the aircraft is very close to the ground that there are quite large differences between the two scaling criteria; the near-field region requires full scale pressures for accurate representation. Away from this region, the Nozzle Pressure Ratio does not greatly affect the flowfield. Testing of a generic aircraft model with a number of different configurations shows that once near-field flowpaths have been eliminated the ingestion levels are underpredicted if the flow-field buoyancy is below full scale. Absolute levels of ingestion are not greatly different between the two scaling criteria, particularly with the large scatter in results which is endemic to the phenomenon. However, it is concluded that for practical configurations, i.e., those with low levels of ingestion, scaling of flowfield buoyancy is more correct than scaling of the pressure field. This method of scaling is appropriate for use in achieving a low ingestion configuration. Author (revised)

N94-28018# Rolls-Royce Ltd., Bristol (England). Powerplant Technology.
INFLUENCE OF HEADWIND ON HOT GAS REINGESTION AND CONSIDERATION OF PRESSURE RATIO SCALING c07
C. J. Penrose *In* AGARD, Computational and Experimental Assessment of Jets in Cross Flow Nov. 1993 9 p (For primary document see N94-28003 07-34)
Copyright Avail: CASI HC A02/MF A04

A major concern affecting the operation of Advanced Short Take-Off and Vertical Landing (ASTOVL) aircraft close to the ground is ingestion by the aircraft intakes of engine hot exhaust gas. This hot gas reingestion (HGR) can produce loss of engine thrust and erode engine stability margins. A prime source of HGR is the flow occupying the region in the 'near' and 'mid' fields around the aircraft. The 'near-field' flow can be controlled by aircraft-mounted anti-HGR devices but these are likely to be less effective in containing the mid-field flow which is greatly influenced by headwind. Near and mid-field ingestion on Harrier-type configurations has, for many years, been studied by means of model-scale experiments. In most cases in the United Kingdom, the experiments have been set up observing scaling procedures which include consideration of the buoyant action of the hot gas and imply tests at low jet velocities with dynamic head similarity maintained. It can be argued that low velocities may not be appropriate for currently-conceived ASTOVL aircraft employing high pressure-ratio supersonic exhausts, and it may be more appropriate to test at full-scale nozzle pressure ratios. This paper reviews the effects of headwind on HGR for Harrier-type configurations during landing maneuvers with tests carried out both at low jet velocities consistent with buoyancy scaling (NPR(sub F) = 1. 07) and at velocities representative of full-scale nozzle pressure ratios (NPR(sub f) = 2.46). The HGR results are examined in relation to expectations of the forward-flowing gas cloud height and penetration distance for the engine exhaust streams while under the influence of headwinds. Author (revised)

N94-28019# Rolls-Royce Ltd., Bristol (England). Powerplant Technology.
UNSTEADY ASPECTS OF HOT GAS REINGESTION AND STATISTICAL ANALYSIS c07
R. Beasley *In* AGARD, Computational and Experimental Assessment of Jets in Cross Flow Nov. 1993 6 p (For primary document see N94-28003 07-34)
Copyright Avail: CASI HC A02/MF A04

The ingestion of engine exhaust gases into an aircraft intake during jet-lift Advanced Short Take-off and Vertical Lift (ASTOVL) aircraft operation close to the ground is an area of considerable concern and has been the subject of much experimental study. The recirculatory flows follow complex paths which are strongly influenced by interference with the ground, aircraft structures, adjacent jet streams, and by the action of an oncoming headwind. The flows are turbulent at a large scale and unsteady with 'streaks' of hot gas entering the intake in a random manner. This Hot Gas Reingestion (HGR) can erode engine stability margins in a region of aircraft operation where reliable engine performance is critical. To ensure engine stability, sophisticated analysis techniques are required to enable prediction of worst-case destabilizing temperature distortion levels for chosen aircraft/engine combination. This paper describes the development and application of statistical analysis techniques designed to examine results of model experiments. These techniques enable quantitative conclusions to be reached as an extension to qualitative examination of trends from observed data. Due to the nature of the flow and distortion parameter, observed HGR data distributions are frequently not normal (Gaussian), and standard statistical techniques cannot be used. Author (revised)

N94-28020# Laboratoire d'Aerothermique du CNRS, Meudon (France).
CONTROL JETS IN INTERACTION WITH HYPERSONIC RAREFIED FLOW [JETS TRANSVERSAUX EN INTERACTION AVEC DES ECOULEMENTS HYPERSONIQUES RAREFIES] c18
J. Allegre and M. Raffin *In* AGARD, Computational and Experimental Assessment of Jets in Cross Flow Nov. 1993 9 p In FRENCH

Sponsored by ESA (For primary document see N94-28003 07-34)
Copyright Avail: CASI HC A02/MF A04

Control jets are used on space vehicles in order to replace or complement mechanical aerodynamic controls at high altitudes. As a matter of fact, the efficiency of mechanical controls decreases drastically with higher rarefaction levels of external flow. Control jets were experimentally investigated in wind-tunnels. The jets interact with external hypersonic rarefied flows. Jet efficiency and associated interaction mechanisms were analyzed for two types of configurations. The first configuration is a delta wing with transverse control jets issuing from sonic nozzles located close to the trailing edge. Tests are performed with an external hypersonic air flow characterized by a Mach number of about 8, a Reynolds number of 11,000, and a rarefaction parameter V = 0.077. The second configuration is a corner flow interacting with a transverse jet issuing from one hypersonic nozzle. This nozzle is inserted in one of the two walls which make up the corner model. Tests are made under external hypersonic nitrogen flows characterized by a Mach number of about 20 and dynamic pressures ranging from 20 Pa to 620 Pa covering rarefaction levels associated with reentry conditions. Author (revised)

N94-28021# Southampton Univ. (England). Dept. of Aeronautics and Astronautics.

COMPARISON OF THE INTERACTIONS OF TWO AND THREE DIMENSIONAL TRANSVERSE JETS WITH A HYPERSONIC FREE STREAM c02

H. E. G. Powrie, G. J. Ball, and R. A. East *In* AGARD, Computational and Experimental Assessment of Jets in Cross Flow Nov. 1993 8 p Sponsored by Defence Research Agency (For primary document see N94-28003 07-34)
Copyright Avail: CASI HC A02/MF A04

The interaction between a three dimensional (circular) sonic jet and a Mach 6.69 cross flow on a flat plate has been investigated experimentally. The results are compared with data from a two dimensional (slot) sonic jet in the same flow. In both cases the undisturbed flow on the plate is laminar. Heat transfer and oil flow visualization have been used to identify separation and reattachment within the flow field which, for the case of circular injection, has revealed a number of vortex cells in the region ahead of the jet. For the two dimensional interaction there is only evidence of one vortex pair in this region; however, a complex flow downstream of the slot jet has been observed. The influence of injectant gas type on the two dimensional interaction flow field is limited to a weak molecular weight dependence implied by separation length data. In contrast, for three dimensional injection, jet gas composition is found to have a marked effect on the size of the interaction flow field, as well as influencing surface heat transfer rate in the vicinity of the injector. Author (revised)

N94-28022# Institut Franco-Allemand de Recherches, Saint-Louis (France).

EXPERIMENTS ON INTERACTION FORCE OF JETS IN HYPERVELOCITY CROSS-FLOW IN A SHOCK TUNNEL c02

K. W. Naumann, H. Ende, G. Mathieu, and A. George *In* AGARD, Computational and Experimental Assessment of Jets in Cross Flow Nov. 1993 12 p (For primary document see N94-28003 07-34)
Copyright Avail: CASI HC A03/MF A04

This paper discusses experiments on side-jet control efficiency in the hypervelocity flow of a shock tunnel. The parameters of the test flow represent the Mach number, Reynolds number, velocity, and density of tropospheric hypervelocity flight. The experiments are carried out with a model, which is equipped with pyrotechnical charges, a settling chamber, laterally blowing jets, and a set of small accelerometers. The pyrotechnically supplied side-jets also are roughly adequate to those used in sound vehicles. Extensive jet gas diagnostics yield the parameters of the gas and the nozzle flow. The accelerometers incorporated in the model allow direct millisecond aerodynamic force measurement. To provide free-flight during the testing time, a fast-acting mounting support releases the model and grips it again when the test flow has passed the model. Using measured acceleration and Pitot pressure histories allows direct straightforward time-dependent evaluation of the aerodynamic coefficients. The procedure is insensitive to disturbances in the starting phase of the flow or moderate flow variations. The results quantify the force, which is produced by interaction of side-jets and ambient flow, and acts on the surface of the model. At the tropospheric hypervelocity conditions of our test, the interaction force on a flat plate substantially increases jet thrust. Moreover, the results quantify the time necessary to establish quasistationary flow for the actual test conditions. Author (revised)

N94-28023*# National Aeronautics and Space Administration. Ames Research Center, Moffett Field, CA.

A NUMERICAL INVESTIGATION OF A SUBSONIC JET IN A CROSSFLOW

Stephen H. Chiu (Space Systems/Loral, Palo Alto, CA.), Karlin R. Roth, Richard J. Margason, and Jin Tso (California Polytechnic State Univ., San Luis Obispo.) *In* AGARD, Computational and Experimental Assessment of Jets in Cross Flow Nov. 1993 14 p Original contains color illustrations (For primary document see N94-28003 07-34)
Copyright Avail: CASI HC A03/MF A04

The flowfield induced by a single, subsonic jet exhausting perpendicularly from a flat plate into a subsonic crossflow has been numerically investigated. The test case was chosen to match available experimental data where the jet Mach number was 0.78, and the freestream Mach number was 0.13. Time-averaged solutions were obtained using the thin-layer Navier-Stokes equations and two overlapping grids. The solutions were sensitive to the radial grid clustering near the edge of the jet and to the far-field boundary conditions. Experimental data comparisons were required to determine the most appropriate jet grid and satisfactory boundary conditions. Globally, the solutions converged in about 6000 iterations. The computational results accurately showed the deflected jet and associated contrarotating vortices. The fine clustered grid in the region upstream of the jet exit allowed the horseshoe vortex in the boundary layer near the jet exit to be captured. Most importantly for aircraft applications, the computed plate pressure distributions compared favorably with the experimental data over most of the surface. However, in the wake region immediately downstream of the jet exit, where there is extensive flow separation, some discrepancies with experimental data were observed. Two turbulence models were used in this study: (1) the zero-equation, two layer Baldwin-Lomax turbulence model; and (2) one-equation Baldwin-Barth turbulence model. The turbulence models gave results which generally compared no better with experimental data than the laminar computation results. Author (revised)

N94-28024# Manchester Coll. of Science and Technology (England). Dept. of Mechanical Engineering.

CALCULATION OF SINGLE AND MULTIPLE JETS IN CROSS-FLOW WITH AND WITHOUT IMPINGEMENT USING REYNOLDS-STRESS-TRANSPORT CLOSURE

N. Z. Ince and M. A. Leschziner *In* AGARD, Computational and Experimental Assessment of Jets in Cross Flow Nov. 1993 14 p Sponsored in part by British Aerospace Public Ltd. Co. (For primary document see N94-28003 07-34)
Copyright Avail: CASI HC A03/MF A04

A finite-volume algorithm, incorporating a non diffusive quadratic scheme for the approximation of convection and full second-moment (Reynolds-stress-transport) turbulence closure, is applied to a free jet in moderately strong cross-flow and three jet configurations combining impingement with weak cross-flow, one geometry involving a twin-jet and another a triple-jet arrangement. The primary objective is to identify the merits and weaknesses of Reynolds-stress modelling, in contrast to one based on the isotropic eddy-viscosity approach, in the present complex 3D environment. While open questions remain, due principally to uncertainties arising from boundary conditions and insufficient numerical resolution in isolated highly sheared regions the present calculations provide clear indications, in accord with earlier studies in both 2D and 3D flows, of the superiority of the anisotropic closure. It is also demonstrated that a careful treatment of the jet-discharge conditions can be highly influential in respect of predictive realism. Author

N94-28025# Imperial Coll. of Science and Technology, London (England). Dept. of Chemical Engineering.

PREDICTIONS OF MOMENTUM AND SCALAR FIELDS IN A JET IN CROSS-FLOW USING FIRST AND SECOND ORDER TURBULENCE CLOSURES

J. Alvarez, W. P. Jones, and R. Seoud (Defence Research Agency, London, England.) *In* AGARD, Computational and Experimental Assessment of Jets in Cross Flow Nov. 1993 10 p Sponsored by Ministry of

Defence (For primary document see N94-28003 07-34)
Copyright Avail: CASI HC A02/MF A04

The k-epsilon model and a second moment closure have been applied to the calculation of a slighted heated jet issuing into a cross-flow. Two jet to cross-flow velocity ratios were considered. An assessment of the model performance is made difficult by the high turbulence intensities observed in the recirculation region in the lee of the jet and consequent uncertainty in the hot-wire measurements. Overall, the second moment closure gives slightly better agreement but the difference between the results obtained with the two model is not large. For the low velocity ratio, results are extremely sensitive to the boundary conditions prevailing at jet inlet. The predicted mean temperature profiles appear to be more strongly dependent on the predicted velocity fields than on the scalar field closure. Author

N94-28026# Middle East Technical Univ., Ankara (Turkey). Dept. of Aeronautical Engineering.

NAVIER-STOKES SIMULATION OF TWO AND THREE DIMENSIONAL JETS IN CROSSFLOW, EFFECTS OF GRID, AND BOUNDARY CONDITIONS

Mehmet Serif Kavsaoglu, Ibrahim Sinan Akmandor, Suleyman Ciray (Turkish Aerospace Industries, Ankara.), and Kozo Fujii (Tokyo Univ., Sagamihara, Japan.) *In* AGARD, Computational and Experimental Assessment of Jets in Cross Flow Nov. 1993 22 p Sponsored by General Dynamics Corp. (For primary document see N94-28003 07-34)
Copyright Avail: CASI HC A03/MF A04

Flowfields of two and three dimensional subsonic jets injected into a crossflow were solved by using a three dimensional Navier-Stokes code (LANS3D). Baldwin-Lomax turbulence model and the algebraic curved jet turbulence model of Oh and Schetz were used depending on the location in the flowfield. Application of characteristic boundary conditions based on Riemann invariants were found to be useful for the convergence of solutions. Computations made using flat bottom grids showed local pressure singularities around the jet exit. It was shown that these singularities could be removed by using grids with a cavity for the jet entrance. Grid skewness was a particularly effective parameter on the prediction of surface pressures. Author

N94-28027# Deutsche Aerospace A.G., Munich (Germany). Military Aircraft Div.

EFFECTS, LIMITS, AND LIMITATIONS OF SPANWISE BLOWING c02

W. H. Staudacher *In* AGARD, Computational and Experimental Assessment of Jets in Cross Flow Nov. 1993 10 p (For primary document see N94-28003 07-34)
Copyright Avail: CASI HC A02/MF A04

Concentrated spanwise blowing over wings is a technique using mainly the secondary (= nonreactive) effects of a jet in crossflow, with the primary intention to generate and/or stabilize and control separated rolled-up leading edge vortex systems. This means an indirect application of a crossflow jet via triggering another crossflow phenomenon, the L.E. vortex. Based on the results of extensive experimental research, the merits and shortcomings of this technique are overviewed concerning aerodynamic performances, and stability and control aspects. The limits of aerodynamics efficiency are established on an empirical/theoretical basis and compared to experimental results. There is found a definite upper and lower boundary. The author's view is given concerning the practical (non-) applicability of this simple technique and the reasons for missing examples in operational aircraft are discussed via comparison to competitive approaches. Author

N94-28028# McDonnell-Douglas Aerospace Information Services Co., Saint Louis, MO.

PNEUMATIC MANAGEMENT OF BLUNTED-FOREBODY FLOW ASYMMETRY FOR HIGH-ANGLE-OF-ATTACK DIRECTIONAL CONTROL c08

Frederick W. Roos, Charles L. Magness, and Daniel V. Brown *In* AGARD, Computational and Experimental Assessment of Jets in Cross Flow Nov. 1993 6 p (For primary document see N94-28003 07-34)
Copyright Avail: CASI HC A02/MF A04

Low-speed experiments have been conducted to explore the effectiveness of combining nose bluntness, which suppresses the tendency toward flowfield asymmetry, and pneumatic flow-separation control, which triggers flow asymmetry, into a system of pneumatic side-force control for a slender forebody shape at high angles of attack (alpha). The basic forebody shape studied, a 20%-blunted, 3.5-caliber tangent ogive, developed no side force over the range 0 less than or = alpha less than or = 60 degrees. Slight blowing through either or two symmetrically positioned orifices at the blunt nose of the forebody produced a degree of flow asymmetry (and a corresponding side force) that depended on jet massflow rate within limits that varied with alpha, the specific jet configuration, and laminar vs. turbulent boundary-layer separation. Forward-blowing jets were found to be generally more effective that nets normal to the forebody surface in producing pneumatic side-force control. Derived from text

N94-28029# Stanford Univ., CA.

THEORETICAL AND EXPERIMENTAL INVESTIGATION OF A DELTA WING WITH TURBULENT LEADING-EDGE JETS c02

K. J. Craig, L. Roberts, D. I. Greenwell (Bath Univ., England.), and N. J. Wood (Bath Univ., England.) *In* AGARD, Computational and Experimental Assessment of Jets in Cross Flow Nov. 1993 13 p (For primary document see N94-28003 07-34)
Copyright Avail: CASI HC A03/MF A04

Control of the separated flow over a delta wing using Tangential Leading-Edge Blowing has been investigated experimentally and computationally. Tangential Leading-Edge Blowing describes the injection of momentum into the cross flow plane of the wing by thin Coanda wall jets located at the point of cross flow separation. The concept is shown to be capable of generating significant asymmetry in the vortical flowfield, and hence a lateral control capability, up to very high angles of attack. The primary effects of jet blowing have been modeled using a Navier-Stokes computation with an algebraic turbulence model. Author

N94-28030# Science Applications International Corp., Fort Washington, PA. Propulsive Sciences Div.

RECENT DEVELOPMENTS IN THE SIMULATION OF STEADY AND TRANSIENT TRANSVERSE JET INTERACTIONS FOR MISSILE, ROTORCRAFT, AND PROPULSIVE APPLICATIONS

S. M. Dash, B. J. York, N. Sinha, R. A. Lee, A. Hosangadi, and D. C. Kenzakowski *In* AGARD, Computational and Experimental Assessment of Jets in Cross Flow Nov. 1993 21 p (For primary document see N94-28003 07-34)
Copyright Avail: CASI HC A03/MF A04

A review of recent activities focused on the simulation of transverse jet interaction problems using advanced time-asymptotic and time-accurate Navier-Stokes methodology is presented. Missile work has involved the simulation of short-duration control jets issued from solid rocket motor nozzles. For the simulation of time-accurate particle-laden flows, a new Eulerian-based upwind/implicit particle-solver was developed and coupled with the gas-phase solver. Rotorcraft work has involved simulating the interaction of the exhaust plumes with the rotor wake and body aerodynamic flow. Hybrid vortex tracking/Navier-stokes methodology has been implemented with gridding of this complex 3D interactive flow being an issue of primary concern. Propulsive work has emphasized turbulence modeling. For scramjet fuel-injection applications, compressible-dissipation extensions to the k-epsilon turbulence model which provided marked improvements in simulating fundamental high-speed shear layers, have proven to work quite well for transverse jet injection. Author

N94-28031# Aerospatiale, Verrieres-L-Buisson (France).

NUMERICAL ASSESSMENT OF AERODYNAMIC INTERACTIONS ON MISSILES WITH TRANSVERSE JETS CONTROL c02

M. Dormieux and R. Marsaa-Poey *In* AGARD, Computational and Experimental Assessment of Jets in Cross Flow Nov. 1993 11 p Sponsored in part by Ministry of Defence (For primary document see N94-28003 07-34)
Copyright Avail: CASI HC A03/MF A04

This paper deals with numerical studies made at AEROSPATIALE-MISSILES about aerodynamic interactions due to the use of pyrotechnical lateral force control. Calculations were performed in order to predict lateral jets interactions on two kinds of missiles: subsonic antitank and supersonic antimissile. In the subsonic case, Euler and Navier-Stokes calculations were compared on a missile body test case. Then, Euler code was applied to an antitank missile configuration, and missile spinning effects were assessed. In the supersonic case, jet stagnation temperature and jet species effects were studied on a surface-to-air missile. Author

N94-28032# Deutsche Forschungs- und Versuchsanstalt fuer Luft- und Raumfahrt, Goettingen (Germany). Inst. for Experimental Fluid Mechanics.

FIRST EXPERIMENTAL ASSESSMENT OF RCS PLUME-FLOW FIELD INTERACTION ON HERMES LEADING EDGE THRUSTER CONFIGURATION c20

T. Poertner *In* AGARD, Computational and Experimental Assessment of Jets in Cross Flow Nov. 1993 13 p (For primary document see N94-28003 07-34)

Copyright Avail: CASI HC A03/MF A04

Glow discharge flow visualization experiments are demonstrated which have been performed to enable a first assessment of the HERMES 1.0 leading edge thruster configuration concerning interference between the thruster plumes of the reaction control system (RCS) and the surrounding flow field. The results of the flow visualization tests are presented in exemplary selected photographs. Additional Pitot pressure measurements support assumptions concerning interference induced pressure changes that may result from the observed significant flow field disturbances. Author

N94-28033*# National Aeronautics and Space Administration. Ames Research Center, Moffett Field, CA.

NUMERICAL SIMULATION OF A POWERED-LIFT LANDING c05

Kalpana Chawla (MCAT Inst., Moffett Field, CA.) and William R. VanDalsem *In* AGARD, Computational and Experimental Assessment of Jets in Cross Flow Nov. 1993 10 p (For primary document see N94-28003 07-34)

Copyright Avail: CASI HC A02/MF A04

The flow field about a delta wing equipped with thrust reverse jets in slow speed flight near the ground has been computed. Results include the prediction of the flow about the delta wing at four fixed heights above the ground, and simulated landing, in which the delta wing descends towards the ground. Comparison of computed and experimental lift coefficients indicates that the simulations can capture at least the qualitative trends in lift-loss encountered by thrust-vectoring aircraft operating in ground effect. Author

N94-28034# Wright Lab., Wright-Patterson AFB, OH.

A STUDY OF JET EFFECT AND GROUND EFFECT INTERFERENCE ON A STOL FIGHTER c05

David J. Moorhouse, James G. Reinsberg (McDonnell-Douglas Aerospace Information Services Co., Saint Louis, MO.), and Frank J. Shirk (McDonnell-Douglas Aerospace Information Services Co., Saint Louis, MO.) *In* AGARD, Computational and Experimental Assessment of Jets in Cross Flow Nov. 1993 10 p (For primary document see N94-28003 07-34)

Copyright Avail: CASI HC A02/MF A04

The STOL and Maneuver Technology Demonstrator (S/MTD) program was structured to investigate, develop and validate through analysis, experiment and flight test, four specific technologies related to providing current and future high performance fighters with both STOL capability and enhanced combat mission performance. The four technologies are: (1) Two-dimensional thrust vectoring and reversing exhaust nozzle, (2) Integrated Flight/Propulsion Control (IFPC) System, (3) Advanced Pilot Vehicle Interface, and (4) Rough/soft field landing gear. In addition to the required technologies, all-moving canard surfaces were also incorporated into the baseline F-15B. As stated previously, the intent of the demonstration program was to validate specific technologies, it was neither a prototype nor an explicit research program. Starting with an existing aircraft, many wind tunnel tests were performed to define the incremental effects of the specific technology items. Thrust reversing was achieved by blocking the nozzle exit area and exhausting the flow through vane packs on top and bottom of the engine. In the Short Landing (SLAND) mode the engines were at full military RPM and all exhaust flow was diverted through final approach with the reverse vanes pointed aft to provide forward thrust. At touchdown, the vanes quickly swing forward to orient the exhaust flow to provide reverse thrust for the rollout. A significant amount of wind tunnel testing was devoted to measuring jet effects at all conditions but definition of jet effects in ground effect received particular emphasis. Reference 1 documented the development of the S/MTD configuration with details on the wind tunnel data and control laws. Data was presented on the jet effects in ground effect that were predicted. Special control logic was defined to mitigate strong nose-up pitching moments as thrust reversing was initiated after touchdown. A special ground-handling mode was also incorporated for the rollout phase. The flight testing produced some surprising results. The object of the present paper is to document that experience. Data will be summarized briefly for completeness. Pertinent flight test experience will be presented, with results of an innovative analysis technique developed by the contractor. Lastly, future requirements will be discussed. Author

N94-28035*# National Aeronautics and Space Administration. Ames Research Center, Moffett Field, CA.

TRANSITIONAL FLIGHT CHARACTERISTICS OF A GEOMETRICALLY SIMPLIFIED STOVL MODEL c05

Karlin R. Roth *In* AGARD, Computational and Experimental Assessment of Jets in Cross Flow Nov. 1993 10 p (For primary document see N94-28003 07-34)

Copyright Avail: CASI HC A02/MF A04

The transitional flight characteristics of a geometrically simplified Short Take-Off Vertical Landing (STOVL) aircraft configuration were measured in the NASA Ames 7- by 10-Foot Wind Tunnel. The experiment was designed to provide detailed data for evaluating the capability of computational fluid dynamics methods to predict the important powered lift flow parameters. The model consists of a 60 deg cropped delta wing planform; a blended fuselage; and tandem, circular, high pressure air jets that exit perpendicular to the flat lower surface. Freestream Mach number is limited to a maximum 0.2. Model angle of attack ranges from -10 deg to +20 deg. The nozzle pressure ratios of both jets are varied between 1 and 3, and the jet exit temperatures are maintained at near ambient conditions. Detailed surface pressure measurements show that suction pressure peaks located on the upper surface of the wing during conventional wingborne flight for angles of attack greater than 5 deg move to the wing lower surface at angles of attack less than 0 deg. A reduction in these suction pressure peaks is observed when the lift jets are operating. With sonic jet exit conditions, a freestream Mach number of 0.14, and 0 deg angle of attack, the jet-induced suckdown is equivalent to a 3.7 deg reduction in angle of attack. Schlieren, laser light sheet flow visualization and total pressure measurements in the jet plumes provide a description of the three-dimensional jet efflux flowfield. Author

N94-28036# Hertfordshire Univ., Hatfield (England). Dept. of Aeronautics.

EFFECTS OF FREE-STREAM TURBULENCE ON A JET IN A CROSS FLOW

T. H. Toften, A. E. Holdo, and D. Kapfer *In* AGARD, Computational and Experimental Assessment of Jets in Cross Flow Nov. 1993 10 p Sponsored by Royal Norwegian Council for Scientific and Industrial Research and Dept. of Scientific and Industrial Research (For primary document see N94-28003 07-34)

Copyright Avail: CASI HC A02/MF A04

At present there is limited information available on effects of free-stream turbulence intensities and scale on both the time average and instantaneous development of a jet in a cross flow. The aim of this study was to investigate such effects on both entrainment and mean path of the jet using primarily experimental methods. The experimental part consisted of measurements using hot wire anemometers, thermocouples and a nine hole vortex probe as well as observations with a color Schlieren system on a jet issuing from a circular aperture in a flat plate. The jet Reynolds numbers of the tests were in the region 2x10(exp 4) to 8x10(exp 4) and the flow could be considered as incompressible for all cases tested. The use of both visualization technique as well as quantitative measurements have proven to be helpful in the description of free-stream turbulence effects. Although it should be noted that some quantitative data can be inferred from the Schlieren observations. The results show that there are clear effects due to variations in free-stream turbulence on the development of the jet. The effects within the range of variation in free-stream turbulence intensity and length scale of the investigation are manifest in terms of all main jet characteristics. These characteristics are the rate of entrainment, the mean jet path and the strength of the main jet vortices. The observed effects are significant, but at present there are no direct trends in the results with increasing or decreasing turbulence scales or intensity to help propose the primary mechanisms involved in the effects. This is the subject of further investigations at the present time. Author

N94-28037# Karlsruhe Univ. (Germany).

ANALYSIS OF COOLING JETS NEAR THE LEADING EDGE OF TURBINE BLADES **c07**

E. Benz, S. Wittig, A. Beeck (ABB Power Generation, Inc., Baden, Switzerland.), and L. Fottner (Universitaet der Bundeswehr Muenchen, Neubiberg, Germany.) *In* AGARD, Computational and Experimental Assessment of Jets in Cross Flow Nov. 1993 12 p (For primary document see N94-28003 07-34)

Copyright Avail: CASI HC A03/MF A04

Film-cooling air ejection affects the aerodynamics of turbine blades by the mixing of the coolant with the mainstream as well as by the interaction between the jet and the boundary layer. In the present paper, these effects are studied experimentally and numerically. The results show that the flow in the coolant channel is strongly affected by the main flow around the blade, leading to significant deflection of the coolant air jets. To account for these interactions between the cooling jet and the main flow in the numerical predictions, a multi-block technique is applied. With this technique very complex but structured geometries can be modelled by simply attaching grids of the different sub-domains. For the present investigations, these sub-domains are the two coolant channels at the leading edge and the main flow around the blade. For adaption to the curved geometry of such a turbine blade, a non-orthogonal body fitted grid is used for solving the time average two- or three-dimensional compressible Navier-Stokes equations by a finite volume method. The turbulence is taken into account by the standard k-epsilon model. For discretization of the convective terms the Monotonized-Linear-Upwind scheme (MLU) is used. The pressure-velocity coupling is achieved by the SIMPLEC-algorithm for compressible flows. The calculated results are compared with experimental investigation performed with a L2F-system at a large scaled turbine blade. Three typical blowing ratios are presented. Due to the simultaneous calculation of the coolant flow and the main flow, good agreement was obtained. Author

N94-28038# Turkish Aerospace Industries, Ankara.

NAVIER-STOKES ANALYSIS OF A SWIRLING JET IN CROSSFLOW

Huseyin Yagci and Mehmet Serif Kavsaoglu (Middle East Technical Univ., Ankara, Turkey.) *In* AGARD, Computational and Experimental Assessment of Jets in Cross Flow Nov. 1993 7 p (For primary document see N94-28003 07-34)

Copyright Avail: CASI HC A02/MF A04

Flowfield of a subsonic swirling jet injected into a subsonic crossflow was computed by using a three dimensional Navier-Stokes code (LANS3D). Baldwin-Lomax turbulence model and the algebraic curved jet turbulence model of Oh and Schetz were used depending on the location in the flowfield. Characteristic boundary conditions based on Riemann invariants were utilized for the flow in and out planes. A single block grid with a cavity at the jet entrance was used. Author

N94-28039# Office National d'Etudes et de Recherches Aerospatiales, Paris (France). Direction de l'Aerodynamique.

EXPERIMENTAL STUDY ON THE INTERACTIONS BETWEEN A TRANSVERSE HEATED SUPERSONIC JET AND AN EXTERNAL SUPERSONIC FLOW [ETUDE EXPERIMENTALE SUR LES INTERACTIONS ENTRE UN JET SUPERSONIQUE CHAUFFE TRANSVERSAL ET UN ECOULEMENT SUPERSONIQUE EXTERNE] **c02**

R. Gaillard, P. Geffroy, L. Jacquin, and G. Losfeld *In* AGARD, Computational and Experimental Assessment of Jets in Cross Flow Nov. 1993 12 p In FRENCH (For primary document see N94-28003 07-34)

Copyright Avail: CASI HC A03/MF A04

This paper presents the techniques implemented as well as a collection of the results obtained during an experimentation leading to the S5 wind tunnel of ONERA in the case of a transverse jet of Mach number equal to 2, strongly heated, emerging in a perpendicular flow of the same Mach number. The flow is qualified by means of a miniature 5 hole probe, by thermocouples and tridirectional laser velocimetry. The effects of the temperature on the average and turbulent properties of the jet are discussed. Clear strioscopies are also presented. They highlight the strongly nonstationary nature of this interaction. Transl. by FLS

N94-28040# City Univ., London (England). Dept. of Mechanical Engineering and Aeronautics.

INCLINED AIR-JETS USED AS VORTEX GENERATORS TO SUPPRESS SHOCK-INDUCED SEPARATION **c02**

H. H. Pearcey, K. Rao, and D. M. Sykes *In* AGARD, Computational and Experimental Assessment of Jets in Cross Flow Nov. 1993 10 p Sponsored by British Aerospace Defence Ltd. (For primary document see N94-28003 07-34)

Copyright Avail: CASI HC A02/MF A04

Experiments have been performed to assess the effectiveness of air-jet vortex generators as alternative to vanes in suppressing shock-induced separation. It is shown that a single jet inclined to the plane of the surface and skewed to the direction of the undisturbed stream produces a single strong vortex and can therefore be treated as the equivalent of a single vane. It follows that jets can be installed in arrays to correspond to arrays of vane vortex generators. A spanwise array of jets is shown to produce closely similar results to an array of co-rotating vane vortex generators of the type that has now been used in very many applications to suppress the effects of shock-induced separation. Air-jet vortex generators should therefore be equally effective in practice and may have significant inherent advantages for many applications. The vortex generators were effective for shock upstream Mach numbers up to and beyond 1.6. The maximum effectiveness occurred close to the generators but they remained reasonably effective for a range of shock positions of up to 50% chord. Some initial pointers are given on the influence of certain design parameters and on what considerations would apply in tailoring the jets to specific applications. Author

N94-28064 ESDU International Ltd., London (England).

CONDENSATION INSIDE TUBES: COMPUTER PROGRAM FOR PRESSURE DROP IN STRAIGHT TUBES (HORIZONTAL AND VERTICAL WITH DOWNFLOW)

Dec. 1993 16 p

(ISSN 0141-402X)

(ESDU-93014; ISBN-0-85679-865-5) Avail: ESDU

ESDU 93014 introduces a Fortran program that implements the calculation procedures of ESDU 90024 and 91023 respectively for vertical and horizontal cases. Those documents should be consulted for details of the empirical correlation used. Since vapor density is an important variable in the calculation and is usually available as a function of saturation temperature, the relationship between pressure and saturation temperature is required at points along the tube, although a constant value of vapor density may be used if the user wishes. The program provides options to use an Antoine or Wagner equation, or to provide a set of values of saturation pressure and temperature; for the vapor density the options are to use the ideal gas law, to provide a set of values of saturation temperature and density or to use a specific correlation equation (log density as a fraction of critical as a five term polynomial function of reciprocal reduced temperature minus one). For a wide range of pure compounds the ESDU Physical Data, Chemical Engineering Sub-series provides values of the constants in the correlation equations for saturation temperature and vapor density. The program (ESDUpac A9314) is provided on disc (uncompiled) in the software volume, and also compiled within ESDUview, a user-friendly shell running under MS DOS that prompts on screen for the input data. A worked example illustrates the use of the program and the formats of the input data and the output. ESDU

N94-28095 ESDU International Ltd., London (England).

VORTEX GENERATORS FOR CONTROL OF SHOCK-INDUCED SEPARATION. PART 1: INTRODUCTION AND AERODYNAMICS

Dec. 1993 63 p

(ISSN 0141-4356)

(ESDU-93024-Pt-1; ISBN-0-85679-877-0) Avail: ESDU

ESDU 93024 summarizes situations where vortex generators have been used to control shock-induced separation. It is suggested that their use should be considered at the design stage and not only as a fix for undesirable characteristics found post-flight. Types of vortex generators are reviewed and the aerodynamic principles of their operation considered. Attention is focused on vane types: co- or counter-rotating and biplane. By applying simplifying assumptions, the degree and range of mixing effectiveness, and the rate of vortex decay, are studied and offer some guidance on the streamwise extent of control, the lateral spacing and the height above the surface that are appropriate for both co- and counter-rotating types. The degree of control achievable on aerofoils is considered, and calculations also show the possible adverse effects on drag. The use of multiple arrays and the use of vortex generators to control shock-induced separation in corners are briefly discussed. The use of wind-tunnel tests to assess the effects of vortex generators is considered. ESDU

N94-28096 ESDU International Ltd., London (England).

VORTEX GENERATORS FOR CONTROL OF SHOCK-INDUCED SEPARATION. PART 3: EXAMPLES OF APPLICATIONS OF VORTEX GENERATORS TO AIRCRAFT

Dec. 1993 35 p
(ISSN 0141-4356)
(ESDU-93026-Pt-3; ISBN-0-85679-879-7) Avail: ESDU

ESDU 93026 illustrates by case studies the use of the information in Parts 1 and 2 on the use of vortex generators to control shock-induced separation. The examples are the control of internal noise by the application of vortex generators on the forward cabin roof of a business aircraft (Gulfstream III), the control of separation associated with a three-shock pattern near the tip of a highly swept and tapered model wing in a wind-tunnel, and the improvement of the buffet maneuver boundary on a straight wing interceptor aircraft of the fifties. In each case the geometric details of the arrays of vortex generators tested are provided, the results obtained are described, and the aerodynamic principles involved that influence those results are assessed. ESDU

N94-28099 Heidelberg Univ. (Germany). Dept. of Mathematics.

A PARALLEL MULTIGRID ALGORITHM FOR SOLVING THE NAVIER-STOKES EQUATIONS ON A TRANSPUTER SYSTEM

Friedhelm Schieweck (Technical Univ. of Magdeburg, Germany.) 4 Nov. 1992 39 p Sponsored by DFG Limited Reproducibility: More than 20% of this document may be affected by microfiche quality
(Preprint-699; ETN-94-95085) Avail: CASI HC A03

The numerical solution of the stationary incompressible Navier-Stokes equations for a wide range of Reynolds numbers is considered. A nonconforming finite element discretization of upwind type is used. For solving the discrete systems of equations within an outer nonlinear iteration, a robust multigrid algorithm, which admits a slightly modified parallel version with nearly the same good properties, is proposed. The parallel efficiency for an implementation on a transputer system, when changing the number of employed processors and the number of used grid levels, is studied. ESA

N94-28139 ESDU International Ltd., London (England).

FORCED CONVECTION HEAT TRANSFER IN STRAIGHT TUBES. PART 2: LAMINAR AND TRANSITIONAL FLOW

Aug. 1993 27 p Supersedes ESDU-68006
(ISSN 0141-402X)
(ESDU-93018-Pt-2; ESDU-68006; ISBN-0-85679-870-3) Avail: ESDU

ESDU 93018 presents Nusselt number data in laminar flow for conditions of either uniform wall temperature or uniform heat flux in fully-developed flow, flow that is thermally-developing (where the heated section is preceded by an isothermal length exceeding the hydrodynamic entry length), and flow that is developing simultaneously both thermally and hydrodynamically. The effect of variable fluid properties is considered and a correction for radial viscosity variation in liquids is recommended, but no correction is felt necessary for gases, following an assessment of the available data. For mixed convection conditions only a uniform wall temperature condition is considered. Nusselt number data are given for buoyancy-assisted flow in vertical tubes (heated upflow and cooled downflow) and for buoyancy-opposed flow. Data are also provided for flow in horizontal tubes. The ranges of conditions for which the recommended correlations have been tested are tabulated for the mixed convection conditions. For transitional flow an interpolation function in Nusselt number is suggested to be used between the limiting values in laminar and turbulent flow at Reynolds numbers (based on tube diameter) of 2000 and 8000, respectively. Worked examples illustrate the use of the equations and methods. ESDU 92003 provides guidance on the boundaries between the flow regimes. ESDU

N94-28172 Southampton Univ. (England). Inst. of Sound and Vibration Research.

ACOUSTIC BUBBLE SIZING, USING ACTIVE AND PASSIVE TECHNIQUES TO COMPARE AMBIENT AND ENTRAINED POPULATIONS

A. D. Phelps, T. G. Leighton, M. F. Schneider, and P. R. White Mar. 1994 11 p
(ISVR-TR-229) Copyright Avail: Issuing Activity (Inst. of Sound and Vibration Research, Univ. of Southampton, Southampton SO9 5NH, England)

Details of the progress into sizing bubbles actively by means of the two frequency insonation method are included and the success of examining the subharmonic sum-and-difference coupling is outlined. In addition, preliminary results are presented which relate to investigations into the variation of the subharmonic response with differing excitation amplitude and step size between successive interrogating signals, and examinations into the reproducibility of the response. Work was also done on the passive sizing of bubbles upon entrainment with the Gabor transform technique, which gives a fast and accurate representation of the bubble's resonant frequency, of the time at which entrainment occurs and of the amplitude of the signal. Author (revised)

N94-28173 Southampton Univ. (England). Inst. of Sound and Vibration Research.

A MODELLING OF THE NOISE FROM SIMPLE COAXIAL JETS. PART 3: WITH HOT PRIMARY FLOW

M. J. Fisher and G. A. Preston Jan. 1994 42 p
(ISVR-TR-230-Pt-3) Copyright Avail: Issuing Activity (Inst. of Sound and Vibration Research, Univ. of Southampton, Southampton SO9 5NH, England)

The third part of a continuing study of the noise of coaxial jets is described and modifications to the model developed previously to allow for the effect of heated flow from the primary nozzle are described. The essential feature of the model developed for the prediction of the noise from isothermal coaxial jets was the identification of three flow regions whose noise production could be obtained from single stream jet prediction methods. In particular it was shown that noise from the principal interaction zone could be calculated using single jet prediction methods as long as account was taken of the fact that measured turbulence levels in this region were lower than those observed in a single isolated jet at the same center-line velocity. For isothermal flows, within which only quadruple sources exist, allowance for the reduced turbulence is straightforward. However for heated flows both dipole and quadruple sources exist which have different dependencies on turbulence level. Hence to predict the noise one needs to know the relative contributions of the dipole and quadruple sources. Use was made of previously published results for these relative contributions, as a function of velocity and temperature, for single jets. This then permits prediction of the noise from the interaction zone which is subsequently combined with that from the secondary jet and the fully mixed flow region, as before. Comparison between data and prediction over a range of angles of observation, velocities and temperatures shows a very acceptable level of agreement. Author (revised)

N94-28175 Southampton Univ. (England). Inst. of Sound and Vibration Research.

ON THE USE OF FEEDBACK TO CONTROL SOUND RADIATION FROM A PLATE EXCITED BY A TURBULENT BOUNDARY LAYER

D. R. Thomas and P. A. Nelson Jan. 1994 60 p
(ISVR-TR-227) Copyright Avail: Issuing Activity (Inst. of Sound and Vibration Research, Univ. of Southampton, Southampton SO9 5NH, England)

It is shown that the problem of applying active control to simply supported plate excited by a turbulent boundary layer can be presented in a form which allows the application of optimal control theory. Linear regulator theory and stochastic linear regulator theory are briefly summarized and the application of the latter to sound radiation from a vibrating structure is illustrated by the simple example of a rigid piston excited by a random force. It is shown that the optimal control theory can be applied to such a problem if the sound power radiated by the structure is estimated from the vibration signal by means of a 'radiation filter'. A modal model for the vibration of an elastic structure is presented and the state space realization of the model is given. It is shown that a simple Corcos model of the turbulent boundary layer excitation can be modeled as a number of 'excitation filters'. The state space realization of these filters can be combined with the state space model of a vibrating plate to give a state space model of a turbulent boundary layer excited plate to which optimal control theory can be applied. In similar fashion the sound power radiated by the plate can be estimated by means of a 'radiation filter matrix'. A detailed account of the calculation of such a 'radiation filter matrix' is given. Hence, the state space forms of the 'excitation filters' and 'radiation filter matrix' can be combined with the state space model of the plate to give a system state space realization which can be used in the solution of a linear quadratic regulator problem. Once in such a form optimal control analysis is applied to the state equations and optimal reductions in the far field radiated power are obtained for various arrangements of control forces. These results give insight into the possibilities for obtaining useful reductions in turbulent boundary layer induced noise in aircraft by the application of feedback control. They do not, however, enable the simple design of practical controllers. Author (revised)

N94-28180*# High Technology Corp., Hampton, VA.
LOCALIZED AND DISTRIBUTED BOUNDARY-LAYER RECEPTIVITY TO CONVECTED UNSTEADY WAKE IN FREE STREAM
Meelan Choudhari Apr. 1994 22 p
(Contract NAS1-19299; RTOP 538-05-15-03)
(NASA-CR-4578; NAS 1.26:4578) Avail: CASI HC A03/MF A01

Receptivity to a model convected disturbance in the presence of localized and distributed variations in wall geometry and wall-suction velocity is examined. The model free-stream disturbance corresponds to the time-harmonic wake of a vibrating ribbon that is placed at a suitable distance above the surface of a thin airfoil. The advantages of using this disturbance for experiments on receptivity to convected disturbances are outlined. A brief parametric study is presented for a flat-plate boundary layer. The study quantifies the effect of wake position as well as wake width; in addition, it should be helpful in the choice of an optimal setting for a controlled experiment of the above type, which the above parametric study shows as feasible. Author

N94-27899*# Pennsylvania State Univ., University Park. Dept. of Mechanical Engineering.
A COMPREHENSIVE COMPARISON OF TURBULENCE MODELS IN THE FAR WAKE
John M. Cimbala *In* Old Dominion Univ., The 1993 NASA-ODU American Society for Engineering Education (ASEE) Summer Faculty Fellowship Program Dec. 1993 p 80-82 (For primary document see N94-27893 07-80)
Avail: CASI HC A01/MF A03

N94-27911*# Old Dominion Univ., Norfolk, VA. Dept. of Mechanical Engineering and Mechanics.
A NUMERICAL STUDY OF MIXING AND COMBUSTION IN HYPERVELOCITY FLOWS THROUGH A SCRAMJET COMBUSTOR MODEL
Ramesh Krishamurthy *In its* The 1993 NASA-ODU American Society for Engineering Education (ASEE) Summer Faculty Fellowship Program Dec. 1993 p 123-125 (For primary document see N94-27893 07-80)
Avail: CASI HC A01/MF A03

N94-28326 Ecole Polytechnique, Montreal (Quebec). Dept. of Mechanical Engineering.
UNIFIED APPROACH FOR DIRECT AND INVERSE BOUNDARY LAYER PREDICTION USING CUBIC SPLINE COLLOCATION
A. Ilinca, B. C. Basu, and J. Godin *In* Canadian Aeronautics and Space Inst., Abstracts of Papers Presented at the 4th CASI Aerodynamics Symposium 1993 p 41-44 (For primary document see N94-28315 07-02)
Avail: Issuing Activity (Canadian Aeronautics and Space Inst., 130 Slater Street, Suite 818, Ottawa, ON K1P 6E2 Canada)

N94-28327 Ecole Polytechnique, Montreal (Quebec). Dept. of Mechnical Engineering.
TRANSITION FOR THREE-DIMENSIONAL, COMPRESSIBLE BOUNDARY LAYERS
R. Martinuzzi, F. Lamarre, and I. Paraschivoiu *In* Canadian Aeronautics and Space Inst., Abstracts of Papers Presented at the 4th CASI Aerodynamics Symposium 1993 p 45-48 (For primary document see N94-28315 07-02)
Avail: Issuing Activity (Canadian Aeronautics and Space Inst., 130 Slater Street, Suite 818, Ottawa, ON K1P 6E2 Canada)

N94-28342 Ecole Polytechnique, Montreal (Quebec). Dept. of Mechanical Engineering.
TECHNIQUES FOR ACCURATELY SOLVING UNSTEADY SHOCK WAVES AND CONTACT DISCONTINUITIES
M. Paraschivoiu, J. Y. Trepanier, and R. Camarero *In* Canadian Aeronautics and Space Inst., Abstracts of Papers Presented at the 4th CASI Aerodynamics Symposium 1993 p 106-109 (For primary document see N94-28315 07-02)
Avail: Issuing Activity (Canadian Aeronautics and Space Inst., 130 Slater Street, Suite 818, Ottawa, ON K1P 6E2 Canada)

N94-28343 Ecole Polytechnique, Montreal (Quebec). Dept. of Mechanical Engineering.
A NEW FLUX VECTOR SPLITTING SCHEME
G.-C. Zha and E. Bilgen *In* Canadian Aeronautics and Space Inst., Abstracts of Papers Presented at the 4th CASI Aerodynamics Symposium 1993 p 110-113 (For primary document see N94-28315 07-02)
Avail: Issuing Activity (Canadian Aeronautics and Space Inst., 130 Slater Street, Suite 818, Ottawa, ON K1P 6E2 Canada)

N94-28347 Ecole Polytechnique, Montreal (Quebec). Dept. of Mechanical Engineering.
UNSTEADY THREE DIMENSIONAL EULER SOLUTIONS ON MOVING GRIDS
A. Ilinca, J. Y. Trepanier, M. Reggio, and R. Camarero *In* Canadian Aeronautics and Space Inst., Abstracts of Papers Presented at the 4th CASI Aerodynamics Symposium 1993 p 126-129 (For primary document see N94-28315 07-02)
Avail: Issuing Activity (Canadian Aeronautics and Space Inst., 130 Slater Street, Suite 818, Ottawa, ON K1P 6E2 Canada)

N94-28348 George Washington Univ., Washington, DC. Dept. of Civil, Mechanical and Environmental Engineering.
RECENT ADVANCES IN THE SPECTRAL ELEMENT METHOD
Catherine Mavriplis *In* Canadian Aeronautics and Space Inst., Abstracts of Papers Presented at the 4th CASI Aerodynamics Symposium 1993 p 130-133 (For primary document see N94-28315 07-02)
Avail: Issuing Activity (Canadian Aeronautics and Space Inst., 130 Slater Street, Suite 818, Ottawa, ON K1P 6E2 Canada)

N94-28349 Canadair Ltd., Montreal (Quebec).
MULTIGRID SOLUTIONS OF THE 2D EULER/NAVIER-STOKES EQUATIONS ON UNSTRUCTURED MESHES
Farzad Mokhtarian *In* Canadian Aeronautics and Space Inst., Abstracts of Papers Presented at the 4th CASI Aerodynamics Symposium 1993 p 134-135 (For primary document see N94-28315 07-02)
Avail: Issuing Activity (Canadian Aeronautics and Space Inst., 130 Slater Street, Suite 818, Ottawa, ON K1P 6E2 Canada)

N94-28350 Institute for Aerospace Research, Ottawa (Ontario).
EXPERIMENTAL INVESTIGATIONS INTO THE WALL INTERFERENCE AND SIDEWALL BOUNDARY LAYER EFFECTS IN THE NATIONAL RESEARCH COUNCIL/INST. FOR AEROSPACE RESEARCH HIGH REYNOLDS NUMBER 2-D TEST FACILITY
Y. Nishimura and K. A. Schippers *In* Canadian Aeronautics and Space Inst., Abstracts of Papers Presented at the 4th CASI Aerodynamics Symposium 1993 p 136-139 (For primary document see N94-28315 07-02)
Avail: Issuing Activity (Canadian Aeronautics and Space Inst., 130 Slater Street, Suite 818, Ottawa, ON K1P 6E2 Canada)

N94-28351 Institute for Aerospace Research, Ottawa (Ontario).
COMPUTATION OF WIND-TUNNEL SIDE-WALL INTERFERENCE USING 3D NAVIER-STOKES CODE
D. F. Hawken *In* Canadian Aeronautics and Space Inst., Abstracts of Papers Presented at the 4th CASI Aerodynamics Symposium 1993

p 140-143 (For primary document see N94-28315 07-02)
Avail: Issuing Activity (Canadian Aeronautics and Space Inst., 130 Slater Street, Suite 818, Ottawa, ON K1P 6E2 Canada)

N94-28352 Institute for Aerospace Research, Ottawa (Ontario). High Speed Aerodynamics Lab.
EVALUATION OF THE BUOYANCY DRAG ON AUTOMOBILE MODELS IN LOW SPEED WIND TUNNELS
Miroslav Mokry *In* Canadian Aeronautics and Space Inst., Abstracts of Papers Presented at the 4th CASI Aerodynamics Symposium 1993 p 144-147 (For primary document see N94-28315 07-02)
Avail: Issuing Activity (Canadian Aeronautics and Space Inst., 130 Slater Street, Suite 818, Ottawa, ON K1P 6E2 Canada)

35 INSTRUMENTATION AND PHOTOGRAPHY

Includes remote sensors; measuring instruments and gages; detectors; cameras and photographic supplies; and holography.

For aerial photography see *43 Earth Resources and Remote Sensing*. For related information see also *06 Aircraft Instrumentation*, and *19 Spacecraft Instrumentation*.

N94-25599# Fermi National Accelerator Lab., Batavia, IL.
DISTRIBUTING FUNCTIONALITY IN THE DRIFT SCAN CAMERA SYSTEM
T. Nicinski, P. Constanta-Fanourakis, B. MacKinnon, D. Petravick, C. Pluquet, R. Rechenmacher, and G. Sergey Nov. 1993 4 p Presented at the 3rd Annual Conference on Astronomical Data Analysis Software and Systems, Victoria, Ontario, 13-15 Oct. 1993
(Contract DE-AC02-76CH-03000)
(DE94-003640; FNAL/C-93/339; CONF-9310239-1) Avail: CASI HC A01/MF A01

The Drift Scan Camera (DSC) System acquires image data from a CCD camera. The DSC is divided physically into two subsystems which are tightly coupled to each other. Functionality is split between these two subsystems: the front-end performs data acquisition; and the host subsystem performs near real-time data analysis and control. Yet, through the use of backplane-based Remote Procedure Calls, the feel of one coherent system is preserved. Observers can control data acquisition, archiving to tape, and other functions from the host, but, the front-end can accept these same commands and operate independently. The DSC meets the needs for such robustness and cost-effective computing. DOE

N94-25637# Nationaal Inst. voor Kernfysica en Hoge Energiefysica, Amsterdam (Netherlands).
ALIGNMENT OF THE AMSTERDAM PULSE STRETCHER (AmPS) [UITLIJNING VAN DE AMSTERDAM PULSSTRETCHER (AMPS)]
J. A. Heemskerk May 1993 34 p In DUTCH
(MTG-93-02; ETN-94-94954) Avail: CASI HC A03/MF A01

The alignment procedure carried out during the construction of the AmPS ring (Amsterdam Pulse Stretcher) is described. The main lines were fixed using theodolites, water leveling instruments, and measuring tape. The installation and mounting sequence of the different components is discussed and the measured data are tabulated. ESA

N94-25662# California Univ., Berkeley. Lawrence Berkeley Lab.
DETECTION GEOMETRY AND RECONSTRUCTION ERROR IN MAGNETIC SOURCE IMAGING
Paul Hughett and Thomas F. Budinger Nov. 1993 4 p Presented at the IEEE Medical Imaging Conference, San Francisco, CA, 4-6 Nov. 1993
(Contract DE-AC03-76SF-00098)
(DE94-004012; LBL-34841; CONF-9311114-3) Avail: CASI HC A01/MF A01

A recently developed reconstruction algorithm for magnetic source imaging exploits prior knowledge about source location, source power density, detector geometry, and detector noise power to obtain an explicit estimate of the reconstruction error. This paper demonstrates the application of the new algorithm to the optimal design of practical detector arrays to minimize the reconstruction error in specific applications. For a representative configuration for magnetocardiography, the optimal array width (for minimum reconstruction error) varies from 19 to 28 cm depending on the assumed source depth, number of detectors, source power and noise power. The reconstruction accuracy ranges from 5% of the a priori standard deviation for the sources nearest the detector plane to 95% of the a priori deviation for the deepest sources. The reconstruction error was found to depend on accidental alignments between dipole sources and point detectors, indicating that a more sophisticated model is required for accurate estimates of reconstruction error. The error calculation is fast, taking about a second for this problem on a workstation-class computer. The availability of a method for rapidly computing the reconstruction error for any given source characteristics and detector geometry will facilitate the optimal design of magnetometer array size, element spacing, and orientation for specific applications in biomagnetic and geomagnetic source imaging. DOE

N94-25735 Joint Inst. for Nuclear Research, Dubna (USSR). Lab. of High Energy.
AN ELECTROMAGNETIC CALORIMETER WITH WAVELENGTH SHIFTING FIBER READOUT
S. V. Afanasev, V. I. Kolesnikov, A. I. Malakhov, V. A. Gladyshev (Academy of Sciences, USSR, Moscow.), and A. L. Proskuryakov (Academy of Sciences, USSR, Moscow.) 1991 17 p Limited Reproducibility: More than 20% of this document may be affected by microfiche quality
(DE93-616664; JINR-R-13-91-380) Avail: CASI HC A03 (US Sales Only)

The response of an electromagnetic calorimeter using wavelength shifting fibers for the readout have been investigated. The calorimeter has been built as a sandwich of lead and scintillator plates. The fibers have been inserted into holes perpendicular to the plates. This calorimeter has been exposed to electrons, hadrons and muons in the energy range between 0.5 and 4.5 GeV, obtaining an average energy resolution of 11.4%/(radical)E for electrons. Two algorithms for reconstruction the central position of an electromagnetic shower have been applied. The better algorithm has given a spatial resolution of 3.9 mm. Also light yield, uniformity of response and (pi)-e separation have been studied. DOE

N94-25967 Carnegie-Mellon Univ., Pittsburgh, PA. Robotics Inst.
REAL-TIME 3-D POSE ESTIMATION USING A HIGH-SPEED RANGE SENSOR
David A. Simon, Martial Hebert, and Takeo Kanade Nov. 1993 17 p Limited Reproducibility: More than 20% of this document may be affected by microfiche quality
(AD-A273873; CMU-RI-TR-93-24) Avail: CASI HC A03

A system which can perform full 3-D pose estimation of a single arbitrarily shaped, rigid object at rates up to 10Hz is described. A triangular mesh model of the object to be tracked is generated offline using conventional range sensors. Real-time range data of the object is sensed by the CMU high speed VLSI range sensor. Pose estimation is performed by registering the real-time range data to the triangular mesh model using an enhanced implementation of the Iterative Closest Point (ICP) Algorithm introduced by Besl and McKay. The method does not require explicit feature extraction or specification of correspondence. Pose estimation accuracies on the order of 1mm in translation and 1 degree in rotation were measured. DTIC

N94-26150*# National Aeronautics and Space Administration. Marshall Space Flight Center, Huntsville, AL.
SURVEY OF VISUALIZATION AND ANALYSIS TOOLS
P. J. Meyer Jan. 1994 38 p
(NASA-TM-108436; NAS 1.15:108436) Avail: CASI HC A03/MF A01

A large number of commercially available visualization and analysis tools are available to the researcher. Some of the strengths and limitations of some of these tools, from the viewpoint of the earth sciences discipline, are discussed. Visualization and analysis tools fall into one of two categories: those that are designed to a specific purpose and are non-extensive and those that are generic visual programming tools that are extensible. Most of the extensible packages examined incorporate a data flow paradigm. Author (revised)

N94-26358# Materials Research Labs., Ascot Vale (Australia).
BREAKWIRE TECHNIQUE FOR HYPERVELOCITY MEASUREMENT
Michael Podlesak Sep. 1993 44 p
(AD-A274779; MRL-TR-92-39; DODA-AR-008-223) Avail: CASI HC A03/MF A01

An electrical breakwire technique for measuring the speed of hypervelocity projectiles is described and assessed, using Boomer, a large scale exploding foil flying plate generator. Two techniques were tested, a dual breakwire method and a single breakwire method. The dual breakwire method is the simpler of the two, but it was found to be less reliable than the single breakwire approach. With the single breakwire method, a reasonable approximation to the projectile's velocity-time-history can be obtained by conducting a series of experiments where a range of times of arrival of the flyer is measured as a function of the breakwire position only. However, accuracy of this technique depends on shot-to-shot consistency and the velocity versus time resolution is limited by the number of different positions of the projectile's trajectory at which the firings can be performed. Compared with other velocity measurement techniques, the breakwire method was found reasonably consistent and effective, in terms of simplicity, turnaround time, low cost and ability to operate within an environment containing high levels of electromagnetic noise in the radio-frequency and optical spectrum. Analysis of the breakwire data from Boomer experiments has indicated a possibility of improvement in the accuracy of the single breakwire technique through correlation of the time-of-break with variations in the Boomer-current waveform. DTIC

N94-26378 Gosudarstvennyi Komitet po Ispolzovaniyu Atomnoi Energii, Serpukhov (USSR). Inst. Fiziki Vysokikh Ehnergij.
CALORIMETER WITH WLS FIBERS AND PARALLEL TO BEAM SCINTILLATORS
V. I. Kryshkin, V. G. Lapshin, A. I. Mysnik, V. A. Polyakov, A. I. Ronzhin, and B. V. Chujko 1992 4 p Limited Reproducibility: More than 20% of this document may be affected by microfiche quality
(DE93-634188; IHEP-OEF-92-95) Avail: CASI HC A01 (US Sales Only)

A sandwich calorimeter with scintillating tiles placed parallel to the beam and light collection by optical fibers doped with a wave length shifter is described. The results on beam test of the electromagnetic calorimeter module are presented and a structure for barrel hadron calorimeter is proposed. DOE

N94-26394 Gosudarstvennyi Komitet po Ispolzovaniyu Atomnoi Energii, Serpukhov (USSR). Inst. Fiziki Vysokikh Ehnergij.
THE 1024 SCINTILLATION HODOSCOPE [STSINTILLYATSIONNYJ GODOSKOP NA 1024 KANALA]
A. V. Vasilev, A. N. Galyaev, V. I. Kotov, and I. Z. Mandzhavidze 1992 8 p In RUSSIAN Limited Reproducibility: More than 20% of this document may be affected by microfiche quality
(DE93-634183; IFVE-ONF-92-42) Avail: CASI HC A02 (US Sales Only)

The main characteristics of the 1024 channel scintillation hodoscope and the measurement methods are given. The number of photoelectrons from the farthest point of scintillator respect to PM is 4-7; the effective speed of light across the scintillator is 15 cm/nsec; the hodoscope efficiency is 98%. The coincidence curves are measured for different H.V. values. DOE

N94-26395 Gosudarstvennyi Komitet po Ispolzovaniyu Atomnoi Energii, Serpukhov (USSR). Inst. Fiziki Vysokikh Ehnergij.
PHYSICAL CHARACTERISTICS OF POLYMETHYLMETHACRYLATE SCINTILLATOR SOFG-120 [FIZICHESKIE KHARAKTERISTIKI POLIMETILMETAKRILATNOGO STSINTILLYATORA SOFG-120]
S. V. Belikov, S. N. Gurzhiev, and A. P. Dyachkov et al 1992 8 p In RUSSIAN Submitted for publication Limited Reproducibility: More than 20% of this document may be affected by microfiche quality
(DE93-634184; IFVE-ONF-92-47) Avail: CASI HC A02 (US Sales Only)

Characteristics of the polimethylmetacrylate scintillator which is used for the fast scintillating trigger in the liquid argon neutrino detector of the Tagged Neutrino Facility are studied. Scintillator SOFG-120 consists of PMMA-85%, naphtalene-14%, PPO-0.8%, and POPOP-0.08%. As main characteristics, spectral emission, light output (50% NE-110), time resolution 4.8 ns, and attenuation length (for sheet 1265x333x22 mm(exp 3)) lambda approximately = m were obtained. DOE

N94-26396 Gosudarstvennyi Komitet po Ispolzovaniyu Atomnoi Energii, Serpukhov (USSR). Inst. Fiziki Vysokikh Ehnergij.
UNSEGMENTED ELECTROMAGNETIC CALORIMETER PROTOTYPE. ENERGY AND COORDINATE RESOLUTION [PROTOTIP NESEGMENTIROVANNOGO EHLEKTROMAGNITNOGO KALORIMETRA. EHNERGETICHESKOE I KOORDINATNOE RAZRESHENIYA]
V. V. Babintsev, A. P. Vorobev, E. A. Eremchenko, Eh. P. Kistenev, A. A. Neushkin, V. F. Perelygin, V. N. Ryadovikov, and A. G. Kholodenko 1992 11 p In RUSSIAN Limited Reproducibility: More than 20% of this document may be affected by microfiche quality
(DE93-634185; IFVE-ONF-92-9) Avail: CASI HC A03 (US Sales Only)

Energy and coordinate resolutions of unsegmented layered uranium calorimeters with the scintillator with cross sections of 40 x 20 cm and 15 x 15 cm have been determined. The obtained experimental data are compared with the results of the calorimeter simulation using the GEANT3.13 program. The obtained results are in a good agreement with the analytical predictions both for the calorimeter with the 0.5 cm uranium plate and that with a 0.2 cm uranium plate. The conclusion is made on a possibility to use those type calorimeters in physical experiments. DOE

N94-26397 Gosudarstvennyi Komitet po Ispolzovaniyu Atomnoi Energii, Serpukhov (USSR). Inst. Fiziki Vysokikh Ehnergij.
HADRON GAS IONIZATION CALORIMETERS [ADRONNYJ GAZOVYJ IONIZATSIONNYJ KALORIMETR]
Yu. V. Gilitskij, S. P. Denisov, and A. Yu. Dushkin et al 1992 15 p In RUSSIAN Submitted for publication Limited Reproducibility: More than 20% of this document may be affected by microfiche quality
(DE93-634186; IFVE-ONF-92-98) Avail: CASI HC A03 (US Sales Only)

The characteristics dependence of the hadron gas ionization calorimeter with flat parallel geometry of electrodes on energy, electric field strength and operating gas pressure (95%Ar+5%C F4 mixture) has been studied. Electron/hadron ratio has been measured to be 1.13 +/- 0.03. The ionization signal duration is equal to 40 ns. The formula, describing the energy resolution dependence on energy in the 30-60 GeV range under 40 atm pressure, is given. DOE

N94-26439 Gosudarstvennyi Komitet po Ispolzovaniyu Atomnoi Energii, Serpukhov (USSR). Inst. Fiziki Vysokikh Ehnergii.
STUDY ON THE COMPENSATED LEAD HADRON CALORIMETER CHARACTERISTICS BY MEANS OF HADRON AND ELECTRON BEAMS [IZUCHENIE KHARAKTERISTIK KOMPENSIROVANNOGO SVINTSOVOGO ADRONNOGO KALORIMETRA NA PUCHKAKH ADRONOV I EHLEKTRONOV]
G. A. Alekseev, V. D. Apokin, and O. V. Buyanov et al 1992 14 p In RUSSIAN Limited Reproducibility: More than 20% of this document may be affected by microfiche quality
(DE93-634176; IFVE-OEF-92-36) Avail: CASI HC A03 (US Sales Only)

The results on measuring the basic characteristics of a compensated lead calorimeter (NEPTUN experiment) in a hadron and electron beam are presented. A prototype consisting of 30 modulus was used in the measurements. The energy resolution follows the dependence approximately = 57%/sq. root of E, the detector uniformity is (+-)5%, the measured e/h ratio is close to unity. DOE

N94-26525# Lawrence Livermore National Lab., CA.
ON THE APPLICATION OF ALLAN VARIANCE METHOD FOR RING LASER GYRO PERFORMANCE CHARACTERIZATION
L. C. Ng 15 Oct. 1993 29 p
(Contract W-7405-eng-48)
(DE94-003880; UCRL-ID-115695) Avail: CASI HC A03/MF A01

The method of Allan variance and its application to the characterization of a Ring Laser Gyro's (RLG) performance is described. Allan variance, a time domain analysis technique, is an accepted IEEE standard for gyro specifications. The method was initially developed by David Allan of the National Bureau of Standards to quantify the error statistics of a Cesium beam frequency standard employed as the U.S. Frequency Standards in the 1960's. The method can, in general, be applied to analyze the error characteristics of any precision measurement instrument. The key attribute of the method is that it allows for a finer, easier characterization and identification of error sources and their contribution to the overall noise statistics. An overview of the method is presented, the relationship between Allan variance and power spectral density distribution of underlying noise sources is explained, the batch and recursive implementation approaches are described, the Allan variance computation is validated with a simulation model, and the Allan variance method is illustrated using data collected from several Honeywell LIMU units. DOE

N94-26568# HITEC Products, Inc., Ayer, MA.
ATTACHMENT TECHNIQUES FOR HIGH TEMPERATURE STRAIN Final Report, Nov. 1990 - Jan. 1993
Steve P. Wnuk, Jr. Jan. 1993 147 p
(Contract F33615-90-C-3215)
(AD-A274766; WL-TR-93-3020) Avail: CASI HC A07/MF A02

Attachment methods for making resistive strain measurements to 2500 F were studied. A survey of available strain gages and attachment techniques was made, and the results are compiled for metal and carbon composite test materials. A theoretical analysis of strain transfer into a bonded strain gage was made, and the important physical parameters of the strain transfer medium, the ceramic matrix, were identified. A pull tester to measure pull-out tests on commonly used strain gage cements indicated that all cements tested displayed adequate strength for good strain transfer. Rokide flame sprayed coatings produced significantly stronger bonds than ceramic cements. An in-depth study of the flame spray process produced simplified installation procedures which also resulted in greater reliability and durability. Application procedures incorporating improvements made during this program are appended to the report. Strain gages installed on carbon composites, Rene' 41, 316 stainless steel, and TZM using attachment techniques developed during this program were successfully tested to 2500 F. Photographs of installation techniques, test procedures, and graphs of the test data are included in this report. DTIC

N94-26647 Prins Maurits Lab. TNO, Rijswijk (Netherlands). Pulse Physics Lab.
FLASH UNIT FOR HIGH SPEED PHOTOGRAPHY Final Report [FLITSEENHEID VOOR ULTRA SNELLE FOTOGRAFIE]
M. Koops and T. Huijser Sep. 1992 52 p In DUTCH Sponsored by DWOO, The Hague, Netherlands; TNO Defence Research, Delft, Netherlands; and DOD, Washington, DC Original contains color illustrations
(Contract A87/K/046)
(PML-1992-91; TD92-1511; ETN-94-94937) Copyright Avail: Issuing Activity (TNO-Prins Maurits Lab., P. O Box 45, 2280 AA Rijswijk, Netherlands)

A high energy pulsed light source for application in high speed photography was developed. The flash unit uses a xenon flash tube and a pulsed energy source, consisting of a semi-transmission line. The flash unit supplies a square light pulse of 1 ms duration and with 4 kJ electrical energy. Relevant technical data of the components is added. The report is also meant as an operation manual for the flash unit. ESA

N94-26662 University of Western Ontario, London. Dept. of Physics.
THE RESPONSE OF AN HYPERPURE Ge DETECTOR TO IONIZING RADIATION Ph.D. Thesis
Shaoying Tong Jul. 1993 172 p
(ISBN-0-315-83968-6; CTN-94-61044) Copyright Avail: Micromedia Ltd., Technical Information Centre, 240 Catherine Street, Suite 305, Ottawa, Ontario, K2P 2G8, Canada HC/MF

The detailed response of a hyperpure Ge detector to ionizing radiation was studied with regard to the radiation ionization energy ratio Ei/E0, using radioactive alpha and gamma sources and accelerated ion beams. Effects of temperature and bias voltage variation were investigated. The response to charged particles and gamma rays was measured simultaneously by using 152Eu, 60Co, and 137Cs gamma ray sources. Contrary to earlier conclusions, a difference of about 1 percent between E0 and E(alpha or proton) was found in Ge, often showing results qualitatively in accord with the observed behavior for Si semiconductor detectors. The functional behavior of E(alpha)/E0 and E(proton)/E0 exhibits a nonlinear response of the Ge detector as a function of ion energy for a given projectile, similar to the results observed for Si detectors. The energy loss in the window of the Ge detector is found to vary with the energy of the incident particle in a manner that does not agree with the stopping power curve. Pronounced channeling effects are evident in the pulse height spectra as the incidence angle of the ions is rotated with respect to the detector surface normal. Monte Carlo calculations of the projectile energy loss under channeling conditions are in qualitative agreement with experimental observations. Author (CISTI)

N94-26707*# National Aeronautics and Space Administration. Langley Research Center, Hampton, VA.
EVALUATION OF THE PROTOTYPE DUAL-AXIS WALL ATTITUDE MEASUREMENT SENSOR
Douglas T. Wong Feb. 1994 46 p
(RTOP 505-59-54-02)
(NASA-TM-109056; NAS 1.15:109056) Avail: CASI HC A03/MF A01

A prototype dual-axis electrolytic tilt sensor package for angular position measurements was built and evaluated in a laboratory environment. The objective was to investigate the use of this package for making wind tunnel wall attitude measurements for the National Transonic Facility (NTF) at NASA Langley Research Center (LaRC). The instrumentation may replace an existing, more costly, and less rugged servo accelerometer package (angle-of-attack package) currently in use. The dual-axis electrolytic tilt sensor package contains two commercial electrolytic tilt sensors thermally insulated with NTF foam, all housed within a stainless steel package. The package is actively heated and maintained at 160 F using foil heating elements. The laboratory evaluation consisted of a series of tests to characterize the linearity, repeatability, cross-axis interaction, lead wire effect, step response, thermal time constant, and rectification errors. Tests revealed that the total RMS errors for the x-axis sensor is 0.084 degree, and 0.182 degree for the y-axis sensor. The RMS errors are greater than the 0.01 degree specification required for NTF wall attitude measurements. It is therefore not a viable replacement for the angle-of-attack package in the NTF application. However, with some physical modifications, it can be used as an inexpensive 5-degree range dual-axis inclinometer with overall accuracy approaching 0.01 degree under less harsh environments. Also, the data obtained from the tests can be valuable for wind tunnel applications of most types of electrolytic tilt sensors. Author (revised)

N94-26787# Brookhaven National Lab., Upton, NY.
DESIGN OF A HIGH-PRECISION DOUBLE CRYSTAL TUNABLE MONOCHROMATOR
M. Shleifer, S. Sharma, M. Woodle, E. Rotela, and C. Brite 1993 4 p Presented at the Annual Meeting of the Society of Photo-Optical Instrumentation Engineers (SPIE), San Diego, CA, 11-16 Jul. 1993
(Contract DE-AC02-76CH-00016)
(DE94-003004; BNL-49661; CONF-930722-52) Avail: CASI HC A01/MF A01

This paper describes a UHV-compatible double crystal monochromator with independent drives for 2 linear and 2 angular crystal motions. Precise angular crystal positioning is achieved by using a spindle with a double gimbal mechanism which converts linear motion of 0.1 micron to an angular motion of 0.042 arcsec. In order to decrease thermal distortions the crystal intercepting white beam is watercooled. DOE

N94-27044# Swedish Inst. for Materials Testing, Boras. Div. of Fire Technology.
SP INDUSTRY CALORIMETER FOR RATE OF HEAT RELEASE MEASUREMENTS UP TO 10MW
Martin Dahlberg 1993 23 p
(PB94-124211; SP-RAPP-1992:43; ISBN-91-7848-361-1) Avail: CASI HC A03/MF A01

The Swedish National Testing and Research Institute (SP) has installed a 10 MW fire calorimeter for rate of heat release measurements, similar to the one at Factory Mutual Research Corporation (FMRC). It can be used to classify commodities with respect to their fire hazard, to evaluate the efficiency of sprinkler systems, for chemical analysis of the combustion gases from hazardous fires, to produce input data for the fire modelling, etc. A large hood collects the fire gases and leads them into a duct where gas velocity, gas temperature, smoke density, and contents of oxygen, carbon dioxide, and carbon monoxide are measured. On the basis of these measurements, mass flow and rate of heat release are calculated. The rate of heat release is calculated according to the oxygen consumption principle. The upper limit for measurements is approximately 10 MW and the lower is 0.1 MW. NTIS

N94-27134# Physics and Electronics Lab. TNO, The Hague (Netherlands).
CCD-CAMERA IMAGES OF BEST-TWO AND PROCESSING RESULTS Final Report [CCD-CAMERABEELDEN VAN BEST-TWO EN RESULTATEN VAN BEELDBEWERKING]

J. A. Boden, M. Deutekom, and M. J. Wilmink Apr. 1993 136 p
(AD-A274140; FEL-93-A057; TDCK-93-0466) Avail: CASI HC A07/MF A02

A survey is presented of the 'still video' pictures that have been recorded with 3 CCD-cameras during the BEST-TWO trial in Mourmelon, France. The composition of and selection for two databases is described, and the results of processing with the FELimage processing algorithm are given. A statistical analysis of these processing results is carried out and described. For each scenario, one or more examples of processed images are given. DTIC

N94-27160 Sveriges Lantbruksuniv., Uppsala. Inst. foer Virkeslaera.
CALIBRATING/TESTING METERS IN HOT WATER TEST BENCH VM7 [KALIBRERING/PROVNING AV MAETARE I UTRUSTNING VARM-VATTENBAENK VM7]
E. Kling, K. Stolt, P. Lau, and K. Mattiasson 1993 44 p In SWEDISH
(PB94-124294; SP-RAPP-1993:26) Avail: Issuing Activity (National Technical Information Service (NTIS))

A Hot Water Test Bench, VM7, has been developed and constructed for the calibration and testing of volume and flowmeters, in a project at the National Volume Measurement Laboratory at the Swedish National Testing and Research Institute. The intended area of use includes use as a reference at audit measurements, e.g. for accredited laboratories, calibration of meters for the industry and for the testing of hot water meters. The objective of the project, which was initiated in 1989, was to design equipment with stable flow and with a minimal temperature drop even at very low flow rates. The principle of the design is a closed system with two pressure tanks at different pressures. The water is led from the high pressure tank through the test object and the volume standard, in the form of master meters or a piston prover alternatively, to the low pressure tank. Calibrations/tests are made comparing the indication of the test object to that of master meters covering the current flow rate. These are, in the same test cycle, calibrated to the piston prover. Alternatively, the test object can be calibrated directly to the piston prover. NTIS

N94-27214*# Pennsylvania State Univ., University Park. Materials Research Lab.
HIGH TEMPERATURE SENSOR/MICROPHONE DEVELOPMENT FOR ACTIVE NOISE CONTROL Final Technical Report, 1 Dec. 1990 - 30 Nov. 1993
Thomas R. Shrout 1993 165 p
(Grant NAG3-1225)
(NASA-CR-195214; NAS 1.26:195214) Avail: CASI HC A08/MF A02

The industrial and scientific communities have shown genuine interest in electronic systems which can operate at high temperatures, among which are sensors to monitor noise, vibration, and acoustic emissions. Acoustic sensing can be accomplished by a wide variety of commercially available devices, including: simple piezoelectric sensors, accelerometers, strain gauges, proximity sensors, and fiber optics. Of the several sensing mechanisms investigated, piezoelectrics were found to be the most prevalent, because of their simplicity of design and application and, because of their high sensitivity over broad ranges of frequencies and temperature. Numerous piezoelectric materials are used in acoustic sensors today; but maximum use temperatures are imposed by their transition temperatures (T(sub c)) and by their resistivity. Lithium niobate, in single crystal form, has the highest operating temperature of any commercially available material, 650 C; but that is not high enough for future requirements. Only two piezoelectric materials show potential for use at 1000 C; AlN thin film reported to be piezoactive at 1150 C, and perovskite layer structure (PLS) materials, which possess among the highest T(sub c) (greater than 1500 C) reported for ferroelectrics. A ceramic PLS composition was chosen. The solid solution composition, 80% strontium niobate (SN) and 20% strontium tantalate (STa), with a T(sub c) approximately 1160 C, was hot forged, a process which concurrently sinters and renders the plate-like grains into a highly oriented configuration to enhance piezo properties. Poled samples of this composition showed coupling (k33) approximately 6 and piezoelectric strain constant (d33) approximately 3. Piezoactivity was seen at 1125 C, the highest temperature measurement reported for a ferroelectric ceramic. The high temperature piezoelectric responses of this, and similar PLS materials, opens the possibility of their use in electronic devices operating at temperatures up to 1000 C. Concurrent with the materials study was an effort to define issues involved in the development of a microphone capable of operation at temperatures up to 1000 C; important since microphones capable of operation above 260 C are not generally available. The distinguishing feature of a microphone is its diaphragm which receives sound from the atmosphere: whereas, most other acoustic sensors receive sound through the solid structure on which they are installed. In order to gain an understanding of the potential problems involved in designing and testing a high temperature microphone, a prototype was constructed using a commercially available lithium niobate piezoelectric element in a stainless steel structure. The prototype showed excellent frequency response at room temperature, and responded to acoustic stimulation at 670 C, above which temperature the voltage output rapidly diminished because of decreased resistivity in the element. Samples of the PLS material were also evaluated in a simulated microphone configuration, but their voltage output was found to be a few mV compared to the 10 output of the prototype. Author (revised)

N94-27216 National Defence Research Establishment, Linkoeping (Sweden). Huvudavdelning foer Informationsteknologi.
CMT-SI [IR-CCD KAMERA]
S. Lindstroem Jun. 1993 72 p In SWAHILI
(PB94-123619; FOA-C-30716-8.3) Avail: Issuing Activity (National Technical Information Service (NTIS))

The specification of and problems met with the realization of an infrared camera (IR-camera) with an IR-charge coupled device (IR-CCD) sensor of CMT-Si type, and the hardware construction are described. The construction of a digital data collection unit for a Personal Computer (PC) is described. In addition to the IR-camera, an implementation of a seeker algorithm (correlation) in real time is described. The seeker algorithm is processed in the signal processing unit UMISIL (acronym from Swedish 'Universellt bildMInne med SIgnaLprocessor') connected to a gyro-stabilized platform. NTIS

N94-27229*# Alabama Univ., Huntsville. Center for Applied Optics.
ADVANCED TECHNOLOGY DEVELOPMENT MULTI-COLOR HOLOGRAPHY Final Report, 1 Feb. 1993 - 31 Jan. 1994
Chandra S. Vikram 19 Jan. 1994 36 p
(Contract NAS8-38609)
(NASA-CR-193931; NAS 1.26:193931; UAH5-33157) Avail: CASI HC A03/MF A01

Several key aspects of multi-color holography and some non-conventional ways to study the holographic reconstructions are considered. The error analysis of three-color holography is considered in detail with particular example of a typical triglycine sulfate crystal growth situation. For the numerical analysis of the fringe patterns, a new algorithm is introduced with experimental verification using sugar-water solution. The role of the phase difference among component holograms is also critically considered with examples of several two- and three-color situations. The status of experimentation on two-color holography and fabrication of a small breadboard system is also reported. Finally, some successful demonstrations of unconventional ways to study holographic reconstructions are described. These methods are deflectometry and confocal optical processing using some Spacelab III holograms. Author (revised)

N94-27257 Carleton Univ., Ottawa (Ontario). Dept. of Physics.
THE OPAL VERTEX DETECTOR Ph.D. Thesis
J. Michael Roney Feb. 1989 264 p
(ISBN-0-315-51152-4; CTN-94-60971) Copyright Avail: Micromedia Ltd., Technical Information Centre, 240 Catherine Street, Suite 305, Ottawa, Ontario, K2P 2G8, Canada HC/MF

A high resolution charged particle tracking detector has been developed to measure vertex topologies of the subatomic particles produced in e+ e- collisions. The vertex detector is a cylindrical drift chamber segmented radially into an axial and stereo layer, each divided into 36 jet cells. A detector prototype containing four axial and two stereo cells was built to measure various characteristics of the detector design and to determine the limitations of spatial resolution in this design. It was studied using a pion test beam under a variety of operating conditions with two types of chamber gas. The prototype experiments showed that the detector drift time resolutions were limited mainly by chamber pulse nonuniformities. If a gas having a reduced drift velocity is used, the design has a potential for obtaining resolutions better than 30 micrometers. A simple calibration technique that preserved most of the intrinsic resolution was developed.

Under optimal conditions, the end-to-end difference technique provided a measurement with a resolution of 100 ps, equivalent to a spatial resolution of 2 cm. The OPAL vertex detector was built on the basic prototyped design with some modifications that would optimize the detector for operation with a low drift velocity gas. The results of the prototype studies were verified in early tests with the complete OPAL detector. Author (CISTI)

N94-27317 Calian Communications, Kanata (Ontario).
ACOUSTO-OPTICAL POST-PROCESSOR TIME-INTEGRATING CORRELATOR CALIBRATION UPDATES Final Report
P. Baker 12 Feb. 1992 11 p Limited Reproducibility: More than 20% of this document may be affected by poor print
(DSIS-94-00053; CTN-94-61092) Avail: Issuing Activity

The acousto-optical signal processing facility and time integrating correlator system has been updated to allow proper handling of multiple peaks and to increase the readout rate. These modifications are described. In the supervisor task, a phase shift dialog box has been added to the phase shift menu items. This dialog box allows the operator to limit the area examined while searching for peaks or to specify the peak location directly. An amplitude offset calibration dialog box has been added to the amplitude offset menu item. This dialog box allows the operator to limit the area examined during the amplitude offset calibration, which is designed to perform calculations on a portion of the correlogram that does not contain a peak. In addition, the interface between the photodetector and personal computer has been modified to double the maximum pixel clock rate to 10 MHz. Author (CISTI)

N94-27597 Defence Research Establishment, Ottawa (Ontario). Electromagnetics Section.
TEST AND EVALUATION OF THE LITTON (CANADA) CANADIAN STRAPDOWN GYROSCOPE (CSG-2) PERFORMANCE EVALUATION UNIT (PEU)
M. F. Vinnins and L. D. Gallop Sep. 1988 43 p
(DREO-1010; DSIS-94-00101; CTN-94-61115) Avail: CASI HC A03/MF A01

A prototype gyroscope used for evaluation purposes in an experimental attitude and heading reference system employs unique fabrication methods including laser welding and advanced electro-discharge machining. The result is a two degree of freedom, tuned rotor gyroscope which is highly stable yet inexpensive, capable of random drift rates of under 0.01 deg/hour. Two gyroscopes were integrated into a performance evaluation unit (PEU) containing three accelerometers in order to verify gyroscope performance in a harsh system environment. Extensive laboratory tests included measurements of drift coefficients, instrument misalignments, temperature sensitivity, and scale factor stability and deviation. System effects on instrument performance were evaluated. Individual gyroscope performance was well within specification although a relatively low torquer scale factor resulted in a predicted large scale factor deviation over the desired rate range due to torquer heating effects. System performance was seriously impaired due to the wheel noise caused by poor filtering and shielding within the package and poor temperature control of the PEU. In addition, since little effort was put into sensor modeling, software error compensation within the PEU is inadequate to demonstrate the instrument performance capabilities in a convincing manner. Author (CISTI)

N94-27615# Oak Ridge Inst. for Science and Education, TN.
RESONANT HOLOGRAPHIC MEASUREMENTS OF LASER ABLATION PLUME EXPANSION IN VACUUM AND ARGON GAS BACKGROUNDS Ph.D. Thesis
Roger Alan Lindley (Michigan Univ., Ann Arbor.) 1993 189 p
(Contract DE-AC05-76OR-00033)
(DE94-001407; DOE/OR-00033/T564) Avail: CASI HC A09/MF A02

This thesis discusses the following on resonant holographic measurements of laser ablation plume expansion: Introduction to laser ablation; applications of laser ablation; the study of plume expansion; holographic interferometry; resonant holographic interferometry; accounting for finite laser bandwidth; the solution for doppler broadening and finite bandwidth; the main optical table; the lumonics laser spot shape; developing and reconstructing the holograms; plume expansion in RF/plasma environments; determining lambda(sub o); resonant refraction effects; fringe shift interpretation; shot-to-shot consistency; laser ablation in vacuum and low pressure, inert, background gas; theoretically modeling plume expansion in vacuum and low pressure, inert, background gas; and laser ablation in higher pressure, inert, background gas. DOE

N94-27624# Los Alamos National Lab., NM.
ADVANCES IN GAMMA RAY FIELD INSTRUMENTATION AT LOS ALAMOS
J. K. Halbig, S. F. Klosterbuer, P. A. Russo, J. K. Sprinkle, Jr., and S. E. Smith (Oak Ridge Y-12 Plant, TN.) 1993 2 p Presented at the International Symposium on Nuclear Material Safeguards, Vienna, Austria, 14-18 Mar. 1994
(Contract W-7405-eng-36)
(DE93-040264; LA-UR-93-2784; CONF-940307-2) Avail: CASI HC A01/MF A01

A prototype miniature and modular multi-channel analyzer (M3CA) has been developed. The prototype brings together hardware and software technologies in an instrument that can be effectively used in many safeguards, arms control, nuclear industry, and environmental applications. The design uses modular building blocks for both hardware and software. It is much easier to interface to external controllers than previous instruments. The prototype instrument demonstrates that low-power instruments now have the capabilities and performance required in many applications where, previously, only mains-powered instruments have been used. This paper will summarize performance results of the prototype with regard to the first application as well as the ultimate performance of such an instrument. Derived from text

N94-27651# Waterloo Univ. (Ontario). Dept. of Systems Design Engineering.
FLEXIBLE RANGE FINDING APPLIED TO 3D SURFACE SYNTHESIS: A PSEUDO-TRINOCULAR APPROACH Ph.D. Thesis
Tongminh Hong 1992 219 p
(ISBN-0-315-84616-X; CTN-94-61067) Copyright Avail: Micromedia Ltd., Technical Information Centre, 240 Catherine Street, Suite 305, Ottawa, Ontario, K2P 2G8, Canada HC/MF

An important area in machine vision and computer graphics is surface modeling, which involves the issue of data acquisition. A new range finding system is proposed which exploits perspective invariance (cross ratio), the targeting capability of structural lighting (slide projector), and epipolar planes' geometry (trinocular strategy). The system allows a fully autonomous calibration process and is highly efficient in terms of speed and accuracy. The system eliminates the ambiguity in disparity matching experienced in stereopsis, the extra image processing encountered in the trinocular system, the tedious reorganization of range data into a rectangular domain for surface modeling, and the scanning process of most active range finders that are not suitable for moving objects. Research described includes the development of several new camera calibration techniques, reformulation of the epipolar lines geometry method, and a rigorous study of the orientation constraints of the sensors (cameras and projector) in order to enhance the robustness of the vision system. The superiority of this new pseudo trinocular approach over the active structural lighting method and the passive binocular and/or trinocular techniques is convincing. It is believed that the proposed range finder has considerable potential for surface modeling. Author (CISTI)

N94-27703# Japan Atomic Energy Research Inst., Tokyo.
MODE ANALYSIS OF GYROTRON OSCILLATION USING A k-SPECTROMETER
Atsushi Kasugai (Japan Atomic Energy Research Inst., Naka.), Keishi Sakamoto (Japan Atomic Energy Research Inst., Naka.), Sunao Maebara (Japan Atomic Energy Research Inst., Naka.), Masaki Tsuneoka (Japan Atomic Energy Research Inst., Naka.), and Takashi Nagashima (Japan Atomic Energy Research Inst., Naka.) May 1993 35 p In JAPANESE; In JAPANESE
(DE94-701195; JAERI-M-93-101) Avail: CASI HC A03/MF A01

Experimental analysis of an oscillation mode 500 kW gyrotron at 120 GHz with a TE12,2 whispering gallery mode is reported. Using a k-spectrometer, the oscillation mode was measured. As a result, the oscillation mode was confirmed to be TE12,2 whispering gallery mode, which coincides with the designed value. Also, it is recognized the gyrotron is operated at TE9,3 or TE6,4 mode by adjusting the axial magnetic field. In addition to the major mode, some spurious modes were observed.

These modes are considered to be caused by a mode conversion from the main mode in the transmission line between the gyrotron cavity and the k-spectrometer. DOE

N94-27763 LASIRIS, Inc., Saint-Laurent (Quebec).
DEVELOPMENT OF A HOLOGRAPHIC ILLUMINATION SYSTEM FOR A TIME-INTEGRATING CORRELATOR Final Report
Mar. 1992 11 p
(DSIS-94-00111; CTN-94-61124) Avail: CASI HC A03/MF A01

Work was performed to design and fabricate a special type of diffraction grating called a Dammann grating to be used as a precision beamsplitter for the illumination of a time integrating correlator. Dammann gratings are a type of binary phase computer generated hologram with a periodic fringe structure. The gratings had to show a very precise diffraction behavior. The reconstruction (or zero order) beam had to be almost eliminated while the first orders were maximized. The three steps in producing the grating include design of the diffractive structure, recording of the diffractive structure by E-beam, and recording of the Dammann gratings by microlithographic techniques. The optical performance of the Dammann gratings is compared to specifications, showing that the gratings are either very close to the required specifications or surpass them. Author (CISTI)

N94-27779# California Univ., Berkeley. Lawrence Berkeley Lab.
THE X RAY HOLOGRAPHIC MICROSCOPY USING THE ATOMIC-FORCE MICROSCOPE
M. R. Howells, C. J. Jacobsen (State Univ. of New York, Stony Brook.), and S. Lindaas (State Univ. of New York, Stony Brook.) Sep. 1993 15 p Presented at the 4th International Conference on X Ray Microscopy, Chenogolovka, Russia, 20-24 Sep. 1993
(Contracts DE-AC03-76SF-00098; DE-FG02-89ER-60858)
(DE94-004003; LBL-34663; CONF-9309290-1) Avail: CASI HC A03/MF A01

The present authors have been seeking for some time to improve the resolution of holographic microscopy and have engaged in a continuing series of experiments using the X1A soft x-ray undulator beam line at Brookhaven. The principle strategy for pushing the resolution lower in these experiments has been the use of polymer resists as x-ray detectors and the primary goal has been to develop the technique to become useful for examining wet biological material. The authors report on progress in the use of resist for high-spatial-resolution x-ray detection. This is the key step in in-line holography and the one which sets the ultimate limit to the image resolution. The actual recording has always been quite easy, given a high-brightness undulator source, but the difficult step was the readout of the recorded pattern. The authors describe how they have built a special instrument: an atomic force microscope (AFM) to read holograms recorded in resist. They report the technical reasons for building, rather than buying, such an instrument and they give details of the design and performance of the device. The authors also describe the first attempts to use the system for real holography and the authors show results of both recorded holograms and the corresponding reconstructed images. Finally, the authors try to analyze the effect that these advances are likely to have on the future prospects for success in applications of x-ray holography and the degree to which the other technical systems that are needed for such success are available or within reach. DOE

N94-27981*# National Aeronautics and Space Administration. Goddard Space Flight Center, Greenbelt, MD.
NIMBUS-7 EARTH RADIATION BUDGET CALIBRATION HISTORY. PART 2: THE EARTH FLUX CHANNELS
H. Lee Kyle, Douglas Richard R. Hucek (Research and Data Systems, Inc., Greenbelt, MD.), Philip E. Ardanuy (Research and Data Systems, Inc., Greenbelt, MD.), John R. Hickey (Eppley Lab., Inc., Newport, RI.), Robert H. Maschhoff (Computer Sciences Corp., Lanham, MD.), Lanning M. Penn (Research and Data Systems, Inc., Greenbelt, MD.), Brian S. Groveman (Gulton Industries, Inc., Albuquerque, NM.), and Brenda J. Vallette (Research and Data Systems, Inc., Greenbelt, MD.) Washington Mar. 1994 114 p
(Contract NAS5-31331; RTOP 665-10-70)
(NASA-RP-1335-Pt-2; Rept-94B00047; NAS 1.61:1335-Pt-2) Avail: CASI HC A06/MF A02

Nine years (November 1978 to October 1987) of Nimbus-7 Earth radiation budget (ERB) products have shown that the global annual mean emitted longwave, absorbed shortwave, and net radiation were constant to within about + 0.5 W/sq m. Further, most of the small annual variations in the emitted longwave have been shown to be real. To obtain this measurement accuracy, the wide-field-of-view (WFOV) Earth-viewing channels 12 (0.2 to over 50 micrometers), 13 (0.2 to 3.8 micrometers), and 14 (0.7 to 2.8 micrometers) have been characterized in their satellite environment to account for signal variations not considered in the prelaunch calibration equations. Calibration adjustments have been derived for (1) extraterrestrial radiation incident on the detectors, (2) long-term degradation of the sensors, and (3) thermal perturbations within the ERB instrument. The first item is important in all the channels; the second, mainly in channels 13 and 14, and the third, only in channels 13 and 14. The Sun is used as a stable calibration source to monitor the long-term degradation of the various channels. Channel 12, which is reasonably stable to both thermal perturbations and sensor degradation, is used as a reference and calibration transfer agent for the drifting sensitivities of the filtered channels 13 and 14. Redundant calibration procedures were utilized. Laboratory studies complemented analyses of the satellite data. Two nearly independent models were derived to account for the thermal perturbations in channels 13 and 14. The global annual mean terrestrial shortwave and longwave signals proved stable enough to act as secondary calibration sources. Instantaneous measurements may still, at times, be in error by as much as a few Wm(exp -2), but the long-term averages are stable to within a fraction of a Wm(exp -2). Author

N94-28098 Nationaal Inst. voor Kernfysica en Hoge Energiefysica, Amsterdam (Netherlands).
A PROTOTYPE PRESAMPLER FOR THE URANIUM-SCINTILLATOR CALORIMETER IN ZEUS
H. Grabosch (Deutsches Elektronen-Synchrotron, Zeuthen, Germany.), U. Holm (Hamburg Univ., Germany.), H. Kammerlocher (Hamburg Univ., Germany.), W. Kroeger (Hamburg Univ., Germany.), A. Meyer (Deutsches Elektronen-Synchrotron, Zeuthen, Germany.), T. Neumann (Hamburg Univ., Germany.), C. Rethfeldt, S. Schlenstedt (Deutsches Elektronen-Synchrotron, Zeuthen, Germany.), H. Tiecke, and M. Vreeswijk (Deutsches Elektronen-Synchrotron, Zeuthen, Germany.) 1993 26 p Limited Reproducibility: More than 20% of this document may be affected by microfiche quality
(NIKHEF-H/93-11; ZEUS-Note-93-059; ETN-94-95043) Avail: CASI HC A03

The design and test of a prototype presampler suitable for the Zeus calorimeter is described. The energy loss due to the presence of inactive material positioned in front of the Zeus calorimeter prototype is studied for electrons and hadrons in the energy range 10 to 100 GeV. A method to recover the energy loss is described. The correction of the energy loss for electrons and hadrons where the amount of inactive material is not exactly known is calculated. It is shown that the calorimetric energy measurements, after correction with the presampler signal, agrees to within about 1% of the nominal beam energy, with only a minor deterioration in the energy resolution. The presampler information can contribute to the electron hadron identification and position determination in regions where inactive material is positioned in front of the calorimeter. ESA

N94-25562# National Research Inst. for Metals, Tokyo (Japan). Chemical Processing Div.
DEVELOPMENT OF SO(x) AND NO(x) SOLID ELECTROLYTE SENSORS [SO(X), NO(X) KOTAI DENKAISHITSU SENSA NO KAIHATSU NI KANSURU KENKYU]
Hiroaki Nakamura, Mikihiko Kobayashi, Akira Kasahara, Yoichi Ogawa, Hiroaki Isago, and Isao Morinaka *In its* Bulletin of National Research Institute for Metals in Fiscal Year 1993, No. 14 29 Jan. 1993 p 153-164 In JAPANESE (For primary document see N94-25544 07-26)
Avail: CASI HC A03/MF A04

N94-27389# Tohoku Univ., Sendai (Japan). Inst. for Chemical Reaction Science.
VARIABLE TEMPERATURE COLD STAGE FOR MICROSCOPE OBSERVATION [ONDO KAHEN KENBIKYO TEION SUTEJI NO SHISAKU]
Hirosi Yamada, Minoru Hanaya (Tokyo Inst. of Tech., Japan.), Youichi Kanno, Takemitu Kikuchi, and Shinji Onodera *In its* Bulletin of the

Institute for Chemical Reaction Science, Tohoku University, Volume 2 30 Sep. 1992 p 39-40 In JAPANESE (For primary document see N94-27385 07-25)
Avail: CASI HC A01/MF A02

N94-27390# Tohoku Univ., Sendai (Japan). Inst. for Chemical Reaction Science.
HIGH-TEMPERATURE AND HIGH-PRESSURE FLOW CALORIMETER [KOON KOATSU RYUTSUSHIKI NETSURYOKEI]
Yoshio Abe, Yoichi Kanno, Minoru Takahashi, and Chiaki Yokoyama *In its* Bulletin of the Institute for Chemical Reaction Science, Tohoku University, Volume 2 30 Sep. 1992 p 41-45 In JAPANESE (For primary document see N94-27385 07-25)
Avail: CASI HC A01/MF A02

N94-27391# Tohoku Univ., Sendai (Japan). Inst. for Chemical Reaction Science.
GLASS CYLINDRICAL FILTER FOR ELECTROLYSIS CELL [DENKAISOYO GARASU ENTO FIRUTA NO SEISAKU]
Shinichi Abe and Fuminori Akiyama *In its* Bulletin of the Institute for Chemical Reaction Science, Tohoku University, Volume 2 30 Sep. 1992 p 47-48 In JAPANESE (For primary document see N94-27385 07-25)
Avail: CASI HC A01/MF A02

N94-27392# Tohoku Univ., Sendai (Japan). Inst. for Chemical Reaction Science.
POROUS VYCOR GLASS TUBE JOINED TO BOROSILICATE GLASS [TAKOSHITSU BAIKORU GARASUKAN NO YOSETSU]
Shinichi Abe, Takemitsu Kikuchi, and Shinji Onodera *In its* Bulletin of the Institute for Chemical Reaction Science, Tohoku University, Volume 2 30 Sep. 1992 p 49-50 In JAPANESE (For primary document see N94-27385 07-25)
Avail: CASI HC A01/MF A02

N94-27895*# Hampton Univ., VA. Dept. of Mass Media Arts.
RIAD VISUAL IMAGING BRANCH ASSESSMENT
Sherilee F. Beam *In* Old Dominion Univ., The 1993 NASA-ODU American Society for Engineering Education (ASEE) Summer Faculty Fellowship Program Dec. 1993 p 68-70 (For primary document see N94-27893 07-80)
Avail: CASI HC A01/MF A03

N94-27907*# Christopher Newport Coll., Newport News, VA. Dept. of Physics and Computer Science.
SPACECRAFT OPTICAL DISK RECORDER MEMORY BUFFER CONTROL
Robert F. Hodson *In* Old Dominion Univ., The 1993 NASA-ODU American Society for Engineering Education (ASEE) Summer Faculty Fellowship Program Dec. 1993 p 109-113 (For primary document see N94-27893 07-80)
Avail: CASI HC A01/MF A03

N94-27921*# Virginia Polytechnic Inst. and State Univ., Blacksburg. Dept. of Mechanical Engineering.
EVALUATION OF HIGH TEMPERATURE SUPERCONDUCTIVE THERMAL BRIDGES FOR SPACE-BORNE CRYOGENIC INFRARED DETECTORS
Elaine P. Scott *In* Old Dominion Univ., The 1993 NASA-ODU American Society for Engineering Education (ASEE) Summer Faculty Fellowship Program Dec. 1993 p 162-165 (For primary document see N94-27893 07-80)
Avail: CASI HC A01/MF A03

36 LASERS AND MASERS

Includes parametric amplifiers.
For related information see also *76 Solid-State Physics.*

N94-25616 Air Force Inst. of Tech., Wright-Patterson AFB, OH.
FAILURE MECHANISMS OF HIGH TEMPERATURE SEMICONDUCTOR LASERS M.S. Thesis
David H. Leicester Dec. 1993 185 p Limited Reproducibility: More than 20% of this document may be affected by microfiche quality
(AD-A273833; AFIT/GE/ENP/93D-01) Avail: CASI HC A09

The primary intent of this research was to determine the influence of three common degradation mechanisms--dark area defects, facet degradation, and contact degradation--on the operational lifetime of GaAs edge-emitting semiconductor lasers driven by continuous current at 100 C. Inherent to this work was the quantified characterization of the lasers during their operation. This characterization arose as the power output as a function of driving current at room temperature before and after laser exposure to 100 C ambient temperature. These power vs. current characterizations were conducted at room temperature on each laser before and after exposure to 100 C as well as at the beginning and end of each laser's exposure to 100 C. An additional means of examining laser degradation came from measuring the current required over time to maintain a constant power output of 5,7, or 10mW at the elevated temperature. The research demonstrated that facet degradation and contact degradation were minor contributors to the bulk of the data base's degradation. Dark area defects were thus the primary degradation mechanism as the data's gradually increasing current necessary to maintain constant output will attest. An HF acid rinse on one laser, reacting aggressively to local crystal defects, highlighted the growth of dark area defects toward the lasing cavity due to continued lasing. One trend in the data was left unexlained. As a whole, the lasers performed with higher slope efficiencies at elevated temperature, contrary to previously documented research. This topic deserves future research. DTIC

N94-25744# Air Force Inst. of Tech., Wright-Patterson AFB, OH.
CHARACTERIZATION OF NONLINEAR EFFECTS IN OPTICALLY PUMPED VERTICAL CAVITY SURFACE EMITTING LASERS M.S. Thesis
Scott L. Brown Dec. 1993 93 p
(AD-A273840; AFIT/GEO/ENP/93D-01) Avail: CASI HC A05/MF A01

The nonlinear characteristics of optically pumped Vertical Cavity Surface Emitting Lasers (VCSEL's) are identified, isolated, and quantified. Three different VCSEL's are evaluated including two with gain regions of bulk GaAs operating at 875nm and one multi-quantum well (MQW) InGaAs VCSEL operating at 950nm. The nonlinearities evaluated include those due to cavity temperature, carrier injection, and internal lasing field. The VCSEL's are pumped by a picosecond/femtosecond Ti:Sapphire laser which is configured to operate in CW, gated CW (minimum gate width was 200ns), picosecond, and gated picosecond modes. A linear relationship is shown between wavelength and substrate temperature, cavity temperature, and injected carriers. It is shown that heating is the dominate nonlinearity in the bulk gain region VCSEL's for the pump duty cycles which could be achieved. The MQW VCSEL was dominated by nonlinearities due to carrier population at duty cycles of 10% or less causing the VCSEL to blueshift. A nonlinear relationship is shown between input power and output power and is attributed to the optical Kerr effects in the mirror layers and gain region. DTIC

N94-25756# Stanford Univ., CA. Lab. of Physics.
ULTRA-HIGH AGGREGATE BANDWIDTH TWO-DIMENSIONAL MULTIPLE-WAVELENGTH DIODE LASER ARRAYS Semiannual Progress Report, 10 Apr. - 9 Dec. 1993
Connie Chang-Hasnain 9 Dec. 1993 12 p
(Contract N00014-93-1-0558)
(AD-A274018) Avail: CASI HC A03/MF A01

Two-dimensional (2D) multi-wavelength vertical cavity surface emitting laser (VCSEL) arrays is promising for ultrahigh aggregate capacity optical networks. A 2D VCSEL array emitting 140 distinct wavelengths was reported by implementing a spatially graded layer in the VCSEL structure, which in turn creates a wavelength spread. Concentrtion was on epitaxial growth techniques to make reproducible and repeatable multi-wavelength VCSEL arrays. Our approach to fabricate the spatially graded layer involves creating a nonuniform substrate surface temperature across the wafer during the growth of the cavity spacer region using the fact that the molecular beam epitaxy growth of GaAs is highly sensitive to the substrate temperature. Growth is investigated with the use of a patterned spacer (either a Ga or Si substrate) placed in-between the substrate and its heater. The temperature distribution on such wafers is used to guide our experiments. A reflectivity measurement apparatus that is capable of mapping a 2 in. wafer with a

100 microns diameter resolution was built for diagnosing our wafers. In this first six-month report, our calculations, the various experimental results, and a discussion on future directions are presented. DTIC

N94-26020# Lawrence Livermore National Lab., CA.
IMAGING WITH X RAY LASERS
L. B. DaSilva, B. Cauble, G. Frieders, J. A. Koch, B. J. MacGowan, D. L. Matthews, S. Mrowka, D. Ress, J. E. Trebes, and T. L. Weiland Nov. 1993 9 p Presented at the Annual Meeting of the Society of Photo-Optical Instrumentation Engineers (SPIE), San Diego, CA, 11-16 Jul. 1993
(Contract W-7405-eng-48)
(DE94-002844; UCRL-JC-114478; CONF-930722-54) Avail: CASI HC A02/MF A01

Collisionally pumped soft x-ray lasers now operate over a wavelength range extending from 35-300 Angstrom. These sources have high peak brightness and are now being utilized for x-ray imaging and plasma interferometry. In this paper we will describe our efforts to probe long scalelength plasmas using Moire deflectrometry and soft x-ray imaging. The progress in the development of short pulse x-ray lasers using a double pulse irradiation technique which incorporates a travelling wave pump will also be presented. DOE

N94-26112# National Lab. for High Energy Physics, Tsukuba (Japan).
THE PROCEEDINGS OF THE KEK FEL SIMULATION CODE WORKSHOP
Takuya Kamitani, ed. Nov. 1992 217 p In ENGLISH and JAPANESE Workshop held in Tsukuba, Japan, 15 Mar. 1991
(DE93-520378; KEK-Proc-92-12; CONF-9103277) Avail: CASI HC A10/MF A03

This is the record of the lectures given at the free electron laser simulation code workshop held at the National Laboratory for High Energy Physics on 15 Mar. 1991. As a result of the fact that free electron lasers can generate especially powerful and coherent light in the wide wavelength region from long wavelengths, such as microwaves, to short wavelengths, such as X-rays and gamma rays, the interest in free electron lasers has grown in Japan and foreign countries, and new experimentation has been carried out actively. As a result, the necessity for quantitative theoretical calculations using simulations has become paramount. This workshop was held for the express purpose of exchanging information and discussion. Thirty-nine persons took part in the workshop, and 11 lectures were presented. DOE

N94-26126# Los Alamos National Lab., NM.
ELASTIC BACKSCATTERING LIDAR FOR A MSTI SATELLITE
T. W. Meyer, D. M. Alde, and J. L. Banger et al 1993 6 p Presented at the Integrated Record Input System (IRIS) Meeting on Active Systems, Monterey, CA, 2-4 Nov. 1993
(Contract W-7405-eng-36)
(DE94-002701; LA-UR-93-3838; CONF-9311120-1) Avail: CASI HC A02/MF A01 (US Sales Only)

An elastic backscattering lidar is being built for the Ballistic Missile Defense Organization to fly on a MSTI (Miniature Seeker Technology Integration) satellite in low-earth orbit. It is planned that the 90-kg payload be designed, constructed, and tested in a two-year time interval. It features a 76-cm diameter primary light collection mirror and a diode-pumped Nd:YAG laser (1064 nm) emitting 1.5 joules per pulse at a repetition frequency of 50 Hz. The telescope, fixed with respect to the satellite, has a 6 deg field-of-regard, within which a scanning mirror will select the laser beam direction and the field-of-view of 0.5 mr. Other payload elements are the detector (avalanche photodiode) and the R3081-microprocessor-based payload control electronics. This payload will demonstrate the capability of a lidar system on a small satellite to track a theater missile both during boost phase and after burnout. Expected signal amplitudes will be presented, based on available data and on our own measurements of missile plumes with a ground-based lidar. Finally, missile tracking accuracies will be discussed. DOE

N94-26130# California Univ., Berkeley. Lawrence Berkeley Lab.
IMPROVED MEASUREMENT ACCURACY IN A LONG TRACE PROFILER: COMPENSATION FOR LASER POINTING INSTABILITY
S. C. Irick 2 Aug. 1993 9 p Presented at the Synchrotron Radiation Instrumentation, Gaithersburg, MD, 23-26 Aug. 1993
(Contract DE-AC03-76SF-00098)
(DE94-003408; LBL-34603; CONF-930824-27) Avail: CASI HC A02/MF A01

Laser pointing instability adds to the error of slope measurements taken with the Long Trace Profiler (LTP). As with carriage pitch error, this laser pointing error must be accounted for and subtracted from the surface under test (SUT) slope measurement. In the past, a separate reference beam (REF) allowed characterization of the component of slope error from carriage pitch. However, the component of slope error from laser pointing manifests itself differently in the SUT measured slope. An analysis of angle error propagation is given, and the effect of these errors on measured slope is determined. Then a method is proposed for identifying these errors and subtracting them from the measured SUT slope function. Separate measurements of carriage pitch and laser pointing instability isolate these effects, so that the effectiveness of the error identification algorithm may be demonstrated. DOE

N94-26157 Korean Atomic Energy Research Inst., Daeduk (Republic of Korea).
BROAD BAND TUNABLE DYE LASER DEVELOPMENT
Jong Min Lee, Jung Bog Kim, Sung Ho Kim, Do Kyung Go, Chang Hwan Lim, Si Pyo Rho, Kyu Seok Song, Byung Cheol Lee, Jong Hoon Rhi, and Jae Min Han et al Dec. 1992 81 p In KOREAN Limited Reproducibility: More than 20% of this document may be affected by microfiche quality
(DE93-632978; KAERI/RR-1143/92) Avail: CASI HC A05 (US Sales Only)

The technical goal and objectives are the development of a tunable laser which can be tuned from UV to near IR and commercialization for uses in various fields. Two kinds of resonators are developed. The user can select one resonator and change into the other without changing other parts. GIM type has a linewidth of 5 GHz which is able to be used usually, and a SLM type which has a very narrow linewidth of less than 1 GHz. Each system can have one or two amplifiers depending on output power or cost. High stability and safety, cost-down, and modules into about 30 components have been tried. We hope that this laser can help developments in researches of university, industry, and institute. DOE

N94-26178# Schwartz Electro-Optics, Inc., Concord, MA. Research Div.
THE DEVELOPMENT OF Cr, Tm, Ho:YAG LASERS FOR AIRBORNE LIDAR Final Report, 22 Jul. 1991 - 21 Jan. 1993
John H. Flint 22 Feb. 1993 29 p
(Contract F19628-91-C-0119)
(AD-A274895; PL-TR-93-2035; AD-E201724) Avail: CASI HC A03/MF A01

A research effort was conducted to determine the physical principles limiting the performance of pulsed Cr,Tm,Ho:YAG (CTH:YAG) lasers. The project was to conclude with the design of an eye-safe, aircraft-based transmitter for LIDAR and other remote sensing applications. The target specifications of the laser were: 100 mJ at 10 Hz repetition rate, single longitudinal mode, with a minimum pulse width of 500 ns. The research program investigated Q-switched operation of CTH:YAG lasers, flashlamp-pumped amplifiers, and injection seeding using diode-laser-pumped, single-frequency TH-YAG lasers. Up to 30 mJ was extracted in a TEM(sub 00) pulse at 10 Hz from both linear and ring resonators. The pulse widths at 30 mJ ranged from 200 ns to 400 ns. Injection-seeding of a ring resonator operating at 10 mJ per pulse at 7 Hz was demonstrated, and the output of this laser was amplified by a factor of three. The final task of this research program, the design of an aircraft-based transmitter, was incomplete at the end of the contract period. DTIC

N94-26184 Korean Atomic Energy Research Inst., Daeduk (Republic of Korea).
DEVELOPMENT OF AN INDUSTRIAL CO2 LASER FOR MASK MARKING
Cheol Jung Kim, Chin Mann Jung, Jeong Mook Kim, Kwang Suk Kim, Seong Ouk Kwon, Sang Mock Lee, and Duk Hyun Kim Jun. 1992 84 p In KOREAN Limited Reproducibility: More than 20% of this document may be affected by microfiche quality
(DE93-632901; KAERI/RR-1125/92) Avail: CASI HC A05 (US Sales Only)

We developed and commercialized an industrial pulsed TEA CO2 laser with high power and high repetition rate for printing characters and figures. Several commercial models have been investigated in design and performance. We improved its quality to the level of commercial TEA CO2 laser by an endurance test for each parts of laser system. The maximum pulse energy and repetition rate of our laser were above 5 J/pulse and 20 pps, respectively. Moreover, we designed the resolving power could be possible to 10 line/mm. Many optical parts were localized and lowered much in cost. Only few parts were imported and almost 90% in cost were localized. Also, to accelerate the commercialization by the joint company, the training and transfer of technology were pursued in the joint participation in design and assembly by company researchers from the early stage. DOE

N94-26185 Korean Atomic Energy Research Inst., Daeduk (Republic of Korea).

DEVELOPMENT OF SURGICAL CW Nd:YAG LASER WITH OPTICAL FIBER DELIVERY SYSTEM

Cheol Jung Kim, Jeong Mook Kim, Chin Mann Jung, Kwang Suk Kim, Min Suk Kim, Jae Wan Cho, and Duk Hyun Kim Jun. 1992 114 p In KOREAN Limited Reproducibility: More than 20% of this document may be affected by microfiche quality

(DE93-632902; KAERI/RR-1126/92) Avail: CASI HC A06 (US Sales Only)

We developed a surgical CW Nd:YAG laser with optical fiber delivery system. Several commercial models have been investigated in design and performance. We improved its quality to the level of commercial Nd:YAG laser by an endurance test for each parts of laser system. The maximum power of our surgical laser was 150 W and the laser pulse width could be controlled to 99 sec continuously by 0.1 sec. Many optical parts were localized and lowered much in cost. Only a few parts were imported and almost 90% in cost were localized. Also, to find out the maintenance problem of this surgical laser, it was applicated to the production line of our joint company. DOE

N94-26203# Norwegian Defence Research Establishment, Kjeller.

LASER-BASED COMMUNICATION LINK [LASERBASERT KOMMUNIKASJONSLINK]

Knut Stenersen, Stig Landroe, and Oeyvind Christensen 15 Apr. 1993 17 p In NORWEGIAN

(FFI-93/7023; ETN-94-95210) Avail: CASI HC A03/MF A01

A prototype of a laser based communication link for point to point transmission of data through the atmosphere is described. The link has a laser transmitter and a receiver at each end, which allows full duplex communication. The link has a EUROCOM B interface and can be used for transmission of 512 kbit/s data between two switches in the Norwegian military tactical communication system TADKOM. The data are transmitted through the air as FSK (Frequency Shift Keying) modulated laser light. The laser transmitter is an eyesafe 10 mW diode laser with 1.55 micrometer wavelength. The transmitter and receiver lobes have an angular divergence of about 1.5 mrad, and the system requires an alignment accuracy of better than 0.5 mrad for good performance. The maximum range of the link is slightly larger than the optical visibility for optical visibilities below 2 km. For 10 km visibility the maximum range is about 5 km. Based on available visibility statistics, it was calculated that a 1 km link should be in operation 97 to 99% of the time (average over one year) for typical locations in Norway. The link was tested with TADKOM equipment in laboratory. ESA

N94-26225# Technische Univ., Eindhoven (Netherlands). Dept. of Physics.

LASER MANIPULATION OF METASTABLE NEON ATOMS Ph.D. Thesis

Maarten Dirk Hoogerland 1993 96 p Sponsored by Stichting voor Fundamenteel Onderzoek der Materie

(ETN-94-95344) Avail: CASI HC A05/MF A01

The force that laser light exerts on neutral atoms is studied. The design, the tests and the operation of an atomic beam brightener are discussed. Doppler cooling to intensify a beam of metastable ((3s)-3(P(sub 2))) neon atoms by applying it into two dimensions is used. In order to increase the capture range of the cooling processs, curved wavefronts, keeping the angle between the laser beam and the atom trajectory at a fixed value, are used. The effects of running and standing laser fields on an ensemble of atoms with a well defined initial velocity by atomic beam deflection are studied. The deflection of a well collimated atomic beam of metastable neon atoms by a running laser wave is considered. Results giving the deviation of photon statistics of the resonance fluorescence from Poissonian statistics as a function of laser detuning and laser intensity are given. The results are compared to the results of a numerical simulation, showing excellent agreement. The first force and diffusion measurements on sub Doppler cooling processes are presented. The deflection of a well collimated atomic beam of metastable neon atoms by a short interaction with a (quasi) standing wave is investigated. ESA

N94-26271# Medox Research, Inc., Dexter, MI.

COMPACT, SOLID-STATE FEMTOSECOND SOURCE Final Report, Nov. 1992 - May 1993

Philippe Bado Oct. 1993 80 p

(Contract F30602-93-C0041)

(AD-A273932; RL-TR-93-188) Avail: CASI HC A05/MF A01

The goal of this program was to demonstrate that femtosecond laser sources (1 femtosecond = 10(exp -15) sec) can be made to be extremely compact and robust. We demonstrated the generation of ultrashort pulses using compact diode-pumped lasers. Our latest pump source is 300 times smaller and weighs only a fraction of today's commercial equivalent. It runs on 110 VAC and requires no water cooling. The commercial availability of robust sources will have a broad commercial impact. A brief listing includes: industry (3D imaging, ranging, thin-film monitoring, optical memory), medical (confocal microscopy, real-time assessment of surgical procedure), and military (sensor fusion, high-power THz beam generation, phase-array radars). We are pursuing the development of a general laboratory instrument, as well as several specific applications. This large market has not gone unnoticed: Japan's Ministry of International Trade and Industry (MITT) has very recently recommended Femtosecond Technology as one of Japan's only six priority research areas. DTIC

N94-26402# Korean Atomic Energy Research Inst., Daeduk (Republic of Korea).

STUDY ON LASER ATOMIC SPECTROSCOPY

Hyung Ki Cha, Kyu Seok Song, Do Young Jeong, Jong min Lee, Jong Hoon Yi, and Jung Bok Kim Jan. 1993 124 p In KOREAN

(DE93-633328; KAERI/RR-1166/92) Avail: CASI HC A06/MF A02 (US Sales Only)

Laser atomic spectroscopic study on actinium element has been performed in many areas of spectroscopy. The study on characteristic of atomic vapor has been proceeded for copper atom and the spatial density distribution of copper vapor is measured. This experimental data has been compared with the theoretically calculated data. In spectroscopic experiment, the first and second excited states for actinium element are identified and the most efficient ionization scheme for actinium element is identified. In addition, the corrosion problem for filament material due to the heating of the actinium element has been studied. DOE

N94-26403 Korean Atomic Energy Research Inst., Daeduk (Republic of Korea).

DEVELOPMENT OF REAL-TIME PULSE SHAPING TECHNOLOGY IN SOLID-STATE LASERS

Cheol Jung Kim, Jeong Mook Kim, Chin Mann Jung, Kwang Suk Kim, Min Suk Kim, Jae Wan Cho, and Duk Hyun Kim Feb. 1993 147 p In KOREAN Limited Reproducibility: More than 20% of this document may be affected by microfiche quality

(DE93-633438; KAERI/RR-1207/92) Avail: CASI HC A07 (US Sales Only)

Real-time pulse shaping technology in solid state lasers was developed for special cutting and welding applications. The real-time pulse shaping unit has the capability of 20 step variation in laser intensity, 200 steps in laser pulse width, and 16 pulse shape patterns with MOSFET pulse width modulation method. Also, a previous 250 W class Nd:YAG laser system was improved by using this new technology. Many optical parts were localized and lowered in cost. Only a few parts were imported and almost 90% of costs were localized. Also, to accelerate the commercialization by the joint company, the training and transfer of technology were pursued in the joint participation in design and assembly by company researchers from the early stage. Two Nd:YAG lasers have been assembled and will be tested in industrial manufacturing processes to prove the capability of developed Nd:YAG laser with potential users. DOE

N94-26498# Naval Postgraduate School, Monterey, CA.
LASER DOPPLER VELOCIMETRY IN A LOW SPEED MULTISTAGE COMPRESSOR M.S. Thesis
Joseph M. Utschig 23 Sep. 1993 97 p
(AD-A274836) Avail: CASI HC A05/MF A02

Two-dimensional Laser Doppler Velocimetry (LDV) measurements were taken in the Low Speed Multistage Compressor (LSMSC) with data indexed to the rotor position. Laser measurements were conducted at two axial positions downstream of the second rotor and one axial position downstream of the second stator. The entire rotor periphery was measured at fixed radial displacements at each location and ensemble averaged. The survey downstream of the stator attempted to quantify the unsteady flow of the stator passage. Attempts were made to quantify the absolute flow angle behind both the rotor and the stator and compare them to pneumatic data collected at the same axial and circumferential positions, respectively. Absolute flow angles calculated from the laser measurements were in agreement with pneumatic probe data. In addition, the surveys were conducted in an attempt to quantify the velocity profile from the rotor passage. The laser surveys indicated distinct and repeatable patterns in both the axial and circumferential components of the rotor exit velocity. Data downstream of the stator proved inconclusive. DTIC

N94-26520# Korean Atomic Energy Research Inst., Daeduk (Republic of Korea).
DEVELOPMENT OF HIGH AVERAGE POWER INDUSTRIAL Nd:YAG LASER WITH PEAK POWER OF 10 kW CLASS
Cheol Jung Kim, Jeong Mook Kim, Chin Mann Jung, Soo Sung Kim, Kwang Suk Kim, Min Suk Kim, Jae Wan Cho, and Duk Hyun Kim Mar. 1992 273 p In KOREAN
(DE93-633201; KAERI/RR-1106/91) Avail: CASI HC A12/MF A03 (US Sales Only)

We developed and commercialized an industrial pulsed Nd:YAG laser with peak power of 10 kW class for fine cutting and drilling applications. Several commercial models have been investigated in design and performance. We improved its quality to the level of commercial Nd:YAG laser by an endurance test for each parts of laser system. The maximum peak power and average power of our laser were 10 kW and 250 W, respectively. Moreover, the laser pulse width could be controlled from 0.5 msec to 20 msec continuously. Many optical parts were localized and lowered much in cost. Only few parts were imported and almost 90% in cost were localized. Also, to accelerate the commercialization by the joint company, the training and transfer of technology were pursued in the joint participation in design and assembly by company researchers from the early stage. Three Nd:YAG lasers have been assembled and will be tested in industrial manufacturing process to prove the capability of developed Nd:YAG laser with potential users. DOE

N94-26605# Los Alamos National Lab., NM.
DISTRIBUTED Nd:YAG LASER WELDING AND PROCESS CONTROL IN INERT GLOVE BOXES
J. O. Milewski, G. K. Lewis, M. R. Barbe, and D. A. Cremers 1993 7 p Presented at the American Welding Society International Conference on Modeling and Control of Joining Processes, Orlando, FL, 8 Dec. 1993
(Contract W-7405-eng-36)
(DE94-002629; LA-UR-93-3545; CONF-931234-3) Avail: CASI HC A02/MF A01

The authors have fabricated and assembled a fiber optic delivered Nd:YAG laser welding work station that consists of three glove boxes served by a single 1 kw laser. Processing considerations related to the welding of special nuclear materials, toxic materials, and complex part geometry are addressed within each work cell. The authors are proceeding with a development effort to integrate the equipment capabilities with remote sensing, process monitoring, and control systems. These systems will provide real time data acquisition during welding, monitoring and verification of weld parameters, and CAD/CAM to computer numerical control generated positioning paths. Computerized information storage, retrieval, and network methods are used for weld process documentation and data analysis. A virtual control panel is being configured to integrate the monitoring and control operation of individual subsystems, such as laser and motion control, into a single graphical interface. Development work on sensors to monitor laser beam characteristics and weld depth in real time with potential for adaptive control is in progress. System capabilities and results of these development efforts are presented. DOE

N94-26698# Lawrence Livermore National Lab., CA.
CALCULATIONS OF POPULATION TRANSFER DURING INTENSE LASER PULSES
K. J. Schafer and K. C. Kulander Aug. 1993 8 p Presented at the 6th International Conference on Multiphoton Processes, Quebec City, Quebec, 25-30 Jun. 1993
(Contract W-7405-eng-48)
(DE94-001060; UCRL-JC-114310; CONF-9306125-6) Avail: CASI HC A02/MF A01

Recent experiments by several groups have examined the question of population transfer to resonantly excited states during intense short laser pulses, in particular the amount of population that remains 'trapped' in excited states at the end of a laser pulse. Calculations of population transfer and resonant ionization in xenon at both 660 and 620 nm are presented. At the longer wavelength, the seven photon channel closes at 2.5 x 10(exp 13) W/cm(exp 2). Pulses with peak intensities higher than this result in 'Rydberg trapping', the resonant transfer of population to a broad range of high-lying states. The amount of population transferred depends on both the peak intensity and pulse duration. At 620 mm there are numerous possible six photon resonances to states with p or f angular momentum. A large number of calculations were performed for 40 fs pulses at different peak intensities and the population transferred to these low-lying resonant states were examined as a function of the peak laser intensity. We do not have room to comment upon the resonantly enhanced ionized electron energy spectra that we also determine in the same calculations. Our calculations involve the direct numerical integration of the time-dependent Schroedinger equation for an atom interacting with a strong laser field. The time-dependent wave function of a given valence electron is calculated on a spatial grid using a one-electron pseudo potential. This single active electron approximation (SAE) was shown to be a good approximation for the rare gases at the intensities and wavelengths that we will consider. The SAE potential used has an explicit angular momentum dependence which allows us to reproduce all of the excited state energies for xenon quite well. DOE

N94-26699# Lawrence Livermore National Lab., CA.
PHASE CONJUGATION AND PULSE COMPRESSION OF HIGH ENERGY LASERS: FROM NANOSECONDS TO MICROSECONDS
C. B. Dane and L. A. Hackel 1 Jun. 1993 5 p Presented at the 2nd International School and Topical Meeting on Applications of Nonlinear Optics, Prague, Czechoslovakia, 16-20 Aug. 1993
(Contract W-7405-eng-48)
(DE94-001061; UCRL-JC-114059; CONF-9308186-1) Avail: CASI HC A01/MF A01

SBS phase conjugation is playing a crucial role in the scaling of solid state laser systems to high average power. Amplifier systems with near diffraction limited beam quality were demonstrated with average power outputs of 100W in Nd:glass and Nd:YAG. Wavefront correction provided by an SBS phase conjugate mirror not only significantly lowers the output divergence of the laser, it also increases the maximum average power obtainable by preventing damage to optical components caused by distortion of the beam profile due to uncorrected thermally induced aberrations. The output pulsewidth format required for applications of high average power pulsed solid state lasers is extremely varied, ranging from below a nanosecond to many microseconds. However, most demonstrated applications of SBS phase conjugation to high average power laser systems have involved the amplification of typical Q-switched oscillator pulses of 7-30 ns in duration. Based on the requirements imposed by specific applications for high average power solid state laser systems, the operation of SBS phase conjugated amplifier systems with output pulsewidths ranging from 1 ns to 1 microns were investigated and demonstrated. The specific considerations for the various pulsewidth regimes as well as details of the experimental investigations are presented. DOE

N94-26705*# Schwartz Electro-Optics, Inc., Concord, MA. Research Div.
DEVELOPMENT OF LASERS OPTIMIZED FOR PUMPING Ti:Al2O3 LASERS Final Technical Report, 10 Apr. 1991 - 17 Dec. 1993

Glen A. Rines and Richard A. Schwarz Mar. 1994 103 p
(Contract NAS1-19304; RTOP 324-02-03)
(NASA-CR-4573; NAS 1.26:4573) Avail: CASI HC A06/MF A02

Laboratory demonstrations that were completed included: (1) an all-solid-state, broadly tunable, single-frequency, Ti:Al2O3 master oscillator, and (2) a technique for obtaining 'long' (nominally 100- to 200-ns FWHM) laser pulses from a Q-switched, Nd oscillator at energy levels commensurate with straightforward amplification to the joule level. A diode-laser-pumped, Nd:YLF laser with intracavity SHG was designed, constructed, and evaluated. With this laser greater than 0.9 W of CW, output power at 523.5 nm with 10 W of diode-laser pump power delivered to the Nd:YLF crystal was obtained. With this laser as a pump source, for the first time, to our knowledge, an all solid-state, single frequency, Ti:Al203 laser with sufficient output power to injection seed a high-energy oscillator over a 20-nm bandwidth was demonstrated. The pulsed laser work succeeded in demonstrating pulse-stretching in a Q-switched Nd:YAG oscillator. Pulse energies greater than 50-mJ were obtained in pulses with 100- to 200-ns pulsewidths (FWHM). Author (revised)

N94-26811# Sandia National Labs., Albuquerque, NM.
BEAM-QUALITY MEASUREMENTS FOR MATERIALS PROCESSING LASERS AND THE PROPOSED ISO STANDARD
P. W. Fuerschbach and M. Essien 1993 12 p Presented at the 1993 International Congress on Application of Lasers and Electro-Optics, Orlando, FL, 24-28 Oct. 1993
(Contract DE-AC04-94AL-85000)
(DE94-002738; SAND-93-1331C; CONF-9310194-2) Avail: CASI HC A03/MF A01

Laser beam-quality can indicate the maximum power density that can be obtained with a specific laser and serves as a figure-of-merit when comparing lasers, calibrating lasers, and in assessing a laser's operating condition. Measurements of laser beam-quality for a 1000 watt continuous wave CO2 laser and a 400 watt pulsed Nd:YAG laser have been completed. These measurements were made with two different type instruments: (1) a specially constructed apparatus that uses an integrating sphere and diamond apertures and (2) a commercially available instrument that incorporates a scanning and spinning hollow needle. Laser beam-quality and the propagation constants have been determined using a non-linear curve-fitting technique and the new proposed ISO standard for measuring laser beam-quality. The curve fitting analysis and the ISO analysis were found to produce approximately the same values for beam-quality and the propagation constants. However, a comparison of the experimental procedures required with the two techniques showed significant differences. The utility of the ISO technique was limited by it's experimental procedural restrictions. The importance of spherical aberration in distorting laser beam-quality measurements and in limiting the application of beam-quality to laser spotsize prediction is also detailed. DOE

N94-26940# Air Force Systems Command, Wright-Patterson AFB, OH. Foreign Aerospace Science and Technology.
OPTIMUM FOR THE GASDYNAMIC SYSTEM IN A FAST-AXIAL-FLOW CO2 LASER
Chengwu An, Shimin Li, Qisheng He, and Zaiguang Li 9 Dec. 1993 15 p Transl. into ENGLISH from Jiguang Zazhi (China), v. 10, no. 2, 1989 p 53-56
(AD-A274305; FASTC-ID(RS)T-0123-93) Avail: CASI HC A03/MF A01

It is reported that the temperature rise of the discharge mixture, in a fast-axial-flow CO2 laser, can be decreased by increasing both the mass flow rate and the speed of the mixture through the laser tube. However, increasing the mixture speed, in a practical gas dynamic system, will lead to decreasing the mass flow rate, and thus the discharge tube with appropriate cross section, which matches the properties of the given blower driving the mixture to flow, should be chosen to obtain the optimal operation of the laser. DTIC

N94-26941# Air Force Systems Command, Wright-Patterson AFB, OH. Foreign Aerospace Science and Technology Center.
PRACTICAL DESIGN OF RESONANT CAVITY FOR A RF FREE ELECTRON LASER
Mingchang Wang, Zhijiang Wang, Huifen Zhou, and Chengshi Feng 9 Dec. 1993 15 p Transl. into ENGLISH from Chinese Jnl. of Lasers (China), v. 17, no. 7, Jul. 1990 p 386-389
(AD-A274306; FASTC-ID(RS)T-0120-93) Avail: CASI HC A03/MF A01

Practical design of the resonant cavity for a RF free electron laser at 10.6 micrometers is proposed. For a given cavity length, the parameters, including the curvature of reflector, waist radius and spot size on reflectors, are calculated according to the Gaussian profile. The problem of spatial match between the radiation and the beam in a long narrow waveguide has been solved and the synchronization is discussed. DTIC

N94-27018# Lawrence Livermore National Lab., CA.
PHASE CONJUGATED LASERS APPLIED TO COMMERCIAL X RAY LITHOGRAPHY
L. A. Hackel, C. B. Dane, M. R. Hermann, and L. E. Zapata 1 Jun. 1993 6 p Presented at the 2nd International School and Topical Meeting on Applications of Nonlinear Optics, Prague, Czechoslovakia, 16-20 Aug. 1993
(Contract W-7405-eng-48)
(DE94-001529; UCRL-JC-114058; CONF-9308186-2) Avail: CASI HC A02/MF A01

Over the last 20 years lasers have been a useful tool in the generation of x-ray radiation. Recent technology advances have allowed solid state lasers to be designed as a drive source for proximity print x-ray lithography systems as well as in the longer term for soft x-ray projection lithography systems. In addition the ability to build multi-hundred joule per pulse, several nanosecond pulselength lasers with repetition rate capability and table top size now allow us to design table top x-ray sources and x-ray lasers. Within our laboratory several high power solid state lasers are being built for direct application to these systems. It was found that the best performance of these high power lasers is obtained when non-linear phase conjugate mirrors are included. These mirrors function in two important respects; they provide a means to obtain very high beam brightness without the generation of hot spots which damage optical components and in addition because of their threshold activation characteristic they function in the role of multistage gain isolators. The design and performance of two systems which are being hardened for commercialization and a third system which is in the design phase and will be used as a pump source for an x-ray laser are described in detail. DOE

N94-27179 Tel-Aviv Univ. (Israel).
LASER PHASE INDUCED INTENSITY NOISE IN FIBER-OPTIC SIGNAL PROCESSING AND SENSING SYSTEMS Ph.D. Thesis
Ady Arie Mar. 1991 142 p
(ITN-94-85234) Copyright Avail: Issuing Activity (Tel-Aviv Univ., Exact Sciences Library, Ramat Aviv 69978, Israel)

The effects of random phase fluctuations in laser output on the performance of optical systems was studied. The statistical nature of phase induced intensity noise (PIIN) was measured and analysed by studying its probability density function and the second and fourth moments of the optical field at the output of several multiple path systems. The properties of the semiconductor laser, including broad spectral linewidth and non-Lorentzian line shape were shown to have significant influence on the generated PIIN. The PIIN statistics was first studied via the probability density function (PDF) of the beat signal obtained from a two-beam interferometer fed by the laser. Two distinct operating regimes could be defined, according to the ratio between the interferometer delay and the laser coherence time. Analytical expressions were obtained for statistical averages of the PIIN at the output of a general multiple path system; they represent the variance and autocovariance, and the power spectral density of the PIIN at the system output. The non-Lorentzian lineshape of the semiconductor laser was taken into account and the results obtained were found to differ from the Lorentzian model predictions; power spectrum measurements by means of a Mach-Zehnder interferometer confirmed the theoretical model. Analysis of the PIIN for complex signal processing systems comprising several subsystems showed that the PIIN spectrum was determined by two mechanisms: noise generation and noise filtration. ISA

N94-27262 Sandia National Labs., Albuquerque, NM.
KINOFORM/LENS SYSTEM FOR INJECTING A HIGH POWER LASER BEAM INTO AN OPTICAL FIBER
W. C. Sweatt and M. W. Farn (Massachusetts Inst. of Tech., Lexington.) 1993 29 p Presented at the 25th Boulder Damage Symposium: Annual Symposium on Optical Materials for High-Power Lasers, Boulder, CO, 27-29 Oct. 1993 Limited Reproducibility: More than 20% of this document may

be affected by poor print
(Contract DE-AC04-94AL-85000)
(DE94-003226; SAND-93-2144C; CONF-931054-1) Avail: Issuing Activity (Department of Energy (DOE))

A method for injecting a high peak power multimode YAG laser beam into an optical fiber has been developed. The design minimizes the peak irradiance on the fiber's entrance face and reduces its dependence on the laser's mode structure and the system alignment. A simple lens and a specially designed kinoform (or binary optics element) operate together to transform a 5 mm diameter laser beam into two concentric ring foci that fit on the 400 micron diameter fiber face. DOE

N94-27339# Tokyo Univ. (Japan). Ist. for Solid State Physics.
TECHNICAL REPORT OF ISSP. SER. A, NO. 2685: ASE-FREE TERAWATT KrF/Ti : SAPPHIRE HYBRID LASER SYSTEM
Yasuo Nabekawa, Kiminori Kondo, Nobuhiko Sarukura (Institute of Physical and Chemical Research, Tokyo, Japan.), Kazuaki Sajiki (Komatsu Ltd., Tokyo, Japan.), and Shuntaro Watanabe Jun. 1993 14 p
(ISSN 0082-4798)
(JTN-94-80571) Avail: CASI HC A03/MF A01

A terawatt KrF/Ti:sapphire hybrid laser system free from Amplified Spontaneous Emission (ASE) was developed with an output energy of 130 mJ in 130 fs. An efficient frequency-tripling scheme with Ti:sapphire is demonstrated with an efficiency of 11 percent at a 100-fs regime using LiB3O5 (LBO) and BaB2O4 (BBO). Author (NASDA)

N94-27605# Tokyo Univ. (Japan). Inst. for Solid State Physics.
TECHNICAL REPORT OF ISSP. SER. A, NO. 2686: HIGH-ORDER HARMONIC GENERATION AND IONIZATION USING ULTRASHORT KrF AND Ti:SAPPHIRE LASERS
Kiminori Kondo, Taichiro Tamida, Nabekawa Yasuo, and Shuntaro Watanabe Jun. 1993 39 p
(ISSN 0082-4798)
(JTN-94-80572) Avail: CASI HC A03/MF A01

High-order harmonic generation in KrF and Ti:sapphire lasers is analyzed with an emphasis on the contribution of multiple-charged ions. It is confirmed that the intensity dependence of the ion yield of multiple-charge states is explained by ADK (Ammosov-Delone-Krainov) tunneling theory, regardless of the wavelength. The harmonic distributions are compared with the single-atom responses calculated using the short-range potential model with the effective interaction intensity determined by ADK tunneling theory. From this analysis, the harmonics above the 21st in Ne and above the 13th in Ar for the KrF laser are found to be due to double-charged ions. Author (NASDA)

N94-27668 Defence Research Establishment Atlantic, Dartmouth (Nova Scotia).
LASER SURFACE MODIFICATION OF INTERMETALLIC COMPOUNDS
M. P. Graham, H. W. Kerr, and D. C. Weckman Feb. 1992 90 p
(DREA-CR-92-416; DSIS-94-00040; CTN-94-61127) Avail: CASI HC A05/MF A01

The rare earth compound Terfenol-D (Tb(x)Dy(1-x)Fe(y), where x = 0.3 and y = 1.95) has highly magnetostrictive strain properties, but is very brittle and can be difficult to manufacture into functional components. A study was conducted to investigate the effects of laser surface modification of this intermetallic compound in order to determine if the rapid solidification following laser melting could produce a surface with improved toughness. The effects of various pulsed Nd:Y-Al garnet laser process parameters on the resultant surface pool diameter, penetration, and quality were studied experimentally. Individual spots were made on a carefully prepared butt joint at a mean laser power of 180 W. Conduction mode and keyhole mode pools were observed, and the quality of the specimens was poor. Experiments at 60 W and 180 W laser power were also conducted on bulk material. Different processing approaches were used, including manipulating focal position, temporal pulse shaping, using multiple pulses per shot, and preheating the specimens. Surface quality was improved in specimens processed with a temporal pulse shape consisting of a gentle pre-pulse followed by the balance of energy, and by specimens preheated to 150 and 450 C. Multiple pulses per shot on preheated (150 C) specimens also improved surface quality. Author (CISTI)

N94-27670# Department of the Navy, Washington, DC.
HIGH REPETITION RATE, MODE LOCKED, FIGURE EIGHT LASER WITH EXTRACAVITY FEEDBACK Patent Application
Michael L. Dennis, inventor (to Navy) and Irl N. Duling, III, inventor (to Navy) 29 Sep. 1993 20 p
(AD-D016053; US-Patent-Appl-SN-128187; Navy-Case-74823) Avail: CASI HC A03/MF A01

The present invention relates to fiber laser generators of soliton pulses and more particularly to a figure eight fiber laser with extracavity feedback to obtain pulse shortening, initiation of mode locking, and repetition rate control. DTIC

N94-27671# Department of the Navy, Washington, DC.
SYSTEM FOR CONDITIONING AN ELECTRON BEAM FOR IMPROVED FREE-ELECTRON LASER OPERATION Patent Application
P. Sprangel, inventor (to Navy), B. Hafizi, inventor (to Navy), Glenn Joyce, inventor (to Navy), and Philip Serafim, inventor (to Navy) 29 Jul. 1993 17 p
(AD-D016054; US-Patent-Appl-SN-098989; Navy-Case-75311) Avail: CASI HC A03/MF A01

This invention relates generally to a system for generating an electron beam for a free-electron laser and, more specifically, to a system for conditioning an electron beam to enhance the operation of a free-electron laser. DTIC

N94-27701# Nagoya Univ. (Japan). Dept. of Electrical Engineering and Plasma Science Center.
LASER BLOW-OFF LITHIUM BEAM PROBING WITH HIGH TEMPORAL RESOLUTION FOR EDGE PLASMA DIAGNOSTICS
S. Sasaki, S. Takamura, Y. Uesugi, Y. Ohkouchi, and K. Kadota Apr. 1993 22 p
(DE94-701176; PSC-28) Avail: CASI HC A03/MF A01

Laser blow-off neutral lithium beam probing with high temporal resolution has been developed to measure edge electron density profiles in a plasma. A new electron density reconstruction method, taking account of the transport of a laser blow-off beam in the plasma, improved the accuracy of the density measurement. The use of a camera system with gate function makes it possible to measure the density profile with high temporal resolution of approximately 10 to 50 microseconds. The optimum condition for shuttering timing and period to observe Li I emission profile is discussed from the viewpoints of the beam penetration into the plasma and the accuracy of measurement. A rapid temporal evolution of edge electron density profile during the limiter biasing in a small tokamak HYBTOK-II is successfully obtained by this system. DOE

N94-27781# Argonne National Lab., IL.
MULTIPLE EXPOSURE CCD DETECTOR FOR HIGH-SPEED LASER PUMP, X RAY PROBE LAUE SCATTERING
B. Rodricks 1993 6 p Presented at the International Conference on Lasers and Applications, Lake Tahoe, NV, 6-10 Dec. 1993
(Contract W-31-109-eng-38)
(DE94-004618; ANL/XFD/CP-81491; CONF-931237-2) Avail: CASI HC A02/MF A01

Four charge coupled devices (CCD) fiber-optic coupled detector and detector control electronics and image displays are discussed. DOE

N94-28068# KJT, Inc., Rochester, NY.
FIBER LASER AMPLIFIERS AND OSCILLATORS Final Technical Report, Feb. 1992 - 1993
Kenneth J. Teegarden Sep. 1993 7 p
(Contract F30602-92-C-0037)
(AD-A274231; RL-TR-93-186) Avail: CASI HC A02/MF A01

A tunable erbium doped fiber ring laser, pumped with a 980 nm diode laser, was constructed. Output power as a function of pump power and output wavelength for a given fiber length was measured. Spectral and temporal analysis of the signal showed mode-locked pulses of short duration and broad frequency content, as well as a continuous wave (CW) component confined to a relatively narrow optical frequency range. The mechanisms for this type of mode-locking are discussed as well as the limitations placed on the lasing line width and spectral tunability. DTIC

37 MECHANICAL ENGINEERING

Includes auxiliary systems (nonpower); machine elements and processes; and mechanical equipment.

N94-25782# Case Western Reserve Univ., Cleveland, OH.
A BIOLOGICALLY-INSPIRED AUTONOMOUS ROBOT
Randall D. Beer 13 Dec. 1993 4 p
(Contract N00014-90-J-1545)
(AD-A273909) Avail: CASI HC A01/MF A01

A treadmill has been developed to support our cockroach locomotion studies. We have developed a small treadmill with a transparent belt for studying leg joint movements along with EMG's as the animal walks or runs at various speeds. This allows us to match the electrical activity in muscles with the kinematics of joint movement. Along with intracellular stimulation studies performed previously, the tools are now in place to make major advances in understanding how the insect's walking movements are actually accomplished. DTIC

N94-25794# Army Combat Systems Test Activity (Provisional), Aberdeen Proving Ground, MD.
TEST OPERATIONS PROCEDURE (TOP) 2-2-800 WHEELED VEHICLE CENTER OF GRAVITY Final Report
31 Dec. 1993 18 p
(AD-A273937; ITOP-2-2-800) Avail: CASI HC A03/MF A01

Describes procedures for determining the center of gravity (CG) of wheeled vehicles. The CG provides information relative to roll stability, transportability, and input for mobility model programs. Author

N94-25811# Sandia National Labs., Albuquerque, NM.
STRUCTURAL ANALYSIS OF A FRANGIBLE NUT USED ON THE NASA SPACE SHUTTLE
K. E. Metzinger Nov. 1993 23 p
(Contract DE-AC04-94AL-85000)
(DE94-003672; SAND-93-1720) Avail: CASI HC A03/MF A01

A structural analysis methodology has been developed for the NASA 2.5-inch frangible nut used on the Space Shuttle. Two of these nuts are used to secure the External Tank to the aft end of the Orbiter. Both nuts must completely fracture before the Orbiter can safely separate from the External Tank. Ideally, only one of the two explosive boosters contained in each nut must detonate to completely break a nut. However, after an uncontrolled change in the Inconel 718 material processing, recent tests indicate that in certain circumstances both boosters may be required. This report details the material characterization and subsequent structural analyses of nuts manufactured from two lots of Inconel 718. The nuts from the HSX lot were observed to consistently separate with only one booster, while the nuts from the HBT lot never completely fracture with a single booster. The material characterization requires only tensile test data and the determination of a tearing parameter based on a computer simulation of a tensile test. Subsequent structural analyses using the PRONTO2D finite element code correctly predict the differing response of nuts fabricated from these two lots. This agreement is important because it demonstrates that this technique can be used to screen lots of Inconel 718 before manufacturing frangible nuts from them. To put this new capability to practice, Sandia personnel have transferred this technology to the Pyrotechnics Group at NASA-JSC. DOE

N94-25878 Carnegie-Mellon Univ., Pittsburgh, PA. Robotics Inst.
BALANCING OF A PLANAR BOUNCING OBJECT
Nina B. Zumel 1993 29 p Limited Reproducibility: More than 20% of this document may be affected by microfiche quality
(Grant NSF GER-92-55691)
(AD-A273805; CMU-RI-TR-93-26) Avail: CASI HC A03

While most previous work in planning manipulation tasks has relied on the assumption of quasi-static conditions, there can be situations where the quasistatic assumption may not hold, and the assumptions about the environment must be relaxed. This is true, for example, in a situation where objects are making and breaking contact at high enough velocities that contact dynamics play a significant effect in the motion of the colliding objects. There has been some work studying models of collision, in particular for the design and analysis of systems with intermittent constraints, and for the design of juggling robots. Our work extends previous studies in planar juggling to the case of a polygonal object, using the model of rigid body impulsive collision. Simulations verify the results of a linearized analysis. DTIC

N94-25970# Sandia National Labs., Albuquerque, NM. Intelligent Systems and Robotics Center.
AUTOMATIC ASSEMBLY PLANNING AND ITS ROLE IN AGILE MANUFACTURING: A SANDIA PERSPECTIVE
R. E. Jones and S. G. Kaufman 1993 6 p Presented at the 1st Annual Agile Manufacturing Conference, Albuquerque, NM, 14-15 Oct. 1993
(Contract DE-AC04-94AL-85000)
(DE94-002291; SAND-93-2360C; CONF-9310217-1) Avail: CASI HC A02/MF A01

Sandia was studying automatic assembly planning of electromechanical devices for some years, based on an implemented system called Archimedes. Work done to date has focused on automatic generation of high-level plans, and translation of these plans into robotic control code and workcell layout. More recently, the importance of an assembly planning capability as a design aid has been emphasized, as it could potentially provide early feedback to a designer on the manufacturability of the design. The work done on assembly planning to date, plans for extending it, and its applications to agile manufacturing are described. In particular, an agile manufacturing demonstration project underway at Sandia, and the role the Archimedes assembly planning system will play in it are described. DOE

N94-25980# Los Alamos National Lab., NM.
DIGITAL CONTROL AND DATA ACQUISITION FOR HIGH-VALUE GTA WELDING
T. G. George and E. A. Franco-Ferreira (Westinghouse Savannah River Co., Aiken, SC.) 1993 11 p Presented at the American Welding Society International Conference on Modeling and Control of Joining Processes, Orlando, FL, 8 Dec. 1993
(Contract W-7405-eng-36)
(DE94-000885; LA-UR-93-3425; CONF-931234-1) Avail: CASI HC A03/MF A01

Electric power for the Cassini space probe will be provided by radioisotope thermoelectric generators (RTG's) thermally driven by General-Purpose Heat Source (GPHS) modules. Each GPHS module contains four, 150-g, pellets of Pu-238O2, and each of the four pellets is encapsulated within a thin-wall iridium-alloy shell. GTA girth welding of these capsules is performed at Los Alamos National Laboratory (LANL) on an automated, digitally-controlled welding system. Baseline design considerations for system automation and strategies employed to maximize process yield, improve process consistency, and generate required quality assurance information are discussed. Design of the automated girth welding system was driven by a number of factors which militated for precise parametric control and data acquisition. Foremost among these factors was the extraordinary value of the capsule components. In addition, DOE order 5700.6B, which took effect on 23 Sep. 1986, required that all operations adhere to strict levels of process quality assurance. A detailed technical specification for the GPHS welding system was developed on the basis of a joint LANL/Westinghouse Savannah River Company (WSRC) design effort. After a competitive bidding process, Jetline Engineering, Inc., of Irvine, California, was selected as the system manufacturer. During the period over which four identical welding systems were fabricated, very close liason was maintained between the LANL/WSRC technical representatives and the vendor. The level of rapport was outstanding, and the end result was the 1990 delivery of four systems that met or exceeded all specification requirements. DOE

N94-26110# Sandia National Labs., Albuquerque, NM.
RECENT DEVELOPMENTS IN THE ROBOTIC ALL TERRAIN LUNAR EXPLORATION ROVER (RATLER) PROGRAM
P. R. Klarer 1993 8 p Presented at the Space 94: International Conference and Exposition on Engineering, Construction, and Operations in Space, Albuquerque, NM, 26 Feb. - 3 Mar. 1994
(Contract DE-AC04-76DP-00789)
(DE93-040342; SAND-93-1760C; CONF-940214-4) Avail: CASI HC A02/MF A01

The Robotic All-Terrain Lunar Exploration Rover (RATLER) is a four wheeled all-wheel-drive dual-body vehicle. A uniquely simple method of chassis articulation is employed which allows all four wheels to remain in contact with the ground, even while climbing over step-like obstacles as large as 1.3 wheel diameters. The RATLER design concept began at Sandia National Laboratories in late 1991 with a series of small, proof-of-principle, working scale models. The models proved the viability of the concept for high mobility through mechanical simplicity, and eventually received internal funding at Sandia National Laboratories for full scale, proof-of-concept prototype development. Whereas the proof-of-principle models demonstrated the mechanical design's capabilities for mobility, the full scale for experiments in telerobotics, autonomous robotic operations, and telerobotic field geology is described, including an outline of the program's work over the past year, recent accomplishments, and plans for follow-on development work. DOE

N94-26174# Naval Postgraduate School, Monterey, CA.

THE STUDY OF SINGLE-PASS GMA WELDS WITH DIFFERENT COVER GAS COMPOSITIONS ON HSLA-100 STEEL M.S. Thesis

Ricky A. Seravia 23 Sep. 1993 73 p
(AD-A274857) Avail: CASI HC A04/MF A01

This study investigated the effect of varying cover gas compositions on the microstructure and mechanical properties of single run gas-metal arc welds (GMAW) on HSLA-100 plate. Seven different cover gas compositions containing varying amounts of argon, oxygen, and carbon dioxide were evaluated. A statistical and quantitative analysis of the nonmetallic inclusions in the weld metal was performed by scanning electron microscopy (SEM) and energy dispersive analysis of x rays (EDX). These results show that increasing the oxygen content of the cover gas reduces the inclusion size but increases the number density compared with pure argon cover gas, and that this is reflected in the weld metal microstructure since increasing amounts of acicular ferrite were detected predominantly to be of the spessartite composition (3MnO, Al2O3, 3SiO2). As a result of increasing cover gas oxygen, the strength of the weld metal appeared to be lowered due to the oxidation of aluminum, silicon, manganese, and possibly titanium. In addition, the toughness was improved for weld metal generated from cover gases containing oxygen because the ductile-to-brittle transition temperature was lowered by the increasing amounts of acicular ferrite. DTIC

N94-26306# Technical Research Centre of Finland, Espoo. Heating and Ventilation Lab.

A METHOD FOR TESTING OF HVAC AUTOMATION EQUIPMENT USING THE EMULATOR AND THE APPLICATION OF THE METHOD [LVI-AUTOMAATIOLAITTEIDEN EMULAATTORITESTAUKSEN TESTAUSMENETTELY JA SEN SOVELTAMINEN]

Satu Kaerki Dec. 1992 160 p In FINNISH Sponsored by Ministry of Trade and Industry, Finland
(ISSN 1235-0605)
(VTT-TIED-1435; ISBN-951-38-4329-7; ETN-94-95262) Copyright Avail: CASI HC A08/MF A02

A testing method for testing HVAC automation equipment with the emulator is presented. The testing method is applied to two alternative supervisory control strategies of an air conditioning plant. In the testing method the advance of testing is described step by step from determining processes to evaluation of the behavior of automation equipment. For testing automation equipment with the emulator, an evaluation method was developed based on weighting factors for grading automation equipment and for tested equipment to make it easier for builders and designers to compare the equipment of different manufactures. The evaluation method is mainly intended for use in testing, but it can possibly be used also as a basis for developing evaluation methods for other purposes. Evaluation methods and criteria that appeared in international literature were used as starting points for developing the evaluation method. In the comparison tests between the supervisory control strategies of an air conditioning plant, the testing method was found to advance in a logical, easily observable order. The results of the comparison tests were analyzed both in the conventional way with the help of graphical formulas and statistical values as well as with the evaluation method developed. The same kinds of conclusions were obtained with both analyzing methods. Hence at least on the basis of these tests, the evaluation method developed gives a rather reliable image of the control functions of automation equipment. ESA

N94-26465# Oak Ridge National Lab., TN.

COMPUTER VISUALIZATIONS IN ENGINEERING APPLICATIONS

K. C. Bills 1993 4 p Presented at the 7th Deneb Robotics User Group Meeting, Troy, MI, 12-15 Oct. 1993
(Contract DE-AC05-84OR-21400)
(DE94-003589; CONF-9310216-2) Avail: CASI HC A01/MF A01

The use of computerized simulations of various robotic tasks via IGRIP software is reported. The projects include underwater activities demonstrating clean up of a quarry; time study of methods to store waste drums inside a facility; design walk-through of a new facility; plant layout flyover; and conceptual development and layout of new mechanisms. DOE

N94-26597*# Rockwell International Corp., Canoga Park, CA. Rocketdyne Div.

PUMP CFD CODE VALIDATION TESTS Final Report, May 1991 - Dec. 1993

L. A. Brozowski 15 Dec. 1993 30 p Original contains color illustrations
(Contract NAS8-38864)
(NASA-CR-193939; NAS 1.26:193939; RI/RD-93-195) Avail: CASI HC A03/MF A01

Pump CFD code validation tests were accomplished by obtaining nonintrusive flow characteristic data at key locations in generic current liquid rocket engine turbopump configurations. Data were obtained with a laser two-focus (L2F) velocimeter at scaled design flow. Three components were surveyed: a 1970's-designed impeller, a 1990's-designed impeller, and a four-bladed unshrouded inducer. Two-dimensional velocities were measured upstream and downstream of the two impellers. Three-dimensional velocities were measured upstream, downstream, and within the blade row of the unshrouded inducer. Author

N94-26642 Simon Fraser Univ., Burnaby (British Columbia). School of Engineering Science.

MOTION PLANNING FOR SERIAL MANIPULATORS WITH MANY DEGREES OF FREEDOM: IMPLEMENTATION OF A SEQUENTIAL SEARCH STRATEGY M.S. Thesis

Zhenping Guo Jan. 1992 118 p
(ISBN-0-315-83682-2; CTN-94-61032) Copyright Avail: Micromedia Ltd., Technical Information Centre, 240 Catherine Street, Suite 305, Ottawa, Ontario, K2P 2G8, Canada HC/MF

A motion planner has been developed and implemented which can plan collision-free motions for serial manipulator arms with many degrees of freedom among stationary obstacles. The planner is based on a sequential search strategy that exploits the serial nature of manipulator arms. The motion of each link is planned successively starting from the base link. Given that the motion of links until link i has been planned, the motion of link i+1 is now planned along this collision-free path by controlling the degree of freedom associated with it. In the simplest case, this strategy results in one one-dimensional (the first link is degenerate) and n-1 two-dimensional planning problems instead of one n-dimensional problem for an n-link manipulator arm. The search strategy leads to a fast and efficient algorithm, and is especially suited for manipulator arms with many degrees of freedom. Furthermore, a backtracking mechanism has been incorporated in the planner which makes it more effective, but slower, in cluttered environments. This mechanism provides a parameter which can be used to trade off completeness of the planner with its speed. The effectiveness of the planner strategy is demonstrated with examples of motion planning for several arms with many degrees of freedom. Author (CISTI)

N94-26657 Victoria Univ. (British Columbia). Dept. of Mechanical Engineering.

OPTIMAL ARCHITECTURAL DESIGN OF PARALLEL AND HYBRID MANIPULATORS M.S. Thesis

Kenneth H. Pittens 1992 175 p
(ISBN-0-315-84351-9; CTN-94-61023) Copyright Avail: Micromedia Ltd., Technical Information Centre, 240 Catherine Street, Suite 305, Ottawa, Ontario, K2P 2G8, Canada HC/MF

A study is presented of the optimial design of a class of six degree of freedom (DOF) closed-chain manipulators consisting of serial branches, each with joints acting in parallel on a common end effector. Dexterity measures based on instantaneous kinematic characteristics of the manipulator are used as the primary objective in isolating optimum designs. The fully parallel Stewart platform is first examined and a two-parameter family of optimal configurations is shown to exist. A unique optimum Stewart platform architecture is isolated from those possessing optimum local dexterity. The resulting optimum manipulator architecture is one in which the dimensions of the base are twice those of the platform and the linear actuator attachment points at the base and the platform meet in alternating pairs. Hybrid manipulators are then examined. A specific hybrid chain structure is selected from possible six-DOF structures for further investigation. A class of serial chain branches suitable for this structure is defined and it is shown that only five unique branch structures belong to the kinematically simple class. A novel approach to manipulator configuration optimization for optimal local dexterity objectives is introduced and applied to find optimal configurations of hybrid manipulators utilizing the previously identified branch structures. Author (CISTI)

N94-26658 Toronto Univ. (Ontario). Dept. of Mechanical Engineering.
IMPLEMENTATION OF INTEGRAL MANIFOLD CONTROL ON A TWO DEGREE OF FREEDOM FLEXIBLE JOINT MANIPULATOR: THEORY AND EXPERIMENTS M.S. Thesis
Raymond Wai-Man Tsang 1993 160 p
(ISBN-0-315-83572-9; CTN-94-61039) Copyright Avail: Micromedia Ltd., Technical Information Centre, 240 Catherine Street, Suite 305, Ottawa, Ontario, K2P 2G8, Canada HC/MF

Recently, singular perturbation theory and the integral manifold concept were applied to flexible joint modeling. The dynamic model obtained is of the same order as the rigid joint robot and is feedback linearizable with only the joint position and velocity feedback. To verify the feasibility of this approach, an experimental facility was designed and built for the implementation of integral manifold control. The facility consists of a two degree of freedom robot with the distal joint actuated by a 2N tendon-pulley system. A new type of inflatable actuator called a Rubbertuator, developed in Japan, is used in the tendon-pulley system to control the stiffness of the force transmission line. An electronic interface and a system control software which consists of about 8,000 lines of C code were designed. The results of the experimental implementation of the integral manifold control law are reported. These results confirm the published theoretical results and agree with the computer simulation work done by Spong et al. Several limitations of the proposed control are noted. Author (CISTI)

N94-26849 Swedish Inst. for Materials Testing, Boras.
UNSCREENED LOW TENSION CABLES SCRAPE ABRASION TESTING
L. Spilg 1992 18 p Limited Reproducibility: More than 20% of this document may be affected by microfiche quality
(PB94-123767; SP-RAPP-1992:17; ISBN-91-7848-335-2) Avail: CASI HC A03

A proposal for revision of ISO 6722/1--Road vehicles: Unscreened low tension cables, Part 1: General requirements and test methods--specifies a method for scrape abrasion testing. Tests at different laboratories indicate large variations in the results obtained using this method. It is evident that a number of parameters influence the results. In an effort to clarify the influence of some of these parameters, the ISO/TC 22/SC3/WG4-Low Tension Cables decided to undertake an interlaboratory test focusing on different equipment, different conductor types, and different insulating materials. This report presents the method used and the result of the interlaboratory test. It is concluded that it is not possible to compare data obtained on different equipment although they are made according to standard and that further investigations have to be done before including this method in an international standard. NTIS

N94-26976# Notre Dame Univ., IN. Dept. of Civil Engineering and Geological Sciences.
AIRCRAFT WHEEL LIFE ASSESSMENT Final Report, 1 Oct. 1991 - 1 Sep. 1992
B. F. Spencer, Jr., D. J. Kirkner, E. E. Schudt, and S. Kandarpa Jul. 1993 62 p
(AD-A274378; WL-TR-93-3065) Avail: CASI HC A04/MF A01

The important part of wheel life assessment problems is the accurate determination of the tire/wheel interface pressure distribution under various loading conditions. A combined analytical/experimental methodology for obtaining this pressure distribution was developed. The principal analytical tool in this methodology is the finite element program ANTWILL (Analysis of Tire Wheel Interface Loads) which recovers the pressure distribution given a number of experimental strain measurements on the wheel. The major activity consisted of a study of the F-16 Block 30 and the Block 40 main landing gear wheels to determine the optimal number and location of the strain gages for subsequent experiments. Experiments to be conducted will record strains at the specified locations and this data will be used to determine tire/wheel interface pressures. DTIC

N94-26986# Arnold Engineering Development Center, Arnold AFS, TN.
AN ALGORITHM FOR DETERMINATION OF BEARING HEALTH THROUGH AUTOMATED VIBRATION MONITORING Final Report, 1 Oct. 1992 - 30 Sep. 1993
Sid W. Hite, III Dec. 1993 67 p
(AD-A274591; AEDC-TR-93-19) Avail: CASI HC A04/MF A01

This report investigates considerations involved in designing an expert system capable of real-time monitoring of turbine engine vibration data to detect rolling element bearing faults. Topics include development of the fundamental bearing fault frequencies, data analysis techniques, results of manual analysis, and considerations in bearing health criteria and monitoring. Methodologies are described for characterization of engine family vibration across the engine's envelope, and a bearing health monitoring algorithm is discussed in detail. Work reported will be extended and automated to encompass a complete vibration based turbine engine Health Monitoring System (HEMOS). When completely developed, HEMOS will likely augment the multifaceted capabilities of the Computer Assisted Dynamic Data Monitoring and Analysis System (CADDMAS) under development by the Directorate of Technology - Propulsion Division (DOTP) of Arnold Engineering Development Center (AEDC), Air Force Materiel Command (AFMC), Arnold AFB, TN. DTIC

N94-27104# California Univ., San Diego, La Jolla. Dept. of Applied Mechanics and Engineering Sciences.
COMPUTER SIMULATION AND EXPERIMENTS ON THE QUASI-STATIC MECHANICS AND TRANSPORT PROPERTIES OF GRANULAR MATERIALS Annual Report, 1 Oct. 1992 - 30 Sep. 1993
Xue-Jin Zhuang and J. D. Goddard 1 Oct. 1993 153 p
(Contract F49620-92-J-0037)
(AD-A274192; RR-GR-93-01; AFOSR-93-0912TR) Avail: CASI HC A08/MF A02

This report presents the results of a new quasi-static algorithm developed to compute the mechanical and scalar transport properties of three dimensional sphere assemblages. The algorithm incorporates several new techniques, including a shuffling algorithm for generation of initial random granular packings, an improved microcell-adjacency method to accelerate particle-contact search, and a relaxation method to overcome a singularity in the quasilinear system of equilibrium equations. The calculated Reynolds dilatancy for random dense-packed granular assemblages is found to depend on the interparticle friction, contrary to Reynolds' original hypothesis, and the use of linear contact mechanics is found to be valid near the ideal rigid-particle limit. Triaxial compression tests, employing steel balls as electrically conductive granular particles, confirm the simulation of both mechanical and transport properties, when account is taken of the actual electrical contact resistance between steel balls. The latter is much higher than for Hertzian contact and exhibits a strong dependence on normal load, probably due to asperities and oxide films on the steel-ball surfaces. A major conclusion is that scalar transport can serve as a useful macroscopic probe for stress anisotropy and particle-contact topology in granular media. DTIC

N94-27149*# Spectra Research Systems, Inc., Huntsville, AL. Systems Technology Group.
INTERCHANGEABLE END EFFECTOR TOOLS UTILIZED ON THE PFMA Final Report, Sep. 1988 - Jun. 1991
Joe Cody, John Carroll, George Crow, Paul Gierow, Jay Littles, Michael Maness, and Jim Morrison 27 Feb. 1992 44 p
(Contract NAS8-36307)
(NASA-CR-193925; NAS 1.26:193925; SRS/STG-TR92-14; Rept-5490-08) Avail: CASI HC A03/MF A01

An instrumented task board, used for measuring forces applied by the Protoflight Manipulator Arm (PFMA) to the task board, was fabricated and delivered to Marshall Space Flight Center. SRS Technologies phased out the existing IBM compatible data acquisition system, used with a instrumented task board, and integrated the force measuring electronic hardware in with the Macintosh II data acquisition system. The purpose of this change was to acquire all data with the same time tag, allowing easier and more accurate data reduction in addition to real-time graphics. A three-dimensional optical position sensing system for determining the location of the PFMA's end effect or in reference to the center of the instrumented task board was also designed and delivered under. An improved task board was fabricated which included an improved instrumented beam design. The modified design of the task board improved the force/torque measurement system by increasing the sensitivity, reliability, load range and ease of maintenance. A calibration panel for the optical position system was also designed and fabricated. The calibration method developed for the position sensors enhanced the performance of the sensors as well as simplified the installation and calibration procedures required. The modifications made under this effort expanded the capabilities of the task board system. The system developed determines the arm's position relative to the task board and measures the signals to the joints resulting from the operator's control signals in addition to the task board forces. The software and hardware required to calculate and record the position of the PFMA during the performance of tasks with the instrumented task board were defined, designed and delivered to MSFC. PFMA joint input signals can be measured from a breakout box to evaluate the sensitivity or response of the arm operation to control commands. The data processing system provides the capability for post processing of time-history graphics and plots of the PFMA positions, the operator's actions, and the PFMA servo reactions in addition to realtime force and position sensor data presentation. Derived from text

N94-27181# Oak Ridge Y-12 Plant, TN.

EVALUATING NON-CHLORINATED SOLVENTS FOR WELDING APPLICATIONS

T. M. Mustaleski, Jr., comp. (Martin Marietta Energy Systems, Inc., Oak Ridge, TN.) 11 Aug. 1993 8 p Presented at the 1993 Environmentally Conscious Manufacturing Congress, Arlington, VA, 30 Aug. - 1 Sep. 1993
(Contract DE-AC05-84OR-21400)
(DE94-003332; Y/DV-1275; CONF-93-08150-12) Avail: CASI HC A02/MF A01

There is interest in eliminating the use of chlorinated solvents such as methyl chloroform at the Oak Ridge Y-12 Plant for environmental reasons. Solvent 140 has been offered as an acceptable replacement. Methyl chloroform has frequently been used for the final cleaning of materials just prior to welding. Electron beam welds were made in an aluminum alloy to compare the potential contamination effect of Solvent 140 to that of methyl chloroform. Tests indicated that the Solvent 140 did not have an adverse effect on pump-down time of electron beam welding equipment during normal handling. Solvent 140 resulted in significantly less weld porosity than methyl chloroform in this test. DTIC

N94-27221*# Alabama Univ., Huntsville. Mechanical and Aerospace Engineering.

UAH MATHEMATICAL MODEL OF THE VARIABLE POLARITY PLASMA ARC WELDING SYSTEM CALCULATION Final Report

R. J. Hung Jan. 1994 197 p
(Contract NAS8-38609)
(NASA-CR-193926; NAS 1.26:193926) Avail: CASI HC A09/MF A03

Significant advantages of Variable Polarity Plasma Arc (VPPA) welding process include faster welding, fewer repairs, less joint preparation, reduced weldment distortion, and absence of porosity. A mathematical model is presented to analyze the VPPA welding process. Results of the mathematical model were compared with the experimental observation accomplished by the GDI team. Author (revised)

N94-27224 Southwest Research Inst., San Antonio, TX. Engine, Fuel, and Vehicle Research Div.

SEQUENTIAL MULTI-POINT INJECTION OF A NATURAL GAS ENGINE. TOPICAL REPORT, NOVEMBER 1991 - APRIL 1992

Corwin Snyder and Carina Boschi (Gaz de France, La Plaine Saint Denis.) Apr. 1993 225 p See also PB92-101468 and PB92-123694
(Contract GRI-5086-293-1848)
(PB94-126794; SWRI-3178-4.12; GRI-93/0182) Avail: Issuing Activity (National Technical Information Service (NTIS)

The objective of the project was to evaluate an electronic sequential multi-point injection fuel system on a natural gas-fueled automotive medium-duty engine. This included an evaluation of gaseous fuel injectors, cylinder-to-cylinder fuel-air distribution measurement, performance measurements, exhaust emissions measurements (pre- and post-catalyst), and an oxygen sensor comparison. One additional objective was to run the fuel system in a 'pre-mix' configuration, where fuel and air are mixed for a homogeneous-charge prior to cylinder admission, for comparison to the sequential multi-point fuel system. NTIS

N94-27228*# Rockwell International Corp., Canoga Park, CA. Rocketdyne Div.

DESIGN AND EXPERIMENTAL PERFORMANCE OF A TWO STAGE PARTIAL ADMISSION TURBINE. TASK B.1/B.4 Final Report, Dec. 1984 - Jun. 1986

R. F. Sutton, J. L. Boynton, R. A. Akian, Dan Shea, Edmund Roschak, Lou Rojas, Linsey Orr, Linda Davis, Brad King, and Bill Bubel et al 14 Dec. 1992 168 p
(Contract NAS3-23773)
(NASA-CR-179548; NAS 1.26:179548; RI/RD92-214) Avail: CASI HC A08/MF A02

A three-inch mean diameter, two-stage turbine with partial admission in each stage was experimentally investigated over a range of admissions and angular orientations of admission arcs. Three configurations were tested in which first stage admission varied from 37.4 percent (10 of 29 passages open, 5 per side) to 6.9 percent (2 open, 1 per side). Corresponding second stage admissions were 45.2 percent (14 of 31 passages open, 7 per side) and 12.9 percent (4 open, 2 per side). Angular positions of the second stage admission arcs with respect to the first stage varied over a range of 70 degrees. Design and off-design efficiency and flow characteristics for the three configurations are presented. The results indicated that peak efficiency and the corresponding isentropic velocity ratio decreased as the arcs of admission were decreased. Both efficiency and flow characteristics were sensitive to the second stage nozzle orientation angles. Author (revised)

N94-27238*# National Aeronautics and Space Administration, Washington, DC.

ROBOTICS HANDBOOK. VERSION 1: FOR THE INTERESTED PARTY AND PROFESSIONAL

Dec. 1993 46 p
(NASA-TM-109690; NAS 1.15:109690) Avail: CASI HC A03/MF A01

This publication covers several categories of information about robotics. The first section provides a brief overview of the field of Robotics. The next section provides a reasonably detailed look at the NASA Robotics program. The third section features a listing of companies and organization engaging in robotics or robotic-related activities; followed by a listing of associations involved in the field; followed by a listing of publications and periodicals which cover elements of robotics or related fields. The final section is an abbreviated abstract of referred journal material and other reference material relevant to the technology and science of robotics, including such allied fields as vision perception; three-space axis orientation and measurement systems and associated inertial reference technology and algorithms; and physical and mechanical science and technology related to robotics. Derived from text

N94-27254 Motor Industry Research Association, Nuneaton (England).

OPTIMISING BMW FOUR-CYLINDER TWO-VALVE ENGINES

R. Flierl, F. Kramer, H. Rech, U. Stanski, and M. Wenzel Nov. 1993 35 p
(PB94-125101; MIRA TRANS-93/13) Avail: Issuing Activity (National Technical Information Service (NTIS))

In model year 1994, BMW will present two essentially redesigned 4-cylinder, 2-valve engines. BMW has upgraded its 1.6 1 and 1.8 1 2-valve engines using technical features previously reserved for the 4-valve engines, such as knock control system, distributorless semiconductor ignition, variable induction system (DISA) and ribbed V-belt accessory drive, along with measures to reduce power losses, noise levels and exhaust emissions. BMW models equipped with these two engines offer customers improved response characteristics and fuel consumption, as well as reduced emissions and maintenance requirements. NTIS

N94-27322 National Physical Lab., Teddington (England). Div. of Materials Metrology.
GUIDELINES FOR UNLUBRICATED SLIDING WEAR TESTS. PART 1: GENERAL APPROACH
M. G. Gee 1993 16 p
(PB94-119666; NPL-DMM(A)-96-Pt-1) Copyright Avail: Issuing Activity (National Technical Information Service (NTIS))

This document has been prepared by the author on behalf of the UK Forum on Friction and Wear Testing. The Forum has the overall objectives of improving the reproducibility and repeatability of friction and wear testing in the UK by open discussion and participation in national and international pre-standardization activities. This document serves as a general introduction to friction and wear testing in sliding. It contains a discussion on the most effective approach to friction and wear testing, and it considers the different aspects that should be considered when designing a program of friction and wear testing. NTIS

N94-27324 National Physical Lab., Teddington (England). Div. of Materials Metrology.
GUIDELINES FOR UNLUBRICATED SLIDING WEAR TESTS. PART 2: PROCEDURES FOR PIN-ON-DISC TESTING
M. G. Gee 1993 22 p See also PB94-119666
(PB94-123270; NPL-DMM(A)-97-Pt-2) Copyright Avail: Issuing Activity (National Technical Information Service (NTIS))

These guidelines describe procedures for the conduction of unlubricated pin-on-disc wear tests. They have been prepared for the UK Forum on Friction and Wear Testing and are based in part on results from interlaboratory exercises conducted by Technical Working Area 1, Wear Test Methods of VAMAS. NTIS

N94-27343 Concordia Univ., Montreal (Quebec). Dept. of Mechanical Engineering.
GENERALIZED FINITE ELEMENT DYNAMIC MODELLING AND SIMULATION FOR FLEXIBLE ROBOT MANIPULATORS M.S. Thesis
Feng Zhou Jan. 1993 158 p
(ISBN-0-315-84623-2; CTN-94-61079) Copyright Avail: Micromedia Ltd., Technical Information Centre, 240 Catherine Street, Suite 305, Ottawa, Ontario, K2P 2G8, Canada HC/MF

The finite element approach is used to model multi-link flexible robotic manipulators. The kinematic character of flexible manipulators is analyzed using body-fixed and link element attached coordinates. Dynamic equations for flexible robot manipulators are then derived. The position of each point on the link is expressed using a transformation matrix, and the kinetic and potential energy for each element is computed and summed over all the elements. The Lagrangian formulation is applied to set up the dynamic equations of the system. Computational simulations are performed on single- and two-link manipulators with and without torque to check the validity and correctness of the derived dynamic equations. The Runge-Kutta method is used to solve the dynamic equations for flexible manipulators on which all the joints are revolute. Author (CISTI)

N94-27344 Concordia Univ., Montreal (Quebec). Dept. of Electrical and Computer Engineering.
DYNAMIC CONTROL OF KINEMATICALLY REDUNDANT MANIPULATORS Ph.D. Thesis
Zhengcheng Lin Mar. 1993 195 p
(ISBN-0-315-84627-5; CTN-94-61080) Copyright Avail: Micromedia Ltd., Technical Information Centre, 240 Catherine Street, Suite 305, Ottawa, Ontario, K2P 2G8, Canada HC/MF

A robot manipulator is said to be kinematically redundant when it has more degrees of freedom than are necessary to accomplish a particular task. Useful control strategies are designed for kinematically redundant manipulators in order to enhance their performance. Following the impedance control approach, the problem of minimizing redundant manipulator collision impacts is addressed. The configuration control approach is used to reduce impulsive forces, while a simplified impedance control scheme is formulated to minimize rebound effects. A new Cartesian control strategy for redundant flexible-joint manipulators is proposed. The main idea in this hybrid scheme is to control not only the manipulator's end-effector but also its links, so as to achieve specified positions and velocities for the end-effector and the links. Finally, a new application of kinematically redundant manipulators is proposed: using redundancy resolution to compensate for joint flexibility. This redundancy resolution scheme is incorporated in a control strategy for redundant flexible-joint manipulators. The problem of possible algorithmic singularities is considered, and a scheme is suggested which makes the controller robust with respect to such singularities. Author (CISTI)

N94-27351# Electrotechnical Lab., Tsukuba (Japan).
RESEARCHES OF THE ELECTROTECHNICAL LABORATORY. NO. 52: STUDIES OF EXTERNALLY PRESSURIZED POROUS GAS BEARINGS [DENSHI GIJUTSU SOGO KENKYUSHO KENKYU HOKOKU DAI 52 GO: SEIATSU TAKOSHITSU KITAI JIKUUKE NO KOSEINOKA NO KENKYU]
Makoto Okano 30 Jul. 1993 152 p In JAPANESE
(ISSN 0366-9106)
(JTN-94-80549) Avail: CASI HC A08/MF A02

The results of the studies to solve problems related to manufacturing techniques and calculation methods on externally pressurized porous gas bearings are presented. The following aspects of the studies are outlined: (1) historical backgrounds of studies on the gas lubricated bearings; (2) the machining process of attaining the accuracy required for the gas lubricated bearings; (3) the theoretical analysis on the static performance of this porous gas bearing; (4) the performance under the rotational speed on this type of bearing; and (5) the low-temperature rotating machines for helium refrigerator and the precision measuring instruments with the externally pressurized porous gas bearings which are designed according to the above theoretical and experimental results. Author (NASDA)

N94-27383*# Alabama Univ., Huntsville.
ENHANCED SIMULATION SOFTWARE FOR ROCKET TURBOPUMP, TURBULENT, ANNULAR LIQUID SEALS Final Report
Satya Padavala (Texas A&M Univ., College Station.) and Alan Palazzolo (Texas A&M Univ., College Station.) 26 Jan. 1994 291 p
(Grant NAG8-212; TAMU Proj. 41670-ME)
(NASA-CR-195239; NAS 1.26:195239) Avail: CASI HC A13/MF A03

One of the main objectives of this work is to develop a new dynamic analysis for liquid annular seals with arbitrary profile and to analyze a general distorted interstage seal of the space shuttle main engine high pressure oxygen turbopump (SSME-ATD-HPOTP). The dynamic analysis developed is based on a method originally proposed by Nelson and Nguyen. A simpler scheme based on cubic splines is found to be computationally more efficient and has better convergence properties at higher eccentricities. The first order solution of the original analysis is modified by including a more exact solution that takes into account the variation of perturbed variables along the circumference. A new set of equations for dynamic analysis are derived based on this more general model. A unified solution procedure that is valid for both Moody's and Hirs' friction models is presented. Dynamic analysis is developed for three different models: constant properties, variable properties, and thermal effects with variable properties. Arbitrarily varying seal profiles in both axial and circumferential directions are considered. An example case of an elliptical seal with varying degrees of axial curvature is analyzed in detail. A case study based on predicted clearances of an interstage seal of the SSME-ATD-HPOTP is presented. Dynamic coefficients based on external specified load are introduced to analyze seals that support a preload. The other objective of this work is to study the effect of large rotor displacements of SSME-ATD-HPOTP on the dynamics of the annular seal and the resulting transient motion. One task is to identify the magnitude of motion of the rotor about the centered position and establish limits of effectiveness of using current linear models. This task is accomplished by solving the bulk flow model seal governing equations directly for transient seal forces for any given type of motion, including motion with large eccentricities. Based on the above study, an equivalence is established between linearized coefficients based transient motion and the same motion as predicted by the original governing equations. An innovative method is developed to model nonlinearities in an annular seal based on dynamic coefficients computed at various static eccentricities. This method is thoroughly tested for various types of transient motion using bulk flow model results as a benchmark. Derived from text

N94-27560*# National Aeronautics and Space Administration. Marshall Space Flight Center, Huntsville, AL.
DEVELOPMENT OF A NEW SEAL FOR USE ON LARGE OPENINGS OF PRESSURIZED SPACECRAFT
B. Weddendorf Mar. 1994 30 p

(Proj. 92-11)
(NASA-TM-108444; NAS 1.15:108444) Avail: CASI HC A03/MF A01

The goal of this project was to design, build, and test an example of the seal invented by the author for use on Space Station Freedom and patented in 1991. The seal features a metallic spring core and replaceable elastomeric sealing elements. The metallic spring is designed to retain the sealing force of the elastomeric element against both sides of face seal gland for any specified amount of waviness or separation of the glands. A seal able to tolerate at least 1.3 mm (0.05 in) of flange distortion or separation and a test fixture of this seal which allowed direct comparison testing of O-rings were built. These designs were tested to compare leakage at different amounts of flange deflection. Results of the testing show the development seal exceeded its requirement to seal 1.3 mm of flange separation by 1 mm. This compared with the O-ring leakage, increasing dramatically at 0.5 mm of separation. The development seal also leaked at a lower rate than the O-ring seals in all tests. Author (revised)

N94-27589# Deutsche Forschungsanstalt fuer Luft- und Raumfahrt, Lampoldshausen (Germany). Inst. fuer Chemische Antriebe und Verfahrenstechnik.

CONTROL OF A HYDROGEN/OXYGEN STEAM GENERATOR [REGELUNG EINES H2/O2-DAMPFERZEUGERS]

Stefan Beer and Herbert Willms Sep. 1992 119 p In GERMAN
(ISSN 0939-2963)
(DLR-FB-93-02; ETN-94-95491) Avail: CASI HC A06/MF A02

An H2/O2 steam generator, which is capable of producing steam at a given thermal capacity and state after a very short period of time, is described. The main components of the system are the reactor and the storage for H2, O2, and H2O. The mathematical model should not be very complex in order to keep the computation time small, but it should be capable of directly describing the main features of the system. Different strategies are proposed for the controller which need different computation times due to their inherent complexity. For the measurement of steam temperature and the ratio of propellant supply, different methods were developed and tested. Results derived from the experimental program are presented and discussed. ESA

N94-27591# Deutsche Forschungsanstalt fuer Luft- und Raumfahrt, Goettingen (Germany). Abt. Gitterstroemungen.

STREAMWISE VORTICITY IN A TURBINE ROTOR WITH CONICAL ENDWALLS Ph.D. Thesis - Goettingen Univ. [LAENGSWIRBELENTSTEHUNG IM EINEM TURBINENLAUFRAD MIT KONISCHEN SEITENWAENDEN]

Friedrich Kost Apr. 1993 113 p In GERMAN
(ISSN 0939-2963)
(DLR-FB-93-13; ETN-94-95493) Avail: CASI HC A06/MF A02

To investigate the spatial flow structure caused by sweep and dihedral effects in turbomachinery blade rows, detailed measurements were conducted in a windtunnel for rotating annular cascades. The special configuration consisted of a turbine rotor equipped with straight blades, a conical hub, and a conical casing with a cone half angle of 30 deg. Numerous flow data were obtained from surface pressure distributions at seven radial blade sections and from laser velocimetry upstream, downstream, and inside the rotor. It is shown that large deviations from an axisymmetric surface exist in conical flow. The conical flow gives rise to the production of streamwise vorticity which results in increased flow losses. It is furthermore shown that the secondary flow structure is mainly determined by the rotation of the turbine. ESA

N94-27596 Queens Univ., Kingston (Ontario). Dept. of Electrical Engineering.

DESIGN, IMPLEMENTATION AND EXPERIMENTAL RESULTS OF ROBOTIC ENVIRONMENT INPUT INTO THE ROBOT CONTROLLER TEST STATION (RCTS) M.S. Thesis

Michael A. Ramsay Aug. 1993 192 p
(ISBN-0-315-85355-7; CTN-94-61106) Copyright Avail: Micromedia Ltd., Technical Information Centre, 240 Catherine Street, Suite 305, Ottawa, Ontario, K2P 2G8, Canada HC/MF

The Robot Controller Test Station (RCTS) was developed to provide a tool for facilitating the development and integration of robot research for sensor-based robot systems. RCTS software is designed on a modular basis, and each module is a separate entity sharing the same structure as the other modules. Six functional types of modules exist in the original RCTS version and are classified according to whether they perform control or sensing functions. To advance the RCTS system, research was conducted on the inclusion of sensory inputs from the workspace environment surrounding the robot. Such information allows flexible manufacturing control algorithms, multi-robot coordination, and multi-robot avoidance to be tested on the RCTS. The design and implementation of RCTS versions 3 and 4 is described. Version 3 operates on a UNIX-based workstation and a programmable logic controller is used in Version 4 to collect and process information. Implementation of the versions is detailed along with experiments conducted to evaluate RCTS performance. Author (CISTI)

N94-27599*# National Aeronautics and Space Administration. Lewis Research Center, Cleveland, OH.

DEVELOPMENT OF HYPERSONIC ENGINE SEALS: FLOW EFFECTS OF PRELOAD AND ENGINE PRESSURES

Zhong Cai (Drexel Univ., Philadelphia, PA.), Rajakkannu Mutharasan (Drexel Univ., Philadelphia, PA.), Frank K. Ko (Drexel Univ., Philadelphia, PA.), and Bruce M. Steinetz Apr. 1993 13 p Presented at the 29th Joint Propulsion Conference and Exhibit, Monterey, CA, 28-30 Jun. 1993; sponsored by AIAA, SAE, ASME, and ASEE
(RTOP 763-22-41)
(NASA-TM-106333; E-7400; NAS 1.15:106333; AIAA Paper 93-1998)
Avail: CASI HC A03/MF A01

A new type of engine seal is being developed to meet the needs of advanced hypersonic engines. A seal braided of emerging high temperature ceramic fibers comprised of a sheath-core construction was selected for study based on its low leakage rates. Flexible, low-leakage, high temperature seals are required to seal the movable engine panels of advanced ramjet-scramjet engines either preventing potentially dangerous leakage into backside engine cavities or limiting the purge coolant flow rates through the seals. To predict the leakage through these flexible, porous seal structures as a function of preload and engine pressures, new analytical flow models are required. An empirical leakage resistance/preload model is proposed to characterize the observed decrease in leakage with increasing preload. Empirically determined compression modulus and preload factor are used to correlate experimental leakage data for a wide range of seal architectures. Good agreement between measured and predicted values are observed over a range of engine pressures and seal preloads. Author

N94-27652 Waterloo Univ. (Ontario). Dept. of Electrical Engineering.

ADVANCED CONTROL OF A FLEXIBLE SPHERICAL WRIST M.S. Thesis

Louis Alexander Gorgenyi 1993 141 p
(ISBN-0-315-84424-8; CTN-94-61068) Copyright Avail: Micromedia Ltd., Technical Information Centre, 240 Catherine Street, Suite 305, Ottawa, Ontario, K2P 2G8, Canada HC/MF

A flexible spherical wrist, susceptible to nonlinear torsional vibrations, was developed which utilizes controllers to provide position control and vibration rejection. The issue of robust performance and stability for this robot wrist is examined while adhearing to practical implementation limits. System identification techniques are used to obtain linear models of the dynamic equations of motion. These models contain physical information such as friction and cable drag, and several different parametric forms are presented. Asymptotic stability of the wrist under proportional derivative control is proven using a linearized set of dynamical equations. Experimental results show only stability rather than asymptotic stability due to friction and unmodeled dynamics. In addition, poor robustness of this control methodology is demonstrated when the orientation and payload are varied. One- and two-parameter Hardy space controllers are designed to address the robustness and implementation issues. Variations in wrist orientation and payload are modeled as multiplicative uncertainties. Simulation and experimental results are presented and compared to those of a tracking controller. The Hardy space controllers are shown to have superior robustness properties but poorer performance. Author (CISTI)

N94-27657*# State Univ. of New York, Binghamton. Dept. of Mechanical and Industrial Engineering.

STUDY OF THE KINEMATIC AND DYNAMIC CHARACTERISTICS OF A WORMGEAR TRANSMISSION FOR HELICOPTER APPLICATIONS Final Report

D. C. Sun and Qin Yuan Mar. 1994 138 p
(Grant NAG3-1316; DA Proj. 1L1-61102-AH-45; RTOP 505-62-0K-00)
(NASA-CR-195287; E-8633; NAS 1.26:195287; ARL-CR-78) Avail: CASI HC A07/MF A02

The first phase of the study of the performance of a wormgear transmission is reported. In this phase the work included the selection of a double-enveloping wormgear type, and its dimensions, suitable for use in helicopter transmissions; the 3-D graphics representation of the selected wormgear using the I-DEAS software; the analysis of the kinematics of meshing; the analysis of load sharing among the meshing teeth; and the implementation of the analyses in a computer program. The report describes the analyses, their results, and the use of the computer programs. Author

N94-27665# Instituto de Pesquisas Espaciais, Sao Jose dos Campos (Brazil).
USING FERRO-MAGNETIC FLUIDS TO LUBRICATE NON-CONFORMAL ISOTHERMAL CONTACTS Ph.D. Thesis - Cranfield Inst. of Technology, 1992
Petronio Noronha deSouza 1993 204 p
(INPE-5520-TAE/021) Avail: CASI HC A10/MF A03

Magnetic fluids are synthetic materials that combine in a single medium the properties of fluids and magnetic materials. The action of a magnetic field on the magnetic fluid allows the design of new types of bearings and also provides conventional ones with new properties. This work presents a contribution to the study of the lubrication of linear isothermal non-conformal contacts with magnetic fluids under the action of a nonuniform magnetic field perpendicular to the plane of the contact. The fluid is assumed to present extrinsic superparamagnetism. The regime of lubrication considered is the isoviscous-rigid. The analytical approach adopted considers small perturbations of the classical analytical solution already known for this type of contact. The main objectives of the work are: to establish the equations and assumptions that are necessary to treat the proposed lubrication problem; to analyze the impact of the change in the apparent viscosity of the magnetic fluid on the thickness of the lubricating film due to the presence of the magnetic field; and to develop an experimental technique able to deal with the problems that arise with the use of magnetic fluids in the lubrication of a two-disc machine. The mathematical treatment of the proposed problem brings together the analytical methods adopted in fluid film lubrication to the analysis of long isothermal hydrodynamic bearings and those from the magnetic-liquid fluid dynamics (ferrohydrodynamics) usually adopted to study the flow of magnetic fluids that present extrinsic superparamagnetism. The result is a coherent system of equations supported by a well defined set of assumptions. The solution obtained allows the study of the eventual change of the film thickness that can be achieved by the application of a magnetic field across the contact. The work also discusses the experimental technique necessary to study the problem in a two-disc machine that runs with minute amounts of lubricant, applies a magnetic field across the contact and measures the film thickness by a capacitance method. The work concludes by showing theoretically that the film thickness can be either increased or reduced depending on the magnetic and viscous properties of the fluid and the intensity of the magnetic field. These conclusions are supported by experiments with a magnetic oil in a two-disc machine. Author

N94-27722# California Univ., Berkeley. Lawrence Berkeley Lab. Dept. of Technology Transfer.
OPPORTUNITIES FOR HIGH ASPECT RATIO MICRO-ELECTRO-MAGNETIC-MECHANICAL SYSTEMS (HAR-MEMMS) AT LAWRENCE BERKELEY LABORATORY
Steven Hunter, ed. Oct. 1993 260 p Presented at the Opportunities for HAR-MEMMS at Lawrence Berkeley Laboratory, Berkeley, CA, 3 Aug. 1993
(Contract DE-AC03-76SF-00098)
(DE94-003499; LBL-34767; CONF-9308178) Avail: CASI HC A12/MF A03

This report contains viewgraphs on the following topics: Opportunities for HAR-MEMMS at LBL; Industrial Needs and Opportunities; Deep Etch X-ray Lithography; MEMS Activities at BSAC; DNA Amplification with Microfabricated Reaction Chamber; Electrochemistry Research at LBL; MEMS Activities at LLNL; Space Microsensors and Microinstruments; The Advanced Light Source; Institute for Micromaching; IBM MEMS Interests; and Technology Transfer Opportunities at LBL. DOE

N94-27780# Pacific Northwest Lab., Richland, WA.
COMPARISON OF DYNAMIC ANALYSIS OF A SCHILLING HYDRAULIC MANIPULATOR WITH EXPERIMENTAL RESULTS
C. P. Baker, J. Y. Lew, M. S. Evans, and D. P. Magee (Georgia Inst. of Tech., Atlanta.) Jul. 1993 7 p Presented at the 9th International Conference on Mathematical and Computer Modelling, Berkeley, CA, 26-29 Jul. 1993
(Contract DE-AC06-76RL-01830)
(DE94-004597; PNL-SA-22415; CONF-9307159-1) Avail: CASI HC A02/MF A01

Two independent models of the dynamics of a Schilling Titan II hydraulic manipulator were developed and compared in order to obtain an accurate model of the manipulator dynamics. These models will be used in the development of feedback control laws and active damping algorithms. One of the models is an analytical model which was developed 'by hand' with the assistance of computer symbolic manipulation. The other is a numerical model developed using a commercially available dynamics code. The data from these models were then compared with experimental data from an actual Titan II manipulator. DOE

N94-27874# Solar Turbines, Inc. San Diego, CA. Research Dept.
GAS FIRED ADVANCED TURBINE SYSTEM
R. T. LeCren and D. J. White 1993 9 p Presented at the Joint Contractors Meeting on Advanced Turbine Systems, Fuel Cells and Coal-Fired Heat, Morgantown, WV, 3-5 Aug. 1993
(Contract DE-AC21-86MC-23166)
(DE94-003193; DOE/MC-23166/94/C0236; CONF-930893-37) Avail: CASI HC A02/MF A01

The basic concept thus derived from the Ericsson cycle is an intercooled, recuperated, and reheated gas turbine. Theoretical performance analyses, however, showed that reheat at high turbine rotor inlet temperatures (TRIT) did not provide significant efficiency gains and that the 50 percent efficiency goal could be met without reheat. Based upon these findings, the engine concept adopted as a starting point for the gas-fired advanced turbine system is an intercooled, recuperated (ICR) gas turbine. It was found that, at inlet temperatures greater than 2450 F, the thermal efficiency could be maintained above 50%, provided that the turbine cooling flows could be reduced to 7% of the main air flow or lower. This dual and conflicting requirement of increased temperatures and reduced cooling will probably force the abandonment of traditional air cooled turbine parts. Thus, the use of either ceramic materials or non-air cooling fluids has to be considered for the turbine nozzle guide vanes and turbine blades. The use of ceramic components for the proposed engine system is generally preferred because of the potential growth to higher temperatures that is available with such materials. DOE

N94-27984*# Caterpillar Tractor Co., Peoria, IL.
DEVELOPMENT OF ADVANCED HIGH TEMPERATURE IN-CYLINDER COMPONENTS AND TRIBOLOGICAL SYSTEMS FOR LOW HEAT REJECTION DIESEL ENGINES, PHASE 1 Final Report
C. A. Kroeger and H. J. Larson Mar. 1992 78 p
(Contracts DEN3-374; DE-A101-91CE-50306)
(NASA-CR-187158; NAS 1.26:187158; DOE/NASA/0374-1) Avail: CASI HC A05/MF A01

Analysis and concept design work completed in Phase 1 have identified a low heat rejection engine configuration with the potential to meet the Heavy Duty Transport Technology program specific fuel consumption goal of 152 g/kW-hr. The proposed engine configuration incorporates low heat rejection, in-cylinder components designed for operation at 24 MPa peak cylinder pressure. Water cooling is eliminated by selective oil cooling of the components. A high temperature lubricant will be required due to increased in-cylinder operating temperatures. A two-stage turbocharger air system with intercooling and aftercooling was selected to meet engine boost and BMEP requirements. A turbocompound turbine stage is incorporated for exhaust energy recovery. The concept engine cost was estimated to be 43 percent higher compared to a Caterpillar 3176 engine. The higher initial engine cost is predicted to be offset by reduced operating costs due the lower fuel consumption. Author (revised)

N94-28041# Korea Research Inst. of Standards and Science, Taejon (Republic of Korea).
A NEW METHOD FOR TORSIONAL CRITICAL SPEED CALCULATION OF PRACTICAL INDUSTRIAL ROTORS
Oh-Sung Jun and Paul Y. Kim (National Research Council of Canada, Vancouver, British Columbia.) Jul. 1993 78 p
(IMR-T&M-TR-001; CTN-94-61010) Avail: CASI HC A05/MF A01

A new approach to calculating the torsional critical speed of rotors is presented. The governing equations for these speeds and the method of solutions differ from existing methods such as Holzer's, and the theory and numerical algorithm are straight forward, without any change in the field variables. The rotor studied has a distributed mass and rigid disks, and consists of many shaft segments of different diameters. The exact solution for undamped torsional motion of a uniform shaft segment is applied to a practical rotor-bearing system to generate the simultaneous governing equations for the torsional critical speeds. Within the framework of the theory, the set of governing equations is completely analytical and explicit, and it does not include any approximations, such as discretization of shaft mass and polynomial approximations. A computer program for the torsional critical speeds and the related mode shapes is developed by introducing a simple recurring numerical algorithm for a 3 by 4 submatrix in calculating the determinant generated by the simultaneous equations. The numerical algorithm essentially eliminates the necessity of constructing a huge matrix. The effectiveness of the new method is demonstrated in analyses of three rotors. Author (CISTI)

N94-28043# Von Karman Inst. for Fluid Dynamics, Rhode-Saint-Genese (Belgium).
GAS TURBINE ENGINE TRANSIENT BEHAVIOUR
1993 227 p Lecture series held in Rhode-Saint-Genese, Belgium, 10-12 May 1993
(ISSN 0377-8312)
(VKI-LS-1993-06; ETN-94-95454) Copyright Avail: CASI HC A11/MF A03

Information and data that are intended to provide an in depth understanding of gas turbine engine transient behavior, the modeling methods that are applied to transient events, and the simulation technology that supports the transient analysis process are presented. The diverse nature of the disciplines that are applied to the study of transient behavior makes it necessary to examine the subject from at least three perspectives: the application of the underlying technology to specific design and development concerns; the development of the mathematical models that support the various applications; and the computer programs that implement the models and provide the analytical capability required by the different applications. For individual titles, see N94-28044 through N94-28054.

N94-28044# Rolls-Royce Ltd., Derby (England).
GAS-TURBINE ENGINE STEADY-STATE BEHAVIOR
Barry Curnock *In* VKI, Gas Turbine Engine Transient Behaviour 1993 35 p (For primary document see N94-28043 07-37)
Copyright Avail: CASI HC A03/MF A03

A set of graphics with explanations illustrating gas turbine engine steady state behavior are presented. Typical combinations of compressors and nozzles which occur in a gas turbine engine are shown. The basic effect of a nozzle is explained by considering a compressor on a test rig: typical compressor, fan, and turbine characteristics are illustrated. The following are discussed: the degrees of freedom of an aeroengine (the flow and the power); the 'working lines' of components (the locus of the off design steady state operating points of a component plotted on a chart of that components characteristics); bleed and whirl; offtakes; P1 effects (performance changes which modify the basic nondimensional behavior an engine (caused by the effect on Reynolds number levels and on engine mechanical configuration of basic engine inlet pressure level)), and T1 effects (performance changes which modify the basic nondimensional behavior of an engine and are caused by the effects of engine inlet temperature level on Reynolds number level, on engine mechanical configuration and on specific heat level); variable nozzles; and turbojet matching. ESA

N94-28045# Rolls-Royce Ltd., Derby (England).
TRANSIENT PERFORMANCE
Barry Curnock *In* VKI, Gas Turbine Engine Transient Behaviour 1993 32 p (For primary document see N94-28043 07-37)
Copyright Avail: CASI HC A03/MF A03

Gas turbine engine transient behavior, that which is concerned with the changes in engine parameters during acceleration or decceleration of an engine from one steady state point to a different steady state point, is considered. An engine can also experience cyclic aerodynamic phenomena which occur at a nominally steady condition; examples are compressor rotator stall and intake or afterburner buzz. The following are discussed: certification requirements; mechanism of acceleration; compressor working lines and surge; and some important factors (pressure level, moment of inertia, heat soakage, clearances, measurement of transients, thrust reversal, and transient maneuvers which involve significant changes to the shaft speeds of the engine). A set of graphics illustrating transient performance is presented. ESA

N94-28046# Rolls-Royce Ltd., Derby (England).
COMPRESSOR STABILITY
Barry Curnock *In* VKI, Gas Turbine Engine Transient Behaviour 1993 29 p (For primary document see N94-28043 07-37)
Copyright Avail: CASI HC A03/MF A03

Various operating modes and conditions of the gas turbine which may cause compressor stall are considered. The behavior of a compressor in stall is explained because the engineer, although designing to avoid stall, must consider the possibility of stall and what control measures must be taken to recover engine operability. A major cause of stall is inlet distortion, that is a nonuniform pressure and/or temperature profile at entry to the compressor. The causes and effects of distortion are discussed. A set of graphics illustrating the above is also presented. ESA

N94-28047# Rolls-Royce Ltd., Derby (England).
ENGINE STARTING AND STOPPING
Barry Curnock *In* VKI, Gas Turbine Engine Transient Behaviour 1993 36 p (For primary document see N94-28043 07-37)
Copyright Avail: CASI HC A03/MF A03

Different starter systems for jet engines are discussed: electric, cartridge, iso-propyl-nitrate, air, gas turbine, and hydraulic. The fuel system, ignition system, air flow control system, and actual starting mechanism of an air starter motor system are considered. The variation of engine parameters throughout a typical starting sequence are described, with reference to examples for an RB211-535 engine. Physical constraints on engine starting are considered: rotating stall, light up, the window between hang and stall, hang, compressor stall, and the effects of ambient conditions. The following are also discussed: contractual and airworthiness requirements; windmilling; inflight relighting; afterburning light up; combustion stability; and broken shafts. Graphics illustrating the above are presented. ESA

N94-28048# General Electric Co., Owensboro, KY. Engine Simulation Technology.
TRANSIENT MODEL APPLICATIONS. 1: COMPRESSOR HEAT SOAK/CLEARANCE EFFECTS MODELING
Peter W. McDonald *In* VKI, Gas Turbine Engine Transient Behaviour 1993 16 p (For primary document see N94-28043 07-37)
Copyright Avail: CASI HC A03/MF A03

One of the potentially many ways in which expanding the objectives, requirements, and capabilities of engine simulation might improve the cost and time effectiveness of the engineering process in aircraft engine design is examined. The engine simulation developed for the analysis of heat soak and clearance effects on compressor performance and stability required technology interactions between heat transfer, mechanical design, and compressor aerodynamics. The objective and requirements of the models provided by the interacting technical disciplines were limited to the objectives of determining the compressors internal flow path heat transfer rates and clearances and the effect of these on the compressor performance and stability. The compressor aerodynamics model computes the performance of each compressor stage both at the stall line and the operating line with and without the stage heat addition and clearance variation. Boundary conditions for the aerodynamics model are required from the engine model as well as from the heat transfer and clearance models. ESA

N94-28049# General Electric Co., Owensboro, KY. Engine Simulation Technology.
TRANSIENT MODEL APPLICATIONS. 2: COMPRESSOR STALL MODELING METHODS
Peter W. McDonald and J. L. Moulton *In* VKI, Gas Turbine Engine Transient Behaviour 1993 18 p (For primary document see N94-28043 07-37)
Copyright Avail: CASI HC A03/MF A03

A series of stall capable models which support the engine operability design effort for variable cycle engines is discussed. These models were derived from existing transient simulations which included the control, sensor, and actuator models. The process of constructing the stall models was accomplished in two steps. The first step was the addition of volume dynamics elements throughout the engine simulation. The core and bypass flows were partitioned into several volumes and the compression components were defined as sources and sinks of mass, momentum and energy at boundaries of these volumes. The second step was the extension of compression component performance representations to include in-stall operation. The methods used to accomplish these steps are illustrated with a simple model of a compressor test rig. Graphs showing the variation of compressor power, compressor momentum capability and system response and inlet corrected speed during a repeatable surge cycle and simulation are presented. The compressor inlet and exit pressure, the air flow and the temperature response during surge cycle simulation are graphically illustrated. In-stall and unstalled performance and efficiency are graphically illustrated at 70 to 75% corrected speed, and at 50 and 60% corrected speed. The temperature and momentum variation during a nonrecoverable stall simulation are also graphically illustrated. All graphs are discussed. ESA

N94-28050# General Electric Co., Owensboro, KY. Engine Simulation Technology.
TRANSIENT MODEL APPLICATIONS. 3: TRANSIENT ENGINE SIMULATION AND ANALYSIS OF AN ICE INGESTION TEST
Peter W. McDonald *In* VKI, Gas Turbine Engine Transient Behaviour 1993 15 p (For primary document see N94-28043 07-37)
Copyright Avail: CASI HC A03/MF A03

A transient engine model capable of simulating the transient response of an aircraft engine ice ingestion is examined. This model is required to simulate a controlled test which would provide data with which the model could be verified. Ice ingestion testing is routinely conducted with the objective of demonstrating the ability of an aircraft engine to safely operate while an aircraft passes through a hail storm. The most critical test condition is at a flight idle power setting where the engine power is low (or the capability to melt ice and evaporate water is limited) and the concentration of hail relative to the engine inlet airflow is high. The ice ingestion test was accomplished with a set of ice guns which shot large quantities of uniformly distributed ice at the fan hub region (into the core of the engine). The ice was crushed and filtered to match the size of hail stones and fired at a velocity consistent with the air speed being represented by the test. The response of certain engine parameters, as predicted by the model, to the ice ingestion test, is graphically illustrated and discussed. Examples include fuel flow, fan speed, core speed, compressor discharge pressure, compressor discharge temperature. ESA

N94-28051# McLaughlin (Peter), Glastonbury, CT.
ENGINE SIMULATION TECHNOLOGY
Peter McLaughlin *In* VKI, Gas Turbine Engine Transient Behaviour 1993 14 p (For primary document see N94-28043 07-37)
Copyright Avail: CASI HC A03/MF A03

A discussion of engine simulation technology which is intended to provide an overview of the continuous system simulation process as it has been applied in the gas turbine engine industry is presented. The topics include: devices employed in simulation, numerical and programming methods used; high level languages, applications toward which the simulation process is directed, organizational requirements, and future trends predicted by the current practice. ESA

N94-28052# McLaughlin (Peter), Glastonbury, CT.
TRANSIENT ENGINE SIMULATION
Peter McLaughlin *In* VKI, Gas Turbine Engine Transient Behaviour 9 p(SEE N94-28043 07-37) 1993 (For primary document see N94-28043 07-37)
Copyright Avail: CASI HC A02/MF A03

The specific steps that are taken in the creation of a transient engine simulation program are presented. The types of models used in transient engine simulation are discussed: linear methods such as linear simulation background and Laplace transforms, nonlinear methods, and finite element methods. The process by which the simulation is used to generate useful data is discussed. ESA

N94-28053# McLaughlin (Peter), Glastonbury, CT.
NONLINEAR SOLVERS
Peter McLaughlin *In* VKI, Gas Turbine Engine Transient Behaviour 1993 10 p (For primary document see N94-28043 07-37)
Copyright Avail: CASI HC A02/MF A03

A typical example of a nonlinear solver used in several different engine simulation programs is described, including its interaction with the dynamic and discontinuous aspects of the model. The model equations are solved using the Newton-Raphson technique augmented by a matrix update based on Broyden's method. This solver is applied in both transient and steady state cases and provides reliable convergence of the set of implicit relationships required by the model. Broyden's method provides efficient convergence on component based engine models operating in the normal power range. However, several computations in a quasi Newton Broyden solver utilizing normalized parameters become indeterminate when the iteration variables, for example rotor speeds and flows, approach zero during starting or shutdown. REPLICAS (Rational, Effective Procedures and Logic for the Implementation of Computerized Analysis and Simulation), is a collection of algorithms that is intended to provide convergence properties that are independent of the magnitudes of the iteration variables. In REPLICAS, a unique algorithm is employed which automatically provides an additive bias on the iteration variable. This bias is chosen in such a way as to maintain the magnitudes of the matrix elements at relatively constant values, independent of the absolute magnitude of the actual iteration variables. ESA

N94-28054# McLaughlin (Peter), Glastonbury, CT.
ENGINE SIMULATION SYSTEMS
Peter McLaughlin *In* VKI, Gas Turbine Engine Transient Behaviour 7 p(SEE N94-28043 07-37) 1993 (For primary document see N94-28043 07-37)
Copyright Avail: CASI HC A02/MF A03

The development and utilization of gas turbine engine simulation systems, which are important elements of the process that supports design, development and product support activities, are described. A wide range of program requirements are described including user interfaces, numerical methods, software quality assurance, model and problem definition, model validation, program architecture, training, portability, reliability, error detection and documentation. ESA

N94-28055 ESDU International Ltd., London (England).
CONTACT STRESS IN DISC CAMS WITH ROLLER FOLLOWERS
Mar. 1993 48 p
(ISSN 0141-4046)
(ESDU-93001; ISBN-0-85679-843-6) Avail: ESDU

ESDU 93001 presents a Fortran program that calculates the compressive stress in the contact region of a barrelled roller translating (radial or offset) or swinging arm follower at 1 degree intervals during the cam cycle. Also output are the dimensions of the contact zone and the decrease in separation of the cam and the roller centers. The method applies to unlubricated surfaces or situations where the lubrication regime is elastohydrodynamic or boundary. The method calculates the force at the cam/roller interface due to follower system inertia, action of the return spring and the externally applied load which can be specified at 1 degree intervals of cam rotation, at a few points, or by a sine function. Six cam laws are treated but an option is provided for a user-specified law to be input. The values of contact force, together with cam profile radius of curvature, roller dimensions, and Young's modulus and Poisson's ratio of the cam and roller materials are used to calculate the contact stress following the method of ESDU 78035. An option is included to determine suitable values of spring rate and preload to ensure that contact between cam and follower is maintained. A description of the mathematical model programmed is provided together with guidance on the use of the program, a full description of the input and output formats illustrated by three realistic worked examples, and an explanation of warning messages that may be generated. The program, ESDUpac A9301, is provided on disc (uncompiled) in the software volume and also compiled within ESDUview, a user-friendly shell running under MS DOS that prompts on screen for the input data. ESDU

N94-28056 ESDU International Ltd., London (England).
BLENDING PROFILES OF DISC CAMS WITH RADIAL TRANSLATING ROLLER FOLLOWERS. PART 2: TO INCORPORATE AN INTERMEDIATE PRECISION POINT OR A CONSTANT VELOCITY COMPONENT
Sep. 1993 47 p
(ISSN 0141-4046)
(ESDU-93002-Pt-2; ISBN-0-85679-844-4) Avail: ESDU

ESDU 93002 uses a method by which each motion segment (rise or return) is formed by blending together components of two single-law segments at the point of maximum follower velocity. A hand calculation method may be used, based on the graphs of ESDU 92005 relating to six commonly-used cam laws, or Fortran programs (ESDUpac A9302 for the precision point and ESDUpac B9302 for the constant velocity component), and both techniques yield the minimum allowable size of cam (based on the requirements that the maximum pressure angle does not exceed a specified value and that profile undercutting is avoided). The program also uses the six common cam laws but a user-specified law may also be input provided the maximum velocity occurs at the mid-point of a single segment. The output from the programs can if required include the follower motion at 1 degree intervals for a full cam rotation (displacement, velocity, acceleration and jerk). The theoretical background to the method is explained, step-by-step design procedures are detailed, and guidance on the use of the programs is given. A full description of the input and output formats is illustrated by practical worked examples. The programs are provided on disc (uncompiled) in the software volume and also compiled within ESDUview, a user-friendly shell running under MS DOS that prompts on screen for input data. ESDU 83027 also provides a hand calculation method for blending that applies to both translating and swinging arm followers but provides no information on minimum cam size. ESDU

N94-28073 ESDU International Ltd., London (England).
CALCULATION METHODS FOR STEADILY LOADED CENTRAL CIRCUMFERENTIAL GROOVE HYDRODYNAMIC JOURNAL BEARINGS (GUIDE TO USE OF COMPUTER PROGRAM A9304)
Aug. 1993 25 p
(ISSN 0141-2590)
(ESDU-93004; ISBN-0-85679-856-8) Avail: ESDU

ESDU 93004 introduces a Fortran program that implements the calculation method of ESDU 90027. The program predicts the minimum lubricant film thickness (taking any misalignment into account), eccentricity ratio, the power loss, the lubricant flow rate, and the bearing and lubricant temperatures. It can, optionally, provide a preliminary design to satisfy specified requirements and constraints. The preliminary design method incorporates recommendations for lubricant grade and feed pressure, bearing overall size and proportions, running clearance, and groove dimensions. The program applies for any liquid acting as a lubricant that can be regarded as Newtonian and lubricant properties are held in a database that can be edited or to which further lubricants may be added. The program provides warnings if the bearing temperature is too high, the outlet temperature is too high, the lubricant temperature is outside the usable range, the film thickness is too small, or if there is a risk of half-speed whirl. Suggestions for remedial action in each case are made. The input and output format is fully explained and illustrated with worked examples. The program is available on disc (uncompiled) in the software volume as ESDUpac A9304. ESDU

N94-28074 ESDU International Ltd., London (England).
CALCULATION METHODS FOR STEADILY LOADED AXIAL GROOVE HYDRODYNAMIC JOURNAL BEARINGS (GUIDE TO USE OF COMPUTER PROGRAM A9305)
Aug. 1993 31 p
(ISSN 0141-2590)
(ESDU-93005; ISBN-0-85679-857-6) Avail: ESDU

ESDU 93005 introduces a Fortran program that implements the calculation methods of ESDU 84031 and 85028 and so considers both laminar and turbulent flow in a bearing with one or two grooves. The program predicts, in either case, the minimum film thickness (taking any misalignment into account), the eccentricity ratio, the power loss, the lubricant flow rate, and the bearing and lubricant temperatures. It can, optionally, provide a preliminary design to satisfy specified requirements and constraints. The preliminary design method incorporates recommendations for lubricant grade and feed pressure, bearing overall size and proportions, running clearance and groove dimensions. The program applies to mineral oil lubricants and properties are held in a database that can be edited or to which further lubricants may be added. The program provides warnings if the bearing temperature is too high, the outlet temperature is too high, the lubricant temperature is outside the usable range, the film thickness is too small, or there is a risk of half speed whirl. Suggestions for remedial action in each case are made. The input and output format is fully explained and illustrated with worked examples. The program is available on disc (uncompiled) in the software volume as ESDUpac A9305. ESDU

N94-28075 ESDU International Ltd., London (England).
CALCULATION METHODS FOR STEADILY LOADED AXIAL GROOVE HYDRODYNAMIC JOURNAL BEARINGS. LOW VISCOSITY PROCESS FLUID LUBRICATION (GUIDE TO USE OF COMPUTER PROGRAM A9306)
Aug. 1993 25 p
(ISSN 0141-2590)
(ESDU-93006; ISBN-0-85679-858-4) Avail: ESDU

ESDU 93006 introduces a Fortran program that implements the calculation methods of ESDU 84031, 85028, and 86008 for laminar or turbulent flow in a bearing with one or two grooves. The program predicts the minimum film thickness (taking any misalignment into account), the eccentricity ratio, the power loss, the lubricant flow rate, and the bearing and lubricant temperatures. It can, optionally, provide a preliminary design to satisfy specified requirements and constraints. The preliminary design method incorporates recommendations for bearing overall size and proportions, running clearance and groove dimensions. The program applies for any liquid acting as a lubricant that can be regarded as Newtonian and lubricant properties are held in a database that can be edited or to which further lubricants may be added. The program provides warnings if the bearing temperature is too high, the outlet temperature is too high, the lubricant temperature is outside the usable range, the film thickness is too small, or there is a risk of half-speed whirl. Suggestions for remedial action in each case are made. The input and output format is fully explained and illustrated with worked examples. The program is available on disc (uncompiled) in the software volume as ESDUpac A9306. ESDU

N94-28077# Von Karman Inst. for Fluid Dynamics, Rhode-Saint-Genese (Belgium).
COMBINED CYCLES FOR POWER PLANTS
1993 496 p Lecture series held in Rhode-Saint-Genese, Belgium, 5-9 Jul. 1993
(ISSN 0377-8312)
(VKI-LS-1993-08; ETN-94-95455) Copyright Avail: CASI HC A21/MF A04

Papers which aim to provide an in depth understanding of the principles and practices of combined cycle power generating systems are presented. The increased use of natural gas and the development of clean coal technology has led to a renewed interest in combined cycles to maximize plant efficiency. The fundamentals of cycle thermodynamics and the design of plant components are covered, with particular reference to the design of industrial gas turbines and the associated steam plant and heat rejection system. Plant control and monitoring, methods of reducing emissions, and measurement of performance are also included. Plants fired by natural gas and developments of combined cycles for clean coal combustion systems such as fluidized beds and integrated gasification systems are addressed. For individual titles, see N94-28078 through N94-28090.

N94-28078# Moore (M. J.) (England).
INTRODUCTION TO COMBINED CYCLES c33
M. J. Moore *In* VKI, Combined Cycles for Power Plants 1993 49 p
(For primary document see N94-28077 07-37)
Copyright Avail: CASI HC A03/MF A04

Ideas and concepts underlying the technology of combined cycles including the scientific principles involved and the reasons these cycles are in fashion at the present time, are presented. A cycle is a steady flow process for conversion of heat energy into work, in which a working medium passes through a range of states, returning to its original state. Cycles for power production are the steam cycle, which is a closed cycle, and the gas turbine, which represents an open cycle. Combined cycle thermodynamic parameters, are discussed. The general arrangement of the plant is outlined and important features of their component parts described. The scope for future development is discussed. It is concluded that for the next few years the natural gas fired combined cycle will be the main type of plant installed for electricity generation and cogeneration. Whilst gas turbines may not increase substantially in unit size, there remains scope for further increase in firing temperature with consequent increase in cycle performance. However the larger global reserves of coal are providing an incentive to the development of plant for clean coal combustion using the inherent advantage of the combined cycle to attain high efficiencies. ESA

N94-28079# Imperial Coll. of Science and Technology, London (England). Dept. of Mechanical Engineering.
THERMODYNAMICS OF COMBINED CYCLE PLANT **c77**
R. I. Crane *In* VKI, Combined Cycles for Power Plants 1993 73 p
(For primary document see N94-28077 07-37)
Copyright Avail: CASI HC A04/MF A04

The fundamental thermodynamics of power plants including definitions of performance criteria and an introduction to exergy are reviewed, and treatments of simplified performance calculations for the components which form the major building blocks and a gas/steam combined cycle plant are given: the gas turbine, the heat recovery steam generator, and the remainder of the steam plant. Efficiency relationships and energy and exergy analyses of combined cycle plant are presented, with examples. Among the aspects considered are gas turbine performance characteristics and fuels, temperature differences for heat recovery, multiple steam pressures and reheat, supplementary firing and feed water heating. Attention is drawn to points of thermodynamic interest arising from applications of combined cycle plant to repowering of existing steam plant and to combined heat and power (cogeneration); some advances, including coal firing, are also introduced. ESA

N94-28080# General Electric Co., Schenectady, NY.
DEVELOPMENT OF THE GAS TURBINE. PART 1: DESIGN PHILOSOPHY AND PERFORMANCE
Leroy O. Tomlinson *In* VKI, Combined Cycles for Power Plants 1993 65 p (For primary document see N94-28077 07-37)
Copyright Avail: CASI HC A04/MF A04

The development of the gas turbine from its conception in the 1930's up until present day is outlined. Focus is on the industrial gas turbines which were designed specifically for large combined cycle power generation applications. The materials used, which have to be cost effective, reliable, and have a long life, are discussed. The gas turbine controls, which have almost universally developed to a computer based system to perform control logic sequencing and protective logic, are also considered. The information given includes development, in firing temperature, compressor pressure ratio, efficiency, NO(x) emission, and compressor air flow. ESA

N94-28081# General Electric Co., Schenectady, NY.
DEVELOPMENT OF THE GAS TURBINE. PART 2: MANUFACTURING, COMMISSIONING, AND OPERATION
Leroy O. Tomlinson *In* VKI, Combined Cycles for Power Plants 1993 42 p (For primary document see N94-28077 07-37)
Copyright Avail: CASI HC A03/MF A04

Major accomplishments in the development of gas turbine manufacturing are considered including the important manufacture of high temperature turbine buckets by precision casting. Other developments considered are as follows: directional solidification, applications of coatings in a vacuum, forging, quality checks, and casings. The factory packaging of gas turbines and their accessories, which simplifies and speeds field installation, is considered. The economic power generation cost is also considered. The elements of power generation cost include the fixed charges that are usually a fixed fraction of the installed cost, fuel, operation, and maintenance. The ways in which these elements are influenced by the design of the equipment are discussed. ESA

N94-28082# Siemens A.G., Muelhein-Ruhr (Germany).
GAS TURBINE COMBUSTION AND EMISSION CONTROL
B. Schetter *In* VKI, Combined Cycles for Power Plants 1993 42 p
(For primary document see N94-28077 07-37)
Copyright Avail: CASI HC A03/MF A04

The fundamentals of combustion are discussed in the context of gaseous and liquid fuels and gas turbine fuels. Methods for reducing the emission of pollutants in gas turbines are considered. These emissions are carbon monoxide, unburnt hydrocarbons, smoke/soot, nitrogen oxides, sulphur oxides, and carbon dioxide. The focus is on nitrogen oxides. The general principles of combustor and burner design are considered: aero/can type combustors, silo combustors, and annular combustors. Premix and diffusion flames are discussed. ESA

N94-28083# Stork Ketels B.V., Hengelo (Netherlands).
STEAM PLANT FOR COMBINED CYCLES: HEAT RECOVERY STEAM GENERATORS, DESIGN PRINCIPLES, AND CONSTRUCTION DETAILS
A. vanManen *In* VKI, Combined Cycles for Power Plants 1993 25 p
(For primary document see N94-28077 07-37)
Copyright Avail: CASI HC A03/MF A04

The design of heat recovery steam generators (HRSG) is discussed. The design of the HRSG plays an important role in overall design of a steam and gas turbine (STAG) unit. Focus is on two major items: the influence of the boiler on total efficiency of the STAG unit and the design of the boiler. The growing importance of HRSGs is of course based on the fact that with a STAG unit the efficiency of power generation is high compared to other power generation units. ESA

N94-28084# Stork Ketels B.V., Hengelo (Netherlands).
SIMULATION: A TOOL FOR STEAM PLANT DYNAMIC ANALYSIS
H. Anneveld *In* VKI, Combined Cycles for Power Plants 1993 7 p
(For primary document see N94-28077 07-37)
Copyright Avail: CASI HC A02/MF A04

Stringent requirements of combined cycles makes design and operation of process plants increasingly complex. The behavior of the complete controlled process is studied by way of simulation. By utilizing this method, process conditions can be optimized with reduced risk. This will lead to greater financial benefits. There is a large range of simulation programs which make it possible to study realistically the dynamic behavior of a wide range of complex process conditions and problematic interactions. The steam generation and distribution, the pressure limitation controls, and the dynamic behavior of a steam plant are discussed. ESA

N94-28085# Delaval-Stork V.O.F., Hengelo (Netherlands).
STEAM PLANT: STEAM TURBINES FOR COMBINED CYCLES
J. Schrieken *In* VKI, Combined Cycles for Power Plants 1993 20 p
(For primary document see N94-28077 07-37)
Copyright Avail: CASI HC A03/MF A04

Parameters affecting steam turbines design are discussed and it is concluded that steam turbines for combined cycles are suitable for: powers between 1 and 250 MW; driving a generator, via a gearbox if necessary; drive through of powers which can be up to three times their own power; and ground level installation with up, side, or axial exhaust for condensing turbine applications. Parameters affecting the steam turbine performance are discussed: inlet conditions and flows, sliding inlet conditions, reheat cycles, fired and unfired heat recovery steam generators, cogeneration systems, and combined cycle for process steam supply. Aerodynamic design aspects of steam turbines for combined cycles are discussed. It is concluded that steam turbines for combined cycles have a large range of special requirements. Some typical aspects are: large exhaust annular areas and special exhaust arrangements for condensing steam turbines, drive through of the power of the gas turbines, high influence on the total cycle performance optimization, and a wide variety of extraction systems for cogeneration. ESA

N94-28086# ABB Power Generation, Inc., Baden (Switzerland).
CONTROLS, MONITORING AND PERFORMANCE MEASUREMENTS
J.-P. Rickli *In* VKI, Combined Cycles for Power Plants 1993 30 p
(For primary document see N94-28077 07-37)
Copyright Avail: CASI HC A03/MF A04

Reasons for the increasing complexity of systems due to the desire to improve their efficiency, reliability, and safety are given, and means of keeping this evolution under control, with appropriate control systems, are discussed. The main features of a modern control system - configuration, automation, operation, and monitoring - are discussed. Application is made to the combined cycle power plant. The monitoring of plant operation, essentially used in day to day operation and supervision of the plant, is discussed. The performance, for example power and efficiency, of a combined cycle power plant, which depends very much on the ambient conditions as external parameters and on the gas turbine load as cycle dependent internal factor, is also discussed. The monitoring requirements, performance measurements, and performance measurement standards are addressed. ESA

N94-28087# Hamon-Sobelco (Belgium).
COOLING TOWERS FOR COMBINED CYCLES: DESIGN PHILOSOPHY, PERFORMANCE TESTING, AND OPERATING PROBLEMS
J. Bauthier *In* VKI, Combined Cycles for Power Plants 1993 44 p
(For primary document see N94-28077 07-37)
Copyright Avail: CASI HC A03/MF A04

The characteristics and parameters affecting the choice of a type of cooling tower and its installation in the circuit of a combined cycle are discussed. The different possibilities of water circuits that are encountered are defined. Two modes of exchange and two types of fill are discussed. The various types of wet towers are described and their advantages and disadvantages considered. Factors affecting the selection of a cooling tower include: cost of energy versus cost of tower; performances; water availability and quality; emissions (water, noise, air, and vapor); site locations; and operating conditions. ESA

N94-28088# Hamon-Lummus (Belgium).
COOLING TOWERS FOR COMBINED CYCLES: NEW DEVELOPMENTS TO MEET ENVIRONMENTAL REQUIREMENTS
M. Vouche, F. Bouton (Hamon-Sobelco, Belgium.), and P. Lemmens (Hamon-Sobelco, Belgium.) *In* VKI, Combined Cycles for Power Plants 1993 43 p (For primary document see N94-28077 07-37)
Copyright Avail: CASI HC A03/MF A04

Two new developments in dry cooling systems are presented: the single row condenser (SRC) finned tube and the natural draft air-cooled condenser (NDC). The SRC tube is a flat finned tube based on a technology used for compact heat exchangers. This tube was specifically developed for vacuum air-cooled condensers. The serpentine fins of the SRC tube could be made in aluminum or in galvanized steel. The special technique of the brazing of the aluminum fins is described. A technical and economical comparison is made between the classical dry cooling equipment and the NDC. This comparison concludes with the high economic interest in combining the NDC and the single row design. The mechanical draught wet cooling towers with plume abatement are introduced and compared to classical parallel hybrid and reduced plume towers. The environmental impact of wet cooling towers is discussed with regard to heat and mass transfer, plume, bulkiness, and noise. ESA

N94-28089# Shell Internationale Petroleum Maatschappij B.B. (Netherlands).
CLEAN COAL TECHNOLOGY
P. C. Richards, J.-B. Wijffels, and P. L. Zuideveld *In* VKI, Combined Cycles for Power Plants 1993 24 p (For primary document see N94-28077 07-37)
Copyright Avail: CASI HC A03/MF A04

The different commercially available clean coal technologies are introduced with particular emphasis on their efficiency and environmental performance. The technologies in question are: pulverized fuel combustion with flue gas desulphurization; circulating fluidized bed combustion; integrated coal gasification combined cycle; pressurized fluidized bed combustion. Consideration is also be given to emerging coal combustion technologies. ESA

N94-28090# Shell Internationale Petroleum Maatschappij B.B. (Netherlands).
INTEGRATED COAL GASIFICATION COMBINED CYCLE
P. C. Richards, J.-B. Wijffels, and P. L. Zuideveld *In* VKI, Combined Cycles for Power Plants 1993 26 p (For primary document see N94-28077 07-37)
Copyright Avail: CASI HC A03/MF A04

Features of the integrated coal gasification combined cycle power plants are described against the backdrop of the development and first commercial application of the shell coal gasification process. Focus is on the efficiency and excellent environmental performance of the integrated coal gasification combined power plants. Current IGCC projects are given together with an outline of some of the options for integrating coal gasification with combined cycles and also other applications of synthesis gas. ESA

N94-28093 ESDU International Ltd., London (England).
EJECTORS AND JET PUMPS: COMPUTER PROGRAM FOR DESIGN AND PERFORMANCE FOR LIQUID FLOW
Dec. 1993 50 p
(ISSN 0141-4011)
(ESDU-93022; ISBN-0-85679-875-4) Avail: ESDU

ESDU 93022 introduces a Fortran program (ESDUpac A9322) for ejectors in which the primary and secondary flows are of non-reacting miscible liquids. Inlet conditions for both primary and secondary flows can be either constant pressure or provided by a pump. In the latter case it is assumed that the head can be expressed as a quadratic in pump speed and flow rate. Two procedures are provided: a Design Procedure and Performance Prediction. For the first the input is a selection of entry and required exit pressures and flow rates, together with estimates of loss coefficients in the primary and secondary nozzles, mixing duct and diffuser. The program will optimize the ejector, calculating the primary nozzle, secondary inlet and ejector exit dimensions. For the second case, the ejector dimensions are input together with the loss factors again and a range of entry flow conditions and the program will calculate flow conditions throughout the ejector and at exit. The equations on which the program is based are fully specified, the input format required is set out in clear tables, and two worked examples illustrate the use of both procedures. The program is provided on disc (uncompiled) in the software volume, and compiled within ESDUview, a user-friendly shell running under MS-DOS that prompts on screen for input data. ESDU

N94-28174 Southampton Univ. (England). Inst. of Sound and Vibration Research.
WEAK COUPLING IN STATISTICAL ENERGY ANALYSIS ION RESEARCH, UNIV. OF SOUTHAMPTON, SOUTHAMPTON SO9 5NH, ENGLAND)
P. James and F. J. Fahy Feb. 1994 20 p
(ISVR-TR-228) Copyright Avail: Issuing Activity (Inst. of Sound and Vibration Research, Univ. of Southamapton, Southampton SO9 5NH, England)

The sensitivity to small physical changes of the vibrational response of a mechanical system to external excitation increases with frequency. In time-stationary vibration, with conservative coupling, Statistical Energy Analysis (SEA) aims at providing a reliable tool not only to assess the gross distribution of energy within a system but also to give an idea of this distribution among quasi-similar systems. Derived from text

N94-28209# Northrop Corp., Pico Rivera, CA. B-2 Div.
ADVANCED METALLIC EXHAUST IMPINGED STRUCTURAL CONCEPTS DEMONSTRATION Interim Technical Report No. 2, 7 Nov. 1992 - 5 May 1993
J. W. Bohlen, M. T. Hahn, and J. O. Bunch Jun. 1993 110 p
(Contract F33615-92-C-3201)
Avail: CASI HC A06/MF A02

The goal of the program is to design, develop, and test an advanced metallic exhaust impinged structure. The technology developed will provide a generic solution that can be applied to future advanced aircraft. Phase 1 preliminary design was initiated for two film-cooled concepts using either slots or small holes (transpiration cooling). Both designs were based on the same loft lines, loading requirements, and thermal/pressure profiles (from computational fluid dynamics). Finite element, dynamic, and thermal analyses were begun for the designs and for an uncooled baseline design. The functionality and scalability of the designs were assessed. Preliminary design testing of the candidate structural materials was begun. Author (revised)

N94-28229# Westinghouse Savannah River Co., Aiken, SC. Technology Center.
UPSET WELDING PROCESS FOR 21-6-9 SPHERICAL VESSELS

W. R. Kanne, Jr. Feb. 1993 16 p
(Contract DE-AC09-89SR-18035)
(DE93-018194; WSRC-TR-93-015) Avail: CASI HC A03/MF A01

An upset resistance welding process which was developed to fabricate high quality spherical vessels from forged 21-6-9 stainless steel is discussed. The two hemishells of the vessels were joined at the girth using solid-state upset welding. Vessels passed nondestructive examinations (X-ray radiography, proof and leak tests, volume and dimensional measurements) and destructive examinations (burst tests and metallography). A set of six high quality vessels was produced. These vessels are 1.86 inches in diameter with a threaded boss and tube on top. DOE

N94-28265*# National Aeronautics and Space Administration. Marshall Space Flight Center, Huntsville, AL.
SPACE SHUTTLE MAIN ENGINE TURBOPUMP BEARING ASSESSMENT PROGRAM
B. Spiegel Breithaupt Mar. 1994 39 p
(NASA-TM-108447; NAS 1.15:108447) Avail: CASI HC A03/MF A01

This report documents the work done on the bearing assessment program over the past two and a half years. The objective of the program is to develop a nondestructive evaluation system for the SSME HPOTP's which would be used to detect anomalies in installed bearings without engine disassembly. Data bases of various signatures are obtained by slowly turning the pump shafts before and after an engine firing. These signatures are then analyzed and compared to the original signatures to more accurately predict bearing wear. Author (revised)

N94-28375# Technical Research Centre of Finland, Espoo.
WELDABILITY ASPECTS IN THE DESIGN AND FABRICATION OF ALUMINIUM STRUCTURES SUBJECTED TO FATIGUE LOADS. PART 2: WELDABILITY OF ALUMINIUM ALLOYS USING ADVANCED MIG AND TIG TECHNIQUES. EFFECT OF THE WELD BEAD GEOMETRICAL FACTORS ON THE FATIGUE BEHAVIOR OF THE WELDED JOINT
Pekka Nevasmaa, Jorma Peltonen, Risto Kuitunen, and Klaus Rahka 1993 28 p See also PB94-132487
(ISSN 1235-0605)
(PB94-132446; VTT/RN-1480; ISBN-951-38-4374-2) Copyright Avail: CASI HC A03/MF A01

The project explored experimentally the weldability of high-strength aluminum alloys and suitable welding techniques. Part 2 of the report will examine welding procedures suitable for high-strength 5xxx (AlMg) and 6xxx (AlSiMg) series aluminum alloys using advanced MIG and TIG techniques and evaluate the weldability of these alloys, as well as the importance of the shape of the weld bead for fatigue strength of the welded joint. NTIS

N94-28378# Technical Research Centre of Finland, Espoo.
WELDABILITY ASPECTS IN THE DESIGN AND FABRICATION OF ALUMINIUM STRUCTURES SUBJECTED TO FATIGUE LOADS. PART 1: EFFECT OF WELDING ON THE STRUCTURAL INTEGRITY OF JOINT TYPES DESIGNED FOR REPAIRING ALUMINIUM SHIP SECTIONS
P. Nevasmaa, J. Peltonen, R. Kuitunen, and K. Rahka 1993 34 p See also PB94-132446
(ISSN 1235-0605)
(PB94-132487; VTT/RN-1479; ISBN-951-38-4373-4) Copyright Avail: CASI HC A03/MF A01

The Laboratory of Production Engineering and the Metals Laboratory of the Technical Research Center of Finland (VTT) have participated in a Nordic research project entitled 'New methods for joining of aluminium'. The results from Finnish work of the project will be presented in a report to be published in two parts. Part 1 of the report will evaluate the effects of welding on the structural integrity of some joint types primarily designed for repairing ship sections and sea crafts made from 6xxx (AlSiMg) series alloys. NTIS

N94-25668*# California Univ., Los Angeles. Dept. of Mechanical, Aerospace and Nuclear Engineering.
HARDWARE DESIGN OF A GRAPPLING/DOCKING DEVICE ACCOMMODATING LARGE LATERAL AND ANGULAR MISALIGNMENTS
Myles Baker *In* USRA, Proceedings of the 8th Annual Summer Conference: NASA/USRA Advanced Design Program 1992 p 18-19 (For primary document see N94-25665 07-80)
Avail: CASI HC A01/MF A04

N94-25669*# California Univ., Los Angeles. Dept. of Mechanical, Aerospace and Nuclear Engineering.
HARDWARE DESIGN OF A SPHERICAL MINI-ROVER
John Tarlton *In* USRA, Proceedings of the 8th Annual Summer Conference: NASA/USRA Advanced Design Program 1992 p 19-21 (For primary document see N94-25665 07-80)
Avail: CASI HC A01/MF A04

N94-25675*# Georgia Inst. of Tech., Atlanta. School of Mechanical Engineering.
THE ENABLER: A CONCEPT FOR A LUNAR WORK VEHICLE
James W. Brazell, Craig Campbell, Ken Kaser, James A. Austin, Clark Beard, Glenn Ceniza, Thomas Hamby, Anne Robinson, and Dana Wooters *In* USRA, Proceedings of the 8th Annual Summer Conference: NASA/USRA Advanced Design Program 1992 p 74-79 (For primary document see N94-25665 07-80)
Avail: CASI HC A02/MF A04

N94-25683*# Idaho Univ., Moscow. Dept. of Mechanical Engineering.
PLANETARY SURFACE EXPLORATION MESUR/AUTONOMOUS LUNAR ROVER
Larry Stauffer, Matt DiLorenzo, Dave Austin, Raymond Ayers, David Burton, Joe Gaylord, Jim Kennedy, Richard Laux, Dale Lentz, and Preston Nance et al *In* USRA, Proceedings of the 8th Annual Summer Conference: NASA/USRA Advanced Design Program 1992 p 124-136 (For primary document see N94-25665 07-80)
Avail: CASI HC A03/MF A04

N94-25686*# Maryland Univ., College Park. Dept. of Electrical Engineering.
THE 1991-1992 WALKING ROBOT DESIGN
Shapour Azarm, Wijesurija Dayawansa, Lung-Wen Tsai, and Jon Peritt *In* USRA, Proceedings of the 8th Annual Summer Conference: NASA/USRA Advanced Design Program 1992 p 159-169 (For primary document see N94-25665 07-80)
Avail: CASI HC A03/MF A04

N94-25689*# Minnesota Univ., Minneapolis. Dept. of Aerospace Engineering and Mechanics.
MARS TRANSPORTATION SYSTEM
William Garrard, Andrew Vano, and Dave Rutherford *In* USRA, Proceedings of the 8th Annual Summer Conference: NASA/USRA Advanced Design Program 1992 p 188-195 (For primary document see N94-25665 07-80)
Avail: CASI HC A02/MF A04

N94-25691*# Old Dominion Univ., Norfolk, VA. Dept. of Mechanical Engineering and Mechanics.
EXTRATERRESTRIAL SURFACE PROPULSION SYSTEMS
Robert L. Ash, Dexter L. Blackstock, K. Barnhouse, Z. Charalambous, J. Coats, J. Danagan, T. Davis, J. Dickens, P. Harris, and G. Horner et al *In* USRA, Proceedings of the 8th Annual Summer Conference: NASA/USRA Advanced Design Program 1992 p 209-215 (For primary document see N94-25665 07-80)
Avail: CASI HC A02/MF A04

N94-25704*# Virginia Polytechnic Inst. and State Univ., Blacksburg. Dept. of Aerospace Engineering.
PRESSURIZED LUNAR ROVER (PLR)
Kenneth Creel, Jeffrey Frampton, David Honaker, Kerry McClure, Mazyar Zeinali, Manoj Bhardwaj, Vatsal Bulsara, David Kokan, Shaun Shariff, and Eric Svarverud et al *In* USRA, Proceedings of the 8th Annual Summer Conference: NASA/USRA Advanced Design Program 1992 p 316-324 (For primary document see N94-25665 07-80)
Avail: CASI HC A02/MF A04

N94-26281*# Rensselaer Polytechnic Inst., Troy, NY. Dept. of Electrical, Computer, and Systems Engineering.
INERTIAL-SPACE DISTURBANCE REJECTION FOR SPACE-BASED MANIPULATORS
Kevin Holt and Alan A. Desrochers *In* NASA. Langley Research Center, Selected Topics in Robotics for Space Exploration Dec. 1993 p 37-43 (For primary document see N94-26278 07-12)
Avail: CASI HC A02/MF A03

N94-26282*# Rensselaer Polytechnic Inst., Troy, NY. Dept. of Electrical, Computer and Systems Engineering.
DIRECT MODEL REFERENCE ADAPTIVE CONTROL OF ROBOTIC ARMS
Howard Kaufman, David C. Swift, Steven T. Cummings, and Jeffrey R. Shankey *In* NASA. Langley Research Center, Selected Topics in Robotics for Space Exploration Dec. 1993 p 45-71 (For primary document see N94-26278 07-12)
Avail: CASI HC A03/MF A03

N94-26292*# Sandia National Labs., Albuquerque, NM. Advanced Vehicle Development Dept.
A MULTITASKING BEHAVIORAL CONTROL SYSTEM FOR THE ROBOTIC ALL-TERRAIN LUNAR EXPLORATION ROVER (RATLER)
Paul Klarer *In* NASA. Langley Research Center, Selected Topics in Robotics for Space Exploration Dec. 1993 p 269-278 (For primary document see N94-26278 07-12)
Avail: CASI HC A02/MF A03

N94-27361*# Carnegie-Mellon Univ., Pittsburgh, PA. Robotics Inst.
THE UNIVERSAL ROBOT
Hans Moravec *In* NASA. Lewis Research Center, Vision 21: Interdisciplinary Science and Engineering in the Era of Cyberspace Dec. 1993 p 35-41 (For primary document see N94-27358 07-12)
Avail: CASI HC A02/MF A03

38 QUALITY ASSURANCE AND RELIABILITY

Includes product sampling procedures and techniques; and quality control.

N94-25727# Raytheon Co., Sudbury, MA. Equipment Div.
PACKAGE INTEGRITY MEASUREMENT TECHNOLOGY AND QUALITY ASSURANCE Final Report, Oct. 1989 - Mar. 1992
Aaron DerMarderosian and Vincent Gionet Sep. 1993 100 p
(Contract F30602-89-C-0213)
(AD-A273881; RL-TR-93-159) Avail: CASI HC A05/MF A02

This report is the result of a study to evaluate two procedures in MIL-STD-883D, Test Method 1014.9 (Seal) and Test method 1018.2 (Internal Water-Vapor Content). The first portion of this report reviews and investigates the current test procedures included in Test Method 1014 and explores new test methods for recommendation of incorporation into a new revision of the test method. Included in Appendix-B are the results of a survey of industry for comments and recommendations for improving and clarifying the present test method. Appendix A of this report presents the proposed new version of Test Method 1014. The second portion of this report details the results of a study that provided and distributed Test Method 1018 moisture measurement correlation samples to various Residual Gas Analysis (RGA) laboratories. This was done in order to determine the accuracy and precision of mass spectrometric measurement of moisture in microelectronics packages at facilities deemed suitable or candidates to be deemed suitable by the Defense Electronic Supply Center (DESC) to perform MIL-STD-883D, Test Method 1018.2, Procedure 1 (Mass Spectrometry), moisture testing. DTIC

N94-25896# Air Force Inst. of Tech., Wright-Patterson AFB, OH.
AN EXPLORATORY SURVEY OF METHODS USED TO DEVELOP MEASURES OF PERFORMANCE M.S. Thesis
Kenneth L. Hamner and Charles A. LaFleur Sep. 1993 111 p
(AD-A273945; AFIT/GSM/LAS/93S-6) Avail: CASI HC A06/MF A02

Nonmanufacturing organizations are being challenged to provide high-quality products and services to their customers, with an emphasis on continuous process improvement. Measures of performance, referred to as metrics, can be used to foster process improvement. The application of performance measurement to nonmanufacturing processes can be very difficult. This research explored methods used to develop metrics in nonmanufacturing organizations. Several methods were formally defined in the literature, and the researchers used a two-step screening process to determine the OMB Generic Method was most likely to produce high-quality metrics. The OMB Generic Method was then used to develop metrics. A few other metric development methods were found in use at nonmanufacturing organizations. The researchers interviewed participants in metric development efforts to determine their satisfaction and to have them identify the strengths and weaknesses of, and recommended improvements to, the metric development methods used. Analysis of participants' responses allowed the researchers to identify the key components of a sound metrics development method. Those components were incorporated into a proposed metric development method that was based on the OMB Generic Method, and should be more likely to produce high-quality metrics that will result in continuous process improvement. DTIC

N94-26003# Technische Univ., Eindhoven (Netherlands).
HIERARCHICAL TEST DEVELOPMENT AND DESIGN-FOR-TESTABILITY FOR (A)SYNCHRONOUS SEMI-CUSTOM ASIC'S Ph.D. Thesis
Jentje Leenstra 1993 207 p
(ISBN-9-09-005928-8; ETN-94-95343) Copyright Avail: CASI HC A10/MF A03

The work is concerned with test program development and with design for test techniques for low volume semi custom Application Specific Integrated Circuits (ASIC's). Semi custom ASIC design and the growing problems in test development are discussed. The test development problems are growing due to the increasing complexity of the semi custom ASIC's and the need to reach 100% fault coverage in safety critical applications. The design for test techniques and associated automated test development approaches are presented. Test application costs for semi custom ASIC's are considered. Integrated design and test development are discussed. A Design For Testability (DFT) technique for the design of scan testable (a)synchronous control circuits and dedicated test development techniques for purely synchronous circuits parts are presented. ESA

N94-26008# Technische Univ., Eindhoven (Netherlands). Dept. of Mathematics and Computing Science.
STATISTICAL QUALITY MANAGEMENT
Paul vanderLaan Oct. 1992 17 p In DUTCH Presented at GEWIS voor Wiskunde en Informatica Lecture, Eindhoven, Netherlands, 21 Oct. 1992
(ISSN 0926-4493)
(MEMO-COSOR-92-43; ETN-94-94804) Avail: CASI HC A03/MF A01

Some aspects of statistical quality management are discussed. Quality has to be defined as a concrete, measurable quantity. The concepts of Total Quality Management (TQM), Statistical Process Control (SPC), and inspection are explained. In most cases SPC is better than inspection. It can be concluded that statistics has great possibilities in the field of TQM. ESA

N94-26199*# National Aeronautics and Space Administration. Lewis Research Center, Cleveland, OH.
AN APPROACH TO STUDYING THE RELIABILITY OF MICROGRAVITY EXPERIMENTS
Michael Thaggard (Science Applications International Corp., Brook Park, OH.) and Daniel P. Morilak Mar. 1994 14 p Presented at the Aerospace Design Conference, Irvine, CA, 16-19 Feb. 1993; sponsored by AIAA, AHS, and ASEE See also A93-30937
(Contract NAS3-25515; RTOP 323-42-04)
(NASA-TM-106489; E-8476; NAS 1.15:106489) Avail: CASI HC A03/MF A01

The identification of key factors that influence the nonsuccess of experiments conducted under microgravity conditions will aid in the planning, design, and implementation of future space shuttle experiments, as well as other microgravity experiments (i.e., experiments conducted on the space station). Similarly, knowledge of the experiments' reliability will assist in forecasting the success of forthcoming experiments. Since a relatively large number of space shuttle experiments have been conducted to date, a substantial pool of data exists for assessing the possible causes or factors which influence experiment nonsuccesses. This report details the task being undertaken at NASA Lewis Research Center (LeRC) to measure the space shuttle experiments' nonsuccess trends and identify causes that significantly affect their performance. It addresses the activities associated with correlating experiment macro-factors with experiment nonsuccesses. The development and implementation of a microgravity database to be used for tracking and correlating experiment nonsuccess factors, as well as the criteria for measuring experiment success and nonsuccess, are also discussed. Author (revised)

N94-26257# Technical Research Centre of Finland, Espoo. Metals Lab.
NON-CONTACT ULTRASONIC INSPECTION [KONTAKTITON ULTRAAEAENILUOTAUS]
Kari Lahdenperae and Jorma Pitkaenen Mar. 1993 32 p In FINNISH
(ISSN 1235-0605)
(VTT-TIED-1454; ISBN-951-38-4347-8; ETN-94-95268) Copyright Avail: CASI HC A03/MF A01

A literature study of Electromagnetic Acoustic Transducers (EMAT's) which can be used to excite and receive ultrasonic pulses without acoustical contact to the specimen is presented. Special attention is paid to different transducer constructions necessary to induce different ultrasonic modes. The effect of ferromagnetism on the structure of the transducer is also studied. The block diagram and electrical specifications of the equipment acquired by the metals laboratory are presented. With this equipment, ultrasonic pulses can be received and generated by using EMAT's. Applications of this method are described. ESA

N94-26399 Korean Atomic Energy Research Inst., Daeduk (Republic of Korea).
DEVELOPMENT OF NON-DESTRUCTIVE TESTING TECHNOLOGY FOR THE CRACK OF STEAM GENERATOR TUBES
Yong Moo Cheong, Tae Eon Chung, Chang Jae Yim, and Ki Won Kang Jan. 1993 56 p In KOREAN Limited Reproducibility: More than 20% of this document may be affected by microfiche quality
(DE93-632953; KAERI/RR-1183/92) Avail: Issuing Activity (Department of Energy (DOE)) (US Sales Only)

The artificial defects of slot type with width of 0.2 mm were manufactured by EDM to simulate the axial and the circumferential cracks located at the region of expansion transition of the steam generator tubes. The defect signals of ECT using MRPC were analyzed. It is possible to suppress satisfactorily the malign effects of the variation of the geometry of the tubes on the inspection of cracks by using the MRPC probe. The optimum exciting frequency for the detection of cracks by MRPC is greater than 200 kHz and is less than 400 kHz. The direction of crack has little effect on the detectability of the defect. DOE

N94-26644# Institute for Aerospace Research, Ottawa (Ontario).
A COMPARISON OF PROBABILITY OF DETECTION (POD) DATA DETERMINED USING DIFFERENT STATISTICAL METHODS
A. Fahr, D. Forsyth, and M. Bullock Dec. 1993 18 p
(LTR-ST-1947; CTN-94-61063) Avail: CASI HC A03/MF A01

Different statistical methods have been suggested for determining probability of detection (POD) data for nondestructive inspection (NDI) techniques. A comparative assessment of various methods of determining POD was conducted using results of three NDI methods obtained by inspecting actual aircraft engine compressor disks which contained service induced cracks. The study found that the POD and 95 percent confidence curves as a function of crack size as well as the 90/95 percent crack length vary depending on the statistical method used and the type of data. The distribution function as well as the parameter estimation procedure used for determining POD and the confidence bound must be included when referencing information such as the 90/95 percent crack length. The POD curves and confidence bounds determined using the range interval method are very dependent on information that is not from the inspection data. The maximum likelihood estimators (MLE) method does not require such information and the POD results are more reasonable. The log-logistic function appears to model POD of hit/miss data relatively well and is easy to implement. The log-normal distribution using MLE provides more realistic POD results and is the preferred method. Although it is more complicated and slower to calculate, it can be implemented on a common spreadsheet program. Author (CISTI)

N94-26691*# Physical Research, Inc., Torrance, CA.
OPTICAL SURFACE CONTOURING FOR NON-DESTRUCTIVE INSPECTION OF TURBOMACHINERY Status Report No. 1, 6 Dec. 1993 - 5 Feb. 1994
Dariush Modarress and David F. Schaack 9 Mar. 1994 24 p
(Contract NAS3-27214)
(NASA-CR-195245; NAS 1.26:195245; PRI-200) Avail: CASI HC A03/MF A01

Detection of stress cracks and other surface defects during maintenance and in-service inspection of propulsion system components, including turbine blades and combustion compartments, is presently performed visually. There is a need for a non-contact, miniaturized, and fully fieldable instrument that may be used as an automated inspection tool for inspection of aircraft engines. During this SBIR Phase 1 program, the feasibility of a ruggedized optical probe for automatic and nondestructive inspection of complex shaped objects will be established. Through a careful analysis of the measurement requirements, geometrical and optical constraints, and consideration of issues such as manufacturability, compactness, simplicity, and cost, one or more conceptual optical designs will be developed. The proposed concept will be further developed and a prototype will be fabricated during Phase 2. Derived from text

N94-26833# Clemson Apparel Research, Pengleton, SC.
AUTOMATED FABRIC INSPECTION SYSTEM Final Report, 30 Jan. 1990 - 15 May 1993
Christine W. Jarvis 1 Oct. 1993 20 p
(Contract DLA900-87-D-0017)
(AD-A274522) Avail: CASI HC A03/MF A01

The Automatic Fabric Inspection System developed by Systronics Inc. for Clemson Apparel Research uses vision technology to acquire images of the fabric two thousand times per second. Each image-video line consisting of 2048 picture elements is analyzed by a signal processing module and a decision on defect presence and location is made. A product norm signal is first established by having the system acquire an image of an unflawed stripe of the product. The output of each picture element (pixel) is digitized to a grey scale value in the 0-255 range. Threshold levels for defects with grey scale values higher and lower than product norm can then be established and set. The system will then compare all subsequent images against the set thresholds. DTIC

N94-27042# Swedish Inst. for Materials Testing, Boras.
BASELINE FOR A NORDTEST METHOD. RELIABILITY STRESS SCREENING OF COMPONENTS. A GUIDE FOR COMPONENT USERS
Arne Boerjesson, Valter Loll, and Allan Moller Kristensen 1993 119 p
(Nordtest Proj. 1034-92)
(PB94-123775; SP-RAPP-1993:48) Avail: CASI HC A06/MF A02

A method for reliability stress screening (RSS) of components has been developed and is proposed to form a baseline for a Nordtest-method. Before issuance as a Nordtest-method, it is proposed to supplement this report regarding possible failure modes and to make some editorial changes. The development work has been done in cooperation between the Swedish National Testing and Research Institute (SP) and Elektronikcentralen (EC) and was financed by Nordtest. The method makes use of methods described in IEC standard 1163. It is complementary to Nordtest-method NT ELEC 018 which defines a method for RSS of printed wiring assemblies. The purpose of the method is to give guidance to the component user and equipment manufacturer for the specification and the performance of screening for different cases. Five cases based on the users' different aims for the screening are defined in the method. Examples of the design of a screening program are given for 4 different component generic families. These are chosen as being the component families with the highest rate of early failures as defined by a questionnaire performed during the work with the Nordtest-method NT ELEC 018. NTIS

N94-27613# Los Alamos National Lab., NM.
AN UNAVAILABILITY MODEL FOR ERRORS MADE DURING SURVEILLANCE TESTING
Terry F. Bott 1993 5 p Presented at the 2nd Probabilistic Safety Assessment and Management Conference, San Diego, CA, 20-24 Mar. 1994
(Contract W-7405-eng-36)

(DE94-000816; LA-UR-93-3423; CONF-940312-13) Avail: CASI HC A01/MF A01

Periodic testing or examination is conducted routinely for some critical standby equipment or instrumentation, in an attempt to increase its availability. This is often called 'surveillance testing.' There is a finite probability that tested equipment will be left in a degraded or nonfunctioning state because of an error, and this important type of human error is often called a 'restoration error' in probabilistic safety analysis (PSA) parlance. One would expect a trade-off between the reduction in unavailability gained by a surveillance testing and the increase in unavailability incurred by surveillance testing errors. In this paper, a mathematical model of the effect of errors made during surveillance testing on equipment unavailability is described. DOE

N94-27289*# Ohio Univ., Athens.

FAULT DETECTION AND ISOLATION

Greg Bernath *In* NASA. Langley Research Center, FAA/NASA Joint University Program for Air Transportation Research, 1992-1993 Feb. 1994 p 35-43 Sponsored in part by FAA (For primary document see N94-27284 07-01)

(Grant NGR-36-009-17)

Avail: CASI HC A02/MF A02

N94-27925*# Miami Univ., Coral Gables, FL. Electrical and Computer Engineering.

COMPARATIVE ANALYSIS OF DIFFERENT CONFIGURATIONS OF PLC-BASED SAFETY SYSTEMS FROM RELIABILITY POINT OF VIEW

Moiez A. Tapia *In* Old Dominion Univ., The 1993 NASA-ODU American Society for Engineering Education (ASEE) Summer Faculty Fellowship Program Dec. 1993 p 187-188 (For primary document see N94-27893 07-80)

Avail: CASI HC A01/MF A03

39 STRUCTURAL MECHANICS

Includes structural element design and weight analysis; fatigue; and thermal stress.

For applications see *05 Aircraft Design, Testing and Performance* and *18 Spacecraft Design, Testing and Performance.*

N94-25650# Technical Research Centre of Finland, Espoo. Ship Lab.

EXPERIMENTAL AND NUMERICAL VIBRATION ANALYSES OF A STIFFENED PANEL

Timo Holopainen and Ismo Vessonen Jan. 1993 56 p

(ISSN 1235-0621)

(VTT-PUBS-129; ISBN-951-38-4247-9; ETN-94-95237) Copyright Avail: CASI HC A04/MF A01

The vibration behavior of a stiffened panel is investigated. The finite element method is employed for the computational analysis. The example structure is modeled using three different approaches. The main difference between the approaches is the way the stiffeners are modeled: as stiffener elements; or as flat shell elements. To estimate the errors, three element meshes on different levels of accuracy are used. The resulting natural frequencies and mode shapes are compared. Modal testing of the actual panel is performed. The resonant frequencies and modes of the panel are compared with numerical results. To get an idea of the effect of geometrical imperfections and residual stresses on the vibration characteristics of this kind of structure, the panel is tested both in the natural post welding state and after being straightened. ESA

N94-25732# Army Test and Evaluation Command, Aberdeen Proving Ground, MD.

FR/GE/UK/US INTERNATIONAL TEST OPERATIONS PROCEDURE (ITOP) 1-1-050 DEVELOPMENT OF LABORATORY VIBRATION TEST SCHEDULES Final Report

14 May 1993 87 p

(AD-A273887; ITOP-1-1-050) Avail: CASI HC A05/MF A01

This ITOP presents the considerations and techniques involved in developing laboratory vibration schedules simulate the field transportation vibration environment associated with tactical vehicles. DTIC

N94-25754# Army Research Lab., Watertown, MA. Materials Directorate.

DETERMINATION OF FRACTURE STRESS AND EFFECTIVE CRACK TIP RADIUS FROM TOUGHNESS (KIc) AND YIELD STRENGTH (Y) Final Report

Reinier Beeuwkes, Jr. Nov. 1993 62 p

(AD-A274014; ARL-SR-3) Avail: CASI HC A04/MF A01

This is the last of several reports in which K(sub Ic) toughness is not considered basic, but dependent on two metallurgically controllable parameters, the tensile nil-ductility fracture stress and an effective crack tip radius formed by straining at the sharp crack tip which is shown by examples not to be uniquely dependent on load as would the mathematical increase in radius of a rounded tip no matter how small, in a homogeneous material but also dependent metallurgically on micromechanical structure. How to determine the fracture stress and the radius from K(sub Ic) tests with the aid of a postulated fracture criterion characteristic of the material and a curve derived from the solution for the state of stress in the yielded region of a short elliptically shaped flat crack lying across the center of a plate under uniform tensile loading are described. A more exact solution by Colin E. Freese and Dennis M. Tracey supplants the approximate ones used previously and it is shown that dependent on tempering or test temperature, radius determinations remain unchanged to 20% larger although fracture stress determinations are 75% to 85% as large. DTIC

N94-26032# Sandia National Labs., Albuquerque, NM.

TESTING COMPOSITE-TO-METAL TUBULAR LAP JOINTS

T. R. Guess, E. D. Reedy, Jr., and A. M. Slavin 1993 26 p Presented at the American Society for Testing Materials (ASTM) Symposium on Bolted and Bonded Joints in Composite Materials, Ft. Worth, TX, 16-17 Nov. 1993

(Contract DE-AC04-94AL-85000)

(DE94-003225; SAND-93-0018C; CONF-9311124-1) Avail: CASI HC A03/MF A01

Procedures were developed to fabricate, nondestructively evaluate, and mechanically test composite-to-metal tubular joints. The axially loaded tubular lap joint specimen consisted of two metal tubes bonded within each end of a fiberglass composite tube. Joint specimens with both tapered and untapered aluminum adherends and a plain weave E-glass/epoxy composite were tested in tension, compression, and flexure. Other specimens with tapered and untapered steel adherends and a triaxially reinforced E-glass/epoxy composite were tested in tension and compression. Test results include joint strength and failure mode data. A finite element analysis of the axially loaded joints explains the effect of adherend geometry and material properties on measured joint strength. The flexural specimen was also analyzed; calculated surface strains are in good agreement with measured values, and joint failure occurs in the region of calculated peak peel stress. DOE

N94-26129# California Univ., Berkeley. Lawrence Berkeley Lab.

GROWTH OF SMALL FATIGUE CRACKS IN INCOLOY-908

Z. Mei, C. Krenn, and J. W. Morris, Jr. Jul. 1993 8 p Presented at the International Cryogenic Engineering Conference and International Cryogenic Materials Conference, Albuquerque, NM, 12-16 Jul. 1993

(Contract DE-AC03-76SF-00098)

(DE94-003406; LBL-34018; CONF-930703-39) Avail: CASI HC A02/MF A01

Incoloy-908 was designed as a structural alloy for the conduit of cable-in-conduit superconductors. The conduit is a thin-wall tube that encloses superconducting cables. Since the conduit may be as thin as 3 to 12 mm in thickness and is subject to cyclic loads, fatigue crack growth behavior at liquid helium temperature, especially in the small crack regime, is a critical issue for magnet design. Because it is difficult to perform small fatigue crack propagation tests at 4.2 K, we have studied mechanisms of small crack propagation at room temperature and 77 K, and use the results to propose a feasible method for estimating small crack propagation at 4.2 K. DOE

N94-26186# Federal Aviation Administration, Cambridge, MA. National Transportation Systems Center.

DAMAGE TOLERANCE ASSESSMENT HANDBOOK. VOLUME 1: INTRODUCTION FRACTURE MECHANICS FATIGUE CRACK PROPAGATION Final Report, Jun. 1990 - Dec. 1992

Oct. 1993 164 p
(AD-A274777; DOT-VNTSC-FAA-93-13-Vol-1; DOT/FAA/CT-93/69-Vol-1)
Avail: CASI HC A08/MF A02

This 'Damage Tolerance Assessment Handbook' consists of two volumes: vol. 1 and vol. 2. Volume 1 introduces the damage tolerance concept with a historical perspective followed by the fundamentals of fracture mechanics and fatigue crack propagation. Various fracture criteria and crack growth rules are studied. Volume 2 exclusively treats the subject of damage tolerance evaluation of airframes. DTIC

N94-26214# Technische Univ., Delft (Netherlands). Faculty of Technical Mathematics and Informatics.
THE RAILWAY TRACK RESPONSE FUNCTION
J. J. Kalker 1993 14 p
(ISSN 0922-5641)
(Rept-93-40; ETN-94-95395) Copyright Avail: CASI HC A03/MF A01

The response function of the railway track due to a traveling vertical point load running over the track with constant velocity is calculated. The rail is modeled as a Euler beam. The most important feature of the study is that the traveling of the load is fully taken into account. The complex Fourier transform is used. The response is specialized to the contact point. The expression takes the form of a convolution equation, with the vertical displacement left, and the intensity of the vertical point load and an influence function right. An integral representation of the influence function is given. The calculation should be extended to tangential loads. ESA

N94-26233# Norwegian Defence Research Establishment, Kjeller.
RESULTS FROM A FRACTURE MECHANICAL SERIAL INVESTIGATION OF BREECHRINGS ON THE M109A3GN HOWITZER [RESULTATER FRA EN BRUDDMEKANISK SERIEUNDERSOEKELSE AV BAKSTYKKER TIL M109A3GN HAUBITZ]
Bjoern Bergersen and Ole Edvard Hjortland 12 May 1993 115 p In NORWEGIAN
(FFI-93/8002; ETN-94-95213) Avail: CASI HC A06/MF A02

A serial investigation performed on breechrings from the M109A3GN howitzer is described. A classification based on fracture mechanical tests is given. It was found that one breechring should be replaced. In addition an inspection and follow up procedure is advised for some of the other breechrings. ESA

N94-26255# Technical Research Centre of Finland, Espoo. Metals Lab.
HYPERMEDIA SUPPORT FOR ENGINEERING DESIGN SYSTEMS: APPLICATION TO FATIGUE ANALYSIS
Juha Saeaeski, Sisko Sipilae, and Gary Marquis Dec. 1992 26 p
Sponsored by Technical Research Centre of Finland, Espoo
(ISSN 1235-0605)
(VTT-TIED-1432; ISBN-951-38-4326-2; ETN-94-95259) Copyright Avail: CASI HC A03/MF A01

The possibilities of using hypermedia for supporting engineering design systems are discussed. The application selected to test the hypermedia ideas was fatigue analysis. In addition, the possibility of combining hypermedia and expert system ideas into a fatigue expert system is reported. Hypermedia's underlying notion of linking nodes of information and its capability to handle these information entities stored appear to be well suited for engineering system support systems, especially in those engineering design systems where there exists a great demand for representing graphical information in a convenient way. This can be realized using hypermedia tools that are based on hypermedia techniques. The resulting fatigue handbook covers only part of the hypermedia's possibilities. The development of a prototype application indicates the efficiency of a hypermedia tool to create an electronic manual. ESA

N94-26262# Technical Research Centre of Finland, Espoo. Metals Lab.
GUIDELINES FOR CONTROLLING STRESS CORROSION CRACKING AND CORROSION FATIGUE OF STAINLESS STEELS: A LITERATURE REVIEW [RUOSTUMATTOMIEN TERAESTEN JAENNITYSKORROOSION JA KORROOSIOVAESYMISEN ESTAEMINEN: KIRJALLISUUSTUTKIMUS]
Pekka Pohjanne and Hannu Haenninen Nov. 1992 192 p In FINNISH
Sponsored by Outokumpu Oy, Finland, and Technical Research Centre of Finland, Espoo
(ISSN 1235-0605)
(VTT-TIED-1420; ISBN-951-38-4314-9; ETN-94-95274) Copyright Avail: CASI HC A09/MF A02

Guidelines for obtaining and using Environmentally Assisted Cracking (EAC) test data for stainless steels, which are used in a wide range of industrial applications, are presented. Both fracture mechanics and non fracture mechanics tests and test results for Stress Corrosion Cracking (SCC) and Corrosion Fatigue (CF) are considered, but the emphasis is on using fracture mechanics as part of an overall strategy (a fracture control plan) to prevent or control EAC in service. Various threshold values for cracking to occur are reviewed based on loading, electrochemistry, solution chemistry, and temperature. ESA

N94-26265# Comision Nacional de Energia Atomica, Buenos Aires (Argentina). Gerencia de Desarrollo.
FRACTURE TOUGHNESS ROUND ROBIN TEST INTERNATIONAL IN PRESSURE TUBE MATERIALS [PROGRAMA INTERNACIONAL DE ENSAYOS INTERLABORATORIOS DE TENACIDAD A LA FRACTURA DE MATERIALES PARA TUBOS DE PRESION]
M. P. Villagarcia and M. F. Liendo 1993 6 p In SPANISH Presented at the SAM 1993: 17th Metallurgical Sessions of the Argentine Metals Association; 2nd Argentine Meeting on Ceramics and Refractories, San Carlos de Bariloche, Argentina, 13-16 Apr. 1993
(DE93-634140; INIS-AR-020; CONF-9304174) Avail: CASI HC A02/MF A01 (US Sales Only)

Part of the pressure tubes surveillance program of CANDU type reactors is to determine the fracture toughness using a special fracture specimen and test procedure. Atomic Energy of Canada Limited decided to hold a Round Robin Test International and 9 laboratories participated worldwide in which several pressure tube materials were selected: Zircaloy-2, Zr-2.5%Nb cold worked and Zr-2.5%Nb heat treated. The small specimens used held back the thickness and curvature of the tube. J-R curves at room temperature were obtained and the crack extension values were determined by electrical potential drop techniques. These values were compared with results generated from other laboratories and a bid scatter was founded. It could be due to slight variations in the test method or inhomogeneity of the materials and a statistical study must be done to see if there is any pattern. The next step for the Round Robin Test would be to make some modifications in the test method in order to reduce the scatter. DOE

N94-26307# Technical Research Centre of Finland, Espoo. Structural Engineering Lab.
THE STRUCTURAL BEHAVIOUR OF THE STEEL OR COMPOSITE CONCRETE AND STEEL FRAMES AND THE CONNECTIONS OF FRAME MEMBERS DURING THE FIRE: A LITERATURE REVIEW [TERAES- SEKAE TERAES-BETONILIITTORAKENTEISTEN KEHIEN PALONKESTAEVYYS JA NIIDEN RAKENNEOSIEN VAELISTEN LIITOSTEN TOIMINTA TULIPALOSSA. KIRJALLISUUSTUTKIMUS]
Tapio Leino Jan. 1993 131 p In FINNISH Sponsored by Technical Research Centre of Finland, Espoo, and Ministry of Environment, Finland
(ISSN 1235-0605)
(VTT-TIED-1437; ISBN-951-38-4331-9; ETN-94-95263) Copyright Avail: CASI HC A07/MF A02

Fire safety is discussed in general terms, together with some other factors affecting the fire resistance of a structure and structural elements. Neither the development of fire nor temperature dependent material properties are discussed. Many research reports presented dealing with the behavior of structures and structural elements during fire as well as the behavior of connections in a fire contain valuable advice on how to design structures and element connections so that in the case of fire they are better protected, both with regard to the users of the building and the fire brigade. Studies concerning real fires and experience obtained from large scale fire tests are presented. A report in which the real need and possibilities for repairing structures or structural elements after a fire are discussed is presented. The repair methods are also presented. ESA

N94-26357# Federal Aviation Administration, Cambridge, MA. National Transportation Systems Center.
DAMAGE TOLERANCE ASSESSMENT HANDBOOK. VOLUME 2: AIRCRAFT DAMAGE TOLERANCE EVALUATION Final Report, Jun. 1990 - Dec. 1992

Oct. 1993 198 p
(AD-A274778; DOT-VNTSC-FAA-93-13-Vol-2; DOT/FAA/CT-93/69-Vol-2)
Avail: CASI HC A09/MF A03

This 'Damage Tolerance Assessment Handbook' consists of two volumes: Volume 1 introduces the damage tolerance concept with a historical perspective followed by the fundamentals of fracture mechanics and fatigue crack propagation. Various fracture criteria and crack growth rules are studied. Volume 2 treats exclusively the subject of damage tolerance evaluation of airframes. DTIC

N94-26400 Korean Atomic Energy Research Inst., Daeduk (Republic of Korea).
DEVELOPMENT OF DETECTION TECHNIQUE FOR FATIGUE CRACK DUE TO THERMAL STRATIFICATION PHENOMENA IN RCS PIPING
Sam Lai Lee, Byoung Chul Kim, Hyung Taik Lim, Chi Sung Park, Jong Po Lee, and Kee Ok Chang Jan. 1993 86 p In KOREAN Limited Reproducibility: More than 20% of this document may be affected by microfiche quality
(DE93-632968; KAERI/RR-1182/92) Avail: Issuing Activity (Department of Energy (DOE)) (US Sales Only)

Area highly vulnerable to crack generation has been chosen by calculating the stress and deformation using computer program ANSYS considering thermal stratification phenomena, and for weld area, stress distribution has been investigated in order to perform the intensive ISI. The manufacturing of specimens with inside natural cracks has been done and basic procedure to manufacture mechanical fatigue crack by implanting fatigue cracked specimen into parent metal has been set up. This is a distribution that meets the requirement of ASME code Sec.XI, App.VII and VIII (1989 edition). DOE

N94-26448# Edgewood Arsenal, Aberdeen Proving Ground, MD. Reseach Development and Engineering Center.
RESPONSE SURFACE DESIGN COMPARISONS Final Report, May 1992 - 1993
Ronald B. Crosier Oct. 1993 19 p
(DA Proj. 1O1-61102-A-71-A)
(AD-A274690; ERDEC-TR-126) Avail: CASI HC A03/MF A01

Response surface designs are often compared by optimal design theory criteria, such as the D- and G-efficiencies. For designs over spherical regions such criteria are calculated after scaling the designs to have the same diameter. But in practice designs are applied by scaling the coded factor ranges (not the diameter) to the ranges of the experimental factors. The result of this discrepancy between theory and practice is that the mathematical efficiencies may apply to regions of varying sizes. Further, there are practical objectives, such as minimizing the number of runs or testing for lack of fit, that are ignored by optimal design theory. Two examples were given to show the limitations of optimal design theory comparisons. For many symmetric second-order designs, a table giving the following items was provided: number of noncentral design points, number of levels, number of orthogonal blocks, diameter/range ratio, and G-efficiency. DTIC

N94-26501# Aeronautical Research Labs., Melbourne (Australia).
STRESS ANALYSIS OF A SECONDARY-BENDING SPECIMEN Technical Note
R. L. Evans and M. Heller Nov. 1993 31 p
(AD-A274842; ARL-TN-58; DODA-AR-008-404) Avail: CASI HC A03/MF A01

This note describes a two-dimensional finite-element elastic analysis of a uniaxially-loaded bolted secondary-bending specimen which was conducted to provide information relevant to a recent ARL fatigue testing program. Three different approaches were employed to model the bolt/plate interface and the results are compared with thermoelastic stress measurements. DTIC

N94-26524# Pacific Northwest Lab., Richland, WA.
EARLY STAGES IN THE DEVELOPMENT OF STRESS CORROSION CRACKS
R. H. Jones and E. P. Simonen 1993 29 p Presented at the 4th International Conference on Fundamentals of Fracture, Urabandai, Japan, 30 May - 4 Jun. 1993
(Contract DE-AC06-76RL-01830)
(DE94-003867; PNL-SA-21753; CONF-9305312-1) Avail: CASI HC A03/MF A01

Processes in growth of short cracks and stage 1 of long stress corrosion cracks were identified and evaluated. There is evidence that electrochemical effects can cause short stress corrosion cracks to grow at rates faster or slower than long cracks. Short cracks can grow at faster rates than long cracks for a salt film dissolution growth mechanism or from reduced oxygen inhibition of hydrolytic acidification. An increasing crack growth rate with increasing crack length could result from a process of increasing crack tip concentration of a critical anion, such as Cl(-), with increasing crack length in a system where the crack velocity is dependent on the Cl(-) or some other anion concentration. An increasing potential drop between crack tip and mouth would result in an increased anion concentration at the crack tip and hence an increasing crack velocity. Stage 1 behavior of long cracks is another early development stage in the life of a stress corrosion crack which is poorly understood. This stage can be described by da/dt = AK(sup m) where da/dt is crack velocity, A is a constant, K is stress intensity and m ranges from 2 to 24 for a variety of materials and environments. Only the salt film dissolution model was found to quantitatively describe this stage; however, the model was only tested on one material and its general applicability is unknown. DOE

N94-26563# Sandia National Labs., Albuquerque, NM.
USER'S GUIDE FOR THE FREQUENCY DOMAIN ALGORITHMS IN THE LIFE2 FATIGUE ANALYSIS CODE
H. J. Sutherland and R. L. Linker (New Mexico Univ., Albuquerque.) Oct. 1993 53 p
(Contract DE-AC04-94AL-85000)
(DE94-004678; SAND-93-1900) Avail: CASI HC A04/MF A01

The LIFE2 computer code is a fatigue/fracture analysis code that is specialized to the analysis of wind turbine components. The numerical formulation of the code uses a series of cycle count matrices to describe the cyclic stress states imposed upon the turbine. However, many structural analysis techniques yield frequency-domain stress spectra and a large body of experimental loads (stress) data is reported in the frequency domain. To permit the analysis of this class of data, a Fourier analysis is used to transform a frequency-domain spectrum to an equivalent time series suitable for rainflow counting by other modules in the code. This paper describes the algorithms incorporated into the code and their numerical implementation. Example problems are used to illustrate typical inputs and outputs. DOE

N94-26622 University of Western Ontario, London. Dept. of Mechanical Engineering.
THE FREE VIBRATION OF PLATES, SHALLOW SHELLS AND SOLIDS Ph.D. Thesis
Philippe Georges Young Jul. 1993 191 p
(ISBN-0-315-83931-7; CTN-94-61045) Copyright Avail: Micromedia Ltd., Technical Information Centre, 240 Catherine Street, Suite 305, Ottawa, Ontario, K2P 2G8, Canada HC/MF

The Ritz approach is used to study the free structural vibration problem of a wide class of plates, shallow shells, and solids. The boundaries and/or internal supports of the systems are considered and described by polynomials in Cartesian coordinates. The geometric boundary conditions at these boundaries or supports are enforced by including in a simple polynomial trial series the polynomial equation describing the position of the support raised to the appropriate power. For plates and shallow shells, in some instances, the displacement field is discretized into several domains or elements, and continuity conditions along the connecting boundaries are enforced using a penalty method approach. Complicating effects such as point masses, stepped geometry, cutouts, and internal point supports are also considered. The natural frequencies and mode shapes of isotropic rectangular plates are obtained, then isotropic and orthotropic plates of more general form are considered. The approach is extended to shallow shells of differing shapes and curvatures, as well as complicating effects. The approach is finally applied to studying free vibration of a class of solids including a sphere, cylinders, a cone, and a prismatic solid of more general cross-section. Author (CISTI)

N94-26639 Victoria Univ. (British Columbia). Dept. of Mechanical Engineering.
DYNAMICS OF A FLEXIBLE EXTENDIBLE BEAM Ph.D. Thesis

Marinos Costa Stylianou 1993 192 p
(ISBN-0-315-84278-4; CTN-94-61018) Copyright Avail: Micromedia Ltd., Technical Information Centre, 240 Catherine Street, Suite 305, Ottawa, Ontario, K2P 2G8, Canada HC/MF

Axially moving materials arise in problems associated with spacecraft antennas, pipes conveying fluid, and telescopic robotic manipulators. Hamilton's principle is used to derive the governing differential equation of motion and system invariant properties of a flexible extendible beam (FEB) protruding from a rigid wall with prescribed extrusion profile. Numerical solutions are obtained using finite element analysis in which the number of elements is fixed while the sizes of the elements change with time. To this end, a variable domain beam finite element whose size is a prescribed function of time is formulated. The accuracy of this variable domain beam element is demonstrated through the time integration of equations of motion using various extrusion profiles. Additional verification is performed by the evaluation of the system's invariant quantities, comparison with special analytical solution, and the dynamic stability analysis of pipes conveying fluid. The effects of wall flexibility, tip mass, and high frequency axial motion perturbations to the transverse response of the FEB are also examined. The versatility and power of the finite element formulation is demonstrated in a simulation of an extruding FEB which carries a tip mass and protrudes from a flexible envelope beam which imparts three dimensional rigid-body rotations to the system. Author (CISTI)

N94-26692*# Pratt and Whitney Aircraft, East Hartford, CT.
THERMAL/STRUCTURAL TAILORING OF ENGINE BLADES (T/STAEBL). USER'S MANUAL Final Report
K. W. Brown, W. B. Clevenger, and J. D. Arel Mar. 1994 98 p
(Contract NAS3-22525; RTOP 505-63-5B)
(NASA-CR-194463; E-8496; NAS 1.26:194463; PWA-5774-119) Avail: CASI HC A05/MF A02

The Thermal/Structural Tailoring of Engine Blades (T/STAEBL) system is a family of computer programs executed by a control program. The T/STAEBL system performs design optimizations of cooled, hollow turbine blades and vanes. This manual contains an overview of the system, fundamentals of the data block structure, and detailed descriptions of the inputs required by the optimizer. Additionally, the thermal analysis input requirements are described as well as the inputs required to perform a finite element blade vibrations analysis. Author

N94-26754# Swedish Inst. for Materials Testing, Boras.
PROCEEDINGS OF THE FOURTH EUROSEMINAR ON MICROSCOPY APPLIED TO BUILDING MATERIALS
Jan Erik Lindqvist and Bo Nitz 1993 202 p
(PB94-119807) Avail: CASI HC A10/MF A03

The following topics are covered: lime renderings and masonry - influence of the brick suction on the microstructure of cement-mortars and microstructure in mortar; image analysis - microcracking analysis of permeability specimens in high performance concrete and possible applications of image analysis techniques in the field of microscopy of building materials; cracking - long distance optical microscopy and image processing applied to concrete and rock and microcracking in high-performance concrete; microscopy applied to cement clinker and other materials - quantification of analytical data relating to cement clinker and decay of natural building stones; concrete microstructure - microstructural studies of calcium aluminate cement concretes from structures and effective w/c ratio of cement paste in concrete; concrete mortar damage and restoration - concrete failure caused by delayed ettringite formation and diagnosis of expansive processes in concrete. NTIS

N94-26810# Sandia National Labs., Albuquerque, NM.
IDENTIFICATION AND H(INFINITY)/(MU)-SYNTHESIS CONTROL OF THE SANDIA TRUSS
James J. Allen and James P. Lauffer 1993 15 p Presented at the 4th International Conference on Adaptive Structure, Cologne, Germany, 2-3 Nov. 1993
(Contract DE-AC04-94AL-85000)
(DE94-002735; SAND-93-1119C; CONF-9311119-1) Avail: CASI HC A03/MF A01

This paper presents an overview of an analytical and experimental system identification and control design study performed on a controlled structure test bed, the Sandia Truss. The purpose of this project was to assess the capability of several identification and control methods for vibration suppression of large structures. The Sandia Truss, like most structures, represents a challenge to the existing identification and control methods due to high modal density, closely coupled dynamics, external unmeasured inputs, and frequency regimes with poor signal-to-noise characteristics. Because large space structures will require a coordinated control involving multiple disturbances and control objectives, such as line of sight or system quiescence at a specified location, this study focused on multiple-input/multiple-output identification and control. For the study reported in this paper, control design models were developed from experimentally obtained data using the Eigensystem Realization Algorithm with Data Correlation (ERADC); and, the control design was performed using the H(infinity)/(mu)-synthesis technique. DOE

N94-26825# Polish Academy of Sciences, Warsaw. Inst. Podstawowych Problemow Techniki.
GEOMETRY CHANGES IN THE ELASTIC-PLASTIC ANALYSIS OF STEEL SPATIAL SKELETAL STRUCTURES Ph.D. Thesis
Hosain Mohamed H. Bondok 1993 162 p
(IFTR-37/1993) Avail: CASI HC A08/MF A02

The principal objective is to furnish a tool for aunified formulation and numerical analysis of all the history-independent classes of response of elastic perfectly plastic space skeletal structures. We aim at determination of load domains corresponding to elastic, shakedown and collapse behavior for structures in initial and deformed configurations. Numerical program SDLAS for post-yield and inadaptation (non-shakedown) analysis of elastic-plastic space skeletal structures was prepared. It accounts for biaxial bending, torsion and axial forces contributing to yielding of beam elements. The program permits to determine a safe domain for either proportional or variable repeated loads. The proposed method accounts for nonlinear geometrical effects. In the post-yield analysis the conditions for plastic now are considered at subsequent deformed configurations. For the inadaptation analysis the similar procedure is applied. Automatic generation of all possible plastic deformation modes allows to select the most dangerous mechanisms and to determine a critical plastic deformation path. Finally, the post-yield or inadaptation curve is obtained showing the dependence of load (load domain) multiplier on the plastic deformation. These problems are formulated as a sequence of linear programming tasks and are solved by a step by step procedure. The proposed method allows to determine the limit multiplier and the shakedown (adaptation) multiplier accounting for geometric effects. Author

N94-26859 Materials Research Labs., Ascot Vale (Australia).
EVALUATION OF CRACK ARREST FRACTURE TOUGHNESS OF PARENT PLATE, WELD METAL AND HEAT AFFECTED ZONE OF BIS 812 EMA SHIP PLATE STEEL
I. A. Burch Oct. 1993 22 p Limited Reproducibility: More than 20% of this document may be affected by microfiche quality
(AD-A274871; MRL-TR-93-9; DODA-AR-008-267) Avail: CASI HC A03

The steel chosen for the pressure hull of the Collins class submarine has undergone evaluation to compare the crack arrest fracture toughness, K(Ia), of the parent plate with that of weld metal and heat affected zone. The tests were conducted over a range of subzero temperatures on specimens slightly outside the ASTM standard test method specimen configuration. Shallow face grooved specimens were used to vary the propagating crack velocity from that of non face grooved specimens and determine if K(Ia), is sensitive to changes in crack velocity. The weld metal, heat affected zone (HAZ), and parent plate were assessed to determine if the welding process had a deleterious effect on the crack arrest properties of this particular steel. Tests on each of these regions revealed that, for the combination of parent plate, welding procedure and consumables, no adverse effect on crack arrest properties was encountered. Crack arrest fracture toughness of the weld metal and HAZ was superior to that of the parent plate at comparable temperatures. DTIC

N94-26875# Technische Univ., Delft (Netherlands).
REFINED TRIANGULAR PLATE AND SHELL ELEMENTS Ph.D. Thesis
F. vanKeulen 26 Jan. 1993 128 p
(PB94-126356) Avail: CASI HC A07/MF A02

In this work several refinements of small strain triangular plate and shallow shell elements are discussed. These element types are closely connected in the present work, because the shell elements are formulated on the basis of the plate bending elements. In Chapter 3, a family of plate bending elements is discussed, based upon the Kirchhoff-Love and the Mindlin-Reissner plate models. Refinements of the facet element, which is a combination of the constant strain and the constant bending moment triangle, are presented in Chapter 4. In Chapter 5 an alternative finite rotation formulation is presented, which is applicable to arbitrary rotational increments. Based upon the plate bending elements with linear variations for the bending moments, more complex elements are established in Chapter 6. Throughout the work several numerical examples are given. These examples show characteristic features of the refined elements and yield a comparison with former formulations and some elements known from literature. NTIS

N94-26910 Technische Univ., Delft (Netherlands). Faculty of Aerospace Engineering.

COMPUTATION OF STRESS INTENSITY FACTORS BY THE MODE ENRICHMENT TECHNIQUE WITH APPLICATIONS TO GEOMETRICALLY NONLINEAR PROBLEMS

H. A. J. Knops Feb. 1993 67 p Limited Reproducibility: More than 20% of this document may be affected by microfiche quality
(PB94-126513; LR-712) Avail: Issuing Activity (National Technical Information Service (NTIS))

Standard computational methods for the determination of crack tip stress intensity factors need adaptation if they are to be used for crack problems that are governed by geometrically nonlinear effects. This is also true for the so-called mode enrichment technique, a technique whereby (generalized) local crack tip solutions are used as additional trial functions in a finite element modeling scheme. The paper discusses some of the fine points of this adaptation. One of the advantages of the mode enrichment method is that it produces the complete set of intensity factors that belong to the various modes of cracking. From the practical evaluation of this approach it appears that the method is versatile and accurate, attributes that make it an attractive alternative amongst rival methods. NTIS

N94-26911 Technische Univ., Delft (Netherlands). Faculty of Aerospace Engineering.

FORMULAE FOR THE BUCKLING OF SIMPLY-SUPPORTED CORRUGATED PANELS OF ORTHOTROPIC MATERIAL UNDER SHEAR LOAD

P. G. VanBladel Mar. 1993 28 p Limited Reproducibility: More than 20% of this document may be affected by microfiche quality
(PB94-126547; LR-716) Avail: Issuing Activity (National Technical Information Service (NTIS))

This report presents formulae for the shear buckling of corrugated panels made of orthotropic materials. The formulae developed are to be incorporated in COPANO, a computer program for corrugated panel analysis and optimization. The corrugated panels considered in COPANO can be made of composite material, with orthotropic properties. Both the buckling analysis and the optimization are then much more involved than if isotropic material was used. The buckling analysis then has to take into account more stiffness parameters. Also, the optimization necessitates simple buckling calculations without recourse to numerical iteration procedures, to limit the time consumed in the analysis. These characteristics determine to a large extent the type of buckling formulae developed here. NTIS

N94-26922# CSA Engineering, Inc., Palo Alto, CA.

PROCEEDINGS OF DAMPING 1993, VOLUME 1 Final Interim Report, 1-28 Feb. 1993

Bonnie L. Portis Jun. 1993 387 p Conference held in San Francisco, CA, 24-26 Feb. 1993
(Contract F33615-89-C-3201)
(AD-A274226; WL-TR-93-3103-Vol-1) Avail: CASI HC A17/MF A04

Presented are individual papers of Damping '93 held 24-26 February, 1993, in San Francisco. The subjects included: passive damping concepts; passive damping analysis and design techniques; optimization; damped control/structure interaction; viscoelastic material testing and characterization; highly damped materials; vibration suppression techniques; damping identification and dynamic testing; application to aircraft; space structures; marine structures; commercial products; defense applications; and payoffs of vibration suppression. DTIC

N94-26953# CSA Engineering, Inc., Palo Alto, CA.

PROCEEDINGS OF DAMPING 1993, VOLUME 2 Final Interim Report, 1-28 Feb. 1993

Bonnie L. Portis Jun. 1993 425 p Conference held in San Francisco, CA, 24-26 Feb. 1993
(Contract F33615-89-C-3201)
(AD-A274227; WL-TR-93-3104-Vol-2) Avail: CASI HC A18/MF A04

Presented are individual papers of Damping '93, held 24-26 Feb. 1993 in San Francisco. The subjects included the following: passive damping concepts; passive damping analysis and design techniques; optimization; damped control/structure interaction; viscoelastic material testing and characterization; highly damped materials; vibration suppression techniques; damping identification and dynamic testing; applications to aircraft; space structures; marine structures; and commercial products; defense applications; and payoffs of vibration suppression. DTIC

N94-26960 Technische Univ., Delft (Netherlands). Faculty of Industrial Design Engineering.

FAILURE BEHAVIOUR OF HIGH DENSITY POLYETHYLENE WITH AN EMBRITTLED SURFACE LAYER DUE TO WEATHERING Ph.D. Thesis

J. C. M. deBruijn 23 Dec. 1992 181 p See also PB92-138494 Limited Reproducibility: More than 20% of this document may be affected by microfiche quality
(PB94-126406) Avail: Issuing Activity (National Technical Information Service (NTIS))

Weathering often leads to brittle failure of otherwise ductile plastic products and hence may strongly reduce the service life of plastic products used or stored outdoors. Therefore, the ultimate objective of the research was to predict the mechanical failure behavior of outdoor weathered products on the basis of results of artificially weathered samples. NTIS

N94-26961# Technische Univ., Delft (Netherlands). Faculty of Aerospace Engineering.

DESIGN AND TEST OF POSTBUCKLED STIFFENED CURVED PLATES: A LITERATURE SURVEY

J. L. Verolme Feb. 1993 35 p
(PB94-126521; LR-711) Avail: CASI HC A03/MF A01

A designer's tool for compressive buckling of aircraft fuselage panels, currently being developed at the Structures and Materials Laboratory of the Faculty of Aerospace Engineering of Delft University of Technology, must be validated with experimental results. The tested materials will be either isotropic (metal), orthotropic (GLARE, a fiber-metal laminate), or anisotropic (fibre reinforced plastics). For the formulation of a test matrix, a literature survey concentrating on tests of flat and curved, stiffened and unstiffened plates is performed. At the same time, simple semi-empirical formulas are collected to construct a design procedure based on these formulas. The design procedure can be checked and validated with the results of the literature survey. NTIS

N94-27008# CSA Engineering, Inc., Palo Alto, CA.

PROCEEDINGS OF DAMPING 1993, VOLUME 3 Final Interim Report, 1-28 Feb. 1993

Bonnie L. Portis Jun. 1993 383 p Conference held in San Francisco, CA, 24-26 Feb. 1993
(Contract F33615-89-C-3201)
(AD-A274228; WL-TR-93-3105-Vol-3) Avail: CASI HC A17/MF A03

Presented are individual papers of Damping '93, held 24-26 February 1993 in San Francisco. The subjects included: passive damping concepts; passive damping analysis and design techniques; optimization; damped control/structure interaction; viscoelastic material testing and characterization; highly damped materials; vibration suppression techniques; damping identification and dynamic testing; applications to aircraft; space structures; Marine structures; and commercial products; defense applications; and payoffs of vibration suppression. DTIC

N94-27034# Fairfax Materials Research, Inc., Alexandria, VA.

COMPUTER MODELLING OF CYCLIC DEFORMATION OF HIGH-TEMPERATURE MATERIALS Technical Progress Report, 1 Sep. - 30 Nov. 1993

M. S. Duesbery 30 Nov. 1993 37 p
(Contract N00014-91-C-0067)
(AD-A274504) Avail: CASI HC A03/MF A01

This program aims at improving current methods of lifetime assessment by building in the characteristics of the micromechanisms known to be responsible for damage and failure. The broad approach entails the integration and, where necessary, augmentation of the microscale research results currently available in the literature into a macroscale model with predictive capability. In more detail, the program will develop a set of hierarchically structured models at different length scales, from atomic to macroscopic, at each level taking as parametric input the results of the model at the next smaller scale. In this way the known microscopic properties can be transported by systematic procedures to the unknown macroscale region. It may not be possible to eliminate empiricism completely, because some of the quantities involved cannot yet be estimated to the required degree of precision. In this case the aim will be at least to eliminate functional empiricism. Restriction of empiricism to the choice of parameters to be input to known functional forms permits some confidence in extrapolation procedures and has the advantage that the models can readily be updated as better estimates of the parameters become available.
DTIC

N94-27110# Department of the Navy, Washington, DC.
SAG COMPENSATED VIBRATION ISOLATION MOUNT Patent Application
Stuart Dickinson, inventor (to Navy) 2 Aug. 1993 15 p
(AD-D016040; US-Patent-Appl-SN-100798) Avail: CASI HC A03/MF A01

A sag-compensated vibration isolation mount includes a cylindrical rubber body element and a circular band extending around the body element. The band is formed from a shape-memory alloy metal which has a predetermined transition temperature. The band is operative for restricting, outward bulging and sagging of the body element when the body element is subjected to an axial load at a temperature above the transition temperature. The band has a first length at a temperature above the transition temperature and it is stretchable to a second length at a temperature below the transition temperature. At temperatures below the transition temperature, the body element normally stretches the band to its second length. However, when the band is heated above its transition temperature, the band rapidly decreases in length to its first length to forcibly compress the body element and restrict outward bulging of the body element.
DTIC

N94-27186# Technical Research Centre of Finland, Espoo. Ship Lab.
NUMERICAL ANALYSIS METHODS OF SURFACE CRACKS Ph.D. Thesis - Helsinki Univ. of Technol., Espoo, Finland
Timo P. J. Mikkola Oct. 1992 130 p Sponsored by Teollisuuden Voima Oy, Finland; Imatran Voima Oy, Helsinki, Finland; Technical Research Centre of Finland, Espoo; Ministry of Trade and Industry, Finland; and Tekniikan Edistaemissaeaetioe, Finland
(ISSN 1235-0621)
(VTT-PUBS-119; ISBN-951-38-4237-1; ETN-94-95246) Copyright Avail: CASI HC A07/MF A02

Methods for practical engineering fracture and fatigue analysis of flawed thick walled components were developed. Aims are at improving the applicability of the three dimensional finite element method in calculating fracture mechanical parameters for surface flaws. A method for approximating weight functions for flawed structures is developed. The ACR (automatic finite element model generation for part through cracks) program was developed for modeling a surface crack in a structure with a three dimensional finite element model. The modeling of the crack area was tested by analyzing a large matrix of surface crack sizes in a plate of finite thickness. A local mesh refinement procedure was developed for systematic improvement of the accuracy of the fracture parameters. The weight function method developed was implemented in the VTTSIF (Technical Research Center of Finland Stress Intensity Factor) program. For individual titles, see N94-27187 through N94-27190.

N94-27187# Technical Research Centre of Finland, Espoo. Nuclear Engineering Lab.
DEVELOPMENT OF AN AUTOMATED FRACTURE ASSESSMENT SYSTEM FOR NUCLEAR STRUCTURES (APPENDIX 1/1)
Timo P. J. Mikkola and Heikki Raiko *In its* Numerical Analysis Methods of Surface Cracks Oct. 1992 21 p Repr. from International Journal of Pressure Vessels and Piping, v. 52, no. 3, 1992 p 357-377 Sponsored by Teollisuuden Voima Oy, Finland, and Imatran Voima Oy, Helsinki, Finland (For primary document see N94-27186 07-39)
Copyright Avail: CASI HC A03/MF A02

A program system for fracture assessment of nuclear power plant structures was developed. The system consists of a program for engineering analysis and an automated finite element program system for accurate analysis with solid three dimensional models. The VTTSIF (Technical Research Center of Finland Stress Intensity Factor) program for engineering fracture assessment applies either the weight function method or superposition method in calculating the stress intensity factor. The fatigue crack growth analysis is based on the Paris equation. The generation of a three dimensional finite element model of a cracked structure is automated by the ACR (automatic finite element model generation for part through cracks) program. The finite element analyses are created with commercial programs. The virtual crack extension method is used for fracture parameter evaluation by the VTTVIRT postprocessor program (program for J-integral evaluation using virtual crack extension method). The test cases demonstrated that the accuracy of the system is satisfactory.
ESA

N94-27188# Technical Research Centre of Finland, Espoo. Nuclear Engineering Lab.
METHOD FOR CALCULATING STRESS INTENSITY FACTORS FOR SURFACE CRACKS (APPENDIX 2/1)
Timo P. J. Mikkola *In its* Numerical Analysis Methods of Surface Cracks Oct. 1992 18 p Repr. from Engineering Fracture Mechanics, v. 42, no. 5, 1992 p 713-730 Sponsored by Teollisuuden Voima Oy, Finland, and Imatran Voima Oy, Helsinki, Finland (For primary document see N94-27186 07-39)
Copyright Avail: CASI HC A03/MF A02

An approximate weight function method for calculating stress intensity factors for semi elliptical surface cracks under arbitrary loads is presented. The crack face displacement field required for the calculation is approximated by using one or more known stress intensity factor solutions. The method is applied to surface cracks in a wide plate using published analytical solutions for tension and bending loads as reference solutions. The results were compared with other published results. Different displacement approximation functions were tested. The two parameter displacement approximation gave good accuracy when the tension solution was used as the reference case. The addition of the third parameter improved the results for several load cases. The accuracy of the method is best at the deepest position of the crack. The stress intensity factor for the analyzed load case is interpolated along the crack front with only two interpolation functions. More than two interpolation functions can be used if the weight function equation is applied several times using more than one linearly independent reference solution. This was tested with the two currently available reference solutions, but the tests were not successful.
ESA

N94-27189# Technical Research Centre of Finland, Espoo. Nuclear Engineering Lab.
QUALITY ASSURANCE FOR FRACTURE MECHANICAL FINITE ELEMENT ANALYSES (APPENDIX 3/1)
Timo P. J. Mikkola and H. Niemi *In its* Numerical Analysis Methods of Surface Cracks Oct. 1992 9 p Repr. from Computers and Structures, v. 40, no. 2, 1991 p 271-279 Sponsored by Teollisuuden Voima Oy, Finland, and Imatran Voima Oy, Helsinki, Finland (For primary document see N94-27186 07-39)
Copyright Avail: CASI HC A02/MF A02

A program system for automated fracture mechanical analyses with three dimensional finite element models was developed. The main application was safety analyses of pressurized components of nuclear power stations such as pipes and pipe bends containing surface cracks. The system is extended to surface cracks in reactor pressure vessel nozzle area. A large matrix of varying surface crack sizes in a plate under tension is analyzed and the automatically generated mesh obtained good accuracy. The tests do not guarantee the same accuracy for general loading conditions and geometries. Methods for the accuracy assessment of the results and for directing the mesh refinement are developed. Results of a test series with plane models are promising. In the mesh refinement element subdivision was used. The same accuracy assessment approach is applied to three dimensional models.
ESA

N94-27190# Technical Research Centre of Finland, Espoo. Ship Lab.
APPLICATIONS OF THE WEIGHT FUNCTION METHOD (APPENDIX 4/1)
Timo P. J. Mikkola *In its* Numerical Analysis Methods of Surface Cracks Oct. 1992 37 p Submitted for publication Sponsored by Teollisuuden Voima Oy, Finland, and Imatran Voima Oy, Helsinki, Finland (For primary document see N94-27186 07-39)
Copyright Avail: CASI HC A03/MF A02

New solutions for the stress intensity factor and the crack opening displacement at the crack center for the semi elliptical surface crack in a wide plate under remote tension and bending loads were developed. The solutions were based on results of finite element analyses made by an automated program system. The accuracy of the results was studied. The solutions were used for developing weight functions for the structure. The accuracy of these weight functions were tested. The present automated finite element analysis of surface cracks can be applied to practically any structural geometry. A weight function for a surface crack in a weld connecting a nozzle to a pressure vessel was developed. The accuracy of the present weight function method is sufficient for practical applications. ESA

N94-27197 Swedish Inst. for Materials Testing, Boras.
CRACK CLOSURE, A LITERATURE STUDY [SPRICKSLUTNING, EN LITTERATURSTUDIE]
M. Holmgren 1993 40 p In SWAHILI
(PB94-123361; SP-RAPP-1993-45) Avail: Issuing Activity (National Technical Information Service (NTIS))

In this report crack closure is treated. The state of the art is reviewed. Different empirical formulas for determining the crack closure are compared with each other, and their benefits are discussed. Experimental techniques for determining the crack closure stress are discussed, and some results from fatigue tests are also reported. Experimental data from the literature are reported. NTIS

N94-27198 Swedish Inst. for Materials Testing, Boras.
MODIFICATION OF A MODEL FOR FATIGUE LIFE PREDICTIONS BASED ON LEVEL-CROSSING [MODIFIERAD MODELL FOER LIVSLAENGDSBERAEKNING UTGAENDE FRAN NIVAOEVERSKRIDANDE]
T. Svensson 1993 43 p In SWAHILI
(PB94-123395; SP-RAPP-1993-46) Avail: Issuing Activity (National Technical Information Service (NTIS))

In this report, a method of fatigue life prediction is presented. The method is based on level-crossing and is a modification of a model by Holm and de Mare (HdM). The HdM-model is modified by taking crack closure into account. Variable amplitude and constant amplitude tests are performed on both stainless steel and structural steel. The test results are used to compare the HdM-method, the modified HdM-method, and the RFC-method for load spectra with various irregularities and shapes. Life predictions made with the modified HdM-method are at least as good as the life predictions made with the traditional RFC-method. The original HdM-method often predicts the fatigue life in a conservative way. NTIS

N94-27207# National Aerospace Lab., Tokyo (Japan). Airframe Div.
DEVELOPMENT OF AN AUTOMATIC FATIGUE-DATA ACQUISITION SYSTEM USING COMMERCIAL SOFTWARE [HANYO SOFUTOUEA NIYORU HIRO DETA JIDO KEISOKU SHISUTEMO NO KOCHIKU]
Yasumasa Hamaguchi, Toshiyuki Shimokawa, and Yoshiaki Kakuta Nov. 1992 17 p In JAPANESE
(ISSN 0452-2982)
(NAL-TM-650; JTN-94-80618) Avail: CASI HC A03/MF A01

Using the commercial software, 'LABTECH NOTE BOOK' and Lotus 1-2-3, an automatic fatigue-data acquisition system was developed. This system collects data on fatigue load, actuator position, and strain of a specimen at user-defined intervals and stores them in a personal computer. This system displays this information graphically on a CRT (Cathode Ray Tube) on a real-time basis during a fatigue test. Author (NASDA)

N94-27272 Waterloo Univ. (Ontario). Dept. of Mathematics.
THE ONSET OF CHAOS IN A PERIODICALLY FORCED NONLINEAR OSCILLATOR M.S. Thesis
Michael E. Lunney 1993 195 p
(ISBN-0-315-84564-3; CTN-94-61077) Copyright Avail: Micromedia Ltd., Technical Information Centre, 240 Catherine Street, Suite 305, Ottawa, Ontario, K2P 2G8, Canada HC/MF

The chaotic behavior of a parametrically forced Holmes-Duffing oscillator is studied using methods of nonlinear dynamics. By employing the Poincare map, it is shown that a qualitative understanding of chaotic oscillations can be obtained by studying the discrete dynamics of two-dimensional diffeomorphisms. Both numerical and perturbation methods are used to justify the application of several known theoretical results which describe the onset of chaos in one-parameter families of maps, in particular the Poincare map of the Holmes-Duffing oscillator. Author (CISTI)

N94-27278 Queens Univ., Kingston (Ontario). Dept. of Materials and Metallurgical Engineering.
HIGH INTENSITY X RAY INSTRUMENTATION FOR RESIDUAL STRAIN MEASUREMENTS IN COMPOSITES AND TEXTURED MATERIALS Ph.D. Thesis
Alexander Perry Clarke Aug. 1993 189 p
(ISBN-0-315-85169-4; CTN-94-61100) Copyright Avail: Micromedia Ltd., Technical Information Centre, 240 Catherine Street, Suite 305, Ottawa, Ontario, K2P 2G8, Canada HC/MF

The geometry of equipment and x-ray diffraction criteria were examined to optimize for precision in measurements of residual stress/strain in composite materials while maintaining tolerable measurement times. The resulting diffractometer and a cohabiting texture acquisition system were applied in measuring residual stress states in three composite systems. In SiC-reinforced Al, non-isotropic and triaxial tensile stresses were measured, with the stress magnitude increasing with decreasing reinforcement size. In TiB2-reinforced NiAl, slightly non-isotropic, triaxial, and tensile stresses were found in the matrix. The stress magnitudes were lower than expected, possibly due to the presence of alpha alumina. In a specimen of ridged AISi 430 ferritic stainless steel, stresses were measured in two texture components. A strong compressive stress was found in the transverse direction in the component supporting the buckling model for ridge formation. The development of techniques for precise low angle measurements allowed application to triaxial stress determination as a function of temperature in thin film metallization structures. A modified interfacial diffusion controlled relaxation model was proposed to explain the greater relaxation observed in Al(Cu) films compared to pure Al films. Author (CISTI)

N94-27309# Concordia Univ., Montreal (Quebec). Dept. of Mechanical Engineering.
RESPONSE OF STRUCTURES TO IMPACT LOADS USING ELASTIC AND PLASTIC ANALYSIS M.S. Thesis
Gautam Mundkur May 1992 145 p
(ISBN-0-315-84647-X; CTN-94-61084) Copyright Avail: Micromedia Ltd., Technical Information Centre, 240 Catherine Street, Suite 305, Ottawa, Ontario, K2P 2G8, Canada HC/MF

The response of beams and rectangular plates to impact loads is examined. When the deformations are in the elastic region, normal mode analysis is used to find the response. The Rayleigh-Ritz method is employed to obtain the natural frequency and mode shape coefficients. Different types of displacement shape functions are used in the analysis, functions such as beam characteristic functions and beam characteristic orthogonal polynomials. An approximate plate function is determined by reduction of the plate partial differential equation and solving the resulting ordinary differential equation as in the Kantarovich method, then using the Rayleigh-Ritz method. The same reduction procedure is also used along with successive iteration until convergence to obtain the natural frequencies and mode shape functions directly. Structural response to impact loads is also examined using rigid plastic analysis. A cantilever beam with impulsive load applied at the free end, and with finite blade radius and varying centrifugal forces, is considered. Experimental simulation of impact loading used a mass falling from a known height onto the structure under investigation. The elastic response of a plate with two adjacent edges clamped and the other two free was studied. An equivalent mathematical model was formulated by using flexible edge supports. Author (CISTI)

N94-27315 Concordia Univ., Montreal (Quebec). Centre for Building Studies.
BEHAVIOUR MODIFICATION OF SPACE TRUSSES Ph.D. Thesis
Gargari Mousa Tabatabai Jan. 1993 191 p

(ISBN-0-315-84701-8; CTN-94-61090) Copyright Avail: Micromedia Ltd., Technical Information Centre, 240 Catherine Street, Suite 305, Ottawa, Ontario, K2P 2G8, Canada HC/MF

A space truss is a three dimensional structural system assembled of linear elements arranged so that forces are transferred in a three dimensional manner. Space trusses are used where large unobstructed spaces are required, such as aircraft hangars. Space trusses have the advantages of light weight, ease of assembly, ability to create multipurpose architectural spaces, and aesthetic appeal. Space trusses are designed using linear elastic theory, and their load carrying capacity is considered to be limited by the failure of a few critical members. Due to high redundancy and practical constraints, only a portion of the truss member strength is used. Modification of space truss behavior is studied by introducing nonlinearity in the chord members prior to attaining their maximum load. The amount of nonlinearity required to increase the load capacity of the truss by an economically justifiable amount is determined, and the feasibility of the proposed system was confirmed by tests on the elements and an assembled truss. Alternatively, transfer of load to understressed elements can be achieved by selective removal of internal bracing members. A means to determine the optimum selection of diagonals to be removed has been established. The above techniques were applied to four similar space trusses with different support conditions and member size distribution.

Author (CISTI)

N94-27553 National Aerospace Lab., Amsterdam (Netherlands). Fluid Dynamics Div.

VIBRATIONS IN ENGINEERING STRUCTURES: A REVIEW OF MODEL AND FULL-SCALE TEST OF A CABLE-STAYED BRIDGE AND A TRAFFIC SIGN GANTRY

A. J. Persoon 21 Aug. 1992 24 p Presented at the 2nd International Colloquium on Bluff Body Aerodynamics and Applications, Melbourne, Australia, 7-10 Dec. 1992 Limited Reproducibility: More than 20% of this document may be affected by microfiche quality
(NLR-TP-92321-U; ETN-94-95451) Avail: CASI HC A03

As an example of investigations performed on different slender structures submitted to dynamic wind loading, research on a cable stayed bridge and a traffic sign gantry is discussed. The bridge was primarily investigated in the wind tunnel on 'vortex induced' vibrations. Afterwards, full scale measurements were carried out. The sign gantry appeared to be sensitive to 'galloping' oscillations at the site. This was confirmed by wind tunnel tests.

ESA

N94-27559*# National Aeronautics and Space Administration. Lewis Research Center, Cleveland, OH.

STRUCTURAL DESIGN FEASIBILITY STUDY OF SPACE STATION LONG SPACER TRUSS

Sasan C. Armand, Gregory P. Funk, and Caroline A. Dohogne Feb. 1994 28 p Original contains color illustrations
(RTOP 474-46-10)
(NASA-TM-106346; E-8117; NAS 1.15:106346) Avail: CASI HC A03/MF A01; 2 functional color pages

The structural design and configuration feasibility of the long spacer truss assembly that will be used as part of the Space Station Freedom is the focus of this study. The structural analysis discussed herein is derived from the transient loading events presented in the Space Transportation System Interface Control Document (STS ICD). The transient loading events are liftoff, landing, and emergency landing loads. Quasi-static loading events were neglected in this study since the magnitude of the quasi-static acceleration factors is lower than that of the transient acceleration factors. Structural analysis of the proposed configuration of the long spacer truss with four longerons indicated that negative safety margins are possible. As a result, configuration changes were proposed. The primary configuration change suggested was to increase the number of truss longerons to six. The six-longeron truss appears to be a more promising structure than the four-longeron truss because it offers a positive margin of safety and more volume in its second bay (BAY2). This additional volume can be used for resupply of some of the orbital replacement units (such as a battery box). Note that the design effort on the long spacer truss has not fully begun and that calculations and reports of the negative safety margins are, to date, based on concept only.

Author

N94-27585 McMaster Univ., Hamilton (Ontario). School of Graduate Studies.

FINITE ELEMENT ANALYSIS OF DAMPED VIBRATIONS OF LAMINATED COMPOSITE PLATES Ph.D. Thesis

Baogang Hu Nov. 1992 190 p
(ISBN-0-315-84928-2; CTN-94-61114) Copyright Avail: Micromedia Ltd., Technical Information Centre, 240 Catherine Street, Suite 305, Ottawa, Ontario, K2P 2G8, Canada HC/MF

Damped free vibrations of composite laminates are subjected to macromechanical analysis. Two models are developed: a viscoelastic damping model and a specific damping capacity model. The important symmetry property of the damping matrix is retained in both models. A modified modal strain energy method is proposed for evaluating modal damping in the viscoelastic model using a real (instead of a complex) eigenvalue problem solution. Numerical studies of multidegree of freedom systems are conducted to illustrate the improved accuracy of the method compared to the modal strain energy method. The experimental data reported in the literature for damped free vibrations in both polymer matrix and metal matrix composites were used in finite element analysis to test and compare the damping models. The natural frequencies and modal damping were obtained using both the viscoelastic and specific models. Results from both models are in satisfactory agreement with experimental data. Both models were found to be reasonably accurate for systems with low damping. Parametric studies were conducted to examine the effects on damping of the side to thickness ratio, the principal moduli ratio, the total number of layers, the ply angle, and the boundary conditions.

Author (CISTI)

N94-27656*# Applied Research Associates, Inc., Albuquerque, NM.

PARALLEL COMPUTING FOR PROBABILISTIC RESPONSE ANALYSIS OF HIGH TEMPERATURE COMPOSITES Final Report

R. H. Sues, Y. J. Lua, and M. D. Smith Mar. 1994 59 p
(Contract NAS3-26576; RTOP 505-63-5B)
(NASA-CR-194467; E-8550; NAS 1.26:194467) Avail: CASI HC A04/MF A01

The objective of this Phase I research was to establish the required software and hardware strategies to achieve large scale parallelism in solving PCM problems. To meet this objective, several investigations were conducted. First, we identified the multiple levels of parallelism in PCM and the computational strategies to exploit these parallelisms. Next, several software and hardware efficiency investigations were conducted. These involved the use of three different parallel programming paradigms and solution of two example problems on both a shared-memory multiprocessor and a distributed-memory network of workstations.

Author

N94-27765*# Alabama Univ., Tuscaloosa. Bureau of Engineering Research.

USE OF PHOTOSTRESS AND STRAIN GAGES TO ANALYZE BEHAVIOR OF WELDMENTS Final Report

S. C. Gambrell, Jr. 1993 246 p Prepared for Alabama Univ., Huntsville Original contains color illustrations
(Grant NAG8-293)
(NASA-CR-195269; NAS 1.26:195269; BER-591-97) Avail: CASI HC A11/MF A03; 16 functional color pages

Tensile and pure bending tests were conducted on specimens having welded joints made from 2219-T87 aluminum alloy and 2319 filler. Data were collected using photoelastic coatings and strain gages. Stress-strain relationships and contraction ratios were determined at several points in a grid covering the weld material and heat affected zone. Material behavior was nonlinear and nonuniform at all points in the grid and contraction ratios did not conform to those predicted by Chakrabarty's plasticity theory. Yielding in joints made using four new welding procedures was examined. None of the new procedures produced more uniform yielding in the joint.

Author (revised)

N94-27776*# United Technologies Corp., East Hartford, CT.

THERMAL/STRUCTURAL TAILORING OF ENGINE BLADES (T/STAEBL): USER'S MANUAL Final Report

K. W. Brown Mar. 1994 43 p
(Contract NAS3-22525; RTOP 505-63-5B)
(NASA-CR-194461; E-8494; NAS 1.26:194461) Avail: CASI HC A03/MF A01

The Thermal/Structural Tailoring of Engine Blades (T/STAEBL) system is a computer code that is able to perform numerical optimizations of cooled jet engine turbine blades and vanes. These optimizations seek an airfoil design of minimum operating cost that satisfies realistic design constraints. This report documents the organization of the T/STAEBL computer program, its design and analysis procedure, its optimization procedure, and provides an overview of the input required to run the program, as well as the computer resources required for its effective use. Additionally, usage of the program is demonstrated through a validation test case. Author

N94-27808 British Columbia Univ., Vancouver. Dept. of Civil Engineering.

SUPER FINITE ELEMENTS FOR NONLINEAR STATIC AND DYNAMIC ANALYSIS OF STIFFENED PLATE STRUCTURES Ph.D. Thesis

Tamunoiyala Stanley Koko Oct. 1990 225 p
(ISBN-0-315-63903-2; CTN-94-60998) Copyright Avail: Micromedia Ltd., Technical Information Centre, 240 Catherine Street, Suite 305, Ottawa, Ontario, K2P 2G8, Canada HC/MF

New plate and stiffener beam finite elements are developed for the nonlinear static and dynamic analysis of stiffened plate structures. The elements are specially designed to contain all the basic modes of deformation response which occur in stiffened plates. Only one plate element per bay or one beam element per span is needed to achieve engineering design level accuracy at minimum cost. The Von Karman large deflection theory is used to model the nonlinear geometric behavior. Material nonlinearities are modeled by Von Mises yield criterion and associated flow rule using a bilinear stress strain law. The finite element equations are derived using the virtual work principle and the matrix quantities are evaluated by Gauss quadrature. Temporal integration is carried out using the Newmark-beta method with Newton-Raphson iteration. A computer code was written to implement the theory. This was applied to the static, vibration, and transient analysis of unstiffened plates, beams, and plates stiffened in one or two orthogonal directions. Good approximations were obtained for both linear and nonlinear problems. The displacement and stress responses obtained compare well with experimental, analytical, or other numerical results. Author (CISTI)

N94-27810 Ottawa Univ. (Ontario). Dept. of Mechanical Engineering.

SERIES SOLUTION FOR A CYLINDRICAL COMPOSITE SHELL SUBJECT TO AXISYMMETRIC LOADINGS Ph.D. Thesis

D. W. Lindstrom Jul. 1990 204 p
(ISBN-0-315-60559-6; CTN-94-61000) Copyright Avail: Micromedia Ltd., Technical Information Centre, 240 Catherine Street, Suite 305, Ottawa, Ontario, K2P 2G8, Canada HC/MF

Elasticity equations were solved to an arbitrary degree of precision for a thick-walled orthotropic cylinder subject to axisymmetric loading. The theory is directly applicable to a layered composite material where each layer is orthotropic in character. The solution proceeds by representing the deformations of the cylinder wall as a power series in a nondimensional radial parameter. By introducing a generalized stress resultant and a generalized stiffness for the material, a series of coupled second order differential equations in the coefficients of the deformation series results. These were solved using a generalized eigenvalue technique for an infinitely long cylinder, a simply held cylinder, and a rigidly clamped cylinder. The solution was shown to reduce to standard shell solutions for thin cylinders. A thick-walled filament wound test specimen is also described that when fabricated and pressurized would experimentally verify the refined theory developed. Author (CISTI)

N94-27824*# Auburn Univ., AL. Dept. of Space Power.

SILICON DEVICE PERFORMANCE MEASUREMENTS TO SUPPORT TEMPERATURE RANGE ENHANCEMENT Final Report, 7 May 1990 - 31 Jan. 1994

James Bromstead, Bennett Weir, R. Mark Nelms, R. Wayne Johnson, and Ray Askew 28 Mar. 1994 84 p
(Contract NCC3-175)
(NASA-CR-195265; NAS 1.26:195265) Avail: CASI HC A05/MF A01

Silicon based power devices can be used at 200 C. The device measurements made during this program show a predictable shift in device parameters with increasing temperature. No catastrophic or abrupt changes occurred in the parameters over the temperature range. As expected, the most dramatic change was the increase in leakage currents with increasing temperature. At 200 C the leakage current was in the milliAmp range but was still several orders of magnitude lower than the on-state current capabilities of the devices under test. This increase must be considered in the design of circuits using power transistors at elevated temperature. Three circuit topologies have been prototyped using MOSFET's and IGBT's. The circuits were designed using zero current or zero voltage switching techniques to eliminate or minimize hard switching of the power transistors. These circuits have functioned properly over the temperature range. One thousand hour life data have been collected for two power supplies with no failures and no significant change in operating efficiency. While additional reliability testing should be conducted, the feasibility of designing soft switched circuits for operation at 200 C has been successfully demonstrated. Author

N94-27830*# National Aeronautics and Space Administration. Langley Research Center, Hampton, VA.

RELIABILITY-BASED STRUCTURAL OPTIMIZATION: A PROPOSED ANALYTICAL-EXPERIMENTAL STUDY

W. Jefferson Stroud and Efstratios Nikolaidis (Virginia Polytechnic Inst. and State Univ., Blacksburg.) Dec. 1993 24 p
(RTOP 505-63-53-01)
(NASA-TM-109055; NAS 1.15:109055) Avail: CASI HC A03/MF A01

An analytical and experimental study for assessing the potential of reliability-based structural optimization is proposed and described. In the study, competing designs obtained by deterministic and reliability-based optimization are compared. The experimental portion of the study is practical because the structure selected is a modular, actively and passively controlled truss that consists of many identical members, and because the competing designs are compared in terms of their dynamic performance and are not destroyed if failure occurs. The analytical portion of this study is illustrated on a 10-bar truss example. In the illustrative example, it is shown that reliability-based optimization can yield a design that is superior to an alternative design obtained by deterministic optimization. These analytical results provide motivation for the proposed study, which is underway. Author

N94-27841# Institute of Plasma Physics, Prague (Czechoslovakia).

A NUMERICAL APPROACH TO STEFAN PROBLEM

Pavel Kotalik Jul. 1993 12 p
(IPPCZ-334) Avail: CASI HC A03/MF A01

A one-dimensional Stefan problem for a thin plate which is heated by laser pulses is solved by approximating the enthalpy formulation of the problem by C(sup O) piecewise linear finite elements in space combined with a semi-implicit scheme in time. Author

N94-27851*# Virginia Univ., Charlottesville. Dept. of Materials Science and Engineering.

NASA-UVA LIGHT AEROSPACE ALLOY AND STRUCTURES TECHNOLOGY PROGRAM (LA2ST) Progress Report, 1 Jul. - 31 Dec. 1993

Richard P. Gangloff, John R. Scully, Edgar A. Starke, Jr., Glenn E. Stoner, Earl A. Thornton, Franklin E. Wawner, Jr., and John A. Wert 15 Mar. 1994 218 p
(Grant NAG1-745)
(NASA-CR-195275; NAS 1.26:195275; UVA/528266/MSE94/114) Avail: CASI HC A10/MF A03

The NASA-UVA Light Aerospace Alloy and Structures Technology (LA2ST) Program was initiated in 1986, and continues a high level of activity, with projects being conducted by graduate students and faculty advisors in the Departments of Materials Science and Engineering, and Mechanical and Aerospace Engineering at the University of Virginia. This work is funded by the NASA-Langley Research Center under Grant NAG-1-745. Here, we report on progress achieved between July 1 and December 31, 1993. The objective of the LA2ST Program is to conduct interdisciplinary graduate student research on the performance of next generation, light weight aerospace alloys, composites and thermal gradient structures in collaboration with NASA-Langley researchers. Specific technical objectives are presented for each research project. We generally aim to produce relevant data and basic understanding of material mechanical response, environmental/corrosion behavior, and microstructure; new monolithic and composite alloys; advanced processing methods; new solid and fluid mechanics analyses; measurement and modeling advances; and critically, a pool of educated graduate students for aerospace technologies. Derived from text

N94-27865*# National Aeronautics and Space Administration. Lewis Research Center, Cleveland, OH.

AN OPTIMIZATION PROGRAM BASED ON THE METHOD OF FEASIBLE DIRECTIONS: THEORY AND USERS GUIDE

Ashok D. Belegundu (Pennsylvania State Univ., University Park.), Laszlo Berke, and Surya N. Patnaik (Ohio Aerospace Inst., Brook Park.) Washington Jan. 1994 15 p
(RTOP 505-63-5B)
(NASA-TM-4552; E-8124; NAS 1.15:4552) Avail: CASI HC A03/MF A01

The theory and user instructions for an optimization code based on the method of feasible directions are presented. The code was written for wide distribution and ease of attachment to other simulation software. Although the theory of the method of feasible direction was developed in the 1960's, many considerations are involved in its actual implementation as a computer code. Included in the code are a number of features to improve robustness in optimization. The search direction is obtained by solving a quadratic program using an interior method based on Karmarkar's algorithm. The theory is discussed focusing on the important and often overlooked role played by the various parameters guiding the iterations within the program. Also discussed is a robust approach for handling infeasible starting points. The code was validated by solving a variety of structural optimization test problems that have known solutions obtained by other optimization codes. It has been observed that this code is robust: it has solved a variety of problems from different starting points. However, the code is inefficient in that it takes considerable CPU time as compared with certain other available codes. Further work is required to improve its efficiency while retaining its robustness. Author

N94-27954# Defence Research Agency, Farnborough (England). Intellectual Property Dept.

THE DEVELOPMENT OF STRESS INTENSITY FACTORS

D. P. Rooke Aug. 1993 36 p Presented at the International Conference on Fretting Fatigue, Sheffield, England, 19-22 Apr. 1993
(DRA-TR-93057; ICAF-1948) Avail: CASI HC A03/MF A01

Cracks are costly: their presence increases the time and effort spent on maintenance and repair and they may ultimately lead to component fracture and subsequent structural failure, which in extreme cases can endanger human life. A US National Committee estimated that the cost of fracture amounted to as much as 4 percent of the gross National Product: it is therefore imperative to try and reduce these effects. Since cracks cannot be eliminated, procedures must be devised to quantify and predict the behavior of cracked structures under service conditions. The cracks, themselves, may be present as small flaws in the material manufacturing stage; they may arise during fabrication; or they may be the result of damage (fatigue, impact, corrosion etc.) to the completed structure. Systematic scientific rules must be devised to characterize cracks and their effects and to predict if and when they may become unsafe during the structures operational service life. This science has come to be called Fracture Mechanics and the prime characterization and prediction parameter is the stress intensity factor. This report outlines the sources and theoretical methods for obtaining stress intensity factors for a wide range of structural configurations in both two and three dimensions. Author (revised)

N94-28061 ESDU International Ltd., London (England).

FLAT RECTANGULAR ORTHOTROPIC PLATES UNDER UNIFORMLY DISTRIBUTED NORMAL PRESSURE. ELASTIC STRESSES AND DEFLECTIONS FOR VARIOUS FORMS OF EDGE RESTRAINT

Feb. 1994 30 p
(ISSN 0141-4097; ISSN 0958-0360)
(ESDU-93011; ISBN-0-85679-863-0) Avail: ESDU

ESDU 93011 introduces a Fortran program which gives (1) the detailed distribution of deflection and either the moments and in-plane forces, or the stresses, or the strains, throughout the plate for a given pressure load or (2) the maximum deflection and the peak values of moments, forces, stresses and strains and their location for a range of pressure loads. The differential equations formed in terms of stress and displacement functions apply to elastic, large deflection, moderate rotation, thin plate theory and are solved by a finite difference technique for edge conditions of elastic rotation, translation or shear restraint. The plate must be specially-orthotropic, is considered homogeneous, is rigidly restrained in its own plane, and its properties are input as in-plane and flexural stiffness matrices. The plate is treated as symmetrical and so behavior in one quarter only is considered with a grid chosen by the user of 4x4, 6x6 or 8x8 points. Output of the distributions can be chosen to be at every point or at alternate points. The program input and output are fully described, error messages that may be output are explained, and a worked example illustrates its use. The program is available on disc (uncompiled) in the software volume as ESDUpac A9311. ESDU

N94-28143 ESDU International Ltd., London (England).

THREE-DIMENSIONAL ELASTIC STRESS CONCENTRATION FACTORS: PLAIN OR COUNTERSUNK HOLE IN A WIDE PLATE SUBJECTED TO TENSION, BENDING, OR PIN LOADING

Dec. 1993 16 p
(ISSN 0141-4089; ISSN 0144-2805; ISSN 0958-0379; ISSN 0141-4097)
(ESDU-93030; ISBN-0-85679-883-5) Avail: ESDU

ESDU 93030 introduces a Fortran program, ESDUpac A9330, that calculates the stress concentration factors from polynomial equations that were fitted to a wide range of finite element calculations and reproduces them within two percent. For plain and countersunk holes, stresses due to remote tension and out-of-plane bending are considered. In addition, for plain holes the effect of pin loading is simulated by a cosine pressure distribution constant through the plate thickness and unaffected by any distortion. For countersunk holes, the ratio of shank length to plate thickness can vary from 0 to 1 (pure conical hole to constant diameter hole) and for both hole types the diameter-to-plate thickness can vary from 0.5 to 5. The program is provided on disk (uncompiled) in the software volume and compiled within ESDUview, a user-friendly shell running under MS-DOS that prompts on screen for input data. A worked example shows the format of the input and output data; the latter gives stress concentration values at 21 equally-spaced positions along the bore, and maximum and minimum values with their exact locations. Graphs illustrate the effect of varying the major parameters on the distribution of stress along the bore. Comparison of the results with other available data is made. ESDU

N94-28145 ESDU International Ltd., London (England).

FATIGUE PROPAGATION BEHAVIOUR OF SHORT CRACKS (1-2 mm) IN STEELS

Dec. 1993 57 p
(ISSN 0141-4089; ISSN 0958-0387)
(ESDU-93033; ISBN-0-85679-886-X) Avail: ESDU

ESDU 93033 presents data that compare the behavior of long and short cracks which are longer than the typical microstructural dimension but are not substantially larger than the radius of the plastic zone at the crack tip. Experimental data extracted from the literature for crack growth rate under constant amplitude loading are presented graphically against stress intensity factor range for both long and short cracks at various stress ratios in air for AISI 4340, HY 130, AISI 1045, SAE 0030 (UNS J 03010), and AISI 1020. In addition, there are data obtained in vacuum for E460, and in salt solution and sea water for HY 130. Data in air for E460, A508, QIN, and 304 are for only one stress ratio (but include the effect of sea water for QIN). Data for AISI 316 are for short cracks only in air at two stress ratios and for EN5 are for short and long cracks in sea water and one stress ratio only. No consistent relationship between yield strength and either short or long crack growth behavior was found, but where a short crack effect was evident the threshold value of stress intensity factor range was lower than for long cracks, and the crack growth rate at low values of stress intensity factor range was greater. ESDU

N94-28181*# Colorado Univ., Boulder. Dept. of Aerospace Engineering Sciences and Center for Space Structures and Controls.

HIGH-PERFORMANCE PARALLEL ANALYSIS OF COUPLED PROBLEMS FOR AIRCRAFT PROPULSION Final Report

C. A. Felippa, C. Farhat, S. Lanteri, U. Gumaste, and M. Ronaghi Mar. 1994 38 p
(Grant NAG3-1273; RTOP 505-10-11)
(NASA-CR-195292; E-8658; NAS 1.26:195292; CU-CSSC-93-16) Avail: CASI HC A03/MF A01

Applications are described of high-performance parallel, computation for the analysis of complete jet engines, considering its multi-discipline coupled problem. The coupled problem involves interaction of structures with gas dynamics, heat conduction and heat transfer in aircraft engines. The methodology issues addressed include: consistent discrete formulation of coupled problems with emphasis on coupling phenomena; effect of partitioning strategies, augmentation and temporal solution procedures; sensitivity of response to problem parameters; and methods for interfacing multiscale discretizations in different single fields. The computer implementation issues addressed include: parallel treatment of coupled systems; domain decomposition and mesh partitioning strategies; data representation in object-oriented form and mapping to hardware driven representation, and tradeoff studies between partitioning schemes and fully coupled treatment. Author

N94-28227*# National Aeronautics and Space Administration. Lewis Research Center, Cleveland, OH.

A REVIEW OF RECENT AEROELASTIC ANALYSIS METHODS FOR PROPULSION AT NASA LEWIS RESEARCH CENTER

T. S. R. Reddy (Toledo Univ., OH.), Milind A. Bakhle (Toledo Univ., OH.), R. Srivastava (Toledo Univ., OH.), Oral Mehmed, and George L. Stefko Sep. 1993 25 p
(Grants NAG3-1137; NAG3-1234; NAG3-1230; RTOP 535-03-01; RTOP 505-63-5B)
(NASA-TP-3406; E-7535; NAS 1.60:3406) Avail: CASI HC A03/MF A01

This report reviews aeroelastic analyses for propulsion components (propfans, compressors and turbines) being developed and used at NASA LeRC. These aeroelastic analyses include both structural and aerodynamic models. The structural models include a typical section, a beam (with and without disk flexibility), and a finite-element blade model (with plate bending elements). The aerodynamic models are based on the solution of equations ranging from the two-dimensional linear potential equation to the three-dimensional Euler equations for multibladed configurations. Typical calculated results are presented for each aeroelastic model. Suggestions for further research are made. Many of the currently available aeroelastic models and analysis methods are being incorporated in a unified computer program, APPLE (Aeroelasticity Program for Propulsion at LEwis). Author (revised)

N94-28266*# Texas Univ., Austin. Inst. for Computational Mechanics.

ANALYSIS AND CONTROL OF HOURGLASS INSTABILITIES IN UNDERINTEGRATED LINEAR AND NONLINEAR ELASTICITY Final Report

Olivier P. Jacquotte and J. Tinsley Oden Mar. 1994 127 p
(Grant NAG3-329; RTOP 509-10-11)
(NASA-CR-195293; E-8659; NAS 1.26:195293; TICOM-85-10) Avail: CASI HC A07/MF A02

Methods are described to identify and correct a bad finite element approximation of the governing operator obtained when under-integration is used in numerical code for several model problems: the Poisson problem, the linear elasticity problem, and for problems in the nonlinear theory of elasticity. For each of these problems, the reason for the occurrence of instabilities is given, a way to control or eliminate them is presented, and theorems of existence, uniqueness, and convergence for the given methods are established. Finally, numerical results are included which illustrate the theory. Author (revised)

N94-25548# National Research Inst. for Metals, Tokyo (Japan). Environmental Performance Div.

PREPARATION OF CREEP DATA SHEET: MATERIAL STRENGTH DATA SHEET Report No. 3 [KURIPU DETA SHITO NO SAKUSEI: ZAIRYO KYODO DETA SHITO]

Chiaki Tanaka, Koichi Yagi, Sadao Ikeda, Hiroshi Ito, Eiji Baba, Masaru Shimizu, Hideo Tanaka, Kenji Yokokawa, Hideo Nagai, and Osamu Kanamaru et al *In its* Bulletin of National Research Institute for Metals in Fiscal Year 1993, No. 14 29 Jan. 1993 p 43-63 In JAPANESE (For primary document see N94-25544 07-26)
Avail: CASI HC A03/MF A04

N94-25581# National Research Inst. for Metals, Tokyo (Japan). Failure Physics Div.

STUDY ON ELUCIDATION OF DAMAGE GENERATION PROCESS BY ELECTRON BEAM LITHOGRAPHY [DENSHISEN RISOGURAFI NI YORU SONSHO KATEI NO KAIMEI NI KANSURU KENKYU]

Norio Shinya, Satoshi Kishimoto, Mitsuru Egashira, Junro Kyono, and R. A. Carolan *In its* Bulletin of National Research Institute for Metals in Fiscal Year 1993, No. 14 29 Jan. 1993 p 355-361 In JAPANESE (For primary document see N94-25544 07-26)
Avail: CASI HC A02/MF A04

N94-25583# National Research Inst. for Metals, Tokyo (Japan). Environmental Performance Div.

STUDY ON EVALUATION OF CRACK GENERATION AND CRACK GROWTH BEHAVIORS UNDER STATIC LOADING AT HIGH TEMPERATURE AND UNDER COMBINED LOADING [KOON SEIKAJU OYOBI KURIKAESHI KAJUKA NO KIRETSU HASSEI OYOBI SEICHO KYODO NO HYOKA NI KANSURU KENKYU]

Koichi Yagi, Masaaki Tabuchi, Kenji Yokokawa, Osamu Kanamaru, Kiyoshi Kubo, Toshio Oba, and Fusayuki Suzuki (Yokohama National Univ., Japan.) *In its* Bulletin of National Research Institute for Metals in Fiscal Year 1993, No. 14 29 Jan. 1993 p 369-377 In JAPANESE (For primary document see N94-25544 07-26)
Avail: CASI HC A02/MF A04

N94-25584# National Research Inst. for Metals, Tokyo (Japan). Environmental Performance Div.

STUDY ON FATIGUE CRACK PROPAGATION CHARACTERISTICS AROUND WELDED JOINT INTERFACE IN COMPLEXED CONDITIONS [KANKYOKA NI OKERU SETSUGO KAIMEN KINBO NO HIRO KIRETSU DENPA TOKUSEI HYOKA NI KANSURU KENKYU]

Akihiko Ota, Naoyuki Suzuki, Yoshio Maeda, Toshio Mawari, Saburo Matsuoka, and Satoshi Nishijima *In its* Bulletin of National Research Institute for Metals in Fiscal Year 1993, No. 14 29 Jan. 1993 p 379-386 In JAPANESE (For primary document see N94-25544 07-26)
Avail: CASI HC A02/MF A04

N94-26285*# National Aeronautics and Space Administration. Langley Research Center, Hampton, VA.

STATUS REPORT OF RMS ACTIVE DAMPING AUGMENTATION

Mike Gilbert and Martha E. Demeo (Vigyan Research Associates, Inc., Hampton, VA.) *In its* Selected Topics in Robotics for Space Exploration Dec. 1993 p 149-172 (For primary document see N94-26278 07-12)
Avail: CASI HC A03/MF A03

N94-27920*# Virginia Polytechnic Inst. and State Univ., Blacksburg. Dept. of Mechanical Engineering.

DEVELOPMENT OF METHODOLOGIES FOR THE ESTIMATION OF THERMAL PROPERTIES ASSOCIATED WITH AEROSPACE VEHICLES

Elaine P. Scott *In* Old Dominion Univ., The 1993 NASA-ODU American Society for Engineering Education (ASEE) Summer Faculty Fellowship Program Dec. 1993 p 158-161 (For primary document see N94-27893 07-80)
Avail: CASI HC A01/MF A03

42 GEOSCIENCES (GENERAL)

No abstracts in this category.

43 EARTH RESOURCES AND REMOTE SENSING

Includes remote sensing of earth resources by aircraft and spacecraft; photogrammetry; and aerial photography.

For instrumentation see *35 Instrumentation and Photography.*

N94-25656# Army Topographic Engineering Center, Fort Belvoir, VA.
THE POTENTIAL FOR THE DEPARTMENT OF DEFENSE TO USE SPACE-BASED REMOTE SENSING TO SUPPORT DOD AND OTHER GOVERNMENT AGENCIES' ENVIRONMENTAL PROGRAMS
Donald R. Artis, Jr. Dec. 1993 11 p
(AD-A273895; TEC-R-198) Avail: CASI HC A03/MF A01

This paper describes the potential for the Department of Defense (DoD) to support other Government agencies in the management of national and worldwide environmental programs while continuing to conduct the traditional role of DoD as the military arm of the Federal Government. The DOD space-based remote sensing program must complement other programs, rather than replace or duplicate those programs. This may include defense-related remote sensing applying technologies to civil applications and environmental functions and ecological information needs; using DoD sensors for civil applications; and expanding the role of the Environmental Task Force (ETF). DTIC

N94-25741# Air Force Inst. of Tech., Wright-Patterson AFB, OH.
OBJECTIVE IMAGE QUALITY METRICS: APPLICATIONS FOR PARTIALLY COMPENSATED IMAGES OF SPACE OBJECTS M.S. Thesis
David J. Lee Dec. 1993 90 p
(AD-A273837; AFIT/GSO/ENP/93D-03) Avail: CASI HC A05/MF A01

Digital image reconstruction tasks currently require human intervention for a subjective evaluation of image quality. A method for unsupervised measurement of digital image quality is desired. This research investigated various parameters (metrics) that can be automatically extracted from a digital image and tested how well they correlated with image quality. Specifically, images of orbiting satellites captured by a partially compensated adaptive optics telescope were dealt with. Two different types of quantities were investigated: (1) Fourier spectral parameters, based on the spatial-frequency sensitivities of the HVS; and (2) Histogram shape parameters (i.e., image statistical moments) giving quantitative insight into the structural content, information content, and brightness distribution of an image. An atmospheric imaging simulator was used to generate a test database of images. The use of simulated imagery allowed precise control of the imaging parameters directly relating to image quality: (1) Root Mean Square Error; (2) Seeing conditions (Fried Parameter, ro); and (3) Target magnitude. This in turn allowed quantitative testing of candidate image quality metrics. Metrics could also be tested against the user defined parameters of the reconstruction process, as a proof-of-concept for totally unsupervised image reconstruction. Finally, based on tnis testing, two successful image quality metrics are recommended. DTIC

N94-25746# Technische Univ., Delft (Netherlands). Sectie Fysische, Meetkundige en Ruimtegeodesie.
GEOID DETERMINATION: WITH HELP OF THE ALTERNATIVE SCATTERING METHOD Thesis [GEOIDEBEPALING: MET BEHULP VAN EEN ALTERNATIEVE SCHATTINGSMETHODE]
Mario G. Burger Feb. 1993 97 p In DUTCH
(ETN-94-95375) Avail: CASI HC A05/MF A02

Use of the Stokes formula and the least squares collocation method for geoid height determination is addressed, and an alternative method proposed by R. Rummel (1982) with the purpose of combining the advantages of the first two methods while eliminating the disadvantages is investigated. The alternative method has three important components: derivation of the so called global estimator that must be seen as the limiting case of the collocation; the derived estimator must be evaluated by a numerical integration (discretization); the numerical investigation. From the test calculations realized, the following conclusions can be made. A partially applied alternative method gives similar results to those of the classical Stokes method where the surface weights are given by block anomalies with mean gravity. The more unregularly distributed the points are, the bigger the differences between the treated triangulations get. This means that the differences in surface weights will grow as well, leading to different geoid heights. At regularly distributed points the triangulations are almost identical and the calculation of the weights becomes independent of the chosen triangulation method. In the innermost zone, integration has to be made over the surface assigned to each gravity anomaly. ESA

N94-26107# Technische Univ., Delft (Netherlands). Werkeenheid Fotogrammetrie en Remote Sensing.
GEOMETRIC CORRECTION OF SPOT IMAGES WITH USE OF DIGITAL ELEVATION MODELS Thesis [GEOMETRISCH CORRECTIE VAN SPOT-BEELDEN MET BEHULP VAN DIGITALE HOOGTE MODELLEN]
Ron Oosterwijk Aug. 1992 105 p In DUTCH
(ETN-94-95033) Avail: CASI HC A06/MF A02

Modeling and eliminating of distortions caused by not taking into account relief and the geometrical correction of SPOT images are addressed. Resulting from these corrections is an image which is an orthogonal projection of the terrain on a reference system. This orthogonal projection is called an ORTHO-image. A method which uses multispectral SPOT images with a resolution of 20 by 20 m and Digital Elevation Models (DEM's) with a spatial resolution of approximately 100 by 100 m is presented. The reference system used is UTM (Universal Transversal Mercator) projection. The results could only be visually inspected due to the absence of control and checkpoints. The effects of the relief correction are clearly made visible with specially constructed composite grid images by comparing a system corrected image with an ORTHO-image. A stereocouple is generated consisting of a system corrected image and an ORTHO-image. This stereocouple shows an excellent view of the relief. ESA

N94-26222*# Florida State Univ., Tallahassee. Dept. of Meteorology.
DIFFERENTIATING THE ROLE OF LAND SURFACE VARIABILITY AND CLOUDINESS VARIABILITY ON GLOBAL ENERGY TRANSPORT WITHIN THE ATMOSPHERE AND OCEANS Final Report
Eric A. Smith Mar. 1993 8 p
(Grant NAGw-1840)
(NASA-CR-195229; NAS 1.26:195229) Avail: CASI HC A02/MF A01

The following provides the final report on NASA IDP Project NAGW-1840 'Differentiating the Role of Land Surface Variability on Global Energy Transport within the Atmosphere and Oceans'. The project was designed to investigate the role of regional perturbations in the earth radiation budget on atmospheric and oceanic energy transports on an interannual basis. We proposed a modeling strategy based on an entropy extremum principle that could be used to separate the transports into oceanic and atmospheric components so as to better understand the effects of regional perturbations at the distinct atmospheric and oceanic time scales. The original focus was to consider the maintenance and year-to-year modulation of a large-scale, low-latitude North African-West Pacific Ocean net radiation dipole, which we had detected in the Nimbus 6 and 7 record of earth radiation budget measurements, and which necessitated significant cross-meridional energy transports to maintain global equilibrium. In addition, perturbations in the radiation balance term were to be partitioned into cloud-induced and surface-induced components to better understand the feedbacks between clouds and surface boundary conditions on interannual variability of the radiation balance. Derived from text

N94-26228 Beleidscommissie Remote Sensing, Delft (Netherlands).
REMOTE SENSING AND GIS FOR THE MANAGEMENT AND INVESTIGATION OF THE WADDEN SEA [REMOTE SENSING EN GIS TEN BEHOEVE VAN HET BEHEER VAN EN ONDERZOEK IN DE WADDENZEE]
J. vandenBerg (Rijkswaterstaat Dienst Getijdewateren, The Hague, Netherlands.) and A. J. deLeeuw (Rijkswaterstaat Dienst Getijdewateren, The Hague, Netherlands.) Jan. 1993 25 p In DUTCH Limited Reproducibility: More than 20% of this document may be affected by microfiche quality
(BCRS-92-20; ISBN-9-05-411062-7; ETN-94-94821) Avail: CASI HC A03

The use of Remote Sensing (RS) techniques combined with GIS (Geographic Information Systems) for the operational management of the wet part of the Wadden Sea was investigated. The available RS and GIS techniques, data and applications, as well as the possible management problems where RS and GIS techniques can be useful, are reviewed. A proposal for the sequence of the project is given, including a time schedule and cost estimates. The applicability of RS in the Wadden water is limited. The large scale of the Wadden region favorizes RS recording techniques.

The use of GIS has already started with the development of the WADGIS demonstration model for the Dutch Wadden Sea and the WAT is for the German Wadden region. ESA

N94-26236*# Miami Univ., FL.
REMOTE EARTH SCIENCES DATA COLLECTION USING ACTS Final Report
Robert H. Evans Oct. 1992 34 p
(Grant NAGw-2330)
(NASA-CR-195227; NAS 1.26:195227) Avail: CASI HC A03/MF A01

Given the focus on global change and the attendant scope of such research, we anticipate significant growth of requirements for investigator interaction, processing system capabilities, and availability of data sets. The increased complexity of global processes requires interdisciplinary teams to address them; the investigators will need to interact on a regular basis; however, it is unlikely that a single institution will house sufficient investigators with the required breadth of skills. The complexity of the computations may also require resources beyond those located within a single institution; this lack of sufficient computational resources leads to a distributed system located at geographically dispersed institutions. Finally the combination of long term data sets like the Pathfinder datasets and the data to be gathered by new generations of satellites such as SeaWiFS and MODIS-N yield extra-ordinarily large amounts of data. All of these factors combine to increase demands on the communications facilities available; the demands are generating requirements for highly flexible, high capacity networks. We have been examining the applicability of the Advanced Communications Technology Satellite (ACTS) to address the scientific, computational, and, primarily, communications questions resulting from global change research. As part of this effort three scenarios for oceanographic use of ACTS have been developed; a full discussion of this is contained in Appendix B. Author

N94-26253# Technical Research Centre of Finland, Espoo. Instrument Lab.
SOLID ESTIMATION FEATURE BASED CORRELATION METHOD FOR MEASURING CONTROL POINTS REQUIRED FOR CORRECTING SATELLITE IMAGES [PIIRREPOHJAINEN VANKAN ESTIMOINNIN YHTEENSOVITUSMENETELMAE SATELLIITTIKUVIEN OIKAISUSSA TARVITTAVIEN TUKIPISTEIDEN MITTAAMISEEN]
Mikael Holm Nov. 1992 89 p In FINNISH
(ISSN 1235-0613)
(VTT-JULK-772; ISBN-951-38-4120-0; ETN-94-95244) Copyright Avail: CASI HC A05/MF A01

An image correlation method for finding the control points required for satellite image correction is presented. Different methods of correlation are reviewed, focusing on feature based methods. The feature based correlation method developed is described with examples. The method is concluded to be at least as accurate as the traditional manual solution, but gives many more control points in shorter time lapse. It is equally reliable in circumstances where only the data transmitted simultaneously with the image is available. ESA

N94-26258# Joensuu Univ. (Finland). Faculty of Forestry.
SIMA: A MODEL FOR FOREST SUCCESSION BASED ON THE CARBON AND NITROGEN CYCLES WITH APPLICATION TO SILVICULTURAL MANAGEMENT OF THE FOREST ECOSYSTEM
Seppo Kellomaeki, Hannu Vaeisaenen, Heikki Haenninen, Taneli Kolstroem, Risto Lauhanen, Ulla Mattila, and Brita Pajari 1992 90 p
(ISSN 0780-8232)
(Silva-Carelica-22; ISBN-951-708-060-3; ETN-94-95270) Avail: CASI HC A05/MF A01

A model for succession in the forest ecosystem is described. The growth and development of trees and ground cover are controlled by temperature and light conditions and the availability of nitrogen and water. In addition, the effects of the annual cycle of trees, wild fire, and windblow are included in the model as factors which control the survival and productivity of trees. The model makes it also possible to evaluate the risk of insect attack assuming that the risk of insect attack is inversely related to the growth efficiency of trees. ESA

N94-26277# Sandia National Labs., Albuquerque, NM.
A COMPARATIVE EVALUATION OF SAR AND SLAR
G. A. Mastin, J. J. Manson, J. D. Bradley, R. M. Axline, and G. L. Hover 1993 11 p Presented at the 2nd Thematic Conference on Remote Sensing for Marine and Coastal Environments, New Orleans, LA, 31 Jan. - 2 Feb. 1994
(Contract DE-AC04-94AL-85000)
(DE94-002922; SAND-93-2616C; CONF-940123-1) Avail: CASI HC A03/MF A01

Synthetic aperture radar (SAR) was evaluated as a potential technological improvement over the Coast Guard's existing side-looking airborne radar (SLAR) for oil-spill surveillance applications. The US Coast Guard Research and Development Center (R&D Center), Environmental Branch, sponsored a joint experiment including the US Coast Guard, Sandia National Laboratories, and the Naval Oceanographic and Atmospheric Administration (NOAA), Hazardous Materials Division. Radar imaging missions were flown on six days over the coastal waters off Santa Barbara, CA, where there are constant natural seeps of oil. Both the Coast Guard SLAR and the Sandia National Laboratories SAR were employed to acquire simultaneous images of oil slicks and other natural sea surface features that impact oil-spill interpretation. Surface truth and other environmental data were also recorded during the experiment. The experiment data were processed at Sandia National Laboratories and delivered to the R&D Center on a computer workstation for analysis by experiment participants. Issues such as optimal spatial resolution, single-look vs. multi-look SAR imaging, and the utility of SAR for oil-spill analysis were addressed. Finally, conceptual design requirements for a possible future Coast Guard SAR were outlined and evaluated. DOE

N94-26446# Army Topographic Engineering Center, Fort Belvoir, VA.
OPTIMIZATION OF VECTOR PRODUCT FORMAT (VPF) DATA FOR MAP BACKGROUND DISPLAY IN ARMY TACTICAL SYSTEMS
William Kannawin and Karl Koklauner Jan. 1994 14 p
(AD-A274687; USATEC-R-205) Avail: CASI HC A03/MF A01

The U.S. Army currently relies on raster products as source data for map background displays in tactical systems. In the future, The Defense Mapping Agency would prefer to support these requirements with vector products to reduce production costs and take better advantage of their new Digital Production System. Creative and innovative solutions are needed to allow map-like symbolized displays to be generated on current generation computers, within acceptable time tolerances, using vector source data. Science Applications International Corporation (SAIC) under contract with the U.S. Army Topographic Engineering Center (TEC) has demonstrated that this can be done effectively using special indexing techniques. DTIC

N94-26651# Technische Univ., Delft (Netherlands). Sectie Vastgoedinformatie en Kartografie.
CONSTRUCTION AND APPLICATIONS OF THE TWO DIMENSIONAL DELAUNAY TRIANGULATED IRREGULAR NETWORK AND THE THREE DIMENSIONAL DELAUNAY TETRAHEDRON MODEL Thesis [CONSTRUCTIE EN TOEPASSINGEN VAN HET 2-DIMENSIONALE DELAUNAY DRIEHOEKSMODEL EN HET 3-DIMENSIONALE DELAUNAY TETRAEDERMODEL]
Edward Verbree Aug. 1992 73 p In DUTCH
(ETN-94-95034) Avail: CASI HC A04/MF A01

Two topological models are presented: the two dimensional Triangulated Irregular Network (2D-TIN) and the tetrahedron model (3D-TIN). These models have several advantages with respect to the regular grid structured terrain model. In the Delaunay 2D-TIN model the triangles are as equilateral as possible; for a good visualization sharp triangles are avoided. The program P2DTIN constructs the Delaunay model according to the boundary conditions. Several applications of the model are outlined. The tetrahedron model overcomes the restriction that the terrain points have to be univocally projected in a plane. The program P3DTIN constructs such a model starting from a set of three dimensional data points. A number of applications are given. ESA

N94-26664 Victoria Univ. (British Columbia). Dept. of Geography.
MAPPING COASTAL HABITATS USING AN IMAGING SPECTROMETER M.S. Thesis
Mark Zacharias 1993 126 p
(ISBN-0-315-84362-4; CTN-94-61024) Copyright Avail: Micromedia Ltd., Technical Information Centre, 240 Catherine Street, Suite 305, Ottawa, Ontario, K2P 2G8, Canada HC/MF

Research was conducted to determine whether airborne multispectral data acquired using an imaging spectrometer can be used for accurate mapping of the vegetation and substrates in the intertidal and nearshore environments. The imaging spectrometer used in the study allows the user to tailor the spectral bandwidths of the instrument to the spectral properties of the physical and biological features under study. The spectral characteristics of the intertidal environment are examined and an eight-channel bandset is designed that allows insight into certain phenomena or processes that are only evident in narrow spectral ranges. Previous coastal remote sensing studies are reviewed and the data collection methodology is described along with the evaluation, classification, and accuracy assessment of imagery obtained on Vancouver Island, British Columbia. Radiance plots, between-band correlations, and a principal components analysis were used to examine two physically and biologically distinct littoral regions. Five of the eight bands were found to contribute significant unique information pertaining to intertidal vegetation and substrate identification. Classification of these bands showed that different substrates and algal genera could be identified, and spectrally similar green algae could be differentiated. Author (CISTI)

N94-26667 Victoria Univ. (British Columbia). Dept. of Geography.

AN EVALUATION OF AN AIRBORNE REMOTE SENSING SYSTEM USED TO DETERMINE ICE THICKNESS AND GEOMETRY OF A FIRST YEAR SEA ICE RIDGE LOCATED IN THE BEAUFORT SEA M.S. Thesis

Robert Bowen 1993 209 p

(ISBN-0-315-84383-7; CTN-94-61027) Copyright Avail: Micromedia Ltd., Technical Information Centre, 240 Catherine Street, Suite 305, Ottawa, Ontario, K2P 2G8, Canada HC/MF

One- and two-dimensional interpretation techniques were applied to the electromagnetic (EM) anomalies obtained from a state of the art airborne remote sensing system field tested over a first-year ice ridge. This airborne system combines the technology of a laser altimeter, an impulse radar and an electromagnetic induction sounding system in an attempt to measure irregular ice geometry accurately. The EM component of the airborne system is evaluated based on a volumetric comparison of the airborne EM interpreted data with extensive ground truth data obtained from submersible sonar surveys and surface theodolite surveys. The overall form of the ridge geometry at the study site was obtained by generating digital terrain models from the ground truth data. Two interpolation routines were used, both yielding similar form and volumetric results. Comparison of the ground truth data with the EM interpreted data indicate that the interpretation techniques poorly resolve ice feature definition. However, raw EM anomalies records overlaid onto appropriate cross sections of the ridge suggest that the resolution of the system is far better than the interpreted data would suggest. Author (CISTI)

N94-26668 York Univ., Toronto (Ontario). Graduate Programme in Earth and Space Science.

RESPONSE OF AN AIRBORNE SYNTHETIC APERTURE RADAR TO SEA ICE IN THE MARGINAL ICE ZONE Ph.D. Thesis

Michael John Collins May 1993 207 p

(ISBN-0-315-84243-1; CTN-94-61028) Copyright Avail: Micromedia Ltd., Technical Information Centre, 240 Catherine Street, Suite 305, Ottawa, Ontario, K2P 2G8, Canada HC/MF

Theory on statistical scattering from rough surfaces and synthetic aperture radar (SAR) imaging is reviewed and a theoretical model is developed for a particular measure of image texture, the autocorrelation function (ACF). It is proposed that SAR intensity images of sea ice are spatially non-Gaussian, and that the predominant types and forms of marginal ice zone (MIZ) sea ice may be discriminated based on estimated ACF model parameters. Experimental data were collected from the Labrador MIZ, with the primary data set being SAR imagery collected from an airborne platform at two frequencies (5.3 and 9.25 GHz) and four polarizations. To verify the theoretical foundations of the ACF model, imaging system basis experiments measured system focus, examined its effect on image texture, and verified the derived system impulse response. Scattering basis experiments examined speckle development and the extent of non-Gaussian image texture. The model was found to provide an excellent fit to measured ACFs. The parameter measuring non-Gaussian image texture agreed with the scattering basis experiments. The image texture was found to depend on the form of the sea ice as much as its type. For a given type, the various forms could be discriminated with single SAR channels; for full discrimination of all types and forms, a two-channel combination was necessary. Author (CISTI)

N94-26827# Instituto de Pesquisas Espaciais, Sao Jose dos Campos (Brazil).

DIGITAL FILTER DESIGN FOR SENSOR SIMULATION: APPLICATION TO THE BRAZILIAN REMOTE SENSING SATELLITE

Gerald Jean Francis Banon and Ailton Cruz dosSantos Oct. 1993 52 p

(INPE-5523-RPQ/665) Avail: CASI HC A04/MF A01

A model of the interaction between a large-field-of-view low-resolution sensor on board an earth observation satellite and the earth surface is presented. The simulated sensor is obtained through the composition of a digital simulation algorithm by a smaller field-of-view and higher resolution sensor. A new digital filter design technique is proposed to approximate an ideal Gaussian filter. The resulting filter can be implemented on any existing image processing platform. Finally, two image patches as they would be produced by the SSR (Remote Sensing Satellite) of MECB (Brazilian Complete Spatial Mission) from a LANDSAT-TM (Thematic Mapper) scene are presented as an example. Author (revised)

N94-26848 Foerenade Fabriksverken, Linkoeping (Sweden). Huvudavdelning foer Informationsteknologi.

TRAPEZOID-ORIENTED COMPRESSION OF RUN LENGTH CODED MAP DATA

Daniel Joensson and Erland Jungert Apr. 1993 45 p Limited Reproducibility: More than 20% of this document may be affected by microfiche quality

(PB94-123312; FOA-C-30711-3.4) Avail: CASI HC A03

The method for compressing a set of Run Length Code (RLC) items described here is called Generalized Sequential Trapezoids (GST). It is part of an optimization process with the objective to minimize the size of a spatial database intended for a Geographical Information System (GIS). A major advantage of the proposed method, apart from the extensive saving of space, is the scale independence of the representation. The main concern of this work is the general aspects of the structure. Other aspects such as speed of the algorithms and other performance measures are disregarded, as well as the efficiency and space requirements of the internal representation. The new representation is usable for the same applications as the RLC structure, with only a few modifications. NTIS

N94-26866 Technische Univ., Delft (Netherlands). Faculty of Technical Mathematics and Informatics.

TOPOLOGICAL CONDITIONS FOR THE EXISTENCE OF INVARIANT MEASURES FOR UNIMODAL MAPS

H. Bruin 1992 23 p Limited Reproducibility: More than 20% of this document may be affected by microfiche quality

(ISSN 0922-5641)

(PB94-123296; Rept-92-87) Copyright Avail: CASI HC A03/MF A01

We present a class of S-unimodal maps having an invariant measure which is absolutely continuous with respect to Lebesgue measure. This measure can often be proved to be finite. We give an example of a map which has such a finite measure and for which the liminf of the derivatives of the iterates of the map in the critical value is finite. It will be shown that all topologically conjugate non-flat S-unimodal maps have these same properties. NTIS

N94-27069# Army Topographic Engineering Center, Fort Belvoir, VA.

CONIFER TREE INFLUENCE ON DIGITAL TERRAIN ELEVATION DATA (DTED): A CASE STUDY AT DULLES INTERNATIONAL AIRPORT Final Report, Mar. - Aug. 1991

Kevin R. Slocum Sep. 1993 27 p

(AD-A274213; TEC-0038) Avail: CASI HC A03/MF A01

Conifer tree influence on the collection and portrayal of Digital Terrain Elevation Data (DTED) is presented. Study sites are investigated which had dense conifer canopy closure. Two separate DTED collection techniques are examined in the context of studying conifer tree influence: (1) photo source auto-correlated, and (2) photo source operator assisted (floating dot). Field surveying is the mechanism used for collecting accurate, verifiable ground elevation data subsequently compared against the elevations of corresponding DTED positions. Estimated conifer tree stand heights (at the time of DTED photo source) are compared against the difference in value between DTED and field surveyed elevations. A close relationship between stand height and difference values demonstrates the potential for conifer tree height inclusion within DTED 'ground' elevations. Terrain modelling impacts caused by the addition of tree heights within the DTED are addressed. DTIC

N94-27182# Joensuu Univ. (Finland). Faculty of Forestry.
ASSESSMENT OF TROPICAL FORESTS USING SATELLITE DATA
Sipi Jaakkola, Risto Paeivinen, Juho Pitkaenen, Ron Witt, Timo Pukkala, ed., Veli Pohjonen, and Eero Muinonen Jan. 1992 111 p Sponsored by FinnIDA, Finland; Enso Forest Development Oy Ltd., Finland; United Nations Environment Program, Geneva, Switzerland; and Joensuu Univ., Finland Original contains color illustrations
(ISSN 0780-8232)
(Silva-Carelica-21; ISBN-951-78-038-7; ETN-94-95269) Copyright Avail: CASI HC A06/MF A02

Forest assessment activities being carried out in remote sensing laboratories around the world are addressed. The use of satellite imagery in these assessments is focused upon. The status of tropical forest resources is examined. The use of data from NOAA/AVHRR (advanced very high resolution radiometer) is compared to that from LANDSAT thematic mapper and SPOT. The application of geographic information systems (GIS) is also considered. Different methods of processing the data and analyzing the satellite images are considered. Particular emphasis is given to the mapping of closed tropical forest cover in west Africa using NOAA/AVHRR-local area coverage (LAC), and the analysis of LANDSAT images to assess the changes in woody biomass density in the Tendelti area of central Sudan. For individual titles, see N94-27183 through N94-27185.

N94-27183# United Nations Environment Programme, Geneva (Switzerland). Global Resource Information Database.
GLOBAL TROPICAL FOREST COVER ASSESSMENTS USING SATELLITE IMAGERY
Sipi Jaakkola *In* Joensuu Univ., Assessment of Tropical Forests Using Satellite Data Jan. 1992 p 3-26 (For primary document see N94-27182 07-43)
Copyright Avail: CASI HC A03/MF A02

Key concepts such as tropical forests, deforestation, and forest degradation are defined. Objectives in global assessments are considered. The status of tropical forest resources is examined. The development of remote sensing methodology for tropical forest assessments is discussed. The remote sensing methodology for global forest cover assessments is largely based on NOAA/AVHRR (advanced very high resolution radiometer). The two interrelated branches of methodology are mapping and monitoring. The potential of the methodology discussed is now being recognized in the international debate on tropical forest issues. Many have realized than an objective record of forest cover at a single moment in time was impossible until the advent of satellite imagery. A number of remote sensing oriented projects dedicated to tropical forest assessment at global and continental scales are summarized. The status in 1991 of the following regions is assessed: South America, west Africa, central Africa, and south-east Asia. Experience gained in forest cover asessment projects in the tropical zone using digital AVHRR data analysis is summarized. A case study of a geographic information system (GIS) application is presented. The compilation of a global tropical forest cover map is considered. Problems remaining to be solved in the remote sensing of deforestation are addressed. ESA

N94-27184# Joensuu Univ. (Finland).
MAPPING CLOSED TROPICAL FOREST COVER IN WEST AFRICA USING NOAA/AVHRR-LAC DATA
Risto Paeivinen, Juho Pitkaenen, and Ron Witt (United Nations Environment Programme, Geneva, Switzerland.) *In* Joensuu Univ., Assessment of Tropical Forests Using Satellite Data Jan. 1992 p 27-52 (For primary document see N94-27182 07-43)
Copyright Avail: CASI HC A03/MF A02

A project to map the remaining closed tropical forest cover in west Africa is reported. The major purpose of the project is the use of one kilometer NOAA satellite data from the advanced very high resolution radiometer (AVHRR) sensor local area coverage (LAC) for mapping forested and non-forested regions, and other broad vegetation categories, within the humid tropical forest zone of west Africa. The results were compared with high resolution satellite data from LANDSAT and SPOT, which in turn had been classified using information obtained in field visits. The best results for mapping closed tropical forest (more than 40 percent canopy cover) versus surrounding vegetation classes were obtained using a supervised classification and a segmented approach to mapping across the AVHRR scenes used. A total of four scenes were used to produce a map of closed tropical forest cover in west Africa. ESA

N94-27185# Joensuu Univ. (Finland).
WOODY BIOMASS DENSITY IN THE TENDELTI AREA OF THE CENTRAL SUDAN
T. Pukkala, V. Pohjonen, and E. Muinonen *In its* Assessment of Tropical Forests Using Satellite Data Jan. 1992 p 53-92 (For primary document see N94-27182 07-43)
Copyright Avail: CASI HC A03/MF A02

Based on LANDSAT images from 1986, 1988, and 1990, changes in the woody biomass density were analyzed in the Tendelti area of central Sudan. Methods based on regression and stratification were compared within three circular areas with 30 km, 18 km, and 3 km radii, centered on a town or a big village. The method based on regression used the normalized difference vegetation index as a predictor of woody biomass. In the other method, the images were stratified by the maximum likelihood technique, and the woody biomass densities for each class were measured in the field by sampling with circular plots. The study areas included bare sand dunes, moister clay areas with and without tree cover, natural Acacia senegal vegetation on the dunes, and some planted Prosopis juliflora stands. In the two largest circles, no temporal changes in the woody biomass were detected between the three time points. Inside the smallest circle the woody biomass density doubled between 1988 and 1990, due to succcessful establishment of Prosopis plantations. The average woody biomass density in the Tendelti area was very low, about 0.7 tons dry mass per hectare, which is only 12 percent of the Sudanese national average. Both methods to utilize successive satellite imagery were feasible for monitoring the success of reforestation, especially with species that remain green during the dry season. ESA

N94-27331 Tel-Aviv Univ. (Israel). Dept. of Geophysics and Planetary Sciences.
MAPPING OF SEAWATER INTRUSION INTO THE COASTAL AQUIFER OF ISRAEL (THE SEAWATER-FRESHWATER INTERFACE) BY TDEM (TIME DOMAIN ELECTROMAGNETIC) METHOD M.S. Thesis
Amit Ronen Jan. 1991 233 p
(ITN-94-85238) Copyright Avail: Issuing Activity (Tel-Aviv Univ., Exact Sciences Library, Ramat Aviv 69978, Israel)

An extensive TDEM (Time Domain Electromagnetic) survey, which covered almost the whole Mediterranean coastal strip of Israel, was carried out during the summer of 1989 in order to make a quantitative evaluation of the TDEM method in detecting seawater intrusion into the coastal aquifer. To achieve statistical significance of the results, a total of approximately 100 TDEM stations was established, some in close proximity to existing observation wells. In order to realize the most objective evaluation of the TDEM results, respective data interpretation was carried out prior to the use of, or even acquaintance with, any geological or hydrological information from the wells. The two main objects of the survey were as follows: (1) statistical corroboration of an extremely important feature of seawater-bearing aquifers, namely their consistent resistivity values which are completely different from those of any known lithology in the area; and (2) quantitative evaluation of the accuracy level of the TDEM method and assessment of its applicability to solving various hydrological problems. It was found that the resistivity values of the seawater-intruded aquifers vary within a range of 1.1 to 2.9 ohm-meter, whereas low-resistivity lithologies have minimum values of approximately 10 ohm-meter. Author (ISA)

N94-27384# Instituto de Pesquisas Espaciais, Sao Jose dos Campos (Brazil).
TRAINING ON ASSESSMENT AND MAPPING OF DEFORESTATION: WFW CONFERENCE, BRAZIL
Tania Maria Sausen 1993 6 p Presented at the Asia Pacific ISY Conference: The Earth in Space, 16-20 Nov. 1992
(INPE-5482-PRE/1781) Avail: CASI HC A02/MF A01

At an ISY Conference on Education and Applications held in Deauville, France, Brazil proposed a training program for assessment and mapping of deforestation in the Pan-Amazonian region. The intent was to train project managers so as to establish and conduct national or regional forest monitoring of the Pan-Amazonian region using remote sensing data. The success of the PRODES deforestation project and the acceptance of the Pan-Amazonian proposal inspired the design of this training course which was extended to cover rain forest regions all over the world. The objective of the course, which was part of the activities of the World Forest Watch Conference held in Sao Jose dos Campos, Sao Paulo State, Brazil, on 27-29 May 1992, was to train project managers in subregion (state and country level) deforestation mapping, assessment, and monitoring by using remote sensing and geographic information system techniques. This paper presents an overview of the course schedule, its participants and training staff, and some of the problems addressed in the course. CASI

N94-27555 National Aerospace Lab., Amsterdam (Netherlands). Remote Sensing Dept.

MORPHODYNAMICS OF INTER-TIDAL AREAS: THE WADDEN SEA

H. H. S. Noorbergen 21 Aug. 1992 18 p Presented at A Coastal Congress, Kiel, Germany, 7-13 Sep. 1992 Sponsored by Beleidcommissie Remote Sensing, Delft, Netherlands Limited Reproducibility: More than 20% of this document may be affected by microfiche quality
(NLR-TP-92356-U; ETN-94-95453) Avail: CASI HC A03

The use of LANDSAT MSS (Multi Spectral Scanner) satellite images in order to determine the geomorphology of the Dutch Wadden Sea at one certain moment is presented. By using more satellite images of different acquisition dates, geomorphological changes can be detected. By 1991, LANDSAT MSS imagery from the whole world was available for two decades. The present database of 20 years of remote sensing data provides a useful potential for multitemporal research. Three mosaics of LANDSAT MSS images were composed, all taken at the same low water levels but of different acquisition years: 1975, 1982, and 1987. After geometric coregistration it was possible to detect morphological changes between these years. Several image processing methods were used: spatial gradient filtering, and three color composition of the three different years. The remote sensing analysis can be considered operational in the sense that well defined basic image processing routines suffice to obtain the information, and that the project satisfies immediate information needs of a large area leading to direct application in hydrological studies and engineering work. ESA

N94-27727# Los Alamos National Lab., NM.

SPECTRUM ANALYSIS OF MULTISPECTRAL IMAGERY IN CONJUNCTION WITH WAVELET/KLT DATA COMPRESSION

Jonathan N. Bradley and Christopher M. Brislawn 1993 6 p Presented at the IEEE Asilomar Conference on Signals, Systems, and Computers, Pacific Grove, CA, 1-3 Nov. 1993
(Contract W-7405-eng-36)
(DE94-003961; LA-UR-93-3951; CONF-9311135-2) Avail: CASI HC A02/MF A01

The data analysis program, SPECTRUM, is used for fusion, visualization, and classification of multi-spectral imagery. The raw data used in this study is Landsat Thematic Mapper (TM) 7-channel imagery, with 8 bits of dynamic range per channel. To facilitate data transmission and storage, a compression algorithm is proposed based on spatial wavelet transform coding and KLT decomposition of interchannel spectral vectors, followed by adaptive optimal multiband scalar quantization. The performance of SPECTRUM clustering and visualization is evaluated on compressed multispectral data. 8-bit visualizations of 56-bit data show little visible distortion at 50:1 compression and graceful degradation at higher compression ratios. Two TM images were processed in this experiment: a 1024 x 1024-pixel scene of the region surrounding the Chernobyl power plant, taken a few months before the reactor malfunction, and a 2048 x 2048 image of Moscow and surrounding countryside. DOE

N94-27787*# Alaska Univ., Fairbanks. Geophysical Inst.

REMOTE SENSING OF GLOBAL SNOWPACK ENERGY AND MASS BALANCE: IN-SITU MEASUREMENTS ON THE SNOW OF INTERIOR AND ARCTIC ALASKA Semiannual Report

Carl S. Benson Mar. 1994 7 p
(Grant NAG5-887)
(NASA-CR-195704; NAS 1.26:195704) Avail: CASI HC A02/MF A01

This project is continuing along the lines of the semiannual report dated January 1993. Four major tasks have been addressed: analysis of variability in the seasonal snow of interior and arctic Alaska, the interpretation of microwave brightness temperature across Alaska on transects from south to north, study of nonclimatic controls which affect glaciers, and the location of glacier facies boundaries. Derived from text

N94-27849*# Colorado Univ., Boulder. Cooperative Inst. for Research in Environmental Sciences.

ICE SURFACE TEMPERATURE RETRIEVAL FROM AVHRR, ATSR, AND PASSIVE MICROWAVE SATELLITE DATA: ALGORITHM DEVELOPMENT AND APPLICATION Annual Report

Jeff Key, James Maslanik, and Konrad Steffen 23 Mar. 1994 20 p
(Grant NAGw-3437)
(NASA-CR-195276; NAS 1.26:195276) Avail: CASI HC A03/MF A01

One essential parameter used in the estimation of radiative and turbulent heat fluxes from satellite data is surface temperature. Sea and land surface temperature (SST and LST) retrieval algorithms that utilize the thermal infrared portion of the spectrum have been developed, with the degree of success dependent primarily upon the variability of the surface and atmospheric characteristics. However, little effort has been directed to the retrieval of the sea ice surface temperature (IST) in the Arctic and Antarctic pack ice or the ice sheet surface temperature over Antarctica and Greenland. The reason is not one of methodology, but rather our limited knowledge of atmospheric temperature, humidity, and aerosol vertical, spatial and temporal distributions, the microphysical properties of polar clouds, and the spectral characteristics of snow, ice, and water surfaces. Over the open ocean the surface is warm, dark, and relatively homogeneous. This makes SST retrieval, including cloud clearing, a fairly straightforward task. Over the ice, however, the surface within a single satellite pixel is likely to be highly heterogeneous, a mixture of ice of various thicknesses, open water, and snow cover in the case of sea ice. Additionally, the Arctic is cloudy - very cloudy - with typical cloud cover amounts ranging from 60-90 percent. There are few observations of cloud cover amounts over Antarctica. The goal of this research is to increase our knowledge of surface temperature patterns and magnitudes in both polar regions, by examining existing data and improving our ability to use satellite data as a monitoring tool. Four instruments are of interest in this study: the AVHRR, ATSR, SMMR, and SSM/I. Our objectives are as follows. Retine the existing AVHRR retrieval algorithm defined in Key and Haefliger (1992; hereafter KH92) and applied elsewhere. Develop a method for IST retrieval from ATSR data similar to the one used for SST. Further investigate the possibility of estimating surface temperature from passive microwave data (in conjunction with AVHRR clear sky samples) through the use of 'effective emissivities' and physical relationships between skin temperature and subsurface temperature. Use the general method outlined in MK93 to calculate a 12-year record of clear sky equivalent surface temperatures, or possibly all-sky snow-ice interface physical temperatures, from SMMR and SSM/I, compare these temperatures to climatologies, ECMWF modeled surface temperatures, and surface temperatures predicted by a 2-D ice model. And intercompare several ice surface retrieval methods and validate them against ground measurements from the Swiss Camp on the Greenland ice sheet. Additionally, we intend to develop a surface temperature product based on AVHRR data and possibly blended with drifting buoy and meteorological station temperatures. Derived from text

N94-27863 Sherbrooke Univ. (Quebec). Dept. of Geography and Remote Sensing.

MULTISPECTRAL AND TEXTURAL CLASSIFICATIONS OF A SPOT HRV-1 IMAGE, REGION OF SHERBROOKE, QUEBEC, CANADA M.S. Thesis [CLASSIFICATIONS MULTISPECTRALE ET TEXTURALE D'UNE IMAGE S.P.O.T. HRV.1 REGION DE SHERBROOKE, QUEBEC, CANADA]

Thierry Baulu Nov. 1993 76 p In FRENCH
(ISBN-0-315-84978-9; CTN-94-61112) Copyright Avail: Micromedia Ltd., Technical Information Centre, 240 Catherine Street, Suite 305, Ottawa, Ontario, K2P 2G8, Canada HC/MF

A new method of analyzing multispectral SPOT satellite images of urban areas is presented. A panchromatic and a multispectral image were acquired from the SPOT HRV-1 detector for the area of Sherbrooke, Quebec. A new non-directed classification algorithm developed by Wang et al. was applied to the image, with the sole variable to specify being the final number (k) of classes desired. A number of classifications were carried out by introducing different values of k in order to evaluate the performance of the algorithm. The algorithm was applied to three multispectral channels of the image. In a second step, a textural analysis was conducted to improve the results obtained in the first step. The gray level of each pixel was replaced by the unit value of the corresponding texture. Using a variable magnitude mobile window, the spectrum of textures assigned to the central pixel of this window was constructed. The rest of the image was then swept while basing the classification on the distance established between each dynamic spectral cloud. Data from the two steps were integrated to produce a final classification. The bands from the first two steps were added to subdivide, according to texture, the classes obtained during the multispectral classification. CISTI

N94-27870 New Brunswick Univ., Fredericton. Dept. of Surveying Engineering.

FRACTALS AND THEIR APPLICATIONS TO REMOTE SENSING AND DIGITAL MAPPING M.S. Thesis

Mark Phillips Jun. 1990 142 p
(ISBN-0-315-59469-1; CTN-94-60989) Copyright Avail: Micromedia Ltd., Technical Information Centre, 240 Catherine Street, Suite 305, Ottawa, Ontario, K2P 2G8, Canada HC/MF

The basic concepts and properties of fractals are reviewed. Insight is provided into various types of fractals and how they are constructed, implemented, and applied. It is then seen how fractals can be applied specifically to remote sensing and digital mapping by examining existing algorithms and techniques, as well as by presenting some original ideas, suggestions, and proposals. For the purpose of this report, remote sensing is considered to mean the electromagnetic remote sensing via satellite of earth resources, and the subsequent operations performed on the acquired imagery. The remote sensing applications covered include digital image compression, evaluation of digital image magnification techniques, and analysis of digital images. Map symbolization through the use of fractals is proposed, namely the use of realistic fractal perspective images to supplement normal map symbols and the use of fractal symbols to denote feature attribute values. Finally, the fractal interpolation and generalization of cartographic linear and surface features is described. Existing algorithms are discussed and reviewed, and an algorithm is proposed for the fractal generalization of surfaces. The proposed method is implemented on fractally simulated terrain surfaces. Author (CISTI)

N94-27875# Brookhaven National Lab., Upton, NY. Oceanographic and Atmospheric Sciences.

THE VALIDATION OF ATSR MEASUREMENTS WITH IN SITU SEA TEMPERATURES

P. J. Minnett and K. L. Stansfield (State Univ. of New York, Stony Brook.) Oct. 1993 6 p Presented at the 2nd ERS Symposium on Space at the Service of Our Environment, Hamburg, Germany, 11-14 Oct. 1993
(Contract DE-AC02-76CH-00016)
(DE94-003195; BNL-49690; CONF-9310231-1) Avail: CASI HC A02/MF A01

The largest source of uncertainty in the retrieval of SST (sea-surface) temperature from space-borne infrared radiometric measurements is in the correction for the effects of the intervening atmosphere. During a research cruise of the R/V Alliance, measurements of sea surface temperature, surface meteorological variables, and surface infrared radiances were taken. SST fields were generated from the ATSR data using pre-launch algorithims derived by the ATSR Instrument Team, and the initial comparison between ATSR measurements and SST taken along the ship's track indicate that the dual-angle atmospheric correction is accurate in mid-latitude conditions. DOE

N94-27878 Sherbrooke Univ. (Quebec). Dept. of Geography and Remote Sensing.

MAPPING OF SOIL HUMIDITY USING C-BAND RADAR IMAGES M.S. Thesis

Huaibin Geng Aug. 1993 92 p
(ISBN-0-315-85076-0; CTN-94-61113) Copyright Avail: Micromedia Ltd., Technical Information Centre, 240 Catherine Street, Suite 305, Ottawa, Ontario, K2P 2G8, Canada HC/MF

Synthetic aperture radar (SAR) data were examined as a function of soil moisture and roughness, as well as vegetation cover. Single-look airborne C-band SAR data with three polarizations (HH, VV, and HV) from May 1990 were successfully calibrated using forest lots as a reference target. An analysis of linear regression results shows that radar backscatter strongly depends on soil moisture. The C-HH data show the highest correlation with the soil moisture on bare fields. In this experiment, the soils were in the transition zone from smooth to rough. More importantly, they were relatively uniform between fields and especially within a field. Furthermore, the dynamic range of soil moisture data was relatively low. These factors may combine to reduce the roughness factor for this data set. The roughness was therefore considered as a constant. For mapping soil moisture, the effect of roughness could be ignored. For incidence angles over 45 deg, SAR backscatter over vegetation covered fields was controlled mainly by vegetation conditions. In this case, correlation between radar, data, and moisture was absent. A map of soil moisture distribution was created using the inverse of the regression laws. The accuracy of moisture estimation was 90 percent. Author (CISTI)

N94-27957# Instituto de Pesquisas Espaciais, Sao Jose dos Campos (Brazil).

ROLE OF REMOTE SENSING IN ENERGY, WATER, AND CARBON CYCLE STUDIES OVER THE AMAZON

Getulio Teixeira Batista and Bruce W. Nelson (Instituto Nacional de Pesquisas da Amazonia, Manaus, Brazil.) 1993 11 p Presented at the 25th International Symposium, Remote Sensing and Global Environmental Change, Graz, Austria, 4-8 Apr. 1993
(INPE-5486-PRE/1786) Avail: CASI HC A03/MF A01

Landsat data have been recorded continuously for the Brazilian Amazon Basin since 1973. Examination of these data in yearly intervals has brought out their value for the following synoptic scale evaluations: quantification of total deforestation and deforestation rates; forest recovery; biomass estimation; water and energy balance; and detection of natural disturbances. Considering the uncertainties involving carbon fluxes from tropical forests, the role of GIS based remote sensing techniques is apparent for improving knowledge of past rates of deforestation, monitoring future forest conversions and getting best sampling and extrapolating approaches for biomass estimations, especially for secondary forests for which there are no data available currently. Models of forest change in response to human interference require a prior characterization of the background noise of natural change. We have found four types of natural change visible over just eight years of TM recording: Large forest fires associated with the 1982/83 El Nifio; natural change in bamboo forests of Acre and SW Amazonas; mortality from anomalous flooding of terra firme forest; and large blowdowns (greater than 30 hectares). Although naturally disturbed areas may offer a unique opportunity for remote sensing studies of 'untouched' forest recover, their ecological impacts are far less important than the anthropogenic activities. This paper reviews several experiments that have explored the use of remote sensing for water, energy, and carbon balance studies of the Amazon Region and discusses several approaches for future experiments designed to understand the role of the Amazon in global climatic change. Author (revised)

N94-28070*# Institute of Ecosystem Studies, Millbrook, NY.

LANDSCAPE DYNAMICS OF NORTHEASTERN FORESTS Annual Report No. 1

Charles D. Canham, John A. Silander, Jr. (Connecticut Univ., Storrs.), and Daniel L. Civco (Connecticut Univ., Storrs.) 29 Mar. 1994 3 p
(Grant NAGw-3703)
(NASA-CR-195272; NAS 1.26:195272) Avail: CASI HC A01/MF A01

This project involves collaborative research with Stephen W. Pacala and Simon A. Levin of Princeton University to calibrate, test, and analyze models of heterogeneous forested landscapes containing a diverse array of habitats. The project is an extension of previous, NASA-supported research to develop a spatially-explicit model of forest dynamics at the scale of an individual forest stand (hectares to square kilometer spatial scales). That model (SORTIE) has been thoroughly parameterized from field studies in the modal upland environment of western Connecticut. Under our current funding, we are scaling-up the model and parameterizing it for the broad range of upland environments in the region. Our most basic goal is to understand the linkages between stand-level dynamics (as revealed in our previous research) and landscape-level dynamics of forest composition and structure. Derived from text

N94-27990# Japan Weather Association, Kojimachi.
DEVELOPMENT OF A METHOD FOR PREDICTING SNOWFALL INTENSITY AND COMPACTED SNOW ON ROADS [KOSETSU KYODO TO ROMEN ASSETSU YOSOKU SHUHO NO KAIHATSU]
Hisayuki Funada, Kuniyuki Senkuro, Muneo Matsukawa, and Tadashi Ishisaka (Toyama Prefectural Office, Japan.) *In* the National Research Inst. for Earth Science and Disaster Prevention, Report of the National Research Institute for Earth Science and Disaster Prevention, No. 51 31 Mar. 1993 p 209-219 In JAPANESE (For primary document see N94-27985 07-46)
Avail: CASI HC A03/MF A03

N94-27991# MTS Inst., Inc., Tokyo (Japan).
CONCEPTION OF SNOW INFORMATION NETWORK SYSTEM IN YAMAGATA PREFECTURE [YAMAGATA-KEN NAI NO YUKI SHORI JOHO SHISUTEMU NO KOSO]
Masuyoshi Matsuda, Hiroshi Nishimura, and Tsugio Nakashima (Yamagata Prefectural Office, Japan.) *In* the National Research Inst. for Earth Science and Disaster Prevention, Report of the National Research Institute for Earth Science and Disaster Prevention, No. 51 31 Mar. 1993 p 221-246 In JAPANESE (For primary document see N94-27985 07-46)
Avail: CASI HC A03/MF A03

N94-28269# Science and Technology Agency, Tokyo (Japan). Office of Earth Science and Technology.
ROLE AND ACTIVITY OF STA ON ASIAN PACIFIC REGIONAL COOPERATION
Yoshiaki Takeuchi *In its* Asia-Pacific Seminar on Global Change Research Cooperation 1992 p 5-23 Original contains color illustrations (For primary document see N94-28268 07-45)
Avail: CASI HC A03/MF A03

N94-28270# National Research Inst. for Earth Science and Disaster Prevention, Tsukuba (Japan). Advanced Measurement and Analysis Technology Div.
COOPERATIVE RESEARCH PROJECTS ON SATELLITE REMOTE SENSING FOR THE HYDROLOGICAL SUBJECTS
Shinkichi Kishi *In* Science and Technology Agency, Asia-Pacific Seminar on Global Change Research Cooperation 1992 p 25-3 (For primary document see N94-28268 07-45)
Avail: CASI HC A02/MF A03

N94-28271# Meteorological Research Inst., Tsukuba (Japan).
RESEARCH ACTIVITIES ON THE METEOROLOGY OVER THE ASIA-PACIFIC REGION
Masato Murakami *In* Science and Technology Agency, Asia-Pacific Seminar on Global Change Research Cooperation 1992 p 33-3 (For primary document see N94-28268 07-45)
Avail: CASI HC A01/MF A03

N94-28273# National Space Development Agency, Ohashi (Japan). Earth Observation Center.
NASDA CONTRIBUTION PLAN TO ASIAN COUNTRIES
Hiroshi Kikuchi *In* Science and Technology Agency, Asia-Pacific Seminar on Global Change Research Cooperation 1992 p 47-6 (For primary document see N94-28268 07-45)
Avail: CASI HC A03/MF A03

N94-28274# Remote Sensing Technology Center, Tokyo (Japan).
ACTIVITIES OF REMOTE SENSING TECHNOLOGY CENTER OF JAPAN (RESTEC)
Keiji Maruo *In* Science and Technology Agency, Asia-Pacific Seminar on Global Change Research Cooperation 1992 p 67-7 (For primary document see N94-28268 07-45)
Avail: CASI HC A02/MF A03

44 ENERGY PRODUCTION AND CONVERSION

Includes specific energy conversion systems, e.g., fuel cells; global sources of energy; geophysical conversion; and windpower.

For related information see also *07 Aircraft Propulsion and Power, 20 Spacecraft Propulsion and Power,* and *28 Propellants and Fuels.*

N94-25946# Sandia National Labs., Albuquerque, NM.
RENEWABLE ENERGY SYSTEMS IN MEXICO: INSTALLATION OF A HYBRID SYSTEM
Ronald C. Pate 12 May 1993 11 p
(Contract DE-AC04-76DP-00789)
(DE93-013716; DOE/FTR-93013716) Avail: CASI HC A03/MF A01 (US Sales Only)

Sandia has been providing technical leadership on behalf of DOE and CORECT on a working level cooperative program with Mexico on renewable energy (PROCER). As part of this effort, the Sandia Design Assistance Center (DAC) and the solar energy program staff at Instituto de Investigaciones Electricas (IIE) in Cuernavaca, Mexico, recently reached agreement on a framework for mutually beneficial technical collaboration on the monitoring and field evaluation of renewable energy systems in Mexico, particularly village-scale hybrid systems. This trip was made for the purpose of planning the details for the joint installation of a data acquisition system (DAS) on a recently completed PV/Wind/Diesel hybrid system in the village of Xcalac on the Southeast coast of the state of Quintana Roo, Mexico. The DAS installation will be made during the week of March 15, 1993. While in Mexico, discussions were also held with personnel from.the National Autonomous University of Mexico (UNAM) Solar Energy Laboratory and several private sector companies with regard to renewable energy project activities and technical and educational support needs in Mexico. DOE

N94-26050 Ministry of Energy and Infrastructure, Jerusalem (Israel).
THE FIRST ENERGY CONFERENCE: ISRAEL AND THE FORMER USSR
Sophie Zamkow, ed. Gefen Publishing House Ltd. 15 May 1991 171 p Conference held in Beer-Sheva, Israel, 13-15 May 1991; sponsored by Moscow International Energy Club and Ben Gurion Univ. of the Negev
(ISBN-965-229-098-X; ITN-94-85228) Copyright Avail: Issuing Activity (Office of the Chief Scientist, Ministry of Energy and Infrastructure, PO Box 13106, 91130 Jerusalem, Israel)

Subjects covered by the 18 papers include: electric power systems; oil shale and coal utilization in Israel and the former U.S.S.R.; solar energy; nuclear power; energy and the environment; gas turbines; R&D in magnetohydrodynamic systems; and high-temperature superconductors. Abstracts of eight papers have been included here, as being relevant to NASA's fields of interest. For individual titles, see N94-26051 through N94-26068.

N94-26051 Technion - Israel Inst. of Tech., Haifa.
SOLAR ENERGY IN ISRAEL: UTILIZATION AND RESEARCH
Y. Zvirin and Sophie Zamkow (Ministry of Energy and Infrastructure, Jerusalem, Israel.) *In* Ministry of Energy and Infrastructure, The First Energy Conference: Israel and the Former USSR 15 May 1991 p 39-58 (For primary document see N94-26050 07-44)
Copyright Avail: Issuing Activity (Office of the Chief Scientist, Ministry of Energy and Infrastructure, PO Box 13106, 91130 Jerusalem, Israel)

The State of Israel has been a pioneer in solar energy development and utilization since it was founded. In the 50's, solar domestic hot water heaters (DHWS) became commercially available. At the same time, research work was started in different areas of solar energy, which led to more advanced solar systems for additional applications. The presentation includes some details on commercial utilization of solar energy and a brief description of the main R&D projects in industry, universities and research institutes. ISA

N94-26052 Academy of Sciences (USSR), Moscow. Inst. of High Temperatures.
SOLAR ENERGY UTILIZATION IN THE USSR
E. E. Shpilrain *In* Ministry of Energy and Infrastructure, The First Energy Conference: Israel and the Former USSR 15 May 1991 p 59-64 (For

primary document see N94-26050 07-44)
Copyright Avail: Issuing Activity (Office of the Chief Scientist, Ministry of Energy and Infrastructure, PO Box 13106, 91130 Jerusalem, Israel)

The conditions for solar energy utilization in the USSR are not too favorable. Only in the country's southern regions is there sufficient insolation to make solar energy utilization economic. In higher latitudes, only seasonal use of solar energy is reasonable. Up to now, the main application of solar energy has been to produce low-temperature heat for hot water production, drying of agricultural goods, space heating and thermal treatment of concrete. A substantial proportion of the solar heating installations are flat plate solar collectors. The total installed area of solar collectors slightly exceeds 100,000 square meters. The collectors are produced by large- and small-scale industry. Where selective coatings are applied to the absorber plates, black nickel or chromium are the main coating materials. Recently launched new projects aim to develop and produce advanced collectors, with enhanced efficiency and reliability. There has been substantial progress in developing photovoltaic (PV) cells for space applications, but terrestrial application of PV is still in a very early stage. Annual production of PV cells totals about 100 kW, based on mono- or polycrystalline silicon. R&D work on thin-film PV cells is in progress. Work is in progress on the development of automated production lines to manufacture 1 MW/yr of crystalline and amorphous silicon. A 5-MW tower-type demonstration plant, with a circular heliostat field, uses steam as the working fluid. Experience with this plant has revealed several disadvantages, including commonwealth of independent states. ISA

N94-26053 Technion - Israel Inst. of Tech., Haifa. Faculty of Mechanical Engineering.
ABSORPTION TECHNOLOGY FOR SOLAR AND WASTE HEAT UTILIZATION
G. Grossman *In* Ministry of Energy and Infrastructure, The First Energy Conference: Israel and the Former USSR 15 May 1991 p 83-92 (For primary document see N94-26050 07-44)
Copyright Avail: Issuing Activity (Office of the Chief Scientist, Ministry of Energy and Infrastructure, PO Box 13106, 91130 Jerusalem, Israel)

Absorption heat pumps, first developed in the 19th century, have received renewed and growing attention in the past two decades. With the increasing cost of oil and electricity, the particular features of this heat-powered cycle have made it attractive for both residential and industrial applications. Solar-powered temperature boosters are among the applications on which intensive research was conducted. The operation of absorption systems is described and several practical applications are discussed. It surveys recent advances in absorption technology, including the selection of working fluids, cycle improvements and multi-staging, and fundamentals of the combined heat and mass transfer in absorption processes. ISA

N94-26054 Academy of Sciences (USSR), Moscow. Inst. of Energy Problems of Chemical Physics.
RADIATION APPLICATIONS OF PHYSICAL CHEMISTRY
V. L. Talrose *In* Ministry of Energy and Infrastructure, The First Energy Conference: Israel and the Former USSR 15 May 1991 p 93-105 (For primary document see N94-26050 07-44)
Copyright Avail: Issuing Activity (Office of the Chief Scientist, Ministry of Energy and Infrastructure, PO Box 13106, 91130 Jerusalem, Israel)

Many chemical energy problems have a physical chemistry nature connected with chemical kinetics and thermodynamics. In the USSR, the development in this field is associated with the name of N. N. Semenov, who was involved in a large number of fundamental and applied physical chemistry problems. The new Institute of Energy Problems of Chemical Physics of the USSR Academy of Sciences is dealing with some of them. An overview of the Institute's work on radiation applications is presented. Examples of the use of radiation in the power industry (e.g., in coal gasification), tire production, mechanical joints, metal powder production, and sterilization of pharmaceutical products are given. Methods and problems involved in these applications are discussed and the great potential for extensive utilization is demonstrated. ISA

N94-26055 Ben Gurion Univ. of the Negev, Beersheva (Israel). Center for Systematic Magneto-Hydrodynamic Studies.
LIQUID METAL MHD RESEARCH AND DEVELOPMENT IN ISRAEL
H. Branover *In* Ministry of Energy and Infrastructure, The First Energy Conference: Israel and the Former USSR 15 May 1991 p 127-134 (For primary document see N94-26050 07-44)
Copyright Avail: Issuing Activity (Office of the Chief Scientist, Ministry of Energy and Infrastructure, PO Box 13106, 91130 Jerusalem, Israel)

The study and development of liquid-metal magnetohydrodynamics (MHD) in Israel, from 1973 to the present, are reviewed. Following extensive research and evaluation, it was established that the most promising concept for a relatively short development time was the gravitational system, using lead or lead alloys as the magnetohydrodynamic fluid and steam or gases as the working fluid. The Etgar Program, set up to investigate such systems, is comprised of seven segments, of which the first six have been completed; work on the last segment has been started. The segments are as follows: studies of the physical phenomena; development of a universal numerical code for parametric studies and optimization and design of the system; materials studies; development of engineering components; construction and testing of small-scale Etgar-type systems; economic evaluation and comparison with conventional technologies; and development of an industrial demonstration plant. ISA

N94-26056 Academy of Sciences (USSR), Moscow. Inst. of High Temperatures.
WAYS TO IMPROVE MHD POWER PLANTS AND PROSPECTS OF THEIR APPLICATION
V. M. Batenin, S. I. Pistchikov, J. N. Sokolov, and E. M. Shelkov *In* Ministry of Energy and Infrastructure, The First Energy Conference: Israel and the Former USSR 15 May 1991 p 135-140 (For primary document see N94-26050 07-44)
Copyright Avail: Issuing Activity (Office of the Chief Scientist, Ministry of Energy and Infrastructure, PO Box 13106, 91130 Jerusalem, Israel)

The characteristics of magnetohydrodynamic (MHD) power plants, their modification possibilities, and their areas of application are analyzed. The analysis is based on the status of available power plants including steam turbine and combined-cycle steam/gas power plants. Conventional MHD power plants, based on existing technical solutions and various novel schemes are discussed. The main directions for improvement of energy conversion efficiency are presented, together with ways to modify MHD systems so as to reduce their capital costs. The conclusion is that MHD power plants could be competitive with most advanced power generation technologies. ISA

N94-26057 Kurchatov (I. V.) Inst. of Atomic Energy, Moscow (USSR).
PROSPECTS FOR UTILIZATION OF SUPERCONDUCTORS IN THE POWER INDUSTRY
N. A. Chernoplekov *In* Ministry of Energy and Infrastructure, The First Energy Conference: Israel and the Former USSR 15 May 1991 p 141-149 (For primary document see N94-26050 07-44)
Copyright Avail: Issuing Activity (Office of the Chief Scientist, Ministry of Energy and Infrastructure, PO Box 13106, 91130 Jerusalem, Israel)

Utilization of superconducting technology is greatly influenced by the discovery of the so-called high-temperature superconductors (HTS). This paper considers to what extent there is a need for HTS in up-to-date engineering and to what extent the industry is prepared for practical applications. The work on practical use of superconductors was started about 30 years ago. As a result, two fields of high-current superconductivity have emerged. The first category is the field in which other alternatives are inconceivable from the techno-economic point of view, e.g., magnets of large thermo-nuclear installations, MHD generators, inductive energy storage systems, etc. The second category comprises areas in which superconductors must compete with existing technologies, e.g., electrical devices, magnetic separators, etc. This paper discusses the development of various low-temperature superconducting devices, estimates their potential and evaluates future applications of HTS, based on the experience accumulated in the USSR and elsewhere. ISA

N94-26058 Tel-Aviv Univ. (Israel). School of Physics and Astronomy.
THE POTENTIAL FOR LARGE CRITICAL CURRENTS IN THE HIGH T(SUB c) OXIDES
G. Deutscher *In* Ministry of Energy and Infrastructure, The First Energy Conference: Israel and the Former USSR 15 May 1991 p 150-155 (For primary document see N94-26050 07-44)
Copyright Avail: Issuing Activity (Office of the Chief Scientist, Ministry of Energy and Infrastructure, PO Box 13106, 91130 Jerusalem, Israel)

The potential for high critical current densities is examined. On a thermodynamical basis, the energy scale for vortex pinning can be derived from a measurement of the width of the critical region. This energy scale is on the order of 0.1 eV in YBCO, which is sufficient for practical applications. Another important parameter is the short coherence length. The inner plane length, of the order of a few lattice spacings, is favorable for pinning by point defects. But the very short outer plane length gives rise to anomalous magnetic behavior, unfavorable for high-field applications at high temperature; this is true in particular in the most anisotropic oxides, such as the Bi compounds. ISA

N94-26114# Pacific Northwest Lab., Richland, WA.
ALTERNATIVE MATERIALS FOR SOLID OXIDE FUEL CELLS: PROCESSING AND INTERACTIONS OF MATERIALS
J. L. Bates, T. R. Armstrong, and L. A. Chick 1993 13 p Presented at the Joint Contractors Meeting on Advanced Turbine Systems, Fuel Cells and Coal-Fired Heat, Morgantown, WV, 3-5 Aug. 1993
(Contract DE-AC06-76RL-01830)
(DE94-000016; CONF-930893-35) Avail: CASI HC A03/MF A01

The purpose of this research is to develop alternative materials for solid oxide fuel cell (SOFC) interconnections and electrodes with improved electrical, thermal, and electrochemical properties. The overall approach for this research and development is as follows: minimize the number of cations in the electrode, electrolyte, and interconnection by developing yttrium compounds, such as Y(Ca)CrO3 as the interconnection, and Y(M')MnO3 as the air electrode; develop advanced synthesis and fabrication processes for air sintering, below 1,500 C, of chromite interconnections through: (1) the use of sintering aids, and (2) the synthesis of submicrometer powders; establish methods for the simultaneous processing and consolidation of air-sinterable powders; electrochemically evaluate interface reactions (in reproducible and controlled laboratory tests) for both the alternate and state-of-the-art materials and cell components developed under this program; and evaluate the chemical reactivity and interdiffusion effects that take place between the various fuel cell components--electrolyte/cathode, interconnect/cathode, and interconnect/anode. This paper describes a comprehensive study that assessed the processing of air-sinterable chromites, the sintering mechanism of chromites, and the chemical reactivity and interdiffusional effects between the interconnect, air, and fuel electrodes. Materials evaluated were La(0.7)Ca(0.31)CrO3, La(0.7)Ca(0.29)CrO3, (Y(0.6)Ca(0.4))(1.05)-Cr(0.95)O3, La(1-x)Sr(x)MnO3, La(1-x)Ca(x)MnO3, Y(1-x)Ca(x)MnO3, and Y(1-x)Sr(x)MnO3. DOE

N94-26115# Midwest Research Inst., Golden, CO.
THE STATE OF THE ART OF THIN-FILM PHOTOVOLTAICS
T. Surek Oct. 1993 12 p Presented at the Symposium on Balancing Energy, the Economy, and Ecology: The Solar Energy Contribution, Newark, DE, 16 Feb. 1993
(Contract DE-AC02-83CH-10093)
(DE94-000224; NREL/TP-410-6049; CONF-9302150-1) Avail: CASI HC A03/MF A01

Thin-film photovoltaic technologies, based on materials such as amorphous or polycrystalline silicon, copper indium diselenide, cadmium telluride, and gallium arsenide, offer the potential for significantly reducing the cost of electricity generated by photovoltaics. The significant progress in the technologies, from the laboratory to the marketplace, is reviewed. The common concerns and questions raised about thin films are addressed. Based on the progress to date and the potential of these technologies, along with continuing investments by the private sector to commercialize the technologies, one can conclude that thin-film PV will provide a competitive alternative for large-scale power generation in the future. DOE

N94-26240# Kauppa-ja Teollisuusministerio, Helsinki (Finland).
NEMO 2: NEW ENERGY SYSTEMS AND TECHNOLOGIES
P. Lund (Helsinki Univ. of Technology, Otaniemi, Finland.) 1993 29 p
(DE94-702060; KTM/E-B-132) Avail: CASI HC A03/MF A01

The Advanced Energy Systems and Technologies Research Program (NEMO 2) is one of the main energy research programs of the Ministry of Trade and Industry of Finland for the period of 1993-1998. The main emphasis in NEMO 2 is on solar energy and wind power. These are followed by other small power production, energy storage, and hydrogen technologies. The total budget is about 120 million FIM. The main objective in Nemo 2 is to increase the use of solar and wind energy in Finland and to promote industrial export in this field. Technology research and development is strongly supported and an international leadership role is envisioned for some niche areas. New energy technology is developed as a whole in close cooperation with industry and universities. To enhance the commercialization of these technologies, a small demonstration program is suggested to be realized in connection with the research program. Furthermore, international cooperation is considered important in reaching the program goals. As to wind energy research, basic research on wind meteorology and arctic wind technology will be continued. A series of pilot plants to demonstrate the achievements from wind technology developments is promoted. In solar energy, the NEMO 2 program looks for more efficient and cheaper photovoltaic systems and applications. Manufacturing of new photovoltaic cells is under consideration. Solar heating technologies are also supported with emphasis on improved system demonstrations. Energy storage questions are also dealt with indirectly in connection with solar research and development. DOE

N94-26242# Kauppa-ja Teollisuusministerio, Helsinki (Finland).
PROGRAMME FOR THE PROMOTION OF WIND POWER PRODUCTION
1993 34 p
(DE94-702065; KTM/E-C-35) Avail: CASI HC A03/MF A01

Promotion of renewable energies has a pretty long history in Finnish energy policy. In its energy policy report to Parliament in the spring of 1992, the Council of State expressed the intention to draw up a long-term program for expanding the wind power capacity in Finland. In the Energy Department of the Finnish Ministry of Trade and Industry, a group of civil servants has been surveying the present status of wind power, the chances for expanding it, and how this energy has been promoted in different countries. The survey is to provide a basis for a first goal-oriented Wind Power Program for Finland. Finland's existing wind power capacity approximates 1.5 MW. The Wind Power Program suggests this to be raised to 100 MW by the year 2005. Even so, less than 0.5% of the estimated electricity requirements would be supplied through wind power. To achieve this modest target, a systematic program would already be necessary. Key actions according to the proposed program would include the continuation of research and development efforts, subsidized construction of installations, different options relating to land use planning, and voluntary agreements between the government and the power producers. Information will also have to be supplied to ensure its implementation. Under the proposed program, the Ministry of Trade and Industry would go on contributing investment aid toward the building of wind power installations. Those to be erected in some early years would be looked upon as 'new technology' ones, which would enable them to be assisted at more than 30% of the total cost if necessary. Installations' improved competitiveness would decrease the aid percentage. DOE

N94-26329# California Univ., Berkeley. Lawrence Berkeley Lab.
EXPLORATORY TECHNOLOGY RESEARCH PROGRAM FOR ELECTROCHEMICAL ENERGY STORAGE
K. Kinoshita, ed. Oct. 1993 13 p
(Contract DE-AC03-76SF-00098)
(DE94-003480; LBL-34080) Avail: CASI HC A03/MF A01

This summary denotes the progress made by the Exploratory Technology Research (ETR) Program for Electrochemical Energy Storage during calendar year 1992. The primary objective of the ETR program, which is sponsored by the US Department of Energy (DOE) and managed by Lawrence Berkeley Laboratory (LBL), is to identify electrochemical technologies that can satisfy stringent performance, durability, and economic requirements for electric vehicles (EV's). The ultimate goal is to transfer the most promising electrochemical technologies to the private sector or to another DOE program (e.g., SNL's Electric Vehicle Advanced Battery Systems Development Program, EVABS) for further development and scale-up. Besides LBL, which has overall responsibility for the ETR program, LANL and BNL have participated in the ETR program by providing key research support in several of the program elements. Program consists of three major elements: exploratory eesearch; applied science research; and air systems research. The objectives and the specific battery and electrochemical systems addressed by each program element are discussed. Financial information that relates to the various programs and a description of the management activities for the ETR Program are described. DOE

N94-26426# Midwest Research Inst., Golden, CO. National Renewable Energy Lab.

OVERVIEW OF THE PHOTOVOLTAIC MANUFACTURING TECHNOLOGY (PVMaT) PROJECT

C. E. Witt, R. L. Mitchell, and G. D. Mooney Aug. 1993 7 p Presented at the National Conference and Exposition on Heat Transfer, Atlanta, GA, 8-11 Aug. 1993
(Contract DE-AC02-83CH-10093)
(DE93-018234; NREL/TP-411-5361; CONF-930830-31) Avail: CASI HC A02/MF A01

The Photovoltaic Manufacturing Technology (PVMaT) project is a historic government/industry photovoltaic (PV) manufacturing R&D partnership composed of joint efforts between the federal government (through the US Department of Energy) and members of the US PV industry. The project's ultimate goal is to ensure that the US industry retains and extends its world leadership role in the manufacture and commercial development of PV components and systems. PVMaT is designed to do this by helping the US PV industry improve manufacturing processes, accelerate manufacturing cost reductions for PV modules, improve commercial product performance, and lay the groundwork for a substantial scale-up of US-based PV manufacturing capacities. Phase 1 of the project, the problem identification phase, was completed in early 1991. Phase 2, the problem solution phase, which addresses process-specific problems of specific manufacturers, is now underway with an expected duration of 5 years. Phase 3 addresses R&D problems that are relatively common to a number of PV companies or the PV industry as a whole. These 'generic' problem areas are being addressed through a teamed research approach. DOE

N94-26463# Sandia National Labs., Albuquerque, NM.

LOW-COST PHOTOVOLTAIC INVERTERS INCORPORATING APPLICATION-SPECIFIC INTEGRATED CIRCUITS

George A. OSullivan (Abacus Controls, Inc., Somerville, NJ.) and Joseph A. OSullivan (Washington Univ., Saint Louis, MO.) Oct. 1993 22 p
(Contract DE-AC04-94AL-85000)
(DE94-003270; SAND-93-7076) Avail: CASI HC A03/MF A01

The positive impact of designing a power conditioner control system for photovoltaic applications with an application-specific integrated circuit (ASIC) as the main control element was demonstrated with detailed computer simulations in Phase 1 of a two phase Small Business Innovative Research Grant issued by the US Department of Energy. Completion of the design, building and testing of three prototypes using different power semiconductors was successfully accomplished in Phase 2. The power rating for the residential utility intertied Sunverters Model 753-4-200 is 5 kW. A stand-alone inverter suitable for operation from a photovoltaic array with or without a battery for energy storage was also developed in this effort. A much needed intermediate power level 50-kW three-phase power conditioner, Sunverter Model 759-4-200, was the third product to evolve from the research and development. All designs take advantage of the ASIC and a complementary microprocessor sampled-data control system. The ASIC-controlled power conditioners provide the high reliability, high efficiency, and low cost needed for photovoltaic applications. They cover the power range from the residential level to utility-sized installations. DOE

N94-26464# Case Western Reserve Univ., Cleveland, OH.

THE REACTIVITY OF LITHIUM TOWARD NON-AQUEOUS SOLVENTS OF RELEVANCE TO ENERGY STORAGE APPLICATIONS AS STUDIED BY SURFACE ANALYTICAL TECHNIQUES

K. Wang, G. S. Chottiner, and D. A. Scherson Jun. 1993 26 p
(Contract DE-AC03-76SF-00098)
(DE94-003483; LBL-34312) Avail: CASI HC A03/MF A01

The interactions between metallic lithium and perdeuterated tetrahydrofuran (TDF) have been examined in ultrahigh vacuum (UHV) by X-ray photoelectron and Auger electron spectroscopies (XPS and AES, respectively) and temperature programmed desorption (TPD). The AES, XPS, and TPD spectra of thick layers of Li vapor deposited on clean polycrystalline silver (Ag(poly)) foils exposed to up to 100 L TDF at room temperature showed no evidence for features other than those associated with clean Li/Ag(poly) surfaces. This indicates that the sticking coefficient of (gaseous) TDF on Li at 300 K is negligibly small. Clearly defined C(1s) and O(1s) XPS features were observed, however, for submonolayer coverages of TDF on Li/Ag(poly), obtained by first condensing a thick layer of TDF below 140 K and later gently warming the specimen to 300 K. The binding energies of these peaks were smaller than those for condensed TDF at 135 K. The m/e = 48 TPD spectra of TDF condensed on Ag(poly) yielded for O(TDF) less than 1 a well defined peak centered in the range of 210-240 K, a temperature much higher than that associated with the desorption of bulk-like TDF (ca. 170 K). The fragmentation patterns of adsorbed TDF were consistent with cyclopropane and formaldehyde as the most likely thermally desorbed species. Unlike the behavior observed for TDF/Ag(poly) for which no TPD features were detected for T greater than 300 K, the m/e = 4 TPD spectra for TDF/Li/Ag(poly) displayed a prominent peak centered at about 600 K attributed to D2 generated by the thermal decomposition of LiD. This provides rather unambiguous evidence that TDF reacts with Li at temperatures lower than 350 K to yield LiD as the main product. DOE

N94-26480# Midwest Research Inst., Golden, CO. National Renewable Energy Lab.

SOLAR RESOURCE-UTILITY LOAD MATCHING ASSESSMENT: NREL PHOTOVOLTAIC PROJECT SUMMARY

Nov. 1993 4 p
(Contract DE-AC02-83CH-10093)
(DE94-000232; NREL/TP-411-5836) Avail: CASI HC A01/MF A01

Many utility planners may be unfamiliar with the potential for the development of photovoltaics (PV) in their service areas. The goal of the research summarized in this document is to provide information on the match existing between the output of PV powder plants and the load requirements of U.S. utilities. This material indicates whether or not the effective capacity (hence the value) of this renewable resource should be higher than that traditionally assigned to an intermittent resource. DOE

N94-26513# Midwest Research Inst., Golden, CO.

AN OVERVIEW OF DOE'S WIND TURBINE DEVELOPMENT PROGRAMS

A. Laxson, D. Dodge, L. Flowers, R. Loose (Department of Energy, Washington, DC.), and P. Goldman (Department of Energy, Washington, DC.) Sep. 1993 10 p Presented at the 9th Annual Conference and Exhibition of the Canadian Wind Energy Association, Pincher Creek, Canada, 20-22 Sep. 1993
(Contract DE-AC02-83CH-10093)
(DE93-018224; NREL/TP-441-5761; CONF-9309131-1) Avail: CASI HC A02/MF A01

The development of technologically advanced, higher efficiency wind turbines continues to be a high priority activity of the US wind industry. The United States Department of Energy (DOE) is conducting and sponsoring a range of programs aimed at assisting the wind industry with system design, development, and testing. The overall goal is to develop systems that can compete with conventional electric generation for $.05/kWh at 5.8 m/s (13 mph sites) by the mid-1990's and with fossil-fuel-based generators for $.04/kWh at 5.8 m/s sites by the year 2000. These goals will be achieved through several programs. The Value Engineered Turbine Program will promote the rapid development of US capability to manufacture wind turbines with known and well documented records of performance, cost, and reliability, to take advantage of near-term market opportunities. The Advanced Wind Turbine Program will assist US industry to develop and integrate innovative technologies into utility-grade wind turbines for the near-term (mid 1990's) and to develop a new generation of turbines for the year 2000. The collaborative Electric Power Research Institute (EPRI)/DOE Utility Wind Turbine Performance Verification Program will deploy and evaluate commercial-prototype wind turbines in typical utility operating environments, to provide a bridge between development programs currently underway and commercial purchases of utility-grade wind turbines. A number of collaborative efforts also will help develop a range of small systems optimized to work in a diesel hybrid environment to provide electricity for smaller non-grid-connected applications. DOE

N94-26581# Energy Research Corp., Danbury, CT.

DESIGN OF GASIFIERS TO OPTIMIZE FUEL CELL SYSTEMS

Aug. 1993 54 p
(Contract DE-AC21-90MC-27227)
(DE94-000010; DOE/MC-27227/3471) Avail: CASI HC A04/MF A01

Pursuing the key national goal of clean and efficient utilization of the abundant domestic coal resources for power generation, this study was conducted to evaluate the potential of optimizing the integrated catalytic gasification/carbonate fuel cell power generation system. ERC in close collaboration with Fluor Daniel (providing engineering design and costing), conducted a detailed system configuration study to evaluate various catalytic gasification/carbonate fuel cell power plant configurations and compared them to present day, as well as emerging, alternate coal-based power plant technologies to assess their competitive position. A Topical Report was submitted documenting this effort, and the three catalytic gasification case studies are summarized in Appendix A. Results indicate that system efficiencies approaching 55% (HHV) can be achieved by integrating low temperature catalytic gasification with high efficiency carbonate fuel cells. Thermal balance in the gasifier is achieved without oxygen by recycling hydrogen from the fuel cell anode exhaust. A small amount of air is added to the gasifier to minimize hydrogen recycle. In order to validate the assumptions made in the case configurations, experimental studies were performed to determine the reactivity of Illinois No. 6 coal with the gasification catalysts. The reactivity of the catalyzed coal has significant bearing on gasifier sizing and hence system cost and efficiency. DOE

N94-26583# Argonne National Lab., IL.

RESEARCH AND DEVELOPMENT OF ALTERNATIVE COMPONENTS AT ARGONNE NATIONAL LABORATORY FOR MOLTEN CARBONATE FUEL CELLS

K. M. Myles, M. Krumpelt, G. H. Kucera, M. Roche, and E. Indacochea 1993 9 p Presented at the Joint Contractors Meeting on Advanced Turbine Systems, Fuel Cells and Coal-Fired Heat, Morgantown, WV, 3-5 Aug. 1993
(Contract W-31-109-eng-38)
(DE94-000014; DOE/NBM-94000014; CONF-930893-29) Avail: CASI HC A02/MF A01

Effort was focused on assessing conductive ceramic oxides as electrode materials and determining effectiveness of alternative electrolyte formulations at reducing NiO solubility, minimizing differential electrolyte migration, and reducing component corrosion. Full-cell tests are being carried out with Co-doped and doubly doped $LiFeO_2$ cathodes and undoped $LiCoO_2$ cathodes. Nb-doped CeO_2 anodes were also tested. Effect of a $CaCO_3$-Li_2CO_3-K_2CO_3 electrolyte on components was studied. DOE

N94-26584# Argonne National Lab., IL.

SEALANT RESEARCH FOR SOLID OXIDE FUEL CELLS

K. M. Myles, I. Bloom, M. Krumpelt, K. L. Ley, S. E. Dorris, and A. S. Wagh 1993 7 p Presented at the Joint Contractors Meeting on Advanced Turbine Systems, Fuel Cells and Coal-Fired Heat, Morgantown, WV, 3-5 Aug. 1993
(Contract W-31-109-eng-38)
(DE94-000015; DOE/NBM-94000015; CONF-930893-28) Avail: CASI HC A02/MF A01

A suitable sealant must form strong, dense bonds with SOFC components, be compatible, be stable at 1000 C in SOFC operating environment (H_2 and H_2O on anode side, O_2 on cathode side), and be electrically insulating. Two types of sealants are being developed: Rigid (Mg ammonium phosphate cement) for the cell edge, and compliant (borate-based glass-ceramic) for stack-to-manifold joining. Testing of both is reported. Shrinkage of the rigid sealant needs to be reduced. Further testing is underway. DOE

N94-26612# Sandia National Labs., Albuquerque, NM.

MERGING PHOTOVOLTAIC HARDWARE DEVELOPMENT WITH HYBRID APPLICATIONS IN THE USA

W. Bower 1993 8 p Presented at the Solar 1993 Conference, Perth, Australia, 1-5 Dec. 1993
(Contract DE-AC04-94AL-85000)
(DE94-002682; SAND-93-2145C; CONF-931236-1) Avail: CASI HC A02/MF A01

The use of multi-source power systems, 'hybrids,' is one of the fastest growing, potentially significant markets for photovoltaic (PV) system technology today. Cost-effective applications today include remote facility power, remote area power supplies, remote home and village power, and power for dedicated electrical loads such as communications systems. This market sector is anticipated to be one of the most important growth opportunities for PV over the next five years. The U.S. Department of Energy (USDOE) and Sandia National Laboratories (SNL) are currently engaged in an effort to accelerate the adoption of market-driven PV hybrid power systems and to effectively integrate PV with other energy sources. This paper provides details of this development and the ongoing hybrid activities in the United States. Hybrid systems are the primary focus of this paper. DOE

N94-26617# Sandia National Labs., Albuquerque, NM.

SIMPLIFIED HIGH-EFFICIENCY SILICON CELL PROCESSING

P. A. Basore, J. M. Gee, M. E. Buck, W. K. Schubert, and D. S. Ruby 1993 5 p Presented at the 7th International Photovoltaic Science and Engineering Conference, Nagoya, Japan, 22-26 Nov. 1993
(Contracts DE-AC04-94AL-85000; DE-AC04-76DP-00789)
(DE94-002683; SAND-93-1435C; CONF-931120-1) Avail: CASI HC A01/MF A01

The authors developed an emitter diffusion process that yields a near-ideal doping profile with a passivating oxide in a single furnace step. Because this process subjects the material to only one high-temperature thermal excursion, bulk lifetime is better preserved. This is especially true for lower-cost silicon materials containing a high concentration of oxygen or carbon. Using this process, one-sun cell efficiencies over 19% on float-zone material and over 18% on Czochralski material are routinely obtained. Using solar-grade Czochralski material, record efficiencies of 17.6% at one sun and 20.0% under concentration are demonstrated. Simple processes that yield high-performance diffusion profiles are expected to become increasingly important as manufacturers adopt improved techniques for ohmic contacts. DOE

N94-26700# Sandia National Labs., Albuquerque, NM.

ANALYSIS/TEST CORRELATION USING VAWT-SDS ON A STEP-RELAXATION TEST FOR THE ROTATING SANDIA 34 m TEST BED

J. G. Argueello, C. R. Dohrmann, T. G. Carne, and P. S. Veers 1993 7 p Presented at the 13th Energy-sources Technology Conference and Exhibition (ETCE) on Wind Energy, New Orleans, LA, 23-26 Jan. 1994
(Contract DE-AC04-76DP-00789)
(DE94-002290; SAND-93-1656C; CONF-940113-3) Avail: CASI HC A02/MF A01

The combined analysis/test effort described compares predictions with measured data from a step-relaxation test in the absence of significant wind-driven aerodynamic loading. The process described is intended to illustrate a method for validation of time domain codes for structural analysis of wind turbine structures. Preliminary analyses were performed to investigate the transient dynamic response that the rotating Sandia 34 m Vertical Axis Wind Turbine (VAWT) would undergo when one of the two blades was excited by step-relaxation. The calculations served two purposes. The first was for pretest planning to evaluate the relative importance of the various forces that would be acting on the structure during the test and to determine if the applied force in the step-relaxation would be sufficient to produce an excitation that was distinguishable from that produced by the aerodynamic loads. The second was to provide predictions that could subsequently be compared to the data from the test. The test was carried out specifically to help in the validation of the time-domain structural dynamics code, VAWT-SDS, which predicts the dynamic response of VAWT's subject to transient events. Post-test comparisons with the data were performed and showed a qualitative agreement between pretest predictions and measured response. However, they also showed that there was significantly more damping in the measurements than included in the predictions. Efforts to resolve this difference, including post-test analyses, were undertaken and are reported. The overall effort described represents a major step in the process of arriving at a validated structural dynamics code. DOE

N94-26747# Missouri Univ., Rolla. Dept. of Ceramic Engineering.

PROCESSING OF $LaCrO_3$ FOR SOLID OXIDE FUEL CELL APPLICATIONS

W. Huebner, M. M. Nasrallah, and H. U. Anderson 1993 12 p Presented at the Joint Contractors Meeting on Advanced Turbine Systems, Fuel Cells and Coal-fired Heat, Morgantown, WV, 3-5 Aug. 1993
(Contract DE-FG21-93MC-29224)
(DE94-002981; DOE/MC-29224/94/C0262; CONF-930893-23) Avail: CASI HC A03/MF A01

Objectives of this project is to produce $LaCrO_3$ for the interconnect in solid oxide fuel cells. The project is divided into three areas: reproducible powder synthesis, sintering of $LaCrO_3$-based powders, and co-sintering of

LaCrO3-based powders with cathode and electrolyte materials. The project has been in place for 3 months; construction is underway for the spray pyrolysis system and studies initiated on the organometallic precursor. DOE

N94-26785# Technology Management, Inc., Cleveland, OH.
LOW COST, RADIAL FLOW, SOLID OXIDE FUEL CELL
M. A. Petrik 1993 8 p Presented at the Joint Contractors Meeting on Advanced Turbine Systems, Fuel Cells and Coal-Fired Heat, Morgantown, WV, 3-5 Aug. 1993
(Contract DE-FG02-92ER-81453)
(DE94-002982; DOE/ER-81453/94/C0261; CONF-930893-24) Avail: CASI HC A02/MF A01

The Interscience Radial Flow (IRF) SOFC is designed to minimize problems in high-temperature operation and for low-cost fabrication. The cell has planar, non-sintered construction, uses particulate materials to form porous electrodes, and has internal radial flow. The object of this phase was to demonstrate feasibility of multi-cell stack operation. Performance milestone was 15% DC HHV efficiency with hydrogen at greater than 50 mW/sq cm over 100 h. DOE

N94-26792# Allied-Signal Aerospace Co., Torrance, CA.
MSOFC DEVELOPMENT STATUS
R. A. Gibson and N. Q. Minh 1993 7 p Presented at the Joint Contractors Meeting on Advanced Turbine Systems, Fuel Cells and Coal-Fired Heat, Morgantown, WV, 3-5 Aug. 1993
(Contract DE-AC21-89MC-26006)
(DE94-003192; DOE/MC-26006/94/C0252; CONF-930893-38) Avail: CASI HC A02/MF A01

The objective is to develop materials and fabrication methodologies to develop a monolithic solid oxide fuel cell (MSOFC) system capable of meeting performance, life, and cost goals for coal-derived fuel applications. The program is aimed at fabrication and testing of a 100-W stack. The MSOFC is an all-ceramic structure in which the cell components are configured in a compact, corrugated array; the electrolyte is zirconia, the anode is Ni/Y2O3-ZrO2 cermet, the cathode is doped LaMnO3, and the interconnects are doped LaCrO3. The fabrication sequence is shown, along with electrochemical performance. Baseline anode formulation shrinks when exposed to hydrogen causing cell curvature and stack delamination; new anode compositions are being developed. Sealants are being developed at Argonne. Thermal expansion mismatches need to be taken into account. DOE

N94-26813# Deutsche Forschungsanstalt fuer Luft- und Raumfahrt, Stuttgart (Germany). Abt. Bauteilgestaltung.
THE PLVCR 500 AND HCPC, TESTS AND RESULTS
Volker Leuchsner Sep. 1991 44 p
(ISSN 0939-298X)
(DLR-Mitt-93-04; ETN-94-95206) Avail: CASI HC A03/MF A01

Developments of volumetric receivers during the last decade which have pointed out the advantages and the wide range of applications in comparison with tube receivers are reported. During three test periods in 1990 the 500 kW version of the Pressure Loaded Volumetric Ceramic Receiver (PLVCR 500) and the Hexagonal Compound Parabolic Concentrator (HCPC) were mounted on the Small Solar Power System (SSPS) tower. Concerning the size of the experiment, it represents the most extensive research and development work on pressure loaded volumetric receivers until now. The receiver and the secondary concentrator were tested together and separately. A gauge pressure of 4.2 bars at air outlet temperatures of 960 C was reached. The secondary concentrator was tested under various flux conditions, the inlet and outlet flux distributions were measured. With this test the feasibility of a modular design of receiver and secondary concentrator could be shown. ESA

N94-26838 New Energy and Industrial Technology Development Organization, Tokyo (Japan).
FEASIBILITY STUDY ON INTRODUCTION OF THE BIO-FUEL POWER GENERATION IN TROPICAL REGIONS
Mar. 1993 168 p In JAPANESE Limited Reproducibility: More than 20% of this document may be affected by microfiche quality
(DE94-725203; NEDO-P-9214) Avail: CASI HC A08

Study is made on feasibility of introducing the bio-fuel power generation in tropical regions, especially in South East Asia including Okinawa and South America. Biomass promising as bio-fuel is bagasse and palm oil mill dregs; and bagasse is found to be advantageous to the use for large-scaled power generation. Prospective uses of bagasse are a combined use of gasification process and gas turbine power generation, an effective use of gas turbine exhaust heat at sugar cane factories, and a use of the system to be developed which totalizes these two. As to how to carry out the R and D project, since the gasification power generation process itself is a high technology and has partially unknown fields, it is desirable that research and development are conducted in such technologically developed countries as Japan (Okinawa). A developmental plan, therefore, is worked out as such that a pilot plant of approximately 3000kW is to be constructed in Okinawa because the period for bagasse production is at least 3 months there, and a commercial-scale plant is to be constructed and operated in such big bagasse-producing countries as Brazil. DOE

N94-26869# Westinghouse Electric Corp., Pittsburgh, PA. Science and Technology Center.
HIGH TEMPERATURE SOLID OXIDE FUEL CELL: CUSTOMER TEST UNITS
E. R. Ray and S. E. Veyo 1993 11 p Presented at the Joint Contractors Meeting on Advanced Turbine Systems, Fuel Cells and Coal-fired Heat, Morgantown, WV, 3-5 Aug. 1993
(Contract DE-FC21-91MC-28055)
(DE94-002961; DOE/MC-28055/94/C0253; CONF-930893-34) Avail: CASI HC A03/MF A01

There are three 25-kW class solid oxide fuel cell (SOFC) customer test unit programs; two are in Japan (utility joint ventures), one for Southern California Edison Co. The two in Japan are described: Startup, testing, modifications, and operational performance are discussed. DOE

N94-26871# Westinghouse Electric Corp., Pittsburgh, PA.
HIGH TEMPERATURE SOLID OXIDE FUEL DEVELOPMENT ACTIVITIES
E. R. Ray 1993 8 p Presented at the Joint Contractors Meeting on Advanced Turbine Systems, Fuel Cells and Coal-fired Heat, Morgantown, WV, 3-5 Aug. 1993
(Contract DE-FC21-91MC-28055)
(DE94-002973; DOE/MC-28055/94/C0251; CONF-930893-27) Avail: CASI HC A02/MF A01

An overview of the Westinghouse tubular solid oxide fuel cell (SOFC) development activities and current program status is presented. The goal is to develop a cell that can operate for 50,000 to 100,000 h. Test results are presented for multiple single cell tests which have now successfully exceeded 40,000 hours of continuous power operation at temperature. Two 25-kW SOFC customer tests units were delivered in 1992; a 20-kW SOFC system is bein manufactured and will be operated by Southern California Edison in 1995. Megawatt class generators are being developed. DOE

N94-26913# New Energy and Industrial Technology Development Organization, Tokyo (Japan).
HANDBOOK OF PHOTOVOLTAIC POWER GENERATING DESIGN FOR INTRODUCTION
Mar. 1993 49 p
(DE94-725199; ETDE/JP-mf-94725199) Avail: CASI HC A03/MF A01

The purpose of this handbook is to survey the ways to introduce photovoltaic power generation with specifying a certain region of introduction by international cooperation. Various cases of load requirements and load patterns are taken up for more efficient designing of equipment. When actually introducing photovoltaic power generating facilities, more detailed analyses of the situation would be necessary, but this handbook is effective in investigating and comparing basic designs and possible regions of introduction. Presented are illustrated overall designing procedures of photovoltaic power generating facilities and examples in cases of DC load and AC load. This handbook includes assumed load formats, calculation of storage battery capacity, required capacity of photovoltaic cell, selection of photovoltaic cell module, selection of storage battery, selection of inverter, selection of charge controller, list of possible regions, and amounts and durations of insolation in the selected regions, as data for designing photovoltaic power generation for introduction. DOE

N94-27004# Sandia National Labs., Albuquerque, NM.
EXTRACTION OF MODAL PARAMETERS FROM AN OPERATING HAWT USING THE NATURAL EXCITATION TECHNIQUE (NExT)
G. H. James 1993 17 p Presented at the 13th Energy-Sources Technology Conference and Exhibition (ETCE) on Wind Energy, New Orleans, LA, 23-26 Jan. 1994
(Contract DE-AC04-94AL-85000)
(DE94-001831; SAND-93-2271C; CONF-940113-1) Avail: CASI HC A03/MF A01

The Natural Excitation Technique (NExT) is used to extract modal parameters (natural frequencies, modal damping, and mode shapes) from an operating Horizontal Axis Wind Turbine (HAWT). NExT uses the measured response from the turbine excited by the assumed broad-band, random wind input even though the excitation cannot be directly measured. The damping, measured using NExT, generally increased in the system as the wind speed increased. Such information can be used to aid in the verification and upgrade of codes which predict structural response of operating HAWT's and aid our understanding of the dynamics of wind turbines. The Northern Power Systems 100-kW machine is addressed. Strain data is available from this machine while operating at 72 rpm in 10, 15, 20, 25, and 30 mph winds. The operational modal frequencies and mode shapes were measured for this machine. Reconstructions of the auto and cross spectra are used to verify the validity of the extracted parameters. The modal damping for two modes are presented for this range of wind speeds.
DOE

N94-27005# Eltron Research, Inc., Boulder, CO.
PEROVSKITE SOLID ELECTROLYTES FOR SOFC
A. F. Sammells 1993 7 p Presented at the Joint Contractors Meeting on Advanced Turbine Systems, Fuel Cells and Coal-Fired Heat, Morgantown, WV, 3-5 Aug. 1993
(Contract DE-FG02-90ER-80910)
(DE94-001923; DOE/ER-80910/94/C0267; CONF-930893-5) Avail: CASI HC A02/MF A01

A new series of brownmillerite solid electrolyte phases Ba2GdIn(1-x)Ga(x)O(5) (x = 0,0.2,0.4) with the x = 0.2 phase exhibiting an unusually low E were synthesized. Relative to both the observed ionic conductivity in this phase and to E(sub a)s observed in similar compounds. We attribute measured ionic conductivities to a lack of available charge carriers in Ba2GdIn(0.8)Ga(0.2)O(5). However, the low E(sub a) supports the premise that brownmillerite solid electrolyte structures are suitable for supporting high ionic conductivity. Current work is focusing on enhancing the amount of charge carriers in these materials by systematically introducing disorder into the brownmillerite lattice. DOE

N94-27048# Energy Information Administration, Washington, DC. Office of Coal, Nuclear, Electric and Alternate Fuels.
SOLAR COLLECTOR MANUFACTURING ACTIVITY, 1992
Nov. 1993 70 p
(DE94-003401; DOE/EIA-0174(92)) Avail: CASI HC A04/MF A01

This report presents data provided by US-based manufacturers and importers of solar collectors. Summary data on solar thermal collector shipments are presented for the years 1974 through 1992. Summary data on photovoltaic cell and module shipments are presented for the years 1982 through 1992. Detailed information for solar thermal collectors and photovoltaic cells and modules are presented for 1992. Appendix A describes the survey methodology. Appendix B contains the 1992 survey forms and instructions. Appendices C and D list the companies that responded to the 1992 surveys and granted permission for their names and addresses to appear in the report. Appendix E provides selected tables from this report with data shown in the International System of Units (SI) metric units. Appendix F provides an estimate of installed capacity and energy production from solar collectors for 1992. DOE

N94-27204# Ministry of International Trade and Industry, Tsukuba (Japan). Biomass Div.
REPORT OF NATIONAL INSTITUTE FOR RESOURCES AND ENVIRONMENT. NO. 5: STUDY ON DIRECT LIQUEFACTION OF WOODY BIOMASS [SHIGEN KANKYO GIJUTU SOGO KENKYUSHO HOKOKU DAI 5 GO: MOKUSHITSUKEI BAIOMASU NO CHOKUSETSU EKIKA HANNO NI KANSURU KENKYU]
Tomoko Ogi, Shinya Yokoyama, Tomoaki Minowa, Yutaka Dote, and Katsuya Koguchi 26 Mar. 1993 99 p In JAPANESE Sponsored by Hayashi Memorial Foundation for Female Natural Scientists, Tokyo, Japan
(ISSN 0916-9989)
(JTN-94-80551) Avail: CASI HC A05/MF A02

Various researches on the production of liquid fuels from biomass were undertaken. Carbon monoxide and/or hydrogen were used in most cases, while processes using a little or none of these reducing gas were investigated. The following results on thermochemical conversion of wood biomass are presented, in which wood is reacted in aqueous solution in the presence of an alkali catalyst without reducing gases, which yielded a liquid product: (1) the optimum reaction condition is determined from systematic studies carried out with reaction parameter and variety of catalyst; (2) the optimum organic solvents are determined from investigations concerning production of heavy oil which is easily separable from an aqueous layer; (3) the effectiveness of the repeated use of reaction solvent is indicated by experiments in which water or a 2-propanol/water mixture is used repeatedly as a reaction solvent; and (4) heavy oil obtained by the liquefaction process was analyzed by (1) H-NMR (Nuclear Magnetic Resonance), GC (Gas Chromatography) - MS (Mass Spectrometry), and acid-base extraction. The liquefaction technology may be evaluated as one of the highly promising biomass conversion technologies, although some technical problems, such as separation or upgrading of heavy oils need to be solved. For the promotion of a total system, in which biomass is planted and grown and then the biomass is used as fuel and/or chemicals, further development of technologies are needed not only for conversion itself but also for plantation, afforestation, and irrigation. Author (NASDA)

N94-27225 Tecogen, Inc., Waltham, MA.
FIBROUS EMISSIVE BURNERS SELECTIVE AND BROAD BAND Annual Report, Aug. 1992 - Jul. 1993
Robert E. Nelson Oct. 1993 40 p See also PB93-114411
(Contract GRI-5091-260-2180)
(PB94-128329; TR-4527-029-93; GRI-93/0384) Avail: Issuing Activity (National Technical Information Service (NTIS)

A supported continuous fiber emitter comprised of ytterbia fibers is evaluated for a gas-fired thermophotovoltaic energy conversion application. Optical recuperation as an efficiency enhancer is considered. Photo-convertible radiation efficiency and ytterbia volatility establish the operating temperature of the fibrous emitter. Gas-fired emitters exhibiting a high luminous output are proposed. NTIS

N94-27610# Energy Conversion Devices, Inc., Troy, MI.
CONTINUOUS ROLL-TO-ROLL a-Si PHOTOVOLTAIC MANUFACTURING TECHNOLOGY
M. Izu Dec. 1993 84 p Prepared for Midwest Research Inst., Golden, CO
(Contract DE-AC02-83CH-10093)
(DE94-000260; NREL/TP-411-6003) Avail: CASI HC A05/MF A01

This report describes work done under a 3-year program to advance ECD's roll-to-roll, triple-junction photovoltaic manufacturing technologies, to reduce the module production costs, to increase the stabilized module performance, and to expand commercial capacity utilizing ECD technology. The specific 3-year goal is to develop advanced large-scale manufacturing technology incorporating ECD's earlier research advances with the capability of producing modules with stable 11% efficiency at a cost of approximately $1.00 per peak watt. Accomplishments during Phase 1 included: (1) ECD successfully incorporated a high-performance Ag/metal-oxide back-reflector system into its continuous roll-to-roll commercial production operation. (2) High-quality a-Si-Ge narrow-band-gap solar cells were incorporated into the manufacturing. (3) ECD demonstrated the continuous roll-to-roll production of high-efficiency, triple-junction, two-band-gap solar cells consistently and uniformly throughout a 762-m (2500-ft) run with high yield. (4) ECD achieved 11.1% initial sub-cell efficiency of triple-junction, two-band-gap a-Si alloy solar cells in the production line. (5) The world's first 0.37-sq m (4-sq ft) PV modules were produced utilizing triple-junction spectrum-splitting solar cells manufactured in the production line. (6) As a result of process optimization to reduce the layer thickness and to improve the gas utilization, ECD achieved a 77% material cost reduction for germane and 58% reduction for disilane. Additionally, ECD developed a new low-cost module that saves approximately 30% in assembly material costs. DOE

N94-27625# Kopin Corp., Taunton, MA.
HIGH-EFFICIENCY, THIN-FILM SOLAR CELLS
Ronald P. Gale Jan. 1994 40 p Prepared in cooperation with Midwest Research Inst., Golden, CO
(Contract DE-AC02-83CH-10093)
(DE94-000250; NREL/TP-451-5746) Avail: CASI HC A03/MF A01

This report describes work on a 3-year research program to investigate thin-film GaAs/GaInP cells using the cleavage of lateral epitaxial film for transfer (CLEFT) technique, and to determine the process to enable overgrowth of GaAs films using organometallic chemistry. Application of the CLEFT thin-film technique to GaInP/GaAs solar cells and organometallic overgrowth was investigated. A problem of alloy contamination was identified and controlled, leading to higher quality layers. Solar cell structures were grown and fabricated using previously determined growth parameters for GaAs and GaInP. With the improved materials developed significant improvements were made in solar cell performance. Conditions for in-situ overgrowth by organometallic chemical vapor deposition (OMCVD) were determined and continuous GaAs layers were grown over a separation mask layer. The layers were successfully separated from their substrate using the CLEFT process, demonstrating the application of overgrowth using OM chemistry with HCl. DOE

N94-28100*# National Aeronautics and Space Administration. Marshall Space Flight Center, Huntsville, AL.
THE 1993 NASA AEROSPACE BATTERY WORKSHOP
Jeffrey C. Brewer, comp. Washington Feb. 1994 817 p Workshop held in Huntsville, AL, 16-18 Nov. 1993
(NASA-CP-3254; M-739; NAS 1.55:3254) Avail: CASI HC A99/MF A10

This document contains the proceedings of the 26th annual NASA Aerospace Battery Workshop, hosted by the Marshall Space Flight Center on 16-18 Nov. 1993. The workshop was attended by scientists and engineers from various agencies of the U.S. Government, aerospace contractors, and battery manufacturers, as well as international participation in like kind from a number of countries around the world. The subjects covered included nickel-cadmium, nickel-hydrogen, nickel-metal hydride, and lithium based technologies, as well as advanced technologies including various bipolar designs. For individual titles, see N94-28101 through N94-28136.

N94-28101*# National Aeronautics and Space Administration. Lewis Research Center, Cleveland, OH.
SUMMARY OF NASA AEROSPACE FLIGHT BATTERY SYSTEMS PROGRAM ACTIVITIES
Michelle Manzo and Patricia ODonnell *In* NASA. Marshall Space Flight Center, The 1993 NASA Aerospace Battery Workshop Feb. 1994 p 3-81 (For primary document see N94-28100 07-44)
Avail: CASI HC A04/MF A10

A summary of NASA Aerospace Flight Battery Systems Program Activities is presented. The NASA Aerospace Flight Battery Systems Program represents a unified NASA wide effort with the overall objective of providing NASA with the policy and posture which will increase the safety, performance, and reliability of space power systems. The specific objectives of the program are to: enhance cell/battery safety and reliability; maintain current battery technology; increase fundamental understanding of primary and secondary cells; provide a means to bring forth advanced technology for flight use; assist flight programs in minimizing battery technology related flight risks; and ensure that safe, reliable batteries are available for NASA's future missions. Derived from text

N94-28102*# Naval Surface Warfare Center, Crane, IN. Aerospace Power Systems Branch.
NSWC CRANE AEROSPACE CELL TEST HISTORY DATABASE
Harry Brown and Bruce Moore *In* NASA. Marshall Space Flight Center, The 1993 NASA Aerospace Battery Workshop Feb. 1994 p 83-89 (For primary document see N94-28100 07-44)
Avail: CASI HC A02/MF A10

The Aerospace Cell Test History Database was developed to provide project engineers and scientists ready access to the data obtained from testing of aerospace cell designs at Naval Surface Warfare Center, Crane Division. The database is intended for use by all aerospace engineers and scientists involved in the design of power systems for satellites. Specifically, the database will provide a tool for project engineers to review the progress of their test at Crane and to have ready access to data for evaluation. Additionally, the database will provide a history of test results that designers can draw upon to answer questions about cell performance under certain test conditions and aid in selection of a cell for a satellite battery. Viewgraphs are included. Derived from text

N94-28103*# Jet Propulsion Lab., California Inst. of Tech., Pasadena.
ADVANCED ENERGY STORAGE FOR SPACE APPLICATIONS: A FOLLOW-UP
Gerald Halpert and Subbarao Surampudi *In* NASA. Marshall Space Flight Center, The 1993 NASA Aerospace Battery Workshop Feb. 1994 p 91-109 (For primary document see N94-28100 07-44)
Avail: CASI HC A03/MF A10

Viewgraphs on advanced energy storage for space applications are presented. Topics covered include: categories of space missions using batteries; battery challenges; properties of SOA and advanced primary batteries; lithium primary cell applications; advanced rechargeable battery applications; present limitations of advanced battery technologies; and status of Li-TiS2, Ni-MH, and Na-NiCl2 cell technologies. Author (revised)

N94-28104*# Defence Research Establishment, Ottawa (Ontario).
EXPERIMENTAL EVALUATION OF BATTERY CELLS FOR SPACE-BASED RADAR APPLICATION
Craig A. Maskell and John R. Metcalfe (Canadian Astronautics Ltd., Ottawa, Ontario.) *In* NASA. Marshall Space Flight Center, The 1993 NASA Aerospace Battery Workshop Feb. 1994 p 111-118 (For primary document see N94-28100 07-44)
Avail: CASI HC A02/MF A10

A test program was conducted to characterize five space-quality nickel-hydrogen (NiH2) battery cells. A subset of those tests was also done on five commercial nickel-cadmium (NiCd) cells, for correlation to the characteristics of an Energy Storage Unit Simulator. The test program implemented the recommendations of a 1991 study, as reported to IECEC-92. The findings of the tests are summarized, and expected impacts on the performance of the electrical power system (EPS) of a large space-based radar (SBR) surveillance satellite are derived. The main characteristics examined and compared were terminal voltage (average and transient) and capacity through discharge, equivalent series resistance, derived inductance and capacitance, charge return efficiency, and inter-pulse charge effectiveness. Author (revised)

N94-28105*# Jet Propulsion Lab., California Inst. of Tech., Pasadena.
BATTERY STUDY FOR THE MARS ENVIRONMENTAL SURVEY (MESUR) PATHFINDER
Stephen F. Dawson, B. Otzinger, D. Perrone, Sal DiStefano, and Gerald Halpert *In* NASA. Marshall Space Flight Center, The 1993 NASA Aerospace Battery Workshop Feb. 1994 p 119-131 (For primary document see N94-28100 07-44)
Avail: CASI HC A03/MF A10

Viewgraphs on the battery study for the Mars Environmental Survey (MESUR) Pathfinder are presented. Topics covered include: MESUR pathfinder introduction; power subsystem concept; battery technology selection; mission battery performance; cell/battery baseline design; charge methodology; and proposed testing. CASI

N94-28106*# Aerospace Corp., El Segundo, CA.
SCREEN TEST FOR CADMIUM AND NICKEL PLATES
Angie H. Phan and Albert H. Zimmerman *In* NASA. Marshall Space Flight Center, The 1993 NASA Aerospace Battery Workshop Feb. 1994 p 133-140 Sponsored by NASA. Lewis Research Center (For primary document see N94-28100 07-44)
Avail: CASI HC A02/MF A10

A new procedure is described which was recently developed to quantify loading uniformity of nickel and cadmium plates and to screen finished electrodes prior to cell assembly. The technique utilizes the initial solubility rates of the active material in a standard chemical deloading solution at fixed conditions. The method can provide a reproducible indication of plate loading uniformity in situations where high surface loading limits the free flow of deloading solution into the internal porosity of the sinter plate. A preliminary study indicates that 'good' cell performance is associated with higher deloading rates. Author

N94-28107*# Naval Surface Warfare Center, Crane, IN.
ANALYSIS FOR NICKEL (3 AND 4) IN POSITIVE PLATES FROM NICKEL-CADMIUM CELLS
Harlan L. Lewis *In* NASA. Marshall Space Flight Center, The 1993 NASA Aerospace Battery Workshop Feb. 1994 p 141-146 (For primary document see N94-28100 07-44)
Avail: CASI HC A02/MF A10

The NASA-Goddard procedure for destructive physical analysis (DPA) of nickel-cadmium cells contains a method for analysis of residual charged nickel as NiOOH in the positive plates at complete cell discharge, also known as nickel precharge. In the method, the Ni(III) is treated with an excess of an Fe(II) reducing agent and then back titrated with permanganate. The Ni(III) content is the difference between Fe(II) equivalents and permanganate equivalents. Problems have arisen in analysis at NAVSURFWARCENDIV, Crane because for many types of cells, particularly AA-size and some 'space-qualified' cells, zero or negative Ni(III) contents are recorded for which the manufacturer claims 3-5 percent precharge. Our approach to this problem was to reexamine the procedure for the source of error, and correct it or develop an alternative method.
Author (revised)

N94-28108*# National Aeronautics and Space Administration. Lewis Research Center, Cleveland, OH.
SPACE STATION FREEDOM NIH2 CELL TESTING PROGRAM
Bruce Moore (Naval Surface Warfare Center, Crane, IN.) and Dave Frate *In* NASA. Marshall Space Flight Center, The 1993 NASA Aerospace Battery Workshop Feb. 1994 p 149-239 (For primary document see N94-28100 07-44)
Avail: CASI HC A05/MF A10

Testing for the Space Station Freedom Nickel Hydrogen Cell Test Program began in 1990 at Crave Division, Naval Surface Warfare Center. The program has included receipt inspection, random vibration, acceptance, characterization, and life cycle testing of Ni-H2 cells in accordance with the NASA LeRC Interagency Order C-31001-J. A total of 400 Ni-H2 cells have been received at NAVSURFWARCENDIV Crane from three separate manufacturers; Yardney Technical Products (Yardney), Eagle Picher Industries (Eagle Picher), and Gates Energy Products (Gates). Of those, 308 cells distributed among 39 packs have undergone life cycle testing under a test regime simulating low earth orbit conditions. As of 30 September 1993, there are 252 cells assembled into 32 packs still on life cycle test. Since the beginning of the program, failed cells have been detected in all phases of testing. The failures include the following; seven 65 AmpHr and 81 AmpHr Yardney cells were found to be leaking KOH on receipt, one 65 AmpHr Eagle Picher cell failed the acceptance test, one 65 AmpHr Gates cell failed during the characterization test, and six 65 AmpHr Gates cells failed the random vibration test. Of the 39 life cycle packs, testing on seven packs, 56 cells, has been suspended because of low end of discharge voltages. All of the failed life cycle packs were cycled at 60% depth of discharge.
Author

N94-28109*# International Telecommunications Satellite Organization, Washington, DC.
NI-H2 CELL CHARACTERIZATION FOR INTELSAT PROGRAMS
Andrew F. Dunnet and Martin W. Earl (Communications Satellite Corp., Clarksburg, MD.) *In* NASA. Marshall Space Flight Center, The 1993 NASA Aerospace Battery Workshop Feb. 1994 p 241-259 (For primary document see N94-28100 07-44)
Avail: CASI HC A03/MF A10

Various Ni/H2 cell designs manufactured for INTELSAT Programs during the past decade have been characterized electrically as a function of temperature. The resulting data for these INTELSAT V, VI, VII and VIIA cells are assembled in a manner which allows ready comparison of performance. Also included is a detailed description of each design.
Author

N94-28110*# Societe des Accumulateurs Fixes et de Traction, Poitiers (France).
SAFT NICKEL HYDROGEN CELL CYCLING STATUS
Yannick Borthomieu and Didier Duquesne *In* NASA. Marshall Space Flight Center, The 1993 NASA Aerospace Battery Workshop Feb. 1994 p 261-288 (For primary document see N94-28100 07-44)
Avail: CASI HC A03/MF A10

An overview of the NiH2 cell development is given. The NiH2 SAFT system is an electrochemical (single or dual) stack (IPV). The stack is mounted in an hydroformed Inconel 718 vessel operating at high pressure, equipped with 'rabbit ears' ceramic brazed electrical feedthroughs. The cell design is described: positive electrode, negative electrode, and stack configuration. Overviews of low earth orbit and geostationary earth orbit cyclings are provided. DPA results are also provided. The cycling and DPA results demonstrate that SAFT NiH2 is characterized by high reliability and very stable performances.
CASI

N94-28111*# Aerospace Corp., El Segundo, CA.
CALCULATION OF THE THERMONEUTRAL POTENTIAL OF NICd AND NIH2 CELLS
Albert H. Zimmerman *In* NASA. Marshall Space Flight Center, The 1993 NASA Aerospace Battery Workshop Feb. 1994 p 289-293 (For primary document see N94-28100 07-44)
Avail: CASI HC A01/MF A10

The thermoneutral potential of a nickel cadmium or nickel hydrogen cell is the potential at which the cell charge or discharge process puts out zero heat, and thus is the potential corresponding to the enthalpy change of the charge/discharge reaction, delta H. A relatively straightforward method for obtaining the thermoneutral potential E(sub tn), is based on the measured potential and temperature derivative of the cell reactions, which are related to the free energy change delta G, and entropy change delta S, respectively. Particularly in the nickel hydrogen cell, the pressure of hydrogen can often vary over an order of magnitude or more during the course of a charge or discharge. In a nickel cadmium cell, although significant changes in oxygen pressure can occur during charge or discharge, since oxygen does not enter into the charge/discharge reaction, these pressure changes are related to the heat generated from oxygen evolution and recombination. However, the entropy changes due to changes in hydrogen pressure relative to the 1 atm standard state must be included to apply this method to the nickel hydrogen cell.
Author

N94-28112*# Aerospace Corp., El Segundo, CA.
PERFORMANCE MODEL OF A RECIRCULATING STACK NICKEL HYDROGEN CELL
Albert H. Zimmerman *In* NASA. Marshall Space Flight Center, The 1993 NASA Aerospace Battery Workshop Feb. 1994 p 295-327 (For primary document see N94-28100 07-44)
Avail: CASI HC A03/MF A10

A theoretical model of the nickel hydrogen battery cell has been utilized to describe the chemical and physical changes during charge and overcharge in a recirculating stack nickel hydrogen cell. In particular, the movement of gas and electrolyte have been examined as a function of the amount of electrolyte put into the cell stack during cell activation, and as a function of flooding in regions of the gas screen in this cell design. Additionally, a two-dimensional variation on this model has been utilized to describe the effects of non-uniform loading in the nickel-electrode on the movement of gas and electrolyte within the recirculating stack nickel hydrogen cell. The type of nonuniform loading that has been examined here is that associated with higher than average loading near the surface of the sintered nickel electrode, a condition present to some degree in many nickel electrodes made by electrochemical impregnation methods. The effects of high surface loading were examined primarily under conditions of overcharge, since the movement of gas and electrolyte in the overcharging condition was typically where the greatest effects of non-uniform loading were found. The results indicate that significant changes in the capillary forces between cell components occur as the percentage of free volume in the stack filled by electrolyte becomes very high. These changes create large gradients in gas-filled space and oxygen concentrations near the boundary between the separator and the hydrogen electrode when the electrolyte fill is much greater than about 95 percent of the stack free volume. At lower electrolyte fill levels, these gaseous and electrolyte gradients become less extreme, and shift through the separator towards the nickel electrode. Similarly, flooding of areas in the gas screen cause higher concentrations of oxygen gas to approach the platinum/hydrogen electrode that is opposite the back side of the nickel electrode. These results illustrate the need for appropriate pore size distributions, and the maintenance of both convective electrolyte and gas flow paths through the stack, if the recirculating stack nickel hydrogen cell design is to work properly.
Author

N94-28113*# Societe des Accumulateurs Fixes et de Traction, Poitiers (France).
THERMAL MODELING OF NIH2 BATTERIES
Agnes-Marie Ponthus and Alain Alexandre (TSR, France.) *In* NASA. Marshall Space Flight Center, The 1993 NASA Aerospace Battery Workshop Feb. 1994 p 329-360 (For primary document see N94-28100 07-44)
Avail: CASI HC A03/MF A10

The following are discussed: NiH2 battery mission and environment; NiH2 cell heat dissipation; Nodal software; model development general philosophy; NiH2 battery model development; and NiH2 experimental developments. CASI

N94-28114*# TRW, Inc., Redondo Beach, CA. Space and Electronics Group.
NICKEL-HYDROGEN CELL REVERSAL CHARACTERISTICS
Charles Lurie *In* NASA. Marshall Space Flight Center, The 1993 NASA Aerospace Battery Workshop Feb. 1994 p 361-375 (For primary document see N94-28100 07-44)
Avail: CASI HC A03/MF A10

Nickel-hydrogen cell reversal characteristics are being studied as part of a TRW program directed towards development of a high current battery cell bypass switch. The following are discussed: cell bypass switch; nickel-hydrogen cell reversal characteristics; and nickel-hydrogen cell chemistry: discharge/reversal and overdischarge (reversal) with nickel and hydrogen precharge. CASI

N94-28115*# Aerospace Corp., Los Angeles, CA. Energy Technology Dept.
CYCLE LIFE VERSUS DEPTH OF DISCHARGE UPDATE ON MODELING STUDIES
Lawrence H. Thaller *In* NASA. Marshall Space Flight Center, The 1993 NASA Aerospace Battery Workshop Feb. 1994 p 377-395 (For primary document see N94-28100 07-44)
Avail: CASI HC A03/MF A10

The topics are presented in viewgraph form and cycle life vs. depth of discharge data for the following are presented: data as of three years ago; Air Force/Crane-Fuhr-Smithrick; Ken Fuhr's Data; Air Force/Crane Data; Eagle-Pitcher Data; Steve Schiffer's Data; John Smithrick's Data; temperature effects; and E-P, Yardney, and Hughes 26% Data. Other topics covered include the following: LeRC cycling tests of Yardney Space Station Cells; general statements; general observations; two different models of cycle life vs. depth of discharge; and other degradation modes. CASI

N94-28116*# Aerospace Corp., El Segundo, CA.
AIR FORCE STANDARDS FOR NICKEL HYDROGEN BATTERY
Warren Hwang and Martin Milden *In* NASA. Marshall Space Flight Center, The 1993 NASA Aerospace Battery Workshop Feb. 1994 p 397-403 (For primary document see N94-28100 07-44)
Avail: CASI HC A02/MF A10

The topics discussed are presented in viewgraph form and include Air Force nickel hydrogen standardization goals, philosophy, project outline, cell level standardization, battery level standardization, and schedule. CASI

N94-28117*# Bell Telephone Labs., Inc., Cranbury, NJ.
CHARGE EFFICIENCY OF NI/H2 CELLS DURING TRANSFER ORBIT OF TELSTAR 4 SATELLITES
W. C. Fang, Dean W. Maurer, B. Vyas, and M. N. Thomas *In* NASA. Marshall Space Flight Center, The 1993 NASA Aerospace Battery Workshop Feb. 1994 p 405-422 (For primary document see N94-28100 07-44)
Avail: CASI HC A03/MF A10

The TELSTAR 4 communication satellites being manufactured by Martin Marietta Astro Space (Astro Space) for AT&T are three axis stabilized spacecraft scheduled to be launched on expendable vehicles such as the Atlas or Ariane rockets. Typically, these spacecraft consist of a box that holds the electronics and supports the antenna reflectors and the solar array wings. The wings and reflectors are folded against the sides of the box during launch and the spacecraft is spun for attitude control in that phase; they are then deployed after achieving the final orbit. The launch phase and transfer orbits required to achieve the final geosynchronous orbit typically take 4 to 5 days during which time the power required for command, telemetry, attitude control, heaters, etc., is provided by two 50 AH nickel hydrogen batteries augmented by the exposed outboard solar panels. In the past, this situation has presented no problem since there was a considerable excess of power available from the array. In the case of large high powered spacecraft such as TELSTAR 4, however, the design power levels in transfer orbit approach the time-averaged power available from the exposed surface area of the solar arrays, resulting in a very tight power margin. To compound the difficulty, the array output of the spinning spacecraft in transfer orbit is shaped like a full wave rectified sine function and provides very low charging rates to the batteries during portions of the rotation. In view of the typically low charging efficiency of alkaline nickel batteries at low rates, it was decided to measure the efficiency during a simulation of the TELSTAR 4 conditions at the expected power levels and temperatures on three nickel hydrogen cells of similar design. The unique feature of nickel hydrogen cells that makes the continuous measurement of efficiency possible is that hydrogen is one of the active materials and thus, cell pressure is a direct measure of the state of charge or available capacity. The pressure is measured with a calibrated strain gage mounted on the outside of the pressurized cell. Author

N94-28118*# Martin Marietta Corp., Denver, CO. Astronautics Group.
ORBITAL MANAGEMENT AND DESIGN CONSIDERATIONS FOR NiCd SATELLITE POWER SYSTEMS
Benjamin J. Tausch, II *In* NASA. Marshall Space Flight Center, The 1993 NASA Aerospace Battery Workshop Feb. 1994 p 425-437 (For primary document see N94-28100 07-44)
Avail: CASI HC A03/MF A10

Several recently manufactured 50 and 60 ampere hour aerospace NiCd battery cell lots, produced by Gates Aerospace Batteries, are prone to premature on orbit performance degradation. The failure mechanism is cadmium migration, and the consequent development of soft shorts. A Martin Marietta Astronautics satellite program instituted an orbital management strategy for a set of these batteries that reduced the rate of degradation and brought the system to stable operation. This strategy involves: (1) minimizing the accumulated battery overcharge; (2) regular discharge exercises; and (3) periodic battery reconditioning. Because of changes in the NiCd cell manufacturing process, the actual performance of subsequent lots of NiCd cells is open to question. Future NiCd based power system designs should therefore allow for fine control of charge parameters, and an on orbit battery reconditioning capability. To minimize risk, it is much better to perform a full life test to qualify the cells before launch, rather than in parallel with orbital operations. If there are any changes in the manufacturing process of cells, it is extremely important to maintain very strong cognizance of secondary subcontractors, recognizing that the cell and battery manufacturing discipline is easily atrophied. Author

N94-28119*# Jet Propulsion Lab., California Inst. of Tech., Pasadena.
TOPEX/POSEIDON BATTERY PERFORMANCE DURING THE FIRST YEAR OF OPERATION
Frank Deligiannis, Sal DiStefano, Eric Lopez, and Rob Sherwood *In* NASA. Marshall Space Flight Center, The 1993 NASA Aerospace Battery Workshop Feb. 1994 p 439-458 (For primary document see N94-28100 07-44)
Avail: CASI HC A03/MF A10

The topics are presented in viewgraph form and include the following: cell/battery history, operational strategy, and spacecraft data. CASI

N94-28120*# National Aeronautics and Space Administration. Goddard Space Flight Center, Greenbelt, MD.
NICKEL CADMIUM BATTERY OPERATIONS ON-ORBIT: TRIALS, TRIBULATIONS, AND SUCCESS ON THE UPPER ATMOSPHERE RESEARCH SATELLITE
Gopalakrishna M. Rao and Scott D. Miller (Martin Marietta Services, Inc., Goddard, MD.) *In* NASA. Marshall Space Flight Center, The 1993 NASA Aerospace Battery Workshop Feb. 1994 p 459-489 (For primary document see N94-28100 07-44)
Avail: CASI HC A03/MF A10

The Upper Atmosphere Research Satellite (UARS), designed, built, integrated, tested, and operated by NASA and Martin Marietta is a low-Earth orbiting, Earth-observing spacecraft which was launched via Space Shuttle

Discovery on September 12, 1991 and deployed three days later. The Modular Power Subsystem (MPS) onboard the satellite is equipped with three NASA Standard 50 Ampere-hour (Ah) nickel-cadmium (NiCd) batteries. McDonnell Douglas Electronics Systems Company fabricated the MPS, and batteries from Gates Aerospace Batteries cells. Nominal battery performance was achieved for the first four months of spacecraft operation. First evidence of anomalous battery performance was observed in January 1992, after the first maximum beta angle (low Depth of Discharge) period. Since then, the Flight Operations Team (FOT), under the direction of Goddard Space Flight Center's UARS Project and Space Power Application Branch, has monitored and managed battery performance by adjusting solar array offset angle, conducting periodic deep discharge, and controlling battery recharge ratio. This paper covers a brief overview of the UARS, the FOT's operational battery management, and the observed spacecraft battery performance. Author

N94-28121*# Sanyo Electric Co. Ltd., Sumoto (Japan).
PERFORMANCE TEST RESULTS OF ETS-6 Ni-Cd CELLS
Kensuke Nakatani, Y. Yano, S. Kuwajima (Tsukuba Space Center, Japan.), and Hiroaki Kusawake (Tsukuba Space Center, Japan.) *In* NASA. Marshall Space Flight Center, The 1993 NASA Aerospace Battery Workshop Feb. 1994 p 491-511 (For primary document see N94-28100 07-44)
Avail: CASI HC A03/MF A10

The topics covered are presented in viewgraph form and include the following: development schedule; main specification; cell design; production flow; acceptance test (1); acceptance test (2); cell weight; 20 C performance; canacity; overcharge pressure; end of charge voltage; -5 C performance; ETS-VI simulation cycle test; and battery storage. CASI

N94-28122*# Naval Surface Warfare Center, Crane, IN.
AF Ni-Cd CELL QUALIFICATION PROGRAM
Steve Hall, Harry Brown, G. Collins (Aerospace Corp., El Segundo, CA.), and Warren Hwang (Aerospace Corp., El Segundo, CA.) *In* NASA. Marshall Space Flight Center, The 1993 NASA Aerospace Battery Workshop Feb. 1994 p 513-544 (For primary document see N94-28100 07-44)
Avail: CASI HC A03/MF A10

The present status of the USAF NiCd cell qualification program, which is underway at the Naval Surface Warfare Center-Crane Division, is summarized. The following topics are discussed: overview; background; purpose; stress tests; results for super Ni-Cd; results for SAFT cells; GPS stress test; GPS simulated orbit; and results for gates cells. The discussion is presented in viewgraph format. Author (revised)

N94-28123*# McDonnell-Douglas Corp., Saint Charles, MO. Defense and Electronic Systems.
DISCRIMINATING PERFORMANCE PARAMETERS FOR 50 AMP-HOUR AND 60 AMP-HOUR NICKEL-CADMIUM PLATES AND BATTERY CELLS
Mark R. Toft *In* NASA. Marshall Space Flight Center, The 1993 NASA Aerospace Battery Workshop Feb. 1994 p 545-576 (For primary document see N94-28100 07-44)
Avail: CASI HC A03/MF A10

This is a follow-up of studies of the NASA standard 50 AH cell presented at the NASA battery workshop each of the last two years. This is a dynamic study. Data trends continue to be developed and analyzed for their utility in judging NiCd performance. The trends and parameters presented here may bear relevance to many designs of conventional NiCd batteries, not just the 50 AH and 60 AH sizes. Author (revised)

N94-28124*# TRW, Inc., Redondo Beach, CA. Space and Electronics Group.
BATTERY CHARGE CONTROL: WHICH APPROACH IS BEST?
Charles Lurie *In* NASA. Marshall Space Flight Center, The 1993 NASA Aerospace Battery Workshop Feb. 1994 p 585-588 (For primary document see N94-28100 07-44)
Avail: CASI HC A01/MF A10

The question of the best approach for battery charge control is addressed from two points of view: from the battery point-of-view; and from the spacecraft/mission point-of-view. In terms of performance, more aggressive charging can result in higher discharge voltage and capacity; however, aggressive charging usually implies more overcharge at higher rates and a concomitant higher end of charge temperature (higher stress, shorter life). In terms of life, benign charging can result in lower discharge voltage and capacity (poorer performance). Additionally, benign, or low stress charging, usually implies less overcharge at lower rates with lower end of charge temperature (lower stress, longer life). A discussion of these topics is presented in viewgraph form. Author (revised)

N94-28125*# Methlie (George), Falls Church, VA.
SOME OBSERVATIONS ON BATTERY CHARGE CONTROL
George J. Methlie *In* NASA. Marshall Space Flight Center, The 1993 NASA Aerospace Battery Workshop Feb. 1994 p 589-598 (For primary document see N94-28100 07-44)
Avail: CASI HC A02/MF A10

The following topics are discussed: NiCd charge control; GSFC TCVL control; program specific TCVL's; and v/t changes with time/temperature/cycling. The discussion is presented in viewgraph format. Author (revised)

N94-28126*# National Aeronautics and Space Administration. Goddard Space Flight Center, Greenbelt, MD.
CONSTRUCTION OF TEMPERATURE COMPENSATED CONSTANT VOLTAGE (VT) CURVES FOR SUPER Ni-Cd (TM) CELLS
David A. Baer (Hughes Aircraft Co., Torrance, CA.), David F. Pickett (Hughes Aircraft Co., Torrance, CA.), James M. Pearce (Hughes Aircraft Co., Torrance, CA.), and Gopalakrishna Rao *In* NASA. Marshall Space Flight Center, The 1993 NASA Aerospace Battery Workshop Feb. 1994 p 599-606 (For primary document see N94-28100 07-44)
Avail: CASI HC A02/MF A10

Tests to establish current-voltage characteristics at selected temperatures for 9 a-h Super Nickel-Cadmium cells were conducted at Hughes Industrial Electronics Company's Electron Dynamics Division (HIEC/EDD) under sponsorship of NASA/GSFC through their prime spacecraft contractors Fairchild Space (SMEX/SAMPEX) and TRW (TOMSEP). Curves were constructed using techniques established by Webster, Ford, et al, at NASA/GSFC in the late 1960's - early 1970's time period for conventional nickel cadmium cells used on OAO and OSO aircraft. The NASA/GSFC techniques were slightly modified by HIEC/EDD to fit the Super Ni-Cd situation. Author (revised)

N94-28127*# Naval Research Lab., Washington, DC.
A PRESSURE BASED CHARGE CONTROL SYSTEM FOR THE DSPSE NiH2 CPV BATTERY
Chris Garner, W. Barnes, and G. Hickman *In* NASA. Marshall Space Flight Center, The 1993 NASA Aerospace Battery Workshop Feb. 1994 p 607-626 (For primary document see N94-28100 07-44)
Avail: CASI HC A03/MF A10

The following topics are discussed: the Electrical Power Subsystem; the Eclipse Energy Requirements; the NiH2 CPV battery; and the battery pressure transducer. The discussion is presented in viewgraph format. Author (revised)

N94-28128*# Boeing Defense and Space Group, Seattle, WA.
USE OF CALORIMETRY FOR END OF CHARGE DETERMINATION
Chris J. Johnson *In* NASA. Marshall Space Flight Center, The 1993 NASA Aerospace Battery Workshop Feb. 1994 p 627-639 (For primary document see N94-28100 07-44)
Avail: CASI HC A03/MF A10

To perform heat flow measurements on batteries, it is necessary to consider the following requirements: establish thermal neutral potential; identify inefficient charging; understand self discharge mechanisms; and provide accurate voltage/temperature data. A discussion is provided in viewgraph format. Author (revised)

N94-28129*# Eagle-Picher Industries, Inc., Joplin, MO. Advanced Systems Operation.
ADVANCED NICKEL-HYDROGEN SPACECRAFT BATTERY DEVELOPMENT
Dwaine K. Coates, Chris L. Fox, D. J. Standlee, and B. K. Grindstaff *In* NASA. Marshall Space Flight Center, The 1993 NASA Aerospace Battery Workshop Feb. 1994 p 643-651 (For primary document see N94-28100 07-44)
Avail: CASI HC A02/MF A10

Eagle-Picher currently has several advanced nickel-hydrogen (NiH2) cell component and battery designs under development including common pressure vessel (CPV), single pressure vessel (SPV), and dependent pressure vessel (DPV) designs. A CPV NiH2 battery, utilizing low-cost 64 mm (2.5 in.) cell diameter technology, has been designed and built for multiple smallsat programs, including the TUBSAT B spacecraft which is currently scheduled (24 Nov. 93) for launch aboard a Russian Proton rocket. An advanced 90 mm (3.5 in.) NiH2 cell design is currently being manufactured for the Space Station Freedom program. Prototype 254 mm (10 in.) diameter SPV batteries are currently under construction and initial boilerplate testing has shown excellent results. NiH2 cycle life testing is being continued at Eagle-Picher and IPV cells have currently completed more than 89,000 accelerated LEO cycles at 15% DOD, 49,000 real-time LEO cycles at 30 percent DOD, 37,800 cycles under a real-time LEO profile, 30 eclipse seasons in accelerated GEO, and 6 eclipse seasons in real-time GEO testing at 75 percent DOD maximum. Nickel-metal hydride battery development is continuing for both aerospace and electric vehicle applications. Eagle-Picher has also developed an extensive range of battery evaluation, test, and analysis (BETA) measurement and control equipment and software, based on Hewlett-Packard computerized data acquisition/control hardware. Author (revised)

N94-28130*# Tsukuba Space Center (Japan).

DEVELOPMENT OF NICKEL-METAL HYDRIDE CELL: AN UPDATE

S. Kuwajima, Hiroaki Kusawake, Kensuke Nakatani (Sanyo Electric Co. Ltd., Sumoto, Japan.), and Y. Yano (Sanyo Electric Co. Ltd., Sumoto, Japan.) *In* NASA. Marshall Space Flight Center, The 1993 NASA Aerospace Battery Workshop Feb. 1994 p 653-685 (For primary document see N94-28100 07-44)

Avail: CASI HC A03/MF A10

This paper presents in viewgraph format an overview of NASDA's evaluation of commercial nickel metal-hydride (Ni-MH) cells and the development and testing of Ni-MH cells for use in space. The commercial cells are concluded to be feasible and suitable for use in LEO; for GEO, the durability for overcharge is needed because long-term charge retention is required. For the aerospace Ni-MH cell design, two activation procedures are applied to evaluate the effect of the difference in the amount of overcharge protection and precharge. Specific energy of the Ni-MH cell is nearly accomplished at 50 Wh/kg. Initial characteristics indicate the effect derived from precharge. Thirty-five amp-hour class Ni-MH cells have good performance for LEO cycle of 25 and 40 percent DOD up to 3000 cycles as similar to commercial cells. The effect of the difference in the amount of overcharge protection will appear in life test. CASI

N94-28131*# Gates Aerospace Batteries, Gainesville, FL.

NI-MH STORAGE TEST AND CYCLE LIFE TEST

R. Dan Dell, Glenn C. Klein, and David F. Schmidt *In* NASA. Marshall Space Flight Center, The 1993 NASA Aerospace Battery Workshop Feb. 1994 p 687-700 (For primary document see N94-28100 07-44)

Avail: CASI HC A03/MF A10

Gates Aerospace Batteries is conducting two long term test programs to fully characterize the NiMH cell technology for aerospace applications. The first program analyzes the effects of long term storage upon cell performance. The second program analyzes cycle life testing and preliminary production lot testing. This paper summarizes these approaches to testing the NiMH couple and culminates with initial storage and testing recommendations. Long term storage presents challenges to deter the adverse condition of capacity fade in NiMH cells. Elevated but stabilized pressures and elevated but stabilized end-of-charge voltages also appear to be a characteristic phenomenon of long term storage modes. However, the performance degradation is dependent upon specific characteristics of the metal-hydride alloy. To date, there is no objective evidence with which to recommend the proper method for storage and handling of NiMH cells upon shipment. This is particularly critical due to limited data points that indicate open circuit storage at room temperature for 60 to 90 days will result in irrecoverable capacity loss. Accordingly a test plan was developed to determine what method of mid-term to long-term storage will prevent irrecoverable capacity loss. The explicit assumption is that trickle charging at some rate above the self-discharge rate will prevent the irreversible chemical changes to the negative electrode that result in the irrecoverable capacity loss. Another premise is that lower storage temperatures, typically 0 C for aerospace customers, will impede any negative chemical reactions. Three different trickle charge rates are expected to yield a fairly flat response with respect to recoverable capacity versus baseline cells in two different modes of open circuit. Specific attributes monitored include: end-of-charge voltage, end-of-charge pressure, mid-point discharge voltage, capacity, and end-of-discharge pressure. Cycle life testing and preliminary production lot testing continue to dominate the overall technology development effort at GAB. The cell life test program reflects continuing improvements in baseline cell designs. Performance improvements include lower and more stable charge voltages and pressures. The continuing review of production lot testing assures conformance to the design criteria and expectations. This is especially critical during this period of transferring technology from research and development status to production. Author (revised)

N94-28132*# National Aeronautics and Space Administration. Lyndon B. Johnson Space Center, Houston, TX.

DETERMINATION OF THERMAL PROPERTIES OF COMMERCIAL NI-MH CELLS

Eric C. Darcy *In* NASA. Marshall Space Flight Center, The 1993 NASA Aerospace Battery Workshop Feb. 1994 p 701-716 (For primary document see N94-28100 07-44)

Avail: CASI HC A03/MF A10

The test objectives were to evaluate the electrical and thermal performance of commercial Ni-MH cells, evaluate the effectiveness of commercial charge control circuits, assess the abuse tolerance of these cells, and correlate performance and abuse tolerances to cell design via disassembly. Design objectives were to determine which cell designs are most suitable for scale-up and to guide the design of future shuttle and space station based battery chargers. Results, displayed in viewgraph format, include: reflex charging with ICS circuit resulted in premature charge termination; Ni-MH cells appear very tolerant to overcharge at low rates; Enstore's charger is more electrically and thermally efficient at high rates; and Ni-MH cycles much more efficiently than Ni-Cd with the delta-V/delta-t termination. CASI

N94-28133*# Yardney Technical Products, Inc., Pawcatuck, CT.

HIGH RATE LITHIUM/THIONYL CHLORIDE BIPOLAR BATTERY DEVELOPMENT

Philip G. Russell and F. Goebel *In* NASA. Marshall Space Flight Center, The 1993 NASA Aerospace Battery Workshop Feb. 1994 p 717-751 (For primary document see N94-28100 07-44)

(Contract N60921-91-C-0124)

Avail: CASI HC A03/MF A10

Presented in viewgraph format are results and accomplishments on the development of lithium/thionyl chloride bipolar batteries. Results include the development of manufacturing capability for producing large quantities of uniform cathodes and bipolar plates; the development of assembly, sealing, and activation procedures for fabrication of battery modules containing up to 150 cells in bipolar configuration; and the successful demonstration of a 10.7 kW 150-cell module with constant power pulse discharge, 20 second pulse, and 10 percent duty cycle. CASI

N94-28134*# National Aeronautics and Space Administration. Marshall Space Flight Center, Huntsville, AL.

BIPOLAR LEAD-ACID BATTERIES FOR ELECTRICAL ACTUATION APPLICATIONS

Douglas C. Pierce (Johnson Controls, Inc., Milwaukee, WI.), William O. Gentry (Johnson Controls, Inc., Milwaukee, WI.), and David Hall *In its* The 1993 NASA Aerospace Battery Workshop Feb. 1994 p 753-771 (For primary document see N94-28100 07-44)

Avail: CASI HC A03/MF A10

This document presents in viewgraph format information on bipolar battery development at Johnson Controls, Incorporated. The organization structure, goals, progress to date, future plans, and battery parameters and electrical properties are given. CASI

N94-28135*# Eagle-Picher Co., Joplin, MO.

BIPOLAR Ag-Zn BATTERY

L. John Giltner *In* NASA. Marshall Space Flight Center, The 1993 NASA Aerospace Battery Workshop Feb. 1994 p 773-774 (For primary document see N94-28100 07-44)

Avail: CASI HC A01/MF A10

The silver-zinc (AgZn) battery system has been unique in its ability to safely satisfy high power demand applications with low mass and volume.

However, a new generation of defense, aerospace, and commercial applications will impose even higher power demands. These new power demands can be satisfied by the development of a bipolar battery design. In this configuration the power consuming, interelectrode current conductors are eliminated while the current is then conducted via the large cross-section electrode substrate. Negative and positive active materials are applied to opposite sides of a solid silver foil substrate. In addition to reducing the weight and volume required for a specified power level, the output voltage performance is also improved as follows. Reduced weight through: elimination of the plastic cell container; elimination of plate leads and intercell connector; and elimination of internal plate current collector. Increased voltage through: elimination of resistance of current collector; elimination of resistance of plate lead; and elimination of resistance of intercell connector. EPI worked previously on development of a secondary bipolar silver zinc battery. This development demonstrated the electrical capability of the system and manufacturing techniques. One difficulty with this development was mechanical problems with the seals. However, recent improvements in plastics and adhesives should eliminate the major problem of maintaining a seal around the periphery of the bipolar module. The seal problem is not as significant for a primary battery application or for a requirement for only a few discharge cycles. A second difficulty encountered was with activation (introducing electrolyte into the cell) and with venting gas from the cell without loss of electrolyte. During previous work, the following projections for energy density were made from test data for a high power system which demonstrated in excess of 50 discharge/charge cycles. Projected system power = 100 kilowatts; discharge time = 30 seconds; discharge current density = 1.75 amps/sq in.; system weight = 86 lbs (9.7 WH/lb); and system volume = 1071 cu. in. (.78 WH/cu. in.). EPI is currently working on a development program to produce a bipolar silver-zinc battery design for NASA. The potential application would be to power electromechanical actuators for space launch vehicles. Derived from text

N94-28136*# BST Systems, Inc., Plainfield, CT.
ADVANCED SILVER ZINC BATTERY DEVELOPMENT FOR THE SRB AND ET RANGE SAFETY SUBSYSTEMS
Zoe Adamedes *In* NASA. Marshall Space Flight Center, The 1993 NASA Aerospace Battery Workshop Feb. 1994 p 775-831 (For primary document see N94-28100 07-44)
Avail: CASI HC A04/MF A10

This document presents in viewgraph format the design and development of silver zinc (AgZn) batteries for the solid rocket booster (SRB) and external tank (ET) range safety subsystems. Various engineering techniques, including composite separator systems, new electrode processing techniques, and new restraint techniques, were used to meet difficult requirements. CASI

45 ENVIRONMENT POLLUTION

Includes atmospheric, noise, thermal, and water pollution.

N94-25609# Air Force Inst. of Tech., Wright-Patterson AFB, OH.
AIR POLLUTION TRANSPORT MODELING M.S. Thesis
David M. Paal Dec. 1993 123 p
(AD-A273863; AFIT/ENC/GCS/93D-1) Avail: CASI HC A06/MF A02

This research effort addresses modeling of the transportation of air pollution in the atmosphere and the numerical analysis of the partial differential equations used in such modeling. Three Gaussian models are examined and compared using example problems. Several finite difference schemes are developed to solve the partial differential equations used in air pollution transport modeling. Three Gaussian models: SCREEN, AFTOX, and the program GAUSPLUM are studied. The model GAUSPLUM is developed and uses the Ada programming language and the analytic solution to the advection-diffusion equation. Numerical analysis of the partial differential equations (PDE) used in air pollution modeling is also examined. The equations are generally parabolic or hyperbolic PDE's. The following are examined in this research: the advection equation; the one-, two-, and three-dimensional advection-diffusion equations; and the two-dimensional steady-state equation. DTIC

N94-25755# Air Force Inst. of Tech., Wright-Patterson AFB, OH. School of Systems and Logistics.
ANALYSIS AND DEVELOPMENT OF AN F-5 POLLUTION PREVENTION MANAGEMENT PROGRAM WITH RECOMMENDATIONS FOR CREATION OF SIMILAR PROGRAMS FOR OTHER AIRCRAFT M.S. Thesis
Janice M. Gavern Sep. 1993 154 p
(AD-A274016; AFIT/GLM/LSY/93S-19) Avail: CASI HC A08/MF A02

A pollution prevention program for the F-5 aircraft was developed, and its utility and applicability as a generic framework for similar programs is described. A representative set of F-5 technical orders was analyzed by hand, and the identified chemicals, materials, and processes were loaded into a spreadsheet data base for additional analysis. The Environmental Protection Agency EPA 17 chemical list, and lists of ozone depleting chemicals (ODC's) were used as criteria to identify, for minimization, reduction, or elimination from use on the F-5, a hazardous material (hazmat) subset of those chemicals and materials which had already been identified. The identified hazmat substances were then 'rolled-up' into an F-5 Pollution Prevention Management Plan. Program management use and implementation of the information set out in such a plan were also described. Recommendations for additional research and development, and for required tools were included. Finally, actual examples of all of the material created were attached to the document. DTIC

N94-25760# Technische Univ., Delft (Netherlands). Faculty of Technical Mathematics and Informatics.
SELFSIMILAR SOLUTIONS OF A NONLINEAR TRANSPORT EQUATION
Mark A. Peletier 1993 38 p
(ISSN 0922-5641)
(Rept-93-42; ETN-94-95397) Copyright Avail: CASI HC A03/MF A01

The contamination of the soil with hazardous chemicals which affect people's health is investigated. The contamination may be direct, by diffusion, or indirect, by polluting the ground water and the water supply. Knowledge concerning the propagation of these chemicals is of great importance. The following situation is considered: water, where chemicals are dissolved, is injected into the soil; the injection of water induces a flow field; the chemicals undergo various reactions with the soil particles; and the adsorption reaction is assumed very fast in comparison to the ground water flow. Concentration equations are given, and the concentration profile near the well is obtained. ESA

N94-25789# Brown Univ., Providence, RI.
SENSITIVITY OF CLIMATE MODELS: COMPARISON OF SIMULATED AND OBSERVED PATTERNS FOR PAST CLIMATES
J. Kutzbach, R. J. Oglesby, W. L. Prell, and T. Webb, III Aug. 1993 17 p
(Contract DE-FG02-85ER-60304)
(DE93-019934; DOE/ER-60304/9) Avail: CASI HC A03/MF A01

Predicting the potential climatic effects of increased concentrations of atmospheric carbon dioxide requires the continuing development of climate models. Confidence in the predictions will be much enhanced once the models are thoroughly tested in terms of their ability to simulate climates that differ significantly from today's climate. During the past several years, the authors have used paleoclimatic data to test the accuracy of the NCAR CCM0 (National Center for Atmospheric Research, Community Climate Model, Version 0), after changing its boundary conditions to those appropriate for past climates. Research has shown that comparing the model results with the data is an evolutionary process, because the models, the data, and the methods for comparison are continually being improved. From 1991 to 1993 the authors have completed new modeling experiments, further analyzed previous model experiments, updated existing sets of paleoclimatic data, made new comparisons between data and model results, and participated in workshops on paleoclimatic modeling. DOE

N94-25790# California Univ., Davis.
METHANE EMISSIONS FROM NATURAL WETLANDS
J. L. Meyer (Georgia Univ., Athens.) and R. A. Burke, Jr. (Environmental Protection Agency, Athens, GA.) 1993 19 p
(Contract DE-FC03-90ER-61010)
(DE93-040796; DOE/ER-61010/T10) Avail: CASI HC A03/MF A01

Analyses of air trapped in polar ice cores, in conjunction with recent atmospheric measurements, indicate that the atmospheric methane concentration increased by about 250% during the past two or three hundred years. Because methane is a potent 'greenhouse' gas, the increasing concentrations are expected to contribute to global warming. The timing of the methane increase suggests that it is related to the rapid growth of the human population and associated industrialization and agricultural development. The specific causes of the atmospheric methane concentration increase are not well known, but may relate to either increases in methane sources, decreases in the strengths of the sinks, or both. DOE

N94-25809# National Defence Research Establishment, Umea (Sweden). Dept. of NBC Defence.
EVALUATION OF A CANADIAN MINITUBE AIR SAMPLING SYSTEM [UTVAERDERING AV KANADENSISK UTRUSTNING FOER PROVTAGNING OCH ANALYS AV ORGANISKA LUFTFOERORENINGAR]
Lars Rittfeldt Feb. 1993 25 p In SWAHILI
(ISSN 0347-2124)
(FOA-C-40307-4.6; ETN-94-95283) Avail: CASI HC A03/MF A01

The evaluation of a 'Minitube air sampling system' is described. The system is designed for automatic low level measurements of organic substances in air. It makes use of cassettes with fifty 'Tenax Minitubes' for the sampling and analysis. The performance of the system was tested and evaluated. The results indicate that most volatile organic substances can easily be analyzed down to the ppb level. At lower concentrations measures must be taken to eliminate the contamination of the Tenax tubes that occurs due to passive sampling (the tubes have open ends and are not completely sealed). ESA

N94-25927# Atmospheric and Environmental Research, Inc., Cambridge, MA.
ASSESSING THE CLIMATIC EFFECT OF CARBON DIOXIDE AND OTHER TRACE GASES USING AN INTERACTIVE TWO-DIMENSIONAL CLIMATE-CHEMISTRY MODEL
M. K. W. Ko, G. I. Molnar, and Shun-Tai Zhou 1993 13 p
(Contract DE-FG02-86ER-60485)
(DE94-001741; DOE/ER-60485/5) Avail: CASI HC A03/MF A01

This report covers work on grant DE-FG02-86ER60485 and consists of two parts: progress for the period 1 Dec. 1992 - 31 May 1993 and the work plan for the remaining period 1 Jun. - 30 Nov. 1993. The project includes four tasks, two of which are addressed in the first project year: model interface and climate sensitivity. DOE

N94-25948# Pacific Northwest Lab., Richland, WA.
IMPLICATIONS OF POLICIES AND PREVENT CLIMATE CHANGE FOR FUTURE FOOD SECURITY
N. J. Rosenberg and M. J. Scott Jul. 1993 49 p Presented at the North Atlantic Treaty Organization Advanced Study Workshop on Climate Change and World Food Security, Oxford, England, 11-16 Jul. 1993
(Contract DE-AC06-76RL-01830)
(DE93-018872; PNL-SA-22762; CONF-9307134-1) Avail: CASI HC A03/MF A01

Measures to reduce the use of fossil fuels, suppression of on-farm emissions of methane (CH4) and nitrous oxide (N2O), afforestation, and geoengineering 'fixes' have been proposed to mitigate or eliminate greenhouse-forced climate change. These measures will impact agriculture and other sectors of the economy. this report discusses the above impacts. DOE

N94-26026# Colorado State Univ., Fort Collins.
GRASSLAND/ATMOSPHERE RESPONSE TO CHANGING CLIMATE: COUPLING REGIONAL AND LOCAL SCALES
M. B. Coughenour, T. G. F. Kittel, R. A. Pielke, and J. Eastman Oct. 1993 63 p
(Contract DE-FG02-90ER-60932)
(DE94-003111; DOE/ER-60932/3) Avail: CASI HC A04/MF A01

The objectives of the study were: to evaluate the response of grassland ecosystems to atmospheric change at regional and site scales, and to develop multiscaled modeling systems to relate ecological and atmospheric models with different spatial and temporal resolutions. A menu-driven shell was developed to facilitate use of models at different temporal scales and to facilitate exchange information between models at different temporal scales. A detailed ecosystem model predicted that C3 temperate grasslands wig respond more strongly to elevated CO2 than temperate C4 grasslands in the short-term while a large positive N-PP response was predicted for a C4 Kenyan grassland. Long-term climate change scenarios produced either decreases or increases in Colorado plant productivity (NPP) depending on rainfall, but uniform increases in N-PP were predicted in Kenya. Elevated CO2 is likely to have little effect on ecosystem carbon storage in Colorado while it will increase carbon storage in Kenya. A synoptic climate classification processor (SCP) was developed to evaluate results of GCM climate sensitivity experiments. Roughly 80% agreement was achieved with manual classifications. Comparison of 1x and 2xCO2 GCM Simulations revealed relatively small differences. DOE

N94-26077# Columbia Univ., New York, NY.
THE IMPACT OF RECENT MODEL IMPROVEMENTS ON GISS GCM PREDICTIONS OF CLIMATE CHANGE Annual Report, 15 Sep. 1992 - 14 Sep. 1993
L. M. Druyan May 1993 4 p
(Contract DE-FG02-92ER-61477)
(DE93-019458; DOE/ER-61477/1) Avail: CASI HC A01/MF A01

Multiple year simulations of the GISS GCM at 4 x 5 deg resolution were made for the standard Model 2 and also for alternative versions of the GCM which incorporate new formulations of the planetary boundary layer (PBL), the moist convection, ground hydrology, and C-grid numerics. Five-year Jan. and Jul. mean fields from each simulation, representing each version's basic climatology, each showed certain improvements when compared to analyses based on observed data and to each other. DOE

N94-26123# Oak Ridge National Lab., TN.
ENVIRONMENTAL BENEFITS OF DIFFERENT TYPES OF HEAT PUMPS, AVAILABLE AND EXPECTED
P. J. Hughes 1993 29 p Presented at the 2nd International Conference on Heat Pumps in Cold Climates, Moncton, New Brunswick, 16-17 Aug. 1993
(Contract DE-AC05-84OR-21400)
(DE94-002440; CONF-9308189-1) Avail: CASI HC A03/MF A01

A brief overview of integrated resource planning (IRP) is provided, with emphasis on how stakeholders interact within the process and where the opportunities may lie for heat pump advocates in cold climates. Five heat pump options that represent various approaches for improving heat pump cold weather performance are included here in a comparative analysis: 2-speed electric air source heat pumps, variable-speed electric air source heat pumps, electric ground-source heat pumps, natural gas engine-driven heat pumps, and natural gas absorption heat pumps. The comparative analysis addresses seasonal performance, seasonal peak demand, air pollutant emissions, customer energy costs, and recognition of environmental externalities in IRP, all in the context of a residential application in the Great Lakes region of the U.S. Several actions that may be in the interest of heat pump stakeholders in cold climates were identified: development of improved software for utility planners, advocacy of a practical form of the Societal Test for use in IRP that credits heat pumps for the residential air pollutant emissions that they avoid, and development of practical methods to credit heat pumps with other environmental benefits for which they may be responsible. DOE

N94-26163 United Nations Environment Programme, Nairobi (Kenya). Global Environment Monitoring System.
MEETING OF THE EIGHTH SESSION OF THE SCIENTIFIC ADVISORY COMMITTEE OF THE WORLD CLIMATE IMPACT ASSESSMENT AND RESPONSE STRATEGIES PROGRAMME
Mar. 1992 29 p Meeting held in Budapest, Hungary, 1 Oct. 1991
Limited Reproducibility: More than 20% of this document may be affected by microfiche quality
(DE93-633954; INIS-MF-13601; CONF-9110503) Avail: CASI HC A03 (US Sales Only)

The World Climate Data and Monitoring Program continued its help in improving climate data management. The World Climate Applications and Services Program has developed an inventory of climate application related activities in WMO member countries. Other developments have been the encouragement of national climate program development and projects related to mitigation of drought. The World Climate Research Program is organized through seven main projects: Climate model development; Research on climate processes; Global Energy and Water Cycle Experiments (GEWEX); Tropical Ocean and Global Atmosphere (TOGA); World Ocean Circulation Experiment (WOCE); Study of global change; Scientific exploration of satellite data, in particular in the areas of clouds and the hydrological cycle, transport of greenhouse gases and their distribution in the atmosphere, global ocean circulation and transport of heat and chemicals, polar climate and sea ice, surface hydrological processes and their relation to vegetation. The World Climate Impact Studies Program (WCIP) in 1990/91 was structured to give to: (1) Greenhouse Gases/Climate Change; (2) Coordination of Climate Impact Activities; (3) Methods of Climate Impact Assessment; and (4) Monitoring of erosion, flooding, desertification and high urban atmospheric pollution. DOE

N94-26216# Center for Mathematics and Computer Science, Amsterdam (Netherlands). Dept. of Numerical Mathematics.
A POSITIVE FINITE-DIFFERENCE ADVECTION SCHEME APPLIED ON LOCALLY REFINED GRIDS
W. H. Hundsdorfer, B. Koren, M. vanLoon, and J. G. Verwer Apr. 1993 31 p Submitted for publication Sponsored by Rijksinst. voor Volksgezondheid en Milieuhygiene, Bilthoven, Netherlands
(ISSN 0169-0388)
(CWI-NM-R9309; ETN-94-95413) Copyright Avail: CASI HC A03/MF A01

A class of explicit finite difference advection schemes derived along the method of lines is examined. An important problem field is large scale atmospheric transport, and therefore focus is on the demand of positivity and on the use of locally refined grids. For the spatial discretization, attention is confined to directionally split schemes in conservation form using five points per direction. The fourth order central scheme and the family of k-schemes comprising the second order central, the second order upwind, and the third order upwind biased discretization are studied. Positivity is enforced through flux limiting. The limited third order upwind discretization is concluded to be the best candidate from the four examined. For the time integration, attention is confined to a number of explicit Runge-Kutta methods of orders two up to four. With regard to the demand of positivity, these integration methods turn out to behave almost equally and no best method could be identified. For solutions with steep gradients, a local uniform grid refinement technique is proposed as an effective tool to speed up computations. ESA

N94-26241# Kauppa-ja Teollisuusministerio, Helsinki (Finland).
SIHTI 2: ENERGY AND ENVIRONMENTAL TECHNOLOGY
K. Saviharju and A. Johansson 1993 47 p
(DE94-702061; KTM/E-B-134) Avail: CASI HC A03/MF A01

The program is divided into system and technology parts. The aim of system studies is to determine, on the basis of life cycle analyses, long-term environmental / technological aims for various fields (energy, industry) and to find out an optimum strategy for reaching these aims. The analysis will give data on emission reduction costs and on fields where technical improvements are required, and will determine the limits set by environmental factors for future technical development. Environmental impacts will be discussed from national and economic viewpoints. Technological development is dependent on new ideas. The aim is to indicate possibilities for reducing emissions from energy use of peat and wood, for low-emission production at least in one industrial field (wood-processing industry), to establish emission measuring and control methods, to indicate utilization alternatives for solid matter separated at power plants, and to find out operable alternatives for the energy use of wastes. Other ventures of significance will also be financed: survey of 'new' emissions and development of their measuring and purification methods. The field of the program will be divided into synergic sub-fields: systematics of emission chains, fields of operation (energy and environment problems in the wood-processing industries), development of flue gas purification technology, measuring and control technology, by-products of power plants, emissions from peat production, etc. DOE

N94-26419# California Univ., Berkeley. Lawrence Berkeley Lab.
A CONCEPTUAL FRAMEWORK FOR THE EVALUATION OF COST-EFFECTIVENESS OF PROJECTS TO REDUCE GHG EMISSIONS AND SEQUESTER CARBON
J. Sathaye, R. Norgaard, and W. Makundi Jul. 1993 29 p
(Contract DE-AC03-76SF-00098)
(DE93-040448; LBL-33859) Avail: CASI HC A03/MF A01

This paper proposes a conceptual framework for evaluating the cost of projects to reduce atmospheric greenhouse gases (GHG's). The evaluation of cost-effectiveness should account for both the timing of carbon emissions and the damage caused by the atmospheric stock of carbon. We develop a conceptual basis to estimate the cost-effectiveness of projects in terms of the cost of reducing atmospheric carbon (CRAC) and other GHG's. CRAC accounts for the economic discount rate, alternative functional forms of the shadow price, the residence period of carbon in the atmosphere, and the multiple monetary benefits of projects. The last item is of particular importance to the developing countries. DOE

N94-26474# National Inst. for Resources and Environment, Ibaraki (Japan).
AN OBSERVATIONAL STUDY OF AIR POLLUTION TRANSPORT OVER A LARGE URBAN COMPLEX [DAITOSHIIKI JOKU NI OKERU OSEN BUSSHITSU YUSO NO KANSOKUTEKI KENKUY]
Hiroshi Yoshikado, Tateki Mizuno, Hiroaki Kondo, Koji Kitabayashi, Shigeo Shimogata, and Susumu Yamamoto 28 May 1993 139 p In JAPANESE
(ISSN 0926-9989)
(Rept-6; ETN-94-80513) Avail: CASI HC A07/MF A02

A series of intensive wide range observations of local meteorology and air pollution was carried out during six years from 1986 to 1991 in the western portion of the Kanto Plain, including the Tokyo metropolitan area. The following two important meteorological structures closely related with the air pollution in large urban areas were clarified: (1) local wind system characteristics in summer; and (2) air stagnation frequently occurring in early winter. The following subjects are discussed: (1) the significance of the present research from the historical point of view and in the current field of research of air pollution forecasting and assessment; (2) introduction of data obtained and the general description of weather conditions during each observation periods of 1986 through 1991; (3) analysis of the vertical structure of the sea breeze which penetrates inland from Tokyo Bay; and (4) analysis of the meteorological conditions which are concerned with the very high level of pollutants frequently occurring in early winter in the Tokyo area. Author (NASDA)

N94-26670 York Univ. (Ontario). Dept. of Physics.
A THREE-DIMENSIONAL CHEMICAL TRANSPORT MODEL STUDY OF THE 1991 ANTARCTIC OZONE HOLE USING OBJECTIVELY ANALYSED DATA M.S. Thesis
John Wade Sandilands Jul. 1993 179 p
(ISBN-0-315-84250-4; CTN-94-61030) Copyright Avail: Micromedia Ltd., Technical Information Centre, 240 Catherine Street, Suite 305, Ottawa, Ontario, K2P 2G8, Canada HC/MF

The development of the ozone hole over the Antarctic was investigated using a three dimensional spectral chemical transport model at R-15 resolution for the period of September 15 to October 15, 1991. The model is driven by objectively analyzed wind fields and uses the chemical module developed by Kaminski (1993), which contains simplified stratospheric chemistry. A rudimentary temperature flag is also included to initiate the heterogeneous reactions essential to large ozone reductions during the austral spring. Initial chemical conditions are based on the two-dimensional fields of Garcia and Solomon (1983). Four model experiments that involve varying the temperature flags for the heterogeneous chemistry and altering some of the model's dynamical and chemical code all show that, although extensive processing of NO(y) and Cl(x) occurs within the model, the ozone hole that develops appears shallow and ephemeral. Analysis of components of the equation governing the model's evolution indicates that meridional ozone transport suffices to overwhelm the substantial chemical depletion that does occur. It is concluded that the objectively analyzed data improperly represent the dynamical conditions of the southern polar region and are unable to capture the essential isolated nature of the vortex. CISTI

N94-26757# Environmental Protection Agency, Research Triangle Park, NC.
COMPILATION OF AIR POLLUTANT EMISSION FACTORS. VOLUME 1: STATIONARY POINT AND AREA SOURCES. SUPPLEMENT F

Jul. 1993 630 p See also Supplement E
(PB94-121431; AP-42-Suppl-F) Avail: CASI HC A99/MF A06

The following are covered: external combustion sources, solid waste disposal, stationary internal combustion sources, evaporation loss sources, chemical process industry, food and agricultural industry, metallurgical industry, mineral products industry, petroleum industry, wood products industry, miscellaneous sources, and storage of organic liquids. NTIS

N94-26774# Center for Mathematics and Computer Science, Amsterdam (Netherlands). Dept. of Numerical Mathematics.

A ROBUST UPWIND DISCRETIZATION METHOD FOR ADVECTION, DIFFUSION AND SOURCE TERMS

Barry Koren Apr. 1993 24 p Submitted for publication
(ISSN 0169-0388)
(CWI-NM-R9308; ETN-94-9512) Avail: CASI HC A03/MF A01

A finite volume discretrization for advection diffusion equations with source term is described and applied. The complete space discretization is second to third order accurate and monotone. Good accuracy and monotonicity are guaranteed by an appropriate limiter function in the upwind advection operator. The discretization of diffusion is standard, second order central. For source terms, an evaluation is proposed which is consistent with that of the advection terms. It leads to improved accuracy, as well as to improved residual convergence for steady problems. The complete space discretization works well for both smooth and non smooth problems. This good robustness is considered to be the method's main property. Except for two novelties (the limiter function and the source term evaluation), the space discretization is standard and well proven in for example aircraft aerodynamics computations. In air pollution transport computations it is not. It is thought that it can be successfully applied in the latter field as well. ESA

N94-26817# Virginia Polytechnic Inst. and State Univ., Blacksburg. Center for Environmental and Hazardous Materials Studies.

MEASURING VARIATION IN ECOSYSTEM SENSITIVITY TO STRESS Annual Technical Report, Oct. 1992 - Nov. 1993

John Cairns, Jr., Paul V. McCormick, Matthew E. Arnegard, and Eric P. Smith 29 Nov. 1993 84 p
(Grant AF-AFOSR-0379-91)
(AD-A274232; AFOSR-93-0905TR) Avail: CASI HC A05/MF A01

This report presents the results of field studies which were designed to investigate the variability in periphyton sensitivity to stress. Chlorine and sulfuric acid were experimentally delivered to periphyton communities using chemical-diffusing substrates. Significant variations in chlorine sensitivity among ecosystems were generally not explained by differences in water quality characteristics, but may be related to differences in the inherent tolerance of algal taxa to chlorine exposure. Periphyton community biomass and oxygen consumption did not respond to decreases in pH as low as pH=3; taxonomic responses to this manipulation are still being analyzed. The report also describes a study of stress induced tolerance of periphyton communities to novel copper stress using chemical diffusers. DTIC

N94-26843# Pennsylvania State Univ., University Park. Dept. of Mechnical Engineering.

NUMERICAL ANALYSIS OF THE PHOTO-DISSOCIATION/RADICAL OXIDATION OF FORMALDEHYDE BY ULTRAVIOLET LIGHT IN A PHOTOLYTIC REACTOR M.S. Thesis

Robert O. Fetter Dec. 1993 73 p
(AD-A274539) Avail: CASI HC A04/MF A01

The release of volatile organic compounds (VOC's) into the atmosphere has come under fire by the Environmental Protection Agency (EPA) and state regulatory agencies in the past several years. These releases come from a wide variety of sources from gasoline filling stations to industrial and military operations. A new pollution control technology currently under development utilizes ultraviolet (UV) light to break down the volatile organic compounds (VOC's) contained in an airstream. One pollution control equipment manufacturer has already employed this method in an installation in California. DTIC

N94-26888# Naval Research Lab., Monterey, CA.

LEADEX ENVIRONMENTAL PHENOMENA AND EFFECTS OBSERVED BY DMSP, NOAA, AND ERS-1 SATELLITES Final Report, 25 Mar. - 24 Apr. 1992

Robert W. Fett Nov. 1993 106 p
(Contract N00014-92-C-6018)
(AD-A274596; NRL/PU/7530-93-0008) Avail: CASI HC A06/MF A02

This report examines notable atmospheric and cryospheric conditions observed by satellites over the Beaufort Sea region surrounding the Leadex ice camp position. DMSP and NOAA direct readout high resolution data include visible and infrared scenes in a variety of discrete channels. The special sensor microwave imager (SSM/I) data of DMSP and the synthetic aperture radar (SAR) data of the European ERS-1 satellite are of special interest and value in evaluating changes in ice appearance and configuration noted during the period of Leadex from 25 March to 24 April 1992. Multi-channel comparisons of the various data types over the same location and correlation with available ground truth data yield significant insights into the nature and state of the phenomena observed. DTIC

N94-26904# New Energy and Industrial Technology Development Organization, Tokyo (Japan).

FEASIBILITY STUDY ON CONSTRUCTION OF A GLOBAL ENVIRONMENT RESEARCH AND DEVELOPMENT INFORMATION NETWORK

Mar. 1993 193 p In ENGLISH and JAPANESE
(DE94-725198; ETDE/JP-mf-94725198) Avail: CASI HC A09/MF A03

Investigations are made for effective connection of a greenhouse gas technology information exchange system (Green-TIE) plan with a technology transfer scheme by the Asia Pacific Economic Cooperation Organization. Information in the energy/environmental field has not been used very effectively, or the personnel network has not yet been formed in the local area. Technology information on the Green-TIE plan has already been demonstrated and is greatly needed in developing countries in terms of liability, cost, and access method. In providing policy information as the other value-added service, it is mainly administrative organizations that provide policy information on technology already demonstrated. As to support of technology information exchange which is original to developing countries, construction of the developing country information source database is supported by cooperation with administrative organization. Direct technology transfer support is realized by heightening adjusting function of the joint project in liaison with each country. It is necessary for Japan to cooperate in promotion and arrangement of the system so as to make these international technology information networks useful. DOE

N94-26952# Argonne National Lab., IL.

ADVANCES IN PASSIVE-REMOTE AND EXTRACTIVE FOURIER TRANSFORM INFRARED SPECTROSCOPIC SYSTEMS

J. C. Demirgian, C. Hammer, E. Hwang, and Zhuo-Xiong Mao 1993 11 p Presented at the Air and Waste Management Association's (AWMA) International Specialty Conference, Atlanta, GA, 11-14 Oct. 1993
(Contract W-31-109-eng-38)
(DE94-001424; ANL/CMT-ACL/CP-80970; CONF-9310197-1) Avail: CASI HC A03/MF A01

The Clean Air Act of 1990 requires the monitoring of air toxics including those from incinerator emissions. Continuous emission monitors (CEM) would demonstrate the safety of incinerators and address public concern about emissions of hazardous organic compounds. Fourier transform infrared (FTIR) spectroscopy can provide the technology for continuous emission monitoring of stacks. Stack effluent can be extracted and analyzed in less than one minute with conventional FTIR spectrometers. Passive-remote FTIR spectrometers can detect certain emission gases over 1 km away from a stack. The authors discuss advances in both extractive and passive-remote FTIR technology. Extractive systems are being tested with EPA protocols, which will soon replace periodic testing methods. Standard operating procedures for extractive systems are being developed and tested. Passive-remote FTIR spectrometers have the advantage of not requiring an extracted sample; however, they have less sensitivity. We have evaluated the ability of commercially available systems to detect fugitive plumes and to monitor carbon monoxide at a coal-fired power plant. DOE

N94-27200# Nederlands Inst. voor Onderzoek der Zee, Texel.

MACROBENTHIC FAUNA IN THE DUTCH SECTOR OF THE NORTH SEA IN 1991

G. C. A. Duineveld 1992 23 p
(PB94-126414; NIOZ-1992-6) Avail: CASI HC A03/MF A01

The present report describes and discusses the results of a macrobenthic survey made in spring 1991 in the Dutch Sector of the North Sea. The survey is meant to be a part of a long term biological monitoring program of the benthic fauna in the area, an initiative of the Tidal Water Division of Rijkswaterstaat (RWS). The common interest of the participants is to obtain an insight into the year-to-year variations of the macrobenthos and in the factors governing these fluctuations. The stations for the present survey were selected from current as well as previous benthic research programs in the area. One set of stations was provided by the Tidal Water Division. At these particular stations, ongoing measurements on water and sediment quality are being conducted in the framework of a chemical monitoring program, and, moreover, some of the stations were sampled for macrofauna on earlier occasions. NTIS

N94-27267# Lawrence Livermore National Lab., CA.
INITIAL ULTRAVIOLET-B INTENSITY DATA AT LAWRENCE LIVERMORE NATIONAL LABORATORY
Kenneth O. Patten, Jr., Donald J. Wuebbles, and Gerald J. Smith (New Zealand Inst. for Industrial Research and Development, Lower Hutt.) Oct. 1993 25 p
(Contract W-7405-eng-48)
(DE94-004279; UCRL-ID-115334) Avail: CASI HC A03/MF A01

A measurement of UV-B reaching the ground has been established at the Lawrence Livermore National Laboratory. The instrument is the same as those operated by the National Institute for Water and Atmospheric Research in their network in New Zealand. The wavelength response of the radiometer is similar to the response of human skin to UV-B. Intensity data are collected by averaging meter readings over 10 minutes from 6:00 am to 6:00 pm Pacific Standard Time, then converting to effective UV-B intensity normalized at 310 nm. This report checks the intensities obtained at LLNL from November 1992 to July 1993 against the expected results: increased solar zenith angle, whether from the daily cycle or from the yearly cycle in solar position, should decrease UV-B intensity at the ground due to increased optical path; and intervening cloud cover should decrease ground UV-B intensity. Three additional findings are reported here: maximum UV-B intensity on cloudless days does not always follow a smooth curve, but instead varies either high or low to some extent; morning UV-B intensities are less than those in the afternoon at comparable solar zenith angles at certain times of year; LLNL wintertime daily-averaged UV-B intensities are somewhat higher than those observed at Auckland, New Zealand in their winter of 1992. DOE

N94-27430*# Alabama Univ., Huntsville.
GLOBAL CHANGE RESEARCH RELATED TO THE EARTH'S ENERGY AND HYDROLOGIC CYCLE Report No. 1, 1 Sep. 1993 - 28 Feb. 1994
Donald J. Perkey 10 Mar. 1994 72 p
(Contract NCC8-22)
(NASA-CR-195270; NAS 1.26:195270) Avail: CASI HC A04/MF A01

The following are discussed: Geophysical Modeling and Processes; Land Surface Processes and Atmospheric Interactions; Remote Sensing Technology and Geophysical Retrievals; and Scientific Data Management and Visual Analysis. CASI

N94-27601# Pacific Northwest Lab., Richland, WA.
AN OVERVIEW OF THE ASCOT PROGRAM
J. C. Doran Sep. 1993 15 p Presented at the Topical Meeting on Environmental Transport and Dosimetry, Charleston, SC, 31 Aug. - 3 Sep. 1993
(Contract DE-AC06-76RL-01830)
(DE94-004356; PNL-SA-22351; CONF-930810-13) Avail: CASI HC A03/MF A01

ASCOT (Atmospheric Studies in Complex Terrain) is a multi-laboratory U.S. Department of Energy research program studying the properties of atmospheric boundary layers over non-uniform terrain and the interactions among various scales of motion that influence those properties. Within this context, one of the principal goals of the ASCOT program is to provide information necessary for an accurate description of transport and diffusion processes for atmosphere pollutants that may be released in regions of complex terrain. Three examples from past ASCOT research relevant to this goal are presented. Current and proposed research in the Front Range region of Colorado in the vicinity of the Rocky Flats Plant is also described. DOE

N94-27691# Oak Ridge National Lab., TN.
COASTAL ZONE MANAGEMENT ACT AND RELATED LEGISLATION, REVISION 3
15 Oct. 1993 135 p
(Contract DE-AC05-84OR-21400)
(DE94-004180; ORNL/M-3027-Rev-3) Avail: CASI HC A07/MF A02

In recognition of the increasing pressures upon the nation's coastal resources, Congress enacted the Coastal Zone Management Act in 1972. Its purpose is to encourage states to preserve, protect, develop, and, where possible, restore or enhance such valuable natural resources as wetlands, floodplains, estuaries, beaches, dunes, barrier islands, and coral reefs, as well as the fish and wildlife utilizing those habitats. A unique feature of the act is that participation by states is voluntary. One key provision for encouraging states to participate is the availability of federal financial assistance to any coastal state or territory, including those on the Great Lakes, which is willing to develop and implement a comprehensive coastal management program. Additionally, the Coastal Barrier Resources Act (CBRA) was passed in 1983. This report contains the legislative history and statutes associated with each act. Regulations for implementation and other guidance are included. DOE

N94-27958*# National Aeronautics and Space Administration, Washington, DC.
MISSION TO PLANET EARTH: A PROGRAM TO UNDERSTAND GLOBAL ENVIRONMENTAL CHANGE
Feb. 1994 11 p
(NASA-PAM-556; NAS 1.75:556) Avail: CASI HC A03/MF A01

A description of Mission to Planet Earth, a program to understand global environmental change, is presented. Topics discussed include: changes in the environment; global warming; ozone depletion; deforestation; and NASA's role in global change research. CASI

N94-28147# National Inst. for Resources and Environment, Ibaraki (Japan).
JOURNAL OF NIRE, VOLUME 2, NUMBER 4 [SHIGEN TO KANKYO, VOLUME 2, NUMBER 4]
Takeshi Usami, ed., Yoshihiro Ogisu, ed., Masahiro Saito, ed., Nobuo Kido, ed., Koichi Mizuno, ed., Akira Miyazaki, ed., Hiroaki Kondo, ed., Yoshio Yamada, ed., Mikio Kobayashi, ed., and Katsuya Tsurusaki, ed. et al 26 Jul. 1993 97 p In JAPANESE
(ISSN 0916-9997)
(JTN-94-80554) Avail: CASI HC A05/MF A02

The following topics were discussed: earth environments, environmental monitoring, environmental protection, water quality, quality regulation, organic compounds, waste disposal, waste treatment, waste utilization, oxidation, bioconversion, microorganisms, bacteria, coastal water, coastal sediments, sulfate reduction inhibition, p-chlorophenol, microanalysis, lead compounds, GC (Gas Chromatography), MS (Mass Spectroscopy), lead isotope abundance, international cooperation, buckwheat stillage, oils, percussive rock excavation, water jet, slot, pre-stress analysis, DRA (Deformation Rate Analysis), numerical simulation, free turbulent shear flow, jet flow, rotational flow, TF (Two Fluid) models, ML (Mixing Length) models, and k-epsilon models. For individual titles, see N94-28148 through N94-28157.

N94-28148# National Inst. for Resources and Environment, Ibaraki (Japan). Hydrospheric Environmental Protection Dept.
RECENT LEGAL MOVEMENT ON WATER QUALITY REGULATION IN JAPAN [WAGA KUNI NI OKERU SUISHITSU KISEI NO SAIKIN NO DOKO]
Masanao Hirai *In its* Journal of NIRE, Volume 2, Number 4 26 Jul. 1993 p 1-9 In JAPANESE (For primary document see N94-28147 07-45)
Avail: CASI HC A02/MF A02

Various chemical substances have come to be detected in ambient water, following recent industrial activities and diversification of life style. Since quite a few of those substances are harmful to health, measures to assure the safety of water, such as drinking water, have been considered among various countries of which the industrialized countries take a leading part, and the new standards and the guiding principles were presented. With such international movements for a background, amendment of laws concerning preservation of the quality of ambient water and measures for such quality control are going to be practiced also in Japan. To begin with, water quality standards were drastically revised after 34 years, and they will be enforced in December 1993. Environmental standards have been reviewed as well, reflecting the changes in water quality standards, for the purpose of quality assurance of water for public use, which is, the fundamental source of waterworks. A total of 15 new items such as organic chlorides and pesticides have been added to be regulated in the environmental standards. Requisites for lead and arsenic became more strict. 'Audit items' were established for water quality maintenance. In addition to these revisions and amendments, a new environmental standard will be set on a basis of quantitative relations between nitrogen/phosphorus concentration and water quality index. Author (NASDA)

N94-28149# National Inst. for Resources and Environment, Ibaraki (Japan). Advanced Water Treatment Div.

COLLABORATION OF CHEMICAL OXIDATION AND BIOLOGICAL TREATMENT FOR REMOVAL OF REFRACTORY ORGANIC SUBSTANCES [NAN BUNKAISEI YUGAI YUKI KAGAKU BUSSHITSU NO KAGAKU SANKA TO SEIBUTSU SHORI NO HEIYO NI YORU SHORI]

Hiroyasu Ichikawa, Shinji Wada, and Kenji Tatsumi *In its* Journal of NIRE, Volume 2, Number 4 26 Jul. 1993 p 11-2 In JAPANESE (For primary document see N94-28147 07-45)

Avail: CASI HC A02/MF A02

Various refractory organic substances such as aromatic chloro and nitro compounds are present at significant concentrations in wastewater from organic chemical industries. These chemicals are hardly removed by the activated sludge method and are discharged into the environment where they remain since they are hard to decompose by microorganisms and inhibit microorganism activity. The accumulation of these chemicals in the environment pollutes and destroys the ecosystem. To remove refractory substances in wastewater from the chemical industry, it is necessary to establish a chemical oxidation and biological treatment to be used in combination. For this purpose, the oxidative decomposition of refractory chemicals and biodegradability of the reaction products were studied. This report gives an outline of the treatment of refractory organic substances with combined use of chemical oxidation and biological treatment. Author (NASDA)

N94-28150# National Inst. for Resources and Environment, Ibaraki (Japan). Ecological Chemistry and Microbiology Div.

EFFECTS OF p-CHLOROPHENOL ON SULFATE REDUCTION IN MARINE SEDIMENTS [ENGAN KAIYO TAISEKIBUTSUCHU NO RYUSAN KANGEN KASSEI NI OYOBOSU PARAKUROROFENORU NO EIKYO]

Manabu Fukui, Junln Suh (Shimane Univ., Matsue, Japan.), Yoshitaka Yonezawa, and Yoshikuni Urushigawa *In its* Journal of NIRE, Volume 2, Number 4 26 Jul. 1993 p 21-2 In JAPANESE (For primary document see N94-28147 07-45)

Avail: CASI HC A02/MF A02

The effects of p-chlorophenol (concentration; zero, 10, 100, 500, and 1,000 micro-M) on bacterial sulfate reduction were examined in three coastal sediments of Ise Bay, Japan. Sulfate reduction rate (13 nmol per ml day) at A3 point (34 deg 59 min 00 sec N, 136 deg 44 min 05 sec E, water depth, 20.5 m) was similar to that at E3 point (34 deg 51 min 55 sec N, 136 deg 44 min 20 sec E, water depth, 36 m) and higher than that at B1 point (34 deg 56 min 50 sec N, 136 deg 40 min 30 sec E, water depth, 16 m). At A3 point, sulfate reduction rates were stimulated by p-chlorophenol up to 100 micro-M, but inhibited at 500 and 1,000 micro-M. At E3 point, p-chlorophenol did not affect sulfate reduction rates up to 500 micro-M and inhibited slightly the activity at 1,000 micro-M. p-Chlorophenol stimulated sulfate reduction at B1 point up to 1,000 micro-M. Sulfate-reducing bacteria would, thus, appear to utilize low concentrations of p-chlorophenol as a substrate in coastal sediment. Author (NASDA)

N94-28151# National Inst. for Resources and Environment, Ibaraki (Japan). Advanced Water Treatment Div.

TREATMENT OF REFRACTORY ORGANIC SUBSTANCES WITH COMBINED USE OF CHEMICAL OXIDATION AND BIOLOGICAL TREATMENT. PART 2: BIODEGRADABILITY OF OZONATION PRODUCTS OF CHLOROPHENOL [KAGAKU SANKA TO SEIBUTSU SHORI NO HEIYO NI YORU NANBUNKAISEI YUKI KAGAKU BUSSHITSU NO SHORI. DAI 2 HO: KUROROFENORU NO OZON SANKABUTSU NO SEIBUNKAISEI]

Hiroyasu Ichikawa, Shinji Wada, and Kenji Tatsumi *In its* Journal of NIRE, Volume 2, Number 4 26 Jul. 1993 p 29-3 In JAPANESE (For primary document see N94-28147 07-45)

Avail: CASI HC A02/MF A02

To remove refractory substances in wastewater from the chemical industry, it is necessary to establish a chemical oxidation and biological treatment to be used in combination. For this purpose, the oxidative decomposition of refractory chemicals and biodegradability of the reaction products were studied. The solution of p-chlorophenol and 2,4-dichlorophenol were ozonated in the ozone concentration range, 24.2 to 26.5 mg/l. Chlorophenols were rapidly reduced and after 45 - 60 minutes ozonation could no longer be detected. However, Dissolved Organic Carbon (DOC) was only reduced to about 50 percent even after 120 minutes ozonation. Ozonation of chlorophenols led to the formation of oxalic and formic acids as major products and small amounts of acetic acid. A mixture of the ozonated solution with non-acclimated sludge culture was incubated for four days at 25 C, and the biodegradability was evaluated using DOC reduction. DOC of chlorophenols was hardly reduced even after a four-day incubation, indicating little biodegradability. For the ozonation solution of p-chlorophenol in which most of them was decomposed, DOC removal of more than 80 percent was attained and DOC in the solution was less than 10 ppm. Author (NASDA)

N94-28152# National Inst. for Resources and Environment, Ibaraki (Japan). Water Analysis Div.

DETERMINATION OF LEAD ISOTOPE RATIOS IN SEAWATER BY PURGE AND TRAP GC/MS AFTER ETHYLATION [PAJI ANDO TORAPPU GC/MS NI YORU BIRYO NAMARI NO DOITAIHI BUNSEKI]

Takashi Imagawa, Hiroaki Tao, and Akira Miyazaki *In its* Journal of NIRE, Volume 2, Number 4 26 Jul. 1993 p 37-4 In JAPANESE (For primary document see N94-28147 07-45)

Avail: CASI HC A02/MF A02

A 1-ml portion of sodium tetraethylborate was added to sample water and heated from room temperature to 100 C to convert inorganic lead to tetraethyllead. Tetraethyllead was purged by helium for 18 min at a flow rate of 15 ml/min and trapped on fused silica tube cooled at -10 C. The tube was heated rapidly to 220 C and the tetraethyllead was introduced to ion source of GC (Gas Chromatography)/MS (Mass Spectroscopy). Ion intensities of Pb(C2H5)3(+) were measured at m/z from 291 to 295. The effects of fragment ions and C-13 containing ions were corrected by calculation to obtain the isotopic ratios of Pb-204, 206, 207 and 208. The isotopic ratio of NIST (National Institute of Standards and Technology) SRM (Standard Reference Materials) 81 and 82, measured by the present method agreed with the certified value within one percent. By this method, it was possible to determine the isotopic ratio of lead in a seawater sample whose concentration was 0.1 ppb. The effect of the blank and other causes of systematic errors should be removed to obtain more accurate results required in the case of discussing the differences in environmental samples. Author (NASDA)

N94-28153# National Inst. for Resources and Environment, Ibaraki (Japan).

ENVIRONMENTAL MANAGEMENT AND AUDIT [KANKYO KANRI - KANSA NI TSUITE]

Tateki Mizuno *In its* Journal of NIRE, Volume 2, Number 4 26 Jul. 1993 p 45-5 In JAPANESE (For primary document see N94-28147 07-45)

Avail: CASI HC A02/MF A02

Environmental audit which started in the late 80's has recently been introduced to Japan. Although Japan has been a leading country in environmental pollution prevention, its environmental management has been just a risk management dealing with only a part of the whole issue, not covering global environmental problems. In Europe and the United States, where the controls of governments are not so strong, environmental management does not penetrate private companies very much. Under these circumstances, European countries started introducing environmental audit to companies, and Japan is expected to keep pace with them. ISO (International Standarization Organization) and IEC (International Electrotechnical Commission) have been considering international standardization of environmental management and audit, and established a devoted technical committee. Such ISO standards may be incorporated with JIS (Japanese Industrial Standards) in Japan. IEC proposes to conduct both internal audit (audit by a third party within a company) and external audit (audit by a third party outside a company), whereas ICC (International Chamber of Commerce) as well as ILO (International Labor Organization), UNEP (United Nations Environment Program), WHO (World Health Organization), and OECD (Organization for Economic Cooperation and Development) propose only internal audits. Author (NASDA)

N94-28154# National Inst. for Resources and Environment, Ibaraki (Japan). Biomass Div.

OIL PRODUCTION FROM BUCKWHEAT STILLAGE BY THERMOCHEMICAL LIQUEFACTION [NETSU KAGAKU HANNO NI YORU SOBAJOCHU ZANSA KARA NO OIRU NO SEIZO]

Tomoaki Minowa, Yutaka Dote, Tomoko Ogi, and Shinya Yokoyama *In its* Journal of NIRE, Volume 2, Number 4 26 Jul. 1993 p 53-6 In JAPANESE (For primary document see N94-28147 07-45)

Avail: CASI HC A02/MF A02

Stillage from the ethanol fermentation of buckwheat was converted directly into oil by thermochemical liquefaction for the recovery of energy in the form of liquid fuel. The stillage with moisture content of 83 weight percent was heated under pressurized nitrogen at reaction temperature of 200 - 325 C and holding time of zero to 60 min with or without sodium carbonate as catalyst. Oil yield decreased by catalyst addition and increased with increasing reaction temperature. The oil yield obtained at holding time of 30 min had the highest value among the yield at zero to 60 min. The oil was obtained in the maximum yield of 58 percent on an organic basis at reaction temperature of 325 C, operating pressure of 15 MPa and holding time of 30 min without catalyst. This oil had a calorific value of 38.1 MJ/kg, viscosity of 320 mPa sec., carbon content of 74.1 percent, hydrogen content of 10.3 percent, oxygen content of .9 percent, and nitrogen content of 5.8 percent. These values satisfy the specification of No. 3-2 fuel oil in JIS (Japanese Industrial Standards). Buckwheat stillage is an ideal raw material of liquefaction in terms of oil yield and its properties, compared to sweet potato stillage, barley stillage, and rice stillage. The high crude fat content and low crude fiber content of buckwheat stillage may possibly be the reasons for its high oil yield. Author (NASDA)

N94-28155# National Inst. for Resources and Environment, Ibaraki (Japan). Mining System Engineering Div.

EFFECTS OF SLOT ON ROCK SURFACE FOR PERCUSSIVE ROCK EXCAVATION: WATER JET ASSISTED PERCUSSIVE ROCK EXCAVATION Report No. 1 [DAGEKI KUSSAKU NI OYOBOSU SESSAKUKO NO EIKYO: SUI FUNRYU HEIYO DAGEKI KUSSAKU GIJUTSU NI KANSURU KENKYU]

Keiji Hanada, Norio Yamakado (Japan Foundation Engineering Co. Ltd., Osaka.), Hirohide Hayamizu (Japan Foundation Engineering Co. Ltd., Osaka.), Masanobu Sanai (Japan Foundation Engineering Co. Ltd., Osaka.), and Masato Utsumi (Japan Foundation Engineering Co. Ltd., Osaka.) *In its* Journal of NIRE, Volume 2, Number 4 26 Jul. 1993 p 63-7 In JAPANESE (For primary document see N94-28147 07-45)

Avail: CASI HC A03/MF A02

To evaluate the effects of slot cut on rock surface for water jet assisted percussive rock excavation, a laboratory investigation was performed. The main results are summarized as follows: (1) slot cut on the rock surface is very effective for water jet assisted percussive rock excavation by hitting a certain point, though there is an effective distance between the slot and blow point; (2) empirical equations are proposed to express the relationship among weight of rock breakage, distance from the slot and depth of the slot, and that among width of rock breakage, distance from the slot and depth of the slot; and (3) an empirical equation expressing the relationship among maximum effective distance from the slot, depth of the slot, and blow energy is proposed. Author (NASDA)

N94-28156# National Inst. for Resources and Environment, Ibaraki (Japan). Fracture Mechanics and Explosives Div.

THE ESTIMATION OF PRE-STRESS BY DEFORMATION RATE ANALYSIS AND SUGGESTION OF A MECHANISM FROM THE ELAST-PLASTICAL THEORY [HENKEIRITSU HENKAHO NI YORU SHOKI CHIATSU NO SUITEI TO DANSOSEIGAKUTEKI ICHI KOSATSU]

Manabu Utagawa, Masahiro Seto, and Kunihisa Katsuyama *In its* Journal of NIRE, Volume 2, Number 4 26 Jul. 1993 p 75-8 In JAPANESE (For primary document see N94-28147 07-45)

Avail: CASI HC A02/MF A02

Cyclic loading tests of pre-stressed rocks were conducted to estimate the pre-stress of rocks. In these tests, four strain gages were used to average the inclination of the value of each gage. The results showed a shorter elapsed time after applied pre-stress loading, and a clearer bend of the DRA (Deformation Rate Analysis) curve. With the increase in elapsed time, the DRA curve became less clear. However in that case, the clear bend of the DRA curve appeared at the pre-stress point on and after the second loading. Therefore, it was possible to estimate the pre-stress even when the bend point of the DRA curve was not observed clearly in the first loading. Not only axial prestress but also lateral ones could be estimated for one axial loading test by DRA. The pre-stress estimation method using the DRA curve in cyclic loading is recommended. Also, a theoretical model regarding the bend point of the DRA curve is examined. Author (NASDA)

N94-28157# National Inst. for Resources and Environment, Ibaraki (Japan). Combustion Engineering Div.

NUMERICAL SIMULATION OF TURBULENT FREE JET BY TFKE MODEL [TFKE MODERU NI YORU RANRYU JIYU FUNRYU NO SUCHI SHIMYURESHON]

Masakazu Yamazaki and Shinya Kamiyama *In its* Journal of NIRE, Volume 2, Number 4 26 Jul. 1993 p 85-9 In JAPANESE (For primary document see N94-28147 07-45)

Avail: CASI HC A02/MF A02

Free turbulent shear flows such as turbulent jets are characterized by the intermittent phenomenon that rotational and irrotational states appear randomly and separately. In a turbulent jet flame, momentum, mass and heat transport between the fluid fragments of fuel and air resulting from the intermittent fluid motion inside the jet plays a dominant role in determining its structure and combustion characteristics. In this report, the TFKE (Two-Fluid Kappa Epsilon Two-Equation) turbulence model constructed for the prediction of the intermittency by integrating the two-fluid model and kappa epsilon two-equation model is described and the numerical calculations based on the TFKE model for the intermittency and diffusion characteristics of a unburnt axisymmetric turbulent free jet are discussed. It is presented that the numerical predictions satisfy quite well the existing experimental results and the TFKE model can provide the zone averages as well as time averages of the turbulence properties and the length scale distribution. This suggests, therefore, that the TFKE model is one of the promising turbulence models for further numerical simulation of turbulent jet flames. Author (NASDA)

N94-28268# Science and Technology Agency, Tokyo (Japan).

ASIA-PACIFIC SEMINAR ON GLOBAL CHANGE RESEARCH COOPERATION

1992 257 p Seminar held in Tokyo, Japan, 4-5 Dec. 1992 Prepared in cooperation with Research Development Corporation of Japan, Tokyo (JTN-94-80517) Avail: CASI HC A12/MF A03

The following topics were discussed: earth environment, environmental monitoring, environmental quality, environmental effects, change detection, global change, earth atmosphere, earth ozonosphere, climate change, atmospheric sounding, ocean currents, air sea interactions, hydrological cycles, greenhouse effect, air pollution, water pollution, water quality, ozone depletion, vegetation index, earth resources, coastal water, sea ice, phytoplankton, biomass, resources management, land management, remote sensing, satellite observation, satellite imagery, information systems, data systems, ground station, earth terminals, image analysis, image processing, international cooperation, Asia, Pacific Ocean, project planning, and project management. For individual titles, see N94-28269 through N94-28293.

N94-28269# Science and Technology Agency, Tokyo (Japan). Office of Earth Science and Technology.

ROLE AND ACTIVITY OF STA ON ASIAN PACIFIC REGIONAL COOPERATION c43

Yoshiaki Takeuchi *In its* Asia-Pacific Seminar on Global Change Research Cooperation 1992 p 5-23 Original contains color illustrations (For primary document see N94-28268 07-45)

Avail: CASI HC A03/MF A03

Promotion of the earth science technology and role and activities on Asian Pacific regional cooperation of the Science and Technology Agency of Japan (STA) are outlined. Topics included are as follows: (1) the National Space Development Agency of Japan (NASDA) and the Japan Marine Science and Technology Center (JAMSTEC) are massive organization for development of the infrastructure necessary for earth observation; (2) STA promotes the research projects in cooperation with other ministries and agencies; (3) STA has two kinds of funds for these research, that is, special funds for investigation and research of earth science and technology and the Special Coordination Funds for Promoting Science and Technology (SCF); (4) intergovernmental cooperation and international cooperation on STA projects; and (5) some projects associated with Asia-Pacific cooperation, such as Japanese Pacific Climate Studies (JAPACS), research program on the changes of tropical forests and their influences, Japan-China Joint Study on Desertification (JC-JOSDES), Japanese experiment on Asian monsoon, and Japanese study on the behavior of greenhouse gases and aerosols. The start of an international cooperative research program on construction of the global data set from FY (Fiscal Year) 1993 with the coordination funds is proposed. Author (NASDA)

N94-28270# National Research Inst. for Earth Science and Disaster Prevention, Tsukuba (Japan). Advanced Measurement and Analysis Technology Div.

COOPERATIVE RESEARCH PROJECTS ON SATELLITE REMOTE SENSING FOR THE HYDROLOGICAL SUBJECTS c43

Shinkichi Kishi *In* Science and Technology Agency, Asia-Pacific Seminar on Global Change Research Cooperation 1992 p 25-3 (For primary document see N94-28268 07-45)
Avail: CASI HC A02/MF A03

Subjects of the cooperative hydrological research projects on satellite remote sensing were outlined. The subjects mentioned are as follows: (1) Japanese Experiment on Asian Monsoon (JEXAM) (1989 to 1998), including studies on air-sea-land interactions and their long term variation and theoretical experimental study by numerical simulations; (2) research for the enhancement of remote sensing technology in earth observation using advanced sensor systems (1992 to 1994); (3) Japan-China Joint Study on Desertification (JC-JOSDES) (1989 to 1992), including studies on the formation of the desert and simulation study on the desertification; and (4) Japanese Pacific Climate Studies (JAPACS) (1990 to 1992), including observation in the sea ice zone and analytical studies on air-sea interaction by the use of the Marine Observation Satellite-1 (MOS-1) data and relevant data. Author (NASDA)

N94-28271# Meteorological Research Inst., Tsukuba (Japan).

RESEARCH ACTIVITIES ON THE METEOROLOGY OVER THE ASIA-PACIFIC REGION c43

Masato Murakami *In* Science and Technology Agency, Asia-Pacific Seminar on Global Change Research Cooperation 1992 p 33-3 (For primary document see N94-28268 07-45)
Avail: CASI HC A01/MF A03

International joint research projects on the meteorology over Asia-Pacific region, such as the Tropical Ocean Global Atmosphere (TOGA)-Coupled Ocean-Atmosphere Response Experiment (COARE) and the Tropical Rainfall Measuring Mission (TRMM) are outlined. Among the proposed collaboration in the late 1990's, the Global Energy and Water Cycle Experiment (GEWEX) will be the major project which requires both international and interdisciplinary collaboration. GEWEX should pursue the global scale analysis which includes the three dimensional distribution of the wind and water vapor over the ocean, the global climate of clouds and precipitation, the global ocean monitoring and the global monitoring of land and its vegetation. The GEWEX will bring an opportunity to deploy a new earth observing system by satellites in order to monitor, investigate and predict the climate changes. It will give a prototype of the future routine observation network by satellites. In the late 1990's, marine observing satellites related to the TOGA and the World Ocean Circulation Experiment (WOCE) will be realized. Japan should, cooperating with other countries to build up a satellite observation network, develop new sensors capable to observe the important components such as the water vapor, wind, precipitation and the soil moisture over the globe. Author (NASDA)

N94-28272# Japan Marine Science and Technology Center, Tokyo.

AN OCEANOGRAPHICAL OBSERVATION IN THE WESTERN PACIFIC AND INTERNATIONAL COOPERATIONS c48

Kei Muneyama *In* Science and Technology Agency, Asia-Pacific Seminar on Global Change Research Cooperation 1992 p 35-4 (For primary document see N94-28268 07-45)
Avail: CASI HC A03/MF A03

Outline of Kuroshio research to study the following subjects are explained: (1) the dynamical oceanography of Kuroshio; (2) the biogeochemical processes; (3) the biological activities; (4) ocean-atmosphere interaction; and (5) development of the observation system. The Japan Marine Science and Technology Center (JAMSTEC) and Badan Pengkajian dan Penerapen Teknologi (BPPT) of Indonesia started a cooperative oceanographical study in waters off Taraud to Halmahera to Irian Java in 1992. The western Pacific is not only the origin of Kuroshio but also the epicenter of El Nino. The warm water is piled up in the western Pacific to form warmpool by the trade wind prevailing in equatorial Pacific. This movement of the convection center eastward means the drought in Southeast Asia and Australia. The role of the Indonesian through-flow has been speculated for past years to be related to the evolution of the warmpool but no direct observation data concerning it's transport volume has been given. The observation of the Indonesian through-flow seems to give valuable data because it has linked directly to the several years scale phenomena such as El Nino and seasonal change such as a monsoon. The most distinctive feature is that the current flows southward at the northern part and flows northward at the southern part at the moment of observation. This result clearly shows the necessity of the seasonal observations. Author (NASDA)

N94-28273# National Space Development Agency, Ohashi (Japan). Earth Observation Center.

NASDA CONTRIBUTION PLAN TO ASIAN COUNTRIES c43

Hiroshi Kikuchi *In* Science and Technology Agency, Asia-Pacific Seminar on Global Change Research Cooperation 1992 p 47-6 (For primary document see N94-28268 07-45)
Avail: CASI HC A03/MF A03

The following aspects of the National Space Development Agency of Japan's (NASDA) contribution plan to Asian countries are outlined: (1) background; (2) purpose; (3) total system, including ground station network, regional data center network, and national data center network; (4) activities, including Asian Pacific International Space Year (ISY) conference, international sub-committee of earth environmental observation, tropical ecosystem seminar, Committee for Earth Observation Satellites (CEOS) IDN, cooperative research projects with Mongolia, China, Thailand, and Australia, next generation satellite program study for Asian Pacific region; and (5) NASDA's new data policy for research and commercial purposes. This presentation is represented in viewgraphs only. Author (NASDA)

N94-28274# Remote Sensing Technology Center, Tokyo (Japan).

ACTIVITIES OF REMOTE SENSING TECHNOLOGY CENTER OF JAPAN (RESTEC) c43

Keiji Maruo *In* Science and Technology Agency, Asia-Pacific Seminar on Global Change Research Cooperation 1992 p 67-7 (For primary document see N94-28268 07-45)
Avail: CASI HC A02/MF A03

The activities of the Remote Sensing Technology Center of Japan (RESTEC) are introduced. The following fields of activities are outlined: (1) education and training on the remote sensing technologies, especially on the data processing technology, commissioned by the Science and Technology Agency (STA) of Japan, the Japan International Cooperation Agency (JICA), and the National Space Development Agency of Japan (NASDA); (2) data distribution and marketing of the remote sensing data from satellites, such as LANDSAT, the Marine Observation Satellite (MOS), the SPOT, and the Japanese Earth Resources Satellite-1 (JERS-1); (3) data network system called the Earth Observation Center (EOC)-Information System (IS), including the Committee for Earth Observation Satellites (CEOS) IDN and a data inventory system; (4) researches and developments conducted by RESTEC; and (5) national and regional (Asian Pacific) seminars, symposia, and publicity. Author (NASDA)

N94-28275# Ministry of Environment and Forest, Dhaka (Bangladesh).

GLOBAL CONCERN ON RESEARCH COOPERATION FOR ENVIRONMENT

Mohammed Sirajul Anwar *In* Science and Technology Agency, Asia-Pacific Seminar on Global Change Research Cooperation 1992 p 81-9 (For primary document see N94-28268 07-45)
Avail: CASI HC A03/MF A03

Activities carried out for solving environmental problems in Bangladesh are outlined. Topics included are as follows: (1) the problems of overpopulation, poverty, recurring floods, natural disasters, rapid deforestation threatened wildlife, trend of desertification in the northern part of the country, and increasing salinity in southern Bangladesh; (2) the flow of water from major rivers which originated in different countries; (3) environmental issues related to urbanization, industrial pollution, and agrochemicals; (4) few important steps to reduce the environmental problems in the country; (5) improvements of capability and expertise to deal with problems of disaster management, and plans to improve environmental training and education programs; (6) the Department of Environment (DOE); (7) governmental research organizations, universities, and non-governmental organization responsible for environmental activities; (8) environment policy including related laws and regulations; and (9) full endorsement for the formation of Asian-Pacific network. Author (NASDA)

N94-28276# National Environmental Protection Agency, Beijing (China).

PROGRESS IN THE STUDY OF GLOBAL CHANGE IN CHINA

Ruqiu Ye *In* Science and Technology Agency, Asia-Pacific Seminar on Global Change Research Cooperation 1992 p 95-102 (For primary document see N94-28268 07-45)

Avail: CASI HC A02/MF A03

The Chinese government's efforts to cope with the global change are outlined. The following topics are included: (1) global climate change, including setting up historic climate data bank, developments of the model for prediction of climate change, inauguration of the inventory of CO2 emission sources, influence of methane emission from paddy fields to climate change, climate change observation and greenhouse gas monitoring throughout the country; (2) protection of biological diversity, of which serious loss is caused by human activity, such as biological resources exploration; (3) research on acid precipitation; and (4) stratospheric ozone layer protection, including active part played by Chinese government in the montreal protocol on ozone depleting substances. Author (NASDA)

N94-28277# Agency for Assessment and Application of Technology, Jakarta (Indonesia).

RESEARCH AND OBSERVATION PROGRAMMES ON GLOBAL CHANGES IN INDONESIA

Ir. Sri Woro B. Harijono *In* Science and Technology Agency, Asia-Pacific Seminar on Global Change Research Cooperation 1992 p 103-113 (For primary document see N94-28268 07-45)

Avail: CASI HC A03/MF A03

An overview of the activities related to global changes in Indonesia is presented. The Indonesian view on the Asia Pacific research network concept is also explained. The following topics are included: (1) existing facilities and capability relevant to global change research and planned programs; (2) national research and observation programs, including activities related to global and regional forecast of human activities, global and regional models of geophysical global change, ecosystem, social and economic impact, and technological countermeasures; (3) international research and observation programs, including activities related to climate, environment, and participation in international forums such as International Forum on Climate Change (IPCC), Global Weather Climate Change (GWCC), Tropical Ocean Global Atmosphere (TOGA), European Center for Medium-Range Weather Forecast (ECMWF), joint research on climate between Indonesia and the US, and International Center for Equatorial Atmosphere Research (ICEAR); and (4) Indonesian concept for Asia Pacific research network, including data network, joint research network, and human resource development. Author (NASDA)

N94-28278# Ministry of Environment, Seoul (Republic of Korea). Global Environment Div.

COUNTRY REPORT ON GLOBAL CHANGE RESEARCH FOR THE REPUBLIC OF KOREA

Boo-Ho Noh *In* Science and Technology Agency, Asia-Pacific Seminar on Global Change Research Cooperation 1992 p 115-119 (For primary document see N94-28268 07-45)

Avail: CASI HC A01/MF A03

The aspects of global change activities in the Republic of Korea (ROK) are outlined. The following topics are explained: (1) various environmental research projects related to environmental problems inaugurated by the Ministry of Environment mostly focusing on the identification of air and water pollution sources and the development of control technologies; (2) a new Highly Advanced National (HAN) projects for environmental science and technology with inter-ministerial cooperation and coordination launched by the ROK government (mainly to develop clean technologies for reducing or minimizing pollutants emissions and wastes, and to establish cost-effective national strategies to cope with global environmental issues); (3) the environmental part of HAN projects coordinated by the National Institute of Environment Research (NIER) (related to climate change, acid precipitation, and marine pollution); and (4) major on going and planned projects related to global changes. The Korean government's announcement of its commitment to the global and regional environmental cooperation to actively join the international efforts for the preservation of the global environment is expressed. Author (NASDA)

N94-28279# Department of Environment and Natural Resources, Quezon City (Philippines). Environmental Management Bureau.

PHILIPPINE THRUST ON ENVIRONMENTAL RESEARCH RELATING TO GLOBAL CHANGE

Rodrigo U. Fuentes *In* Science and Technology Agency, Asia-Pacific Seminar on Global Change Research Cooperation 1992 p 120-122 (For primary document see N94-28268 07-45)

Avail: CASI HC A01/MF A03

An overview of Philippine environmental research related to global change is presented. Topics included are as follows: (1) the Philippine activities related to global climate change; (2) the preparation of the Framework Convention on Climate Change which was one of the products of the Earth Summit in Rio de Janiero by the Philippines; (3) the Philippines council for substantial development which will serve as a coordinative body that will overseas the integration of environmental considerations in every sector of the society; and (4) policy and research studies related to climate change. The main agencies involved in the discussion and research in climate change are as follows: (1) Department of Environment and Natural Resources (DENR); (2) Department of Science and Technology (DOST); (3) Department of Agriculture (DA); (4) some established academic institution such as the University of the Philippines, Ateneo University, Silliman University, and Xavier University; and (5) non-government agencies which partakes advocacy roles. The above agencies and institutions undertake researches on the following areas: (1) land use and land cover changes; (2) coastal resource management; (3) marine pollution; (4) industrial and water pollution; (5) soil and water conservation; (6) deforestation; (7) climate and weather monitoring; (8) biodiversity researches; and (9) marine ecosystem research. Author (NASDA)

N94-28280# Ministry of Science, Technology and Environment, Bangkok (Thailand). Pollution Control Dept.

THE ENVIRONMENTAL RESEARCH AND TRAINING CENTRE

Pornchai Taranatham *In* Science and Technology Agency, Asia-Pacific Seminar on Global Change Research Cooperation 1992 p 123-127 (For primary document see N94-28268 07-45)

Avail: CASI HC A01/MF A03

The following aspects of the Environmental Research and Training Center (ERTC) are introduced: (1) Thailand took responsibility for land preparation, construction of access roads and fences, extension of electricity, telephone, and water supplies to the site and other services for issuing visas to Japanese personnel; (2) the five year Japanese technical liason to the ERTC to allow the government of Japan to take necessary measures through the Japan International Cooperation Agency (JICA) to support at its own expense, services of the Japanese experts, machinery, equipment, and other materials including those to Thai staff in Japan; and (3) the status of ERTC building and equipment installation. The ERTC functions are as follows: (1) undertaking practical research on environmental management; (2) promoting and encouraging research activities on environmental quality; (3) strengthening environmental monitoring programs; (4) providing training programs to staff in national and local governments, and inter-governmental organizations focussing on environmental management; and (5) providing environmental education programs for staff at all levels and training people with an appropriate expertise. Author (NASDA)

N94-28281# Commonwealth Scientific and Industrial Research Organization, Lyneham (Australia). Div. of Wildlife and Ecology.

GLOBAL CHANGE AND TERRESTRIAL ECOSYSTEMS (GCTE): PROGRESS REPORT AND PROSPECTS FOR ASIAN CONTRIBUTIONS Progress Report

Will Steffen *In* Science and Technology Agency, Asia-Pacific Seminar on Global Change Research Cooperation 1992 p 131-141 (For primary document see N94-28268 07-45)

Avail: CASI HC A03/MF A03

The objectives and structure of the Global Change and Terrestrial Ecosystems (GCTE) in Australia, its implementation strategy, and the present status are outlined. The topics included are summarized as follows: (1) the objectives of GCTE are to predict the effects of changes in climate, atmospheric composition, and land use on terrestrial ecosystems and to determine how these effects lead to feedbacks to the atmosphere and the physical climate system; and (2) GCTE is organized into a hierarchy of foci, activities, and tasks. The four foci are divided into the ecosystem philosophy, the change in ecosystem structure, the global change impact on agriculture and forestry, and the global change and ecological complexity (proposed). The GCTE operational plan provides the framework for its core research program. The individual projects which contribute to the core research program come primarily from the following two sources: (1) national and regional contributions; and (2) GCTE-initiated research. GCTE has made a strong progress during 1992 with the publication in Apr. 1992 of the GCTE operation plan and the approval of the first set of contributing research projects. A recent meeting of the GCTE Scientific Steering Committee continued the strong progress with the evaluation and acceptance of an additional set of contributing research projects to bring the total of 16 projects involving scientists from 21 countries. There are many opportunities for Asian scientists to contribute to GCTE. Author (NASDA)

N94-28282# Commonwealth Scientific and Industrial Research Organization, Lyneham (Australia). Div. of Wildlife and Ecology.

GLOBAL CHANGE: A RESEARCH STRATEGY FOR AUSTRALIA 1992-1996 Progress Report

Will Steffen *In* Science and Technology Agency, Asia-Pacific Seminar on Global Change Research Cooperation 1992 p 142-146 (For primary document see N94-28268 07-45)

Avail: CASI HC A01/MF A03

An overview of the current status and new initiatives for the global change program conducted in Australia is presented. The Australian global change research program consists of 10 major projects, each involving a multi-disciplinary team of scientists from several Australian research institutions. The projects are as follows: (1) atmospheric chemistry, biogeochemistry, and ecosystem dynamics in tropical northern Australia; (2) energy and water exchanges between atmosphere and land; (3) impact of changes in carbon dioxide, climate, and land use on agriculture and the environment; (4) ozone depletion and the impact of ultraviolet-B radiation on terrestrial and marine plants; (5) nature and causes of climate change over the past 20,000 years in Australia and Antarctica; (6) past response of vegetation and surface water to Australian climates; (7) circulation, heat transport, and sea ice changes in the southern ocean; (8) eastern Indian Ocean circulation and process study; (9) carbon fluxes in the subtropical convergence and the southern ocean; and (10) the carbon cycle in the monsoonal marine tropics. The present status of and new initiatives for the program are also described. Author (NASDA)

N94-28283# Institute of Atmospheric Physics, Beijing (China).

A PROGRESS REPORT ON GLOBAL CHANGE STUDIES IN CHINA Progress Report

Congbin Fu *In* Science and Technology Agency, Asia-Pacific Seminar on Global Change Research Cooperation 1992 p 147-155 (For primary document see N94-28268 07-45)

Avail: CASI HC A02/MF A03

The progress in the global change research activities in China since the Asian Planning Meeting for International Geosphere-Biosphere Program (IGBP) is outlined. Subjects outlined are as follows: (1) the nature, objectives, and main research activities of a research project on future trend of changing eco-environmental system in China in next 20 to 50 years; (2) other related projects in global change studies, such as climate dynamics and the theory of climate prediction, experiment and demonstration researches on the ecological research network, biological resources and ecological environment of Antarctic and global change, and others; and (3) progress in preparation to establish the global change research network in the East Asia and West Pacific region. Author (NASDA)

N94-28284# National Physical Lab., New Delhi (India).

INDIAN ACTIVITIES ON THE CORE PROGRAMME IGAP AND PROPOSALS FOR NETWORK ACTIVITIES

A. P. Mitra *In* Science and Technology Agency, Asia-Pacific Seminar on Global Change Research Cooperation 1992 p 156-159 (For primary document see N94-28268 07-45)

Avail: CASI HC A01/MF A03

Indian activities on the core program 'International Geosphere-Biosphere Program (IGBP)' and proposals for network activities are outlined. Subjects presented are as follows: biogenic emission measurement campaigns - 1991 methane campaign for measurement of methane gas from rice paddy fields in India, wetland campaign to measure methane emission from wetlands, and measurement of N2O emissions from river discharge and polluted water; biomass burning - study on CO2 emissions from deforestation, shifting cultivation, accidental and controlled fire, and firewood burning in India; acid chemistry; Gas Laboratory (GASLAB) sampling in the Arabian Sea primarily focusing on carbon dioxide isotope fractionation; ozone program; and water vapor measurements. An important question concerns reliable measurement of water vapor profiles up to stratospheric heights. Author (NASDA)

N94-28285# University of Science of Malaysia, Penang. Astronomy and Atmospheric Research Unit.

ATMOSPHERIC SCIENCE RESEARCH IN MALAYSIA: PERSPECTIVES ON INTERNATIONAL COOPERATION

Mohammed Ilyas *In* Science and Technology Agency, Asia-Pacific Seminar on Global Change Research Cooperation 1992 p 160-164 (For primary document see N94-28268 07-45)

Avail: CASI HC A01/MF A03

An overview of atmospheric science research in Malaysia is presented. Three institutions playing a key role in atmospheric studies are introduced. Malaysian Meteorological Service is involved in the traditional monitoring and data collection of a wide range of parameters. The Department of Environment is involved in environmental control such as ozone depleting substance control and legislative aspects. The department is also participating in regional and international research programs through the Association of South-East Asian Nations (ASEAN) system, International Geosphere-Biosphere Program (IGBP), World Climate Research Program (WCRP), and World Meteorological Organization. And the University of Science Malaysia is specialized in atmospheric science research. The university is playing a leading role through two major developments. The first one is the physical infrastructure development at the university for a special research focused on atmospheric ozone, minor constituents, and ultraviolet radiation by establishing the Atmospheric Research Unit. The second one is the completion of the Sheikh Tahir Astronomical Observatory to provide a cooperative research base for tropical atmospheric studies. The present status of the tropical network of ozone, ultraviolet (UV), and related atmospheric research and international cooperation is described. Author (NASDA)

N94-28286# NAST Secretariat, Taguig (Philippines).

HDGEC ACTIVITY IN ASIA PACIFIC REGION

Filomena F. Campos *In* Science and Technology Agency, Asia-Pacific Seminar on Global Change Research Cooperation 1992 p 165-167 Sponsored by Science and Technology Agency and Japan and Research Development Cooperation of Japan (For primary document see N94-28268 07-45)

Avail: CASI HC A01/MF A03

The Human Dimensions of Global Environment Change (HDGEC) activities by the social scientists in close collaboration with the natural scientists are outlined. The following subjects identified by one of the workshop missions during the Global Change System for Analysis, Research, and Training (START) are presented: human dimensions of natural resource management affecting land use change, coastal resource management, and inland resource management; and urbanization and industrialization related to environmental problems. Human response to projected sea level change in Southeastern Asia, one example of global environment change research within the HDGEC, is exemplified. It was agreed by the workshop members that regional collaboration can be strengthened through the following mechanisms: developing closer interaction between the natural and social scientists to establish clear understanding of the integral role of social science in environmental research related to global change; creation of a working group with appropriate representatives in social sciences; establishing and developing a database on socioeconomic and physical science; appointment of social scientists as members of the national International Geosphere-Biosphere Program (IGBP) committee; and inclusion of social scientists in the START organization. Current status of the HDGEC in South Asia is presented. Author (NASDA)

N94-28287# Chulalongkorn Univ., Bangkok (Thailand). Environmental Research Inst.

CHANGES IN PHYTOPLANKTON POPULATION IN THE CHAO PHRAYA ESTUARY, THAILAND, DURING THE EUTROPHICATION MECHANISMS STUDIES

Twesukdi Piyakarnchana, S. Boonyapiwat (Ministry of Agriculture and Cooperatives, Bangkok, Thailand.), T. Okaichi (Kagawa Univ., Japan.), S. Wisessang, and G. Wattayakorn *In* Science and Technology Agency, Asia-Pacific Seminar on Global Change Research Cooperation 1992 p 168-191 (For primary document see N94-28268 07-45)
Avail: CASI HC A03/MF A03

The changes in abundance and species compositions of the phytoplankton populations in the estuarine region of the Chao Phraya river mouth were observed. The other environmental parameters such as water temperature, salinity, dissolved oxygen, ammonia, nitrite, nitrate, phosphate, and silicate were also measured. The samples were taken at nine fixed stations within one day, and at one or two selected stations for twenty four hours at every two hours. The results clearly indicate that phytoplankton populations varied with the sampling times and water quality. The number of species compositions in the wet season (August) showed less abundance than in the dry season (December). The differences were greater at the up-river stations with low salinity and high turbidity than at the seaward ones. Phytoplankton species composition differences between wet and dry season and between high and low tide are outlined. Author (NASDA)

N94-28288# Chiang Mai Univ. (Thailand). Dept. of Geography.

LAND USE CHANGE IN THAILAND AND ITS IMPACT ON ENVIRONMENTAL CHANGE: JOINT THAI-JAPANESE RESEARCH PROJECT (1993-1995)

Vanpen Surarerks *In* Science and Technology Agency, Asia-Pacific Seminar on Global Change Research Cooperation 1992 p 192-211 (For primary document see N94-28268 07-45)
Avail: CASI HC A03/MF A03

The significance, background, objectives, methodology, anticipated benefits, and time schedule of the joint Thai-Japanese research project to study land use change and its impact on environmental change are outlined. The objectives are to study and characterize the human activities affecting environmental change, problems in the farming system, and land use, and then to propose suitable land use management. The methodology includes the following subjects: collection of physical and socioeconomic data; data preparation, such as organizing maps for raw data for use in geographic information systems (GIS), tables, models, diagrams, and descriptive data organized from data collected from documents and field surveys; and data analysis, such as mapping from GIS techniques and documentary data interpreted and analyzed as well as data from surveys, observations, and field interviews. Anticipated benefits of recommendations for proposing a suitable land use management at present and in the future, and the time schedule, are presented. Author (NASDA)

N94-28289# Satellite Meteorological Center, Beijing (China).

STUDY ON ENVIRONMENT MONITORING OVER WHOLE CHINA USING NDVI FROM AVHRR DATA AND FUTURE PROJECT

Zongyi Fang, Qianguang Xiao, Xuanji Wang, and Yongwei Sheng *In* Science and Technology Agency, Asia-Pacific Seminar on Global Change Research Cooperation 1992 p 215-225 Original contains color illustrations (For primary document see N94-28268 07-45)
Avail: CASI HC A03/MF A03

The following aspects of study on environmental monitoring over whole China using Non-Dimensional Vegetation Indices (NDVI) from Advanced Very High-Resolution Radiometer (AVHRR) are outlined: (1) data processing; (2) application analysis; (3) main research contents; (4) subject planning arrangement; and (5) data processing requirements. The following conclusions can be obtained through analysis of remote sensing vegetation indices during the years of 1987 to 1991: (1) the basic conditions for vegetation growth are light, temperature, and water; (2) the climate divisions identified by satellite vegetation index maps match with those identified by temperature; (3) the monthly anomaly of satellite vegetation index matches that of precipitation in general; and (4) the remote sensing monitoring on environment of the vulnerable area is very important because it is quite sensitive to the environmental change. Author (NASDA)

N94-28290# Malayan Meteorological Service, Petaling Jaya.

UTILIZATION OF REMOTE SENSING DATA FOR GLOBAL CLIMATE CHANGE RESEARCH IN MALAYSIA

Subramaniam Moten *In* Science and Technology Agency, Asia-Pacific Seminar on Global Change Research Cooperation 1992 p 226-237 (For primary document see N94-28268 07-45)
Avail: CASI HC A03/MF A03

The global climate change research utilizing remote sensing data in Malaysia is presented. The following aspects of global climate change are outlined: (1) greenhouse effect gases and climate change; (2) global warming and its impact on the regional climate; (3) change in rainfall and impacts due to changes of precipitation; (4) change in sea level and impact of sea level rise; (5) utilization of remote sensing data; and (6) remote sensing activities in Malaysia. Global warming affected by increase in greenhouse effect gases is a potential threat to the environment and society. The consequences will be far reaching and the impact will be felt slowly but surely if model simulations are used as indicators. The impact in the tropics may be greater because of increased rainfall during the wet season and possible decrease during the dry season, increase in tropical storm activities and damage to the coastal regions which sustains the economy of many countries. Monitoring the environment is important for checking the trends in climate and detecting changes that are consequences of global warming. Remote sensing can play a useful role by providing data at a high resolution, on timely basis and fraction of the cost for obtaining data from conventional methods. Author (NASDA)

N94-28291# National Research Council, Bangkok (Thailand).

THAILAND SATELLITE GROUND RECEIVING STATION IN GLOBAL CHANGE RESEARCH COOPERATION

Suvit Vibulsresth *In* Science and Technology Agency, Asia-Pacific Seminar on Global Change Research Cooperation 1992 p 238-244 (For primary document see N94-28268 07-45)
Avail: CASI HC A02/MF A03

An overview of the Thailand's satellite ground station for global change research cooperation is presented. The following subjects related to the above are outlined: (1) features of the related activities in Thailand; (2) Malaysian organizational system for remote sensing oriented activities; (3) organization of the National Research Council; (4) the effect of sea level rise on Indonesia; (5) carbon emission due to fossil fuel consumption and the carbon dioxide concentration at Maunaroa in Hawai Island; and (6) temporal sea level change. Viewgraphs only are presented.
Author (NASDA)

N94-28292# National Inst. of Aeronautics and Space, Jakarta (Indonesia). Data Processing Technology Div.

UTILIZATION OF REMOTE SENSING DATA FOR GLOBAL CHANGE RESEARCH

Mahdi Kartasasmita *In* Science and Technology Agency, Asia-Pacific Seminar on Global Change Research Cooperation 1992 p 245-250 (For primary document see N94-28268 07-45)
Avail: CASI HC A02/MF A03

An overview of the remote sensing data utilization for global change research in Indonesia is presented. The following aspects of Indonesian activities related to global change research are outlined: (1) satellite remote sensing data characteristics, including the earth parameters to become input to the global environment change model for monitoring and prediction; (2) Indonesian geographic features and remote sensing (satellite) facilities; and (3) international and regional cooperations for strengthening the human resources and the facilities in the region, and performing joint research using as much as possible the capabilities of each country (indigenous capabilities, scientists and experts as well as facilities), which are aimed toward the following areas: (1) change of tropical forest cover and other land covers; (2) monitoring sea surface temperature and other oceanic parameters; (3) vertical atmospheric and upper atmosphere profiles; and (4) study of the effects of the above three board types of parameters toward global environment change in the region. Viewgraphs only are presented. Author (NASDA)

N94-28293# National Research Inst. for Earth Science and Disaster Prevention, Tsukuba (Japan).
CONTRIBUTION OF SATELLITE OBSERVATION TO GLOBAL CHANGE RESEARCH
Atsushi Takeda *In* Science and Technology Agency, Asia-Pacific Seminar on Global Change Research Cooperation 1992 p 251 (For primary document see N94-28268 07-45)
Avail: CASI HC A01/MF A03

An overview of the contribution of satellite observation to global change research is presented. Satellite observation of the earth can make an outstanding contribution to the research of global change. Satellite observations need to be supplemented by in situ or ground truth observations. Developments in optical sensors are expected to make much improvement in the interpretation of land image. Loss due to cloud cover should be reduced by use of microwave image sensors like Synthetic Aperture Radar (SAR) which can see the earth surface through the cloud layer. Receiving stations and other ground system should also be reinforced particularly in those developing countries and regions. Improved analyzing techniques should be developed quickly to extract more information from the existing data sets and to reduce the cost and time of data processing. Coordination of world satellite programs is strongly recommended to produce effective data sets for global change research of every region over the earth surface. Author (NASDA)

N94-28383# Helsinki Univ. of Technology, Espoo (Finland). Inst. of Energy Engineering.
FIBROUS CERAMIC CANDLE FILTER FOR PARTICLE REMOVAL IN PRESSURIZED FLUIDIZED BED COMBUSTION
J. Jalovaara, I. Hippinen, and A. Jahkola Aug. 1993 53 p See also PB94-133071
(PB94-133089; ISBN-951-22-1719-8) Avail: CASI HC A04/MF A01

A fibrous, layered Al2O3/SiO2-based ceramic candle filter has been tested for pressurized fluidized bed combustion (PFBC) hot gas cleaning at the Otaniemi PFBC test rig. The fuels used have been bituminous coal and peat. The exhaust gas from a pressurized fluidized bed reactor was passed through two cyclones before entering the ceramic filter unit, which was operated at a temperature range from 580 to 740 C and at a pressure range from 6 to 10 br (abs.). Total exposure time of the two candle filter elements was about 340 hours. This paper presents measured data and operating experiences of the ceramic filter. NTIS

N94-28394# Helsinki Univ. of Technology, Espoo (Finland). Inst. of Energy Engineering.
EXPERIMENTAL STUDIES OF PRESSURISED FLUIDISED BED COMBUSTION AT HELSINKI UNIVERSITY OF TECHNOLOGY, 1991-1992
I. Hippinen and A. Jahkola Aug. 1993 45 p
(PB94-133063; ISBN-951-22-1717-1) Avail: CASI HC A03/MF A01

The report is a general part of the research project 'Nitrogen oxide, alkali metal and particle emissions in pressurized fluidized bed combustion,' which was carried out as a two-year project 1991-92 at Helsinki University of Technology. The main subjects of the project were the emissions of nitrogen oxides and nitrous oxide and their reduction, the release of sodium and potassium, and hot gas clean-up with fibrous ceramic filters. This report presents the project and test arrangements and the results of material balances, sulfur capture, and combustion performance. NTIS

N94-28395# Helsinki Univ. of Technology, Espoo (Finland). Inst. of Energy Engineering.
EMISSIONS OF NITROGEN OXIDES (NO(x) AND N2O) IN PRESSURIZED FLUIDIZED BED COMBUSTION
Y. Lu, I. Hippinen, J. Jalovaara, and A. Jahkola Aug. 1993 52 p See also PB94-133089
(PB94-133071; ISBN-951-22-1718-X) Avail: CASI HC A04/MF A01

This report presents the experimental studies of nitrogen oxide (NO(x) and N2O) emissions and their reduction in pressurized fluidized bed combustion (PFBC). It includes two parts: one is the emissions of nitrogen oxides and their reduction in PFBC at the Otaniemi PFBC pilot reactor; and the other is the formation of nitrogen oxides in PFB-combustion and PFB-pyrolysis that were carried out at the batch PFBC reactor. NTIS

N94-28307*# Virginia Polytechnic Inst., Blacksburg. Dept. of Geological Sciences.
PROPOSED LAW OF NATURE LINKING IMPACTS, PLUME VOLCANISM, AND MILANKOVITCH CYCLES TO TERRESTRIAL VERTEBRATE MASS EXTINCTIONS VIA GREENHOUSE-EMBRYO DEATH COUPLING Abstract Only
D. M. McLean *In* Houston Univ., New Developments Regarding the KT Event and Other Catastrophes in Earth History 1994 p 82-83 (For primary document see N94-28294 07-46)
Avail: CASI HC A01/MF A02

N94-28312*# Houston Univ., TX.
OZONE CONTROL OF BIOLOGICAL ACTIVITY DURING EARTH'S HISTORY, INCLUDING THE KT CATASTROPHE Abstract Only
W. R. Sheldon *In* Houston Univ., New Developments Regarding the KT Event and Other Catastrophes in Earth History 1994 p 112-113
Sponsored by NSF (For primary document see N94-28294 07-46)
(Grant NSF ATM-92-06417)
Avail: CASI HC A01/MF A02

46 GEOPHYSICS

Includes aeronomy; upper and lower atmosphere studies; ionospheric and magnetospheric physics; and geomagnetism.

For space radiation see *93 Space Radiation.*

N94-25752# Massachusetts Univ., Lowell. Center for Atmospheric Research.
COHERENT HF RADAR SYSTEM FOR THE STUDY OF NATURAL AND HEATER INDUCED IONOSPHERIC IRREGULARITIES Final Report, Aug. 1991 - May 1993
Bodo W. Reinisch, James L. Scali, and D. M. Haines Jun. 1993 50 p
(Contract F19628-91-K-0036)
(AD-A273804; AD-E201727; PL-TR-93-2128) Avail: CASI HC A03/MF A01

The highly irregular polar ionosphere requires sophisticated sensing techniques to identify and monitor the ionospheric characteristics. The deployment of a new ionospheric sounder, the Digisonde Portable Sounder (DPS), at Svalbard (78.2 deg N) is described and the first results obtained with this instrument are discussed. The most important new feature in the DPS, not available in the old Digisondes, is the capability of high precision incidence angle measurements and spectral characterization at up to 128 ranges. While Svalbard rotated from the polar cap (at magnetic midnight) through the reversal boundaries and the auroral oval to the cusp region, the DPS was able to monitor the different features of a highly stressed ionosphere. It is demonstrated that the DPS can characterize the behavior of the background ionosphere while simultaneously measuring the motion of irregular plasma structures. This capability can be applied to identify and track irregularities generated by high power HF transmitters as planned for HAARP (HF Active Auroral Research Program) experiments in Alaska. How the DPS identifies different plasma structures in a naturally stressed ionosphere within the field of view of the instrument which extends over several hundred kilometers in the ionosphere is shown. DTIC

N94-25807# Norwegian Defence Research Establishment, Kjeller.
NORWEGIAN IONOSPHERIC SATELLITE EXPERIMENT: HIGH LATITUDE, LOW EARTH ORBIT PLASMA MEASUREMENTS
K. Svenes, B. T. Narheim, J. Troeim, U.-P. Hope, E. V. Thrane, and W. T. Armstrong 15 Apr. 1993 21 p
(FFI-93/7025; ETN-94-95211) Avail: CASI HC A03/MF A01

A possible Norwegian microsatellite is described. It is envisioned that the satellite will be fully developed and tested in Norway. The launch should occur after a short (approximately three years) project period, preferably from Andoya, and operation as well as data archiving should be accomplished in Norway. The main scientific objective of the satellite will be to study ion outflow both from the auroral oval as well as the polar cap. These measurements will in addition be related to the particle precipitation and optical auroral activity in the oval and over the polar cap. A secondary objective will be to do a global survey, with the prerequisite that foreign participation is enlisted for some of the instrument development. ESA

N94-25847# Colorado School of Mines, Golden. Center for Wave Phenomena.
EFFICIENT MODELING IN TRANSVERSELY ISOTROPIC INHOMOGENEOUS MEDIA
T. Alkhalifah Nov. 1993 35 p
(Contract DE-FG02-89ER-14079)
(DE94-003394; DOE/ER-14079/29; CWP-129P) Avail: CASI HC A03/MF A01

An efficient modeling technique for transversely isotropic, inhomogeneous media is developed using a mix of analytical equations and numerical calculations. The analytic equation for the ray path in a factorized transversely isotropic (FTI) media with linear velocity variation, derived by Shearer and Chapman, is used to trace between two points. In addition, an analytical equation is derived for geometrical spreading in FTI media that aids in preserving program efficiency; however, the travel time is calculated numerically. The method is generalized to treat general transversely isotropic (TI) media that are not factorized anisotropic inhomogeneous by perturbing the FTI travel times, following the perturbation ideas of Cerveny and Filho. A Kirchhoff summation based program relying on Trorey's diffraction method is used to generate synthetic seismograms for such a medium. For the type of velocity models treated, the program is much more efficient than finite difference and general ray-trace modeling techniques. DOE

N94-25877# Northwest Research Associates, Inc., Bellevue, WA.
COMPARATIVE INVESTIGATION OF HIGH-LATITUDE IONOSPHERIC STRUCTURE AND EFFECTS NEAR SOLAR MAXIMUM Final Report, 7 Dec. 1990 - 1 Jan. 1993
C. C. Andreasen, Elizabeth A. Holland, James A. Secan, and John M. Lansinger 31 Mar. 1993 92 p
(Contract F19628-91-C-0004)
(AD-A273799; NWRA-CR-93-R092; PL-TR-93-2088) Avail: CASI HC A05/MF A01

Northwest Research Associates (NWRA) has recorded a database containing measurements of the intensities of two L-band signals transmitted by satellites of the Global Positioning System and the differential carrier phase and differential group delay between them. Data collection was carried out during the period Dec. 1990 to Dec. 1992, which immediately followed the recent solar maximum. Data collection equipment, operated and serviced by NWRA, was located at Hanscom AFB, MA; Lerwick, Shetland Island, UK; and Thule AB, Greenland. Software tools to test, quality check, reduce, analyze, and display the data were developed. The total electron content data from the sub-auroral station (Lerwick, Shetland Island, UK) have been well analyzed and are shown to provide extremely detailed morphology for all times, seasons, and levels of magnetic activity. A log detailing the availability of data according to date, site, receiver type, and data quality is included herein. DTIC

N94-25979# Oak Ridge Inst. for Science and Education, TN.
INTERACTIONS BETWEEN A TROPICAL MIXED BOUNDARY LAYER AND CUMULUS CONVECTION IN A RADIATIVE-CONVECTIVE MODEL Ph.D. Thesis
C. L. Dean May 1993 142 p Prepared in cooperation with Pennsylvania State Univ., University Park
(Contract DE-AC05-76OR-00033)
(DE94-000848; DOE/OR-00033/T554) Avail: CASI HC A07/MF A02

A radiative-convective model, combining previously developed cumulus, stable cloud and radiation parameterizations with a boundary layer scheme, which was developed in the current study is detailed. The cloud model was modified to incorporate the effects of both small and large clouds. The boundary layer model which was adapted from a mixed layer model was only slightly modified to couple it with the more sophisticated cloud model. The model was tested for a variety of imposed divergence profiles, which simulate the regions of the tropical ocean from approximately the Intertropical Convergence Zone (ITCZ) to the subtropical high region. The sounding used to initialize the model for most of the runs is from the trade wind region of ATEX. For each experiment, the model was run with a timestep of 300 seconds for a period of 7 days. DOE

N94-26015# California Univ., San Diego.
ISOTOPICALLY LABELED CO2 FROM STRATOSPHERE: A TRACER OF CARBON BIOGEOCHEMISTRY
Yuk L. Yung (California Inst. of Tech., Pasadena.) and M. H. Thiemens 1993 4 p
(Contract DE-FC03-90ER-61010)
(DE94-002777; DOE/ER-61010/T14) Avail: CASI HC A01/MF A01

It has been recently discovered that the stratosphere is a source of isotopically enriched CO2: CO(sup 18)O and CO(sup 17)O. The cause of this isotopic enrichment is exchange between heavy O3 and CO2 via the excited radical O((sup 1)D). The research effort consists of a coordinated laboratory and model surfaces of isotopomers of CO2. The laboratory study yields data on the chemical kinetics of oxygen exchange between CO2 and O3. The modeling study uses the laboratory results as well as atmospheric measurements to model the source and sinks of CO2 isotopomers in the stratosphere and troposphere. It is expected that this combined study will bring new insights on the exchange of CO2 between the atmosphere and the biosphere. The goals of this study are to study the kinetic pathways for isotopic exchange between O2 and CO2 and to study O3: the exchange rate of isotopically labelled CO2 between the stratosphere and the troposphere. DOE

N94-26152*# National Aeronautics and Space Administration. Goddard Space Flight Center, Greenbelt, MD.
LASER ALTIMETRY SIMULATOR. VERSION 3.0: USER'S GUIDE
James B. Abshire, Jan F. McGarry, Linda K. Pacini, J. Bryan Blair, and Gregory C. Elman (Science Systems and Applications, Inc., Lanham, MD.) Jan. 1994 71 p
(NASA-TM-104588; NAS 1.15:104588; Rept-94B00039) Avail: CASI HC A04/MF A01

A numerical simulator of a pulsed, direct detection laser altimeter has been developed to investigate the performance of space-based laser altimeters operating over surfaces with various height profiles. The simulator calculates the laser's optical intensity waveform as it propagates to and is reflected from the terrain surface and is collected by the receiver telescope. It also calculates the signal and noise waveforms output from the receiver's optical detector and waveform digitizer. Both avalanche photodiode and photomultiplier detectors may be selected. Parameters of the detected signal, including energy, the 50 percent rise-time point, the mean timing point, and the centroid, can be collected into histograms and statistics calculated after a number of laser firings. The laser altimeter can be selected to be fixed over the terrain at any altitude. Alternatively, it can move between laser shots to simulate the terrain profile measured with the laser altimeter. Author (revised)

N94-26201# Aerospace Corp., El Segundo, CA. Engineering and Technology Group.
QUIET-TIME INTENSIFICATIONS ALONG THE POLEWARD AURORAL BOUNDARY NEAR MIDNIGHT
O. DeLaBeaujardiere, L. R. Lyons, J. M. Ruohoniemi, E. Friis-Christensen, C. Danielsen, F. J. Rich, and P. T. Newel 15 Mar. 1994 15 p
Original contains color illustrations
(ATR-93(7248)-2) Avail: CASI HC A03/MF A01

Radar and optical measurements from Sondrestrom are combined with satellite and Goose Bay data in a study of the poleward edge of the nightside auroral oval during a quiet period. The B(sub y) and B(sub z) components of the interplanetary magnetic field were close to zero, and the B(sub x) component was approximately 8 nT for more than 24 hours. On a large scale, the convection and precipitation patterns remained almost constant during this period; on a small scale, however, the conditions were quite dynamic. At 10- to 20-minute intervals, the arc that marked the poleward auroral boundary intensified, and a new arc appeared poleward of it. About once per hour, stronger intensifications were observed. One such event is examined in detail. The auroral arcs first appeared to dim, and then they brightened, with a factor of ten increase in E region electron density. At the time of the brightening, a new arc formed poleward of all the arcs. The arcs then drifted southward at velocities of approximately 70 m/s. A plasma drift disturbance, characterized by a doubling of the southward velocity and a reversal in the east-west component, propagated westward at 900 m/s through the fields of view of the Sondrestrom and Goose Bay radars. A simultaneous satellite overpass close to the radars revealed the presence of an energetic ion event similar to the 'velocity dispersed ion structures' observed on the Aureol satellite and presumed to be the signature of fast ion beams within the plasma sheet boundary layer. The stronger arc intensification events observed by the Sondrestrom radar are associated with an increase in plasma flow across the boundary between open and closed magnetic field lines. This increased flow is interpreted as the ionospheric signature of abrupt, localized increases in the reconnection rate in the midnight sector. Author (revised)

N94-26204*# Michigan Univ., Ann Arbor. Dept. of Atmospheric, Oceanic and Space Sciences.
DYNAMICS EXPLORER INTERDISCIPLINARY SCIENTIST INVESTIGATIONS Final Report, 1 Oct. 1990 - 30 Jan. 1994
Janet U. Kozyra and A. F. Nagy 1994 11 p
(Grant NAG5-472)
(NASA-CR-195226; NAS 1.26:195226; UMICH-021979) Avail: CASI HC A03/MF A01

This document is a final report on research activities and accomplishments that occurred during the funding period of 10-1-90 through 1-30-94. The focus of our interdisciplinary investigation during the Dynamics Explorer Mission was on the complex coupling processes that tap the magnetic-storm energy, stored in the ring current particle reservoir, and transport this energy into the subauroral, midlatitude and even equatorial ionospheric regions. The transport of energy through the inner magnetosphere and into the underlying ionospheric regions is a critical element in our understanding of the impact of solar and magnetic disturbances on upper atmospheric and ionospheric regions equatorward of the auroral zone. Author

N94-26224 Massachusetts Univ., Lowell. Center for Atmospheric Research.
IONOSPHERIC MODIFICATION BY HIGH POWER, OBLIQUELY PROPAGATED HF RADIO WAVE TRANSMISSIONS. PART 1: EXPERIMENTAL
Gary S. Sales Jul. 1993 28 p Limited Reproducibility: More than 20% of this document may be affected by microfiche quality
(Contract F19628-90-K-0039)
(AD-A273746; AD-E201706; PL-TR-93-2171-Pt-1; SR-6-Pt-1) Avail: CASI HC A03

Published material on the heating of electrons in the ionosphere using high power transmissions at high frequencies typically used for communications and OTH radar systems is reviewed. Although the emphasis of the reviewed experimental papers involves the oblique nature of radio transmissions, actually the important factor that differentiates these measurements from typical high power plasma heating studies is the fact that these involve underdense heating, i.e., at frequencies above the maximum plasma frequency in the ionosphere. The process of inclusion into this report necessitated a critical judgement of the published experimental results, requiring of them, either a degree of credibility and repeatability or when they have become part of the folk lore in the field of oblique heating. In the latter case, a critical review of the reported results is undertaken in light of the current and best understanding of 'heating' phenomenology. DTIC

N94-26304# Pacific-Sierra Research Corp., Santa Monica, CA.
EXCITATION OF EARTH-IONOSPHERE WAVEGUIDE IN THE ELF AND LOWER VLF BANDS BY MODULATED IONOSPHERIC CURRENT
E. C. Field and R. M. Bloom 21 May 1993 33 p
(Contract F19628-90-C-0100)
(AD-A274969; SR-3; PL-TR-93-2024) Avail: CASI HC A03/MF A01

In this report, the principal of reciprocity is used in conjunction with a full-wave propagation code to calculate ground-level fields excited by ionospheric currents modulated at frequencies between 50 and 100 Hz with HF heaters. Results show the dependence on source orientation, altitude, and dimension and therefore pertain to experiments using the HIPAS or HAARP ionospheric heaters. In the end-fire mode, the waveguide excitation efficiency of an ELF HED in the ionosphere is up to 20 dB greater than for a ground-based antenna, provided its altitude does not exceed 80 to 90 km. The highest efficiency occurs for a source altitude of around 70 km; if that altitude is raised to 100 km, the efficiency drops by about 20 dB in the day and 10 dB at night. That efficiency does not account for the greater conductivity modulation that might be achieved at altitudes greater than 70 km, however. The trade-off between the altitude dependencies of the excitation efficiency and maximum achievable modulation depends on the ERP of the HF heater, the optimum altitude increasing with increasing ERP. For HIPAS the best modulation altitude is around 70 km, whereas for HAARP there might be marginal value in modulating at attitudes as high as 100 km. DTIC

N94-26338# Boston Coll., Chestnut Hill, MA. Inst. for Space Research.
CRRES HIGH ENERGY PROTON FLUX MAP
M. S. Gussenhoven, E. G. Mullen, C. Hein, J. Bass, and D. Madden Jan. 1994 9 p
(Contract F19628-92-K-0003)
(AD-A274803; PL-TR-94-2004) Avail: CASI HC A02/MF A01

Proton flux maps of near-Earth space are presented using the Proton Telescope (PROTEL) detector on CRRES. The proton energy range covered is 1 - 100 MeV. Contamination of PROTEL measurements due to more than 100 MeV protons is corrected using loss cone data, resulting on consistency with dosimeter measurements and a Monte Carlo computer model of PROTEL. Two states of the inner magnetosphere were found during the CRRES mission, a quiet state having a single proton belt, and an active state with a double belt. The properties of the new population in the second belt are presented. Comparisons with NASA proton codes are made. DTIC

N94-26365# International Centre for Theoretical Physics, Trieste (Italy).
DETERMINATION OF THE GEOMAGNETIC EXTERNAL CONTRIBUTION BY NONLINEAR OPTIMIZATION METHODS
H. Comisel and L. Popa Jul. 1993 16 p
(DE94-600882; IC-93/225) Avail: CASI HC A03/MF A01 (US Sales Only)

The fluctuations of the Geomagnetic Field have been determined from magnetometric data in the framework of AKTIVE experiment. Using an approximate model which describes the oscillating motional of the satellite, the parameters of motion have also been calculated. DOE

N94-26418# International Centre for Theoretical Physics, Trieste (Italy).
ORTHODOX GRAVITY
A. Y. Shiekh Jul. 1993 7 p
(DE94-601560; IC-93/196) Avail: CASI HC A02/MF A01 (US Sales Only)

A scalar filed theory is investigated within the context of orthodox quantum gravity. DOE

N94-26433# California Univ., Berkeley. Seismographic Station.
ELASTIC SCATTERING BY A SPHERICAL INCLUSION Final Report, 12 Sep. 1990 - 31 Aug. 1993
Valeri A. Korneev and Lane R. Johnson 30 Aug. 1993 54 p
(Contract F19628-90-K-0055)
(AD-A274713; PL-TR-93-2193) Avail: CASI HC A04/MF A01

The scattering problem of an arbitrary elastic wave incident upon a spherically symmetric inclusion is considered. General results expressed in the form of canonical scattering coefficients are obtained for the cases of incident P waves and incident S waves. Optical theorems relating the scattering cross-section to the amplitude of the scattered field in the forward direction are also derived for both of these cases. Analytical expressions for scattering coefficients of a homogeneous elastic sphere, a sphere filled by fluid, and a spherical cavity are presented, and scattering cross-sections are calculated for these different types of obstacles. It is shown that the scattering scale factor for low frequencies is defined by the wavelength of the scattered wave rather than the wavelength of the incident wave. Low velocity fluid inclusions have a resonant type of scattering with numerous peaks in the spectrum. Various approximate solutions are derived from the exact solutions, including the low contrast (Born) case and the low frequency (Rayleigh) case. The modifications of the low contrast solution necessary to maintain conservation of energy are discussed. Low-frequency asymptotics of the scattering coefficients for a homogeneous sphere of arbitrary contrast are obtained together with expressions for the scattered fields from both P and S incident waves. These expressions can be used for energy absorbing inclusions by assigning complex values to the elastic parameters. Waves scattered by the earth's core are examined as an example of high-frequency scattering. DTIC

N94-26475# National Inst. for Resources and Environment, Ibaraki (Japan). Fracture Mechanics and Explosives Div.

STUDIES ON THE MEASUREMENT OF SUBSURFACE FRACTURES AND GEOSTRESS USING ACOUSTIC EMISSION TECHNIQUE FOR DEEP COALBED DEVELOPMENT [CHIKA SHINBU TANSO KAIHATSU NI KAKAWARU AE HO NI YORU CHIKA KIRETSU TO CHIKA ORYOKU NO KEISOKU NI KANSURU KENKYU]

Masahiro Seto, Manabu Utagawa, Kunihisa Katsuyama, Tamotsu Kiyama, Takashi Narita, and Makoto Kono 11 Jun. 1993 131 p In JAPANESE (ISSN 0916-9989)
(Rept-7; JTN-94-80514) Avail: CASI HC A07/MF A02

Acoustic Emission (AE) technique was applied to the estimation of fractures and geostress using three kinds of AE measuring systems. One is for measuring AE parameters, other one is for measuring AE waves, and another is for measuring AE parameters in combination with two dimensional source location. The results of the study on the following subjects are as follows: (1) AE measuring systems and experimental consideration on the AE behavior of coal under the compressive stress; (2) experimental considerations on the propagation of hydrofracture in the discontinuous rocks, the propagation of hydrofracture in the coal measure rock, the mechanism of the Kaiser effect of AE, and the effect of elapsed time on the Kaiser effect; and (3) the practical application of the new suggested method to the estimation of geostress using cored rocks. It was confirmed that the new method for estimating geostress using acoustic emission was applicable to the estimation of geostress from cored rocks. Author (NASDA)

N94-26502 Joint Inst. for Nuclear Research, Dubna (USSR). Lab. of Computing Techniques and Automation.

ABOUT STOCHASTIZATION OF MOTION OF CHARGED PARTICLES IN GEOMAGNETIC FIELD AND IN THE FIELD OF A WAVE PACKET [O STOKHASTIZATSII DVIZHENIYA ZARYAZHENNYKH CHASTITS V GEOMAGNITNOM POLE I POLE VOLNOVOGO PAKETA]

I. V. Amirkhanov, E. P. Zhidkov, V. V. Ignatov (Academy of Sciences, USSR, Moscow.), A. N. Ilina (Moscow State Univ., Russia.), and I. V. Ilin (Moscow State Univ., Russia.) 1992 11 p In RUSSIAN Limited Reproducibility: More than 20% of this document may be affected by microfiche quality
(DE93-634309; JINR-R-11-92-288) Avail: Issuing Activity (Department of Energy (DOE)) (US Sales Only)

The mechanism of stochastic acceleration of the particles in magnetic field and in the field of a wave packet in the conditions of geomagnetic trap is considered. A short survey of the latest works on the problem of stochastic heating of the particles and their resonance interaction with a wave packet in constant magnetic field is given. The simple conclusion of twist mapping is given. DOE

N94-26504 Joint Inst. for Nuclear Research, Dubna (USSR).

THE GRAVITY EQUATIONS IN THE LOBACHEVSKIJ SPACE [URAVNENIYA TYAGOTENIYA V PROSTRANSTVE LOBACHEVSKOGO]

N. A. Chernikov 1992 20 p In RUSSIAN Limited Reproducibility: More than 20% of this document may be affected by microfiche quality
(DE93-634334; JINR-R-2-92-192) Avail: CASI HC A03 (US Sales Only)

The gravity equations in the Lobachevskij space are derived. The problem of the gravitational field of point mass in the Lobachevskij space is solved. DOE

N94-26515# Geological Survey, Denver, CO.

VOLCANOLOGY AND VOLCANIC ACTIVITY WITH A PRIMARY FOCUS ON POTENTIAL HAZARD IMPACTS FOR THE HAWAII GEOTHERMAL PROJECT

R. B. Moore, P. T. Delaney, and J. P. Kauahikaua (Hawaiian Volcano Observatory.) 1993 10 p
(Contract DE-AI05-93OR-22089)
(DE94-001614; DOE/OR-22089/3; USGS-OFR-93-512A) Avail: CASI HC A02/MF A01

This annotated bibliography reviews published references about potential volcanic hazards on the Island of Hawaii that are pertinent to drilling and operating geothermal wells. The first two sections of this annotated bibliography list the most important publications that describe eruptions of Kilauea volcano, with special emphasis on activity in and near the designated geothermal subzones. References about historic eruptions from Mauna Loa's northeast rift zone, as well as the most recent activity on the southern flank of dormant Mauna Kea, adjacent to the Humu'ula Saddle are described. The last section of this annotated bibliography lists the most important publications that describe and analyze deformations of the surface of Kilauea and Mauna Loa volcanoes. DOE

N94-26569# Boston Univ., MA.

UPPER ATMOSPHERE NEUTRAL AND PLASMA DENSITY MODELING Final Report, 25 May 1990 - 26 May 1993

Jeffrey M. Forbes and Matthew Fox 31 Mar. 1993 43 p
(Contract F19628-90-K-0014)
(AD-A274768; PL-TR-93-2115) Avail: CASI HC A03/MF A01

The neutral density studies described in this report concentrate on specifying tidal aspects of the thermosphere. Firstly, HME's were used to describe the variations in a database of tidal measurements providing improved thermospheric specification. Similar techniques were used to derive diurnal and semi-diurnal density corrections to the Grove/MSIS83 model currently used by the AWS. Finally, the variations of satellite-based (SETA) wind and density measurements in the 170-220 km high latitude region have been described. The plasma modeling work described in this report includes both the development and application of semi-empirical ionospheric models and the application of theoretical models. A simple model was derived for storm-time middle-latitude perturbation in TEC. A simple model of slab thickness was developed leading to a simple successful model of TEC. Slab thickness was also used as a constraint in a new profile formalism that was both validated against an ICS database and extended into a SLIM-like profile model. The PLIM was applied in diagnostic modeling studies to investigate the nature of diurnal double maxima and to derive relationships between ionospheric parameters and satellite-based UV nightglow measurements providing additional ionospheric monitoring at AWS. DTIC

N94-26576# Lawrence Livermore National Lab., CA. Global Climate Research Div.

NUMERICAL PROCEDURE FOR PLANETARY WAVE SOLUTION

Woo Kap Choi and D. J. Wuebbles Sep. 1993 12 p
(Contract W-7405-eng-48)
(DE94-004280; UCRL-ID-115335) Avail: CASI HC A03/MF A01

The newly-developed LLNL two-dimensional chemical-radiative-transport model requires a knowledge of the EP flux divergence as an input momentum forcing. The major contributions for this forcing term come from the synoptic wave in the troposphere, the planetary wave in the stratosphere and mesosphere and the gravity wave in the upper mesosphere. The major source of the zonal momentum forcing in the middle atmosphere is the nonlinear planetary wave breaking. This planetary wave breaking also plays a significant role of mixing the chemical tracers. Garcia suggested a way of parameterizing the planetary wave breaking by using linear damping of the primary wave. In this note we describe the procedure of obtaining the wave solution for the parameterization. DOE

N94-26599*# Southwest Research Inst., San Antonio, TX. Dept. of Space Sciences.

INVESTIGATION OF PLASMA INSTABILITIES IN THE POLAR CUSP Annual Progress Report, 1 Sep. 1993 - 28 Feb. 1994

H. K. Wong 1994 10 p
(Grant NAGw-1620; SwRI Proj. 15-2779)
(NASA-CR-195212; NAS 1.26:195212) Avail: CASI HC A02/MF A01

During the last six months, considerable progress was made in studying the excitation of electromagnetic waves in the whistler frequency range by an anisotropic or gyrating electron beam. A paper entitled 'Electron Cyclotron Wave Generation by Relativistic Electrons' was published in the Journal of Geophysical Research. Another paper entitled 'Electron Beam Excitation of Upstream Waves in the Whistler Mode Frequency Range' was submitted for publication in Journal of Geophysical Research. This paper is in collaboration with Dr. C. W. Smith at Bartol Research Institute. In this paper, it was shown that an anisotropic electron beam (or gyrating electron beam) is capable of generating both left-hand and right-hand polarized electromagnetic waves in the whistler frequency range. Our earlier paper 'Electromagnetic Components of Auroral Hiss and Lower Hybrid Waves in the Polar Magnetosphere' was accepted for publication in the AGU Chapman Conference on Micro and Meso Scale Phenomena in Space Plasmas. Electromagnetic waves in the lower hybrid and whistler waves regime were identified and a mechanism of how these waves are generated was suggested. Author (revised)

N94-26752 Australian National Univ., Canberra. Research School of Earth Sciences.

A PRELIMINARY SHEAR VELOCITY MODEL FOR CENTRAL ASIA Final Report, Jan. - 31 Dec. 1993

Alet Zielhuis and Brian L. Kennett 24 Dec. 1993 9 p Limited Reproducibility: More than 20% of this document may be affected by microfiche quality
(Grant AF-AFOSR-0352-90)
(AD-A274972; AFOSR-94-0003TR) Avail: CASI HC A02

Waveforms of S body waves and Rayleigh waves are analyzed with the method of partitioned waveform inversion, with the objective to develop a three dimensional S-velocity model for the crust and upper mantle below Central Asia. Thus far, 103 seismograms have been processed. Using starting models with crustal thicknesses representative for the source-receiver path, good predictions of the observed waveforms, and good fits, have been obtained. The preliminary model, constructed on the basis of the data collected, shows that the Indian craton is marked by distinctly higher velocities than the rest of the region between 45 and at least 100 km depth. The Tarim craton and the Sino-Korean craton do not show high velocities at this depth. The Tibetan Plateau shows low velocities between 70 and 200 km depth. DTIC

N94-26762# Pacific Northwest Lab., Richland, WA.

RECENT ASCOT EXPERIMENTS IN MULTI-LAYERED FLOWS

C. E. Elderkin Sep. 1993 5 p Presented at the Topical Meeting on Environmental Transport and Dosimetry, Charleston, SC, 31 Aug. - 3 Sep. 1993
(Contract DE-AC06-76RL-01830)
(DE94-002360; PNL-SA-22598; CONF-930810-11) Avail: CASI HC A01/MF A01

The US Department of Energy's (DOE's) Atmospheric Studies in Complex Terrain (ASCOT) program has conducted its most recent research along the mountain-plains interface near DOE's Rocky Flats Plant in Colorado. ASCOT meteorological experiments in January and February 1991 were coordinated with Rocky Flats tracer releases for airflow and dispersion evaluations. It was found that dispersion was controlled by multiple scales of motion that created interacting layers of flow varying significantly in three dimensions and on an hourly basis. Plume dispersion at night was held close to the surface within a stable drainage-layer that followed regional flow features, intermittently interrupted by evolving mountain-canyon flows. Further implications of the highly variable flow features are that releases into shear zones above shallow surface layers or into canyon outflows, undetected by conventional measurement networks, could be transported unexpected directions diverging widely from predictions. DOE

N94-26806# Los Alamos National Lab., NM.

ELECTRICAL CONDUCTIVITY OF PEROVSKITE-MAGNESIOWUESTITE AS A FUNCTION OF PRESSURE AND TEMPERATURE

J. Peyronneau (Institut de Physique du Globe, Paris, France.), J. P. Poirier (Institut de Physique du Globe, Paris, France.), and T. J. Shankland 1993 5 p Presented at the 14th International Conference of the International Association for the Advancement of High Pressure Science and Technology, Colorado Springs, CO, 27 Jun. - 2 Jul. 1993
(Contract W-7405-eng-36)
(DE94-002714; LA-UR-93-3654; CONF-930676-61) Avail: CASI HC A01/MF A01

The high pressure transformation products of olivine, (Mg(sub 1-x),Fe(sub x))(sub 2)SiO4--the most abundant mineral in the Earth's upper mantle--are perovskite (Mg,Fe)SiO3 and magnesiowuestite (Mg,Fe)O. These materials are considered the principal components of the lower mantle, which comprises about 2/3 of Earth's volume. We measured the electrical conductivity (sigma) of a perovskite-magnesiowuestite mixture transformed by laser heating in a diamond anvil cell. From a starting material of San Carlos olivine having x=0.16 the high pressure phases were (Mg(sub 1-x),Fe(sub x))SiO3 with x=0.08 and (Mg(sub 1-x),Fe(sub x))O with x=0.24. Iron-magnesium partitioning was determined by TEM and x-ray microanalysis. During conductivity measurements the sample was heated to 400C by an external heater at different pressures to 40 GPa. To derive activation energy and activation volume the data were simultaneously fitted to the equation (sigma)=(sigma)(sub o)exp(-(Delta)U-P(delta)V)/kT. Conductivities extrapolated to lower mantle conditions are of order 1-10 S/m, in good agreement with geophysical models. DOE

N94-26828# Army Research Lab., Adelphi, MD.

A PRELIMINARY METHOD FOR ATMOSPHERIC SOUNDINGS IN REAL TIME USING SATELLITE AND GROUND-BASED REMOTELY SENSED DATA Final Report

James Cogan and Aldo Izaguirre Jul. 1993 45 p
(AD-A274381; ARL-TR-240) Avail: CASI HC A03/MF A01

A near-real-time sounding of the atmosphere from the surface to less than or equal to 30 km may be obtained by combining atmospheric profiles from meteorological (met) satellite and a ground-based system for remotely sensing wind and temperature. This type of capability is essential for optimum use of Army assets such as artillery and defense against biological and chemical attack. This report describes the method for merging data from satellite and ground-based remote-sensing systems and briefly discusses the algorithms used to evaluate the combined soundings. The current software allows the user to generate output in a standard form or in the format of an artillery met message. Initial results of this merging method are compared with data from nearly coincident rawinsondes. Preliminary comparisons of individual combined and rawinsonde sounding pairs, and individual met message zones for a number of sounding pairs, give an initial insight into the technique and the satellite/ground-based system concept. DTIC

N94-26855# Scripps Institution of Oceanography, La Jolla, CA. Inst. of Geophysics and Planetary Physics.

NONLINEAR HYSTERESIS IN AN ENDOCHRONIC SOLID Final Report, 3 Nov. 1991 - 3 Nov. 1993

Jean-Bernard Minster 4 Jan. 1994 17 p
(Contract F19628-88-K-0039)
(AD-A274594) Avail: CASI HC A03/MF A01

Propagation of seismic waves in the nearfield where rock rheology is demonstrably nonlinear raises unique difficulties. Nonlinearity arises primarily in two forms at intermediate to large strains: (1) nonlinear elasticity, and (2) amplitude-dependent attenuation. The proper representation of nonlinear constitutive equations for rocks in this regime is a potentially important ingredient of quantitative source models. We have shown previously that nonlinear one-dimensional wave propagation can result in spectral distortions at all wavelengths. This effect is strongly pulse-shape dependent, and therefore, calls for a 3-D capability. More recently, we found that our approximate description of the phenomenology in the nonlinear regime was inadequate and unable to simulate new laboratory observations. We describe an intrinsically nonlinear rheological model, based on the endochronic framework of K. Valanis, which replicates the main features of observed hysteresis loops in the strain regime of interest and is easily reduced to differential form. The resulting differential equations can be readily solved numerically. Thus, this model is suitable for finite difference and finite element stress wave codes. Ultimately, a complete description of the rheology in terms of a thermodynamically valid constitutive equation is really what should be used in numerical simulations, if it can be developed and validated experimentally. DTIC

N94-26874 Universidad Nacional Autonoma de Mexico, Mexico City.

GEOLOGICAL DATING BY Ar-40 - Ar-39 METHOD Ph.D. Thesis [FECHAMIENTO GEOLOGICO POR EL METODO: 40 AR - 39 AR]

M. E. VollbertRomero 1992 90 p In SPANISH Limited Reproducibility: More than 20% of this document may be affected by microfiche quality
(DE94-601975; INIS-mf-13617) Avail: CASI HC A05 (US Sales Only)

The isotope K40 is radioactive, it decays to Ar-40 stable. The number of Ar-40 atoms produced from K-40, permits to calculate the date of rocks and minerals. This dating technique is named 'Conventional K-Ar Dating Method'. The Ar-40 - Ar-39 dating method permits to calculate the age of rocks and minerals eliminating the limitation of the K-Ar method by calculating potassium and argon concentrations in a single measurement of the ratio of argon isotopes. The irradiation of the sample with fast neutrons in the nuclear reactor was established. Ar-39 is obtained from the induced reaction K-39 (n,p) Ar-39. Thus the ratio of (Ar-39)-(Ar-39) allows to obtain the date of rocks and minerals. This ratio was measured in a mass spectrometer. If the measurement of argon concentration in the sample is carried out at different increasing temperature values, it is possible to get information of paleotemperatures. The number of atoms Ar-39 is a function of the number K-39 atoms, irradiation time, neutrons flux, its energy E and the capture cross section sigma of K-39. These parameters are calculated indirectly by obtaining the so called 'J value ' by using a standard mineral with known age (HD-BI y Biot-133), this mineral is irradiated together with the unknown age sample. The values of 'J' obtained are in the interval of 2.85 to 3.03 x 10(exp -3)J/h. Rocks from 'Tres Virgenes' were dated by the method described, showing an agreement with previous values of different authors. The age of these rocks are from Cenozoico era, mainly in the miocene period. DOE

N94-26880 Technische Univ., Delft (Netherlands). Lab. of Electromagnetic Research.
ELASTIC WAVE UP/DOWN DECOMPOSITION IN INHOMOGENEOUS AND ANISOTROPIC MEDIA: AN OPERATOR APPROACH AND ITS APPROXIMATIONS
Maarten V. deHoop (Schlumberger Cambridge Research, England.) and Adrianus T. deHoop 1993 56 p Limited Reproducibility: More than 20% of this document may be affected by microfiche quality
(PB94-126497; ET/EM-1993-16) Copyright Avail: CASI HC A04/MF A01

A structural operator approach to the up/down decomposition of elastic waves in inhomogeneous and anisotropic media is presented. First, the up/down decomposition is carried out; next, a decomposition of the wave field into its polarization constituents is worked out. The procedure is discussed in detail for the class of orthorhombic media and includes lateral variations. The high-frequency approximation to the operator approach is shown to be amenable to matrix manipulations in the horizontal Fourier transform domain. Two-level parabolic approximations are carried out to find sparse matrix (finite-difference) representations of the relevant operators. Finally, the space-time peculiarities and artifacts associated with the parabolic approximation to the particle velocity of the wave motion generated by a point force in a homogeneous and isotropic solid are discussed. NTIS

N94-27039# Swedish Inst. of Space Physics, Kiruna.
KIRUNA GEOPHYSICAL DATA. DATA SUMMARY 93/4-6, APRIL-JUNE 1993
Sheila Kirkwood, ed. 1993 57 p See also PB93-210771
(ISSN 0453-9478)
(PB94-123700) Avail: CASI HC A04/MF A01

This is a collection of results of ground-based more or less continuous measurements of upper atmosphere variables carried out at the Swedish Institute of Space Physics. The objective with this data summary is to present current geophysical data, related to polar upper atmospheric conditions, to those who require it for their research work. Contents: Legend--Geomagnetic data, All-sky camera data, and Ionospheric absorption data; Tables of April-June 1993--Geomagnetic K-indices, and All-sky camera; Reproductions for April-June 1993--Magnetogram plots, and Riometer recordings. NTIS

N94-27040# Swedish Inst. of Space Physics, Kiruna.
AURORAL TOMOGRAPHY WORKSHOP PROCEEDINGS
Ake Steen, ed. Aug. 1993 100 p Workshop held in Kiruna, Sweden, 9-11 March, 1993
(ISSN 0284-1703)
(PB94-123718; IRF-SR-213) Avail: CASI HC A05/MF A02

In ionospheric and atmospheric physics, the importance of multi-station imaging has grown as a consequence of the availability of scientific grade CCD cameras with digital output and affordable massive computing power. Tomographic inversion techniques are used in many different areas, e.g. medicine, plasma research, and space physics. The tomography workshop was announced to gather a limited group of people interested in auroral tomography or tomographic inversion methods in general. ALIS (Auroral Large Imaging System) is a multi-station ground-based system developed primarily for three-dimensional auroral imaging, however, other non-auroral objects can be studied with ALIS, e.g. stratospheric clouds. Several of the contributions in the workshop dealt with problems related to geometries similar to the ALIS-configuration. NTIS

N94-27043# Swedish Inst. of Space Physics, Kiruna.
KIRUNA GEOPHYSICAL DATA. DATA SUMMARY 93/1-3, JANUARY-MARCH, 1993
Sheila Kirkwood, ed. 1993 60 p See also PB93-210771
(ISSN 0453-9478)
(PB94-123791) Avail: CASI HC A04/MF A01

This is a collection of results of ground-based more or less continuous measurements of upper atmosphere variables carried out at the Swedish Institute of Space Physics. The objective with this data summary is to present current geophysical data, related to polar upper atmospheric conditions, to those who require it for their research work. Contents: Legend--Geomagnetic data, All-sky camera data, and Ionospheric absorption data; Tables of January-March 1993--Geomagnetic K-indices, and All-sky camera; Reproductions for January-March 1993--Magnetogram plots, and Riometer recordings. NTIS

N94-27052# Wageningen Agricultural Univ. (Netherlands).
TIME DOMAIN REFLECTOMETRY FOR MEASURING BULK SOIL ELECTRICAL CONDUCTIVITY AND COMPARISON WITH THE EM38 INSTRUMENT
P. C. Slik May 1993 71 p
(PB94-125432; REPT-35) Avail: CASI HC A04/MF A01

The purpose of the report is to investigate the capability of Time Domain Reflectometry (TDR) to measure water content and bulk soil electrical conductivity (EC(sub a)) simultaneously and to compare these values with electromagnetic (EM38) induction measurements for five different soil profiles. The study sites all had a natural vegetation. Horizontal and vertical EM38 measurements were taken at intervals of 10 cm above soil surface to a height of 1.3 meter. TDR is found to be a quick method for determining an EC(sub a) profile in comparison with soil sampling. NTIS

N94-27143# Massachusetts Inst. of Tech., Cambridge. Dept. of Earth Atmospheric and Planetary Sciences.
CRUSTAL DEFORMATION MEASUREMENTS IN THE VICINITY OF VANDENBERG AIR FORCE BASE Final Report, 1 Jun. 1989 - 28 Feb. 1993
Robert W. King 16 Aug. 1993 6 p
(Grant AF-AFOSR-0400-89)
(AD-A274166; AFOSR-93-0882TR) Avail: CASI HC A02/MF A01

Recent geological and geodetic studies have suggested that the region surrounding Vandenberg AFB is undergoing active crustal deformation. This has important implications for both the geodetic stability and the seismogenic potential of the Western Test Range (WTR). Part of the evidence for significant deformation was obtained from GPS measurements which we carried out in cooperation with other university and government scientists beginning in late 1986. These measurements were made annually through 1991 over a broad region of central and southern California but were of insufficient spatial and temporal density to answer important questions about the seismogenic potential of Vandenberg. DTIC

N94-27237*# New Hampshire Univ., Durham. Dept. of Physics.
IONOSPHERE-MAGNETOSPHERE COUPLING Final Technical Report, 1 Mar. 1991 - 31 Jan. 1994
Richard L. Kaufmann 1994 5 p
(Grant NAGw-1625)
(NASA-CR-195222; NAS 1.26:195222) Avail: CASI HC A01/MF A01

Principal results are presented for the four papers that were supported from this grant. These papers include: 'Mapping and Energization in the Magnetotail. 1. Magnetospheric Boundaries; 'Mapping and Energization in the Magnetotail. 2. Particle Acceleration'; 'Cross-Tail Current: Resonant Orbits'; and 'Cross-Tail Current, Field-Aligned Current, and B(sub y)'. CASI

N94-27299# National Inst. of Polar Research, Tokyo (Japan).
JARE DATA REPORTS. NO. 186: UPPER ATMOSPHERE PHYSICS DATA. SYOWA AND ASUKA STATIONS, 1990
Takayuki Ono, Hideaki Nakajima, Masaki Satoh (Ministry of Posts and Telecommunications, Kashima, Japan.), Kazuhiro Ohtaka (Ministry of Posts and Telecommunications, Tokyo, Japan.), Masatoshi Kawahara (Ministry of Posts and Telecommunications, Tokyo, Japan.), and Akinori Kumade et al Mar. 1993 224 p

(ISSN 0075-3343)
(JTN-94-80594) Avail: CASI HC A10/MF A03

This data book summarizes upper atmosphere physics data acquired by the Upper Atmosphere Physics Monitoring System at Syowa Station in 1990. The items of observations at Syowa Station are geomagnetism (H-, D-, and Z-components of magnetic variations, total force of the geomagnetic field, H-, D- and Z-components of magnetic pulsations), ELF (Extremely Low Frequency)-VLF (Very Low Frequency) wave (intensities and wide-band signal of ELF-VLF emissions), ionosphere (cosmic noise absorption) and aurora (all sky camera, scanning photometer, fixed directional photometer, multi-channel photometer, all sky TV, monochromatic CCD (Charged Coupled Device) TV (Television) and Fabry-Perot Doppler Imaging System), and those at Asuka Station are geomagnetism (H-, D- and Z-components of magnetic variations and magnetic pulsations), ionosphere (cosmic noise absorption and differential doppler measurement of NNSS (National Navigation Satellite System) telemetry signals) and aurora (all sky camera and fixed directional photometer). It contains an outline of Upper Atmosphere Physics Monitoring System, specifications of the observation instruments and the data acquisition system, recording periods, the format of the compiled digital data, and magnetograms in the period of January 1 to December 31, 1990 at Syowa Station and Asuka Station. Author (NASDA)

N94-27300# National Inst. of Polar Research, Tokyo (Japan).
THE SIXTEENTH SYMPOSIUM ON COORDINATED OBSERVATIONS OF THE IONOSPHERE AND THE MAGNETOSPHERE IN THE POLAR REGIONS: PROGRAM AND ABSTRACTS [DAI 16 KAI KYOKUIKI NI OKERU DENRIKEN JIKIKEN SOGO KANSOKU SHINPOJIUMU PUROGURAMU]
15 Dec. 1992 82 p In ENGLISH and JAPANESE Symposium held in Tokyo, Japan, 15-16 Dec. 1992
(JTN-94-80601) Avail: CASI HC A05/MF A01

This symposium concerns ionosphere and magnetosphere in the polar regions based on data acquired by satellite observation, tethered rocket, atmospherics, ground observation, balloon observation, computer simulation, etc. The presentation included studies on High Frequency (HF) wave, Very Low Frequency (VLF) wave and Ultra Low Frequency (ULF) wave observation, and Pi2 cavity and global Pc5 pulsation concerning ULF wave. For phenomena relating substorm, polar cap, polar shower, aurora oval, plasma regime, Birkeland currents, plasmapheric disturbances are presented. Magnetosphere-ionosphere coupling included topics concerning observation of aurora, field-aligned potential drop structure and ion temperature. For heliosphere and magnetopause study, structure of the polar region of the outer heliosphere and solar coronal region, observation by Geophysical Tail (GEOTAIL) satellite, and stratospheric and tropospheric changes were presented. Geomagnetic storms concerning statistical study, polar cap absorption, thermosphere, airglow emission enhancements, electric field enhancements, and low-latitude aurorae were reported. There were presentations of stratospheric balloon experiments and polar patrol balloon project, phenomena relating aurorae, and future observation plans. Author (NASDA)

N94-27330 Tel-Aviv Univ. (Israel).
WAVE PROPAGATION IN THE SHALLOW REGIONS OF THE EARTH'S CRUST AND THE BOREHOLE VICINITY Ph.D. Thesis
David Kessler Sep. 1991 127 p
(ITN-94-85237) Copyright Avail: Issuing Activity (Tel-Aviv Univ., Exact Sciences Library, Ramat Aviv 69978, Israel)

New numerical methods are developed for the simulation of wave propagation in the vicinity of a cylindrical object. These methods are suitable for the solution of wave propagation problems in a completely heterogeneous medium. A review of the mathematical methods used in numerical seismic modeling serves as a background to the new methods developed in this work. It includes the basic principles which lead to the creation of numerical solutions for the acoustic as well as the elastic wave equations. The 2-dimensional Chebyshev-Fourier cylindrical numerical grid is presented. It comprises the non-periodic Chebyshev expansion in the radial direction and the periodic Fourier expansion in the angular direction. We solve the acoustic wave equation using this same grid. The boundary conditions are applied using one-dimensional considerations, namely the characteristic variables of the wave equation. An elastic rheology is introduced. The elastic wave equation is solved on the 2-dimensional Chebyshev-Fourier cylindrical numerical grid. In order to stabilize the numerical scheme, we have to adopt a multi-domain approach. The numerical mesh is constructed from a few smaller ring shaped grids. The mesh that results is the 2-D multi-domain Chebyshev-Fourier cylindrical grid. The different subdomains can represent either solid or liquid material. The solution to the problem of wave propagation in the vicinity of a borehole is presented. Author (ISA)

N94-27334# Instituto de Pesquisas Espaciais, Sao Jose dos Campos (Brazil).
PHOTOCHEMICAL PROCESSES AND THE ATMOSPHERIC AIRGLOW EMISSIONS OF OH AND Na IN THE MESOSPHERIC REGION [PROCESSOS FOTOQUIMICOS E EMISSOES DE LUMINESCENCIA ATMOSFERICA DE OH E NA REGIAO DA MESOFERA]
Stella Maris Ludovic Melo Feb. 1992 37 p In PORTUGESE
(INPE-5380-PUD/050) Avail: CASI HC A03/MF A01

The Na and OH emissions in the mesosphere region of the atmosphere were known for more than three decades. Despite the great amount of work that has been carried out, an adequate comprehension of the physical-chemical processes involved has not been achieved yet. A brief review of the present state of knowledge in this area, with emphasis on historical aspects and on the main problems under study today, is presented. Author (revised)

N94-27342# National Inst. of Polar Research, Tokyo (Japan).
MEMORIES OF NATIONAL INSTITUTE OF POLAR RESEARCH. SERIES A-19. UPPER ATMOSPHERE PHYSICS: ELF EMISSION IN HIGH LATITUDES: RAY PATH CALCULATION AND GROUND-SATELLITE OBSERVATIONS
Hisao Yamagishi, Takao Hoshiai, Masaki Ejiri, Takeo Hirasawa, Yoshikuni Hiroi, Katsutada Kaminuma, Sadao Kawaguchi, Susumu Kokubun, Ikuo Kushiro, and Shinji Mae et al Mar. 1989 126 p
(ISSN 0386-5517)
(JTN-94-80592) Avail: CASI HC A07/MF A02

Results are presented of the study of the two kinds of the Extremely Low Frequency (ELF) ray propagation from the equatorial plane to the polar region with the observation of ELF and Very Low Frequency (VLF) waves by the International Satellite for Ionosphere Studies (ISIS) over Antarctica, ELF waves at Showa Station, Antarctica, and Bremsstrahlung X-rays by balloons. Conditions for the existence of penetrating ray paths are obtained from a two-dimensional ray tracing. Wave normal directions and arriving latitudes at low altitudes are also calculated. The calculated characteristics of ELF wave normals are compared with those from ISIS satellite observation in the altitude range of 1,450 to 3,500 km by means of spin-modulated characteristics and multi-ion cutoff characteristics of received ELF signals. Seasonal variation of ELF emission intensity at the ISIS satellite altitude and on the ground is attributable to a north-south asymmetry in the penetrating ray paths depending on a field-aligned electron density gradient in the both hemispheres. Another mode of ELF wave propagation, i.e., ducted propagation outside the plasmapause, is investigated for periodic emissions. ELF emissions observed on the ground are compared with Bremsstrahlung X-rays observed by balloons. Three balloon experiments were carried out in northern Norway and at Showa Station, Antarctica, and the observed Bremsstrahlung X-rays and ELF emissions were compared for three characteristic time scales: slow variations (a few tens of minutes), pulsations (from a few tens of seconds to several minutes) and bursts (less than 10 seconds). Author (NASDA)

N94-27380*# National Center for Atmospheric Research, Boulder, CO.
[SOLAR AND AIRGLOW MEASUREMENTS ABOARD THE TWO SUBORBITAL FLIGHTS NASA 36.098 AND 36.107] Final Report, 1993
Thomas N. Woods 31 Mar. 1994 8 p Original contains color illustrations
(Grant NAG5-676)
(NASA-CR-195279; NAS 1.26:195279) Avail: CASI HC A02/MF A01; 2 functional color pages

This suborbital program, involving the University of Colorado (CU), National Center for Atmospheric Research (NCAR), University of California at Berkeley (UCB), and Boston University (BU), has resulted in two rocket flights from the White Sands Missile Range, one in 1992 and one in 1993 as NASA 36.098 and 36.107 respectively. The rocket payload includes five solar instruments and one airglow instrument from CU/NCAR and one solar instrument and two airglow instruments from UCB/BU. This report discusses results on solar radiation measurements and the study of thermospheric airglow, namely the photoelectron excited emissions from N2 and O, for the CU/NCAR program. CASI

N94-27393*# Computational Physics, Inc., Fairfax, VA.
ANALYSIS OF EUV/FUV DAYGLOW AND AURORAL MEASUREMENTS Final Report
T. Majeed, D. J. Strickland, and R. Link Jan. 1994 80 p
(Contract NASw-4744)
(NASA-CR-195237; NAS 1.26:195237) Avail: CASI HC A05/MF A01

This report documents investigations carried out over the twelve month period which commenced in November 1992. The contract identifies the following three tasks: analysis of the O II 83.4 nm dayglow and comparison with incoherent scatter radar data, analysis of the EUV spectrum of an electron aurora, and analysis of the EUV spectrum of a proton-hydrogen-electron aurora. The analysis approach, data reduction methods, and results, including plots of O I 98.9 nm versus time and average spectra, are presented for the last two tasks. The appendices contain preprints of two papers written under the first task. The first paper examines the effect of new O(3P) photoionization cross sections, N2 photoabsorption cross sections, and O(+) oscillator strengths and transition probabilities on the O II 83.4 nm dayglow. The second addresses the problem of remotely sensing the dayside F2 region using limb O II 83.4 nm data. CASI

N94-27438*# Boston Univ., MA. Center for Space Physics.
CONFIGURATION OF THE NEAR-EARTH PLASMA SHEET Status Report, 1 Apr. 1993 - 31 Mar. 1994
Gary M. Erickson 1994 3 p
(Grant NAGw-2627)
(NASA-CR-195271; NAS 1.26:195271) Avail: CASI HC A01/MF A01

During the past year, research has continued in improving understanding in three related areas: the mechanisms responsible for magnetospheric substorm onset, a fundamental description of field-aligned currents and parallel electric fields, and consequences of dawn-side depletion and the physics of the Harang discontinuity. Derived from text

N94-27852*# SRI International Corp., Menlo Park, CA. Geoscience and Engineering Center.
MODELING OF THE COUPLED MAGNETOSPHERIC AND NEUTRAL WIND DYNAMOS Annual Technical Status Report No. 1, 1 Apr. 1993 - 30 Mar. 1994
Jeffrey P. Thayer 30 Mar. 1994 11 p
(Grant NAGw-3508; SRI Proj. 4604)
(NASA-CR-195273; NAS 1.26:195273) Avail: CASI HC A03/MF A01

This report summarizes the progress made in the first year of NASA Grant No. NAGW-3508 entitled 'Modeling of the Coupled Magnetospheric and Neutral Wind Dynamos.' The approach taken has been to impose magnetospheric boundary conditions with either pure voltage or current characteristics and solve the neutral wind dynamo equation under these conditions. The imposed boundary conditions determine whether the neutral wind dynamo will contribute to the high-latitude current system or the electric potential. The semi-annual technical report, dated December 15, 1993, provides further detail describing the scientific and numerical approach of the project. The numerical development has progressed and the dynamo solution for the case when the magnetosphere acts as a voltage source has been evaluated completely using spectral techniques. The simulation provides the field-aligned current distribution at high latitudes due to the neutral wind dynamo. A number of geophysical conditions can be simulated to evaluate the importance of the neutral wind dynamo contribution to the field-aligned current system. On average, field-aligned currents generated by the neutral wind dynamo contributed as much as 30 percent to the large-scale field-aligned current system driven by the magnetosphere. A term analysis of the high-latitude neutral wind dynamo equation describing the field aligned current distribution has also been developed to illustrate the important contributing factors involved in the process. The case describing the neutral dynamo response for a magnetosphere acting as a pure current generator requires the existing spectral code to be extended to a pseudo-spectral method and is currently under development. Derived from text

N94-27883*# Colorado Univ., Boulder. Dept. of Aerospace Engineering Sciences.
IONOSPHERIC CALIBRATION FOR SINGLE FREQUENCY ALTIMETER MEASUREMENTS Final Report
William S. Schreiner, George H. Born, and Robert E. Markin 21 Mar. 1994 26 p
(Grant NAG1-1491)
(NASA-CR-195709; NAS 1.26:195709) Avail: CASI HC A03/MF A01

This study is a preliminary analysis of the effectiveness (in terms of altimeter calibration accuracy) of various ionosphere models and the Global Positioning System (GPS) to calibrate single frequency altimeter height measurements for ionospheric path delay. In particular, the research focused on ingesting GPS Total Electron Content (TEC) data into the physical Parameterized Real-Time Ionospheric Specification Model (PRISM), which estimates the composition of the ionosphere using independent empirical and physical models and has the capability of adjusting to additional ionospheric measurements. Two types of GPS data were used to adjust the PRISM model: GPS receiver station data mapped from line-of-sight observations to the vertical at the point of interest and a grid map (generated at the Jet Propulsion Laboratory) of GPS derived TEC in a sun-fixed longitude frame. The adjusted PRISM TEC values, as well as predictions by the International Reference Ionosphere (IRI-90), a climatological (monthly mean) model of the ionosphere, were compared to TOPEX dual-frequency TEC measurements (considered as truth) for a number of TOPEX sub-satellite tracks. For a 13.6 GHz altimeter, a Total Electron Content (TEC) of 1 TECU 10(exp 16) electrons/sq m corresponds to approximately 0.218 centimeters of range delay. A maximum expected TEC (at solar maximum or during solar storms) of 10(exp 18) electrons/sq m will create 22 centimeters of range delay. Compared with the TOPEX data, the PRISM predictions were generally accurate within the TECU when the sub-satellite track of interest passed within 300 to 400 km of the GPS TEC data or when the track passed through a night-time ionosphere. If neither was the case, in particular if the track passed through a local noon ionosphere, the PRISM values differed by more than 10 TECU and by as much as 40 TECU. The IRI-90 model, with no current ability to unseat GPS data, predicted TEC to a slightly higher error of 12 TECU. The performance of PRISM is very promising for predicting TEC and will prove useful for calibrating single frequency altimeter height measurements for ionospheric path delay. When adjusted to the GPS line-of-sight data the PRISM URSI empirical model predicted TEC over a day's period to within a global error of 8.60 TECU rms during a nighttime ionosphere and 9.74 TECU rms during the day. When adjusted to the GPS derived TEC grid, the PRISM parametrized model predicted TEC to within an error of 8.47 TECU rms for a nighttime ionosphere and 12.83 TECU rms during the day. However, the grid cannot be considered globally due to the lack of sufficient numbers of GPS stations and large latitude gaps in GPS data. It is the opinion of the authors that using the PRISM model and adjusting to the global sun-fixed TEC grid regenerated with a localized weighted interpolation offers the best possibility of meeting the 10 TECU global rms (or 2 cm at 13.6 GHz) ionosphere range correction accuracy requirement of TOPEX/Poseidon and should be the subject of further study. However, it is clear that the anticipated requirement of 34 TECU global rms for TOPEX/Poseidon Follow-On (corresponding to the TOPEX/Poseidon performance) can not be met with any realizable combination of existing models and data assimilation schemes. Author

N94-27963# National Inst. of Polar Research, Tokyo (Japan).
ANTARCTIC RECORD, VOL. 36, NO. 2 [NANKYOKU SHIRYO VOL. 36, NO. 2]
Takao Hoshiai, ed., Masaki Ejiri, ed., Takeo Hirasawa, ed., Yoshikuni Hiroi, ed. (Chiba Univ., Japan.), Katsutada Kaminuma, ed., Sadao Kawaguchi, ed., Shunichi Kobayashi, ed. (Niigata Univ., Japan.), Susumu Kokubun, ed. (Tokyo Univ., Japan.), Yasuhiko Naito, ed., and Nobuo Ono, ed. et al 30 Jul. 1992 185 p In ENGLISH and JAPANESE
(ISSN 0085-7289)
(Rept-107; JTN-94-80590) Avail: CASI HC A09/MF A02

The following topics were discussed: Antarctica, antarctic region, atmospheric sounding, earth atmosphere, earth stratosphere, earth ionosphere, ice floes, auroras, auroral adsorption, electron energy, radio transmission, radio noise, ionospheric noise, solar activity, ice dome, core samples, clathrate hydrates, crystal structure, climate change, annual variation, penguin colony, breeding colony, moss colonies, vegetation growth, radio receivers, antenna design, image analysis, image processing, imaging techniques, data acquisition, computer programs, photometers, riometers, imaging riometers, photometers, cameras, data recorders, magnetometers, artificial earthquakes, seismometers, and penetrators. For individual titles, see N94-27964 through N94-27973.

N94-27964# National Inst. of Polar Research, Tokyo (Japan).

ENERGY PARAMETERS OF THE INCIDENT AURORAL ELECTRONS DERIVED BY THE INTENSITY RATIO OF AURORAL EMISSIONS [TAHACHO FOTO META KANSOKU NI YORU KOKA DENSHI ENERUGI PARAMETA NO SUITEI] **c32**

Takayuki Ono, Ryusuke Satake (University of Electro-Communications, Chofu, Japan.), Takeo Yoshino (University of Electro-Communications, Chofu, Japan.), and Takeo Hirasawa *In its* Antarctic Record, Vol. 36, No. 2 30 Jul. 1992 p 163-180 In JAPANESE (For primary document see N94-27963 07-46)
Avail: CASI HC A03/MF A02

Average energy and total energy flux of the incident electrons in active auroras are estimated by using the intensity ratio of auroral emissions measured with a multi-channel photometer at Showa Station, Antarctica, in 1990. To avoid possible ambiguities which are mainly caused by quenching effects on metastable species and complex excitation processes, the intensity ratios of the emissions of allowed transitions were used such as 844.6 nm (OI), 670.5 nm (N2 1PG (Positive Bands)), and 427.8 nm (N2(+) 1NG (Negative Bands). Measured intensity ratios were directly compared with the result of model calculation of auroral emissions. The estimated energy parameters in active auroras showed a rapid change of average energy as well as total energy flux of electrons associated with pulsating auroras and intense auroral arcs. Average energy and total energy flux of the auroral electrons determined by the present method were consistent with the result of the previous insitu observations of precipitating electrons. These data analyses on active arcs in break-up phase showed that usage of the 427.8 nm emission has difficulty due to a scattering effect of the atmosphere. Usage of 670.5 nm emission in place of 427.8 nm made it possible to evaluate the energy parameters of electrons even in the vicinity intense auroral arcs. Author (NASDA)

N94-27965# Kyoto Univ., Sakyoku (Japan). Faculty of Science.

CHARACTERISTICS OF 30-MHz INTERFERENCE NOISES OBSERVED BY RIOMETERS [RIOMETA DE KANSOKU SARETA 30 MHZ KONSHIN NO SEISHITSU]

Akira Yukimatsu *In* National Inst. of Polar Research, Antarctic Record, Vol. 36, No. 2 30 Jul. 1992 p 181-202 In JAPANESE (For primary document see N94-27963 07-46)
Avail: CASI HC A03/MF A02

In 1989, when the sun was highly active, interference noises were often observed by 30 MHz riometers at Asuka and Showa Stations in Antarctica. The noises showed a systematic diurnal and seasonal variation. The noises were global phenomena because they were also seen in other riometer data at high and middle latitudes in the Northern Hemisphere. These noises were investigated in connection with ionospheric f(sub 0)F(sub 2) data, geomagnetic K(sub p) indices and sunspot numbers. The results are summarized as follows: (1) interference noises consist mainly of ground radio waves reflected by the ionosphere; (2) the interference noise occurrence shows a good correlation with f(sub 0)F(sub 2); and (3) the noise intensity shows a tendency of decreasing on weekends, and [illegible] feature suggests that the noises are mainly of artificial origins. It is concluded, therefore, that the occurrence feature of the interference noises reflects the condition of the ionosphere, and can be used as an indicator of the global electromagnetic wave environment in HF (High Frequency) range. Author (NASDA)

N94-27966# Nihon Univ., Tokyo (Japan). Coll. of Science and Technology.

A LABORATORY TEST ON CONSTRUCTION OF ICE DOMES AND THEIR LOAD-CARRYING CAPACITY [AISU DOMU MOKEI NO SHISAKU TO KYODO SHIKEN]

Toshio Hannuki, Kenji Ishizawa (National Inst. of Polar Research, Tokyo, Japan.), Kenji Futami, and Keita Tsukui *In* National Inst. of Polar Research, Antarctic Record, Vol. 36, No. 2 30 Jul. 1992 p 203-226 In JAPANESE (For primary document see N94-27963 07-46)
Avail: CASI HC A03/MF A02

Ice domes will be useful as a shelter of depot and laboratory space without heating systems which will be constructed on the ice field in the Arctic or Antarctic. Efficacious use of ice domes is discussed for facilities of research camp in the Antarctic. Some experiments on construction technique of ice domes and their load-carrying capacity were carried out in a low temperature laboratory. It was confirmed experimentally that ice domes could be made by spraying water onto a spherically inflated membrane form under the condition of holding a temperature below -18 C. Mechanical property of artificial ice made in the laboratory was examined by some bending tests of simply supported ice beams so as to discuss a constitutive model of ice for numerical analysis. Load-carrying capacity and creep behavior of ice dome models were examined in the laboratory and analytical models of ice structure for a numerical procedure of the design were discussed and compared with the tests. A usefulness of elastic-plastic model for the mechanical behavior of ice structures in a short term loading and a convenience of Maxwell model for the long time creep of ice structure were confirmed in the discussion. These laboratory tests and analytical applications led to the first step of realization of the ice dome construction in the Antarctic. Author (NASDA)

N94-27967# National Inst. of Polar Research, Tokyo (Japan).

DEVELOPMENT OF IMAGING RIOMETERS [IMEJINGU RIOMETA NO KAIHATSU] **c74**

Hisao Yamagishi, Masanori Nishino (National Inst. of Polar Research, Tokyo, Japan.), Mitsugi Sato, Yasuo Kato, Masayoshi Kojima, Natsuo Sato, and Takashi Kikuchi *In its* Antarctic Record, Vol. 36, No. 2 30 Jul. 1992 p 227-250 In JAPANESE Sponsored by Ministry of Education, Science and Culture, Tokyo, Japan Prepared in cooperation with Solar-Terrestrial Environment Lab., Nagoya Univ., Aichi, Japan and Communications Research Lab., Tokyo, Japan (For primary document see N94-27963 07-46)
Avail: CASI HC A03/MF A02

An eight by eight beam imaging riometer with a view field of 180 km by 180 km, spatial resolution of 20 km, and time resolution of 1 to 4 s was developed in Japan. System design is described with some stress on the difference from the first Imaging Riometer System (IRIS), developed by the University of Maryland. This system has a unique capability of displaying absorption image on the real time basis with the aid of QL (Quick Look) software, which is summarized in a separate paper. The performance of the array antenna system is confirmed by simulation calculations using the galactic radio noise map at 30 MHz obtained by Cane. Procedures for absorption image forming are also described. Some of the absorption images obtained by this system are compared with optical auroral images observed at the same location at the same time. It is found that the both images show a good similarity for morning-side auroras. It is, therefore, concluded that the imaging riometer is a very useful tool for monitoring the auroral form when the optical aurora observation is difficult by the sunlit, or weather condition. Author (NASDA)

N94-27968# Nagoya Univ., Toyokawa (Japan). Solar-Terrestrial Environment Lab.

QUICK-LOOK SYSTEM OF AURORAL ABSORPTION IMAGES BY IMAGING RIOMETER [IMEJINGA RIOMETA KYUSHU GAZO KYU ERU SHISUTEMU NO KAIHATSU] **c74**

Mitsugi Sato, Hisao Yamagishi, Yasuo Kato, and Masanori Nishino *In* National Inst. of Polar Research, Antarctic Record, Vol. 36, No. 2 30 Jul. 1992 p 251-267 In JAPANESE Original contains color illustrations (For primary document see N94-27963 07-46)
Avail: CASI HC A03/MF A02

Imaging riometer of two-dimensional multi-narrow beams is a powerful radio instrument to investigate the structure of CNA (Cosmic Noise Absorption) in the auroral ionosphere caused by the precipitation of energetic electrons. However, the instrument has a demerit of delay-look for imaging because of the use of a large capacity computer for data processing. QL (Quick-Look) system of the imaging riometer was developed by using a personal computer. This system has a function to view the CNA images in real time. QDC's (Quiet Day Curves) which indicate the condition of quiet ionosphere are determined from daily variations of cosmic noise intensity obtained during the initial ten days. Thereafter the QDC's are set into real-time data processing as a reference. The QL system has an advantage for real-time comparison with auroral images by the all-sky TV (Television) camera. Author (NASDA)

N94-27969# Hokkaido Univ., Sapporo (Japan). Inst. of Low Temperature Science.

CRYSTALLOGRAPHYIC ANALYSES OF CLATHRATE HYDRATES INCLUDED IN VOSTOK ICE CORES [BOSUTOKU KOA NI FUKUMARERU KURASURETO SUIWABUTSU NO KESSHOGAKUTEKI KAISEKI]

Takeo Hondo, Tsutomu Uchida (Hokkaido Univ., Sapporo, Japan.), Shinji Mae (Hokkaido Univ., Sapporo, Japan.), P. Duval (Centre National de la Recherche Scientifique, Saint Martin d'Heres, France.), and V. Y. Lipenkov (Arkticheskii i Antarkticheskii Nauchno-Issledovatelskii Inst., Leningrad, USSR.) *In* National Inst. of Polar Research, Antarctic Record, Vol. 36, No. 2 30 Jul. 1992 p 268-278 In JAPANESE (For primary document see N94-27963 07-46)

Avail: CASI HC A03/MF A02

Purpose and methods of crystallographic analyses of clathrate hydrates included in ice cores recovered at Vostok, Antarctica are briefly reviewed. The clathrate hydrate is a crystal composed of a cage structure formed by water molecules, and includes individual air molecules in the molecular cages. The crystallographic structure of the clathrate hydrate crystals found in deep ice cores determined by x ray diffraction and Raman scattering measurements is described, and the formation process of the crystals in the ice sheet is discussed. It is also discussed as a future prospect in core analysis that what kind of information and knowledge relating to climatic changes can be deduced from the crystallographic analysis of the clathrate hydrates. Author (NASDA)

N94-27970# National Inst. of Polar Research, Tokyo (Japan).

COUNTING ADELIE PENGUINS AT COLONIES: SEASONAL AND ANNUAL CHANGES [KORONI DENO ADERI PENGIN NO KAUNTO: KISETSU HENKA TO NEN HENKA] c51

In its Antarctic Record, Vol. 36, No. 2 30 Jul. 1992 p 279-284 In JAPANESE (For primary document see N94-27963 07-46)

Avail: CASI HC A02/MF A02

The number of Adelie penguin (Pygoscelis adeliae) adults at colonies around Showa Station changes seasonally. The penguins started to arrive at the colonies on October 20-25. The number of adults at each colony reached its maximum on November 10-20, decreased until late November and was stable on December 1-10. This seasonal pattern was consistent over years and colonies. Censuses in mid-November and early December are recommended since they could give reliable numbers of breeding pairs. Author (NASDA)

N94-27971# Hiroshima Univ. (Japan). Dept. of Environmental Studies.

NOTE ON THE STRUCTURE OF MOSS COLONIES COMPOSED OF TWO SPECIES ON KING GEORGE ISLAND, THE SOUTH SHETLAND ISLANDS [KINGUJOJITO NO NI SHU YORI NARU SENRUI KORONI NO KOZO NI TSUITE] c51

Takayuki Nakatsubo and Shuji Otani (National Inst. of Polar Research, Tokyo, Japan.) *In* National Inst. of Polar Research, Antarctic Record, Vol. 36, No. 2 30 Jul. 1992 p 285-293 Sponsored by Ministry of Education, Science and Culture, Tokyo, Japan (For primary document see N94-27963 07-46)

Avail: CASI HC A02/MF A02

Moss colonies composed of two species Sanionia uncinata and Bryum pseudotriquetrum are abundant in the vicinity of Great Wall Station on King George Island. Vertical cross-sections of these colonies were examined to know the colony structure indicating the interaction between the two species. In several colonies, a layer composed of Bryum pseudotriquetrum was partially covered with shoots of Sanionia uncinata. In some other colonies, a layer composed of Sanionia uncinata was partially covered with shoots of Bryum pseudotriquetrum. For the rest of the colonies, both species coexisted without covering each other. It is concluded that the proportion of the two species in a colony has changed through the colony growth, but the direction of the change varies among the colonies at each site. Author (NASDA)

N94-27972# Kyoto Univ., Sakyoku (Japan). Faculty of Science.

OBSERVATION OF THE UPPER ATMOSPHERE PHYSICS AT ASUKA STATION BY THE 30TH JAPANESE ANTARCTIC RESEARCH EXPEDITION IN 1989 [DAI 30 JI NANKYOKU CHIIKI KANSOKUTAI ASUKA KANSOKU KYOTEN ETTOTAI (1989): CHUKUKEI HOKOKU]

Akira Yukimatsu *In* National Inst. of Polar Research, Antarctic Record, Vol. 36, No. 2 30 Jul. 1992 p 294-309 In JAPANESE (For primary document see N94-27963 07-46)

Avail: CASI HC A03/MF A02

Observations of the upper atmosphere physics at Asuka Station from 1 Jan. to 24 Dec. 1989, carried out by the 30th Japanese Antarctic Research Expedition (JARE-30) are described. In JARE-30 one research member of the upper atmosphere physics was wintering at Asuka Station, and several instruments were newly installed so as to observe auroral phenomena in conjunction with Showa Station, Iceland observations, and scientific satellites. Characteristics of the JARE-30's observations at Asuka Station are as follows: (1) the observation of Cosmic Noise Absorption (CNA) with a 30 MHz riometer was made throughout the year; (2) a fixed direction and a tracking photometers were newly installed, and spatial and temporal developments of aurora photo emissions in various wave lengths were observed; (3) an all sky camera used in JARE-28 was re-installed; (4) an all sky SIT (Silicon Intensifier Target)-TV (Television) camera was newly installed so as to observe auroral motions with high time resolution; (5) a digital data recorder was installed for the auroral photometric data; (6) Z-component of an Ultra Low Frequency (ULF) induction magnetometer which had been in trouble was recovered, so the three components of both a fluxgate magnetometer and the induction magnetometer could be observed; and (7) in 1989, the solar activity was very high and there were many interesting geophysical events, and auroral phenomena. Author (NASDA)

N94-27973# National Inst. of Polar Research, Tokyo (Japan).

STATUS REPORT FOR THE DEVELOPMENT OF THE ANTARCTIC PENETRATOR: 1990-YEAR PROGRAM Report No. 2 [NANKYOKU JINKO JISHIN KANSOKUYO PENETORETA NO KAIHATSU: 1990 NENDO KEIKA HOKOKU]

Kazuo Shibuya, Katsutada Kaminuma, Masahiko Hayakawa (Ministry of Education, Science and Culture, Sagamihara, Japan.), Akio Fujimura (Ministry of Education, Science and Culture, Sagamihara, Japan.), Shigeki Tsukamoto (Ministry of Education, Science and Culture, Sagamihara, Japan.), Hitoshi Mizutani (Ministry of Education, Science and Culture, Sagamihara, Japan.), Isao Yamada, Junji Koyama, Minoru Kasahara, and Kiyoshi Ito et al *In its* Antarctic Record, Vol. 36, No. 2 30 Jul. 1992 p 310-340 In JAPANESE Sponsored by Ministry of Education, Science and Culture, Tokyo, Japan (For primary document see N94-27963 07-46)

Avail: CASI HC A03/MF A02

GPS (Global Positioning System) differential positioning test on the Antarctic penetrator was made at the Aoyama Pasture in Hokkaido. The reference GPS receiving site was chosen at 200 km southwest of the Aoyama Pasture, taking the planned operation on the Soer Rondane Mountains 400 km profile in Antarctica into consideration. Three dummy penetrators were dropped twice by changing the release height in the range from 160 to 1,000 m above the ground. Six impact positions of the deployed penetrators were determined by a relative carrier phase measurement to an accuracy of 0.1 m, and the position results were compared with the post-processed GPS differential positions. When 10 to 20 sec duration GPS position data could be acquired at an interval of 1 sec before and after the release instance of the penetrator, the estimated impact position by tracing the falling trajectory was found to be within 30 m offset from the actual impact location determined by the relative carrier phase measurement. When the GPS hovering data could be acquired for at least 1 minute duration just above the impact crater, the calculated impact location via the hovering-helicopter GPS position data was found to be within 10 m offset from the actual impact location. The height accuracy of GPS differential positioning was +/- 10 m which is considered to degrade to +/- 20 m when the coordinates of the reference GPS receiving site were determined by the time-average of point-positioning results. Author (NASDA)

N94-27985# National Research Inst. for Earth Science and Disaster Prevention, Tsukuba (Japan).
REPORT OF THE NATIONAL RESEARCH INSTITUTE FOR EARTH SCIENCE AND DISASTER PREVENTION, NO. 51 [BOSAI KAGAKU GIJUTSU KENKYUSHO KENKYU HOKOKU]
31 Mar. 1993 249 p In JAPANESE
(ISSN 0916-6564)
(JTN-94-80509) Avail: CASI HC A11/MF A03

The following topics were discussed: earthquakes, seismic waves, P waves, S waves, underground structure, Japan, wave propagation, inhomogeneity, seismometers, seismographs, tiltmeters, data acquisition system, data systems, data reduction, personal computers, computer programs, on-line systems, information systems, statistical analysis, rms (root mean square) method, optical measurement, light scattering, optical polarization, polarized light, water, wetness, snow, snow cover, ice formation, road condition, hazards, traffic control, remote sensing, rotating polarizers, meteorological parameters, atmospheric temperature, and skin temperature. For individual titles, see N94-27986 through N94-27991.

N94-27986# National Research Inst. for Earth Science and Disaster Prevention, Tsukuba (Japan).
OBSERVATION WITH STS SEISMOMETER AT NAKAIZU, CENTRAL JAPAN: OBSERVATION SYSTEM AND COMPARISON WITH TILTMETER [NAKAIZU NI OKERU STS JISHIN KANSOKU: KANSOKU HOSHIKI OYOBI KEISHAKEI TONO HIKAKU]
Yoshimitsu Okada and Mizuho Ishida *In its* Report of the National Research Institute for Earth Science and Disaster Prevention, No. 51 31 Mar. 1993 p 1-22 In JAPANESE (For primary document see N94-27985 07-46)
Avail: CASI HC A03/MF A03

A broad-band seismometer, STS-1 was equipped in the vault of Nakaizu Observatory, central Japan, in March, 1988. To record and transmit the observed seismic waveform, a data acquisition system, PDAS-100, was introduced for its ability of flexible data recording schedule, resolution enhancement by over-sampling and off-line telemetry with dial-out mode. To utilize the obtained data, some basic software systems are developed as well as those for routine data processing. They include the functions to store the data, to list the files, to operate filtering, differentiation, and integration, and to display the processed waveforms with arbitrary scaling and time interval. As tilt observation by pendulum-type tiltmeter continued in the same vault, both records were compared with each other. This tiltmeter is adopting a force balanced feed back system which is the same principle as that employed in STS seismometer. It was confirmed that the waveforms for local and global earthquakes are almost identical in both time and frequency domains. It is expected that borehole tiltmeters of this type can work as excellent horizontal broad-band seismometers.
Author (NASDA)

N94-27987# National Research Inst. for Earth Science and Disaster Prevention, Tsukuba (Japan).
UNDERGROUND STRUCTURE IN THE EASTERN PART OF KANAGAWA PREFECTURE INFERRED FROM EXPLOSION SEISMIC OBSERVATIONS [JINKO JISHIN NI YORU KANAGAWA-KEN TOBU CHIKI NO CHIKA KOZO CHOSA]
Hiroyoshi Suzuki, Ryosuke Hirobe (Japan International Cooperation Agency, Shinjuku.), and Takeshi Watanabe (Daiwa Exploration and Consulting Co. Ltd., Meguro, Japan.) *In its* Report of the National Research Institute for Earth Science and Disaster Prevention, No. 51 31 Mar. 1993 p 23-40 In JAPANESE (For primary document see N94-27985 07-46)
Avail: CASI HC A03/MF A03

To study the underground structure in the south-eastern part of the Kanto Plain and the Miura Peninsular, a seismic prospecting survey traverse with a length of 42 km was carried out between Midori Ward in Yokohama City and Miura City, Kanagawa Prefecture. There were three explosion sites and sixty observation sites. The results can be divided into four groups. First, the underground structure of the investigated area is approximately divided into two parts: the south and the north near the roots of the Miura Peninsular. Second, the north is characterized by a simple structure consisting of three gently sloping, almost horizontal layers with P-wave seismic velocities of 2.0, 2.3, and 3.0 km/s respectively (top to bottom) and a layer with a P-velocity of 4.7 km/s under these layers. The 4.7 km/s layer, whose lowermost point is 4 km beneath the surface, is located in the vicinity of Konan Ward in Yokohama City. Third, in the south there are three layers with P-wave velocities of 2.3-2.4, 3.6, and 4.7 km/s respectively. The 3.0 km/s layer found in the north disappears and is assumed to change to the 3.6 km/s layer instead. The uppermost depth of the 3.6 km/s layer is about 0.5 km, which displays upheaval structure near the middle of the Miura Peninsular. Finally, the underground structure obtained from the P-wave velocity profile in this study is in harmony with the supposed geological structure.
Author (NASDA)

N94-27988# National Research Inst. for Earth Science and Disaster Prevention, Tsukuba (Japan).
ANALYSIS OF S-WAVE SEISMOGRAM ENVELOPE OF DEEP EARTHQUAKES AND ESTIMATION OF RANDOM INHOMOGENEITIES IN THE KANTO-TOKAI AREA [KANTO TOKAI CHIKI NI OKERU SHINKAI JISHIN NO S HA ENBEROPU NO TOKUCHO TO FUKINSHITSU KOZO NO SUITEI]
Kazushige Obara *In its* Report of the National Research Institute for Earth Science and Disaster Prevention, No. 51 31 Mar. 1993 p 41-202 In JAPANESE (For primary document see N94-27985 07-46)
Avail: CASI HC A08/MF A03

Seismogram envelopes around direct S waves of deep earthquakes which occurred in the subducting Pacific plate were analyzed based on the parabolic approximation and random inhomogeneity of the upper mantle and the crust. The upper mantle and the crust were investigated in the Kanto-Tokai area, Japan. The time lags of the maximum peak arrival and the half-maximum arrival were measured from the S wave onset of Band Path Filter (BPF)-Root Mean Square (RMS) traces of a horizontal seismogram at some frequency bands. The dependence of shape of the envelopes on frequency and travel distance was examined. The random inhomogeneity beneath the east edge of the seismic network was estimated to be represented by the Gaussian Autocorrelation Function (ACF). The function type is a little bit close to the exponential type in the west part of the volcanic front. The difference in the ACF type might be attributed to the difference in the short wavelength component's inhomogeneity.
Author (NASDA)

N94-27989# National Research Inst. for Earth Science and Disaster Prevention, Shinjo (Japan). Branch of Snow and Ice Studies.
DETECTION OF WATER ON ROAD SURFACE BY THE POLARIZED LIGHT [HENKO NI YORU ROMEN NO NURE NO KANSHUTSU] c74
Tadashi Kimura *In its* Report of the National Research Institute for Earth Science and Disaster Prevention, No. 51 31 Mar. 1993 p 203-208 In JAPANESE (For primary document see N94-27985 07-46)
Avail: CASI HC A02/MF A03

This report explains the working principle, structure, and performance of a new detector of water on a road surface paved with concrete by polarized light. Near the polarizing angle, reflected light from the road surface includes vertical and horizontal polarized components. Intensity difference of the two polarized lights is very small on the dry road surface. On the wet road surface, the vertical component decreases much more than horizontal component. Based on the above mentioned fact, experiments to detect water on a road surface were carried out using a rotating polarizer (41.3 rps) and a silicon pinphotodiode under the sunlight. Experimental results showed that this system could remotely detect water on the road surface over the area of a few square meters.
Author (NASDA)

N94-27990# Japan Weather Association, Kojimachi.
DEVELOPMENT OF A METHOD FOR PREDICTING SNOWFALL INTENSITY AND COMPACTED SNOW ON ROADS [KOSETSU KYODO TO ROMEN ASSETSU YOSOKU SHUHO NO KAIHATSU] c43
Hisayuki Funada, Kuniyuki Senkuro, Muneo Matsukawa, and Tadashi Ishisaka (Toyama Prefectural Office, Japan.) *In* the National Research Inst. for Earth Science and Disaster Prevention, Report of the National Research Institute for Earth Science and Disaster Prevention, No. 51 31 Mar. 1993 p 209-219 In JAPANESE (For primary document see N94-27985 07-46)
Avail: CASI HC A03/MF A03

Heat balance analysis was carried out using the data which were obtained during three winter seasons, 1988-1991. After classifying measurements of traffic counter according to weekday, Monday-Friday and holiday, Saturday, Sunday, and national holiday, figures were made showing relation between snowfall intensity, the road surface minimum temperature, and compacted snow. An on-line system, in which variables such as present temperature and situation of a road surface at fixed points were automatically gathered, was made. It has been possible to predict road surface minimum temperature by connecting these variables with some other variables given by an existing system, MICOS (Meteorological Information Confidential On-line System)-LAN (local area network). As a result, a method for predicting icing and compacted snow on roads was developed. Author (NASDA)

N94-27991# MTS Inst., Inc., Tokyo (Japan).

CONCEPTION OF SNOW INFORMATION NETWORK SYSTEM IN YAMAGATA PREFECTURE [YAMAGATA-KEN NAI NO YUKI SHORI JOHO SHISUTEMU NO KOSO] **c43**

Masuyoshi Matsuda, Hiroshi Nishimura, and Tsugio Nakashima (Yamagata Prefectural Office, Japan.) *In* the National Research Inst. for Earth Science and Disaster Prevention, Report of the National Research Institute for Earth Science and Disaster Prevention, No. 51 31 Mar. 1993 p 221-246 In JAPANESE (For primary document see N94-27985 07-46)

Avail: CASI HC A03/MF A03

Yamagata Prefecture, located in the northern portion of the main island of Japan, is covered with snow for four months during winter. Heavy snowfall, blizzards, and road-surface freezing cause not only hazards to traffic, but suffering to all aspects of people's daily life and socioeconomic activities. This study aims at elaborating the plan of the network system regarding snow information in Yamagata Prefecture and building up its prototype, after careful inspection of the meteorological and snow/ice hazard conditions in this prefecture. Author (NASDA)

N94-28206# RADEX, Inc., Bedford, MA.

PERSISTENCE OF AURORAL ELECTRON FLUX EVENTS FROM DMSP/F9 ELECTRON MEASUREMENTS Report No. 3

K. H. Bounar and W. J. McNeil 31 Jan. 1992 54 p

(Contract F19628-90-C-0191)

(RXR-92012; PL-TR-92-2019) Avail: CASI HC A04/MF A01

The persistence of auroral electron activity is examined and correlated to the geomagnetic activity, which is measured by the Kp index. To study this correlation, the superposed epoch analysis technique was implemented. Epoch zero is the time at which Kp values persisted above a specified threshold value for a specified duration. It was found that a high correlation between enhanced Kp and the number of bright arcs can be achieved for a limited time. The waiting time to increase the chance of observing bright auroral arcs after enhanced Kp values are observed should be between 3 to 6 hours. Further, the substantial increase in the number of observations of intense events as a result of enhanced Kp lingers a maximum of 36 to 48 hours. After this time period, this number drops to the average number of random observations. Author (revised)

N94-28214# Texas Univ., Austin. Inst. for Geophysics.

AN INTEGRATED APPROACH TO SEISMIC EVENT LOCATION: 1. EVALUATING HOW METHOD OF LOCATION AFFECTS THE VOLUME OF GROUPS OF HYPOCENTERS Report No. 1

Clifford A. Frohlich 12 Nov. 1992 34 p

(Contract F19628-91-K-0026)

(PL-TR-92-2323) Avail: CASI HC A03/MF A01

When seismic events occur in spatially compact clusters, the volume and geometric characteristics of these clusters often provides information about the relative effectiveness of different location methods, or about physical processes occurring within the hypocentral region. This report defines and explains how to determine the convex polyhedron of minimum volume (CPMV) surrounding a set of points. We evaluate both single-event and joint hypocenter determination (JHD) relocations for three rather different clusters of seismic events: (1) nuclear explosions from Muroroa relocated using P and PKP phases reported by the ISC; (2) intermediate depth earthquakes near Bucaramanga, Colombia, relocated using P and PKP phases reported by the ISC; and (3) shallow earthquakes near Vanuatu (formerly, the New Hebrides), relocated using P and S phases from a local station network. This analysis demonstrates that different location methods markedly affect the volume of the CPMV, however, volumes for JHD relations are not always smaller than volumes for single-event relocations. Author

N94-28218*# Aerospace Corp., El Segundo, CA. Engineering and Technology Group.

PROTON AURORA AND SUBSTORM INTENSIFICATIONS

J. C. Samson (Alberta Univ., Edmonton.), B. Xu (Alberta Univ., Edmonton.), L. R. Lyons, P. T. Newell (Johns Hopkins Univ., Baltimore, MD.), and F. Creutzberg (National Research Council of Canada, Ottawa, Ontario.) 15 Oct. 1993 9 p See also A93-16191 Prepared in cooperation with National Science Foundation, Washington, DC

(Grants NAG5-1541; NSF ATM-90-17637; NSF ATM-90-16941)

(ATR-93(7248)-1) Copyright Avail: CASI HC A02/MF A01

Ground based measurements from the CANOPUS array of meridian scanning photometers and precipitating ion and electron data from the DMSP F9 satellite show that the electron arc which brightens to initiate substorm intensifications is formed within a region of intense proton precipitation that is well equatorward (approximately four to six degrees) of the nightside open-closed field line boundary. The precipitating protons are from a population that is energized via earthward convection from the magnetotail into the dipolar region of the magnetosphere and may play an important role in the formation of the electron arcs leading to substorm intensifications on dipole-like field lines. Author (revised)

N94-28294*# Houston Univ., Clear Lake, TX. Lunar and Planetary Inst.

NEW DEVELOPMENTS REGARDING THE KT EVENT AND OTHER CATASTROPHES IN EARTH HISTORY

1994 150 p Proceedings held in Houston, TX, 9-12 Feb. 1994

(Contract NASw-4574)

(NASA-CR-195169; NAS 1.26:195169; LPI-CONTRIB-825) Avail: CASI HC A07/MF A02

Papers presented at the conference on New Developments Regarding the KT Event and Other Catastrophes in Earth History are included. Topics covered include: trajectories of ballistic impact ejecta on a rotating earth; axial focusing of impact energy in the earth's interior: proof-of-principle tests of a new hypothesis; in search of Nemesis; impact, extinctions, volcanism, glaciations, and tectonics: matches and mismatches. For individual titles, see N94-28295 through N94-28314.

N94-28295*# California Univ., Berkeley. Dept. of Geology and Geophysics.

TRAJECTORIES OF BALLISTIC IMPACT EJECTA ON A ROTATING EARTH Abstract Only

W. Alvarez *In* Houston Univ., New Developments Regarding the KT Event and Other Catastrophes in Earth History 1994 p 2-3 (For primary document see N94-28294 07-46)

Avail: CASI HC A01/MF A02

On an airless, slowly rotating planetary body like the Moon, ejecta particles from an impact follow simple ballistic trajectories. If gaseous interactions in the fireball are ignored, ejecta particles follow elliptical orbits with the center of the planetary body at one focus until they encounter the surface at the point of reimpact. The partial elliptical orbit of the ejecta particle lies in a plane in inertial (galactic) coordinates. Because of the slow rotation rate (for example, 360 degrees/28 days for the Moon), the intersection of the orbital plane and the surface remains nearly a great circle during the flight time of the ejecta. For this reason, lunar rays, representing concentrations of ejecta with the same azimuth but different velocities and/or ejecta angles, lie essentially along great circles. Ejecta from airless but more rapidly rotating bodies will follow more complicated, curving trajectories when plotted in the coordinate frame of the rotating planet or viewed as rays on the planetary surface. The curvature of trajectories of ejecta particles can be treated as a manifestation of the Coriolis effect, with the particles being accelerated by Coriolis pseudoforces. However, it is more straightforward to calculate the elliptical orbit in inertial space and then determine how far the planet rotates beneath the orbiting ejecta particle before reimpact. The Earth's eastward rotation affects ballistic ejecta in two ways: (1) the eastward velocity component increases the velocity of eastbound ejecta and reduces the velocity of westbound ejecta; and (2) the Earth turns underneath inflight ejecta, so that although the latitude of reimpact is not changed, the longitude is displaced westward, with the displacement increasing as a function of the time the ejecta remains aloft. Author (revised)

N94-28296*# Sandia National Labs., Albuquerque, NM.

AXIAL FOCUSING OF IMPACT ENERGY IN THE EARTH'S INTERIOR: PROOF-OF-PRINCIPLE TESTS OF A NEW HYPOTHESIS Abstract Only

M. B. Boslough, E. P. Chael, T. G. Trucano, M. E. Kipp, and D. A. Crawford *In* Houston Univ., New Developments Regarding the KT Event and Other Catastrophes in Earth History 1994 p 14-16 (For primary document see N94-28294 07-46)
(Contract DE-AC04-76DP-00789)
Avail: CASI HC A01/MF A02

A causal link between major impact events and global processes would probably require a significant change in the thermal state of the Earth's interior, presumably brought about by coupling of impact energy. One possible mechanism for such energy coupling from the surface to the deep interior would be through focusing due to axial symmetry. Antipodal focusing of surface and body waves from earthquakes is a well-known phenomenon which has previously been exploited by seismologists in studies of the Earth's deep interior. Antipodal focusing from impacts on the Moon, Mercury, and icy satellites has also been invoked by planetary scientists to explain unusual surface features opposite some of the large impact structures on these bodies. For example, 'disrupted' terrains have been observed antipodal to the Caloris impact basis on Mercury and Imbrium Basin on the Moon. Very recently there have been speculations that antipodal focusing of impact energy within the mantle may lead to flood basalt and hotspot activity, but there has not yet been an attempt at a rigorous model. A new hypothesis was proposed and preliminary proof-of-principle tests for the coupling of energy from major impacts to the mantle by axial focusing of seismic waves was performed. Because of the axial symmetry of the explosive source, the phases and amplitudes are dependent only on ray parameter (or takeoff angle) and are independent of azimuthal angle. For a symmetric and homogeneous Earth, all the seismic energy radiated by the impact at a given takeoff angle will be refocused (minus attenuation) on the axis of symmetry, regardless of the number of reflections and refractions it has experienced. Mantle material near the axis of symmetry will experience more strain cycles with much greater amplitude than elsewhere and will therefore experience more irreversible heating. The situation is very different than for a giant earthquake, which in addition to having less energy, has an asymmetric focal mechanism and a larger area. Two independent proof-of-principle approaches were used. The first makes use of seismic simulations, which are being performed with a realistic Earth model to determine the degree of focusing along the axis and to estimate the volume of material, if any, that experiences significant irreversible heating. The second involves two-dimensional hydrodynamic code simulations to determine the stress history, internal energy, and temperature rise as a function of radius along the axis. Author (revised)

N94-28297*# California Univ., Berkeley. Lawrence Berkeley Lab.

IN SEARCH OF NEMESIS Abstract Only

c89

S. Carlson, T. Culler, R. A. Muller, M. Tetreault, and S. Perlmutter *In* Houston Univ., New Developments Regarding the KT Event and Other Catastrophes in Earth History 1994 p 19-20 (For primary document see N94-28294 07-46)
Avail: CASI HC A01/MF A02

The parallax of all stars of visual magnitude greater than about 6.5 has already been measured. If Nemesis is a main-sequence star 1 parsec away, this requires Nemesis's mass to be less than about 0.4 solar masses. If it were less than about 0.05 solar masses its gravity would be too weak to trigger a comet storm. If Nemesis is on the main sequence, this mass range requires it to be a red dwarf. A red dwarf companion would probably have been missed by standard astronomical surveys. Nearby stars are usually found because they are bright or have high proper motion. However, Nemesis's proper motion would now be 0.01 arcsec/yr, and if it is a red dwarf its magnitude is about 10 - too dim to attract attention. Unfortunately, standard four-color photometry does not distinguish between red dwarfs and giants. So although surveys such as the Dearborn Red Star Catalog list stars by magnitude and spectral type, they do not identify the dwarfs. Every star of the correct spectral type and magnitude must be scrutinized. Our candidate list is a hybrid; candidate red stars are identified in the astrometrically poor Dearborn Red Star Catalog and their positions are corrected using the Hubble Guide Star Catalog. When errors in the Dearborn catalog make it impossible to identify the corresponding Hubble star, the fields are split so that we have one centering on each possible candidate. We are currently scrutinizing 3098 fields, which we believe contain all possible red dwarf candidates in the northern hemisphere. Since our last report the analysis and database software has been completely rebuilt to take advantage of updated hardware, to make the data more accessible, and to implement improved methods of data analysis. The software is now completed and we are eliminating stars every clear night. Author

N94-28298*# Texas Univ., Austin. Inst. for Geophysics.

IMPACTS, EXTINCTIONS, VOLCANISM, GLACIATIONS, AND TECTONICS: MATCHES AND MISMATCHES Abstract Only

I. W. D. Dalziel *In* Houston Univ., New Developments Regarding the KT Event and Other Catastrophes in Earth History 1994 p 28-29 (For primary document see N94-28294 07-46)
Avail: CASI HC A01/MF A02

The debate concerning possible reactions between impacts, extinction events, and volcanism has recently taken a new turn. Diamictites and associated sedimentary deposits long regarded by geologists as glaciogenic, have been reinterpreted as impact-related. Going further, the Permo-Carboniferous diamictites that are widespread in the southern continents and India are not put forward as evidence that fragmentation of the Gondwana supercontinent in the Mesozoic was a direct result of meteorite impact. In an abstract at a meeting of the American Geophysical Union, and in an article in the popular press, one member of the earth science community has made a specific claim to identify the site of the supercontinent-destroying bolide on the Falkland/Malvinas Plateau. It is claimed by this scientist that the Cape Fold belt in Africa represents a 'breaking wave' of deformation resulting from this impact, and that fractures in the clasts of the Dwyka diamictite in southern Africa represent impact-induced cataclasis of the target rock. These hypotheses fly in the face of the well-established tectonic history of the Gondwana supercontinent in several respects. Author (revised)

N94-28299*# National Museum of Natural History, Washington, DC. Dept. of Paleobiology.

THE END-PERMIAN MASS EXTINCTION: A COMPLEX, MULTICAUSAL EXTINCTION Abstract Only

D. H. Erwin *In* Houston Univ., New Developments Regarding the KT Event and Other Catastrophes in Earth History 1994 p 33-34 (For primary document see N94-28294 07-46)
Avail: CASI HC A01/MF A02

The end-Permian mass extinction was the most extensive in the history of life and remains one of the most complex. Understanding its causes is particularly important because it anchors the putative 26-m.y. pattern of periodic extinction. However, there is no good evidence for an impact and this extinction appears to be more complex than others, involving at least three phases. The first began with the onset of a marine regression during the Late Permian and resulting elimination of most marine basins, reduction in habitat area, and increased climatic instability; the first pulse of tetrapod extinctions occurred in South Africa at this time. The second phase involved increased regression in many areas (although apparently not in South China) and heightened climatic instability and environmental degradation. Release of gas hydrates, oxidation of marine carbon, and the eruption of the Siberian flood basalts occurred during this phase. The final phase of the extinction episode began with the earliest Triassic marine regression and destruction of nearshore continental habitats. Some evidence suggests oceanic anoxia may have developed during the final phase of the extinction, although it appears to have been insufficient to the sole cause of the extinction. Derived from text

N94-28300*# Stanford Univ., CA.

SCIENCE OBSERVED: THE MASS-EXTINCTION DEBATES Abstract Only

W. Glen *In* Houston Univ., New Developments Regarding the KT Event and Other Catastrophes in Earth History 1994 p 44-45 (For primary document see N94-28294 07-46)
Avail: CASI HC A01/MF A02

The upheaval triggered in 1980 by the Alvarez-Berkeley group impact hypothesis transformed the literature of mass extinctions from an unfocused, sporadic collection of papers that virtually ignored extraterrestrial causes and treated endogenous ones only sparingly better to an integrated, diverse body of literature. Research programs organized seemingly overnight spawned collaborative teams whose members, often from distant, isolated disciplines, redirected their careers in order to address the captivating, high-stakes issues. The initial, generally skeptical, cool reception of the impact hypothesis might have been predicted for any of a number of reasons: such an instantaneous catastrophe contravened earth science's reigning philosophy of uniformitarianism; it was formulated from a form of evidence - siderophile element anomalies - alien to the community charged with its appraisal; it advanced a causal mechanism that was improbable in terms of canonical knowledge; and it was proffered mainly by specialists alien to earth and biological science, especially paleobiology. Early on it became clear that irrespective of which causal hypothesis was chosen, the chosen one would be the strongest predictor of how the chooser would select and apply standards in assessing evidence bearing on all such hypothesis. Less strong correlation also appeared between disciplinary speciality and the assessment of evidence. Such correlations varied with the level of specialization; the most robust correlations appeared in the broadest areas of science practice. The gestalt (mindset) seemingly engendered by the embrace of an extinction hypothesis overrode, or was stronger than, the intellectual predispositions attributable to disciplinary specialty. Derived from text

N94-28301*# Los Alamos National Lab., NM. Theoretical Div.
CONSEQUENCES OF IMPACTS OF SMALL ASTEROIDS AND COMETS WITH EARTH Abstract Only
J. G. Hills *In* Houston Univ., New Developments Regarding the KT Event and Other Catastrophes in Earth History 1994 p 50 (For primary document see N94-28294 07-46)
Avail: CASI HC A01/MF A02

The fragmentation of a small asteroid in the atmosphere greatly increases its cross sections for aerodynamic braking and energy dissipation. At a typical impact velocity of 22 km/s, the atmosphere absorbs more than half the kinetic energy of stony meteoroids with diameters, D(sub m), less than 220 m and iron meteoroids with D(sub m) less than 80 m. The corresponding diameter for comets with impact velocity 50 km/s is D(sub m) less than 1600 m. Most of the atmospheric energy dissipation occurs in a fraction of a scale height, so large meteors appear to 'explode' or 'flare' at the end of their visible paths. This dissipation of energy in the atmosphere protects the earth from direct impact damage (e.g., craters), but it produces a blast wave that can do considerable damage. The area of destruction around the impact point in which the over-pressure in the blast wave exceeds 4 lb/sq in = 2.8 x 10(exp 5) dynes/cu cm, which is enough to knock over trees and destroy buildings, increases rapidly from zero for chondritic meteoroids less than 56 m in diameter (15 megatons) to about 200 sq km for those 80 m in diameter (48 megatons); the probable diameter of the tunguska impactor of 1908 is about 80 m. Crater formation and earthquakes are not significant in land impacts by stony asteroids less than about 200 m in diameter because of the air protection. A tsunami is probably the most devastating type of damage for asteroids 200 m to 1 km in diameter. An impact by an asteroid this size anywhere in the Atlantic would devastate coastal areas on both sides of the ocean. An asteroid a few kilometers across would produce a tsunami that would reach the foothills of the Appalachian Mountains in the upper half of the East Coast of the United States. Most of Florida is protected from a tsunami by the gradual slope of the ocean off its coast, which causes most of the tsunami energy to be reflected back into the Atlantic. The atmosphere plume produced by asteroids with diameters exceeding about 120 m cannot be contained by the atmosphere, so this bubble of high-temperature gas forms a new layer on top of the atmosphere. The dust entrapped in this hot gas is likely to have optical depths exceeding tau = 10 for asteroids with diameters exceeding about 0.5 to 1 km. The optical flux from asteroids 60 m or more in diameter is enough to ignite pine forests. However, the blast wave from an impacting asteroid goes beyond the radius in which the fire starts. The blast wave tends to blow out the fire, so it is likely that the impact will char the forest, as at Tunguska, but the impact will not produce a sustained fire. Because comets dissipate their energy much higher in the atmosphere than asteroids, they illuminate a much larger region and their blast wave is weaker. So they are much more effective in producing large fires. This suggests that the KT impactor was a comet rather than an asteroid. Author (revised)

N94-28302*# Chicago Univ., IL. Dept. of the Geophysical Sciences.
MASS EXTINCTIONS: PERSISTENT PROBLEMS AND NEW DIRECTIONS Abstract Only
D. Jablonski *In* Houston Univ., New Developments Regarding the KT Event and Other Catastrophes in Earth History 1994 p 56-57 (For primary document see N94-28294 07-46)
Avail: CASI HC A01/MF A02

Few contest that mass extinctions have punctuated the history of life, or that those events were so pervasive environmentally, taxonomically, and geographically that physical forcing factors were probably involved. However, consensus remains elusive on the nature of those factors, and on how a given perturbation - impact, volcanism, sea-level change, or ocean anoxic event - could actually generate the observed intensity and selectivity of biotic losses. At least two basic problems underlie these long-standing disagreements: difficulties in resolving the fine details of taxon ranges and abundances immediately prior to and after an extinction boundary and the scarcity of simple, unitary cause-and-effect relations in complex biological systems. Derived from text

N94-28303*# Smithsonian Institution, Washington, DC. Dept. of Paleobiology.
THE BIOSTRATIGRAPHY AND PALEOGEOGRAPHY OF MAASTRICHTIAN INOCERAMIDS Abstract Only
K. G. MacLeod, B. T. Huber, and P. D. Ward (Washington Univ., Seattle.) *In* Houston Univ., New Developments Regarding the KT Event and Other Catastrophes in Earth History 1994 p 74-75 (For primary document see N94-28294 07-46)
Avail: CASI HC A01/MF A02

The global distribution of Maastrichtian inoceramids is now known in enough detail that the patterns of disappearance can be used to place first-order constraints on paleoceanographic changes that may have occurred during that age. The Inoceramidae is an excellent group to focus on in a study of Maastrichtian events for the following reasons: (1) they were globally distributed in the early Maastrichtian; (2) they did not survive the age (i.e., they undergo change during the interval); and (3) they have left a rich microfossil and macrofossil record. Some inoceramids grew to be very large; however, even the largest often passively disaggregated and are preserved as hundreds of millions of characteristic, columnar, polygonal prisms of calcite approximately 100 microns across. This taphonomic process has greatly increased the inoceramid fossil record and provides a means of objectively estimating changes in their standing population. In addition, because these prisms commonly occur in Deep Sea Drilling Project (DSDP) and Ocean Drilling Program (ODP) cores, it is relatively easy to generate a truly global database. The existing macrofossil record of inoceramids has less temporal and spacial resolution but greater taxonomic resolution than the microfossil record. In concert the microfossil and macrofossil records of inoceramids demonstrate that important changes occurred during the Maastrichtian. These changes are distinct from the KT boundary catastrophe but are part of the larger KT transition. Author (revised)

N94-28304*# Princeton Univ., NJ. Dept. of Geological and Geophysical Sciences.
AN EVALUATION OF CRITERIA THAT MAY BE USED TO IDENTIFY SPECIES SURVIVING A MASS EXTINCTION Abstract Only c51
N. MacLeod *In* Houston Univ., New Developments Regarding the KT Event and Other Catastrophes in Earth History 1994 p 75-77 (For primary document see N94-28294 07-46)
Avail: CASI HC A01/MF A02

One of the most difficult obstacles to establishing a causal connection between mass extinctions and large body impacts is the existence of what appear to be many more KT survivor species than previously suspected. Though interpretations of 'Cretaceous' faunal elements in lowermost Danian sediments differ, this enigmatic fauna has not been recovered from every biozone-complete boundary section, including the El Kef stratotype. In terms of their potential for providing constraints on scenarios seeking to account for the KT extinction event, the significance of such observations cannot be overstated. Owing to the consistency with which these observations have been made over the last several years, the possibility of widespread trans-KT biotic survivorship can no longer be dismissed. Rather, the survivorship hypothesis must be tested alongside its alternative (the reworking hypothesis) to determine which explains the available data in the most complete yet parsimonious manner. Moreover, valid tests for survivorship cannot be based on negative evidence or on the assumption that only a small cohort of species could have survived the KT boundary event. Several authors have recently proposed various criteria that might be used to test alternative interpretations for this aspect lowermost Danian biotic record. Author (revised)

N94-28305*# University of Southwestern Louisiana, Lafayette. Dept. of Physics.

MODULATING TERRESTRIAL IMPACTS FROM OORT CLOUD COMETS BY THE ADIABATICALLY CHANGING GALACTIC TIDES Abstract Only

J. J. Matese, P. G. Whitman, K. A. Innanen (York Univ., Toronto, Ontario.), and M. J. Valtonen (Turku Univ., Finland.) *In* Houston Univ., New Developments Regarding the KT Event and Other Catastrophes in Earth History 1994 p 78-80 (For primary document see N94-28294 07-46)

Avail: CASI HC A01/MF A02

Time modulation of the flux of new Jupiter-dominated Oort cloud comets is the subject of interest here. The major perturbation of these comets during the present epoch is due to the tidal field of the relatively smooth distribution of matter in the galactic disk. A secondary source of the near-parabolic comet flux are stars penetrating the inner Oort cloud and providing impulses that create brief comet showers. Substantial stellar-induced showers occur approximately every 100 m.y. Less frequent (but stronger) impulses due to giant molecular clouds can also perturb comets from the inner cloud. These occur on timescales of approximately equal to 500 m.y. In contrast to these infrequent stochastic shower phenomena is the continuously varying tidal-induced flux due to the galaxy. As the Sun orbits the galactic center it undergoes quasiharmonic motion about the galactic midplane, which is superimposed on the small eccentricity, near-Keplerian motion in the plane having epicycle period approximately equal to 150 m.y. In the process the galactic tidal field on the Sun/cloud system will vary causing a modulation of the observable Oort cloud flux. We have created a model of the galactic matter distribution as it affects the solar motion over a time interval ranging from 300 m.y. in the past to 100 m.y. into the future. As constraints on the disk's compact dark matter component we require consistency with the following: (1) the observed galactic rotation curve, (2) today's flux distribution of new comets, (3) the studies of K-giant distributions, and (4) the periodicity found in the terrestrial cratering record. The adiabatically varying galactic tidal torque is then determined and used to predict the time dependence of the flux. We find that a model in which approximately half the disk matter is compact is consistent with these constraints. Under such circumstances the peak-to-trough flux variation will be approx. equal to 5:1 with a full width of 9 m.y. This variability will manifest in the terrestrial cratering record and is consistent with the observed cratering periodicity, if over half of the impacts on Earth are caused by comets or asteroids that originate in the outer Oort cloud. Author (revised)

N94-28306*# Washington Univ., Saint Louis, MO. Dept. of Earth and Planetary Sciences.

SOME IMPLICATIONS OF LARGE IMPACT CRATERS AND BASINS ON VENUS FOR TERRESTRIAL RINGED CRATERS AND PLANETARY EVOLUTION Abstract Only c91

W. B. McKinnon and J. S. Alexopoulos *In* Houston Univ., New Developments Regarding the KT Event and Other Catastrophes in Earth History 1994 p 81-82 (For primary document see N94-28294 07-46)

Avail: CASI HC A01/MF A02

Approximately 950 impact craters have been identified on the surface of Venus, mainly in Magellan radar images. From a combination of Earth-based Arecibo, Venera 15/1, and Magellan radar images, we have interpreted 72 as unequivocal peak-ring craters and four as multiringed basins. The morphological and structural preservation of these craters is high owing to the low level of geologic activity on the venusian surface (which is in some ways similar to the terrestrial benthic environment). Thus these craters should prove crucial to understanding the mechanics of ringed crater formation. They are also the most direct analogs for craters formed on the Earth in Phanerozoic time, such as Chicxulub. We summarize our findings to date concerning these structures. Author (revised)

N94-28307*# Virginia Polytechnic Inst., Blacksburg. Dept. of Geological Sciences.

PROPOSED LAW OF NATURE LINKING IMPACTS, PLUME VOLCANISM, AND MILANKOVITCH CYCLES TO TERRESTRIAL VERTEBRATE MASS EXTINCTIONS VIA GREENHOUSE-EMBRYO DEATH COUPLING Abstract Only c45

D. M. McLean *In* Houston Univ., New Developments Regarding the KT Event and Other Catastrophes in Earth History 1994 p 82-83 (For primary document see N94-28294 07-46)

Avail: CASI HC A01/MF A02

A greenhouse-physiological coupling killing mechanism active among mammals, birds, and reptiles has been identified. Operating via environmental thermal effects upon the maternal core-skin blood flow critical to the survival and development of embryos, it reduces the flow of blood to the uterine tract. Today, during hot summers, this phenomena kills embryos on a vast, global scale. Because of sensitivity of many mammals to modern heat, a major modern greenhouse could reduce population numbers on a global scale, and potentially trigger population collapses in the more vulnerable parts of the world. In the geological past, the killing mechanism has likely been triggered into action by greenhouse warming via impact events, plume volcanism, and Earth orbital variations (Milankovitch cycles). Earth's biosphere is maintained and molded by the flow of energy from the solar energy source to Earth and on to the space energy sink (SES). This SES energy flow maintains Earth's biosphere and its living components, as open, intermediate, dissipative, nonequilibrium systems whose states are dependent upon the rate of energy flowing through them. Greenhouse gases such as CO2 in the atmosphere influence the SES energy flow rate. Steady-state flow is necessary for global ecological stability (autopoiesis). Natural fluctuations of the C cycle such as rapid releases of CO2 from the mantle, or oceans, disrupt steady-state SES flow. These fluctuations constantly challenge the biosphere; slowdown of SES energy flow drives it toward thermodynamical equilibrium and stagnation. Fluctuations induced by impact event, mantle plume volcanism, and Milankovitch cycles can grow into structure-breaking waves triggering major perturbations of Earth's C cycle and mass extinctions. A major C cycle perturbation involves readjustment of the outer physiochemical spheres of the Earth: the atmosphere, hydrosphere, and lithosphere; and by necessity, the biosphere. A greenhouse, one manifestation of a major C cycle perturbation, is the most dangerous natural phenomenon that life on Earth can experience. Greenhouse conditions existed during the KT mass extinctions of 65 m.y. ago, and the Pleistocene-Holocene (P-H) mammalian extinctions of 10,000-12,000 yr ago. Coupling climatology to reproductive physiology via effects of ambient air temperature upon uterine blood flow to developing embryos accounts for the extinctions via established physiological principles. Author (revised)

N94-28308*# California Univ., Berkeley. Lawrence Berkeley Lab. Dept. of Physics.

EXTRATERRESTRIAL ACCRETION AND GLACIAL CYCLES Abstract Only c90

R. A. Muller *In* Houston Univ., New Developments Regarding the KT Event and Other Catastrophes in Earth History 1994 p 85-86 (For primary document see N94-28294 07-46)

Avail: CASI HC A01/MF A02

We propose that the approx. 100-k.y. cycle seen in terrestrial glaciation is due to changes in meteor flux that come from changes in the Earth's orbit. This model can explain a 70-k.y. 'anomalous' period in climate data and the apparent discrepancy between present extraterrestrial fluxes and those in oceanic sediments. It can be tested by measuring Ir densities in sediments and ice during glacials and interglacials. Author

N94-28309*# First Inst. of Oceanography, Qingdao (China). State Oceanic Administration.

AN EXTRATERRESTRIAL EVENT AT THE TERTIARY-QUATERNARY BOUNDARY Abstract Only c90

H. Peng *In* Houston Univ., New Developments Regarding the KT Event and Other Catastrophes in Earth History 1994 p 88-89 (For primary document see N94-28294 07-46)

Avail: CASI HC A01/MF A02

During the North Pacific Manganese Nodules Investigation in 1983, we collected a large-diameter core M14 (8 deg. 00.15 N, 176 deg, 10.65 W; 3991-m depth of water). This gravity core is 420 cm long in total. It is composed of calcureous ooze at 0-320 cm and siliceous ooze at 320-420 cm of depth. A great number of microtektites were found at 270-300 cm (average content is 15 microtektites per 100-g sediment). Because abundant microtektites are restricted to a 30-m-thick zone of deep-sea core, we called this zone the microtektite layer. The age of the sedimentary stratum containg microtektites is 2.14-2.30 m.y., corresponding to the Pliocene to

Pleistocene Periods as indicated by paleomagnetic and paleontologic analysis. We can give the following two primary conclusions: (1) the core M14 microtektites are products of a major meteorite or asteroid impact 2.14-2.30 m.y. ago; and (2) the age of 2.14-2.30 m.y. is an important geological age; perhaps it is just a correct age for dividing the Tertiary/Quarternary boundary. This result is quite close to previous data. Author

N94-28310*# New York Univ., New York. Dept. of Earth System Science.

A GENERAL THEORY OF IMPACTS AND MASS EXTINCTIONS, AND THE CONSEQUENCES OF LARGE-BODY IMPACT ON THE EARTH Abstract Only

M. R. Rampino *In* Houston Univ., New Developments Regarding the KT Event and Other Catastrophes in Earth History 1994 p 91-92 (For primary document see N94-28294 07-46)
Avail: CASI HC A01/MF A02

The theory that large-body impacts are the primary cause of mass extinctions of life on the Earth now has a sound theoretical and observational foundation. A convergence of evidence suggests that the biosphere may be a sensitive detector of large impact events, which result in the recorded global mass extinction pulses. The astronomically observed flux of asteroids and comets in the neighborhood of the Earth, and the threshold impact size calculated to produce a global environment catastrophe, can be used to predict a time history of large impact events and related mass extinctions of life that agrees well with the record of approx. 24 extinction events in the last 540 m.y. Derived from text

N94-28311*# Wisconsin Univ., Milwaukee. Dept. of Geology.

WERE ALL EXTINCTION EVENTS CAUSED BY IMPACTS? Abstract Only

P. M. Sheehan and P. J. Coorough *In* Houston Univ., New Developments Regarding the KT Event and Other Catastrophes in Earth History 1994 p 110-112 Sponsored by NSF (For primary document see N94-28294 07-46)
(Grant NSF EAR-90-04589)
Avail: CASI HC A01/MF A02

Extraterrestrial impacts are firmly implicated in several of the five major Phanerozoic extinction events. A critical issue now is whether extraterrestrial events have been the only mechanism that produced physical changes of sufficient magnitude to cause major extinction events. While we believe the evidence is overwhelming that the KT extinction event was caused by an impact, we also find that an event of similar or larger size near the end of the Ordovician is best explained by terrestrial causes. The Ordovician extinction event (End-O extinction event) occurred near the end of the Ordovician, but the interval of extinction was completed prior to the newly established Ordovician-Silurian boundary. In spite of extensive field studies, a convincing signature of an associated impact has not been found. However, a prominent glaciation does coincide with the End-O extinction event. Author

N94-28312*# Houston Univ., TX.

OZONE CONTROL OF BIOLOGICAL ACTIVITY DURING EARTH'S HISTORY, INCLUDING THE KT CATASTROPHE Abstract Only c45

W. R. Sheldon *In* Houston Univ., New Developments Regarding the KT Event and Other Catastrophes in Earth History 1994 p 112-113 Sponsored by NSF (For primary document see N94-28294 07-46)
(Grant NSF ATM-92-06417)
Avail: CASI HC A01/MF A02

There have been brief periods since the beginning of the Cambrian some 600 m.y. ago when mass extinctions destroyed a significant fraction of living species. The most widely studied of these events is the catastrophe at the KT boundary that ended the long dominance of the dinosaurs. In addition to mass extinctions, there is another profound discontinuity in the history of Earth's biota, the explosion of life at the end of the Precambrian era which is an episode that is not explained well at all. For some 3 b.y. before the Cambrian, life had been present on Earth, but maintained a low level of activity which is an aspect of the biota that is puzzling, especially during the last two-thirds of that period. During the last 2 b.y. before the Cambrian, conditions at the Earth's surface were suitable for a burgeoning of the biota, according to most criteria: the oceans neither boiled nor were fozen solid during this time, and the atmosphere contained sufficient O for the development of animals. The purpose of this paper is to suggest that mass extinctions and the lackluster behavior of the Precambrian biota share a common cause: an inadequate amount of ozone in the atmosphere. Author

N94-28313*# Lowell Observatory, Flagstaff, AZ.

THE CRASH OF P/SHOEMAKER-LEVY 9 INTO JUPITER AND ITS IMPLICATIONS FOR COMET BOMBARDMENT ON EARTH Abstract Only c91

E. M. Shoemaker and C. S. Shoemaker *In* Houston Univ., New Developments Regarding the KT Event and Other Catastrophes in Earth History 1994 p 113-114 (For primary document see N94-28294 07-46)
Avail: CASI HC A01/MF A02

Periodic Comet Shoemaker/Levy 9 will impact Jupiter in late July 1994. The comet, which broke into more than 20 telescopically detectable fragments when it passed with the Roche lobe of Jupiter on July 8, 1992, is captured in a highly eccentric orbit about Jupiter. The 21 recognized nuclei will be spread out in a train of the order 7 x 10(exp 6) km long at the time of impact, and the impacts will be spread in time over about 5 1/2 days centered on about July 21.2 UT. In addition to the train of recognized bright nuclei, the comet consists of 'wings' of unresolved bodies that are the source of a very broad composite dust tail. The linear extent of the wings is about an order of magnitude greater than that of the train of recognized discrete nuclei. Collision of the wings will be spread in time over several months. Thus the impact of P/S-L 9 with Jupiter will be an event of appreciable duration. Derived from text

N94-28314*# Dominion Astrophysical Observatory, Victoria (British Columbia).

SUPERNOVAE AND MASS EXTINCTIONS Abstract Only

S. vandenBergh *In* Houston Univ., New Developments Regarding the KT Event and Other Catastrophes in Earth History 1994 p 127 (For primary document see N94-28294 07-46)
Avail: CASI HC A01/MF A02

Shklovsky and others have suggested that some of the major extinctions in the geological record might have been triggered by explosions of nearby supernovae. The frequency of such extinction events will depend on the galactic supernova frequency and on the distance up to which a supernova explosion will produce lethal effects upon terrestrial life. In the present note it will be assumed that a killer supernova has to occur so close to Earth that it will be embedded in a young, active, supernova remnant. Such young remnants typically have radii approximately less than 3 pc (1 x 10(exp 19) cm). Larger (more pessimistic?) killer radii have been adopted by Ruderman, Romig, and by Ellis and Schramm. From observations of historical supernovae, van den Bergh finds that core-collapse (types Ib and II) supernovae occur within 4 kpc of the Sun at a rate of 0.2 plus or minus 0.1 per century. Adopting a layer thickness of 0.3 kpc for the galacitc disk, this corresponds to a rate of approximately 1.3 x 10(exp -4) supernovae pc(exp -3) g.y.(exp -1). Including supernovae of type Ia will increase the total supernovae rate to approximately 1.5 x 10(exp -4) supernovae pc(exp -3) g.y.(exp -1). For a lethal radius of R pc the rate of killer events will therefore be 1.7 (R/3)(exp 3) x 10(exp -2) supernovae per g.y. However, a frequency of a few extinctions per g.y. is required to account for the extinctions observed during the phanerozoic. With R (extinction) approximately 3 pc, the galactic supernova frequency is therefore too low by 2 orders of magnitude to account for the major extinctions in the geological record. Author

47 METEOROLOGY AND CLIMATOLOGY

Includes weather forecasting and modification.

N94-25722# Organisatie voor Toegepast Natuurwetenschappelijk Onderzoek, The Hague (Netherlands). Physics and Electronics Lab.

WIND MEASUREMENTS WITH AN INCOHERENT LIDAR

G. J. Kunz 12 Jul. 1993 76 p
(AD-A273756; FEL-93-A040; TDCK-TD-93-0485) Avail: CASI HC A05/MF A01

Atmospheric structures can be measured with incoherent optical radars (lidars). Because these structures drift with the wind, they can serve as a tracer for remote sensing of the wind vector. For this purpose, a dual monostatic scanning lidar system is available to measure the atmosphere simultaneously in two different directions over a maximum range of about 1 km. The transit time of identified patterns between two sensing points in the horizontal plane provides in combination with the geometry of the lidar, sufficient information to derive the horizontal wind vector. The method is based on cross-correlation techniques. To determine the spatial wind vector as a function of altitude it is sufficient to measure in three different upward directions. This can be realized with a triple lidar or with a single lidar by measuring consecutively in three different directions and using an equivalent but more extended inversion method. DTIC

N94-25793# Naval Research Lab., Monterey, CA.
DEVELOPMENT AND TESTING OF THE COUPLED Ocean/Atmosphere MESOSCALE PREDICTION SYSTEM (COAMPS) Final Report
Richard M. Hodur Nov. 1993 84 p
(AD-A273925; NRL/MR/7533-93-7213) Avail: CASI HC A05/MF A01

A three-dimensional coupled ocean/atmosphere mesoscale prediction system (COAMPS) has been developed, consisting of a nonhydrostatic atmospheric model and a hydrostatic ocean model. The models can be integrated simultaneously so that the surface fluxes of heat, momentum, and moisture are exchanged across the air-water interface every time step. Optionally, either the atmospheric model or the ocean model can be used as a stand-alone system. Two idealized simulations of a hurricane are performed In the first simulation, only the atmospheric model is used, assuming a fixed sea surface temperature. A realistic hurricane structure with spiral bands develops. Evidence is found of concentric eye walls interacting to modify the intensification of the hurricane. In the second simulation, the ocean model is run simultaneously with the atmospheric model. After 84 hours, the sea surface temperature decreases more than 8 C within the radius of maximum winds. While this has a large impact on the intensity of the system (i.e., the strength of the maximum winds), there is little change in the overall structure of the system as measured by the tangential velocities outside the radius of maximum winds. DTIC

N94-25861# Air Force Inst. of Tech., Wright-Patterson AFB, OH. School of Engineering.
DEVELOPING PREDICTION REGIONS FOR A TIME SERIES MODEL FOR HURRICANE FORECASTING M.S. Thesis
William Cheman Dec. 1993 68 p
(AD-A273777; AFIT/GSO/ENS/93D-03) Avail: CASI HC A04/MF A01

In this thesis, a class of time series models for forecasting a hurricane's future position based on its previous positions and a generalized model of hurricane motion are examined and extended. Results of a literature review suggest that meteorological models continue to increase in complexity while few statistical approaches, such as linear regression, have been successfully applied. An exception is provided by a certain class of time series models that appear to forecast storms almost as well as current meteorological models without their tremendous complexity. A suggestion for enhancing the performance of these time series models is pursued through an examination of the forecast errors produced when these models are applied to historical storm tracks. The results uncover no patterns that can be exploited in developing an improved model and suggest that there are meteorological processes or factors at work beyond those that can be modeled with the available historical data base. The statistical structure of the time series approach is exploited to develop a practical method for determining prediction regions which probabilistically describe a hurricane's likely future position. The Monte Carlo approach used to develop these prediction ellipses is seen to be applicable for predicting areas subject to risk from hurricane landfall. DTIC

N94-25873 Phillips Lab., Edwards AFB, CA.
CATALOG OF ABSOLUTELY CALIBRATED, RANGE NORMALIZED, WIDEBAND, ELECTRIC FIELD WAVEFORMS FROM TRIGGERED LIGHTNING FLASHES IN FLORIDA Interim Report
Yataka Izumi and John C. Willett 22 Jun. 1993 106 p Limited Reproducibility: More than 20% of this document may be affected by microfiche quality
(AD-A273793; AD-E201708; PL-TR-93-2151; ERP-1124) Avail: CASI HC A06

During the summer of 1987, a rocket-triggered-lightning program was conducted at NASA KSC, Florida. The rocket triggering was performed from two trigger platforms--one over water and the other over land. The propagation paths from the two sites were almost entirely over brackish water. This report presents waveform plots of the electric-field time derivative, the electric field, and the high-frequency spectral density at 5 MHz. DTIC

N94-25936# Lawrence Livermore National Lab., CA.
THE EFFECT OF ELEVATION DATA REPRESENTATION ON NOCTURNAL DRAINAGE WIND SIMULATIONS
H. Walker and J. M. Leone, Jr. Aug. 1993 12 p Presented at the 2nd International Workshop in Integrating Geographic Information Systems and Environmental Modeling, Breckenridge, CO, 27-29 Sep. 1993
(Contract W-7405-eng-48)
(DE94-003624; UCRL-JC-112788; CONF-9309230-3) Avail: CASI HC A03/MF A01

A critical requirement for accurately representing surface-atmosphere interactions within an atmospheric model is to realistically characterize the land surface. Data must be extracted from a geographical database and transformed so that it is consistent with the needs of the numerical model. In such a process, there are two major classes of error that must be understood and minimized whenever possible. The first class involves the accuracy, precision, and resolution of the geographical data itself. The second is error introduced by the transformations used to assimilate the data into the atmospheric model. Thus, this research has two coupled objectives: to understand the effects of errors within the geographical data base upon the accuracy of the atmospheric model simulation; and to design optimal techniques for the transformation of the data. Such transformations are often constrained by the conflicting needs of representing physically important spatial and temporal scales while eliminating scales that cannot be resolved by the model. DOE

N94-25939# Alaska Univ., Fairbanks. Geophysical Inst.
SEASONAL SNOW OF ARCTIC ALASKA R4D INVESTIGATIONS
C. S. Benson Feb. 1993 46 p
(Contract DE-FG06-84ER-60245)
(DE93-040082; DOE/ER-60245/T2) Avail: CASI HC A03/MF A01

Seasonal snow is present on the Arctic Slope of Alaska for nine months each year. Its presence or absence determines whether 80% of the solar radiation is reflected or absorbed, respectively. Although life on the Arctic Slope is adapted to, and in some cases dependent upon seasonal snow, little is known about it from a scientific point of view. Its quantity has been grossly underestimated, and knowledge of its distribution and the extent of wind transport and redistribution is very limited. This research project dealt with the amount, regional distribution and physical properties of wind blown snow and its biological role in the R4D area of the Arctic Slope. Physical processes which operate within the snow that were studied included the flux of heat and vapor and the fractionation of stable isotopes through it during fall and winter, and the complex heat and mass transfer within the snow and between snow, its substrate and the overlying atmosphere during the melt period. DOE

N94-25951# Alaska Univ., Fairbanks.
ACTIVE LAYER DYNAMICS AND ARCTIC HYDROLOGY AND METEOROLOGY
1993 18 p
(Contracts DE-FG06-92ER-61457; DE-FG06-84ER-60247)
(DE94-001724; DOE/ER-61457/T1) Avail: CASI HC A03/MF A01

Man's impact on the environment is increasing with time. To be able to evaluate anthropogenic impacts on an ecosystems, it is necessary first to understand all facets of how the ecosystems works: what the main processes (physical, biological, chemical) are, at what rates they proceed, and how they can be manipulated. Arctic ecosystems are dominated by physical processes of energy exchange. This project has concentrated on a strong program of hydrologic and meteorologic data collection, to better understand dominant physical processes. Field research focused on determining the natural annual and diurnal variability of meteorologic and hydrologic variables, especially those which may indicate trends in climatic change. Comprehensive compute models are being developed to simulate physical processes occurring under the present conditions and to simulate processes under the influence of climatic change. DOE

N94-26013# Organisatie voor Toegepast Natuurwetenschappelijk Onderzoek, The Hague (Netherlands). Physics and Electronics Lab.
CONVERSION OF THE CLUSE MODEL FOR APPLICATIONS OVER OPEN OCEAN Final Report, Jun. 1991 - Dec. 1992
A. M. VanEijk, P. G. Mestayer, and G. DeLeeuw Aug. 1993 80 p
(AD-A273750; FEL-93-A035; TDCK-TD-930758) Avail: CASI HC A05/MF A01

The CLUSE model has been developed to describe the dynamics of (fresh water) spray droplets in the homogeneous boundary layer of an air-sea interaction simulation tunnel, and their influence on humidity and temperature profiles. Extension to open ocean conditions requires that the fresh water droplets are replaced by sea-salt aerosol, and that the influence of waves is taken into account. In this report we describe the progress on the development of the SeaCluse model that applies to open ocean conditions. The calculation of the profiles of the mean wind velocity and turbulent diffusivity has been changed to take into account the characteristics of the marine atmosphere and of the wave field. A module was added to the initialization routines that models the air flow over the waves in a non-turbulent and non-evaporative atmosphere. This module yields vertical profiles of droplet concentrations that enter in the relaxation term that models the mean movement of the particles. These profiles are then modified in the iterative budget calculation that accounts for droplet transport by atmospheric turbulence and their interaction with the humidity field by evaporation. In this part of the code, the evaporation module was changed to describe the evaporation of sea salt aerosols in the marine atmosphere. The output of the new SeaCluse model consists of vertical profiles of temperature, humidity and aerosol concentration from the sea surface up to the top of the marine atmospheric boundary layer. DTIC

N94-26016# Organisatie voor Toegepast Natuurwetenschappelijk Onderzoek, The Hague (Netherlands). Physics and Electronics Lab.
AN OVERVIEW OF THE TNO CONTRIBUTION TO VAST 92
G. J. Kunz and M. M. Moerman 2 Sep. 1993 42 p
(AD-A273751; FEL-93-A039; TDCK-TD-930480) Avail: CASI HC A03/MF A01

The 'Vertical Atmospheric Structure Trail' (VAST92) took place from September 28 to October 16, 1992 at the Wehr Technische Dienststelle (WTD 52), Oberjettenberg, Germany, in the framework of NATO working group AC/243 (Panel 4/RSG.8) on atmospheric propagation effects on electro-optical systems. The experiment was designed to quantify the influence of the atmospheric vertical structure variations on infrared propagation and imaging and on lidar means of remotely sensing the variations. The TNO-Physics and Electronics Laboratory participated with a lidar system, meteo and aerosol equipment. The lidar was stationed in the valley. An altimeter and meteo-equipment were mounted on the cable car. Aerosol spectrometers and meteorological equipment were used, including a sonic anemometer and a fast hygrometer to measure turbulence on the mountain. A large part of the data from these instruments is of crucial importance for the evaluation and interpretation of the data obtained by the other participants. In this report, we present an overview of the TNO instrumentation and experiments. A number of data sets have been processed to demonstrate the possibilities of the different instruments. Interpretation of the results is postponed to later reports. This report is also a guideline for processing the TNO data in conjunction with data from other participants. DTIC

N94-26082# Atmospheric and Environmental Research, Inc., Cambridge, MA.
TESTBED MODEL AND DATA ASSIMILATION FOR ARM
J. F. Louis 28 Apr. 1993 12 p
(Contract DE-FG02-90ER-61065)
(DE94-000432; DOE/ER-61065/3) Avail: CASI HC A03/MF A01

The ultimate objectives of this research are to further develop the ALFA (AER Local Forecast and Assimilation) model originally designed at AER for local weather prediction and apply it to several related purposes in connection with the Atmospheric Radiation Measurement (ARM) program: (1) to provide a testbed that simulates a global climate model in order to facilitate the development and testing of new cloud parametrizations and radiation models; (2) to assimilate the ARM data continuously at the scale of a climate model, using the adjoint method, thus providing the initial conditions and verification data for testing parametrizations; and (3) to study the sensitivity of a radiation scheme to cloud parameters, again using the adjoint method, thus demonstrating the usefulness of the testbed model. The data assimilation uses a variational technique that minimizes the difference between the model results and the observation during the analysis period. The adjoint model is used to compute the gradient of a measure of the model errors with respect to nudging terms that are added to the equations to force the model output closer to the data. DOE

N94-26134*# Alabama Univ., Huntsville. Dept. of Chemistry.
FNAS LIGHTNING DETECTION Final Report, 28 Sep. 1992 - 27 Oct. 1993
George P. Miller and Melanie A. Alzmann 27 Oct. 1993 20 p
(Contract NAS8-38609)
(NASA-CR-193927; NAS 1.26:193927; UAH-5-33068) Avail: CASI HC A03/MF A01

A review of past and future investigations into lightning detection from space was incorporated into a brochure. Following the collection of background information, a meeting was held to discuss the format and contents of the proposed documentation. An initial outline was produced and decided upon. Photographs to be included in the brochure were selected. Quotations with respect to printing the document were requested. In the period between 28 March and June 1993, work continued on compiling the text. Towards the end of this contract, a review of the brochure was undertaken by the technical monitor. Photographs were being revised and additional areas of lightning research were being considered for inclusion into the brochure. Included is a copy of the draft (and photographs) which is still being edited by the technical monitor at the time of this report.
Derived from text

N94-26138*# Texas A&M Univ., College Station.
PROPERTIES OF THE CENTRAL AMERICAN COLD SURGE
James P. McGuirk, Philip J. Reding, and Yuxia Zhang 1993 4 p
Presented at the 20th AMF Conference on Hurricanes and Tropical Meteorology and the 9th AMF Conference on Atmospheric and Oceanic Waves and Stability, San Antonio, TX, May 1993
(Grant NAG8-845)
(NASA-CR-194849; NAS 1.26:194849) Avail: CASI HC A01/MF A01

The Central American cold surge (CACS) is a frontal incursion from the United States into Central America and resembles the East Asian cold surge. They occur more frequently than analyzed by NMC or by published results, based on our observations between 1979 and 1990. Climatology and structure are quantified, based on surface and upper air stations throughout Central America and satellite products from GOES visible and infrared sensors and SSM/I precipitable water and rain rate sensors.
Derived from text

N94-26168# Phillips Lab., Hanscom AFB, MA.
A MODELING STUDY OF THE MESOCYCLONE Interim Report
Paul R. Desrochers 4 Dec. 1992 50 p
(AD-A274889; PL-TR-92-2330; ERP-1113) Avail: CASI HC A03/MF A01

The mesocyclone is a strongly-rotating column of air associated with the updraft of a severe thunderstorm. The size and shape of the phenomenon allows ready detection with a single Doppler radar. Quantitative evaluation of the mesocyclone has been shown to be useful for the prediction of large hail and tornadoes. Accuracy in mesocyclone interpretation is of course critical to these endeavors. A limitation with single-Doppler observation of the mesocyclone is that the flow field is measured directly in only one dimension. Therefore, the shape and spatial variation of intensity can be difficult to determine. For this reason, it is common practice to assume the mesocyclone flow is circularly symmetric when interpreting the single-Doppler image. The problem is that mesocyclone flows are generally not circular, and the deviation from circular can be considerable. This report presents an improved model for the interpretation of single-Doppler mesocyclone observations. The model describes an elliptical flow pattern of any eccentricity. Some examples of highly distorted, single-Doppler, mesocyclone flows are presented which are well simulated by the model. DTIC

N94-26183# Naval Postgraduate School, Monterey, CA.
MESOSCALE FRONTAL EVOLUTION OF THE ERICA IOP-5A CYCLONE M.S. Thesis

Steven R. Cameron Sep. 1993 81 p
(AD-A274906) Avail: CASI HC A05/MF A01

A synoptic investigation was conducted of the rapid coastal cyclogenesis that occurred during Intensive Observation Period (IOP) 5A of the Experiment on Rapidly Intensifying Cyclones over the Atlantic (ERICA). Navy Operational Regional Analysis and Prediction System (NORAPS) forecasts were examined in order to study the mesoscale frontal evolution associated with this rapidly deepening coastal cyclone. The ability of the NORAPS forecasts to accurately depict the frontal positions and intensity was also investigated. The frontal evolution showed characteristics of a classical occlusion, similar to the Norwegian cyclone model and of marine frontal structure as discussed by Shapiro and Keyser. The frontal evolution was highly influenced by the prior existence of strong arctic and coastal fronts. These fronts intensified during the course of the storm development and did not develop as a result of the cyclogenesis. DTIC

N94-26195# South Dakota School of Mines and Technology, Rapid City.
THE NUMERICAL SIMULATION OF MARINE BOUNDARY LAYER CLOUDS
Harold D. Orville 1993 3 p
(Contract N00014-91-J-4017)
(AD-A273669) Avail: CASI HC A01/MF A01

The primary objectives of the research are to numerically simulate stratus, stratocumulus, and cumulus clouds in the marine boundary layer. The research included the formation, evolution, and dissolution of the clouds and the area covered. Next, the change of convection type and the formation of cloud streets could be investigated. Another objective is to increase our understanding of conditions in the marine boundary layer. What determines the vertical profiles of humidity, temperature, and cloud characteristics in space and time? What causes the changing depth of the boundary layer? What are its interaction with the clouds in and out of the boundary layer? A third objective is to compare various numerical models among themselves and with observations. Such comparisons should indicate ways to improve the model and whether practical predictive cloud models for the marine boundary layer can be constructed. DTIC

N94-26313# California Univ., Davis.
A PRELIMINARY ANALYSIS OF THE US WEST CLIMATOLOGY
J. O. Roads, S. C. Chen, K. Ueyoshi, J. Bossert, and J. Winterkamp 1992 4 p Presented at the 17th Annual Climate Diagnostics Conference, Norman, OK, 19-23 Oct. 1992
(Contract DE-FC03-90ER-61010)
(DE94-003028; CONF-9210334-4) Avail: CASI HC A01/MF A01

In a previous paper, Roads et al. discussed the forecast accuracy of the National Meteorological Center's (NMC's) medium-range forecasts (MRF's) of various near-surface meteorological elements, such as temperature, relative humidity, and wind speed in terms of NMC's global analysis. Although these global analyses are most applicable for global perspectives, the authors are interested in more regional scales. Here one might expect the large-scale global analyses to only grossly simulate various regional effects, especially in regions that are strongly influenced by topography. At regional scales, a mesoscale model, which is overlying mesoscale topography and which is forced at the boundary and initialized with a large scale analysis, could provide an even better representation of the regional behavior. In a similar manner, a regional model initialized and forced at the horizontal boundaries by general circulation model (GCM) variables might provide more detailed spatial representation of climatic change than is available from statistical interpolations or simple linear interpolations of the large-scale GCM output to the regional scale. DOE

N94-26431# Florida State Univ., Tallahassee. Dept. of Meteorology.
ANALYSIS AND INTERPRETATION OF THE METEOROLOGY OF THE 1988 COASTAL TRANSITION ZONE EXPERIMENT Final Report
David W. Stuart 31 Dec. 1993 24 p
(Contract N00014-89-J-1578)
(AD-A274710) Avail: CASI HC A03/MF A01

Coastal Transition Zone (CTZ) Experiments were conducted off the California Coast near Pt. Arena by the Office of Naval Research (ONR). One of the basic goals of these experiments was: 'To understand the role of the atmosphere in driving coastal ocean currents and to learn of possible ocean-atmosphere feedback.' This principal investigator acted as a focal person for the meteorology of the CTZ experiments providing meteorological expertise to the other investigators. Our basic objectives were: (1) Documentation of the meteorological conditions during each field study; and (2) Data reduction plus analysis-synthesis of the meteorological conditions for each field study. DTIC

N94-26469 Korean Atomic Energy Research Inst., Daeduk (Republic of Korea).
OVERALL ANALYSIS OF METEOROLOGICAL INFORMATION IN THE DAEDUK NUCLEAR COMPLEX
Byung Woo Kim, Young Bok Lee, Moon Hee Han, Eun Han Kim, Kyung Suk Suh, Won Tae Hwang, and Suk Boong Hong Dec. 1992 116 p In KOREAN Limited Reproducibility: More than 20% of this document may be affected by microfiche quality
(DE93-632594; KAERI/RR-1175/92) Avail: Issuing Activity (Department of Energy (DOE)) (US Sales Only)

Trouble shooting of the tower structure, sensor installation, and grounding and cabling were completed in an integrated field-test. Establishment of the data acquisition system and instrument calibration have been finished since the completion of the main tower construction earlier this year. A procedure guide covering instrument operation, calibration, and repair was also completed. Actual measurements were performed during Oct. and Nov. after the system equipment integration was completed. The occurrence of nocturnal inversion layers, fog, and frequent conditions of atmospheric stability were shown as the analysis results of measured data which represent the seasonal and regional characteristics of the site. Wireless data transmission to the MIPS (Meteorological Information Processing System) was performed after the information was collected by the DAS (data acquisition system). At MIPS, the environmental assessment can be done by the simulation programs for cases of emergency and normal operation. DOE

N94-26506*# Oregon State Univ., Corvallis. Coll. of Oceanic and Atmospheric Sciences.
SCIENCE SUPPORT FOR THE EARTH RADIATION BUDGET EXPERIMENT Final Report
James A. Coakley, Jr. 7 Mar. 1994 44 p
(Contract NAS1-18992; RTOP 665-45-20-01)
(NASA-CR-191600; NAS 1.26:191600) Avail: CASI HC A03/MF A01

The work undertaken as part of the Earth Radiation Budget Experiment (ERBE) included the following major components: The development and application of a new cloud retrieval scheme to assess errors in the radiative fluxes arising from errors in the ERBE identification of cloud conditions. The comparison of the anisotropy of reflected sunlight and emitted thermal radiation with the anisotropy predicted by the Angular Dependence Models (ADM's) used to obtain the radiative fluxes. Additional studies included the comparison of calculated longwave cloud-free radiances with those observed by the ERBE scanner and the use of ERBE scanner data to track the calibration of the shortwave channels of the Advanced Very High Resolution Radiometer (AVHRR). Major findings included: the misidentification of cloud conditions by the ERBE scene identification algorithm could cause 15 percent errors in the shortwave flux reflected by certain scene types. For regions containing mixtures of scene types, the errors were typically less than 5 percent, and the anisotropies of the shortwave and longwave radiances exhibited a spatial scale dependence which, because of the growth of the scanner field of view from nadir to limb, gave rise to a view zenith angle dependent bias in the radiative fluxes. Author (revised)

N94-26628 Victoria Univ. (British Columbia). Dept. of Computer Science.
NUMERICAL MODELLING OF PRECIPITATION OVER COMPLEX TERRAIN M.S. Thesis
Xi Huang 1993 87 p
(ISBN-0-315-84327-6; CTN-94-61021) Copyright Avail: Micromedia Ltd., Technical Information Centre, 240 Catherine Street, Suite 305, Ottawa, Ontario, K2P 2G8, Canada HC/MF

Two models are described for calculating topographical effects on precipitation in complex terrain. One is a three dimensional variational model, and the other is a three dimensional initial value model. The initial value model is the best in principle since it incorporates the most physics, but it requires an accurately defined initial state and is computationally expensive. The variational model is comparatively simple and easy to compute. The three dimensional variational model is applied to calculate the precipitation for 11 Jul. 1983 in the upper Columbia River watershed in

southeastern British Columbia as an experiment. The experimental results strongly show that the model gives realistic results and that the initial wind velocities can be adjusted by different methods. Theoretically speaking, adjusting velocities by two functions is the best, but this result cannot be proven from these experiments since the functions were chosen randomly.
Author (CISTI)

N94-26678# Air Force Systems Command, Wright-Patterson AFB, OH. Foreign Aerospace Science and Tehcnology Center.
INVESTIGATION OF MESOSCALE CONVECTIVE CLOUD CLUSTERS IN SOUTH CHINA
Jixi Jiang, Huiming Ye, and Meizhen Chen 3 Nov. 1993 26 p Transl. into ENGLISH from Yingyong Qixiang Xuebao (China), v. 1, no. 3, Aug. 1990 p 232-241
(AD-A274303; FASTC-ID(RS)T-0369-93) Avail: CASI HC A03/MF A01

The statistical characteristics of 176 mesoscale convective cloud clusters in South China, which are classified into three types in terms of their size, are analyzed based on the short interval GMS images and conventional data during April-October, 1980-1988. Two composite model charts are presented for their formation and development, and two typical cases are studied. Some conclusions can be drawn as follow: (1) Mesoscale convective systems in South China; (2) The convergences of wind and moisture fields in the surface layer and orographic forcing are the trigger mechanism for the genesis of cloud clusters: and (3) Low-level jet and monsoon cloud swell are the most important factors for the development of cloud clusters.
DTIC

N94-26697# Wisconsin Univ., Madison.
ARM FOURIER TRANSFORM SPECTROMETER DATA ANALYSIS TOOLS
W. L. Smith 13 Sep. 1993 23 p
(Contract DE-FG02-92ER-61365)
(DE94-000865; DOE/ER-61365/T1) Avail: CASI HC A03/MF A01

Research activities in the following task areas are summarized: (1) improve infrared radiative transfer model under clear and cloud conditions based on the ARM spectral measurements; (2) model the effects of cloud microphysical properties on the radiative properties of a cloud from interpreting FTIR observations and developing remote sensing technologies; (3) develop a method of inferring effective cloud optical properties from FTIR observations for application to cloud radiative parameterizations; (4) develop a classification method for screening spectral radiance into categories to facilitate atmospheric radiative transfer studies; and (5) develop algorithms for retrieving temperature and constituent concentration profiles from the FTIR observations. Figures depicting coincident radiosonde and AERI downwelling radiance observations are included. DOE

N94-26761# Pacific Northwest Lab., Richland, WA.
MESOSCALE METEOROLOGICAL MEASUREMENTS CHARACTERIZING COMPLEX FLOWS
J. M. Hubbe and K. J. Allwine Sep. 1993 10 p Presented at the Topical Meeting on Environmental Transport and Dosimetry, Charleston, SC, 31 Aug. - 3 Sep. 1993
(Contract DE-AC06-76RL-01830)
(DE94-002359; PNL-SA-22559; CONF-930810-10) Avail: CASI HC A02/MF A01

Meteorological measurements are an integral and essential component of any emergency response system for addressing accidental releases from nuclear facilities. An important element of the US Department of Energy's (DOE's) Atmospheric Studies in Complex Terrain (ASCOT) program is the refinement and use of state-of-the-art meteorological instrumentation. ASCOT is currently making use of ground-based remote wind sensing instruments such as doppler acoustic sounders (sodars). These instruments are capable of continuously and reliably measuring winds up to several hundred meters above the ground, unattended. Two sodars are currently measuring the winds, as part of ASCOT's Front Range Study, in the vicinity of DOE's Rocky Flats Plant (RFP) near Boulder, Colorado. A brief description of ASCOT's ongoing Front Range Study is given followed by a case study analysis that demonstrates the utility of the meteorological measurement equipment and the complexity of flow phenomena that are experienced near RFP. These complex flow phenomena can significantly influence the transport of the released material and consequently need to be identified for accurate assessments of the consequences of a release.
DOE

N94-26798 Analytic Sciences Corp., Reading, MA.
SHORT-RANGE CLOUD AMOUNT FORECASTING WITH MODEL OUTPUT STATISTICS Final Report, Feb. 1992 - Sep. 1993
M. E. Cianciolo Sep. 1993 167 p Limited Reproducibility: More than 20% of this document may be affected by microfiche quality
(Contract F19628-91-C-0185)
(AD-A274769; PL-TR-93-2205) Avail: Issuing Activity (Defense Technical Information Center (DTIC))

TASC conducted a feasibility study of the utility of short-range (3-, 6-, and 9-hour) forecasts of total cloud amount and probability of cloud cover categories using the Model Output Statistics (MOS) approach. The MOS models were built using output from the Air Force Global Spectral Model (GSM) and the Real-Time NEPHanalysis (RTNEPH) model. The RTNEPH total cloud amount fields were also used as ground truth. Models were developed on the eighth-mesh RTNEPH grid (approximately 40 km resolution) for 71 data sets covering a range of locations (tropics and midlatitudes), seasons, and times of day. Results were compared with persistence forecasts using the Brier score, 20/20 score, and sharpness measure. The MOS-based forecasts outperformed persistence with respect to the overall reduction in mean square error, but forecast sharpness was sacrificed. Estimates for future model performance for total cloud cover and probabilities of cloud cover categories were determined for two sample cases. Considering the short data records used to develop the equations, the MOS-based forecast models were remarkably robust in most cases. Recommendations for model improvements and additional performance assessment included: using higher spatial resolution model data that better match the resolution of the eighth-mesh forecasts, using cloud layer variables in model development, developing regression coefficients using additional seasons of data, using non-linear models, and continuing model evaluation using independent cloud data. DTIC

N94-26846# Army Research Lab., White Sands Missle Range, NM.
SURFACE ROUGHNESS LENGTHS Final Report
Frank V. Hansen Aug. 1993 34 p
(AD-A274550; ARL-TR-61) Avail: CASI HC A03/MF A01

The surface roughness length is the meteorological equivalent of an aerodynamic drag coefficient. The surface morphology and terrain relief contribute to the roughness, have a large effect upon surface drag, and influence the analysis of wind, temperature, and specific humidity profiles in the surface boundary layer, as well as the examination of the surface energy balance. Roughness lengths effectively determine the vertical wind shear just above the surface with atmospheric stability almost a direct function of shear and roughness. Experimentally, roughness lengths over many natural surfaces have been determined. Many summaries of estimated surface roughness have been prepared, with most listing only a few typical values. One comprehensive study tabulated all values according to the year the data were collected. In this current effort, an attempt has been made to list roughness as a function of five categories, that is, natural surfaces, including seasonal variations, agricultural lands, urban roughness, effective roughness, and land-use categories. DTIC

N94-26850# Air Force Systems Command, Wright-Patterson AFB, OH. Foreign Aerospace Science and Technology Center.
PROPAGATION OF COLD AIR MASSES IN EAST ASIA AND ITS ASSOCIATED PLANETARY-SCALE FUNCTION
Yihui Ding 3 Nov. 1993 23 p Transl. into ENGLISH from Yingyong Qixiang Xuebao (China), v. 2, no. 2, May 1991 p 124-132
(AD-A274304; FASTC-ID(RS)T-0370-93) Avail: CASI HC A03/MF A01

The present paper has delt with the characteristics of propagation of the winter monsoon during cold air outbreaks for 19 cases of 1980-1984 in East Asia as well as the associated planetary-scale effect. It has been revealed that the propagation of cold air mainly shows a mode of 10-20 day period oscillation. Furthermore, the Siberian cold high associated with outbreaks of cold air may lead to the response of a chain of planetary-scale events. This mainly shows up in the fact that the branch of upward motion of the divergent circulation rapidly shifts from the Indonesia-Malaysian region eastward to the eastern Pacific, thus causing the normal-type Walker circulation to reverse its sense. This condition is very similar to the movement of divergent circulation from non-El Nino year to El Nino year. From the dynamic viewpoint, this kind of divergent circulation is favorable to the synoptic development over the eastern Pacific and the western coast of North America. DTIC

N94-26959# National Oceanic and Atmospheric Administration, Boulder, CO. Environmental Technology Lab.
CLOUD LIQUID WATER CONTENT MEASUREMENT TESTS USING DUAL-WAVELENGTH RADAR Technical Memo
Brooks E. Martner, Robert A. Kropfli, L. Edward Ash (Colorado Univ., Boulder.), and Jack B. Snider Oct. 1993 53 p See also PB91-131839 and PB92-133800 Prepared in cooperation with Colorado Univ., Boulder
(PB94-125960; NOAA-TM-ERL-ETL-235) Avail: CASI HC A04/MF A01

The first field test of a dual-wavelength differential attenuation radar technique for providing range-resolved measurements of cloud liquid water content (LWC) was conducted in Colorado during and shortly after the 1991 Winter Icing and Storms Project (WISP91). A dual-wavelength system was improvised from existing radars of 3.2 cm and 0.87 cm wavelengths. The radar antennas were electronically slaved together and scanned in synchronization with each other and with a steerable microwave radiometer which was used for comparisons. The experiment had mixed results. LWC values computed by the radar technique for several cases during WISP91 were erratic and included negative values. These clouds were relatively dry, however, and did not provide a suitable sample for evaluating the technique's performance in the more hazardous aircraft icing conditions of high LWC. Radar measurements obtained alone shortly after the end of WISP91 yielded reasonable LWC values and patterns, but without independent data for verification. The analyses suggest the radar technique may work best for long path lengths through high-LWC clouds of small droplets that contain some moderately large ice crystals and for clouds containing large droplets up to drizzle sizes. NTIS

N94-27025# Naval Oceanography Command Center/Joint Typhoon Warning Center, FPO San Francisco, CA.
TROPICAL CYCLONE REPORT, 1992 Annual Report, Jan. - Dec. 1992
Donald A. Mautner and Charles P. Guard 1992 271 p
(AD-A274464) Avail: CASI HC A12/MF A03

This annual publication summarizes tropical cyclone activity in the Western North Pacific, Bay of Bengal, Arabian Sea, Western South Pacific, and South Indian Ocean. A best track is provided for each significant tropical cyclone. A brief narrative is given for all tropical cyclones in the Western North Pacific and North Indian Oceans. Forecast verification data and statistics for the Joint Typhoon Warning Center (JTWC) are included. DTIC

N94-27169# National Research Inst. for Earth Science and Disaster Prevention, Tsukuba (Japan).
METEOROLOGICAL DATA AT THE NAGAOKA INSTITUTE OF SNOW AND ICE STUDIES Report No. 1, Dec. 1981 - Apr. 1991 [NAGAOKA NI OKERU KISHO KANSOKU SHIRYO]
Masujiro Shimizu, Tadashi Kimura, and Masayoshi Nakao 30 Mar. 1993 68 p In JAPANESE
(ISSN 0917-057X)
(Rept-158; JTN-94-80511) Avail: CASI HC A04/MF A01

Meteorological data have been collected since March 1971 as an important basis for the snow and ice studies at the Nagaoka Institute of Snow and Ice Studies. It is located at 37 deg 25 min N, 138 deg 53 min E, and 7 cm above sea level in the south of the Echigo plain, the central portion of Japan's main island. This report contains the daily data of 10 winters from December 1981 to April 1991, on the following elements: barometric pressure, air temperature, soil temperatures, wind direction and speed, global solar radiation, radiation balance, duration of sunshine, and amount of precipitation. Author (NASDA)

N94-27356# Instituto de Pesquisas Espaciais, Sao Jose dos Campos (Brazil).
AN OBSERVATIONAL STUDY OF THE EXTRATROPICAL ANTICYCLONES IN THE SOUTH AMERICAN CONTINENT [UM ESTUDO OBSERVACIONAL DA FORMACAO E TRAJETORIAS DE ANTICICLONES EXTRATROPICAIS NA AMERICA DO SUL]
Luiz Claudio Ermida Lima Dec. 1991 91 p In PORTUGESE
(INPE-5387-TDI/476) Avail: CASI HC A05/MF A01

In this study, South American extratropical anticyclones have been studied in the period between 1979 and 1989 for the weak and moderate ones, and between 1953 and 1990 for the most intense ones (in which average pressure was greater or equal to 1030 hPa) by using daily synoptic charts. The main goal of this work was to show the tracks of the anticyclones and the regions where the first closed isobar appeared more frequently in the area between 15 deg S and 55 deg S over the South American Continent. Initially we estimated the number of days in which inner anticyclonic curved isobars crossed the 5x5 degrees areas. Then all tracks of the migratory anticyclones were followed by using daily surface charts. The highest pressure located in the interior of the anticyclones or ridges and temperature was interpolated. We concluded that orography plays an important role in the distribution of anticylonic isobars, with a higher number of days to the west of the Andes cordillera than to the east of the mountains. It was observed that the anticyclogenetic area for the moderate and weak ones is located in an area to the south of Paraguay and North Argentina, while the most intense ones have their first closed isobar in Central Argentina. The weak anticyclones follow a zonal track and the moderate or intense ones follow a path oriented in the SW-NE direction. Author

N94-27408*# Texas A&M Univ., College Station.
GLOBAL BAROTROPIC RESPONSE TO A TROPICAL FORCING
Yuxia Zhang and James P. McGuirk 1993 2 p Presented at the 9th AMS Conference on Atmospheric and Oceanic Waves and Stability, San Antonio, TX, May 1993
(Grant NAG8-912)
(NASA-CR-195256; NAS 1.26:195256) Avail: CASI HC A01/MF A01

Zonally varying flow has been used to initialize numerical models and has been shown to play an important role in strong localized responses both in extratropics and the tropics. In this study, a climatological 200 mb January mean is used as a steady basic state of a barotropical model which consists of shallow water equations and a mass source centered at 4 deg S/120 deg E to simulate convective heating over Indonesia region. In the experiment, tropical responses appear not only over the western Pacific, where the forcing is located, but also over the eastern Pacific where the response is related to the zonally varying basic state. The westward propagating equatorial Rossby waves excited by the forcing interact with waves out of and into the tropics and the positive and negative phase of the Rossby waves result in blocking circulation over North America and tropical plumes over equatorial eastern Pacific, respectively. Derived from text

N94-27422# Instituto de Pesquisas Espaciais, Sao Jose dos Campos (Brazil).
A SYNOPTIC STUDY ON PERIODS OF DEFICIENCY OVER RIO GRANDE DO SUL/BRAZIL [ESTUDO SINOTICO DE PERIODOS DEFICIENTES DE CHUVAS NO RIO GRANDE DO SUL]
Humberto Conrado Feb. 1992 155 p In PORTUGESE
(INPE-5456-TDI/498) Avail: CASI HC A08/MF A02

The rainfall regime in the State of Rio Grande do Sul (Brazil) is characterized by a homogeneous monthly distribution and a low interannual variability. A spatial series considering 39 years of precipitation data (1952-1990) was used to analyze the years which had periods of rain deficiency. In the years 1988 and 1989 the annual precipitation presented meaningful negative deviation. Two summer seasons (January and February) which presented negative anomalous behavior during these years were selected. A synoptical study, using geopotential fields, vertical velocity, relative vorticity, vorticity advection, and divergence fields was performed to analyze this period of rain deficiency. The South Atlantic Convergence Zone (SACZ) was observed to persist during the February months which registered a significant negative deviation precipitation. Related to the SACZ, the presence of a trough was noticed over to the east of Rio Grande do Sul state. At the same time, a trough in the Pacific Ocean was found about 120 deg W. This atmospheric pattern showed to be stationary in February, suggesting effects similar to a blocking situation. As a result, the frontal systems were deviated from their usual path over the State of Rio Grande do Sul. The position of the trough axis, to the east of Rio Grande do Sul induced a persistent subsidence which contributed to inhibiting the convective activity over the region. This period with anomalous negative precipitation coincided with the presence of a positive Southern Oscillation Index in the Pacific Ocean. Author (revised)

N94-27571# Lawrence Livermore National Lab., CA.
SIMULATION OF THE INDIAN AND EAST-ASIAN SUMMER MONSOON IN THE ECMWF MODEL: SENSITIVITY TO HORIZONTAL RESOLUTION
K. R. Sperber, G. L. Potter, J. S. Boyle, and S. Hameed (State Univ. of New York, Stony Brook.) Nov. 1993 37 p
(Contract W-7405-eng-48)
(DE94-004276; UCRL-ID-115322; PCMDI-12) Avail: CASI HC A03/MF A01

The ability of the ECMWF model (Cycle 33) to simulate the Indian and East Asian summer monsoon is evaluated at four different horizontal resolutions: T21, T42, T63, and T106. Generally, with respect to the large scale features of the circulation, the largest differences among the simulations occur at T42 relative to T21. However, on regional scales, important differences among the high frequency temporal variability serve as a further critical test of the model's ability to simulate the monsoon. More generally, the results indicate the importance of evaluating high frequency time scales as a component of the climate system. T106 best captures both the spatial and temporal characteristics of the Indian and East Asian monsoon, while T42 fails to correctly simulate the sequence and development of synoptic scale milestones that characterize the monsoon flow. In particular, T106 is superior at simulating the development and migration of the monsoon trough over the Bay of Bengal. In the T42 simulation, the development of the monsoon occurs one month earlier than typically observed. At this time the trough is incorrectly located adjacent to the east coast of India which results in an underestimate of precipitation over the Burma/Thailand region. This early establishment of the monsoon trough affects the evolution of the East-Asian monsoon and yields excessive preseason rainfall over the Mei-yu region. EOF analysis of precipitation over China indicates that T106 best simulates the Mei-yu mode of variability associated with an oscillation of the rainband that gives rise to periods of enhanced rainfall over the Yangize River Valley. The coarse resolution of T21 precludes simulation of the aforementioned regional scale monsoon flows. DOE

N94-27751# Deutsche Forschungsanstalt fuer Luft- und Raumfahrt, Oberpfaffenhofen (Germany). Abt. Wolkenphysik.
EXAMINATION OF MICRO- AND MACRO-PHYSICAL STRUCTURES AND PROCESSES IN HAILSTORMS WITH RESPECT TO THEIR MODIFICATION [UNTERSUCHUNG VON MIKRO- UND MAKROPHYSIKALISCHEN STRUKTUREN UND PROZESSEN IN HAGELWOLKEN IM HINBLICK AUF DEREN BEEINFLUSSBARKEIT]
Hartmut Hoeller and Peter F. Meischner Jul. 1993 75 p In GERMAN Original contains color illustrations
(ISSN 0939-2963)
(DLR-FB-93-25; ETN-94-95501) Avail: CASI HC A04/MF A01

The internal structure of thunderstorms occurring in Southern Germany is investigated using a polarization diversity Doppler radar (POLDIRAD). The discrimination of different kinds of hydrometeors such as raindrops, graupel or hail was possible by polarimetric measurements. Following the temporal evolution of the particles allows the basic processes involved in hail formation to be inferred, as exemplified by a case study. Based on these processes as well as on statistics of storm types and potential damage, an assessment was made on the probable effects of cloud seeding for hail prevention as performed operationally in the counties of Rosenheim and Miesbach. Considering a variety of possible factors of influence, cloud seeding turned out to have negligible influence on potential hail damages on the ground. In accordance with this finding, six year statistics of the regional distribution of the radar determined hailfalls does not show any effects attributable to cloud seeding. ESA

N94-27884*# Mitre Corp., Bedford, MA.
THUNDERSTORM HYPOTHESIS REASONER Final Report
Alice M. Mulvehill Jan. 1994 29 p
(Contract NAS10-11572)
(NASA-CR-195714; NAS 1.26:195714) Avail: CASI HC A03/MF A01

THOR is a knowledge-based system which incorporates techniques from signal processing, pattern recognition, and artificial intelligence (AI) in order to determine the boundary of small thunderstorms which develop and dissipate over the area encompassed by KSC and the Cape Canaveral Air Force Station. THOR interprets electric field mill data (derived from a network of electric field mills) by using heuristics and algorithms about thunderstorms that have been obtained from several domain specialists. THOR generates two forms of output: contour plots which visually describe the electric field activity over the network and a verbal interpretation of the activity. THOR uses signal processing and pattern recognition to detect signatures associated with noise or thunderstorm behavior in a near real time fashion from over 31 electrical field mills. THOR's AI component generates hypotheses identifying areas which are under a threat from storm activity, such as lightning. THOR runs on a VAX/VMS at the Kennedy Space Center. Its software is a coupling of C and FORTRAN programs, several signal processing packages, and an expert system development shell. Author (revised)

N94-28146# Los Alamos National Lab., NM.
MUSIC FOR LOCALIZATION OF THUNDERSTORM CELLS
J. C. Mosher, P. S. Lewis, and T. M. Rynne (Science Applications and Research Associates, Inc., Huntington, Beach, CA.) 1993 6 p Presented at the Institute of Electrical and Electronic Engineers (IEEE) Asilomar Conference on Signals, Systems, and Computers, Pacific Grove, CA, 1-3 Nov. 1993
(Contract W-7405-eng-36)
(DE94-004985; LA-UR-93-4265; CONF-9311135-4) Avail: CASI HC A02/MF A01

Lightning represents an event detectable optically, electrically, and acoustically, and several systems are already in place to monitor such activity. Unfortunately, such detection of lightning can occur too late, since operations need to be protected in advance of the first lightning strike. Additionally, the bolt itself can traverse several kilometers before striking the ground, leaving a large region of uncertainty as to the center of the storm and its possible strike regions. NASA Kennedy Space Center has in place an array of electric field mills that monitor the effectively DC electric field. Prior to the first lightning strike, the surface electric fields rise as the storm generator within a thundercloud begins charging. Extending methods developed for an analogous source localization problem in magnetoencephalography, Cramer-Rao lower bounds and MUSIC scans for fitting a point-charge source model to the electric field mill data are presented. Such techniques can allow for the identification and localization of charge centers in cloud structures. DOE

N94-28179*# National Aeronautics and Space Administration. Goddard Space Flight Center, Greenbelt, MD.
MODIS AIRBORNE SIMULATOR VISIBLE AND NEAR-INFRARED CALIBRATION, 1992 ASTEX FIELD EXPERIMENT. CALIBRATION VERSION: ASTEX KING 1.0
G. Thomas Arnold (Applied Research Corp., Landover, MD.), Michael Fitzgerald (Analytical Technology Applications Corp., Mountain View, CA.), Patrick S. Grant (Analytical Technology Applications Corp., Mountain View, CA.), and Michael D. King Mar. 1994 22 p
(RTOP 913-00-00)
(NASA-TM-104599; NAS 1.15:104599; Rept-94B00055) Avail: CASI HC A03/MF A01

Calibration of the visible and near-infrared (near-IR) channels of the MODIS Airborne Simulator (MAS) is derived from observations of a calibrated light source. For the 1992 Atlantic Stratocumulus Transition Experiment (ASTEX) field deployment, the calibrated light source was the NASA Goddard 48-inch integrating hemisphere. Tests during the ASTEX deployment were conducted to calibrate the hemisphere and then the MAS. This report summarizes the ASTEX hemisphere calibration, and then describes how the MAS was calibrated from the hemisphere data. All MAS calibration measurements are presented and determination of the MAS calibration coefficients (raw counts to radiance conversion) is discussed. In addition, comparisons to an independent MAS calibration by Ames personnel using their 30-inch integrating sphere is discussed. Derived from text

N94-28182*# National Aeronautics and Space Administration. Goddard Space Flight Center, Greenbelt, MD.
MODIS AIRBORNE SIMULATOR VISIBLE AND NEAR-INFRARED CALIBRATION, 1991 FIRE-CIRRUS FIELD EXPERIMENT. CALIBRATION VERSION: FIRE KING 1.1
G. Thomas Arnold (Applied Research Corp., Landover, MD.), Michael Fitzgerald (Analytical Technology Applications Corp., Mountain View, CA.), Patrick S. Grant (Analytical Technology Applications Corp., Mountain View, CA.), and Michael D. King Mar. 1994 26 p

(RTOP 913-00-00)
(NASA-TM-104600; NAS 1.15:104600; Rept-94B00054) Avail: CASI HC A03/MF A01

Calibration of the visible and near-infrared channels of the MODIS Airborne Simulator (MAS) is derived from observations of a calibrated light source. For the 1991 FIRE-Cirrus field experiment, the calibrated light source was the NASA Goddard 48-inch integrating hemisphere. Laboratory tests during the FIRE Cirrus field experiment were conducted to calibrate the hemisphere and from the hemisphere to the MAS. The purpose of this report is to summarize the FIRE-Cirrus hemisphere calibration, and then describe how the MAS was calibrated from observations of the hemisphere data. All MAS calibration measurements are presented, and determination of the MAS calibration coefficients (raw counts to radiance conversion) is discussed. Thermal sensitivity of the MAS visible and near-infrared calibration is also discussed. Typically, the MAS in-flight is 30 to 60 degrees C colder than the room temperature laboratory calibration. Results from in-flight temperature measurements and tests of the MAS in a cold chamber are given, and from these, equations are derived to adjust the MAS in-flight data to what the value would be at laboratory conditions. For FIRE-Cirrus data, only channels 3 through 6 were found to be temperature sensitive. The final section of this report describes comparisons to an independent MAS (room temperature) calibration by Ames personnel using their 30-inch integrating sphere. Author

N94-28223# Atmospheric and Environmental Research, Inc., Cambridge, MA.

AN ENHANCED GLOBAL SPECTRAL MODEL Final Report, Sep. 1989 - Nov. 1991

Thomas Nehrkorn, Ross Hoffman, Jean-Francois Louis, and Marina Zivkovic 27 Feb. 1992 85 p
(Contract F19628-89-C-0112)
(PL-TR-92-2011) Avail: CASI HC A05/MF A01

This report describes the development of a vectorized, multiprocessing global spectral model (GSM) with enhanced physical parameterizations. The starting point was the Phillips Laboratory GSM, in its GL90 version, which contained an enhanced suite of physical parameterizations. The latitude tasking scheme for multiprocessing the loop over latitude in the calculation of the spectral tendencies and adjusted model variables was implemented, using the general truncation version of the hydrodynamics code. Wavenumber calculations were vectorized over wavenumber and multiprocessed over vertical level. All grid point calculations were vectorized over longitude, and the physics packages were brought into closer compliance with plug-compatibility rules. Speedups due to the optimization were demonstrated in single- and multiprocessing timing tests on a dedicated Cray 2 and Cray Y-MP. The enhanced physics GSM was evaluated in forecast tests and contrasted with the simpler physics GSM used at GWC. Minimization of errors in the computation of the horizontal pressure gradient force was investigated using a perturbation temperature instead of full temperature in the integration of the hydrostatic equation. Several schemes were tested in an idealized model atmosphere. Author (revised)

48 OCEANOGRAPHY

Includes biological, dynamic, and physical oceanography; and marine resources.

For related information see also *43 Earth Resources and Remote Sensing.*

N94-25635# National Inst. for Resources and Environment, Ibaraki (Japan).

A STUDY ON STRUCTURE OF BENTHIC BOUNDARY LAYER IN COASTAL WATERS [ENGAN KAIIKI NI OKERU KAITEI KYOKAISO NO KOZO NI KANSURU KENKYU]

Eichi Sumi 25 Feb. 1993 121 p In JAPANESE
(ISSN 0916-9989)
(Rept-4; JTN-94-80512) Avail: CASI HC A06/MF A02

A three dimensional ultrasonic current meter capable of measuring turbulent characteristics was developed and used to study the turbulent structure of the benthic boundary layer. The results obtained by the system are as follows: (1) the current system of coastal waters is the same as other natural current systems and originally has a three dimensional structure; and (2) it is demonstrated that the turbulent structure near the sea bottom is distributed in the turbulent level. A tidal flow was considered to be a field of the unsteady flow study and many unsteady phenomena were studied. The study results are as follows: (1) nearly 10 minutes were required for the assumption of quasi-steadiness to be established and the friction velocity could be measured with extreme precision at the sampling time of 3 minutes; and (2) the results of studying the temporal similarities and hysteresis effects of the turbulent structure of tidal flow near the sea bottom showed that the turbulent characteristics change with respect to the average horizontal flow velocity. The similarities between the benthic boundary layer and the atmospheric boundary layer were studied, and the study results were as follows: (1) in coastal waters which include shallow waters, it was shown that the friction velocity, not the Reynold's stress, decreases linearly with respect to the height and that the Reynold's stress had a nonlinear distribution; and (2) the vertical eddy viscosity coefficient in shallow waters was estimated from the results of field tests on various assumptions. Author (NASDA)

N94-25791# Bern Univ. (Switzerland).

SIMULATION OF THE CARBON CYCLE IN THE OCEANS

U. Siegenthaler 1993 4 p
(Contract DE-FG02-90ER-61054)
(DE94-000780; DOE/ER-61054/3) Avail: CASI HC A01/MF A01

In this report, the authors conclude that the average oceanic uptake of anthropogenic CO2, as determined from four different ocean models and normalized to the observed mean penetration depth of bomb-C-14 (analogue to anthropogenic CO2), is 2.0 +/- 0.5 GtC/yr (decade 1980-1989). This oceanic uptake plus the year-to-year growth of the atmospheric CO2 content together are less by 1.8 +/- 1.2 GtC/yr than the estimated anthropogenic CO2 emissions from fossil fuels and land use. DOE

N94-26072# Lawrence Livermore National Lab., CA.

INTERPRETING THE IMPLIED MERIDIONAL OCEANIC ENERGY TRANSPORT IN AMIP

D. A. Randall (Colorado State Univ., Fort Collins.) and P. J. Gleckler Sep. 1993 4 p Presented at the 74th American Meteorological Society Annual Meeting, Nashville, TN, 23-28 Jan. 1994
(Contract W-7405-eng-48)
(DE94-001538; UCRL-JC-114683; CONF-940115-8) Avail: CASI HC A01/MF A01

The Atmospheric Model Intercomparison Project (AMIP) was outlined in Paper No. CLIM VAR 2.3 (entitled 'The validation of ocean surface heat fluxes in AMIP') of these proceedings. Preliminary results of AMIP subproject No. 5 were also summarized. In particular, zonally averaged ocean surface heat fluxes resulting from various AMIP simulations were intercompared, and to the extent possible they were validated with uncertainties in observationally-based estimates of surface heat fluxes. The intercomparison is continued in this paper by examining the Oceanic Meridional Energy Transport (OMET) implied by the net surface heat fluxes of the AMIP simulations. As with the surface heat fluxes, the perspective here will be very cursory. The annual mean implied ocean heat transport can be estimated by integrating the zonally averaged net ocean surface heat flux, N(sub sfc), from one pole to the other. In AGCM simulations (and perhaps reality), the global mean N(sub sfc) is typically not in exact balance when averaged over one or more years. Because of this, an important assumption must be made about changes in the distribution of energy in the oceans. Otherwise, the integration will yield a non-zero transport at the endpoint of integration (pole) which is not physically realistic. Here the authors will only look at 10-year means of the AMIP runs, and for simplicity they assume that any long term imbalance in the global averaged N(sub sfc) will be sequestered (or released) over the global ocean. Tests have demonstrated that the treatment of how the global average energy imbalance is assumed to be distributed is important, especially when the long term imbalances are in excess of 10 W m(exp -2). However, this has not had a substantial impact on the qualitative features of the implied heat transport of the AMIP simulations examined thus far. DOE

N94-26076# Naval Postgraduate School, Monterey, CA. Dept. of Oceanography.

HYDROGRAPHIC AND ACOUSTIC DOPPLER CURRENT PROFILER (ADCP) DATA FROM THE ONR EASTERN BOUNDARY CURRENT

ACCELERATED RESEARCH INITIATIVE, 9-16 JUNE 1992
Paul F. Jessen and Steven R. Ramp Nov. 1993 157 p
(AD-A274115; NPS-OC-93-006) Avail: CASI HC A08/MF A02

This data report presents hydrographic (CTD) and Acoustic Doppler Current Profiler (ADCP) data from a cruise to the continental slope region near Point Arena, CA during 9-16 Jun. 1992. The study area encompassed a region from about 38 deg 0.0 min N to 39 deg 0.0 min N from 20 to 90 km offshore. The sampling grid consisted of five along-shore transects 15 km apart, with five CTD stations 15 km apart in each transect. A total of 28 CTD casts were made. ADCP data were collected throughout the cruise. The data are presented as vertical sections, property distributions on horizontal surfaces, and waterfall plots. DTIC

N94-26108# Technische Univ., Delft (Netherlands). Sectie Fysische, Meetkundige en Ruimte Geodesie.
CORRELATION BETWEEN THE GRAVITY FIELD AND THE BATHYMETRY IN THE NORTH ATLANTIC OCEAN Thesis [CORRELATIE TUSSEN HET ZWAARTEKRACHTVELD EN DE BATHYMETRIE IN DE NOORDATLANTISCHE OCEAAN]
Baptist Welting Jun. 1992 92 p In DUTCH
(ETN-94-95036) Avail: CASI HC A05/MF A01

The correlation between the gravity field and the topography/bathymetry in a limited regional area is addressed. The gravity implied by the mass distribution inside the Earth is described by Newton's law of gravity. The Newtonian integral is evaluated in two steps. The influence of the long wave topography is calculated, and the influence of the residual topography is examined. The North Atlantic Ocean is chosen as a test area. For the calculation of the gravity implied by the residual topography, the Newtonian integral is expressed as a convolution integral in terms of the Fourier theory. This convolution integral is evaluated using fast Fourier techniques. The correlation analysis shows that the long wavelength gravity agrees perfectly with an isostatic compensated topography model. The short wave gravity field correlates almost directly with the topography itself. The method is concluded to be convenient to model the gravity influence of the local topography. Only the Airy-Heiskanen model is used to describe the topography and its isostatic compensation. It will be interesting to investigate whether it is possible to expand the derived model, using Fourier techniques, for more complex topography/isostasy models, which are expected to provide even more realistic results for the local influence. ESA

N94-26149# Scripps Institution of Oceanography, La Jolla, CA.
COUPLING OF PELAGIC AND BENTHIC COMMUNITIES OVER A SEAMOUNT IN THE EASTERN NORTH PACIFIC Final Report, 1 Oct. 1988 - 30 Sep. 1993
Kenneth L. Smith, Jr. 1994 9 p
(Contract N00014-89-J-1540)
(AD-A274750) Avail: CASI HC A02/MF A01

Recent studies indicate that seamounts can be sites of enriched biological activity with enhanced biomass of pelagic and benthic organisms relative to the surrounding water. We undertook a study to examine the interaction of micronekton/nekton and benthopelagic animals/epibenthic megafauna over a deep oceanic seamount, Fieberling Guyot, located in the eastern North Pacific. We monitored the number and movements of acoustically detectable targets within the bottom 100 m of the water column over the summit using a vertically-profiling acoustic array developed for this study. A large multiple opening-closing net system (10 sq m) and free-vehicle baited traps were used to collect the pelagic fauna for identification, sizing and gut content analysis. A total of 26 acoustic targets were detected, dispersed non-randomly with a skewed distribution between 65 and 85 m above bottom. Temporal distribution of targets was random but revealed higher numbers in the morning than in the evening. The micronekton/nekton consisted of 114 species which were gravimetrically dominated by fish, especially the macrourid, Malacocephalus laevis. Four species of benthopelagic animals/epibenthic megafauna were collected including a new macrourid species, Nezumia n.sp. There are no strong trends in the diel distribution of the micronekton/nekton and the limited data on acoustic targets shows a random temporal distribution. Alternative explanations of trophic coupling over Fieberling Guyot are discussed.
DTIC

N94-26354# Colorado Univ., Boulder.
NONLINEAR OCEAN WAVES Progress Report, 1 Jan. - 31 Dec. 1993
Harvey Segur 6 Jan. 1994 3 p
(Contract N00014-92-J-1274)
(AD-A274651) Avail: CASI HC A01/MF A01

Two major papers were written during the last year. The papers describe our work under this contract in our two main areas of research: (1) numerically induced chaos, and (2) waves in shallow water. This progress report summarizes the contents of those two papers. DTIC

N94-26361# Naval Postgraduate School, Monterey, CA.
TOPICS IN LONGSHORE CURRENTS Ph.D. Thesis
John C. Church Sep. 1993 130 p
(AD-A274788) Avail: CASI HC A07/MF A02

The momentum equation governing mean longshore currents on straight beaches is a balance of forcing from the momentum transfer of the oscillatory wave motion, turbulent momentum transfer (mixing), and bottom stress. Of these, the wave's contribution is well understood, but the remaining two are not, principally due to the complicated hydrodynamics of the surf-zone. Addressing the bottom stress term, a longshore current model is developed which includes a modification of the bottom stress due to the effects of breaking-wave induced turbulence. A one-dimensional turbulent kinetic energy equation is used to model this breaking-wave induced turbulence, producing a spatially varying bottom friction coefficient. The modeled longshore current cross-shore profiles show improved agreement with field observations. In a second bottom stress study, vertical profiles of mean longshore currents are examined using field data obtained with vertically stacked electromagnetic current meters with the goal of measuring the bottom stress and its associated drag coefficient. The profiles are observed to become vertically uniform whenever the ratio of wave height to depth exceeds 0.3, indicating that nearly all of the waves passing a given location are breaking. Finally, horizontal turbulent momentum transfer (mixing) is examined for the case of shear instabilities of the longshore current.
DTIC

N94-26567# Sverdrup Technology, Inc., Bay Saint Louis, MS.
BATHYMETRIC DATA SET EXTRACTION PROGRAM. USERS GUIDE Final Report
Wesley J. Youtsey and Robert L. Woodyard 8 Nov. 1993 19 p
(DA Proj. X05-13)
(AD-A274761; NRL-FR/7323-93-9431) Avail: CASI HC A03/MF A01

This report is a users guide for a suite of programs that can be used to generate, plot, and modify bathymetric data files. This software has evolved over several years to meet the needs of the Naval Layered Ocean Model development. Each facet of the program is discussed, and examples are provided to show typical entries to the program. DTIC

N94-26853# Sverdrup Technology, Inc., Bay Saint Louis, MS.
THE HOUGH TRANSFORM ALGORITHM FOR SEA ICE LEAD ANALYSIS: AN EVALUATION Final Report
Denise J. Gineris and Florence M. Fetterer 15 Nov. 1993 32 p
(AD-A274535; NRL-MR/7240-93-7072) Avail: CASI HC A03/MF A01

An algorithm for sea ice lead analysis using a Hough transform technique has been developed at the Naval Research Laboratory (NRL) Remote Sensing Applications Branch and is currently in use at NRL and the Navy/National Oceanic and Atmospheric Administration (NOAA) Joint Ice Center (JIC). The algorithm resides on a Sun microcomputer system as part of a larger image processing package (the NRL Satellite Image Processing System or NSIPS) developed at NRL. Currently, the algorithm functions on Advanced Very High Resolution Radiometer (AVHRR) and Operational Line Scan imagery. Algorithm performance was evaluated by comparing results from the Hough transform technique to those obtained through manual analysis for a set of five AVHRR infrared images. The algorithm operated well, but there is still room for improvement. Details of the evaluation and recommendations for improvement are contained in this report. DTIC

N94-26886# Washington Univ., Seattle. Applied Physics Lab.
SOUND, SPEED, REFLECTIVITY, ABSORPTION, AND THERMAL DIFFUSIVITY MEASUREMENTS IN ARCTIC ICE IN 1990
G. R. Garrison, K. L. Williams, P. D. Mourad, R. E. Francois, and T. Wen Nov. 1993 172 p
(Contract N00039-91-C-0072)
(AD-A274326; APL-UW-TR-9208) Avail: CASI HC A08/MF A02

Detailed measurements of internal properties of Arctic ice were made in Spring 1990 to relate acoustic properties to the physical properties of the ice. This report presents the procedures, analyses, and results of those studies. Some basic parameters measured in previous field studies were remeasured; consistency between individual experiments strengthens our confidence in the results and the techniques used. Novel techniques were used to measure properties of growing ice, which was later cored, submerged, and remeasured. Results reported here have been summarized in the open literature. The basic data and their processing are described here in detail. In the ice-growth and submergence study, a 2-m-square hole was cut through the ice canopy. Strings of hydrophones and thermistors were then suspended vertically in the hole, and the water froze around them. Frequent monitoring of ice temperature and the receipt of sound pulses from below, along with salinities determined from ice cores obtained a short distance away, gave insight into the freezing process and the formation of a skeletal layer above the ice/water interface. Periodic measurements of the reflectivity of the growing ice at 37-150 kHz gave further information on the skeletal structure. The sound speed in the skeletal layer varied from that of the water at the ice/water interface to that of bulk ice at about 3 cm into the ice. Absorption of sound (in decibels per meter) was about three times greater near the interface, decreasing to that for bulk ice at 15-20 cm into the ice. DTIC

N94-26887# Naval Research Lab., Monterey, CA.
THE NOGAPS TEN YEAR AMIP INTEGRATION Final Report
Thomas E. Rosmond Oct. 1993 60 p
(DA Proj. 7W0-513)
(AD-A274332; NRL/MR/7532-93-7212) Avail: CASI HC A04/MF A01

This report is a user's guide to the 10 year model history data set from an integration of the Navy Operational Global Atmospheric Prediction System (NOGAPS). NRL Monterey is participating in the Atmospheric Model Intercomparison Project (AMIP) sponsored by the Department of Energy. Nearly every major atmospheric modeling center in the world has run their model for the years 1979 through 1988 with sea surface temperature and sea ice boundary conditions provided by AMIP. The NOGAPS AMIP data set has great potential for use in a wide variety of atmosphere/ocean studies that require the high time and space resolution available from a global atmospheric model. DTIC

N94-27090# Washington Univ., Seattle. Applied Physics Lab.
AN XCP USER'S GUIDE AND REFERENCE MANUAL
Thomas B. Sanford, Eric A. DAsaro, Eric L. Kunze, John H. Dunlap, and Robert G. Drever Aug. 1993 120 p
(Contracts N00014-90-J-1100; N00014-84-C-0111; N00014-87-K-0004)
(AD-A274519; APL-UW-TR-9309) Avail: CASI HC A06/MF A02

This report describes expendable current profiler (XCP) instrumentation, equipment testing procedures, data acquisition methods, and data processing. It also provides a guide to XCP field operations. DTIC

N94-27156 Foerenade Fabriksverken, Linkoeping (Sweden). Huvudavdelning foer Informationsteknologi.
COMPILATION OF CORRECTIONS FOR POSTPROCESSING OF LASER BATHYMETRY DATA [SAMMANSTAELLNING AV KORREKTIONER FOER EFTERBEHANDLING AV LASERBATYMETRIDATA]
O. Steinvall, K. Koppari, and U. Karlsson May 1993 41 p In SWAHILI
(PB94-123668; FOA-30079-3.1) Avail: Issuing Activity (National Technical Information Service (NTIS))

The report shortly reviews the most important corrections which have to be applied in the post-processing of the raw data from a laser bathymetry system. These corrections include absolute positioning of the depth sounding as well as corrections for the measured depth. The depth corrections consist of system dependent parameters as well as environmental factors such as the influence of waves and multiple scattering in the water. Many of the corrections are hard to apply with great accuracy, e.g. those corrections which depend on wave slopes as these slopes are hard to measure. An analysis of the total error budget indicates that a depth sounding laser system during most weather and water conditions can meet the demand on depth accuracy set by the International Hydrographic Bureau (IHB) as being no larger than + or - 30 cm down to 30 m depth and no larger than 1 m down to 100 m depth. NTIS

N94-27208 National Defence Research Establishment, Linkoeping (Sweden). Huvudavdelning foer Informationsteknologi.
SCANVIEW: A GRAFICAL PROGRAM FOR ANALYSIS OF LASERBATHYMETRY DATA [SCANVIEW: ETT GRAFIKPROGRAM FOER ANALYS AV LASERBATYMETRIDATA]
S. Kulldorff Mar. 1993 73 p In SWAHILI; Text in SWEDISH; summary in ENGLISH
(PB94-124443; FOA-C-30707-3.1) Avail: Issuing Activity (National Technical Information Service (NTIS))

The report describes the development of a program called ScanView. The program is supposed to simplify the postprocessing of water depth data collected with the FLASH-system. ScanView consists of a number of windows and dialogs that present swath and echos graphicly. With the program one can study collected bathymetry data as a color scaled map describing depth of water. Various settings can be made to make out interesting shots. The individual laser shots may then be selected and studied for instance by its waveform. The program is written in the programming language Ada with help of the window system Motif. NTIS

N94-28393# Helsinki Univ. of Technology, Espoo (Finland). Lab. for Strength of Materials.
STUDIES IN ICE MECHANICS
J. Kaemaeraeinen Jun. 1993 192 p
(PB94-133055; ISBN-951-22-1550-0) Avail: CASI HC A09/MF A02

The intention of the study is to provide a general review on the formation of natural ice, the structure of natural ice, and the strength of ice as a material. The knowledge is important for example when problems related to ice bearing capability, ice-structure interaction, or ship ice resistance are studied. Most of the material given in the study is based on direct quotations of the literature. NTIS

N94-28272# Japan Marine Science and Technology Center, Tokyo.
AN OCEANOGRAPHICAL OBSERVATION IN THE WESTERN PACIFIC AND INTERNATIONAL COOPERATIONS
Kei Muneyama *In* Science and Technology Agency, Asia-Pacific Seminar on Global Change Research Cooperation 1992 p 35-4 (For primary document see N94-28268 07-45)
Avail: CASI HC A03/MF A03

51 LIFE SCIENCES (GENERAL)

N94-25593# Edgewood Arsenal, Aberdeen Proving Ground, MD. Research Development and Engineering Center.
PROCEEDINGS OF THE SYMPOSIUM ON CURRENT CONCEPTS AND APPROACHES ON ANIMAL TEST ALTERNATIVES Final Report, period ending Feb. 1992
Harry Salem, comp. Sep. 1993 407 p
(DA Proj. 101-62622-A-553)
(AD-A273926; ERDEC-SP-012) Avail: CASI HC A18/MF A04

Biological and medical research has historically been conducted primarily with animal experimentation. The advances in biological scientific knowledge and medicine have been dependent and resulted from these animal experiments, supplemented with in vitro studies. Over the last decade, advocates for animal rights, and the skyrocketing cost of animal experimentation, have intensified the search for more alternatives to animal biomedical research and testing. Although to replace animal research is a noble quest, realistically this may never be accomplished since the final proof will require testing in an integrated whole animal system. However, the scientific and animal activist communities, sensitive to all of these issues, are advocating the adoption of three goals: replacement of animals, reduction in the number of animals, and refinement by getting more information from fewer animals and using animals lower on the phylogenetic tree. A fourth task is taking responsibility for implementation. These proceedings describe the current state of the art in these approaches. Alternative methods (in vitro, chemical, computer) are described for not only eye and skin, but also for inhalation, aquatic, environmental and noncarcinogenic endpoints. In addition, the regulatory status is discussed since this is a major prerequisite to validation and acceptance. DTIC

N94-26086*# National Aeronautics and Space Administration. Ames Research Center, Moffett Field, CA.

AN AUTOMATIC 14-DAY PASTE DIET FEEDER FOR ANIMALS

Marilyn Vasques, Jerry Mulenburg, Dan Gundo, and Jon Griffith (Bionetics Corp., Moffett Field, CA.) Jan. 1994 13 p
(RTOP 199-08-12-06)
(NASA-TM-108804; A-94037; NAS 1.15:108804) Avail: CASI HC A03/MF A01

During a centrifuge experiment, any interruption that requires stopping the centrifuge may influence the results. Centrifuges often must be stopped for animal maintenance (food, water and waste removal), especially in cases of timed feedings. To eliminate the need for stopping the centrifuge while still providing timed feeding, an automatic paste diet feeder was developed. The feeder is based on a constant volume concept and can deliver a predetermined amount of paste diet at specified time intervals. This unit was supported by water delivery and waste collection systems. The entire system performed reliably and maintained the animals well for a continuous centrifugation experiment of 14 days. Author

N94-26093*# National Aeronautics and Space Administration. Ames Research Center, Moffett Field, CA.

PLASMA VOLUME SHIFTS AND EXERCISE THERMOREGULATION WITH WATER IMMERSION AND SIX-DEGREE HEAD-DOWN TILT

Andrew Carl Ertl Jan. 1994 32 p
(Grant NGT-50686; RTOP 199-18-12-07)
(NASA-TM-108781; A-93097; NAS 1.15:108781) Avail: CASI HC A03/MF A01

The hypothesized fluid shifts and resultant responses that occur during spaceflight are simulated by six-degree head down tilt (HDT) and water immersion (WI). The purpose of this study was to compare exercise thermoregulation before and after physiologic mechanisms reduce plasma volume (PV) in response to 24-hr HDT (HDT24). A secondary study utilized WI to reproduce the PV reduction of HDT24. Seven males were studied in two conditions: during 70 minutes of supine cycling ergometry at 58 percent of peak oxygen consumption following 1-hr HDT (HDT1) and HDT24; and up to 6 hr WI at 34.5 C. Plasma volume was reduced by 10.4 percent in HDT24 when compared to HDT1. Pre-exercise rectal temperature, T(sub re), was an average 0.22 C higher after HDT24. Rectal temperature increased during exercise with no interaction between time and treatment. The reduced PV and elevated pre-exercise T(sub re) had offsetting effects on thermoregulatory mechanisms, suggesting no alteration in the response at a given T(sub re). Plasma volume was reduced by 4.3 +/- 2.3 percent and 1.1 +/- 1.8 percent following HDT24 and WI, respectively, compared to upright chair rest. Although the reductions in PV were not significantly different, great intra-individual variability was evident. The ability to reproduce PV changes consistently with HDT and WI is limited by this variability. Author (revised)

N94-26210*# National Aeronautics and Space Administration. Ames Research Center, Moffett Field, CA.

THERMOREGULATORY EFFECTS OF CAFFEINE INGESTION DURING REST AND EXERCISE IN MEN

Nancy Dunagan, John E. Greenleaf, and Craig J. Cisar Jan. 1994 47 p
(RTOP 199-18-12-07)
(NASA-TM-108783; A-93099; NAS 1.15:108783) Avail: CASI HC A03/MF A01

Body temperatures and thermoregulatory responses were measured at rest and during submaximal exercise under normal ambient conditions in 11 aerobically-conditioned men (age = 29.2 +/- 6.2 yr, VO2(max) = 3.73 +/- 0.46 min(sup -1), relative body fat = 12.3 +/- 3.7 percent, mean +/- SD) with (CT) and without (NCT) the ingestion of 10 mg of caffeine per kg of body weight. Oxygen uptake (VO2), heart rate (HR), and rectal (T(sub re)) and mean skin (T-bar(sub sk)) temperatures were recorded for 100 minutes starting one minute after ingestion of caffeine or a placebo. Data were collected throughout 30 minutes of rest (sitting) and the following 70 minutes of sitting leg ergometer exercise using the same constant load (1,088 +/- 153 kgm/min) in both NCT and CT. The load resulted in a mean relative exercise intensity equal to approximately 68 percent of VO2(sub max). Skin heat conductance (H(sub sk)) and sweat rate were calculated. Two-way analysis of covariance revealed no significant (P greater than 0.05) differences between NCT and CT in VO2, HR, T(sub re), T-bar(sub sk), or H(sub sk). A dependent t-test indicated no significant difference between NCT and CT in sweat rate. Thus, a high level of caffeine ingestion has no detrimental effects on body temperatures and thermoregulatory responses during moderately heavy exercise in normal ambient conditions. Author (revised)

N94-26470 Korean Atomic Energy Research Inst., Daeduk (Republic of Korea).

STUDIES ON THE APPLICATION OF RADIATION FOR GENETIC TRANSFORMATION IN HIGHER PLANTS

Young Il Lee, Hi Sup Song, Jae Sung Kim, In Chul Shin, Sang Jae Lee, Ki Woon Lee, and Yong Tack Lim Feb. 1993 70 p In KOREAN
Limited Reproducibility: More than 20% of this document may be affected by microfiche quality
(DE93-632656; KAERI/RR-1214/92) Avail: Issuing Activity (Department of Energy (DOE)) (US Sales Only)

The present research discusses the use of radiation in genetic engineering to increase productivity. Some variants were selected from the M2 generation of Namzack and the M3 generation of Sumi. The variants were derived from the plantlet of the microtuber culture of two potato cultivars irradiated with gamma rays. The rate of variation in the irradiated microtuber indicated that there were very few differences among the cultivars. The optimum gamma ray dosage for inducing mutations was found to be in the range of 30-50 Gy of gamma rays. DOE

N94-26517# Texas Univ. Health Science Center, San Antonio. Dept. of Radiology.

THE ROLE OF HYPERBARIC OXYGEN AS A PROPHYLAXIS FOR RADIATION ENTERITIS Final Report, 15 Feb. 1992 - 14 Feb. 1993

John J. Feldmeier 14 Feb. 1993 6 p
(Contract F49620-92-J-0183)
(AD-A274974; AFOSR-94-0016TR) Avail: CASI HC A02/MF A01

C3H mice were used to study the effects of post radiation treatments of hyperbaric oxygen (HBO) on preventing onset of radiation enteritis. Fifty mice were irradiated in the abdominal pelvic regions with identical radiation doses of 3000 CGY in 10 fractions over two weeks. The mice were randomly divided into a control and a study group of 25 each. The control group received no other treatment while being maintained with standard nutritional support. The study group preceived 30 HBO treatments (90 min of 100% oxygen at 2.4 ATA for 5 days/week for 6 weeks) starting 7 weeks after radiation therapy. All mice were sacrificed at 7 months and examined for signs of radiation damage. A numerical scoring system was used to quantitatively evaluate radiation damage to tissue. A score of +30 was determined for the radiation control group consisting of 21 surviving animals while a score of only +3 was noted for the HBO treated study group consisting of 25 surviving animals. Stretch meter examination showed that 7 of 21 control animals possessed stenotic lesions while only 4 of 25 HBO-treated animals were affected. Histological examination for submucosal fibrosis is presently in progress with no apparent differences noted thus far. This study indicates that post-radiation HBO treatments can significantly reduce small bowel radiation damage in mice. DTIC

N94-26623# Los Alamos National Lab., NM.

NEUTRON AND X RAY SCATTERING STUDIES OF THE INTERACTIONS BETWEEN Ca(2+)-BINDING PROTEINS AND THEIR REGULATORY TARGETS: COMPARISONS OF TROPONIN C AND CALMODULIN

J. Trewhella and G. A. Olah 1993 15 p Presented at the 4th International Conference on Biophysics and Synchrotron Radiation, Tsukuba, Japan, 30 Aug. - 5 Sep. 1992
(Contract W-7405-eng-36)
(DE94-002706; LA-UR-93-3851; CONF-920821-4) Avail: CASI HC A03/MF A01

The regulatory proteins calmodulin and troponin C share a strikingly unusual overall structure. Their crystal structures show each protein consists of two structurally homologous globular domains connected by an extended, solvent exposed alpha-helix of approximately eight turns. Calmodulin regulates a variety of enzymes that show remarkable functional and structural diversity. This diversity extends to the amino acid sequences of the calmodulin-binding domains in the target enzymes. In contrast with calodulin, troponin C appears to have a single very specialized function. It is an integral part of the troponin complex, and Ca(2+) binding to troponin c results in the release of the inhibitory function of troponin I, which eventually leads to actin-binding to myosin and the triggering of muscle contraction. Small-angle scattering has been particularly useful for studying the dumbbell shaped proteins because the technique is very sensitive to changes in the relative dispositions of the two globular domains. Small-angle scattering, using x rays or neutrons, gives information on the overall shapes of proteins in solution. Small-angle scattering studies of calmodulin and its complexes with calmodulin-binding domains from various target enzymes have played an important role in understanding the functional role of its unusual solvent exposed helix. Likewise, small-angle scattering has been used to study troponin C with various peptides, to shed light on the similarities and differences between calmodulin and troponin C. DOE

N94-26991# Aerospace Medical Research Labs., Brooks AFB, TX. Crew Systems Directorate.

PERFORMANCE RECOVERY IN THE BABOON FOLLOWING (+)G SUB z-INDUCED LOSS OF CONSCIOUSNESS Final Report, Jul. 1985 - Sep. 1990

John W. Burns, Paul M. Werchan, John W. Fanton, and Andrew B. Dollins Dec. 1993 17 p
(AF Proj. 7930)
(AD-A274411; AL/CF-TR-1993-0110) Avail: CASI HC A03/MF A01

Seven male baboons (avg. wt. 20.6 +/- 1.6 kg) were trained in a simple shock-avoidance performance task on the Armstrong Laboratory human/animal centrifuge for subsequent (+)G sub z-induced loss of consciousness (G-LOC) exposure. A red light was presented to the baboon at approximate 2-s intervals. The animal was allowed 1 s to turn off the light or receive a 1-s shock. The shock could be abbreviated by a late trigger pull (escape). Thus, the animal could avoid, escape, or accept the full shock. EEG was monitored from three transcranial stainless steel electrodes. Loss of consciousness (LOC) was induced by a rapid onset (4 or 6 G/s) exposure to 8 (+)G sub z, (head-to-feet inertial load), and sustained until LOC was identified by a near isoelectric EEG signal. Performance recovery time was measured from the return of EEG activity to the time when the animal resumed the performance task. These data were compared with previously obtained human data and found to be very similar. Also, it was found that performance recovery time significantly (p less than .001) increased with increased duration of unconsciousness. This study demonstrates the utility of the baboon as an animal model for G-LOC research. DTIC

N94-27045# National Defence Research Establishment, Umea (Sweden). Huvudavdelning foer ABC-Skydd.

BAKTERIELLA TOXINER-MORGONDAGENS HOT (BACTERIAL TOXINS-THE THREAT OF TOMORROW)

Karin Hjalmarrsson, Lena Norlander, and Roland Rosqvist May 1993 62 p In SWAHILI
(PB94-124229; FOA-C-40310-4.4) Avail: CASI HC A04/MF A01

Toxins from pathogenic bacteria have been studied for the last century and have remained objects for intense research over the last decade. The power of gene technology has been used to increase the understanding of structure and mechanism of action of bacterial toxins. This review describes what is known for some of the most potent bacterial toxins. Aspects that are discussed are production of toxins in different systems, the use of toxins as new therapeutic agents and vaccines, and methods for identification of toxins. NTIS

N94-27165# Iowa Univ., Iowa City.

NCVS, VOLUME 5 Status and Progress Report, Nov. 1993

Ingo Titze, ed., Julie Lenke, ed., Julie Ostrem, ed., and Martin Milder, ed. Nov. 1993 106 p Sponsored by National Inst. on Deafness and Other Communication Disorders Prepared in cooperation with Denver Center for the Performing Arts, CO; Wisconsin Univ., Madison; and Utah Univ., Salt Lake City
(AD-A274975) Avail: CASI HC A06/MF A02

This 5th Status and Progress Report comes at a time when we are all thinking of the long term future of the National Center for Voice and Speech. Many things are changing right now in the health science arena. All of us are familiar, of course, with the day to day developments of President Clinton's health care package. One thing is certain - each year we have to become more clever as researchers. The Advisory Board to NIDCD wishes us to get deeper into the molecular structure of all the organs of the human body involved in speech communication. At the same time, they wish us to understand the whole body as a system. Yet it is becoming more and more difficult to do invasive procedures, either on humans or on animals. This means that the critical data that we all need have to come from very carefully conducted experiments, those that have a high benefit to risk (or cost) ratio. On the one hand, we need large numbers of human subjects or animals to make our results statistically reliable; on the other hand, we need to conserve and protect humans and animals involved in research. This puts all of the pressure on the experimenter to obtain only those pieces of information that are absolutely vital and then to integrate the fragments in the most clever ways. DTIC

N94-27171 National Defence Research Establishment, Umea (Sweden). Huvudavdelning foer ABC-Skydd.

MICROBIOLOGY RESEARCH AT SOME RESEARCH INSTITUTES IN THE FORMER SOVIET UNION: A SURVEY OF SCIENTIFIC PUBLICATIONS [MIKROBIOLOGISK FORSKNING VID ETT ANTAL FORSKNINGSINSTITUT I DET FORNA SOVJETUNIONEN: EN SAMMANFATTNING AV LITTERATURDATA]

G. Bostroem, B. Engberg, L. Norlander, A. Norqvist, and A. Osterman May 1993 22 p In SWAHILI
(PB94-123320; FOA-C-40309-4.4) Avail: Issuing Activity (National Technical Information Service (NTIS))

The survey of the publications of some research institutes of the former Soviet Union has been performed. The study has focused on scientific publications found in the bibliographic database BIOSIS during 1980-89. NTIS

N94-27227*# National Aeronautics and Space Administration. Ames Research Center, Moffett Field, CA.

PROPRIOCEPTIVE ISOKINETIC EXERCISE TEST

P. T. Dempster (Loredan Biomedical, Inc., Davis, CA.), E. M. Bernauer (California Univ., Davis.), M. Bond (Loredan Biomedical, Inc., Davis, CA.), and J. E. Greenleaf Jun. 1993 12 p
(RTOP 199-18-12-07)
(NASA-TM-104015; A-93070; NAS 1.15:104015) Avail: CASI HC A03/MF A01

Proprioception, the reception of stimuli within the body that indicates position, is an important mechanism for optimal human performance. People exposed to prolonged bed rest, microgravity, or other deconditioning situations usually experience reduced proprioceptor and kinesthetic stimuli that compromise body balance, posture, and equilibrium. A new proprioceptive test is described that utilizes the computer-driven LIDO isokinetic ergometer. An overview of the computer logic, software, and testing procedure for this proprioceptive test, which can be performed with the arms or legs, is described. Author

N94-27411*# National Aeronautics and Space Administration. John F. Kennedy Space Center, Cocoa Beach, FL.

EFFECT OF CARBON DIOXIDE ENRICHMENT ON RADISH PRODUCTION USING NUTRIENT FILM TECHNIQUE (NFT)

C. L. Mackowiak (Bionetics Corp., Cocoa Beach, FL.), L. M. Ruffe (Bionetics Corp., Cocoa Beach, FL.), N. C. Yorio (Bionetics Corp., Cocoa Beach, FL.), and R. M. Wheeler (Bionetics Corp., Cocoa Beach, FL.) Mar. 1994 17 p
(NASA-TM-107198; NAS 1.15:107198) Avail: CASI HC A03/MF A01

Radish plants (Raphanus sativus L. cvs. Cherry Belle, Giant White Globe, and Early Scarlet Globe) were grown in four different CO2 enriched environments, 0.04, 0.10, 0.50, and 1.00 kPa (400, 1000, 5000, 10000 ppm). Cultivar responses to CO2 treatments varied, where cv. Cherry Belle showed no significant response to CO2 enrichment, cv. Giant White Globe was moderately affected and Early Scarlet Globe was strongly affected. Enrichment at 0.10 kPa led to greater root dry matter (DM) than 1.00 kPa for cv. Giant White Glove, whereas 0.10 kPa produced greater storage root, shoot, and root DM than 1.00 kPa for cv. Early Scarlet Globe. The data suggest that 1.00 kPa CO2 may be detrimental to the growth of certain radish cultivars. Root:shoot ratios tended to increase with increasing CO2 concentration. Water use efficiency (g biomass/kg H2O) increased with increasing CO2 enrichment, up to 0.5 kPa but then declined at the 1.00 kPa treatment. The total nitric acid used to maintain nutrient solution pH was lowest at the 1.00 kPa treatment as well, suggesting a decreased demand of nutrients by the plants at the highest CO2 level. Author

N94-27412*# National Aeronautics and Space Administration. John F. Kennedy Space Center, Cocoa Beach, FL.
DEVELOPMENT OF A SPARGING TECHNIQUE FOR VOLATILE EMISSIONS FROM POTATO (SOLANUM TUBEROSUM)
Elizabeth Berdis (Bionetics Corp., Cocoa Beach, FL.), Barbara Vieux Peterson (Bionetics Corp., Cocoa Beach, FL.), Neil C. Yorio (Bionetics Corp., Cocoa Beach, FL.), Jennifer Batten (Bionetics Corp., Cocoa Beach, FL.), and Raymond M. Wheeler 8 Dec. 1993 23 p
(Contract NAS10-11624)
(NASA-TM-109199; NAS 1.15:109199) Avail: CASI HC A03/MF A01

Accumulation of volatile emissions from plants grown in tightly closed growth chambers may have allelopathic or phytotoxic properties. Whole air analysis of a closed chamber includes both biotic and abiotic volatile emissions. A method for characterization and quantification of biogenic emissions solely from plantlets was developed to investigate this complex mixture of volatile organic compounds. Volatile organic compounds from potato (Solanum tuberosum L. cv. Norland) were isolated, separated and identified using an in-line configuration consisting of a purge and trap concentrator with sparging vessels coupled to a GC/MS system. Analyses identified plant volatile compounds: transcaryophyllene, alpha-humulene, thiobismethane, hexanal, cis-3-hexen-1-ol, and cis-3-hexenyl acetate. Author

N94-27743# Deutsche Forschungsanstalt fuer Luft- und Raumfahrt, Cologne (Germany). Abt. Strahlenbiologie.
CONSTRUCTION AND TEST OF EXPERIMENT HARDWARE FOR A SPACE EXPERIMENT ON SPACELAB MISSION IML-2 Ph.D. Thesis - Fachhochschule Aachen [KONSTRUKTION UND PRUEFUNG VON EXPERIMENT-HARDWARE EIN WELTRAUMEXPERIMENT AUF DER SPACELAB-MISSION IML-2]
Ute Schlengermann Mar. 1993 83 p In GERMAN
(ISSN 0939-2963)
(DLR-FB-93-23; ETN-94-95499) Avail: CASI HC A05/MF A01

The space experiment KINETICS onboard of the Spacelab mission IML-2 (International Microgravity Laboratory) deals with cellular repair processes of radiation injured DNA (Deoxyribo Nucleic Acid) in microgravity. The biological samples consist of irradiated cultures of bacteria and human cells in nine Typ-1-containers of the Biorack. They are kept frozen except for the active phase in the 37 C incubator. The experiment hardware comprises nine sample carriers and three passive thermal units to keep the samples frozen during the first 30 h of the mission. The sample carriers are constructed from rectangular aluminum profiles with holes to accommodate eighteen 200 micrometers tubes with bacteria and ten 600 micrometers tubes with cell cultures, each. The passive thermal units are stainless steel vacuum flasks. Their interior is divided into an inner part, accommodating three sample carriers, and an outer part with phase changing material. A total of 550 ml of a water salt solution as phase changing material will keep the samples frozen for 42 h. ESA

N94-27754# Deutsche Forschungsanstalt fuer Luft- und Raumfahrt, Cologne (Germany). Abt. Strahlenbiologie.
VACUUM-UV-EFFECTS ON E. COLI PLASMID pUC19: INACTIVATION, STRAND BREAK INDUCTION AND MUTATION INDUCTION Ph.D. Thesis - Bonn Univ. [VAKUUM-UV-EFFEKTE AUF DAS E. COLI PLASMID PUC19: INAKTIVIERUNG, STRANGBRUCHINDUKTION UND MUTATIONSINDUKTION]
Joerg Wehner Jul. 1993 111 p In GERMAN
(ISSN 0939-2963)
(DLR-FB-93-26; ETN-94-95502) Avail: CASI HC A06/MF A02

On Escherichia coli plasmid pUC19 the UV action spectra of inactivation, mutation induction and strand break induction are compared between wet and dry state. The cross sections of inactivation and mutation induction show similar dependence on wavelength strand in the range 190 to 254 nm, whereas the cross sections of inactivation and break induction show similar dependence on wavelength in the range 160 to 190 nm. The mutation spectrum was detected after irradiation with V-UV (Vacuum UV) (160 nm) and V-UV (254 nm). In both cases, more than 60 of the detected mutations were transitions. After irradiation with V-UV (254 nm) a significant amount of frame-shift mutations could be detected. ESA

N94-27862# Japan Atomic Energy Research Inst., Tokyo.
NEUTRONS IN BIOLOGY
Satoru Funahashi (Japan Atomic Energy Research Inst., Tokai.) and Nobuo Niimura (Toho Univ., Tokyo, Japan.) Jan. 1993 104 p
(DE94-701085; JAERI-M-92-213) Avail: CASI HC A06/MF A02

The start of JRR-3M in 1990 was a great epoch to the neutron scattering research in Japan. Abundant neutron beam generated by the JRR-3M made it possible to widen the research field of neutron scattering in Japan. In the early days of neutron scattering, biological materials were too difficult to be studied by neutrons not only because of their complexity but also because of the strong incoherent scattering by hydrogen. However, the remarkable development of the recent neutron scattering and its related sciences, as well as the availability of higher flux, has made biological materials one of the most attractive subjects to be studied by neutrons. In early September 1992, an intensive workshop titled 'Neutrons in Biology' was held in Hitachi City by making use of the opportunity of the 4th International Conference on Biophysics and Synchrotron Radiation (BSR92) held in Tsukuba. The workshop was organized by volunteers who are eager to develop the research in this field in Japan. Numbers of outstanding neutron scattering biologists from U.S., Europe, and Asian countries met together and enthusiastic discussions were held all day long. The editors believe that the presentations at the workshop were so invaluable that it is absolutely adequate to put them on record as an issue of JAERI-M and to make them available for scientists to refer to in order to further promote the research in the future. DOE

N94-27940*# Ohio State Univ., Columbus.
ROOT GRAVITROPISM IN MAIZE AND ARABIDOPSIS Final Report, 1 Mar. 1992 - 30 Nov. 1993
Michael L. Evans 30 Nov. 1993 4 p
(Grant NAG10-84)
(NASA-CR-195710; NAS 1.26:195710) Avail: CASI HC A01/MF A01

Research during the period 1 March 1992 to 30 November 1993 focused on improvements in a video digitizer system designed to automate the recording of surface extension in plants responding to gravistimulation. The improvements included modification of software to allow detailed analysis of localized extension patterns in roots of Arabidopsis. We used the system to analyze the role of the postmitotic isodiametric growth zone (a region between the meristem and the elongation zone) in the response of maize roots to auxin, calcium, touch and gravity. We also used the system to analyze short-term auxin and gravitropic responses in mutants of Arabidopsis with reduced auxin sensitivity. In a related project, we studied the relationship between growth rate and surface electrical currents in roots by examining the effects of gravity and thigmostimulation on surface potentials in maize roots. Derived from text

N94-25672*# Colorado Univ., Boulder. Dept. of Aerospace Engineering Sciences.
AUTONOMOUS SUPPORT FOR MICROORGANISM RESEARCH IN SPACE
M. W. Luttges, D. M. Klaus, M. L. Fleet, M. S. Miller, D. E. Shipley, and J. D. Smith *In* USRA, Proceedings of the 8th Annual Summer Conference: NASA/USRA Advanced Design Program 1992 p 40-52 (For primary document see N94-25665 07-80)
Avail: CASI HC A03/MF A04

N94-25673*# Florida Univ., Gainesville. Dept. of Aerospace Engineering, Mechanics and Engineering Sciences.
BIOREGENERATIVE SYSTEM COMPONENTS FOR MICROGRAVITY
Gale E. Nevill, Jr. and Michael I. Hessel, Jr. *In* USRA, Proceedings of the 8th Annual Summer Conference: NASA/USRA Advanced Design Program 1992 p 53-66 (For primary document see N94-25665 07-80)
Avail: CASI HC A03/MF A04

N94-27444# Nagoya Women's Univ. (Japan).
ENDOCRINOLOGICAL EVALUATIONS OF MUSCLE AND BONE ATROPHY IN TAIL-SUSPENDED RATS [BIBU KENSUI RATTO NI OKERU KIN-KOTSU ISHUKU NO NAIBUNPIGAKU TEKI KENTO]
Setsuko Kawano, Kazumi Kanda (Sanwa Kagaku Kenkyusho Co. Ltd., Kasugai, Japan.), Yoshiharu Murata (Nagoya Univ., Japan.), Sachiko Omori (Nagoya Univ., Japan.), Norihiro Miyamoto (Nagoya Univ., Japan.), Kaori Sueda (Nagoya Univ., Japan.), and Hisao Seo (Nagoya Univ., Japan.) *In* Nagoya Univ., Annals of the Research Inst. of Environmental Medicine,

Nagoya Univ., Volume 44 25 Mar. 1993 p 5-8 In JAPANESE (For primary document see N94-27442 07-52)
Avail: CASI HC A01/MF A04

N94-27464# Nagoya Univ. (Japan). Research Inst. of Environmental Medicine.
MODULATION BY GALACTOSAMINE-INDUCED HEPATITIS OF BIOLOGICAL RESPONSES OF THE RAT EXPOSED TO HIGH ALTITUDE HYPOXIA [KYUSEI TEIATSU-TEISANSO KANKYOKA NI OKERU GARAKUT OSAMIN YUHATSU KANEN RATTO NO SEITAI HANNO]
Chikashi Yamamoto, Masataka Yoshino (Institute for Developmental Research, Kasugai, Japan.), Shigeo Mori, and Hisao Seo *In its* Annals of the Research Inst. of Environmental Medicine, Nagoya Univ., Volume 44 25 Mar. 1993 p 97-98 In JAPANESE (For primary document see N94-27442 07-52)
Avail: CASI HC A01/MF A04

N94-27465# Nagoya Univ. (Japan). Research Inst. of Environmental Medicine.
PROTECTIVE ACTION OF PLATELET-ACTIVATING FACTOR ANTAGONIST, TCV-309, AGAINST ISCHEMIA REPERFUSION INJURY IN ISOLATED RABBIT HEARTS [KESSHOBAN KASSEIKA INSHI (PAF) KIKKOZAI TCV-309 NO KYOKETSU SHINKIN HOGO KOKA: IEUSAGI TEKISHUTSU KANRYUSHIN O MOCHITA JIKKENTEKI KENTO]
Satoru Kato, Akira Koike, Toshio Abe, Itsuo Kodama, and Junji Toyama *In its* Annals of the Research Inst. of Environmental Medicine, Nagoya Univ., Volume 44 25 Mar. 1993 p 99-101 In JAPANESE (For primary document see N94-27442 07-52)
Avail: CASI HC A01/MF A04

N94-27466# Nagoya Univ. (Japan). Dept. of Cardiol-Surgery.
PROTECTIVE ACTION OF AN AMILORIDE DERIVATIVE (AMILORIDE, 5-(N, N-DIMETHYL) HYDROCHLORIDE) AGAINST IN ISOLATED ISCHEMIA/REPERFUSION NEWBORN RABBIT HEARTS [MIJUKU SHINKIN NO KYOKETSU SAIKANRYU SHOGAI NI TAISURU AMIRORAIDO YUDOTAI (AMIRORAIDO,5-(N-, N-JIMECHIRU) HIDOROKURORAIDO) NO HOGO KOKA]
Akira Koike, Satoru Kato, Toshiaki Akita, Toshio Abe, Itsuo Kodama, and Junji Toyama *In* Nagoya Univ., Annals of the Research Inst. of Environmental Medicine, Nagoya Univ., Volume 44 25 Mar. 1993 p 102-104 In JAPANESE (For primary document see N94-27442 07-52)
Avail: CASI HC A01/MF A04

N94-27467# Nagoya Univ. (Japan). Research Inst. of Environmmental Medicine.
EFFECTS OF HIGH-INTENSITY ELECTRIC FIELD STIMULATION ON THE ELECTROMECHANICAL PERFORMANCE OF CARDIAC MUSCLE: INFLUENCE OF FIBER ORIENTATION Report No. 6 [KOENERUGI DENKI SHIKKU GA SHINKIN NO MAKU KATSUDO DENI TO CHORYOKU NI OYOBOSU SAYO: SHINKIN SENI SOKO NO EIKYO]
Itsuo Kodama, Akiko Arai, Ryoko Suzuki, Nitaro Shibata (Tokyo Woman's Medical Coll., Japan.), Kiyomi Niki (Tokyo Woman's Medical Coll., Japan.), Ichiro Sakuma (Tokyo Woman's Medical Coll., Japan.), Tadashi Haraguchi (Tokyo Denki Univ., Japan.), Kenji Furukawa, Yasuhiko Fukui, and Saichi Hosoda (Tokyo Woman's Medical Coll., Japan.) et al *In its* Annals of the Research Inst. of Environmental Medicine, Nagoya Univ., Volume 44 25 Mar. 1993 p 105-109 In JAPANESE (For primary document see N94-27442 07-52)
Avail: CASI HC A01/MF A04

N94-27468# Nagoya Univ. (Japan). Research Inst. of Environmental Medicine.
ON THE MECHANISM OF REENTRANT ARRHYTHMIAS FOLLOWING DC DEFIBRILLATION: INFLUENCE OF FIBER ORIENTATION TO THE EFFECTS OF LOW-ENERGY ELECTRIC FIELD STIMULATION ON THE EFFECTIVE REFRACTORY PERIOD OF CARDIAC MUSCLE [CHOKURYU JOSAIDO GO NO RIENTORI HUSEIMYAKU HASSEI KIJO NI KANSURU KENKYU: TEI ENERUGI DENBA SHIGEKI NIYORU SINKIN FUOKI ENCHO TO SENI SOKO NO KANKEI]
Itsuo Kodama, Nitaro Shibata (Tokyo Woman's Medical Coll., Japan.), Ichiro Sakuma (Tokyo Denki Univ., Japan.), Kiyomi Niki (Tokyo Woman's Medical Coll., Japan.), Akiko Arai, Ryoko Suzuki, Tadashi Haraguchi (Tokyo Denki Univ., Japan.), Kenji Furukawa (Tokyo Denki Univ., Japan.), Yasuhiko Fukui (Tokyo Denki Univ., Japan.), and Saichi Hosoda (Tokyo Woman's Medical Coll., Japan.) et al *In its* Annals of the Research Inst. of Environmental Medicine, Nagoya Univ., Volume 44 25 Mar. 1993 p 110-113 In JAPANESE (For primary document see N94-27442 07-52)
Avail: CASI HC A01/MF A04

N94-27469# Nagoya Univ. (Japan). Research Inst. of Environmental Medicine.
POSITIVE CHRONOTROPIC EFFECT OF MECHANICAL STRETCH ON THE SINOATRIAL NODE: ROLES OF NEUROTRANSMITTERS AND STRETCH ACTIVATED CHANNELS [KIKAITEKI SHINTEN NI YORU DOKESSETSU JIDONO KOSHIN NO KIJO NI KANSURU KENKYU]
Akiko Arai, Ryoko Suzuki, Itsuo Kodama, and Junji Toyama *In its* Annals of the Research Inst. of Environmental Medicine, Nagoya Univ., Volume 44 25 Mar. 1993 p 114-116 In JAPANESE (For primary document see N94-27442 07-52)
Avail: CASI HC A01/MF A04

N94-27470# Nagoya Univ. (Japan). Research Inst. of Environmental Medicine.
DISTURBED NEURONAL MIGRATION IN THE CEREBRAL CORTEX OF MICE BY LOW-DOSE GAMMA RADIATION [TEISENRYO HOSHASEN NI YORU MAUSU DAINO HISHITSU SHINKEI SAIBO NO YUSO SHOGAI]
Minoru Inoue, Shizu Hayasaka, Xue-Zhi Sun, and Hideki Yamamura *In its* Annals of the Research Inst. of Environmental Medicine, Nagoya Univ., Volume 44 25 Mar. 1993 p 117-121 In JAPANESE (For primary document see N94-27442 07-52)
(Grant MOE-03680181)
Avail: CASI HC A01/MF A04

N94-27471# Nagoya Univ. (Japan). Research Inst. of Environmental Medicine.
DISTRIBUTION OF GABA IMMUNOREACTIVE NEURONS IN THE BRAIN OF ROLLING MOUSE NAGOYA AND GAMMA-IRRADIATED MOUSE [IDENSEI UNDO SHICCHO MAUSU TO GANMASEN HIBAKU MAUSU NO NO NI OKERU GABA NYURON NO BUNPU]
Takayoshi Imai, Yoshiko Takagishi, Shizu Hayasaka, Minoru Inouye, and Hideki Yamamura *In its* Annals of the Research Inst. of Environmental Medicine, Nagoya Univ., Volume 44 25 Mar. 1993 p 122-124 In JAPANESE (For primary document see N94-27442 07-52)
Avail: CASI HC A01/MF A04

N94-27472# Suzuka Univ. of Medical Science and Technology (Japan).
EFFECTS OF GAMMA RAY RADIATION ON THE DEVELOPING MOUSE CEREBELLUM: APOPTOTIC CELL DEATH AND INDUCTION OF TISSUE TRANSGLUTAMINASE [GANMASEN SHOSHA NO MAUSU SHINSEISHI NO SHONO GENKI NI OYOBOSU EIKYO: SAIBOSHI TO SOSHIKI TORANSUGURUTAMINAZE NO YUDO]
Masao Tamaru, Masato Ando (Fujita Health Univ., Toyohashi, Japan.), Yutaka Nagata (Fujita Health Univ., Toyohashi, Japan.), and Minoru Inoue (Nagoya Univ., Japan.) *In* Nagoya Univ., Annals of the Research Inst. of Environmental Medicine, Nagoya Univ., Volume 44 25 Mar. 1993 p 125-127 In JAPANESE (For primary document see N94-27442 07-52)
Avail: CASI HC A01/MF A04

N94-27477# Nagoya Univ. (Japan). Research Inst. of Environmental Medicine.
THE INTRACELLULAR SECOND MESSENGER SYSTEM IN c-fos GENE INDUCTION BY ACTH [ACTH NI YORU C-FOS IDENSHI YUDO NO SAIBONAI SEKANDO MESSENJA]
Norihiro Miyamoto, Kazumi Kanda, Hiroyoshi Hidaka, and Hisao Seo *In its* Annals of the Research Inst. of Environmental Medicine, Nagoya Univ., Volume 44 25 Mar. 1993 p 145-147 In JAPANESE (For primary document see N94-27442 07-52)
(Grant MOE-04671469)
Avail: CASI HC A01/MF A04

N94-27479# Nagoya Univ. (Japan). Dept. of Surgery.
CLONING OF RAT RXR ALPHA cDNA AND THE EXPRESSION OF ITS mRNA IN REGENERATING LIVER AND PRIMARY CULTURED HEPATOCYTES [RATTO RXR ARUFA CDNA NO KURONINGU TO SAISEIKAN OYOBI SHODAI BAIYO SAIBO NI OKERU MRNA NO HATSUGEN]
Masafumi Menjo, Yoshiharu Murata, Fukushi Kambe, Taichi Kato, Tsuyoshi Kato, and Hisao Seo *In its* Annals of the Research Inst. of Environmental Medicine, Nagoya Univ., Volume 44 25 Mar. 1993 p 151-15 In JAPANESE (For primary document see N94-27442 07-52)
(Grant MOE-03807084)
Avail: CASI HC A01/MF A04

N94-27480# Nagoya Univ. (Japan). Research Inst. of Environmental Medicine.
CLONING OF A NOVEL POU FAMILY GENE BY RT-PCR METHOD [RT-PCR HO O MOCHIITA ATARASHII POU IDENSHI NO KURONINGU NO KOKOROMI]
Fukushi Kambe, Shinichiro Tsukahara, Taichi Kato, Norihiro Miyamoto, Yoshiharu Murata, and Hisao Seo *In its* Annals of the Research Inst. of Environmental Medicine, Nagoya Univ., Volume 44 25 Mar. 1993 p 154-157 In JAPANESE (For primary document see N94-27442 07-52)
(Grant MOE-04454559)
Avail: CASI HC A01/MF A04

N94-27482# Nagoya Univ. (Japan). Dept. of Internal Medicine.
EXPRESSION ANALYSIS OF THYROXINE-BINDING GLOBULIN COMPLETE DEFICIENCY IN JAPANESE (TBG-CDJ) [NIHONJIN NO TBG KANZEN KESSONSHO (TBG-CDJ) NO HASSHO KIJO NI KANSURU KENKYU]
Yoshitaka Miura, Fukushi Kanbe, Yuichi Mori, Ikuo Yamamori, Yoshiyuki Tani, Yoshiharu Murata, Yutaka Oiso, and Hisao Seo *In its* Annals of the Research Inst. of Environmental Medicine, Nagoya Univ., Volume 44 25 Mar. 1993 p 161-165 In JAPANESE (For primary document see N94-27442 07-52)
(Grant MOE-04671468)
Avail: CASI HC A01/MF A04

N94-27483# Nagoya Univ. (Japan). Research Inst. of Environmental Medicine.
DEVELOPMENT OF PURKINJE CELLS IN VITRO [BAIYOKEI NI OKERU PURUKINE SAIBO NO BUNKA]
Yoshiko Takagishi, Manabu Inoue (Mie Univ., Japan.), Takahito Sugimoto (Mie Univ., Japan.), and Hideki Yamamura *In its* Annals of the Research Inst. of Environmental Medicine, Nagoya Univ., Volume 44 25 Mar. 1993 p 166-169 In JAPANESE (For primary document see N94-27442 07-52)
Avail: CASI HC A01/MF A04

N94-27484# Nagoya Univ. (Japan). Research Inst. of Environmental Medicine.
DEVELOPMENTAL EXPRESSION OF PROTEIN KINASE C TYPE 1 ISOZYME IN SUNCUS AND RAT CEREBELLA [SUNKUSU TO RATTO NO SHONO NI OKERU PUROTEINKINAZE C1 GATA AISOZAIMU NO HATSUGEN]
Shizu Hayasaka, Yoshiko Takagishi, Senichi Oda, Minoru Inoue, and Hideki Yamamura *In its* Annals of the Research Inst. of Environmental Medicine, Nagoya Univ., Volume 44 25 Mar. 1993 p 170-173 In JAPANESE (For primary document see N94-27442 07-52)
Avail: CASI HC A01/MF A04

N94-27485# Nagoya Univ. (Japan). School of General Education.
ABNORMAL DEVELOPMENT OF SEROTONIN NERVE FIBERS IN THE CEREBRAL CORTEX OF YOUNG RATS WITH METHYLAZOXYMETHANOL INDUCED MICROCEPHALY [MECHIRUAZOKISHIMETANORU NI YORU JIKKENTEKI SHOTOSHO RATTO NO DAINO HISHITSU NI OKERU SEROTONIN SHINKEI SENI NO SEIGO SHOKI HATTATSU IJO]
Atsushi Funahashi, Minoru Inoue, and Hideki Yamamura *In its* Annals of the Research Inst. of Environmental Medicine, Nagoya Univ., Volume 44 25 Mar. 1993 p 174-176 In JAPANESE (For primary document see N94-27442 07-52)
Avail: CASI HC A01/MF A04

N94-27486# Nagoya Univ. (Japan). Research Inst. of Environmental Medicine.
EFFECTS OF ML-9, A MYOSIN LIGHT-CHAIN KINASE INHIBITOR, ON PREIMPLANTATION DEVELOPMENT OF THE MOUSE [MAUSU NO CHAKUSHOMAE HASSEI NI OYOBOSU MIOSHIN KEISA KINAZE SOGAIZAI ML-9 NO EIKYO]
Nurul Kabir, Hideki Yamamura, Yoshiko Takagishi, Minoru Inoue, Senichi Oda, and Hiroyoshi Hidaka *In its* Annals of the Research Inst. of Environmental Medicine, Nagoya Univ., Volume 44 25 Mar. 1993 p 177-179 In JAPANESE (For primary document see N94-27442 07-52)
(Grant MOE-04670012)
Avail: CASI HC A01/MF A04

N94-27487# Nagoya Univ. (Japan). Research Inst. of Environmental Medicine.
COMPACTION-LIKE BLASTOMERE AGGREGATION CAUSED BY 1-OLEOYL-2-ACETYLGLYCEROL IN MOUSE EMBRYOS: AN ELECTRON MICROSCOPIC OBSERVATION [1-OREOIRU-2-ASECHIRUGURISERORU NI YORI CONPAKUSHON YO NO KAKKYU GYOSHU O OKOSHITA MAUSUHAI NO DENKENTEKI KANSATSU]
Toshihiko Kumazawa, Yoshiko Takagishi, Mami Osugi (Mie Univ., Japan.), and Hideki Yamamura *In its* Annals of the Research Inst. of Environmental Medicine, Nagoya Univ., Volume 44 25 Mar. 1993 p 180-182 In JAPANESE (For primary document see N94-27442 07-52)
Avail: CASI HC A01/MF A04

N94-27488# Seinan Gakuin Univ., Fukuoka (Japan).
INDUCTIVE DIFFERENTIATION OF NERVE CELLS IN MOUSE EMBRYONIC ECTODERM AT EARLY PRIMITIVE STREAK STAGE BY RETINOIC ACID [RECHINOINSAN NI YORU SHOKI GENSHI SENJOKI HAISEIGAIHAIYO KARANO SHIMKEI SAIBO NO YUDOTEKI BUNKA]
Kiyoko Yamamoto and Hideki Yamanura (Nagoya Univ., Japan.) *In* Nagoya Univ., Annals of the Research Inst. of Environmental Medicine, Nagoya Univ., Volume 44 25 Mar. 1993 p 183-185 In JAPANESE Sponsored by Narishige Zoological Science Award (For primary document see N94-27442 07-52)
Avail: CASI HC A01/MF A04

N94-27489# Nagoya Univ. (Japan). Research Inst. of Environmental Medicine.
ANORECTAL MALFORMATIONS INDUCED BY INTRAPERITONEAL INJECTION OF ALL-TRANS RETINOIC ACID IN SUNCUS [SUNKUSU NI OKERU ORU TORANSU RECHINOIN SAN FUKUKONAI TOYO NI YORU SAKO NO YUHATSU]
Ryozo Hashimoto, Senichi Oda, Minoru Inoue, and Hideki Yamamura *In its* Annals of the Research Inst. of Environmental Medicine, Nagoya Univ., Volume 44 25 Mar. 1993 p 186-188 In JAPANESE (For primary document see N94-27442 07-52)
Avail: CASI HC A01/MF A04

N94-27490# Eisai Co. Ltd., Hashima (Japan). Dept. of Drug Safety Research.
CROSS-SECTIONAL ANATOMY OF DAY 30 SUNCUS FETUSES [SUNKUSU 30 NICHI TAIJI NI OKERU ODAMEN NI YORU NAIBU KIKAN KANSATSU]
Nobuhiro Niwa, Takao Matsubara, Senichi Oda (Nagoya Univ., Japan.), Minoru Inoue (Nagoya Univ., Japan.), and Hideki Yamamura (Nagoya Univ., Japan.) *In* Nagoya Univ., Annals of the Research Inst. of Environmental Medicine, Nagoya Univ., Volume 44 25 Mar. 1993 p 189-192 In JAPANESE (For primary document see N94-27442 07-52)
Avail: CASI HC A01/MF A04

N94-27491# Aichi Agricultural Research Center, Naga (Japan).
SKELETAL DEVELOPMENT AND OSSIFICATION OF THE SWINE FETUSES [BUTA TAIJI NO KOKKAKU KEISEI KATEI NO KANSATSU]
Ayumi T. Ichikawa, Senichi Oda (Nagoya Univ., Japan.), and Minoru Inoue (Nagoya Univ., Japan.) *In* Nagoya Univ., Annals of the Research Inst. of

Environmental Medicine, Nagoya Univ., Volume 44 25 Mar. 1993 p 193-196 In JAPANESE (For primary document see N94-27442 07-52)
Avail: CASI HC A01/MF A04

N94-27492# Yagi Memorial Park, Mitake (Japan). Inst. of Applied Biochemistry.
DEVELOPMENT OF INBRED STRAINS FROM JAPANESE WILD RATS (RATTUS NORVEGICUS) [NIHONSAN YASEI RATTO (RATUSU NORUBEGIKUSU) KARANO KEITO IKUSEI]
Kyoko Ono, Yoshiki Niwa, Shizuka Kato, Senichi Oda (Nagoya Univ., Japan.), Kyoji Kondo, and Hideki Yamamura (Nagoya Univ., Japan.) *In* Nagoya Univ., Annals of the Research Inst. of Environmental Medicine, Nagoya Univ., Volume 44 25 Mar. 1993 p 197-201 In JAPANESE (For primary document see N94-27442 07-52)
Avail: CASI HC A01/MF A04

N94-27493# Academy of Sciences (USSR), Novosibirsk. Inst. of Cytology and Genetics.
ELECTRON MICROSCOPIC ANALYSIS OF MEIOTIC CHROMOSOME PAIRING IN MALE HOUSE MUSK SHREW, SUNCUS MURINUS [SUNKUSU OSU NI OKERU SENSHOKUTAI TAIGO NO DENSHI KENBIKYO NI YORU KAISEKI]
Pavel M. Borodin, Senichi Oda (Nagoya Univ., Japan.), Yoshiko Takagishi (Nagoya Univ., Japan.), Minoru Inoue (Nagoya Univ., Japan.), and Hideki Yamamura (Nagoya Univ., Japan.) *In* Nagoya Univ., Annals of the Research Inst. of Environmental Medicine, Nagoya Univ., Volume 44 25 Mar. 1993 p 202-204 In JAPANESE (For primary document see N94-27442 07-52)
Avail: CASI HC A01/MF A04

N94-27494# Nagoya Univ. (Japan). Research Inst. of Environmental Medicine.
EFFECT OF PGE2 RECEPTOR AGONISTS BUTAPROST, M AND B 28767 AND AN ANTAGONIST AH 6809 ON THE BK RESPONSE OF VISCERAL POLYMODAL RECEPTORS [NAIZO PORIMODARU JUYOKI NO BURAJIKININ HANNO NI TAISURU PUROSUTAGURANJIN E2 JUYOTAI NO AGONISUTO BUTAPUROSUTO, M/B 28767, OYOBI ANTAGONISUTO AH 6809 NO KOKA]
Hisashi Koda, Kazue Mizumura, and Takao Kumazawa *In its* Annals of the Research Inst. of Environmental Medicine, Nagoya Univ., Volume 44 25 Mar. 1993 p 205-207 In JAPANESE (For primary document see N94-27442 07-52)
(Grant MOE-04255103)
Avail: CASI HC A01/MF A04

N94-27495# Nagoya Univ. (Japan). Research Inst. of Environmental Medicine.
EXCITATION OF CUTANEOUS POLYMODAL RECEPTOR INDUCED BY SYMPATHETIC STIMULATION IN ADJUVANT-INDUCED ARTHRITIS RATS [AJUBANTO KANSETSUEN RATTO NI MIRARETA KOKAN SHINKEI SHIGEKI NI YORU HIFU PORIMODARU JUYOKI KOFUN]
Jun Sato, Shigeyuki Suzuki, Tomoko Iseki, and Takao Kumazawa *In its* Annals of the Research Inst. of Environmental Medicine, Nagoya Univ., Volume 44 25 Mar. 1993 p 208-210 In JAPANESE Sponsored by Uehara Memorial Foundation and Research Foundation for Oriental Medicine (For primary document see N94-27442 07-52)
(Grants MOE-04770070; MOE-04255103)
Avail: CASI HC A01/MF A04

N94-27496# Nagoya Univ. (Japan). Research Inst. of Environmental Medicine.
SELECTION OF SITE INJECTING ADJUVANT IN CHRONIC INFLAMMATION MODEL [MANSEI ENSHO MODERU NI OKERU KIENZAI TOYO BUI NO SENTAKU]
Shigeyuki Suzuki, Tomoko Iseki, Kazue Mizumura, and Takao Kumazawa *In its* Annals of the Research Inst. of Environmental Medicine, Nagoya Univ., Volume 44 25 Mar. 1993 p 211-213 In JAPANESE (For primary document see N94-27442 07-52)
(Grant MOE-04255103)
Avail: CASI HC A01/MF A04

N94-27497# Nagoya Univ. (Japan). Research Inst. of Environmental Medicine.
INFLUENCE OF MECHANICAL STIMULATION ON INFLAMMATORY EDEMA [UNDO SHIGEKI NO ENSHOSEI FUSHU NI TAISURU EIKYO]
Shigeyuki Suzuki, Tomoko Iseki, Kazue Mizumura, and Takao Kumazawa *In its* Annals of the Research Inst. of Environmental Medicine, Nagoya Univ., Volume 44 25 Mar. 1993 p 214-216 In JAPANESE (For primary document see N94-27442 07-52)
(Grant MOE-04255103)
Avail: CASI HC A01/MF A04

N94-27498# Nagoya Univ. (Japan). Coll. of Medical Technology.
THE EFFECT OF NALOXONE ON SLEEPING TIME IN ADJUVANT ARTHRITIC RATS [CHOKI AJUBANTO KANSETSUEN RATTO NO MASUI KOKA JIKAN NI TAISURU NAROKISON ZENTOYO NO EIKYO]
Tomoko Iseki, Shigeyuki Suzuki, Kazue Mizumura, and Takao Kumazawa *In its* Annals of the Research Inst. of Environmental Medicine, Nagoya Univ., Volume 44 25 Mar. 1993 p 217-218 In JAPANESE (For primary document see N94-27442 07-52)
(Grant MOE-04255103)
Avail: CASI HC A01/MF A04

N94-27499# Nagoya Univ. (Japan). Research Inst. of Environmental Medicine.
EFFECTS OF CAPSAICIN ON FRESHLY DISSOCIATED RAT DORSAL ROOT GANGLION CELLS [RATTO SEKIZUI GOKON SHINKEISETSU BUNRI SAIBO NI TAISURU KAPUSAISHIN NO KOKA]
Masanori Kasai, Kazue Mizumura, and Takao Kumazawa *In its* Annals of the Research Inst. of Environmental Medicine, Nagoya Univ., Volume 44 25 Mar. 1993 p 219-220 In JAPANESE (For primary document see N94-27442 07-52)
(Grant MOE-04255103)
Avail: CASI HC A01/MF A04

N94-27500# Nagoya Univ. (Japan). Research Inst. of Environmental Medicine.
SIZE DISTRIBUTION OF RETROGRADELY LABELED DORSAL ROOT GANGLION CELLS: TEST OF NORMALITY [GYAKKOSEI TORESAHO NI YORI HYOSHIKI SARETA GOKON SHINKEISETSU SAIBO NO OKISA NO BUNPU: SEIKISEI NO KENTEI]
Ryoko Tamura, Kazue Mizumura, and Takao Kumazawa *In its* Annals of the Research Inst. of Environmental Medicine, Nagoya Univ., Volume 44 25 Mar. 1993 p 221-223 In JAPANESE (For primary document see N94-27442 07-52)
(Grant MOE-04255103)
Avail: CASI HC A01/MF A04

N94-27502# Kinjo Gakuin Univ., Nagoya (Japan). Dept. of Home Economics.
INTERACTION BETWEEN ENDOGENOUS OPIOID AND CHOLECYSTOKININ (CCK) IN MODULATING RESPIRATORY RESPONSES INDUCED BY THIN-FIBER MUSCULAR AFFERENTS [KI SAIKEI SHINKEI NYURYOKU NI YORU KOKYU HANNO NO SHUSHOKU NI OKERU NAIINSEI OPIOIDO TO KORESHISUTOKININ (CCK) NO SOGO SAYO]
Eiko Tadaki, Yasuko Kozaki (Nagoya Univ., Japan.), and Takao Kumazawa (Nagoya Univ., Japan.) *In* Nagoya Univ., Annals of the Research Inst. of Environmental Medicine, Nagoya Univ., Volume 44 25 Mar. 1993 p 227-229 In JAPANESE (For primary document see N94-27442 07-52)
(Grant MOE-04255103)
Avail: CASI HC A01/MF A04

N94-27503# Nagoya Univ. (Japan). Research Inst. of Environmental Medicine.
EFFECTS OF PERFUSION OF AMIODARONE ON ELECTROPHYSIOLOGICAL PROPERTIES IN SINGLE RABBIT VENTRICULAR MYOCYTES [AMIODARONE KYUSEI TOYO GA IEUSAGI TANRI SHINSHITSUKIN SAIBO NI OYOBOSU DENKI SEIRIGAKUTEKI SAYO]
Kaichiro Kamiya, Jianhua Cheng, Itsuo Kodama, and Junji Toyama *In its* Annals of the Research Inst. of Environmental Medicine, Nagoya Univ.,

Volume 44 25 Mar. 1993 p 230-232 In JAPANESE (For primary document see N94-27442 07-52)
Avail: CASI HC A01/MF A04

N94-27504# Nagoya Univ. (Japan). Research Inst. of Environmental Medicine.
FAST AND SLOW ONSETS OF Na CHANNEL BLOCKING ACTIONS DUE TO LIDOCAINE AND DISOPYRAMIDE USING CONCENTRATION-CLAMP METHOD [NODO KOTEIHO NI YORU ENUE NATORIUMU CHANERU YOKUSEIYAKU NO SAYO HATSUGEN KIJO NI KANSURU KENTO]
Takafumi Anno, Eiichi Watanabe, Akihiko Taniguchi, Itsuo Kodama, and Junji Toyama *In its* Annals of the Research Inst. of Environmental Medicine, Nagoya Univ., Volume 44 25 Mar. 1993 p 233-235 In JAPANESE (For primary document see N94-27442 07-52)
Avail: CASI HC A01/MF A04

N94-27505# Nagoya Univ. (Japan). Research Inst. of Environmental Medicine.
ELECTROPHYSIOLOGICAL EFFECTS OF MS-551, A NEW CLASS 3 ANTIARRHYTHMIC AGENT, ON ISOLATED RABBIT VENTRICULAR MUSCLES [KURASU 3 KOFUSEIMYAKUYAKU MS-551 NO IEUSAGI SHINSHITSUKIN NI TAISURU DENKI SEIRIGAKUTEKI SAYO]
Ryoko Suzuki, Itsuo Kodama, and Junji Toyama *In its* Annals of the Research Inst. of Environmental Medicine, Nagoya Univ., Volume 44 25 Mar. 1993 p 236-238 In JAPANESE (For primary document see N94-27442 07-52)
Avail: CASI HC A01/MF A04

N94-27506# Nagoya Univ. (Japan). Research Inst. of Environmental Medicine.
COMPARATIVE INVESTIGATION OF NEW CLASS 3 ANTIARRHYTHMIC DRUGS, E-4031 AND MS-551, ON ELECTROPHYSIOLOGICAL PROPERTIES IN ISOLATED RABBIT VENTRICULAR MYOCYTES [DAI 3 GUN KOFUSEIMYAKUYAKU E-4031, MS-551 GA IEUSAGI TANRI SHINSHITSUKIN SAIBO NI OYOBOSU DENKI SEIRIGAKUTEKI SAYO NO HIKAKU KENTO]
Jianhua Cheng, Kaichiro Kamiya, Itsuo Kodama, and Junji Toyama *In its* Annals of the Research Inst. of Environmental Medicine, Nagoya Univ., Volume 44 25 Mar. 1993 p 239-241 In JAPANESE (For primary document see N94-27442 07-52)
Avail: CASI HC A01/MF A04

N94-27507# Nagoya Univ. (Japan). Research Inst. of Environmental Medicine.
EFFECTS OF CLASS 1 ANTIARRHYTHMIC DRUGS ON THE INTRAVENTRICULAR CONDUCTION: INFLUENCE OF FIBER ORIENTATION [KURASU 1 KOFUSEIMYAKUYAKU NIYORU SHINSHITSUNAI DENDO YOKUSEI TO SHINKIN SENI SOKO]
Masato Iida, Itsuo Kodama, and Junji Toyama *In its* Annals of the Research Inst. of Environmental Medicine, Nagoya Univ., Volume 44 25 Mar. 1993 p 242-244 In JAPANESE (For primary document see N94-27442 07-52)
Avail: CASI HC A01/MF A04

N94-27508# Nagoya Univ. (Japan). Research Inst. of Environmental Medicine.
EFFECTS OF CLASS 3 ANTIARRHYTHMIC AGENTS, E-4031 AND MS-551 ON VENTRICULAR REPOLARIZATION IN ISOLATED RABBIT HEARTS [IEUSAGI SHINSHITSU NO SAI BUNKYOKU NI TAISURU KURASU 3 KOFUSEIMYAKUZAI E-4031 TO MS-551 NO SAYO]
Hirokazu Iwata, Ryoko Suzuki, Kaichiro Kamiya, Itsuo Kodama, and Junji Toyama *In its* Annals of the Research Inst. of Environmental Medicine, Nagoya Univ., Volume 44 25 Mar. 1993 p 245-247 In JAPANESE (For primary document see N94-27442 07-52)
Avail: CASI HC A01/MF A04

N94-27509# Nagoya Univ. (Japan). Research Inst. of Environmental Medicine.
ELECTRICAL COUPLING BETWEEN THE SINO-ATRIAL NODE AND ATRIAL MUSCLE: CELL TO CELL INTERACTION THROUGH AN EXTERNAL CIRCUIT AND ITS SIMULATION BY COMPUTER MODELING [DOBO KESSETSU TO SHINBOKAN NO DENKITEKI KETSUGO NI KANSURU KENKYU: GAIBU KAIRO O MOCHIITA SAIBO KETSUGO JIKKEN]
Eiichi Watanabe, Takafumi Anno, Itsuo Kodama, and Junji Toyama *In its* Annals of the Research Inst. of Environmental Medicine, Nagoya Univ., Volume 44 25 Mar. 1993 p 248-250 In JAPANESE (For primary document see N94-27442 07-52)
Avail: CASI HC A01/MF A04

N94-27510# Nagoya Univ. (Japan). Research Inst. of Environmental Medicine.
A STUDY ON TISSUE EXCITATION OF CARDIAC MUSCLE UNDER ELECTRICAL FIELD STIMULATION [FIRUDO SHIGEKIKA SHINKIN NO KATSUDO DENI SAIDAI TACHIAGARI SOKUDO]
Akihiko Taniguchi, Takafumi Anno, Masaki Shirakawa (Toyohashi Univ. of Technology, Aichi, Japan.), Shiro Usui (Toyohashi Univ. of Technology, Aichi, Japan.), Itsuo Kodama, and Junji Toyama *In its* Annals of the Research Inst. of Environmental Medicine, Nagoya Univ., Volume 44 25 Mar. 1993 p 251-254 In JAPANESE (For primary document see N94-27442 07-52)
Avail: CASI HC A01/MF A04

N94-27511# Nagoya Univ. (Japan). Research Inst. of Environmental Medicine.
BLOCK OF CARDIAC SODIUM CHANNELS BY Ro 22-9194 (R), A NEW ANTIARRHYTHMIC AGENT: EFFECTS ON THE MAXIMUM UPSTROKE VELOCITY (Vmax) OF SINGLE GUINEA PIG VENTRICULAR MYOCYTES [KOFUSEIMYAKUYAKU RO 22-9194 (R) NO SHINKIN NA CHANERU YOKUSEI SAYO: MORUMOTTO TANRI SHINSHITSUKIN SAIBO NO KATSUDO DENI SAIDAI TACHIAGARI SOKUDO (VMAX) NIYORU KENTO]
Kazuyasu Maruyama, Ryoko Suzuki, Takafumi Anno, Itsuo Kodama, and Junji Toyama *In its* Annals of the Research Inst. of Environmental Medicine, Nagoya Univ., Volume 44 25 Mar. 1993 p 255-258 In JAPANESE (For primary document see N94-27442 07-52)
Avail: CASI HC A01/MF A04

N94-27512# Nagoya Univ. (Japan). Research Inst. of Environmental Medicine.
ELECTROPHYSIOLOGICAL EFFECTS OF AN ANTIARRHYTHMIC DRUG, MORICIZINE ON ISOLATED GUINEA PIG VENTRICULAR MUSCLES [KO FUSEIMYAKUYAKU MORISHIJIN NO MORUMOTTO SHINSHITSUKIN NI TAISURU DENKI SEIRIGAKUTEKI SAYO]
Kazuyasu Maruyama, Ryoko Suzuki, Takafumi Anno, Itsuo Kodama, and Junji Toyama *In its* Annals of the Research Inst. of Environmental Medicine, Nagoya Univ., Volume 44 25 Mar. 1993 p 259-261 In JAPANESE (For primary document see N94-27442 07-52)
Avail: CASI HC A01/MF A04

N94-27513# Nagoya Univ. (Japan). Research Inst. of Environmental Medicine.
CORRELATION BETWEEN ELECTRICAL ACTIVITY AND THE SIZE OF SINGLE SINOATRIAL NODE CELLS [DOBO KESSETSU HOCHODORI SAIBO NO OKISA TO DENKITEKI TOKUSEI TONO KANKEI]
Haruo Honjo, M. R. Boyett (Leeds Univ., England.), Itsuo Kodama, and Junji Toyama *In its* Annals of the Research Inst. of Environmental Medicine, Nagoya Univ., Volume 44 25 Mar. 1993 p 262-265 In JAPANESE (For primary document see N94-27442 07-52)
Avail: CASI HC A01/MF A04

N94-27514# Nagoya Univ. (Japan). Research Inst. of Environmental Medicine.
THE IONIC MECHANISM UNDERLYING THE NEGATIVE CHRONOTROPIC EFFECT OF ACETYLCHOLINE: EXPERIMENTAL STUDY IN RABBIT SINGLE SINOATRIAL NODE CELLS Report No. 1 [DOBO KESSETSU NI TAISURU ASECHIRUKORIN INSEI HENJI SAYO NO ION KIJO NI KANSURU KENKYU: TANRI DOBO KESSETSU SAIBOU O MOCHIITA JIKKEN]
Haruo Honjo, M. R. Boyett (Leeds Univ., England.), Itsuo Kodama, and Junji Toyama *In its* Annals of the Research Inst. of Environmental Medicine, Nagoya Univ., Volume 44 25 Mar. 1993 p 266-268 In JAPANESE (For primary document see N94-27442 07-52)
Avail: CASI HC A01/MF A04

N94-27515# Nagoya Univ. (Japan). Research Inst. of Environmental Medicine.
THE IONIC MECHANISM UNDERLYING THE NEGATIVE CHRONOTROPIC EFFECT OF ACETYLCHOLINE: EXPERIMENTS USING SMALL SINOATRIAL NODE TISSUE PREPARATIONS ISOLATED FROM RABBIT HEARTS Report No. 2 [DOBO KESSETSU NI TAISURU ASECHIRUKORIN INSEI HENJI SAYO NO ION KIJO NI KANSURU KENKYU: TASAIBO BISHO HYOHON O MOCHIITA JIKKEN]
Itsuo Kodama, M. R. Boyett (Leeds Univ., England.), Akiko Arai, Ryoko Suzuki, Haruo Honjo, and Junji Toyama *In its* Annals of the Research Inst. of Environmental Medicine, Nagoya Univ., Volume 44 25 Mar. 1993 p 269-271 In JAPANESE (For primary document see N94-27442 07-52)
Avail: CASI HC A01/MF A04

N94-27516# Nagoya Univ. (Japan). Research Inst. of Environmental Medicine.
THE IONIC MECHANISM UNDERLYING THE NEGATIVE CHRONOTROPIC EFFECT OF ACETYLCHOLINE: POSTGANGLIONIC VAGAL STIMULATION IN ISOLATED RABBIT HEARTS Report No. 3 [DOBO KESSETSU NI TAISURU ASECHIRUKORIN INSEI HENJI SAYO NO ION KIJO NI KANSURU KENKYU: MEISO SHINKEISETSUGO SENI SHIGEKI NO KOKA]
Itsuo Kodama, Akiko Arai, Ryoko Suzuki, Haruo Honjo, M. R. Boyett (Leeds Univ., England.), and Junji Toyama *In its* Annals of the Research Inst. of Environmental Medicine, Nagoya Univ., Volume 44 25 Mar. 1993 p 272-275 In JAPANESE (For primary document see N94-27442 07-52)
Avail: CASI HC A01/MF A04

N94-27519# Nagoya Univ. (Japan). Dept. of Ophthalomology.
ANALYSIS OF THE ELECTRICALLY EVOKED RESPONSE (EER) OF THE CAT [NEKO EER (EREKUTORIKARI EBOKUTO RESUPONSU) NO KISOTEKI KENKYU: 17, 18 YA HISHITSU NI OKERU EER NO NYURON KIGEN NO KENKYU]
Kazuhiro Shimazu, Yozo Miyake, Yasuhiro Fukatsu (Fukatsu Eye Clinic, Nagoya, Japan.), and Satoru Watanabe *In* Nagoya Univ., Annals of the Research Inst. of Environmental Medicine, Nagoya Univ., Volume 44 25 Mar. 1993 p 282-287 In JAPANESE (For primary document see N94-27442 07-52)
Avail: CASI HC A02/MF A04

N94-27530# Nagoya Univ. (Japan). Research Inst. of Environmental Medicine.
THE MEASUREMENTS OF MUSCLE BLOOD FLOW BY LASER DOPPLER FLOWMETRY WITH NEEDLE TYPE PROBE [HARIGATA PUROBE O MOCHIITA REZA DOPPURA KETSURYURYOKEI NIYORU KIN SOSHIKI KETSURYURYO NO SOKUTEI]
Kiyohito Yamamoto, Yasuhiro Oba, Tadaaki Mano, and Shigehiko Shionoya *In its* Annals of the Research Inst. of Environmental Medicine, Nagoya Univ., Volume 44 25 Mar. 1993 p 335-339 In JAPANESE (For primary document see N94-27442 07-52)
Avail: CASI HC A01/MF A04

N94-27537# Nagoya Univ. (Japan). Dept. of Circulation.
DESENSITIZATION TO ACETHYLCHOLINE IN PACEMAKER CELLS OF THE SINOATRIAL NODE [DOBO KESSETSU SAIBO HOCHODORI SAIBO NI OKERU ASECHIRUKORIN INSEI HENJI SAYO NO DATSU KANSA GENSHO]
Haruo Honjo, Itsuo Kodama, and Mark R. Boyett (Leeds Univ., England.) *In its* Annals of the Research Inst. of Environmental Medicine, Nagoya Univ., Volume 44 25 Mar. 1993 p 367-369 In JAPANESE Presented at the 13th Symposium on Environmental Medicine, Aichi, Japan, 11 Nov. 1992 (For primary document see N94-27442 07-52)
Avail: CASI HC A01/MF A04

N94-27539# Nagoya Univ. (Japan). Dept. of Neural Regulation.
THE POLYMODAL RECEPTOR [PORIMODARU RESEPUTA]
Kazue Mizumura *In its* Annals of the Research Inst. of Environmental Medicine, Nagoya Univ., Volume 44 25 Mar. 1993 p 373-374 In JAPANESE Presented at the 13th Symposium on Environmental Medicine, Aichi, Japan, 11 Nov. 1992 (For primary document see N94-27442 07-52)
Avail: CASI HC A01/MF A04

N94-27970# National Inst. of Polar Research, Tokyo (Japan).
COUNTING ADELIE PENGUINS AT COLONIES: SEASONAL AND ANNUAL CHANGES [KORONI DENO ADERI PENGIN NO KAUNTO: KISETSU HENKA TO NEN HENKA]
In its Antarctic Record, Vol. 36, No. 2 30 Jul. 1992 p 279-284 In JAPANESE (For primary document see N94-27963 07-46)
Avail: CASI HC A02/MF A02

N94-27971# Hiroshima Univ. (Japan). Dept. of Environmental Studies.
NOTE ON THE STRUCTURE OF MOSS COLONIES COMPOSED OF TWO SPECIES ON KING GEORGE ISLAND, THE SOUTH SHETLAND ISLANDS [KINGUJOJITO NO NI SHU YORI NARU SENRUI KORONI NO KOZO NI TSUITE]
Takayuki Nakatsubo and Shuji Otani (National Inst. of Polar Research, Tokyo, Japan.) *In* National Inst. of Polar Research, Antarctic Record, Vol. 36, No. 2 30 Jul. 1992 p 285-293 Sponsored by Ministry of Education, Science and Culture, Tokyo, Japan (For primary document see N94-27963 07-46)
Avail: CASI HC A02/MF A02

N94-28198*# Oceanographic Consultants.
SONIC BOOMS AND MARINE MAMMALS: INFORMATIONAL STATUS AND RECOMMENDATIONS
William C. Cummings *In* NASA. Ames Research Center, High-Speed Research: Sonic Boom, Volume 1 Feb. 1994 p 219-231 (For primary document see N94-28188 07-02)
Avail: CASI HC A03/MF A03

N94-28304*# Princeton Univ., NJ. Dept. of Geological and Geophysical Sciences.
AN EVALUATION OF CRITERIA THAT MAY BE USED TO IDENTIFY SPECIES SURVIVING A MASS EXTINCTION Abstract Only
N. MacLeod *In* Houston Univ., New Developments Regarding the KT Event and Other Catastrophes in Earth History 1994 p 75-77 (For primary document see N94-28294 07-46)
Avail: CASI HC A01/MF A02

52 AEROSPACE MEDICINE

Includes physiological factors; biological effects of radiation; and effects of weightlessness on man and animals.

N94-25871# Institute for Perception RVO-TNO, Soesterberg (Netherlands).
ENDOGENEOUS AND EXOGENOUS CONTROL OF VISUAL SELECTION: A REVIEW OF THE LITERATURE Final Report
J. Theeuwes 15 Jul. 1993 23 p
(AD-A273761; IZF-1993-B-9; TDCK-TD-93-1361) Avail: CASI HC A03/MF A01

Among the most fundamental issues of visual attention research is the extent to which visual selection is controlled by properties of the stimulus or by the intentions, goals and beliefs of the observer. Before selective attention operates, preattentive processes perform some basic analyses segmenting the visual field into functional perceptual units. The crucial question is whether the allocation of attention to these perceptual units is under the endogenous control of the observer (intentions, goals, beliefs) or under the exogenous control of stimulation. This report discusses evidence regarding the endogenous and exogenous control of attention in tasks in which subjects search for a particular 'basic' feature (e.g., search for a unique color, shape, brightness). The present review suggests that selectivity in these type of search tasks is dependent on the relative saliency of the stimulus attributes. It is concluded that the visual system automatically calculates differences in basic features (e.g., difference in shape, color, brightness) and that visual information occupying the position of the highest saliency across stimulus dimensions is exogenously passed on to the 'central representation' that is responsible for further stimulus analysis. Alternative explanations of the present findings and tentative speculations resulting from the present approach are discussed. DTIC

N94-25909 Selskapet for Industriell og Teknisk Forskning, Trondheim (Norway).
ECARHEART2 VERSION 1.0: PROGRAMMERS DOCUMENTATION
S. Stoeren and P. Neksae 1 Jul. 1993 44 p
(PB94-124633; STF23-A93028) Avail: Issuing Activity (National Technical Information Service (NTIS))

EcarHeart2 is a program for analysis of the cardiac function and the systematic and pulmonal arterial tree. It is an EchoDisp Custom Analysis Routine (ECAR) and runs under EchoDisp. This documentation is the programmers documentation of the EcarHeart2 code. It covers the core of EcarHeart2 and the calculation modules: Aortic pressure and flow; Wall stress; and Proximal inflow convergence. NTIS

N94-25943# Air Force Inst. of Tech., Wright-Patterson AFB, OH. School of Engineering.
THE AFIT MULTIELECTRODE ARRAY FOR NEURAL RECORDING AND SIMULATION: DESIGN, TESTING, AND ENCAPSULATION M.S. Thesis
James R. Reid, Jr. Dec. 1993 105 p
(AD-A274086; AFIT/GE/Eng/93D-33) Avail: CASI HC A06/MF A02

A two-dimensional, X-Y addressable, multiplexed array of 256 electrodes (16 x 16) has been fabricated using conventional semiconductor processing techniques. The individual electrodes are 160 microns x 160 microns approximating the size of the cortical columns; the overall array size is 3910 microns x 3910 microns. The array has been fitted to a chronically implantable package and tested for several days in a simulated neural environment. EEG-like data were collected successfully from individual electrodes in the array. This array improves on a previous design of a 16 electrode (4 x 4) array that was chronically implanted on the cortex of a laboratory beagle (Canis familiaris) in 1982. The original implant, located approximately over primary visual cortex, recorded both EEG and visually evoked response (VER) data. It proved the feasibility of multiplexing data directly from the surface of the cortex, thereby opening the possibility of very large arrays of electrodes since only a single wideband signal channel could address significant numbers of electrodes. DTIC

N94-26173# Naval Health Research Center, San Diego, CA.
REWARMING METHODOLOGIES IN THE FIELD
S. Feith, R. Hesslink, J. Reading, P. Kincaid, and R. Pozos 17 Nov. 1993 20 p
(NR Proj. M00-96)
(AD-A274744; NHRC-93-4) Avail: CASI HC A03/MF A01

The Heatpac is currently used by the U.S. Marine Corps to warm cold-stressed infantry personnel in the field. Recently, this system has been modified so a small wetting chamber called Humipac can be attached to the Heatpac so personnel can breathe warm humidified air. The air is saturated to 95-99% humidity with a temperature range of 45.3 to 49.4 C. In a series of experiments using a USMC issue sleeping bag, the effectiveness of the Heatpac was compared to the combined Heatpac/Humipac and to rewarming by shivering. Subjects wearing only swimming trunks were placed in 12.8 C water for one hour. At the end of that period, any of the three interventions were randomly assigned. In all conditions, the subject was placed in a sleeping bag. Heart rate, T(sub re) and T(sub es) temperatures, and metabolic rates were monitored during the cooling phase and for 120 minutes during the rewarming phase. Breathing the warm humidified air did not significantly alter the rate of body rewarming. In some cases, normal shivering induced as large an increase in core temperature as did the active interventions. Additional studies are underway to investigate the relative role that these various rewarming systems have on thermogenesis. DTIC

N94-26179# Naval Aerospace Medical Research Lab., Pensacola, FL.
EFFECTS OF METHAMPHETAMINE ON VIGILANCE AND TRACKING DURING EXTENDED WAKEFULNESS Interim Report
R. R. Stanny, A. H. McCardie, and D. F. Neri Sep. 1993 36 p
(NR Proj. M00-96)
(AD-A274896; NAMRL-1386) Avail: CASI HC A03/MF A01

The effects of a 10 mg/70 kg oral dose of d-methamphetamine HCl on high-event-rate vigilance and tracking performance in a 13.5-hour sustained-performance session during a night of sleep loss are examined. At 0116 hours, seven subjects were administered d-methamphetamine, double-blind. The remaining six subjects were given a placebo. Values of sensitivity (d) in the vigilance task declined markedly during the night in the placebo group. The methamphetamine treatment reversed an initial decline in d' within approximately two hours of administration. The methamphetamine treatment also reversed increases in nonresponses (lapses) within approximately two hours of administration. Tracking performance also declined markedly during the night in the placebo group. The methamphetamine treatment reversed the decline in tracking performance. An analysis of fast guesses in the vigilance experiment disclosed no evidence to suggest that methamphetamine tended to increase impulsive responding. In fact, the methamphetamine treatment was associated with a small and nonsignificant reduction in fast guesses. The overall pattern of the results suggests that methamphetamine at 10 mg/70 kg produces genuine increases in efficiency that effectively counteract the effects of continuous work during a night of sleep loss. DTIC

N94-26360# Army Health Care Studies and Clinical Investigation Activity, Fort Sam Houston, TX.
PRACTICE PATTERNS OF US ARMY MEDICAL DEPARTMENT PSYCHIATRISTS AND PSYCHOLOGISTS Final Report, May 1991 - Dec. 1993
Nancy K. Willcockson and James M. Georgoulakis Jan. 1994 27 p
(AD-A274787; HCSCIA-HR-94-002) Avail: CASI HC A03/MF A01

The present study is an evaluation of psychiatrist and psychologist patient care services from the Army's Ambulatory Care Data Base. The data from the present study did not reveal any evidence that psychiatrists performed patient care or medical services in any manner different from psychologists, with the exception that they prescribed medication. Psychologists were found (1) to spend more time with patients, (2) to provide a wider variety of patient care services, (3) to treat more patients with concurrent medical disorders, (4) to perform nearly all psychological testing evaluations, and (5) to be the sole medical professionals performing biofeedback and behavioral assessment. Both provider groups treated all of the same patient diagnostic categories, with some variation in patient diagnostic frequency, and neither group utilized ancillary medical procedures to any significant extent in its evaluation and management of patients. This data revealed that psychologists' are the almost exclusive providers of psychological testing evaluation, which is a work intensive, lengthy, and complex diagnostic process. Four significant variations were found: (1) time spent in evaluation, depended upon the type of assessment performed (e.g., personality, intellectual, neuropsychological, or a combination thereof; (2) the amount of direct provider time required by psychologists, which depended upon three factors--the complexity of the case, the type of assessment undertaken, and whether a psychological assistant was utilized; (3) the frequency with which types of evaluations were performed, with personality assessments accounting for almost one-half half of all psychological testing evaluations; and (4) the average number of visit days involved in an assessment, which, again, varied with the complexity of the evaluation. DTIC

N94-26377# Naval Health Research Center, San Diego, CA.
MONITORING ACTIVITY WITH A WRIST-WORN ACTIGRAPH: EFFECTS OF AMPLIFIER PASSBAND AND THRESHOLD VARIATIONS Final Report, Nov. 1990 - Oct. 1992

Timothy F. Elsmore and Paul Naitoh Feb. 1993 63 p
(Contract MIPR-91MM1505)
(AD-A274705; NHRC-93-18) Avail: CASI HC A04/MF A01

This project investigated some properties of the AMA-32 wrist-worn activity monitor. In the first phase of this project, a software program for the analysis of activity data was developed. The program permits rapid statistical and graphical summaries of activity data. The second phase of the project investigated effects of varying the sensitivity of the actigraph. Three different frequency passbands were investigated. The ability to differentiate sleep from wake was optimized with a 2 to 3 Hz passband, particularly with a high trigger threshold. Increasing sensitivity by lowering the trigger threshold or by broadening the passband reduced sleep/wake discriminability. The optimal sleep/wake discrimination parameters for the AMA-32 approximate those of earlier generations of wrist-worn actigraphs. The work in this report suggests research to investigate the utility of other actigraph sensitivity settings for differentiating movement patterns during sleep or for assessments of daytime workload. DTIC

N94-26432# Army Aeromedical Research Lab., Fort Rucker, AL.

US ARMY AVIATION EPIDEMIOLOGY DATA REGISTRY: INCIDENCE AND OUTCOMES OF AVIATOR FLYING EVALUATION BOARDS Final Report

Kevin T. Mason and S. G. Shannon Oct. 1993 21 p
(DA Proj. 3M1-62787-A-879)
(AD-A274711; USAARL-94-2) Avail: CASI HC A03/MF A01

The Aviation Epidemiology Data Registry (AEDR) is a family of databases storing history and physical information on Army aircrewmembers. The AEDR lacks some aviation career endpoints, one being the outcome of flying evaluation boards (FEB's) for nonmedical disqualifications. The outcomes of 170 new FEB actions from 1985 through 1992 in active duty and U.S. Army Reserve aviators were reviewed. The overall incidence was 1.13 per 1,000 aviator-years. Aviators aged 25 through 39 were twice as likely to undergo FEB actions. The likelihood of restoration to flying duties after FEB was significantly lower if the FEB was for habits, character, and motivation, than if the FEB was for poor flying proficiency or failure to follow flight rules. Many nonmedical disqualifications leading to FEB require medical evaluation to rule out underlying mental disorders. DTIC

N94-26435# Air Force Systems Command, Brooks AFB, TX. Armstrong Lab.

AEROMEDICAL ISSUES RELATED TO POSITIVE PRESSURE BREATHING FOR +Gz PROTECTION Interim Report, 1 Apr. - 31 Oct. 1992

Larry P. Krock Dec. 1993 13 p
(AF Proj. 7930)
(AD-A274717; AL-TP-1992-0024) Avail: CASI HC A03/MF A01

Positive pressure breathing as a method to enhance aircrew tolerance for repeated and sustained high +Gz exposures (PBG) was first considered many years ago. Use of Combined Advanced Technology Enhanced Design G Ensemble (COMBAT EDGE) as a G-protection measure increases overall tolerance to +Gz acceleration by reducing the fatigue associated with performing straining maneuvers during extended or repeated exposures to acceleration stress. Physiologically, PBG exerts its effects upon both the cardiovascular and respiratory systems. The principal benefit of PBG is the maintenance of elevated intrathoracic pressure with minimal voluntary effort on behalf of the individual. Some confusion exists with regard to the potential impact COMBAT EDGE may have on the physical health of aircrew. A certain unknown probability exists suggesting acute and/or long-term exposure to PBG may produce certain undesirable changes in the cardiopulmonary physiology of a pilot. This issue has resulted in the need to provide information regarding the current state of our understanding. Described herein are the principal physiologic issues raised concerning use of COMBAT EDGE, looking to the available literature, past experience, and current and future research answers. DTIC

N94-26549 Korean Atomic Energy Research Inst., Daeduk (Republic of Korea).

MOLECULAR BIOLOGICAL STUDIES ON THE HUMAN RADIORESISTANCE AND DRUG RESISTANCE

Chang Min Kim and Weon Seon Hong Apr. 1992 20 p In KOREAN
Limited Reproducibility: More than 20% of this document may be affected by microfiche quality
(DE93-632682; KAERI/RR-1114/91) Avail: CASI HC A03 (US Sales Only)

We irradiated the MKN45 and PC14 cell lines with 500 rads and also established the adriamycin-resistant and cis-platinum resistant cell line. The genomic DNA and total RNA were extracted and subjected to the Southern and Northern analysis using various probes including heat shock protein 70, MDR1, fos, TGFb, etc. The mRNA transcript was increased 1 hour after the irradiation and sustained during the 48 hours and returned to the level of pre-irradiation. No significant change was observed with the drug resistant cell lines at the level of gene dosage. We suggest that the marked increase of the hsp70 transcript is a very important finding and is believed to be a good candidate for the modulation of the cellular response to irradiation and the radioresistance. DOE

N94-26748# Army Aeromedical Research Lab., Fort Rucker, AL.

A COMPARISON OF SLEEP SCORED FROM ELECTROENCEPHALOGRAPHY TO SLEEP SCORED BY WRIST ACTIGRAPHY Technical Report, Nov. 1989 - Feb. 1990

J. L. Caldwell and John A. Caldwell, Jr. Sep. 1993 33 p
(AD-A273739; USAARL-93-32) Avail: CASI HC A03/MF A01

During military operations, it has been found that soldiers often are required to work for long periods of time without rest. In order to assist commanders in determining how much rest soldiers receive, various methods of monitoring activity have been used. One unobtrusive method is to use wrist activity monitors (WAM's) to determine how long soldiers are required to work with little or no sleep. This study compared data from traditionally scored sleep using electroencephalographs (EEG's) to data from WAM's to determine the ability of WAMs to measure sleep. Based on this limited comparison study, it appears that the WAM is a good instrument to use to estimate sleep time when an EEG is not possible. The percent agreement between WAM sleep time and EEG sleep time is very high, with an average of almost 89 percent. The error tended to be in the direction of overestimation of sleep time by the WAM. Also, the current method of scoring using a set cutoff of counts is a suitable method. However, an overestimation of sleep most likely will occur when this method is used. Therefore, whenever actigraphs are used, a conservative interpretation of the data is to discuss 'rest time' instead of 'sleep time.' In addition, the quality of sleep as determined by normal EEG sleep staging cannot be assessed by the WAM. DTIC

N94-26847# Air Force Flight Test Center, Edwards AFB, CA.

THE USE OF EEG AS A WORKLOAD ASSESSMENT TOOL IN FLIGHT TEST Technical Report

Bruce P. Hunn Oct. 1993 79 p
(AD-A274568; AFFTC-TIM-93-02) Avail: CASI HC A05/MF A01

This report examines the use of EEG (Electroencephalography) as a tool to assess aircrew mental workload in-flight. It contains a brief history of EEG methods and a detailed analysis section. It also contains a large reference section for additional research purposes. Analysis methods, both historical and current are discussed. Statistical and graphic presentation of continuous EEG data is reviewed and recommendations are made for future testing of EEG technologies. DTIC

N94-26973# Systems Research Labs., Inc., Dayton, OH.

PASSIVE AND ACTIVE BEHAVIOR OF THE CARDIOVASCULAR SYSTEM UNDER INCREASED GRAVITATIONAL LOADS IN A CHRONICALLY INSTRUMENTAL CONSCIOUS BABOON MODEL Final Report, 1 Feb. 1991 - 1 Jun. 1993

David A. Self, Curtis D. White, Richard W. Owens, John W. Fanton, and Ricky D. Latham Nov. 1993 27 p
(AF Proj. 2312)
(AD-A274344; AL/AO-TR-1993-0103) Avail: CASI HC A03/MF A01

Simultaneous recordings of right atrial, left atrial, left ventricular (LV) and aortic pressure (AOP), aortic root flow and LV dimensions were recorded in chronically instrumented baboons at rest and undergoing centrifugation that mimicked military aviation acceleration environments. We separated the early and late hemodynamic responses to increased +Gz loads during acceleration using a rapid onset-rapid return (ROR) (greater than 4.5 G/s) centrifugation protocol. +Gz onset resulted in immediate changes in vascular pressure from hydrostatic effects, followed by passive shifting of blood volume to dependent regions causing declines in systemic pressure above the hydrostatic indifference point (HIP) and in venous return. Stroke volume (SV) and mean cardiac power output fell. Distending carotid level pressure routinely fell during acceleration to levels well outside threshold values previously reported for carotid baroreflex function. Active compensation consisted of increases in heart rate, AOP and decreases in aortic flow. Previous +Gz load history had enormous impact on blood pressure regulation during increased +Gz loads and on baseline pressures existing prior to exposure to a second +Gz onset. Animals exposed to a conditioning run that saturated their short-term pressure regulatory mechanisms 5 min before a second +Gz exposure, displayed significantly higher mean aortic root pressures and consistently overshot their baseline operating points during centrifugation. We conclude that hemodynamic consequences of rapid-onset acceleration are extremely complex and may provide conflicting error signal information during compensatory adjustments. DTIC

N94-26985# Army Aeromedical Research Lab., Fort Rucker, AL.
MONOGRAPH OF THE AVIATION EPIDEMIOLOGY DATA REGISTER FOR CALENDAR YEAR 1988 Final Report
Robert H. Schrimsher and Samuel G. Shannon Aug. 1993 99 p
(Contract DAMD17-92-C-2062)
(AD-A274589) Avail: CASI HC A05/MF A02

The purpose of this monograph is to provide the reader with descriptive statistics from the Aviation Epidemiology Data Register (AEDR). Data are presented for class 2/2A Flying Duty Medical Examinations (FDMES) based on information received by the AEDR during calendar year 1988. It is our purpose to provide these data with little discussion so as to encourage comparisons with other monographs. DTIC

N94-27088# Wright State Univ., Dayton, OH.
PULSE WAVEFORM AND TRANSCRANIAL DOPPLER ANALYSIS DURING LOWER BODY NEGATIVE PRESSURE Interim Report, Jan. - Oct. 1992
Rainer K. Effenhauser and Lloyd D. Tripp, Jr. Apr. 1993 83 p
(AF Proj. 7231)
(AD-A274516; AL/CF-TR-1993-0097) Avail: CASI HC A05/MF A01

The use of lower body negative pressure (LBNP) as an acceleration pre-conditioning technique for space applications was investigated. The purpose was to evaluate changes in cephalic blood flow during LBNP. The intent was to see if detection or warning of impending syncope was possible, and to simulate effects which occur under exposure to +Gz. Ten subjects underwent the following LBNP profile while in a standing position: Five minutes of baseline at ambient pressure, followed by increments of -10 mm Hg every three minutes to a minimum of -50 mm Hg. They remained at -50 mm Hg for a maximum of twenty minutes or until presyncopal symptoms occurred. An additional five minutes of post-LBNP baseline data were collected. The analog pulse waveform, obtained from a pulse oximeter sensor located approximately at eye level on the subject's ear lobe. The pulse waveform analysis included pulse area, amplitude, and duration. Other physiological variables included: middle cerebral artery blood flow velocity using transcranial Doppler (TCD) sonography, and oxygen saturation obtained from a pulse oximeter. Six of the ten subjects experienced presyncopal symptoms during the LBNP profile. Significant changes were observed in several variables at the presyncopal endpoint and included: pulse waveform area ($P=0.0048$), pulse waveform amplitude ($P=0.0236$), cerebral artery blood flow velocity ($P=0.0001$), and cerebral artery pulsatility index ($P=0.0357$). DTIC

N94-27097# Army Aeromedical Research Lab., Fort Rucker, AL.
AVIATION EPIDEMIOLOGY DATA REGISTER: INDEXING THE AEDR DOCUMENT LASER OPTIC ARCHIVE Final Report
Kevin T. Mason, Samuel G. Shannon, and Robert E. Post Oct. 1993 20 p
(DA Proj. 3M1-62787-A-879)
(AD-A274185; USAARL-94-1) Avail: CASI HC A03/MF A01

The Aviation Epidemiology Data Register (AEDR) is a family of databases storing health and physical parameters of Army aircrew. The components are administratively linked by social security number (SSN). A new component is an upgrade of the medical document microfiche archive to laser optic CD-ROM. The U.S. Army Aeromedical Activity requested assistance in creating an indexing scheme for the new system. They wanted to use a single SSN digit, the disks to fill at a uniform rate, and to keep the same aircrew member on the same disk even if multiple entries were made for the same patient. The SSN of each case in the microfiche archive was extracted as a reference population. Analysis of the frequency distribution of decimal values for selected SSN digits showed the last SSN digit would meet the stated requirements. Any of the first five SSN digits should not be used for indexing. DTIC

N94-27130# Army Aeromedical Research Lab., Fort Rucker, AL.
MONOGRAPH OF THE AVIATION EPIDEMIOLOGY DATA REGISTER FOR CY 1992 Final Report
Robert H. Schrimsher and Samuel G. Shannon Aug. 1993 109 p
(DA Proj. 3M1-62787-A-879)
(AD-A274400; USAARL-93-35) Avail: CASI HC A06/MF A02

The purpose of this monograph is to provide the reader with descriptive statistics from the Aviation Epidemiology Data Register (AEDR). Data are presented for class 2/2A flying Duty Medical Examinations (FDME) based on information received by the AEDR during calendar year 1992. It is our purpose to provide these data with little discussion so as to encourage comparisons with other monographs. DTIC

N94-27442# Nagoya Univ. (Japan). Research Inst. of Environmental Medicine.
ANNALS OF THE RESEARCH INST. OF ENVIRONMENTAL MEDICINE, NAGOYA UNIV., VOLUME 44 [KANKYO IGAKU KENKYUJO NENPO]
25 Mar. 1993 401 p In JAPANESE
(ISSN 0369-3570)
(Rept-44-Vol-44; JTN-94-80524) Avail: CASI HC A18/MF A04

The following topics were discussed: space environments, microgravity, low oxygen, metabolism, posture control, space activity, eye movement, temperature effect, thermoregulation, water immersion, sensory reception, stresses, visual reception, heart, cardiac muscle, pace-maker cells, electric stimuli, gamma radiation, brain, neurons, nervous cells, nervous systems, autonomic nervous system, receptors, circulatory system, neurotransmitters, enzymes, proteins, hormones, genes, electric potential, RNA (Ribonucleic Acid), DNA (Deoxyribonucleic Acid), cultivation, cloning, electron microscopy, acetylcholine, prostaglandin, Na ion channel, K ion channel, Ca(2+), ion current, antiarrhythmic agents, blood flow, saccade system, microneurography, and hypotension. For individual titles, see N94-27443 through N94-27541.

N94-27443# Sanwa Kagaku Kenkyusho Co. Ltd., Kasugai (Japan).
CHANGES IN CIRCADIAN VARIATIONS OF URINE EXCRETION IN TAIL-SUSPENDED RATS [RATTO BIBU KENSUI NI OKERU CHUYA NO NYO HAISETSU RIZUMU NO HENKA]
Kazumi Kanda, Sachiko Ohmori (Nagoya Univ., Japan.), Chikashi Yamamoto (Nagoya Univ., Japan.), Setsuko Kawano (Nagoya Women's Univ., Japan.), Sayoko Hayamizu (Nagoya Univ., Japan.), Norihiro Miyamoto (Nagoya Univ., Japan.), Yoshiharu Murata (Nagoya Univ., Japan.), and Hisao Seo (Nagoya Univ., Japan.) *In* Nagoya Univ., Annals of the Research Inst. of Environmental Medicine, Nagoya Univ., Volume 44 25 Mar. 1993 p 1-4
In JAPANESE (For primary document see N94-27442 07-52)
Avail: CASI HC A01/MF A04

In this study, urine excretion was examined using tail-suspended rats as a model of muscle and bone atrophy in a weightless state. Subjects were 30 Wistar strain rats, classified into a control group, and suspended groups. In suspended groups, rats were suspended from the ceilings of the cages with wires pierced through the coccygeal bone for seven days, and urine was collected every 12 hours, as well as the amount of diets and water ingested was measured. As a result, the amount of diet and water ingestion was significantly decreased in the tail-suspended groups. Urine excretion in day was increased in all suspended groups, while that in night was different by when the suspension started; i.e. rats suspended at 19:00 increased in urine excretion, but those suspended at 7:00 did not show remarkable change. Comparing the ratios of urine excretion in night to that in day, they were significantly decreased in the suspended groups, whereas no observable change was detected in the control group. These results suggest that the circadian change of urine excretion may result from secretion and modification of Atrial Natriuretic Polypeptide (ANP) by glucocorticoids. Author (NASDA)

N94-27444# Nagoya Women's Univ. (Japan).
ENDOCRINOLOGICAL EVALUATIONS OF MUSCLE AND BONE ATROPHY IN TAIL-SUSPENDED RATS [BIBU KENSUI RATTO NI OKERU KIN-KOTSU ISHUKU NO NAIBUNPIGAKU TEKI KENTO] **c51**
Setsuko Kawano, Kazumi Kanda (Sanwa Kagaku Kenkyusho Co. Ltd., Kasugai, Japan.), Yoshiharu Murata (Nagoya Univ., Japan.), Sachiko Omori (Nagoya Univ., Japan.), Norihiro Miyamoto (Nagoya Univ., Japan.), Kaori Sueda (Nagoya Univ., Japan.), and Hisao Seo (Nagoya Univ., Japan.) *In* Nagoya Univ., Annals of the Research Inst. of Environmental Medicine, Nagoya Univ., Volume 44 25 Mar. 1993 p 5-8 In JAPANESE (For primary document see N94-27442 07-52)
Avail: CASI HC A01/MF A04

Metabolic change and endocrine variation of tail-suspended rats were studied as a model of atrophy in weightless state or long term bedding. Subjects were Wistar strain rats, suspended from the ceilings of the cages by wires pierced through the tails, and urine was collected every 12 hours. Seven days after the suspension, all rats were killed, and wet weight of associated organs, and testosterone, activated vitamin D3, hydroxyproline, Ca and Pi (Inorganic Phosphorus) concentration were measured, as well as Alkali Phosphatase (ALP) activity. As a result, in suspension groups, significant decrease was observed in body weight and in wet weights of the thymus, testicle and bones, whereas the adrenal gland weight was significantly increased. In suspension groups, there was also significant decrease in testosterone concentration, as well as tendency of decrease in vitamin D3. Ca and Pi concentrations in blood were significantly decreased within the normal range. In the bones of suspended group, ALP activity, the amounts of hydroxyproline, Ca and Pi were all decreased. These results suggest the correlation of muscle and bone atrophy with decrease of testosterone. The change of the bone components also reveals the decrease of bone density, which may result from the decrease of vitamin D3 in blood. Author (NASDA)

N94-27445# Nagoya Univ. (Japan). Research Inst. of Environmental Medicine.
CHANGES IN FLUID AND ELECTROLYTE METABOLISM DURING WATER IMMERSION AT HIGH OR THERMONEUTRAL TEMPERATURE [KOON OYOBI CHUSEION SUISHINJI NI OKERU MIZU-DENKAISHITSU TAISHA NO HENDO]
Sachiko Omori, Kazumi Kanda, Chikashi Yamamoto, Sayoko Hayamizu, K. A. Kirsch (Freie Univ., Berlin, Germany.), Satoshi Iwase, Chihiro Miwa, Junichi Sugenoya (Aichi Medical Univ., Nagakute, Japan.), Tadaaki Mano, and Yoshiharu Murata *In its* Annals of the Research Inst. of Environmental Medicine, Nagoya Univ., Volume 44 25 Mar. 1993 p 9-17 In JAPANESE (For primary document see N94-27442 07-52)
Avail: CASI HC A02/MF A04

It is known that water and electrolyte metabolism changes due to movement of fluid from lower part to upper part of the body when astronauts are in a weightless state. In addition, stress might effect on astronauts' metabolism during space travel. To study metabolic changes in this condition, subjects were immersed in thermoneutral water or hot water to load stress, and blood and urine samples were collected. As a result, Ht (Hematocrit), total protein and Ca concentration was decreased by immersion in thermoneutral water bath, which suggests that blood was diluted by fluid transferred into the vessel in a weightless state. In addition, decrease of aldosterone that was also observed may cause increase of Na in urine and urine flow. Contrastingly, by immersion in high temperature water, it was revealed that blood was condensed by sweating, and aldosterone was increased. These results suggests that stress loaded by high temperature might stimulate the hypothalamus that controls the secretion of the adrenal grand. Author (NASDA)

N94-27446# Nagoya Univ. (Japan). Research Inst. of Environmental Medicine.
STUDY ON POSTURE CONTROL AND ADAPTION MECHANISM UNDER WEIGHTLESSNESS: RESULTS OF SECOND REHEARSAL FOR SPACE EXPERIMENT USING CARP Progress Report No. 45 [MUJURYOKU KANKYO KA NO UNDO SEIGYO TO SONO JUNNO NI KANSURU KENKYU: KOI NO UCHU JIKKEN, DAINIKAI RIHASARU SEIKA HOKOKU] **c54**
Shigeo Mori, Sadaharu Takagi, Satoru Watanabe, Akira Takabayashi (Fujita Health Univ., Toyohashi, Japan.), and Shiro Usui *In its* Annals of the Research Inst. of Environmental Medicine, Nagoya Univ., Volume 44 25 Mar. 1993 p 18-21 In JAPANESE (For primary document see N94-27442 07-52)
Avail: CASI HC A01/MF A04

The 2nd rehearsal of the space experiment on posture control and adaption mechanism under weightless condition using carp was performed in April to May 1992, in order to simulate and practice the ground operation of the experiment. This rehearsal included transportation and breeding of carp in the pool of Kennedy Space Center (KSC) and examination of conductivity of implanted electrodes for brain wave. As a result, many carp died from encephalic infection after implantation of the electrode in KSC, especially in carp that had undergone statolithis extirpation in Japan. For this reason, several countermeasures were proposed, such as improvement of statolithis extirpation, prompt transportation system, suitable breeding procedure in KSC, selection of adaptable carp to a experimental unit, preparation for carp implantation, and supply system of carp. Above all, sufficient duration seems to be important for carp to recover from stress of operation or transportation. Therefore, a time table was prepared on the basis of these findings. Author (NASDA)

N94-27447# Nagoya Univ. (Japan). Research Inst. of Environmental Medicine.
STUDY ON POSTURE CONTROL AND ADAPTATION MECHANISM UNDER WEIGHTLESSNESS: SUMMARY REPORT OF GROUND OPERATIONS PERFORMED FOR CARP EXPERIMENT (FMPT/L-2) IN SPACE SHUTTLE MISSION Report No. 46 [MUJURYOKU KANKYO KA NO UNDO SEIGYO TO SONO JUNNO NI KANSURU KENKYU: SUPESUSHATORU RIYO NI YORU KOI NO UCHU JIKKEN (FMPT/L-2) JISSHI KEIKA HOKOKU] **c54**
Shigeo Mori, Sadaharu Takagi, Satoru Watanabe, Akira Takabayashi (Fujita Health Univ., Toyohashi, Japan.), Shiro Usui (Toyohashi Univ. of Technology, Aichi, Japan.), and Genyo Mitarai (Chukyo Univ., Toyota, Japan.) *In its* Annals of the Research Inst. of Environmental Medicine, Nagoya Univ., Volume 44 25 Mar. 1993 p 22-26 In JAPANESE (For primary document see N94-27442 07-52)
Avail: CASI HC A01/MF A04

An experiment on posture control and adaptation mechanism under weightless condition using carp was performed in Space Shuttle, Endeavor, in aviation of September 12-20, 1992 (FMPT (First Material Processing Test)/L-2). Although unexpected troubles occurred in ground operation, preparation could be completed thanks to the support system organized for this mission and the time schedule based on the results of two rehearsals that suggested importance of time margin for rest and adaption of carp. During aviation, there were several accidents such as entanglement of cables, but the experiment was completed and brain wave of carp could be recorded. The post-aviation test was also performed on the carp used in the space experiment that seemed healthy when returned from space travel, but at the end of all these experiments, the carp were demonstrated to be anoxia from analysis of water in the tank. As the data recorded during aviation were not obtained at this time, this report describes mainly preparation and process of experiment performed in the Space Shuttle and post-aviation. Author (NASDA)

N94-27448# Fujita Health Univ., Toyohashi (Japan). School of Hygiene.
STUDY ON POSTURE CONTROL AND ADAPTION MECHANISM UNDER WEIGHTLESSNESS: DIFFERENCES IN WEIGHT AND SHAPE OF UTRICULAR OTOLITH OF CARP Report No. 47 [MUJURYOKU KANKYO KA NO UNDO SEIGYO TO SONO JUNNO NI KANSURU KENKYU: KOI NO RANKEINO JISEKI NO JURYO TO KEITAI NI OKERU SA NI TSUITE] **c54**
Akira Takabayashi, Sadaharu Takagi (Nagoya Univ., Japan.), Shigeo Mori (Nagoya Univ., Japan.), and Satoru Watanabe (Nagoya Univ., Japan.) *In* Nagoya Univ., Annals of the Research Inst. of Environmental Medicine, Nagoya Univ., Volume 44 25 Mar. 1993 p 27-29 In JAPANESE (For primary document see N94-27442 07-52)
Avail: CASI HC A01/MF A04

The Space Adaptation Syndrome (SAS) is one functional abnormality in a weightless state which leads to autonomic disorder. The cause of SAS is considered to be disorder of sensory coordination. Not only human beings but also other animals show abnormal behavior in a weightless state. Both of them can control movement and posture by three senses; i.e. sight, vestibule and somatesthesia. Among these senses, vestibule seems to be most affected under weightless condition, especially by disappearance of stimulation of statoliths. Therefore, it can be considered that SAS may result from sensory disorder by unbalance between the right and left vestibule senses. To review this possibility, right and left statolithses extirpated from carp in preparation of the Space Shuttle experiment were compared in respect to the shape and weight. As a result, right and left statoliths was similar in shape and weight, so that sensory disorder might not be caused by the difference between the weight of right and left statolithses. Author (NASDA)

N94-27449# Kawasaki Heavy Industries Ltd., Kobe (Japan).

TELESCIENCE TESTBEDDING FOR PHYSIOLOGICAL EXPERIMENTS UNDER HYPOBARIC HYPOXIC CONDITIONS [TEIATSU TEISANSO KANKYOKA DENO SEIRIGAKU JIKKEN ENO TERESAIENSU-SHISUTEMU NO TEKIYO]

Seiji Nishio, Satoru Watanabe (Nagoya Univ., Japan.), Masamichi Yamashita (Ministry of Education, Kanagawa, Japan.), Shigeo Mori (Nagoya Univ., Japan.), Sokichi Sakuragi (Aichi Univ. of Education, Japan.), Yoshiro Wada (Nagoya Univ., Japan.), Hiroyuki Suzuki (Aichi Univ. of Education, Japan.), Mitsuhiro Koeda (Chukyo Univ., Toyota, Japan.), and Takatoshi Shoji *In* Nagoya Univ., Annals of the Research Inst. of Environmental Medicine, Nagoya Univ., Volume 44 25 Mar. 1993 p 30-34 In JAPANESE (For primary document see N94-27442 07-52)
Avail: CASI HC A01/MF A04

Physiological experiments in outer space requires special knowledge and technique. However the limited number of Payload Specialists (PS) cannot cover all the special fields, so that the role of telescience has become important in order to communicate experimental sequences or manipulation with Principal Investigators (PI), especially in experiments with flexible sequences. Several preliminary studies to simulate space experiments using testbedding revealed that human factors may provide an important effect on space experiments. Therefore, this study focused on operation ability of PS's under hypobaric hypoxic conditions that was evaluated by Kraepelin census, results of a video game, brain wave and heart rate. As a result, operation ability was not decreased in this condition, which suggests effectiveness of the teletool as a means of communication with PI's on ground and PS's in space. The method that direction by PI's was given as necessary was proved to be useful to optimize the time line if PS's have enough level of skill. In addition, several PI's directed two PS's to perform two experiments parallely. This parallel system seemed to be useful to save time, but it should be prudent to introduce it, because both PI's and PS's felt anxiety in the parallel system. Author (NASDA)

N94-27450# Aichi Univ. of Education (Japan). Dept. of Nursing.

TELESCIENCE TESTBEDDING UNDER HYPOBARIC HYPOXIC CONDITIONS: EVALUATION BY OPERATION ABILITY AND RECOGNITION ABILITY [TEIATSU TEISANSO KANKYOKA DENO TERESAIENSU-TESUTOBEDDO: SAGYO NORYOKU OYOBI JOHO NINSHIKINORYOKU NI YORU HYOKA]

Sokichi Sakuragi, Satoru Watanabe (Nagoya Univ., Japan.), Shigeo Mori (Nagoya Univ., Japan.), Yoshiro Wada (Nagoya Univ., Japan.), Hiroyuki Suzuki (Nagoya Univ., Japan.), Takatoshi Shoji (Kawasaki Heavy Industries Ltd., Kobe, Japan.), and Seiji Nishio (Kawasaki Heavy Industries Ltd., Kobe, Japan.) *In* Nagoya Univ., Annals of the Research Inst. of Environmental Medicine, Nagoya Univ., Volume 44 25 Mar. 1993 p 35-37 In JAPANESE (For primary document see N94-27442 07-52)
Avail: CASI HC A01/MF A04

Telescience is a remote operation support system which enables Principal Investigators (PI) on ground to direct a Payload Specialist (PS) and to manipulate directly the experimental system in outer space through teletools. In order to complete this system, simulation tests were performed on ground using testbedding. This report concerns the 4th simulation test, that focused on human factors under a particular condition of outer space, hypobaric hypoxia. In this test, operation and recognition ability was evaluated by results of Kraepelin census, results of a video game, scoring of subjective symptoms and measurements of brain wave and heart rate, for two subjects. As a result, no difference was observed in these abilities between normal and hypobaric hypoxic condition in one subject, probably because of experience of a decompression chamber that the subjects already had. The other subject, who had no such experience, revealed decrease in operation ability, while no or slight decrease was observed in recognition ability. These results suggests that a PS can respond to clear directions even in a particular condition that could decrease operation ability. Author (NASDA)

N94-27451# Nagoya Univ. (Japan). Research Inst. of Environmental Medicine.

TELESCIENCE TESTBEDDING FOR PHYSIOLOGICAL EXPERIMENTS UNDER HYPOBARIC HYPOXIC CONDITIONS: DEVELOPMENT AND EVALUATION IN CNV MEASURING [TEIATSU TEISANSO KANKYOKA DENO SEIRIGAKU JIKKEN ENO TERESAIENSU-SHISUTEMU NO TEKIYO: CNV KEISOKU KARA MITA HYOKA]

Hiroyuki Suzuki, Satoru Watanabe, Shigeo Mori, Yoshiro Wada, Masamichi Yamashita (Ministry of Education, Kanagawa, Japan.), Sokichi Sakuragi (Aichi Univ. of Education, Japan.), Mitsuhiro Koeda (Chukyo Univ., Toyota, Japan.), Seiji Nishio (Kawasaki Heavy Industries Ltd., Kobe, Japan.), and Takatoshi Shoji (Kawasaki Heavy Industries Ltd., Kobe, Japan.) *In its* Annals of the Research Inst. of Environmental Medicine, Nagoya Univ., Volume 44 25 Mar. 1993 p 38-44 In JAPANESE (For primary document see N94-27442 07-52)
Avail: CASI HC A02/MF A04

Telescience is a system to achieve highly credible experiment in outer space, directed by Principal Investigators (PI) on ground through teletools, and is inevitable to perform complicated physiological experiments that require flexible experimental sequences. For development and operation of telescience, preliminary experiments were performed under the hypobaric hypoxic condition in a testbedding. In this study, Contigent Negative Variation (CNV) was used as an objective index of attentiveness to evaluate credibility and adequacy of telescience experiments. In addition, a teletool which has been developed to determine CNV, was also evaluated in respect to operational effectiveness. As a result, it was demonstrated that CNV was a useful index to evaluate operation ability. In evaluation of the teletool, the up link image was effective in presenting, directing and discussing data from ground, especially in a phase requiring sophisticated manipulation. The down link data was improved to send only status data of device and statistic data on physiological and behavior indexes, which enabled: (1) reduction of information to 1/200; (2) decrease of PI's work; and (3) visualization and facilitation of data by making a graph. On the other hand, as the system largely depends on the computer support, several problems occurred due to less communication with PS's. Author (NASDA)

N94-27452# Nagoya Univ. (Japan). Research Inst. of Environmental Medicine.

THE ELECTROGASTROGRAM DURING PARABOLIC FLIGHT [PARABORIKKU FURAITO NI OKERU EGG (EREKUTOROGASUTOROGURAFI) SOKUTEI]

Yoshiro Wada, Hiroyuki Suzuki, Satoru Watanabe, and Yoshiki Kaneoke *In its* Annals of the Research Inst. of Environmental Medicine, Nagoya Univ., Volume 44 25 Mar. 1993 p 45-48 In JAPANESE (For primary document see N94-27442 07-52)
Avail: CASI HC A01/MF A04

Motion sickness is a disease caused by vehicles with symptoms of digestive system, as well as pale and cold sweat. It is often observed in parabolic flight which produces microgravity and hypergravity. Recently, Electrogastrography (ECG) has been developed to record gastric electroactivity percutaneously. In order to examine whether ECG was available as an index of nausia and vomitting in motion sickness, ECG was measured during parabolic flight in this study. As a result, from scoring of motion sickness according to the diagnosis table, four in eight subjects were diagnosed as motion sickness. Although there was individual difference in amplitude and frequency of ECG, motion sickness occurred in subjects who had large amplitude before vomiting, or high frequency as nausea became worse. It was also observed that trajectory of ECG turned to the opposite direction when gravity shifted from 0 to 2 G. Therefore, ECG might be useful as an objective index of motion sickness, however, further studies with large population would be necessary in order to remove individual differences. Author (NASDA)

N94-27453# Nagoya Univ. (Japan). Research Inst. of Environmental Medicine.

VERTICAL GAZE DIRECTION DURING PARABOLIC FLIGHT [PARABORIKKU FURAITO JI NO SUICHOKUSEI GANSHIN]

Hiroyuki Suzuki, Satoru Watanabe, Shiro Usui (Toyohashi Univ. of Technology, Aichi, Japan.), Akira Miyamoto (National Space Development

Agency, Tokyo, Japan.), and Shunji Nagaoka (National Space Development Agency, Tokyo, Japan.) *In its* Annals of the Research Inst. of Environmental Medicine, Nagoya Univ., Volume 44 25 Mar. 1993 p 49-51 In JAPANESE Sponsored by NASDA (For primary document see N94-27442 07-52)
Avail: CASI HC A01/MF A04

There are many reports that variation of gravity causes vertical nystagmus, probably resulting from changes of vertical acceleration sensed by statoliths system. This report concerns some findings obtained from simultaneous measurement of acceleration and vertical eye movement by Electronystagmography (ENG) in the parabolic flight under the following three conditions: (1) open eyed gaze with sitting position; (2) dark field with sitting position; and (3) dark field with reclining position. As a result, under the condition (1), no eye movement was detected during vertical gravity (Gz) altered from 2.3 to 0 G, while upward shift of eye position and downward nystagmus were observed during Gz changing from hypergravity to microgravity under the condition (2). On the other hand, while the eye position was shifted upwards under the condition (3), slight downward nystagmus was observed from hypergravity to microgravity. In both sitting and reclining positions, eye position was shifted before Gz decreased below 1 G. In addition, the posture or the direction that subjects were facing may affect the eye movement in parabolic flight, so that these factors should be considered in the study concerning sense of equilibrium. Author (NASDA)

N94-27454# Aichi Univ. of Education (Japan). Dept. of Nursing.
HEART RATE CHANGE IN NORMAL AND LABYRINTHECTOMIZED HAMSTERS DURING PARABOLIC FLIGHT [HOBUTSUSEN HIKOCHU NO SEIJO OYOBI ZENTEI HAKAI HAMUSUTA NO SHINPAKUSU HENKA]
Sokichi Sakuragi, Satoru Watanabe (Nagoya Univ., Japan.), Yoshiro Wada (Nagoya Univ., Japan.), and Hiroyuki Suzuki (Nagoya Univ., Japan.) *In* Nagoya Univ., Annals of the Research Inst. of Environmental Medicine, Nagoya Univ., Volume 44 25 Mar. 1993 p 52-54 In JAPANESE (For primary document see N94-27442 07-52)
Avail: CASI HC A01/MF A04

Usually, circulatory system is regulated under a constant gravity. However, in outer space, microgravity causes fluid to move to the upper part of the body, and the regulation of the fluid movement results in circulatory hypometabolism after returning in normal gravity. There is no effective countermeasure for this hypometabolism at present. In this study, adaptation of circulatory system under microgravity was examined by Electrogastrography (ECG) in parabolic flight using eight hamsters, including three normal, three hemilateral labyrinthectomized and two bilateral labyrinthectomized hamsters. ECG data was sent by telemetric transmitter implanted in the hamsters, with data of vertical gravity. As a result, two in three normal hamsters increased heart rate under the microgravity, while the other [illegible]thectomized hamsters did not reveal any change by variation of gravity [illegible]ultaneous human experiment demonstrated that although human h[illegible] was decreased under microgravity, and was increased under hy[illegible]vity in sitting position, it was not affected in supine position. This could be because in sitting position the fluid movement by change of gravity stimulates baroreceptor, leading to decrease of heart rate, while in supine position the change of gravity may not move fluid. As hamsters' posture is considered to be similar to human supine position, the effect of fluid can be excluded, so that the change of heart rate in hamster may be caused by change of vestibular sense or somatasthenia. Author (NASDA)

N94-27455# Nagoya Univ. (Japan). Research Inst. of Environmental Medicine.
FREQUENCY ANALYSIS OF BODY SWAY INDUCED BY OPTOKINETIC STIMULATION [SHIUNDO SHIGEKI YUHATSUSEI SHINTAI DOYO NO SHUHASU KAISEKI] c54
Masumi Ichikawa, Hiroyasu Jijiwa (Institute for Developmental Research, Kasugai, Japan.), Takako Kawaguchi, and Satoru Watanabe *In its* Annals of the Research Inst. of Environmental Medicine, Nagoya Univ., Volume 44 25 Mar. 1993 p 55-58 In JAPANESE (For primary document see N94-27442 07-52)
Avail: CASI HC A01/MF A04

It is known that optokinetic stimulation of extensive field causes body sway and inclination, probably because regulatory system works for the change of posture. In this study, body sway caused by optokinetic stimulation and inclining board was examined using frequency analysis. For optokinetic stimulation, random dot patterns was projected on the screen, moving downwards, and the body sway was recorded as the displacement of the center of the gravity. The locus of longitudal sway was analyzed by frequency analysis. As a result, power spectrum during the optokinetic stimulation was increased in the frequency from 0.2 to 0.7 Hz, while power spectrum variation was not varied markedly in this range by intentional inclining on the tilt board. Because previous studies revealed that the displacement of center of gravity was increased in the frequency of less than 0.1 Hz when eyes closed, the increase of frequency in 0.2 to 0.7 Hz may reflect the direct intervention of sight into the regulation of orthostatic position. In addition, it was suggested that the increase of power spectrum in the frequency of 3 to 4 Hz was in response to the posture regulation mainly caused by stretch reflex of the crural muscles. Author (NASDA)

N94-27456# Nagoya City Univ. (Japan). Dept. of Othorhinolaryngology.
EFFECTS OF IMAGINARY TARGET ON INDUCED EYE MOVEMENTS BY LINEAR ACCELERATION [CHOKUSEN KASOKUDO NI YORI YUHATSU SARERU GANKYU UNDO NI TAISURU KASO KOSHITEN NO EIKYO] c54
Motoyuki Hashiba, Hirotaka Watabe, Toru Matsuoka, Shunkichi Baba, Satoru Watanabe (Nagoya Univ., Japan.), Yoshiro Wada (Nagoya Univ., Japan.), Hiroyuki Suzuki (Nagoya Univ., Japan.), Chiharu Sekiguchi (National Space Development Agency, Tokyo, Japan.), Sei Yumikura (National Space Development Agency, Tokyo, Japan.), and K. Hofstetter-Degen (Mainz Univ., Germany.) *In* Nagoya Univ., Annals of the Research Inst. of Environmental Medicine, Nagoya Univ., Volume 44 25 Mar. 1993 p 59-63 In JAPANESE (For primary document see N94-27442 07-52)
Avail: CASI HC A01/MF A04

Under microgravity, the gravity does not effect on the vestibular organ, especially on vestibulo-ocular reflex that senses the change of acceleration, which could be a dominant cause of space sickness. In vestibulo-ocular reflex system, the vertical acceleration (Y-axis) can elicit eye movement most effectively, while head position also plays an important role; i.e. prone position induces eye movement more than supine position. This can be explained by the effect of gazing at an imaginary target, because it has been reported that an imaginary target near to the head increased the reflex. In this report, the effect of imaginary fixed targets on vestibulo-ocular reflex was examined using a linear accelerator. Subjects imagined either body fixed target or space fixed target in prone position or supine position. The results revealed that imaginary target had remarkable effect on vestibulo-ocular reflex system. Especially, space fixed targets increased the reflex largely, probably because of non-visual smooth eye movement by senses other than sight, that is, acceleration or sound by the accelerator. Therefore, the body fixed target seems more appropriate to evaluate vestibulo-ocular reflex. Author (NASDA)

N94-27457# Nagoya Univ. (Japan). Research Inst. of Environmental Medicine.
THE MECHANISM OF CALORIC NYSTAGMUS UNDER MICROGRAVITY. 1: CHANGES OF ENDOLYMPHATIC PRESSURE IN THE SEMICIRCULAR CANAL OF PIGEON BY CALORIC STIMULATION [MUJURYOKU KA NI OKERU ONDOSEI GANSHIN HATSUGEN KIJO. 1: HATO NO ONDO SHIGEKI NI TAISURU SUIHEI HANKIKANNAI RINPA ATSU HENKA]
Yoshiro Wada, Hiroyuki Suzuki, and Satoru Watanabe *In its* Annals of the Research Inst. of Environmental Medicine, Nagoya Univ., Volume 44 25 Mar. 1993 p 64-67 In JAPANESE (For primary document see N94-27442 07-52)
Avail: CASI HC A01/MF A04

The caloric nystagmus is a nystagmus caused by pouring cold or hot water in the external auditory meatus, which is extensively practiced in clinical test of equilibrium function. The cause might be change of endolymphatic pressure in the semicircular canal according to caloric stimulation. This study examined the variation of endolymphatic pressure in response to caloric stimulation in pigeons in order to verify the hypothesis. The endolymphatic pressure was measured with a thermosensor directly on the semicircular canal, around which a silicon tube was twisted to stimulate by hot or cold water flowing through it. It was observed that the endolymphatic pressure of pigeons increased when stimulated by cold water and decreased by hot water, and the pressure was varied in proportion to the change of temperature. In addition, because this change was not affected by posture of a pigeon's head which fixed to keep the semicircular canal in horizontal or 45 degree-inclining position, the effect of gravity could be excluded. Author (NASDA)

N94-27458# Nagoya Univ. (Japan). Research Inst. of Environmental Medicine.

CARDIOVASCULAR FUNCTION DURING THERMONEUTRAL HEAD-OUT WATER IMMERSION IN THE ELDERLY [KOREISHA NI OKERU CHURITSUON KEIKA SUISHIN FUKAJI NO JUNKAN DOTAI]

Yoshiki Sugiyama, Chihiro Miwa, Hatsue Suzuki, Ye-Xiang Xue, Toshiyoshi Matsukawa, Satoshi Iwase, and Tadaaki Mano *In its* Annals of the Research Inst. of Environmental Medicine, Nagoya Univ., Volume 44 25 Mar. 1993 p 68-71 In JAPANESE (For primary document see N94-27442 07-52)

Avail: CASI HC A01/MF A04

Circulation system is regulated mainly by autonomic nerve system including pressor-receptor reflex. However, in the elderly, this regulation system did not seem to function, probably because of degeneration of baroreceptor and less fluid movement which may lower the suppression of muscular intension via sympathetic nervous system. The purpose of this study is to review circulatory regulation in the elderly. For examination of circulatory function, heart rate, blood pressure, mean stroke volume and cardiac output were compared between the elderly and the youth when immersed in thermoneutral water up to the level of navel or shoulder, or in standing position before the immersion. As a result, during immersion, heart rate was significantly decreased in the youth, while no decrease was observed in the elderly. Blood pressure was significantly increased in the elderly, but stroke volume was significantly increased in the youth. Cardiac output was increased only in the youth. These results reveal that in the elderly the blood pressure was increased significantly in spite of less cardiac output, which should be suppressed by negative feedback of sympathetic nervous system stimulated by the baroreceptor. However the function of pressor-receptor reflex may degenerate in the elderly. In addition, during immersion, water pressure moves fluid toward upper part of the body, and this fluid movement may stimulate the baroreceptor. However, the mechanism might not work sufficiently in the elderly. Author (NASDA)

N94-27459# Nagoya Univ. (Japan). Research Inst. of Environmental Medicine.

EFFECTS OF 40 C HOT WATER IMMERSION FOR AN HOUR ON THERMOREGULATORY FUNCTIONS IN HUMANS: COMPARISON WITH 34 C THERMONEUTRAL IMMERSION [40 C ICHI JIKANNO SUISHIN GA TAION CHOSETSU KINO NI OYOBOSU EIKYO: 34 C NO CHURITSUON SUISHIN TONO HIKAKU]

Chihiro Miwa, Satoshi Iwase, Toshiyoshi Matsukawa, Junichi Sugenoya (Aichi Medical Univ., Nagakute, Japan.), Koji Yamaguchi (Toho Gas Co. Ltd., Nagoya, Japan.), Tadaaki Mano, Yoshiki Sugiyama, Ye-Xiang Xue, and Karl A. Kirsch (Freie Univ., Berlin, Germany.) *In its* Annals of the Research Inst. of Environmental Medicine, Nagoya Univ., Volume 44 25 Mar. 1993 p 72-75 In JAPANESE (For primary document see N94-27442 07-52)

Avail: CASI HC A01/MF A04

This study examined the effects of temperature in water immersion by measuring skin temperature, core temperature, sweat rate, blood flow, body weight loss and urine volume, and compared the data between 34 C and 40 C water immersion. As a result, skin temperature and blood flow in forearms and precordia was increased, and blood flow in fingertips was decreased, during immersion in hot water. After immersion for 10 minutes, the core temperature and sweat rate was rapidly increased in high temperature water. During thermoneutral water immersion, skin temperature, sweat rate and blood flow did not change, and core temperature was lowered. Body weight loss in hot water immersion was larger by 300 g, while urine volume in thermoneutral water immersion was five times as much as that in hot water immersion. The sweat rate in the palm which represents psychogenic sweat was observed 20 minutes after the hot water immersion, probably because of stress by high temperatrue. In addition, in hot water, blood flow and skin temperature was increased by two steps; one is immediately after the immersion and the other is about 10 minutes after that. The first step might be the direct effect of water temperature, and the second might result from dilation of peripheral vessels by the change of core temperature that could stimulate thermoregulation system. It is suggested that the body weight loss might result from increased sweat in the case of high temperature, and from endocrine variation in the case of thermoneutral immersion. Author (NASDA)

N94-27460# Nagoya Univ. (Japan). Research Inst. of Environmental Medicine.

DEVELOPMENT OF STIMULUS-SEEKING SCALE FOR EXPECTING INDIVIDUAL DIFFERENCES AGAINST CONFINEMENT STRESS [HEISA KANKYO SUTORESU NI TAISURO TAISEI YOSOKU NO TAMENO SHIGEKI KIKYU SHAKUDO NO SAKUSEI]

Mitsuro Kida, Masafumi Tanaka, Tetsuji Ito, and Kazuaki Kawano *In its* Annals of the Research Inst. of Environmental Medicine, Nagoya Univ., Volume 44 25 Mar. 1993 p 76-83 In JAPANESE (For primary document see N94-27442 07-52)

(Grant MOE-04551001)

Avail: CASI HC A02/MF A04

Confinement stress is a current issue caused by an extremely few stimuli such as life in a satellite station or polar base. There are several levels of optimal stimulus for each individual, and if the individual difference could be measured, the confinement stress will be predicted. The purpose of this study was to develop a new stimulus-seeking scale based on Zuckerman's scale. In this stimulus-seeking scale, two levels were presumed; i.e. external stimulus-seeking that seeks external or physical stimulus, and internal stimulus-seeking that seeks internal or mental stimulus. Based on the two stimulus-seeking levels, a questionnaire was prepared to verify whether this classification was appropriate or not, as well as to review this scale by comparing the established scale of anxiety and disposition. From results of about 200 subjects, each 10 items were selected for internal and external stimulus-seeking level as appropriate items to distinguish individual features. Analytical study revealed the credibility and propriety of these items. Comparing scores of characteristic anxiety scale and disposition scale, there was correlation with external stimulus-seeking scale, while slight or no correlation was observed with internal stimulus-seeking scale. Author (NASDA)

N94-27461# Osaka Prefecture Univ., Sakai (Japan). Coll. of Integrated Arts and Sciences.

THE EFFECT OF BODY ORIENTATION ON THE PERCEPTION OF VERTICAL AND HORIZONTAL DISTANCE IN AN OUTDOOR SETTING [HIKENSHA NO SHISEI TO YAGAI NI OKERU SUICHOKU-SUIHEI KYORI NO CHIKAKU] c54

Atsuki Higashiyama and Kazuo Koga (Nagoya Univ., Japan.) *In* Nagoya Univ., Annals of the Research Inst. of Environmental Medicine, Nagoya Univ., Volume 44 25 Mar. 1993 p 84-87 In JAPANESE (For primary document see N94-27442 07-52)

Avail: CASI HC A01/MF A04

It is known that vertical distance appears longer than horizontal distance although they are the same length. The purpose of this study was to examine whether this effect depends on a subject's postures. 28 subjects were classified into upright-position group and lie-down position group, and three-story white building was used as a vertical scale. Subjects were told to move where they thought the distance from the building to the subject (horizontal distance) matched that from a mark on the side of the building to the ground (vertical distance). As a result, the longer the actual distance was, the longer the visual vertical distance appeared. Generally, vertical distance appeared longer in upright-position, whereas difference between visual vertical and horizontal distance was not observed in lie-down position as far as the actual distance was less than 6 m, and, even in the case that the actual distance is longer than 6 m, the differences between visual vertical and horizontal distance was not so much as those of upright-position. The most important finding was that the posture of subjects affected only the sense of vertical distance, rather than that of horizontal distance. Author (NASDA)

N94-27462# Kanazawa Univ. (Japan). Dept. of Psychology.

EYE-HEAD COORDINATION AND SWINGING OF THE VISUAL SCENE WHEN WEARING VISUALLY UP-DOWN REVERSING MIRROR FOR 14 DAYS [JOGEHANTENKYO CHAKUYOCHU NO GANKYU-TOBU UNDO TO SHIYA NO DOYO] c54

Hirokazu Yoshimura and Kazuo Koga (Nagoya Univ., Japan.) *In* Nagoya Univ., Annals of the Research Inst. of Environmental Medicine, Nagoya Univ., Volume 44 25 Mar. 1993 p 88-92 In JAPANESE (For

primary document see N94-27442 07-52)
(Grant NOE-03551003)
Avail: CASI HC A01/MF A04

In this study, one subject wore a visually up-down reversing mirror for 14 days and recorded the subjective impression. During the period, eye-head movement and swinging of the visual scene were measured every three days. For eye-head movement, eye position and head position were recorded while the subject shook the head every one second. This experiment was performed in a dark room under the following two conditions: one is not to intend to fix the head or eyes in a particular position, the other is to intend to fix eyes at an imaginary point. As a result, on the second day, the eye movement traced in a reverse phase with the head movement, probably due to compensating the head movement, in both conditions. However, this tendency became decreased, and spikes of saccade began to be observed in the trace of eye movement. On the 15th day, the decrease of amplitude was obvious even in a trace under the condition of no intention, and, in condition of intention to fixate an imaginary point, the eye movement that showed saccade instead of pursuit movement coordinated with the phase of the head movement. For the swinging of the scene, critical fusion frequency of on-and-off light was measured under head-fixed condition and head-movement condition that shook the head every one second. As a result, the critical frequency did not change remarkably under the head-fixed condition, whereas it was increased once, then, after the 12th day, decreased under the head-movement condition.
Author (NASDA)

N94-27463# Nagoya Univ. (Japan). Research Inst. of Environmental Medicine.
COMPARATIVE MEASUREMENT OF VISUAL STABILITY IN COSMIC SPACE: ONBOARD EXPERIMENT AND PRE-FLIGHT ACTIVITIES Quick Report [UCHU KUKAN NI OKERU SHIKAKU ANTEISEI NO KENKYU: JIKKEN UNYO TO UNYO NI ITARU SHOKATEI] c54
Kazuo Koga, Tadaaki Mano, Mitsuro Kida, Yoshihiro Ota, Keiichiro Tsuji, Takuo Goto, and Ryoji Osaka (Aichigakuin Univ., Nisshin, Japan.) *In its* Annals of the Research Inst. of Environmental Medicine, Nagoya Univ., Volume 44 25 Mar. 1993 p 93-96 In JAPANESE (For primary document see N94-27442 07-52)
Avail: CASI HC A01/MF A04

It is expected that visual recognition and coordination of eye-hand or eye-head movement would be somewhat different in cosmic space. To examine the human behavior in space, a study was planned and operated as a part of the First Material Processing Test (FMPT) in the Space Shuttle Endeavor. In this study, saccadic eye movement and anti-gravity muscle activity of a Payload Specialist (PS) was recorded. This article reports the process and operation of this experiment. For the mission operation, staff training was started in 1991, in order to master general operation of the control facilities, technical terms used in flight control, and the downlink display, etc. In 1992, several simulation training were performed using the facilities of NASA. During the flight, three experiments were scheduled to operate, with support of downlink image data. Communication with PS was also capable; however, the number of circuit was limited so that it was permitted only when necessary. The experiment was completed almost as scheduled, although several changes were added.
Author (NASDA)

N94-27464# Nagoya Univ. (Japan). Research Inst. of Environmental Medicine.
MODULATION BY GALACTOSAMINE-INDUCED HEPATITIS OF BIOLOGICAL RESPONSES OF THE RAT EXPOSED TO HIGH ALTITUDE HYPOXIA [KYUSEI TEIATSU-TEISANSO KANKYOKA NI OKERU GARAKUT OSAMIN YUHATSU KANEN RATTO NO SEITAI HANNO] c51
Chikashi Yamamoto, Masataka Yoshino (Institute for Developmental Research, Kasugai, Japan.), Shigeo Mori, and Hisao Seo *In its* Annals of the Research Inst. of Environmental Medicine, Nagoya Univ., Volume 44 25 Mar. 1993 p 97-98 In JAPANESE (For primary document see N94-27442 07-52)
Avail: CASI HC A01/MF A04

Under hypobaric hypoxic condition, liver function is expected to be affected by induction of enzymes to adapt anaerobic condition. These biological responses were studied using rats induced hepatitis by galactosamine under the condition with altitude of 8,000 m. To examine liver metabolism, the activity of mitochondrial enzymes (citrate synthase, fumarase), cytosol glycolysis enzyme (hexokinase), glyconeogenesis enzyme FBPase (Fructose 1,6-bisphosphatase Steroid-Induced Enzyme) (tyrosine aminotransgerase) were measured. As a result, the activity of mitochondrial enzymes were decreased in hepatitis group, whereas that of hexokinase and FBPase was not changed by galactosamine. Both hepatitis and control group were not affected by exposure of high altitude hypoxia. However, tyrosine aminotransferase activity was increased twice as much as that of control group by exposure of high altitude hypoxia, while no change was observed in hepatitis group. The fact that mitochondrial enzymes were changed but not cytosol glycolysis enzymes in hepatitis group suggests that mitochondrial membrane could be damaged by galactosamine. In addition, galactosamine inhibited the steroidal induction of tyrosine aminotransferase under the condition of high altitude hypoxia. This implies that galactosamine was damaged endoplasmic reticulum, too. These results suggests that galactosamine-induced hepatitis is useful to examine how to switch the anaerobic metabolism to aerobic metabolism. Author (NASDA)

N94-27465# Nagoya Univ. (Japan). Research Inst. of Environmental Medicine.
PROTECTIVE ACTION OF PLATELET-ACTIVATING FACTOR ANTAGONIST, TCV-309, AGAINST ISCHEMIA REPERFUSION INJURY IN ISOLATED RABBIT HEARTS [KESSHOBAN KASSEIKA INSHI (PAF) KIKKOZAI TCV-309 NO KYOKETSU SHINKIN HOGO KOKA: IEUSAGI TEKISHUTSU KANRYUSHIN O MOCHITA JIKKENTEKI KENTO] c51
Satoru Kato, Akira Koike, Toshio Abe, Itsuo Kodama, and Junji Toyama *In its* Annals of the Research Inst. of Environmental Medicine, Nagoya Univ., Volume 44 25 Mar. 1993 p 99-101 In JAPANESE (For primary document see N94-27442 07-52)
Avail: CASI HC A01/MF A04

It has been revealed that Platelet Activating Factor (PAF) has a direct effect on the heart, as well as possibility to be associated with reperfusion injury in the heart. This study examined the effect of TCV-309, an PAF antagonist, on isolated rabbit heart and on CPK (Creatine Phosphokinase) release during reperfusion. For this study, isolated rabbit hearts were perfused aerobically for 30 minutes, followed by blocking of perfusion for 120 minutes, then, reperfused again for 60 minutes. TCV-309 was administered in perfusate before and after the block. In this experiment, Left Ventricular Developed Pressure (LVDP) and the amount of CPK released in perfusate for 5 minutes after the reperfusion were measured. As a result, LVDP recovery rate was 54.3 percent in control group, whereas it was remarkably improved up to 77.6 percent in TCV-309 administered group. The amount of CPK was significantly decreased in TCV-309 administered group. From these results, it can be concluded that TCV-309 can improve cardiac function after ischemia and inhibit CPK release. These results support the possibility that PAF might be associated with reperfusion injury of cardiac ischemia.
Author (NASDA)

N94-27466# Nagoya Univ. (Japan). Dept. of Cardiol-Surgery.
PROTECTIVE ACTION OF AN AMILORIDE DERIVATIVE (AMILORIDE, 5-(N, N-DIMETHYL) HYDROCHLORIDE) AGAINST IN ISOLATED ISCHEMIA/REPERFUSION NEWBORN RABBIT HEARTS [MIJUKU SHINKIN NO KYOKETSU SAIKANRYU SHOGAI NI TAISURU AMIRORAIDO YUDOTAI (AMIRORAIDO,5-(N-, N-JIMECHIRU) HIDOROKURORAIDO) NO HOGO KOKA] c51
Akira Koike, Satoru Kato, Toshiaki Akita, Toshio Abe, Itsuo Kodama, and Junji Toyama *In* Nagoya Univ., Annals of the Research Inst. of Environmental Medicine, Nagoya Univ., Volume 44 25 Mar. 1993 p 102-104 In JAPANESE (For primary document see N94-27442 07-52)
Avail: CASI HC A01/MF A04

It is known that excess intracellular Ca(2+) causes cytotoxic reaction after reperfusion of cardiac ischemia. Ca(2+) is transported into the cell by Na(+)/Ca(2+) exchange propelled by H(+) concentration gradient, followed by Na(+)/H(+) exchange. It was reported that amiloride improved cardiac function in newborn rabbit hearts where intracellular Na(+) might be accumulated more than matured hearts probably due to anaerobic glycolysis. This effect depends on inhibition of Na(+)/H(+) and Na(+)/Ca(2+) exchanger. This study concerns protective action of a amiloride derivative, amiloride, 5-(N, N-dimethyl) hydrochloride (DMA) against reperfusion injury after ischemia, which can inhibit Na(+)/H(+) exchanger selectively. In this study, perfusion was blocked for 45 minutes after 15 minutes of preperfusion in isolated newborn rabbit heart, followed by reperfusion for 30 minutes, and Left Ventricular Developed Pressure (LVDP) was measured, as well as the amount of CPK (Creatine Phosphokinase) in perfusate for 15 minutes after the reperfusion was determined. It was also revealed that DMA barely effected non-ischemic heart from one to 10 micromoles, but 100 micromoles of DMA caused cardiac arrest. LVDP recovery rate was 51 percent in control group, whereas DMA improved it up to 1 percent. Comparing the amount of CPK, DMA group was decreased significantly than control group (68 unit/g vs. 10 unit/g). These results suggest that DMA improved LVDP recovery rate after reperfusion, and decreased CPK release, without any adverse effect on the heart. This effect was as much strong as amiloride. Author (NASDA)

N94-27467# Nagoya Univ. (Japan). Research Inst. of Environmmental Medicine.

EFFECTS OF HIGH-INTENSITY ELECTRIC FIELD STIMULATION ON THE ELECTROMECHANICAL PERFORMANCE OF CARDIAC MUSCLE: INFLUENCE OF FIBER ORIENTATION Report No. 6 [KOENERUGI DENKI SHIKKU GA SHINKIN NO MAKU KATSUDO DENI TO CHORYOKU NI OYOBOSU SAYO: SHINKIN SENI SOKO NO EIKYO] **c51**

Itsuo Kodama, Akiko Arai, Ryoko Suzuki, Nitaro Shibata (Tokyo Woman's Medical Coll., Japan.), Kiyomi Niki (Tokyo Woman's Medical Coll., Japan.), Ichiro Sakuma (Tokyo Woman's Medical Coll., Japan.), Tadashi Haraguchi (Tokyo Denki Univ., Japan.), Kenji Furukawa, Yasuhiko Fukui, and Saichi Hosoda (Tokyo Woman's Medical Coll., Japan.) et al *In its* Annals of the Research Inst. of Environmental Medicine, Nagoya Univ., Volume 44 25 Mar. 1993 p 105-109 In JAPANESE (For primary document see N94-27442 07-52)

Avail: CASI HC A01/MF A04

This study examined the responses of a cardiac muscle in the longitudinal (L) direction and transverse (T) direction stimulated by electric shock pulses (SP) using the cardiac muscles of guinea pigs. As a result, it was revealed that they responded differently by orientation of muscle fibers; i.e., the diastolic threshold of excitation in L direction was 1.4 - 1.6 times the strength as that in T direction. This suggests that L direction was more responsive to high intensity electric stimulation than T direction, probably resulting from electric potential (membrane potential) that is varied by the length of conductor in the same direction as electric field. However, in case of stimulating by 25 V/cm or more of SP's, the delayed responses were contrary to these results; i.e., decrease of resting potential and increase of contractility were larger in T direction than L direction, and vibration of membrane potential and spontaneous activity tend to occur in T direction. This is probably because electroporation that can pass ions unselectively after high-intensity electric stimulation does not present or presents slightly at the ends of longitudinal axis. Thus, electric coupling via gap junction of intercellular constitution that are different by orientation of muscle fibers may cause the different conductivity between T and L direction. Author (NASDA)

N94-27468# Nagoya Univ. (Japan). Research Inst. of Environmental Medicine.

ON THE MECHANISM OF REENTRANT ARRHYTHMIAS FOLLOWING DC DEFIBRILLATION: INFLUENCE OF FIBER ORIENTATION TO THE EFFECTS OF LOW-ENERGY ELECTRIC FIELD STIMULATION ON THE EFFECTIVE REFRACTORY PERIOD OF CARDIAC MUSCLE [CHOKURYU JOSAIDO GO NO RIENTORI HUSEIMYAKU HASSEI KIJO NI KANSURU KENKYU: TEI ENERUGI DENBA SHIGEKI NIYORU SINKIN FUOKI ENCHO TO SENI SOKO NO KANKEI] **c51**

Itsuo Kodama, Nitaro Shibata (Tokyo Woman's Medical Coll., Japan.), Ichiro Sakuma (Tokyo Denki Univ., Japan.), Kiyomi Niki (Tokyo Woman's Medical Coll., Japan.), Akiko Arai, Ryoko Suzuki, Tadashi Haraguchi (Tokyo Denki Univ., Japan.), Kenji Furukawa (Tokyo Denki Univ., Japan.), Yasuhiko Fukui (Tokyo Denki Univ., Japan.), and Saichi Hosoda (Tokyo Woman's Medical Coll., Japan.) et al *In its* Annals of the Research Inst. of Environmental Medicine, Nagoya Univ., Volume 44 25 Mar. 1993 p 110-113 In JAPANESE (For primary document see N94-27442 07-52)

Avail: CASI HC A01/MF A04

In this study, the correlation between effects of low energy electric field stimulation on Effective Refractory Period (ERP) and cardiac fiber orientation was reviewed in order to clarify the mechanism of reentrant arrhythmias following DC (direct current) defibrillation. The ERP was measured using a cardiac muscle of guinea pigs stimulated by shock pulses (PS) provided to the longitudinal (L) direction and the transverse (T) direction. As a result, it was revealed that repolarization and ERP were delayed according to the intervals between basic stimulation and PS and intensity of low energy electric field stimulations. This effect was marked in the L direction than the T direction, probably resulting from the shape of cardiac fibers. They are usually longer in the L direction than the T direction by 8 - 10 times so that the maximum membrane potential in the L direction is estimated to be several times as much as that in the T direction. The difference of conductivity by directions causes anisotropy of tissue resistance. In addition, electrical coupling occurred effectively and extracellular resistance was lowered in the L direction, which might also cause the difference of electric density by the directions. Low energy DC electric field stimulation can delay ERP and repolarization, and the delay was modified by strength of electric field, interval of stimulation, and orientation of cardiac fibers, leading to inequal refractory period in different sites. This could be a cause of reentrant arrhythmias. Author (NASDA)

N94-27469# Nagoya Univ. (Japan). Research Inst. of Environmental Medicine.

POSITIVE CHRONOTROPIC EFFECT OF MECHANICAL STRETCH ON THE SINOATRIAL NODE: ROLES OF NEUROTRANSMITTERS AND STRETCH ACTIVATED CHANNELS [KIKAITEKI SHINTEN NI YORU DOKESSETSU JIDONO KOSHIN NO KIJO NI KANSURU KENKYU] **c51**

Akiko Arai, Ryoko Suzuki, Itsuo Kodama, and Junji Toyama *In its* Annals of the Research Inst. of Environmental Medicine, Nagoya Univ., Volume 44 25 Mar. 1993 p 114-116 In JAPANESE (For primary document see N94-27442 07-52)

Avail: CASI HC A01/MF A04

It is known that stretch stimulation causes positive chronotropic effect on the sinoatrial node probably mediated by Stretch-Activated (SA) channels. This study examined the mechanism using the SA-channel blocker, gadolinium (Gd(3+)). The sinoatrial node of rabbit was extracted and the Spontaneous Cycle Length (SPCL) was determined during and after the stretch stimulation. As a result, it was revealed that the mechanical stretch caused positive chronotropic effect in proportion to the strength of the tension. The maximum effect was achieved immediately after the stretch stimulation and then decreased exponentially. When the neurotransmitter in the tissue was blocked pharmacologically by propranolol and atropine, residual effect after the stimulation disappeared. However, Gd(3+) did not decrease the positive chronotropic effect. These results suggests that this effect might result from not only neurotransmitters, especially noradrenaline, but also another factor. However, Gd(3+) sensitive SA channel might not play an important role in this process. Author (NASDA)

N94-27470# Nagoya Univ. (Japan). Research Inst. of Environmental Medicine.

DISTURBED NEURONAL MIGRATION IN THE CEREBRAL CORTEX OF MICE BY LOW-DOSE GAMMA RADIATION [TEISENRYO HOSHASEN NI YORU MAUSU DAINO HISHITSU SHINKEI SAIBO NO YUSO SHOGAI] **c51**

Minoru Inoue, Shizu Hayasaka, Xue-Zhi Sun, and Hideki Yamamura *In its* Annals of the Research Inst. of Environmental Medicine, Nagoya Univ., Volume 44 25 Mar. 1993 p 117-121 In JAPANESE (For primary document see N94-27442 07-52)

(Grant MOE-03680181)

Avail: CASI HC A01/MF A04

There is a possibility that gamma-radiation may affect a development of nerve cells by disturbance of neuronal migration. In the cerebral cortex, ganglionic layer is formed from inside to outside, and young nerve cells developed in the ventricule migrate through the primodial cortex to form the outer layer. This study examined the effect of low dose gamma-radiation on this migration using mice. Proliferative cells in S stage were labeled by Bromodeoxy Uridine (BrdU) at the 16th or 17th day of pregnancy, and 0.26 Gy of gamma-ray was radiated at the 17th day. These mice were killed at hours after the radiation or two days or six weeks after the birth, and each brain was examined. As a result, cell death was not observed in the ventricle hours after radiation. However, in the cerebral cortex of two day-old mice, migration of nerve cells in S-stage were disturbed, while those in G1 or G2 stage migrated normally. In six week-old mice, migration was disturbed in cells in both S-stage and G0/G2 stage. These results suggest that low-dose gamma-radiation disturbs the migration of premature nerve cells to the cerebral cortex. In this process, cells during DNA (Deoxyribonucleic Acid) replication were more sensitive to the radiation effect than those during differentiation. Author (NASDA)

N94-27471# Nagoya Univ. (Japan). Research Inst. of Environmental Medicine.
DISTRIBUTION OF GABA IMMUNOREACTIVE NEURONS IN THE BRAIN OF ROLLING MOUSE NAGOYA AND GAMMA-IRRADIATED MOUSE [IDENSEI UNDO SHICCHO MAUSU TO GANMASEN HIBAKU MAUSU NO NO NI OKERU GABA NYURON NO BUNPU] **c51**
Takayoshi Imai, Yoshiko Takagishi, Shizu Hayasaka, Minoru Inouye, and Hideki Yamamura *In its* Annals of the Research Inst. of Environmental Medicine, Nagoya Univ., Volume 44 25 Mar. 1993 p 122-124 In JAPANESE (For primary document see N94-27442 07-52)
Avail: CASI HC A01/MF A04

A rolling mouse Nagoya has been used as a model of human spinocerebellar degeneration presenting hereditary ataxia. In this study, distribution of neurons containing Gamma-Aminobutyric Acid (GABA) in the brain of a rolling mouse Nagoya was determined immunologically using anti-GABA antibodies. In addition, mice with microcephaly by embryonal gamma-irradiation was also studied in the same manner. The brain of both mice were sliced, immunostained and observed microscopically. As a result, the cerebrum of the rolling mice appeared normal, and no histological abnormality was observed in the cerebellum in spite of some reports that presented the possibility of hypoplasia of the frontal lobe and decrease of granule cells. On the contrary, the gamma-irradiation mice had obviously smaller cerebrum and thinner cortex layer than control, but other parts of the brain was histologically normal. In the immunostain study, GABA-positive neurons were mainly observed in the cerebral cortex in both mice, striate body, thalamus and cerebellar cortex. In the cerebral cortex, they were distributed predominantly in the two and four layers of control mice, whereas they were distributed in all layers of the gamma-irradiated mice and rolling mice. In other parts of the brain, no particular difference was observed in the distribution of GABA-positive neurons between control group and gamma-irradiated and rolling mice group. Author (NASDA)

N94-27472# Suzuka Univ. of Medical Science and Technology (Japan).
EFFECTS OF GAMMA RAY RADIATION ON THE DEVELOPING MOUSE CEREBELLUM: APOPTOTIC CELL DEATH AND INDUCTION OF TISSUE TRANSGLUTAMINASE [GANMASEN SHOSHA NO MAUSU SHINSEISHI NO SHONO GENKI NI OYOBOSU EIKYO: SAIBOSHI TO SOSHIKI TORANSUGURUTAMINAZE NO YUDO] **c51**
Masao Tamaru, Masato Ando (Fujita Health Univ., Toyohashi, Japan.), Yutaka Nagata (Fujita Health Univ., Toyohashi, Japan.), and Minoru Inoue (Nagoya Univ., Japan.) *In* Nagoya Univ., Annals of the Research Inst. of Environmental Medicine, Nagoya Univ., Volume 44 25 Mar. 1993 p 125-127 In JAPANESE (For primary document see N94-27442 07-52)
Avail: CASI HC A01/MF A04

It is known that developing nerve cells are so sensitive to radiation that apoptotic death often occurs. In this process, condensation of chromatin and pykonosis, followed by reduction of cells, finally results in destruction of cells. It is considered that Transglutaminase (TG) plays an important role to form apoptotic body via cross-link of protein. In order to reveal the TG function, it was examined whether the TG activity was changed or induced during the apoptosis. One-day old mice were irradiated by gamma-rays to cause apoptosis in the outer granule layer of the cerebellum. As a result, pykonosis increased 3 hours after the radiation, achieved the peak after 5 hours, then gradually decreased in the cerebellum, while the TG activity was changed in accordance with the change of pyknosis. TG activation and induction might strengthen the cross-link of protein which stabilizes apoptotic body and prevent leak of intracellular substances. Thus, these results support the idea that TG may function in occurrence of apoptosis. Author (NASDA)

N94-27473# Nagoya Univ. (Japan). Research Inst. of Environmental Medicine.
EFFECTS OF BATHING AT 40 C ON CARDIOVASCULAR SYSTEM IN HUMANS: COMPARISON WITH 34 C THERMONEUTRAL BATHING [40 C NO NYUYOKU GA HITO NO JUNKANKIKEI NI OYOBOSU EIKYO]
Toshiyoshi Matsukawa, Chihiro Miwa, Satoshi Iwase, Yoshiki Sugiyama, Ye-Xiang Xue, Tadaaki Mano, Junichi Sugenoya (Aichi Medical Univ., Nagakute, Japan.), Koji Yamaguchi (Toho Gas Co. Ltd., Nagoya, Japan.), and Karl A. Kirsch (Freie Univ., Berlin, Germany.) *In its* Annals of the Research Inst. of Environmental Medicine, Nagoya Univ., Volume 44 25 Mar. 1993 p 128-130 In JAPANESE (For primary document see N94-27442 07-52)
Avail: CASI HC A01/MF A04

The incidence of stroke and cardiac infarction increases during and immediately after bathing; however, it is not sufficiently understood what is the effect of bathing, especially on the circulatorysystem. In this study, the changes of core temperature, skin blood flow, blood pressure and heart rate were measured to compare the effect of bathing in 34 C water and 40 C water on healthy human subjects. As a result, in 34 C bathing, skin blood flow and systolic pressure did not change, while core temperature, diastolic pressure, mean blood pressure and heart rate were decreased. On the contrary, in 40 C bathing, core temperature, skin blood flow and heart rate were significantly increased, and systolic, diastolic and mean pressure were decreased significantly. Generally, bathing effects circulatory system by static water pressure and water temperature, but 34 C bathing receives only static water pressure. Therefore, the difference between 34 C and 40 C bathing could result from the effect of water temperature. This effect includes an increase of peripheral blood that may decrease the amount of central blood, leading to decrease of blood pressure in 40 C bathing. The reverse response of heart rate was explained as follows: in 34 C bathing, increase of central blood by static water pressure may stimulate baroreceptor to decrease heart rate, whereas, in 40 C bathing, baroreceptor was stimulated oppositely, as well as stimulation of the hypothalamus by high core temperature also functioned to increase heart rate via sympathetic nerve system. Author (NASDA)

N94-27474# Nagoya Univ. (Japan). Research Inst. of Environmental Medicine.
EFFECTS OF 41 C BATHING FOR 20 MINUTES ON CARDIOVASCULAR AND THERMOREGULATORY FUNCTIONS IN HUMANS [HITO NO SHIN JUNKAN KINO TO ONDO CHOSETSU KINO NI OYOBOSU 41 C 20 PUNKAN NYUYOKU NO EIKYO]
Chihiro Miwa, Satoshi Iwase, Toshiyoshi Matsukawa, Yoshiki Sugiyama, Tadaaki Mano, Mitsuro Kida, Hiroshi Yamaguchi (Toho Gas Co. Ltd., Nagoya, Japan.), Seishi Okuyama (Toho Gas Co. Ltd., Nagoya, Japan.), Toshiya Mizuno, and Teruyuki Saito et al *In its* Annals of the Research Inst. of Environmental Medicine, Nagoya Univ., Volume 44 25 Mar. 1993 p 131-134 In JAPANESE (For primary document see N94-27442 07-52)
Avail: CASI HC A01/MF A04

The Japanese prefers hot water bathing of 41 - 43 C; however, it was reported that cardiovascular and cerebrovascular diseases often occurs during hot water bathing. This study examined physiological effects of 41 C bathing for 20 minutes on healthy human subjects. As a result, heart and respiration rate, skin temperature and skin blood flow were increased, while blood pressure was decreased. When bathing, the first response could be dilation of peripheral vessels that decreases circulatory blood and cardiac output, which might result in immediate decrease of blood pressure and rise of heart and respiration rate. The second response which occurred 10 minutes after bathing was increase of heart rate and respiration rate, probably resulting from elevation of core temperature that also stores blood in peripheral vessels and decrease circulatory blood, and from stimulation of the hypothalamus by high core temperature to activate sympathetic nerve system. Sweat was observed 10 minutes after the bathing, which would be thermoregulation against core temperature elevation. Author (NASDA)

N94-27475# Nagoya Univ. (Japan). School of Engineering.
MONTHLY VARIATION OF PHYSIOLOGICAL AND PSYCHOLOGICAL RESPONSES UNDER UNSTEADY THERMAL CONDITIONS Report No. 2 [HITEIJO ONNETSU KANKYOKA DENO SEIRI-SHINRI HANNO NI OKERU NENNAI HENDO]
Teruyuki Saito, Satoru Kuno, Mitsuro Kida, Kazuo Koga, Hatsue Suzuki, Toshiya Mizuno, Hideo Ono (Sugiyama Jogakuin Univ., Nagoya, Japan.), and Nobuo Nakahara *In its* Annals of the Research Inst. of Environmental Medicine, Nagoya Univ., Volume 44 25 Mar. 1993 p 135-139 In JAPANESE (For primary document see N94-27442 07-52)
Avail: CASI HC A01/MF A04

This study examined physiological response (mean skin temperature)

and psychological response (feeling of hot and cold, cool and warm, comfort and desire for elevating or lowering room temperature) of human subjects for every month in case of changing room temperature from 18 to 26 C and from 34 to 26 C. For each response parameters, linear regression line was obtained from the relation of the response with change of room temperature. Concerning skin temperature, regression lines of each month were compared between rising and lowering temperature condition, and the inclines in the two conditions differed remarkably during June to August. This suggests that during summer sweat lowers skin temperature in 34 C condition so that the incline becomes gentler around the temperature. The incline of hot and cold feelings was not varied by seasonal changes, but generally, the inclines were steeper in rising temperature than lowering temperature. This is because at 18 C subjects complained coldness more than the degree of complain of hotness in lowering temperature. In the desire for room temperature, the Y intercepts were smaller in winter, which suggests that a man is satisfied to higher temperature during winter.
Author (NASDA)

N94-27476# Sugiyama Jogakuin Univ., Nagoya (Japan). Dept. of Human Environment.

MAN'S ABILITY TO ADAPT HIMSELF FOR THE SEASONAL CLIMATIC CHANGES: FROM VIEWPOINT OF ANTICIPATION AND SEASONABLE BEHAVIOR [DOTEKI NA ONNETSU KANKYO NI TAISURU NINGEN NO TSUIJUSEI NI KANSURU KOSATSU: YOCHIKODO ANCHISHIPESHON TO KISETSU SOOSEI NO KANKEI NI TSUITE]

Hideo Ono and Mitsuro Kida (Nagoya Univ., Japan.) *In* Nagoya Univ., Annals of the Research Inst. of Environmental Medicine, Nagoya Univ., Volume 44 25 Mar. 1993 p 140-144 In JAPANESE (For primary document see N94-27442 07-52)
Avail: CASI HC A01/MF A04

The purpose of this article is to review the studies on environmental evaluation and changes of comfortability by dynamic thermal conditions, especially on a effect of seasonal changes, in order to achieve a coordinated environments not depending on large energy consumption but considering ecological system on the entire earth. From these studies, it was revealed that the change of room temperature caused physiological and psychological changes. The similar physiological changes were also observed in seasonal changes, although the peak of hot or cold temperature preceded the peak of physiological responses by about two months. The senses of warm or cool seem to largely depend on a physiological factor (hormone or metabolism), and a mental factor (scenary or color). The adaptability is a behavior to reach such warm or cool condition by anticipating the seasonal changes. There are two factors that effect thermo-comfortability: seasonal factor, such as metabolism, meteorological condition, or scenary, and seasonable factor, such as admiration of seasons. It seems to be important to consider both factors for design and management of comfortable environment.
Author (NASDA)

N94-27477# Nagoya Univ. (Japan). Research Inst. of Environmental Medicine.

THE INTRACELLULAR SECOND MESSENGER SYSTEM IN c-fos GENE INDUCTION BY ACTH [ACTH NI YORU C-FOS IDENSHI YUDO NO SAIBONAI SEKANDO MESSENJA] c51

Norihiro Miyamoto, Kazumi Kanda, Hiroyoshi Hidaka, and Hisao Seo *In its* Annals of the Research Inst. of Environmental Medicine, Nagoya Univ., Volume 44 25 Mar. 1993 p 145-147 In JAPANESE (For primary document see N94-27442 07-52)
(Grant MOE-04671469)
Avail: CASI HC A01/MF A04

In the previous report, it was demonstrated that Adrenocorticotroic Hormone (ACTH) induced to express the c-fos gene, a cellular tumor gene, transiently in the early stage in hypophysectomy rats. Several intracellular second messengers might participate in the c-fos gene induction, including cAMP (cyclic Adenosine 3', 5'-monophosphate) dependent kinase (A-kinase), proteinkinase C (C-kinase), and Ca(2+)/calmodulin-dependent kinase (CaM-kinase). This study examined the function of these messengers in c-fos gene induction. To the primary culture of rat's adrenal cells, an activator of either A-kinase, C-kinase or CaM-kinase was added, as well as an A-kinase inhibitor. As a result, c-fos mRNA (messenger Ribonucleic Acid) was remarkably increased 60 minutes after A-kinase activator, cAMP, addition, and decreased to the level before the addition at 180 minutes. The amount of corticosterone in the culture was increased in proportion to time. The A-kinase inhibitor, H-89, inhibited the increase of mRNA, as well as production of corticosterone, in dose-dependent manner. However, the activators of C-kinase and CaM-kinase did not increase the mRNA and corticosterone. These results suggest that the c-fos gene induction by ACTH may mediated by cAMP as a intracellular second messenger, and that C-kinase and CaM-kinase may not participate in c-fos gene induction as a second messenger.
Author (NASDA)

N94-27478# Nagoya Univ. (Japan). Research Inst. of Environmental Medicine.

THYROID HORMONE ACTION IN CULTURED HUMAN SKIN FIBROBLASTS: EVALUATION USING SPHEROID CULTURE [HITO HIFU SENIGA SAIBO NI OKERU KOJOSEN HORUMON SAYO: SUFEROIDO BAIYO O MOCHITA KENTO]

Yoshiharu Murata, Masafumi Menjo, Takashi Miyazaki, Hisao Seo, Manabu Yamazaki (Japan Research Center, Atsugi.), and Yuichi Mori (Japan Research Center, Atsugi.) *In its* Annals of the Research Inst. of Environmental Medicine, Nagoya Univ., Volume 44 25 Mar. 1993 p 148-150 In JAPANESE (For primary document see N94-27442 07-52)
(Grant MOE-04671470)
Avail: CASI HC A01/MF A04

This article presents the responses of human skin fibroblasts to the stimulus of thyroid hormone. In previous studies, the mechanism was examined with monolayer culture, however, different stages of cell cycle were observed among cells. On the other hand, cells are considered to stay at G(sub 0)-stage in the spheroid culture. In this study, this spheroid culture was applied using a thermo-sensitive polymer which has a property to become insoluble above 30 C and soluble below the temperature. Human skin fibroblasts were cultured in solid medium at 37 C, and when confluent, it was cooled to 4 C to melt the polymer so that the cells were suspended in the medium and gradually formed spheroids. Triiodothyronine (T(sub 3)) was added to the culture when spheroid was formed and Fibronectin (FN) mRNA (Messenger Ribonucleic Acid) and collagenase mRNA was determined as indices of the response. As a result, FN mRNA was decreased to two-thirds by T(sub 3) addition, while collagenase mRNA was not changed by T(sub 3). There is some contradictions between these results and those from monolayer culture, because the effect of proteinkinase C cannot be excluded from the latter system due to containing cells with different cell cycles. Therefore, the spheroid culture may be superior in examining the pure effect of thyroid hormone.
Author (NASDA)

N94-27479# Nagoya Univ. (Japan). Dept. of Surgery.

CLONING OF RAT RXR ALPHA cDNA AND THE EXPRESSION OF ITS mRNA IN REGENERATING LIVER AND PRIMARY CULTURED HEPATOCYTES [RATTO RXR ARUFA CDNA NO KURONINGU TO SAISEIKAN OYOBI SHODAI BAIYO SAIBO NI OKERU MRNA NO HATSUGEN] c51

Masafumi Menjo, Yoshiharu Murata, Fukushi Kambe, Taichi Kato, Tsuyoshi Kato, and Hisao Seo *In its* Annals of the Research Inst. of Environmental Medicine, Nagoya Univ., Volume 44 25 Mar. 1993 p 151-15 In JAPANESE (For primary document see N94-27442 07-52)
(Grant MOE-03807084)
Avail: CASI HC A01/MF A04

It was demonstrated that the response to thyroid hormone was weakened in hepatocytes of proliferation phase due to inhibiting the expression of T(sub 3) response genes. This study examined the gene expression of rat alpha-Retinoid X Receptor (RXR-alpha) cDNA (complementary Deoxyribonucleic Acid) that is a T(sub 3) receptor auxiliary protein presenting in the liver, in order to clarify the mechanism of the thyroid hormone response in hepatocytes. For cDNA, RXR alpha cDNA was amplified by RT (Reverse Transcription)-PCR (Polymerase Chain Reaction) from total mRNA extracted from mice liver, and was cloned, and the sequence was determined. As a result, it was proved that the cDNA was homologous to the human RXR alpha DNA in 2.1 percent. Gene expression of RXR alpha was examined using regenerating liver, primary cultured hepatocytes, and sham-operated liver. The three cells were cultivated by monolayer culture and spheroid culture, amplified by PCR, and the RXR alpha mRNA was identified on electrophoresis. As a result, no difference was observed in respect to mRNA expression among three kinds of cells, and between two culture methods. Therefore, it can be concluded that gene expression of

RXR alpha mRNA (messenger Ribonucleic Acid) are not related with the decrease of the thyroid hormone response in proliferating hepatocytes.
Author (NASDA)

N94-27480# Nagoya Univ. (Japan). Research Inst. of Environmental Medicine.
CLONING OF A NOVEL POU FAMILY GENE BY RT-PCR METHOD [RT-PCR HO O MOCHIITA ATARASHII POU IDENSHI NO KURONINGU NO KOKOROMI] **c51**
Fukushi Kambe, Shinichiro Tsukahara, Taichi Kato, Norihiro Miyamoto, Yoshiharu Murata, and Hisao Seo *In its* Annals of the Research Inst. of Environmental Medicine, Nagoya Univ., Volume 44 25 Mar. 1993 p 154-157 In JAPANESE (For primary document see N94-27442 07-52)
(Grant MOE-04454559)
Avail: CASI HC A01/MF A04

Recently, it has been demonstrated that expression of Pit-1, an homeobox gene, is necessary for differentiation and proliferation of growth hormone, prolactin and thyroid-stimulating hormone in the anterior pituitary of rats, and that Pit-1 functioned as a transcription regulatory factor for the expression of hormone genes in each cell. Furthermore, a group of proteins called the POU family, that have a highly homologous domain with the Pit-1 gene, were found in the central nerve system, testicle, and B-cells. In this study, mRNA's (Messenger Ribonucleic Acid) were extracted from several organs, to find new POU gene. As a result, mRNA's of the hypothalamus, thyroid gland, thymus, adrenal grand and testicle were amplified by RT (Reverse Transcription)-PCR (Polymenase Chain Reaction), and their cDNA (complementary Deoxyribonucleic Acid) were revealed to be highly homologous to the human Oct-1 gene, which is of the POU family. The cDNA amplified from mRNA of the pituitary was identified as the Pit-1 POU domain. The mRNA of the pancreas could not be amplified. These results suggest that the cDNA's cloned in this study were rat Oct-1 cDNA, and that the Oct-1 POU domain sequence could be ubiquitous in vertebrates. In respect to organs, the Oct-1 gene was found in almost all organs except for the pancreas.
Author (NASDA)

N94-27481# Nagoya Univ. (Japan). Research Inst. of Environmental Medicine.
EFFECT OF SERA FROM PATIENTS TREATED WITH LONG-TERM HEMODIALYSIS ON mRNA'S FOR COLLAGENASE, STROMELYSIN, AND TISSUE INHIBITOR OF METALLOPROTEASE IN CULTURED HUMAN SYNOVIAL CELLS [BAIYO HITO KATSUMAKU SAIBO NI OKERU KORAGENAZE, SUTOMERAISHIN, OYOBI SOSHIKI METAROPUROTEAZE INHIBITA NO KAKUIDENSHI HATSUGEN NI OYOBOSU TOSEKI KANJA KESSEI TENKA NO EIKYO]
Takash Miyazaki, Motoyoshi Sato, Yoshiharu Murata, Kenji Maeda, and Hisao Seo *In its* Annals of the Research Inst. of Environmental Medicine, Nagoya Univ., Volume 44 25 Mar. 1993 p 158-160 In JAPANESE Sponsored by the Aichi Kidney Foundation and Kowa Life Science Foundation (For primary document see N94-27442 07-52)
Avail: CASI HC A01/MF A04

Long-term hemodialysis usually causes dialysis amyloid arthropathy. It was demonstrated in the previous studies that sera from long-term hemodialysis patients promoted the production of Collagenase (CS) that plays an important role in degradation of interstitial tissue in synovial cells. This study examined whether this sera varies the expression of mRNA of Stomelysin (SN) and Tissue Inhibitor of Metalloprotease (TIMP). It is known that SN promotes degradation of interstitial tissue together with CS synergistically, and TIMP inhibits such degradation by blocking both proteases to reconstitute interstitial tissue. Sera from long-term dialysis patient was added to subcultured synovial cells, and the mRNA (messenger Ribonucleic Acid) was extracted and determined. As a result, mRNA of CS and SN was increased three times as much as that of control in which sera from healthy person was added. On the contrary, at the most, only a slight difference was observed in TIMP mRNA expression between sera from patient and a healthy person. This suggests that sera from the dialysis patient change synovial cells to promote degradation of surrounding interstitial tissue.
Author (NASDA)

N94-27482# Nagoya Univ. (Japan). Dept. of Internal Medicine.
EXPRESSION ANALYSIS OF THYROXINE-BINDING GLOBULIN COMPLETE DEFICIENCY IN JAPANESE (TBG-CDJ) [NIHONJIN NO TBG KANZEN KESSONSHO (TBG-CDJ) NO HASSHO KIJO NI KANSURU KENKYU] **c51**
Yoshitaka Miura, Fukushi Kanbe, Yuichi Mori, Ikuo Yamamori, Yoshiyuki Tani, Yoshiharu Murata, Yutaka Oiso, and Hisao Seo *In its* Annals of the Research Inst. of Environmental Medicine, Nagoya Univ., Volume 44 25 Mar. 1993 p 161-165 In JAPANESE (For primary document see N94-27442 07-52)
(Grant MOE-04671468)
Avail: CASI HC A01/MF A04

Thyroxine-binding globulin complete deficiency is a hereditary disease that is defined by a serum Thyroxine-Binding Globulin (TBG) level of less than 5 mg/l. It has several subtypes including Thyroxine-Binding Globulin Complete Deficiency in Japanese (TBG-CDJ) which produces TBG with a deficit of 22 amino acids from the C-terminal, probably because of mistranslation of genetic code resulting from a deficit of one base. The purpose of this study was to reveal the mechanism of TBG-CDJ by examining the synthesis and release of TBG in COS-1 cells derived from a monkey's renal cells to which normal TBG (TBG-N) or mutant TBG (TBG-CDJ) was induced. As a result, the presence of intracellular TBG was identified in the cell induced TBG-CDJ for a relative long period. This suggests that something interfered with the release of normal TBG in the TBG-CDJ cells. From results of cell fractionation and sensitivity to endoglycosidase H, it was revealed that TBG was stored in RER (Rough-Surfaced Endoplasmic Reticulum) and was not transported to Golgi bodies. This is probably due to the C-terminal which might be important for intracellular transportation was varied in TBG-CDJ, and the tertiary structure was also considered to be changed.
Author (NASDA)

N94-27483# Nagoya Univ. (Japan). Research Inst. of Environmental Medicine.
DEVELOPMENT OF PURKINJE CELLS IN VITRO [BAIYOKEI NI OKERU PURUKINE SAIBO NO BUNKA] **c51**
Yoshiko Takagishi, Manabu Inoue (Mie Univ., Japan.), Takahito Sugimoto (Mie Univ., Japan.), and Hideki Yamamura *In its* Annals of the Research Inst. of Environmental Medicine, Nagoya Univ., Volume 44 25 Mar. 1993 p 166-169 In JAPANESE (For primary document see N94-27442 07-52)
Avail: CASI HC A01/MF A04

This study examined the development of Purkinje cells in a serum-free medium. The cerebellum of newborn mice or one week-old mice were trypsinized, and the free cells were cultivated in the serum-free medium at 37 C and under 5 percent CO2. To identify Purkinje cells, the antibodies for vitamin D-dependent Ca Binding Protein (CaBP) that are present in Purkinje cells were used for immunostain. As a result, slightly large sphere cells were stained at the first day of the cultivation. At the seventh day, Purkinje cells were observed with long axons and short dendrites that became longer at the 14th day and at the 21st day. Purkinje cells with branched axons were observed. The process of cell development in vitro was almost similar to that in vivo. It was reported that synapses of granule cells and Purkinje cells were observed electrophysiologically in vitro. Therefore cultivation of undeveloped Purkinje cells might be a useful model system to study the developing of nerve cells in the cerebellum.
Author (NASDA)

N94-27484# Nagoya Univ. (Japan). Research Inst. of Environmental Medicine.
DEVELOPMENTAL EXPRESSION OF PROTEIN KINASE C TYPE 1 ISOZYME IN SUNCUS AND RAT CEREBELLA [SUNKUSU TO RATTO NO SHONO NI OKERU PUROTEINKINAZE C1 GATA AISOZAIMU NO HATSUGEN] **c51**
Shizu Hayasaka, Yoshiko Takagishi, Senichi Oda, Minoru Inoue, and Hideki Yamamura *In its* Annals of the Research Inst. of Environmental Medicine, Nagoya Univ., Volume 44 25 Mar. 1993 p 170-173 In JAPANESE (For primary document see N94-27442 07-52)
Avail: CASI HC A01/MF A04

This study compared the development of the cerebellum between suncuses and rats by the expression of protein kinase C type 1 isozyme which is only present in the nervous system, especially in the Purkinje cells of rats and rabbits. The expression was identified by immunohistological method and immuno-blot method; i.e., the cerebellums were extracted from zero, one, three, five, 10, 15, 21, and 42 day-old suncuses and rats were sliced, immunostained, and observed microscopically, or homogenated and analyzed by electrophoresis. Purkinje cells were observed in the cerebellum of newborn suncuses, and their numbers increased as time passed, while they were not found until the third day in rats. In the immunohistological study, Purkinje cells were identified by type 1 isozyme in newborn suncuses and in 15 day-old rats. In the immuno-blot study, these cells were expressed in newborn suncuses and in 10 day-old rats. This suggests that the development of Purkinje cells was underway in suncuses at birth because their pregnancy period is longer than rats. Author (NASDA)

N94-27485# Nagoya Univ. (Japan). School of General Education.

ABNORMAL DEVELOPMENT OF SEROTONIN NERVE FIBERS IN THE CEREBRAL CORTEX OF YOUNG RATS WITH METHYLAZOXYMETHANOL INDUCED MICROCEPHALY [MECHIRUAZOKISHIMETANORU NI YORU JIKKENTEKI SHOTOSHO RATTO NO DAINO HISHITSU NI OKERU SEROTONIN SHINKEI SENI NO SEIGO SHOKI HATTATSU IJO] c51

Atsushi Funahashi, Minoru Inoue, and Hideki Yamamura *In its* Annals of the Research Inst. of Environmental Medicine, Nagoya Univ., Volume 44 25 Mar. 1993 p 174-176 In JAPANESE (For primary document see N94-27442 07-52)

Avail: CASI HC A01/MF A04

In a previous study, it was demonstrated that rats in which microcephaly was induced by intraperitoneal injection of Methylazoxymethanol (MAM) on the 15th day of pregnancy (MAM rat) had underdeveloped serotonin nerve fibers in the raphe nuclei. There are some reports that monoamine concentration, including serotonin, is increased in the cerebral cortex and other subcortex regions of MAM rats. This study compared the distribution of serotonin nerve fibers in the visual cortex between a MAM rat group and control group. Both groups rats were killed on the first, third, or fifth day after birth, the brain was extracted, and the brain was examined for abnormal development of serotonin nerve fibers and nerve endings in the visual cortex by immunohistological method. Author (NASDA)

N94-27486# Nagoya Univ. (Japan). Research Inst. of Environmental Medicine.

EFFECTS OF ML-9, A MYOSIN LIGHT-CHAIN KINASE INHIBITOR, ON PREIMPLANTATION DEVELOPMENT OF THE MOUSE [MAUSU NO CHAKUSHOMAE HASSEI NI OYOBOSU MIOSHIN KEISA KINAZE SOGAIZAI ML-9 NO EIKYO] c51

Nurul Kabir, Hideki Yamamura, Yoshiko Takagishi, Minoru Inoue, Senichi Oda, and Hiroyoshi Hidaka *In its* Annals of the Research Inst. of Environmental Medicine, Nagoya Univ., Volume 44 25 Mar. 1993 p 177-179 In JAPANESE (For primary document see N94-27442 07-52)

(Grant MOE-04670012)

Avail: CASI HC A01/MF A04

The purpose of this study is to reveal whether myosin light-chain kinase participates in preimplantaion development. Rat embryos were extracted 44 hours after fertilization, and they were cultivated for four days at 37 C in air containing 5 percent CO2. In the medium, an inhibitor of myosin light-chain kinase, 1-(5-chloronaphthalene 1-sulfonyl) 1H-hexahydro 1,4-diazepine hydrochloride (ML-9), was added at concentrations of 1, 10, or 50 micro M. The development was expressed by biological ages corresponding to each developing stage, and the relation with the biological age and time was examined. As a result, development of the embryo was inhibited by ML-9 in a dose-dependent manner. This implies that myosin light-chain kinase may participate in the preimplantation development of a mouse, and the intracellular regulation may be mediated by Ca-calmodulin-myosin light-chain kinase pathway. Author (NASDA)

N94-27487# Nagoya Univ. (Japan). Research Inst. of Environmental Medicine.

COMPACTION-LIKE BLASTOMERE AGGREGATION CAUSED BY 1-OLEOYL-2-ACETYLGLYCEROL IN MOUSE EMBRYOS: AN ELECTRON MICROSCOPIC OBSERVATION [1-OREOIRU-2-ASECHIRUGURISERORU NI YORI CONPAKUSHON YO NO KAKKYU GYOSHU O OKOSHITA MAUSUHAI NO DENKENTEKI KANSATSU] c51

Toshihiko Kumazawa, Yoshiko Takagishi, Mami Osugi (Mie Univ., Japan.), and Hideki Yamamura *In its* Annals of the Research Inst. of Environmental Medicine, Nagoya Univ., Volume 44 25 Mar. 1993 p 180-182 In JAPANESE (For primary document see N94-27442 07-52)

Avail: CASI HC A01/MF A04

It is known that 1-oleolyl-2-acetylglycerol (1,2-OAG), an activator of proteinkinase, causes compaction-like aggregation in embryos in two, four, and eight-celled stages. This study examined the compaction-like aggregation induced by 1,2-OAG using an electron microscopy, especially the boundary surface of the blastomere and the microvillus on the outer surface, and compared it with physiological compaction. Embryos were extracted from B6C3F1 mice, cultivated till two, four, eight, or compaction stage, and 1,2-OAG was added. The embryos cultivated in the 1,2-OAG free medium had microvillus on the surface of blastomeres in two, four, and eight-celled stages, but they did not have a intracellular junction. In the 1,2-OAG treated embryos, microvillus was observed on the outer surface of blastomeres but not in the boundary surface, and the intracellular junction was not observed. The embryos with physiologically induced compaction had microvillus on the outer surface, and the intracellular junction was formed between the boundary surfaces. Author (NASDA)

N94-27488# Seinan Gakuin Univ., Fukuoka (Japan).

INDUCTIVE DIFFERENTIATION OF NERVE CELLS IN MOUSE EMBRYONIC ECTODERM AT EARLY PRIMITIVE STREAK STAGE BY RETINOIC ACID [RECHINOINSAN NI YORU SHOKI GENSHI SENJOKI HAISEIGAIHAIYO KARANO SHIMKEI SAIBO NO YUDOTEKI BUNKA] c51

Kiyoko Yamamoto and Hideki Yamanura (Nagoya Univ., Japan.) *In* Nagoya Univ., Annals of the Research Inst. of Environmental Medicine, Nagoya Univ., Volume 44 25 Mar. 1993 p 183-185 In JAPANESE Sponsored by Narishige Zoological Science Award (For primary document see N94-27442 07-52)

Avail: CASI HC A01/MF A04

Retinoic acid has a strong teratogenic effect, and it participates in embryonic development extensively. In previous studies, the mouse embryonic ectoderm was cultivated in vitro at the early primitive streak stage, and it was found that most embryos differentiated to epithelial cells and fibroblasts but did not seem to be committed to nerve cells. This study examined whether the embryonic ectoderm can differentiate to nerve cells in the presence of Retinoic Acid (RA). The embryos were extracted from mice at the early primitive streak stage, cultivated in a medium with RA for 20 hours, then removed to an RA-free medium. Cell differentiation was observed morphologically, and nerve cells were identified by the immunohistological method using anti-neurofilament monoclonal antibodies. As a result, the differentiation of nerve cells was observed at the fifth day of cultivation, and this was identified immunohistologically. However, the number of differentiated nerve cells was not constant among each culture. Author (NASDA)

N94-27489# Nagoya Univ. (Japan). Research Inst. of Environmental Medicine.

ANORECTAL MALFORMATIONS INDUCED BY INTRAPERITONEAL INJECTION OF ALL-TRANS RETINOIC ACID IN SUNCUS [SUNKUSU NI OKERU ORU TORANSU RECHINOIN SAN FUKUKONAI TOYO NI YORU SAKO NO YUHATSU] c51

Ryozo Hashimoto, Senichi Oda, Minoru Inoue, and Hideki Yamamura *In its* Annals of the Research Inst. of Environmental Medicine, Nagoya Univ., Volume 44 25 Mar. 1993 p 186-188 In JAPANESE (For primary document see N94-27442 07-52)

Avail: CASI HC A01/MF A04

All-trans Retinoic Acid (RA) is a strong teratogenic agent that causes several malformations including anorectal malformation. The incidence of human anorectal malformation is reported to be relatively high (0.02 percent), so that it is important to study the development mechanism using animal models. The purpose of this study was to clarify whether a suncus is available for a experimental model of malformation development. Therefore, the suitable amount and timing of RA administration was determined to achieve high incidence of anorectal malformation. RA was injected 50, 100, or 200 mg/g weight to suncuses intraperitoneally at the 10th, 11th, 12th, or 13th day of pregnancy. Corn oil was injected as a control in the same way. The fetuses were extracted at the 27th day and observed microscopically. The highest incidence of anorectal malformation was observed in the group administered 100 mg/g weight RA at 12th day (88.2 percent). Administration at 10th day did not cause anorectal malformation. Administration at the 13th day caused tail malformation and only one case of anorectal malformation. In the case of 200 mg/g weight RA administration, all of the fetuses were dead. As a result, anorectal malformation can be induced by RA in suncuses with high incidence. This could be useful for pathological study of the development of anorectal malformation. Author (NASDA)

N94-27490# Eisai Co. Ltd., Hashima (Japan). Dept. of Drug Safety Research.

CROSS-SECTIONAL ANATOMY OF DAY 30 SUNCUS FETUSES [SUNKUSU 30 NICHI TAIJI NI OKERU ODAMEN NI YORU NAIBU KIKAN KANSATSU] **c51**

Nobuhiro Niwa, Takao Matsubara, Senichi Oda (Nagoya Univ., Japan.), Minoru Inoue (Nagoya Univ., Japan.), and Hideki Yamamura (Nagoya Univ., Japan.) *In* Nagoya Univ., Annals of the Research Inst. of Environmental Medicine, Nagoya Univ., Volume 44 25 Mar. 1993 p 189-192 In JAPANESE (For primary document see N94-27442 07-52)

Avail: CASI HC A01/MF A04

The study of the safe administration of drugs is important in the area of preclinical studies. Rats are usually used to evaluate teratogeny of drugs, and the test methods have already been established. Although teratogeny has been observed in suncuses, the use of suncuses in safety studies has not been established. This report describes the observation of cross-sectional anatomy using normal 30 day suncus fetuses. Author (NASDA)

N94-27491# Aichi Agricultural Research Center, Naga (Japan).

SKELETAL DEVELOPMENT AND OSSIFICATION OF THE SWINE FETUSES [BUTA TAIJI NO KOKKAKU KEISEI KATEI NO KANSATSU] **c51**

Ayumi T. Ichikawa, Senichi Oda (Nagoya Univ., Japan.), and Minoru Inoue (Nagoya Univ., Japan.) *In* Nagoya Univ., Annals of the Research Inst. of Environmental Medicine, Nagoya Univ., Volume 44 25 Mar. 1993 p 193-196 In JAPANESE (For primary document see N94-27442 07-52)

Avail: CASI HC A01/MF A04

Recently, the experimental demand for swine has increased, especially in the field of medicinal biology. For experimental use, it is necessary to understand normal fetal development, and ossification can be used as an index after organogenesis. This report presents the observational results of the timing of ossification and order in swine fetuses. The fetuses were extracted from the 32nd to 53rd day of pregnancy, fixed in ethanol, stained for the bones, and observed microscopically. As a result, ossification began in the mandible and the regions around the orbits on the 34th day. Until the 39th day, ossification of the cranium and facial bones had begun except for hyoid bone which began after the 52nd day. In the spine, ossification of the cervical vertebrae, ribs, and lumbar vertebrae was observed on the 39th day. Other vertebrae began to develop from anterior to posterior. For the limb bones, the humeri ossified on the 34th day. The scapulae, ulnae, radii, ilium, femora, tibiae, and fibrae ossified on the 39th day. The order of skeletogeny of feet and hooves was also determined in detail. Author (NASDA)

N94-27492# Yagi Memorial Park, Mitake (Japan). Inst. of Applied Biochemistry.

DEVELOPMENT OF INBRED STRAINS FROM JAPANESE WILD RATS (RATTUS NORVEGICUS) [NIHONSAN YASEI RATTO (RATUSU NORUBEGIKUSU) KARANO KEITO IKUSEI] **c51**

Kyoko Ono, Yoshiki Niwa, Shizuka Kato, Senichi Oda (Nagoya Univ., Japan.), Kyoji Kondo, and Hideki Yamamura (Nagoya Univ., Japan.) *In* Nagoya Univ., Annals of the Research Inst. of Environmental Medicine, Nagoya Univ., Volume 44 25 Mar. 1993 p 197-201 In JAPANESE (For primary document see N94-27442 07-52)

Avail: CASI HC A01/MF A04

This report discusses the development of inbred strains of Japanese wild rats (Rattus norvegicus) and the characteristics of these strains. Twelve pairs of wild rats were bred, and inbred strains were developed by sibling mating. The gene of hair color was analyzed for each of the strains, and a biological marker gene was detected by electrophoresis. As a result, five inbred strains were developed: A, B, C, D, and E. Strain A rats were gentle, docile, and seemed most suitable for experimental rats. They have stable breeding potential. Strain B rats have the mutant gene for hair color and eye color, and their characteristics and fertility are similar to those of strain A rats. Strain C rats were undersized, and may have a maker gene--transferrin mutant. Strain D rats showed marked maternal aggression. Strain E rats were developed from a different pair of captured rats from the other four strains. They are slightly gentle and docile, and their breeding potential is unstable. Author (NASDA)

N94-27493# Academy of Sciences (USSR), Novosibirsk. Inst. of Cytology and Genetics.

ELECTRON MICROSCOPIC ANALYSIS OF MEIOTIC CHROMOSOME PAIRING IN MALE HOUSE MUSK SHREW, SUNCUS MURINUS [SUNKUSU OSU NI OKERU SENSHOKUTAI TAIGO NO DENSHI KENBIKYO NI YORU KAISEKI] **c51**

Pavel M. Borodin, Senichi Oda (Nagoya Univ., Japan.), Yoshiko Takagishi (Nagoya Univ., Japan.), Minoru Inoue (Nagoya Univ., Japan.), and Hideki Yamamura (Nagoya Univ., Japan.) *In* Nagoya Univ., Annals of the Research Inst. of Environmental Medicine, Nagoya Univ., Volume 44 25 Mar. 1993 p 202-204 In JAPANESE (For primary document see N94-27442 07-52)

Avail: CASI HC A01/MF A04

It has been reported that crossbred suncuses express a high frequency of mutation in size, shape, or number of chromosomes. Hence, they are an appropriate model for studying pairing or reconstitution of chromosomes. This study examines the chromosome pairing and shape of nucleolus from zygotene stage to diplotene stage of meiosis using spermatocyte of crossbred suncuses. The subjects were 17 mature male suncuses from eight breeding groups. The testicles were extracted, separated with a thin needle, fixed on a slide, and staind by silver staining. The spermatocyte chromosomes were observed by an electron microscopy and compared with other mammals, such as the Chinese hamster or mouse. As a result, no difference was observed between suncus and other mammals in respect to the behavior of chromosomes and shape of spermatocytes in prophase of meiosis. However, the behavior of the sex chromosome was apparently different from other mammals; i.e., the sex vesicle appeared in early prophase in the suncus, as opposed to late prophase in other mammals. Detail observation of pairing and shape of nucleolus in prophase of meiosis may be useful to study complicated meiosis in crossbreeding suncus with various number or shape of chromosomes. Author (NASDA)

N94-27494# Nagoya Univ. (Japan). Research Inst. of Environmental Medicine.

EFFECT OF PGE2 RECEPTOR AGONISTS BUTAPROST, M AND B 28767 AND AN ANTAGONIST AH 6809 ON THE BK RESPONSE OF VISCERAL POLYMODAL RECEPTORS [NAIZO PORIMODARU JUYOKI NO BURAJIKININ HANNO NI TAISURU PUROSUTAGURANJIN E2 JUYOTAI NO AGONISUTO BUTAPUROSUTO, M/B 28767, OYOBI ANTAGONISUTO AH 6809 NO KOKA] **c51**

Hisashi Koda, Kazue Mizumura, and Takao Kumazawa *In its* Annals of the Research Inst. of Environmental Medicine, Nagoya Univ., Volume 44 25 Mar. 1993 p 205-207 In JAPANESE (For primary document see N94-27442 07-52)

(Grant MOE-04255103)

Avail: CASI HC A01/MF A04

The polymodal receptor is one of the noxious receptors and can respond to extensive noxious stimulation including mechanical stimulation, heat, and dolorogenic substances. An inflammatory mediator, Prostaglandin E2 (PGE2), does not stimulate the polymodal receptor by itself; however, it strengthens the effects of heat or Bradykinin (BK) on the receptor. This study examined subtypes of the PGE2 receptor that might be associated with BK responses. Author (NASDA)

N94-27495# Nagoya Univ. (Japan). Research Inst. of Environmental Medicine.

EXCITATION OF CUTANEOUS POLYMODAL RECEPTOR INDUCED BY SYMPATHETIC STIMULATION IN ADJUVANT-INDUCED ARTHRITIS RATS [AJUBANTO KANSETSUEN RATTO NI MIRARETA KOKAN SHINKEI SHIGEKI NI YORU HIFU PORIMODARU JUYOKI KOFUN] **c51**

Jun Sato, Shigeyuki Suzuki, Tomoko Iseki, and Takao Kumazawa *In its* Annals of the Research Inst. of Environmental Medicine, Nagoya Univ., Volume 44 25 Mar. 1993 p 208-210 In JAPANESE Sponsored by Uehara Memorial Foundation and Research Foundation for Oriental

Medicine (For primary document see N94-27442 07-52)
(Grants MOE-04770070; MOE-04255103)
Avail: CASI HC A01/MF A04

It was demonstrated that the polymodal receptor, one of the pain receptors, causes paralgesia via the sympathetic nerve, and that catecholamine alpha-2 receptors participate in this pain transmission. This report presents the effect of sympathetic nerves on polymodal receptors using adjuvant-induced arthritis rats. Author (NASDA)

N94-27496# Nagoya Univ. (Japan). Research Inst. of Environmental Medicine.

SELECTION OF SITE INJECTING ADJUVANT IN CHRONIC INFLAMMATION MODEL [MANSEI ENSHO MODERU NI OKERU KIENZAI TOYO BUI NO SENTAKU] **c51**

Shigeyuki Suzuki, Tomoko Iseki, Kazue Mizumura, and Takao Kumazawa *In its* Annals of the Research Inst. of Environmental Medicine, Nagoya Univ., Volume 44 25 Mar. 1993 p 211-213 In JAPANESE (For primary document see N94-27442 07-52)
(Grant MOE-04255103)
Avail: CASI HC A01/MF A04

As an experimental model for chronic inflammation, rats with arthritis induced by adjuvant are used extensively. A phologogenic agent is usually administered to these rats at the base of the tail or the foot. A severe inflammatory response with marked swelling usually occurs at the administration site on the first day. This rapid and severe response is not suitable for experiments that measure the foot volume as an index of inflammation. Therefore, injecting the adjuvant at the one-third distal site of the tail was used in thisstudy. The purpose was to clarify whether the injection causes suitable inflammatory response as a model of chronic inflammation and to prepare control data on these rats. Author (NASDA)

N94-27497# Nagoya Univ. (Japan). Research Inst. of Environmental Medicine.

INFLUENCE OF MECHANICAL STIMULATION ON INFLAMMATORY EDEMA [UNDO SHIGEKI NO ENSHOSEI FUSHU NI TAISURU EIKYO] **c51**

Shigeyuki Suzuki, Tomoko Iseki, Kazue Mizumura, and Takao Kumazawa *In its* Annals of the Research Inst. of Environmental Medicine, Nagoya Univ., Volume 44 25 Mar. 1993 p 214-216 In JAPANESE (For primary document see N94-27442 07-52)
(Grant MOE-04255103)
Avail: CASI HC A01/MF A04

In previous studies, it was shown that inflammatory edema could be affected by a neurogenic inflammation caused by polymodal receptor stimulation using adjuvant-induced arthritis rats. This study examined the effect of mechanical stimulus on inflammatory edema while varying the concentration of the phlogogenic agent. The subjects were 13 Lewis strain rats, to which either 0.6 ($N = 3$), 0.4 ($N = 3$), 0.2 ($N = 5$), or 0.1 mg ($N = 2$) of adjuvant was administered at the one-third distal site of the tail. Each rat was forced to move everyday after the administration, and the foot volume was measured before and after the movement and compared with non-movement group. As a result, the foot volume is not different between the movement group and non-movement group in the case of administered 0.4 mg and 0.6 mg adjuvant; however, 0.2 mg adjuvant rats revealed remarkably larger foot volume in the movement group than the non-movement group. The 0.1 mg adjuvant rats, however, showed the opposite response to 0.2 mg adjuvant rats; the foot volume was smaller in the movement group. Assuming that the greater the concentration of phlogogenic agent gets, the more severe the inflammation becomes, these results suggest that polymodal receptors may be stimulated by mechanical stimulus in a certain inflammatory state and may result in occurrence of edema by neurogenic inflammation. Author (NASDA)

N94-27498# Nagoya Univ. (Japan). Coll. of Medical Technology.

THE EFFECT OF NALOXONE ON SLEEPING TIME IN ADJUVANT ARTHRITIC RATS [CHOKI AJUBANTO KANSETSUEN RATTO NO MASUI KOKA JIKAN NI TAISURU NAROKISON ZENTOYO NO EIKYO] **c51**

Tomoko Iseki, Shigeyuki Suzuki, Kazue Mizumura, and Takao Kumazawa *In its* Annals of the Research Inst. of Environmental Medicine, Nagoya Univ., Volume 44 25 Mar. 1993 p 217-218 In JAPANESE (For primary document see N94-27442 07-52)
(Grant MOE-04255103)
Avail: CASI HC A01/MF A04

It was known that the narcotic effect was prolonged in adjuvant-induced arthritic rats, probably due to decrease of the liver microsome activity. Recently, a finding was obtained that opioid analgesics prolongs the narcotic effect of pentobarbital. This suggests that the opioid pathway might be related to the prolongation in adjuvant-induced arthritic rats, and this possibility was examined in this study. The subjects were six Lewis strain rats classified into the control group ($N = 3$) and the adjuvant-induced arthritis group ($N = 3$). In both subjects the narcotics were administered intraperitoneally, and the period that wink reflex disappeared was measured as the effective time of the narcotics. The same measurement was performed on subjects preadministered with naloxone. As a result, the effective time of adjuvant group was longer than that before adjuvant administration; however, in case of preadministration of naroxone, the effective time became shorter. In the control group, the effective time became slightly shorter in case of naroxone preadministration. Author (NASDA)

N94-27499# Nagoya Univ. (Japan). Research Inst. of Environmental Medicine.

EFFECTS OF CAPSAICIN ON FRESHLY DISSOCIATED RAT DORSAL ROOT GANGLION CELLS [RATTO SEKIZUI GOKON SHINKEISETSU BUNRI SAIBO NI TAISURU KAPUSAISHIN NO KOKA] **c51**

Masanori Kasai, Kazue Mizumura, and Takao Kumazawa *In its* Annals of the Research Inst. of Environmental Medicine, Nagoya Univ., Volume 44 25 Mar. 1993 p 219-220 In JAPANESE (For primary document see N94-27442 07-52)
(Grant MOE-04255103)
Avail: CASI HC A01/MF A04

It was demonstrated that polymodal receptors responsive to noxious stimuli are sensitive to capsaicin (CAP), a phlogogenic agent, in peripheral levels. The fact that polymodal receptors present in Dorsal Root Ganglions (DRG) and the cells in DRG can bind with and be stimulated by CAP suggests that the membrane of DRG cells might respond to CAP. Author (NASDA)

N94-27500# Nagoya Univ. (Japan). Research Inst. of Environmental Medicine.

SIZE DISTRIBUTION OF RETROGRADELY LABELED DORSAL ROOT GANGLION CELLS: TEST OF NORMALITY [GYAKKOSEI TORESAHO NI YORI HYOSHIKI SARETA GOKON SHINKEISETSU SAIBO NO OKISA NO BUNPU: SEIKISEI NO KENTEI] **c51**

Ryoko Tamura, Kazue Mizumura, and Takao Kumazawa *In its* Annals of the Research Inst. of Environmental Medicine, Nagoya Univ., Volume 44 25 Mar. 1993 p 221-223 In JAPANESE (For primary document see N94-27442 07-52)
(Grant MOE-04255103)
Avail: CASI HC A01/MF A04

In this study, the size of dosal root ganglion cells was compared with other ganglion cells using a retrograde tracer method. Fast Blue (FB) was injected to the testicle and epididymis or the left superior testicular nerve of male dogs, and the diameter of the cells in the first and second lumber vertebra (L1 and L2) was measured. In case of administering FB at the testicle, the mean diameter of labelled cells was 35.7 micrometers, whereas it was 31.7 micrometers when administered at the superior testicular nerve. The results of the normality test revealed that the cells labelled at the testicle were intermingled with several sizes of cells. It is known that the dorsal root ganglion cells can be morphologically classified into small cell and large cell. The cells labelled at the superior testicular nerve were small cells, which implies that afferent neurons that control the testicle via superior testicular nerve may correspond to small cells. When FB was administered at the testicle, the fluorochrome may stain not only afferent neurons but also other cells. Therefore, the size of afferent neuron could be determined by the FB-labelled cells administered at the superior testicular cells. It can be concluded that the test of normality is useful to detect intermingled cells in the study using retrograde tracer method. Author (NASDA)

N94-27501# Yasui Acupuncture Clinic, Nagoya (Japan).

CHANGES IN PAIN SENSATION INDUCED BY REPETITIVE APPLICATION OF NOXIOUS HEAT PULSES TO THE HUMAN SKIN [SHINGAITEKI FUKUSHANETSU SHIGEKI NO KURIKAESHI NI YORU HITO HIFU TSUKAKU NO HENKA]

Hirotaka Yasui, Kazuhiko Kumazawa (Aichi Medical Univ., Nagakute, Japan.), Kazue Mizumura (Nagoya Univ., Japan.), and Takao Kumazawa (Nagoya Univ., Japan.) *In* Nagoya Univ., Annals of the Research Inst. of Environmental Medicine, Nagoya Univ., Volume 44 25 Mar. 1993 p 224-226 In JAPANESE (For primary document see N94-27442 07-52)
(Grant MOE-04255103)
Avail: CASI HC A01/MF A04

Pain can be classified into two types: primary pain, which is weakened by repetitive stimuli; and secondary pain, which is dull and strengthened by repetitive stimuli. The purpose of this study was to examine the change of primary pain sensation when repetitive stimuli of noxious heat pulses was applied to the human skin. Author (NASDA)

N94-27502# Kinjo Gakuin Univ., Nagoya (Japan). Dept. of Home Economics.

INTERACTION BETWEEN ENDOGENOUS OPIOID AND CHOLECYSTOKININ (CCK) IN MODULATING RESPIRATORY RESPONSES INDUCED BY THIN-FIBER MUSCULAR AFFERENTS [KI SAIKEI SHINKEI NYURYOKU NI YORU KOKYU HANNO NO SHUSHOKU NI OKERU NAIINSEI OPIOIDO TO KORESHISUTOKININ (CCK) NO SOGO SAYO] **c51**

Eiko Tadaki, Yasuko Kozaki (Nagoya Univ., Japan.), and Takao Kumazawa (Nagoya Univ., Japan.) *In* Nagoya Univ., Annals of the Research Inst. of Environmental Medicine, Nagoya Univ., Volume 44 25 Mar. 1993 p 227-229 In JAPANESE (For primary document see N94-27442 07-52)
(Grant MOE-04255103)
Avail: CASI HC A01/MF A04

It was reported that Cholecystokinin (CCK) participates in tachyphylaxy of opioid analgesics. The CCK receptor is classified into two subtypes; type A and type B. The effect of a type B receptor was examined using highly selective inhibitors, L-365 and 260, because B receptors are present mainly in the brain. The thin-fiber muscular afferent nerves of cats were stimulated every 35 minutes and L-365 or 260 was injected slowly for 1 minute intravenously, while respiratory response was monitored, and respiratory output was determined as an index. The concentration of inhibitor was 0.03, 0.1, 0.2, 0.3, 1.0 mg/kg, in the order of administration, and, at the last of them, naroxone, an inhibitor of opioids, was administered. As a result, the tachyphylaxis of Aspiratory Suppression (AS) that was induced by repetitive stimulation of thin-fiber muscular afferent nerves was inhibited by CCK-B (CCK Type-B) receptor inhibitor, L-365 and 260, in dose-dependent manner. It was also revealed that there is high correlation between the degree of tachyphylaxy and degree of inhibition. Therefore, this tachyphylaxy may be mediated by CCK-B receptors. L-365 and 260 dominantly affect the respiratory rate. This suggests that tachyphylaxy of AS may not result from deletion of endogenous opioid, but from activation of CCK receptors by excitation of thin-fiber muscular afferent nerve which modulates respiratory rate. Author (NASDA)

N94-27503# Nagoya Univ. (Japan). Research Inst. of Environmental Medicine.

EFFECTS OF PERFUSION OF AMIODARONE ON ELECTROPHYSIOLOGICAL PROPERTIES IN SINGLE RABBIT VENTRICULAR MYOCYTES [AMIODARONE KYUSEI TOYO GA IEUSAGI TANRI SHINSHITSUKIN SAIBO NI OYOBOSU DENKI SEIRIGAKUTEKI SAYO] **c51**

Kaichiro Kamiya, Jianhua Cheng, Itsuo Kodama, and Junji Toyama *In its* Annals of the Research Inst. of Environmental Medicine, Nagoya Univ., Volume 44 25 Mar. 1993 p 230-232 In JAPANESE (For primary document see N94-27442 07-52)
Avail: CASI HC A01/MF A04

The acute administration of amiodarone, an antiarrhythmic agent, was studied and the data was compared with chronic administration. The ventricular myocytes were isolated from rabbit hearts, perfusated with perfusate containing amiodarone, and action potential was measured under steady stimulating frequency. As a result, Action Potential Duration (APD) was shortened by amiodarone acute administration, and this did not depend on the stimulating frequency. The previous study demonstrated that APD was remarkably prolonged by chronic administration of amiodarone. Therefore, electrophysiologically reverse effects were observed in rabbit ventricular myocytes by the two administration methods. In respect to ion current, amiodarone acute administration interfered Na current and Ca current, and the suppression of these inward currents may result in the shortening of APD. In addition, transient outward current induced by repetitive depolarization was not affected by amiodarone acute administration, whereas it was decreased by chronic administration. Author (NASDA)

N94-27504# Nagoya Univ. (Japan). Research Inst. of Environmental Medicine.

FAST AND SLOW ONSETS OF Na CHANNEL BLOCKING ACTIONS DUE TO LIDOCAINE AND DISOPYRAMIDE USING CONCENTRATION-CLAMP METHOD [NODO KOTEIHO NI YORU ENUE NATORIUMU CHANERU YOKUSEIYAKU NO SAYO HATSUGEN KIJO NI KANSURU KENTO] **c51**

Takafumi Anno, Eiichi Watanabe, Akihiko Taniguchi, Itsuo Kodama, and Junji Toyama *In its* Annals of the Research Inst. of Environmental Medicine, Nagoya Univ., Volume 44 25 Mar. 1993 p 233-235 In JAPANESE (For primary document see N94-27442 07-52)
Avail: CASI HC A01/MF A04

The purpose was to examine the change of Na current by lidocaine and disopyramide using concentration-clamp method, and to consider how the drugs bind the channel protein. The ventricular myocytes were isolated from guinea pig hearts and the Na current was measured using whole-cell clamp method. As a result, Na current was interfered slowly, at the time constant of 10 seconds, when disopyramide was added extracellularly. In case that lidocaine was added, Na channel was blocked by two steps; one is rapid block with the time constant of less than 0.1 seconds, and another is slow block that reached steady state for 60 to 120 seconds. The concentration of both drugs were so high that the Na current suppression depended not on electric potential or stimulating rate, but on binding the drug with the channel protein. If binding site of lidocaine presents on the only outer surface of the cell membrane, the time constant can be expressed using binding constant (k) and dissociation constant (l) as the following formula; $1/(k(D) + l)$. In order to bind the channel protein, drugs must pass through a extracellular hydrophilic path as well as intermembrane hydrophobic path. This suggests that the slow time constant of disopyramide and lidocaine may correspond to the hydrophobic pathway, and the rapid time constant of lidocaine, to the hydrophilic pathway. Author (NASDA)

N94-27505# Nagoya Univ. (Japan). Research Inst. of Environmental Medicine.

ELECTROPHYSIOLOGICAL EFFECTS OF MS-551, A NEW CLASS 3 ANTIARRHYTHMIC AGENT, ON ISOLATED RABBIT VENTRICULAR MUSCLES [KURASU 3 KOFUSEIMYAKUYAKU MS-551 NO IEUSAGI SHINSHITSUKIN NI TAISURU DENKI SEIRIGAKUTEKI SAYO] **c51**

Ryoko Suzuki, Itsuo Kodama, and Junji Toyama *In its* Annals of the Research Inst. of Environmental Medicine, Nagoya Univ., Volume 44 25 Mar. 1993 p 236-238 In JAPANESE (For primary document see N94-27442 07-52)
Avail: CASI HC A01/MF A04

MS-511, 1, 3-dimethyl 6-(2-(N-(2-hydroxethyl) 3-(4-nitrophenyl) propylamino) ethylamino) 2, 4-(1H, 3H)-pyrimidinedione hydrochloride, is a newly developed antiarrhythmic agent that can prolong the Action Potential Duration (APD) and effective refractory period mainly due to K channel blockage. The MS-551 was compared with sotalol and E-4031 in respect to prolongation of effective refractory period. Rabbit ventricular muscles were extracted, perfusated with perfusate containing MS-551, and the membrane potential was measured. As a result, MS-551 prolonged APD significantly at the concentration of 0.3 micro-M or more, without suppressing maximum upstroke velocity. The APD prolongation caused by sotalol and E-4031 showed remarkable reverse use-dependency within the range of 0.1 to 3.0 Hz of stimulus, whereas that by MS-551 showed diphasic rate-dependency. This suggests that MS-511 may suppress a different K channel from other drug suppression. Among various K channels in the myocytes, slow rectifying K channel may participate in the rate-dependent APD prolongation, and MS-551 may bind with the activated K channel because the effect emerged not at the first stimulating pulse but at the second pulse after a long pause. Author (NASDA)

N94-27506# Nagoya Univ. (Japan). Research Inst. of Environmental Medicine.

COMPARATIVE INVESTIGATION OF NEW CLASS 3 ANTIARRHYTHMIC DRUGS, E-4031 AND MS-551, ON ELECTROPHYSIOLOGICAL PROPERTIES IN ISOLATED RABBIT VENTRICULAR MYOCYTES [DAI 3 GUN KOFUSEIMYAKUYAKU E-4031, MS-551 GA IEUSAGI TANRI SHINSHITSUKIN SAIBO NI OYOBOSU DENKI SEIRIGAKUTEKI SAYO NO HIKAKU KENTO] c51

Jianhua Cheng, Kaichiro Kamiya, Itsuo Kodama, and Junji Toyama *In its* Annals of the Research Inst. of Environmental Medicine, Nagoya Univ., Volume 44 25 Mar. 1993 p 239-241 In JAPANESE (For primary document see N94-27442 07-52)

Avail: CASI HC A01/MF A04

The effect of newly developed Class 3 antiarrhythmic agents, E-4031 and MS-551 on electrophysiological property of myocytes, especially on action potential and transient outward current was examined. The ventricular myocytes were extracted from rabbit hearts, and membrane potential was measured using whole cell clamp method. As a result, Action Potential Duration (APD) was prolonged by E-4031 under low frequency stimulus in reverse use-dependent manner. On the other hand, MS-511 prolonged APD under high frequency stimulus in use dependent manner. However both drugs were similar in respect to APD prolongation without affecting maximum upstroke potential or action potential amplitude. In addition, they did not affect transient outward current that is an important factor to cause the notch in the first phase of the action potential and to regulate APD. Therefore, the APD prolongation by low frequency stimulus using E-4031 may not result from the effect on transient outward current. MS-511 prolongs APD with premature contraction which shows shorter coupling duration than E-4031, so that they may have different association and dissociation constants of drug and channel. Author (NASDA)

N94-27507# Nagoya Univ. (Japan). Research Inst. of Environmental Medicine.

EFFECTS OF CLASS 1 ANTIARRHYTHMIC DRUGS ON THE INTRAVENTRICULAR CONDUCTION: INFLUENCE OF FIBER ORIENTATION [KURASU 1 KOFUSEIMYAKUYAKU NIYORU SHINSHITSUNAI DENDO YOKUSEI TO SHINKIN SENI SOKO] c51

Masato Iida, Itsuo Kodama, and Junji Toyama *In its* Annals of the Research Inst. of Environmental Medicine, Nagoya Univ., Volume 44 25 Mar. 1993 p 242-244 In JAPANESE (For primary document see N94-27442 07-52)

Avail: CASI HC A01/MF A04

Class 1 drugs, such as Na channel blockers, were used for ventricular arrhythmia to lower the conductivity and excitability of the ventricle. Recently, it was revealed that the inhibition of conductivity caused reentry in the ventricle. The conduction and fiber orientation of ventricular epicardium surface when lidocaine or flecainide was added, in order to clarify the mechanism of arrhythmia caused by class 1 antiarrhythmic agents was examined. The ventricle was extracted from rabbit hearts, and the extracellular potential was recorded and mapped to draw isochronic lines of conduction on the surface. These lines became stable after 2 hours of perfusion, and drew ellipses extended to the longitudinal direction of the fibers (L-direction). Lidocaine inhibited the L-direction conduction at the stimulating frequency of 2.0 Hz or more, and flecainide showed the similar inhibition within the range of 0.2 to 3.0 Hz. These inhibitions augmented with increase of stimulating frequency. This rate-dependency may result from use-dependent block of Na channel. However, both lidocaine and flecainanide did not inhibit the conduction to the transversal direction of the fibers. Author (NASDA)

N94-27508# Nagoya Univ. (Japan). Research Inst. of Environmental Medicine.

EFFECTS OF CLASS 3 ANTIARRHYTHMIC AGENTS, E-4031 AND MS-551 ON VENTRICULAR REPOLARIZATION IN ISOLATED RABBIT HEARTS [IEUSAGI SHINSHITSU NO SAI BUNKYOKU NI TAISURU KURASU 3 KOFUSEIMYAKUZAI E-4031 TO MS-551 NO SAYO] c51

Hirokazu Iwata, Ryoko Suzuki, Kaichiro Kamiya, Itsuo Kodama, and Junji Toyama *In its* Annals of the Research Inst. of Environmental Medicine, Nagoya Univ., Volume 44 25 Mar. 1993 p 245-247 In JAPANESE (For primary document see N94-27442 07-52)

Avail: CASI HC A01/MF A04

It is known that class 3 antiarrhythmic agents can prolong action potential duration and refractory period, however it is uncertain whether these effects are different by each ventricular site, or how these drugs modify the repolarization in the entire ventricle. The effects of newly developed class 3 drugs, E-4031 and MS-551, were examined by mapping the electric potential of the heart surface. The hearts were extracted from rabbits, and heart surface potential were recorded and conductivity was mapped using a distant bipolar electrogram. As a result, it was demonstrated that E-4031 had a different effect from E-4031 prolonged the APD (Action Potential Duration) mainly in the apex, and increased spatial inequality of repolarization, whereas MS-551 did not cause inequality of ADP and repolarization in the entire left ventricle. It is known that class 3 drugs prolong APD and refractory period by inhibiting three types of K current, i.e., slow rectifying K(+) current, inward rectifying K(+) current, and transient outward current. The channels of these current are distributed unequally on the heart surface. This may be the reason why ADP and E-4031 effect was different by the sites of ventricle. Author (NASDA)

N94-27509# Nagoya Univ. (Japan). Research Inst. of Environmental Medicine.

ELECTRICAL COUPLING BETWEEN THE SINO-ATRIAL NODE AND ATRIAL MUSCLE: CELL TO CELL INTERACTION THROUGH AN EXTERNAL CIRCUIT AND ITS SIMULATION BY COMPUTER MODELING [DOBO KESSETSU TO SHINBOKAN NO DENKITEKI KETSUGO NI KANSURU KENKYU: GAIBU KAIRO O MOCHIITA SAIBO KETSUGO JIKKEN] c51

Eiichi Watanabe, Takafumi Anno, Itsuo Kodama, and Junji Toyama *In its* Annals of the Research Inst. of Environmental Medicine, Nagoya Univ., Volume 44 25 Mar. 1993 p 248-250 In JAPANESE (For primary document see N94-27442 07-52)

Avail: CASI HC A01/MF A04

Electric coupling between a multicellular sample or isolated myocyte and an external circuit simulating a gap junction able to change the conductivity was examined, and the electric coupling between sinoatrial node and atrial muscle was reviewed. The external circuit was consist of a voltage converter connected with an amplifier with membrane potential to membrane current converter, which can couple certain cells with other cells or a membrane model that can change the conductance like gap junction. Using this system, two experiments were performed. In one experiment, sinoatrial node cells were connected with a membrane model, however, spontaneous exciting cycle, depolarization velocity of the fourth phase, and action potential duration were not modified by the membrane model. This is probably because of insufficient space clamp due to low input resistance of the cells. Another experiment was that a single atrial cell of a guinea pig was connected with recorded action potential of the sinoatrial node. As a result, the atrial cell was excited, and as conductance increased, the action potential became similar to action potential in the sinoatrial node. Therefore, it can be concluded that this system is useful for quantitative evaluation of the cell-to-cell interaction and cellular excitability by electric coupling between a cell and a membrane model. Author (NASDA)

N94-27510# Nagoya Univ. (Japan). Research Inst. of Environmental Medicine.

A STUDY ON TISSUE EXCITATION OF CARDIAC MUSCLE UNDER ELECTRICAL FIELD STIMULATION [FIRUDO SHIGEKIKA SHINKIN NO KATSUDO DENI SAIDAI TACHIAGARI SOKUDO] c51

Akihiko Taniguchi, Takafumi Anno, Masaki Shirakawa (Toyohashi Univ. of Technology, Aichi, Japan.), Shiro Usui (Toyohashi Univ. of Technology, Aichi, Japan.), Itsuo Kodama, and Junji Toyama *In its* Annals of the Research Inst. of Environmental Medicine, Nagoya Univ., Volume 44 25 Mar. 1993 p 251-254 In JAPANESE (For primary document see N94-27442 07-52)

Avail: CASI HC A01/MF A04

Whether action potential by electrical field stimulation is affected by intercellular electrical interaction was examined. The right ventricular papillary muscles were extracted from guinea pig hearts, to which electrical field stimulation was given, and the upstroke phase of action potential was recorded, as well as the activation time was determined as a time to reach the maximum upstroke velocity (V(sub max)) for each phase. As a result, V(sub max) was similar to that of one-point stimulation at any part of the muscle, which was about half of the V(sub max) in a single cell. The activation time was dispersed within the range of approximately 2-3 msec. In this experiment, a two-dimensional sheet model was developed to simulate cell membrane with dispersed excitation stages. Using this model, it was revealed that when electrical field stimulation was given, the cells were not excited synchronously, but the excitation was propagated among cells. The change of field stimulation may vary the direction of conduction, and cause unequal excitation, because isochronic line of conduction was obviously changed according to the change of stimulus strength, and because there were sites that V(sub max) was changed largely by abrupt change of activation time. Therefore, it can be concluded that V(sub max) was affected by various intercellular interaction when electric field stimulation was given, so that V(sub max) should not be used as an index of availability of Na channels. Author (NASDA)

N94-27511# Nagoya Univ. (Japan). Research Inst. of Environmental Medicine.

BLOCK OF CARDIAC SODIUM CHANNELS BY Ro 22-9194 (R), A NEW ANTIARRHYTHMIC AGENT: EFFECTS ON THE MAXIMUM UPSTROKE VELOCITY (Vmax) OF SINGLE GUINEA PIG VENTRICULAR MYOCYTES [KOFUSEIMYAKUYAKU RO 22-9194 (R) NO SHINKIN NA CHANERU YOKUSEI SAYO: MORUMOTTO TANRI SHINSHITSUKIN SAIBO NO KATSUDO DENI SAIDAI TACHIAGARI SOKUDO (VMAX) NIYORU KENTO] **c51**

Kazuyasu Maruyama, Ryoko Suzuki, Takafumi Anno, Itsuo Kodama, and Junji Toyama *In its* Annals of the Research Inst. of Environmental Medicine, Nagoya Univ., Volume 44 25 Mar. 1993 p 255-258 In JAPANESE (For primary document see N94-27442 07-52)
Avail: CASI HC A01/MF A04

Ro 22-9194 (R), (2R)-2-amino N-(2, 6-dimethylphenyl) N-(3-(3-pyridyl) propyl) propionamiade D-tartrate is a newly developed antiarrhythmic agent. In previous study, it was demonstrated that the effect was dependent on blockage of Na channels of myocytes, because the drug inhibited the maximum upstroke velocity (V(sub max)) in rate-dependent manner. The membrane potential dependency of Na channel blockage by Ro 22-9194 (R) was examined. Venticular myocytes were isolated from guinea pig hearts, membrane potential was clamped by the whole cell clamp method, and the membrane potential and V(sub max) was determined. From the relation between resting potential of a single cell and V(sub max), it was revealed that the membrane potential that decreases V(sub max) by 50 percent was lowered by .0 mV by adding 30 micro-M Ro 22-9194 (R). This suggests that the drug may bind inactivated Na channels. In order to examine the participation of Na channel in detail, clamp pulses were given, which can shift the Na channel to resting state to inactivated state via activated state, and the duration of inactivated state is changeable. When a single pulse was given, V(sub max) inhibition was apparently increased by prolongation of pulse duration, so that Na block may occur both in the upstroke phase and in the plateau phase. From the experiment using train pulses, it was revealed that Ro 22-9194 blocked Na channels in use dependent manner by repetitive activation, and the drug could bind both activated and inactivated channel. Author (NASDA)

N94-27512# Nagoya Univ. (Japan). Research Inst. of Environmental Medicine.

ELECTROPHYSIOLOGICAL EFFECTS OF AN ANTIARRHYTHMIC DRUG, MORICIZINE ON ISOLATED GUINEA PIG VENTRICULAR MUSCLES [KO FUSEIMYAKUYAKU MORISHIJIN NO MORUMOTTO SHINSHITSUKIN NI TAISURU DENKI SEIRIGAKUTEKI SAYO] **c51**

Kazuyasu Maruyama, Ryoko Suzuki, Takafumi Anno, Itsuo Kodama, and Junji Toyama *In its* Annals of the Research Inst. of Environmental Medicine, Nagoya Univ., Volume 44 25 Mar. 1993 p 259-261 In JAPANESE (For primary document see N94-27442 07-52)
Avail: CASI HC A01/MF A04

Moricizine is an oral antiarrhythmic agent that has an effect to block Na channel. Rate-dependent and membrane potential-dependent Na channel inhibition by moricizine using maximum upstroke velocity (V(sub max)) as an index was studied. The right papillary muscles were extracted from guinea pig hearts, and the action potential was recorded when electric stimuli were given. As a result, moricizine decreased the V(sub max) in dose-dependent manner without affecting the resting potential at the concentration of 1 micro-M or more. The concentration to inhibit the V(sub max) by 20 percent (IC(sub 20)) was 1.3 micro-M under basic stimulus of 1 Hz, and under three or more micro-M, the action potential duration was shortened significantly. These results suggest that main effect of moricizine on cardiac muscles might depend on inhibition of Na channels. In case of train stimuli, V(sub max) was inhibited use-dependently, and the inhibition was augmented as the frequency of stimulus was increased. The recovery time constant and onset rate of Use-Dependent Block (UDB) were similar to flecainide that shows slow Na channel blockage. From experiments using isolated ventricular myocytes, V(sub max) was decreased significantly when the duration of 0 mV conditioning clamp was prolonged to 400 msec or more, and the longer the duration was prolonged, the more the V(sub max) decreased. 0 mV conditioning clamp shifts Na channel from resting state to inactivating state via activating state. From these results, it can be concluded that moricizine may have high affinity to inactivated Na channel. Author (NASDA)

N94-27513# Nagoya Univ. (Japan). Research Inst. of Environmental Medicine.

CORRELATION BETWEEN ELECTRICAL ACTIVITY AND THE SIZE OF SINGLE SINOATRIAL NODE CELLS [DOBO KESSETSU HOCHODORI SAIBO NO OKISA TO DENKITEKI TOKUSEI TONO KANKEI] **c51**

Haruo Honjo, M. R. Boyett (Leeds Univ., England.), Itsuo Kodama, and Junji Toyama *In its* Annals of the Research Inst. of Environmental Medicine, Nagoya Univ., Volume 44 25 Mar. 1993 p 262-265 In JAPANESE (For primary document see N94-27442 07-52)
Avail: CASI HC A01/MF A04

In the sinoatrial node, various sizes of pacemaker cells are present. The purpose is to compare the cell size with spontaneous action potential pulses and ion current densities in pacemaker cells. The sinoatrial myocytes were isolated from rabbit hearts, and the cells which contract spontaneously were clamped by the whole cell clamp method. The action potential was recorded and membrane current was measured under membrane potential clamp. As a result, there was correlation between the size of these cells and spontaneous action potential; i.e., the small cells showed shallow maximum diastolic membrane potential and low maximum upstroke velocity and diastolic depolarization velocity compared by the large cells. In addition, small cells tended to be slow in spontaneous excitation. It is known that small cells present in the central part of the sinoatrial node, so that pacemaker cells in the central sinoatrial node may have shallow maximum diastolic potential, slow maximum upstroke velocity and diastolic depolarization velocity, and slow spontaneous activity. In respect to correlation between ion current density and cell size, no significant correlation was observed between the density of L-type Ca current and cell size, however, the density of non-selective current activated by hyperpolarization tended to augment the large cells. Therefore, this current may participate in rapid spontaneous activity and diastolic depolarization velocity in larger cells. Author (NASDA)

N94-27514# Nagoya Univ. (Japan). Research Inst. of Environmental Medicine.

THE IONIC MECHANISM UNDERLYING THE NEGATIVE CHRONOTROPIC EFFECT OF ACETYLCHOLINE: EXPERIMENTAL STUDY IN RABBIT SINGLE SINOATRIAL NODE CELLS Report No. 1 [DOBO KESSETSU NI TAISURU ASECHIRUKORIN INSEI HENJI SAYO NO ION KIJO NI KANSURU KENKYU: TANRI DOBO KESSETSU SAIBOU O MOCHIITA JIKKEN] **c51**

Haruo Honjo, M. R. Boyett (Leeds Univ., England.), Itsuo Kodama, and Junji Toyama *In its* Annals of the Research Inst. of Environmental Medicine, Nagoya Univ., Volume 44 25 Mar. 1993 p 266-268 In JAPANESE (For primary document see N94-27442 07-52)
Avail: CASI HC A01/MF A04

Acetylcholine (Ach) has a negative chronotropic effect on the heart due to suppressing automatism of the pacemaker in the sinoatrial node. How selective inhibition of ion channels can influence the Ach negative chronotropic effect was examined. The sinoatrial myocytes were isolated from rabbit hearts, and spontaneous cycle length was measured. In order to distinguish Ach effects on K current and on non-selective current activated by hyperdepolarization, each current was inhibited selectively using Ba(2+) and Cs(+); 0.5 mM Ba(2+) can inhibit K current by 80 - 0 percent, and 1 mM Cs(+) can inhibit the non-selective current by 50 - 60 percent. Both inhibitors do not affect other currents. A 1 mM Cs(+) did not show any effect on spontaneous excitation rate of the sinoatrial node, and on inhibition by Ach. This suggests that the negative chronotropic effect of Ach is not related to the non-selective current. On the other hand, although 0.5 mM Ba(2+) did not affect the spontaneous excitation rate when Ach was not present, it suppressed the Ach effect on spontaneous excitation. Therefore, the K current may participate in negative chronotropic effect of Ach. Author (NASDA)

N94-27515# Nagoya Univ. (Japan). Research Inst. of Environmental Medicine.

THE IONIC MECHANISM UNDERLYING THE NEGATIVE CHRONOTROPIC EFFECT OF ACETYLCHOLINE: EXPERIMENTS USING SMALL SINOATRIAL NODE TISSUE PREPARATIONS ISOLATED FROM RABBIT HEARTS Report No. 2 [DOBO KESSETSU NI TAISURU ASECHIRUKORIN INSEI HENJI SAYO NO ION KIJO NI KANSURU KENKYU: TASAIBO BISHO HYOHON O MOCHIITA JIKKEN] c51

Itsuo Kodama, M. R. Boyett (Leeds Univ., England.), Akiko Arai, Ryoko Suzuki, Haruo Honjo, and Junji Toyama *In its* Annals of the Research Inst. of Environmental Medicine, Nagoya Univ., Volume 44 25 Mar. 1993 p 269-271 In JAPANESE (For primary document see N94-27442 07-52)

Avail: CASI HC A01/MF A04

The inhibition of automatism and change of membrane potential pulses in multicellular samples under wide range of Acetylcholine (Ach) concentration using selective inhibitors of channels associated with Ach was studied. Small sinoatrial node tissues were extracted from rabbit hearts, and perfused with perfusate containing Ach, Ba(2+), or Cs(+). Ba(2+) was used as a selective inhibitor of Ach sensitive K current (I(sub k)), and Cs(+), as a inhibitor of inward current activated by hyperdepolarization (I(sub f)). As a result, 2 mM Cs(+) decreased spontaneous excitation rate by 12.8 percent, while 2 mM Cs(+) did not affect the negative chronotropic effect of Ach; i.e., the dose-response curve and IC(sub 50) (the concentration inhibiting Ach effect by 50 percent) was not changed by Cs(+) addition. This implies that I(sub f) may not play an important role in pacemaker function, and that the negative chronotropic effect by Ach may not be associated with I(sub f). 0.5mM Ba(2+) prolonged the action potential duration, and decreased the maximum diastolic potential by 8-10 mV, as well as slight promotion of spontaneous excitation was observed. This is probably because of decrease of slow rectifying K current, and partially due to decrease of I(sub f) current secondary to the depolarization. In addition, Ba(2+) shifted the dose-response curve of Ach to the right, and increase IC(sub 50) (Ach) 3.5 times, which implies that Ach effect was inhibited. Therefore, the negative chronotropic effect of Ach may be caused by the activation of K current. Author (NASDA)

N94-27516# Nagoya Univ. (Japan). Research Inst. of Environmental Medicine.

THE IONIC MECHANISM UNDERLYING THE NEGATIVE CHRONOTROPIC EFFECT OF ACETYLCHOLINE: POSTGANGLIONIC VAGAL STIMULATION IN ISOLATED RABBIT HEARTS Report No. 3 [DOBO KESSETSU NI TAISURU ASECHIRUKORIN INSEI HENJI SAYO NO ION KIJO NI KANSURU KENKYU: MEISO SHINKEISETSUGO SENI SHIGEKI NO KOKA] c51

Itsuo Kodama, Akiko Arai, Ryoko Suzuki, Haruo Honjo, M. R. Boyett (Leeds Univ., England.), and Junji Toyama *In its* Annals of the Research Inst. of Environmental Medicine, Nagoya Univ., Volume 44 25 Mar. 1993 p 272-275 In JAPANESE (For primary document see N94-27442 07-52)

Avail: CASI HC A01/MF A04

In a previous study, it was demonstrated that the negative chronotropic effect of Acetylcholine (Ach) on sinoatrial node was owed to activation of K current (I(sub k)) rather than inward current activated by hyperpolarization (I(sub f)). The negative chronotropic effect of Ach released from postganglionic vagal ending on the entire sinoatrial node was studied. The sample tissues extracted from rabbit hearts were stimulated by electric field stimulus, and the response disappeared when atropine was added. Therefore, this response may be caused by binding muscarinic receptor with Ach released from postganglionic vagal ending. The vagal nerves responded with three phases; early automatism inhibition, secondary post-inhibitory rebound, and late artomatism inhibition. The post-inhibitory rebound can not be explained by the shift of pace-making site to other site in the sinoatrial node, because there is a finding that the post-inhibitory rebound was observed after the pacemaker site returned to the original site. When Cs(2+), an inhibitor of I(sub f), was added, the post-inhibitory rebound disappeared or decreased, which implies that automatism may be promoted by I(sub f) activation following hyperpolarization in vagal endings. Although Cs(2+) did not change the relation between early automatism inhibition and vagal stimulus compared with control, Ba(2+) decreased the negative chronotropic effect. It can be concluded that I(sub k) may play a more important role than I(sub f) in the negative chronotropic effect by Ach. Author (NASDA)

N94-27517# Nagoya Univ. (Japan). Research Inst. of Environmental Medicine.

A STUDY OF PSYCHOLOGICAL FACTORS AFFECTING AN EXTREMELY ISOLATED ENVIRONMENT [HEISA KAKURI KANKYOKA NI OKERU SHINRI YOSO NO KENKYU] c53

Masafumi Tanaka *In its* Annals of the Research Inst. of Environmental Medicine, Nagoya Univ., Volume 44 25 Mar. 1993 p 276-278 In JAPANESE (For primary document see N94-27442 07-52)

Avail: CASI HC A01/MF A04

This study was performed as a part of a three-year project of international comparison of human behavior and psychology under extremely isolated environment, advocated by the Scientific Committee on Antarctic Research (SCAR) to Canada, Italy, Australia, France, and Japan. The subjects were 31 Japanese male members of the 32nd Antarctic wintering party, consisting of 16 observation members and 15 construction members. The age was ranging from 25 to 45, and the average age was 33.9. The duration was from November 1990 to March 1992. This test can be divided into two phases. The first phase was the test using questionnaires that was delivered to each members who were told to answer it within one week. Although this test was not compulsive, the recovery rate was as high as 1.3 percent. Another test was observation of particular members in some opportunities where every member was present at one time, such as meetings or dinner. In this test, the behavior, conversation, and others were recorded. These data are being analyzed now, and are scheduled to be compared at the international working group next year. What was interesting in this test was apparent contrast between observation members and construction members. Construction members answered to try external self-control rather than internal self-control when self-control was required, and included many inadaptable members. Author (NASDA)

N94-27518# Nagoya Univ. (Japan). Research Inst. of Environmental Medicine.

INTERHEMISPHERIC PHASE RELATIONSHIP OF ALPHA WAVES AND CEREBRAL DOMINANCE [ARUFAHA NO HANKYUKAN ISO RENKAN TO HANKYU YUISEI] c53

Takako Kawaguchi, Hiroyasu Jijiwa (Institute for Developmental Research, Kasugai, Japan.), and Satoru Watanabe *In its* Annals of the Research Inst. of Environmental Medicine, Nagoya Univ., Volume 44 25 Mar. 1993 p 279-281 In JAPANESE (For primary document see N94-27442 07-52)

Avail: CASI HC A01/MF A04

In previous studies, phase of alpha wave was compared between the right and left hemispheres during loading mental work. Whether the interhemispheric difference could be changed by linguistic load and acoustic load was examined. The subjects were healthy 20 students. They sat relaxed with closed eyes, and brain waves were recorded, during the following two mental loadings; one is 10 questions on proverbs previously recorded by a cassette tape recorder, and another was to sing or follow seven musics in mind. The music included three children's songs with words and four melodies without words. As a result, the phase of alpha waves were significantly increased in temporal and frontal regions under linguistic loads and in temporal regions under acoustic loads, compared with those during closed-eyed relaxation. The time ratio of preceding phase in the left hemisphere to the right hemisphere was significantly larger in the temporal, frontal and central regions under linguistic loading, whereas it was not changed during acoustic loading and relaxation. This suggests that the left hemisphere of the brain may have a function of the linguistic process. No significant interhemispheric difference was observed between the music with and without words. Author (NASDA)

N94-27519# Nagoya Univ. (Japan). Dept. of Ophthalomology.

ANALYSIS OF THE ELECTRICALLY EVOKED RESPONSE (EER) OF THE CAT [NEKO EER (EREKUTORIKARI EBOKUTO RESUPONSU) NO KISOTEKI KENKYU: 17, 18 YA HISHITSU NI OKERU EER NO NYURON KIGEN NO KENKYU] c51

Kazuhiro Shimazu, Yozo Miyake, Yasuhiro Fukatsu (Fukatsu Eye Clinic, Nagoya, Japan.), and Satoru Watanabe *In* Nagoya Univ., Annals of the Research Inst. of Environmental Medicine, Nagoya Univ., Volume 44 25 Mar. 1993 p 282-287 In JAPANESE (For primary document see N94-27442 07-52)

Avail: CASI HC A02/MF A04

Phosphene is a sense obtained by electric stimulus of eyeball, and it can be applied as an evoked potential in the brain. The basic pulses of EER (Electricaly Evoked Response) and responses of a single neuron in the area 17 and 18 of the cerebral cortex were studied. The subjects were cats whose cerebral cortex was exposed, and extracellular potential was recorded. 54 units of cortex neurons were identified in the area 17, including 41 simple cells and 13 complex cells, and, 48 units, in the area 18. It is known that discharge occurs corresponding to two negative waves in Lateral Geniculate Neurons (LGN); i.e., latency ms (N1) and latency 20 ms (N2) stimulus. As a result of neuronal responses in the area 17, simple cells discharged by either N1, N2 or N1 and N2, and the response was less periodical compared with LGN, while the complex cells tended to slightly respond to the N1 and N2 stimuli. In the area 18, a few neurons discharged by the N1 stimulus, and no neuron could respond to both N1 and N2 stimuli. However, the neurons discharging by 30 ms or more stimulus presented in the area 18. In addition, by stimuli of 20 ms or more given twice at the interval of 20 ms, the responses were inhibited, which implies that these responses may be mediated by multiple synapses in the cortex, and the responses to 20 ms of stimuli may be a single synaptic response. Author (NASDA)

N94-27520# Nagoya Univ. (Japan). Research Inst. of Environmental Medicine.

IMPAIRED ASSOCIATED MOVEMENT IN PARKINSON'S DISEASE: AN EVALUATION OF BELL'S PHENOMENON [PAKINSONBYO NI OKERU RENGO UNDO SHOGAI: BERU GENSHO NI TSUITE NO KENTO]

Minoru Hoshiyama, Satoru Watanabe, Seiji Yoshino (Suzuka Univ. of Medical Science and Technology, Japan.), and Kaneo Mori *In its* Annals of the Research Inst. of Environmental Medicine, Nagoya Univ., Volume 44 25 Mar. 1993 p 288-291 In JAPANESE (For primary document see N94-27442 07-52)

Avail: CASI HC A01/MF A04

One of the dyskinesia in Parkinson's disease is a kinesia with impaired associated movement. This impairment includes Bell's phenomenon which is an upward movement of eye balls accompanied with eye close movement. The purpose is to observe the Bell's phenomenon in patients with Parkinson's disease. The subjects were seven patients with Parkinson's disease and eight healthy persons in the similar ages, who sat in resting position, with the head fixed, and closed the eyes while gazing at the front. Movement of eye ball and eye lid was recorded by an Electrooculogram (EOG). As a result, the Bell's phenomenon was observed in both groups. However, vertical movement of eye balls was significantly smaller in movement angle and the maximum angle in patient group, although no difference was observed in horizontal movement and distance of eye lid movement between both groups. There was a correlation between distance and velocity of eye lid movement in both groups, which implies that the duration of close eye movement was constant. In addition, duration from the beginning to the end of upward movement of eye ball was not different between two groups. Therefore, the difference of upward movement of eye balls could result from the difference of eye movement velocity. Author (NASDA)

N94-27521# Nagoya Univ. (Japan). Research Inst. of Environmental Medicine.

HYPERALGESIA TO COLD IN PATIENTS WITH SUBACUTE MYELO-OPTICO-NEUROPATHY (SMON) [SUMON KANJA NO HIFU TSUKAKU KABIN: SAMO TESUTO NI YORU KENTO]

Yoshiki Sugiyama, Satoshi Iwase, Tadaaki Mano, Yasuo Koike, Kimiya Sugimura, and Akira Takahashi *In its* Annals of the Research Inst. of Environmental Medicine, Nagoya Univ., Volume 44 25 Mar. 1993 p 292-294 In JAPANESE (For primary document see N94-27442 07-52)

Avail: CASI HC A01/MF A04

In previous studies, it was demonstrated that hyperalgesia was manifested by ischemic block in the brachium. Blocking for 2 minutes causes spontaneous discharge of myelinated thick-fibers, resulting in tingling pain, and in case of blocking more than 10 minutes, dull pain hypersensitive to coldness occurred at the level of less than the threshold stimulus probably due to excitation of unmyelinated fibers, both of which are similar to the pain in a patient with Subacute Myelo-Optico-Neuropathy (SMON). The functional disorder of myelinated thick-fibers and afferent thin-fibers in hyperalgesia observed in SMON were examined. The subjects were 17 patients with SMON, to whom caloric stimulus and vibration were given. As a result, hyperalgesia by vibration was observed in seven cases, and thermoparesthesia was eight cases in the hand and nine cases in the thigh. What is interesting was abnormal sensitivity to coldness was observed in 11 cases. The threshold of these stimuli was within the non-pain range, and the response has a property of secondary pain with sense of ardor. These results suggest that hyperalgesia in SMON may be mediated by unmyelinated fibers. Author (NASDA)

N94-27522# Nagoya Univ. (Japan). Research Inst. of Environmental Medicine.

CONTRIBUTION OF MUSCLE SPINDLE AFFERENT ACTIVITY TO TRANSIENT PAUSE IN EMG DURING VOLUNTARY TONIC CONTRACTION [JIZOKUSEI KIN SHUSHUKUCHU NI MIRARERU KIN HODEN NO KYUSHI NI KAKAWARU KIN BOSUI KYUSHINSEI HASSHA KATSUDO]

Reiko Tsukahara, Hisashi Aoki (Institute for Developmental Research, Kasugai, Japan.), Kyonosuke Yabe, and Tadaaki Mano *In its* Annals of the Research Inst. of Environmental Medicine, Nagoya Univ., Volume 44 25 Mar. 1993 p 295-298 In JAPANESE (For primary document see N94-27442 07-52)

Avail: CASI HC A01/MF A04

The purpose of this study is to examine how discharge of afferent fibers contributes to the pause emerging incidently in electromyogram (EMG) during voluntary tonic contraction. The subjects were five healthy adults, who lied in the prone position with isometric plantar flexion, and EMG and electroneurogram were recorded to identify afferent discharge of muscle spindle and Golgi tendon organ. As a result, the afferent discharge of muscle spindle was paused or grouped before muscle discharge paused. The muscle spindle afferent discharge was not relevant to restart of muscle discharge, at least through spinal reflex pathway. In addition, although discharge of muscle spindle tended to group before pauses of muscle discharge, the tendency disappeared after the pauses. The EMG of Golgi tendon organ revealed that discharge was decreased during muscle discharge pause as well as before restart of muscle discharge. This suggests that decrease of inhibitory stimulus from Golgi tendon organ may contribute to muscle discharge after the restart. Author (NASDA)

N94-27523# Tokyo Univ. (Japan). Dept. of Psychology.

FUNCTION OF SELECTIVE ATTENTION INTRINSIC TO THE SACCADE SYSTEM: DOES THE VOLUNTARY CONTROL OVERRIDE THE STIMULUS DRIVEN CONTROL? [SAKKADO SHISUTEMU NI NAIZAISURU SENTAKUTEKI CHUI KINO: ZUIITEKI SEIGYO WA SHIGEKI KUDO SEIGYO OSEISURUKA] c53

Hiromi Imai and Kazuo Koga (Nagoya Univ., Japan.) *In* Nagoya Univ., Annals of the Research Inst. of Environmental Medicine, Nagoya Univ., Volume 44 25 Mar. 1993 p 299-303 In JAPANESE (For primary document see N94-27442 07-52)

Avail: CASI HC A01/MF A04

From many studies on spatial attention, it was revealed that subjects can maintain selective attention to a particular target with ignoring distractors. However, the mechanism of this selective attention is not understood. The purpose of this study is to examine which is the dominant control, voluntary control or stimulus driven control, and, in the case that one control was dominant, whether the other control could affect the control or not. Three subjects were told to gaze at a target dot on a display and to ignore a distractor that appeared after a short interval, and the horizontal movement of the left eye was recorded. As a result, saccade to the targets was mainly observed, and the distractor scarcely caused saccade even in emergence immediately after the emergence of the target. This suggests that voluntary control may override stimulus driven control. However, because duration from emergence of target to occurrence of saccade was prolonged by a distractor, the presence of a distractor may interfere with saccade programming to some extent. Author (NASDA)

N94-27524# Nagoya Univ. (Japan). Research Inst. of Environmental Medicine.

EFFECT OF PROSTAGLANDIN E1 ON THE RELATIONSHIP BETWEEN SKIN SYMPATHETIC NERVE ACTIVITY AND REDUCTION IN SKIN BLOOD FLOW [PUROSUTAGURANJIN E1 GA HIFU KOKAN SHINKEI KATSUDO TO HIFU KETSURYURYO TONO KANKEI NI ATAERU EIKYO]

Satoshi Iwase, Yoshiki Sugiyama, Toshiyoshi Matsukawa, Chihiro Miwa, Shigeo Takeuchi, and Tadaaki Mano *In its* Annals of the Research Inst. of Environmental Medicine, Nagoya Univ., Volume 44 25 Mar. 1993 p 304-308 In JAPANESE (For primary document see N94-27442 07-52)

Avail: CASI HC A01/MF A04

It is known that skin sympathetic nerve activity causes vasoconstriction and decrease of skin blood flow. This study examined the effect of a peripheral vasodilator, Prostaglandin E1 (PGE1), on the skin sympathetic nerve activity. The subjects were five healthy male adults to whom skin sympathetic nerve activity burst was induced by several stimuli with or without PGE1, and the nerve activity and skin blood flow were recorded. It had been proved that there is a positive correlation between the intensity of the nerve activity and decrease of skin blood flow. In this study, it was demonstrated that PGE1 does not change the blood flow in resting condition, while it inhibites vasoconstriction in a dose-dependent manner under such stimuli as to cause burst activity in skin sympathetic nerve. These results suggest that it may be useful to test sympathetic nerve activity pharmacologically for examination of the vasoconstrictive action of drugs. Author (NASDA)

N94-27525# Nagoya Univ. (Japan). Research Inst. of Environmental Medicine.

DIFFERENCE IN SKIN BLOOD FLOW REDUCTION DEPENDING ON ACTIVATING MANEUVER OF SKIN SYMPATHETIC NERVE ACTIVITY [KAKUSHU HIFU KOKAN SHINKEI KATSUDO FUKATSUKAHO GA MASSHO HIFU KETSURYURYO GENSHO NI OYOBOS EIKYO]

Satoshi Iwase, Yoshiki Sugiyama, Toshiyoshi Matsukawa, Chihiro Miwa, and Tadaaki Mano *In its* Annals of the Research Inst. of Environmental Medicine, Nagoya Univ., Volume 44 25 Mar. 1993 p 309-313 In JAPANESE (For primary document see N94-27442 07-52)

Avail: CASI HC A01/MF A04

It is known that activity burst can be induced in skin sympathetic nerve by various stimuli. This study examined the change of skin blood flow during occurrence of the activity burst to reveal the participation of activity burst in vasoconstrictive and sweating effect of sympathetic nerve. The subjects were four healthy male adults, to whom activity burst was induced by mental arithmetic, acoustic stimulus, electric stimulus, and sudden and deep inspiration, while skin nerve activity, skin blood flow, and sweating were measured. As a result, linear relation was observed between skin sympathetic nerve activity and reduction of blood flow, when activity burst was induced by mental arithmetic, acoustic stimulus, electric stimulus, or in resting condition. Under activity burst by deep breathing, reduction of blood flow was larger than other stimuli. The stimuli, such as acoustic or electric stimulus, can activate the sympathetic nerve system via the cerebral cortex, while inspiratory stimulus activates afferent vagus nerve directly through Hering-Breuer reflex. These results indicate that the decrease of skin blood flow was larger when the response was mediated by afferent vagus nerve via Hering-Breuer reflex than mediated through cerebral cortex. Therefore, the activation via afferent vagus nerve may stimulate vasoconstrictive activity more vividly during skin sympathetic nerve activity. Author (NASDA)

N94-27526# Nagoya Univ. (Japan). Research Inst. of Environmental Medicine.

EFFECT OF L-DOPA ON HEMODYNAMIC FUNCTIONS IN HUMANS [L-DOPA GA HITO NO JUNKAN DOTAI NI OYOBOSU EIKYO]

Shigeo Takeuchi, Yoshiki Sugiyama, Satoshi Iwase, Tadaaki Mano, Toshiyoshi Matsukawa, and Reiko Tsukahara *In its* Annals of the Research Inst. of Environmental Medicine, Nagoya Univ., Volume 44 25 Mar. 1993 p 314-320 In JAPANESE (For primary document see N94-27442 07-52)

Avail: CASI HC A02/MF A04

L-dopa often causes orthostatic hypotension in patients with Parkinson's disease. This study examined the effect of L-dopa on human circulatory system to clarify the mechanism of this adverse reaction. The subjects were eight healthy adults, who lied in supine position on a tilting bed which was inclined 20, 40, and 60 degrees for head-up tilt before and after administration of L-dopa. To evaluate cardiovascular functions, the associated cardiovascular parameters and sympathetic nerve activity were measured. As a result, burst activity of muscle sympathetic nerve was increased significantly in every tilt by L-dopa administration, so that the effect of L-dopa may result from inhibition of sympathetic nerve activity at the peripheral level. This is supported by the fact that the increase of muscle sympathetic nerve activity was lowered by L-dopa as flow resistance in the leg was increased during tilting. Therefore, L-dopa may cause vasodilation or inhibit vasoconstriction at the peripheral level. Flow resistance was significantly decreased at 60 degrees tilt after L-dopa administration, probably because decrease of blood pressure by peripheral vasodilation surpasses central sympathetic nerve activity. Author (NASDA)

N94-27527# Toyota Coll. of Technology (Japan). Dept. of Applied Physiology.

SYMPATHETIC NERVE ACTIVITY DURING DYNAMIC LEG EXERCISE [DOTEKI KYAKU UNDOJI NO KOKAN SHINKEI KATSUDO]

Mitsuru Saito and Tadaaki Mano (Nagoya Univ., Japan.) *In* Nagoya Univ., Annals of the Research Inst. of Environmental Medicine, Nagoya Univ., Volume 44 25 Mar. 1993 p 321-324 In JAPANESE (For primary document see N94-27442 07-52)

Avail: CASI HC A01/MF A04

It has been suggested that sympathetic nerve activity may be affected by the muscles that participate in the motive activity and by exercise patterns. The purpose of this study is to observe sympathetic nerve activity during dynamic leg exercise that increased oxygen consumption up to 70 percent of the maximum oxygen consumption. The subjects were five healthy male adults, 22 to 27 years old, who were loaded with an ergometer by four stages; i.e., Warming-up stage (W-Up), load less than anaerobic metabolic threshold, load corresponding to anaerobic metabolic threshold, and load more than anaerobic metabolic threshold, and sympathetic nerve activity, heart rate, blood pressure, and electromyogram (EMG) of femur muscle surface were recorded. As a result, the heart rate, EMG, and blood pressure were all increased as the load increased. As an index of sympathetic nerve activity, discharge burst rate (BR) was determined by the number of peak bursts from the analysis of muscle sympathetic nerve activity, which indicated that BR was once decreased in W-Up, then increased linearly as the exercise load was increased. In other words, sympathetic nerve activity was increased in heavy exercise, although it was suppressed in light exercise. Author (NASDA)

N94-27528# Nagoya Univ. (Japan). Research Inst. of Environmental Medicine.

ANALYSIS ON ONE MINUTE WAVE IN BODY FLUID VOLUME AND MUSCLE PUMPING REFERRED TO BODY PARTS GENERATING THE ONE MINUTE WAVE DURING HUMAN ACTIVE STANDING [HITO NO NODOTEKI SEISHI RITSUI NI OKERU TAIEKIRYO HENDO ICHI FUNHA NO HASSEI BUI OYOBI SONO ICHI FUNHA TO KIN PONPU SAYO TONO KANKEI]

Kinsaku Inamura, Tadaaki Mano, and Satoshi Iwase *In its* Annals of the Research Inst. of Environmental Medicine, Nagoya Univ., Volume 44 25 Mar. 1993 p 325-330 In JAPANESE (For primary document see N94-27442 07-52)

Avail: CASI HC A02/MF A04

It is known that muscle pumping and sympathetic nerve response can regulate one-minute waves that are generated by automatic vasoconstriction in venous blood congestive sites in order to circulate congestive blood. The purpose of this study is to reveal the generating site and propagation of one-minute waves in active standing by measuring body fluid volume and surface electromyography in detail, and to reveal the relationship between muscle pumping and one-minute waves in body fluid volume. The subjects were 14 healthy adults, 18 to 20 years old, who maintained active standing for 40 minutes, and circumferences of each body parts, electromyograms, and foot pressure centers were measured. As a result, it was revealed that the one-minute waves in body fluid volume were generated not only in the lower thigh but also in the abdomen and upper thigh and propagated upwards. The one-minute waves were generated at one site each in the lower thigh, upper thigh, and upper body, and they were usually observed in the soleus muscle, central calf, upper thigh, and navel and stomach level of the abdomen. In addition, as soon as muscle constriction occurred, one-minute waves were observed on this site, and the wave was coupled with one-minute wave of foot pressure center resulting from body sway in active standing. This implies that the muscle pumping caused by body sway may circulate blood by one-minute waves in body fluid volume. Author (NASDA)

N94-27529# Aichi Medical Univ., Nagakute (Japan). Dept. of Physiology.

AN ATTEMPT OF INTRANEURAL STIMULATION BY MICROELECTRODE INSERTED IN SKIN SYMPATHETIC NERVE FASCICLE [BISHO DENKYOKU NI YORU HIFU KOKAN SHINKEINAI SHIGEKI NO KOKOROMI]

Junichi Sugenoya, Satoshi Iwase (Nagoya Univ., Japan.), Yoshiki Sugiyama (Nagoya Univ., Japan.), and Tadaaki Mano (Nagoya Univ., Japan.) *In* Nagoya Univ., Annals of the Research Inst. of Environmental Medicine, Nagoya Univ., Volume 44 25 Mar. 1993 p 331-334 In JAPANESE (For primary document see N94-27442 07-52)
Avail: CASI HC A01/MF A04

Recently, microelectrode techniques have enabled selective stimulation of a nerve by inserting a stimulating electrode into the target nerve fascicle percutaneously. In this study, a new technique was attempted using a microelectrode to stimulate skin sympathetic nerve selectively. The subjects were four healthy male adults, to whom a microelectrode was inserted into the tibial nerve percutaneously, and skin sympathetic nerve activity (SSNA) was recorded. Sweating and skin blood flow were also recorded in the soles which have effecters of the tibial nerve. Before insertion, the nerve was blocked by lidocaine at 5 cm proximal from the insertion site, and stimulated with various strengths of current, duration, and stimulating patterns. Although the nerve was not blocked completely, the latency of sweating response was shortened by 1.5 seconds when stimulated, which indicates that the electrode directly stimulated the sweat controlling nerve. This response was increased by repetitive stimuli. In addition, the more the current strength was, the more the sweating responses became. Even when the stimulus was so weak that sweating response did not occur, it tended to occur by repetitive stimuli with more frequent cycle. The latency tended to be shortened when large response occurred by strong stimulus. However, no change was observed in skin blood flow. Author (NASDA)

N94-27530# Nagoya Univ. (Japan). Research Inst. of Environmental Medicine.

THE MEASUREMENTS OF MUSCLE BLOOD FLOW BY LASER DOPPLER FLOWMETRY WITH NEEDLE TYPE PROBE [HARIGATA PUROBE O MOCHIITA REZA DOPPURA KETSURYURYOKEI NIYORU KIN SOSHIKI KETSURYURYO NO SOKUTEI] c51

Kiyohito Yamamoto, Yasuhiro Oba, Tadaaki Mano, and Shigehiko Shionoya *In its* Annals of the Research Inst. of Environmental Medicine, Nagoya Univ., Volume 44 25 Mar. 1993 p 335-339 In JAPANESE (For primary document see N94-27442 07-52)
Avail: CASI HC A01/MF A04

Laser Doppler velocimetry is an easy method to measure continuous skin blood flow. However, for muscle blood flow measurement, the probe must touch directly to the operationally exposed muscle, and the performance has not been determined yet. The newly developed needle type probe for laser Doppler velocimetry can be inserted into the target muscle without operation, so that simple and continuous measurement of muscle blood flow might be achieved. In order to examine this possibility, the laser Doppler velocimeter was compared with an ultrasonic velocimeter in respect to suitability of continuous measurement and reproducibility. The subjects were three dogs, in which an ultrasonic velocimeter was equipped to the popliteal artery, and a laser Doppler velocimeter was inserted into the musculus gastrocnemius, and blood flow was varied by papaverin and reactive hyperemia. As a result, there was a linear relationship between measurements of the two velocimeters when blood flow increased, whereas when blood flow decreased, no linear relationship was observed between the two methods. However, in short-period blood flow decrease, the two methods were correlated positively, although the incline was different between papaverin and reactive hyperemia. These results suggest that the laser Doppler velocimeter could be useful to measure muscle blood flow with high reproducibility; however the measurements should be evaluated as relative values. Author (NASDA)

N94-27531# Nagoya Univ. (Japan). Research Inst. of Environmental Medicine.

MUSCLE SYMPATHETIC NERVE ACTIVITY IN PATIENTS WITH HYPER-AND HYPOTHYROIDISM: A MICRONEUROGRAPHIC STUDY [KOJOSEN KINO KOSHINSHO OYOBI TEIKASHO KANJA NI OKERU KIN KOKAN SHINKEI KATSUDO: MAIKURONYUROGURAFI O MOCHIITA KENKYU]

Toshiyoshi Matsukawa and Tadaaki Mano *In its* Annals of the Research Inst. of Environmental Medicine, Nagoya Univ., Volume 44 25 Mar. 1993 p 340-342 In JAPANESE (For primary document see N94-27442 07-52)
Avail: CASI HC A01/MF A04

Clinical manifestations of hyper- and hypothyroidism are similar to those of hyper- and hypoactivity of sympathetic nerves. In order to clarify the relation between muscle sympathetic nerve activity (MSNA) and thyroid function, action potential of sympathetic nerve was measured directly using microneurography, and the data were compared with control and patients with hyper- and hypothyroidism. The subjects were eight healthy persons, six patients with hyperthyroidism, and six patients with hypothyroidism. Blood pressure, cardiac rate, and MSNA were measured and at the same time free triiodothyronine (F-T3), free thyroxine (F-T4), and thyroid-stimulating hormone (TSH) in venous blood were determined. As a result, it was revealed that sympathetic nerve was hyperactive in patients with hypothyroidism, while it was hypoactive in patients with hyperthroidism. In addition, there was a negative correlation between thyroid hormone concentration and MSNA, probably because thyrotropin releasing hormone (TRH) that can activate MSNA may be lowered in hyperthyroidism, and increased in hypothyroidism. Moreover, this negative relation may be relevant to beta-receptor which can be increased in number and affinity by thyroid hormone. Author (NASDA)

N94-27532# Aichi Medical Univ., Nagakute (Japan).

ENHANCEMENT OF SKIN SYMPATHETIC NERVE ACTIVITY IN AMYOTROPHIC LATERAL SCLEROSIS [KIN ISHUKUSEI SOKUSAKU KOKASHO NI OKERU HIFU KOKAN SHINKEI KATSUDO NO KENTO]

Koji Yamamoto, Gen Sobue, Satoshi Iwase (Nagoya Univ., Japan.), Tetsuya Okamoto (Nagoya Univ., Japan.), Tadaaki Mano (Nagoya Univ., Japan.), and Terunori Mitsuma *In* Nagoya Univ., Annals of the Research Inst. of Environmental Medicine, Nagoya Univ., Volume 44 25 Mar. 1993 p 343-347 In JAPANESE (For primary document see N94-27442 07-52)
Avail: CASI HC A01/MF A04

Amyotrophic lateral sclerosis (ALS) is a disease that degenerates motor neurons systematically. Several studies suggest that sympathetic nerve activity may be activated in ALS patients. The purpose of this study is to examine the skin sympathetic nerve activity (SSNA) in ALS using microneurography. The subjects were five patients with ALS and 10 healthy adults, to whom a microelectrode was inserted into the efferent sympathetic nerve, tibial nerve, and SSNA was determined using burst activity as an index. Blood flow and sweating were measured in the sole, an effector of the efferent nerve, during rest and sympathetic nerve stimulation. As a result, SSNA was higher in patients with ALS than the control group in rest. However, under stimulation, SSNA was not changed in ALS patients, whereas it was activated in the control group. This implies that the sympathetic nerve was hyperactivated in ALS patients. There were individual differences in SSNA among ALS patients. Whether these differences may be associated with individual severity or stages of the disease cannot be determined because only a few subjects participated in this study.
Author (NASDA)

N94-27533# Red Cross Hospital, Nagoya (Japan).

TREATMENT OF ORTHOSTATIC HYPOTENSION BY NASAL ADMINISTRATION OF VASOPRESSIN [BASOPURESHIN SEIZAI TENBI TOYO NI YORU KIRITSUSEI TEIKETSUATSU NO CHIRYO KOKA]

Shigetaka Hakusui, Yoshiki Sugiyama (Nagoya Univ., Japan.), Satoshi Iwase (Nagoya Univ., Japan.), and Tadaaki Mano (Nagoya Univ., Japan.) *In* Nagoya Univ., Annals of the Research Inst. of Environmental Medicine, Nagoya Univ., Volume 44 25 Mar. 1993 p 348-350 In JAPANESE (For primary document see N94-27442 07-52)
Avail: CASI HC A01/MF A04

Orthostatic hypotension (OH) is an important symptom in patients with autonomic disorder; however, definitive treatment has not established yet.

The purpose of this study is to examine the effect of two drugs, arginine vasopressin (AVP) and lysine vasopressin (LVP), on OH. The subject was a 41 year-old male patient with multisystemic atrophy presenting marked OH, to whom orthostatic load was applied by a tilting bed, and the blood pressure and heart rate were measured before and after the loading. The load was also applied after nasal administration of AVP and LVP. In resting, blood pressure was significantly increased by AVP and LVP. Under orthostatic load, the subject complained of the symptoms of OH at the incline of 70 degrees without AVP or LVP, whereas such symptoms did not appear after administration of AVP or LVP, and blood pressure was improved in each incline. Unpublished data revealed that AVP increased the blood pressure in patients with OH or post-prandial hypotension, although it did not affect the blood pressure of healthy subjects. These results suggest that patients with autonomic disorder may be supersensitive to vasopressin, which may be a reason for effectiveness of AVP on OH.

Author (NASDA)

N94-27534# Tokyo Univ. (Japan). Inst. for Brain Research of Biochemistry.

ACTIVATION BY G PROTEIN BETA GAMMA SUBUNITS OF G PROTEIN-COUPLED RECEPTOR KINASE [G TANPAKUSHITSU KYOEKI JUYOTAI KINAZE NO G TANPAKUSHITSU BETA GANMA SABUYUNITTO NI YORU KASSEIKA]

Tatsuya Haga, Kazuko Haga, Kimihiko Kameyama, and Hiroko Nakata *In* Nagoya Univ., Annals of the Research Inst. of Environmental Medicine, Nagoya Univ., Volume 44 25 Mar. 1993 p 352-354 In JAPANESE Presented at the 13th Symposium on Environmental Medicine, Aichi, Japan, 11 Nov. 1992; sponsored by Research Inst. of Environmental Medicine (For primary document see N94-27442 07-52)

Avail: CASI HC A01/MF A04

This study examined the regulation of G protein-coupled receptor kinase by G protein. Musucarinic acetylcholine receptor (mAChR) kinase purified from swine brains was proved to be able to regulate phosphorylation of muscarinic receptors by G protein; i.e., the mAChR kinase was activated by alpha, beta, and gamma subunits of G protein, and inhibited by beta and gamma subunits. The beta and gamma subunits also activated the phosphorylation of rhodopsin and beta-AR (adrenergic receptor), although it did not affect the activity of rhodopsin kinase. Comparing the beta and gamma subunits of G protein with beta and gamma subunits of transducin, the former activated mAChR, rhodopsin, and beta-AR in low concentration, while the latter showed low activation in high concentration. These results suggest that beta and gamma subunits of G protein may activate phosphorylation in general. The experiment to express cDNA (complementary deoxyribonucleic acid) of beta-AR kinase support that mAChR kinase may be identical with beta-AR kinase. Comparing the amino acid sequence between beta-AR and rhodopsin kinase, beta-AR was longer in the C-terminal with which beta and gamma subunits may interact. Therefore, it can be concluded that mAChR kinase could be an effector of G protein, and be activated by beta and gamma subunits. It is also suggested that beta and gamma subunits may promote desensitization of such a receptor kinase via phosphorylation. Author (NASDA)

N94-27535# Shizuoka Saiseikai General Hospital (Japan). Dept. of Circulation.

POSTNATAL CHANGES IN THE AUTONOMIC MODULATION OF L-TYPE Ca(EXP 2+) CURRENTS OF RABBIT VENTRICULAR CELLS [JIRITSU SINKEI NI YORU SHINKIN CA(2+) DENRYU SHUSHOKU KIKO NO SEIGO HENKA]

Toshiyuki Osaka and Ronald W. Joyner (Emory Univ., Atlanta, GA.) *In* Nagoya Univ., Annals of the Research Inst. of Environmental Medicine, Nagoya Univ., Volume 44 25 Mar. 1993 p 355-361 In JAPANESE Presented at the 13th Symposium on Environmental Medicine, Aichi, Japan, 11 Nov. 1992; sponsored by Research Inst. of Environmental Medicine (For primary document see N94-27442 07-52)

Avail: CASI HC A02/MF A04

This article presents findings on postnatal development of autonomic modulation of L type Ca(2+) current, I(sub ca). Firstly, participation of beta-adrenergic receptor and muscarinic acetylcholine (mACh) receptor was examined in a single myocyte of adult rabbit (AD) and newborn rabbit (NB) using beta-agonist (isoproterenol (ISO)) and musucarinic agonist (carbacol (CCh)). As a result, ISO increased I(sub ca) to similar extent in AD and NB, while CCh inhibited the ISO effect more remarkably in NB than AD. Secondly, the effect of adenylate cyclase (AC) activator, forskolin (FOR), was examined in AD and NB, and it was revealed that FOR increased I(sub ca) to similar extent in AD and NB, and this increase was slightly inhibited by CCh in AD, while it was completely inhibited in NB. Thirdly, FOR effect was examined with presence of GTP (guamosine 5'-triphosphate) analog, 5'-guanulylimido diphosphate (GppNHp). As a result, FOR effect on I(sub ca) was slightly decreased by GppNHp in AD, while it was largely decreased in NB. Finally, pertussis toxin (PTX) that blocks interaction of mACh receptor and GTP binding protein, Gi, was used to examine the effect of both Gi activator, CCh and GppNHp, and Gi inactivator, PTX, on either ISO or FOR, and it was demonstrated that the effect was more remarkable in NB than AD. These results suggest that in immature hearts, AC is inhibited by parasympathetic nerve system via a tonic effect of Gi even when musucarinic agonist does not exist. Author (NASDA)

N94-27536# Yamagata Univ. (Japan). Dept. of Pharmacology.

MECHANISM FOR REGULATION OF MYOCARDIAL CONTRACTILITY BY AUTONOMIC DRUGS: PATHOPHYSIOLOGICAL RELEVANCE IN CONGESTIVE HEART FAILURE [JIRITSU SHINKEI SADO BUSSHITSU NI YORU SHINKIN SAIBO SHUSHUKU NO SEIGYO KIKO: SHINFUZEN NI OKERU BYOTAI SEIRIGAKUTEKI IGI]

Masao Endo *In* Nagoya Univ., Annals of the Research Inst. of Environmental Medicine, Nagoya Univ., Volume 44 25 Mar. 1993 p 362-366 In JAPANESE Presented at the 13th Symposium on Environmental Medicine, Aichi, Japan, 11 Nov. 1992; sponsored by Research Inst. of Environmental Medicine (For primary document see N94-27442 07-52)

Avail: CASI HC A01/MF A04

This article outlines second messengers that regulates cardiac myocyte function via alpha and beta receptors, and the pathophysiological relevance to congestive heart failure. In respect to beta receptors, the mechanism to regulate cardiac function and relevance to heart failure has been considerably understood. Beta receptors which consist of beta 1 receptor and beta 2 receptor couple with G protein, Gs, and activate catalytic subunits (CS). The CS promotes cardiac function via second messenger, cAMP (adenosine 3', 5'-cyclic monophosphate). In patients with congestive heart failure, receptor down-regulation (R-DO) occurs by exposure to high level of catecholamine in blood, and lessen the number of beta-receptors on myocyte surfaces so that cardiac function is degraded. Beta receptor blockers can recover the number of beta receptors. In addition to R-DO, heart failure results from insufficient coupling with Gs, against which phospho diesterase-3 (PDE-3) inhibitor is used to increase intracellular cAMP. However, some reports recently presented data that such inhibitors increased mortality of severe heart failure patients. In respect to alpha receptors, the mechanism to regulate cardiac function seems so complicated that the relevance to congestive heart failure has not been understood well. It was revealed that cardiac alpha receptor may increase Ca(2+)(sub i) and sensitivity to Ca(2+) by prolongation of action potential due to decrease of transient outward current and activation of Na(+)/H(+) exchangers.

Author (NASDA)

N94-27537# Nagoya Univ. (Japan). Dept. of Circulation.

DESENSITIZATION TO ACETHYLCHOLINE IN PACEMAKER CELLS OF THE SINOATRIAL NODE [DOBO KESSETSU SAIBO HOCHODORI SAIBO NI OKERU ASECHIRUKORIN INSEI HENJI SAYO NO DATSU KANSA GENSHO] **c51**

Haruo Honjo, Itsuo Kodama, and Mark R. Boyett (Leeds Univ., England.) *In its* Annals of the Research Inst. of Environmental Medicine, Nagoya Univ., Volume 44 25 Mar. 1993 p 367-369 In JAPANESE Presented at the 13th Symposium on Environmental Medicine, Aichi, Japan, 11 Nov. 1992 (For primary document see N94-27442 07-52)

Avail: CASI HC A01/MF A04

The most important effect of acetylcholine (Ach) on the heart is negative chronotropic effect that decreases heart rate by inhibiting autonomic activity of sinoatrial pacemaker. This article presents experimental findings on the desensitization of negative chronotropic effect by Ach. It is reported that the negative chronotropic effect is caused by three ion currents; i.e., activation of Ach sensitive inward rectifying K current, i(sub k, Ach), inhibition of L type Ca current, i(sub Ca), and non-selective current activated by hyperdepolarization, i(sub f). Therefore, it was examined which current participates in Ach desensitization, using a single sinoatrial myocytes of rabbit hearts with clamped membrane potential. As a result, i(sub k, Ach) was activated by Ach, then decayed biphasically, while Ach inhibited i(sub Ca) and i(sub f) under stimulation of beta receptor, but this inhibition did not decay. I(sub Ca) and i(sub f) are inhibited by decrease of cAMP (adenosine 3', 5'-cyclic monophosphate) resulting from adenylate cyclase suppression via inhibitory G protein. These results suggest that adenylate cyclase inhibition by Ach may not cause desensitization of ion currents, but that the desensitization may result from change of Ach sensitive K channels. Author (NASDA)

N94-27538# Nagoya Univ. (Japan). Dept. of Autonomic and Behavioral Neurosciences.

MUSCLE SYMPATHETIC NERVE ACTIVITY IN HUMANS [KIN KOKAN SHINKEI KATSUDO]

Toshiyoshi Matsukawa *In its* Annals of the Research Inst. of Environmental Medicine, Nagoya Univ., Volume 44 25 Mar. 1993 p 370-372 In JAPANESE Presented at the 13th Symposium on Environmental Medicine, Aichi, Japan, 11 Nov. 1992 (For primary document see N94-27442 07-52)

Avail: CASI HC A01/MF A04

This article describes regulation of muscle sympathetic nerve activity by endogenous reflex, especially on measuring method of reflex function, and its relevance to essential hypertension. The endogenous reflex includes arterial baroreceptor reflex, cardiopulmonary baroreceptor reflex, arterial chemoreceptor reflex, and skeletal muscle chemoreceptor reflex. These reflexes sense changes of blood pressure, CO2 or O2 partial pressure, or pH by baroreceptors or chemoreceptors, and regulate them by negative feedback via sympathetic nerve activity. These reflexes are modified in patients with essential hypertension. From measurements of muscle sympathetic nerve activity (MSNA), it was revealed that occurrence and development of essential hypertension may be relevant to activation of MSNA. In young boundary hypertension patients, the arterial baroreceptor reflex was decreased, while cardiopulmonary baroreceptor reflex was increased. These contradictory results imply that the two reflexes compensate each other. In addition, arterial chemoreceptor reflex was increased probably due to decrease of arterial baroreceptor reflex. Author (NASDA)

N94-27539# Nagoya Univ. (Japan). Dept. of Neural Regulation.

THE POLYMODAL RECEPTOR [PORIMODARU RESEPUTA] c51

Kazue Mizumura *In its* Annals of the Research Inst. of Environmental Medicine, Nagoya Univ., Volume 44 25 Mar. 1993 p 373-374 In JAPANESE Presented at the 13th Symposium on Environmental Medicine, Aichi, Japan, 11 Nov. 1992 (For primary document see N94-27442 07-52)

Avail: CASI HC A01/MF A04

The polymodal receptor is a noxious receptor that not only causes the sense of pain, but also affects autonomic functions, and is sensitized by inflammatory mediators. This article presents the findings on the sensitization of polymodal receptors examined by prostaglandin E2 (PGE2). The PGE2 scarcely causes discharge on polymodal receptor; however, it augments the discharge caused by Bradykinin (BK) or caloric stimulus in different concentrations. This suggests that the polymodal receptor has at least two binding sites for prostaglandin. Therefore, antagonists of each three subtypes of PGE receptors (EP1, EP2, and EP3) were added to the polymodal receptor, and it was revealed that EP3 receptor might participate in augmentation of BK effect, and EP2 receptor may be relevant to caloric stimulus. In order to identify the second messengers of these receptors, the relation between adenosine 3', 5'-cyclic monophosphate (cAMP) concentration and responses to BK and caloric stimulus was examined. As a result, BK response was slightly suppressed by increase of intracellular cAMP, which may imply that EP3 receptor inhibited adenylate cyclase via inhibitory G protein. On the contrary, the thermoresponse was obviously increased by cAMP increase, and it was also decreased by adenylate cyclase inhibitor, which supports the idea that cAMP participates in thermoresponse via PGE2 receptor. Author (NASDA)

N94-27540# Tokyo Woman's Medical Coll. (Japan). Dept. of Internal Medicine.

AUTONOMIC NERVOUS SYSTEM AND CARDIOVASCULAR CONTROL: CLINICAL IMPLICATIONS OF THE 1/f FLUCTUATIONS OF HEART RATE [JIRITSU SHINKEI NI YORU SHINZO CHOSETSU]

Kuniaki Otsuka and Haruo Watanabe *In* Nagoya Univ., Annals of the Research Inst. of Environmental Medicine, Nagoya Univ., Volume 44 25 Mar. 1993 p 375-379 In JAPANESE Presented at the 13th Symposium on Environmental Medicine, Aichi, Japan, 11 Nov. 1992; sponsored by Research Inst. of Environmental Medicine (For primary document see N94-27442 07-52)

Avail: CASI HC A01/MF A04

The 1/f fluctuation is observed extensively in nature, from the rhythm of music or vibration of vehicles to magnetic field of the galactic system. This article presents findings concerning the 1/f fluctuation of autonomic nerve activity. To examine the relation between heart rate and 1/f fluctuation, electrocardiograms were recorded and analyzed in healthy volunteers. Natural fluctuation includes 1/f fluctuation, white fluctuation, and 1/f(exp 2) fluctuation, which can be identified by incline of linear regression line of power spectral density against frequency. As a result, circadian rhythm was observed in 1/f fluctuation of healthy subjects, and the 1/f fluctuation gradually shifted to white fluctuation when subjects got older or in patients with Parkinson's disease. The same tendency was also observed in a patient with severe pseudo aldosteronism, in whom white fluctuation shifted to 1/f fluctuation as the patient recovered. These results support the notion that 1/f fluctuation may be a basic fluctuation of organisms. Author (NASDA)

N94-27541# Osaka Univ. (Japan). Dept. of Internal Medicine.

THE ROLE OF BETA-ADRENOCEPTOR STIMULATION IN THE PROGRESSION OF CHRONIC HEART FAILURE [SHINFUZEN NO SHINTEN NI OKERU KOKAN SHINKEI BETA JUYOTAI SHIGEKI NO IGI]

Masatsugu Hori, Hideyuki Sato, Hiroshi Sato, and Takenobu Kamada *In* Nagoya Univ., Annals of the Research Inst. of Environmental Medicine, Nagoya Univ., Volume 44 25 Mar. 1993 p 380-383 In JAPANESE Presented at the 13th Symposium on Environmental Medicine, Aichi, Japan, 11 Nov. 1992; sponsored by Research Inst. of Environmental Medicine (For primary document see N94-27442 07-52)

Avail: CASI HC A01/MF A04

In heart failure, sympathetic nerve activity is activated in proportion to severity of the disease. This activation may be a compensatory mechanism in order to increase blood supply to muscles in motion by stimulating cardiac muscles. Norepinephrine released in sympathetic nerve activation stimulates beta-receptors to increase heart rate, stroke volume, and cardiac output, as well as alpha-receptor to increase blood pressure and blood supply. However, alpha-receptor stimulation also decreases renal blood flow, and beta-receptor stimulation activates renin, angiotensin, and aldosterone, which contradicts with cardiac alpha-receptor response in vasoconstriction. These excess sympathetic nerve activations may exacerbate heart failure by down-regulation of beta-receptor and destruction of microtubules. For these patients, beta blocker is chronically administered to protect cardiac muscles from excess catecholamine effects. In administration, it is important to start with a low dose and increase it little by little. Author (NASDA)

N94-27556*# National Aeronautics and Space Administration, Washington, DC.

SPACE RADIATION HEALTH RESEARCH, 1991-1992

M. H. Jablin, comp., C. Brooks, comp., G. Ferraro, comp., K. J. Dickson, comp. (George Washington Univ., Washington, DC.), J. V. Powers, comp. (George Washington Univ., Washington, DC.), J. Wallace-Robinson, comp. (George Washington Univ., Washington, DC.), and B. Zafren, comp. (George Washington Univ., Washington, DC.) Washington Oct. 1993 149 p Prepared in cooperation with Lockheed Engineering and Sciences Co., Washington, DC

(NASA-TM-109721; NAS 1.15:109721) Avail: CASI HC A07/MF A02

The present volume is a collection of 227 abstracts of radiation research sponsored by the NASA Space Radiation Health Program for the period 1991-1992. Each abstract has been categorized within one of three discipline areas: Physics, Biology and Risk Assessment. Topic areas within each discipline have been assigned as follows: Physics - Atomic Physics, Theory, Cosmic Ray and Astrophysics, Experimental, Environments and Environmental Models, Solar Activity and Prediction, Experiments, Radiation Transport and Shielding, Theory and Model Development, Experimental Studies, and Instrumentation. Biology - Biology, Molecular Biology, Cellular Radiation Biology, Transformation, Mutation, Lethality, Survival, DNA Damage and Repair, Tissue, Organs, and Organisms, In Vivo/In Vitro Systems,

Carcinogenesis and Life Shortening, Cataractogenesis, Genetics/ Developmental, Radioprotectants, Plants, and Other Effects. Risk Assessment - Risk Assessment, Radiation Health and Epidemiology, Space Flight Radiation Health Physics, Inter- and Intraspecies Extrapolation and Radiation Limits and Standards. Section I contains refereed journals; Section II contains reports/meetings. Keywords and author indices are provided. A collection of abstracts spanning the period 1986-1990 was previously issued as NASA Technical Memorandum 4270. Author

N94-27744# Los Alamos National Lab., NM.
TEMPORAL STOCHASTICITY LEADS TO NONDETERMINISTIC CHAOS IN A MODEL FOR BLOOD CELL PRODUCTION
Ramit Mehr and Zvia Agur 1993 12 p Presented at the Fluctuations and Order: The New Synthesis Workshop, Los Alamos, NM, 9-12 Sep. 1993
(Contract W-7405-eng-36)
(DE94-003943; LA-UR-93-4088; CONF-9309185-5) Avail: CASI HC A03/MF A01

All types of blood cells are formed by differentiation from a small population of pluripotent stem cells in the bone marrow. This population should maintain the balance between self-renewal and differentiation, even under severe perturbations, e.g. the massive cell death caused by chemotherapy or irradiation. The authors constructed a cellular-automata model for bone marrow dynamics, which retrieves its homeostatic capabilities even under periodic perturbations with constant or random amplitude. However, temporally stochastic perturbations result in a chaotic-like behavior. Several methods of analysis failed to distinguish between the time series in this case and a chaotic time series, although the chaotic-like behavior has no deterministic source. DOE

N94-27942# Japanese Air Self-Defense Force, Tokyo. Aeromedical Lab.
THE REPORTS OF AEROMEDICAL LABORATORY, VOLUME 33, NUMBER 4 [KOKU IGAKU JIKKENTAI HOKOKU, DAI 33 KAN DAI 4 GO]
Akio Nakamura, Miyako Okaue, Hideo Tarui, Akihiko Onozawa, and Shoichi Tachibana et al 1 Dec. 1992 73 p In JAPANESE
(ISSN 0023-2858)
(JTN-94-80586) Avail: CASI HC A04/MF A01

The following topics were discussed: aircraft pilots, pilot training, flight training, flight control, aircraft control, attitude control, pilot performance, experience, flight simulators, roll, pitch, high acceleration, acceleration effect, gravitational effect, blood flow, blood circulation, blood flow rate, hemoglobin, near infrared spectroscopy, low atmospheric pressure, high altitude pressure, low oxygen pressure, consciousness, hypoxia, symptoms, and physiological effects. For individual titles, see N94-27943 through N94-27945.

N94-27943# Japanese Air Self-Defense Force, Tokyo. Aeromedical Lab.
COMPARISON OF PERFORMANCE IN SIMULATOR FLIGHT AMONG SUBJECTS WITH DIFFERENT SIMULATOR EXPERIENCES [FURAITO SHIMYURETA SOJU NI OKERU MIKEIKENSHA TO KEIKENSHA NO SOI NI TSUITE] c54
Miyako Okaue, Atsushi Kadoo, Syuji Nishi, Kyouichi Nagatsuka, and Zoujirou Katoh *In its* The Reports of Aeromedical Laboratory, Volume 33, Number 4 1 Dec. 1992 p 87-101 In JAPANESE (For primary document see N94-27942 07-52)
Avail: CASI HC A03/MF A01

A comparison of flight simulator control was made among three subject groups: Japan Air Self Defence Force (JASDF) personnel in their 20's, who had not applied to become pilots and are currently engaged in non-flight duties (Group 1); flight students (in their 20's) with only 4 hours of flight experience (Group 2); and non-pilots ranging in age from 28 to 48 (mean age, 38) (Group 3). The data-gathering flight patterns included seven segments. Each segment began from straight and level flight, proceeded to the aircraft maneuver in question, and ended in straight and level flight. The aircraft maneuvers were as follows: straight climb and descend for segment 1; right and left level turn for segment 2; left climbing turn for segment 3; right climbing turn for segment 4; left descending turn for Segment 5; right descending turn for Segment 6; and landing for Segment 7. As was expected, Group 3 performed the best overall. Author (NASDA)

N94-27944# Japanese Air Self-Defense Force, Tokyo. Aeromedical Lab.
EVALUATION OF NEAR-INFRARED SPECTROPHOTOMETRIC METHOD FOR INDIVIDUAL TOLERANCE TO +Gz ACCELERATION [KIN SEKIGAI BUNKOHO NI YORU TAI JISEI HYOKA]
Yoshinori Miyamoto, Chieko Mizumoto, Ken Shimizu, Asao Kobayashi, Akio Nakamura, and Shigeyuki Yagura *In its* The Reports of Aeromedical Laboratory, Volume 33, Number 4 1 Dec. 1992 p 103-109 In JAPANESE (For primary document see N94-27942 07-52)
Avail: CASI HC A02/MF A01

A technique for measurement of cerebral oxygen status was evaluated on volunteer subjects in the Aeromedical Laboratory centrifuge. Eight males were exposed to a 0.1 G sec(exp -1) onset rate profile until grayout. By using near infrared oxygenation monitor, this instrumentation is capable of measuring the concentrations in the brain of oxygenated Hemoglobin (HbO2), reduced Hemoglobin (Hb), oxidized cytochrome aa(sub 3)-reduced Cytochrome aa(sub 3) (CtO2) and total Hemoglobin (BV, HbO2+Hb). Results showed changes within the brain, as generally expected, during increased Gz with reductions in HbO2 and BV. Hb and CtO2 measurements were inconclusive. There were high correlations (R = -0.95 +/- 0.02, n = 18) between the change of the cerebral HbO2 concentration and the +Gz value. This correlation may be used as a criterion of individual subject +Gz tolerance. Author (NASDA)

N94-27945# Japanese Air Self-Defense Force, Tokyo. Aeromedical Lab.
SYMPTOMS OF HYPOXIA AT SIMULATED ALTITUDE OF 25,000 FEET [KODO 25,000 FITO NI OKERU TEI SANSOSHO NO SHOJO NI TSUITE]
Nobuyuki Fujita, Hideki Sonoda, Makoto Komizu, Kiyoaki Fujii, Shoichi Tachibana, and Akio Nakamura *In its* The Reports of Aeromedical Laboratory, Volume 33, Number 4 1 Dec. 1992 p 111-138 In JAPANESE (For primary document see N94-27942 07-52)
Avail: CASI HC A03/MF A01

The signs and symptoms experienced by the 500 trainees who took the chamber flight training in 1990 at Tachikawa were reviewed. The trainees were asked to answer the questionnaire of 14 items and evaluate their hypoxic conditions into five grades of seriousness by themselves after hypoxia experience (maximum duration of 5 minutes). These data were evaluated in terms of the duties and ages of the trainees. The time during the trainee was without his oxygen mask was recorded as 'Time of Useful Consciousness (T.U.C.).' Occurrence of hypoxic signs and symptoms showed similar tendency regardless of their duties or ages. Each individual experienced more than four symptoms out of 12 items. The most common symptom was burning sensation (or hot flashes) that was complained by 85.8 percent of all trainees. This symptom is considered to be one of the important alarming signs for hypoxia since it appears in early stage. Judgment impairment was observed in 79.4 percent and visual disturbance was complained by 58.9 percent. Both of these problems are critical for controlling the aircraft. Average TUC was 2 minutes and 53 seconds. TUC of inexperienced trainees was approximately 1 minute longer than that of experienced trainees. This proves the effectiveness of repeating chamber training. Author (NASDA)

N94-28208* National Aeronautics and Space Administration, Washington, DC.
AEROSPACE MEDICINE AND BIOLOGY: A CONTINUING BIBLIOGRAPHY WITH INDEXES (SUPPLEMENT 386)
Mar. 1994 56 p
(NASA-SP-7011(386); NAS 1.21:7011(386)) Avail: CASI HC A04

This bibliography lists 117 reports, articles and other documents introduced into the NASA Scientific and Technical Information System during Mar. 1994. Subject coverage includes: aerospace medicine and physiology, life support systems and man/system technology, protective clothing, exobiology and extraterrestrial life, planetary biology, and flight crew behavior and performance. Derived from text

N94-28213* National Aeronautics and Space Administration, Washington, DC.
AEROSPACE MEDICINE AND BIOLOGY: A CONTINUING BIBLIOGRAPHY WITH INDEXES (SUPPLEMENT 387)
Apr. 1994 33 p
(NASA-SP-7011(387); NAS 1.21:7011(387)) Avail: CASI HC A03

This bibliography lists 60 reports, articles and other documents introduced into the NASA Scientific and Technical Information System during Apr.

1994. Subject coverage includes: aerospace medicine and physiology, life support systems and man/system technology, protective clothing, exobiology and extraterrestrial life, planetary biology, and flight crew behavior and performance. Derived from text

N94-28219* National Aeronautics and Space Administration, Washington, DC.

AEROSPACE MEDICINE AND BIOLOGY: A CUMULATIVE INDEX TO A CONTINUING BIBLIOGRAPHY (SUPPLEMENT 384)

Jan. 1994 245 p
(NASA-SP-7011(384); NAS 1.21:7011(384)) Avail: CASI HC A11

This publication is a cumulative index to the abstracts contained in Supplements 372 through 383 of Aerospace Medicine and Biology: A Continuing Bibliography. It includes seven indexes: subject, personal author, corporate source, foreign technology, contract number, report number, and accession number. Author (revised)

N94-28361*# National Aeronautics and Space Administration. Lyndon B. Johnson Space Center, Houston, TX.

WORKSHOP ON COUNTERING SPACE ADAPTATION WITH EXERCISE: CURRENT ISSUES

Bernard A. Harris, ed. and Steven F. Siconolfi, ed. Feb. 1994 234 p
Workshop held in Houston, TX, 1989 Sponsored by NASA, Washington
(NASA-CP-3252; S-755; NAS 1.55:3252) Avail: CASI HC A11/MF A03

The proceedings represent an update to the problems associated with living and working in space and the possible impact exercise would have on helping reduce risk. The meeting provided a forum for discussions and debates on contemporary issues in exercise science and medicine as they relate to manned space flight with outside investigators. This meeting also afforded an opportunity to introduce the current status of the Exercise Countermeasures Project (ECP) science investigations and inflight hardware and software development. In addition, techniques for physiological monitoring and the development of various microgravity countermeasures were discussed. For individual titles, see N94-28362 through N94-28374.

N94-28362*# Ariel Dynamics.

MUSCULAR ACTIVITY AND ITS RELATIONSHIP TO BIOMECHANICS AND HUMAN PERFORMANCE

Gideon Ariel *In* NASA. Johnson Space Center, Workshop on Countering Space Adaptation with Exercise: Current Issues Feb. 1994 p 1-97
(For primary document see N94-28361 07-52)
Avail: CASI HC A05/MF A03

The purpose of this manuscript is to address the issue of muscular activity, human motion, fitness, and exercise. Human activity is reviewed from the historical perspective as well as from the basics of muscular contraction, nervous system controls, mechanics, and biomechanical considerations. In addition, attention has been given to some of the principles involved in developing muscular adaptations through strength development. Brief descriptions and findings from a few studies are included. These experiments were conducted in order to investigate muscular adaptation to various exercise regimens. Different theories of strength development were studied and correlated to daily human movements. All measurement tools used represent state of the art exercise equipment and movement analysis. The information presented here is only a small attempt to understand the effects of exercise and conditioning on Earth with the objective of leading to greater knowledge concerning human responses during spaceflight. What makes life from nonliving objects is movement which is generated and controlled by biochemical substances. In mammals, the controlled activators are skeletal muscles and this muscular action is an integral process composed of mechanical, chemical, and neurological processes resulting in voluntary and involuntary motions. The scope of this discussion is limited to voluntary motion. Derived from text

N94-28363*# Massachusetts Univ., Amherst. Dept. of Exercise Science.

ECCENTRIC EXERCISE TESTING AND TRAINING

Priscilla M. Clarkson *In* NASA. Johnson Space Center, Workshop on Countering Space Adaptation with Exercise: Current Issues Feb. 1994 p 99-110 (For primary document see N94-28361 07-52)
Avail: CASI HC A03/MF A03

Some researchers and practitioners have touted the benefits of including eccentric exercise in strength training programs. However, others have challenged its use because they believe that eccentric actions are dangerous and lead to injuries. Much of the controversy may be based on a lack of understanding of the physiology of eccentric actions. This review will present data concerning eccentric exercise in strength training, the physiological characteristics of eccentric exercise, and the possible stimulus for strength development. Also a discussion of strength needs for extended exposure to microgravity will be presented. Not only is the use of eccentric exercise controversial, but the name itself is fraught with problems. The correct pronunciation is with a hard 'c' so that the word sounds like ekscentric. The confusion in pronunciation may have been prevented if the spelling that Asmussen used in 1953, excentric, had been adopted. Another problem concerns the expressions used to describe eccentric exercise. Commonly used expressions are negatives, eccentric contractions, lengthening contractions, resisted muscle lengthenings, muscle lengthening actions, and eccentric actions. Some of these terms are cumbersome (i.e., resisted muscle lengthenings), one is slang (negatives), and another is an oxymoron (lengthening contractions). Only eccentric action is appropriate and adoption of this term has been recommended by Cavanagh. Despite the controversy that surrounds eccentric exercise, it is important to note that these types of actions play an integral role in normal daily activities. Eccentric actions are used during most forms of movement, for example, in walking when the foot touches the ground and the center of mass is decelerated and in lowering objects, such as placing a bag of groceries in the car. Author (revised)

N94-28364*# Texas Univ., Austin. Dept. of Kinesiology and Health.

EXERCISE DETRAINING: APPLICABILITY TO MICROGRAVITY

Edward F. Coyle *In* NASA. Johnson Space Center, Workshop on Countering Space Adaptation with Exercise: Current Issues Feb. 1994 p 111-118 (For primary document see N94-28361 07-52)
Avail: CASI HC A02/MF A03

Physical training exposes the various systems of the body to potent physiologic stimuli. These stimuli induce specific adaptations that enhance an individual's tolerance for the type of exercise encountered in training. The level of adaptation and the magnitude of improvement in exercise tolerance is proportional to the potency of the physical training stimuli. Likewise, our bodies are stimulated by gravity, which promotes adaptations of both the cardiovascular and skeletal muscles. Exposure to microgravity removes normal stimuli to these systems, and the body adapts to these reduced demands. In many respects the cessation of physical training in athletes and the transition from normal gravity to microgravity represent similar paradigms. Inherent to these situations is the concept of the reversibility of the adaptations induced by training or by exposure to normal gravity. The reversibility concept holds that when physical training is stopped (i.e., detraining) or reduced, or a person goes from normal gravity to microgravity, the bodily systems readjust in accordance with the diminished physiologic stimuli. The focus of this chapter is on the time course of loss of the adaptations to endurance training as well as on the possibility that certain adaptations persist, to some extent, when training is stopped. Because endurance exercise training generally improves cardiovascular function and promotes metabolic adaptations within the exercising skeletal musculature, the reversibility of these specific adaptations is considered. These observations have some applicability to the transition from normal to microgravity. Author (revised)

N94-28365*# Medical Coll. of Wisconsin, Milwaukee. Dept. of Anesthesiology and Physiology.

AEROBIC FITNESS AND ORTHOSTATIC TOLERANCE: EVIDENCE AGAINST AN ASSOCIATION

Thomas J. Ebert *In* NASA. Johnson Space Center, Workshop on Countering Space Adaptation with Exercise: Current Issues Feb. 1994 p 121-128 (For primary document see N94-28361 07-52)
Avail: CASI HC A02/MF A03

This presentation will focus on only one side of the debate as to whether high levels of aerobic fitness have a deleterious effect on tolerance to gravitational stress. This issue was raised in the early 1970's as a result of two research publications. The first work investigated the carotid sinus baroreflex of humans with an airtight chamber that surrounded the head and neck. The steady-state reflex changes in blood pressure that were recorded 3 minutes after application of the head and neck stimuli, were attenuated in an athletic group compared to a sedentary group of volunteers. A second report in the NASA literature indicated that five endurance-trained runners were less tolerant to LBNP than five nonrunners.

These early research findings have stimulated a considerable amount of interest that has lead to a growing number of research efforts seeking an association between aerobic fitness and orthostatic tolerance in humans. I will briefly review some of the more pertinent published research information which suggests that there is no relationship between aerobic fitness and orthostatic tolerance in humans. Author (revised)

N94-28366*# Texas Coll. of Osteopathic Medicine, Fort Worth. Dept. of Physiology.

DOES TRAINING-INDUCED ORTHOSTATIC HYPOTENSION RESULT FROM REDUCED CAROTID BAROREFLEX RESPONSIVENESS?

James A. Pawelczyk and Peter B. Raven *In* NASA. Johnson Space Center, Workshop on Countering Space Adaptation with Exercise: Current Issues Feb. 1994 p 129-140 (For primary document see N94-28361 07-52)

Avail: CASI HC A03/MF A03

As manned space travel has steadily increased in duration and sophistication, the answer to a simple, relevant question remains elusive. Does endurance exercise training - high intensity rhythmic activity, performed regularly for extended periods of time - alter the disposition to, or severity of, postflight orthostatic hypotension? Research results continue to provide different views; however, data are difficult to compare because of the following factors that vary between investigations: the type of orthostatic stress imposed (+Gz, lower body negative pressure (LBNP), head-up tilt); pretest perturbations used (exercise, heat exposure, head-down tilting, bed rest, water immersion, hypohydration, pharmacologically-induced diuresis); the length of the training program used in longitudinal investigations (days versus weeks versus months); the criteria used to define fitness; and the criteria used to define orthostatic tolerance. Generally, research results indicate that individuals engaged in aerobic exercise activities for a period of years have been reported to have reduced orthostatic tolerance compared to untrained control subjects, while the results of shorter term longitudinal studies remain equivocal. Such conclusions suggest that chronic athletic training programs reduce orthostatic tolerance, whereas relatively brief (days to weeks) training programs do not affect orthostatic tolerance to any significant degree (increase or decrease). A primary objective was established to identify the alterations in blood pressure control that contribute to training-induced orthostatic hypotension (TIOH). Although any aspect of blood pressure regulation is suspect, current research has been focused on the baroreceptor system. Reductions in carotid baroreflex responsiveness have been documented in exercise-trained rabbits, reportedly due to an inhibitory influence from cardiac afferent, presumably vagal, nerve fibers that is abolished with intrapericardiac denervation. The purpose of this investigation was to attempt to determine if similar relationships existed in men with varied levels of fitness, using maximal aerobic power, VO2 max, as the marker of fitness. Derived from text

N94-28367*# Minnesota Univ., Minneapolis. Dept. of Physical Medicine and Rehabilitation.

CARDIAC OUTPUT AND CARDIAC CONTRACTILITY BY IMPEDANCE CARDIOGRAPHY DURING EXERCISE OF RUNNERS

W. G. Kubicek and R. A. Tracy *In* NASA. Johnson Space Center, Workshop on Countering Space Adaptation with Exercise: Current Issues Feb. 1994 p 141-149 (For primary document see N94-28361 07-52)

Avail: CASI HC A02/MF A03

Most of the solid state electronic engineering of the system now generally known as the Minnesota Impedance Cardiograph was performed with the support of a five-year contract, NAS9-4500, with the NASA Lyndon B. Johnson Space Center, Houston, Texas. This contract ran from 1965 to 1970. In addition to the engineering design and development of the hardware, the contract called for testing on both animals and human subjects. This project also provided funds to construct twenty impedance cardiographs and place them in selected research and clinical facilities for further evaluation. This, then, led to the First Symposium on Impedance Cardiography, held at the NASA Lyndon B. Johnson Space Center, Houston, Texas, 2-4 June 1969. Twenty-four excellent papers were presented. Derived from text

N94-28368*# Boston Univ., MA. School of Medicine.

WEIGHTLESSNESS AND THE HUMAN SKELETON: A NEW PERSPECTIVE

Michael F. Holick *In* NASA. Johnson Space Center, Workshop on Countering Space Adaptation with Exercise: Current Issues Feb. 1994 p 153-168 (For primary document see N94-28361 07-52)

Avail: CASI HC A03/MF A03

It is now clear after more than two decades of space exploration that one of the major short- and long-term effects of microgravity on the human body is the loss of bone. The purpose of this presentation will be to review the data regarding the impact of microgravity and bed rest on calcium and bone metabolism. The author takes the position in this Socratic debate that the effect of microgravity on bone metabolism can be either reversed or mitigated. As we begins to contemplate long-duration space flight and habitation of Space Station Freedom and the moon, one of the issues that needs to be addressed is whether humans need to maintain a skeleton that has been adapted for the one-g force on earth. Clearly, in the foreseeable future, a healthy and structurally sound skeleton will be required for astronauts to shuttle back and forth from earth to the moon, space station, and Mars. Based on most available data from bed-rest studies and the short- and long-duration microgravity experiences by astronauts and cosmonauts, bone loss is a fact of life in this environment. With the rapid advances in understanding of bone physiology it is now possible to contemplate measures that can prevent or mitigate microgravity-induced bone loss. Will the new therapeutic approaches for enhancing bone mineralization be useful for preventing significant bone loss during long-term space flight? Are there other approaches such as exercise and electrical stimulation that can be used to mitigate the impact of microgravity on the skeleton? A recent study that evaluated the effect of microgravity on bone modeling in developing chick embryos may perhaps provide a new perspective about the impact of microgravity on bone metabolism. Derived from text

N94-28369*# Ford (Henry) Hospital, Detroit, MI. Bone and Mineral Research Lab.

IRREVERSIBILITY OF ADVANCED OSTEOPOROSIS: LIMITED ROLE FOR PHARMACOLOGIC INTERVENTION

A. M. Parfitt *In* NASA. Johnson Space Center, Workshop on Countering Space Adaptation with Exercise: Current Issues Feb. 1994 p 169-174 (For primary document see N94-28361 07-52)

Avail: CASI HC A02/MF A03

Osteoporosis is of medical interest only because it increases bone fragility and risk of fracture, and except for relief of symptoms, preventing fracture is the only purpose of intervention. To prevent the first fracture, adequate bone density must be accumulated and conserved, but to prevent subsequent fracture, bone density must be augmented so that the supportive function of the skeleton can be restored. Almost 50 years after the recognition of post menopausal osteoporosis as a clinical entity, not one of the many treatments that have been used has been demonstrated to be efficacious in reducing subsequent fracture risk. My purpose is not to recite this chronicle of disappointment, but to account for it in terms of bone biology, to consider some possible exceptions, and to reiterate the importance of preventing damage to the skeleton rather than belatedly attempting its repair. Author

N94-28370*# California Univ., San Francisco. Dept. of Radiology.

EXERCISE AND OSTEOPOROSIS: METHODOLOGICAL AND PRACTICAL CONSIDERATIONS

Jon E. Block, Anne L. Friedlander, Peter Steiger, and Harry K. Genant *In* NASA. Johnson Space Center, Workshop on Countering Space Adaptation with Exercise: Current Issues Feb. 1994 p 175-180 (For primary document see N94-28361 07-52)

Avail: CASI HC A02/MF A03

Physical activity may have important implications for enhancing bone density prior to the initiation of space flight, for preserving bone density during zero gravity, and for rehabilitating the skeleton upon return to Earth. Nevertheless, the beneficial effects of exercise upon the skeleton have not been proven by controlled trials and no consensus exists regarding the type, duration, and intensity of exercise necessary to make significant alterations to the skeleton. The following sections review our current understanding of exercise and osteoporosis, examine some of the methodological shortcomings of these investigations, and make research recommendations for future clinical trials. Author

N94-28371*# Massachusetts Univ., Amherst. Dept. of Exercise Science.

ELECTRICAL STIMULATION IN EXERCISE TRAINING

Walter Kroll *In* NASA. Johnson Space Center, Workshop on Countering Space Adaptation with Exercise: Current Issues Feb. 1994 p 183-186 (For primary document see N94-28361 07-52)
Avail: CASI HC A02/MF A03

Electrical stimulation has a long history of use in medicine dating back to 46 A.D. when the Roman physician Largus found the electrical discharge of torpedo fishes useful in the treatment of pain produced by headache and gout. A rival Greek physician, Dioscorides, discounted the value of the torpedo fish for headache relief but did recommend its use in the treatment of hemorrhoids. In 1745, the Leyden jar and various sized electrostatic generators were used to treat angina pectoris, epilepsy, hemiplegia, kidney stones, and sciatica. Benjamin Franklin used an electrical device to treat successfully a young woman suffering from convulsive fits. In the late 1800's battery powered hydroelectric baths were used to treat chronic inflammation of the uterus while electrified athletic supporters were advertised for the treatment of male problems. Fortunately, such an amusing early history of the simple beginnings of electrical stimulation did not prevent eventual development of a variety of useful therapeutic and rehabilitative applications of electrical stimulation. Over the centuries electrical stimulation has survived as a modality in the treatment of various medical disorders with its primary application being in the rehabilitation area. Recently, a surge of new interest in electrical stimulation has been kindled by the work of a Russian sport scientist who reported remarkable muscle strength and endurance improvements in elite athletes. Yakov Kots reported his research on electric stimulation and strength improvements in 1977 at a Canadian-Soviet Exchange Symposium held at Concordia University in Montreal. Since then an explosion of new studies has been seen in both sport science and in medicine. Based upon the reported works of Kots and the present surge of new investigations, one could be misled as to the origin of electrical stimulation as a technique to increase muscle strength. As a matter of fact, electric stimulation has been used as a technique to improve muscle strength for over a century. Bigelow reported in 1894, for example, the use of electrical stimulation on a young man for the purpose of increasing muscle strength. Employing a rapidly alternating sinusoidal induced current and a dynamometer for strength testing, Bigelow reported that the total lifting capacity of a patient increased from 4328 pounds to 4639 pounds after only 25 minutes of stimulation. In 1965, Massey et al. reported on the use of an Isotron electrical stimulator that emitted a high frequency current. Interestingly enough, the frequencies used by Massey et al. and the frequencies used by Bigelow in 1894 were in the same range of frequencies reported by Kots as being the most effective in strength development. It would seem the Russian secret of high frequency electrical stimulation for strength development, then, is not a modern development at all. Author

N94-28372*# Kentucky Univ., Lexington. Dept. of Physical Therapy.
THE VALUE OF ELECTRICAL STIMULATION AS AN EXERCISE TRAINING MODALITY
Dean P. Currier, J. Michael Ray, John Nyland, and Tim Noteboom *In* NASA. Johnson Space Center, Workshop on Countering Space Adaptation with Exercise: Current Issues Feb. 1994 p 187-191 (For primary document see N94-28361 07-52)
Avail: CASI HC A01/MF A03

Voluntary exercise is the traditional way of improving performance of the human body in both the healthy and unhealthy states. Physiological responses to voluntary exercise are well documented. It benefits the functions of bone, joints, connective tissue, and muscle. In recent years, research has shown that neuromuscular electrical stimulation (NMES) simulates voluntary exercise in many ways. Generically, NMES can perform three major functions: suppression of pain, improve healing of soft tissues, and produce muscle contractions. Low frequency NMES may gate or disrupt the sensory input to the central nervous system which results in masking or control of pain. At the same time NMES may contribute to the activation of endorphins, serotonin, vasoactive intestinal polypeptides, and ACTH which control pain and may even cause improved athletic performances. Soft tissue conditions such as wounds and inflammations have responded very favorably to NMES. NMES of various amplitudes can induce muscle contractions ranging from weak to intense levels. NMES seems to have made its greatest gains in rehabilitation where directed muscle contractions may improve joint ranges of motion correct joint contractures that result from shortening muscles; control abnormal movements through facilitating recruitment or excitation into the alpha motoneuron in orthopedically, neurologically, or healthy subjects with intense sensory, kinesthetic, and proprioceptive information; provide a conservative approach to management of spasticity in neurological patients; by stimulation of the antagonist muscle to a spastic muscle stimulation of the agonist muscle, and sensory habituation; serve as an orthotic substitute to conventional bracing used with stroke patients in lieu of dorsiflexor muscles in preventing step page gait and for shoulder muscles to maintain glenohumeral alignment to prevent subluxation; and of course NMES is used in maintaining or improving the performance or torque producing capability of muscle. NMES in exercise training is our major concern. Author (revised)

N94-28373*# California Univ., Los Angeles. Human Biomechanics Lab.
THE USE OF BIOMECHANICS IN THE STUDY OF MOVEMENT IN MICROGRAVITY
R. J. Gregor, J. P. Broker, and M. M. Ryan *In* NASA. Johnson Space Center, Workshop on Countering Space Adaptation with Exercise: Current Issues Feb. 1994 p 195-201 (For primary document see N94-28361 07-52)
Avail: CASI HC A02/MF A03

As biomechanists interested in the adaptability of the human body to microgravity conditions, it appears that our job is not only to make sure that the astronauts can function adequately in space but also that they can function upon their return to Earth. This is especially significant since many of the projects now being designed at NASA concern themselves with humans performing for up to 3 years in microgravity. While the Extended Duration Orbiter flights may last 30 to 60 days, future flights to Mars using current propulsion technology may last from 2 to 3 years. It is for this range of time that the adaptation process must be studied. Specifically, biomechanists interested in space travel realize that human performance capabilities will change as a result of exposure to microgravity. The role of the biomechanist then is to first understand the nature of the changes realized by the body. These changes include adaptation by the musculoskeletal system, the nervous system, cardiorespiratory system, and the cardiovascular system. As biomechanists, it is also our role to take part in the development of countermeasure programs that involve some form of regular exercise. Exercise countermeasure programs should include a variety of modalities with full knowledge of the loads imposed on the body by these modalities. Any exercise programs that are to be conducted by the astronauts during space travel must consider the fact that the musculoskeletal and neuromuscular systems degrade as a function of flight duration. Additionally, it must be understood that the central nervous system modifies its output in the control of the human body during space flight and most importantly, we must prepare the astronauts for their return to one g. Author (revised)

N94-28374*# North Carolina Univ., Chapel Hill. Exercise Physiology Lab.
PSYCHOPHYSIOLOGY IN MICROGRAVITY AND THE ROLE OF EXERCISE
J. M. Shaw and A. C. Hackney *In* NASA. Johnson Space Center, Workshop on Countering Space Adaptation with Exercise: Current Issues Feb. 1994 p 205-213 (For primary document see N94-28361 07-52)
Avail: CASI HC A02/MF A03

The Space Transportation-Shuttle (STS) Program has greatly expanded our capabilities in space by allowing for missions to be flown more frequently, less expensively, and to encompass a greater range of goals than ever before. However, the scope of the United State's role and involvement in space is currently at the edge of a new and exciting era. The National Aeronautics and Space Administration (NASA) has plans for placing an orbiting space station (Space Station Freedom) into operation before the year 2000. Space Station Freedom promises to redefine the extent of our involvement in space even further than the STS program. Space Station crewmembers will be expected to spend extended periods of time (approximately 30 to 180 days) in space exposed to an extremely diverse and adverse environment (e.g., the major adversity being the chronic microgravity condition). Consequently, the detrimental effects of exposure to the microgravity environment is of primary importance to the biomedical community responsible for the health and well-being of the crewmembers. Space flight and microgravity exposure present a unique set of stressors for the crewmember; weightlessness, danger, isolation/confinement, irregular work-rest cycles, separation from family/friends, and mission/ground crew interrelationships. A great deal is beginning to be known about the physiological changes associated with microgravity exposure, however, limited objective psychological findings exist. Examination of this latter area will become of critical concern as NASA prepares to place crewmembers on the longer space missions that will be required on Space Station Freedom. Psychological factors, such as interpersonal relations will become increasingly important issues, especially as crews become more heterogeneous in the way of experience, professional background, and assigned duties. In an attempt to minimize the detrimental physiological effects of prolonged space flight and microgravity exposure, the United States and Russian space agencies have taken steps to implement various countermeasure programs. One of the principle countermeasures used by both nations is exercise during space flight. The purpose is to present a brief overview of the major research findings examining the psychophysiological changes associated with microgravity exposure, and to address the potential role of exercise as a countermeasure in affecting these psychophysiological changes. Author (revised)

N94-28392# Research Inst. of National Defence, Stockholm (Sweden). Huvudadelning foer Maensklig Prestation och Funktion.
VISIT TO CERMA: CENTRE D'ETUDES ET DE RECHERCHES DE MEDECINE AEROSPATIALE, CENTRE FOR STUDIES AND RESEARCH IN AVIATION AND SPACE MEDICINE, BRETIGNY SUR ORGE, FRANCE, NOVEMBER 16-18, 1992 [BESOEK VID CERMA-CENTRE D'ETUDES ET DE RECHERCHES DE MEDECINE AEROSPATIALE, CENTRUM FOER STUDIER OCH FORSKNING I FLYG- OCH RYMDMEDICIN, BREGTIGNY SUR ORGE, FRANKRIKE, 1992-11-16-18]
G. Derefeldt and B. Schantz Nov. 1993 38 p In SWEDISH
(PB94-132990; FOA-A-50019-5.5) Avail: CASI HC A03/MF A01

A visit to CERMA is reported. The purpose of the journey was to visit the division for space and aviation ergonomics at CERMA to discuss cooperation between FOA and CERMA within the agreements now being established between FOA and DRET concerning co-operation within defense research. DRET is the organization for defense research in France and is the equivalent to FOA in Sweden. There are four research themes: (1) effects of variations in gravitation (acceleration, space) on the cardiovascular and musculoskeletal systems; (2) man-machine interfaces (MMI) in complex systems; (3) perturbations in vigilance; and (4) nutrition. At the division for space and aviation ergonomics, research is carried out on the following themes: (1) vision, (2) man-machine dialog, and (3) applied neurophysiology. The main result of the journey was a proposal to co-operate in visual information retrieval, color perception, and colorcoding. NTIS

53 BEHAVIORAL SCIENCES

Includes psychological factors; individual and group behavior; crew training and evaluation; and psychiatric research.

N94-25774# Air Force Inst. of Tech., Wright-Patterson AFB, OH. School of Engineering.
DEVELOPING REALISTIC COOPERATIVE BEHAVIORS FOR AUTONOMOUS AGENTS IN AIR COMBAT SIMULATION M.S. Thesis
Dean P. Hipwell Dec. 1993 169 p
(AD-A274077; AFIT/GCE/Eng/93D-05) Avail: CASI HC A08/MF A02

This thesis investigated, developed, and implemented cooperative decision-making behaviors in an air combat simulation by using a knowledge-based system. Knowledge-based systems were well suited for this task because of built-in features such as inference engines and rule-based constructs. This thesis addresses the specific problem of generating autonomous forces for inclusion in the Advanced Research Projects Agency Distributed Interactive Simulation program. Existing autonomous forces implementations lacked flexibility, realistic behaviors, real-time planning, and other features. The simulation system in this thesis addresses the problem of realistic behavior by modeling pilot decision processes rather than aircraft platforms. The system is based on phased control of a blackboard architecture. Modular knowledge bases partition rules to process decision data. Cooperative behaviors are based on a leader-follower relationship. Agents share the workload in assessing threats. Leaders make the initial decision, but followers react independently if necessary. The simulator described in this thesis provides an architecture and design for modeling combat pilot decision processes. The system was developed using the C Language Integrated Production System Object Oriented Language. DTIC

N94-25897# Air Force Inst. of Tech., Wright-Patterson AFB, OH. School of Logistics and Acquisition Management.
A TEST OF THE THEORY OF REASONED ACTION AT THE GROUP LEVEL OF ANALYSIS M.S. Thesis
Thomas A. Fitch and Edward A. McCarty Sep. 1993 52 p
(AD-A273965; AFIT/GLM/LAR/93S-16) Avail: CASI HC A04/MF A01

A vast array of studies exist which have sought to explore the relationships between behavioral intentions, job satisfaction, turnover and performance at the individual level of analysis. Recent efforts to move to the group level of analysis have shown some promise, but few exist. The crux of the issue under consideration here was whether or not there was utility in treating attitude-intention-behavior linkages as group level phenomena. Both Schneider (1987) and George (1990' contend that, while individual analysis cannot be discounted as a means of understanding behavior, there is also value in examining group-level phenomena. The purpose of this study was to test the generalizability of Fishbein and Ajzen's (1975) model to the group level of analysis by assessing the pattern of relationships among attitudinal, intentional, and behavioral variables. The objective of the project was to determine whether or not the basic assumptions of the theory held at the group level of analysis. DTIC

N94-25965 Ohio State Univ., Columbus. Dept. of Psychology.
PACING VISUAL ATTENTION: TEMPORAL STRUCTURE EFFECTS Ph.D. Thesis
June J. Skelly Jun. 1993 194 p Limited Reproducibility: More than 20% of this document may be affected by microfiche quality
(AF Proj. 7184)
(AD-A273859; AL-TR-1993-0024) Avail: CASI HC A09

The role of temporal relationships in how we attend to dynamic visual events was investigated. Specifically, those factors that are temporal in nature, i.e., the rate and rhythm of event sequences, were the primary variables of interest. The research explored the possibility that persisting temporal relationships may be an important factor in the external (exogenous) control of visual attention, at least to some extent, was the focus of the current research. Five experiments attempted to identify the respective roles of rate and rhythm time parameters in a simple selective attention task involving two differently timed streams of information. Results from these experiments indicated that the rhythmic structure of integrated streams was a more powerful 'pacing' factor than either of the rhythm or rate of single stream. Together, these experiments suggest that there may be two kinds of temporal 'pacing' in visual attention: (1) a passive entrainment with external time patterns, and (2) the active 'use' of timing relationships to shift and direct the focus of attention. DTIC

N94-26346# Naval Aerospace Medical Research Lab., Pensacola, FL.
A COMPARISON OF TWO HARDWARE IMPLEMENTATIONS OF A CREW SELECTION SYSTEM Special Report
T. Nontasak and K. T. Helton Oct. 1993 16 p
(AD-A274913; NAMRL-SR-93-3) Avail: CASI HC A03/MF A01

A number of disadvantages existed within the Apple IIe version of the Landing Craft Air Cushion vehicle Crew Selection System (LCSS). These disadvantages included slow processing speed, memory constraints, and cumbersome test administration. The system was also less conducive to future test development. The LCSS was upgraded to an IBM PC compatible Zenith 248 system. A comparison of 48 single and composite subtest scores between like measures of the two systems yielded significant positive correlations (p less than .0001). The majority of the correlations ranged from .60 to .89. A small percentage of the associations were less robust. Overall, however, the Apple IIe and Zenith 248 versions of the LCSS proved to be comparable testing systems. DTIC

N94-26430# Naval Health Research Center, San Diego, CA.
PERFORMANCE ASSESSMENT IN SUSTAINED OPERATIONS USING A COMPUTER-BASED SYNTHETIC WORK TASK
Timothy F. Elsmore, Paul Naitoh, and Steven Linnville 1993 32 p
(DA Proj. M00-96; DA Proj. MM3-P-30)
(AD-A274707; NHRC-92-30) Avail: CASI HC A03/MF A01

Prediction of the effects of stressors on military performance from laboratory tests frequently involves use of procedures simulating critical functional aspects of military jobs. This paper presents a computerized 'Synthetic Work' test, SYNWORKI, as a prototypical alternative to traditional Performance Assessment Batteries. This test simulates complex operational environments by requiring subjects to work on four simultaneous tasks, and assigns explicit consequences for work on each component task. As illustrations of the utility of this technique, data are presented from three applications of SYNWORK1, a laboratory study of sleep deprivation, a test of extended exposure to a simulated sonar 'ping', and the use of the same task during army operations in Operation Desert Storm. DTIC

N94-26600# Federal Aviation Administration, Oklahoma City, OK. Civil Aeromedical Inst.

VALIDATION OF THE FEDERAL AVIATION ADMINISTRATION AIR TRAFFIC CONTROL SPECIALIST PRE-TRAINING SCREEN Final Report

Dana Broach and Jan Brecht-Clark (Federal Aviation Administration, Washington, DC.) Feb. 1994 15 p

(DOT/FAA/AM-94/4) Avail: CASI HC A03/MF A01

Two formal validation studies of the Air Traffic Control Specialist Pre-Training Screen (ATCS/PTS), a 5-day computer-administered test battery, are described. The ATCS/PTS was designed to replace the 9-week U.S. Federal Aviation Administration (FAA) Academy ATCS Nonradar Screen program that served as the second major test in the ATCS selection system. Review of ATCS job analyses suggested that predictor tests should assess cognitive constructs such as spatial reasoning and short-term memory, and require dynamic, concurrent performance. A proposed test battery was developed, consisting of 2 computer-administered information processing tests and a simplified radar-based air traffic control work sample. In study 1, predictive, criterion-related validation (N = 438) found that the proposed test battery explained additional variability in scores earned in the 9-week FAA Academy program, after taking into account student aptitude. In study 2, criterion-related validation (N = 297) demonstrated that the proposed test battery was as valid as the 9-week FAA Academy ATCS Nonradar Screen for predicting progress in field training. Preliminary data from a third study conducted after validation of the ATCS/PTS seem to suggest that the abilities assessed by the new computerized tests reflect the abilities required on the job. However, implementation of the ATCS/PTS for actual employment decision-making in June 1992 was based on results obtained in the second concurrent, criterion-related validation study. The U.S. controller selection system since June 1992 consisted of the 4-hour written ATCS aptitude test battery followed by, for those applicants earning a qualifying score and dependent upon agency manpower requirements, second-level screening on the ATCS/PTS. Additional research requirements as part of an aviation program are described. Author (revised)

N94-26683# Medical Research Council, Cambridge (England). Applied Psychology Unit.

THE CENTRAL EXECUTIVE COMPONENT OF WORKING MEMORY Final Report, 1 Sep. 1990 - 31 Aug. 1993

A. Baddeley, J. Duncan, and H. Emslie 31 Oct. 1993 47 p

(Grant AF-AFOSR-0343-90)

(AD-A274295; AFOSR-93-0896TR) Avail: CASI HC A03/MF A01

A distinction between voluntary/controlled and stimulus-driven/automatic behavior has been separately applied to the effects of frontal lobe lesions, individual differences in general intelligence or Spearman's g, and interference between dissimilar, concurrent tasks. We suggest that these three problems are indeed closely linked, all concerning a process of selection between alternative goals or abstract requirements on behavior, especially under conditions of novelty and /or weak environmental cues to action. Among our findings are: (1) Executive deficits following frontal lesions are specifically associated with losses in fluid intelligence; (2) Conventional frontal tests have little in common besides g. (3) Across a wide range of spatial and verbal tasks, dual task interference is closely related to both g correlations and frontal lobe involvement. This may only be true, however, when the secondary task is random sequence generation, designed to avoid stereotype. (4) Frontal patients and people from the lower part of the g distribution share a tendency to goal neglect, or disregard of a task requirement even though that requirement has been understood. Neglect is confined to novel behavior, eliminated by verbal prompts, and sensitive to the number of concurrent goals. (5) In speeded stimulus classification, switching classification rules produces high g correlations. Correlations rapidly decrease, however, with practice on a fixed rule. The results begin to clarify the role of executive control in the organization of behavior. DTIC

N94-26749# Army Command and General Staff Coll., Fort Leavenworth, KS.

FEMALE COMBAT HELICOPTER PILOT SELECTION CRITERIA M.S. Thesis

Wendy R. Mullins 4 Jun. 1993 112 p

(AD-A273935) Avail: CASI HC A06/MF A02

This study investigates selection criteria for selecting female aviators for training in combat helicopters (AH-64, AH-1, OH-58D, and RAH-66). Selection for such training would occur as either a part of the multitrack program of instruction used in the current Initial Entry Rotary Wing flight training course, or as transition training for already qualified aviators. Analysis included a review of: current Army regulations governing prerequisites for combat helicopter training and combat helicopter maintenance test pilot training; Initial Entry Rotary Wing selection criteria for combat helicopter tracks (AH-1 and OH-58); Aviation Branch personnel manager interviews; combat helicopter manprint/anthropometric restrictions; standards of medical fitness; anthropometric standards; and previous reports on female performance in Initial Entry Rotary Wing training. Conclusion supports selecting females for combat helicopter training using the same selection criteria currently used for choosing males for such training. Study recommends additional research in aircraft accommodation measurements, social-psychological aspects, and physical body strength requirements. DTIC

N94-26873 Groningen Rijksuniv. (Netherlands). Dept. of Computing Science.

INTERACTING CORTICAL FILTERS FOR OBJECT RECOGNITION

N. Petkov and T. Lourens 1994 19 p See also PB94-125366 Sponsored by Nederlandse Organisatie voor Wetenschappelijk Onderzoek, The Hague Limited Reproducibility: More than 20% of this document may be affected by microfiche quality

(PB94-125374; CS-9303) Avail: Issuing Activity (National Technical Information Service (NTIS))

It is shown how cortical filters can be used for image analysis and object recognition. Similarly to previous work in this area, we compute functional inner products of a two-dimensional input signal (image) with a set of two-dimensional Gabor functions which fit the receptive fields of simple cells in the primary visual cortex of mammals. We propose a method in which these inner products become the subject of thresholding, orientation competition and lateral inhibition. Each of the resulting cortical images contains only edge lines of a particular orientation and a particular light-to-dark transition direction. In this way, the information which is present in the original image is split in different channels and we show how this splitting can be used for object recognition. Each cortical image is reduced to a single number so that a set of cortical images that emanate from the same input image is reduced to a set of descriptors of the input image which are robust for translations of an object in the visual field. Multi-scale resolution and dynamic programming are used to compensate for size variations, rotations and non-topologic form differences. The method discriminates between simple geometrical figures, e.g. polygons with different numbers of edges, with reliability of 100% and a recognition rate of 99% has been achieved when the method was applied to a large database of face images. NTIS

N94-26882# Arizona State Univ., Tempe. Dept. of Industrial Management Systems Engineering.

BENEFITS ESTIMATION FOR SIMULATION SYSTEMS USED FOR AIRCREW TRAINING IN A MULTISHIP ENVIRONMENT Final Report, Jul. - Oct. 1992

William C. Moor and Dee H. Andrews Nov. 1993 44 p

(AD-A274313; AL/HR-TR-1993-0158) Avail: CASI HC A03/MF A01

A general model for the benefit evaluation of multiship training simulation systems is presented. The benefit measures derived are oriented toward allowing benefit-cost evaluations of proposed alternative simulation systems. The model is based on empirical data drawn from evaluation studies of simulators as well as analytical approaches. The focus of the approach using this model is selecting the most appropriate and economic simulators for use at the operational level. The model does not attempt to compare, or justify the comparison of, the training value of a specific simulator versus a specific aircraft. The model allows for full sensitivity analysis and variation of all important parameters. A set of LOTUS 1-2-3 spreadsheets are presented which facilitate the use of the model. The model is demonstrated by means of an application which is based on actual data. DTIC

N94-27001# Groningen Rijksuniv. (Netherlands). Dept. of Computing Science.
ORIENTATION COMPETITION IN CORTICAL FILTERS
N. Petkov, T. Lourens, and P. Kruizinga 1994 15 p See also PB94-125374
(PB94-125366; CS-9302) Avail: CASI HC A03/MF A01

This work presents explorations in the microstructure of natural vision systems based on large scale computer simulations. Similarly to previous work in this area, we compute the functional inner products of a two-dimensional input signal (image) with a set of two-dimensional Gabor functions which have been shown to fit the receptive fields of simple cells in the primary visual cortex of mammals. These inner products are then considered as net inputs to the cortical cells and used to compute the cell activations as non-linear functions. A previously used model is extended with a pixel-wise winner-takes-all competition between different Gabor filters which is introduced in order to increase the orientation sensitivity of computed cortical cell responses. The effect of this competition is qualitatively estimated by visualization of computed cortical images and quantitatively evaluated by applying the model to a face recognition problem. Recognition rate of 97% was achieved on a database of 205 face images of 30 persons vs 94% achieved with a previously used model. NTIS

N94-27012# Stanford Univ., CA. Dept. of Psychology.
INDUCED PICTORIAL REPRESENTATIONS Final Technical Report, 1 Nov. 1988 - 30 Nov. 1993
Barbara G. Tversky 30 Nov. 1993 31 p
(Grant AF-AFOSR-0076-89)
(AD-A274251; AFOSR-93-0887TR) Avail: CASI HC A03/MF A01

Language is often used to describe environments or to give directions. This project investigated how spatial language describing large and small scale environments is comprehended and produced. The research on large scale environments, such as a town, has shown that in descriptions, people adopt either a route or a survey perspective or a mixture of both. In comprehension of such descriptions, people form spatial mental models that are more abstract than either perspective. The research on small scale environments investigated people's mental models of the objects surrounding them. People are faster to access objects at some directions from their bodies than others. Accessibility depends on enduring characteristics of the perceptual world and the relation of the body to it. Several variations and extensions of each project are described. The research has implications for spatial cognition as well as language comprehension and production. DTIC

N94-27056# Walter Reed Army Inst. of Research, Washington, DC.
HUMAN DIMENSIONS RESEARCH TEAM, OPERATION RESTORE HOPE Report, 26 Jan. - 5 Mar. 1993
Robert K. Gifford, James N. Jackson, and Kathleen B. DeShazo 5 Mar. 1993 14 p
(AD-A274340) Avail: CASI HC A03/MF A01

The purpose of this investigation was to assess soldier coping and adaptation to the stresses of operation Restore Hope. Interviews, observations, and command consultation generated the data necessary to delineate key themes. Perhaps the most important of the investigation's findings was that current Army doctrine and practices provided the support necessary for the deployed force to successfully adapt to the unique challenges of operation Restore Hope. The Human Dimensions Research Team detected no problems that were severe enough to threaten/comprise the Army's ability to perform its mission, or that would portend significant future mental health problems (e.g., post-traumatic stress disorder). While there were numerous, identifiable stressors (e.g., redeployment uncertainty, mission ambiguity, restrictive rules of engagement, slow mail, limited phone access), none were unexcepted, and more importantly, none were beyond the soldiers' or units' capacity to cope. DTIC

N94-27072# Massachusetts Inst. of Tech., Cambridge. Dept. of Brain and Cognitive Sciences.
TOP DOWN INFLUENCES ON BOTTOM-UP PROCESSING Final Report, Sep. 1989 - Sep. 1993
Whitman Richards 27 Oct. 1993 34 p
(Grant AF-AFOSR-0504-89)
(AD-A274220; AFOSR-93-0893TR) Avail: CASI HC A03/MF A01

Although integrated computational and psychophysical studies have considerably advanced our understanding of early visual processing (up to Marr's 2 1/2 D Sketch), much less research, by comparison, is being conducted on intermediate and higher-level vision. One reason for the scarcity is that high-level vision includes goal-directed, context-sensitive, top-down knowledge. However, little is known about these aspects of vision and how they are organized in the visual knowledge base (for example, how default preferences and categorical states are organized and related). Hence, plausible, detailed computational models can't be formulated. These studies begin to reveal the structure of some aspects of cognitive visual knowledge. DTIC

N94-27094# State Univ. of New York, Stony Brook. Dept. of Psychology.
SIGNAL- AND LISTENER-BASED FACTORS IN COMPLEX AUDITORY PATTERN PERCEPTION Annual Technical Report, 15 Sep. 1992 - 15 Sep. 1993
Arthur G. Samuel 9 Nov. 1993 13 p
(Grant AF-AFOSR-0378-91)
(AD-A274148; AFOSR-93-0906TR) Avail: CASI HC A03/MF A01

The research conducted during the second year of AFOSR grant 91-0378 investigated fundamental issues in the early processing of speech and similarly complex acoustic signals. The research pursued the information processing goal of specifying the levels of analysis that occur between the initial sensory coding of the signal and the recognition of the phonetic sequence it conveys. Five experiments provided evidence for the existence of at least three qualitatively different levels of perceptual analysis. The data help to specify the properties of each level, including a locus (peripheral versus central), a stimulus domain, and the mechanisms affected by repeated stimulation. The convergence across several different approaches used to determine levels of analysis supports the three-level model. DTIC

N94-27138 Institute for Perception RVO-TNO, Soesterberg (Netherlands).
ON THE DEVELOPMENT OF MOTOR CHUNKS AND CONCURRENT PROCESSING IN A STRUCTURED CONTINUOUS KEYPRESSING TASK Final Report
W. B. Verwey and Y. Dronkert Jun. 1993 26 p Limited Reproducibility: More than 20% of this document may be affected by microfiche quality
(AD-A274153; IZF-1993-B-6; TDCK-93-1348) Avail: Issuing Activity (Defense Technical Information Center (DTIC))

This report describes an experiment designed to assess the effects of practice in performing a structured sequence of keypresses. The task consisted of pressing a sequence of nine keys with nine fingers, each in response to a corresponding stimulus. Each response was followed by a response-stimulus interval (RSI), which sometimes was zero ms, before the next stimulus was presented. Upon completion of one sequence, production of the identical sequence was immediately repeated. One group of 18 subjects - the 333 group - practiced with three regularly spaced, non-negligible RSI's while the remaining RSI's were zero. This divided the sequence into three groups of three keypresses each. Another group of 18 subjects - the 45 group - practiced with two non-negligible RSI's partitioning the sequence into a four- and a five-key group. These conditions were coined structured conditions. On occasion all subjects carried out a condition in which all RSI's were zero. This was the unstructured condition. The results show that interkey times in this condition clearly reflected the position of the long RSI's in the structured condition. This suggests that motor chunks had developed in the structured condition which were also used in the unstructured condition. More detailed analyses suggest that preparing one chunk concurred with execution of the preceding chunk in the unstructured and probably also in the structured condition. Concurrent preparation of the next chunk slowed down execution of the preceding chunk in the unstructured condition. In the structured condition it concealed effects of chunk-size on initiating each chunk (i.e. the complexity effect). DTIC

N94-27141# Hahnemann Medical Coll. and Hospital, Philadelphia, PA. Dept. of Physiology and Biophysics.

CORTICAL MECHANISMS OF ATTENTION, DISCRIMINATION, AND MOTOR RESPONSE TO SOMESTHETIC STIMULI Final Report, 1 Apr. 1990 - 31 Mar. 1993

John K. Chapin 31 Mar. 1993 9 p
(Grant AF-AFOSR-0266-90)
(AD-A274163; AFOSR-93-0897TR) Avail: CASI HC A02/MF A01

Work carried out on AFOSR 90-0266 made major progress in several areas: (1) development of technology for recording large numbers of single neurons (up to 64) simultaneously through microwires implanted at multiple levels of the somatosensory system in awake rats; (2) utilization of an operant conditioning paradigm for investigating the detection and processing of sensory cues which trigger an active motor response; (3) demonstration that neuronal responses in the SI and MI cortices to such sensory cues are increased when they are used to trigger a conditioned motor response; (4) demonstration that this conditioning increases the prevalence of functional connections between neurons in the SI and MI cortices; (5) used quantitative techniques to defined dynamic and distributed properties of receptive fields in the somatosensory cortex and thalamus; (6) developed the use of multivariate statistical techniques to define population coding within ensembles of recorded neurons; and (7) continued to define neuroanatomical substrates for processing within this system. DTIC

N94-27584# National Aerospace Lab., Tokyo (Japan). Computational Sciences Div.

AN ALGORITHM FOR STEREO CORRESPONDENCE PROBLEMS ON THE ANALOGY OF HUMAN VISION [HITO NO SHIKAKU NI MANANDA BIDEO KAMERA NO SHISEN SEIGYO NIYORU TAIOTEN TANSAKU]

Hiromi Gomi Nov. 1992 32 p In JAPANESE
(ISSN 0389-4010)
(NAL-TR-1185; JTN-94-80614) Avail: CASI HC A03/MF A01

An approach for solving stereo correspondence problems that imitates human vision is proposed and verified by directing two cameras to the same point in experiments. The algorithm is based on the fact that the illuminance difference between images on left and right human retinal foveae is minimized when both eyes look at the same point. This is due to the fact that the difference between the images is smaller than the resolution. The algorithm is robust against camera discrepancies and has an operating range similar to that of human vision. The algorithm is an area-based method using 256 x 256 picture elements, which is greater than ordinary template matchings, and is not affected by the relative illuminance of the lens because of convergence control of the cameras. Author (NASDA)

N94-27517# Nagoya Univ. (Japan). Research Inst. of Environmental Medicine.

A STUDY OF PSYCHOLOGICAL FACTORS AFFECTING AN EXTREMELY ISOLATED ENVIRONMENT [HEISA KAKURI KANKYOKA NI OKERU SHINRI YOSO NO KENKYU]

Masafumi Tanaka *In its* Annals of the Research Inst. of Environmental Medicine, Nagoya Univ., Volume 44 25 Mar. 1993 p 276-278 In JAPANESE (For primary document see N94-27442 07-52)
Avail: CASI HC A01/MF A04

N94-27518# Nagoya Univ. (Japan). Research Inst. of Environmental Medicine.

INTERHEMISPHERIC PHASE RELATIONSHIP OF ALPHA WAVES AND CEREBRAL DOMINANCE [ARUFAHA NO HANKYUKAN ISO RENKAN TO HANKYU YUISEI]

Takako Kawaguchi, Hiroyasu Jijiwa (Institute for Developmental Research, Kasugai, Japan.), and Satoru Watanabe *In its* Annals of the Research Inst. of Environmental Medicine, Nagoya Univ., Volume 44 25 Mar. 1993 p 279-281 In JAPANESE (For primary document see N94-27442 07-52)
Avail: CASI HC A01/MF A04

N94-27523# Tokyo Univ. (Japan). Dept. of Psychology.

FUNCTION OF SELECTIVE ATTENTION INTRINSIC TO THE SACCADE SYSTEM: DOES THE VOLUNTARY CONTROL OVERRIDE THE STIMULUS DRIVEN CONTROL? [SAKKADO SHISUTEMU NI NAIZAISURU SENTAKUTEKI CHUI KINO: ZUIITEKI SEIGYO WA SHIGEKI KUDO SEIGYO OSEISURUKA]

Hiromi Imai and Kazuo Koga (Nagoya Univ., Japan.) *In* Nagoya Univ., Annals of the Research Inst. of Environmental Medicine, Nagoya Univ., Volume 44 25 Mar. 1993 p 299-303 In JAPANESE (For primary document see N94-27442 07-52)
Avail: CASI HC A01/MF A04

N94-27901*# Old Dominion Univ., Norfolk, VA. Dept. of Psychology.

BRAIN WAVE CORRELATES OF ATTENTIONAL STATES: EVENT RELATED POTENTIALS AND QUANTITATIVE EEG ANALYSIS DURING PERFORMANCE OF COGNITIVE AND PERCEPTUAL TASKS

Frederick G. Freeman *In its* The 1993 NASA-ODU American Society for Engineering Education (ASEE) Summer Faculty Fellowship Program Dec. 1993 p 85-88 (For primary document see N94-27893 07-80)
Avail: CASI HC A01/MF A03

54 MAN/SYSTEM TECHNOLOGY AND LIFE SUPPORT

Includes human engineering; biotechnology; and space suits and protective clothing.

For related information see also *16 Space Transportation.*

N94-25611# Air Force Inst. of Tech., Wright-Patterson AFB, OH.

CREATION OF PROTOTYPE AIRCREW PROTECTION EQUIPMENT BASED ON FACE ANTHROPOMETRY M.S. Thesis

Martin E. Piccus, Gary A. Smith, Brian K. Standley, Tami L. Volk, and Linda B. Wildes Dec. 1993 325 p
(AD-A273865; AFIT/GSE/ENY/93D-2) Avail: CASI HC A14/MF A03

The objective of this research is to develop a process which will analyze and group human faces, concentrating on the oxygen mask seal area, into a minimum number of generic yet distinct face types. The shape and size, or form, of the face is described by bending energies. This bending energy provides the features for the grouping of similar face types, while distinguishing representatives for each cluster. The face tariffs are the percentage of faces grouped under a representative face. The representative faces are then transformed into three-dimensional solids using computer-aided design. A rapid prototype creates the solids or plugs from which MBU5/P masks are made and tested. The two major outcomes of this research are a formal morphological method which allows the comparison between multiple faces, and a process to transform anthropomorphic surfaces into a prototype mask mold. DTIC

N94-25724# Institute for Perception RVO-TNO, Soesterberg (Netherlands).

THE EFFECT OF PLATFORM MOTION ON HUMAN ENERGY EXPENDITURE DURING WALKING. AN EXPLORATORY EXPERIMENT Final Report

A. H. Wertheim, R. Heus, T. G. Vrijkotte, and J. T. Marcus 11 Aug. 1993 20 p
(AD-A273760; IZF-1993-B-10; TDCK-TD-93-1366) Avail: CASI HC A03/MF A01

An experiment was performed in which various physiological measures of energy expenditure were taken with subjects walking for periods of 10 minutes (either freely or on a treadmill) on a moving platform (Ship Motion Simulator). Platform motion was either in a heave, pitch or roll mode, or it was stationary. The results show that during pitch and roll movements of the platform energy expenditure is larger than during heave motions and when the platform remained stationary. Pitch and roll did not differ from each other, and neither did heave and stationary conditions. The results are interpreted as indicating that the muscular effort needed for the maintenance of balance when walking on a pitching or rolling platform requires a significant increase in energy expenditure. DTIC

N94-26136# Federal Aviation Administration, Oklahoma City, OK. Civil Aeromedical Inst.

HUMAN FACTORS IN AIRWAY FACILITIES MAINTENANCE: DEVELOPMENT OF A PROTOTYPE OUTAGE ASSESSMENT INVENTORY Final Report

Robert E. Blanchard and Jennifer J. Vardaman Feb. 1994 25 p
Prepared for FAA, Atlantic City, NJ
(DOT/FAA/AM-94/5) Avail: CASI HC A03/MF A01

The airway facilities (AF) maintenance community is concerned with identifying ways of reducing both the incidence of equipment failure and the amount of time required to restore equipment to operational status following a failure. It is vitally important to identify the many components of downtime and contributors to a particular outage (equipment failure). Thus, the primary objective was to develop a technique or tool with which to identify and map within a 'systems' structure all potentially-significant contributors to AF maintenance downtime. The technique was designed to facilitate (1) the collection of maintenance-related data during an actual outage; (2) the entry of this data into a data base; and (3) the analysis of the data base in order to identify causal relationships. The secondary objective was to be able to make use of past outage data as a means for building the data base by determining whether overall outage time values can be apportioned among the contributors to downtime using subject matter experts (SME's) who were intimately involved in restoring a given outage. SME's from the Oklahoma City (OKC) General National Airspace System (GNAS) Airway Facilities Sector (AFS) and the Memphis GNAS AFS assisted in the iterative design and review process that produced the Airway Facilities Outage Assessment Inventory - Form A (AFOAI). Ten previous OKC GNAS outages and four previous Memphis GNAS outages were analyzed using the AFOAI - Form A, thus confirming that the inventory is a useful tool in identifying specific contributors to AF maintenance downtime. Recommendations were to continue to refine the format of the AFOAI and to install it on a trial basis to test its usefulness in collecting and analyzing data on factors and conditions contributing to facility outages. Author (revised)

N94-26339# Naval Air Warfare Center, Warminster, PA. Air Vehicle and Crew Systems Technology Dept.

A CRITICAL ANALYSIS OF WORKLOAD PREDICTIONS GENERATED BY MULTIPLE RESOURCE THEORY DURING EARLY CREWSTATION DESIGN Final Report

David Cohen, Robert J. Wherry, Jr., and Floyd Glenn 1 Jun. 1993 35 p
(AD-A274804; NAWCADWAR-TN-93043-60) Avail: CASI HC A03/MF A01

Subjective workload ratings based on multiple resource theory were independently collected from two highly experienced pilots for 225 different tasks of an anticipated mission for a future advanced strike aircraft. Factor analysis of their responses suggest that while such ratings could have little actual validity in and even high inter-rater reliabilities, the ratings have high face validity and even high inter-rater reliabilities, the ratings could have little actual validity in terms of efforts required to utilize the seven postulated resource channels (visual or auditory input, spatial, verbal, or analytical cognition, and manual or speech output). Ratings of efforts required for various postulated cognitive resource channels were particularly suspect. Four independent factors were identified for each pilot which accounted for virtually all of the intercorrelations among the seven resource channels. Three factors (visual-spatial, verbal communications, and manual and speech output) were identical for both pilots and accounted for most of their explainable variance. DTIC

N94-26555# Pacific Northwest Lab., Richland, WA.

EMERGING HUMAN-COMPUTER INTERFACE (HCI) DESIGN GUIDELINES FOR GRAPHICAL USER INTERFACE (GUI)

S. E. Bowser and S. M. Adams Oct. 1993 8 p Presented at the Human Factors and Ergonomics Society Meeting, Seattle, WA, 11-15 Oct. 1993
(Contract DE-AC06-76RL-01830)
(DE94-004293; PNL-SA-22009; CONF-9310100-7) Avail: CASI HC A02/MF A01

The requirement to establish baseline style references for Graphical User Interfaces (GUI's) is recognized. The ability to obtain consensus among user communities was limited to nonexistent. The authors are part of a team that developed a generic baseline human-computer interface (HCI) style guide for the U.S. Department of Defense (DoD). The DoD HCI Style Guide has its origin in a style guide developed by the intelligence community and in human factors design guidelines developed for Army tactical command and control systems. The DoD HCI Style Guide is intended to be a baseline style reference for the design of HCI's within DoD. The needs of specific user communities were addressed by including addenda that expand on the baseline and address focus areas of interest. The conclusion is that an overall or general style guide should be adopted for GUI's with allowance for specialized user group requirements and additions. The anticipated results would be higher productivity and reduced training and development time. DOE

N94-26788*# Boeing Defense and Space Group, Huntsville, AL.

SPACE STATION EVOLUTION STUDY OXYGEN LOOP CLOSURE Final Report

M. G. Wood and D. DeLong 17 Nov. 1993 40 p
(Contract NAS8-38783)
(NASA-CR-193938; NAS 1.26:193938) Avail: CASI HC A03/MF A01

In the current Space Station Freedom (SSF) Permanently Manned Configuration (PMC), physical scars for closing the oxygen loop by the addition of oxygen generation and carbon dioxide reduction hardware are not included. During station restructuring, the capability for oxygen loop closure was deferred to the B-modules. As such, the ability to close the oxygen loop in the U.S. Laboratory module (LAB A) and the Habitation A module (HAB A) is contingent on the presence of the B modules. To base oxygen loop closure of SSF on the funding of the B-modules may not be desirable. Therefore, this study was requested to evaluate the necessary hooks and scars in the A-modules to facilitate closure of the oxygen loop at or subsequent to PMC. The study defines the scars for oxygen loop closure with impacts to cost, weight and volume and assesses the effects of byproduct venting. In addition, the recommended scenarios for closure with regard to topology and packaging are presented. Author (revised)

N94-26964 National Academy of Sciences - National Research Council, Washington, DC. Committee on Human Factors.

WORKLOAD TRANSITION: IMPLICATIONS FOR INDIVIDUAL AND TEAM PERFORMANCE

Beverly M. Huey and Christopher D. Wickens 1993 301 p Limited Reproducibility: More than 20% of this document may be affected by microfiche quality
(AD-A274538) Avail: Issuing Activity (Defense Technical Information Center (DTIC))

The work of this study was performed by a small group of experts from key areas in workload, training, vigilance, circadian rhythms and performance effects of sleep loss and fatigue, cognitive switching, situation awareness, and crew communication and coordination. DTIC

N94-26984# Kent State Univ., OH.

A MULTIVARIATE ANTHROPOMETRIC METHOD FOR CREW STATION DESIGN: ABRIDGED Interim Report, Jan. 1989 - Dec. 1992

Gregory F. Zehner, Richard S. Meindl, and Jeffrey A. Hudson Apr. 1993 30 p
(Contract F33615-85-C-0541)
(AD-A274588; AL-TR-1992-0164) Avail: CASI HC A03/MF A01

Body size accommodation in USAF cockpits is still a significant problem despite all the years of experience and the many aircraft designs that have been developed. Adequate reach to controls, body clearances (particularly during escape) and vision (internal and external), are all functions of pilot body size and position in the cockpit. One of the roots of this problem is the way cockpit accommodation is specified and tested. For many years the percentile pilot has been used. This paper describes the errors inherent in the 'percentile man' approach, and presents a multivariate alternative for describing the body size variability existing in a given flying population. A number of body size representative cases are calculated which, when used properly in specifying, designing, and testing new aircraft, should ensure the desired level of accommodation. The approach can be adapted to provide anthropometric descriptions of body size variability for a great many designs or for computer models of the human body by altering the measurements of interest and/or selecting different data sets describing the anthropometry of a user population. DTIC

N94-27089# South Dakota Univ., Vermillion. Human Factors Lab.
CONTROL PANEL DIMENSIONS FOR GLOVED OPERATION STUDY 2: TOGGLE SWITCHES MINIMUM SPACING REQUIRED BETWEEN TOGGLE Final Report
Michelle McCleerey, Jan Berkhout, Glen Anderson, and Michael Granaas
Oct. 1993 102 p
(Contract DAAA15-90-C-1025; DA Proj. 1L1-62716-AH-70)
(AD-A274518; ARL-CR-122) Avail: CASI HC A06/MF A02

This study was to confirm the military specification of toggle switch spacing for gloved operators. An examination of toggle switch operations with five different glove types was conducted: a butyl and cotton glove assembly, a butyl and nomex glove assembly, a leather and wool glove assembly, a fire-fighting glove, and a vinyl glove. Subjects were required to operate a sequence of four switches in a 3 by 3 array. Three switch spacings were investigated: 15 mm, 20 mm, and 25 mm. Half the subjects operated toggle switches located directly in front of them, and the other half operated switches located behind them, in a position where the switches could not be seen. Subjects were required to activate the toggle switches in specific sequences as quickly and as accurately as possible. The task was machine-paced, and the time allowed for operation of a sequence of switches became progressively shorter as the subject was able to continue correct operation. Each subject performed the task both gloved and bare-handed. DTIC

N94-27114# Department of the Navy, Washington, DC.
HELMET HEAD TRACKING MOUNTING DEVICE Patent Application
Christine Horvat, inventor (to Navy), Gary F. Bradley, inventor (to Navy), and Carroll L. Rhodes, inventor (to Navy) 23 Feb. 1993 14 p
(AD-D016048; US-Patent-Appl-SN-021388) Avail: CASI HC A03/MF A01

A unified, low-profile, lightweight, and strong component mounting system for an aircrew member's helmet is disclosed. The system includes a substantially rectangular mounting bracket that carries necessary power, communications, and optical inputs to the components, mounting hardware and specially designed interface pieces for each component. The system is designed to securely and easily snap-lock onto the helmet and is positioned to stay balanced while attached to eliminate crewmember discomfort. DTIC

N94-27155 National Defence Research Establishment, Stockholm (Sweden).
TASK DEMAND, WORKLOAD, AND PERFORMANCE
B. Bergstroem Jul. 1993 31 p
(PB94-123627; FOA-A-50016-5.2) Avail: Issuing Activity (National Technical Information Service (NTIS))

The measurement of mental workload has become increasingly important as systems have become more complex and sophisticated. In this report workload and related concepts are discussed. Three dimensions of workload are recognized: task demand, operator workload (OWL), and performance. In order to measure OWL, the concepts capacity, resource, and effort must be defined and also related to a cognitive model of the brain. Four regions of workload operation are described: underload, resource dependent, maximum capacity, and overload. Satisfactory system function can only take place in the underload and resource dependent regions. It is finally concluded that to yield meaningful workload results the experimenter must control and measure task demand, OWL, and performance at the same time. NTIS

N94-27320# Air Force Inst. of Tech., Wright-Patterson AFB, OH. School of Logistics and Acquisition Management.
AN INVESTIGATION OF INTEGRATED PRODUCT DEVELOPMENT IMPLEMENTATION ISSUES: A CASE STUDY OF BOSMA MACHINE AND TOOL CORP. M.S. Thesis
F. P. Khuri and Howard M. Plevyak, Jr. Sep. 1993 108 p
(AD-A273917; AFIT/GSM/LAS/93S-11) Avail: CASI HC A06/MF A02

This thesis investigated integrated product development (IPD) implementation issues. Research emphasis focused on teams used in IPD, particularly self-directed work teams (SDWT's). The areas addressed in the study were: work environment, team organization, training and education, group dynamics and communication, motivation, rewards and incentives, measurements, and contracts. Data was collected using interviews and presented as a case study. The most significant findings on work environment were that the organization's leadership should commit to the teaming idea and sell it to the organization's members. Teams should be organized by choosing members carefully and defining all roles. Personnel should be trained in technical skills and human relations. Group interaction should be ensured by establishing open communication in a non-attribution setting. The greatest motivator of personnel is pride of ownership. A measurement baseline should be established at the outset against which productivity, efficiency, and morale may be measured. Finally, team members should be allowed to provide inputs to any contract which involves them. Author (revised)

N94-27410*# Texas Univ., Dallas. Southwestern Medical Center.
SPACELAB LIFE SCIENCES 2 POST MISSION REPORT Final Report, 16 Jan. - 30 Nov. 1993
Jay C. Buckey 14 Jan. 1994 10 p
(Contract NAS9-18736)
(NASA-CR-195544; NAS 1.26:195544; Rept-1) Avail: CASI HC A02/MF A01

Jay C. Buckey, M.D., Assistant Professor of Medicine at The University of Texas Southwestern Medical Center at Dallas served as an alternate payload specialist astronaut for the Spacelab Life Sciences 2 Space Shuttle Mission from January 1992 through December 1993. This report summarizes his opinions on the mission and offers suggestions in the areas of selection, training, simulations, baseline data collection and mission operations. The report recognizes the contributions of the commander, payload commander and mission management team to the success of the mission. Dr. Buckey's main accomplishments during the mission are listed. Author

N94-27437*# National Aeronautics and Space Administration. Marshall Space Flight Center, Huntsville, AL.
DESIGNING FOR HUMAN PRESENCE IN SPACE: AN INTRODUCTION TO ENVIRONMENTAL CONTROL AND LIFE SUPPORT SYSTEMS
Paul Wieland Jan. 1994 355 p Sponsored by NASA, Washington
(NASA-RP-1324; M-735; NAS 1.61:1324) Avail: CASI HC A15/MF A03

Human exploration and utilization of space requires habitats to provide appropriate conditions for working and living. These conditions are provided by environmental control and life support systems (ECLSS) that ensure appropriate atmosphere composition, pressure, and temperature; manage and distribute water, process waste matter, provide fire detection and suppression; and other functions as necessary. The functions that are performed by ECLSS are described and basic information necessary to design an ECLSS is provided. Technical and programmatic aspects of designing and developing ECLSS for space habitats are described including descriptions of technologies, analysis methods, test requirements, program organization, documentation requirements, and the requirements imposed by medical, mission, safety, and system needs. The design and development process is described from initial trade studies through system-level analyses to support operation. ECLSS needs for future space habitats are also described. Extensive listings of references and related works provide sources for more detailed information on each aspect of ECLSS design and development. Author

N94-27683 Defence and Civil Inst. of Environmental Medicine, Downsview (Ontario). Human Factors Div.
ONE FROM MANY: SELECTING AN APPROPRIATE HUMAN PERFORMANCE MODEL
Mary Margaret Schuck 1993 8 p
(DCIEM-93-25; DSIS-94-00071; CTN-94-61117) Avail: CASI HC A02/MF A01

A wide variety of approaches exist for representing human behavior within an overall model of system performance. In modelling human performance, a model must be selected which not only answers the human performance problem identified, but which is also compatible with the overall system model. Blanchard and Fabrycky have suggested a six-step framework for selecting models for systems engineering studies. The first four steps of this framework are critical, and modifications are suggested to make them appropriate for models of human performance which are incorporated into an overall systems model. These steps are problem definition, identification of alternatives, selection of evaluation criteria, and application of modelling techniques. It is proposed to classify models according to their complexity, flexibility and generality, and to whether they have been validated successfully. This classification relies on a tradeoff between

complexity and the model's ability to be generalized into any system. This classification system, and the other modifications proposed, allow designers of human performance models to apply an existing engineering framework to the unique problems inherent in selecting human performance models.
Author (CISTI)

N94-27934*# Jet Propulsion Lab., California Inst. of Tech., Pasadena.
LUNAR BASE HABITAT DESIGNS: CHARACTERIZING THE ENVIRONMENT, AND SELECTING HABITAT DESIGNS FOR FUTURE TRADE-OFFS
Gani B. Ganapathi, Joseph Ferrall, and P. K. Seshan May 1993 78 p
(Contract NAS7-918; RTOP 506-49-21-00)
(NASA-CR-195687; JPL-Publ-93-20; NAS 1.26:195687) Avail: CASI HC A05/MF A01

A survey of distinct conceptual lunar habitat designs covering the pre- and post-Apollo era is presented. The impact of the significant lunar environmental challenges such as temperature, atmosphere, radiation, soil properties, meteorites, and seismic activity on the habitat design parameters are outlined. Over twenty habitat designs were identified and classified according to mission type, crew size; total duration of stay, modularity, environmental protection measures, and emplacement. Simple selection criteria of (1) post-Apollo design, (2) uniqueness of the habitat design, (3) level of thoroughness in design layout, (4) habitat dimensions are provided, and (5) materials of construction for the habitat shell are specified, are used to select five habitats for future trade studies. Habitat emplacement scenarios are created to examine the possible impact of emplacement of the habitat in different locations, such as lunar poles vs. equatorial, above ground vs. below ground, etc. Author (revised)

N94-27952*# National Aeronautics and Space Administration. Marshall Space Flight Center, Huntsville, AL.
EXTRA-VEHICULAR ACTIVITY (EVA) GLOVE EVALUATION TEST PROTOCOL
E. M. Hinman-Sweeney Mar. 1994 153 p
(NASA-TM-108442; NAS 1.15:108442) Avail: CASI HC A08/MF A02

One of the most critical components of a space suit is the gloves, yet gloves have traditionally presented significant design challenges. With continued efforts at glove development, a method for evaluating glove performance is needed. This paper presents a pressure-glove evaluation protocol. A description of this evaluation protocol, and its development is provided. The protocol allows comparison of one glove design to another, or any one design to bare-handed performance. Gloves for higher pressure suits may be evaluated at current and future design pressures to drive out differences in performance due to pressure effects. Using this protocol, gloves may be evaluated during design to drive out design problems and determine areas for improvement, or fully mature designs may be evaluated with respect to mission requirements. Several different test configurations are presented to handle these cases. This protocol was run on a prototype glove. The prototype was evaluated at two operating pressures and in the unpressurized state, with results compared to bare-handed performance. Results and analysis from this test series are provided, as is a description of the configuration used for this test. Author (revised)

N94-25678*# Georgia Inst. of Tech., Atlanta. School of Textile and Fiber Engineering.
VARIABLE SPEED CONTROLLER
Christa Estes, Charles Spiggle, Shannon Swift, Stephen VanGeffen, and Frank Younger *In* USRA, Proceedings of the 8th Annual Summer Conference: NASA/USRA Advanced Design Program 1992 p 90-95 (For primary document see N94-25665 07-80)
Avail: CASI HC A01/MF A04

N94-25679*# Georgia Inst. of Tech., Atlanta. School of Textile and Fiber Engineering.
ENABLER OPERATOR STATION
Andrea Bailey, John Kietzman, Shirlyn King, Rae Stover, and Torsten Wegner *In* USRA, Proceedings of the 8th Annual Summer Conference: NASA/USRA Advanced Design Program 1992 p 96-10 (For primary document see N94-25665 07-80)
Avail: CASI HC A01/MF A04

N94-25680*# Georgia Inst. of Tech., Atlanta. School of Textile and Fiber Engineering.
DUST CONTROL FOR ENABLER
Kevin Hilton, Chad Karl, Mark Litherland, David Ritchie, and Nancy Sun *In* USRA, Proceedings of the 8th Annual Summer Conference: NASA/USRA Advanced Design Program 1992 p 101-107 (For primary document see N94-25665 07-80)
Avail: CASI HC A02/MF A04

N94-25681*# Houston Univ., TX. International Center for Space Architecture.
PORTABLE HABITAT FOR ANTARCTIC SCIENTIFIC RESEARCH (PHASR)
Samantha S. Griswold *In* USRA, Proceedings of the 8th Annual Summer Conference: NASA/USRA Advanced Design Program 1992 p 108-113 (For primary document see N94-25665 07-80)
Avail: CASI HC A02/MF A04

N94-25684*# Kansas State Univ., Manhattan. Dept. of Mechanical Engineering.
AUTOMATION OF CLOSED ENVIRONMENTS IN SPACE FOR HUMAN COMFORT AND SAFETY
Allen C. Cogley and Nathan P. Tucker *In* USRA, Proceedings of the 8th Annual Summer Conference: NASA/USRA Advanced Design Program 1992 p 137-145 (For primary document see N94-25665 07-80)
Avail: CASI HC A02/MF A04

N94-25693*# Prairie View Agricultural and Mechanical Coll., TX. Dept. of Architecture.
DESIGN AND DEVELOPMENT OF THE SECOND GENERATION MARS HABITAT
Ikhlas Sabouni, Roy Smith, Steven Taylor, Brock Harrell, and Earnest Crawford *In* USRA, Proceedings of the 8th Annual Summer Conference: NASA/USRA Advanced Design Program 1992 p 228-236 (For primary document see N94-25665 07-80)
Avail: CASI HC A02/MF A04

N94-25694*# Puerto Rico Univ., Rio Piedras. School of Architecture.
FIRST LUNAR OUTPOST
Aureo F. Andino, Daniel Silva, Nelson Ortiz, Omar Alvarez, Julio A. Colon, Myrelle Colon, Alicia Diaz, Xochiquetzal Y. Escobar, Alberto Garcia, and Isabel C. Gonzalez et al *In* USRA, Proceedings of the 8th Annual Summer Conference: NASA/USRA Advanced Design Program 1992 p 237-249 (For primary document see N94-25665 07-80)
Avail: CASI HC A03/MF A04

N94-25698*# Texas Univ., Austin. Dept. of Mechanical Engineering.
THE 1991-1992 PROJECT SUMMARIES
Steven P. Nichols and Hank Kleespies *In* USRA, Proceedings of the 8th Annual Summer Conference: NASA/USRA Advanced Design Program 1992 p 267-270 (For primary document see N94-25665 07-80)
Avail: CASI HC A01/MF A04

N94-25706*# Wisconsin Univ., Milwaukee. Dept. of Architecture.
PAX: A PERMANENT BASE FOR HUMAN HABITATION OF MARS
Gary T. Moore, Patrick J. Rebholz, Joseph P. Fieber, Janis Huebner-Moths, and Kerry L. Paruleski *In* USRA, Proceedings of the 8th Annual Summer Conference: NASA/USRA Advanced Design Program 1992 p 343-357 (For primary document see N94-25665 07-80)
Avail: CASI HC A03/MF A04

N94-27374*# Brubaker Group, Los Angeles, CA.
A WIDELY ADAPTABLE HABITAT CONSTRUCTION SYSTEM UTILIZING SPACE RESOURCES
Harry B. Wykes *In* NASA. Lewis Research Center, Vision 21: Interdisciplinary Science and Engineering in the Era of Cyberspace Dec. 1993 p 231-240 (For primary document see N94-27358 07-12)
Avail: CASI HC A02/MF A03

N94-27376*# Carnegie-Mellon Univ., Pittsburgh, PA. Robotics Inst.
PIGS IN CYBERSPACE
Hans Moravec *In* NASA. Lewis Research Center, Vision 21: Interdisciplinary

Science and Engineering in the Era of Cyberspace Dec. 1993 p 259-264 (For primary document see N94-27358 07-12)
Avail: CASI HC A02/MF A03

N94-27446# Nagoya Univ. (Japan). Research Inst. of Environmental Medicine.
STUDY ON POSTURE CONTROL AND ADAPTION MECHANISM UNDER WEIGHTLESSNESS: RESULTS OF SECOND REHEARSAL FOR SPACE EXPERIMENT USING CARP Progress Report No. 45 [MUJURYOKU KANKYO KA NO UNDO SEIGYO TO SONO JUNNO NI KANSURU KENKYU: KOI NO UCHU JIKKEN, DAINIKAI RIHASARU SEIKA HOKOKU]
Shigeo Mori, Sadaharu Takagi, Satoru Watanabe, Akira Takabayashi (Fujita Health Univ., Toyohashi, Japan.), and Shiro Usui *In its* Annals of the Research Inst. of Environmental Medicine, Nagoya Univ., Volume 44 25 Mar. 1993 p 18-21 In JAPANESE (For primary document see N94-27442 07-52)
Avail: CASI HC A01/MF A04

N94-27447# Nagoya Univ. (Japan). Research Inst. of Environmental Medicine.
STUDY ON POSTURE CONTROL AND ADAPTATION MECHANISM UNDER WEIGHTLESSNESS: SUMMARY REPORT OF GROUND OPERATIONS PERFORMED FOR CARP EXPERIMENT (FMPT/L-2) IN SPACE SHUTTLE MISSION Report No. 46 [MUJURYOKU KANKYO KA NO UNDO SEIGYO TO SONO JUNNO NI KANSURU KENKYU: SUPESUSHATORU RIYO NI YORU KOI NO UCHU JIKKEN (FMPT/L-2) JISSHI KEIKA HOKOKU]
Shigeo Mori, Sadaharu Takagi, Satoru Watanabe, Akira Takabayashi (Fujita Health Univ., Toyohashi, Japan.), Shiro Usui (Toyohashi Univ. of Technology, Aichi, Japan.), and Genyo Mitarai (Chukyo Univ., Toyota, Japan.) *In its* Annals of the Research Inst. of Environmental Medicine, Nagoya Univ., Volume 44 25 Mar. 1993 p 22-26 In JAPANESE (For primary document see N94-27442 07-52)
Avail: CASI HC A01/MF A04

N94-27448# Fujita Health Univ., Toyohashi (Japan). School of Hygiene.
STUDY ON POSTURE CONTROL AND ADAPTION MECHANISM UNDER WEIGHTLESSNESS: DIFFERENCES IN WEIGHT AND SHAPE OF UTRICULAR OTOLITH OF CARP Report No. 47 [MUJURYOKU KANKYO KA NO UNDO SEIGYO TO SONO JUNNO NI KANSURU KENKYU: KOI NO RANKEINO JISEKI NO JURYO TO KEITAI NI OKERU SA NI TSUITE]
Akira Takabayashi, Sadaharu Takagi (Nagoya Univ., Japan.), Shigeo Mori (Nagoya Univ., Japan.), and Satoru Watanabe (Nagoya Univ., Japan.) *In* Nagoya Univ., Annals of the Research Inst. of Environmental Medicine, Nagoya Univ., Volume 44 25 Mar. 1993 p 27-29 In JAPANESE (For primary document see N94-27442 07-52)
Avail: CASI HC A01/MF A04

N94-27455# Nagoya Univ. (Japan). Research Inst. of Environmental Medicine.
FREQUENCY ANALYSIS OF BODY SWAY INDUCED BY OPTOKINETIC STIMULATION [SHIUNDO SHIGEKI YUHATSUSEI SHINTAI DOYO NO SHUHASU KAISEKI]
Masumi Ichikawa, Hiroyasu Jijiwa (Institute for Developmental Research, Kasugai, Japan.), Takako Kawaguchi, and Satoru Watanabe *In its* Annals of the Research Inst. of Environmental Medicine, Nagoya Univ., Volume 44 25 Mar. 1993 p 55-58 In JAPANESE (For primary document see N94-27442 07-52)
Avail: CASI HC A01/MF A04

N94-27456# Nagoya City Univ. (Japan). Dept. of Othorhinolaryngology.
EFFECTS OF IMAGINARY TARGET ON INDUCED EYE MOVEMENTS BY LINEAR ACCELERATION [CHOKUSEN KASOKUDO NI YORI YUHATSU SARERU GANKYU UNDO NI TAISURU KASO KOSHITEN NO EIKYO]
Motoyuki Hashiba, Hirotaka Watabe, Toru Matsuoka, Shunkichi Baba, Satoru Watanabe (Nagoya Univ., Japan.), Yoshiro Wada (Nagoya Univ., Japan.), Hiroyuki Suzuki (Nagoya Univ., Japan.), Chiharu Sekiguchi (National Space Development Agency, Tokyo, Japan.), Sei Yumikura (National Space Development Agency, Tokyo, Japan.), and K. Hofstetter-Degen (Mainz Univ., Germany.) *In* Nagoya Univ., Annals of the Research Inst. of Environmental Medicine, Nagoya Univ., Volume 44 25 Mar. 1993 p 59-63 In JAPANESE (For primary document see N94-27442 07-52)
Avail: CASI HC A01/MF A04

N94-27461# Osaka Prefecture Univ., Sakai (Japan). Coll. of Integrated Arts and Sciences.
THE EFFECT OF BODY ORIENTATION ON THE PERCEPTION OF VERTICAL AND HORIZONTAL DISTANCE IN AN OUTDOOR SETTING [HIKENSHA NO SHISEI TO YAGAI NI OKERU SUICHOKU-SUIHEI KYORI NO CHIKAKU]
Atsuki Higashiyama and Kazuo Koga (Nagoya Univ., Japan.) *In* Nagoya Univ., Annals of the Research Inst. of Environmental Medicine, Nagoya Univ., Volume 44 25 Mar. 1993 p 84-87 In JAPANESE (For primary document see N94-27442 07-52)
Avail: CASI HC A01/MF A04

N94-27462# Kanazawa Univ. (Japan). Dept. of Psychology.
EYE-HEAD COORDINATION AND SWINGING OF THE VISUAL SCENE WHEN WEARING VISUALLY UP-DOWN REVERSING MIRROR FOR 14 DAYS [JOGEHANTENKYO CHAKUYOCHU NO GANKYU-TOBU UNDO TO SHIYA NO DOYO]
Hirokazu Yoshimura and Kazuo Koga (Nagoya Univ., Japan.) *In* Nagoya Univ., Annals of the Research Inst. of Environmental Medicine, Nagoya Univ., Volume 44 25 Mar. 1993 p 88-92 In JAPANESE (For primary document see N94-27442 07-52)
(Grant NOE-03551003)
Avail: CASI HC A01/MF A04

N94-27463# Nagoya Univ. (Japan). Research Inst. of Environmental Medicine.
COMPARATIVE MEASUREMENT OF VISUAL STABILITY IN COSMIC SPACE: ONBOARD EXPERIMENT AND PRE-FLIGHT ACTIVITIES Quick Report [UCHU KUKAN NI OKERU SHIKAKU ANTEISEI NO KENKYU: JIKKEN UNYO TO UNYO NI ITARU SHOKATEI]
Kazuo Koga, Tadaaki Mano, Mitsuro Kida, Yoshihiro Ota, Keiichiro Tsuji, Takuo Goto, and Ryoji Osaka (Aichigakuin Univ., Nisshin, Japan.) *In its* Annals of the Research Inst. of Environmental Medicine, Nagoya Univ., Volume 44 25 Mar. 1993 p 93-96 In JAPANESE (For primary document see N94-27442 07-52)
Avail: CASI HC A01/MF A04

N94-27943# Japanese Air Self-Defense Force, Tokyo. Aeromedical Lab.
COMPARISON OF PERFORMANCE IN SIMULATOR FLIGHT AMONG SUBJECTS WITH DIFFERENT SIMULATOR EXPERIENCES [FURAITO SHIMYURETA SOJU NI OKERU MIKEIKENSHA TO KEIKENSHA NO SOI NI TSUITE]
Miyako Okaue, Atsushi Kadoo, Syuji Nishi, Kyouichi Nagatsuka, and Zoujirou Katoh *In its* The Reports of Aeromedical Laboratory, Volume 33, Number 4 1 Dec. 1992 p 87-101 In JAPANESE (For primary document see N94-27942 07-52)
Avail: CASI HC A03/MF A01

55 SPACE BIOLOGY

Includes exobiology; planetary biology; and extraterrestrial life.

N94-26098*# National Aeronautics and Space Administration. Ames Research Center, Moffett Field, CA.
INTERMITTENT GRAVITY: HOW MUCH, HOW OFTEN, HOW LONG?
Joan Vernikos and David A. Ludwig (North Carolina Univ., Greensboro.) Jan. 1994 106 p
(RTOP 199-14-12-11)
(NASA-TM-108800; A-94027; NAS 1.15:108800) Avail: CASI HC A06/MF A02

Continuous exposure to gravity may not be necessary to prevent the deconditioning effects of microgravity. It is not known, however, what the minimum gravity (G) exposure requirements are, whether they vary for different physiological systems, or whether passive Gz (gravity in the head-to-toe vector) or activity in a G field is more effective in preventing deconditioning. It is also not known what the optimal characteristics of the

G stimulus should be in terms of amplitude, duration, and frequency. To begin to address these questions, a 4-day -6 deg head-down bed rest (HDBR) study was conducted. Nine males (aged 30-50 yr) were subjected, over a period of seven months, to four different +1 Gz exposure protocols (periodic standing or controlled walking each for a total of 2 or 4 hr/day in individual 15-min doses), plus a control (0 Gz) of continuous HDBR. The study consisted of one ambulatory control day, 4 full days of -6 deg HDBR, and a recovery day when subjects were released at the end of HDBR after completion of tests. A battery of tests was selected and standardized in order to evaluate the known early responses to HDBR. Dependent variables of interest included orthostatic tolerance (30 min at 60 deg head-up tilt) and hemodynamics during head-up tilt, peak oxygen consumption (VO2(sub peak)) plasma volume (PV), and urinary calcium (Ca). The results were as follows: 4 hr standing completely prevented and 2 hr walking partially prevented post-HDBR orthostatic intolerance. Walking at 3 mi/hr for 4 hr/day provided no additional benefit. Intermittent walking attenuated, but did not prevent, the decrease in VO2(sub peak). Both 4 hr conditions showed less PV loss by the end of HDBR; both 2 hr conditions were without effect. Both 2 and 4 hr walking essentially prevented urinary Ca excretion and were more effective than standing. It is concluded that different physiological systems benefit differentially from passive +1 Gz or activity in +1 Gz, and the intensity of the stimulus may be an important contributing factor. Author (revised)

N94-27370*# Sverdrup Technology, Inc., Cleveland, OH.
THE FERMI PARADOX: AN APPROACH BASED ON PERCOLATION THEORY
Geoffrey A. Landis *In* NASA. Lewis Research Center, Vision 21: Interdisciplinary Science and Engineering in the Era of Cyberspace Dec. 1993 p 163-167 (For primary document see N94-27358 07-12)
Avail: CASI HC A01/MF A03

59 MATHEMATICAL AND COMPUTER SCIENCES (GENERAL)

N94-28251*# National Aeronautics and Space Administration. Goddard Space Flight Center, Greenbelt, MD.
THE 1994 SPACE AND EARTH SCIENCE DATA COMPRESSION WORKSHOP
James C. Tilton, ed. Washington Apr. 1994 139 p Workshop held in Salt Lake City, UT, 2 Apr. 1994
(RTOP 930-00-00)
(NASA-CP-3255; Rept-94B00043; NAS 1.55:3255) Avail: CASI HC A07/MF A02

This document is the proceedings from the fourth annual 'Space and Earth Science Data Compression Workshop,' which was held on April 2, 1994, at the University of Utah in Salt Lake City, Utah. This workshop was held in cooperation with the 1994 Data Compression Conference, which was held at Snowbird, Utah, March 29-31 1994. The Workshop explored opportunities for data compression to enhance the collection and analysis of space and Earth science data. It consisted of 13 papers presented in 4 sessions. The papers focus on data compression research that is integrated into, or has the potential to be integrated into, a particular space and/or Earth science data information system. Presenters were encouraged to take into account the scientist's data requirements, and the constraints imposed by the data collection, transmission, distribution, and archival system. For individual titles, see N94-28252 through N94-28264.

N94-28252*# National Aeronautics and Space Administration. Ames Research Center, Moffett Field, CA.
AN IMAGE ASSESSMENT STUDY OF IMAGE ACCEPTABILITY OF THE GALILEO LOW GAIN ANTENNA MISSION c91
S. L. Chuang, R. F. Haines (RECOM Technologies, Inc., Moffett Field, CA.), T. Grant, Yaron Gold (RECOM Technologies, Inc., Moffett Field, CA.), and Kar-Ming Cheung (Jet Propulsion Lab., California Inst. of Tech., Pasadena.) *In* NASA. Goddard Space Flight Center, The 1994 Space and Earth Science Data Compression Workshop Apr. 1994 p 3-10 (For primary document see N94-28251 07-59)
Avail: CASI HC A02/MF A02

This paper describes a study conducted by NASA Ames Research Center (ARC) in collaboration with the Jet Propulsion Laboratory (JPL), Pasadena, California on the image acceptability of the Galileo Low Gain Antenna mission. The primary objective of the study is to determine the impact of the Integer Cosine Transform (ICT) compression algorithm on Galilean images of atmospheric bodies, moons, asteroids and Jupiter's rings. The approach involved fifteen volunteer subjects representing twelve institutions involved with the Galileo Solid State Imaging (SSI) experiment. Four different experiment specific quantization tables (q-table) and various compression stepsizes (q-factor) to achieve different compression ratios were used. It then determined the acceptability of the compressed monochromatic astronomical images as evaluated by Galileo SSI mission scientists. Fourteen different images were evaluated. Each observer viewed two versions of the same image side by side on a high resolution monitor, each was compressed using a different quantization stepsize. They were requested to select which image had the highest overall quality to support them in carrying out their visual evaluations of image content. Then they rated both images using a scale from one to five on its judged degree of usefulness. Up to four pre-selected types of images were presented with and without noise to each subject based upon results of a previously administered survey of their image preferences. Fourteen different images in seven image groups were studied. The results showed that: (1) acceptable compression ratios vary widely with the type of images; (2) noisy images detract greatly from image acceptability and acceptable compression ratios; and (3) atmospheric images of Jupiter seem to have higher compression ratios of 4 to 5 times that of some clear surface satellite images. Author

N94-28253*# Allied-Signal Corp., Morristown, NJ. Technical Services.
IMAGE COMPRESSION SOFTWARE FOR THE SOHO LASCO AND EIT EXPERIMENTS c61
Mitchell R. Grunes, Russell A. Howard (Naval Research Lab., Washington, DC.), Karl Hoppel (Naval Research Lab., Washington, DC.), Stephen A. Mango (Naval Research Lab., Washington, DC.), and Dennis Wang (Interferometrics, Inc., Greenbelt, MD.) *In* NASA. Goddard Space Flight Center, The 1994 Space and Earth Science Data Compression Workshop Apr. 1994 p 11-22 (For primary document see N94-28251 07-59)
Avail: CASI HC A03/MF A02

This paper describes the lossless and lossy image compression algorithms to be used on board the Solar Heliospheric Observatory (SOHO) in conjunction with the Large Angle Spectrometric Coronograph and Extreme Ultraviolet Imaging Telescope experiments. It also shows preliminary results obtained using similar prior imagery and discusses the lossy compression artifacts which will result. This paper is in part intended for the use of SOHO investigators who need to understand the results of SOHO compression in order to better allocate the transmission bits which they have been allocated. Author

N94-28254*# Technische Univ., Aachen (Germany).
COMPARISON OF THE LOSSY IMAGE DATA COMPRESSIONS FOR THE MESUR PATHFINDER AND FOR THE HUYGENS TITAN PROBE c61
P. Rueffer, F. Rabe, F. Gliem, and H.-U. Keller (Max-Planck-Inst. fuer Aeronomie, Katlenburg-Lindau, Germany.) *In* NASA. Goddard Space Flight Center, The 1994 Space and Earth Science Data Compression Workshop Apr. 1994 p 23-30 (For primary document see N94-28251 07-59)
Avail: CASI HC A02/MF A02

The commercial JPEG standard complies well with the specific requirements of exploratory space missions. Therefore, JPEG has been chosen to be the baseline for a series of spaceborne image data compressions (e.g. MARS94-HRSC, -WAOSS, HUYGENS-DISR, MESUR-IMP). One S/W-implementation (IMP) and one H/W-implementation (DISR) of image data compression are presented. Details of the modifications applied to standard JPEG are outlined. Finally, a performance comparison of the two implementations is given. Author (revised)

N94-28255*# Jet Propulsion Lab., California Inst. of Tech., Pasadena.
ADVANCED END-TO-END SIMULATION FOR ON-BOARD PROCESSING (AESOP) c61
Alan S. Mazer *In* NASA. Goddard Space Flight Center, The 1994

Space and Earth Science Data Compression Workshop Apr. 1994 p 31-41 (For primary document see N94-28251 07-59)
Avail: CASI HC A03/MF A02

Developers of data compression algorithms typically use their own software together with commercial packages to implement, evaluate and demonstrate their work. While convenient for an individual developer, this approach makes it difficult to build on or use another's work without intimate knowledge of each component. When several people or groups work on different parts of the same problem, the larger view can be lost. What's needed is a simple piece of software to stand in the gap and link together the efforts of different people, enabling them to build on each other's work, and providing a base for engineers and scientists to evaluate the parts as a cohesive whole and make design decisions. AESOP (Advanced End-to-end Simulation for On-board Processing) attempts to meet this need by providing a graphical interface to a developer-selected set of algorithms, interfacing with compiled code and standalone programs, as well as procedures written in the IDL and PV-Wave command languages. As a proof of concept, AESOP is outfitted with several data compression algorithms integrating previous work on different processors (AT&T DSP32C, TI TMS320C30, SPARC). The user can specify at run-time the processor on which individual parts of the compression should run. Compressed data is then fed through simulated transmission and uncompression to evaluate the effects of compression parameters, noise and error correction algorithms. The following sections describe AESOP in detail. Section 2 describes fundamental goals for usability. Section 3 describes the implementation. Sections 4 through 5 describe how to add new functionality to the system and present the existing data compression algorithms. Sections 6 and 7 discuss portability and future work. Derived from text

N94-28256*# Naval Postgraduate School, Monterey, CA. Dept. of Electrical and Computer Engineering.
PERFORMANCE CONSIDERATIONS FOR THE APPLICATION OF THE LOSSLESS BROWSE AND RESIDUAL MODEL **c61**
Walter D. Abbott, III, Robert T. Kay, and Ron J. Pieper *In* NASA. Goddard Space Flight Center, The 1994 Space and Earth Science Data Compression Workshop Apr. 1994 p 43-54 (For primary document see N94-28251 07-59)
Avail: CASI HC A03/MF A02

A hybrid lossless compression model employing both the (lossy) JPEG DCT algorithm and one of a selection of lossless image compression methods has been tested. The hybrid model decomposes the original image into a low-loss quick-look browse and a residual image. The lossless compression methods tested in the model are Huffman, arithmetic, LZW, lossless JPEG, and diagonal coding. For both the direct and the hybrid application of these lossless methods, the compression ratios (CR's) are calculated and compared on three test images. For each lossless method tested, the hybrid model had no more than a nominal loss in compression efficiency relative to the direct approach. In many cases, the hybrid model provided a significant compression gain. When used in the hybrid model, lossless JPEG outperformed the other lossless methods over a broad range of browse image qualities. Author (revised)

N94-28257*# University of North Texas, Denton. Dept. of Computer Sciences.
IMAGE QUALITY MEASURES AND THEIR PERFORMANCE **c61**
Ahmet M. Eskicioglu, Paul S. Fisher, and Si-Yuan Chen *In* NASA. Goddard Space Flight Center, The 1994 Space and Earth Science Data Compression Workshop Apr. 1994 p 55-67 (For primary document see N94-28251 07-59)
Avail: CASI HC A03/MF A02

A number of quality measures are evaluated for gray scale image compression. They are all bivariate exploiting the differences between corresponding pixels in the original and degraded images. It is shown that although some numerical measures correlate well with the observers' response for a given compression technique, they are not reliable for an evaluation across different techniques. The two graphical measures (histograms and Hosaka plots), however, can be used to appropriately specify not only the amount, but also the type of degradation in reconstructed images. Author (revised)

N94-28258*# Hughes Research Labs., Malibu, CA.
A COMPARISON OF SPECTRAL DECORRELATION TECHNIQUES AND PERFORMANCE EVALUATION METRICS FOR A WAVELET-BASED, MULTISPECTRAL DATA COMPRESSION ALGORITHM **c61**
Roy M. Matic and Judith I. Mosley (Santa Barbara Research Center, Goleta, CA.) *In* NASA. Goddard Space Flight Center, The 1994 Space and Earth Science Data Compression Workshop Apr. 1994 p 69-80 (For primary document see N94-28251 07-59)
Avail: CASI HC A03/MF A02

Future space-based, remote sensing systems will have data transmission requirements that exceed available downlinks necessitating the use of lossy compression techniques for multispectral data. In this paper, we describe several algorithms for lossy compression of multispectral data which combine spectral decorrelation techniques with an adaptive, wavelet-based, image compression algorithm to exploit both spectral and spatial correlation. We compare the performance of several different spectral decorrelation techniques including wavelet transformation in the spectral dimension. The performance of each technique is evaluated at compression ratios ranging from 4:1 to 16:1. Performance measures used are visual examination, conventional distortion measures, and multispectral classification results. We also introduce a family of distortion metrics that are designed to quantify and predict the effect of compression artifacts on multi spectral classification of the reconstructed data. Author (revised)

N94-28259*# Centre National d'Etudes Spatiales, Toulouse (France).
A COMPARATIVE STUDY OF SAR DATA COMPRESSION SCHEMES **c61**
C. Lambert-Nebout, O. Besson (Ecole Nationale Superieure d'Ingenieurs de Constructions Aeronautiques, Toulouse, France.), D. Massonnet, and B. Rogron *In* NASA. Goddard Space Flight Center, The 1994 Space and Earth Science Data Compression Workshop Apr. 1994 p 81-91 (For primary document see N94-28251 07-59)
Avail: CASI HC A03/MF A02

The amount of data collected from spaceborne remote sensing has substantially increased in the last years. During same time period, the ability to store or transmit data has not increased as quickly. At this time, there is a growing interest in developing compression schemes that could provide both higher compression ratios and lower encoding/decoding errors. In the case of the spaceborne Synthetic Aperture Radar (SAR) earth observation system developed by the French Space Agency (CNES), the volume of data to be processed will exceed both the on-board storage capacities and the telecommunication link. The objective of this paper is twofold: to present various compression schemes adapted to SAR data; and to define a set of evaluation criteria and compare the algorithms on SAR data. In this paper, we review two classical methods of SAR data compression and propose novel approaches based on Fourier Transforms and spectrum coding. Author (revised)

N94-28260*# Environmental Research Inst. of Michigan, Ann Arbor.
PERCEPTUAL COMPRESSION OF MAGNITUDE-DETECTED SYNTHETIC APERTURE RADAR IMAGERY **c61**
John D. Gorman and Susan A. Werness *In* NASA. Goddard Space Flight Center, The 1994 Space and Earth Science Data Compression Workshop Apr. 1994 p 93-103 (For primary document see N94-28251 07-59)
Avail: CASI HC A03/MF A02

A perceptually-based approach for compressing synthetic aperture radar (SAR) imagery is presented. Key components of the approach are a multiresolution wavelet transform, a bit allocation mask based on an empirical human visual system (HVS) model, and hybrid scalar/vector quantization. Specifically, wavelet shrinkage techniques are used to segregate wavelet transform coefficients into three components: local means, edges, and texture. Each of these three components is then quantized separately according to a perceptually-based bit allocation scheme. Wavelet coefficients associated with local means and edges are quantized using high-rate scalar quantization while texture information is quantized using low-rate vector quantization. The impact of the perceptually-based multiresolution compression algorithm on visual image quality, impulse response, and texture properties is assessed for fine-resolution magnitude-detected SAR imagery; excellent image quality is found at bit rates at or above 1 bpp along with graceful performance degradation at rates below 1 bpp. Author (revised)

N94-28261*# David Sarnoff Research Center, Princeton, NJ.
COMPRESSION OF MULTISPECTRAL LANDSAT IMAGERY USING THE EMBEDDED ZEROTREE WAVELET (EZW) ALGORITHM **c61**
Jerome M. Shapiro, Stephen A. Martucci, and Martin Czigler *In* NASA. Goddard Space Flight Center, The 1994 Space and Earth Science Data Compression Workshop Apr. 1994 p 105-113 (For primary document see N94-28251 07-59)
Avail: CASI HC A02/MF A02

The Embedded Zerotree Wavelet (EZW) algorithm has proven to be an extremely efficient and flexible compression algorithm for low bit rate image coding. The embedding algorithm attempts to order the bits in the bit stream in numerical importance and thus a given code contains all lower rate encodings of the same algorithm. Therefore, precise bit rate control is achievable and a target rate or distortion metric can be met exactly. Furthermore, the technique is fully image adaptive. An algorithm for multispectral image compression which combines the spectral redundancy removal properties of the image-dependent Karhunen-Loeve Transform (KLT) with the efficiency, controllability, and adaptivity of the embedded zerotree wavelet algorithm is presented. Results are shown which illustrate the advantage of jointly encoding spectral components using the KLT and EZW. Author (revised)

N94-28262*# Environmental Research Inst. of Michigan, Ann Arbor.
VECTOR QUANTIZER DESIGNS FOR JOINT COMPRESSION AND TERRAIN CATEGORIZATION OF MULTISPECTRAL IMAGERY **c61**
John D. Gorman and Daniel F. Lyons (Mitre Corp., McLean, VA.) *In* NASA. Goddard Space Flight Center, The 1994 Space and Earth Science Data Compression Workshop Apr. 1994 p 115-121 (For primary document see N94-28251 07-59)
Avail: CASI HC A02/MF A02

Two vector quantizer designs for compression of multispectral imagery and their impact on terrain categorization performance are evaluated. The mean-squared error (MSE) and classification performance of the two quantizers are compared, and it is shown that a simple two-stage design minimizing MSE subject to a constraint on classification performance has a significantly better classification performance than a standard MSE-based tree-structured vector quantizer followed by maximum likelihood classification. This improvement in classification performance is obtained with minimal loss in MSE performance. The results show that it is advantageous to tailor compression algorithm designs to the required data exploitation tasks. Applications of joint compression/classification include compression for the archival or transmission of Landsat imagery that is later used for land utility surveys and/or radiometric analysis. Author (revised)

N94-28263*# TRW Systems Group, Redondo Beach, CA. Data Technologies Div.
WAVELET COMPRESSION TECHNIQUES FOR HYPERSPECTRAL DATA **c61**
Bruce Evans, Brian Ringer, and Mathew Yeates *In* NASA. Goddard Space Flight Center, The 1994 Space and Earth Science Data Compression Workshop Apr. 1994 p 123-133 (For primary document see N94-28251 07-59)
Avail: CASI HC A03/MF A02

Hyperspectral sensors are electro-optic sensors which typically operate in visible and near infrared bands. Their characteristic property is the ability to resolve a relatively large number (i.e., tens to hundreds) of contiguous spectral bands to produce a detailed profile of the electromagnetic spectrum. In contrast, multispectral sensors measure relatively few non-contiguous spectral bands. Like multispectral sensors, hyperspectral sensors are often also imaging sensors, measuring spectra over an array of spatial resolution cells. The data produced may thus be viewed as a three dimensional array of samples in which two dimensions correspond to spatial position and the third to wavelength. Because they multiply the already large storage/transmission bandwidth requirements of conventional digital images, hyperspectral sensors generate formidable torrents of data. Their fine spectral resolution typically results in high redundancy in the spectral dimension, so that hyperspectral data sets are excellent candidates for compression. Although there have been a number of studies of compression algorithms for multispectral data, we are not aware of any published results for hyperspectral data. Three algorithms for hyperspectral data compression are compared. They were selected as representatives of three major approaches for extending conventional lossy image compression techniques to hyperspectral data. The simplest approach treats the data as an ensemble of images and compresses each image independently, ignoring the correlation between spectral bands. The second approach transforms the data to decorrelate the spectral bands, and then compresses the transformed data as a set of independent images. The third approach directly generalizes two-dimensional transform coding by applying a three-dimensional transform as part of the usual transform-quantize-entropy code procedure. The algorithms studied all use the discrete wavelet transform. In the first two cases, a wavelet transform coder was used for the two-dimensional compression. The third case used a three dimensional extension of this same algorithm. Author (revised)

N94-28264*# Martin Marietta Astro Space, Princeton, NJ.
SOME PRACTICAL ASPECTS OF LOSSLESS AND NEARLY-LOSSLESS COMPRESSION OF AVHRR IMAGERY **c61**
David B. Hogan, Chris X. Miller, Than Lee Christensen, and Raj Moorti *In* NASA. Goddard Space Flight Center, The 1994 Space and Earth Science Data Compression Workshop Apr. 1994 p 135-142 (For primary document see N94-28251 07-59)
Avail: CASI HC A02/MF A02

Compression of Advanced Very high Resolution Radiometers (AVHRR) imagery operating in a lossless or nearly-lossless mode is evaluated. Several practical issues are analyzed including: variability of compression over time and among channels, rate-smoothing buffer size, multi-spectral preprocessing of data, day/night handling, and impact on key operational data applications. This analysis is based on a DPCM algorithm employing the Universal Noiseless Coder, which is a candidate for inclusion in many future remote sensing systems. It is shown that compression rates of about 2:1 (daytime) can be achieved with modest buffer sizes (less than or equal to 2.5 Mbytes) and a relatively simple multi-spectral preprocessing step. Author (revised)

60 COMPUTER OPERATIONS AND HARDWARE

Includes hardware for computer graphics, firmware, and data processing.

For components see *33 Electronics and Electrical Engineering.*

N94-25648# Air Force Inst. of Tech., Wright-Patterson AFB, OH. School of Engineering.
DEVELOPMENT OF A 4-BIT PARALLEL ANALOG-TO-DIGITAL CONVERTER AND A FOUR-QUADRANT DOUBLE-BALANCED MIXER USING HETEROJUNCTION BIPOLAR TRANSISTOR TECHNOLOGY M.S. Thesis
Scott F. Jokerst Dec. 1993 123 p
(AD-A274074; AFIT/GE/Eng/93D-16) Avail: CASI HC A06/MF A02

A four-bit parallel analog-to-digital converter (ADC) and a four-quadrant double-balanced mixer were designed and simulated using heterojunction bipolar transistor (HBT) technology to test the dc and high-frequency characteristics of HBT's. HSPICE simulations of small-scale components and the large-scale ADC operated within expected ranges. The ADC implemented with the Rockwell HBT model operated at a sampling rate of over 1 GHz, and the Fellows model also operated at a 1 GHz sampling rate. The mixer produced an intermediate frequency (IF) signal using radio frequency (RF) and local oscillator (LO) inputs. The circuit produced a +9 dB power gain with less than one percent harmonic distortion and shows potential for microwave applications. In order to facilitate the fabrication of HBT circuits, a Magic technology file was developed to lay out HBT's and extract the transistors for the purpose of doing a layout versus schematic check. The extraction software was altered to recognize HBT's in the extracted file. The program ext2spice successfully identified HBT's and converted the transistors, as well as parasitic capacitances, into an HSPICE netlist. Since load resistors determine the output logic swing in current-mode logic, an attempt was made to extract resistors using the HBT technology file for Magic. The configuration of the HBT within Magic and the methods used for resistance extraction offer ways to extract HSPICE netlists for accurate simulations. DTIC

N94-25720# Organisatie voor Toegepast Natuurwetenschappelijk Onderzoek, The Hague (Netherlands). Physics and Electronics Lab.
INTERFACE TECHNICAL SPECIFICATION OF THE V.25 BIS EMULATOR Final Report
P. P. Copeland Jun. 1993 31 p
(AD-A273754; FEL-93-A103; TDCK-TD-93-0753) Avail: CASI HC A03/MF A01

This document contains the interface technical specification for the V.25 bis Emulator developed by TNO-FEL under the contract number A93KL626, in support of the RNLA's VLOTATS project. The V.25 bis Emulator is capable of emulating a subset of the CCITT Recommendation V.25 bis interface protocols in both DTE and DCE mode of operation. The Emulator will be used during the conformance testing of the following equipments to be employed in the VLOTATS project: (1) Communications Gateway; (2) Message Terminal Communicatie Kaart; (3) Digitaal Beveiligd Telefoontoestel; and (4) Data Communication Card. DTIC

N94-25864# Educational Testing Service, Princeton, NJ.
EXTENDING THE RULE SPACE MODEL TO A SEMANTICALLY-RICH DOMAIN: DIAGNOSTIC ASSESSMENT IN ARCHITECTURE Final Report, Apr. 1989 - Aug. 1993
Irvin R. Katz, Michael E. Martinez, Kathleen Sheehan, and Kikumi K. Tatsuoka Oct. 1993 40 p
(Contract N00014-90-J-1307)
(AD-A273789; ETS-RR-93-42-ONR) Avail: CASI HC A03/MF A01

A technique is presented for applying the Rule Space model of cognitive diagnosis to assessment in a semantically-rich domain. Responses to 22 architecture test items, developed to assess a range of architectural knowledge, were analyzed using Rule Space. Verbal protocol analyses guided the construction of a model of examinee performance, consisting of processes for constructing an initial representation of an item - labeled understand; forming goals and performing actions based on those goals - solve; and determining whether goals have been attempted and satisfied - check. Item attributes, derived from these processes, formed the basis for diagnosis. The technique extends Rule Space's applicability by defining attributes in terms of item characteristics and the causal relations between characteristics and the problem-solving model. Data were collected from 122 architects of various ability levels (students, architecture interns, and professional architects). Rule Space successfully classified approximately 65%, 90%, and 40% of examinees based, respectively, on attributes associated with the understand, solve, and check processes of the problem-solving model. The findings support the effectiveness of Rule Space in a complex domain and suggest directions for developing new architecture items by using attributes particularly effective at distinguishing among examinees of different ability levels. DTIC

N94-26111# Sandia National Labs., Albuquerque, NM.
TEMPERATURE DEPENDENCE OF STATIC RAM VOLATILITY
T. L. Meisenheimer, D. M. Fleetwood, and P. S. Winokur 1993 5 p
Presented at the Hardened Electronics and Radiation Technology, Monterey, CA, 14-18 Feb. 1994
(Contract DE-AC04-76DP-00789)
(DE93-040345; SAND-93-1926C; CONF-940217-1) Avail: CASI HC A01/MF A01

We have measured the temperature dependence of the volatility of a wide variety of static RAMS. The temperature dependence is directly related to the memory cell design and device processing or fabrication parameters. We have seen the volatility change by approximately 10 orders of magnitude when the absolute temperature is changed by a factor of approximately 2. We present physical reasons for such a large temperature dependence and derive an analytical model which accurately predicts the volatility. Neutron irradiation is seen to increase the low-temperature volatility. DOE

N94-26266# Gosudarstvennyi Komitet po Ispolzovaniyu Atomnoi Energii, Serpukhov (USSR). Inst. Fiziki Vysokikh Ehnergij.
AUXILIARY CONTROLLER FOR TIME-TO-DIGITAL CONVERTER MODULE READOUT [DOPOINTEL'NYJ KONTROLLER DIYA S'EMA INFORMATSII S MODULEJ VTSP]
Yu. V. Ermolin 1992 6 p In RUSSIAN
(DE93-634172; IFVE-OEA-92-19) Avail: CASI HC A02/MF A01 (US Sales Only)

The KD-225 auxiliary controller for time-to-digital converter module readout in the SUMMA crate is described. After readout and preliminary processing the data are written in the P-140 buffer memory module. The controller is used in the FODS-2 experimental setup data acquisition system. DOE

N94-26381 Gosudarstvennyi Komitet po Ispolzovaniyu Atomnoi Energii, Serpukhov (USSR). Inst. Fiziki Vysokikh Ehnergij.
FAST GENERATOR OF PROGRAM WAVEFORMS SIGNALS [BYSTRODEJSTVUYUSHCHIJ GENERATOR SIGNALOV PROGRAMMIRUEMOJ FORMY]
V. G. Korolev and V. N. Rychenkov 1992 8 p In RUSSIAN Limited Reproducibility: More than 20% of this document may be affected by microfiche quality
(DE93-634230; IFVE-OEA-92-75) Avail: CASI HC A02 (US Sales Only)

The module intended for generation of complex shape nanosecond and microsecond test signals using digital method is described. The generator is designed on the base of fast integrated circuits DAC, ECL-memory, and amplifiers. It has 10 bits, 1024 discrete values, 66 MHz maximum discretization frequency, and settling time within +/- 5 V output voltage range is less than 30 ns. Maximum output current is 100 mA. DOE

N94-26578# Lawrence Livermore National Lab., CA.
THE HIGH PERFORMANCE STORAGE SYSTEM
R. A. Coyne (IBM Federal Systems Div., Houston, TX.), H. Hulen (IBM Federal Systems Div., Houston, TX.), and R. Watson Sep. 1993 12 p
Presented at the Supercomputing Conference on High Performance Computing and Communications, Portland, OR, 15-19 Nov. 1993
(Contract W-7405-eng-48)
(DE94-004351; UCRL-JC-115318; CONF-931115-13) Avail: CASI HC A03/MF A01

The National Storage Laboratory (NSL) was organized to develop, demonstrate and commercialize technology for the storage system that will be the future repositories for our national information assets. Within the NSL four Department of Energy laboratories and IBM Federal System Company have pooled their resources to develop an entirely new High Performance Storage System (HPSS). The HPSS project concentrates on scalable parallel storage system for highly parallel computers as well as traditional supercomputers and workstation clusters. Concentrating on meeting the high end of storage system and data management requirements, HPSS is designed using network-connected storage devices to transfer data at rates of 100 million bytes per second and beyond. The resulting products will be portable to many vendor's platforms. The three year project is targeted to be complete in 1995. This paper provides an overview of the requirements, design issues, and architecture of HPSS, as well as a description of the distributed, multi-organization industry and national laboratory HPSS project. DOE

N94-26713 Centre National d'Etudes Spatiales, Toulouse (France).
REAL-TIME EMBEDDED PROCESSING FOR SPACE APPLICATIONS [SYSTEMES INFORMATIQUES TEMPS REEL POUR LES APPLICATIONS SPATIALES]
Apr. 1993 426 p In ENGLISH and FRENCH Symposium held in Saintes-Maries-de-la-Mer, France, 3-6 Nov. 1992
(ISBN-2-85428-335-X; ETN-94-95199) Copyright Avail: Issuing Activity (CEPADUES-Editions, 111, Rue Nicolas-Vauquelin, 31100 Toulouse, France)

Papers from a symposium addressing computer architectures on board spacecraft are presented. In the context of real time onboard applications and computer technology developments, the papers aimed to encourage information transfer between research and industry, taking into consideration the general techniques for onboard applications or those used on the ground. The main themes which emerged were scheduling, architectures, applications, development methods, and validation techniques. For individual titles, see N94-26714 through N94-26746.

N94-26714* Jet Propulsion Lab., California Inst. of Tech., Pasadena.
COMPUTING IN SPACE: ISSUES AND ANSWERS **c61**
John M. Davidson and Ravishankar K. Iyer (Illinois Univ., Urbana.) *In* CNES, Real-Time Embedded Processing for Space Applications Apr. 1993 p 21-28 (For primary document see N94-26713 07-60)
(Grant NAG1-613)

Copyright Avail: Issuing Activity (CEPADUES-Editions, 111, Rue Nicolas-Vauquelin, 31100 Toulouse, France)

Future plans for space exploration call for scientific instruments whose data is increasingly voluminous, far exceeding constraints set by telemetry rates, and therefore, an increased role for spaceborne computing. Three issues that greatly influence the realization of spaceborne computing systems are addressed. The first involves the identification of those research problems which are unique to space computing. Resources must be expended on these problems if efforts are to add value to, and have impact on, the technology of computing in space. The second addresses the transfer of new technology from the research laboratory to use in space. What can be done to expedite this process and shrink the technology gap that separates Earth and space based systems must be assessed. The third issue involves the user's point of view of what is required of new space computing systems. That is, what are the driving forces that most influence customers' decisions to use or not use new technology? Issues of design environment for spaceborne computers, tools for modeling and evaluation of flight systems, and validation of space flight hardware and software are also discussed. ESA

N94-26715 GEC-Plessey Semiconductors, Lincoln (England).

DEVELOPMENT OF A MIL-STD-1750 MICROPROCESSOR SYSTEM FOR SPACE APPLICATIONS

D. Mead and A. L. R. Pouponnot (European Space Agency. European Space Research and Technology Center, ESTEC, Noordwijk, Netherlands.) *In* CNES, Real-Time Embedded Processing for Space Applications Apr. 1993 p 29-40 (For primary document see N94-26713 07-60)

Copyright Avail: Issuing Activity (CEPADUES-Editions, 111, Rue Nicolas-Vauquelin, 31100 Toulouse, France)

An overview of the ESA development program for the MA31750 microprocessor system is presented. Objectives were to design and manufacture a high performance radiation hard microprocessor for onboard space applications with a computing power of 3 million instructions per second, a low pin count to minimize the board area, and power consumption of less than 0.5 W. The justification for the selected approach, the main characteristics of the microprocessor system, the present status of the development, and the continuation of the development work are described. The development of complementary elements is outlined: an Error Detection and Correction unit (EDAC) named MA31752, a Direct Memory Access Controller (DMAC) named MA31753, and a Processor Support Circuit (PSC) named MA31754; VHDL (VHSIC (Very High Speed Integrated Circuit) Hardware Description Language) for the MA31750 chip set; a Software Development Environment (SDE) for the microprocessor system. ESA

N94-26716 National Space Development Agency, Tokyo (Japan).

ON-BOARD COMPUTER FOR CONTROL SUBSYSTEM OF SATELLITE

Shunsuke Tanaka, Shin-Ichiro Ichikawa, Yasuhiro Kawada, Masaya Mine (Toshiba Corp., Kawasaki, Japan.), Yasuo Ishige (Toshiba Corp., Kawasaki, Japan.), Atsushi Itsukaichi (Toshiba Corp., Kawasaki, Japan.), and Kotaro Moritani (Toshiba Corp., Kawasaki, Japan.) *In* CNES, Real-Time Embedded Processing for Space Applications Apr. 1993 p 41-49 (For primary document see N94-26713 07-60)

Copyright Avail: Issuing Activity (CEPADUES-Editions, 111, Rue Nicolas-Vauquelin, 31100 Toulouse, France)

Two types of computer design are presented. One is a highly reliable computer which applies fault tolerant techniques on an Attitude Control Electronics (ACE) of the ETS-4 (Engineering Test Satellite 4). The other is a high performance computer which applies parallel processing techniques on an Arm Control Unit (ACU), for space robots. Both of them use radiation hardened CMOS gate arrays, and they have multi-CPU (Central Processing Unit) configurations. ETS-4 ACE is applicable to all kinds of satellite and the ACU is applicable to Orbital Maneuvering Vehicles (OMV) or high performance computers. ESA

N94-26717 Sextant Avionique, Velizy-Villacoublay (France).

REAL TIME AVIONICS CONSTRAINTS: SILICON SOLUTIONS [CONTRAINTES DE L'AVIONIQUE TEMPS REEL: SOLUTIONS SILICIUM]

Jean-Marie Sers *In* CNES, Real-Time Embedded Processing for Space Applications Apr. 1993 p 51-62 In FRENCH (For primary document see N94-26713 07-60)

Copyright Avail: Issuing Activity (CEPADUES-Editions, 111, Rue Nicolas-Vauquelin, 31100 Toulouse, France)

The timing, safety, and economic constraints of avionics systems and the RTO (Real Time Operation) solution in the context of intensively connected multiprocessor systems are described. RTO behaves, with regard to a processor, like a coprocessor specialized in real time processing, in the same way as a floating coprocessor relieves the processor of all its numerical calculations. It is just as adaptable to a multiprocessor as to a monoprocessor. The processing carried out by RTO, its hardware and software interfaces, and its advantages are described. The IMA (Integrated Modular Avionics) concept and the SMARK (Secure Multiapplication Ada Real Time Kernel) are described. ESA

N94-26718* Jet Propulsion Lab., California Inst. of Tech., Pasadena.

HIGH PERFORMANCE FLIGHT COMPUTER DEVELOPED FOR DEEP SPACE APPLICATIONS

Robert L. Bunker *In* CNES, Real-Time Embedded Processing for Space Applications Apr. 1993 p 63-81 Sponsored by NASA, Washington (For primary document see N94-26713 07-60)

Copyright Avail: Issuing Activity (CEPADUES-Editions, 111, Rue Nicolas-Vauquelin, 31100 Toulouse, France)

The development of an advanced space flight computer for real time embedded deep space applications which embodies the lessons learned on Galileo and modern computer technology is described. The requirements are listed and the design implementation that meets those requirements is described. The development of SPACE-16 (Spaceborne Advanced Computing Engine) (where 16 designates the databus width) was initiated to support the MM2 (Marine Mark 2) project. The computer is based on a radiation hardened emulation of a modern 32 bit microprocessor and its family of support devices including a high performance floating point accelerator. Additional custom devices which include a coprocessor to improve input/output capabilities, a memory interface chip, and an additional support chip that provide management of all fault tolerant features, are described. Detailed supporting analyses and rationale which justifies specific design and architectural decisions are provided. The six chip types were designed and fabricated. Testing and evaluation of a brass/board was initiated. ESA

N94-26719 Phillips Lab., Kirtland AFB, NM.

QUALIFIED MANUFACTURING AND INTEROPERABILITY FOR SPACE APPLICATIONS

Russell R. Herndon *In* CNES, Real-Time Embedded Processing for Space Applications Apr. 1993 p 83-88 (For primary document see N94-26713 07-60)

Copyright Avail: Issuing Activity (CEPADUES-Editions, 111, Rue Nicolas-Vauquelin, 31100 Toulouse, France)

The Advanced Spaceborne Computer Module (ASCM) program, a program which is designed to extend and validate the Qualification Manufacturers Listing (QML) methodology for producing space qualified Very High Speed Integrated Circuit (VHSIC) devices, is described. The ASCM program is a flagship Total Quality Management (TQM) program to validate a major change in qualification methods. The QML methodology significantly reduces destructive end of line testing, thereby, reducing overall individual circuit costs, while maintaining no less a quality product. The program includes some extensive end of line testing formerly performed for the Qualified Product List (QPL), Class S qualification. This information was used for correlation between the two methodologies. The development and demonstration of the qualification methodology was performed by producing devices on the commercial fabrication line for space qualified flight hardware. The first deliverables were based on an advanced MIL-STD-1750A processor with post radiation throughput requirements of 3 to 5 million instructions per second. This product was structured to allow for use of technologies such as radiation hardened 64 K Static Random Access Memories (SRAM's) and the Generic VHSIC Spaceborne Computer (GVSC) class MIL-STD-1750A processors. The physical, electrical package, and interoperability requirements for ASCM were defined. The principal elements are: intramodule bus; spacecraft bus; host interface; and telemetry. ESA

N94-26720 Nippon Electric Co. Ltd., Tokyo (Japan).

FAULT TOLERANT REAL-TIME PROCESSING SYSTEM FOR SPACE USE

Tamotsu Onozawa, Yasuo Morimoto, Tsunekazu Kimura, and Nobuyoshi Hayashi *In* CNES, Real-Time Embedded Processing for Space Applications Apr. 1993 p 89-99 (For primary document see N94-26713 07-60)
Copyright Avail: Issuing Activity (CEPADUES-Editions, 111, Rue Nicolas-Vauquelin, 31100 Toulouse, France)

The Fault tolerant Real time Processing System (FRPS) for onboard space applications, such as for the Japanese HOPE (H2 Orbiting Plane), is described. The FRPS meets requirements by the following design concepts: powerful microprocessor with a general purpose architecture; fault tolerant functions organized systematically and hierarchically; balanced hardware and software; software functions controlling hardware realized by support programs such as outer OS (Operating System); and upward compatible extension of C language called 'real time C' for concurrent programming. The performance and configuration, architecture, fault tolerant feature, system software, software development environment, and verification environment are described. ESA

N94-26721 R-Tech A.B., Lund (Sweden).
A COMPLETE VERSION OF THE Ada TASKING COPROCESSOR
J. Roos and F. Gomez-Molinero *In* CNES, Real-Time Embedded Processing for Space Applications Apr. 1993 p 101-110 Sponsored by ESA/ESTEC (For primary document see N94-26713 07-60)
Copyright Avail: Issuing Activity (CEPADUES-Editions, 111, Rue Nicolas-Vauquelin, 31100 Toulouse, France)

A study to redefine and reimplement the Ada Tasking Coprocessor (ATAC) is described. The resulting ATAC 2.0 architecture and its VLSI (Very Large Scale Integration) implementation are outlined. The ATAC 2.0 architecture is neutral enough to allow efficient integration in existing lines of compilers and has a high degree of transparency with respect to hardware environments. The ATAC is a memory mapped device, to permit flexibility of use with various types of microprocessors. Exception handling, internal interrupt management, and managing time are described. The ATAC does not implement general exception handling support, but it handles exception 'propagation' between tasks and detection of the task related predefined exceptions. The purpose of integrating an interrupt controller with the ATAC was to cut down on the three interrelated problem areas: lock-out, latency, and priority inversion. The desire was also to support interrupts in a way that is fully in line with the Ada tasking model. An internal time manager handles delays and the time-of-day needed to implement the Calendar and the Clock, using the same 64 bit clock. For the VLSI implementation, the main building blocks, signal interface, bus transactions, instruction sequencing, and external task data base memories, are described. ESA

N94-26722 Centre National d'Etudes Spatiales, Toulouse (France).
DESIGN PRINCIPLES OF ONBOARD MANAGEMENT OF A SUN SYNCHRONOUS SATELLITE [PRINCIPES DE CONCEPTION DE LA GESTION BORD D'UN SATELLITE HELIO-SYNCHRONE]
Eric Boussarie, Alain Julhe, and Bernard Olalainty *In its* Real-Time Embedded Processing for Space Applications Apr. 1993 p 113-124 In FRENCH Prepared in cooperation with MATRA Marconi Space, Toulouse, France (For primary document see N94-26713 07-60)
Copyright Avail: Issuing Activity (CEPADUES-Editions, 111, Rue Nicolas-Vauquelin, 31100 Toulouse, France)

The choices presiding in the specification of the onboard computer (software and hardware) architecture of the SPOT 4 satellite are presented, and the software architecture is described. The three principles which guided the SPOT 4 designers are described: requirements related to system security; system observability requirements; and onboard software predictability and determinism requirements. The onboard architecture of SPOT 4 is characterized by the following: modularity of hardware architecture, which ensures on-board safety by minimal dimensioning of onboard software, and on-ground investigations in the case of breakdowns; and the finest possible reconfigurations. The structure of its central software, its cyclical character, guarantee of its predictability, introduces a high testability level, without any mission limitation. ESA

N94-26723* National Aeronautics and Space Administration. Goddard Space Flight Center, Greenbelt, MD.
NASA'S SPACECRAFT DATA SYSTEM **c61**
Alan Cudmore and Mark Flanegan *In* CNES, Real-Time Embedded Processing for Space Applications Apr. 1993 p 125-139 (For primary document see N94-26713 07-60)
Copyright Avail: Issuing Activity (CEPADUES-Editions, 111, Rue Nicolas-Vauquelin, 31100 Toulouse, France)

The NASA Small Explorer Data System (SEDS), a space flight data system developed to support the Small Explorer (SMEX) project, is addressed. The system was flown on the Solar Anomalous Magnetospheric Particle Explorer (SAMPEX) SMEX mission, and with reconfiguration for different requirements will fly on the X-ray Timing Explorer (XTE) and the Tropical Rainfall Measuring Mission (TRMM). SEDS is also foreseen for the Hubble repair mission. Its name was changed to Spacecraft Data System (SDS) in view of expansions. Objectives, SDS hardware, and software are described. Each SDS box contains two computers, data storage memory, uplink (command) reception circuitry, downlink (telemetry) encoding circuitry, Instrument Telemetry Controller (ITC), and spacecraft timing circuitry. The SDS communicates with other subsystems over the MIL-STD-1773 data bus. The SDS software uses a real time Operating System (OS) and the C language. The OS layer, communications and scheduling layer, application task layer, and diagnostic software, are described. Decisions on the use of advanced technologies, such as ASIC's (Application Specific Integrated Circuits) and fiber optics, led to technical improvements, such as lower power and weight, without increasing the risk associated with the data system. The result was a successful SAMPEX development, integration and test, and mission using SEDS, and the upgrading of that system to SDS for TRMM and XTE. ESA

N94-26724 Aerospatiale, Les Mureaux (France). Espace et Defense.
THE ARIANE 5 DATA MANAGEMENT SYSTEM
Yves Durand, Jean-Marie Pasquet, and Jean-Noel Monfort *In* CNES, Real-Time Embedded Processing for Space Applications Apr. 1993 p 141-151 (For primary document see N94-26713 07-60)
Copyright Avail: Issuing Activity (CEPADUES-Editions, 111, Rue Nicolas-Vauquelin, 31100 Toulouse, France)

The various classes of real time constraints associated with the Ariane 5 onboard avionics are introduced, and the architecture that was found adequate to meet these specifications, as well as the associated industrial constraints, are described. The Ariane 5 program is still midpoint in its development and the real time system characteristics, depending on final hardware and software performances, are not available yet. However, the design drivers and the methods used to specify, control, and validate the real time system performances of the onboard avionics are outlined. ESA

N94-26725 Centre National d'Etudes Spatiales, Toulouse (France). Projet PRONAOS.
PRONAOS FLIGHT SOFTWARE: A REAL-TIME APPLICATION FOR A BALLOONBORNE SCIENTIFIC GONDOLA **c61**
Andre Laurens *In its* Real-Time Embedded Processing for Space Applications Apr. 1993 p 153-168 In FRENCH (For primary document see N94-26713 07-60)
Copyright Avail: Issuing Activity (CEPADUES-Editions, 111, Rue Nicolas-Vauquelin, 31100 Toulouse, France)

The flight software for PRONAOS (French acronym for national program of submillimeter astronomy) is addressed. Space applications use more and more sophisticated (and expensive) onboard computers. The PRONAOS project (as well as other science projects) cannot afford such architectures and is to use only classical, almost old fashioned, solutions. The main effort is made on software and methodology, to realize the required functions with the required performance. PRONAOS scientific aims, environment, and global architecture are presented, and the main onboard software (called LV NAPS (NAPS (French acronym for PRONAOS stabilized balloon gondola))), the associated computer architecture, and its main algorithms, are described. The main methodological principles in use for the software development are presented, and how they helped to reach the project's goals is discussed. ESA

N94-26726 MATRA Marconi Space (England).
MATRA MARCONI SPACE: THE SILEX ON-BOARD PROCESSOR AND ON-BOARD SOFTWARE **c61**
L. T. Daryanani, C. Cantenot (MATRA Marconi Space, Toulouse, France.), and J. P. Roussel (MATRA Marconi Space, Toulouse, France.) *In* CNES, Real-Time Embedded Processing for Space Applications Apr. 1993 p 169-183 (For primary document see N94-26713 07-60)

Copyright Avail: Issuing Activity (CEPADUES-Editions, 111, Rue Nicolas-Vauquelin, 31100 Toulouse, France)

The Silex (Semiconductor laser Intersatellite Link Experiment) On Board Processor (OBP) is a real time processing equipment designed for SPOT 4 and Artemis (Advanced Relay Technological Mission Satellite) platforms. The OBP unit is in charge of the management, control, and measurement of the Silex equipments. The Silex On Board Software (OBS) provides classical mission management facilities, and supports pointing control loops, where stringent multitasking and real time performance are required. The OBP terminal data bus supports asynchronous data exchange with reference to the CPU (Central Processing Unit) real time process. In case of major failure, the OBP is tasked to switch the entire Silex experiment to a safe position. The requirements imposed on the OBP equipment, the resulting architecture of the unit, and the various advanced state of the art technologies employed to meet these functions, such as thick film hybrids, ceramic mounted high density RAM (Random Access Memory), and FPGA (Field Programmable Gate Arrays)devices, are described. The OBP and OBS design and development philosophy to arrive at cost effective solutions which, owing to their modular construction, could be reused with little or no modification for other projects, are described. These are assets which make the OBP/OBS concept versatile, and thus it could be considered as a baseline product for future projects, including those in other fields of applications. ESA

N94-26727 Birmingham Univ. (England). School of Physics and Space Research.

ON-BOARD SOFTWARE FOR THE JET-X TELESCOPE ON THE SPECTRUM-X MISSION **c61**

M. D. Bull, C. J. Eyles, and O. Emam *In* CNES, Real-Time Embedded Processing for Space Applications Apr. 1993 p 185-200 Sponsored by Science Research Council (For primary document see N94-26713 07-60)

Copyright Avail: Issuing Activity (CEPADUES-Editions, 111, Rue Nicolas-Vauquelin, 31100 Toulouse, France)

JET-X, the Joint European X Ray Telescope, is one of the core instruments on the Russian Spectrum Roentgen (x ray) Gamma (SRG) high energy astrophysics mission. The instrument comprises two coaligned grazing incidence x ray telescopes, using x ray sensitive charge coupled devices (CCD's) as focal plane detectors. The SRG spacecraft will be launched into a highly eccentric four day orbit with ground contacts for periods of approximately 2 hours every 24 hours. The JET-X onboard data handling system is based on a network of four 80C86 processors, interconnected via serial links, and includes a 60 Mbyte mass memory to store data between ground contacts. The embedded software performs real time processing of the image data from the various CCD detectors in order to reduce the very high data rates produced to a value consistent with the size of the mass memory. It was designed with particular attention to the requirement for reliable, autonomous operation during the 24 hour periods between ground contacts. ESA

N94-26728 Ecole Centrale de Nantes (France). Lab. d'Automatique.

SCHEDULING TASKS WITH UNPREDICTABLE TIMING PARAMETERS IN HARD REAL-TIME SYSTEMS **c61**

Maryline Silly *In* CNES, Real-Time Embedded Processing for Space Applications Apr. 1993 p 203-210 (For primary document see N94-26713 07-60)

Copyright Avail: Issuing Activity (CEPADUES-Editions, 111, Rue Nicolas-Vauquelin, 31100 Toulouse, France)

The problem of guaranteeing response times to periodic and sporadic tasks even under transient overloads and a solution using the deadline mechanism to provide tradeoffs among time and precision are addressed. Hard real time systems are characterized by their timing constraints because they are responsible for safety and time critical control systems such as aircraft, nuclear systems, etc. The software of such systems features a large number of tasks said to be time critical because they must start at a required time and produce results before a certain deadline. One of the most important design issues in a real time system is to schedule tasks to meet their deadlines, which requires a formal performance evaluation of the system. Solutions used today for a large proportion of systems are static in that they assume complete and prior knowledge of all the tasks and make static decisions. Unfortunately, next generation systems are more complex and dynamic. Notably, determination of task execution time is very difficult and arrival time of sporadic tasks is unpredictable. In these systems, the fluctuations in both the rate and magnitude of service demands may dynamically overload the computing system and thus entail deadline misses which is inacceptable in a hard real time environment. One approach to cope with the problem of transient system overload is to use the deadline mechanism combined with an efficient scheduling strategy so all deadlines are guaranteed to be met under all circumstances. The deadline mechanism provides two implementation versions for a task which differ only in the amount of processor time they consume and the precision of the results that they return. ESA

N94-26729 CR2A, Nanterre (France).

STANDARDIZE Ada HARD REAL-TIME SERVICES? **c61**

Dominique L. R. Chandesris, Vincent Celier, and Nasser Kettani *In* CNES, Real-Time Embedded Processing for Space Applications Apr. 1993 p 211-221 (For primary document see N94-26713 07-60)

Copyright Avail: Issuing Activity (CEPADUES-Editions, 111, Rue Nicolas-Vauquelin, 31100 Toulouse, France)

Technical issues raised by the use of Ada for hard real time (HRT) systems are examined: All the solutions proposed for increasing the success of this programming language within the HRT community are not examined, only the secondary standard solution is analyzed. The International Standards Organization (ISO) Real Time Rapporteur Group (RRG) goals and objectives are presented, and the RRG proposal approach is illustrated by an example: distribution and multiprogramming. The secondary standard approach is understood to be the best pragmatic compromise between continuous language changes and conservative and strict language maintenance. Belief is that the Ada HRT community needs standardized HRT services for Ada and that the secondary standard approach is the best one. This secondary standard must have a validation process, including metrics, for the users to be able trust the future products implementing the RRG standard. An implementation of the future secondary standard is under development. ESA

N94-26730 Alsys, Inc., Saint Cloud (France).

Ada MULTIPLE-PROGRAMMING FOR HARD REAL TIME APPLICATIONS IN SPACE SYSTEMS **c61**

Marc Richard-Foy *In* CNES, Real-Time Embedded Processing for Space Applications Apr. 1993 p 223-233 In FRENCH (For primary document see N94-26713 07-60)

Copyright Avail: Issuing Activity (CEPADUES-Editions, 111, Rue Nicolas-Vauquelin, 31100 Toulouse, France)

Ada implementation of the integrated modular avionics (IMA) is addressed. IMA puts the accent on three types of requirements found in avionic and space projects: hard real time, safety systems, and multiprogramming. The principal results of the formal method rate monotonic analysis (RMA) are outlined. In applying RMA to an Ada multiprogram system, a scheduling method simultaneously for programs and tasks satisfying IMA criteria must be developed. A multiprogram scheduling conforming to RMA analysis is proposed and a second model more appropriate to the IMA concept is described. The real time executive certification procedures and current and future standards of the IMA support concept and RMA with the Ada language are discussed. ESA

N94-26731 British Aerospace Public Ltd. Co., Stevenage (England). Communication Satellites Div.

IMPLEMENTING HARD REAL-TIME SYSTEMS: A CASE STUDY **c61**

C. M. Bailey, A. Burns (York Univ., England.), E. Fyfe, F. Gomez-Molinero (European Space Agency. European Space Research and Technology Center, ESTEC, Noordwijk, Netherlands.), and A. J. Wellings (York Univ., England.) *In* CNES, Real-Time Embedded Processing for Space Applications Apr. 1993 p 235-249 (For primary document see N94-26713 07-60)

(Contract ESTEC-9198/90/NL/SF)

Copyright Avail: Issuing Activity (CEPADUES-Editions, 111, Rue Nicolas-Vauquelin, 31100 Toulouse, France)

A case study implementation of a proposed scheduling approach for single processor space applications is presented. The use of a modification of the Ada tasking model, using asynchronous communication via a passive monitor-like abstraction and supporting 'time-fences' to prevent an application from executing more CPU cycles than was allowed for in the prerun time analysis of its worst case execution time, was investigated. The approach to scheduling is based on preemptive priority based dispatching. Priorities are assigned according to the deadline monotonic scheme. To support the proposed scheduling, a hard real time hierarchical object oriented design (HRT-HOOD) method was developed. HRT-HOOD, which builds on the foundations of HOOD, recognizes sporadic and cyclic objects, and 'protected' objects which facilitate object interactions but only in ways that can be analyzed for their temporal behavior. A proof of concept implementation of the normal mode of operation of the Olympus AOCS (Attitude and Orbital Control System), that is the attitude control loops and associated telemetry and telecommand handling, is described and the scheduling approach is assessed. ESA

N94-26732 Ecole Centrale de Nantes (France). Lab. d'Automatique.
TOOL FOR PERFORMANCE ANALYSIS AND OFF-LINE PREDICTION OF TIMING BEHAVIOUR
E. Mesnard and Y. Trinquet *In* CNES, Real-Time Embedded Processing for Space Applications Apr. 1993 p 251-259 In FRENCH (For primary document see N94-26713 07-60)
Copyright Avail: Issuing Activity (CEPADUES-Editions, 111, Rue Nicolas-Vauquelin, 31100 Toulouse, France)

An analysis of real time system timing behavior, to provide a design aid for such systems to enable them to verify a priori if certain timing characteristics conform to their specifications, is presented. The study is part of a more general framework enabling a characteristic graph of program execution to be obtained using a program written in the C language (program dependance graph). The approach described belongs to the asynchronous system framework but an application model imposing constraints in the algorithmic description of the application and an execution model using a non-preemptive scheduling mode are described. An analysis model, using a graph, allows the offline study of timing behavior of the application and the verification of whether the timing constraints are verified. ESA

N94-26733 Intecs Sistemi S.p.A., Pisa (Italy) Operating System Section.
A REAL-TIME EXECUTIVE IMPLEMENTING PRIORITY INHERITANCE PROTOCOLS **c61**
S. Sabina, R. Chiaverini, and C. Migliorini *In* CNES, Real-Time Embedded Processing for Space Applications Apr. 1993 p 261-271 (For primary document see N94-26713 07-60)
Copyright Avail: Issuing Activity (CEPADUES-Editions, 111, Rue Nicolas-Vauquelin, 31100 Toulouse, France)

A priority model and a task model of an 'executive' suitable for hard real time environments are presented. Preemptive scheduling algorithms are generally used for managing concurrency on large and complex monoprocessor systems. However, they lead to nondeterministic system execution times and unpredictable system timing behavior. The main cause of unpredictability is the so called priority inversion problem. It occurs when a high priority task is forced to wait for the execution of a lower priority task. To overcome the drawback of unpredictability, the use of hard real time scheduling algorithms, for example the rate monotonic, or the deadline monotonic with priority inheritance, is required. This class of scheduling algorithms sets upper bounds to the duration of priority inversion, and thus leads to analyzable systems. A priority model and a task model suitable for the implementation of hard real time scheduling algorithms in an executive, and the main design issues to be taken into account in the implementation of the basic priority inheritance protocol, are presented. ESA

N94-26734 Vrije Univ., Brussels (Belgium).
SCHEDULING APPROACHES WITH Ada **c61**
R. Devillers, D. DeLucca, J. Beaufays (TRASYS Space, Brussels, Belgium.), and E. Snyers (TRASYS Space, Brussels, Belgium.) *In* CNES, Real-Time Embedded Processing for Space Applications Apr. 1993 p 273-283 (For primary document see N94-26713 07-60)
Copyright Avail: Issuing Activity (CEPADUES-Editions, 111, Rue Nicolas-Vauquelin, 31100 Toulouse, France)

A project aiming to analyze and compare different approaches for hard real time scheduling in Ada is reported. Three different approaches for process scheduling were analyzed and implemented in Ada: the traditional cyclic executive; the rate monotonic scheduling; and the deadline monotonic sheduling. To perform this comparison, a reference application was developed involving the cyclic execution of a set of periodic processes with different frequencies and the response of the system to aperiodic requests with different response times. The practical application of the three different scheduling approaches in Ada, with respect to their time correctness, flexibility, and complexity, is discussed. ESA

N94-26735 Institut Univ. de Technologie, Nantes (France).
FAULT-TOLERANT SCHEDULING IN DISTRIBUTED CRITICAL REAL-TIME SYSTEMS **c61**
Houssine Chetto *In* CNES, Real-Time Embedded Processing for Space Applications Apr. 1993 p 285-295 (For primary document see N94-26713 07-60)
Copyright Avail: Issuing Activity (CEPADUES-Editions, 111, Rue Nicolas-Vauquelin, 31100 Toulouse, France)

A real time system is said to be hard if a failure to meet the timing constraints imposed on the software will result in property damage or even in a loss of human life. A key issue in the design of such a system is to determine an appropriate fault tolerant mechanism so that the occurrence of any erroneous state does not result in a timing failure (deadline missing) and, consequently, allows an acceptable although degraded performance to be guaranteed. A study in which the deadline mechanism, which is a variation of the recovery block scheme and is used to support timing fault tolerance, is presented. The deadline mechanism and implementation considerations in a distributed system are considered and a strategy for task allocation and dynamic reconfiguration is presented. ESA

N94-26736 MATRA Marconi Space, Toulouse (France).
EARLY REAL-TIME PERFORMANCE MEASUREMENTS ON THE COLUMBUS PROCESSOR SYSTEM
G. Birnbaum, P. Humbert, T. Jourdan, and C. Renoux *In* CNES, Real-Time Embedded Processing for Space Applications Apr. 1993 p 299-317 (For primary document see N94-26713 07-60)
Copyright Avail: Issuing Activity (CEPADUES-Editions, 111, Rue Nicolas-Vauquelin, 31100 Toulouse, France)

To fulfill its 30 year space station mission with regard to the variety of its users (crew work station, data storage and retrieval, mission management, and subsystem control), the Columbus processor system, called Processing Node Drawer (PND), provides a large set of powerful and reliable processing, communications, and peripheral interface building blocks. The PND is a catalyst which allows the standardization offered by commercial techniques and products to be applied to space applications and users. The full range of space environmental conditions and design rules are incorporated, not added afterwards. All PND dynamic performance predictions take into account an operation in worst case conditions and an in-orbit lifetime of ten years. Predevelopment of common building blocks such as the Network Interface Unit, the Columbus Operating System, the Space NuBus, and associated hardware and software have increased confidence in the feasibility of this distributed and open computing solution. ESA

N94-26737 Centre National d'Etudes Spatiales, Toulouse (France).
TEST OF ONBOARD REAL TIME APPLICATIONS (LICE (TM)) [LE TEST DES APPLICATIONS TEMPS REEL EMBARQUEES (LA METHODE LICE (TM))] **c61**
J. L. Carayon *In its* Real-Time Embedded Processing for Space Applications Apr. 1993 p 319-328 In FRENCH (For primary document see N94-26713 07-60)
Copyright Avail: Issuing Activity (CEPADUES-Editions, 111, Rue Nicolas-Vauquelin, 31100 Toulouse, France)

The different phases encountered during the integration of a real time embedded application using software are described. The needs of specific tools for monitoring the real time behavior of the application are presented. An approach addressing the observability problem of complex software during its integration phase is proposed. This approach is based upon the LICE (French acronym for onboard applications control software and interface) tools. ESA

N94-26738 Centre National d'Etudes Spatiales, Toulouse (France).
ARITHMETIC PERFORMANCES OF ONBOARD COMPUTERS [PERFORMANCES ARITHMETIQUES DES CALCULATEURS EMBARQUES]
J. C. Berges *In its* Real-Time Embedded Processing for Space Applications Apr. 1993 p 329-339 In FRENCH (For primary

document see N94-26713 07-60)
Copyright Avail: Issuing Activity (CEPADUES-Editions, 111, Rue Nicolas-Vauquelin, 31100 Toulouse, France)

A study within the greater framework of developing AQUARELS (French acronym for workshop on numerical quality for scientific software realization) is presented. The trajectory determination of a space vehicle is generally computed by ground stations with mainframes or workstations. However, for future projects, this 'scientific processing' component (extended Kalman filter, ordinary differential equations, and intensive use of the elementary functions: sin, cos, sqrt, e to the power x, etc.) will be on board and it is important to evaluate the arithmetic performances of the onboard processors available for these missions. Tools to evaluate the basic parameters of an arithmetic unit, and a synthesis of results of the microprocessor evaluation for the Hermes project are described. ESA

N94-26739 MATRA Marconi Space, Toulouse (France).
VERIFICATION AND VALIDATION OF THE ON-BOARD SOFTWARE REAL TIME REQUIREMENTS [LA VERIFICATION ET LA VALIDATION DES EXIGENCES TEMPS REEL DU LOGICIEL TEMPS SPATIAL EMBARQUE] **c61**
Jean-Louis Dega, Jean Jacques Montiel, and Bruno Vatan *In* CNES, Real-Time Embedded Processing for Space Applications Apr. 1993 p 341-353 In FRENCH (For primary document see N94-26713 07-60)
Copyright Avail: Issuing Activity (CEPADUES-Editions, 111, Rue Nicolas-Vauquelin, 31100 Toulouse, France)

An assessment of the verification and validation of space embedded software and ground segment facilities is presented. Focus is on: the generic philosophy of the actual software validation facilities to test the operational requirements (and particularly the real time requirements) at each step of the building of a software component from the low level ones to the complete software; the constraints imposed on the test environment by the real time code under test; positioning for reducing cost and time consumption in the verification and validation process of these real time requirements. This flashback on the verification and validation process covers the satellite software such as those of the telecommunication satellites, the SPOT family, Hipparcos, and ERS. It shows how this experience gained during more than 10 years permits tackling of the new generation of these complex systems such as Hermes and Columbus. To allow the test of the real time requirements of these more and more large and complex softwares and to avoid an excessive increase of costs, it is necessary: to build the verification tools of these requirements and to use it early in the development cycle; to reuse these tools along the development and the verification in order to update the requirements as soon as first tests results appear; and to define a new generic philosophy of reusing verification and validation components from the low level software test facilities to the complete software test facilities including in house facilities to large test result analysis. ESA

N94-26740* SRI International Corp., Menlo Park, CA. Computer Science Lab.
FORMAL METHODS FOR DEPENDABLE REAL-TIME SYSTEMS
John Rushby *In* CNES, Real-Time Embedded Processing for Space Applications Apr. 1993 p 355-366 (For primary document see N94-26713 07-60)
(Contracts NAS1-18266; NAS1-18969; N00014-92-C-2177)
Copyright Avail: Issuing Activity (CEPADUES-Editions, 111, Rue Nicolas-Vauquelin, 31100 Toulouse, France)

The motivation for using formal methods to specify and reason about real time properties is outlined and approaches that were proposed and used are sketched. The formal verifications of clock synchronization algorithms are concluded as showing that mechanically supported reasoning about complex real time behavior is feasible. However, there was significant increase in the effectiveness of verification systems since those verifications were performed, at it is to be expected that verifications of comparable difficulty will become fairly routine. The current challenge lies in developing perspicuous and economical approaches to the formalization and specification of real time properties. ESA

N94-26741 Dornier System G.m.b.H., Friedrichshafen (Germany).
DEVELOPING WITH Ada USING HOOD DESIGN METHODOLOGY **c61**
K. Baeuerle, U. Denskat, and J. Garbers *In* CNES, Real-Time Embedded Processing for Space Applications Apr. 1993 p 369-379 (For primary document see N94-26713 07-60)
Copyright Avail: Issuing Activity (CEPADUES-Editions, 111, Rue Nicolas-Vauquelin, 31100 Toulouse, France)

Experiences gained when developing Ada software for a high reliable application on a real time embedded system using the HOOD (Hierarchical Object Oriented Design) design methodology are described. A two way approach is used in summarizing the encountered problems. Discrepancies existing between requirements for high performance, high reliability and hierarchical object oriented design, are identified, and experience gained and problems encountered during implementation of this kind of software, especially those raised by the use of heterogeneous CASE toolset together with an APSE, are described. The experience is mainly based on developing communications and low level services software for the Ariane 5 onboard computer. The software was designed using the HOOD version 2.1 methodology and implemented in Ada and assembler. A large discrepancy must be seen presently between new development concepts and their applicability in real projects. ESA

N94-26742 Sextant Avionique, Velizy-Villacoublay (France).
USE OF HOOD COUPLED TO REAL TIME MONITORS [UTILISATION DE HOOD COUPLEE A DES MONITEURS TEMPS REEL] **c61**
Thierry Gohon and Philippe Guedou *In* CNES, Real-Time Embedded Processing for Space Applications Apr. 1993 p 381-398 In FRENCH (For primary document see N94-26713 07-60)
Copyright Avail: Issuing Activity (CEPADUES-Editions, 111, Rue Nicolas-Vauquelin, 31100 Toulouse, France)

The Hierarchical Object Oriented Design (HOOD) method and Ada are both widely used for large embedded real time software. This design method is oriented toward Ada programming. It uses the Ada tasking to map the dynamical properties of objects. Some particular critical real time requirements may today be hardly compatible with the implementation of Ada tasking. A real time silicon executive RTO (Real Time Operation) providing real time services that can be called from the software was developed. The capability of using this microchip early in the HOOD design phase while keeping the high level of abstraction of the HOOD real time features is addressed. The RTO silicon executive is seen as an alternative to the Ada implementation of the HOOD. The use of HOOD with RTO to provide an efficient implementation of cyclic tasks is examined. The HOOD/RTO connection is seen as a step leading to validation of the use of HOOD with IMAGES (Integrated Modular Avionics General Executive Software). ESA

N94-26743 THARSYS (France).
Ada REUSABLE SOFTWARE FOR SATELLITE ON-BOARD DATA HANDLING **c61**
P. Tarabbia *In* CNES, Real-Time Embedded Processing for Space Applications Apr. 1993 p 399-407 (For primary document see N94-26713 07-60)
Copyright Avail: Issuing Activity (CEPADUES-Editions, 111, Rue Nicolas-Vauquelin, 31100 Toulouse, France)

With the increasing success of Ada in aerospace systems, attention focused recently on software reuse: reusing software components can imply substantial costs savings, sometimes up to 90%. Software components tend to become safer as they are reused, thus implying that a system built with reusable components is potentially more reliable than one developed from the scratch. However reusability has so far been implemented as local 'recovery' actions out of former projects, but hardly as an investment policy. The onboard data handling division of ESA initiated an activity to develop a set of reusable software modules for satellite onboard data handling. The results of this project are described. The project confirmed that using reusable software components can lead to an 80% reduction of the development effort. ESA

N94-26744 Centre National d'Etudes Spatiales, Toulouse (France).
THE CODE-TOP (CONCURRENT SYSTEM DEVELOPMENT USING TRANSFORMATIONS OF PREDICATE-TRANSITION NETS) METHOD: EXAMPLES OF USING IT FOR SYSTEM ARCHITECTURE SPECIFICATION, SOFTWARE SPECIFICATION, AND CODE GENERATION **c61**
Patrick deBondeli *In its* Real-Time Embedded Processing for Space Applications Apr. 1993 p 409-427 (For primary document see N94-26713

07-60)
Copyright Avail: Issuing Activity (CEPADUES-Editions, 111, Rue Nicolas-Vauquelin, 31100 Toulouse, France)

The CODE-TOP method for specifying concurrent systems modeled as asynchronous processes cooperating through the use of common synchronization/communication objects is presented. CODE-TOP can be regarded as an extension of the 'transformational approach' to software development for concurrent systems. CODE-TOP relies basically on three techniques: data abstraction or object oriented programming; formal specifications; and transformational programming. Examples of CODE-TOP are given, and the case of the ABSTRACT BUS COMMMUNICATION abstract data type, a nontrivial real life component, is used to illustrate CODE-TOP specification techniques and to give hints on the CODE-TOP Ada83 code generation technique. ESA

N94-26745 Institut National de Recherche d'Informatique et d'Automatique, Le Chesnay (France).

SPECIFICATION PERFORMANCE OPTIMIZATION AND EXECUTIVE GENERATION FOR ONBOARD MULTIPROCESSOR REAL TIME APPLICATION WITH SynDEx [SPECIFICATION, OPTIMISATION DE PERFORMANCES ET GENERATION D'EXECUTIF POUR APPLICATION TEMPS-REEL EMBARQUEE MULTI-PROCESSEUR AVEC SYNDEX] c62

Christophe Lavarenne and Yves Sorel *In* CNES, Real-Time Embedded Processing for Space Applications Apr. 1993 p 429-437 In FRENCH (For primary document see N94-26713 07-60)
Copyright Avail: Issuing Activity (CEPADUES-Editions, 111, Rue Nicolas-Vauquelin, 31100 Toulouse, France)

SIGNAL, an example of synchronous languages, and SynDEx (Synchronous Distributed Executive), which is designed to meet needs of multiprocessor executive optimization and generation, are presented. SynDEx is a graphical interactive development environment, offering: interface with SIGNAL for specification and verification of the application algorithm for achieving program reliability; specification and dimensioning of the multiprocessor machine in view of hardware optimization; optimized placement-arranging of the application algorithm on the multiprocessor with performance evaluation and visualization; and generation of the distributed executive for real time execution, relieving the user, at maximum, of heavy tasks of low level programming. ESA

N94-26746 European Space Agency. European Space Research and Technology Center, ESTEC, Noordwijk (Netherlands). On-Board Data Div.

ASYNCHRONOUS AND PACKETIZED SYSTEMS ENGINEERING TOOLS

F. Teston and T. Vardanega *In* CNES, Real-Time Embedded Processing for Space Applications Apr. 1993 p 439-452 (For primary document see N94-26713 07-60)
Copyright Avail: Issuing Activity (CEPADUES-Editions, 111, Rue Nicolas-Vauquelin, 31100 Toulouse, France)

The achievement of a high degree of efficiency is one of the most critical aspect in the overall economy of spacecraft design. Emerging technologies however provide the means to significantly increase the achievable efficiency in the utilization of processing and communication resources. These emerging technologies are centered around the concept of packet based services for the end to end communications on board and with ground, and the concept of deadline monotonic analysis for the scheduling of onboard software activities. Systems based upon such concepts operate according to a virtually asynchronous processing paradigm, as opposed to current systems which mostly operate in a rigidly synchronous fashion. The design of such new 'asynchronous' systems however, presents a higher number of free variable parameters and interdependencies among system components. The net result is thus an increased overall complexity. Mastering such complexity, and offering the means to tailor the system around specific application requirements is thus the key issue in the effective exploitation of this new system technology. Advanced engineering tools are needed for this purpose. A simulation based approach is discussed. ESA

N94-27016# California Univ., San Diego, La Jolla. Dept. of Electrical and Computer Engineering.

DESIGN AND EVALUATION OF FAULT TOLERANCE IN OPTO-ELECTRONIC COMPUTING Semiannual Report

Ting-Ting Y. Lin 3 Dec. 1993 13 p
(Contract N00014-93-1-0698)
(AD-A274281) Avail: CASI HC A03/MF A01

The first area of research is Data-Flow Clustering. In synchronous circuits (described in terms of registers and combinational nodes), it is known that the feedback loops are dominant in determining the achievable clock period for the circuit. More precisely, the maximum delay to register ratio over all loops in the circuit (called the iteration bound) is a lower bound on the clock period. Furthermore, if the combinational nodes are fine-grained in nature, the iteration bound very closely reflects the achievable clock period through retiming. However, because of size constraints it is often necessary to partition such a circuit into multiple modules (for example FPGA's). The second area of research is network partitioning. The classical problem of finding the Minimum-Cut in an undirected graph, given source and sink nodes, s and t was studied. The problem is reformulated as a continuous placement problem. The correspondence between the Min-Cut problem and the placement problem which is then solved iteratively using gradient methods is shown. In addition, this method has good potential for efficient parallel implementation. Experimental data on the effectiveness of our approach is provided. DTIC

N94-27152# Air Force Inst. of Tech., Wright-Patterson AFB, OH. School of Engineering.

VIRTUAL MEMORY MANAGEMENT AND VIRTUAL BUS OVERLOADING ON MULTIPLE CHANNEL ARCHITECTURES M.S. Thesis

John N. Armitstead Dec. 1993 73 p
(AD-A274127; AFIT/GCS/Eng/93D-1) Avail: CASI HC A04/MF A01

Today's computational environment requires the processing capabilities available only through parallel architectures. The bottleneck that limits the potential of parallel processing is communication between processors, memories, and other hardware devices. A proposed multiple channel architecture (MCA) utilizes tunable semiconductor lasers and fiber optic cables that serve as the communication medium between processor, memory, and I/O nodes. A memory management unit (MMU) was completely described and implemented in a multiprocessor simulator. A permutation-based interleaving (PBI) scheme was utilized to reduce the chance of memory access collisions. Virtual bus utilization, number of collisions, and message traffic patterns were studied under various amounts of overloading. Results show that it is possible to maintain processor efficiency while reducing demand for channel availability. DTIC

N94-27191# Technische Univ., Eindhoven (Netherlands). Faculty of Electrical Engineering.

PROCEEDINGS OF THE THIRD WORKSHOP COMPUTERSYSTEMS: RESEARCH FORUM ON DESIGN, REALIZATION AND USE OF COMPUTERSYSTEMS

Willem Jan Withagen, ed. 1991 72 p Workshop held in Eindhoven, Netherlands, 15 May 1991
(ISBN-90-6144-995-2; ETN-94-95284) Avail: CASI HC A04/MF A01

A language for the description and analysis of digital systems at a behavioral and structural level of abstraction, named DALIA, is presented. A parallel object oriented computer system, named POOMA, and a parallel object oriented language to express programs for execution on this are designed and implemented. A model to analyze the inherent parallelism of a simulation, and a survey of existing strategies to perform simulation in parallel are presented. A model for calculating the required amount of redundancy and the necessary degree of partitioning of the circuit to achieve a maximum efficiency is proposed. A compile time technique for determining if a set of procedures within a parallel program can be executed sequentially without causing deadlock is described. For individual titles, see N94-27192 through N94-27196.

N94-27192# Technische Univ., Eindhoven (Netherlands). Faculty of Electrical Engineering.

DALIA: A LANGUAGE FOR THE DESCRIPTION AND ANALYSIS OF DIGITAL SYSTEMS c61

Henk vanderWeij *In its* Proceedings of the 3rd Workshop Computersystems: Research Forum on Design, Realization and Use of Computersystems 1991 p 1-16 (For primary document see N94-27191 07-60)
Avail: CASI HC A03/MF A01

DALIA is a formal language for the description and analysis of digital systems at a behavioral as well as a structural level of abstraction. It is based on a functional style of programming, extended with annotations for indicating system structure, accessability, and signal flow direction. Program transformation rules are defined for rewriting DALIA descriptions to behaviorally equivalent alternatives. The language is developed to be used as a formal basis for automated system design, adopting the following philosophy: the requirements for the system to be designed are formalized in the DALIA notation. The formal specification is stepwise transformed to a structural description of the system realization. Formal descriptions and transformations, allowing a correctness by construction methodology, are considered. ESA

N94-27193# Philips International B.V., Eindhoven (Netherlands). Natuurkundig Lab.
PARALLEL COMPUTERS FOR ADVANCED INFORMATION PROCESSING Abstract Only **c62**
E. Odijk *In* Technische Univ., Proceedings of the 3rd Workshop Computersystems: Research Forum on Design, Realization and Use of Computersystems 1991 p 17 (For primary document see N94-27191 07-60)
Avail: CASI HC A01/MF A01

A parallel object oriented computer system, POOMA, and a parallel object oriented language to express programs for execution on this system were designed and implemented. A survey of the systems concepts, the rationale of a number of the design choices, and the lessons learned during the design are included. POOMA is a distributed memory, scalable, computer that consists of self contained computers, each with their own central processing unit, main memory and a communication unit. These computers communicate via a sparsely connected, packet switching, topology of bidirectional communication links that are serviced by the communication unit. The architecture designed to meet the requirements of the parallel object oriented language, and the match of the conceptual and operational models are described. ESA

N94-27194# Amsterdam Univ. (Netherlands). Dept. of Computer Systems.
PARALLEL DISCRETE EVENT SIMULATION **c62**
Benno Overeinder, Bob Hertzberger, and Peter Sloot *In* Technische Univ., Proceedings of the 3rd Workshop Computersystems: Research Forum on Design, Realization and Use of Computersystems 1991 p 19-30 (For primary document see N94-27191 07-60)
Avail: CASI HC A03/MF A01

A model to analyze the inherent parallelism of a simulation, together with a survey of existing strategies to perform the simulation in parallel are presented. Extensions to this model are discussed, resulting in reliable evaluation of the effectiveness of these strategies. In simulating applications for execution on specific computing systems, the simulation performance figures must be known in a short period of time. One basic approach to the problem of reducing the required simulation time is the exploitation of parallelism. Due to the distributed generation of events causality errors can occur; as a result, the sequence in which to process the events is essentially indeterminated. An introduction to discrete event simulation is given. A parallel view to the sequential simulation is proposed. Methods for parallel simulation are described and their effectiveness is considered. These methods are evaluated and some suggestions for further research are presented. ESA

N94-27195# Universiteit Twente, Enschede (Netherlands). Dept. of Computer Science.
A PARTITIONING AND REDUNDANCY MODEL FOR WAFER-SCALE INTEGRATED CIRCUITS
Martin F. Beusekamp *In* Technische Univ., Proceedings of the 3rd Workshop Computersystems: Research Forum on Design, Realization and Use of Computersystems 1991 p 31-49 (For primary document see N94-27191 07-60)
Avail: CASI HC A03/MF A01

A general, architecture independent model to calculate the required amount of redundancy and the necessary degree of partitioning of the circuit to achieve a maximum efficiency are presented. In wafer scale integration, a certain amount of redundancy is required to achieve an acceptable yield. It is shown that in practical cases, the efficiency curve around the maximum is relatively flat. The model presents the optimal degree of partitioning, rate of redundancy, total area, yield and efficiency for any desired circuit. It is shown that, for every technological environment, there exists a critical circuit size, below which the implementation of partitioning and redundancy is undesirable. Above this critical circuit size, partitioning into rather small cells leads to optimal efficiency, in spite of the fact that small cells require a considerable overhead of reconfiguration wiring and switches. It was shown that the model can be adapted to any specific architecture by adjusting parameters and limiting possible solutions to restricted, architecture dependent values. By a mathematical substitution, the model can be made completely analytic. ESA

N94-27196# Technische Univ., Delft (Netherlands). Dept. of Electrical Engineering.
EFFICIENT IMPLEMENTATION OF HIGH-LEVEL PARALLEL SYMBOLIC LANGUAGES **c61**
Mark Korsloot (Oregon Univ., Portland.) and E. Tick *In* Technische Univ., Proceedings of the 3rd Workshop Computersystems: Research Forum on Design, Realization and Use of Computersystems 1991 p 51-69 (For primary document see N94-27191 07-60)
Avail: CASI HC A03/MF A01

A compile time technique for determining if a set of procedures within a parallel program can be executed sequentially without causing deadlock is presented. The analysis and methods are described for committed choice parallel logic programming languages. The concepts are general enough for any concurrent languages with fine grain communicating processes. Methods for ensuring that sequential evaluation of a program module cannot result in producer-consumer suspension within the module itself, resulting in deadlock, are derived. The advantages of sequentializing fine grain languages include the use of 'traditional' compiler optimizations, and continuation stacking procedure invocation. ESA

N94-27547# Center for Mathematics and Computer Science, Amsterdam (Netherlands). Dept. of Computer Science/Dept. of Algorithmics and Architecture.
BINARY SNAPSHOTS
Jaap-Henk Hoepman and John T. Tromp Mar. 1993 11 p
(ISSN 0169-118X)
(CWI-CS-R9319; ETN-94-95432) Copyright Avail: CASI HC A03/MF A01

The shared memory wait-free 'atomic snapshot' object in its simplest form where each cell contains a single bit is considered. The 'universality' of this binary snapshot object is demonstrated by presenting an efficent linear time implementation of the general multibit atomic snapshot object using an atomic binary snapshot object as a primitive. Thus, the search for an efficient (subquadratic or linear time) wait-free atomic snapshot implementation may be restricted to the binary case. ESA

N94-27769*# National Aeronautics and Space Administration. Lyndon B. Johnson Space Center, Houston, TX.
HUMAN COMPUTER INTERFACE GUIDE, REVISION A
Jul. 1993 253 p
(NASA-TM-109708; NAS 1.15:109708; SSP-30540-Rev-A) Avail: CASI HC A12/MF A03

The Human Computer Interface Guide, SSP 30540, is a reference document for the information systems within the Space Station Freedom Program (SSFP). The Human Computer Interface Guide (HCIG) provides guidelines for the design of computer software that affects human performance, specifically, the human-computer interface. This document contains an introduction and subparagraphs on SSFP computer systems, users, and tasks; guidelines for interactions between users and the SSFP computer systems; human factors evaluation and testing of the user interface system; and example specifications. The contents of this document are intended to be consistent with the tasks and products to be prepared by NASA Work Package Centers and SSFP participants as defined in SSP 30000, Space Station Program Definition and Requirements Document. The Human Computer Interface Guide shall be implemented on all new SSFP contractual and internal activities and shall be included in any existing contracts through contract changes. This document is under the control of the Space Station Control Board, and any changes or revisions will be approved by the deputy director. Derived from text

N94-28267*# Odyssey Research Associates, Inc., Ithaca, NY.
USING FORMAL SPECIFICATION IN THE GUIDANCE AND CONTROL SOFTWARE (GCS) EXPERIMENT. FORMAL DESIGN AND VERIFICATION TECHNOLOGY FOR LIFE CRITICAL SYSTEMS Final Report
Doug Weber and Damir Jamsek 5 Apr. 1994 114 p
(Contract NAS1-18972; RTOP 505-64-10-51)
(NASA-CR-194884; NAS 1.26:194884; TM-92-0046) Avail: CASI HC A06/MF A02

The goal of this task was to investigate how formal methods could be incorporated into a software engineering process for flight-control systems under DO-178B and to demonstrate that process by developing a formal specification for NASA's Guidance and Controls Software (GCS) Experiment. GCS is software to control the descent of a spacecraft onto a planet's surface. The GCS example is simplified from a real example spacecraft, but exhibits the characteristics of realistic spacecraft control software. The formal specification is written in Larch. Author

N94-26287*# Prairie View Agricultural and Mechanical Coll., TX.
MODELING AND EXPERIMENTAL VERIFICATION OF SINGLE EVENT UPSETS
T. N. Fogarty, J. O. Attia, A. A. Kumar, T. S. Tang (Texas A&I Univ., Kingsville.), and J. S. Lindner (Texas A&I Univ., Kingsville.) *In* NASA. Langley Research Center, Selected Topics in Robotics for Space Exploration Dec. 1993 p 193-211 Sponsored in part by NASA. Johnson Space Center (For primary document see N94-26278 07-12)
(Grants NAG9-659; NAG9-331)
Avail: CASI HC A03/MF A03

N94-27362*# National Aeronautics and Space Administration. Lewis Research Center, Cleveland, OH.
VENI, VIDEO, VICI: THE MERGING OF COMPUTER AND VIDEO TECHNOLOGIES
Jay G. Horowitz *In its* Vision 21: Interdisciplinary Science and Engineering in the Era of Cyberspace Dec. 1993 p 43-50 (For primary document see N94-27358 07-12)
Avail: CASI HC A02/MF A03

N94-27372*# Sverdrup Technology, Inc., Brook Park, OH.
EMERGING COMPUTER TECHNOLOGIES AND THE NEWS MEDIA OF THE FUTURE
Debra A. Vrabel *In* NASA. Lewis Research Center, Vision 21: Interdisciplinary Science and Engineering in the Era of Cyberspace Dec. 1993 p 181-183 (For primary document see N94-27358 07-12)
Avail: CASI HC A01/MF A03

61 COMPUTER PROGRAMMING AND SOFTWARE

Includes computer programs, routines, alogorithms, and specific applications, e.g., CAD/CAM.

N94-25588 RTware, Inc., Durham, NC.
MODULE INTERCONNECTION FRAMEWORKS FOR A REAL-TIME SPREADSHEET Final Report
Richard Clarke 19 Oct. 1993 59 p Limited Reproducibility: More than 20% of this document may be affected by microfiche quality
(AD-A273853) Avail: CASI HC A04

Phase 1 research into a modular real-time spreadsheet has yielded a significant result: a spreadsheet can be used to completely simulate, completely prototype, and completely implement distributed control systems. A usable implementation of such a system will be done in Phase 2. Commercialization will begin in the middle of Phase 2, with the release of a set of distributed processing options for RTware's ControlCalc product. Demonstration applications in Naval applications will be done in cooperation with RTware's existing Naval customers. A real-time spreadsheet will be used to build nodes in a software module interconnection framework (MIF), allowing interactive, on-line construction of distributed control applications. Due to major advances in spreadsheet software technology already implemented in ControlCalc, the commercially-available spreadsheet to be used, the system will allow prototyping, simulation, top down design, and implementation down to the final, lowest-level runtime machine code. The MIF is Polylith, which provides a remote function calling and message-passing abstraction that can be used by any language, including a spreadsheet. A graphical diagram editor will provide visualization of and navigation through the module framework. The major spreadsheet advances are as follows: on-the-fly expression compilation, multi-threading evaluation, and multi-tasking text or graphical user interface sessions. Important supporting capabilities include the following: in-line I/O functions for direct access to analog or digital hardware and file or network protocols, strong typing, direct mapping to the output of graphical user interface editors, and extensibility through calling user-supplied functions in other languages directly from compiled spreadsheet expressions. DTIC

N94-25602# Jet Propulsion Lab., California Inst. of Tech., Pasadena.
SYSTEM SOFTWARE AND TOOLS FOR HIGH PERFORMANCE COMPUTING ENVIRONMENTS: A REPORT ON THE FINDINGS OF THE PASADENA WORKSHOP
1 Apr. 1993 223 p Workshop held in Pasadena, CA, 14-16 Apr. 1992
(Contract DE-AI02-92ER-25118)
(DE94-003918; DOE/ER-25118/1; JPL-Publ-93-15) Avail: CASI HC A10/MF A03

The Pasadena Workshop on System Software and Tools for High Performance Computing Environments was held at the Jet Propulsion Laboratory from 14-16 Apr. 1992. The workshop was sponsored by a number of Federal agencies committed to the advancement of high performance computing (HPC) both as a means to advance their respective missions and as a national resource to enhance American productivity and competitiveness. Over a hundred experts in related fields from industry, academia, and government were invited to participate in this effort to assess the current status of software technology in support of HPC systems. The overall objectives of the workshop were to understand the requirements and current limitations of HPC software technology and to contribute to a basis for establishing new directions in research and development for software technology in HPC environments. This report includes reports written by the participants of the workshop's seven working groups. Materials presented at the workshop are reproduced in appendices. Additional chapters summarize the findings and analyze their implications for future directions in HPC software technology development. DOE

N94-25606*# Mississippi State Univ., Mississippi State. Center for Air Sea Technology.
NAVAL INTERACTIVE DATA ANALYSIS SYSTEM (NIDAS), SOFTWARE USER'S MANUAL Technical Note
Dharmesh Krishnamagaru, Leana Dusang, Vishnumohan Das, and M. S. Foster, ed. 29 Nov. 1993 53 p
(Contract NAS13-564)
(NASA-CR-195179; NAS 1.26:195179; AD-A273847; CAST-TN-03-94)
Avail: CASI HC A04/MF A01

NIDAS provides interactive blending and overlay capabilities for a broad range of environmental data types and formats. The product output of NIDAS is a three-dimensional gridded field of temperature and salinity constructed from (1) data derived by the user internally within NIDAS by synthesis, and (2) data obtained from external numerical models, observations, and climatological databases. NIDAS operate using numerous oceanographic data categories stored in an installed version of the Naval Environmental Operational Nowcast System (NEONS), a relational database management system (rdbms) which employs the EXPRESS proprietary rbdms engine. Data management, configuration, and control functions for the supporting rdbms are performed externally. NIDAS retrieves and stores data to/from the rdbms but exercises no direct internal control over the rbdms or its configuration. Data is also ingested into the rbdms, for use by NIDAS, by external data acquisition processes. DTIC

N94-25610# Air Force Inst. of Tech., Wright-Patterson AFB, OH.
HIGH RESOLUTION FOURIER TRANSFORM ABSORPTION SPECTRUM OF 79Br2 B3 Pi(Ou+) X1 SIGMA g+ M.S. Thesis
Robert E. Franklin Dec. 1993 78 p
(AD-A273864; AFIT/GAP/ENP/93D-02) Avail: CASI HC A05/MF A01

High Resolution Fourier Transform Spectroscopy was conducted for the B(sub 3)Pi(O(sub u)(+)) yields X(sub 1)Sigma(sub g)(+) system of (Br2)-79.

A total of 64 vibrational levels, including v'' = 0-3 and v' = 10-33, were observed and assigned. Rotational levels as high as J=76 were observed. A global fitting routine was developed to fit the rotational spectra to the Dunham Expansion. Using B(sub v) and D(sub v) for both the X and B state, rotational transitions were calculated to within 0.02 cm(sub -1). The expansions of these terms required five coefficients for the B state and three coefficients for the X state. Attempts to fit the vibrational spectrum to an equation in terms of (v+1/2) were only accurate to within 0.03 cm(sub -1) when five molecular constants were used on the upper level and three were used on the ground state. However, direct calculation of the vibrational energy levels was able to fit all vibrational bandheads to less than 0.02 cm(sub -1). Recommendations are made for attempting a global fit over many more vibrational bands. DTIC

N94-25642# Technical Research Centre of Finland, Espoo. Computer Technology Lab.
CALCULATION OF A 3-D POSE OF A KNOWN OBJECT IN A SINGLE PERSPECTIVE VIEW Ph.D. Thesis - Oulu Univ.
Kari Pehkonen Nov. 1992 105 p Sponsored by Technology Development Center of Finland
(ISSN 1235-0621)
(VTT-PUBS-122; ISBN-951-38-4240-1; ETN-94-95235) Copyright Avail: CASI HC A06/MF A02

An algorithm for determining the three dimensional (3D) pose of a known object in a single two dimensional view is described. The pose calculation algorithm consists of four main stages: pose candidate generation, candidate verification, optimization, and reliability analysis. Pose candidates are generated by matching model and image triangles. The three point perspective pose estimation problem is solved numerically. Pose candidates are verified by matching model and image features. The first accepted candidate is optimized. Three optimization methods are considered: Newton-Raphson, simulated annealing, and robust M estimate using Lorenzian distribution. The reliability estimates are based on covariance analysis. Uncertainties due to both model and image noise are taken into account. A structure optimization method to reduce modeling noise is presented. The speed and accuracy of the algorithm were estimated. ESA

N94-25646# Army Research Lab., Aberdeen Proving Ground, MD.
SHIVA: A UNIX-BASED, MENU-DRIVEN, COLOR IMAGE PROCESSING SOFTWARE PACKAGE Final Report, May 1992 - May 1993
Michael J. McQuaid, Gary C. Bliesener, Eric Prather, and Avi Birk Oct. 1993 26 p
(AD-A274071; ARL-TR-294) Avail: CASI HC A03/MF A01

A user-friendly 'point and click' program named SHIVA has been developed to facilitate processing and analysis of digital color images. SHIVA, an acronym for simple heuristic interactive visualization and animation, provides access to a full range of image processing and analysis tools via a graphical interface and with minimal instruction. This technical report describes the main hierarchy and functionality of SHIVA. The program has been used to process color images of burning monopropellant sprays illuminated by a copper vapor laser. Though SHIVA was developed to support the spray research effort, it should be useful in a wide range of U.S. Army Research Laboratory (ARL) research applications where color image processing and analysis is employed. DTIC

N94-25649# Air Force Inst. of Tech., Wright-Patterson AFB, OH. School of Engineering.
VULNERABILITY ASSESSMENT USING A FUZZY LOGIC BASED METHOD M.S. Thesis
Richard W. Fleming Dec. 1993 102 p
(AD-A274075; AFIT/GCE/Eng/93D-03) Avail: CASI HC A06/MF A02

This thesis demonstrates the feasibility of using qualitative analysis methods to evaluate computer security vulnerabilities. Although many risk analysis systems exist, few provide for the adequate analysis of identified vulnerabilities. While the main focus of this thesis is to evaluate computer security vulnerabilities, the methods involved have application in other areas requiring evaluation using qualitative methods. It is proposed, and demonstrated by this thesis, that the use of qualitative analysis using linguistic variables to describe the impact of computer security vulnerabilities is not only feasible, but intrinsically easier to understand and use than quantitative methods. DTIC

N94-25661# Wright Lab., Wright-Patterson AFB, OH.
PROPOSED OBJECT ORIENTED PROGRAMMING (OOP) ENHANCEMENTS TO THE VERY HIGH SPEED INTEGRATED CIRCUITS (VHSIC) HARDWARE DESCRIPTION LANGUAGE (VHDL) Final Report, 4 May 1992 - 4 Aug. 1993
Michael T. Mills Aug. 1993 22 p
(AD-A274004; WL-TR-93-5025) Avail: CASI HC A03/MF A01

This report describes an integrated set of Object Oriented Programming (OOP) enhancements proposed for a future revision of the VHSIC Hardware Description Language (VHDL). It offers inheritance with extension for VHDL record, array and private type declarations, plus multiple inheritance with extension for entities and corresponding architecture bodies, and a class wide dispatching capability for all tagged types and tagged entities. If these three enhancements are accepted by the IEEE, VHDL based design automation tools can possess new abstract design capabilities for developing and enhancing electronic hardware. Current software languages with OOP capability increase productivity and reuse by enabling the design process to inherit and extend existing data structures and functionality. By selectively inheriting what already exists, the designer minimizes duplication. Functional capabilities and characteristics can be inherited and extended without affecting existing portions of a design. DTIC

N94-25663# California Univ., Berkeley. Lawrence Berkeley Lab.
AN OPTIMAL CONSTRAINED LINEAR INVERSE METHOD FOR MAGNETIC SOURCE IMAGING
Paul Hughett Nov. 1993 5 p Presented at the IEEE Medical Imaging Conference, San Francisco, CA, 4-6 Nov. 1993
(Contract DE-AC03-76SF-00098)
(DE94-004014; LBL-34512-Summ; CONF-9311114-4) Avail: CASI HC A01/MF A01

The optimal constrained linear inverse method (OCLIM) is a new algorithm for magnetic source imaging that approximates an unknown continuous current distribution as a weighted sum of current sources in fixed positions, uses prior information about the expected source power density and measurement noise, and can be efficiently computed. It achieves the minimum possible mean square reconstruction error for any linear estimator and provides statistical confidence limits on the reconstructed source amplitudes. The minimum-norm least squares and weighted pseudoinverse methods are included as special cases. However, OCLIM can produce reconstruction artifacts if the true current distribution is inconsistent with the assumed priors. DOE

N94-25753# Army Research Lab., Aberdeen Proving Ground, MD.
IGES 4.0 TO LCAD TRANSLATOR FOR CSG MODELS
John R. Anderson, Earl P. Weaver, and Susanne L. Muuss Dec. 1993 24 p
(DA Proj. 1L1-62618-AH-80)
(AD-A274013; ARL-TR-315) Avail: CASI HC A03/MF A01

The subject of importing IGES 4.0 format (Initial Graphics Exchange Specification Version 4.0) computer-aided design (CAD) constructive solid geometry (CSG) models into the former Ballistic Research Laboratory's Computer-Aided Design (BRLCAD) package is discussed and the results of a software development project to implement an IGES-to-BRLCAD translator that conforms to the ASME Y14.26M-1989 Standard are described. A brief description of the IGES philosophy and specification, the relationship between IGES and the American National Standards Institute (ANSI) standard on the exchange of product definition data, limitations of the current specifications/standards and BRLCAD, suggested solutions for overcoming those limitations, and recommendations for future work are also included. DTIC

N94-25761# Technische Hogeschool, Delft (Netherlands). Faculty of Technical Mathematics and Informatics.
A LOGARITHMIC BARRIER CUTTING PLANE METHOD FOR CONVEX PROGRAMMING
D. denHertog, C. Roos, J. Kaliski, and T. Terlaky 1993 29 p Sponsored by Shell
(Contract OTKA-2116) (ISSN 0922-5641)
(Rept-93-43; ETN-94-95398) Copyright Avail: CASI HC A03/MF A01

A logarithmic barrier cutting plane algorithm for convex programming is presented. Most cutting plane methods solve a linear approximation of the problem and generate an additional cut to remove the linear program's optimal point. Other methods calculate a center of the linear approximation and adjust the level of the objective or separate the current center from the feasible set. A method which does not solve the linear relaxations till optimality, but stays in the interior of the feasible set, is described. The iterates follow the central path of a linear relaxation until the current iterate either leaves the feasible set or is too close to the boundary. When this occurs, a new cut is generated and the algorithm iterates. The tools developed to analyze the effect of adding and deleting contraints in long step logarithmic barrier methods for linear programming are used. Implementation issues and computational results are presented. The test problems come from the classes of convex geometric and semi infinite programming problems. ESA

N94-25762 Technische Hogeschool, Delft (Netherlands). Faculty of Technical Mathematics and Informatics.
A NOTE ON CENTRAL CUTTING PLANE METHODS FOR CONVEX PROGRAMMING
D. denHertog, C. Roos, J. Kaliski, and T. Terlaky 1993 12 p Sponsored by Shell Limited Reproducibility: More than 20% of this document may be affected by microfiche quality
(Contract OTKA-2116) (ISSN 0922-5641)
(Rept-93-44; ETN-94-95399) Copyright Avail: CASI HC A03

A unified treatment of Elzinga and Moore's and Goffin and Vial's central cutting plane methods is presented. It is shown that Goffin and Vial's method enjoys the same convergence properties as Elzinga and Moore's method. Cutting plane methods, like that of Kelley and Cheney and Goldstein, solve a linear approximation (localization) of the problem and then generate an additional cut to remove the linear program's optimal point. Other methods, like the 'central cutting' plane methods, calculate a center of the linear approximation and then adjust the level of the objective or separate the current center from the feasible set. ESA

N94-25764# Technische Univ., Delft (Netherlands). Faculty of Technical Mathematics and Informatics.
A SIMPLICIAL APPROACH TO INTEGER PROGRAMMING, PART 2
Chuangyin Dang and Hans vanMaaren 1993 29 p
(ISSN 0922-5641)
(Rept-93-47-Pt-2; ETN-94-95401) Copyright Avail: CASI HC A03/MF A01

An algorithm to compute an integral point in a polytope is presented. It is based on an integer labeling and a triangulation of R(sup n). The idea is as follows. The algorithm subdivides R(sup n) into n + 1 cones and assigns to each point in R(sup n) an integer according to the cones and the polytope. It generates a sequence of adjacent simplices of varying dimension along each of n + 1 rays. The sequence terminates within a finite number of iterations at either a socalled complete n dimensional simplex or a so-called 0 complete n dimensional simplex that yields an integral point in the polytope. Numerical tests show the efficiency of the algorithm. ESA

N94-25767# Air Force Inst. of Tech., Wright-Patterson AFB, OH.
ObjectSim: A REUSABLE OBJECT ORIENTED DIS VISUAL SIMULATION M.S. Thesis
Mark I. Snyder Dec. 1993 106 p
(AD-A274030; AFIT/GCS/ENG/93D-20) Avail: CASI HC A06/MF A02

This research designed and implemented a reusable distributed interactive simulation (DIS) visual simulation architecture for Silicon Graphics platforms. The goal was to research software architecture technologies and to create a design and implementation using these ideas. The architecture was designed using object oriented techniques to provide the ability to customize it via inheritance extension. The resulting design was implemented using C++ and applied to several DIS visual simulation projects in the Graphics Lab at AFIT. The architecture, named ObjectSim, was successful in its goal of providing a reusable core for the DIS visual simulation projects in the Graphics Lab at AFIT. It provides simulation developers reusable capabilities in the areas of rendering, data display, device interfacing, and DIS network interfacing. The projects designed and implemented with ObjectSim exceeded their research goals. Data on reuse effectiveness and several different performance areas was collected. DTIC

N94-25777*# Carnegie-Mellon Univ., Pittsburgh, PA. Robotics Inst.
DESIGN OF DYNAMICALLY RECONFIGURABLE REAL-TIME SOFTWARE USING PORT-BASED OBJECTS
David B. Stewart, Richard A. Volpe, and Pradeep K. Khosla 1 Jul. 1993 28 p
(Contract NAG1-1075; DAAA21-89-C-0001)
(NASA-CR-195178; NAS 1.26:195178; AD-A273717; CMU-RI-TR-93-11) Avail: CASI HC A03/MF A01

The current development of applications for sensor-based robotic and automation (R&A) systems is typically a 'one-of-a-kind' process, where most software is developed from scratch, even though much of the code is similar to code written for other applications. The cost of these systems can be drastically reduced and the capability of these systems improved by providing a suitable software framework for all R&A systems. A software framework, based on the notion of dynamically reconfigurable software for sensor-based control systems was described. Tools to support the implementation of this framework were built into the Chimera 3.0 Real-Time Operating System. The framework provides for the systematic development and predictable execution of flexible R&A applications while maintaining the ability to reuse code from previous applications. It combines object-oriented design of software with port-automaton design of digital control systems. A control module is an instance of a class of port-based objects. DTIC

N94-25783# Air Force Inst. of Tech., Wright-Patterson AFB, OH. School of Engineering.
DOMAIN ANALYSIS AND MODELING OF A MODEL-BASED SOFTWARE EXECUTIVE M.S. Thesis
Robert L. Welgan Dec. 1993 160 p
(AD-A274087; AFIT/GCS/Eng/93D-25) Avail: CASI HC A08/MF A02

This research adapted the domain analysis techniques of Prieto-Diaz and Tracz to specify a domain analysis process which was used to conduct domain analysis over the domain of software executives. This analysis created a set of informal and formal domain model artifacts. The domain model artifacts were instantiated into two application executive subsystems. These executive subsystems operated in Architect, a domain-oriented application composition system based on the object connection update (OCU) model. This research demonstrated and evaluated execution of the instantiated executive domain model in a series of event-driven and time-driven applications. As a consequence of developing the application executive for Architect, this research proposes additions to the OCU model. DTIC

N94-25799# Air Force Inst. of Tech., Wright-Patterson AFB, OH.
SOURCE CODE FOR THE OO1 BENCHMARK AND THE AFIT SIMULATION BENCHMARK
Timothy J. Halloran 5 Nov. 1993 145 p
(AD-A274035; AFIT/EN-TR-93-09) Avail: CASI HC A07/MF A02

This paper contains the source code for implementations of the OO1 benchmark and the AFIT simulation benchmark. OO1 benchmark implementations are listed for the Itasca, Matisse, and ObjectStore object-oriented database management systems (DBMS). An AFIT simulation benchmark implementation is listed for the ObjectStore object-oriented DBMS. DTIC

N94-25818# Sandia National Labs., Albuquerque, NM.
GRAPHICAL PROGRAMMING AT SANDIA NATIONAL LABORATORIES
Michael J. McDonald, Robert D. Palmquist, and Lisa Desjarlais (New Mexico Univ., Albuquerque.) Sep. 1993 4 p Presented at the 7th Deneb Robotics User Group Meeting, Troy, MI, 12-15 Oct. 1993
(Contract DE-AC04-94AL-85000)
(DE94-003803; SAND-93-2742C; CONF-9310216-4) Avail: CASI HC A01/MF A01

Sandia has developed an advanced operational control system approach, called Graphical Programming, to design, program, and operate robotic systems. The Graphical Programming approach produces robot systems that are faster to develop and use, safer in operation, and cheaper overall than alternative teleoperation or autonomous robot control systems. Graphical Programming also provides an efficient and easy-to-use interface to traditional robot systems for use in setup and programming tasks. This paper provides an overview of the Graphical Programming approach and lists key features of Graphical Programming systems. Graphical Programming uses 3-D visualization and simulation software with intuitive operator interfaces for the programming and control of complex robotic systems. Graphical Programming Supervisor software modules allow an operator to command and simulate complex tasks in a graphic preview mode and, when acceptable, command the actual robots and monitor their motions with the graphic system. Graphical Programming Supervisors maintain registration with the real world and allow the robot to perform tasks that cannot be accurately represented with models alone by using a combination of model and sensor-based control. DOE

N94-25821# Maryland Univ., Baltimore.
RESEARCH ON PRIMAL-DUAL INTERIOR POINT ALGORITHMS FOR MATHEMATICAL PROGRAMMING
Yin Zhang Sep. 1993 7 p
(Contract DE-FG05-91ER-25100)
(DE94-003982; DOE/ER-25100/2) Avail: CASI HC A02/MF A01

Today interior-point methods of choice for general linear programming are primal-dual infeasible interior-point algorithms. There is a big gap between theoretical algorithms and practical algorithms. Major goals of the project were to narrow the gaps between theory and practice of primal-dual interior-point methods. The PI (principal investigator) played a leading role in joint work with Richard Tapia on constructing the first superlinear and polynomial primal-dual algorithm. The PI's recent work on infeasible interior-point methods established the first polynomial result for today's interior-point methods of device. More recently, the PI established polynomial complexities for Mehrotra-type predictor-corrector methods which have been widely regarded today as the most practically efficient methods. This work has laid a solid theoretical foundation for these methods. DOE

N94-25855# Carnegie-Mellon Univ., Pittsburgh, PA. Software Engineering Inst.
THE USE OF ASN.1 AND XDR FOR DATA REPRESENTATION IN REAL-TIME DISTRIBUTED SYSTEMS Final Report
B. C. Myers and Gary Chastek Oct. 1993 70 p
(Contract F19628-90-C-0003)
(AD-A273769; CMU/SEI-93-TR-10; ESC-TR-93-187) Avail: CASI HC A04/MF A01

This report provides an overview of two standards that are used for data specification and representation in distributed systems. The standards considered are the Abstract Syntax Notation One (ASN.1) and the external data representation (XDR). Standards for data representation are appropriate for the development of real-time distributed systems, particularly loosely coupled, heterogeneous systems. The report presents an example of the use of each standard. Several performance metrics are also introduced that are suitable for comparing the space and time costs of using the different standards. Several issues are discussed that are appropriate to a system designer. An Ada implementation of ASN.1 encode and decode routines for floating point types is included in an appendix. DTIC

N94-25879# RADEX, Inc., Bedford, MA.
IRMA: A PROGRAM FOR THREE-DIMENSIONAL COLOR DISPLAY OF DATA
M. F. Tautz 30 May 1993 45 p
(Contract F19628-89-C-0068)
(AD-A273811; PL-TR-93-2116; SR-13) Avail: CASI HC A03/MF A01

This report describes the input, output, and interactive capabilities of the IRMA plotting program. Actual FORTRAN or C coding is not given. The IRMA program was designed for displaying data from spacecraft charging and contamination codes in three dimensions and in color. The user interface features interactive control of viewing position and perspective by keyboard and mouse input. Text ports are available so that figure captions can be typed directly to the screen. The current graphics state can be saved in a parameter file for later restoration. The many data visualization options include drawing complex polygon objects, displaying particle trajectories, creating contour level surfaces, and building random dot plots to represent number density. Column density images can be obtained by integrating along an arbitrary line of sight. Image files can be written out to create a set of frames depicting the time sequence of events. DTIC

N94-25917 Joint Inst. for Nuclear Research, Dubna (USSR). Lab. of Nuclear Problems.
FAST VERTEX SEARCH (IN PLANE)
A. A. Glazov, I. V. Kisel, E. V. Konotopskaja, and S. M. Korenchenko 1991 13 p Limited Reproducibility: More than 20% of this document may be affected by microfiche quality
(DE93-616655; JINR-E-10-91-374) Avail: CASI HC A03 (US Sales Only)

The fast vertex search method is suggested for plane geometry. The search for the vertex reduces to comparison of values of the functional in a few easy-to-find points. This method also provides a simple procedure for 'pulling' the vertex to the target. These properties are extremely important for processing the data, obtained in experiments on the search for rare and forbidden decays, when registered events are accidental in most cases. If necessary, the vertex found by this method may be used as an initial approximation for the least square method, which is important for experiments with a big target. The method was examined on three-track events, obtained in the experiment of the search for the forbidden decay mu yields 3e on the ARES facility. DOE

N94-25942# Air Force Inst. of Tech., Wright-Patterson AFB, OH. School of Engineering.
OBJECT INTERACTION IN A PARALLEL OBJECT-ORIENTED DISCRETE-EVENT SIMULATION M.S. Thesis
Walter G. Trachsel 15 Dec. 1993 131 p
(AD-A274084; AFIT/GCS/Eng/93D-22) Avail: CASI HC A07/MF A02

This thesis investigates object interaction issues involved in developing an object-oriented parallel discrete-event simulation and develops a simulation model that provides object interaction capabilities. The research covers issues in object representation, object interaction, object management, discrete-event simulation, and parallel simulation. There are three primary types of objects that the research discusses. The first type is a basic simulation object, whose size and behavior is insignificant compared to the size of the simulation as a whole. The second type is an aggregate object which consists of smaller component objects that interact and affect the performance of the larger object as a whole. Finally, there are environmental objects, such as terrain and weather, whose size and impact are significant to the entire simulation environment. This research addresses issues about whether these objects can be represented the same in the simulation or whether a special case must exist for each type of object. As a result of the research, a simulation model is designed that allows interaction between simulation objects. The design goals used to develop the model were strict use of object-oriented practices, ease of simulation modification, and reuse across other applications in the same class of simulations. In this case, the class of simulations is interacting objects in a spatially partitioned discrete-event simulation. The model is then implemented using AFIT's Battlesim program, which is a parallel discrete-event simulation that has a battlefield divided into partitions and allows objects to move and interact. DTIC

N94-25963# Organization for Industrial Research, TNO, The Hague (Netherlands). Physics and Electronics Lab.
A REAL-TIME CONVOLUTION ALGORITHM AND ARCHITECTURE WITH APPLICATIONS IN SAR PROCESSING
L. H. Bierens Oct. 1993 28 p
(AD-A273817; FEL-93-B113; TDCK-TD93-2788) Avail: CASI HC A03/MF A01

An algorithm that maps a large one-dimensional linear convolution problem onto a small two-dimensional linear convolution problem is proposed. It was shown that this property can be derived from a signal flow representation of a sectioned convolution. The introduction of short length FFT processor elements into the signal flow graph results in a structure that can be efficiently implemented in a dedicated hardware architecture. Although the performance of the architecture is not optimal in terms of computational complexity, the performance in terms of data rate, input data sequence lengths and amount of required hardware is high. The architecture design is illustrated with a configuration suitable for real-time on-board airborne synthetic aperture radar (SAR) processing for the Phased Array Universal Sar (PHARUS), which is currently under development at TNO-FEL. DTIC

N94-25968 Duke Univ., Durham, NC. Dept. of Computer Science.
STUDIES IN NONLINEAR NUMERICAL ANALYSIS Report, 1 Oct. 1992 - 30 Sep. 1993
Donald J. Rose 19 Aug. 1993 4 p Limited Reproducibility: More than

20% of this document may be affected by microfiche quality
(Contract N00014-89-J-1644)
(AD-A273911) Avail: CASI HC A01

The quantum optimal control (QOC) problem was worked on. A complete algorithmic strategy, capable of higher order convergence was devised, and this strategy was implemented in a prototype code. Special implicit ordinary differential equations (ODE) were devised or tuned for this problem. The next step in the QOC problem is to resolve 1-D and 2-D problems in space to get a more realistic assessment of our algorithmic strategy than the simple problems we have solved can provide. CASI

N94-25986# Clarkson Univ., Potsdam, NY. Dept. of Chemical Engineering.
ANALYSIS AND COMPUTER TOOLS FOR SEPARATION PROCESSES INVOLVING NONIDEAL MIXTURES
A. Lucia 12 Jul. 1993 5 p
(Contract DE-FG02-86ER-13552)
(DE94-004162; DOE/ER-13552/10) Avail: CASI HC A01/MF A01

This research is concerned with developing mathematical analysis, numerical analysis, and computer tools for separation processes involving nonideal, homogeneous, and heterogeneous multi-component mixtures. Progress organized in terms of mathematical analysis, numerical analysis, and algorithmic development is summarized. DOE

N94-25994# Air Force Inst. of Tech., Wright-Patterson AFB, OH. School of Engineering.
DEVELOPING A SOPHISTICATED USER INTERFACE TO SUPPORT DOMAIN-ORIENTED APPLICATION COMPOSITION AND GENERATION SYSTEMS M.S. Thesis
Jay A. Cossentine 15 Dec. 1993 128 p
(AD-A274080; AFIT/GCS/Eng/93D-04) Avail: CASI HC A07/MF A02

This research refined the visual presentation and usability of a previously developed visual interface for a domain-oriented application composition and generation system. The refined visual interface incorporated domain-specific bit-mapped graphics and sophisticated user interface design concepts to reduce user workload. User workload was reduced by the following methods: object layout, window design, and color utilization techniques; by combining repetitive procedures into single commands; and reusing, rather than recreating, composition information throughout the application composition process. The Software Refinery environment, including its graphical interface tool INTERVISTA, was used to develop techniques for visualizing and manipulating objects contained in a formal object base. INTERVISTA was supplemented with graphical routines provided by Common Windows, a Lisp-based graphical environment that serves as the foundation for INTERVISTA. The interface was formally validated with a well-understood application domain, digital logic-circuits, and users of the interface were polled to ascertain the subjective usability of the interface. A comparative analysis of the application composition process with the previous visual interface was conducted to quantify the workload reduction realized by the new interface. Workload was measured as the number of user interactions (mouse or keyboard) required to compose an application. On average, application composition effort was reduced 44.0% for the test cases. DTIC

N94-26018# Air Force Inst. of Tech., Wright-Patterson AFB, OH.
DEVELOPING A GRAPHICAL USER INTERFACE TO SUPPORT A REAL-TIME DIGITAL SIGNAL PROCESSING SYSTEM M.S. Thesis
Jeffrey C. Miller Dec. 1993 163 p
(AD-A274032; AFIT/GCS/ENG/93D-16) Avail: CASI HC A08/MF A02

A graphical software user interface for a VME bus-based real-time digital signal processing system was designed. User requirements were defined and the Rumbaugh object-oriented analysis and design technique was applied to analyze the requirements and produce an object-oriented design. The software design includes a graphical, mouse-, and keyboard-driven user interface; specialized hardware driver modules; and operating system interfaces. An implementation plan was also developed to map the design into the C programming language using existing system code, automatically generated code, and newly written code. Based on the implementation plan, a limited software system prototype was successfully developed and demonstrated. The system can be used to analyze signals previously recorded on disk or sampled in real time. Analyzed signals can be displayed either as a set of discrete samples or as a graph in either the time or frequency domains. The system includes real-time sampling hardware, specialized DSP hardware, general-purpose computing hardware based on the Motorola 68030 microprocessor, mass storage media, and a high-resolution graphical display. DTIC

N94-26048# Pacific Northwest Lab., Richland, WA.
SOFTWARE REDESIGN FOR USABILITY: A CASE STUDY
J. A. Sanchez and M. D. Adickes Oct. 1993 4 p Presented at the Human Factors and Ergonomics Society Meeting, Seattle, WA, 11-15 Oct. 1993
(Contract DE-AC06-76RL-01830)
(DE94-003704; PNL-SA-23116; CONF-9310100-4) Avail: CASI HC A01/MF A01

In an ideal software development environment, the use of a programming language such as C allows developers the ability to create an application that matches the requirements and needs of a client. Recent breakthroughs and advances in software design and graphical user interfaces, however, make it much more difficult to justify, from either a cost or time perspective, developing an application completely from scratch using such a language. By using commercial development packages (prototyping development tools), developers are freed from many of the time consuming tasks that would ordinarily be involved in creating an application, and are able instead to concentrate on what should be the two most important areas of an application, what it should do and how it should look. This poster session illustrates the significant benefits that can be achieved by creating an application using a commercial data base package with a graphical user interface developer along with a multidisciplinary team of developers. The primary emphasis of the display focuses on the ability of the developer to incorporate human factors considerations to ensure that the program is both easy to use and easy to change, given additional client inputs and requests. DOE

N94-26106 Technische Univ., Delft (Netherlands). Werkeenheid Fotogrammetrie en Remote Sensing.
IMAGE SEGMENTATION BY A COMBINATION OF EDGE DETECTION AND REGION GROWING Thesis [BEELDSEGMENTATIE DOOR EEN COMBINATIE VAN RANDDETECTIE EN REGION GROWING]
R. J. Wicherson Jul. 1992 85 p In DUTCH Limited Reproducibility: More than 20% of this document may be affected by microfiche quality
(ETN-94-95032) Avail: CASI HC A05

The development of a two stage image segmentation method is reported. In stage one, the edge based region growing stage, adjacent pixels with gray values which have a nonsignificant difference are merged into one segment through the use of a predictor. In this stage, special attention is payed to the localization of the segment borders. In stage two, the region growing stage, all the incorrect placed segment borders are eliminated. If the difference between the medians of the pixels of two segments is non significant, these segments are merged. Segments which have a nonsignificant size and segments existing of mixed pixels are removed by merging these with the best fitting adjacent segment. All the decision rules are based on statistical tests. The developed method was programmed and tested on three artificial and three real images. The method results in segments with closed contours. The segmented test images show after visual assessment that the edges are located accurately. The number of detected segments corresponds to the correct number of segments. ESA

N94-26118# Sandia National Labs., Albuquerque, NM.
THE NATIONAL CENTER FOR ADVANCED INFORMATION COMPONENTS MANUFACTURING: PROGRAM UPDATE
J. L. Jorgensen 1993 3 p Presented at the Defense Manufacturing Conference, San Francisco, CA, 29 Nov. - 2 Dec. 1993
(Contract DE-AC04-94AL-85000)
(DE94-002647; SAND-93-2508C; CONF-9311113-1) Avail: CASI HC A01/MF A01

The National Center for Advanced Information Components Manufacturing (NCAICM) was established by congressional appropriation in the FY93 Defense Appropriation Bill. The Center, located at Sandia National Laboratories in Albuquerque, NM, is funded through the Advanced Research Projects Agency (ARPA). The technical focus of NCAICM is emissive flat panel displays and associated microelectronics, specifically targeting manufacturing issues such as materials, processes, equipment, and software tools. This Center is a new avenue of collaboration between ARPA and the Department of Energy (DOE). It will help the government meet its obligation to develop dual-use capabilities for the defense and civilian sectors of the economy and provide a new method for cooperation and collaboration between the federal government and American industry. In particular, one of NCAICM's goals is to provide industry access to the broad resource base available at three DOE Defense Programs laboratories -- Sandia National Laboratories, Los Alamos National Laboratory, and Lawrence Livermore National Laboratory. DOE

N94-26146# Sandia National Labs., Albuquerque, NM.
PARAMETER ESTIMATION BY GENETIC ALGORITHMS
G. M. Reese 1993 3 p Presented at the 1993 MATLAB Conference, Boston, MA, 18-20 Oct. 1993
(Contract DE-AC04-94AL-85000)
(DE94-002924; SAND-93-1298C; CONF-9310196-2) Avail: CASI HC A01/MF A01

Test/analysis correlation, or structural identification, is a process of reconciling differences in the structural dynamic models constructed analytically (using the finite element (FE) method) and experimentally (from modal tests). This is a methodology for assessing the reliability of the computational model, and it is very important in building models of high integrity, which may be used as predictive tools in design. Both the analytic and experimental models evaluate the same quantities: the natural frequencies (or eigenvalues, (omega(sub i)), and the mode shapes (or eigenvectors, (var phi)). In this paper, selected frequencies are reconciled in the two models by modifying physical parameters in the FE model. A variety of parameters may be modified such as the stiffness of a joint member or the thickness of a plate. Engineering judgement is required to identify important frequencies and to characterize the uncertainty of the model design parameters. DOE

N94-26148# Naval Surface Warfare Center, Dahlgren, VA.
AN ALGORITHM TO FIND THE INTERSECTION OF TWO CONVEX POLYGONS Final Report
Armido R. DiDonato Sep. 1993 26 p
(AD-A274722; NSWCDD/TR-93/345) Avail: CASI HC A03/MF A01

An algorithm is given that finds the intersection of two convex polygons. It is coded in FORTRAN for the IBM PC desktop computer. The program is robust and fast. It has been used successfully in targeting applications that require a rapid determination of the common intersection of more than 100 convex polygons, each specified by more than 150 vertices. DTIC

N94-26207*# Rutgers - The State Univ., Piscataway, NJ. Dept. of Electrical and Computer Engineering.
FEATURE ISOLATION AND QUANTIFICATION OF EVOLVING DATASETS Semiannual Status Report, Oct. 1993 - Feb. 1994
Feb. 1994 23 p
(Grant NAG2-829)
(NASA-CR-195230; NAS 1.26:195230) Avail: CASI HC A03/MF A01

Identifying and isolating features is an important part of visualization and a crucial step for the analysis and understanding of large time-dependent data sets (either from observation or simulation). In this proposal, we address these concerns, namely the investigation and implementation of basic 2D and 3D feature based methods to enhance current visualization techniques and provide the building blocks for automatic feature recognition, tracking, and correlation. These methods incorporate ideas from scientific visualization, computer vision, image processing, and mathematical morphology. Our focus is in the area of fluid dynamics, and we show the applicability of these methods to the quantification and tracking of three-dimensional vortex and turbulence bursts. Author

N94-26218# Center for Mathematics and Computer Science, Amsterdam (Netherlands). Dept. of Computer Science.
MULTIMEDIA IN VIEWS
Monica Bordegoni Dec. 1992 50 p Sponsored by European Research Consortium in Informatics and Mathematics, Netherlands
(ISSN 0169-118X)
(CWI-CS-R9263; ETN-94-95415) Copyright Avail: CASI HC A03/MF A01

Work aimed at defining and implementing a multimedia model within the TAXATA (things are exactly as they appear) model used in the Views project, which supplies a consistent and integrated open architecture application environment, is presented. Dynamic objects, having a time dimension, structuring operators, and presentation and accessing methods were integrated into the current Views model. Relationships among the media objects were defined using temporal relations instead of a time line approach. ESA

N94-26219# Center for Mathematics and Computer Science, Amsterdam (Netherlands). Dept. of Computer Science.
EDITING TREE STRUCTURES
Lon G. Barfield Dec. 1992 20 p
(ISSN 0169-118X)
(CWI-CS-R9264; ETN-94-95416) Copyright Avail: CASI HC A03/MF A01

An interactive editor that operates on a projection of a tree structure can offer the user many possible commands. An attempt to catalog and classify, in a rigorous way, the commands that can be offered is made. A simple tree and more complex trees are discussed. It is assumed that the reader has some familiarity with the basics of structured editors. ESA

N94-26221# Center for Mathematics and Computer Science, Amsterdam (Netherlands). Dept. of Computer Science.
THE ERGONOMICS OF SOFTWARE PORTING: AUTOMATICALLY CONFIGURING SOFTWARE TO THE RUNTIME ENVIRONMENT OR EVERYTHING YOU WANTED TO KNOW ABOUT YOUR C COMPILER BUT DIDN'T KNOW WHO TO ASK
Steven Pemberton Dec. 1992 23 p
(ISSN 0169-118X)
(CWI-CS-R9266; ETN-94-95418) Copyright Avail: CASI HC A03/MF A01

Techniques used in a program called 'enquire.c,' which calculates and prints out details of the target machine and the C compiler, are presented. The program can be used for interest, to see the properties of the particular target machine, and to produce the two header files 'float.h' and 'limits.h,' which give target machine values such as word length, byte order, minimum and maximum values for a range of types, etc., which need to be known when porting C programs. An additional option allows a check to see if the compiler reads the header files correctly: many read the minimum floating point number back as zero, or get the last few digits of floating point numbers wrong. ESA

N94-26254# Technical Research Centre of Finland, Espoo. Computer Technology Lab.
DEVELOPMENT AND ANALYSIS OF SECURE EMBEDDED SOFTWARE [TURVALLISTEN SULAUTETTUJEN OHJELMISTOJEN KEHITTAEMINEN JA ANALYSOINTI]
Jukka Korhonen and Jarmo Kalaoja Nov. 1992 74 p In FINNISH
(ISSN 1235-0605)
(VTT-TIED-1430; ISBN-951-38-4324-6; ETN-94-95258) Copyright Avail: CASI HC A04/MF A01

Information on the best design methods for secure software is presented. Procedures and instruments applicable to the analysis of embedded software security were developed for the case where the software development was based on the Yourdon real time structure analysis procedure. The analysis technique chosen was that of fault trees, completed by an instrument to draw the fault trees and by a code generator. During system testing, the code generated using the fault trees reacts to danger situations and signals, via the test environment, the software behavior presenting a danger to security. ESA

N94-26298# Naval Postgraduate School, Monterey, CA.
NPSNET-4: A REAL-TIME, 3D DISTRIBUTED INTERACTIVE VIRTUAL WORLD M.S. Thesis
Roy D. Young Sep. 1993 76 p
(AD-A274942) Avail: CASI HC A05/MF A01

The problems addressed by this research are to develop a new NPSNET simulator to allow simulations with any simulator that complies with the Distributed Interactive Simulation (DIS) protocol; to provide a more realistic simulation by maximizing the use of the Silicon Graphics Inc. (SGI) Reality Engine; and to provide for future extensions to the system. The approach taken for this research was to develop a DIS based simulator. To provide greater realism, Performer, a 3-D toolkit made by SGI, was used to take advantage of its multiprocessing management capabilities, real-time scene management, and other rapid rending tools. To enhance the systems extensibility, C++ object classes were used to encapsulate entity behaviors and user inputs. The result of this work is the NPSNET-IV simulation system. This system uses the DIS protocol to interact with other heterogeneously developed simulators as was demonstrated in a week long simulation between NPSNET-IV and two different simulation systems written by the Air Force Institute of Technology. Performer's direct access to the Reality Engine hardware and real-time scene management allows integration of more realistic models and higher rates of movement in the virtual world. The extensibility of the system is enhanced through the use of C++ objects, which was proven by the addition of a submersible vehicle type to the simulation. DTIC

N94-26303# Stanford Univ., CA. Dept. of Computer Science.
DEDUCTIVE COMPUTER PROGRAMMING Final Technical Report, 1 Nov. 1989 - 31 Dec. 1992
Zohar Manna 23 Mar. 1993 14 p
(Grant AF-AFOSR-0057-90)
(AD-A274966; AFOSR-94-0025TR) Avail: CASI HC A03/MF A01

Research has been conducted on the following related topics: automated deduction - new inference rules have been developed to facilitate reasoning about ordering relations, which pervade all software-development applications; program synthesis - a deductive approach to program synthesis has been developed, cased on the application of theorem-providing techniques; automated planning - the deductive Tableau system, extended to situational logic, has been applied to the formation of robotic and engineering plans; temporal logic - research into the foundational questions of temporal logic has yielded several techniques for reasoning about temporal concepts; reactive systems - a methodology based on temporal based logic was developed for the specification and verification of reactive systems, i.e., a system whose role is to maintain an ongoing interaction with its environment; real-time system - the temporal methodology has been extended to deal with real-time systems by introducing a time parameter into the state; and hybrid systems - the temporal methodology, the specification language, and the proof system have been extended to deal with hybrid systems. DTIC

N94-26318# Lawrence Livermore National Lab., CA.
RED'S NATURAL EDITOR: A PROGRAM DESIGNED TO EDIT FORTRAN PROGRAMS
D. E. Cullen 1 Sep. 1993 17 p
(Contract W-7405-eng-48)
(DE94-003271; UCRL-ID-115226) Avail: CASI HC A03/MF A01

This program allows the user to edit files using a completely natural method. You don't need a lot of time to learn how to use this program; it's as simple as using a typewriter. Even while you are reading this report you can start editing files. Although it is as simple as using a typewriter, this is a full screen editor, so that you can overwrite (replace) anything, delete or insert characters or lines, copy or move lines, and find or change anything. All of this can be done without using any complicated combinations of key strokes (as you are forced to memorize with other editors). This program is written in standard FORTRAN. Although it was designed and implemented on an IBM-PC, it can be easily adapted for use on virtually any graphics terminal. DOE

N94-26327# California Univ., Berkeley. Lawrence Berkeley Lab.
OPM SCHEME EDITOR 2: A GRAPHICAL EDITOR FOR SPECIFYING OBJECT-PROTOCOL STRUCTURES
I-Min A. Chen, Victor Markowitz, Francis Pang, and Ofer Ben-Shachar Jul. 1993 81 p
(Contract DE-AC03-76SF-00098)
(DE94-003477; LBL-33410) Avail: CASI HC A05/MF A01

This document describes an X-window based Schema Editor for the Object-Protocol Model (OPM). OPM is a data model that supports the specification of complex object and protocol classes. Objects and protocols are qualified in OPM by attributes that are defined over (associated with) value classes. Connections of object and protocol classes are expressed in OPM via attributes. OPM supports the specification (expansion) of protocols in terms of alternative and sequences of component (sub) protocols. The OPM Schema Editor allows specifying, displaying, modifying, and browsing through OPM schemas. The OPM Schema Editor generates an output file that can be used as input to an OPM schema translation tool that maps OPM schemas into definitions for relational database management systems. The OPM Schema Editor was implemented using C++ and the X11 based Motif toolkit, on Sun SPARCstation under Sun Unix OS 4.1. This document consists of the following parts: a tutorial consisting of seven introductory lessons for the OPM Schema Editor; a reference manual describing all the windows and functions of the OPM Schema Editor; and an appendix with an overview of OPM. DOE

N94-26370# Sandia National Labs., Albuquerque, NM.
THE CHACO USER'S GUIDE
B. Hendrickson and R. Leland Nov. 1993 28 p
(Contract DE-AC04-94AL-85000)
(DE94-003669; SAND-93-2339) Avail: CASI HC A03/MF A01

Graph partitioning is a fundamental problem in many scientific settings. This document describes the capabilities and operation of Chaco, a software package designed to partition graphs. Chaco allows for recursive application of any of several different methods for finding small edge separators in weighted graphs. These methods include inertial, spectral, Kernighan-Lin, and multilevel methods in addition to several simpler strategies. Each of these methods can be used to partition the graph into two, four or eight pieces at each level of recursion. In addition, the Kernighan-Lin method can be used to improve partitions generated by any of the other methods. Brief descriptions of these methods are provided, along with references to relevant literature. The user interface, input/output formats and appropriate settings for a variety of code parameters are discussed in detail, and some suggestions on algorithm selection are offered. DOE

N94-26371# Sandia National Labs., Albuquerque, NM.
USERS MANUAL FOR CATNIP: A COMPUTER ANALYSIS TOOL FOR NORMAL IMPACT PENETRATION
B. S. Altman Sep. 1993 16 p
(Contract DE-AC04-94AL-85000)
(DE94-003671; SAND-93-1749) Avail: CASI HC A03/MF A01

This program was developed to provide a computer based framework for analytical models to predict depth of penetration and temporal quantities for rigid non-deforming ogive-nose projectiles penetrating into a wide variety of targets. CATNIP provides results for penetration into semi-infinite targets, but does not provide for perforation events. The program has a graphical user interface to facilitate operation so that people unfamiliar with the analytical models can use the code with a minimum of training. CATNIP runs on Apple Macintosh computers using the Hypercard program. The Hypercard program is included with the system software on all Macintosh computers. A familiarity with the Macintosh use of pointing and clicking with the mouse is assumed for the use of this program. DOE

N94-26373# Software Productivity Consortium, Herndon, VA.
SOFTWARE ERROR ESTIMATION PROGRAM (SWEEP), VERSION 02.00.00 USER MANUAL
23 Dec. 1993 1 p
(Contract MDA972-92-J-1018)
(AD-A274697; SPC-92017-CMC) Avail: CASI HC A01/MF A01

One of the difficult challenges in today's software development environment is controlling and managing software errors. An error is defined as a detected failure; a failure is defined as a manifestation of the software product's inability to conform to requirements. Errors can also be referred to as defects; many people and projects use the terms interchangeably. SWEEP was developed to aid with the control and management of error data for software projects. It allows software error estimates that are useful in setting project goals and monitoring the quality of the software as it is developed. SWEEP uses software error data available early in the development cycle to project both the number of errors that will be found in later stages of development and the errors contained in the software when it is delivered (latent error content). Latent error content is expressed as an error density; however, if the user knows the size of the software code, the latent error content can easily be converted to the number of errors at delivery. SWEEP is useful to anyone involved with metrics (data collection and monitoring) or verification activities within a software life cycle. SWEEP can be used to make cost-effective decisions. DTIC

N94-26386# International Centre for Theoretical Physics, Trieste (Italy).
ON THE RELIABILITY OF A WINDOW LEAST SQUARES ALGORITHM

G. Adam and S. Adama Jun. 1993 28 p
(DE93-634666; IC-93/147) Avail: CASI HC A03/MF A01 (US Sales Only)

Reliability evaluation of a piecewise continuous window least squares (WLS) method devoted to the statistical noise smoothing of two-dimensional data is reported. DOE

N94-26407# Argonne National Lab., IL.
PROGRAMMING IN FORTRAN M
I. T. Foster, R. D. Olson, and S. J. Tuecke Oct. 1993 61 p
(Contract W-31-109-eng-38)
(DE94-002756; ANL-93/26-Rev-1) Avail: CASI HC A04/MF A01

Fortran M is a small set of extensions to Fortran that supports a modular approach to the construction of sequential and parallel programs. Fortran M programs use channels to plug together processes which may be written in Fortran M or Fortran 77. Processes communicate by sending and receiving messages on channels. Channels and processes can be created dynamically, but programs remain deterministic unless specialized nondeterministic constructs are used. Fortran M programs can execute on a range of sequential, parallel, and networked computers. This report incorporates both a tutorial introduction to Fortran M and a users guide for the Fortran M compiler developed at Argonne National Laboratory. The Fortran M compiler, supporting software, and documentation are made available free of charge by Argonne National Laboratory, but are protected by a copyright which places certain restrictions on how they may be redistributed. See the software for details. The latest version of both the compiler and this manual can be obtained by anonymous ftp from Argonne National Laboratory in the directory pub/fortran-m at info.mcs.anl.gov. DOE

N94-26466*# National Aeronautics and Space Administration. Langley Research Center, Hampton, VA.
PARALLEL GRID GENERATION ALGORITHM FOR DISTRIBUTED MEMORY COMPUTERS
Stuti Moitra and Anutosh Moitra (High Technology Corp., Hampton, VA.) Feb. 1994 20 p
(RTOP 505-90-53-02)
(NASA-TP-3429; L-17249; NAS 1.60:3429) Avail: CASI HC A03/MF A01

A parallel grid-generation algorithm and its implementation on the Intel iPSC/860 computer are described. The grid-generation scheme is based on an algebraic formulation of homotopic relations. Methods for utilizing the inherent parallelism of the grid-generation scheme are described, and implementation of multiple levELs of parallelism on multiple instruction multiple data machines are indicated. The algorithm is capable of providing near orthogonality and spacing control at solid boundaries while requiring minimal interprocessor communications. Results obtained on the Intel hypercube for a blended wing-body configuration are used to demonstrate the effectiveness of the algorithm. Fortran implementations bAsed on the native programming model of the iPSC/860 computer and the Express system of software tools are reported. Computational gains in execution time speed-up ratios are given. Author

N94-26521# Texas Univ., Austin. Inst. for Fusion Studies.
DELTA f ALGORITHM
R. E. Denton (Dartmouth Coll., Hanover, NH.) and M. Kotschenreuther Nov. 1993 34 p
(Contract DE-FG05-80ET-53088)
(DE94-003120; IFSR-629; DOE/ET-53088/629) Avail: CASI HC A03/MF A01

The (delta)f Algorithm is a low noise particle code algorithm. The perturbation of the distribution function ((delta)f) away from a large equilibrium is evolved rather than the total distribution function. 'Particles' in the code are actually Lagrangian markers at which the value of the distribution functaion is known. The magnitude of the numerical noise is characteristic of the size of the perturbation rather than the equilibrium, and scales roughly as the inverse of the number of particles. The algorithm is described and conserved energies are derived for linear and nonlinear sets of equations. Two different forms of the energy principle test separately adequate resolution in time and space and adequacy of the number of simulation particles. A semi-implicit time step method is described which allows violation of the Courant condition. Low noise capabilities of a linear code using the algorithm are demonstrated. DOE

N94-26530# Naval Postgraduate School, Monterey, CA.
USEFULNESS OF COMPILE-TIME RESTRUCTURING OF LGDF PROGRAMS IN THROUGHPUT-CRITICAL APPLICATIONS M.S. Thesis
David M. Cross Sep. 1993 56 p
(AD-A274915) Avail: CASI HC A04/MF A01

In this thesis, the Large Grain Data Flow (LGDF) representation of parallelism is applied to throughput-critical applications that process periodically arriving data. The applications are represented by directed acyclic graphs in which a vertex represents an indivisible node program execution and an arc represents data flow from its source node to sink node. The machine and graph parameters are assumed to be such that the time to transfer one unit of data is comparable to the time to execute one operation at a processor. The machine model consists of a set of processors connected to a set of memory modules by a cross-bar interconnection network. Execution of LGDF graphs on such machines either requires a run-time mechanism to dispatch executable nodes on available processors or a compile-time static scheduling of nodes to processors. The former approach, although flexible and robust, suffers from contention-related overhead and the latter, although capable of eliminating contention, is rigid and computationally intensive. It is shown by simulation that throughput can be improved when compile-time graph restructuring is coupled with simple first-come-first-serve dispatching. The restructuring is based on selectively adding control dependencies between graph nodes. This technique, called the revolving cylinder analysis, is shown to be an effective framework for achieving communication/computation overlap and reducing memory contention. DTIC

N94-26615 Simon Fraser Univ., Burnaby (British Columbia). School of Engineering Science.
EXTRACTING COMPLETE 3-DIMENSIONAL BOUNDARY REPRESENTATION FROM MULTIPLE RANGE IMAGES M.S. Thesis
Zukang Xu Jun. 1992 119 p
(ISBN-0-315-83776-4; CTN-94-61034) Copyright Avail: Micromedia Ltd., Technical Information Centre, 240 Catherine Street, Suite 305, Ottawa, Ontario, K2P 2G8, Canada HC/MF

An important problem in computer vision is that of generating a three dimensional (3D) description of objects from sensed data. In robotics applications, 3D descriptions require explicit geometric and topological relations between faces, edges, and vertices, and are very similar to boundary representation (b-rep) used in solid modeling. An approach is presented for extracting a complete b-rep description of a polyhedral object from range images taken from multiple viewpoints. The system starts from basic face models of visible surfaces of objects in each local view, extracts features, matches those features, generates rigid body transformations that relate the local views, and finally merges these views into a complete 3D b-rep description of the object. In a matching algorithm, a triple branch structure is defined as the main feature to determine correspondence. A coarse-to-fine search stragegy and a prioritizing procedure are designed to reduce the search time even further. The b-rep model is incrementally updated by merging each of the local views in a global description. A convenient and effective termination criterion is designed to monitor the integration process. The system has been implemented in C, and a synthetic range image generator has also been implemented. The system has been tested on several synthetic range images. Author (CISTI)

N94-26616 Regina Univ. (Saskatchewan). Dept. of Computer Science.
AN INTERACTIVE, PHYSICALLY-BASED SIMULATION SYSTEM M.S. Thesis
Allan Neill Snider Jul. 1992 129 p
(ISBN-0-315-83884-1; CTN-94-61035) Copyright Avail: Micromedia Ltd., Technical Information Centre, 240 Catherine Street, Suite 305, Ottawa, Ontario, K2P 2G8, Canada HC/MF

A system to animate dynamic deformable models incorporates physically based techniques to determine motion. Models understood by the system consist of simple text format descriptions of non-rigid bodies composed of spring-mass and torque-spring constructions with surface tessellations providing geometric shape. Numerical integration techniques including a second order Runge-Kutta technique (improved Euler's or Heun's method) are used to advance these models in time, using small regular increments, and their motion is graphically displayed. Real-time interaction with the system is provided by means of control panels. A general purpose implementation of the system is given, as well as additional components used to render and produce realistic video animations. Model display modes, model definitions, animation control, and animation production aspects of the implementation (the ANIM computer program) are presented and illustrated with test experiments. Author (CISTI)

N94-26632 Toronto Univ. (Ontario). Dept. of Electrical Engineering.
APPLICATION OF MARKOV RANDOM FIELD THEORY TO IMAGE CODING AND MOTION ESTIMATION M.S. Thesis
Peifang Zhou 1993 83 p
(ISBN-0-315-83435-8; CTN-94-61042) Copyright Avail: Micromedia Ltd., Technical Information Centre, 240 Catherine Street, Suite 305, Ottawa, Ontario, K2P 2G8, Canada HC/MF

Two applications of Markov random field theory to image coding and motion estimation are presented. Markov random fields are first used to model the correlation in the image intensity fields. A noncausal and nonlinear image coding scheme is proposed in which the estimation of present pixel is based on both past and future neighboring pixels. Two decoding algorithms are developed. Open-loop and closed-loop quantizer structures are implemented for noncausal prediction. Secondly, Markov random fields are used to model the smoothness inherent in the image motion fields. The motion estimation problem is formulated in the framework of maximum a posteriori estimation and smoothness constraints are imposed to regulate the motion fields. A deterministic multipass prediction algorithm is developed as an alternative to stochastic simulated annealing. A multi workstation version of both multipass prediction and simulated annealing algorithms is implemented. Author (CISTI)

N94-26655 National Physical Lab., Teddington (England). Information Technology and Computing Div.
AUTOMATIC TEST CASE GENERATION USING PROLOG
S. J. Ashford 12 Jan. 1993 32 p
(ISSN 0262-5369)
(NPL-DITC-215/93; ETN-94-95282) Copyright Avail: Issuing Activity (National Physical Lab., Teddington, Middlesex, TW11 OLW, England)

A method for generating tests using a formalized test purpose notation to guide the system is reported. The automatic derivation of test cases from formalized protocol specifications is an increasingly important research topic. The means by which the number and type of test cases output from such a generator may be controlled is of importance. The work described is a development from earlier work on test generation, based on the Class 0 protocol and a limited Class 4 subset. The general principles developed in those projects were used as the basis for the new work. The main limitation of the earlier work was that the Class 4 specification used omitted many of the features of the protocol, and could only deal with a small set of example test purposes. The new specification covers all the main Class 4 features, excluding network layer events and network connection management. This was developed by extending the original specification, while retaining essentially the same structure. ESA

N94-26663 Carleton Univ., Ottawa (Ontario). School of Computer Science.
INTEGRATING AUTOMATA WITH GENETIC ALGORITHMS IN ORDER TO PROVIDE ADAPTIVE OPERATORS M.S. Thesis
Anthony Richard Phil White 12 May 1993 215 p
(ISBN-0-315-84094-3; CTN-94-61052) Copyright Avail: Micromedia Ltd., Technical Information Centre, 240 Catherine Street, Suite 305, Ottawa, Ontario, K2P 2G8, Canada HC/MF

Genetic algorithms are loosely based on the principles of the survival of the fittest and exploitation of genetic material from one generation to the next. Genetic algorithms have shown themselves to be successful in solving a wide range of combinatorial problems. Genetic algorithms have traditionally required the specification of a number of parameters that control the evolutionary process, two of these being related to the probability of applying the mutation and crossover operators. Extensions are proposed to the classical genetic algorithm model. In the classical model, the aforementioned mutation and crossover operator probabilities are specified before the start of a genetic algorithm run and remain unchanged, a so-called static model. In the extended model, automata are used to allow the adaptation of these operator probabilities as the run progresses in order to improve the quality of the solutions found. Favorable results have been achieved for a wide range of function minimization problems. Author (CISTI)

N94-26680*# Illinois Univ., Urbana. Center for Reliable and High-Performance Computing.
FAST INCREMENTAL COMPILER TRANSFORMATIONS FOR MULTIPLE INSTRUCTION RETRY
Shyh-Kwei Chen, Neal J. Alewine, W. K. Fuichs, and Wen-Mei W. Hwu Jul. 1992 25 p
(Contract NAG1-613; N00014-91-J-1283)
(NASA-CR-195209; NAS 1.26:195209; AD-A274290) Avail: CASI HC A03/MF A01

Previous work on compiler-assisted multiple instruction retry has utilized a series of compiler transformations, loop protection, node splitting, and loop expansion, to eliminate anti-dependencies of length less than N in the pseudo register, machine register, and the post-pass resolver phases of compilation. The results have provided a means of rapidly recovering from transient processor failures by rolling back N instructions. This paper presents techniques for improving compilation and runtime performance in compiler-assisted multiple instruction retry. Incremental updating enhances compilation time when new instructions are added to the program. Post-pass code rescheduling and spill register reassignment algorithms improve the run-time performance and decrease the code growth across the application programs studied. Branch hazards axe also shown to be resolvable by simple modifications to the incremental updating schemes during the pseudo register phase and to the spill register reassignment algorithm during the post-pass phase. DTIC

N94-26682# Georgia Inst. of Tech., Atlanta. School of Mathematics.
PROBABILISTIC METHODS FOR IMAGE GENERATION AND ENCODING Final Report, 15 May 1990 - 14 May 1993
Marc A. Berger 15 Oct. 1993 9 p
(Grant AF-AFOSR-0288-90)
(AD-A274294; AFOSR-93-0894TR) Avail: CASI HC A02/MF A01

The research described herein involves a new digital image compression algorithm. A hybrid low-pass filter/fractal technique was developed, taking advantage of the fact that fractals afford a remarkable way of compressing high frequency data. The low frequency content of the image is stored without loss, and then fractal image processing is used to touch-up the high frequency features, with some loss. An image compression software system has been built around this. The system handles 24-bit digital images of arbitrary resolution. Compression is quick - for example, the system compresses a still 1280 x 1024 (high-definition) image in a few seconds on a Personal Iris (6 MFlops); and also decompresses in a few seconds. At low compression (around 15:1), the compression is visually lossless. At high compression (around 100:1), there is some loss, but not much. DTIC

N94-26764# Oak Ridge National Lab., TN.
PARALLEL MATRIX TRANSPOSE ALGORITHMS ON DISTRIBUTED MEMORY CONCURRENT COMPUTERS
J. Choi, D. W. Walker, and J. J. Dongarra (Tennessee Univ., Knoxville.) Oct. 1993 27 p
(Contract DE-AC05-84OR-21400)
(DE94-002424; ORNL/TM-12309) Avail: CASI HC A03/MF A01

This paper describes parallel matrix transpose algorithms on distributed memory concurrent processors. It is assumed that the matrix is distributed over a P x Q processor template with a block scattered data distribution. P, Q, and the block size can be arbitrary, so the algorithms have wide applicability. The communication schemes of the algorithms are determined by the greatest common divisor (GCD) of P and Q. If P and Q are relatively prime, the matrix transpose algorithm involves complete exchange communication. If P and Q are not relatively prime, processors are divided into GCD groups and the communication operations are overlapped for different groups of processors. Processors transpose GCD wrapped diagonal blocks simultaneously, and the matrix can be transposed with LCM/GCD steps, where LCM is the least common multiple of P and Q. The algorithms make use of non-blocking, point-to-point communication between processors. The use of nonblocking communication allows a processor to overlap the messages that it sends to different processors, thereby avoiding unnecessary synchronization. Combined with the matrix multiplication routine, C = A(center dot)B, the algorithms are used to compute parallel multiplications of transposed matrices, C = A(sup T)(center dot)B(sup T), in the PUMMA package. Details of the parallel implementation of the algorithms are given, and results are presented for runs on the Intel Touchstone Delta computer. DOE

N94-26772# Center for Mathematics and Computer Science, Amsterdam (Netherlands). Dept. of Numerical Mathematics.
VLUGR2: A VECTORIZED LOCAL UNIFORM GRID REFINEMENT CODE FOR PDE'S IN 2D
J. G. Blom and J. G. Verwer Mar. 1993 31 p
(Grant CRG-92.05) (ISSN 0169-0388)
(CWI-NM-R9306; ETN-94-95410) Copyright Avail: CASI HC A03/MF A01

An ANSI FORTRAN 77 code, VLUGR2, vectorized for the Cray YMP, that is based on an adaptive grid finite difference method to solve time dependent two dimensional (2D) systems of partial differential equations, is described. The performance of VLUGR2 and MOORKOP (an adaptive grid code for initial boundary value problems in two space dimensions) on ground water flow problems were compared. ESA

N94-26775# Lawrence Livermore National Lab., CA.
COMPUTATIONAL MECHANICS
G. L. Goudreau Mar. 1993 38 p
(Contract W-7405-eng-48)
(DE94-003015; UCRL-ID-112772) Avail: CASI HC A03/MF A01

The Computational Mechanics thrust area sponsors research into the underlying solid, structural, and fluid mechanics and heat transfer necessary for the development of state-of-the-art general purpose computational software. The scale of computational capability spans office workstations, departmental computer servers, and Cray-class supercomputers. The DYNA, NIKE, and TOPAZ codes have achieved world-wide fame, through our broad collaborators program, in addition to their strong support of on-going Lawrence Livermore National Laboratory (LLNL) programs. Several technology transfer initiatives have been based on these established codes teaming LLNL analysts and researchers with counterparts in industry and extending code capability to specific industrial interests of casting, metalforming, and automobile crash dynamics. The next-generation solid/structural mechanics code, ParaDyn, is targeted toward massively parallel computers, which will extend performance from gigaflop to teraflop power. Our work for FY-92 is described in the following eight articles: (1) Solution Strategies: New Approaches for Strongly Nonlinear Quasistatic Problems Using DYNA3D; (2) Enhanced Enforcement of Mechanical Contact: The Method of Augmented Lagrangians; (3) ParaDyn: New Generation Solid/Structural Mechanics Codes for Massively Parallel Processors; (4) Composite Damage Modeling; (5) HYDRA: A Parallel/Vector Flow Solver for Three-Dimensional, Transient, Incompressible Viscous Flow; (6) Development and Testing of the TRIM3D Radiation Heat Transfer Code; (7) A Methodology for Calculating the Seismic Response of Critical Structures; and (8) Reinforced Concrete Damage Modeling. DOE

N94-26784# Oak Ridge National Lab., TN.
NEW FORTRAN COMPUTER PROGRAMS TO ACQUIRE AND PROCESS ISOTOPIC MASS SPECTROMETRIC DATA: OPERATOR'S MANUAL
D. H. Smith and H. S. McKown Sep. 1993 117 p
(Contract DE-AC05-84OR-21400)
(DE94-003174; ORNL/TM-12196) Avail: CASI HC A06/MF A02

This TM is one of a pair that describes ORNL-developed software for acquisition and processing of isotope ratio mass spectral data. This TM is directed at the laboratory analyst. No technical knowledge of the programs and programming is required. It describes how to create and edit files, how to acquire and process data, and how to set up files to obtain the desired results. The aim of this TM is to serve as a utilitarian instruction manual, a 'how to' approach rather than a 'why?'. DOE

N94-26816 National Physical Lab., Teddington (England). Materials Metrology Div.
DUSOL: IMPROVED SOFTWARE FOR ANALYSIS OF ULTRASONIC VELOCITY DATA ON ANISOTROPIC MATERIALS
A. Woolf Jun. 1993 26 p
(NPL-DMM(A)-104; ETN-94-95225; PB94-105061) Copyright Avail: Issuing Activity

The program for computing stiffness components, compliances, and engineering elastic constants for composite materials was developed. Velocity measurements taken from the ultrasonic immersion method were used. The method is applicable to transversely isotropic, tetragonal, and orthotropic materials. An example is included. The ultrasonic method, the stages of the computation, and how the data is prepared for each stage are presented. Operating instructions and examples are given. Notes on the mathematics for computing the compliances and engineering elastic constants are included. ESA

N94-26831# Naval Research Lab., Washington, DC.
VCALC: A 3-SPACE VECTOR CALCULATOR
Harold M. Greenwald and Frank J. Pipitone 15 Dec. 1993 16 p
(AD-A274520; NRL/MR/5511-93-7422) Avail: CASI HC A03/MF A01

Vcalc is a 3-space vector calculator providing graphic displays for vector and scalar operations. Designed to operate on a Sun Workstation, the program may be run stand-alone or as a debugging tool linked to a C program. It is a straightforward and useful tool whose development was motivated by the difficulty of debugging geometric programs. DTIC

N94-26852 Vrije Univ., Amsterdam (Netherlands). Faculteit der Wiskunde en Informatica.
A FORMALIZATION OF OBJECTS USING EQUATIONAL DYNAMIC LOGIC
R. J. Wieringa Feb. 1993 25 p Submitted for publication Limited Reproducibility: More than 20% of this document may be affected by microfiche quality
(PB94-125218; IR-324) Avail: Issuing Activity (National Technical Information Service (NTIS))

Order-sorted equational logic is extended with dynamic logic to a specification language for dynamic objects. Special attention is paid to different concepts of encapsulation that play a role in object-orientation. It is argued that the resulting language, CMSL, meets those requirements of the object-oriented database system manifesto that are applicable to object-oriented conceptual models (as opposed to object-oriented databases). NTIS

N94-26862# Lawrence Livermore National Lab., CA.
AN AUTOMATIC CONTACT ALGORITHM IN DYNA3D FOR IMPACT PROBLEMS
R. G. Whirley and B. E. Engelmann 23 Jul. 1993 11 p Presented at the IMPACT-4: Structural Mechanics in Reactor Technology Conference, Berlin, Germany, 23-24 Aug. 1993
(Contract W-7405-eng-48)
(DE94-002856; UCRL-JC-114820; CONF-9308161-2) Avail: CASI HC A03/MF A01

A new approach for the automatic definition and treatment of mechanical contact in explicit nonlinear finite element analysis is presented. Automatic contact offers the benefits of significantly reduced model construction time and fewer opportunities for user error, but faces significant challenges in reliability and computational costs. Key aspects of the proposed new method include automatic identification of adjacent and opposite surfaces in the global search phase, and the use of a well-defined surface normal which allows a consistent treatment of shell intersection and corner contact conditions without an ad-hoc rules. Three examples which illustrate the performance of the newly proposed algorithm in the public DYNA3D code are given. DOE

N94-26908# Vrije Univ., Amsterdam (Netherlands).
COMBINING LOGICS
Agoston Eiben, Andras Janossy (Hungarian Academy of Sciences, Budapest.), and Agnes Kurucz (Hungarian Academy of Sciences, Budapest.) Dec. 1993 33 p Prepared in cooperation with Magyar Tudomanyos Akademia, Budapest. Mathematical Inst.
(PB94-125242; IR-319) Avail: CASI HC A03/MF A01

In this paper, we investigate connections between different logics. In particular, we are interested in a special kind of connection, when a logic is a 'mixture' of other logics. We give four natural and intuitive criteria that need to be satisfied by 'mixtures' of logics and an additional fifth one for the method of combination. We rely on a general notion of a logic and we study two frameworks for combining logics in connection with the above criteria. The first concept is a reformulation of Gabbay's fibered semantics, whereas the second one defines the 'mixture' of logics as a colimit construction in the category of logics. NTIS

N94-26919# Technische Univ., Eindhoven (Netherlands). Dept. of Mathematics and Computing Science.
PROCESS ALGEBRA OF CONCURRENT CONSTRAINT PROGRAMMING
Frank S. deBoer and Catuscia Palamidessi (Pisa Univ., Italy.) Jun. 1993 26 p Prepared in cooperation with Pisa Univ.
(PB94-126695; COMPUTING SCIENCE NOTES-93/20) Avail: CASI HC A03/MF A01

The authors develop an algebraic theory for the observational equivalence of concurrent constraint programs which identifies processes which have the same final results for all possible executions. NTIS

N94-26920# Technische Univ., Eindhoven (Netherlands). Dept. of Mathematics and Computing Science.
HARD REAL-TIME RELIABLE MULTICAST IN THE DEDOS SYSTEM
D. Alstein and P. vanderStok Jun. 1993 32 p
(PB94-126745; COMPUTING SCIENCE NOTES-93/17) Avail: CASI HC A03/MF A01

Two protocols for reliable multicast in a multiprocessor system are presented. The protocols use mailboxes located in common memory to exchange messages, instead of relying on communication channels. The mailboxes are replicated for reliability. The protocols have bounded completion time, making them suitable for use in hard real-time systems. Multiple source ordering is imposed on the messages that pass through a mailbox. The protocols are shown to be tolerant of memory crashes, and of process or processor failures. The basic protocol tolerates only crash failures of processes, while the second protocol can also handle timing failures. The protocols can be extended so that multicast group membership is dynamic. NTIS

N94-26921# Helsinki Univ. of Technology, Espoo (Finland). Control Engineering Lab.
NEW MIXED INTEGER ALGORITHM FOR CLASSIFICATION AND PLACEMENT OF MEASUREMENTS IN PROCESS FLOW NETWORKS
P. J. Immonen Aug. 1993 61 p
(PB94-126752; ISBN-951-22-1742-2) Avail: CASI HC A04/MF A01

The purpose of this report is to introduce a new approach to the assessment of metering systems through flowsheet analysis. The method determines an index called the degree of calculability for each process quantity, providing a unified classification method for both measured and unmeasured variables. The computation of the index is done through mixed integer programming, utilizing the linear or linearized plant model in a straight-forward fashion. Single-component flow systems form a special class of applications that can be transformed into network linear programming problems, facilitating much faster solutions. The classification algorithms also identify the new measurements that would increase the degree of calculability. A practical plant example is also given. - NTIS

N94-26955 Technische Univ., Eindhoven (Netherlands). Dept. of Mathematics and Computing Science.
DESIGN OF AN ONLINE HELP FACILITY FOR EXSPECT
G. J. Houben Jun. 1993 30 p See also PB91-234989 Limited Reproducibility: More than 20% of this document may be affected by microfiche quality
(PB94-126687; CSN-93/19) Avail: Issuing Activity (National Technical Information Service (NTIS))

In this paper we briefly discuss general principles and guidelines for the design of online documentation and we illustrate them by evaluating the design of an online help facility for ExSpect, a software tool for writing executable specifications. NTIS

N94-26956 Technische Univ., Eindhoven (Netherlands). Dept. of Mathematics and Computing Science.
FREENESS ANALYSIS FOR LOGIC PROGRAMS-AND CORRECTNESS
Michael Codish, Dennis Dams, Gilberto File, and Maurice Bruynooghe Jun. 1993 33 p Limited Reproducibility: More than 20% of this document may be affected by microfiche quality
(PB94-126703; CSN-93/21) Avail: CASI HC A03

Several proposals for computing freeness information for logic programs have been put forward in recent literature. This paper introduces a novel domain of abstract equation systems describing possible sharing and definite freeness of terms in a system of equations. A simple and intuitive abstract unification algorithm is presented, providing the core of a correct and precise sharing and freeness analysis for logic programs. Our contribution is not only a correct algorithm, but perhaps primarily, the systematic approach in which it is derived by mimicking each step in a suitable concrete unification algorithm. Consequently, the abstract algorithm is intuitive--as it resembles the concrete algorithm. It is easy to justify--as the proof of correctness boils down to showing that each step in the concrete algorithm is mimicked by a corresponding step in the abstract algorithm. Finally, it is precise--as each step mimics only those situations which can arise in the concrete algorithm. NTIS

N94-26966 Technische Univ., Delft (Netherlands). Faculty of Technical Mathematics and Informatics.
CENTRAL DYNAMIC SHARE SCHEDULING IN DISTRIBUTED SYSTEMS
J. F. C. M. deJongh 1993 50 p Limited Reproducibility: More than 20% of this document may be affected by microfiche quality
(ISSN 0922-5641)
(Rept-93-48; ETN-94-95402) Copyright Avail: CASI HC A03

The objectives for share scheduling policies in distributed computing systems are reported. Performance measures to evaluate such policies are defined. The major objectives of share scheduling are: compliance with share objectives, and avoidance of capacity loss. Shares are defined as fractions of the processing capacity that are used to serve a group of jobs. Capacity loss occurs if at least one processor is idle while at another processor two or more jobs are present. A number of central dynamic initial placement policies for share scheduling in homogeneous distributed computing systems are proposed. A scheduling policy consists of two components: a global scheduling policy, which decides which processor serves which job, and a local scheduling policy, which decides when to serve a job on the processor it is assigned to. Jobs arrive according to independent Poisson processes, one for each group. Service times for 'all' jobs are identically distributed exponential random variables. The results indicate that if the system consists of only one processor, a scheduling policy called group priority processor sharing can be effectively used for share scheduling. ESA

N94-26970# Technische Univ., Eindhoven (Netherlands). Dept. of Mathematics and Computing Science.
CONGRUENCE THEOREM FOR STRUCTURED OPERATIONAL SEMANTICS WITH PREDICATES AND NEGATIVE PREMISES
C. Verhoef Jun. 1993 31 p See also PB93-225274
(ISSN 0926-4515)
(PB94-126729; CSN-93/18) Avail: CASI HC A03/MF A01

We proposed a syntactic format, the panth format, for structured operational semantics. In addition to ordinary transitions, predicates, negated predicates, and negated transitions may occur if the rules are stratifiable, and the strong bisimulation equivalence is a congruence for all the operators that can be defined within the panth format. To show the utility of this format, we took some examples from the literature. The examples touch upon issues such as priorities, termination, convergence, discrete time, recursion, (infinitary) Hennessy-Milner logic, and universal quantification. NTIS

N94-26971# Technische Univ., Eindhoven (Netherlands). Dept. of Mathematics and Computing Science.
TRACE-BASED COMPOSITIONAL PROOF THEORY FOR FAULT TOLERANT DISTRIBUTED SYSTEMS
Henk Schepers and Jozef Hooman Jun. 1993 36 p
(ISSN 0926-4515)
(PB94-126737; CSN-93/16) Avail: CASI HC A03/MF A01

We present a compositional network proof theory to specify and verify safety properties of fault tolerant distributed systems. In this proof, we abstract from the precise nature and occurrence of faults, but model their effect on the externally visible input and output behavior. To this end, we formalize a fault hypothesis as a reflexive relation between the normal behavior (i.e. the behavior when no faults occur) of a system and its acceptable behavior, that is, the normal behavior together with the exceptional behavior (i.e. the behavior whose abnormality should be tolerated). The method is compositional to allow for the reasoning with the specifications of processes while ignoring their implementation details. This compositionality is achieved by starting from a SAT formalism to reason about the normal behavior and extending it with a single rule to obtain a specification of the acceptable behavior from the specification of the normal behavior and a predicate characterizing the fault hypothesis. We prove soundness and relative network completeness of the method. Our approach is illustrated by applying it to a triple modular redundant component and the alternating bit protocol. NTIS

N94-26997# Vrije Univ., Amsterdam (Netherlands). Faculteit der Wiskunde en Informatica.

WHAT CAN WE LEARN FROM GENETIC ALGORITHMS: A NEW PERSPECTIVE FOR SEARCH METHODS

Agoston Eiben Dec. 1992 27 p
(PB94-125234; IR-320) Avail: CASI HC A03/MF A01

This paper is concerned with search methods, in particular with genetic algorithms (GA's) and their status in artificial intelligence (AI). We describe and study GA's in the context of classic AI search techniques, such as depth-first or A*. By systematically studying similarities and differences between general search methods and genetic algorithms, we have established a place for GA's in the AI search family. GA's are distinguished by relying on a fixed data structure of the search space and a standard child construction mechanism. In the second part of this paper we surpass GA traditions concerning these aspects and generalize along two axes. We discuss non-standard data types and child construction mechanisms with an arbitrary number of parents. Hereby we also achieve a general framework, a shell, to define basic search operators. Finally, we summarize what we can learn from genetic algorithms and sketch the outlines of a scientific program for developing and investigating new kinds of search methods. NTIS

N94-27020# Virginia Polytechnic Inst. and State Univ., Blacksburg.

PARALLEL MATHEMATICAL SOFTWARE

L. T. Watson and C. J. Ribbens 17 May 1993 9 p
(Contract DE-FG05-88ER-25068)
(DE94-001587; DOE/ER-25068/3) Avail: CASI HC A02/MF A01

Parallel software for nonlinear systems of equations are discussed. Topics covered include: mathematical background for homotopy algorithms, polynomial systems, small dense nonlinear systems, large sparse nonlinear systems, parallel software for elliptic partial differential equations, and domain decomposition, DOE

N94-27031# Technische Univ., Delft (Netherlands). Faculty of Technical Mathematics and Informatics.

UNIFYING INVESTIGATION OF INTERIOR-POINT METHODS FOR CONVEX PROGRAMMING

D. denHertog, F. Jarre, C. Roos, and T. Terlaky 1992 20 p See also AD-A239457
(PB94-126463; Rept-92-89) Copyright Avail: CASI HC A03/MF A01

In the recent past a number of papers were written that present low complexity interior-point methods for different classes of convex programs. The goal of this article is to show that the logarithmic barrier function associated with these programs is self-concordant, and that the analyses of interior-point methods for these programs can thus be reduced to the analysis of interior-point methods with self-concordant barrier functions. NTIS

N94-27049# California Univ., Berkeley. Lawrence Berkeley Lab.

OBJECT-ORIENTED SOFTWARE CONSTRUCTION AT ALS

H. Nishimura Oct. 1993 3 p Presented at the International Conference on Accelerator and Large Experimental Control Systems, Berlin, Germany, 18-22 Oct. 1993
(Contract DE-AC03-76SF-00098)
(DE94-003418; LBL-34720; CONF-931023-8) Avail: CASI HC A01/MF A01

New C++ class libraries have been developed and used for accelerator modeling and machine control at the Advanced Light Source. A class library for accelerator modeling is portable and supports multiple instances dynamically at run time. A class library for machine control covers fields from virtual devices to simulation studies. DOE

N94-27060# Maryland Univ., College Park.

CMSC-130 INTRODUCTORY COMPUTER SCIENCE, LECTURE NOTES

Duane J. Jarc and Eric Fendler Jul. 1993 166 p
(Contract MDA972-92-J-1021)
(AD-A274369; CMSC-130) Avail: CASI HC A08/MF A02

The CMSC 130 Introductory Computer Science lecture notes are used in the classroom for teaching CMSC 130, an introductory computer science course, using the Ada programming language. DTIC

N94-27063# Carnegie-Mellon Univ., Pittsburgh, PA. Dept. of Computer Science.

MEMORY SUBSYSTEM PERFORMANCE OF PROGRAMS WITH INTENSIVE HEAP ALLOCATION

Amer Diwan, David Tarditi, and Eliot Moss 13 Dec. 1993 46 p
(Contract F19628-91-C-0168; ARPA Order 8313)
(AD-A274122; CMU-CS-93-227) Avail: CASI HC A03/MF A01

Heap allocation with copying garbage collection is a general storage management technique for modern programming languages. It is believed to have poor memory subsystem performance. To investigate this, we conducted an in-depth study of the memory subsystem performance of heap allocation for memory subsystems found on many machines. We studied the performance of mostly-functional Standard ML programs which made heavy use of heap allocation. We found that most machines support heap allocation poorly. However, with the appropriate memory subsystem organization, heap allocation can have good performance. The memory subsystem property crucial for achieving good performance was the ability to allocate and initialize a new object into the cache without a penalty. This can be achieved by having subblock placement with a subblock size of one word with a write allocate policy, along with fast page-mode writes or a write buffer. For caches with subblock placement, the data cache overhead was under 9% for a 64-K of larger data cache: without subblock placement the overhead was often higher than 50%. DTIC

N94-27064# Carnegie-Mellon Univ., Pittsburgh, PA. Dept. of Computer Science.

COMBINING SHAPE AND COLOR INFORMATION FOR 3D OBJECT RECOGNITION

Kazunori Higuchi, Martial Hebert, and Katsushi Ikeuchi Dec. 1993 19 p
(Contracts F33615-90-C-1465; F33615-93-1-1282; NSF IRI-92-24521)
(AD-A274123; CMU-CS-93-215) Avail: CASI HC A03/MF A01

Both photometric and geometric information are important for 3D object recognition. Traditionally, however, few systems utilized both types of information. This is because no single representation is suitable for both types of information. This paper proposes a method for representing both color and geometric information using a common framework, the Spherical Attribute Image (SAI). The SAI maps the values of curvature and color computed at every node of a mesh approximating the object surface onto a spherical image. A model object and an observed surface are computed by finding the rotation that brings their spherical images into correspondence. We show how this matching algorithm can be used for object recognition using both geometric and photometric information. In addition, we describe how the two types of information can be combined in a way that takes into account their actual distribution on the surface. DTIC

N94-27065# Carnegie-Mellon Univ., Pittsburgh, PA. Dept. of Computer Science.

DEFERRED COMPILATION: THE AUTOMATION OF RUN-TIME CODE GENERATION

Mark Leone and Peter Lee Dec. 1993 21 p
(Grant NSF CCR-90-57567)
(AD-A274124; CMU-CS-93-225) Avail: CASI HC A03/MF A01

This paper describes deferred compilation, an alternative and complement to compile-time program analysis and optimization. By deferring aspects of compilation to run time, exact information about programs can be exploited, leading to greater opportunities for code improvement. This is in contrast to the use of static analyses, which are inherently conservative. Deferred compilation automates the translation of ordinary programs into native machine code that performs fast optimization and native-code generation at run time. Automation is obtained through the use of a compile-time staging analysis, which determines the portions of a program that may be safely and profitably compiled at run time. Fast run-time optimization is obtained by trading space for time: compile-time specialization yields numerous run-time code generators, each customized to optimize a small portion of the source program based on run-time information.

Implementation strategies developed for a prototype compiler are discussed, and the results of preliminary experiments demonstrating significant overall speedup are presented. DTIC

N94-27075# Air Force Inst. of Tech., Wright-Patterson AFB, OH. School of Engineering.
AN OBJECT-ORIENTED DATABASE INTERFACE FOR Ada M.S. Thesis
Anthony D. Moyers Dec. 1993 67 p
(AD-A274391; AFIT/GCE/Eng/93D-11) Avail: CASI HC A04/MF A01

Object data management (ODM) is currently at the forefront of research and development efforts in the database community. In order to take advantage of ODM technology, the Department of Defense (DoD) needs to ensure that these systems are accessible to Ada programmers. The Air Force Institute of Technology (AFIT) is conducting research towards the development of an Ada ODM interface to existing ODM systems. The design goals are portability, transparency, and completeness for Ada programmers. Portability means that the ODM system can be changed without affecting any existing application programs. Transparency means that Ada programmers can use the interface without having to know different programming languages or specifics about the different systems being used. Completeness means that all of the functionality of the ODM systems are available to Ada application developers. This thesis defines requirements for an Ada ODM interface and proposes a design. In addition, the challenges associated with implementation are investigated using commercial ODM systems at AFIT. Implementation of the interface is based on the use of Ada bindings to the existing application program interfaces (API's) of the ODM systems. A preprocessor will be necessary in order to achieve transparency. DTIC

N94-27120# Air Force Inst. of Tech., Wright-Patterson AFB, OH. School of Engineering.
GENETIC ALGORITHMS APPLIED TO A MISSION ROUTING PROBLEM M.S. Thesis
James B. Olsan Dec. 1993 125 p
(AD-A274130; AFIT/GCE/Eng/93-12) Avail: CASI HC A06/MF A02

This thesis applies genetic algorithms to a mission routing problem. The mission routing problem involves determining an aircraft's best route between a staging base and a target. The goal is to minimize the route distance and the exposure to radar. Potential routes are mapped to a 3-dimensional mesh where the nodes correspond to checkpoints in the route and the arcs correspond to partial paths of the route. Each arc is weighted with respect to distance and exposure to radar. A genetic algorithm is a probabilistic search technique loosely based on theories of biological evolution. Genetic crossover and survival of the fittest are the basis of a genetic algorithm's control structure and can be used for general problems. Encoding and evaluation of the data structure is problem specific. This thesis focuses on approaches to mapping the mission routing problem's mesh to a data structure which the genetic algorithm's control structure can effectively and efficiently manipulate. Three broad methods are proposed: Bounded Progress, Free Progress, and Restricted Progress. The Bounded Progress method uses a tightly-coupled mesh while the Free Progress method uses a loosely-coupled mesh. The Restricted Progress method is a hybrid of the other two methods. DTIC

N94-27128# Air Force Inst. of Tech., Wright-Patterson AFB, OH. School of Engineering.
ALTERNATIVE ARCHITECTURES FOR DOMAIN-ORIENTED APPLICATION COMPOSITION AND GENERATION SYSTEMS M.S. Thesis
Warren E. Gool Dec. 1993 130 p
(AD-A274180; AFIT/GCS/Eng/93D-11) Avail: CASI HC A07/MF A02

This thesis presents a formalized framework for comparing the structure and semantics of software architectures. The framework uses object diagrams for analyzing the structure of the architectures and the axiomatic approach for analyzing the semantics. This framework is used to compare the Object Connection Update (OCU) model (developed by the Software Engineering Institute) against four other software architectures: VHDL defined by Lipsett, MetaH defined by Honeywell, microRapide defined by Luckham, and hierarchical software systems as defined by Batory. The goal of the comparison was to evaluate the OCU model for suitability within prototype application composition and generation systems. This research concluded that the OCU model has all the elements necessary for use in application composition and generation systems. Additionally, the framework identified several common elements in all the software architectures. These common elements may lead to the development of a meta-model for software architectures. DTIC

N94-27140# George Washington Univ., Washington, DC. Dept. of Operations Research.
RESEARCH IN IMPROVED ASSESSMENT OF SOFTWARE RELIABILITY Final Report, 1 Nov. 1991 - 31 Oct. 1993
N. D. Singpurwalla 31 Oct. 1993 3 p
(Contract F49620-92-J-0030)
(AD-A274161; AFOSR-93-0901TR) Avail: CASI HC A01/MF A01

The objective of this research was to develop novel and realistic statistical models and experimental schemes for software development and testing. The proposed research was directed towards the development of improved techniques for assessing the reliability and quality of computer software. There were 12 technical reports and two publications in referred journals written under this grant. DTIC

N94-27154 National Defence Research Establishment, Stockholm (Sweden). Dept. of Weapon Systems, Effects and Protection.
USERS GUIDE FOR GRIKURV: A CODE FOR DRAWING GRAPHS [ANVAENDARHANDLEDNING TILL GRIKURV: ETT PROGRAM FOER DIAGRAMRITNING]
A. Collin Jun. 1993 14 p In SWAHILI
(PB94-123593; FOA-C-20933-2.7) Avail: Issuing Activity (National Technical Information Service (NTIS))

GRIKURV is a c(K)URV drawing-code for xy-data and designed for personal computers with MS-DOS. The programming language is TURBO-PASCAL, and the code consists of a main program and a number of separately compiled units. It is possible to choose the columns that should compose coordinates with a table editor, and there is also an opportunity to edit data. Curves can be drawn by certain methods, such as the least-square-method, the method of Bezier-fitting, or by interpolation with splines. Formulas with one variable and parameters can also be fed to the code by the means of an editor of formulas. Several curves can be included in the graph and text can be inserted by a cursor. This is all done in dialog with the user. The graph can be written out in the format of HPGL, the format of PostScript or through a file. NTIS

N94-27157 Foerenade Fabriksverken, Linkoeping (Sweden).
TRANSLATION AND ROTATION INVARIANT PATTERN RECOGNITION [TRANSLATIONS- OCH ROTATIONSINVARIANT MOENSTERIGENKAENNING]
S. Posluk and M. Bengtsson Feb. 1993 50 p In SWEDISH
(PB94-123676; FOA-C-30702-8.4,3.4) Avail: Issuing Activity (National Technical Information Service (NTIS))

This report introduces a method for 2D pattern representations, which has explicit and simultaneous translation and rotation invariance. In contrast to previous efforts in this direction, we do not rely on center of gravity calculations and subsequent resampling of the image. Instead the fourier transformed image is used as input to a rotation invariant operator, i.e., the image is transformed twice. This results in a translation and rotation invariant representation since the rotation operator commutes with the fourier transform. The invariant features are then used as input to a neural network classifier. The result is a robust and noise insensitive system. NTIS

N94-27168*# Mississippi State Univ., Mississippi State. Dept. of Electrical and Computer Engineering.
THE COMMUNICATION LINK AND ERROR ANALYSIS (CLEAN) SIMULATOR Semiannual Report, 1 Jul. 1993 - 30 Jun. 1994
William J. Ebel, Frank M. Ingels, and Shane Crowe Dec. 1993 47 p
(Grant NAG5-2006)
(NASA-CR-195243; NAS 1.26:195243) Avail: CASI HC A03/MF A01

During the period July 1, 1993 through December 30, 1993, significant developments to the Communication Link and Error ANalysis (CLEAN) simulator were completed and include: (1) Soft decision Viterbi decoding; (2) node synchronization for the Soft decision Viterbi decoder; (3) insertion/deletion error programs; (4) convolutional encoder; (5) programs to investigate new convolutional codes; (6) pseudo-noise sequence generator; (7) soft decision data generator; (8) RICE compression/decompression (integration of RICE code generated by Pen-Shu Yeh at Goddard Space Flight Center); (9) Markov Chain channel modeling; (10) percent complete indicator when a program is executed; (11) header documentation; and (12) help utility. The CLEAN simulation tool is now capable of simulating a very wide variety of satellite communication links including the TDRSS downlink with RFI. The RICE compression/decompression schemes allow studies to be performed on error effects on RICE decompressed data. The Markov Chain modeling programs allow channels with memory to be simulated. Memory results from filtering, forward error correction encoding/decoding, differential encoding/decoding, channel RFI, nonlinear transponders and from many other satellite system processes. Besides the development of the simulation, a study was performed to determine whether the PCI provides a performance improvement for the TDRSS downlink. There exist RFI with several duty cycles for the TDRSS downlink. We conclude that the PCI does not improve performance for any of these interferers except possibly one which occurs for the TDRS East. Therefore, the usefulness of the PCI is a function of the time spent transmitting data to the WSGT through the TDRS East transponder. Author

N94-27311 Concordia Univ., Montreal (Quebec). Dept. of Electrical and Computer Engineering.
MOTION ANALYSIS FROM A SEQUENCE OF RANGE IMAGES Ph.D. Thesis
Peiying Zhu Apr. 1993 232 p
(ISBN-0-315-84684-4; CTN-94-61086) Copyright Avail: Micromedia Ltd., Technical Information Centre, 240 Catherine Street, Suite 305, Ottawa, Ontario, K2P 2G8, Canada HC/MF

The feasibility of recovering motion from a sequence of range images is investigated as an alternate solution to the complex motion problem. An approach to finding matching features in two or more successive images is proposed using a Hopfield neural network. A model is developed to convert the correspondence problem to the problem of minimizing an energy function. After establishing the feature matching, a delta-bound matching concept is introduced to detect the reliable matching features. The algorithm used is tolerant to noise due to feature detection or occlusion. For the case of a single rigid moving object, a simple but powerful algorithm is proposed to estimate motion. The motion problem is modelled as solving a set of linear equations. A weighted least squares technique provided the best performance. For more complicated motion such as nonrigid motion, low-level processing was considered. An algorithm was developed which uniquely estimates three dimensional velocities of points on smooth surfaces, and another algorithm based on the correlation of the local structure of principal curvatures was developed to provide reliable estimates of velocities near edge points. The former algorithm is computationally fast while the latter is computationally intensive. It is suggested that the two algorithms be combined to give the best performance. Author (CISTI)

N94-27316 Concordia Univ., Montreal (Quebec). Dept. of Education.
PRODUCTION OF A COMPUTER BASED LESSON TEACHING EMPLOYEES HOW TO USE AN AIR DATA TESTER M.S. Thesis
Deborah Lynn Barker Oct. 1992 140 p
(ISBN-0-315-84708-5; CTN-94-61091) Copyright Avail: Micromedia Ltd., Technical Information Centre, 240 Catherine Street, Suite 305, Ottawa, Ontario, K2P 2G8, Canada HC/MF

A computer-based lesson was developed in order to provide aircraft maintenance personnel with quality and timely training concerning the operation of a new air data tester. These new-generation testers are used for checking and calibrating certain aircraft systems and operate in a manner significantly different from the ones they replace. Dick and Carey's (1985) instructional design model was used to guide the design of the lesson. Using Air Canada equipment and the WISE authoring system, a portion of the lesson was produced. Three types of people participated in a formative evaluation of the lesson. An instructional design expert evaluated the design of the lesson and found it acceptable. A subject matter expert evaluated the programmed portion of the lesson for technical accuracy. A few minor changes were required. Eight members of the target population worked through the lesson's programmed portion. Oral and written comments were positive, and some technical errors were identified. There was a statistically significant improvement between the pre-test (35 percent) and post-test (93 percent) mean scores indicating that the students learned from the program. Author (CISTI)

N94-27318 JASCO Research Ltd., Sidney (British Columbia).
DEVELOPMENT OF DIGITAL RESAMPLING AND PULSE COMPRESSION COMPUTER SOFTWARE
P. Scrimger, I. Schumacher, R. L. Kirlin (Victoria Univ., British Columbia.), and W. Du (Victoria Univ., British Columbia.) 1992 51 p Limited Reproducibility: More than 20% of this document may be affected by poor print
(DREP-92-32; DSIS-94-00230; CTN-94-61093) Avail: Issuing Activity

Five digital resampling and pulse compression computer programs are described. These include a program for generating maximum length binary sequences (M-sequences), a digital resampling program, a data rescaling program, a program for demodulating a phase modulated signal of known frequency, and a signal cross correlation program. The use of these programs is also outlined and program examples are included. The five programs can be used to examine M-sequences which are often used when measuring propagation delays under extremely noisy multipath conditions such as those which existed in the Heard Island Feasibility Test. An appendix is included which describes a technique for carrier frequency estimation and phase unwrapping. Author (CISTI)

N94-27346 Queens Univ., Kingston (Ontario). Dept. of Electrical Engineering.
ESTIMATION OF IMAGE MOTION IN SCENES CONTAINING MULTIPLE MOVING OBJECTS Ph.D. Thesis
Heyun Zheng Jul. 1993 158 p
(ISBN-0-315-85208-9; CTN-94-61101) Copyright Avail: Micromedia Ltd., Technical Information Centre, 240 Catherine Street, Suite 305, Ottawa, Ontario, K2P 2G8, Canada HC/MF

An error weighted regularization algorithm for image motion field estimation is proposed as a computationally attractive alternative to stochastic optimization based schemes. Block matching errors in the local motion measurement process are used in the regularization functional to avoid oversmoothing across motion boundaries. A second algorithm, anisotropic regularization, improves on the local measurement process by employing alternative matching criteria and matching window organization. A selective confidence measure derived from local anisotropic measurements is used to further improve the error weighted regularization. For moving object estimation needed in object oriented video coding applications, a new optimality criterion based on the minimum description length (MDL) principle is developed. In the proposed MDL estimator, the cost to be minimized is the sum of the ideal coding lengths for the motion parameters, boundaries, and motion compensated predictive errors of all moving objects in a scene. An optimization procedure to obtain a suboptimal MDL estimator is proposed based on a region-merging framework. A number of experimental comparisons has shown a significant ideal coding rate reduction of the object oriented coding scheme using an MDL estimator over a standard block-oriented scheme. Author (CISTI)

N94-27396# Technische Univ., Eindhoven (Netherlands). Dept. of Mathematics and Computing Science.
POLYHEDRAL CHARACTERIZATION OF THE ECONOMIC LOT-SIZING PROBLEM WITH START-UP COSTS
C. P. M. vanHoesel, A. P. M. Wagelmans (Erasmus Univ., Rotterdam, Netherlands.), and L. A. Wolsey (CORE International, Inc., Louvain-la-Neuve, Belgium.) Nov. 1992 23 p
(ISSN 0926-4493)
(MEMO-COSOR-92-46; ETN-94-94807) Avail: CASI HC A03/MF A01

A class of strong valid inequalities for the single item uncapacitated economic lot sizing problem with start up costs is described. It is shown that these inequalities yield a complete polyhedral characterization of the problem. The corresponding separation problem is formulated as a shortest path problem. A reformulation as a plant location problem is shown to imply the class of strong valid inequalities. The polynomial size uncapacitated facility location reformulation is shown to be tight. These results are of a purely theoretical nature. Computational testing should reveal which of the two formulations is best used in practical problems in which the economic lot sizing problem with start up costs appears as a relaxation. ESA

N94-27416*# Institute for Computer Applications in Science and Engineering, Hampton, VA.
SHARED VIRTUAL MEMORY AND GENERALIZED SPEEDUP Final Report

Xian-He Sun and Jianping Zhu Jan. 1994 24 p Submitted for publication
(Contract NAS1-19480; RTOP 505-90-52-01)
(NASA-CR-191592; ICASE-94-2; NAS 1.26:191592) Avail: CASI HC A03/MF A01

Generalized speedup is defined as parallel speed over sequential speed. The generalized speedup and its relation with other existing performance metrics, such as traditional speedup, efficiency, scalability, etc., are carefully studied. In terms of the introduced asymptotic speed, it was shown that the difference between the generalized speedup and the traditional speedup lies in the definition of the efficiency of uniprocessor processing, which is a very important issue in shared virtual memory machines. A scientific application was implemented on a KSR-1 parallel computer. Experimental and theoretical results show that the generalized speedup is distinct from the traditional speedup and provides a more reasonable measurement. In the study of different speedups, various causes of superlinear speedup are also presented. Author (revised)

N94-27417*# Institute for Computer Applications in Science and Engineering, Hampton, VA.
INTERACTIVE SHAPE METAMORPHOSIS Final Report
David T. Chen (North Carolina Univ., Chapel Hill.), Andrei State (North Carolina Univ., Chapel Hill.), and David Banks Jan. 1994 10 p Submitted for publication
(Contract NAS1-19480; RTOP 505-90-52-01)
(NASA-CR-191597; NAS 1.26:191597; ICASE-94-7) Avail: CASI HC A02/MF A01

A technique for controlled metamorphosis between surfaces in 3-space is described. Well-understood techniques to produce shape metamorphosis between models in a 2D parametric space is applied. The user selects morphable features interactively, and the morphing process executes in real time on a high-performance graphics multicomputer. Author (revised)

N94-27542*# National Aeronautics and Space Administration. Ames Research Center, Moffett Field, CA.
THIRTEEN WAYS TO SAY NOTHING WITH SCIENTIFIC VISUALIZATION
Al Globus (Computer Sciences Corp., Moffett Field, CA.) and E. Raible 25 Feb. 1992 5 p
(Contract NAS2-12961; RTOP 536-01-11)
(NASA-CR-195280; NAS 1.26:195280; RNR-92-006) Avail: CASI HC A01/MF A01

Scientific visualization can be used to produce very beautiful images. Frequently, users and others not properly initiated into mysteries of visualization research fail to appreciate the artistic qualities of these images. Scientists will frequently use our work to needlessly understand the data from which it is derived. This paper describes a number of effective techniques to confound such pernicious activity. Author (revised)

N94-27543 Center for Mathematics and Computer Science, Amsterdam (Netherlands). Dept. of Computer Science/Dept. of Software Technology.
A CHARACTERIZATION OF STABLE MODELS USING A NON-MONOTONIC OPERATOR
Frank Teusink Mar. 1993 24 p Sponsored by SION Limited Reproducibility: More than 20% of this document may be affected by microfiche quality
(ISSN 0169-118X)
(CWI-CS-R9315; ETN-94-95428) Copyright Avail: CASI HC A03

Stable models seem to be a natural way to describe the beliefs of a rational agent. However, the definition of stable models itself is not constructive. It is therefore interesting to find a constructive characterization of stable models, using a fixpoint construction. The operator defined is based on the work of F. Fages (among others). For this operator, every total stable model of a general logic program will coincide with the limit of some (infinite) sequence of interpretations generated by it. The set of all stable models will coincide with certain interpretations in these sequences. The least fixpoint of the Fitting operator and the well founded model is characterized using the operator. ESA

N94-27544# Center for Mathematics and Computer Science, Amsterdam (Netherlands). Dept. of Computer Science/Dept. of Software Technology.
MODULAR TERMINATION PROOFS FOR LOGIC AND PURE PROLOG PROGRAMS
Krzysztof R. Apt (Amsterdam Univ., Netherlands.) and Dino Pedreschi (Pisa Univ., Italy.) Mar. 1993 37 p Submitted for publication Sponsored in part by EEC
(ISSN 0169-118X)
(CWI-CS-R9316; ETN-94-95429) Copyright Avail: CASI HC A03/MF A01

A uniform and simplified presentation of the methods of Bezem and of Apt and Pedreschi for proving termination of logic and PROLOG programs is presented. It is shown how these methods can be refined so that they can be used in a modular way. ESA

N94-27545# Center for Mathematics and Computer Science, Amsterdam (Netherlands). Dept. of Computer Science/Dept. of Software Technology.
A STRATEGY FOR DYNAMIC INTERPRETATION: A FRAGMENT AND AN IMPLEMENTATION
Olivier Bouchez, D. Jan N. vanEijck (OTS, Utrecht, Netherlands.), and Olivier Istace Mar. 1993 26 p Presented at the Association for Computational Linguistics' European Chapter 6th Conference, Utrecht, Netherlands, 21-23 Apr. 1993 Submitted for publication
(ISSN 0169-118X)
(CWI-CS-R9317; ETN-94-95430) Copyright Avail: CASI HC A03/MF A01

A strategy for natural language interpretation which implements the dynamics of context change by translating natural language texts into a meaning representation language consisting of (descriptions of) programs, in the spirit of Dynamic Predicate Logic (DPL), is presented. The difference with DPL is that the usual DPL semantics is replaced by an error state semantics. This allows for the treatment of unbound anaphors, as in DPL but also of presuppositions and presupposition projection. The use of this dynamic interpretation strategy is demonstrated in an implementation of a small fragment of natural language which handles unbound pronoun antecedent links, where it is assumed that the intended links are indicated in the input string, and uniqueness presuppositions of definite descriptions. The implementation consists of a syntax module which outputs parse trees, a semantic module mapping parse trees to DPL representations, a representation processor which determines truth conditions, falsity conditions and presupposition failure conditions, and an evaluator of these conditions in a database model. The implementation uses the logic programming language GOEDEL, an experimental successor of PROLOG, with similar functionality and expressiveness, but with an improved declarative semantics. ESA

N94-27548# Center for Mathematics and Computer Science, Amsterdam (Netherlands). Dept. of Computer Science/Dept. of Algorithmics and Architecture.
SCHEMA INTEGRATION IN OBJECT-ORIENTED DATABASES
Christiaan J. E. Thieme and Arno P. J. M. Siebes Mar. 1993 33 p
(ISSN 0169-118X)
(CWI-CS-R9320; ETN-94-95433) Copyright Avail: CASI HC A03/MF A01

A formal appproach to support schema integration in object oriented databases is presented. The basis of the approach is a synthetic subclass order, which is defined in terms of a weak subtype relation on underlying types of classes and a subfunction relation on functional forms of methods. Classes are identified using an equivalence relation induced by the subclass order and factorized using a join operator with respect to the subclass order. Class hierarchies are integrated by repeatedly identifying and factorizing classes. Both attributes and methods are used to compare classes and behavior of methods is used to compare attributes. ESA

N94-27549 Center for Mathematics and Computer Science, Amsterdam (Netherlands). Dept. of Computer Science/Dept. of Software Technology.
MODAL LOGIC, TRANSITION SYSTEMS AND PROCESSES
Johan vanBenthem (Amsterdam Univ., Netherlands.), D. Jan N. vanEijck (OTS, Utrecht, Netherlands.), and Vera Stebletsova Mar. 1993 46 p Limited Reproducibility: More than 20% of this document may be affected by microfiche quality

(ISSN 0169-118X)
(CWI-CS-R9321; ETN-94-95434) Copyright Avail: CASI HC A03

Transition systems can be viewed either as process diagrams or as Kripke structures. The first perspective is that of process theory, the second that of modal logic. It is shown how formalisms of modal logic can be brought to bear on processes. Notions of bisimulation can not only be motivated by operations on transition systems, but they can also be suggested by investigations of modal formalisms. To show that the equational view of processes from process algebra is closely related to modal logic, various ways of looking at the relation between the calculus of basic process algebra and propositional dynamic logic are considered. Preservation results for various bisimulation notions, a result on the expressive power of propositional dynamic logic, and a definition of bisimulation which is the proper notion of invariance for concurrent propositional dynamic logic are given. ESA

N94-27550 Center for Mathematics and Computer Science, Amsterdam (Netherlands). Dept. of Computer Science/Dept. of Algorithmics and Architecture.

SAVING COMPARISONS IN THE CROCHEMORE-PERRIN STRING MATCHING ALGORITHM

Dany Breslauer Mar. 1993 16 p Sponsored in part by IBM Fellowship, and European Research Consortium for Informatics and Mathematics, Netherlands Limited Reproducibility: More than 20% of this document may be affected by microfiche quality
(ISSN 0169-118X)
(CWI-CS-R9322; ETN-94-95435) Copyright Avail: CASI HC A03

The modification of an algorithm discovered by Crochemore and Perrin, which is a linear time constant space string matching algorithm that makes at most 2n - m symbol comparison, to make fewer comparisons is presented. Given any fixed epsilon greater than zero, the new algorithm takes linear time, uses constant space, and makes at most n + (((1 + epsilon)/2)(n - m)) symbol comparisons. If O(log m) space is available, then the algorithm makes at most n + ((1/2)(n - m)) symbol comparisons. The pattern preprocessing step also takes linear time and uses constant space. These are the first string matching algorithms that make fewer than 2n - m symbol comparisons and use sublinear space. ESA

N94-27552 Center for Mathematics and Computer Science, Amsterdam (Netherlands). Dept. of Computer Science/Dept. of Interactive Systems.

AN OBJECT MODEL FOR MULTIMEDIA PROGRAMMING

F. Arbab, I. Herman, and G. J. Reynolds Apr. 1993 16 p Submitted for publication Sponsored by EEC Limited Reproducibility: More than 20% of this document may be affected by microfiche quality
(ISSN 0169-118X)
(CWI-CS-R9327; ETN-94-95439) Copyright Avail: CASI HC A03

The development of multimedia applications is a complex task. Much of this complexity stems from requirements associated with programming multiple media objects and the control of dependences and interrelationships between these media objects and the user(s). It is clearly necessary to have a basic framework on which to build multimedia appplications in the face of such complexities. Such a conceptual model, called an object model, is addressed. The MADE (Multimedia Application Development Environment) object model represents a novel approach to multimedia application programming that is founded on the two principal concepts of 'active objects' and 'delegation.' Although these concepts are not novel in themselves, it is believed that their combined use in a multimedia development environment represents a substantial enhancement to more traditional approaches to programming in this area. ESA

N94-27558*# Institute for Computer Applications in Science and Engineering, Hampton, VA.

EFFICIENT MASSIVELY PARALLEL SIMULATION OF DYNAMIC CHANNEL ASSIGNMENT SCHEMES FOR WIRELESS CELLULAR COMMUNICATIONS Final Report

Albert G. Greenberg, Boris D. Lubachevsky, David M. Nicol, and Paul E. Wright Jan. 1994 15 p Submitted for publication
(Contract NAS1-19480; RTOP 505-90-52-01)
(NASA-CR-191593; ICASE-94-3; NAS 1.26:191593) Avail: CASI HC A03/MF A01

Fast, efficient parallel algorithms are presented for discrete event simulations of dynamic channel assignment schemes for wireless cellular communication networks. The driving events are call arrivals and departures, in continuous time, to cells geographically distributed across the service area. A dynamic channel assignment scheme decides which call arrivals to accept, and which channels to allocate to the accepted calls, attempting to minimize call blocking while ensuring co-channel interference is tolerably low. Specifically, the scheme ensures that the same channel is used concurrently at different cells only if the pairwise distances between those cells are sufficiently large. Much of the complexity of the system comes from ensuring this separation. The network is modeled as a system of interacting continuous time automata, each corresponding to a cell. To simulate the model, conservative methods are used; i.e., methods in which no errors occur in the course of the simulation and so no rollback or relaxation is needed. Implemented on a 16K processor MasPar MP-1, an elegant and simple technique provides speedups of about 15 times over an optimized serial simulation running on a high speed workstation. A drawback of this technique, typical of conservative methods, is that processor utilization is rather low. To overcome this, new methods were developed that exploit slackness in event dependencies over short intervals of time, thereby raising the utilization to above 50 percent and the speedup over the optimized serial code to about 120 times. Author (revised)

N94-27572*# Institute for Computer Applications in Science and Engineering, Hampton, VA.

ILLUMINATION IN DIVERSE CODIMENSIONS Final Report

David C. Banks Jan. 1994 23 p Submitted for publication
(Contract NAS1-19480; RTOP 505-90-52-01)
(NASA-CR-191596; NAS 1.26:191596; ICASE-94-6) Avail: CASI HC A03/MF A01

This paper derives a model of diffuse and specular illumination in arbitrarily large dimensions, based on a few characteristics of material and light in three-space. It then describes how to adjust for the anomaly of excess brightness in large codimensions. If a surface is grooved or furry, it can be illuminated with a hybrid model that incorporates both the one dimensional geometry (the grooves or fur) and the two dimensional geometry (the surface). Author (revised)

N94-27573*# National Aeronautics and Space Administration. Langley Research Center, Hampton, VA.

ELECTRONIC DOCUMENT DISTRIBUTION: DESIGN OF THE ANONYMOUS FTP LANGLEY TECHNICAL REPORT SERVER

Michael L. Nelson and Gretchen L. Gottlich Mar. 1994 18 p
(RTOP 505-90-53-02)
(NASA-TM-4567; L-17355; NAS 1.15:4567) Avail: CASI HC A03/MF A01

An experimental electronic dissemination project, the Langley Technical Report Server (LTRS), has been undertaken to determine the feasibility of delivering Langley technical reports directly to the desktops of researchers worldwide. During the first six months, over 4700 accesses occurred and over 2400 technical reports were distributed. This usage indicates the high level of interest that researchers have in performing literature searches and retrieving technical reports at their desktops. The initial system was developed with existing resources and technology. The reports are stored as files on an inexpensive UNIX workstation and are accessible over the Internet. This project will serve as a foundation for ongoing projects at other NASA centers that will allow for greater access to NASA technical reports. Author (revised)

N94-27575 Center for Mathematics and Computer Science, Amsterdam (Netherlands). Dept. of Computer Science/Dept. of Interactive Systems.

SEMANTICS OF MANIFOLD: SPECIFICATION IN ASF+SDF AND EXTENSION

E. P. B. M. Rutten and S. Thiebaux Dec. 1992 106 p Limited Reproducibility: More than 20% of this document may be affected by microfiche quality
(ISSN 0169-118X)
(CWI-CS-R9269; ETN-94-95421) Copyright Avail: Issuing Activity (European Space Agency (ESA))

MANIFOLD is a parallel programming language where processes called 'manifolds' use broadcast events to coordinate the dynamic data flow communications among other processes. A specification of the event driven mechanisms of MANIFOLD in the ASF+SDF formalism, and its implementation in the ASF+SDF system, providing automatically a programming environment for MANIFOLD, with syntax directed editor, parser, static checker, and interpreter, are presented. This subset of the language is augmented with a detailed specification of the unit exchange mechanism of the language: the streams, carrying units of data, that compose the data flow networks in MANIFOLD. ESA

N94-27576# Center for Mathematics and Computer Science, Amsterdam (Netherlands). Dept. of Computer Science/Dept. of Algorithmics and Architecture.
DESIGN AND IMPLEMENTATION OF A DBMS PERFORMANCE ASSESSMENT TOOL
M. L. Kersten and F. Kwakkel Dec. 1992 16 p
(ISSN 0169-188X)
(CWI-CS-R9270; ETN-94-95422) Copyright Avail: CASI HC A03/MF A01

The increasing number of advanced Data Base Management Systems (DBMS's) offered on the market require tools to quickly assess their performance and to assure their quality. Performance measurement involves running a set of representative workloads, such as benchmarks, and quality assurance, which involves extensive testing. The Software Testpilot described greatly simplifies both jobs by enabling a compact specification of the workload search space, a flexible mechanism to interact with a system under study, and a fast algorithm to expose the performance bottlenecks or software instabilities. ESA

N94-27578 Center for Mathematics and Computer Science, Amsterdam (Netherlands). Dept. of Computer Science/Dept. of Software Technology.
A THEORY FOR SIMULATOR TOOLS
Henri P. Korver Jan. 1993 24 p Sponsored in part by EEC Limited Reproducibility: More than 20% of this document may be affected by microfiche quality
(ISSN 0169-118X)
(CWI-CS-R9302; ETN-94-95424) Copyright Avail: CASI HC A03

A possible formalization of the notion simulator tool for process languages like ACP, CCS, (mu)CRL, LOTOS and PSF, is presented. Precise definitions for the notions simulator and simulation are given, and the equivalence that a simulator induces on the explored process terms is investigated. This is done by considering two processes, say p and q, equivalent if each simulation of p is also a simulation of q and vice versa. It is proven that there is no 'reasonable' simulator inducing bisimulation equivalence. It is demonstrated that simulators inducing coarser equivalences, for example ready, failure and trace equivalences, are unlikely to be computationally tractable. The conclusion is that a practical simulator induces an equivalence that is finer (less identifying) than bisimulation and even finer than graph isomorphism. ESA

N94-27580# Center for Mathematics and Computer Science, Amsterdam (Netherlands). Dept. of Computer Science/Dept. of Software Technology.
FORWARD AND BACKWARD SIMULATIONS. PART 1: UNTIMED SYSTEMS
Nancy A. Lynch (Massachusetts Inst. of Tech., Cambridge.) and Frits W. Vaandrager Mar. 1993 38 p Sponsored in part by EEC
(Contracts N00014-85-K-0168; N00014-91-J-1988; N00014-89-J-1988; NSF CCR-89-15206) (ISSN 0169-118X)
(CWI-CS-R9313-Pt-1; ETN-94-95426) Copyright Avail: CASI HC A03/MF A01

A comprehensive presentation of simulation techniques is given in terms of a simple (untimed) automation model. In particular, refinements, forward and backward simulations, forward-backward and backward-forward simulations, and history and prophecy relations, are discussed. History and prophecy relations are new and are abstractions of the history and prophecy variables of Abadi and Lamport, as well as the auxiliary variables of Owicki and Gries. Elegant and short proofs of soundness and completeness results for complicated simulations in terms of soundness and (partial) completeness results for simple simulations are given. ESA

N94-27581 Center for Mathematics and Computer Science, Amsterdam (Netherlands). Dept. of Computer Science/Dept. of Software Technology.
FORWARD AND BACKWARD SIMULATIONS. PART 2: TIMING-BASED SYSTEMS
Nancy A. Lynch (Massachusetts Inst. of Tech., Cambridge.) and Frits W. Vaandrager (Amsterdam Univ., Netherlands.) Mar. 1993 39 p Sponsored in part by EEC Limited Reproducibility: More than 20% of this document may be affected by microfiche quality
(Contracts N00014-85-K-0168; N00014-91-J-1988; N00014-89-J-1988; N00014-92-J-4033) (ISSN 0169-118X)
(CWI-CS-R9314-Pt-2; ETN-94-95427) Copyright Avail: Issuing Activity (European Space Agency (ESA))

A general automaton model for timing based systems is presented and is used as the context for developing a variety of simulation proof techniques for such systems. These techniques include refinements, forward and backward simulations, forward-backward and backward-forward simulations, and history and prophecy relations. Soundness and completeness results are given for these simulations. These results are largely analogous to the results in part 1 for untimed systems. In fact, many of the results for the timed case are obtained as consequences of the analogous results for the untimed case. ESA

N94-27582# European Space Agency. European Space Research and Technology Center, ESTEC, Noordwijk (Netherlands).
VALIDATION TESTS OF TOPSIM 4
Erwin Bayha (ANT Nachrichtentechnik, Backnang, Germany.), Renato LoCigno (Politecnico di Torino, Italy.), Sander Rasmussen (ANT Nachrichtentechnik, Backnang, Germany.), and W. R. Burke, ed. Jul. 1993 32 p
(Contract ESTEC-9357/91/NL/US) (ISSN 0379-4067)
(ESA-STM-249; ISBN-9-29-092216-8; ETN-94-95456) Copyright Avail: CASI HC A03/MF A01

The purpose of the work is a detailed validation of the new TOPSIM 4 functionalities. The TOPSIM 4 is a system simulator package which needs validation for establishing the reliability of the tool itself. The validation of some selected library blocks covering coding, digital system processing subsystems, and digital filters is presented. Block processing, multirate simulation, and special features intended to enhance the performance of the simulator are taken into account. All the procedures tested showed behavior that was in good agreement with theoretical results, hardware measurements, and results from the literature. The actual version of the simulator is powerful and user friendly for the analysis of design and communication systems. ESA

N94-27595 Queens Univ., Kingston (Ontario). Dept. of Electrical Engineering.
A MODULAR APPROACH TO EVALUATION CRYPTOGRAPHIC PROTOCOLS USING PETRI NETS M.S. Thesis
Cynthia Mae Morton Jun. 1993 111 p
(ISBN-0-315-85354-9; CTN-94-61105) Copyright Avail: Micromedia Ltd., Technical Information Centre, 240 Catherine Street, Suite 305, Ottawa, Ontario, K2P 2G8, Canada HC/MF

In a methodology used to evaluate the security properties of cryptographic protocols, a protocol is converted to a colored Petri net model with an intruder, capable of intercepting and modifying messages, placed between communicating protocol entities. All reachable model states in a reachability tree are checked to determine whether a path through the tree violates the security properties of the protocol. If a path contains a security violation, then an identifiable flaw has been found in the protocol. A modular approach is developed to simplify the reachability analysis and to reduce the search for security violations. This approach decomposes the Petri net model into component modules, and reachability analysis results from these modules are used to compose the overall reachability analysis results. In conjunction with the module reachability analysis, message acceptance criteria are used to eliminate unsuccessful intruder attacks from the reachability tree. The versatility of the Petri net method is illustrated in the analysis of the authentication and key agreement protocol of the European mobile network GSM, a proposed public key authentication and key distribution protocol and a modified Needham Schroeder key distribution protocol with multiple role entities. The security weaknesses and flaws of these protocols are discussed. Author (CISTI)

N94-27655*# National Aeronautics and Space Administration. Langley Research Center, Hampton, VA.
PATRAN 2.5/EAL INTERFACE GUIDE
Winifred S. Feldhaus Feb. 1994 49 p
(RTOP 237-02-02-03)
(NASA-TM-109053; NAS 1.15:109053) Avail: CASI HC A03/MF A01

The PATRAN/EA interface guide describes two programs, EALPAT and PATEAL. EALPAT reads an EAL LO1 file and translates the model and results into a PATRAN 2.5 neutral file, element results file, and nodal results file. An EAL model can be color coded in PATRAN, and geometry, loads, boundary conditions, section and material properties, rigid masses, springs, and beam orientations can be plotted and debugged. EAL results can be brought into PATRAN as element or nodal quantities and displayed as deformed plots, animated shapes, color coded elements, or color filled contour plots. PATEAL converts a PATRAN 2.5 data base into an EAL runstream. Geometry, including all element types, alternate coordinate systems, material properties, section properties, loads and boundary conditions are all converted. EALPAT and PATEAL can also be used together with the PATNAS translator from PDA Engineering to convert an EAL runstream to an MSC/NASTRAN bulk data file. Author

N94-27663*# Stevens Inst. of Tech., Hoboken, NJ.
HARDWARE AND SOFTWARE RELIABILITY ESTIMATION USING SIMULATIONS
Frederic L. Swern Feb. 1994 160 p
(Grant NAG1-587; RTOP 505-66-21)
(NASA-CR-187588; NAS 1.26:187588) Avail: CASI HC A08/MF A02

The simulation technique is used to explore the validation of both hardware and software. It was concluded that simulation is a viable means for validating both hardware and software and associating a reliability number with each. This is useful in determining the overall probability of system failure of an embedded processor unit, and improving both the code and the hardware where necessary to meet reliability requirements. The methodologies were proved using some simple programs, and simple hardware models. Author

N94-27702# Japan Atomic Energy Research Inst., Tokyo.
DEVELOPMENT OF CALCOMP COMPATIBLE INTERFACE LIBRARY 'PIFLIB' ON X WINDOW SYSTEM
Hidenobu Tanabe (Nuclear Energy Data Center, Japan.), Mitsuo Yokokawa (Japan Atomic Energy Research Inst., Tokai.), and Yoshio Onuma (Japan Atomic Energy Research Inst., Tokai.) May 1993 45 p In JAPANESE; In JAPANESE
(DE94-701190; JAERI-M-93-110) Avail: CASI HC A03/MF A01

Graphics processing at JAERI mainly has been executed on mainframe computers with Calcomp compatible graphics libraries. With spread of engineering workstations (EWS), it is important that those enormous graphics software be able to be carried out on EWS. The Calcomp compatible interface library 'piflib' has been developed on the X Window System, which is the most popular window environments on EWS. In this report, specifications of the library 'piflib' and its usage are presented. The cooperative processing with mainframe computers is also described. DOE

N94-27717# Argonne National Lab., IL.
THE PRISM PROJECT: INFRASTRUCTURE AND ALGORITHMS FOR PARALLEL EIGENSOLVERS
C. Bischof, X. Sun, S. Huss-Lederman (Supercomputer Research Center, Bowie, MD.), and A. Tsao (Supercomputer Research Center, Bowie, MD.) 1993 10 p Presented at the Institute of Electrical and Electronic Engineers (IEEE) Meeting on Scalable Parallel Libraries, Starkville, MS, 6-8 Oct. 1993
(Contract W-31-109-eng-38)
(DE94-005125; ANL/MCS/CP-81643; CONF-9310220-4) Avail: CASI HC A02/MF A01

The goal of the PRISM project is the development of the infrastructure and algorithms for the parallel solution of eigenvalue problems. We are currently investigating a complete eigensolver based on the Invariant Subspace Decomposition Algorithm for dense symmetric matrices (SYISDA). After briefly reviewing the SYISDA approach, we discuss the algorithmic highlights of a distributed-memory implementation of an eigensolver based on this approach. These include a fast matrix-matrix multiplication algorithm, a new approach to parallel band reduction and tridiagonalization, and a harness for coordinating the divide-and-conquer parallelism in the problem. We also present performance results of these kernels as well as the overall SYISDA implementation on the Intel Touchstone Delta prototype and the IBM SP/1. DOE

N94-27732# Japan Atomic Energy Research Inst., Tokyo.
INVERTED PENDULUM CONTROL APPARATUS USING TRANSPUTERS
Shinji Inomata (Japan Atomic Energy Research Inst., Tokai.) and Katuo Suzuki (Japan Atomic Energy Research Inst., Tokai.) Jun. 1993 50 p In JAPANESE; In JAPANESE
(DE94-701224; JAERI-M-93-119) Avail: CASI HC A03/MF A01

An inverted pendulum control apparatus is is controlled by a personal computer with transputer, analog-to-digital converter (A/D), and digital-to-analog converter (D/A) boards. For the apparatus, it is necessary to shorten the program processing time for input of data by A/D and output of calculation results by D/A. In order to implement control algorithms, we investigated three programming methods for interfacing between the transputer and A/D or D/A converters: (1) by expanding I/O server, (2) by port-accessing using I/O server, and (3) without use of I/O server. Each programming method is evaluated from the view point of their applicability to the inverted pendulum control which requires millisecond-order response. It is concluded that for the inverted pendulum control experiment the first method is the most suitable one because of the advantages of short processing time and easy programming of control algorithm in spite of the complexity of interface programming. These advantages are also confirmed by the control experiment. DOE

N94-27737 Center for Mathematics and Computer Science, Amsterdam (Netherlands). Dept. of Computer Science/Dept. of Algorithmics and Architecture.
A STRANGE APPLICATION OF KOLMOGOROV COMPLEXITY
Alexander Shen (Institute for Problems of Information Transmission, Moscow, USSR.) Apr. 1993 7 p Limited Reproducibility: More than 20% of this document may be affected by microfiche quality
(ISSN 0169-118X)
(CWI-CS-R9328; ETN-94-95440) Copyright Avail: CASI HC A02

Two similar inequalities are addressed: 2K((A, B, C)) is less than or equal to K((A, B)) + K((A, C)) + K((B, C)) + O(log n) and 2KP((A, B, C)) is less than or equal to KP((A, B)) + KP((A, C)) + KP ((B, C)) + O(1), where K denotes simple Kolmogorov entropy and KP denotes prefix entropy. It turns out from the first inequality that the following well known geometric fact can be inferred: the (absolute value of v) squared is less than or equal to the absolute value of S(sub xy) times the absolute value of S(sub yz) times the absolute value of S(sub xz), where V is a set in three dimensional space, S(sub xy), S(sub yz), S(sub xz) are its three two dimensional projections, and the absolute value of W is the volume (or the area) of W. The second inequality is a corollary of the well known Cauchy-Schwarz inequality. The connection between geometry and Kolmogorov complexity therefore works in both directions. ESA

N94-27761 Calian Communications, Kanata (Ontario).
MODULATION SIMULATION PROGRAM: PROGRAMMER'S MANUAL, VERSION 1.00
Kenneth Lazaris-Brunner 16 Oct. 1990 45 p
(Contract DSS-W7714-0-9883)
(DREO-16; DSIS-94-00051; CTN-94-61121) Copyright Avail: CASI HC A03/MF A01

A programmer manual is presented for software developed to digitally simulate various types of modulations, both analog and digital, of interest in the field of modulation identification and recognition. The software can simulate amplitude, frequency, and single and double sideband suppressed carrier modulation, plus amplitude shift keying, phase shift keying (binary, quadrature, and offset quadrature), frequency shift keying, on-off keying, and continuous wave plus noise. For each simulation, the user can select the modulator parameters or let the program randomly select them within user-defined limits. The software can also automatically generate as many files as desired without requiring any operator intervention. This feature is useful for creating a large data bank of signals. Author (CISTI)

N94-27762 Software Kinetics Ltd., Stittsville (Ontario).
ACES SPECTRAL DISPLAY SOFTWARE: USER MANUAL
30 Apr. 1992 17 p Revised
(Contract DREO-W7714-1-0007)
(SKL-1600-99-002; DSIS-94-00056; CTN-94-61123) Avail: CASI HC A03/MF A01

The user interface to the prototype Advanced Communications Electronic Support Measures System spectral display software is described. The

software provides the user with a real-time spectral display of a portion of the radio frequency spectrum based on signal data produced by a high speed digital signal processor. The prototype system is based on a 80486 personal computer and the software was developed using Microsoft C version 6.0. After program startup, the user specifies whether a two- or three-dimensional display is required, then enters the sampling frequency and the minimum and maximum signal strength. The resulting spectral display is then shown on a high resolution monitor. A list of software source files and their contents is appended, along with a procedure for compiling and linking the source files and modifying the software to change the color pallet, scrolling of data, and display size and location.
Author (CISTI)

N94-27767*# Cornell Univ., Ithaca, NY. Dept. of Computer Science.
SIMULATING FAIL-STOP IN ASYNCHRONOUS DISTRIBUTED SYSTEMS
Laura Sabel and Keith Marzullo Mar. 1994 26 p Sponsored by DARPA, IBM, and Siemens
(Grant NAG2-593)
(NASA-CR-195698; NAS 1.26:195698; TR-94-1413) Avail: CASI HC A03/MF A01

The fail-stop failure model appears frequently in the distributed systems literature. However, in an asynchronous distributed system, the fail-stop model cannot be implemented. In particular, it is impossible to reliably detect crash failures in an asynchronous system. In this paper, we show that it is possible to specify and implement a failure model that is indistinguishable from the fail-stop model from the point of view of any process within an asynchronous system. We give necessary conditions for a failure model to be indistinguishable from the fail-stop model, and derive lower bounds on the amount of process replication needed to implement such a failure model. We present a simple one-round protocol for implementing one such failure model, which we call simulated fail-stop.
Author

N94-27794# Center for Mathematics and Computer Science, Amsterdam (Netherlands). Dept. of Computer Science/Dept. of Software Technology.
ARM: ABSTRACT REWRITING MACHINE
J. F. T. Kamperman and H. R. Walters Apr. 1993 26 p Sponsored in part by EEC
(ISSN 0169-118X)
(CWI-CS-R9330; ETN-94-95441) Copyright Avail: CASI HC A03/MF A01

Term rewriting is frequently used as an implementation technique for algebraic specifications. The Abstract Term Rewriting Machine (ARM), which has an extremely compact instruction set and imposes no restrictions on the implemented TRS's, is presented. Apart from standard conditional term rewriting, associative lists are supported. ARM code is translated to ANSI C; the resulting execution speeds are good: on a Sun 4, an average of 80,000 rewriting steps per second and a maximum of 416,000 r/s were measured. Several benchmarks are shown, and related work is discussed.
ESA

N94-27805 British Columbia Univ., Vancouver. Dept. of Computer Science.
A THEORY OF MULTI-SCALE, CURVATURE AND TORSION BASED SHAPE REPRESENTATION FOR PLANAR AND SPACE CURVES Ph.D. Thesis
Farzin Mokhtarian Oct. 1990 184 p
(ISBN-0-315-63894-X; CTN-94-60996) Copyright Avail: Micromedia Ltd., Technical Information Centre, 240 Catherine Street, Suite 305, Ottawa, Ontario, K2P 2G8, Canada HC/MF

A theory of shape representation for planar and space curves was developed to satisfy various criteria considered useful for evaluating shape representation methods in computer vision. Two regular representations and two variants are proposed. Experiments were carried out on the representations which show that they are very stable under severe noise conditions and very useful for tasks which call for recognition of a noisy curve of arbitrary shape at an arbitrary scale or orientation. Planar or space curves are described at varying levels of detail by convolving their parametric representations with Gaussian functions of varying standard deviations. The curvature or torsion of each such curve is then computed using equations expressing curvature and torsion in terms of the convolutions of derivatives of Gaussian functions and parametric representations of the input curves. Curvature or torsion zero crossing points of those curves are then located and combined to form one of the representations mentioned. A number of theorems about describing a curve at increasing levels of abstraction are presented to provide a sound theoretical foundation for the representation methods proposed.
Author (CISTI)

N94-27823 Software Kinetics Ltd., Stittsville (Ontario).
SMALLTALK: A TOOL FOR DEVELOPMENT OF AN Ada IMPLEMENTATION OF EWCAC
I. Graham 6 Dec. 1988 26 p Submitted for publication
(SKL-1600-46-003-01-0; DSIS-94-00054; CTN-94-61125) Avail: CASI HC A03

The Electronic Warfare Control and Analysis Centre (EWCAC) will support tactical electronic warfare units in their intercept, collection, and analysis tasks. The EWCAC system will be implemented in the Ada language in accordance with requirements. A preliminary EWCAC design has already been done, and prototyping techniques may be used during the design phase to allow ongoing verification. For prototyping to be cost-effective, it is important to ensure that a suitable programming language be used. The use of Smalltalk and its environment as a tool to aid in EWCAC development is examined. Smalltalk is compared to Ada in order to identify the strengths of each language. The EWCAC development process is then studied and the usefulness of Smalltalk during each phase is assessed. It is concluded that Smalltalk would be a valuable tool in a number of areas including EWCAC simulation, contracting, design, prototyping, training, and future support. Of special importance is the reusability, at each stage, of Smalltalk software developed in previous stages. The flexibility of Smalltalk would also be advantageous in easing each phase of EWCAC development.
Author (CISTI)

N94-27835# Instituto de Pesquisas Espaciais, Sao Jose dos Campos (Brazil).
RANKING ALTERNATIVES USING FUZZY NUMBERS: A COMPUTATIONAL APPROACH SHORT COMMUNICATION
Oscar Pereira Dias, Jr. 1993 11 p
(INPE-5483-PRE/1782) Avail: CASI HC A03/MF A01

The method presented for ranking alternatives by using fuzzy numbers is discussed as far as computational aspects are concerned. An alternative procedure is presented which allows for the use of any convex and normalized fuzzy set to assess the contribution of each alternative to some of the criteria. The procedure also allows the criteria to be structured in n-level hierarchies. An example is presented to illustrate the algorithm.
Author

N94-27869 Royal Military Coll. of Canada, Kingston (Ontario). Dept. of Electrical and Computer Engineering.
A PROPOSED SOFTWARE ENGINEERING ENVIRONMENT FOR SYSTEMS LIFE CYCLE MANAGEMENT M.S. Thesis
J. J. P. Tremblay May 1990 131 p
(ISBN-0-315-60634-7; CTN-94-60988) Copyright Avail: Micromedia Ltd., Technical Information Centre, 240 Catherine Street, Suite 305, Ottawa, Ontario, K2P 2G8, Canada HC/MF

A research project was established to address deficiencies in off-the-shelf tools used to help automate source file management. The background work necessary to initiate the research project is provided, along with general guidelines for future research activities. The type of tool which is considered can be labelled as a software engineering environment (SEE) or an integrated project support environment (IPSE). This SEE uses a process programming language to define the software engineering process to be enforced. A process is modelled as a set of activities which must occur according to a predetermined sequence. An event-driven approach is used to determine the sequencing of activities. The completion of an activity is an example of an event which can be used. Whenever an event occurs, the SEE determines what activity, if any, must be released next and then assigns them to users. A user performs software engineering work through the activities found in this activity list. The user is presented with a list of options whenever an activity is selected from that list. Selecting an option invokes a software tool which in turn performs a subactivity required to fulfill the parent activity. The requirements and the design of the first prototype of the SEE is presented. A simple process programming language is also introduced and evaluation issues are discussed.
Author (CISTI)

N94-27872 Windsor Univ. (Ontario). Dept. of Electrical Engineering.
VISUAL SURFACE PERCEPTION: SURFACE RECONSTRUCTION FROM SHADING AND STEREO Ph.D. Thesis
Srinivasan Raghavan 1990 143 p
(ISBN-0-315-60974-5; CTN-94-60992) Copyright Avail: Micromedia Ltd., Technical Information Centre, 240 Catherine Street, Suite 305, Ottawa, Ontario, K2P 2G8, Canada HC/MF

Using stereo vision to compute depth, stereo correspondence between points in left and right images can be reliably achieved only at points of intensity changes. Due to the need for computing depth at every point in the image, interpolation of this sparse depth data becomes necessary. A class of interpolants known as Shepard's surfaces is shown to satisfy the required constraints on interpolation. Shepard's interpolants were implemented and results from testing on random dot stereograms show that stereo vision can function alone without any additional visual cues. Even when intensity changes are sparse, the reconstruction preserves the shape of the natural stereo pair. Besides depth from stereopsis, shape information also becomes important in reconstructing the surface. An important shape cue is provided by shading. A method is proposed to compute relative depth, normals, and principal curvatures of a surface, involving minimization of a global objective function formulated by imposing certain constraints. The principal curvatures are shown computable from the shape descriptor used. It is also shown that depth information at an arbitrary set of points can be included as additional set constraints in the shape computing algorithm, and any known set of normals can be used to improve the convergence of the shape from shading algorithm.
Author (CISTI)

N94-27936# Universiteit Twente, Enschede (Netherlands). Dept. of Computer Science.
COMPARISON OF OBJECT-ORIENTED ANALYSIS AND DESIGN METHODS: A COLLECTION OF PAPERS
Sjaak Brinkkemper, Geert vandenGoor (Nijmegen Univ., Netherlands.), and Shuguang Hong (Georgia State Univ., Atlanta.) Nov. 1992 41 p In DUTCH and ENGLISH
(ISSN 0924-3755)
(MEMO-INF-92-69; ETN-94-94111) Copyright Avail: CASI HC A03/MF A01

A formal approach in order to compare information systems development methods is presented. For each of the methods, a formal representation of it is constructed as a metaprocess model and a metadata model. The metamodels represent the steps of the analysis and design, the concepts, and the techniques provided by this method. The six methods are compared and the results are given. The implications of the transition to object oriented methods for the systems development practice and its CASE (computer aided systems engineering) tool support are presented. For individual titles, see N94-27937 through N94-27939.

N94-27937# Georgia State Univ., Atlanta. Dept. of Computer Information Systems.
A FORMAL APPROACH TO THE COMPARISON OF OBJECT-ORIENTED ANALYSIS AND DESIGN METHODOLOGIES
Shuguang Hong, Geert vandenGoor (Nijmegen Univ., Netherlands.), and Sjaak Brinkkemper (Universiteit Twente, Enschede, Netherlands.) *In* Univ. Twente, Comparison of Object-Oriented Analysis and Design Methods: A Collection of Papers Nov. 1992 p 1-10 Submitted for publication (For primary document see N94-27936 07-61)
Copyright Avail: CASI HC A02/MF A01

A formal approach for comparing six object oriented analysis and design methodologies is presented. For each of the methodologies, a formal representation of it is constructed as a metaprocess model and a metadata model. The metamodels represent the steps of the analysis and design, the concepts, and the techniques provided by this methodology. The six methodologies are compared and the results are presented. The approach enables an accurate comparison of the methodologies to be performed.
ESA

N94-27938# Nijmegen Univ. (Netherlands). Dept. of Information Systems.
OBJECT-ORIENTED DEVELOPMENT METHODS [OBJECT-GEORIENTEERDE ONTWERPMETHODEN]
Geert vandenGoor, Sjaak Brinkkemper (Universiteit Twente, Enschede, Netherlands.), and Shuguang Hong (Georgia State Univ., Atlanta.) *In* Univ. Twente, Comparison of Object-Oriented Analysis and Design Methods: A Collection of Papers Nov. 1992 p 11-26 In DUTCH (For primary document see N94-27936 07-61)
Copyright Avail: CASI HC A03/MF A01

Object oriented analysis and design methods are introduced. In contrast with the traditional Structured Analysis/Structured Design (SA/SD) approach, the object oriented paradigm describes and designs systems as much as possible as they occur in the real world. The background and concepts are overviewed. Results of comparative studies of object oriented methods are described. The relation between these methods and some object oriented programming languages is outlined. These methods are difficult to implement in a traditional programming language with maintenance of their advantages.
ESA

N94-27939# Nijmegen Univ. (Netherlands). Dept. of Information Systems.
CASE TOOLS FOR THE SUPPORT OF OBJECT-ORIENTED ANALYSIS AND DESIGN METHODS
Geert vandenGoor, Sjaak Brinkkemper (Universiteit Twente, Enschede, Netherlands.), and Shuguang Hong (Georgia State Univ., Atlanta.) *In* Univ. Twente, Comparison of Object-Oriented Analysis and Design Methods: A Collection of Papers Nov. 1992 p 27-36 (For primary document see N94-27936 07-61)
Copyright Avail: CASI HC A02/MF A01

Six Object Oriented Analysis and Design Methods (OOADM's) are compared by metamodeling. Metadata models of the development data and metaprocess models of the methods steps are obtained. CASE (Computer Aided Systems Engineering) tools were applied. Three scenarios for the adoption of OOADM's are discussed: the singular scenario that is chosen for one method; the synthetic scenario that tries to integrate OO analysis and design techniques into the more conventional approaches; and the open scenario that supports as many different OO techniques as possible. The transition of OO analysis and design products to OO programming environments and OO database management systems is considered.
ESA

N94-27951 Calian Communications, Kanata (Ontario).
MODULATION SIMULATION PROGRAM: OPERATOR'S MANUAL, VERSION 1.00
Kenneth Lazaris-Brunner 16 Oct. 1990 48 p
(Contract DSS-W7714-0-9883)
(DREO-16; DSIS-94-00110; CTN-94-61122) Copyright Avail: CASI HC A03

An operator manual is presented for software developed to digitally simulate various types of modulations, both analog and digital, of interest in the field of modulation identification and recognition. The software can simulate amplitude, frequency, and single and double sideband suppressed carrier modulation, plus amplitude shift keying, phase shift keying (binary, quadrature, and offset quadrature), frequency shift keying, on-off keying, and continuous wave plus noise. Each type of modulation has its own separate program, and program files and inputs are described. For each simulation, the user can select the modulator parameters or let the program randomly select them within user-defined limits. Bandwidth estimation algorithms can be added to all programs. The software can also automatically generate as many files as desired without requiring any operator intervention. This feature is useful for creating a large data bank of signals.
Author (CISTI)

N94-27992*# National Aeronautics and Space Administration, Washington, DC.
SOFTWARE ASSURANCE STANDARD
10 Nov. 1992 25 p
(NASA-TM-109705; NAS 1.15:109705; NASA-STD-2201-93) Avail: CASI HC A03/MF A01

This standard specifies the software assurance program for the provider of software. It also delineates the assurance activities for the provider and the assurance data that are to be furnished by the provider to the acquirer. In any software development effort, the provider is the entity or individual that actually designs, develops, and implements the software product, while the acquirer is the entity or individual who specifies the requirements and accepts the resulting products. This standard specifies at a high level an overall software assurance program for software developed for and by NASA. Assurance includes the disciplines of quality assurance, quality engineering, verification and validation, nonconformance reporting and corrective action, safety assurance, and security assurance. The application of these disciplines during a software development life cycle is called software assurance. Subsequent lower-level standards will specify the specific processes within these disciplines. Derived from text

N94-28137 ESDU International Ltd., London (England).
PARAMETER ESTIMATION OF LINEAR SYSTEMS FROM FREQUENCY RESPONSE MEASUREMENTS (COMPUTER PROGRAM)
Jul. 1993 24 p
(ISSN 0141-3988)
(ESDU-93016; ISBN-0-85679-868-1) Avail: ESDU

ESDU 93016 introduces a Fortran program that implements the method of ESDU 90006 but modified to take into account the residual gain and phase variation effects of modes whose resonant frequencies lie outside the range of analysis. The system is modeled as a set of lightly-damped coupled second order differential equations with constant coefficients; the response determined from those equations is equivalent to the sum of the responses of a related set of single degree-of-freedom systems. The program requires initial estimates of the resonant frequency of each response mode together with an associated frequency range and they are obtained from a visual inspection of the Nyquist or Bode diagram of the measurement data. From those initial values, the program determines the damping ratio of the modes. These values provide a starting point for a nonlinear parameter estimation procedure using a Newton-Gauss algorithm from which the mode characteristics that satisfy the complete measurement data are found. The program will handle up to 3000 measurement points and nine separate response modes. Examples illustrate the use of the program for systems with two and four degrees-of-freedom, and show clearly the input format required and the output provided. The program is available on disc (uncompiled) in the software volume as ESDUpac A9316. ESDU

N94-28356# Helsinki Univ. of Technology, Espoo (Finland). Dept. of Computer Science.
ACTORSTUDIO: AN INTERACTIVE USER INTERFACE EDITOR
Marja-Riitta Koivunen, Ora Lassila, Juha Ahvo, Minna Rankinen, Sirpa Riihiaho, and Bodil Riihinen 1993 13 p
(PB94-132859; TKO-B103) Avail: CASI HC A03/MF A01

ActorStudio is a graphical, interactive user interface editor targeted for creating application specific interaction techniques. These techniques can be defined on different abstraction levels. ActorStudio offers components that define the basic and the reactive appearances, and the behavior of the user interface. The components in turn can be joined into sophisticated hierarchies describing complicated user interfaces. As result from editing actions, ActorStudio produces a description of a developed user interface in a language called Screenplay. ActorStudio has been implemented for Macintoshes using Common Lisp and CLOS. It also uses an object oriented toolkit called WimperActors developed in Helsinki University of Technology. NTIS

N94-28377# Technical Research Centre of Finland, Espoo. Lab. of Electrical and Automation Engineering.
OPEN COMMUNICATION IN MANUFACTURING AUTOMATION [AVION TIEDONSIIRTO TUOTANTOAUTOMAATIOSSA]
Arto Visala 1993 128 p In FINNISH
(ISSN 1235-0605)
(PB94-132479; VTT/RN-1471; ISBN-951-38-4365-3) Copyright Avail: CASI HC A07/MF A02

Specific requirements for communication in manufacturing are discussed. The benefits of standardization of communication protocols are analyzed. The guidelines for protocol layering defined in the Open System Interconnection (OSI) reference model of the International Organization for Standardization (ISO) are presented. The historical backgrounds and the status of the Manufacturing Automation Protocol/Technical and Office Protocol (MAP/TOP) and the so-called field bus process are analyzed. Important application layer OSI protocols for manufacturing are discussed: Directory Services, Network Management, File Transfer and Access Management (FTAM) and Manufacturing Message Specification (MMS). The MMS service sets, services and protocol are described. The MAP implementation classes and ISO/IEC (International Electrotechnical Commission) MMS Companion Standards are viewed. The MAP/TOP product markets and installations are analyzed. It is highly probable that the use of OSI/MAP/TOP and particularly MMS products will increase and the market share will grow. NTIS

N94-25666*# Alabama Univ., Huntsville. Dept. of Mechanical Engineering.
SYSTEMATIC PROPULSION OPTIMIZATION TOOLS (SPOT)
Mark Bower and John Celestian *In* USRA, Proceedings of the 8th Annual Summer Conference: NASA/USRA Advanced Design Program 1992 p 3-5 (For primary document see N94-25665 07-80)
Avail: CASI HC A01/MF A04

N94-26289*# SET Group, Denver, CO.
TECHNOLOGY DRIVERS FOR FLIGHT TELEROBOTIC SYSTEM SOFTWARE
Robert Labaugh *In* NASA. Langley Research Center, Selected Topics in Robotics for Space Exploration Dec. 1993 p 223-232 (For primary document see N94-26278 07-12)
Avail: CASI HC A02/MF A03

N94-26714* Jet Propulsion Lab., California Inst. of Tech., Pasadena.
COMPUTING IN SPACE: ISSUES AND ANSWERS
John M. Davidson and Ravishankar K. Iyer (Illinois Univ., Urbana.) *In* CNES, Real-Time Embedded Processing for Space Applications Apr. 1993 p 21-28 (For primary document see N94-26713 07-60)
(Grant NAG1-613)
Copyright Avail: Issuing Activity (CEPADUES-Editions, 111, Rue Nicolas-Vauquelin, 31100 Toulouse, France)

N94-26723* National Aeronautics and Space Administration. Goddard Space Flight Center, Greenbelt, MD.
NASA'S SPACECRAFT DATA SYSTEM
Alan Cudmore and Mark Flanegan *In* CNES, Real-Time Embedded Processing for Space Applications Apr. 1993 p 125-139 (For primary document see N94-26713 07-60)
Copyright Avail: Issuing Activity (CEPADUES-Editions, 111, Rue Nicolas-Vauquelin, 31100 Toulouse, France)

N94-26725 Centre National d'Etudes Spatiales, Toulouse (France). Projet PRONAOS.
PRONAOS FLIGHT SOFTWARE: A REAL-TIME APPLICATION FOR A BALLOONBORNE SCIENTIFIC GONDOLA
Andre Laurens *In its* Real-Time Embedded Processing for Space Applications Apr. 1993 p 153-168 In FRENCH (For primary document see N94-26713 07-60)
Copyright Avail: Issuing Activity (CEPADUES-Editions, 111, Rue Nicolas-Vauquelin, 31100 Toulouse, France)

N94-26726 MATRA Marconi Space (England).
MATRA MARCONI SPACE: THE SILEX ON-BOARD PROCESSOR AND ON-BOARD SOFTWARE
L. T. Daryanani, C. Cantenot (MATRA Marconi Space, Toulouse, France.), and J. P. Roussel (MATRA Marconi Space, Toulouse, France.) *In* CNES, Real-Time Embedded Processing for Space Applications Apr. 1993 p 169-183 (For primary document see N94-26713 07-60)
Copyright Avail: Issuing Activity (CEPADUES-Editions, 111, Rue Nicolas-Vauquelin, 31100 Toulouse, France)

N94-26727 Birmingham Univ. (England). School of Physics and Space Research.
ON-BOARD SOFTWARE FOR THE JET-X TELESCOPE ON THE SPECTRUM-X MISSION
M. D. Bull, C. J. Eyles, and O. Emam *In* CNES, Real-Time Embedded Processing for Space Applications Apr. 1993 p 185-200 Sponsored by Science Research Council (For primary document see N94-26713 07-60)
Copyright Avail: Issuing Activity (CEPADUES-Editions, 111, Rue Nicolas-Vauquelin, 31100 Toulouse, France)

N94-26728 Ecole Centrale de Nantes (France). Lab. d'Automatique.
SCHEDULING TASKS WITH UNPREDICTABLE TIMING PARAMETERS IN HARD REAL-TIME SYSTEMS
Maryline Silly *In* CNES, Real-Time Embedded Processing for Space Applications Apr. 1993 p 203-210 (For primary document see N94-26713 07-60)
Copyright Avail: Issuing Activity (CEPADUES-Editions, 111, Rue Nicolas-Vauquelin, 31100 Toulouse, France)

N94-26729 CR2A, Nanterre (France).
STANDARDIZE Ada HARD REAL-TIME SERVICES?
Dominique L. R. Chandesris, Vincent Celier, and Nasser Kettani *In* CNES, Real-Time Embedded Processing for Space Applications Apr. 1993 p 211-221 (For primary document see N94-26713 07-60)
Copyright Avail: Issuing Activity (CEPADUES-Editions, 111, Rue Nicolas-Vauquelin, 31100 Toulouse, France)

N94-26730 Alsys, Inc., Saint Cloud (France).
Ada MULTIPLE-PROGRAMMING FOR HARD REAL TIME APPLICATIONS IN SPACE SYSTEMS
Marc Richard-Foy *In* CNES, Real-Time Embedded Processing for Space Applications Apr. 1993 p 223-233 In FRENCH (For primary document see N94-26713 07-60)
Copyright Avail: Issuing Activity (CEPADUES-Editions, 111, Rue Nicolas-Vauquelin, 31100 Toulouse, France)

N94-26731 British Aerospace Public Ltd. Co., Stevenage (England). Communication Satellites Div.
IMPLEMENTING HARD REAL-TIME SYSTEMS: A CASE STUDY
C. M. Bailey, A. Burns (York Univ., England.), E. Fyfe, F. Gomez-Molinero (European Space Agency. European Space Research and Technology Center, ESTEC, Noordwijk, Netherlands.), and A. J. Wellings (York Univ., England.) *In* CNES, Real-Time Embedded Processing for Space Applications Apr. 1993 p 235-249 (For primary document see N94-26713 07-60)
(Contract ESTEC-9198/90/NL/SF)
Copyright Avail: Issuing Activity (CEPADUES-Editions, 111, Rue Nicolas-Vauquelin, 31100 Toulouse, France)

N94-26733 Intecs Sistemi S.p.A., Pisa (Italy) Operating System Section.
A REAL-TIME EXECUTIVE IMPLEMENTING PRIORITY INHERITANCE PROTOCOLS
S. Sabina, R. Chiaverini, and C. Migliorini *In* CNES, Real-Time Embedded Processing for Space Applications Apr. 1993 p 261-271 (For primary document see N94-26713 07-60)
Copyright Avail: Issuing Activity (CEPADUES-Editions, 111, Rue Nicolas-Vauquelin, 31100 Toulouse, France)

N94-26734 Vrije Univ., Brussels (Belgium).
SCHEDULING APPROACHES WITH Ada
R. Devillers, D. DeLucca, J. Beaufays (TRASYS Space, Brussels, Belgium.), and E. Snyers (TRASYS Space, Brussels, Belgium.) *In* CNES, Real-Time Embedded Processing for Space Applications Apr. 1993 p 273-283 (For primary document see N94-26713 07-60)
Copyright Avail: Issuing Activity (CEPADUES-Editions, 111, Rue Nicolas-Vauquelin, 31100 Toulouse, France)

N94-26735 Institut Univ. de Technologie, Nantes (France).
FAULT-TOLERANT SCHEDULING IN DISTRIBUTED CRITICAL REAL-TIME SYSTEMS
Houssine Chetto *In* CNES, Real-Time Embedded Processing for Space Applications Apr. 1993 p 285-295 (For primary document see N94-26713 07-60)
Copyright Avail: Issuing Activity (CEPADUES-Editions, 111, Rue Nicolas-Vauquelin, 31100 Toulouse, France)

N94-26737 Centre National d'Etudes Spatiales, Toulouse (France).
TEST OF ONBOARD REAL TIME APPLICATIONS (LICE (TM)) [LE TEST DES APPLICATIONS TEMPS REEL EMBARQUEES (LA METHODE LICE (TM))]
J. L. Carayon *In its* Real-Time Embedded Processing for Space Applications Apr. 1993 p 319-328 In FRENCH (For primary document see N94-26713 07-60)
Copyright Avail: Issuing Activity (CEPADUES-Editions, 111, Rue Nicolas-Vauquelin, 31100 Toulouse, France)

N94-26739 MATRA Marconi Space, Toulouse (France).
VERIFICATION AND VALIDATION OF THE ON-BOARD SOFTWARE REAL TIME REQUIREMENTS [LA VERIFICATION ET LA VALIDATION DES EXIGENCES TEMPS REEL DU LOGICIEL TEMPS SPATIAL EMBARQUE]
Jean-Louis Dega, Jean Jacques Montiel, and Bruno Vatan *In* CNES, Real-Time Embedded Processing for Space Applications Apr. 1993 p 341-353 In FRENCH (For primary document see N94-26713 07-60)
Copyright Avail: Issuing Activity (CEPADUES-Editions, 111, Rue Nicolas-Vauquelin, 31100 Toulouse, France)

N94-26741 Dornier System G.m.b.H., Friedrichshafen (Germany).
DEVELOPING WITH Ada USING HOOD DESIGN METHODOLOGY
K. Baeuerle, U. Denskat, and J. Garbers *In* CNES, Real-Time Embedded Processing for Space Applications Apr. 1993 p 369-379 (For primary document see N94-26713 07-60)
Copyright Avail: Issuing Activity (CEPADUES-Editions, 111, Rue Nicolas-Vauquelin, 31100 Toulouse, France)

N94-26742 Sextant Avionique, Velizy-Villacoublay (France).
USE OF HOOD COUPLED TO REAL TIME MONITORS [UTILISATION DE HOOD COUPLEE A DES MONITEURS TEMPS REEL]
Thierry Gohon and Philippe Guedou *In* CNES, Real-Time Embedded Processing for Space Applications Apr. 1993 p 381-398 In FRENCH (For primary document see N94-26713 07-60)
Copyright Avail: Issuing Activity (CEPADUES-Editions, 111, Rue Nicolas-Vauquelin, 31100 Toulouse, France)

N94-26743 THARSYS (France).
Ada REUSABLE SOFTWARE FOR SATELLITE ON-BOARD DATA HANDLING
P. Tarabbia *In* CNES, Real-Time Embedded Processing for Space Applications Apr. 1993 p 399-407 (For primary document see N94-26713 07-60)
Copyright Avail: Issuing Activity (CEPADUES-Editions, 111, Rue Nicolas-Vauquelin, 31100 Toulouse, France)

N94-26744 Centre National d'Etudes Spatiales, Toulouse (France).
THE CODE-TOP (CONCURRENT SYSTEM DEVELOPMENT USING TRANSFORMATIONS OF PREDICATE-TRANSITION NETS) METHOD: EXAMPLES OF USING IT FOR SYSTEM ARCHITECTURE SPECIFICATION, SOFTWARE SPECIFICATION, AND CODE GENERATION
Patrick deBondeli *In its* Real-Time Embedded Processing for Space Applications Apr. 1993 p 409-427 (For primary document see N94-26713 07-60)
Copyright Avail: Issuing Activity (CEPADUES-Editions, 111, Rue Nicolas-Vauquelin, 31100 Toulouse, France)

N94-27192# Technische Univ., Eindhoven (Netherlands). Faculty of Electrical Engineering.
DALIA: A LANGUAGE FOR THE DESCRIPTION AND ANALYSIS OF DIGITAL SYSTEMS
Henk vanderWeij *In its* Proceedings of the 3rd Workshop Computersystems: Research Forum on Design, Realization and Use of Computersystems 1991 p 1-16 (For primary document see N94-27191 07-60)
Avail: CASI HC A03/MF A01

N94-27196# Technische Univ., Delft (Netherlands). Dept. of Electrical Engineering.
EFFICIENT IMPLEMENTATION OF HIGH-LEVEL PARALLEL SYMBOLIC LANGUAGES
Mark Korsloot (Oregon Univ., Portland.) and E. Tick *In* Technische Univ., Proceedings of the 3rd Workshop Computersystems: Research Forum on Design, Realization and Use of Computersystems 1991 p 51-69 (For primary document see N94-27191 07-60)
Avail: CASI HC A03/MF A01

N94-27295*# Princeton Univ., NJ. Lab. for Control and Automation.
DESIGNING ROBUST CONTROL LAWS USING GENETIC ALGORITHMS
Chris Marrison *In* NASA. Langley Research Center, FAA/NASA Joint University Program for Air Transportation Research, 1992-1993 Feb. 1994 p 99-109 (For primary document see N94-27284 07-01)
Avail: CASI HC A03/MF A02

N94-27364*# Bradford Univ. (England).
PARALLEL ALGORITHM FOR DOMINANT POINTS CORRESPONDENCES IN ROBOT BINOCULAR STEREO VISION
A. Al-Tammami and B. Singh *In* NASA. Lewis Research Center, Vision 21: Interdisciplinary Science and Engineering in the Era of Cyberspace Dec. 1993 p 71-81 (For primary document see N94-27358 07-12)
Avail: CASI HC A03/MF A03

N94-27906*# Moravian Coll., Bethlehem, PA. Dept. of Computer Science.
LOCATING TIE-POINTS ON A GRID
Jim Green *In* Old Dominion Univ., The 1993 NASA-ODU American Society for Engineering Education (ASEE) Summer Faculty Fellowship Program Dec. 1993 p 104-108 (For primary document see N94-27893 07-80)
Avail: CASI HC A01/MF A03

N94-27916*# Tuskegee Inst., AL. Dept. of Computer Science.
REVIEW AND ANALYSIS OF DENSE LINEAR SYSTEM SOLVER PACKAGE FOR DISTRIBUTED MEMORY MACHINES
H. N. Narang *In* Old Dominion Univ., The 1993 NASA-ODU American Society for Engineering Education (ASEE) Summer Faculty Fellowship Program Dec. 1993 p 140-145 (For primary document see N94-27893 07-80)
Avail: CASI HC A02/MF A03

N94-27927*# Paul D. Camp Community Coll., Suffolk, VA. Dept. of Computer Information Systems.
ADP ANALYSIS PROJECT FOR THE HUMAN RESOURCES MANAGEMENT DIVISION
Robert L. Tureman, Jr. *In* Old Dominion Univ., The 1993 NASA-ODU American Society for Engineering Education (ASEE) Summer Faculty Fellowship Program Dec. 1993 p 190-191 (For primary document see N94-27893 07-80)
Avail: CASI HC A01/MF A03

N94-28253*# Allied-Signal Corp., Morristown, NJ. Technical Services.
IMAGE COMPRESSION SOFTWARE FOR THE SOHO LASCO AND EIT EXPERIMENTS
Mitchell R. Grunes, Russell A. Howard (Naval Research Lab., Washington, DC.), Karl Hoppel (Naval Research Lab., Washington, DC.), Stephen A. Mango (Naval Research Lab., Washington, DC.), and Dennis Wang (Interferometrics, Inc., Greenbelt, MD.) *In* NASA. Goddard Space Flight Center, The 1994 Space and Earth Science Data Compression Workshop Apr. 1994 p 11-22 (For primary document see N94-28251 07-59)
Avail: CASI HC A03/MF A02

N94-28254*# Technische Univ., Aachen (Germany).
COMPARISON OF THE LOSSY IMAGE DATA COMPRESSIONS FOR THE MESUR PATHFINDER AND FOR THE HUYGENS TITAN PROBE
P. Rueffer, F. Rabe, F. Gliem, and H.-U. Keller (Max-Planck-Inst. fuer Aeronomie, Katlenburg-Lindau, Germany.) *In* NASA. Goddard Space Flight Center, The 1994 Space and Earth Science Data Compression Workshop Apr. 1994 p 23-30 (For primary document see N94-28251 07-59)
Avail: CASI HC A02/MF A02

N94-28255*# Jet Propulsion Lab., California Inst. of Tech., Pasadena.
ADVANCED END-TO-END SIMULATION FOR ON-BOARD PROCESSING (AESOP)
Alan S. Mazer *In* NASA. Goddard Space Flight Center, The 1994 Space and Earth Science Data Compression Workshop Apr. 1994 p 31-41 (For primary document see N94-28251 07-59)
Avail: CASI HC A03/MF A02

N94-28256*# Naval Postgraduate School, Monterey, CA. Dept. of Electrical and Computer Engineering.
PERFORMANCE CONSIDERATIONS FOR THE APPLICATION OF THE LOSSLESS BROWSE AND RESIDUAL MODEL
Walter D. Abbott, III, Robert T. Kay, and Ron J. Pieper *In* NASA. Goddard Space Flight Center, The 1994 Space and Earth Science Data Compression Workshop Apr. 1994 p 43-54 (For primary document see N94-28251 07-59)
Avail: CASI HC A03/MF A02

N94-28257*# University of North Texas, Denton. Dept. of Computer Sciences.
IMAGE QUALITY MEASURES AND THEIR PERFORMANCE
Ahmet M. Eskicioglu, Paul S. Fisher, and Si-Yuan Chen *In* NASA. Goddard Space Flight Center, The 1994 Space and Earth Science Data Compression Workshop Apr. 1994 p 55-67 (For primary document see N94-28251 07-59)
Avail: CASI HC A03/MF A02

N94-28258*# Hughes Research Labs., Malibu, CA.
A COMPARISON OF SPECTRAL DECORRELATION TECHNIQUES AND PERFORMANCE EVALUATION METRICS FOR A WAVELET-BASED, MULTISPECTRAL DATA COMPRESSION ALGORITHM
Roy M. Matic and Judith I. Mosley (Santa Barbara Research Center, Goleta, CA.) *In* NASA. Goddard Space Flight Center, The 1994 Space and Earth Science Data Compression Workshop Apr. 1994 p 69-80 (For primary document see N94-28251 07-59)
Avail: CASI HC A03/MF A02

N94-28259*# Centre National d'Etudes Spatiales, Toulouse (France).
A COMPARATIVE STUDY OF SAR DATA COMPRESSION SCHEMES
C. Lambert-Nebout, O. Besson (Ecole Nationale Superieure d'Ingenieurs de Constructions Aeronautiques, Toulouse, France.), D. Massonnet, and B. Rogron *In* NASA. Goddard Space Flight Center, The 1994 Space and Earth Science Data Compression Workshop Apr. 1994 p 81-91 (For primary document see N94-28251 07-59)
Avail: CASI HC A03/MF A02

N94-28260*# Environmental Research Inst. of Michigan, Ann Arbor.
PERCEPTUAL COMPRESSION OF MAGNITUDE-DETECTED SYNTHETIC APERTURE RADAR IMAGERY
John D. Gorman and Susan A. Werness *In* NASA. Goddard Space Flight Center, The 1994 Space and Earth Science Data Compression Workshop Apr. 1994 p 93-103 (For primary document see N94-28251 07-59)
Avail: CASI HC A03/MF A02

N94-28261*# David Sarnoff Research Center, Princeton, NJ.
COMPRESSION OF MULTISPECTRAL LANDSAT IMAGERY USING THE EMBEDDED ZEROTREE WAVELET (EZW) ALGORITHM
Jerome M. Shapiro, Stephen A. Martucci, and Martin Czigler *In* NASA. Goddard Space Flight Center, The 1994 Space and Earth Science Data Compression Workshop Apr. 1994 p 105-113 (For primary document see N94-28251 07-59)
Avail: CASI HC A02/MF A02

N94-28262*# Environmental Research Inst. of Michigan, Ann Arbor.
VECTOR QUANTIZER DESIGNS FOR JOINT COMPRESSION AND TERRAIN CATEGORIZATION OF MULTISPECTRAL IMAGERY
John D. Gorman and Daniel F. Lyons (Mitre Corp., McLean, VA.) *In* NASA. Goddard Space Flight Center, The 1994 Space and Earth Science Data Compression Workshop Apr. 1994 p 115-121 (For primary document see N94-28251 07-59)
Avail: CASI HC A02/MF A02

N94-28263*# TRW Systems Group, Redondo Beach, CA. Data Technologies Div.
WAVELET COMPRESSION TECHNIQUES FOR HYPERSPECTRAL DATA
Bruce Evans, Brian Ringer, and Mathew Yeates *In* NASA. Goddard Space Flight Center, The 1994 Space and Earth Science Data Compression Workshop Apr. 1994 p 123-133 (For primary document see N94-28251

07-59)
Avail: CASI HC A03/MF A02

N94-28264*# Martin Marietta Astro Space, Princeton, NJ.
SOME PRACTICAL ASPECTS OF LOSSLESS AND NEARLY-LOSSLESS COMPRESSION OF AVHRR IMAGERY
David B. Hogan, Chris X. Miller, Than Lee Christensen, and Raj Moorti *In* NASA. Goddard Space Flight Center, The 1994 Space and Earth Science Data Compression Workshop Apr. 1994 p 135-142 (For primary document see N94-28251 07-59)
Avail: CASI HC A02/MF A02

62 COMPUTER SYSTEMS

Includes computer networks and special application computer systems.

N94-25786# Syracuse Univ., NY.
PARALLEL ASSESSMENT WINDOW SYSTEM (PAWS) ENHANCEMENTS Final Technical Report
Daniel J. Pease Oct. 1993 49 p
(Contract F30602-91-D-0001)
(AD-A274094; RL-TR-93-200) Avail: CASI HC A03/MF A01

This final technical report documents work conducted under the Expert Engineering and Science Program (ES&E) entitled Parallel Architecture Assessment Tool. This report contains a summary of the activities conducted under this effort which included the enhancement of the Parallel Assessment Window System (PAWS). PAWS is an experimental system for performing machine evaluation and comparisons of parallel architecture computers against programmed algorithms. This report provides a comprehensive users manual for the PAWS tool. DTIC

N94-25802# Argonne National Lab., IL.
USING A TRANSFER FUNCTION TO DESCRIBE THE LOAD-BALANCING PROBLEM
A. J. Conley Nov. 1993 5 p
(Contract W-31-109-eng-38)
(DE94-004218; ANL-93/40) Avail: CASI HC A01/MF A01

The dynamic load-balancing problem for mesh-connected parallel computers can be clearly described by introducing a function that identifies how much work is to be transmitted between neighboring processors. This function is a solution to an elliptic problem for which a wealth of knowledge exists. The nonuniqueness of the solution to the load-balancing problem is made explicit. DOE

N94-25860# Air Force Inst. of Tech., Wright-Patterson AFB, OH. School of Engineering.
A NUMERICAL STUDY OF HIGH-SPEED MISSILE CONFIGURATIONS USING A BLOCK-STRUCTURED PARALLEL ALGORITHM M.S. Thesis
Douglas C. Blake Dec. 1993 119 p
(AD-A273776; AFIT/GAE/ENY/93D-4) Avail: CASI HC A06/MF A02

A numerical analysis of the aerodynamic phenomena associated with the high speed flight of a sharp-nosed, four-finned, high fineness ratio missile using a block-structured, parallel computer algorithm is presented. The algorithm, PANS-3EM, utilizes a second order accurate, shock-capturing, total variation diminishing scheme and incorporates a Baldwin-Lomax turbulence model. PANS-3EM allows for extreme flexibility in the choice of computational domain decomposition and computing machine of implementation. Developmental work consists of conceptualization and verification of the algorithm as well as parallel performance and scalability studies conducted on a variety of computing platforms. Using PANS-3EM, the aerodynamic characteristics of the missile are investigated. Drag and pitching moment coefficients are computed and compared against experimental flight data. Trends in the numerical data agree with experimental results with the exception that an unexpected reversal of the stability characteristics exhibited by the missile at speeds in excess of Mach 3.75 are not confirmed by the computer code. DTIC

N94-25906# Air Force Inst. of Tech., Wright-Patterson AFB, OH. School of Engineering.
OBJECT-ORIENTED DESIGN AND IMPLEMENTATION OF A PARALLEL Ada SIMULATION SYSTEM M.S. Thesis
James T. Belford Nov. 1993 113 p
(AD-A274119; AFIT/GCE/Eng/93D-01) Avail: CASI HC A06/MF A02

Simulations which model the behavior 'real world' entities are often large and complex, and require frequent changes to the configuration. This research effort examines the benefits of using object-oriented techniques to develop a distributed simulation environment which supports modularity, modifiability, and portability. The components of the Parallel Discrete Event Simulation (PDES) environment are identified and modeled using the Rumbaugh modeling technique. From the model, a prototype implementation of a Parallel Ada Simulation Environment (PASE) is accomplished using Classic Ada. A system interface for the Intel ipsc/2 Hypercube was developed to illustrate the concepts of modularity and portability. In addition, the prototype environment uses a filter which implements the basic Chandy-Misra time synchronization protocol. Finally, to test the correct operation of the environment, a simple battlefield application model is developed. PASE is tested in the sequential mode on both a Sun Sparc station and the Hypercube. The ability to distribute across n-nodes is demonstrated using various configurations on the Hypercube. The parallel test demonstrates the ability for objects on separate processors to interact with each other by passing messages, and to execute events generated by remote objects in the proper time stamp order. DTIC

N94-25918 Joint Inst. for Nuclear Research, Dubna (USSR).
USE OF PARALLEL COUNTERS FOR TRIGGERING
N. M. Nikityuk 1991 23 p Limited Reproducibility: More than 20% of this document may be affected by microfiche quality
(DE93-616656; JINR-E-10-91-567) Avail: CASI HC A03 (US Sales Only)

Results of investigation of using parallel counters, majority coincidence schemes, parallel compressors for triggering in multichannel high energy spectrometers are described. Concrete examples of methods of constructing fast and economic new devices used to determine multiplicity hits t greater than 900 registered in a hodoscopic plane and a pixel detector are given. For this purpose the author uses the syndrome coding method and cellular arrays. In addition, an effective coding matrix has been created which can be used for light signal coding. For example, such signals are supplied from scintillators to photomultipliers. DOE

N94-25952# Sandia National Labs., Albuquerque, NM.
OUT OF CORE, OUT OF MIND: PRACTICAL PARALLEL I/O
D. E. Womble, D. S. Greenberg, R. E. Riesen, and S. R. Wheat 1993 7 p Presented at the Institute of Electrical and Electronic Engineers (IEEE) Meeting on Scalable Parallel Libraries, Starkville, MS, 6-8 Oct. 1993
(Contract DE-AC04-94AL-85000)
(DE94-003107; SAND-93-2595C; CONF-9310220-2) Avail: CASI HC A02/MF A01

Parallel computers are becoming more powerful and more complex in response to the demand for computing power by scientists and engineers. Inevitably, new and more complex I/O systems will be developed for these systems. In particular we believe that the I/O system must provide the programmer with the ability to explicitly manage storage, despite the trend toward complex parallel file systems and caching schemes. One method of doing so is to have a partitioned secondary storage in which each processor owns a logical disk. Along with operating system enhancements which allow overheads such as buffer copying to be avoided and libraries to support optimal remapping of data, this sort of I/O system meets the needs of high performance computing. DOE

N94-25953# Sandia National Labs., Albuquerque, NM.
ACHIEVING HIGH PERFORMANCE ON THE INTEL PARAGON
D. S. Greenberg, B. Maccabe, R. Riesen, S. Wheat, and D. Womble 1993 6 p Presented at the Intel Super Computer Users Group Meeting, St. Louis, MO, 4 Oct. 1993
(Contract DE-AC04-94AL-85000)
(DE94-003108; SAND-93-2597C; CONF-9310232-1) Avail: CASI HC A02/MF A01

When presented with a new supercomputer most users will first ask 'How much faster will my applications run?' and then add a fearful 'How much effort will it take me to convert to the new machine?' This paper describes some lessons learned at Sandia while asking these questions about the new 1800+ node Intel Paragon. The authors conclude that the operating system is crucial to both achieving high performance and allowing easy conversion from previous parallel implementations to a new machine. Using the Sandia/UNM Operating System (SUNMOS) they were able to port a LU factorization of dense matrices from the nCUBE2 to the Paragon and achieve 92% scaled speed-up on 1024 nodes. Thus on a 44,000 by 44,000 matrix which had required over 10 hours on the previous machine, they completed in less than 1/2 hour at a rate of over 40 GFLOPS. Two keys to achieving such high performance were the small size of SUNMOS (less than 256 kbytes) and the ability to send large messages with very low overhead. DOE

N94-25984# Superconducting Super Collider Lab., Dallas, TX.
REAL-TIME TRACKING WITH A 3D-FLOW PROCESSOR ARRAY
D. Crosetto Jun. 1993 5 p Presented at the Workshop on B Physics At Hadron Colliders, Snowmass, CO, 21 Jun. - 2 Jul. 1993 Submitted for publication
(Contract DE-AC35-89ER-40486)
(DE94-003981; SSCL-Preprint-516; CONF-9306258-14) Avail: CASI HC A01/MF A01

The problem of real-time track-finding was performed to date with CAM (Content Addressable Memories) or with fast coincidence logic, because the processing scheme was thought to have much slower performance. Advances in technology together with a new architectural approach make it feasible to also explore the computing technique for real-time track finding thus giving the advantages of implementing algorithms that can find more parameters such as calculate the sagitta, curvature, pt, etc., with respect to the CAM approach. Real-time track finding using new computing approach technique based on the 3D-Flow array processor system was described. This system consists of a fixed interconnection architecture scheme, allowing flexible algorithm implementation on a scalable platform. The 3D-Flow parallel processing system for track finding is scalable in size and performance by either increasing the number of processors, or increasing the speed or else the number of pipelined stages. The conceptual idea and the design stage of the project are described. DOE

N94-26009# Wright Lab., Wright-Patterson AFB, OH.
A VHDL REGISTER TRANSFER LEVEL MODEL OF THE LINEAR TOKEN PASSING MULTIPLEX DATA BUS PROTOCOL FOR THE HIGH SPEED DATA BUS Interim Report, 1 Jun. 1992 - 15 Jul. 1993
Jerry A. Myers Sep. 1993 74 p
(AF Proj. 2003)
(AD-A273734; WL-TR-93-1125) Avail: CASI HC A04/MF A01

The research project abstract presented will describe the design process to develop a partial simulatable specification model written in VHDL at the register transfer level to describe the linear token passing multiplex data bus protocol ('PROTOCOL') specification. The PROTOCOL is a distributed token passing computer protocol which operates over a dual redundant bus. The PROTOCOL is used as the communications standard to implement the high speed data bus (HSDB) module specification. The PROTOCOL and HSDB specifications are two of the pave pillar avionics architecture bus specifications being developed for the F-22, LHX, and future military aircraft. While this model does not implement the entire HSDB protocol specification, it does implement enough of the referenced specifications to give credence to the concept of hardware simulation modeling of avionics specifications. This concept is applicable for both military and commercial applications written in the VHDL language at a specification level of detail. DTIC

N94-26120# Los Alamos National Lab., NM.
RUN-TIME RECOGNITION OF TASK PARALLELISM WITHIN THE P++ PARALLEL ARRAY CLASS LIBRARY
R. Parsons and D. Quinlan 1993 11 p Presented at the Institute of Electrical and Electronic Engineers (IEEE) Meeting on Scalable Parallel Libraries, Starkville, MS, 6-8 Oct. 1993
(Contract W-7405-eng-36)
(DE94-002707; LA-UR-93-3856; CONF-9310220-1) Avail: CASI HC A03/MF A01

The use of a run-time system to recognize task parallelism with a C++ array class library was explored. Run-time systems currently support data parallelism in P++, FORTRAN 90 D, and High Performance FORTRAN. But data parallelism is insufficient for many applications, including adaptive mesh refinement. Without access to both data and task parallelism, such applications exhibit several orders of magnitude more message passing and poor performance. A C++ array class library is used to implement deferred evaluation and run-time dependence for task parallelism recognition, to obtain task parallelism through a data flow interpretation of data parallel array statements. Performance results show that analysis and optimizations are both efficient and practical, allowing us to consider more substantial optimizations. DOE

N94-26473 Sandia National Labs., Albuquerque, NM.
A DOUBLY LOGARITHMIC COMMUNICATION ALGORITHM FOR THE COMPLETELY CONNECTED OPTICAL COMMUNICATION PARALLEL COMPUTER
L. A. Goldberg, M. Jerrum (Edinburgh Univ., Scotland.), T. Leighton (Massachusetts Inst. of Tech., Cambridge.), and S. Rao (NEC Research Inst., Princeton, NJ.) 20 Jan. 1993 19 p Presented at the 5th Annual Association for Computing Machinery on Parallel Algorithms and Architectures, Velen, Germany Limited Reproducibility: More than 20% of this document may be affected by poor print
(Contract DE-AC04-76DP-00789)
(DE93-019408; SAND-93-0205C; CONF-9306220-1) Avail: Issuing Activity (Department of Energy (DOE))

In this paper we consider the problem of interprocessor communication on a Completely Connected Optical Communication Parallel Computer (OCPC). The problem in question is that of realizing an h-relation. In this problem, each processor has at most h messages to send and at most h messages to receive. It is clear that any 1-relation can be realized in one communication step on an OCPC. However, the best known p-processor OCPC algorithm for realizing an arbitrary h-relation for h greater than 1 requires theta(h + log p) expected communication steps. The algorithm is optimal only for h = omega(log p) and it is an open question as to whether or not there is a faster algorithm for h = o(log p). In this paper we answer this question in the affirmative by presenting a theta(h + log log p) communication step algorithm that realizes an arbitrary h-relation on a p-processor OCPC. We show that if h is less than or equal to (log p), then the failure probability can be made as small as p(sup -(alpha)) for any positive constant alpha. DOE

N94-26635 Carleton Univ., Ottawa (Ontario). School of Computer Science.
PARALLEL COMPUTATIONAL GEOMETRY ON ANALOG HOPFIELD NETWORKS M.S. Thesis
Natana Valiveti 23 Nov. 1992 140 p
(ISBN-0-315-84093-5; CTN-94-61051) Copyright Avail: Micromedia Ltd., Technical Information Centre, 240 Catherine Street, Suite 305, Ottawa, Ontario, K2P 2G8, Canada HC/MF

A novel approach to solving computational geometry problems in parallel is presented, using analog Hopfield neural networks. The use of massively parallel analog networks requires a radically different approach to geometric problem solving because time is continuous and geometric data are represented by analog components. Analog network algorithms are presented for the following geometrical problems: minimum weight triangulation of planar point sets or of polygons with holes; finding the smallest E so that two given point sets are E-congruent via translation; and partition of a set of points into K clusters such that the maximum diameter of the clusters is minimized. An improvement is also given to Hopfield's solution for the Euclidean travelling salesman problem. For each network, the network's parameters are analyzed in detail and it is proven that the networks indeed produce feasible solutions. Experimental results demonstrate the performance of the analog Hopfield neural networks. CISTI

N94-26674 Carleton Univ., Ottawa (Ontario). Dept. of Electronics.
DESIGN AND IMPLEMENTATION OF A MULTIPROCESSOR FOR DSP AND COMMUNICATIONS SYSTEMS ALGORITHM EVALUATION M.S. Thesis
George Nicolas Yaremchuk May 1993 110 p
(ISBN-0-315-84128-1; CTN-94-61060) Copyright Avail: Micromedia Ltd., Technical Information Centre, 240 Catherine Street, Suite 305, Ottawa, Ontario, K2P 2G8, Canada HC/MF

It is proposed to create a test bed to ease algorithm and hardware development tasks. The advances in very large scale integration have created a situation in which complex signal processing algorithms are considered even for high speed, high computational complexity applications. For these applications for which only an incomplete analytical performance evaluation can be made, the problem of signal processing algorithm verification becomes a bottleneck in both research and development stages. A programmable hardware algorithm evaluation system capable of operating at or near real-time for the data rates of interest is required. A multiprocessor system based on a slotted ring bus communication scheme has been adopted as a compromise between interconnection bus complexity and bus transfer efficiency. A review of selected digital signal processing (DSP) system algorithms has been used to verify the design choices. The hardware has been implemented on the TMS320C30 microprocessor and tested, and benchmark results are given. The test bed discussed can serve for testing complex DSP algorithms. The speedup in evaluation time creates for the user a nearly final-product testing situation, providing results at or near real time. Author (CISTI)

N94-26903 Bhabha Atomic Research Centre, Bombay (India).
A MULTITRANSPUTER PARALLEL PROCESSING SYSTEM (MTPPS)
A. K. Jethra, S. S. Pande, S. P. Borkar, A. N. Khare, M. D. Ghodgaonkar, and B. R. Bairi 1993 69 p Limited Reproducibility: More than 20% of this document may be affected by microfiche quality
(DE94-604652; BARC-1993/E/009) Avail: CASI HC A04 (US Sales Only)

This report describes the design and implementation of a 16 node multitransputer parallel processing system (MTPPS) which is a platform for parallel program development. It is a MIMD machine based on message passing paradigm. The basic compute engine is an Inmos Transputer Ims T800-20. Transputer with local memory constitutes the processing element (node) of this MIMD architecture. Multiple nodes can be connected to each other in an identifiable network topology through the high speed serial links of the transputer. A network configuration unit (NCU) incorporates the necessary hardware to provide software controlled network configuration. System is modularly expandable and more nodes can be added to the system to achieve the required processing power. The system is back-end to the IBM-PC which has been integrated into the system to provide user I/O interface. PC resources are available to the programmer. Interface hardware between the PC and the network of transputers is INMOS compatible. Therefore, all the commercially available development software compatible to INMOS products can run on this system. While giving the details of design and implementation, this report briefly summarizes MIMD architectures, transputer architecture, and parallel processing software development issues. LINPACK performance evaluation of the system and solutions of neutron physics and plasma physics problem have been discussed along with results. DOE

N94-26998# Technische Univ., Twente (Netherlands). Dept. of Computer Science.
PARSING SCHEMATA: A FRAMEWORK FOR PARALLEL AND SEQUENTIAL PARSING
Klaas Sikkel May 1993 103 p See also PB93-211118
(PB94-125267; Memo-INF-93-28) Avail: CASI HC A06/MF A02

A parsing schema is an abstract specification of a parser. It can be seen as a generalization of a chart parser for context-free languages. A parsing system for a particular grammar and string is a logical deduction system. It consists of a domain of items, an initial set of items, and rules that allow one to deduce new items from already known ones. A parsing schema yields a parsing system for any given grammar and input string. Two types of operations on parsing schemata are treated extensively. A schema can be refined into another schema by making smaller deduction steps and storing the intermediate results. A schema can be filtered by discarding items and deduction steps that cannot contribute to the construction of a valid parse. Filtering is particularly useful for sequential implementations. This paper has a dual purpose. On the one hand, the theoretical foundations of parsing schemata and relations between schemata are worked out. On the other hand, by giving a range of nontrivial examples, we show that the approach can successfully be used to define, compare, and improve practical parsers. NTIS

N94-27070# Air Force Inst. of Tech., Wright-Patterson AFB, OH. School of Engineering.
INTERACTIVE CONTROL OF A PARALLEL SIMULATION FROM A REMOTE GRAPHICS WORKSTATION M.S. Thesis
Douglas C. Looney 14 Dec. 1993 82 p
(AD-A274217; AFIT/GCE/Eng/93D-9) Avail: CASI HC A05/MF A01

Modern military commanders are faced with an overwhelming amount of intelligence data concerning the disposition of engaging forces. The sheer volume of data produced for a single planning scenario is an obstacle to the user as well as the computer. Today's commander requires a real-time, three-dimensional representation of the battlefield in order to assimilate the data for the management of a conflict. Parallel computation is required to complete the processing of this information in a timely manner. The improvement of user interaction through graphical representation of a parallel simulation is the purpose of this study. The requirements for the user's control commands and the effect of these requirements upon the entire system are developed and demonstrated. This research provides an increased capability to assist in battlefield management and critical decision making processes. DTIC

N94-27092# Lawrence Livermore National Lab., CA.
IMPLEMENTATION AND PERFORMANCE OF A DOMAIN DECOMPOSITION ALGORITHM IN SISAL
T. DeBoni, J. Feo, G. Rodrigue (California Univ., Livermore.), and J. Muller (State Univ. of New York, Stony Brook.) 23 Sep. 1993 12 p Presented at the 27th Hawaii International Conference on System Sciences, Maui, HI, 4-7 Jan. 1994
(Contract W-7405-eng-48)
(DE94-002012; UCRL-JC-115029; CONF-940136-3) Avail: CASI HC A03/MF A01

Sisal is a general-purpose functional language that hides the complexity of parallel processing, expedites parallel program development, and guarantees determinacy. Parallelism and management of concurrent tasks are realized automatically by the compiler and runtime system. Spatial domain decomposition is a widely-used method that focuses computational resources on the most active, or important, areas of a domain. Many complex programming issues are introduced in paralleling this method including the following: dynamic spatial refinement, dynamic grid partitioning and fusion, task distribution, data distribution, and load balancing. In this paper, we describe a spatial domain decomposition algorithm programmed in Sisal. We explain the compilation process, and present the execution performance of the resultant code on two different multiprocessor systems: a multiprocessor vector supercomputer, and cache-coherent scalar multiprocessor. DOE

N94-27100# Rome Lab., Griffiss AFB, NY.
STATIC TASK ALLOCATION FOR PARALLEL PROCESSING SYSTEMS DURING SOFTWARE DEVELOPMENT Report, Jul. 1992 - Apr. 1993
Richard C. Metzger, John K. Antonio, and Loretta S. Auvil Sep. 1993 39 p
(AD-A274204; RL-TR-93-158) Avail: CASI HC A03/MF A01

In the sequential world, the mapping of processes to a computer system was not a problem because of the classic Von Newman architecture. However, in the parallel world, the mapping of processes to nodes and the balancing of the load on each node becomes an issue that needs to be addressed. This problem enters software development in the implementation phase and remains an issue through the testing and system integration phases. This report describes a new method developed to improve the mapping on a hypercube system. This new hypersphere mapping approach performs an optimal mapping based on the geometry of the physical system and the communication patterns of the processes. The hypersphere mapper can map processes to nodes where the number of processes exceeds the number of nodes. Other mapping approaches rely on heuristics to cluster the communication graphs into subgraphs to accomplish this mapping. The hypersphere mapper can be instrumental in the implementation phase of software development by specifying an optimal mapping that will improve the performance of the system. This method also provides a transparent programming environment, where the programmer does not need to know about the interconnection network of the physical computer system. The hypersphere mapper was tested using simulated directed and undirected random communication graphs. DTIC

N94-27117# Carnegie-Mellon Univ., Pittsburgh, PA. Dept. of Computer Science.
AUTOMATIC MAPPING OF TASK AND DATA PARALLEL PROGRAMS FOR EFFICIENT EXECUTION ON MULTICOMPUTERS
Jaspal Subhlok Nov. 1993 17 p
(Contract MDA972-90-C-0035; ARPA Order 7330)
(AD-A274125; CMU-CS-93-212) Avail: CASI HC A03/MF A01

For a wide variety of applications, both task and data parallelism must be exploited to achieve the best possible performance on a multicomputer. Recent research has underlined the importance of exploiting task and data parallelism in a single complier framework, and such a complier can map a single source program in many different ways onto a parallel machine. There are several complex trade offs between task and data parallelism, depending on the characteristics of the program to be executed and the performance parameters of the target parallel machine. This makes it very difficult for a programmer to select a good mapping for a task and data parallel program. In this paper we isolate and examine specific characteristics of executing programs that determine the performance for different mappings on a parallel machine, and present an automatic system to obtain good mappings. The process consists of two steps: First, an instrumented input program is executed a fixed number of times with different mappings, to build an execution model of the program. Next, the model is analyzed to obtain a good final mapping of the program on to the processors of the parallel machine. DTIC

N94-27123# Air Force Inst. of Tech., Wright-Patterson AFB, OH. School of Engineering.
DESIGN OF A PARALLEL DISCRETE EVENT SIMULATION COPROCESSOR M.S. Thesis
Jacob L. Berlin Dec. 1993 132 p
(AD-A274135; AFIT/GCS/Eng/93D-02) Avail: CASI HC A07/MF A02

A Parallel Discrete Event Simulation Coprocessor was designed to off-load the synchronization overhead from the processors executing the application. In a multiprocessor architecture, one coprocessor executes the synchronization routines for each host processor. Speedup can be achieved when the host processor executes the application and the coprocessor concurrently executes synchronization routines. The coprocessor uses a programmable microcode control store to guarantee flexibility in the synchronization routines. The coprocessor uses an Extreme Search Associative Memory to support fast Next Event Queue (NEQ) management. This associative memory uses bit-serial word-parallel search logic to provide 0(1) insert and retrieval time of events in the NEQ. The coprocessor was completely described in the VHSIC Hardware Description Language (VHDL), and several components were fabricated and tested. Timing measurements of the fabricated components were back-annotated into the VHDL description to improve model accuracy. Synchronization overhead of a parallel VHDL simulation was measured using the AFIT Algorithm Animation Research Facility, and this data was used for a conceptual performance analysis of the coprocessor. A four-fold speedup was achieved for the NEQ management of the simulation; however, the total speedup was only 1.02 since less than 2% of the application was accelerated. DTIC

N94-27332 Carleton Univ., Ottawa (Ontario). School of Computer Science.
GARBAGE COLLECTION IN A MULTIPROCESSOR SMALLTALK SYSTEM Ph.D. Thesis
John Duimovich 12 Jan. 1989 112 p
(ISBN-0-315-51159-1; CTN-94-60980) Copyright Avail: Micromedia Ltd., Technical Information Centre, 240 Catherine Street, Suite 305, Ottawa, Ontario, K2P 2G8, Canada HC/MF

In modern programming systems, dynamic memory allocation and deallocation is provided through the use of system primitives. The responsibility for the use of these is left wholly up to the programmer. To ease this burden, some systems such as Smalltalk provide automatic storage reclamation mechanisms known as garbage collection. With the increasing attractiveness of multiprocessor systems, projects such as Multiprocessor Smalltalk require high performance multiprocessor garbage collection strategies optimized for the system in question. A multiprocessor garbage collection algorithm is presented for use in Actra, a multiprocessor Smalltalk system. The algorithm uses entry tables to determine interprocessor object reachability. The use of tables reduces interprocessor synchronization requirements, allowing processors to garbage collect independently. This technique differs from other multiprocessor algorithms which require that all processors stop during garbage collection. A prototype of this collector has been implemented and is described. Author (CISTI)

N94-27579# Center for Mathematics and Computer Science, Amsterdam (Netherlands). Dept. of Computer Science/Dept. of Algorithmics and Architecture.
FAST PARALLEL PERMUTATION ALGORITHMS
Joerg Keller Jan. 1993 10 p
(Contract NF-62-376) (ISSN 0169-118X)
(CWI-CS-R9303; ETN-94-95425) Copyright Avail: CASI HC A02/MF A01

The problem of permuting n data items, each covering D global memory cells, on an EREW PRAM with n/(log n) processors and less than Dn additional storage is investigated. A family of algorithms (A(sub k))(sub k), where k = 1, 2, ..., log* n, such that A(sub k) needs time Dlog nlog(sup k)n, is presented. Here, log(sup k)n, denotes k times application of log to n, and log* n = min(k such that log(sup k)n less than or equal to 1). All algorithms need Theta(n) operations, which is optimal. The storage requirements for A(sub k) are n global bits, n/log(sup k - 1)n global memory cells if k is greater than or equal to 2, and Dlog n/log(sup k - 1)n (respectively D) local memory cells per processor if k is greater than or equal to 2 (respectively k = 1). The family A(sub k) hence reveals a time-space tradeoff. The result can be generalized to machines with p less n/log n processors such that the run time is (Dn/p)log(sup k)n, (Dn/p)/log(sup k - 1)n local cells per processor are needed, and the global storage requirements remain as given above. ESA

N94-27600# Pacific Northwest Lab., Richland, WA.
HIGH PERFORMANCE COMPUTING IN CHEMISTRY AND MASSIVELY PARALLEL COMPUTERS: A SIMPLE TRANSITION?
R. A. Kendall Mar. 1993 22 p Presented at the 1993 Sanible Symposia, St. Augustine, FL, 15-19 Mar. 1993
(Contract DE-AC06-76RL-01830)
(DE94-004318; PNL-SA-21769; CONF-9303248-1) Avail: CASI HC A03/MF A01

A review of the various problems facing any software developer targeting massively parallel processing (MPP) systems is presented. Issues specific to computational chemistry application software will be also outlined. Computational chemistry software ported to and designed for the Intel Touchstone Delta Supercomputer will be discussed. Recommendations for future directions will also be made. DOE

N94-27644 Alberta Univ., Edmonton. Dept. of Computing Science.
MIMD PARALLEL APPROACHES TO OBJECT LABELING M.S. Thesis
R. M. Gregorish 1990 103 p
(ISBN-0-315-60198-1; CTN-94-60986) Copyright Avail: Micromedia Ltd., Technical Information Centre, 240 Catherine Street, Suite 305, Ottawa, Ontario, K2P 2G8, Canada HC/MF

Efficient solution of the consistent (unambiguous) labeling problem has applications in fields including image processing, computer vision, graph theory, cryptography, and other areas which can be posed as constraint satisfaction problems. It was shown that the labeling problem is inherently suited to implementation on parallel architectures. It is suggested that the unique aspects of multiple instruction multiple data stream (MIMD) architectures can be exploited for efficient solution of the consistent labeling problem. The behavior of three parallel algorithms for object labeling is investigated. These algorithms attempt to take advantage of the strengths of MIMD architectures. The algorithms are implemented on the Myrias SPS-2 multiprocessor architecture using the Myrias model of parallel computation and the pardo programming construct. An analysis of the behavior of these algorithms and recommendations for their improvement are presented. In addition, a method of ordering the search using characteristics of the problem to eliminate inconsistent labelings early in the search is proposed. This ordering technique has a significant effect on the behavior of labeling algorithms by increasing the effective use of available parallel resources. Author (CISTI)

N94-27649 Carleton Univ., Ottawa (Ontario). Dept. of Electronics.
A FAST FOURIER TRANSFORM RADIX-2 COMPLEX BUTTERFLY WITH BUILT-IN SELF-TEST M.S. Thesis
Wilson W. K. Wong Dec. 1992 74 p

(ISBN-0-315-84139-7; CTN-94-61065) Copyright Avail: Micromedia Ltd., Technical Information Centre, 240 Catherine Street, Suite 305, Ottawa, Ontario, K2P 2G8, Canada HC/MF

A high speed very large scale integration architecture is proposed for computing the radix-2 complex butterfly algorithm. The architecture employs redundant binary arithmetics, parallel pipelining, and Booth's algorithm. A 16-by-12-bit radix-2 complex butterfly was implemented in a 15,000-gate, 180-pin pin-grid-array application specific integrated circuit (ASIC). The ASIC technology is a 1.5-micron complementary metal oxide silicon gate-array. The 20 ASIC prototypes were a first-pass success, and test results show an average complex data sampling rate of 12.3 MHz. Pairs of radix-2 complex butterfly ASIC and the switch ASIC can be grouped to form a high-speed, 49.2 Msamples/sec parallel pipeline fast Fourier transform (FFT) processor of sizes up to 32-point with some external memory integrated circuits. The target application of the high-speed FFT is in the multi-carrier group demodulator of an on-board satellite processor system. The complex butterfly ASIC also was built-in self-test circuitry to assist chip-level and board-level testing. The complex butterfly architecture allows an easy migration path for increasing the data sampling rate to 75 MHz.
Author (CISTI)

N94-27685 Carleton Univ., Ottawa (Ontario). School of Computer Science.
UNIFIED DISTRIBUTED SIMULATION M.S. Thesis
J. McAffer Mar. 1990 93 p
(ISBN-0-315-59019-X; CTN-94-60987) Copyright Avail: Micromedia Ltd., Technical Information Centre, 240 Catherine Street, Suite 305, Ottawa, Ontario, K2P 2G8, Canada HC/MF

A method is proposed for generalizing existing distributed simulation algorithms such as Time Warp and Chandy-Misra to create a unified distributed simulation (UDS) algorithm. Models from different paradigms can be mixed within one simulation, resulting in a more powerful environment for creating complex simulations. It is shown that UDS extends the functionality of the current distributed simulation techniques. UDS allows components to describe how and when they are willing to receive and process messages and as a result gives the user more power and flexibility. Current distributed simulation techniques are presented and contrasted. Computational reflection and speculation are related to the UDS algorithm and the concurrent object oriented programming environment created to support Rival, its implementation, is detailed. Rival is implemented in Smalltalk and uses ideas from computational reflection and actor theory to create a sound and flexible model of concurrency. Author (CISTI)

N94-27713# Sandia National Labs., Albuquerque, NM.
COMMUNICATION ON THE PARAGON
David Greenberg, Barney Maccabe, Kevin S. McCurley, Rolf Riesen, and Stephen Wheat 15 Oct. 1993 8 p Presented at the Intel Super Computer Users Group Meeting, St. Louis, MO, 4 Oct. 1993
(Contract DE-AC04-94AL-85000)
(DE94-003103; SAND-93-2596C; CONF-9310232-2) Avail: CASI HC A02/MF A01

In this note the authors describe the results of some tests of the message-passing performance of the Intel Paragon. These tests have been carried out under both the Intel-supplied OSF/1 operating system with an NX library and also under an operating system called SUNMOS (Sandia UNM Operating System). For comparison with the previous generation of Intel machines, they have also included the results on the Intel Touchstone Delta. The source code used for these tests is identical for all systems. As a result of these tests, the authors can conclude that SUNMOS demonstrates that the Intel Paragon hardware is capable of very high bandwidth communication and that the message coprocessor on Paragon nodes can be used to give quite respectable latencies. Further tuning can be expected to yield even better performance. DOE

N94-27804 National Lab. for High Energy Physics, Tsukuba (Japan).
PROCEEDINGS OF WORKSHOP ON DISTRIBUTED COMPUTING AND NETWORK
F. Abe, ed. and F. Yuasa, ed. Feb. 1993 294 p In ENGLISH and JAPANESE Workshop held in Tsukuba, Japan, 27-28 Feb. 1992 Limited Reproducibility: More than 20% of this document may be affected by microfiche quality
(DE94-701165; KEK-Proc-92-19; CONF-9202194) Avail: CASI HC A13 (US Sales Only)

'Distributed Computing and Network' is a hot topic in the field of computing. Recent progress in the computer technology is providing new paradigm for computing even in High Energy Physics. Particularly the workstation based computer system is opening new active field of computer application to sciences. The major topics discussed in this symposium are distributed computing and wide area research network for domestic and international link. The two days symposium provided enough topics to foresee the next direction of our computing environment. 70 people got together to discuss these interesting themes as well as information exchange on the computer technologies. DOE

N94-28042 NR/NS, Inc., Kanata (Ontario).
PLANNING FOR THE FUTURE OF THE DREnet: THE WAY AHEAD
T. Symchych 31 Mar. 1993 58 p Sponsored by National Defence Headquarters
(NRNS-002-00-001-01; DSIS-94-00165; CTN-94-61120) Avail: CASI HC/04

In the 1970's and 1980's, Canadian Department of National Defense staff from several Defence Research Establishments (DRE's) obtained accounts on computer systems connected to the U.S. Department of Defense ARPANET. The favorable experiences gained resulted in requests to provide similar technology within Canada. An experimental network was established at the Communications Research Centre Ottawa to address this need, and this network evolved into the current DREnet, which connects over 20 sites through a central gateway at DRE Ottawa. DREnet is now used as a testbed for examination of new services and technologies available in the Internet world. Work was carried out in message handling, directory services, application and network level protocols, and audio/video services. Information is given on where the DREnet resides in the international research network community, the defense research community, and the national research network community. Various issues that must be addressed by the DREnet community in planning for the future are discussed, including DREnet's relations with Internet, standards, resource sharing, security, new transmission technologies, and bandwidth. Recommendations are made regarding future DREnet infrastructure, services, management, research projects, and interaction with other communities. CISTI

N94-28354 Helsinki Univ. of Technology, Espoo (Finland). Digital Systems Lab.
SHEAF SEMANTICS FOR PETRI NETS
J. Lilius Jun. 1993 17 p Sponsored by Information-Technology Promotion Agency Limited Reproducibility: More than 20% of this document may be affected by microfiche quality
(PB94-132826; ISBN-951-22-1639-6) Avail: CASI HC A03

The semantics of Petri Nets are discussed within the 'Objects are sheaves' paradigm. Transitions and places are represented as sheaves and nets are represented as diagrams of sheaves. Both an interleaving semantics, and a non-interleaving semantics are shown to arise as the limit of the sheaf diagram representing the net. NTIS

N94-26745 Institut National de Recherche d'Informatique et d'Automatique, Le Chesnay (France).
SPECIFICATION PERFORMANCE OPTIMIZATION AND EXECUTIVE GENERATION FOR ONBOARD MULTIPROCESSOR REAL TIME APPLICATION WITH SynDEx [SPECIFICATION, OPTIMISATION DE PERFORMANCES ET GENERATION D'EXECUTIF POUR APPLICATION TEMPS-REEL EMBARQUEE MULTI-PROCESSEUR AVEC SYNDEX]
Christophe Lavarenne and Yves Sorel *In* CNES, Real-Time Embedded Processing for Space Applications Apr. 1993 p 429-437 In FRENCH (For primary document see N94-26713 07-60)
Copyright Avail: Issuing Activity (CEPADUES-Editions, 111, Rue Nicolas-Vauquelin, 31100 Toulouse, France)

N94-27193# Philips International B.V., Eindhoven (Netherlands). Natuurkundig Lab.
PARALLEL COMPUTERS FOR ADVANCED INFORMATION PROCESSING Abstract Only
E. Odijk *In* Technische Univ., Proceedings of the 3rd Workshop Computersystems: Research Forum on Design, Realization and Use of

Computersystems 1991 p 17 (For primary document see N94-27191 07-60)
Avail: CASI HC A01/MF A01

N94-27194# Amsterdam Univ. (Netherlands). Dept. of Computer Systems.
PARALLEL DISCRETE EVENT SIMULATION
Benno Overeinder, Bob Hertzberger, and Peter Sloot *In* Technische Univ., Proceedings of the 3rd Workshop Computersystems: Research Forum on Design, Realization and Use of Computersystems 1991 p 19-30
(For primary document see N94-27191 07-60)
Avail: CASI HC A03/MF A01

N94-27365*# Carnegie-Mellon Univ., Pittsburgh, PA. Studio for Creative Inquiry.
SCULPTING IN CYBERSPACE: PARALLEL PROCESSING THE DEVELOPMENT OF NEW SOFTWARE
Rob Fisher *In* NASA. Lewis Research Center, Vision 21: Interdisciplinary Science and Engineering in the Era of Cyberspace Dec. 1993 p 83-99
(For primary document see N94-27358 07-12)
Avail: CASI HC A03/MF A03

63 CYBERNETICS

Includes feedback and control theory, artificial intelligence, robotics and expert systems.

For related information see also *54 Man/System Technology and Life Support.*

N94-25591# Carnegie-Mellon Univ., Pittsburgh, PA. Robotics Inst.
DETECTING ACTIN FIBERS IN CELL IMAGES USING MINIMAL SPANNING TREES
Andrew E. Johnson and Raul E. Valdes-Perez 21 Sep. 1993 21 p
(Grants NSF BIR-89-20118; NSF ASC-92-17091)
(AD-A273914; CMU-RI-TR-93-18) Avail: CASI HC A03/MF A01

The quantitative description of cell structures in light microscope images is an important task in biological research. The inclusion of digital image processing techniques and fluorescent markers into light microscope imaging has recently made this task feasible. In this paper, we present a method for detection of filamentary structures in cell images that have been highlighted with fluorescent markers. The method has three stages. First, pixels belonging to fiber contours are extracted from the image. Then these pixels are grouped together based on proximity by a minimal spanning tree. Finally, the fiber contours are determined as sub-trees of the minimal spanning tree. Once the pixels belonging to individual fibers contours have been determined, quantitative statistics describing the fibers in the cell can be calculated. DTIC

N94-25743# Air Force Inst. of Tech., Wright-Patterson AFB, OH.
OPTIMAL CONTROL DESIGN ADVANTAGES UTILIZING TWO-DEGREE-OF-FREEDOM CONTROLLERS M.S. Thesis
Michael J. Stephens Dec. 1993 188 p
(AD-A273839; AFIT/GAE/ENY/93D-27) Avail: CASI HC A09/MF A02

The purpose was to investigate and describe the differences between a one-degree-of-freedom (1-DOF) controller, in which a controller is placed in a single location in the control loop, and a two-degree-of-freedom (2-DOF) controller, in which two separate controllers are designed - one in the feedback loop and the other as a prefilter in the forward loop. The approach involved summarizing the major rules governing loop shaping for performance and robustness in the 1-DOF case and then extending the concepts to the 2-DOF case. H(sub 2) optimization was utilized to perform several types of SISO examples and one MIMO example to verify the concepts. In all cases, the 2-DOF controller exhibited superior tracking performance over a wide range of plant disturbances and measurement noises compared to the 1-DOF model. DTIC

N94-25759# Air Force Inst. of Tech., Wright-Patterson AFB, OH.
COLOR IMAGE SEGMENTATION M.S. Thesis
Kimberley A. McCrae Dec. 1993 65 p
(AD-A274027; AFIT/GEO/ENG/93D-02) Avail: CASI HC A04/MF A01

The most difficult stage of automated target recognition (ATR) is segmentation. Current AFIT segmentation problems include faces and tactical targets; previous efforts to segment these objects have used intensity and motion cues. A color preprocessing scheme to be used with the other segmentation techniques was developed. A neural network is trained to identify the color of a desired object, eliminating all but that color from the scene. Gabor correlations and 2D wavelet transformations will be performed on stationary images; and 3D wavelet transforms on multispectral data will incorporate color and motion detection into the machine visual system. It was demonstrated that color and motion cues can enhance a computer segmentation system. Results from segmenting faces both from the AFIT data base and from video taped television are presented; results from tactical targets such as tanks and airplanes are also given. Color preprocessing is shown to greatly improve the segmentation in most cases. DTIC

N94-25898# Carnegie-Mellon Univ., Pittsburgh, PA. Robotics Inst.
THE TELEVISION AS ROBOT SERVANT
Robert Thibadeau Aug. 1993 10 p
(Contract MDA972-92-J-1010; ARPA Order 6873)
(AD-A273985; CMU-RI-TR-93-22) Avail: CASI HC A02/MF A01

Television and computing have an interesting intersection in the topic of how to put computer software into the television infrastructure. It is widely recognized that the result is a home information appliance. However, despite previous commercial experimentation, such an appliance has not emerged as successful. Perhaps there is only a deficiency in properly conceptualizing the appliance. In keeping with this theme, this paper presents a theory of why people value information. Using this theory as a design aid in the creation of future home information appliances should improve their chances of commercial success. DTIC

N94-25899# Georgia Inst. of Tech., Atlanta. Center for Human-Machine Systems Research.
KNOWLEDGE ORGANIZATION IN INTELLIGENT TUTORING SYSTEMS FOR DIAGNOSTIC PROBLEM SOLVING IN COMPLEX DYNAMIC DOMAINS
Vijay Vasandani and T. Govindaraj Sep. 1993 53 p
(Contract N00014-87-K-0482; DA Proj. RM3-3-M-20)
(AD-A273986; CHMSR-93-1) Avail: CASI HC A04/MF A01

Turbinia-Vyasa is a computer-based instructional system that trains operators to troubleshoot and diagnose faults in marine power plants. It is implemented on Apple Macintosh 2 computers. The simulator, Turbinia, is based on a hierarchical representation of subsystems, components, and primitives. Vyasa is the computer-based tutor that teaches the troubleshooting task using Turbinia. The simulator, an interactive, direct manipulation interface, and the tutor (with its expert, student, and instructional modules) comprise the architecture for the instructional system. In this paper, we discuss the details of knowledge organization that supports the functions of the three major elements of the intelligent tutoring system. DTIC

N94-25900# Carnegie-Mellon Univ., Pittsburgh, PA. Robotics Inst.
THE DETERMINATION OF SURFACE ROUGHNESS FROM REFLECTED STEP EDGES
Ronald A. Stone and Steven A. Shafer Nov. 1993 39 p
(Contract F33615-90-C-1465; ARPA Order 7597)
(AD-A273987; CMU-RI-TR-93-25) Avail: CASI HC A03/MF A01

The ability to measure the roughness of surfaces will be important for general purpose machine vision systems, in which a robot attempts to passively gain information about its environment. Although the traditional study of profilometry is well developed, its methods are unsuitable for this endeavor, since they require specialized apparatuses such as laser interferometers and styluses. We propose a method for the visual determination of surface roughness which does not require strong environmental constraints such as coherent light and small samples of the surface in question. We determine surface roughness by the measurement of the sharpness of the edges of an image reflected in a rough surface. We choose step edges since they will be present in many environments, and because the methods of edge detection and localization are mature. For these initial experiments, we assume a common surface roughness model of simple form, which we believe models milled or rolled surfaces. We show that if we also assume a known shape for the reflective surface and a known position for the viewer, we may calculate a roughness parameter. For our surface roughness model, we show that the resulting intensity distribution may be given in closed form. We then show the results of experiments performed with planar surfaces in a controlled environment and give the calculated roughness parameter. We compare these results with the values of the roughness as measured with a stylus profilometer, and find that the results are quite different. We discuss the possibilities that this difference is due to the non-Gaussian character of the surface height distribution, and the possibility that the difference arises from the difference in measurement procedures. DTIC

N94-25966 Georgia Inst. of Tech., Atlanta. Center for Human-Machine Systems Research.

INTEGRATION OF INTERACTIVE INTERFACES WITH INTELLIGENT TUTORING SYSTEMS: AN IMPLEMENTATION

Vijay Vasandani and T. Govindaraj Sep. 1993 42 p Limited Reproducibility: More than 20% of this document may be affected by microfiche quality
(Contract N00014-87-K-0482; DA Proj. RM3-3-M-20)
(AD-A273869; CHMSR-TR-93-2) Avail: CASI HC A03

Turbinia-Vyasa is an instructional system that trains operators in diagnostic problem solving in the domain of marine power plants. It is comprised of a steam power plant simulator and an intelligent tutoring system. The simulator, Turbinia, is based on a hierarchical representation of subsystems, components, and primitives together with necessary physical and logical linkages among them. Vyasa is the computer-based tutor that teaches the troubleshooting task using Turbinia. The simulator, an interactive, direct manipulation interface, and the tutor (with its expert, student, and instructional modules) comprise the instructional system. The interactive interface to the system and the tutor forms an integral and essential component of the instructional system. The interface, including important features and implementation details is discussed. The presentation includes details of the interactions. DTIC

N94-25983# Los Alamos National Lab., NM.

ADAPTIVE OPTIMIZATION AND CONTROL USING NEURAL NETWORKS

W. C. Mead, S. K. Brown, R. D. Jones, P. S. Bowling, and C. W. Barnes 22 Oct. 1993 18 p Presented at the International Conference on Accelerator and Large Experimental Control Systems, Berlin, Germany, 18-22 Oct. 1993
(Contract W-7405-eng-36)
(DE94-003941; LA-UR-93-4102; CONF-931023-9) Avail: CASI HC A03/MF A01

Recent work has demonstrated the ability of neural-network-based controllers to optimize and control machines with complex, non-linear, relatively unknown control spaces. A brief overview of neural networks via a taxonomy illustrating some capabilities of different kinds of neural networks is presented. Some successful control examples, particularly the optimization and control of a small-angle negative ion source, are presented. DOE

N94-26006*# Carnegie-Mellon Univ., Pittsburgh, PA. Dept. of Computer Science.

RATIONAL HANDLING OF MULTIPLE GOALS FOR MOBILE ROBOTS

Richard Goodwin and Reid Simmons 1 Nov. 1993 18 p
(Grant NAGw-1175)
(NASA-CR-195177; NAS 1.26:195177; AD-A273733; CMU-CS-93-204)
Avail: CASI HC A03/MF A01

This report examines a method for handling multiple active goals for mobile robots. Specifically, the focus is on asynchronous goal activation and on how to incorporate the accomplishment of a newly active goal into a partially executed plan. A utility based decision theoretic approach is adopted for investigating the tradeoffs that must be made. The applicability of decision theory to problems in artificial intelligence and planning in particular has long been recognized. In his review of the use of decision theory, Horvitz argues for its use as a basis for making choices in artificial intelligence. In an early example, Feldman and Sproull, in their analysis of planning for the hungry monkey problem, used utility based decision theory to evaluate plans taking into account uncertainty and risk. More recent work has focused on time dependent planning and on applying decision theory to search. The work presented here differs from these in that it focuses on plan evaluation when all goals are not initially known and the plan must be reformulated as goals become active. In such cases, the time dependent utility of goal satisfaction, as well as the time distribution of utilities and resource use, must be taken into account. DTIC

N94-26336# Air Force Inst. of Tech., Wright-Patterson AFB, OH. School of Engineering.

INVESTIGATION INTO MODEL-BASED FUZZY LOGIC CONTROL M.S. Thesis

Michael W. Logan Dec. 1993 193 p
(AD-A274660; AFIT/GE/ENG/93D-25) Avail: CASI HC A09/MF A03

The following topics are discussed: Plant Development and Current Approaches; Model-Based Fuzzy Logic Control Linear Design Considerations; Model-based Fuzzy Logic Control Nonlinear Design Considerations; and Development of a model-based Fuzzy Logic Controller. DTIC

N94-26462# Sandia National Labs., Albuquerque, NM.

ADAPTIVE PATH PLANNING IN CHANGING ENVIRONMENTS

Pang C. Chen Oct. 1993 15 p
(Contract DE-AC04-94AL-85000)
(DE94-003269; SAND-92-2744) Avail: CASI HC A03/MF A01

Path planning needs to be fast to facilitate real-time robot programming. Unfortunately, current planning techniques are still too slow to be effective, as they often require several minutes, if not hours of computation. To overcome this difficulty, we present an adaptive algorithm that uses previous experience to speed up future performance. It is a learning algorithm suitable for incrementally-changing environments such as those encountered in manufacturing of evolving products and waste-site remediation. The algorithm extends our previous work for stationary environments in two directions: (1) for minor environmental change, an object-attached experience abstraction scheme is introduced to increase the flexibility of the learned experience; and (2) for major environmental change, an on-demand experience repair scheme is also introduced to retain those experiences that remain valid and useful. In addition to presenting this algorithm, we identify three other variants with different repair strategies. To compare these algorithms, we develop an analytic model to compare the costs and benefits of the corresponding repair processes. Using this model, we formalize the concept of incremental change, and prove the optimality of our proposed algorithm under such change. Empirically, we also characterize the performance curve of each variant, confirm our theoretical optimality results, and demonstrate the practicality of our algorithm. DOE

N94-26629 Victoria Univ. (British Columbia). Dept. of Electrical and Computer Engineering.

ASYMPTOTICALLY STABLE NEURAL NETWORKS FOR IDENTIFICATION OF NONLINEAR DYNAMIC SYSTEMS M.S. Thesis

Chris M. Jubien 1993 130 p
(ISBN-0-315-84328-4; CTN-94-61022) Copyright Avail: Micromedia Ltd., Technical Information Centre, 240 Catherine Street, Suite 305, Ottawa, Ontario, K2P 2G8, Canada HC/MF

Neural networks have the advantage that they are extremely flexible and, once trained, provide accurate and fast modelling of complex systems. Stable neural networks are studied for application in the identification of nonlinear dynamic systems. A novel approach to system identification is used. The approach is based on a class of recurrent neural networks which has been proven to be asymptotically stable. A neural network was shown which could implement an arbitrary linear system, and a neural network was also designed which had a peaked response suitable for the task of scheduling various models for different input and output levels. These two neural networks were then combined to produce an architecture suitable for identification of nonlinear systems. Equations for training these neural networks to model the complex behavior that nonlinear systems exhibit were developed. Computer simulations were used to test the theory. In a simulated system, the neural network is found to provide good modelling. The equations were also applied to train a neural network to model the dynamic behavior of a boat and a PUMA-560 two-link robot arm. Author (CISTI)

N94-26660 Toronto Univ. (Ontario). Dept. of Electrical and Computer Engineering.

DESIGNING AND OPTIMIZING FUZZY-LOGIC CONTROLLERS M.S. Thesis

Sanjiv K. Lakhanpal 1993 161 p

(ISBN-0-315-83505-2; CTN-94-61041) Copyright Avail: Micromedia Ltd., Technical Information Centre, 240 Catherine Street, Suite 305, Ottawa, Ontario, K2P 2G8, Canada HC/MF

Fuzzy logic is an approximate reasoning model aimed at characterizing the modes of reasoning humans use to make rational decisions in environments of uncertainty and imprecision. It incorporates elements of expert systems, approximate reasoning, multiple valued logic, and probability theory. The fuzzy logic controller provides a means of converting a linguistic control strategy based on expert knowledge into an automatic control strategy. An optimized fuzzy logic controller is presented to meet the needs of real-time fuzzy signal processing. The architecture is optimized towards increasing the rate of inference, allowing for easy reconfiguration and reprogramming in order to speed the evaluation and development stages, and decreasing the cost of resources. Discussions are provided on fuzzification strategies and the effects of transducer error, inference engine architectures, a heuristic methodology for determining physical parameters of a fuzzy controller, defuzzification methods and architectures, the composition of the knowledge base, and the interface with and the control of the fuzzy controller. Author (CISTI)

N94-26807# Los Alamos National Lab., NM.
VIRTUAL DATA
E. Bjorklund 1993 7 p Presented at the International Conference on Accelerator and Large Experimental Control Systems, Berlin, Germany, 18-22 Oct. 1993
(Contract W-7405-eng-36)
(DE94-002718; LA-UR-93-3697; CONF-931023-7) Avail: CASI HC A02/MF A01

In the 1970's, when computers were memory limited, operating system designers created the concept of 'virtual memory' which gave users the ability to address more memory than physically existed. In the 1990's, many large control systems have the potential for becoming data limited. We propose that many of the principles behind virtual memory systems (working sets, locality, caching, and clustering) can also be applied to data-limited systems - creating, in effect, 'virtual data systems.' At the Los Alamos National Laboratory's Clinton P. Anderson Meson Physics Facility (LAMPF), we have applied these principles to a moderately sized (10,000 data points) data acquisition and control system. To test the principles, we measured the system's performance during tune-up, production, and maintenance periods. In this paper, we present a general discussion of the principles of a virtual data system along with some discussion of our own implementation and the results of our performance measurements. DOE

N94-26916# Technische Univ., Twente (Netherlands). Dept. of Applied Mathematics.
SINGLE-SERVER QUEUES WITH SPATIALLY DISTRIBUTED ARRIVALS
D. P. Kroese and V. Schmidt (Ulm Univ., Germany.) Jun. 1993 32 p Prepared in cooperation with Ulm Univ.
(PB94-126638; MEMO-1142) Avail: CASI HC A03/MF A01

Consider a queueing system where customers arrive at a circle according to a homogeneous Poisson process. After choosing their positions on the circle, according to a uniform distribution, they wait for a single server who travels on the circle. The server's movement is modeled by a Brownian motion with drift. Whenever the server encounters a customer, he stops and serves this customer. The service times are independent, but arbitrarily distributed. The model generalizes the continuous cyclic polling system (the diffusion coefficient of the Brownian motion is zero in this case) and can be interpreted as a continuous version of a Markov polling system. Using Tweedie's lemma for positive recurrence of Markov chains with general state space, it is shown that the system is stable if and only if the traffic intensity is less than one. Moreover, a stochastic decomposition result is derived which leads to equilibrium equations for the stationary configuration of customers on the circle. Steady-state performance characteristics are determined, in particular the expected number of customers in the system as seen by a travelling server and at an arbitrary point in time. NTIS

N94-26948# Oak Ridge National Lab., TN.
SENSOR-BASED NAVIGATION OF A MOBILE ROBOT USING AUTOMATICALLY CONSTRUCTED FUZZY RULES
Y. Watanabe and F. G. Pin 1993 8 p Presented at the ICAR 1993: 6th International Conference on Advanced Robotics, Tokyo, Japan, 1-2 Nov. 1993
(Contract DE-AC05-84OR-21400)
(DE94-001137; CONF-9311107-2) Avail: CASI HC A02/MF A01

A system for automatic generation of fuzzy rules is proposed which is based on a new approach, called 'Fuzzy Behaviorist,' and on its associated formalism for rule base development in behavior-based robot control systems. The automated generator of fuzzy rules automatically constructs the set of rules and the associated membership functions that implement reasoning schemes that have been expressed in qualitative terms. The system also checks for completeness of the rule base and independence and/or redundancy of the rules to ensure that the requirements of the formalism are satisfied. Examples of the automatic generation of fuzzy rules for cases involving suppression and/or inhibition of fuzzy behaviors are given and discussed. Experimental results obtained with the automated fuzzy rule generator applied to the domain of sensor-based navigation in a priori unknown environments using one of our autonomous test-bed robots are then presented and discussed to illustrate the feasibility of large-scale automatic fuzzy rule generation using our proposed 'Fuzzy Behaviorist' approach. DOE

N94-26992# National Defence Research Establishment, Stockholm (Sweden). Dept. of Weapon Systems, Effects and Protection.
BLURRED FOCAL ELEMENTS GENERALIZATION OF DEMPSTER'S RULE [EN GENERALISERING AV DEMPSTERS REGEL FOR OTYDLIGA FOKALELEMENT]
Johan Schubert Aug. 1993 15 p In SWAHILI See also PB92-151455
(PB94-124278; FOA-C-20938-2.7) Avail: CASI HC A03/MF A01

When propositions are poorly specified it is uncertain if two propositions of different pieces of evidence are in logical conflict, i.e., it is uncertain whether the intersection between their corresponding focal elements is empty. To distinguish between normal focal elements and these poorly represented focal elements, the latter shall be called blurred focal elements. In order to resolve the ambiguity, this uncertainty is modeled by creating an additional piece of evidence against the simultaneous belief in both propositions and treating the two original pieces of evidence as non-conflicting. A generalization of Dempster's rule for evidence with blurred focal elements based on this methodology is presented. NTIS

N94-27029# Technische Univ., Delft (Netherlands).
GREY-BOX MODELLING AND IDENTIFICATION TOPICS Ph.D. Thesis
Herbert Johannes Ant Franciscus 21 Dec. 1992 176 p
(PB94-126380; ISBN-90-9005644-0) Avail: CASI HC A09/MF A02

The first part of this thesis presents an industrial view on intelligent adaptive control, aiming at the development of multivariable adaptive control methods for slowly-varying, nonlinear, stochastic, dynamic processes in the petrochemical industry. Continuous adaptation is often unfeasible, as it is too expensive or too risky under difficult circumstances. An 'at-request tuner' concept is propagated, which features automated modeling and controller retuning at user's request only and which is especially suitable for mode-switch processes. Chapter two deals with the architecture of the at-request tuner, which consists of a supervisor with performance monitor and library modules, and modules for control design, model identification, and test-signal generation. Chapter three is devoted to possible improvements in experiment design. In chapter four, an adaptive forgetting strategy (AFS) for use in on-line identification is highlighted. Chapter five contains the central topic of this thesis: grey-box modeling and identification. Conventional identification methods postulate a statistical, black-box input-output model for the process dynamics. This approach has important advantages, the most prominent being that no 'expensive' physical model is required. It is argued that a compromise between the full-blown physical and the statistical approach is more attractive. Such a compromise would lead to a 'grey-box' model class where strategic process characteristics, such as stability, are forced upon a family of suitable statistical models. Chapter six elaborates upon the topic of the previous chapter. In chapter seven, grey-box estimators are applied to linearized physicochemical reactor models. NTIS

N94-27032# Carnegie-Mellon Univ., Pittsburgh, PA. Dept. of Computer Science.
BUILDING 3-D MODELS FROM UNREGISTERED RANGE IMAGES

Kazunori Higuchi, Martial Hebert, and Katsushi Ikeuchi Nov. 1993 23 p
(Contracts F33615-90-C-1465; F33615-93-1-1282; NSF IRI-92-24521)
(AD-A274126; CMU-CS-93-214) Avail: CASI HC A03/MF A01

In this paper, a new approach is described for building a three-dimensional model from a set of range images. The approach is able to build models of free-form surfaces obtained from arbitrary viewing directions, with no initial estimate of the relative viewing directions. The approach is based on building discrete meshes representing the surfaces observed in each of the range images, mapping each of the meshes to a spherical image, and computing the transformations between the views by matching the spherical images. The meshes are built using an iterative fitting algorithm previously developed; the spherical images are built by mapping the nodes of the surface meshes to the nodes of a reference mesh on the unit sphere and by storing a measure of curvature at every node. The algorithms used for building such models from range images and for matching them are described. Results obtained using range images of complex objects are shown. DTIC

N94-27077# Dayton Univ. Research Inst., OH.
ALUMINUM ALLOY 8090-T8771 THICK PLATE MATERIAL CHARACTERIZATION Interim Report, Oct. 1991 - May 1993
Russell R. Cervay Oct. 1993 64 p
(Contract F33615-90-C-5915)
(AD-A274146; UDR-TR-93-71; WL-TR-93-4111) Avail: CASI HC A04/MF A01

The purpose of this study was to evaluate the mechanical properties of Al-Li alloy 8090, 1.750 inch thick plate thermally processed to the T8771 condition. Room temperature properties evaluated were: tensile, compression, bearing, and shear strengths, fracture toughness, notched and smooth fatigue, and constant amplitude and variable amplitude fatigue crack growth rate. Constant amplitude fatigue crack growth rate test data was generated at two load-ratios, 0.1 and 0.33, and in both laboratory air and saturated air environments. As expected, tensile properties were acceptable for the various specimen orientations removed from the plate's rolling plane: there was a significant drop in yield strength for in-plane specimens oriented 45 degrees off the rolling direction. Also, through-the-thickness ductility was quite low. Compression, bearing, shear, and fatigue properties were all good for the specimen orientations examined. The fracture toughness was acceptable for specimens with a L-T and T-L orientations: for through-the-thickness loading, i.e. S-L orientation, the toughness was cut in half. The material showed superior fatigue crack resistance attributable to considerable crack closure induced by very course crack faces. The exceptional surface roughness is characteristic of a mostly unrecrystallized grain structure in Al-Li materials. The high level of closure is manifested as a plateau of nearly constant fatigue crack growth rate over the normally linear log-da/dN versus log delta K mid-range seen in conventional high strength aluminum products and Al-Li materials having a recrystallized grain structure. DTIC

N94-27093# CSA Engineering, Inc., Palo Alto, CA.
SMART STRUCTURES, AN OVERVIEW Final Report, Sep. 1991 - Jul. 1993
Kenneth B. Lazarus and Kevin L. Napolitano Sep. 1993 67 p
(Contract F33615-90-C-3211)
(AD-A274147; ASIAC-TR-93-9; WL-TR-93-3101) Avail: CASI HC A04/MF A01

This report assesses the current status and maturity of smart structures technology. The report contains sections on smart materials, neural networks, health monitoring, and smart structures component technologies such as actuators, sensory elements, control methodologies and algorithms, controller architecture and implementation hardware, and signal conditioning and power amplification. A strategic research and development plan is suggested for the Air Force. Eleven specific problems with Air Force aircraft structure and weapons systems are identified which have the potential for being alleviated or reduced by application of smart structures technologies. DTIC

N94-27121# Air Force Inst. of Tech., Wright-Patterson AFB, OH. School of Engineering.
USING DISCOVERY-BASED LEARNING TO PROVE THE BEHAVIOR OF AN AUTONOMOUS AGENT M.S. Thesis
David N. Mezera Dec. 1993 144 p
(AD-A274131; AFIT/GCE/Eng/93D-10) Avail: CASI HC A07/MF A02

Computer-generated autonomous agents in simulation often behave predictably and unrealistically. These characteristics make them easy to spot and exploit by human participants in the simulation, when we would prefer the behavior of the agent to be indistinguishable from human behavior. An improvement in behavior might be possible by enlarging the library of responses, giving the agent a richer assortment of tactics to employ during a combat scenario. Machine learning offers an exciting alternative to constructing additional responses by hand by instead allowing the system to improve its own performance with experience. This thesis presents NOSTRUM, a discovery-based learning (DBL) system designed to work in tandem with the MAXIM air combat simulator. Through a process of repeated experimentation modeled after the scientific method, NOSTRUM was able to discover many responses that were more appropriate than the single mode of agent control implemented in the original MAXIM program. NOSTRUM often found responses that dramatically improved the offensive position of the agent, and it sometimes placed the agent in position for an extended shot on the target when one was not available before. DTIC

N94-27122# Air Force Inst. of Tech., Wright-Patterson AFB, OH. School of Engineering.
MULTIPLE MODEL ADAPTIVE CONTROL OF A LARGE FLEXIBLE SPACE STRUCTURE WITH PURPOSEFUL DITHER FOR ENHANCED IDENTIFIABILITY M.S. Thesis
James A. Fitch Dec. 1993 142 p
(AD-A274132; AFIT/GA/Eng/93D-01) Avail: CASI HC A07/MF A02

Dithering techniques for enhancing uncertain parameter identification with moving-bank Multiple Model Adaptive Estimation (MMAE) and Control (MMAC) algorithms are analyzed in this thesis. The dithering techniques and multiple-model adaptive algorithms are applied to the SPICE 2 flexible space structure. The dithering techniques studied include purposefully constructed square wave, sine wave (fixed and swept frequency) and wide-band noise wave forms. Purposeful rigid-body slew commands are also used in order to excite the structure's flexible bending modes. Dither inputs into the structure are performed in an effort to enhance the open-loop identifiability of the uncertain parameter, namely a scalar multiplier on the undamped natural frequencies of the flexible bending modes. Correct identification of this parameter enables the MMAE and MMAC algorithms to quell any vibrations induced into the structure, in the face of varying parameter values. The results of this study indicate that purposefully constructed dither signals do enhance parameter identification significantly. The parameter identification enhancement due to rigid-body slew command input was shown to be less effective than that with sinusoid and wide band noise dither inputs, however. DTIC

N94-27124# Northeastern Univ., Boston, MA.
CONTROL ORIENTED SYSTEM IDENTIFICATION Final Report, 1 Jun. 1991 - 14 Jun. 1993
Clas A. Jacobson Aug. 1993 7 p
(Grant AF-AFOSR-0222-91)
(AD-A274162; AFOSR-93-0898TR) Avail: CASI HC A02/MF A01

The research goals for this grant were to obtain algorithms for control oriented system identification to construct dynamical models of systems based primarily on measured data that are compatible with robust control design techniques. The research carried out under this grant has continued the research on control oriented identification originated by the PI and his collaborators, has extended control oriented identification methods to new classes of dynamical systems and has initiated a study unifying identification and control laws design. The research that has extended existing problem formulation concerns the construction of algorithms for linear shift invariant systems using a combination of apriori and experimental information. Algorithms for the identification of continuous time systems and efficient linear algorithms have been constructed. The research that has extended the existing problem formulation concerns the development of algorithms for the construction of parameterized linear families from a combination of apriori and measured information. Algorithms for this type of nonlinear system identification have been given that produce models suitable for gain scheduled controllers. Finally research into the integration control oriented identification and robust control for slowly time varying systems was initiated under this grant. DTIC

N94-27139# Minnesota Univ., Minneapolis. Dept. of Electrical Engineering.

OPERATOR THEORETIC METHODS IN THE CONTROL OF DISTRIBUTED AND NONLINEAR SYSTEMS Final Report, 1 Oct. 1989 - 30 Sep. 1993

Allen R. Tannenbaum 2 Nov. 1993 38 p
(Grant AF-AFOSR-0024-90)
(AD-A274160; AFOSR-93-0899TR) Avail: CASI HC A03/MF A01

In this final technical report, we outline a number of problems in robust and nonlinear control theory which we have studied using an operator theoretic methodology. In particular, we discuss an approach to the structured singular value and u-synthesis procedure in robust control which is based on a new type of interpolation method. We consider nonlinear extension of H-infinity optimization theory and investigate corresponding question in causality which arise in this area. Moreover, we discuss a saddle-point, game-theoretic approach to such problems. Further, we sketch the application of our skew Toeplitz methods to distributed (infinite dimensional) H-infinity control. We also consider and h-infinity of approach to sampled data systems based on a lifting method, as well as consider problem using h-infinity-H(sup 2) combined suboptimal controller. Finally, we list some of our results in image processing and computer vision as applied to visual tracking. DTIC

N94-27271 Waterloo Univ. (Ontario). Dept. of Mathematics.

IMPULSIVE CONTROL AND STABILIZATION M.S. Thesis

Allan Richard Willms 1993 143 p
(ISBN-0-315-84563-5; CTN-94-61076) Copyright Avail: Micromedia Ltd., Technical Information Centre, 240 Catherine Street, Suite 305, Ottawa, Ontario, K2P 2G8, Canada HC/MF

A system of ordinary differential equations subject to an impulsive (discrete-time) controller is considered. The question of controllability is answered for linear systems and, for the case where the system has constant coefficients, the controllability criteria are shown to be the same as that for classical continuous control functions. Two optimal control problems are analyzed and a set of equations is presented which constitutes a set of necessary and sufficient conditions that must be satisfied by the optimal solution. The question of stabilizability of any state is studied for nonlinear autonomous systems. Both necessary and sufficient conditions for a particular state to be stabilizable are established using the notion of an impulsive invariant set and the method of Liapunov functions. Finally, the stability properties of a general nonautonomous impulsive system are analyzed. This analysis yields a method of testing whether a particular impulsive program will stabilize a given system. Further, Liapunov stability results for impulsive systems are extended to large scale systems in a manner analogous to extensions for purely continuous or purely discrete systems. Author (CISTI)

N94-27277 Queens Univ., Kingston (Ontario). Dept. of Mathematics and Statistics.

FINITE TIME DIFFERENTIAL EQUATIONS AND THEIR APPLICATION TO CONTROL SYSTEMS M.S. Thesis

Evelyn Marie Baylis Aug. 1993 72 p
(ISBN-0-315-85158-9; CTN-94-61099) Copyright Avail: Micromedia Ltd., Technical Information Centre, 240 Catherine Street, Suite 305, Ottawa, Ontario, K2P 2G8, Canada HC/MF

A proposition is presented that allows finding one-dimensional finite time differential equations. A proposition is then considered which can be used to determine whether or not an n-dimensional equation is finite time. The proposition is employed to state two Lyapunov-like finite time theorems. Some results of two-dimensional finite time differential equations are studied and extended to an n-dimensional theorem. An example of this theorem for $n=2$ is presented and it is shown how it might be used to demonstrate that a multi dimensional system is finite time. Sliding mode control is then discussed, and the sliding mode method is used to find a smooth two-dimensional differential equation that is finite time. The method could possibly be generalized to create an n-dimensional finite time differential equation, and an imperfect answer to this problem is stated along with how it may be used in a practical sense. Finally, application of the above theories to finite time controllers is discussed. Finite time controllers can be used in many of the same areas already occupied by bang-bang controllers and sliding mode controllers, such as in robot manipulators. CISTI

N94-27641 Toronto Univ. (Ontario).

TOOLS FOR QUANTITATIVE STABILITY ROBUSTNESS ANALYSIS Ph.D. Thesis

Li Qiu 1990 218 p
(ISBN-0-315-59950-2; CTN-94-60982) Copyright Avail: Micromedia Ltd., Technical Information Centre, 240 Catherine Street, Suite 305, Ottawa, Ontario, K2P 2G8, Canada HC/MF

Stability is a crucial requirement for any control system. Since the modeling of a physical system is always inexact, this implies that the effect of model uncertainty on system stability must be considered. Stability robustness analysis has the purpose of considering such effects. The stability robustness of linear time-invariant finite dimensional systems, focusing on three types of objects fundamental in the stability analysis of such systems. The stability robustness analysis is carried out quantitatively and new mathematical tools are introduced. For matrices subject to unstructured uncertainties, the stability radius of a stable matrix is defined as the distance of the matrix to the set of unstable matrices. A tensor product method is then used to study the properties of the stability radius. For polynomials with affine uncertainties, a general solution is obtained using tools from convex analysis. For real rational matrices, a new family of metrics called pointwise gap metrics is defined on the space of all real rational matrices of the same size. Using this metric, quantitative measures for the open loop and closed loop stability robustness are obtained. Author (CISTI)

N94-27645 British Columbia Univ., Vancouver. Dept. of Electrical Engineering.

AN INVESTIGATION OF METHODS FOR DETERMINING DEPTH FROM FOCUS Ph.D. Thesis

John E. Ens Jul. 1990 201 p
(ISBN-0-315-64015-4; CTN-94-60990) Copyright Avail: Micromedia Ltd., Technical Information Centre, 240 Catherine Street, Suite 305, Ottawa, Ontario, K2P 2G8, Canada HC/MF

The concept of depth from focus involves calculating distances to points in an observed scene by modeling the effect that the camera's focal parameters have on images acquired with a small depth of field. This technique does not require special scene illumination and needs only a single camera. Deconvolving and modeling the defocus operator is the most difficult segment of calculating depth from focus. Some fundamental problems with the conventional method of isolating the defocus operator are exposed, such as inaccuracies in finding the frequency domain representation and the presence of border effects. To solve the general depth from focus problem, an application of an iterative matrix based method is presented. This uses two images of the same scene, obtained under different conditions of defocus. The defocus operator may be assumed using a parametric model or experimentally measured. Tradeoffs in implementation are resolved through regularization. The method is theoretically justified, and shown to eliminate problems mentioned above. A constrained inverse filtering method and the iterative matrix based method are experimentally implemented on four scenes. The experiments show that the iterative matrix solution consistently yields more accurate results. Author (CISTI)

N94-27706# Oak Ridge National Lab., TN.

ON MODELING AND CONTROLLING INTELLIGENT SYSTEMS

W. B. Dress 1993 8 p Presented at the 2nd International Conference on Information and Knowledge Management, Washington, DC, 1-5 Nov. 1993
(Contract DE-AC05-84OR-21400)
(DE94-002446; CONF-9311112-1) Avail: CASI HC A02/MF A01

The aim of this paper is to show how certain diverse and advanced techniques of information processing and system theory might be integrated into a model of an intelligent, complex entity capable of materially enhancing an advanced information management system. To this end, we first examine the notion of intelligence and ask whether a semblance thereof can arise in a system consisting of ensembles of finite-state automata. Our goal is to find a functional model of intelligence in an information-management setting that can be used as a tool. The purpose of this tool is to allow us to create systems of increasing complexity and utility, eventually reaching the goal of an intelligent information management system that provides and anticipates needed data and information. We base our attempt on the ideas of general system theory where the four topics of system identification, modeling, optimization, and control provide the theoretical framework for constructing a complex system that will be capable of interacting with complex systems in the real world. These four key topics are discussed within the purview of cellular automata, neural networks, and evolutionary programming. This is a report of ongoing work, and not yet a success story of a synthetic intelligent system. DOE

N94-27773*# National Aeronautics and Space Administration. Langley Research Center, Hampton, VA.
LOCAL PERFORMANCE OPTIMIZATION FOR A CLASS OF REDUNDANT EIGHT-DEGREE-OF-FREEDOM MANIPULATORS
Robert L. Williams, II Mar. 1994 23 p
(RTOP 586-02-11)
(NASA-TP-3417; L-17289; NAS 1.60:3417) Avail: CASI HC A03/MF A01

Local performance optimization for joint limit avoidance and manipulability maximization (singularity avoidance) is obtained by using the Jacobian matrix pseudoinverse and by projecting the gradient of an objective function into the Jacobian null space. Real-time redundancy optimization control is achieved for an eight-joint redundant manipulator having a three-axis spherical shoulder, a single elbow joint, and a four-axis spherical wrist. Symbolic solutions are used for both full-Jacobian and wrist-partitioned pseudoinverses, partitioned null-space projection matrices, and all objective function gradients. A kinematic limitation of this class of manipulators and the limitation's effect on redundancy resolution are discussed. Results obtained with graphical simulation are presented to demonstrate the effectiveness of local redundant manipulator performance optimization. Actual hardware experiments performed to verify the simulated results are also discussed. A major result is that the partitioned solution is desirable because of low computation requirements. The partitioned solution is suboptimal compared with the full solution because translational and rotational terms are optimized separately; however, the results show that the difference is not significant. Singularity analysis reveals that no algorithmic singularities exist for the partitioned solution. The partitioned and full solutions share the same physical manipulator singular conditions. When compared with the full solution, the partitioned solution is shown to be ill-conditioned in smaller neighborhoods of the shared singularities. Author (revised)

N94-27800 National Aerospace Lab., Amsterdam (Netherlands). Informatics Div.
MULTI-SENSOR DATA FUSION IN A DISTRIBUTED ENVIRONMENT: ARCHITECTURAL SOLUTIONS
R. G. Zuidgeest 17 Jun. 1992 47 p Limited Reproducibility: More than 20% of this document may be affected by microfiche quality
(Contract MOD-01689029811)
(NLR-TP-92243-U; ETN-94-95450) Avail: CASI HC A03

The human operator observing the real world is confronted with a huge amount of data from multiple sensors observing that world. Multisensor data fusion (MSDF) is one of the emerging fields in advanced information processing, concerned with fusing sensor data from these multiple sensors. Automated MSDF can help the operator by processing sensor data into concise and surveyable information that is more useful than any sensor can separately provide. The merit of MSDF can be increased by employing the knowledge of the human operator about the real world, the sensor systems, and the fusion process. With the aid of this knowledge, automated MSDF can assign meaning to sensor data and is able to reason about the observed world at a high level as humans do. Often, MSDF has an inherent distributed character, spatially as well as functionally. Architectural solutions should cope with this characteristic. The possibility of employing distributed artificial intelligence techniques in MSDF applications, in particular command and control applications such as battlefield surveillance, is focused on. Candidate architectures are proposed in which MSDF functions and aspects of distributed networks are demonstrated. ESA

N94-27809 Japan Atomic Energy Research Inst., Tokyo.
PULSE CONTROL METHOD AND ITS CHARACTERISTICS
Junya Shimazaki (Japan Atomic Energy Research Inst., Tokai.) and Nobuyuki Ishikawa (Japan Atomic Energy Research Inst., Tokai.) May 1993 36 p In JAPANESE Limited Reproducibility: More than 20% of this document may be affected by microfiche quality
(DE94-701187; JAERI-M-93-063) Avail: CASI HC A03 (US Sales Only)

Pulse control is defined as one of digital control techniques and acts during part of time-sampling period of control. A design method of the pulse control and its characteristics are discussed on the basis of simple control system model for three types of modern control such as pole assignment control with state variable feedback, linear quadratic optimal control and dead-beat digital control. Control performances of the pulse control corresponding to the above mentioned controls are compared to continuous and ordinary digital controls. As the results, the pulse controls are shown to have as good control performances as the other controls, although the former has strong restrictions on the control variables. Applications of the pulse control to real plants will be useful for the short time of control by a flexible design of pulse width. DOE

N94-27833# Instituto de Pesquisas Espaciais, Sao Jose dos Campos (Brazil).
A HYBRID FORMALISM FOR REPRESENTATION AND INTERPRETATION OF IMAGE KNOWLEDGE
Francisco deAssisTavaresFerreiradaSilva 1993 7 p Presented at the ISPRS Congress, Washington, DC, 2-14 Aug. 1992
(INPE-5485-PRE/1784) Avail: CASI HC A02/MF A01

A blackboard-base knowledge representation, adapted to maintain information about images using method of frame, is proposed. This representation is to be used in the development of artificial intelligence applications to help human operators in the radar images and related informations. This project is part of the development of artificial intelligence applications in the image processing area. Author

N94-27975 McMaster Univ., Hamilton (Ontario). School of Graduate Studies.
TOPICS IN THE DESIGN, ANALYSIS AND IMPLEMENTATION OF FEEDBACK CONTROL SYSTEMS Ph.D. Thesis
Nathaniel Leonard Segall 1993 291 p
(ISBN-0-315-84934-7; CTN-94-61110) Copyright Avail: Micromedia Ltd., Technical Information Centre, 240 Catherine Street, Suite 305, Ottawa, Ontario, K2P 2G8, Canada HC/MF

A new definition of robustness for continuous feedback control systems is advanced: the region of the joint allowable variation in the gain and the dead-time of the process. This region is constructed from the open loop system frequency response. The continuous time proportional integral derivative (PID), internal model control (IMC), and linear quadratic optimal control (LQOC) design procedures for a first order plus dead-time process are compared for integral square error (ISE) performance when tuned for the same level of robustness. Highest performance is achieved by PID, followed by IMC and LQOC. The continuous ISE performance of the discrete LQOC and state deadbeat IMC controllers are compared as the size of the control interval is changed. A new modified LQOC controller and a new extended horizon controller are proposed. The robustness analysis is extended to discrete systems. The state deadbeat IMC with an augmented filter and modified LQOC controllers are shown to have better ISE performance than the LQOC controller when tuned for the same level of robustness. A procedure is presented for saturation correction in multivariable one-step optimal controllers. A simultaneous correction is included which adjusts the remaining control inputs if some inputs saturate. Results on saturation correction for PID controllers are also given. Author (CISTI)

N94-28065*# National Aeronautics and Space Administration. Ames Research Center, Moffett Field, CA.
ARTIFICIAL INTELLIGENCE RESEARCH BRANCH FUTURE PLANS Progress Report, 1992
Helen Stewart, ed. Mar. 1992 78 p
(NASA-TM-109733; NAS 1.15:109733; FIA-92-07) Avail: CASI HC A05/MF A01

This report contains information on the activities of the Artificial Intelligence Research Branch (FIA) at NASA Ames Research Center (ARC) in 1992, as well as planned work in 1993. These activities span a range from basic scientific research through engineering development to fielded NASA applications, particularly those applications that are enabled by basic research carried out in FIA. Work is conducted in-house and through collaborative partners in academia and industry. All of our work has research themes with a dual commitment to technical excellence and applicability to NASA short, medium, and long-term problems. FIA acts as the Agency's lead organization for research aspects of artificial intelligence, working closely with a second research laboratory at the Jet Propulsion Laboratory (JPL) and AI applications groups throughout all NASA centers. This report is organized along three major research themes: (1) Planning and Scheduling: deciding on a sequence of actions to achieve a set of complex goals and determining when to execute those actions and how to allocate resources to carry them out; (2) Machine Learning: techniques for forming theories about natural and man-made phenomena; and for improving the problem-solving performance of computational systems over time; and (3) Research on the acquisition, representation, and utilization of knowledge in support of diagnosis design of engineered systems and analysis of actual systems. Derived from text

N94-26280*# Rensselaer Polytechnic Inst., Troy, NY. Dept. of Mechanical Engineering, Aeronautical Engineering, and Mechanics.
APPLICATION OF THE CIRSSE COOPERATING ROBOT PATH PLANNER TO THE NASA LANGLEY TRUSS ASSEMBLY PROBLEM
Jonathan M. Weaver and Stephen J. Derby *In* NASA. Langley Research Center, Selected Topics in Robotics for Space Exploration Dec. 1993 p 28-35 Sponsored by NASA, Washington (For primary document see N94-26278 07-12)
(Grant NAGw-1333)
Avail: CASI HC A02/MF A03

N94-27896*# Colorado Univ., Denver. Dept. of Electrical Engineering.
ON IDENTIFIED PREDICTIVE CONTROL
Jan T. Bialasiewicz *In* Old Dominion Univ., The 1993 NASA-ODU American Society for Engineering Education (ASEE) Summer Faculty Fellowship Program Dec. 1993 p 71-73 (For primary document see N94-27893 07-80)
Avail: CASI HC A01/MF A03

N94-27913*# Missouri Univ., Columbia. Electrical and Computer Engineering.
AN OVERVIEW ON DEVELOPMENT OF NEURAL NETWORK TECHNOLOGY Abstract Only
Chun-Shin Lin *In* Old Dominion Univ., The 1993 NASA-ODU American Society for Engineering Education (ASEE) Summer Faculty Fellowship Program Dec. 1993 p 129 (For primary document see N94-27893 07-80)
Avail: CASI HC A01/MF A03

64 NUMERICAL ANALYSIS

Includes iteration, difference equations, and numerical approximation.

N94-25594# Naval Postgraduate School, Monterey, CA. Dept. of Mathematics.
REPEATED KNOTS IN LEAST SQUARES MULTIQUADRIC FUNCTIONS Technical Report, Aug. - Oct. 1993
Richard Franke, Hans Hagen, and Gregory M. Nielson 14 Oct. 1993 18 p
(AD-A273866; NPS-MA-94-004) Avail: CASI HC A03/MF A01

A previous paper by the authors noted that there was a strong tendency to obtain near-repeated knots in their algorithm for least squares approximation of scattered data by multiquadric functions. It was observed that this leads naturally to the inclusion of derivatives of the multiquadric basis function in the approximation, and an algorithm for accomplishing this is given. A comparison of the results obtained with this algorithm and the previous one is made. While the multiple knot algorithm usually has the advantage in terms of accuracy and computational stability, there are datasets for which this is reversed. DTIC

N94-25733# Technical Research Centre of Finland, Espoo. Fire Technology Lab.
PIECEWISE LEAST SQUARES FITTING TECHNIQUE USING FINITE INTERVAL METHOD WITH HERMITE POLYNOMIALS
Djebar Baroudi Apr. 1993 30 p
(ISSN 1235-0621)
(VTT-PUBS-135; ISBN-951-38-4253-3; ETN-94-95240) Copyright Avail: CASI HC A03/MF A01

A fitting technique based on the approximation technique of the finite element method is presented. The confidence interval for the fitted function and its first and second derivatives are calculated. The approximation assumes the fitted function and its derivatives up to the second order to be continuous. The fitting problem is formulated as an unconstrained optimization problem. The unknowns to be determined are found by minimizing the sum of squared errors. A performing software package programmed in standard FORTRAN 77 is presented. Given a set of data points, this software performs the fitting and calculates the confidence intervals of the fitted function, and its first and second derivatives. ESA

N94-25829 International Centre for Theoretical Physics, Trieste (Italy).
ON THE OSCILLATION OF A CLASS OF HYPERBOLIC EQUATIONS OF NEUTRAL TYPE
M. Kirane and N. Parhi Oct. 1992 18 p Limited Reproducibility: More than 20% of this document may be affected by microfiche quality
(DE93-616815; IC-92/306) Avail: CASI HC A03 (US Sales Only)

Sufficient conditions have been obtained for oscillations of all solutions of a class of hyperbolic differential equations of neutral type. DOE

N94-25830 International Centre for Theoretical Physics, Trieste (Italy).
OSCILLATORY BEHAVIOUR OF SOLUTIONS OF COUPLED HYPERBOLIC DIFFERENTIAL EQUATIONS OF NEUTRAL TYPE
N. Parhi and M. Kirane Oct. 1992 15 p Limited Reproducibility: More than 20% of this document may be affected by microfiche quality
(DE93-616816; IC-92/333) Avail: CASI HC A03 (US Sales Only)

Sufficient conditions have been obtained for oscillation of all solutions of a class of coupled hyperbolic differential equations of neutral type. DOE

N94-25834# Air Force Inst. of Tech., Wright-Patterson AFB, OH.
PREDICTING NONLINEAR TIME SERIES M.S. Thesis
James C. Gainey, Jr. Dec. 1993 13 p
(AD-A274051; AFIT/GEO/Eng/93D-05) Avail: CASI HC A03/MF A01

Predicting future values of a time series has many practical uses in real-time signal processing and understanding. This thesis implements an Adaptive Time Delay Neural Network (ATNN) capable of user-defined degeneration to the more common Time Delay Neural Network (TDNN). Time delays along axons or at the synapses, which vary in biological systems, motivate this research. The ATNN/TDNN test results and time series prediction capabilities are compared to those of the Real-Time Recurrent Learning (RTRL) algorithm. To show the advantages and disadvantages of using TDNN and ATNN for prediction versus the RTRL, the networks were applied to two problems: incommensurate sum of sine waves and financial time series. These data sets represent examples of nonlinear data with known and unknown mathematical functions, respectively. Although the RTRL predicted better than the ATNN for a known predictable function, this ATNN approach proved competitive in determining the direction of the future values for this function and outperforms the RTRL on the more difficult prediction task. The ATNN program, developed in C++ with an object-oriented framework, also takes much less computation time than the RTRL during training. DTIC

N94-25838# Melbourne Univ., Parkville (Australia). School of Physics.
A POSSIBLE WAY OF CONNECTING THE GRASSMANN VARIABLES AND THE NUMBER OF GENERATION
Xiao-Gang He Apr. 1993 7 p
(DE94-601624; UM-P-93/40; OZ-93/10) Avail: CASI HC A02/MF A01 (US Sales Only)

A Left-Right symmetric model is constructed in which the number of generation is related to Grassmann variables. Two sets of complex Grassmann variables (theta(sup 1)(sub 2), theta(sup 2)(sub 2)), (theta(sup 1)(sub l), theta(sup 2)(sub l)) are associated with left-and right-handed quark and lepton fields, respectively. Expanding quark and lepton fields in powers of the Grassmann variables, it was found that there are exactly three generations of quarks and leptons. Integrating out the Grassmann variables, phenomenologically acceptable fermion mass matrices were obtained. DOE

N94-25865 International Centre for Theoretical Physics, Trieste (Italy).
CONDITIONALLY EXPONENTIAL CONVEX FUNCTIONS ON LOCALLY COMPACT GROUPS

A. S. OkbEl-Bab Sep. 1992 9 p Limited Reproducibility: More than 20% of this document may be affected by microfiche quality
(DE93-613025; IC-92/275) Avail: CASI HC A02 (US Sales Only)

The main results of the thesis are: (1) the construction of a compact base for the convex cone of all conditionally exponential convex functions; and (2) the determination of the extreme parts of this cone. Some supplementary lemmas are proved for this purpose. DOE

N94-25867 International Centre for Theoretical Physics, Trieste (Italy).
(2,0) SUPERCONFORMAL ANOMALY
T. Lhallabi Aug. 1992 20 p Limited Reproducibility: More than 20% of this document may be affected by microfiche quality
(DE93-613046; IC-92/182) Avail: CASI HC A03 (US Sales Only)

The (2,0) supersymmetric Wess-Zumino-Polyakov, action is constructed and the (2,0) superconformal anomaly is given. The anomalous Ward-identity in the right sector is derived and the known operator product expansion of the N = 2 superstress energy tensor is recovered. DOE

N94-25880 International Centre for Theoretical Physics, Trieste (Italy).
APPROXIMATE SOLUTION OF THE FOURTH ORDER INITIAL VALUE PROBLEM USING DEFICIENT SPLINE POLYNOMIALS
M. N. AbouEl-Ela Sep. 1992 10 p Limited Reproducibility: More than 20% of this document may be affected by microfiche quality
(DE93-613023; IC-92/269) Avail: CASI HC A02 (US Sales Only)

We investigate in this paper the existence, uniqueness, consistency relations, and convergence for approximating the solution of the fourth order initial value problem using a spline of degree m and continuity class C(sup m-4)(0,b) and a step of length H = 4h. DOE

N94-25881 International Centre for Theoretical Physics, Trieste (Italy).
SOME PROPERTIES OF GENERALIZED BIREGULAR FUNCTIONS WITH VALUES IN A CLIFFORD ALGEBRA
Le Hung Son and Tran Quyet Thang Sep. 1992 11 p Limited Reproducibility: More than 20% of this document may be affected by microfiche quality
(DE93-613024; IC-92/270) Avail: CASI HC A03 (US Sales Only)

In this paper, some properties of holomorphic functions such as the Identity Theorem, the Maximum Modulus Principle, and the Hartogs Extension Theorem are proved for a class of more general functions taking values in a Clifford algebra than the regular and biregular functions. DOE

N94-25884# International Centre for Theoretical Physics, Trieste (Italy).
THE ALGEBRA OF NON-LOCAL CHARGES IN NON-LINEAR SIGMA MODELS
E. Abdalla, M. C. B. Abdalla, J. C. Brunelli (Universidade Estadual de Paulista, Sao Paulo, Brazil.), and A. Zadra (Universidade Estadual de Paulista, Sao Paulo, Brazil.) Jul. 1993 30 p
(DE94-601563; IC-93/220) Avail: CASI HC A03/MF A01 (US Sales Only)

The exact Dirac algebra obeyed by the conserved non-local charges in bosonic non-linear sigma models was obtained. Part of the computation is specialized for a symmetry group O(N). As it turns out the algebra corresponds to a cubic deformation of the Kac-Moody algebra. The non-linear terms are computed in closed form. In each Dirac bracket only highest order terms (as explained), defining a saturated algebra are found. The results for the presence of a Wess-Zumino term was generalized. The algebra is very similar to the previous one, containing now a calculable correction of order one unit lower. DOE

N94-25928# Minnesota Univ., Minneapolis.
CENTER FOR COMPUTATION AND VISUALIZATION OF GEOMETRIC STRUCTURES
12 Feb. 1993 28 p
(Contract DE-FG02-92ER-25137)
(DE94-001882; DOE/ER-25137/1) Avail: CASI HC A03/MF A01

The mission of the center is to establish a unified environment promoting research, education, and software and tool development. The work is centered on computing, interpreted in a broad sense to include the relevant theory, development of algorithms, and actual implementation. The research aspects of the center are focused on geometry; correspondingly the computational aspects are focused on three dimensional, and higher, visualization. The educational aspects are likewise centered on computing and focused on geometry. A broader term than education is 'communication' which encompasses the challenge of explaining to the world current research in mathematics, and specifically geometry. DOE

N94-26079# Los Alamos National Lab., NM.
TOWARDS A THEORY OF GROWING SURFACES: MAPPING TWO-DIMENSIONAL LAPLACIAN GROWTH ONTO HAMILTONIAN DYNAMICS AND STATISTICS
R. Blumenfeld 1993 17 p Presented at the Fluctuations and Order: The New Synthesis Workshop, Los Alamos, NM, 9-12 Sep. 1993
(Contract W-7405-eng-36)
(DE94-002636; LA-UR-93-3591; CONF-9309185-4) Avail: CASI HC A03/MF A01

I show that the evolution of a two dimensional surface in a Laplacian field can be described by Hamiltonian dynamics. First the growing region is mapped conformally to the interior of the unit circle, creating in the process a set of mathematical zeros and poles that evolve dynamically as the surface grows. Then the dynamics of these quasi-particles are transformed into a separable action-angle Hamiltonian that describes an orbital motion on a torus. A specific case is discussed explicitly, which demonstrates the integrability of the surface-tension-free Laplacian growth process. This formulation holds as long as the singularities of the map are confined to within the unit circle. This approach further allows for surface tension to be introduced as an energetic term in the resulting Hamiltonian which effects repulsion between the quasi-particles and the surface. These results are used here to formulate a first-principles statistical theory of pattern formation in stochastic growth, where noise is a key player. DOE

N94-26215# Technische Univ., Delft (Netherlands). Faculty of Technical Mathematics and Informatics.
PHASE PORTRAITS OF QUADRATIC SYSTEMS WITH FINITE MULTIPLICITY THREE AND ONE CRITICAL POINT OF INFINITY
J. W. Reyn and X. Huang 1993 22 p
(ISSN 0922-5641)
(Rept-93-41; ETN-94-95396) Copyright Avail: CASI HC A03/MF A01

A quadratic system is an autonomous system of ordinary differential equations. An approach to investigate the phase portraits of multiplicity 3, being characterized by the most complicated infinite critical points that can occur in multiplicity 3, is presented. A multiple infinite critical point is indicated by M(sub p, q)(sup i), where i indicates the index of the point, p the number of finite critical points and q the number of infinite critical points that can bifurcate from it. If p is different from zero, the point is transversally nonhyperbolic, and for multiplicity 3 there is one such point and p = 1. The most complicated infinite critical point is then a M(sub 1,3)(sup i), a fourth order saddle node with index 0, and the only critical point at infinity possible in the systems to be studied. Investigation of these systems should serve as a stepping stone toward the study of systems in multiplicity 3 with critical point M(sub 1,2)(sup i) and finally with a M(sub 1,1)(sup i). ESA

N94-26217# Center for Mathematics and Computer Science, Amsterdam (Netherlands). Dept. of Numerical Mathematics.
PRECONDITIONING IN PARALLEL RUNGE-KUTTA METHODS FOR STIFF INITIAL VALUE PROBLEMS
P. J. vanderHouwen and B. P. Sommeijer May 1993 17 p
(ISSN 0169-0388)
(CWI-NM-R9310; ETN-94-95414) Copyright Avail: CASI HC A03/MF A01

From a theoretical point of view, Runge-Kutta methods of collocation type belong to the most attractive step by step methods for integrating stiff problems. These methods combine excellent stability features with the property of superconvergence at the step points. Like the initial value problem itself, they only need the given initial value without requiring additional starting values, and therefore are a natural discretization of the initial value problem. On the other hand, from a practical point of view, these methods have the drawback of requiring in each step the solution of a system of equations of dimension sd, s and d being the number of stages and the dimension of the initial value problem, respectively. In contrast, linear multistep methods, the main competitor of Runge-Kutta methods, require the solution of systems of dimension d. However, parallel computers have changed the scene and motivated the design of parallel iteration methods for solving the implicit systems in such a way that the resulting methods become efficient step by step methods for integrating stiff initial value problems. ESA

N94-26226# Technische Univ., Eindhoven (Netherlands). Dept. of Mathematics and Computing Science.
THE GENERAL PICKUP AND DELIVERY PROBLEM
M. Sol and M. W. P. Savelsbergh Nov. 1992 26 p
(ISSN 0926-4493)
(MEMO-COSOR-92-44; ETN-94-94805) Avail: CASI HC A03/MF A01

In pickup and delivery problems vehicles have to transport loads from origins to destinations without transshipment at intermediate locations. Several characteristics that distinguish them from standard vehicle routing problems are presented. A survey of the problem types and solution methods found in the literature is given. The main problem in solving multiple vehicle pickup and delivery problems is the assignment of transportation requests to vehicles. Pickup and delivery problems, as well as other routing and scheduling problems, seem to be well suited for solution approaches based on set partitioning with column generation. An important obstacle in the development of effective and efficient approximation algorithms is the lack of a reliable measure of closeness. In vehicle routing problems, customers that are geographically close to each other are likely to be served by the same vehicle. A concept similar to that of geographical closeness in vehicle routing problems does not exist for pickup and delivery problems. None of the alternatives proposed turned out to be entirely satisfactory. The development of a useful closeness concept seems crucial for progress in approximation algorithms. ESA

N94-26227 Technische Univ., Eindhoven (Netherlands). Dept. of Mathematics and Computing Science.
A LINEAR DESCRIPTION OF THE DISCRETE LOT-SIZING AND SCHEDULING PROBLEM
C. P. M. vanHoesel and Antoon Kolen (Limburg State Univ., Maastricht, Netherlands.) Nov. 1992 21 p Limited Reproducibility: More than 20% of this document may be affected by microfiche quality
(ISSN 0926-4493)
(MEMO-COSOR-92-47; ETN-94-94808) Avail: CASI HC A03

An integer linear programming formulation for the discrete lot sizing and scheduling problem is presented. This polynomial size formulation is obtained from the model with the natural variables by splitting these variables. Its linear programming relaxation is shown to be tight, by reformulating it as a shortest path problem. A dynamic programming formulation for the discrete lot sizing and scheduling problem is provided. Both the linear description and the dynamic programming recursion can be generalized to the multi-item case. The shortest path model then extends to an $(N + 1)$ dimensional network, N being the number of items. The model grows quickly with the number of items and the most practical way to use this formulation is to split a multi-item discrete lot sizing and scheduling problem in N single item problems and solve each with the linear program. The separation problem for the single item can also be modeled as a shortest path problem. By then, if any nonintegral variables are still left specific multi-item constraints may be added. ESA

N94-26229 Leiden Univ. (Netherlands). Dept. of Mathematics and Computer Science.
ON THE ERROR COMMITTED BY STOPPING THE NEWTON ITERATION IN IMPLICIT RUNGE-KUTTA METHODS
M. N. Spijker Feb. 1993 16 p Submitted for publication Limited Reproducibility: More than 20% of this document may be affected by microfiche quality
(TW-93-02; ETN-94-94833) Avail: CASI HC A03

The numerical solution of initial value problems for nonlinear ordinary differential equations by implicit Runge-Kutta methods is considered. For stiff problems, Picard iteration is not appropriate and some variant of the Newton method is used. The problem of estimating the stopping error of Newton like iterations is discussed. An understanding of this error comparable to what is known about Picard iterations is obtained. Because of stiffness, the theory is more delicate than for Picard iterations. Various estimates of the Newton stopping errors are reviewed. The effect of these errors on the Runge-Kutta approximations to the solution of the given initial value problem is analyzed. Most of the error estimates established reflect order reduction phenomena in the presence of stiffness. This order reduction is confirmed by numerical experiments. ESA

N94-26252 Technische Univ., Delft (Netherlands). Faculty of Technical Mathematics and Informatics.
ON THE ROBUSTNESS OF A MULTIPLE SEMI-COARSENED GRID METHOD
C. W. Oosterlee and P. Wesseling 1993 16 p Limited Reproducibility: More than 20% of this document may be affected by microfiche quality
(ISSN 0922-5641)
(Rept-93-51; ETN-94-95405; PB94-125309) Avail: CASI HC A03

The robustness of a non standard multigrid method called Multiple Semi-coarsened Grids (MSG) is investigated. The smoother is a damped point Jacobi relaxation method. Three different coarse grid correction strategies are implemented and compared. Roboustness is investigated by solving the rotated anisotropic diffusion equation and the convection diffusion equation. Good convergence results are obtained for the reference problems, the rotated anisotropic diffusion equation and the convection diffusion equation, solved with MSG on a very fine mesh. Interesting future developments will be the investigation for three dimensional problems and the investigation of the performance on a massive parallel computer. ESA

N94-26267# International Centre for Theoretical Physics, Trieste (Italy).
ON POISSON BRACKETS AND SYMPLECTIC STRUCTURES FOR THE CLASSICAL AND QUANTUM ZITTERBEWEGUNG
A. O. Barut and N. Unal Jun. 1993 6 p
(DE93-634305; IC-93/134) Avail: CASI HC A02/MF A01 (US Sales Only)

The symplectic structures (brackets, hamilton's equations and Lagrange's equations) for Dirac electron and its classical model have exactly the same form. We give explicitly the Poisson brackets in the dynamical variables (chi(sup mu), p(sup mu), nu(sup nu), S(sup mu nu)). The only difference is in the normalization of Dirac velocities gamma(sub mu)(gamma(sup mu)) = 4 which has significant consequences. DOE

N94-26302# Arizona State Univ., Tempe. Dept. of Mathematics.
CONTINUATION AND MULTI-GRID FOR BIFURCATION PROBLEMS Final Report, 1 Dec. 1989 - 15 Aug. 1993
Hans D. Mittelmann 31 Dec. 1993 13 p
(Grant AF-AFOSR-0080-90)
(AD-A274965; AFOSR-94-0018TR) Avail: CASI HC A03/MF A01

An overview is given of the work completed under grant AFOSR-90-0080 since December 1989. The research concerned the numerical solution of bifurcation and nonlinear eigenvalue problems for parameter-dependent partial differential equations and systems. The scope of the research is rather wide, stressing the development, study, and implementation of computational methods for several classes of difficult nonlinear problems, but also including the derivation of analytic results in cases where these questions had not been settled before. This grant was a continuation and extension of grant AFOSR-84-315. The earlier grant has resulted in 26 papers over a five-year period. The present grant resulted in the publication of 18 papers in refereed journals or refereed high-quality proceedings volumes and of one book. Several of the 26 papers generated under the earlier grant were listed as to appear in the final report for that grant. They all have appeared but are not listed here again. Instead, for simplicity, the papers and books produced under the present grant are referred to by giving the corresponding number in the list of all publications which is a part of the attached curriculum vitae. DTIC

N94-26366# International Centre for Theoretical Physics, Trieste (Italy).
MATRIX NEAR RINGS AND PSEUDO DISTRIBUTIVITY
S. J. Abbasi Jun. 1993 5 p
(DE94-601505; IC-93/150) Avail: CASI HC A01/MF A01 (US Sales Only)

This paper shows the insights picture of matrix near rings constructed over pseudo distributive near rings. The main result says that pseudo distributive matrix near rings, are, in fact, rings. DOE

N94-26367# International Centre for Theoretical Physics, Trieste (Italy).
WINDING NUMBERS IN HOMOTOPY THEORY FROM INTEGERS TO REALS

M. Mekhfi Jul. 1993 12 p
(DE94-601510; IC-93/223) Avail: CASI HC A03/MF A01 (US Sales Only)

In Homotopy Theory (HT), we define paths on a given topological space. Closed paths prove to be construction elements of a group (the fundamental group) Pi(sub 1) and carry charges, the winding numbers. The charges are integers as they indicate how many times closed paths encircle a given hole (or set of holes). Open paths, as they are defined in (HT), do not possess any groups structure and as such they are less useful in topology. In the present paper, we enlarge the concept of a path in such a way that both types of paths do possess a group structure. In this broad sense we have two fundamental groups the Pi(sub i) = Z group and the SO(2) group of rotations but the latter has the global property that there is no periodicity in the rotation angle. There is also two charge operators W and W(sub lambda) whose eigenvalues are either integers or reals depending respectively on the paths being closed or open. Also the SO(2) group and the real charge operator, W(sub lambda), are not independently defined but directly related respectively to the Pi(sub i) group and to the integer charge operator W. Thus, well defined links can be established between seemingly different groups and charges. DOE

N94-26408 International Centre for Theoretical Physics, Trieste (Italy).
STABILITY OF LARGE SCALE INTERCONNECTED DYNAMICAL SYSTEMS
E. P. Akpan Jul. 1993 9 p Limited Reproducibility: More than 20% of this document may be affected by microfiche quality
(DE94-601536; IC-93/176) Avail: CASI HC A02 (US Sales Only)

Large scale systems modeled by a system of ordinary differential equations are considered and necessary and sufficient conditions are obtained for the uniform asymptotic connective stability of the systems using the method of cone-valued Lyapunov functions. It is shown that this model significantly improves the existing models. DOE

N94-26409 International Centre for Theoretical Physics, Trieste (Italy).
CHARACTERIZATION OF SELF-CONJUGATE MINIMAL SURFACES IN R(SUP 3)
Weihuan Chen Jul. 1993 14 p Limited Reproducibility: More than 20% of this document may be affected by microfiche quality
(DE94-601538; IC-93/199) Avail: CASI HC A03 (US Sales Only)

In this paper, we continue to consider self-conjugate minimal surfaces in R(sup 3), i.e., minimal surfaces which congruent with their conjugate ones, and we want to characterize them in terms of their metrics and to study their further properties. DOE

N94-26410# International Centre for Theoretical Physics, Trieste (Italy).
NUMERICAL SOLUTION OF SINGULARITY-PERTURBED TWO-POINT BOUNDARY-VALUE PROBLEMS
R. W. P. Masenge Jul. 1993 11 p
(DE94-601542; IC-93/209) Avail: CASI HC A03/MF A01 (US Sales Only)

Physical processes which involve transportation of slowly diffusing substances in a fast-flowing medium are mathematically modelled by so-called singularly-perturbed second order convection diffusion differential equations in which the convective first order terms dominate over the diffusive second order terms. In general, analytical solutions of such equations are characterized by having sharp solution fronts in some sections of the interior and/or the boundary of the domain of solution. The presence of these (usually very narrow) layer regions in the solution domain makes the task of globally approximating such solutions by standard numerical techniques very difficult. In this expository paper we use a simple one-dimensional prototype problem as a vehicle for analysing the nature of the numerical approximation difficulties involved. In the sequel, we present, without detailed derivation, two practical numerical schemes which succeed in varying degrees in numerically resolving the layer of the solution to the prototype problem. DOE

N94-26412# International Centre for Theoretical Physics, Trieste (Italy).
ENUMERATION OF n-FOLD TANGENT HYPERPLANES TO A SURFACE
I. Vainsencher Aug. 1993 21 p
(DE94-601544; IC-93/232) Avail: CASI HC A03/MF A01 (US Sales Only)

For each 1 (less than or = n less than or = 6) we present formulas for the number of n-nodal curves in an n-dimensional linear systems on a smooth, projective surface. The method yields in particular the numbers of rational curves in the system of hyperplane sections of a generic K3-surface imbedded in P(sup n) by a complete system of curves of genus n as well as the number 17,601,000 of rational (singular) plane quintic curves in a generic quintic threefold. DOE

N94-26425# International Centre for Theoretical Physics, Trieste (Italy).
GAUGING OF CHERN-SIMONS p-BARNES
R. P. Zaikov Aug. 1993 9 p
(DE94-601553; IC-93/236) Avail: CASI HC A02/MF A01 (US Sales Only)

The Chern-Simons membranes and in general the Chern-Simons p-branes moving in D-dimensional target space admit an infinite set of secondary constraints. With respect to the Poisson bracket these constraints form a closed algebra which contains classical W(sub 1 + infinity) algebra in p-dimensions as a superalgebra. Corresponding gauged theory in the phase-space is constructed in a Hamilton gauge as an analogue of the ordinary W-gravity. DOE

N94-26440 International Centre for Theoretical Physics, Trieste (Italy).
FINITE DIMENSIONAL REPRESENTATIONS OF THE QUANTUM SUPERALGEBRA U(SUB q)(gl(3/2))
T. D. Palev and N. I. Stoilova (Ghent Univ., Belgium.) Jun. 1993 8 p Limited Reproducibility: More than 20% of this document may be affected by microfiche quality
(DE93-634303; IC-93/123) Avail: CASI HC A02 (US Sales Only)

For generic q, we give expressions for the transformations of all essentially typical finite-dimensional modules of the Hopf superalgebra U(sub q)(gl(3/2)). The latter is a deformation of the universal enveloping algebra of the Lie superalgebra gl(3/2). The basis within each module is similar to the Gel'fand-Zetlin basis for gl(5). We write down expressions for the transformations of the basis under the action of the Chevalley generators. DOE

N94-26441 International Centre for Theoretical Physics, Trieste (Italy).
ON THE PHI(SUB 0)-STABILITY OF PERTURBED NONLINEAR DIFFERENTIAL SYSTEMS
E. P. Akpan Jun. 1993 13 p Limited Reproducibility: More than 20% of this document may be affected by microfiche quality
(DE93-634304; IC-93/132) Avail: CASI HC A03 (US Sales Only)

In this paper, we investigate the exponential Phi(sub 0)-stability and total Phi(sub 0)-stability of perturbed nonlinear differential systems. We assume that an invariant set u = 0 of the unperturbed system has exponential and total Phi(sub 0)-stability properties, we then study the effect of the perturbation of u = 0. We give conditions under which these Phi(sub 0)-stability properties are preserved under certain perturbations. DOE

N94-26442 Instituto de Fisica Teorica, Sao Paulo (Brazil).
QUANTUM HAMILTONIAN DIFFERENTIAL GEOMETRY: HOW DOES QUANTIZATION AFFECT SPACE?
R. Aldrovandi Jan. 1993 52 p Limited Reproducibility: More than 20% of this document may be affected by microfiche quality
(DE93-634306; IFT-P-004/93) Avail: CASI HC A04 (US Sales Only)

Quantum phase space is given a description which entirely parallels the usual presentation of Classical Phase Space. A particular Schwinger unitary operator basis, in which the expansion of each operator is its own Weyl expression, is specially convenient for the purpose. The quantum Hamiltonian structure obtains from the classical structure by the conversion of the classical pointwise product of dynamical quantities into the noncommutative star product of Wigner functions. The main qualitative difference in the general structure is that, in the quantum case, the inverse symplectic matrix is not simply antisymmetric. This difference leads to the presence of braiding in the backstage of Quantum Mechanics. DOE

N94-26457# Gosudarstvennyi Komitet po Ispolzovaniyu Atomnoi Energii, Serpukhov (USSR). Inst. Fiziki Vysokikh Ehnergij.
STATISTICAL MECHANICAL PROPERTIES OF Z(N)(SUP n-1) BROKEN MODEL
S. M. Sergeev 1992 9 p

(DE93-634344; IHEP-OTF-92-46) Avail: CASI HC A02/MF A01 (US Sales Only)

The formulation of the Z(sub N)(sup n-1) broken model is given. The partition function is obtained under an assumption of analyticity. A string function for the local state probabilities was also found. DOE

N94-26458 International Centre for Theoretical Physics, Trieste (Italy).
CONE-VALUED LYAPUNOV FUNCTIONS AND THE STABILITY OF STOCHASTIC DIFFERENTIAL EQUATIONS
E. P. Akpan Jul. 1993 14 p Limited Reproducibility: More than 20% of this document may be affected by microfiche quality
(DE94-601504; IC-93/121) Avail: CASI HC A03 (US Sales Only)

Stochastic differential equations of Ito-type are considered and the theory of stochastic differential inequalities is systematically developed. Sufficient conditions for stability in probability, with probability one and in the mean of the Ito-type stochastic differential equations are given, using the method of cone-valued Lyapunov functions. Necessary conditions for the construction of stochastic cone-valued Lyapunov functions are obtained for the cases where the Ito-type stochastic differential equations have uniform asymptotic stability in probability and uniform asymptotic stability in the mean. DOE

N94-26459 International Centre for Theoretical Physics, Trieste (Italy).
THE HAMILTONIAN STRUCTURES OF THE SUPER KP HIERARCHY ASSOCIATED WITH AN EVEN PARITY SUPERLAX OPERATOR
J. Barcelos-Neto, Sasanka Ghosh, and Shibaji Roy Jul. 1993 14 p Limited Reproducibility: More than 20% of this document may be affected by microfiche quality
(DE94-601506; IC-93/179) Avail: CASI HC A03 (US Sales Only)

The even parity superLax operator for the supersymmetric KP hierarchy of the form L = D(sup 2) + (Sigma)(sup infinity)(sub i = 0) u(sub i-2)D(sup -i+1) was considered and the two Hamiltonian structures following the standard method of Gelfand and Dikii were obtained. It was observed that the first Hamiltonian structure is local and linear whereas the second Hamiltonian structure is non-local and nonlinear among the superfields appearing in the Lax operator. Their connections with the super omega(sub infinity) algebra are discussed briefly. DOE

N94-26471 Joint Inst. for Nuclear Research, Dubna (USSR). Lab. of Computing Techniques and Automation.
ON A SPLINE-APPROXIMATION METHOD FOR SOLVING ORDINARY DIFFERENTIAL EQUATIONS [O METODE SPLAJN-APPROKSIMATSII RESHENIYA OBYKNOVENNYKH DIFFERENTSIAL'NYKHURAVNENIJ]
T. Zhanlav 1992 14 p In RUSSIAN Limited Reproducibility: More than 20% of this document may be affected by poor print and microfiche quality
(DE93-634290; JINR-R-5-92-111) Avail: Issuing Activity (Department of Energy (DOE)) (US Sales Only)

The properties of the collocating spline method for approximating the solution of boundary value problems of second order differential equations are studied. The expansion of coefficients of the spline, in degrees of step of the uniform mesh, is obtained. A method of solving the five-point spline scheme with higher accuracy is suggested, and the convergence of approximate solution and its derivatives is established. DOE

N94-26601*# Institute for Computer Applications in Science and Engineering, Hampton, VA.
RECONSTRUCTION OF MULTIPLE CRACKS FROM EXPERIMENTAL ELECTROSTATIC BOUNDARY MEASUREMENTS Final Report
Kurt Bryan (Rose-Hulman Inst. of Tech., Terre Haute, IN.), Valdis Liepa (Michigan Univ., Ann Arbor.), and Michael Vogelius (Rutgers Univ., New Brunswick, NJ.) Dec. 1993 31 p Submitted for publication
(Contracts NAS1-18605; NAS1-19480; NSF DMS-92-02042; RTOP 505-90-52-01)
(NASA-CR-191584; NAS 1.26:191584; ICASE-93-96) Avail: CASI HC A03/MF A01

An algorithm for recovering a collection of linear cracks in a homogeneous electrical conductor from boundary measurements of voltages induced by specified current fluxes is described. The technique is a variation of Newton's method and is based on taking weighted averages of the boundary data. An apparatus that was constructed specifically for generating laboratory data on which to test the algorithm is also described. The algorithm is applied to a number of different test cases and the results are discussed. Author (revised)

N94-26614 Simon Fraser Univ., Burnaby (British Columbia). School of Computing Science.
COLOUR OBJECT RECOGNITION M.S. Thesis
G. D. Finlayson Apr. 1992 82 p
(ISBN-0-315-83684-9; CTN-94-61033) Copyright Avail: Micromedia Ltd., Technical Information Centre, 240 Catherine Street, Suite 305, Ottawa, Ontario, K2P 2G8, Canada HC/MF

Since color characterizes local surface properties and is largely viewpoint insensitive, it is a useful cue for object recognition. A simple color indexing scheme that identifies objects by matching color-space histograms fails if the intensity or spectral characteristics of the incident illuminant varies. Two strategies for rectifying this failure are examined. A color constancy transform is first applied to each image prior to color indexing. Several color constancy algorithms are reviewed and in almost all cases it is concluded that their assumptions are too limiting. The exception, a discrete implementation of Forsyth's CRULE, successfully solves the color constancy problem for sets of simple objects viewed under constant illumination. To circumvent the need for color constancy preprocessing and to recognize more complex object sets, indexing on illuminant invariants (volumetric, ratio, and opponent) is considered. An algorithm is developed which identifies objects by matching color ratio-space histograms. In general, this algorithm performs comparably with color indexing under fixed illumination, but substantially better than color indexing under varying illumination. Author (CISTI)

N94-26640 York Univ. (Ontario). Dept. of Physics and Astronomy.
A NUMERICAL SOLUTION TO THE ONE AND TWO DIMENSIONAL LINE RADIATIVE TRANSFER EQUATION Ph.D. Thesis
Erik Griffioen Jul. 1993 149 p
(ISBN-0-315-84258-X; CTN-94-61031) Copyright Avail: Micromedia Ltd., Technical Information Centre, 240 Catherine Street, Suite 305, Ottawa, Ontario, K2P 2G8, Canada HC/MF

A new, simple, and powerful technique for solving radiative transfer problems has been developed and coded for a two level (bound state) atom in one- and two-dimensional Cartesian coordinate systems. Scattering is assumed to be isotropic in angle, with either monochromatic or complete frequency redistribution (CFR), and has been broadened to include angle averaged frequency redistribution (AAFR). The formal solution is based on the lambda operator method. For optically thick scattering media, convergence is very slow using straight lambda iteration. Rapid and robust convergence is attained using an intermediate operator which is readily evaluated. Linear extrapolation based on previous iterates increases the convergence rate further. The one-dimensional model intensity versus frequency profiles are found to compare favorably with those using other proven models. Two-dimensional results are presented in terms of an auroral source in an optically thick scattering isothermal medium. The effect of angle quadrature, auroral source location, CFR versus AAFR, and conservative versus nonconservative scattering on the results are explored. The effect of lateral spreading of the OI 1304 A triplet auroral emissions in the Earth's thermosphere has been modelled and was found to be quite significant. Author (CISTI)

N94-26659 Toronto Univ. (Ontario). Inst. for Aerospace Studies.
SIMULATION DYNAMICS OF A MULTIBODY CHAIN: RECURSION BASED ON CHAIN MODAL COORDINATES M.S. Thesis
Anne Marie Christine Bornath 1993 85 p
(ISBN-0-315-83555-9; CTN-94-61040) Copyright Avail: Micromedia Ltd., Technical Information Centre, 240 Catherine Street, Suite 305, Ottawa, Ontario, K2P 2G8, Canada HC/MF

A computer implementation of a new method for the solution of the simulation dynamics of a chain of bodies is presented. The simulation dynamics was developed by D'Eleuterio and utilizes chain coordinates and the implementation uses the LSODE software package and a finite element procedure. The algorithm is recursive in the sense that it deals with the rigid coordinates on a body-by-body basis and then solves for the elastic coordinates as an additional step. The computer code is applicable to chains of rigid and/or flexible bodies connected by joints of up to three rotational degrees of freedom. Numerical results of applying the procedure to an example manipulator similar to the space shuttle Canadarm are presented. These results are compared to numerical results obtained from an implementation of a recursive algorithm based on body modes. This comparison shows that the new method allows fewer elastic degrees of freedom to be used without a significant loss in accuracy of the results. The use of fewer elastic coordinates is accompanied by a significant reduction in computational time required. Thus the chain coordinate method is a potential improvement over existing procedures. Author (CISTI)

N94-26768 Gosudarstvennyi Komitet po Ispolzovaniyu Atomnoi Energii, Serpukhov (USSR).

KINETIC EQUATION IDENTIFICATION FROM MEASUREMENT OF A PARTICULAR SOLUTION

M. Z. Tarasko 1992 15 p Limited Reproducibility: More than 20% of this document may be affected by microfiche quality
(DE93-634585; FEI-2291) Avail: CASI HC A03 (US Sales Only)

The problem of kinetic identification is stated as an estimation of differential equation parameters by the measured values of the process to be observed. The technique of parameter evaluation is presented with the recurrent calculational formulas input. Step-by-step algorithm of technique implementation is presented. Algorithm efficiency is illustrated by a numerical example of kinetic processes identification in nuclear-excited plasma. DOE

N94-26773# Center for Mathematics and Computer Science, Amsterdam (Netherlands). Dept. of Numerical Mathematics.

LOCAL UNIFORM GRID REFINEMENT AND SYSTEMS OF COUPLED PARTIAL DIFFERENTIAL EQUATIONS

Ron A. Trompert Mar. 1993 32 p
(ISSN 0169-0388)
(CWI-NM-R9307; ETN-94-95411) Copyright Avail: CASI HC A03/MF A01

An adaptive grid method based on local uniform grid refinement applied to systems of coupled time dependent PDE's (Partial Differential Equations) is considered. Local uniform grid refinement means that the PDE's are solved on a series of nested, uniform, increasingly finer subgrids which cover only a part of the domain. These subgrids are created up to a level of refinement where sufficient spatial accuracy is obtained and their location and shape is adjusted after each time step in order to follow the moving steep fronts. When a system of coupled PDE's is solved, the behavior of the local and global error associated with each separate PDE can be very different from one PDE to another. A refinement strategy based on a global error analysis, which takes these differences into account, was developed. This refinement strategy aims at the domination of the global space error by the space discretization error at the finest subgrid. ESA

N94-26776# Center for Mathematics and Computer Science, Amsterdam (Netherlands). Dept. of Computer Science.

SEMANTICS, ORDERINGS AND RECURSION IN THE WEAKEST PRECONDITION CALCULUS

Marcello Bonsangue and Joost N. Kok (Utrecht State Univ., Netherlands.) Dec. 1992 61 p Sponsored in part by Milan Univ., Italy, and CNR
(ISSN 0169-118X)
(CWI-CS-R9267; ETN-94-95419) Copyright Avail: CASI HC A04/MF A01

An extension of Dijkstra's guarded command language is studied, including sequential composition, demonic choice and a backtrack operator. Three orderings on this language are considered: a refinement ordering defined by Back, a deadlock ordering, and an approximation ordering of Nelson. The deadlock ordering is in between the two other orderings. All operators are monotonic in Nelson's ordering, but backtracking is not monotonic in Back's ordering and sequential composition is not monotonic for the deadlock ordering. At first sight recursion can only be added using Nelson's ordering. By extending the theory of fixed points in partial orderings, it is shown that, under certain circumstances, least fixed points for non monotonic functions can be obtained by iteration from the least element. This permits the addition of recursion even using Back's ordering or the deadlock ordering. In order to give a semantic characterization of the three orderings that relates initial states to possible outcomes of the computation, the relations between predicate transformers and discrete powerdomains are studied. Three powerdomains are considered: two versions of the Smyth powerdomain and the Egli-Milner powerdomain. For each of them an isomorphism is proved with a suitable domain of predicate transformers. ESA

N94-26812# Nationaal Inst. voor Kernfysica en Hoge Energiefysica, Amsterdam (Netherlands).

SIMPLE CURRENTS VERSUS ORBIFOLDS WITH DISCRETE TORSION: A COMPLETE CLASSIFICATION

M. Kreuzer (European Organization for Nuclear Research, Geneva, Switzerland.) and A. N. Schellekens 1993 28 p
(NIKHEF-H/93-13; CERN-TH.6912/93; ETN-94-95045) Avail: CASI HC A03/MF A01

Simple current modular invariants, extending results for (Z(sub p))(sup k) to arbitrary centers are classified. An explicit formula for the most general case is obtained. Using orbifold techniques, a one to one correspondence between simple current invariants and subgroups of the center with discrete torsions is found. The conjectured monodromy independence of the total number of such invariants is proven. The orbifold approach works in a straightforward way for symmetries of odd order. Modifications are required to deal with symmetries of even order. With these modifications the orbifold construction with discrete torsion is complete within the class of simple current invariants. ESA

N94-26818# Technische Univ., Delft (Netherlands). Faculty of Technical Mathematics and Informatics.

NESTED KRYLOV METHODS BASED ON GCR

E. deSturler 1993 28 p Sponsored by Shell Research B.V., Netherlands, and STIPT
(ISSN 0922-5641)
(PB94-125317; Rept-93-50; ETN-94-95404) Copyright Avail: CASI HC A03/MF A01

The GMRESR method for the solution of linear systems of equations is presented. The GMRESR involves an inner and an outer method. The outer method is GCR, which is used to compute the optimal approximation over a given set of direction vectors in the sense that the residual is minimized. The inner method is GMRES, which at each step computes a new direction vector by approximately solving the residual equation. This direction vector is then used by the outer algorithm to compute a new approximation. The optimality of the approximation over the space of search directions is ignored in the inner GMRES algorithm. This leads to suboptimal corrections to the solution in the outer algorithm. The orthogonality relations of GCR in the inner GMRES algorithm is preserved. Some of the Krylov method properties are discussed. The results show that in terms of matrix vector multiplications this modification always leads to better convergence. Because of the additional orthogonalizations, it does not always give an improved performance in time. The experimental results indicate, that especially for such methods it is advantageous to preserve the orthogonality in the inner method. ESA

N94-26829# Air Force Inst. of Tech., Wright-Patterson AFB, OH. School of Engineering.

THREE DIMENSIONAL OBJECT RECOGNITION USING A COMPLEX AUTOREGRESSIVE MODEL M.S. Thesis

David E. Chelen Dec. 1993 112 p
(AD-A274388; AFIT/GE/ENG/93D-04) Avail: CASI HC A06/MF A02

Based on an autoregressive model, Complex Partial Correlation (CPARCOR) features are known to provide exceptional Position, Scale, and Rotation Invariant (PSRI) properties for planar 2-dimensional (2-D) object recognition. Although autogressive models have been successfully applied to numerous spatio-temporal recognition tasks, the effects of out-of-plane image rotations were never considered. This study investigates application of the CPAR-COR model to a five class problem of nonplanar 2-D views of 3-D objects. Recognition based on CPAR-COR features is evaluated using a Template Matching algorithm, two K-Nearest-Neighbor (KNN) classifiers, and a Hidden Markov Model (HMM). Direct comparisons to recognition based on Fourier features are made. Results indicate that the CPAR-COR model parameters provide useful shape-features for recognition of out-of-plane rotations. Displaying exceptional PSRI properties, the features are shown capable of classification by simple nonadaptive recognition schemes. Relatively successful results are obtained for a variety of tests. The advantage of classification by a multiple-look technique over the traditional single-look method is clearly demonstrated. Feature space crowding is noted as the cause of unusual recognition rates for occluded-view tests. Although general trends are noted, optimal model order and selection of CPARCOR versus Fourier features are considered application dependent. DTIC

N94-26898 International Centre for Theoretical Physics, Trieste (Italy).
DEFORMATION OF THE EXTERIOR ALGEBRA AND THE GL(SUB q) (r, INCLUDED IN) ALGEBRA
A. ElHassouni, Y. Hassouni, and M. Zakkari Jun. 1993 7 p Limited Reproducibility: More than 20% of this document may be affected by microfiche quality
(DE94-602558; IC-93/156) Avail: CASI HC A02

The deformation of the associative algebra of exterior forms is performed. This operation leads to a Yang-Baxter (Y.B.) equation. Its relation with the braid group B(sub n-1) is analyzed. The correspondence of this deformation with the GL(sub q)(r, included in) algebra is developed. DOE

N94-26915 Technische Univ., Twente (Netherlands). Dept. of Applied Mathematics.
CLASSIFICATION OF LINEAR DIFFERENTIAL OPERATORS WITH AN INVARIANT SUBSPACE IN MONOMIALS
G. F. Post and A. Turbiner (Institute for Theoretical and Experimental Physics, Moscow, USSR.) Jun. 1993 14 p Prepared in cooperation with Gosudarstvennyi Komitet po Ispol'zovaniyu Atomnoi Energii SSSR, Moscow. Inst. Teoreticheskoi i Eksperimental'noi Fiziki Limited Reproducibility: More than 20% of this document may be affected by microfiche quality
(PB94-126620; MEMO-1143) Avail: CASI HC A03

A complete classification of linear differential operators, possessing finite-dimensional invariant subspace with a basis in monomials, is presented. NTIS

N94-26917# Technische Univ., Twente (Netherlands). Dept. of Applied Mathematics.
COMMUNICATION COMPLEXITY OF t-INTERSECTION PROBLEMS IN GENERALIZED BOOLEAN ALGEBRAS
U. Faigle, W. Kern, and B. Spieker Jun. 1993 20 p
(PB94-126646; MEMO-1141) Avail: CASI HC A03/MF A01

The following game is considered: Two players independently choose a chain in a partially ordered set. How many bits of information have to be communicated until at least one of the players knows whether the chains have exactly t elements in common? This model generalizes the t-intersection problem for subsets of a finite set. The deterministic communication complexity is established in general. For the special cases of generalized Boolean algebras, improved nondeterministic and probabilistic protocols are presented that are of optimal order of complexity for classes with fixed width q. NTIS

N94-26936# California Univ., Berkeley. Lawrence Berkeley Lab.
AN OPTIMAL CONSTRAINED LINEAR INVERSE METHOD FOR MAGNETIC SOURCE IMAGING
P. Hughett Sep. 1993 42 p
(Contract DE-AC03-76SF-00098)
(DE94-002264; LBL-34512) Avail: CASI HC A03/MF A01

Magnetic source imaging is the reconstruction of the current distribution inside an inaccessible volume from magnetic field measurements made outside the volume. If the unknown current distribution is expressed as a linear combination of elementary current distributions in fixed positions, then the magnetic field measurements are linear in the unknown source amplitudes and both the least square and minimum mean square reconstructions are linear problems. This offers several advantages: The problem is well understood theoretically and there is only a single, global minimum. Efficient and reliable software for numerical linear algebra is readily available. If the sources are localized and statistically uncorrelated, then a map of expected power dissipation is equivalent to the source covariance matrix. Prior geological or physiological knowledge can be used to determine such an expected power map and thus the source covariance matrix. The optimal constrained linear inverse method (OCLIM) derived in this paper uses this prior knowledge to obtain a minimum mean square error estimate of the current distribution. OCLIM can be efficiently computed using the Cholesky decomposition, taking about a second on a workstation-class computer for a problem with 64 sources and 144 detectors. Any source and detector configuration is allowed as long as their positions are fixed a priori. Correlations among source and noise amplitudes are permitted. OCLIM reduces to the optimally weighted pseudo-inverse method of Shim and Cho if the source amplitudes are independent and identically distributed and to the minimum-norm least squares estimate in the limit of no measurement noise or no prior knowledge of the source amplitudes. In the general case, OCLIM has better mean square error than either previous method. OCLIM appears well suited to magnetic imaging, since it exploits prior information, provides the minimum reconstruction error, and is inexpensive to compute. DOE

N94-26962 Technische Univ., Twente (Netherlands). Dept. of Applied Mathematics.
SOME PROPERTIES OF GRAPHS WITH LOCAL ORE CONDITIONS
A. S. Asratian Jun. 1993 16 p Sponsored by Nederlandse Organisatie voor Wetenschappelijk Onderzoek, The Hague Limited Reproducibility: More than 20% of this document may be affected by microfiche quality
(PB94-126612; MEMO-1140) Avail: CASI HC A03

It is shown that a connected graph G of order at least 3 is hamiltonian if for each vertex x the subgraph G(sub 1)(x) induced by x and its neighbors in G is an Ore graph. We prove here that a graph G satisfying the above conditions is fully cycle extendable. Moreover, G is panconnected if and only if G is 3-connected and G does not = K(sub n) (joint operation symbol) (bar-K(sub n)) for some n greater than or equal to 3. The paper is concluded with two conjectures. NTIS

N94-26967# Technische Univ., Delft (Netherlands). Faculty of Technical Mathematics and Informatics.
A NON-LINEAR MATHEMATICAL MODEL OR FINITE, PERIODIC RAIL CORRUGATIONS
J. Piotrowski (Warsaw Univ., Poland.) and J. J. Kalker 1993 16 p
(ISSN 0922-5641)
(Rept-93-49; ETN-94-95403) Copyright Avail: CASI HC A03/MF A01

A nonlinear mathematical model of rail corrugations which takes into account nonlinear contact mechanical and geometrical properties of wheel/rail contact is presented. The contact area is approximated by an ellipse and a steady state rolling contact code is used for the description of creep forces. The preliminaries of a theory in which nonlinearity of the contact problem is fully taken into account are summarized. The following aspects are considered: the contact formation on sinusoidal corrugation in its dependence on load and position; the corrugation formation taking place as a consequence of abrasive wear, which is assumed linearly proportional to the frictional work performed in the contact area. ESA

N94-26972# Army Research Lab., Adelphi, MD.
THE MORPHOLOGICAL PROCESSING OF BINARY IMAGES Interim Report, Sep. 1991 - Feb. 1993
Dennis W. McGuire Oct. 1993 70 p
(AD-A274310; ARL-TR-283) Avail: CASI HC A04/MF A01

The morphological processing of binary images is treated in depth from the viewpoint of ordered topology. The basic ideas of Nachbin arid Birkhoff concerning when a partial ordering of a set that has a topology is compatible with that topology are used to obtain a definition of an order resolvable topological ordered space. This abstraction is then used to define semicontinuity in a sufficiently general way to unify its treatment in mathematical morphology. This is followed by a detailed review of the basic concepts of closed-set morphology. In this review, a more thorough treatment than is available elsewhere is given of the several limit concepts used in morphology; likewise, the continuity properties of the erosion, dilation, and homothesis operations are more thoroughly treated than is usual. The morphological transformation and transformation space theory of closed-set morphology is presented in a systematic way that incorporates the relevant contributions of Matheron and Maragos, as well as the recent important work of Banon and Barrera. Finally, a class of countable closed-set bases for the underlying hit-miss topology is used to derive a novel representation of morphological transformations. DTIC

N94-26993# Institut des Hautes Etudes Scientifiques, Bures-sur-Yvette (France).
SPACES OF ALGEBRAIC CYCLES
H. Blaine Lawson, Jr. Aug. 1993 93 p Prepared for NSF, Washington, DC
(PB94-124369; IHES/M-93/46) Avail: CASI HC A05/MF A01

A recent body of work is reviewed which is concerned with the structure of the spaces of algebraic cycles on an algebraic variety. Topics covered include: Algebraic Cycles; Suspension and Join; Cycles on P(sup n) and Classifying Spaces; the Functor L(sub *)H(sub *); The Functor L(sup *)H(sup *) (Morphic Cohomology); and Duality. NTIS

N94-26994# Institut des Hautes Etudes Scientifiques, Bures-sur-Yvette (France).
LYAPUNOV EXPONENTS FOR SOME QUASI-PERIODIC COCYCLES
L. S. Young Aug. 1993 31 p Prepared for NSF, Washington, DC
(PB94-124377; IHES/M-93/42) Avail: CASI HC A03/MF A01

SL(2,R)-valued cocycles over rotations of the circle are considered and it is proved that they are likely to have Lyapunov exponents approximately equal to + or - log(lambda) if the norms of all of the matrices are approximately equal to lambda. This is proved for lambda sufficiently large. The ubiquity of elliptic behavior is also observed. NTIS

N94-26995# Institut des Hautes Etudes Scientifiques, Bures-sur-Yvette (France).
ESTIMATES FOR CONE MULTIPLIERS
Jean Bourgain Sep. 1993 21 p
(PB94-124385; IHES/M-93/52) Avail: CASI HC A03/MF A01

A technique to improve on Mockenhaupt's 1/16 result for the boundedness on L(sup 4)(R(sup 3)) of cone multipliers is developed. NTIS

N94-26996# Institut des Hautes Etudes Scientifiques, Bures-sur-Yvette (France).
POISSON-LIE GROUP OF PSEUDODIFFERENTIAL SYMBOLS
Boris Khesin and Ilya Zakharevich 25 Sep. 1993 69 p See also PB93-117737
(PB94-124393; IHES/M-93/53) Avail: CASI HC A04/MF A01

A Lie bialgebra structure on the central extension of the Lie algebra of differential operators on the line and the circle (with scalar or matrix coefficients) is introduced. This defines a Poisson-Lie structure on the dual group of pseudodifferential symbols of an arbitrary real (or complex) order. It was shown that the usual (second) Benney, GL(sub n)-KdV (or GL(sub n)-Adler-Gelfand-Dickey) and KP Poisson structures are naturally realized as restrictions of this Poisson structure to submanifolds of this 'universal' Poisson-Lie group. Moreover, the reduced (= SL(sub n)) versions of these manifolds (or W(sub n)-algebras in physical terminology) can be viewed as certain subspaces of the quotient of this Poisson-Lie group by the dressing action of the group of functions on the circle (or as a result of a Poisson reduction). Finally, an infinite set of commuting functions on this Poisson-Lie group that give the standard families of Hamiltonians when restricted to the submanifolds mentioned above are defined. The Poisson structure and Hamiltonians on the whole group interpolate between the Poisson structures and Hamiltonians of Benney, KP, and KdV flows. We also discuss the geometrical meaning of W(sub infinity) as a limit of Poisson algebras W(sub epsilon) when epsilon approached 0. NTIS

N94-26999# Groningen Rijksuniv. (Netherlands). Dept. of Mathematics.
NECESSARY AND SUFFICIENT CONDITIONS FOR THE EXISTENCE OF THE STABILIZING SOLUTION OF THE RICCATI EQUATION IN A HILBERT SPACE: A POPOV FUNCTION APPROACH
Martin Weiss 1993 30 p
(PB94-125341; W-9311) Avail: CASI HC A03/MF A01

A necessary and sufficient condition was given for the existence of the stabilizing solution of a general Riccati equation in an abstract Hilbert space setting where the input operators are assumed to be bounded. This result allowed an extension of a known criterion for J-spectral factorizations. Two particular cases are then considered. Both cases enjoy the property that the solutions to the Riccati equations have an 'optimality' property. The first case is related to the well-known Positivity Theorem and gives the solution to the LQ problem. The second case is shown to give the solution to a max-min quadratic problem. A sufficient condition was given for existence of a positive stabilizing solution of the Riccati equation in this second case. As an application, a central result in H(infinity)-control theory was re-derived. NTIS

N94-27000# Groningen Rijksuniv. (Netherlands). Dept. of Mathematics.
GRID-INDEPENDENT CONVERGENCE BASED ON PRECONDITIONING TECHNIQUES
A. VanderPloeg, E. F. F. Botta, and F. W. Wubs 1994 35 p
(PB94-125358; W-9310) Avail: CASI HC A03/MF A01

A preconditioning technique is described which shows grid-independent convergence when combined with any conjugate gradient-like method. This technique is relatively easy to implement. Only an incomplete LU-decomposition of A has to be made. Essential to the method is the choice of a drop tolerance controlling the size of R = A - LU and the ordering of the unknowns. The ordering is similar to that in multigrid approaches and makes it possible to construct an incomplete LU-decomposition which can be used in eliminating effectively both high- and low-frequency errors. For model problems, an expression for the drop tolerance has been derived such that the condition number of the preconditioned matrix does not depend on the dimension of the system. Similar expressions for less trivial problems seem to be possible. The method is tested on a variety of well-known elliptic test problems described in the literature. These include strongly varying coefficients, advective terms, and grid refinement. In all cases, the method is much cheaper than standard ICCG. NTIS

N94-27015# California Inst. of Tech., Pasadena.
ROLE OF ANTICAUSAL INVERSES IN MULTIRATE FILTER-BANKS. PART 1: SYSTEM THEORETIC FUNDAMENTALS
P. P. Vaidyanathan and Tsuhan Chen Sep. 1993 33 p
(Contract N00014-93-1-0231)
(AD-A274279) Avail: CASI HC A03/MF A01

In a maximally decimated filter bank with identical decimation ratios for all channels, the perfect reconstructibility properties depend on the properties of the polyphase matrix. Various properties and capabilities of the filter bank depend on the properties of the polyphase matrix as well as the nature of its inverse. A study of the types of inverses was undertaken and they were characterized according to their system theoretic properties (i.e., properties of state-space descriptions, McMillan degree, degree of determinant, and so forth). It was found in particular that causal polyphase matrices with anticausal inverses have an important role in filter bank theory. Their properties both for the FIR and IIR cases were studied. Techniques for implementing anticausal IIR inverses based on state space descriptions are outlined. It is found that causal FIR matrices with anticausal FIR inverses (abbreviated cafacafi) have a key role in the characterization of FIR filter banks. In a companion paper these results are applied for the factorization of biorthonormal FIR filter banks, and a generalization of the lapped orthogonal transform called the biorthonormal lapped transform (BOLT) developed. DTIC

N94-27023 International Centre for Theoretical Physics, Trieste (Italy).
Q - DIFFERENCE INTERTWINING OPERATORS FOR A LORENTZ QUANTUM ALGEBRA
L. Dabrowski (International School for Advanced Studies, Trieste, Italy.), V. K. Dobrev, and R. Floreanini (Istituto Nazionale di Fisica Nucleare, Trieste, Italy.) Jun. 1993 21 p Limited Reproducibility: More than 20% of this document may be affected by microfiche quality
(DE94-602559; IC-93/159; UTS-DFT-17-93; SISSA-92/93/FM) Avail: CASI HC A03 (US Sales Only)

The authors construct representations pi-circumflex(sub r, r) of a Lorentz quantum algebra U labelled by two complex numbers r, r and acting in the space of formal power series of two non-commuting variables eta, eta. These variables are built from elements of the matrix Lorentz quantum group L which is dual to U. The conditions for reducibility of pi-circumflex(sub r, r) are given. The authors construct explicitly q - difference intertwining operators in eta, eta-bar which realize partial equivalencies of the representations pi-circumflex(sub r, r). The whole construction is a generalization of a known procedure for q = 1. The case when q is a root of unity is also considered in detail. DOE

N94-27028# Groningen Rijksuniv. (Netherlands). Dept. of Mathematics.
BIFURCATION SEQUENCES AT 1:4 RESONANCE: AN INVENTORY
Bernd Krauskopf 1994 30 p
(PB94-125408; W-9308) Avail: CASI HC A03/MF A01

The problem of 1:4 resonance of a closed orbit of a vector field in R(sup 3) leads to the study of the Z(sub 4)-equivariant planar vector field, in complex notation, z-dot = e(sup i*alpha)*z + A*z*(absolute value of z)(exp 2) + z-bar(exp 3), where A is a member of C and alpha is a member of R are parameters. This system has been studied in other papers. The parameter A-plane is divided in at least 48 different regions with topologically different bifurcation sequences under variation of the parameter alpha. An inventory of computer generated pictures of the bifurcation sequences is presented. In contrast to sketches, the pictures show the physical appearance of the system. For example, some limit cycles are square-shaped and some saddle-node bifurcations are cusp-like. The knowledge of these interesting features can stimulate further research. They are discussed along with the problems of the computation. NTIS

N94-27030# Technische Univ., Delft (Netherlands). Faculty of Technical Mathematics and Informatics.
SYMMETRIC AND ASYMMETRIC DIOPHANTINE APPROXIMATION BY CONTINUED FRACTIONS
Cornelis Kraaikamp 1992 28 p
(ISSN 0922-5641)
(PB94-126455; Rept-92-88) Copyright Avail: CASI HC A03/MF A01

Let (P(sub n)/Q(sub n))(sub n greater than or equal to 0) be the sequence of regular continued fraction convergents of the real irrational number x. Define the approximation constants d(sub n), n greater than or equal to 0, by d(sub n) = d(sub n)(x) := Q(sub n+1) absolute value of (Q(sub n)x - P(sub n)), n greater than or equal to 0. In this paper the distribution for almost all x of the sequences (d(sub n-1), d(sub n))(sub n greater than or equal to 1) and (d(sub n-1), d(sub n), d(sub n+1))(sub n greater than or equal to 1) is discussed. Furthermore, two recent theorems by Jingcheng Tong concerning arithmetical properties of the d(sub n)'s are generalized. NTIS

N94-27035# California Inst. of Tech., Pasadena. Dept. of Electrical Engineering.
CAUSAL FIR MATRICES WITH ANTICAUSAL FIR INVERSES, AND APPLICATION IN CHARACTERIZATION OF BIORTHONORMAL FILTER BANKS
P. P. Vaidyanathan 1993 4 p
(Contract N00014-93-1-0231)
(AD-A274509) Avail: CASI HC A01/MF A01

Causal FIR matrices with anticausal FIR inverses have a key role in the theory of FIR perfect reconstruction filter banks. The theory of such matrices is explored. Some general results on the nature of inverses of first order causal FIR matrices are then presented. This leads, in particular, to a complete parameterization of the biorthonormal lapped transform (BOLT) reported earlier. DTIC

N94-27103# Wisconsin Univ., Madison. Center for Mathematical Sciences.
RADIAL BASIS FUNCTION APPROXIMATION: FROM GRIDDED CENTERS TO SCATTERED CENTERS
Nira Dyn and Amos Ron Dec. 1993 32 p
(Contract DAAL03-90-G-0090; NSF DMS-90-00053)
(AD-A274184; CMS-TSR-94-3) Avail: CASI HC A03/MF A01

The paper studies L-infinity-norm approximations from a space spanned by a discrete set of translates of a basis function theta. Attention here is restricted to functions phi whose Fourier transform is smooth and has a singularity at the origin. Examples of such basis functions are the thin-plate splines and the multiquadrics, as well as other types of radial basis functions that are employed in Approximation Theory. The above approximation problem is well-understood in case the set of points used for translating theta forms a lattice, and many optimal and quasi-optimal approximation schemes can already be found in the literature. In contrast, only few, mostly specific, results are known for a set of scattered points. The main objective of this paper is to provide a general tool for extending approximation schemes that use integer translates of a basis function to the non-uniform case. We introduce a single, relatively simple, conversion method that preserves the approximation orders provided by a large number of schemes presently in the literature (more precisely, to almost all stationary schemes). In anticipation of future introduction of new schemes for uniform grids, an effort is made to impose only a few mild conditions on the function theta, which still allow for a unified error analysis to hold. In the course of the discussion here, the recent results of BuDL on scattered center approximation are reproduced and improved upon. DTIC

N94-27115 Rutherford Appleton Lab., Chilton (England).
Ma42: A NEW FRONTAL CODE FOR SOLVING SPARSE UNSYMMETRIC SYSTEMS
I. S. Duff and J. A. Scott 1993 43 p See also PB93-179588
(PB94-124302; RAL-93-064) Copyright Avail: Issuing Activity (National Technical Information Service (NTIS))

We describe the design, implementation, and performance of a frontal code for the solution of large sparse unsymmetric systems of linear equations. The resulting software package, MA42, is included in Release 11 of the Harwell Subroutine Library and is intended to supersede the earlier MA32 package. We discuss in detail design changes from the earlier code indicating the way in which they aid clarity, maintainability, and portability. The new design also permits extensive use of higher level BLAS (Basic Linear Algebra Subprograms) kernels, which aid both modularity and efficiency. We illustrate the performance of our new code on practical problems on a CRAY Y-MP, an IBM 3090, and an IBM RISC System/6000. We indicate some directions for future development. NTIS

N94-27116# Groningen Rijksuniv. (Netherlands). Dept. of Mathematics.
CHEBYSHEV-MARKOV RATIONAL FUNCTIONS OVER SEVERAL INTERVALS
A. L. Lukashov 6 May 1993 19 p
(PB94-125333; W-9312) Avail: CASI HC A03/MF A01

Let K be a compact subset of the real line. Let C be its complement R/K. Considering a Chebyshev (T-) system phi = (phi(sub 0), phi(sub 1),...,phi(sub n)) of continuous functions over K, one calls the Chebyshev polynomial T(sub N)(K,phi,x) a polynomial c(sub 0)phi(sub 0) + ... + c(sub N-1)phi(sub N-1)(x) + phi(x) such that its uniform norm over K is the minimal one among all polynomials of such a form with real c(sub i). The ramifications of this assertion are explored. NTIS

N94-27162 International Centre for Theoretical Physics, Trieste (Italy).
MAPPING BETWEEN THE SINH-GORDON AND ISING MODELS
C. Ahn, G. Delfino (International School for Advanced Studies, Trieste, Italy.), and G. Mussardo (International School for Advanced Studies, Trieste, Italy.) Jun. 1993 9 p Limited Reproducibility: More than 20% of this document may be affected by microfiche quality
(DE94-601535; IC-93/143; ISAS/EP-93/89) Avail: CASI HC A02 (US Sales Only)

The S-matrix of the Ising Model can be obtained as a particular limit of the roaming trajectories associated to the S-matrix of the Sinh-Gordon model. Using the form factors of Sinh-Gordon, the correspondence between the operators of the two theories is analyzed. DOE

N94-27269 Waterloo Univ. (Ontario).
FAST METHODS FOR COMPUTATION WITH ALGEBRAIC NUMBERS Ph.D. Thesis
Trevor Janathan Smedley 1989 109 p
(ISBN-0-315-57888-2; CTN-94-60979) Copyright Avail: Micromedia Ltd., Technical Information Centre, 240 Catherine Street, Suite 305, Ottawa, Ontario, K2P 2G8, Canada HC/MF

Algebraic numbers commonly arise in the solution of polynomial equations and in many integration problems. As these are quite common problems in symbolic computation, it is necessary to have efficient algorithms for dealing with algebraic numbers symbolically. Many standard algorithms for working with algebraic numbers are quite slow. The problems of detecting dependencies between algebraic numbers and computation of algebraic number polynomial greatest common divisors are addressed, and a method for efficiently detecting all dependencies between unnested radicals is presented. A new modular heuristic method for doing operations in algebraic number fields is then given. This method can be used for most polynomial operations involving algebraic numbers, but is most useful for calculating greatest common divisors. Techniques of using this method for factorization and for multiple extensions are discussed, as well as the way in which the heuristic can be used as an algorithm. Author (CISTI)

N94-27312 Concordia Univ., Montreal (Quebec). Dept. of Computer Science.
ROBUST ESTIMATION FOR RANGE IMAGE SEGMENTATION AND FITTING Ph.D. Thesis
Xinming Yu Feb. 1993 220 p

(ISBN-0-315-84686-0; CTN-94-61087) Copyright Avail: Micromedia Ltd., Technical Information Centre, 240 Catherine Street, Suite 305, Ottawa, Ontario, K2P 2G8, Canada HC/MF

A new robust estimation technique for range image segmentation and fitting has been developed. Its performance has been improved considerably by incorporating a genetic algorithm (GA). The new robust estimation method randomly samples range image points and solves equations determined by these points for parameters of selected primitive type. From K samples a residual consensus (RESC) is measured by a compressed histogram method in order to choose one set of sample points which determines an equation best fitting the largest homogeneous surface patch in the current processing region. A boundary list searching method is used to extract the surface patch out of the processing region. The RESC method can tolerate over 80 percent outliers, segments range image into planar and quadratic surfaces, and works well even in smoothly connected curve regions. A GA was used to accelerate the random search. A large number of offline average performance experiments on GA's were conducted to examine different types of GA's and the influence of control parameters. A steady state GA was found to work better than a generational replacement GA. The algorithms have been validated on a large set of synthetic and real range images. Author (CISTI)

N94-27349 Technische Univ., Eindhoven (Netherlands). Dept. of Mathematics and Computing Science.

FRACTIONAL CALCULUS, GEGENBAUER TRANSFORMATIONS AND INTEGRAL EQUATIONS

C. A. M. vanBerkel and S. J. L. vanEijndhoven Mar. 1993 22 p
Limited Reproducibility: More than 20% of this document may be affected by microfiche quality
(ISSN 0926-4507)
(PB93-237683; RANA-93-04) Avail: CASI HC A03

Starting from the Riemann-Liouville and the Weyl calculus, compositions of fractional integral and fractional differential operators are studied. These composite operators and their inverses admit descriptions as integral transformations with Gegenbauer functions in their kernel. Rodriques type formulas for Gegenbauer functions and new relations for fractional differential and integral operators are derived. Thus classical results on integral equations of Mellin convolution type are extended and unified. NTIS

N94-27404 Waterloo Univ. (Ontario). Dept. of Mathematics.

COMPUTATION OF NUMERICAL SOLUTION OF PARABOLIC PDES BY MONOTONE ITERATIVE METHODS M.S. Thesis

Ying Chen 1993 125 p
(ISBN-0-315-84553-8; CTN-94-61074) Copyright Avail: Micromedia Ltd., Technical Information Centre, 240 Catherine Street, Suite 305, Ottawa, Ontario, K2P 2G8, Canada HC/MF

By using a weighted difference scheme and the method of upper-lower solutions proposed by Liu et al. to study elliptic differential equations, a monotone iteration scheme has been developed for the computation of solutions to nonlinear parabolic boundary initial value problems (NPBIVP) and coupled NPBIVP. In each iteration, it is only needed to solve a linear system of which the coefficient matrix is an M-matrix. The proposed scheme and method allows the nonlinearity of the first order partial differential terms which generalizes several previous results related to the same types of problems. In particular, the results presented cover Sattinger's 1972 results about the parabolic boundary initial value problem and some of Pao's 1982 results about the coupled parabolic boundary value problem. Examples are presented to illustrate the efficiency of implementation and applicability of the proposed scheme, as well as its convergence in a test problem. To keep computational costs reasonable, nonuniform grids in time and space can be used, but this will make programming more complicated. Author (CISTI)

N94-27405 Waterloo Univ. (Ontario). Dept. of Mathematics.

SOLVING THE LINEAR QUADRATIC OPTIMAL CONTROL PROBLEM FOR INFINITE-DIMENSIONAL SYSTEMS M.S. Thesis

Janet Rose Grad 1993 197 p
(ISBN-0-315-84562-7; CTN-94-61075) Copyright Avail: Micromedia Ltd., Technical Information Centre, 240 Catherine Street, Suite 305, Ottawa, Ontario, K2P 2G8, Canada HC/MF

Solutions of the linear quadratic regulator (LQR) problem for infinite dimensional systems are considered. A sequence of approximating finite dimensional LQR problems is shown to converge under certain stabilizability assumptions. Rather than attempting to solve an infinite dimensional system, the problem is formulated in terms of this convergent sequence. An iterative method for computing the Riccati matrix and associated feedback gains is proposed. The method is based on mapping the feedback gains and Riccati matrix between successive approximating spaces. In this manner, prior information is conveyed to the next larger space and is used as an initial estimate for the current solution. Advantages of the proposed algorithm over the standard eigenvector approaches (Potter's method and the Laub-Schur method) are discussed and illustrated using two examples: control of the heat distribution in a one-dimensional rod and control of acoustic pressure in a two-dimensional cavity. The latter problem has physical applications in such fields as noise reduction in airplanes. Author (CISTI)

N94-27415*# Institute for Computer Applications in Science and Engineering, Hampton, VA.

A SENSITIVITY EQUATION APPROACH TO SHAPE OPTIMIZATION IN FLUID FLOWS Final Report

Jeff Borggaard (Virginia Polytechnic Inst. and State Univ., Blacksburg.) and John Burns (Virginia Polytechnic Inst. and State Univ., Blacksburg.) Jan. 1994 35 p Submitted for publication
(Contracts NAS1-19480; NAS1-18605; F49620-92-J-0078; F49620-93-1-0280; NSF INT-89-22490; RTOP 505-90-52-01)
(NASA-CR-191598; NAS 1.26:191598; ICASE-94-8) Avail: CASI HC A03/MF A01

A sensitivity equation method to shape optimization problems is applied. An algorithm is developed and tested on a problem of designing optimal forebody simulators for a 2D, inviscid supersonic flow. The algorithm uses a BFGS/Trust Region optimization scheme with sensitivities computed by numerically approximating the linear partial differential equations that determine the flow sensitivities. Numerical examples are presented to illustrate the method. Author (revised)

N94-27434*# Institute for Computer Applications in Science and Engineering, Hampton, VA.

PARALLEL IMPLICIT UNSTRUCTURED GRID EULER SOLVERS Final Report

V. Venkatakrishnan Jan. 1994 21 p Submitted for publication
(Contracts NAS1-19480; NAS2-12961; RTOP 505-90-52-01)
(NASA-CR-191594; NAS 1.26:191594; ICASE-94-4) Avail: CASI HC A03/MF A01

A mesh-vertex finite volume scheme for solving the Euler equations on triangular unstructured meshes is implemented on an MIMD (multiple instruction/multiple data stream) parallel computer. An explicit four-stage Runge-Kutta scheme is used to solve two-dimensional flow problems. A family of implicit schemes is also developed to solve these problems, where the linear system that arises at each time step is solved by a preconditioned GMRES algorithm. Two partitioning strategies are employed, one that partitions triangles and the other that partitions vertices. The choice of the preconditioner in a distributed memory setting is discussed. All the methods are compared both in terms of elapsed times and convergence rates. It is shown that the implicit schemes offer adequate parallelism at the expense of minimal sequential overhead. The use of a global coarse grid to further minimize this overhead is also investigated. The schemes are implemented on a distributed memory parallel computer, the iPSC/860. Author

N94-27557*# Institute for Computer Applications in Science and Engineering, Hampton, VA.

AGGLOMERATION MULTIGRID FOR THE THREE-DIMENSIONAL EULER EQUATIONS Final Report

V. Venkatakrishnan and D. J. Mavriplis Jan. 1994 29 p Submitted for publication
(Contract NAS1-19480; RTOP 505-90-52-01)
(NASA-CR-191595; NAS 1.26:191595; ICASE-94-5) Avail: CASI HC A03/MF A01

A multigrid procedure that makes use of coarse grids generated by the agglomeration of control volumes is advocated as a practical approach for solving the three dimensional Euler equations on unstructured grids about complex configurations. It is shown that the agglomeration procedure can be tailored to achieve certain coarse grid properties such as the sizes of the coarse grids and aspect ratios of the coarse grid cells. The agglomeration is done as a preprocessing step and runs in linear time. The implications for multigrid of using arbitrary polyhedral coarse grids are discussed. The agglomeration multigrid technique compares very favorably with existing multigrid procedures both in terms of convergence rates and elapsed times. The main advantage of the present approach is the ease with which coarse grids of any desired degree of coarseness may be generated in three dimensions, without being constrained by considerations of geometry. Inviscid flows over a variety of complex configurations are computed using the agglomeration multigrid strategy. Author (revised)

N94-27564# Sandia National Labs., Albuquerque, NM.
MULTIPLE WEIGHT STEPWISE REGRESSION
Joel Atkins (California Univ., Berkeley.) and James Campbell 1993 6 p
Presented at the 2nd Probabilistic Safety Assessment and Management Conference, San Diego, CA, 20-24 Mar. 1994
(Contract DE-AC04-94AL-85000)
(DE94-001602; SAND-93-2419C; CONF-940312-29) Avail: CASI HC A02/MF A01

In many science and engineering applications, there is an interest in predicting the outputs of a process for given levels of inputs. In order to develop a model, one could run the process, or a simulation of the process, at a number of points (a point would be one run at one set of possible input values) and observe the values of the outputs at those points. These observations can be used to predict the values of the outputs for other values of the inputs. Since the outputs are a function of the inputs, a surface in the space of possible inputs and outputs can be generated. This surface is called a response surface. In some cases, collecting data needed to generate a response surface can be very expensive. Thus, in these cases, there is a powerful incentive to minimize the sample size while building better response surfaces. One such case is the semiconductor equipment manufacturing industry. Semiconductor manufacturing equipment is complex and expensive. Depending upon the type of equipment, the number of control parameters may range from 10 to 30 with perhaps 5 to 10 being important. Since a single run can cost hundreds or thousands of dollars, it is very important to have efficient methods for building response surfaces. A current approach to this problem is to do the experiment in two stages. First, a traditional design, such as fractional factorial, is used to screen variables. After deciding which variables are significant, additional runs of the experiment are conducted. The original runs and the new runs are used to build a model with the significant variables. However, the original (screening) runs are not as helpful for building the model as some other points might have been. This paper presents a point selection scheme that is more efficient than traditional designs. DOE

N94-27569# Pacific Northwest Lab., Richland, WA.
ITERATIVE METHODS FOR THE WLS STATE ESTIMATION ON RISC, VECTOR, AND PARALLEL COMPUTERS
J. Nieplocha and C. C. Carroll (Alabama Univ., Tuscaloosa.) Oct. 1993 9 p Presented at the 1993 North American Power Symposium, Washington, DC, 11-12 Oct. 1993
(Contract DE-AC06-76RL-01830)
(DE94-004260; PNL-SA-23064; CONF-9310246-1) Avail: CASI HC A02/MF A01

The authors investigate the suitability and effectiveness of iterative methods for solving the weighted-least-square (WLS) state estimation problem on RISC, vector, and parallel processors. Several of the most popular iterative methods are tested and evaluated. The best performing preconditioned conjugate gradient (PCG) is very well suited for vector and parallel processing as is demonstrated for the WLS state estimation of the IEEE standard test systems. A new sparse matrix format for the gain matrix improves vector performance of the PCG algorithm and makes it competitive to the direct solver. Internal parallelism in RISC processors, used in current multiprocessor systems, can be taken advantage of in an implementation of this algorithm. DOE

N94-27577 Center for Mathematics and Computer Science, Amsterdam (Netherlands). Dept. of Computer Science/Dept. of Software Technology.
EXPRESSIVENESS RESULTS FOR PROCESS ALGEBRAS
Frits W. Vaandrager (Amsterdam Univ., Netherlands.) Jan. 1993 33 p Submitted for publication Sponsored in part by EEC Prepared in cooperation with MIT, Cambridge, MA Limited Reproducibility: More than 20% of this document may be affected by microfiche quality
(Contract N00014-85-K-0168) (ISSN 0169-118X)
(CWI-CS-R9301; ETN-94-95423) Copyright Avail: CASI HC A03

The expressive power of process algebras is investigated in a general setting of Structural Operational Semantics (SOS). The notion of an effective operational semantics is introduced and it is observed that no effective operational semantics for an enumerable language can specify all effective process graphs up to trace equivalence. A natural class of Plotkin style SOS specifications is identified, containing the guarded versions of calculi like CCS (Calculus of Communicating Systems), SCCS, MEIJE and ACP, and it is proved that any specification in this class induces an effective operational semantics. Using techniques introduced by Bloom, it is shown that for the guarded versions of CCS like calculi, there is a double exponential bound on the speed with which the number of outgoing transitions in a state can grow. As a corollary of this result it follows that two expresiveness results of De Simone for MEIJE and SCCS depend in a fundamental way on the use of unguarded recursion. A final result is that all operators definable via a finite number of rules in a format due to De Simone, are derived operators in the simple Process Calculus (PC). ESA

N94-27632# International Centre for Theoretical Physics, Trieste (Italy).
FIXED POINT TYPE THEOREMS AND PROJECTION-INTERACTION APPROXIMATION
Tran Quoc Binh (Institute of Mathematics, Hanoi, Viet Nam.) and Nguyen Minh Chuong Aug. 1993 8 p
(DE94-603669; IC-93/241) Avail: CASI HC A02/MF A01 (US Sales Only)

The existence of solutions of equations $T(x, x) = x$ for nonexpansive mappings and their approximation by a projection-iteration method are studied. The differences between $T(x, x) = x$ and $Tx = x$, including a new Edelstein fixed point type theorem, will be shown. DOE

N94-27637 International Centre for Theoretical Physics, Trieste (Italy).
JOINT ESSENTIAL MAXIMAL NUMERICAL RANGE
G. A. Khan Jun. 1993 10 p Limited Reproducibility: More than 20% of this document may be affected by microfiche quality
(DE94-603674; IC-93/99) Avail: CASI HC A02 (US Sales Only)

The notion of essential maximal numerical range of a single operator was introduced by Fong and was further studied by Khan. The aim of this paper is to generalize this notion to n-tuple of operators and prove certain results analogous to the single operator case. DOE

N94-27731# Japan Atomic Energy Research Inst., Tokyo.
NUMERICAL EXPERIMENT ON FINITE ELEMENT METHOD FOR MATCHING DATA
Shinji Tokuda, Toshimasa Kumakura, and Koichi Yoshimura Mar. 1993 37 p In JAPANESE; In JAPANAESE
(DE94-701208; JAERI-M-93-075) Avail: CASI HC A03/MF A01

Numerical experiments are presented on the finite element method by Pletzer-Dewar for matching data of an ordinary differential equation with regular singular points by using a model equation. Matching data play an important role in nonideal MHD stability analysis of a magnetically confined plasma. In the Pletzer-Dewar method, the Frobenius series for the 'big solution', the fundamental solution which is not square-integrable at the regular singular point, is prescribed. The experiments include studies of the convergence rate of the matching data obtained by the finite element method and of the effect on the results of computation by truncating the Frobenius series at finite terms. It is shown from the present study that the finite element method is an effective method for obtaining the matching data with high accuracy. DOE

N94-27818 International Centre for Theoretical Physics, Trieste (Italy).
STUDY OF THE CRITICAL POINTS AT INFINITY ARISING FROM THE FAILURE OF THE PALAIS-SMALE CONDITION FOR N-BODY TYPE PROBLEMS
H. Riahi Aug. 1993 71 p Limited Reproducibility: More than 20% of this document may be affected by microfiche quality
(DE94-603656; IC-93/247) Avail: CASI HC A04 (US Sales Only)

This paper is a study of these critical points at infinity and of the topology of their stable and unstable manifolds. The potential considered here satisfies the strong force hypothesis which eliminates collision orbits.

The details are given for 4-body type problems then generalized to n-body type problems. DOE

N94-27839 International Centre for Theoretical Physics, Trieste (Italy).
THE gl(n/m) AND RELATED q-IDENTITIESEMATICS AND COMPUTER SCIENCE ENDS IN NUCLEAR AND RELATED q-IDENTITIES
T. D. Palev, N. I. Stoilova, and J. VanDerJeugt Jun. 1993 12 p Limited Reproducibility: More than 20% of this document may be affected by microfiche quality
(DE94-603653; IC-93/157) Avail: CASI HC A03 (US Sales Only)

Explicit expressions for the generators of the quantum superalgebra U(sub q)(gl(n/m)) acting on a class of irreducible representations are given. The class under consideration consists of all essentially typical representations: for these a Gel'fand Zetlin basis is known. The verification of the quantum superalgebra relations to be satisfied is shown to reduce to a set of q-number identities. DOE

N94-27846# Joint Inst. for Nuclear Research, Dubna (USSR). Lab. of Theoretical Physics.
A METHOD FOR OBTAINING QUANTUM DOUBLES FROM THE YANG-BAXTER R-MATRICES
A. A. Vladimirov 1992 7 p
(DE94-606300; JINR-E-2-92-506) Avail: CASI HC A02/MF A01 (US Sales Only)

The approach is developed earlier that enables one to associate a quasitriangular Hopf algebra to every regular invertible constant solution of the quantum Yang-Baxter equations. DOE

N94-27948 Waterloo Univ. (Ontario). Dept. of Mechanical Engineering.
ON THE LAGRANGIAN AND UPDATED LAGRANGIAN NONLINEAR FINITE ELEMENT FORMULATIONS Ph.D. Thesis
Abdelfattah Soliman 1990 138 p
(ISBN-0-315-61111-1; CTN-94-61002) Copyright Avail: Micromedia Ltd., Technical Information Centre, 240 Catherine Street, Suite 305, Ottawa, Ontario, K2P 2G8, Canada HC/MF

An increasing demand for the solution of various engineering problems with geometric and/or material nonlinearities in such areas as metal forming and aircraft industries has contributed to the rapid growth in popularity of finite element methods. Of the various methods of formulation of those nonlinearities, the updated Lagrangian formulation is considered. The formulations are derived from the virtual work principle expressed in the current configuration, then transferred to the proper reference configuration. Explicit forms for the stiffness matrices are given in each case. It is shown that nonlinear stiffness matrices must be included in the formulations if they are to be consistent with the constitutive assumptions. The Lagrangian formulations are rederived in the rate form using the objective Jaumann stress-rate and the principal axes technique. Specific forms of constitutive equations for elastic and elastic-plastic material response are presented. The use of stress rates to derive acceptable constitutive equations is also discussed. The Lagrangian and updated Lagrangian rate formulations are expressed in incremental forms and used to solve three sample problems involving large deformation, large rotation, and large strain for elastic-plastic solids. Author (CISTI)

N94-28216# New Mexico State Univ., Las Cruces. Dept. of Mathematical Science.
HOTINE'S (OMEGA, PHI, NU) COORDINATE SYSTEM Report No. 5
J. D. Zund 13 Aug. 1993 28 p
(Contract F19628-89-K-0044)
(PL-TR-93-2174) Avail: CASI HC A03/MF A01

This report is an extensive reworking of the material in Chapter 12 of Hotine's treatise 'Mathematical Geodesy' (U.S. Department of Commerce, Washington D.C. 1969) which dealt with the basic properties of the (omega, phi, nu) coordinate system. In 1990, the author showed that Hotine's derivation of this coordinate system was incomplete, and the present document contains the full details of that work as well as the material required to rigorously complete Hotine's analysis. The latter material has not been previously published. Author

N94-28228 International Centre for Theoretical Physics, Trieste (Italy).
ON THE ZEROS OF SOLUTIONS OF FORCED PARABOLIC DIFFERENTIAL EQUATIONS OF NEUTRAL TYPE
N. Parhi Sep. 1992 17 p Limited Reproducibility: More than 20% of this document may be affected by microfiche quality
(DE93-613019; IC-92/260) Avail: CASI HC A03 (US Sales Only)

Sufficient conditions were obtained for the oscillation of all solutions of a class of forced parabolic differential equations of neutral type. DOE

N94-28353# National Aerospace Lab., Amsterdam (Netherlands).
THE DETERMINISTIC POWER-SPECTRAL-DENSITY-METHOD FOR NONLINEAR SYSTEMS
R. Noback 25 Aug. 1992 58 p
(Contract OV/RLD-132)
(AD-B179687; NLR-TP-92342-U) Avail: CASI HC A04/MF A01

The deterministic power spectral density (P.S.D.) method can be derived from the design envelope analysis of the continuous P.S.D. method. It provides a method to determine a deterministic function that gives a maximum response equal to the P.S.D. design load for linear systems. The P.S.D. design load is undefined for nonlinear systems. In this report a 'reasonable extrapolation' of the deterministic P.S.D. method has been proposed for nonlinear systems. Design loads for a simple nonlinear aircraft model have been calculated. The results have been compared with results obtained with a 'reasonable extrapolation' of the P.S.D method using simulation. Author (revised)

N94-28389# Helsinki Univ. of Technology, Espoo (Finland). Inst. of Mathematics.
HESSENBERG MATRICES IN KRYLOV SUBSPACES AND THE COMPUTATION OF THE SPECTRUM
O. Nevanlinna Jun. 1993 26 p
(PB94-133170; ISBN-951-22-1658-2) Avail: CASI HC A03/MF A01

The paper discusses the possibility to find the spectrum of a limit operator, or rather the polynomially convex hull of it, from a sequence of operators. The tools are applied to Hessenberg matrices which are implicitly created in Krylov subspace approximations. NTIS

N94-28398# Helsinki Univ. of Technology, Espoo (Finland). Lab. of Information Processing Science.
LISP INTERFACE TO GEOMETRIC MODELLING OPERATIONS
T. Laakko and M. Maentylae 1993 51 p
(PB94-133121; TKK-TKO-C62) Avail: CASI HC A04/MF A01

A Lisp programming interface to basic geometric modeling operations typically available in solid modeling systems is described. The geometric modeling interface operations include different sweeping operations, profile combination, Boolean set operations, and a special geometry definition schema, which is a symbolic description of a boundary representation solid model. The interface provides parametric feature geometry definitions embedded in feature frames. NTIS

65 STATISTICS AND PROBABILITY

Includes data sampling and smoothing; Monte Carlo method; and stochastic processes.

N94-25607# Air Force Inst. of Tech., Wright-Patterson AFB, OH. School of Engineering.
THE APPLICATION OF SIMULATED ANNEALING TO STOCHASTIC SYSTEMS M.S. Thesis
Charles B. Warrender 18 Nov. 1993 222 p
(AD-A273850; AFIT/GSO/ENS/93D-16) Avail: CASI HC A10/MF A03

Simulated Annealing was used to optimize three constrained simulation models. For each of these models, seven different acceptance functions were evaluated and compared against the performance of Local Search. These comparisons demonstrated the affect that different acceptance functions have on the performance of the algorithm. The performance was measured by the average solution quality and average efficiency obtained from several runs. The first model facilitated the implementation of Simulated Annealing using the SLAM simulation language. The configuration space was small, described by only two decision variables. It demonstrated the viability of using Simulated Annealing to optimize the variable settings in a simulation model. The second model, with six decision variables, provided greater insight to the advantages and limitations of Simulated Annealing. This model was implemented as an open queuing network. The third model, similar to the second, was implemented as a closed queuing network. The results from this variation were completely unexpected. They showed a wide performance separation among the different acceptance functions that was not present in the first two models. No attempt was made to justify the use of Simulated Annealing from a theoretical perspective. Rather, empirical results from the three models were used to infer the practical utility of the algorithm. DTIC

N94-25903# Carnegie-Mellon Univ., Pittsburgh, PA. Dept. of Computer Science.

SET BASED ANALYSIS OF ARITHMETIC

Nevin Heintze Dec. 1993 19 p
(Contract F19628-91-C-0168)
(AD-A274112; CMU-CS-93-221) Avail: CASI HC A03/MF A01

Set based analysis is an approach to compile-time program analysis that is based on a simple approximation: all dependencies between variables are ignored. In effect, program variables are treated as sets of values. Thus far, set based analysis techniques have focussed on data-constructor languages. The main reason for this is algorithmic: the equality for data-constructor values is structural. This has important implications for how sets of such values can be represented during the computation of a set based analysis. In contrast, the equality theory of arithmetic is much richer. Two terms with very different structure can be equal. Correspondingly, the manipulation and representation of sets of arithmetic values is significantly more complex. In this paper, we extend the ideas of set based analysis to arithmetic expression in such a way that the analysis yields descriptions of how arithmetic values are computed. Importantly, this extended analysis yields useful information about the arithmetic components of a program while maintaining the efficiency of the basic set constraint approach. We show how this information can be exploited during compilation with two examples involving array bounds elimination. While this work is carried out in the context of the ML, the techniques developed appear to be applicable to other languages. DTIC

N94-25910 Weizmann Inst. of Science, Rehovoth (Israel). Dept. of Physics.

SURFACES ALLOWING FOR FRACTIONAL STATISTICS

Charilaos Aneziris Jul. 1992 18 p Limited Reproducibility: More than 20% of this document may be affected by microfiche quality
(DE93-614526; WIS-PH-92-55) Avail: CASI HC A03 (US Sales Only)

In this paper we give a necessary condition in order for a geometrical surface to allow for Abelian fractional statistics. In particular, we show that such statistics is possible only for two-dimentional oriented surfaces of genus zero, namely the sphere S(sup 2), the plane R(sup 2) and the cylindrical surface R(sup 1)xS(sup 1), and in general the connected sum of n planes R(sup 2)R(sup 2)R(sup 2)...R(sup 2). DOE

N94-25962# Educational Testing Service, Princeton, NJ.

PROFICIENCY SCALING BASED ON CONDITIONAL PROBABILITY FUNCTIONS FOR ATTRIBUTES Final Report, Apr. 1989 - Aug. 1993

Kikumi Tatsuoka, Menucha Birenbaum, Charles Lewis, and Kathleen Sheehan Oct. 1993 72 p
(Contract N00014-90-J-1307; DA Proj. RR0-4204)
(AD-A273816; ETS-RR-93-50-ONR) Avail: CASI HC A04/MF A01

Procedures for constructing a proficiency scale for a large-scale test by applying Tatsuoka's Rule Space Model are introduced. The SAT Mathematics (SAT M), Section 2, is used for illustrating the process and the results. A task analysis is summarized in a mapping sentence, and then 14 processes and content attributes are identified for explaining the underlying cognitive aspects of the examinees' performance on the SAT M. Analysis results show that almost 98% of 2,334 examinees are successfully classified into one of 468 cognitive states. The cognitive states are characterized by mastery or non-mastery of the 14 attributes. Attribute Characteristic Curves, which are conditional probability functions defined on the SAT Scale, are introduced and used for interpreting an examinee's proficiency. Prototypes of a student's performance report and a group performance report are given as examples of possible ways for summarizing the analysis results. DTIC

N94-25992# Air Force Inst. of Tech., Wright-Patterson AFB, OH. School of Engineering.

MULTIPLE MODEL ADAPTIVE ESTIMATION APPLIED TO THE LAMBDA URV FOR FAILURE DETECTION AND IDENTIFICATION M.S. Thesis

David W. Lane 2 Dec. 1993 237 p
(AD-A274078; AFIT/GE/Eng/93D-23) Avail: CASI HC A11/MF A03

Multiple Model Adaptive Estimation (MMAE) is a method of estimating unknown system parameters by modeling all possible parameter configurations in several models. The parameters for this research are failure status conditions associated with flight control actuators and sensors on the LAMBDA Unmanned Research Vehicle. The LAMBDA URV is an experimental aircraft operated by Wright Laboratory Flight Controls Division at Wright-Patterson Air Force Base, Ohio. Six actuator failures and eight sensor failures are modeled, along with the fully functional aircraft, in fifteen elemental Kalman filters. These filters propagate and update their own aircraft state estimates in real time. A probability computation representing the likelihood of each elemental filter's match to the true condition of the aircraft is used to generate relative probabilities for each filter's hypothesis. In this research, the MMAE algorithm is extended for the identification of dual failures through the use of a hierarchical structure of filter banks. The ability of the MMAE to identify dual failures in the face of wind gust uncertainty and sensor noise is investigated. Aircraft state excitation is required for effective MMAE performance. Therefore, the form of an optimal input dither signal is derived through extensive experimentation. Dither signals are applied to the command inputs of a Quantitative Feedback Theory flight control system which controls pitch rate, roll rate, and sideslip angle. In particular, the MMAE performance is studied as sinusoidal dither inputs are varied in frequency and magnitude. An analysis of tuning techniques for the elemental filters within the MMAE is presented. DTIC

N94-26000# Technische Univ., Eindhoven (Netherlands). Precision Engineering Group.

ACCURACY ANALYSIS OF MULTI-AXIS MACHINES Ph.D. Thesis

Johannes Augustinus Soons 1993 220 p
(ETN-94-95341) Avail: CASI HC A10/MF A03

A general strategy to estimate and describe the quasi static errors of multi axis machines is presented. The goal is a model for the errors in the position and orientation of the end effector relative to the workpiece during an arbitrary task. A model of the machine errors is developed. The unknown parameters in this model are estimated using artifact measurements. The model is verified by simulating and compensating the machine errors. The modeling strategy is applied to a five axis milling machine and a three axis coordinate measuring machine. For the milling machine, the models for the geometric and finite stiffness errors are validated by predicting the errors of hole plate measurements executed by the machine. The models for the thermal errors are validated by predicting the observed zero point drift of the tool during characteristic duty cycles of the spindle. The accuracy of the machine is improved by software error compensation of the geometric errors. The geometric errors of the coordinate measuring machine are estimated by three different methods, all using length measurements. The respective models are validated by predicting the observed errors of a large number of length measurements executed by the machine. ESA

N94-26038# Gosudarstvennyi Komitet po Ispolzovaniyu Atomnoi Energii, Serpukhov (USSR).

SPATIAL SYMMETRY, LOCAL INTEGRABILITY AND TETRAHEDRON EQUATIONS IN THE BAXTER-BAZHANOV MODEL

R. M. Kashaev, V. V. Mangazeev, and Yu. G. Stroganov 1992 16 p
(DE93-634348; IHEP-TD-92-63) Avail: CASI HC A03/MF A01 (US Sales Only)

It is shown that the Baxter-Bazhanov model is invariant under the action of the cube symmetry group. The three-dimensional star-star relations, proposed by Baxter and Bazhanov as local integrability conditions, correspond to a particular transformation from this group. Invariant Boltzmann weights, parameterized in terms of the Zamolodchikov's angle variables, apparently satisfy the tetrahedron equations. DOE

N94-26213# Technische Univ., Delft (Netherlands). Faculty of Technical Mathematics and Informatics.

ISOTONIC ESTIMATION AND RATES OF CONVERGENCE IN WICKSELL'S PROBLEM

Piet Groeneboom and Geurt Jongbloed 1993 28 p
(ISSN 0922-5641)
(Rept-93-39; ETN-94-95394) Copyright Avail: CASI HC A03/MF A01

It is shown that, in the nonparametric setting for the so-called Wicksell problem, the distribution function of the squared radii of the balls cannot be estimated at a rate faster than (1/square root of n)(square root of log n). An isotonic estimator of the distribution function which attains this rate is presented. Its asymptotic distribution is derived. It is shown that the variance of this limiting distribution is exactly half the asymptotic variance of the naive plug-in estimator. The violation of both monotonicity and the range constraints for distribution functions by the estimators are discussed. An isotonized naive estimator is defined. ESA

N94-26355# Victoria Univ., Wellington (New Zealand).
PARAMETER ESTIMATION FOR ARMA MODELS WITH INFINITE VARIANCE INNOVATIONS
Thomas Mikosch, Tamar Gadrich, Claudia Kluppelberg, and Robert J. Adler 30 Dec. 1993 40 p
(Contract N00014-89-J-1870)
(AD-A274654) Avail: CASI HC A03/MF A01

We consider a standard ARMA process of the form phi(B)X(sub t) = Theta(B)Z(sub t), where the innovations Z(sub t) belong to the domain of attraction of a stable law, so that neither the Z(sub t) nor the X(sub t) have a finite variance. Our aim is to estimate the coefficients of phi and theta). Since maximum likelihood estimation is not a viable possibility (due to the unknown form of the marginal density of the innovation sequence) we adopt the so-called Whittle estimator, based on the sample periodogram of the X sequence. Despite the fact that the periodogram does not, a priori, seem like a logical object to study in this non-L' situation, we show that our estimators are consistent, obtain their asymptotic distributions, and show that they converge to the true values faster than in the usual L2 case. DTIC

N94-26385# International Centre for Theoretical Physics, Trieste (Italy).
WINDOW LEAST SQUARES METHOD APPLIED TO STATISTICAL NOISE SMOOTHING OF POSITRON ANNIHILATION DATA
Gh. Adam, S. Adam, B. Barbiellini (Geneva Univ., Switzerland.), L. Hoffmann (Geneva Univ., Switzerland.), A. A. Manuel (Geneva Univ., Switzerland.), and M. Peter (Geneva Univ., Switzerland.) Jun. 1993 40 p
(DE93-634665; IC-93/146) Avail: CASI HC A03/MF A01 (US Sales Only)

The paper deals with the off-line processing of experimental data obtained by two-dimensional angular correlation of the electron-positron annihilation radiation (2D-ACAR) technique on high-temperature superconductors. A piecewise continuous window least squares (WLS) method devoted to the statistical noise smoothing of 2D-ACAR data, under close control of the crystal reciprocal lattice periodicity, is derived. Reliability evaluation of the constant local weight WLS smoothing formula (CW-WLSF) shows that consistent processing 2D-ACAR data by CW-WLSF is possible. CW-WLSF analysis of 2D-ACAR data collected on untwinned Y Ba2Cu3O(7-delta) single crystals yields a significantly improved signature of the Fermi surface ridge at second Umklapp processes and resolves, for the first time, the ridge signature at third Umklapp processes. DOE

N94-26436# Naval Undersea Warfare Center, Newport, RI.
FUZZY ROBUST STATISTICS FOR APPLICATION TO THE FUZZY c-MEANS CLUSTERING ALGORITHM Technical Report
P. R. Kersten 1 Dec. 1993 17 p
(AD-A274719; NUWC-NPt-TR-10298) Avail: CASI HC A03/MF A01

This report introduces two robust statistics -- the fuzzy median and the fuzzy median absolute deviation from the median -- that have been developed for use with fuzzy data sets. The two statistics were applied to the fuzzy c-Means algorithm, a powerful clustering algorithm that normally employs linear statistics. The modified algorithm showed improved performance, being able to cluster data sets generated by heavy-tailed distributions like the Cauchy and Slash distributions. DTIC

N94-26445# Wisconsin Univ., Madison. Center for Mathematical Sciences.
RADIAL BASE FUNCTIONS: L(SUP p)-APPROXIMATION ORDERS WITH SCATTERED CENTERS Technical Summary Report
Martin D. Buhmann and Amos Ron Jan. 1994 22 p
(Contracts DMS-9224748; DAAL03-90-G-0090)
(AD-A274682; CMS-94-5) Avail: CASI HC A03/MF A01

In this paper we generalize several results on uniform approximation orders with radial basis functions in (Buhmann, Dyn and Levin, 1993) and (Dyn and Ron, 1993) to L(sup p)-approximation orders. These results apply, in particular, to approximants from spaces spanned by translates of radial basis functions by scattered centers. Examples to which our results apply include quasi-interpolation and least-squares approximation from radial function spaces. DTIC

N94-26485# Stanford Univ., CA. Dept. of Statistics.
SUBGRAPH APPROXIMATIONS FOR LARGE DIRECTED GRAPHICAL MODELS
Constantin T. Yiannoutsos and Alan E. Gelfand 27 Sep. 1993 39 p
(Contract N00014-92-J-1264)
(AD-A274813; TR-473) Avail: CASI HC A03/MF A01

Graphical Models provide a powerful tool for the formulation of general statistical models. In a previous paper, the authors argued that sampling-based techniques provide a unified approach for the analysis of graphical models under general distributional specifications. These techniques include both noniterative and iterative Monte Carlo. Our concern here is with very large graphical models whose size and complexity may prohibit analysis within a reasonable time frame. Typically in large systems, however, interest focuses on the behavior of only a few critical nodes. Our proposal is to develop, for a particular node, an approximating subgraph which contains virtually as much information about the variable as the full network, but by virtue of its reduced size, enables rapid computational investigation. We provide an illustration using a 40-node graph. Though this is not as large as we would envision in practice, it is convenient in permitting full model calculations to enable assessment of our approximations. DTIC

N94-26494# Stanford Univ., CA. Dept. of Statistics.
SIMULATION APPROACHES FOR CALCULATIONS IN DIRECTED GRAPHICAL MODELS
Constantin T. Yiannoutsos and Alan E. Gelfand 12 Oct. 1993 35 p
(Contract N00014-92-J-1264)
(AD-A274825; TR-475) Avail: CASI HC A03/MF A01

In formulating models for a complex system, graphical representation is an effective tool. When the components of the system are viewed as random variables, directed graphical models detail the nature of the dependence among them. Moreover, if for each variable the conditional distribution is provided according to the graph, the joint distribution is uniquely determined. Natural questions arise about the static behavior of the system under such specification as well as its response to information (observed levels of some of the variables). Answers to these questions require the ability to calculate arbitrary marginal and conditional distributions. In complex cases (high dimensional structures) such calculations require high dimensional integrations and/or summations. Most of the work to date has taken advantage of properties of directed graphs to facilitate exact calculations but is limited with regard to distributional assumptions and feasible system size. Monte Carlo methods for such calculations can accommodate much larger system size with arbitrary dependence structure and distributional forms yielding approximations which can be as accurate as desired. It is the objective of this paper to detail such methodology. An illustration is provided using a diagnostic system for congenital heart disease in neonates. DTIC

N94-26495# Stanford Univ., CA. Dept. of Statistics.
ASPECTS OF GOODNESS-OF-FIT
Michael A. Stephens 30 Sep. 1993 17 p
(Contract N00014-92-J-1264)
(AD-A274826; TR-474) Avail: CASI HC A03/MF A01

In this article, two important methods of testing fit to a distribution are discussed and compared. They are the family of tests based on the empirical distribution function of a random sample, and the family based on plotting the order statistics against a suitable set of constants and examining the fit of a line through the plotted points. The two sets will be called EDF tests and Regression tests respectively. DTIC

N94-26496# Stanford Univ., CA. Dept. of Statistics.
ESTIMATION AND TESTS-OF-FIT FOR THE THREE PARAMETER WEIBULL DISTRIBUTION
Richard A. Lockhart and Michael A. Stephens 27 Oct. 1993 40 p
(Contract N00014-92-J-1264)
(AD-A274827; TR-476) Avail: CASI HC A03/MF A01

Estimation techniques are given for the three-parameter Weibull distribution, with the location (or origin) parameter unknown, and possibly also the shape and/or scale parameters unknown. Tests of fit are described, and tables are given for the EDF statistics A(2), W(2) and U(2), to make the tests. Several examples are discussed. DTIC

N94-26867 Technische Univ., Twente (Netherlands). Tele-Informatics and Open Systems Group.
MODELING SYSTEMS BY PROBABILISTIC PROCESS ALGEBRA: AN EVENT STRUCTURES APPROACH
Joost-Pieter Katoen, Rom Langerak, and Diego Latella (Consiglio Nazionale delle Ricerche, Pisa, Italy.) 10 May 1993 25 p Limited Reproducibility: More than 20% of this document may be affected by microfiche quality
(ISSN 0924-3755)
(PB94-125259; TIOS-93/17) Copyright Avail: Issuing Activity (National Technical Information Service (NTIS))

Performance and reliability analysis of distributed systems based on formal specifications is an important and widely recognized issue. This paper treats a probabilistic version of the process algebra LOTOS. It incorporates a probabilistic choice assigning a probability of occurrence to each of its alternatives. Opposed to the traditional interleaving semantics used for existing probabilistic process algebras the presented language is based on a true concurrency semantics. This enables us to distinguish between non-determinism and parallelism, to reduce the state explosion problem and, moreover, to analyze part of the system without considering other (irrelevant) parts. In this paper the language is presented and the formal semantics is defined by using an extension of bundle event structures. A short example illustrates the novelties of the language and links the language to stochastic analysis based on semi-Markov chains. NTIS

N94-26870 Technische Univ., Twente (Netherlands). Tele-Informatics and Open Systems Group.
RECURSIVE BUNDLE EVENT STRUCTURES
Diego Latella (Consiglio Nazionale delle Ricerche, Pisa, Italy.) 23 Apr. 1993 30 p Limited Reproducibility: More than 20% of this document may be affected by microfiche quality
(ISSN 0924-3755)
(PB94-125275; TIOS-93/16) Copyright Avail: Issuing Activity (National Technical Information Service (NTIS))

In this paper we propose a model, recursive bundle event structures (recBES), of finite, graph-based representations for a class of (possibly) infinite bundle event structures. The model must be at least as powerful as Finite State Automata (FSA). This is because we want to use it as a basis for a probabilistic model which can fully and effectively exploit Markov Theory. This is a minimal requirement in the sense that recBES are indeed more powerful than FSA and can give rise to probabilistic models which can represent stochastic processes which are not Markovian, but the stochastic behavior of which can still be effectively studied. NTIS

N94-26939# Consiglio Nazionale delle Ricerche, Milan (Italy).
INTRODUCTION TO BAYESIAN NONPARAMETRIC THEORY
E. Regazzini 1994 33 p
(PB94-125002) Avail: CASI HC A03/MF A01

The paper provides a basic framework for a Bayesian nonparametric approach to statistical inference when observables form a sequence of exchangeable random elements. NTIS

N94-27051 Consiglio Nazionale delle Ricerche, Milan (Italy).
SOME CONTRIBUTIONS TO THE THEORY OF MONOTONE DEPENDENCE
D. M. Cifarelli and E. Regazzini 1994 33 p
(PB94-124922) Avail: CASI HC A03/MF A01

During the 1914-1916 three-year period, the Italian statistician Corrado Gini published a certain number of papers concerning the measure of the concordance (positive dependence) and discordance (monotone dependence) between two ordered characters. The present paper aims at providing an accurate, analytical representation of Gini's original idea of index of homophily. In the Ginian statistical framework, the concept of cograduation is strictly connected with that of homophily. In fact, the first is the counter-part of the second when ranks are considered in the place of true values. We will deal with cograduation in Section 3. There it will be shown, for example, that the well-known Gini's cograduation index and Spearman's rank correlation coefficient are the expression of the general index of Section 2 in very specific cases. Furthermore, we will use the index of Section 2 to define a general class of cograduation indices which work when ties are present. Section 4 deals with some miscellaneous results relating to the analytical expression of the index of homophily under specific conditions. NTIS

N94-27106# California Univ., Santa Barbara.
LIMIT THEOREMS FOR FUNCTIONALS OF MARKOV PROCESSES AND RENORMALIZABLE STABLE FIELDS
Raisa E. Feldman and Nagamani Krishnakumar 1993 18 p
(Contract N00014-89-J-1870)
(AD-A274645) Avail: CASI HC A03/MF A01

We study the limiting distribution of the amount of charge left in some set by an infinite system of charged Markovian particles, when the charge distribution belongs to the domain of attraction of a symmetric alpha-stable law. The limits are symmetric alpha-stable generalized random fields. Their multiple integrals are built in a similar manner. We also study the renormalizability of these families of random fields and use the construction to simulate stable fields on R1 and R2. DTIC

N94-27211 Technische Univ., Twente (Netherlands). Faculty of Applied Mathematics.
WHITE NOISE THEORY OF ROBUST NONLINEAR FILTERING WITH CORRELATED STATE AND OBSERVATION NOISES
A. Bagchi and R. Karandikar Jun. 1993 19 p
(PB94-126661; MEMO-1138) Avail: Issuing Activity (National Technical Information (NTIS)

One purpose of the paper is to remove the asymmetry in the existing 'direct' white noise theory by modeling the state process as the solution of a stochastic differential equation with a 'directly modelled' white noise as the input. It is shown that the solution of such a stochastic differential equation is, indeed, a Markov process. With this formulation, it is straightforward to introduce correlation between the state and observation noises. The other purpose of the paper is to obtain robust nonlinear filtering equation for stochastic dynamical systems with correlated state and observation noises. NTIS

N94-27223# Technische Univ., Twente (Netherlands). Faculty of Applied Mathematics.
WIEAND'S THEOREM
W. C. M. Kallenberg and A. J. Koning Jul. 1993 18 p Prepared in cooperation with Erasmus Univ.
(PB94-126711; MEMO-1144) Avail: CASI HC A03/MF A01

Wieand's theorem on the equivalence of limiting approximate Bahadur efficiency and limiting Pitman efficiency is extended in several ways. Conditions on monotonicity and continuity are obviated, composite null hypotheses are incorporated, and the implications of a weaker form of Wieand's Condition 3 are investigated. NTIS

N94-27612# Los Alamos National Lab., NM.
IS PROBABILITY OF FREQUENCY TOO NARROW?
Harry F. Martz 1993 9 p Presented at the 2nd Probabilistic Safety Assessment and Management Conference, San Diego, CA, 20-24 Mar. 1994
(Contract W-7405-eng-36)
(DE94-000687; LA-UR-93-3461; CONF-940312-12) Avail: CASI HC A02/MF A01

Modern methods of statistical data analysis, such as empirical and hierarchical Bayesian methods, should find increasing use in future Probabilistic Risk Assessment (PRA) applications. In addition, there will be a more formalized use of expert judgment in future PRA's. These methods require an extension of the probabilistic framework of PRA, in particular, the popular notion of probability of frequency, to consideration of frequency of frequency, frequency of probability, and probability of probability. The genesis, interpretation, and examples of these three extended notions are discussed. DOE

N94-27816# Los Alamos National Lab., NM.
ESTIMATORS FOR THE CAUCHY DISTRIBUTION
K. M. Hanson and D. R. Wolf 1993 9 p Presented at the 13th MAXENT Workshop, Santa Barbara, CA, 1-3 Aug. 1993
(Contract W-7405-eng-36)
(DE94-004990; LA-UR-93-4251; CONF-9308205-1) Avail: CASI HC A02/MF A01

The properties of various estimators of the central position of the Cauchy distribution are discussed. The performance of these estimators is evaluated for a set of simulated experiments. Estimators based on the maximum and mean of the posterior probability density function are empirically found to be well behaved when more than two measurements are available. On the contrary, because of the infinite variance of the Cauchy distribution, the average of the measured positions is an extremely poor estimator of the location of the source. However, the median of the measured positions is well behaved. The rms errors for the various estimators are compared to the Fisher-Cramer-Rao lower bound. It was found that the square root of the variance of the posterior density function is predictive of the rms error in the mean posterior estimator. DOE

66 SYSTEMS ANALYSIS

Includes mathematical modeling; network analysis; and operations research.

N94-26802# Los Alamos National Lab., NM.
PRE-ORBITAL CRITICALITY SAFETY FOR THE NEPSTP MISSION
Joseph Sapir, Denise Pelowitz, J. Robert Streetman, Yevgeny S. Glushkov (Kurchatov, I. V. Inst. of Atomic Energy, Moscow, USSR.), Nikolai N. Ponomarev-Stepnoi (Kurchatov, I. V. Inst. of Atomic Energy, Moscow, USSR.), Georgiy V. Kompanietz (Kurchatov, I. V. Inst. of Atomic Energy, Moscow, USSR.), and Vyacheslav A. Lobynstev (Kurchatov, I. V. Inst. of Atomic Energy, Moscow, USSR.) 1993 11 p Presented at the 11th Symposium on Space Nuclear Power Systems, Albuquerque, NM, 9-13 Jan. 1994
(Contract W-7405-eng-36)
(DE94-002600; LA-UR-93-3213; CONF-940101-22) Avail: CASI HC A03/MF A01

In December 1991, the Strategic Defense Initiative Organization (SDIO) proposed investigating whether launching a Russian Topaz-II space nuclear power system could be done safely and within budget constraints. Functional safety requirements developed for the U.S. Topaz mission mandated that the reactor remain subcritical when immersed in water. Topaz-II is an epithermal, enriched-uranium-fueled, NaK- (liquid metal alloy with 22% sodium and 78% potassium) cooled, and zirconium hydride-moderated reactor. A radial beryllium reflector containing 12 rotatable control drums surrounds the core. The authors prepared a computer model of the Topaz reactor that explicitly represented all major reactor components. Initial analyses indicated that in several water-immersion scenarios, the reactor would not remain subcritical. After additional calculations, modifications were proposed that would assure subcriticality under such conditions. This paper describes the analyses and the proposed modifications. DOE

N94-27172 National Defence Research Establishment, Linkoeping (Sweden). Huvudavdelning foer Informationsteknologi.
COMPUTER MODEL FOR GENERATION OF INFRARED IMAGES [DATORMODELL FOER GENERERING AV IR-BILDER]
L. Berglund Apr. 1993 34 p In SWAHILI
(PB94-123551; FOA-C-30713-8.3) Avail: Issuing Activity (National Technical Information Service (NTIS))

When simulating the duels between optoelectronically guided weapons and different kinds of objects protected by countermeasures, images of objects and countermeasures are used. In lack of available images, a computer model can be used to create the images needed for the simulation. The images generated are in general infrared images showing the heat radiation from the object. A software package has been developed to generate images which show different kinds of objects within the infrared wavelength bands. The report describes the computer model which is used for the generation of the infrared images. The structure of the computer model and its possibilities are given. NTIS

N94-27173 National Defence Research Establishment, Stockholm (Sweden). Dept. of Weapon Systems, Effects and Protection.
DATA ANALYSIS AND DATA FUSION FOR INTELLIGENCE ANALYSIS AND DECISION SUPPORT. RESEARCH PLAN 1993-2000 [DATAANALYS OCH DATAFUSION FOER UNDERRAETTELSEBEARBETNING OCH BESLUTSSTOED. FORSKNINGSPLAN 1993-2000]
P. Svensson and J. Schubert Jun. 1993 45 p In SWAHILI
(PB94-123569; FOA-A-20054-2.7) Avail: Issuing Activity (National Technical Information Service (NTIS))

This report is a research plan for 1993 - 2000 for a research group active in the field of intelligence analysis and decision support. The research of the group concerns the development of methodologies for data analysis, in particular spatial analysis, and data fusion, among other things with the aid of Dempster-Shafer's theory of evidence, for applications within these fields. The group has also been active in the field of advanced graphic interaction. This report mainly addresses scientists and engineers with an interest in data analysis and data fusion. NTIS

67 THEORETICAL MATHEMATICS

Includes topology and number theory.

N94-25781# Cranfield Inst. of Tech., Bedford (England). Dept. of Aerospace Science.
ARBITRARY-ORDER NUMERICAL SCHEMES FOR MODEL PARABOLIC EQUATIONS
Jian Shi Sep. 1992 27 p
(Cranfield-Aero-9210; ISBN-1-871564-493; ETN-94-95217) Avail: CASI HC A03/MF A01

The general theory and methodology of high order numerical schemes for one dimensional model parabolic equations are investigated. The universal formula from which a two level explicit arbitrary order numerical methods for diffusion equation can be derived is developed. Using the universal formula some high order numerical methods are constructed. Important features of numerical methods are revealed through the construction of high order numerical methods and stability analysis. Subject to the limitation of diffusion number, d, being positive, only the method that satisfies positive stable region is relevant. Because of the limitation of the diffusion number, some numerical schemes are physically violating. In order to obtain a physically correct and numerically stable method, a numerical method which possesses a positive stable region in terms of diffusion number d was selected. The results indicate that the ideal numerical schemes for the model parabolic equation are central point schemes which have the largest stable region. ESA

N94-25823# Cranfield Inst. of Tech., Bedford (England). Dept. of Aerospace Science.
ARBITRARY-ORDER HIGH RESOLUTION SCHEMES FOR MODEL HYPERBOLIC CONSERVATION LAWS
Jian Shi Jul. 1992 94 p
(Cranfield-Aero-9209; ISBN-1-871564-514; ETN-94-95216) Avail: CASI HC A05/MF A01

The general theory and methodology of high resolution numerical schemes for one dimensional hyperbolic conservation laws are investigated. The universal formula from which two level explicit conservative arbitrary order numerical methods can be derived is developed. The issue of linear stability is considered. A new approach to linear stability analysis is presented. The generalized formulation for total variation diminishing methods with stable region of c between -1 and 1 is proposed. To demonstrate the theories, third order and fourth order total variation diminishing methods are generated. Computational results of these schemes show features of high resolution methods. ESA

N94-25868 International Centre for Theoretical Physics, Trieste (Italy).
DUALITY FOR MULTIPARAMETRIC QUANTUM GL(n) AND FOR A LORENTZ QUANTUM GROUP

V. K. Dobrev and P. Parashar Jul. 1992 20 p Limited Reproducibility: More than 20% of this document may be affected by microfiche quality
(DE93-613048; IC-92/189) Avail: Issuing Activity (Department of Energy (DOE)) (US Sales Only)

We show that the algebra U(sub uq) dual to the multiparametric deformation GL(sub uq)(n,C) may be realized a la Sudbery, viz, tangent vectors at the identity. Furthermore, we give the Cartan-Weyl basis of U(sub uq) and show that this is consistent with Sudbery duality. We also give the algebra dual to the matrix Lorentz quantum group of Podles-Woronowicz and Watamura et al. DOE

N94-25886# Melbourne Univ., Parkville (Australia). School of Physics.
THE DIRAC EQUATION IN KERR SPACETIME, SPHEROIDAL COORDINATES AND THE M.I.T. BAG MODEL OF HADRONS
Bruce H. J. McKellar, Mark J. Thomson, and G. J. Stephenson, Jr. (Los Alamos National Lab., NM.) Mar. 1993 13 p
(DE94-601566; UM-P-93/22; OZ-93/08) Avail: CASI HC A03/MF A01 (US Sales Only)

The Dirac equation in Kerr spacetime is separated using the rotating tetrad formalism. This allows solutions of the Dirac equation, in flat spacetime, written in oblate and prolate spheroidal coordinates to be extracted. The usual M.I.T. bag boundary condition is then found to be incompatible with a nonvanishing separated wave function except in the spherical limit. However, it is shown that an alternative boundary condition can arise naturally in scalar-pseudoscalar potential models, that is physically motivated and allows for a non-trivial solution. DOE

N94-26193 Joint Inst. for Nuclear Research, Dubna (USSR). Lab. of Theoretical Physics.
DIMENSIONAL CROSSOVER FROM NON-RENORMALIZABILITY TO RENORMALIZABILITY
Yu. A. Kubyshin, D. OConnor, and C. R. Stephens 1991 15 p Limited Reproducibility: More than 20% of this document may be affected by microfiche quality
(DE93-613052; JINR-E-2-91-497) Avail: CASI HC A03 (US Sales Only)

It is shown for one loop that a (lambda)(Phi)(exp 4) theory contracts from being a non-renormalizable theory above four dimensions to a renormalizable theory in the limit of zero size of the additional dimensions above four dimensions. This provides an example of the decoupling of an infinite number of modes in the infrared domain of the theory. The results have applications to statistical mechanical systems above the critical point in the context of finite size effects and Kaluza-Klein theories in high energy physics. DOE

N94-26270 International Centre for Theoretical Physics, Trieste (Italy).
CLASSICAL SOLUTIONS OF YANG-MILLS-CHERN-SIMONS THEORY IN 2+1 DIMENSIONS: A QUASI-LINEAR SUPERPOSITION
R. Teh Jun. 1993 12 p Limited Reproducibility: More than 20% of this document may be affected by microfiche quality
(DE93-634335; IC-93/139) Avail: CASI HC A03 (US Sales Only)

We pointed out that there exists a critical frequency of oscillation for the vortex-like solution above which the system switches to the fields of an alternating current inside a solenoid. We also show the existence a non-abelian gauge for which the fields can alternate periodically in space between the abelian fields and another abelian (or non-abelian) field pointing in a different isospin space direction. The solution discussed here are real, zero-action Minkowski space configurations. DOE

N94-26368# International Centre for Theoretical Physics, Trieste (Italy).
ANALYTICAL SOLUTION OF MORI'S EQUATION WITH SECANT HYPERBOLIC MEMORY
K. Tankeshwar and K. N. Pathak (Panjab Univ., Chandigarh, India.) Jul. 1993 20 p
(DE94-601541; IC-93/206) Avail: CASI HC A03/MF A01 (US Sales Only)

The equation of motion of the auto-correlation function has been solved analytically using a secant-hyperbolic form of the memory function. The analytical results obtained for the long time expansion together with the short time expansion provide a good description over the whole time domain as judged by their comparison with the numerical solution of Mori's equation of motion. We also find that the time evolution of the auto-correlation function is determined by a single parameter (tau) which is related to the frequency sum rules up to the fourth order. The auto-correlation function has been found to show simple decaying or oscillatory behavior depending on whether the parameter (tau) is greater than or less than some critical values. Similarities as well as differences in time evolution of the auto-correlation have been discussed for exponential, secant-hyperbolic, and Gaussian approaches of the memory function. DOE

N94-26411# International Centre for Theoretical Physics, Trieste (Italy).
HOW RELIABLE IS THE HMSA INTEGRAL EQUATION FOR THE PAIR STRUCTURE OF SUPERCOOLED AND AMORPHOUS MIXTURES?
F. O. Kaddour and G. Pastore (Trieste Univ., Italy.) Jul. 1993 13 p
(DE94-601543; IC-93/215) Avail: CASI HC A03/MF A01 (US Sales Only)

Accurate Molecular Dynamics calculations on highly asymmetric Lennard-Jones mixtures have been performed to check, in rather extreme cases, the ability of the self-consistent HMSA integral equation to predict the pair correlations in supercooled and glassy mixtures. We find that, in the supercooled region, the HMSA is a reasonable approximation for the structural properties and thermodynamics properties, but systematic deviations from MD data appear when the glass transition is approached. DOE

N94-26413# International Centre for Theoretical Physics, Trieste (Italy).
THE MASSLESS REPRESENTATIONS OF THE CONFORMAL QUANTUM ALGEBRA
V, K. Dobrev and R. Floreanini (Istituto Nazionale di Fisica Nucleare, Trieste, Italy.) Jun. 1993 14 p
(DE94-601555; IC-93/158; UTS-DFT-16-93) Avail: CASI HC A03/MF A01 (US Sales Only)

The massless representations of the conformal quantum algebra U(sub q)(su(2,2)) for complex q such that module q = 1 are studied in detail. By factorizing out all singular vectors of the corresponding Verma modules, a simple basis for these representations is explicitly constructed. This basis is new also for the usual conformal algebra su(2,2). This construction allows a straightforward treatment of the case q a root of unity, when the representations are unitary and finite-dimensional. DOE

N94-26414# International Centre for Theoretical Physics, Trieste (Italy).
AFFINE ALGEBRAS ON THE TORUS
M. Zakkari Jul. 1993 8 p
(DE94-601556; IC-93/170) Avail: CASI HC A02/MF A01 (US Sales Only)

The analysis of the Kac-Moody 'like' algebra L-circumflex(sup 2)(G) on the torus is performed. It will be seen that the root systems construction leading to a Cartan matrix is not possible. Different twist of L-circumflex(sup 2)(sub lambda)(G) are discussed. Connections with known results are done. DOE

N94-26415# International Centre for Theoretical Physics, Trieste (Italy).
HIGHER SPIN EXTENSIONS OF THE VIRASORO ALGEBRA, AREA-PRESERVING ALGEBRAS AND THE MATRIX ALGEBRA A-BAR(SUB (INFINITY))
M. Zakkari Jul. 1993 6 p
(DE94-601557; IC-93/173) Avail: CASI HC A02/MF A01 (US Sales Only)

The generating functional of Kac-Moody, Virasoro algebra and area preserving diffeomorphism on the torus T(sup 2) is given. Realization of higher integer spin symmetries is discussed. The correspondence between the area preserving diffeomorphism on the torus T(sup k) and the algebra a-bar(sub infinity) is pointed out. DOE

N94-26460 International Centre for Theoretical Physics, Trieste (Italy).
ON THE (PHI)(SUB 0)-STABILITY OF FUNCTIONAL DIFFERENTIAL EQUATIONS
E. P. Akpan Jul. 1993 29 p Limited Reproducibility: More than 20% of this document may be affected by microfiche quality
(DE94-601507; IC-93/180) Avail: CASI HC A03 (US Sales Only)

The theory of functional differential inequalities through cones is developed and comparison theorems in the framework of cone-valued Lyapunov functions were obtained. The (Phi)(sub 0)-stability theory for functional differential equations of comparison type was developed and results giving sufficient conditions for various stability concepts for more general functional differential equations using comparison technique of the method of cone-valued Lyapunov functions was obtained. Necessary and sufficient conditions for exponential stability and uniform asymptotic stability are obtained for hereditary systems and perturbed functional differential systems respectively. DOE

N94-26472# Joint Inst. for Nuclear Research, Dubna (USSR).
HOW TO BUILD ANALOGUES OF THE BESSEL-CLIFFORD EXPANSIONS FOR THE SUM OF THE REPULSIVE COULOMB POTENTIAL AND CENTRAL POTENTIAL DECREASING MORE RAPIDLY THAN THE CENTRIFUGAL ONE?
V. V. Pupyshev 1992 15 p
(DE93-634308; JINR-E-4-92-213) Avail: CASI HC A03/MF A01 (US Sales Only)

The suggested algorithm is based on a linear version of the variable phase approach. The regular and irregular wave-functions of scattering are represented as an infinite series in which the distance and momentum are separated from each other as well as in the Bessel-Clifford expansions for the Coulomb functions. The construction of the finite sums uniformly approximating these series under well-defined conditions is reduced to the solution of the simplest differential problems. DOE

N94-26552 International Centre for Theoretical Physics, Trieste (Italy).
STRING HYPOTHESIS AND CHARACTERS OF COSET CFTs
S. Dasmahapatra Jun. 1993 13 p Limited Reproducibility: More than 20% of this document may be affected by microfiche quality
(DE93-634337; IC-93/91) Avail: Issuing Activity (Department of Energy (DOE)) (US Sales Only)

An algorithm for the construction of the branching functions in the vacuum sector for affine Lie algebras based on the string hypothesis solution to a system of Bethe equations for generalized RSOS models is presented. It is also mentioned how the ground state structure and features of the excitation spectra like the Brillouin zone schemes of these models (and those in the same universality classes) can be extracted from combinatoric arguments and encoded in Lie algebraic terms. DOE

N94-26928 Melbourne Univ., Parkville (Australia). School of Physics.
ASYMPTOTICS FOR KUMMER FUNCTIONS, BOSE PLASMAS, AND RELATED SPECIAL FUNCTIONS
V. Kowalenko (Australian National Univ., Canberra.) and N. E. Frankel (Australian National Univ., Canberra.) 1993 33 p Limited Reproducibility: More than 20% of this document may be affected by microfiche quality
(DE94-601853; UM-P-93/02) Avail: CASI HC A03 (US Sales Only)

New asymptotic expansions for the Kummer functions are presented. These expansions play a determining role in the behavior of magnetized Bose plasmas in the limit that the external magnetic field B approaches zero. The technique for establishing these expansions is also used to study other related special functions and series. The purpose is not to consider the physical properties of these systems but to establish the mathematical machinery for such studies to follow. DOE

N94-27222# Technische Univ., Twente (Netherlands). Faculty of Applied Mathematics.
GRAPHS SATISFYING A LOCAL ORE-TYPE CONDITION
A. S. Asratian, H. J. Broersma, J. vandenHeuvel, and H. J. Veldman Jun. 1993 14 p Sponsored by Nederlandse Organisatie voor Wetenschappelijk Onderzoek, The Hague
(PB94-126679; MEMO-1139) Avail: CASI HC A03/MF A01

The report presents topological theorems and proofs concerning linear graphs G which satisfy a local Ore-type condition. Classical results on Hamiltonian graphs are initially given, followed by toughness, Hamiltonian properties, and perfect matchings of L2-graphs. NTIS

N94-27264 University of Western Ontario, London.
OPERATOR REGULARIZATION AND RENORMALIZATION THEORY
Ph.D. Thesis
Louis B. Culumovic Feb. 1989 140 p
(ISBN-0-315-49334-8; CTN-94-60976) Copyright Avail: Micromedia Ltd., Technical Information Centre, 240 Catherine Street, Suite 305, Ottawa, Ontario, K2P 2G8, Canada HC/MF

The operator regularization (o.r.) technique is extended beyond one-loop order in perturbation theory, and some two-loop calculations in o.r. are performed. First, the Schwinger expansion is used to calculate the general coefficients of the DeWitt expansion, which enables using this expansion beyond one-loop order. An approach to calculating renormalization group functions based on examining finite Green functions is then presented. Explicit calculations of the renormalization group functions to develop two-loop order are performed in scalar models using the new DeWitt expansion coefficients. Two other applications are included, one being the computation of the divergence of the U(1) axial current in the presence of constant U(1) and SO(3) gauge fields to two-loop order. This combines o.r. with a functional technique, and a result compatible with the Adler-Bardeen result is obtained. The other application is to massive Yang-Mills theory. Introducing a mass breaks gauge invariance and makes the theory non-renormalizable. Since o.r. always gives finite results, it presents the opportunity to examine a non-renormalizable theory without the usual difficulties. It turns out that the arbitrary mass scale parameter loses its arbitrariness and becomes fixed by the strength of a radiatively induced four-point interaction. Author (CISTI)

N94-27633 International Centre for Theoretical Physics, Trieste (Italy).
SOME REMARKS ON THE SYMMETRY OF SELF-CONJUGATE MINIMAL SURFACES IN R3
Weihuan Chen and M. S. Rahman Aug. 1993 8 p Limited Reproducibility: More than 20% of this document may be affected by microfiche quality
(DE94-603670; IC-93/244) Avail: CASI HC A02 (US Sales Only)

Symmetry properties of self-conjugate minimal surfaces, i.e. minimal surfaces which are congruent with their conjugate ones in R(sup 3), are studied. DOE

N94-27777# Los Alamos National Lab., NM.
A SURVEY OF OPEN PROBLEMS IN SYMPLECTIC INTEGRATION
Robert I. McLachlan (Colorado Univ., Boulder.) and Clint Scovel 15 Oct. 1993 27 p Presented at the Integration Algorithms for Classical Mechanics, Ontario, 14-27 Oct. 1993
(Contract W-7405-eng-36)
(DE94-003966; LA-UR-93-3914; CONF-9310235-1) Avail: CASI HC A03/MF A01

In the past few years there has been a substantial amount of research on symplectic integration. The subject is only part of a program concerned with numerically preserving a system's inherent geometrical structures. Volume preservation, reversibility, local conservation laws for elliptic equations, and systems with integral invariants are but a few examples of such invariant structures. In many cases one requires a numerical method to stay in the smallest possible appropriate group of phase space maps. It is not the authors' opinion that symplecticity, for example, automatically makes a numerical method superior to all others, but it is their opinion that it should be taken seriously and that a conscious, informed decision be made in that regard. A survey of open problems in symplectic integration, including other problems from the larger program are presented. This is not intended as a review of symplectic integration and is naturally derived from the authors' own research interests. At present, this survey is incomplete, but the authors hope the help of the colleagues to be able to include in the proceedings of this conference a more comprehensive survey. Many of the problems mentioned call for numerical experimentation, some for application of suggested but untested methods, some for new methods, and some for theorems. Some envisage large research programs. DOE

70 PHYSICS (GENERAL)

For precision time and time interval (PTTI) see *35 Instrumentation and Photography;* for geophysics, astrophysics or solar physics see *46 Geophysics, 90 Astrophysics,* or *92 Solar Physics.*

N94-25603 Joint Inst. for Nuclear Research, Dubna (USSR).
ON THE FIRST INTEGRALS OF GEODESICS
S. I. Kaleva (Bulgarian Academy of Sciences, Sofia.) 1992 12 p Limited Reproducibility: More than 20% of this document may be affected by microfiche quality
(DE93-612974; JINR-E-2-92-20) Avail: Issuing Activity (Department of Energy (DOE)) (US Sales Only)

The first integrals of the geodesics in the Riemann spaces which admit various geometric symmetries are considered. Some possibilities of their physical interpretation and application are investigated. DOE

N94-25831 International Centre for Theoretical Physics, Trieste (Italy).
STOCHASTIC RESONANCE IN A PERIODIC POTENTIAL SYSTEM UNDER A CONSTANT FORCE
Hu Gang Oct. 1992 8 p Limited Reproducibility: More than 20% of this document may be affected by microfiche quality
(DE93-616817; IC-92/339) Avail: CASI HC A02 (US Sales Only)

An overdamped particle moving in a periodic potential, and subject to a constant force and a stochastic force (i.e., x = -sin(2(pi)(chi)) + B + (Gamma)(t), (Gamma)(t) is a white noise) is considered. The mobility of the particle, d(x(t))/dt, is investigated. The stochastic resonance type of behaviour is revealed. The study of the SR problem can thus be extended to systems with periodic force. DOE

N94-25988# Rochester Univ., NY.
THEORETICAL AND EXPERIMENTAL STUDIES OF ELEMENTARY PHYSICS
A. Bodek, T. Ferbel, A. C. Melissinos, P. Slattery, P. Tipton, A. Das, C. R. Hagen, S. G. Rajeev, S. Okubo, and L. Orr 1 May 1993 166 p
(Contract DE-FG02-91ER-40685)
(DE94-002310; DOE/ER-40685/759) Avail: CASI HC A08/MF A02

The various components of the high-energy physics research program at the University of Rochester are presented. Fixed-target experimentation at FNAL includes studies of direct photon production by p and (pi) on H, Be, and Cu, and hybrid mesons and other physics issues in Coulomb excitation at high energies. The status of the GEM (Gammas, Electrons, and Muons) Experiment at the SSC is given. The D-Zero experiment at FNAL is reviewed. Deep inelastic lepton--nucleon scattering experiments are summarized: electron scattering experiments at SLAC, FNAL neutrino quad triplet runs, FNAL neutrino sign selected experiments, and SDC cosmic ray test and test beam calibration. Studies of nonlinear QED at SLAC concentrated on a study of QED at critical field strength in intense laser--high-energy electron collisions. Development work on the Collider Detector at Fermilab (CDF) emphasized the CDF silicon vertex detector, the end plug calorimeter, and the SDC tile/fiber calorimetry. The theoretical physics effort is sketched. DOE

N94-26256# Technical Research Centre of Finland, Espoo. Fire Technology Lab.
A TRANSIENT SYMMETRICAL METHOD FOR THE MEASUREMENT OF TEMPERATURE DEPENDENT THERMAL DIFFUSIVITY
Matti Kokkala and Djebar Baroudi Apr. 1993 27 p Sponsored by Finnish Fire Research Board, Finland
(ISSN 1235-0605)
(VTT-TIED-1452; ISBN-951-38-4345-9; ETN-94-95267) Copyright Avail: CASI HC A03/MF A01

Measurement of temperature dependent thermal diffusivities using a transient symmetrical method is studied. The thermal diffusivity is determined from the temperature profile in a specimen constructed of thin slabs and heated symmetrically from both sides. The thermal diffusivity is determined as the ratio of the time derivative and the second spatial derivative at the position of the extremum of temperature. A numerical method was developed to calculate the thermal diffusivity as a function of time. The confidence interval of the diffusivity is determined. The numerical methods were validated by using numerically calculated temperature profiles for a material with known thermal diffusivity. The practical applicability of the method was investigated. The method proved to work for an inert material when no changes of geometry of the sample occurred. If reactions, convection, or substantial thermal expansions causing gaps inside the specimen occur, the assumptions of the method do not hold, and the results will not be well defined. ESA

N94-26374# Technion - Israel Inst. of Tech., Haifa. Faculty of Industrial and Management Engineering.
BISEXUAL BRANCHING DIFFUSIONS
Leonid Mytnik and Robert J. Adler 30 Dec. 1993 38 p
(Contract N00014-89-J-1870)
(AD-A274698) Avail: CASI HC A03/MF A01

The limiting behavior of large systems of two types of Brownian particles undergoing bisexual branching is studied. Particles of each type generate individuals of both types, and the respective branching law is asymptotically critical for the two dimensional system, while being subcritical for each individual population. The main result of the paper is that the limiting behavior of suitably scaled sums and differences of the two populations is given by a pair of measure and distribution valued processes which, together, determine the limit behaviors of the individual populations. Proofs are based on the martingale problem approach to general state space processes. The fact that the limit involves both measure and distribution valued processes requires the development of some new methodologies of independent interest. DTIC

N94-26376# Army Armament Research, Development and Engineering Center, Watervliet, NY. Benet Lab.
POWER LAWS, FLICKER NOISE, AND THE BARKHAUSEN EFFECT Final Report
L. V. Meisel and P. J. Cote Oct. 1993 25 p
(AD-A274702; ARCCB-TR-93038) Avail: CASI HC A03/MF A01

The Barkhausen effect was studied in three ferromagnetic metals: an amorphous alloy, iron, and alumel. The data exhibit all the characteristics of self-organized critical behavior enumerated by Bak, Tang, and Weisenfeld: The distributions of pulse durations, areas, and energies have the form of power laws, which have been modified to account for finite-size effects, and the power spectral densities have the form of flicker noise. Furthermore, the parameters describing the Barkhausen noise pulse distributions are consistent with those characterizing the power spectral density in the light of the results of Jensen, Christensen, and Fogedby. The data are also consistent with a model based on an inherent static fractal structure, independent of a self-organizing principle. DTIC

N94-26421# Argonne National Lab., IL.
CORRELATION OF EXPERIMENTAL DATA AND THREE-DIMENSIONAL FINITE ELEMENT MODELING OF A SPINNING QUADRUPOLE
W. L. Lorimer (California Univ., Berkeley.), D. K. Lieu (California Univ., Berkeley.), J. R. Hull, T. M. Mulcahy, and T. D. Rossing 1993 3 p Presented at the Conference on Computation of Electromagnetic Fields, Miami, FL, 31 Oct. - 4 Nov. 1993
(Contract W-31-109-eng-38)
(DE93-041173; ANL/MCT/CP-79097; CONF-931013-1) Avail: CASI HC A01/MF A01

A permanent magnet quadrupole spinning over an aluminum disk was constructed, and drag torque was measured for various speeds and gap sizes. The experiment was modeled using a three-dimensional finite element program. Experimental and analytical results were compared, and the effect of magnet polarity was determined. DOE

N94-26484# Aerospace Corp., El Segundo, CA. Technology Operations.
DIODE-LASER-PUMPED, GAS-CELL ATOMIC CLOCKS
R. E. Drullinger, Csaba Szekely, and James C. Camparo 1 Nov. 1993 8 p
(Contract F04701-88-C-0089)
(AD-A274812; TR-92(2925)-3; SMC-TR-93-58) Avail: CASI HC A02/MF A01

Recent theoretical calculations suggest that the short-term stability of rubidium, atomic, gas-cell frequency standards could be improved by several orders of magnitude if diode lasers were used for optical pumping. Moreover, the theoretical results predict that rubidium, as opposed to cesium, is the best alkali atom to choose for gas cell atomic clock operation. This report describes strategies for developing such clocks for space applications and as local oscillators for other high-accuracy atomic clocks. DTIC

N94-26851 Swedish Inst. for Materials Testing, Boras.
REFRACTIVE AND DIELECTRIC PROPERTIES OF HELIUM, ARGON AND NITROGEN GASES
Leslie Pendrill 1993 18 p Limited Reproducibility: More than 20% of this document may be affected by microfiche quality
(PB94-123783; SP-Rept-1993:23) Avail: Issuing Activity (National Technical Information Service (NTIS))

A review has been made of experimental and theoretical values of the refractive and dielectric properties of macroscopic gases of helium, argon, and nitrogen and corresponding microscopic parameters such as the atomic (or molecular) polarizability. In addition to absolute values, these quantities are expressed as functions of optical wavelength, pressure, and temperature. Also given are relations governing the density of each gas. NTIS

N94-26968# Groningen Rijksuniv. (Netherlands). Dept. of Mathematics.
NORMAL FORMS FOR PERTURBATIONS OF THE EULER TOP
Heinz Hanssmann 28 Mar. 1993 34 p
(PB94-125390; W-9309) Avail: CASI HC A03/MF A01

A method for studying the behavior of a rigid body in a general force field is proposed. The study is restricted to the case of a perturbation of the Euler top by a small external force. A normal form approach yields a formal 2-torus symmetry, which in turn leads to the reduction to a one-degree-of-freedom system. The behavior of this system is used to identify quasi-periodic motions of the rigid body with two or three independent frequencies. The method is tested in the integrable cases of Lagrange and Kirchhoff. Furthermore, it is applied to some nonintegrable cases in which two of the principle moments of inertia of the rigid body are equal. NTIS

N94-27108# Technion - Israel Inst. of Tech., Haifa. Faculty of Industrial and Management Engineering.
A SUPERPROCESS WITH A DISAPPEARING SELF-INTERACTION
Robert J. Adler and Lidia Ivanitskaya 1993 15 p
(Contract N00014-89-J-1870)
(AD-A274647) Avail: CASI HC A03/MF A01

We start with a system of independent branching Brownian motions which, properly organized and normalized, generate a super Brownian motion in the high density limit. We introduce a weak interaction between the particles, that affects the diffusion but not the branching. The interaction is chosen in such a way that the infinite density limit is absolutely continuous with respect to the non-interacting system. We find that, despite the fact that the interaction mechanism never completely disappears, the limiting superprocesses are identical. We study what actually happens to the interaction mechanism, or ghost-process. DTIC

N94-27126# Howard Univ., Washington, DC.
CENTER FOR NONLINEAR PHENOMENA AND MAGNETIC MATERIALS Final Report, Jul. 1991 - Jun. 1992
Tepper L. Gill 4 Dec. 1992 55 p
(Contract F49620-89-C-0079)
(AD-A274176) Avail: CASI HC A04/MF A01

In previous work we have proved existence and obtained estimates for the (finite) Huasdorff and fractal dimensions of global (maximal compact) attractors for the Landau-Lifschitz equations. These are the fundamental equations of the classical theory ferromagnetism. In order to obtain more detailed information about these attractors, we are currently developing approximation methods based on the theory of inertial manifolds. Inertial manifolds are finite dimensional manifolds which attract all solutions at an exponential rate. They contain the global attractor and have the advantage that they are manifolds whereas the attractors generally are not(they can be complicated fractal sets). The equations reduce to a finite-dimensional system of O.D.E.'s on the inertial manifolds. DTIC

N94-27131 National Physical Lab., Teddington (England). Div. of Quantum Metrology.
FRONTIERS OF SCIENCE AND MEASUREMENT: REPORT ON A SEMINAR JOINTLY ORGANIZED BY THE NATIONAL PHYSICAL LABORATORY AND THE INSTITUTE OF PHYSICS
C. C. Hodge and D. W. Robinson 1993 9 p Conference held in Teddington, England, 26 May 1993
(PB94-124310; NPL-QU-97) Copyright Avail: Issuing Activity (National Technical Information Service (NTIS))

A seminar entitled 'Frontiers of Science and Measurement' was held at the National Physical Laboratory (NPL) on 26 May 1993. It was aimed at facilitating the exchange of ideas and research interests in the expectation of encouraging future collaborative activities. Many expressed the wish for closer links with NPL and the need for follow-on meetings to explore the more promising areas identified at the Seminar. NTIS

N94-27268 Waterloo Univ. (Ontario). Dept. of Computer Science.
COHERENCE AND SATISFIABILITY OF WAVEFORM TIMING SPECIFICATIONS Ph.D. Thesis
Anthony Joseph Gahlinger 1990 132 p
(ISBN-0-315-57769-X; CTN-94-60978) Copyright Avail: Micromedia Ltd., Technical Information Centre, 240 Catherine Street, Suite 305, Ottawa, Ontario, K2P 2G8, Canada HC/MF

Hardware designers often use digital waveforms to specify critical device timing. Several problems related to the use of such specifications are analyzed. These include the verification of the coherence of specifications; the determination of whether each device's timing requirements are satisfied by the timing of other devices in the system, given the timing specifications of devices in a system; and derivation of the conditions that must be met for the timing of a system to be considered reliable, when specifications are incomplete. Timing specifications are formulated as sets of linear constraints, and it is shown that the problems can be solved with optimization techniques. Several algorithms are presented along with open problems concerning efficient solutions. In addition, a model is proposed for the propagation of events in a digital circuit that can serve as a basis for the timing bounds found in specifications. This model is used to show that the method used to test the satisfiability of specifications is safe in the sense that affirmative answers are trustworthy while negative answers may be conservative. The work reported can serve as a basis for the design of computer aided design tools for validating timing specifications, analyzing the timing of device connections, and synthesizing the conditions that ensure reliability. Author (CISTI)

N94-27924*# Tuskegee Inst., AL. Dept. of Aerospace and Mechanical Engineering.
INVESTIGATION OF SPECTRAL ANALYSIS TECHNIQUES FOR RANDOMLY SAMPLED VELOCIMETRY DATA
Dave Sree *In* Old Dominion Univ., The 1993 NASA-ODU American Society for Engineering Education (ASEE) Summer Faculty Fellowship Program Dec. 1993 p 183-186 (For primary document see N94-27893 07-80)
Avail: CASI HC A01/MF A03

71 ACOUSTICS

Includes sound generation, transmission and attenuation.
For noise pollution see *45 Environmental Pollution.*

N94-25731# Federal Aviation Administration, Cambridge, MA.
INM, INTEGRATED NOISE MODEL. VERSION 4.11: USER'S GUIDE, SUPPLEMENT Final Report
Gregg G. Fleming and John R. DAprile Dec. 1993 85 p
(AD-A273885; DOT-VNTSC-FAA-93-19; DOT/FAA/EE-93-03) Avail: CASI HC A05/MF A01

The John A. Volpe National Transportation Systems Center (Volpe Center), in support of the Federal Aviation administration, Office of Environment and Energy, has developed Version 4.11 of the Integrated Noise Model (INM). The User's Guide for the Version 4.11 computer software is a supplement to INM, Version 3, User's Guide - Revision 1 for the Version 3.10 computer software released in June, 1992. The Version 4.11 supplement, prepared by the Volpe Center's Acoustics Facility, presents computer system requirements as well as installation procedures and enhancements. Specific enhancements discussed include: (1) the introduction of a takeoff profile generator; (2) the ability to account for terrain elevation around a specified airport; (3) the ability to compute the CNEL, WECPNL, LEQDAY, and LEQNIGHT noise metrics; (4) the ability to account for airplane runup operations; (5) the ability to account for displaced runway thresholds during approach operations; (6) an enhancement to the noise contour computations: (7) an increase in the number of takeoff profile segments; and (8) enhancements to the echo file. DTIC

N94-25737# Air Force Inst. of Tech., Wright-Patterson AFB, OH.
BINAURAL ROOM SIMULATION M.S. Thesis
Brian A. Smith Dec. 1993 127 p
(AD-A273823; AFIT/GAM/ENC/93D-1) Avail: CASI HC A07/MF A02

Research in binaural and spatial hearing is of particular interest to the Air Force. Applications in cockpit communication, target recognition, and aircraft navigation are being explored. Human auditory localization cues are examined and a mathematical model for the transfer function of a sound signal traveling from an isotropic point source through a rectangular room to both ears of a listener is developed. Using this model as a guide, non-head coupled binaural sound signals are generated in a binaural room simulation. Reflection and attenuation cues included in the computer generated signals are varied in order to determine which cues enhance the listener's degree of extracranialization. Results of this research indicate that the addition of three or more attenuated reflections into a non-head coupled binaural signal provide the listener with a binaural sound that is localized extracranially. DTIC

N94-26889# Georgia Inst. of Tech., Atlanta. School of Mechanical Engineering.
NEW VARIATIONAL TECHNIQUES FOR ACOUSTIC RADIATION AND SCATTERING FROM ELASTIC SHELL STRUCTURES Final Report
Jerry H. Ginsberg 20 Dec. 1993 24 p
(Contract N00014-91-J-1187)
(AD-A274599) Avail: CASI HC A03/MF A01

The interaction between a vibrating submerged structure and the surrounding fluid, which features coupling between the surface pressure distribution and the structural displacement, is an inherent feature for sound radiation and target strength analyses. A variety of approaches have been implemented in the past, but each suffers from serious limitations. Formal mathematical analysis using separation of variables or integral transform techniques is suitable only for the simplest structural models, while full finite element descriptions of realistic structures and the surrounding medium lead to excessively large computer simulations. One approach uses approximate impedance-type boundary condition of uncertain accuracy to model the fluid response. Boundary element formulations rationally represent the interaction phenomena without explicitly solving field equations for the fluid, at the expense of an enormous increase in computational effort due to the need to cover the surface with a reasonably fine mesh. DTIC

N94-26923# Naval Undersea Warfare Center, Newport, RI.
PREWHITENING OF COLORED NOISE FIELDS FOR DETECTION OF THRESHOLD SOURCES Final Report
Alain C. Barthelemy 7 Nov. 1993 54 p
(AD-A274346; NUWC-NPT-TR-10495) Avail: CASI HC A04/MF A01

This report presents an algorithm for the estimation of noise correlations for an array of sensors. The algorithm assumes a mixed spectra model composed of discrete sinusoidal sources and continuous noise components. A spatial autoregressive (AR) process models the continuous component. Previous methods use spatial AR models with real coefficients, restricting the utility of the model to noise sources that impinge on an array at broadside. The complex formulation presented here solves the general problem of arbitrarily oriented noise sources. The technique uses a gradient algorithm for maximization of a likelihood functional to solve for the complex AR coefficients. Once the algorithm determines the noise covariance matrix, prewhitening techniques allow detection of threshold sources. The multiple signal classification (MUSIC) direction finder when applied to the prewhitened observed correlation matrix illustrates the usefulness in detecting low signal-to-noise ratio (SNR) sources. Computational examples use the standardized test case (STC), a realistic model with a challenging range of SNR and difficult source locations. DTIC

N94-26983# Texas Univ., Austin. Dept. of Mechanical Engineering.
PROBLEMS IN NONLINEAR ACOUSTICS: RAYLEIGH WAVES, PULSED SOUND BEAMS, AND WAVEGUIDES Annual Summary Report No. 5, 15 Aug. 1992 - 31 Aug. 1993
Mark F. Hamilton 31 Aug. 1993 26 p
(Contract N00014-89-J-1003)
(AD-A274587) Avail: CASI HC A03/MF A01

Three project topics, all in the area of nonlinear acoustics, are discussed in this annual summary report: (1) Nonlinear Rayleigh Waves (including diffraction effects in Rayleigh wave beams, local and nonlocal nonlinearity in Rayleigh waves, pulsed nonlinear Rayleigh waves, and nonlinear Stoneley waves); (2) Pulsed Finite Amplitude Sound Beams (including a uniformly valid axial solution for self-demodulation, and measurements of pulsed sound beams in water); and (3) Finite Amplitude Sound in Waveguides. Nonlinear acoustics, Rayleigh waves, Stoneley waves, Diffraction, Pulses, Self-demodulation, Waveguides. DTIC

N94-27037# Foersvarets Materialverk, Stockholm (Sweden). Dept. of Weapon Systems, Effects and Protection.
HYDROACOUSTIC WAVE-FIELDS GENERATED BY DIFFERENT SOURCE TYPES, A COMPUTATIONAL STUDY
Joacim Tegnesjoe Jun. 1993 59 p
(ISSN 0347-3694)
(PB94-123536; FOA-C-20929-2.2) Avail: CASI HC A04/MF A01

This report treats hydroacoustic wave field computations from different source types. The numerical method used to solve the hydroacoustic wave equations is the propagator matrix method. Three different kinds of point sources are considered. Simulations are carried out for each one of them. In addition, an array of symmetric point sources is considered. The basic theory of the propagator matrix method is explained and the source conditions for all source types are given. Low frequency wave fields have a rapid attenuation in the liquid. At higher frequencies, the simulations show a more complex pattern. The wave fields from the vertical point force give zero pressure along a horizontal line out from the source. The dipole gives a wave field that has zero pressure along a vertical line through the source. The array of symmetric point sources is used to excite modes and to compute reflections of a Gaussian plane wave at the sea bed. Mode excitation was carried out with different numbers of sources. Modes are excited with as few sources as six. Especially in cases with a rigid bottom excitation of modes, it is possible even with few sources. A beam incident to the sea bed excites a lateral wave field in the sediment. This wave field causes a horizontal displacement and a splitting of the reflected beam. NTIS

N94-27067# Connecticut Univ., Farmington. Health Center.
MONAURAL AND BINAURAL PROCESSING OF COMPLEX WAVEFORMS Annual Technical Report, 1 Nov. 1992 - 31 Oct. 1993
Constantine Trahiotis and Leslie R. Bernstein 30 Nov. 1993 11 p
(Contract F49620-92-J-0062)
(AD-A274209; AFOSR-93-0907TR) Avail: CASI HC A03/MF A01

During the past year of the granting period, we have continued to make substantial progress consistent with the objectives outlined in our latest proposal. (1) We have completed an extensive analysis of and succeeded in publishing a very comprehensive set of data concerning the amount of 'comodulation masking release' (CMR) that can be obtained when the coherent envelope information is presented successively rather than simultaneously. It was determined that 'off-frequency' information, such as that which usually produces a CMR, can provide only a very small release from masking when it is presented prior and subsequent to the temporal interval containing the signal. The most striking finding was that the threshold for detecting a 1-kHz tone masked by an 50-Hz-wide band of noise centered on 1 kHz, was reduced by 7 dB when an identical, 'on frequency', masking noise was presented in all four intervals of our two-cue, two-interval, forced-choice procedure. (2) We finished three other papers, one of which was published and two of which have been revised and resubmitted. (3) We are currently collecting data concerning how varying the forward fringe of a masker affects the magnitude of the binaural masking-level difference. The experiments are being conducted with low-frequency signals where the interaural cues are conveyed by the fine-structure of the waveform and with high-frequency signals where the interaural cues are conveyed via the envelope of the waveform. DTIC

N94-27282# Tokyo Inst. of Tech., Yokahama (Japan). Precision and Intelligence Lab.
BULLETIN OF PRECISION AND INTELLIGENCE LABORATORY, NO. 68
Sep. 1993 174 p
(ISSN 0916-8311)
(JTN-94-80609) Avail: CASI HC A08/MF A02

The following topics were discussed: silence amenity engineering, historical review, philosophy, silence amenity, noise, noise reduction, noise control, noise quality, environmental quality, habitability, noise propagation, aerodynamic noise, vibration noise, and noise source. This material also contains bibliographies which lists 163 abstracts. In these abstracts, the following topics were discussed: speech recognition, sound propagation, molecular beam epitaxy, artificial reality, image processing, image analysis, crystal structure, crystal growth, laser devices, semiconductor devices, ultrasonic motors, accurate control techniques, materials processing, alloys, and materials properties. For individual title, see N94-27283.

N94-27283# Tokyo Inst. of Tech., Yokahama (Japan). Precision and Intelligence Lab.
SILENCE AMENITY ENGINEERING: PAST AND PRESENT
Hajime Fujita and Yasuyuki Yokono *In its* Bulletin of Precision and Intelligence Laboratory, No. 68 Sep. 1993 p 1-7 (For primary document see N94-27282 07-71)
Avail: CASI HC A02/MF A02

Recent historical development of the noise control engineering, from mere noise reduction to silence amenity engineering, is reviewed, with social and psychological backgrounds behind it. Philosophical view points for fundamental approach to the silence amenity engineering and examples of noise source control in vibration and aerodynamic noises are described.
Author (NASDA)

N94-27659*# National Aeronautics and Space Administration. Langley Research Center, Hampton, VA.
NUMERICAL AND EXPERIMENTAL ANALYSES OF THE RADIANT HEAT FLUX PRODUCED BY QUARTZ HEATING SYSTEMS
Travis L. Turner and Robert L. Ash (Old Dominion Univ., Norfolk, VA.) Mar. 1994 40 p
(RTOP 505-63-50-10)
(NASA-TP-3387; L-17081; NAS 1.60:3387) Avail: CASI HC A03/MF A01

A method is developed for predicting the radiant heat flux distribution produced by tungsten filament, tubular fused-quartz envelope heating systems with reflectors. The method is an application of Monte Carlo simulation, which takes the form of a random walk or ray tracing scheme. The method is applied to four systems of increasing complexity, including a single lamp without a reflector, a single lamp with a Hat reflector, a single lamp with a parabolic reflector, and up to six lamps in a six-lamp contoured-reflector heating unit. The application of the Monte Carlo method to the simulation of the thermal radiation generated by these systems is discussed. The procedures for numerical implementation are also presented. Experiments were conducted to study these quartz heating systems and to acquire measurements of the corresponding empirical heat flux distributions for correlation with analysis. The experiments were conducted such that several complicating factors could be isolated and studied sequentially. Comparisons of the experimental results with analysis are presented and discussed. Good agreement between the experimental and simulated results was obtained in all cases. This study shows that this method can be used to analyze very complicated quartz heating systems and can account for factors such as spectral properties, specular reflection from curved surfaces, source enhancement due to reflectors and/or adjacent sources, and interaction with a participating medium in a straightforward manner.
Author (revised)

N94-28141 ESDU International Ltd., London (England).
METHODS OF TESTING FOR ENDURANCE OF STRUCTURAL ELEMENTS USING SIMULATED ACOUSTIC LOADING
Oct. 1993 27 p
(ISSN 0141-3961)
(ESDU-93027; ISBN-0-85679-880-0) Avail: ESDU

ESDU 93027 discusses methods of testing structural elements, designed to represent features of the full-size structure, using random-amplitude narrowband loading to simulate response to acoustic loading. A wide range of element geometries is included with information on probable failure locations, typical sizes, and any inherent limitations. Mounting methods are considered with examples of multiple specimen tests to allow the scatter in fatigue life to be determined in minimum elapsed time. Guidance is provided on excitation requirements, the measurement and monitoring instrumentation, specimen tuning, and the assessment of structural damping and response linearity. The means of defining a failure are considered, with particular reference to composite structures, and the use of residual strength assessment is discussed. The application of the techniques to obtain endurance data at elevated temperature is addressed. Finally, guidance is included on the interpretation of the results. ESDU

N94-28195*# National Aeronautics and Space Administration. Langley Research Center, Hampton, VA.
EXPERIMENTAL STUDIES OF LOUDNESS AND ANNOYANCE RESPONSE TO SONIC BOOMS
Brenda M. Sullivan (Lockheed Engineering and Sciences Co., Hampton, VA.) and Jack D. Leatherwood *In* NASA. Ames Research Center, High-Speed Research: Sonic Boom, Volume 1 Feb. 1994 p 153-175 (For primary document see N94-28188 07-02)
Avail: CASI HC A03/MF A03

N94-28196*# Bolt, Beranek, and Newman, Inc., Canoga Park, CA. BBV Systems and Technologies.
COMPARISON OF METHODS OF PREDICTING COMMUNITY RESPONSE TO IMPULSIVE AND NONIMPULSIVE NOISE
Sanford Fidell and Karl S. Pearsons *In* NASA. Ames Research Center, High-Speed Research: Sonic Boom, Volume 1 Feb. 1994 p 177-189 (For primary document see N94-28188 07-02)
Avail: CASI HC A03/MF A03

N94-28197*# McDonnell-Douglas Aerospace, Long Beach, CA. Transport Aircraft.
VARIABILITY OF MEASURED SONIC BOOM SIGNATURES
K. R. Elmer and M. C. Joshi *In* NASA. Ames Research Center, High-Speed Research: Sonic Boom, Volume 1 Feb. 1994 p 191-218 (For primary document see N94-28188 07-02)
(Contract NAS1-19060)
Avail: CASI HC A03/MF A03

N94-28318 De Havilland Aircraft Co. of Canada Ltd., Downsview (Ontario). Structures Research and Development.
ASSESSING THE EFFECTS OF TUNED VIBRATION ABSORBERS (TVAs) ON INTERIOR CABIN NOISE LEVELS: A CORRELATION BETWEEN ANALYTICAL ACOUSTIC PREDICTIONS AND FLIGHT TEST MEASUREMENTS
Ralph Garcea *In* Canadian Aeronautics and Space Inst., Abstracts of Papers Presented at the 4th CASI Aerodynamics Symposium 1993 p 9-12 (For primary document see N94-28315 07-02)
Avail: Issuing Activity (Canadian Aeronautics and Space Inst., 130 Slater Street, Suite 818, Ottawa, ON K1P 6E2 Canada)

72 ATOMIC AND MOLECULAR PHYSICS

Includes atomic structure, electron properties, and molecular spectra.

N94-25589# Air Force Inst. of Tech., Wright-Patterson AFB, OH. School of Engineering.
VIBRATIONAL ENERGY TRANSFER WITHIN THE B 3PI (O(+) SUB u) STATE OF 79BR2 UPON COLLISION WITH N2, O2, NO, AND SF6 M.S. Thesis
Gregory S. Williams Dec. 1993 75 p
(AD-A273905; AFIT/GAP/ENP/93D-10) Avail: CASI HC A04/MF A01

Vibrational transfer and electronic quenching in the lower vibrational levels of the (79)Br2(B; v' less than or equal to three) were investigated using spectrally resolved, temporally resolved pulsed laser induced fluorescence techniques. Spectrally resolved emissions from collisionally populated Br2(B) vibrational levels were observed for N2, O2, NO, and SF6 collision partners. The vibrational transfer was efficient in the non-predissociative vibrational levels and is adequately described by the Montroll-Shuler model. DTIC

N94-25598# Superconducting Super Collider Lab., Dallas, TX.
SECONDARY PARTICLE IN BACKGROUND LEVELS AND EFFECTS ON DETECTORS AT FUTURE HADRON COLLIDERS
T. Pal Jun. 1993 23 p Presented at the Workshop on B Physics at Hadron Colliders, Snowmass, CO, 21 Jun. - 2 Jul. 1993 Submitted for publication
(Contract DE-AC35-89ER-40486)
(DE94-003378; SSCL-520; CONF-9306258-8) Avail: CASI HC A03/MF A01

The next generation of hadron colliders, the Superconducting Super Collider (SSC) and the Large Hadron Collider (LHC), will operate at high center-of-mass energies and luminosities. Namely, for the SSC (LHC) the square root of s = 40 TeV (the square root of s = 16 TeV) and L = 10(exp 33) cm(exp -2)s(exp -1) (L = 3 x 10(exp 34) cm(exp -2)s(exp -1)). These conditions will result in the production of large backgrounds as well as radiation environments. Ascertaining the backgrounds, in terms of the production of secondary charged and neutral particles, and the radiation environments are important considerations for the detectors proposed for these colliders. An initial investigation of the radiation levels in the SSC detectors was undertaken by D. Groom and colleagues, in the context of the 'task force on radiation levels in the SSC interaction regions.' The method consisted essentially of an analytic approach, using standard descriptions of average events in conjunction with simulations of secondary processes. Following Groom's work, extensive Monte Carlo simulations were performed to address the issues of backgrounds and radiation environments for the GEM and SD C3 experiments proposed at the SSC and for the ATLAS and CMS experiments planned for the LHC. The purpose of the present article is to give a brief summary of some aspects of the methods, assumptions, and calculations performed to date (principally for the SSC detectors) and to stress the relevance of such calculations to the detectors proposed for the study of B-physics in particular. DOE

N94-25612# Los Alamos National Lab., NM.

BACK-REACTION BEYOND THE MEAN FIELD APPROXIMATION

Y. Kluger 1993 14 p Presented at the NATO Advanced Study Institute on Hot and Dense Nuclear Matter, Bodrum, Turkey, 26 Sep. - 9 Oct. 1993
(Contract W-7405-eng-36)
(DE94-003936; LA-UR-93-4147; CONF-930999-2) Avail: CASI HC A03/MF A01

A method for solving an initial value problem of a closed system consisting of an electromagnetic mean field and its quantum fluctuations coupled to fermions is presented. By tailoring the large N(sub f) expansion method to the Schwinger-Keldysh closed time path (CTP) formulation of the quantum effective action, the causality of the resulting equations of motion is ensured, and a systematic energy conserving and gauge invariant expansion about the electromagnetic mean field in powers of 1/N(sub f) is developed. The resulting equations may be used to study the quantum nonequilibrium effects of pair creation in strong electric fields and the scattering and transport processes of a relativistic e(+)e(-) plasma. Using the Bjorken ansatz of boost invariance initial conditions in which the initial electric mean field depends on the proper time only, we show numerical results for the case in which the N(sub f) expansion is truncated in the lowest order and compare them with those of a phenomenological transport equation. DOE

N94-25636# Tokyo Univ. (Japan). Inst. for Solid State Physics.

ATOMIC-SCALE CHEMISTRY OF METAL SURFACES

Kenichi Tanaka Feb. 1993 24 p Sponsored by Asahi Glass Foundation, Tokyo, Japan
(ISSN 0082-4798)
(Rept-A-2657; JTN-94-80528) Avail: CASI HC A03/MF A01

The concept of pseudo-molecules is derived from reviewing the results of Scanning Tunneling Microscopy (STM) of metal surfaces. Ni(110), Cu(110), and Ag(110) surfaces exposed to H2 or O2 at room temperature reveal the formation of one-dimensional pseudo-molecules. This is essentially different from the phenomenon of adsorption. The pseudo-molecules produced on the surface are in an ordered arrangement on these metal surfaces. The ordering style is influenced by their lateral interaction. The -Cu-O- chains oriented along the group of zone (001) zone axes direction coalesce to form a p(2 x 1) arrangement on the Cu(110), but the added -Ag-O- rows on the Ag(110) surface may not prefer the p(2 x 1) structure, because the p (2 x 1) -Ag-O- added row induces a large distortion of the substrate Ag atoms. As a result, the added -Ag-O- rows undergo sequential change of the p(n x 1) structures. When the p(2 x 1) -Cu-O- island is annealed at 550 - 640 K, the p(2 x 1) overlayer bunches into regular-sized in-phase p(2 x 1) -Cu-O- islands. In contrast, reordering of the (2 x 1) -Ag-O- overlayer to (4 x 1) at 500 K yields narrow out-of-phase (4 x 1) domains with the wavering domain boundaries. Based on these results, the influence of pseudo-molecules on catalysis is predicted. Author (NASDA)

N94-25655# Naval Postgraduate School, Monterey, CA. Dept. of Electrical and Computer Engineering.

PREDICTING ANTENNA PARAMETERS FROM ANTENNA PHYSICAL DIMENSIONS Final Report

Steven E. Lundholm, R. C. Robertson, and Randy L. Borchardt Dec. 1993 269 p
(AD-A273893; NPS-EC-93-019) Avail: CASI HC A12/MF A03

This report details the development and provides the documentation for custom computer software applications that evaluate antenna parameters. The applications are written in Mathcad 3.1 for the following antenna types: linear, planar, and circular arrays; folded dipole; caged dipole; parabolic reflectors with helical and spiral feeds. Inputs to the applications are limited to the antenna's physical dimensions. In some cases, ground parameters are required. The chapters are structured to provide the user with the necessary information needed to use and interpret the software for each antenna type. The software applications are proved as appendices and give examples of each antenna type. Outputs of the applications provide various numerical and performance predictions, as well as fax-field radiation patterns. The results computed are consistent with predictions provided in applicable publications, as well as those calculated by numerical antenna analysis programs such as ELNEC. DTIC

N94-25726# Visidyne, Inc., Burlington, MA.

CHARACTERIZATION OF THE ENERGY DEPOSITION PRODUCED BY THE PRIMARY ELECTRON BEAM ON THE EXCEDE 3 PROGRAM. APPENDIX B AND C

R. J. Rieder, R. L. McNutt (Johns Hopkins Univ., Laurel, MD.), and S. A. Rappaport May 1993 144 p
(Contract F19628-90-C-0187)
(AD-A273878; VI-2067; PL-TR-93-2132(2); SR-3) Avail: CASI HC A07/MF A02

The primary goal of the EXCEDE III (Excitation by Electron Deposition) atmospheric energy deposition experiment was to monitor the spatial distribution of the energy deposition profile produced by the approx. 18 Ampere approx. 2.5 keV electron beam. During the rocket flight on April 27, 1990, prompt emission at 3914 A from the N2+ (1N) 0-0 transition were measured by a UV scanning photometer. We have inverted the intensity profiles to obtain profiles of energy deposition by the beam. DTIC

N94-25750 Joint Inst. for Nuclear Research, Dubna (USSR).

A DOUBLE ARM TIME-OF-FLIGHT SPECTROMETER BASED ON POSITION-SENSITIVE PARALLEL-GRID AVALANCHE COUNTERS

G. G. Chubaryan, V. A. Gorshkov, V. E. Zhuchko, S. M. Lukyanov, Kh. G. Ortlepp, V. S. Salamatin, and D. Wohlfarth 1992 16 p Limited Reproducibility: More than 20% of this document may be affected by microfiche quality
(DE93-616665; JINR-R-13-92-18) Avail: CASI HC A03 (US Sales Only)

A double arm time-of-flight spectrometer, built-up at the Laboratory of Nuclear Reactions JINR, intended to register and study the characteristics of fission-like products produced in heavy-ion reactions with complex nuclei are presented. The basis part of spectrometer are two identical mobile position-sensitive time-of-flight arms. Each arm consists of a parallel-plate avalanche 'start' counter and of position-sensitive, large area parallel-grid avalanche 'stop' counters. The spectrometer is mounted on a beam-line of the U-400 heavy-ion accelerator. DOE

N94-25795# Brookhaven National Lab., Upton, NY.

PRODUCTION OF (PHI) MESONS IN CENTRAL Si + Au COLLISIONS AT 14.6 AGeV/c

Yufeng Wang 1993 4 p Presented at the 10th International Conference on Ultra-Relativistic Nucleus-Nucleus Collisions, Boprlaenge, Sweden, 20-24 Jun. 1993
(Contract DE-AC02-76CH-00016)
(DE94-003196; BNL-49665; CONF-930636-10) Avail: CASI HC A01/MF A01

The production of phi mesons from central Si + Au collisions was measured by E859 at the BNL-AGS by selecting events with identified K(+)K(-) pairs. The values for the mass and width of the phi obtained from the invariant mass of the kaon pairs are consistent with those of the Particle Data Book. Preliminary results for the invariant (1/2(pi)m(sub T))(d(sup 2)n/dm(sub T)dy) distribution and dN/dy are presented. DOE

N94-25800# Ohio Univ., Athens. Dept. of Physics and Astronomy.

THEORETICAL AND COMPUTATIONAL STUDIES IN INTERMEDIATE ENERGY NUCLEAR PHYSICS

C. Elster Aug. 1993 9 p
(Contract DE-FG02-93ER-40756)
(DE94-004177; DOE/ER-40756/1) Avail: CASI HC A02/MF A01

The research includes applications of many-body scattering theory to nuclear systems and studies of few-body systems described by effective hadronic field theories. Progress was made in bringing all first-order effects into the nonrelativistic elastic nucleon-nucleus scattering in a consistent fashion. This work is directed towards completely and reliably calculating the first-order term in a Watson expansion including a modification through the nuclear medium. The research effort in few-body physics was concentrated on nucleon-nucleon (NN) scattering below pion production threshold, where recent measurements indicated that the backward-angle neutron-proton (np) differential cross section may show sensitivity to the size of the pion-nucleon coupling constant. DOE

N94-25816# Argonne National Lab., IL.
THREE METHODS TO MEASURE RH BOND ENERGIES
Joseph Berkowitz, G. Barney Ellison (Colorado Univ., Boulder.), and David Gutman (Catholic Univ. of America, Washington, DC.) 21 Mar. 1993 100 p
(Contract W-31-109-eng-38)
(DE94-003795; ANL/CHM/PP-80545) Avail: CASI HC A05/MF A02

In this paper, the authors compare and contrast three powerful methods for experimentally measuring bond energies in polyatomic molecules. The methods are: radical kinetics; gas phase acidity cycles; and photoionization mass spectroscopy. The knowledge of the values of bond energies are a basic piece of information to a chemist. Chemical reactions involve the making and breaking of chemical bonds. It has been shown that comparable bonds in polyatomic molecules, compared to the same bonds in radicals, can be significantly different. These bond energies can be measured in terms of bond dissociation energies. DOE

N94-25820# Los Alamos National Lab., NM.
DATA ON PARITY VIOLATION IN THE COMPOUND NUCLEUS AND ITS INTERPRETATION
J. D. Bowman, C. M. Frankle, J. N. Knudson, S. I. Penttila, S. J. Seestrom, J. J. Szymanski, Yen Yi-Fen, S. H. Yoo, V. W. Yuan, and B. Crawford (Duke Univ., Durham, NC.) et al 1993 23 p Presented at the International Workshop/Time Reversal Invariance and Parity Violation in Neutron Physics, Dubna, Russia, 4-7 May 1993
(Contracts W-7405-eng-36; DE-FG05-88ER-40441; DE-FG05-91ER-40619)
(DE94-003965; LA-UR-93-3920; CONF-9305235-5) Avail: CASI HC A03/MF A01

This report discusses the measurement of parity-violating asymmetries in the compound nucleus; summary of data on this process; theories of the random asymmetry, M(sup 2); and theories of the constant asymmetry. DOE

N94-25826 Joint Inst. for Nuclear Research, Dubna (USSR). Lab. of Theoretical Physics.
QUARK-ANTIQUARK BOUND STATES
W. Lucha and F. Schoeberl 1991 32 p Limited Reproducibility: More than 20% of this document may be affected by microfiche quality
(DE93-613054; JINR-E-4-91-500) Avail: CASI HC A03 (US Sales Only)

This brief review discusses various aspects of the description of hadrons as bound states of quarks at the simpler example of mesons, which are regarded as composite of a constituent quark and antiquark. It is shown how a recently derived relativistic virial theorem may be used in order to cast some light on the interplay between the semi-relativistic and, maybe only effective, nonrelativistic treatment of bound states. Furthermore, a new relativistic approach to fermion-antifermion bound states is briefly sketched and applied in order to predict analytically a few selected general features of the meson spectrum. DOE

N94-25827 International Centre for Theoretical Physics, Trieste (Italy).
A STUDY OF VIBRATIONAL RELAXATION OF ELECTRONICALLY-EXCITED MOLECULES
V. V. Datsyuk (Kiev State Univ., USSR.), I. A. Izmailov (Academy of Sciences of the Ukraine, Kiev.), and V. A. Kochelap Sep. 1992 27 p Limited Reproducibility: More than 20% of this document may be affected by microfiche quality
(DE93-613553; IC-92/261) Avail: Issuing Activity (Department of Energy (DOE)) (US Sales Only)

The time kinetics of the vibrational relaxation of excimers is studied in the diffusional approximation. Simple formulae for functions of nonstationary vibrational distribution are found for the electronically excited molecules. Some spectral-kinetic dependencies of the excimer luminescence are explained in a new way. The possibilities of the determination of excimer parameters are discussed. The dependence of energetical characteristics of excimer lasers on these parameters is particularly emphasized. DOE

N94-25828 Joint Inst. for Nuclear Research, Dubna (USSR).
A DATA PROCESSING SYSTEM AT THE HYBRID SPECTROMETER
A. U. Abdurakhimov, V. G. Ivanov, L. S. Okhrimenko, I. S. Saitov, and T. Ehrdehnehdehlgehr 1992 25 p In RUSSIAN Limited Reproducibility: More than 20% of this document may be affected by microfiche quality
(DE93-616801; JINR-R-10-92-1) Avail: CASI HC A03 (US Sales Only)

A system for data processing at hybrid spectrometer is described. A set of the programs for sorting and recording measurements as well as geometrical reconstruction of events is considered. Different service procedures of experimental data processing are presented. The system is designed for the operating on the ES computers under the control of the VM operating system. DOE

N94-25835 Moscow State Univ. (Russia).
PRINCIPLES OF GAUGE THEORY OF REAL HADRONS
L. M. Slad 1992 26 p Limited Reproducibility: More than 20% of this document may be affected by microfiche quality
(DE93-613096; INP-MSU-92-15-264; NIIYaF-MGU-92-15-264) Avail: CASI HC A03 (US Sales Only)

Complete analysis of Lagrangian structure of hadron three-particle interaction, invariant as to gauge transformations, generated by vector representation of the Lorentz complete group, was carried out. Qualitative evaluations of several problems of particle physics in the framework of the Lorentz-vector gauge theory of hadrons are provided. DOE

N94-25836 Joint Inst. for Nuclear Research, Dubna (USSR). Lab. of Theoretical Physics.
WEAK INTERACTIONS IN A BILOCAL CHIRAL THEORY
Yu. L. Kalinovskij, W. Kallies, L. Muenchow, and V. N. Pervushin 1991 19 p Limited Reproducibility: More than 20% of this document may be affected by microfiche quality
(DE93-613097; JINR-E-4-91-501) Avail: CASI HC A03

Relativistic covariant equations for quarkonia in the framework of a bilocal description are obtained. These equations can be used to find the solutions for the bound state functions for any given angular momentum. DOE

N94-25837# International Centre for Theoretical Physics, Trieste (Italy).
COSMOPARTICLE PHYSICS OF FAMILY SYMMETRY BREAKING
Maxim Yu. Khlopov Jul. 1993 12 p
(DE94-601623; IC-93/198) Avail: CASI HC A03/MF A01 (US Sales Only)

The foundations of both particle theory and cosmology are hidden at super energy scale and can not be tested by direct laboratory means. Cosmoparticle physics is developed to probe these foundations by the proper combination of their indirect effects, thus providing definite conclusions on their reliability. Cosmological and astrophysical tests turn to be complementary to laboratory searches of rare processes, induced by new physics, as it can be seen in the case of gauge theory of broken symmetry of quark and lepton families, ascribing to the hierarchy of the horizontal symmetry breaking the observed hierarchy of masses and the mixing between quark and lepton families. DOE

N94-25839# International Centre for Theoretical Physics, Trieste (Italy).
OUT OF EQUILIBRIUM PHASE TRANSITIONS AND A TOY MODEL FOR DISORIENTED CHIRAL CONDENSATES
P. F. Bedaque and A. Das Jul. 1993 17 p
(DE94-601642; IC-93/178; UR-1315; ER-40685-765) Avail: CASI HC A03/MF A01 (US Sales Only)

We study the dynamics of a second order phase transition in a situation that mimics a sudden quench to a temperature below the critical temperature in a model with dynamical symmetry breaking. In particular we show that the domains of correlated values of the condensate grow as (radical)t and that this result seems to be largely model independent. DOE

N94-25840# Melbourne Univ., Parkville (Australia). School of Physics.
EXPERIMENTAL STUDY OF THE NEAR THRESHOLD pi(SUP +)p YIELDS (pi(SUP +))(pi(SUP +))(n) CROSS SECTION AND CHIRAL SYMMETRY
M. E. Sevior, A. Ambardar (British Columbia Univ., Vancouver.), J. T. Brack (British Columbia Univ., Vancouver.), F. Duncan (British Columbia Univ., Vancouver.), A. Feltham (British Columbia Univ., Vancouver.), R. R. Johnson (British Columbia Univ., Vancouver.), G. Koch (British Columbia Univ., Vancouver.), P. Camerini (Trieste Univ., Italy.), R. Rui (Trieste Univ., Italy.), and J. Ernst (Bonn Univ., Germany.) et al 1993 28 p
(DE94-601671; UM-P-93/18) Avail: CASI HC A03/MF A01 (US Sales Only)

Total cross section measurements of the pi(sup +)p yields (pi(sup +))(pi(sup +))(n) reaction at pion kinetic energies of 180,184,190 and 200 MeV are reported. The threshold value for the amplitude, a(pi(sup +) pi(sup +)), as well as the s-wave, isospin 2, pi(pi) scattering length, a(sup 0)(sub 2), were determined. The results were found to be in agreement with chiral perturbation theory and inconsistent with the calculations of Jacob and Scadron and the model of dominance by quark loop anomalies. DOE

N94-25841# Melbourne Univ., Parkville (Australia). School of Physics.
CP VIOLATING FORM FACTORS FOR THREE GAUGE BOSON VERTEX IN THE TWO HIGGS DOUBLET AND LEFT-RIGHT SYMMETRIC MODELS
X. G. He, J. P. Ma, and B. H. J. McKellar 1993 14 p
(DE94-601704; UM-P-92/75; OZ-92/26) Avail: CASI HC A03/MF A01 (US Sales Only)

In this paper we calculate the one loop contributions to the CP violating three gauge boson coupling in two-Higgs doublet and Left-Right symmetric models. In the two-Higgs doublet model only a P conserving and CP violating coupling is generated, and it can be large as 10(sup -3). In the Left-Right symmetric model both P conserving and violating couplings are generated. Due to constraints on the W(sub L)-W(sub R) mixing, these couplings are small. DOE

N94-25842# Flinders Univ., Adelaide (Australia). Electronic Structure of Materials Centre.
CONVERGENT CLOSE-COUPLING CALCULATION OF ELECTRON-SODIUM SCATTERING
Igor Bray Apr. 1993 6 p
(DE94-601815; ESM-54) Avail: CASI HC A02/MF A01 (US Sales Only)

Calculations up to 45 state close-coupling were performed of electrons scattering on atomic sodium, where the target states have been obtained by diagonalizing the target Hamiltonian in a Laguerre basis. Convergence is established by variation of the size of the basis. It is shown that the results are in excellent quantitative agreement at most scattering angles with the measurements of spin asymmetries and L, the angular momentum transferred to the atom perpendicular at the two projectile energies considered of 10 and 20 eV. This demonstrates that the very large effects of the target continuum, in particular on the spin asymmetries, are very accurately represented using square-integrable states. DOE

N94-25853 Joint Inst. for Nuclear Research, Dubna (USSR). Lab. of Theoretical Physics.
ON THE CLASSIFICATION SCHEME FOR RESONANT STATES OF MUONIC MOLECULES
A. V. Matveenko 1991 23 p Limited Reproducibility: More than 20% of this document may be affected by microfiche quality
(DE93-613645; JINR-E-4-91-370) Avail: CASI HC A03 (US Sales Only)

The hyperradial adiabatic one-state calculation of resonant states of (dd(mu))(sup +) and (dt(mu))(sup +) below the n = 2 level of muonic atoms have been performed. The results are used to produce a new classification scheme for these states. Comparing these calculation with the recent full variational calculation by S.Hara and T.Ishihara it is concluded that the classical Born-Oppenheimer classification scheme can be misleading. DOE

N94-25869 Joint Inst. for Nuclear Research, Dubna (USSR). Lab. of Theoretical Physics.
THE AMPLITUDE OF THE ELASTIC HADRON-HADRON SCATTERING IN THE COULOMBIC RANGE OF TRANSFER MOMENTA
O. V. Selyugin 1991 23 p Limited Reproducibility: More than 20% of this document may be affected by microfiche quality
(DE93-613183; JINR-E-2-91-356) Avail: CASI HC A03 (US Sales Only)

The questions of the determination of sigma(sub tot)(s), the slope of differential cross sections, B(s,t), rho(s,t)=Re T(s,t)/Im T(s,t) and the phase of the coulomb-nuclear scattering, Phi(s,t), from the experimental data are examined. It is shown that there is significant indeterminacy in the knowledge of sigma(sub tot)(s), B(s,t) and rho(s,t) and it is necessary that the next experiments would be performed at t=-1.10(sup -5)-1.10(sup -3) GeV(sup 2). DOE

N94-25875# Air Force Inst. of Tech., Wright-Patterson AFB, OH. School of Engineering.
SPECTROSCOPIC AND VIBRATIONAL ENERGY TRANSFER STUDIES IN MOLECULAR BROMINE Ph.D. Thesis
Courtney D. Holmberg Dec. 1993 194 p
(AD-A273795; AFIT/DS/ENP-93-04) Avail: CASI HC A09/MF A03

Vibrational transfer and electronic quenching in the lower vibrational levels (v' less than or equal to 3) of the B(sup 3)pi(O(u)(+)) state of (79)Br2 were investigated using spectrally resolved, temporally resolved laser induced fluorescence techniques. Spectrally resolved emissions from collisionally populated Br2(B) vibrational levels were observed for Br2 and rare gas collision partners. Vibrational transfer was efficient in the non-predissociative vibrational levels and was adequately described by the Montroll-Shuler model for harmonic oscillators. A single fundamental rate coefficient for vibrational transfer from v' = 1 to v'= 0, kv(1,0), characterizes vibrational relaxation. For Br2, the value was kv(1,0) = 3.6 +/- 0.4 x 10(exp -11) cu cm/molec(sec). For rare gas collisions, values ranged from kv(1,0) = 2.5 +/- 0.3 x 10(exp -11) cu cm/molec(sec) for helium to kv(1,0) = 3.1 +/- 0.4 x 10(exp -11) cu cm/molec(sec) for xenon.Electronic quenching rates for the observed vibrational levels were obtained from the same data. For Br2, the quenching rate coefficient was kq = 3.7 +/- 1.2 x 10(exp -11) cu cm/molec(sec). Quenching rate coefficients for the rare gases were smaller, kq = 8.0 +/- 1.2 x 10(exp -12) cu cm/molec(sec). DTIC

N94-25887# International Centre for Theoretical Physics, Trieste (Italy).
VECTOR MESON EXCHANGES AND CP ASYMMETRY IN K(SUP +/-) YIELDS pi(SUP +/-)pi(SUP 0)
Riazuddin, N. Paver (Trieste Univ., Italy.), and F. Simeoni (Trieste Univ., Italy.) Jul. 1993 10 p
(DE94-601605; IC-93/186; UTS-DFT-93-18) Avail: CASI HC A02/MF A01 (US Sales Only)

Using a current algebra framework, the contribution of vector meson exchanges to the CP violating asymmetry in the decay K(sup +/-) yields pi(sup +/-)pi(sup 0), resulting from the interference of the K yields (pi)(pi) amplitude with the radiative correction K yields (pi)(pi)(gamma) is discussed. DOE

N94-25888# Melbourne Univ., Parkville (Australia). School of Physics.
CP VIOLATION IN HIGGS DECAYS
Xiao-Gang He, J. P. Ma, and Bruce McKellar Feb. 1993 9 p
(DE94-601607; UM-P-93/11; OZ-93/5) Avail: CASI HC A02/MF A01 (US Sales Only)

This contribution deals with CP violation in fermion pair decays of Higgs boson. Some CP odd observables related to the tree level decay amplitude are identified. It was found that a few thousand Higgs boson decay events can already provide important information about CP violation. If the Higgs boson is produced, such an analysis could be carried out at the new generation of colliders such as SCC, LHC, and NLC. DOE

N94-25889# Melbourne Univ., Parkville (Australia). School of Physics.
CP TEST IN THE W PAIR PRODUCTION BY WAY OF PHOTON FUSION AT NLC
J. P. Ma and B. H. J. McKellar 1993 12 p
(DE94-601608; UM-P-93/16; OZ-93/06) Avail: CASI HC A03/MF A01 (US Sales Only)

The possibility to test CP invariance in the W(+)W(-) production via photon fusion at NLC was studied. The predictions of the CP violation effects are made within two Higgs doublet extensions of the minimal standard model, where CP violation is introduced by a neutral Higgs exchange in s channel. The width effect in the Higgs propagator on the CP violation effects is discussed in detail. The CP violation effects can be measured in some parameter region of the extensions. DOE

N94-25890# Melbourne Univ., Parkville (Australia). School of Physics.
SEPARABLE EXPANSIONS OF THE NN t-MATRIX BY WAY OF EXACT HALF OFF THE ENERGY SHELL METHODS
G. Pisent, K. Amos, P. J. Dortmans, and L. Canton 1992 44 p
(DE94-601615; UM-P-92/76) Avail: CASI HC A03/MF A01 (US Sales Only)

Recently a method was proposed by which one can obtain rank 1 (for uncoupled channels) and rank 2 (for coupled channels), energy dependent t-matrix representations which are exact on- and half off of the energy shell. Fully off shell, this representation, though accurate at low energies, is flawed. For uncoupled channels, if the phase shift passes through zero, the representation has a pathology. Two methods which overcome this are investigated, one due to Haberzettl which was extended to coupled channels, and the second which is based upon selective combination of the elements of Sturmian expansions. All methods of separation over a range of energies up to 250 MeV for the (sup 1)S(sub 0) and (sup 3)S(sub 1) channels are compared with the Paris interaction. Special attention is paid to the convergence of the higher order Haberzettl expansion and to the comparison of the extended methods for energies around the zero phase shift pathology for the (sup 1)S(sub 0) channel. The method describes well the fully off-shell properties of the t-matrices up to quite high energies, while keeping the rank of the separation as low as possible in order to be used in three or more body calculations. DOE

N94-25891# Melbourne Univ., Parkville (Australia). School of Physics.
UNRAVELLING THE STRUCTURE OF MATTER ON HIGH-PERFORMANCE COMPUTERS
T. D. Kieu and B. H. J. McKellar Nov. 1992 10 p
(DE94-601620; UM-P-92/94; OZ-92/34) Avail: CASI HC A02/MF A01 (US Sales Only)

The various phenomena and the different forms of matter in nature are believed to be the manifestation of only a handful set of fundamental building blocks - the elementary particles - which interact through the four fundamental forces. In the study of the structure of matter at this level, one has to consider forces which are not sufficiently weak to be treated as small perturbations to the system, an example of which is the strong force that binds the nucleons together. High-performance computers, both vector and parallel machines, have facilitated the necessary non-perturbative treatments. The principles and the techniques of computer simulations applied to Quantum Chromodynamics are explained, examples include the strong interactions, the calculation of the mass of nucleons and their decay rates. Some commercial and special-purpose high-performance machines for such calculations are also mentioned. DOE

N94-25916 Joint Inst. for Nuclear Research, Dubna (USSR).
ON RADIATION DEFECTS IN STRIP DETECTORS
V. S. Barashenkov, A. N. Sosnin, and S. Yu. Shmakov 1991 8 p Limited Reproducibility: More than 20% of this document may be affected by microfiche quality
(DE93-616646; JINR-R-2-91-505) Avail: CASI HC A02 (US Sales Only)

Radiation defects production in microstrip silicon detector under irradiation by means of protons, alpha-particles and Si-28 ions at energies from dozens of MeV up to several GeVxA and neutron flux at energy 10.5 MeV is calculated by means of the Monte Carlo method. Comparison of these data allows one to derive conclusions on possibility of imitation of the defect production by means of change-over from one beam to the other, more convenient from the point of view of the experimental procedure. DOE

N94-25919 Joint Inst. for Nuclear Research, Dubna (USSR). Lab. of Computing Techniques and Automation.
ALGORITHMS OF THE VERTEX COORDINATE RECONSTRUCTION FOR STRAIGHT TRACKS OF SHORT-LIVED PARTICLES
Yu. A. Budagov, L. A. Kulyukina, G. A. Ososkov, L. A. Permyakova, S. Tokar, and N. I. Chernov 1991 21 p Limited Reproducibility: More than 20% of this document may be affected by microfiche quality
(DE93-616661; JINR-R-10-91-311) Avail: CASI HC A03 (US Sales Only)

For space reconstruction of secondary vertices in a fixed target experiment several algorithms are proposed. They are based on experimental design and random search technique. The algorithms are tested by data of B-meson decays simulated in TeV range of energy by standard programs - Pythia, Geant and Gheisha. The study of the algorithm reliability and accuracy showed satisfactory results. DOE

N94-25920 Moscow State Univ. (Russia). Nauchno-Issledovatel'skij Inst. Yader.
PRINCIPLES OF GAUGE THEORY OF REAL HADRONS
L. M. Slad 1992 12 p Limited Reproducibility: More than 20% of this document may be affected by microfiche quality
(DE93-616857; INP-MSU-92-12-261; NIIYaF-MGU-92-12-261) Avail: CASI HC A03 (US Sales Only)

Physical interpretation and mathematic formulation of gauge transformation concept as the one generated by any representation of the given group are given. An assumption is made, that the hadron theory is invariant relative to the gauge transformations generated by vector representation of a complete Lorentz group. DOE

N94-25922# Tokyo Univ., Tanashi (Japan). Inst. for Nuclear Study.
NUCLEON-NUCLEON SCATTERING LENGTHS IN QCD SUM RULES
Y. Kondo and O. Morimatsu Feb. 1993 14 p
(DE93-520239; INS-965) Avail: CASI HC A03/MF A01 (US Sales Only)

Nucleon-nucleon scattering lengths are calculated using QCD sum rules. The calculation is based on the observation that the coefficient of the second-order pole term of the nucleon correlation function is proportional to the nucleon-nucleon scattering length at the threshold. By applying the Borel sum rules, we express the scattering length in terms of the expectation values of the quark-gluon field operators with respect to the one-nucleon state. The scattering lengths calculated are in qualitative agreement with the experiment. It is also shown that in the linear density approximation the nucleon mass shift in nuclear matter is related to the nucleon-nucleon scattering length. It is concluded that the recent calculations of the effective nucleon mass in nuclear matter using QCD sum rules with linear density approximation for the condensates should be interpreted in this way. DOE

N94-25935# Fermi National Accelerator Lab., Batavia, IL.
HEAVY QUARK PRODUCTION AND SPECTROSCOPY
J. A. Appel Nov. 1993 22 p Presented at the 16th International Symposium on Lepton and Photon Interactions, Ithaca, NY, 10-15 Aug. 1993
(Contract DE-AC02-76CH-03000)
(DE94-003619; FNAL/C-93/328; CONF-930823-16) Avail: CASI HC A03/MF A01

This review covers many new experimental results on heavy flavor production and spectroscopy. It also shows some of the increasingly improved theoretical understanding of results in light of basic perturbative QCD and heavy quark symmetry. At the same time, there are some remaining discrepancies among experiments as well as significant missing information on some of the anticipated lowest lying heavy quark states. Most interesting, perhaps, are some clearly measured production effects awaiting full explanation. DOE

N94-25955# Argonne National Lab., IL. High Energy Physics Div.
MONTE CARLO EVENT GENERATORS FOR HADRON-HADRON COLLISIONS
I. G. Knowles and S. D. Protopopescu (Brookhaven National Lab., Upton, NY.) Jun. 1993 29 p Presented at the Workshop on Physics At Current Accelerators and the Supercollider, Argonne, IL, 2-5 Jun. 1993
(Contract W-31-109-eng-38)
(DE94-003212; ANL-HEP-CP-93-95; CONF-9306176-14) Avail: CASI HC A03/MF A01

A brief review of Monte Carlo event generators for simulating hadron-hadron collisions is presented. Particular emphasis is placed on comparisons of the approaches used to describe physics elements and identifying their relative merits and weaknesses. This review summarizes a more detailed report. DOE

N94-25957# Fermi National Accelerator Lab., Batavia, IL.
A DEPENDENCE OF EXCLUSIVE VECTOR MESON PRODUCTION IN MUON-NUCLEUS SCATTERING
Guang Yin Fang (Harvard Univ., Cambridge, MA.) Oct. 1993 5 p
Presented at the 13th International Conference on Particles and Nuclei, Perugia, Italy, 27 Jun. - 3 Jul. 1993
(Contract DE-AC02-76CH-03000)
(DE94-003363; FNAL/C-93/305; CONF-930637-11) Avail: CASI HC A01/MF A01

Preliminary results on the cross section ratios of exclusive rho(sup 0) and phi meson production off carbon, calcium, and lead to that off deuterium in deep-inelastic muon-nucleon scattering are reported. The data were taken with the E665 spectrometer using the Fermilab Tevatron muon beam. The mean beam energy was 470 GeV. Significant increases in the cross section ratios are seen as the four-momentum squared of the virtual photon increases. The results support the idea of color transparency. DOE

N94-26002# Technische Univ., Eindhoven (Netherlands).
SPIN-POLARIZED ATOMIC HYDROGEN: DEVICES AND PHENOMENA Ph.D. Thesis
Anthonius Cornelis Maan 1993 122 p
(ETN-94-95342) Avail: CASI HC A06/MF A02

Several questions in which the spin-polarization of atomic hydrogen is involved are discussed. The effect of a permanent magnetic field on the collisions between two hydrogen atoms and the subsequent influence on the stability of the cryogenic hydrogen maser are treated. It is shown that the introduction of a magnetic field does not produce the hoped for increase in frequency stability. The hydrogen maser is not only used for very precise time keeping, but due to the very narrow linewidth of the maser output it is also suited to obtain information on the hydrogen gas. A variation on the cryogenic hydrogen maser is proposed: the surface cryogenic hydrogen maser. This proposed maser operates at lower temperatures and has an increased area to volume ratio of the storage bulb compared to the cryogenic hydrogen maser. The operating conditions for such a maser are evaluated. It is pointed out that the output characteristics are determined by the two dimensional gas of hydrogen atoms at the surface of the storage bulb. The operation of the cryogenic hydrogen maser is described in a regime of operation which is characterized by a pulsed output power. A method to calculate the recombination rate is proposed. ESA

N94-26010# International Centre for Theoretical Physics, Trieste (Italy).
THE CHERENKOV HADRONIC LIKE-JETS
A. El-Naghy, K. S. Abdel-Khalek, M. Tag El-DinKamal (National Research Centre, Cairo, Egypt.), and M. T. Hussein (Cairo Univ., Egypt.) Jun. 1993 13 p
(DE93-634525; IC-93/148) Avail: CASI HC A03/MF A01 (US Sales Only)

A new mechanism of multiparticle production implying emission of hadronic jets due to Cherenkov gluon radiation was investigated. The present work reports on a systematic study of high multiplicity events in central collisions of Ne-22 + Ag(Br) and Si-28 + Ag(Br) at 4.1 - 4.5A GeV/c. From the analysis, it was shown that 13 events display the characteristic features (ring-like) of Cherenkov or deconfinement hadronic emission. The angles of emission correspond to the formation length of hadrons approximately = 1 fm. The cross section of this phenomena is about 1/100 of total inelastic interaction cross section of Si-28 (Ne-22) with emulsion nuclei at 4.5A GeV/c. DOE

N94-26033# Sandia National Labs., Albuquerque, NM.
FAST PARALLEL ALGORITHMS FOR SHORT-RANGE MOLECULAR DYNAMICS
S. Plimpton May 1993 40 p
(Contract DE-AC04-76DP-00789)
(DE93-018519; SAND-91-1144) Avail: CASI HC A03/MF A01

Three parallel algorithms for classical molecular dynamics are presented: the first assigns each processor a subset of atoms; the second assigns each a subset of inter-atomic forces to compute; and the third assigns each a fixed spatial region. The algorithms are suitable for molecular dynamics models which can be difficult to parallelize efficiently--those with short-range forces where the neighbors of each atom change rapidly. They can be implemented on any distributed-memory parallel machine which allows for message-passing of data between independently executing processors. The algorithms are tested on a standard Lennard-Jones benchmark problem for system sizes ranging from 500 to 10,000,000 atoms on three parallel supercomputers: the nCUBE 2, the Intel iPSC/860, and the Intel Delta. Comparing the results to the fastest reported vectorized Cray Y-MP and C90 algorithm shows that the current generation of parallel machines is competitive with conventional vector supercomputers even for small problems. For large problems, the spatial algorithm achieves parallel efficiencies of 90%, and the Intel Delta performs about 30 times faster than a single Y-MP processor and 12 times faster than a single C90 processor. Trade-offs between the three algorithms and guidelines for adapting them to more complex molecular dynamics simulations are also discussed. DOE

N94-26034# International Atomic Energy Agency, Vienna (Austria).
INDEX TO BROND-2, CENDL-2, ENDF/B-6, JEF-2, JENDL-3
H. D. Lemmel Apr. 1993 19 p
(DE93-634500; IAEA-NDS-107(Rev-7)) Avail: CASI HC A03/MF A01 (US Sales Only)

This document contains a brief index to the five main data libraries for evaluated neutron reaction data, including BROND-2 from USSR, CENDL-2 from China, ENDF/B-6 from USA, JEF-2 from OECD/NEA, and JENDL-3 from Japan. DOE

N94-26035# Gosudarstvennyi Komitet po Ispolzovaniyu Atomnoi Energii, Serpukhov (USSR).
ON THE GLUON PROPAGATOR IN THE INFRARED REGION
V. V. Kiselev 1992 9 p
(DE93-634345; IHEP-OTF-92-51) Avail: CASI HC A02/MF A01 (US Sales Only)

A model for the gluon propagator based on the one-loop renormalization group calculation is considered in the infrared region. DOE

N94-26040# Instituto de Fisica Teorica, Sao Paulo (Brazil).
LEPTON MASSES IN AN SU(3)(SUB L) X U(1)(SUB N) GAUGE MODEL
R. Foot (Southampton Univ., England.), O. F. Hernandez (McGill Univ., Montreal, Quebec.), F. Pisano, and V. Pleitez Jul. 1992 10 p
(DE93-634366; IFT-P-025/92) Avail: CASI HC A02/MF A01 (US Sales Only)

The SU(3)(sub c) x SU(3)(sub L) x U(1)(sub N) model of Pisano and Pleitez extends the Standard Model in a particularly nice way, so that the example the anomalies cancel only when the number of generations is divisible by three. The original version of the model has some problems accounting for the lepton masses. This problem was solved by modifying the details of the symmetry breaking sector in the model. DOE

N94-26041 Instituto de Fisica Teorica, Sao Paulo (Brazil).
HEAVY CHARGED LEPTONS IN AN SU(3)(SUB L) X U(1)(SUB N) MODEL
V. Pleitez and M. D. Tonasse Dec. 1992 11 p Limited Reproducibility: More than 20% of this document may be affected by poor print
(DE93-634367; IFT-P-050/92) Avail: Issuing Activity (Department of Energy (DOE)) (US Sales Only)

An SU(3)(sub L) x U(1)(sub N) model for the electroweak interactions which includes additional heavy charged leptons is considered. These leptons have not strong constraints on their masses since they do not couple in the same way as the lightest leptons to the neutral-currents and also because new contributions to the muon g-2 factor already suppressed because of the massive new vector boson present in this model. DOE

N94-26042# Gosudarstvennyi Komitet po Ispolzovaniyu Atomnoi Energii, Serpukhov (USSR).
PSEUDOSCALAR GLUEBALL IN THE COMPOSITE INTERPOLATING FIELDS APPROACH
M. L. Nekrasov 1992 26 p
(DE93-634374; IHEP-OTF-92-35) Avail: CASI HC A03/MF A01 (US Sales Only)

The problem of the PS-glueball is revised in the light of the altered experimental situation: instead of one in the i(1440) region there are two or more PS-states. Besides, the production of each of these states in J/(phi) radiative decays is not more effective than that of (eta)'-meson. From the point of view of the conventional understanding, this last property considerably impedes, if not eliminates, the possibility of a glueball interpretation of some of the detected PS-states. The present paper solves this problem within the composite interpolating fields approach using the concept of current quarks and gluons and the N(sub c)(sup -1)-expansion methods. DOE

N94-26043# Instituto de Fisica Teorica, Sao Paulo (Brazil).

DECIPHERING THE QUARK-GLUON STRUCTURE OF THE PHOTON IN ELECTRON(GAMMA) COLLISIONS

O. J. P. Eboli, M. C. Gonzalez-Garcia, F. Halzen, and S. F. Novaes Nov. 1992 21 p
(DE93-634386; IFT-P-049/92) Avail: CASI HC A03/MF A01 (US Sales Only)

The capability of an electron(gamma) collider to unravel the hadronic content of the photon is investigated. The experimental problem for probing the gluonic structure of the photon is that small-x triggers overwhelmingly select soft photons rather than soft gluons in hard photons. It is showed that the problem can be finessed in experiments where laser back-scattering is used to prepare a source of very hard photons. It is illustrated their power for studying the parton distribution of the photon and, specifically, for separating the quark and gluon components in events where dijets, jet-(gamma) pairs, and heavy quark pairs are produced. DOE

N94-26045# Gosudarstvennyi Komitet po Ispolzovaniyu Atomnoi Energii, Serpukhov (USSR).

MESON X(1814) AS A CANDIDATE FOR A HYBRID STATE

G. V. Borisov, S. S. Gershtejn, and A. M. Zajtsev 1992 4 p
(DE93-634447; IHEP-OTF-92-14) Avail: CASI HC A01/MF A01 (US Sales Only)

The experimental data on resonance X(1814) are compared with the theoretical models. The properties of this object are shown to be close to those expected for the J(sup PC) = 2(sup -+) hybrid meson. DOE

N94-26049# Pacific Northwest Lab., Richland, WA.

MODELING DEFECT PRODUCTION IN HIGH ENERGY COLLISION CASCADES

H. L. Heinisch, B. N. Singh (Risoe National Lab., Roskilde, Denmark.), and T. DiazdelaRubia (Lawrence Livermore National Lab., CA.) 1993 16 p Presented at the 6th International Conference on Fusion Reactor Materials, Stresa, Italy, 27 Sep. - 1 Oct. 1993
(Contract DE-AC06-76RL-01830)
(DE94-003810; PNL-SA-22489; CONF-930928-11) Avail: CASI HC A03/MF A01

A multi-model approach (MMA) to simulating defect production processes at the atomic scale is described that incorporates molecular dynamics (MD), binary collision approximation (BCA) calculations, and stochastic annealing simulations. The central hypothesis of the MMA is that the simple, fast computer codes capable of simulating large numbers of high energy cascades (e.g., BCA codes) can be made to yield the correct defect configurations when their parameters are calibrated using the results of the more physically realistic MD simulations. The calibration procedure is investigated using results of MD simulations of 25 keV cascades in copper. The configurations of point defects are extracted from the MD cascade simulations at the end of the collisional phase, similar to the information obtained with a binary collision model. The MD collisional phase defect configurations are used as input to the ALSOME annealing simulation code, and values of the ALSOME quenching parameters are determined that yield the best fit to the post-quenching defect configurations of the MD simulations. DOE

N94-26078# Argonne National Lab., IL.

CROSSOVER BETWEEN BCS AND PERFORMED-BOSON THEORIES WITH INCREASING INTERACTIONS

M. Randeria Aug. 1993 8 p Presented at the International Conference on Strongly Correlated Electron Systems, La Jolla, CA, 16-19 Aug. 1993
(Contract W-31-109-eng-38)
(DE93-019018; ANL/MSD/CP-80489; CONF-930865-1) Avail: CASI HC A02/MF A01

The author reviews recent work on Fermi systems with attractive interactions of arbitrary strength. First, he describes the results of a functional integral formulation to study the crossover from cooperative Cooper pairing to independent bound state formation and condensation. The inadequacy of a saddle point approximation with increasing coupling is pointed out, and the importance of temporal (quantum) fluctuations for normal state properties at intermediate and strong coupling is emphasized. Next, results from a quantum Monte Carlo simulation of the 2D attractive Hubbard model are described. The intermediate coupling normal state is found to deviate markedly from a canonical Fermi liquid; 'spin-gap' behavior, with 1/T(sub 1)T is approximately (chi)(T), is found in a degenerate Fermi system. DOE

N94-26083# California Univ., Berkeley. Lawrence Berkeley Lab.

THE STAR EXPERIMENT AT THE RELATIVISTIC HEAVY ION COLLIDER

J. W. Harris Sep. 1993 9 p Presented at the 10th International Conference on Ultra-Relativistic Nucleus-nucleus Collisions, Borlaenge, Sweden, 20-24 Jun. 1993
(Contract DE-AC03-76SF-00098)
(DE94-003409; LBL-34726; CONF-930636-9) Avail: CASI HC A02/MF A01

The STAR experiments will concentrate on measurements of hadron production over a large solid angle to be able to study observables on an event-by-event basis. STAR will search for signatures of QGP formation and investigate the behavior of strongly interacting matter at high energy density. Since there is no single definitive signature for the QGP, it is essential to use a flexible detection system at RHIC. STAR will simultaneously measure many experimental observables to study signatures of the phase transition and the space-time evolution of the collision process. This requires an understanding of the microscopic structure of hadronic interactions, at the level of quarks and gluons, at high energy densities. The experiment will utilize two aspects of hadron production that are fundamentally new at RHIC: correlations between global observables on an event-by-event basis and the use of hard scattering of partons as a probe of the properties of high density nuclear matter. DOE

N94-26101# Stanford Linear Accelerator Center, CA.

THE DELTA (1232) RESONANCE TRANSITION FORM FACTOR

L. M. Staurt (California Univ., Davis.), P. E. Bosted (American Univ., Washington, DC.), and A. Lung (American Univ., Washington, DC.) Aug. 1993 4 p Presented at the Conference on Exclusive Reactions At High Momentum Transfer, Elba, Italy, 24-26 Jun. 1993
(Contracts DE-AC03-76SF-00515; W-7405-eng-48; DE-FG02-88ER-40415; DE-AC02-76ER-13065; DE-FG06-90ER-40537)
(DE94-003442; SU-SLAC-PUB-6316; CONF-9306260-3) Avail: CASI HC A01/MF A01

Old and new measurements of inclusive e-p cross sections in the Delta(1232) resonance region have been combined, and a global data fit has been made. Using this fit to parameterize the nonresonant background, the transition form factors have been extracted out to a four-momentum transfer, Q(sup 2), of 9.8 (GeV/c)(exp 2). The results are systematically higher than those from a previous analysis, but agree within errors. A similar analysis has been done with e-d cross sections, and sigma(sub n)/sigma(sub p) in the Delta(1232) resonance region has been extracted out to a Q(sup 2) of 7.9 (GeV/c)(exp 2). Sigma(sub n)/sigma(sub p) for Delta(1232) production is consistent with unity, while sigma(sub n)/sigma(sub p) for the nonresonant background is constant with Q(sup 2) at approximately 0.4. DOE

N94-26116# Korean Atomic Energy Research Inst., Daeduk (Republic of Korea).

STUDY ON NEUTRON ACTIVATION ANALYSIS

Yong Sam Chung and Seung Yeon Cho Jan. 1993 69 p In KOREAN
(DE93-632191; KAERI/RR-1160/92) Avail: CASI HC A04/MF A01 (US Sales Only)

Environmental samples were analyzed quantitatively by neutron activation analysis using high resolution gamma-ray spectrometry. The accuracy and precision of the method were checked by the analysis of reference materials, Urban Particulate Matter (NBS SRM 1648), and Coalfly ash (NBS SRM 1633a). Airborne particulates collected for 6 months with a low volume air sampler at the outer area of Seoul were analyzed as the start of full scale airborne particulates research. We analyzed 19 trace elements from the samples, and the NAA method was accepted as a viable method for environmental pollution research. DOE

N94-26133# Stanford Linear Accelerator Center, CA.
A STUDY OF LPM SUPPRESSION OF BREMSSTRAHLUNG AT 25 GeV
P. Anthony (Lawrence Livermore National Lab., CA.), R. Becker-Szendy, and P. Bosted (American Univ., Washington, DC.) Mar. 1993 4 p
Presented at the International Cosmic Ray Conference, Calgary, Alberta, 19-20 Jul. 1993
(Contract DE-AC03-76SF-00515)
(DE94-003457; SU-SLAC-PUB-6096; CONF-930779-18) Avail: CASI HC A01/MF A01

This paper describes progress to date in making accurate measurements of the LPM suppression of bremsstrahlung with 25 GeV electrons. By using a 120 pulses per second beam, a precise BGO calorimeter, and spectrometer to tag the outgoing electrons, an accurate measurement of the bremsstrahlung photons was made in the 0-400 MeV region, where the Bethe Heitler and LPM predictions differ. Data was taken with targets made of carbon, uranium, tungsten, and iron, with thicknesses in the two to six percent X(sub 0) range. In addition, data was taken with two very thin gold targets. The latter have thicknesses that are comparable to or less than the LPM formation zone length, and so should not exhibit LPM suppression. Photons of a few MeV in energy were studied to test the closely related longitudinal density effect predicted by Ter-Mikaelian in which very low energy photon emission is suppressed due to dielectric effects of the medium. DOE

N94-26145# Argonne National Lab., IL.
RESCATTERING AND ENERGY LOSS OF FAST PARTONS IN NUCLEAR MATTER
T. Fields and M. Corcoran (Rice Univ., Houston, TX.) 1993 3 p
Presented at the International Europhysics Conference on High-Energy Physics, Marseille, France, 22-28 Jul. 1993
(Contract W-31-109-eng-38)
(DE94-002918; ANL-HEP-CP-93-86; CONF-930761-4) Avail: CASI HC A01/MF A01

We compare nuclear rescattering and energy loss effects as seen in dijet production in Fermilab fixed target experiment E609 with theoretical estimates and with data from Drell-Yan dilepton production. Possible explanations for these effects being unusually large in dijet production are briefly discussed. DOE

N94-26172# New Orleans Univ., LA. Dept. of Chemistry.
COMPUTATIONAL STUDIES OF ENERGETIC ORGANIC MOLECULES
Peter Politzer and Jane S. Murray 27 Dec. 1993 49 p
(Contract N00014-91-J-4057)
(AD-A274726; TR-65) Avail: CASI HC A03/MF A01

First-principles calculations have been carried out for organic energetic molecules of the following types: nitroaromatics; aliphatic and alicyclic nitramines; highly strained cage-like systems; and high-nitrogen-content molecules. The scope includes both ab initio molecular orbital methods and also density functional procedures, with a specific emphasis on the understanding of factors influencing shock/impact sensitivities and relative stabilities. For each class of compounds mentioned above, structural and electronic properties are discussed, followed generally by a review of calculations relating to the decompositions of some specific members of these classes. The discussion of sensitivity and its relationship to molecular properties focuses upon general correlations that exist within separate categories of compounds, e.g. nitroaromatics and nitramines, and upon exceptions to these relationships which suggest that other factors may play key roles in specific instances. In the area of high-nitrogen-content molecules, the presence of localized N-N bonds appears to be a factor favoring instability/high sensitivity. DTIC

N94-26244# Louisiana State Univ., Baton Rouge.
A SEARCH FOR THE PRODUCTION OF DIRECT LEPTONS IN NUCLEON-NUCLEUS AND NUCLEUS-NUCLEUS COLLISIONS
P. N. Kirk 15 Dec. 1993 31 p
(Contract DE-FG05-88ER-40445)
(DE94-004640; DOE/ER-40445/43) Avail: CASI HC A03/MF A01

The purpose of this report is to describe activities performed by the Intermediate Energy Nuclear Physics Group (IENPG) at the Louisiana State University (LSU) under the terms of grant FG05-88ER40445. The report will cover, for the most part, the period of time between April 1, 1991, and the present. The principal focus of activities is currently the muon subgroup of the PHENIX Collaboration. Other activities, however, are being concluded, specifically memberships in the Di-Lepton Spectrometer (DLS) collaboration at LBL and the AMY collaboration at KEK. A few examples are cited of contributions to these collaborations. DOE

N94-26245# Fermi National Accelerator Lab., Batavia, IL.
PHOTON AND HADRON PRODUCTION OF HEAVY FLAVORS
F. DeJongh Nov. 1993 15 p Presented at the 5th International Symposium on Heavy Flavor Physics, Montreal, Canada, 6-10 Jul. 1993
(Contract DE-AC02-76CH-03000)
(DE94-004655; FNAL/C-93/330-E; CONF-9307143-6) Avail: CASI HC A03/MF A01

Recent experiments have obtained large, clean samples of charmed and bottom hadrons, and have measured both single-quark inclusive cross sections and quark-antiquark correlations. Predictions for these production properties are available from next-to-leading order QCD. We review recent results from fixed target hadroproduction of charm and bottom, fixed target photoproduction of charm, and production of bottom at proton-antiproton colliders. DOE

N94-26325# California Univ., Berkeley. Lawrence Berkeley Lab.
MEASUREMENT OF TAU LEPTON BRANCHING FRACTIONS Ph.D. Thesis
N. A. Nicol 30 Sep. 1993 79 p
(Contract DE-AC03-76SF-00098)
(DE94-003423; LBL-34784) Avail: CASI HC A05/MF A01

Presented are tau(sup -) lepton branching fraction measurements based on data from the TPC/two-gamma detector at PEP. Using a sample of tau(sup -) yields nu(sub tau)K(sup -)pi(sup +)pi(sup -) events, the resonance structure of the K(sup -)pi(sup +)pi(sup -) system is examined and the first measurements of branching fractions for tau(sup -) yields nu(sub tau)K(sub 1)(sup -)(1270) and tau(sup -) yields nu(sub tau)K(sub 1)(sup -)(1400) are obtained. Also described are a complete set of branching fraction measurements in which all the decays of the tau(sup -) lepton are separated into classes defined by the identities of the charged particles and an estimate of the number of neutrals. This is the first such global measurement with decay classes defined by the four possible charged particle species, e, mu, pi, and K. DOE

N94-26333 International Centre for Theoretical Physics, Trieste (Italy).
WHY IS THE HIGGS DOUBLET LIGHT?
G. Dvali Jun. 1993 12 p Limited Reproducibility: More than 20% of this document may be affected by microfiche quality
(DE94-601711; IC-93/151) Avail: CASI HC A03 (US Sales Only)

We consider a possible mechanism for the explanation of the doublet-triplet mass hierarchy in the grand unified theories. The Higgs doublet is automatically light since it is related by a certain 'custodial' SU(2)(sub C) symmetry to another doublet which after GUT symmetry breaking becomes an unphysical Higgs. Custodial symmetry may or may not be a part of GUT symmetry. An explicit example of SUSY GUT is constructed. DOE

N94-26334 Melbourne Univ., Parkville (Australia). School of Physics.
ELECTRON ENERGY LOSS SPECTROSCOPY IN A CRYSTALLINE ENVIRONMENT USING INNER SHELL IONIZATION
L. J. Allen 1993 23 p Limited Reproducibility: More than 20% of this document may be affected by microfiche quality
(DE94-601820; UM-P-92/104) Avail: CASI HC A03 (US Sales Only)

A theory for electron energy loss spectroscopy (EELS) is presented. The focus is on inner shell ionization in a crystalline environment under dynamical electron diffraction conditions which includes dechanneling due to inelastic scattering and in particular to thermal diffuse scattering (TDS). It incorporates ionization kinematics and the associated localization of the interaction from first principles. Appropriate integration over the possible final states of the detected scattered fast electron as well as the ejected target electron is catered for. The theory accounts for ionization by the dechanneled thermally scattered electrons as well as delocalization due to thermal fluctuations in target atom position. This formulation extends previous work which did not explicitly incorporate inelastic scattering into the ionization cross section. The dependence of the EELS cross section on the orientation, thickness and temperature of the specimen will be discussed. Also the influence of incident energy, energy window for the detected energy loss electrons and the acceptance angle of the detector on the cross section will be considered. In a simpler version of the formalism given here, with channeling limited to the incident electron, was successfully applied to energy dispersive x-ray emission spectroscopy and the related technique of atom location by channeling enhanced microanalysis (ALCHEM). DOE

N94-26393 Gosudarstvennyi Komitet po Ispolzovaniyu Atomnoi Energii, Serpukhov (USSR). Inst. Fiziki Vysokikh Ehnergij.
SEPARATION AND RECONSTRUCTION OF ELECTRON NEUTRINO INTERACTION IN THE IHEP-JINR NEUTRINO DETECTOR AND BARS DETECTOR [SEPARATSIYA I REKONSTRUKTSIYA VZAIMODEJSTVIJ EHLEKTRONNYKH NEJTRINO V NEJTRINNOM DETEKTORE IFVEH-OLYAL I V DETEKTORE BARS]
M. M. Kirsanov 1992 20 p In RUSSIAN Limited Reproducibility: More than 20% of this document may be affected by microfiche quality
(DE93-634182; IFVE-ONF-92-33) Avail: CASI HC A03 (US Sales Only)

The algorithm for the search and reconstruction of deep inelastic interactions of electron neutrino in the IHEP-JINR neutrino detector was created. The algorithm is used in the experiment on the search for prompt neutrino, where the electron neutrino flux comprises 7% out of the muon neutrino flux. The 46 events have been found, the background from muon neutrino is 25%. In the WBB exposure and the focusing system off where nu(sub e)/nu(sub mu) approximately = 2.5%, 600 events were found, and the background from muon neutrino was 40%. Possibilities to use the similar algorithm for the BARS detector are considered. DOE

N94-26416# International Centre for Theoretical Physics, Trieste (Italy).
DIFFERENTIAL REGULARIZATION OF A NON-RELATIVISTIC ANYON MODEL
D. Z. Freedman, G. Lozano, and N. Rius (Massachusetts Inst. of Tech., Cambridge.) Jul. 1993 16 p
(DE94-601558; IC-93/183; CTP-2216) Avail: CASI HC A03/MF A01 (US Sales Only)

Differential regularization is applied to a field theory of a non-relativistic charged boson field phi with lambda(phi)(sup *)(phi)(sup 2) self-interaction and coupling to a statistics-changing 0(1) Chern-Simons gauge field. Renormalized configuration-space amplitudes for all diagrams contributing to the phi(sup *)(phi)(sup *)(phi)(phi) 4-point function, which is the only primitively divergent Green's function, are obtained up to 3-loop order. The renormalization group equations are explicitly checked, and the scheme dependence of the beta-function is investigated. If the renormalization scheme is fixed to agree with a previous 1-loop calculation, the 2- and 3-loop contributions to beta(lambda, e) vanish, and beta(lambda, epsilon) itself vanishes when the 'self-dual' condition relating lambda to the gauge coupling e is imposed. DOE

N94-26423# International Centre for Theoretical Physics, Trieste (Italy).
C-PERIODICITY AND THE PHYSICAL MASS IN THE 3-STATE POTTS MODEL
R. V. Gavai and L. Polley (Oldenburg Univ., Germany.) Jul. 1993 17 p
(DE94-601551; IC-93/131; TIFR/TH-93-28) Avail: CASI HC A03/MF A01 (US Sales Only)

The standard infinite-volume definition of connected correlation function and particle mass in the 3-state Potts model can be implemented in Monte Carlo simulations by using C-periodic spatial boundary conditions. This avoids both the breaking of translation invariance (cold wall b.c.) and the phase-dependent and thus possible biased evaluation of data (periodic b.c.). The numerical feasibility of the standard definitions is demonstrated by sample computations on a 24 x 24 x 48 lattice. DOE

N94-26424# International Centre for Theoretical Physics, Trieste (Italy).
SPINOR AND ISOSPINOR STRUCTURE OF RELATIVISTIC PARTICLE PROPAGATORS
D. M. Gitman and Sh. M. Shvartsman (Case Western Reserve Univ., Cleveland, OH.) Jul. 1993 8 p
(DE94-601552; IC-93/197) Avail: CASI HC A02/MF A01 (US Sales Only)

Representations by means of path integrals are used to find spinor and isospinor structure of relativistic particle propagators in external fields. For a Dirac propagator in an external electromagnetic field, all Grassmannian integrations are performed and a general result is presented via a bosonic path integral. The spinor structure of the integrand is given explicitly by its decomposition in the independent gamma-matrix structures. A similar technique is used to get the isospinor structure of the scalar particle propagator in an external non-Abelian field. DOE

N94-26454 Gosudarstvennyi Komitet po Ispolzovaniyu Atomnoi Energii, Serpukhov (USSR).
SPIN FROM ISOSPIN: THE MODEL OF SUPERPARTICLE IN A NON-GRASSMANNIAN APPROACH
M. S. Pljushchay 1992 12 p Limited Reproducibility: More than 20% of this document may be affected by microfiche quality
(DE93-634341; IHEP-OTF-92-13) Avail: CASI HC A03 (US Sales Only)

Within a non-Grassmannian approach, the (3+1)-dimensional model of a massless spinning particle with internal even degrees of freedom, described by the isospin vector, is constructed. It is shown that quantization of the model leads to the massless supermultiplet. The generalization of the model to the case of N-extended supersymmetry is carried out. The connection of the proposed model with the supertwistor model of superparticles is traced. DOE

N94-26455# Gosudarstvennyi Komitet po Ispolzovaniyu Atomnoi Energii, Serpukhov (USSR). Inst. Fiziki Vysokikh Ehnergij
DYNAMIC BREAKING OF U(N) AND APPEARANCE OF CHERN-SIMONS TERM IN 4-FERMION THEORIES
K. G. Klimenko 1992 6 p
(DE93-634342; IHEP-OTF-92-2) Avail: CASI HC A02/MF A01 (US Sales Only)

The phase structure of the four-fermion field theory is considered in three dimensions. Both parity and the U(N)-invariance of the model are shown to break at g less than 0. At odd N's, this leads to the appearance of the Chern-Simons term, provided there is an interaction between fermions and the gauge field. DOE

N94-26456# Gosudarstvennyi Komitet po Ispolzovaniyu Atomnoi Energii, Serpukhov (USSR). Inst. Fiziki Vysokikh Ehnergij.
ON THE RELATIVISTIC INVARIANT REPRESENTATION OF ARBITRARY BILINEAR COMBINATIONS OF DIRAC SPINORS
A. V. Shchelkachev 1992 19 p
(DE93-634343; IHEP-OTF-92-45) Avail: CASI HC A03/MF A01 (US Sales Only)

It is demonstrated that, generally, a bilinear combination of two arbitrary four-spinors with one of the sixteen Dirac matrices cannot be expressed via the momentum and spin four-vectors (Pauli and Lubanski vectors). The universal general formula derived contains more four-vectors, corresponding to two three-dimensional base vectors in a particle rest frame perpendicular to the direction of the particle spin. The limit transition to zero masses is discussed. Presented are some specific formulas describing the binary combinations of spinors in the case of elastic scattering for helicity and the 'transversal' amplitudes. DOE

N94-26478# Technische Univ., Eindhoven (Netherlands).
MERGED-BEAM STUDIES OF ELECTRON-RECOMBINATION AND EXCITATION OF ATOMIC AND MOLECULAR HYDROGEN IONS Ph.D. Thesis
Petrus Johannes T. vanderDonk 1993 134 p Sponsored by U.S. Air Force, and Natural Sciences and Engineering Research Council, Canada Prepared in cooperation with Univ. of Western Ontario, London, Canada
(ETN-94-95339) Avail: CASI HC A07/MF A02

The cross sections for dissociative recombination and dissociative excitation of positive small molecular ions and electrons are presented. An overview of some electron-ion interactions is given. Results of a high resolution dissociative recombination experiment on H2(+) and an attempt to fit the experimental data with a model are presented. The smallest tri-atomic molecular ion, H3(+), is investigated. The dissociative excitation and recombination of D3(+) is described. Several field-ionization experiments, performed to analyze Rydberg products formed in the dissociative recombination of H2(+) are explained. Ionization models are evaluated using the results of a unique experiment, where the quantization of the electron-energy is observed. Some measured cross sections for the production of the negative ion are presented. The results of the measurements of stimulated radiative combination of protons and considerations for the calculation of production gain are included. ESA

N94-26505 Joint Inst. for Nuclear Research, Dubna (USSR). Lab. of Theoretical Physics.
MESONS AND DIQUARKS IN A NJL-MODEL AT FINITE TEMPERATURE AND CHEMICAL POTENTIAL
D. Ebert, Yu. L. Kalinovskij, L. Muenchow, and M. K. Volkov 1992 26 p Limited Reproducibility: More than 20% of this document may be affected by microfiche quality
(DE93-634375; JINR-E-2-92-134) Avail: CASI HC A03 (US Sales Only)

An extended NJL model with (qantiq) and (qq)-interactions is studied at finite temperature and baryon density. DOE

N94-26507 Joint Inst. for Nuclear Research, Dubna (USSR). Lab. of Theoretical Physics.
CHANCE TO USE W-DECAY LEPTON CHANNELS FOR WIDTH DETERMINATION
A. V. Ivkin (Academy of Sciences, USSR, Alma-Ata.), M. T. Nazirov (Academy of Sciences, USSR, Alma-Ata.), T. V. Kukhto (Belorussian State Univ., Minsk, Belarus.), and E. A. Kuraev 1992 8 p Limited Reproducibility: More than 20% of this document may be affected by microfiche quality
(DE93-634438; JINR-E-2-92-90) Avail: CASI HC A02 (US Sales Only)

The prosess of W(+)W(-)-production at e(+)e(-)-collisions as well as the process of single W-boson production in (gamma)e-collision with subsequent W decay via lepton channel were considered. Due to resonance nature of W-boson propagator in an intermediate state, lepton yield has a sharp rise in the region of W-boson production threshold. Lepton-inclusive cross sections were calculated. In the case of two-lepton production their energy fractions and the angle between their momenta in c.m.s. for the majority of events are found to be connected by the condition confining a certain body in 3 dimensional space of these parameters. For the case of single W production the decay lepton energy fraction and its angle with respect to a beam axis play a role of such parameters; their allowed regions being a plane figure. It is shown that measurement of 'smearing' of lepton distribution due to W-boson resonance nature would give quite reliable information on the ratio of the W-boson total width to its mass. Influence of radiation corrections on this distributions is analyzed. DOE

N94-26508 Joint Inst. for Nuclear Research, Dubna (USSR). Lab. of Computing Techniques and Automation.
ABOUT POSSIBLE TYPES OF NEUTRINO OSCILLATIONS
Kh. M. Beshtoev 1992 6 p Limited Reproducibility: More than 20% of this document may be affected by microfiche quality
(DE93-634449; JINR-E-2-92-318) Avail: CASI HC A02 (US Sales Only)

Possible types of neutrino oscillations are considered. Together with neutrino oscillations based on analogies with oscillations of K(sup 0) and K-tilde(sup 0) mesons, virtual neutrino oscillations (neutrinos produced in the oscillations do not undergo transition to the mass surface) are considered. Conditions in which such oscillations occur are studied. DOE

N94-26509 Joint Inst. for Nuclear Research, Dubna (USSR). Lab. of Nuclear Reactions.
ON THE WAVE AND CORPUSCULAR PROPERTIES OF MICROPARTICLES [K VOLNOVYM I KORPUSKULYARNYM SVOJSTVAM MIKROCHASTITS]
B. A. Klenin 1992 18 p In RUSSIAN Limited Reproducibility: More than 20% of this document may be affected by microfiche quality
(DE93-634450; JINR-R-2-92-163) Avail: Issuing Activity (Department of Energy (DOE)) (US Sales Only)

It is shown that a spring of the properties of the electron is its zero oscillations with the Doppler frequency in the vacuum zero electromagnetized field. DOE

N94-26511 Joint Inst. for Nuclear Research, Dubna (USSR).
MEASUREMENTS OF THE p (MU)d-MOLECULE FORMATION RATE AT DIFFERENT HYDROGEN TEMPERATURE
V. P. Dzhelepov, V. V. Filchenkov, and S. A. Ivanovskij et al 1992 16 p Limited Reproducibility: More than 20% of this document may be affected by microfiche quality
(DE93-634636; JINR-E-15-92-82) Avail: CASI HC A03 (US Sales Only)

In an experiment with a cryogenic target of high pressure (0.6 kbar) on the muon beam of the JINR phasotron, the time distributions of (gamma)-quanta from the reaction pd(mu) yields H-3(mu) + (gamma) + 5.5 MeV were measured in the temperature region T = 21-300 K. DOE

N94-26527# Los Alamos National Lab., NM.
RELATIVISTIC COLLISION RATE CALCULATIONS FOR ELECTRON-AIR INTERACTIONS
Gerald Graham and Robert Roussel-Dupre (EG and G Energy Measurements, Inc., Los Alamos, NM.) Dec. 1993 51 p
(Contracts W-7405-eng-36; DE-AC08-93NV-11265)
(DE94-004204; LA-12604-MS) Avail: CASI HC A04/MF A01

The most recent data available on differential cross sections for electron-air interactions are used to calculate the avalanche, momentum transfer, and energy loss rates that enter into the fluid equations. Data for the important elastic, inelastic, and ionizing processes are generally available out to electron energies of 1-10 keV. Prescriptions for extending these cross sections to the relativistic regime are presented. The angular dependence of the cross sections is included where data are available as is the doubly differential cross section for ionizing collisions. The collision rates are computed by taking moments of the Boltzmann collision integrals with the assumption that the electron momentum distribution function is given by the Juettner distribution function which satisfies the relativistic H-theorem and which reduces to the familiar Maxwellian velocity distribution in the nonrelativistic regime. The distribution function is parameterized in terms of the electron density, mean momentum, and thermal energy and the rates are therefore computed on a two dimensional grid as a function of mean kinetic energy and thermal energy. DOE

N94-26540 Nationaal Inst. voor Kernfysica en Hoge Energiefysica, Amsterdam (Netherlands).
CONSTRUCTION OF A NEW ELECTROWEAK SPHALERON
F. R. Klinkhamer Jun. 1993 16 p Limited Reproducibility: More than 20% of this document may be affected by microfiche quality
(NIKHEF-H/93-09; ETN-94-95042) Avail: CASI HC A03

A self consistent ansatz for a new sphaleron in the electroweak standard model is presented. The resulting field equations are solved numerically. This sphaleron sets the height of the energy barrier for the global SU(2) anomaly. A simple procedure to arrive at a new self consistent ansatz was employed: the maximum configuration of a noncontractible sphere, was generated while keeping the symmetries of the configurations of the noncontractible sphere. It is important to note that our maximum configuration is distinguished by an additional symmetry. This construction method can probably also be used to discover other classical solutions. ESA

N94-26562# Pennsylvania Univ., Philadelphia. Dept. of Chemistry.
A SEMICLASSICAL REACTIVE FLUX METHOD FOR THE CALCULATION OF CONDENSED PHASE ACTIVATED RATE CONSTANTS
Diane E. Sagnella, Jianshu Cao, and Gregory A. Voth 11 Jan. 1994 33 p
(Contract N00014-92-J-1243)
(AD-A274850; TR-7) Avail: CASI HC A03/MF A01

A semiclassical reactive flux algorithm for calculating thermally activated rate constants is presented which is based on a semiclassical transition state theory due to Chapman, Garrett, and Miller J. This reactive flux technique, when combined with the semiclassical TST, enables one to describe dynamical recrossings of the transition state on the same footing as tunneling effects. Most importantly, the method is readily applied to nonlinear multidimensional systems over a wide range of temperatures. It will be shown that the method works very well for a variety of existing models. DTIC

N94-26574# Oak Ridge National Lab., TN.
SIGNATURES FOR HYBRIDS
T. Barnes 1993 13 p Presented at the Conference on Exclusive Reactions at High Momentum Transfer, Elba, Italy, 24-26 Jun. 1993
(Contract DE-AC05-84OR-21400)
(DE94-004244; CONF-9306260-5) Avail: CASI HC A03/MF A01

In this review talk I summarize theoretical expectations for properties of hybrid mesons and baryons, and discuss the prospects for identifying these states experimentally. DOE

N94-26577# Lawrence Livermore National Lab., CA.
A CONCURRENT, MULTIGROUP, DISCRETE ORDINATES MODEL OF NEUTRON TRANSPORT
M. R. Dorr and C. H. Still 22 Oct. 1993 12 p Presented at the

Institute of Electrical and Electronic Engineers (IEEE) Meeting on Scalable Parallel Libraries, Starkville, MS, 6-8 Oct. 1993
(Contract W-7405-eng-48)
(DE94-004334; UCRL-JC-115601; CONF-9310220-3) Avail: CASI HC A03/MF A01

The authors present an algorithm for the concurrent solution of the linear system arising from a multigroup, discrete ordinates model of neutron transport. The target architectures consist of distributed memory computers ranging from workstation clusters to massively parallel computers. Based on an analysis of the memory requirement and floating point complexity of matrix-vector multiplication in the iterative solution of the linear system, the authors propose a data layout and communication strategy designed to achieve scalability with respect to all phase space variables. Numerical results are presented to demonstrate the performance of the algorithm on the nCUBE/2. DOE

N94-26586# Texas Univ., Austin. Dept. of Physics.
PION-NUCLEUS INTERACTIONS AND THE STAR EXPERIMENT AT RHIC
C. F. Moore Sep. 1993 75 p
(Contract DE-FG05-87ER-40343)
(DE94-000658; DOE/ER-40343/7) Avail: CASI HC A04/MF A01

The work carried out by personnel from the University of Texas at Austin at the Los Alamos Clinton P. Anderson Meson Physics Facility (LAMPF) during the calendar years 1990-1993 and on the STAR experiment at RHIC between the University of Texas at Austin and the United States Department of Energy is summarized. A brief overview of work supported by this grant is given in Section 2. An account of the study of the double giant resonances in pion double charge exchange forms Section 3. A list of published papers and preprints in Section 6, invited talks in Section 7, and abstracts in Section 8 are included. These papers summarize experiments involving participants supported by this grant and indicate the work accomplished by these participants in this program of medium energy nuclear physics research. Section 9 contains a list of personnel who have participated in this research program. DOE

N94-26620# Los Alamos National Lab., NM.
AN ANTIPROTON-PROTON PARTIAL-WAVE ANALYSIS
R. Timmermans, T. A. Rijken (Nijmegen Univ., Netherlands.), and J. J. deSwart (Nijmegen Univ., Netherlands.) 1993 10 p Presented at the 14th European Conference on Few-body Problems in Physics, Amsterdam, Netherlands, 22-27 Aug. 1993
(Contract W-7405-eng-36)
(DE94-002690; LA-UR-93-3728; CONF-9308164-5) Avail: CASI HC A02/MF A01

Partial-wave analyses (PWA's) have a long history in the fields of pi N and NN scattering. Due to the poor quality of low-energy antiproton beams and the resulting absence of accurate experimental data, analogous model-independent studies of the much more complex bar-p p system have in the past always been impossible. In the pre-LEAR era spin-dependent observables and charge-exchange (bar-p p yields bar-n n) data were almost nonexistent, the situation between 400 and 925 MeV/c is now quite good. High-quality analyzing-power data have been obtained for the elastic and charge-exchange reactions. Very recently, even charge-exchange depolarization data have become available. Unfortunately, the practical difficulties involved in constructing a high-quality 'cooled' antiproton beam of lower momentum are large. Consequently, the bar-p p database below about 400 MeV/c is still by far not as good as one would like, in striking contrast to the pp case where very accurate data exist as low as T(sub L) = 0.35 MeV. It also remains an outstanding experimental challenge to construct a polarized antiproton beam to further probe the spin structure of the interaction. A new method has been developed by the Nijmegen group to perform PWA's of the abundant and accurate NN scattering data below T(sub L) = 350 MeV. With the now available high-quality data from LEAR and KEK, the authors have been able to extend the methods used in these NN PWA's to perform an energy-dependent PWA of all bar-p p scattering data below p(sub L) = 925 MeV/c. The same methods of PWA have also been applied to the strangeness-exchange reaction bar-p p yields bar-Lambda Lambda, for which the PS185 group at LEAR has obtained beautiful data. Theoretical ideas behind these Nijmegen PWA's are reviewed and these ideas and methods are applied to the case of bar-p p scattering. Some results of this bar-p p PWA are presented and discussed. DOE

N94-26665 Victoria Univ. (British Columbia). Dept. of Physics and Astronomy.
MEASURING THE TIME DEPENDENCE OF B(SUB S)(SUP 0) MESON - ANTI B(SUB S)(SUP 0) MESON OSCILLATIONS M.S. Thesis
Manuella Greta Vincter 1992 176 p
(ISBN-0-315-84367-5; CTN-94-61025) Copyright Avail: Micromedia Ltd., Technical Information Centre, 240 Catherine Street, Suite 305, Ottawa, Ontario, K2P 2G8, Canada HC/MF

A Monte Carlo study was made of the possibility of measuring the frequency of oscillation of B/anti-B meson mixing (each meson consisting of an anti-b quark and an s quark), given existing detector technology. A measurement of this oscillation frequency is important since it leads to the determination of one of the elements of the Cabibbo Kobayashi Maskawa quark mixing matrix. The present values of the elements of this matrix suggest that the oscillation frequency lies in the range Delta M/Gamma approximately 2 to 265, although the current best estimates give Delta M/Gamma about equal to 15. The OPAL silicon microvertex detector is used as an example of present-day detector technology. The energy lost by an ionizing particle in a silicon wafer is studied in detail. The phenomenon of B meson oscillations was simulated by computer using a simple model. These simulated events were analyzed by three different methods in an attempt to quantify the number of events needed to achieve a given precision for the measurement of the B meson oscillation frequency. With 200 B mesons detected, a measurement of Delta M/Gamma up to 10 can be made with good precision. CISTI

N94-26677# Ohio State Univ., Columbus. Research Foundation.
STRONGLY INTERACTING FERMION SYSTEMS
1993 11 p
(Contract DE-FG02-88ER-45347)
(DE94-002674; DOE/ER-45347/33) Avail: CASI HC A03/MF A01

Success was obtained in three fields: Optical properties in electronic structure program (optical activity--Se, Si); quasi-one-dimensional systems (CH(x), fullerene tubule, polyaniline, etc.); and other strongly interacting fermion systems (Kondo impurities interacting with conduction bands, phonon-induced decay rates for quasi-particle cyclotron orbits in simple metals, fluctuation conductivity above superconducting transition). DOE

N94-26759# Superconducting Super Collider Lab., Dallas, TX.
LIGHT-QUARK, HEAVY-QUARK SYSTEMS: AN UPDATE
B. Grinstein Jun. 1993 21 p Presented at the Workshop on B Physics At Hadron Colliders, Snowmass, CO, Jun. 1993
(Contract DE-AC35-89ER-40486)
(DE94-002298; SSCL-Preprint-514; CONF-9306258-5) Avail: CASI HC A03/MF A01

We review many of the recently developed applications of Heavy Quark Effective Theory techniques. After a brief update on Luke's theorem, we describe striking relations between heavy baryon form factors, and how to use them to estimate the accuracy of the extraction of (vert bar)V(sub cb)(vert bar). We discuss factorization and compare with experiment. An elementary presentation, with sample applications, of reparametrization invariance comes next. The final and most extensive chapter in this review deals with phenomenological lagrangians that incorporate heavy-quark spin-flavor as well as light quark chiral symmetries. We compile many interesting results and discuss the validity of the calculations. DOE

N94-26760# Notre Dame Univ., IN.
RYDBERG STATES IN MULTIPLY CHARGED IONS
A. E. Livingston May 1993 5 p
(Contract DE-FG02-92ER-14283)
(DE94-002335; DOE/ER-14283/1) Avail: CASI HC A01/MF A01

This report summarizes research progress in accelerator-based studies of atomic structure and decay characteristics of excited states in multiply charged ions. This work involves spectroscopic measurements in visible to extreme ultraviolet wavelength regions of atomic transitions involving Rydberg states and low-lying excited states in multiply charged ions. These investigations are of both fundamental and applied interest. Of fundamental importance are trusts of long range electron-ion interactions and many-body electron correlations in Rydberg states, sensitivity to relativistic effects in the energy structures of few-electron ions, and tests of accurate many-body calculations of transition probabilities. This has application to understanding of laboratory and astrophysical plasmas and of detailed atomic structure and decay properties in highly charged ions. DOE

N94-26766 Instituto de Fisica Teorica, Sao Paulo (Brazil).
CONSTRAINTS ON SINGLET RIGHT-HANDED NEUTRINOS COMING FROM THE Z(0)-WIDTH
C. O. Escobar, O. L. G. Peres, and V. Pleitez Dec. 1992 12 p
Limited Reproducibility: More than 20% of this document may be affected by microfiche quality
(DE93-634393; IFT-P-040/92) Avail: CASI HC A03 (US Sales Only)

The constraints on masses and missing angles imposed by the measured Z(sup 0) invisible width, in a model in which a singlet right-handed neutrino mixes with all the Standard model neutrinos are studied. If neutrinos are massive an important question to be answered concerns the way the Z-pole observables constraint their masses and mixing parameters. In particular the measured Z-invisible width, Gamma(sup inv), implies that the number of families is compatible with three. On the other hand, it is well known that this number need not to be an integer number if right-handed neutrinos transformed as singlets under SU(2)(sub L) x U(1)(sub Y) are added to the particle content of the theory. Experimental searches for sequential neutron leptons beyond the three generations exclude stable Dirac neutrinos below 41.8 GeV and stable Majorana neutrinos below 34.8 GeV. For the unstable cases these values are 46.4 and 45.1 GeV respectively. However, it is worth stressing that these limits are valid for sequential leptons and do not apply to the case of singlets of right-handed neutrinos. Here we will consider the simplest extension of the standard electroweak model with the addition of the one right-handed singlet neutral fermion, resulting in 4 physical neutrinos two of them massless and two massive ones. DOE

N94-26767 Gosudarstvennyi Komitet po Ispolzovaniyu Atomnoi Energii, Serpukhov (USSR).
LEPTONIC DECAY CONSTANTS OF HEAVY MESONS IN QCD
A. V. Tkabladze 1992 8 p Limited Reproducibility: More than 20% of this document may be affected by microfiche quality
(DE93-634426; IHEP-OTF-92-71) Avail: CASI HC A02 (US Sales Only)

The formula for calculating the axial decay constant of heavy-light quark mesons has been obtained by means of the QCD sum rules. The calculations are based on the use of excited state mass spectrum of the corresponding system. The calculated values for the charmed mesons are f(sub D) = 145 MeV and f(sub F) = 160 MeV. For B and B(sub s) mesons, the dependences of the decay constants on the b-quark mass are presented. At m(sub b) = 4.55 GeV the results are f(sub B) = 165 MeV and f(sub Bs) = 177 MeV. DOE

N94-26769# Brookhaven National Lab., Upton, NY.
STRANGE DIBARYONS
G. B. Franklin (Carnegie-Mellon Univ., Pittsburgh, PA.), M. Athanas (Cornell Univ., Ithaca, NY.), P. D. Barnes (Los Alamos National Lab., NM.), B. Bassalleck (New Mexico Univ., Albuquerque.), A. Berdoz (Carnegie-Mellon Univ., Pittsburgh, PA.), M. Murger (Freiburg Univ., Germany.), T. Burger (Freiburg Univ., Germany.), M. Chapman (New Mexico Univ., Albuquerque.), R. Chrien, and C. Davis (Manitoba Univ., Winnipeg.) et al 1993 6 p
Presented at the Future Directions in Particle and Nuclear Physics at Multi-GeV Hadron Beam Facilities, Upton, NY, 4-6 Mar. 1993
(Contract DE-AC02-76CH-00016)
(DE94-003005; BNL-49659; CONF-930389-26) Avail: CASI HC A02/MF A01

Strange Dibaryons, six valence-quark hadrons constructed from one or more strange quarks, are predicted to have greater binding than dibaryons in the non-strange sector. The flavor-singlet dibaryon with quark structure 'uuddss' is of particular theoretical and experimental interest. A brief review of the status of H dibaryon studies is presented with emphasis on experiment E813, which is currently taking data at the AGS. DOE

N94-26793# Argonne National Lab., Idaho Falls, ID.
PROGRESS IN SSC HIGGS PHYSICS: REPORT OF THE HIGGS WORKING GROUP
J. F. Gunion (California Univ., Davis.) and S. Geer (Fermi National Accelerator Lab., Batavia, IL.) Jun. 1993 33 p Presented at the Workshop on Physics at Current Accelerators and the Supercollider, Argonne, IL, 2-5 Jun. 1993
(Contract W-31-109-eng-38)
(DE94-003224; ANL-HEP-CP-93-96; CONF-9306176-13) Avail: CASI HC A03/MF A01

I review new developments in Higgs physics and electroweak symmetry breaking that have resulted from the Madison-Argonne workshops on SSC physics. DOE

N94-26809# Washington Univ., Seattle. Dept. of Physics.
NUCLEAR THEORY GROUP, UNIVERSITY OF WASHINGTON RECENT AND PLANNED RESEARCH
1993 40 p
(Contract DE-FG06-88ER-40427)
(DE94-002729; DOE/ER-40427/10-N93) Avail: CASI HC A03/MF A01

The work of the five staff members is presented individually in turn. (1) Nonperturbative aspects of quantum chromodynamics and its implication for phenomena involving nucleon structure, nuclear structure, and relativistic heavy-ion collisions. (2) Symmetries and the connection of the quark-gluon description of nucleons and nuclei with the nucleon-meson degrees of freedom-parity nonconservation, time reversal invariance, chiral symmetry and charge symmetry, QCD sum rules. (3) The relation between nuclear physics and quantum chromodynamics-physics of color transparency, fundamental symmetries, physics of confinement and hadronic form factors, EMC effect. (4) Chirally invariant chromo-dielectric soliton model, many-nucleon system in models of QCD, flux tube dynamics, (anti p)-p to (anti Lambda)-Lambda and (anti Lambda)-Sigma collisions, isotopic effects in atomic parity nonconservation, quantum molecular dynamics. (5) Numerical work related to lattice QCD simulations, and analytical work related to model studies of hadronic phenomenology and the development and understanding of new methods. DOE

N94-26894# New Orleans Univ., LA. Dept. of Chemistry.
MOLECULAR SURFACE ELECTROSTATIC POTENTIALS IN THE ANALYSIS OF NON-HYDROGEN-BONDING NONCOVALENT INTERACTIONS
Jane S. Murray, Kim Paulsen, and Peter Politzer 27 Dec. 1993 16 p
(Contract N00014-91-J-4057)
(AD-A274612; TR-66) Avail: CASI HC A03/MF A01

Electrostatic potentials computed on molecular surfaces are used to analyze some noncovalent interactions that are not in the category of hydrogen bonding, e.g. halogen bonding. The systems examined include halogenated methanes, substituted benzenes, s-tetrazine, and 1,3-bisphenylurea. The data were obtained by ab initio SCF calculations. DTIC

N94-26899 International Centre for Theoretical Physics, Trieste (Italy).
FLAVOR CHANGING NEUTRAL CURRENTS IN SU(3) X U(1) MODELS
F. Pisano and V. Pleitez (Instituto de Fisica Teorica, Sao Paulo, Brazil.) Jul. 1993 8 p Limited Reproducibility: More than 20% of this document may be affected by microfiche quality
(DE94-602576; IC-93/174) Avail: CASI HC A02 (US Sales Only)

We consider flavor changing neutral current effects coming from the Z' exchange in 3-3-1 models. We show that the mass of this extra neutral vector boson may be less than 2 TeV. DOE

N94-26900 International Centre for Theoretical Physics, Trieste (Italy).
LOW-ENERGY HADRONIC INTERACTIONS BEYOND THE CURRENT ALGEBRA APPROACH
A. N. Ivanov (Saint Petersburg Technical Univ., Russia.), N. I. Troitskaya (Saint Petersburg Technical Univ., Russia.), and M. Nagy Jun. 1993 11 p Limited Reproducibility: More than 20% of this document may be affected by microfiche quality
(DE94-602600; IC-93/145) Avail: CASI HC A03 (US Sales Only)

The new low-energy AP(sup 3)-interaction, which is produced by convergent box-constituent-quark-loop diagrams, is obtained within chiral perturbation theory at the quark level (CHPT)(sub q) with linear realization of chiral U(3) x U(3) symmetry. Its contributions to processes of low-energy interactions of low-lying mesons are investigated. The new interaction goes beyond the framework of the low-energy current algebra approach and of the effective chiral Lagrangians with linear realization of chiral symmetry, constructed at the hadronic level. DOE

N94-26926# Florida Univ., Gainesville.
INTERNATIONAL JOURNAL OF QUANTUM CHEMISTRY. QUANTUM CHEMISTRY SYMPOSIUM NUMBER 27: PROCEEDINGS OF THE INTERNATIONAL SYMPOSIUM ON ATOMIC, MOLECULAR, AND CONDENSED MATTER THEORY AND COMPUTATIONAL METHODS
Per-Olov Lowdin, N. Y. Ohrn, John R. Sabin, and Michael C. Zerner 20 Mar. 1993 860 p Proceedings held in St. Augustine, FL, 13-20 Mar. 1993
(Contracts N00014-93-1-0343; DAAH04-93-G-0072)
(AD-A274352) Avail: CASI HC A99/MF A10

The topics covered at the 33rd annual Sanibel Symposium, organized by the faculty and staff of the Quantum Theory Project of the University of Florida, and held March 13 - 20, 1993, include advanced scientific computing, interaction of photons and matter, quantum molecular dynamics, electronic structure methods, polymeric systems, and quantum chemical methods for extended systems. DTIC

N94-26929 Melbourne Univ., Parkville (Australia). School of Physics.
DISINTEGRATION OF (C60) BY Xe ION IRRADIATION
R. Kalish (Technion - Israel Inst. of Tech., Haifa.), A. Samoiloff (Technion - Israel Inst. of Tech., Haifa.), A. Hoffman (Technion - Israel Inst. of Tech., Haifa.), C. Uzan-Saguy (Technion - Israel Inst. of Tech., Haifa.), S. Prawer, and D. McCulloch (Royal Melbourne Inst. of Tech., Australia.) 1993 13 p Limited Reproducibility: More than 20% of this document may be affected by microfiche quality
(DE94-601913; UM-P-93/26) Avail: CASI HC A03 (US Sales Only)

The changes in resistivity of fullerene (C60) films subject to 320 keV Xe ion irradiation are investigated as a function of ion dose. From a comparison of this dependence with similar data on other Xe irradiated C containing insulating materials and with data on C implanted fused quartz, it is concluded that upon ion impact, C60 clusters completely disintegrate. This disintegration releases about 60 C atoms which disperse amongst the remaining intact C60 spheres giving rise to hopping conductivity between isolated C atoms. DOE

N94-26938# Fermi National Accelerator Lab., Batavia, IL.
D0 RESULTS ON SEARCHES FOR THE TOP QUARK
S. Abachi Sep. 1993 10 p Presented at the 5th International Symposium on Heavy Flavor Physics, Montreal, 6-10 Jul. 1993
(Contract DE-AC02-76CH-03000)
(DE94-003361; FNAL/C-93/287; CONF-9307143-4) Avail: CASI HC A02/MF A01

A search for creation of the top quark in p bar-p collisions was performed at square root of s = 1.8 GeV at Tevatron, Fermilab. Production of t bar-t followed by top decay to W + b quark is assumed. The decay channels were searched for with both W's decaying leptonically, and with one W decay to an electron and the other to quarks. A preliminary report on the status of one interesting event is presented. By combining the results from the ee and e mu channels, a lower top mass limit of 99 GeV on the 95% confidence level is obtained. DOE

N94-26942 Flinders Univ., Adelaide (Australia).
CALCULATION OF ELECTRON-POTASSIUM SCATTERING
I. Bray, D. V. Fursa, and I. E. McCarthy Dec. 1992 26 p Limited Reproducibility: More than 20% of this document may be affected by microfiche quality
(DE94-601812; ESM-50) Avail: CASI HC A03 (US Sales Only)

Elastic through to 7(sup 2)F differential, integrated, and total cross sections for electrons scattering from the ground state of potassium atoms are presented. Spin asymmetries, L perpendicular for singlet, triplet, and spin-averaged scattering, optical excitation cross sections, and various photon polarization observables for elastic channel and 4(sup P) channel are also discussed. These are calculated using the Coupled-Channel Optical method. A total of 17 target states are explicitly coupled with the effect of the continuum included in the first 6 of these. The calculations have been performed at a range of energies from 1 to 100 eV. The results are generally in good agreement with available experiment data. It was found that the effect of the inclusion of the continuum is most evident in calculating spin asymmetries and singlet spin-resolved L parameter. DOE

N94-26943 Flinders Univ., Adelaide (Australia).
SPIN ASYMMETRY IN RESONANT ELECTRON-HYDROGEN ELASTIC SCATTERING
I. E. McCarthy and Bo Shang Feb. 1993 7 p Limited Reproducibility: More than 20% of this document may be affected by microfiche quality
(DE94-601813; ESM-52) Avail: CASI HC A02 (US Sales Only)

Differential cross sections and asymmetries at 90 deg and 30 deg are calculated for electron-hydrogen elastic scattering over the energies of the lowest (sup 1)S and (sup 3)P resonances using a nine-state coupled-channels calculation with and without continuum effects, which are represented by an equivalent-local polarization potential. The polarization potential improves agreement with experiment in general for the spin-averaged cross sections. It is suggested that continuum effects would be critically tested by asymmetry measurement at 30 deg over the (sup 1)S resonance. DOE

N94-26944 Flinders Univ., Adelaide (Australia).
CALCULATION OF TOTAL CROSS SECTIONS FOR ELECTRON AND POSITRON SCATTERING ON SODIUM AND POTASSIUM
I. E. McCarthy, K. Ratnavelu, and Y. Zhou Feb. 1993 7 p Limited Reproducibility: More than 20% of this document may be affected by microfiche quality
(DE94-601814; ESM-53) Avail: CASI HC A02 (US Sales Only)

Total cross sections for electron and positron scattering on sodium and potassium are calculated at various energies and compared with experiment. The method use is the coupled-channels-optical method with the equivalent-local polarization potential, which takes all channels into account. For electrons the calculations are checked by comparison with coupled-channels-optical calculations using a detailed polarization potential that makes only one approximation, that of weak coupling in the ionization space. The polarization potential for positrons includes effects of ionization and positronium formation. DOE

N94-26945 Flinders Univ., Adelaide (Australia).
CALCULATIONS OF ASYMMETRIES IN ELECTRON-ALKALI SCATTERING
I. Bray May 1993 5 p Limited Reproducibility: More than 20% of this document may be affected by microfiche quality
(DE94-601816; ESM-55) Avail: CASI HC A01 (US Sales Only)

In this work it is shown that in order to calculate spin asymmetries at projectile energies above the ionization threshold, the target continuum needs to be taken into account. However, this does not imply that in the experiment, intermediate excitation into the continuum plays a major role. Rather, any theory, such as the standard close-coupling method, that does not allow for electron flux to be in all open channels is likely to have difficulty in reproducing the measured spin asymmetries. DOE

N94-26947 International Atomic Energy Agency, Vienna (Austria). Atomic and Molecular Data Unit.
INTERNATIONAL BULLETIN ON ATOMIC AND MOLECULAR DATA FOR FUSION. NO. 46
J. Botero, ed. Jun. 1993 208 p Limited Reproducibility: More than 20% of this document may be affected by microfiche quality
(DE94-601818; INIS-mf-4754(no-46); IBAMD-46) Avail: CASI HC A10 (US Sales Only)

The bulletin is published by the International Atomic Energy Agency to provide atomic and molecular data relevant to fusion research and technology. In Part 1 the indexed papers are listed separately for (1) structure and spectra (energy levels, wavelengths; transition probabilities, oscillator strengths; interatomic potentials); (2) atomic and molecular collisions (photon collisions; electron collisions; heavy-particle collisions; homonuclear sequences; isoelectronic sequences); and (3) surface interactions (sputtering; chemical reactions; trapping and detrapping; surface damage; blistering, flaking; secondary electron emission). Part 2 contains the bibliographic data for the above listed topics and for high energy laser- and beam-matter interaction; interaction of atomic particles with fields. The atomic and molecular data needs in fusion research, as identified during the IAEA Consultants' Meeting on 'Atomic and Molecular Database for Hydrogen Recycling and Helium Exhaust from Fusion Reactors', June 1992, Vienna, are listed, covering (1) atomic and molecular collision processes, (2) particle-surface interaction processes, and (3) the status of data bases on atomic and molecular data and plasma-surface interactions.

News on the ALADDIN (A labelled Atomic Data INterface) system is provided. Finally, a list of evaluated atomic and molecular data bases is provided.
DOE

N94-26949# City Coll. of the City Univ. of New York, NY. Dept. of Physics.
EXPERIMENTAL INVESTIGATIONS OF STRONG INTERACTION IN THE NON-PERTURBATIVE QCD REGION
S. J. Lindenbaum and S. Samuel Sep. 1993 26 p
(Contract DE-FG02-92ER-40698)
(DE94-001178; DOE/ER-40698/2) Avail: CASI HC A03/MF A01

A critical investigation of non-perturbative QCD require investigating glueballs, search for a Quark Gluon Plasma (OGP), and search for strangelets. In the glueball area the data obtained (E-881) at 8 GeV/c were analyzed for pi(sup -) + p yields phi(phi)n (OZI forbidden), (phi)K(sup +)K(sup -)n (OZI allowed), K(sup -)p yields phi(phi)((Lambda)(Sigma)) (OZI allowed), and (bar p)p yields phi(phi)pi(sup 0) (OZI forbidden), (phi)K(sup +)K(sup -)pi(sup 0) (OZI allowed). By comparing the OZI forbidden (glueball filter reactions) with the OZI allowed and previous 22 GeV/c pi(sup -)p yields phi(phi)n or (phi)K(sup +)K(sup -)n data a further critical test of the so far unsuccessfully challenged hypothesis that our g(sup T)(2010), g(sub T')(2300) and g(sub T")(2340) all with I(sup G)J(sup PC) = 0(sup +)2(sup ++) are produced by 1-3 2(sup ++) glueballs will be made. In the QGP search with a large-solid-angle TPC a good Xi signal was observed. The ratio of Xi to single strange quark particles such as lambda is a better indication of strangeness enhancement in QGP formation. The data indicate enhancement by a factor approximately equal to 2 over cascade model (corrected to observed strangeness) predictions, but it is definitely far from conclusive at this stage since the result is model dependent. Double lambda topologies of the type needed to discover light strangelets in the nanosecond lifetime region were found. In addition, research has been accomplished in three main areas: bosonic technicolor and strings, buckministerfullerene C(sub 60) and neutrino oscillations in a dense neutrino gas. DOE

N94-27011# Harvard Univ., Cambridge, MA. Dept. of Physics.
ANTIPROTON STUDIES IN PENNING TRAPS Final Report, 1 Jul. 1988 - 30 Sep. 1993
Gerald Gabrielse 30 Sep. 1993 19 p
(Grant AF-AFOSR-0306-88)
(AD-A274250; AFOSR-93-0889TR) Avail: CASI HC A03/MF A01

Antiprotons are produced in giant accelerators with typical energies measured in GeV. In the unique LEAR facility of CERN, such antiprotons are decelerated to and cooled at an energy of 5 MeV. The experiments described in this proposal made it possible to slow, store, and study antiprotons at dramatically lower energies, 10(exp 10) times lower than ever realized before. Antiprotons from LEAR are slowed to several KeV by sending them through a metal degrader window of a precisely chosen thickness. They are then captured in a specially designed Penning trap. Once inside the trap, collisions with extremely cold electrons dramatically lower the energy of the trapped antiprotons to thermal equilibrium at 4.2 K. Antiprotons have now been stored for months in thermal equilibrium at 4.2 K, which requires a vacuum better than 5 x 10(exp -17) Torr. The first precision measurement at this new, low energy frontier is a comparison of the inertial masses of the antiproton and proton at an accuracy more than 1000 times greater than was achieved in earlier experiments. The accurate mass spectroscopy is greatly facilitated by the invention of self-shielding superconducting solenoid system which has likely applications to MRI imaging. DTIC

N94-27050# Stanford Linear Accelerator Center, CA.
THE CHALLENGES OF EXCLUSIVE PROCESSES IN QCD
S. J. Brodsky Sep. 1993 8 p Presented at the Conference on Exclusive Reactions At High Momentum Transfer, Elba, Italy, 24-26 Jun. 1993
(Contract DE-AC03-76SF-00515)
(DE94-003429; SU-SLAC-PUB-6356; CONF-9306260-4) Avail: CASI HC A02/MF A01

This report reviews some of the outstanding theoretical and experimental issues confronting the application of perturbative quantum chromodynamics to large momentum transfer exclusive reactions. DOE

N94-27133# California Univ., Los Angeles. Dept. of Physics.
COMPUTER SIMULATIONS OF RADIATION GENERATION FROM RELATIVISTIC ELECTRON BEAMS Final Report, 1 Oct. 1992 - 30 Sep. 1993
Anthony T. Lin 30 Sep. 1993 56 p
(Grant AF-AFOSR-0006-91)
(AD-A274139; AFOSR-93-0892TR) Avail: CASI HC A04/MF A01

This is the Final Technical Report on work performed under the support of the Air Force Office of Scientific Research under Grant AFOSR 91-0006 for the period 1 Oct. 1992 to 30 Sep. 1993. The objective of this work was to carry out basic physics research on the generation of coherent, tunable radiation from relativistic electron beams and exploring means of improving performance. DTIC

N94-27199 Rutherford Appleton Lab., Chilton (England).
CHARMONIUM PHYSICS AT A TAU-CHARM FACTORY
T. Barnes Sep. 1993 15 p The Third Workshop on a Tau-Charm Factory held in Marbella, Spain, 1-6 Jun. 1993 See also PB93-204485 Prepared in cooperation with Oak Ridge National Lab., TN, Tennessee Univ., Knoxville, TN, and DOE, Washington, DC
(Contract DE-AC05-84OR-21400)
(PB94-124344; RAL-93-065) Avail: Issuing Activity (National Technical Information Service (NTIS))

This talk summarizes the status of the charmonium system. Particular emphasis is given to the outstanding problems in QCD spectroscopy which a tau charm factory can address. NTIS

N94-27250# Gosudarstvennyi Komitet po Ispolzovaniyu Atomnoi Energii, Serpukhov (USSR).
STUDY OF THE PROCESS (PI)(SUP -)A(YIELDS)(PI)(SUP -)(ETA)'(ETA)A AT THE MOMENT 36 GeV/c
S. I. Bityukov, G. V. Borisov, N. K. Vishnevskij, E. V. Vlasov, Yu. P. Gouz, R. I. Dzhelyadin, A. M. Zaitsev, Yu. M. Ivanyushenkov, A. N. Karyukhin, and I. A. Kachaev et al 1992 13 p
(DE93-634530; IHEP-OEIUNK-92-37) Avail: CASI HC A03/MF A01 (US Sales Only)

Reaction pi(-)A yields pi (-)(eta)'(eta)A has been studied at 36 GeV/c beam momentum. The new state near the threshold of pi(-)(eta)'(eta) decaying through the pi(-)f(sub0)(1590) has been observed. The combined analysis of two channels pi(-)(eta)'(eta) and pi(-)(eta)'(eta) gives for branching ratio: Br(X yields pi(-)(eta)'(eta)) /Br(X yields pi(-)(eta)(eta)) = 029 +/- 0.07. DOE

N94-27258 Concordia Univ., Montreal (Quebec). Dept. of Physics.
SPECTROSCOPY AND STRONG DECAYS OF BARYONS Ph.D. Thesis
Bao N. Tran Mar. 1989 191 p
(ISBN-0-315-49073-X; CTN-94-60972) Copyright Avail: Micromedia Ltd., Technical Information Centre, 240 Catherine Street, Suite 305, Ottawa, Ontario, K2P 2G8, Canada HC/MF

A quark model, suggested by quantum chromodynamics, is used to calculate the entire spectrum of baryons, containing u, d, s, c, and b quarks. A short-range Coulomb potential is used, together with a long-range linear potential, modified by a harmonic oscillator potential. This combination leads to a good description of the masses of both positive and negative parity baryons, based on the five quark masses and four additional parameters related to the chosen potential. The quark pair creation model of Le Yaouanc et al. is then used to study the decay processes N, Delta yielding N pi and Lambda, Sigma yielding NK(-). The pair creation strength gamma is replaced by k raised to the gamma. Beside the meson radius, this is the only parameter of the model. The result is in good agreement with experimental data and confirms the assignment of baryons in the mass calculation. Author (CISTI)

N94-27259 McGill Univ., Montreal (Quebec). Dept. of Physics.
FINDING THE MISSING PIECES OF THE STANDARD MODEL Ph.D. Thesis
David Atwood Jun. 1989 175 p
(ISBN-0-315-57174-8; CTN-94-60973) Copyright Avail: Micromedia Ltd., Technical Information Centre, 240 Catherine Street, Suite 305, Ottawa, Ontario, K2P 2G8, Canada HC/MF

The standard model is discussed in general and the predicted, but as yet unobserved, Higgs boson and top quark described. Detection of a top

quark at electron positron colliders and hadron colliders is considered for top-quark mass of under 80 GeV. The detection of the Higgs boson is considered at the Z peak in electron positron annihilation for Higgs-boson masses equal to or less than 60 GeV, as well as in the continuum 100-200 GeV (intermediate mass range). For this range of the Higgs-boson mass, consideration is also given to its detection at the Superconducting Supercollider through the tau-lepton decay mode. A dispersive approach is considered for Higgs boson with large mass, equal to or greater than 500 GeV, in order to estimate nonperturbative self interaction effects.
Author (CISTI)

N94-27260 McGill Univ., Montreal (Quebec). Dept. of Physics.
A STUDY OF THE GLOBAL PROPERTIES OF HADRONIC MATTER AT LARGE DENSITIES Ph.D. Thesis
Francois Lamarche 14 May 1989 201 p
(ISBN-0-315-57234-5; CTN-94-60974) Copyright Avail: Micromedia Ltd., Technical Information Centre, 240 Catherine Street, Suite 305, Ottawa, Ontario, K2P 2G8, Canada HC/MF

A study is presented of the properties of nuclear matter under extreme conditions of density and temperature, using collisions of heavy nuclei measured in the NA34 experiment at the CERN super proton synchrotron. The emphasis is on the study of the variation of the properties of average central collisions with the sizes of the colliding nuclei. The projectiles used are 200 GeV protons, 60 and 200 GeV/nucleon O-16 nuclei, and 200 GeV/nucleon S-32 nuclei. The targets are thin disks of Al, Cu, Ag, W, Pt, Pb, and U nuclei. The energy density achieved in these collisions, on the order of 10 GeV/fm(exp 3), is a necessary but not sufficient condition to create a plasma of quarks and gluons. The appropriateness of a hydrodynamic description of the data is examined. From the observation of the work done by the hydrodynamic forces, constraints are obtained on the properties of the hypothetical plasma. Author (CISTI)

N94-27266 University of Western Ontario, London.
A JET CALCULUS APPROACH INCLUDING COHERENCE EFFECTS AND THE ASSOCIATED PROBLEM OF MOMENT INVERSION Ph.D. Thesis
Kumbakonan S. Sowmyanarayanan May 1989 229 p
(ISBN-0-315-51715-8; CTN-94-60977) Copyright Avail: Micromedia Ltd., Technical Information Centre, 240 Catherine Street, Suite 305, Ottawa, Ontario, K2P 2G8, Canada HC/MF

The production of colorless clusters (CC) in high-energy e+ e- collisions in the framework of perturbative quantum chromodynamics (QCD) is studied using jet calculus. This approach enables treatment of the cascade of successively generated partons initiated by the virtual photon in terms of quantum mechanical probabilities. Special attention is given to the presence of soft gluons in the cascade, which produce non-negligible quantum mechanical interference contributions. The Crespi-Jones (CJ) approach, ideally suited for studying gluons in a CC, is used throughout. Mueller's criterion of angle-ordered gluon emission is invoked to redefine the evolution variable in the conventional CJ equations to account for soft gluon effects. The method of moments is used to solve the CJ equations. Results are presented in both moment space and longitudinal momentum (x) space. The zeroth moment of the CC distribution in gluon jets is evaluated under certain asymptotic approximations and results for low x are shown to be in fair agreement with other work. Several new algorithms for numerical inversion of moments are presented which are relevant to the study of the low-x region in QCD. Finally, a method based on Gaussian quadrature and singular value decomposition is discussed. The methods are tested on a wide variety of trial functions. Author (CISTI)

N94-27310 Concordia Univ., Montreal (Quebec). Dept. of Chemistry and Biochemistry.
MOLECULAR DYNAMICS SIMULATION AND CRYSTAL-FIELD THEORY: PREDICTING THE OPTICAL SPECTRA AND STRUCTURE OF RARE-EARTH DOPED INORGANIC GLASSES Ph.D. Thesis
Guy Cormier Apr. 1993 242 p
(ISBN-0-315-84679-8; CTN-94-61085) Copyright Avail: Micromedia Ltd., Technical Information Centre, 240 Catherine Street, Suite 305, Ottawa, Ontario, K2P 2G8, Canada HC/MF

Simulated structural models were developed for two doped inorganic glasses, Na2O-2SiO2-Eu(III) and SiO2-Eu(III). The simulated structure of the base glasses and the local environment of the doped Eu(III) ions were investigated with the help of radial distribution functions, cumulative distribution functions, and bond angle distributions of the various atomic species found in both glasses. A successful validation of the simulated structural model of the Na-Si-Eu glass was performed through a comparison between room temperature absorption and broadband emission spectra of an experimental glass and calculated absorption and emission spectra of the simulated glass. The validation culminated in creation of an indirect link between the simulated model and the corresponding glass, allowing investigation of various spectral properties of rare-earth doped glasses. It is concluded that rare-earth environments are composed of a continuous distribution of local fields which satisfy energetic bonding requirements of the Eu(III) ions. Overall electrostatic and covalent energy of the individual sites has the greatest influence on the electronic spectra. An experimental technique, dilution narrowed laser spectroscopy, was also examined. This technique could eventually lead to the observation of the optical spectrum of isolated rare-earth ions doped in glass fibers. Author (CISTI)

N94-27333 York Univ., Toronto (Ontario).
A RELATIVISTIC QUARK MODEL Ph.D. Thesis
Tao Zhang Sep. 1990 162 p
(ISBN-0-315-60926-5; CTN-94-60981) Copyright Avail: Micromedia Ltd., Technical Information Centre, 240 Catherine Street, Suite 305, Ottawa, Ontario, K2P 2G8, Canada HC/MF

Color singlet bound states of quark-antiquark systems, which incorporate transverse gluon degrees of freedom, are studied by means of a variational principle within the framework of relativistic quantum field theory. An effective Hamiltonian for quark-antiquark systems which incorporates the effects of a Coulomb plus linear potential and gluon exchange is constructed. Momentum-space integral eigenvalue equations for the bound states are obtained by using a variational principle. The equations are decoupled within an approximation and then solved numerically. Both the variational and basis state expansion methods are used to solve the equations. The method is applied to the charmonium and bottomonium systems. A good fit to the experimental data is obtained. Author (CISTI)

N94-27337# Tokyo Science Univ. (Japan). Inst. for Solid State Physics.
TECHNICAL REPORT OF ISSP. SER. A, NO. 2683: ITINERANT CHARACTER OF 5f ELECTRONS IN UNi2Ga
Tetsuo Ohama, Hiroshi Yasuoka, Yasuomi Maeda, Toshiro Takabatake, and Hironobu Fujii Jun. 1993 15 p
(ISSN 0082-4798)
(JTN-94-80569) Avail: CASI HC A03/MF A01

NMR (Nuclear Magnetic Resonance) and NQR (Nuclear Quadrupole Resonance) measurements were made for Pauli paramagnetic UNi2Ga. The temperature dependence of the Knight shift and the nuclear relaxation rate 1/T(sub 1) at the Ga sites were measured between 4.2 K and 290 K. Fermi liquid behavior, that is, temperature-independent Knight shift and 1/T(sub 1) proportional to temperature, was observed over the measured temperature range. A quantitative analysis suggests that the enhancement of the wave-vector dependent susceptibility chi(q) is fairly localized near q approximately zero in the q space. Author (NASDA)

N94-27338# Tokyo Univ. (Japan). Inst. for Solid State Physics.
TECHNICAL REPORT OF ISSP. SER. A, NO. 2684: WAVELENGTH DEPENDENCE OF NONSEQUENTIAL DOUBLE IONIZATION IN He
Kiminori Kondo, Akihiko Sagisaka, Taichiro Tamida, Yasuo Nabekawa, and Shuntaro Watanabe Jun. 1993 14 p
(ISSN 0082-4798)
(JTN-94-80570) Avail: CASI HC A03/MF A01

An enhancement of He(2+) yield near the appearance intensity was not observed by linearly polarized KrF laser light (248 nm), whereas a significant enhancement was observed by linearly polarized Ti:sapphire laser light (745 nm). These results are consistent with the quasi-static model proposed by Corkum. Author (NASDA)

N94-27348 Amsterdam Univ. (Netherlands).
HIGH GAS-EFFICIENCY HYDROGEN NEGATIVE ION SOURCES Ph.D. Thesis
R. M. A. Heeren 4 Dec. 1992 107 p Prepared in cooperation with Stichting voor Fundamenteel Onderzoek der Materie, Amsterdam, Netherlands and Inst. voor Atoom en Molecuulfyusica; sponsored by Nederlandse Organisatie voor Wetenschappelijk Onderzoek, The Hague,

Netherlands and Euratom, Brussels, Belgium Limited Reproducibility: More than 20% of this document may be affected by microfiche quality
(PB93-232163) Avail: CASI HC A06

The work described in the thesis was undertaken to gain insight into processes contributing to the formation of hydrogenous negative ions in a barium surface conversion source and to optimize the gas-efficiency of such a ion source. The interest in these negative ion source originates from the need for additional heating and current drive of next generation fusion plasmas by 1-1.3 MeV D(sup 0) injection. These high energy neutral deuterium beams can only be produced by the neutralization of fast negative deuterium ions. In chapter two an extensive calculation of the magnetic configuration necessary for a good confinement of the source plasma of the surface conversion source is presented. Chapter three examines the build up of the hydrogen and deuterium concentration in the barium surface more closely. In chapter four, measurements on the energy distributions of surface produced negative ions clearly show a substantial amount of negative ions leaving the surface with an energy up to a value approaching the energy of the incoming particles. In chapter five an experiment is presented which can improve both the gas-efficiency and negative ion output of the driver region of a high power density multicusp volume source. NTIS

N94-27399 McGill Univ., Montreal (Quebec). Dept. of Physics.
OMEGA OMEGA AND RHO+ RHO- PRODUCTION IN TWO PHOTON INTERACTIONS AT ARGUS Ph.D. Thesis
George Tsipolitis 1990 155 p
(ISBN-0-315-63748-X; CTN-94-60966) Copyright Avail: Micromedia Ltd., Technical Information Centre, 240 Catherine Street, Suite 305, Ottawa, Ontario, K2P 2G8, Canada HC/MF

The two-photon reactions gamma gamma yielding 2pi+ 2pi- 2pi0 and gamma gamma yielding pi+ pi- pi0 pi0 have been studied by using the ARGUS detector at the e+e- storage ring DORIS 2 at the Deutsches Elektronen Synchrotron. In the 2pi+ 2pi- 2pi0 final state, the production of omega-mesons is observed and in particular the reaction gamma gamma yielding omega omega is seen for the first time. The cross section for gamma gamma yielding omega omega is found to have an enhancement at around 19 GeV/c-squared of about 12 nb. The topological cross sections for the reactions gamma gamma yielding 2pi+ 2pi- 2pi0 and gamma gamma yielding omega pi+ pi- pi0 are also measured. The production of charged rho-mesons is observed in the pi+ pi- pi0 pi0 final state. The cross section for the reaction gamma gamma yielding rho+ rho- is measured for the first time. The cross section did not show a threshold enhancement similar to that found in the reaction gamma gamma yielding rho0 rho0 and is about a factor of four smaller. A spin parity analysis of the rho+ rho- system shows that the cross section is dominated by the two amplitudes J(P) = 0+ and J(P) = 2+ with helicity 2. Author (CISTI)

N94-27400 Toronto Univ. (Ontario).
OBSERVATION OF EXCITED CHARMED MESONS Ph.D. Thesis
Scott Robert Menary 23 Aug. 1989 120 p
(ISBN-0-315-57014-8; CTN-94-60967) Copyright Avail: Micromedia Ltd., Technical Information Centre, 240 Catherine Street, Suite 305, Ottawa, Ontario, K2P 2G8, Canada HC/MF

Using a tagged photon spectrometer and a high energy photon beam, Fermilab experiment E691 was able to collect a large sample of fully reconstructed charmed particles. The resulting data set is used to search for P-wave charmed mesons, called D**s. Evidence is found for a state of mass 2459 MeV/c-squared and width 21 MeV/c-squared, which decays to the mesons D+ pi-. The statistical significance of the signal is measured to be greater than five standard deviations. Various arguments suggest that the state is the J(P) = 2+ P-wave charmed meson but neither the spin nor parity is measured directly. The fraction of D+ coming from D**0(2459) is .07 + or - .02. Also, the D**0(2420) yielding D*+ pi- decay observed previously in e+e- experiments is confirmed. Finally, a four standard deviation signal is observed in the D0 pi+ spectrum. This is interpreted as evidence for the decay of the charged counterpart of the D**0(2420) to D*0 pi+, with the neutral from the D*0 decay going unobserved. The mass and width of the state are 2443 MeV/c-squared and 41 MeV/c-squared, respectively. The fraction of D*+ coming from D**0(2420) and the fraction of D*0 coming from the charged counterpart of the D**0(2420) are measured to be consistent. Author (CISTI)

N94-27402 Alberta Univ., Edmonton. Dept. of Physics.
WEAK HADRONIC DECAYS OF HEAVY FLAVOR MESONS Ph.D. Thesis
Nita Sinha 1989 195 p
(ISBN-0-315-55542-4; CTN-94-60969) Copyright Avail: Micromedia Ltd., Technical Information Centre, 240 Catherine Street, Suite 305, Ottawa, Ontario, K2P 2G8, Canada HC/MF

A coupled multichannel calculation was performed for various two-body hadronic decays of charmed mesons, with particular attention to the role of the weak annihilation term. A two channel calculation of Cabibbo angle favored D(S)+ yielding vector pseudoscalar meson (VP) results in a satisfactory fit to experimental data. An extension of this to include the omega pi+ mode also satisfies the recent experimental limit. For Cabibbo angle favored D-VP decays, a three channel calculation is performed, coupling the K* pi, K rho and K0 phi states in isospin 1/2. For the Cabibbo angle favored D/D(s) yielding double vector meson decay modes, a similar treatment is followed. Cabbibo angle suppressed modes are also studied in a coupled channel formalism. The D+ yielding rho0 pi+ branching ratio can be fitted in this approach, whereas its un-unitarized amplitude yields a very small value. Some of the other models proposed to study heavy flavor decays are also discussed. An attempt is made to incorporate the effect of final state interactions. The possibility of large D(s)+ yielding eta pi+, eta' pi+ branching ratios is investigated in a theoretical framework. Finally, the effect of final state scattering phases on two-body B decays are studied in view of a possible measurement of the mixing angle from the noncharmed, nonstrange hadronic decays of the bottom mesons. Author (CISTI)

N94-27565# Wisconsin Univ., Madison.
AN ANALYSIS OF MONOJET DATA IN p(BAR-p) COLLISIONS AT SQUARE ROOT OF s EQUAL TO 1.8 TEV Ph.D. Thesis
R. Markeloff 1992 179 p
(Contract DE-AC02-76ER-00881)
(DE94-001822; DOE/ER-00881/T3) Avail: CASI HC A09/MF A02

An analysis is presented of events with a single jet and significant missing transverse energy selected from 4.7 pb(exp -1) of data collected at the Fermilab Tevatron with the CDF detector. The goal is to identify events of the type p bar-p yields Z(sup 0) + jet; Z(sup 0) yields nu bar-nu. Event selection and backgrounds are discussed. The number of observed monojet events is compared to the number of observed Z(sup 0) yields e(+) e(-) events in which the Z(sup 0) is accompanied by a jet. The number of light neutrino species is measured to be N(sub nu) = 2.2 +/- 1.5 and an upper limit on the number of neutrino species is placed at N(sub nu) less than five (90% C.L.). DOE

N94-27604# Duke Univ., Durham, NC. Dept. of Physics.
QUANTUM CHROMODYNAMICS AND NUCLEAR PHYSICS AT EXTREME ENERGY DENSITY
B. Mueller 15 May 1993 56 p
(Contract DE-FG05-90ER-40592)
(DE94-004418; DOE/ER-40592/3) Avail: CASI HC A04/MF A01

This report discusses research in the following areas: Hadron structure physics; relativistic heavy ion collisions; finite-temperature QCD; real-time lattice gauge theory; and studies in quantum field theory. DOE

N94-27620# Argonne National Lab., IL.
DOUBLE EXCITATION OF He AND H(-) BY FAST PROTON AND ANTI-PROTON IMPACT
Ken-Ichi Hino (University of Electro-Communications, Chofu, Japan.), K. Moribayashi, M. Nagase (University of Electro-Communications, Chofu, Japan.), and M. Matsuzawa (University of Electro-Communications, Chofu, Japan.) 1993 11 p
(Contract W-31-109-eng-38)
(DE94-004581; ANL/ER/PP-77881) Avail: CASI HC A03/MF A01

A theoretical investigation has been made on the double excitation processes of He and H(-) by fast proton and anti-proton impact in the MeV/u-energy region. The cross sections are calculated by use of both the close-coupling and the perturbation expansion methods, and the wave functions of target atoms are generated based on the hyperspherical coordinate method. The excitation to the 2p(sup 2) (sup 1)D(sup e) state of H(-) by anti-proton impact is dominant by about three times in comparison with that by proton impact at the incident energy of 0.1 MeV/u. The spectral shape of an ejected electron from the 2s2p (sup 1)p(sup o) state of H(-) at the incident energy of 1.5 MeV/u is consistent with the line profile of the H(-) photodetachment observed by Bryant et al. DOE

N94-27629 International Centre for Theoretical Physics, Trieste (Italy).
ALL-COUPLING POLARON GROUND STATE ENERGY IN D-DIMENSION
G. Ganbold and G. V. Efimov (Joint Inst. for Nuclear Research, Dubna, USSR.) Aug. 1993 25 p Limited Reproducibility: More than 20% of this document may be affected by microfiche quality
(DE94-603666; IC-93/228) Avail: CASI HC A03 (US Sales Only)

An extension of the Feynman's path integral treatment for polaron ground state energy to an electron moving in D-dimension is obtained for the entire range of electron-phonon coupling constant. The method of equivalent representation of functional integrals was used. In the approach, the leading term of polaron self-energy gives an upper bound of polaron ground state energy and represents an improvement over the known Feynman's variational estimation. A result of this paper is the obtained all-coupling second correction to the leading term, which slightly lowers the polaron energy. Obtained results are in good agreement with known published data. DOE

N94-27631 International Centre for Theoretical Physics, Trieste (Italy).
GEOMETRICAL RESONANCES IN THE NYQUIST NOISE SPECTRUM FOR BALLISTIC CONDUCTORS
O. M. Bulashenko and V. A. Kochelap Aug. 1993 16 p Limited Reproducibility: More than 20% of this document may be affected by microfiche quality
(DE94-603668; IC-93/240) Avail: CASI HC A03 (US Sales Only)

The equilibrium current fluctuations (thermal noise) for low-dimensional degenerate electron gas (one dimensional, two dimensional) bounded in a narrow (short) channel, or in a thin film (three dimensional) have been calculated within the semiclassical Boltzmann-equation approach. The analytical formulas for the autocorrelation functions have been derived for the complete degenerate case. The noise spectrum under ballistic regime of electron transport was found to be non-Lorentzian with decreased zero-frequency plateau and geometrical resonances at high frequencies depending on the size of the channel. The formulas for the conductivity (conductance) derived from the obtained analytical expressions for C(sub 1)(t) are exactly identical to the known formulas, e.g., to Fuchs size-effect formula for the three dimensional case. DOE

N94-27681# Joint Inst. for Nuclear Research, Dubna (USSR). Lab. of Theoretical Physics.
PROTON ELECTROMAGNETIC FORM FACTOR NEAR THE PROTON-ANTIPROTON THRESHOLD AND QUASINUCLEAR BOUND STATE
G. V. Meshcheryakov and V. A. Meshcheryakov 1993 8 p
(DE94-606458; JINR-E-2-93-88) Avail: CASI HC A02/MF A01 (US Sales Only)

The influence of the PP-bar-state in the unitarity condition on the behavior of the proton form factor in the time-like region is considered. The result obtained earlier on existence of a quasinuclear bound state in the elastic PP-bar-channel is used to estimate its contribution to electromagnetic form factor of the proton. The obtained expression well describes the high precision data of the experiment PS-170 performed at LEAR at CERN and indicates the quantum numbers of the quasinuclear PP-bar bound state near threshold. DOE

N94-27682# Joint Inst. for Nuclear Research, Dubna (USSR). Lab. of Theoretical Physics.
NEUTRON-NEUTRON SCATTERING: POSSIBILITY OF IN-BEAM EXPERIMENT
Yu. N. Pokotilovskij and G. G. Takhtamyshev 1992 7 p
(DE94-606459; JINR-E-3-92-417) Avail: CASI HC A02/MF A01 (US Sales Only)

The possibility experiment on a direct measurement of the neutron-neutron scattering length is discussed, consisting in registration of both neutrons after their scattering in a collimated thermal neutron beam from the reactor. Some results of the Monte-Carlo simulation of the experiment are given and peculiarities and advantages of this approach are discussed and compared with the earlier suggested one. DOE

N94-27684 McGill Univ., Montreal (Quebec). Dept. of Physics.
PI PLUS PI MINUS GAMMA AND K+ K- PRODUCTION IN TWO PHOTON COLLISIONS AT ARGUS Ph.D. Thesis
Kenneth William McLean Jun. 1990 236 p
(ISBN-0-315-63598-3; CTN-94-60964) Copyright Avail: Micromedia Ltd., Technical Information Centre, 240 Catherine Street, Suite 305, Ottawa, Ontario, K2P 2G8, Canada HC/MF

The production of the final states K+K- and eta' yielding pi-plus pi-minus in two-photon collisions has been measured using the ARGUS detector. The product of the two-photon width of the eta' meson and the (eta' yielding rho gamma) branching ratio has been determined. The topological cross section for the production of charged kaon pairs in two-photon collisions has been measured and the two-photon widths and interference parameters for the tensor mesons f2(1270), a2(1320), and f2'(1525) have been extracted. The helicity structure assumed for the K+K- continuum contribution has a significant effect on the result. Upper limits have been obtained for the two-photon widths of the glueball candidate states f2(1720) and X(2230). Author (CISTI)

N94-27689# Rensselaer Polytechnic Inst., Troy, NY. Dept. of Physics.
ELECTROWEAK AND OTHER INTERACTIONS IN MEDIUM-ENERGY NUCLEAR PHYSICS Progress Report, Apr. 1991 - Mar. 1993
Nimai C. Mukhopadhyay 1993 43 p
(Contract DE-FG02-88ER-40448)
(DE94-004161; DOE/ER-40448/6) Avail: CASI HC A03/MF A01

This report discusses the following topics: spectrum generating algebra; vibrational spectra in the heavy quarkonia; chiral soliton model; pion neutral photoproduction from proton with polarized photons in the delta-1232 region; Compton scattering in the delta-1232 region; nucleon magnetic polarizability and the role of the delta resonance; eta photo- and electroproduction; perturbative QCD; and nuclear muon capture. DOE

N94-27711# Brookhaven National Lab., Upton, NY.
FUTURE DIRECTIONS IN PARTICLE AND NUCLEAR PHYSICS AT MULTI-GeV HADRON BEAM FACILITIES
Donald F. Geesaman, ed. (Argonne National Lab., IL.) 1993 618 p Presented at the Future Directions in Particle and Nuclear Physics at Multi-GeV Hadron Beam Facilities, Upton, NY, 4-6 Mar. 1993
(Contract DE-AC02-76CH-00016)
(DE94-002946; BNL-52389; CONF-930389) Avail: CASI HC A99/MF A06

This report contains papers on the following topics in particle and nuclear physics: hadron dynamics; lepton physics; spin physics; hadron and nuclear spectroscopy; hadronic weak interactions; and Eta physics. These papers have been indexed separately elsewhere. DOE

N94-27718# Japan Atomic Energy Research Inst., Tokyo.
SECONDARY ELECTRON EMISSION FROM COPPER SURFACE DUE TO NEODYMIUM AND GADOLINIUM ION BOMBARDMENT
Takemasa Shibata (Japan Atomic Energy Research Inst., Tokai.) and Koichi Ogura (Japan Atomic Energy Research Inst., Tokai.) Mar. 1993 18 p In JAPANESE; In JAPANESE
(DE94-701115; JAERI-M-93-092) Avail: CASI HC A03/MF A01

The electron emission yields gamma of a copper surface have been measured under bombardment with Nd(+) and Gd(+) in the energy range 0.1 to 2.6 keV. The ions are extracted from a new laser ion source. For both cases of Nd(+) and Gd(+), gammas are about linear functions of ion energies with threshold about 300 eV and are equal to 0.8 at the bombardment energy of 2 keV. The obtained yields are much higher and the thresholds are lower than many secondary electron emission data reported in the literature. DOE

N94-27733# Osaka Univ., Ibaraki (Japan).
PROCEEDINGS OF THE WORKSHOP ON (PI), K, (ETA)-NUCLEON INTERACTIONS
Apr. 1992 117 p In JAPANESE Presented at the Workshop on (pi), K, (eta)-nucleon Interactions, Ibaraki (Japan), 18-20 Feb. 1991
(DE94-701314; RCNP-P-124; CONF-9102201) Avail: CASI HC A06/MF A02

This workshop was held at the Research Center for Nuclear Physics, Osaka University, from 18 - 20 Feb. 1991. The understanding of atomic nuclei as a many body nucleon system is inseparable from the deeper understanding of the structures of nucleonsand mesons and their interaction. This workshop is going to investigate the hadron physics of atomic nuclei centering on the elementary processes of various interactions of (pi) and nuclei, K and nuclei, and(eta) and nuclei. More than 50 people took part in the workshop. This book contains 22 papers. DOE

N94-27736# Stanford Research Inst., Menlo Park, CA. Linear Accelerator Center.

HIGH ENERGY PARTON-PARTON ELASTIC SCATTERING IN QCD

W. K. Tang Aug. 1993 3 p Presented at the 19th International Conference on Elastic and Diffractive Scattering, 5th Blois Workshop, Providence, RI, 8-12 Jun. 1993
(Contract DE-AC03-76SF-00515)
(DE94-003432; SU-SLAC-PUB-6340; CONF-9306221-9) Avail: CASI HC A01/MF A01

We show that the high energy limit of quark-quark or gluon-gluon elastic scattering is calculable in terms of the BFKL pomeron when (-)t (much greater than) (Lambda)(sub QCD)(sup 2). Surprisingly, this on-shell amplitude does not have infrared divergences in the high energy limit. DOE

N94-27748# Fermi National Accelerator Lab., Batavia, IL.

A MEASUREMENT OF THE W MASS USING ELECTRONS AT CDF

D. Saltzberg Nov. 1993 15 p Presented at the 9th Workshop on Proton-Antiproton Collider Physics, Tsukuba, Japan, 18-22 Oct. 1993
(Contract DE-AC02-76CH-03000)
(DE94-004656; FNAL/C-93/355-E; CONF-9310247-2) Avail: CASI HC A03/MF A01

A preliminary measurement of the mass of the boson using electron data from the 1992-93 collider run at the Fermilab Tevatron is presented. The result is Mw = 80.47 +/- 0.15 (stat) +/- 0.25 (syst.) GeV. Current predictions agree with this value. DOE

N94-27749# Fermi National Accelerator Lab., Batavia, IL.

SEARCH FOR THE TOP QUARK IN THE SINGLE LEPTON + JETS CHANNEL AT D0

H. B. Greenlee Nov. 1993 10 p Presented at the 9th Workshop on Proton-Antiproton Collider Physics, Tsukuba, Japan, 18-22 Oct. 1993
(Contract DE-AC02-76CH-03000)
(DE94-004660; FNAL/C-93/363-E; CONF-9310247-3) Avail: CASI HC A02/MF A01

Standard model top quark pair production at (radical)s = 1.8 TeV was searched. Preliminary results of searches in the single lepton decay modes (i.e. where one top quark decays semileptonically to an electron or a muon and the other top quark decayed hadronically) are presented. We do not find evidence for top quark production in these decay channels. By combining this negative result with our negative result from the dilepton decay channels, a 95% confidence level upper limit on the top quark production cross section for top masses between 80 and 140 GeV/c(sup 2) was obtained. By comparing this cross section upper limit curve with a theoretical production cross section, a lower limit on the top quark mass of 124 GeV/c(sup 2) is obtained. DOE

N94-27752# Fermi National Accelerator Lab., Batavia, IL.

JET PRODUCTION IN MUON SCATTERING AT FERMILAB E665

C. W. Salgado Nov. 1993 5 p Presented at the 23rd International Symposium on Multiparticle Dynamics, Aspen, CO, 13-17 Sep. 1993
(Contract DE-AC02-76CH-03000)
(DE94-004663; FNAL/C-93-345-E; CONF-9309297-1) Avail: CASI HC A01/MF A01

Measurements of multi-jet production rates from Muon-Nucleon and Muon-Nuclei scattering at Fermilab-E665 are presented. Jet rates are defined by the JADE clustering algorithm. Rates in Muon-Nucleon deep-inelastic scattering are compared to Monte Carlo model predictions. Preliminary results from jet production on heavy targets, in the shadowing region, show a higher suppression of two-forward jets as compared to one-forward jet production. DOE

N94-27758# Ben Gurion Univ. of the Negev, Beersheva (Israel). Dept. of Physics.

TECHNICAL REPORT OF ISSP. SER. A, NO. 2687: QUANTIZED PERSISTENT CURRENTS OF A QUANTUM DOT IN A STRONG MAGNETIC FIELD

Yshai Avishai and Mahito Kohmoto (Tokyo Univ., Japan.) Jun. 1993 17 p Sponsored by Ministry of Education, Science and Culture, Tokyo, Japan and Ministry of Science and Development, Jerusalem, Israel
(ISSN 0082-4798)
(JTN-94-80573) Avail: CASI HC A03/MF A01

Equilibrium electron currents and magnetization in an ideal two-dimensional disc of radius R placed in a strong magnetic field H are investigated. The most striking results emerge when the conditions for the existence of edge and bulk states are met, namely R is much greater than a(sub H) = square root of (h-c/eH). When the Fermi energy is locked on a Landau level, the current as a function of electron density is quantized in units of (e/h)(h-omega(sub c)/2), where omega(sub c) is the cyclotron frequency. It is argued that this effect survives against weak disorder. It is also shown that the persistent current has an approximately periodic dependence on 1/H. The calculated magnetization as a function of the magnetic field displays de Haas-van Alphen oscillations modified by finite size effects, thus confirming the earlier results of Sivan and Imry. Author (NASDA)

N94-27759# Tokyo Univ. (Japan). Inst. for Solid State Physics.

STUDY OF INVISIBLE NUCLEON DECAY, N APPROACHES NU NU NU BAR, AND A FORBIDDEN NUCLEAR TRANSITION IN THE KAMIOKANDE DETECTOR

Y. Suzuki, Y. Fukuda, K. S. Hirata, K. Inoue, T. Ishida, T. Kajita, K. Kihara, M. Nakahata, K. Nakamura, and A. Sakai et al May 1993 16 p Sponsored by Ministry of Education, Science and Culture, Tokyo, Japan and University of Pennsylvania, Philadelphia, PA Prepared in cooperation withKamiokanade Collaboration, Kamioka, Gifu, Japan
(ICRR-299-93-11; JTN-94-80576) Avail: CASI HC A03/MF A01

A search was made for anomalous gamma-rays in the energy range between 19 and 50 MeV in the large underground water Cherenkov detector, Kamiokande. No significant excess was found above the known backgrounds. The result was used to set a limit on invisible nucleon decay through n approaches (nu(sub mu))(nu(sub mu))(bar-nu(sub mu)), n approaches (nu(sub e))(nu(sub e))(nu(sub e)), and n approaches (nu(sub tau))(nu(sub tau))(bar-nu(sub tau)). A lower limit on the partial life time tau(sub B) is given by tau(sub B)/Br(gamma) = 1.8 x 10(exp 31) years (90 percent C. L. (Confindence Level)), where Br(gamma) = Gamma(sub gamma)/Gamma(sub tot) is the branching fraction of the gamma-decay to the particle emission of the deexcitation of O-15(sup *). The life time limit becomes tau(sub B) = 4.9 x 10(exp 26) years (90 percent C. L.) for a conservative estimate of B(gamma) = 2.7 x 10(exp -5) assuming a nuclear single particle model. The result was also used for studying forbidden transitions in the O-16 nucleus. The limit for the relative strength of the forbidden transition to the normal transition is less than 2.3 x 10(exp -57) (90 percent C. L.). Author (NASDA)

N94-27760 Tel-Aviv Univ. (Israel).

DYNAMICS OF METASTABLE STATES IN SUPERSONIC BEAMS Ph.D. Thesis

Ofer Sneh May 1991 141 p
(ITN-94-85232) Copyright Avail: Issuing Activity (Tel-Aviv Univ., Exact Sciences Library, Ramat Aviv 69978, Israel)

Experimental studies are presented of triplet-state dynamics in molecules isolated in supersonic beams, including the application of new experimental techniques to the quantitative investigation of several questions related to intersystem singlet-triplet dynamics and intratriplet-manifold reactions. The experiments were performed in a differentially pumped collimated supersonic beam apparatus. The main detector used for the interrogation of excited triplet states was based on Surface-Electron Ejection by Laser Excited Metastables (SEELEM). Other experimental techniques used included Laser Induced Fluorescence (LIF); Laser Induced Phosphorescence (LIP); and Multi-Photon Ionization (MPI). Experimental procedures included: measurements of triplet lifetimes, ranging from 3 to 3,500 microsec; measurements of the relative quantum yields in triplet formation of triplet excitations formed by intersystem crossing (ISC) of excited singlet states;

measurements of the relative radiation rates of excited triplet states; and spectroscopy of directly laser-excited triplet states. ISA

N94-27783# Rochester Univ., NY.

STUDIES OF HEAVY-ION REACTIONS AND TRANSURANIC NUCLEI

W. U. Schroeder Aug. 1993 353 p
(Contract DE-FG02-88ER-40414)
(DE94-004642; DOE/ER-40414/6) Avail: CASI HC A16/MF A03

Papers on the following topics are included: The Cold-Fusion Saga; Decay Patterns of Dysprosium Nuclei Produced in S-32 + Sn-118,124 Fusion Reactions; Unexpected Features of Reactions Between Very Heavy Ions at Intermediate Bombarding Energies; Correlations Between Neutrons and Charged Products from the Dissipative Reaction Au-197 + Pb-208 at E/A = 29 MeV; Dissipative Dynamics of Projectile-Like Fragment Production in the Reaction Bi-209 + Xe-136 at E/A = 28.2 MeV; Dynamical Production of Intermediate-Mass Fragments in Peripheral Bi-209 + Xe-136 Collisions at E(sub lab)/A = 28.2 MeV; The Rochester 960-Liter Neutron Multiplicity Meter; A Simple Pulse Processing Concept for a Low-Cost Pulse-Shape-Based Particle Identification; A One-Transistor Preamplifier for PMT Anode Signals; A Five-Channel Multistop TDC/Event Handler for the SuperBall Neutron Multiplicity Meter; Construction of the SuperBall - a 16,000-Liter Neutron Detector for Calorimetric Studies of Intermediate-Energy Heavy-Ion Reactions; A Computer Code for Light Detection Efficiency Calculations for Photo-multipliers of a Neutron Detector; Evaluation of Gd-Loaded Liquid Scintillators for the SuperBall Neutron Calorimeter; and Measurement of the Interaction of Cosmic-Ray mu(-) with a Muon Telescope. DOE

N94-27811# Ames Lab., IA.

TOPICS IN ELECTROWEAK BARYOGENESIS: THE SPHALERON AND T-VIOLATION Ph.D. Thesis

L. SeungKoog Dec. 1993 121 p
(Contract W-7405-eng-82)
(DE94-004886; IS-T-1684) Avail: CASI HC A06/MF A02

Assuming that beyond the standard model, physics can be parametrized in terms of high dimensional operators, their effects on the energy of the sphaleron and the classical solution of the gauge and Higgs fields are examined. In the absence of fermions, all of the six dimension 6 operators which are SU(2) symmetric have a small effect when calculated perturbatively. However, calculated non-perturbatively, one of the operators alters the boundary conditions of the equations of motion of the Higgs and gauge fields involved, and another operator gives rise to an abrupt change in the sphaleron energy at a small but definite Higgs quartic coupling. The magnitude of the T-violating muon polarization induced by electromagnetic final state interaction in the radiative Kaon decay K(+) yields (mu)(+)(nu)(sub mu)(gamma) is order of 10(exp -3). DOE

N94-27814# Brookhaven National Lab., Upton, NY.

SURFACE MODES AND CHIRAL SYMMETRY (WILSON FERMIONS IN A BOX)

M. Creutz and I. Horvath Dec. 1993 4 p Presented at the Lattice 1993: International Symposium on Lattice Field Theory, Dallas, TX, 12-17 Oct. 1993
(Contract DE-AC02-76CH-00016)
(DE94-004946; BNL-49782; CONF-9310250-2) Avail: CASI HC A01/MF A01

A Hamiltonian discussion of surface states in an extra dimension as a basis for chiral fermions in lattice models is given. Such modes appear with the Wilson fermion action when the hopping parameter exceeds a critical value. The association of such states with the closing and reopening of a band gap was noted by Shockley in 1939. DOE

N94-27815# Illinois Univ., Urbana. Physics Lab.

RESEARCH ON ELEMENTARY PARTICLE PHYSICS, PART 2

L. E. Holloway May 1993 57 p
(Contract DE-FG02-91ER-40677)
(DE94-004956; DOE/ER-40677/2-Pt-2) Avail: CASI HC A04/MF A01

The activities of the University of Illinois Experimental High Energy Physics Group are described. The physicists in the University of Illinois High Energy Physics Group are engaged in a wide variety of experiments at current and future accelerator laboratories. These include: (1) the CDF experiment at the Fermilab Tevetron p(bar p) collider; (2) design and developmental work for the SDC group at SSCL; (3) experiments at the wide band photon beam at Fermilab, (4) e(+)e(-) experiments, the Mark III and SLD at SLAC and CLEO at Cornell; (5) CP violation experiments at Fermilab; (6) the HiRes cosmic ray experiment at Dugway Proving Grounds, Utah; (7) computational facilities; and (8) electronics systems development. DOE

N94-27820# Japan Atomic Energy Research Inst., Tokyo.

MEASUREMENT OF METASTABLE POPULATION DISTRIBUTION IN GADOLINIUM ATOMIC BEAM BY LASER RESONANCE PHOTOIONIZATION METHOD

Koichi Ogura (Japan Atomic Energy Research Inst., Tokai.) and Takemasa Shibata (Japan Atomic Energy Research Inst., Tokai.) Mar. 1993 29 p In JAPANESE; In JAPANESE
(DE94-701194; JAERI-M-93-098) Avail: CASI HC A03/MF A01

Population distribution of metastable state of gadolinium atoms produced by electron beam heating was measured using resonance photoionization. The population distributions followed the Boltzmann distribution and the atomic excitation temperature was determined. The excitation temperature is far lower than that of evaporation surface and nearly equal to the translational temperature of gadolinium atomic beam. This suggests that the excitation energy and the kinetic energy of atoms exchange at high reaction rate in the atomic vapor expanding from the evaporation surface into vacuum. DOE

N94-27834# Comision Nacional de Energia Atomica, Buenos Aires (Argentina).

FULLERENE FABRICATION USING AN ARC FURNACE. CHARACTERIZATION OF THE PRODUCT

E. E. Pasqualini 1993 2 p Presented at the 2nd Argentine Sessions on Materials Science, La Plata, Argentina, 25-28 Oct. 1993
(DE94-603006; INIS-AR-041; CONF-9310181) Avail: CASI HC A01/MF A01 (US Sales Only)

The first studies about fullerenes were based on the clusters formed by laser heating of graphite; later they were produced in gram quantities with carbon evaporation equipment. They were also produced in flames and by induction heating of graphite. In the present work a commercial arc furnace with graphite spectral electrodes three millimeters in diameter, d.c. current 50 Amperes and helium pressure between 40 and 180 torr, was used. The decomposition of electrodes of 40 mm in length was done in 1 minute to obtain 0.3 grams of soot. loluene dissolution with the help of a soxblet was used for the extraction of fullerenes with a yield of 8%. With the evaporation, a solid residue of precipitates was obtained. The precipitates were analyzed with X rays, electronic microscopy, chromatography, mass spectroscopy, nuclear magnetic resonance, FTIR and UV. The quantitative analyses of the fullerene mixture is shown. DOE

N94-27847# Joint Inst. for Nuclear Research, Dubna (USSR). Lab. of Nuclear Problems.

THE THREE-DIMENSIONAL HYDROGEN ATOM IN CROSSED MAGNETIC AND ELECTRIC FIELDS

V. S. Melezhik 1993 20 p
(DE94-606301; JINR-E-4-93-94) Avail: CASI HC A03/MF A01 (US Sales Only)

The authors give a solution of the three-dimensional Schroedinger equation for the electron of a hydrogen atom in external electric and magnetic fields of arbitrary mutual orientation. The rearrangement of the energy spectrum due to changing in the mutual orientation of the fields is evaluated by using n=2 multiplet as an example. The calculations agree with the second-order perturbation formulas that exist for the special cases of mutually parallel and orthogonal fields. For another special two-dimensional case which is currently being extensively investigated, namely the hydrogen atom in a strong magnetic field, the approach agrees with advanced calculations by other authors and yields more accurate binding energies for certain of the low-lying excited states that have been considered. DOE

N94-27848 Joint Inst. for Nuclear Research, Dubna (USSR). Lab. of Theoretical Physics.

ON THE MODEL OF THE RELATIVISTIC PARTICLE WITH CURVATURE AND TORSION

V. V. Nesterenko 1992 10 p Limited Reproducibility: More than 20% of this document may be affected by microfiche quality
(DE94-606330; JINR-E-2-92-479) Avail: CASI HC A02 (US Sales Only)

Two integrals along the world trajectory of its curvature and torsion are added to the standard action for the point-like spinless relativistic particle. This enables one to quantize the model canonically and to derive exactly the relation between the spin and mass of the states. DOE

N94-27860# Joint Inst. for Nuclear Research, Dubna (USSR). Lab. of Theoretical Physics.
DECAY CONSTANTS OF HEAVY MESONS IN THE RELATIVISTIC POTENTIAL MODEL WITH VELOCITY DEPENDENT CORRECTIONS
I. S. Avaliani (Tbilisi State Univ., USSR.), A. N. Sisakyan, and L. A. Slepchenko 1992 10 p
(DE94-606495; JINR-E-2-92-547) Avail: CASI HC A02/MF A01 (US Sales Only)

In the relativistic model with the velocity dependent potential, the masses and leptonic decay constants of heavy pseudoscalar and vector mesons are computed. The possibility of using this potential is discussed. DOE

N94-27861# Joint Inst. for Nuclear Research, Dubna (USSR).
MUON TRANSFER RATES IN COLLISIONS OF HYDROGEN ISOTOPE MESIC ATOMS ON BARE NUCLEI: MULTICHANNEL ADIABATIC APPROACH
V. I. Korobov, V. S. Melezhik, and L. I. Ponomarev (Kurchatov, I. V. Inst. of Atomic Energy, Moscow, USSR.) 1992 15 p
(DE94-606752; JINR-E-4-92-358) Avail: CASI HC A03/MF A01 (US Sales Only)

A numerical scheme for solving the problem of slow collisions in the three-body adiabatic approach is applied for calculation of muon transfer rates in collisions of hydrogen isotope atoms on bare nuclei. It is demonstrated that the multichannel adiabatic approach allows one to reach high accuracy results (approximately three percent) estimating the cross sections of charge transfer processes. The method is applicable in a wide range of energies (0.001-50 eV) which is of interest for analysis of muon catalyzed fusion experiments. DOE

N94-27877 Tokyo Univ., Tanashi (Japan). Inst. for Nuclear Study.
FIRST OBSERVATION OF NEUTRAL CURRENT PROTON ELECTRON SCATTERING AT THE SQUARE ROOT OF s = 300 GeV
Takuya Hasegawa (Tokyo Univ., Japan.) Feb. 1993 138 p Limited Reproducibility: More than 20% of this document may be affected by microfiche quality
(DE94-701107; INS-J-175) Avail: CASI HC A07 (US Sales Only)

Neutral current proton electron scattering at center of mass energy 295 GeV was observed for the first time, using the newly built proton electron collider HERA (Hadron Elektron Ring Anlage) and the general purpose detector ZEUS. The distributions of Q(sup 2), Bjorken-x(x), and Bjorken-y(y) were compared with the expectation based on the standard electroweak theory and QCD. Regarding the investigation of high-Q(sup 2) region, an event of Q(sup 2) approximately 1000 GeV(exp 2) was observed for the first time. From the x-distribution of the events, a limit on the mass and the coupling of an exotic s-channel resonance of a quark-lepton system (leptoquark) was obtained. The mass limit is 72 GeV (97 GeV) at 95% confidence level for a scalar type leptoquark with a left-handed (right-handed) electromagnetic coupling to ordinary leptons. The leptoquark is assumed to be weak-isoscalar. To realize this experiment, a uranium scintillator sandwich type calorimeter was developed. Equal response to electrons and hadrons (e/h = 1), which is essential for the good energy resolution for hadrons, has been achieved. One of the main characteristics of this calorimeter is a possibility of calibration utilizing its own uranium radioactivity. The grain variation of each channel can be detected with an accuracy of plus or minus one percent. DOE

N94-27994# International Centre for Theoretical Physics, Trieste (Italy).
CORRELATIONS IN INELASTIC COLLISIONS OF RELATIVISTIC NUCLEI WITH EMULSION AT (4.1 - 4.5) A GeV/c
A. El-Naghy, M. T. Ghoniem (Cairo Univ., Giza, Egypt.), M. T. Hussein (Cairo Univ., Giza, Egypt.), S. Ramadan (Cairo Univ., Giza, Egypt.), N. M. Sadek (Cairo Univ., Giza, Egypt.), N. N. Abdel-Allah (Assiut Univ., Sohag, Egypt.), S. A. Krasnov (Joint Inst. for Nuclear Research, Dubna, USSR.), K. D. Tolstov (Joint Inst. for Nuclear Research, Dubna, USSR.), S. Vokal (Joint Inst. for Nuclear Research, Dubna, USSR.), and D. M. Semverstov (Leningrad Nuclear Physics Inst., USSR.) et al Jun. 1993 27 p
(DE93-634526; IC-93/149) Avail: CASI HC A03/MF A01 (US Sales Only)

Presented are a systematic study and statistically significant results of different types of correlations in angles, rapidities, and rapidity intervals, between various charged secondary particles produced in inelastic interactions of relativistic nuclei with emulsion at (4.1 to 4.5) A GeV/c. All types of particles are found to be emitted asymmetrically in the azimuthal plane. This asymmetry increases with the decrease of impact parameter. The two particle correlation function is found to be positive except in the extreme projectile fragmentation region. Particles from different kinematical regions are emitted back-to-back in the azimuthal plane. A multiparticle correlation is observed between created particles as well as target fragments. This assumes production of clusters. These clusters seem to be formed during the decoloring process. Investigations are being carried out to reveal the characteristics of these clusters. DOE

N94-28001# Los Alamos National Lab., NM.
COMPUTER SIMULATION OF AQUEOUS Na-Cl ELECTROLYTES
G. Hummer, D. M. Soumpasis (Max-Planck-Inst. fuer Biophysikalische Chemie, Goettingen, Germany.), and M. Neumann (Wien Univ., Austria.) 1993 13 p Presented at the 2nd Liquid Matter Conference, Florence, Italy, 18-22 Sep. 1993
(Contract W-7405-eng-36)
(DE94-002622; LA-UR-93-3570; CONF-9309267-1) Avail: CASI HC A03/MF A01

Equilibrium structure of aqueous Na-Cl electrolytes between 1 and 5 mol/l is studied by means of molecular dynamics computer simulation using interaction site descriptions of water and ionic components. Electrostatic interactions are treated both with the newly developed charged-clouds scheme and with Ewald summation. In the case of a 5 mol/l electrolyte, the results for pair correlations obtained by the two methods are in excellent agreement. However, the charged-clouds technique is much faster than Ewald summation and makes simulations at lower salt concentrations feasible. It is found that both ion-water and ion-ion correlation functions depend only weakly on the ionic concentration. Sodium and chloride ions exhibit only a negligible tendency to form contact pairs. In particular, no chloride ion pairs in contact are observed. DOE

N94-27898*# Christopher Newport Coll., Newport News, VA. Dept. of Biology, Chemistry, and Environmental Science.
PROTON IRRADIATION ON MATERIALS
C. Ken Chang *In* Old Dominion Univ., The 1993 NASA-ODU American Society for Engineering Education (ASEE) Summer Faculty Fellowship Program Dec. 1993 p 78-79 (For primary document see N94-27893 07-80)
Avail: CASI HC A01/MF A03

N94-27910*# College of William and Mary, Williamsburg, VA. Dept. of Mathematics.
THE MOLECULAR MATCHING PROBLEM
Rex K. Kincaid *In* Old Dominion Univ., The 1993 NASA-ODU American Society for Engineering Education (ASEE) Summer Faculty Fellowship Program Dec. 1993 p 120-122 (For primary document see N94-27893 07-80)
Avail: CASI HC A01/MF A03

N94-27915*# University of Southern Illinois, Carbondale. Dept. of Physics.
RADIATIONS FROM HOT NUCLEI
F. Bary Malik *In* Old Dominion Univ., The 1993 NASA-ODU American Society for Engineering Education (ASEE) Summer Faculty Fellowship Program Dec. 1993 p 137-139 (For primary document see N94-27893 07-80)
Avail: CASI HC A01/MF A03

73 NUCLEAR AND HIGH-ENERGY PHYSICS

Includes elementary and nuclear particles; and reactor theory.
For space radiation see *93 Space Radiation.*

N94-25619# Nationaal Inst. voor Kernfysica en Hoge Energiefysica, Amsterdam (Netherlands).
BUNDLE INTENSITY AND BEAMGATE LENGTH RECORDER (BIBL) [BUNDEL INTENSITEITS- EN BEAMGATE LENGTE-RECORDER (BIBL)]
J. D. Schipper and J. Stolte 1993 28 p In DUTCH
(DIGEL-1993-7; ETN-94-94955) Avail: CASI HC A03/MF A01

A module was developed for the storage ring AmPS (Amsterdam pulse stretcher) to measure the bundle intensity as a function of time in the bundle, and to measure the average burst duration. During the burst pulse the beam intensity recorder samples the signal on the input 'beam-in' and adds the measured value to the sum of the previous measurements. In the beamgate module the signal beam gate length is deduced from the start and stop extraction pulses. ESA

N94-25621# Technical Research Centre of Finland, Espoo. Fire Technology Lab.
HDR REACTOR CONTAINMENT FIRE MODELING WITH BRI2
John A. Rockett (National Bureau of Standards, Washington, DC.), Olavi Keski-Rahkonen, and Liisa Heikkila Sep. 1992 89 p Sponsored by Ministry of Trade and Industry, Finland; Finnish Center of Radiation and Nuclear Safety, Helsinki; Imatran Voima Oy, Finland; Teollisuuden Voima Oy, Finland; and Suomen Atomivakuutuspooli, Finland
(ISSN 1235-0621)
(VTT-PUBS-113; ISBN-951-38-4231-2; ETN-94-95232) Copyright Avail: CASI HC A05/MF A01

Fire tests at the German test reactor, HDR, were simulated using a Japanese zone model code, BR12. For potential users of fire models, the process by which model inputs for a complex building are developed and debugged, are illustrated. Eight and ten room models of the containment building were developed. Critical phenomena occurring during simulation were explored. BR12 must be exercised where a side wind increases entrainment by the fire plume. Horizontal vents were described by effective vertical vents. Effect of location of the vent to ambient was found critical during severely oxygen limited burning. The importance of blowing of the fire by the door jet generated. ESA

N94-25850 Joint Inst. for Nuclear Research, Dubna (USSR). Lab. of High Energy
HADRON JETS AND NUCLEON CLUSTERS IN THE RELATIVISTIC NUCLEAR COLLISIONS
L. A. Didenko, V. G. Grishin, and A. A. Kuznetsov 1991 20 p Limited Reproducibility: More than 20% of this document may be affected by microfiche quality
(DE93-613434; JINR-E-1-91-323) Avail: CASI HC A03 (US Sales Only)

The production of hadron jets and nucleon clusters has been investigated in different hadron and nuclear reactions over an energy range from 4.0 to 205 GeV. The characteristics of hadron jets and nucleon clusters are studied in terms of a new relativistic invariant approach in a relative four-velocity space. It has been observed that the properties of hadron jets in soft and hard interactions and nucleon clusters with temperature T(sub 1) = 60-70 MeV are universal, i.e. independent of neither the type of fragmenting system nor collision energy. The asymptotic regime occurs at (radical)S greater than or approximately equal to 6 GeV for hadron jets and at p greater than or approximately equal to 4.2 x AGeV for nucleon clusters. The dependence of cluster temperature on proton multiplicity in the nucleon cluster was obtained. It was also shown that nucleon clusters under consideration can be interpreted as a decay product of multinucleon resonances with a width of about a few MeV. DOE

N94-25870 Joint Inst. for Nuclear Research, Dubna (USSR). Lab. of Theoretical Physics.
STRUCTURE FUNCTIONS OF SEA QUARKS, KOGUT-SUSSKIND POLE AND DYNAMICS OF PP- AND PP-BAR-INTERACTIONS AT HIGH ENERGIES
A. E. Dorokhov, N. I. Kochelev (Academy of Sciences, USSR, Alma-Ata.), and Yu. A. Zubov (Academy of Sciences, USSR, Alma-Ata.) 1991 24 p Limited Reproducibility: More than 20% of this document may be affected by microfiche quality
(DE93-613184; JINR-E-2-91-375) Avail: Issuing Activity (Department of Energy (DOE)) (US Sales Only)

It is shown that anomalous behavior of the spin-dependent proton structure function g(sub 1)(sup P)(x) is defined by the contribution to this structure function as x(yields)0 of a new Regge trajectory caused by Kogut-Susskind pole. It is pointed out that manifestation of a new trajectory in pp- and pp-bar-interactions allows us to explain some peculiarities of these reactions at high energies. DOE

N94-25931# Brown Univ., Providence, RI. Dept. of Physics.
A RESEARCH PROGRAM IN EXPERIMENTAL AND THEORETICAL HIGH ENERGY PHYSICS Progress Report, 1 Jun. 1992 - 31 May 1993
R. Brandenberger, D. Cutts, and H. M. Fried et al 1 Jun. 1993 80 p
(Contract DE-FG02-91ER-40688)
(DE94-002156; DOE/ER-40688/2) Avail: CASI HC A05/MF A01

The main emphasis in the theoretical program has been in the area of string theory; also investigated were confinement and other aspects of QCD, electroweak symmetry breaking, and electroweak baryogenesis. The research program in computational physics concentrated on the development of the source Galerkin method of numerical quantum field theory. One portion of the experimental program dealt with interactions of leptons and hadrons from accelerator and strophysics sources. A description of the Large Volume Detector at Gran Sasso and its use as a stellar collapse monitor is given, along with an account of research and development on resistive plate counters. The rest of the experimental program concerns hadron collider and neutrino physics, with major emphasis on the D0 experiment at the Tevatron. The commissioning of the D0 detector and its operation are described, along with D0 analysis. Also reported is a novel cryogenic technique utilizing superfluid helium for neutrino calorimetry. DOE

N94-26044# Gosudarstvennyi Komitet po Ispolzovaniyu Atomnoi Energii, Serpukhov (USSR).
SPIN EFFECTS IN HARD INTERACTIONS (INTEREST IN ACCELERATED POLARIZED BEAM)
S. M. Troshin and N. E. Tyurin 1992 28 p
(DE93-634398; IHEP-OTF-92-76) Avail: CASI HC A03/MF A01 (US Sales Only)

The dynamics of spin effects in hard hadron processes is discussed along with some suggestions for experimental study of these effects with use of the accelerated polarized proton beam. DOE

N94-26097 Iowa State Univ. of Science and Technology, Ames. Dept. of Physics and Astronomy.
RELATIVISTIC HEAVY ION PHYSICS
J. C. Hill and F. K. Wohn 1993 42 p Limited Reproducibility: More than 20% of this document may be affected by poor print
(Contract DE-FG02-92ER-40692)
(DE94-003161; DOE/ER-40692/2) Avail: Issuing Activity (Department of Energy (DOE))

This is a progress report for the period May 1992 through April 1993. The first section, entitled 'Purpose and Trends,' gives background on the recent trends in the research program and its evolution from an emphasis on nuclear structure physics to its present emphasis on relativistic heavy ion and RHIC physics. The next section, entitled 'Physics Research Progress,' is divided into four parts: participation in the program to develop a large detector named PHENIX for the RHIC accelerator; joining E864 at the AGS accelerator and the role in that experiment; progress made in the study of electromagnetic dissociation, the highlight of this endeavor being an experiment carried out with the Au-197 beam from the AGS accelerator in April 1992; and progress in completion of the nuclear structure studies. In the final section a list of publications, invited talks, and contributed talks is given. DOE

N94-26113# National Lab. for High Energy Physics, Tsukuba (Japan).
JLC-1
Dec. 1992 249 p
(DE93-520380; KEK-92-16) Avail: CASI HC A11/MF A03

The JLC project is the post-Tristan high energy physics program that was recommended by the High Energy Committee in 1986. The project consists of the construction of a linear collider and the development of the experiments that will use it, at an initial center of mass energy around 500 GeV. The machine will eventually reach 1.5 TeV through planned upgrades. According to the recommendation, a systematic research and development program was begun, and many remarkable results have been produced. The recent precision measurement at LEP has greatly enhanced the importance of an e(+)e(-) linear collider to explore the energy region just above LEP. The construction of the JLC-1 is proposed. The main purpose of the JLC-1 is to search for the Higgs boson and the top quark which are the two missing constituents of the Standard Model. The physics related to this search is described. The technical feasibility of the construction of the JLC-1 accelerator is considered. The klystrons that can emit a peak power of about 100 MW and experimentally verify the high acceleration gradient of 100 Mv/m are the target of the research and development. The physics, detectors, the accelerator, the time schedule, the cost estimation, and other factors are described. DOE

N94-26119# Harvard Univ., Cambridge, MA.
HARVARD UNIVERSITY HIGH ENERGY PHYSICS
1993 44 p
(Contract DE-FG02-91ER-40654)
(DE94-002406; DOE/ER-40654/3) Avail: CASI HC A03/MF A01

The mainly experimental research program in high energy physics at Harvard is summarized in a descriptive fashion according to the following outline: Proton-antiproton colliding beam program at Fermilab--CDF; forward/backward electromagnetic calorimeters--FEM; central muon extension--CMX; gas calorimetry and electronics development; front-end electronics upgrades; software development; physics analysis; electron-positron collisions in the upsilon region--CLEO; search for nu(sub (mu)) to nu(sub (tau)) oscillations with the NOMAD experiment at CERN; the solenoidal detector collaboration at the SSC; muon scattering at FNAL--E665; the L3 experiment; and phenomenological analysis of high-energy (bar-p)p cross sections. DOE

N94-26164 Gosudarstvennyi Komitet po Ispolzovaniyu Atomnoi Energii, Serpukhov (USSR). Inst. Fiziki Vysokikh Ehnergij.
REGROUPING OF THE BEAM IN THE IHEP PS FOR THE UNK p-p PROGRAMS
E. A. Myae, E. S. Nelipovich, P. T. Pashkov, and A. V. Smirnov 1992 12 p Limited Reproducibility: More than 20% of this document may be affected by microfiche quality
(DE93-634021; IHEP-OKU-92-83) Avail: CASI HC A03 (US Sales Only)

Possibilities to form particle bunches in the IHEP machine whose longitudinal parameters would satisfy the requirements imposed by the UNK p-p programs are analyzed. In the case of the 3 x 3 TeV p-p program the accelerated proton beam in the IHEP PS after preliminary quasiadiabatic debunching process will be recaptured into a stable oscillating mode at 33.3 MHz. The peculiarities of the RF system designed for these purposes with an account of strong beam loading are discussed. For the 0.4 x 3 TeV UNK colliding beam regime, it is necessary to compress the accelerated proton bunches in the IHEP PS so that their length will be 4 times less. The main difficulties arising during 'RF gymnastics' which is used for beam compressing, are caused by nonlinearities of the external accelerating field and also the fields induced in the RF cavities by the beam. The compensation of such effects with the help of the special RF system is discussed. DOE

N94-26165 Gosudarstvennyi Komitet po Ispolzovaniyu Atomnoi Energii, Serpukhov (USSR). Inst. Fiziki Vysokikh Ehnergij.
LONGITUDINAL DIFFUSION OF A PROTON BUNCH UNDER EXTERNAL NOISE
S. V. Ivanov 1992 38 p In RUSSIAN Limited Reproducibility: More than 20% of this document may be affected by microfiche quality
(DE93-634022; IHEP-UNK-92-43) Avail: CASI HC A03 (US Sales Only)

Evolution of longitudinal distribution of a proton bunch subjected to stationary (amplitude or phase) RF-noises is governed by a diffusion equation. Its diffusion coefficient is essentially nonlinear and, possibility, diverges near separatrix. The paper deals with the dynamical foundations of this diffusive approximation. Treated in detail is the motion of particles located either inside, or outside stationary buckets (beam halo). The formal statement of boundary-value problem for the noise-induced diffusion of a bunch (zero boundary conditions at separatrix, or at infinity) is discussed. Both these problems are solved numerically for arbitrarily long bunches. Use is made of the Finite Element Technique (spatial discretization), and of the Crank-Nicolson's scheme (time-domain integration). Computed estimates of the representative bunch life-times for the wide-band (white) noise approximation are presented. These emerge from the criteria of either bunch quality degradation, or of its population loss. DOE

N94-26330# California Univ., Berkeley. Lawrence Berkeley Lab.
ON A THEORY OF TWO-BEAM MECHANISMS OF CHARGED PARTICLE ACCELERATION IN ELECTRODYNAMIC STRUCTURES
A. O. Ostrovsky (Kharkov State Univ., USSR.) Sep. 1993 29 p
(Contract DE-AC03-76SF-00098)
(DE94-003482; LBL-34729) Avail: CASI HC A03/MF A01

This work is devoted to the theoretical studies of two-beam mechanisms of charged particle acceleration in electronic structures. The first section continues the outline of results of theoretical studies commenced in the intermediate report and considers the two-beam scheme of acceleration in the plasma waveguide. According to this scheme the strong current relativistic electron beam (REB) excites the intensive plasma waves accelerating the electrons of the second beam. The driving beam is assumed to be density modulated. The preliminary modulation of the driving REB is shown to enhance substantially the acceleration efficiency of relativistic electrons of the driven beam. The second section deals with the two-beam acceleration in the vacuum corrugated waveguide. According to this scheme the excitation of electromagnetic waves and acceleration of driven beam electrons by them is accomplished under different Cherenkov resonances between the particles of beams and the corrugated waveguide field. The electromagnetic field in the periodic structure is known to be the superposition of spatial harmonics. With the small depth of the periodic nonuniformity, the amplitudes of these harmonics decrease fast with their number increasing. Therefore, if the driving beam is in the Cherenkov resonance with the first spatial harmonic and the driven beam is in resonance with the zero space harmonic then the force accelerating the driven beam would be considerably bigger than the force decelerating the driving beam electrons. DOE

N94-26405# Gosudarstvennyi Komitet po Ispolzovaniyu Atomnoi Energii, Serpukhov (USSR). Inst. Fiziki Vysokikh Ehnergij.
PROBLEMS OF APPLICATION OF CHARGED PARTICLES CHANNELING EFFECTS IN CRYSTALS IN HIGH-ENERGY PHYSICS [PROBLEMY PRIMENIYA EHFFEKTOV KANALIROVANIYA CHASTITS KRISTALLAMI V FIZIKE VYSOKIKH EHNERGIJ]
A. A. Aseev 1992 132 p In RUSSIAN
(DE93-634023; INIS-RU-355) Avail: CASI HC A07/MF A02 (US Sales Only)

This document contains brief papers presented at the All-Union meeting on problems of application of charged particles channelling effects in crystals in high energy physics, Protvino, 26-28 February 1991. DOE

N94-26543 National Lab. for High Energy Physics, Tsukuba (Japan).
PROCEEDINGS OF THE SECOND EGS4 USER'S MEETING IN JAPAN
Hideo Hirayama, ed., Yoshihito Namito, ed., and Syuichi Ban, ed. Dec. 1992 70 p Meeting held in Tsukuba, Japan, 20-22 Jul. 1992 Limited Reproducibility: More than 20% of this document may be affected by microfiche quality
(DE93-520383; KEK-Proc-92-16; CONF-9207216) Avail: CASI HC A04

This report is the summary of the lectures in second EGS4 study meeting held under the auspices of the Radiation Safety Management Center at National Laboratory for High Energy Physics, from July 20 to 22, 1992. In the study meeting, 79 people took part, and the new users of EGS4 seem to expand, taking the opportunity of this study meeting. In 13 lectures on the research using EGS4, the stories in wide fields were able to be heard. The interchange of the researches in various fields was able to be carried out through the common means of EGS4, and it was significant. DOE

N94-26881# Rome Lab., Griffiss AFB, NY.
A CURRENT EVALUATION OF THE DIGITAL BEAMFORMING TESTBED AT ROME LABORATORY Technical Report, Jul. 1992 - Jul. 1993
William R. Humbert and Hans Steyskal Sep. 1993 42 p
(AD-A274311; RL-TR-93-198) Avail: CASI HC A03/MF A01

The purpose of this report is to provide a recent evaluation of the digital beamforming (DBF) testbed at Rome Laboratory, Hanscom AFB, MA. Section 1 of the report provides a brief introduction to digital beamforming and some of the associated concepts. Section 2 briefly discusses each component of the digital beamforming system (form and function) in a top-down fashion. Section 3 discusses some system limitations associated with the receiver architecture and outlines the techniques used to investigate these limitations. Section 4 contains the measurement results, which show in-phase and quadrature errors approximately 27 dB below the signal, and dc offsets approximately 37 dB below the signal. Third order harmonics are also approximately equal 37 dB below the signal. Amplitude variation among the channels is + or -2 dB. Removal of the dc offset error had little effect on a 40 dB Taylor pattern. However, removal of the in-phase and quadrature errors (the dominant errors) greatly improved the pattern. Also included are simple examples of super-resolution of two sources spaced about 1/2 beamwidth apart, and of open-loop adaptive nulling for a 20 dB Taylor pattern. DTIC

N94-27078# Austin Research Associates, Inc., TX.
ANALYTICAL STUDY OF BEAM HANDLING AND EMITTANCE CONTROL Final Report
James R. Thompson and M. L. Sloan Dec. 1993 142 p
(Contract N00014-88-C-0542)
(AD-A274412; I-ARA-93-U-60) Avail: CASI HC A07/MF A02

The thrust of our research on beam handling and emittance control was to explore how one might design high current electron accelerators, with the preservation of high beam quality designed as the primary design consideration. We considered high current, induction linacs in the parameter class of the ETA/ATA accelerators at LLNL, but with improvements to the accelerator gap design and other features to permit a significant increase in the deliverable beam brightness. Our approach for beam quality control centered on the use of solenoidal magnetic focusing through such induction accelerators, together with gently-shaped (adiabatic) acceleration gaps. This approach offers several tools for the control of beam quality. The strength and axial variation in the solenoidal magnetic field may be designed, as may the length and shape of the acceleration gaps, the loading of the gaps, and the axial spacing from gap to gap. This research showed that each of these design features may individually be optimized to contribute to improved beam quality control, and by exploiting these features, it appears feasible to produce high current, high energy electron beams possessing breakthrough beam quality and brightness. Applications which have been technologically unachievable may for the first time become possible. One such application is the production of high performance free electron lasers at very short wavelengths, extending down to the optical (less than 1 micron) regime. DTIC

N94-27082# Naval Research Lab., Washington, DC.
IMPLEMENTATION OF A COMPACT MAGNETIC ELECTRON ENERGY SPECTROMETER FOR INTENSE RELATIVISTIC ELECTRON BEAMS Interim Report
J. A. Gregor and J. A. Antoniades 5 Nov. 1993 23 p
(AD-A274451; NRL/MR/6756-93-7406) Avail: CASI HC A03/MF A01

A diagnostic used for measuring the energy of 1 to 5 MEV pulsed electron beams by means independent of the beam generating device is investigated. The method employed is capable of collecting the required data optically in a single pulse. The beam energy is measured using a magnetic electron spectrometer coupled with a scintillating material. Using a polaroid camera to collect data, the energy of electron beams from two field emission diode accelerators is measured. The first is a nominal 1 MEV, 16 kA, 25 ns FWHM electron beam and the second is a nominal 5 MEV, 20 kA, 50 ns FWHM electron beam. A detailed study of measurement accuracy and possible sources of error was accomplished. DTIC

N94-27083# Phillips Lab., Edwards AFB, CA.
PROCEEDINGS OF THE HIGH ENERGY DENSITY MATTER (HEDM) CONTRACTOR'S CONFERENCE Special Report, May - Jun. 1992
T. L. Thompson Nov. 1993 466 p Conference held in Woods Hole, MA, 6-8 Jun. 1993
(AD-A274452; PL-TR-93-3041) Avail: CASI HC A20/MF A04

The information presented at the seventh annual High Energy Density Matter (HEDM) Contractors Conference held 6-8 June 1993 in Woods Hole, MA is presented. This report contains the extended abstracts of the oral, workshop and poster presentations given by the Air Force funded contractors and by the in-house researchers from the Phillips Laboratory. Topics covered include: HIDM, high energy density matter, propellant, solid hydrogen, cryogenic matrices, energetic materials, and potential energy surfaces. DTIC

N94-27084# Visidyne, Inc., Burlington, MA.
CHARACTERIZATION OF THE ENERGY DEPOSITION PRODUCED BY THE PRIMARY ELECTRON BEAM ON THE EXCEDE 3 PROGRAM Scientific Report No. 3
R. J. Rieder, R. L. McNutt (Johns Hopkins Univ., Laurel, MD.), and S. A. Rappaport May 1993 38 p
(Contract F19628-90-C-0187)
(AD-A274453; VI-2067; SR-3; PL-TR-93-2132(1)) Avail: CASI HC A03/MF A01

The primary goal of the EXCEDE III (Excitation by Electron Deposition) atmospheric energy deposition experiment was to monitor the spatial distribution of the energy deposition profile produced by the approximately 18 Ampere approximately 2.5 keV electron beam. During the rocket flight on April 27, 1990, prompt emission at 391 4 A from the N2(+) (1N) 0-0 transition were measured by a UV scanning photometer. The intensity profiles were inverted to obtain profiles of energy deposition by the beam. DTIC

N94-27614# Indiana Univ., Bloomington. Dept. of Physics.
INDIANA UNIVERSITY HIGH ENERGY PHYSICS, TASK A
B. Brabson, R. Crittenden, A. Dzierba, G. Hanson, H. Martin, T. Marshall, R. Mir, H. Ogren, D. Rust, and S. Teige et al 1993 110 p
(Contract DE-FG02-91ER-40661)
(DE94-000961; DOE/ER-40661/5) Avail: CASI HC A06/MF A02

This report discusses research at Indiana University on the following high energy physics experiments: A search for mesons with unusual quantum numbers; hadronic states produced in association with high-mass dimuons; FNAL E740 (D0); superconducting super collider; and OPAL experiment at CERN. DOE

N94-27646*# Wisconsin Univ., La Crosse. Dept. of Physics.
STOPPING POWERS AND CROSS SECTIONS DUE TO TWO-PHOTON PROCESSES IN RELATIVISTIC NUCLEUS-NUCLEUS COLLISIONS Final Report
Wang K. Cheung and John W. Norbury Mar. 1994 64 p See also N92-30012
(Grant NAG1-1457; RTOP 199-45-16-11)
(NASA-CR-4574; NAS 1.26:4574) Avail: CASI HC A04/MF A01

The effects of electromagnetic-production processes due to two-photon exchange in nucleus-nucleus collisions are discussed. Feynman diagrams for two-photon exchange are evaluated using quantum electrodynamics. The total cross section and stopping power for projectile and target nuclei of identical charge are found to be significant for heavy nuclei above a few GeV per nucleon-incident energy. Author

74 OPTICS

Includes light phenomena; and optical devices.
For lasers see *36 Lasers and Masers.*

N94-25721# Organisatie voor Toegepast Natuurwetenschappelijk Onderzoek, The Hague (Netherlands). Physics and Electronics Lab.
THEORY AND MODELING OF STIMULATED RAMAN SCATTERING
J. C. VandenHeuvel Jun. 1993 86 p
(AD-A273755; FEL-93-A135; TDCK-TD-92-1737) Avail: CASI HC A05/MF A01

A three-dimensional finite difference method is presented for the propagation through a gain medium of beams focused by an astigmatic lens. The method is used for the modeling of a Raman amplifier that uses astigmatic lenses. With this method, the effect of gain focusing on the amplification is studied. The numerical results show a good correspondence with analytical models in the range where these models are applicable. The threshold power of stimulated Raman scattering (SRS) has been calculated for various nondiffraction-limited pump beams using the numerical model. It is shown that the threshold power, for a tightly focused beam, depends on the M squared factor that is related to the pump beam quality. Additionally, the influence of the exact pump beam profile on the threshold is small. Therefore, the M squared factor is a useful parameter for analyzing the experimental threshold. We show that the measured SRS thresholds in methane correspond with the calculated thresholds. DTIC

N94-25729# Air Force Inst. of Tech., Wright-Patterson AFB, OH. School of Engineering.
CHARACTERIZATION OF AN LCD FOR USE AS A PROGRAMMABLE PHASE SHIFTER TO PRODUCE A SINGLE-LOBED FAR-FIELD PATTERN IN A PHASED ARRAY M.S. Thesis
Gregory S. Kenyon Dec. 1993 71 p
(AD-A273883; AFIT/GAP/ENP/93D-05) Avail: CASI HC A04/MF A01

The liquid crystal display (LCD) from an inexpensive pocket television was converted to a spatial light modulator (SLM) for the purpose of altering the phase front of a ten element diode laser array to produce a single lobe far field pattern. Characterization of the SLM determined the amount of phase shift, amplitude modulation and polarization rotation properties. Nonuniformities within the phase shifter and insufficient phase shift prevented the formation of a single lobe. However, a very limited phase grating was created and analyzed. LCDs from inexpensive commercial pocket televisions were found unsuitable for use as phase shifting spatial light modulators. DTIC

N94-25730# Air Force Inst. of Tech., Wright-Patterson AFB, OH. School of Engineering.
IMPROVED QUALITY OF RECONSTRUCTED IMAGES THROUGH SIFTING OF DATA IN STATISTICAL IMAGE RECONSTRUCTION M.S. Thesis
Craig A. Stoudt Dec. 1993 151 p
(AD-A273884; AFIT/GEO/ENP/93D-03) Avail: CASI HC A08/MF A02

The U.S. Air Force employs adaptive optics systems to produce images of exo-atmospheric objects. Typically, a large set of short exposure images are collected, re-centered to compensate for random image motion, averaged together to improve the signal to noise ratio, and then processed to form a reconstructed image. It is known that some short exposure images will be better than others, so some researchers have suggested that image quality can be improved by selecting a subset of the short exposure images according to some quality criterion, and then processing the average of this subset to form a single, high quality image. This thesis investigates the statistical implications of using frame selection as a post-processing technique to enhance images of exo-atmospheric objects measured by Air Force adaptive optics systems. The results demonstrate that frame selection narrows the optical system point spread function, which reduces image blurring, and increases the frequency spectrum signal to noise ratio, particularly in the mid-frequency range. For extended objects, the technique is light level dependent: for a 1 meter adaptive optics telescope, frame selection will yield an increase in signal to noise ratio for objects brighter than visual magnitude +2.3. DTIC

N94-25742# Air Force Inst. of Tech., Wright-Patterson AFB, OH.
PERFORMANCE IMPACTS FOR ACTUATOR MISALIGNMENTS AND FAILURES IN LARGE-APERTURE ADAPTIVE-OPTIC TELESCOPES M.S. Thesis
Timothy D. Hogan Dec. 1993 106 p
(AD-A273838; AFIT/GSO/ENP/93D-01) Avail: CASI HC A06/MF A02

Large-aperture telescopes require adaptive optics in order to compensate for atmospheric turbulence which would otherwise negate the resolution advantages of using large apertures. This investigation analyzes the impacts of misalignments and failures, in the deformable mirror actuators, upon the performance of such systems. A numerical simulation of a standard adaptive optics system is used to generate characteristic optical transfer function (OTF) and signal-to-noise ratio (SNR) performance metrics. The performance impacts of the misalignments are shown to be dependent upon the Fried parameter (effective telescope diameter), the source object brightness, and the control system time delay. The degree of performance degradation is directly related to the relative value of the Fried parameter to the deformable mirror displacement (misalignment cases) and the effective actuator spacing (actuator failure cases). The results indicate that the impact of misalignments and failures is small when seeing conditions are good or the percentage misalignments and failures are small. DTIC

N94-25758# Air Force Inst. of Tech., Wright-Patterson AFB, OH.
DESIGN OF A SHARED COHERENT CACHE FOR A MULTIPLE CHANNEL ARCHITECTURE M.S. Thesis
John A. Reisner Dec. 1993 112 p
(AD-A274026; AFIT/GCS/ENG/93D-19) Avail: CASI HC A06/MF A02

The Multiple Channel Architecture (MCA) is a recently proposed computer architecture which uses fiber optic communications to overcome many of the problems associated with interconnection networks. There exists a detailed MCA simulator which faithfully simulates an MCA system, however, the original version of the simulator did not cache shared data. In order to improve the performance of the MCA, a cache coherency protocol was developed and implemented in the simulator. The protocol has two features which are significant: (1) a time-division multiplexed (TDM) communication bus is used for coherency traffic, and (2) the shared data is cached in an independent cache. The modified simulator was then used to test the protocol. Two applications and six test configurations were used throughout the testing. Experiment results showed that the protocol consistently improved system performance. Also, a proof-of-concept experiment indicated that performance improvements can be attained by varying cache parameters between the independent shared and private data caches. DTIC

N94-25768# Air Force Inst. of Tech., Wright-Patterson AFB, OH.
PERFORMANCE COMPARISON OF SHEARING INTERFEROMETER AND HARTMANN WAVE FRONT SENSORS M.S. Thesis
Timothy L. Pennington Dec. 1993 91 p
(AD-A274031; AFIT/GE/ENG/93D-31) Avail: CASI HC A05/MF A01

The resolution of optical imaging systems is severely degraded from the diffraction limit by the random effects of the atmosphere. Techniques exist to compensate for the atmospheric turbulence, one of which is adaptive optics. A critical component in the adaptive optics system is the wavefront sensor. Presently, two types of sensors are being used: the Hartmann-Shack wavefront sensor and the shearing interferometer. Previous studies have compared these two sensors and found them to perform identically for a point source. However, to date, no comparison has been performed for an extended source and subaperture spacing larger than the correlation length of the atmosphere, ro. This thesis has examined this problem and compared these two sensors for the above conditions. Results indicate that the sensors have comparable performance when an infinite number of photons are available. However, the photon limited cases indicate superior performance by the Hartmann sensor. DTIC

N94-25902# Rockwell International Corp., Thousand Oaks, CA. Science Center.
STUDIES OF NON-LINEAR OPTICAL EFFECTS FOR AGILE BEAM STEERING Final Report, 1 May 1988 - 31 Jul. 1991
F. Vachss, I. McMichael, and P. Yeh Nov. 1993 28 p
(Contract N00014-88-C-0231)
(AD-A273998; SC5545.FR) Avail: CASI HC A03/MF A01

The objective of this program is the demonstration of a new technique for massless beam steering of high energy laser radiation. Using the effect of nonlinear electrostriction in acousto-optic devices, we show large improvements in diffraction efficiency and resolution. These results are obtained through the development of a novel geometry for acousto-optic beam steering and of a prototype device designed to take advantage of this geometry. Theoretical and experimental results of this effort establish the validity of large aperture, high frequency nonlinear acousto-optic beam steering. The results are found to be applicable to steering of high power laser beams. DTIC

N94-25940# Army Research Lab., Adelphi, MD.
MITSUBISHI 3-5 MICROMETERS IR IMAGER FOR MACHINE-VISION/ATA APPLICATIONS Final Report, 1990 - 1993
David B. Hillis Nov. 1993 17 p
(AD-A273812; ARL-TR-304) Avail: CASI HC A03/MF A01

Presented in this report are the results of a study conducted to test the performance of the Mitsubishi model 5120C IR Imager as part of an automatic target acquisition (ATA) system. The study was conducted in two phases. The first was directed toward a detailed analysis of the images produced by the Mitsubishi sensor, with the aim of identifying any artifacts or characteristics that might elude the human observer but still affect the ATA system's performance. The second phase involved extensive field testing using the Mitsubishi sensor with two ATA systems: one based on the VME (Versa Module European) bus standard and the other based on a PC. The Mitsubishi sensor showed very good performance in almost all tests and appears to be an excellent choice for ATA/machine-vision applications. Frame-by-frame analysis of digitized image sequences from the Mitsubishi sensor failed to uncover any hidden problems, and several weeks of field testing with two different ATA systems demonstrated high-quality performance. DTIC

N94-25941# Southwest Research Inst., San Antonio, TX.
MICROTUBULES FOR NONLINEAR OPTICAL LIMITING Final Report
Stephen T. Wellinghoff, Charles K. Baker, Martin J. Sablik, Ralph H. Hill, and David W. Naegeli 3 Dec. 1993 98 p
(SwRI Proj. 01-3165)
(AD-A273940) Avail: CASI HC A05/MF A02

The effort in visible laser eye and sensor protection has focussed on several problems, one of which was the threshold for laser eye damage of 1.0-0.1 microjoule (micro J)/sq cm (or 1000-100 W/sq cm for a nanosecond pulse) over a broad wavelength range form 400-700 nm. This value is the so-called 'clamping threshold' which is the maximum intensity permitted to exit the optical device, regardless of the input intensity. The most interest was concentrated in finding a solution for nanosecond threats by a retrofit of existing equipment (binoculars, periscope viewers, etc.,) or by fabrication into a simple set of goggles or a visor. This very low clamping threshold, or course, requires a very highly nonlinear material that is fast and operates over a wide frequency range. The nonlinear materials work can be classified into the following types: (1) liquid crystals; (2) organometallics and polymers; (3) ultrarapid crystallizing alloys and other thermally induced phase changes; and (4) phase conjugate mirrors. DTIC

N94-26100# University of Southern Mississippi, Bay Saint Louis.
DEVELOPMENT OF A MULTI-SENSOR IN SITU FIBER OPTIC FLUOROMETER
S. E. Lohrenz, V. L. Asper, M. J. Morris (Ocean Optics, Inc., Dunedin, FL.), and R. A. Walters (Ocean Optics, Inc., Dunedin, FL.) Nov. 1993 27 p
(Contract DE-FG02-92ER-61443)
(DE94-003399; DOE/ER-61443/2) Avail: CASI HC A03/MF A01

The objective is to develop and evaluate a multi-sensor in situ fiber optic fluorometer. The instrument is designed to sample and store in vivo strobe-stimulated fluorescence data at multiple depths and high frequencies (1 Hz). This information may be used for estimating the distribution and abundance of particulate pigment biomass, for supporting models of water column primary production, and as a complement to remotely sensed ocean color estimates of pigment biomass. The instrument is unique in that it uses fiber optic technology to increase vertical resolution. While it is theoretically possible to accomplish this task using a large number of commercially available fluorometers, the proposed design would provide a less expensive approach. Two prototype instruments have been built and are being tested. The first, a single sensor instrument interfaced with a 486 personal computer, has been used to optimize hardware and sensor design and to evaluate fiber performance and instrument detection limits. The second instrument, containing eight sensors and capable of autonomous operation with time-series data acquisition and storage, was recently deployed in a cruise in the Gulf of Mexico. Preliminary results indicate that the instrument meets all the project goals and that low cost, high frequency, high spatial resolution fluorescence data are obtainable with the current design. DOE

N94-26246# Sandia National Labs., Albuquerque, NM.
PECULIARITIES AND APPLICATION PERSPECTIVES OF METAL-ION IMPLANTS IN GLASSES
P. Mazzoldi (Padua Univ., Italy.), F. Gonella (Padua Univ., Italy.), G. W. Arnold, G. Battaglin (Venice Univ., Italy.), and R. Bertoncello (Padua Univ., Italy.) 1993 50 p Presented at the Nuclear Instruments and Methods in Physics Research on Radiation Effects in Insulators, Nagoya, Japan, Sep. 1993
(Contract DE-AC04-94AL-85000)
(DE94-004671; SAND-93-3826C; CONF-9309259-3) Avail: CASI HC A03/MF A01

Ion implantation in insulators causes modifications in the refractive index as a result of radiation damage, phase separation, or compound formation. As a consequence, light waveguides may be formed with interesting applications in the field of optoelectronics. Recently, implantation of metals ions (e.g. silver, copper, gold, lead) showed the possibility of small radii colloidal particles formation in a thin surface layer of the glass substrate. These particles exhibit an electron plasmon resonance which depends on the optical constants of the implanted metal and on the refractive index of the glass host. The nonlinear optical properties of such colloids, in particular the enhancement of optical Kerr susceptibility, suggest that the ion implantation technique may play an important role for the production of all-optical switching devices. In this paper an analysis of the state-of-the-art of the research in this field will be presented in the framework of ion implantation in glass physics and chemistry. DOE

N94-26276# Argonne National Lab., IL.
COMPARISON OF TECHNOLOGY FOR HIGH-POWER LASER MIRRORS AND SYNCHROTRON RADIATION MIRRORS
H. E. Bennett (Naval Air Warfare Center, China Lake, CA.) and A. M. Khounsary 1993 18 p Presented at the Annual Meeting of the Society of Photo-Optical Instrumentation Engineers, San Diego, CA, 11-16 Jul. 1993
(Contract W-31-109-eng-38)
(DE94-002913; ANL/XFD/CP-81152; CONF-930722-53) Avail: CASI HC A03/MF A01

There are obvious differences but some surprising similarities between high-power laser mirrors designed for use in the visible and infrared wavelengths and synchrotron mirrors designed for use at x-ray wavelengths. The use of synchrotron mirrors at grazing incidence results in a relaxation of figure, surface microroughness, and thermal heating tolerances relative to the wavelength of nearly two orders of magnitude. As a result, the tolerances become roughly comparable to those desired for high-power laser mirrors for the visible region of the spectrum. Experience gained over the years by laser mirror designers in substrate design, the influence of metallic coatings on thermal and optical performance and limiting values for surface microroughness may be helpful to designers of synchrotron systems, but exploitation of the promise of the new synchrotron systems still represents a challenging problem for researchers. The specifications and operational approaches to meeting them for the new Advanced Photon Source at Argonne National Laboratory are given. DOE

N94-26383 International Centre for Theoretical Physics, Trieste (Italy).
CAD OF GeO2-SiO2 DOUBLE-LAYER CORE DISPERSION-SHIFTED SINGLE-MODE FIBRE
Jing Huang (China Scientific and Technical Univ., Hofei.) and Zhen-Yuan Liu (China Scientific and Technical Univ., Hofei.) Apr. 1993 7 p Limited Reproducibility: More than 20% of this document may be affected by microfiche quality
(DE93-634325; IC-93/119) Avail: CASI HC A02 (US Sales Only)

A numerical method of double-layer core dispersion-shifted single-mode fibre without central dip is shown. The refractive-index profile parameter of 10 micron core diameter fiber is calculated, when zero dispersion wavelength equals 1.55 microns. This method is simple and convenient. DOE

N94-26572# Science Applications International Corp., Albuquerque, NM.
LONG DURATION EXPOSURE FACILITY SPACE OPTICS HANDBOOK Final Report, 6 Jan. 1992 - 31 Aug. 1993
William T. Kemp (Phillips Lab., Kirtland AFB, NM.), Edward Taylor (Phillips Lab., Kirtland AFB, NM.), Carl Bloemker, Frank White, Gary Rensner, and Alan Watts (POD Associates, Inc., Albuquerque, NM.) Sep. 1993 406 p
(Contract F29601-91-C-0071)
(AD-A274831; PL-TN-93-1067) Avail: CASI HC A18/MF A04

This handbook provides a user a space optics design guide to materials based on the Long Duration Exposure Facility (LDEF) Space Optics Experiments. The materials covered are refractive optics, coatings, filters, mirrors, second surface mirrors, quartz microbalances, and fiber optics. The guide presents the data and the experience learned from the LDEF Space Optics Experiments in one volume in a user-friendly fashion. The data reported in the handbook are a compilation of the data published by the individual experimenters. Natural space environment data with an emphasis on the microparticle environment are also presented. DTIC

N94-26648 Physics and Electronics Lab. TNO, The Hague (Netherlands).
FOCAL PLANE ARRAYS IN ADVANCED THERMAL IMAGES Review Report [FOCAL PLANES ARRAYS IN GEAVANCEERDE WARMTEBEELDCAMERASYSTEMEN]
J. S. deVries and H. M. A. Schleijpen Mar. 1993 54 p In DUTCH and ENGLISH Sponsored by DMKL/OMAT/KIO, The Hague, Netherlands
(Contract A90/KL/654)
(AD-B174292; FEL-93-A009; TD92-3837; ETN-94-94941) Copyright Avail: Issuing Activity (TNO Physics and Electronics Lab., P. O. Box 96864, 2509 JG The Hague, Netherlands)

The development of infrared focal plane array detectors (IR-FPA's) during the last decade is summarized. The different aspects of the IR-FPA's are discussed. Each type of IR-FPA detector system, and hence each camera system in which the FPA is used, has advantages and disadvantages. The status of IR-FPA techniques is outlined. Advanced systems are presented. The expected developments and applications of IR-FPA's in thermal imaging systems are given. ESA

N94-26649 Physics and Electronics Lab. TNO, The Hague (Netherlands).
ANALYSIS OF THE INFLUENCE OF WEATHER ON INFRARED IMAGERY [ANALYSE VAN DE WEERSINVLOED OP INFRAROOD-BEELDEN]
A. J. Maas and J. S. deVries Feb. 1993 36 p In DUTCH
(Contract A90/KL/655)
(FEL-92-A421; TD92-3836; ETN-94-94944) Copyright Avail: Issuing Activity (TNO Physics and Electronics Lab., P. O. Box 96864, 2509 JG The Hague, Netherlands)

The behavior of the contrast characteristics in IR images as a function of weather parameters was investigated in order to gain insight into the dependence of detectability of targets with IR sensors as a function of environmental parameters. IR images in the 10 micron band acquired with the DuDa sensor were used. The images consist of a series of 325 recordings of various objects situated in a natural background. For every pixel, the observed apparent temperatures are fitted as a function of the measured environmental parameters using the multilinear regression method. The derived empirical model can be used to simulate imagery for other sets of environmental parameters which have not been observed. ESA

N94-26666 Victoria Univ. (British Columbia). Dept. of Mechanical Engineering.
CAPTURE AND LOCATION OF BLOBS IN DIGITAL IMAGES M.S. Thesis
Sven Alexander Steelemann 1993 170 p
(ISBN-0-315-84382-9; CTN-94-61026) Copyright Avail: Micromedia Ltd., Technical Information Centre, 240 Catherine Street, Suite 305, Ottawa, Ontario, K2P 2G8, Canada HC/MF

Three methods of detecting the location of active targets using machine vision are described. In the field of visual servoing, the detection and location of targets is the first step in controlling the motion of a platform with respect to the target. In certain long-range outdoor settings, active targets are the only feasible target type. For each method (centroid, linear parameter estimation, and nonlinear parameter estimation), a theoretical resolution and accuracy analysis is performed. This analysis is followed by an experimental suite that determines real resolution and accuracy of each method. Results show that the linear parameter estimation technique does not properly locate active targets. Both the centroid and nonlinear parameter estimation techniques can achieve accuracies of 0.25 pixels in locating active targets. Author (CISTI)

N94-26834# Emory Univ., Atlanta, GA. Dept. of Chemistry.
MECHANISTIC STUDIES OF OPTO-ELECTRONIC MATERIALS AND SYNTHESES USING MULTIPLE LASER AND SURFACE DIAGNOSTICS Final Report, 1 Dec. 1988 - 31 Dec. 1993
M. C. Lin 31 Dec. 1993 20 p
(Contract N00014-89-J-1235)
(AD-A274528) Avail: CASI HC A03/MF A01

The objective of this program was the development of novel OMCVD/LCVD processes for preparation of wide band-gap semiconductors and the elucidation of the basic reaction mechanisms in these processes, so as to control the deposition rates and to improve the opto-electronic properties of the materials. The synthesis and the mechanistic elucidation of wide band-gap III/V metal nitrides by OMCVD and LCVD, the dry-passivation of GaAs and the deposition of carbon nitride films, have been carried out with a unique UHV surface reaction system equipped with multiple gas-phase and surface species analyses. The system was constructed with joint support from the ONR and Emory University. Gas-phase species were detected by EI- and REMPI-MS, whereas surface species and structure were characterized by multiple surface diagnostic tools: AES, UPS, XPS, LEED, SEM and HREELS. The systematic elucidation of the spectroscopy and the mechanisms for the thermal and photochemical decomposition reactions of individual source molecules involved in the OMCVD/LCVD processes were first carried out before the actual deposition processes were conducted. We used a new nitrogen source, hydrazoic acid (HN3), for the preparation of InN films with 1:1 elemental ratio by low-pressure CVD. The prepared films were characterized by AES, UPS, XPS, SEM, LEED and HREELS, and optical techniques such as UV/visible adsorption and photo-luminescence. InN films with very high quality SEM and UPS characteristics have been deposited on GaAs substrates without a buffer layer. Over 20 technical papers (with 23 presentations) were completed from these studies. DTIC

N94-26857# Honeywell, Inc., Minneapolis, MN. Systems and Research Center.
OPTOELECTRONIC TECHNOLOGY CONSORTIUM Quarterly Report No. 5, 1 Jul. - 30 Sep. 1993
Mary Hibbs-Brenner 15 Oct. 1993 10 p
(Contract MDA972-92-C-0071; ARPA Order 8351C)
(AD-A274595) Avail: CASI HC A02/MF A01

The Optoelectronic Technology Consortium has been established to position U.S. industry as the world leader in optical interconnect technology by developing, fabricating, integrating and demonstrating the producibility of optoelectronic components for high-density/high-data-rate processors and accelerating the insertion of this technology into military and commercial applications. This objective will be accomplished by a program focused in three areas. Demonstrated performance: OETC will demonstrate an aggregate data transfer rate of 16 Gb/s between single transmitter and receiver packages, as well as the expandability of this technology by combining four links in parallel to achieve a 64 Gb/s link. Accelerated development: By collaborating during the precompetitive technology development stage, OETC will advance the development of optical components and produce links for a multiboard processor testbed demonstration. Producibility: OETC's technology will achieve this performance by using components that are affordable and reliable. DTIC

N94-26981# Naval Surface Warfare Center, Crane, IN.
CHARACTERIZATION AND CALIBRATION OF THE AGEMA 880+ IMAGING RADIOMETER Final Report, 1 Jan. - 23 Aug. 1993
Tim Bradley and Jeff Hendrixson 23 Aug. 1993 96 p
(AD-A274417; NSWCCR/RDTR-93/040) Avail: CASI HC A05/MF A01

With traditional flare measurements, a flare is assumed to be a point source since it is a relatively small target viewed at a relatively long range. However, when the flare area becomes sufficiently large in relation to the viewing range, the flare must be treated as an extended source, and the spatial characteristics of the flare must be considered. The ability of an imaging radiometer to provide spatial information makes this instrument ideal for area type flare measurements. This report outlines a series of calibration and characterization procedures performed on the AGEMA 880+ thermal imager. The project objectives were to do the following: (1) Verify the accuracy of 880+ measurements; (2) Perform an external calibration of the 880+ system; and (3) Reduce radiometric data and produce false color images. DTIC

N94-26982# Wright Lab., Wright-Patterson AFB, OH.
OPTICAL CHARACTERIZATION AND GUIDED WAVE LOSS MEASUREMENTS FOR END-CAPPED 6F-POLYBENZOXAZOLE Final Report, 1 Nov. 1990 - 1 Jun. 1993
Angela L. McPherson and Jeffery W. Baur Sep. 1993 94 p
(AF Proj. 2305)
(AD-A274586; WL-TR-93-4098) Avail: CASI HC A05/MF A01

A Mathematica software package to model the behavior of light inside an optical waveguide is discussed. Examples of package features are presented and discussed. Possible new waveguide materials are investigated with this package as a baseline for material evaluation. The use of the polymer 6F-PBO-IE as a possible candidate for high temperature optical waveguide material based in its high Tg of 300C and its optical clarity is discussed. Theoretical studies are performed with the Mathematica package. Slab waveguide samples are fabricated by spin-coating on oxidizO5 silicon wafers and characterized through measurements of the index of refraction and waveguide loss. Results show that the material exhibits its lowest loss of 4.5 db/cm at a wavelength of 700nm. We conclude, based on experimental results, that this material, 6F-PBO-1E, while it may be useful for some optical applications, does not meet the Air Force specification of 1 db/cm or less performance guideline for optical waveguide materials and therefore is not appropriate for Air Force applications in its present form. DTIC

N94-26990# Colorado Univ., Boulder.
AN OPTOELECTRONIC GRAPHICS DISPLAY PROCESSOR Quarterly Report, 15 Sep. - 14 Dec. 1993
Vincent P. Heuring 15 Dec. 1993 4 p
(Contract N00014-93-1-0419)
(AD-A274401) Avail: CASI HC A01/MF A01

We are continuing to make significant progress toward an Optoelectronic Graphics Display Processor. During this period we have designed and are having fabricated, at no cost to ONR, some small prototype OEIC high-speed detector amplifiers and microlaser driver circuits. We are proceeding with our calculations of system bit error rate due to crosstalk and power loss, and we have redesigned our system visualization and animation CAD component. Most importantly, we are extending our architecture to handle 3D scenes, that is, incorporation of a Z-buffer, and we are also extending it to handle color/gray scale. DTIC

N94-27010# SRI International Corp., Menlo Park, CA.
HIGH-SPEED, HIGH-DENSITY, COHERENT TIME-DOMAIN OPTICAL MEMORY Final Report, 1 Sep. 1990 - 31 Aug. 1993
Ravinder Kachru and Xiao-An Shen Nov. 1993 60 p
(Contract F49620-90-C-0083)
(AD-A274249; MP-93-225; AFOSR-93-0900TR) Avail: CASI HC A04/MF A01

The objective of this research was to quantitatively evaluate the concept of time-domain optical memory (TDOM) using the hole-burning mechanism. The TDOM concept offers both high speed and high memory density. The advantage of TDOM over traditional semiconductor memory is its inherent parallelism, which allows data to be stored and retrieved from the memory at much higher speed. The practical success of the proposed memory, therefore, depends critically on-among other issues-the storage, retrieval, and processing of images. In addition, new data storage techniques are needed to implement a practical memory. The last three years of this research program focused on (1) development of new phase modulation techniques to enhance the storage, retrieval, and integrity of the stored information; (2) experimental studies of image storage and phase conjugate retrieval; (3) image processing; and (4) practical holographic storage of images by using the hybrid time-frequency approach. Specifically, SRI demonstrated data encryption by phase modulating the read and write pulses. Image correlation and convolution was demonstrated and its implication for pattern recognition examined. Finally, this laboratory demonstrated high-fidelity random access and retrieval using holographic storage in Pr3+: YA103 with a single-frequency ring laser. These experiments have clearly demonstrated the practical viability of TDOM with existing technology. In the next stage of the research, the performance issues such as bit-error-rates, signal-to-noise ratios, and laser stability need to be addressed. DTIC

N94-27046# National Defence Research Establishment, Linkoeping (Sweden). Huvudavdelning foer Informationsteknologi.
RESEARCH AND DEVELOPMENT WITHIN NONLINEAR OPTICS FOR PROTECTION OF OPTICAL SENSORS AGAINST LASER IRRADIATION ON OF OPTICAL SENSORS AGAINST LASER IRRADIATION. QUARTERANNUAL REPORT 1 (APRIL 1993)) Quarterly Annual Report No. 1, Apr. 1993 [FORSKNING OCH UTVECKLING INOM OMRADET ICKELINJAER OPTIK FOER SKYDD AV OPTISKA SENSORER MOT IASERSTRALNING. KVARTALSRAPPORT 1, APRIL 1993]
Mikael Lindgren Apr. 1993 15 p In SWAHILI
(ISSN 0281-0212)
(PB94-124245; FOA-A-30083-3.1) Avail: CASI HC A03/MF A01

This is the first in a series of five periodic reports concerning research and development within nonlinear optics at FOA3. Results are obtained in four distinct activity areas: (1) Development of techniques for determination of nonlinear index of refraction and two photon absorption. Equipment for z-scan measurements has been built and development of theory and computer programs for analysis has started. (2) Preparation and characterization of electrooptically active (liquid crystalline) polymer films. Equipment for m-line spectroscopy and associated analysis programs are developed at FOA2. (3) Theoretical calculations of nonlinear optical properties of organic materials. Several classes of organic materials (molecules) have been examined theoretically and from the results a series of test materials has been purchased. (4) Literature studies and seminars. A database for materials (organics) and applications/techniques of nonlinear optics has been created. NTIS

N94-27062# Air Force Inst. of Tech., Wright-Patterson AFB, OH. School of Engineering.
DETECTION OF LOW-INTENSITY MAGNETIC FIELDS WITH A MAGNETOSTRICTIVE FIBER OPTIC SENSOR M.S. Thesis
Laura L. Picon Dec. 1993 262 p
(AD-A274120; AFIT/GE/Eng/93D-32) Avail: CASI HC A12/MF A03

This thesis presents the fabrication, evaluation, and performance results of a magnetostrictive fiber optic sensor. The sensor was fabricated using a Mach-Zehnder interferometric arrangement. Four classes of sensing arms were fabricate as: ribbons, cylinders, sandwiches, and sputter coated sheaths. The four classes of sensing arms were evaluated using Metglas(TM), nickel, and a combination of Metglas(TM) and nickel. Optimization techniques were applied to the sensor to maximize its sensitivity. These techniques included: annealing the magnetostrictive material, operating the magnetic field at a range of frequencies, enclosing the sensor in a shielded chamber, and fabricating the sensing arms with polarization maintaining fiber optic cable. The lowest magnetic flux density that could be detected was 0.3 mG. This was achieved using a Metglas ribbon-fiber configuration with the ribbon's magnetization direction aligned perpendicularly with the applied 52 kHz AC magnetic field with a 5 volt DC bias. When operating this configuration at a 10 Hz AC magnetic field with a 5 volt DC bias, the lowest magnetic flux density that could be achieved was 8.9 mG. DTIC

N94-27066# Naval Surface Warfare Center, Crane, IN.
RADIOMETRIC, SPECTRAL, AND EFFECTIVENESS EQUIPMENT Final Report
Bernard E. Douda and Henry A. Webster 24 Sep. 1993 22 p
(AD-A274208; NSWCCR/RDTN-93/010) Avail: CASI HC A03/MF A01

This is a description of an assortment of infrared radiometric, spectral, and effectiveness equipment used for measurement of the radiative output and effectiveness of assorted devices. These instruments are installed and routinely operated at this center and on field flight test. The contents describe some of the instrument parameters and measurement capability. DTIC

N94-27102# Air Force Inst. of Tech., Wright-Patterson AFB, OH. School of Engineering.
ENHANCED TRACKING OF AIRBORNE TARGETS USING FORWARD LOOKING INFRARED AND LASER RETURN MEASUREMENTS M.S. Thesis
Patrick J. Grondin Dec. 1993 441 p
(AD-A274181; AFIT/GE/Eng/93D-11) Avail: CASI HC A19/MF A04

The Air Force Institute of Technology has been involved in developing Kalman filter based trackers of ballistic missiles for 15 years. The goal of this thesis is to develop a Multiple Model Adaptive Estimator (MMAE) that tracks the missile plume (using a forward looking infrared sensor) and the missile hardbody center-of-mass (using low energy laser returns) for the purpose of directing a high power laser to incapacitate the missile. The missile plume 'pogos' about an offset equilibrium point (relative to the hardbody center-of-mass) with an amplitude and frequency of oscillation that are not precisely known a priori. The MMAE algorithm estimates these parameters to improve performance in tracking the hardbody center-of-mass. To accomplish this MMAE structure, single Kalman filters were developed and tested at the different parameter values. A Kalman filter residual analysis was used on these working single filters to define the MMAE structure that provided the most effective adaptation and most

accurate target tracking. A three-filter MMAE structure gave the lowest hardbody center-of-mass tracking errors. The two-dimensional parameter space, pogo amplitude and frequency, was successfully partitioned according to the frequency of oscillation. When the plume pogo amplitude is large, the MMAE structure substantially reduces the tracking errors of the hardbody center-of-mass, compared to a tracker without adaptive pogo estimation.
DTIC

N94-27137 Physics and Electronics Lab. TNO, The Hague (Netherlands).
LIGHT EMITTING POROUS SILICON Final Report
H. H. Bekman, K. W. Benoist, J. L. Joppe, and H. J. VanWeerden May 1993 32 p Limited Reproducibility: More than 20% of this document may be affected by microfiche quality
(AD-A274152; FEL-93-B047; TDCK-93-0302) Avail: Issuing Activity (Defense Technical Information Center (DTIC))

After a review of the basic properties of porous silicon, the fabrication method used to produce visible light emission from silicon is described. The photoluminescence spectra were recorded using a room temperature spectrometer. Initial attempts producing electrically stimulated light emission are described. Two pressure experiments were carried out to unravel the origin of light emission in porous silicon. DTIC

N94-27153# Department of the Navy, Washington, DC.
METHOD OF MEASURING LIQUID LEVEL Patent Application
Lloyd Bobb, inventor (to Navy) 24 Nov. 1993 25 p
(AD-D016049; US-Patent-Appl-SN-159962) Avail: CASI HC A03/MF A01

A method of measuring the position of a liquid surface vessel is described. An optical fiber is provided which has first and second ends and has an energy-absorbing element of a predetermined length disposed upon a portion of the cladding thereof such that there is a thermal interface between the energy-absorbing element and the cladding. The optical fiber is then positioned in the vessel so that the energy-absorbing element disposed thereon extends a known distance into the vessel along a known depth gradient of the vessel and so that the energy-absorbing element will intersect the liquid surface over the anticipated range of positions. Single-frequency, coherent light is then transmitted through the core of the optical fiber by launching it into the first end of the optical fiber. A pulse of energy is applied across the entire length of the energy-absorbing element to heat it, and then the transmitted light is received from the second end of the optical fiber. The change in phase of the transmitted light resulting from applying the pulse of energy is then measured, and the position of the liquid surface is then determined in accordance with the change in phase. DTIC

N94-27178 Tel-Aviv Univ. (Israel). School of Physics and Astronomy.
EVANESCENT FIELD INFRARED SPECTROSCOPY USING CHALCOGENIDE GLASS FIBER M.S. Thesis
Moti Katz Mar. 1992 127 p In HEBREW
(ITN-94-85233) Copyright Avail: Issuing Activity (Tel-Aviv Univ., Exact Sciences Library, Ramat Aviv 69978, Israel)

A study was made of the interaction between infrared radiation in an optical fiber and a specimen in which the fiber was embedded. The interaction involves the evanescent field which extends outside the fiber, and the present study concentrated on the absorption of this field by the specimen, which behaves as cladding on the fiber. A theoretical model of the absorption process was developed, which expresses the absorption by an infinite cladding in terms of fiber and sample parameters and radiation coupling conditions. Experimental checks showed that the model could predict the radiation absorption within a 5% error range. A second model was developed, to predict the signal to noise ratio as a function of fiber and sample parameters and radiation coupling conditions. The predictions of the model were confirmed experimentally and the model was used to develop a novel fiber-bundle sensor. This sensor combines a large energy-collecting capacity with high responsivity, so that the signal to noise ratio for weak signals can be improved five-fold compared with a single-fiber sensor. The model developed for absorption in a single-fiber sensor is valid also for the fiber-bundle sensor. Another novel sensor, developed and studied in the course of the present investigation, is the bitapered fiber sensor, which improves the signal to noise ratio for weak signals by up to two orders of magnitude, compared with a single-fiber sensor of the same interaction length. The model for absorption by an infinite cladding layer was extended for the case of thin cladding layers. An experiment characterizing the absorption spectrum of a thin layer is presented and the model is used to calculate its thickness (160 A). In the last part of the study, two unique experiments are presented, one being the measurement of a gas by a bitapered fiber sensor in an FTIR spectrometer and the other being the monitoring of the steps of a polymer layer growth by infrared spectroscopy. ISA

N94-27209 National Defence Research Establishment, Linkoeping (Sweden). Huvudavdelning foer Informationsteknologi.
Ir-FIBERS IN A LASER THREAT WARNING SYSTEM AND ROBOT SHOT WARNING SYSTEM [IR-FIBRER I LASERVARNARE OCH ROBOTSKOTTVARNARE]
S. Oedman and J. P. Bengtsson Mar. 1993 36 p In SWAHILI
(PB94-124476; FOA-C-30697-9.4,3.1) Avail: Issuing Activity (National Technical Information Service (NTIS))

The report contains a literature survey of research on optical and mechanical properties and the aging of IR fibers. Many glasses and crystals have their lowest attenuation in the infrared, IR, region. The attenuation in these materials has a theoretical value, 10(exp -3) (dB/km), that is much lower than in optical quartz fibers, 0.15 (dB/km). IR fibers may therefore give better performance, economy and novel technical solutions for fiber optic sensors and communication systems. Transmission of IR radiation in laser warning systems and imaging IR systems is potentially possible using IR-fibers. A field of regard of 360 deg can be realized by transmitting IR radiation from various strategic points at a platform to a central detector or imaging system. There are, however, uncertainties about long term mechanical and optical properties. The authors have also calculated theoretical detection distances for laser threat and missile warning systems. NTIS

N94-27441 Concordia Univ., Montreal (Quebec). Dept. of Electrical and Computer Engineering.
A STUDY OF MULTIPLE GUIDE OPTICAL COUPLERS M.S. Thesis
Edward Milczarek Mar. 1993 153 p
(ISBN-0-315-84633-X; CTN-94-61082) Copyright Avail: Micromedia Ltd., Technical Information Centre, 240 Catherine Street, Suite 305, Ottawa, Ontario, K2P 2G8, Canada HC/MF

Coupled mode theory is introduced and used to study the transfer characteristics of multiple guide optical couplers. Two- and three-guide couplers are examined to determine their effectiveness as power transfer devices, and the implementation of two- and three-guide switches is discussed. An approach to designing a three-guide coupler is introduced, in which a feedback loop is placed around one of the guides. It is demonstrated that this device exhibits desirable characteristics unavailable in current passive coupler designs: splitting any fraction of a signal while maintaining a zero-phase shift between the outputs, as well as combining two signals of arbitrary amplitude and phase. The wavelength dependence of this device is examined, and its potential as a wavelength selective filter or wavelength division multiplexer is demonstrated. Various computer programs were developed to aid in the analysis of optical couplers, including one that animates the eigensolutions of the device as signals propagate through its length. The technique of eigensolution decomposition is used to illustrate the relationship between coupling parameters of multiple N-guide couplers such that they may either achieve complete transfer of power between guides or act as interferometers. Author (CISTI)

N94-27598 Defence Research Establishment Valcartier (Quebec).
ANALYTIC APPROXIMATION TO RANDOMLY ORIENTED SPHEROID EXTINCTION
B. T. N. Evans and G. R. Fournier Dec. 1993 50 p
(DREV-4712-93; DSIS-94-00102; CTN-94-61116) Avail: CASI HC A03/MF A01

The estimation of electromagnetic extinction through dust or other nonspherical atmospheric aerosols and hydrosols is an essential first step in the evaluation of the performance of all electro-optic systems. Investigations were conducted to reduce the computational burden in calculating the extinction from nonspherical particles. An analytic semi-empirical approximation to the extinction efficiency Q(sub ext) for randomly oriented spheroids, based on an extension of the anomalous diffraction formula, is given and compared with the extended boundary condition or T-matrix method. This will allow for better and more general modeling of obscurants. Using this formula, Q(sub ext) can be evaluated over 10,000 times faster than with previous methods. This approximation has been verified for complex refractive indices m=n-ik, where n ranges from one to infinity and k from zero to infinity, and aspect ratios of 0.2 to 5. It is believed that the approximation is uniformly valid over all size parameters and aspect ratios. It has the correct Rayleigh, refractive index, and large particle asymptotic behaviors. The accuracy and limitations of this formula are extensively discussed. Author (CISTI)

N94-27603# Alabama Agricultural and Mechanical Coll., Normal. Dept. of Physics.
PREDOCTORAL TRAINING GRANT IN THE AREA OF PHYSICAL SCIENCES
P. Venkateswarlu Nov. 1993 55 p
(Contract DE-FG05-89ER-75531)
(DE94-004406; DOE/ER-75531/1) Avail: CASI HC A04/MF A01

This final technical report represents the results of the research in nonlinear optics (optical phase conjugation) obtained by five (5) predoctoral students in the department of physics at Alabama Agricultural and Mechanical University (AAMU). DOE

N94-27643 Royal Military Coll. of Canada, Kingston (Ontario). Dept. of Mechanical Engineering.
BINARY OPTICAL ELEMENTS: STUDIES IN DESIGN, MANUFACTURE AND PERFORMANCE M.S. Thesis
Norman Douglas Bell May 1990 196 p
(ISBN-0-315-60643-6; CTN-94-60985) Copyright Avail: Micromedia Ltd., Technical Information Centre, 240 Catherine Street, Suite 305, Ottawa, Ontario, K2P 2G8, Canada HC/MF

Binary optical elements made from computer generated holographic masks were designed and fabricated using e-beam and pattern generation mask writers and standard photoresist techniques. These 10.6 micrometer wavelength diffractive elements include F/6 and F/10, 50-mm diameter, cylindrical elements and a F/24, 12.4-mm diameter spherical element on thin Si substrates for use with a plane wave incident at 45 deg. A relatively simple hybrid mechanical binary reflective element was fabricated by deforming the straight ridges of the F/6 cylindrical element in the other direction to give spherical focusing. The Si wafer was pressure mounted onto an Al base, milled to yield an elliptically curved surface requiring maximum wafer deflections of 0.79-0.83 mm across the aperture. All elements were tested, utilizing computer controlled data acquisition, for relative focusing abilities by scanning a detector, apodized with a 15 micrometer pinhole, over the focal region. The F/10 cylindrical element blur width dimension was 279 micrometers and the F/24 spherical element gave blur spot dimensions of 483 by 635 micrometers, both within 10 percent of their predicted values. The F/6 hybrid element yielded an unsymmetrical blur spot 254 by 343 micrometers, compared to its ideal value of 155 by 155 micrometers. These deviations are discussed. Author (CISTI)

N94-27674# Department of the Navy, Washington, DC.
FIBER OPTIC FARADAY FLUX TRANSFORMER SPECIFICATION Patent Application
Frank Bucholtz, inventor (to Navy) 22 Oct. 1993 25 p
(AD-D016058; US-Patent-Appl-SN-140389; Navy-Case-74807) Avail: CASI HC A03/MF A01

A fiber optic Faraday flux transformer sensor is disclosed which comprises: a closed loop of wire being responsive to a first time-varying magnetic field from a remote source for producing a secondary time-varying magnetic field which varies as a function of the first time-varying magnetic field, and an optical fiber loop having a plurality of turns arranged in a preselected configuration adjacent to the closed loop of wire and adapted to receive and pass there through input light having a fixed state of linear polarization. The optical fiber loop is responsive to the secondary time-varying magnetic field and to the input light for producing light having a polarization state which changes as a function of the secondary time-varying magnetic field applied thereto. Author (DTIC)

N94-27676# Department of the Navy, Washington, DC.
REFLECTOMETER EMPLOYING AN INTEGRATING SPHERE AND LENS-MIRROR CONCENTRATOR Patent Application
Keith Snail, inventor (to Navy) and Roy Schiff, inventor (to Navy) 29 Oct. 1993 19 p
(AD-D016061; US-Patent-Appl-SN-143098; Navy-Case-75057) Avail: CASI HC A03/MF A01

A reflectometer wherein a light having a predetermined wavelength is projected into an integrating sphere containing a sample whose reflectance is to be measured. As the projected light strikes the sample, rays are reflected back the walls of the integrating sphere; some of which strike the area within the field-of-view of a concentrator. The rays striking within the field-of-view of the contractor upon a detector element which allows one to determine the reflectance of the sample. A control means is utilized to control the wavelength of the projected light through a spectrophotometer, and to calculate the reflectance of the sample. DTIC

N94-27721# Sandia National Labs., Albuquerque, NM.
DEVELOPMENT OF A 2f OPTICAL PERFORMANCE MEASUREMENT SYSTEM
J. W. Grossman 1993 8 p Presented at the ASME International Solar Energy Conference, San Francisco, CA, 27-30 Mar. 1994
(Contract DE-AC04-94AL-85000)
(DE94-003489; SAND-93-1533C; CONF-940326-2) Avail: CASI HC A02/MF A01

Commercialization of faceted stretched-membrane concentrators has created the need for quality control measurements for facet optical performance. High-volume production scenarios require a test method that is quick, can be performed on the production floor, and does not require laboratory-grade equipment. At Sandia, we are developing an optical test method that can be done in a relatively short period of time, requires little space, uses 'off the shelf' test equipment, and provides a quantitative measure adequate to address quality control requirements. The test method is based on common ray trace calculations for targets and images at the radius of curvature for spherical and parabolic (f/D greater than 3) concentrators. The initial development work was done using a monochrome television camera and the beam characterization system. Twenty-four 3-meter facets built for a faceted stretched-membrane dish were characterized using this system. Other smaller facets have also been tested with the system to help establish a correlation with this method and other optical characterization tests. Current work involves adapting a color camera to the system and developing custom software to reduce analysis time and make the system viable for the production floor. This paper discusses the development of the monochrome system, reviews the results of testing, and presents plans for the development of a color system. DOE

N94-27962 McMaster Univ., Hamilton (Ontario). Faculty of Graduate Studies.
THE OPTICAL PROPERTIES OF HIGH-T(c) SUPERCONDUCTORS GROWN BY PULSED LASER DEPOSITION Ph.D. Thesis
Robert Alan Hughes Sep. 1992 152 p
(ISBN-0-315-84917-7; CTN-94-61108) Copyright Avail: Micromedia Ltd., Technical Information Centre, 240 Catherine Street, Suite 305, Ottawa, Ontario, K2P 2G8, Canada HC/MF

Superconducting Pb-Cu-Sr-Y-Ca-O films were successfully grown in-situ by pulsed laser deposition on LaAlO3 at 620 C. The growth procedure yields relatively sharp superconducting transitions and by substituting Ca for Y it is possible to vary the superconducting transition temperature from 10 K to a maximum of 86 K. The laser deposition system was also used to deposit superconducting Nd-Ce-CuO thin films. By carefully controlling the film's oxygen content through high temperature vacuum anneals, it is possible to obtain a superconductor with a transition temperature onsetting at 21 K. The far infrared optical properties of these films were measured using Michelson interferometry. The optical conductivity obtained from Kramers-Kronig analysis is divided into two components, the first fitted to a Drude model and the second described by a model which couples phonons to a midinfrared band. The far infrared reflectance of partially transparent Pb-Cu-Sr-Y-Ca-O films was measured, and normal state results were also described in terms of the two component model. The Drude component again showed a constant plasma frequency and a scattering rate which closely follows the temperature dependence of the direct current resistivity, while the second component showed only a small change as the temperature was varied. Author (CISTI)

N94-27999# Sandia National Labs., Albuquerque, NM.
OPTICAL PARAMETRIC OSCILLATOR MODELING WITH DIFFRACTION, DEPLETION, AND DOUBLE REFRACTION
M. S. Bowers (Aculight Corp., Bellevue, WA.) and A. V. Smith 1993 4 p Presented at the 9th Advanced Solid-State Lasers Meeting, Salt Lake City, UT, 7-10 Feb. 1994
(Contract DE-AC04-94AL-85000)
(DE94-001504; SAND-93-2226C; CONF-940226-1) Avail: CASI HC A01/MF A01 (US Sales Only)

Advancement in the growth and fabrication of nonlinear materials along with continual improvements in the performance of solid-state lasers have led to a resurgence of interest in the development of optical parametric oscillators (OPO's). While many experimental results have been recently reported, very little attention has been given to the development of detailed models to simulate the output characteristics (such as beam quality, efficiency, and threshold) of nanosecond-pumped OPO's. Such models are necessary for understanding experiments and for developing advanced OPO designs that enhance the overall performance of these devices. In this work, we describe a time-dependent model of pulsed OPO's that includes diffraction, depletion, and double refraction (walkoff) in the parametric amplification process. The model is used to predict output beam profiles, beam quality, and conversion efficiency of an injection-seeded KTP ring OPO. Predicted output beam profiles in the near and intermediate fields are in qualitative agreement with the experimental results reports in a companion paper. Our results show that diffraction and double refraction must be included in models of pulsed OPO's to predict realistic beam profiles. DOE

N94-28000# Sandia National Labs., Albuquerque, NM.
SUM FREQUENCY GENERATION USING AN OPTICAL PARAMETRIC OSCILLATOR
W. J. Alford, T. D. Raymond, A. V. Smith, D. D. Lowenthal (Aculight Corp., Bellevue, WA.), and R. D. Mead (Aculight Corp., Bellevue, WA.) 1993 4 p Presented at the 9th Advanced Solid-State Lasers Meeting, Salt Lake City, UT, 7-10 Feb. 1994
(Contract DE-AC04-94AL-85000)
(DE94-001827; SAND-93-2206C; CONF-940226-2) Avail: CASI HC A01/MF A01 (US Sales Only)

A number of applications would benefit from sources of tunable coherent ultraviolet (uv) radiation in the 250 to 400 nm range. Among these are uv fluorescence laser detection and ranging (LIDAR). Other applications such as photolithography could use a fixed-frequency solid-state equivalent to excimer lasers. Broad tunability in this wavelength region has generally been accessed by frequency doubling tunable visible or near infrared lasers or by frequency mixing these lasers with the harmonics of a Nd:YAG laser. Unfortunately, to cover the full wavelength range requires multiple dye changes and/or multiple nonlinear crystals because of the relatively narrow tuning range of any one laser medium. The use of optical parametric oscillators (OPO's) with their wide tuning range as a tunable source of near infrared light coupled with a single (beta)-barium borate (BBO) crystal for sum frequency mixing with the Nd:YAG harmonics should yield a convenient alternative to cover this wavelength range. In this paper we demonstrate that an OPO can be efficiently sum frequency mixed with the Nd:YAG harmonics to produce tunable uv radiation in the 250-400 nm range. This is significant because OPO's generally have poor beam quality which limits their nonlinear conversion in critically phase matched processes. Specifically, we have mixed the 780 nm signal beam from a potassium tytanyl phosphate (KTP) OPO with the second harmonic from a Nd:YAG laser in BBO converting up to 50% of the OPO photons into 316 nm photons. We have also demonstrated the generation of narrow bandwidth 248 nm by mixing 827 nm from the OPO with the third harmonic of the Nd:YAG. DOE

N94-28202# RADEX, Inc., Bedford, MA.
THE PROTEL CONTAMINATION CODE Report No. 4
C. A. Hein 31 Jul. 1993 31 p
(Contract F19628-90-C-0090)
(RXR-93071; PL-TR-93-2178) Avail: CASI HC A03/MF A01

The Proton Telescope (PROTEL) was one of several instruments used to measure the proton populations encountered by the Combined Radiation and Release Experimental Satellite (CRRES) in its 15 months of successful operation. In the radiation environment encountered by CRRES, the PROTEL instrument was subjected to contamination caused by the penetration of high energy protons passing through the instrument outside its nominal aperture, falsely trigger a valid detection response. The PROTEL contamiation code was written to model the performance of the PROTEL High Energy Head (HEH) which is designed to respond to protons in the 10-100 MeV range. This report provides a brief description of the contamination code, the methodology underlying the modeling used, together with a summary of results. Tables and graphs describing the PROTEL contamination response for isotropic and mirror plane proton distributions are provided. The results of the modeling have been successfully used to compare PROTEL observations with observations made by the CRRES radiation dosimeter and proton instruments aboard other satellites. Author (revised)

N94-28224 Department of the Navy, Washington, DC.
OPTICAL PATTERN RECOGNITION SYSTEM UTILIZING RESONATOR ARRAY Patent
Joseph P. Garcia, inventor (to Navy) 31 Aug. 1993 20 p Filed 31 Aug. 1992
(AD-D016071; US-Patent-5,241,616; US-Patent-Appl-SN-937098; US-Patent-Class-385-126) Avail: US Patent and Trademark Office

Separate features of a composite image in a field of view illuminated by a laser beam are respectively monitored by low level optical cavity resonators of an array from which optical data outputs are distributed to high level resonators for optical data correlation. Adjacent low level resonators of the array are coupled by controllers for modal interaction modified by feedback to the controllers from the high level resonators through optical signal transforming means for signal correction purposes in pattern recognition of the composite image. DTIC

N94-27923*# Hampton Univ., VA. Dept. of Engineering.
FIBER OPTIC SENSORS FOR CORROSION DETECTION
Alphonso C. Smith *In* Old Dominion Univ., The 1993 NASA-ODU American Society for Engineering Education (ASEE) Summer Faculty Fellowship Program Dec. 1993 p 179-182 (For primary document see N94-27893 07-80)
Avail: CASI HC A01/MF A03

N94-27967# National Inst. of Polar Research, Tokyo (Japan).
DEVELOPMENT OF IMAGING RIOMETERS [IMEJINGU RIOMETA NO KAIHATSU]
Hisao Yamagishi, Masanori Nishino (National Inst. of Polar Research, Tokyo, Japan.), Mitsugi Sato, Yasuo Kato, Masayoshi Kojima, Natsuo Sato, and Takashi Kikuchi *In its* Antarctic Record, Vol. 36, No. 2 30 Jul. 1992 p 227-250 In JAPANESE Sponsored by Ministry of Education, Science and Culture, Tokyo, Japan Prepared in cooperation with Solar-Terrestrial Environment Lab., Nagoya Univ., Aichi, Japan and Communications Research Lab., Tokyo, Japan (For primary document see N94-27963 07-46)
Avail: CASI HC A03/MF A02

N94-27968# Nagoya Univ., Toyokawa (Japan). Solar-Terrestrial Environment Lab.
QUICK-LOOK SYSTEM OF AURORAL ABSORPTION IMAGES BY IMAGING RIOMETER [IMEJINGA RIOMETA KYUSHU GAZO KYU ERU SHISUTEMU NO KAIHATSU]
Mitsugi Sato, Hisao Yamagishi, Yasuo Kato, and Masanori Nishino *In* National Inst. of Polar Research, Antarctic Record, Vol. 36, No. 2 30 Jul. 1992 p 251-267 In JAPANESE Original contains color illustrations (For primary document see N94-27963 07-46)
Avail: CASI HC A03/MF A02

N94-27989# National Research Inst. for Earth Science and Disaster Prevention, Shinjo (Japan). Branch of Snow and Ice Studies.
DETECTION OF WATER ON ROAD SURFACE BY THE POLARIZED LIGHT [HENKO NI YORU ROMEN NO NURE NO KANSHUTSU]
Tadashi Kimura *In its* Report of the National Research Institute for Earth Science and Disaster Prevention, No. 51 31 Mar. 1993 p 203-208 In JAPANESE (For primary document see N94-27985 07-46)
Avail: CASI HC A02/MF A03

N94-28325 De Havilland Aircraft Co. of Canada Ltd., Downsview (Ontario). Research and Development Methods Group.
INFRARED IMAGING FOR TRANSITION DETECTION IN A TRANSONIC BLOWDOWN WIND TUNNEL
I. Fejtek, G. D. Jones, and R. Panza-Giosa *In* Canadian Aeronautics and Space Inst., Abstracts of Papers Presented at the 4th CASI Aerodynamics Symposium 1993 p 37-40 (For primary document see N94-28315 07-02)
Avail: Issuing Activity (Canadian Aeronautics and Space Inst., 130 Slater Street, Suite 818, Ottawa, ON K1P 6E2 Canada)

75 PLASMA PHYSICS

Includes magnetohydrodynamics and plasma fusion.
For ionospheric plasmas see *46 Geophysics*. For space plasmas see *90 Astrophysics*.

N94-25792# Texas Univ., Austin. Inst. for Fusion Studies.
TOROIDAL PLASMA BETA-FLR LIMIT IN A TOROIDALLY LINKED MIRROR SYSTEM
H. V. Wong, H. L. Berk, V. I. Ilgisonis, and V. P. Pastukhov Oct. 1993 27 p
(Contract DE-FG05-80ET-53088)
(DE94-003119; DOE/ET-53088/627; IFSR-627) Avail: CASI HC A03/MF A01

The ballooning stability limit in one toroidal section of the recently proposed toroidally linked neutron source is investigated in the context of finite Larmor radius effects. The ideal ballooning instability limits the toroidal plasma beta to less than 1% for a reasonable set of design parameters. The inclusion of stabilizing kinetic effects predicts an improvement in the toroidal plasma beta limit to approximately 2 percent. DOE

N94-25801# General Atomic Co., San Diego, CA.
REVIEW OF TOKAMAK EXPERIMENTS ON DIRECT ELECTRON HEATING AND CURRENT DRIVE WITH FAST WAVES
R. I. Pinsker Dec. 1993 13 p Presented at the 10th Topical Conference on Radio Frequency Power in Plasmas, Boston, MA, 1-3 Apr. 1993
(Contract DE-AC03-89ER-51114)
(DE94-004185; GA-A-21286; CONF-9304112-24) Avail: CASI HC A03/MF A01

Results from tokamak experiments on direct electron interaction with the compressional Alfven wave (fast wave) are reviewed. Experiments aimed at electron heating as well as those in which fast wave electron current drive was investigated are discussed. A distinction is drawn between experiments employing the lower hybrid range of frequencies, where both the lower hybrid wave (slow wave) and the fast wave can propagate in much of the plasma, and those experiments using the fast wave in the range of moderate to high ion cyclotron harmonics, where only the fast wave can penetrate to the plasma core. Most of the early tokamak experiments were in the lower hybrid frequency regime, and the observed electron interaction appeared to be very similar to that obtained with the slow wave at the same frequency. In particular, electron interaction with the fast wave was observed only below a density limit nearly the same as the well known slow wave density limit. In the more recent lower frequency fast wave experiments, electron interaction (heating and current drive) is observed at the center of the discharge, where slow waves are not present. DOE

N94-25846# InterScience, Inc., Troy, NY.
HEAVY NEUTRAL BEAM PROBE FOR EDGE PLASMA ANALYSIS IN TOKAMAKS
J. Castracane, E. Saravia, J. Beckstead, and S. Aceto 3 Sep. 1993 19 p
(Contract DE-FG02-91ER-54111)
(DE94-003391; DOE/ER-54111/3) Avail: CASI HC A03/MF A01

The contents of this report present the progress achieved to date on the Heavy Neutral Beam Probe project. This effort is an international collaboration in magnetic confinement fusion energy research sponsored by the US Department of Energy, Office of Energy Research (Confinement Systems Division) and the Centre Canadien de Fusion Magnetique (CCFM). The overall objective of the effort is to develop and apply a neutral particle beam to the study of edge plasma dynamics in discharges on the Tokamak de Varennes (TdeV) facility in Montreal, Canada. To achieve this goal, a research and development project was established to produce the necessary hardware to make such measurements and meet the scheduling requirements of the program. At present the project is in the middle of its second budget period with the instrumentation on-site at TdeV. The first half of this budget period was used to complete total system tests at InterScience, Inc., dismantle and ship the hardware to TdeV, and reassemble and install the HNBP on the tokamak. Integration of the diagnostic into the TdeV facility has progressed to the point of first beam production and measurement on the plasma. At this time, the HNBP system is undergoing final debugging prior to restart of machine operation in early Fall of this year. DOE

N94-25923# Texas Univ., Austin. Inst. for Fusion Studies.
KINETIC RESONANCE DAMPING RATE OF THE TOROIDAL ION TEMPERATURE GRADIENT MODE
J. Y. Kim, Y. Kishimoto, W. Horton, and T. Tajima Nov. 1993 36 p Revised
(Contract DE-FG05-80ET-53088)
(DE94-003511; DOE/ET-53088/623; IFSR-623) Avail: CASI HC A03/MF A01

The linear damping rates of the toroidal ion temperature gradient ((eta)(sub i)) mode due to the toroidal resonance are calculated in the local kinetic limit. The well-known Landau contour method is generalized to treat the analytic continuation problem of the guiding center dispersion function in the toroidal resonance system where the resonance occurs from both the magnetic (del)B-curvature drift and the parallel ion transit drift. A detailed numerical analysis is presented for the dependence of the damping rate of the toroidal (eta)(sub i) mode on various parameters such as (epsilon)(sub n), (kappa)(sub y), and the rapped electron fraction. In addition, a consideration is presented on the decay problem of the ballistic response by phase mixing in the toroidal system, which is directly related to the kinetic damping problem of the wave normal modes by the toroidal resonance. DOE

N94-25933# Oak Ridge National Lab., TN.
RF MODELING AND DESIGN OF A FOLDED WAVEGUIDE LAUNCHER FOR THE ALCATOR C-MOD TOKAMAK
T. S. Bigelow, C. F. Fogelman, F. W. Baity, M. D. Carter, D. J. Hoffman, P. M. Ryan, J. J. Yugo, S. N. Golovato (Massachusetts Inst. of Tech., Cambridge.), and P. Bonoli (Massachusetts Inst. of Tech., Cambridge.) 1993 5 p Presented at the Symposium on Fusion Engineering, Hyannis, MA, 11-15 Oct. 1993
(Contract DE-AC05-84OR-21400)
(DE94-003588; CONF-931018-64) Avail: CASI HC A01/MF A01

The folded waveguide (FWG) launcher is being investigated as an improved antenna configuration for plasma heating in the ion cyclotron range of frequencies (ICRF). A development FWG launcher was successfully tested at Oak Ridge National Laboratory (ORNL) with a low-density plasma load and found to have significantly greater power density capability than current strap-type antennas operating in similar plasmas. To further test the concept on a high density tokamak plasma, a collaboration has been set up between ORNL and Massachusetts Institute of Technology (MIT) to develop and test an 80-MHz, 2-MW FWG on the Alcator C-Mod tokamak at MIT. The radio frequency (rf) electromagnetic modeling techniques and laboratory measurements used in the design of this antenna are described in this paper. A companion paper describes the mechanical design of the FWG. DOE

N94-25949# Oak Ridge Inst. for Science and Education, TN.
INTERACTION BETWEEN A HIGH DENSITY-LOW TEMPERATURE PLASMA AND A FROZEN HYDROGEN PELLET IN A RAILGUN INJECTOR Ph.D. Thesis
Michael James Grapperhaus (Illinois Univ., Urbana.) 1993 82 p
(Contract DE-AC05-76OR-00033)
(DE94-000846; DOE/OR-00033/T552) Avail: CASI HC A05/MF A01

A model has been developed which describes the ablation process of frozen hydrogen pellets in an electromagnetic railgun. The model incorporates the neutral gas shielding model in which the pellet surface is heated by incident electrons from the plasma arc. The heated surface then ablates, forming a neutral cloud which attenuates the incoming electrons. The energy lost in the cloud by the electrons heats the ablatant material as it flows into the plasma arc. Under steady-state conditions, a scaling law for the ablation rate was derived as a function of plasma-arc temperature and density. In addition, flow conditions and the criteria for the existence of a steady-state solution were formulated and subsequently examined under simplifying assumptions. Comparison with experimentally observed ablation rates shows good qualitative agreement. DOE

N94-25958# Texas Univ., Austin. Inst. for Fusion Studies.
NONLINEAR GROWTH OF STRONGLY UNSTABLE TEARING MODES
F. L. Waelbroeck Nov. 1993 29 p
(Contract DE-FG05-80ET-53088)
(DE94-003366; IFSR-633; DOE/ET-53088/633) Avail: CASI HC A03/MF A01

Rutherford's theory of the tearing instability is extended to cases where current nonlinearities are important, such as long wavelength modes in current slabs and the m = 1 instability in tokamaks with moderately large aspect ratios. Of particular interest is the possibility that the associated magnetic islands, as a result of secondary instabilities, have a singular response to the ohmic diffusion of the current. A family of islands is used to test this possibility; it is found that the response remains bounded. DOE

N94-25976# General Atomics Technologies Corp., San Diego, CA.
EVALUATION OF HELIUM COOLING FOR FUSION DIVERTORS
C. B. Baxi Sep. 1993 12 p Presented at the International Atomic Energy Agency (IAEA) Meeting on Fusion Studies, Los Angeles, CA, 13-17 Sep. 1993
(Contract DE-AC03-89ER-51114)
(DE94-002680; GA-A-21448; CONF-9309274-1) Avail: CASI HC A03/MF A01

The divertors of future fusion reactors will have a power throughput of several hundred MW. The peak heat flux on the diverter surface is estimated to be 5 to 15 MW/sq m at an average heat flux of 2 MW/sq m. The divertors have a requirement of both minimum temperature (100 C) and maximum temperature. The minimum temperature is dictated by the requirement to reduce the absorption of plasma, and the maximum temperature is determined by the thermo-mechanical properties of the plasma facing materials. Coolants that have been considered for fusion reactors are water, liquid metals, and helium. Helium cooling has been shown to be very attractive from safety and other considerations. Helium is chemically and neutronically inert and is suitable for power conversion. The challenges associated with helium cooling are as follows: (1) manifold sizes; (2) pumping power; and (3) leak prevention. In this paper the first two of the above design issues are addressed. A variety of heat transfer enhancement techniques are considered to demonstrate that the manifold sizes and the pumping power can be reduced to acceptable levels. A helium-cooled diverter module was designed and fabricated by GA for steady-state heat flux of 10 MW/sq m. This module was recently tested at Sandia National Laboratories. At an inlet pressure of 4 MPa, the module was tested at a steady-state heat flux of 10 MW/sq m. The pumping power required was less than 1% of the power removed. These results verified the design prediction. DOE

N94-26081# Los Alamos National Lab., NM.
HOOK SPECTROSCOPY AS AN ATOMIC NUMBER DENSITY DIAGNOSTIC APPLIED TO LASER-ABLATED COPPER PLASMAS
D. K. Zerkle, A. D. Sappey, and T. K. Gamble 1993 13 p Presented at the Fall Meeting of the Western States Section of the Combustion Institute, Menlo Park, CA, 18-19 Oct. 1993
(Contract W-7405-eng-36)
(DE94-002645; LA-UR-93-3624; CONF-931076-2) Avail: CASI HC A03/MF A01

Hook spectroscopy has been used to determine the absolute number density of ground state copper atoms in laser-ablated plasma plumes. An ablation laser power flux of approximately 1.5 GW/cm(exp 2) is applied to a solid copper target in a background gas, producing a plasma plume suitable for studying homogeneous copper vapor condensation. Density is measured at post-ablation time delays ranging from 10 to 3 microseconds with 25 torr of argon as the background gas. Planar laser-induced fluorescence (PLEF) images containing relative density information are used in conjunction with the hook spectra to resolve spatially the absolute density within the plume. Copper atom densities thus measured ranged from 1.9 x 10(exp 15) cm(exp -3) at a delay of 10 microseconds to 2.7 x 10(exp 13) cm(exp -3) at 3 microsecond delay in 25 torr of argon. The decrease in density is due to the condensation of copper vapor to form fine particulate. As a combustion diagnostic, the hook method may prove extremely useful for the determination of metal impurity density in coal fired flames as well as a single-shot OH density and temperature diagnostic. DOE

N94-26132# Wisconsin Univ., Madison. Dept. of Physics.
MEASUREMENT OF MAGNETIC FLUCTUATION INDUCED ENERGY TRANSPORT
G. Fiksel, S. C. Prager, W. Shen, and M. Stoneking Nov. 1993 16 p
(Contract DE-FG02-85ER-53198)
(DE94-003846; DOE/ER-53198/227) Avail: CASI HC A03/MF A01

The local electron energy flux produced by magnetic fluctuations has been measured directly in the MST reversed field pinch (over the radial range r/a greater than 0.75). The flux, produced by electrons traveling parallel to a fluctuating magnetic field, is obtained from correlation between the fluctuations in the parallel heat flux and the radial magnetic field. The fluctuation induced flux is large (100 kW/sq cm) in the 'core' (r/a less than 0.85) and small (less than 10-30 kW/sq cm) in the edge. DOE

N94-26140# Oak Ridge National Lab., TN.
HIGH-SPEED REPETITIVE PELLET INJECTOR FOR PLASMA FUELING OF MAGNETIC CONFINEMENT FUSION DEVICES
S. K. Combs, L. R. Baylor, and C. R. Foust et al 1993 9 p Presented at the Symposium on Fusion Engineering, Hyannis, MA, 11-15 Oct. 1993
(Contract DE-AC05-84OR-21400)
(DE94-002792; CONF-931018-48) Avail: CASI HC A02/MF A01

The projected fueling requirements of future magnetic confinement devices for controlled thermonuclear research (e.g., the International Thermonuclear Experimental Reactor (ITER)) indicate that a flexible plasma fueling capability is required. This includes a mix of traditional gas puffing and low- and high-velocity deuterium-tritium pellets. Conventional pellet injectors (based on light gas guns or centrifugal accelerators) can reliably provide frozen hydrogen pellets (1- to 6-mm-diam sizes tested) up to approximately 1.3-km/s velocity at the appropriate pellet fueling rates (1 to 10 Hz or greater). For long-pulse operation in a higher velocity regime (greater than 2 km/s), an experiment in collaboration between Oak Ridge National Laboratory (ORNL) and ENEA Frascati is under way. This activity will be carried out in the framework of a collaborative agreement between the U.S. Department of Energy and European Atomic Energy Community--ENEA Association. In this experiment, an existing ORNL hydrogen extruder (equipped with a pellet chambering mechanism/gun barrel assembly) and a Frascati two-stage light gas gun driver have been combined on a test facility at ORNL. Initial testing has been carried out with single deuterium pellets accelerated up to 2.05 km/s with the two-stage driver; in addition, some preliminary repetitive testing (to commission the diagnostics) was performed at reduced speeds, including sequences at 0.5 to 1 Hz and 10 to 30 pellets. The primary objective of this study is to demonstrate repetitive operation (up to approximately 1 Hz) with speeds in the 2- to 3-km/s range. In addition, the strength of extruded hydrogen ice as opposed to that produced in situ by direct condensation in pipe guns can be investigated. The equipment and initial experimental results are described. DOE

N94-26159 Korean Atomic Energy Research Inst., Daeduk (Republic of Korea).
DEVELOPMENT OF FUSION TECHNOLOGY
Churl Kew Hwang, Kwang Won Lee, Sang Ryul In, Soon Mo Hwang, Byung Hoon Oh, Seung Ho Jeong, Byeong Joo Youn, Jae Sung Yoon, and Woo Sup Song Jun. 1992 172 p In KOREAN Limited Reproducibility: More than 20% of this document may be affected by microfiche quality
(DE93-633444; KAERI/RR-1122/92) Avail: CASI HC A08 (US Sales Only)

Total inspections over the most components of KAERIT are made with respect to every details including vacuum, mechanical, and electrical ones during the period of reassembling of main body to reinforce the mechanical strength of toroidal field coils. The manufacturing of power supplies for the magnetic field coils is completed as their control system constructions and electrical connections to the main body of the tokamak have been finished this year. Power supply systems for the toroidal field coils, the ohmic heating transformer, and equilibrium field coils are connected to each coil assembly, and the basic circuit characteristics are tested individually. A study on the vacuum technology has been conducted to develop a vacuum regulating system and to establish the KAERIT vacuum cycles. The vacuum vessel is cleaned and examined thoroughly during the period of tokamak disassembling. Also, the remote control systems for vacuum regulation and gas injection have been composed and experiments on their system characteristics are conducted. To initiate the developments of data acquisition system and plasma diagnostics, active integrators are developed and a receiver system for electron cyclotron emission is designed as a first step. DOE

N94-26274# General Atomic Co., San Diego, CA.
NEW THOMSON SCATTERING LASER CONTROL FOR D3-D
C. C. Makariou, R. E. Stockdale, T. N. Carlstrom, C. L. Hsieh, and G. Bramson Oct. 1993 4 p Presented at the Symposium on Fusion Engineering, Hyannis, MA, 11-15 Oct. 1993
(Contract DE-AC03-89ER-51114)
(DE94-002890; GA-A-21427; CONF-931018-45) Avail: CASI HC A01/MF A01

A Laser Control system has been built for the D3-D Scattering Diagnostic. This new system has provided the capability to place the laser probe pulses with one microsecond timing precision throughout the D3-D shot. The new system fires the eight lasers with a programmable sequence which repeats ever 50 ms. If one wants to probe the plasma at a higher rate to study a fast paced event, the new control circuit can fire all charged lasers in rapid succession (BURST MODE). This burst rate is programmable. The new Laser Control system successfully replaced the previous control scheme which consisted of three VME Motorola 68030 computers (one host under UNIX VME V/68 and two interrupt driven targets under VME Exec. The old system was not successful due to the many VME interrupts needed to service the lasers. The new hardware approach is much more reliable. The old system still controls data acquisition and as a monitoring system since it does not have the burden of controlling the lasers. A brief description of the Thomson Scattering diagnostic will be presented with emphasis in the new upgraded laser firing control system and data acquisition timing control. DOE

N94-26321# Los Alamos National Lab., NM.
SCALING OF SUSTAINED ZT-40 M REVERSED FIELD PINCHES
J. Graham, ed. Dec. 1993 61 p
(Contract W-7405-eng-36)
(DE94-003318; LA-12567-MS) Avail: CASI HC A04/MF A01

Experiments aimed at evaluating the scaling properties of the ZT-40M Reversed-Field Pinch (RFP) facility were conducted in 1983 at Los Alamos. Sustained discharges were produced at nominal toroidal currents ranging from 60 to 240 kA. The standard fill pressure was kept close to the lower limit of the usable pressure range, and the scaling data were acquired at a fixed time in the discharges while the plasma was in a quasi-steady state. Scalings of the diameter-averaged electron density, electron temperature on axis, product of these two parameters, and of various definitions of the electrical resistivity are presented. Trends of the toroidal voltage, energy containment time, and poloidal beta are shown. The impurity contents, particle containment time, and total radiation losses are described, and results obtained with and without poloidal limiters are compared. In addition, the performance of the facility at higher than standard density and at a constant ratio of the toroidal current over the electron line density is examined. DOE

N94-26323# General Atomics Technologies Corp., San Diego, CA.
A ROBUST HELIUM-COOLED SHIELD/BLANKET DESIGN FOR ITER
C. P. C. Wong, R. F. Bourque, C. B. Baxi, A. P. Colleraine, H. J. Grunloh, T. Letchenberg, J. A. Leuer, E. E. Reis, K. Redler, and R. Will et al Nov. 1993 4 p Presented at the Symposium on Fusion Engineering, Hyannis, MA, 11-15 Oct. 1993
(Contract DE-AC03-89ER-51114)
(DE94-003402; GA-A-21485; CONF-931018-61) Avail: CASI HC A01/MF A01

General Atomics Fusion and Reactor Groups have completed a helium-cooled, conceptual shield/blanket design for ITER. The configuration selected is a pressurized tubes design embedded in radially oriented plates. This plate can be made from ferritic steel or from V-alloy. Helium leakage to the plasma chamber is eliminated by conservative, redundant design and proper quality control and inspection programs. High helium pressure at 18 MPa is used to reduce pressure drop and enhance heat transfer. This high gas pressure is believed practical when confined in small diameter tubes. Ample industrial experience exists for safe high gas pressure operations. Inboard shield design is highlighted in this study since the allowable void fraction is more limited. Lithium is used as the thermal contacting medium and for tritium breeding; its safety concerns are minimized by a modular, low inventory design that requires no circulation of the liquid metal for the purpose of heat removal. This design is robust, conservative, reliable, and meets all design goals and requirements. It can also be built with present-day technology. DOE

N94-26324# General Atomics Technologies Corp., San Diego, CA.
LIMITATIONS OF POWER CONVERSION SYSTEMS UNDER TRANSIENT LOADS AND IMPACT ON THE PULSED TOKAMAK POWER REACTOR
G. T. Sager, C. P. C. Wong, D. D. Kapich, C. F. McDonald, and R. W. Schleicher Nov. 1993 4 p Presented at the Symposium on Fusion Engineering, Hyannis, MA, 11-15 Oct. 1993
(Contract DE-AC03-89ER-52153)
(DE94-003404; GA-A-21474; CONF-931018-60) Avail: CASI HC A01/MF A01

The impact of cyclic loading of the power conversion system of a helium-cooled, pulsed tokamak power plant is assessed. Design limits of key components of heat transport systems employing Rankine and Brayton thermodynamic cycles are quantified based on experience in gas-cooled fission reactor design and operation. Cyclic loads due to pulsed tokamak operation are estimated. Expected performance of the steam generator is shown to be incompatible with pulsed tokamak operation without load leveling thermal energy storage. The close cycle gas turbine is evaluated qualitatively based on performance of existing industrial and aeroderivative gas turbines. Advances in key technologies which significantly improve prospects for operation with tokamak fusion plants are reviewed. DOE

N94-26356# Science Applications International Corp., McLean, VA.
LABORATORY PLASMA STUDIES Final Report, 25 Mar. 1989 - 30 Sep. 1993
Arne Fliflet 30 Nov. 1993 752 p
(Contract N00014-89-C-2111)
(AD-A274655; SAIC-93/1229) Avail: CASI HC A99/MF A06

The contents of the document are as follows: NIKE KrF Laser Support; Microwave and Millimeter Wave Experiments; Studies of Novel Accelerator Concepts and Free Electron Lasers; Studies for the Modified Betatron Accelerator (MBA); PHAROS 3 Studies; Electron Beam Diagnostics; Microwave Energy Deposition in the Upper Atmosphere; and Visualization Tools and Parallel Processing for Physics Applications. DTIC

N94-26428# Department of Energy, Washington, DC. Office of Energy Research.
FUSION ENERGY ADVISORY COMMITTEE: ADVICE AND RECOMMENDATIONS TO THE US DEPARTMENT OF ENERGY IN RESPONSE TO THE CHARGE LETTER OF SEPTEMBER 1, 1992
Apr. 1993 125 p
(DE93-019842; DOE/ER-0593T; FEAC-93-I) Avail: CASI HC A06/MF A02

This document is a compilation of the written records that relate to the Fusion Energy Advisory Committee's deliberations with regard to the Letter of Charge received from the Director of Energy Research, dated 1 Sep. 1992. During its sixth meeting, held in Mar. 1993, the FEAC provided a detailed response to the charge contained in the letter of 1 Sep. 1992. In particular, it responded to the paragraph: I would like the Fusion Energy Advisory Committee (FEAC) to evaluate the Neutron Interactive Materials Program of the Office of Fusion Energy (OFE). Materials are required that will satisfy the service requirements of components in both inertial and magnetic fusion reactors including the performance, safety, economic, environmental, and recycle/waste management requirements. Given budget constraints, is our program optimized to achieve these goals for DEMO, as well as to support the near-term ITER program? Before FEAC could generate its response to the charge in the form of a letter report, one member, Dr. Parker, expressed severe concerns over one of the conclusions that the committee had reached during the meeting. It proved necessary to resolve the issue in public debate, and the matter was reviewed by FEAC for a second time, during its seventh meeting, held in mid-Apr. 1993. In order to help it to respond to this charge in a timely manner, FEAC established a working group, designated Panel No. 6, which reviewed the depth and breadth of the US materials program, and its interactions and collaborations with international programs. The panel prepared background material, included in this report as Appendix 1, to help FEAC in its deliberations. DOE

N94-26510 Nauchno-Issledovatelskii Inst. Ehlekt- Rofizicheskoj Apparatury, Leningrad (USSR).
NUMERICAL SIMULATION OF PLASMA VERTICAL POSITION STABILIZATION IN ITER [CHISLENNOE MODELIROVANIE STABILIZATSII VERTIKAL'NOGO POLOZHENIYA PLAZMY V ITEHR]
A. M. Astapkovich and S. N. Sadakov 1992 21 p In RUSSIAN Limited Reproducibility: More than 20% of this document may be affected by microfiche quality
(DE93-634586; NIIEFA-P-B-0900) Avail: CASI HC A03 (US Sales Only)

Numerical simulation of plasma vertical position stabilization in ITER is addressed. The calculations are performed using EDDY C-2 code by the method of direct numerical simulation of transient electromagnetic processes taking into account the evolution of plasma position, cross-section shape and full plasma current. When simulating free vertical plasma drift in ITER with twin passive stabilization loops, it was shown that account of the effects of cross-section deformation and plasma current alternations results in almost two fold degradation of passive stabilization parameters as compared to the calculations for 'rigid displacement' model. In terms of methodology, the account of the effects of cross section deformation and plasma current alternations requires clarification of the definitions for reverse increment of vertical instability and for stability margin coefficient. The simulation of plasma pinch return to equilibrium position after the closure of control coils allows to assess the required parameters of active control system and demonstrate the effect of screen current reverse in twin loops. The obtained results were used to develop the ITER conceptual design and affected the choice of the concept of twin passive loops and new positron of control coils as the basis approaches. DOE

N94-26523# Maryland Univ., College Park.
MARYLAND CONTROLLED FUSION RESEARCH PROGRAM
T. M. Antonsen, Jr., J. F. Drake, J. M. Finn, P. Guzdar, A. Hassam, C. S. Liu, and E. Ott May 1993 16 p
(Contract DE-FG02-93ER-54197)
(DE94-003533; DOE/ER-54197/1) Avail: CASI HC A03/MF A01

In recent years, members of the Maryland Plasma Theory Group have made significant contributions to the national fusion theory program, and, in many cases, these theoretical developments helped to interpret experimental results and to design new experimental programs. The technical progress in four major areas of tokamak research are summarized: (1) L/H transition and edge turbulence and transport; (2) active control of micro-turbulence and transport; (3) major disruptions; and (4) the sawtooth crash. DOE

N94-26579# Illinois Univ., Urbana. Fusion Technology Lab.
APPLICATION OF RAILGUN PRINCIPLE TO HIGH-VELOCITY HYDROGEN PELLET INJECTION FOR MAGNETIC FUSION REACTOR FUELING
Kyekyoon Kim and Jianhua Zhang 1993 85 p
(Contract DE-FG02-84ER-52111)
(DE94-004411; DOE/ER-52111/6) Avail: CASI HC A05/MF A01

This report discusses research being conducted on hydrogen pellet acceleration by railgun accelerators for fueling magnetic fusion reactors. DOE

N94-26694# Oak Ridge National Lab., TN.
PROBABILITY OF ACCESSING THE MULTIPLE SATURATED STATES IN THE RESISTIVE INTERCHANGE INSTABILITY
L. Garcia (Universidad Complutense, Madrid, Spain.), B. A. Carreras, and V. E. Lynch 1993 4 p Presented at the 20th European Conference on Controlled Fusion and Plasma Physics, Lisbon, Portugal, 26-30 Jul. 1993
(Contract DE-AC05-84OR-21400)
(DE94-000478; CONF-930720-21) Avail: CASI HC A01/MF A01

The probability of accessing the multiple saturated states for the full 3/2 helicity was studied. The presence of an external flow can induce Kelvin-Helmholtz type instabilities for relatively low beta values. This seems to be the case for the low-m modes with the equilibrium parameters used in our calculations. To separate this effect, a simplified electrostatic model in the numerical calculations was employed. DOE

N94-26820# Hampton Univ., VA.
CRITICAL SURVEY OF PLASMA PROCESSING Final Report
William P. Marable 28 Sep. 1993 9 p
(Contract MDA972-91-J-1006)
(AD-A274233) Avail: CASI HC A02/MF A01

Low temperature plasmas represent an expansive region in the density-temperature parameter space of experimentally generated plasmas. With densities ranging from 10(exp 6) to 10(exp 17) cu cm, and temperatures ranging from 10(exp -2) to 10 eV, these plasmas exhibit a variety of collective behaviors, supporting many physical states and interactions among the particle species within the plasma. It is precisely this variety in physical conditions that lends the plasma environment so well to the myriad of applications that have developed in plasma processing. Examples of these applications are: processing of solid state materials by ion implantation, thin film deposition, plasma enhanced chemical vapor deposition, plasma etching, and hardening and improving wear and corrosion resistance of refractory metals and composites. These applications have enjoyed great advancement in technological development. DTIC

N94-26858# Oak Ridge National Lab., TN.
CONCEPTUAL DESIGN OF THE TOKAMAK RADIATION SHIELDING FOR THE TOKAMAK PHYSICS EXPERIMENT (TPX)
M. J. Cole, B. E. Nelson, G. H. Jones, P. L. Goranson, Y. Gohar (Argonne National Lab., IL.), and S. L. Liew (Princeton Univ., NJ.) 1993 5 p Presented at the Symposium on Fusion Engineering, Hyannis, MA, 11-15 Oct. 1993
(Contract DE-AC05-84OR-21400)
(DE94-002791; CONF-931018-52) Avail: CASI HC A01/MF A01

The tokamak radiation shielding includes the neutron and gamma shielding around the torus and penetrations required to (1) limit activation of components outside the shield to levels that permit hands-on maintenance, and (2) limit the nuclear heating of the superconducting coils and cold structure. The primary design drivers are space, the 350 C bakeout temperature, and cost; therefore, different shield materials were used for different shield components and locations. The shielding is divided into three areas: (1) torus shielding around the vacuum vessel, (2) duct shielding around the vacuum pumping ducts and vertical diagnostic ducts, and (3) penetration shielding in and around the radial ports. The major shield components include water between the walls of the vacuum vessel, lead monosilicate/boron carbide tiles that are attached to the exterior of the vacuum vessel, shield plugs that fill the openings of the large radial ports, and polyethylene/lead/boron shield blocks for duct shielding. A description of the shielding configuration and the performance and operational requirements are discussed. DOE

N94-26860# Oak Ridge National Lab., TN.
POTENTIAL OF COMMERCIAL TOKAMAK REACTORS WITH IMPROVED PHYSICS
J. D. Galambos, L. J. Perkins (Lawrence Livermore National Lab., CA.), S. Haney (Lawrence Livermore National Lab., CA.), and J. Mandrekas (Georgia Inst. of Tech., Atlanta.) 1993 4 p Presented at the Symposium on Fusion Engineering, Hyannis, MA, 11-15 Oct. 1993
(Contract DE-AC05-84OR-21400)
(DE94-002794; CONF-931018-51) Avail: CASI HC A01/MF A01

The impact of improvements in plasma confinement and beta on commercial tokamak embodiments was systematically investigated. Cases were investigated for both steady-state and pulsed reactors. A narrow range of useful confinement enhancement (H factors over the ITER-89 Power scaling) and Troyon beta limit coefficients g are found to be beneficial for reducing the cost of electricity (COE). Improvements in the beta limit (i.e., g) offer the greatest improvement in reactors. For g limited to about

4, H factors of only 2 are needed. If g of 6 is attainable, H factors up to 2.5 are useful. Pulsed reactors have slightly higher useful H factors, ranging from 2.5 for g near 4 to 3 for g near 6. DOE

N94-26861# Oak Ridge National Lab., TN.
METHODOLOGY FOR FIRST WALL DESIGN
J. D. Galambos, D. L. Conner, P. L. Goranson, D. C. Lousteau, D. E. Williamson, B. E. Nelson, and F. C. Davis 1993 4 p Presented at the Symposium on Fusion Engineering, Hyannis, MA, 11-15 Oct. 1993
(Contract DE-AC05-84OS-21400)
(DE94-002795; CONF-931018-47) Avail: CASI HC A01/MF A01

An analytic parametric scoping tool was developed for application to first wall (FW) design problems. Both thermal and disruption force effects are considered. For the high heat flux and high disruption load conditions expected in the International Thermonuclear Experimental Reactor (ITER) device, Vanadium alloy and dispersion-strengthened copper offer the best stress margins using a somewhat flattened plasma-facing configuration. Ferritic steels also appear to have an acceptable stress margin, whereas the conventional stainless steel 316 does not appear feasible. If a full semicircle shape FW is required, only the Vanadium and ferritic steel alloy have acceptable solutions. DOE

N94-26863# Lawrence Livermore National Lab., CA.
THE TPX CRYOSTAT CONCEPTUAL DESIGN
D. Ravenscroft, A. Posey, P. Heitzenroeder (Princeton Univ., NJ.), and T. Brown (Grumman Aerospace Corp., Princeton, NJ.) Oct. 1993 6 p Presented at the Symposium on Fusion Engineering, Hyannis, MA, 11-15 Oct. 1993
(Contracts W-7405-eng-48; DE-AC02-76CH-03073)
(DE94-002857; UCRL-JC-114267; CONF-931018-57) Avail: CASI HC A02/MF A01

The TPX (Tokamak Physics Experiment) will be the first tokamak to employ both superconducting TF (toroidal field) and PF (poloidal field) magnets. Consequently, the entire device is located within an evacuated cryostat to provide the necessary thermal barrier between the ambient temperature test cell and the magnets that are cooled by supercritical liquid helium at 5 K. The cryostat design requirements, design concepts, and the cryostat fabrication and installation are described. DOE

N94-26865# General Atomics Technologies Corp., San Diego, CA.
NEW CONDITIONING PROCEDURE DERIVED FROM OPERATING EXPERIENCE WITH THE COMMON LONG-PULSE ION SOURCE
B. G. Scoville, M. Madruga, R. M. Hong, and J. C. Phillips Oct. 1993 3 p Presented at the Symposium on Fusion Engineering, Hyannis, MA, 11-15 Oct. 1993
(Contract DE-AC03-89ER-51114)
(DE94-002891; GA-A-21422; CONF-931018-59) Avail: CASI HC A01/MF A01

The DIII-D neutral beam system utilizes an 80 kV version of the Common Long-Pulse Ion Source designed by Lawrence Berkeley Laboratories (LBL) and originally built by RCA. Eight of these ion sources are mounted on four beamlines to provide a total of 20 MW of injected deuterium neutral power to the DIII-D tokamak. To support the DIII-D one-shift operation, neutral beams must be readied in a relatively short period of time each day, typically one hour. During non-operating periods conditioning time for the ion sources is limited, due to the costs of associated support services and the need to perform corrective and preventive maintenance. The experience gained over a six year period resulted in finely tuned procedures for the conditioning and operation of these ion sources. Recently, an ion source was conditioned which had been accidentally filled with water for several days, resulting in surface corrosion and deconditioning of the grids and surfaces. The method of successful recovery along with data, experience and procedures derived this event and normal operations are detailed and discussed. DOE

N94-26946 International Atomic Energy Agency, Vienna (Austria). Atomic and Molecular Data Unit.
INTERNATIONAL BULLETIN ON ATOMIC AND MOLECULAR DATA FOR FUSION. NO. 42-45, MAR. 1991 - DEC. 1992
J. Botero, ed. Dec. 1992 595 p Limited Reproducibility: More than 20% of this document may be affected by poor print and microfiche quality
(DE94-601817; INIS-mf-4754(no-42-45); IBAMD-42-45) Avail: Issuing Activity (Department of Energy (DOE)) (US Sales Only)

The bulletin is published by the International Atomic Energy Agency to provide atomic and molecular data relevant to fusion research and technology. In Part 1 the indexed papers are listed separately for (1) structure and spectra (energy levels, wavelengths; transition probabilities, oscillator strengths; polarizabilities, electric moments; interatomic potentials); (2) atomic and molecular collisions (photon collisions; electro collisions; heavy-particle collisions; homonuclear sequences); and (3) surface interactions (sputtering; trapping, detrapping; adsorption, desorption; surface damage; blistering, flaking; chemical reactions). Part 2 contains the bibliographic data for the above listed topics and for plasma composition and impurities; plasma heating, cooling and fuelling; fusion research of general interest; high energy laser- and beam-matter interaction; interaction of atomic particles with fields. A list of evaluated data bases on atomic and molecular collisions and on particle-surface interactions is also given. DOE

N94-26950# General Atomic Co., San Diego, CA.
ROLE OF CORE TOROIDAL ROTATION SHEAR ON TURBULENCE AND TRANSPORT IN THE IMPROVED CONFINEMENT REGIMES OF THE D3-D TOKAMAK
R. J. LaHaye, C. M. Greenfield, R. J. Groebner, A. W. Hyatt, L. L. Lao, T. H. Osborne, J. T. Scoville, and C. L. Rettig (California Univ., Los Angeles.) Aug. 1993 6 p Presented at the Workshop on Local Transport Studies in Fusion Plasmas, Varenna, Italy, 30 Aug. - 3 Sep. 1993
(Contract DE-AC03-89ER-51114)
(DE94-001215; GA-A-21431; CONF-9308183-2) Avail: CASI HC A02/MF A01

This a brief report which discusses the role of core toroidal rotation shear on turbulence and transport in the improved confinement regimes of the doublet-3 tokamak. DOE

N94-27019# Lawrence Livermore National Lab., CA.
TOKAMAK PHYSICS EXPERIMENT POLOIDAL FIELD DESIGN
R. H. Bulmer Oct. 1993 6 p Presented at the Symposium on Fusion Engineering, Hyannis, MA, 11-15 Oct. 1993
(Contract W-7405-eng-48)
(DE94-001542; UCRL-JC-114268; CONF-931018-16) Avail: CASI HC A02/MF A01

The Tokamak Physics Experiment (TPX) will have a poloidal field system capable of full inductive operation poloidal for approximately a 20-s flattop and, with superconducting toroidal and poloidal field coils and non-inductive current drive, it will be capable of true steady-state operation. The poloidal field design is based on the ideal magnetohydrodynamic (MHD) equilibrium model as implemented in the TEQ code developed at LLNL. The PF coils are arranged in an up-down symmetric configuration, external to the TF coils. The TPX diverted plasma will have an aspect ratio of 4.5 and is highly shaped with a nominal elongation of 2 and triangularity of approximately 0.8 as measured at the separatrix. The tokamak design is based on a high-current (q(sub (psi))=3) plasma scenario and a low current scenario. Each scenario has an operational flexibility requirement which is defined as a region of plasma pressure and inductivity (beta(sub N) - l(sub i)) space, where the plasma shape is constrained to keep the divertor configuration operational. Single-null plasma configurations are feasible, even with the same divertor hardware, by operating the PF coils asymmetrically. Recently applied optimization techniques have improved the capability of the PF system without additional cost. DOE

N94-27074 JAYCOR, Vienna, VA.
RESEARCH IN PULSED POWER PLASMA PHYSICS Final Report
David Hinshelwood and David Rose Nov. 1993 629 p Limited Reproducibility: More than 20% of this document may be affected by microfiche quality
(Contract N00014-89-C-2134)
(AD-A274323) Avail: CASI HC A99

The research was conducted in support of light-ion-driven inertial confinement fusion (ICF) for the Department of Energy (DOE), and nuclear weapon effects simulation (NWES) for the Defense Nuclear Agency (DNA). Accomplishments related to ion beams include: development of a practical backup approach to ion beam transport; the first studies of ion-beam interaction with a neutral gas; initial investigations of a promising industrial application of ion beam technology; and detailed theoretical evaluation of several different ion beam transport schemes. Major accomplishments relating to opening switches include: the first direct measurement of the electron density in an opening switch; detailed studies of switch conduction-time scaling; evaluation of several different switch plasma sources; and extensive studies of switch performance into diode loads, leading to the development of a new (and now generally accepted) model of switch behavior. DTIC

N94-27098# Maryland Univ., College Park.
EXPERIMENTAL AND THEORETICAL INVESTIGATION OF RF ABSORPTION AND REFLECTION FROM PREFORMED PLASMAS Final Report, 30 Sep. 1989 - 30 Sep. 1993
William W. Destler 30 Sep. 1993 71 p
(Grant AF-AFOSR-0488-89)
(AD-A274189; AFOSR-93-0883TR) Avail: CASI HC A04/MF A01

This report constitutes the final progress report for a program of experimental and theoretical research on the reflection, absorption, and scattering of VHF and microwave radiation from plasma-covered conductors. A principal goal of this research is to determine to what extent plasmas can be used to reduce the radar cross-section of highly RF-reflective objects. The major goals of this program were: to study RF absorption and reflection from a plasma-covered plane conductor to determine under what conditions the presence of the plasma can result in a significant reduction in the backscattered RF; to conduct such studies under a wide range of plasma (overdense and underdense) and RF (frequency, power density, and pulse duration) conditions; and to establish a solid theoretical foundation for the understanding of experimental observations. DTIC

N94-27261# Oak Ridge National Lab., TN.
DESIGN AND CONTROL OF PHASED ICRF ANTENNA ARRAYS
R. H. Goulding, F. W. Baity, D. J. Hoffman, P. M. Ryan, J. S. deGrassie (General Atomics Technologies Corp., San Diego, CA.), C. C. Petty (General Atomics Technologies Corp., San Diego, CA.), R. I. Pinsker (General Atomics Technologies Corp., San Diego, CA.), M. Bures (Joint European Torus Project, Abingdon, England.), J. A. Dobbing (Joint European Torus Project, Abingdon, England.), and D. F. H. Start (Joint European Torus Project, Abingdon, England.) et al 1993 5 p Presented at the Symposium on Fusion Engineering, Hyannis, MA, 11-15 Oct. 1993
(Contract DE-AC05-84OR-21400)
(DE94-002796; CONF-931018-50) Avail: CASI HC A01/MF A01

Phased antenna arrays operating in the ion cyclotron range of frequencies (ICRF) are used to produce highly directional wave spectra, primarily for use in current drive experiments. RF current drive using phased antennas has been demonstrated in both the JET and DIII-D tokamaks, and both devices are planning to operate new four-element arrays beginning early next year. Features of antenna design that are relevant to phased operation and production of directional spectra are reviewed. Recent advances in the design of the feed circuits and the related control systems for these arrays should substantially improve their performance, by reducing the coupling seen by the matching networks and rf power supplies caused by the mutual impedance of the array elements. The feed circuit designs for the DIII-D and JET phased antenna arrays are compared. The two configurations differ significantly due to the fact that one power amplifier is used for the entire array in the former case, and one per element in the latter. The JET system uses automatic feedback control of matching, phase and amplitude of antenna currents, and the transmitter power balance. The design of this system is discussed, and a time dependent model used to predict its behavior is described. DOE

N94-27350# Electrotechnical Lab., Tsukuba (Japan).
RESEARCHES OF THE ELECTROTECHNICAL LABORATORY. NO. 51: STUDY OF FORMATION AND SUSTAINMENT OF REVERSED FIELD PINCH BY SLOW CONTROL OF MAGNETIC FIELD [DENSHI GIJUTSU SOGO KENKYUSHO KENKTU HOKOKU DAI 51 GO: TEISOKU TACHIAGE GYAKU JIKAI PINCHI NO HAII KEISEI TO SONO IJI NI KANSURU KENKYU]
Yoichi Hirano 30 Jul. 1993 143 p In JAPANESE Sponsored by Science and Technology Agency, Tokyo, Japan
(ISSN 0366-9106)
(JTN-94-80548) Avail: CASI HC A07/MF A02

Experimental results of controlled thermonuclear fusion research on Reversed Field Pinch (RFP) machines, TPE-1RM and TPE-1RM15, are presented. The main experimental results of TPE-1RM, such as RFP configuration formation conditions, insensitivity of RFP configuration to the initial conditions, its dependency on the instantaneous boundary condition, very high temperature measured by Thomson scattering of ruby laser, the ion temperature measured by Doppler broadening of C(4+) line, proportionality of the electron temperature and density to the plasma current, and the linear increase of the ion temperature with the plasma current are outlined. The main experiment results of TPE-1RM15 are as follows: (1) the RFP configuration can be formed by magnetic field control much slower than that in TPE-1RM; (2) the RFP configuration can be sustained by maintaining the plasma current and the reversal of toroidal field; (3) the electron temperature and density are kept nearly constant by sustaining the configuration; (4) the equilibrium position control by the quasi-DC (Direct Current) vertical field is essential for reducing the toroidal loop voltage; (5) the confinement property in the large current region is greatly improved by using purified molybdenum limiters; and (6) the electron density and temperature are roughly proportional to the plasma current. It is demonstrated that the theoretically predicted relaxation towards the RFP configuration exists and the RFP configuration can be formed with the slow formation whose current rise time is in the range of milli-second. Author (NASDA)

N94-27568# Oak Ridge National Lab., TN.
FAST WAVE CURRENT DRIVE TECHNOLOGY DEVELOPMENT AT ORNL
F. W. Baity, D. B. Batchelor, R. H. Goulding, D. J. Hoffman, E. F. Jaeger, P. M. Ryan, J. S. deGrassie (General Atomic Co., San Diego, CA.), C. C. Petty (General Atomic Co., San Diego, CA.), R. I. Pinsker (General Atomic Co., San Diego, CA.), and R. Prater (General Atomic Co., San Diego, CA.) 1993 11 p Presented at the IAEA Meeting on Radio-Frequency Launchers for Plasma Heating and Current Drive, Naka, Japan, 10-12 Nov. 1993
(Contract DE-AC05-84OR-21400)
(DE94-004243; CONF-9311140-1) Avail: CASI HC A03/MF A01

The technology required for fast wave current drive (FWCD) systems is discussed. Experiments are underway on DIII-D, JET, and elsewhere. Antennas for FWCD draw heavily upon the experience gained in the design of ICRF heating systems with the additional requirement of launching a directional wave spectrum. Through collaborations with DIII-D, JET, and Tore Supra, rapid progress is being made in the demonstration of the physics and technology of FWCD needed for TPX and ITER. DOE

N94-27630 International Centre for Theoretical Physics, Trieste (Italy).
NONLINEAR TRANSVERSE PROPAGATION OF PHOTONS IN A ULTRARELATIVISTICALLY HOT AND MAGNETIZED ELECTRON-POSITRON PLASMA: COUPLING OF LANGMUIR AND ELECTROMAGNETIC SOLITONS
U. A. Mofiz, N. L. Tsintsadze, and L. N. Tsintsadze (Georgian Polytechnic Inst., Tbilisi.) Aug. 1993 9 p Limited Reproducibility: More than 20% of this document may be affected by microfiche quality
(DE94-603667; IC-93/230) Avail: CASI HC A02 (US Sales Only)

Nonlinear propagation of electromagnetic waves across the ambient magnetic field immersed in an ultrarelativistically hot electron-positron plasma is considered. A system of nonlinear equations is obtained. Coupled Langmuir and electromagnetic solitons are found to propagate across the magnetic field and its relevance to pulsar magnetosphere is outlined. DOE

N94-27686# Wisconsin Univ., Madison. Fusion Technology Inst.
FUSION REACTOR SYSTEMS STUDIES
Sep. 1993 142 p
(Contract DE-FG02-89ER-52158)
(DE94-003162; DOE/ER-52158/11) Avail: CASI HC A07/MF A02

Fusion Technology Institute personnel actively participated in the ARIES/PULSAR project during the present contract period. Numerous presentations were made at PULSAR project meetings, major contributions were written for the ARIES-2/4 Final Report presentations, and papers were given at technical conferences. Additionally, contributions were written for the ARIES Lessons Learned report, and a very large number of electronic-mail and regular-mail communications were sent. The remaining sections of this progress report will summarize the work accomplished and in progress for the PULSAR project during the contract period. The main areas of effort are as follows: PULSAR Research; ARIES-2/4 Report Contributions; ARIES Lessons Learned Report Contributions; and Stellarator Study. DOE

N94-27690# Wisconsin Univ., Madison.
TFTR EXPERIMENTAL DATA ANALYSIS COLLABORATION Annual Progress Report, 15 Nov. 1992 - 14 Nov. 1993
J. D. Callen 1993 13 p
(Contract DE-FG02-92ER-54139)
(DE94-004166; DOE/ER-54139/2) Avail: CASI HC A03/MF A01

The research performed under the second year of this three-year grant has concentrated on a few key TFTR experimental data analysis issues: magnetohydrodynamic (MHD) mode identification and effects on supershots, identification of new MHD modes, MHD mode theory-experiment comparisons, local electron heat transport inferred from impurity-induced cool pulses, and some other topics. Progress in these areas and activities undertaken in conjunction with this grant are summarized briefly in this report. DOE

N94-27698 Technical Univ. of Prague (Czechoslovakia).
PROCEEDINGS OF THE 16TH SYMPOSIUM ON PLASMA PHYSICS AND TECHNOLOGY
1993 356 p Symposium held in Prague, Czechoslovakia, 27-29 Apr. 1993 Prepared in cooperation with Ceskoslovenska Akademie Ved, Prague Limited Reproducibility: More than 20% of this document may be affected by microfiche quality
(DE94-604181; INIS-MF-13714; CONF-9304218) Avail: CASI HC A16 (US Sales Only)

Among 53 papers collected in the proceedings, 28 papers deal with the theory and modelling (8 papers), experimental research (11 papers), and diagnostics of high temperature plasmas. These include lower hybrid current drive in tokamaks, plasma heating by electron beams, laser plasma interaction, and z-pinch experiments. In the diagnostic papers, attention is mostly paid to x ray and optical plasma spectroscopy and to advanced Langmuir probe diagnostics. The remaining papers discuss low temperature plasmas and their applications. In this group, 8 papers deal with low pressure electric discharges; 5 papers with high pressure arcs, glidarcs, and plasma torches; and 12 papers with various plasma technology topics, such as thin film deposition, plasma spraying, and plasma chemistry. DOE

N94-27699# Japan Atomic Energy Research Inst., Tokyo.
SHINE THROUGH MEASUREMENTS WITH HYDROGEN BEAM IN JT-60
Masaaki Kuriyama (Japan Atomic Energy Research Inst., Naka.), Shunsuke Kunieda (Japan Atomic Energy Research Inst., Naka.), Mamoru Matsuoka (Japan Atomic Energy Research Inst., Naka.), Makoto Mizuno (Japan Atomic Energy Research Inst., Naka.), Yoshihiro Ohara (Japan Atomic Energy Research Inst., Naka.), Hiroshi Oohara (Japan Atomic Energy Research Inst., Naka.), and Kazuhiko Mogaki (Japan Atomic Energy Research Inst., Naka.) Mar. 1993 18 p
(DE94-701113; JAERI-M-93-059) Avail: CASI HC A03/MF A01

The shine through rate with hydrogen beams in the JT-60 neutral beam injection experiments was measured in a beam energy range of 40-75 keV and plasma densities of 1-7 x 10(exp 19) m(exp -3) for the estimation of absorbed beam power in the plasma. The shine through rate was calculated from the temperature rise measurement with thermocouples installed in an armor plate. The shine through depends on the plasma density inverse-exponentially and the beam energy linearly. Additionally, the rate changes with the plasma species and the plasma facing materials which effect impurity contamination of the plasma. An enhancement of beam stopping cross section by multistep collisions was also found even in a beam energy range of 40-75 keV. DOE

N94-27715# Los Alamos National Lab., NM.
ATOMIC PROCESSES IN INERTIAL ELECTROSTATIC CONFINEMENT (IEC) DEVICES
R. A. Nebel, L. Turner, T. N. Tiouririne, D. C. Barnes, W. D. Nystrom, R. W. Bussard (Energy/Matter Conversion Corp., Manassas, VA.), G. H. Miley (Illinois Univ., Urbana.), J. Javedani (Illinois Univ., Urbana.), and Y. Yamamoto (Illinois Univ., Urbana.) 1993 10 p Presented at the 9th Biennial Topical Conference on Atomic Processes in Plasmas, San Antonio, TX, 19-23 Sep. 1993
(Contract W-7405-eng-36)
(DE94-005015; LA-UR-93-4482; CONF-9309119-2) Avail: CASI HC A02/MF A01

Inertial Electrostatic Confinement (IEC) is one of the earliest plasma confinement concepts, having first been suggested by P. T. Farnsworth in the 1950's. The concept involves a simple apparatus of concentric spherical electrostatic grids or a combination of grids and magnetic fields. An electrostatic structure is formed from the confluence of electron or ion beams. Gridded IEC systems have demonstrated neutron yields as high as 2(10)(exp 10) neutrons/sec. These systems have considerable potential as small, inexpensive, portable neutron sources for assaying applications. Neutron tomography is also a potential application. Atomic physics effects strongly influence the performance of all of these systems. Important atomic effects include elastic scattering, ionization, excitation, and charge exchange. This paper discusses how an IEC system is influenced by these effects and how to design around them. Theoretical modeling and experimental results are presented. DOE

N94-27720# Rensselaer Polytechnic Inst., Troy, NY.
ADVANCED DEVELOPMENT OF PARTICLE BEAM PROBE DIAGNOSTIC SYSTEM Progress Report, 15 Dec. 1992 - 15 Oct. 1993
T. P. Crowley, P. M. Schoch, and K. A. Connor 1993 10 p
(Contract DE-FG02-85ER-53211)
(DE94-002316; DOE/ER-53211/12) Avail: CASI HC A02/MF A01

This progress report under DOE Grant DE-FG02-85ER3211 covers the period 15 Dec. 1992 through 15 Oct. 1993. The major accomplishments of this period are summarized. The basic TEXT heavy ion beam probe including the primary beam line, the upper secondary beam line with the old 500 keV analyzer, and the lower secondary beam line with the new 2 MeV analyzer is operational, and system shake-down is now beginning. Several subsystems of the complete system design are still under development including secondary beam line sweeps, primary beam detectors, the digital control, and data acquisition system. The lower analyzer entrance aperture and detector plates also have very limited capabilities to make it possible to more rapidly obtain satisfactory initial alignment and calibration conditions. We have performed a variety of high voltage tests that establish the basic efficacy of the 2 MeV analyzer design. We have upgraded the ion optics and added vacuum chambers in our vertical test stand facility to allow us to test the 2 MeV analyzers. We have also constructed a facility for testing ion source characteristics. We analyzed data on primary beam modulation taken during the last run period and confirmed the accuracy of our simulation code. Analysis of magnetic field measurements continued. DOE

N94-27723# Texas Univ., Austin. Inst. for Fusion Studies.
REDUCED BRAGINSKII EQUATIONS
M. Yagi and W. Horton Nov. 1993 12 p
(Contract DE-FG05-80ET-53088)
(DE94-003510; DOE/ET-53088/632; IFSR-632) Avail: CASI HC A03/MF A01

A set of reduced Braginskii equations is derived without assuming flute ordering and the Boussinesq approximation. These model equations conserve the physical energy. It is crucial at finite (beta) that we solve the perpendicular component of Ohm's law to conserve the physical energy while ensuring the relation (del) (center dot) j = 0. DOE

N94-27735# Columbia Univ., New York, NY. Plasma Physics Lab.
PASSIVE STABILIZATION OF MHD INSTABILITIES AT HIGH (BETA)n IN THE HBT-EP TOKAMAK Ph.D. Thesis
D. A. Gates 1993 133 p
(Contract DE-FG02-86ER-53222)
(DE94-003317; DOE/ER-53222/108) Avail: CASI HC A07/MF A02

The HBT-EP Tokamak has been designed, built, and is now fully operational in the Columbia University Plasma Physics Laboratory. One of the primary purposes of this facility is to study the effects of a conducting wall on the MHD modes that lead up to plasma disruptions. Of particular interest are the types of instabilities that are driven by the kinetic pressure of the plasma, because these instabilities are believed to be responsible for the present limit to plasma Beta with Beta proportional to (p)/B(exp 2), where the (p) is the volume averaged pressure and B is the magnetic field. To this end, a movable conducting wall has been installed inside the HBT-EP vacuum chamber. The primary result of this thesis is the initial results from experiments that study the effect of this wall on plasma instabilities. The experiment shows that the conducting wall significantly reduces the growth rate of instabilities that precede a plasma disruption that occurs when the value of (beta) is near the Troyon limit. The location of the wall required for significant stabilization is b/a approximately 1.2 where a is the minor radius of the plasma and b is the minor radial location of the wall. Moving the wall closer than $b/a = 1.2$ slightly degrades the stabilizing effect, which is consistent with recent theories. DOE

N94-27785# Oak Ridge National Lab., TN.
HELIUM TRANSPORT AND EXHAUST STUDIES OF H-MODE DISCHARGES IN THE D3-D TOKAMAK
D. L. Hillis, M. R. Wade, J. T. Hogan, W. P. West (General Atomic Co., San Diego, CA.), K. H. Burrell (General Atomic Co., San Diego, CA.), R. Maingi, C. C. Klepper, M. M. Menon, P. K. Mioduszewski, and M. A. Mahdavi (General Atomic Co., San Diego, CA.) et al 1993 6 p Presented at the IAEA Meeting on H-Mode Physics, Naka, Japan, 15-17 Nov. 1993
(Contracts DE-AC05-84OR-21400; DE-AC03-89ER-51114)
(DE94-004744; CONF-9311147-1) Avail: CASI HC A02/MF A01

A collaborative program was initiated to measure helium (He) transport and exhaust on DIII-D in L-mode, ELM-free H-mode, and ELMing H-mode. These diverted plasmas operating in enhanced confinement regimes should provide valuable information for the International Thermonuclear Experimental Reactor (ITER). To simulate the presence of He ash in DIII-D, a 50 ms He puff is injected into a DIII-D plasma, resulting in a He concentration of approximately 15%. The time dependence of the He density profiles in the plasma core is measured with charge-exchange recombination spectroscopy and the He spatial distribution on the diverter floor is studied with an impurity monitor array. The dependence of core transport diffusivities as a function of ELM frequency were studied and the first demonstration made of He exhaust from an H-mode plasma in a diverted tokamak. The exhaust rate of He from these ELMing H-mode plasmas appears to be within the acceptable range for a fusion reactor, like ITER, based on a measured value of (tau)*(sub He)/(tau)E approximately 14. DOE

N94-27791# General Atomic Co., San Diego, CA.
FUEL ION ROTATION MEASUREMENT AND ITS IMPLICATIONS ON H-MODE THEORIES
J. Kim, K. H. Burrell, P. Gohil, R. J. Groebner, F. L. Hinton, Y. B. Kim, R. Seraydarian, W. Mandl (Max-Planck-Inst. fuer Plasmaphysik, Garching, Germany.), and M. R. Wade (Oak Ridge National Lab., TN.) Oct. 1993 6 p Presented at the IAEA Meeting on H-Mode Physics, Naka, Japan, 15-17 Nov. 1993
(Contract DE-AC03-89ER-51114)
(DE94-004860; GA-A-21507; CONF-9311147-2) Avail: CASI HC A02/MF A01

Poloidal and toroidal rotation of the fuel ions (He(2+)) and the impurity ions (C(6+) and B(5+)) in H-mode helium plasmas were investigated in the DIII-D tokamak by means of charge exchange recombination spectroscopy, resulting in the discovery that the fuel ion poloidal rotation is in the ion diamagnetic drift direction while the impurity ion rotation is in the electron diamagnetic drift direction. The radial electric field obtained from radial force balance analysis of the measured pressure gradients and rotation velocities is shown to be the same regardless of which ion species is used and therefore is a more fundamental parameter than the rotation flows in studying H-mode phenomena. It is shown that the three contributions to the radial electric field (diamagnetic, poloidal rotation, and toroidal rotation terms) are comparable and consequently the poloidal flow does not solely represent the E x B flow. In the high-shear edge region, the density scale length is comparable to the ion poloidal gyroradius, and thus neoclassical theory is not valid there. In view of this new discovery that the fuel and impurity ions rotate in opposite sense, L-H transition theories based on the poloidal rotation may require improvement. DOE

N94-27825# Los Alamos National Lab., NM.
PERFORMANCE OF A 14-MeV NEUTRON GENERATOR AS AN IN SITU CALIBRATION SOURCE FOR TFTR
A. L. Roquemore (Princeton Univ., NJ.), D. L. Jassby (Princeton Univ., NJ.), L. C. Johnson (Princeton Univ., NJ.), J. D. Strachan (Princeton Univ., NJ.), and C. W. Barnes 14 Oct. 1993 6 p Presented at the Symposium on Fusion Engineering, Hyannis, MA, 11-15 Oct. 1993
(Contracts W-7405-eng-36; DE-AC02-76CH-03073)
(DE94-004993; LA-UR-93-4234; CONF-931018-77) Avail: CASI HC A02/MF A01

TFTR will soon enter its D-T phase with the introduction of tritium. This will result in the production of neutrons having 14-MeV energy which is significantly greater than the 2.5-MeV neutrons encountered during D-D operation. In preparation for the D-T phase, a calibration of the four neutron detection systems was performed using a 14-MeV neutron generator producing 10(exp 8) n/sec. To account for the spatial extent of the toroidally shaped plasma and for neutrons scattered from surrounding structures, detector responses were determined with the source positioned at many locations inside the vacuum vessel. Before the generator could be used as a calibration source, a characterization of its total yield and angular emission properties was obtained. The total yield was determined by aluminum activation methods to within +/- 6%, while the angular emission was found to be anisotropic in the forward and reverse cones along the generator axis. After the characterization was performed, the generator was mounted on a moveable track inside the vacuum vessel, where it could be remotely moved across the view of each detector. This paper presents details of the methods and results of the source characterization, together with initial results of the in-vessel D-T neutron calibration. DOE

N94-27836# Institute of Plasma Physics, Prague (Czechoslovakia).
FAST H-ALPHA LINE BROADENING DURING THE 100 ns REB INJECTION INTO A PLASMA
K. Kolacek, M. Ripa, J. Ullschmied, K. Jungwirth, and P. Sunka Jun. 1992 7 p
(IPPCZ-322) Avail: CASI HC A02/MF A01

Profiles of the H-alpha line emitted from the hot electron plasma Te much greater than Ti during the 100 ns REB injection resemble the Gaussian ones from neutrals with a temperature Tn(t) approximately equal to Ti(t) approximately equal to Te(t) rapidly growing up to 30 eV. Combination of Doppler and Stark effects of the intense ion sound waves - remnants of the burned out Langmuir cavitons - is suggested for plausible explanation of this fast H-alpha line broadening. Reliability of the basic ideas of strong Langmuir turbulence for description of REB-plasma systems is thus indirectly supported, too. Author

N94-27840# Institute of Plasma Physics, Prague (Czechoslovakia).
ON HELICON WAVE INDUCED RADIAL PLASMA TRANSPORT
V. Petrzilka Apr. 1993 13 p
(IPPCZ-333) Avail: CASI HC A03/MF A01

Estimates of helicon wave induced radial plasma transport are presented. The wave induced transport growths or decreases in dependence on the sign of the azimuthal wave number; these changes in transport may be important for helicon wave plasma sources. Author

N94-27842# Institute of Plasma Physics, Prague (Czechoslovakia).
PRELIMINARY CONSIDERATIONS ON THE DIFFRACTION (QUASI-OPTICAL) GRILL IN CASTOR TOKAMAK
R. Klima Sep. 1993 9 p
(IPPCZ-335) Avail: CASI HC A02/MF A01

An original system for launching lower hybrid waves (LHW) into tokamak plasmas has been suggested. The purpose of the present note is to give simple estimates of possibility to verify this new quasi-optical grill at the CASTOR tokamak. We briefly estimate the accessibility, the spectrum expected, and the directivity in connection with the penetration through the evanescence layer. A schematic sketch of the proposed launching system in CASTOR tokamak is included in this document. Derived from text

N94-27844 Universidad Autonoma Metropolitana de Mexico (Mexico). Unidad Azcapotzalco.
DETERMINATION OF THE PLASMA COLUMN SHAPE IN THE TOKAMAK NOVILLO CROSS SECTION BY MAGNETIC PROBES Ph.D. Thesis
Adrian Hernandez Omana 1993 77 p Limited Reproducibility: More than 20% of this document may be affected by microfiche quality
(DE94-604986; INIS-mf-13724) Avail: CASI HC A05 (US Sales Only)

The determination of plasma cross section shape in tokamaks is an important diagnostic method for equilibrium conditions analysis. In this work, a time dependent variation of the plasma column cross section in the Novillo Tokamak is obtained. The experimental method is based on using one magnetic probe, which is installed inside of the vacuum vessel in a 1 mm wall thickness stainless steel tube, in the protected region of the limiter shadow. The plasma column cross section is determined by measuring the poloidal magnetic field produced by the plasma current. This method, now running for determining the plasma column shape, requires the measurement of magnetic field present outside plasma column. The measurements are carried out from a set of small coils, which are located inside the vacuum chamber in the radial and poloidal direction, so the magnetic field with no current attenuations produced by the penetration time of the stainless steel vacuum chamber can be measured. The magnetic probes detect a real time variation of magnetic flux passing through them. In order to obtain the magnetic field values, it is required that the electric signals coming from the magnetic probe be integrated; this operation is carried out by active circuits located between the probe signal and one oscilloscope. The integrated signals can be exhibited by photographs of the oscilloscope display. DOE

N94-27855 China Nuclear Information Centre, Beijing.
THE CALCULATION FOR ENERGY BALANCE OF HEATING PLASMAS BY ALFVEN WAVES
Yong-Xing Long (Southwest Inst. of Physics, Sichuan, China.), Ning Ding (Southwest Inst. of Physics, Sichuan, China.), Qi-Bing He (Southwest Inst. of Physics, Sichuan, China.), Wen-Xiao Qu (Southwest Inst. of Physics, Sichuan, China.), Lin Huang (Southwest Inst. of Physics, Sichuan, China.), and Xiao-Ming Qiu (Southwest Inst. of Physics, Sichuan, China.) Oct. 1992 8 p In CHINESE Limited Reproducibility: More than 20% of this document may be affected by microfiche quality
(DE94-604994; CNIC-00658; SIP-0050) Avail: CASI HC A02 (US Sales Only)

A numerical method for computing the energy balance of heating tokamak plasmas by Alfven waves is introduced. The results are in agreement with experiments. This method is not only simpler and more distinct but also quicker in computation. It also can be used in kinetic problems with other types of radio frequency (RF) heating. DOE

N94-27856 China Nuclear Information Centre, Beijing.
ANALYSIS OF DENSITY LIMIT AND EFFICIENCY IN LOWER HYBRID CURRENT DRIVE
Yong-Xiang Yin (Southwest Inst. of Physics, Sichuan, China.) and Xiao-Dong Li (Southwest Inst. of Physics, Sichuan, China.) Jul. 1992 8 p Limited Reproducibility: More than 20% of this document may be affected by microfiche quality
(DE94-604995; CNIC-00665; SIP-0053) Avail: CASI HC A02 (US Sales Only)

The conditions of accessibility and parameter decay instability as well as the power spectrum are used to analyze the density limit and efficiency of lower hybrid current drive (LHCD). For convenience of the analysis, an equal-N(sub parallel) curve and an operation curve are defined, where N(sub parallel) is the refractive index of lower hybrid wave parallel to toroidal magnetic field. By means of the two kinds of curves, the dependences of density limit and efficiency of LHCD on toroidal magnetic field B(sub 0) pump frequency f(sub 0), electron density n(sub c), and electron temperature T(sub e) are obtained, which are in good agreement with LHCD experiments on most tokamaks. DOE

N94-27949 Saskatchewan Univ., Saskatoon. Dept. of Electrical Engineering.
MODELLING AND CONTROL OF PLASMA POSITION IN THE STOR-M TOKAMAK Ph.D. Thesis
Majid Emaami-Khonsaari Apr. 1990 152 p
(ISBN-0-315-58891-8; CTN-94-61004) Copyright Avail: Micromedia Ltd., Technical Information Centre, 240 Catherine Street, Suite 305, Ottawa, Ontario, K2P 2G8, Canada HC/MF

A new tokamak model is presented in which the tokamak components are treated together as an electrical circuit and the effects of turbulent heating (TH) on the circuit elements are included. The plasma dynamics is approximated with linear time-invariant state equations. The simple model was used to study the behavior of the system around an operating point of interest. Based on this study, a control system was designed. Simulation results showed that the plasma position is rather insensitive to variation in the time constant of the control current driver system as long as it is under 1.4 ms. It was also shown that the presence of the iron core results in unstable roots in the open loop plasma position Laplace transfer function. A least squares error algorithm was used to determine improved estimates of the model parameters. A control strategy for plasma position using analog control during ohmic heating (OH) was developed and successfully demonstrated. However, rapid changes in plasma parameters during and after TH were shown to require adaptive control. A suitable digital controller was designed, built, and verified for controlling plasma position after a TH pulse. The final result is a stably controlled plasma that can be maintained for the entire duration of a plasma discharge, for both the OH and TH modes. Author (CISTI)

N94-25576# National Research Inst. for Metals, Tokyo (Japan). Materials Characterization Div.
STUDY ON DEVELOPMENT OF CHEMICAL MEASUREMENT METHOD UTILIZING PLASMAS [PURAZUMA O RIYO SHITA KAGAKU KEISOKUHO NO KAIHATSU NI KANSURU KENKYU]
Morimasa Saito and Fumio Hirose *In its* Bulletin of National Research Institute for Metals in Fiscal Year 1993, No. 14 29 Jan. 1993 p 299-307 In JAPANESE (For primary document see N94-25544 07-26)
Avail: CASI HC A02/MF A04

76 SOLID-STATE PHYSICS

Includes superconductivity.

For related information, see also *33 Electronics and Electrical Engineering* and *36 Lasers and Masers.*

N94-25601# Sandia National Labs., Albuquerque, NM.
MOLECULAR BEAM MASS SPECTROMETRY STUDIES OF THE CHEMICAL VAPOR DEPOSITION OF DIAMOND
Wen L. Hsu, Mark C. McMaster, Michael E. Coltrin, and David S. Dandy (Colorado State Univ., Fort Collins.) 1993 30 p Presented at the 15th Dry Processing Symposium, Tokyo, Japan, 1-2 Nov. 1993
(Contract DE-AC04-94AL-85000)
(DE94-003802; SAND-93-2678C; CONF-9311142-1) Avail: CASI HC A03/MF A01

We have developed a novel molecular beam mass spectrometry technique that can quantitatively analyze the gas-phase composition in a CVD reactor. The technique simultaneously monitors a wide variety of radical and stable species, and their concentrations can be determined with sensitivities approaching 1 ppM. Measurements performed in a diamond deposition system have given us keen insights into the important phenomena that affect the growth environment. This paper first discusses the primary gas sampling design issues. In the second part, the details of the experimental results and their implications will be described. DOE

N94-25614# Tokyo Univ. (Japan). Inst. for Solid State Physics.
HEAVY-ELECTRON BEHAVIOR IN LARGE COORDINATION COMPOUNDS CeZn11 AND UZn12
Yasuhiro Nakazawa, Masayasu Ishikawa, Satoru Noguchi (Osaka Prefecture Univ., Sakai, Japan.), and Kiichi Okuda (Osaka Prefecture Univ., Sakai, Japan.) Mar. 1993 16 p Sponsored by Ministry of Education, Science and Culture, Tokyo, Japan
(ISSN 0082-4798)
(Rept-A-2663; JTN-94-80534) Avail: CASI HC A03/MF A01

Two intermetallic compounds, CeZn11 and UZn12, were investigated, for heavy-electron behavior and found that the gamma value of low-temperature specific heat amounts to about 1.5 J/(mol sq K) for CeZn11 and 850 - 900 mJ/(mol sq K) for UZn12. CeZn11 exhibited an antiferromagnetic long-range order at 2.0 K evidenced by a large peak of specific heat and a broad maximum in the susceptibility, while UZn12 did neither superconducting nor magnetic phase transition down to 0.4 K. Author (NASDA)

N94-25645# Massachusetts Inst. of Tech., Lexington. Lincoln Lab.
SOLID STATE RESEARCH Quarterly Report, 1 Feb. - 30 Apr. 1993
Alan L McWhorter 15 May 1993 62 p
(Contract F19628-90-C-0002)
(AD-A274063; Rept-1993.2; ESC-TR-93-254) Avail: CASI HC A04/MF A01

This report covers in detail the research work of the Solid State Division at Lincoln Laboratory for the period 1 February - 30 April 1993. The topics covered are electrooptical devices, quantum electronics, materials research, submicrometer technology, high speed electronics, microelectronics, and analog device technology. Funding is provided primarily by the Air Force, with additional support provided by the Army, DARPA, Navy, SDIO, and NASA. DTIC

N94-25814# Sandia National Labs., Albuquerque, NM.

BINDING OF COPPER AND NICKEL TO CAVITIES IN SILICON FORMED BY HELIUM ION IMPLANTATION

S. M. Myers, D. M. Follstaedt, and D. M. Bishop 1993 6 p Presented at the Fall Meeting of the Materials Research Society, Boston, MA, 29 Nov. - 3 Dec. 1993
(Contract DE-AC04-94AL-85000)
(DE94-003769; SAND-93-1453C; CONF-931108-7) Avail: CASI HC A02/MF A01

Cavities formed in Si by He ion implantation and annealing are shown to be strong traps for Cu and Ni impurities. Experiments utilizing ion-beam analysis and transmission electron microscopy indicate that Cu is trapped at the internal surfaces of cavities up to approximately 1 monolayer coverage with a binding energy of 2.2 +/- 0.2 eV relative to solution. This is greater than the heat of solution from the precipitated Cu3Si phase, determined to be 1.7 eV in agreement with earlier work. Copper at cavity-wall sites is reversibly replaced by H during heating in H2 gas, indicating the relative stability of the two surface terminations. Initial results for Ni impurities indicate that trapping at cavities is again energetically preferred to silicide formation. The saturation coverage of Ni on the internal surfaces, however, is an order of magnitude smaller for Ni than Cu, consistent with published studies of external-surface adsorption. These results suggest that cavity trapping may getter metallic impurities in Si more effectively than methods based on silicide precipitation. DOE

N94-25815# Sandia National Labs., Albuquerque, NM.

HYDROGEN UPTAKE INTO SILICON FROM AN ECR PLASMA

W. R. Wampler and J. C. Barbour 1993 19 p Presented at the 40th National Symposium of the American Vacuum Society, Orlando, FL, 15-19 Nov. 1993
(Contract DE-AC04-94AL-85000)
(DE94-003771; SAND-93-1159C; CONF-9311104-14) Avail: CASI HC A03/MF A01

The concentration of hydrogen in solution near the surface of silicon exposed to an electron cyclotron resonance (ECR) plasma was determined by measuring the flux of hydrogen permeating to subsurface microcavities. The energy and flux of hydrogen impinging onto the surface from the plasma was also measured. A model is described which predicts the concentration of hydrogen in solution from the energy and flux of the impinging hydrogen. The measured solution concentrations were approximately 10(exp -9) H/Si at 600 C and approximately 10(exp -8) H/Si at 400 C, in fairly good agreement with the model. The absence of accumulation of immobile hydrogen near the surface indicates that lattice defects, which strongly trap hydrogen, were not produced by the ECR plasma. This study establishes a connection between the properties of the ECR plasma and the concentration of hydrogen in silicon samples exposed to the plasma, which allows improved control over passivation of defects and dopants. DOE

N94-25817# Sandia National Labs., Albuquerque, NM. Condensed Matter and Thermal Physics Group.

MICROSCOPIC STUDY OF LOCAL STRUCTURE AND CHARGE DISTRIBUTION IN METALLIC La2CuO(4+DELTA)

P. C. Hammel (Los Alamos National Lab., NM.), A. P. Reyes (Los Alamos National Lab., NM.), E. T. Ahrens (Los Alamos National Lab., NM.), Z. Fisk (Los Alamos National Lab., NM.), P. C. Canfield (Los Alamos National Lab., NM.), J. D. Thompson (Los Alamos National Lab., NM.), and J. E. Schirber 29 Oct. 1993 22 p Presented at the 2nd Workshop on Phase Separation in Cuprate Superconductors, Cottbus, Germany, 4-10 Sep. 1993
(Contract DE-AC04-94AL-85000)
(DE94-003801; SAND-93-2709C; LA-UR-93-3836; CONF-9309283-2) Avail: CASI HC A03/MF A01

The authors employ NMR and NQR spectroscopy as probes of local structure and charge environments in metallic La2CuO(4+delta) (Tc= 38 K). They discuss the effect of annealing the sample at various temperatures T(sub a) (Tc less than T(sub a) less than 300 K) on the superconducting (Tc). The dependence of (Tc) on annealing indicates that annealing allows the development of structural order which is important for (Tc). The La-139 quadrupole frequency, nu(sub Q) is smaller than in undoped materials. This is unexpected and may indicate a smaller charge on the apex oxygen in the doped material and thus a different distribution of charge between the La-O layer to the planes. The further, rapid decrease in nu(sub Q) just above (Tc) indicates that temperature dependent charge redistribution is occurring. The presence of doped holes induces a distribution of displacements of the apex oxygen off of the vertical La-Cu bond axis. These vary from zero to the value observed in lightly doped (antiferromagnetic) La2CuO(4+delta). These measurements demonstrate a striking degree of inhomogeneity in the crystal structure of the La-O layer. Copper NQR spectroscopy shows that there are two distinct copper sites in the CuO2 planes and thus that either the structure or the charge distribution in the planes is inhomogeneous as well. These inhomogeneities are the intrinsic response of the crystal to doped holes; they are not the result of distortions of the lattice due to the presence of interstitial oxygen atoms. DOE

N94-25825 Joint Inst. for Nuclear Research, Dubna (USSR). Lab. of Computing Techniques and Automation.

COHERENT STATE APPROACH FOR THE (PHI)(SUP 6)-LATTICE MODEL AND PHASE TRANSITIONS

M. A. Aguero-Granados and V. G. Makhankov 1991 19 p Limited Reproducibility: More than 20% of this document may be affected by microfiche quality
(DE93-613053; JINR-E-2-91-506) Avail: CASI HC A03 (US Sales Only)

Phase transitions in the lattice version of the Phi(sup 6)-field theory are studied. The generalized coherent states approach is used. In such a way the roles of kinks and bubbles in phase transitions have been reexamined. It is shown via a numerical analysis that first and second order phase transitions appear due to the behavior of kink and bubble excitations. DOE

N94-25843# International Centre for Theoretical Physics, Trieste (Italy).

VOLUME DEPENDENCE OF VANADIUM MAGNETISM

M. E. Elzain Jul. 1993 11 p
(DE94-601838; IC-93/224) Avail: CASI HC A03/MF A01 (US Sales Only)

The first principle discrete variational method in the spin polarized local density approximation is used to calculate the local properties of 15 atom clusters representing variable crystal size bcc vanadium. Four distinct magnetic configurations are recognized as the lattice constant varies from 5.4 to 8.4 (a.u.). At the lowest end the clusters are paramagnetic (PM) whereas at the upper end clusters are ferromagnetic (FM). In between antiferromagnetic couplings prevail. The local magnetic moment increases, in a fashion not unlike second order transitions, from zero in the PM range to non-zero values in the AFM region. Transitions between other phases are first order. The systematics of these transitions are ascribed to the general shape of the density of states. The contact magnetic hyperfine field, charge density and 3d partial occupations at the central sites are also calculated. DOE

N94-25848# Rochester Univ., NY. Dept. of Physics and Astronomy.

FLUX FLOW, PINNING, AND RESISTIVE BEHAVIOR IN SUPERCONDUCTING NETWORKS

S. Teitel Oct. 1993 9 p
(Contract DE-FG02-89ER-14017)
(DE94-003400; DOE/ER-14017/5) Avail: CASI HC A02/MF A01

The behavior of fluctuation effects in superconducting systems was studied using numerical simulations of XY and Coulomb gas models. The fluctuation of vortex lines in high temperature superconductors, in the presence of an external magnetic field, has been studied using a three dimensional XY model. The existence of two distinct phase transitions was verified in this model. As the vortex line lattice is heated, it melts first into a line liquid where superconductivity is destroyed for currents perpendicular to the applied magnetic field, but persists for currents parallel to the field. As heating continues, the thermal excitation of closed vortex line loops links all the lines together, leading to completely normal metal properties in all directions. Upon cooling of the vortex line liquid, as the system width increases, one can get trapped into an entangled nonequilibrium state in which vortex line cuttings are frozen out on measurable time scales. Simulations were continued of the two dimensional Coulomb gas, as a model for vortex fluctuations in two dimensional arrays of Josephson junctions, and thin film superconductors. Preliminary results support the accepted view of a Kosterlitz-Thouless melting of the vortex lattice, in the limit of a uniform continuous film. DOE

N94-25851 International Centre for Theoretical Physics, Trieste (Italy).
ON THE ESTIMATION OF MATRIX ELEMENTS FOR OPTICAL TRANSITIONS IN SEMICONDUCTORS
A. R. Hassan Sep. 1992 12 p Limited Reproducibility: More than 20% of this document may be affected by microfiche quality
(DE93-613550; IC-92/221) Avail: CASI HC A03 (US Sales Only)

A semi-empirical method is used to calculate the numerical values of the interband momentum matrix elements of the allowed optical transitions in semiconductors. This method is based on the evaluation of the ratio of the two-photon and one-photon absorption coefficients and the compare the result with the corresponding experimental values in a number of semiconductors both for direct and indirect transition processes. The numerical values of the momentum matrix elements are compared with the convenient theoretical calculations available. The result is found to agree fairly well with the corresponding values computed using the k-vector (center dot) p-vector perturbation theory. DOE

N94-25856# Air Force Inst. of Tech., Wright-Patterson AFB, OH. School of Engineering.
ELECTRICAL PROPERTIES OF p-TYPE GaInP2 M.S. Thesis
Roy S. Calfas Dec. 1993 52 p
(AD-A273771; AFIT/GAP/ENP/93D-01) Avail: CASI HC A04/MF A01

The GaInP2 n(+)-p junction diode has recently become important to the development of high efficiency GaInP2/GaAs dual junction solar cells, which have a demonstrated air mass 1.5 conversion efficiencies in excess of 27%. In order to study the effects of long term exposure to the space environment, the GaInP2 n(+)-p junction diodes were irradiated with a 1 MeV electron beam with a fluence of 10(exp 16) electrons/sq cm. Since little is known about deep level defects (traps) in GaInP2, a deep level transient spectroscopy (DLTS) study was made to characterize the traps that are thought to dominate the dark current in GaInP2 solar cells. The measurements indicated that there are a number of majority carrier traps in the p-type base of the GaInP2 n(+)-p junction diode. Traps that are identified are located 0.12 to 0.55 eV above the valence band and are attributed to phosphorous vacancies in the lattice. DTIC

N94-25885# Melbourne Univ., Parkville (Australia). School of Physics.
FERMIONIC FIELD THEORY AND GAUGE INTERACTIONS ON RANDOM LATTICES
C. J. Griffin and T. D. Kieu 1993 16 p
(DE94-601565; UM-P-93/05) Avail: CASI HC A03/MF A01 (US Sales Only)

Random-lattice fermions were shown to be free of the doubling problem if there are no interactions or interactions of a non-gauge nature. However, gauge interactions impose stringent constraints as expressed by the Ward-Takahashi identities which could revive the free-field suppressed doubler modes in loop diagrams. After introducing a formulation for fermions on a new kind of random lattice, random, naive and Wilson fermions are compared in two dimensional Abelian background gauge theory. It is shown that the doublers are revived for random lattices in the continuum limit, while demonstrating that gauge invariance plays the critical role in this revival. Some implications of the persistent doubling phenomenon on random lattices are also discussed. DOE

N94-25912 Comision Nacional de Energia Atomica, Buenos Aires (Argentina).
THE LATIN AMERICAN CONFERENCE ON THE APPLICATIONS OF THE MOESSBAER EFFECT
1992 168 p Conference held in Buenos Aires, Argentina, 5-9 Oct. 1992 Limited Reproducibility: More than 20% of this document may be affected by microfiche quality
(DE93-615942; INIS-mf-13436; CONF-9210294) Avail: CASI HC A08 (US Sales Only)

This work includes all the papers presented at the LACAME'92 Latin American conference on the applications of the Moessbauer effect, held in Buenos Aires (Argentine Republic), from 5th through 9th, 1992. DOE

N94-25914 International Centre for Theoretical Physics, Trieste (Italy).
LIGHTER ALKALI HYDRIDE AND DEUTERIDE 1: ELECTRONIC PROPERTIES OF PURE SOLIDS
A. K. M. A. Islam Oct. 1992 61 p Limited Reproducibility: More than 20% of this document may be affected by microfiche quality
(DE93-616188; IC-92/344) Avail: CASI HC A04 (US Sales Only)

The properties of lighter alkali hydrides of metals which crystallize in the rock-salt structure are discussed. First, the properties of pure crystals which are dominated by the electrons, in particular the energy levels and the eigenstates of the electrons in the absence of lattice defects are considered. After that, the optical properties of the solids excited at photon energies larger than those appropriate to lattice vibration and dominated by the transition of electron from the occupied core and valence levels to the normally empty conduction states, are discussed. DOE

N94-25921# Tokyo Univ. (Japan). Inst. for Solid State Physics.
SUCCESSIVE STRUCTURAL PHASE TRANSITIONS IN STOICHIOMETRIC La2NiO4 OBSERVED BY X RAY DIFFRACTION
Akihiko Hayashi, Hiroyasu Tamura, and Yutaka Ueda Apr. 1993 18 p
Sponsored by Ministry of Education, Science and Culture, Tokyo, Japan
(ISSN 0082-4798)
(Rept-A-2665; JTN-94-80536) Avail: CASI HC A03/MF A01

Phase transition in La2NiO4+delta near stoichiometric oxygen content has been studied between 10 and 800 K by powder X-ray diffraction. In addition to a second-order transition from a High-Temperature Tetragonal (HTT) phase into a Low-Temperature Orthorhombic (LTO1) phase at 700 K on cooling, a transition into another orthorhombic (LTO2) phase was observed at 75 K. The LTO2 phase developed into domains large enough for X-ray powder diffraction. The study made it evident that the LTO2 phase is apparently an orthorhombic one and the second transition is of first-order. The nature of phase transitions in La2MO4 (M = Ni, Cu) is also discussed in relation to the temperature dependence of the orthorhombicity. Author (NASDA)

N94-25944# Sandia National Labs., Albuquerque, NM.
IN SITU X RAY REFLECTIVITY MEASUREMENTS OF THIN FILM STRUCTURAL EVOLUTION
E. Chason and M. Chason (Motorola, Inc., Schaumburg, IL.) 1993 17 p
Presented at the 40th National Symposium of the American Vacuum Society (AVS), Orlando, FL, 15-19 Nov. 1993
(Contract DE-AC04-94AL-85000)
(DE94-002289; SAND-93-1146C; CONF-9311104-7) Avail: CASI HC A03/MF A01

X ray reflectivity using energy dispersive x ray detection has been used to investigate vacuum deposited thin films. A resolution of 0.3 nm for thickness in the range of 3 to 200 nm and of 0.05 nm for roughness in the range of 0.1 to 3 nm has been demonstrated. Further, it is shown that by using energy dispersive detection, spectra can be obtained in less than 500 s allowing real time studies to be performed. Thin, discrete Cr/Al deposits on quartz substrates have been investigated and the presence of a 1.5 nm thick Al/Cr intermetallic layer formed during room temperature deposition has been determined. During annealing at 250 C, the Cr layer thickness decreases linearly with time until approximately 4 nm is consumed in additional intermetallic formation; further annealing does not change the Cr layer thickness. DOE

N94-25945 International Centre for Theoretical Physics, Trieste (Italy).
OPTICAL CONDUCTIVITY AND RESISTIVITY IN THE TWO-BAND EMERY MODEL
Tran Minh-Tien Jul. 1993 16 p Limited Reproducibility: More than 20% of this document may be affected by microfiche quality
(DE94-601943; IC-93/177) Avail: CASI HC A03 (US Sales Only)

The temperature and frequency-dependent conductivity due to the scattering of oxygen holes by antiferromagnetic spin fluctuations of the copper spins in the two-band Emery model is calculated by means of the memory function method. Using the dynamic spin susceptibility obtained in mean field Schwinger boson approach, the resistivity reveals a crossover from a quadratic to a linear temperature dependence. The scattering rate

of quasiparticles appears to be proportional to frequency. At the same time, the optical conductivity contains a Druke peak around zero frequency. From these results it is concluded that the normal-state basal-plane resistivity and optical conductivity of high-Tc superconductors may be explained by two dimensional spin-fluctuation scattering in the Fermi-liquid picture.
DOE

N94-25947# Lawrence Livermore National Lab., CA.
TRAPPED ELECTRONS IN SOLID HYDROGEN
G. W. Collins, F. Magnotta, E. R. Mapoles, and H. E. Lorenzana Jun. 1993 15 p Presented at the AFOSR) High Energy Density Materials Contractors Conference, Woods Hole, MA, 6-8 Jun. 1993
(Contract W-7405-eng-48)
(DE93-018628; UCRL-JC-114006; CONF-9306212-1) Avail: CASI HC A03/MF A01

We report here a relatively large increase in emission of the integrated 800 nm line when pumping the UV absorption and a much smaller increase (by a factor of approximately 15) upon pumping the IR absorption band in solid D-T at 4.6 K. These data show the 800 run emission is most likely the result of an electron bubble transition. We also present ESR data for electrons in D2 and H2 doped with 2% T2 and pure T2. We find there are two components to this absorption, a narrow line component which we attribute to trapped electrons and a broad line component which we attribute to delocalized electrons. The narrow ESR linewidth in the H2 and D2 samples are commensurate with the idea of electrons localized in vacancy seeded traps. In solid T2 the broad line dominates, implying that most electrons are delocalized due to the large concentration of electrons and other impurities. We find that the temperature and time dependence of the electron concentration from the 800 nm line is similar to the unpaired atoms as measured previously with ESR. DOE

N94-25971# Sandia National Labs., Albuquerque, NM.
THE STRUCTURAL, CHEMICAL, AND ELECTRICAL PROPERTIES OF He-IMPLANTATION-INDUCED NANOCAVITIES IN SILICON
C. H. Seager, S. M. Myers, D. M. Follstaedt, H. J. Stein, and W. R. Wampler 1993 20 p Presented at the 3rd Workshop on the Role of PointDefects/Defect Complexes in Silicon Device Fabrication, Vail, CO, 16-18 Aug. 1993
(Contract DE-AC04-94AL-85000)
(DE94-002681; SAND-93-1725C; CONF-9308191-1) Avail: CASI HC A03/MF A01

Si implanted with He to doses of about 2 x 10(exp 16) cm(sup -2) and greater and annealed at high temperatures develops a layer of internal nanocavities near the end of the He range. Above an annealing temperature of 700 C, all the implanted He escapes from these implanted samples, and the resultant internal cavity surfaces can be shown to possess a high density of chemically reactive Si dangling orbitals. These structures, in addition to possessing a variety of interesting electronic properties, were recently shown to hold great promise as getters for removing undesirable impurities from the silicon matrix. Some of the structural features of these nanocavities and studies which were used to accurately determine the binding energy of H and Cu to Si atoms at the cavity walls are described. Recently, they also demonstrated that these nanocavities capture large densities of majority carriers in n- and p-type silicon. These electrical measurements demonstrated that the nanocavity electronic states possess both acceptor and donor levels in the Si forbidden gap. The approximate location of these levels was determined by a variety of different types of capacitance transient spectroscopy. DOE

N94-25972# Los Alamos National Lab., NM.
TEMPERATURE DEPENDENCE OF THE RADIATION INDUCED CHANGE OF DEPLETION VOLTAGE IN SILICON PIN DETECTORS
H. J. Ziock, K. Holzscheiter, A. Morgan, A. P. T. Palounek, J. Ellison (California Univ., Riverside.), A. P. Heinson (California Univ., Riverside.), M. Mason (California Univ., Riverside.), S. J. Wimpenny (California Univ., Riverside.), E. Barberis (California Univ., Santa Cruz.), and N. Cartiglia (California Univ., Santa Cruz.) et al 1993 9 p Presented at the Nuclear Science Symposium, San Francisco, CA, 2-5 Nov. 1993
(Contract W-7405-eng-36)
(DE94-002705; LA-UR-93-3811; CONF-931107-8) Avail: CASI HC A02/MF A01

The silicon microstrip detectors that will be used in the SDC experiment at the Superconducting Super Collider (SSC) will be exposed to very large fluences of charged particles, neutrons, and gammas. A study of how temperature affects the change in the depletion voltage of silicon PIN detectors damaged by radiation is presented. The initial radiation damage and the short-term and long-term annealing of that damage as a function of temperature in the range from -10 C to +50 C, and as a function of 800 MeV proton fluence up to 1.5 x 10(exp 14) p/cm(sup 2) was studied. They express the pronounced temperature dependencies in a simple model in terms of two annealing time constants which depend exponentially on the temperature. DOE

N94-25989# Sandia National Labs., Albuquerque, NM.
INVESTIGATION OF PLASMA ETCH INDUCED DAMAGE IN COMPOUND SEMICONDUCTOR DEVICES
R. J. Shul, M. L. Lovejoy, D. L. Hetherington, D. J. Rieger, G. A. Vawter, J. F. Klem, and M. R. Melloch (Purdue Univ., West Lafayette, IN.) 1993 19 p Presented at the 40th National Symposium of the American Vacuum Society, Orlando, FL, 15-19 Nov. 1993
(Contract DE-AC04-94AL-85000)
(DE94-002849; SAND-93-1171C; CONF-9311104-10) Avail: CASI HC A03/MF A01

We have investigated the electrical performance of mesa-isolated GaAs pn-junction diodes to determine the plasma-induced damage effects from reactive ion and reactive ion beam etching. A variety of plasma chemistries (SiCl4, BCl3, BCl3/Cl2, and Cl2) and ion energies ranging from 100 to 400 eV were studied. We have observed that many of the RIE BCl3/Cl2 plasmas and RIBE Cl2 plasmas yield diodes with low reverse-bias currents that are comparable to the electrical characteristics of wet-chemical-etched devices. The reverse-bias leakage currents are independent of surface morphology and sidewall profiles. DOE

N94-25993# Wright Lab., Wright-Patterson AFB, OH.
THREE-WAVE NONLINEAR INTERACTIONS IN KTiOPO4 (KTP) AND KTP ISOMORPHS Final Report, May - Sep. 1993
Dale L. Fenimore and Kenneth L. Schepler 14 Sep. 1993 119 p
(AD-A274079; WL-TR-93-5029) Avail: CASI HC A06/MF A02

This document reports an investigation of three-wave interactions in positive (nonlinear) biaxial crystals-specifically, the crystal KTiOPO4 (KTP) and its crystallographic isomorphs: RbTiOPO4 (RTP), KTiOAsO4 (KTA), RbTiOAsO4 (RTA), and CsTiOAsO4 (CTA). The results are characterized in terms of phase matching angles, effective nonlinear coefficients, and walkoff angles for the optical beams. In phase matching angles, RTP and CTA showed larger variations in theta (i.e., were more birefringent) than the other isomorphs (which were more uniaxial-like). Where KTP did not have the largest d(eff) the difference from the isomorph which did was typically no more than 0.7 pm/V. Although overall walkoff was less than 3 deg for all isomorphs; the arsenates had around half the walkoff of the phosphates. Strictly from a performance characteristics basis, for uses at wavelengths less than 2.75 microns there is little reason to select one of the other isomorphs over KTP. RTP is acceptable for OPO usage to 3.17 microns, though an arsenate, CTA, is a better choice (higher d(eff) less walkoff, and negligible absorption). Above 3.2 microns, the arsenates, with their smaller walkoff angles and minimal absorption losses, are considerably better choices than the phosphates. DTIC

N94-26012# International Centre for Theoretical Physics, Trieste (Italy).
FIRST PRINCIPLE CALCULATION FOR MAGNETO-CRYSTALLINE ANISOTROPY
Z. Zeng, Q. Q. Zheng (Academia Sinica, Hefei, China.), and W. Y. Lai (Academia Sinica, Beijing, China.) Jun. 1993 12 p
(DE93-634653; IC-93/140) Avail: CASI HC A03/MF A01 (US Sales Only)

Magneto-crystalline anisotropy of permanent magnetic material has been discussed based on the first principle electronic structure calculations. Three methods are applied to evaluate the magneto-crystalline anisotropy of the R2Fe17A(delta) compounds. The crystal field parameters are obtained from correcting the point charge model by (1) using the real space charge distribution from the cluster model calculation; (2) directly calculating the crystal field parameters from the crystal field potential in the embedded cluster model; and (3) taking into account the spin-orbit coupling by perturbation calculation in a semi-relativistic embedded cluster approach. The obtained results are in agreement with the experiments. DOE

N94-26025# Sandia National Labs., Albuquerque, NM.
ORIENTED LEAD ZIRCONATE TITANATE THIN FILMS: CHARACTERIZATION OF FILM CRYSTALLIZATION
J. A. Voigt, B. A. Tuttle, T. J. Headley, M. O. Eatough, D. L. Lamppa, and D. Goodnow 1993 8 p Presented at the Spring Meeting of the Materials Research Society, San Francisco, CA, 12-16 Apr. 1993
(Contract DE-AC04-94AL-85000)
(DE94-003104; SAND-92-2905C; CONF-930405-50) Avail: CASI HC A02/MF A01

Film processing temperature and time was varied to characterize the pyrochlore-to-perovskite crystallization of solution-derived PZT 20/80 thin films. 3000 (Angstrom) thick films were prepared by spin deposition using group of zone axes (100) single crystal MgO as substrate. By controlled rapid thermal processing, films at different stages in the perovskite crystallization process were prepared with the tetragonal PZT 20/80 phase being group of z one axes (100)/(001) oriented relative to the MgO surface. An activation energy for the conversion process of 326 kJ/mole was determined by use of an Arrhenius expression using rate constants found by application of the method of Avrami. Activation energy for formation of the PZT 20/80 perovskite phase of the solution-derived films compared favorably with that calculated from data by Kwok and Desu for sputter-deposited 3500 (Angstrom) thick PZT 55/45 films. Similarity in activation energies indicates that the energetics of the conversion process are not strongly dependent on the method used for film deposition. DOE

N94-26029# Argonne National Lab., Idaho Falls, ID.
GRAIN BOUNDARY DEGRADATION OF YBCO SUPERCONDUCTORS SINTERED IN CO2-CONTAINING ATMOSPHERES
U. Balachandran, K. L. Merkle, J. N. Mundy, Y. Gao (New Mexico Inst. of Mining and Technology, Socorro.), C. Zhang (San Jose State Univ., CA.), D. Xu (San Jose State Univ., CA.), and G. Selvaduray (San Jose State Univ., CA.) Nov. 1993 18 p Presented at the 1st Meeting of the Pacific Rim Ceramic Societies, Honolulu, HI, 7-10 Nov. 1993
(Contract W-31-109-eng-38)
(DE94-003206; ANL/ET/CP-78725; CONF-931142-4) Avail: CASI HC A03/MF A01

The transport critical current density (J(sub c)) of YBCO superconductors decreased with increasing CO2 partial pressure in the sintering atmosphere and ultimately reached zero, even though magnetization measurements showed that the bulk of the samples with zero J(sub c) remained superconducting. The microstructure and composition of the samples was investigated by high resolution transmission electron microscopy and secondary-ion mass spectroscopy (SIMS). Microbeam SIMS indicated carbon segregation at grain boundaries (GB's). Approximately 10% of the GB's were coated with a thin layer of a second phase, deduced to be BaCuO2 and BaCu2O2. Near some grain boundaries, the structure was tetragonal within several tens of nm of the boundaries. The degradation of J(sub c) is discussed in terms of the partial pressure of CO2 and the processing temperatures. Detailed examination of GB microstructures is given in this paper. DOE

N94-26031# Argonne National Lab., IL.
BUCKYBALL MICROWAVE PLASMAS: FRAGMENTATION AND DIAMOND-FILM GROWTH
D. M. Gruen, Shengzhong Liu, A. R. Krauss, and Xianzheng Pan Aug. 1993 22 p
(Contract W-31-109-eng-38)
(DE94-003209; ANL/CHM/PP-80544) Avail: CASI HC A03/MF A01

Microwave discharges (2.45 GHz) have been generated in C60-containing Ar produced by flowing Ar over fullerene-containing soot. Optical spectroscopy shows that the spectrum is dominated by the d(sup 3)(Pi)g-a(sup 3)(Pi)u Swan bands of C2 and particularly the (Delta)v = -2, -1, 0, +1, and +2 sequences. These results give direct evidence that C2 is one of the products of C60 fragmentation brought about, at least in part, by collisionally induced dissociation (CID). C60 has been used as a precursor in a plasma-enhanced chemical vapor deposition (PECVD) experiment to grow diamond-thin films. The films, grown in an Ar/H2 gas mixture (0.14% carbon content, 100 Torr, 20 sccm Ar, 4 sccm H2, 1500 W, 850 C substrate temperature), were characterized with SEM, XRD, and Raman spectroscopy. Growth rate was found to be approximately 0.6 (mu)/hr. Assuming a linear dependence on carbon concentration, a growth rate at least six times higher than commonly observed using methane as a precursor, would be predicted at a carbon content of 1% based on C60. Energetic and mechanistic arguments are advanced to rationalize this result based on C2 as the growth species. DOE

N94-26071# Tokyo Univ. (Japan). Inst. for Solid State Physics.
FORMATION OF THREE TYPES OF QUASI-CRYSTALS IN Al-Pd-Mg SYSTEM
Naokiyo Koshikawa, Keiichi Edagawa, Yuko Honda, and Shin Takeuchi Apr. 1993 18 p
(ISSN 0082-4798)
(Rept-A-2667; JTN-94-80538) Avail: CASI HC A03/MF A01

In the Al-Pd-Mg system, a Mackay-Icosahedron (MI) type Icosahedral (I) phase with the F-type superlattice order and a Decagonal (D) phase were found to form in a melt-quenched state, in addition to the Frank-Kasper (FK) type stable I-phase reported previously. This is the first example in which the three types of quasi-crystalline phases are formed in the same alloy system. The formation range of the FK-type I-phase in melt-quenched state is rather wide: 5 - 20 at percent Pd and 20 - 45 at percent Mg. In contrast, the MI-type, I-phase and D-phase are formed in small composition ranges around Al52Pd31Mg17 and Al74Pd21Mg5, respectively. Electron diffraction studies showed that the period along the tenfold axis of the D-phase is about 1.6 nm. The formation and stability of the MI-type and FK-type I-phases were discussed in terms of a Hume-Rothery rule. Author (NASDA)

N94-26089# Tokyo Univ. (Japan). Inst. for Solid State Physics.
PHASE DIAGRAM OF La2NiO(4+DELTA) (0 LESS THAN OR EQUAL TO DELTA LESS THAN OR EQUAL TO 0.18). 1: PHASES AT ROOM TEMPERATURE AND PHASE TRANSITION ABOVE DELTA EQUAL TO 0.15
Hiroyasu Tamura, Akihiko Hayashi, and Yutaka Ueda Mar. 1993 21 p Sponsored by Ministry of Education, Science and Culture, Tokyo, Japan and Ogasawara Foundation for the Promotion of Science and Engineering, Japan
(ISSN 0082-4798)
(Rept-A-2661; JTN-94-80532) Avail: CASI HC A03/MF A01

La2NiO(4+delta) was prepared in the range of 0.00 less than or equal to delta less than or equal to 0.18. Oxygen stoichiometry, structure and phase transition were studied by TG-DTA (Thermogravimetric and Differential Thermal Analysis) and powder X-ray diffraction measurements. Five phases, orthorhombic Bmab (delta = 0.00), pseudo-tetragonal (delta = 0.02), orthorhombic (0.05 less than delta less than 0.09), tetragonal I4/mmm (0.1 less than delta less than 0.15) and orthorhombic Fmmm (delta greater than or equal to 0.15), appear in sequence of delta with intervals of coexistence range at room temperature. The orthorhombic phase (Fmmm) shows a first-order phase transition to a tetragonal phase (I4/mmm) with elevating transition temperatures from 320 K for delta = 0.15 to 430 K for delta = 0.18. A tentative phase diagram of La2NiO(4+delta) is also shown. Author (NASDA)

N94-26094# California Univ., Berkeley. Lawrence Berkeley Lab.
DETERMINATION OF SURFACE RECOMBINATION VELOCITY AND BULK LIFETIME IN DETECTOR GRADE SILICON AND GERMANIUM CRYSTALS
N. Derhacobian, P. Fine, J. T. Walton, Y. K. Wong, C. S. Rossington, and P. N. Luke Oct. 1993 5 p Presented at the Nuclear Science Symposium, San Francisco, CA, 2-5 Nov. 1993
(Contract DE-AC03-76SF-00098)
(DE94-003886; LBL-34022; CONF-931107-17) Avail: CASI HC A01/MF A01

Utility of a noncontact photoconductive decay (PCD) technique is demonstrated in measuring bulk lifetime, tau(sub B), and surface recombination velocity, S, in detector grade silicon and germanium crystals. We show that the simple analytical equations which relate the observed effective lifetimes in PCD transients to tau(sub B) and S have a limited range of applicability. The noncontact PCD technique is used to determine the effect of several surface treatments on the observed effective lifetimes in Si and Ge. A degradation of the effective lifetime in Si is reported as result of the growth of a thin layer of native oxide at room temperature under atmospheric conditions. DOE

N94-26095# California Univ., Berkeley. Lawrence Berkeley Lab.
LITHIUM DRIFTED SILICON DETECTOR FABRICATION ON GETTERED FLOATING-ZONE SILICON
J. T. Walton, Y. K. Wong, N. Derhacobian, and E. E. Haller Nov. 1993 6 p Presented at the Nuclear Science Symposium, San Francisco, CA, 2-5 Nov. 1993
(Contract DE-AC03-76SF-00098)
(DE94-003890; LBL-33967; CONF-931107-15) Avail: CASI HC A02/MF A01

A gettering procedure using phosphorus doped glass is shown to remove lithium-ion precipitation sites from p-type Floating-Zone (FZ) silicon. A model involving interaction between grown-in vacancies and oxidation-injected silicon interstitials is proposed to explain the gettering procedure. Examples of silicon lithium-drifted detectors fabricated on ungettered and gettered FZ silicons are presented. DOE

N94-26109# Kyoto Univ., Kumatori (Japan). Research Reactor Inst.
RADIATION-INDUCED STRUCTURAL CHANGES, 2
M. Ogasawara, ed. (Hokkaido Univ., Sapporo, Japan.) and T. Matsuyama, ed. Nov. 1992 102 p In JAPANESE Seminar held in Kumatori, Japan, 13-14 Feb. 1992
(DE93-520314; KURRI-TR-368) Avail: CASI HC A06/MF A02

This seminar is aimed at investigating both the physical and chemical aspects of the structural changes of materials induced by photons or ionizing radiation. The seminar was held on 19 Dec. 1991 and from 13-14 Feb. 1992 in this institute. The most active areas of the material science, in addition to the previous subjects, such as organic superconductors, silicon-based polymers, and fullerenes, were included in this seminar. DOE

N94-26125# California Univ., Berkeley. Lawrence Berkeley Lab.
Se EXAFS STUDY OF THE ELEVATED WURTZITE TO ROCK SALT STRUCTURAL PHASE TRANSITION IN CdSe NANOCRYSTALS
S. H. Tolbert (California Univ., Berkeley.) and A. P. Alivisatos (California Univ., Berkeley.) Sep. 1993 12 p Presented at the North Atlantic Treaty Organization (NATO) Advanced Study Meeting of Institute on Nanophas Materials, Corfu, Greece, 20 Jun. - 2 Jul. 1993
(Contract DE-AC03-76SF-00098)
(DE94-003247; LBL-34763; CONF-9306223-2) Avail: CASI HC A03/MF A01

High pressure Se EXAFS data has been obtained on 2.7 nm radius CdSe semiconductor nanocrystals. This system is observed to undergo a solid-solid phase transition at 6.5 GPa which is approximately twice the reported value for bulk CdSe. In combination with high pressure optical absorption experiments, EXAFS data can be used to identify the high-pressure phase structure as rock salt. EXAFS data can be fit with equations of state to yield pressure volume curves. Resultant values of bulk modulus and its derivative with respect to pressure are B(sub o) = 37 +/- 5 GPa and B(sub o)' = 11 +/- 3. A thermodynamic model for the data is presented in which the internal energy in each phase is modified by a surface energy term. Differences in surface energy are used to explain the elevation in phase transition pressure. The model can be used to estimate a value for the surface energy in the rock salt phase; 1.9 +/- 0.3 N/m is obtained in comparison to 0.9 +/- 0. 1 N/m for the wurtzite phase. DOE

N94-26128# California Univ., Berkeley. Lawrence Berkeley Lab.
INSTANTANEOUS AMPLITUDE AND FREQUENCY DYNAMICS OF COHERENT WAVE MIXING IN SEMICONDUCTOR QUANTUM WELLS
D. S. Chemla 30 Jun. 1993 31 p Presented at the International School of Physics on Enrice Fermi, Varenna, Italy, 20-30 Jul. 1993
(Contract DE-AC03-76SF-00098)
(DE94-003262; LBL-34433; CONF-9307155-1) Avail: CASI HC A03/MF A01

This article reviews recent investigations of nonlinear optical processes in semiconductors. Section 2 discusses the theory of coherent wave mixing in semiconductors, with emphasis on resonant excitation with only one exciton state. Section 3 reviews recent experimental investigations of amplitude and phase of coherent wave-mixing resonant with quasi-2d excitons in GaAs quantum wells. DOE

N94-26137# Oak Ridge National Lab., TN.
ION IMPLANTATION OF DIAMOND: DAMAGE, DOPING, AND LIFT-OFF
N. R. Parikh (North Carolina Univ., Chapel Hill.), E. McGucken (North Carolina Univ., Chapel Hill.), M. L. Swanson (North Carolina Univ., Chapel Hill.), J. D. Hunn, C. W. White, and R. A. Zuhr Sep. 1993 6 p Presented at the International Union of Materials Research Societies on Advanced Materials, Tokyo, Japan, 31 Aug. - 4 Sep. 1993
(Contract DE-AC05-84OR-21400)
(DE94-001133; CONF-9308122-12) Avail: CASI HC A02/MF A01

In order to make good quality economical diamond electronic devices, it is essential to grow films and to dope these films to obtain n- and p-type conductivity. This review discusses doping by ion implantation and the production of large area single crystal diamonds. The C implantation damage below an estimated Frenkel defect concentration of 7% could be recovered by annealing at 950 C. For a defect concentration between 7 and 10%, a stable damage form of diamond ('green diamond') was formed by annealing. At still higher damage levels, the diamond graphitized. To introduce p-type doping, we have co-implanted B and C into natural diamond at 77K, followed with annealing up to 1100 C. The resulting semiconducting material has electrical properties similar to those of natural B-doped diamond. To create n-type diamond, we have implanted Na(+), P(+), and As(+) ions and have observed semiconducting behavior. This has been compared with carbon or noble element implantation in an attempt to isolate the effect of radiation damage. Recently, in order to obtain large area signal crystals, we have developed a novel technique for removing thin layers of diamond from bulk or homoepitaxial films. This method consists of ion implantation, followed by selective etching. High energy (4-5 MeV) implantation of carbon or oxygen ions creates a well-defined layer of damaged diamond buried at a controlled depth. This layer is graphitized and selectivity etched either by heating at 550 C in an oxygen ambient or by electrolysis. This process successfully lifts off the diamond plate above the graphite layer. The lift-off method, combined with well-established homoepitaxial growth processes, has potential for fabrication of large area single-crystal diamond sheets. DOE

N94-26139# Argonne National Lab., IL.
FAST PHOTOCONDUCTOR CdTe DETECTORS FOR SYNCHROTRON X RAY STUDIES
Sung-Shik Yoo (Illinois Univ., Chicago.), J. P. Faurie (Illinois Univ., Chicago.), Kemei Wang (Illinois Univ., Chicago.), P. A. Montano (Illinois Univ., Chicago.), Qiang Huang, and Brian Rodricks Sep. 1993 14 p Presented at the 3rd London Conference on Position-Sensitive Detectors, London, England, 6-10 Sep. 1993
(Contract W-31-109-eng-38)
(DE94-001334; ANL/XFD/CP-80819; CONF-9309256-3) Avail: CASI HC A03/MF A01

The Advanced Photon Source will be the brightest source of synchrotron x-rays when it becomes operational in 1996. During normal operation, the ring will be filled with 20 bunches of positrons with an interbunch spacing of 177 ns and a bunch width of 119 ps. To perform experiments with x-rays generated by positrons on these time scales one needs extremely high speed detectors. To achieve the necessary high speed we are developing MBE-grown CdTe-base photoconductive position sensitive array detectors. The arrays fabricated have 64 pixels with a gap of 100 microns between pixels. The high speed response of the devices was tested using a short pulse laser. X-ray static measurements were performed using an x-ray tube and synchrotron radiation to study the device's response to flux and wavelength changes. This paper presents the response of the devices to some of these tests and discusses different physics aspects to be considered when designing high speed detectors. DOE

N94-26147# Pacific Northwest Lab., Richland, WA.
OXYGEN REDUCTION AT A YSZ INTERFACE WITH CATHODE MATERIALS La(1-x)(Ca OR Sr)(x)MnO3(1-x)CaMnO3
G. E. Youngblood, C. F. Windisch, Jr., and J. L. Bates Sep. 1993 7 p Presented at the 14th International Symposium on Materials Science, Roskilde, Denmark, 6-10 Sep. 1993
(Contract DE-AC06-76RL-01830)
(DE94-002954; PNL-SA-22654; CONF-9309106-2) Avail: CASI HC A02/MF A01

Impedance spectroscopy combined with an unbonded interface cell (UIC) design, was used to assess oxygen reduction at an yttria-stabilized zirconia electrolyte interface with several substituted yttrium and lanthanum manganite cathode compositions. By analyzing impedance spectra taken using the UIC, the effective length of the reaction zone at the solid-gas triple phase boundary can be estimated and used to normalize the oxygen reduction reaction rate for each cell, thus effectively removing the effects of interface morphology. Intrinsic reaction rates (specific oxygen activities) were determined from spectra as function of temperature and oxygen partial pressure for cathodes La(1-x)(Ca or Sr)(x)(x)MnO3 and Y(1-x)Ca(x)MnO3 (LCM, LSM, and YCM, respectively) and for Pt. Specific activities in the temperature and P(O2) ranges of an operating solid oxide fuel cell (SOFC) cathode, 1173-1273 K and 10(exp 5)-10(exp 3) Pa, were highest for LCM intermediate for YCM and lowest for LSM. For LCM and YCM, compositions with x = 0.5 gave highest specific activities. Specific activities for all of the tested manganite compositions exceeded the platinum specific activities by at least an order of magnitude. Shapes of impedance spectra for all the manganite systems were similar. Examination of spectra shapes revealed that the overall cathodic polarization process was rather complex and made up of at least two or more fundamental steps. DOE

N94-26171 Melbourne Univ., Parkville (Australia). School of Physics.
CRYSTAL POTENTIAL RETRIEVAL IN HRTEM
M. J. Beeching and A. E. C. Spargo 1993 12 p Limited Reproducibility: More than 20% of this document may be affected by microfiche quality
(DE94-601883; UM-P-93/10) Avail: CASI HC A03 (US Sales Only)

A possible method for obtaining the crystal potential by inversion of the complex wave-field at the exit surface of the specimen, based on reversal of the multi-slice algorithm, is outlined. Results from preliminary testing of the method using computer simulated data are presented and appear promising, although the limits of applicability of the method are yet to be defined. DOE

N94-26188# Florida Univ., Gainesville.
INVESTIGATION OF A NORMAL INCIDENCE HIGH-PERFORMANCE p-TYPE STRAINED LAYER In(0.3)Ga(0.7)As / In(0.52)Al(0.48) AS QUANTUM WELL INFRARED PHOTODETECTOR Semiannual Progress Report No. 1, 15 Jul. 1993 - 15 Jan. 1994
Jerome T. Chu and Sheng S. Li 15 Jan. 1994 25 p
(Contract N00014-93-1-0827)
(AD-A274854; Rept-92129712) Avail: CASI HC A03/MF A01

During this reporting period, we have made significant strides towards the program goals. A major breakthrough was made in the development of a new strained layer p-type InGaAs/InAlAs QWIP grown on InP by MBE. This new QWIP achieved an ultra-low dark current and a very high detectivity at 8.1 micrometers and 77 K. This detector is under background limited performance (BLIP) at temperatures up to 100 K, which is the highest BLIP temperature reported for a QWIP. A dark current density of 7 x 1O(exp -8) A/sq cm and a BLIP detectivity of 5.9 x 10(exp 10) Jones were measured for this QWIP at 77 K. Currently, we are investigating other possible p-type QWIP structures with different performance parameters. These include the design and fabrication of a GaAs/InGaAs p-type QWIP grown on GaAs via MBE and a new dual strained InGaAs/InAlAs p-type QWIP. Additional consideration is being given towards the reliability of p-type contacts for these QWIP structures. DTIC

N94-26194 Valladolid Univ. (Spain). Materia Convensada.
STUDY OF THE HOMOGENEITY OF InP WAFERS Final Report, 15 Jul. 1991 - 14 Jul. 1993
J. Jimenez, P. Martin, and M. Avella Jul. 1993 79 p Limited Reproducibility: More than 20% of this document may be affected by microfiche quality
(Grant AF-AFOSR-0278-91)
(AD-A273658; EOARD-TR-94-01) Avail: CASI HC A05

The homogeneity of InP substrate at both microscope and microscopic scale has been studied by Raman microprobe and photocurrent mapping. Raman microprobe was used for any type of substrate revealing different structural and electronic properties of different extended defects. This study was correlated with photoetching and a relationship between revealed defects and Raman features was established. Semi-insulating substrates were analyzed by photocurrent mapping. Three excitation wavelengths were used revealing different sources of non-uniformity in these wafers. The technique is shown to be quite sensitive to electrical non- homogeneities concerning the iron distribution across the wafer. DTIC

N94-26238# Lawrence Livermore National Lab., CA.
GENERALIZED PERTURBATION METHOD EXPANSIONS OF THE TOTAL ENERGY OF AN ALLOY
A. Gonis, P. P. Singh, and P. E. A. Turchi Aug. 1993 9 p Presented at the NATO Advanced Study Workshop on Metallic Alloys: Experimental and Theoretical Perspectives, Boca Raton, FL, 16-21 Jul. 1993
(Contract W-7405-eng-48)
(DE94-003865; UCRL-JC-114733; CONF-930759-6) Avail: CASI HC A02/MF A01

The generalized perturbation method, commonly used in connection with the band energy contribution to the energy of a solid to approximate the total energy of an ordered configuration of an alloy, is reformulated with respect to total energy. The connection of the results derived here to those obtained based on the band energy is pointed out, and possible applications of the method is discussed. DOE

N94-26239# California Univ., Berkeley. Lawrence Berkeley Lab.
STRESS RELAXATION IN SPUTTERED W FILMS AND W/GeSi/Si HETEROSTRUCTURES
F. M. Ross, R. R. Kola (Bell Telephone Labs., Inc., Murray Hill, NJ.), R. Hull (Bell Telephone Labs., Inc., Murray Hill, NJ.), and J. C. Bean (Bell Telephone Labs., Inc., Murray Hill, NJ.) Nov. 1993 6 p Presented at the Fall Meeting of the Materials Research Society (MRS), Boston, MA, 29 Nov. - 3 Dec. 1993
(Contract DE-AC03-76SF-00098)
(DE94-004007; LBL-34856; CONF-931108-11) Avail: CASI HC A02/MF A01

Stress relaxation was investigated in GeSi/Si heterostructures on which thin W films have been sputtered with different stress states. Real-time electron microscope observations of the relaxation process demonstrate that the presence of the stressed metal film changes the relaxation kinetics of the GeSi/Si heterostructures. The significance of this result is discussed for the processing of strained layer heterostructures into devices. The relationship between microstructure and stress in these sputtered W films is discussed, and, by developing a novel specimen geometry for the transmission electron microscope (TEM), dynamic observations are made of the evolution of microstructure and stress during the beta-W yields alpha-W transformation. DOE

N94-26243# Argonne National Lab., IL.
THE EFFECT OF PROCESSING ON THE MICROSTRUCTURE OF Ag-SHEATHED Bi-2223 WIRES
D. J. Miller, J. G. Hu, P. Kostic, U. Balachandran, and P. Haldar (Intermagnetics General Corp., Guilderland, NY.) Nov. 1993 12 p Presented at the Fall Meeting of the Minerals, Metals and Materials Society: Physical Metallurgy and Materials, Pittsburgh, PA, 17-21 Oct. 1993
(Contract W-31-109-eng-38)
(DE94-004627; ANL/MSD/CP-81484; CONF-931009-15) Avail: CASI HC A03/MF A01

Studies using TEM and SEM focused on effect of final heat treatment conditions on microstructure of (Bi,Pb)2Sr2Ca2Cu3O(x) (Bi-2223) wires and corresponding variations in critical currents I(sub c). It is found that variations in I(sub c) for segments cut from various points along length of a wire can be correlated with variations in volume fraction and nature of second phases. Similar variations are observed between wires processed under different final annealing conditions. A common feature found in all of the wire segments with lower I(sub c) values was presence of the Pb3Sr2Ca2CuO(x) phase (Pb-3221). Microchemical analysis suggests that formation of this phase leads to variations in composition of Bi-2223 grains. As a result, the wires which exhibit the Pb-3221 phase consist of an assemblage of grains with a range of transition temperatures based on composition. Thus, in these segments, the current carrying capacity of individual grains at 77K varies from very good to poor, and a significant reduction in the overall I(sub c) of the segment is observed. DOE

N94-26275# Argonne National Lab., IL.
STUDIES OF THIN-FILM GROWTH, ADSORPTION, AND OXIDATION BY IN SITU, REAL-TIME, AND EX SITU ION BEAM ANALYSIS
Y. Lin, A. R. Krauss, D. M. Gruen, and Y. Nishino 1993 25 p Presented at the 40th National Symposium of the American Vacuum Society, Orlando, FL, 15-19 Nov. 1993

(Contract W-31-109-eng-38)
(DE94-002907; ANL/CHM/CP-81119; CONF-9311104-8) Avail: CASI HC A03/MF A01

We have developed a time-of-flight (TOF) ion scattering and direct recoil spectrometer (ISS/DRS) to study the surface composition and reconstruction of metals, metal-oxides, and semiconductors, and to provide in situ characterization of the thin-film deposition process. In situ, real-time study of Pb, Zr, and Ru ultrathin films produced by ion beam sputter deposition is presented as a demonstration of pulsed ion beam surface analysis (PIBSA) as a means of characterizing monolayer and submonolayer growth, both in UHV and in mTorr oxygen background. The capability of performing surface analysis at pressures greater than 10(exp -3) Torr is unique to pulsed ion beam surface analysis among surface analytical methods and enables the in situ monitoring of oxide thin-film growth processes and surface-gas phase reactions. Using angular-resolved ISS (ARISS), combined with Auger electron spectroscopy (AES), we studied the oxygen adsorption and reconstruction of (001) oriented InSb thin-film surfaces. It was found that the adsorption of molecular oxygen on the InSb (001) surface is consistent with the Langmuir model. Oxygen adsorption preferentially occurs on the antimony sites corresponding to the extension of the lattice into the vacuum and reduces the inward contraction of the first two layers of the clean InSb (001) surface relative to the bulk atomic spacing. DOE

N94-26308# Sandia National Labs., Albuquerque, NM.
MBE GROWN 3 TO 5 STRAIN RELAXED BUFFER LAYERS AND SUPERLATTICES CHARACTERIZED BY ATOMIC FORCE MICROSCOPY
A. J. Howard, I. J. Fritz, T. J. Drummond, J. A. Olsen, B. E. Hammons, S. R. Kurtz, and T. M. Brennan 1993 20 p Presented at the 40th National Symposium of the American Vacuum Society, Orlando, FL, 15-19 Nov. 1993
(Contract DE-AC04-94AL-85000)
(DE94-002931; SAND-93-1126C; CONF-9311104-12) Avail: CASI HC A03/MF A01

Using atomic force microscopy (AFM), the authors have investigated the effects of growth temperature and dopant incorporation on the surface morphology of MBE grown graded buffer layers and strained layer superlattices (SLS's) in the InGaAlAs/GaAs and InAsSb/InSb material systems. The AFM results show quantitatively that over the temperature range from 380 to 545 C, graded In(x)Al(1-x)As (x = 0.05 - 0.32) buffer layers grown at high temperatures (approximately 520 C), and graded In(x)Ga(1-x)As (x = 0.05 - 0.33) buffer layers and In(0.4)Ga(0.6)As/In(0.26)Al(0.35)Ga(0.39)As SLS's grown at low temperatures (approximately 400 C) have the lowest RMS roughness. Also, for SLS's InAs(0.21)Sb(0.79)/InSb, undoped layers grown at 470 C were smoother than undoped layers grown at 420 C and Be-doped layers grown at 470 C. These results illustrate the role of surface tension in the growth of strained layer materials near the melting temperature of the InAs(x)Sb(1-x)/InSb superlattice. Nomarski interference and transmission electron microscopies, IR photoluminescence, x-ray diffraction, and photocurrent spectroscopy were also used to evaluate the relative quality of the material but usually, the results were not conclusive. DOE

N94-26326# Stanford Linear Accelerator Center, CA.
THE EPITAXIAL GROWTH OF Ge ON Si(100) USING Te AS A SURFACTANT
X. Yang, J. Wu, R. Cao, J. Terry, P. Pianetta, and J.-S. Li (Stanford Univ., CA.) Oct. 1993 6 p Presented at the Spring Meeting of the Materials Research Society, San Francisco, CA, 12-16 Apr. 1993
(Contract DE-AC03-76SF-00515)
(DE94-003437; SU-SLAC-PUB-6300; SLAC/SSRL-0041; CONF-930405-51)
Avail: CASI HC A02/MF A01

Epitaxial growth of Ge on Si using Te as a surfactant was studied with high resolution photoemission, low energy electron diffraction, and cross-sectional transmission electron microscopy. The growth mode of Ge on Si changed from Stranski-Krastanov to layer-by-layer mode when 1/4 ML Te atoms were on the surface. During the growth, Te atoms segregated to the top of the surface. If the growth temperature is too high, above approximately 450 C, the Te coverage was less than the necessary coverage to keep the layer by layer growth, and the growth mode of Ge on Si is still S-K. DOE

N94-26352# Sandia National Labs., Albuquerque, NM.
ORDERING AND PHASE SEPARATION IN MOCVD InGaP ALLOYS AND UNICOMPOSITIONAL QUANTUM WELLS
D. M. Follstaedt, R. P. Schneider, Jr., and E. D. Jones 1993 6 p Presented at the Fall Meeting of the Materials Research Society (MRS), Boston, MA, 29 Nov. - 3 Dec. 1993
(Contract DE-AC04-94AL-85000)
(DE94-004693; SAND-93-1493C; CONF-931108-24) Avail: CASI HC A02/MF A01

The microstructures of In(0.5)Ga(0.5)P alloys grown on (100) GaAs by MOVPE have been characterized with cross-section TEM and their optical emission examined with photoluminescence at low temperatures. All the alloys exhibit spinodal-like decomposition with compositional modulations along directions in the growth plane. Alloys grown at 775 C have the highest emission energy, 2.0 eV, while those at 675 C have the lowest, 1.89 eV, due to strong CuPt-type ordering of In and Ga. The ordered domains are platelets 20 to 200 nm wide and 10-20 nm thick with antiphase boundaries 1-2 nm apart. We have also formed 'unicompositional' quantum wells of thin (1.3-20 nm) ordered layers grown at 675 C between disordered barriers grown at 775 C. Ordering is found only in the active layer, with domains similar to those of thick layers. The emission energy increases by 90 meV as the well thickness is decreased from 10 to 1.3 nm, thus demonstrating quantum size effects solely through disorder-order phenomena. DOE

N94-26363# Melbourne Univ., Parkville (Australia). School of Physics.
POLAR AND CHEMICAL DOMAIN STRUCTURES OF LEAD SCANDIUM TANTALATE (PST)
J. L. Peng and L. A. Bursill 1993 18 p
(DE94-600760; UM-P-93/25) Avail: CASI HC A03/MF A01 (US Sales Only)

The local structure of chemical and polar domains and domain walls is determined directly by atomic resolution high-resolution electron microscopy. Thus, the Pb, Ta, and Sc atomic positions may be located in the images of very thin crystals. Furthermore, the Pb cation displacements away from the ideal perovskite A-site have been measured directly for the first time. Local variations in polarization direction may be mapped directly off the images, provided certain electron optical conditions are met. Results are relevant to recent theories of polar-glass behavior in relaxor-type complex oxide functional ceramics. DOE

N94-26364# Melbourne Univ., Parkville (Australia). School of Physics.
REGROWTH ZONES IN LASER ANNEALED RADIATION DAMAGED DIAMOND
D. N. Jamieson, S. Prawer, S. P. Dooley, and R. Kalish (Technion - Israel Inst. of Tech., Haifa.) 1993 21 p Presented at the 3rd International Conference on Nuclear Microprobe Technology and Applications, Uppsala, Sweden, 8-12 Jan. 1992
(DE94-600821; UM-P-92/74; CONF-9201160) Avail: CASI HC A03/MF A01 (US Sales Only)

Focused laser annealing of ion implanted diamond with a 15 micron diameter laser spot produces as variety of effects that depend on the power density of the laser. Channeling Contrast Microscopy (CCM) provides a relatively straight forward, rapid, method to analyze the annealed regions of the diamond to characterize the effects. In order of increasing laser power density, effects that are observed include: regrowth of the end of range damage of the ion implantation, formation of a buried graphitic layer, and complete graphitization of the surface of the diamond down to the bottom of the original damage layer. Information provided by CCM leads to an understanding the causes of these effects and provides insight into the carbon phase diagram in the neighborhood of the graphite to diamond phase transition. Analysis of the effects of laser annealing by CCM are complicated by the swelling of the diamond lattice caused by the original ion implantation, compaction following regrowth, and the effect of the analysis beam irradiation itself. DOE

N94-26379 Gosudarstvennyi Komitet po Ispolzovaniyu Atomnoi Energii, Serpukhov (USSR). Inst. Fiziki Vysokikh Ehnergij.
EXPLORATION OF GaAs STRUCTURES FOR SOLID-STATE DETECTORS
V. B. Chmil, A. V. Chuntonov, and V. A. Sergeev et al 1992 10 p

Limited Reproducibility: More than 20% of this document may be affected by microfiche quality
(DE93-634191; IHEP-ONF-92-59) Avail: CASI HC A02 (US Sales Only)

The work describes the results on systematic search of GaAs structures for the solid-state detectors that should be exploited in a high flux of high energy particles and low energy neutrons. Three types of GaAs structures were found that can separate well a noise and signal spectra. The GaAs samples have been irradiated with a source of gamma ray and results of the response to the action of beta-source are also presented. DOE

N94-26384 International Centre for Theoretical Physics, Trieste (Italy).
THE EFFECT OF HIGH FREQUENCY ELECTRIC FIELD ON HYPERSOUND AMPLIFICATION IN SUPERLATTICE
S. Y. Mensah, F. K. A. Allotey, and S. K. Adjepong May 1993 13 p
Limited Reproducibility: More than 20% of this document may be affected by microfiche quality
(DE93-634326; IC-93/95) Avail: CASI HC A03 (US Sales Only)

Propagation of hypersound in a semiconductor superlattice (SL) in the presence of an external electric field of the form E = E(sub 0) + E(sub 1) cos(omega)t has been studied theoretically. The analytical expressions obtained for the absorption coefficient, gamma, are presented graphically. It is observed that in the absence of a.c. electric field the dependence of gamma on E(sub 0) is nonlinear unlike the homogeneous bulk material where the dependence of gamma on E(sub 0) is linear. The inclusion of a.c. electric field affects the elation gamma on E(sub 0) depending on the values of E(sub 1) and omega(tau). For a given E(sub 1), the peaks of the curve gamma(sub 0) on E(sub 0) decrease, shift and eventually oscillate for increasing values of omega(tau) i.e. from omega(tau) much less than 1 to omega(tau) much greater than 1. DOE

N94-26387# International Centre for Theoretical Physics, Trieste (Italy).
ON THE ELECTRON MOBILITY IN SLIGHTLY COMPENSATED HEAVILY DOPED GALLIUM ARSENIDE AT LOW TEMPERATURES
Doan Nhat Quang, Nguyen Nhu Dat (Institute of Theoretical Physics, Hanoi, Viet Nam.), and Dinh Van An (Hue Coll., Viet Nam.) Jun. 1993 9 p
(DE93-634712; IC-93/138) Avail: CASI HC A02/MF A01 (US Sales Only)

The electron mobility at low temperatures is calculated for a slightly compensated heavily doped sample of GaAs which undergoes a thermal treatment. Account is taken of high-temperature ionic correlation and low-temperature electronic screening as well. The numerical result is found to be in very good agreement with experimental data, especially at the highest impurity concentrations. DOE

N94-26388# International Centre for Theoretical Physics, Trieste (Italy).
HOLES IN A TWO-DIMENSIONAL QUANTUM ANTIFERROMAGNET
Yu Lu, Su Zhao-Bin (Academia Sinica, Beijing, China.), and Li Yan-Min (Warwick Univ., Coventry, England.) Jun. 1993 53 p
(DE93-634753; IC-93/135) Avail: CASI HC A04/MF A01 (US Sales Only)

A brief review is presented on the studies of the hole motion in a two-dimensional quantum antiferromagnetic. An extended introduction is given to cover the background of the problem. The quantum Bogoliubov-de Gennes formalism which treats the local distortion of the spin configuration and the quantum renormalization process on an equal footing, is outlined. The latest development on the central issue, whether a hole can freely propagate on an antiferromagnetic background, is overviewed. DOE

N94-26389# International Centre for Theoretical Physics, Trieste (Italy).
MULTI-CHANNEL KONDO NECKLACE
P. Fazekas and Haeyoung Kee Jun. 1993 29 p
(DE93-634754; IC-93/136) Avail: CASI HC A03/MF A01 (US Sales Only)

A multi-channel generalization of Doniach's Kondo necklace model is formulated, and its phase diagram studied in the mean-field approximation. Our intention is to introduce the possible simplest model which displays some of the features expected from the overscreened Kondo lattice. The N conduction electron channels are represented by N sets of pseudospins tau(sub J), j = 1 1,..., N which are all antiferromagnetically coupled to a periodic array of modul S = 1/2 spins. Exploiting permutation symmetry in the channel index j allows us to write down the self-consistency equation for general N. For N greater than 2, we find that the critical temperature is rising with increasing Kondo interaction; we interpret this effect by pointing out that the Kondo coupling creates the composite pseudospin objects which undergo an ordering transition. The relevance of our findings to the underlying fermionic multi-channel problem is discussed. DOE

N94-26390# International Centre for Theoretical Physics, Trieste (Italy).
ISING CRITICAL BEHAVIOUR IN THE ONE-DIMENSIONAL FRUSTRATED QUANTUM XY MODEL
E. Granato Jun. 1993 18 p
(DE93-634755; IC-93/137) Avail: CASI HC A03/MF A01 (US Sales Only)

A generalization of the one-dimensional frustrated quantum XY model is considered in which the inter and intra-chain coupling constants of the two infinite XY (planar rotor) chains have different strengths. The model can describe the superconductor-insulator transition due to charging effects in a ladder of Josephson junctions in a magnetic field with half a flux quantum per plaquette. From a fluctuation-effective action, this transition is expected to be in the universality class of the two-dimensional classical XY-Ising model. The critical behavior is studied using a Monte Carlo transfer matrix applied to the path-integral representation of the model and a finite-size-scaling analysis of data on small system sizes. It is found that, unlike the previous studied case of equal inter- and intra-chain coupling constants, the XY and Ising-like excitations of the quantum model decouple for large interchain coupling, giving rise to pure Ising model critical behavior for the chirality order parameter in good agreement with the results for the XY-Ising model. DOE

N94-26404 Korean Atomic Energy Research Inst., Daeduk (Republic of Korea).
A STUDY ON THE DEVELOPMENT OF HIGH T(SUB c) SUPERCONDUCTING MATERIALS
D. Y. Won, G. W. Hong, H. G. Lee, H. J. Lee, C. J. Kim, S. D. Park, W. G. Kim, K. B. Kim, S. C. Kwon, and I. S. Chang et al Jan. 1993 101 p
In KOREAN Limited Reproducibility: More than 20% of this document may be affected by microfiche quality
(DE93-633529; KAERI/RR-1169/92) Avail: CASI HC A06 (US Sales Only)

As a kind of high T(sub c) superconductor application technique, a study on the development of energy storage flywheel system using Y-Ba-Cu-O superconductor was performed. Quasi-melt process was developed to fabricate the high magnetization superconductor which is needed to develop the flywheel system and the effects of various process variables on the superconducting properties of the specimens were tested and analyzed. Magnetomechanical interactions between superconductor and permanent magnet was also studied. A small prototype flywheel system in which the disc shape permanent magnet is rotated above the Y-Ba-Cu-O superconductor pellets was designed and a test device for the prototype design was assembled to test its basic properties. DOE

N94-26420# Sandia National Labs., Albuquerque, NM.
DEVELOPMENTS IN CRYSTALLOGRAPHIC PHASE ANALYSIS IN THE SEM: BACKSCATTERED ELECTRON KIKUCHI PATTERNS
J. R. Michael, R. P. Goehner, and C. R. Hills 1993 3 p Presented at the 2nd Interamerican Congress on Electron Microscopy, Cancun, Mexico, 26 Sep. - 2 Oct. 1993
(Contract DE-AC04-76DP-00789)
(DE93-040755; SAND-93-1808C; CONF-9309241-1) Avail: CASI HC A01/MF A01

The recent development of a charge coupled device (CCD)-based detector for the acquisition of backscattered electron Kikuchi patterns has enabled on-line crystallographic phase identification studies to be conducted in the scanning electron microscope. High quality patterns have been obtained from a wide variety of materials with relatively little specimen preparation compared to electron diffraction in the transmission electron microscope (TEM). Crystallographic phase identification through a combination of BEKP and energy dispersive x-ray spectrometry is demonstrated by the identification of precipitates in a high temperature Ni-based alloy containing Cr and W. The precipitates that formed in this alloy were identified as M6C or M23C6. DOE

N94-26512 Joint Inst. for Nuclear Research, Dubna (USSR). Lab. of High Energy.

THE INFLUENCE OF ENERGY LOSSES WITH TIME IN NbTi SUPERCONDUCTORS IN PULSED MAGNETIC FIELDS [IZMENENIE SO VREMENEM POTER' EHNERGII V NBTI-SVERKHPROVODNIKAKH V IMPUL'SNYKH MAGNITNYKH POLYAKH]

N. M. Vladimirova, V. M. Drobin, and E. I. Dyachkov 1992 6 p In RUSSIAN Limited Reproducibility: More than 20% of this document may be affected by microfiche quality
(DE93-634761; JINR-R-8-92-223) Avail: CASI HC A02 (US Sales Only)

The influence of time factor on energy losses of a NbTi multifilamentary superconductor in a pulsed magnetic field was investigated. The observed decrease of eddy current losses by a factor of 1.4-3.4 is probably associated with increasing an effective transverse resistivity of the matrix due to diffusion between NbTi and copper. Processes of obsolescence did not result in decreasing current-carrying capability. DOE

N94-26514# Los Alamos National Lab., NM.

A NEW MATERIALS DATA COMPILATION CAN HELP IN ACTINIDE PHASE-DIAGRAM RESEARCH

P. L. Wallace, L. D. Calvert, M. H. Mueller (Argonne National Lab., IL.), T. C. Huang (International Business Machines Corp., San Jose, CA.), J. N. Dann (Sylvania Electric Products, Inc., Towanda, PA.), and S. Weissmann (Rutgers Univ., Piscataway, NJ.) 1993 17 p Presented at the International Symposium on Actinides: Processing and Materials, San Francisco, CA, 27 Feb. - 3 Mar. 1994
(Contract W-7405-eng-36)
(DE94-000797; LA-UR-93-3244; CONF-940215-2) Avail: CASI HC A03/MF A01

New metals and alloys (M&A) indexes to the Powder Diffraction File (PDF) were developed. All index data were critically reviewed, and the organization, selection of materials, and use of alphabetical formulae are similar to those of Villars and Calvert. The book contains four indexes. The Permuted-Sort Alphabetical Formula Index collects all entries containing a given element in alphabetical formula order. Within phase diagrams, phases are listed in compositional order. The Structure Type Index has entries arranged in Pearson symbol order. Hence, one can easily find all the materials with a given structure. The Common Names Index links common metallurgical names to PDF data. The Strukturbericht Symbol Index links Strukturbericht symbols to the equivalent Pearson symbols and prototype structures. DOE

N94-26516# California Univ., Berkeley. Lawrence Berkeley Lab.

SUBMILLIMETER RESIDUAL LOSSES IN HIGH-(Tc) SUPERCONDUCTORS Ph.D. Thesis

D. Miller Sep. 1993 156 p
(Contract DE-AC03-76SF-00098)
(DE94-003241; LBL-34665) Avail: CASI HC A08/MF A02

Bolometry was used to obtain accurate submillimeter residual loss data for epitaxial films of YBa2Cu3O7 (YBCO), Tl2Ca2Ba2Cu3O10, Tl2CaBa2Cu2O8 (TCBCO), and Ba(0.6)K(0.4)BiO3 (BKBO). The absorptivity measured for Nb films was fit to an Eliashberg strong coupling calculation; excellent agreement resulted between parameters from best fits and measured Residual Resistivity Ratio. Microwave surface resistance measurements made on the same YBCO and TCBCO films are in excellent agreement with submillimeter measurements. Absorptivities for all YBCO films studied are qualitatively similar, increasing smoothly with frequency, with no gap-like features below the well known absorption edge at 450 cm(sup -1). Losses in YBCO films were fit to a weakly coupled grain model for the a-b plane conductivity. Strong phonon structure was observed in TCBCO films between 60 and 700 cm(sup -1) (2 THz and 23 THz); these losses could not be fitted to the simple weakly coupled grain model, in contrast to the case for other high-(T(sub c)) superconductors where phonon structure observed in ceramics is absent in epitaxial oriented films and crystals because of electronic screening due to high conductivity of a-b planes. Absorptivity data for the BKBO films all show a strong absorption onset near the BCS tunneling gap of 3.5 k(sub B)(T(sub c)). Comparison with strong coupling Eliashberg predictions and of a Kramers-Kronig analysis indicate that the absorption onset is consistent with a superconducting energy gap. Effects of magnetic field on residual losses in YBCO films show a resonant absorption feature in vicinity of predicted. DOE

N94-26526# Columbia Univ., New York, NY.

TRANSLATIONAL-ENERGY-RESOLVED STUDIES OF PHOTOGENERATED CARRIER-INDUCED REACTIONS ON UHV SEMICONDUCTOR SURFACES

R. M. Osgood, Jr. 1993 28 p
(Contract DE-FG02-90ER-14104)
(DE94-004169; DOE/ER-14104/4) Avail: CASI HC A03/MF A01

The central phenomena of adsorbate photochemistry of semiconductor-adsorbate interfaces was observed and understood. In particular, it was observed that a major channel of photochemistry on a semiconductor surface is through the transfer of photoexcited substrate electrons to the adsorbed molecules. In contrast, photochemical processes by direct intra-adsorbate excitation are largely quenched for molecules in direct contact with the surface. The electron-transfer mediated process leads to both desorption and intra-adsorbate bond cleavage. The transfer may be by hot electrons or thermalized electrons in the conduction band. Dynamics of the electron-transfer reaction vary greatly for molecules in the first and second layer and for molecules of different orientations in the first layer. While molecules in the second layer can be dissociated only through the transfer of hot electrons or direct photon bond cleavage, those in the first layer react by thermalized electrons as well as hot electrons, depending on the orientation of the molecules. The two processes are differentiated experimentally by the different characteristic energy and angular distribution of the photofragments. In addition, it was discovered that reaction self-quenching can be an important process in thermalized electron-induced reactions on semiconductor surfaces. This behavior stems from effects on lifetime of the thermalized carriers by reaction products left on the surface. Finally, importance of electron-transfer-induced reactions at surfaces arises in part from shift in lowering of unoccupied electronic orbitals of adsorbates in image region of semiconductor surfaces. This latter effect is also largely responsible for a red shift observed for photochemical processes on surfaces. DOE

N94-26545# Technical Research Centre of Finland, Espoo. Metals Lab.

MAGNETOSTRICTION AND MAGNETOSTRICTIVE MATERIALS [MAGNETOSTRIKTIIVISYYS JA MAGNETOSTRIKTIIVISET MATERIAALIT]

Pekka Ruuskanen Dec. 1992 50 p In FINNISH
(ISSN 1235-0605)
(VTT-TIED-1434; ISBN-951-38-4328-9; ETN-94-95261) Copyright Avail: CASI HC A03/MF A01

When ferromagnetic material is under the influence of a stress the magnetization of the material is observed to change. This phenomenon is called magnetostriction. Magnetostriction is defined as a relation lambda = (Delta 1)/1. Here 1 is the initial length of the material and Delta 1 is the increase in the length caused by the magnetic field. All the theories of magnetostriction are based on the experimental results and there is no common theory which could explain all the properties of magnetostriction. Also the internal magnetization of ferromagnetic material is not understood in details. Magnetostriction can be exploited in many industrial applications like transducers, motors and measuring equipments. In high frequency applications magnetostriction causes energy losses. In these cases low magnetostrictive materials have to be used. ESA

N94-26565# Sandia National Labs., Albuquerque, NM.

MICROSTRUCTURES OF SI SURFACE LAYERS IMPLANTED WITH Cu

D. M. Follstaedt and S. M. Myers 1993 7 p Presented at the Fall Meeting of the Materials Research Society (MRS), Boston, MA, 29 Nov. - 3 Dec. 1993
(Contract DE-AC04-94AL-85000)
(DE94-004690; SAND-93-1471C; CONF-931108-26) Avail: CASI HC A02/MF A01

Microstructures of Si ion-implanted with Cu have been characterized by TEM after annealing. For 1.2 at.%, the Cu is trapped at planar defects, but for 10 at.%, (eta)-Cu3Si forms and Cu diffuses at its equilibrium solubility. These observations allow proper evaluation of the binding energies of Cu to previously formed internal cavities (2.2 eV) and (eta)-Cu3Si (1.7 eV). The 10 at.% Cu layer promotes oxidation of Si catalyzed by (eta)-Cu3Si. The microstructures also indicate that Si implanted with (approximately)2 at.% Cu reforms epitaxially with embedded defects after 8 hr at 700C, but for (approximately)10 at.% Cu, epitaxy is not recovered after 6 hours at 600C. DOE

N94-26566# Naval Command, Control and Ocean Surveillance Center, San Diego, CA. RDT and E Div.
DEMONSTRATION OF MONOLITHIC CO-FABRICATION OF Y1Ba2Cu3O7-SIGMA AND CMOS DEVICES ON THE SAME SAPPHIRE SUBSTRATE
P. R. DeLaHoussaye, M. J. Burns, W. S. Ruby, S. D. Russell, and S. R. Clayton Oct. 1993 4 p
(AD-A274757) Avail: CASI HC A01/MF A01

This paper reports the first fabrication of active semiconductor and high temperature superconducting (HTS) devices on the same substrate. Complementary Metal-Oxide-Semiconductor (CMOS) transistors were fabricated on the same sapphire substrate as either YBCO flux-flow transistors (FFT's) or YBCO superconducting quantum interference devices (SQUID's). All devices functioned as expected at 77 K without degradation demonstrating that a compatible process has been found to monolithically integrate adjacent CMOS and HTS devices. DTIC

N94-26571# Pennsylvania Univ., Philadelphia. Dept. of Chemistry.
OCTAHEDRAL METALLOMESOGENS: LIQUID CRYSTALLINITY IN LOW ASPECT RATIO MATERIALS
Hanxing Zheng and Timothy M. Swager 8 Jan. 1994 3 p
(Contract N00014-92-J-1416)
(AD-A274830; TR-5) Avail: CASI HC A01/MF A01

A new class of metallomesogens with octahedral structures are described. The observation of liquid crystallinity in these materials was unexpected as a result of their low aspect ratios. To better understand these materials, the dependence of the mesomorphism upon the number of sidechains (N) and metal center (Fe, Mn, Cr) was investigated. Complexes of Fe (N=6) appear to exhibit a highly ordered smectic phase. However, all of the complexes investigated with N= 12, 15, and 18 display columnar mesomorphism. Columnar phases with hexagonal and rectangular symmetry were observed which display optical textures similar to known discotic phases. In addition it was found that the conformational preferences of the alkoxyphenyl groups attached to the 1,3-diketone ligands are coupled to the stability of different phases. Although these phases show textural and structural similarities with known discotic columnar phases, they are not miscible with discotic compounds having similar lattice parameters and regions of mesomorphism. It is proposed that the octahedral complexes exhibit clefts necessary to accommodate sidechains which can not be directed outside the columns core. As a result of the differences from regular discotics, these new columnar phases have been labeled as octahedral hexagonal O(h) and octahedral rectangular O(r). DTIC

N94-26591# Argonne National Lab., IL. Materials Science Div.
MODULATION WAVELENGTH DEPENDENCE OF ION MIXING IN METALLIC SUPERLATTICES
Dale E. Alexander, Eric E. Fullerton, P. M. Baldo, C. H. Sowers, and L. E. Rehn Nov. 1993 7 p Presented at the Fall Meeting of the Materials Research Society, Boston, MA, 29 Nov. - 3 Dec. 1993
(Contract W-31-109-eng-38)
(DE94-004608; ANL/MSD/CP-80134; CONF-931108-16) Avail: CASI HC A02/MF A01

Ion mixing was studied in polycrystalline Nb/V and single-crystal Mo/V superlattices and in bilayers of the same materials. Systematic variation in the modulation wavelength, Lambda, revealed a factor of three decrease in mixing efficiency at small Lambda for Nb/V. The decrease appears to coincide with a structural transition in which the Nb/V superlattices become coherent. The results are consistent with a diffusion-induced grain boundary migration interpretation of mixing during irradiation. DOE

N94-26681# Yale Univ., New Haven, CT. Dept. of Applied Physics.
PREPARATION AND CHARACTERIZATION OF HIGH TEMPERATURE SUPERCONDUCTOR FILM SURFACES Final Report, 1 Jun. 1990 - 31 May 1993
Daniel E. Prober 27 Oct. 1993 4 p
(Grant AF-AFOSR-0306-90)
(AD-A274293; AFOSR-93-0891TR) Avail: CASI HC A01/MF A01

Research during this period was conducted at Westinghouse Science and Technology Center on deposition and production of microbridges of SNS high T sub c superconductor devices. DC and microwave properties were measured at Westinghouse. At Yale University, an electronic test system was constructed to allow flexible testing of devices produced at Westinghouse. DTIC

N94-26695# Los Alamos National Lab., NM.
MODELING GROUP 4 ELEMENTS WITH NEW TRANSFERABLE TIGHT-BINDING MODELS
I. Kwon and R. Biswas (Iowa State Univ. of Science and Technology, Ames.) 1993 4 p Presented at the Interatomic Potentials for Large-Scale Simulations of Non-Equilibrium Phenomena in SiC Meeting, Santa Barbara, CA, 15-17 Aug. 1993
(Contract W-7405-eng-36)
(DE94-000770; LA-UR-93-3359; CONF-9308182-1) Avail: CASI HC A01/MF A01

An outstanding problem in the computer-based microscopic description of Group IV materials is the need for an accurate transferable model of the energetic and electronic properties of semiconductor structures. The three complementary approaches were the ab-initio method including Car-Parinello simulations, the classical molecular dynamics method, and tight-binding molecular dynamics. While being very accurate, the ab-initio molecular dynamics was performed on small systems (approximately 100 atoms) for short time scales (approximately 10 ps). On the other hand, classical potential models had much success in describing melting of silicon, amorphous silicon structures, thin film growth and a variety of computationally intensive molecular dynamics simulations. However, the classical based models do not contain important electronic information which is essential in a variety of problems in electronic materials such as determining the gap states for structural defects. The accuracy of the classical models in configurations, far from the fitting database, may be uncertain. Our approach is to find transferable tight-binding models for silicon that are in between the ab-initio simulations and the classical models for molecular dynamics in level of sophistication. DOE

N94-26703 Carleton Univ., Ottawa (Ontario). Dept. of Electronics.
DEVELOPMENT OF GaAs CHARGE-COUPLED DEVICES M.S. Thesis
Robert I. James Mar. 1993 52 p
(ISBN-0-315-84116-8; CTN-94-61056) Copyright Avail: Micromedia Ltd., Technical Information Centre, 240 Catherine Street, Suite 305, Ottawa, Ontario, K2P 2G8, Canada HC/MF

The design, fabrication, and operation of GaAs cermet- and capacitive-gate charge coupled devices (CCD's) are described. Performance tradeoffs in the design of GaAs CCD's for signal processing applications are evaluated in terms of physical design parameters (mark/space ratio) and substrate material specifications. An in-depth examination of the influence of the cermet-gate structure on device performance is provided. The incorporation of this structure has been shown to improve the charge transfer efficiency and dynamic range of the CCD, thereby extending the bandwidth and range of useful operation of these devices. Experimental characterization of the charge transfer efficiency and dynamic range has been performed at clock frequencies up to 1 GHz, the upper limit being imposed by available test circuitry. These devices exhibit transfer efficiency in excess of 0.996 at 1 GHz with a sensitivity of -30 dBm and approximately 40 dB of dynamic range. The demonstration of fair performance of a cermet-gate CCD fabricated on a metal semiconductor field effect transistor (MESFET) compatible substrate indicates the potential for successful monolithic integration of these devices with GaAs D-MESFET circuitry. Author (CISTI)

N94-26765# Oak Ridge National Lab., TN.
ELECTRON MICROSCOPY OF AlN-SiC INTERFACES AND SOLID SOLUTIONS
J. Bentley, S. Tanaka (North Carolina State Univ., Raleigh.), and R. F. Davis (North Carolina State Univ., Raleigh.) 1993 5 p Presented at the Biennial Conference of the Electron Microscopy and Analysis Group of the Institute of Physics: Recent Advances in Electron Microscopy and Related Microanalytical Techniques, Liverpool, United Kingdom, 14-17 Sep. 1993
(Contracts DE-AC05-84OR-21400; DE-AC05-76OR-00033)
(DE94-002449; CONF-930956-1) Avail: CASI HC A01/MF A01

In a 2H AlN-SiC solid solution grown by MBE on alpha(6H)-SiC (3 degrees) from (0001), the epilayer contained a high density of basal faults related to approximately 5 nm steps on the growth surface: no compositional inhomogeneity was detected by PEELS. In diffusion couples of polycrystalline, sintered AlN on SiC annealed at 1600 and 1700 degrees C. 8H sialon (nominally (AlN)2Al2O3) formed at the interface of SiC and recrystallized epitactic AlN grains, and Si3N4-rich (beta)(prime) sialon particles formed in the SiC. No interdiffusion was detected by PEELS in diffusion couples of MBE-grown AlN on SiC annealed at 1700 and 1850 degrees C. Irregular epilayer thickness explains companion Auger depth profile results. DOE

N94-26771# Brookhaven National Lab., Upton, NY.
A MECHANISM FOR RESISTIVE DISSIPATION IN Ag SHEATHED Bi2Sr2CaCu2O8 AND Bi2Sr2Ca2Cu3O10
M. Suenaga, Q. Li, R. L. Sabatini, K. Shibutani (Kobe Steel Ltd., Japan.), S. Hayoashi (Kobe Steel Ltd., Japan.), R. Ogawa (Kobe Steel Ltd., Japan.), Y. Kawate (Kobe Steel Ltd., Japan.), L. Motowidlo (IGC/Advanced Supercomputers, Inc., Waterbury, CT.), and P. Hadlar (Intermagnetics General Corp., Guilderland, NY.) 1993 5 p Presented at the 6th International Symposium on Superconductivity, Hiroshima, Japan, 26-29 Oct. 1993
(Contract DE-AC02-76CH-00016)
(DE94-003009; BNL-49652; CONF-931073-3) Avail: CASI HC A01/MF A01

Detailed measurements of the V-I curves for a number of Bi2Sr2CaCu2O8 and Bi2Sr2Ca2Cu3O10/Ag composite tapes were made at 4.2, 27, and 64-77 K as a function of applied magnetic field as well as the angle between the tape face and the direction of applied field. Results suggest that the weak vortex-pinning strength and the amount of the weakly coupled grain boundaries and of the non-superconducting volume are the primary limiting factors for critical current densities in Bi(2212)/Ag and Bi(2223)/Ag, respectively. Furthermore, in both cases, the dissipative voltages arise from the interior of the gains. DOE

N94-26780# City Coll. of the City Univ. of New York, NY. Dept. of Physics.
NONLINEAR DYNAMICS AND PATTERN SELECTION AT THE CRYSTAL-MELT INTERFACE
H. Z. Cummins 1993 7 p
(Contract DE-FG02-84ER-45132)
(DE94-003112; DOE/ER-45132/8) Avail: CASI HC A02/MF A01

Progress is reported on the following: dendritic sidebranching (pivalic acid), subcritical/supercritical bifurcation crossover in directional solidification (succinonitrile coumarin 152), and evolution of planar-cellular-dendritic interface (succinonitrile rhodamine 6G). DOE

N94-26782# Pennsylvania State Univ., University Park.
INFLUENCE OF POINT DEFECTS ON GRAIN BOUNDARY DIFFUSION IN OXIDES
V. S. Stubican 1993 83 p
(Contract DE-FG02-90ER-45414)
(DE94-003164; DOE/ER-45414/3) Avail: CASI HC A05/MF A01

Grain boundary diffusion coefficients of Co-57 and Co-59 in polycrys. NiO, NiO bicrystal, and polycrys. Fe3O4 were determined at various oxygen pressures at 750 C. For NiO, the low oxygen pressure region (less than 10(exp -10) MPa) displayed constant grain boundary diffusion coefficients as the oxygen pressure decreased indicating an extrinsic region in which the impurity-induced defects dominated the intrinsic defects. At greater oxygen pressures, the intrinsic defects (Ni vacancies) dominated the extrinsic defects causing the diffusion to increase with pressure. For Fe3O4, at low oxygen pressures (less than 10(exp -16) MPa), the grain boundary diffusion coefficient increased when the pressure decreased owing to interstitial type diffusion; at greater than 10(exp -15) MPa, the diffusion increased with pressure owing to vacancy type diffusion. D(sub gb) of Co ions in Fe3O4 is proportional to pO2(exp -2/3) in the low pressure region and to pO2(exp 2/3) in the high pressure region, indicating similar mechanisms in the grain boundary diffusion and volume diffusion. Ratio of D(sub gb)/D was about 10(exp 3). DOE

N94-26795# California Univ., Berkeley. Lawrence Berkeley Lab.
EVALUATION OF APC NbTi SUPERCONDUCTOR IN A MODEL DIPOLE MAGNET
R. M. Scanlan, A. Lietzke, J. Royet, A. Wandesforde, C. E. Taylor, J. Wong (Supercon, Inc., Shrewsbury, MA.), and M. K. Rudziak (Supercon, Inc., Shrewsbury, MA.) 20 Sep. 1993 7 p Presented at the 13th International Conference on Magnet Technology, Victoria, 20-24 Sep. 1993
(Contract DE-AC03-76SF-00098)
(DE94-003258; LBL-33439; SC-MAG-417; CONF-930926-22) Avail: CASI HC A02/MF A01

The artificial pinning center (APC) approach to NbTi superconductor fabrication offers the potential benefits of higher current density and lower cost than the conventional process for NbTi. We have been evaluating several approaches for fabricating NbTi via the APC approach to determine whether these advantages can be realized in a practical conductor. The study began with the fabrication by several vendors of 10kg size samples which were evaluated as short samples. This was followed by the scale-up of one process to 150mm diameter billets. This material was evaluated first in a solenoid configuration and recently in a one-meter long dipole. We will report here on the results of these coil tests and other characterization results for this new material. We will also describe the plans to continue the scale-up to full size billets and we will discuss the potential cost savings of this approach compared with conventional NbTi fabrication. DOE

N94-26839# North Carolina State Univ., Raleigh. Dept. of Materials Science and Engineering.
GROWTH, CHARACTERIZATION AND DEVICE DEVELOPMENT IN MONOCRYSTALLINE DIAMOND FILMS Quarterly Technical Report, 1 Oct. - 31 Dec. 1993
Robert F. Davis, Jeffrey T. Glass, and R. J. Nemanich Dec. 1993 66 p
(Contract N00014-93-I-0437)
(AD-A274245) Avail: CASI HC A04/MF A01

Biased enhanced nucleation of diamond on beta-SiC(100) and Si(100) has been achieved but not on Cu(100). Carbide formation is an apparent attribute to the nucleation. The refractory metals of Hf, Ti, Ta, Ni, and W were thus explored as substrates. Diamond nucleation density was found to be directly related to the carbide heat of formation without scratching these substrates. TEM of highly oriented diamond films on Si(100) showed dislocations at low angle boundaries formed from coalesced grains. The azimuthal rotation between grains was between zero to six degrees. Negative electron affinity (NEA) has been found experimentally and theoretically for the two by one reconstructed diamond surface. Theoretical results indicate that the observed NEA is associated with a monohydride terminated surface, while the hydrogen-free surface exhibits a positive electron affinity. Raman and various photoluminescence (PL) techniques were used to investigate the role of N doping on the optical centers in CVD diamond films. The PL transitions attributed to the zero-phonon lines of N centers are observed at 1.945 eV and 2.154 eV. A new N center at 1.967 eV and the band A luminescence were also observed. The presence of an in-gap state distribution resulting from the sp(sup 2) disordered phase has been established. BN films have been grown on 100 oriented Si, diamond, Cu, and Ni substrates via IBAD and characterized via FTIR and HRTEM. DTIC

N94-26840# North Carolina State Univ., Raleigh. Dept. of Materials Science and Engineering.
NITRIDE SEMICONDUCTORS FOR ULTRAVIOLET DETECTION Semiannual Report, 1 Jul. - 31 Dec. 1993
Robert F. Davis, K. Gruss, D. Hanser, B. Perry, and L. Smith Dec. 1993 55 p
(Contract N00014-92-J-1720)
(AD-A274246) Avail: CASI HC A04/MF A01

Monocrystalline thin films of AlN and GaN have been deposited on vicinal alpha(6H)-SiC(0001) wafers via gas-source MBE and cold-wall metalorganic (MO) CVD and extensively investigated via high-resolution TEM. Elemental metal sources combined with activated nitrogen generated using an ECR plasma were employed in the MBE system; triethylgallium, triethylaluminum and ammonia were used in the MOCVD system. The MBE research has also included n-(Si) and p-type(Mg) doping and the creation of p-n junctions. The effects on growth of T, P, and MO flux have been investigated in the MOCVD work. Below the critical thickness, AlN only contains threading dislocations emanating from the misfit dislocations; above this thickness, defects parallel to the growth surface greatly increase. The defect density of AlN grown on SiC at 1100 C is much lower than that contained in materials deposited at 700 C. Deposition of GaN on an AlN buffer layer previously deposited on sapphire or SiC results in a larger number of dislocations parallel to the growth surface. A system for the deposition of InN and its solid solutions which addresses the problems of the low decomposition pressure has also been designed. The feasibility of designing an ammonia cracker cell for the MBE system to provide an alternative source of activated nitrogen is being investigated. DTIC

N94-26841# North Carolina State Univ., Raleigh. Dept. of Materials Science and Engineering.
PSEUDOMORPHIC SEMICONDUCTING HETEROSTRUCTURES FROM COMBINATIONS OF AlN, GaN AND SELECTED SiC POLYTYPES: THEORETICAL ADVANCEMENT AND ITS COORDINATION WITH EXPERIMENTAL STUDIES OF NUCLEATION, GROWTH, CHARACTERIZATION AND DEVICE DEVELOPMENT Semiannual Report, 1 July - 31 Dec. 1993
Robert F. Davis, S. Kern, K. Linthicum, S. Roberson, and S. Tanaka Dec. 1993 22 p
(Contract N00014-90-J-1427)
(AD-A274247) Avail: CASI HC A03/MF A01

Thin epitaxial films of SiC/AlN multilayers and (AlN)(x)(SiC)(1-x) solid solutions have been grown by plasma-assisted, molecular beam epitaxy between 1050 to 1300 C using the gas sources of Si2H6, C2H4, and N2, the last decomposed using a compact electron cyclotron resonance plasma source, and the solid source of Al. Vicinal alpha(6H)-SiC(0001) was used for the substrates. Electron diffraction and high resolution TEM revealed monocrystalline layers and pseudomorphic growth. Additional studies have shown that the off-axis orientation of the substrate affects the film morphology, surface cleaning is very important, and Si/C gas flow ratios may be used to control the SiC polytype. Both Beta(3C)- and alpha(6H)-SiC have been successfully deposited on alpha(6H)-SiC substrates. The chemical interdiffusion between monocrystalline AlN films and alpha(6H)-SiC wafers is also under study. The results of the successful research regarding multilayer heterostructures in the AlN/GaN system are now being used to guide the fabrication of a double heterostructure ultraviolet light emitting diode based on suitably doped AlGaN confinement layers with improved carrier confinement and mobility. DTIC

N94-26856# Sandia National Labs., Albuquerque, NM.
FERROELECTRIC THIN FILM MICROSTRUCTURE DEVELOPMENT AND RELATED PROPERTY ENHANCEMENT
B. Tuttle, J. A. Voigt, T. J. Headley, B. G. Potter, D. Dimos, R. W. Schwartz, M. T. Dugger, J. Michael, R. D. Nasby, and T. J. Garino et al 1993 11 p Presented at the 8th International Meeting on Ferroelectricity, Gaithersburg, MD, 8-13 Aug. 1993
(Contract DE-AC04-94AL-85000)
(DE94-002741; SAND-93-2248C; CONF-930852-4) Avail: CASI HC A03/MF A01

Factors that control phase evolution, microstructural development, and ferroelectric domain assemblage are evaluated for chemically prepared lead zirconate titanate (PZT) thin films. Zirconium to titanium stoichiometry is shown to strongly influence microstructure. As Ti content increases, there is an apparent enhancement of the perovskite phase nucleation rate, grain size becomes smaller, and the amount of pyrochlore phase, if present, decreases. While the pyrochlore matrix microstructure for near morphotropic phase boundary composition thin films consists of two interpenetrating nanophases (pyrochlore and an amorphous phase), the pyrochlore microstructure for PZT 20/80 films deposited on MgO substrates is single phase and consists of 10nm grains. Zirconium to titanium stoichiometry also has a substantial influence on process integration. Near morphotropic phase boundary films exhibit extensive reaction with underlying TiO2 diffusion barriers; conversely, there is no chemical reaction for identically processed PZT 20/80 thin films. The authors have attempted to directly correlate the optical quality of PZT thin films to the following microstructural features: (1) presence of a second phase, (2) domain orientation, and (3) nanometer surface morphology. DOE

N94-26868# Edgerton, Germeshausen and Grier, Inc., Idaho Falls, ID.
CALCULATION OF THE ELECTROMAGNETIC CRITICAL STATE RESPONSE OF HIGH T(SUB c) SUPERCONDUCTOR TAPE
L. S. Koo and K. L. Telschow 1993 6 p Presented at the 20th Annual Review of Progress in Quantitative Nondestructive Evaluation (NDE), Brunswick, ME, 1-6 Aug. 1993
(Contract DE-AC07-76ID-01570)
(DE94-002894; EGG-M-93127; CONF-9308167-4) Avail: CASI HC A02/MF A01

The new superconducting materials are being fabricated into long lengths in the form of thin tapes clad in silver for applications such as magnets. Variations in critical current as a function of position along the tape is a constant fabrication problem. An important nondestructive evaluation (NDE) task is to develop methods for determining critical current density with high spatial resolution along the tape in order to aid the fabrication process. Typically, critical currents are measured by contact four point voltage-current measurements. Although widely used, this technique averages results over long measurement regions, typically centimeters, and requires physical contact. An alternative method uses a probe similar to those used for eddy current measurements in normal metals to induce the critical state locally under the coil. The local critical current can be determined from the measured tape response and the critical state model. Previously, this model was developed only for experimental situations involving uniform externally applied magnetic fields. It was successfully used to predict the electromagnetic response, even as to harmonic content, of samples in slab or cylindrical geometry. Tape geometries and the need for high-resolution local measurements dictate that nonuniform external fields be used, such as those produced by small coils of only a few turns. Recently, this type of probe was used to measure critical currents as a function of position along tapes utilizing an empirical analysis of the critical state. Progress toward establishing a direct calculational method that can be used to predict the critical state response for nonuniform external fields generated by cylindrically symmetric current loops is outlined. An integral equation is developed describing the critical state that can be solved exactly in lowest order, iterated for higher precision, and that may be useful for other geometries. DOE

N94-26878# International Centre for Theoretical Physics, Trieste (Italy).
AB-INITIO CALCULATION OF THE VALENCE-BAND OFFSET AT STRAINED GaAs/InAs (001) HETEROJUNCTION
Nacir Tit, Maria Peressi (Trieste Univ., Italy.), and Stefano Baroni (International School for Advanced Studies, Trieste, Italy.) Jun. 1993 22 p
(DE94-602538; IC-93/153) Avail: CASI HC A03/MF A01 (US Sales Only)

A self consistent pseudopotential calculation of the valence band offset (VBO) at GaAs/InAs (001) strained heterojunction, which is chosen as an example of the isovalent polar with common-anion lattice mismatched heterojunctions, is presented. The effects of strain are studied by looking at the variation of the VBO versus the inplane lattice constant, which is imposed by the substrate. Our results show that the VBO can be tuned by about 0.17 eV going from GaAs to InAs substrates. Comparison of our work with the available experimental and theoretical results is also discussed. DOE

N94-26879 International Centre for Theoretical Physics, Trieste (Italy).
EFFECT OF IMPURITY CORRELATION ON THE DENSITY OF STATES IN SLIGHTLY COMPENSATED HEAVILY DOPED SEMICONDUCTORS
Doan Nhat Quang, Nguyen Nhu Dat (Institute of Theoretical Physics, Hanoi, Viet Nam.), and Dihn Van An (Hue Coll., Viet Nam.) Jul. 1993 25 p
Limited Reproducibility: More than 20% of this document may be affected by microfiche quality
(DE94-602539; IC-93/175) Avail: CASI HC A03 (US Sales Only)

A theory is developed of the electron density of states (DOS) in slightly compensated heavily doped semiconductors which undergo a thermal treatment. The calculation is carried out within the semiclassical approach to the random impurity field, taking adequately into account high-temperature correlation among the impurities and low temperature screening due to the free carriers as well. Then, a simple analytic expression for the DOS is obtained which exhibits the same energy dependence as in the case of a random impurity distribution, but now with some correlation-induced changes in the coefficients. A numerical estimation on non-compensated n-type sample of GaAs at a doping level of 5 x 10(exp 18) cm(sup -3) shows that in the tail region the correlated DOS turns out to be somewhat larger and cut less sharply than the random one. DOE

N94-26885# North Carolina State Univ., Raleigh.
ATOMIC LAYER EPITAXY OF GROUP 4 MATERIALS: SURFACE PROCESSES, THIN FILMS, DEVICES AND THEIR CHARACTERIZATION Semiannual Report, 1 Jul. - 31 Dec. 1993
Robert F. Davis, Salah Bedair, Nadina El-Masry, and Jeffrey T. Glass

Dec. 1993 34 p
(Contract N00014-91-J-1416)
(AD-A274325) Avail: CASI HC A03/MF A01

Atomic layer epitaxy of monocrystalline Beta-SiC on Si(100) and alpha (6H)-SiC(0001) substrates has been accomplished at 850 C by alternating the supplies of Si2H6, C2H4, and atomic hydrogen without the use of a carbonizing step. Conformal deposition of SiC has been demonstrated within trenches etched into Si(100) wafers. P-type films have also been achieved using Al as a dopant. Devices including HBT's with Beta-SiC emitters have been designed. Hydrogen plasma cleaning of SiC surfaces has been studied. XPS has shown that this process effectively removes C-O, C-F and C-H bonding at the surface. Temperature programmed desorption has been used to look at the amount of subsurface hydrogen generated during plasma cleaning. The diamond precursors of chlorinated methylsilanes and the substrate of Si(100) were subjected to bias enhanced high-frequency CVD. No difference in diamond nucleation density between the precursors was observed. An interface structure of single crystal CeO2/Si(111) grown by laser ablation has been investigated. An interfacial reaction occurred between these phases during deposition which resulted in the formation of an oxygen deficient amorphous (a) CeOx layer and an SiO2 layer. Post annealing in O2 caused the disappearance of the a-CeOx and the regrowth of crystalline CeO2. DTIC

N94-26892# Lehigh Univ., Bethlehem, PA.
CONTROLLED HETEROGENEOUS NUCLEATION OF MELT-TEXTURED YBa2Cu3O(6+x) BY ADDITION OF Al2O3 PARTICLES
Yan L. Chen, Lijie Zhang, Helen M. Chan, and Martin P. Harmer 1992 20 p
(AD-A274605) Avail: CASI HC A03/MF A01

The reaction between alumina and yttrium barium cuprate subjected to a melt-texturing heat-treatment was studied. Microstructural examination of quenched, partially transformed samples revealed that at approximately 1050 C (which is above the incongruent melting temperature of YBa2Cu3O(6+x), a reaction layer forms at the alumina interface. The reaction products were identified as Ba6Y2Al4O15 and a copper-rich liquid phase. On cooling below the peritectic temperature, aligned domains of YBa2Cu3O(6+x) (123) were observed to preferentially nucleate at the reaction layer. For samples of melt-textured 123 deliberately seeded with alumina particles, it was found that nucleation and growth of 123 occurred exclusively at the particles. A reaction sequence for the formation of the Ba6Y2Al4O15 is put forward, together with a discussion of the possible nucleation mechanisms for the 123. DTIC

N94-26897 International Centre for Theoretical Physics, Trieste (Italy).
POLAR OPTICAL OSCILLATION MODES IN GaAs-BASED DOUBLE HETEROSTRUCTURES: LONG WAVELENGTH LIMIT
F. Comas (Havana Univ.,, Cuba.), R. Perez-Alvarez (Havana Univ.,, Cuba.), and C. Trallero-Giner Jul. 1993 28 p Limited Reproducibility: More than 20% of this document may be affected by microfiche quality
(DE94-601874; IC-93/189) Avail: CASI HC A03 (US Sales Only)

Applying a theory developed in previous works we calculated the polar oscillation modes of a DHS (double heterostructure) of the GaAs/AlAs prototype in the long wavelength limit. The material for each layer of the structure is modeled as an isotropic continuum. We report general analytical solutions of the fundamental equations involved in the theory, allowing in principle to study an arbitrary structure of the same type with N interfaces. For the DHS case, we report amplitudes and potentials as a function of coordinates for the various oscillation modes, as well as dispersion-relation curves. Our results show good agreement with experimental data and also an excellent coincidence with ab initio microscopic calculations even for relatively large values of the in-plane wavevector. DOE

N94-26901 International Centre for Theoretical Physics, Trieste (Italy).
ELECTRONIC STRUCTURE OF A SINGLE OXYGEN VACANCY IN RUTILE TiO2
N. Tit Jun. 1993 21 p Limited Reproducibility: More than 20% of this document may be affected by microfiche quality
(DE94-602717; IC-93/154) Avail: CASI HC A03 (US Sales Only)

I report calculations of the electronic structure of an ideal (undistorted) oxygen vacancy in rutile TiO2 using the equation-of-motion method. I use a full phenomenological tight-binding Hamiltonian due to Vos to describe the electronic structure. The bulk band structure is also discussed in detail using the traditional Green-function method. I illustrate an efficient way to calculate the perfect crystal Green function matrix elements for any structure, including those that belong to non-symmorphic space groups. The results show that the oxygen vacancy in rutile TiO2 results in deeply localized states in its vicinity. DOE

N94-26902# International Centre for Theoretical Physics, Trieste (Italy).
LENGTH-SCALE DEPENDENT ENSEMBLE-AVERAGED CONDUCTANCE OF A 1D DISORDERED CONDUCTOR: CONDUCTANCE MINIMUM
Nacir Tit, N. Kumar, and Prabhakar Pradhan (Indian Inst. of Science, Bangalore.) Jul. 1993 10 p
(DE94-602732; IC-93/162) Avail: CASI HC A02/MF A01 (US Sales Only)

Exact numerical calculation of ensemble averaged length-scale dependent conductance for the 1D Anderson model is shown to support an earlier conjecture for a conductance minimum. Numerical results can be understood in terms of the Thouless expression for the conductance and the Wigner level-spacing statistics. DOE

N94-26927 Melbourne Univ., Parkville (Australia). School of Physics.
DELOCALIZATION IN ELECTRON IMPACT IONIZATION IN A CRYSTALLINE ENVIRONMENT
L. J. Allen and C. J. Rossouw (Commonwealth Scientific and Industrial Research Organization, Melbourne, Australia.) 1993 23 p Limited Reproducibility: More than 20% of this document may be affected by microfiche quality
(DE94-601819; UM-P-92/103) Avail: CASI HC A03 (US Sales Only)

A theory for variations in cross section with diffraction conditions for electron impact ionization of atoms in a crystalline environment is presented. This takes into account, for the first time, total interaction delocalization, due both to long range Coulombic interaction and thermal smearing of the target position, by integration over all scattering angles and ejected electron momenta as well as attenuation of dynamical effects by inelastic scattering, particularly thermal diffuse scattering. These results are of fundamental importance for atom location by channeling enhanced microanalysis using energy dispersive x ray or electron energy loss spectroscopy techniques. Agreement between this theory and various energy dispersive x ray experiments reported in the literature under dynamical electron diffraction conditions is satisfactory. DOE

N94-26932# Oak Ridge National Lab., TN.
ION IMPLANTATION AND DYNAMIC RECOVERY OF TIN-DOPED INDIUM OXIDE FILMS
Yuzo Shigesato (Brown Univ., Providence, RI.), D. C. Paine (Brown Univ., Providence, RI.), and T. E. Haynes Sep. 1993 5 p Presented at the International Union of Materials Research Societies on Advanced Materials, Tokyo, Japan, 31 Aug. - 4 Sep. 1993
(Contracts DE-AC05-84OR-21400; N00014-91-J-1837; NSF DMR-91-15054)
(DE94-001126; CONF-9308122-14) Avail: CASI HC A01/MF A01

The effect of O(+) ion implantation on the electronic (carrier density, mobility, resistivity) and microstructural properties of thin film Sn-doped In2O3 (ITO) was studied. Both polycrystalline (c-) and amorphous (a-) ITO thin films, 200 nm thick, were implanted at substrate temperatures ranging from -196 to 300 C with 80 keV O(+) at doses ranging from 0 to 4.0 x 10(exp 15) cm(exp -2). X ray diffraction studies show that polycrystalline ITO remains crystalline even after implantation with 80 keV O(+) at -196 C to a dose of 4.0 x 10(exp 15) cm(exp -2) which suggests that dynamic recovery processes are active in ITO at this low temperature. Although the x ray diffraction pattern of the polycrystalline ITO remains unchanged with implant dose, the electrical properties were seen to degrade when implanted to a dose of 1.0 x 10(exp 15) cm(exp -2) below 200 C. In contrast, amorphous ITO films remain amorphous upon ion implantation and shows almost no degradation in resistivity when implanted below 16 C. The recrystallization temperature of amorphous ITO is about 150 C in the absence of ion implantation. DOE

N94-26934# Argonne National Lab., IL.
FABRICATION AND CHARACTERIZATION OF NANO-CRYSTALLINE DIAMOND FILMS
D. M. Gruen, X. Pan, A. R. Krauss, S. Liu, J. Luo, and C. M. Foster 1993 18 p Presented at the 40th National Symposium of the American Vacuum Society (AVS), Orlando, FL, 15-19 Nov. 1993

(Contract W-31-109-eng-38)
(DE94-002202; ANL/CHM/CP-81063; CONF-9311104-5) Avail: CASI HC A03/MF A01

Highly uniform, smooth nano-crystalline diamond films have been fabricated with a magneto-active microwave CVD system. Top and bottom magnet currents were 145 A and 60 A, while microwave power and substrate temperature were controlled at 1500 W and 850 C during deposition. Total processing pressure was regulated at 40 Pa (300 mTorr), with gas flow rates of 30 sccm of hydrogen, 2.4 sccm of methane, and 1 sccm of oxygen. Diamond films obtained under the above conditions have grain sizes between 0.1 to 0.3 micro-m, a growth rate of 0.1 micro-m/hr, and a mean roughness of 14.95 nm. Characterization techniques have involved XRD, Raman spectroscopy, SEM, AFM, and TEM. Both x ray and electron diffraction patterns show no evidence of non-diamond phases. Although a high density of twins and stacking faults were revealed by HREM, compact diamond grains and clean intergranular boundaries (no graphitic or amorphous phases) were observed. DOE

N94-26958# Oregon State Univ., Corvallis. Dept. of Physics.
INDIUM DONOR COMPLEXES WITH CATION VACANCIES IN CdTe AND ZnSe
J. W. Griffith, R. Lundquist, R. Platzer, J. A. Gardner, G. Karczewski (Notre Dame Univ., IN.), and J. K. Furdyna (Notre Dame Univ., IN.) 1993 6 p Presented at the 17th International Conference on Defects in Semiconductors, Gmunden, Austria, 18-23 Jul. 1993
(Contract DE-FG06-85ER-45191)
(DE94-002731; DOE/ER-45191/23; CONF-9307124-3) Avail: CASI HC A02/MF A01

Very dilute (10(exp 12) cm(exp -3)) indium donors in CdTe and ZnSe powders and in CdTe single crystals were investigated using (sup 111)In perturbed angular correlation spectroscopy. Most indium atoms are in uncomplexed sites but can form weakly-bound complexes with native defects in very defective material. The only complex observed in CdTe is an indium-Cd vacancy pair. The CdTe in which these pairs occur is apparently n-type, most Cd vacancies are free and doubly-charged, and the binding energy with indium is 0.15 eV. In ZnSe, indium can pair with a Zn vacancy or with some other presently unidentified defect. These complexes form in ZnSe containing large concentrations of both free Zn vacancies and complexes of Zn vacancies with other defects. In CdTe, the pair formation equilibration time constant is two days at 15 C, an implication that Cd vacancies are mobile at room temperature. Lattice relaxation around a Cd vacancy in CdTe was probed by single crystal PAC experiments. DOE

N94-26965 Cornell Univ., Ithaca, NY. Dept. of Physics.
THE GROWTH AND CHARACTERIZATION OF GaN AS A PHOTODETECTOR Semiannual Technical Report, 1 May - 31 Oct. 1993
Wilson Ho 21 Dec. 1993 4 p Limited Reproducibility: More than 20% of this document may be affected by microfiche quality
(Contract N00014-92-1-0499)
(AD-A274570) Avail: Issuing Activity (Defense Technical Information Center (DTIC))

A unique apparatus incorporating four independent supersonic jets and a substrate transfer mechanism for the growth of thin films in an ultrahigh vacuum chamber is under construction. The four jets are the continuous flow type and can be turned on and off with computer control allowing precise control of the reactants for atomic layer epitaxy. The supersonic jet configuration prepares the reactants with high translational energies to overcome activation barriers, enhances the impinging flux, and reduces the growth temperature and by about six orders of magnitude the growth pressure. Growth of high quality films is expected. Thin films of gallium nitride (GaN) will be grown on Si(100) using triethylgallium and ammonia as the precursors. Photodetector of GaN will be fabricated at the Cornell National Nanofabrication Facility. Second harmonic generation and atomic force microscopy measurements have been performed on GaN films on sapphire grown by Asif Khan of APA Optics. A new experiment measuring the thin film interference and band gap absorption of GaN film on sapphire has been set up in the Advanced Laboratory at Cornell University. DTIC

N94-26987 Melbourne Univ., Parkville (Australia). School of Physics.
He(+) AND H(+) MICROBEAM DAMAGE, SWELLING AND ANNEALING IN DIAMONDS
S. P. Dooley, D. N. Jamieson, and S. Prawer 1992 22 p Presented at the 3rd International Conference on Nuclear Microprobe Technology and Applications, Uppsala, Sweden, 8-12 Jan. 1992 Limited Reproducibility: More than 20% of this document may be affected by microfiche quality
(DE94-601912; UM-P-92/72; CONF-9201160) Avail: CASI HC A03 (US Sales Only)

The effects of scanned 2 MeV He(+) and 1.4 MeV H(+) microbeam irradiation on unimplanted and P implanted diamond are discussed. Although diamond was found to be resistant to lattice defect production, it was found to swell very rapidly in comparison with other materials, giving rise to serious swelling induced dechanneling at scan edges at relatively low doses (10(exp 17)/cm(exp 2) for 2 MeV He(+)). Microbeams annealed the damage due to a 1.5 microns deep Phosphorus implantation at a dose of 10(exp 15)P(+)/cm(sup 2). The implantation damage was reduced at a dose of (1.6 x 10(exp 17)/cm(sup 2)) by up to 21% for 2 MeV He(+) irradiation, up to 16% for high flux 1.4 MeV H(+) irradiation and 12% for low flux H(+) irradiation. For the choice of analysis beam, all these beam effects were found to be most significant for He(+) microbeams, so H(+) microbeams should be used for analysis of diamond unless high depth resolution is required. DOE

N94-27017 International Centre for Theoretical Physics, Trieste (Italy).
A MODEL OF ELECTRIC BREAKDOWN IN POLYCRYSTALLINE SEMICONDUCTORS WITH HIGHLY NONLINEAR I - V CHARACTERISTICS
E. H. Yildirim, B. Tanatar (Bilkent Univ., Ankara, Turkey.), and E. Canessa Jul. 1993 20 p Limited Reproducibility: More than 20% of this document may be affected by microfiche quality
(DE94-601537; IC-93/182) Avail: CASI HC A03 (US Sales Only)

A deterministic algorithm to study the nonlinear current-voltage characteristics of polycrystalline semiconductors, such as ZnO-based metal oxide varistors, under dc bias and at room temperature is developed based on the electrical properties of individual grain boundaries. Assuming a thermionic emission type mechanism between individual grains and a nonuniform distribution of barrier heights at grain boundaries, the set of nonlinear Kirchhoff equations that determines the macroscopic current across the specimen and the nonlinearity coefficient alpha is solved numerically. The applied voltage dependence of the barrier height is found to be crucial to obtain alpha values reaching approximately 50, indicating high nonlinearity as required by potential commercial applications. DOE

N94-27047# Superconducting Super Collider Lab., Dallas, TX.
MEASUREMENTS OF THE B(SUP 0)(BAR B)(SUP 0)CP ASYMMETRY
V. Lueth Jun. 1993 7 p Presented at the Workshop on B Physics At Hadron Colliders, Snowmass, CO, Jun. 1993
(Contract DE-AC35-89ER-40486)
(DE94-003379; SSCL-Preprint-527; CONF-9306258-7) Avail: CASI HC A02/MF A01

This report discusses B(sup 0) and (bar-B)(sup 0) production rates, B(sup 0) branching ratios, detection efficiency of B(sup 0), and the dilution factors of the CP asymmetry. DOE

N94-27055# Crystal Associates, Inc., Waldwick, NJ.
DEVELOPMENT OF K(1-x)Na(x)TiOPO4 CRYSTALS FOR NONLINEAR APPLICATIONS
G. M. Loiacono 6 Dec. 1993 4 p
(Contract N00014-93-C-0225)
(AD-A274336) Avail: CASI HC A01/MF A01

During this first quarter, the raw materials, crucibles and furnace parts required for this program were purchased and received. The initial crystal growth of Na doped KTP requires seeds of identical composition in order to minimize strain effects. For each composition examined, a preliminary crystal growth run to obtain these seeds utilized the spontaneous nucleation method. A saturated solution of proper composition is superheated to 950 C. The saturation temperature of the solution was estimated based on previously determined solubility data. The solution was programmed at 5 C/day to obtain nucleation. This process was repeated for each new composition. DTIC

N94-27058# North Carolina State Univ., Raleigh.
INTERFACE PROPERTIES OF WIDE BANDGAP SEMICONDUCTOR STRUCTURES Semiannual Technical Report
Robert F. Davis, R. J. Nemanich, Salah Bedair, Jerry Bernholc, R. J.

Nemanich, and Jeffrey T. Glass Dec. 1993 212 p
(Contract N00014-92-J-1477)
(AD-A274356) Avail: CASI HC A10/MF A03

Ab initio molecular dynamics calculations have shown that the 1x1:2H and the 2x1:H surfaces of diamond (C)(100) have a negative electron affinity (EA); the clean (100) surface has a positive EA. This is in agreement with experiment. Biased nucleation of C on beta-SiC(100) and Si(100) has been achieved but not on Cu(100). C nucleation densities on Hf, Ti, Ta, Ni, and W were directly related to the carbide heat of formation. The precursors of chlorinated methylsilanes coupled with bias were used to deposit C films on Si(100). Textured C(111) films were also achieved using an oxyacetylene torch. Cu forms an epitaxial rectifying contact to diamond with a Schottky barrier height (SBH) of approximately 1.1 eV. Hydrogen plasma was used to remove hydrocarbons from SiC surface at 400 C. Controlled growth of single crystal beta(3C)-and alpha(6H)-SiC films has been achieved on alpha(6H)-SiC wafers at 1050 C by gas source (GS) MBE. The growth mode of each polytype has been investigated. Rectifying Ti contacts with low ideality factors (n less than 1.09) and leakage currents (5 x 10(exp -7) A/sq cm at 10 V) and SBH's of 0.79 to 0.88 have been achieved. The three-dimensional nucleation and coalescence of islands of AlN on alpha(6H)-SiC has been discerned via TEM. Multilayers and solid solutions of AlN and SiC have been achieved and characterized. DTIC

N94-27095# Chicago Univ., IL. Dept. of Chemistry.
SPECTROSCOPY AND DYNAMICS OF MOLECULAR AND IONIC IMPURITIES EMBEDDED IN SOLID HYDROGEN Final Report, 13 Apr. 1990 - 12 Apr. 1993
Takeshi Oka Sep. 1993 73 p
(Contract F33615-90-C-2035)
(AD-A274149; WL-TR-93-2099) Avail: CASI HC A04/MF A01

The research involved high resolution infrared spectroscopy to measure the crystalline field and intermolecular interactions in solid hydrogen coupled with a variety of methods, including bombardment by high energy electrons and gamma ray irradiation, to energize and ionize solid hydrogen and obtain solid plasmas. Simultaneous absorption and stimulated Raman measurements are reported. The infrared spectrum of the trimer hydrogen ion (protonated hydrogen) was also measured. A review was completed of the spectroscopy of H3(+) and of its occurrence and importance in laboratory and space plasmas. DTIC

N94-27174# Tokyo Univ. (Japan). Inst. for Solid State Physics.
TECHNICAL REPORT OF ISSP. SER. A, NO. 2678: MAGNETIC PROPERTIES OF CARBON NANOTUBES
Hiroshi Ajiki and Tsuneya Ando May 1993 15 p
(ISSN 0082-4798)
(JTN-94-80564) Avail: CASI HC A03/MF A01

Magnetic properties of carbon nanotubes (CN's) are calculated in the effective-mass theory. The magnetic moment in a magnetic flux parallel to the tube axis oscillates as a function of the flux with period determined by the flux quantum and phase depending on whether CN is metallic or semiconducting. For a magnetic field perpendicular to the axis, CN's exhibit a large diamagnetism independent of metallic or semiconducting properties. The magnetic moment induced by a perpendicular field is about three order of magnitude as large as that by a parallel field. Author (NASDA)

N94-27175# Tokyo Univ. (Japan). Inst. for Solid State Physics.
TECHNICAL REPORT OF ISSP. SER. A, NO. 2679: NOVEL ELECTRONIC STATES OF PARTIALLY DEUTERATED (DMe-DCNQI)2Cu
Hiroshi Sawa, Masafumi Tamura, Shuji Aonuma, Reizo Kato, Minoru Kinoshita, and Hayao Kobayashi (Toho Univ., Tokyo, Japan.) Jun. 1993 13 p Sponsored by Ministry of Education, Science and Culture, Tokyo, Japan
(ISSN 0082-4798)
(JTN-94-80565) Avail: CASI HC A03/MF A01

Magnetic and structural studies of giant metal (M)-insulator (I)-metal reentrant transitions in the partially deuterated molecular conductors (DMe-DCNQI-d(sub n))2Cu (n=2,3) are presented. In the insulating phase, Curie-Weiss-like susceptibilities with reduced Curie constants and diffusive satellite reflections showing a three-fold superstructure were observed. The results are discussed in terms of novel electronic states associated with the three-dimensional narrow 'd-band' in the one-dimensional 2p pi conduction band. Author (NASDA)

N94-27176# Tokyo Univ. (Japan). Inst. for Solid State Physics.
TECHNICAL REPORT OF ISSP. SER. A, NO. 2680: DETERMINATION OF INTERVALLEY SCATTERING TIME IN GERMANIUM BY SUBPICOSECOND TIME-RESOLVED RAMAN SPECTROSCOPY
Koichiro Tanaka, Hideyuki Otake, and Toru Suemoto Jun. 1993 17 p
(ISSN 0082-4798)
(JTN-94-80566) Avail: CASI HC A03/MF A01

Time-resolved Raman scattering measurements were made by 110 fs laser pulses in germanium under the condition of the collision limited regime, initial carrier density approximately 10(exp 18) cm(exp -3). The Raman scattering from photo-excited electrons in L-valleys was clearly observed along with hot luminescence. The Raman signal was found to increase with a time constant of 1.1 +/- 0.1 ps. The result means that the intervalley scattering time of photo-excited electrons from gamma-valley to L-valleys is 1.1 +/- 0.1 ps. Author (NASDA)

N94-27177# National Research Inst. for Metals, Tokyo (Japan).
TECHNICAL REPORT OF ISSP. SER. A, NO. 2681: ORBITAL AND SPIN SUSCEPTIBILITIES OF THE PLANE COPPER SITES IN YBa2Cu3O(x) SYSTEM
Tadashi Shimizu, Haruyoshi Aoki, Hiroshi Yasuoka, Toshinobu Tsuda, Yutaka Ueda, Kazuyoshi Yoshimura, and Koji Kosuge Jun. 1993 31 p Sponsored by Ministry of Education, Science and Culture, Tokyo, Japan
(ISSN 0082-4798)
(JTN-94-80567) Avail: CASI HC A03/MF A01

The tensor components of the magnetic susceptibility, chi, and the Knight shift, K, at the plane Cu(2) sites have been precisely measured in YBa2Cu3O(x) with x = 6.98, 6.48 and 6.0. By using the temperature dependent chi and K observed in YBa2Cu3O(6.48), the analysis of K(sub -chi) diagram has been carried out to make a separation of the observed susceptibility into orbital and spin contributions. The obtained spin susceptibility is discussed in comparison with the theories of the Heisenberg model, the Stoner model, and a band structure calculation. A complete set of the parameter values used in the crystal field model of a Cu(2+) ion - the crystal field splittings, the orbital reduction factor, the spin-orbit coupling, and the g-factors - has been determined from the K(sub -chi) analysis. Author (NASDA)

N94-27231# Utah Univ., Salt Lake City. Dept. of Physics.
TECHNICAL REPORT OF ISSP. SER. A, NO. 2671: QUASI-LOCALIZATION OF LIGHT WAVES IN FIBONACCI DIELECTRIC MULTILAYERS
W. Gellermann, M. Kohmoto (Tokyo Univ., Japan.), B. Sutherland, and P. C. Taylor Apr. 1993 15 p
(ISSN 0082-4798)
(JTN-94-80557) Avail: CASI HC A03/MF A01

It has been measured that the optical transmission of quasiperiodic dielectric multilayer stacks of SiO2 (A) and TiO2 (B) thin films which are ordered according to a Fibonacci sequence S(sub (j+1)) = (S(sub (j-1)), S(sub j)), with S(sub 0) = (B) and S(sub 1) = (A) up to the sequence S9 which consists of 55 layers. A scaling of the transmission coefficient with increasing Fibonacci sequences at quarter-wavelength optical thicknesses is observed. This behavior is in good agreement with theory and can be considered as experimental evidence for the quasi-localization of the light waves. Author (NASDA)

N94-27232# Tokyo Univ. (Japan). Inst. for Solid State Physics.
TECHNICAL REPORT OF ISSP. SER. A, NO. 2674: HIGH-FIELD CYCLOTRON RESONANCE AND IMPURITY TRANSITION IN n- AND p-3C-SIC AT MAGNETIC FIELDS UP TO 175 T
Junichiro Kono, Shojiro Takeyama, Hiroyuki Yokoi, Noboru Miura, Mitsugu Yamanaka, Mikiya Shinohara, and Keiko Ikoma Apr. 1993 31 p
(ISSN 0082-4798)
(JTN-94-80560) Avail: CASI HC A03/MF A01

Magneto-transmission experiments have been carried out on 3C-SiC thin films grown on Si(100) substrates, using the combination of pulsed high magnetic fields up to 175 T generated by the single-turn coil technique and pulsed far-infrared radiations from an H2O(D2O) laser at photon energies up to 73.2 meV. In n-type 3C-SiC, two Cyclotron Resonance (CR) peaks have been observed for B parallel to k parallel to greater than 100 less than over a wide range of photon energy 10.4 - 53.8 meV, corresponding to the light- and heavy-mass valleys at the X-points, i.e., m(sub t)(sup *)

= (0.25 +/- 0.01)m(sub 0) and (m(sub t)(sup *) m(sub 1)(sup *))(exp 1/2) = (0.41 +/- 0.01)m(sub 0). These values are in agreement with those of Kaplan obtained from CR at low fields. This leads to a conclusion that the conduction band in 3C-SiC is very parabolic up to 53.8 meV, and that unlike GaP the effect of camel's back structure is unobservable. A number of impurity transitions were observed for the first time at temperatures below 100 K with photon energies ranging from 34.4 to 73.2 meV. It was found that the observed lines originate from three different donor states which have different binding energies, E(sub d) = 19, 35 and 53 meV. The first observation of hole CR was also made in p-type 3C-SiC. A broad but prominent peak was observed with an effective mass of 0.45m(sub 0), at temperatures around 210 K and at wavelength of 119 micrometers.
Author (NASDA)

N94-27239# Tokyo Univ. (Japan). Synchrotron Radiation Lab.

TECHNICAL REPORT OF ISSP. SER. A, NO. 2670: ELECTRONIC STRUCTURE OF LIGHT TRANSITION METAL COMPOUNDS STUDIED BY PHOTOEMISSION

S. Shin, Y. Tezuka, T. Ishii, and Y. Ueda Apr. 1993 15 p
(ISSN 0082-4798)
(JTN-94-80556) Avail: CASI HC A03/MF A01

The valence band photoemission has been measured on ScF3, TiO2 and V2O5 which have no 3d electron nominally. The charge-transfer satellites are found in the region from 11 eV to 17 eV below the top of the valence band. It is concluded from the resonant photoemission that the charge-transfer-type configuration is manifest to form the valence state in the ground state in addition to the originally filled-up 2p state of ligand.
Author (NASDA)

N94-27240# Tokyo Univ. (Japan). Inst. for Solid State Physics.

TECHNICAL REPORT OF ISSP. SER. A, NO. 2672: MAGNETO-OPTICAL EFFECTS OF EXCITONS IN BiI3 CRYSTALS UNDER PULSED HIGH MAGNETIC FIELDS. 3: EXCITONS CONFINED AROUND A STACKING DISORDER FORMED BY A BENDING STRESS

Katsuyoshi Watanabe, Shojiro Takeyama, Noboru Miura, Teruo Komatsu, Takenori Higashimura, and Takeshi Iida Apr. 1993 30 p Sponsored by Ministry of Education, Science and Culture, Tokyo, Japan
(ISSN 0082-4798)
(JTN-94-80558) Avail: CASI HC A03/MF A01

It has been observed that a series of new lines in the absorption and luminescence spectra of BiI3 crystals are strained by a bending stress. The magnetic field effects on these lines were investigated in pulsed high magnetic fields up to 47 T. The magneto-optical spectra were well explained by the cationic exciton model. The origin of the lines was concluded to be an exciton state confined around a stacking disorder, which was formed by the deformation. The quantum size effect of the excitons in the specific region of the stacking disorder is discussed. Author (NASDA)

N94-27243 Tel-Aviv Univ. (Israel). School of Physics and Astronomy.

MORPHOLOGY TRANSITIONS DURING NON-EQUILIBRIUM GROWTH PROCESSES M.S. Thesis

Ofer Shochet Apr. 1992 107 p
(ITN-94-85236) Copyright Avail: Issuing Activity (Tel-Aviv Univ., Exact Sciences Library, Ramat Aviv 69978, Israel)

The diffusion-transition scheme was developed to study interfacial pattern formation during diffusion-limited growth in systems described by a conserved order parameter. The new approach is inspired by the specific example of solidification from supersaturated solutions, for which advantage was taken of new experimental observations in surface kinetics. The time dependence in the metastable phase (the concentration of solute) is evaluated by solving the continuous linear diffusion equation. The motion of the interface is described by the statistical mechanics of discrete phase transitions (solidification and melting) at the interface. Both processes are simulated alternately, each for a time period which is shorter than the characteristic time of both processes. The new approach enables us to investigate both equilibrium and non-equilibrium situations. The model can be related both to experimental results and to those of the phenomenological free boundary model. It also enables us to simulate very large systems in a reasonable time and so to investigate generic features of late-stage growth. The new scheme enables us to investigate different kinetics of phase transition at the interface. Complete information of the concentration field is gained. First, the average equilibrium shapes are compared with those evaluated by the Wulff construction. The fluctuations of the interface about the average shape as well as the temporal fluctuation in the diffusion field were calculated.
Author (ISA)

N94-27245# Tokyo Univ. (Japan). Inst. for Solid State Physics.

TECHNICAL REPORT OF ISSP. SER. A, NO. 2675: HIGH-FIELD CYCLOTRON RESONANCE AND VALENCE-BAND STRUCTURE IN SEMICONDUCTING DIAMOND

Junichiro Kono, Shojiro Takeyama, T. Takamasu, Noboru Miura, Naoji Fujimori, Yoshiki Nishibayashi, Takeshi Nakajima, and Kazuo Tsuji Apr. 1993 33 p
(ISSN 0082-4798)
(JTN-94-80561) Avail: CASI HC A03/MF A01

Cyclotron resonance of thermally excited free holes has been observed in synthetic semiconducting diamond at ultra-high magnetic fields up to 150 T generated by the single-turn coil technique with pulsed far-infrared laser radiations of 28, 36 and 119 micrometers. Three absorption peaks were observed at and above room temperature for the magnetic fields parallel to (100), (111), and (110) crystallographic directions. The typical value of omega(sub c) tau was as small as two at 40 C even in ultra-high fields. One of the three peaks was observed in the Cyclotron Resonance Inactive (CRI) circular polarization for holes, whilst the other two lines were observed in Cyclotron Resonance Active (CRA) for holes. Assuming that these resonance absorption lines are due to three holes of the valence-bands at the gamma-point, i.e. light-hole, heavy-hole, and split-off-hole, it is able to be concluded that the band dispersion curve for one of the three bands has a negative (electron-like) curvature in some directions. Author (NASDA)

N94-27248# Tokyo Univ. (Japan). Inst. for Solid State Physics.

TECHNICAL REPORT OF ISSP. SER. A, NO. 2676: CHARGE MASS SINGULARITY IN TWO-DIMENSIONAL HUBBARD MODEL

Nobuo Furukawa and Masatoshi Imada May 1993 13 p
(ISSN 0082-4798)
(JTN-94-80562) Avail: CASI HC A03/MF A01

Two-dimensional Hubbard model with both the nearest and the next-nearest neighbor transfer is studied. A singularity in the charge susceptibility at the Mott transition point delta approaches 0 is observed, leading to the anomaly of the charge mass m(sub c)(sup *) in the form m(sub c)(sup *) varies with (absolute value of delta)(exp -1)(sup *), where delta is the doping concentration. The singularity is similar to the case without the next-nearest neighbor transfer. It indicates that the singularity in the charge mass is a universal nature of this model irrespective of its band structure. Author (NASDA)

N94-27251# Oak Ridge National Lab., TN.

EXPERIMENTAL MEASUREMENT OF LOCAL DISPLACEMENT AND CHEMICAL PAIR CORRELATIONS IN CRYSTALLINE SOLID SOLUTIONS

C. L. Sparks, G. E. Ice, J. L. Robertson, and L. B. Shaffer (Anderson Univ., IN.) 1993 10 p Presented at the NATO Advanced Study Workshop on Metallic Alloys: Experimental and Theoretical Perspectives, Boca Raton, FL, 16-21 Jul. 1993
(Contract DE-AC05-84OR-21400)
(DE94-001124; CONF-930759-3) Avail: CASI HC A02/MF A01

Measurement of near-neighbor atomic arrangements in crystalline solid solutions is well established and provides meaningful values for chemical preference of atoms for their near neighbors to beyond the first ten neighboring shells. Static displacements (atomic size) between these atom pairs have mostly been either ignored in the recovery of the local pair preferences or removed by making use of the displacement scattering dependence on momentum transfer. With intense and energy tunable x-ray synchrotron sources, our ability to recover these static displacements between atoms has greatly improved. Data taken with multiple x-ray energies to obtain the contrast necessary to separate like from unlike neighbor pair distances are discussed for the two cases studied to date: a locally ordered Ni(77.5)Fe(22.5) crystal and a locally clustered Fe53Cr47 crystal. Analysis of experimental parameters and data gives the systematic and statistical errors on the recovered parameters. Meaningful atomic displacements from the mean lattice can be measured and recovered. These displacements help us understand material properties and will provide theorists with tests for their calculations. DOE

N94-27276 Coors Porcelain Co., Golden, CO.
TRANSPARENT POLYCRYSTALLINE BODY WITH HIGH ULTRAVIOLET TRANSMITTANCE, PROCESS FOR MAKING AND APPLICATIONS THEREOF Patent
Donald W. Roy, inventor (to Coors), James L. Hastert, inventor (to Coors), Lawrence Coubrough, inventor (to Coors), Kenneth E. Green, inventor (to Coors), and Aurelio Trujillo, inventor (to Coors) 28 Dec. 1993 52 p
(CA-Patent-1325511; Int-Patent-Class-C04B-035/44;
Int-Patent-Class-F41F-003/04; Int-Patent-Class-H01Q-001/42;
CTN-94-61097) Copyright Avail: Micromedia Ltd., Technical Information Centre, 240 Catherine Street, Suite 305, Ottawa, Ontario, K2P 2G8, Canada HC/MF

A sintered polycrystalline body is disclosed which consists essentially of magnesia alumina spinel having an in-line transmittance per 1.88 mm thickness of not less than about 62.5 percent at a wavelength of about 0.2 microns and not less than 85 percent at a wavelength of about 0.3 microns. The material retains at least about 90 percent of its original transmissivity after as much as 240 hours or more of exposure to ultraviolet light in the 0.2-0.4 micron wavelength range. The sintered body has a flexural strength of at least about 15,000 psi. The sintered transparent body can be produced by a two-step process in which a spinel powder is formed into a closed porosity body by hot pressing or pressureless sintering. The closed porosity body is then hot isostatic pressed at a temperature of at least about 1,400 C under a pressure of at least about 15,000 psi. The sintered body so produced has a grain size under about 150 microns, a porosity less than about 0.001 percent, and a transmittance previously specified. Substantially larger grain sizes result in reduced strength, while substantially smaller grain sizes result in unacceptable ultraviolet transmission. The invention relates in particular to a missile dome and a launch tube window which has high ultraviolet transmittance properties and is stable under high temperatures, corrosive environments, and resistant to abrasion or erosion. Author (CISTI)

N94-27329# Instituto de Pesquisas Espaciais, Sao Jose dos Campos (Brazil).
SYNTHESIS OF DIAMOND FILM ASSISTED BY AN ARCJET PLASMA SOURCE, PART 2 [SINTETIZACAO DE FILMES DE DIAMANTE ASSISTIDO POR JATO DE PLASMA GERADO POR UMA DESCARGA ELETRICA TIPO ARCO EM BAIXA PRESSAO, PARTE 2]
Patricia Regina Pere Barreto and Edson DelBosco Oct. 1993 53 p In PORTUGESE
(INPE-5527-PRP/178-Pt-2) Avail: CASI HC A04/MF A01

This report presents the results of the initial characterization of a plasma jet projected for diamond thin film deposition. The temperature and density profiles were measured with a double electrostatic probe. A conceptual project involving the design of a new plasma jet based on gas dynamic theory is also discussed. Author (revised)

N94-27347 International Centre for Theoretical Physics, Trieste (Italy).
FIRST PRINCIPLES CALCULATIONS FOR THE CLEAVED AND ANNEALED Ge(111) SURFACES
N. Takeuchi, E. Tosatti, and A. Selloni (International School for Advanced Studies, Trieste, Italy.) Nov. 1992 14 p Limited Reproducibility: More than 20% of this document may be affected by microfiche quality
(DE93-617048; IC-92/367) Avail: CASI HC A03 (US Sales Only)

Ab initio Molecular Dynamics was used to study the structural and electronic properties of cleaved and annealed Ge(111) surfaces. New features emerge for both structures. For the (2x1) it is found that even though the stable state has a pi-bonded chain structure, there are two isomers with the tilt angle of the chain in opposite directions. For the c(2x8) an asymmetry was found in the surface unit cell, in agreement with Low Energy Electron Diffraction (LEED) experiments that show weak quarter-order spots. This inequivalence also produces a splitting of the rest atom and adatom dangling bond, which explains recent STM experiments. DOE

N94-27353# Tokyo Univ. (Japan). Inst. for Solid State Physics.
TECHNICAL REPORT OF ISSP. SER. A, NO. 2669: RELATIONS BETWEEN OXYGEN DEFICIENCY AND STRUCTURES IN THE La-Sr-Cu-O SYSTEM. 3: OXYGEN CONTENTS AND STRUCTURE OF (La, Sr)8Cu8O(16+DELTA) PHASE
Kenji Otzschi, Keiichi Koga, and Yutaka Ueda Apr. 1993 39 p Sponsored by Ministry of Education, Science and Culture, Tokyo, Japan
(ISSN 0082-4798)
(JTN-94-80555) Avail: CASI HC A03/MF A01

The oxygen content of (La(1-x)Sr(x))8Cu8O(16 + delta) was determined for variously heat-treated samples. It increases with increasing partial pressure of oxygen, for example, x = 0.75 and delta = 0.08 (annealed in Ar at 810 C), 0.27 (quenched from 1050 C in air), 2.29 (annealed in O2 at 800 C), and 2.54 (treated under O2 high-pressure 300 atm). X-ray diffraction studies indicate that there are two distinct phases, the oxygen-poor phase (delta approx. = 0.0--the 8-8-16 phase) and the oxygen-rich phase (delta greater than or equal to 2.0--the 8-8-18 phase). Author (NASDA)

N94-27354# Tokyo Univ. (Japan). Inst. for Solid State Physics.
TECHNICAL REPORT OF ISSP. SER. A, NO. 2682: PRESSURE DEPENDENCE OF Sm:YAG FLUORESCENCE TO 50 GPa: A NEW CALIBRATION AS A HIGH PRESSURE SCALE
Hitoshi Yusa, Takehiko Yagi, and Haruo Arashi Jun. 1993 18 p
(ISSN 0082-4798)
(JTN-94-80568) Avail: CASI HC A03/MF A01

The pressure-induced wavelength shift of laser excited fluorescence in Samarium doped Yttrium Aluminum Garnet (Sm:YAG) was measured at up to 50 GPa at room temperature. The intense peaks between 618 nm and 611 nm were analyzed as a triplet, Y1, Y2, and Y3, by curve fitting analysis using Lorentzian function. The Y1 (lambda(sub 0) = 618 nm) peak was the strongest peak up to 40 GPa while the Y2 (lambda(sub 0) = 616 nm) peak became the strongest above it. As the temperature dependence of the fluorescence shift of Sm:YAG is negligibely small, these pressure scales will be useful for high pressure and high temperature experiments using diamond anvil cell. Author (NASDA)

N94-27561*# Akron Univ., OH. Dept. of Mechanical Engineering.
ON LINE QUANTIFICATION OF CRYSTAL SURFACES BY STEREO IMAGING Final Technical Report
Celal Batur 1992 29 p
(Contract NCC3-211)
(NASA-CR-195277; NAS 1.26:195277) Avail: CASI HC A03/MF A01

The shape of an interface while a crystal is growing inside a crystal growth furnace is an important measurement to assess the crystal quality on-line. If the crystal surface can be visualized by video or x ray imaging, the interface shape can be determined by the stereo image processing techniques. This paper presents a methodology to determine the shape of the solid-melt interface by stereo based imaging techniques while the crystal is growing inside a transparent furnace. The methodology generates qualitative shape information provided that a good pair of stereo images of the interface can be captured. For a quantitative shape description, i.e., for the determination of interface points with respect to a fixed coordinate frame, both cameras must be calibrated. This paper illustrates the methodology for qualitative shape determination of lead bromide crystal interface. Author (revised)

N94-27590# Deutsche Forschungsanstalt fuer Luft- und Raumfahrt, Stuttgart (Germany). Inst. fuer Technische Physik.
FLOAT ZONE CRYSTAL GROWTH USING LASER RADIATION [LASERGESTUTZTE KRISTALLZUCHT NACH DEM ZONENSCHMELZVERFAHREN]
Josef Muckenschnabel, Uwe Becker, Uwe Brauch, and Alexander Cohen May 1993 43 p
(ISSN 0939-2963)
(DLR-FB-93-10; ETN-94-95492) Avail: CASI HC A03/MF A01

A float zone crystal growth apparatus was developed and built. To evaluate the influences of different laser wavelengths on crystal growth, the molten zone was heated either by CO2 (10 micrometers) or CO (5 micrometers) laser radiation. Transparent single crystals of Ti:Al2O3, Nd:YAG (Yttrium Aluminum Garnet), and Yb:YAG with diameters up to 6 mm were obtained. In an oxygen containing atmosphere of 100 to 200 Torr, YAG crystals could be grown with a flat interface. This was achieved either by heating the molten zone with the CO laser or at high counterrotation rates with the CO2 laser. In the Al2O3, no significant influence of laser wavelength on the interface shape was noticed. To reduce the high temperature gradients, an afterheater in the form of an 'ellipsoidal' reflector was installed. ESA

N94-27602# Pacific Northwest Lab., Richland, WA.
EFFECT OF TEMPERATURE AND RECOIL-ENERGY SPECTRA ON IRRADIATION-INDUCED AMORPHIZATION IN Ca2La8(SiO4)6O2
W. J. Weber and L. M. Wang (New Mexico Univ., Albuquerque.) Sep. 1993 16 p Presented at the Nuclear Instruments and Methods in Physics Research on Radiation Effects in Insulators, Nagoya, Japan, Sep. 1993
(Contract DE-AC06-76RL-01830)
(DE94-004371; PNL-SA-22525; CONF-9309259-2) Avail: CASI HC A03/MF A01

Single crystals of Ca2La8(SiO4)6O2 have been irradiated with different ions/energies in an in situ study of the effects of temperature and recoil-energy spectra on irradiation-induced amorphization. The dose for complete amorphization increases with temperature in two stages. The low-temperature stage (below 250 K) has an activation energy of 0.01 +/- 0.003 eV and is believed to be associated with simultaneous close-pair recombination. The high-temperature stage (above 250 K) has an activation energy of 0.13 +/- 0.02 eV and may be associated with irradiation-enhanced defect mobility. The critical temperature for amorphization increases from approximately 360 K for 0.8 MeV Ne(+) to approximately 710 K for 1.5 MeV Kr(+). At 15 K, the amorphization dose is approximately 0.36 dpa and is independent of recoil-energy spectra. The amorphization dose increases more rapidly with temperature for Ne(+) due to the larger fraction of mobile defects produced by the low energy recoils. The temperature dependence is similar for 1.0 MeV Ar(+), 1.5 MeV Kr(+), and 1.5 MeV Xe(+). DOE

N94-27609# Midwest Research Inst., Golden, CO.
RESEARCH ON HIGH-EFFICIENCY, LARGE-AREA, CuInSe2 BASED THIN-FILM MODULES
K. E. Knapp and R. R. Gay Jan. 1994 39 p Prepared in cooperation with Siemens Solar Industries, Camarillo, CA
(Contract DE-AC02-83CH-10093)
(DE94-000259; NREL/TP-413-6216) Avail: CASI HC A03/MF A01

This report describes work to demonstrate 12.5% aperture efficient, large-area (3900-sq cm) encapsulated thin-film CuInSe2 (CIS) photovoltaic modules. Module design consists of 53 series-connected ZnO/CdS/CIS/Mo/glass cells fabricated on a 4141-sq cm (128.6 x 32.2 cm) glass substrate with a nominal aperture area of 3895 sq cm (127.3 x 30.6 cm). Four CIS modules were shipped to NREL under the terms of the subcontract. Phase 2 consisted of fabricating large-area (3900-sq cm) modules for high-performance module processing. The large-area parts proved to be cumbersome, and we decided to use smaller substrates (100 sq cm) to accelerate the progress in solving the types of technical challenges that were discovered in processing large-area parts, and then to apply these solutions to larger areas to meet the objectives of the investigation. Most critical issues determining module yield losses can be grouped into three major categories: (1) Uniformity and reproducibility of the absorber formation process dominates the fundamental performance of the material over a large area, (2) interaction of the substrate with the Mm requires appropriate selection criteria and preparation techniques for minimizing defects that lead to shunting and areas of poor photoresponse, and (3) performance losses near interconnects reduce module performance and can cause inadequate performance through module durability testing. DOE

N94-27623 Instituto de Pesquisas Energeticas e Nucleares, Sao Paulo (Brazil).
STUDY OF THE HYPERFINE MAGNETIC FIELD AT Ta-181 SITE IN THE HEUSLER Co2ScSn, Co2ScGa, AND Co2HfSn ALLOYS
Roberta Nunes Attili 1992 101 p Limited Reproducibility: More than 20% of this document may be affected by microfiche quality
(DE94-603989; INIS-BR-3149) Avail: CASI HC A06 (US Sales Only)

The hyperfine magnetic fields acting on Ta-181 nuclei at the Sc and Hf sites have been measured in Heusler alloys Co2ScSn, Co2ScGa, and Co2HfSn using the time differential perturbed gamma-gamma angular correlation (TDPAC) technique. The measurements were carried out using an automatic spectrometer consisting of two BaF2 detectors and the conventional electronics. The magnitude of hyperfine magnetic field at Ta-181 was measured for all the alloys. The signs of the field were determined in the cases of Co2ScSn and Co2HfSn alloys by performing the perturbed angular correlation measurements with an external polarizing magnetic field of approximately equal to 5 k Gauss. The hyperfine magnetic fields obtained are -187.6 +/- 3.3 and 90.0 +/- 2.1 kOe measured at 77 K for Co2ScSn and Co2ScGa alloys respectively, and -342.4 +/- 10.1 kOe measured at the room temperature for Co2HfSn alloy. These results are discussed and compared with the hyperfine magnetic field systematics in Co-based Heusler alloy. DOE

N94-27634 International Centre for Theoretical Physics, Trieste (Italy).
CORRELATED MEAN FIELD ANSATZ FOR THE KONDO NECKLACE
H. Y. Kee and P. Fazekas Aug. 1993 26 p Limited Reproducibility: More than 20% of this document may be affected by microfiche quality
(DE94-603671; IC-93/248) Avail: CASI HC A03 (US Sales Only)

The ground state phase diagram of the pseudospin model introduced by Doniach to describe the essential physics of Kondo lattices is studied. Variational trial states are used which augment the usual mean field solution by incorporating various intersite correlations. A composite spin correlation describing the antiparallel alignment of fluctuating triplets is found to be particularly favorable for large Kondo couplings. With this trial state, the magnetic-to-Kondo transition is suppressed and the strong coupling ground state is ordered with strongly reduced moments. The relevance of the findings is discussed. DOE

N94-27635 International Centre for Theoretical Physics, Trieste (Italy).
LOCALIZATION PROPERTIES OF ONE-DIMENSIONAL ELECTRIFIED CHAINS
R. Ouasti, A. Brezini, and N. Zekri Aug. 1993 17 p Limited Reproducibility: More than 20% of this document may be affected by microfiche quality
(DE94-603672; IC-93/249) Avail: CASI HC A03 (US Sales Only)

A Kronig-Penney model with a constant electric field for a noninteracting electron is used to study the transmission properties of Anderson transition in one-dimensional systems with disordered strengths of delta-function potentials. The authors examined the cases where the potential varies uniformly from O to W (barriers) or from -W to O (wells) for a given disorder W. Mainly, the authors observe unexpected abrupt transition at the points E + Fx = n(exp 2) pi(exp 2). However, these transitions are related to the small oscillations observed by Soukoulis et al. in the mixed case (wells and barriers). An interesting feature in the wells is that in the presence of a small field the states become more localized and the localization length decrease up to a minimum for a critical value F(sub m). In the end, the authors have studied the effect of the disorder on the Anderson transition by the mean of the participation ratio and the localization length. DOE

N94-27638 International Centre for Theoretical Physics, Trieste (Italy).
SECOND-ORDER PHASE TRANSITION IN (g(PHI)4)2 THEORY
G. Ganbold and G. V. Efimov Aug. 1993 10 p Limited Reproducibility: More than 20% of this document may be affected by microfiche quality
(DE94-603677; IC-93/227) Avail: CASI HC A02 (US Sales Only)

The authors suggest a regular scheme for calculating systematically the leading term and next corrections to it up to the fourth order for the effective potential in the scalar phi(sup 4)(sub 2) theory. The obtained results give evidence in favor of a second-order phase transition at (g/2 pi m(exp 2))(sub crit) approximately equal to 0.9 in the theory under consideration. DOE

N94-27647 International Centre for Theoretical Physics, Trieste (Italy).
RELATIVISTIC TWO-BODY SYSTEM IN 1+1-DIMENSIONAL QED. 1: ON THE CIRCLE S1
A. O. Barut and F. M. Saradzhev Jun. 1993 22 p Limited Reproducibility: More than 20% of this document may be affected by microfiche quality
(DE94-603716; IC-93/167) Avail: CASI HC A03 (US Sales Only)

From the coupled Maxwell-Dirac equations for two fermions fields psi(sub 1) and psi(sub 2), the authors derive a covariant two-body equation for the composite field Phi(chi(sub 1), chi(sub 2)) in configuration space which includes radiative self energy effects. Both Coulomb gauge and covariant gauge have been used and their equivalence is proved. For the space S(sup 1), the two-body equation with mutual interactions is solved exactly and the mass spectrum is obtained in the case of massless fermions. DOE

N94-27677 International Centre for Theoretical Physics, Trieste (Italy).
GAUGE INVARIANCE AND TRANSPORT PROPERTIES IN SUPERCONDUCTORS ABOVE T(c)
A. G. Aronov, S. Hikami (Tokyo Univ., Japan.), and A. I. Larkin (Weizmann Inst. of Science, Rehovoth, Israel.) Jun. 1993 13 p Limited Reproducibility: More than 20% of this document may be affected by microfiche quality
(DE94-604013; IC-93/129) Avail: CASI HC A03 (US Sales Only)

We have developed a theory of transport phenomena for superconductors above T(sub c) in the fluctuations region in dirty and clean limits. We show that it is possible to construct a phenomenological theory based on Ginzburg-Landau equation and its gauge invariance, and as a result we can express the fluctuation corrections to the conductivity tensor in a magnetic field in terms of the classical conductivity and coherence lengths. We find that the sign of the Hall conductivity is universal, and we present the method by which it is determined. DOE

N94-27678 International Centre for Theoretical Physics, Trieste (Italy).
DECAY OF NON-EQUILIBRIUM POLARITON CONDENSATE IN SEMICONDUCTORS
Igor V. Beloussov (Academy of Sciences of the Moldavian SSR, Kishinev.) and Yuri M. Shvera Aug. 1993 6 p Limited Reproducibility: More than 20% of this document may be affected by microfiche quality
(DE94-604016; IC-93/235) Avail: CASI HC A02 (US Sales Only)

Excitation dynamics of polariton quantum fluctuations arising in direct-gap semi-conductor as a result of parametric decay of non-equilibrium polariton condensate with non-zero wave vector is studied. The predominant mechanism of polariton scattering is supposed to be exciton-exciton interaction. Steady state, which corresponds to the case of dynamic equilibrium between the polariton condensate and quantum fluctuations, is obtained. Distribution functions of non-condensate polaritons are localized in the resonant regions, corresponding to two-particle excitation of polaritons from the condensate. The spectrum of elementary excitations in steady state coincides with usual polariton energy with the shift proportional to initial density of polariton condensate. DOE

N94-27679# Joint Inst. for Nuclear Research, Dubna (USSR).
EXCITED LANDAU LEVELS, ORBITAL ANGULAR MOMENTUM AND AXIAL ANOMALY
O. V. Teryaev 1993 7 p
(DE94-606407; JINR-E-2-93-56) Avail: CASI HC A02/MF A01 (US Sales Only)

The IR cutoff via the exclusion of the high orbital momentum components for the excited Landau levels leads to the physical interpretation of the cancellation between the explicitly and anomalous chiral symmetry breaking. DOE

N94-27693# Sandia National Labs., Albuquerque, NM.
INFLUENCE OF LATTICE DAMAGE ON RETENTION AND TRANSPORT OF DEUTERIUM IN BETA SILICON CARBIDE
W. R. Wampler and R. A. Causey Oct. 1993 18 p
(Contract DE-AC04-76DR-00789)
(DE94-005206; SAND-93-2007) Avail: CASI HC A03/MF A01

Experiments were done to determine the effect of lattice damage on solubility and transport of deuterium (D) in silicon carbide. Beta SiC samples were irradiated with energetic ions to produce lattice damage, and were then soaked in D2 gas at 1000 C. Concentration of D versus depth was then measured by nuclear reaction analysis. Very near the surface (less than 0.5 micron), concentration of D was larger in irradiated than in unirradiated, but beyond 1 micron the D concentrations were similar (approximately 20 +/- 10 atomic ppM), even though the damage extended to 2.2 micron in most of the samples. Results from this study of ion irradiated SiC together with a previous study of tritium migration in undamaged SiC point to the conclusion that uptake of D from gas into SiC occurs by transport along grain boundaries, whereas uptake of D into lattice damage produced by ion irradiation and release of energetically implanted D both require permeation of D within grains which is much slower. DOE

N94-27697 Universidade Estadual de Paulista, Sao Paulo (Brazil). Inst. de Quimica.
PREPARATION, CHARACTERIZATION, AND THERMAL BEHAVIOUR STUDY OF LANTHANIDES (3) AND YTTRIUM (3) 4-METHOXY BENZYLIDENE PYRUVATE IN SOLID STATE M.S. Thesis [PREPARACAO, CARACTERIZACAO E ESTUDO DO COMPORTAMENTO TERMICO DOS 4-METOXIBENZALPIRUVATOS DE LANTANIDEOS (3) E DE ITRIO (3) NO ESTADO SOLIDO]
L. C. S. deOliveira 1992 64 p In PORTUGESE Limited Reproducibility: More than 20% of this document may be affected by microfiche quality
(DE94-604079; INIS-BR-3169) Avail: CASI HC A04 (US Sales Only)

Solid state compounds involving Ln and 4-MeO-BP, where Ln = trivalent lanthanides (except promethium) and yttrium and 4-MeO-BP = 4-methoxy benzylidene pyruvate, were prepared by addition of ligand to the corresponding metal ions chlorides, both in aqueous solution. The precipitates were washed with distilled water and dried at ambient temperature in a forced circulation oven. Complexometry with EDTA, thermogravimetry (TG), differential scanning calorimetry (DSC), and x ray diffraction have been used in the study of these compounds. DOE

N94-27704# University of Western Washington, Bellingham. Dept. of Physics and Astronomy.
CHARACTERIZATION OF SEMI-INSULATING GALLIUM ARSENIDE Final Report, 18 Nov. 1992 - 17 Nov. 1993
John S. Blakemore 29 Nov. 1993 22 p
(Contract N00014-93-P-2005)
(AD-A273781; N93-015) Avail: CASI HC A03/MF A01

The project was established 18 Nov. 1992 to continue for 12 months. Its purpose has been electrical and optical characterization of samples from semi-insulating (SI) melt-grown crystals of gallium arsenide (GaAs). As a further definition of the project's purpose, the primary goal has been to assist NRL in assessing the properties of SI GaAs crystals grown at NRL by the vertical zone melt (VZM) method. A second aspect of this characterization work has involved samples from SI GaAs crystals grown by various commercial vendors including samples of pre-synthesized GaAs evaluated for its suitability as starting 'feedstock' for VZM growth. Measurements made at Western Washington University (WWU) under the terms of this project accord with a Statement of Work provided at the outset. These have included the following: (1) low-field dc electrical transport data for SI GaAs samples, as functions of temperature; (2) near-infrared (NIR) transmittance/absorption spectra of polished slabs, with data concerning the well-known EL2 defect determined from NIR absorption strength and spectral form; and (3) mid-IR data on absorption caused by carbon acceptors in SI GaAs. DTIC

N94-27724# Lawrence Livermore National Lab., CA.
OBSERVATION OF STIMULATED EMISSION FROM AN MBE GROWN GaN FILM ON SAPPHIRE
K. Yung, J. Yee, J. Koo, M. Rubin (California Univ., Berkeley. Lawrence Berkeley Lab.), N. Newman (California Univ., Berkeley. Lawrence Berkeley Lab.), T. Fu (California Univ., Berkeley. Lawrence Berkeley Lab.), and J. Ross (California Univ., Berkeley. Lawrence Berkeley Lab.) 12 Nov. 1993 8 p Presented at the NOVEL Laser Sources and Applications Workshop, San Jose, CA, 12-13 Nov. 1993
(Contract W-7405-eng-48)
(DE94-003638; UCRL-JC-115682; CONF-9311138-1) Avail: CASI HC A02/MF A01

The authors report the first observation of optically pumped stimulated emission from an GaN epilayer at 77K and at room temperature grown by reactive ion-beam molecular beam epitaxy. The observed UV optical emission profile was a nonlinear function of the pump power density, with line narrowing at threshold power densities. The similarity in the emission profile as compared with those of films grown with low-pressure metal-organic chemical vapor deposition and metal-organic vapor phase epitaxy techniques will be noted. DOE

N94-27729# International Centre for Theoretical Physics, Trieste (Italy).
HYPERFINE STRUCTURE OF POSITRONIUM ENERGY LEVELS IN A CRYSTAL
I. V. Bondarev and S. A. Kuten Jul. 1993 8 p
(DE94-603898; IC-93/226) Avail: CASI HC A02/MF A01 (US Sales Only)

Hyperfine structure of positronium energy levels in crystal solids with noncubic lattice is considered. It is shown that due to the hyperfine interaction between the electron and the positron positronium atom in a crystal can have effective quadrupole moment and tensor polarizability. In such a case the effective quadrupole interaction with intracrystalline fields leads to the quadrupole splitting of triplet level and also to the positronium magnetic quenching anisotropy in the presence of external magnetic field. The possibilities of experimental observation of such anisotropy are discussed.
DOE

N94-27753# Sandia National Labs., Albuquerque, NM.
HIGH TEMPERATURE GRAIN GROWTH AND OXIDATION OF Fe-29Ni-17Co (KOVAR (TM)) ALLOY LEADS
J. J. Stephens, F. A. Greulich, and L. C. Beavis 1993 34 p Presented at the Minerals, Metals, and Materials Society/American Society for Metals (TMS/ASM) Materials Week 1992, Chicago, IL, 2-5 Nov. 1992
(Contract DE-AC04-94AL-85000)
(DE94-004691; SAND-93-2168C; CONF-9211117-12) Avail: CASI HC A03/MF A01

One important application for the Fe-29Ni-17Co (Kovar(trademark)) alloy in wire form is in brazed feed through assemblies which are integral parts of vacuum electronic devices. Since Cu metal brazes are performed at process temperatures of about 1100 C, there is opportunity for significant grain growth to occur during the brazing operation. Additional high temperature exposure includes decarburization of the Fe-29Ni-17Co alloy wire in wet hydrogen for 30 min. at 1000 C prior to the Cu brazing operation. Two approaches were used to characterize grain growth in two lots of Fe-29Ni-17Co alloy: (1) a once-through processing study to study the effect of one-time-only device thermal processing on the resulting grain size, and (2) an isothermal grain growth study involving various times at 800-1100 C. The results of the once-through processing study indicate that acceptable grain sizes are obtained from both cold worked and mill-annealed wire lots following Cu brazing. The isothermal grain growth study indicates that the linear intercept distance for Fe-29Ni-17Co can be described with a power law function of time, and that thermal exposure must be controlled at temperatures in excess of 900 C in order to avoid excessive grain growth. A second study characterized the oxidation kinetics of Fe-29Ni-17Co alloy wire in air at temperatures ranging from 550-700 C. This study indicates the parabolic growth law applies for this material, and between 550 and 700 C, oxidation in this alloy occurs at an activation energy of 27.9 kcal/mole. Other oxidation studies at higher temperatures (greater than 750 C) indicate an activation energy of 52.2 kcal/mole for oxidation of Fe-29Ni-17Co alloy at temperatures greater than 790 C. Quantitative point analyses of the oxide scale formed at 600 C suggest that a significant fraction of the scale is close to the stoichiometry of the Fe2O3-type oxide.
DOE

N94-27756# Tokyo Univ. (Japan). Inst. for Solid State Physics.
TECHNICAL REPORT OF ISSP. SER. A, NO. 2677: OCTA-TWIN MODEL OF TETRAPOD ZnO CRYSTALS
Shin Takeuchi, Hiroshi Iwanaga, and Mitsuhiro Fujii (Nagasaki Univ., Japan.) May 1993 15 p
(ISSN 0082-4798)
(JTN-94-80563) Avail: CASI HC A03/MF A01

The characteristic morphology of tetrapod-shaped ZnO particles grown by oxidizing zinc vapor in air has been thoroughly interpreted by the growth process from octahedral multiple-twin embryos. The origin of the tetrapod-shape consists in: (1) formation of the octahedral multiple-twin due to small c/a ratio of the wurtzite ZnO; (2) inversion-type twin boundaries; and (3) a large growth anisotropy with respect to the crystal polarity.
Author (NASDA)

N94-27757# Oak Ridge National Lab., TN.
ELECTRON MICROSCOPY STUDIES OF UNDOPED AND PHOSPHORUS DOPED Si:H AND Si,C:H FILMS
Y. L. Chen (North Carolina State Univ., Raleigh.), C. Wang (North Carolina State Univ., Raleigh.), G. Lucovsky (North Carolina State Univ., Raleigh.), D. M. Maher (North Carolina State Univ., Raleigh.), and J. Bentley 1993 7 p Presented at the Spring Meeting of the Materials Research Society, San Francisco, CA, 12-16 Apr. 1993
(Contracts DE-AC05-84OR-21400; DE-AC05-76OR-00033)
(DE94-004738; CONF-930405-52) Avail: CASI HC A02/MF A01

Microstructure of undoped and phosphorus doped Si:H and Si,C:H films was analyzed by selected-area diffraction, conical dark-field imaging, energy-dispersive x-ray spectroscopy, and electron energy-loss spectroscopy in transmission electron microscopes. Thin films were synthesized by remote plasma-enhanced chemical vapor deposition and characterized in terms of degree of crystallinity. Distribution of phosphorus in Si:H and Si,C:H films, and of carbon in Si,C:H films was evaluated. Results indicate that (1) the microstructure of a film may be two phase, consisting of silicon microcrystallites in an amorphous matrix, (2) phosphorus doping as well as the presence of carbon influences the degree of crystallinity by reducing the average size and volume fraction of microcrystallites, (3) the presence of carbon and phosphorus doping completely suppresses the crystalline phase, (4) phosphorus is distributed at approximately the same concentration in both the crystalline and amorphous phases of diphasic films, and (5) carbon is detected in the amorphous phase of the Si,C:H films. DOE

N94-27790# Sandia National Labs., Albuquerque, NM.
THERMALLY STABLE OXYGEN AND NITROGEN IMPLANT ISOLATION OF C-DOPED Al(0.35)Ga(0.65)As
J. C. Zolper, M. E. Sherwin, A. G. Baca, and R. P. Schneider, Jr. 1993 6 p Presented at the Fall Meeting of the Materials Research Society (MRS), Boston, MA, 29 Nov. - 3 Dec. 1993
(Contract DE-AC04-94AL-85000)
(DE94-004799; SAND-93-1509C; CONF-931108-28) Avail: CASI HC A02/MF A01

Oxygen and nitrogen ion implantation were applied to C-doped Al(0.35)Ga(0.65)As layers to produce high resistivity regions (rho)(sub s) greater than or equal to 1 x 10(exp 10) (Omega)/(open square) that are stable after annealing at 900 C. A dose threshold for stable compensation for both O and N ions was found above 8 x 10(exp l3) cm(sup -2) for samples doped at 2 x 10(exp l8) cm(sup -3). Although O implantation was reported to form stable compensation in Si-doped and Be-doped AlGaAs, the ability of nitrogen implantation to produce thermally stable compensation was not previously reported and may be due to a C-N complex. The existence of this C-N complex is supported by results for O- and N-implants into C-doped GaAs where N formed thermally stable compensation but O did not. Sheet resistance data versus anneal temperature and estimates of the depth of the defect levels are reported. This result will have application to heterojunction bipolar transistors and complementary heterostructure field effect transistor technologies that employ C-doped AlGaAs or GaAs layers along with high temperature post-isolation processing. DOE

N94-27819 International Centre for Theoretical Physics, Trieste (Italy).
IMAGE POTENTIAL OF A TUNNELLING ELECTRON MOVING NEAR TWO DIFFERENT METALS
Do Nam Aug. 1993 11 p Limited Reproducibility: More than 20% of this document may be affected by microfiche quality
(DE94-603657; IC-93/251) Avail: CASI HC A03 (US Sales Only)

The image potential of a tunnelling electron near two metal surfaces is studied by calculating its self-energy, applying hydrodynamic model for two different metals separated by a narrow vacuum gap. The self-energy is calculated for its motion in every metal and in the vacuum gap between them. The most important limiting cases for the self-energy are also derived. Agreement between our results in corresponding limits with previous ones is shown.
DOE

N94-27828# Los Alamos National Lab., NM.
DAMAGE GROWTH IN MgAl2O4 CRYSTALS BY Xe ION IRRADIATIONS
Ning Yu, M. Nastasi, M. G. Hollander, C. R. Evans, C. J. Maggiore, K. E. Sickafus, and J. R. Tesmer 1993 6 p Presented at the Fall Meeting of the Materials Research Society (MRS), Boston, MA, 29 Nov. - 3 Dec. 1993
(Contract W-7405-eng-36)
(DE94-005009; LA-UR-93-4326; CONF-931108-31) Avail: CASI HC A02/MF A01

We have studied damage kinetics in single crystal MgAl2O4 (spinel) with (100) orientation under 370 keV Xe ion irradiations at temperatures of -100 and 400 C. In-situ Rutherford Backscattering Spectrometry (RBS) and ion channeling have been used to monitor the damage accumulation in spinel following sequential Xe ion irradiations. A significant temperature effect on the irradiation damage has been found. Channeling data show that at -100 C, the irradiated spinel layer reaches the same level as in a random spectrum at a dose of 8 x 10(exp 15) Xe/cm(exp 2) (20 DPA for peak damage), while at 400 C, the near surface region (50 nm) remains single-crystalline up to 2 x 10(exp I6) Xe/cm(exp 2). DOE

N94-27843 China Nuclear Information Centre, Beijing.
HYPERSENSITIVE TRANSITION SPECTRUM OF f-ELEMENT AND COORDINATION STRUCTURE
Cao Xuan (Tsinghua Univ., Bejing, China.), Song Chongli (Tsinghua Univ., Bejing, China.), and Zhu Yongjun (Tsinghua Univ., Bejing, China.) Oct. 1992 12 p Limited Reproducibility: More than 20% of this document may be affected by microfiche quality
(DE94-604133; CNIC-00673; TSHUNE-0053) Avail: CASI HC A03 (US Sales Only)

Some f-f transitions of Ln(An) metallic ions have particular super-sensitivity to the change of coordination environments. This is called super-sensitive transitions. Based on the irreducible tensor operator method, a computation model and corresponding computer program for calculating the hypersensitive transition spectrum of f-element were developed. By comparing the theoretical spectra of all possible coordination structures with the experimental one, the possible coordination structures of complex can be determined. The coordination structures of Nd(3+), Er(3+) hydrate, and their extraction complex with H(DEHP) were successfully determined by this method, and the experimental spectra were also assigned. DOE

N94-27859# Joint Inst. for Nuclear Research, Dubna (USSR). Lab. of Theoretical Physics.
AXIAL ANOMALY IN e(+)e(-) YIELDS GAMMA GAMMA AND ANYON SUPERCONDUCTIVITY
O. V. Teryaev 1993 8 p
(DE94-606406; JINR-E-2-93-25) Avail: CASI HC A02/MF A01 (US Sales Only)

The spin-dependent total cross-section of e(+) e(-) yields gamma gamma is shown to have a delta (q(exp 2)) singularity for m(sub e) approaches 0. The relation to some problems of anion superconductivity is discussed. DOE

N94-27974 McMaster Univ., Hamilton (Ontario). Faculty of Graduate Studies.
ANISOTROPY IN THE ELECTRICAL, MAGNETIC AND OPTICAL PROPERTIES OF Pb2Sr2RCu3O8 Ph.D. Thesis
Maureen Reedyk Sep. 1992 259 p
(ISBN-0-315-84930-4; CTN-94-61109) Copyright Avail: Micromedia Ltd., Technical Information Centre, 240 Catherine Street, Suite 305, Ottawa, Ontario, K2P 2G8, Canada HC/MF

Measurements of anisotropy in the magnetization, direct current resistivity, and optical properties of Pb2Sr2(Y/Ca) Cu3O8 (PSYCCO) superconductors are presented. The in-plane and c-axis fundamental superconducting parameters of the material were extracted from analysis of the magnetization measurements. The optically derived plasma frequency is considerably smaller while the resistivity is an order of magnitude larger than in both Bi-Sr-Ca and Y-Ba cuprate superconductors. Along with large penetration depth, this suggests that the carrier concentration is unusually small given the high (about 80 K) transition temperature (Tc) and represents a significant deviation from a proposed universal relationship between the level of doping and Tc. The extent of anisotropy in this system is similar to that in YBa2Cu3O(7-x). The doping dependence of the ab-plane optical properties is investigated via the Ca-free Pb2Sr2RCu3O8 series, which exhibits a metal to insulator transition with increasing ionic radius of the rare earth R. In this progression, phonons in the far infrared reflectance of the insulating members become weaker while new phonon modes appear. Examination of several high-Tc superconductors with similar structure leads to the hypothesis that these features are due to the coupling of longitudinal c-axis phonons to the ab-plane mid infrared continuum. Author (CISTI)

N94-27995# International Centre for Theoretical Physics, Trieste (Italy).
FERMI SURFACE RIDGE AT SECOND AND THIRD UMKLAPP POSITRON ANNIHILATIONS IN Y Ba2Cu3O(7-DELTA)
G. Adam, S. Adam, B. Barbiellini (Geneva Univ., Switzerland.), L. Hoffmann (Geneva Univ., Switzerland.), A. A. Manuel (Geneva Univ., Switzerland.), S. Massidda (Institut Romand de Recherche Numerique en Physique des Materiaux, Lausanne, Switzerland.), and M. Peter (Institute of Physics and Nuclear Engineering, Bucharest, Romania.) Jun. 1993 12 p
(DE93-634760; IC-93/155) Avail: CASI HC A03/MF A01 (US Sales Only)

Results of statistical noise smoothing of the electron momentum distribution obtained by two-dimensional angular correlation of the electron-positron annihilation radiation technique on untwinned YBa2Cu3O(7-delta) single crystals are reported. Two distinct signatures of the sheet of Fermi surface related to the CuO chains (the ridge) are resolved. The first occurs at second Umklapp processes, in agreement with previous evidence. The second one, identified for the first time, occurs at third Umklapp processes. Comparison with FLAPW calculations confirms this result. DOE

N94-28067# Sandia National Labs., Albuquerque, NM.
ADSORPTION AND DESORPTION STUDIES OF CESIUM ON SAPPHIRE SURFACES
K. R. Zavadil and J. L. Ing (AEA Technology, Albuquerque, NM.) 1993 8 p Presented at the 11th Symposium on Space Nuclear Power Systems, Albuquerque, NM, 9-13 Jan. 1994
(Contract DE-AC04-94AL-85000)
(DE94-003798; SAND-93-2545C; CONF-940101-27) Avail: CASI HC A02/MF A01

Adsorption/desorption were studied using combined surface analytical techniques. An approximate initial sticking coefficient for Cs on sapphire was measured using reflection mass spectrometry and found to be 0.9. Thermal desorption mass spectrometry (TDMS) and auger electron spectroscopy (AES) were used to verify that a significant decrease in sticking coefficient occurs as the Cs coverage reaches a critical submonolayer value. TDMS analysis demonstrates that Cs is stabilized on a clean sapphire surface at temperatures (1200 K) in excess of the temperatures experienced by sapphire in a TOPAZ-2 thermionic fuel element (TFE). Surface contaminants on sapphire can enhance Cs adsorption relative to the clean surface. C contamination eliminates the high temperature state of Cs desorption found on clean sapphire but shifts the bulk of the Cs desorption from 400 to 620 K. Surface C is a difficult contaminant to remove from sapphire, requiring annealing above 1400 K. Whether Cs is stabilized on sapphire in a TFE environment will most likely depend on relation between surface contamination and surface structure. DOE

N94-28225 Department of the Navy, Washington, DC.
SUPERCONDUCTING FIBERS MADE WITH YTTRIUM AND YTTRIUM OXIDE INTERLAYERS AND BARIUM CUPRATE COVER LAYERS Patent
Amarnath P. Divecha, inventor (to Navy) and James M. Kerr, inventor (to Navy) 19 Oct. 1993 4 p Filed 31 Oct. 1991
(AD-D016073; US-Patent-5,254,529; US-Patent-Appl-SN-790725; US-Patent-Class-505-1) Avail: US Patent and Trademark Office

A high temperature superconducting wire or yarn is presented. The wire is coated with three layers: (1) yttria, (2) barium cuprate, and (3) superconducting YBa2Cu3O(7-x) formed at the interface between the first and third layers. The wire can be yttrium, and the yarn can be alumina. DTIC

N94-25564# National Research Inst. for Metals, Tokyo (Japan). Materials Physics Div.
STUDY ON COMPUTERIZED EXPERIMENT OF AMORPHOUS TRANSFORMATION PROCESS BY SOLID PHASE REACTION [KOSO HANNO NI YORU AMORUFASU SEISEI KATEI NO KEISANKI JIKKEN NI KANSURU KENKYU]
Katsuyuki Kusunoki, Masato Enomoto, and Tamio Oguchi *In its* Bulletin of National Research Institute for Metals in Fiscal Year 1993, No. 14 29 Jan. 1993 p 173-185 In JAPANESE (For primary document see N94-25544 07-26)
Avail: CASI HC A03/MF A04

N94-25571# National Research Inst. for Metals, Tokyo (Japan). Surface and Interface Div.
STUDY ON MICROSCOPIC STRUCTURAL CONTROLS AND ELECTRONIC PROPERTIES AT MATERIAL SURFACES BY ION BEAMS [BIMUHO NI YORU HYOMEN KAIMEN NO BISHITEKI KOZO SEIGYO TO DENSHI BUSSEI NI KANSURU KISOTEKI KENKYU]
Kazuo Saito, Masatsugu Kaise, Tadahisa Matsushima, Mitsuru Uehara, Shozo

Ikeda, and Kazunori Hayashi *In its* Bulletin of National Research Institute for Metals in Fiscal Year 1993, No. 14 29 Jan. 1993 p 253-257 In JAPANESE (For primary document see N94-25544 07-26)
Avail: CASI HC A01/MF A04

N94-25572# National Research Inst. for Metals, Tokyo (Japan). Advanced Materials Processing Div.
STUDY ON PRODUCTION OF MATERIALS WITH ONE DIRECTION SOLIDIFICATION TEXTURE [ICHIHOKO GYOKO SOSHIKI ZAIRYO NO SOSEI NI KANSURU KENKYU]
Akira Sato, Toru Namai, Yoshiaki Osawa, and Goro Aragane *In its* Bulletin of National Research Institute for Metals in Fiscal Year 1993, No. 14 29 Jan. 1993 p 259-268 In JAPANESE (For primary document see N94-25544 07-26)
Avail: CASI HC A02/MF A04

N94-27367*# Rutgers Univ., New Brunswick, NJ. Dept. of Computer Science.
UTILITY FOG: A UNIVERSAL PHYSICAL SUBSTANCE
J. Storrs Hall *In* NASA. Lewis Research Center, Vision 21: Interdisciplinary Science and Engineering in the Era of Cyberspace Dec. 1993 p 115-126 (For primary document see N94-27358 07-12)
Avail: CASI HC A03/MF A03

N94-28160# Tohoku Univ., Sendai (Japan). Inst. for Advanced Materials Processing.
STRUCTURAL STUDY OF Cu/Co MULTILAYER BY ANOMALOUS SMALL-ANGLE X RAY SCATTERING
Eiichiro Matsubara and Yoshio Waseda *In its* The Science Reports of the Research Institutes, Tohoku University. Series A: Physics, Chemistry, and Metallurgy. Volume 38, No. 1: Amorphous Materials 14 29 Mar. 1993 p 14-23 (For primary document see N94-28158 07-26)
Avail: CASI HC A02/MF A02

N94-28161# Tohoku Univ., Sendai (Japan). Inst. for Materials Research.
DIFFERENTIAL SCANNING CALORIMETRIC STUDY OF SOLID STATE AMORPHIZATION AND CRYSTALLIZATION IN Zr/Co AND Zr/Ni MULTILAYERS
Tomoyasu Aihara, Jr., Kiyoshi Aoki, and Tsuyoshi Masumoto *In its* The Science Reports of the Research Institutes, Tohoku University. Series A: Physics, Chemistry, and Metallurgy. Volume 38, No. 1: Amorphous Materials 14 29 Mar. 1993 p 24-33 (For primary document see N94-28158 07-26)
Avail: CASI HC A02/MF A02

N94-28162# Tohoku Univ., Sendai (Japan). Inst. for Materials Research.
NMR STUDY OF QUASICRYSTAL Al(70)Pd(20)T(M10) ALLOY (T(M):Cr, Mn, Fe, AND Co)
Takeshi Shinohara and Takashi Sato *In its* The Science Reports of the Research Institutes, Tohoku University. Series A: Physics, Chemistry, and Metallurgy. Volume 38, No. 1: Amorphous Materials 14 29 Mar. 1993 p 34-42 (For primary document see N94-28158 07-26)
Avail: CASI HC A02/MF A02

N94-28163# Tohoku Univ., Sendai (Japan). Inst. for Materials Research.
FORMATION AND CRYSTALLIZATION OF HYDROGEN-INDUCED AMORPHOUS Ti3InH(4.5) ALLOY
Katsuhiko Mori, Kiyoshi Aoki, and Tsuyoshi Masumoto *In its* The Science Reports of the Research Institutes, Tohoku University. Series A: Physics, Chemistry, and Metallurgy. Volume 38, No. 1: Amorphous Materials 14 29 Mar. 1993 p 43-52 (For primary document see N94-28158 07-26)
Avail: CASI HC A02/MF A02

77 THERMODYNAMICS AND STATISTICAL PHYSICS

Includes quantum mechanics; theoretical physics; and Bose and Fermi statistics.

For related information see also *25 Inorganic and Physical Chemistry* and *34 Fluid Mechanics and Heat Transfer.*

N94-25852 International Centre for Theoretical Physics, Trieste (Italy).
BIEXCITON FORMATION BY TWO-PHOTON ABSORPTION IN QUANTUM WELLS
A. R. Hassan Sep. 1992 7 p Limited Reproducibility: More than 20% of this document may be affected by microfiche quality
(DE93-613551; IC-92/222) Avail: CASI HC A02 (US Sales Only)

Direct creation of biexciton states by two-photon absorption in quantum well structure semiconductors is investigated theoretically. The two-photon transition rate to biexciton as a final state is analytically calculated for both photon polarization configurations. The biexciton matrix element has been estimated adopting a more accurate variational parameters wave functions. A numerical application for GaAs Quantum Well (QW) shows that the biexciton two-photon absorption coefficient, alpha(sup 2) (bie(chi)) for both polarization is enhanced over the exciton two-photon absorption coefficient, alpha(sup 2) (e(chi)), by an order of magnitude. This enhancement is, essentially, found to arise from the resonance effect and the structure of the matrix elements involved in the two processes. Furthermore, alpha(sup 2) (bie(chi)), in GaAs QW is four order of magnitude larger than alpha(sup 2) (bie(chi)) in bulk GaAs. This large increase is due to the spatial confinement of the carriers in the QW. DOE

N94-25882# International Centre for Theoretical Physics, Trieste (Italy).
TOPOLOGICAL AMPLITUDES IN STRING THEORY
I. Antoniadis (Ecole Polytechnique, Palaiseau, France.), E. Gava, K. S. Narain, and T. R. Taylor (Northeastern Univ., Boston, MA.) Jul. 1993 33 p
(DE94-601561; IC-93/202; NUB-3071; CPTH-A258/0793) Avail: CASI HC A03/MF A01 (US Sales Only)

It was shown that certain type II string amplitudes at genus g are given by the topological partition F(sub g) discussed recently by Bershadsky, Cecotti, Ooguri and Vafa. These amplitudes give rise to a term in the four-dimensional effective action of the form Sigma(sub g)F(sub g)W(sup 2g), where W is the chiral superfield of N = 2 supergravitational multiplet. The holomorphic anomaly of F(sub g) is related to non-localities of the effective action due to the propagation of massless states. This result generalizes the holomorphic anomaly of the one loop case which is known to lead to non-harmonic gravitational couplings. DOE

N94-25883# International Centre for Theoretical Physics, Trieste (Italy).
ON STRING THEORY INTERACTING WITH TWO-DIMENSIONAL GRAVITY
I. L. Buchbinder (Tomsk State Univ., USSR.), I. L. Shapiro, and A. G. Sibiryakov (Tomsk State Univ., USSR.) Jul. 1993 11 p
(DE94-601562; IC-93/206) Avail: CASI HC A03/MF A01 (US Sales Only)

The approach to the unification of the string theory and the two-dimensional gravity is proposed. It is shown that, up to the one-loop order, the nonlinear D-dimensional sigma-model coupled to the induced local quantum gravity is equivalent to some special (renormalizable) D + 2-dimensional nonlinear sigma-model on the classical gravitational background. The requirement of the Weyl invariance of the effective action leads to some consistency equations for the D + 2-model background fields. These equations may be reduced to the equations for the D-dimensional-sigma-model. DOE

N94-25911 Weizmann Inst. of Science, Rehovoth (Israel).
ASPECTS OF NONRENORMALIZABLE TERMS IN A SUPERSTRING STANDARD-LIKE MODELS
Alon E. Faraggi Jun. 1992 28 p Limited Reproducibility: More than 20% of this document may be affected by microfiche quality
(DE93-614530; WIS-PH-92-48; SLAC-PUB-5845) Avail: CASI HC A03 (US Sales Only)

I investigate the role of nonrenormalizable terms, up to order N=8, in a superstring derived standard-like model. I argue that nonrenormalizable terms restrict the gauge symmetry, at the Planck scale, to be SU(3)xSU(2)xU(1)(sub B-L)xU(1)(sub T(sub 3R)) rather than SU(3)xSU(2)xU(1)(sub Y). I show that the breaking the gauge symmetry directly to the Standard Model leads to breaking the supersymmetry at the Planck scale, or to dimension four, baryon and lepton violating, operators. I show that if the gauge symmetry is broken directly to the Standard Model the cubic level solution to the F and D flatness constraints is violated by higher order terms, while if U(1)(sub Z') remains unbroken at the Planck scale, the cubic level solution is valid to all orders of nonrenormalizable terms. I discuss the Higgs and fermion mass spectrum. I demonstrate that realistic, hierarchical, fermion mass spectrum can be generated in this model. DOE

N94-26036# Gosudarstvennyi Komitet po Ispolzovaniyu Atomnoi Energii, Serpukhov (USSR).
QUANTIZABLE CONFIGURATIONS OF THE RELATIVISTIC STRING
I. N. Nikitin 1992 24 p
(DE93-634346; IHEP-OTF-92-74) Avail: CASI HC A03/MF A01 (US Sales Only)

In a phase space of the classical bosonic string submanifolds have been found, whose quantization is free of anomaly. Such submanifolds consist of string configurations with axial symmetry and some of their superpositions. DOE

N94-26037# Gosudarstvennyi Komitet po Ispolzovaniyu Atomnoi Energii, Serpukhov (USSR).
DYNAMICAL GROUP OF RELATIVISTIC STRAIGHT-LINE STRING
G. P. Pronko and O. L. Zorin 1992 12 p
(DE93-634347; IHEP-OTF-92-92) Avail: CASI HC A03/MF A01 (US Sales Only)

The relativistic straight-line string is described in terms of orbits of co-adjoint representation of non-compact groups. The description is based on the Kirillov construction. A formulation of the straight-line string analogous to Bargmann-Wigner formalism for high spin particles is found. DOE

N94-26039# Gosudarstvennyi Komitet po Ispolzovaniyu Atomnoi Energii, Serpukhov (USSR).
Z(SUB N)(SUP n-1) BROKEN MODEL
S. M. Sergeev 1992 4 p
(DE93-634357; IHEP-TD-92-7) Avail: CASI HC A01/MF A01 (US Sales Only)

Using the psi-vectors method for the Belavin elliptic R matrix the A(sub n-1) generalization of the Kashiwara-Miwa model is obtained. DOE

N94-26417# International Centre for Theoretical Physics, Trieste (Italy).
VORTICES IN CURVED SPACETIME
J. D. Edelstein, F. A. Schaposnik, and G. Lozano Jul. 1993 11 p
(DE94-601559; IC-93/185) Avail: CASI HC A03/MF A01 (US Sales Only)

We study an Abelian Higgs model coupled to a background metric. We find Bogomol'nyi equations when the coupling is achieved through an R(phi)(sup 2) term (R being the scalar curvature and phi the Higgs scalar). Remarkably, these equations coincide with those arising in models where the gauge field dynamics is governed by a Chern-Simons term so that vortex solutions in our system can be related to self-dual Chern-Simons vortices. DOE

N94-26453# Gosudarstvennyi Komitet po Ispolzovaniyu Atomnoi Energii, Serpukhov (USSR). Inst. Fiziki Vysokikh Ehnergij.
COMPONENT STRUCTURE OF THE N = 2 SUPER-YANG-MILLS THEORY IN THE HARMONIC SUPERSPACE
A. A. Maslikov and G. G. Volkov 1992 14 p
(DE93-634340; IHEP-OTF-92-100) Avail: CASI HC A03/MF A01 (US Sales Only)

The specific features of massless and massive N=2 super-Yang-Mills theories are studied. In the frame of the harmonic superspace formalism, the component of the superstrength and free Lagrangian of the vector multiplet will be found without fixing a concrete supergauge for the Abelian case. Starting with the Abelian superstrength, find the form of the non-Abelian superstrength in the first order of the coupling constant g, not fixing the supergauge. In conclusion the approach analogous to the Stueckelberg method, was used to obtain the component Lagrangian of the massive N=2 Yang-Mills theory in the first order of the couplig constant g. DOE

N94-26461 International Centre for Theoretical Physics, Trieste (Italy).
QUANTUM GROUP AND MANIN PLANE RELATED TO A COLORED BRAID GROUP REPRESENTATION
B. Basu-Mallick Jul. 1993 20 p Limited Reproducibility: More than 20% of this document may be affected by microfiche quality
(DE94-601509; IC-93/219) Avail: CASI HC A03 (US Sales Only)

By considering 'colored' braid group representation, a quantum group was obtained, which reduces to the standards GL(sub q)(2) and GL(sub pq)(2) cases at some particular limits of the 'color' parameters. In spite of quite complicated nature, all of these new quantum group relations can be expressed neatly in the Heisenberg-Weyl form, for a nontrivial choice of the basis elements. Furthermore, it is possible to associate invariant Manin planes, parametrized by the 'color' variables, with such quantum group structure. DOE

N94-26503 Joint Inst. for Nuclear Research, Dubna (USSR). Lab. of Theoretical Physics.
GRAVITATIONAL FIELD OF A POINT MASS IN THE LOBACHEVSKIJ SPACE [GRAVTATSIONNOE POLE SOSREDOTOCHENNOJ MASY V PROSTRANSTVE LOBACHEVSKOGO]
N. A. Chernikov 1992 26 p In RUSSIAN Limited Reproducibility: More than 20% of this document may be affected by microfiche quality
(DE93-634333; JINR-R-2-92-108) Avail: CASI HC A03 (US Sales Only)

The problems of the gravitational field of point mass in the Lobachevskij space is solved. In the nonrelativistic case this problems was solved by Lobacheskij himself. The obtained metric depends on the Lobachevskij constant k for the visible world and turns into the known Schwarzchild metric in the limit k tends to infinity. DOE

N94-26541# Nationaal Inst. voor Kernfysica en Hoge Energiefysica, Amsterdam (Netherlands).
ANOMALY CANDIDATES AND INVARIANTS OF D 4, N 1 SUPERGRAVITY THEORIES
Friedemann Brandt (Technische Univ., Hanover, Germany.) 1993 19 p
Sponsored by DFG
(NIKHEF-H/93-12; ITP-UH-07/93; ETN-94-95044) Avail: CASI HC A03/MF A01

Anomaly candidates and the form of the most general invariant local action are given. Old and new minimal supergravity, including the cases where additional Yang-Mills and Chiral matter multiplets are present, are discussed. Nonmininal supergravity is discussed. In this case local supersymmetry itself may be anomalous. Some of the corresponding anomaly candidates are given. The results are obtained by solving the descent equations. The BRS operator for supergravity is given. The basic features and the field content of old, new, and nonminimal supergravity are stressed. ESA

N94-26551 International Centre for Theoretical Physics, Trieste (Italy).
THE EXTENSIONS OF SPACE-TIME. PHYSICS IN THE 8-DIMENSIONAL HOMOGENEOUS SPACE D IS EQUAL TO SU(2,2)/K
A. O. Barut Jul. 1993 15 p Limited Reproducibility: More than 20% of this document may be affected by microfiche quality
(DE93-634336; IC-93/166) Avail: CASI HC A03 (US Sales Only)

The Minkowski space-time is only a boundary of a bigger homogeneous space of the conformal group. The conformal group is the symmetry group of our most fundamental massless wave equations. These extended groups and spaces have many remarkable properties and physical implications. DOE

N94-26553# Gosudarstvennyi Komitet po Ispolzovaniyu Atomnoi Energii, Serpukhov (USSR). Inst. Fiziki Vysokikh Ehnergij.
ON KINETIC EXPANSION IN SCALAR FIELD THEORY [O KINETICHESKOM RAZLOZHENII V SKALYARNOJ TEORII POLYA]
V. E. Rochev 1992 18 p In RUSSIAN
(DE93-634338; IFVE-OTF-92-103) Avail: CASI HC A03/MF A01 (US Sales Only)

A method kinetic expansion summation based on the self-consistent expansion with the help of second Legendre transform was proposed. The self-consistent kinetic expansion solves two principal problems of the strong coupling expansion: the interpretation problem and the problem of ultraviolet cutoff removal (renormalization). DOE

N94-26758 International Centre for Theoretical Physics, Trieste (Italy).
WIGNER QUANTUM OSCILLATORS
T. D. Palev and N. I. Stoilova (Ghent Univ., Belgium.) Jul. 1993 8 p Limited Reproducibility: More than 20% of this document may be affected by microfiche quality
(DE94-601508; IC-93/190) Avail: CASI HC A02 (US Sales Only)

We present three groups of noncanonical oscillators. The position and the momentum operators of each of the groups generate basic Lie superalgebras, namely sl(1/3), osp(1/6) and osp(3/2). The sl(1/3)-oscillators have finite energy spectrum and finite-dimensions. The osp(1/6)-oscillators are related to the para-Bose statistics. The internal angular momentum s of the osp(3/2)-oscillators takes no more than three (half)integer values. In a particular representation $s = 1/2$. DOE

N94-26805# Los Alamos National Lab., NM.
QUANTUM STATISTICAL INFERENCE FOR DENSITY ESTIMATION
R. N. Silver, H. F. Martz, and T. Wallstrom 1993 10 p Presented at the Joint American Statistical Association (ASA), Institute of Mathematics, Statistics, and Biometrics Society Conference, San Francisco, CA, 8-12 Aug. 1993
(Contract W-7405-eng-36)
(DE94-002625; LA-UR-93-3552; CONF-9308107-4) Avail: CASI HC A02/MF A01

A new penalized likelihood method for non-parametric density estimation is proposed, which is based on a mathematical analogy to quantum statistical physics. The mathematical procedure for density estimation is related to maximum entropy methods for inverse problems; the penalty function is a convex information divergence enforcing global smoothing toward default models, positivity, extensivity and normalization. The novel feature is the replacement of classical entropy by quantum entropy, so that local smoothing may be enforced by constraints on the expectation values of differential operators. Although the hyperparameters, covariance, and linear response to perturbations can be estimated by a variety of statistical methods, we develop the Bayesian interpretation. The linear response of the MAP estimate is proportional to the covariance. The hyperparameters are estimated by type-II maximum likelihood. The method is demonstrated on standard data sets. DOE

N94-26837 International Centre for Theoretical Physics, Trieste (Italy).
CALCULATING THE SURFACE PROPERTIES FOR THE LIQUID-VAPOUR INTERFACE: ILLUSTRATING THE THERMODYNAMIC STABILITY OF THE SPHERICAL MICROSTRUCTURES
S. M. Osman Jun. 1993 13 p Limited Reproducibility: More than 20% of this document may be affected by microfiche quality
(DE94-601992; IC-93/152) Avail: CASI HC A03 (US Sales Only)

Results of calculations of the equilibrium density profile and related surface properties for liquid-vapor interface of simple fluids are presented. The interface was considered (1) Planar, (2) Spherical, with some attention to the stability of small liquid droplets. These calculations are based on the Density Functional Theory (DFT), in particular, the gradient approximation, in conjunction with the simplified Random Phase Approximation (RPA) Bhatia-Young model for the bulk liquid. DOE

N94-26876# International Centre for Theoretical Physics, Trieste (Italy).
QUANTUM SUBGROUPS AND QUANTUM CO-SET SPACES AND DIFFERENTIAL CALCULI ON THEM
Xiaodong Sun, Shikun Wang (Academia Sinica, Beijing, China.), and Ke Wu (Academia Sinica, Beijing, China.) Jul. 1993 10 p
(DE94-602520; IC-93/195) Avail: CASI HC A02/MF A01 (US Sales Only)

Quantum subgroups and quantum co-set spaces including corresponding differential calculi are discussed. DOE

N94-26896# International Centre for Theoretical Physics, Trieste (Italy).
THERMODYNAMICS AND FORM FACTORS OF SUPERSYMMETRIC INTEGRABLE FIELD THEORIES
Changrim Ahn Jun. 1993 47 p
(DE94-602557; IC-93/144) Avail: CASI HC A03/MF A01 (US Sales Only)

On-shell and off-shell properties of the supersymmetric Sinh-Gordon and perturbed SUSY Yang-Lee models using the thermodynamic Bethe ansatz and form factors were studied. Identifying the supersymmetric models with the Eight Vertex Free Fermion Model, the inversion relation for the inhomogeneous transfer matrix and TBA equations were derived and correct UV results were obtained. Two-point form factors of the trace of energy-momentum tensor using the Watson equations and their SUSY transformations were obtained. As an application, the UV central charge using these form factors and spectral representation of the C-theorem were computed. DOE

N94-27002# New York Univ., New York. Dept. of Physics.
IMPROVED NUMERICAL METHODS FOR QUANTUM FIELD THEORY (OUTSTANDING JUNIOR INVESTIGATOR AWARD)
A. D. Sokal 1 Sep. 1993 6 p
(Contract DE-FG02-90ER-40581)
(DE94-001793; DOE/ER-40581/3) Avail: CASI HC A02/MF A01

New and more efficient numerical methods for problems in quantum field theory are being developed. Our principal goal is to achieve radical reductions in critical slowing-down. At present concentration is on three new families of algorithms: multi-grid Monte Carlo (MGMC), Swendsen-Wang (SW), and generalized Wolff-type embedding algorithms. In addition, a high-precision numerical study of the hyperscaling conjecture for the self-avoiding walk, which is closely related to the triviality problem for (var phi)(sup 4) quantum field theory is in progress. DOE

N94-27024 International Centre for Theoretical Physics, Trieste (Italy).
A NOTE ON RIEMANNIAN 2-SPACE
M. S. Rahman Jul. 1993 6 p Limited Reproducibility: More than 20% of this document may be affected by microfiche quality
(DE94-602560; IC-93/161) Avail: CASI HC A02 (US Sales Only)

A variety of the leading properties of a Riemannian two-space is furnished. The reason why a Ricci flat two-space may be looked upon as a flat space is given. It is established that the Ricci tensor is semi-covariantly constant and that the tensor satisfies a covariantly differential equation or its equivalent an ordinary one with the condition, similar to the latter, involving the derivatives of the components of the fundamental tensors. The necessity and sufficiency of the conditions for the scalar curvature to be constant and for the covariant derivative of a vector to be commutative are found. DOE

N94-27263 Toronto Univ. (Ontario).
QCD CORRECTIONS TO INCLUSIVE B - S PROCESSES IN THE STANDARD MODEL Ph.D. Thesis
Mark M. Sutherland 6 Oct. 1989 138 p
(ISBN-0-315-54572-0; CTN-94-60975) Copyright Avail: Micromedia Ltd., Technical Information Centre, 240 Catherine Street, Suite 305, Ottawa, Ontario, K2P 2G8, Canada HC/MF

The quark-level decays b yields s gamma and b yields s e+ e- are loop induced processes in the Standard Model. They are therefore potentially sensitive to the presence of the top quark as well as to many kinds of new physics beyond that model. The effect of short-distance strong interaction corrections can be large, and a calculation of these leading logarithmic corrections is presented. Three issues of theoretical interest are discussed in detail. First, an examination is made of the validity of applying equations of motion to certain effective operators at an early stage, in order to reduce the size of the operator bias. It is shown that the equations of motion are indeed commutative with renormalization group scaling. Second, a full computation is performed that includes all contributions to the b yields s gamma process which arise from the b yields s gluon process via operator mixing. It is found that all such effects are indeed negligible and that the b yields s gluon process is strongly supported by quantum chromodynamics (QCD). Third, dimensional reduction is proposed as an alternative to dimensional regularization. QCD corrections using both techniques show that results differ. A four dimensional method is discovered by which the discrepancy is resolved in favor of dimensional regularization. Author (CISTI)

N94-27398 McGill Univ., Montreal (Quebec). Dept. of Physics.
ASPECTS OF PERTURBATIVE CORRECTIONS IN QUANTUM CHROMODYNAMICS Ph.D. Thesis
Stavros Papadopoulos Dec. 1989 189 p
(ISBN-0-315-63607-6; CTN-94-60965) Copyright Avail: Micromedia Ltd., Technical Information Centre, 240 Catherine Street, Suite 305, Ottawa, Ontario, K2P 2G8, Canada HC/MF

The perturbative regime of quantum chromodynamics (QCD) is considered, and certain aspects related with higher order corrections (HOC) are studied. Certain large correction terms in the perturbative expansion are determined, in particular, for large transverse momentum direct photon production. The origin of these terms is specified and simple forms called K-factors are provided (soft gluon approach). Furthermore, for processes initiated by 2-2 particle subprocesses, the structure of the complete HOC is analyzed. It is shown that when structure functions and/or fragmentation functions are involved, there is a gauge invariant part that dominates HOC over a sizable kinematic range. Simple and general expressions are derived, allowing an easy calculation of this part. It is also shown that under certain approximations, this part reduces to the form of the simple K-factors. Other aspects of HOC, particularly the dependence on the choice of scales, are considered. Using complete HOC, detailed analysis of recent and old data on large transverse momentum direct photon production is performed. The dependence of the form of the gluon distribution on the choice of the scales is discussed. It is concluded that appreciable ambiguity in this distribution still remains. Author (CISTI)

N94-27401 York Univ. (Ontario).
A VARIATIONAL APPROACH TO THE QUANTUM FIELD THEORETIC BOUND-STATE PROBLEM Ph.D. Thesis
William Peter Dykshoorn Sep. 1990 80 p
(ISBN-0-315-60960-5; CTN-94-60968) Copyright Avail: Micromedia Ltd., Technical Information Centre, 240 Catherine Street, Suite 305, Ottawa, Ontario, K2P 2G8, Canada HC/MF

The bound-state problem in quantum field theory provides a stringent test of ideas about the nature of particle interactions. Most calculational schemes have relied on perturbative methods where an expansion parameter of small magnitude was used. With the advent of quantum chromodynamics (QCD), it quickly became apparent that traditional methods would not suffice to calculate the spectrum of the theory. The variational method was applied to the two-particle bound-state problem in quantum electrodynamics. The coupling constant is allowed to become large in order to study the bound states in the ultra relativistic region. Coupled nonperturbative integral equations are developed variationally and solved numerically. The ansatz does not initially contain explicit photon degrees of freedom, but by systematically improving the calculation they are incorporated. In the latter case, the resulting equations, when perturbatively reduced, yield the correct coefficients. The eigenvalue curves show parity doubling in the spectrum in the ultra relativistic region, pointing to the fact that the massive theory behaves as a massless one in this region. The large spin-dependent splittings which appear in the spectrum are of interest as they are present in the highly relativistic bound systems of QCD. Author (CISTI)

N94-27403 British Columbia Univ., Vancouver.
FINITE DENSITY EFFECTS IN GAUGE THEORIES Ph.D. Thesis
Andre Roberge Jan. 1989 118 p
(ISBN-0-315-50637-7; CTN-94-60970) Copyright Avail: Micromedia Ltd., Technical Information Centre, 240 Catherine Street, Suite 305, Ottawa, Ontario, K2P 2G8, Canada HC/MF

Various effects of finite fermionic densities in gauge theories are studied. The phase structure of SU(N) gauge theories with fermions as a function of imaginary chemical potential is related to the confining properties of the theory. This phase structure is controlled by a remnant of the Z(N) symmetry which is present in the absence of fermions. At high temperature, the theory has a first-order phase transition as a function of imaginary chemical potential. This transition is expected to be absent in the low-temperature phase. It is shown that properties of the theory at nonzero fermion density can be deduced from its behavior at finite imaginary chemical potential. Anomalies in gauge theories are introduced using various two-dimensional models. In particular, the chiral Schwinger model is shown to be consistent despite being anomalous. The effects of finite densities in anomalous gauge theories are investigated. It is found that, contrary to some recent claims, an effective Hamiltonian (obtained by integrating out the fermions) cannot be obtained by the simple inclusion of a Chern-Simons term multiplying the fermionic chemical potential. The importance of dynamical effects is stressed and a mechanism for producing primordial magnetic field is suggested. Author (CISTI)

N94-27626 International Centre for Theoretical Physics, Trieste (Italy).
THE EINSTEIN TENSOR CHARACTERIZING SOME RIEMANN SPACES
M. S. Rahman Jul. 1993 7 p Limited Reproducibility: More than 20% of this document may be affected by microfiche quality
(DE94-603663; IC-93/204) Avail: CASI HC A02 (US Sales Only)

A formal definition of the Einstein tensor is given. Mention is made of how this tensor plays a role of expressing certain conditions in a precise form. The cases of reducing the Einstein tensor to a zero tensor are studied on its merit. An account of results, formulated as theorems, on Einstein symmetric and Einstein recurrent spaces is then presented. DOE

N94-27627 International Centre for Theoretical Physics, Trieste (Italy).
THE SUPER WEIERSTRASS (ZETA)-FUNCTION AND OPERATOR PRODUCT EXPANSIONS IN 2D-INDUCED SUPERGRAVITY ON THE SUPERTORUS
H. Kachkachi and M. Kachkachi Jul. 1993 10 p Limited Reproducibility: More than 20% of this document may be affected by microfiche quality
(DE94-603664; IC-93/210) Avail: CASI HC A02 (US Sales Only)

In order to solve the super Beltrami equations (SBE) on the supertorus, the quasielliptic Weierstrass zeta-function is constructed as the delta-Cuachy kernel thereon. Using this solution the stress-energy tensor is computed, as well as Green functions corresponding to induced supergravity in Polyakov's path integral formalism. This allows the corresponding results to be recovered on the supercomplex plane and the torus. Finally, generalizations to super Riemann surfaces of higher genus are discussed. DOE

N94-27636 International Centre for Theoretical Physics, Trieste (Italy).
COSMIC NO-HAIR IN BRANS-DICKE THEORY
E. Guzman and S. Alam Aug. 1993 6 p Limited Reproducibility: More than 20% of this document may be affected by microfiche quality
(DE94-603673; IC-93/250) Avail: CASI HC A02 (US Sales Only)

Within the context of alternative version of the Brans-Dicke theory, for omega greater than or equal to -3/2, where omega is the Brans-Dicke parameter, the anisotropic Bianchi type cosmological models evolve towards the de Sitter isotropic universe. It is shown that during inflation there is no difference between the Brans-Dicke theory and general relativity. The result can thus be viewed as a generalization of the Wald's theorem for general relativity. DOE

N94-27680# Joint Inst. for Nuclear Research, Dubna (USSR). Lab. of Theoretical Physics.
STOCHASTIC SPACE-TIME, CONFINEMENT POTENTIAL AND PARTICLE PROPAGATOR
Kh. Namsrai 1993 8 p
(DE94-606415; JINR-E-2-93-118) Avail: CASI HC A02/MF A01 (US Sales Only)

Stochastic space-time caused by random strings is considered. Confinement potential and particle propagator are calculated in this induced gravitation. It turns out that force-transmitting quanta become nonlocal and unobservable. Quantum field theory of such objects is nonlocal and free from ultraviolet divergences. DOE

N94-27696 International Centre for Theoretical Physics, Trieste (Italy).
ENHANCEMENT OF THE RATE OF RADIATIVE PROCESSES IN THE FIELD OF A MAGNETIC MONOPOLE
A. O. Barut, Ya. M. Shnir, M. A. Knyazev (Akademiya Nauk BSSR, Minsk.), and E. A. Tolkachev (Akademiya Nauk BSSR, Minsk.) Jul. 1993 9 p Limited Reproducibility: More than 20% of this document may be affected by microfiche quality
(DE94-603717; IC-93/187) Avail: CASI HC A02 (US Sales Only)

The spontaneous emission rate for the bound system charge-dyon is calculated. It is shown that the magnetic monopole field leads to the significant increase of the rate of radiative processes. DOE

N94-27858# Joint Inst. for Nuclear Research, Dubna (USSR). Lab. of Theoretical Physics.

SOLUTION OF THE HEISENBERG EQUATION FOR THE FOUR-FERMION CONTACT INTERACTION BY THE METHOD OF DYNAMICAL MAPPINGS

A. N. Vall (Irkutsk State Univ., USSR.), V. M. Leviant (Irkutsk State Univ., USSR.), and A. V. Sinitskaya (Irkutsk State Univ., USSR.) 1992 22 p
(DE94-606341; JINR-E-2-92-497) Avail: CASI HC A03/MF A01 (US Sales Only)

The paper considers the non-relativistic analog of the Nambu-Jona-Lasinio model and demonstrates, by this most simplified example, the method of dynamical mappings of Heisenberg fields on physical fields. The expressions for one particle eigen-excitation spectrum of full Hamiltonian (spectrum of clad fermions), the wave function of two excitations bound state and its mass, and the Bethe-Solpither amplitude are obtained. The relation for the density of vacuum energy is derived as well as a function of mapping parameters. The minimization of energy leads to the fixation of these parameters. The method admits the generalization of the relativistic case.
DOE

N94-28079# Imperial Coll. of Science and Technology, London (England). Dept. of Mechanical Engineering.

THERMODYNAMICS OF COMBINED CYCLE PLANT

R. I. Crane *In* VKI, Combined Cycles for Power Plants 1993 73 p
(For primary document see N94-28077 07-37)
Copyright Avail: CASI HC A04/MF A04

80 SOCIAL SCIENCES (GENERAL)

Includes educational matters.

N94-25665*# Universities Space Research Association, Houston, TX.

PROCEEDINGS OF THE 8TH ANNUAL SUMMER CONFERENCE: NASA/USRA ADVANCED DESIGN PROGRAM

1992 493 p Conference held in Washington, DC, 15-19 Jun. 1992
(Contract NASw-4435)
(NASA-CR-195118; NAS 1.26:195118) Avail: CASI HC A21/MF A04

Papers presented at the 8th Annual Summer Conference are categorized as Space Projects and Aeronautics projects. Topics covered include: Systematic Propulsion Optimization Tools (SPOT), Assured Crew Return Vehicle Post Landing Configuration Design and Test, Autonomous Support for Microorganism Research in Space, Bioregenerative System Components for Microgravity, The Extended Mission Rover (EMR), Planetary Surface Exploration MESUR/Autonomous Lunar Rover, Automation of Closed Environments in Space for Human Comfort and Safety, Walking Robot Design, Extraterrestrial Surface Propulsion Systems, The Design of Four Hypersonic Reconnaissance Aircraft, Design of a Refueling Tanker Delivering Liquid Hydrogen, The Design of a Long-Range Megatransport Aircraft, and Solar Powered Multipurpose Remotely Powered Aircraft. For individual titles, see N94-25666 through N94-25719.

N94-25666*# Alabama Univ., Huntsville. Dept. of Mechanical Engineering.

SYSTEMATIC PROPULSION OPTIMIZATION TOOLS (SPOT) c61

Mark Bower and John Celestian *In* USRA, Proceedings of the 8th Annual Summer Conference: NASA/USRA Advanced Design Program 1992 p 3-5 (For primary document see N94-25665 07-80)
Avail: CASI HC A01/MF A04

This paper describes a computer program written by senior-level Mechanical Engineering students at the University of Alabama in Huntsville which is capable of optimizing user-defined delivery systems for carrying payloads into orbit. The custom propulsion system is designed by the user through the input of configuration, payload, and orbital parameters. The primary advantages of the software, called Systematic Propulsion Optimization Tools (SPOT), are a user-friendly interface and a modular FORTRAN 77 code designed for ease of modification. The optimization of variables in an orbital delivery system is of critical concern in the propulsion environment. The mass of the overall system must be minimized within the maximum stress, force, and pressure constraints. SPOT utilizes the Design Optimization Tools (DOT) program for the optimization techniques. The SPOT program is divided into a main program and five modules: aerodynamic losses, orbital parameters, liquid engines, solid engines, and nozzles. The program is designed to be upgraded easily and expanded to meet specific user needs. A user's manual and a programmer's manual are currently being developed to facilitate implementation and modification.
Author

N94-25667*# Arizona Univ., Tucson. Dept. of Aerospace and Mechanical Engineering.

AUTONOMOUS SPACE PROCESSOR FOR ORBITAL DEBRIS ADVANCED DESIGN PROJECT IN SUPPORT OF SOLAR SYSTEM EXPLORATION c18

Kumar Ramohalli, Dominique Mitchell, Brett Taft, Paul Chinnock, and Bjoern Kutz *In* USRA, Proceedings of the 8th Annual Summer Conference: NASA/USRA Advanced Design Program 1992 p 6-17 (For primary document see N94-25665 07-80)
Avail: CASI HC A03/MF A04

This paper is regarding a project in the Advanced Design Program at the University of Arizona. The project is named the Autonomous Space Processor for Orbital Debris (ASPOD) and is a NASA/Universities Space Research Association (USRA) sponsored design project. The development of ASPOD and the students' abilities in designing and building a prototype spacecraft are the ultimate goals of this project. This year's focus entailed the development of a secondary robotic arm and end-effector to work in tandem with an existent arm in the removal of orbital debris. The new arm features the introduction of composite materials and a linear drive system, thus producing a light-weight and more accurate prototype. The main characteristic of the end-effector design is that it incorporates all of the motors and gearing internally, thus not subjecting them to the harsh space environment. Furthermore, the arm and the end-effector are automated by a control system with positional feedback. This system is composed of magnetic and optical encoders connected to a 486 PC via two servo-motor controller cards. Programming a series of basic routines and sub-routines has allowed the ASPOD prototype to become more autonomous. The new system is expected to perform specified tasks with a positional accuracy of 0.5 cm.
Author

N94-25668*# California Univ., Los Angeles. Dept. of Mechanical, Aerospace and Nuclear Engineering.

HARDWARE DESIGN OF A GRAPPLING/DOCKING DEVICE ACCOMMODATING LARGE LATERAL AND ANGULAR MISALIGNMENTS c37

Myles Baker *In* USRA, Proceedings of the 8th Annual Summer Conference: NASA/USRA Advanced Design Program 1992 p 18-19 (For primary document see N94-25665 07-80)
Avail: CASI HC A01/MF A04

In this hardware project, continued from last year, the students developed ideas for a new grappling and docking mechanism that would be able to accommodate a very large initial misalignment (up to one half of the spacecraft radius) and simultaneously a large angular misalignment (up to 20 degrees) between space tug and space vehicle. The students were made familiar with the project by visiting TRW, where they could study the prototype of the NASA Orbiting Maneuvering Vehicle (OMV, since canceled). The students' objective was to design a model, built in the University machine shop, that would demonstrate the potential for much larger misalignments than was possible with the OMV.
Author

N94-25669*# California Univ., Los Angeles. Dept. of Mechanical, Aerospace and Nuclear Engineering.

HARDWARE DESIGN OF A SPHERICAL MINI-ROVER c37

John Tarlton *In* USRA, Proceedings of the 8th Annual Summer Conference: NASA/USRA Advanced Design Program 1992 p 19-21 (For primary document see N94-25665 07-80)
Avail: CASI HC A01/MF A04

In this hardware project the students designed the prototype of a novel mini-rover for the exploration of a planetary surface. In an actual application, a large number of such miniature roving devices would be released from a landing craft. Each rover would be equipped with a Cd 109 radio-isotope source (a gamma ray emitter) irradiating the planetary surface below the rover, and an x-ray fluorescence detector for a quantitative assay of high atomic weight elements in the planet's surface. (Similar, miniaturized, hand-held devices have recently been developed for use in gold mines). The device developed by the students was limited to demonstrating the mechanical and electrical drive. The geometric external shape is a sphere; hence there is no danger of the rover being turned on its back and stopped. Propulsion is by means of an interior mass, eccentric to the sphere and driven by an electric motor. In an inter-disciplinary effort in mechanical and electrical engineering, the students designed the mechanical parts, built the transistorized circuit board, and tested the device. Author

N94-25670*# California Univ., Los Angeles. Dept. of Mechanical, Aerospace and Nuclear Engineering.

MANNED MISSION TO MARS WITH PERIODIC REFUELING FROM ELECTRICALLY PROPELLED TANKERS **c12**

Laura Gogan, Joseph Melko, Fritz Wang, Daniel Lourme, Sophie Ben Moha, Christele Lardon, and Muriel Richard *In* USRA, Proceedings of the 8th Annual Summer Conference: NASA/USRA Advanced Design Program 1992 p 22-30 Prepared in cooperation with Ecole Polytechnique Feminine, Sceaux, France (For primary document see N94-25665 07-80)
Avail: CASI HC A02/MF A04

In a joint study by students from the Ecole Polytechnique Feminine, France, and the University of California, Los Angeles, a mission concept that had the objective of evaluating the feasibility of a non-nuclear, yet fast, manned mission to Mars was considered. Ion-engine propelled tankers are postulated that would provide mid-coarse refueling of LOX and LH2 to the manned ship. The scenario is therefore one of a 'split mission', yet with the added feature that the cargo ships include tankers for mid-course refueling. The present study is a continuation of one first conducted last year. Emphasis this year was on the design of the tanker fleet. Author

N94-25671*# University of Central Florida, Orlando. Dept. of Mechanical and Aerospace Engineering.

ASSURED CREW RETURN VEHICLE POST LANDING CONFIGURATION DESIGN AND TEST **c18**

Loren A. Anderson and Pamela Kay Armitage *In* USRA, Proceedings of the 8th Annual Summer Conference: NASA/USRA Advanced Design Program 1992 p 31-39 (For primary document see N94-25665 07-80)
Avail: CASI HC A02/MF A04

The 1991-1992 senior Mechanical and Aerospace Engineering Design class continued work on the post landing configurations for the Assured Crew Return Vehicle (ACRV) and the Emergency Egress Couch (EEC). The ACRV will be permanently docked to Space Station Freedom, fulfilling NASA's commitment of Assured Crew Return Capability in the event of an accident or illness aboard Space Station Freedom. The EEC provides medical support and a transportation surface for an incapacitated crew member. The objective of the projects was to give the ACRV Project Office data to feed into their feasibility studies. Four design teams were given the task of developing models with dynamically and geometrically scaled characteristics. Groups one and two combined effort to design a one-fifth scale model of the Apollo Command Module derivative, an on-board flotation system, and a lift attachment point system. This model was designed to test the feasibility of a rigid flotation and stabilization system and to determine the dynamics associated with lifting the vehicle during retrieval. However, due to priorities, it was not built. Group three designed a one-fifth scale model of the Johnson Space Center (JSC) benchmark configuration, the Station Crew Return Alternative Module (SCRAM) with a lift attachment point system. This model helped to determine the flotation and lifting characteristics of the SCRAM configuration. Group four designed a full scale EEC with changeable geometric and dynamic characteristics. This model provided data on the geometric characteristics of the EEC and on the placement of the CG and moment of inertia. It also gave the helicopter rescue personnel direct input to the feasibility study. Author

N94-25672*# Colorado Univ., Boulder. Dept. of Aerospace Engineering Sciences.

AUTONOMOUS SUPPORT FOR MICROORGANISM RESEARCH IN SPACE **c51**

M. W. Luttges, D. M. Klaus, M. L. Fleet, M. S. Miller, D. E. Shipley, and J. D. Smith *In* USRA, Proceedings of the 8th Annual Summer Conference: NASA/USRA Advanced Design Program 1992 p 40-52 (For primary document see N94-25665 07-80)
Avail: CASI HC A03/MF A04

A preliminary design for performing on-orbit, autonomous research on microorganisms and cultured cells/tissues is presented. An understanding of gravity and its effects on cells is crucial for space exploration as well as for terrestrial applications. The payload is designed to be compatible with the COMmercial Experiment Transported (COMET) launch vehicle, an orbiter middeck locker interface, and with Space Station Freedom. Uplink/downlink capabilities and sample return through controlled reentry are available for all carriers. Autonomous testing activities are preprogrammed with inflight reprogrammability. Sensors for monitoring temperature, pH, light, gravity levels, vibration, and radiation are provided for environmental regulation and experimental data collection. Additional experiment data acquisition includes optical density measurement, microscopy, video, and file photography. Onboard full data storage capabilities are provided. A fluid transfer mechanism is utilized for inoculation, sampling, and nutrient replenishment of experiment cultures. In addition to payload design, representative experiments were developed to ensure scientific objectives remained compatible with hardware capabilities. The project is defined to provide biological data pertinent to extended duration crewed space flight including crew health issues and development of a Controlled Ecological Life Support System (CELSS). In addition, opportunities are opened for investigations leading to commercial applications of space, such as pharmaceutical development, modeling of terrestrial diseases, and material processing. Author

N94-25673*# Florida Univ., Gainesville. Dept. of Aerospace Engineering, Mechanics and Engineering Sciences.

BIOREGENERATIVE SYSTEM COMPONENTS FOR MICROGRAVITY **c51**

Gale E. Nevill, Jr. and Michael I. Hessel, Jr. *In* USRA, Proceedings of the 8th Annual Summer Conference: NASA/USRA Advanced Design Program 1992 p 53-66 (For primary document see N94-25665 07-80)
Avail: CASI HC A03/MF A04

The goal of the class was to design, fabricate, and test prototype designs that were independent, yet applicable to a Closed Loop Life Support System. The three prototypes chosen were in the areas of agar plant growth, regnerative filtration, and microgravity food preparation. The plant growth group designed a prototype agar medium growth system that incorporates nutrient solution replenishment and post-harvest refurbishment. In addition, the unit emphasizes material containment and minimization of open interfaces. The second project was a filter used in microgravity that has the capability to clean itself. The filters are perforated plates which slide through a duct and are cleaned outside of the flow with a vacuum system. The air in the duct is prevented from flowing outside of the duct by a network of sliding seals. The food preparation group developed a device which dispenses and mixes ingredients and then cooks the mixture in microgravity. The dry ingredients are dispensed from a canister by a ratchet-operated piston. The wet ingredients are dispensed from plastic bags through tubing attached to a syringe. Once inside the mixing chamber, the ingredients are mixed using a collapsible whisk and then pushed into the cooking device. Author

N94-25674*# Florida Agricultural and Mechanical Univ., Tallahassee. Dept. of Mechanical Engineering.

THE EXTENDED MISSION ROVER (EMR) **c12**

W. Shields, Anthony Halecki, Manh Chung, Ken Clarke, Kevin Frankle, Fariba Kassemkhani, John Kuhlhoff, Josh Lenzini, David Lobdell, and Sam Morgan et al *In* USRA, Proceedings of the 8th Annual Summer Conference: NASA/USRA Advanced Design Program 1992 p 67-73 Prepared in cooperation with Florida State Univ., Tallahassee (For primary document see N94-25665 07-80)
Avail: CASI HC A02/MF A04

A key component in ensuring America's status as a leader in the global community is its active pursuit of space exploration. On the twentieth anniversary of Apollo 11, President George Bush challenged the nation to place a man on the moon permanently and to conduct human exploration of Mars in the 21st century. The students of the FAMU/FSU College of Engineering hope to make a significant contribution to this challenge, America's Space Exploration Initiative (SEI), with their participation in the NASA/USRA Advanced Design Program. The project selected by the 1991/1992 Aerospace Design group is the design of an Extended Mission Rover (EMR) for use on the lunar surface. This vehicle will serve as a mobile base to provide future astronauts with a 'shirt-sleeve' living and working environment. Some of the proposed missions are planetary surface exploration, construction and maintenance, hardware setup, and in situ resource experimentation. This vehicle will be put into use in the 2010-2030 time frame. Author

N94-25675*# Georgia Inst. of Tech., Atlanta. School of Mechanical Engineering.
THE ENABLER: A CONCEPT FOR A LUNAR WORK VEHICLE c37
James W. Brazell, Craig Campbell, Ken Kaser, James A. Austin, Clark Beard, Glenn Ceniza, Thomas Hamby, Anne Robinson, and Dana Wooters *In* USRA, Proceedings of the 8th Annual Summer Conference: NASA/USRA Advanced Design Program 1992 p 74-79 (For primary document see N94-25665 07-80)
Avail: CASI HC A02/MF A04

The Enabler is an earthbound prototype designed to model an actual lunar work vehicle and is able to perform many of the tasks that might be expected of a lunar work vehicle. The vehicle will be constructed entirely from parts made by students and from standard stock parts. The design utilizes only four distinct chassis pieces and sixteen moving parts. The Enabler has non-orthogonal articulating joints that give the vehicle a wide range of mobility and reduce the total number of parts. Composite wheels provide the primary suspension system for the vehicle. Author

N94-25676*# Georgia Inst. of Tech., Atlanta. School of Textile and Fiber Engineering.
DESIGN FOR PRODUCING FIBERGLASS FABRIC IN A LUNAR ENVIRONMENT c31
Rafer M. Benson, Dana R. Causby, Michael C. Johnson, Mark A. Storey, Dai T. Tran, and Thomas A. Zahr *In* USRA, Proceedings of the 8th Annual Summer Conference: NASA/USRA Advanced Design Program 1992 p 80-85 (For primary document see N94-25665 07-80)
Avail: CASI HC A02/MF A04

The purpose of this project was to design a method of producing a fabric material on the lunar surface from readily available glass fibers. Various methods for forming fabrics were analyzed to determine which methods were appropriate for the lunar conditions. A nonwoven process was determined to be the most suitable process for making a fabric material out of fiberglass under these conditions. Various resins were considered for adhering the fibers. A single thermoplastic resin (AURUM) was found to be the only applicable resin. The end product of the process was determined to be suitable for use as a roadway surfacing material, canopy material, reflective material, or packaging material. A cost analysis of the lunar process versus shipping the end-product from the Earth suggests that the lunar formation is highly feasible. A design for a lunar, nonwoven process was determined and is included. Author

N94-25677*# Georgia Inst. of Tech., Atlanta. School of Textile and Fiber Engineering.
LUNAR PREFORM MANUFACTURING c31
Gregory N. Leong, Sandra Nease, Vicky Lager, Raffy Yaghjian, and Chris Waller *In* USRA, Proceedings of the 8th Annual Summer Conference: NASA/USRA Advanced Design Program 1992 p 86-90 (For primary document see N94-25665 07-80)
Avail: CASI HC A01/MF A04

A design for a machine to produce hollow, continuous fiber-reinforced composite rods of lunar glass and a liquid crystalline matrix using the pultrusion process is presented. The glass fiber will be produced from the lunar surface, with the machine and matrix being transported to the moon. The process is adaptable to the low gravity and near-vacuum environment of the moon through the use of a thermoplastic matrix in fiber form as it enters the pultrusion process. With a power consumption of 5 kW, the proposed machine will run unmanned continuously in fourteen-day cycles, matching the length of lunar days. A number of dies could be included that would allow the machine to produce rods of varying diameter, I-beams, angles, and other structural members. These members could then be used for construction on the lunar surface or transported for use in orbit. The benefits of this proposal are in the savings in weight of the cargo each lunar mission would carry. The supply of glass on the moon is effectively endless, so enough rods would have to be produced to justify its transportation, operation, and capital cost. This should not be difficult as weight on lunar mission is at a premium. Author

N94-25678*# Georgia Inst. of Tech., Atlanta. School of Textile and Fiber Engineering.
VARIABLE SPEED CONTROLLER c54
Christa Estes, Charles Spiggle, Shannon Swift, Stephen VanGeffen, and Frank Younger *In* USRA, Proceedings of the 8th Annual Summer Conference: NASA/USRA Advanced Design Program 1992 p 90-95 (For primary document see N94-25665 07-80)
Avail: CASI HC A01/MF A04

This report details a new design for a variable speed controller which can be used to operate lunar machinery without the astronaut using his or her upper body. In order to demonstrate the design, a treadle for an industrial sewing machine was redesigned to be used by a standing operator. Since the invention of an electrically powered sewing machine, the operator has been seated. Today, companies are switching from sit down to stand up operation involving modular stations. The old treadle worked well with a sitting operator, but problems have been found when trying to use the same treadle with a standing operator. Emphasis is placed on the ease of use by the operator along with the ergonomics involved. Included with the design analysis are suggestions for possible uses for the speed controller in other applications. Author

N94-25679*# Georgia Inst. of Tech., Atlanta. School of Textile and Fiber Engineering.
ENABLER OPERATOR STATION c54
Andrea Bailey, John Kietzman, Shirlyn King, Rae Stover, and Torsten Wegner *In* USRA, Proceedings of the 8th Annual Summer Conference: NASA/USRA Advanced Design Program 1992 p 96-10 (For primary document see N94-25665 07-80)
Avail: CASI HC A01/MF A04

The objective of this project was to design an onboard operator station for the conceptual Lunar Work Vehicle (LWV). The LWV would be used in the colonization of a lunar outpost. The details that follow, however, are for an Earth-bound model. The operator station is designed to be dimensionally correct for an astronaut wearing the current space shuttle EVA suit (which include life support). The proposed operator station will support and restrain an astronaut as well as to provide protection from the hazards of vehicle rollover. The threat of suit puncture is eliminated by rounding all corners and edges. A step-plate, located at the front of the vehicle, provides excellent ease of entry and exit. The operator station weight requirements are met by making efficient use of rigid members, semi-rigid members, and woven fabrics. Author

N94-25680*# Georgia Inst. of Tech., Atlanta. School of Textile and Fiber Engineering.
DUST CONTROL FOR ENABLER c54
Kevin Hilton, Chad Karl, Mark Litherland, David Ritchie, and Nancy Sun *In* USRA, Proceedings of the 8th Annual Summer Conference: NASA/USRA Advanced Design Program 1992 p 101-107 (For primary document see N94-25665 07-80)
Avail: CASI HC A02/MF A04

The dust control group designed a system to restrict dust that is disturbed by the Enabler during its operation from interfering with astronaut or camera visibility. This design also considers the many different wheel positions made possible through the use of artinuation joints that provide the steering and wheel pitching for the Enabler. The system uses a combination of brushes and fenders to restrict the dust when the vehicle is moving in either direction and in a turn. This design also allows for ease of maintenance as well as accessibility of the remainder of the vehicle. Author

N94-25681*# Houston Univ., TX. International Center for Space Architecture.
PORTABLE HABITAT FOR ANTARCTIC SCIENTIFIC RESEARCH (PHASR) c54
Samantha S. Griswold *In* USRA, Proceedings of the 8th Annual Summer Conference: NASA/USRA Advanced Design Program 1992 p 108-113 (For primary document see N94-25665 07-80)
Avail: CASI HC A02/MF A04

The Portable Habitat for Antarctic Scientific Research, PHASR, is designed as a versatile, general purpose habitat system that addresses the problem of functional space and environmental soundness in a partially fabric-covered shelter. PHASR is used for remote field site applications that can be quickly deployed. PHASR will also provide four scientists with a comfortable and efficient use of interior space. PHASR is a NASA/USRA Advanced Design Program project conducted at the University of Houston College of Architecture, Sasadawa International Center for Space Architecture (SICSA). This report is prepared for NASA/USRA. Author

N94-25682*# Houston Univ., TX. International Center for Space Architecture.
LOWEST COST, NEAREST TERM OPTIONS FOR A MANNED MARS MISSION **c12**
Bob Sauls, Michael Mortensen, Renee Myers, Giovanni Guacci, and Fred Montes *In* USRA, Proceedings of the 8th Annual Summer Conference: NASA/USRA Advanced Design Program 1992 p 114-123 (For primary document see N94-25665 07-80)
Avail: CASI HC A02/MF A04

This study is part of a NASA/USRA Advanced Design Program project executed for the purpose of examining the requirements of a first manned Mars mission. The mission, classified as a split/sprint mission, has been designed for a crew of six with a total manned trip time of one year. Author

N94-25683*# Idaho Univ., Moscow. Dept. of Mechanical Engineering.
PLANETARY SURFACE EXPLORATION MESUR/AUTONOMOUS LUNAR ROVER **c37**
Larry Stauffer, Matt DiLorenzo, Dave Austin, Raymond Ayers, David Burton, Joe Gaylord, Jim Kennedy, Richard Laux, Dale Lentz, and Preston Nance et al *In* USRA, Proceedings of the 8th Annual Summer Conference: NASA/USRA Advanced Design Program 1992 p 124-136 (For primary document see N94-25665 07-80)
Avail: CASI HC A03/MF A04

Planetary surface exploration micro-rovers for collecting data about the Moon and Mars have been designed by the Department of Mechanical Engineering at the University of Idaho. The goal of both projects was to design a rover concept that best satisfied the project objectives for NASA/Ames. A second goal was to facilitate student learning about the process of design. The first micro-rover is a deployment mechanism for the Mars Environmental Survey (MESUR) Alpha Particle/Proton/X-ray (APX) Instrument. The system is to be launched with the 16 MESUR landers around the turn of the century. A Tubular Deployment System and a spiked-legged walker have been developed to deploy the APX from the lander to the Martian Surface. While on Mars, the walker is designed to take the APX to rocks to obtain elemental composition data of the surface. The second micro-rover is an autonomous, roving vehicle to transport a sensor package over the surface of the moon. The vehicle must negotiate the lunar terrain for a minimum of one year by surviving impacts and withstanding the environmental extremes. The rover is a reliable track-driven unit that operates regardless of orientation that NASA can use for future lunar exploratory missions. This report includes a detailed description of the designs and the methods and procedures which the University of Idaho design teams followed to arrive at the final designs. Author

N94-25684*# Kansas State Univ., Manhattan. Dept. of Mechanical Engineering.
AUTOMATION OF CLOSED ENVIRONMENTS IN SPACE FOR HUMAN COMFORT AND SAFETY **c54**
Allen C. Cogley and Nathan P. Tucker *In* USRA, Proceedings of the 8th Annual Summer Conference: NASA/USRA Advanced Design Program 1992 p 137-145 (For primary document see N94-25665 07-80)
Avail: CASI HC A02/MF A04

For prolonged missions into space and colonization outside the Earth's atmosphere, development of Environmental Control and Life Support Systems (ECLSS) are essential to provide astronauts with habitable environments. The Kansas State University Advanced Design Team have researched and designed a control system for an ECLSS like that on Space Station Freedom. The following milestones have been accomplished: (1) completed computer simulation of the CO2 Removal Assembly; (2) created a set of rules for the expert control system of the CO2 Removal Assembly; (3) created a classical controls system for the CO2 Removal Assembly; (4) established a means of communication between the mathematical model and the two controls systems; and (5) analyzed the dynamic response of the simulation and compared the two methods of control. Author

N94-25685*# Maryland Univ., College Park. Dept. of Aerospace Engineering.
MINOTAUR (MARYLAND'S INNOVATIVE ORBITAL TECHNOLOGICALLY ADVANCED UNIVERSITY ROCKET) **c20**
Mark J. Lewis, Dave Akin, Charles Lind, T. Rice, ed., and W. Vincent, ed. *In* USRA, Proceedings of the 8th Annual Summer Conference: NASA/USRA Advanced Design Program 1992 p 146-158 (For primary document see N94-25665 07-80)
Avail: CASI HC A03/MF A04

Over the past decade, there has been an increasing interest in designing small commercial launch vehicles. Some of these designs include OSC's Pegasus, and AMROC's Aquila. Even though these vehicles are very different in their overall design characteristics, they all share a common thread of being expensive to design and manufacture. Each of these vehicles has an estimated production and operations cost of over $15000/kg of payload. In response to this high cost factor, the University of Maryland is developing a cost-effective alternative launch vehicle, Maryland's Innovative Orbital Technologically Advanced University Rocket (MINOTAUR). A preliminary cost analysis projects that MINOTAUR will cost under $10000/kg of payload. MINOTAUR will also serve as an enriching project devoted to an entirely student-designed-and-developed launch vehicle. This preliminary design of MINOTAUR was developed entirely by undergraduates in the University of Maryland's Space Vehicle Design class. At the start of the project, certain requirements and priorities were established as a basis from which to begin the design phase: (1) carry a 100 kg payload into a 200 km circular orbit; (2) provide maximum student involvement in the design, manufacturing, and launch phases of the project; and (3) use hybrid propulsion throughout. The following is the list of the project's design priorities (from highest to lowest): (1) safety, (2) cost, (3) minimum development time, (4) maximum use of the off-the-shelf components, (5) performance, and (6) minimum use of pyrotechnics. Author

N94-25686*# Maryland Univ., College Park. Dept. of Electrical Engineering.
THE 1991-1992 WALKING ROBOT DESIGN **c37**
Shapour Azarm, Wijesurija Dayawansa, Lung-Wen Tsai, and Jon Peritt *In* USRA, Proceedings of the 8th Annual Summer Conference: NASA/USRA Advanced Design Program 1992 p 159-169 (For primary document see N94-25665 07-80)
Avail: CASI HC A03/MF A04

The University of Maryland Walking Machine team designed and constructed a robot. This robot was completed in two phases with supervision and suggestions from three professors and one graduate teaching assistant. Bob was designed during the Fall Semester 1991, then machined, assembled, and debugged in the Spring Semester 1992. The project required a total of 4,300 student hours and cost under $8,000. Mechanically, Bob was an exercise in optimization. The robot was designed to test several diverse aspects of robotic potential, including speed, agility, and stability, with simplicity and reliability holding equal importance. For speed and smooth walking motion, the footpath contained a long horizontal component; a vertical aspect was included to allow clearance of obstacles. These challenges were met with a leg design that utilized a unique multi-link mechanism which traveled a modified tear-drop footpath. The electrical requirements included motor, encoder, and voice control circuitry selection, manual controller manufacture, and creation of sensors for guidance. Further, there was also a need for selection of the computer, completion of a preliminary program, and testing of the robot. Author

N94-25687*# Massachusetts Inst. of Tech., Cambridge. Dept. of Aeronautics and Astronautics.
PROJECT COLUMBIAD: REESTABLISHMENT OF HUMAN PRESENCE ON THE MOON **c12**
Joseph Shea, Stanley Weiss, Harold Alexander, Peter Belobaba, Greg Loboda, Maresi Berry, Mark Bower, Charles Bruen, Patrick Cazeau, and Michael Clarke et al *In* USRA, Proceedings of the 8th Annual Summer Conference: NASA/USRA Advanced Design Program 1992 p 170-177 (For primary document see N94-25665 07-80)
Avail: CASI HC A02/MF A04

In response to the Report of the Advisory Committee on the future of the U.S. Space Program and a request from NASA's Exploration Office, the MIT Hunsaker Aerospace Corporation (HAC) conducted a feasibility study, known as Project Columbiad, on reestablishing human presence on the Moon before the year 2000. The mission criteria established were to transport a four person crew to the lunar surface at any latitude and back to Earth with a 14-28 day stay on the lunar surface. Safety followed by cost of the Columbiad Mission were the top level priorities of HAC. The resulting design has a precursor mission that emplaces the required surface payloads before the piloted mission arrives. Both the precursor and piloted missions require two National Launch System (NLS) launches. Both the precursor and piloted missions have an Earth orbit rendezvous (EOR) with a direct transit to the Moon post-EOR. The piloted mission returns to Earth via a direct transit. Included among the surface payloads preemplaced are a habitat, solar power plant (including fuel cells for the lunar night), lunar rover, and mecanisms used to cover the habitat with regolith (lunar soil) in order to protect the crew members from severe solar flare radiation. Author (revised)

N94-25688*# Michigan Univ., Ann Arbor. Dept. of Aerospace Engineering.

PROJECT APEX: ADVANCED MANNED EXPLORATION OF THE MARTIAN MOON PHOBOS **c91**

Joe G. Eisley and Jim Akers *In* USRA, Proceedings of the 8th Annual Summer Conference: NASA/USRA Advanced Design Program 1992 p 178-187 (For primary document see N94-25665 07-80)

Avail: CASI HC A02/MF A04

A preliminary design has been developed for a manned mission to the Martian moon Phobos. The spacecraft is to carry a crew of five and will be launched from Low Earth Orbit in the year 2010. The outbound trajectory to Mars uses a gravitational assisted swingby of Venus and takes eight months to complete. The stay at Phobos is scheduled for 60 days. During this time, the crew will be busily engaged in setting up a prototype fuel processing facility. The vehicle will then return to Earth orbit after a total mission duration of 656 days. The spacecraft is powered by three nuclear thermal rockets which also provide the primary electrical power via dual mode operation. The overall spacecraft length is 110 m, and the total mass departing from Low Earth Orbit is 900 metric tons. Author (revised)

N94-25689*# Minnesota Univ., Minneapolis. Dept. of Aerospace Engineering and Mechanics.

MARS TRANSPORTATION SYSTEM **c37**

William Garrard, Andrew Vano, and Dave Rutherford *In* USRA, Proceedings of the 8th Annual Summer Conference: NASA/USRA Advanced Design Program 1992 p 188-195 (For primary document see N94-25665 07-80)

Avail: CASI HC A02/MF A04

The University of Minnesota Advanced Space Design Program has developed a sample Mars exploration scenario. The purpose of the design project is to enhance NASA and university interaction, to provide fresh ideas to NASA, and to provide real world design problems to engineering students. The Mars Transportation System in this paper is designed to transport a crew of six astronauts to the Martian surface and return them to Low Earth Orbit (LEO) starting in the year 2016. The proposed vehicle features such advanced technologies as nuclear propulsion, nuclear power generation, and aerobraking. Three missions are planned. Orbital trajectories are of the conjunction class with an inbound Venus swingby providing a 60-day surface stay at Mars and an average total trip time of 520 days. Author

N94-25690*# Ohio State Univ., Columbus. Dept. of Aeronautical and Astronautical Engineering.

PROJECT WISH: THE EMERALD CITY **c20**

Hayrani Oz, Jim Dunne, Stan Butchar, Tommy George, Rob Hellstrom, Tricia Kringen, George Owens, Mike Perrea, Paul Semeraro, and Phil Thorndike *In* USRA, Proceedings of the 8th Annual Summer Conference: NASA/USRA Advanced Design Program 1992 p 196-208 (For primary document see N94-25665 07-80)

Avail: CASI HC A03/MF A04

Phase 3 of Project WISH saw the evolution of the Emerald City (E-City) from a collection of specialized independent analyses and ideas to a working structural design integrated with major support systems and analyses. Emphasis was placed on comparing and contrasting the closed and open cycle gas core nuclear rocket engines to further determine the optimum propulsive system for the E-City. Power and thermal control requirements were then defined and the question of how to meet these requirements was addressed. Software was developed to automate the mission/system/configuration analysis so changes dictated by various subsystem constraints could be managed efficiently and analyzed interactively. In addition, the liquid hydrogen propellant tank was statically designed for minimum mass and shape optimization using a finite element modeling package called SDRC I-DEAS. Spoke and shaft cross-sectional areas were optimized on ASTROS (Automated Structural Optimization System) for mass minimization. A structural dynamic analysis of the optimal structure also conducted using ASTROS enabled a study of the modes, frequencies, displacements, and accelerations of the E-City. Finally, the attitude control system design began with an initial mass moment of inertia analysis and was then designed and optimized using linear quadratic regulator control theory. Author (revised)

N94-25691*# Old Dominion Univ., Norfolk, VA. Dept. of Mechanical Engineering and Mechanics.

EXTRATERRESTRIAL SURFACE PROPULSION SYSTEMS **c37**

Robert L. Ash, Dexter L. Blackstock, K. Barnhouse, Z. Charalambous, J. Coats, J. Danagan, T. Davis, J. Dickens, P. Harris, and G. Horner et al *In* USRA, Proceedings of the 8th Annual Summer Conference: NASA/USRA Advanced Design Program 1992 p 209-215 (For primary document see N94-25665 07-80)

Avail: CASI HC A02/MF A04

Lunar traction systems, Mars oxygen production, and Mars methane engine operation were the three topics studied during 1992. An elastic loop track system for lunar construction operations was redesigned and is being tested. A great deal of work on simulating the lunar environment to facilitate traction testing has been reported. Operation of an oxygen processor under vacuum conditions has been the focus of another design team. They have redesigned the processor facility. This included improved seals and heat shields. Assuming methane and oxygen can be produced from surface resources on Mars, a third design team has addressed the problem of using Mars atmospheric carbon dioxide to control combustion temperatures in an internal combustion engine. That team has identified appropriate tests and instrumentation. They have reported on the test rig that they designed and the computer-based system for acquiring data. Author (revised)

N94-25692*# Pennsylvania State Univ., University Park. Dept. of Aerospace Engineering.

COMET NUCLEUS AND ASTEROID SAMPLE RETURN MISSIONS **c12**

Robert G. Melton, Roger C. Thompson, Thomas F. Starchville, Jr., C. Adams, A. Aldo, K. Dobson, C. Flotta, J. Gagliardino, M. Lear, and C. McMillan et al *In* USRA, Proceedings of the 8th Annual Summer Conference: NASA/USRA Advanced Design Program 1992 p 216-227 (For primary document see N94-25665 07-80)

Avail: CASI HC A03/MF A04

During the 1991-92 academic year, the Pennsylvania State University has developed three sample return missions: one to the nucleus of comet Wild 2, one to the asteroid Eros, and one to three asteroids located in the Main Belt. The primary objective of the comet nucleus sample return mission is to rendezvous with a short period comet and acquire a 10 kg sample for return to Earth. Upon rendezvous with the comet, a tethered coring and sampler drill will contact the surface and extract a two-meter core sample from the target site. Before the spacecraft returns to Earth, a monitoring penetrator containing scientific instruments will be deployed for gathering long-term data about the comet. A single asteroid sample return mission to the asteroid 433 Eros (chosen for proximity and launch opportunities) will extract a sample from the asteroid surface for return to Earth. To limit overall mission cost, most of the mission design uses current technologies, except the sampler drill design. The multiple asteroid sample return mission could best be characterized through its use of future technology including an optical communications system, a nuclear power reactor, and a low-thrust propulsion system. A low-thrust trajectory optimization code (QuickTop 2) obtained from the NASA LeRC helped in planning the size of major subsystem components, as well as the trajectory between targets. Author (revised)

N94-25693*# Prairie View Agricultural and Mechanical Coll., TX. Dept. of Architecture.

DESIGN AND DEVELOPMENT OF THE SECOND GENERATION MARS HABITAT **c54**

Ikhlas Sabouni, Roy Smith, Steven Taylor, Brock Harrell, and Earnest Crawford *In* USRA, Proceedings of the 8th Annual Summer Conference: NASA/USRA Advanced Design Program 1992 p 228-236 (For primary document see N94-25665 07-80)
Avail: CASI HC A02/MF A04

The second generation of Mars Habitat is to be utilized as an advanced permanent base for 20 crew members to live on Mars for a period of 6-12 months. It is designed to be a self-contained environment accommodating five main facilities: living, working, service, medical, and a greenhouse. The objective of the design is to create a comfortable, safe, living environment. Hexamars-2 and Lavapolis-2 are two different concepts for the advanced Mars Habitat. The design team assumes there will be an initial habitat located near or on the site from earlier missions that satisfies the requirement for a short-term habitation for the crew to use while constructing Hexamars-2 or Lavapolis-2. Prefabricated structures and materials will be shipped to the site before the long-term crew members arrive. Partial construction and preparation for the long-term habitat will be done by crew members or robotics from a previous mission. The construction of the long-term base will occur in phases. Hexamars-2 consists of six sphere-shaped inflatable modules that will be partially buried below the Martian surface. The construction of each sphere will occur in ten steps. Shape charges will be used to create the crater in which the spherical structure will be placed. The interior core will be unloaded and put into place followed by the exterior structure. The foundation will be filled, the interior bladder will be inflated, floor-to-floor joists connected, and sand pockets filled. Finally, the life support system and interior partitions are put in place. Each sphere consists of three levels of which the lower level will be safe haven. Particular attention is given to structural support, the dominance of internal pressure, the process of construction, and human factors.
Author (revised)

N94-25694*# Puerto Rico Univ., Rio Piedras. School of Architecture.
FIRST LUNAR OUTPOST **c54**
Aureo F. Andino, Daniel Silva, Nelson Ortiz, Omar Alvarez, Julio A. Colon, Myrelle Colon, Alicia Diaz, Xochiquetzal Y. Escobar, Alberto Garcia, and Isabel C. Gonzalez et al *In* USRA, Proceedings of the 8th Annual Summer Conference: NASA/USRA Advanced Design Program 1992 p 237-249 (For primary document see N94-25665 07-80)
Avail: CASI HC A03/MF A04

Design and research efforts at the University of Puerto Rico have focused on the evaluation and refinement of the Habitability Criteria for a prolonged human presence in space during the last four years. Living quarters for a Mars mission and a third generation lunar base concept were proposed. This academic year, 1991-92, work on further refinement of the habitability criteria and design of partial gravity furniture was carried on. During the first semester, design alternatives for furniture necessary in a habitat design optimized for lunar and Martian environments were developed. Designs are based on recent research data from lunar and Mars gravity simulations, and current NASA standards. Artifacts will be submitted to NASA architects to be tested in KC-135 flights. Test findings will be submitted for incorporation in future updates to NASA habitat design standards. Second semester work was aimed at integrating these findings into the First Lunar Outpost (FLO), a mission scenario currently being considered by NASA. The mission consists of a manned return to the moon by crews of four astronauts for periods of 45 days. The major hardware components of the mission are as follows: (1) a Crew Module for the delivery of the crew and their supplies, and (2) the Habitat Module, which will arrive on the Moon unmanned. Our design efforts concentrated on this Habitat Module and on application of habitability criteria. Different geometries for the pressure vessel and their impact on the interior architecture were studied. Upon the selection of a geometry, a more detailed analysis of the interior design was performed, taking into consideration the reduced gravity, and the protection against radiation, micrometeorites, and the extreme temperature variation. A proposal for a FLO was submitted by the students, consisting essentially of a 24-feet (7.3 m.) by 35-feet (10.67 m) high vertical cylinder with work areas, crew quarters, galley, wardroom, leisure facilities, health maintenance, waste management, EVA operations facilities, and safe havens.
Author (revised)

N94-25695*# Rensselaer Polytechnic Inst., Troy, NY. Dept. of Mechanical Engineering, Aerospace Engineering, and Mechanics.
THE LIGHTCRAFT PROJECT: FLIGHT TECHNOLOGY FOR A HYPERSONIC MASS TRANSIT SYSTEM Abstract Only **c05**
Leik Myrabo and Kenneth Bouchard *In* USRA, Proceedings of the 8th Annual Summer Conference: NASA/USRA Advanced Design Program 1992 p 250 (For primary document see N94-25665 07-80)
Avail: CASI HC A01/MF A04

Rensselaer Polytechnic Institute has been developing transatmospheric 'Lightcraft' technology aimed at creating an efficient, economically affordable, hypersonic mass transportation system. The system utilizes laser-energized airbreathing engines to accelerate minimum-volume passenger capsules. The system gains a high level of reliability by using remote 'centralized' space power sources, e.g., satellite solar power stations. The most critical portion of the Lightcraft's acceleration trajectory involves flight propulsion at hypersonic velocities within the Earth's atmosphere, using a 'Magneto-Hydro-Dynamic (MHD) Fanjet' mode. Of all the propulsion modes proposed for the Lightcraft's combined-cycle engine, the MHD-Fanjet mode has received the least critical inquiry, largely because of its complexity. During the 1991-1992 academic year, Rensselaer's ADP teams produced a detailed conceptual design for the MHD-Fanjet engine, including the specific details of its integration with the other three propulsive modes. To facilitate this process, students built a full-scale mockup of a 1/12th section of this annular engine, complete with a working model of the shroud translation system. The class also made preliminary design calculations for the double-dipole, 'cuspfield' superconducting magnets that provide the external magnetic field needed by the MHD air accelerator, as well as for an onboard microwave power system to enhance the electrical conductivity of the air plasma working fluid. In addition, a large hypersonic model of the MHD accelerator was designed for future tests in RPI's Hypersonic Shock Tunnel in order to validate present analytical performance models. Another group continued design work on a full-sized prototype of a one-person 'Mercury Lightcraft' (a transatmospheric flight simulator), with major emphasis on the detailed design of the major structure, robotic landing gear, and exterior aeroshell. Author (revised)

N94-25696*# Texas Univ., Austin. Dept. of Aerospace Engineering and Engineering Mechanics.
SPACE HABITAT, ASSEMBLY AND REPAIR FACILITY **c14**
Todd A. Colangelo, Debora C. Hoetger, Addison C. Kuo, Michael C. Lo, Leland R. Marcus, Phillip P. Tran, Chris J. Tutt, Chad M. Wassmuth, and Gregory M. Wildgrube *In* USRA, Proceedings of the 8th Annual Summer Conference: NASA/USRA Advanced Design Program 1992 p 251-263 (For primary document see N94-25665 07-80)
Avail: CASI HC A03/MF A04

Integrated Space Systems (ISS) has designed a Low Earth Orbit Assembly Facility for submission in the 1992 AIAA/LORAL Team Space Design Competition. This facility, the Space Habitat, Assembly, and Repair Center (SHARC), will be used to construct, assemble, and service space vehicles. SHARC's primary mission will be the construction of interplanetary vehicles, but it will also be able to perform repair and refueling operations of craft which are in an Earth orbit. This facility has been designed using only present and near-present technology. The emphasis is on minimizing cost.
Author (revised)

N94-25697*# Texas Univ., Austin. Dept. of Aerospace Engineering and Engineering Mechanics.
ASTEROID EXPLORATION AND UTILIZATION **c90**
Brian M. Radovich, Alan E. Carlson, Medha D. Date, Manny G. Duarte, Neil F. Erian, George K. Gafka, Peter H. Kappler, Scott J. Patano, Martin Perez, and Edgar Ponce et al *In* USRA, Proceedings of the 8th Annual Summer Conference: NASA/USRA Advanced Design Program 1992 p 264-266 (For primary document see N94-25665 07-80)
Avail: CASI HC A01/MF A04

The Earth is nearing depletion of its natural resources at a time when human beings are rapidly expanding the frontiers of space. The resources possessed by asteroids have enormous potential for aiding and enhancing human space exploration as well as life on Earth. Project STONER (Systematic Transfer of Near Earth Resources) is based on mining an asteroid and transporting raw materials back to Earth. The asteroid explorer/sample return mission is designed in the context of both scenarios and is the first phase of a long range plan for humans to utilize asteroid resources. Project STONER is divided into two parts: asteroid selection and explorer spacecraft design. The spacecraft design team is responsible for the selection and integration of the subsystems: GNC, communications, automation, propulsion, power, structures, thermal systems, scientific instruments, and mechanisms used on the surface to retrieve and store asteroid regolith. The sample return mission scenario consists of eight primary phases that are critical to the mission. Author (revised)

N94-25698*# Texas Univ., Austin. Dept. of Mechanical Engineering.
THE 1991-1992 PROJECT SUMMARIES **c54**
Steven P. Nichols and Hank Kleespies *In* USRA, Proceedings of the 8th Annual Summer Conference: NASA/USRA Advanced Design Program 1992 p 267-270 (For primary document see N94-25665 07-80)
Avail: CASI HC A01/MF A04

The Department of Mechanical Engineering at The University of Texas at Austin participated in seven cooperative design projects this year. Six of the projects were associated with the Johnson Space Center and include the design of a thermal control system for an inflatable lunar habitat module, a vibration isolation system for a space shuttle cycle ergometer, a radiator shading device for a lunar outpost, a reusable astronaut safety tether, a resistive exercise device for use on the space shuttle, and a fleet of autonomous regolith throwing devices for radiation shielding of lunar habitats. The seventh project is associated with the Jet Propulsion Lab and involves the design of a shock absorbing wheel for a small six-wheeled Martian rover vehicle. Author (revised)

N94-25699*# Naval Academy, Annapolis, MD. Dept. of Aerospace Engineering.
LOW-COST UNMANNED LUNAR LANDER **c18**
Walter K. Daniel *In* USRA, Proceedings of the 8th Annual Summer Conference: NASA/USRA Advanced Design Program 1992 p 271-273 (For primary document see N94-25665 07-80)
Avail: CASI HC A01/MF A04

Two student groups designed unmanned landers to deliver 200 kilogram payloads to the lunar surface. Payloads could include astronomical telescopes, small lunar rovers, and experiments related to future human exploration. Requirements include the use of existing hardware where possible, use of a medium-class launch vehicle, an unobstructed view of the sky for the payload, and access to the lunar surface for the payload. The projects were modeled after Artemis, a project that the NASA Office of Exploration is pursuing with a planned first launch in 1996. The Lunar Scout design uses a Delta 2 launch vehicle with a Star 48 motor for insertion into the trans-lunar trajectory. During the transfer, the solar panels will be folded inward and the spacecraft will be powered by rechargeable nickel-cadmium batteries. The lander will use a combination of a solid rocket motor and hydrazine thrusters for the descent to the lunar surface. The solar arrays will be deployed after landing. The lander will provide power for operations to the payload during the lunar day; batteries will provide 'stay-alive' power during the lunar night. A horn antenna on the lander will provide communications between the payload and the earth. Author (revised)

N94-25700*# Naval Postgraduate School, Monterey, CA. Space Systems Academic Group.
HIGH TEMPERATURE SUPERCONDUCTING INFRARED IMAGING SATELLITE **c18**
B. Angus, J. Covelli, N. Davinic, J. Hailey, E. Jones, V. Ortiz, J. Racine, D. Satterwhite, T. Spriesterbach, and D. Sorensen et al *In* USRA, Proceedings of the 8th Annual Summer Conference: NASA/USRA Advanced Design Program 1992 p 274-286 (For primary document see N94-25665 07-80)
Avail: CASI HC A03/MF A04

A low earth orbiting platform for an infrared (IR) sensor payload is examined based on the requirements of a Naval Research Laboratory statement of work. The experiment payload is a 1.5-meter square by 0.5-meter high cubic structure equipped with the imaging system, radiators, and spacecraft mounting interface. The orbit is circular at 509 km (275 nmi) altitude and 70 deg. inclination. The spacecraft is three-axis stabilized with pointing accuracy of plus or minus 0.5 deg. in each axis. The experiment payload requires two 15-minute sensing periods over two contiguous orbit periods for 30 minutes of sensing time per day. The spacecraft design is presented for launch via a Delta 2 rocket. Subsystem designs include attitude control, propulsion, electric power, telemetry, tracking and command, thermal design, structure, and cost analysis. Author (revised)

N94-25701*# Naval Postgraduate School, Monterey, CA. Space Systems Academic Group.
LOW EARTH ORBIT COMMUNICATIONS SATELLITE **c18**
D. Moroney, D. Lashbrook, B. McKibben, N. Gardener, T. Rivers, G. Nottingham, B. Golden, B. Barfield, J. Bruening, and D. Wood et al *In* USRA, Proceedings of the 8th Annual Summer Conference: NASA/USRA Advanced Design Program 1992 p 287-297 (For primary document see N94-25665 07-80)
Avail: CASI HC A03/MF A04

A current thrust in satellite communication systems considers a low-Earth orbiting constellations of satellites for continuous global coverage. Conceptual design studies have been done at the time of this design project by LORAL Aerospace Corporation under the program name GLOBALSTAR and by Motorola under their IRIDIUM program. This design project concentrates on the spacecraft design of the GLOBALSTAR low-Earth orbiting communication system. Overview information on the program was gained through the Federal Communications Commission licensing request. The GLOBALSTAR system consists of 48 operational satellites positioned in a Walker Delta pattern providing global coverage and redundancy. The operational orbit is 1389 km (750 nmi) altitude with eight planes of six satellites each. The orbital planes are spaced 45 deg., and the spacecraft are separated by 60 deg. within the plane. A Delta 2 launch vehicle is used to carry six spacecraft for orbit establishment. Once in orbit, the spacecraft will utilize code-division multiple access (spread spectrum modulation) for digital relay, voice, and radio determination satellite services (RDSS) yielding position determination with accuracy up to 200 meters. Author (revised)

N94-25702*# Utah State Univ., Logan. Dept. of Mechanical and Aerospace Engineering.
COPERNICUS: LUNAR SURFACE MAPPER **c91**
Frank J. Redd and Shaun D. Anderson *In* USRA, Proceedings of the 8th Annual Summer Conference: NASA/USRA Advanced Design Program 1992 p 298-308 (For primary document see N94-25665 07-80)
Avail: CASI HC A03/MF A04

The Utah State University (USU) 1991-92 Space Systems Design Team has designed a Lunar Surface Mapper (LSM) to parallel the development of the NASA Office of Exploration lunar initiatives. USU students named the LSM 'Copernicus' after the 16th century Polish astronomer, for whom the large lunar crater on the face of the moon was also named. The top level requirements for the Copernicus LSM are to produce a digital map of the lunar surface with an overall resolution of 12 meters (39.4 ft). It will also identify specified local surface features/areas to be mapped at higher resolutions by follow-on missions. The mapping operation will be conducted from a 300 km (186 mi) lunar-polar orbit. Although the entire surface should be mapped within six months, the spacecraft design lifetime will exceed one year with sufficient propellant planned for orbit maintenance in the anomalous lunar gravity field. The Copernicus LSM is a small satellite capable of reaching lunar orbit following launch on a Conestoga launch vehicle which is capable of placing 410 kg (900 lb) into translunar orbit. Upon orbital insertion, the spacecraft will weigh approximately 233 kg (513 lb). This rather severe mass constraint has insured attention to component/subsystem size and mass, and prevented 'requirements creep.' Transmission of data will be via line-of-sight to an earth-based receiving system. Author (revised)

N94-25703*# Virginia Polytechnic Inst. and State Univ., Blacksburg. Dept. of Aerospace Engineering.
PROJECT PARAS: PHASED ARRAY RADIO ASTRONOMY FROM SPACE **c89**
Kenneth Nuss, Christopher Hoffmann, Michael Dungan, Michael Madden, and Monia Bendakhlia (Ecole Polytechnique Feminine, Sceaux, France.) *In* USRA, Proceedings of the 8th Annual Summer Conference: NASA/USRA Advanced Design Program 1992 p 309-316 (For primary document see N94-25665 07-80)
Avail: CASI HC A02/MF A04

An orbiting radio telescope is proposed which, when operated in a very long baseline interferometry (VLBI) scheme, would allow higher than

currently available angular resolution and dynamic range in the maps and the ability to observe rapidly changing astronomical sources. Using passive phased array technology, the proposed design consists of 656 hexagonal modules forming a 150-m diameter antenna dish. Each observatory module is largely autonomous, having its own photovoltaic power supply and low-noise receiver and processor for phase shifting. The signals received by the modules are channeled via fiber optics to the central control computer in the central bus module. After processing and multiplexing, the data are transmitted to telemetry stations on the ground. The truss frame supporting each observatory panel is a novel hybrid structure consisting of a bottom graphite/epoxy tubular triangle and rigidized inflatable Kevlar tubes connecting the top observatory panel and the bottom triangle. Attitude control and station keeping functions will be performed by a system of momentum wheels in the bus and four propulsion modules located at the compass points on the periphery of the observatory dish. Each propulsion module has four monopropellant thrusters and four hydrazine arcjets, the latter supported by either a photovoltaic array or a radioisotope thermoelectric generator. The total mass of the spacecraft is about 20,500 kg.
Author (revised)

N94-25704*# Virginia Polytechnic Inst. and State Univ., Blacksburg. Dept. of Aerospace Engineering.
PRESSURIZED LUNAR ROVER (PLR) c37
Kenneth Creel, Jeffrey Frampton, David Honaker, Kerry McClure, Mazyar Zeinali, Manoj Bhardwaj, Vatsal Bulsara, David Kokan, Shaun Shariff, and Eric Svarverud et al *In* USRA, Proceedings of the 8th Annual Summer Conference: NASA/USRA Advanced Design Program 1992 p 316-324 (For primary document see N94-25665 07-80)
Avail: CASI HC A02/MF A04

The objective of this project was to design a manned pressurized lunar rover (PLR) for long-range transportation and for exploration of the lunar surface. The vehicle must be capable of operating on a 14-day mission, traveling within a radius of 500 km during a lunar day or within a 50-km radius during a lunar night. The vehicle must accommodate a nominal crew of four, support two 28-hour EVA's, and in case of emergency, support a crew of six when near the lunar base. A nominal speed of ten km/hr and capability of towing a trailer with a mass of two mt are required. Two preliminary designs have been developed by two independent student teams. The PLR 1 design proposes a seven meter long cylindrical main vehicle and a trailer which houses the power and heat rejection systems. The main vehicle carries the astronauts, life support systems, navigation and communication systems, lighting, robotic arms, tools, and equipment for exploratory experiments. The rover uses a simple mobility system with six wheels on the main vehicle and two on the trailer. The nonpressurized trailer contains a modular radioisotope thermoelectric generator (RTG) supplying 6.5 kW continuous power. A secondary energy storage for short-term peak power needs is provided by a bank of lithium-sulfur dioxide batteries. The life support system is partly a regenerative system with air and hygiene water being recycled. A layer of water inside the composite shell surrounds the command center allowing the center to be used as a safe haven during solar flares. The PLR 1 has a total mass of 6197 kg. It has a top speed of 18 km/hr and is capable of towing three metric tons, in addition to the RTG trailer. The PLR 2 configuration consists of two four-meter diameter, cylindrical hulls which are passively connected by a flexible passageway, resulting in the overall vehicle length of 11 m. The vehicle is driven by eight independently suspended wheels. The dual-cylinder concept allows articulated as well as double Ackermann steering. The primary power of 8 kW is supplied by a dynamic isotope system using a closed Brayton cycle with a xenon-hydrogen mixture as the working fluid. A sodium-sulfur battery serves as the secondary power source. Excess heat produced by the primary power system and other rover systems is rejected by radiators located on the top of the rear cylinder. The total mass of the PLR 2 is 7015 kg. Simplicity and low total weight have been the driving principles behind the design of PLR 1. The overall configuration consists of a 7-m-long, 3-m-diameter cylindrical main vehicle and a two-wheeled trailer. The cylinder of the main body is capped by eight-section, faceted, semi-hemispherical ends. The trailer contains the RTG power source and is not pressurized. The shell of the main body is constructed of a layered carbon fiber/foam/Kevlar sandwich structure. Included in the shell is a layer of water for radiation protection. The layer of water extends from the front of the rover over the crew compartment and creates a safe haven for the crew during a solar flare-up. The carbon fiber provides the majority of the strength and stiffness and the Kevlar provides protection from micrometeoroids. The Kevlar is covered with a gold foil and multi-layer insulation (MLI) to reduce radiation degradation and heat transfer through the wall. A thin thermoplastic layer seals the fiber and provides additional strength.
Author (revised)

N94-25705*# Washington Univ., Seattle. Dept. of Aeronautics and Astronautics.
PROJECT MINERVA: A LOW-COST MANNED MARS MISSION BASED ON INDIGENOUS PROPELLANT PRODUCTION c28
Adam P. Bruckner, Hobie Anderson, Kelly Caviezel, Todd Daggert, Mike Folkers, Mark Fornia, Steven Hamling, Bryan Johnson, Martin Kalberer, and Mike Machula et al *In* USRA, Proceedings of the 8th Annual Summer Conference: NASA/USRA Advanced Design Program 1992 p 325-342 (For primary document see N94-25665 07-80)
Avail: CASI HC A03/MF A04

Project Minerva is a low-cost manned Mars mission designed to deliver a crew of four to the Martian surface, using only two sets of two launches. Key concepts which make this mission realizable are the use of near-term technologies and in-situ propellant production, following the senario originally proposed by R. Zubrin of Martin Marietta. The first set of launches delivers two unmanned payloads into low earth orbit (LEO): one consists of an Earth Return Vehicle (ERV), a propellant production plant, and a set of robotic vehicles, and the second consists of the upper stage/trans-Mars injection (TMI) booster. In LEO, the two payloads are joined and inserted into a Mars transfer orbit. The landing on Mars is performed with the aid of multiple aerobraking maneuvers. On the Martian surface, the propellant production plant uses a Sabatier/electrolysis-type process to combine six tons of hydrogen brought from earth with carbon dioxide from the Martian atmosphere to produce 100 tons of liquid oxygen and methane, which are later used as the propellants for the rover expeditions and the manned return journey of the ERV. Once the in-situ propellant production is completed, approximately two years after the first set of launches, the manned portion of the mission leaves earth. This set of two launches is similar to that of the unmanned vehicles; the two payloads are the Manned Transfer Vehicle (MTV) and the upper stage/TMI booster. The MTV contains the manned rover and the habitat which houses the astronauts enroute to Mars and on the Martian surface. During the 180-day trip to Mars, artificial gravity is created by tethering the MTV to the TMI booster and inducing rotation. Upon arrival the MTV performs aerobraking maneuvers to land near the fully-fueled ERV, which will be used by the crew a year and a half later to return to earth. The mission entails moderate travel times with relatively low-energy conjunction-class trajectories and allows ample time for scientific exploration. This set of missions can be repeated every two years in order to continue exploration at a variety of sites and gradually establish the infrastructure for a permanent base on Mars.
Author (revised)

N94-25706*# Wisconsin Univ., Milwaukee. Dept. of Architecture.
PAX: A PERMANENT BASE FOR HUMAN HABITATION OF MARS c54
Gary T. Moore, Patrick J. Rebholz, Joseph P. Fieber, Janis Huebner-Moths, and Kerry L. Paruleski *In* USRA, Proceedings of the 8th Annual Summer Conference: NASA/USRA Advanced Design Program 1992 p 343-357 (For primary document see N94-25665 07-80)
Avail: CASI HC A03/MF A04

The Advanced Design Program in Space Architecture at the University of Wisconsin-Milwaukee supported the synthesis report and two of its scenarios - 'Architecture 1' and 'Architecture 4' - and the Weaver ExPO report on near-term extraterrestrial explorations during the spring of 1992. The project investigated the implications of different mission scenarios, the Martian environment, supporting technologies, and especially human factors and environment-behavior considerations for the design of the first permanent Martian base. This paper presents the results of that investigation. The paper summarizes site selection, development of habitability design requirements based on environment-behavior research, construction sequencing, and a full concept design and design development for a first permanent Martian base and habitat. The proposed design is presented in terms of an integrative mission scenario and master plan phased through initial operational configuration, base site plan, and design development details of a complete Martian habitat for 18 crew members including all laboratory, mission control, and crew support spaces. Author (revised)

N94-25707*# Worcester Polytechnic Inst., MA. Dept. of Mechanical Engineering.

MICROGRAVITY IGNITION EXPERIMENT **c29**

Vahid Motevalli, William Elliott, Keith Garrant, and Ryan Marcotte *In* USRA, Proceedings of the 8th Annual Summer Conference: NASA/USRA Advanced Design Program 1992 p 358-364 (For primary document see N94-25665 07-80)

Avail: CASI HC A02/MF A04

The purpose of this project is to develop a flight-ready apparatus of the microgravity ignition experiment for the GASCAN 2 program. The microgravity ignition experiment is designed to study how a microgravity environment affects the time to ignition of a sample of alpha-cellulose paper. A microgravity environment will result in a decrease in the heat transferred from the sample due to a lack of convection currents, which would decrease time to ignition. A lack of convection current would also cause the oxygen supply at the sample not to be renewed, which could delay or even prevent ignition. When this experiment is conducted aboard GASCAN 2, the dominant result of the lack of ignition will be determined. The experiment consists of four canisters containing four thermocouples and a sensor to detect ignition of the paper sample. This year the interior of the canister was redesigned and a mathematical model of the heat transfer around the sample was developed. This heat transfer model predicts an ignition time of approximately 5.5 seconds if the decrease of heat loss from the sample is the dominant factor of the lack of convection currents.

Author (revised)

N94-25708*# Auburn Univ., AL. Dept. of Aerospace Engineering.

DESIGN OF THE ADVANCED REGIONAL AIRCRAFT, THE DART-75 **c05**

Steve Elliot, Jason Gislason, Mark Huffstetler, Jon Mann, Ashley Withers, and Mark Zimmerman *In* USRA, Proceedings of the 8th Annual Summer Conference: NASA/USRA Advanced Design Program 1992 p 367-373 (For primary document see N94-25665 07-80)

Avail: CASI HC A02/MF A04

The need for regional aircraft stems from the problem of hub airport congestion. Regional travel will allow a passenger to commute from one spoke city to another spoke city without entering the congested hub airport. In addition, those people traveling longer routes may begin the flight at home instead of traveling to the hub airport. At this time, there is no American aerospace company that produces a regional transport for under 100 passengers. The intention of the Developmental Advanced Regional Transport (DART-75) is to fill this void with a modern, efficient regional aircraft. This design achieves the efficiency through a number of advanced features including three lifting surfaces, partial composite construction, and an advanced engine design. Efficiency is not the only consideration. Structural integrity, fatigue life, ease of maintenance, passenger comfort and convenience, and environmental aspects must all be considered. These factors force the design team to face many tradeoffs that are studied to find the best solution. The final consideration that cannot be overlooked is that of cost. The DART-75 is a 75-passenger medium-range regional transport intended for spoke-to-spoke, spoke-to-hub, and some hub-to-hub operations. Included are the general descriptions of the structures, weight and balance, stability and control, performance, and engine design.

Derived from text

N94-25709*# Auburn Univ., AL. Dept. of Aerospace Engineering.

EAGLE RTS: A DESIGN OF A REGIONAL TRANSPORT **c05**

Paul Bryer, Jon Buckles, Paul Lemke, and Kirk Peake *In* USRA, Proceedings of the 8th Annual Summer Conference: NASA/USRA Advanced Design Program 1992 p 373-378 (For primary document see N94-25665 07-80)

Avail: CASI HC A02/MF A04

The Eagle RTS (Regional Transport System) is a 66-passenger aircraft designed to satisfy the need for accessible and economical regional travel. The first design objective for the Eagle RTS is safety. Safety results primarily from avoidance of the hub airport air traffic, implementation of anti-stall characteristics by tailoring the canard, and proper positioning of the engines for blade shedding. To provide the most economical aircraft, the Eagle RTS will use existing technology to lower production and maintenance costs by decreasing the amount of new training required. In selecting the propulsion system, the effects on the environment were a main consideration. Two advantages of turbo-prop engines are the high fuel efficiency and low noise levels produced by this type of engine. This ensures the aircraft's usage during times of rising fuel costs and growing aircraft noise restrictions. The design of the Eagle RTS is for spoke-to-spoke transportation. It must be capable of landing on shorter runways and have speeds comparable to that of the larger aircraft to make its service beneficial to the airlines. With the use of turbo-prop engines and high lift devices, the Eagle RTS is highly adaptable to regional airports. The design topics discussed include: aerodynamics, stability, structures and materials, propulsion, and cost.

Author

N94-25710*# California Polytechnic State Univ., San Luis Obispo. Dept. of Aeronautical Engineering.

PRELIMINARY DESIGN OF NINE HIGH SPEED CIVIL TRANSPORTS **c05**

Doral Sandlin, Robert vantRiet, Dani Soban, and Ty Hoang *In* USRA, Proceedings of the 8th Annual Summer Conference: NASA/USRA Advanced Design Program 1992 p 379-390 (For primary document see N94-25665 07-80)

Avail: CASI HC A03/MF A04

Sixty senior design students at Cal Poly, SLO have completed a year-long project to design the next generation of High Speed Civil Transports (HSCT). The design process was divided up into three distinct phases. The first third of the project was devoted entirely to research into the special problems associated with an HSCT. These included economic viability, airport compatibility, high speed aerodynamics, sonic boom minimization, environmental impact, and structures and materials. The result of this research was the development of nine separate Requests for Proposal (RFP) that outlined reasonable yet challenging design criteria for the aircraft. All were designed to be technically feasible in the year 2015. The next phase of the project divided the sixty students into nine design groups. Each group, with its own RFP, completed a Class 1 preliminary design of an HSCT. The nine configurations varied from conventional double deltas to variable geometry wings to a pivoting oblique wing design. The final phase of the project included a more detailed Class 2 sizing as well as performance and stability and control analysis. Cal Poly, San Luis Obispo presents nine unique solutions to the same problem: that of designing an economically viable, environmentally acceptable, safe and comfortable supersonic transport.

Author

N94-25711*# California State Polytechnic Univ., Pomona. Dept. of Aerospace Engineering.

SUPERCRUISER ARROW HS-8 **c05**

Paul Lord, Edward Kao, Joey B. Abobo, Todd A. Collins, Leong Ma, Adnan Murad, Hitesh Naran, Thuan P. Nguyen, Timithy I. Nuon, and Dimitri D. Thomas *In* USRA, Proceedings of the 8th Annual Summer Conference: NASA/USRA Advanced Design Program 1992 p 391-405 (For primary document see N94-25665 07-80)

Avail: CASI HC A03/MF A04

Technology in aeronautics has advanced dramatically since the last design of a production High Speed Civil Transport (HSCT) aircraft. Newly projected requirements call for a new High Speed Civil Transport aircraft with a range of approximately 550 nm and at least 275 passenger capacity. The aircraft must be affordable and marketable. The new HSCT must be able to sustain long-duration flights and to absorb the abuse of daily operation. The new aircraft must be safe and simple to fly and require a minimum amount of maintenance. This aircraft must meet FAA certification criteria of FAR Part 25 and environmental constraints. Several design configurations were examined and two designs were selected for further investigation. The first design employs the delta planform wings and conventional empennage layout. The other design uses a swing wing layout and conventional empennage. Other engineering challenges, including materials and propulsion are also discussed. At a cruise flight speed between Mach 2.2 and Mach 3.0, no current generation of materials can endure the thermal loading of supersonic flight and satisfy the stringent weight requirements. A new generation of lightweight composite materials must be developed for the HSCT. With the enforcement of stage 3 noise restrictions, these new engines must be able to propel the aircraft and satisfy the noise limit. The engine with the most promise is the variable cycle engine. At low subsonic speeds the engine operates like a turbofan engine, providing the most efficient performance. At higher speeds the variable cycle engine operates as a turbojet power plant. The two large

engine manufacturers, General Electric and Pratt & Whitney in the United States, are combining forces to make the variable cycle engine a reality.
Author (revised)

N94-25712*# California State Univ., Northridge. Dept. of Mechanical Engineering.
PROJECT ARES 3 c05
Dan Raymer, Phyllis Russell, Tim Fox, Doug Meyers, Steven Lovric, Robert Grabow, Manfred Epp, Warren Wynn, Jr., Zoltan Mako, and Gunther Linzner et al *In* USRA, Proceedings of the 8th Annual Summer Conference: NASA/USRA Advanced Design Program 1992 p 406-412 (For primary document see N94-25665 07-80)
Avail: CASI HC A02/MF A04

The mission of Project Ares is to design and fabricate an Earth prototype, autonomous flying rover capable of flying on the Martian surface. The project was awarded to California State University, Northridge (CSUN) in 1989 where an in-depth paper study was completed. The second year's group, Project Ares 2, designed and fabricated a full-scale flight demonstration aircraft. Project Ares 3, the third and final group, is responsible for propulsion system design and installation, controls and instrumentation, and high altitude testing. The propulsion system consists of a motor and its power supply, geartrain, and propeller. The motor is a four-brush DC motor powered by a 50-V NiCd battery supply. A pulley and belt arrangement is used for the geartrain and includes light weight, low temperature materials. The propeller is constructed from composite materials which ensures high strength and light weight, and is specifically developed to provide thrust at extremely high altitudes. The aircraft is controlled with a ground-based radio control system and an autopilot which will activate in the event that the control signal is lost. A transponder is used to maintain radar contact for ground tracking purposes. The aircraft possesses a small, onboard computer for collecting and storing flight data. To safeguard the possibility of computer failure, all flight data is transmitted to a ground station via a telemetry system. An initial, unpowered, low-level test flight was completed in August of 1991. Testing of systems integration in the second low-level test flight resulted in loss of elevator control which caused considerable damage on landing. Complete failure analysis and repairs are scheduled for September of 1992. Author

N94-25713*# Case Western Reserve Univ., Cleveland, OH. Dept. of Mechanical and Aerospace Engineering.
TESSERACT SUPERSONIC BUSINESS TRANSPORT c05
Eli Reshotko, Gary Garbinski, James Fellenstein, Mary Botting, Joan Hooper, Michael Ryan, Peter Struk, Ben Taggart, Maggie Taillon, and Gary Warzynski *In* USRA, Proceedings of the 8th Annual Summer Conference: NASA/USRA Advanced Design Program 1992 p 413-424 (For primary document see N94-25665 07-80)
Avail: CASI HC A03/MF A04

This year, the senior level Aerospace Design class at Case Western Reserve University developed a conceptual design of a supersonic business transport. Due to the growing trade between Asia and the United States, a transpacific range was chosen for the aircraft. A Mach number of 2.2 was chosen, too, because it provides reasonable block times and allows the use of a large range of materials without a need for active cooling. A payload of 2,500 lbs. was assumed corresponding to a complement of nine passengers and crew, plus some light cargo. With these general requirements set, the class was broken down into three groups. The aerodynamics of the aircraft were the responsibility of the first group. The second developed the propulsion system. The efforts of both the aerodynamics and propulsion groups were monitored and reviewed for weight considerations and structural feasibility by the third group. Integration of the design required considerable interaction between the groups in the final stages. The fuselage length of the final conceptual design was 107.0 ft, while the diameter of the fuselage was 7.6 ft. The delta wing design consisted of an aspect ratio of 1.9 with a wing span of 47.75 ft and mid-chord length of 61.0 ft. A SNECMA MCV 99 variable-cycle engine design was chosen for this aircraft. Author (revised)

N94-25714*# Kansas Univ., Lawrence. Dept. of Aerospace Engineering.
A REVOLUTIONARY APPROACH TO COMPOSITE CONSTRUCTION AND FLIGHT MANAGEMENT SYSTEMS FOR SMALL, GENERAL AVIATION AIRPLANES c05
Jan Roskam and Ed Wenninger *In* USRA, Proceedings of the 8th Annual Summer Conference: NASA/USRA Advanced Design Program 1992 p 425-436 (For primary document see N94-25665 07-80)
Avail: CASI HC A03/MF A04

The design studies for two composite general aviation airplanes are presented. The main consideration for both of the designs was to avoid the typical 'metal replacement' philosophy that has hindered the widespread use of composites in general aviation aircraft. The first design is for a low wing aircraft based on the Smith Aircraft Corporation GT-3 Global Trainer. The second aircraft is a composite version of the Cessna 152. The project was conducted as a graduate level design class under the auspices of the KU/NASA/USRA Advanced Design Program in aeronautics. The results obtained from the Fall semester of 1991 and the Spring semester of 1992 are presented. Author (revised)

N94-25715*# Notre Dame Univ., IN. Dept. of Aerospace and Mechanical Engineering.
DESIGN STUDY TO SIMULATE THE DEVELOPMENT OF A COMMERCIAL FREIGHT TRANSPORTATION SYSTEM c05
Stephen M. Batill, Kevin Costello, and Jim Pinkelman *In* USRA, Proceedings of the 8th Annual Summer Conference: NASA/USRA Advanced Design Program 1992 p 437-452 (For primary document see N94-25665 07-80)
Avail: CASI HC A03/MF A04

The Notre Dame Aerospace Engineering senior class was divided into six design teams. A request for proposals (RFP) asking for the design of a remotely piloted vehicle (RPV) was given to the class, and each design team was responsible for designing, developing, producing, and presenting an RPV concept. The RFP called for the design of commercial freight transport RPV. The RFP provided a description of a fictitious world called 'Aeroworld'. Aeroworld's characteristics were scaled to provide the same types of challenges for RPV design that the real world market provides for the design of commercial aircraft. Fuel efficiency, range and payload capabilities, production and maintenance costs, and profitability are a few of the challenges that were addressed in this course. Each design team completed their project over the course of a semester by designing and flight testing a prototype, freight-carrying remotely piloted vehicle. Author

N94-25716*# Ohio State Univ., Columbus. Dept. of Aeronautical and Astronautical Engineering.
THE DESIGN OF FOUR HYPERSONIC RECONNAISSANCE AIRCRAFT c05
G. M. Gregorek and D. T. Detwiler *In* USRA, Proceedings of the 8th Annual Summer Conference: NASA/USRA Advanced Design Program 1992 p 453-462 (For primary document see N94-25665 07-80)
Avail: CASI HC A02/MF A04

Four different hypersonic reconnaissance aircraft were designed by separate student teams. These aircraft were designed to provide the U.S. with a system to acquire aerial tactical reconnaissance when satellite reconnaissance proved unobtainable or ineffective. The design requirements given for this project stated that these aircraft must carry a 7500 lb, 250 cu ft payload of electronic and photographic intelligence gathering equipment over a target area at speeds between Mach 4-7 and at altitudes above 80,000 ft. Two of the aircraft were required to be manned by a crew of two and have a range of 12,000 nmi. One of these was to use airborne refueling to complete its mission while the other was not to use any refueling. The other two aircraft were required to be unmanned with a range of 6,000 nmi. One of these was to take off from another aircraft. The final details of all four aircraft designs along with an overview of the design process is provided. Author (revised)

N94-25717*# Ecole Polytechnique Feminine, Sceaux (France).
DESIGN OF A REFUELING TANKER DELIVERING LIQUID HYDROGEN c05
Daniel Lourme, Caroline Barnier, Sabine Faure, Marie-Helene Pompei, and Karine Pruniaux *In* USRA, Proceedings of the 8th Annual Summer Conference: NASA/USRA Advanced Design Program 1992 p 463-466 (For primary document see N94-25665 07-80)
Avail: CASI HC A01/MF A04

A refueling tanker that could deliver 155,000 lb of liquid hydrogen to a hypersonic tanker in 15 min was designed. A flying boom system was chosen to fit strict delivery criteria. Tank design and material specification were also addressed. To assure the flow required, it was important to cancel the pressure drop phenomenon. Geometry, aerodynamics, weight considerations, propulsion, stability, and performance for the tanker were also considered. Finally, the cost of developing three prototypes was estimated. Author

N94-25718*# Purdue Univ., West Lafayette, IN. School of Aeronautics and Astronautics.

THE DESIGN OF A LONG-RANGE MEGATRANSPORT AIRCRAFT c05

Terrence A. Weisshaar and Carl L. Allen *In* USRA, Proceedings of the 8th Annual Summer Conference: NASA/USRA Advanced Design Program 1992 p 467-476 (For primary document see N94-25665 07-80)

Avail: CASI HC A02/MF A04

Aircraft manufacturers are examining the market and feasibility of long-range passenger aircraft carrying more than 600 passengers. These aircraft would carry travelers at reduced cost and, at the same time, reduce congestion around major airports. The design of a large, long-range transport involves broad issues such as: the integration of airport terminal facilities; passenger loading and unloading; trade-offs between aircraft size and the cost to reconfigure these existing facilities; and, defeating the 'square-cube' law. Thirteen Purdue design teams generated RFP's that defined passenger capability and range, based upon team perception of market needs and infrastructure constraints. Turbofan engines were designed by each group to power these aircraft. The design problem and the variety of solutions developed are reviewed. Author (revised)

N94-25719*# Worcester Polytechnic Inst., MA. Dept. of Mechanical Engineering.

SOLAR POWERED MULTIPURPOSE REMOTELY POWERED AIRCRAFT c05

A. N. Alexandrou, W. W. Durgin, R. F. Cohn, D. J. Olinger, Charlotte K. Cody, Agnes Chan, Kwok-Hung Cheung, Kristin Conley, Paul M. Crivelli, and Christian T. Javorski et al *In* USRA, Proceedings of the 8th Annual Summer Conference: NASA/USRA Advanced Design Program 1992 p 477-489 (For primary document see N94-25665 07-80)

Avail: CASI HC A03/MF A04

Increase in energy demands coupled with rapid depletion of natural energy resources have deemed solar energy as an attractive alternative source of power. The focus was to design and construct a solar powered, remotely piloted vehicle to demonstrate the feasibility of solar energy as an effective, alternate source of power. The final design included minimizing the power requirements and maximizing the strength-to-weight and lift-to-drag ratios. Given the design constraints, Surya (the code-name given to the aircraft), is a lightweight aircraft primarily built using composite materials and capable of achieving level flight powered entirely by solar energy. Author

N94-27893*# Old Dominion Univ., Norfolk, VA. Dept. of Mechanical Engineering.

THE 1993 NASA-ODU AMERICAN SOCIETY FOR ENGINEERING EDUCATION (ASEE) SUMMER FACULTY FELLOWSHIP PROGRAM

Final Report, 7 Jun. - 13 Aug. 1993

Surendra N. Tiwari, comp. and Deborah B. Young, comp Dec. 1993 238 p Fellowship program held in Norfolk, VA, 1993 Sponsored in part by NASA. Langley Research Center

(Grant NGT-47-003-029)

(NASA-CR-191544; NAS 1.26:191544) Avail: CASI HC A11/MF A03

Since 1964, the National Aeronautics and Space Administration has supported a program of summer faculty fellowships for engineering and science educators. In a series of collaborations between NASA research and development centers and nearby universities, engineering faculty members spend 10 weeks working with professional peers on research. The Summer Faculty Program Committee of the American Society for Engineering Education supervises the programs. Objectives are: to further the professional knowledge of qualified engineering and science faculty members; to stimulate and exchange ideas between participants and NASA; to enrich and refresh the research and teaching activities of participants' institutions; and to contribute to the research objectives of the NASA center. For individual titles, see N94-27894 through N94-27930.

N94-27894*# Arizona State Univ., Tempe. Dept. of Electrical Engineering.

HYBRID TECHNIQUES FOR COMPLEX AEROSPACE ELECTROMAGNETICS PROBLEMS c32

Jim Aberle *In* Old Dominion Univ., The 1993 NASA-ODU American Society for Engineering Education (ASEE) Summer Faculty Fellowship Program Dec. 1993 p 65-67 (For primary document see N94-27893 07-80)

Avail: CASI HC A01/MF A03

Important aerospace electromagnetics problems include the evaluation of antenna performance on aircraft and the prediction and control of the aircraft's electromagnetic signature. Due to the ever increasing complexity and expense of aircraft design, aerospace engineers have become increasingly dependent on computer solutions. Traditionally, computational electromagnetics (CEM) has relied primarily on four disparate techniques: the method of moments (MoM), the finite-difference time-domain (FDTD) technique, the finite element method (FEM), and high frequency asymptotic techniques (HFAT) such as ray tracing. Each of these techniques has distinct advantages and disadvantages, and no single technique is capable of accurately solving all problems of interest on computers that are available now or will be available in the foreseeable future. As a result, new approaches that overcome the deficiencies of traditional techniques are beginning to attract a great deal of interest in the CEM community. Among these new approaches are hybrid methods which combine two or more of these techniques into a coherent model. During the ASEE Summer Faculty Fellowship Program a hybrid FEM/MoM computer code was developed and applied to a geometry containing features found on many modern aircraft. Author (revised)

N94-27895*# Hampton Univ., VA. Dept. of Mass Media Arts.

RIAD VISUAL IMAGING BRANCH ASSESSMENT c35

Sherilee F. Beam *In* Old Dominion Univ., The 1993 NASA-ODU American Society for Engineering Education (ASEE) Summer Faculty Fellowship Program Dec. 1993 p 68-70 (For primary document see N94-27893 07-80)

Avail: CASI HC A01/MF A03

Every year the demand to visualize research efforts increases. The visualization provides the means to effectively analyze data and present the results. The technology support for visualization is constantly changing, improving, and being made available to users everywhere. As such, many researchers are entering into the practice of doing their own visualization in house - sometimes successfully, sometimes not. In an effort to keep pace with the visualization needs of researchers, the Visual Imaging Branch of the Research, Information, and Applications Division at NASA Langley Research Center has conducted an investigation into the current status of imaging technology and imaging production throughout the various research branches at the center. This investigation will allow the branch to evaluate its current resources and personnel in an effort to identify future directions for meeting the needs of the researchers at the center. The investigation team, which consisted of the ASEE fellow, the head of the video section, and the head of the photo section, developed an interview format that could be accomplished during a short interview period with researchers, and yet still provide adequate statistics about items such as in-house equipment and usage. Derived from text

N94-27896*# Colorado Univ., Denver. Dept. of Electrical Engineering.

ON IDENTIFIED PREDICTIVE CONTROL c63

Jan T. Bialasiewicz *In* Old Dominion Univ., The 1993 NASA-ODU American Society for Engineering Education (ASEE) Summer Faculty Fellowship Program Dec. 1993 p 71-73 (For primary document see N94-27893 07-80)

Avail: CASI HC A01/MF A03

Self-tuning control algorithms are potential successors to manually tuned PID controllers traditionally used in process control applications. A very attractive design method for self-tuning controllers, which has been developed over recent years, is the long-range predictive control (LRPC). The success of LRPC is due to its effectiveness with plants of unknown order and dead-time which may be simultaneously nonminimum phase and unstable or have multiple lightly damped poles (as in the case of flexible structures or flexible robot arms). LRPC is a receding horizon strategy and can be, in general terms, summarized as follows. Using assumed long-range (or multi-step) cost function the optimal control law is found in terms of unknown parameters of the predictor model of the process, current input-output sequence, and future reference signal sequence. The common approach is to assume that the input-output process model is known or separately identified and then to find the parameters of the predictor model. Once these are known, the optimal control law determines control signal at the current time t which is applied at the process input and the whole procedure is repeated at the next time instant. Most of the recent research in this field is apparently centered around the LRPC formulation developed by Clarke et al., known as generalized predictive control (GPC). GPC uses ARIMAX/CARIMA model of the process in its input-output formulation. In this paper, the GPC formulation is used but the process predictor model is derived from the state space formulation of the ARIMAX model and is directly identified over the receding horizon, i.e., using current input-output sequence. The underlying technique in the design of identified predictive control (IPC) algorithm is the identification algorithm of observer/Kalman filter Markov parameters developed by Juang et al. at NASA Langley Research Center and successfully applied to identification of flexible structures. Derived from text

N94-27897*# Northwestern Univ., Evanston, IL. Dept. of Mechanical Engineering.

EFFECTS OF PHYSICAL AGING ON LONG-TERM BEHAVIOR OF COMPOSITES **c24**

L. Catherine Brinson *In* Old Dominion Univ., The 1993 NASA-ODU American Society for Engineering Education (ASEE) Summer Faculty Fellowship Program Dec. 1993 p 74-77 (For primary document see N94-27893 07-80)

Avail: CASI HC A01/MF A03

The HSCT plane, envisioned to have a lifetime of over 60,000 flight hours and to travel at speeds in excess of Mach 2, is the source of intensive study at NASA. In particular, polymer matrix composites are being strongly considered for use in primary and secondary structures due to their high strength to weight ratio and the options of property tailoring. However, an added difficulty in the use of polymer based materials is that their properties change significantly over time, especially at the elevated temperatures that will be experienced during flight, and prediction of properties based on irregular thermal and mechanical loading is extremely difficult. This study focused on one aspect of long-term polymer composite behavior: physical aging. When a polymer is cooled to below its glass transition temperature, the material is not in thermodynamic equilibrium and the free volume and enthalpy evolve over time to approach their equilibrium values. During this time, the mechanical properties change significantly and this change is termed physical aging. This work begins with a review of the concepts of physical aging on a pure polymer system. The effective time theory, which can be used to predict long term behavior based on short term data, is mathematically formalized. The effects of aging to equilibrium are proven and discussed. The theory developed for polymers is then applied first to a unidirectional composite, then to a general laminate. Comparison to experimental data is excellent. It is shown that the effects of aging on the long-term properties of composites can be counter-intuitive, stressing the importance of the development and use of a predictive theory to analyze structures. Author (revised)

N94-27898*# Christopher Newport Coll., Newport News, VA. Dept. of Biology, Chemistry, and Environmental Science.

PROTON IRRADIATION ON MATERIALS **c72**

C. Ken Chang *In* Old Dominion Univ., The 1993 NASA-ODU American Society for Engineering Education (ASEE) Summer Faculty Fellowship Program Dec. 1993 p 78-79 (For primary document see N94-27893 07-80)

Avail: CASI HC A01/MF A03

A computer code is developed by utilizing a radiation transport code developed at NASA Langley Research Center to study the proton radiation effects on materials which have potential application in NASA's future space missions. The code covers the proton energy from 0.01 Mev to 100 Gev and is sufficient for energetic protons encountered in both low earth and geosynchronous orbits. With some modification, the code can be extended for particles heavier than proton as the radiation source. The code is capable of calculating the range, stopping power, exit energy, energy deposition coefficients, dose, and cumulative dose along the path of the proton in a target material. The target material can be any combination of the elements with atomic number ranging from 1 to 92, or any compound with known chemical composition. The generated cross section for a material is stored and is reused in future to save computer time. This information can be utilized to calculate the proton dose a material would receive in an orbit when the radiation environment is known. It can also be used to determine, in the laboratory, the parameters such as beam current of proton and irradiation time to attain the desired dosage for accelerated ground testing of any material. It is hoped that the present work be extended to include polymeric and composite materials which are prime candidates for use as coating, electronic components, and structure building. It is also desirable to determine, for ground testing these materials, the laboratory parameters in order to simulate the dose they would receive in space environments. A sample print-out for water subject to 1.5 Mev proton is included as a reference. Author (revised)

N94-27899*# Pennsylvania State Univ., University Park. Dept. of Mechanical Engineering.

A COMPREHENSIVE COMPARISON OF TURBULENCE MODELS IN THE FAR WAKE **c34**

John M. Cimbala *In* Old Dominion Univ., The 1993 NASA-ODU American Society for Engineering Education (ASEE) Summer Faculty Fellowship Program Dec. 1993 p 80-82 (For primary document see N94-27893 07-80)

Avail: CASI HC A01/MF A03

In the present study, the far wake was examined numerically using an implicit, upwind, finite-volume, compressible Navier-Stokes code. The numerical grid started at 500 equivalent circular cylinder diameters in the wave, and extended to 4000 equivalent diameters. By concentrating only on the far wake, the numerical difficulties and fine mesh requirements near the wake-generating body were eliminated. At the time of this writing, results for the K-epsilon and K-omega turbulence models at low Mach number have been completed and show excellent agreement with previous incompressible results and far-wake similarity solutions. The code is presently being used to compare the performance of various other turbulence models, including Reynolds stress models and the new anisotropic two-equation turbulence models being developed at NASA Langley. By increasing our physical understanding of the deficiencies and limits of these models, it is hoped that improvements to the universality of the models can be made. Future plans include examination of two-dimensional momentumless wakes as well. Author (revised)

N94-27900*# Norfolk State Univ., VA. Dept. of Chemistry and Physics.

AN EXPERIMENTAL INVESTIGATION OF FATIGUE DAMAGE IN ALUMINUM 2024-T3 ALLOYS **c26**

Milton W. Ferguson *In* Old Dominion Univ., The 1993 NASA-ODU American Society for Engineering Education (ASEE) Summer Faculty Fellowship Program Dec. 1993 p 83-84 (For primary document see N94-27893 07-80)

Avail: CASI HC A01/MF A03

Aluminum alloys are finding increasing use in the aerospace and automobile industries due to their attractive low density-high modulus and low density-high strength characteristics. Unfortunately, cyclic stress-strain deformation alters the microstructure of the material. These structural changes can lead to fatigue damage and ultimately service failure. Therefore, in order to assess the integrity of the alloy, a correlation between fatigue damage and a measurable microstructural property is needed. Aluminum 2024-T3, a commonly used commercial alloy, contains many grains (individual crystals) of various orientations. The sizes and orientations of these grains are known to affect the strength, hardness, and magnetic permeability of polycrystalline alloys and metals; therefore, perhaps a relationship between a grain property and the fatigue state can be established. Tension-compression cycling in aluminum alloys can also induce changes in their dislocation densities. These changes can be studied from measurements of the electrical resistivities of the materials. Consequently, the goals of this investigation were: to study the grain orientation of aluminum 2024-T3 and to seek a correlation between the grain orientation and the fatigue state of the material; and to measure the electrical resistivities of fatigued samples of aluminum 2024-T3 and to interpret the findings. Derived from text

N94-27901*# Old Dominion Univ., Norfolk, VA. Dept. of Psychology.

BRAIN WAVE CORRELATES OF ATTENTIONAL STATES: EVENT RELATED POTENTIALS AND QUANTITATIVE EEG ANALYSIS DURING PERFORMANCE OF COGNITIVE AND PERCEPTUAL TASKS c53

Frederick G. Freeman *In its* The 1993 NASA-ODU American Society for Engineering Education (ASEE) Summer Faculty Fellowship Program Dec. 1993 p 85-88 (For primary document see N94-27893 07-80)

Avail: CASI HC A01/MF A03

The increased use of automation in the cockpits of commercial planes has dramatically decreased the workload requirements of pilots, enabling them to function more efficiently and with a higher degree of safety. Unfortunately, advances in technology have led to an unexpected problem: the decreased demands on pilots have increased the probability of inducing 'hazardous states of awareness.' A hazardous state of awareness is defined as a decreased level of alertness or arousal which makes an individual less capable of reacting to unique or emergency types of situations. These states tend to be induced when an individual is not actively processing information. Under such conditions a person is likely to let his/her mind wander, either to internal states or to irrelevant external conditions. As a result, they are less capable of reacting quickly to emergency situations. Since emergencies are relatively rare, and since the high automated cockpit requires progressively decreasing levels of engagement, the probability of being seduced into a lowered state of awareness is increasing. This further decreases the readiness of the pilot to react to unique circumstances such as system failures. The HEM Lab at NASA-Langley Research Center has been studying how these states of awareness are induced and what the physiological correlates of these different states are. Specifically, they have been interested in studying electroencephalographic (EEG) measures of different states of alertness to determine if such states can be identified and, hopefully, avoided. The project worked on this summer involved analyzing the EEG and the event related potentials (ERP) data collected while subjects performed under two conditions. Each condition required subjects to perform a relatively boring vigilance task. The purpose of using these tasks was to induce a decreased state of awareness while still requiring the subject to process information. Each task involved identifying an infrequently presented target stimulus. In addition to the task requirements, irrelevant tones were presented in the background. Research has shown that even though these stimuli are not attended, ERP's to them can still be elicited. The amplitude of the ERP waves has been shown to change as a function of a person's level of alertness. ERP's were also collected and analyzed for the target stimuli for each task. Brain maps were produced based on the ERP voltages for the different stimuli. In addition to the ERP's, a quantitative EEG (QEEG) was performed on the data using a fast Fourier technique to produce a power spectral analysis of the EEG. This analysis was conducted on the continuous EEG while the subjects were performing the tasks. Finally, a QEEG was performed on periods during the task when subjects indicated that they were in an altered state of awareness. During the tasks, subjects were asked to indicate by pressing a button when they realized their level of task awareness had changed. EEG epochs were collected for times just before and just after subjects made this reponse. The purpose of this final analysis was to determine whether or not subjective indices of level of awareness could be correlated with different patterns of EEG. Derived from text

N94-27902*# Texas A&M Univ., College Station. Dept. of Aerospace Engineering.

INVESTIGATION OF AERODYNAMIC DESIGN ISSUES WITH REGIONS OF SEPARATED FLOW c02

Tom Gally *In* Old Dominion Univ., The 1993 NASA-ODU American Society for Engineering Education (ASEE) Summer Faculty Fellowship Program Dec. 1993 p 89-90 (For primary document see N94-27893 07-80)

Avail: CASI HC A01/MF A03

Existing aerodynamic design methods have generally concentrated on the optimization of airfoil or wing shapes to produce a minimum drag while satisfying some basic constraints such as lift, pitching moment, or thickness. Since the minimization of drag almost always precludes the existence of separated flow, the evaluation and validation of these design methods for their robustness and accuracy when separated flow is present has not been aggressively pursued. However, two new applications for these design tools may be expected to include separated flow and the issues of aerodynamic design with this feature must be addressed. The first application of the aerodynamic design tools is the design of airfoils or wings to provide an optimal performance over a wide range of flight conditions (multipoint design). While the definition of 'optimal performance' in the multipoint setting is currently being hashed out, it is recognized that given a wide range of flight conditions, it will not be possible to ensure a minimum drag constraint at all conditions, and in fact some amount of separated flow (presumably small) may have to be allowed at the more demanding flight conditions. Thus a multipoint design method must be tolerant of the existence of separated flow and may include some controls upon its extent. The second application is in the design of wings with extended high speed buffet boundaries of their flight envelopes. Buffet occurs on a wing when regions of flow separation have grown to the extent that their time varying pressures induce possible destructive effects upon the wing structure or adversely effect either the aircraft controllability or passenger comfort. A conservative approach to the expansion of the buffet flight boundary is to simply expand the flight envelope of nonseparated flow under the assumption that buffet will also thus be alleviated. However, having the ability to design a wing with separated flow and thus to control the location, extent and severity of the separated flow regions may allow aircraft manufacturers to gain an advantage in the early design stages of an aircraft, when configuration changes are relatively inexpensive to make. The goal of the summer research at NASA Langley Research Center (LaRC) was twofold: first, to investigate a particular airfoil design problem observed under conditions of strong shock induced flow separation on the upper surface of an airfoil at transonic conditions; and second, to suggest and investigate design methodologies for the prediction (or detection) and control of flow separation. The context of both investigations was to use an existing two dimensional Navier-Stokes flow solver and the constrained direct/iterative surface curvature (CDISC) design algorithm developed at LaRC. As a lead in to the primary task, it was necessary to gain a familiarity with both the design method and the computational analysis and to perform the FORTRAN coding needed to couple them together. Derived from text

N94-27903*# Wilkes Coll., Wilkes-Barre, PA. Dept. of Mechanical and Material Engineering.

MICROSPHERES FOR LASER VELOCIMETRY IN HIGH TEMPERATURE WIND TUNNEL c09

Anthony Ghorieshi *In* Old Dominion Univ., The 1993 NASA-ODU American Society for Engineering Education (ASEE) Summer Faculty Fellowship Program Dec. 1993 p 91-99 (For primary document see N94-27893 07-80)

Avail: CASI HC A02/MF A03

The introduction of non-intrusive measurement techniques in wind tunnel experimentation has been a turning point in error free data acquisition. Laser velocimetry has been progressively implemented and utilized in various wind tunnels; e.g. subsonic, transonic, and supersonic. The success of the laser velocimeter technique is based on an accurate measurement of scattered light by seeding particles introduced into the flow stream in the wind tunnel. Therefore, application of appropriate seeding particles will affect, to a large extent the acquired data. The seeding material used depends on the type of experiment being run. Among the seeding material for subsonic tunnel are kerosene, Kaolin, and polystyrene. Polystyrene is known to be the best because of being solid particles, having high index of refraction, capable of being made both spherical and monodisperse. However for high temperature wind tunnel testing seeding material must have an additional characteristic that is high melting point. Typically metal oxide powders such as Al2O3 with melting point 3660 F are used. The metal oxides are, however polydispersed, have a high density, and a tendency to form large agglomerate that does not closely follow the flow velocity. The addition of flame phase silica to metal oxide helps to break up the agglomerates, yet still results in a narrow band of polydispersed seeding. The less desirable utility of metal oxide in high temperature wind tunnels necessitates the search for a better alternative particle seeding which this paper addresses. The Laser Velocimetry (LV) characteristic of polystyrene makes it a prime candidate as a base material in achieving the high temperature particle seeding inexpensively. While polystyrene monodisperse seeding particle reported has been successful in a subsonic wind tunnel, it lacks the high melting point and thus is not practically usable in a high temperature wind tunnel. It is well known that rise in melting point of polystyrene can be achieved by a cross-linking technique. Since polystyrene already possesses all the desired characteristics for LV, to circumvent the low melting point, a cross-linking technique was investigated. Author

N94-27904*# Mary Washington Coll., Fredricksburg, VA. Dept. of Chemistry.

NEW MONOMERS FOR HIGH PERFORMANCE POLYMERS **c27**

Roy F. Gratz *In* Old Dominion Univ., The 1993 NASA-ODU American Society for Engineering Education (ASEE) Summer Faculty Fellowship Program Dec. 1993 p 100-101 (For primary document see N94-27893 07-80)

Avail: CASI HC A01/MF A03

This laboratory has been concerned with the development of new polymeric materials with high thermo-oxidative stability for use in the aerospace and electronics industries. Currently, there is special emphasis on developing matrix resins and composites for the high speed civil transport (HSCT) program. This application requires polymers that have service lifetimes of 60,000 hr at 350 F (177 C) and that are readily processible into void-free composites, preferably by melt-flow or powder techniques that avoid the use of high boiling solvents. Recent work has focused on copolymers which have thermally stable imide groups separated by flexible arylene ether linkages, some with trifluoromethyl groups attached to the aromatic rings. The presence of trifluoromethyl groups in monomers and polymers often improves their solubility and processibility. The goal of this research was to synthesize several new monomers containing pendant trifluoromethyl groups and to incorporate these monomers into new imide/arylene ether copolymers. Initially, work was begun on the synthesis of three target compounds. The first two, 3,5-dihydroxybenzo trifluoride and 3-amino 5-hydroxybenzo trifluoride, are intermediates in the synthesis of more complex monomers. The third, 3,5-bis (3-amino-phenoxy) benzotrifluoride, is an interesting diamine that could be incorporated into a polyimide directly. Author

N94-27905*# Drexel Univ., Philadelphia, PA. Dept. of Electrical and Computer Engineering.

NEURAL CONTROL OF MAGNETIC SUSPENSION SYSTEMS **c09**

W. Steven Gray *In* Old Dominion Univ., The 1993 NASA-ODU American Society for Engineering Education (ASEE) Summer Faculty Fellowship Program Dec. 1993 p 102-103 (For primary document see N94-27893 07-80)

Avail: CASI HC A01/MF A03

The purpose of this research program is to design, build and test (in cooperation with NASA personnel from the NASA Langley Research Center) neural controllers for two different small air-gap magnetic suspension systems. The general objective of the program is to study neural network architectures for the purpose of control in an experimental setting and to demonstrate the feasibility of the concept. The specific objectives of the research program are: (1) to demonstrate through simulation and experimentation the feasibility of using neural controllers to stabilize a nonlinear magnetic suspension system; (2) to investigate through simulation and experimentation the performance of neural controllers designs under various types of parametric and nonparametric uncertainty; (3) to investigate through simulation and experimentation various types of neural architectures for real-time control with respect to performance and complexity; and (4) to benchmark in an experimental setting the performance of neural controllers against other types of existing linear and nonlinear compensator designs. To date, the first one-dimensional, small air-gap magnetic suspension system has been built, tested and delivered to the NASA Langley Research Center. The device is currently being stabilized with a digital linear phase-lead controller. The neural controller hardware is under construction. Two different neural network paradigms are under consideration, one based on hidden layer feedforward networks trained via back propagation and one based on using Gaussian radial basis functions trained by analytical methods related to stability conditions. Some advanced nonlinear control algorithms using feedback linearization and sliding mode control are in simulation studies. Author (revised)

N94-27906*# Moravian Coll., Bethlehem, PA. Dept. of Computer Science.

LOCATING TIE-POINTS ON A GRID **c61**

Jim Green *In* Old Dominion Univ., The 1993 NASA-ODU American Society for Engineering Education (ASEE) Summer Faculty Fellowship Program Dec. 1993 p 104-108 (For primary document see N94-27893 07-80)

Avail: CASI HC A01/MF A03

A robust software method is described for analyzing a digitized image of a calibration grid in order to determine the location of the intersections of its grid lines or tie-points. Derived from text

N94-27907*# Christopher Newport Coll., Newport News, VA. Dept. of Physics and Computer Science.

SPACECRAFT OPTICAL DISK RECORDER MEMORY BUFFER CONTROL **c35**

Robert F. Hodson *In* Old Dominion Univ., The 1993 NASA-ODU American Society for Engineering Education (ASEE) Summer Faculty Fellowship Program Dec. 1993 p 109-113 (For primary document see N94-27893 07-80)

Avail: CASI HC A01/MF A03

This paper discusses the research completed under the NASA-ASEE summer faculty fellowship program. The project involves development of an Application Specific Integrated Circuit (ASIC) to be used as a Memory Buffer Controller (MBC) in the Spacecraft Optical Disk System (SODR). The SODR system has demanding capacity and data rate specifications requiring specialized electronics to meet processing demands. The system is being designed to support Gigabit transfer rates with Terabit storage capability. The complete SODR system is designed to exceed the capability of all existing mass storage systems today. The ASIC development for SODR consist of developing a 144 pin CMOS device to perform format conversion and data buffering. The final simulations of the MBC were completed during this summer's NASA-ASEE fellowship along with design preparations for fabrication to be performed by an ASIC manufacturer. Author

N94-27908*# Old Dominion Univ., Norfolk, VA. Dept. of Mechanical Engineering.

SYSTEM IDENTIFICATION OF THE LARGE-ANGLE MAGNETIC SUSPENSION TEST FACILITY (LAMSTF) **c09**

Jen-Kuang Huang *In its* The 1993 NASA-ODU American Society for Engineering Education (ASEE) Summer Faculty Fellowship Program Dec. 1993 p 114-115 (For primary document see N94-27893 07-80)

Avail: CASI HC A01/MF A03

The Large-Angle Magnetic Suspension Test Facility (LAMSTF), a laboratory-scale research project to demonstrate the magnetic suspension of objects over wide ranges of attitudes, has been developed. This system represents a scaled model of a planned Large-Gap Magnetic Suspension System (LGMSS). The LAMSTF system consists of a planar array of five copper electromagnets which actively suspend a small cylindrical permanent magnet. The cylinder is a rigid body and can be controlled to move in five independent degrees of freedom. Five position variables are sensed indirectly by using infra-red light-emitting diodes and light-receiving phototransistors. The motion of the suspended cylinder is in general nonlinear and hence only the linear, time-invariant perturbed motion about an equilibrium state is considered. One of the main challenges in this project is the control of the suspended element over a wide range of orientations. An accurate dynamic model plans an essential role in controller design. The analytical model of the LAMSTF system includes highly unstable real poles (about 10 Hz) and low-frequency flexible modes (about 0.16 Hz). Projection filters are proposed to identify the state space model from closed-loop test data in time domain. A canonical transformation matrix is also derived to transform the identified state space model into the physical coordinate. The LAMSTF system is stabilized by using a linear quadratic regulator (LQR) feedback controller. The rate information is obtained by calculating the back difference of the sensed position signals. The reference inputs contain five uncorrelated random signals. This control input and the system reponse are recorded as input/output data to identify the system directly from the projection filters. The sampling time is 4 ms and the model is fairly accurate in predicting the step responses for different controllers while the analytical model has a deficiency in the pitch axis. Author

N94-27909*# College of William and Mary, Williamsburg, VA. Dept. of Chemistry.

KINETIC PARAMETERS FROM THERMOGRAVIMETRIC ANALYSIS **c25**

Richard L. Kiefer *In* Old Dominion Univ., The 1993 NASA-ODU American

Society for Engineering Education (ASEE) Summer Faculty Fellowship Program Dec. 1993 p 116-119 (For primary document see N94-27893 07-80)
Avail: CASI HC A01/MF A03

High performance polymeric materials are finding increased use in aerospace applications. Proposed high speed aircraft will require materials to withstand high temperatures in an oxidative atmosphere for long periods of time. It is essential that accurate estimates be made of the performance of these materials at the given conditions of temperature and time. Temperatures of 350 F (177 C) and times of 60,000 to 100,000 hours are anticipated. In order to survey a large number of high performance polymeric materials on a reasonable time scale, some form of accelerated testing must be performed. A knowledge of the rate of a process can be used to predict the lifetime of that process. Thermogravimetric analysis (TGA) has frequently been used to determine kinetic information for degradation reactions in polymeric materials. Flynn and Wall studied a number of methods for using TGA experiments to determine kinetic information in polymer reactions. Kinetic parameters, such as the apparent activation energy and the frequency factor, can be determined in such experiments. Recently, researchers at the McDonnell Douglas Research Laboratory suggested that a graph of the logarithm of the frequency factor against the apparent activation energy can be used to predict long-term thermo-oxidative stability for polymeric materials. Such a graph has been called a kinetic map. In this study, thermogravimetric analyses were performed in air to study the thermo-oxidative degradation of several high performance polymers and to plot their kinetic parameters on a kinetic map. Author

N94-27910*# College of William and Mary, Williamsburg, VA. Dept. of Mathematics.
THE MOLECULAR MATCHING PROBLEM **c72**
Rex K. Kincaid *In* Old Dominion Univ., The 1993 NASA-ODU American Society for Engineering Education (ASEE) Summer Faculty Fellowship Program Dec. 1993 p 120-122 (For primary document see N94-27893 07-80)
Avail: CASI HC A01/MF A03

Molecular chemistry contains many difficult optimization problems that have begun to attract the attention of optimizers in the Operations Research community. Problems including protein folding, molecular conformation, molecular similarity, and molecular matching have been addressed. Minimum energy conformations for simple molecular structures such as water clusters, Lennard-Jones microclusters, and short polypeptides have dominated the literature to date. However, a variety of interesting problems exist and we focus here on a molecular structure matching (MSM) problem. Author

N94-27911*# Old Dominion Univ., Norfolk, VA. Dept. of Mechanical Engineering and Mechanics.
A NUMERICAL STUDY OF MIXING AND COMBUSTION IN HYPERVELOCITY FLOWS THROUGH A SCRAMJET COMBUSTOR MODEL **c34**
Ramesh Krishamurthy *In its* The 1993 NASA-ODU American Society for Engineering Education (ASEE) Summer Faculty Fellowship Program Dec. 1993 p 123-125 (For primary document see N94-27893 07-80)
Avail: CASI HC A01/MF A03

Interest in high speed, air-breathing propulsion systems such as scramjets has revived in recent years fueled to a large extent by the National Aerospace Plane (NASP) program. These vehicles are expected to fly trans-atmospheric and as a consequence, the Mach number level within the engine/combustor would be rather high (M greater than 5). Ground based testing of such scramjet engines requires a facility that can not only achieve the right Mach number, but also have the proper pressures and temperatures to simulate the combustion processes. At present, only pulse type facilities can provide such high enthalpy flows. The newest of these is the free-piston shock tunnel, T5 located at GALCIT. Recently, a generic combustor model was tested in T5, and the experimental data from that study is analyzed in the present report. The available experimental data from T5 are essentially the static pressures on the injection wall and the one opposite to it. Thus, a principal aim of the present study was to validate the available experimental data by using a proven CFD tool and then investigate the performance characteristics of the combustor model, such as, the mixing efficiency and combustion efficiency. For this purpose, in this study, the code GASP has been used. Author

N94-27912*# Old Dominion Univ., Norfolk, VA. Dept. of Engineering Technology.
EXPERIMENTAL APPARATUS FOR OPTIMIZATION OF FLAP POSITION FOR A THREE-ELEMENT AIRFOIL MODEL **c09**
Drew Landman *In its* The 1993 NASA-ODU American Society for Engineering Education (ASEE) Summer Faculty Fellowship Program Dec. 1993 p 126-128 (For primary document see N94-27893 07-80)
Avail: CASI HC A01/MF A03

It is proposed to design and build a wind tunnel model comprising a Douglas Aircraft Company three-element high-lift airfoil with internal actuators to move the flap vertically and horizontally under computer control. The model will be used to find the optimum flap location for a fixed angle of attack, slat position and flap deflection angle. The model will span the full tunnel width and lift will be measured by integration of pressure readings taken from midspan taps. It is proposed to conduct experiments in the NASA Langley EFPB 2' x 3' low speed wind tunnel. This report serves as a project overview and a review of work completed to date through funding by the 1993 NASA/ASEE Summer Faculty Fellowship Program. Author

N94-27913*# Missouri Univ., Columbia. Electrical and Computer Engineering.
AN OVERVIEW ON DEVELOPMENT OF NEURAL NETWORK TECHNOLOGY Abstract Only **c63**
Chun-Shin Lin *In* Old Dominion Univ., The 1993 NASA-ODU American Society for Engineering Education (ASEE) Summer Faculty Fellowship Program Dec. 1993 p 129 (For primary document see N94-27893 07-80)
Avail: CASI HC A01/MF A03

The study has been to obtain a bird's-eye view of the current neural network technology and the neural network research activities in NASA. The purpose was two fold. One was to provide a reference document for NASA researchers who want to apply neural network techniques to solve their problems. Another one was to report out survey results regarding NASA research activities and provide a view on what NASA is doing, what potential difficulty exists and what NASA can/should do. In a ten week study period, we interviewed ten neural network researchers in the Langley Research Center and sent out 36 survey forms to researchers at the Johnson Space Center, Lewis Research Center, Ames Research Center and Jet Propulsion Laboratory. We also sent out 60 similar forms to educators and corporation researchers to collect general opinions regarding this field. Twenty-eight survey forms, 11 from NASA researchers and 17 from outside, were returned. Survey results were reported in our final report. In the final report, we first provided an overview on the neural network technology. We reviewed ten neural network structures, discussed the applications in five major areas, and compared the analog, digital and hybrid electronic implementation of neural networks. In the second part, we summarized known NASA neural network research studies and reported the results of the questionnaire survey. Survey results show that most studies are still in the development and feasibility study stage. We compared the techniques, application areas, researchers' opinions on this technology, and many aspects between NASA and non-NASA groups. We also summarized their opinions on difficulties encountered. Applications are considered the top research priority by most researchers. Hardware development and learning algorithm improvement are the next. The lack of financial and management support is among the difficulties in research study. All researchers agree that the use of neural networks could result in cost saving. Fault tolerance has been claimed as one important feature of neural computing. However, the survey indicates that very few studies address this issue. Fault tolerance is important in space mission and aircraft control. We believe that it is worthy for NASA to devote more efforts into the utilization of this feature. Author

N94-27914*# Arizona Univ., Tucson. Dept. of Aerospace and Mechanical Engineering.
MECHANICALLY FASTENED COMPOSITE LAMINATES SUBJECTED TO COMBINED BEARING-BYPASS AND SHEAR LOADING **c24**
Erdogan Madenci *In* Old Dominion Univ., The 1993 NASA-ODU American Society for Engineering Education (ASEE) Summer Faculty Fellowship Program Dec. 1993 p 130-136 (For primary document see N94-27893 07-80)
Avail: CASI HC A02/MF A03

Bolts and rivets provide a means of load transfer in the construction of aircraft. However, they give rise to stress concentrations and are often the source and location of static and fatigue failures. Furthermore, fastener holes are prone to cracks during take-off and landing. These cracks present the most common origin of structural failures in aircraft. Therefore, accurate determination of the contact stresses associated with such loaded holes in mechanically fastened joints is essential to reliable strength evaluation and failure prediction. As the laminate is subjected to loading, the contact region, whose extent is not known, develops between the fastener and the hole boundary through this contact region, which consists of slip and no-slip zones due to friction. The presence of the unknown contact stress distribution over the contact region between the pin and the composite laminate, material anisotropy, friction between the pin and the laminate, pin-hole clearance, combined bearing-bypass and shear loading, and finite geometry of the laminate result in a complex non-linear problem. In the case of bearing-bypass loading in compression, this non-linear problem is further complicated by the presence of dual contact regions. Previous research concerning the analysis of mechanical joints subjected to combined bearing-bypass and shear loading is non-existent. In the case of bearing-bypass loading only, except for the study conducted by Naik and Crews (1991), others employed the concept of superposition which is not valid for this non-linear problem. Naik and Crews applied a linear finite element analysis with conditions along the pin-hole contact region specified as displacement constraint equations. The major shortcoming of this method is that the variation of the contract region as a function of the applied load should be known a priori. Also, their analysis is limited to symmetric geometry and material systems, and frictionless boundary conditions. Since the contact stress distribution and the contact region are not known a priori, they did not directly impose the boundary conditions appropriate for modelling the contact and on-contact regions between the fastener and the hole. Furthermore, finite element analysis is not suitable for iterative design calculations for optimizing laminate construction in the presence of fasteners under complex loading conditions. In this study, the solution method developed by Madenci and Ileri (1992a,b) has been extended to determine the contact stresses in mechanical joints under combined bearing-bypass and shear loading, and bearing-bypass loading in compression resulting in dual contact regions. Author

N94-27915*# University of Southern Illinois, Carbondale. Dept. of Physics.

RADIATIONS FROM HOT NUCLEI **c72**

F. Bary Malik *In* Old Dominion Univ., The 1993 NASA-ODU American Society for Engineering Education (ASEE) Summer Faculty Fellowship Program Dec. 1993 p 137-139 (For primary document see N94-27893 07-80)

Avail: CASI HC A01/MF A03

The investigation indicates that nuclei with excitation energy of a few hundred MeV to BeV are more likely to radiate hot nuclear clusters than neutrons. These daughter clusters could, furthermore, de-excite emitting other hot nuclei, and the chain continues until these nuclei cool off sufficiently to evaporate primarily neutrons. A few GeV excited nuclei could radiate elementary particles preferentially over neutrons. Impact of space radiation with materials (for example, spacecraft) produces highly excited nuclei which cool down emitting electromagnetic and particle radiations. At a few MeV excitation energy, neutron emission becomes more dominant than gamma-ray emission and one often attributes the cooling to take place by successive neutron decay. However, a recent experiment studying the cooling process of 396 MeV excited Hg-190 casts some doubt on this thinking, and the purpose of this investigation is to explore the possibility of other types of nuclear emission which might out-compete with neutron evaporation. Author

N94-27916*# Tuskegee Inst., AL. Dept. of Computer Science.

REVIEW AND ANALYSIS OF DENSE LINEAR SYSTEM SOLVER PACKAGE FOR DISTRIBUTED MEMORY MACHINES **c61**

H. N. Narang *In* Old Dominion Univ., The 1993 NASA-ODU American Society for Engineering Education (ASEE) Summer Faculty Fellowship Program Dec. 1993 p 140-145 (For primary document see N94-27893 07-80)

Avail: CASI HC A02/MF A03

A dense linear system solver package recently developed at the University of Texas at Austin for distributed memory machine (e.g. Intel Paragon) has been reviewed and analyzed. The package contains about 45 software routines, some written in FORTRAN, and some in C-language, and forms the basis for parallel/distributed solutions of systems of linear equations encountered in many problems of scientific and engineering nature. The package, being studied by the Computer Applications Branch of the Analysis and Computation Division, may provide a significant computational resource for NASA scientists and engineers in parallel/distributed computing. Since the package is new and not well tested or documented, many of its underlying concepts and implementations were unclear; our task was to review, analyze, and critique the package as a step in the process that will enable scientists and engineers to apply it to the solution of their problems. All routines in the package were reviewed and analyzed. Underlying theory or concepts which exist in the form of published papers or technical reports, or memos, were either obtained from the author, or from the scientific literature; and general algorithms, explanations, examples, and critiques have been provided to explain the workings of these programs. Wherever the things were still unclear, communications were made with the developer (author), either by telephone or by electronic mail, to understand the workings of the routines. Whenever possible, tests were made to verify the concepts and logic employed in their implementations. A detailed report is being separately documented to explain the workings of these routines. Author

N94-27917*# Mississippi State Univ., Mississippi State. Dept. of Aerospace Engineering.

WING DESIGN FOR A CIVIL TILTROTOR TRANSPORT AIRCRAFT: A PRELIMINARY STUDY **c05**

Masoud Rais-Rohani *In* Old Dominion Univ., The 1993 NASA-ODU American Society for Engineering Education (ASEE) Summer Faculty Fellowship Program Dec. 1993 p 147-148 (For primary document see N94-27893 07-80)

Avail: CASI HC A01/MF A03

A preliminary study was conducted on the design of the wing-box structure for a civil tiltrotor transport aircraft. The wing structural weight is to be minimized subject to structural and aeroelastic constraints. The composite wing-box structure is composed of skin, stringers, ribs, and spars. The design variables include skin ply thicknesses and orientations and spar cap and stringer cross-sectional areas. With the total task defined, an initial study was conducted to learn more about the intricate dynamic and aeroelastic characteristics of the tiltrotor aircraft and their roles in the wing design. Also, some work was done on the wing finite-element modeling (via PATRAN) which would be used in structural analysis and optimization. Initial studies indicate that in order to limit the wing/rotor aeroelastic and dynamic interactions in the preliminary design, the cruise speed, rotor system, and wing geometric attributes must all be held fixed. Author (revised)

N94-27918*# Saint Cloud State Coll., MN. Dept. of Electrical Engineering.

A SIMULATION OF GPS AND DIFFERENTIAL GPS SENSORS **c04**

James M. Rankin *In* Old Dominion Univ., The 1993 NASA-ODU American Society for Engineering Education (ASEE) Summer Faculty Fellowship Program Dec. 1993 p 149-153 (For primary document see N94-27893 07-80)

Avail: CASI HC A01/MF A03

The Global Positioning System (GPS) is a revolutionary advance in navigation. Users can determine latitude, longitude, and altitude by receiving range information from at least four satellites. The statistical accuracy of the user's position is directly proportional to the statistical accuracy of the range measurement. Range errors are caused by clock errors, ephemeris errors, atmospheric delays, multipath errors, and receiver noise. Selective Availability, which the military uses to intentionally degrade accuracy for non-authorized users, is a major error source. The proportionality constant relating position errors to range errors is the Dilution of Precision (DOP) which is a function of the satellite geometry. Receivers separated by relatively short distances have the same satellite and atmospheric errors. Differential GPS (DGPS) removes these errors by transmitting pseudorange corrections from a fixed receiver to a mobile receiver. The corrected pseudorange at the moving receiver is now corrupted only by errors from the receiver clock, multipath, and measurement noise. This paper describes a software package that models position errors for various GPS and DGPS systems. The error model is used in the Real-Time Simulator and Cockpit Technology workstation simulations at NASA-LaRC. The GPS/DGPS sensor can simulate enroute navigation, instrument approaches, or on-airport navigation. Author (revised)

N94-27919*# Virginia State Univ., Petersburg. Dept. of Engineering Technology.
AERODYNAMIC HEATING IN HYPERSONIC FLOWS c02
C. Subba Reddy *In* Old Dominion Univ., The 1993 NASA-ODU American Society for Engineering Education (ASEE) Summer Faculty Fellowship Program Dec. 1993 p 154-155 (For primary document see N94-27893 07-80)
Avail: CASI HC A01/MF A03

Aerodynamic heating in hypersonic space vehicles is an important factor to be considered in their design. Therefore the designers of such vehicles need reliable heat transfer data in this respect for a successful design. Such data is usually produced by testing the models of hypersonic surfaces in wind tunnels. Most of the hypersonic test facilities at present are conventional blow-down tunnels whose run times are of the order of several seconds. The surface temperatures on such models are obtained using standard techniques such as thin-film resistance gages, thin-skin transient calorimeter gages and coaxial thermocouple or video acquisition systems such as phosphor thermography and infrared thermography. The data are usually reduced assuming that the model behaves like a semi-infinite solid (SIS) with constant properties and that heat transfer is by one-dimensional conduction only. This simplifying assumption may be valid in cases where models are thick, run-times short, and thermal diffusivities small. In many instances, however, when these conditions are not met, the assumption may lead to significant errors in the heat transfer results. The purpose of the present paper is to investigate this aspect. Specifically, the objectives are as follows: (1) to determine the limiting conditions under which a model can be considered a semi-infinite body; (2) to estimate the extent of errors involved in the reduction of the data if the models violate the assumption; and (3) to come up with correlation factors which when multiplied by the results obtained under the SIS assumption will provide the results under the actual conditions. Author (revised)

N94-27920*# Virginia Polytechnic Inst. and State Univ., Blacksburg. Dept. of Mechanical Engineering.
DEVELOPMENT OF METHODOLOGIES FOR THE ESTIMATION OF THERMAL PROPERTIES ASSOCIATED WITH AEROSPACE VEHICLES c39
Elaine P. Scott *In* Old Dominion Univ., The 1993 NASA-ODU American Society for Engineering Education (ASEE) Summer Faculty Fellowship Program Dec. 1993 p 158-161 (For primary document see N94-27893 07-80)
Avail: CASI HC A01/MF A03

Thermal stress analyses are an important aspect in the development of aerospace vehicles such as the National Aero-Space Plane (NASP) and the High-Speed Civil Transport (HSCT) at NASA-LaRC. These analyses require knowledge of the temperature within the structures which consequently necessitates the need for thermal property data. The initial goal of this research effort was to develop a methodology for the estimation of thermal properties of aerospace structural materials at room temperature and to develop a procedure to optimize the estimation process. The estimation procedure was implemented utilizing a general purpose finite element code. In addition, an optimization procedure was developed and implemented to determine critical experimental parameters to optimize the estimation procedure. Finally, preliminary experiments were conducted at the Aircraft Structures Branch (ASB) laboratory. Author (revised)

N94-27921*# Virginia Polytechnic Inst. and State Univ., Blacksburg. Dept. of Mechanical Engineering.
EVALUATION OF HIGH TEMPERATURE SUPERCONDUCTIVE THERMAL BRIDGES FOR SPACE-BORNE CRYOGENIC INFRARED DETECTORS c35
Elaine P. Scott *In* Old Dominion Univ., The 1993 NASA-ODU American Society for Engineering Education (ASEE) Summer Faculty Fellowship Program Dec. 1993 p 162-165 (For primary document see N94-27893 07-80)
Avail: CASI HC A01/MF A03

The focus of this research is on the reduction of the refrigeration requirements for infrared sensors operating in space through the use of high temperature superconductive (HTS) materials as electronic leads between the cooled sensors and the relatively warmer data acquisition components. Specifically, this initial study was directed towards the design of an experiment to quantify the thermal performance of these materials in the space environment. First, an intensive review of relevant literature was undertaken, and then, design requirements were formulated. From this background information, a preliminary experimental design was developed. Additional studies will involve a thermal analysis of the experiment and further modifications of the experimental design. Author (revised)

N94-27922*# Hampton Univ., VA. Dept. of Mathematics.
A TRI-STATE OPTICAL SWITCH FOR LOCAL AREA NETWORK COMMUNICATIONS c33
Garfield Simms *In* Old Dominion Univ., The 1993 NASA-ODU American Society for Engineering Education (ASEE) Summer Faculty Fellowship Program Dec. 1993 p 170-176 (For primary document see N94-27893 07-80)
Avail: CASI HC A02/MF A03

This novel structure is a heterojunction phototransistor which can be used as an emitter-detector, and when placed in a quiescent mode, the device becomes a passive transmitter. By varying the voltage bias, this novel device will switch between all three modes of operation. Such a device has broad application in network environments with operation speeds of less than 50 MHz and distances of less than 1 km, e.g. automobiles, airplanes, and intra-instrumentation. During this period, the emission mode for this device was studied and mathematically modeled. Author (revised)

N94-27923*# Hampton Univ., VA. Dept. of Engineering.
FIBER OPTIC SENSORS FOR CORROSION DETECTION c74
Alphonso C. Smith *In* Old Dominion Univ., The 1993 NASA-ODU American Society for Engineering Education (ASEE) Summer Faculty Fellowship Program Dec. 1993 p 179-182 (For primary document see N94-27893 07-80)
Avail: CASI HC A01/MF A03

The development of fiber optic sensors for the detection of a variety of material parameters has grown tremendously over the past several years. Additionally, the potential for analytical applications of fiber optic sensors have become more widely used. New pH sensors have also been developed using fiber optic techniques to detect fluorescence characteristics from immobilized fluorogenic reagent chemicals. The primary purpose of this research was to investigate the feasibility of using fiber optic sensors to detect the presence of Al(sup 3+) ions made in the process of environmental corrosion of aluminum materials. The Al(sup 3+) ions plus a variety of other type of metal ions can be detected using analytical techniques along with fiber optic sensors. Author (revised)

N94-27924*# Tuskegee Inst., AL. Dept. of Aerospace and Mechanical Engineering.
INVESTIGATION OF SPECTRAL ANALYSIS TECHNIQUES FOR RANDOMLY SAMPLED VELOCIMETRY DATA c70
Dave Sree *In* Old Dominion Univ., The 1993 NASA-ODU American Society for Engineering Education (ASEE) Summer Faculty Fellowship Program Dec. 1993 p 183-186 (For primary document see N94-27893 07-80)
Avail: CASI HC A01/MF A03

It is well known that velocimetry (LV) generates individual realization velocity data that are randomly or unevenly sampled in time. Spectral analysis of such data to obtain the turbulence spectra, and hence turbulence scales information, requires special techniques. The 'slotting' technique of Mayo et al, also described by Roberts and Ajmani, and the 'Direct Transform' method of Gaster and Roberts are well known in the LV community. The slotting technique is faster than the direct transform method in computation. There are practical limitations, however, as to how a high frequency and accurate estimate can be made for a given mean sampling rate. These high frequency estimates are important in obtaining the microscale information of turbulence structure. It was found from previous studies that reliable spectral estimates can be made up to about the mean sampling frequency (mean data rate) or less. If the data were evenly samples, the frequency range would be half the sampling frequency (i.e. up to Nyquist frequency); otherwise, aliasing problem would occur. The mean data rate and the sample size (total number of points) basically limit the frequency range. Also, there are large variabilities or errors associated with the high frequency estimates from randomly sampled signals. Roberts and Ajmani proposed certain pre-filtering techniques to reduce these variabilities, but at the cost of low frequency estimates. The prefiltering acts as a high-pass filter. Further, Shapiro and Silverman showed theoretically that, for Poisson sampled signals, it is possible to obtain alias-free spectral estimates far beyond the mean sampling frequency. But the question is, how far? During his tenure under 1993 NASA-ASEE Summer Faculty Fellowship Program, the author investigated from his studies on the spectral analysis techniques for randomly sampled signals that the spectral estimates can be enhanced or improved up to about 4-5 times the mean sampling frequency by using a suitable prefiltering technique. But, this increased bandwidth comes at the cost of the lower frequency estimates. The studies further showed that large data sets of the order of 100,000 points, or more, high data rates, and Poisson sampling are very crucial for obtaining reliable spectral estimates from randomly sampled data, such as LV data. Some of the results of the current study are presented. Author

N94-27925*# Miami Univ., Coral Gables, FL. Electrical and Computer Engineering.

COMPARATIVE ANALYSIS OF DIFFERENT CONFIGURATIONS OF PLC-BASED SAFETY SYSTEMS FROM RELIABILITY POINT OF VIEW c38

Moiez A. Tapia *In* Old Dominion Univ., The 1993 NASA-ODU American Society for Engineering Education (ASEE) Summer Faculty Fellowship Program Dec. 1993 p 187-188 (For primary document see N94-27893 07-80)

Avail: CASI HC A01/MF A03

The study of a comparative analysis of distinct multiplex and fault-tolerant configurations for a PLC-based safety system from a reliability point of view is presented. It considers simplex, duplex and fault-tolerant triple redundancy configurations. The standby unit in case of a duplex configuration has a failure rate which is k times the failure rate of the standby unit, the value of k varying from 0 to 1. For distinct values of MTTR and MTTF of the main unit, MTBF and availability for these configurations are calculated. The effect of duplexing only the PLC module or only the sensors and the actuators module, on the MTBF of the configuration, is also presented. The results are summarized and merits and demerits of various configurations under distinct environments are discussed. Author (revised)

N94-27926*# College of William and Mary, Williamsburg, VA. Dept. of Chemistry.

PROPERTY ENCHANCEMENT OF POLYIMIDE FILMS BY WAY OF THE INCORPORATION OF LANTHANIDE METAL IONS Abstract Only c27

David W. Thompson *In* Old Dominion Univ., The 1993 NASA-ODU American Society for Engineering Education (ASEE) Summer Faculty Fellowship Program Dec. 1993 p 189 (For primary document see N94-27893 07-80)

Avail: CASI HC A01/MF A03

Lanthanide metal ions were incorporated into the polyimide derived from 2,2-bis(3,4-dicarboxyphenyl) hexafluoropropane dianhydride (6FDA) and 1,3-bis(aminophenoxy) benzene (APB) in an attempt to produce molecular level metal-polymer composites. The lanthanide series of metal ions (including aluminum, scandium, and yttrium) provide discrete and stable metal ions in the 3+ oxidation state. Throughout the series there is a uniform variation in ionic size ranging from 50 pm for aluminum to a maximum of 103.4 pm for cerium and gradually decreasing again to 84.8 pm for lutetium. The high charge-to-size ratio for these ions as well as the ability to obtain large coordination numbers makes them excellent candidates for interacting with the polymer substructure. The distinct lack of solubility of simple lanthanide salts such as the acetates and halides has made it difficult to obtain metal ions distributed in the polymer framework as discrete ions or metal complexes rather than microcomposites of metal clusters. (Lanthanum nitrates are quite soluble, but the presence of the strongly oxidizing nitrate ion leads to serious degradation of the polymer upon thermal curing. This work was successful at extending the range of soluble metals salts by using chelating agents derived from the beta-diketones dipivaloylmethane, dibenzoylmethane, trifluoroacetylacetone, and hexafluoroacetylacetone. Metal acetates which are insoluble in dimethylacetamide dissolve readily in the presence of the diketones. Addition of the polyimide yields a homogeneous resin which is then cast into a clear film. Upon curing clear films were obtained with the dibenzoylmethane and trifluoroacetylacetone ligands. The dipavaloylmethane precipitates the metal during the film casting process, and hexafluoroacetylacetone gives cured films which are deformed and brittle. These clear films are being evaluated for the effect of the metal ions on the coefficient of thermal expansion, resistance to atomic oxygen, and on selective gas permeability. Much more commonly than above, polyimide films are prepared by casting the film as the poly(amic acid) precursor which is then converted to the imidized form during the thermal cure cycle. Very limited success was achieved in the past in adding lanthanide metal ions to the amide precursors because of gellation and lack of solubility. With the use of the diketone ligands cited above, the solubility and gellation problems were overcome. However, the films after curing were clear but unacceptably brittle. Attempts to overcome this cure embrittlement problem are in progress.

Author (revised)

N94-27927*# Paul D. Camp Community Coll., Suffolk, VA. Dept. of Computer Information Systems.

ADP ANALYSIS PROJECT FOR THE HUMAN RESOURCES MANAGEMENT DIVISION c61

Robert L. Tureman, Jr. *In* Old Dominion Univ., The 1993 NASA-ODU American Society for Engineering Education (ASEE) Summer Faculty Fellowship Program Dec. 1993 p 190-191 (For primary document see N94-27893 07-80)

Avail: CASI HC A01/MF A03

The ADP (Automated Data Processing) Analysis Project was conducted for the Human Resources Management Division (HRMD) of NASA's Langley Research Center. The three major areas of work in the project were computer support, automated inventory analysis, and an ADP study for the Division. The goal of the computer support work was to determine automation needs of Division personnel and help them solve computing problems. The goal of automated inventory analysis was to find a way to analyze installed software and usage on a Macintosh. Finally, the ADP functional systems study for the Division was designed to assess future HRMD needs concerning ADP organization and activities. Author

N94-27928*# Old Dominion Univ., Norfolk, VA.

SPACE TRANSPORTATION VEHICLE DESIGN EVALUATION USING SATURATED DESIGNS c16

Resit Unal *In its* The 1993 NASA-ODU American Society for Engineering Education (ASEE) Summer Faculty Fellowship Program Dec. 1993 p 192-193 (For primary document see N94-27893 07-80)

Avail: CASI HC A01/MF A03

An important objective in the preliminary design and evaluation of space transportation vehicles is to find the best values of design variables that optimize the performance characteristic (e.g. dry weight). For a given configuration, the vehicle performance can be determined by the use of complex sizing and performance evaluation computer programs. These complex computer programs utilize iterative algorithms and they are generally too expensive and/or difficult to use directly in multidisciplinary design optimization. An alternative is to use response surface methodology (RSM) and obtain quadratic polynomial approximations to the functional relationships between performance characteristics and design variables. In RSM, these approximation models are then used to determine optimum design parameter values and for rapid sensitivity studies. Constructing a second-order model requires that 'n' design parameters be studied at least at 3 levels (values) so that the coefficients in the model can be estimated. There, 3(n) factorial experiments (point designs or observations) may be necessary. For small values of 'n' such as two or three, this design works well. However, when a large number of design parameters are under study, the number of design points required for a full-factorial design may become excessive. Fortunately, these quadratic polynomial approximations can be obtained by selecting an efficient design matrix using central composite designs (CCD) from design of experiments theory. Each unique point design from the CCD matrix is then conducted using computerized analysis tools (e.g. POST, CONSIZ, etc.). In the next step, least squares regression analysis is used to calculate the quadratic polynomial coefficients from the data. However, in some multidisciplinary applications involving a large number of design variables and several disciplines, the computerized performance synthesis programs may get too time consuming and expensive to run even with the use of efficient central composite designs. In such cases, it may be preferable to keep the number of design points to an absolute minimum and trade some model accuracy with cost. For this purpose, another class of experimental designs, called saturated D-optimal designs may be utilized for generating a matrix of vehicle designs. A design is called saturated when the number of design points is exactly equal to the number of terms in the model to be fitted. As a result, saturated designs require the absolute minimum number of design points $((n+1)(n+2)/s)$ to estimate the quadratic polynomial model coefficients. Saturated designs can be generated using the D-optimality criterion. A good saturated design should give rise to least squares estimates with minimum generalized variance. Author (revised)

N94-27929*# California Univ., Davis. Dept. of Mechanical and Aeronautical Engineering.

PREDICTION OF LEADING-EDGE TRANSITION AND RELAMINARIZATION PHENOMENA ON A SUBSONIC MULTI-ELEMENT HIGH-LIFT SYSTEM **c02**

C. P. vanDam *In* Old Dominion Univ., The 1993 NASA-ODU American Society for Engineering Education (ASEE) Summer Faculty Fellowship Program Dec. 1993 p 194-195 (For primary document see N94-27893 07-80)

Avail: CASI HC A01/MF A03

Boundary-layer transition and relaminarization may have a critical effect on the flow development about multi-element high-lift systems of subsonic transport jets with swept wings. The purpose of the research is to study these transition phenomena in the leading-edge region of the various elements of a high-lift system. The flow phenomena studied include transition to the attachment-line flow, relaminarization, and crossflow instability, and transition. The calculations are based on pressure distributions measured in flight on the NASA Transport Systems Research Vehicle (Boeing 737-100) at a wing station where the flow approximated infinite swept wing conditions. The results indicate that significant regions of laminar flow can exist on all flap elements in flight. In future flight experiments (planned for January-February, 1994) the extent of these regions, the transition mechanisms and the effect of laminar flow on the high-lift characteristics of the multi-element system will be further explored. Author (revised)

N94-27930*# California State Univ., Los Angeles. Dept. of Mechanical Engineering.

COMPUTATION OF TRANSONIC VISCOUS FLOW PAST THE NTF 65-DEGREE DELTA WING **c02**

Chivey Wu *In* Old Dominion Univ., The 1993 NASA-ODU American Society for Engineering Education (ASEE) Summer Faculty Fellowship Program Dec. 1993 p 196-199 (For primary document see N94-27893 07-80)

Avail: CASI HC A01/MF A03

This project is a continuation of the work performed in the summers of 1991 and 1992, during which a 9-block structured grid for the computational domain around each of the four NTF 65-degree Delta Wing models with the sting mount were created. The objective of the project is to validate and supplement the test data on the wing models by computing the viscous flow field about the models. Author

81 ADMINISTRATION AND MANAGEMENT

Includes management planning and research.

N94-25796# Air Force Inst. of Tech., Wright-Patterson AFB, OH.

A COST MODEL FOR USAF ACQUISITION OF COMMERCIAL AIRCRAFT FOR SERVICE IN THE SPECIAL AIR MISSION FLEET M.S. Thesis

C. G. McVicker, III and Michael T. Roche 4 Jun. 1993 102 p

(AD-A274012; AFIT/GCA/LAS/93S-8) Avail: CASI HC A06/MF A02

The purpose of this research was to develop a cost estimating model which would allow cost estimators the ability to quickly and accurately estimate the acquisition of Air Force Special Air Mission fleet aircraft. The literature review revealed studies, government contracts, and trade publications which served as source data. This information was supplemented by interviews with acquisition specialists and contractors and incorporated into a database. Several estimating techniques were created and used to estimate the various cost elements. The Commercial Aircraft Integrated Cost Estimating Tool (CAICET) model was then developed to incorporate the estimating techniques with the database. This was accomplished by integrating dialog boxes to access the information and estimate the program acquisition. The CAICET model provides the analyst with the ability to estimate an acquisition program based on a few specific parameters concerning the missionization of the aircraft. These parameters include interior configuration, avionics, mission communications, and self-sufficiency items. Once this information is input, the CAICET model provides the analyst with a real-time estimate in standard AF Form 1537 format. DTIC

N94-25895# Air Force Inst. of Tech., Wright-Patterson AFB, OH. School of Logistics and Acquisition Management.

DEVELOPMENT OF THE AIR FORCE CONTINGENCY CONTRACTING COURSE FRAMEWORK M.S. Thesis

David A. Bethany and Michael A. Miller Sep. 1993 117 p

(AD-A273921; AFIT/GCM/LAS/93S-1) Avail: CASI HC A06/MF A02

The objective of this research was to develop a framework for a standardized Air Force Contingency Contracting course. This task was undertaken due to the occurrence of a common recommendation calling for specialized training in Contingency Contracting. The recommendation was found in several AFIT theses, as well as, various after action reports generated due to the experience gained during Operation Desert Shield/Storm and Hurricane Andrew. This thesis answered the basic questions of need, content, and structure for a future course in Contingency Contracting. Using an exploratory research design, the research team was able to conduct an extensive analysis on completed formalized research in the area of Contingency Contracting. The outcome of the research is a four-phased, block of instruction with recommended training topics and first hand accounts of contingency contracting. The blocks of instruction can be used alone or as a segment in current DOD Contracting Courses. DTIC

N94-26181# Naval Postgraduate School, Monterey, CA.

IMPLEMENTING A MULTIPLE CRITERIA MODEL BASE IN CO-OP WITH A GRAPHICAL USER INTERFACE GENERATOR M.S. Thesis

Hsin-Yen Tsai 23 Sep. 1993 85 p

(AD-A274901) Avail: CASI HC A05/MF A01

This thesis designs and implements prototype multiple criteria decision making (MCDM) modules to add into the Cooperative Multiple Criteria Group Decision Support System (Co-op) for Windows. The algorithms and the graphical user interfaces for these modules are implemented using Microsoft Visual Basic under the Windows based environment operating in a IBM compatible microcomputer. Design of the MCDM programs interface is based on general interface design principles of user control, screen design, and layout. DTIC

N94-26206*# Texas A&M Univ., College Station. Dept. of Computer Science.

COORDINATED SCHEDULING FOR DYNAMIC REAL-TIME SYSTEMS Final Report

Swaminathan Natarajan and Wei Zhao 21 Feb. 1994 11 p

(Contract NCC2-770; TEES Proj. 41590-CS)

(NASA-CR-195231; NAS 1.26:195231) Avail: CASI HC A03/MF A01

In this project, we addressed issues in coordinated scheduling for dynamic real-time systems. In particular, we concentrated on design and implementation of a new distributed real-time system called R-Shell. The design objective of R-Shell is to provide computing support for space programs that have large, complex, fault-tolerant distributed real-time applications. In R-shell, the approach is based on the concept of scheduling agents, which reside in the application run-time environment, and are customized to provide just those resource management functions which are needed by the specific application. With this approach, we avoid the need for a sophisticated OS which provides a variety of generalized functionality, while still not burdening application programmers with heavy responsibility for resource management. In this report, we discuss the R-Shell approach, summarize the achievement of the project, and describe a preliminary prototype of R-Shell system. Author

N94-26299# Naval Postgraduate School, Monterey, CA.

BUSINESS PROCESS REDESIGN: DESIGN THE IMPROVED PROCESS M.S. Thesis

Jerry L. Warwick Sep. 1993 155 p

(AD-A274947) Avail: CASI HC A08/MF A02

This thesis reports the results of a business activity modeling exercise to explore how a functional manager in DoD can best improve and redesign one's business processes. The validity of exercise results was assessed and found to be generally accurate with minor modifications. The business activity model was constructed by a faculty/student team in August of 1992, in support of DoD's Corporate Information Management (CIM) initiative. This team used an Integrated Definitions Language (IDEFO) supported software tool (Design/IDEF by Meta Software of Cambridge, Massachusetts) to construct their model. DTIC

N94-26314# Technische Univ., Eindhoven (Netherlands). Dept. of Mathematics and Computing Science.

ONE MACHINE SCHEDULING WITH DELAYED PRECEDENCE CONSTRAINTS

Egon Balas (Carnegie-Mellon Univ., Pittsburgh, PA.), Jan Karel Lenstra (Center for Mathematics and Computer Science, Amsterdam, Netherlands.), and Alkis Vazacopoulos (Carnegie-Mellon Univ., Pittsburgh, PA.) Feb. 1993 40 p
(Contract N00014-85-K-0198; NSF DDM-89-01495) (ISSN 0926-4493)
(PB93-237626; Memo-COSOR-93-04; ETN-94-94812) Avail: CASI HC A03/MF A01

The one machine scheduling problem with release and delivery times and the minimum makespan objective is investigated. The study is performed in the presence of constraints that for certain pairs of jobs require a delay between the completion of the first job and the start of the second. This problem arises in the context of the shifting bottleneck procedure for the general job shop scheduling problem, as a relaxation of the latter, tighter than the standard one machine relaxation. The difference between the two relaxations is explained. A modified longest tail heuristic, whose analysis identifies those situations that permit efficient branching is introduced. An optimization algorithm is developed. Embedding this algorithm into a modified version of the shifting bottleneck procedure that uses the tighter one machine relaxation results in a performance improvement on all classes of job shop scheduling problems. ESA

N94-26814# Air Force Inst. of Tech., Wright-Patterson AFB, OH. School of Logistics and Acquisition Management.

ANALYSIS OF COST AND SCHEDULE GROWTH ON SOLE SOURCE AND COMPETITIVE AIR FORCE CONTRACTS M.S. Thesis

Klaes W. Wandland and Gary P. Wickman Sep. 1993 108 p
(AD-A273920; AFIT/GSM/LAS/93S-20) Avail: CASI HC A06/MF A02

This study investigated if differences exist in the cost and schedule growth of competed versus sole source contracts. Prior studies concentrated mainly on estimated savings from competition at the time of contract award. This study expanded prior analysis by investigating the cost and schedule growth over the contract's period of performance. In addition to an analysis between competed and sole source contracts, this study investigated if differences exist between lower and higher risk contracts as well as lower and higher initial priced contracts. When comparing competed and sole source contracts the results were consistent, with sole source contracts exhibiting an average of 57% higher cost growth in all areas. Sole source contracts also exhibited a schedule growth that was over four times greater than the schedule growth of competed contracts. When comparing lower and higher initial priced contracts, the results were also consistent with higher priced contracts exhibiting higher cost growth than lower price contracts. The results were mixed when measured between lower and higher risk contracts however. DTIC

N94-27180# Naval Postgraduate School, Monterey, CA.

CONCEPTS AND METHODS OF MEASURING PRODUCTIVITY AT THE ORGANIZATION LEVEL M.S. Thesis

Maxie Y. Davis Sep. 1993 66 p
(AD-A273126) Avail: CASI HC A04/MF A01

This thesis addresses the concepts of productivity measurement. Productivity measurements are generally a ratio between outputs and inputs. The criteria for identifying and quantifying the output and input components are explored. The methodology used by the Bureau of Labor and Statistics are examined to provide insight into the application of the concepts of productivity measurement. Business and government sectors outputs are identified and partial and multifactor productivity measurements defined. Common methodologies for measuring productivity at the organization level are also outlined. These methodologies are examined for their applicability to phenomena of the post-industrial society, particularly the rise in the white collar work force, information technology, and process reengineering. Adaptations of these methodologies are proposed as an appropriate measurement technique for DOD functional managers. Author (DTIC)

N94-27661*# National Aeronautics and Space Administration, Washington, DC.

SMALL BUSINESS INNOVATION RESEARCH PROGRAM SOLICITATION

15 Jun. 1994 78 p
(NASA-TM-109695; NAS 1.15:109695; SBIR-94-1) Avail: CASI HC A05/MF A01

The National Aeronautics and Space Administration invites eligible small business concerns to submit Phase 1 proposals for its 1994 Small Business Innovation Research (SBIR) Program, which is described in this twelfth annual NASA SBIR Program Solicitation. The 1994 solicitation period for Phase 1 proposals begins April 4, 1994 and ends June 15, 1994. Eligible firms with research or research and development capabilities (R/R&D) in any of the listed topic and subtopic areas are encouraged to participate. Through SBIR, NASA seeks innovative concepts addressing the program needs described in the SBIR solicitation subtopics and offering commercial application potential. This document contains program background information, outlines eligibility requirements for SBIR participants, describes the three SBIR program phases, and provides the information qualified offerors need to prepare and submit responsive proposals. Derived from text

N94-27707# Los Alamos National Lab., NM.

PRACTICAL PROBLEMS IN AGGREGATING EXPERT OPINIONS

Jane M. Booker, Richard R. Picard, and Mary A. Meyer 1993 6 p
Presented at the 2nd Probabilistic Safety Assessment and Management Conference, San Diego, CA, 20-24 Mar. 1994
(Contract W-7405-eng-36)
(DE94-002623; LA-UR-93-3566; CONF-940312-38) Avail: CASI HC A02/MF A01

Expert opinion is data given by a qualified person in response to a technical question. In these analyses, expert opinion provides information where other data are either sparse or non-existent. Improvements in forecasting result from the advantageous addition of expert opinion to observed data in many areas, such as meteorology and econometrics. More generally, analyses of large, complex systems often involve experts on various components of the system supplying input to a decision process; applications include such wide-ranging areas as nuclear reactor safety, management science, and seismology. For large or complex applications, no single expert may be knowledgeable enough about the entire application. In other problems, decision makers may find it comforting that a consensus or aggregation of opinions is usually better than a single opinion. Many risk and reliability studies require a single estimate for modeling, analysis, reporting, and decision making purposes. For problems with large uncertainties, the strategy of combining as diverse a set of experts as possible hedges against underestimation of that uncertainty. Decision makers are frequently faced with the task of selecting the experts and combining their opinions. However, the aggregation is often the responsibility of an analyst. Whether the decision maker or the analyst does the aggregation, the input for it, such as providing weights for experts or estimating other parameters, is imperfect owing to a lack of omniscience. Aggregation methods for expert opinions have existed for over thirty years; yet many of the difficulties with their use remain unresolved. The bulk of these problem areas are summarized in the sections that follow: sensitivities of results to assumptions, weights for experts, correlation of experts, and handling uncertainties. The purpose of this paper is to discuss the sources of these problems and describe their effects on aggregation. DOE

N94-27772*# National Aeronautics and Space Administration, Washington, DC.

NASA SBIR ABSTRACTS OF 1992, PHASE 1 PROJECTS

F. C. Schwenk (Futron Corp., Bethesda, MD.), J. A. Gilman (Futron Corp., Bethesda, MD.), J. B. Paige (Futron Corp., Bethesda, MD.), and S. M. Sacknoff (Futron Corp., Bethesda, MD.) Washington Sep. 1993 148 p
(NASA-TM-109694; NAS 1.15:109694; SBIR-92-2) Avail: CASI HC A07/MF A02

The objectives of 346 projects placed under contract by the Small Business Innovation Research (SBIR) program of the National Aeronautics and Space Administration (NASA) are described. These projects were selected competitively from among proposals submitted to NASA in response to the 1992 SBIR Program Solicitation. The basic document consists of edited, non-proprietary abstracts of the winning proposals submitted by small businesses. The abstracts are presented under the 15 technical topics within which Phase 1 proposals were solicited. Each project was assigned a sequential identifying number from 001 to 346, in order of its appearance in the body of the report. Appendixes to provide additional information about the SBIR program and permit cross-reference of the 1992 Phase 1 projects by company name, location by state, principal investigator, NASA Field Center responsible for management of each project, and NASA contract number are included. Derived from text

N94-27866*# Rockwell International Corp., Downey, CA. Space Systems Div.
AUTOMATION LIFE-CYCLE COST MODEL Final Technical Report
Thomas P. Gathmann, Arlinda J. Reeves, Rick Cline, Max Henrion, and Corinne Ruokangas 2 Jul. 1992 169 p
(Contract NAS2-13419)
(NASA-CR-195695; NAS 1.26:195695; SSD92D0154) Avail: CASI HC A08/MF A02

The problem domain being addressed by this contractual effort can be summarized by the following list: Automation and Robotics (A&R) technologies appear to be viable alternatives to current, manual operations; Life-cycle cost models are typically judged with suspicion due to implicit assumptions and little associated documentation; and Uncertainty is a reality for increasingly complex problems and few models explicitly account for its affect on the solution space. The objectives for this effort range from the near-term (1-2 years) to far-term (3-5 years). In the near-term, the envisioned capabilities of the modeling tool are annotated. In addition, a framework is defined and developed in the Decision Modelling System (DEMOS) environment. Our approach is summarized as follows: Assess desirable capabilities (structure into near- and far-term); Identify useful existing models/data; Identify parameters for utility analysis; Define tool framework; Encode scenario thread for model validation; and Provide transition path for tool development. This report contains all relevant, technical progress made on this contractual effort. Author (revised)

N94-28176# General Accounting Office, Washington, DC.
NASA: MAJOR CHALLENGES FOR MANAGEMENT. TESTIMONY BEFORE THE LEGISLATION AND NATIONAL SECURITY SUBCOMMITTEE, COMMITTEE ON GOVERNMENT OPERATIONS, HOUSE OF REPRESENTATIVES
Frank C. Conahan 6 Oct. 1993 24 p
(GAO/T-NSIAD-94-18) Avail: CASI HC A03/MF A01

Presented is the statement of Frank C. Conahan before the House of Representatives on management issues and challenges facing the National Aeronautics and Space Administration. Issues covered are: bringing plans in line with likely budgets, managing systems development efforts more efficiently, improving operations and oversight, and preserving U.S. aeronautical leadership. Programs discussed include the space station, the Advanced X Ray Astrophysics Facility, the Earth Observing System, and the National Aerospace Plane. Topics discussed include reporting under the Financial Integrity Act and the need for a Chief Financial Officer, improving shuttle operating efficiency, improving procurement and contract management, space project testing, science data management, facilities maintenance, and environmental protection activities. CASI

N94-28177# General Accounting Office, Washington, DC. National Security and International Affairs Div.
DEFENSE FORCE MANAGEMENT: CHALLENGES FACING DOD AS IT CONTINUES TO DOWNSIZE ITS CIVILIAN WORK FORCE. REPORT TO THE CHAIRMAN, SUBCOMMITTEE ON FEDERAL SERVICES, POST OFFICE, AND CIVIL SERVICE, COMMITTEE ON GOVERNMENTAL AFFAIRS, US SENATE
Feb. 1993 18 p
(GAO/NSIAD-93-123; B-247621) Avail: CASI HC A03/MF A01; also available from GAO, PO Box 6015, Gaithersburg, MD 20884-6015

In testimony given in Feb. 1992, important differences in the approaches that the Department of Defense (DOD) has employed to facilitate force reductions, minimize involuntary separations, and shape its civilian and military work forces were highlighted. This report builds on our statements in these testimonies in the following ways: (1) reporting on the status of DOD's civilian work force reductions, (2) contrasting the DOD's strategy for reducing the military work force with the strategy for reducing the civilian work force, and (3) providing information of DOD's implementation of the new authorizations for separation incentive programs. Author (revised)

N94-28386# Helsinki Univ. of Technology, Espoo (Finland). Systems Analysis Lab.
INTERTEMPORAL BARGAINING AND DYNAMIC CONSISTENCY
H. Ehtamo and J. Ruusunen Jun. 1993 31 p See also PB92-133826
(PB94-133147; ISBN-951-22-1623-X) Avail: CASI HC A03/MF A01

This paper proposes a model for intertemporal bargaining over two periods. At the first period the bargaining game is defined by the set of the decision makers' feasible total gains over the two periods, and the contract is an element of this set. At the second period the contract is renegotiated taking into account the decision makers' gains from the first period. The choice of the contract is made at each period on the basis of an a priori specified axiomatic bargaining model. The paper gives a definition for the dynamic consistency of the contract. This concept is important in intertemporal economic problems, but thus far it has not been considered in the context of multiperiod bargaining. A remarkable result of the paper is the paradoxical conclusion that to obtain dynamic consistency of the bargaining solution, the controversial independence of irrelevant alternatives property of the axiomatization must be accepted. NTIS

82 DOCUMENTATION AND INFORMATION SCIENCE

Includes information management; information storage and retrieval technology; technical writing; graphic arts; and micrography.

For computer documentation see *61 Computer Programming and Software.*

N94-25723# Institute for Perception RVO-TNO, Soesterberg (Netherlands).
THE EFFECT OF THE TIME RESTRICTIONS ON INFORMATION SEARCH AND INFORMATION INTEGRATION IN A DYNAMIC TASK ENVIRONMENT Final Report
J. H. Kerstholt and P. Willems 13 Jul. 1993 20 p
(AD-A273759; IZF-1993-B-8; TDCK-TD-93-1359) Avail: CASI HC A03/MF A01

To date, research has mainly used deadlines in static task environments to investigate the effects of time pressure on decision making behavior. A dynamic environment, on the other hand, changes over time and time pressure may result when time is not used efficiently and negative consequences are rapidly increasing. An experiment was carried out to investigate the effects of time horizon on decision making behavior in a dynamic task environment. Subjects were required to monitor the fitness level of a running athlete, depicted graphically on a computer screen, and to apply a proper treatment whenever necessary. Information could be requested on symptoms, which were probabilistically related to underlying causes. The time horizon was manipulated by the speed at which the athlete's fitness level changed over time. Restrictions in time horizon did not affect the amount and type of information that was requested, and the diagnoses became even better. Nevertheless, more athletes collapsed in the more restricted time horizon conditions. In the short time horizon conditions subjects furthermore employed a more cautious decision strategy. As far as the use of time was concerned it was found that information processing was speeded up, but subjects waited relatively the same amount of time before they started to intervene with the system. DTIC

N94-25751 International Atomic Energy Agency, Vienna (Austria).
STANDARDIZING EXCHANGE FORMATS
H. D. Lemmel and J. J. Schmidt 1992 25 p Presented at the 11th International CODATA Conference: Scientific and Technical Data in A New Era, Karlsruhe, Germany, 26-29 Sep. 1988 Limited Reproducibility: More than 20% of this document may be affected by microfiche quality
(DE93-616798; INIS-mf-13438; CONF-880907) Avail: CASI HC A03 (US Sales Only)

An international network of co-operating data centers is described who maintain identical data bases which are simultaneously updated by an agreed data exchange procedure. The agreement covers 'data exchange formats' which are compatible to the centers' internal data storage and retrieval systems which remain different, optimized at each center to the available computer facilities and to the needs of the data users. Essential condition for the data exchange is an agreement on common procedures for the data exchange is an agreement on common procedures for the data compilation, including critical data analysis and validation. The systems described ('EXFOR', 'ENDF', 'CINDA') are used for 'nuclear reaction data', but the principles used for data compilation and exchange should be valid also for other data types. DOE

N94-25765# Air Force Inst. of Tech., Wright-Patterson AFB, OH.
PERFORMANCE MEASUREMENT OF THREE COMMERCIAL OBJECT-ORIENTED DATABASE MANAGEMENT SYSTEMS M.S. Thesis
Timothy J. Halloran Dec. 1993 260 p
(AD-A274028; AFIT/GCS/ENG/93D-12) Avail: CASI HC A12/MF A03

The goal of this thesis was to study the performance of three commercial object-oriented database management systems. The commercial systems studied included: Itasca, sold by Itasca Systems Incorporated; Matisse, sold by Intellitic International; and ObjectStore, sold by Object Design Incorporated. To examine performance of these database management systems two benchmarks were run: the OO1 benchmark and a new AFIT Simulation benchmark. The OO1 benchmark was designed, implemented, and run on all three database management systems. ObjectStore was our top performer on all configurations of the OO1 benchmark. The AFIT Simulation benchmark was designed, implemented, and run on the ObjectStore database management system. A nonpersistent version of the benchmark was also created in the C++ programming language. There was minimal performance overhead incurred due to the use of ObjectStore, especially when compared to the functional benefits gained. We concluded that there are major differences between the performance levels offered in current commercial object-oriented database management systems. We also concluded that a programming language interface to an object-oriented database management system should not be middle ground. Either it should be closely tied to a specific language or not tied to a specific language at all. DTIC

N94-25813# Pacific Northwest Lab., Richland, WA.
FULL-TEXT INFORMATION SERVICES AT THE DESKTOP
J. R. Judy 1993 6 p Presented at the INFOTECH 1993, Oak Ridge, TN, 20-23 Oct. 1993
(Contract DE-AC06-76RL-01830)
(DE94-003728; PNL-SA-22626; CONF-9310145-5) Avail: CASI HC A02/MF A01

In order to develop true electronic information services, libraries will be called upon to deliver a wide array of full-text documents to users' desktop computers. This requirement can currently be seen in the demands for electronic access to the ever-growing array of federal, state and local regulations covering almost any activity at DOE sites. The Hanford Technical Library has put together a new online statutory and regulatory information service, SARIS, that is described in this paper. SARIS is expected to serve as a platform fort the delivery of additional full-text information sources in the future. DOE

N94-25925# Educational Testing Service, Princeton, NJ.
A DIAGNOSTIC CLASSIFICATION MODEL FOR DOCUMENT PROCESSING SKILLS Final Report, Apr. 1989 - Aug. 1993
Kathleen Sheehan, Kikumi Tatsuoka, and Charles Lewis Oct. 1993 41 p
(Contract N00014-90-J-1307)
(AD-A273790; ETS-RR-93-39-ONR) Avail: CASI HC A03/MF A01

This paper introduces a modification to the Rule Space diagnostic classification procedure which allows for processing of response vectors containing missing data. Rule Space is an approach to diagnostic classification which involves characterizing examinees' performances in terms of an underlying cognitive model of generalized problem-solving skills. It has two components: a procedure for determining a comprehensive set of knowledge states, where each state is characterized in terms of a unique subset of mastered skills; and a procedure for classifying examinees into one or another of the specified states. The procedure for determining a comprehensive set of knowledge states is based on the Boolean descriptive function given in Tatsuoka. The procedure for classifying examinees involves comparing examinees' scored response vectors to the patterns expected within each of the specified knowledge states. Missing data is expected to be a common problem for this approach because, although the procedure for determining the comprehensive set of knowledge states requires a large pool of items, the procedure for examinee classification can be performed with smaller (less expensive) item subsets. This approach to diagnostic classification is illustrated with data collected in the Survey of Young Adult Literacy, a nationwide survey of literacy skills conducted by the National Assessment of Educational Progress (NAEP) in 1985. DTIC

N94-25997# Air Force Inst. of Tech., Wright-Patterson AFB, OH. School of Engineering.
RENDERING OF THREE-DIMENSIONAL DATA SETS DERIVED FROM FINITE-DIFFERENCE AND SPECTRAL METHODS M.S. Thesis
Paul A. Schubert Dec. 1993 81 p
(AD-A273724; AFIT/GAE/ENY/93D-24) Avail: CASI HC A05/MF A01

The timely visualization of three-dimensional data sets and the advantages of using a spectral method solution versus a finite-difference method solution in rendering isosurfaces is described. The Beam-Warming numerical algorithm, which uses implicit-approximate-factorization, is used to generate the steady-state solutions for a model diffusion-convection problem. The Chebyshev collocation operator is used to evaluate the right-hand side of the Beam-Warming algorithm for the spectral solution. Comparing the model problem results with the exact solution, the spectral series solution is truncated to the same degree of accuracy as the finite-difference for comparison of rendering times. The rendering algorithm employs octrees to efficiently traverse the data set to fit the isosurfaces. The actual fitting of polygons to the isosurface uses the marching cubes table look up algorithm. With the spectral series solution, interval math is investigated for guaranteed detection of isosurfaces during the initial octree traversal(s). DTIC

N94-26024# Air Force Inst. of Tech., Wright-Patterson AFB, OH. School of Engineering.
USING DATABASE TECHNOLOGY TO SUPPORT DOMAIN-ORIENTED APPLICATION COMPOSITION SYSTEMS M.S. Thesis
Danny A. Cecil and Joseph A. Fullenkamp Dec. 1993 219 p
(AD-A274091; AFIT/GCS/Eng/93D-03) Avail: CASI HC A10/MF A03

This research designed and prototyped an OODBMS technology base to store and retrieve various types of domain artifacts for domain-oriented application composition systems (DOACS). We developed object-oriented database schemas for a validating domain and the Object-Connection-Update software architecture. We implemented an inheritance relationship between the schemas so a domain model can inherit an architectural structure from an architecture model allowing us to isolate domain-specific knowledge from architecture-specific knowledge. We also developed a meta-model to formally define domain models in the database. We then developed a set of database methods to transform a domain model into a database schema for storing artifacts from the domain and to automatically populate the DOACS object base with the domain definition. Using an OODBMS, the structure and relationships that provide much of the power in object models are retained because the artificial flattening required for storage in traditional databases and file systems is prevented. Isolating domain and architecture models from each other has greatly increased the reusability of the domain artifacts, the domain model, and the architecture model. The inheritance relationship between domain and architecture models allows a domain to be defined once, but used in many different architectural environments and vice versa. DTIC

N94-26180# Naval Postgraduate School, Monterey, CA.
CODE DIVISION MULTIPLE ACCESS LOCAL AREA NETWORK COMMUNICATIONS EMPLOYING FIBER OPTIC SIGNAL PROCESSING TECHNIQUES M.S. Thesis
Bruce A. Legge Sep. 1993 81 p
(AD-A274897) Avail: CASI HC A05/MF A01

This thesis investigated the feasibility of implementing a code division multiple access (CDMA) local area network (LAN) employing all-optical signal processing. A two-user unidirectional data link was built and successfully tested. This data link utilized variations of optical orthogonal code sequences (OOC's) generated by serially connected fiber optic delay lines and 2x2 couplers. A special feature of this network design was use of the same hardware to decode the signal as was used to encode the signal. A detailed review of the various coding techniques and the generation of spread spectrum signals was also performed. The results of the overall system design effort demonstrated that high-data-rate signal traffic can be supported by the network and in a more power efficient and affordable manner than previous designs. DTIC

N94-26220# Center for Mathematics and Computer Science, Amsterdam (Netherlands). Dept. of Computer Science.
THE MUSA DESIGN METHODOLOGY
Steven Pemberton and Lon G. Barfield Dec. 1992 18 p
(ISSN 0169-118X)
(CWI-CS-R9265; ETN-94-95417) Copyright Avail: CASI HC A03/MF A01

MUSA is a multi-user authoring system, planned as an application in the Views system. MUSA's aim is to support concurrent development of 'products' being produced by several people cooperatively or by one person alone. The products are documents in a wide sense: articles, books, software, drawings, etc. ESA

N94-26297# Naval Postgraduate School, Monterey, CA.
DESIGN AND SPECIFICATION OF THE XPRESS TRANSFER HIGH-SPEED PROTOCOL M.S. Thesis
David J. Sacha Sep. 1993 100 p
(AD-A274941) Avail: CASI HC A05/MF A02

The use of fiber optics in high-speed data networks has significantly increased throughput and reliability at the physical layer. Consequently, the transport layer has become a bottleneck to the data transfer potential of high-speed networks. This bottleneck has forced an investigation of transport protocols and standards to be used in future networks. The Xpress Transfer Protocol (XTP) is a transport layer protocol designed to perform efficiently in networks where high data rates, densely packed bit pipes, and low bit error rates are normal operating conditions. However, XTP is a relatively new protocol which has not yet undergone extensive testing and analysis to verify its ability to resolve the transport layer bottleneck. In this thesis the specification and analysis of the XTP protocol using the System of Communicating Machines (SCM) model is presented. A comparison is then made with an alternative high-speed protocol called SNR, originated at AT&T Bell Labs. Based on this study, it is concluded that the XTP protocol provides several mechanisms, such as rate control and extended sequence numbering, that should be included in developing high-speed transport protocols. Furthermore, it is concluded that XTPs flexible characteristics allow for multiple paradigm implementations at the cost of some complexity, making a more complete analysis of this protocol difficult. As work on high-speed transport protocols continues, many of the XTP mechanisms should be considered for inclusion into evolving standards. It is also concluded that there are some critical features for high-speed protocols that are not in XTP. DTIC

N94-26300# Naval Postgraduate School, Monterey, CA. Dept. of Computer Science.
DESIGN AND IMPLEMENTATION OF A QUERY EDITOR FOR THE AMADEUS SYSTEM M.S. Thesis
Turgay Cince Sep. 1993 164 p
(AD-A274955) Avail: CASI HC A08/MF A02

One side effect of the proliferation of relational databases within a single organization is that sharing of data to access a global information base is difficult. People erroneously assume that since almost all of the commercially available RDBMS's support the Structured Query Language (SQL), sharing of data is easy. Unfortunately, currently available systems only support a specific dialect of SQL. The Amadeus front-end system overcomes the data-sharing problem. With the Amadeus front-end system, database users can use one common language called Dataflow Query Language (DFQL) to access heterogeneous RDBMS's. A query specified in DFQL is correctly translated into a SQL dialect that the connected RDBMS recognizes. With this front-end approach, the user can access data from multiple databases by writing a single DFQL query, instead of writing multiple SQL queries. A prototype query builder is re-implemented using an object-oriented design. This component of Amadeus interacts with the user for creating DFQL queries. DTIC

N94-26348# Pacific Northwest Lab., Richland, WA.
SCIENTIFIC AND TECHNICAL INFORMATION (STI)....WHAT'S THE STATUS?
D. A. Varley 1993 7 p Presented at the INFOTECH 1993, Oak Ridge, TN, 20-23 Oct. 1993
(Contract DE-AC06-76RL-01830)
(DE94-003731; PNL-SA-22619; CONF-9310145-3) Avail: CASI HC A02/MF A01

In 1982, the Pacific Northwest Laboratory (PNL) developed an electronic Publications and Presentations Registry designed to track Scientific and Technical Information (STI) products through PNL and Department of Energy (DOE) programmatic reviews. All information forwarded to the Office of Scientific and Technical Information (OSTI) for release (e.g., public, UCNI, Export Control) is included in the database. The database contains client and programmatic information for all STI generated by PNL. This electronic format is currently one of the most comprehensive resources for PNL authored and co-authored documents on the Hanford Site. DOE

N94-26350# Department of Energy, Washington, DC. Office of Science Education and Technical Information.
FEDERAL INFORMATION EXCHANGE (FEDIX) USER'S GUIDE: FALL 1993, VERSION 5.0/RELEASE 1.0
Sep. 1993 58 p
(DE94-003826; DOE/ET-0004-12) Avail: CASI HC A04/MF A01

FEDIX is an on-line information service that links the educational community and the federal government to facilitate research, education, and services. The system provides accurate and timely federal agency information to colleges, universities, and other research organizations. This guide is intended to help users access and utilize the FEDIX system. Because the system is frequently updated, however, some menus and tables used as examples in this text may not exactly match those displayed on the live system. DOE

N94-26375# Defense Information Systems Agency, Arlington, VA. Center for Information Manage Ment.
INFORMATION SYSTEMS CRITERIA FOR APPLYING SOFTWARE REENGINEERING: GUIDELINES FOR IDENTIFYING INFORMATION SYSTEMS FOR SOFTWARE REENGINEERING Final Report
Tamra K. Moore 13 May 1993 97 p
(AD-A274699) Avail: CASI HC A05/MF A02

Knowing when to reengineer is the key to helping managers make decisions that are cost effective and beneficial to reaching their organizational goals. The Software Reengineering Criteria provides assistance in identifying automated information systems (AIS) that are candidates for reengineering and proposes how software reengineering technology can benefit AIS. Experiences in industry, government agencies, and academia fostered the development of this criteria for identifying candidate information systems for software reengineering. This paper presents the Software Reengineering Criteria in four parts. First, a set of terms defines the activities within reengineering technology. An overview summarizes other sources providing guidance for when to reengineer. The criteria characterizes software systems and software engineering environments that exhibit the potential to benefit from reengineering technology and presents recommendations for software reengineering strategies. Finally, potential application areas for the criteria are explored. DTIC

N94-26382 International Centre for Theoretical Physics, Trieste (Italy).
NUMERICAL TREATMENT OF EXPERIMENTAL DATA IN CALIBRATION PROCEDURES
C. Moreno Jun. 1993 17 p Limited Reproducibility: More than 20% of this document may be affected by microfiche quality
(DE93-634289; IC-93/122) Avail: CASI HC A03 (US Sales Only)

A discussion of a numerical procedure to find the proportionality factor between two measured quantities is given in the framework of the least-squares method. Variable, as well as constant, amounts of experimental uncertainties are considered for each variable along their measured range. The variance of the proportionality factor is explicitly given as a closed analytical expression valid for the general case. Limits of the results obtained here have been studied allowing comparisons with those obtained using classical least-squares expressions. Analytical and numerical examples are also discussed. DOE

N94-26398 Energy Technology Data Exchange, Oak Ridge, TN.
INTERNATIONAL ENERGY: RESEARCH ORGANIZATIONS, 1988-1992
P. Hendricks, ed. and S. Jordan, ed. Jun. 1993 579 p Revised Limited Reproducibility: More than 20% of this document may be affected by poor print
(DE93-017267; ETDE/PUB-3-Rev-1) Avail: Issuing Activity (Department of Energy (DOE))

This publication contains the standardized names of energy research organizations used in energy information databases. Involved in this cooperative task are the two following groups: (1) the technical staff of the US DOE Office of Scientific and Technical Information (OSTI) in cooperation with the member countries of the Energy Technology Data Exchange (ETDE); and (2) the International Nuclear Information System (INIS). ETDE member countries are also members of the International Nuclear Information System (INIS). Nuclear organization names recorded for INIS by these ETDE member countries are also included in the ETDE Energy Database. Therefore, these organization names are cooperatively standardized for use in both information systems. This publication identifies current organizations doing research in all energy fields, standardizes the format for recording these organization names in bibliographic citations, assigns a numeric code to facilitate data entry, and identifies report number prefixes assigned by these organizations. These research organization names may be used in searching the databases 'Energy Science & Technology' on DIALOG and 'Energy' on STN International. These organization names are also used in USDOE databases on the Integrated Technical Information System. Research organizations active in the past five years, as indicated by database records, were identified to form this publication. This directory includes approximately 31,000 organizations that reported energy-related literature from 1988 to 1992 and updates the DOE Energy Data Base: Corporate Author Entries. DOE

N94-26451# Army Topographic Engineering Center, Fort Belvoir, VA.
PDEF: A STANDARD FILE FORMAT FOR DATA INTERCHANGE
Michael McDonnell Jan. 1994 11 p
(AD-A274694; TEC-R-203) Avail: CASI HC A03/MF A01

The Protean Data Exchange Format (PDEF) is a set of computer programs which can be used to transform data between different systems which do not understand each other's formats. The problem of data transformation is not restricted to any particular discipline, but those of us concerned with digital terrain data have felt this problem acutely as we have found that different Geographic Information Systems (GIS) cannot use each other's data. Although PDEF was written to alleviate this particular problem, its uses are more general than the specific problem for which it was originally written. PDEF was designed primarily to be easy to use since reformatting decisions must be made by people. This report will examine both the format and the uses of PDEF. DTIC

N94-26490# Cornell Univ., Ithaca, NY. Inst. for the Study of the Continents.
A GEOLOGICAL AND GEOPHYSICAL INFORMATION SYSTEM FOR EURASIA Final Technical Report, 30 Jul. 1991 - 31 Aug. 1993
Eric J. Fielding, Muawia Barazangi, and Bryan L. Isacks 15 Dec. 1993 39 p
(Contract F29601-91-K-DB08)
(AD-A274818) Avail: CASI HC A03/MF A01

Topography and heterogeneous crustal structure have major effects on the propagation of regional seismic phases. We are collecting topographical, geological, and geophysical datasets for Eurasia into an information system that can be accessed via Internet connections. Now available are digital topography, satellite imagery, and data on sedimentary basins and crustal structure thicknesses. New datasets for Eurasia include maps of depth to Moho beneath Europe and Scandinavia. We have created regularly spaced grids of the crustal thickness values from these maps that can be used to create profiles of crustal structure. These profiles can be compared by an analyst or an automatic program with the crustal seismic phases received along the propagation path to better understand and predict the path effects on phase amplitudes, a key to estimating magnitudes and yields, and for understanding variations in travel-time delays for phases such as Pn, which are important for improving regional event locations. The gridded data could also be used to model propagation of crustal phases in three dimensions. DTIC

N94-26500# Naval Postgraduate School, Monterey, CA.
MODELING AND SIMULATION OF A FIBER DISTRIBUTED DATA INTERFACE LOCAL AREA NETWORK M.S. Thesis
Aldo B. Schenone 23 Sep. 1993 54 p
(AD-A274838) Avail: CASI HC A04/MF A01

In this thesis, the performance of the fiber distributed data interface (FDDI) local area network is evaluated by software simulation. The network is modeled with OPNET, a communication network simulation tool. The main focus of the model is on the medium access control (MAC) and the timing requirements that need to be met for the correct behavior of the protocol. Simulation data is presented to support results from previous analytic studies of distinctive features of the protocol, including the behavior of the token rotation time, synchronous frame delays, fairness of channel access for nodes transmitting asynchronous traffic, etc. Comparisons between the simulated and theoretical results confirm the accuracy of the OPNET simulation tools and demonstrate that it may be used to model other protocols of particular interest. DTIC

N94-26559# Westinghouse Hanford Co., Richland, WA.
HANFORD ENVIRONMENTAL INFORMATION SYSTEM (HEIS) SAMPLE/DATA ENTRY FLOW SUMMARY
K. T. Key 1993 22 p
(Contract DE-AC06-87RL-10930)
(DE94-002494; WHC-SD-EN-SD-001) Avail: CASI HC A03/MF A01

The purpose of this summary is to present a unified overview of the processes that ultimately lead to the loading and storage of the Hanford environmental data on the Hanford Environmental Information System (HEIS) database and the Hanford Groundwater Database (HGWDB). The relationships among the various organizations involved in the process and the functions they perform with respect to these databases are delineated. As such, this summary can be used to support the activities of the overall Hanford environmental data management, either by the various WHC departments or by PNL, with the ultimate goal of integrating the totality of the Hanford environmental data onto the HEIS database. DOE

N94-26561# Woods Hole Research Center, MA.
BIBLIOGRAPHY OF TECHNICAL REPORTS, 1992
Susan S. Berteaux Aug. 1993 14 p
(AD-A274849; WHOI-93-37) Avail: CASI HC A03/MF A01

The technical reports prepared by the Woods Hole Oceanographic Institution in 1992 are listed in this bibliography. Inquiries about availability of extra copies will be handled on an individual basis. Initial distribution of the reports is controlled by the funding agencies. Reports listed in this bibliography are available from the: National Technical Information Service NTIS, Order Desk 5285, Port Royal Road, Springfield, VA 22161, USA. NTIS order numbers are included with each report listed. DTIC

N94-26570# Pittsburgh Univ., PA. Learning Research and Development Center.
LONG TERM LEARNING: INTEGRATION OF KNOWLEDGE ACQUISITION AND KNOWLEDGE COMPILATION Quarterly Progress Report No. 4, 1 Apr. - 30 Jun. 1993
Kurt VanLehn 14 Jan. 1994 6 p
(Contract N00014-92-J-1945)
(AD-A274775) Avail: CASI HC A02/MF A01

This Report is the initial quarterly progress report for grant N00014-92-J-1945, entitled 'Long Term Learning: Integration of Knowledge Acquisition and Knowledge Compilation.' It covers the period from 1 Jul. 1992 to 30 Sep. 1992. Two major objectives were achieved during this report period. The first was to consolidate our understanding of the sources of the learning that occurred in the protocols of 9 subjects learning physics over a period of about 5 hours each. These protocols were first analyzed by Micki Chi and her colleagues then modelled by my group. Despite some considerable effort, no one had ever been able to isolate the exact places where the subjects' beliefs shifted. During this report period, we conducted a large number of protocol analyses aimed at isolating and quantifying the subjects' knowledge acquisition. We eventually found evidence for 3 different acquisition processes. DTIC

N94-26598# Argonne National Lab., IL.
DESIGN CONSIDERATIONS WHEN USING EXTERNAL HYPERTEXT ENGINES FROM APPLICATIONS

B. Sutter and J. Vercellone 1993 5 p Presented at the 2nd Annual Workshop on Intelligent Hypertext Conference on Information and Knowledge Management, Washington, DC, 1-5 Nov. 1993
(Contract W-31-109-eng-38)
(DE94-002213; ANL/DIS/CP-81102; CONF-9311118-1) Avail: CASI HC A01/MF A01

More and more applications today are employing the advantages available from the advances in hypertext to better impart information to the user. This position paper addresses experiences with the specific case of an information application using an 'external' hypertext 'engine' to reference large textual documents that are regularly changing. As hypertext engines take on a role of 'text servers' that can appear seamlessly in other applications, we can benefit from lessons learned in code reuse regarding extensibility, expandability and portability. If a text referenced by an application was static, the interface between the application and the hypertext engine would be simple. However, a changing reference document can induce unacceptable life-cycle costs for an application that needs to employ external hypertext engines to display the referenced text. This paper will present solutions to this problem that were developed when building an information system that would run on an 'ordinary' PC. DOE

N94-26891# Search Technology, Inc., Norcross, GA.
AUTOMATED INFORMATION MANAGEMENT FOR DESIGNERS: FUNCTIONAL REQUIREMENTS FOR COMPUTER BASED ASSOCIATES THAT SUPPORT ACCESS AND USE OF TECHNICAL INFORMATION IN DESIGN Final Report, Sep. 1986 - Mar. 1992
William J. Cody, William B. Rouse, and Kenneth R. Boff Mar. 1993 126 p
(Contract F33615-86-C-0542)
(AD-A274603; AL/CF-TR-1993-0069) Avail: CASI HC A07/MF A02

The purpose of this program was to analyze the process of complex system design to determine why designers often fail to consider potentially valuable technical information in making design decisions. Based on this analysis, the goal was to define functional requirements for a new class of supports that will enhance designers' access and use of such information. Termed Designer's Associates, these supports derive from a thorough understanding of designer's tasks and the services that intelligent computing technologies make possible. DTIC

N94-27013# Massachusetts Univ., Amherst.
RETRIEVAL USING PLAUSIBLE INFERENCE Final Technical Report, 15 Aug. 1991 - 14 Aug. 1993
W. B. Croft Oct. 1993 8 p
(Grant AF-AFOSR-0324-91)
(AD-A274252; FTR-528996; AFOSR-93-0886TR) Avail: CASI HC A02/MF A01

The goal of this project was basic research and development in the area of text-based information systems. A new probabilistic model of text retrieval using Bayesian inference nets was proposed and extended. An efficient implementation of this model for large full-text databases resulted in the INQUERY indexing and retrieval engine. Retrieval experiments carried out using INQUERY and a variety of databases have shown that it produces high-quality results compared to other approaches. Significant progress was also made, both conceptually and with prototype implementations, in showing how text retrieval can be integrated with hypertext and database management systems in a single framework. The success of the INQUERY system in ARPA-sponsored evaluations led to a number of technology transfer projects. DTIC

N94-27014# Carnegie-Mellon Univ., Pittsburgh, PA. Dept. of Computer Science.
MEMORY SUBSYSTEM PERFORMANCE OF PROGRAMS USING COPYING GARBAGE COLLECTION
Amer Diwan, David Tarditi, and Eliot Moss 10 Dec. 1993 21 p
(Contract F19628-91-C-0168; ARPA Order 8313)
(AD-A274258; CMU-CS-93-210) Avail: CASI HC A03/MF A01

Heap allocation with copying garbage collection is believed to have poor memory subsystem performance. A study of the memory subsystem performance of heap allocation for memory subsystems found on many machines was conducted. It was found that many machines support heap allocation poorly. However, with the appropriate memory subsystem organization, heap allocation can have good memory subsystem performance. DTIC

N94-27022# Sandia National Labs., Albuquerque, NM.
BIBLIOGRAPHIC RETRIEVAL SYSTEM (BARS) SANDIA SHOCK COMPRESSION (SSC) DATABASE SHOCK PHYSICS INDEX (SPHINX) DATABASE, VOLUME 3
G. M. vonLaven (Advanced Software Engineering, Madison, AL.) and W. Herrmann Sep. 1993 71 p
(Contract DE-AC04-94AL-85000)
(DE94-001705; SAND-93-1422-Vol-3) Avail: CASI HC A04/MF A01

The Bibliographic Retrieval System (BARS) is a database management system specially designed to store and retrieve bibliographic references and track documents. The system uses INGRES to manage this database and user interface. It uses forms for journal articles, books, conference proceedings, theses, technical reports, letters, memos, visual aids, as well as a miscellaneous form which can be used for data sets or any other material which can be assigned an access or file number. Sorted output resulting from flexible BOOLEAN searches can be printed or saved in files which can be inserted in reference lists for use with word processors. DOE

N94-27101# Florida Univ., Gainesville. Dept. of Computer and Information Sciences.
ACTIVE DATABASE ARCHITECTURES AND THE DESIGN OF SENTINEL FOR CONSTRAINT MANAGEMENT Final Report, Mar. 1992 - Jul. 1993
Sharma Chakravarthy, E. Anwar, and L. Maugis Oct. 1993 77 p
(Contract F30602-92-C-0035)
(AD-A274205; RL-TR-93-190) Avail: CASI HC A05/MF A01

Over the last few years active databases have become an important research area geared towards meeting of the requirements of a variety of non-traditional applications. This report concentrates on providing a seamless incorporation of events and rules into an OODBMS with an emphasis on the modularity and extensibility of the resulting system. The report extends the monitoring view point to an external one, thereby allowing objects to monitor and react to changes occurring to their own state as well as changes occurring to other objects. This is accomplished by introducing a reactive asynchronous object interface. This interface enables objects to propagate pre-declared events occurring to their state to other objects, thereby enabling other objects to perform operations. In addition, a subscription and notification mechanism is introduced that allows event notification to be specified dynamically. This mechanism enables objects to selectively monitor other objects at run-time using the reactive interface. A design is proposed for the specification and detection of simple as well as complex events. This report combines the strengths of the approaches taken in Ode and ADAM and extends them in several significant ways. DTIC

N94-27118# Air Force Inst. of Tech., Wright-Patterson AFB, OH. School of Engineering.
A METHOD FOR POPULATING THE KNOWLEDGE BASE OF AFIT'S DOMAIN-ORIENTED APPLICATION COMPOSITION SYSTEM M.S. Thesis
Russell M. Warner Dec. 1993 130 p
(AD-A274128; AFIT/GCS/Eng/93D-24) Avail: CASI HC A07/MF A02

This research developed a formal method for adding new domains to Architect, a domain-oriented application composition system being developed at the Air Force Institute of Technology (AFIT) to explore new software engineering technologies. Using canonical formal specifications of domain objects, Architect rapidly composes these specifications into a software application and executes a prototype of that application as a means to demonstrate its correctness before any programming language specific code is generated. Architect is implemented in the Software Refinery environment, which allows Architect to create and manipulate object-oriented specifications. As a part of this research effort, domain-oriented application composition systems were investigated in general. leading to the development of a general method for populating the knowledge base of systems of this type. This general population method was then used as a basis for creating a specific knowledge base population method for Architect. To validate this method, Architect was populated with the Digital Signal Processing domain. The correct implementation of this domain was verified by creating applications and comparing their execution to expected results. The addition of the Digital Signal Processing domain to Architect also serves to validate the usefulness and correctness of the Architect system. DTIC

N94-27164# Columbia Univ., New York, NY. Dept. of Computer Science.

PARALLEL STRING MATCHING ALGORITHMS

Dany Breslauer and Zvi Galil 1992 28 p
(Grant NSF CCR-90-14605)
(AD-A274502; CUCS-002-92) Avail: CASI HC A03/MF A01

The string matching problem is one of the most studied problems in computer science. While it is very easily stated and many of the simple algorithms perform very well in practice, numerous works have been published on the subject and research is still very active. In this paper recent results on parallel algorithms for the string matching problem are surveyed. DTIC

N94-27336# Electrotechnical Lab., Tsukuba (Japan).

CIRCULARS OF THE ELECTROTECHNICAL LABORATORY. NO. 223: AN EXTENDED SURVEY ON PROVABLE INFORMATION BASE SYSTEMS [DENSHI GIJUTSU SOGO KENKYUSHO CHOSA HOKOKU DAI 223 GO: PURUBABURU JOHO BESU SHISUTEMU NI KANSURU CHOSA HOKOKU]

Ichiro Ogata, Yoshinao Isobe, Koichi Takahashi, Ichiro Ebihara, Isao Kojima, Yutaka Sato, and Kazuhito Omaki 26 Mar. 1993 161 p In JAPANESE
(ISSN 0366-9084)
(JTN-94-80550) Avail: CASI HC A08/MF A02

Each software system on a computer is generally composed from different layered software, such as operating systems, language processors and application programs. Any of those layers have to handle their own structured or organized data by themselves. Therefore, a technology to construct data structures which can be commonly used from different software layers is needed. It is defined that the information base is software which includes both static and dynamic representations of data. The information base should be commonly used by the different software layers. It is also defined that the provable information base is an information base where each software component in the information base is theoretically proved and the construction of a whole system is also theoretically proved. A technology for provable information base systems must be developed, since, by using the provable information base systems as software engines to manipulate all kinds of data, software engineers can only concentrate on the improvement of their own algorithms besides boring data handling problems. This survey includes extended abstracts of selected papers able to contribute to the construction of the provable information base systems. Author (NASDA)

N94-27394 Center for Mathematics and Computer Science, Amsterdam (Netherlands). Dept. of Computer Science, Algorithmics and Architecture.

QUERY OPTIMIZATION STRATEGIES FOR BROWSING SESSIONS

Martin L. Kersten and M. F. N. deBoer Dec. 1992 19 p Sponsored in part by EEC Limited Reproducibility: More than 20% of this document may be affected by microfiche quality
(ISSN 0169-118X)
(CWI-CS-R9268; ETN-94-95420) Copyright Avail: CASI HC A03

Techniques and experiments to obtain response time improvement for a browsing session, that is a sequence of interrelated queries to locate a subset of interest, are described. The optimization technique is based on a symbolic analysis of the query interdependencies and exploitation of (partial) query answers retained automatically. A prototype Browsing Session Optimizer (BSO) was constructed that runs as a front end to the Ingres relational system. Based on the experiments reported, a proposal to extend (existing) DBMS's (Data Base Management Systems) with a mechanism to keep and reuse small answers by default is made. Such investments quickly pay off in sessions with interrelated queries. The optimization techniques are shown to be capable of outperforming ad hoc index construction and repetitive joint evaluations that are already supported by an index. ESA

N94-27413*# National Aeronautics and Space Administration, Washington, DC.

UNIVERSITY PROGRAM MANAGEMENT INFORMATION SYSTEM, FY 1993

1993 662 p
(NASA-TM-109719; NAS 1.15:109719) Avail: CASI HC A99/MF A06

The University Program Report, Fiscal Year 1993, provides current information and related statistics for 7682 grants/contracts/cooperative agreements active during the report period. NASA field centers and certain Headquarters program offices provide funds for those R&D activities in universities which contribute to the mission needs of that particular NASA element. This annual report is one means of documenting the NASA-university relationship, frequently denoted, collectively, as NASA's University Program. Author

N94-27563# Pacific Northwest Lab., Richland, WA.

REINVENTING INFORMATION SERVICES TO INCREASE CUSTOMER SATISFACTION

J. E. Madison 1993 6 p Presented at the INFOTECH 1993, Oak Ridge, TN, 20-23 Oct. 1993
(Contract DE-AC06-76RL-01830)
(DE94-003718; PNL-SA-22938; CONF-9310145-4) Avail: CASI HC A02/MF A01

In this paper, the author presents her view of the role of an information service and proposes means of improving information customer service and satisfaction. The emphasis of the paper is on placing the primary value on the information customer rather than on the information itself. After receiving a request for information, the information service should strive for speed and accuracy of service to provide full-text sources in a language and format convenient to the customer. The author stresses that information professionals need to re-evaluate their roles to correctly assess and rectify customers' information deficiencies. DOE

N94-27700# Japan Atomic Energy Research Inst., Tokyo.

CORRESPONDENCE DICTIONARY FROM FREE ENGLISH TERM TO INIS DESCRIPTORS

Mar. 1993 18 p In ENGLISH and JAPANESE
(DE94-701173; INIS-JP-012) Avail: CASI HC A03/MF A01

This dictionary is intended for the on-line users of INIS database who select controlled terms (INIS descriptors) starting from free terms. The purpose of terminology control is to reduce the ambiguity of the term use among different subject fields and to improve the recall by coordinating the synonyms. The controlled terms are collected in the thesaurus, but it is not always easy to find suitable descriptors. This dictionary has been compiled by analyzing existing records, and provides the specialists' know-how of converting free terms to descriptors. Besides the compilation of this dictionary, the characteristics of the assigned descriptors were also clarified. DOE

N94-28385# Helsinki Univ. of Technology, Espoo (Finland). Lab. of Information Processing Science.

CONCURRENT SHADOW PAGING: SNAPSHOTS, READ-ONLY TRANSACTIONS, AND ON-THE-FLY MULTI-LEVEL INCREMENTAL DUMPING

T. Yloenen, T. Kivinen, H. Suonsivu, and T. Maennistoe 1993 23 p See also PB93-179034
(PB94-133139; TKK-TKO-B104) Avail: CASI HC A03/MF A01

Shadow paging has a number of desirable properties, of which snapshots are discussed in this paper. It is possible to take a transaction consistent snapshot of a database in a few microseconds. This can be used to execute arbitrary read-only transactions with full consistency without any locking and only minimal overhead. A related application is dumping the database; it is shown that the page table allows very efficient multilevel incremental dumping of the database without disturbing normal transaction processing. Algorithms are given to solve the associated problems. Modification of snapshots is also discussed; this may turn out to have some interesting applications. NTIS

N94-28396# Helsinki Univ. of Technology, Espoo (Finland). Dept. of Computer Science.

EFFICIENT REBALANCING OF TREE-TYPE MAIN MEMORY

DICTIONARIES
L. Malmi 1993 32 p
(PB94-133105; TKO-B107) Avail: CASI HC A03/MF A01

Keeping all data and dictionaries in main memory is a way to implement very fast access to data. Traditional data structures for such applications include balanced trees. However, in highly dynamic applications the performance of balanced trees degrades because of the time required for rebalancing the tree after each update. An alternative solution would be to give up rebalancing during peak hours and postpone it till a more peaceful time. Currently this means that the tree has to be rebalanced using algorithms whose running time is Omega(N). A new algorithm is introduced that performs rebalancing more efficiently. It only traverses the modified branches of the tree and runs in O(Mlog(N+M)) time, where N is the number of nodes in the tree and M is the number of updates performed in the tree. The algorithm is based on using chromatic search trees and at most it requires one byte per node extra storage for the information about the performed updates and the needs for rebalancing. Its performance is compared to other rebalancing algorithms and found that it performs much better when the ratio of updates to the size of the tree is below 15%. NTIS

N94-25550# National Research Inst. for Metals, Tokyo (Japan). Materials Design Div.
KNOWLEDGE BASE SYSTEMS FOR CHEMICAL COMPOUNDS DESIGNING SUPPORT [KAGAKU BUSSHITSU SEKKEI TO SHIEN NO TAME NO CHIHSIKI BESU SHISUTEMU NI KANSURU KENKYU]
Michio Yamazaki, Kenichi Hoshimoto, Toshihiro Yamagata, Katsumi Ono, Hidehiro Onodera, Hiroshi Harada, and Tadaharu Yokokawa *In its* Bulletin of National Research Institute for Metals in Fiscal Year 1993, No. 14 29 Jan. 1993 p 75-86 In JAPANESE (For primary document see N94-25544 07-26)
Avail: CASI HC A03/MF A04

N94-25568# National Research Inst. for Metals, Tokyo (Japan). Materials Design Div.
STUDY ON KNOWLEDGE EXTRACTION AND SYSTEMATIZATION FOR MATERIAL DESIGN [ZAIRYO SEKKEI NO TAME NO CHISHIKI NO CHUSHUTSU TO TAIKEIKA NI KANSURU KENKYU]
Kenichi Hoshimoto, Yutaka Kurihara, Akimitsu Miyazaki, Ryuichi Kaneko, Tadaharu Yokokawa, Shuichi Iwata, and Mitsutane Fujita *In its* Bulletin of National Research Institute for Metals in Fiscal Year 1993, No. 14 29 Jan. 1993 p 219-230 In JAPANESE (For primary document see N94-25544 07-26)
Avail: CASI HC A03/MF A04

83 ECONOMICS AND COST ANALYSIS

Includes cost effectiveness studies.

N94-26918 Technische Univ., Twente (Netherlands). Dept. of Applied Mathematics.
SOME ASPECTS OF NONLINEAR DISCRETE-TIME DESCRIPTOR SYSTEMS IN ECONOMICS
T. Fliegner, H. Nijmeuer, and U. Kotta (Academy of Sciences of the Estonian SSR, Tallinn.) Jun. 1993 13 p Prepared in cooperation with Akademiya Nauk Estonskoi SSR, Tallinn. Inst. Kibernetiki Limited Reproducibility: More than 20% of this document may be affected by microfiche quality
(PB94-126653; MEMO-1137) Avail: CASI HC A03

In this paper, nonlinear discrete-time descriptor (or singular, implicit, general) systems are studied. Some of the problems connected with such systems, which arise naturally in economic modeling, are questions concerning existence and uniqueness of solutions. By means of a step by step procedure, under generic conditions, a local reduction mechanism is given yielding a possibly lower dimensional system in state space form. NTIS

84 LAW, POLITICAL SCIENCE AND SPACE POLICY

Includes NASA appropriation hearings; aviation law; space law and policy; international law; international cooperation; and patent policy.

N94-27218 National Defence Research Establishment, Linkoeping (Sweden). Huvudavdelning foer Informationsteknologi.
CONTRIBUTIONS TO CD SPACE COMMITTEE 1992 [CD RYMDKOMMITTEARBETE 1992: SAMMANFATTNING OCH KOMMENTARER]
U. Ekblad Apr. 1993 46 p In SWAHILI See also PB92-195312
(PB94-124401; FOA-A-30081-9.4) Avail: Issuing Activity (National Technical Information Service (NTIS))

A summary of the contributions in the space area to the United Nations Conference on Disarmament in Geneva and its Space Committee, the Ad Hoc Committee on the Prevention of an Arms Race in Outer Space (PAROS), during the 1992 sessions is given, together with commentaries. NTIS

N94-27323 Etablissement Technique Central de l'Armement, Arcueil (France).
HOW TO MAKE GOOD USE OF INTERNATIONAL RESEARCH COLLABORATION, WITH EMPHASIS ON THE EVOLVING SITUATION IN EUROPE [BON USAGE DE LA COOPERATION INTERNATIONALE POUR LES TRAVAUX DE RECHERCHE; NOTAMMENT EVOLUTION DE LA COOPERATION EUROPEENNE DE RECHERCHE]
Dec. 1992 49 p In FRENCH; Text in French; summary in English
(PB94-119690) Avail: Issuing Activity (National Technical Information Service (NTIS))

This report summarizes the work and proposals of group sessions at the second annual seminar on how to make good use of international collaboration in research. The bulk of it is taken up by two speeches by an aeronautical civil engineer and a weapons inspector. Points covered in the working groups include factors that impede and argue in favor of international research, considerations concerning basic research, problems encountered, future directions, the motivations for forming international teams, and proposals and recommendations. The first speech discusses the desirability and barriers to international collaboration in weapons research, national and international tools, legitimate actions for the EC to take, the need for a European weapons policy including an R&D and export component, and innovating by creating a European Weapons Agency. The second speech discusses changes in the General Weapons Delegation. NTIS

N94-28201# National Science Foundation, Washington, DC. Div. of Science Resources Studies.
SELECTED DATA ON FEDERAL SUPPORT TO UNIVERSITIES AND COLLEGES: FY 1991
Sep. 1993 45 p
(NSF-93-320) Avail: CASI HC A03/MF A01

The data presented in this summary are derived from the Survey of Federal Support to Universities, Colleges, Nonprofit Institutions: Fiscal Year 1991 and are being released in advance of the publication that contains more comprehensive detailed statistical tables. Among the available data excluded from this summary are academic totals by type of institutional control, by highest degree granted, and by field of science and engineering (S&E) discipline; data on historically black colleges and universities; data on nonprofit institutions; and data on university and nonprofit-administered federally funded research and development centers. Derived from text

85 URBAN TECHNOLOGY AND TRANSPORTATION

Includes applications of space technology to urban problems; technology transfer; technology assessment; and surface and mass transportation.

For related information see also *03 Air Transportation and Safety, 16 Space Transportation,* and *44 Energy Production and Conversion.*

N94-26023# Lawrence Livermore National Lab., CA.
EMERGING TECHNOLOGIES
Shin-yee Lu Mar. 1993 32 p
(Contract W-7405-eng-48)
(DE94-003022; UCRL-ID-112779) Avail: CASI HC A03/MF A01

The mission of the Emerging Technologies thrust area at Lawrence Livermore National Laboratory is to help individuals establish technology areas that have national and commercial impact, and are outside the scope of the existing thrust areas. We continue to encourage innovative ideas that bring quality results to existing programs. We also take as our mission the encouragement of investment in new technology areas that are important to the economic competitiveness of this nation. In fiscal year 1992, we have focused on nine projects, summarized in this report: (1) Tire, Accident, Handling, and Roadway Safety; (2) EXTRANSYT: An Expert System for Advanced Traffic Management; (3) Odin: A High-Power, Underwater, Acoustic Transmitter for Surveillance Applications; (4) Passive Seismic Reservoir Monitoring: Signal Processing Innovations; (5) Paste Extrudable Explosive Aft Charge for Multi-Stage Munitions; (6) A Continuum Model for Reinforced Concrete at High Pressures and Strain Rates: Interim Report; (7) Benchmarking of the Criticality Evaluation Code COG; (8) Fast Algorithm for Large-Scale Consensus DNA Sequence Assembly; and (9) Using Electrical Heating to Enhance the Extraction of Volatile Organic Compounds from Soil. DOE

88 SPACE SCIENCES (GENERAL)

No abstracts in this category.

89 ASTRONOMY

Includes radio, gamma-ray, and infrared astronomy, and astrometry.

N94-25656# Air Force Inst. of Tech., Wright-Patterson AFB, OH. School of Engineering.
FEASIBILITY STUDY OF A MULTIAPERTURE TELESCOPE FOR DEEP-SPACE EARTH SURVEILLANCE M.S. Thesis
Charles V. Rothermich Dec. 1993 82 p
(AD-A273903; AFIT/GSO/ENP/93D-04) Avail: CASI HC A05/MF A01

Optical systems launched into space currently have a restriction on their size due to the shuttle's payload capacity. The size of optical systems on the shuttle is limited to 3 m in diameter. Multiaperture telescopes can overcome this limitation. Each subaperture of a multiaperture telescope samples the incoming signal. The waves sampled by each subaperture are combined to form a single image. The radiometric model is developed for a geosynchronous orbiting multiaperture telescope used for Earth surveillance. Using the radiometric model, SNR calculations determine if enough signal is present to generate an image. The OTF and PSF are studied to understand the effects of increasing the multiaperture telescope's diameter. Piston and tilt errors are added to the subapertures to provide insight into how these errors can degrade images in a multiaperture telescope. A total of three circular multiaperture telescopes are examined. The results show that 1 m resolution is achieved with a multiaperture telescope consisting of 31 subapertures. Each subaperture is 2.1 m in diameter, and the telescope's overall diameter is 35 m. DTIC

N94-26234*# Tennessee State Univ., Nashville.
ULTRAVIOLET OBSERVATIONS OF ASTRONOMICAL SOURCES Final Technical Report, 1 Jul. 1988 - 14 Feb. 1993
Joel A. Eaton 15 Mar. 1994 5 p
(Grant NAG5-1327)
(NASA-CR-195232; NAS 1.26:195232) Avail: CASI HC A01/MF A01

The final report on 'Ultraviolet Observations of Astronomical Sources,' which ran for a total of three years, roughly between 1 July 1988 and 14 Feb. 1993 is presented. During the first year, I worked at Indiana University; since October, 1989, I have been at Tennessee State University. This grant has supported my studies of archival International Ultraviolet Explorer (IUE) observations of zeta Aur binaries, cool stars that are paired with hot stars in binary systems. Such systems are important as a source of detailed knowledge about the structures of chromospheres and winds in cool giant and supergiant stars, since the hot star serves as a probe of many lines of sight through the cool supergiant star's outer atmosphere. By determining the physical conditions along many such lines of sight, a detailed two-dimensional map of the chromosphere and wind may be constructed. The grant grew out of my analysis of archival IUE observations of 31 Cyg in which I analyzed five epochs of an atmospheric eclipse that occurred in 1982. I fit the attenuation spectra of atmospheric eclipse throughout the ultraviolet (lambda(lambda)1175-1950 and lambda(lambda)2500-3100) with theoretically calculated spectra, thereby determining the physical properties of gas (mass column density of absorbers, temperature, and velocity spread) along each observed line of sight. A similar analysis for other such zeta Aur binaries was accomplished and theoretical models for the chromospheres of these stars based on my observations were constructed. Author (revised)

N94-26528# Lawrence Livermore National Lab., CA.
MODELLING ATMOSPHERIC TURBULENCE EFFECTS ON GROUND-BASED TELESCOPE SYSTEMS
L. W. Bradford (California Univ., Santa Cruz.), S. M. Flatte (California Univ., Santa Cruz.), and C. E. Max 30 Sep. 1993 7 p Presented at the North Atlantic Treaty Organization/Advanced Study Inst. (NATO/ASI) Conference on Adaptive Optics for Astronomy, Cargese, France, 29 Jun. - 9 Aug. 1993
(Contract W-7405-eng-48)
(DE94-004211; UCRL-JC-115309; CONF-9306245-2) Avail: CASI HC A02/MF A01

Questions still exist concerning the appropriate model for turbulence-induced phase fluctuations seen in ground-based telescopes. Bester et al. used a particular observable (slope of the Allan variance) with an infrared interferometer in an attempt to distinguish models. That observable was calculated for Kolmogorov and 'random walk' models with a variety of outer scales and altitude-dependent turbulence and wind velocity. It was found that clear distinction between models requires good data on the vertical distribution of wind and turbulence. Furthermore, measurements at time separations of order 60 s are necessary to distinguish the 'random walk' model from the Kolmogorov model. DOE

N94-26669 York Univ. (Ontario). Graduate Program in Physics and Astronomy.
WOBBLE-NUTATION MODES OF THE EARTH Ph.D. Thesis
Xianhua Jiang Sep. 1993 152 p
(ISBN-0-315-84246-6; CTN-94-61029) Copyright Avail: Micromedia Ltd., Technical Information Centre, 240 Catherine Street, Suite 305, Ottawa, Ontario, K2P 2G8, Canada HC/MF

In view of the rapid improvement in the accuracy of rotational observations of the Earth, a more sophisticated theoretical model of rotational dynamics of the Earth is needed in order to infer new information about the Earth's deep interior from observations. Numerical calculations are presented of wobble and nutation modes of realistic Earth models. The finite element method is used for numerical implementation of a variational principle based on the subseismic approximation to the motion of the outer core. A new prograde free core nutation with a period of 538 solar days for the 1066A Earth model is obtained. It is also found that the period of the retrograde free core nutation is 450 solar days, about 10 days shorter than the period given by previous studies. For the first time, the displacement field of wobble-nutation modes is calculated and plotted out in detail. This allows a comparison with other theoretical modes. A very long base interferometry data set, covering a time interval of about nine years, is analyzed to search for the free core nutation modes predicted by the study. A retrograde free nutation with a period of about 431 days is found significant above the 95% confidence level. Incomplete correction for the retrograde annual term might account for the spectral peak identified as the free core nutation. Author (CISTI)

N94-26789*# Southwest Research Inst., San Antonio, TX. Instrumentation and Space Research Div.
STUDIES OF EXTRA-SOLAR OORT CLOUDS AND THE KUIPER DISK Semiannual Progress Report, Mar. 1994
S. Alan Stern 22 Mar. 1994 61 p Original contains color illustrations
(Grant NAGw-3023; SwRI Proj. 15-4971)
(NASA-CR-195242; NAS 1.26:195242) Avail: CASI HC A04/MF A01; 1 functional color page

The March 1994 Semi-Annual report for Studies of Extra-Solar Oort Clouds and the Kuiper Disk is presented. We are conducting research designed to enhance our understanding of the evolution and detectability of comet clouds and disks. This area holds promise for also improving our understanding of outer solar system formation, the bombardment history of the planets, the transport of volatiles and organics from the outer solar system to the inner planets, and to the ultimate fate of comet clouds around the Sun and other stars. According to 'standard' theory, both the Kuiper Disk and Oort Cloud are (at least in part) natural products of the planetary accumulation stage of solar system formation. One expects such assemblages to be a common attribute of other solar systems. Therefore, searches for comet disks and clouds orbiting other stars offer a new method for inferring the presence of planetary systems. Our three-year effort consists of two major efforts: observational work to predict and search for the signatures of Oort Clouds and comet disks around other stars; and modeling studies of the formation and evolution of the Kuiper Disk (KD) and similar assemblages that may reside around other stars, including beta Pic. Author (revised)

N94-27302 Queens Univ., Kingston (Ontario). Dept. of Electrical Engineering.
PROPERTIES OF THE NEAR-AXIS BISPECTRUM APPLIED TO HIGH-RESOLUTION ASTRONOMICAL IMAGING Ph.D. Thesis
Julian Meng Jul. 1993 267 p
(ISBN-0-315-85247-X; CTN-94-61103) Copyright Avail: Micromedia Ltd., Technical Information Centre, 240 Catherine Street, Suite 305, Ottawa, Ontario, K2P 2G8, Canada HC/MF

A new quasi least-squares (QLS) algorithm has been developed for phase recovery in the triple correlation (TC) process applied to speckle imaging in astronomy. The QLS algorithm is found to provide significant improvement in terms of image reconstruction fidelity over the popular recursive algorithm. Implementing the QLS algorithm using phasors avoids the modulo 2-pi problem inherent to linear least squares solutions. The performance of the QLS algorithm, along with a Knox-Thompson (KT) phase recovery process for comparison, was rigorously studied using second- and third-order noise models. Those models eliminate the need for speckle image simulation and the computation of second- and third-order products required by KT and TC for phase recovery. The validity of the model was confirmed using simulated speckle data. Simulations showed that for the high signal to noise ratio (SNR) case, the near-axis TC transfer function subplanes have lower phase error than the comparable KT transfer function subplanes. Computing subplanes only in the near-axis region is important if computer resources are limited. Because of the lower phase error, the TC process was found to produce better images than the KT algorithm with high-SNR input data. This previously unreported difference is analyzed in detail. Author (CISTI)

N94-27750# Fermi National Accelerator Lab., Batavia, IL.
SLOAN DIGITAL SKY SURVEY
S. M. Kent Nov. 1993 4 p Presented at the Science With Infrared Surveys Conference, Les Houches, France, 21-24 Sep. 1993
(Contract DE-AC02-76CH-03000)
(DE94-004662; FNAL/C-93/346; CONF-9309298-1) Avail: CASI HC A01/MF A01

The Solan Digital Sky Survey is a project which will produce a detailed digital phometric map of half the northern sky to about 23 magnitude using a special purpose wide field telescope of 2.5 meter aperture. This map will be used to select about a million galaxies and 100,000 quasars, for which high resolution spectra will be obtained using the same telescope. A catalog will be produced of all the detected objects, about 100 million galaxies and a similar number of stars, and a million quasar candidates. DOE

N94-27933*# Smithsonian Astrophysical Observatory, Cambridge, MA.
WEAK BUMP QUASARS Final Report, 15 Sep. 1991 - 14 Dec. 1993
B. J. Wilkes and J. McDowell Jan. 1994 14 p
(Grant NAG5-1771)
(NASA-CR-195267; NAS 1.26:195267) Avail: CASI HC A03/MF A01

Research into the optical, ultraviolet and infrared continuum emission from quasars and their host galaxies was carried out. The main results were the discovery of quasars with unusually weak infrared emission and the construction of a quantitative estimate of the dispersion in quasar continuum properties. One of the major uncertainties in the measurement of quasar continuum strength is the contribution to the continuum of the quasar host galaxy as a function of wavelength. Continuum templates were constructed for different types of host galaxy and individual estimates made of the decomposed quasar and host continua based on existing observations of the target quasars. The results are that host galaxy contamination is worse than previously suspected, and some apparent weak bump quasars are really normal quasars with strong host galaxies. However, the existence of true weak bump quasars such as PHL 909 was confirmed. The study of the link between the bump strength and other wavebands was continued by comparing with IRAS data. There is evidence that excess far infrared radiation is correlated with weaker ultraviolet bumps. This argues against an orientation effect and implies a probable link with the host galaxy environment, for instance the presence of a luminous starburst. However, the evidence still favors the idea that reddening is not important in those objects with ultraviolet weak bumps. The same work has led to the discovery of a class of infrared weak quasars. Pushing another part of the envelope of quasar continuum parameter space, the IR-weak quasars have implications for understanding the effects of reddening internal to the quasars, the reality of ultraviolet turnovers, and may allow further tests of the Phinney dust model for the IR continuum. They will also be important objects for studying the claimed IR to x-ray continuum correlation. Author (revised)

N94-25703*# Virginia Polytechnic Inst. and State Univ., Blacksburg. Dept. of Aerospace Engineering.
PROJECT PARAS: PHASED ARRAY RADIO ASTRONOMY FROM SPACE
Kenneth Nuss, Christopher Hoffmann, Michael Dungan, Michael Madden, and Monia Bendakhlia (Ecole Polytechnique Feminine, Sceaux, France.) *In* USRA, Proceedings of the 8th Annual Summer Conference: NASA/USRA Advanced Design Program 1992 p 309-316 (For primary document see N94-25665 07-80)
Avail: CASI HC A02/MF A04

N94-28297*# California Univ., Berkeley. Lawrence Berkeley Lab.
IN SEARCH OF NEMESIS Abstract Only
S. Carlson, T. Culler, R. A. Muller, M. Tetreault, and S. Perlmutter *In* Houston Univ., New Developments Regarding the KT Event and Other Catastrophes in Earth History 1994 p 19-20 (For primary document see N94-28294 07-46)
Avail: CASI HC A01/MF A02

90 ASTROPHYSICS

Includes cosmology; celestial mechanics; space plasmas; and interstellar and interplanetary gases and dust.

For related information see also *75 Plasma Physics.*

N94-26046# International Centre for Theoretical Physics, Trieste (Italy).
DIBARYON-INDUCED INSTABILITY OF NEUTRON STARS
L. Popa and V. Popa Apr. 1993 7 p
(DE93-634453; IC-93/74) Avail: CASI HC A02/MF A01 (US Sales Only)

The possibility of spontaneous production of non-strange dibaryonic states inside the core of neutron stars is discussed. Some untrivial predictions concerning the instability of the rotation period of such objects are derived. DOE

N94-26268 International Centre for Theoretical Physics, Trieste (Italy).
TEV EMISSION FROM CLOSE BINARIES
I. V. Moskalenko Jun. 1993 13 p Limited Reproducibility: More than 20% of this document may be affected by microfiche quality
(DE93-634330; IC-93/160) Avail: CASI HC A03 (US Sales Only)

It is commonly accepted that candidates to very high energy gamma-ray sources are neutron stars (NS's), binary systems, black holes, etc. Close binary systems containing a normal hot star and a NS (or a black hole) form an important class of very high energy gamma-ray sources. Such systems are variable in any region of the electromagnetic spectrum and they enable us to study various stages of stellar evolution, accretion processes, mechanisms of particle acceleration etc. Phenomena connected with this class of very high energy gamma-ray sources are discussed, the particular emphasis has been placed on the TeV region. DOE

N94-26269 International Centre for Theoretical Physics, Trieste (Italy).
MAGNETIC FIELD INDUCED CONTRIBUTIONS OF SUPERSYMMETRIC PARTICLES TO ENERGY LOSSES OF NEUTRON STAR
G. G. Likhachev and A. I. Studenikin Jul. 1993 7 p Limited Reproducibility: More than 20% of this document may be affected by microfiche quality
(DE93-634331; IC-93/168) Avail: CASI HC A02 (US Sales Only)

Using recent results for the probabilities of emission of pairs of supersymmetric particles by the electron in strong magnetic field we have considered the contribution of these processes to neutron star energy losses. The comparison of these new proposed mechanisms of energy losses with the standard neutrino mechanism is presented. DOE

N94-26311# Fermi National Accelerator Lab., Batavia, IL.
THE MEANING OF EROS/MACHO
M. S. Turner 1993 17 p
(Contract DE-AC02-76CH-03000)
(DE94-003003; FNAL/Pub-93/298-A) Avail: CASI HC A03/MF A01

Most of the mass density in the Universe and in the halo of our own galaxy exists in the form of dark matter. Overall, the contribution of luminous matter (in stars) to the mass density of the Universe is less than 1%. Primordial nucleosynthesis indicates that baryons contribute between 1% and 10% of the critical density (0.01 h(exp -2) is approximately less than Omega(sub B) is approximately less than 0.02 h(exp -2); h = the Hubble constant in units of 100 kms(exp -1) Mpc(exp -1)). Other evidence indicates that the total mass density is at least 10% of critical density and is likely much greater. If the universal density is as low as 10% of the critical density, there may be but one kind of dark matter. More likely, the universal density is greater than 10%, and there are two kinds of dark matter and thus, two dark matter problems: In what form does the baryonic dark matter exist? and In what form does the nonbaryonic dark matter exist? The MACHO and EROS collaborations have presented evidence for the microlensing of stars in the LMC by 10(exp -1+/-1) solar mass dark objects in the halo of our own galaxy and may well have solved one of the dark matter puzzles by identifying the form of the baryonic dark matter. It is too early to make precise statements about the fraction of the mass density in the halo of our galaxy contributed by lensing objects (= f(sub m)), though the EROS/MACHO data suggest that f(sub m) is probably 0.1 or larger. Taking our galaxy to be typical and taking account a fraction f(sub m) of the mass in the portion of the halo that contributes most significantly to microlensing (within 20 kpc of the galactic center), I estimate that lensing objects contribute a fraction 0.008f (sub m)/h of the critical density, and clearly cannot account for the bulk of the dark matter if Omega(sub 0)is much greater than 0.1. DOE

N94-26638 Victoria Univ. (British Columbia). Dept. of Physics and Astronomy.
A COSMOLOGICAL FIELD THEORY Ph.D. Thesis
Steven Paul Starkovich 1992 101 p
(ISBN-0-315-84271-7; CTN-94-61017) Copyright Avail: Micromedia Ltd., Technical Information Centre, 240 Catherine Street, Suite 305, Ottawa, Ontario, K2P 2G8, Canada HC/MF

In an oscillating cosmological model, the cosmological fluid is described by a classical scalar field undergoing a series of phase transitions over the lifetime of the universe. In general, for a standard model universe and a given equation of state, it is shown that the field potential V may be derived from the solution of Riccati's equation. The resulting expression for V includes parameters whose values are determined from the boundary conditions. The scalar field Lagrangian is thus determined for the entire history of the universe. The resulting cosmological model is free of singularities and describes a universe that is very cold at minimum radius and heats up rapidly in an initial inflationary era. The temperature increase of the scalar field during inflation is a direct consequence of applying classical thermodynamics and does not depend on fine tuning of free parameters. Inflation continues until the Planck temperature is attained, when a phase transition occurs and the standard model era begins. By relating the temperature of the scalar field in the theory to the radiation temperature in the standard model universe, it is possible to establish a thermodynamic constraint on a more complete theory of matter for the early universe. It is found that the value of the Hubble parameter least sensitive to the initial equation of state is 33-44 km/sec/megaparsec. Author (CISTI)

N94-26786# Fermi National Accelerator Lab., Batavia, IL.
COSMOLOGICAL PHASE TRANSITIONS
E. W. Kolb Oct. 1993 18 p Presented at the 37th Yamada Conference, Tokyo, Japan, 8-12 Jun. 1993
(Contract DE-AC02-76CH-03000)
(DE94-003001; FNAL/C-93/321-A; CONF-9306277-1) Avail: CASI HC A03/MF A01

If modern ideas about the role of spontaneous symmetry breaking in fundamental physics are correct, then the Universe should have undergone a series of phase transitions early in its history. The study of cosmological phase transitions has become an important aspect of early-Universe cosmology. In this lecture I review some very recent work on three aspects of phase transitions: the electroweak transition, texture, and axions. DOE

N94-27265# General Research Corp., Danvers, MA.
ZODIACAL LIGHT DATA INVESTIGATION. INTERIM RESULTS FOR THE EARTHLIMB CLUTTER EXPERIMENT
Wesley K. Cobb, Shawn V. Burdick, and Thomas L. Murdock 15 Jul. 1993 74 p
(Contract F19628-91-C-0104)
(AD-A274461; Rept-1949-01-93-TR; SR-1; PL-TR-93-2179) Avail: CASI HC A04/MF A01

Zodiacal light data from the Earth Limb Clutter experiment (ELC) have been analyzed and compared with IRAS observations in order to bring the former into a common calibration framework with COBE and IRAS. There were 9 ELC spectral bands, 2 of which were broad (12 and 26 microns), and 7 of which were narrow (5.6, 9.6, 10.6, 11.5, 12.5, 13.7, 15.2 microns). The ELC data appeared to show considerable spectral structure in the zodiacal light for 9-15 micron regime. The recalibrated ELC data are also important because they contain zodiacal plane crossings at low (190) and high (1670) solar elongations -- regions not accessible to IRAS or COBE. The antisolar crossing is particularly interesting because it is associated with nearly symmetrically placed secondary peaks at + 280 ecliptic latitude. Possible origins for these peaks are discussed. DTIC

N94-27407*# TRW Space Technology Labs., Redondo Beach, CA. Applied Technology Div.
COLLISIONLESS SHOCK STRUCTURES OF EARTH AND OTHER PLANETS Final Report, Aug. 1992 - Oct. 1993
Eugene W. Greenstadt and Stewart L. Moses Nov. 1993 65 p
(Contract NASw-4749)
(NASA-CR-195257; NAS 1.26:195257; HQROM93.WR1) Avail: CASI HC A04/MF A01

This report summarizes the closing segment of our multi-spacecraft, multi-instrument study of collisionless shock structure. In this last year of our study, we have necessarily concentrated on subjects that limited time and remaining resources could be expected to bring to reasonable stopping points, if not full conclusions. Our attention has been focused therefore on matters that were either well underway when the year began or that could be expected to yield rapidly completed reports publishable quickly in abbreviated versions. Contemporary publication delays prevent any new initiatives from reaching the literature within the year in the best of circumstances. The topics that fell into these categories were detailed plasma wave (pw) phenomenology in slow shocks in the Earth's distant geomagnetic tail, instantaneous orientations of theta(sub Bn) in quasiparallel (Q(sub parallel)) shock structure, and a comprehensive overview of the relationship between structural ULF waves in the QII shock environment and waves in the magnetosphere, i.e. geomagnetic ULF pulsations. The remainder of this report describes our freshly completed results, discusses two related investigations of pw waves in the foreshock and magnetosheath, and appends the abstracts of published papers and the texts of papers in press. Derived from text

N94-27428*# Smithsonian Astrophysical Observatory, Cambridge, MA.
INVESTIGATIONS OF THE DYNAMICAL EVOLUTION OF PROTOPLANETARY NEBULAE Annual Status Report No. 1, 1 Nov. 1992 - 31 Oct. 1993
Lee W. Hartmann Mar. 1994 7 p
(Grant NAGw-2306)
(NASA-CR-195278; NAS 1.26:195278) Avail: CASI HC A02/MF A01

The spectral energy distributions (SED's) of all the known Class I (protostellar) sources in the Taurus molecular cloud were modelled. The Tereby, Shu, & Cassen (1984, TSC) density distribution for a rotating, infalling envelope was adopted. The radiative equilibrium temperature distribution from the spherical average of the TSC density distribution was calculated. The resulting spherically-symmetric temperature distribution then provides the source function to obtain the emergent spectrum at a given inclination angle i from the formal solution of the transfer equation, using the exact density (opacity) distribution. Results showed that the SED's of the protostar candidates in Taurus can be reproduced with TSC models having infall rates close to the values predicted by the theory of isothermal cloud collapse. Flat Spectrum T Tauri Stars were studied. The mid- to far-infrared fluxes of 'flat spectrum' T Tauri stars can be explained by radiative equilibrium emission from infalling dusty envelopes. This explanation indicated that models employing 'active' disks, in which the temperature distribution is a parameterized power law, should be invoked with caution. Infall also naturally explains the scattered light nebulae detected around many flat-spectrum sources. Results showed that the SED's of the protostar candidates in Taurus can be reproduced with TSC models having infall rates close to the values predicted by the theory of isothermal cloud collapse. Flattened infalling envelope models are also being studied. Derived from text

N94-27932*# Colorado Univ., Boulder. Dept. of Computer Science.
VISUALIZATION TECHNIQUES TO AID IN THE ANALYSIS OF MULTISPECTRAL ASTROPHYSICAL DATA SETS Final Report
E. W. Brugel, Gitta O. Domik, and T. R. Ayres Sep. 1993 51 p
(Grant NAGw-1902)
(NASA-CR-195268; NAS 1.26:195268) Avail: CASI HC A04/MF A01

The goal of this project was to support the scientific analysis of multi-spectral astrophysical data by means of scientific visualization. Scientific visualization offers its greatest value if it is not used as a method separate or alternative to other data analysis methods but rather in addition to these methods. Together with quantitative analysis of data, such as offered by statistical analysis, image or signal processing, visualization attempts to explore all information inherent in astrophysical data in the most effective way. Data visualization is one aspect of data analysis. Our taxonomy as developed in Section 2 includes identification and access to existing information, preprocessing and quantitative analysis of data, visual representation and the user interface as major components to the software environment of astrophysical data analysis. In pursuing our goal to provide methods and tools for scientific visualization of multi-spectral astrophysical data, we therefore looked at scientific data analysis as one whole process, adding visualization tools to an already existing environment and integrating the various components that define a scientific data analysis environment. As long as the software development process of each component is separate from all other components, users of data analysis software are constantly interrupted in their scientific work in order to convert from one data format to another, or to move from one storage medium to another, or to switch from one user interface to another. We also took an in-depth look at scientific visualization and its underlying concepts, current visualization systems, their contributions and their shortcomings. The role of data visualization is to stimulate mental processes different from quantitative data analysis, such as the perception of spatial relationships or the discovery of patterns or anomalies while browsing through large data sets. Visualization often leads to an intuitive understanding of the meaning of data values and their relationships by sacrificing accuracy in interpreting the data values. In order to be accurate in the interpretation, data values need to be measured, computed on, and compared to theoretical or empirical models (quantitative analysis). If visualization software hampers quantitative analysis (which happens with some commercial visualization products), its use is greatly diminished for astrophysical data analysis. The software system STAR (Scientific Toolkit for Astrophysical Research) was developed as a prototype during the course of the project to better understand the pragmatic concerns raised in the project. STAR led to a better understanding on the importance of collaboration between astrophysicists and computer scientists. Twenty-one examples of the use of visualization for astrophysical data are included with this report. Sixteen publications related to efforts performed during or initiated through work on this project are listed at the end of this report. Author

N94-28184*# Michigan Univ., Ann Arbor. Dept. of Atmospheric, Oceanic and Space Sciences.
THE KINETICS AND DYNAMICS OF THE COMA OF HALLEY'S COMET Final Report
Michael R. Combi Jan. 1994 64 p
(Grants NAGw-1946; NAGw-695; NAGw-3319)
(NASA-CR-194828; NAS 1.26:194828) Avail: CASI HC A04/MF A01

This grant to the University of Michigan supported the efforts of Michael R. Combi to serve as a co-investigator in collaboration with a larger effort by the principal investigator, William Smyth of Atmospheric and Environmental Research, Inc. The overall objective of this project was to analyze in a self-consistent manner unique optical O((sup 1)D) and NH2 ultra-high resolution line profile data of excellent quality and other supporting lower-resolution spectral data for the coma of comet P/Halley by using highly developed and physically-based cometary coma models in order to determine and explain in terms of physical processes the actual dynamics and photochemical kinetics that occur in the coma. The justification for this work is that it provides a valuable and underlying physical base from which to interpret significantly different types of coma observations in a self-consistent manner and hence bring into agreement (or avoid) apparent inconsistencies that arise from non-physically based interpretations. The level of effort for the Michigan component amounted to less than three person-months over a planned period of three years. The period had been extended at no extra cost to four years because the Michigan grant and the AER contract did not have coincident time periods. An effort of somewhat larger scope was undertaken by the PI. The importance of the O((sup 1)D) profiles is that they provide a direct trace of the water distribution in comets. The line profile shape is produced by the convolution of the outflow velocity and thermal dispersion of the parent water molecules with the photokinetic ejection of the oxygen atoms upon photodissociation of the parent water molecules. Our understanding of the NH2 and its precursor ammonia are important for comet-to-comet composition variations as they relate to the cosmo-chemistry of the early solar nebula. Modeling of the distribution of NH2 is necessary in order to infer the ammonia production rates from NH2 observations. Derived from text

N94-25697*# Texas Univ., Austin. Dept. of Aerospace Engineering and Engineering Mechanics.
ASTEROID EXPLORATION AND UTILIZATION
Brian M. Radovich, Alan E. Carlson, Medha D. Date, Manny G. Duarte, Neil F. Erian, George K. Gafka, Peter H. Kappler, Scott J. Patano, Martin Perez, and Edgar Ponce et al *In* USRA, Proceedings of the 8th Annual Summer Conference: NASA/USRA Advanced Design Program 1992 p 264-266 (For primary document see N94-25665 07-80)
Avail: CASI HC A01/MF A04

N94-28308*# California Univ., Berkeley. Lawrence Berkeley Lab. Dept. of Physics.
EXTRATERRESTRIAL ACCRETION AND GLACIAL CYCLES Abstract Only
R. A. Muller *In* Houston Univ., New Developments Regarding the KT Event and Other Catastrophes in Earth History 1994 p 85-86 (For primary document see N94-28294 07-46)
Avail: CASI HC A01/MF A02

N94-28309*# First Inst. of Oceanography, Qingdao (China). State Oceanic Administration.
AN EXTRATERRESTRIAL EVENT AT THE TERTIARY-QUATERNARY BOUNDARY Abstract Only
H. Peng *In* Houston Univ., New Developments Regarding the KT Event and Other Catastrophes in Earth History 1994 p 88-89 (For primary document see N94-28294 07-46)
Avail: CASI HC A01/MF A02

91 LUNAR AND PLANETARY EXPLORATION

Includes planetology; and manned and unmanned flights.

For spacecraft design or space stations see *18 Spacecraft Design, Testing and Performance.*

N94-25981# Wisconsin Univ., Madison.
AN EVALUATION OF THE UTILITY OF GROUND-BASED HIGH RESOLUTION INTERFEROMETER (GB-HIS) SOUNDINGS OF THE PLANETARY BOUNDARY LAYER Ph.D. Thesis
Han-Jun Ding 1993 84 p
(Contract DE-FG02-92ER-61365)
(DE94-000960; DOE/ER-61365/T2) Avail: CASI HC A05/MF A01

Atmospheric soundings generated from the ground-based high resolution interferometer sounder (GB-HIS) are evaluated. The two goals are (1) to estimate the accuracy of GB-HIS temperature and dew point soundings using statistical analysis and comparison against observation from simultaneous radiosondes, and (2) to exploit the high temporal resolution of GB-HIS data set to analyze planetary boundary layer (PBL) thermodynamic properties. Five additional sections are included. Section 2 describes the methodology of GB-HIS retrieval. Section 3 provides a statistical error analysis of the GB-HIS system. Section 4 shows the utility of GB-HIS data in monitoring the PBL evolution, while Section 5 discusses and validates a simple mixed-layer growth model. Finally, Section 6 offers conclusions and suggestions for further studies. DOE

N94-26237*# Colorado Univ., Boulder. Lab. for Atmospheric and Space Physics.
SULFUR DIOXIDE IN THE ATMOSPHERE OF VENUS 1 SOUNDING ROCKET OBSERVATIONS Final Technical Report, 1 Feb. 1976 - 31 Mar. 1994
William E. McClintock, Charles A. Barth, and Richard A. Kohnert 1994 53 p
(Grant NsG-5103)
(NASA-CR-195224; NAS 1.26:195224) Avail: CASI HC A04/MF A01

In this paper we present ultraviolet reflectance spectra obtained during two sounding rocket observations of Venus made during September 1988 and March 1991. We describe the sensitivity of the derived reflectance to instrument calibration and show that significant artifacts can appear in that spectrum as a result of using separate instruments to observe both the planetary radiance and the solar irradiance. We show that sulfur dioxide is the primary spectral absorber in the 190 - 230 nm region and that the range of altitudes probed by these wavelengths is very sensitive to incidence and emission angles. In a following paper Na et. al. (1994) show that sulfur monoxide features are also present in these data. Accurate identification and measurement of additional species require observations in which both the planetary radiance and the solar irradiance are measured with the same instrument. The instrument used for these observations is uniquely suited for obtaining large phase angle coverage and for studying transient atmospheric events on Venus because it can observe targets within 18 deg of the sun while earth orbiting instruments are restricted to solar elongation angles greater than or equal to 45 deg. Author

N94-27007# California Univ., Berkeley. Lawrence Berkeley Lab.
CRATERING RATES FROM LUNAR XENOSPHERULES
R. A. Muller 25 May 1993 7 p
(Contract DE-AC03-76SF-00098)
(DE94-003481; LBL-34168) Avail: CASI HC A02/MF A01

The goal of this project is to obtain the time history of impacts on the moon, with emphasis on recent impacts. In particular, the project could prove (or disprove) the existence of comet sores and provide the dates when they occurred. DOE

N94-27406*# Atmospheric and Environmental Research, Inc., Cambridge, MA.
STUDIES FOR IO'S EXTENDED ATMOSPHERE AND NEUTRAL CLOUDS AND THEIR IMPACT ON THE LOCAL SATELLITE ATMOSPHERE AND ON THE PLANETARY MAGNETOSPHERE Final Report, 10 Dec. 1992 - 9 Dec. 1993
William H. Smyth 9 Dec. 1993 127 p
(Contract NASw-4771)
(NASA-CR-195255; NAS 1.26:195255) Avail: CASI HC A07/MF A02

The research performed in this project is divided in two main investigations: (1) the synthesis and analysis of a collection of independent observations for Io's sodium corona, its sodium extended atmosphere, and the sodium cloud, and (2) the analysis of a (System III longitude correlated) space-time 'bite-out' near western elongation in the 1981 sodium cloud images from the JPL Table Mountain Sodium Cloud Data Set. For the first investigation, modeling analysis of the collective observed spatial profiles has shown that they are reproduced by adopting at Io's exobase a modified sputtering flux speed distribution function which is peaked near 0.5 km/s and has a small high-speed (15-20 km/s) nonisotropic component. The nonisotropic high-speed component is consistent with earlier modeling of the trailing directional feature. For the second investigation, modeling analysis of the 'bite-out' observed near western elongation (but not eastern elongation) has shown that it is reproduced in model calculation by adopting a plasma torus description for the sodium lifetime that is inherently asymmetric in System III longitudes of the active sector and that also has an east-west asymmetry. The east-west and System III longitude asymmetries were determined from independent observations for the plasma torus in 1981. The presence of the 'bite-out' feature only near western elongation may be understood in terms of the relative value for sodium of its lifetime and its transport time through the System III enhanced plasma torus region. Author

N94-27409*# SETS Technology, Inc., Mililani, HI.
PLANETARY INSTRUMENT DEFINITION AND DEVELOPMENT PROGRAM (PIDDP). INSTRUMENT FOR FUTURE PLANETARY FLIGHT MISSIONS: A VISIBLE-INFRARED IMAGING SPECTROMETER FOR PLANETARY MISSIONS Final Report
Thomas B. McCord 12 Oct. 1993 13 p
(Contract NASw-4739)
(NASA-CR-195254; NAS 1.26:195254) Avail: CASI HC A03/MF A01

The objective of this project is to develop and prove a small, light-weight, efficient imaging spectrometer design to cover the VIS/NIR spectral range for applications particularly but not exclusively to NASA inner solar system space missions. A design and a brassboard prototype will be developed and tested. Progress over the first year of this project includes design specification, optical design layout, grating specifications, infrared detector selection, and mechanical design. Mechanical and grating manufacturing drawings were begun. We developed an agreement in principle to cooperate with the German space group, DLR, to apply some of their electronics microminiaturization technology to this imaging spectrometer project, mostly or entirely at their expense. Funds from NASA for the second year of this effort have been received and the effort is on track. Release of funds for the third year of this award will be requested later this year in order to accelerate this work and bring it to a conclusion in time for new NASA missions considerations as well as to make effective use of the DLR contributions. Derived from text

N94-27418# General Accounting Office, Washington, DC.
SPACE SCIENCE: CAUSES AND IMPACTS OF CUTBACKS TO NASA'S OUTER SOLAR SYSTEM EXPLORATION MISSIONS. REPORT TO THE CHAIRMAN, SUBCOMMITTEE ON INVESTIGATIONS AND OVERSIGHT, COMMITTEE ON SCIENCE, SPACE, AND TECHNOLOGY, HOUSE OF REPRESENTATIVES
Frank Degnan 29 Dec. 1993 39 p
(GAO/NSIAD-94-24; B-254122) Avail: CASI HC A03/MF A01; GAO, P.O. Box 6015, Gaithersburg, MD 20877 HC

The Comet Rendezvous Asteroid Flyby (CRAF)/Cassini program was first funded by the Congress in fiscal year 1990. Since then, it has encountered difficulties that resulted in the cancellation of CRAF, reduction of Cassini's original scientific capabilities, and extension of its launch date. At the request of the former Chairman of the Investigations and Oversight Subcommittee, House Committee on Science, Space, and Technology, GAO reviewed the program to identify the factors that led to the cancellation of the CRAF project and the prospects for continuation of the Cassini project. Author (revised)

N94-27784*# California Inst. of Tech., Pasadena. Space Radiation Lab.
ANALYSIS OF ENERGETIC PROTON AND ELECTRON DATA IN NEPTUNE'S MAGNETOSPHERE Final Report, 1 Jan. 1992 - 31 Dec. 1993
Edward C. Stone 5 Apr. 1994 3 p
(Grant NAGw-2402)
(NASA-CR-195707; NAS 1.26:195707) Avail: CASI HC A01/MF A01

This grant was for the analysis and interpretation of data obtained by the cosmic ray system (CRS) on Voyager 2 in the magnetosphere of Neptune. The research goals included the following: characterize the distribution and intensity of trapped electrons and protons; relate them to theoretical models of particle transport; study the particle absorption signatures of Neptune's moons and rings; develop planetary magnetic field models based on the particle data; and study Neptune's cosmic ray cutoff. Derived from text

N94-27850*# Brown Univ., Providence, RI. Dept. of Geological Sciences.
EXPERIMENTAL STUDY OF LUNAR AND SNC (MARS) MAGMAS Progress Report, 1 Apr. 1992 - 31 Mar. 1994
Malcolm J. Rutherford 1994 4 p
(Grant NAG9-575)
(NASA-CR-195274; NAS 1.26:195274) Avail: CASI HC A01/MF A01

The overall objectives of this research were to evaluate the role of C-O-S-Cl degassing processes in explaining vesiculation, oxidation state and fire-fountaining of lunar magmas by analysis of individual lunar glass spherules, and by experimental determination of equilibrium abundances and diffusion rates of C, S and Cl melt species in lunar glass compositions; and to determine possible primitive SNC magma compositions and the mineralogy of the mantle from which they were derived, and to evaluate P, T, XH2O etc. conditions at which they crystallize to form the SNC meteorites. After funding for one year, a project on the A15 volcanic green glass has been completed to the point of writing a first manuscript. Carbon-oxygen species C-O and CO2 are below detection limits (20 ppm) in these glasses, but there is up to 500 ppm S with concentrations both increasing and decreasing toward the spherule margins. Calculations and modeling indicate that C species could have been present in the volcanic gases, however. In a second project, experiments with low PH2O have resulted in refined estimates of the early intercumulus melt composition in the Chassigny meteorite which is generally accepted as a sample from Mars. Author

N94-27885*# Atmospheric and Environmental Research, Inc., Cambridge, MA.
REANALYSIS OF MARINER 9 UV SPECTROMETER DATA FOR OZONE, CLOUD, AND DUST ABUNDANCES, AND THEIR INTERACTION OVER CLIMATE TIMESCALES Final Report, 1 May 1991 - 31 Dec. 1993
Bernhard Lee Lindner 7 Feb. 1994 138 p
(Contract NASw-4614)
(NASA-CR-195244; NAS 1.26:195244) Avail: CASI HC A07/MF A02

Mariner 9 UV spectrometer data have been reinverted for the ozone abundance. The spectra were fit by models which covered the full range in observed solar zenith angle, cloud, dust and ozone amount, ice albedo and look angles. Errors in ozone retrieval with this data are tabulated over a range in theses conditions and are shown graphically. This work shows that significant underestimation of ozone occurred in earlier analysis of Mariner 9 data, and that much of the observed variability in Mars ozone is due to masking of ozone by clouds and dust. An in-situ measurement by balloon is recommended as it is the only technique capable of accurately inferring the ozone abundance in all conditions. Recommendations for future research are also presented. 7 manuscripts have been published in refereed journals, and three are in review. A review of these publications and presentations is in the report. For individual titles, see N94-27886 through N94-27892.

N94-27886*# Atmospheric and Environmental Research, Inc., Cambridge, MA.
COOLING THE MARTIAN ATMOSPHERE: THE SPECTRAL OVERLAP OF THE C02 15 MICROMETERS BAND AND DUST
Bernhard Lee Lindner *In its* Reanalysis of Mariner 9 UV Spectrometer Data for Ozone, Cloud, and Dust Abundances, and Their Interaction Over Climate Timescales 7 Feb. 1994 4 p (For primary document see N94-27885 07-91)
(Contract NASw-4614; NAGw-389; NAGw-552; NSF ATM-83-05841)
Avail: CASI HC A01/MF A02

Careful consideration must be given to the simultaneous treatment of the radiative transfer of the CO2 15 micron band and dust calculations for the Martian winter polar region show that a simple sum of separately calculated CO2 cooling rates and dust cooling rates can easily result a 30 percent error in the net cooling particularly near the surface. CO2 and dust hinder each others ability to cool the atmosphere. Even during periods of low dust opacity, dust still reduces the efficacy of CO2 at cooling the atmosphere. At the other extreme, when dust storms occur, CO2 still significantly impedes the ability of dust to cool the atmosphere. Hence, both CO2 and dust must be considered in radiative transfer models. Author (revised)

N94-27887*# Atmospheric and Environmental Research, Inc., Cambridge, MA.
MARTIAN ATMOSPHERIC RADIATION BUDGET
Bernhard Lee Lindner *In its* Reanalysis of Mariner 9 UV Spectrometer Data for Ozone, Cloud, and Dust Abundances, and Their Interaction Over Climate Timescales 7 Feb. 1994 32 p Revised Submitted for publication (For primary document see N94-27885 07-91)
(Contract NASw-4614; NAGw-389; NAGw-552; NSF ATM-83-05841)
Avail: CASI HC A03/MF A02

A computer model is used to study the radiative transfer of the martian winter-polar atmosphere. Solar heating at winter-polar latitudes is provided predominately by dust. For normal, low-dust conditions, CO2 provides almost as much heating as dust. Most heating by CO2 in the winter polar atmosphere is provided by the 2.7 micron band between 10 km and 30 km altitude, and by the 2.0 micron band below 10 km. The weak 1.3 micron band provides some significant heating near the surface. The minor CO2 bands at 1.4, 1.6, 4.8 and 5.2 micron are all optically thin, and produce negligible heating. O3 provides less than 10 percent of the total heating. Atmospheric cooling is predominantly thermal emission by dust, although CO2 15 micron band emission is important above 20 km altitude. Author (revised)

N94-27888*# Atmospheric and Environmental Research, Inc., Cambridge, MA.
MARS OZONE: MARINER 9 REVISITED
Bernhard Lee Lindner *In its* Reanalysis of Mariner 9 UV Spectrometer Data for Ozone, Cloud, and Dust Abundances, and Their Interaction Over Climate Timescales 7 Feb. 1994 15 p Submitted for publication (For primary document see N94-27885 07-91)
(Contract NASw-4614)
Avail: CASI HC A03/MF A02

The efficacy of the UV spectroscopy technique used by Mariner 9 to remotely measure ozone abundance at Mars is discussed. Previously-inferred ozone abundances could be underestimated by as much as a factor of 3, and much of the observed variability in the ozone abundance could be due to temporal and spatial variability in cloud and dust amount. Author

N94-27889*# Atmospheric and Environmental Research, Inc., Cambridge, MA.
WHY IS THE NORTH POLAR CAP ON MARS DIFFERENT THAN THE SOUTH POLAR CAP?
Bernhard Lee Lindner *In its* Reanalysis of Mariner 9 UV Spectrometer Data for Ozone, Cloud, and Dust Abundances, and Their Interaction Over Climate Timescales 7 Feb. 1994 2 p (For primary document see N94-27885 07-91)
Avail: CASI HC A01/MF A02

One of the most puzzling mysteries about the planet Mars is the hemispherical asymmetry in the polar caps. Every spring the seasonal polar cap of CO2 recedes until the end of summer, when only a small part, the residual polar cap, remains. During the year that Viking observed Mars, the residual polar cap was composed of water ice in the northern hemisphere but was primarily carbon dioxide ice in the southern hemisphere. Scientists have sought to explain this asymmetry by modeling observations of the latitudinal recession of the polar cap and seasonal variations in atmospheric pressure (since the seasonal polar caps are primarily frozen atmosphere, they are directly related to changes in atmospheric mass). These models reproduce most aspects of the observed annual variation in atmospheric pressure fairly accurately. Furthermore, the predicted latitudinal recession of the northern polar cap in the spring agrees well with observations, including the fact that the CO2 ice is predicted to completely sublime away. However, these models all predict that the carbon dioxide ice will also sublime away during the summer in the southern hemisphere, unlike what is observed. This paper will show how the radiative effects of ozone, clouds, airborne dust, light penetration into and through the polar cap, and the dependence of albedo on solar zenith angle affect CO2 ice formation and sublimation, and how they help explain the hemispherical asymmetry in the residual polar caps. These effects have not been studied with prior polar cap models. Derived from text

N94-27890*# Atmospheric and Environmental Research, Inc., Cambridge, MA.

PROBING THE MARTIAN ATMOSPHERE IN THE ULTRAVIOLET

Bernhard Lee Lindner *In its* Reanalysis of Mariner 9 UV Spectrometer Data for Ozone, Cloud, and Dust Abundances, and Their Interaction Over Climate Timescales 7 Feb. 1994 4 p (For primary document see N94-27885 07-91)
Avail: CASI HC A01/MF A02

Ozone is a key to understanding atmospheric chemistry on Mars. The O3 abundance has been inferred from UV spectra by several spacecraft, with the most complete coverage provided by Mariner 9. The Mariner 9 UV spectrometer scanned from 2100 to 3500 Angstroms in one of its two spectral channels every 3 seconds with a spectral resolution of 15 Angstroms and an effective field-of-view of approximately 300 sq km. The only atmospheric absorption in the 2000 to 3000 Angstrom region was assumed to come from the Hardey band system of ozone, which has an opacity of order unity. Therefore, the amount of ozone was inferred by fitting this absorption feature with laboratory data of ozone absorption, as shown in Fig 1. Mars O3 shows strong seasonal and latitudinal variation, with column abundances ranging from 0.2 micron-atm at equatorial latitudes to 60 micron-atm over the northern winter polar latitudes (1 micron-atm is a column abundance of 2.689 x 10(exp 15) molecules cm(exp -2). However, the O3 abundance is never great enough to significantly affect atmospheric temperatures or surface temperatures and frost budgets. Author (revised)

N94-27891*# Atmospheric and Environmental Research, Inc., Cambridge, MA.

HOW WELL WAS TOTAL OZONE ABUNDANCE INFERRED WITH MARINER 9?

Bernhard Lee Lindner *In its* Reanalysis of Mariner 9 UV Spectrometer Data for Ozone, Cloud, and Dust Abundances, and Their Interaction Over Climate Timescales 7 Feb. 1994 7 p (For primary document see N94-27885 07-91)
Avail: CASI HC A02/MF A02

Ozone is a key to understanding atmospheric chemistry on Mars. Over 20 photochemical models of the martian atmosphere have been published, and O3 is often used as a benchmark for these models. O3 abundance has been inferred from instrumentation on several spacecraft, with the most complete coverage provided by Mariner 9. The Mariner 9 UV spectrometer scanned from 2100 to 3500 Angstroms with a spectral resolution of 15 Angstroms and an effective field-of-view of approximately 300 sq km. The only atmospheric absorption in the 2000 to 3000 A wavelength region was previously assumed to come from the Hartley band system of ozone, which has an opacity of order unity at winter polar latitudes. Therefore, the amount of ozone was inferred by fitting this absorption feature with laboratory data of ozone absorption. Mars O3 shows strong seasonal and latitudinal variation, with column abundances ranging from 0.2 micron-atm at equatorial latitudes to 60 micron-atm over northern winter polar latitudes (1 micron-atm is a column abundance of 2.689 x 10 exp 15 molecules cm(exp -2)). However, the O3 abundance is never great enough to significantly affect atmospheric temperatures or surface temperatures and frost amounts. Some of the previously-inferred O3 abundances are shown. A radiative transfer computer model is used to re-examine the Mariner 9 UV spectra. Assuming a constant mixing ratio for O3 and no chemical or radiative interaction between O3 and clouds/dust, it is shown that when typical amounts of dust and cloud are present that significant underestimation of O3 abundance occurs. A factor of 3 times as much O3 is needed to generate the same spectrum the spacecraft would measure for a cloudy, dusty atmosphere as for a clear atmosphere. If the scattering properties of martian clouds and dust were well known, then their appearance would not be a problem, as a model would be capable of retrieving the O3 abundance. However, these properties are not well known, which raises doubts about the effectiveness of the UV reflectance spectroscopy technique for measuring O3 abundance on Mars. Derived from text

N94-27892*# Atmospheric and Environmental Research, Inc., Cambridge, MA.

IN SITU MARS OZONE DETECTOR

Bernhard Lee Lindner and Elliot M. Weinstock (Harvard Univ., Cambridge, MA.) *In its* Reanalysis of Mariner 9 UV Spectrometer Data for Ozone, Cloud, and Dust Abundances, and Their Interaction Over Climate Timescales 7 Feb. 1994 1 p (For primary document see N94-27885 07-91)
Avail: CASI HC A01/MF A02

We propose sending a balloon-borne UV photometer sensor package to measure atmospheric ozone on Mars, and this package could be a Discovery Program sensor candidate. Past measurements of ozone on Mars are highly uncertain, perhaps a factor of 3 or so uncertain, due primarily to interference and masking by cloud and dust. In-situ balloon measurements would avoid these problems, and would provide 'ground truth' which remote sensing techniques cannot. We have explored this approach to measure ozone abundance in the terrestrial stratosphere with a balloon-borne UV absorption photometer. Atmospheric pressures and temperatures and ozone concentrations near the surface of Mars are similar to those in the terrestrial stratosphere. Derived from text

N94-27935*# Washington Univ., Seattle. Dept. of Atmospheric Sciences.

THE MARTIAN ATMOSPHERIC PLANETARY BOUNDARY LAYER STABILITY, FLUXES, SPECTRA, AND SIMILARITY Final Report

James E. Tillman 23 Mar. 1994 1 p
(Grant NAGw-2041)
(NASA-CR-195711; NAS 1.26:195711) Avail: CASI HC A01/MF A01

This is the first analysis of the high frequency data from the Viking lander and spectra of wind, in the Martian atmospheric surface layer, along with the diurnal variation of the height of the mixed surface layer, are calculated for the first time for Mars. Heat and momentum fluxes, stability, and z(sub O) are estimated for early spring, from a surface temperature model and from Viking Lander 2 temperatures and winds at 44 deg N, using Monin-Obukhov similarity theory. The afternoon maximum height of the mixed layer for these seasons and conditions is estimated to lie between 3.6 and 9.2 km. Estimations of this height is of primary importance to all models of the boundary layer and Martian General Circulation Models (GCM's). Model spectra for two measuring heights and three surface roughnesses are calculated using the depth of the mixed layer, and the surface layer parameters and flow distortion by the lander is also taken into account. These experiments indicate that z(sub O), probably lies between 1.0 and 3.0 cm, and most likely is closer to 1.0 cm. The spectra are adjusted to simulate aliasing and high frequency rolloff, the latter caused both by the sensor response and the large Kolmogorov length on Mars. Since the spectral models depend on the surface parameters, including the estimated surface temperature, their agreement with the calculated spectra indicates that the surface layer estimates are self consistent. This agreement is especially noteworthy in that the inertial subrange is virtually absent in the Martian atmosphere at this height, due to the large Kolmogorov length scale. These analyses extend the range of applicability of terrestrial results and demonstrate that it is possible to estimate the effects of severe aliasing of wind measurements, to produce a models which agree well with the measured spectra. The results show that similarity theory developed for Earth applies to Mars, and that the spectral models are universal. Author (revised)

N94-27941*# Michigan Univ., Ann Arbor. Dept. of Atmospheric, Oceanic, and Space Science.

STUDIES FOR THE LOSS OF ATOMIC AND MOLECULAR SPECIES FROM IO Annual Report, 1 May 1993 - 30 Apr. 1994

Michael R. Combi 7 Apr. 1994 72 p
(Grant NAGw-3585)
(NASA-CR-195702; NAS 1.26:195702) Avail: CASI HC A04/MF A01

The general objective of this project is to advance theoretical understanding of Io's atmosphere and how various atomic and molecular species are lost from this atmosphere and are distributed in the circumplanetary environment of Jupiter. The major task for the University of Michigan portion of this work is the generalization of the Io sodium cloud model to simulate the ion-precursor of sodium that is the apparent source of the fast sodium jet observed by Schneider et al. (1991). The goal is a quantitative test of the molecular ion hypothesis with a model that is comparable to a general sodium cloud model published previously. A detailed comparison of observations with such a model will help to probe the feasibility of such a source and to examine the rates and scale lengths associated with the decay of the ion precursor so as to possibly uncover the identity of the parent ion. Another important task to be performed at Michigan is more support of AER in the general area of modeling the Na and SO2-family clouds. Derived from text

N94-27982*# McDonnell-Douglas Space Systems Co., Cocoa Beach, FL.
LUNAR TRANSPORTATION FACILITIES AND OPERATIONS STUDY, OPTION 1 Annual Report
May 1991 444 p Original contains color illustrations
(Contract NAS10-11567)
(NASA-CR-195700; NAS 1.26:195700) Avail: CASI HC A19/MF A04; 1 functional color page

Throughout the Option I period of the Lunar Transportation Facilities and Operations Study (LTFOS), McDonnell Douglas Space Systems Company - Kennedy Space Center (MDSSC-KSC) provided support to both the Planetary Surface Systems (PSS) Office at the National Aeronautics and Space Administration (NASA) at the Johnson Space Center and to the Flight and Ground Systems Projects Office (Payload Projects Management) at the Kennedy Space Center. The primary objective of the Option I phase of the study was to assist the above NASA centers in developing Space Exploration Initiative (SEI) concepts. MDSSC-KSC conducted three analyses which provided launch and landing detail to the proposed exploration concepts. One analysis, the Lunar Ejecta Assessment, was conducted to determine the effects of launch and landing a vehicle in a dusty environment. A second analysis, the Thermal/Micrometeoroid Protection Trade Study, was refined to determine the impacts that Reference Architecture Option 5A would have on thermal/micrometeoroid protection approaches. The third analysis, the Centaur Prelaunch Procedure Analysis, used a Centaur prelaunch test and checkout flow to identify key considerations that would be important if a Lunar Excursion Vehicle (LEV) was to use an expander cycle liquid oxygen-liquid hydrogen engine. Several 'quick look' assessments were also conducted. One quick look assessment, the Storable Propellant Quick Look Assessment, was conducted to identify design considerations that should be made if storable propellants were to be used instead of liquid oxygen and liquid hydrogen. The LEV Servicer Maintenance Analysis provided an early look at the effort required to maintain an LEV Servicer on the lunar surface. Also, support was provided to the PSS Logistics Manager to develop initial LEV Servicer cost inputs. Consideration was given to the advanced development that must be provided to accomplish a lunar and/or Mars mission. MDSS-KSC also provided support to both MASE and PSS by reviewing and commenting on architecture documents and concept definitions to ensure adequate considerations were given to the launch and landing function of an exploration initiative. Author

N94-27983*# McDonnell-Douglas Space Systems Co., Cocoa Beach, FL.
LUNAR TRANSPORTATION FACILITIES AND OPERATIONS STUDY, OPTION 2 Annual Report
Feb. 1992 254 p Original contains color illustrations
(Contract NAS10-11567)
(NASA-CR-195701; NAS 1.26:195701) Avail: CASI HC A12/MF A03; 1 functional color page

During the Option 2 period of the Lunar Transportation Facilities and Operations Study (LTFOS), a joint McDonnell Douglas Space Systems Company Kennedy Space Center (MDSSC-KSC) and National Aeronautics and Space Administration Kennedy Space Center (NASA-KSC) Study team conducted a comparison of the functional testing of the RL-10 and Space Shuttle Main Engine, a quick-look impact assessment of the Synthesis Group Report, and a detailed assessment of the Synthesis Group Report. The results of these KSC LTFOS team efforts are included. The most recent study task effort was a detailed assessment of the Synthesis Group Report. The assessment was conducted to determine the impact on planetary launch and landing facilities and operations. The result of that effort is a report entitled 'Analysis of the Synthesis Group Report, its Architectures and their Impacts on PSS Launch and Landing Operations' and is contained in Appendix A. The report is structured in a briefing format with facing pages as opposed to a narrative style. A quick-look assessment of the Synthesis Group Report was conducted to determine the impact of implementing the recommendations of the Synthesis Group on KSC launch facilities and operations. The data was documented in a presentation format as requested by Kennedy Space Center Technology and Advanced Projects Office and is included in Appendix B. Appendix C is a white paper on the comparison of the functional testing of the RL-10 and Space Shuttle Main Engine. The comparison was undertaken to provide insight regarding common test requirements that would be applicable to Lunar and Mars Excursion Vehicles (LEV and MEV). Author (revised)

N94-25688*# Michigan Univ., Ann Arbor. Dept. of Aerospace Engineering.
PROJECT APEX: ADVANCED MANNED EXPLORATION OF THE MARTIAN MOON PHOBOS
Joe G. Eisley and Jim Akers *In* USRA, Proceedings of the 8th Annual Summer Conference: NASA/USRA Advanced Design Program 1992 p 178-187 (For primary document see N94-25665 07-80)
Avail: CASI HC A02/MF A04

N94-25702*# Utah State Univ., Logan. Dept. of Mechanical and Aerospace Engineering.
COPERNICUS: LUNAR SURFACE MAPPER
Frank J. Redd and Shaun D. Anderson *In* USRA, Proceedings of the 8th Annual Summer Conference: NASA/USRA Advanced Design Program 1992 p 298-308 (For primary document see N94-25665 07-80)
Avail: CASI HC A03/MF A04

N94-26290*# National Aeronautics and Space Administration. Langley Research Center, Hampton, VA.
EARLY LUNAR ROVER MISSION STUDIES
V. P. Gillespie *In its* Selected Topics in Robotics for Space Exploration Dec. 1993 p 233-246 (For primary document see N94-26278 07-12)
Avail: CASI HC A03/MF A03

N94-26291*# Sandia National Labs., Albuquerque, NM.
THE ROBOTIC ALL-TERRAIN LUNAR EXPLORATION ROVER (RATLER): INCREASED MOBILITY THROUGH SIMPLICITY
J. Bryan Pletta *In* NASA. Langley Research Center, Selected Topics in Robotics for Space Exploration Dec. 1993 p 247-267 (For primary document see N94-26278 07-12)
Avail: CASI HC A03/MF A03

N94-27360*# National Aeronautics and Space Administration. Ames Research Center, Moffett Field, CA.
TELEPRESENCE IN THE HUMAN EXPLORATION OF MARS: FIELD STUDIES IN ANALOG ENVIRONMENTS
Carol R. Stoker *In* NASA. Lewis Research Center, Vision 21: Interdisciplinary Science and Engineering in the Era of Cyberspace Dec. 1993 p 23-34 (For primary document see N94-27358 07-12)
Avail: CASI HC A03/MF A03

N94-27366*# Scotter Research and Development Ltd., Thunder Bay (Ontario).
SPIRAL SURVEY EXPEDITION: A PROPOSAL TO ORGANIZE FOR THE SURVEY, EXPLORATION AND EVENTUAL COLONIZATION OF THE MILKY WAY GALAXY
Scott Galloway *In* NASA. Lewis Research Center, Vision 21: Interdisciplinary Science and Engineering in the Era of Cyberspace Dec. 1993 p 101-114 (For primary document see N94-27358 07-12)
Avail: CASI HC A03/MF A03

N94-28252*# National Aeronautics and Space Administration. Ames Research Center, Moffett Field, CA.
AN IMAGE ASSESSMENT STUDY OF IMAGE ACCEPTABILITY OF THE GALILEO LOW GAIN ANTENNA MISSION
S. L. Chuang, R. F. Haines (RECOM Technologies, Inc., Moffett Field, CA.), T. Grant, Yaron Gold (RECOM Technologies, Inc., Moffett Field, CA.), and Kar-Ming Cheung (Jet Propulsion Lab., California Inst. of Tech., Pasadena.) *In* NASA. Goddard Space Flight Center, The 1994 Space and Earth Science Data Compression Workshop Apr. 1994 p 3-10 (For primary document see N94-28251 07-59)
Avail: CASI HC A02/MF A02

N94-28306*# Washington Univ., Saint Louis, MO. Dept. of Earth and Planetary Sciences.
SOME IMPLICATIONS OF LARGE IMPACT CRATERS AND BASINS ON VENUS FOR TERRESTRIAL RINGED CRATERS AND PLANETARY EVOLUTION Abstract Only
W. B. McKinnon and J. S. Alexopoulos *In* Houston Univ., New Developments Regarding the KT Event and Other Catastrophes in Earth History 1994 p 81-82 (For primary document see N94-28294 07-46)
Avail: CASI HC A01/MF A02

N94-28313*# Lowell Observatory, Flagstaff, AZ.
THE CRASH OF P/SHOEMAKER-LEVY 9 INTO JUPITER AND ITS IMPLICATIONS FOR COMET BOMBARDMENT ON EARTH Abstract Only
E. M. Shoemaker and C. S. Shoemaker *In* Houston Univ., New Developments Regarding the KT Event and Other Catastrophes in Earth History 1994 p 113-114 (For primary document see N94-28294 07-46)
Avail: CASI HC A01/MF A02

92 SOLAR PHYSICS

Includes solar activity, solar flares, solar radiation and sunspots.
For related information see *93 Space Radiation.*

N94-26590*# Lockheed Missiles and Space Co., Palo Alto, CA. Research and Development.
PHOTOSPHERIC ORIGINS OF CHROMOSPHERIC AND CORONAL ACTIVITY Progress Report, 1 Nov. 1993 - 1 Feb. 1994
Theodore Tarbell 1994 3 p
(Contract NAS8-39746)
(NASA-CR-195215; NAS 1.26:195215) Avail: CASI HC A01/MF A01

This contract is for a two-year research study of the origins of activity in the upper atmosphere of the sun. The approach is to collect high resolution images of the lower atmosphere on observing runs at the Swedish Solar Observatory on La Palma, Canary Islands, Spain. The best observations are analyzed and compared with data from other telescopes and/or theoretical models, to study magnetic flux emergence, coronal heating, and various dynamic phenomena and transients. Software for analysis and visualization of the data is developed as needed. The contract is being performed by the Solar and Astrophysics Laboratory, part of the Lockheed Palo Alto Research Laboratory (LPARL) of the Research and Development Division (RDD) of Lockheed Missiles and Space Co., Inc. (LMSC).
Derived from text

N94-26696# Los Alamos National Lab., NM.
CORONAL HEATING VIA NANOFLARES
G. Poletto (Osservatorio Astrofisico di Arcetri, Florence, Italy.) and R. Kopp 1993 7 p Presented at the 7th European Meeting on Solar Physics, Catania, Italy
(Contract W-7405-eng-36)
(DE94-000773; LA-UR-93-3343; CONF-9305294-1) Avail: CASI HC A02/MF A01

It has been recently proposed that the coronae of single late-type main sequence stars represent the radiative output from a large number of tiny energy release events, the so-called nanoflares. Although this suggestion is attractive and order of magnitude estimates of the physical parameters involved in the process are consistent with available data, nanoflares have not yet been observed and theoretical descriptions of these phenomena are still very crude. The temporal behavior of a magnetic flux tube subject to the repeated occurrence of energy release events, randomly distributed in time are examined, and it was shown that an originally empty cool loop may, in fact, reach typical coronal density and temperature values via nanoflare heating. By choosing physical parameters appropriate to solar conditions, the possibilities for observationally detecting nanoflares were also examined. Although the Sun is the only star where nanoflares might be observed, present instrumentation appears to be inadequate for this purpose. DOE

N94-26755# National Oceanic and Atmospheric Administration, Boulder, CO. Space Environment Lab.
REGION 5395 OF MARCH 1989
Willow Cliffswallow, ed., Michael S. Abbott, Christopher C. Balch, Robert L. Bass, Timothy J. Brown, Norman L. Cohen, Larry Combs, Kent A. Doggett, Howard Garcia, and Paul A. Gehred et al Nov. 1993 46 p Prepared in cooperation with Department of the Air Force, Washington, DC
(PB94-120714; NOAA-TM-ERL-SEL-82) Avail: CASI HC A03/MF A01

Large solar events and geomagnetic disturbances can affect satellites and people in space as well as earth-based systems. The activity of solar region 5395 is an example of how events on the sun can interfere with systems we all depend on. The report outlines the potential effects of large and active sunspot regions and provides examples of how this particular region affected many human-made systems. A summary plot is provided of the x-ray, energetic particle, and geomagnetic activity for the period 6 March - 19 March 1989, most of which was produced by region 5395.
NTIS

N94-26883# Columbia Univ., New York, NY. Astrophysics Lab.
CHAOTIC DYNAMICS OF THE SOLAR CYCLE Annual Report, 1 Nov. 1992 - 31 Oct. 1993
Edward A. Spiegel 31 Oct. 1993 29 p
(Contract F49620-92-J-0061)
(AD-A274315; AFOSR-93-0909TR) Avail: CASI HC A03/MF A01

A dynamical model of the solar activity cycle has been developed that incorporates the key chaotic mechanism of on/off intermittence. It has been proposed that the solar butterfly diagram represents the motion of activity waves which are very stable nonlinear solitary waves. The waves are driven by an instability under the convection zone in a layer called the tachocline. The result are for one wave in one solar hemisphere but show the correct spatio-temporal dynamics. A new approach to dynamo theory is being developed based on theoretical techniques developed in chaos theory called the thermodynamic formalism. Possible sources of activity in other turbulent, rotating stars has been studied. DTIC

N94-27053# National Geophysical Data Center, Boulder, CO.
SOLAR-GEOPHYSICAL DATA NUMBER 590, OCTOBER 1993. PART 1: (PROMPT REPORTS). DATA FOR SEPTEMBER, AUGUST 1993, AND LATE DATA
H. E. Coffey Oct. 1993 123 p See also PB94-125911 and PB94-117082
(PB94-125903; SGD-590-Pt-1) Avail: CASI HC A06/MF A02

The contents of this document are as follows: Detailed index for 1993; Data for Sep. 1993--Solar-terrestrial environment, IUWDS alert periods (Advance and worldwide), Solar activity indices, Solar flares, Solar radio emission, and Stanford mean solar magnetic field; Data for Aug. 1993--Solar active regions, Sudden ionospheric disturbances, Solar radio spectral observations, Solar radioheliograph-164 MHz-Nancay, Cosmic ray measurements by neutron monitor, and Geomagnetic indices; and Late data--Dst provisional hourly values Jan.-Feb. 88. NTIS

N94-27054# National Geophysical Data Center, Boulder, CO.
SOLAR-GEOPHYSICAL DATA NUMBER 590, OCTOBER 1993. PART 2: (COMPREHENSIVE REPORTS). DATA FOR APRIL 1993, AND MISCELLANEOUS
H. E. Coffey Oct. 1993 53 p See also PB94-125903 and PB94-117405
(PB94-125911; SGD-590-Pt-2) Avail: CASI HC A04/MF A01

The contents of this document are as follows: Detailed index for 1993; and Data for Apr. 1993--Solar flares, Solar radio bursts at fixed frequencies, Solar x-ray radiation from GOES satellite graphs, Mass ejections from the sun, Active prominences, and filaments. NTIS

N94-27096# New Jersey Inst. of Tech., Newark. Dept. of Physics.
OBSERVATION OF IMPULSIVE ACOUSTIC EVENTS AND THE EXCITATION OF SOLAR OSCILLATIONS Final Report, 1 Nov. 1992 - 31 Oct. 1993
Philip R. Goode 31 Oct. 1993 18 p
(Contract F49620-92-J-0094)
(AD-A274159; AFOSR-93-0910TR) Avail: CASI HC A03/MF A01

A new set of observations has been made of the intensity and Doppler shift in the 543.4 nm Fe I line consisting of 356 spatial points in a row 1024 arc seconds long. For these observations, new data acquisition software and new data reduction routines were developed. Wave number versus frequency diagrams have been obtained at several altitudes in the photosphere. It has been shown that the changes in the sun's internal rotation over the sun's activity cycle occurs just above the base of the convection zone. A seismic method has been developed to directly determine the sun's internal angular momentum, and seismic limits have been placed on the sun's internal magnetic field. DTIC

N94-27099# Stanford Univ., CA. Center for Space Science and Astrophysics.
ENVIRONMENTAL CONDITIONS RESPONSIBLE FOR SOLAR ACTIVITY Annual Technical Report, 1 Oct. 1992 - 1 Oct. 1993
Peter A. Sturrock 30 Nov. 1993 8 p
(Contract F49620-92-J-0015)
(AD-A274191; AFOSR-93-0908TR) Avail: CASI HC A02/MF A01

During the past year, the Stanford group has continued its investigations into the origins of solar coronal activity. Solar activity occurs within a complex magnetic environment, which is determined by the entire history of magnetic flux emergence and surface flows at the underlying photosphere. One of the main achievements has been the development of a technique to reconstruct the coronal magnetic field above active regions from measurements of the magnetic field at the photosphere. To complement this empirical tool, the authors have continued theoretical work on the influence of photospheric shearing motions on the configuration and energy content of coronal fields. This work is shedding light on the nature of eruptive phenomena such as coronal mass ejections. They have also intensively evaluated the role of magnetohydrodynamic waves and reconnection in heating the solar atmosphere, and identified a number of promising coronal heating scenarios that will require detailed numerical modeling. DTIC

N94-27321*# Lockheed Missiles and Space Co., Palo Alto, CA. Research and Development.
HIGH RESOLUTION STUDIES OF SUNSPOTS AND FLUX TUBES Progress Report, 1 Nov. 1993 - 1 Feb. 1994
Alan Title 1994 7 p
(Contract NAS8-39747)
(NASA-CR-195216; NAS 1.26:195216) Avail: CASI HC A02/MF A01

This contract is for a three-year research study of sunspots and magnetic flux tubes in the solar atmosphere, using tunable filter images collected with a CCD camera during observing runs at the Canary Islands observatories in Spain. The best observations are analyzed and compared with theoretical models, to study the structure and dynamics of sunspots, their connections with surrounding magnetic fields, and the properties and evolution of smaller flux tubes in plage and quiet sun. Scientific results are reported at conferences and published in the appropriate journals. The contract is being performed by the Solar and Astrophysics Laboratory, part of the Lockheed Palo Alto Research Laboratory (LPARL) of the Research and Development Division (RDD) of Lockheed Missiles and Space Co., Inc. (LMSC). The principal investigator is Dr. Alan Title, and the research is done by him and other scientific staff at LPARL and Solar Physics Research Corporation (SPRC), often in collaboration with visiting scientists and students from other institutions. Highlights during this reporting period include completing the final version of a paper on the Evershed effect, writing a paper on magnetic diffusion, continuing work on contrast of small flux tubes, and work on the development of new models to interpret our sunspots observations. Derived from text

N94-27742# Los Alamos National Lab., NM.
THE STATUS OF THE SOLAR NEUTRINO PROBLEM
Thomas J. Bowles 1993 17 p Presented at the 16th Meeting on Elementary Particle Physics, Kazimierz, Poland, 24-28 May 1993
(Contract W-7405-eng-36)
(DE94-003934; LA-UR-93-4173; CONF-9305309-1) Avail: CASI HC A03/MF A01

Perhaps the most outstanding discrepancy between prediction and measurements in current particle physics comes from the solar neutrino problem, in which a large deficit of high-energy solar neutrinos is observed. Many Nonstandard Solar Models have been invoked to try to reduce the predicted flux, but all have run into problems in trying to reproduce other measured parameters (e.g., the luminosity) of the Sun. Other explanations involving new physics such as neutrino decay and neutrino oscillations, etc. have also been proffered. Again, most of these explanations have been ruled out by either laboratory or astrophysical measurements. It appears that perhaps the most likely particle physics solution is that of matter enhanced neutrino oscillation, the Mikheyev - Smirnov - Wolfenstein (MSW) oscillations. Two new radiochemical gallium experiments, which have a low enough threshold to be sensitive to the dominant flux of low-energy p-p neutrinos, now also report a deficit and also favor a particle physics solution. The next generation of solar experiments promise to finally resolve the source of the 'solar neutrino problem' by the end of this decade. DOE

N94-27953*# National Aeronautics and Space Administration. Goddard Space Flight Center, Greenbelt, MD.
ACCELERATION OF ELECTRONS AND IONS BY STRONG LOWER-HYBRID TURBULENCE IN SOLAR FLARES
D. S. Spicer, R. Bingham (Rutherford Appleton Lab., Chilton, England.), J. J. Su (National Central Univ., Chung-Li, Taiwan.), V. D. Shapiro (California Univ., San Diego, La Jolla.), V. Shevchenko (California Univ., San Diego, La Jolla.), S. Ma (California Univ., Los Angeles.), J. M. Dawson (California Univ., Los Angeles.), and K. G. McClements (United Kingdom Atomic Energy Authority, Culham, England.) Mar. 1994 31 p
(NASA-TM-109723; NAS 1.15:109723; RAL-94-022) Avail: CASI HC A03/MF A01

One of the outstanding problems in solar flare theory is how to explain the 10-20 keV and greater hard x-ray emissions by a thick target bremsstrahlung model. The model requires the acceleration mechanism to accelerate approximately 10(exp 35) electrons sec(exp -l) with comparable energies, without producing a large return current which persists for long time scales after the beam ceases to exist due to Lenz's law, thereby, producing a self-magnetic field of order a few mega-Gauss. In this paper, we investigate particle acceleration resulting from the relaxation of unstable ion ring distributions, producing strong wave activity at the lower hybrid frequency. It is shown that strong lower hybrid wave turbulence collapses in configuration space producing density cavities containing intense electrostatic lower hybrid wave activity. The collapse of these intense nonlinear wave packets saturate by particle acceleration producing energetic electron and ion tails. There are several mechanisms whereby unstable ion distributions could be formed in the solar atmosphere, including reflection at perpendicular shocks, tearing modes, and loss cone depletion. Numerical simulations of ion ring relaxation processes, obtained using a 2 1/2-D fully electromagnetic, relativistic particle in cell code are discussed. We apply the results to the problem of explaining energetic particle production in solar flares. The results show the simultaneous acceleration of both electrons and ions to very high energies: electrons are accelerated to energies in the range 10-500 keV, while ions are accelerated to energies of the order of MeVs, giving rise to x-ray emission and gamma-ray emission respectively. Our simulations also show wave generation at the electron cyclotron frequency. We suggest that these waves are the solar millisecond radio spikes. The strong turbulence collapse process leads to a highly filamented plasma producing many localized regions for particle acceleration and resulting in approximately 10(exp 17) electron 'beamlets' of width approximately equal to 10 lambda sub De which eliminates the production of large magnetic fields. In this paper, we demonstrate that the model produces an energetic electron spectrum with the right flux to account for the hard x-ray observations. Author (revised)

N94-28360# National Geophysical Data Center, Boulder, CO.
SOLAR-GEOPHYSICAL DATA NUMBER 591, NOVEMBER 1993. PART 2: (COMPREHENSIVE REPORTS). DATA FOR MAY 1993 AND MISCELLANEOUS
Helen E. Coffey, ed. Nov. 1993 59 p See also PB92-158898
(PB94-134830; SGD-591-Pt-2) Avail: CASI HC A04/MF A01

Contents of the document include: data for May 1993 - solar flares, solar radio bursts at fixed frequencies, solar x ray radiation from GOES satellite graphs, mass ejections from the sun, and active prominences and filaments; interplanetary phenomena; and international geophysical calendar 1994. NTIS

93 SPACE RADIATION

Includes cosmic radiation; and inner and outer earth's radiation belts.

For biological effects of radiation see *52 Aerospace Medicine.* For theory see *73 Nuclear and High-Energy Physics.*

N94-25624# Tokyo Univ., Tanashi (Japan). Inst. for Cosmic Ray Research.

CONTRIBUTIONS TO THE 23RD ICRC FROM EMULSION CHAMBER EXPERIMENTS AT MT. CHACALTAYA AND PAMIRS

Jun. 1993 42 p Conference held in Calgary, Alberta, 19-30 Jul. 1993
(ICRR-Rept-295-93-7; JTN-94-80541) Avail: CASI HC A03/MF A01

The following topics were discussed: high energy particles, charged particles, cosmic ray showers, cosmic ray families, hadrons, high energy interactions, high energy shower clusters, space observation, high altitude, high altitude environments, radiation measuring instruments, energy distribution, gamma rays, hadron-gamma family, flux, pt particle, air showers, Centauro species interactions, incident angles, size spectrum, computerized simulation, Monte-Carlo method, Feynman scaling law, lead emulsion chamber, and Chacaltaya and Pamir chambers, and International Conference on Cosmic Rays (ICRC). For individual titles, see N94-25625 through N94-25634.

N94-25625# Academy of Sciences (USSR), Moscow. Inst. of Physics.

A STUDY OF VERY HIGH ENERGY HADRON INTERACTIONS THROUGH OBSERVATION OF COSMIC-RAY FAMILIES OF VISIBLE ENERGY GREATER THAN 500 TeV, 1

L. T. Baradzei, A. S. Borisov, K. V. Cherdyntseva, Z. M. Guseva, V. G. Denisova, N. A. Dobrotin, A. M. Dunaevsky, E. A. Kanevskaya, S. A. Karpova, and V. M. Maximenko et al *In* Tokyo Univ., Contributions to the 23rd ICRC from Emulsion Chamber Experiments at Mt. Chacaltaya and Pamirs Jun. 1993 p 1-4 (For primary document see N94-25624 07-93)
Avail: CASI HC A01/MF A01

A summary of the study on the global characteristics of very high energy cosmic-ray hadron interactions is presented. The study is carried out on the basis of 75 families recorded during the total of up to 1,400 sq m per year exposure at the Chacaltaya and the Pamir. The first striking encountered feature is those highest energy cosmic-ray families' wonderful variety in configurations. The second feature is the scantiness in frequency of the families at the Chacaltaya and Pamir altitudes. It will be convincing to assume that the higher energy portion of the constituent showers will reflect the characteristics of the family-generating main interaction directly. The scatter diagram of the number of hadrons against energy fraction of hadron component is shown. There are large differences between the observational and the simulational distributions which are of the same character as already noticed previously for the families with E(sub family) greater than or equal to 100 TeV. There exist families which are extremely rich in hadrons, in both multiplicity and energy fraction. They represent no other than the manifest indication that there exist exotic families with the characteristics similar to those of the 'Centauro-species'. Author (NASDA)

N94-25626# Academy of Sciences (USSR), Moscow. Inst. of Physics.

A STUDY OF VERY HIGH ENERGY HADRON INTERACTIONS THROUGH OBSERVATION OF COSMIC-RAY FAMILIES OF VISIBLE ENERGY GREATER THAN 500 TeV, 2

L. T. Baradzei, A. S. Borisov, K. V. Cherdyntseva, Z. M. Guseva, V. G. Denisova, N. A. Dobrotin, A. M. Dunaevsky, E. A. Kanevskaya, S. A. Karpova, and V. M. Maximenko et al *In* Tokyo Univ., Contributions to the 23rd ICRC from Emulsion Chamber Experiments at Mt. Chacaltaya and Pamirs Jun. 1993 p 5-8 (For primary document see N94-25624 07-93)
Avail: CASI HC A01/MF A01

This report presents the experimental results on cosmic-ray families of unusually small lateral spread, indicate the production of extremely small pt particles. Families of that kind have ever been reproduced well by the simulation calculations based on the ordinary multiple pion production models. The experimental results have been obtained on statistics of the 75 cosmic-ray families of the highest energy range, i.e., those with the visible energy sums not less than 500 TeV, recorded in the Chacaltaya two-story chambers, the Pamir and Pamir-joint chambers of carbon type, with the total exposure of the analyzed part amounting to up to 1,400 m2yr. The structure of energy flow, including the degree of sharpness in energy concentration on the above 75 families, and comparison of the results with those of the simulation calculation based on the model were studied. A systematic study on such type of high energy clusters of visible energy not less than 100 TeV has been carried out in nuclear emulsion plates under microscope for the families observed in the Chacaltaya chambers. Author (NASDA)

N94-25627# Academy of Sciences (USSR), Moscow. Inst. of Physics.

A STUDY OF VERY HIGH ENERGY HADRON INTERACTIONS THROUGH OBSERVATION OF COSMIC-RAY FAMILIES WITH VISIBLE ENERGY NOT LESS THAN 500 TeV, 3

L. T. Baradzei, A. S. Borisov, K. V. Cherdyntseva, Z. M. Guseva, V. G. Denisova, N. A. Dobrotin, A. M. Dunaevsky, E. A. Kanevskaya, S. A. Karpova, and V. M. Maximenko et al *In* Tokyo Univ., Contributions to the 23rd ICRC from Emulsion Chamber Experiments at Mt. Chacaltaya and Pamirs Jun. 1993 p 9-12 (For primary document see N94-25624 07-93)
Avail: CASI HC A01/MF A01

This report presents the clean and/or quasi-clean examples which show characteristics of extremely large pt(gamma) particle production among 75 families of the highest energy range--those with visible energy sum greater than 500 TeV. It is possible to select clean and/or quasi-clean families by looking for the events which show an absent or very minor contribution of lower energy showers over the family area, since such lower energy showers near the threshold energy must come from secondary and/or tertiary effects during the passage through the atmosphere. Examples are given of such quasi-clean families with extreme large lateral spread and where the interaction must occur near the chambers. This indicates abnormal large pt particle production. The studies have been continuously made on the nature of high energy secondaries from 'Centauro-species' in Chacaltaya two-story chambers. Striking characteristics have been noticed on the nature of high energy secondaries from Chiron-type families. They are the existence of penetrating 'mini-clusters' of small pt(gamma) particle productions and the short collision mean free path of high energy secondaries in not only in atmosphere but also in the chamber material. The results of a systematic study on interaction mean free path of high energy secondaries from Chiron-type interactions by measuring the distribution of shower starting position in Chacaltaya two-story chambers are outlined. Author (NASDA)

N94-25628# Waseda Univ., Tokyo (Japan). Science and Engineering Research Lab.

OBSERVATION OF CHARACTERISTICS OF COSMIC-RAY HADRON INTERACTIONS IN UNIFORM-TYPE THICK LEAD CHAMBERS AT PAMIR, 1

T. Arisawa, Y. Fujimoto, S. Hasegawa, K. Honda, H. Ito, M. Tamada (Kinki Univ., Osaka, Japan.), H. Fujiwara (Aoyamagakuin Univ., Tokyo, Japan.), K. Izaki (Aoyamagakuin Univ., Tokyo, Japan.), K. Yokoi (Aoyamagakuin Univ., Tokyo, Japan.), and V. V. Kopenkin (Moscow State Univ., Russia.) et al *In* Tokyo Univ., Contributions to the 23rd ICRC from emulsion Chamber Experiments at Mt. Chacaltaya and Pamirs Jun. 1993 p 13-16 (For primary document see N94-25624 07-93)
Avail: CASI HC A01/MF A01

The experimental procedures and the experimental results of the observation of characteristics of cosmic-ray hadron interactions in uniform-type thick lead chambers at Pamir are outlined. The structure of the 60 cm-thick uniform-type lead chambers used in this experiment and that of the 120 cm-thick lead chambers which the Moscow State University (MSU) group analyzed previously are presented. The chambers are composed of three units, and each of them has an area of 10 sq m. After exposure, the X-ray films were processed in Russia and then sent to Japan for analysis. Experimental results based on the exposure of 16 sq myr and the comparison with MSU results based on the exposure of 26 sq myr are described. The routine naked-eye scanning of the dark spots due to electron showers is applied on X-ray film to measure the direction

and energy of electron showers. The origin of the observed showers is either a gamma-ray or a hadron. A shower which starts deep in the chamber, or whose transition curve deviates much from that of a pure electromagnetic cascade shower, is identified as a hadron-induced shower. The basic results on cosmic-ray hadrons at the altitude of the Pamir (590 g/sq cm) are presented, and excellent mutual agreement is observed between the present results and those of the MSU group.
Author (NASDA)

N94-25629# Waseda Univ., Tokyo (Japan). Science and Engineering Research Lab.

OBSERVATION OF CHARACTERISTICS OF COSMIC-RAY HADRON INTERACTIONS IN UNIFORM-TYPE THICK LEAD CHAMBERS AT PAMIR, 2

T. Arisawa, Y. Fujimoto, S. Hasegawa, K. Honda, H. Ito, M. Tamada (Kinki Univ., Osaka, Japan.), H. Fujiwara (Aoyamagakuin Univ., Tokyo, Japan.), K. Izaki (Aoyamagakuin Univ., Tokyo, Japan.), K. Yokoi (Aoyamagakuin Univ., Tokyo, Japan.), and V. V. Kopenkin (Moscow State Univ., Russia.) et al *In* Tokyo Univ., Contributions to the 23rd ICRC from emulsion Chamber Experiments at Mt. Chacaltaya and Pamirs Jun. 1993 p 17-20 (For primary document see N94-25624 07-93)
Avail: CASI HC A01/MF A01

This report describes the experimental results on the characteristics of atmospheric and local hadron interactions through the observation of high energy cosmic-ray hadrons in uniform-type thick lead chambers (containing 60 cm-thick lead) exposed at Pamir. The global feature of atmospheric hadron interactions through the observed cosmic-ray hadron flux were studied by comparing it with the simulation calculation results. The simulations are conducted on the models constructed on the basis of the knowledge obtained in lower energy accelerator experiments. Two of the models, both of which assume scaling type pion multiple production, are studied. Observed hadron-induced showers belong to either of the two categories, due to singly arriving hadrons and those associated with families. A 'family' is defined as a group composed of at least two parallelly arriving showers satisfying the condition in which their respective visible energies are not less than detection threshold energy. The cosmic-ray has been repeatedly studied at high mountain altitudes, Charataya and Pamir, with various types of chambers, and the flux value obtained at the Pamirs in this experiment is consistent. It is quite striking that not only high energy cosmic-ray family flux but also hadron flux is much smaller than expected value on the extrapolation of the knowledge on hadron interactions observed in the lower energy accelerator experiments. Author (NASDA)

N94-25630# Waseda Univ., Tokyo (Japan). Science and Engineering Research Lab.

OBSERVATION OF CHARACTERISTICS OF COSMIC-RAY HADRON INTERACTIONS IN UNIFORM-TYPE THICK LEAD CHAMBERS AT PAMIR, 3

T. Arisawa, Y. Fujimoto, S. Hasegawa, K. Honda, H. Ito, M. Tamada (Kinki Univ., Osaka, Japan.), H. Fujiwara (Aoyamagakuin Univ., Tokyo, Japan.), K. Izaki (Aoyamagakuin Univ., Tokyo, Japan.), K. Yokoi (Aoyamagakuin Univ., Tokyo, Japan.), and V. V. Kopenkin (Moscow State Univ., Russia.) et al *In* Tokyo Univ., Contributions to the 23rd ICRC from Emulsion Chamber Experiments at Mt. Chacaltaya and Pamirs Jun. 1993 p 21-24 (For primary document see N94-25624 07-93)
Avail: CASI HC A01/MF A01

The characteristics of the secondary 'hadrons', produced by a special type 'Chiron', one of the exotic cosmic-ray families named 'Centauro-species', were studied. They have short mean free path, which is as small as one-third to half of the nucleonic geometrical collision mean free path, and they give rise to special shower phenomena named 'mini-clusters', the shower clusters initiated by a group of particles with very small relative production p(sub t). The attenuation of high energy hadrons belonging to the families of highest energy range observed in the uniform-type thick lead chambers was studied, and the results seem to constitute one of the most promising indication for the existence of the type of exotic cosmic-ray interactions, 'Chiron'. Showers of hadronic origin which show anomalous transition behavior were noticed. Examples of the showers indicate that some peculiar fragmentation processes are going on in the forwardmost angular region of the high energy cosmic-ray hadronic collision, giving rise to the emission of small p(sub t) secondaries, which themselves, in turn, induce the showers of anomalous transition behavior. Author (NASDA)

N94-25631# Kinki Univ., Osaka (Japan). Faculty of Science and Technology.

PENETRATING NATURE OF VERY COLLIMATED HIGH-ENERGY SHOWER-CLUSTERS OF HADRONS AND GAMMA RAYS

M. Tamada *In* Tokyo Univ., Contributions to the 23rd ICRC from Emulsion Chamber Experiments at Mt. Chacaltaya and Pamirs Jun. 1993 p 25-28 (For primary document see N94-25624 07-93)
Avail: CASI HC A01/MF A01

Calculation was conducted for the case of shower-clusters with non-vertical incidence, and contribution from hadronic showers was also included in the calculation. The following simulation calculations were conducted: (1) atmospheric nuclear and electromagnetic cascade using Monte Carlo algorithm as a model of nuclear interactions and assuming all secondaries are pions for simplicity; (2) three-dimensional electromagnetic shower development inside the chamber, for each constituent shower particle, using Monte Carlo method taking into account the exact structure of Pamir carbon chamber; and (3) three-dimensional electromagnetic shower development inside the chamber applying the Monte Carlo method to the electrons, photons, and hadrons inside a square area of 22 times 22 sq mm of the family center. Experiment was conducted applying raster scanning over shower-cluster region (5 times 5 sq mm, 10 times 10 sq mm, etc., depending on the size) in x ray film of the four layers by microphotometer. In the simulated gamma and hadron families, hadrons are usually spread out and very small number of hadrons are found in the central part of the families. Penetrating power seen in experimental data was large possibly due to contributions of hadronic component which have interacted inside carbon layer of 60 cm thick. Author (NASDA)

N94-25632# Kinki Univ., Osaka (Japan). Faculty of Science and Technology.

ENERGY CONCENTRATION IN HIGH ENERGY HADRON-GAMMA FAMILIES

M. Tamada *In* Tokyo Univ., Contributions to the 23rd ICRC from Emulsion Chamber Experiments at Mt. Chacaltaya and Pamirs Jun. 1993 p 29-32 (For primary document see N94-25624 07-93)
Avail: CASI HC A01/MF A01

Exotic hadron-gamma families of 'Centauro-species' were observed and how inclusion of exotic processes changes the relation between family intensity and rate of energy concentration was also studied by constructing simple toy-model for exotic processes. The relations in this model are closer to those of experimental data than in the other models of pion multiple production, but this model gives too many events with very large spread. In the present toy-model, secondary nucleons are assumed to be produced with large p(sub t), and then secondaries and tertiaries are spread out. Moreover gamma-rays are tertiary products and the energy dissipation of gamma-ray component becomes very large, and only those events which make interaction near and above the chamber can be detected. Thus low intensity of family observation together with hard spectrum of showers in the families and high rate of energy concentration indicate that the observed families are in a young stage of atmospheric nuclear cascade development. It is assumed that secondaries in Centauro and mini-Centauro interactions are nucleons and anti-nucleons, and these particles make interaction during passage process through the atmosphere.
Author (NASDA)

N94-25633# Tokyo Univ., Tanashi (Japan). Inst. for Cosmic Ray Research.

VIOLATION OF FEYNMAN SCALING LAW IN THE FORWARD REGION

Akinori Ohsawa *In its* Contributions to the 23rd ICRC from Emulsion Chamber Experiments at Mt. Chacaltaya and Pamirs Jun. 1993 p 33-36 Sponsored by Ministry of Education, Science and Culture (For primary document see N94-25624 07-93)
Avail: CASI HC A01/MF A01

Comparison was made on three sets of data from two simulation models, and Chacaltaya experiments, which are at present the whole of the data available to discuss the Feynman scaling law in the forward region at high energy region. Comparison is made without introducing any additional assumptions except the experimental data, and hence the conclusion shows exactly what the data indicate. It is concluded that all of the data, expressed by the different physical quantities, are consistent with one another and show the violation of the law. The degree of the violation, estimated in the present analysis, is stronger than the estimation, but weaker than that by Wdowszyk and Wolfendale. The scale-breaking feature in pion multiple production and the consequent decreasing inelasticity cause detectable effects to the behavior of high energy cosmic rays in the atmosphere. It is concluded that the primary cosmic rays are not necessary to be heavy-dominant, because the violation of the law provides a rapid energy-dissipating process sufficiently. Hence the hypothesis of the heavy-dominant primary cosmic rays should be revised in light of the violation of the Feynman scaling law. Author (NASDA)

N94-25634# Yamanashi Univ., Kofu (Japan). Faculty of Education.

SIMULTANEOUS OBSERVATION OF FAMILIES AND AIR SHOWERS AT MT. CHACALTAYA

Norio Kawasumi, Itsuro Tsushima, Ken Honda, Katsumi Hashimoto, Tsuneo Matano (Fukui Inst. of Tech., Japan.), Kenju Mori (Saitama Univ., Urawa, Japan.), Naoya Inoue (Saitama Univ., Urawa, Japan.), Rolando Ticona (Saitama Univ., Urawa, Japan.), Akinori Osawa (Tokyo Univ., Tanashi, Japan.), and Masanobu Tamada (Kinki Univ., Osaka, Japan.) et al *In* Tokyo Univ., Contributions to the 23rd ICRC from Emulsion Chamber Experiments at Mt. Chacaltaya and Pamirs Jun. 1993 p 37-40 Sponsored by Ministry of Education, Science and Culture (For primary document see N94-25624 07-93)

Avail: CASI HC A01/MF A01

Data of 46 families with the accompanying Air Showers (AS), observed by the combination of the Emulsion Chamber (EC) and the air shower array at Mt. Chacaltaya, are presented. The experimental setup including the AS array which consists of 40 scintillation detectors and the emulsion chamber of 32 units is outlined. Size spectrum of total AS observed and the total energy observed in the family were obtained. The AS, which accompanies the family, is looked for in the list by the following two conditions: (1) the burst size is in proportion with the total energy observed in the family; and (2) both arrival directions of the family and Electromagnetic Air Shower (EAS) are in agreement with each other within the range of errors to examine the correlation between families and AS's. Integral energy spectrum of gamma-rays per family for the different intervals of the total energy observed in the family and the size of AS. Comparison with simulation calculation results concludes that a change is necessary in the characteristics of hadron interactions in high energy region equal to or exceeding 10(exp 15) eV. Author (NASDA)

N94-26550*# National Aeronautics and Space Administration. Langley Research Center, Hampton, VA.

STOCHASTIC SOLUTION TO QUANTUM DYNAMICS

Sarah John (Vigyan Research Associates, Inc., Hampton, VA.) and John W. Wilson Feb. 1994 38 p

(RTOP 199-45-16-11)

(NASA-TP-3408; L-17295; NAS 1.60:3408) Avail: CASI HC A03/MF A01

The quantum Liouville equation in the Wigner representation is solved numerically by using Monte Carlo methods. For incremental time steps, the propagation is implemented as a classical evolution in phase space modified by a quantum correction. The correction, which is a momentum jump function, is simulated in the quasi-classical approximation via a stochastic process. The technique, which is developed and validated in two- and three- dimensional momentum space, extends an earlier one-dimensional work. Also, by developing a new algorithm, the application to bound state motion in an anharmonic quartic potential shows better agreement with exact solutions in two-dimensional phase space. Author (revised)

N94-26685*# Alabama Univ., Huntsville.

BATSE DATA ANALYSIS Final Report, 8 Jul. 1992 - 8 Jan. 1994

Geoffrey N. Pendleton 15 Feb. 1994 9 p

(Contract NAS8-38609)

(NASA-CR-195545; NAS 1.26:195545) Avail: CASI HC A02/MF A01

The four primary tasks of the Burst and Transient Source Experiment (BATSE) were completed. The Detector Response Matrices were maintained and some improvements implemented. The spectral analysis tasks based on the 4 channel lad data were accomplished. The BLOT team effort was completed and the SN1987A balloon flight data analysis paper was submitted. For individual titles, see N94-26686 through N94-26690.

N94-26686*# National Aeronautics and Space Administration. Marshall Space Flight Center, Huntsville, AL.

THE CONTINUUM SPECTRAL CHARACTERISTICS OF GAMMA RAY BURSTS OBSERVED BY BATSE Abstract Only

Geoffrey N. Pendleton (Alabama Univ., Huntsville.), William S. Paciesas (Alabama Univ., Huntsville.), Michael S. Briggs (Alabama Univ., Huntsville.), Robert S. Mallozzi (Alabama Univ., Huntsville.), Tom M. Koshut (Alabama Univ., Huntsville.), Gerald J. Fishman, Charles A. Meegan, Robert B. Wilson, Alan B. Harmon, and Chryssa Kouveliotou *In* Alabama Univ., BATSE Data Analysis 15 Feb. 1994 1 p (For primary document see N94-26685 07-93)

Avail: CASI HC A01/MF A01

Distributions of the continuum spectral characteristics of 260 bursts in the first Burst and Transient Source Experiment (BATSE) catalog are presented. The data are derived from flux ratios calculated from the BATSE Large Area Detector (LAD) four channel discriminator data. The data are converted from counts to photons using a direct spectral inversion technique to remove the effects of atmospheric scattering and the energy dependence of the detector angular response. Although there are intriguing clusterings of bursts in the spectral hardness ratio distributions, no evidence for the presence of distinct burst classes based on spectral hardness ratios alone is found. All subsets of bursts selected for their spectral characteristics in this analysis exhibit spatial distributions consistent with isotropy. The spectral diversity of the burst population appears to be caused largely by the highly variable nature of the burst production mechanisms themselves. Author

N94-26687*# National Aeronautics and Space Administration. Marshall Space Flight Center, Huntsville, AL.

CONTINUUM SPECTRAL CHARACTERISTICS OF BURSTS MEASURED WITH BATSE LARGE AREA DETECTORS Abstract Only

Geoffrey N. Pendleton (Alabama Univ., Huntsville.), William S. Paciesas (Alabama Univ., Huntsville.), Michael S. Briggs (Alabama Univ., Huntsville.), Robert S. Mallozzi (Alabama Univ., Huntsville.), Tom M. Koshut (Alabama Univ., Huntsville.), Gerald J. Fishman, Robert B. Wilson, Charles A. Meegan, and Chryssa Kouveliotou (Universities Space Research Association, Huntsville, AL.) *In* Alabama Univ., BATSE Data Analysis 15 Feb. 1994 1 p (For primary document see N94-26685 07-93)

Avail: CASI HC A01/MF A01

The continuum spectra of bursts are studied with particular emphasis placed on the search for spectral subcomponents. The spectra observed in individual bursts show significant evolution throughout their durations. The degree to which hard and soft spectra are combined in bursts and the effect this has on the complexity of the observed spectra are addressed. In particular the presence of broad cusps in spectra in the 50-100 keV range are studied to determine both the degree to which these features are present in the LAD data and whether superposition of hard and soft spectra simultaneously can account for them. Also the time histories of the power output (ergs/sec) from bursts are studied to investigate the dynamic coupling between hard and soft spectra in bursts as a probe of the autonomy of the hard and soft emission mechanisms. Author (revised)

N94-26688*# National Aeronautics and Space Administration. Marshall Space Flight Center, Huntsville, AL.

A STUDY OF GAMMA RAY BURST CONTINUUM PROPERTIES PRESNTING EVIDENCE FOR TWO SPECTRAL STATES IN BURSTS Abstract Only

Geoffrey N. Pendleton (Alabama Univ., Huntsville.), William S. Paciesas (Alabama Univ., Huntsville.), Robert S. Mallozzi (Alabama Univ., Huntsville.), Tom M. Koshut (Alabama Univ., Huntsville.), Gerald J. Fishman, Charles A. Meegan, Robert B. Wilson, B. A. Harmon, and J. P. Lestrade (Mississippi State Univ., Mississippi State.) *In* Alabama Univ., BATSE Data Analysis 15 Feb. 1994 1 p (For primary document see N94-26685 07-93)

Avail: CASI HC A01/MF A01

Evidence is presented for the existence of two spectral states contributing simultaneously to the total spectrum observed in many gamma-ray bursts (GRB's). An ensemble of 120 GRB's measured by BATSE were studied, using 4 channel spectral data, to determine in which bursts the spectral states can be most effectively resolved. The technique of summing the low intensity spectra together to get an average spectrum allows for precise characterization of the average low intensity spectral behavior. The 4 and

16 channel spectra obtained by the BATSE Large Area Detectors (LAD's) are analyzed using a model-independent spectral inversion technique. The results of these analyses applied to an individual burst are discussed in detail. Author (revised)

N94-26689*# National Aeronautics and Space Administration. Marshall Space Flight Center, Huntsville, AL.

BALLOON-BORNE MEASUREMENTS OF THE SN1987A HARD X RAY CONTINUUM Abstract Only

Geoffrey N. Pendleton (Alabama Univ., Huntsville.), William S. Paciesas (Alabama Univ., Huntsville.), Gerald J. Fishman, Charles A. Meegan, and Robert B. Wilson *In* Alabama Univ., BATSE Data Analysis 15 Feb. 1994 1 p (For primary document see N94-26685 07-93)

Avail: CASI HC A01/MF A01

SN1987A hard x ray continuum spectra obtained on 29 Oct. 1987, 9-10 Apr. 1988, and 11 Nov. 1988, from balloon flight measurements are presented. The spectra, spanning the energy range from 25 keV to 300 keV, were analyzed using a detector response matrix inversion technique that converts the spectra from counts/sec-sq cm-kev to photons/sec-sq cm-kev allowing direct comparison with theoretical models. The results indicate that the bulk of the Co-56 is mixed moderately through the inner regions of the SN envelope but they do not preclude the mixing of a small amount of the Co-56 further out into the envelope necessary to account for the observed Co-56 line fluxes. The effect of the ratio of Co-57 to Co-56 on the 11 Nov. 1988, continuum spectrum is discussed. Author (revised)

N94-26690*# National Aeronautics and Space Administration. Marshall Space Flight Center, Huntsville, AL.

CHANNEL TO ENERGY CALIBRATION RESULTS FOR THE BATSE LARGE AREA DETECTORS Abstract Only

Geoffrey N. Pendleton (Alabama Univ., Huntsville.), William S. Paciesas (Alabama Univ., Huntsville.), Michael S. Briggs (Alabama Univ., Huntsville.), B. A. Harmon, C. A. Wilson, Gerald J. Fishman, Robert B. Wilson, and Charles A. Meegan *In* Alabama Univ., BATSE Data Analysis 15 Feb. 1994 1 p (For primary document see N94-26685 07-93)

Avail: CASI HC A01/MF A01

Continuum 16 channel spectra obtained from in flight data are used to identify and correct for nonlinearities in the channel-to-energy conversion algorithm for the BATSE large area detectors. The Crab Nebula spectra obtained by the BATSE earth occultation technique are used to characterize any nonlinearities inherent in the low energy channel bin widths on a detector by detector basis. The bin widths are optimized to remove distortions from observed gamma ray spectra. The recalibrated bin edges are used in an analysis of Crab Pulsar data to verify the improvements in the calibration. Author (revised)

N94-26790*# Lockheed Missiles and Space Co., Palo Alto, CA. Research Labs.

COMPTON GAMMA RAY OBSERVATORY/BATSE OBSERVATIONS OF ENERGETIC ELECTRONS SCATTERED BY CYCLOTRON RESONANCE WITH WAVES FROM POWERFUL VLF TRANSMITTERS Final Report, 13 Oct. 1992 - 12 Feb. 1994

Dayton W. Datlowe and William L. Imhof 12 Feb. 1994 40 p

(Contract NAS5-32065)

(NASA-CR-195240; NAS 1.26:195240; LMSC-F254276) Avail: CASI HC A03/MF A01

To obtain a better understanding of the wave-particle mechanisms responsible for the loss of electrons from the radiation belts, energetic electron data from the Burst and Transient Source Experiment (BATSE) on the NASA's Compton Gamma Ray Observatory (GRO) was studied. Powerful ground-based VLF transmitters resonantly scatter electrons from the inner radiation belt onto trajectories from which they precipitate into the atmosphere as they drift eastward. 563 instances in which the satellite traversed a cloud of energetic electrons which had been scattered into quasi-trapped trajectories were identified. From the longitude distribution, it was concluded that waves from the VLF transmitter NWC at 114 deg E are the origin of 257 of the events, and waves from UMSat 44 deg E related to 45 more. In another 177 cases the electrons had drifted from the longitude of these transmitters to a location in the western hemisphere. The previously reported seasonal variation in the frequency of occurrence of cyclotron resonance interaction is confirmed with the continuous coverage provided by GRO. The frequency of occurrence of the cyclotron resonance interactions is largest before sunrise, which we attribute to the diurnal variations in the transmission VLF waves through the ionosphere. For the first time, unique very narrow sheets of electrons occurring in the aftermath of a large geomagnetic storm are reported. Author (revised)

N94-27003# Notre Dame Univ., IN. Dept. of Physics.

MESON SPECTROSCOPY AND PARTICLE ASTROPHYSICS

J. M. LoSecco Jul. 1993 27 p

(Contract DE-FG02-91ER-40623)

(DE94-001799; DOE/ER-40623/2) Avail: CASI HC A03/MF A01

Progress in the design and construction of a light meson spectroscopy experiment is reported. The experiment will run in 1993. Some non-accelerator activities and plans for the future are also discussed. Results of a Brookhaven beam test with a subset of the final detector are described. The test was quite promising both in the speed with which results were obtained and in the quality of the data itself. The status of the CsI veto is reported. The target region, in particular the CsI veto experiment is Notre Dame's primary hardware responsibility on this experiment. DOE

N94-27167*# Alabama Univ., Huntsville.

A MEASUREMENT OF THE ENERGY SPECTRA OF COSMIC RAYS FROM 20 TO 1000 GeV PER AMU Semiannual Report, 1 Apr. 1993 - 31 Mar. 1994

John C. Gregory and Arthur Smith 1994 16 p

(Grant NAGw-2023)

(NASA-CR-195246; NAS 1.26:195246) Avail: CASI HC A03/MF A01

During the report period the BUGS-4 instrument was completed, and the maiden voyage took place on 29 September from Fort Sumner, New Mexico. The successful flight of a large spherical drift chamber is a unique first for the sub-orbital balloon program. Unfortunately the instrument was consumed by fire after striking a power line during landing. However, while at float altitude, circa 24 hours of data were telemetered. The pre-flight preparations, and flight operations are described. Author (revised)

N94-27236*# Wisconsin Univ., Madison. Dept. of Physics, Coll. of Letters and Science.

COSMIC X RAY PHYSICS Final Report, 1 Jan. 1985 - 31 Mar. 1992

Dan McCammon, D. P. Cox, W. L. Kraushaar, and W. T. Sanders 1992 18 p

(Grant NAG5-629)

(NASA-CR-195225; NAS 1.26:195225) Avail: CASI HC A03/MF A01

This final report covers the period 1 January 1985 - 31 March 1992. It is divided into the following sections: the soft x-ray background; proportional counter and filter calibrations; sounding rocket flight preparations; new sounding rocket payload: x-ray calorimeter; and theoretical studies. Staff, publications, conference proceedings, invited talks, contributed talks, colloquia and seminars, public service lectures, and Ph. D. theses are listed. CASI

N94-27419*# Wisconsin Univ., Madison. Dept. of Physics.

COSMIC X RAY PHYSICS Annual Progress Report, 1 Jan. - 31 Dec. 1989

Dan McCammon, D. P. Cox, W. L. Kraushaar, and W. T. Sanders Jan. 1990 10 p

(Grant NAG5-629)

(NASA-CR-195218; NAS 1.26:195218) Avail: CASI HC A02/MF A01

The annual progress report on Cosmic X Ray Physics is presented. Topics studied include: the soft x ray background, proportional counter and filter calibrations, the new sounding rocket payload: X Ray Calorimeter, and theoretical studies. CASI

N94-27420*# Wisconsin Univ., Madison. Dept. of Physics.

COSMIC X RAY PHYSICS Annual Progress Report, 1 Jan. - 31 Dec. 1990

Dan McCammon, D. P. Cox, W. L. Kraushaar, and W. T. Sanders Jan. 1991 12 p

(Grant NAG5-629)

(NASA-CR-195219; NAS 1.26:195219) Avail: CASI HC A03/MF A01

The annual progress report on Cosmic X Ray Physics for the period 1 Jan. to 31 Dec. 1990 is presented. Topics studied include: soft x ray background, new sounding rocket payload: x ray calorimeter, and theoretical studies. CASI

N94-27440*# National Aeronautics and Space Administration. Marshall Space Flight Center, Huntsville, AL.
AN APRIL 1991 OUTBURST FROM 4U0115+63 OBSERVED BY BATSE
Lynn Cominsky (Sonoma State Univ., CA.), Mallory Roberts (Sonoma State Univ., CA.), and Mark H. Finger Dec. 1993 3 p
(Contract NAG5-2032; DE-AC03-76SF-00515)
(NASA-CR-195252; NAS 1.26:195252; SLAC-PUB-6406) Avail: CASI HC A01/MF A01

4U0115+63 is a recurrent transient X-ray pulsar in a moderately eccentric orbit with a Be star companion, V635 Cas. Many outbursts from this system have been reported over the past twenty years; yet despite the apparent relation between optical outbursts from the companion star and subsequent X-ray transient events, the physical mechanism for the mass transfer in the system remains unclear. In this paper, we present the preliminary results of analysis of observations made using BATSE during the 1991 April outburst from this system. This outburst does not fit the pattern of three year recurrence intervals previously suggested by Whitlock, Roussel-Dupre and Priedhorsky (1989). The orbital elements of the system have been updated and do not support the claim of Tamura et al., (1992) that apsidal motion was detected in this system based on the 1990 Ginga outburst. Author

N94-27607# Hirosaki Univ. (Japan). Dept. of Physics.
DIRECT EVIDENCE OF THE INTERPLANETARY MAGNETIC FIELD EFFECT ON THE COSMIC-RAY SHADOW BY THE SUN
M. Amenomori, Z. Cao, L. K. Ding, Z. Y. Feng, K. Hibino, N. Hotta, Q. Huang, A. X. Huo, H. Y. Jia, and G. Z. Jiang et al Jun. 1993 19 p Sponsored by Ministry of Education, Science and Culture, Tokyo, Japan and Committee of Natural Science Foundation, Beijing, China Prepared in cooperation with Tibet Asr Collaboration, Tibet, China
(ICRR-296-93-8; JTN-94-80575) Avail: CASI HC A03/MF A01

The Tibet air shower array, which has been successively operated at an altitude of 4,300 m a.s.l. since 1990, has detected the shadows of the sun and moon in the 10 TeV cosmic ray flux. In particular, the shadow of the sun was observed in the direction significantly away from the apparent solar position, under the influence of the solar and interplanetary magnetic fields. A further analysis shows that the shadows by cosmic rays are shifted in opposite directions according to the polarity of the fields. This is the first direct observation of the influence of the interplanetary magnetic field on the shadow's displacement. The results imply that observation of the cosmic ray shadow by the sun can produce new information on the relation between a time variation of the large-scale structure of the solar and interplanetary magnetic fields and the cycle of solar activity. Author (NASDA)

N94-27621# Pacific Northwest Lab., Richland, WA.
MONTE CARLO CALCULATIONS OF LOW BACKGROUND DETECTOR RESPONSE
H. S. Miley Nov. 1993 5 p Presented at the Nuclear Science Symposium, San Francisco, CA, 2-5 Nov. 1993
(Contract DE-AC06-76RL-01830)
(DE94-004593; PNL-SA-22411; CONF-931107-27) Avail: CASI HC A01/MF A01

An implementation of the Electron Gamma Shower 4 code (EGS4) has been developed to allow convenient simulation of typical gamma ray measurement systems. Coincidence gamma rays, beta spectra, and angular correlations have been added to adequately simulate a complete nuclear decay and provide corrections to experimentally determined detector efficiencies. This code has been used to strip certain low-background spectra for the purpose of extremely low-level assay. Monte Carlo calculations of this sort can be extremely successful since low background detectors are usually free of significant contributions from poorly localized radiation sources, such as cosmic muons, secondary cosmic neutrons, and radioactive construction or shielding materials. Validation of this code has been obtained from a series of comparisons between measurements and blind calculations. The singles counting efficiency of a particular counting experiment was reproduced within the accuracy of the known dimensions of the detector components. This allowed the complete simulation of a nuclear decay including two coincident gamma rays with a non-isotropic angular correlation. In addition, text-book efficiency curves have been reproduced for several sizes of sodium iodide detectors. Examples of the use and several spectral results are presented. DOE

N94-27714# Los Alamos National Lab., NM.
BATSE BURST LOCATION ACCURACY AND CONSTRAINTS ON THE FRACTION OF REPEATING GRB SOURCES
T. E. Strohmayer, E. E. Fenimore, and J. A. Miralles (Valencia Univ., Burjassot, Spain.) 1993 10 p Presented at the BATSE Gamma Ray Burst Workshop, Huntsville, AL, 21-23 Oct. 1993
(Contract W-7405-eng-36)
(DE94-004981; LA-UR-93-4279; CONF-9310252-2) Avail: CASI HC A02/MF A01

We use a one parameter model for GRB source repetition to investigate the ability of BATSE to detect source repetition and to place constraints on the fraction of repeating sources. From Monte Carlo simulations, we find that the current uncertainty in BATSE burst locations severely limits our ability to confidently detect source repetition from distributions containing fewer than 10 - 15% repeaters. A fit of our repetition model to 260 BATSE catalog bursts yields a best-fit repeating fraction of f(sub r) = 21% with a 90% confidence region ranging from 5.5 to 32.5%. By modifying the size of the measurement errors in our simulations we show that the location and width of the confidence region depends sensitively on the burst location errors. With BATSE's present location accuracy analysis of larger samples of bursts will not appreciably improve the constraint on the repeating fraction. DOE

N94-27740# Stanford Research Inst., Menlo Park, CA. Linear Accelerator Center.
GAMMA LARGE AREA SILICON TELESCOPE (GLAST): APPLYING SILICON STRIP DETECTOR TECHNOLOGY TO THE DETECTION OF GAMMA RAYS IN SPACE
W. B. Atwood Jun. 1993 15 p Presented at the GLAST Silicon Detector Conference, Hiroshima, Japan, 22-24 May 1993
(Contract DE-AC03-76SF-00515)
(DE94-003451; SU-SLAC-PUB-6267; CONF-9305305-1) Avail: CASI HC A03/MF A01

The recent discoveries and excitement generated by space satellite experiment EGRET (presently operating on the Compton Gamma Ray Observatory (CGRO)) have prompted an investigation into modern detector technologies for the next generation space based gamma ray telescopes. The GLAST proposal is based on silicon strip detectors as the 'technology of choice' for space application: no consumables, no gas volume, robust (versus fragile), long lived, and self triggerable. The GLAST detector basically has two components: a tracking module preceding a calorimeter. The tracking module has planes of crossed strip (x,y) 300 (mu)m pitch silicon detectors coupled to a thin radiator to measure the coordinates of converted electron-positron pairs. The gap between the layers (approximately 5 cm) provides a lever arm for track fitting resulting in an angular resolution of less than 0.1 deg at high energy. The status of this R & D effort is discussed including details on triggering the instrument, the organization of the detector electronics and readout, and work on computer simulations to model this instrument. DOE

N94-27793# Los Alamos National Lab., NM.
DMSP SATELLITES AS GAMMA RAY BURST DETECTORS
J. Terrell, P. Lee, R. W. Klebesadel, and J. W. Griffee (Sandia National Labs., Albuquerque, NM.) 1993 6 p Presented at the BATSE Gamma Ray Burst Workshop, Huntsville, AL, 21-23 Oct. 1993
(Contract W-7405-eng-36)
(DE94-004977; LA-UR-93-4313; CONF-9310252-1) Avail: CASI HC A02/MF A01

Gamma-ray burst detectors are aboard three US Air Force Defense Meteorological Satellite Program (DMSP) spacecraft, in orbit at 800 km altitude, with corresponding fields of view to 117 deg from the zenith. A large number of bursts were detected by DMSP, usually confirming and supplementing data from GRO and other spacecraft. The location of a gamma-ray burst source detected by several DMSP spacecraft is considerably restricted by knowledge of the several fields of view. Often non-detection of a strong burst by one or more DMSP spacecraft is even more informative in narrowing the possible area of the burst. The DMSP data in conjunction with observations by other spacecraft can lead to reasonable positional information when more accurate positions are not available from GRO or other data. DOE

N94-27826# Los Alamos National Lab., NM.
SIMULATIONS OF TERRESTRIAL IN-SITU COSMOGENIC-NUCLIDE PRODUCTION
R. C. Reedy, K. Nishiizumi (California Univ., San Diego, La Jolla.), J. R. Arnold (California Univ., San Diego, La Jolla.), and D. Lal (Scripps Institution of Oceanography, La Jolla, CA.) 1993 6 p Presented at the 6th International Conference on Accelerator Mass Spectrometry, Canberra, Australia, 17 Sep. - 1 Oct. 1993
(Contract W-7405-eng-36)
(DE94-004999; LA-UR-93-4406; CONF-930960-6) Avail: CASI HC A02/MF A01

Targets of silicon and silicon dioxide were irradiated with spallation neutrons to simulate the production of long-lived radionuclides in the surface of the earth. Gamma-ray spectroscopy was used to measure Be-7 and Na-22, and accelerator mass spectrometry was used to measure Be-10, C-14, and Al-26. The measured ratios of these nuclides are compared with calculated ratios and with ratios from other simulations and agree well with ratios inferred from terrestrial samples. DOE

N94-27827# Los Alamos National Lab., NM.
GAMMA RAY BURSTS FROM THE ACCRETION OF SOLID BODIES ONTO HIGH-VELOCITY GALACTIC NEUTRON STARS
S. A. Colgate and P. J. T. Leonard 1993 6 p Presented at the BATSE Gamma Ray Burst Workshop, Huntsville, AL, 21-23 Oct. 1993
(Contract W-7405-eng-36)
(DE94-005006; LA-UR-93-4340; CONF-9310252-4) Avail: CASI HC A02/MF A01

We propose a simple model for the gamma-ray bursts based on high velocity Galactic neutron stars that have accretion disks. The latter are formed from a mixture of material from the supernova shell and that ablated from a pre-supernova binary companion. Accretion onto the neutron star from this disk when the disk is still largely gaseous may result in a soft gamma-ray repeater phase. Much later, after the neutron star has moved away from its birthplace, solid bodies form in the disk, and some are perturbed into hitting the neutron star to create gamma-ray bursts. This model makes several predictions that are consistent with the observations. The observed combination of a high degree of isotropy on the sky coupled with the observed value of (V/V(sub max)) is not, at first glance, predicted, but is not impossible to attain in our model. DOE

N94-27996 International Centre for Theoretical Physics, Trieste (Italy).
A SIMPLE SATELLITE SYSTEM TO LOCATE GAMMA RAY BURSTERS USING SCINTILLATING FIBER TECHNOLOGY
Alberto Colavita, F. Fratnik, and P. Colavita (Universidad Nacional de San Luis, Argentina.) Jul. 1993 14 p Limited Reproducibility: More than 20% of this document may be affected by microfiche quality
(DE94-601287; IC-93/218) Avail: CASI HC A03 (US Sales Only)

A study on the feasibility of using a system of small, light, long-lived and simple satellites in order to locate gamma-ray bursters is presented. Each small satellite possesses only electronics to discriminate gamma rays out of the large background of cosmic rays and to time the arrival of the front of a gamma ray burst. The arrival of a gamma ray strikes a plane made out of scintillating fibers. A layered structure of thin lead foils and scintillating fibers is used to obtain a low trigger threshold of approximately 20 MeV. To locate the burster applying triangulation methods, the system uses the time of arrival of the front of the gamma-ray burst and the position of the satellites at that very moment. The authors review an elementary version of the triangulation method to study the angular error in the determination of the burster position. They show that for almost all nonpathological distances among satellites, the angular location of the source can be determined to better than one arc min. This precision allows the visible counterpart of the burster to be found, if it exists. These simple satellites can be made modular in order to customize their sizes or weights in order to use spare space available during major launches. Also proposed is a block diagram for the satellite architecture as well as a simple and strong detector using scintillating fiber technology. DOE

N94-28066# International Centre for Theoretical Physics, Trieste (Italy).
COSMOLOGICAL CONSTRAINTS ON VERY HEAVY STABLE NEUTRINOS
M. Yu. Khlopov and R. V. Konoplich (Cosmion Ltd., Moscow, Russia.) Jul. 1993 22 p
(DE94-601669; IC-93/192) Avail: CASI HC A03/MF A01 (US Sales Only)

A detailed analysis is carried out on the influence of the effects of the very heavy neutrino annihilation (m(sub nu) greater than 44 GeV) on the cosmic ray production in the galaxy. Also considered are the possibilities of the search for such neutrinos at accelerators in the reaction e(+) e(-) yields nu nu-tilde gamma. DOE

99 GENERAL

N94-26155*# National Aeronautics and Space Administration. Langley Research Center, Hampton, VA.
THE EVOLUTION OF THE HIGH-SPEED CIVIL TRANSPORT
M. Leroy Spearman Feb. 1994 48 p Presented at the AIAA Aircraft Design, Systems and Operations Meeting, Monterey, CA, 11-13 Aug. 1993
(RTOP 505-69-20-01)
(NASA-TM-109089; NAS 1.15:109089) Avail: CASI HC A03/MF A01

Current research directed toward the technology requirements for a high-speed civil transport (HSCT) airplane is an outgrowth of many years of activity related to air transportation. The purpose was to review some of the events that provided the background upon which current research programs are built. The review will include the subsonic era of transport aircraft and some events of the supersonic era that are related to the development of commercial supersonic transport aircraft. These events include the early NASA in-house studies and industry evaluations, the U.S. Supersonic Transport (SST) Program, the follow-on NASA supersonic cruise research programs, and the issuance of the National Aeronautical Research and Development (R&D) goals. Observations are made concerning some of the factors, both technical and nontechnical, that have had an impact on HSCT studies. Author (revised)

N94-26656# Tri-Univ. Meson Facility, Vancouver (British Columbia).
TRIUMF SCIENTIFIC ACTIVITIES Annual Report, 1992
Apr. 1993 263 p
(CTN-94-61062) Avail: CASI HC A12/MF A03

TRIUMF was established in 1968 as a laboratory operated and to be used jointly by a consortium of British Columbia and Alberta universities. Universities from other provinces have since been added as associate members, and the facility is also open to other Canadian and foreign users. The experimental program is based on a cyclotron capable of producing three simultaneous beams of protons, two of which are individually variable in energy from 180 to 520 MeV, and the third which is fixed at 70 MeV. The potential for high beam currents qualifies this machine as a meson factory. Fields of research include medium-energy nuclear physics and chemistry, particle physics, applied research in such fields as radioisotopes and tomography, and nuclear fuel research. A biomedical research facility at TRIUMF uses mesons in cancer research and treatment. Research programs at TRIUMF are reviewed along with activities in its electronics and computing division, applied programs division, engineering division, cyclotron operations division, and in the study being conducted to define various aspects of the KAON project. Lists of publications and experiment proposals are included. CISTI

N94-26701# Toronto Univ., Downsview (Ontario). Inst. for Aerospace Studies.
UNIVERSITY OF TORONTO INSTITUTE FOR AEROSPACE STUDIES Annual Progress Report, 1991 - 1992
1993 124 p
(CTN-94-61013) Avail: CASI HC A06/MF A02

A review is presented of the laboratory facilities and progress in research at the Institute for Aerospace Studies at the University of Toronto. Lists of publications and theses are included. The progress reports are in the fields of flight mechanics, fluid dynamics, solid mechanics, spacecraft mechanics, and engineering physics. Some developments in 1991/92 include the first powered flight of a model ornithopter, development of a novel technique of modeling air cushion dynamics, successful tests of a simple and inexpensive aerostat design, a new semi-empirical method for providing accurate optimum efficiency predictions for propellers, development of a computer program to solve the compressible thin-layer Navier-Stokes equations on high-lift multi-element airfoil configurations, development of a time-of-flight system for measuring velocity and energy distribution of atomic oxygen beams, and commercial development of the first fiber optic strain gauges. CISTI

N94-26709# National Research Council of Canada, Ottawa (Ontario). Inst. for Information Technology.
INSTITUTE FOR INFORMATION TECHNOLOGY Annual Report, 1992-1993
Sep. 1993 56 p
(ISSN 1183-9082)
(NRC-37061; CTN-94-61006) Copyright Avail: CASI HC A04/MF A01

The Institute for Information Technology (IIT) is one of the engineering research and technology sector institutes of the National Research Council of Canada. The mission of IIT is to assist industry across Canada to improve competitiveness through excellence in information technology by supporting and undertaking focused, industry oriented research in software and systems and by applying information technology in partnership with other Council institutes. There are four laboratories within IIT and there are four elements to IIT's research program: software engineering, knowledge based systems, sensor based automation, and systems integration. Institute activities in the IIT laboratories are reviewed, along with IIT management and administration, financial and human resources, publications, awards, patents and licenses, presentations at conferences by IIT members, and IIT participation on committees. Highlights of research include development of the world's first commercial erbium-doped fiber laser, devising of a technique for realtime collision avoidance for robotic manipulators, a demonstration of the BIRIS three dimensional vision system, and building of a simulator to evaluate reliability of a safety critical software demonstration. CISTI

N94-26937# California Univ., Berkeley. Lawrence Berkeley Lab.
HIGHLIGHTS 1993
1993 28 p
(Contract DE-AC03-76SF-00098)
(DE94-002270; LBL-Pub-733) Avail: CASI HC A03/MF A01

Current research programs at Lawrence Berkeley Laboratory are presented. The topics include: the genetic basis for breast cancer, the Advanced Light Source, selenium characterization in soils via x ray absorption spectroscopy, automated colony sorting in efforts to map the human genome, cancer drugs, the Sudbury Neutrino Observatory (SNO), atomic force microscopes (AFM), mapping the radon risk in homes, ketene research, tracking B mesons and the search for the top quark, computerized scientific visualization, technology transfer efforts, and astronomy in the classroom. DOE

N94-27355# Tohoku Univ., Sendai (Japan). Inst. for Materials Resarch.
LIST OF PAPERS PUBLISHED BY THE MEMBERS OF INSTITUTE FOR MATERIALS RESEARCH, TOHOKU UNIVERSITY 1992
Aug. 1993 86 p
(JTN-94-80608) Avail: CASI HC A05/MF A01

This bibliography lists reports published by the members of Institute for Materials Research, Tohoku University, Japan in 1992. This list contains papers on materials, properties and phenomena, instrumentation and experimental methods, and computer science. The category of materials contains ferrous and non-ferrous metals and alloys, semimetals and semiconductors, refractory materials and ceramics, superconductors and superconductivity, magnetic materials and magnetism, nuclear materials and irradiation effects, composite materials, amorphous materials and quasicrystal, and thin film, fine particles, and mesoscopic state. The properties and phenomena contains phase diagram and transformation, thermodynamical properties and diffusion, crystal growth and imperfection, impurity effect, melting and solidification, metal working and joining, high temperature and plasma state, amorphous and liquid state, crystal structure, electronic structure, electrical properties, optical properties magnetic resonance and Mossbauer effects, low temperature and quantum fluids, surface, interface and tunneling, electrochemical properties, corrosion and catalysis, and mechanical properties. The instrumentation and experimental methods includes analytical chemistry and spectroscopy, electron-, ion- and optical microscopy, diffraction and scattering of X-ray, electron, neutron and ion, high magnetic field and high pressure, purification and impurity detection, new method of material development and techniques. The computer science contains materials design by computer simulation, database system and retrieval method, and computer graphics and other applications. Author (NASDA)

N94-27381*# National Aeronautics and Space Administration, Washington, DC.
AEROSPACE SAFETY ADVISORY PANEL Annual Report
Mar. 1994 74 p Original contains color illustrations
(NASA-TM-109692; NAS 1.15:109692) Avail: CASI HC A04/MF A01; 1 functional color page

This report from the Aerospace Safety Advisory Panel (ASAP) contains findings, recommendations, and supporting material concerning safety issues with the space station program, the space shuttle program, aeronautics research, and other NASA programs. Section two presents findings and recommendations, section three presents supporting information, and appendices contain data about the panel membership, the NASA response to the March 1993 ASAP report, and a chronology of the panel's activities during the past year. CASI

N94-27431*# National Aeronautics and Space Administration. Langley Research Center, Hampton, VA.
NASA LANGLEY RESEARCH CENTER SEVENTY-FIFTH ANNIVERSARY PUBLICATIONS, 1992
1992 205 p Original contains color illustrations
(NASA-TM-109691; NAS 1.15:109691; HHR-58) Avail: CASI HC A10/MF A03; 13 functional color pages

The following are presented: The National Advisory Committee for Aeronautics Charter; Exploring NASA's Roots, the History of NASA Langley Research Center; NASA Langley's National Historic Landmarks; The Mustang Story: Recollections of the XP-51; Testing the First Supersonic Aircraft: Memoirs of NACA Pilot Bob Champine; NASA Langley's Contributions to Spaceflight; The Rendezvous that was Almost Missed: Lunar Orbit Rendezvous and the Apollo Program; NASA Langley's Contributions to the Apollo Program; Scout Launch Vehicle Program; NASA Langley's Contributions to the Space Shuttle; 69 Months in Space: A History of the First LDEF; NACA TR No. 460: The Characteristics of 78 Related Airfoil Sections from Tests in the Variable-Density Wind Tunnel; NACA TR No. 755: Requirements for Satisfactory Flying Qualities of Airplanes; 'Happy Birthday Langley' NASA Magazine Summer 1992 Issue. CASI

N94-27566# Lawrence Livermore National Lab., CA.
ENERGY AND TECHNOLOGY REVIEW, JULY 1993
W. J. Quirk Jul. 1993 21 p
(Contract W-7405-eng-48)
(DE94-004219; UCRL-52000-93-7) Avail: CASI HC A03/MF A01

This report discusses the two-stage light-gas gun which was developed by the Super-High-Altitude Research Project (SHARP) and is a step toward realizing a launcher that can deliver payloads at a fraction of the cost of rockets. The SHARP gun is different from other two-stage designs because it is larger and its launch and pump tubes are joined at right angles. This configuration allows the launch tube to point at any angle toward the sky while the pump tube remains horizontal. The authors have demonstrated that this gun can fire projectiles when the launch tube is in the horizontal position. Also included is a discussion about and remarks from Dr. Michael M. May who was the Laboratory's fifth director from 1965 to 1971. CASI

N94-27764*# National Aeronautics and Space Administration. Ames Research Center, Moffett Field, CA.
NAS TECHNICAL SUMMARIES. NUMERICAL AERODYNAMIC SIMULATION PROGRAM, MARCH 1992 - FEBRUARY 1993
Mar. 1994 161 p Original contains color illustrations
(RTOP 536-01-11)
(NASA-RP-1321; A-94015; NAS 1.61:1321) Avail: CASI HC A08/MF A02; 123 functional color pages

NASA created the Numerical Aerodynamic Simulation (NAS) Program in 1987 to focus resources on solving critical problems in aeroscience and related disciplines by utilizing the power of the most advanced supercomputers available. The NAS Program provides scientists with the necessary computing power to solve today's most demanding computational fluid dynamics problems and serves as a pathfinder in integrating leading-edge supercomputing technologies, thus benefitting other supercomputer centers in government and industry. The 1992-93 operational year concluded with 399 high-speed processor projects and 91 parallel projects representing NASA, the Department of Defense, other government agencies, private industry, and universities. This document provides a glimpse at some of the significant scientific results for the year. Author (revised)

N94-27993*# National Aeronautics and Space Administration. Lyndon B. Johnson Space Center, Houston, TX.
RESEARCH AND DEVELOPMENT ANNUAL REPORT, 1992
Aug. 1993 219 p
(NASA-TM-104777; S-731; NAS 1.15:104777) Avail: CASI HC A10/MF A03

Issued as a companion to Johnson Space Center's Research and Technology Annual Report, which reports JSC accomplishments under NASA Research and Technology Operating Plan (RTOP) funding, this report describes 42 additional JSC projects that are funded through sources other than the RTOP. Emerging technologies in four major disciplines are summarized: space systems technology, medical and life sciences, mission operations, and computer systems. Although these projects focus on support of human spacecraft design, development, and safety, most have wide civil and commercial applications in areas such as advanced materials, superconductors, advanced semiconductors, digital imaging, high density data storage, high performance computers, optoelectronics, artificial intelligence, robotics and automation, sensors, biotechnology, medical devices and diagnosis, and human factors engineering. Author

N94-28204*# National Aeronautics and Space Administration. Lyndon B. Johnson Space Center, Houston, TX.
JSC ALMANAC
Jun. 1993 141 p
(NASA-TM-109702; NAS 1.15:109702; JSC-23314-Rev-C) Avail: CASI HC A07/MF A02

During America's space shuttle flights, press and public attention focuses on the Johnson Space Center in Houston. The press and public often put questions to JSC technical and management staff. This fourth JSC Almanac supplies answers for many such questions, and provide an informational resource for speeches to general interest groups. This Almanac is not necessarily comprehensive or definitive. It is not intended as a statement of JSC or NASA policy. However, it does provide a much needed compilation of information from diverse sources. These sources are given as references, permitting the reader to obtain additional information as required. While every effort has been made to ensure accuracy and to reconcile statistics, users requiring the most up-to-date and accurate information should contact the office supplying the information at issue. The Almanac is updated periodically as needed. The following offices were responsible for supplying material for this update. Author (revised)

SUBJECT INDEX

SCIENTIFIC AND TECHNICAL AEROSPACE REPORTS VOLUME 32 NUMBER 7

Typical Subject Index Listing

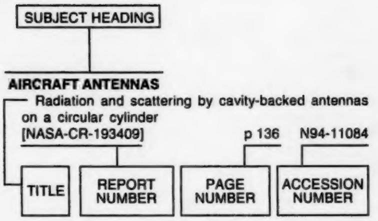

The subject heading is a key to the subject content of the document. Titles, report numbers, and accession numbers of pertinent documents are provided under each subject heading. When the title is insufficiently descriptive of the document content, a title extension is added, separated from the title by three hyphens. The report number helps to indicate the type of document cited (e.g., NASA report, NASA translation, NASA contractor report). The accession number is the number by which the document abstracts are arranged in this journal and by which the document is sold or requested. The page number helps you locate the citation in the abstract section. The titles, with title extensions if present, are arranged under each subject heading in ascending accession number order. The subject headings have been selected from the latest revision of the *NASA Thesaurus.*

A

ABEL FUNCTION

Matrix near rings and pseudo distributivity [DE94-601505] p 2992 N94-26366

ABILITIES

Proficiency scaling based on conditional probability functions for attributes [AD-A273816] p 3002 N94-25962

ABLATION

Ablation of solid-propellant rocket-motor nozzle materials [ESA-TT-1289] p 2699 N94-25638

Interaction between a high density-low temperature plasma and a frozen hydrogen pellet in a railgun injector [DE94-000846] p 3041 N94-25949

ABLATIVE MATERIALS

Ablation of solid-propellant rocket-motor nozzle materials [ESA-TT-1289] p 2699 N94-25638

Materials characterization on efforts for ablative materials [NASA-CR-193929] p 2756 N94-27230

ABNORMALITIES

Effects of expected-value information and display format on recognition of aircraft subsystem abnormalities [NASA-TP-3395] p 2673 N94-27882

ABORTED MISSIONS

STS-51 pad abort. OV103-engine 2033 (ME-2) fuel flowmeter sensor open circuit [NASA-CR-193924] p 2701 N94-26230

ABRASION

Unscreened low tension cables scrape abrasion testing [PB94-123767] p 2823 N94-26849

ABRASION RESISTANCE

Unscreened low tension cables scrape abrasion testing [PB94-123767] p 2823 N94-26849

ABSORPTION COOLING

Absorption technology for solar and waste heat utilization p 2854 N94-26053

ABSORPTION CROSS SECTIONS

Microwave coupling into a slotted cavity [PB94-123742] p 2772 N94-27041

Analysis of EUV/FUV dayglow and auroral measurements [NASA-CR-195237] p 2883 N94-27393

ABSORPTION SPECTRA

Characterization of semi-insulating gallium arsenide [AD-A273781] p 3068 N94-27704

Hypersensitive transition spectrum of f-element and coordination structure [DE94-604133] p 3070 N94-27843

ABSORPTION SPECTROSCOPY

Study on analyzing method establishment for metallic material development p 2729 N94-25578

High resolution fourier transform absorption spectrum of 79Br2 B3 Pi(Ou+) X1 sigma g+ [AD-A273864] p 2956 N94-25610

X ray absorption studies of Ti/polymer and Cr/polymer interfaces [DE94-003008] p 2753 N94-26770

An x ray absorption fine structure study of ordering in polythiophene thin films [AD-A274235] p 2753 N94-26822

Sound, speed, reflectivity, absorption, and thermal diffusivity measurements in Arctic ice in 1990 [AD-A274326] p 2899 N94-26886

In situ Mars ozone detector p 3108 N94-27892

ABSORPTIVITY

The effect of high frequency electric field on hypersound amplification in superlattice [DE93-634326] p 3057 N94-26384

ABUNDANCE

Reanalysis of Mariner 9 UV Spectrometer Data for Ozone, Cloud, and Dust Abundances, and Their Interaction Over Climate Timescales [NASA-CR-195244] p 3107 N94-27885

Probing the Martian atmosphere in the ultraviolet p 3108 N94-27890

How well was total ozone abundance inferred with Mariner 9? p 3108 N94-27891

Determination of lead isotope ratios in seawater by purge and trap GC/MS after ethylation p 2870 N94-28152

ACCELERATED LIFE TESTS

Failure behaviour of high density polyethylene with an embrittled surface layer due to weathering [PB94-126406] p 2840 N94-26960

Kinetic parameters from thermogravimetric analysis p 2721 N94-27909

ACCELERATION (PHYSICS)

Transient performance p 2828 N94-28045

ACCELERATION STRESSES (PHYSIOLOGY)

The electrogastrogram during parabolic flight p 2913 N94-27452

ACCELERATION TOLERANCE

The electrogastrogram during parabolic flight p 2913 N94-27452

Vertical gaze direction during parabolic flight p 2913 N94-27453

Heart rate change in normal and labyrinthectomized hamsters during parabolic flight p 2914 N94-27454

Effects of imaginary target on induced eye movements by linear acceleration p 2914 N94-27456

The Reports of Aeromedical Laboratory, volume 33, number 4 [JTN-94-80586] p 2933 N94-27942

ACCELEROMETERS

Fluid dynamic linear accelerometer [AD-D016042] p 2678 N94-27112

Modelling of the MEA float zone using accelerometer data [NASA-CR-193933] p 2761 N94-27220

ACCEPTABILITY

High-Speed Research: Sonic Boom, Volume 1 [NASA-CP-10132] p 2649 N94-28188

ACCEPTOR MATERIALS

Characterization of semi-insulating gallium arsenide [AD-A273781] p 3068 N94-27704

ACCESS CONTROL

Modeling and simulation of a fiber distributed data interface local area network [AD-A274838] p 3098 N94-26500

ACCESS TIME

A GPS coverage model p 2642 N94-27292

ACCIDENT PREVENTION

Evaluation and improvement of the inquest system on work accidents (TOT) [VTT-TIED-1418] p 2762 N94-26261

ACCIDENTS

Evaluation and improvement of the inquest system on work accidents (TOT) [VTT-TIED-1418] p 2762 N94-26261

A constitutive model for layered wire mesh and aramid cloth fabric [DE94-003275] p 2708 N94-26796

Propellants and explosives in ballistic missiles [UCRL-LR-113578] p 2760 N94-28222

ACCRETION DISKS

Studies of extra-solar Oort Clouds and the Kuiper Disk [NASA-CR-195242] p 3103 N94-26789

Gamma ray bursts from the accretion of solid bodies onto high-velocity Galactic neutron stars [DE94-005006] p 3117 N94-27827

ACCURACY

Accuracy analysis of multi-axis machines [ETN-94-95341] p 3002 N94-26000

Improved measurement accuracy in a Long Trace Profiler: Compensation for laser pointing instability [DE94-003408] p 2816 N94-26130

A simulation of GPS and differential GPS sensors p 2666 N94-27918

ACETONITRILE

Novel oxidizing reagents derived from elemental fluorine [ITN-94-85231] p 2719 N94-27687

ACOUSTIC ATTENUATION

Sound, speed, reflectivity, absorption, and thermal diffusivity measurements in Arctic ice in 1990 [AD-A274326] p 2899 N94-26886

Hydroacoustic wave-fields generated by different source types, a computational study [PB94-123536] p 3010 N94-27037

ACOUSTIC EMISSION

Characterization of acoustic effects on flame structures by beam deflection technique [DE94-003240] p 2714 N94-26122

Studies on the measurement of subsurface fractures and geostress using acoustic emission technique for deep coalbed development [REPT-7] p 2879 N94-26475

ACOUSTIC EXCITATION

Observation of impulsive acoustic events and the excitation of solar oscillations [AD-A274159] p 3111 N94-27096

ACOUSTIC FATIGUE

Methods of testing for endurance of structural elements using simulated acoustic loading [ESDU-93027] p 3011 N94-28141

ACOUSTIC PROPERTIES

Characterization of acoustic effects on flame structures by beam deflection technique [DE94-003240] p 2714 N94-26122

Sound, speed, reflectivity, absorption, and thermal diffusivity measurements in Arctic ice in 1990 [AD-A274326] p 2899 N94-26886

Problems in nonlinear acoustics: Rayleigh waves, pulsed sound beams, and waveguides [AD-A274587] p 3010 N94-26983

Hydroacoustic wave-fields generated by different source types, a computational study [PB94-123536] p 3010 N94-27037

Researches of the Electrotechnical Laboratory. No. 955: Speech recognition by description of acoustic characteristic variations [JTN-94-80604] p 2775 N94-27249

ACOUSTIC SCATTERING

New variational techniques for acoustic radiation and scattering from elastic shell structures [AD-A274599] p 3010 N94-26889

ACOUSTIC VELOCITY

Characterization of acoustic effects on flame structures by beam deflection technique [DE94-003240] p 2714 N94-26122

Iron: What is melt? [DE94-003373] p 2735 N94-26322

Sound, speed, reflectivity, absorption, and thermal diffusivity measurements in Arctic ice in 1990 [AD-A274326] p 2899 N94-26886

ACOUSTICS

Hydrodynamics, acoustics and scaling of traveling bubble cavitation [AD-A273846] p 2789 N94-25605

Characterization of acoustic effects on flame structures by beam deflection technique [DE94-003240] p 2714 N94-26122

Compressibility effects on rotor forces in the leakage path between a shrouded pump impeller and its housing p 2796 N94-27379

ACOUSTO-OPTICS

Studies of non-linear optical effects for agile beam steering [AD-A273998] p 3034 N94-25902

Acousto-optical post-processor time-integrating correlator calibration updates [DSIS-94-00053] p 2813 N94-27317

ACQUISITION

A cost model for USAF acquisition of commercial aircraft for service in the special air mission fleet [AD-A274012] p 3093 N94-25796

ACRYLATES

Dual cure low-VOC coating process [DE94-000365] p 2756 N94-27611

ACTINIDE SERIES

Debye-Waller factors of the light actinide metals [DE94-000685] p 2733 N94-26069

Radiochemistry Division annual progress report : 1991 [DE94-600652] p 2715 N94-26392

Study on laser atomic spectroscopy [DE93-633328] p 2817 N94-26402

A new materials data compilation can help in actinide phase-diagram research [DE94-000797] p 3058 N94-26514

ACTIVATED CARBON

Double layer capacitance of carbon foam electrodes [DE94-002651] p 2780 N94-25975

ACTIVATION (BIOLOGY)

Vacuum-UV-effects on E. coli plasmid pUC19: Inactivation, strand break induction and mutation induction [DLR-FB-93-26] p 2903 N94-27754

ACTIVATION ENERGY

Oriented lead zirconate titanate thin films: Characterization of film crystallization [DE94-003104] p 3053 N94-26025

Effect of temperature and recoil-energy spectra on irradiation-induced amorphization in Ca2La8(SiO4)6O2 [DE94-004371] p 3067 N94-27602

The Science Reports of the Research Institutes, Tohoku University. Series A: Physics, Chemistry, and Metallurgy. Volume 38, No. 1: Amorphous Materials 14 [JTN-94-80610] p 2744 N94-28158

Differential scanning calorimetric study of solid state amorphization and crystallization in Zr/Co and Zr/Ni multilayers p 2745 N94-28161

ACTIVE CONTROL

Module interconnection frameworks for a real-time spreadsheet [AD-A273853] p 2956 N94-25588

Status report of RMS active damping augmentation p 2684 N94-26285

A study on piezoelectric actuators and sensors for vibration control of flexible space structures [AD-A274925] p 2695 N94-26532

Operator theoretic methods in the control of distributed and nonlinear systems [AD-A274160] p 2988 N94-27139

On the use of feedback to control sound radiation from a plate excited by a turbulent boundary layer [ISVR-TR-227] p 2807 N94-28175

ACTIVITY (BIOLOGY)

Coupling of pelagic and benthic communities over a seamount in the Eastern North Pacific [AD-A274750] p 2899 N94-26149

Monitoring activity with a wrist-worn actigraph: Effects of amplifier passband and threshold variations [AD-A274705] p 2909 N94-26377

A comparison of sleep scored from electroencephalography to sleep scored by wrist actigraphy [AD-A273739] p 2910 N94-26748

Ozone control of biological activity during Earth's history, including the KT catastrophe p 2876 N94-28312

ACTIVITY CYCLES (BIOLOGY)

Chaotic dynamics of the solar cycle [AD-A274315] p 3110 N94-26883

ACTS

Remote Earth Sciences data collection using ACTS [NASA-CR-195227] p 2848 N94-26236

ACTUATORS

Performance impacts for actuator misalignments and failures in large-aperture adaptive-optic telescopes [AD-A273838] p 3034 N94-25742

Multiple model adaptive estimation applied to the LAMBDA URV for failure detection and identification [AD-A274078] p 3002 N94-25992

A study on piezoelectric actuators and sensors for vibration control of flexible space structures [AD-A274925] p 2695 N94-26532

Modelling and stability of a shape memory alloy position control system [ISBN-0-315-84467-1] p 2740 N94-27304

Experimental apparatus for optimization of flap position for a three-element airfoil model p 2682 N94-27912

ADA (PROGRAMMING LANGUAGE)

Object-oriented design and implementation of a parallel Ada simulation system [AD-A274119] p 2979 N94-25906

Real-Time Embedded Processing for Space Applications [ISBN-2-85428-335-X] p 2948 N94-26713

Real time avionics constraints: Silicon solutions p 2949 N94-26717

A complete version of the Ada tasking coprocessor p 2950 N94-26721

Standardize Ada hard real-time services? p 2951 N94-26729

Ada multiple-programming for hard real time applications in space systems p 2951 N94-26730

Scheduling approaches with Ada p 2952 N94-26734

Developing with Ada using HOOD design methodology p 2953 N94-26741

Use of HOOD coupled to real time monitors p 2953 N94-26742

Ada reusable software for satellite on-board data handling p 2953 N94-26743

CMSC-130 introductory computer science, lecture notes [AD-A274369] p 2967 N94-27060

An object-oriented database interface for Ada [AD-A274391] p 2968 N94-27075

ADAPTATION

Discovery learning in autonomous agents using genetic algorithms [AD-A274083] p 2677 N94-25998

Human dimensions research team, operation restore hope [AD-A274340] p 2939 N94-27056

ADAPTERS

New rubber qualification for the igniter adapter [NASA-CR-193936] p 2752 N94-26708

ADAPTIVE CONTROL

Adaptive optimization and control using neural networks [DE94-003941] p 2985 N94-25983

Physical modelling and adaptive predictive control of diffusion/LPCVD reactors [PB94-126398] p 2763 N94-26819

Grey-box modelling and identification topics [PB94-126380] p 2986 N94-27029

Development of a performance evaluation tool (MMSOFE) for detection of failures with Multiple Model Adaptive Estimation (MMAE) [AD-A274218] p 2665 N94-27071

Multiple model adaptive control of a large flexible space structure with purposeful dither for enhanced identifiability [AD-A274132] p 2987 N94-27122

Beamforming/null-steering adaptive array [CA-PATENT-1325260] p 2775 N94-27270

On identified predictive control p 2990 N94-27896

Modelling and control of plasma position in the STOR-M tokamak [ISBN-0-315-58891-8] p 3049 N94-27949

ADAPTIVE FILTERS

Evaluation of an Acoustic Charge Transport (ACT) device for adaptive interference suppression in spread spectrum communications systems [AD-A274073] p 2765 N94-25647

Kalman filtering of narrowband interference from direct sequence spread spectrum communications systems [ISBN-0-315-84011-0] p 2784 N94-26627

An adaptive Kalman filter for tactical missiles guidance systems [ISBN-0-315-84115-X] p 2677 N94-26636

Development of a performance evaluation tool (MMSOFE) for detection of failures with Multiple Model Adaptive Estimation (MMAE) [AD-A274218] p 2665 N94-27071

Enhanced adaptive statistical filter providing improved performance for target motion analysis noise discrimination statement of government interest [AD-D016039] p 2786 N94-27109

ADAPTIVE OPTICS

Improved quality of reconstructed images through sifting of data in statistical image reconstruction [AD-A273884] p 3034 N94-25730

Performance impacts for actuator misalignments and failures in large-aperture adaptive-optic telescopes [AD-A273838] p 3034 N94-25742

Performance comparison of shearing interferometer and Hartmann wave front sensors [AD-A274031] p 3034 N94-25768

ADDITIVES

Ion implantation of diamond: Damage, doping, and lift-off [DE94-001133] p 3054 N94-26137

Simplified high-efficiency silicon cell processing [DE94-002683] p 2857 N94-26617

ADHESION

Intelligent material systems and structures. Part 6: Measurements of adhesion between optical fibres and composite materials [PB94-123577] p 2756 N94-27215

ADHESIVE BONDING

Testing composite-to-metal tubular lap joints [DE94-003225] p 2836 N94-26032

Investigation of the bond strength of a discrete skin-stiffener interface [NLR-TP-92183-U] p 2670 N94-27796

ADHESIVES

Design of a computer expert system for adhesive selection using artificial intelligence techniques [AD-A274715] p 2751 N94-26434

Dual cure low-VOC coating process [DE94-000365] p 2756 N94-27611

ADIABATIC EQUATIONS

On the classification scheme for resonant states of muonic molecules [DE93-613645] p 3014 N94-25853

Muon transfer rates in collisions of hydrogen isotope mesic atoms on bare nuclei: Multichannel adiabatic approach [DE94-606752] p 3030 N94-27861

ADRENAL GLAND

The intracellular second messenger system in c-fos gene induction by ACTH p 2904 N94-27477

ADRENOCORTICOTROPIN (ACTH)

The intracellular second messenger system in c-fos gene induction by ACTH p 2904 N94-27477

ADSORPTION

Binding of copper and nickel to cavities in silicon formed by helium ion implantation [DE94-003769] p 3050 N94-25814

Studies of thin-film growth, adsorption, and oxidation by in situ, real-time, and ex situ ion beam analysis [DE94-002907] p 3055 N94-26275

Translational-energy-resolved studies of photogenerated carrier-induced reactions on UHV semiconductor surfaces [DE94-004169] p 3058 N94-26526

Adsorption and desorption studies of cesium on sapphire surfaces [DE94-003798] p 3070 N94-28067

ADVANCED VERY HIGH RESOLUTION RADIOMETER

The Hough transform algorithm for sea ice lead analysis: An evaluation [AD-A274535] p 2899 N94-26853

Ice surface temperature retrieval from AVHRR, ATSR, and passive microwave satellite data: Algorithm development and application [NASA-CR-195276] p 2851 N94-27849

Some practical aspects of lossless and nearly-lossless compression of AVHRR imagery p 2947 N94-28264

ADVECTION

Air pollution transport modeling [AD-A273863] p 2865 N94-25609

A positive finite-difference advection scheme applied on locally refined grids [CWI-NM-R9309] p 2867 N94-26216

A robust upwind discretization method for advection, diffusion and source terms [CWI-NM-R9308] p 2868 N94-26774

AERIAL RECONNAISSANCE

An analysis of multiple sensor system payloads for unmanned aerial vehicles [AD-A274905] p 2667 N94-26182

An evaluation of an airborne remote sensing system used to determine ice thickness and geometry of a first year sea ice ridge located in the Beaufort Sea [ISBN-0-315-84383-7] p 2849 N94-26667

Laboratory of Space Technology [PB94-133204] p 2689 N94-28358

AEROACOUSTICS
Methods in unsteady aerodynamics
[DLR-FB-93-21] p 2648 N94-27741
Coupled 2-dimensional cascade theory for noise an d unsteady aerodynamics of blade row interaction in turbofans. Volume 2: Documentation for computer code CUP2D
[NASA-CR-4506-VOL-2] p 2675 N94-27778
On the aging of sonic booms p 2650 N94-28194
AEROBRAKING
Mars transportation system p 2833 N94-25689
Minimum accommodation for aerobrake assembly, phase 2
[NASA-TM-107608] p 2692 N94-27774
AEROCAPTURE
Nonequilibrium radiation and chemistry models for aerocapture vehicle flowfields
[NASA-CR-195706] p 2648 N94-28071
AERODYNAMIC CHARACTERISTICS
Tesseract supersonic business transport
p 2671 N94-25713
The design of four hypersonic reconnaissance aircraft
p 2671 N94-25716
Design of a flight controller for an unmanned research vehicle with control surface failures using quantitative feedback theory
[AD-A274049] p 2677 N94-25833
Low-speed pressure distribution measurements over the aft-fuselage, fins, and stabilators of a 1/9th scale F/A-18 wind-tunnel model
[AD-A274870] p 2644 N94-26342
Experimental and theoretical study of aerodynamic characteristics of some lifting bodies at angles of attack from -10 degrees to 53 degrees at Mach numbers from 2.30 to 4.62
[NASA-TM-4528] p 2646 N94-26693
Effects, limits, and limitations of spanwise blowing
p 2659 N94-28027
Recent developments in the simulation of steady and transient transverse jet interactions for missile, rotorcraft, and propulsive applications p 2804 N94-28030
A review of recent aeroelastic analysis methods for propulsion at NASA Lewis Research Center
[NASA-TP-3406] p 2846 N94-28227
AERODYNAMIC COEFFICIENTS
Surface roughness lengths
[AD-A274550] p 2895 N94-26846
Numerical simulation of a powered-lift landing
p 2671 N94-28033
An initial investigation into methods of computing transonic aerodynamic sensitivity coefficients
[NASA-CR-195705] p 2648 N94-28072
Program for calculation of maximum lift coefficient of plain aerofoils and wings at subsonic speeds
[ESDU-93015] p 2649 N94-28076
Application of the influence function method using the interference distributed loads code to prediction of store aerodynamic load during separation from the CF-18 fighter aircraft p 2654 N94-28330
AERODYNAMIC CONFIGURATIONS
Control jets in interaction with hypersonic rarefied flow
p 2698 N94-28020
AERODYNAMIC DRAG
Experimental investigation of advanced hub and pylon fairing configurations to reduce helicopter drag
[NASA-TM-4540] p 2668 N94-26604
An investigation into the aerodynamic effects of wing patches
[ISBN-0-315-84121-4] p 2646 N94-26672
Surface roughness lengths
[AD-A274550] p 2895 N94-26846
Examples of flight path optimisation using a multivariate gradient-search method
[ESDU-93021] p 2670 N94-28092
Drag prediction by wake integrals using 3-D multi-grid Euler method (MGAERO) p 2655 N94-28335
Preliminary assessment of aerodynamic effects of wing repair patches p 2657 N94-28346
Evaluation of the buoyancy drag on automobile models in low speed wind tunnels p 2658 N94-28352
AERODYNAMIC FORCES
A finite wake theory for two-dimensional rotary wing unsteady aerodynamics
[AD-A274921] p 2645 N94-26535
Multidisciplinary aeroelastic analysis of a generic hypersonic vehicle
[NASA-TM-4544] p 2691 N94-27868
Experiments on interaction force of jets in hypervelocity cross-flow in a shock tunnel p 2659 N94-28022
AERODYNAMIC HEAT TRANSFER
Program to develop a performance and heat load prediction system for multistage turbines
[NASA-CR-195223] p 2674 N94-26588
AERODYNAMIC HEATING
Aerodynamic heating in hypersonic flows
p 2658 N94-27919
AERODYNAMIC INTERFERENCE
Vectored jets-induced interference on aircraft, prediction and verification p 2801 N94-28012
Experimental investigations into the wall interference and sidewall boundary layer effects in the National Research Council/Inst. for Aerospace Research High Reynolds Number 2-D Test Facility
p 2658 N94-28350
Computation of wind-tunnel side-wall interference using 3D Navier-Stokes code p 2658 N94-28351
Evaluation of the buoyancy drag on automobile models in low speed wind tunnels p 2658 N94-28352
AERODYNAMIC LOADS
Correlation of airloads on a two-bladed helicopter rotor
[NASA-TM-103982] p 2644 N94-26143
Analysis/test correlation using VAWT-SDS on a step-relaxation test for the rotating Sandia 34 m test bed
[DE94-002290] p 2857 N94-26700
Impact tests on fibre metal laminates under a tensile load
[PB94-126570] p 2710 N94-27201
Application of the influence function method using the interference distributed loads code to prediction of store aerodynamic load during separation from the CF-18 fighter aircraft p 2654 N94-28330
AERODYNAMIC NOISE
Silence amenity engineering: Past and present
p 3011 N94-27283
AERODYNAMIC STABILITY
Eagle RTS: A design of a regional transport
p 2671 N94-25709
Low-speed pressure distribution measurements over the aft-fuselage, fins, and stabilators of a 1/9th scale F/A-18 wind-tunnel model
[AD-A274870] p 2644 N94-26342
Effects, limits, and limitations of spanwise blowing
p 2659 N94-28027
AERODYNAMIC STALLING
Computational investigation of the compressible dynamic stall characteristics of the Sikorsky SSC-A09 airfoil
[AD-A274867] p 2644 N94-26191
Compressor stability p 2828 N94-28046
Potential flow modelling of airfoil stall
p 2654 N94-28332
Preliminary assessment of aerodynamic effects of wing repair patches p 2657 N94-28346
AERODYNAMICS
Preliminary design of nine high speed civil transports
p 2671 N94-25710
The identification of inflow fluid dynamics parameters that can be used to scale fatigue loading spectra of wind turbine structural components
[DE94-000231] p 2791 N94-26117
Proceedings of the Non-Linear Aero Prediction Requirements Workshop
[NASA-CP-10138] p 2670 N94-27439
NAS technical summaries. Numerical aerodynamic simulation program, March 1992 - February 1993
[NASA-RP-1321] p 3118 N94-27764
Control jets in interaction with hypersonic rarefied flow
p 2698 N94-28020
Transient model applications. 1: Compressor heat soak/clearance effects modeling p 2828 N94-28048
Examples of excrescence drag prediction for typical wing components of a subsonic transport aircraft at the cruise condition
[ESDU-93032] p 2649 N94-28144
Aeronautical engineering: A continuing bibliography with indexes (supplement 301)
[NASA-SP-7037(301)] p 2643 N94-28203
Abstracts of papers presented at the 4th CASI Aerodynamics Symposium
[ISBN-0-920203-01-9] p 2651 N94-28315
AEROELASTICITY
A comparative study of serial and parallel aeroelastic computations of wings
[NASA-TM-108805] p 2645 N94-26538
Methods in unsteady aerodynamics
[DLR-FB-93-21] p 2648 N94-27741
Understanding and development of a prediction method of transonic limit cycle oscillation characteristics of fighter aircraft
[NLR-TP-92210-U] p 2679 N94-27798
Multidisciplinary aeroelastic analysis of a generic hypersonic vehicle
[NASA-TM-4544] p 2691 N94-27868
Wing design for a civil tiltrotor transport aircraft: A preliminary study p 2671 N94-27917
A review of recent aeroelastic analysis methods for propulsion at NASA Lewis Research Center
[NASA-TP-3406] p 2846 N94-28227
AERONAUTICAL ENGINEERING
Aeronautical engineering: A continuing bibliography with indexes (supplement 301)
[NASA-SP-7037(301)] p 2643 N94-28203
AEROSOLS
The chemical detector paper as a potential alarm
[FFI-93/6007] p 2712 N94-25745
Analytic approximation to randomly oriented spheroid extinction
[DREV-4712-93] p 3038 N94-27598
AEROSPACE ENGINEERING
Technology development in space projects
[VTT-TIED-1438] p 2682 N94-26249
University of Toronto Institute for Aerospace Studies
[CTN-94-61013] p 3117 N94-26701
Proceedings of the Non-Linear Aero Prediction Requirements Workshop
[NASA-CP-10138] p 2670 N94-27439
NAS technical summaries. Numerical aerodynamic simulation program, March 1992 - February 1993
[NASA-RP-1321] p 3118 N94-27764
Laboratory of Space Technology
[PB94-133204] p 2689 N94-28358
AEROSPACE ENVIRONMENTS
Proceedings of the 8th Annual Summer Conference: NASA/USRA Advanced Design Program
[NASA-CR-195118] p 3075 N94-25665
Automation of closed environments in space for human comfort and safety p 2943 N94-25684
Long Duration Exposure Facility space optics handbook
[AD-A274831] p 3035 N94-26572
Physics of debris clouds from hypervelocity impacts
[NASA-CR-193932] p 2696 N94-26791
Development and application of contamination technology for MSFC managed space systems
[NASA-CR-193934] p 2697 N94-27421
Evaluation of high temperature superconductive thermal bridges for space-borne cryogenic infrared detectors
p 2815 N94-27921
Prometheus in space: Research Committee on Functional New Material
[JTN-94-80580] p 2761 N94-28002
AEROSPACE INDUSTRY
Technology development in space projects
[VTT-TIED-1438] p 2682 N94-26249
Future of aerospace
[PB94-120185] p 2669 N94-26906
Thermoplastic or thermosetting composites in aircrafts
[PB94-123809] p 2710 N94-27253
AEROSPACE MEDICINE
Plasma volume shifts and exercise thermoregulation with water immersion and six-degree head-down tilt
[NASA-TM-108781] p 2901 N94-26093
US Army aviation epidemiology data registry: Incidence and outcomes of aviator flying evaluation boards
[AD-A274711] p 2910 N94-26432
Aeromedical issues related to positive pressure breathing for +Gz protection
[AD-A274717] p 2910 N94-26435
Monograph of the Aviation Epidemiology Data Register for CY 1992
[AD-A274400] p 2911 N94-27130
Brain wave correlates of attentional states: Event related potentials and quantitative EEG analysis during performance of cognitive and perceptual tasks
p 2940 N94-27901
The Reports of Aeromedical Laboratory, volume 33, number 4
[JTN-94-80586] p 2933 N94-27942
Aerospace medicine and biology: A continuing bibliography with indexes (supplement 386)
[NASA-SP-7011(386)] p 2933 N94-28208
Aerospace medicine and biology: A continuing bibliography with indexes (supplement 387)
[NASA-SP-7011(387)] p 2933 N94-28213
Aerospace medicine and biology: A cumulative index to a continuing bibliography (supplement 384)
[NASA-SP-7011(384)] p 2934 N94-28219
Workshop on Countering Space Adaptation with Exercise: Current Issues
[NASA-CP-3252] p 2934 N94-28361
Does training-induced orthostatic hypotension result from reduced carotid baroreflex responsiveness?
p 2935 N94-28366
Cardiac output and cardiac contractility by impedance cardiography during exercise of runners
p 2935 N94-28367
Weightlessness and the human skeleton: A new perspective p 2935 N94-28368
Irreversibility of advanced osteoporosis: Limited role for pharmacologic intervention p 2935 N94-28369
Exercise and osteoporosis: Methodological and practical considerations p 2935 N94-28370

Visit to CERMA: Centre d'Etudes et de Recherches de Medecine Aerospatiale, Centre for Studies and Research in Aviation and Space Medicine, Bretigny sur Orge, France, November 16-18, 1992
[PB94-132990] p 2937 N94-28392

AEROSPACE SAFETY
Preliminary reentry safety assessment of the General Purpose Heat Source module for the Cassini mission: Aerospace Nuclear Safety Program
[DE94-001646] p 2699 N94-25926
Aerospace safety advisory panel
[NASA-TM-109692] p 3118 N94-27381
Risks and issues in fire safety on the Space Station
[NASA-TM-106430] p 2692 N94-27436
Summary of NASA Aerospace Flight Battery Systems Program activities p 2860 N94-28101

AEROSPACE SCIENCES
Technical and scientific research for aeronautics and astronautics
[ETN-94-95392] p 2641 N94-26212

AEROSPACE SYSTEMS
Development and application of contamination technology for MSFC managed space systems
[NASA-CR-193934] p 2697 N94-27421
Effects of expected-value information and display format on recognition of aircraft subsystem abnormalities
[NASA-TP-3395] p 2673 N94-27882
Lunar Transportation Facilities and Operations Study, option 1
[NASA-CR-195700] p 3109 N94-27982
Lunar Transportation Facilities and Operations Study, option 2
[NASA-CR-195701] p 3109 N94-27983
Summary of NASA Aerospace Flight Battery Systems Program activities p 2860 N94-28101

AEROSPACE TECHNOLOGY TRANSFER
The proliferation of aerospace weapons technology: Ballistic missiles and the case of Brazil
[ISBN-0-315-84082-X] p 2763 N94-26634
NASA: Major challenges for management. Testimony before the Legislation and National Security Subcommittee, Committee on Government Operations, House of Representatives
[GAO/T-NSIAD-94-18] p 3095 N94-28176

AEROSPACE VEHICLES
Development of methodologies for the estimation of thermal properties associated with aerospace vehicles
p 2846 N94-27920

AEROTHERMOCHEMISTRY
Ablation of solid-propellant rocket-motor nozzle materials
[ESA-TT-1289] p 2699 N94-25638

AFFERENT NERVOUS SYSTEMS
Contribution of muscle spindle afferent activity to transient pause in EMG during voluntary tonic contraction p 2928 N94-27522

AFRICA
Assessment of tropical forests using satellite data
[SILVA-CARELICA-21] p 2850 N94-27182
Mapping closed tropical forest cover in West Africa using NOAA/AVHRR-LAC data p 2850 N94-27184

AFTERBURNING
Engine starting and stopping p 2828 N94-28047

AGING (MATERIALS)
Effects of physical aging on long-term behavior of composites p 2712 N94-27897

AGING (METALLURGY)
Issues for conversion coating of aluminum alloys with hydrotalcite
[DE94-003804] p 2732 N94-25819

AGRICULTURE
Methane emissions from natural wetlands
[DE93-040796] p 2865 N94-25790

AIR CARGO
Integrators: A challenge for air cargo
p 2662 N94-28244

AIR CONDITIONING
Absorption technology for solar and waste heat utilization p 2854 N94-26053
A method for testing of HVAC automation equipment using the emulator and the application of the method
[VTT-TIED-1435] p 2822 N94-26306

AIR CONDUCTIVITY
The Lightcraft project: Flight technology for a hypersonic mass transit system p 2670 N94-25695

AIR COOLING
Cooling towers for combined cycles: New developments to meet environmental requirements
p 2832 N94-28088

AIR DATA SYSTEMS
Pressure distributions on a 0.02-scale Space Shuttle orbiter nose at Mach 21.5 in helium
[NASA-TM-4495] p 2646 N94-26592
Production of a computer based lesson teaching employees how to use an air data tester
[ISBN-0-315-84706-5] p 2969 N94-27316

First Canadair jet flies for Lufthansa city line
p 2662 N94-28243

AIR FLOW
Recent ASCOT experiments in multi-layered flows
[DE94-002360] p 2880 N94-26762
Numerical analysis of the photo-dissociation/radical oxidation of formaldehyde by ultraviolet light in a photolytic reactor
[AD-A274539] p 2868 N94-26843
Propagation of cold air masses in East Asia and its associated planetary-scale function
[AD-A274304] p 2895 N94-26850
An experimental study of plunging liquid jet induced air carryunder and dispersion
[AD-A274414] p 2794 N94-26979
Experimental verification of tomographic reconstruction of turbulent air flow structure using optical wavefront measurements
[AD-A274392] p 2795 N94-27129
An overview of the ASCOT program
[DE94-004356] p 2869 N94-27601

AIR JETS
Transitional flight characteristics of a geometrically simplified STOVL model p 2672 N94-28035
Analysis of cooling jets near the leading edge of turbine blades p 2676 N94-28037
Inclined air-jets used as vortex generators to suppress shock-induced separation p 2659 N94-28040

AIR MASSES
Propagation of cold air masses in East Asia and its associated planetary-scale function
[AD-A274304] p 2895 N94-26850

AIR NAVIGATION
Realtime mitigation of GPS SA errors using Loran-C
p 2642 N94-27291
A sky above Europe p 2661 N94-28234

AIR POLLUTION
Air pollution transport modeling
[AD-A273863] p 2865 N94-25609
Evaluation of a Canadian minitube air sampling system
[FOA-C-40307-4.6] p 2866 N94-25809
Study on neutron activation analysis
[DE93-632191] p 3017 N94-26116
Environmental benefits of different types of heat pumps, available and expected
[DE94-002440] p 2866 N94-26123
SIHTI 2: Energy and environmental technology
[DE94-702061] p 2867 N94-26241
An observational study of air pollution transport over a large urban complex
[REPT-6] p 2867 N94-26474
Compilation of air pollutant emission factors. Volume 1: Stationary point and area sources. Supplement F
[PB94-121431] p 2867 N94-26757
A robust upwind discretization method for advection, diffusion and source terms
[CWI-NM-R9308] p 2868 N94-26774
Numerical analysis of the photo-dissociation/radical oxidation of formaldehyde by ultraviolet light in a photolytic reactor
[AD-A274539] p 2868 N94-26843
Advances in passive-remote and extractive Fourier transform infrared spectroscopic systems
[DE94-001424] p 2868 N94-26952
An overview of the ASCOT program
[DE94-004356] p 2869 N94-27601
The single European market: Economical advance, ecological problem? p 2661 N94-28235
Indian activities on the core programme IGAP and proposals for network activities p 2874 N94-28284
Fibrous ceramic candle filter for particle removal in pressurized fluidized bed combustion
[PB94-133089] p 2876 N94-28383
Experimental studies of pressurised fluidised bed combustion at Helsinki University of Technology, 1991-1992
[PB94-133063] p 2876 N94-28394

AIR QUALITY
Advances in passive-remote and extractive Fourier transform infrared spectroscopic systems
[DE94-001424] p 2868 N94-26952

AIR SAMPLING
Evaluation of a Canadian minitube air sampling system
[FOA-C-40307-4.6] p 2866 N94-25809
Study on neutron activation analysis
[DE93-632191] p 3017 N94-26116

AIR TO AIR REFUELING
Manned mission to Mars with periodic refueling from electrically propelled tankers p 2689 N94-25670
Design of a refueling tanker delivering liquid hydrogen
p 2671 N94-25717

AIR TRAFFIC
Air traffic controller working memory: Considerations in air traffic control tactical operations
[AD-A273722] p 2664 N94-26197
Rotorcraft low altitude IFR benefit/cost analysis: Conclusions and recommendations
[AD-A274241] p 2665 N94-26826
Lufthansa Yearbook 1992
[DSK-9734-H-92] p 2660 N94-28230
The single European market and air traffic chances and risks p 2660 N94-28231
Deregulation of air traffic in America: A model to be initiated? p 2661 N94-28232
Air traffic of the European Community with European neighbors p 2661 N94-28233
The advantages of the location Germany must not be jeopardized in air traffic p 2661 N94-28236
Air traffic administration enroute to Europe
p 2661 N94-28238
Air traffic in recession p 2662 N94-28240
German-American relations in air traffic are to be criticized p 2662 N94-28241

AIR TRAFFIC CONTROL
Air traffic controller working memory: Considerations in air traffic control tactical operations
[AD-A273722] p 2664 N94-26197
Rotorcraft low altitude IFR benefit/cost analysis: Conclusions and recommendations
[AD-A274241] p 2665 N94-26826
An investigation of air transportation technology at the Massachusetts Institute of Technology, 1992-1993
p 2641 N94-27285
Air traffic management as principled negotiation between intelligent agents p 2643 N94-27297
Optical communications for transport aircraft
p 2643 N94-27298
Aircraft accident report: Runway departure following landing American Airlines flight 102, McDonnell Douglas DC-10-30, N139AA, Dallas/Fort Worth International Airport, Texas, April 14, 1993
[PB94-910402] p 2660 N94-27766
Refinement for fault-tolerance: An aircraft hand-off protocol
[NASA-CR-195697] p 2666 N94-27768
Special investigation report: Safety issues related to wake vortex encounters during visual approach to landing
[PB94-917002] p 2660 N94-27881
A sky above Europe p 2661 N94-28234

AIR TRAFFIC CONTROLLERS (PERSONNEL)
Airborne data link operational evaluation test plan
[AD-A274096] p 2664 N94-25788
Air traffic controller working memory: Considerations in air traffic control tactical operations
[AD-A273722] p 2664 N94-26197
Validation of the Federal Aviation Administration air traffic control specialist pre-training screen
[DOT/FAA/AM-94/4] p 2938 N94-26600

AIR TRANSPORTATION
A constitutive model for layered wire mesh and aramid cloth fabric
[DE94-003275] p 2708 N94-26796
FAA/NASA Joint University Program for Air Transportation Research, 1992-1993
[NASA-CP-3246] p 2641 N94-27284
An investigation of air transportation technology at the Massachusetts Institute of Technology, 1992-1993
p 2641 N94-27285
Investigation of air transportation technology at Ohio University, 1992-1993 p 2642 N94-27288
Investigation of air transportation technology at Princeton University, 1992-1993 p 2643 N94-27294
Methodology development of forecasting inter-regional air transport demand in China
[DLR-FB-93-24] p 2660 N94-27746
The 1993 Federal Aviation Administration plan for research, engineering and development
p 2643 N94-27960
Air traffic of the European Community with European neighbors p 2661 N94-28233
Lufthansa facing the single European market
p 2661 N94-28237
Integrators: A challenge for air cargo
p 2662 N94-28244
Powerful selling and sales strategy
p 2662 N94-28245
Lufthansa and Europe p 2663 N94-28247

AIR WATER INTERACTIONS
Development and testing of the Coupled Ocean/Atmosphere Mesoscale Prediction System (COAMPS)
[AD-A273925] p 2892 N94-25793
Conversion of the CLUSE model for applications over open ocean
[AD-A273750] p 2893 N94-26013
Interpreting the implied meridional oceanic energy transport in AMIP
[DE94-001538] p 2898 N94-26072

Meeting of the Eighth Session of the Scientific Advisory Committee of the World Climate Impact Assessment and Response Strategies Programme
[DE93-633954] p 2866 N94-26163

The numerical simulation of marine boundary layer clouds
[AD-A273669] p 2894 N94-26195

Differentiating the role of land surface variability and cloudiness variability on global energy transport within the atmosphere and oceans
[NASA-CR-195229] p 2847 N94-26222

Analysis and interpretation of the meteorology of the 1988 coastal transition zone experiment
[AD-A274710] p 2894 N94-26431

The NOGAPS ten year AMIP integration
[AD-A274332] p 2900 N94-26887

An experimental study of plunging liquid jet induced air carryunder and dispersion
[AD-A274414] p 2794 N94-26979

Acoustic bubble sizing, using active and passive techniques to compare ambient and entrained populations
[ISVR-TR-229] p 2807 N94-28172

Asia-Pacific Seminar on Global Change Research Cooperation
[JTN-94-80517] p 2871 N94-28268

Cooperative research projects on satellite remote sensing for the hydrological subjects
p 2853 N94-28270

An oceanographical observation in the Western Pacific and international cooperations p 2872 N94-28272

AIRBORNE EQUIPMENT

MODIS airborne simulator visible and near-infrared calibration, 1992 ASTEX field experiment. Calibration version: ASTEX King 1.0
[NASA-TM-104599] p 2897 N94-28179

AIRBORNE LASERS

The development of Cr, Tm, Ho:YAG lasers for airborne lidar
[AD-A274895] p 2816 N94-26178

AIRBORNE RADAR

A comparative evaluation of SAR and SLAR
[DE94-002922] p 2848 N94-26277

AIRBORNE/SPACEBORNE COMPUTERS

Technology drivers for flight telerobotic system software p 2684 N94-26289

Real-Time Embedded Processing for Space Applications
[ISBN-2-85428-335-X] p 2948 N94-26713

Computing in space: Issues and answers
p 2948 N94-26714

Development of a MIL-STD-1750 microprocessor system for space applications p 2949 N94-26715

On-board computer for control subsystem of satellite
p 2949 N94-26716

High performance flight computer developed for deep space applications p 2949 N94-26718

Qualified manufacturing and interoperability for space applications p 2949 N94-26719

Fault tolerant real-time processing system for space use p 2949 N94-26720

Design principles of onboard management of a Sun synchronous satellite p 2950 N94-26722

NASA's spacecraft data system p 2950 N94-26723

The Ariane 5 data management system
p 2950 N94-26724

PRONAOS flight software: A real-time application for a balloonborne scientific gondola p 2950 N94-26725

MATRA Marconi Space: The Silex on-board processor and on-board software p 2950 N94-26726

On-board software for the JET-X telescope on the Spectrum-X mission p 2951 N94-26727

Early real-time performance measurements on the Columbus processor system p 2952 N94-26736

Test of onboard real time applications (LICE (tm))
p 2952 N94-26737

Developing with Ada using HOOD design methodology
p 2953 N94-26741

Ada reusable software for satellite on-board data handling p 2953 N94-26743

Center for space microelectronics technology
[NASA-CR-195282] p 2786 N94-27574

AIRCRAFT ACCIDENT INVESTIGATION

Aircraft accident report: Runway departure following landing American Airlines flight 102, McDonnell Douglas DC-10-30, N139AA, Dallas/Fort Worth International Airport, Texas, April 14, 1993
[PB94-910402] p 2660 N94-27766

AIRCRAFT ACCIDENTS

Impact of improved materials and cabin water spray on commuter aircraft postcrash fire survivability
[AD-A274421] p 2660 N94-27081

Aircraft accident report: Runway departure following landing American Airlines flight 102, McDonnell Douglas DC-10-30, N139AA, Dallas/Fort Worth International Airport, Texas, April 14, 1993
[PB94-910402] p 2660 N94-27766

Special investigation report: Safety issues related to wake vortex encounters during visual approach to landing
[PB94-917002] p 2660 N94-27881

AIRCRAFT ANTENNAS

Developments in the application of the geometrical theory of diffraction and computer graphics to aircraft inter-antenna coupling analysis
[ISBN-0-315-84643-7] p 2776 N94-27308

AIRCRAFT APPROACH SPACING

An investigation of air transportation technology at the Massachusetts Institute of Technology, 1992-1993
p 2641 N94-27285

AIRCRAFT COMPARTMENTS

Assessing the effects of Tuned Vibration Absorbers (TVAs) on interior cabin noise levels: A correlation between analytical acoustic predictions and flight test measurements p 2652 N94-28318

AIRCRAFT CONFIGURATIONS

Preliminary design of nine high speed civil transports
p 2671 N94-25710

Design optimization of high-speed proprotor aircraft
[NASA-TM-103988] p 2667 N94-26151

Analysis and optimization of preliminary aircraft configurations in relationship to emerging agility metrics
[NASA-CR-195228] p 2668 N94-26235

A technique for integrating engine cycle and aircraft configuration optimization
[NASA-CR-191602] p 2668 N94-26606

Application of the MBTEC Euler code to the Challenger and the CF-18 complete aircraft configurations
p 2653 N94-28324

AIRCRAFT CONSTRUCTION MATERIALS

A revolutionary approach to composite construction and flight management systems for small, general aviation airplanes p 2671 N94-25714

X ray computed tomography for emerging aerospace materials and processes development
[AD-A273721] p 2705 N94-25779

NASA Lewis Research Center lean-, rich-burn materials test burner rig
[NASA-CR-194437] p 2680 N94-26141

Experimental study of the angled crack in GLARE 3
[PB94-126554] p 2669 N94-26954

Development of fibre-metal laminates, ARALL and GLARE, new fatigue resistant materials
[PB94-126471] p 2669 N94-26969

Thermoplastic or thermosetting composites in aircrafts
[PB94-123809] p 2710 N94-27253

Composite leading edge/spar member for an aircraft control surface
[CA-PATENT-1-325-765] p 2669 N94-27273

Fracture toughness and crack resistance of damage tolerant and high strength Al-Li alloys
[NLR-TP-91249-U] p 2743 N94-27795

Status and prospects for aluminium-lithium alloys in aircraft structures
[NLR-TP-92193-U] p 2743 N94-27797

Development of methodologies for the estimation of thermal properties associated with aerospace vehicles
p 2846 N94-27920

AIRCRAFT CONTROL

The application of a C(star) flight control law to large civil transport aircraft
[CRANFIELD-AERO-9303] p 2676 N94-25640

Report on a visit to the Arvin/Calspan Corporation, Buffalo, New York, USA, September 1992
[CRANFIELD-AERO-9305] p 2676 N94-25653

Design of a flight controller for an unmanned research vehicle with control surface failures using quantitative feedback theory
[AD-A274049] p 2677 N94-25833

Aircraft maneuvers for the evaluation of flying qualities and agility. Volume 3: Simulation data
[AD-A273814] p 2667 N94-25961

Analysis and optimization of preliminary aircraft configurations in relationship to emerging agility metrics
[NASA-CR-195228] p 2668 N94-26235

Research in robust control for hypersonic aircraft
[NASA-CR-195250] p 2678 N94-26821

Standardization of aircraft control and performance symbology on the USAF head-up display
[AD-A274283] p 2673 N94-26989

Reconfigurable aircraft stick control
[AD-D016043] p 2681 N94-27113

Design and flight test of the Propulsion Controlled Aircraft (PCA) flight control system on the NASA F-15 test aircraft
[NASA-CR-186028] p 2674 N94-27432

Aircraft accident report: Runway departure following landing American Airlines flight 102, McDonnell Douglas DC-10-30, N139AA, Dallas/Fort Worth International Airport, Texas, April 14, 1993
[PB94-910402] p 2660 N94-27766

Comparison of performance in simulator flight among subjects with different simulator experiences
p 2933 N94-27943

First experimental assessment of RCS plume-flow field interaction on Hermes leading edge thruster configuration p 2703 N94-28032

AIRCRAFT DESIGN

Proceedings of the 8th Annual Summer Conference: NASA/USRA Advanced Design Program
[NASA-CR-195118] p 3075 N94-25665

Design of the advanced regional aircraft, the DART-75
p 2671 N94-25708

Preliminary design of nine high speed civil transports
p 2671 N94-25710

Supercruiser Arrow HS-8 p 2671 N94-25711

Tesseract supersonic business transport
p 2671 N94-25713

A revolutionary approach to composite construction and flight management systems for small, general aviation airplanes p 2671 N94-25714

Design study to simulate the development of a commercial freight transportation system
p 2671 N94-25715

The design of four hypersonic reconnaissance aircraft
p 2671 N94-25716

Design of a refueling tanker delivering liquid hydrogen
p 2671 N94-25717

The design of a long-range megatransport aircraft
p 2671 N94-25718

Solar powered multipurpose remotely powered aircraft
p 2671 N94-25719

EGADS: A microcomputer program for estimating the aerodynamic performance of general aviation aircraft
[NASA-TM-104013] p 2667 N94-26091

Design optimization of high-speed proprotor aircraft
[NASA-TM-103988] p 2667 N94-26151

A technique for integrating engine cycle and aircraft configuration optimization
[NASA-CR-191602] p 2668 N94-26606

A multivariate anthropometric method for crew station design: Abridged
[AD-A274588] p 2941 N94-26984

Proceedings of the Non-Linear Aero Prediction Requirements Workshop
[NASA-CP-10138] p 2670 N94-27439

Techniques to improve maneuver stability characteristics of a nonlinear wide-body transport airplane in cruise flight
[NASA-TM-4521] p 2679 N94-27660

Wing design for a civil tiltrotor transport aircraft: A preliminary study p 2671 N94-27917

Abstracts of papers presented at the 4th CASI Aerodynamics Symposium
[ISBN-0-920203-01-9] p 2651 N94-28315

The deterministic power-spectral-density-method for nonlinear systems
[AD-B179687] p 3001 N94-28353

AIRCRAFT ENGINES

Evaluation of moderate angle of attack roll of a dual engine, thrust vectoring aircraft using quantitative feedback theory
[AD-A274118] p 2667 N94-25905

Aircraft turbine engine reliability and inspection investigations
[AD-A274860] p 2673 N94-26176

Effects of expected-value information and display format on recognition of aircraft subsystem abnormalities
[NASA-TP-3395] p 2673 N94-27882

Transient model applications. 1: Compressor heat soak/clearance effects modeling p 2828 N94-28048

Transient model applications. 3: Transient engine simulation and analysis of an ice ingestion test
p 2829 N94-28050

AIRCRAFT GUIDANCE

Ground station siting considerations for DGPS
p 2642 N94-27293

AIRCRAFT HAZARDS

The relationship of an integral wind shear hazard to aircraft performance limitations
[NASA-TM-109080] p 2677 N94-26593

AIRCRAFT INDUSTRY

Future of aerospace
[PB94-120185] p 2669 N94-26906

AIRCRAFT LANDING

The application of a C(star) flight control law to large civil transport aircraft
[CRANFIELD-AERO-9303] p 2676 N94-25640

Methods for experimentally determining commercial jet aircraft landing parameters from video image data
[AD-A274207] p 2669 N94-27105

Optimal control of helicopters following power failure
[NAL-TR-1190] p 2678 N94-27206
Ground station siting considerations for DGPS
p 2642 N94-27293
A study of jet effect and ground effect interference on a STOL fighter p 2671 N94-28034

AIRCRAFT MAINTENANCE
Aircraft turbine engine reliability and inspection investigations
[AD-A274860] p 2673 N94-26176
Effects of plastic media blasting on aircraft skin
[AD-A274817] p 2668 N94-26488
An investigation into the aerodynamic effects of wing patches
[ISBN-0-315-84121-4] p 2646 N94-26672
Know-how export: Lufthansa technology at Shannon
p 2663 N94-28248
Preliminary assessment of aerodynamic effects of wing repair patches p 2657 N94-28346

AIRCRAFT MANEUVERS
Aircraft maneuvers for the evaluation of flying qualities and agility. Volume 1: Maneuver development process and initial maneuver set
[AD-A273913] p 2666 N94-25590
Aircraft maneuvers for the evaluation of flying qualities and agility. Volume 3: Simulation data
[AD-A273814] p 2667 N94-25961
Automation of formation flight control
[AD-A274137] p 2678 N94-27132

AIRCRAFT MODELS
Evaluation of moderate angle of attack roll of a dual engine, thrust vectoring aircraft using quantitative feedback theory
[AD-A274118] p 2667 N94-25905
Investigation of the aerodynamic environment for an advanced lightweight rotor in forward flight. Volume 4: Laser velocimeter wake data, advance ratio of 0.037
[NASA-TM-109040-VOL-4] p 2645 N94-26483
Investigation of the aerodynamic environment for an advanced lightweight rotor in forward flight. Volume 1: Laser velocimeter inflow data, advance ratio of 0.37, thrust coefficient of 0.0081 and hover tip speed of 603 feet/second
[NASA-TM-109040-VOL-1] p 2645 N94-26489
Investigation of the aerodynamic environment for an advanced lightweight rotor in forward flight. Volume 2: Laser velocimeter inflow data, advance ratio of 0.37, thrust coefficient of 0.0064 and hover tip speed of 710 feet/second
[NASA-TM-109040-VOL-2] p 2645 N94-26492
Investigation of the aerodynamic environment for an advanced lightweight rotor in forward flight. Volume 3: Laser velocimeter inflow data, advance ratio of 0.37, thrust coefficient of 0.0064 and hover tip speed of 603 feet/second
[NASA-TM-109040-VOL-3] p 2645 N94-26497
Experimental apparatus for optimization of flap position for a three-element airfoil model p 2682 N94-27912
Transient model applications. 1: Compressor heat soak/clearance effects modeling p 2828 N94-28048

AIRCRAFT NOISE
INM, Integrated Noise Model. Version 4.11: User's guide, supplement
[AD-A273885] p 3009 N94-25731
Assessing the effects of Tuned Vibration Absorbers (TVAs) on interior cabin noise levels: A correlation between analytical acoustic predictions and flight test measurements p 2652 N94-28318

AIRCRAFT PARTS
Methods in unsteady aerodynamics
[DLR-FB-93-21] p 2648 N94-27741

AIRCRAFT PERFORMANCE
EGADS: A microcomputer program for estimating the aerodynamic performance of general aviation aircraft
[NASA-TM-104013] p 2667 N94-26091
Analysis and optimization of preliminary aircraft configurations in relationship to emerging agility metrics
[NASA-CR-195228] p 2668 N94-26235
Investigation of the aerodynamic environment for an advanced lightweight rotor in forward flight. Volume 4: Laser velocimeter wake data, advance ratio of 0.037
[NASA-TM-109040-VOL-4] p 2645 N94-26483
Investigation of the aerodynamic environment for an advanced lightweight rotor in forward flight. Volume 1: Laser velocimeter inflow data, advance ratio of 0.37, thrust coefficient of 0.0081 and hover tip speed of 603 feet/second
[NASA-TM-109040-VOL-1] p 2645 N94-26489
Investigation of the aerodynamic environment for an advanced lightweight rotor in forward flight. Volume 2: Laser velocimeter inflow data, advance ratio of 0.37, thrust coefficient of 0.0064 and hover tip speed of 710 feet/second
[NASA-TM-109040-VOL-2] p 2645 N94-26492
Investigation of the aerodynamic environment for an advanced lightweight rotor in forward flight. Volume 3: Laser velocimeter inflow data, advance ratio of 0.37, thrust coefficient of 0.0064 and hover tip speed of 603 feet/second
[NASA-TM-109040-VOL-3] p 2645 N94-26497
The relationship of an integral wind shear hazard to aircraft performance limitations
[NASA-TM-109080] p 2677 N94-26593
A technique for integrating engine cycle and aircraft configuration optimization
[NASA-CR-191602] p 2668 N94-26606
Experiments into the scaling parameters required for exhaust gas ingestion testing of vertical landing aircraft
p 2671 N94-28017
Transitional flight characteristics of a geometrically simplified STOVL model p 2672 N94-28035

AIRCRAFT PILOTS
A critical analysis of workload predictions generated by multiple resource theory during early crewstation design
[AD-A274804] p 2941 N94-26339
US Army aviation epidemiology data registry: Incidence and outcomes of aviator flying evaluation boards
[AD-A274711] p 2910 N94-26432
Female combat helicopter pilot selection criteria
[AD-A273935] p 2938 N94-26749
Comparison of performance in simulator flight among subjects with different simulator experiences
p 2933 N94-27943
Evaluation of near-infrared spectrophotometric method for individual tolerance to +Gz acceleration
p 2933 N94-27944

AIRCRAFT POWER SUPPLIES
Bipolar lead-acid batteries for electrical actuation applications p 2864 N94-28134

AIRCRAFT PRODUCTION
Future of aerospace
[PB94-120185] p 2669 N94-26906

AIRCRAFT RELIABILITY
Engine starting and stopping p 2828 N94-28047
A340 testing p 2662 N94-28242
After thirty years: Farewell of Europa jet
p 2663 N94-28249
A symbol of reliability: Ju 52 p 2663 N94-28250

AIRCRAFT SAFETY
Soft ground arresting system for airports
[DOT/FAA/CT-93/80] p 2680 N94-26202
Impact of improved materials and cabin water spray on commuter aircraft postcrash fire survivability
[AD-A274421] p 2660 N94-27081
Aircraft accident report: Runway departure following landing American Airlines flight 102, McDonnell Douglas DC-10-30, N139AA, Dallas/Fort Worth International Airport, Texas, April 14, 1993
[PB94-910402] p 2660 N94-27766
Special investigation report: Safety issues related to wake vortex encounters during visual approach to landing
[PB94-917002] p 2660 N94-27881
The 1993 Federal Aviation Administration plan for research, engineering and development
p 2643 N94-27960

AIRCRAFT STABILITY
Report on a visit to the Arvin/Calspan Corporation, Buffalo, New York, USA, September 1992
[CRANFIELD-AERO-9305] p 2676 N94-25653
Linear modeling of rotorcraft for stability analysis and preliminary design
[AD-A274869] p 2677 N94-26192

AIRCRAFT STRUCTURES
Formulae for the buckling of simply-supported corrugated panels of orthotropic material under shear load
[PB94-126547] p 2840 N94-26911
Design and test of postbuckled stiffened curved plates: A literature survey
[PB94-126521] p 2840 N94-26961
Smart structures, an overview
[AD-A274147] p 2987 N94-27093
Impact tests on fibre metal laminates under a tensile load
[PB94-126570] p 2710 N94-27201
Multidisciplinary aeroelastic analysis of a generic hypersonic vehicle
[NASA-TM-4544] p 2691 N94-27868
Development of methodologies for the estimation of thermal properties associated with aerospace vehicles
p 2846 N94-27920
Advanced metallic exhaust impinged structural concepts demonstration p 2832 N94-28209

AIRCRAFT TIRES
Aircraft wheel life assessment
[AD-A274378] p 2823 N94-26976

AIRCRAFT WAKES
Special investigation report: Safety issues related to wake vortex encounters during visual approach to landing
[PB94-917002] p 2660 N94-27881
Calculation of unsteady incompressible inviscid flow about wings and bodies using CANAERO-T panel model
p 2655 N94-28334
Drag prediction by wake integrals using 3-D multi-grid Euler method (MGAERO) p 2655 N94-28335

AIRFOIL OSCILLATIONS
Methods in unsteady aerodynamics
[DLR-FB-93-21] p 2648 N94-27741

AIRFOIL PROFILES
Calculation of viscous drag of two low angle of attack supercritical profiles
[FFA-TN-1984-22] p 2644 N94-26104
Comments regarding two upwind methods for solving two-dimensional external flows using unstructured grids
[NASA-TM-109078] p 2644 N94-26154
An investigation of the effects of the high maximum-thickness-to-chord ratio on the performance of nozzle guide vanes in a transonic planar cascade
[ISBN-0-315-84107-9] p 2793 N94-26671
The renewing of the test section of the NAL transonic wind tunnel. Part 1: Reconstruction of the 1st corner turning vanes and aerodynamic stress measurement
[NAL-TM-651] p 2681 N94-27247
Effect of surface finish on turbine airfoil cascade losses p 2652 N94-28320
Potential flow modelling of airfoil stall
p 2654 N94-28332
Viscous airfoil computations using adaptive structured grids p 2655 N94-28337
Solution of the Euler equations using unstructured grids p 2656 N94-28338
A study of blunt trailing edge airfoils using the Navier Stokes code: ARC2D p 2656 N94-28340
Thin-layer Navier-Stokes computations for multi-element airfoils p 2656 N94-28341

AIRFOILS
A finite wake theory for two-dimensional rotary wing unsteady aerodynamics
[AD-A274921] p 2645 N94-26535
Influence of the transonic doublet in the farfield of a lifting airfoil
[IAR-AN-78] p 2647 N94-26702
Control of leading-edge separation on an airfoil by localized excitation
[DLR-FB-93-16] p 2647 N94-27592
Investigation of aerodynamic design issues with regions of separated flow p 2658 N94-27902
Experimental apparatus for optimization of flap position for a three-element airfoil model p 2682 N94-27912
Program for calculation of maximum lift coefficient of plain aerofoils and wings at subsonic speeds
[ESDU-93015] p 2649 N94-28076
Wing lift increment at zero angle of attack due to deployment of single-slotted flaps at low speeds
[ESDU-93019] p 2649 N94-28140
Abstracts of papers presented at the 4th CASI Aerodynamics Symposium
[ISBN-0-920203-01-9] p 2651 N94-28315

AIRFRAMES
Damage tolerance assessment handbook. Volume 1: Introduction fracture mechanics fatigue crack propagation
[AD-A274777] p 2836 N94-26186
Damage tolerance assessment handbook. Volume 2: Aircraft damage tolerance evaluation
[AD-A274778] p 2837 N94-26357
A parametric sensitivity study for single-stage-to-orbit hypersonic vehicles using trajectory optimization
[NASA-CR-195703] p 2697 N94-27789
Know-how export: Lufthansa technology at Shannon
p 2663 N94-28248

AIRGLOW
Photochemical processes and the atmospheric airglow emissions of OH and Na in the mesospheric region
[INPE-5380-PUD/050] p 2882 N94-27334
Solar and airglow measurements aboard the two suborbital flights NASA 36.098 and 36.107
[NASA-CR-195279] p 2882 N94-27380

AIRLINE OPERATIONS
Lufthansa Yearbook 1992
[DSK-9734-H-92] p 2660 N94-28230
The single European market and air traffic chances and risks p 2660 N94-28231
Deregulation of air traffic in America: A model to be initiated? p 2661 N94-28232
The advantages of the location Germany must not be jeopardized in air traffic p 2661 N94-28236
Lufthansa facing the single European market
p 2661 N94-28237
Munich Airport: The new Lufthansa hub
p 2662 N94-28239

Air traffic in recession p 2662 N94-28240

German-American relations in air traffic are to be criticized p 2662 N94-28241

Integrators: A challenge for air cargo p 2662 N94-28244

Powerful selling and sales strategy p 2662 N94-28245

Lufthansa long range services: More simplicity p 2663 N94-28246

Lufthansa and Europe p 2663 N94-28247

Know-how export: Lufthansa technology at Shannon p 2663 N94-28248

After thirty years: Farewell of Europa jet p 2663 N94-28249

AIRPORTS

INM, Integrated Noise Model. Version 4.11: User's guide, supplement
[AD-A273885] p 3009 N94-25731

Machine intelligent gust front algorithm
[AD-A273695] p 2680 N94-26196

Conifer tree influence on Digital Terrain Elevation Data (DTED): A case study at Dulles International Airport
[AD-A274213] p 2849 N94-27069

The advantages of the location Germany must not be jeopardized in air traffic p 2661 N94-28236

Munich Airport: The new Lufthansa hub p 2662 N94-28239

ALASKA

Remote sensing of global snowpack energy and mass balance: In-situ measurements on the snow of interior and Arctic Alaska
[NASA-CR-195704] p 2851 N94-27787

ALCOHOLS

Reactivity of nitrate radical (NO3) toward organic compounds p 2704 N94-27387

Thermal conductivity of liquid aliphatic alcohols
[ESDU-93008] p 2720 N94-28058

ALDEHYDES

Reactivity of nitrate radical (NO3) toward organic compounds p 2704 N94-27387

ALERTNESS

Effects of methamphetamine on vigilance and tracking during extended wakefulness
[AD-A274896] p 2909 N94-26179

Brain wave correlates of attentional states: Event related potentials and quantitative EEG analysis during performance of cognitive and perceptual tasks p 2940 N94-27901

ALGAE

Mapping coastal habitats using an imaging spectrometer
[ISBN-0-315-84362-4] p 2848 N94-26664

Measuring variation in ecosystem sensitivity to stress
[AD-A274232] p 2868 N94-26817

ALGEBRA

Duality for multiparametric quantum GL(n) and for a Lorentz quantum group
[DE93-613048] p 3005 N94-25868

Some properties of generalized biregular functions with values in a Clifford algebra
[DE93-613024] p 2991 N94-25881

Matrix near rings and pseudo distributivity
[DE94-601505] p 2992 N94-26366

The massless representations of the conformal quantum algebra
[DE94-601555] p 3006 N94-26413

Gauging of Chern-Simons p-Barnes
[DE94-601553] p 2993 N94-26425

Finite dimensional representations of the quantum superalgebra U(sub q)(gl(3/2))
[DE93-634303] p 2993 N94-26440

Process algebra of concurrent constraint programming
[PB94-126695] p 2966 N94-26919

Spaces of algebraic cycles
[PB94-124369] p 2996 N94-26993

Modal logic, transition systems and processes
[CWI-CS-R9321] p 2970 N94-27549

Expressiveness results for process algebras
[CWI-CS-R9301] p 3000 N94-27577

A method for obtaining quantum doubles from the Yang-Baxter R-matrices
[DE94-606300] p 3001 N94-27846

Fields and potentials in general uniaxial bianisotropic media I. Axial sources
[PB94-132875] p 2778 N94-28379

ALGORITHMS

Characteristics and control response of the TOPAZ 2 reactor system real-time dynamic simulator
[DE94-003788] p 2699 N94-25600

System software and tools for high performance computing environments: A report on the findings of the Pasadena Workshop
[DE94-003918] p 2956 N94-25602

Calculation of a 3-D pose of a known object in a single perspective view
[VTT-PUBS-122] p 2957 N94-25642

Detection geometry and reconstruction error in magnetic source imaging
[DE94-004012] p 2809 N94-25662

An optimal constrained linear inverse method for magnetic source imaging
[DE94-004014] p 2957 N94-25663

A logarithmic barrier cutting plane method for convex programming
[REPT-93-43] p 2957 N94-25761

A note on central cutting plane methods for convex programming
[REPT-93-44] p 2958 N94-25762

A simplicial approach to integer programming, part 2
[REPT-93-47-PT-2] p 2958 N94-25764

Filtering, coding, and compression with Malvar wavelets
[AD-A274055] p 2780 N94-25770

Research on primal-dual interior point algorithms for mathematical programming
[DE94-003982] p 2959 N94-25821

Algorithms of the vertex coordinate reconstruction for straight tracks of short-lived particles
[DE93-616661] p 3015 N94-25919

Emerging technologies
[DE94-003022] p 3102 N94-26023

Fast parallel algorithms for short-range molecular dynamics
[DE93-018519] p 3016 N94-26033

An algorithm to find the intersection of two convex polygons
[AD-A274722] p 2961 N94-26148

Machine intelligent gust front algorithm
[AD-A273695] p 2680 N94-26196

The general pickup and delivery problem
[MEMO-COSOR-92-44] p 2992 N94-26226

One machine scheduling with delayed precedence constraints
[PB93-237626] p 3094 N94-26314

The Chaco user's guide
[DE94-003669] p 2962 N94-26370

On the reliability of a window least squares algorithm
[DE93-634666] p 2962 N94-26386

Adaptive path planning in changing environments
[DE94-003269] p 2985 N94-26462

A doubly logarithmic communication algorithm for the Completely Connected Optical Communication Parallel Computer
[DE93-019408] p 2980 N94-26473

MIMO recursive least squares control algorithm for the AN/FPN-44A Loran-C transmitter
[AD-A274820] p 2664 N94-26493

Delta f Algorithm
[DE94-003120] p 2963 N94-26521

Integrating automata with genetic algorithms in order to provide adaptive operators
[ISBN-0-315-84094-3] p 2964 N94-26663

Design and implementation of a multiprocessor for DSP and communications systems algorithm evaluation
[ISBN-0-315-84128-1] p 2980 N94-26674

A real-time executive implementing priority inheritance protocols p 2952 N94-26733

Scheduling approaches with Ada p 2952 N94-26734

Combatting inherent vulnerabilities of CFAR algorithms and a new robust CFAR design
[AD-A274918] p 2770 N94-26751

Computation of non-isentropic internal flows with variable density
[AD-A274848] p 2794 N94-26801

Nested Krylov methods based on GCR
[PB94-125317] p 2995 N94-26818

The Hough transform algorithm for sea ice lead analysis: An evaluation
[AD-A274535] p 2899 N94-26853

New mixed integer algorithm for classification and placement of measurements in process flow networks
[PB94-126752] p 2966 N94-26921

Prewhitening of colored noise fields for detection of threshold sources
[AD-A274346] p 3010 N94-26923

An algorithm for determination of bearing health through automated vibration monitoring
[AD-A274591] p 2823 N94-26986

What can we learn from genetic algorithms: A new perspective for search methods
[PB94-125234] p 2967 N94-26997

Grid-independent convergence based on preconditioning techniques
[PB94-125358] p 2997 N94-27000

Symbolic model checking for sequential circuit verification
[AD-A274375] p 2786 N94-27061

Parametric time-scale methods in signal analysis
[AD-A274212] p 2773 N94-27068

Implementation and performance of a domain decomposition algorithm in Sisal
[DE94-002012] p 2981 N94-27092

Parallel string matching algorithms
[AD-A274502] p 3100 N94-27164

A partitioning and redundancy model for wafer-scale integrated circuits p 2955 N94-27195

Fast methods for computation with algebraic numbers
[ISBN-0-315-57888-2] p 2998 N94-27269

Developments in the application of the geometrical theory of diffraction and computer graphics to aircraft inter-antenna coupling analysis
[ISBN-0-315-84643-7] p 2776 N94-27308

Motion analysis from a sequence of range images
[ISBN-0-315-84684-4] p 2969 N94-27311

Parallel algorithm for dominant points correspondences in robot binocular stereo vision p 2686 N94-27364

Saving comparisons in the Crochemore-Perrin string matching algorithm
[CWI-CS-R9322] p 2971 N94-27550

Efficient massively parallel simulation of dynamic channel assignment schemes for wireless cellular communications
[NASA-CR-191593] p 2971 N94-27558

Fast parallel permutation algorithms
[CWI-CS-R9303] p 2982 N94-27579

High performance computing in chemistry and massively parallel computers: A simple transition?
[DE94-004318] p 2982 N94-27600

A fast Fourier transform radix-2 complex butterfly with built-in self-test
[ISBN-0-315-84139-7] p 2982 N94-27649

The PRISM project: Infrastructure and algorithms for parallel eigensolvers
[DE94-005125] p 2973 N94-27717

Inverted pendulum control apparatus using transputers
[DE94-701224] p 2973 N94-27732

A strange application of Kolmogorov complexity
[CWI-CS-R9328] p 2973 N94-27737

Time-step enlargement and optimal smoothing in Runge-Kutta time-integration algorithms by implicit and explicit smoothing
[NLR-TP-92221-U] p 2798 N94-27799

Ice surface temperature retrieval from AVHRR, ATSR, and passive microwave satellite data: Algorithm development and application
[NASA-CR-195276] p 2851 N94-27849

An optimization program based on the method of feasible directions: Theory and users guide
[NASA-TM-4552] p 2845 N94-27865

Thunderstorm Hypothesis Reasoner
[NASA-CR-195714] p 2897 N94-27884

A parallel multigrid algorithm for solving the Navier-Stokes equations on a transputer system
[PREPRINT-699] p 2807 N94-28099

Image compression software for the SOHO LASCO and EIT experiments p 2945 N94-28253

Performance considerations for the application of the lossless browse and residual model p 2946 N94-28256

A comparison of spectral decorrelation techniques and performance evaluation metrics for a wavelet-based, multispectral data compression algorithm p 2946 N94-28258

A comparative study of SAR data compression schemes p 2946 N94-28259

Perceptual compression of magnitude-detected synthetic aperture radar imagery p 2946 N94-28260

Compression of multispectral Landsat imagery using the Embedded Zerotree Wavelet (EZW) algorithm p 2947 N94-28261

Techniques for accurately solving unsteady shock waves and contact discontinuities p 2656 N94-28342

Efficient rebalancing of tree-type main memory dictionaries
[PB94-133105] p 3100 N94-28396

ALIGNMENT

Alignment of the Amsterdam Pulse Stretcher (AmPS)
[MTG-93-02] p 2809 N94-25637

ALIPHATIC COMPOUNDS

Thermal conductivity of liquid aliphatic alcohols
[ESDU-93008] p 2720 N94-28058

Vapour pressures and critical points of liquids: Aliphatic and cyclic ketones
[ESDU-93009] p 2720 N94-28059

Orthobaric densities and molar volumes of liquids: Aliphatic and cyclic ketones
[ESDU-93010] p 2720 N94-28060

ALIPHATIC HYDROCARBONS

Measurement of viscosity, density, and gas solubility of refrigerant blends in selected synthetic lubricants
[DE94-003609] p 2713 N94-25934

Computational studies of energetic organic molecules
[AD-A274726] p 3019 N94-26172

Transition metal activation and functionalization of carbon-hydrogen bonds
[DE94-003650] p 2715 N94-26369

ALKALI METALS

Calculations of asymmetries in electron-alkali scattering
[DE94-601816] p 3023 N94-26945

Experimental studies of pressurised fluidised bed combustion at Helsinki University of Technology, 1991-1992
[PB94-133063] p 2876 N94-28394

ALKENES

Reactivity of nitrate radical (NO3) toward organic compounds p 2704 N94-27387

ALKYL COMPOUNDS

Phosphazene-containing amine as curing agent for phthalonitrile-base polymer
[AD-D016029] p 2755 N94-27147

ALKYNES

The coordination and atom transfer chemistry of titanium porphyrin complexes
[DE94-003091] p 2704 N94-26779

ALLOTROPY

Structure and phase transformations in uranium metal
[DE94-003892] p 2732 N94-26004

ALLOYING

Issues for conversion coating of aluminum alloys with hydrotalcite
[DE94-003804] p 2732 N94-25819

The influence of weld metal alloying additions to extend the heat input range for the submerged arc welding of high strength steels
[AD-A274284] p 2738 N94-26679

Formation of glassy Pd-Ni-P alloys by mechanical alloying and their structure and thermal stability
p 2746 N94-28168

Study on the production of flaky amorphous alloy powders by impact flattening of atomized liquid droplets on a rapidly rotating wheel p 2746 N94-28169

ALLOYS

Bulletin of National Research Institute for Metals in Fiscal Year 1993, no. 14
[REPT-14] p 2722 N94-25544

Generalized perturbation method expansions of the total energy of an alloy
[DE94-003865] p 3055 N94-26238

A new materials data compilation can help in actinide phase-diagram research
[DE94-000797] p 3058 N94-26514

The Science Reports of the Research Institutes, Tohoku University. Series A: Physics, Chemistry, and Metallurgy. Volume 38, No. 1: Amorphous Materials 14
[JTN-94-80610] p 2744 N94-28158

ALPINE METEOROLOGY

Numerical modelling of precipitation over complex terrain
[ISBN-0-315-84327-6] p 2894 N94-26628

ALTERNATING CURRENT

Electromagnetic properties of a toroidal solenoid
[DE93-613032] p 2766 N94-25866

Classical solutions of Yang-Mills-Chern-Simons theory in 2+1 dimensions: A quasi-linear superposition
[DE93-634335] p 3006 N94-26270

Channel model for AC electric arc
[PB94-124591] p 2786 N94-27327

ALTERNATIVES

Proceedings of the symposium on current concepts and approaches on animal test alternatives
[AD-A273926] p 2900 N94-25593

ALTIMETERS

Digital Altimeter Setting Indicator (DASI) Operational Test and Evaluation (OT/E) operational test procedures
[AD-A274100] p 2672 N94-26030

ALUMINIDES

The processing of powder metallurgically produced near gamma-titanium aluminide
[ISBN-0-315-84018-8] p 2738 N94-26633

An investigation of the effect of surface impurities on the adsorption kinetics of hydrogen chemisorbed onto iron
[NASA-CR-195213] p 2716 N94-26643

Microstructure and mechanical behaviour of L1(2) titanium trialuminides
[ISBN-0-315-84488-4] p 2740 N94-27306

Current status of research and development on nickel and iron aluminides
[DE94-004247] p 2741 N94-27616

ALUMINUM

Issues for conversion coating of aluminum alloys with hydrotalcite
[DE94-003804] p 2732 N94-25819

Plasma surface cleaning using microwave plasmas
[DE94-002754] p 2713 N94-26014

Deviatoric stresses and plastic strain rates in strong shock waves for six metals
[DE94-002964] p 2733 N94-26022

Aluminum-ion sputtering from Al surfaces with very-low-energy ions
[REPT-A-2668] p 2733 N94-26073

Effects of post-fabrication processing on the tensile properties of centrifugally cast SiC particulate reinforced aluminum composites
[AD-A274865] p 2707 N94-26190

Effects of plastic media blasting on aircraft skin
[AD-A274817] p 2668 N94-26488

A constitutive model for layered wire mesh and aramid cloth fabric
[DE94-003275] p 2708 N94-26796

The electrochemical behavior of the Al3Fe intermetallic compound and localized corrosion of impure 1100 Al
[DE94-002037] p 2739 N94-26912

Experimental results of 40-kA Nb3Al conductor
[DE94-701207] p 2788 N94-27821

High Quality Aluminium Castings Conference
[PB94-133592] p 2747 N94-28359

Joining of fibre reinforced metal matrix composite materials
[PB94-132453] p 2712 N94-28376

Weldability aspects in the design and fabrication of aluminium structures subjected to fatigue loads. Part 1: Effect of welding on the structural integrity of joint types designed for repairing aluminium ship sections
[PB94-132487] p 2833 N94-28378

ALUMINUM ALLOYS

Study on production of materials with one direction solidification texture p 2727 N94-25572

Study on solidification of non-homogeneous melting/solidification materials p 2728 N94-25573

Study on improvement in physical analysis method of metallic materials p 2728 N94-25577

Issues for conversion coating of aluminum alloys with hydrotalcite
[DE94-003804] p 2732 N94-25819

An investigation of cavitation in a mechanically alloyed 15 volume percent SiCp/IN9021 aluminum composite
[DE94-003371] p 2748 N94-25959

Formation of three types of quasi-crystals in Al-Pd-Mg system
[REPT-A-2667] p 3053 N94-26071

Toward insulating quasicrystalline alloy in Al-Pd-Re icosahedral phase
[REPT-A-2666] p 2736 N94-26477

Effects of plastic media blasting on aircraft skin
[AD-A274817] p 2668 N94-26488

Study of precipitation and recrystallization in Al alloy 2519 by backscattered electron imaging methods
[AD-A274919] p 2736 N94-26533

Deformation twinning: Influence of strain rate
[DE94-002693] p 2738 N94-26621

Experimental study of the angled crack in GLARE 3
[PB94-126554] p 2669 N94-26954

Hot deformation behaviour of Si(p)/Al composites and their matrices and an Al-Mg-Si alloy
[ISBN-0-315-84699-2] p 2711 N94-27314

Process modelling of aluminium alloys. Modelling of the quench sensitivity of alloy AA6082
[PB94-124567] p 2741 N94-27325

Current status of research and development on nickel and iron aluminides
[DE94-004247] p 2741 N94-27616

Use of photostress and strain gages to analyze behavior of weldments
[NASA-CR-195269] p 2843 N94-27765

An anodic dissolution-based mechanism for the rapid cracking, pre-exposure phenomenon demonstrated by Al-Li-Cu alloys
[DE94-004798] p 2742 N94-27788

NASA-UVA light aerospace alloy and structures technology program (LA2ST)
[NASA-CR-195275] p 2844 N94-27851

An experimental investigation of fatigue damage in aluminum 2024-T3 alloys p 2747 N94-27900

The transition from stress corrosion cracking to corrosion fatigue in AA-7075 and AA-8090
[ISBN-0-315-59526-4] p 2744 N94-27950

Low strain behaviour of a particulate reinforced aluminum alloy
[ISBN-0-315-84906-1] p 2744 N94-27961

NMR study of quasicrystal Al(70)Pd(20)T(M10) alloy (T(M):Cr, Mn, Fe, and Co) p 2745 N94-28162

Mechanical behavior of amorphous alloys at elevated temperatures p 2746 N94-28167

Formation and high mechanical strength of Al-based alloys containing a nanoscale icosahedral phase as a main constituent p 2746 N94-28171

High Quality Aluminium Castings Conference
[PB94-133592] p 2747 N94-28359

Weldability aspects in the design and fabrication of aluminium structures subjected to fatigue loads. Part 2: Weldability of aluminium alloys using advanced MIG and TIG techniques. Effect of the weld bead geometrical factors on the fatigue behavior of the welded joint
[PB94-132446] p 2833 N94-28375

Weldability aspects in the design and fabrication of aluminium structures subjected to fatigue loads. Part 1: Effect of welding on the structural integrity of joint types designed for repairing aluminium ship sections
[PB94-132487] p 2833 N94-28378

ALUMINUM ARSENIDES

Polar optical oscillation modes in GaAs-based double heterostructures: Long wavelength limit
[DE94-601874] p 3062 N94-26897

ALUMINUM COMPOUNDS

Study on measurement and evaluation methods for superconductive characteristics p 2725 N94-25560

Study on variation of damage generation mechanism by fatigue on TiAl compounds due to different slip systems p 2729 N94-25579

ALUMINUM GALLIUM ARSENIDES

Optoelectronic technology consortium
[AD-A274595] p 3036 N94-26857

Thermally stable oxygen and nitrogen implant isolation of C-doped Al(0.35)Ga(0.65)As
[DE94-004799] p 3069 N94-27790

Dry etching process development for submicron and nanometer semiconductor devices
[PB94-133196] p 2788 N94-28357

ALUMINUM NITRIDES

Electron microscopy of AlN-SiC interfaces and solid solutions
[DE94-002449] p 3059 N94-26765

Nitride semiconductors for ultraviolet detection
[AD-A274246] p 3060 N94-26840

Pseudomorphic semiconducting heterostructures from combinations of AlN, GaN and selected SiC polytypes: Theoretical advancement and its coordination with experimental studies of nucleation, growth, characterization and device development
[AD-A274247] p 3061 N94-26841

Interface properties of wide bandgap semiconductor structures
[AD-A274356] p 3063 N94-27058

ALUMINUM OXIDES

Study on film generation phenomena by particle deposition p 2728 N94-25575

Fracture behavior of 20% Nb particulate reinforced alumina composite
[DE94-002830] p 2706 N94-26019

Examination of hardness, fracture toughness and microstructure in Al2O3-B4C binary ceramics
[PB94-124237] p 2755 N94-27158

Transparent polycrystalline body with high ultraviolet transmittance, process for making and applications thereof
[CA-PATENT-1325511] p 3066 N94-27276

Superconducting fibers made with yttrium and yttrium oxide interlayers and barium cuprate cover layers
[AD-D016073] p 3070 N94-28225

ALUMINUM-LITHIUM ALLOYS

Aluminum alloy 8090-T8771 thick plate material characterization
[AD-A274146] p 2987 N94-27077

Fracture toughness and crack resistance of damage tolerant and high strength Al-Li alloys
[NLR-TP-91249-U] p 2743 N94-27795

Status and prospects for aluminium-lithium alloys in aircraft structures
[NLR-TP-92193-U] p 2743 N94-27797

AMAZON REGION (SOUTH AMERICA)

Role of remote sensing in energy, water, and carbon cycle studies over the Amazon
[INPE-5486-PRE/1786] p 2852 N94-27957

AMBIENT TEMPERATURE

Effect of loading mode on the fracture toughness of a reduced activation ferritic/martensitic stainless steel
[DE94-004290] p 2732 N94-25987

Cryogenic size reduction of solid propellant
[AD-A274844] p 2759 N94-26800

Computation of static pressure downstream of a normal shock for hypersonic flight (ambient temperature known)
[ESDU-93020] p 2649 N94-28091

AMINES

Computational studies of energetic organic molecules
[AD-A274726] p 3018 N94-26172

Phosphazene-containing amine as curing agent for phthalonitrile-base polymer
[AD-D016029] p 2755 N94-27147

Mechanism for regulation of myocardial contractility by autonomic drugs: Pathophysiological relevance in congestive heart failure p 2931 N94-27536

AMINO RADICAL
The kinetics and dynamics of the coma of Halley's comet
[NASA-CR-194828] p 3105 N94-28184

AMMONIA
High-temperature and high-pressure flow calorimeter
p 2718 N94-27390

AMMONIUM COMPOUNDS
Computational analysis of some aspects of a synthetic route to ammonium dinitramide
[AD-A274648] p 2704 N94-26353

AMORPHOUS MATERIALS
Development of SO(x) and NO(x) solid electrolyte sensors p 2725 N94-25562
Study on computerized experiment of amorphous transformation process by solid phase reaction
p 2726 N94-25564
Characterization of physically vapor deposited AF2400 thin films
[DE94-004019] p 2749 N94-25985
How reliable is the HMSA integral equation for the pair structure of supercooled and amorphous mixtures?
[DE94-601543] p 3006 N94-26411
Magnetostriction and magnetostrictive materials
[VTT-TIED-1434] p 3058 N94-26545
Modelling and predicting properties of polymers in the amorphous glassy state
[ETN-94-95345] p 2752 N94-26645
Ion beam mixing of marker layers into amorphous aluminum oxide
[DE94-000901] p 2752 N94-26676
Fabrication technology
[DE94-003017] p 2763 N94-26778
List of papers published by the members of Institute for Materials Research, Tohoku University 1992
[JTN-94-80608] p 3118 N94-27355
Effect of temperature and recoil-energy spectra on irradiation-induced amorphization in Ca2La8(SiO4)6O2
[DE94-004371] p 3067 N94-27602
Fragmentation of Ge(1-x) Sn(x) Se2 glasses
[DE94-603009] p 2758 N94-27837
The Science Reports of the Research Institutes, Tohoku University. Series A: Physics, Chemistry, and Metallurgy. Volume 38, No. 1: Amorphous Materials 14
[JTN-94-80610] p 2744 N94-28158
Differential scanning calorimetric study of solid state amorphization and crystallization in Zr/Co and Zr/Ni multilayers p 2745 N94-28161
Formation and crystallization of hydrogen-induced amorphous Ti3InH(4.5) alloy p 2745 N94-28163
The electrocatalytic oxidation of ethylene and methane, and reduction of oxygen on gas-diffusion electrodes made of amorphous nickel-valve metal-platinum group metal alloys p 2722 N94-28165
CO2 methanation catalysts prepared from amorphous Ni-valve metal alloys containing platinum group elements
p 2745 N94-28166
Mechanical behavior of amorphous alloys at elevated temperatures p 2746 N94-28167
Formation of glassy Pd-Ni-P alloys by mechanical alloying and their structure and thermal stability
p 2746 N94-28168
Study on the production of flaky amorphous alloy powders by impact flattening of atomized liquid droplets on a rapidly rotating wheel p 2746 N94-28169
Production of an amorphous Fe(75)Si(10)B(15) sheet by a metallic mold casting method and its properties
p 2746 N94-28170

AMORPHOUS SEMICONDUCTORS
Recombination and metastability in amorphous silicon and silicon germanium alloys
[DE94-000237] p 2736 N94-26481

AMORPHOUS SILICON
The state of the art of thin-film photovoltaics
[DE94-000224] p 2855 N94-26115
The fracture behavior of a CVD crystalline Si3N4/amorphous Si3N4 composite
[DE94-002646] p 2750 N94-26124
Multichip module high speed testing
[AD-A274873] p 2782 N94-26343
Recombination and metastability in amorphous silicon and silicon germanium alloys
[DE94-000237] p 2736 N94-26481
Deposition of a-SiC:H using organosilanes in an argon/hydrogen plasma
[DE94-004428] p 2751 N94-26580
Continuous roll-to-roll a-Si photovoltaic manufacturing technology
[DE94-000260] p 2859 N94-27610

AMPLIFICATION
The effect of high frequency electric field on hypersound amplification in superlattice
[DE93-634326] p 3057 N94-26384
Phase conjugation and pulse compression of high energy lasers: From nanoseconds to microseconds
[DE94-001061] p 2818 N94-26699

AMPLIFIER DESIGN
Ultralinear wideband integrated circuit design
[ISBN-0-315-84130-3] p 2784 N94-26675
NASA satellite communications application research, phase 2 addendum. Efficient high power, solid state amplifier for EHF communications
[NASA-CR-195712] p 2777 N94-27946

AMPLIFIERS
Signal amplifier-shapers for multiwire detectors
[DE93-634171] p 2783 N94-26438

AMPLITUDE MODULATION
Parametric time-scale methods in signal analysis
[AD-A274212] p 2773 N94-27068

ANALOG CIRCUITS
Electrical coupling between the sino-atrial node and atrial muscle: Cell to cell interaction through an external circuit and its simulation by computer modeling
p 2907 N94-27509

ANALOG COMPUTERS
Set based analysis of arithmetic
[AD-A274112] p 3002 N94-25903

ANALOG SIMULATION
Parallel computational geometry on analog Hopfield networks
[ISBN-0-315-84093-5] p 2980 N94-26635
Electrical coupling between the sino-atrial node and atrial muscle: Cell to cell interaction through an external circuit and its simulation by computer modeling
p 2907 N94-27509

ANALOG TO DIGITAL CONVERTERS
Development of a 4-bit parallel analog-to-digital converter and a four-quadrant double-balanced mixer using heterojunction bipolar transistor technology
[AD-A274074] p 2947 N94-25648
Auxiliary controller for time-to-digital converter module readout
[DE93-634172] p 2948 N94-26266
The 12-channel flash-ADC FASTBUS module
[DE93-634229] p 2783 N94-26380
ADC test support program
[AD-A274819] p 2783 N94-26491
Users guide for GRIKURV: A code for drawing graphs
[PB94-123593] p 2968 N94-27154
Inverted pendulum control apparatus using transputers
[DE94-701224] p 2973 N94-27732

ANALYSIS (MATHEMATICS)
Computational analysis of some aspects of a synthetic route to ammonium dinitramide
[AD-A274648] p 2704 N94-26353

ANALYTIC FUNCTIONS
Some properties of generalized biregular functions with values in a Clifford algebra
[DE93-613024] p 2991 N94-25881

ANATOMY
Cross-sectional anatomy of day 30 suncus fetuses
p 2905 N94-27490
Skeletal development and ossification of the swine fetuses p 2905 N94-27491

ANDESITE
Effects of slot on rock surface for percussive rock excavation: Water jet assisted percussive rock excavation p 2871 N94-28155

ANESTHESIA
The effect of naloxone on sleeping time in adjuvant arthritic rats p 2906 N94-27498

ANGLE OF ATTACK
Evaluation of moderate angle of attack roll of a dual engine, thrust vectoring aircraft using quantitative feedback theory
[AD-A274118] p 2667 N94-25905
A numerical determination of bifurcation points for low Reynolds number conical flows
[AD-A273984] p 2791 N94-25991
Computational investigation of the compressible dynamic stall characteristics of the Sikorsky SSC-A09 airfoil
[AD-A274867] p 2644 N94-26191
Experimental and theoretical study of aerodynamic characteristics of some lifting bodies at angles of attack from -10 degrees to 53 degrees at Mach numbers from 2.30 to 4.62
[NASA-TM-4528] p 2646 N94-26693
Controlled oscillation of forebody vortices by nozzle jet blowing
[ISBN-0-315-84134-6] p 2678 N94-27648
Normal force of low aspect ratio cropped-delta wings at pre-stall angles of attack and subsonic speeds
[ESDU-93034] p 2648 N94-27955
Pneumatic management of blunted-forebody flow asymmetry for high-angle-of-attack directional control
p 2679 N94-28028
Measurements of steady and dynamic pressure on an F/A-18 wind tunnel model at high angles of attack
p 2653 N94-28323
Aerodynamic performance of novel ducted-tip wings
p 2654 N94-28331

ANGLES (GEOMETRY)
Discrete vacuum ultra violet reflective interference filter
[AD-D016059] p 2756 N94-27675

ANGULAR ACCELERATION
Evaluation of near-infrared spectrophotometric method for individual tolerance to +Gz acceleration
p 2933 N94-27944

ANGULAR CORRELATION
Window least squares method applied to statistical noise smoothing of positron annihilation data
[DE93-634665] p 3003 N94-26385
Fermi surface ridge at second and third Umklapp positron annihilations in Y Ba2Cu3O(7-delta)
[DE93-634760] p 3070 N94-27995

ANGULAR DISTRIBUTION
Modeling the DMSP and CRRES dosimeters using the path length distribution method
[RXR-93051] p 2698 N94-28200

ANGULAR MOMENTUM
Weak interactions in a bilocal chiral theory
[DE93-613097] p 3013 N94-25836
Excited Landau levels, orbital angular momentum and axial anomaly
[DE94-606407] p 3068 N94-27679

ANGULAR VELOCITY
Design of a high-precision double crystal tunable monochromator
[DE94-003004] p 2811 N94-26787

ANILINE
Mechanical properties of polyaniline prepared by polymerization in an organized monolayer
[AD-A274350] p 2753 N94-26925
LB-Deposited, side-chain substituted polyaniline, polypyrrole and the corresponding monomers, studied by STM
[AD-A274405] p 2754 N94-26977
Kinetics of 2-pentadecylaniline polymerizations in monolayers: Relationships between experimental data and a new theoretical model
[AD-A274419] p 2754 N94-27080
Stabilization of polyaniline solutions
[DE94-003958] p 2704 N94-27745

ANIMALS
Proceedings of the symposium on current concepts and approaches on animal test alternatives
[AD-A273926] p 2900 N94-25593
An automatic 14-day paste diet feeder for animals
[NASA-TM-108804] p 2901 N94-26086
Macrobenthic fauna in the dutch sector of the north sea in 1991
[PB94-126414] p 2868 N94-27200
An evaluation of criteria that may be used to identify species surviving a mass extinction
p 2889 N94-28304
Ozone control of biological activity during Earth's history, including the KT catastrophe p 2876 N94-28312

ANIONS
The use of on-line ion chromatography for high temperature and high pressure reaction studies
[DE94-002525] p 2713 N94-26075
Axial anomaly in e(+)e(-) yields gamma gamma and anyon superconductivity
[DE94-606406] p 3070 N94-27859

ANISOTROPIC MEDIA
DUSOL: Improved software for analysis of ultrasonic velocity data on anisotropic materials
[NPL-DMM(A)-104] p 2965 N94-26816
Elastic wave up/down decomposition in inhomogeneous and anisotropic media: An operator approach and its approximations
[PB94-126497] p 2881 N94-26880
Electromagnetic modeling of bi-isotropic media
[PB94-132909] p 2778 N94-28382
Plane wave propagation in an anisotropic chiral medium with isotropic permittivity and permeability
[PB94-133097] p 2778 N94-28384
Analytic solution for the dyadic Green's function of a nonreciprocal uniaxial bianisotropic medium
[PB94-133162] p 2779 N94-28388

ANISOTROPY
First principle calculation for magneto-crystalline anisotropy
[DE93-634653] p 3052 N94-26012
Design and test of postbuckled stiffened curved plates: A literature survey
[PB94-126521] p 2840 N94-26961
Technical report of ISSP. Ser. A, no. 2673: Two successive spin glass transitions in non-diluted Heisenberg-like spin glass Ni(0.42)Mn(0.58) TiO3
[JTN-94-80559] p 2756 N94-27241
Cosmic no-hair in Brans-Dicke theory
[DE94-603673] p 3074 N94-27636
Plane wave propagation in an anisotropic chiral medium with isotropic permittivity and permeability
[PB94-133097] p 2778 N94-28384

Analytic solution for the dyadic Green's function of a nonreciprocal uniaxial bianisotropic medium
[PB94-133162] p 2779 N94-28388

Image theory for DC problems involving a conducting half space bounded by the general anisotropic impedance surface
[PB94-132917] p 2779 N94-28390

Green dyadic and dipole fields for a medium with anisotropic chirality
[PB94-132933] p 2779 N94-28391

Dielectric polarizability of sphere with arbitrary anisotropy
[PB94-133113] p 2779 N94-28397

ANNEALING

Binding of copper and nickel to cavities in silicon formed by helium ion implantation
[DE94-003769] p 3050 N94-25814

Microscopic study of local structure and charge distribution in metallic La2CuO(4+delta)
[DE94-003801] p 3050 N94-25817

Modeling defect production in high energy collision cascades
[DE94-003810] p 3017 N94-26049

Ion implantation of diamond: Damage, doping, and lift-off
[DE94-001133] p 3054 N94-26137

Regrowth zones in laser annealed radiation damaged diamond
[DE94-600821] p 3056 N94-26364

Ferroelectric fluoride memory FET development
[AD-A274341] p 2785 N94-27057

First principles calculations for the cleaved and annealed Ge(111) surfaces
[DE93-617048] p 3066 N94-27347

ANNIHILATION REACTIONS

Window least squares method applied to statistical noise smoothing of positron annihilation data
[DE93-634665] p 3003 N94-26385

An analysis of monojet data in p(bar-p) collisions at square root of s equal to 1.8 TEV
[DE94-001822] p 3026 N94-27565

Cosmological constraints on very heavy stable neutrinos
[DE94-601669] p 3117 N94-28066

ANNUAL VARIATIONS

The impact of recent model improvements on GISS GCM predictions of climate change
[DE93-019458] p 2866 N94-26077

Monthly variation of physiological and psychological responses under unsteady thermal conditions
p 2918 N94-27475

Man's ability to adapt himself for the seasonal climatic changes: From viewpoint of anticipation and seasonable behavior p 2919 N94-27476

Remote sensing of global snowpack energy and mass balance: In-situ measurements on the snow of interior and Arctic Alaska
[NASA-CR-195704] p 2851 N94-27787

Probing the Martian atmosphere in the ultraviolet
p 3108 N94-27890

How well was total ozone abundance inferred with Mariner 9? p 3108 N94-27891

Counting Adelie penguins at colonies: Seasonal and annual changes p 2885 N94-27970

Observation of the upper atmosphere physics at Asuka Station by the 30th Japanese Antarctic Research Expedition in 1989 p 2885 N94-27972

ANODES

MSOFC development status
[DE94-003192] p 2858 N94-26792

Channel model for AC electric arc
[PB94-124591] p 2786 N94-27327

An anodic dissolution-based mechanism for the rapid cracking, pre-exposure phenomenon demonstrated by Al-Li-Cu alloys
[DE94-004798] p 2742 N94-27788

ANOMALIES

(2,0) superconformal anomaly
[DE93-613046] p 2991 N94-25867

ANTARCTIC REGIONS

Portable Habitat for Antarctic Scientific Research (PHASR) p 2943 N94-25681

A three-dimensional chemical transport model study of the 1991 Antarctic ozone hole using objectively analysed data
[ISBN-0-315-84250-4] p 2867 N94-26670

Ice surface temperature retrieval from AVHRR, ATSR, and passive microwave satellite data: Algorithm development and application
[NASA-CR-195276] p 2851 N94-27849

Antarctic Record, Vol. 38, No. 2
[REPT-107] p 2883 N94-27963

ANTENNA ARRAYS

Predicting antenna parameters from antenna physical dimensions
[AD-A273893] p 3012 N94-25655

Project PARAS: Phased array radio astronomy from space p 3081 N94-25703

The application of FD-TD method to antenna radiation patterns
[ISBN-0-315-83893-0] p 2769 N94-26618

A current evaluation of the digital beamforming testbed at Rome Laboratory
[AD-A274311] p 3032 N94-26881

Focal plane antenna array for millimeter waves
[AD-D016034] p 2774 N94-27202

Design and control of phased ICRF antenna arrays
[DE94-002796] p 3046 N94-27261

Beamforming/null-steering adaptive array
[CA-PATENT-1325260] p 2775 N94-27270

Fast wave current drive technology development at ORNL
[DE94-004243] p 3046 N94-27568

Fiber optic true time-delay array antenna feed system
[AD-D016063] p 2777 N94-27734

ANTENNA DESIGN

A study of two dimensional tapered periodic edge treatments to reduce wideband edge diffraction
[AD-A274054] p 2766 N94-25824

RF modeling and design of a folded waveguide launcher for the Alcator C-Mod tokamak
[DE94-003588] p 3041 N94-25933

Design and control of phased ICRF antenna arrays
[DE94-002796] p 3046 N94-27261

ANTENNA FEEDS

Fiber optic true time-delay array antenna feed system
[AD-D016063] p 2777 N94-27734

NASA satellite communications application research, phase 2 addendum. Efficient high power, solid state amplifier for EHF communications
[NASA-CR-195712] p 2777 N94-27946

ANTENNA RADIATION PATTERNS

Predicting antenna parameters from antenna physical dimensions
[AD-A273893] p 3012 N94-25655

The application of FD-TD method to antenna radiation patterns
[ISBN-0-315-83893-0] p 2769 N94-26618

Hybrid techniques for complex aerospace electromagnetics problems p 2779 N94-27894

ANTHROPOMETRY

Creation of prototype aircrew protection equipment based on face anthropometry
[AD-A273865] p 2940 N94-25611

Female combat helicopter pilot selection criteria
[AD-A273935] p 2938 N94-26749

A multivariate anthropometric method for crew station design: Abridged
[AD-A274588] p 2941 N94-26984

ANTICYCLONES

An observational study of the extratropical anticyclones in the South American continent
[INPE-5387-TDI/476] p 2896 N94-27356

ANTIDIURETICS

Treatment of orthostatic hypotension by nasal administration of vasopressin p 2930 N94-27533

ANTIFERROMAGNETISM

Microscopic study of local structure and charge distribution in metallic La2CuO(4+delta)
[DE94-003801] p 3050 N94-25817

Volume dependence of vanadium magnetism
[DE94-601838] p 3050 N94-25843

Structure of the modulated magnetic phase of Mn3Sn
[DE94-002788] p 2733 N94-26092

Holes in a two-dimensional quantum antiferromagnet
[DE93-634753] p 3057 N94-26388

Multi-channel Kondo necklace
[DE93-634754] p 3057 N94-26389

ANTIMONIDES

Study on synthesis and characteristics of intermetallic compound with strong electron correlation
p 2726 N94-25563

ANTIPARTICLES

Measuring the time dependence of B(sub s)(sup 0) meson - anti B(sub s)(sup 0) meson oscillations
[ISBN-0-315-84367-5] p 3021 N94-26665

ANTIPROTONS

An antiproton-proton partial-wave analysis
[DE94-002690] p 3021 N94-26620

Antiproton studies in penning traps
[AD-A274250] p 3024 N94-27011

Double excitation of He and H(-) by fast proton and anti-proton impact
[DE94-004581] p 3026 N94-27620

Proton electromagnetic form factor near the proton-antiproton threshold and quasinuclear bound state
[DE94-606458] p 3027 N94-27681

ANTIREFLECTION COATINGS

Characterization of physically vapor deposited AF2400 thin films
[DE94-004019] p 2749 N94-25985

Long Duration Exposure Facility space optics handbook
[AD-A274831] p 3035 N94-26572

APEXES

Fast vertex search (in plane)
[DE93-616655] p 2959 N94-25917

Algorithms of the vertex coordinate reconstruction for straight tracks of short-lived particles
[DE93-616661] p 3015 N94-25919

An algorithm to find the intersection of two convex polygons
[AD-A274722] p 2961 N94-26148

APPLICATION SPECIFIC INTEGRATED CIRCUITS

Hierarchical test development and design-for-testability for (a)synchronous semi-custom ASIC's
[ISBN-9-09-005928-8] p 2834 N94-26003

Low-cost photovoltaic inverters incorporating application-specific integrated circuits
[DE94-003270] p 2856 N94-26463

Center for space microelectronics technology
[NASA-CR-195282] p 2786 N94-27574

Spacecraft optical disk recorder memory buffer control
p 2815 N94-27907

APPLICATIONS PROGRAMS (COMPUTERS)

SHIVA: A unix-based, menu-driven, color image processing software package
[AD-A274071] p 2957 N94-25646

Systematic Propulsion Optimization Tools (SPOT)
p 2976 N94-25666

Parallel Assessment Window System (PAWS) enhancements
[AD-A274094] p 2979 N94-25786

Source code for the OO1 benchmark and the AFIT simulation benchmark
[AD-A274035] p 2958 N94-25799

EcarHeart2 version 1.0: Programmers documentation
[PB94-124633] p 2909 N94-25909

Coordinated scheduling for dynamic real-time systems
[NASA-CR-195231] p 3093 N94-26206

The MUSA design methodology
[CWI-CS-R9265] p 3097 N94-26220

The ergonomics of software porting: Automatically configuring software to the runtime environment or everything you wanted to know about your C compiler but didn't know who to ask
[CWI-CS-R9266] p 2961 N94-26221

Red's natural editor: A program designed to edit FORTRAN programs
[DE94-003271] p 2962 N94-26318

The Chaco user's guide
[DE94-003669] p 2962 N94-26370

Users manual for CATNIP: A Computer Analysis Tool for Normal Impact Penetration
[DE94-003671] p 2962 N94-26371

Programming in Fortran M
[DE94-002756] p 2963 N94-26407

Design principles of onboard management of a Sun synchronous satellite p 2950 N94-26722

Using the TSAR electromagnetic modeling system
[DE94-002617] p 2771 N94-26803

Optical characterization and guided wave loss measurements for end-capped 6F-polybenzoxazole
[AD-A274586] p 3036 N94-26982

Processing of wide-angle synthetic aperture radar signals for target detection
[AD-A274225] p 2773 N94-27073

An object-oriented database interface for Ada
[AD-A274391] p 2968 N94-27075

Ma42: A new frontal code for solving sparse unsymmetric systems
[PB94-124302] p 2998 N94-27115

Development of digital resampling and pulse compression computer software
[DREP-92-32] p 2969 N94-27318

Rocket engine numerical simulation
p 2688 N94-27375

High performance computing in chemistry and massively parallel computers: A simple transition?
[DE94-004318] p 2982 N94-27600

Thunderstorm Hypothesis Reasoner
[NASA-CR-195714] p 2897 N94-27884

Contact stress in disc cams with roller followers
[ESDU-93001] p 2829 N94-28055

Blending profiles of disc cams with radial translating roller followers. Part 2: To incorporate an intermediate precision point or a constant velocity component
[ESDU-93002-PT-2] p 2830 N94-28056

Flat rectangular orthotropic plates under uniformly distributed normal pressure. Elastic stresses and deflections for various forms of edge restraint
[ESDU-93011] p 2845 N94-28061

Condensation inside tubes: Computer program for pressure drop in straight tubes (horizontal and vertical with downflow)
[ESDU-93014] p 2806 N94-28064

Calculation methods for steadily loaded central circumferential groove hydrodynamic journal bearings (guide to use of computer program A9304)
[ESDU-93004] p 2830 N94-28073
Calculation methods for steadily loaded axial groove hydrodynamic journal bearings (guide to use of computer program A9305)
[ESDU-93005] p 2830 N94-28074
Calculation methods for steadily loaded axial groove hydrodynamic journal bearings. Low viscosity process fluid lubrication (guide to use of computer program A9306)
[ESDU-93006] p 2830 N94-28075
Program for calculation of maximum lift coefficient of plain aerofoils and wings at subsonic speeds
[ESDU-93015] p 2649 N94-28076
Ejectors and jet pumps: Computer program for design and performance for liquid flow
[ESDU-93022] p 2832 N94-28093
Parameter estimation of linear systems from frequency response measurements (computer program)
[ESDU-93016] p 2976 N94-28137
Three-dimensional elastic stress concentration factors: Plain or countersunk hole in a wide plate subjected to tension, bending, or pin loading
[ESDU-93030] p 2845 N94-28143
Application of the MBTEC Euler code to the Challenger and the CF-18 complete aircraft configurations
p 2653 N94-28324

APPROACH CONTROL
The effects of tailwinds and control cross coupling on rotorcraft handling qualities for steep, decelerating instrument approaches and missed approaches
[IAR-AN-77] p 2677 N94-26710
Investigation of air transportation technology at Ohio University, 1992-1993 p 2642 N94-27288
Flight testing of GPS and GPS-aided systems
[NLR-TP-92151-U] p 2666 N94-27831

APPROPRIATIONS
Selected data on Federal support to universities and colleges: FY 1991
[NSF-93-320] p 3101 N94-28201

APPROXIMATION
Back-reaction beyond the mean field approximation
[DE94-003936] p 3012 N94-25612
A comparison of three approximate mathematical models for the gravity gradient stabilized satellite
[AD-A273832] p 2694 N94-25615
Approximate solution of the fourth order initial value problem using deficient spline polynomials
[DE93-613023] p 2991 N94-25880
Set based analysis of arithmetic
[AD-A274112] p 3002 N94-25903
An approximate solution for the spinup dynamics of near axisymmetric axial gyrostats using the method of multiple scales
[AD-A273723] p 2698 N94-26223
Numerical solution of singularity-perturbed two-point boundary-value problems
[DE94-601542] p 2993 N94-26410
Radial base functions: L(sup p)-approximation orders with scattered centers
[AD-A274682] p 3003 N94-26445
On a spline-approximation method for solving ordinary differential equations
[DE93-634290] p 2994 N94-26471
Symmetric and asymmetric diophantine approximation by continued fractions
[PB94-126455] p 2998 N94-27030
Radial basis function approximation: From gridded centers to scattered centers
[AD-A274184] p 2998 N94-27103
Analytic approximation to randomly oriented spheroid extinction
[DREV-4712-93] p 3038 N94-27598

APTITUDE
A comparison of two hardware implementations of a crew selection system
[AD-A274913] p 2937 N94-26346
Validation of the Federal Aviation Administration air traffic control specialist pre-training screen
[DOT/FAA/AM-94/4] p 2938 N94-26600

AQUEOUS SOLUTIONS
Multivariate calibration applied to near-infrared spectroscopy for the quantitative analysis of dilute aqueous solutions
[DE94-003231] p 2716 N94-26794
High-temperature and high-pressure flow calorimeter
p 2718 N94-27390
Effect of different ions on the anodic behaviour of alloy 800 in chloride solutions at high temperature
[DE94-602982] p 2743 N94-27832
Computer simulation of aqueous Na-Cl electrolytes
[DE94-002622] p 3030 N94-28001

AQUIFERS
Mapping of seawater intrusion into the coastal aquifer of Israel (the seawater-freshwater interface) by TDEM (Time Domain Electromagnetic) method
[ITN-94-85238] p 2850 N94-27331

ARABIAN SEA
Tropical cyclone report, 1992
[AD-A274464] p 2896 N94-27025

ARAMID FIBER COMPOSITES
Development of fibre-metal laminates, ARALL and GLARE, new fatigue resistant materials
[PB94-126471] p 2669 N94-26969
Impact tests on fibre metal laminates under a tensile load
[PB94-126570] p 2710 N94-27201

ARC GENERATORS
A study of DC-DC converters with MCT's for arcjet power supplies
[NASA-CR-191204] p 2703 N94-27662

ARC HEATING
Fullerene fabrication using an arc furnace. Characterization of the product
[DE94-603006] p 3029 N94-27834

ARC MELTING
Channel model for AC electric arc
[PB94-124591] p 2786 N94-27327

ARC WELDING
Weldability of Direct-Quenched and Tempered (DQT) high strength steel HT80
[VTT-TIED-1406] p 2731 N94-25623
Weldability of Accelerated-Cooled (AcC) high strength TMCP steel HT50
[VTT-TIED-1410] p 2731 N94-25784
The study of single-pass GMA welds with different cover gas compositions on HSLA-100 steel
[AD-A274857] p 2822 N94-26174
The influence of weld metal alloying additions to extend the heat input range for the submerged arc welding of high strength steels
[AD-A274284] p 2738 N94-26679

ARCHITECTURE (COMPUTERS)
Design of a shared coherent cache for a multiple channel architecture
[AD-A274026] p 3034 N94-25758
Knowledge organization in intelligent tutoring systems for diagnostic problem solving in complex dynamic domains
[AD-A273986] p 2984 N94-25899
Real-time tracking with a 3D-flow processor array
[DE94-003981] p 2980 N94-25984
The High Performance Storage System
[DE94-004351] p 2948 N94-26578
Real-Time Embedded Processing for Space Applications
[ISBN-2-85428-335-X] p 2948 N94-26713
High performance flight computer developed for deep space applications p 2949 N94-26718
Fault tolerant real-time processing system for space use p 2949 N94-26720
A complete version of the Ada tasking coprocessor
p 2950 N94-26721
Design principles of onboard management of a Sun synchronous satellite p 2950 N94-26722
NASA's spacecraft data system p 2950 N94-26723
The Ariane 5 data management system
p 2950 N94-26724
PRONAOS flight software: A real-time application for a balloonborne scientific gondola p 2950 N94-26725
MATRA Marconi Space: The Silex on-board processor and on-board software p 2950 N94-26726
Virtual data
[DE94-002718] p 2986 N94-26807
A Multitransputer Parallel Processing System (MTPPS)
[DE94-604652] p 2981 N94-26903
An optoelectronic graphics display processor
[AD-A274401] p 3037 N94-26990
Design of a parallel discrete event simulation coprocessor
[AD-A274135] p 2982 N94-27123
Alternative architectures for domain-oriented application composition and generation systems
[AD-A274180] p 2968 N94-27128
Virtual memory management and virtual bus overloading on multiple channel architectures
[AD-A274127] p 2954 N94-27152
A partitioning and redundancy model for wafer-scale integrated circuits p 2955 N94-27195
Binary snapshots
[CWI-CS-R9319] p 2955 N94-27547
Communication on the Paragon
[DE94-003103] p 2983 N94-27713
Proceedings of Workshop on Distributed Computing and Network
[DE94-701165] p 2983 N94-27804

ARCTIC REGIONS
Seasonal snow of arctic Alaska R4D investigations
[DE93-040082] p 2892 N94-25939
Active layer dynamics and arctic hydrology and meteorology
[DE94-001724] p 2892 N94-25951
Sound, speed, reflectivity, absorption, and thermal diffusivity measurements in Arctic ice in 1990
[AD-A274326] p 2899 N94-26886
Leadex environmental phenomena and effects observed by DMSP, NOAA, and ERS-1 satellites
[AD-A274596] p 2868 N94-26888
Ice surface temperature retrieval from AVHRR, ATSR, and passive microwave satellite data: Algorithm development and application
[NASA-CR-195276] p 2851 N94-27849

ARGON
Hook spectroscopy as an atomic number density diagnostic applied to laser-ablated copper plasmas
[DE94-002645] p 3042 N94-26081
Physical characteristics of polymethylmethacrylate scintillator SOFG-120
[DE93-634184] p 2810 N94-26395
Ion beam mixing of marker layers into amorphous aluminum oxide
[DE94-000901] p 2752 N94-26676

ARGON ISOTOPES
Geological Dating by Ar-40 - Ar-39 method
[DE94-601975] p 2880 N94-26874

ARGON PLASMA
Two dimensional self-consistent fluid simulation of RF inductive sources
[DE94-003635] p 2767 N94-25937
Plasma surface cleaning using microwave plasmas
[DE94-002754] p 2713 N94-26014

ARIANE LAUNCH VEHICLE
The Ariane 5 data management system
p 2950 N94-26724
Charge efficiency of Ni/H2 cells during transfer orbit of Telstar 4 satellites p 2862 N94-28117

ARITHMETIC
Set based analysis of arithmetic
[AD-A274112] p 3002 N94-25903

ARITHMETIC AND LOGIC UNITS
Arithmetic performances of onboard computers
p 2952 N94-26738

ARMED FORCES
Satellite navigation system GPS: A review of principles and performance and developments in general
[PB94-124534] p 2665 N94-27210

ARMED FORCES (UNITED STATES)
Human dimensions research team, operation restore hope
[AD-A274340] p 2939 N94-27056

ARMOR
Dynamic response of S-2 glass reinforced plastic structural armor
[AD-A273868] p 2747 N94-25596

AROMATIC COMPOUNDS
Analytical method for estimation of the total amount of aromatic and poly aromatic compounds in diesel fuel
[PB94-123692] p 2759 N94-25907

ARRESTING GEAR
Soft ground arresting system for airports
[DOT/FAA/CT-93/80] p 2680 N94-26202

ARRHYTHMIA
On the mechanism of reentrant arrhythmias following DC defibrillation: Influence of fiber orientation to the effects of low-energy electric field stimulation on the effective refractory period of cardiac muscle
p 2904 N94-27468
Effects of perfusion of amiodarone on electrophysiological properties in single rabbit ventricular myocytes p 2906 N94-27503
Electrophysiological effects of MS-551, a new Class 3 antiarrhythmic agent, on isolated rabbit ventricular muscles p 2907 N94-27505
Comparative investigation of new Class 3 antiarrhythmic drugs, E-4031 and MS-551, on electrophysiological properties in isolated rabbit ventricular myocytes
p 2907 N94-27506
Effects of Class 1 antiarrhythmic drugs on the intraventricular conduction: Influence of fiber orientation
p 2907 N94-27507
Effects of Class 3 antiarrhythmic agents, E-4031 and MS-551 on ventricular repolarization in isolated rabbit hearts p 2907 N94-27508
Block of cardiac sodium channels by Ro 22-9194 (R), a new antiarrhythmic agent: Effects on the maximum upstroke velocity (Vmax) of single guinea pig ventricular myocytes p 2907 N94-27511
Electrophysiological effects of an antiarrhythmic drug, moricizine on isolated guinea pig ventricular muscles
p 2907 N94-27512

ARSENATES

Three-wave nonlinear interactions in KTiOPO4 (KTP) and KTP isomorphs
[AD-A274079] p 3052 N94-25993

ARTERIES

EcarHeart2 version 1.0: Programmers documentation
[PB94-124633] p 2909 N94-25909

ARTHRITIS

Excitation of cutaneous polymodal receptor induced by sympathetic stimulation in adjuvant-induced arthritis rats
p 2906 N94-27495

Selection of site injecting adjuvant in chronic inflammation model p 2906 N94-27496

Influence of mechanical stimulation on inflammatory edema p 2906 N94-27497

The effect of naloxone on sleeping time in adjuvant arthritic rats p 2906 N94-27498

ARTIFICIAL INTELLIGENCE

Discovery learning in autonomous agents using genetic algorithms
[AD-A274083] p 2677 N94-25998

Rational handling of multiple goals for mobile robots
[NASA-CR-195177] p 2985 N94-26006

Deductive computer programming
[AD-A274966] p 2962 N94-26303

Design of a computer expert system for adhesive selection using artificial intelligence techniques
[AD-A274715] p 2751 N94-26434

Blurred focal elements generalization of dempster's rule
[PB94-124278] p 2986 N94-26992

What can we learn from genetic algorithms: A new perspective for search methods
[PB94-125234] p 2967 N94-26997

Using discovery-based learning to prove the behavior of an autonomous agent
[AD-A274131] p 2987 N94-27121

Robotics handbook. Version 1: For the interested party and professional
[NASA-TM-109690] p 2824 N94-27238

Vision 21: Interdisciplinary Science and Engineering in the Era of Cyberspace
[NASA-CP-10129] p 2685 N94-27358

The coming technological singularity: How to survive in the post-human era p 2685 N94-27359

The universal robot p 2686 N94-27361

Pigs in cyberspace p 2689 N94-27376

On modeling and controlling intelligent systems
[DE94-002446] p 2988 N94-27706

Multi-sensor data fusion in a distributed environment: Architectural solutions
[NLR-TP-92243-U] p 2989 N94-27800

A hybrid formalism for representation and interpretation of image knowledge
[INPE-5485-PRE/1784] p 2989 N94-27833

Thunderstorm Hypothesis Reasoner
[NASA-CR-195714] p 2897 N94-27884

Artificial Intelligence Research Branch future plans
[NASA-TM-109733] p 2989 N94-28065

ARTIFICIAL SATELLITES

Design analysis of a combined optical/LADAR deep-space surveillance satellite
[AD-A274040] p 2694 N94-25832

Satellite attitude determination using linear combination of models
[AD-A274082] p 2694 N94-25996

Technology development in space projects
[VTT-TIED-1438] p 2682 N94-26249

Mounting of SSM's
[VTT-TIED-1442] p 2695 N94-26250

ARTILLERY

A preliminary method for atmospheric soundings in real time using satellite and ground-based remotely sensed data
[AD-A274381] p 2880 N94-26828

ASIA

A geological and geophysical information system for Eurasia
[AD-A274818] p 3096 N94-26490

A preliminary shear velocity model for Central Asia
[AD-A274972] p 2880 N94-26752

Propagation of cold air masses in East Asia and its associated planetary-scale function
[AD-A274304] p 2895 N94-26850

Global change: A research strategy for Australia 1992-1996 p 2874 N94-28282

ASPECT RATIO

Normal force of low aspect ratio cropped-delta wings at pre-stall angles of attack and subsonic speeds
[ESDU-93034] p 2648 N94-27955

Wing lift increment at zero angle of attack due to deployment of single-slotted flaps at low speeds
[ESDU-93019] p 2649 N94-28140

ASSAYING

Atomic processes in Inertial Electrostatic Confinement (IEC) devices
[DE94-005015] p 3047 N94-27715

ASSEMBLING

Automatic assembly planning and its role in agile manufacturing: A Sandia perspective
[DE94-002291] p 2821 N94-25970

STS-56, RSRM-031, 360L031 KSC processing configuration and data report
[NASA-CR-193922] p 2691 N94-26135

STS-51, RSRM-033, 360T033 KSC processing configuration and data report
[NASA-CR-193923] p 2691 N94-26153

ASSESSMENTS

Measurement of laboratory quality
[VTT-TIED-1427] p 2679 N94-25652

Practical problems in aggregating expert opinions
[DE94-002623] p 3094 N94-27707

ASTEROID MISSIONS

Comet nucleus and asteroid sample return missions
p 2689 N94-25692

Asteroid exploration and utilization
p 3080 N94-25697

ASTEROIDS

Comet nucleus and asteroid sample return missions
p 2689 N94-25692

Asteroid exploration and utilization
p 3080 N94-25697

A widely adaptable habitat construction system utilizing space resources p 2688 N94-27374

Consequences of impacts of small asteroids and comets with Earth p 2889 N94-28301

An extraterrestrial event at the tertiary-quaternary boundary p 2890 N94-28309

A general theory of impacts and mass extinctions, and the consequences of large-body impact on the Earth
p 2891 N94-28310

ASTIGMATISM

Theory and modeling of stimulated Raman scattering
[AD-A273755] p 3033 N94-25721

ASTRONAUT PERFORMANCE

Telescience testbedding for physiological experiments under hypobaric hypoxic conditions
p 2913 N94-27449

Telescience testbedding under hypobaric hypoxic conditions: Evaluation by operation ability and recognition ability p 2913 N94-27450

Telescience testbedding for physiological experiments under hypobaric hypoxic conditions: Development and evaluation in CNV measuring p 2913 N94-27451

ASTRONAUTICS

Technical and scientific research for aeronautics and astronautics
[ETN-94-95392] p 2641 N94-26212

ASTRONOMICAL CATALOGS

The continuum spectral characteristics of gamma ray bursts observed by BATSE p 3114 N94-26686

Sloan Digital Sky Survey
[DE94-004662] p 3103 N94-27750

In search of Nemesis p 2888 N94-28297

ASTRONOMICAL MODELS

Cosmic no-hair in Brans-Dicke theory
[DE94-603673] p 3074 N94-27636

ASTRONOMICAL PHOTOGRAPHY

Properties of the near-axis bispectrum applied to high-resolution astronomical imaging
[ISBN-0-315-85247-X] p 3103 N94-27302

Comparison of the lossy image data compressions for the MESUR Pathfinder and for the Huygens Titan Probe
p 2945 N94-28254

Performance considerations for the application of the lossless browse and residual model
p 2946 N94-28256

ASTRONOMICAL SPECTROSCOPY

Reanalysis of Mariner 9 UV Spectrometer Data for Ozone, Cloud, and Dust Abundances, and Their Interaction Over Climate Timescales
[NASA-CR-195244] p 3107 N94-27885

Visualization techniques to aid in the analysis of multispectral astrophysical data sets
[NASA-CR-195268] p 3105 N94-27932

ASTROPHYSICS

Dibaryon-induced instability of neutron stars
[DE93-634453] p 3103 N94-26046

Visualization techniques to aid in the analysis of multispectral astrophysical data sets
[NASA-CR-195268] p 3105 N94-27932

ASYMMETRY

Data on parity violation in the compound nucleus and its interpretation
[DE94-003965] p 3013 N94-25820

How reliable is the HMSA integral equation for the pair structure of supercooled and amorphous mixtures?
[DE94-601543] p 3006 N94-26411

Spin asymmetry in resonant electron-hydrogen elastic scattering
[DE94-601813] p 3023 N94-26943

Calculations of asymmetries in electron-alkali scattering
[DE94-601816] p 3023 N94-26945

Measurements of the B(sup 0)(bar B)(sup 0)CP asymmetry
[DE94-003379] p 3063 N94-27047

White noise theory of robust nonlinear filtering with correlated state and observation noises
[PB94-126661] p 3004 N94-27211

Why is the north polar cap on Mars different than the south polar cap? p 3107 N94-27889

Pneumatic management of blunted-forebody flow asymmetry for high-angle-of-attack directional control
p 2679 N94-28028

ASYMPTOTIC METHODS

On the phi(sub 0)-stability of perturbed nonlinear differential systems
[DE93-634304] p 2993 N94-26441

Recent developments in the simulation of steady and transient transverse jet interactions for missile, rotorcraft, and propulsive applications p 2804 N94-28030

ASYMPTOTIC PROPERTIES

Stability of large scale interconnected dynamical systems
[DE94-601536] p 2993 N94-26408

ASYMPTOTIC SERIES

Parameter estimation for ARMA models with infinite variance innovations
[AD-A274654] p 3003 N94-26355

Asymptotics for Kummer functions, Bose plasmas, and related special functions
[DE94-601853] p 3007 N94-26928

ATHLETES

Aerobic fitness and orthostatic tolerance: Evidence against an association p 2934 N94-28365

ATLANTIC OCEAN

Correlation between the gravity field and the bathymetry in the North Atlantic Ocean
[ETN-94-95036] p 2899 N94-26108

Mesoscale frontal evolution of the ERICA IOP-5A Cyclone
[AD-A274906] p 2893 N94-26183

ATMOSPHERIC ATTENUATION

Probing the Martian atmosphere in the ultraviolet
p 3108 N94-27890

How well was total ozone abundance inferred with Mariner 9? p 3108 N94-27891

High-Speed Research: Sonic Boom, Volume 1
[NASA-CP-10132] p 2649 N94-28188

Progress in modeling atmospheric propagation of sonic booms p 2650 N94-28189

ATMOSPHERIC BOUNDARY LAYER

Interactions between a tropical mixed boundary layer and cumulus convection in a radiative-convective model
[DE94-000848] p 2877 N94-25979

The numerical simulation of marine boundary layer clouds
[AD-A273669] p 2894 N94-26195

Radar detection of low-altitude targets in a maritime environment. Volume 2: Meteorological and radar data
[AD-A274658] p 2768 N94-26335

Surface roughness lengths
[AD-A274550] p 2895 N94-26846

Modeling of the coupled magnetospheric and neutral wind dynamos
[NASA-CR-195273] p 2883 N94-27852

The Martian atmospheric planetary boundary layer stability, fluxes, spectra, and similarity
[NASA-CR-195711] p 3108 N94-27935

ATMOSPHERIC CHEMISTRY

Simulation of the carbon cycle in the oceans
[DE94-000780] p 2898 N94-25791

Seasonal snow of arctic Alaska R4D investigations
[DE93-040082] p 2892 N94-25939

Isotopically labeled CO2 from stratosphere: A tracer of carbon biogeochemistry
[DE94-002777] p 2877 N94-26015

A conceptual framework for the evaluation of cost-effectiveness of projects to reduce GHG emissions and sequester carbon
[DE93-040448] p 2867 N94-26419

Numerical procedure for planetary wave solution
[DE94-004280] p 2879 N94-26576

A three-dimensional chemical transport model study of the 1991 Antarctic ozone hole using objectively analysed data
[ISBN-0-315-84250-4] p 2867 N94-26670

Probing the Martian atmosphere in the ultraviolet
p 3108 N94-27890

How well was total ozone abundance inferred with Mariner 9? p 3108 N94-27891

Studies for the loss of atomic and molecular species from Io
[NASA-CR-195702] p 3108 N94-27941

ATMOSPHERIC CIRCULATION
The numerical simulation of marine boundary layer clouds
[AD-A273669] p 2894 N94-26195
Investigation of mesoscale convective cloud clusters in South China
[AD-A274303] p 2895 N94-26678
Recent ASCOT experiments in multi-layered flows
[DE94-002360] p 2880 N94-26762
Surface roughness lengths
[AD-A274550] p 2895 N94-26846
Propagation of cold air masses in East Asia and its associated planetary-scale function
[AD-A274304] p 2895 N94-26850
The NOGAPS ten year AMIP integration
[AD-A274332] p 2900 N94-26887
An observational study of the extratropical anticyclones in the South American continent
[INPE-5387-TDI/476] p 2896 N94-27356
Global change research related to the Earth's energy and hydrologic cycle
[NASA-CR-195270] p 2869 N94-27430
Simulation of the Indian and East-Asian summer monsoon in the ECMWF model: Sensitivity to horizontal resolution
[DE94-004276] p 2897 N94-27571
The Martian atmospheric planetary boundary layer stability, fluxes, spectra, and similarity
[NASA-CR-195711] p 3108 N94-27935

ATMOSPHERIC COMPOSITION
Extraterrestrial surface propulsion systems
p 2833 N94-25691
Sensitivity of climate models: Comparison of simulated and observed patterns for past climates
[DE93-019934] p 2865 N94-25789
Methane emissions from natural wetlands
[DE93-040796] p 2865 N94-25790
Assessing the climatic effect of carbon dioxide and other trace gases using an interactive two-dimensional climate-chemistry model
[DE94-001741] p 2866 N94-25927
A conceptual framework for the evaluation of cost-effectiveness of projects to reduce GHG emissions and sequester carbon
[DE93-040448] p 2867 N94-26419
Reanalysis of Mariner 9 UV Spectrometer Data for Ozone, Cloud, and Dust Abundances, and Their Interaction Over Climate Timescales
[NASA-CR-195244] p 3107 N94-27885
Mars ozone: Mariner 9 revisited p 3107 N94-27888
In situ Mars ozone detector p 3108 N94-27892
Studies for the loss of atomic and molecular species from Io
[NASA-CR-195702] p 3108 N94-27941

ATMOSPHERIC CORRECTION
Properties of the near-axis bispectrum applied to high-resolution astronomical imaging
[ISBN-0-315-85247-X] p 3103 N94-27302
The validation of ATSR measurements with in situ sea temperatures
[DE94-003195] p 2852 N94-27875
Ionospheric calibration for single frequency altimeter measurements
[NASA-CR-195709] p 2883 N94-27883

ATMOSPHERIC DENSITY
Upper atmosphere neutral and plasma density modeling
[AD-A274768] p 2879 N94-26569
Trajectories of ballistic impact ejecta on a rotating Earth p 2887 N94-28295

ATMOSPHERIC DIFFUSION
Air pollution transport modeling
[AD-A273863] p 2865 N94-25609

ATMOSPHERIC EFFECTS
System design analysis of a lightweight laser satellite terminal
[AD-A274033] p 2690 N94-25769
An overview of the TNO contribution to VAST 92
[AD-A273751] p 2893 N94-26016
The validation of ATSR measurements with in situ sea temperatures
[DE94-003195] p 2852 N94-27875

ATMOSPHERIC ELECTRICITY
Modeling of the coupled magnetospheric and neutral wind dynamos
[NASA-CR-195273] p 2883 N94-27852

ATMOSPHERIC ENTRY
Preliminary reentry safety assessment of the General Purpose Heat Source module for the Cassini mission: Aerospace Nuclear Safety Program
[DE94-001646] p 2699 N94-25926

ATMOSPHERIC GENERAL CIRCULATION MODELS
Interpreting the implied meridional oceanic energy transport in AMIP
[DE94-001538] p 2898 N94-26072
The impact of recent model improvements on GISS GCM predictions of climate change
[DE93-019458] p 2866 N94-26077
A preliminary analysis of the US west climatology
[DE94-003028] p 2894 N94-26313
Simulation of the Indian and East-Asian summer monsoon in the ECMWF model: Sensitivity to horizontal resolution
[DE94-004276] p 2897 N94-27571

ATMOSPHERIC MODELS
Air pollution transport modeling
[AD-A273863] p 2865 N94-25609
Sensitivity of climate models: Comparison of simulated and observed patterns for past climates
[DE93-019934] p 2865 N94-25789
Development and testing of the Coupled Ocean/Atmosphere Mesoscale Prediction System (COAMPS)
[AD-A273925] p 2892 N94-25793
Assessing the climatic effect of carbon dioxide and other trace gases using an interactive two-dimensional climate-chemistry model
[DE94-001741] p 2866 N94-25927
The effect of elevation data representation on nocturnal drainage wind simulations
[DE94-003624] p 2892 N94-25936
Interactions between a tropical mixed boundary layer and cumulus convection in a radiative-convective model
[DE94-000848] p 2877 N94-25979
Interpreting the implied meridional oceanic energy transport in AMIP
[DE94-001538] p 2898 N94-26072
Testbed model and data assimilation for ARM
[DE94-000432] p 2893 N94-26082
Meeting of the Eighth Session of the Scientific Advisory Committee of the World Climate Impact Assessment and Response Strategies Programme
[DE93-633954] p 2866 N94-26163
A modeling study of the mesocyclone
[AD-A274889] p 2893 N94-26168
Modelling atmospheric turbulence effects on ground-based telescope systems
[DE94-004211] p 3102 N94-26528
Upper atmosphere neutral and plasma density modeling
[AD-A274768] p 2879 N94-26569
Numerical modelling of precipitation over complex terrain
[ISBN-0-315-84327-6] p 2894 N94-26628
A three-dimensional chemical transport model study of the 1991 Antarctic ozone hole using objectively analysed data
[ISBN-0-315-84250-4] p 2867 N94-26670
Investigation of mesoscale convective cloud clusters in South China
[AD-A274303] p 2895 N94-26678
The NOGAPS ten year AMIP integration
[AD-A274332] p 2900 N94-26887
Global barotropic response to a tropical forcing
[NASA-CR-195256] p 2896 N94-27408
An overview of the ASCOT program
[DE94-004356] p 2869 N94-27601
Ionospheric calibration for single frequency altimeter measurements
[NASA-CR-195709] p 2883 N94-27883
The Martian atmospheric planetary boundary layer stability, fluxes, spectra, and similarity
[NASA-CR-195711] p 3108 N94-27935
An enhanced global spectral model
[PL-TR-92-2011] p 2898 N94-28223

ATMOSPHERIC MOISTURE
Investigation of mesoscale convective cloud clusters in South China
[AD-A274303] p 2895 N94-26678
Cloud liquid water content measurement tests using dual-wavelength radar
[PB94-125960] p 2896 N94-26959

ATMOSPHERIC OPTICS
Performance comparison of shearing interferometer and Hartmann wave front sensors
[AD-A274031] p 3034 N94-25768

ATMOSPHERIC PHYSICS
Kiruna geophysical data. Data summary 93/4-6, April-June 1993
[PB94-123700] p 2881 N94-27039
Auroral Tomography Workshop Proceedings
[PB94-123718] p 2881 N94-27040
Kiruna geophysical data. Data summary 93/1-3, January-March, 1993
[PB94-123791] p 2881 N94-27043
Observation of the upper atmosphere physics at Asuka Station by the 30th Japanese Antarctic Research Expedition in 1989 p 2885 N94-27972

ATMOSPHERIC PRESSURE
Digital Altimeter Setting Indicator (DASI) Operational Test and Evaluation (OT/E) operational test procedures
[AD-A274100] p 2672 N94-26030
Symptoms of hypoxia at simulated altitude of 25,000 feet p 2933 N94-27945

ATMOSPHERIC RADIATION
Testbed model and data assimilation for ARM
[DE94-000432] p 2893 N94-26082
Dynamics explorer interdisciplinary scientist investigations
[NASA-CR-195226] p 2878 N94-26204
Differentiating the role of land surface variability and cloudiness variability on global energy transport within the atmosphere and oceans
[NASA-CR-195229] p 2847 N94-26222
JARE data reports. No. 186: Upper atmosphere physics data. Syowa and Asuka Stations, 1990
[JTN-94-80594] p 2881 N94-27299
The Sixteenth Symposium on Coordinated Observations of the Ionosphere and the Magnetosphere in the Polar Regions: Program and abstracts
[JTN-94-80601] p 2882 N94-27300
Martian atmospheric radiation budget
p 3107 N94-27887

ATMOSPHERIC REFRACTION
Over-the-horizon propagation measurements at six radar-frequency bands at the Atlantic Ocean Coast
[AD-A274151] p 2773 N94-27136
Theoretical and experimental analysis of the spatial and temporal behaviour of the intensity of an electro-magnetic wave reflected from a diffuse target after passing through a turbulent atmosphere
[ITN-94-85230] p 2774 N94-27234

ATMOSPHERIC SCATTERING
Performance statistics bulletin: High altitude meteor scatter propagation, August, September, October 1989
[AD-A274455] p 2773 N94-27085
Spectral and temporal correlations of multifrequency waves in the turbulent atmosphere
[ITN-94-85229] p 2774 N94-27233

ATMOSPHERIC SOUNDING
Coherent HF radar system for the study of natural and heater induced ionospheric irregularities
[AD-A273804] p 2876 N94-25752
An evaluation of the utility of ground-based high resolution interferometer (GB-HIS) soundings of the planetary boundary layer
[DE94-000960] p 3106 N94-25981
A preliminary method for atmospheric soundings in real time using satellite and ground-based remotely sensed data
[AD-A274381] p 2880 N94-26828
Zodiacal light data investigation. Interim results for the Earthlimb Clutter Experiment
[AD-A274461] p 3104 N94-27265
The Sixteenth Symposium on Coordinated Observations of the Ionosphere and the Magnetosphere in the Polar Regions: Program and abstracts
[JTN-94-80601] p 2882 N94-27300
Memories of National Institute of Polar Research. Series A-19. Upper atmosphere physics: ELF emission in high latitudes: Ray path calculation and ground-satellite observations
[JTN-94-80592] p 2882 N94-27342
Antarctic Record, Vol. 36, No. 2
[REPT-107] p 2883 N94-27963
Observation of the upper atmosphere physics at Asuka Station by the 30th Japanese Antarctic Research Expedition in 1989 p 2885 N94-27972
Role and activity of STA on Asian Pacific regional cooperation p 2853 N94-28269
Cooperative research projects on satellite remote sensing for the hydrological subjects
p 2853 N94-28270
Atmospheric science research in Malaysia: Perspectives on international cooperation p 2874 N94-28285

ATMOSPHERIC TEMPERATURE
A preliminary analysis of the US west climatology
[DE94-003028] p 2894 N94-26313
Surface roughness lengths
[AD-A274550] p 2895 N94-26846
How well was total ozone abundance inferred with Mariner 9? p 3108 N94-27891

ATMOSPHERIC TURBULENCE
Performance comparison of shearing interferometer and Hartmann wave front sensors
[AD-A274031] p 3034 N94-25768
Conversion of the CLUSE model for applications over open ocean
[AD-A273750] p 2893 N94-26013

Modelling atmospheric turbulence effects on ground-based telescope systems
[DE94-004211] p 3102 N94-26528
Theoretical and experimental analysis of the spatial and temporal behaviour of the intensity of an electro-magnetic wave reflected from a diffuse target after passing through a turbulent atmosphere
[ITN-94-85230] p 2774 N94-27234
The deterministic power-spectral-density method
[AD-B175894] p 2678 N94-27395
High-Speed Research: Sonic Boom, Volume 1
[NASA-CP-10132] p 2649 N94-28188
Progress in modeling atmospheric propagation of sonic booms p 2650 N94-28189
Implications for high speed research: The relationship between sonic boom signature distortion and atmospheric turbulence p 2650 N94-28190
Interaction of the sonic boom with atmospheric turbulence p 2650 N94-28191
The propagation of spark-produced N waves through turbulence p 2650 N94-28193

ATOMIC BEAMS
Heavy neutral beam probe for edge plasma analysis in tokamaks
[DE94-003391] p 3041 N94-25846
Study on laser atomic spectroscopy
[DE93-633328] p 2817 N94-26402
Measurement of metastable population distribution in gadolinium atomic beam by laser resonance photoionization method
[DE94-701194] p 3029 N94-27820

ATOMIC CLOCKS
Diode-laser-pumped, gas-cell atomic clocks
[AD-A274812] p 3008 N94-26484

ATOMIC CLUSTERS
Hadron jets and nucleon clusters in the relativistic nuclear collisions
[DE93-613434] p 3031 N94-25850

ATOMIC COLLISIONS
Convergent close-coupling calculation of electron-sodium scattering
[DE94-601815] p 3014 N94-25842
Spin asymmetry in resonant electron-hydrogen elastic scattering
[DE94-601813] p 3023 N94-26943
Calculation of total cross sections for electron and positron scattering on sodium and potassium
[DE94-601814] p 3023 N94-26944
Calculations of asymmetries in electron-alkali scattering
[DE94-601816] p 3023 N94-26945
International bulletin on atomic and molecular data for fusion. No. 42-45, Mar. 1991 - Dec. 1992
[DE94-601817] p 3045 N94-26946
International bulletin on atomic and molecular data for fusion. No. 46
[DE94-601818] p 3023 N94-26947
A study of the global properties of hadronic matter at large densities
[ISBN-0-315-57234-5] p 3025 N94-27260
Muon transfer rates in collisions of hydrogen isotope mesic atoms on bare nuclei: Multichannel adiabatic approach
[DE94-606752] p 3030 N94-27861
Correlations in inelastic collisions of relativistic nuclei with emulsion at (4.1 - 4.5) A GeV/c
[DE93-634526] p 3030 N94-27994

ATOMIC ENERGY LEVELS
Theoretical and experimental studies of elementary physics
[DE94-002310] p 3008 N94-25988
Excited Landau levels, orbital angular momentum and axial anomaly
[DE94-606407] p 3068 N94-27679

ATOMIC EXCITATIONS
Hook spectroscopy as an atomic number density diagnostic applied to laser-ablated copper plasmas
[DE94-002645] p 3042 N94-26081
Solution of the Heisenberg equation for the four-fermion contact interaction by the method of dynamical mappings
[DE94-606341] p 3075 N94-27858

ATOMIC FORCE MICROSCOPY
MBE grown 3 to 5 strain relaxed buffer layers and superlattices characterized by atomic force microscopy
[DE94-002931] p 3056 N94-26308
The growth and characterization of GaN as a photodetector
[AD-A274570] p 3063 N94-26965

ATOMIC PHYSICS
Frontiers of science and measurement: Report on a seminar jointly organized by the National Physical Laboratory and the Institute of Physics
[PB94-124310] p 3009 N94-27131
Atomic processes in Inertial Electrostatic Confinement (IEC) devices
[DE94-005015] p 3047 N94-27715

ATOMIC SPECTRA
Study on laser atomic spectroscopy
[DE93-633328] p 2817 N94-26402
Spectroscopy Division
[DE94-604074] p 2717 N94-26988

ATOMIC STRUCTURE
Study on characteristics and electronic structures of materials with strong electronic correlations by ferromagnetic fields p 2724 N94-25557
Study on synthesis and characteristics of intermetallic compound with strong electron correlation
p 2726 N94-25563
First principle calculation for magneto-crystalline anisotropy
[DE93-634653] p 3052 N94-26012
Hook spectroscopy as an atomic number density diagnostic applied to laser-ablated copper plasmas
[DE94-002645] p 3042 N94-26081
The origins of ordering in CuPt
[DE94-003864] p 2736 N94-26351
Strongly interacting fermion systems
[DE94-002674] p 3021 N94-26677
Modeling Group 4 elements with new transferable tight-binding models
[DE94-000770] p 3059 N94-26695
Rydberg states in multiply charged ions
[DE94-002335] p 3021 N94-26760
Electronic structure of a single oxygen vacancy in rutile TiO2
[DE94-602717] p 3062 N94-26901
International journal of quantum chemistry. Quantum Chemistry Symposium Number 27: Proceedings of the International Symposium on Atomic, Molecular, and Condensed Matter Theory and Computational Methods
[AD-A274352] p 3023 N94-26926
International bulletin on atomic and molecular data for fusion. No. 42-45, Mar. 1991 - Dec. 1992
[DE94-601817] p 3045 N94-26946
International bulletin on atomic and molecular data for fusion. No. 46
[DE94-601818] p 3023 N94-26947
The growth and characterization of GaN as a photodetector
[AD-A274570] p 3063 N94-26965
Technical report of ISSP. Ser. A, no. 2678: Magnetic properties of carbon nanotubes
[JTN-94-80564] p 3064 N94-27174
Technical report of ISSP. Ser. A, no. 2679: Novel electronic states of partially deuterated (DMe-DCNQI)2Cu
[JTN-94-80565] p 3064 N94-27175
Technical report of ISSP. Ser. A, no. 2681: Orbital and spin susceptibilities of the plane copper sites in YBa2Cu3O(x) system
[JTN-94-80567] p 3064 N94-27177
Technical report of ISSP. Ser. A, no. 2671: Quasi-localization of light waves in Fibonacci dielectric multilayers
[JTN-94-80557] p 3064 N94-27231
Technical report of ISSP. Ser. A, no. 2674: High-field cyclotron resonance and impurity transition in n- and p-3C-SiC at magnetic fields up to 175 T
[JTN-94-80560] p 3064 N94-27232
Technical report of ISSP. Ser. A, no. 2670: Electronic structure of light transition metal compounds studied by photoemission
[JTN-94-80556] p 3065 N94-27239
Technical report of ISSP. Ser. A, no. 2672: Magneto-optical effects of excitons in BiI3 crystals under pulsed high magnetic fields. 3: Excitons confined around a stacking disorder formed by a bending stress
[JTN-94-80558] p 3065 N94-27240
Technical report of ISSP. Ser. A, no. 2675: High-field cyclotron resonance and valence-band structure in semiconducting diamond
[JTN-94-80561] p 3065 N94-27245
Technical report of ISSP. Ser. A, no. 2676: Charge mass singularity in two-dimensional Hubbard model
[JTN-94-80562] p 3065 N94-27248
First principles calculations for the cleaved and annealed Ge(111) surfaces
[DE93-617048] p 3066 N94-27347
Proceedings of the workshop on (pi), K, (eta)-nucleon interactions
[DE94-701314] p 3027 N94-27733
Photoelectron spectroscopic studies of the electronic structure and bonding in TiC and TiN
[ATR-93(8361)-2] p 2746 N94-28185

ATOMIC THEORY
Atomic processes in Inertial Electrostatic Confinement (IEC) devices
[DE94-005015] p 3047 N94-27715

ATOMS
Modaling defect production in high energy collision cascades
[DE94-003810] p 3017 N94-26049
Refractive and dielectric properties of helium, argon and nitrogen gases
[PB94-123783] p 3008 N94-26851

ATROPHY
Endocrinological evaluations of muscle and bone atrophy in tail-suspended rats p 2903 N94-27444

ATTACK AIRCRAFT
Report of the defense science board task force on aircraft assessment
[AD-A274531] p 2669 N94-26835

ATTENTION
Pacing visual attention: Temporal structure effects
[AD-A273859] p 2937 N94-25965

ATTITUDE (INCLINATION)
Evaluation of the prototype dual-axis wall attitude measurement sensor
[NASA-TM-109056] p 2811 N94-26707

ATTITUDE CONTROL
Project WISH: The Emerald City p 2703 N94-25690
Inertial-space disturbance rejection for space-based manipulators p 2683 N94-26281
Berthing of Space Station Freedom using the shuttle remote manipulator system p 2684 N94-26284
Comparison of performance in simulator flight among subjects with different simulator experiences
p 2933 N94-27943

ATTITUDE GYROS
Test and evaluation of the Litton (Canada) Canadian strapdown gyroscope (CSG-2) Performance Evaluation Unit (PEU)
[DREO-1010] p 2813 N94-27597

ATTITUDE INDICATORS
Evaluation of the prototype dual-axis wall attitude measurement sensor
[NASA-TM-109056] p 2811 N94-26707

AUDITORY PERCEPTION
Signal- and listener-based factors in complex auditory pattern perception
[AD-A274148] p 2939 N94-27094

AUDITORY SIGNALS
Monaural and binaural processing of complex waveforms
[AD-A274209] p 3010 N94-27067
Signal- and listener-based factors in complex auditory pattern perception
[AD-A274148] p 2939 N94-27094

AUDITORY STIMULI
Difference in skin blood flow reduction depending on activating maneuver of skin sympathetic nerve activity
p 2929 N94-27525

AUGMENTATION
Status report of RMS active damping augmentation
p 2684 N94-26285

AURORAL ABSORPTION
Development of imaging riometers
p 2884 N94-27967
Quick-look system of auroral absorption images by imaging riometer p 2884 N94-27968

AURORAL ARCS
Quiet-time intensifications along the poleward auroral boundary near midnight
[ATR-93(7248)-2] p 2877 N94-26201
Proton aurora and substorm intensifications
[ATR-93(7248)-1] p 2887 N94-28218

AURORAL IRRADIATION
Energy parameters of the incident auroral electrons derived by the intensity ratio of auroral emissions
p 2779 N94-27964

AURORAL ZONES
Auroral Tomography Workshop Proceedings
[PB94-123718] p 2881 N94-27040

AURORAS
A numerical solution to the one and two dimensional line radiative transfer equation
[ISBN-0-315-84258-X] p 2994 N94-26640
Kiruna geophysical data. Data summary 93/4-6, April-June 1993
[PB94-123700] p 2881 N94-27039
Auroral Tomography Workshop Proceedings
[PB94-123718] p 2881 N94-27040
Kiruna geophysical data. Data summary 93/1-3, January-March, 1993
[PB94-123791] p 2881 N94-27043
JARE data reports. No. 186: Upper atmosphere physics data. Syowa and Asuka Stations, 1990
[JTN-94-80594] p 2881 N94-27299
The Sixteenth Symposium on Coordinated Observations of the Ionosphere and the Magnetosphere in the Polar Regions: Program and abstracts
[JTN-94-80601] p 2882 N94-27300

Analysis of EUV/FUV dayglow and auroral measurements
[NASA-CR-195237] p 2883 N94-27393

Energy parameters of the incident auroral electrons derived by the intensity ratio of auroral emissions
p 2779 N94-27964

Persistence of auroral electron flux events from DMSP/F9 electron measurements
[RXR-92012] p 2887 N94-28206

AUSTENITE

Microstructural development in low activation ferritic alloys irradiated to 200 dpa at 420 C
[DE94-004269] p 2731 N94-25803

AUSTENITIC STAINLESS STEELS

Corrosion resistance at welded zones of nuclear fuel reprocessing system p 2722 N94-25546

Study on phase transformation due to deformation in ferromagnetic fields at cryogenic condition
p 2724 N94-25556

Computer aided simulation of heat treatment
[VTT-PUBS-131] p 2731 N94-25643

Radiation hardening effects on localized deformation and stress corrosion cracking of stainless steels
[DE94-004308] p 2731 N94-25804

Grain boundary chromium concentration effects on the IGSCC and IASCC of austenitic stainless steels
[DE94-004268] p 2741 N94-27570

Cryogenic fracture behavior of 316LN in magnetic fields up to 14.6 T
[DE94-005215] p 2742 N94-27694

Mechanical properties and microstructure of thermomechanically processed, high manganese steel
[ARL-TR-146] p 2747 N94-28212

AUSTRALIA

Global change: A research strategy for Australia 1992-1996 p 2874 N94-28282

AUTOCLAVES

The use of on-line ion chromatography for high temperature and high pressure reaction studies
[DE94-002525] p 2713 N94-26075

AUTOCORRELATION

Analytical solution of Mori's equation with secant hyperbolic memory
[DE94-601541] p 3006 N94-26368

Conifer tree influence on Digital Terrain Elevation Data (DTED): A case study at Dulles International Airport
[AD-A274213] p 2849 N94-27069

Simulating high-frequency wind for long durations
[DE94-002739] p 2682 N94-27997

AUTOMATA THEORY

Integrating automata with genetic algorithms in order to provide adaptive operators
[ISBN-0-315-84094-3] p 2964 N94-26663

Recursive bundle event structures
[PB94-125275] p 3004 N94-26870

Deferred compilation: The automation of run-time code generation
[AD-A274124] p 2967 N94-27065

Forward and backward simulations. Part 1: Untimed systems
[CWI-CS-R9313-PT-1] p 2972 N94-27580

Forward and backward simulations. Part 2: Timing-based systems
[CWI-CS-R9314-PT-2] p 2972 N94-27581

On modeling and controlling intelligent systems
[DE94-002446] p 2988 N94-27706

AUTOMATIC CONTROL

Autonomous space processor for orbital debris advanced design project in support of solar system exploration p 2697 N94-25667

Design of dynamically reconfigurable real-time software using port-based objects
[NASA-CR-195178] p 2958 N94-25777

Graphical programming at Sandia National Laboratories
[DE94-003803] p 2958 N94-25818

Digital control and data acquisition for high-value GTA welding
[DE94-000885] p 2821 N94-25980

Recent developments in the Robotic All Terrain Lunar Exploration Rover (RATLER) program
[DE93-040342] p 2821 N94-26110

A method for testing of HVAC automation equipment using the emulator and the application of the method
[VTT-TIED-1435] p 2822 N94-26306

Designing and optimizing fuzzy-logic controllers
[ISBN-0-315-83505-2] p 2985 N94-26660

Combatting inherent vulnerabilities of CFAR algorithms and a new robust CFAR design
[AD-A274918] p 2770 N94-26751

Automated fabric inspection system
[AD-A274522] p 2835 N94-26833

Automated information management for designers: Functional requirements for computer based associates that support access and use of technical information in design
[AD-A274603] p 3099 N94-26891

Automation of formation flight control
[AD-A274137] p 2678 N94-27132

Automated in-situ inspection systems for underground storage tanks
[AD-A274644] p 2764 N94-27144

Open communication in manufacturing automation
[PB94-132479] p 2976 N94-28377

AUTOMATIC GAIN CONTROL

A feasibility study on bird classification with neural network
[AD-A273753] p 2659 N94-25780

AUTOMATIC PILOTS

Design of a flight controller for an unmanned research vehicle with control surface failures using quantitative feedback theory
[AD-A274049] p 2677 N94-25833

Discovery learning in autonomous agents using genetic algorithms
[AD-A274083] p 2677 N94-25998

AUTOMATION

Automatic assembly planning and its role in agile manufacturing: A Sandia perspective
[DE94-002291] p 2821 N94-25970

AUTOMOBILE ENGINES

Sequential multi-point injection of a natural gas engine. Topical report, November 1991 - April 1992
[PB94-126794] p 2824 N94-27224

Optimising BMW four-cylinder two-valve engines
[PB94-125101] p 2824 N94-27254

AUTOMOBILE FUELS

CRC customer versus rater octane number requirement program (1990)
[AD-A273997] p 2758 N94-25901

Analytical method for estimation of the total amount of aromatic and poly aromatic compounds in diesel fuel
[PB94-123692] p 2759 N94-25907

Natural gas applications for hybrid vehicles.
[PB94-117108] p 2759 N94-26753

AUTOMOBILES

Feasibility study on introduction of transportation-use petroleum substitution energy
[DE94-725205] p 2759 N94-26905

Evaluation of the buoyancy drag on automobile models in low speed wind tunnels p 2658 N94-28352

AUTONOMIC NERVOUS SYSTEM

Annals of the Research Inst. of Environmental Medicine, Nagoya Univ., volume 44
[REPT-44-VOL-44] p 2911 N94-27442

Postnatal changes in the autonomic modulation of L-type Ca(exp 2+) currents of rabbit ventricular cells
p 2931 N94-27535

Desensitization to acethylcholine in pacemaker cells of the sinoatrial node p 2908 N94-27537

Autonomic nervous system and cardiovascular control: Clinical implications of the 1/f fluctuations of heart rate
p 2932 N94-27540

AUTONOMY

Autonomous space processor for orbital debris advanced design project in support of solar system exploration p 2697 N94-25667

Autonomous support for microorganism research in space p 2903 N94-25672

Developing realistic cooperative behaviors for autonomous agents in air combat simulation
[AD-A274077] p 2937 N94-25774

Discovery learning in autonomous agents using genetic algorithms
[AD-A274083] p 2677 N94-25998

Autonomous rendezvous and docking for Space Station Freedom p 2684 N94-26286

Sensor-based navigation of a mobile robot using automatically constructed fuzzy rules
[DE94-001137] p 2986 N94-26948

Using discovery-based learning to prove the behavior of an autonomous agent
[AD-A274131] p 2987 N94-27121

AUTOREGRESSIVE PROCESSES

Three dimensional object recognition using a complex autoregressive model
[AD-A274388] p 2995 N94-26829

AUTOROTATION

Engine starting and stopping p 2828 N94-28047

AVALANCHES

Relativistic collision rate calculations for electron-air interactions
[DE94-004204] p 3020 N94-26527

AVIATION METEOROLOGY

A data fusion algorithm for multi-sensor microburst hazard assessment p 2641 N94-27287

AVIATION PSYCHOLOGY

Task demand, workload, and performance
[PB94-123627] p 2942 N94-27155

AVIONICS

A VHDL register transfer level model of the linear token passing multiplex data bus protocol for the high speed data bus
[AD-A273734] p 2980 N94-26009

Digital systems validation book plan. Volume 3: Handbook
[AD-A274099] p 2672 N94-26028

Research and test facilities
[NASA-TM-109685] p 2681 N94-26684

Real time avionics constraints: Silicon solutions
p 2949 N94-26717

The Ariane 5 data management system
p 2950 N94-26724

Ada multiple-programming for hard real time applications in space systems p 2951 N94-26730

Description of the Experimental Avionics Systems Integration Laboratory (EASILY)
[NASA-TM-109072] p 2681 N94-27425

AXIAL FLOW

The high Reynolds number flow through an axial-flow pump
[AD-A273844] p 2789 N94-25604

An investigation of the surge behavior of a high-speed ten-stage axial flow compressor
[AD-A274910] p 2674 N94-26345

Optimum for the gasdynamic system in a fast-axial-flow CO2 laser
[AD-A274305] p 2819 N94-26940

Circular cylinder in axial flow
[ISBN-0-315-59114-5] p 2798 N94-27873

AXIAL FLOW PUMPS

The high Reynolds number flow through an axial-flow pump
[AD-A273844] p 2789 N94-25604

AXIAL LOADS

The microstructural response of granular soil under uniaxial strain
[AD-A274808] p 2763 N94-26341

SAG compensated vibration isolation mount
[AD-D016040] p 2841 N94-27110

Series solution for a cylindrical composite shell subject to axisymmetric loadings
[ISBN-0-315-60559-6] p 2844 N94-27810

Calculation methods for steadily loaded axial groove hydrodynamic journal bearings (guide to use of computer program A9305)
[ESDU-93005] p 2830 N94-28074

AXIAL STRAIN

The microstructural response of granular soil under uniaxial strain
[AD-A274808] p 2763 N94-26341

AXISYMMETRIC BODIES

A numerical determination of bifurcation points for low Reynolds number conical flows
[AD-A273984] p 2791 N94-25991

AZO COMPOUNDS

Langmuir-Blodgett film of amylose-esters and chiral azo-dyes (structure and second order nonlinear optical behaviour)
[ETN-94-95390] p 2747 N94-25749

AZULENE

Analytical method for estimation of the total amount of aromatic and poly aromatic compounds in diesel fuel
[PB94-123692] p 2759 N94-25907

B

B-70 AIRCRAFT

Variability of measured sonic boom signatures
p 2651 N94-28197

BABOONS

Performance recovery in the baboon following (+)G sub z-induced loss of consciousness
[AD-A274411] p 2902 N94-26991

BACILLUS

Bakteriella toxiner-morgondagens hot (bacterial toxins-the threat of tomorrow)
[PB94-124229] p 2902 N94-27045

BACKGROUND NOISE

Prewhitening of colored noise fields for detection of threshold sources
[AD-A274346] p 3010 N94-26923

VHF-UHF noise surveys at Gulkana, Elmensdorf AFB, Galena AFB, Kotzebue and Cape Lisburne, Alaska and NRL, Pomonkey, Maryland
[PL-TR-93-2136] p 2777 N94-28211

BACKGROUND RADIATION

Secondary particle in background levels and effects on detectors at future hadron colliders
[DE94-003378] p 3011 N94-25598

A space fiber-optic x ray burst detector
[DE94-002722] p 2696 N94-26808

BACKSCATTERING
Elastic backscattering lidar for a MSTI satellite
[DE94-002701] p 2816 N94-26126
Diffusion of substitutional elements in Ti in its hcp phase
[DE93-633762] p 2733 N94-26160
Study of precipitation and recrystallization in Al alloy 2519 by backscattered electron imaging methods
[AD-A274919] p 2736 N94-26533
S-76 high intensity radiated fields, volume 2
[AD-A274572] p 2771 N94-26836
S-76 high intensity radiated fields, volume 3
[AD-A274416] p 2772 N94-26980

BACKWARD WAVES
HPm-tubes: Literature survey comprising 1992
[PB94-123643] p 2785 N94-27038

BACTERIA
Autonomous support for microorganism research in space p 2903 N94-25672
Bakteriella toxiner-morgondagens hot (bacterial toxins-the threat of tomorrow)
[PB94-124229] p 2902 N94-27045

BALANCING
Balancing of a planar bouncing object
[AD-A273805] p 2821 N94-25878
Efficient rebalancing of tree-type main memory dictionaries
[PB94-133105] p 3100 N94-28396

BALL BEARINGS
Space Shuttle main engine turbopump bearing assessment program
[NASA-TM-108447] p 2833 N94-28265

BALLISTIC MISSILES
Elastic backscattering lidar for a MSTI satellite
[DE94-002701] p 2816 N94-26126
The proliferation of aerospace weapons technology: Ballistic missiles and the case of Brazil
[ISBN-0-315-84082-X] p 2763 N94-26634
Enhanced tracking of airborne targets using forward looking infrared and laser return measurements
[AD-A274181] p 3037 N94-27102
Propellants and explosives in ballistic missiles
[UCRL-LR-113578] p 2760 N94-28222

BALLISTIC TRAJECTORIES
Trajectories of ballistic impact ejecta on a rotating Earth p 2887 N94-28295

BALLOON FLIGHT
PRONAOS flight software: A real-time application for a balloonborne scientific gondola p 2950 N94-26725
A measurement of the energy spectra of cosmic rays from 20 to 1000 GeV per AMU
[NASA-CR-195246] p 3115 N94-27167

BALLOON SOUNDING
In situ Mars ozone detector p 3108 N94-27892

BALLOON-BORNE INSTRUMENTS
In situ Mars ozone detector p 3108 N94-27892

BALLOONING MODES
Toroidal plasma beta-FLR limit in a toroidally linked mirror system
[DE94-003119] p 3041 N94-25792

BAND STRUCTURE OF SOLIDS
Technical report of ISSP. Ser. A, no. 2678: Magnetic properties of carbon nanotubes
[JTN-94-80564] p 3064 N94-27174
Technical report of ISSP. Ser. A, no. 2679: Novel electronic states of partially deuterated (DMe-DCNQI)2Cu
[JTN-94-80565] p 3064 N94-27175
Technical report of ISSP. Ser. A, no. 2674: High-field cyclotron resonance and impurity transition in n- and p-3C-SiC at magnetic fields up to 175 T
[JTN-94-80560] p 3064 N94-27232
Technical report of ISSP. Ser. A, no. 2670: Electronic structure of light transition metal compounds studied by photoemission
[JTN-94-80556] p 3065 N94-27239
Technical report of ISSP. Ser. A, no. 2675: High-field cyclotron resonance and valence-band structure in semiconducting diamond
[JTN-94-80561] p 3065 N94-27245
Technical report of ISSP. Ser. A, no. 2676: Charge mass singularity in two-dimensional Hubbard model
[JTN-94-80562] p 3065 N94-27248

BANDSTOP FILTERS
Evaluation of an Acoustic Charge Transport (ACT) device for adaptive interference suppression in spread spectrum communications systems
[AD-A274073] p 2765 N94-25647

BANDWIDTH
Encoding approaches for data link transmission of weather graphics
[AD-A274497] p 2772 N94-26963

BARIUM
High gas-efficiency hydrogen negative ion sources
[PB93-232163] p 3025 N94-27348
Superconducting fibers made with yttrium and yttrium oxide interlayers and barium cuprate cover layers
[AD-D016073] p 3070 N94-28225

BARIUM FLUORIDES
Ferroelectric fluoride memory FET development
[AD-A274341] p 2785 N94-27057

BARIUM OXIDES
Synthesis, rheology, and forming of Y-Ba-Cu-O ceramics
[DE94-005558] p 2757 N94-27695

BARKHAUSEN EFFECT
Power laws, flicker noise, and the barkhausen effect
[AD-A274702] p 3008 N94-26376

BARORECEPTORS
Muscle sympathetic nerve activity in humans
p 2932 N94-27538
Does training-induced orthostatic hypotension result from reduced carotid baroreflex responsiveness?
p 2935 N94-28366

BAROTROPIC FLOW
Global barotropic response to a tropical forcing
[NASA-CR-195256] p 2896 N94-27408

BARRIER LAYERS
Chemical vapor deposition and characterization of tungsten boron alloy films
[DE94-002648] p 2738 N94-26610

BARYONS
Dibaryon-induced instability of neutron stars
[DE93-634453] p 3103 N94-26046
The delta (1232) resonance transition form factor
[DE94-003442] p 3017 N94-26101
The meaning of EROS/MACHO
[DE94-003003] p 3104 N94-26311
Mesons and diquarks in a NJL-model at finite temperature and chemical potential
[DE93-634375] p 3020 N94-26505
Signatures for hybrids
[DE94-004244] p 3020 N94-26574
Strange Dibaryons
[DE94-003005] p 3022 N94-26769
Spectroscopy and strong decays of baryons
[ISBN-0-315-49073-X] p 3024 N94-27258
Topics in electroweak baryogenesis: The sphaleron and T-violation
[DE94-004886] p 3029 N94-27811

BASE PRESSURE
The effects of three-dimensional imposed 3-d disturbances on bluff-body near wake flows
[AD-A274845] p 2791 N94-26187

BATHS
Effects of bathing at 40 C on cardiovascular system in humans: Comparison with 34 C thermoneutral bathing
p 2918 N94-27473
Effects of 41 C bathing for 20 minutes on cardiovascular and thermoregulatory functions in humans
p 2918 N94-27474

BATHYMETERS
Correlation between the gravity field and the bathymetry in the North Atlantic Ocean
[ETN-94-95036] p 2899 N94-26108
Bathymetric data set extraction program. Users guide
[AD-A274761] p 2899 N94-26567
Compilation of corrections for postprocessing of laser bathymetry data
[PB94-123668] p 2900 N94-27156
Scanview: A grafical program for analysis of laserbathymetry data
[PB94-124443] p 2900 N94-27208

BATTERY CHARGERS
Method of optimizing the charging of a battery of storage cells, and apparatus for performing the method
[AD-D016066] p 2781 N94-26102

BAYES THEOREM
Introduction to bayesian nonparametric theory
[PB94-125002] p 3004 N94-26939
Development of a performance evaluation tool (MMSOFE) for detection of failures with Multiple Model Adaptive Estimation (MMAE)
[AD-A274218] p 2665 N94-27071

BEAM CURRENTS
Bundle Intensity and Beamgate Length recorder (BIBL)
[DIGEL-1993-7] p 3031 N94-25619

BEAM INJECTION
Heavy neutral beam probe for edge plasma analysis in tokamaks
[DE94-003391] p 3041 N94-25846
New conditioning procedure derived from operating experience with the Common Long-Pulse Ion Source
[DE94-002891] p 3045 N94-26865
Kinoform/lens system for injecting a high power laser beam into an optical fiber
[DE94-003226] p 2819 N94-27262
High gas-efficiency hydrogen negative ion sources
[PB93-232163] p 3025 N94-27348
Shine through measurements with hydrogen beam in JT-60
[DE94-701113] p 3047 N94-27699
Fast H-alpha line broadening during the 100 ns REB injection into a plasma
[IPPCZ-322] p 3048 N94-27836

BEAM INTERACTIONS
Space Experiments with Particle Accelerators (SEPAC)
[NASA-CR-193935] p 2761 N94-27664

BEAM SPLITTERS
High definition Raman microscopic imaging
[DE94-003158] p 2716 N94-26781
High repetition rate, mode locked, figure eight laser with extracavity feedback
[AD-D016053] p 2820 N94-27670

BEAM WAVEGUIDES
On a theory of two-beam mechanisms of charged particle acceleration in electrodynamic structures
[DE94-003482] p 3032 N94-26330
Design and evaluation of an electromagnetic beam waveguide for measuring electrical properties of materials
[NASA-TP-3418] p 2769 N94-26611

BEAMFORMING
Analyzing adaptive beamformer performance in a stable multipath environment
[AD-A274029] p 2766 N94-25766
Meteor Burst Communications (MBC) throughput improvement tests
[AD-A273941] p 2767 N94-25990
A current evaluation of the digital beamforming testbed at Rome Laboratory
[AD-A274311] p 3032 N94-26881
Beamforming/null-steering adaptive array
[CA-PATENT-1325260] p 2775 N94-27270
Neutron-neutron scattering: Possibility of in-beam experiment
[DE94-606459] p 3027 N94-27682

BEAMS (RADIATION)
Characterization of acoustic effects on flame structures by beam deflection technique
[DE94-003240] p 2714 N94-26122
A current evaluation of the digital beamforming testbed at Rome Laboratory
[AD-A274311] p 3032 N94-26881

BEAMS (SUPPORTS)
Dynamics of a flexible extendible beam
[ISBN-0-315-84278-4] p 2838 N94-26639
Response of structures to impact loads using elastic and plastic analysis
[ISBN-0-315-84647-X] p 2842 N94-27309
On the Lagrangian and updated Lagrangian nonlinear finite element formulations
[ISBN-0-315-61111-1] p 3001 N94-27948

BEARINGS
An algorithm for determination of bearing health through automated vibration monitoring
[AD-A274591] p 2823 N94-26986

BEAUFORT SEA (NORTH AMERICA)
An evaluation of an airborne remote sensing system used to determine ice thickness and geometry of a first year sea ice ridge located in the Beaufort Sea
[ISBN-0-315-84383-7] p 2849 N94-26667
Leadex environmental phenomena and effects observed by DMSP, NOAA, and ERS-1 satellites
[AD-A274596] p 2868 N94-26888

BED REST
Intermittent gravity: How much, how often, how long?
[NASA-TM-108800] p 2944 N94-26098

BEHAVIOR
The central executive component of working memory
[AD-A274295] p 2938 N94-26683

BELL AIRCRAFT
Experimental investigation of advanced hub and pylon fairing configurations to reduce helicopter drag
[NASA-TM-4540] p 2668 N94-26604

BEND TESTS
Structure and properties of intermetallic composites synthesized in situ using solid state displacement reactions
[DE94-004312] p 2705 N94-25805
Stress analysis of a secondary-bending specimen
[AD-A274842] p 2838 N94-26501

BENDING
Use of photostress and strain gages to analyze behavior of weldments
[NASA-CR-195269] p 2843 N94-27765

BENDING MOMENTS
Design of cold-formed HSS channels for bending and eccentric compression: Bending in the plane of symmetry
[VTT-TIED-1403] p 2762 N94-25622

Refined triangular plate and shell elements
[PB94-126356] p 2839 N94-26875

BENDING THEORY
Creation of prototype aircrew protection equipment based on face anthropometry
[AD-A273865] p 2940 N94-25611

BENZENE
Transition metal activation and functionalization of carbon-hydrogen bonds
[DE94-003650] p 2715 N94-26369

BERYLLIUM
Space-R thermionic space nuclear power system: Design and technology demonstration
[DE94-001890] p 2699 N94-25929
An investigation of the effect of surface impurities on the adsorption kinetics of hydrogen chemisorbed onto iron
[NASA-CR-195213] p 2716 N94-26643
Study of the process (pi)(sup -)A(yields)(pi)(sup -)(eta)'(eta)A at the moment 36 GeV/c
[DE93-634530] p 3024 N94-27250
Experiment of neutron multiplication in beryllium
[DE94-604605] p 2742 N94-27730

BESSEL FUNCTIONS
How to build analogues of the Bessel-Clifford expansions for the sum of the repulsive Coulomb potential and central potential decreasing more rapidly than the centrifugal one?
[DE93-634308] p 3007 N94-26472

BETATRONS
Laboratory plasma studies
[AD-A274655] p 3043 N94-26356

BETHE-SALPETER EQUATION
Weak interactions in a bilocal chiral theory
[DE93-613097] p 3013 N94-25836
String hypothesis and characters of coset CFTs
[DE93-634337] p 3007 N94-26552
Solution of the Heisenberg equation for the four-fermion contact interaction by the method of dynamical mappings
[DE94-606341] p 3075 N94-27858

BIBLIOGRAPHIES
International energy: Research organizations, 1988-1992
[DE93-017267] p 3098 N94-26398
Volcanology and volcanic activity with a primary focus on potential hazard impacts for the Hawaii geothermal project
[DE94-001614] p 2879 N94-26515
Bibliography of technical reports, 1992
[AD-A274849] p 3098 N94-26561
International bulletin on atomic and molecular data for fusion. No. 42-45, Mar. 1991 - Dec. 1992
[DE94-601817] p 3045 N94-26946
International bulletin on atomic and molecular data for fusion. No. 46
[DE94-601818] p 3023 N94-26947
Bibliographic Retrieval System (BARS) Sandia Shock Compression (SSC) database Shock Physics Index (SPHINX) database, volume 3
[DE94-001705] p 3099 N94-27022
Microbiology research at some research institutes in the former Soviet Union: A survey of scientific publications
[PB94-123320] p 2902 N94-27171
List of papers published by the members of Institute for Materials Research, Tohoku University 1992
[JTN-94-80608] p 3118 N94-27355
Center for space microelectronics technology
[NASA-CR-195282] p 2786 N94-27574
NASA SBIR abstracts of 1992, phase 1 projects
[NASA-TM-109694] p 3094 N94-27772
Aeronautical engineering: A continuing bibliography with indexes (supplement 301)
[NASA-SP-7037(301)] p 2643 N94-28203
Aerospace medicine and biology: A cumulative index to a continuing bibliography (supplement 384)
[NASA-SP-7011(384)] p 2934 N94-28219

BICRYSTALS
Influence of point defects on grain boundary diffusion in oxides
[DE94-003164] p 3060 N94-26782

BIG BANG COSMOLOGY
Cosmological phase transitions
[DE94-003001] p 3104 N94-26786

BINARY ALLOYS
Reference electrodes for solid polymer electrolytes
[DE94-004583] p 2780 N94-25806
Dissolution of secondary phases during extrusion
[PB94-124583] p 2732 N94-25908
Stress corrosion cracking and dealloying of copper-gold alloy in iodine vapor
[DE93-633790] p 2734 N94-26264
Eutectic transformation L in equilibrium to Zr6Fe23 + Fe(tau) in the Fe-Zr system
[DE93-633766] p 2735 N94-26295
A tri-junction diffusion couple analysis of the Nb-Cr-Ti system at 950 C
[DE94-002637] p 2737 N94-26607
Differential scanning calorimetric study of solid state amorphization and crystallization in Zr/Co and Zr/Ni multilayers p 2745 N94-28161

BINARY DATA
The morphological processing of binary images
[AD-A274310] p 2996 N94-26972
Kinoform/lens system for injecting a high power laser beam into an optical fiber
[DE94-003226] p 2819 N94-27262
Binary snapshots
[CWI-CS-R9319] p 2955 N94-27547

BINARY FLUIDS
Solubility, viscosity, and density of refrigerant/lubricant mixtures
[DE94-004237] p 2721 N94-28069

BINARY INTEGRATION
New binary integration strategies and corresponding R90 calculations
[AD-A274786] p 2769 N94-26359

BINARY MIXTURES
Automated system for gas detectors providing with binary mixtures
[DE93-634192] p 2715 N94-26406

BINARY STARS
Ultraviolet observations of astronomical sources
[NASA-CR-195232] p 3102 N94-26234
TEV emission from close binaries
[DE93-634330] p 3104 N94-26268

BINARY SYSTEMS (MATERIALS)
Bimaterial interfaces and their role in the mechanical performance of the in-situ composites
[AD-A274688] p 2707 N94-26447

BINAURAL HEARING
Binaural room simulation
[AD-A273823] p 3009 N94-25737

BINDERS (MATERIALS)
Polyurethane self-priming topcoats
[AD-D016041] p 2755 N94-27111
Thermoplastic elastomers having alternate crystalline structure for us as high energy binders
[AD-D016035] p 2755 N94-27203

BINOCULAR VISION
Parallel algorithm for dominant points correspondences in robot binocular stereo vision p 2686 N94-27364

BIOACOUSTICS
Comparison of methods of predicting community response to impulsive and nonimpulsive noise
p 2651 N94-28196

BIOASTRONAUTICS
Plasma volume shifts and exercise thermoregulation with water immersion and six-degree head-down tilt
[NASA-TM-108781] p 2901 N94-26093
Spacelab life sciences 2 post mission report
[NASA-CR-195544] p 2942 N94-27410
Aerospace medicine and biology: A cumulative index to a continuing bibliography (supplement 384)
[NASA-SP-7011(384)] p 2934 N94-28219
Does training-induced orthostatic hypotension result from reduced carotid baroreflex responsiveness?
p 2935 N94-28366
Cardiac output and cardiac contractility by impedance cardiography during exercise of runners
p 2935 N94-28367
Weightlessness and the human skeleton: A new perspective p 2935 N94-28368

BIOCHEMISTRY
The 27th Annual Meeting of the Israel Society for Microscopy and the 12th Annual Meeting of the Israel Society for Histochemistry and Cytochemistry
[DE93-632416] p 2716 N94-26519

BIOCONVERSION
Report of National Institute for Resources and Environment. No. 5: Study on direct liquefaction of woody biomass
[JTN-94-80551] p 2859 N94-27204
Collaboration of chemical oxidation and biological treatment for removal of refractory organic substances
p 2870 N94-28149
Treatment of refractory organic substances with combined use of chemical oxidation and biological treatment. Part 2: Biodegradability of ozonation products of chlorophenol p 2870 N94-28151

BIODEGRADABILITY
High impact strength poly(lactide) tough biodegradable materials
[ETN-94-95389] p 2747 N94-25748

BIODEGRADATION
High impact strength poly(lactide) tough biodegradable materials
[ETN-94-95389] p 2747 N94-25748

BIODYNAMICS
A biologically-inspired autonomous robot
[AD-A273909] p 2821 N94-25782
Comparison of methods of predicting community response to impulsive and nonimpulsive noise
p 2651 N94-28196
Workshop on Countering Space Adaptation with Exercise: Current Issues
[NASA-CP-3252] p 2934 N94-28361
Muscular activity and its relationship to biomechanics and human performance p 2934 N94-28362
The use of biomechanics in the study of movement in microgravity p 2936 N94-28373

BIOELECTRIC POTENTIAL
Effects of high-intensity electric field stimulation on the electromechanical performance of cardiac muscle: Influence of fiber orientation p 2904 N94-27467
On the mechanism of reentrant arrhythmias following DC defibrillation: Influence of fiber orientation to the effects of low-energy electric field stimulation on the effective refractory period of cardiac muscle
p 2904 N94-27468

BIOELECTRICITY
Positive chronotropic effect of mechanical stretch on the sinoatrial node: Roles of neurotransmitters and stretch activated channels p 2904 N94-27469
Effects of perfusion of amiodarone on electrophysiological properties in single rabbit ventricular myocytes p 2906 N94-27503
Fast and slow onsets of Na channel blocking actions due to lidocaine and disopyramide using concentration-clamp method p 2907 N94-27504
Electrophysiological effects of MS-551, a new Class 3 antiarrhythmic agent, on isolated rabbit ventricular muscles p 2907 N94-27505
Comparative investigation of new Class 3 antiarrhythmic drugs, E-4031 and MS-551, on electrophysiological properties in isolated rabbit ventricular myocytes
p 2907 N94-27506
Effects of Class 1 antiarrhythmic drugs on the intraventricular conduction: Influence of fiber orientation
p 2907 N94-27507
Effects of Class 3 antiarrhythmic agents, E-4031 and MS-551 on ventricular repolarization in isolated rabbit hearts p 2907 N94-27508
Electrical coupling between the sino-atrial node and atrial muscle: Cell to cell interaction through an external circuit and its simulation by computer modeling
p 2907 N94-27509
A study on tissue excitation of cardiac muscle under electrical field stimulation p 2907 N94-27510
Block of cardiac sodium channels by Ro 22-9194 (R), a new antiarrhythmic agent: Effects on the maximum upstroke velocity (Vmax) of single guinea pig ventricular myocytes p 2907 N94-27511
Electrophysiological effects of an antiarrhythmic drug, moricizine on isolated guinea pig ventricular muscles
p 2907 N94-27512
Correlation between electrical activity and the size of single sinoatrial node cells p 2907 N94-27513
The ionic mechanism underlying the negative chronotropic effect of acetylcholine: Experimental study in rabbit single sinoatrial node cells
p 2908 N94-27514
The ionic mechanism underlying the negative chronotropic effect of acetylcholine: Experiments using small sinoatrial node tissue preparations isolated from rabbit hearts p 2908 N94-27515
The ionic mechanism underlying the negative chronotropic effect of acetylcholine: Postganglionic vagal stimulation in isolated rabbit hearts
p 2908 N94-27516
Desensitization to acethylcholine in pacemaker cells of the sinoatrial node p 2908 N94-27537

BIOINSTRUMENTATION
Monitoring activity with a wrist-worn actigraph: Effects of amplifier passband and threshold variations
[AD-A274705] p 2909 N94-26377
A comparison of sleep scored from electroencephalography to sleep scored by wrist actigraphy
[AD-A273739] p 2910 N94-26748
The measurements of muscle blood flow by laser Doppler flowmetry with needle type probe
p 2908 N94-27530

BIOLOGICAL EFFECTS
Initial ultraviolet-B intensity data at Lawrence Livermore National Laboratory
[DE94-004279] p 2869 N94-27267
Aerospace medicine and biology: A continuing bibliography with indexes (supplement 386)
[NASA-SP-7011(386)] p 2933 N94-28208
Aerospace medicine and biology: A continuing bibliography with indexes (supplement 387)
[NASA-SP-7011(387)] p 2933 N94-28213
Aerospace medicine and biology: A cumulative index to a continuing bibliography (supplement 384)
[NASA-SP-7011(384)] p 2934 N94-28219

Irreversibility of advanced osteoporosis: Limited role for pharmacologic intervention p 2935 N94-28369

BIOLOGICAL MODELS (MATHEMATICS)

Temporal stochasticity leads to nondeterministic chaos in a model for blood cell production [DE94-003943] p 2933 N94-27744

BIOMAGNETISM

Detection geometry and reconstruction error in magnetic source imaging [DE94-004012] p 2809 N94-25662

BIOMASS

Implications of policies and prevent climate change for future food security [DE93-018872] p 2866 N94-25948

Coupling of pelagic and benthic communities over a seamount in the Eastern North Pacific [AD-A274750] p 2899 N94-26149

Feasibility study on introduction of the bio-fuel power generation in tropical regions [DE94-725203] p 2858 N94-26838

Woody biomass density in the Tendelti area of the central Sudan p 2850 N94-27185

Report of National Institute for Resources and Environment. No. 5: Study on direct liquefaction of woody biomass [JTN-94-80551] p 2859 N94-27204

Role of remote sensing in energy, water, and carbon cycle studies over the Amazon [INPE-5486-PRE/1786] p 2852 N94-27957

Note on the structure of moss colonies composed of two species on King George Island, the South Shetland Islands p 2885 N94-27971

Changes in phytoplankton population in the Chao Phraya estuary, Thailand, during the eutrophication mechanisms studies p 2875 N94-28287

BIOMASS ENERGY PRODUCTION

Coupling of pelagic and benthic communities over a seamount in the Eastern North Pacific [AD-A274750] p 2899 N94-26149

Feasibility study on introduction of the bio-fuel power generation in tropical regions [DE94-725203] p 2858 N94-26838

Present situation of the development of petroleum substitution energy (France) [DE94-725201] p 2760 N94-26914

Report of National Institute for Resources and Environment. No. 5: Study on direct liquefaction of woody biomass [JTN-94-80551] p 2859 N94-27204

BIOMEDICAL DATA

Biomedical polyurethane networks [ETN-94-95391] p 2750 N94-26211

BIOPHYSICS

Neutrons in biology [DE94-701085] p 2903 N94-27862

BIOSPHERE

Spiral Survey Expedition: A proposal to organize for the Survey, exploration and eventual colonization of the Milky Way Galaxy p 2686 N94-27366

Proposed law of nature linking impacts, plume volcanism, and Milankovitch cycles to terrestrial vertebrate mass extinctions via greenhouse-embryo death coupling p 2876 N94-28307

BIPOLAR TRANSISTORS

Development of a 4-bit parallel analog-to-digital converter and a four-quadrant double-balanced mixer using heterojunction bipolar transistor technology [AD-A274074] p 2947 N94-25648

A physics-based heterojunction bipolar transistor model for integrated circuit simulation [AD-A274081] p 2781 N94-25995

Silicon device performance measurements to support temperature range enhancement [NASA-CR-195265] p 2844 N94-27824

BIPOLARITY

Bipolar lead-acid batteries for electrical actuation applications p 2864 N94-28134

Bipolar Ag-Zn battery p 2864 N94-28135

BIRD-AIRCRAFT COLLISIONS

A feasibility study on bird classification with neural network [AD-A273753] p 2659 N94-25780

BIRDS

A feasibility study on bird classification with neural network [AD-A273753] p 2659 N94-25780

Antarctic Record, Vol. 36, No. 2 [REPT-107] p 2883 N94-27963

Counting Adelie penguins at colonies: Seasonal and annual changes p 2885 N94-27970

BIREFRINGENCE

Three-wave nonlinear interactions in KTiOPO4 (KTP) and KTP isomorphs [AD-A274079] p 3052 N94-25993

BISMUTH ALLOYS

Research into the microstructure and mechanical behavior of eutectic Bi-Sn and In-Sn [DE94-004558] p 2741 N94-27619

BISMUTH COMPOUNDS

The potential for large critical currents in the high T(sub c) oxides p 2854 N94-26058

Energy Dispersive X ray Diffraction (EDXD) apparatus for liquids at high temperature p 2721 N94-28159

BISMUTH OXIDES

Technical report of ISSP. Ser. A, no. 2672: Magneto-optical effects of excitons in BiI3 crystals under pulsed high magnetic fields. 3: Excitons confined around a stacking disorder formed by a bending stress [JTN-94-80558] p 3065 N94-27240

BIT ERROR RATE

On the performance of trellis coded 8PSK with Reed Solomon codes [ISBN-0-315-84289-X] p 2770 N94-26626

Annex report FEL-92-A163: Description of the Link and BER Test Analysis System (LIBERTAS) for the frequency band V (14.5 - 15.3 GHz) [FEL-92-A442] p 2770 N94-26650

Coded communications with nonideal interleaving [ITN-94-85235] p 2774 N94-27242

BLACKOUT (PHYSIOLOGY)

Performance recovery in the baboon following (+)G sub z-induced loss of consciousness [AD-A274411] p 2902 N94-26991

BLADE TIPS

Behaviour of separation bubbles in sharp-edged gaps of finite dimensions [ISBN-0-315-84113-3] p 2793 N94-26637

BLADE-VORTEX INTERACTION

Correlation of airloads on a two-bladed helicopter rotor [NASA-TM-103982] p 2644 N94-26143

BLANKETS (FUSION REACTORS)

A robust helium-cooled shield/blanket design for ITER [DE94-003402] p 3043 N94-26323

BLAST LOADS

Shock wave interaction with L-shaped structures [AD-A273774] p 2790 N94-25858

Safety standards for aircraft shelter [FFI-92/4003] p 2680 N94-26305

BLOCK COPOLYMERS

Thermoplastic elastomers having alternate crystalline structure for us as high energy binders [AD-D016035] p 2755 N94-27203

BLOOD

Endocrinological evaluations of muscle and bone atrophy in tail-suspended rats p 2903 N94-27444

BLOOD CELLS

Temporal stochasticity leads to nondeterministic chaos in a model for blood cell production [DE94-003943] p 2933 N94-27744

BLOOD CIRCULATION

Analysis on one minute wave in body fluid volume and muscle pumping referred to body parts generating the one minute wave during human active standing p 2929 N94-27528

Evaluation of near-infrared spectrophotometric method for individual tolerance to +Gz acceleration p 2933 N94-27944

BLOOD FLOW

EcarHeart2 version 1.0: Programmers documentation [PB94-124633] p 2909 N94-25909

Pulse waveform and transcranial Doppler analysis during lower body negative pressure [AD-A274516] p 2911 N94-27088

Effect of prostaglandin E1 on the relationship between skin sympathetic nerve activity and reduction in skin blood flow p 2929 N94-27524

Difference in skin blood flow reduction depending on activating maneuver of skin sympathetic nerve activity p 2929 N94-27525

The measurements of muscle blood flow by laser Doppler flowmetry with needle type probe p 2908 N94-27530

Enhancement of skin sympathetic nerve activity in amyotrophic lateral sclerosis p 2930 N94-27532

Evaluation of near-infrared spectrophotometric method for individual tolerance to +Gz acceleration p 2933 N94-27944

Proposed law of nature linking impacts, plume volcanism, and Milankovitch cycles to terrestrial vertebrate mass extinctions via greenhouse-embryo death coupling p 2876 N94-28307

BLOOD GROUPS

Protective action of platelet-activating factor antagonist, TCV-309, against ischemia reperfusion injury in isolated rabbit hearts p 2904 N94-27465

BLOOD PRESSURE

Passive and active behavior of the cardiovascular system under increased gravitational loads in a chronically instrumental conscious baboon model [AD-A274344] p 2910 N94-26973

Aerobic fitness and orthostatic tolerance: Evidence against an association p 2934 N94-28365

BLOOD VOLUME

Plasma volume shifts and exercise thermoregulation with water immersion and six-degree head-down tilt [NASA-TM-108781] p 2901 N94-26093

Passive and active behavior of the cardiovascular system under increased gravitational loads in a chronically instrumental conscious baboon model [AD-A274344] p 2910 N94-26973

BLOWDOWN WIND TUNNELS

Experimental investigation of the flow quality in the GLT20 subsonic-transonic boundary layer wind tunnel [PB94-126539] p 2681 N94-26815

Aerodynamic heating in hypersonic flows p 2658 N94-27919

BLOWING

Controlled oscillation of forebody vortices by nozzle jet blowing [ISBN-0-315-84134-6] p 2678 N94-27648

Theoretical and experimental investigation of a delta wing with turbulent leading-edge jets p 2659 N94-28029

BLUFF BODIES

Flow past a circular cylinder with a permeable wake splitter plate [AD-A273765] p 2790 N94-25872

The effects of three-dimensional imposed 3-d disturbances on bluff-body near wake flows [AD-A274845] p 2791 N94-26187

Nominally 2-dimensional flow about a normal flat plate [AD-A274472] p 2794 N94-27026

Research on bluff body vortex wakes [AD-A273780] p 2796 N94-27319

BLUNT LEADING EDGES

The effect of axial velocity ratio, turbulence intensity, incidence, and leading edge geometry on the midspan performance of a turbine cascade p 2652 N94-28321

BLUNT TRAILING EDGES

A study of blunt trailing edge airfoils using the Navier Stokes code: ARC2D p 2656 N94-28340

BODIES OF REVOLUTION

New variational techniques for acoustic radiation and scattering from elastic shell structures [AD-A274599] p 3010 N94-26889

BODY CENTERED CUBIC LATTICES

Volume dependence of vanadium magnetism [DE94-601838] p 3050 N94-25843

Formation and crystallization of hydrogen-induced amorphous Ti3InH(4.5) alloy p 2745 N94-28163

BODY FLUIDS

Multivariate calibration applied to near-infrared spectroscopy for the quantitative analysis of dilute aqueous solutions [DE94-003231] p 2716 N94-26794

Changes in fluid and electrolyte metabolism during water immersion at high or thermoneutral temperature p 2912 N94-27445

Analysis on one minute wave in body fluid volume and muscle pumping referred to body parts generating the one minute wave during human active standing p 2929 N94-27528

BODY SWAY TEST

Frequency analysis of body sway induced by optokinetic stimulation p 2914 N94-27455

BODY TEMPERATURE

Rewarming methodologies in the field [AD-A274744] p 2909 N94-26173

Effects of 40 C hot water immersion for an hour on thermoregulatory functions in humans: Comparison with 34 C thermoneutral immersion p 2915 N94-27459

BODY VOLUME (BIOLOGY)

Selection of site injecting adjuvant in chronic inflammation model p 2906 N94-27496

BODY-WING CONFIGURATIONS

Euler and Navier-Stokes wing/fuselage computations of the De Havilland Dash 8 aircraft p 2654 N94-28329

BOEING 727 AIRCRAFT

After thirty years: Farewell of Europa jet p 2663 N94-28249

BOEING 757 AIRCRAFT

Special investigation report: Safety issues related to wake vortex encounters during visual approach to landing [PB94-917002] p 2660 N94-27881

BOILERS

Control of a hydrogen/oxygen steam generator [DLR-FB-93-02] p 2826 N94-27589

Steam plant for combined cycles: Heat recovery steam generators, design principles, and construction details p 2831 N94-28083

BOLTS

Mechanically fastened composite laminates subjected to combined bearing-bypass and shear loading
p 2712 N94-27914

BOLTZMANN TRANSPORT EQUATION

Refractive and dielectric properties of helium, argon and nitrogen gases
[PB94-123783] p 3008 N94-26851

BONDED JOINTS

Investigation of the bond strength of a discrete skin-stiffener interface
[NLR-TP-92183-U] p 2670 N94-27796

BONDING

Attachment techniques for high temperature strain
[AD-A274766] p 2811 N94-26568

Sealant research for solid oxide fuel cells
[DE94-000015] p 2857 N94-26584

Molecular surface electrostatic potentials in the analysis of non-hydrogen-bonding noncovalent interactions
[AD-A274612] p 3022 N94-26894

Intelligent material systems and structures. Part 6: Measurements of adhesion between optical fibres and composite materials
[PB94-123577] p 2756 N94-27215

BONE DEMINERALIZATION

Endocrinological evaluations of muscle and bone atrophy in tail-suspended rats p 2903 N94-27444

Workshop on Countering Space Adaptation with Exercise: Current Issues
[NASA-CP-3252] p 2934 N94-28361

Weightlessness and the human skeleton: A new perspective p 2935 N94-28368

Irreversibility of advanced osteoporosis: Limited role for pharmacologic intervention p 2935 N94-28369

BONE MINERAL CONTENT

Endocrinological evaluations of muscle and bone atrophy in tail-suspended rats p 2903 N94-27444

Irreversibility of advanced osteoporosis: Limited role for pharmacologic intervention p 2935 N94-28369

BONES

Skeletal development and ossification of the swine fetuses p 2905 N94-27491

Weightlessness and the human skeleton: A new perspective p 2935 N94-28368

Irreversibility of advanced osteoporosis: Limited role for pharmacologic intervention p 2935 N94-28369

Exercise and osteoporosis: Methodological and practical considerations p 2935 N94-28370

BOOLEAN ALGEBRA

Communication complexity of t-intersection problems in generalized Boolean algebras
[PB94-126646] p 2996 N94-26917

BOREHOLES

Wave propagation in the shallow regions of the earth's crust and the borehole vicinity
[ITN-94-85237] p 2882 N94-27330

BORN APPROXIMATION

Holes in a two-dimensional quantum antiferromagnet
[DE93-634753] p 3057 N94-26388

BORON

An atom probe investigation of the influence of trace impurities on the mechanical behavior of NiAl
[DE94-002797] p 2734 N94-26272

BORON ALLOYS

Chemical vapor deposition and characterization of tungsten boron alloy films
[DE94-002648] p 2738 N94-26610

Production of an amorphous Fe(75)Si(10)B(15) sheet by a metallic mold casting method and its properties
p 2746 N94-28170

BORON CARBIDES

Deformation twinning: Influence of strain rate
[DE94-002693] p 2738 N94-26621

Examination of hardness, fracture toughness and microstructure in Al2O3-B4C binary ceramics
[PB94-124237] p 2755 N94-27158

BORON NITRIDES

R and D for creation, measurement, application of ultra-high vacuum p 2723 N94-25549

High performance fibers
[AD-A274693] p 2707 N94-26450

The deposition of boron nitride and carbon films on silica glass fibers
[DE94-004684] p 2751 N94-26564

BOROSILICATE GLASS

Porous vycor glass tube joined to borosilicate glass
p 2718 N94-27392

BOSON FIELDS

Differential regularization of a non-relativistic anyon model
[DE94-601558] p 3019 N94-26416

BOSONS

CP violating form factors for three gauge boson vertex in the two Higgs doublet and left-right symmetric models
[DE94-601704] p 3014 N94-25841

CP violation in Higgs decays
[DE94-601607] p 3014 N94-25888

Quantizable configurations of the relativistic string
[DE93-634346] p 3072 N94-26036

JLC-1
[DE93-520380] p 3031 N94-26113

Differential regularization of a non-relativistic anyon model
[DE94-601558] p 3019 N94-26416

Progress in SSC Higgs physics: Report of the Higgs working group
[DE94-003224] p 3022 N94-26793

Flavor changing neutral currents in SU(3) x U(1) models
[DE94-602576] p 3022 N94-26899

Finding the missing pieces of the standard model
[ISBN-0-315-57174-8] p 3024 N94-27259

An analysis of monojet data in p(bar-p) collisions at square root of s equal to 1.8 TEV
[DE94-001822] p 3026 N94-27565

A measurement of the W mass using electrons at CDF
[DE94-004656] p 3028 N94-27748

BOUNDARIES

Hydrographic and Acoustic Doppler Current Profiler (ADCP) data from the ONR eastern boundary current accelerated research initiative, 9-16 June 1992
[AD-A274115] p 2898 N94-26076

BOUNDARY CONDITIONS

Extension of On-Surface Radiation Condition (OSRC) theory to full-vector electromagnetic wave scattering by three-dimensional conducting, dielectric, and coated targets
[AD-A274023] p 2766 N94-25757

Sensitivity of climate models: Comparison of simulated and observed patterns for past climates
[DE93-019934] p 2865 N94-25789

On the oscillation of a class of hyperbolic equations of neutral type
[DE93-616815] p 2990 N94-25829

Oscillatory behaviour of solutions of coupled hyperbolic differential equations of neutral type
[DE93-616816] p 2990 N94-25830

The Dirac equation in Kerr spacetime, spheroidal coordinates and the M.I.T. bag model of hadrons
[DE94-601566] p 3006 N94-25886

Prediction of undsteady flows in turbomachinery using the linearized Euler equations on deforming grids
[NASA-CR-195285] p 2675 N94-27654

Uncertainties in the characterization of the thermal environment of a solid rocket propellant fire
[DE94-002023] p 2760 N94-27719

Modeling of the coupled magnetospheric and neutral wind dynamos
[NASA-CR-195273] p 2883 N94-27852

A numerical investigation of a subsonic jet in a crossflow p 2803 N94-28023

Calculation of single and multiple jets in cross-flow with and without impingement using Reynolds-stress-transport closure p 2803 N94-28024

Predictions of momentum and scalar fields in a jet in cross-flow using first and second order turbulence closures p 2803 N94-28025

Navier-Stokes analysis of a swirling jet in crossflow
p 2806 N94-28038

On the zeros of solutions of forced parabolic differential equations of neutral type
[DE93-613019] p 3001 N94-28228

BOUNDARY LAYER EQUATIONS

A study on structure of benthic boundary layer in coastal waters
[REPT-4] p 2898 N94-25635

BOUNDARY LAYER FLOW

A study on structure of benthic boundary layer in coastal waters
[REPT-4] p 2898 N94-25635

Performance of renormalization group algebraic turbulence model on boundary layer transition simulation
[NASA-CR-194466] p 2644 N94-26131

An investigation into the aerodynamic effects of wing patches
[ISBN-0-315-84121-4] p 2646 N94-26672

Experimental investigation of the flow quality in the GLT20 subsonic-transonic boundary layer wind tunnel
[PB94-126539] p 2681 N94-26815

Turbulent boundary layer inner-outer interactions
[AD-A274357] p 2794 N94-27059

Numerical simulation of receptivity and transition in a boundary layer on a flat plate with a suction hole
[NASA-CR-195708] p 2798 N94-27782

Circular cylinder in axial flow
[ISBN-0-315-59114-5] p 2798 N94-27873

An experimental study of siphonal jets in a turbulent boundary layer crossflow p 2802 N94-28015

Analysis of cooling jets near the leading edge of turbine blades p 2676 N94-28037

Unified approach for direct and inverse boundary layer prediction using cubic spline collocation
p 2653 N94-28326

Euler and Navier-Stokes wing/fuselage computations of the De Havilland Dash 8 aircraft p 2654 N94-28329

Viscous airfoil computations using adaptive structured grids p 2655 N94-28337

Attached and separated trailing edge flow measurements with a triple-split hot-film probe
p 2656 N94-28339

A study of blunt trailing edge airfoils using the Navier Stokes code: ARC2D p 2656 N94-28340

Thin-layer Navier-Stokes computations for multi-element airfoils p 2656 N94-28341

Ice accretion on aircraft wings p 2657 N94-28345

Preliminary assessment of aerodynamic effects of wing repair patches p 2657 N94-28346

Experimental investigations into the wall interference and sidewall boundary layer effects in the National Research Council/Inst. for Aerospace Research High Reynolds Number 2-D Test Facility
p 2658 N94-28350

BOUNDARY LAYER SEPARATION

Flow past a circular cylinder with a permeable wake splitter plate
[AD-A273765] p 2790 N94-25872

A numerical investigation of a subsonic jet in a crossflow p 2803 N94-28023

Theoretical and experimental investigation of a delta wing with turbulent leading-edge jets
p 2659 N94-28029

Inclined air-jets used as vortex generators to suppress shock-induced separation p 2659 N94-28040

Experimental study on the shock wave interaction with a hypersonic boundary layer near a convex corner
p 2654 N94-28328

BOUNDARY LAYER STABILITY

Localized and distributed boundary-layer receptivity to convected unsteady wake in free stream
[NASA-CR-4578] p 2808 N94-28180

Transition for three-dimensional, compressible boundary layers p 2653 N94-28327

BOUNDARY LAYER TRANSITION

Performance of renormalization group algebraic turbulence model on boundary layer transition simulation
[NASA-CR-194466] p 2644 N94-26131

Numerical simulation of receptivity and transition in a boundary layer on a flat plate with a suction hole
[NASA-CR-195708] p 2798 N94-27782

Prediction of leading-edge transition and relaminarization phenomena on a subsonic multi-element high-lift system p 2659 N94-27929

Localized and distributed boundary-layer receptivity to convected unsteady wake in free stream
[NASA-CR-4578] p 2808 N94-28180

Infrared imaging for transition detection in a transonic blowdown wind tunnel p 2653 N94-28325

Transition for three-dimensional, compressible boundary layers p 2653 N94-28327

BOUNDARY LAYERS

The numerical simulation of marine boundary layer clouds
[AD-A273669] p 2894 N94-26195

Numerical simulation of receptivity and transition in a boundary layer on a flat plate with a suction hole
[NASA-CR-195708] p 2798 N94-27782

Unsteady wake structures in transverse jets
p 2800 N94-28006

Localized and distributed boundary-layer receptivity to convected unsteady wake in free stream
[NASA-CR-4578] p 2808 N94-28180

BOUNDARY VALUE PROBLEMS

Back-reaction beyond the mean field approximation
[DE94-003936] p 3012 N94-25612

Abstraction in, specification and proof of software for a 1D heat-transfer problem
[REPT-93-45] p 2790 N94-25763

Approximate solution of the fourth order initial value problem using deficient spline polynomials
[DE93-613023] p 2991 N94-25880

Longitudinal diffusion of a proton bunch under external noise
[DE93-634022] p 3032 N94-26165

Preconditioning in parallel Runge-Kutta methods for stiff initial value problems
[CWI-NM-R9310] p 2991 N94-26217

Numerical solution of singularity-perturbed two-point boundary-value problems
[DE94-601542] p 2993 N94-26410

On a spline-approximation method for solving ordinary differential equations
[DE93-634290] p 2994 N94-26471

Computation of numerical solution of parabolic PDEs by monotone iterative methods
[ISBN-0-315-84553-8] p 2999 N94-27404

Time-step enlargement and optimal smoothing in Runge-Kutta time-integration algorithms by implicit and explicit smoothing
[NLR-TP-92221-U] p 2798 N94-27799

BOUSSINESQ APPROXIMATION
Reduced Braginskii equations
[DE94-003510] p 3047 N94-27723

BRACKETS
Helmet head tracking mounting device
[AD-D016048] p 2942 N94-27114

BRAIDED COMPOSITES
Fatigue resistance of unnotched and post impact(+/-30 deg/0 deg) 3-D braided composites
[NASA-CR-191590] p 2711 N94-27433

BRAIN
The AFIT multielectrode array for neural recording and simulation: Design, testing, and encapsulation
[AD-A274086] p 2909 N94-25943
Distribution of GABA immunoreactive neurons in the brain of rolling mouse Nagoya and gamma-irradiated mouse p 2904 N94-27471

BRAIN DAMAGE
The central executive component of working memory
[AD-A274295] p 2938 N94-26683

BRANCHING (MATHEMATICS)
A numerical determination of bifurcation points for low Reynolds number conical flows
[AD-A273984] p 2791 N94-25991
Continuation and multi-grid for bifurcation problems
[AD-A274965] p 2992 N94-26302
Bisexual branching diffusions
[AD-A274698] p 3008 N94-26374
Bifurcation sequences at 1:4 resonance: An inventory
[PB94-125408] p 2997 N94-27028

BRANCHING (PHYSICS)
Measurement of tau lepton branching fractions
[DE94-003423] p 3018 N94-26325

BRAYTON CYCLE
Small low mass advanced PBR's for bi-modal operation
[DE94-003201] p 2699 N94-25798
Limitations of power conversion systems under transient loads and impact on the pulsed tokamak power reactor
[DE94-003404] p 3043 N94-26324

BRAZIL
Digital filter design for sensor simulation: Application to the Brazilian remote sensing satellite
[INPE-5523-RPQ/665] p 2849 N94-26827
A synoptic study on periods of deficiency over Rio Grande do Sul/Brazil
[INPE-5456-TDI/498] p 2896 N94-27422
Role of remote sensing in energy, water, and carbon cycle studies over the Amazon
[INPE-5486-PRE/1786] p 2852 N94-27957

BRAZING
High temperature grain growth and oxidation of Fe-29Ni-17Co (Kovar (tm)) alloy leads
[DE94-004691] p 3069 N94-27753

BREADBOARD MODELS
Planetary Instrument Definition and Development Program (PIDDP). Instrument for future planetary flight missions: A visible-infrared imaging spectrometer for planetary missions
[NASA-CR-195254] p 3106 N94-27409

BREATHING APPARATUS
Rewarming methodologies in the field
[AD-A274744] p 2909 N94-26173

BREEDING (REPRODUCTION)
Development of inbred strains from Japanese wild rats (Rattus norvegicus) p 2906 N94-27492

BREMSSTRAHLUNG
A study of LPM suppression of bremsstrahlung at 25 GeV
[DE94-003457] p 3018 N94-26133
Proceedings of the Second EGS4 User's Meeting in Japan
[DE93-520383] p 3032 N94-26543
Acceleration of electrons and ions by strong lower-hybrid turbulence in solar flares
[NASA-TM-109723] p 3111 N94-27953

BRIDGES (STRUCTURES)
Vibrations in engineering structures: A review of model and full-scale test of a cable-stayed bridge and a traffic sign gantry
[NLR-TP-92321-U] p 2843 N94-27553

BRIGHTNESS
Endogeneous and exogenous control of visual selection: A review of the literature
[AD-A273761] p 2908 N94-25871

BRIGHTNESS TEMPERATURE
Remote sensing of global snowpack energy and mass balance: In-situ measurements on the snow of interior and Arctic Alaska
[NASA-CR-195704] p 2851 N94-27787

BRILLOUIN ZONES
String hypothesis and characters of coset CFTs
[DE93-634337] p 3007 N94-26552

BRITTLE MATERIALS
SP/MSP tests for the evaluation of FGM
[NAL-SP-17] p 2710 N94-27279
SP/MSP tests for the evaluation of FGM
p 2710 N94-27280
Research on the development of fracture characteristics evaluation system for ceramics and metal composite materials p 2710 N94-27281

BRITTLENESS
Numerical simulations of interfacial debonding in ductile-phase reinforced intermetallic matrix composites
[DE94-003639] p 2706 N94-25938
Current status of research and development on nickel and iron aluminides
[DE94-004247] p 2741 N94-27616

BROADBAND
A study of two dimensional tapered periodic edge treatments to reduce wideband edge diffraction
[AD-A274054] p 2766 N94-25824
Catalog of absolutely calibrated, range normalized, wideband, electric field waveforms from triggered lightning flashes in Florida
[AD-A273793] p 2892 N94-25873
Broad band tunable dye laser development
[DE93-632978] p 2816 N94-26157
Electrical analysis of wideband and distributed windows using time-dependent field codes
[DE94-002987] p 2768 N94-26310
Diagnostics and microelectronics
[DE94-003016] p 2784 N94-26777
Multiple model adaptive control of a large flexible space structure with purposeful dither for enhanced identifiability
[AD-A274132] p 2987 N94-27122
Multivariate spectral analysis to extract materials from multispectral data
[AD-A274142] p 2709 N94-27135

BROKEN SYMMETRY
Data on parity violation in the compound nucleus and its interpretation
[DE94-003965] p 3013 N94-25820
Coherent state approach for the (Phi)(sup 6)-lattice model and phase transitions
[DE93-613053] p 3050 N94-25825
Cosmoparticle physics of family symmetry breaking
[DE94-601623] p 3013 N94-25837
Out of equilibrium phase transitions and a toy model for disoriented chiral condensates
[DE94-601642] p 3013 N94-25839
Aspects of nonrenormalizable terms in a superstring standard-like models
[DE93-614530] p 3071 N94-25911
Z(sub N)(sup n-1) broken model
[DE93-634357] p 3072 N94-26039
Lepton masses in an SU(3)(sub L) x U(1)(sub N) gauge model
[DE93-634366] p 3016 N94-26040
Differential regularization of a non-relativistic anyon model
[DE94-601558] p 3019 N94-26416
C-periodicity and the physical mass in the 3-state Potts model
[DE94-601551] p 3019 N94-26423
Statistical mechanical properties of Z(N)(sup n-1) broken model
[DE93-634344] p 2993 N94-26457
Cosmological phase transitions
[DE94-003001] p 3104 N94-26786
Progress in SSC Higgs physics: Report of the Higgs working group
[DE94-003224] p 3022 N94-26793
Measurements of the B(sup 0)(bar B)(sup 0)CP asymmetry
[DE94-003379] p 3063 N94-27047
Second-order phase transition in (g(phi)4)2 theory
[DE94-603677] p 3067 N94-27638
Excited Landau levels, orbital angular momentum and axial anomaly
[DE94-606407] p 3068 N94-27679
Topics in electroweak baryogenesis: The sphaleron and T-violation
[DE94-004886] p 3029 N94-27811
Research on elementary particle physics, part 2
[DE94-004956] p 3029 N94-27815

BROMINE
Vibrational energy transfer within the B 3Pi (O(+) sub u) state of 79BR2 upon collision with N2, O2, NO, and SF6
[AD-A273905] p 3011 N94-25589
High resolution fourier transform absorption spectrum of 79Br2 B3 Pi(Ou+) X1 sigma g+
[AD-A273864] p 2956 N94-25610

BROWNIAN MOVEMENTS
Bisexual branching diffusions
[AD-A274698] p 3008 N94-26374
Single-server queues with spatially distributed arrivals
[PB94-126638] p 2986 N94-26916
A superprocess with a disappearing self-interaction
[AD-A274647] p 3009 N94-27108

BRYOPHYTES
Antarctic Record, Vol. 36, No. 2
[REPT-107] p 2883 N94-27963
Note on the structure of moss colonies composed of two species on King George Island, the South Shetland Islands p 2885 N94-27971

BSCCO SUPERCONDUCTORS
The effect of processing on the microstructure of Ag-sheathed Bi-2223 wires
[DE94-004627] p 3055 N94-26243
Liquid and solid solubility of Ag in Bi2Sr2CaCu2O8
[DE94-002829] p 2735 N94-26273
Processing and properties of Ag-clad Bi-2223 tapes
[DE94-004603] p 2783 N94-26589
Powder synthesis, fabrication, and transport properties of long-length Ag clad Bi-2223 conductors
[DE94-002376] p 2740 N94-26957

BUBBLES
Hydrodynamics, acoustics and scaling of traveling bubble cavitation
[AD-A273846] p 2789 N94-25605
Interfacial area and interfacial transfer in two-phase flow
[DE93-041226] p 2792 N94-26468
Behaviour of separation bubbles in sharp-edged gaps of finite dimensions
[ISBN-0-315-84113-3] p 2793 N94-26637
Numerical studies on the dynamics of bubble, turbulent, free shear flows: Effect of the inter-phase coupling on the global flow evolution
[AD-A274521] p 2794 N94-26832
Acoustic bubble sizing, using active and passive techniques to compare ambient and entrained populations
[ISVR-TR-229] p 2807 N94-28172

BUCKLING
Formulae for the buckling of simply-supported corrugated panels of orthotropic material under shear load
[PB94-126547] p 2840 N94-26911
Design and test of postbuckled stiffened curved plates: A literature survey
[PB94-126521] p 2840 N94-26961

BUFFER STORAGE
Spacecraft optical disk recorder memory buffer control
p 2815 N94-27907

BUFFETING
Lift-curve slope for structural response calculations
[ESDU-93013] p 2648 N94-28063
Examples of flight path optimisation using a multivariate gradient-search method
[ESDU-93021] p 2670 N94-28092

BUILDINGS
Shock wave interaction with L-shaped structures
[AD-A273774] p 2790 N94-25858

BULK MODULUS
Se EXAFS study of the elevated wurtzite to rock salt structural phase transition in CdSe nanocrystals
[DE94-003247] p 3054 N94-26125
Mechanical properties of polyaniline prepared by polymerization in an organized monolayer
[AD-A274350] p 2753 N94-26925

BUMPERS
Physics of debris clouds from hypervelocity impacts
[NASA-CR-193932] p 2696 N94-26791

BUNCHING
Regrouping of the beam in the IHEP PS for the UNK p-p programs
[DE93-634021] p 3032 N94-26164
Longitudinal diffusion of a proton bunch under external noise
[DE93-634022] p 3032 N94-26165

BURGER EQUATION
Recent advances in the spectral element method
p 2657 N94-28348

BURNERS
Characterization of acoustic effects on flame structures by beam deflection technique
[DE94-003240] p 2714 N94-26122

BURNING RATE
An apparatus for measurement of ignition and burning characteristics of metallic particles
[AD-A274815] p 2716 N94-26487
Uncertainties in the characterization of the thermal environment of a solid rocket propellant fire
[DE94-002023] p 2760 N94-27719

BURST TESTS
Upset welding process for 21-6-9 spherical vessels
[DE93-018194] p 2832 N94-28229

BUS CONDUCTORS
A VHDL register transfer level model of the linear token passing multiplex data bus protocol for the high speed data bus
[AD-A273734] p 2980 N94-26009
BYPASS RATIO
The design of a counter rotating ultra-high-bypass fan simulator for windtunnel investigation
[DLR-FB-93-20] p 2675 N94-27739
BYPASSES
Nickel-hydrogen cell reversal characteristics
p 2862 N94-28114

C

C (PROGRAMMING LANGUAGE)
The ergonomics of software porting: Automatically configuring software to the runtime environment or everything you wanted to know about your C compiler but didn't know who to ask
[CWI-CS-R9266] p 2961 N94-26221
Vcalc: A 3-space vector calculator
[AD-A274520] p 2965 N94-26831
C++ (PROGRAMMING LANGUAGE)
Run-time recognition of task parallelism within the P++ parallel array class library
[DE94-002707] p 2980 N94-26120
Object-oriented software construction at ALS
[DE94-003418] p 2967 N94-27049
CABLES
Unscreened low tension cables scrape abrasion testing
[PB94-123767] p 2823 N94-26849
CADMIUM
Screen test for cadmium and nickel plates
p 2860 N94-28106
CADMIUM SELENIDES
Se EXAFS study of the elevated wurtzite to rock salt structural phase transition in CdSe nanocrystals
[DE94-003247] p 3054 N94-26125
CADMIUM TELLURIDES
The state of the art of thin-film photovoltaics
[DE94-000224] p 2855 N94-26115
Indium donor complexes with cation vacancies in CdTe and ZnSe
[DE94-002731] p 3063 N94-26958
CAFFEINE
Thermoregulatory effects of caffeine ingestion during rest and exercise in men
[NASA-TM-108783] p 2901 N94-26210
CALCITE
The biostratigraphy and paleogeography of Maastrichtian inoceramids p 2889 N94-28303
CALCIUM METABOLISM
Weightlessness and the human skeleton: A new perspective p 2935 N94-28368
CALCIUM OXIDES
Proceedings of the Fourth Euroseminar on Microscopy Applied to Building Materials
[PB94-119807] p 2839 N94-26754
CALCULATORS
Vcalc: A 3-space vector calculator
[AD-A274520] p 2965 N94-26831
CALCULI
Quantum subgroups and quantum co-set spaces and differential calculi on them
[DE94-602520] p 3073 N94-26876
CALCULUS
Semantics, orderings and recursion in the weakest precondition calculus
[CWI-CS-R9267] p 2995 N94-26776
Fractional calculus, gegenbauer transformations and integral equations
[PB93-237683] p 2999 N94-27349
CALIBRATING
Evaluation of a concentration probe for application in a supersonic flow field
[AD-A273915] p 2643 N94-25592
Catalog of absolutely calibrated, range normalized, wideband, electric field waveforms from triggered lightning flashes in Florida
[AD-A273793] p 2892 N94-25873
Digital Altimeter Setting Indicator (DASI) Operational Test and Evaluation (OT/E) operational test procedures
[AD-A274100] p 2672 N94-26030
Numerical treatment of experimental data in calibration procedures
[DE93-634289] p 3097 N94-26382
Separation and reconstruction of electron neutrino interaction in the IHEP-JINR neutrino detector and BARS detector
[DE93-634182] p 3019 N94-26393
Study on the compensated lead hadron calorimeter characteristics by means of hadron and electron beams
[DE93-634176] p 2810 N94-26439
Multivariate calibration applied to near-infrared spectroscopy for the quantitative analysis of dilute aqueous solutions
[DE94-003231] p 2716 N94-26794
Characterization and calibration of the Agema 880+ imaging radiometer
[AD-A274417] p 3036 N94-26981
Calibrating/testing meters in hot water test bench VM7
[PB94-124294] p 2812 N94-27160
Acousto-optical post-processor time-integrating correlator calibration updates
[DSIS-94-00053] p 2813 N94-27317
Calibration of SAR systems
[DLR-FB-93-18] p 2777 N94-27738
Performance of a 14-MeV neutron generator as an in situ calibration source for TFTR
[DE94-004993] p 3048 N94-27825
Ionospheric calibration for single frequency altimeter measurements
[NASA-CR-195709] p 2883 N94-27883
Locating tie-points on a grid p 2978 N94-27906
Nimbus-7 Earth radiation budget calibration history. Part 2: The Earth flux channels
[NASA-RP-1335-PT-2] p 2814 N94-27981
Landscape dynamics of northeastern forests
[NASA-CR-195272] p 2852 N94-28070
MODIS airborne simulator visible and near-infrared calibration, 1992 ASTEX field experiment. Calibration version: ASTEX King 1.0
[NASA-TM-104599] p 2897 N94-28179
MODIS airborne simulator visible and near-infrared calibration, 1991 FIRE-Cirrus field experiment. Calibration version: FIRE King 1.1
[NASA-TM-104600] p 2897 N94-28182
CALMODULIN
Neutron and x ray scattering studies of the interactions between Ca(2+)-binding proteins and their regulatory targets: Comparisons of troponin C and calmodulin
[DE94-002706] p 2901 N94-26623
CALORIC STIMULI
The mechanism of caloric nystagmus under microgravity. 1: Changes of endolymphatic pressure in the semicircular canal of pigeon by caloric stimulation
p 2914 N94-27457
Cardiovascular function during thermoneutral head-out water immersion in the elderly p 2915 N94-27458
Effects of 40 C hot water immersion for an hour on thermoregulatory functions in humans: Comparison with 34 C thermoneutral immersion p 2915 N94-27459
Effects of bathing at 40 C on cardiovascular system in humans: Comparison with 34 C thermoneutral bathing
p 2918 N94-27473
Effects of 41 C bathing for 20 minutes on cardiovascular and thermoregulatory functions in humans
p 2918 N94-27474
Monthly variation of physiological and psychological responses under unsteady thermal conditions
p 2918 N94-27475
Man's ability to adapt himself for the seasonal climatic changes: From viewpoint of anticipation and seasonable behavior p 2919 N94-27476
Changes in pain sensation induced by repetitive application of noxious heat pulses to the human skin
p 2924 N94-27501
Hyperalgesia to cold in patients with Subacute Myelo-Optico-Neuropathy (SMON) p 2928 N94-27521
CALORIMETERS
An electromagnetic calorimeter with wavelength shifting fiber readout
[DE93-616664] p 2809 N94-25735
Theoretical and experimental studies of elementary physics
[DE94-002310] p 3008 N94-25988
Harvard University High Energy Physics
[DE94-002406] p 3032 N94-26119
Calorimeter with WLS fibers and parallel to beam scintillators
[DE93-634188] p 2810 N94-26378
Unsegmented electromagnetic calorimeter prototype. Energy and coordinate resolution
[DE93-634185] p 2810 N94-26396
Hadron gas ionization calorimeters
[DE93-634186] p 2810 N94-26397
Thermal conductivity of PAX 2A explosive by DSC
[AD-A274721] p 2759 N94-26437
Study on the compensated lead hadron calorimeter characteristics by means of hadron and electron beams
[DE93-634176] p 2810 N94-26439
SP industry calorimeter for rate of heat release measurements up to 10MW
[PB94-124211] p 2811 N94-27044
Cosmic x ray physics
[NASA-CR-195225] p 3115 N94-27236
Bulletin of the Institute for Chemical Reaction Science, Tohoku University, volume 2
[JTN-94-80602] p 2717 N94-27385
High-temperature and high-pressure flow calorimeter
p 2718 N94-27390
Gamma Large Area Silicon Telescope (GLAST): Applying silicon strip detector technology to the detection of gamma rays in space
[DE94-003451] p 3116 N94-27740
First observation of neutral current proton electron scattering at the square root of s = 300 GeV
[DE94-701107] p 3030 N94-27877
CAMERAS
An apparatus for measurement of ignition and burning characteristics of metallic particles
[AD-A274815] p 2716 N94-26487
Application of Space Shuttle Project Hercules imagery in the investigation of ship cloud tracks
[AD-A274923] p 2692 N94-26529
Methods for experimentally determining commercial jet aircraft landing parameters from video image data
[AD-A274207] p 2669 N94-27105
CCD-Camera images of BEST-TWO and processing results
[AD-A274140] p 2811 N94-27134
CMT-Si
[PB94-123619] p 2812 N94-27216
High resolution studies of sunspots and flux tubes
[NASA-CR-195216] p 3111 N94-27321
An algorithm for stereo correspondence problems on the analogy of human vision
[NAL-TR-1185] p 2940 N94-27584
Flexible range finding applied to 3D surface synthesis: A pseudo-trinocular approach
[ISBN-0-315-84616-X] p 2813 N94-27651
CAMOUFLAGE
Development and evaluation of a near infrared reflecting and low visibility paint scheme for RAAF P-3C Orion aircraft
[AD-A274881] p 2669 N94-26864
Thermoplastic or thermosetting composites in aircrafts
[PB94-123809] p 2710 N94-27253
CAMS
Contact stress in disc cams with roller followers
[ESDU-93001] p 2829 N94-28055
Blending profiles of disc cams with radial translating roller followers. Part 2: To incorporate an intermediate precision point or a constant velocity component
[ESDU-93002-PT-2] p 2830 N94-28056
CANADAIR AIRCRAFT
First Canadair jet flies for Lufthansa city line
p 2662 N94-28243
CANARD CONFIGURATIONS
Design of the advanced regional aircraft, the DART-75
p 2671 N94-25708
Eagle RTS: A design of a regional transport
p 2671 N94-25709
CANCELLATION
Space science: Causes and impacts of cutbacks to NASA's outer solar system exploration missions. Report to the Chairman, Subcommittee on Investigations and Oversight, Committee on Science, Space, and Technology, House of Representatives
[GAO/NSIAD-94-24] p 3106 N94-27418
CANCELLATION CIRCUITS
Equalization and cancellation of nonlinear intersymbol interference in a dispersive satellite communication channel
[ISBN-0-315-85147-3] p 2775 N94-27274
CANCER
The intracellular second messenger system in c-fos gene induction by ACTH p 2904 N94-27477
CANONICAL FORMS
Lyapunov exponents for some quasi-periodic cocycles
[PB94-124377] p 2997 N94-26994
CAPACITANCE
Double layer capacitance of carbon foam electrodes
[DE94-002651] p 2780 N94-25975
CAPILLARY FLOW
Continuation and multi-grid for bifurcation problems
[AD-A274965] p 2992 N94-26302
Thermocapillary flow with evaporation and condensation and its effect on liquid retention in low-G fluid acquisition devices
[NASA-TP-3463] p 2797 N94-27639
CARBIDES
A review of carbide fuel corrosion for nuclear thermal propulsion applications
[DE94-003938] p 2699 N94-25613
Microstructural development in low activation ferritic alloys irradiated to 200 dpa at 420 C
[DE94-004269] p 2731 N94-25803
Examination of hardness, fracture toughness and microstructure in Al2O3-B4C binary ceramics
[PB94-124237] p 2755 N94-27158

CARBON
Simulation of the carbon cycle in the oceans [DE94-000780] p 2898 N94-25791
Advances in preparing and characterizing low density pan-carbon microcellular foam [DE94-002278] p 2748 N94-25932
Hadron gas ionization calorimeters [DE93-634186] p 2810 N94-26397
The deposition of boron nitride and carbon films on silica glass fibers [DE94-004684] p 2751 N94-26564
Mechanistic studies of opto-electronic materials and syntheses using multiple laser and surface diagnostics [AD-A274528] p 3036 N94-26834
Technical report of ISSP. Ser. A, no. 2678: Magnetic properties of carbon nanotubes [JTN-94-80564] p 3064 N94-27174
Technical report of ISSP. Ser. A, no. 2675: High-field cyclotron resonance and valence-band structure in semiconducting diamond [JTN-94-80561] p 3065 N94-27245

CARBON COMPOUNDS
Voltammetric studies of poly(carbon disulfide) [DE94-001385] p 2717 N94-26951

CARBON CYCLE
Simulation of the carbon cycle in the oceans [DE94-000780] p 2898 N94-25791
Role of remote sensing in energy, water, and carbon cycle studies over the Amazon [INPE-5486-PRE/1786] p 2852 N94-27957

CARBON DIOXIDE
Assessing the climatic effect of carbon dioxide and other trace gases using an interactive two-dimensional climate-chemistry model [DE94-001741] p 2866 N94-25927
Implications of policies and prevent climate change for future food security [DE93-018872] p 2866 N94-25948
Isotopically labeled CO2 from stratosphere: A tracer of carbon biogeochemistry [DE94-002777] p 2877 N94-26015
Grassland/atmosphere response to changing climate: Coupling regional and local scales [DE94-003111] p 2866 N94-26026
Grain boundary degradation of YBCO superconductors sintered in CO2-containing atmospheres [DE94-003206] p 3053 N94-26029
A conceptual framework for the evaluation of cost-effectiveness of projects to reduce GHG emissions and sequester carbon [DE93-040448] p 2867 N94-26419
Space Station evolution study oxygen loop closure [NASA-CR-193936] p 2941 N94-26788
Effect of carbon dioxide enrichment on radish production using Nutrient Film Technique (NFT) [NASA-TM-107198] p 2902 N94-27411
Cooling the Martian atmosphere: The spectral overlap of the C02 15 micrometers band and dust p 3107 N94-27886
Martian atmospheric radiation budget p 3107 N94-27887
Why is the north polar cap on Mars different than the south polar cap? p 3107 N94-27889

CARBON DIOXIDE CONCENTRATION
Extraterrestrial surface propulsion systems p 2833 N94-25691
Sensitivity of climate models: Comparison of simulated and observed patterns for past climates [DE93-019934] p 2865 N94-25789
Effect of carbon dioxide enrichment on radish production using Nutrient Film Technique (NFT) [NASA-TM-107198] p 2902 N94-27411

CARBON DIOXIDE LASERS
Development of an industrial CO2 laser for mask marking [DE93-632901] p 2816 N94-26184
An apparatus for measurement of ignition and burning characteristics of metallic particles [AD-A274815] p 2716 N94-26487
Beam-quality measurements for materials processing lasers and the proposed ISO standard [DE94-002738] p 2819 N94-26811
Optimum for the gasdynamic system in a fast-axial-flow CO2 laser [AD-A274305] p 2819 N94-26940

CARBON DIOXIDE REMOVAL
Automation of closed environments in space for human comfort and safety p 2943 N94-25684

CARBON MONOXIDE
A conceptual framework for the evaluation of cost-effectiveness of projects to reduce GHG emissions and sequester carbon [DE93-040448] p 2867 N94-26419
Advances in passive-remote and extractive Fourier transform infrared spectroscopic systems [DE94-001424] p 2868 N94-26952

CARBON STEELS
Isothermal corrosion testing of steels in molten nitrate salts [DE94-004695] p 2742 N94-27755

CARBON-CARBON COMPOSITES
Ablation of solid-propellant rocket-motor nozzle materials [ESA-TT-1289] p 2699 N94-25638

CARBONATES
Issues for conversion coating of aluminum alloys with hydrotalcite [DE94-003804] p 2732 N94-25819
Research and development of alternative components at Argonne National Laboratory for Molten Carbonate Fuel Cells [DE94-000014] p 2857 N94-26583

CARBONIZATION
Double layer capacitance of carbon foam electrodes [DE94-002651] p 2780 N94-25975

CARBOXYLIC ACIDS
Thermal conductivity of liquid carboxylic acids [ESDU-93017] p 2721 N94-28138

CARBURIZING
Effect of nitrocarburizing on shape of titanium alloy parts [DE94-004040] p 2732 N94-25822

CARDIAC OUTPUT
Passive and active behavior of the cardiovascular system under increased gravitational loads in a chronically instrumental conscious baboon model [AD-A274344] p 2910 N94-26973
Cardiac output and cardiac contractility by impedance cardiography during exercise of runners p 2935 N94-28367

CARDIOLOGY
The role of beta-adrenoceptor stimulation in the progression of chronic heart failure p 2932 N94-27541

CARDIOVASCULAR SYSTEM
EcarHeart2 version 1.0: Programmers documentation [PB94-124633] p 2909 N94-25909
Aeromedical issues related to positive pressure breathing for +Gz protection [AD-A274717] p 2910 N94-26435
Passive and active behavior of the cardiovascular system under increased gravitational loads in a chronically instrumental conscious baboon model [AD-A274344] p 2910 N94-26973
Cardiovascular function during thermoneutral head-out water immersion in the elderly p 2915 N94-27458
Effects of bathing at 40 C on cardiovascular system in humans: Comparison with 34 C thermoneutral bathing p 2918 N94-27473
Effects of 41 C bathing for 20 minutes on cardiovascular and thermoregulatory functions in humans p 2918 N94-27474
Workshop on Countering Space Adaptation with Exercise: Current Issues [NASA-CP-3252] p 2934 N94-28361
Exercise detraining: Applicability to microgravity p 2934 N94-28364

CARNOT CYCLE
Introduction to combined cycles p 2789 N94-28078

CARRIER LIFETIME
Low threshold all-optical crossbar switch on GaAs-GaAlAs channel waveguide arrays [AD-A274971] p 2783 N94-26536

CARRIER MOBILITY
The potential for large critical currents in the high T(sub c) oxides p 2854 N94-26058

CASCADE FLOW
Effects of crenulations on three dimensional losses in a linear compressor cascade [AD-A273778] p 2790 N94-25862
Effect of surface finish on turbine airfoil cascade losses p 2652 N94-28320
The effect of axial velocity ratio, turbulence intensity, incidence, and leading edge geometry on the midspan performance of a turbine cascade p 2652 N94-28321
Solution-adaptive simulation of transonic cascade flows p 2657 N94-28344

CASCADE WIND TUNNELS
An investigation of the effects of the high maximum-thickness-to-chord ratio on the performance of nozzle guide vanes in a transonic planar cascade [ISBN-0-315-84107-9] p 2793 N94-26671

CASSINI MISSION
Preliminary reentry safety assessment of the General Purpose Heat Source module for the Cassini mission: Aerospace Nuclear Safety Program [DE94-001646] p 2699 N94-25926
Space science: Causes and impacts of cutbacks to NASA's outer solar system exploration missions. Report to the Chairman, Subcommittee on Investigations and Oversight, Committee on Science, Space, and Technology, House of Representatives [GAO/NSIAD-94-24] p 3106 N94-27418

CASTING
Study on production of materials with one direction solidification texture p 2727 N94-25572
Effect of nitrocarburizing on shape of titanium alloy parts [DE94-004040] p 2732 N94-25822
Technique to predict the curing behaviour of unsaturated polyester materials [PB94-124856] p 2748 N94-25892
Modelling the inhibition cure behaviour of unsaturated polyester moulding materials [PB94-124864] p 2748 N94-25893
Stress relaxation in dough moulding compounds [PB94-124872] p 2748 N94-25894
Solidification modeling of a spiral casting to determine material fluidity [DE94-002212] p 2739 N94-26935
A widely adaptable habitat construction system utilizing space resources p 2688 N94-27374
Production of an amorphous Fe(75)Si(10)B(15) sheet by a metallic mold casting method and its properties p 2746 N94-28170
High Quality Aluminium Castings Conference [PB94-133592] p 2747 N94-28359

CASTINGS
Squeeze casting: A literature review [PB94-124575] p 2741 N94-27326
High Quality Aluminium Castings Conference [PB94-133592] p 2747 N94-28359

CATALYSIS
Design of gasifiers to optimize fuel cell systems [DE94-000010] p 2856 N94-26581

CATALYSTS
Polymer-bound rhodium hydroformylation catalysts [ETN-94-95388] p 2712 N94-25747
Controlled synthesis of polyenes by catalytic methods [DE94-004168] p 2749 N94-25973
Accelerated screening methods for determining chemical and thermal stability of refrigerant-lubricant mixtures. Part 2: Experimental comparison and verification of methods [DE94-003664] p 2749 N94-26007
Exploratory Technology Research Program for Electrochemical Energy Storage [DE94-003479] p 2781 N94-26047
A mimic model of Pt-Rh catalyst prepared by electrochemical deposition of Rh on Pt (100) surface [REPT-A-2664] p 2715 N94-26476
Sol-gel derived silica/siloxane composite materials: The effect of loading level and catalyst activity on silica domain formation [DE94-002734] p 2712 N94-27710
CO2 methanation catalysts prepared from amorphous Ni-valve metal alloys containing platinum group elements p 2745 N94-28166

CATALYTIC ACTIVITY
Polymer-bound rhodium hydroformylation catalysts [ETN-94-95388] p 2712 N94-25747
A mimic model of Pt-Rh catalyst prepared by electrochemical deposition of Rh on Pt (100) surface [REPT-A-2664] p 2715 N94-26476

CATHODES
Oxygen reduction at a YSZ interface with cathode materials La(1-x)(Ca or Sr)(x)MnO3(1-x)CaMnO3 [DE94-002954] p 3054 N94-26147
MSOFC development status [DE94-003192] p 2858 N94-26792
Channel model for AC electric arc [PB94-124591] p 2786 N94-27327

CATHODIC COATINGS
Oxygen reduction at a YSZ interface with cathode materials La(1-x)(Ca or Sr)(x)MnO3(1-x)CaMnO3 [DE94-002954] p 3054 N94-26147
Processing of LaCrO3 for solid oxide fuel cell applications [DE94-002981] p 2857 N94-26747

CATIONS
Morphological analysis of ionomers [DE94-003660] p 2749 N94-26005
The use of on-line ion chromatography for high temperature and high pressure reaction studies [DE94-002525] p 2713 N94-26075
Alternative materials for solid oxide fuel cells: Processing and interactions of materials [DE94-000016] p 2855 N94-26114
Structure of ionic fluids in equilibrium with a microporous ionic matrix [DE94-600563] p 2715 N94-26391

Indium donor complexes with cation vacancies in CdTe and ZnSe
[DE94-002731] p 3063 N94-26958

CAUCHY PROBLEM

Riemann solvers for solving the incompressible Navier-Stokes equations using the artificial compressibility method
[CRANFIELD-AERO-9208] p 2790 N94-25778

Estimators for the Cauchy distribution
[DE94-004990] p 3005 N94-27816

CAUSES

The end-Permian mass extinction: A complex, multicausal extinction p 2888 N94-28299

Mass extinctions: Persistent problems and new directions p 2889 N94-28302

CAVITATION FLOW

Hydrodynamics, acoustics and scaling of traveling bubble cavitation
[AD-A273846] p 2789 N94-25605

An investigation of cavitation in a mechanically alloyed 15 volume percent SiCp/IN9021 aluminum composite
[DE94-003371] p 2748 N94-25959

CAVITIES

Study on high temperature damage control and life improvement p 2729 N94-25580

Binding of copper and nickel to cavities in silicon formed by helium ion implantation
[DE94-003769] p 3050 N94-25814

Hydrogen uptake into silicon from an ECR plasma
[DE94-003771] p 3050 N94-25815

The structural, chemical, and electrical properties of He-implantation-induced nanocavities in silicon
[DE94-002681] p 3052 N94-25971

Microwave coupling into a slotted cavity
[PB94-123742] p 2772 N94-27041

Technical report of ISSP. Ser. A, no. 2688: Suppression of higher-order modes in an RF cavity by resistive material
[JTN-94-80574] p 2787 N94-27606

CAVITY RESONATORS

Regrouping of the beam in the IHEP PS for the UNK p-p programs
[DE93-634021] p 3032 N94-26164

Practical design of resonant cavity for a RF free electron laser
[AD-A274306] p 2819 N94-26941

Optical pattern recognition system utilizing resonator array
[AD-D016071] p 3040 N94-28224

CELL CATHODES

Oxygen reduction at a YSZ interface with cathode materials La(1-x)(Ca or Sr)(x)MnO3(1-x)CaMnO3
[DE94-002954] p 3054 N94-26147

CELL MEMBRANES (BIOLOGY)

Effect of sera from patients treated with long-term hemodialysis on mRNA's for collagenase, stromelysin, and tissue inhibitor of metalloprotease in cultured human synovial cells p 2920 N94-27481

CELLS

Effects of capsaicin on freshly dissociated rat dorsal root ganglion cells p 2906 N94-27499

CELLS (BIOLOGY)

Detecting actin fibers in cell images using minimal spanning trees
[AD-A273914] p 2984 N94-25591

Effects of ML-9, a myosin light-chain kinase inhibitor, on preimplantation development of the mouse
p 2905 N94-27486

Compaction-like blastomere aggregation caused by 1-oleoyl-2-acetylglycerol in mouse embryos: An electron microscopic observation p 2905 N94-27487

Inductive differentiation of nerve cells in mouse embryonic ectoderm at early primitive streak stage by retinoic acid p 2905 N94-27488

Influence of mechanical stimulation on inflammatory edema p 2906 N94-27497

The effect of naloxone on sleeping time in adjuvant arthritic rats p 2906 N94-27498

Effects of capsaicin on freshly dissociated rat dorsal root ganglion cells p 2906 N94-27499

Size distribution of retrogradely labeled dorsal root ganglion cells: Test of normality p 2906 N94-27500

Interaction between endogenous opioid and Cholecystokinin (CCK) in modulating respiratory responses induced by thin-fiber muscular afferents
p 2906 N94-27502

Effects of perfusion of amiodarone on electrophysiological properties in single rabbit ventricular myocytes p 2906 N94-27503

Fast and slow onsets of Na channel blocking actions due to lidocaine and disopyramide using concentration-clamp method p 2907 N94-27504

Electrophysiological effects of MS-551, a new Class 3 antiarrhythmic agent, on isolated rabbit ventricular muscles p 2907 N94-27505

Comparative investigation of new Class 3 antiarrhythmic drugs, E-4031 and MS-551, on electrophysiological properties in isolated rabbit ventricular myocytes
p 2907 N94-27506

Electrical coupling between the sino-atrial node and atrial muscle: Cell to cell interaction through an external circuit and its simulation by computer modeling
p 2907 N94-27509

Correlation between electrical activity and the size of single sinoatrial node cells p 2907 N94-27513

The ionic mechanism underlying the negative chronotropic effect of acetylcholine: Experimental study in rabbit single sinoatrial node cells
p 2908 N94-27514

The ionic mechanism underlying the negative chronotropic effect of acetylcholine: Experiments using small sinoatrial node tissue preparations isolated from rabbit hearts p 2908 N94-27515

The ionic mechanism underlying the negative chronotropic effect of acetylcholine: Postganglionic vagal stimulation in isolated rabbit hearts
p 2908 N94-27516

Mechanism for regulation of myocardial contractility by autonomic drugs: Pathophysiological relevance in congestive heart failure p 2931 N94-27536

Desensitization to acethylcholine in pacemaker cells of the sinoatrial node p 2908 N94-27537

CEMENTS

Attachment techniques for high temperature strain
[AD-A274766] p 2811 N94-26568

Sealant research for solid oxide fuel cells
[DE94-000015] p 2857 N94-26584

Proceedings of the Fourth Euroseminar on Microscopy Applied to Building Materials
[PB94-119807] p 2839 N94-26754

CENSUS

Counting Adelie penguins at colonies: Seasonal and annual changes p 2885 N94-27970

CENTAUR LAUNCH VEHICLE

Lunar Transportation Facilities and Operations Study, option 1
[NASA-CR-195700] p 3109 N94-27982

CENTER OF GRAVITY

Test Operations Procedure (TOP) 2-2-800 wheeled vehicle center of gravity
[AD-A273937] p 2821 N94-25794

CENTER OF MASS

Secondary particle in background levels and effects on detectors at future hadron colliders
[DE94-003378] p 3011 N94-25598

Enhanced tracking of airborne targets using forward looking infrared and laser return measurements
[AD-A274181] p 3037 N94-27102

CENTRAL AMERICA

Properties of the Central American cold surge
[NASA-CR-194849] p 2893 N94-26138

CENTRAL NERVOUS SYSTEM STIMULANTS

Effects of methamphetamine on vigilance and tracking during extended wakefulness
[AD-A274896] p 2909 N94-26179

CENTRAL PROCESSING UNITS

On-board computer for control subsystem of satellite
p 2949 N94-26716

CENTRIFUGAL CASTING

Effects of post-fabrication processing on the tensile properties of centrifugally cast SiC particulate reinforced aluminum composites
[AD-A274865] p 2707 N94-26190

CENTRIFUGAL PUMPS

Experimental contribution to the study of secondary flows in centrifugal turbopump stator components
[ECL-92-35] p 2789 N94-25654

Bulk-Flow Analysis, part A
[NASA-CR-193911-PT-A] p 2796 N94-27377

CENTRIFUGES

An automatic 14-day paste diet feeder for animals
[NASA-TM-108804] p 2901 N94-26086

CENTRIFUGING

An automatic 14-day paste diet feeder for animals
[NASA-TM-108804] p 2901 N94-26086

CENTRIFUGING STRESS

Passive and active behavior of the cardiovascular system under increased gravitational loads in a chronically instrumental conscious baboon model
[AD-A274344] p 2910 N94-26973

CERAMIC BONDING

Ceramic technology project
[DE94-003782] p 2750 N94-26332

CERAMIC COATINGS

Study on substance diffusion in thin films with controlled structures p 2727 N94-25570

Micropyrolysis of polymer thin films for ceramics
[ECL-92-62] p 2750 N94-26088

CERAMIC FIBERS

Fibrous emissive burners selective and broad band
[PB94-128329] p 2859 N94-27225

Development of hypersonic engine seals: Flow effects of preload and engine pressures
[NASA-TM-106333] p 2826 N94-27599

CERAMIC MATRIX COMPOSITES

NASA Lewis Research Center lean-, rich-burn materials test burner rig
[NASA-CR-194437] p 2680 N94-26141

Ceramic technology project
[DE94-003782] p 2750 N94-26332

Investigation of forced and isothermal chemical vapor infiltrated SiC/SiC ceramic matrix composites
[DE94-004544] p 2708 N94-26557

Attachment techniques for high temperature strain
[AD-A274766] p 2811 N94-26568

Structure and properties of composites synthesized in situ using solid state displacement reactions
[DE94-004589] p 2737 N94-26585

Engineering limitations of ceramic composites for high performance and high temperature applications
[DE94-001676] p 2754 N94-27021

Examination of hardness, fracture toughness and microstructure in Al2O3-B4C binary ceramics
[PB94-124237] p 2755 N94-27158

SP/MSP tests for the evaluation of FGM
[NAL-SP-17] p 2710 N94-27279

SP/MSP tests for the evaluation of FGM
p 2710 N94-27280

Research on the development of fracture characteristics evaluation system for ceramics and metal composite materials p 2710 N94-27281

Testing procedure for toughness characterisation of ceramic matrix composites
[REPT-932-430-101] p 2711 N94-27586

CERAMICS

Study on film generation phenomena by particle deposition p 2728 N94-25575

Crystallization and microstructural control of ferroelectric thin-films and glass-ceramics
[AD-A273767] p 2748 N94-25854

Collaborative research on ion implantation of ceramics
[DE93-019177] p 2749 N94-26080

Ceramic technology project
[DE94-003782] p 2750 N94-26332

Bimaterial interfaces and their role in the mechanical performance of the in-situ composites
[AD-A274688] p 2707 N94-26447

Attachment techniques for high temperature strain
[AD-A274766] p 2811 N94-26568

Research and development of alternative components at Argonne National Laboratory for Molten Carbonate Fuel Cells
[DE94-000014] p 2857 N94-26583

Structure and properties of composites synthesized in situ using solid state displacement reactions
[DE94-004589] p 2737 N94-26585

Mechanical properties of nanophase materials
[DE94-004625] p 2751 N94-26594

CEN-VAMAS round robin on grain size measurement for advanced technical ceramics
[VAMAS-TR-12] p 2752 N94-26654

High definition Raman microscopic imaging
[DE94-003158] p 2716 N94-26781

Interface phenomena in metal-ceramic composites
[AD-A274167] p 2709 N94-27125

Examination of hardness, fracture toughness and microstructure in Al2O3-B4C binary ceramics
[PB94-124237] p 2755 N94-27158

List of papers published by the members of Institute for Materials Research, Tohoku University 1992
[JTN-94-80608] p 3118 N94-27355

Resonant holographic measurements of laser ablation plume expansion in vacuum and argon gas backgrounds
[DE94-001407] p 2813 N94-27615

Synthesis, rheology, and forming of Y-Ba-Cu-O ceramics
[DE94-005558] p 2757 N94-27695

Characterization of ZnS-GaP naon-composites
[DE94-004888] p 2712 N94-27813

Gas fired advanced turbine system
[DE94-003193] p 2827 N94-27874

Fibrous ceramic candle filter for particle removal in pressurized fluidized bed combustion
[PB94-133089] p 2876 N94-28383

Experimental studies of pressurised fluidised bed combustion at Helsinki University of Technology, 1991-1992
[PB94-133063] p 2876 N94-28394

CEREBELLUM

Effects of gamma ray radiation on the developing mouse cerebellum: Apoptotic cell death and induction of tissue transglutaminase p 2904 N94-27472

CEREBRAL CORTEX

Interacting cortical filters for object recognition
[PB94-125374] p 2938 N94-26873

Orientation competition in cortical filters
[PB94-125366] p 2939 N94-27001

Cortical mechanisms of attention, discrimination, and motor response to somesthetic stimuli
[AD-A274163] p 2940 N94-27141
Disturbed neuronal migration in the cerebral cortex of mice by low-dose gamma radiation
p 2904 N94-27470
Distribution of GABA immunoreactive neurons in the brain of rolling mouse Nagoya and gamma-irradiated mouse p 2904 N94-27471
Effects of gamma ray radiation on the developing mouse cerebellum: Apoptotic cell death and induction of tissue transglutaminase p 2904 N94-27472
Abnormal development of serotonin nerve fibers in the cerebral cortex of young rats with methylazoxymethanol induced microcephaly p 2905 N94-27485

CEREBRUM
Development of Purkinje cells in vitro
p 2905 N94-27483
Developmental expression of protein kinase C type 1 isozyme in suncus and rat cerebella
p 2905 N94-27484
Interhemispheric phase relationship of alpha waves and cerebral dominance p 2927 N94-27518
Analysis of the Electrically Evoked Response (EER) of the cat p 2908 N94-27519

CERENKOV RADIATION
The Cherenkov hadronic like-jets
[DE93-634525] p 3016 N94-26010
HPm-tubes: Literature survey comprising 1992
[PB94-123643] p 2785 N94-27038

CERIUM COMPOUNDS
Study on synthesis and characteristics of intermetallic compound with strong electron correlation
p 2726 N94-25563
Heavy-electron behavior in large coordination compounds CeZn11 and UZn12
[REPT-A-2663] p 3049 N94-25614

CERMETS
Development of GaAs charge-coupled devices
[ISBN-0-315-84116-8] p 3059 N94-26703
MSOFC development status
[DE94-003192] p 2858 N94-26792
Interface phenomena in metal-ceramic composites
[AD-A274167] p 2709 N94-27125

CERTIFICATION
Digital systems validation book plan. Volume 3: Handbook
[AD-A274099] p 2672 N94-26028
Qualified manufacturing and interoperability for space applications p 2949 N94-26719

CESIUM
Adsorption and desorption studies of cesium on sapphire surfaces
[DE94-003798] p 3070 N94-28067

CESIUM IODIDES
Meson spectroscopy and particle astrophysics
[DE94-001799] p 3115 N94-27003

CESSNA AIRCRAFT
A revolutionary approach to composite construction and flight management systems for small, general aviation airplanes p 2671 N94-25714
Piloted simulation study of an ILS approach of a twin-pusher business/commuter turboprop aircraft configuration
[NASA-TM-4516] p 2646 N94-26602

CHAINS
LB-Deposited, side-chain substituted polyaniline, polypyrrole and the corresponding monomers, studied by STM
[AD-A274405] p 2754 N94-26977

CHALCOGENIDES
Evanescent field infrared spectroscopy using chalcogenide glass fiber
[ITN-94-85233] p 3038 N94-27178

CHANGE DETECTION
Morphodynamics of inter-tidal areas: The Wadden Sea
[NLR-TP-92356-U] p 2851 N94-27555
Global concern on research cooperation for environment p 2872 N94-28275
Progress in the study of global change in China
p 2873 N94-28276
Research and observation programmes on global changes in Indonesia p 2873 N94-28277
Philippine thrust on environmental research relating to global change p 2873 N94-28279
Land use change in Thailand and its impact on environmental change: Joint Thai-Japanese research project (1993-1995) p 2875 N94-28288
Study on environment monitoring over whole China using NDVI from AVHRR data and future project
p 2875 N94-28289
Utilization of remote sensing data for global climate change research in Malaysia p 2875 N94-28290
Utilization of remote sensing data for global change research p 2875 N94-28292
Contribution of satellite observation to global change research p 2876 N94-28293

CHANNEL CAPACITY
Coded communications with nonideal interleaving
[ITN-94-85235] p 2774 N94-27242

CHANNEL FLOW
Unsteady wake structures in transverse jets
p 2800 N94-28006

CHANNELS (DATA TRANSMISSION)
A VHDL register transfer level model of the linear token passing multiplex data bus protocol for the high speed data bus
[AD-A273734] p 2980 N94-26009
Virtual memory management and virtual bus overloading on multiple channel architectures
[AD-A274127] p 2954 N94-27152
Coded communications with nonideal interleaving
[ITN-94-85235] p 2774 N94-27242

CHAOS
Nonlinear ocean waves
[AD-A274651] p 2899 N94-26354
Chaotic dynamics of the solar cycle
[AD-A274315] p 3110 N94-26883
The onset of chaos in a periodically forced nonlinear oscillator
[ISBN-0-315-84564-3] p 2842 N94-27272

CHARACTERIZATION
Failure mechanisms of high temperature semiconductor lasers
[AD-A273833] p 2815 N94-25616
Component characterization and development 2
[AD-A274002] p 2765 N94-25660
Pulse transformer characterization
[PML-1992-73] p 2784 N94-26646
Testing procedure for toughness characterisation of ceramic matrix composites
[REPT-932-430-101] p 2711 N94-27586
Characterization of semi-insulating gallium arsenide
[AD-A273781] p 3068 N94-27704
Bench-scale synthesis of nanoscale materials
[DE94-004787] p 2742 N94-27786

CHARGE CARRIERS
Technical report of ISSP. Ser. A, no. 2680: Determination of intervalley scattering time in germanium by subpicosecond time-resolved Raman spectroscopy
[JTN-94-80566] p 3064 N94-27176

CHARGE COUPLED DEVICES
Design analysis of a combined optical/LADAR deep-space surveillance satellite
[AD-A274040] p 2694 N94-25832
Developments in crystallographic phase analysis in the SEM: Backscattered electron Kikuchi patterns
[DE93-040755] p 3057 N94-26420
Development of GaAs charge-coupled devices
[ISBN-0-315-84116-8] p 3059 N94-26703
CCD-Camera images of BEST-TWO and processing results
[AD-A274140] p 2811 N94-27134
CMT-Si
[PB94-123619] p 2812 N94-27216
High resolution studies of sunspots and flux tubes
[NASA-CR-195216] p 3111 N94-27321
Multiple exposure CCD detector for high-speed laser pump, x ray probe Laue scattering
[DE94-004618] p 2820 N94-27781

CHARGE DISTRIBUTION
Microscopic study of local structure and charge distribution in metallic La2CuO(4+delta)
[DE94-003801] p 3050 N94-25817
First principle calculation for magneto-crystalline anisotropy
[DE93-634653] p 3052 N94-26012
Limit theorems for functionals of Markov processes and renormalizable stable fields
[AD-A274645] p 3004 N94-27106

CHARGE EFFICIENCY
Charge efficiency of Ni/H2 cells during transfer orbit of Telstar 4 satellites p 2862 N94-28117
TOPEX/Poseidon battery performance during the first year of operation p 2862 N94-28119

CHARGE EXCHANGE
Atomic processes in Inertial Electrostatic Confinement (IEC) devices
[DE94-005015] p 3047 N94-27715
Muon transfer rates in collisions of hydrogen isotope mesic atoms on bare nuclei: Multichannel adiabatic approach
[DE94-606752] p 3030 N94-27861

CHARGE TRANSFER
Two dimensional self-consistent fluid simulation of RF inductive sources
[DE94-003635] p 2767 N94-25937
Recombination and metastability in amorphous silicon and silicon germanium alloys
[DE94-000237] p 2736 N94-26481
A semiclassical reactive flux method for the calculation of condensed phase activated rate constants
[AD-A274850] p 3020 N94-26562

CHARGED PARTICLES
Secondary particle in background levels and effects on detectors at future hadron colliders
[DE94-003378] p 3011 N94-25598
CP violating form factors for three gauge boson vertex in the two Higgs doublet and left-right symmetric models
[DE94-601704] p 3014 N94-25841
Problems of application of charged particles channeling effects in crystals in high-energy physics
[DE93-634023] p 3032 N94-26405
About stochastization of motion of charged particles in geomagnetic field and in the field of a wave packet
[DE93-634309] p 2879 N94-26502
Delta f Algorithm
[DE94-003120] p 2963 N94-26521
Limit theorems for functionals of Markov processes and renormalizable stable fields
[AD-A274645] p 3004 N94-27106
The radiation design handbook
[ESA-PSS-01-609-ISSUE-1] p 2696 N94-27397
Helium transport and exhaust studies of H-mode discharges in the D3-D tokamak
[DE94-004744] p 3048 N94-27785
Correlations in inelastic collisions of relativistic nuclei with emulsion at (4.1 - 4.5) A GeV/c
[DE93-634526] p 3030 N94-27994

CHARM (PARTICLE PHYSICS)
Heavy quark production and spectroscopy
[DE94-003619] p 3015 N94-25935
Photon and hadron production of heavy flavors
[DE94-004655] p 3018 N94-26245
Charmonium physics at a tau-charm factory
[PB94-124344] p 3024 N94-27199
Observation of excited charmed mesons
[ISBN-0-315-57014-8] p 3026 N94-27400

CHARRING
Materials characterization on efforts for ablative materials
[NASA-CR-193929] p 2756 N94-27230

CHARTS
Parsing schemata: A framework for parallel and sequential parsing
[PB94-125267] p 2981 N94-26998

CHASSIS
The Enabler: A concept for a lunar work vehicle
p 2833 N94-25675
The Robotic All-Terrain Lunar Exploration Rover (RATLER): Increased mobility through simplicity
p 2685 N94-26291

CHEBYSHEV APPROXIMATION
Rendering of three-dimensional data sets derived from finite-difference and spectral methods
[AD-A273724] p 3096 N94-25997
Chebyshev-Markov rational functions over several intervals
[PB94-125333] p 2998 N94-27116

CHEMICAL ANALYSIS
The Latin American conference on the applications of the Moessbaer effect
[DE93-615942] p 3051 N94-25912
Regrowth zones in laser annealed radiation damaged diamond
[DE94-600821] p 3056 N94-26364
Radiochemistry Division annual progress report : 1991
[DE94-600652] p 2715 N94-26392
New FORTRAN computer programs to acquire and process isotopic mass spectrometric data: Operator's manual
[DE94-003174] p 2965 N94-26784
Liquid crystalline side-chain polysiloxanes with 4-amino-4'-stilbene-carboxylic ester mesogens
[AD-A274510] p 2754 N94-27036
Zeeman laser interferometry for detection and chemical analysis
[DE94-003963] p 2719 N94-27728

CHEMICAL ATTACK
Study on performance evaluation of pressure vessel steel in corrosion environments with sulfide
p 2730 N94-25582
The chemical detector paper as a potential alarm
[FFI-93/6007] p 2712 N94-25745
A materials compatibility study in FM-1, a liquid component of a paste extrudable explosive
[DE94-001166] p 2759 N94-26198
A preliminary method for atmospheric soundings in real time using satellite and ground-based remotely sensed data
[AD-A274381] p 2880 N94-26828

CHEMICAL BONDS
X ray computed tomography for emerging aerospace materials and processes development
[AD-A273721] p 2705 N94-25779

Three methods to measure RH bond energies
[DE94-003795] p 3013 N94-25816
Lighter alkali hydride and deuteride 1: Electronic properties of pure solids
[DE93-616188] p 3051 N94-25914
Computational analysis of some aspects of a synthetic route to ammonium dinitramide
[AD-A274648] p 2704 N94-26353
Transition metal activation and functionalization of carbon-hydrogen bonds
[DE94-003650] p 2715 N94-26369
Molecular surface electrostatic potentials in the analysis of non-hydrogen-bonding noncovalent interactions
[AD-A274612] p 3022 N94-26894
Photoelectron spectroscopic studies of the electronic structure and bonding in TiC and TiN
[ATR-93(8361)-2] p 2746 N94-28185

CHEMICAL CLEANING
Stability of reference masses 2: The effect of environment and cleaning methods on the surfaces of stainless steel and allied materials
[NPL-DMM(A)-95] p 2738 N94-26653

CHEMICAL COMPOSITION
Study on substance diffusion in thin films with controlled structures p 2727 N94-25570
Analytical method for estimation of the total amount of aromatic and poly aromatic compounds in diesel fuel
[PB94-123692] p 2759 N94-25907
Formation of three types of quasi-crystals in Al-Pd-Mg system
[REPT-A-2667] p 3053 N94-26071
Polar and chemical domain structures of lead scandium tantalate (PST)
[DE94-600760] p 3056 N94-26363

CHEMICAL EFFECTS
Effects of plastic media blasting on aircraft skin
[AD-A274817] p 2668 N94-26488

CHEMICAL EXPLOSIONS
Structural analysis of a frangible nut used on the NASA Space Shuttle
[DE94-003672] p 2821 N94-25811
Numerical simulation of the reignition of detonation by reflected shocks
[AD-A274755] p 2795 N94-27252
Propellants and explosives in ballistic missiles
[UCRL-LR-113578] p 2760 N94-28222

CHEMICAL INDICATORS
The chemical detector paper as a potential alarm
[FFI-93/6007] p 2712 N94-25745

CHEMICAL PROPERTIES
Study on substance diffusion in thin films with controlled structures p 2727 N94-25570
The structural, chemical, and electrical properties of He-implantation-induced nanocavities in silicon
[DE94-002681] p 3052 N94-25971
Liquid monopropellants
[AD-D016074] p 2760 N94-28226

CHEMICAL REACTION CONTROL
Combustion synthesis method p 2721 N94-25561

CHEMICAL REACTIONS
Atomic-scale chemistry of metal surfaces
[REPT-A-2657] p 3012 N94-25636
Selfsimilar solutions of a nonlinear transport equation
[REPT-93-42] p 2865 N94-25760
Structure and properties of intermetallic composites synthesized in situ using solid state displacement reactions
[DE94-004312] p 2705 N94-25805
Three methods to measure RH bond energies
[DE94-003795] p 3013 N94-25816
Alternative materials for solid oxide fuel cells: Processing and interactions of materials
[DE94-000016] p 2855 N94-26114
X ray absorption studies of Ti/polymer and Cr/polymer interfaces
[DE94-003008] p 2753 N94-26770
The coordination and atom transfer chemistry of titanium porphyrin complexes
[DE94-003091] p 2704 N94-26779
Molecular surface electrostatic potentials in the analysis of non-hydrogen-bonding noncovalent interactions
[AD-A274612] p 3022 N94-26894
Approximate Riemann solvers: Improvement of the HLLEM scheme and its generalization for chemically reacting flows
[NAL-TR-1189] p 2795 N94-27205
Basic research on natural gas combustion phenomena
[PB94-129046] p 2717 N94-27256
Reactivity of nitrate radical (NO3) toward organic compounds p 2704 N94-27387
Emissions of nitrogen oxides (NO(x) and N2O) in pressurized fluidized bed combustion
[PB94-133071] p 2876 N94-28395

CHEMICAL REACTORS
Physical modelling and adaptive predictive control of diffusion/LPCVD reactors
[PB94-126398] p 2763 N94-26819
Experimental studies of pressurised fluidised bed combustion at Helsinki University of Technology, 1991-1992
[PB94-133063] p 2876 N94-28394

CHEMICAL TESTS
Analytical method for estimation of the total amount of aromatic and poly aromatic compounds in diesel fuel
[PB94-123692] p 2759 N94-25907

CHEMICAL VAPOR INFILTRATION
Investigation of forced and isothermal chemical vapor infiltrated SiC/SiC ceramic matrix composites
[DE94-004544] p 2708 N94-26557

CHEMISORPTION
Hydrogen uptake into silicon from an ECR plasma
[DE94-003771] p 3050 N94-25815
An investigation of the effect of surface impurities on the adsorption kinetics of hydrogen chemisorbed onto iron
[NASA-CR-195213] p 2716 N94-26643

CHEMORECEPTORS
Muscle sympathetic nerve activity in humans
p 2932 N94-27538

CHINA
Investigation of mesoscale convective cloud clusters in South China
[AD-A274303] p 2895 N94-26678

CHIPS (ELECTRONICS)
Multichip module high speed testing
[AD-A274873] p 2782 N94-26343
High performance flight computer developed for deep space applications p 2949 N94-26718
Use of HOOD coupled to real time monitors
p 2953 N94-26742
A fully integrated 16 channel digitally trimmed pulse shaping amplifier
[DE94-004555] p 2787 N94-27618
NASA satellite communications application research, phase 2 addendum. Efficient high power, solid state amplifier for EHF communications
[NASA-CR-195712] p 2777 N94-27946
Microprocessor chip incorporating optical signal coupling transceiver
[AD-D016077] p 2788 N94-28186

CHIPS (MEMORY DEVICES)
The 12-channel flash-ADC FASTBUS module
[DE93-634229] p 2783 N94-26380

CHIRAL DYNAMICS
Out of equilibrium phase transitions and a toy model for disoriented chiral condensates
[DE94-601642] p 3013 N94-25839
Experimental study of the near threshold pi(sup +)p yields (pi(sup +))(pi(sup +))(n) cross section and chiral symmetry
[DE94-601671] p 3014 N94-25840
Anomaly candidates and invariants of D 4, N 1 supergravity theories
[NIKHEF-H/93-12] p 3072 N94-26541
Nuclear Theory Group, University of Washington recent and planned research
[DE94-002729] p 3022 N94-26809
Surface modes and chiral symmetry (Wilson fermions in a box)
[DE94-004946] p 3029 N94-27814
Axial anomaly in e(+)e(-) yields gamma gamma and anyon superconductivity
[DE94-606406] p 3070 N94-27859
Polarizability matrix of layered chiral sphere
[PB94-132834] p 2778 N94-28355

CHLORIDES
Effects of plastic media blasting on aircraft skin
[AD-A274817] p 2668 N94-26488
High rate lithium/thionyl chloride bipolar battery development p 2864 N94-28133

CHLORINE
Structure of ionic fluids in equilibrium with a microporous ionic matrix
[DE94-600563] p 2715 N94-26391
Measuring variation in ecosystem sensitivity to stress
[AD-A274232] p 2868 N94-26817

CHLOROCARBONS
Effects of p-chlorophenol on sulfate reduction in marine sediments p 2870 N94-28150

CHLOROFLUOROCARBONS
Accelerated screening methods for determining chemical and thermal stability of refrigerant-lubricant mixtures. Part 2: Experimental comparison and verification of methods
[DE94-003664] p 2749 N94-26007
Thermophysical properties of refrigerant R-134a (1,1,1,2-tetrafluoroethane)
[ESDU-93001] p 2720 N94-27959

CHOLERA
Bakteriella toxiner-morgondagens hot (bacterial toxins-the threat of tomorrow)
[PB94-124229] p 2902 N94-27045

CHROMATOGRAPHY
The use of on-line ion chromatography for high temperature and high pressure reaction studies
[DE94-002525] p 2713 N94-26075

CHROMIUM
The development of Cr, Tm, Ho:YAG lasers for airborne lidar
[AD-A274895] p 2816 N94-26178
X ray absorption studies of Ti/polymer and Cr/polymer interfaces
[DE94-003008] p 2753 N94-26770
Grain boundary chromium concentration effects on the IGSCC and IASCC of austenitic stainless steels
[DE94-004268] p 2741 N94-27570

CHROMIUM ALLOYS
The role of grain boundary chemistry and structure in the environmentally-assisted intergranular cracking of nickel-base alloys
[DE94-003159] p 2732 N94-25954
Influence of helium generation rate and temperature history on mechanical properties of model Fe-Cr-Ni alloys irradiated in FFTF at relatively low displacement rates
[DE94-004264] p 2737 N94-26575
A tri-junction diffusion couple analysis of the Nb-Cr-Ti system at 950 C
[DE94-002637] p 2737 N94-26607
Experimental measurement of local displacement and chemical pair correlations in crystalline solid solutions
[DE94-001124] p 3065 N94-27251
Thermogravimetric study of oxidation of a PdCr alloy used for high-temperature sensors
[NASA-TM-106473] p 2741 N94-27426
Effect of different ions on the anodic behaviour of alloy 800 in chloride solutions at high temperature
[DE94-602982] p 2743 N94-27832
NMR study of quasicrystal Al(70)Pd(20)T(M10) alloy (T(M):Cr, Mn, Fe, and Co) p 2745 N94-28162
Formation and high mechanical strength of Al-based alloys containing a nanoscale icosahedral phase as a main constituent p 2746 N94-28171

CHROMIUM STEELS
Microstructural development in low activation ferritic alloys irradiated to 200 dpa at 420 C
[DE94-004269] p 2731 N94-25803

CHROMOSOMES
Electron microscopic analysis of meiotic chromosome pairing in male house musk shrew, Suncus murinus
p 2906 N94-27493

CHROMOSPHERE
Ultraviolet observations of astronomical sources
[NASA-CR-195232] p 3102 N94-26234
Photospheric origins of chromospheric and coronal activity
[NASA-CR-195215] p 3110 N94-26590

CHRONIC CONDITIONS
Selection of site injecting adjuvant in chronic inflammation model p 2906 N94-27496
The effect of naloxone on sleeping time in adjuvant arthritic rats p 2906 N94-27498

CHRONOLOGY
Geological Dating by Ar-40 - Ar-39 method
[DE94-601975] p 2880 N94-26874

CIRCADIAN RHYTHMS
Workload transition: Implications for individual and team performance
[AD-A274538] p 2941 N94-26964

CIRCLES (GEOMETRY)
Towards a theory of growing surfaces: Mapping two-dimensional Laplacian growth onto Hamiltonian dynamics and statistics
[DE94-002636] p 2991 N94-26079
Single-server queues with spatially distributed arrivals
[PB94-126638] p 2986 N94-26916

CIRCUIT DIAGRAMS
Signal amplifier-shapers for multiwire detectors
[DE93-634171] p 2783 N94-26438

CIRCUIT RELIABILITY
Symbolic model checking for sequential circuit verification
[AD-A274375] p 2786 N94-27061
Coherence and satisfiability of waveform timing specifications
[ISBN-0-315-57769-X] p 3009 N94-27268

CIRCUITS
Signal amplifier-shapers for multiwire detectors
[DE93-634171] p 2783 N94-26438
ADC test support program
[AD-A274819] p 2783 N94-26491

CIRCULAR CYLINDERS
Flow past a circular cylinder with a permeable wake splitter plate
[AD-A273765] p 2790 N94-25872

CIRCULAR ORBITS
A comparison of three approximate mathematical models for the gravity gradient stabilized satellite [AD-A273832] p 2694 N94-25615
Hill equations for satellite orbit determination [ETN-94-95374] p 2690 N94-25787

CIRCULATORY SYSTEM
Annals of the Research Inst. of Environmental Medicine, Nagoya Univ., volume 44 [REPT-44-VOL-44] p 2911 N94-27442
Effect of L-dopa on hemodynamic functions in humans p 2929 N94-27526

CITIES
Project WISH: The Emerald City p 2703 N94-25690
An observational study of air pollution transport over a large urban complex [REPT-6] p 2867 N94-26474

CIVIL AVIATION
Preliminary design of nine high speed civil transports p 2671 N94-25710
The evolution of the high-speed civil transport [NASA-TM-109089] p 3117 N94-26155
Effects of historical and predictive information on ability of transport pilot to predict an alert [NASA-TM-4547] p 2673 N94-27864
The single European market and air traffic chances and risks p 2660 N94-28231
Deregulation of air traffic in America: A model to be initiated? p 2661 N94-28232
Lufthansa facing the single European market p 2661 N94-28237
Air traffic administration enroute to Europe p 2661 N94-28238
Air traffic in recession p 2662 N94-28240
German-American relations in air traffic are to be criticized p 2662 N94-28241
Lufthansa and Europe p 2663 N94-28247
Know-how export: Lufthansa technology at Shannon p 2663 N94-28248
After thirty years: Farewell of Europa jet p 2663 N94-28249

CLADDING
Corrosion resistance at welded zones of nuclear fuel reprocessing system p 2722 N94-25546

CLASSES
Schema integration in object-oriented databases [CWI-CS-R9320] p 2970 N94-27548

CLASSICAL MECHANICS
On the wave and corpuscular properties of microparticles [DE93-634450] p 3020 N94-26509

CLASSIFICATIONS
A feasibility study on bird classification with neural network [AD-A273753] p 2659 N94-25780
On the classification scheme for resonant states of muonic molecules [DE93-613645] p 3014 N94-25853
A diagnostic classification model for document processing skills [AD-A273790] p 3096 N94-25925
Design considerations when using external hypertext engines from applications [DE94-002213] p 3098 N94-26598
Classification of linear differential operators with an invariant subspace in monomials [PB94-126620] p 2996 N94-26915
New mixed integer algorithm for classification and placement of measurements in process flow networks [PB94-126752] p 2966 N94-26921
Multivariate spectral analysis to extract materials from multispectral data [AD-A274142] p 2709 N94-27135

CLASSIFIERS
Discovery learning in autonomous agents using genetic algorithms [AD-A274083] p 2677 N94-25998
Three dimensional object recognition using a complex autoregressive model [AD-A274388] p 2995 N94-26829
Multivariate spectral analysis to extract materials from multispectral data [AD-A274142] p 2709 N94-27135

CLATHRATES
Crystallographyic analyses of clathrate hydrates included in Vostok ice cores p 2885 N94-27969

CLEAN FUELS
Combined Cycles for Power Plants [VKI-LS-1993-08] p 2830 N94-28077
Clean coal technology p 2832 N94-28089

CLEANING
Plasma surface cleaning using microwave plasmas [DE94-002754] p 2713 N94-26014

CLEARANCES
Transient model applications. 1: Compressor heat soak/clearance effects modeling p 2828 N94-28048

CLEAVAGE
First principles calculations for the cleaved and annealed Ge(111) surfaces [DE93-617048] p 3066 N94-27347

CLIMATE
Sensitivity of climate models: Comparison of simulated and observed patterns for past climates [DE93-019934] p 2865 N94-25789
The effect of elevation data representation on nocturnal drainage wind simulations [DE94-003624] p 2892 N94-25936
Environmental benefits of different types of heat pumps, available and expected [DE94-002440] p 2866 N94-26123
Meeting of the Eighth Session of the Scientific Advisory Committee of the World Climate Impact Assessment and Response Strategies Programme [DE93-633954] p 2866 N94-26163
Overall analysis of meteorological information in the Daeduk nuclear complex [DE93-632594] p 2894 N94-26469
Extraterrestrial accretion and glacial cycles p 2890 N94-28308

CLIMATE CHANGE
Assessing the climatic effect of carbon dioxide and other trace gases using an interactive two-dimensional climate-chemistry model [DE94-001741] p 2866 N94-25927
Implications of policies and prevent climate change for future food security [DE93-018872] p 2866 N94-25948
Grassland/atmosphere response to changing climate: Coupling regional and local scales [DE94-003111] p 2866 N94-26026
The impact of recent model improvements on GISS GCM predictions of climate change [DE93-019458] p 2866 N94-26077
Meeting of the Eighth Session of the Scientific Advisory Committee of the World Climate Impact Assessment and Response Strategies Programme [DE93-633954] p 2866 N94-26163
A preliminary analysis of the US west climatology [DE94-003028] p 2894 N94-26313
Global change research related to the Earth's energy and hydrologic cycle [NASA-CR-195270] p 2869 N94-27430
Asia-Pacific Seminar on Global Change Research Cooperation [JTN-94-80517] p 2871 N94-28268
Role and activity of STA on Asian Pacific regional cooperation p 2853 N94-28269
Research activities on the meteorology over the Asia-Pacific region p 2853 N94-28271
Progress in the study of global change in China p 2873 N94-28276
Research and observation programmes on global changes in Indonesia p 2873 N94-28277
Country report on global change research for the Republic of Korea p 2873 N94-28278
Philippine thrust on environmental research relating to global change p 2873 N94-28279
Global change: A research strategy for Australia 1992-1996 p 2874 N94-28282
A progress report on global change studies in China p 2874 N94-28283
HDGEC activity in Asia Pacific region p 2874 N94-28286
Utilization of remote sensing data for global climate change research in Malaysia p 2875 N94-28290
The end-Permian mass extinction: A complex, multicausal extinction p 2888 N94-28299

CLIMATOLOGY
The impact of recent model improvements on GISS GCM predictions of climate change [DE93-019458] p 2866 N94-26077
Testbed model and data assimilation for ARM [DE94-000432] p 2893 N94-26082
Properties of the Central American cold surge [NASA-CR-194849] p 2893 N94-26138
A preliminary analysis of the US west climatology [DE94-003028] p 2894 N94-26313
Extraterrestrial accretion and glacial cycles p 2890 N94-28308

CLIMBING FLIGHT
Examples of flight path optimisation using a multivariate gradient-search method [ESDU-93021] p 2670 N94-28092
Example of statistical techniques applied to analysis of effects of small changes [ESDU-93023] p 2670 N94-28094

CLINICAL MEDICINE
Biomedical polyurethane networks [ETN-94-95391] p 2750 N94-26211
Monograph of the aviation epidemiology data register for calendar year 1988 [AD-A274589] p 2911 N94-26985
Development of inbred strains from Japanese wild rats (Rattus norvegicus) p 2906 N94-27492

CLOCKS
Formal methods for dependable real-time systems p 2953 N94-26740
Improved modeling of GPS selective availability p 2642 N94-27290

CLOSED CYCLES
Project WISH: The Emerald City p 2703 N94-25690
Small low mass advanced PBR's for bi-modal operation [DE94-003201] p 2699 N94-25798

CLOSED ECOLOGICAL SYSTEMS
Automation of closed environments in space for human comfort and safety p 2943 N94-25684
Effect of carbon dioxide enrichment on radish production using Nutrient Film Technique (NFT) [NASA-TM-107198] p 2902 N94-27411
Development of a sparging technique for volatile emissions from potato (Solanum tuberosum) [NASA-TM-109199] p 2903 N94-27412

CLOSTRIDIUM BOTULINUM
Bakteriella toxiner-morgondagens hot (bacterial toxins-the threat of tomorrow) [PB94-124229] p 2902 N94-27045

CLOUD COVER
Differentiating the role of land surface variability and cloudiness variability on global energy transport within the atmosphere and oceans [NASA-CR-195229] p 2847 N94-26222
Science support for the Earth radiation budget experiment [NASA-CR-191600] p 2894 N94-26506
Short-range cloud amount forecasting with model output statistics [AD-A274769] p 2895 N94-26798
Initial ultraviolet-B intensity data at Lawrence Livermore National Laboratory [DE94-004279] p 2869 N94-27267

CLOUD PHYSICS
ARM Fourier transform spectrometer data analysis tools [DE94-000865] p 2895 N94-26697
Cloud liquid water content measurement tests using dual-wavelength radar [PB94-125960] p 2896 N94-26959

CLOUD SEEDING
Examination of micro- and macro-physical structures and processes in hailstorms with respect to their modification [DLR-FB-93-25] p 2897 N94-27751

CLOUDS
Reanalysis of Mariner 9 UV Spectrometer Data for Ozone, Cloud, and Dust Abundances, and Their Interaction Over Climate Timescales [NASA-CR-195244] p 3107 N94-27885

CLOUDS (METEOROLOGY)
Studies for the loss of atomic and molecular species from Io [NASA-CR-195702] p 3108 N94-27941

CLUSTER ANALYSIS
Fuzzy robust statistics for application to the fuzzy c-means clustering algorithm [AD-A274719] p 3003 N94-26436
An integrated approach to seismic event location: 1. Evaluating how method of location affects the volume of groups of hypocenters [PL-TR-92-2323] p 2887 N94-28214

CLUTTER
Processing of wide-angle synthetic aperture radar signals for target detection [AD-A274225] p 2773 N94-27073

CMOS
Advanced qualification techniques [DE94-003709] p 2780 N94-25812
Demonstration of monolithic co-fabrication of Y1Ba2Cu3O7-Sigma and CMOS devices on the same sapphire substrate [AD-A274757] p 3059 N94-26566
On-board computer for control subsystem of satellite p 2949 N94-26716
Processing, fabrication, and demonstration of HTS integrated microwave circuits, appendix A [AD-A274600] p 2785 N94-26890
A fully integrated 16 channel digitally trimmed pulse shaping amplifier [DE94-004555] p 2787 N94-27618

COAL
Advances in passive-remote and extractive Fourier transform infrared spectroscopic systems [DE94-001424] p 2868 N94-26952
Combined Cycles for Power Plants [VKI-LS-1993-08] p 2830 N94-28077

COAL GASIFICATION
Radiation applications of physical chemistry p 2854 N94-26054

Design of gasifiers to optimize fuel cell systems
[DE94-000010] p 2856 N94-26581
Researches of the Electrotechnical Laboratory. No. 53: Spectral emission from combustion gas containing scattering media
[JTN-94-80603] p 2717 N94-27246
Integrated coal gasification combined cycle
p 2832 N94-28090

COAL UTILIZATION
Clean coal technology p 2832 N94-28089

COANDA EFFECT
Theoretical and experimental investigation of a delta wing with turbulent leading-edge jets
p 2659 N94-28029

COASTAL CURRENTS
Topics in longshore currents
[AD-A274788] p 2899 N94-26361
Analysis and interpretation of the meteorology of the 1988 coastal transition zone experiment
[AD-A274710] p 2894 N94-26431

COASTAL ECOLOGY
Mapping coastal habitats using an imaging spectrometer
[ISBN-0-315-84362-4] p 2848 N94-26664

COASTAL WATER
A study on structure of benthic boundary layer in coastal waters
[REPT-4] p 2898 N94-25635
A comparative evaluation of SAR and SLAR
[DE94-002922] p 2848 N94-26277
Journal of NIRE, volume 2, number 4
[JTN-94-80554] p 2869 N94-28147
Effects of p-chlorophenol on sulfate reduction in marine sediments p 2870 N94-28150

COASTS
Hydrographic and Acoustic Doppler Current Profiler (ADCP) data from the ONR eastern boundary current accelerated research initiative, 9-16 June 1992
[AD-A274115] p 2898 N94-26076
A comparative evaluation of SAR and SLAR
[DE94-002922] p 2848 N94-26277
Coastal Zone Management Act and related legislation, revision 3
[DE94-004180] p 2869 N94-27691

COATING
The formation of conducting gold films by thermal decomposition and direct patterning using electron beam lithography of the gold cluster Au55P(C6H5)312C16
[AD-A273720] p 2749 N94-26074
Bimaterial interfaces and their role in the mechanical performance of the in-situ composites
[AD-A274688] p 2707 N94-26447
Equivalent performance in different helical resonator plasma polymerization coater platforms
[DE94-001517] p 2753 N94-26933
Dual cure low-VOC coating process
[DE94-000365] p 2756 N94-27611

COATINGS
Experiment and research on materials irradiated by plasma radiation
[DE94-605011] p 2758 N94-27845

COBALT
Structural study of Cu/Co multilayer by anomalous small-angle x ray scattering p 2744 N94-28160

COBALT ALLOYS
Study of the hyperfine magnetic field at Ta-181 site in the Heusler Co2ScSn, Co2ScGa, and Co2HfSn alloys
[DE94-603989] p 3067 N94-27623
Differential scanning calorimetric study of solid state amorphization and crystallization in Zr/Co and Zr/Ni multilayers p 2745 N94-28161
NMR study of quasicrystal Al(70)Pd(20)T(M10) alloy (T(M):Cr, Mn, Fe, and Co) p 2745 N94-28162

COBALT ISOTOPES
Balloon-borne measurements of the SN1987A hard x ray continuum p 3115 N94-26689

COCKPIT SIMULATORS
Weapon system sensor integration for a DIS-compatible virtual cockpit
[AD-A274088] p 2672 N94-26021

COCKPITS
Weapon system integration for the AFIT virtual cockpit
[AD-A274058] p 2667 N94-25772
A multivariate anthropometric method for crew station design: Abridged
[AD-A274588] p 2941 N94-26984
Standardization of aircraft control and performance symbology on the USAF head-up display
[AD-A274283] p 2673 N94-26989
A graphical workstation based part-task flight simulator for preliminary rapid evaluation of advanced displays
p 2641 N94-27286
First Canadair jet flies for Lufthansa city line
p 2662 N94-28243

COCKROACHES
A biologically-inspired autonomous robot
[AD-A273909] p 2821 N94-25782

CODE DIVISION MULTIPLE ACCESS
Code division multiple access local area network communications employing fiber optic signal processing techniques
[AD-A274897] p 3096 N94-26180

CODERS
Speech coding at low to medium bit rates
[ISBN-0-315-84012-9] p 2770 N94-26630
Deferred compilation: The automation of run-time code generation
[AD-A274124] p 2967 N94-27065
The Communication Link and Error ANalysis (CLEAN) simulator
[NASA-CR-195243] p 2968 N94-27168

CODING
Filtering, coding, and compression with Malvar wavelets
[AD-A274055] p 2780 N94-25770
The use of ASN.1 and XDR for data representation in real-time distributed systems
[AD-A273769] p 2959 N94-25855
Probabilistic methods for image generation and encoding
[AD-A274294] p 2964 N94-26682
The CODE-TOP (COncurrent system DEvelopment using Transformations Of Predicate-transition nets) method: Examples of using it for system architecture specification, software specification, and code generation p 2953 N94-26744
Trapezoid-oriented compression of run length coded map data
[PB94-123312] p 2849 N94-26848
Encoding approaches for data link transmission of weather graphics
[AD-A274497] p 2772 N94-26963
Genetic algorithms applied to a mission routing problem
[AD-A274130] p 2968 N94-27120
SPECTRUM analysis of multispectral imagery in conjunction with wavelet/KLT data compression
[DE94-003961] p 2851 N94-27727
Compression of multispectral Landsat imagery using the Embedded Zerotree Wavelet (EZW) algorithm
p 2947 N94-28261

COEFFICIENT OF FRICTION
Crystal chemistry and self-lubricating properties of monochalcogenides gallium selenide and tin selenide
[DE93-041177] p 2751 N94-26422

COEFFICIENTS
Filtering, coding, and compression with Malvar wavelets
[AD-A274055] p 2780 N94-25770
On a spline-approximation method for solving ordinary differential equations
[DE93-634290] p 2994 N94-26471

COGNITION
Induced pictorial representations
[AD-A274251] p 2939 N94-27012

COGNITIVE PSYCHOLOGY
Extending the rule space model to a semantically-rich domain: Diagnostic assessment in architecture
[AD-A273789] p 2948 N94-25864
A diagnostic classification model for document processing skills
[AD-A273790] p 3096 N94-25925
Air traffic controller working memory: Considerations in air traffic control tactical operations
[AD-A273722] p 2664 N94-26197
Long term learning: Integration of knowledge acquisition and knowledge compilation
[AD-A274775] p 3098 N94-26570
The central executive component of working memory
[AD-A274295] p 2938 N94-26683

COHERENT LIGHT
The proceedings of the KEK FEL Simulation Code Workshop
[DE93-520378] p 2816 N94-26112

COHERENT RADAR
Coherent HF radar system for the study of natural and heater induced ionospheric irregularities
[AD-A273804] p 2876 N94-25752

COHERENT RADIATION
Computer simulations of radiation generation from relativistic electron beams
[AD-A274139] p 3024 N94-27133
Sum frequency generation using an optical parametric oscillator
[DE94-001827] p 3040 N94-28000

COINCIDENCE CIRCUITS
Use of parallel counters for triggering
[DE93-616656] p 2979 N94-25918

COLD CATHODES
Micro-electron deflector
[AD-D016055] p 2787 N94-27672

COLD FLOW TESTS
Orbit transfer rocket engine technology program enhanced heat transfer combustor technology
[NASA-CR-189236] p 2700 N94-26156

COLD FRONTS
Properties of the Central American cold surge
[NASA-CR-194849] p 2893 N94-26138
Propagation of cold air masses in East Asia and its associated planetary-scale function
[AD-A274304] p 2895 N94-26850

COLD NEUTRONS
Surface physics with cold and thermal neutron reflectometry
[DE94-001447] p 2733 N94-26070

COLD PLASMAS
Critical survey of plasma processing
[AD-A274233] p 3044 N94-26820
Proceedings of the 16th Symposium on Plasma Physics and Technology
[DE94-604181] p 3047 N94-27698

COLD SURFACES
C-periodicity and the physical mass in the 3-state Potts model
[DE94-601551] p 3019 N94-26423

COLD TRAPS
Antiproton studies in penning traps
[AD-A274250] p 3024 N94-27011

COLD WEATHER
Environmental benefits of different types of heat pumps, available and expected
[DE94-002440] p 2866 N94-26123

COLD WORKING
Titanium 1992: Science and Technology, volume 1
[AD-A274798-VOL-1] p 2739 N94-26799
Effect of precipitate structure on hot deformation of Al-Mg-Mn alloys
[DE94-004596] p 2741 N94-27622

COLLIMATION
Regrouping of the beam in the IHEP PS for the UNK p-p programs
[DE93-634021] p 3032 N94-26164
Longitudinal diffusion of a proton bunch under external noise
[DE93-634022] p 3032 N94-26165

COLLIMATORS
Development of a holographic illumination system for a time-integrating correlator
[DSIS-94-00111] p 2814 N94-27763

COLLISION AVOIDANCE
A feasibility study on bird classification with neural network
[AD-A273753] p 2659 N94-25780
A global approach to kinematic path planning to robots with holonomic and nonholonomic constraints
p 2683 N94-26279
Application of the CIRSSE cooperating robot path planner to the NASA Langley truss assembly problem
p 2683 N94-26280

COLLISION RATES
Relativistic collision rate calculations for electron-air interactions
[DE94-004204] p 3020 N94-26527

COLLISIONS
Balancing of a planar bouncing object
[AD-A273805] p 2821 N94-25878
Deciphering the quark-gluon structure of the photon in electron(gamma) collisions
[DE93-634386] p 3017 N94-26043
The crash of P/Shoemaker-Levy 9 into Jupiter and its implications for comet bombardment on Earth
p 2891 N94-28313

COLLOCATION
Geoid determination: With help of the alternative scattering method
[ETN-94-95375] p 2847 N94-25746
Rendering of three-dimensional data sets derived from finite-difference and spectral methods
[AD-A273724] p 3096 N94-25997
On a spline-approximation method for solving ordinary differential equations
[DE93-634290] p 2994 N94-26471

COLLOIDS
Ion implantation in silicate glasses
[DE94-003785] p 2757 N94-27726

COLONIES
The Fermi paradox: An approach based on percolation theory p 2687 N94-27370
Counting Adelie penguins at colonies: Seasonal and annual changes p 2885 N94-27970
Note on the structure of moss colonies composed of two species on King George Island, the South Shetland Islands p 2885 N94-27971

COLOR
SHIVA: A unix-based, menu-driven, color image processing software package
[AD-A274071] p 2957 N94-25646
Color image segmentation
[AD-A274027] p 2984 N94-25759
Endogeneous and exogenous control of visual selection: A review of the literature
[AD-A273761] p 2908 N94-25871
IRMA: A program for three-dimensional color display of data
[AD-A273811] p 2959 N94-25879
Combining shape and color information for 3D object recognition
[AD-A274123] p 2967 N94-27064
COLOR VISION
Endogeneous and exogenous control of visual selection: A review of the literature
[AD-A273761] p 2908 N94-25871
Colour object recognition
[ISBN-0-315-83684-9] p 2994 N94-26614
COLUMNS (PROCESS ENGINEERING)
Analytical method for estimation of the total amount of aromatic and poly aromatic compounds in diesel fuel
[PB94-123692] p 2759 N94-25907
COMBAT
Developing realistic cooperative behaviors for autonomous agents in air combat simulation
[AD-A274077] p 2937 N94-25774
COMBINATIONS (MATHEMATICS)
Blurred focal elements generalization of dempster's rule
[PB94-124278] p 2986 N94-26992
COMBINED CYCLE POWER GENERATION
Combined Cycles for Power Plants
[VKI-LS-1993-08] p 2830 N94-28077
Introduction to combined cycles p 2789 N94-28078
Thermodynamics of combined cycle plant
p 2831 N94-28079
Development of the gas turbine. Part 1: Design philosophy and performance p 2831 N94-28080
Steam plant for combined cycles: Heat recovery steam generators, design principles, and construction details
p 2831 N94-28083
Simulation: A tool for steam plant dynamic analysis
p 2831 N94-28084
Steam plant: Steam turbines for combined cycles
p 2831 N94-28085
Controls, monitoring and performance measurements
p 2831 N94-28086
Cooling towers for combined cycles: Design philosophy, performance testing, and operating problems
p 2832 N94-28087
Cooling towers for combined cycles: New developments to meet environmental requirements
p 2832 N94-28088
Clean coal technology p 2832 N94-28089
Integrated coal gasification combined cycle
p 2832 N94-28090
COMBUSTIBLE FLOW
Gordon Research Conference on the Physics and Chemistry of Laser Diagnostics in Combustion
[AD-A274609] p 2716 N94-26893
COMBUSTION
Combustion synthesis method p 2721 N94-25561
On the thermal ignition with variable pre-exponential factor
[DE93-616009] p 2713 N94-25913
Gordon Research Conference on the Physics and Chemistry of Laser Diagnostics in Combustion
[AD-A274609] p 2716 N94-26893
Annual conference on fire research, 1993: Book of abstracts
[PB94-121324] p 2717 N94-26907
Pressure-gain combustion
[DE94-002975] p 2719 N94-27712
COMBUSTION CHAMBERS
Development and implementation of a scramjet cycle analysis code with a finite-rate-chemistry combustion model for use on a personal computer
[AD-A273834] p 2673 N94-25617
Orbit transfer rocket engine technology program enhanced heat transfer combustor technology
[NASA-CR-189236] p 2700 N94-26156
Gaseous hydrogen/oxygen injector performance characterization
[NASA-CR-194464] p 2701 N94-26208
Computation of non-isentropic internal flows with variable density
[AD-A274848] p 2794 N94-26801
Pressure-gain combustion
[DE94-002975] p 2719 N94-27712
Broad specification fuels combustion technology program, phase 2
[NASA-CR-191066] p 2719 N94-27854
A numerical study of mixing and combustion in hypervelocity flows through a scramjet combustor model
p 2808 N94-27911
COMBUSTION CHEMISTRY
Theoretical determination of chemical rate constants using novel time-dependent methods
[NASA-CR-195221] p 2714 N94-26205
Laser probes of natural gas ignition chemistry
[PB94-128345] p 2717 N94-27226
COMBUSTION PHYSICS
Development and implementation of a scramjet cycle analysis code with a finite-rate-chemistry combustion model for use on a personal computer
[AD-A273834] p 2673 N94-25617
Microgravity ignition experiment p 2761 N94-25707
Characterization of acoustic effects on flame structures by beam deflection technique
[DE94-003240] p 2714 N94-26122
An apparatus for measurement of ignition and burning characteristics of metallic particles
[AD-A274815] p 2716 N94-26487
Gordon Research Conference on the Physics and Chemistry of Laser Diagnostics in Combustion
[AD-A274609] p 2716 N94-26893
Basic research on natural gas combustion phenomena
[PB94-129046] p 2717 N94-27256
The addition of molecular oxygen to hydroperoxy-propyl radicals
[DE94-003662] p 2760 N94-27725
COMBUSTION PRODUCTS
Combustion synthesis method p 2721 N94-25561
SP industry calorimeter for rate of heat release measurements up to 10MW
[PB94-124211] p 2811 N94-27044
Researches of the Electrotechnical Laboratory. No. 53: Spectral emission from combustion gas containing scattering media
[JTN-94-80603] p 2717 N94-27246
Gas turbine combustion and emission control
p 2831 N94-28082
Fibrous ceramic candle filter for particle removal in pressurized fluidized bed combustion
[PB94-133089] p 2876 N94-28383
Experimental studies of pressurised fluidised bed combustion at Helsinki University of Technology, 1991-1992
[PB94-133063] p 2876 N94-28394
Emissions of nitrogen oxides (NO(x) and N2O) in pressurized fluidized bed combustion
[PB94-133071] p 2876 N94-28395
COMBUSTION STABILITY
Technical Report of National Research Institute of Fisheries Engineering: Fishing Boat and Instrument, No. 12
[JTN-94-80595] p 2764 N94-27976
Computer aided data recording and analyzing system for the engine test p 2764 N94-27979
Engine starting and stopping p 2828 N94-28047
COMBUSTION TEMPERATURE
Extraterrestrial surface propulsion systems
p 2833 N94-25691
COMET NUCLEI
Comet nucleus and asteroid sample return missions
p 2689 N94-25692
COMET RENDEZVOUS ASTEROID FLYBY MISSION
Space science: Causes and impacts of cutbacks to NASA's outer solar system exploration missions. Report to the Chairman, Subcommittee on Investigations and Oversight, Committee on Science, Space, and Technology, House of Representatives
[GAO/NSIAD-94-24] p 3106 N94-27418
COMETARY ATMOSPHERES
The kinetics and dynamics of the coma of Halley's comet
[NASA-CR-194828] p 3105 N94-28184
COMETS
Studies of extra-solar Oort Clouds and the Kuiper Disk
[NASA-CR-195242] p 3103 N94-26789
Cratering rates from lunar xenospherules
[DE94-003481] p 3106 N94-27007
Consequences of impacts of small asteroids and comets with Earth p 2889 N94-28301
Modulating terrestrial impacts from Oort cloud comets by the adiabatically changing galactic tides
p 2890 N94-28305
A general theory of impacts and mass extinctions, and the consequences of large-body impact on the Earth
p 2891 N94-28310
The crash of P/Shoemaker-Levy 9 into Jupiter and its implications for comet bombardment on Earth
p 2891 N94-28313
COMFORT
Lufthansa long range services: More simplicity
p 2663 N94-28246
COMMAND AND CONTROL
Component characterization and development 2
[AD-A274002] p 2765 N94-25660
Space Station technology testbed: 2010 deep space transport p 2687 N94-27368
Telecommand decoder specification
[ESA-PSS-04-151-ISSUE-1] p 2693 N94-27583
COMMAND LANGUAGES
Editing tree structures
[CWI-CS-R9264] p 2961 N94-26219
COMMAND MODULES
Assured crew return vehicle post landing configuration design and test p 2697 N94-25671
COMMERCE
Fabrication technology
[DE94-003017] p 2763 N94-26778
COMMERCIAL AIRCRAFT
Eagle RTS: A design of a regional transport
p 2671 N94-25709
A cost model for USAF acquisition of commercial aircraft for service in the special air mission fleet
[AD-A274012] p 3093 N94-25796
Methods for experimentally determining commercial jet aircraft landing parameters from video image data
[AD-A274207] p 2669 N94-27105
Effects of historical and predictive information on ability of transport pilot to predict an alert
[NASA-TM-4547] p 2673 N94-27864
Lufthansa Yearbook 1992
[DSK-9734-H-92] p 2660 N94-28230
Lufthansa long range services: More simplicity
p 2663 N94-28246
A symbol of reliability: Ju 52 p 2663 N94-28250
COMMUNICATION NETWORKS
Development of satellite telecommunications during the period 1990 - 2005
[CRANFIELD-AERO-9301] p 2765 N94-25639
Modeling and simulation of a fiber distributed data interface local area network
[AD-A274838] p 3098 N94-26500
Example of the EXPANSE signalling protocol
[PB94-125283] p 2771 N94-26872
The Communication Link and Error ANalysis (CLEAN) simulator
[NASA-CR-195243] p 2968 N94-27168
MILCOM 92 and standardization for HF-communication. A study tour to the USA in October 1992
[PB94-124427] p 2774 N94-27219
Vision 21: Interdisciplinary Science and Engineering in the Era of Cyberspace
[NASA-CP-10129] p 2685 N94-27358
Efficient massively parallel simulation of dynamic channel assignment schemes for wireless cellular communications
[NASA-CR-191593] p 2971 N94-27558
COMMUNICATION SATELLITES
Low Earth orbit communications satellite
p 2698 N94-25701
Automating satellite range scheduling
[AD-A273829] p 2694 N94-25738
Charge efficiency of Ni/H2 cells during transfer orbit of Telstar 4 satellites p 2862 N94-28117
COMMUNICATION THEORY
Communication complexity of t-intersection problems in generalized Boolean algebras
[PB94-126646] p 2996 N94-26917
COMMUTATION
Quantum group and Manin plane related to a colored braid group representation
[DE94-601509] p 3072 N94-26461
COMMUTER AIRCRAFT
Design of the advanced regional aircraft, the DART-75
p 2671 N94-25708
Impact of improved materials and cabin water spray on commuter aircraft postcrash fire survivability
[AD-A274421] p 2660 N94-27081
COMPARISON
Saving comparisons in the Crochemore-Perrin string matching algorithm
[CWI-CS-R9322] p 2971 N94-27550
COMPATIBILITY
A materials compatibility study in FM-1, a liquid component of a paste extrudable explosive
[DE94-001166] p 2759 N94-26198
Compatibility of refrigerants and lubricants with engineering plastics
[DE94-004959] p 2756 N94-27692
COMPENSATORS
Design of a subsonic envelope flight control system for the Vista F-16 using quantitative feedback theory
[AD-A274057] p 2676 N94-25771
COMPETITION
Space Habitat, assembly and repair facility
p 2691 N94-25696

COMPILERS

The ergonomics of software porting: Automatically configuring software to the runtime environment or everything you wanted to know about your C compiler but didn't know who to ask
[CWI-CS-R9266] p 2961 N94-26221

Programming in Fortran M
[DE94-002756] p 2963 N94-26407

Usefulness of compile-time restructuring of LGDF programs in throughput-critical applications
[AD-A274915] p 2963 N94-26530

Fast incremental compiler transformations for multiple instruction retry
[NASA-CR-195209] p 2964 N94-26680

Deferred compilation: The automation of run-time code generation
[AD-A274124] p 2967 N94-27065

Implementation and performance of a domain decomposition algorithm in Sisal
[DE94-002012] p 2981 N94-27092

ARM: Abstract Rewriting Machine
[CWI-CS-R9330] p 2974 N94-27794

COMPLEX COMPOUNDS

Fundamental study on new synthetic technology by phthalocyanine complexes p 2721 N94-25569

Heavy-electron behavior in large coordination compounds CeZn11 and UZn12
[REPT-A-2663] p 3049 N94-25614

Transition metal activation and functionalization of carbon-hydrogen bonds
[DE94-003650] p 2715 N94-26369

Transition metals in highly correlated discotic phases: Designing metallomesogens with selected intermolecular organizations
[AD-A274695] p 2736 N94-26452

Preparation, characterization, and thermal behaviour study of lanthanides (3) and yttrium (3) 4-methoxy benzylidene pyruvate in solid state
[DE94-604079] p 3068 N94-27697

COMPLEX NUMBERS

Q - difference intertwining operators for a Lorentz quantum algebra
[DE94-602559] p 2997 N94-27023

COMPLEX SYSTEMS

On modeling and controlling intelligent systems
[DE94-002446] p 2988 N94-27706

Practical problems in aggregating expert opinions
[DE94-002623] p 3094 N94-27707

Visit to CERMA: Centre d'Etudes et de Recherches de Medecine Aerospatiale, Centre for Studies and Research in Aviation and Space Medicine, Bretigny sur Orge, France, November 16-18, 1992
[PB94-132990] p 2937 N94-28392

COMPLEX VARIABLES

A possible way of connecting the Grassmann variables and the number of generation
[DE94-601624] p 2990 N94-25838

COMPLEXITY

A strange application of Kolmogorov complexity
[CWI-CS-R9328] p 2973 N94-27737

COMPONENT RELIABILITY

Aircraft turbine engine reliability and inspection investigations
[AD-A274860] p 2673 N94-26176

Investigation of ACC/CCI tunnel diodes
[AD-A274549] p 2785 N94-26845

COMPOSITE MATERIALS

Computer modelling of cyclic deformation of high-temperature materials
[AD-A273852] p 2704 N94-25608

A revolutionary approach to composite construction and flight management systems for small, general aviation airplanes p 2671 N94-25714

Solar powered multipurpose remotely powered aircraft
p 2671 N94-25719

Composite raw materials for the building industry
[VTT-TIED-1433] p 2708 N94-26544

Computational mechanics
[DE94-003015] p 2965 N94-26775

DUSOL: Improved software for analysis of ultrasonic velocity data on anisotropic materials
[NPL-DMM(A)-104] p 2965 N94-26816

Method for improving electromagnetic shielding performance of composite materials by electropulsing
[AD-D016050] p 2709 N94-27076

Method for improving electromagnetic shielding performance of composite materials by electroplating
[AD-D016038] p 2709 N94-27091

High temperature tension test equipment of heat resistant composite materials
[NAL-TM-652] p 2710 N94-27255

List of papers published by the members of Institute for Materials Research, Tohoku University 1992
[JTN-94-80608] p 3118 N94-27355

Series solution for a cylindrical composite shell subject to axisymmetric loadings
[ISBN-0-315-60559-6] p 2844 N94-27810

Mechanically fastened composite laminates subjected to combined bearing-bypass and shear loading
p 2712 N94-27914

Analytic solution for the dyadic Green's function of a nonreciprocal uniaxial bianisotropic medium
[PB94-133162] p 2779 N94-28388

COMPOSITE STRUCTURES

Design and life-time of polymer matrix composite structures: Summary
[VTT-TIED-1415] p 2707 N94-26260

The structural behaviour of the steel or composite concrete and steel frames and the connections of frame members during the fire: A literature review
[VTT-TIED-1437] p 2837 N94-26307

Formulae for the buckling of simply-supported corrugated panels of orthotropic material under shear load
[PB94-126547] p 2840 N94-26911

Proceedings of Damping 1993, volume 2
[AD-A274227] p 2840 N94-26953

Wing design for a civil tiltrotor transport aircraft: A preliminary study p 2671 N94-27917

COMPOSITE WRAPPING

Composite leading edge/spar member for an aircraft control surface
[CA-PATENT-1-325-765] p 2669 N94-27273

COMPRESSIBILITY

Design and test of postbuckled stiffened curved plates: A literature survey
[PB94-126521] p 2840 N94-26961

COMPRESSIBILITY EFFECTS

Compressibility effects on rotor forces in the leakage path between a shrouded pump impeller and its housing
p 2796 N94-27379

COMPRESSIBLE BOUNDARY LAYER

Unified approach for direct and inverse boundary layer prediction using cubic spline collocation
p 2653 N94-28326

Transition for three-dimensional, compressible boundary layers p 2653 N94-28327

Euler and Navier-Stokes wing/fuselage computations of the De Havilland Dash 8 aircraft p 2654 N94-28329

COMPRESSIBLE FLOW

Computational investigation of the compressible dynamic stall characteristics of the Sikorsky SSC-A09 airfoil
[AD-A274867] p 2644 N94-26191

On prediction of equilibrium states in homogeneous compressible turbulence
[NASA-CR-4570] p 2792 N94-26467

New constitutive equation for the volume viscosity in fluids
[NASA-TM-109104] p 2798 N94-27867

Unsteady three dimensional Euler solutions on moving grids p 2657 N94-28347

COMPRESSIBLE FLUIDS

Compressibility effects on rotor forces in the leakage path between a shrouded pump impeller and its housing
p 2796 N94-27379

COMPRESSION LOADS

Design of cold-formed HSS channels for bending and eccentric compression: Bending in the plane of symmetry
[VTT-TIED-1403] p 2762 N94-25622

Investigation of compressive behavior for metal matrix composites with a circular hole
[AD-A273835] p 2705 N94-25739

Investigation of tension-compression fatigue behavior of a cross-ply metal matrix composite at room and elevated temperatures
[AD-A273731] p 2706 N94-25999

An experimental study on the effects of compressive stress on the fatigue crack growth of low-alloy steel
[DE94-004447] p 2737 N94-26582

Behaviour modification of space trusses
[ISBN-0-315-84701-8] p 2842 N94-27315

Contact stress in disc cams with roller followers
[ESDU-93001] p 2829 N94-28055

COMPRESSION TESTS

Influence of embedded optical fibers on compressive strength of advanced composites
[AD-A273775] p 2705 N94-25859

The effects of embedded internal delaminations on composite laminate compression strength; an experimental review
[NASA-TM-108440] p 2707 N94-26127

A constitutive model for layered wire mesh and aramid cloth fabric
[DE94-003275] p 2708 N94-26796

Computer simulation and experiments on the quasi-static mechanics and transport properties of granular materials
[AD-A274192] p 2823 N94-27104

Fatigue resistance of unnotched and post impact(+/-30 deg/0 deg) 3-D braided composites
[NASA-CR-191590] p 2711 N94-27433

COMPRESSION WAVES

Review of tokamak experiments on direct electron heating and current drive with fast waves
[DE94-004185] p 3041 N94-25801

COMPRESSIVE STRENGTH

Investigation of compressive behavior for metal matrix composites with a circular hole
[AD-A273835] p 2705 N94-25739

Influence of embedded optical fibers on compressive strength of advanced composites
[AD-A273775] p 2705 N94-25859

The effects of embedded internal delaminations on composite laminate compression strength; an experimental review
[NASA-TM-108440] p 2707 N94-26127

Fatigue resistance under tension-compression of laminates IM6/5245C and AS4/3501-6
[IAR-CR-25] p 2708 N94-26711

Aluminum alloy 8090-T8771 thick plate material characterization
[AD-A274146] p 2987 N94-27077

COMPRESSOR BLADES

Effects of crenulations on three dimensional losses in a linear compressor cascade
[AD-A273778] p 2790 N94-25862

COMPRESSORS

Dynamic response of a compressor research facility
[AD-A273836] p 2679 N94-25740

Compressor stability p 2828 N94-28046

Transient model applications. 1: Compressor heat soak/clearance effects modeling p 2828 N94-28048

Transient model applications. 2: Compressor stall modeling methods p 2829 N94-28049

A review of recent aeroelastic analysis methods for propulsion at NASA Lewis Research Center
[NASA-TP-3406] p 2846 N94-28227

COMPTON EFFECT

Electroweak and other interactions in medium-energy nuclear physics
[DE94-004161] p 3027 N94-27689

COMPUTATION

Adaptive path planning in changing environments
[DE94-003269] p 2985 N94-26462

Fast methods for computation with algebraic numbers
[ISBN-0-315-57888-2] p 2998 N94-27269

The calculation for energy balance of heating plasmas by Alfven waves
[DE94-604994] p 3049 N94-27855

Computation of static pressure downstream of a normal shock for hypersonic flight (ambient temperature known)
[ESDU-93020] p 2649 N94-28091

Examples of excrescence drag prediction for typical wing components of a subsonic transport aircraft at the cruise condition
[ESDU-93032] p 2649 N94-28144

Hessenberg matrices in Krylov subspaces and the computation of the spectrum
[PB94-133170] p 3001 N94-28389

COMPUTATIONAL CHEMISTRY

High performance computing in chemistry and massively parallel computers: A simple transition?
[DE94-004318] p 2982 N94-27600

COMPUTATIONAL FLUID DYNAMICS

Experimental contribution to the study of secondary flows in centrifugal turbopump stator components
[ECL-92-35] p 2789 N94-25654

Riemann solvers for solving the incompressible Navier-Stokes equations using the artificial compressibility method
[CRANFIELD-AERO-9208] p 2790 N94-25778

Shock wave interaction with L-shaped structures
[AD-A273774] p 2790 N94-25858

A numerical study of high-speed missile configurations using a block-structured parallel algorithm
[AD-A273776] p 2979 N94-25860

Rendering of three-dimensional data sets derived from finite-difference and spectral methods
[AD-A273724] p 3096 N94-25997

Calculation of viscous drag of two low angle of attack supercritical profiles
[FFA-TN-1984-22] p 2644 N94-26104

Performance of renormalization group algebraic turbulence model on boundary layer transition simulation
[NASA-CR-194466] p 2644 N94-26131

Comments regarding two upwind methods for solving two-dimensional external flows using unstructured grids
[NASA-TM-109078] p 2644 N94-26154

Computational investigation of the compressible dynamic stall characteristics of the Sikorsky SSC-A09 airfoil
[AD-A274867] p 2644 N94-26191

Feature isolation and quantification of evolving datasets
[NASA-CR-195230] p 2961 N94-26207

A positive finite-difference advection scheme applied on locally refined grids
[CWI-NM-R9309] p 2867 N94-26216

Modelling of ionisation reactions and of the resulting electric fields in one-dimensional hypersonic shock waves with the direct simulation Monte Carlo method
[IC-AERO-92-01] p 2644 N94-26248

Potential capabilities of Reynolds stress turbulence model in the COMMIX-RSM code
[DE94-003716] p 2792 N94-26331

On prediction of equilibrium states in homogeneous compressible turbulence
[NASA-CR-4570] p 2792 N94-26467

A numerical study of quantized vortices in HeII
[ISBN-9-03-860232-4] p 2792 N94-26479

A comparative study of serial and parallel aeroelastic computations of wings
[NASA-TM-108805] p 2645 N94-26538

Computational prediction of isolated performance of an axisymmetric nozzle at Mach number 0.90
[NASA-TM-4506] p 2646 N94-26547

Program to develop a performance and heat load prediction system for multistage turbines
[NASA-CR-195223] p 2674 N94-26588

Computational strategies for three-dimensional flow simulations on distributed computer systems
[NASA-CR-195249] p 2793 N94-26595

Pump CFD code validation tests
[NASA-CR-193939] p 2822 N94-26597

Influence of the transonic doublet in the farfield of a lifting airfoil
[IAR-AN-78] p 2647 N94-26702

Computation of non-isentropic internal flows with variable density
[AD-A274848] p 2794 N94-26801

New variational techniques for acoustic radiation and scattering from elastic shell structures
[AD-A274599] p 3010 N94-26889

A parallel computational fluid dynamics unstructured grid generator
[AD-A274129] p 2795 N94-27119

A second-order shock-adaptive Godunov scheme based on the generalized Lagrangian formulation
[ISBN-0-315-84549-X] p 2795 N94-27307

Bulk-Flow Analysis, part A
[NASA-CR-193911-PT-A] p 2796 N94-27377

Parallel implicit unstructured grid Euler solvers
[NASA-CR-191594] p 2999 N94-27434

Agglomeration multigrid for the three-dimensional Euler equations
[NASA-CR-191595] p 2999 N94-27557

A study on heat transfer in a scramjet leading edge model
[NAL-TR-1187T] p 2675 N94-27608

Thermocapillary flow with evaporation and condensation and its effect on liquid retention in low-G fluid acquisition devices
[NASA-TP-3463] p 2797 N94-27639

NAS technical summaries. Numerical aerodynamic simulation program, March 1992 - February 1993
[NASA-RP-1321] p 3118 N94-27764

Coupled 2-dimensional cascade theory for noise an d unsteady aerodynamics of blade row interaction in turbofans. Volume 2: Documentation for computer code CUP2D
[NASA-CR-4506-VOL-2] p 2675 N94-27778

Numerical simulation of receptivity and transition in a boundary layer on a flat plate with a suction hole
[NASA-CR-195708] p 2798 N94-27782

Time-step enlargement and optimal smoothing in Runge-Kutta time-integration algorithms by implicit and explicit smoothing
[NLR-TP-92221-U] p 2798 N94-27799

A comprehensive comparison of turbulence models in the far wake p 2808 N94-27899

Computational and Experimental Assessment of Jets in Cross Flow
[AGARD-CP-534] p 2799 N94-28003

Fifty years of jet in cross flow research
p 2799 N94-28004

Numerical investigation of thrust vectoring by injection of secondary air into nozzle flows p 2801 N94-28013

Transitional flight characteristics of a geometrically simplified STOVL model p 2672 N94-28035

Analysis of cooling jets near the leading edge of turbine blades p 2676 N94-28037

Abstracts of papers presented at the 4th CASI Aerodynamics Symposium
[ISBN-0-920203-01-9] p 2651 N94-28315

Application of the MBTEC Euler code to the Challenger and the CF-18 complete aircraft configurations
p 2653 N94-28324

Unified approach for direct and inverse boundary layer prediction using cubic spline collocation
p 2653 N94-28326

Transition for three-dimensional, compressible boundary layers p 2653 N94-28327

Euler and Navier-Stokes wing/fuselage computations of the De Havilland Dash 8 aircraft p 2654 N94-28329

Application of the influence function method using the interference distributed loads code to prediction of store aerodynamic load during separation from the CF-18 fighter aircraft p 2654 N94-28330

COMPUTATIONAL GEOMETRY

Center for computation and visualization of geometric structures
[DE94-001882] p 2991 N94-25928

Parallel computational geometry on analog Hopfield networks
[ISBN-0-315-84093-5] p 2980 N94-26635

Bifurcation sequences at 1:4 resonance: An inventory
[PB94-125408] p 2997 N94-27028

Lisp interface to geometric modelling operations
[PB94-133121] p 3001 N94-28398

COMPUTATIONAL GRIDS

Comments regarding two upwind methods for solving two-dimensional external flows using unstructured grids
[NASA-TM-109078] p 2644 N94-26154

A positive finite-difference advection scheme applied on locally refined grids
[CWI-NM-R9309] p 2867 N94-26216

VLUGR2: A vectorized local uniform grid refinement code for PDE's in 2D
[CWI-NM-R9306] p 2965 N94-26772

Local uniform grid refinement and systems of coupled partial differential equations
[CWI-NM-R9307] p 2995 N94-26773

Using the TSAR electromagnetic modeling system
[DE94-002617] p 2771 N94-26803

Grid-independent convergence based on preconditioning techniques
[PB94-125358] p 2997 N94-27000

Combining shape and color information for 3D object recognition
[AD-A274123] p 2967 N94-27064

A parallel computational fluid dynamics unstructured grid generator
[AD-A274129] p 2795 N94-27119

Genetic algorithms applied to a mission routing problem
[AD-A274130] p 2968 N94-27120

Numerical Analysis Methods of Surface Cracks
[VTT-PUBS-119] p 2841 N94-27186

Development of an automated fracture assessment system for nuclear structures (appendix 1/1)
p 2841 N94-27187

Quality assurance for fracture mechanical finite element analyses (appendix 3/1) p 2841 N94-27189

High-lift system analysis method using unstructured meshes
[NLR-TP-92351-U] p 2647 N94-27554

Agglomeration multigrid for the three-dimensional Euler equations
[NASA-CR-191595] p 2999 N94-27557

Prediction of undsteady flows in turbomachinery using the linearized Euler equations on deforming grids
[NASA-CR-195285] p 2675 N94-27654

Locating tie-points on a grid p 2978 N94-27906

Computation of transonic viscous flow past the NTF 65-degree Delta Wing p 2659 N94-27930

An enhanced global spectral model
[PL-TR-92-2011] p 2898 N94-28223

Viscous airfoil computations using adaptive structured grids p 2655 N94-28337

Solution of the Euler equations using unstructured grids p 2656 N94-28338

Thin-layer Navier-Stokes computations for multi-element airfoils p 2656 N94-28341

Techniques for accurately solving unsteady shock waves and contact discontinuities p 2656 N94-28342

Recent advances in the spectral element method
p 2657 N94-28348

Multigrid solutions of the 2D Euler/Navier-Stokes equations on unstructured meshes
p 2658 N94-28349

COMPUTER AIDED DESIGN

Creation of prototype aircrew protection equipment based on face anthropometry
[AD-A273865] p 2940 N94-25611

Development of a 4-bit parallel analog-to-digital converter and a four-quadrant double-balanced mixer using heterojunction bipolar transistor technology
[AD-A274074] p 2947 N94-25648

Systematic Propulsion Optimization Tools (SPOT)
p 2976 N94-25666

IGES 4.0 to LCAD translator for CSG models
[AD-A274013] p 2957 N94-25753

Object-oriented design and implementation of a parallel Ada simulation system
[AD-A274119] p 2979 N94-25906

Center for computation and visualization of geometric structures
[DE94-001882] p 2991 N94-25928

The MUSA design methodology
[CWI-CS-R9265] p 3097 N94-26220

Hypermedia support for engineering design systems: Application to fatigue analysis
[VTT-TIED-1432] p 2837 N94-26255

Cad of GeO2-SiO2 double-layer core dispersion-shifted single-mode fibre
[DE93-634325] p 3035 N94-26383

Computer code for interactive rotorcraft preliminary design using a harmonic balance method for rotor trim
[AD-A274924] p 2668 N94-26531

Partitioning structural VHDL circuits for parallel execution on hypercubes
[AD-A274390] p 2785 N94-26830

Rapid prototyping of application specific signal processors (RASSP)
[AD-A274324] p 2772 N94-26884

Rocket engine numerical simulation
p 2688 N94-27375

Interactive shape metamorphosis
[NASA-CR-191597] p 2970 N94-27417

Validation tests of TOPSIM 4
[ESA-STM-249] p 2972 N94-27582

Thermal/Structural Tailoring of Engine Blades (T/STAEBL): User's manual
[NASA-CR-194461] p 2843 N94-27776

Engine simulation systems p 2829 N94-28054

A new approach to turboprop forward nacelle design
p 2655 N94-28336

COMPUTER AIDED MANUFACTURING

Automatic assembly planning and its role in agile manufacturing: A Sandia perspective
[DE94-002291] p 2821 N94-25970

The National Center for Advanced Information Components Manufacturing: Program update
[DE94-002647] p 2960 N94-26118

Distributed Nd:YAG laser welding and process control in inert glove boxes
[DE94-002629] p 2818 N94-26605

Open communication in manufacturing automation
[PB94-132479] p 2976 N94-28377

COMPUTER AIDED TOMOGRAPHY

Numerical simulation of tomographic reconstruction for the study of turbulence using optical wavefront sensor measurements
[AD-A273851] p 2789 N94-25587

X ray computed tomography for emerging aerospace materials and processes development
[AD-A273721] p 2705 N94-25779

Materials characterization on efforts for ablative materials
[NASA-CR-193929] p 2756 N94-27230

COMPUTER ANIMATION

An interactive, physically-based simulation system
[ISBN-0-315-83884-1] p 2963 N94-26616

COMPUTER ASSISTED INSTRUCTION

Knowledge organization in intelligent tutoring systems for diagnostic problem solving in complex dynamic domains
[AD-A273986] p 2984 N94-25899

Integration of interactive interfaces with intelligent tutoring systems: An implementation
[AD-A273869] p 2985 N94-25966

Production of a computer based lesson teaching employees how to use an air data tester
[ISBN-0-315-84708-5] p 2969 N94-27316

COMPUTER COMPONENTS

MATRA Marconi Space: The Silex on-board processor and on-board software p 2950 N94-26726

COMPUTER DESIGN

Design of a computer expert system for adhesive selection using artificial intelligence techniques
[AD-A274715] p 2751 N94-26434

High performance flight computer developed for deep space applications p 2949 N94-26718

Fault tolerant real-time processing system for space use p 2949 N94-26720

Design principles of onboard management of a Sun synchronous satellite p 2950 N94-26722

MATRA Marconi Space: The Silex on-board processor and on-board software p 2950 N94-26726

A Multitransputer Parallel Processing System (MTPPS)
[DE94-604652] p 2981 N94-26903

COMPUTER GRAPHICS

Module interconnection frameworks for a real-time spreadsheet
[AD-A273853] p 2956 N94-25588

IGES 4.0 to LCAD translator for CSG models
[AD-A274013] p 2957 N94-25753

ObjectSim: A reusable object oriented DIS visual simulation
[AD-A274030] p 2958 N94-25767
Graphical programming at Sandia National Laboratories
[DE94-003803] p 2958 N94-25818
A virtual environment for satellite modeling and orbital analysis in a distributed interactive simulation
[AD-A274114] p 2694 N94-25904
Center for computation and visualization of geometric structures
[DE94-001882] p 2991 N94-25928
Weapon system sensor integration for a DIS-compatible virtual cockpit
[AD-A274088] p 2672 N94-26021
NPSNET-4: A real-time, 3D distributed interactive virtual world
[AD-A274942] p 2961 N94-26298
Optimization of Vector Product Format (VPF) data for map background display in army tactical systems
[AD-A274687] p 2848 N94-26446
Benefits estimation for simulation systems used for aircrew training in a multiship environment
[AD-A274313] p 2938 N94-26882
Encoding approaches for data link transmission of weather graphics
[AD-A274497] p 2772 N94-26963
Interactive control of a parallel simulation from a remote graphics workstation
[AD-A274217] p 2981 N94-27070
Users guide for GRIKURV: A code for drawing graphs
[PB94-123593] p 2968 N94-27154
Data analysis and data fusion for intelligence analysis and decision support. Research plan 1993-2000
[PB94-123569] p 3005 N94-27173
Developments in the application of the geometrical theory of diffraction and computer graphics to aircraft inter-antenna coupling analysis
[ISBN-0-315-84643-7] p 2776 N94-27308
Interactive shape metamorphosis
[NASA-CR-191597] p 2970 N94-27417
Thirteen ways to say nothing with scientific visualization
[NASA-CR-195280] p 2970 N94-27542
Development of Calcomp compatible interface library 'piflib' on X Window System
[DE94-701190] p 2973 N94-27702
ACES spectral display software: User manual
[SKL-1600-99-002] p 2973 N94-27762
ActorStudio: An interactive user interface editor
[PB94-132859] p 2976 N94-28356

COMPUTER INFORMATION SECURITY
Vulnerability assessment using a fuzzy logic based method
[AD-A274075] p 2957 N94-25649
Development and analysis of secure embedded software
[VTT-TIED-1430] p 2961 N94-26254
An efficient off-line electronic cash system based on the representation problem
[CWI-CS-R9323] p 2776 N94-27551

COMPUTER NETWORKS
Standardizing exchange formats
[DE93-616798] p 3095 N94-25751
Full-text information services at the desktop
[DE94-003728] p 3096 N94-25813
Predicting nonlinear time series
[AD-A274051] p 2990 N94-25834
A VHDL register transfer level model of the linear token passing multiplex data bus protocol for the high speed data bus
[AD-A273734] p 2980 N94-26009
Design and specification of the Xpress transfer high-speed protocol
[AD-A274941] p 3097 N94-26297
Federal Information Exchange (FEDIX) user's guide: Fall 1993, Version 5.0/Release 1.0
[DE94-003826] p 3097 N94-26350
Usefulness of compile-time restructuring of LGDF programs in throughput-critical applications
[AD-A274915] p 2963 N94-26530
The High Performance Storage System
[DE94-004351] p 2948 N94-26578
Vision 21: Interdisciplinary Science and Engineering in the Era of Cyberspace
[NASA-CP-10129] p 2685 N94-27358
Proceedings of Workshop on Distributed Computing and Network
[DE94-701165] p 2983 N94-27804
Planning for the future of the DREnet: The way ahead
[NRNS-002-00-001-01] p 2983 N94-28042

COMPUTER PROGRAM INTEGRITY
Development and analysis of secure embedded software
[VTT-TIED-1430] p 2961 N94-26254
Software assurance standard
[NASA-TM-109705] p 2975 N94-27992

COMPUTER PROGRAMMING
Automating satellite range scheduling
[AD-A273829] p 2694 N94-25738
Graphical programming at Sandia National Laboratories
[DE94-003803] p 2958 N94-25818
The television as robot servant
[AD-A273985] p 2984 N94-25898
Set based analysis of arithmetic
[AD-A274112] p 3002 N94-25903
Developing a sophisticated user interface to support domain-oriented application composition and generation systems
[AD-A274080] p 2960 N94-25994
Software redesign for usability: A case study
[DE94-003704] p 2960 N94-26048
Deductive computer programming
[AD-A274966] p 2962 N94-26303
Adaptive path planning in changing environments
[DE94-003269] p 2985 N94-26462
Scheduling tasks with unpredictable timing parameters in hard real-time systems p 2951 N94-26728
Vcalc: A 3-space vector calculator
[AD-A274520] p 2965 N94-26831
Development of a performance evaluation tool (MMSOFE) for detection of failures with Multiple Model Adaptive Estimation (MMAE)
[AD-A274218] p 2665 N94-27071
Ma42: A new frontal code for solving sparse unsymmetric systems
[PB94-124302] p 2998 N94-27115
A method for populating the knowledge base of AFIT's domain-oriented application composition system
[AD-A274128] p 3099 N94-27118
Sculpting in cyberspace: Parallel processing the development of new software p 2686 N94-27365
Expressiveness results for process algebras
[CWI-CS-R9301] p 3000 N94-27577
A theory for simulator tools
[CWI-CS-R9302] p 2972 N94-27578
ARM: Abstract Rewriting Machine
[CWI-CS-R9330] p 2974 N94-27794
Software assurance standard
[NASA-TM-109705] p 2975 N94-27992

COMPUTER PROGRAMS
Study on knowledge extraction and systematization for material design p 2727 N94-25568
Predicting antenna parameters from antenna physical dimensions
[AD-A273893] p 3012 N94-25655
INM, Integrated Noise Model. Version 4.11: User's guide, supplement
[AD-A273885] p 3009 N94-25731
Graphical programming at Sandia National Laboratories
[DE94-003803] p 2958 N94-25818
A data processing system at the hybrid spectrometer
[DE93-616801] p 3013 N94-25828
IRMA: A program for three-dimensional color display of data
[AD-A273811] p 2959 N94-25879
The television as robot servant
[AD-A273985] p 2984 N94-25898
Set based analysis of arithmetic
[AD-A274112] p 3002 N94-25903
A research program on radiative transfer model development in support of the ARM program
[DE94-001146] p 2767 N94-25950
Technical description of the Vulcano software library
[FFI-93/7024] p 2767 N94-26105
The proceedings of the KEK FEL Simulation Code Workshop
[DE93-520378] p 2816 N94-26112
Analysis and optimization of preliminary aircraft configurations in relationship to emerging agility metrics
[NASA-CR-195228] p 2668 N94-26235
Red's natural editor: A program designed to edit FORTRAN programs
[DE94-003271] p 2962 N94-26318
PDEF: A standard file format for data interchange
[AD-A274694] p 3098 N94-26451
Computer code for interactive rotorcraft preliminary design using a harmonic balance method for rotor trim
[AD-A274924] p 2668 N94-26531
User's guide for the frequency domain algorithms in the LIFE2 fatigue analysis code
[DE94-004678] p 2838 N94-26563
New FORTRAN computer programs to acquire and process isotopic mass spectrometric data: Operator's manual
[DE94-003174] p 2965 N94-26784
A preliminary method for atmospheric soundings in real time using satellite and ground-based remotely sensed data
[AD-A274381] p 2880 N94-26828
Vcalc: A 3-space vector calculator
[AD-A274520] p 2965 N94-26831
Computer program for numerical evaluation of the performance of an overmoded TM01 circular to TE10 rectangular waveguide mode converter
[AD-A274548] p 2771 N94-26844
The NOGAPS ten year AMIP integration
[AD-A274332] p 2900 N94-26887
Alternative architectures for domain-oriented application composition and generation systems
[AD-A274180] p 2968 N94-27128
Users guide for GRIKURV: A code for drawing graphs
[PB94-123593] p 2968 N94-27154
Basic research on natural gas combustion phenomena
[PB94-129046] p 2717 N94-27256
Emerging computer technologies and the news media of the future p 2688 N94-27372
Computer code for controller partitioning with IFPC application: A user's manual
[NASA-CR-195291] p 2678 N94-27414
Design and implementation of a DBMS performance assessment tool
[CWI-CS-R9270] p 2972 N94-27576
PATRAN 2.5/EAL interface guide
[NASA-TM-109053] p 2972 N94-27655
Parallel computing for probabilistic response analysis of high temperature composites
[NASA-CR-194467] p 2843 N94-27656
Study of the kinematic and dynamic characteristics of a wormgear transmission for helicopter applications
[NASA-CR-195287] p 2826 N94-27657
Hardware and software reliability estimation using simulations
[NASA-CR-187588] p 2973 N94-27663
Refinement for fault-tolerance: An aircraft hand-off protocol
[NASA-CR-195697] p 2666 N94-27768
An optimization program based on the method of feasible directions: Theory and users guide
[NASA-TM-4552] p 2845 N94-27865
Proton irradiation on materials p 3030 N94-27898
Space transportation vehicle design evaluation using saturated designs p 2693 N94-27928
Visualization techniques to aid in the analysis of multispectral astrophysical data sets
[NASA-CR-195268] p 3105 N94-27932
Software assurance standard
[NASA-TM-109705] p 2975 N94-27992
Gas Turbine Engine Transient Behaviour
[VKI-LS-1993-06] p 2828 N94-28043
Transient engine simulation p 2829 N94-28052
Engine simulation systems p 2829 N94-28054
Thermal modeling of NiH2 batteries
p 2862 N94-28113
Parameter estimation of linear systems from frequency response measurements (computer program)
[ESDU-93016] p 2976 N94-28137

COMPUTER STORAGE DEVICES
High-speed, high-density, coherent time-domain optical memory
[AD-A274249] p 3037 N94-27010
Ferroelectric fluoride memory FET development
[AD-A274341] p 2785 N94-27057
Interactive control of a parallel simulation from a remote graphics workstation
[AD-A274217] p 2981 N94-27070

COMPUTER SYSTEMS DESIGN
System software and tools for high performance computing environments: A report on the findings of the Pasadena Workshop
[DE94-003918] p 2956 N94-25602
The High Performance Storage System
[DE94-004351] p 2948 N94-26578
Fast incremental compiler transformations for multiple instruction retry
[NASA-CR-195209] p 2964 N94-26680
Computing in space: Issues and answers
p 2948 N94-26714
Development of a MIL-STD-1750 microprocessor system for space applications p 2949 N94-26715
On-board computer for control subsystem of satellite
p 2949 N94-26716
Design principles of onboard management of a Sun synchronous satellite p 2950 N94-26722
PRONAOS flight software: A real-time application for a balloonborne scientific gondola p 2950 N94-26725
Formal methods for dependable real-time systems
p 2953 N94-26740
Developing with Ada using HOOD design methodology
p 2953 N94-26741
Ada reusable software for satellite on-board data handling p 2953 N94-26743

Virtual data
[DE94-002718] p 2986 N94-26807
Trace-based compositional proof theory for fault tolerant distributed systems
[PB94-126737] p 2966 N94-26971
Proceedings of the Third Workshop Computersystems: Research Forum on Design, Realization and Use of Computersystems
[ISBN-90-6144-995-2] p 2954 N94-27191
VENI, video, VICI: The merging of computer and video technologies p 2686 N94-27362
Emerging computer technologies and the news media of the future p 2688 N94-27372
Schema integration in object-oriented databases
[CWI-CS-R9320] p 2970 N94-27548
Proceedings of Workshop on Distributed Computing and Network
[DE94-701165] p 2983 N94-27804
Comparison of Object-Oriented Analysis and Design Methods: A Collection of Papers
[MEMO-INF-92-69] p 2975 N94-27936
A formal approach to the comparison of object-oriented analysis and design methodologies
p 2975 N94-27937
Object-oriented development methods
p 2975 N94-27938

COMPUTER SYSTEMS PERFORMANCE
Performance measurement of three commercial object-oriented database management systems
[AD-A274028] p 3096 N94-25765
Source code for the OO1 benchmark and the AFIT simulation benchmark
[AD-A274035] p 2958 N94-25799
Achieving high performance on the Intel Paragon
[DE94-003108] p 2979 N94-25953
Fast incremental compiler transformations for multiple instruction retry
[NASA-CR-195209] p 2964 N94-26680
Real-Time Embedded Processing for Space Applications
[ISBN-2-85428-335-X] p 2948 N94-26713
Tool for performance analysis and off-line prediction of timing behaviour p 2952 N94-26732
Early real-time performance measurements on the Columbus processor system p 2952 N94-26736
Arithmetic performances of onboard computers
p 2952 N94-26738
Verification and validation of the on-board software real time requirements p 2953 N94-26739
Modeling systems by probabilistic process algebra: An event structures approach
[PB94-125259] p 3004 N94-26867
Shared virtual memory and generalized speedup
[NASA-CR-191592] p 2969 N94-27416
Design and implementation of a DBMS performance assessment tool
[CWI-CS-R9270] p 2972 N94-27576

COMPUTER SYSTEMS PROGRAMS
System software and tools for high performance computing environments: A report on the findings of the Pasadena Workshop
[DE94-003918] p 2956 N94-25602
Developing a sophisticated user interface to support domain-oriented application composition and generation systems
[AD-A274080] p 2960 N94-25994
Developing a graphical user interface to support a real-time digital signal processing system
[AD-A274032] p 2960 N94-26018
Fault tolerant real-time processing system for space use p 2949 N94-26720
NASA's spacecraft data system p 2950 N94-26723
The Ariane 5 data management system
p 2950 N94-26724
PRONAOS flight software: A real-time application for a balloonborne scientific gondola p 2950 N94-26725
MATRA Marconi Space: The Silex on-board processor and on-board software p 2950 N94-26726
On-board software for the JET-X telescope on the Spectrum-X mission p 2951 N94-26727
Early real-time performance measurements on the Columbus processor system p 2952 N94-26736
Test of onboard real time applications (LICE (tm))
p 2952 N94-26737
Arithmetic performances of onboard computers
p 2952 N94-26738
Verification and validation of the on-board software real time requirements p 2953 N94-26739
Garbage collection in a multiprocessor Smalltalk system
[ISBN-0-315-51159-1] p 2982 N94-27332

COMPUTER TECHNIQUES
Extending the rule space model to a semantically-rich domain: Diagnostic assessment in architecture
[AD-A273789] p 2948 N94-25864
The television as robot servant
[AD-A273985] p 2984 N94-25898
Knowledge organization in intelligent tutoring systems for diagnostic problem solving in complex dynamic domains
[AD-A273986] p 2984 N94-25899
EcarHeart2 version 1.0: Programmers documentation
[PB94-124633] p 2909 N94-25909
Focusing properties of a three-element quadrupole lens system and its stigmatic focusing behaviour
[DE93-616534] p 2766 N94-25915
Analysis and computer tools for separation processes involving nonideal mixtures
[DE94-004162] p 2960 N94-25986
A comparison of two hardware implementations of a crew selection system
[AD-A274913] p 2937 N94-26346
Performance assessment in sustained operations using a computer-based synthetic work task
[AD-A274707] p 2937 N94-26430
Optimization of Vector Product Format (VPF) data for map background display in army tactical systems
[AD-A274687] p 2848 N94-26446
Computer visualizations in engineering applications
[DE94-003589] p 2822 N94-26465
Modeling Group 4 elements with new transferable tight-binding models
[DE94-000770] p 3059 N94-26695
An algorithm for determination of bearing health through automated vibration monitoring
[AD-A274591] p 2823 N94-26986
Automatic mapping of task and data parallel programs for efficient execution on multicomputers
[AD-A274125] p 2982 N94-27117
A method for populating the knowledge base of AFIT's domain-oriented application composition system
[AD-A274128] p 3099 N94-27118
The coming technological singularity: How to survive in the post-human era p 2685 N94-27359
Emerging computer technologies and the news media of the future p 2688 N94-27372
NAS technical summaries. Numerical aerodynamic simulation program, March 1992 - February 1993
[NASA-RP-1321] p 3118 N94-27764
Hybrid techniques for complex aerospace electromagnetics problems p 2779 N94-27894
Review and analysis of dense linear system solver package for distributed memory machines
p 2978 N94-27916
ActorStudio: An interactive user interface editor
[PB94-132859] p 2976 N94-28356

COMPUTER VISION
The determination of surface roughness from reflected step edges
[AD-A273987] p 2984 N94-25900
Feature isolation and quantification of evolving datasets
[NASA-CR-195230] p 2961 N94-26207
Colour object recognition
[ISBN-0-315-83684-9] p 2994 N94-26614
Extracting complete 3-dimensional boundary representation from multiple range images
[ISBN-0-315-83776-4] p 2963 N94-26615
Capture and location of blobs in digital images
[ISBN-0-315-84382-9] p 3036 N94-26666
Building 3-D models from unregistered range images
[AD-A274126] p 2986 N94-27032
Top down influences on bottom-up processing
[AD-A274220] p 2939 N94-27072
Operator theoretic methods in the control of distributed and nonlinear systems
[AD-A274160] p 2988 N94-27139
Motion analysis from a sequence of range images
[ISBN-0-315-84684-4] p 2969 N94-27311
Robust estimation for range image segmentation and fitting
[ISBN-0-315-84686-0] p 2998 N94-27312
Parallel algorithm for dominant points correspondences in robot binocular stereo vision p 2686 N94-27364
An algorithm for stereo correspondence problems on the analogy of human vision
[NAL-TR-1185] p 2940 N94-27584
An investigation of methods for determining depth from focus
[ISBN-0-315-64015-4] p 2988 N94-27645
A theory of multi-scale, curvature and torsion based shape representation for planar and space curves
[ISBN-0-315-63894-X] p 2974 N94-27805
Visual surface perception: Surface reconstruction from shading and stereo
[ISBN-0-315-60974-5] p 2975 N94-27872

COMPUTERIZED SIMULATION
Study on computerized experiment of amorphous transformation process by solid phase reaction
p 2726 N94-25564
The application of simulated annealing to stochastic systems
[AD-A273850] p 3001 N94-25607
Computer modelling of cyclic deformation of high-temperature materials
[AD-A273852] p 2704 N94-25608
Computer aided simulation of heat treatment
[VTT-PUBS-131] p 2731 N94-25643
Automation of closed environments in space for human comfort and safety p 2943 N94-25684
Performance measurement of three commercial object-oriented database management systems
[AD-A274028] p 3096 N94-25765
ObjectSim: A reusable object oriented DIS visual simulation
[AD-A274030] p 2958 N94-25767
Weapon system integration for the AFIT virtual cockpit
[AD-A274058] p 2667 N94-25772
Graphical programming at Sandia National Laboratories
[DE94-003803] p 2958 N94-25818
NNN-Ising model simulation of nanodomain textures in relaxor-type lead scandium tantalate
[DE94-601884] p 2748 N94-25844
Unravelling the structure of matter on high-performance computers
[DE94-601620] p 3015 N94-25891
Knowledge organization in intelligent tutoring systems for diagnostic problem solving in complex dynamic domains
[AD-A273986] p 2984 N94-25899
A virtual environment for satellite modeling and orbital analysis in a distributed interactive simulation
[AD-A274114] p 2694 N94-25904
Object-oriented design and implementation of a parallel Ada simulation system
[AD-A274119] p 2979 N94-25906
Object interaction in a parallel object-oriented discrete-event simulation
[AD-A274084] p 2959 N94-25942
Morphological analysis of ionomers
[DE94-003660] p 2749 N94-26005
Technical description of the Vulcano software library
[FFI-93/7024] p 2767 N94-26105
The proceedings of the KEK FEL Simulation Code Workshop
[DE93-520378] p 2816 N94-26112
Feature isolation and quantification of evolving datasets
[NASA-CR-195230] p 2961 N94-26207
NPSNET-4: A real-time, 3D distributed interactive virtual world
[AD-A274942] p 2961 N94-26298
Safety standards for aircraft shelter
[FFI-92/4003] p 2680 N94-26305
How reliable is the HMSA integral equation for the pair structure of supercooled and amorphous mixtures?
[DE94-601543] p 3006 N94-26411
Computer visualizations in engineering applications
[DE94-003589] p 2822 N94-26465
Overall analysis of meteorological information in the Daeduk nuclear complex
[DE93-632594] p 2894 N94-26469
Simulation approaches for calculations in directed graphical models
[AD-A274825] p 3003 N94-26494
Modeling and simulation of a fiber distributed data interface local area network
[AD-A274838] p 3098 N94-26500
A concurrent, multigroup, discrete ordinates model of neutron transport
[DE94-004334] p 3020 N94-26577
An interactive, physically-based simulation system
[ISBN-0-315-83884-1] p 2963 N94-26616
Pre-orbital criticality safety for the NEPSTP mission
[DE94-002600] p 3005 N94-26802
Using the TSAR electromagnetic modeling system
[DE94-002617] p 2771 N94-26803
Partitioning structural VHDL circuits for parallel execution on hypercubes
[AD-A274390] p 2785 N94-26830
Annual conference on fire research, 1993: Book of abstracts
[PB94-121324] p 2717 N94-26907
Interactive control of a parallel simulation from a remote graphics workstation
[AD-A274217] p 2981 N94-27070
Development of a performance evaluation tool (MMSOFE) for detection of failures with Multiple Model Adaptive Estimation (MMAE)
[AD-A274218] p 2665 N94-27071
Ultrastructure processing of macromolecular materials
[AD-A274460] p 2754 N94-27086
Computer simulation and experiments on the quasi-static mechanics and transport properties of granular materials
[AD-A274192] p 2823 N94-27104

Using discovery-based learning to prove the behavior of an autonomous agent
[AD-A274131] p 2987 N94-27121
Computer simulations of radiation generation from relativistic electron beams
[AD-A274139] p 3024 N94-27133
The Communication Link and Error ANalysis (CLEAN) simulator
[NASA-CR-195243] p 2968 N94-27168
Computer model for generation of infrared images
[PB94-123551] p 3005 N94-27172
Parallel discrete event simulation
p 2955 N94-27194
Numerical simulation of the reignition of detonation by reflected shocks
[AD-A274755] p 2795 N94-27252
Basic research on natural gas combustion phenomena
[PB94-129046] p 2717 N94-27256
Interdisciplinary technology p 2686 N94-27363
Sculpting in cyberspace: Parallel processing the development of new software p 2686 N94-27365
Rocket engine numerical simulation
p 2688 N94-27375
A theory for simulator tools
[CWI-CS-R9302] p 2972 N94-27578
Unified distributed simulation
[ISBN-0-315-59019-X] p 2983 N94-27685
Temporal stochasticity leads to nondeterministic chaos in a model for blood cell production
[DE94-003943] p 2933 N94-27744
NAS technical summaries. Numerical aerodynamic simulation program, March 1992 - February 1993
[NASA-RP-1321] p 3118 N94-27764
Comparison of dynamic analysis of a Schilling hydraulic manipulator with experimental results
[DE94-004597] p 2827 N94-27780
An optimization program based on the method of feasible directions: Theory and users guide
[NASA-TM-4552] p 2845 N94-27865
Martian atmospheric radiation budget
p 3107 N94-27887
Computer simulation of aqueous Na-Cl electrolytes
[DE94-002622] p 3030 N94-28001
Navier-Stokes simulation of two and three dimensional jets in crossflow, effects of grid, and boundary conditions p 2804 N94-28026
Recent developments in the simulation of steady and transient transverse jet interactions for missile, rotorcraft, and propulsive applications p 2804 N94-28030
Gas Turbine Engine Transient Behaviour
[VKI-LS-1993-06] p 2828 N94-28043
Engine simulation technology p 2829 N94-28051
Transient engine simulation p 2829 N94-28052
Nonlinear solvers p 2829 N94-28053
Engine simulation systems p 2829 N94-28054
Simulation: A tool for steam plant dynamic analysis
p 2831 N94-28084
Journal of NIRE, volume 2, number 4
[JTN-94-80554] p 2869 N94-28147
Numerical simulation of turbulent free jet by TFKE model p 2871 N94-28157
Advanced End-to-end Simulation for On-board Processing (AESOP) p 2945 N94-28255

CONCENTRATION (COMPOSITION)
Evaluation of a concentration probe for application in a supersonic flow field
[AD-A273915] p 2643 N94-25592
Grain boundary chromium concentration effects on the IGSCC and IASCC of austenitic stainless steels
[DE94-004268] p 2741 N94-27570

CONCENTRATORS
Structural evaluation of concepts for a solar energy concentrator for Space Station advanced development program
[NASA-TP-3375] p 2695 N94-26609
The PLVCR 500 and HCPC, tests and results
[DLR-MITT-93-04] p 2858 N94-26813
Reflectometer employing an integrating sphere and lens-mirror concentrator
[AD-D016061] p 3039 N94-27676
Development of a 2f optical performance measurement system
[DE94-003489] p 3039 N94-27721

CONCRETE STRUCTURES
Emerging technologies
[DE94-003022] p 3102 N94-26023
The structural behaviour of the steel or composite concrete and steel frames and the connections of frame members during the fire: A literature review
[VTT-TIED-1437] p 2837 N94-26307

CONCRETES
Tests of highly loaded skids on a concrete runway
[NASA-TP-3435] p 2669 N94-26608
Proceedings of the Fourth Euroseminar on Microscopy Applied to Building Materials
[PB94-119807] p 2839 N94-26754

Computational mechanics
[DE94-003015] p 2965 N94-26775
A widely adaptable habitat construction system utilizing space resources p 2688 N94-27374

CONCURRENT PROCESSING
The CODE-TOP (COncurrent system DEvelopment using Transformations Of Predicate-transition nets) method: Examples of using it for system architecture specification, software specification, and code generation p 2953 N94-26744
Parallel matrix transpose algorithms on distributed memory concurrent computers
[DE94-002424] p 2964 N94-26764
Modeling systems by probabilistic process algebra: An event structures approach
[PB94-125259] p 3004 N94-26867
Process algebra of concurrent constraint programming
[PB94-126695] p 2966 N94-26919
Binary snapshots
[CWI-CS-R9319] p 2955 N94-27547
An object model for multimedia programming
[CWI-CS-R9327] p 2971 N94-27552
Forward and backward simulations. Part 1: Untimed systems
[CWI-CS-R9313-PT-1] p 2972 N94-27580
Forward and backward simulations. Part 2: Timing-based systems
[CWI-CS-R9314-PT-2] p 2972 N94-27581
Concurrent shadow paging: Snapshots, read-only transactions, and on-the-fly multi-level incremental dumping
[PB94-133139] p 3100 N94-28385

CONDENSATES
Decay of non-equilibrium polariton condensate in semiconductors
[DE94-604016] p 3068 N94-27678

CONDENSED MATTER PHYSICS
International journal of quantum chemistry. Quantum Chemistry Symposium Number 27: Proceedings of the International Symposium on Atomic, Molecular, and Condensed Matter Theory and Computational Methods
[AD-A274352] p 3023 N94-26926

CONDENSERS (LIQUEFIERS)
Gravity dependence or pressure drop and heat transfer in straight two-phase heat transport system condenser ducts
[NLR-TP-92167-U] p 2798 N94-27853
Cooling towers for combined cycles: New developments to meet environmental requirements
p 2832 N94-28088

CONDENSING
Condensation inside tubes: Computer program for pressure drop in straight tubes (horizontal and vertical with downflow)
[ESDU-93014] p 2806 N94-28064

CONDITIONING (LEARNING)
Cortical mechanisms of attention, discrimination, and motor response to somesthetic stimuli
[AD-A274163] p 2940 N94-27141

CONDUCTING POLYMERS
LB-Deposited, side-chain substituted polyaniline, polypyrrole and the corresponding monomers, studied by STM
[AD-A274405] p 2754 N94-26977
Langmuir-Blodgett and STM investigations of conducting polymer thin films
[AD-A274512] p 2755 N94-27087
Corrosion resistant coatings from conducting polymers
[DE94-003959] p 2757 N94-27747

CONDUCTION BANDS
Technical report of ISSP. Ser. A, no. 2678: Magnetic properties of carbon nanotubes
[JTN-94-80564] p 3064 N94-27174
Technical report of ISSP. Ser. A, no. 2674: High-field cyclotron resonance and impurity transition in n- and p-3C-SiC at magnetic fields up to 175 T
[JTN-94-80560] p 3064 N94-27232
Technical report of ISSP. Ser. A, no. 2675: High-field cyclotron resonance and valence-band structure in semiconducting diamond
[JTN-94-80561] p 3065 N94-27245
Technical report of ISSP. Ser. A, no. 2676: Charge mass singularity in two-dimensional Hubbard model
[JTN-94-80562] p 3065 N94-27248

CONDUCTION ELECTRONS
Multi-channel Kondo necklace
[DE93-634754] p 3057 N94-26389

CONDUCTIVE HEAT TRANSFER
Aspects of the circuit board thermal design
[VTT-PUBS-132] p 2779 N94-25644
High-performance parallel analysis of coupled problems for aircraft propulsion
[NASA-CR-195292] p 2845 N94-28181

CONDUCTORS
The effect of Ti conduit on the critical current in (Nb, Ti)3Sn cable-in-conduit conductors
[DE94-701204] p 2788 N94-27817
Electrostatic image solution for the conducting prolate spheroid
[PB94-133154] p 2778 N94-28387

CONFERENCES
Proceedings of the symposium on current concepts and approaches on animal test alternatives
[AD-A273926] p 2900 N94-25593
Proceedings of the 8th Annual Summer Conference: NASA/USRA Advanced Design Program
[NASA-CR-195118] p 3075 N94-25665
The Latin American conference on the applications of the Moessbaer effect
[DE93-615942] p 3051 N94-25912
The First Energy Conference: Israel and the Former USSR
[ISBN-965-229-098-X] p 2853 N94-26050
Collaborative research on ion implantation of ceramics
[DE93-019177] p 2749 N94-26080
The proceedings of the KEK FEL Simulation Code Workshop
[DE93-520378] p 2816 N94-26112
Problems of application of charged particles channeling effects in crystals in high-energy physics
[DE93-634023] p 3032 N94-26405
Eleventh Symposium on Energy Engineering Sciences: Proceedings
[DE93-019930] p 2763 N94-26429
The 27th Annual Meeting of the Israel Society for Microscopy and the 12th Annual Meeting of the Israel Society for Histochemistry and Cytochemistry
[DE93-632416] p 2716 N94-26519
Proceedings of the Second EGS4 User's Meeting in Japan
[DE93-520383] p 3032 N94-26543
Real-Time Embedded Processing for Space Applications
[ISBN-2-85428-335-X] p 2948 N94-26713
Proceedings of the Fourth Euroseminar on Microscopy Applied to Building Materials
[PB94-119807] p 2839 N94-26754
Gordon Research Conference on the Physics and Chemistry of Laser Diagnostics in Combustion
[AD-A274609] p 2716 N94-26893
Annual conference on fire research, 1993: Book of abstracts
[PB94-121324] p 2717 N94-26907
Proceedings of Damping 1993, volume 1
[AD-A274226] p 2840 N94-26922
International journal of quantum chemistry. Quantum Chemistry Symposium Number 27: Proceedings of the International Symposium on Atomic, Molecular, and Condensed Matter Theory and Computational Methods
[AD-A274352] p 3023 N94-26926
Proceedings of Damping 1993, volume 2
[AD-A274227] p 2840 N94-26953
Spectroscopy Division
[DE94-604074] p 2717 N94-26988
Proceedings of Damping 1993, volume 3
[AD-A274228] p 2840 N94-27008
Auroral Tomography Workshop Proceedings
[PB94-123718] p 2881 N94-27040
Proceedings of the High Energy Density Matter (HEDM) Contractor's Conference
[AD-A274452] p 3033 N94-27083
Proceedings of the Third Workshop Computersystems: Research Forum on Design, Realization and Use of Computersystems
[ISBN-90-6144-995-2] p 2954 N94-27191
The Sixteenth Symposium on Coordinated Observations of the Ionosphere and the Magnetosphere in the Polar Regions: Program and abstracts
[JTN-94-80601] p 2882 N94-27300
Vision 21: Interdisciplinary Science and Engineering in the Era of Cyberspace
[NASA-CP-10129] p 2685 N94-27358
Fusion reactor systems studies
[DE94-003162] p 3046 N94-27686
Proceedings of the 16th Symposium on Plasma Physics and Technology
[DE94-604181] p 3047 N94-27698
Proceedings of the workshop on (pi), K, (eta)-nucleon interactions
[DE94-701314] p 3027 N94-27733
Proceedings of Workshop on Distributed Computing and Network
[DE94-701165] p 2983 N94-27804
Hydrogen physics
[DE94-701317] p 2719 N94-27822
Neutrons in biology
[DE94-701085] p 2903 N94-27862
The 1993 NASA Aerospace Battery Workshop
[NASA-CP-3254] p 2860 N94-28100

The 1994 Space and Earth Science Data Compression Workshop
[NASA-CP-3255] p 2945 N94-28251
Asia-Pacific Seminar on Global Change Research Cooperation
[JTN-94-80517] p 2871 N94-28268
Abstracts of papers presented at the 4th CASI Aerodynamics Symposium
[ISBN-0-920203-01-9] p 2651 N94-28315
High Quality Aluminium Castings Conference
[PB94-133592] p 2747 N94-28359
Workshop on Countering Space Adaptation with Exercise: Current Issues
[NASA-CP-3252] p 2934 N94-28361

CONFIDENCE LIMITS
An optimal constrained linear inverse method for magnetic source imaging
[DE94-004014] p 2957 N94-25663
Example of statistical techniques applied to analysis of effects of small changes
[ESDU-93023] p 2670 N94-28094

CONFIGURATION MANAGEMENT
A proposed software engineering environment for systems life cycle management
[ISBN-0-315-60634-7] p 2974 N94-27869

CONFINEMENT
Potential of commercial tokamak reactors with improved physics
[DE94-002794] p 3044 N94-26860
Development of stimulus-seeking scale for expecting individual differences against confinement stress
p 2915 N94-27460
Atomic processes in Inertial Electrostatic Confinement (IEC) devices
[DE94-005015] p 3047 N94-27715
Numerical experiment on finite element method for matching data
[DE94-701208] p 3000 N94-27731

CONFORMAL MAPPING
(2,0) superconformal anomaly
[DE93-613046] p 2991 N94-25867
Towards a theory of growing surfaces: Mapping two-dimensional Laplacian growth onto Hamiltonian dynamics and statistics
[DE94-002636] p 2991 N94-26079
The massless representations of the conformal quantum algebra
[DE94-601555] p 3006 N94-26413
Gauging of Chern-Simons p-Barnes
[DE94-601553] p 2993 N94-26425

CONGENITAL ANOMALIES
Effects of ML-9, a myosin light-chain kinase inhibitor, on preimplantation development of the mouse
p 2905 N94-27486
Anorectal malformations induced by intraperitoneal injection of all-trans retinoic acid in suncus
p 2905 N94-27489

CONGRESSIONAL REPORTS
Report of the defense science board task force on aircraft assessment
[AD-A274531] p 2669 N94-26835
Access to space study
[NASA-TM-109693] p 2685 N94-27151
Defense force management: Challenges facing DOD as it continues to downsize its civilian work force. Report to the Chairman, Subcommittee on Federal Services, Post Office, and Civil Service, Committee on Governmental Affairs, US Senate
[GAO/NSIAD-93-123] p 3095 N94-28177

CONGRUENCES
Congruence theorem for structured operational semantics with predicates and negative premises
[PB94-126729] p 2966 N94-26970

CONICAL BODIES
A numerical determination of bifurcation points for low Reynolds number conical flows
[AD-A273984] p 2791 N94-25991

CONICAL FLOW
A numerical determination of bifurcation points for low Reynolds number conical flows
[AD-A273984] p 2791 N94-25991
Streamwise vorticity in a turbine rotor with conical endwalls
[DLR-FB-93-13] p 2826 N94-27591

CONIFERS
Conifer tree influence on Digital Terrain Elevation Data (DTED): A case study at Dulles International Airport
[AD-A274213] p 2849 N94-27069

CONJUGATE GRADIENT METHOD
Grid-independent convergence based on preconditioning techniques
[PB94-125356] p 2997 N94-27000

CONJUGATES
Characterization of self-conjugate minimal surfaces in R(sup 3)
[DE94-601538] p 2993 N94-26409
Topological conditions for the existence of invariant measures for unimodal maps
[PB94-123296] p 2849 N94-26866
Some remarks on the symmetry of self-conjugate minimal surfaces in R3
[DE94-603670] p 3007 N94-27633

CONNECTICUT
Landscape dynamics of northeastern forests
[NASA-CR-195272] p 2852 N94-28070

CONNECTORS
Alternative materials for solid oxide fuel cells: Processing and interactions of materials
[DE94-000016] p 2855 N94-26114
Characteristics and development report for the T1576 power supply and the MC3935 battery
[DE94-003675] p 2783 N94-26372

CONSECUTIVE EVENTS
Parallel discrete event simulation
p 2955 N94-27194

CONSERVATION
Back-reaction beyond the mean field approximation
[DE94-003936] p 3012 N94-25612
Automation of formation flight control
[AD-A274137] p 2678 N94-27132

CONSERVATION LAWS
On the first integrals of geodesics
[DE93-612974] p 3007 N94-25603
Arbitrary-order high resolution schemes for model hyperbolic conservation laws
[CRANFIELD-AERO-9209] p 3005 N94-25823
Reduced Braginskii equations
[DE94-003510] p 3047 N94-27723

CONSTANTS
A semiclassical reactive flux method for the calculation of condensed phase activated rate constants
[AD-A274850] p 3020 N94-26562

CONSTITUTIVE EQUATIONS
New constitutive equation for the volume viscosity in fluids
[NASA-TM-109104] p 2798 N94-27867

CONSTRAINTS
A global approach to kinematic path planning to robots with holonomic and nonholonomic constraints
p 2683 N94-26279
Real time avionics constraints: Silicon solutions
p 2949 N94-26717
Process algebra of concurrent constraint programming
[PB94-126695] p 2966 N94-26919

CONSTRUCTION
Design and development of the second generation Mars Habitat p 2943 N94-25693
Orbit transfer rocket engine technology program
[NASA-CR-189229] p 2702 N94-26542
A widely adaptable habitat construction system utilizing space resources p 2688 N94-27374
Construction of temperature compensated constant voltage (VT) curves for super Ni-Cd (tm) cells
p 2863 N94-28126

CONSTRUCTION INDUSTRY
Composite raw materials for the building industry
[VTT-TIED-1433] p 2708 N94-26544

CONTACT LOADS
The railway track response function
[REPT-93-40] p 2837 N94-26214
A non-linear mathematical model or finite, periodic rail corrugations
[REPT-93-49] p 2996 N94-26967
Contact stress in disc cams with roller followers
[ESDU-93001] p 2829 N94-28055

CONTAINMENT
HDR reactor containment fire modeling with BRI2
[VTT-PUBS-113] p 3031 N94-25621

CONTAMINANTS
Selfsimilar solutions of a nonlinear transport equation
[REPT-93-42] p 2865 N94-25760
Compilation of air pollutant emission factors. Volume 1: Stationary point and area sources. Supplement F
[PB94-121431] p 2867 N94-26757
An overview of the ASCOT program
[DE94-004356] p 2869 N94-27601
Trace organic chemical detection using an ultraviolet excitation molecular beam fluorometer
[DE94-002649] p 2704 N94-27708

CONTAMINATION
Development and application of contamination technology for MSFC managed space systems
[NASA-CR-193934] p 2697 N94-27421
The PROTEL contamination code
[RXR-93071] p 3040 N94-28202

CONTEXT
Researches of the Electrotechnical Laboratory. No. 955: Speech recognition by description of acoustic characteristic variations
[JTN-94-80604] p 2775 N94-27249

CONTEXT FREE LANGUAGES
Parsing schemata: A framework for parallel and sequential parsing
[PB94-125267] p 2981 N94-26998

CONTINENTAL SHELVES
Hydrographic and Acoustic Doppler Current Profiler (ADCP) data from the ONR eastern boundary current accelerated research initiative, 9-16 June 1992
[AD-A274115] p 2898 N94-26076

CONTINGENCY
Development of the Air Force contingency contracting course framework
[AD-A273921] p 3093 N94-25895

CONTINUITY EQUATION
Computation of non-isentropic internal flows with variable density
[AD-A274848] p 2794 N94-26801
Compressibility effects on rotor forces in the leakage path between a shrouded pump impeller and its housing
p 2796 N94-27379
Reduced Braginskii equations
[DE94-003510] p 3047 N94-27723

CONTINUOUS NOISE
Prewhitening of colored noise fields for detection of threshold sources
[AD-A274346] p 3010 N94-26923

CONTINUOUS RADIATION
Electrical analysis of wideband and distributed windows using time-dependent field codes
[DE94-002987] p 2768 N94-26310
S-76 high intensity radiated fields, volume 2
[AD-A274572] p 2771 N94-26836
S-76 high intensity radiated fields, volume 1
[AD-A274571] p 2771 N94-26854
S-76 high intensity radiated fields, volume 3
[AD-A274416] p 2772 N94-26980

CONTINUOUS SPECTRA
Continuum spectral characteristics of bursts measured with BATSE large area detectors p 3114 N94-26687
A study of gamma ray burst continuum properties presnting evidence for two spectral states in bursts
p 3114 N94-26688
Balloon-borne measurements of the SN1987A hard x ray continuum p 3115 N94-26689

CONTINUOUS WAVE LASERS
Development of surgical CW Nd:YAG laser with optical fiber delivery system
[DE93-632902] p 2817 N94-26185
Beam-quality measurements for materials processing lasers and the proposed ISO standard
[DE94-002738] p 2819 N94-26811

CONTINUUM FLOW
Direct simulation Monte-Carlo of near continuum hypersonic flow with chemical reactions
[DLR-FB-93-01] p 2797 N94-27588

CONTINUUMS
Weak bump quasars
[NASA-CR-195267] p 3103 N94-27933

CONTOURS
IRMA: A program for three-dimensional color display of data
[AD-A273811] p 2959 N94-25879
Optical surface contouring for non-destructive inspection of turbomachinery
[NASA-CR-195245] p 2835 N94-26691

CONTRACT MANAGEMENT
Analysis of cost and schedule growth on sole source and competitive Air Force contracts
[AD-A273920] p 3094 N94-26814
Small business innovation research program solicitation
[NASA-TM-109695] p 3094 N94-27661

CONTRACT NEGOTIATION
Intertemporal bargaining and dynamic consistency
[PB94-133147] p 3095 N94-28386

CONTRACTION
Eccentric exercise testing and training
p 2934 N94-28363
The value of electrical stimulation as an exercise training modality p 2936 N94-28372

CONTROL BOARDS
RF-station control crate
[DIGEL-1992-9] p 2779 N94-25618
Control panel dimensions for gloved operation study 2: Toggle switches minimum spacing required between toggle
[AD-A274518] p 2942 N94-27089

CONTROL EQUIPMENT
Variable speed controller p 2943 N94-25678
Designing and optimizing fuzzy-logic controllers
[ISBN-0-315-83505-2] p 2985 N94-26660
Numerical analysis of the photo-dissociation/radical oxidation of formaldehyde by ultraviolet light in a photolytic reactor
[AD-A274539] p 2868 N94-26843

Fluid dynamic linear accelerometer
[AD-D016042] p 2678 N94-27112
Pulse control method and its characteristics
[DE94-701187] p 2989 N94-27809
Open communication in manufacturing automation
[PB94-132479] p 2976 N94-28377

CONTROL SIMULATION
A method for testing of HVAC automation equipment using the emulator and the application of the method
[VTT-TIED-1435] p 2822 N94-26306

CONTROL STABILITY
The 1991-1992 walking robot design
p 2833 N94-25686
Identification and H(infinity)/(mu)-synthesis control of the Sandia truss
[DE94-002735] p 2839 N94-26810
Impulsive control and stabilization
[ISBN-0-315-84563-5] p 2988 N94-27271
Modelling and stability of a shape memory alloy position control system
[ISBN-0-315-84467-1] p 2740 N94-27304
Tools for quantitative stability robustness analysis
[ISBN-0-315-59950-2] p 2988 N94-27641
Techniques to improve maneuver stability characteristics of a nonlinear wide-body transport airplane in cruise flight
[NASA-TM-4521] p 2679 N94-27660

CONTROL STICKS
Reconfigurable aircraft stick control
[AD-D016043] p 2681 N94-27113

CONTROL SURFACES
Design of a flight controller for an unmanned research vehicle with control surface failures using quantitative feedback theory
[AD-A274049] p 2677 N94-25833
Composite leading edge/spar member for an aircraft control surface
[CA-PATENT-1-325-765] p 2669 N94-27273
Control jets in interaction with hypersonic rarefied flow
p 2698 N94-28020

CONTROL SYSTEMS DESIGN
RF-station control crate
[DIGEL-1992-9] p 2779 N94-25618
Safety analysis in conceptual design of process control
[VTT-PUBS-117] p 2762 N94-25641
Report on a visit to the Arvin/Calspan Corporation, Buffalo, New York, USA, September 1992
[CRANFIELD-AERO-9305] p 2676 N94-25653
The Enabler: A concept for a lunar work vehicle
p 2833 N94-25675
Automation of closed environments in space for human comfort and safety p 2943 N94-25684
Project WISH: The Emerald City p 2703 N94-25690
Optimal control design advantages utilizing two-degree-of-freedom controllers
[AD-A273839] p 2984 N94-25743
Design of a subsonic envelope flight control system for the Vista F-16 using quantitative feedback theory
[AD-A274057] p 2676 N94-25771
Neural networks for dynamic flight control
[AD-A274089] p 2676 N94-25785
Design of a flight controller for an unmanned research vehicle with control surface failures using quantitative feedback theory
[AD-A274049] p 2677 N94-25833
Evaluation of moderate angle of attack roll of a dual engine, thrust vectoring aircraft using quantitative feedback theory
[AD-A274118] p 2667 N94-25905
Direct model reference adaptive control of robotic arms p 2683 N94-26282
A multitasking behavioral control system for the Robotic All-Terrain Lunar Exploration Rover (RATLER)
p 2685 N94-26292
Designing and optimizing fuzzy-logic controllers
[ISBN-0-315-83505-2] p 2985 N94-26660
Identification and H(infinity)/(mu)-synthesis control of the Sandia truss
[DE94-002735] p 2839 N94-26810
Physical modelling and adaptive predictive control of diffusion/LPCVD reactors
[PB94-126398] p 2763 N94-26819
Grey-box modelling and identification topics
[PB94-126380] p 2986 N94-27029
Control oriented system identification
[AD-A274162] p 2987 N94-27124
Finite time differential equations and their application to control systems
[ISBN-0-315-85158-9] p 2988 N94-27277
Dynamics and robust control for uncertain flexible space systems
[INPE-5510-TAE/020] p 2696 N94-27357
Control of a hydrogen/oxygen steam generator
[DLR-FB-93-02] p 2826 N94-27589
Control system for tracking nonlinear systems
[AD-D016057] p 2787 N94-27673
Inverted pendulum control apparatus using transputers
[DE94-701224] p 2973 N94-27732
Pulse control method and its characteristics
[DE94-701187] p 2989 N94-27809
On identified predictive control p 2990 N94-27896
Neural control of magnetic suspension systems
p 2682 N94-27905
System identification of the Large-Angle Magnetic Suspension Test Facility (LAMSTF)
p 2682 N94-27908
Topics in the design, analysis and implementation of feedback control systems
[ISBN-0-315-84934-7] p 2989 N94-27975
Development of the gas turbine. Part 1: Design philosophy and performance p 2831 N94-28080
Controls, monitoring and performance measurements
p 2831 N94-28086

CONTROL THEORY
The application of a C(star) flight control law to large civil transport aircraft
[CRANFIELD-AERO-9303] p 2676 N94-25640
Design of a subsonic envelope flight control system for the Vista F-16 using quantitative feedback theory
[AD-A274057] p 2676 N94-25771
Status report of RMS active damping augmentation
p 2684 N94-26285
Identification and H(infinity)/(mu)-synthesis control of the Sandia truss
[DE94-002735] p 2839 N94-26810
Necessary and sufficient conditions for the existence of the stabilizing solution of the Riccati equation in a Hilbert space: A Popov function approach
[PB94-125341] p 2997 N94-26999
Grey-box modelling and identification topics
[PB94-126380] p 2986 N94-27029
Operator theoretic methods in the control of distributed and nonlinear systems
[AD-A274160] p 2988 N94-27139
Optimal control of helicopters following power failure
[NAL-TR-1190] p 2678 N94-27206
Finite time differential equations and their application to control systems
[ISBN-0-315-85158-9] p 2988 N94-27277
Designing robust control laws using genetic algorithms
p 2643 N94-27295
Air traffic management as principled negotiation between intelligent agents p 2643 N94-27297
Solving the linear quadratic optimal control problem for infinite-dimensional systems
[ISBN-0-315-84562-7] p 2999 N94-27405
Tools for quantitative stability robustness analysis
[ISBN-0-315-59950-2] p 2988 N94-27641
Comparison of dynamic analysis of a Schilling hydraulic manipulator with experimental results
[DE94-004597] p 2827 N94-27780
On identified predictive control p 2990 N94-27896

CONTROLLABILITY
The effects of tailwinds and control cross coupling on rotorcraft handling qualities for steep, decelerating instrument approaches and missed approaches
[IAR-AN-77] p 2677 N94-26710
Impulsive control and stabilization
[ISBN-0-315-84563-5] p 2988 N94-27271

CONTROLLED ATMOSPHERES
Automation of closed environments in space for human comfort and safety p 2943 N94-25684
The determination of surface roughness from reflected step edges
[AD-A273987] p 2984 N94-25900

CONTROLLED FUSION
Development of fusion technology
[DE93-633444] p 3042 N94-26159
Maryland controlled fusion research program
[DE94-003533] p 3044 N94-26523
Research in pulsed power plasma physics
[AD-A274323] p 3045 N94-27074

CONTROLLERS
Autonomous space processor for orbital debris advanced design project in support of solar system exploration p 2697 N94-25667
Variable speed controller p 2943 N94-25678
The 1991-1992 walking robot design
p 2833 N94-25686
Optimal control design advantages utilizing two-degree-of-freedom controllers
[AD-A273839] p 2984 N94-25743
Modal control of a satellite in an unstable periodic orbit about the Earth-Sun interior Lagrange point
[AD-A273707] p 2694 N94-25776
Adaptive optimization and control using neural networks
[DE94-003941] p 2985 N94-25983
Auxiliary controller for time-to-digital converter module readout
[DE93-634172] p 2948 N94-26266
Inertial-space disturbance rejection for space-based manipulators p 2683 N94-26281
Characteristics and development report for the T1576 power supply and the MC3935 battery
[DE94-003675] p 2783 N94-26372
Physical modelling and adaptive predictive control of diffusion/LPCVD reactors
[PB94-126398] p 2763 N94-26819
Research in robust control for hypersonic aircraft
[NASA-CR-195250] p 2678 N94-26821
Control oriented system identification
[AD-A274162] p 2987 N94-27124
Automation of formation flight control
[AD-A274137] p 2678 N94-27132
Operator theoretic methods in the control of distributed and nonlinear systems
[AD-A274160] p 2988 N94-27139
Computer code for controller partitioning with IFPC application: A user's manual
[NASA-CR-195291] p 2678 N94-27414
Neural control of magnetic suspension systems
p 2682 N94-27905
System identification of the Large-Angle Magnetic Suspension Test Facility (LAMSTF)
p 2682 N94-27908
Optical pattern recognition system utilizing resonator array
[AD-D016071] p 3040 N94-28224

CONVECTION
Numerical solution of singularity-perturbed two-point boundary-value problems
[DE94-601542] p 2993 N94-26410

CONVECTION CLOUDS
Investigation of mesoscale convective cloud clusters in South China
[AD-A274303] p 2895 N94-26678

CONVECTION CURRENTS
The numerical simulation of marine boundary layer clouds
[AD-A273669] p 2894 N94-26195
Investigation of mesoscale convective cloud clusters in South China
[AD-A274303] p 2895 N94-26678

CONVECTION-DIFFUSION EQUATION
Rendering of three-dimensional data sets derived from finite-difference and spectral methods
[AD-A273724] p 3096 N94-25997
On the robustness of a multiple semi-coarsened grid method
[REPT-93-51] p 2992 N94-26252
Time-step enlargement and optimal smoothing in Runge-Kutta time-integration algorithms by implicit and explicit smoothing
[NLR-TP-92221-U] p 2798 N94-27799

CONVECTIVE FLOW
Interactions between a tropical mixed boundary layer and cumulus convection in a radiative-convective model
[DE94-000848] p 2877 N94-25979
New constitutive equation for the volume viscosity in fluids
[NASA-TM-109104] p 2798 N94-27867

CONVECTIVE HEAT TRANSFER
Global barotropic response to a tropical forcing
[NASA-CR-195256] p 2896 N94-27408
Forced convection heat transfer in straight tubes. Part 2: Laminar and transitional flow
[ESDU-93018-PT-2] p 2807 N94-28139

CONVERGENCE
A logarithmic barrier cutting plane method for convex programming
[REPT-93-43] p 2957 N94-25761
Approximate solution of the fourth order initial value problem using deficient spline polynomials
[DE93-613023] p 2991 N94-25880
Isotonic estimation and rates of convergence in Wicksell's problem
[REPT-93-39] p 3002 N94-26213
Congruence theorem for structured operational semantics with predicates and negative premises
[PB94-126729] p 2966 N94-26970
Grid-independent convergence based on preconditioning techniques
[PB94-125358] p 2997 N94-27000
Hessenberg matrices in Krylov subspaces and the computation of the spectrum
[PB94-133170] p 3001 N94-28389

CONVERGENT NOZZLES
Transient flow features of a supersonic jet in a low speed cross flow p 2800 N94-28005

CONVERGENT-DIVERGENT NOZZLES
Transient flow features of a supersonic jet in a low speed cross flow p 2800 N94-28005

CONVEXITY

A note on central cutting plane methods for convex programming [REPT-93-44] p 2958 N94-25762

Conditionally exponential convex functions on locally compact groups [DE93-613025] p 2990 N94-25865

An algorithm to find the intersection of two convex polygons [AD-A274722] p 2961 N94-26148

Unifying investigation of interior-point methods for convex programming [PB94-126463] p 2967 N94-27031

CONVOLUTION INTEGRALS

A real-time convolution algorithm and architecture with applications in SAR processing [AD-A273817] p 2959 N94-25963

COOLANTS

Analysis of cooling jets near the leading edge of turbine blades p 2676 N94-28037

COOLING SYSTEMS

A robust helium-cooled shield/blanket design for ITER [DE94-003402] p 3043 N94-26323

Bulletin of the Institute for Chemical Reaction Science, Tohoku University, volume 2 [JTN-94-80602] p 2717 N94-27385

Variable temperature cold stage for microscope observation p 2718 N94-27389

Cooling towers for combined cycles: Design philosophy, performance testing, and operating problems p 2832 N94-28087

Cooling towers for combined cycles: New developments to meet environmental requirements p 2832 N94-28088

COORDINATE TRANSFORMATIONS

Propagation of experimental uncertainties from the tunnel to the body coordinate system in 3-D LDV flow field studies [NASA-CR-191607] p 2680 N94-26603

COORDINATES

On experimental studies of yield surfaces of metals: A more general approach [IFTR-42/1993] p 2739 N94-26824

Users guide for GRIKURV: A code for drawing graphs [PB94-123593] p 2968 N94-27154

COORDINATION

Heavy-electron behavior in large coordination compounds CeZn11 and UZn12 [REPT-A-2663] p 3049 N94-25614

COPOLYMERIZATION

Polymer-bound rhodium hydroformylation catalysts [ETN-94-95388] p 2712 N94-25747

High impact strength poly(lactide) tough biodegradable materials [ETN-94-95389] p 2747 N94-25748

Accordion-like polymers for nonlinear applications [AD-D016031] p 2755 N94-27148

COPOLYMERS

High impact strength poly(lactide) tough biodegradable materials [ETN-94-95389] p 2747 N94-25748

Controlled synthesis of polyenes by catalytic methods [DE94-004168] p 2749 N94-25973

New monomers for high performance polymers p 2758 N94-27904

COPPER

Binding of copper and nickel to cavities in silicon formed by helium ion implantation [DE94-003769] p 3050 N94-25814

Issues for conversion coating of aluminum alloys with hydrotalcite [DE94-003804] p 2732 N94-25819

Deviatoric stresses and plastic strain rates in strong shock waves for six metals [DE94-002964] p 2733 N94-26022

Hook spectroscopy as an atomic number density diagnostic applied to laser-ablated copper plasmas [DE94-002645] p 3042 N94-26081

Microstructures of Si surface layers implanted with Cu [DE94-004690] p 3058 N94-26565

Vapor deposition of copper on stainless steel 304L [DE94-001945] p 2740 N94-27006

Technical report of ISSP. Ser. A, no. 2681: Orbital and spin susceptibilities of the plane copper sites in YBa2Cu3O(x) system [JTN-94-80567] p 3064 N94-27177

The deformation of copper-tungsten composites [ISBN-0-315-84939-8] p 2712 N94-27688

Secondary electron emission from copper surface due to neodymium and gadolinium ion bombardment [DE94-701115] p 3027 N94-27718

Structural study of Cu/Co multilayer by anomalous small-angle x ray scattering p 2744 N94-28160

COPPER ALLOYS

Study on ferromagnetic field magnet using strong and highly conductive material p 2725 N94-25559

Study on production of materials with one direction solidification texture p 2727 N94-25572

Stress corrosion cracking and dealloying of copper-gold alloy in iodine vapor [DE93-633790] p 2734 N94-26264

The origins of ordering in CuPt [DE94-003864] p 2736 N94-26351

An anodic dissolution-based mechanism for the rapid cracking, pre-exposure phenomenon demonstrated by Al-Li-Cu alloys [DE94-004798] p 2742 N94-27788

NASA-UVA light aerospace alloy and structures technology program (LA2ST) [NASA-CR-195275] p 2844 N94-27851

COPPER CHLORIDES

Structure of ionic fluids in equilibrium with a microporous ionic matrix [DE94-600563] p 2715 N94-26391

COPPER COMPOUNDS

Successive structural phase transitions in stoichiometric La2NiO4 observed by x ray diffraction [REPT-A-2665] p 3051 N94-25921

Technical report of ISSP. Ser. A, no. 2679: Novel electronic states of partially deuterated (DMe-DCNQI)2Cu [JTN-94-80565] p 3064 N94-27175

Technical report of ISSP. Ser. A, no. 2669: Relations between oxygen deficiency and structures in the La-Sr-Cu-O system. 3: Oxygen contents and structure of (La, Sr)8Cu8O(16+delta) phase [JTN-94-80555] p 3066 N94-27353

COPPER OXIDES

Atomic-scale chemistry of metal surfaces [REPT-A-2657] p 3012 N94-25636

Preparation and characterization of high temperature superconductor film surfaces [AD-A274293] p 3059 N94-26681

Synthesis, rheology, and forming of Y-Ba-Cu-O ceramics [DE94-005558] p 2757 N94-27695

The optical properties of high-T(c) superconductors grown by pulsed laser deposition [ISBN-0-315-84917-7] p 3039 N94-27962

Anisotropy in the electrical, magnetic and optical properties of Pb2Sr2RCu3O8 [ISBN-0-315-84930-4] p 3070 N94-27974

Fermi surface ridge at second and third Umklapp positron annihilations in Y Ba2Cu3O(7-delta) [DE93-634760] p 3070 N94-27995

COPPER SELENIDES

The state of the art of thin-film photovoltaics [DE94-000224] p 2855 N94-26115

Research on high-efficiency, large-area, CuInSe2 based thin-film modules [DE94-000259] p 3067 N94-27609

CORE SAMPLING

Comet nucleus and asteroid sample return missions p 2689 N94-25692

Crystallographyic analyses of clathrate hydrates included in Vostok ice cores p 2885 N94-27969

CORES

Methane emissions from natural wetlands [DE93-040796] p 2865 N94-25790

CORN

Root gravitropism in maize and Arabidopsis [NASA-CR-195710] p 2903 N94-27940

CORNER FLOW

Control jets in interaction with hypersonic rarefied flow p 2698 N94-28020

CORNERS

Zr-rich corner of the Zr-Sn-O diagram [DE93-633764] p 2734 N94-26161

CORONAS

Studies for Io's extended atmosphere and neutral clouds and their impact on the local satellite atmosphere and on the planetary magnetosphere [NASA-CR-195255] p 3106 N94-27406

CORRELATION

Study on characteristics and electronic structures of materials with strong electronic correlations by ferromagnetic fields p 2724 N94-25557

Advanced qualification techniques [DE94-003709] p 2780 N94-25812

Correlation between the gravity field and the bathymetry in the North Atlantic Ocean [ETN-94-95036] p 2899 N94-26108

Detection of transient vector-fields in additive noise [FFI-93/7028] p 2768 N94-26232

Solid estimation feature based correlation method for measuring control points required for correcting satellite images [VTT-JULK-772] p 2848 N94-26253

Correlation of experimental data and three-dimensional finite element modeling of a spinning quadrupole [DE93-041173] p 3008 N94-26421

C-periodicity and the physical mass in the 3-state Potts model [DE94-601551] p 3019 N94-26423

Experimental measurement of local displacement and chemical pair correlations in crystalline solid solutions [DE94-001124] p 3065 N94-27251

Correlated mean field Ansatz for the Kondo necklace [DE94-603671] p 3067 N94-27634

Practical problems in aggregating expert opinions [DE94-002623] p 3094 N94-27707

Correlations in inelastic collisions of relativistic nuclei with emulsion at (4.1 - 4.5) A GeV/c [DE93-634526] p 3030 N94-27994

Computer simulation of aqueous Na-Cl electrolytes [DE94-002622] p 3030 N94-28001

CORRELATION COEFFICIENTS

Spectral and temporal correlations of multifrequency waves in the turbulent atmosphere [ITN-94-85229] p 2774 N94-27233

CORRELATORS

Acousto-optical post-processor time-integrating correlator calibration updates [DSIS-94-00053] p 2813 N94-27317

Development of a holographic illumination system for a time-integrating correlator [DSIS-94-00111] p 2814 N94-27763

CORROSION

Interactions between corrosion fatigue and stress corrosion crack on steel for light water reactors p 2722 N94-25547

A materials compatibility study in FM-1, a liquid component of a paste extrudable explosive [DE94-001166] p 2759 N94-26198

Guidelines for controlling stress corrosion cracking and corrosion fatigue of stainless steels: A literature review [VTT-TIED-1420] p 2837 N94-26262

Hydrothermal growth and characterization of oxides in zirconium alloys [DE94-602981] p 2743 N94-27829

Fiber optic sensors for corrosion detection p 3040 N94-27923

The corrosion behavior of sputter-deposited magnesium-valve metal alloys p 2745 N94-28164

CORROSION PREVENTION

Issues for conversion coating of aluminum alloys with hydrotalcite [DE94-003804] p 2732 N94-25819

Effect of nitrocarburizing on shape of titanium alloy parts [DE94-004040] p 2732 N94-25822

Guidelines for controlling stress corrosion cracking and corrosion fatigue of stainless steels: A literature review [VTT-TIED-1420] p 2837 N94-26262

Polyurethane self-priming topcoats [AD-D016041] p 2755 N94-27111

Development and application of contamination technology for MSFC managed space systems [NASA-CR-193934] p 2697 N94-27421

Hydrothermal growth and characterization of oxides in zirconium alloys [DE94-602981] p 2743 N94-27829

Effect of different ions on the anodic behaviour of alloy 800 in chloride solutions at high temperature [DE94-602982] p 2743 N94-27832

CORROSION RESISTANCE

Corrosion resistance at welded zones of nuclear fuel reprocessing system p 2722 N94-25546

Issues for conversion coating of aluminum alloys with hydrotalcite [DE94-003804] p 2732 N94-25819

A materials compatibility study in FM-1, a liquid component of a paste extrudable explosive [DE94-001166] p 2759 N94-26198

Method for improving electromagnetic shielding performance of composite materials by electropulsing [AD-D016050] p 2709 N94-27076

Polyurethane self-priming topcoats [AD-D016041] p 2755 N94-27111

Corrosion resistant coatings from conducting polymers [DE94-003959] p 2757 N94-27747

Electrochemical properties of passive films on 440C stainless steel [ISBN-0-315-64248-3] p 2757 N94-27801

The Science Reports of the Research Institutes, Tohoku University. Series A: Physics, Chemistry, and Metallurgy. Volume 38, No. 1: Amorphous Materials 14 [JTN-94-80610] p 2744 N94-28158

The corrosion behavior of sputter-deposited magnesium-valve metal alloys p 2745 N94-28164

CORROSION TESTS

Study on performance evaluation of pressure vessel steel in corrosion environments with sulfide p 2730 N94-25582

A materials compatibility study in FM-1, a liquid component of a paste extrudable explosive [DE94-001166] p 2759 N94-26198

Isothermal corrosion testing of steels in molten nitrate salts
[DE94-004695] p 2742 N94-27755

CORRUGATED PLATES
Formulae for the buckling of simply-supported corrugated panels of orthotropic material under shear load
[PB94-126547] p 2840 N94-26911

CORRUGATING
A non-linear mathematical model or finite, periodic rail corrugations
[REPT-93-49] p 2996 N94-26967

COSMIC BACKGROUND EXPLORER SATELLITE
Zodiacal light data investigation. Interim results for the Earthlimb Clutter Experiment
[AD-A274461] p 3104 N94-27265

COSMIC RAY SHOWERS
Contributions to the 23rd ICRC from emulsion chamber experiments at Mt. Chacaltaya and Pamirs
[ICRR-REPT-295-93-7] p 3112 N94-25624
A study of very high energy hadron interactions through observation of cosmic-ray families of visible energy greater than 500 TeV, 1 p 3112 N94-25625
A study of very high energy hadron interactions through observation of cosmic-ray families of visible energy greater than 500 TeV, 2 p 3112 N94-25626
A study of very high energy hadron interactions through observation of cosmic-ray families with visible energy not less than 500 TeV, 3 p 3112 N94-25627
Observation of characteristics of cosmic-ray hadron interactions in uniform-type thick lead chambers at Pamir, 1 p 3112 N94-25628
Observation of characteristics of cosmic-ray hadron interactions in uniform-type thick lead chambers at Pamir, 2 p 3113 N94-25629
Observation of characteristics of cosmic-ray hadron interactions in uniform-type thick lead chambers at Pamir, 3 p 3113 N94-25630
Penetrating nature of very collimated high-energy shower-clusters of hadrons and gamma rays
p 3113 N94-25631
Energy concentration in high energy hadron-gamma families p 3113 N94-25632
Violation of Feynman scaling law in the forward region
p 3113 N94-25633
Simultaneous observation of families and air showers at Mt. Chacaltaya p 3114 N94-25634
Direct evidence of the interplanetary magnetic field effect on the cosmic-ray shadow by the sun
[ICRR-296-93-8] p 3116 N94-27607
Study of invisible nucleon decay, N approaches nu nu nu bar, and a forbidden nuclear transition in the Kamiokande detector
[ICRR-299-93-11] p 3028 N94-27759

COSMIC RAYS
A measurement of the energy spectra of cosmic rays from 20 to 1000 GeV per AMU
[NASA-CR-195246] p 3115 N94-27167
Simulations of terrestrial in-situ cosmogenic-nuclide production
[DE94-004999] p 3117 N94-27826
Cosmological constraints on very heavy stable neutrinos
[DE94-601669] p 3117 N94-28066

COSMIC X RAYS
Cosmic x ray physics
[NASA-CR-195225] p 3115 N94-27236
Cosmic x ray physics
[NASA-CR-195218] p 3115 N94-27419
Cosmic x ray physics
[NASA-CR-195219] p 3115 N94-27420

COSMOLOGY
Cosmoparticle physics of family symmetry breaking
[DE94-601623] p 3013 N94-25837
A cosmological field theory
[ISBN-0-315-84271-7] p 3104 N94-26638
Cosmic no-hair in Brans-Dicke theory
[DE94-603673] p 3074 N94-27636
Cosmological constraints on very heavy stable neutrinos
[DE94-601669] p 3117 N94-28066

COST ANALYSIS
A cost model for USAF acquisition of commercial aircraft for service in the special air mission fleet
[AD-A274012] p 3093 N94-25796
Rotorcraft low altitude IFR benefit/cost analysis: Conclusions and recommendations
[AD-A274241] p 2665 N94-26826
Automation life-cycle cost model
[NASA-CR-195695] p 3095 N94-27866

COST EFFECTIVENESS
MINOTAUR (Maryland's innovative orbital technologically advanced University rocket)
p 2703 N94-25685
A conceptual framework for the evaluation of cost-effectiveness of projects to reduce GHG emissions and sequester carbon
[DE93-040448] p 2867 N94-26419

COST ESTIMATES
MINOTAUR (Maryland's innovative orbital technologically advanced University rocket)
p 2703 N94-25685
A cost model for USAF acquisition of commercial aircraft for service in the special air mission fleet
[AD-A274012] p 3093 N94-25796
Environmental benefits of different types of heat pumps, available and expected
[DE94-002440] p 2866 N94-26123

COST REDUCTION
Overview of the Photovoltaic Manufacturing Technology (PVMaT) project
[DE93-018234] p 2856 N94-26426
Material optimization and manufacturing development of reduced cost powder metal titanium alloy components for gas turbine engine application, phase 2
[AD-A274410] p 2709 N94-26978
Polyhedral characterization of the economic lot-sizing problem with start-up costs
[MEMO-COSOR-92-46] p 2969 N94-27396
Development of advanced high temperature in-cylinder components and tribological systems for low heat rejection diesel engines, phase 1
[NASA-CR-187158] p 2827 N94-27984

COSTS
Project Columbiad: Reestablishment of human presence on the Moon p 2689 N94-25687
Analysis of cost and schedule growth on sole source and competitive Air Force contracts
[AD-A273920] p 3094 N94-26814
Space projects: Astrophysics facility program contains cost and technical risks. Report to Congressional Requesters
[GAO/NSIAD-94-80] p 2696 N94-27382
Computer code for controller partitioning with IFPC application: A user's manual
[NASA-CR-195291] p 2678 N94-27414
Deregulation of air traffic in America: A model to be initiated? p 2661 N94-28232
German-American relations in air traffic are to be criticized p 2662 N94-28241

COULOMB POTENTIAL
How to build analogues of the Bessel-Clifford expansions for the sum of the repulsive Coulomb potential and central potential decreasing more rapidly than the centrifugal one?
[DE93-634308] p 3007 N94-26472

COUNTERMEASURES
High resolution fourier transform absorption spectrum of 79Br2 B3 Pi(Ou+) X1 sigma g+
[AD-A273864] p 2956 N94-25610
Computer model for generation of infrared images
[PB94-123551] p 3005 N94-27172

COUPLED MODES
A study of multiple guide optical couplers
[ISBN-0-315-84633-X] p 3038 N94-27441
Weak coupling in statistical energy analysis ion Research, Univ. of Southampton, Southampton SO9 5NH, England)
[ISVR-TR-228] p 2832 N94-28174

COUPLERS
Microwave coupling into a slotted cavity
[PB94-123742] p 2772 N94-27041

COUPLING
CP violating form factors for three gauge boson vertex in the two Higgs doublet and left-right symmetric models
[DE94-601704] p 3014 N94-25841
All-coupling polaron ground state energy in D-dimension
[DE94-603666] p 3027 N94-27629

COUPLING CIRCUITS
Microwave coupling into a slotted cavity
[PB94-123742] p 2772 N94-27041

COVARIANCE
Numerical treatment of experimental data in calibration procedures
[DE93-634289] p 3097 N94-26382
Practical problems in aggregating expert opinions
[DE94-002623] p 3094 N94-27707

CRAB NEBULA
Channel to energy calibration results for the BATSE large area detectors p 3115 N94-26690

CRACK ARREST
Evaluation of crack arrest fracture toughness of parent plate, weld metal and heat affected zone of BIS 812 EMA ship plate steel
[AD-A274871] p 2839 N94-26859

CRACK CLOSURE
Crack closure, a literature study
[PB94-123361] p 2842 N94-27197
Modification of a model for fatigue life predictions based on level-crossing
[PB94-123395] p 2842 N94-27198

CRACK GEOMETRY
An experimental study on the effects of compressive stress on the fatigue crack growth of low-alloy steel
[DE94-004447] p 2737 N94-26582
Numerical Analysis Methods of Surface Cracks
[VTT-PUBS-119] p 2841 N94-27186
Applications of the weight function method (appendix 4/1) p 2842 N94-27190

CRACK INITIATION
Computation of stress intensity factors by the mode enrichment technique with applications to geometrically nonlinear problems
[PB94-126513] p 2840 N94-26910
Implementation of thermal residual stresses in the analysis of fiber bridged matrix crack growth in titanium matrix composites
[NASA-TM-109082] p 2711 N94-27658

CRACK PROPAGATION
Bulletin of National Research Institute for Metals in Fiscal Year 1993, no. 14
[REPT-14] p 2722 N94-25544
Interactions between corrosion fatigue and stress corrosion crack on steel for light water reactors
p 2722 N94-25547
Fundamental study on monitoring technology on local surface damages p 2724 N94-25555
Study on high temperature damage control and life improvement p 2729 N94-25580
Study on evaluation of crack generation and crack growth behaviors under static loading at high temperature and under combined loading p 2730 N94-25583
Study on fatigue crack propagation characteristics around welded joint interface in complexed conditions
p 2730 N94-25584
Numerical simulations of interfacial debonding in ductile-phase reinforced intermetallic matrix composites
[DE94-003639] p 2706 N94-25938
Fracture behavior of 20% Nb particulate reinforced alumina composite
[DE94-002830] p 2706 N94-26019
Growth of small fatigue cracks in Incoloy-908
[DE94-003406] p 2836 N94-26129
Grain by grain study of the mechanisms of crack propagation during iodine SCC of Zry-4
[DE93-633765] p 2734 N94-26162
Damage tolerance assessment handbook. Volume 1: Introduction fracture mechanics fatigue crack propagation
[AD-A274777] p 2836 N94-26186
Results from a fracture mechanical serial investigation of breechrings on the M109A3GN howitzer
[FFI-93/8002] p 2837 N94-26233
Damage tolerance assessment handbook. Volume 2: Aircraft damage tolerance evaluation
[AD-A274778] p 2837 N94-26357
Effects of plastic media blasting on aircraft skin
[AD-A274817] p 2668 N94-26488
Early stages in the development of stress corrosion cracks
[DE94-003867] p 2838 N94-26524
An experimental study on the effects of compressive stress on the fatigue crack growth of low-alloy steel
[DE94-004447] p 2737 N94-26582
Fatigue resistance under tension-compression of laminates IM6/5245C and AS4/3501-6
[IAR-CR-25] p 2708 N94-26711
Evaluation of crack arrest fracture toughness of parent plate, weld metal and heat affected zone of BIS 812 EMA ship plate steel
[AD-A274871] p 2839 N94-26859
Computation of stress intensity factors by the mode enrichment technique with applications to geometrically nonlinear problems
[PB94-126513] p 2840 N94-26910
Experimental study of the angled crack in GLARE 3
[PB94-126554] p 2669 N94-26954
Development of fibre-metal laminates, ARALL and GLARE, new fatigue resistant materials
[PB94-126471] p 2669 N94-26969
Engineering limitations of ceramic composites for high performance and high temperature applications
[DE94-001676] p 2754 N94-27021
Aluminum alloy 8090-T8771 thick plate material characterization
[AD-A274146] p 2987 N94-27077
Examination of hardness, fracture toughness and microstructure in Al2O3-B4C binary ceramics
[PB94-124237] p 2755 N94-27156
Development of an automated fracture assessment system for nuclear structures (appendix 1/1)
p 2841 N94-27187
Method for calculating stress intensity factors for surface cracks (appendix 2/1) p 2841 N94-27188

Applications of the weight function method (appendix 4/1) p 2842 N94-27190
Crack closure, a literature study
[PB94-123361] p 2842 N94-27197
Grain boundary chromium concentration effects on the IGSCC and IASCC of austenitic stainless steels
[DE94-004268] p 2741 N94-27570
Testing procedure for toughness characterisation of ceramic matrix composites
[REPT-932-430-101] p 2711 N94-27586
Implementation of thermal residual stresses in the analysis of fiber bridged matrix crack growth in titanium matrix composites
[NASA-TM-109082] p 2711 N94-27658
Fracture toughness and crack resistance of damage tolerant and high strength Al-Li alloys
[NLR-TP-91249-U] p 2743 N94-27795
Status and prospects for aluminium-lithium alloys in aircraft structures
[NLR-TP-92193-U] p 2743 N94-27797
The transition from stress corrosion cracking to corrosion fatigue in AA-7075 and AA-8090
[ISBN-0-315-59526-4] p 2744 N94-27950
Fatigue propagation behaviour of short cracks (1-2 mm) in steels
[ESDU-93033] p 2845 N94-28145

CRACK TIPS
Determination of fracture stress and effective crack tip radius from toughness (KIc) and yield strength (Y)
[AD-A274014] p 2836 N94-25754
Mechanism of mechanical fatigue of silica glass
[DE94-003165] p 2753 N94-26783
Computation of stress intensity factors by the mode enrichment technique with applications to geometrically nonlinear problems
[PB94-126513] p 2840 N94-26910

CRACKING (FRACTURING)
The role of grain boundary chemistry and structure in the environmentally-assisted intergranular cracking of nickel-base alloys
[DE94-003159] p 2732 N94-25954
Micropyrolysis of polymer thin films for ceramics
[ECL-92-62] p 2750 N94-26088
Proceedings of the Fourth Euroseminar on Microscopy Applied to Building Materials
[PB94-119807] p 2839 N94-26754
Development of fibre-metal laminates, ARALL and GLARE, new fatigue resistant materials
[PB94-126471] p 2669 N94-26969
Crack closure, a literature study
[PB94-123361] p 2842 N94-27197
Fracture toughness and crack resistance of damage tolerant and high strength Al-Li alloys
[NLR-TP-91249-U] p 2743 N94-27795

CRACKS
Effect of loading mode on the fracture toughness of a reduced activation ferritic/martensitic stainless steel
[DE94-004290] p 2732 N94-25987
Development of non-destructive testing technology for the crack of steam generator tubes
[DE93-632953] p 2835 N94-26399
Development of detection technique for fatigue crack due to thermal stratification phenomena in RCS piping
[DE93-632968] p 2838 N94-26400
Reconstruction of multiple cracks from experimental electrostatic boundary measurements
[NASA-CR-191584] p 2994 N94-26601
Mechanism of mechanical fatigue of silica glass
[DE94-003165] p 2753 N94-26783
Experimental study of the angled crack in GLARE 3
[PB94-126554] p 2669 N94-26954
Crack closure, a literature study
[PB94-123361] p 2842 N94-27197
An anodic dissolution-based mechanism for the rapid cracking, pre-exposure phenomenon demonstrated by Al-Li-Cu alloys
[DE94-004798] p 2742 N94-27788
Mechanically fastened composite laminates subjected to combined bearing-bypass and shear loading
p 2712 N94-27914

CRASHWORTHINESS
The development of a horizontal impact sled facility and subsequent crashworthiness experiments
[NIAR-93-15] p 2680 N94-26200

CRATERING
Cratering rates from lunar xenospherules
[DE94-003481] p 3106 N94-27007
Modulating terrestrial impacts from Oort cloud comets by the adiabatically changing galactic tides
p 2890 N94-28305

CREEP PROPERTIES
Bulletin of National Research Institute for Metals in Fiscal Year 1993, no. 14
[REPT-14] p 2722 N94-25544
Preparation of creep data sheet: Material strength data sheet p 2723 N94-25548
Study on high temperature damage control and life improvement p 2729 N94-25580
Study on elucidation of damage generation process by electron beam lithography p 2729 N94-25581
Study on evaluation of crack generation and crack growth behaviors under static loading at high temperature and under combined loading p 2730 N94-25583
Characterization of fatigue damage in a metal matrix composite (SCS-6/Ti-15-3) at elevated temperature
[AD-A273797] p 2706 N94-25876
Research into the microstructure and mechanical behavior of eutectic Bi-Sn and In-Sn
[DE94-004558] p 2741 N94-27619
Creep rupture properties of a nickel-base heat-resistant alloy Hastelloy XR under varying temperature/stress condition
[DE94-701175] p 2743 N94-27807
Effects of physical aging on long-term behavior of composites p 2712 N94-27897
A laboratory test on construction of ice domes and their load-carrying capacity p 2884 N94-27966

CREEP RUPTURE STRENGTH
Preparation of creep data sheet: Material strength data sheet p 2723 N94-25548

CREEP STRENGTH
Preparation of creep data sheet: Material strength data sheet p 2723 N94-25548
Interface phenomena in metal-ceramic composites
[AD-A274167] p 2709 N94-27125
Creep rupture properties of a nickel-base heat-resistant alloy Hastelloy XR under varying temperature/stress condition
[DE94-701175] p 2743 N94-27807

CREEP TESTS
Space-R thermionic space nuclear power system design and technology demonstration
[DE94-002017] p 2700 N94-25930
The role of grain boundary chemistry and structure in the environmentally-assisted intergranular cracking of nickel-base alloys
[DE94-003159] p 2732 N94-25954
Compatibility of refrigerants and lubricants with engineering plastics
[DE94-004959] p 2756 N94-27692

CRETACEOUS-TERTIARY BOUNDARY
New Developments Regarding the KT Event and Other Catastrophes in Earth History
[NASA-CR-195169] p 2887 N94-28294
The biostratigraphy and paleogeography of Maastrichtian inoceramids p 2889 N94-28303
An evaluation of criteria that may be used to identify species surviving a mass extinction
p 2889 N94-28304
Were all extinction events caused by impacts?
p 2891 N94-28311
Ozone control of biological activity during Earth's history, including the KT catastrophe p 2876 N94-28312

CREW PROCEDURES (INFLIGHT)
An analysis of the loads applied to a heavy Space Station rack during translation and rotation tasks
[NASA-TM-104790] p 2697 N94-28183

CREW WORKSTATIONS
A critical analysis of workload predictions generated by multiple resource theory during early crewstation design
[AD-A274804] p 2941 N94-26339

CREWS
Workload transition: Implications for individual and team performance
[AD-A274538] p 2941 N94-26964

CRITICAL FREQUENCIES
Classical solutions of Yang-Mills-Chern-Simons theory in 2+1 dimensions: A quasi-linear superposition
[DE93-634335] p 3006 N94-26270

CRITICAL LOADING
Grain by grain study of the mechanisms of crack propagation during iodine SCC of Zry-4
[DE93-633765] p 2734 N94-26162

CRITICAL POINT
Dimensional crossover from non-renormalizability to renormalizability
[DE93-613052] p 3006 N94-26193
Vapour pressures and critical points of liquids: Aliphatic and cyclic ketones
[ESDU-93009] p 2720 N94-28059
Orthobaric densities and molar volumes of liquids: Fused ring compounds
[ESDU-93029] p 2721 N94-28097
Thermal conductivity of liquid carboxylic acids
[ESDU-93017] p 2721 N94-28138
Vapour pressures and critical points of liquids: Fused ring compounds
[ESDU-93028] p 2721 N94-28142

CRITICAL PRESSURE
Orthobaric densities and molar volumes of liquids: Fused ring compounds
[ESDU-93029] p 2721 N94-28097

CRITICAL TEMPERATURE
Multi-channel Kondo necklace
[DE93-634754] p 3057 N94-26389
Process modelling of aluminium alloys. Modelling of the quench sensitivity of alloy AA6082
[PB94-124567] p 2741 N94-27325
Effect of temperature and recoil-energy spectra on irradiation-induced amorphization in Ca2La8(SiO4)6O2
[DE94-004371] p 3067 N94-27602
Orthobaric densities and molar volumes of liquids: Fused ring compounds
[ESDU-93029] p 2721 N94-28097
Thermal conductivity of liquid carboxylic acids
[ESDU-93017] p 2721 N94-28138

CRITICAL VELOCITY
Numerical investigation of thrust vectoring by injection of secondary air into nozzle flows p 2801 N94-28013
A new method for torsional critical speed calculation of practical industrial rotors
[IMR-T&M-TR-001] p 2828 N94-28041

CROP GROWTH
Effect of carbon dioxide enrichment on radish production using Nutrient Film Technique (NFT)
[NASA-TM-107198] p 2902 N94-27411
Development of a sparging technique for volatile emissions from potato (Solanum tuberosum)
[NASA-TM-109199] p 2903 N94-27412

CROSS CORRELATION
Monaural and binaural processing of complex waveforms
[AD-A274209] p 3010 N94-27067

CROSS FLOW
Computational and Experimental Assessment of Jets in Cross Flow
[AGARD-CP-534] p 2799 N94-28003
Fifty years of jet in cross flow research
p 2799 N94-28004
Transient flow features of a supersonic jet in a low speed cross flow p 2800 N94-28005
Separated flow generated by a vectored jet in a crossflow p 2800 N94-28007
Scalar mixing in the subsonic jet in crossflow
p 2800 N94-28008
The interaction region associated with twin jets and a normal crossflow p 2800 N94-28009
Experimental data for CFD validation of impinging jets in crossflow with application to ASTOVL flow problems
p 2801 N94-28010
Topological structure of a jet in a cross flow
p 2801 N94-28014
An experimental study of siphonal jets in a turbulent boundary layer crossflow p 2802 N94-28015
Experiments on the ground vortex formed by an impinging jet in cross flow p 2802 N94-28016
Comparison of the interactions of two and three dimensional transverse jets with a hypersonic free stream p 2659 N94-28021
Experiments on interaction force of jets in hypervelocity cross-flow in a shock tunnel p 2659 N94-28022
A numerical investigation of a subsonic jet in a crossflow p 2803 N94-28023
Calculation of single and multiple jets in cross-flow with and without impingement using Reynolds-stress-transport closure p 2803 N94-28024
Predictions of momentum and scalar fields in a jet in cross-flow using first and second order turbulence closures p 2803 N94-28025
Navier-Stokes simulation of two and three dimensional jets in crossflow, effects of grid, and boundary conditions p 2804 N94-28026
Effects, limits, and limitations of spanwise blowing
p 2659 N94-28027
Theoretical and experimental investigation of a delta wing with turbulent leading-edge jets
p 2659 N94-28029
Recent developments in the simulation of steady and transient transverse jet interactions for missile, rotorcraft, and propulsive applications p 2804 N94-28030
Effects of free-stream turbulence on a jet in a cross flow p 2805 N94-28036
Navier-Stokes analysis of a swirling jet in crossflow
p 2806 N94-28038

CROSSED FIELDS
The three-dimensional hydrogen atom in crossed magnetic and electric fields
[DE94-606301] p 3029 N94-27847

CRRES (SATELLITE)
CRRES high energy proton flux map
[AD-A274803] p 2878 N94-26338
Modeling the DMSP and CRRES dosimeters using the path length distribution method
[RXR-93051] p 2698 N94-28200
The PROTEL contamination code
[RXR-93071] p 3040 N94-28202

CRUCIBLES
Basic research on levitation fusing/solidification technology p 2723 N94-25552
Study on reactions between molten metal and oxide by magnetic flotation dissolution method p 2725 N94-25558
CRUDE OIL
Feasibility study on introduction of transportation-use petroleum substitution energy [DE94-725205] p 2759 N94-26905
CRUSHING
Effects of slot on rock surface for percussive rock excavation: Water jet assisted percussive rock excavation p 2871 N94-28155
CRUSTAL FRACTURES
Crustal deformation measurements in the vicinity of Vandenberg Air Force Base [AD-A274166] p 2881 N94-27143
CRYOGENIC COOLING
A compact 150 GHz SIS receiver cooled by 4 K GM refrigerator [REPT-36] p 2776 N94-27340
CRYOGENIC EQUIPMENT
Experimental analysis of heat transfer characteristics and pressure drop through screen regenerative heat exchangers [AD-A273902] p 2790 N94-25657
CRYOGENIC TEMPERATURE
Study on phase transformation due to deformation in ferromagnetic fields at cryogenic condition p 2724 N94-25556
Study on characteristics and electronic structures of materials with strong electronic correlations by ferromagnetic fields p 2724 N94-25557
Influence of grain structure and solute composition on the work hardening behavior of aluminium at cryogenic temperatures [DE94-003415] p 2733 N94-26087
Cryogenic size reduction of solid propellant [AD-A274844] p 2759 N94-26800
Cryogenic fracture behavior of 316LN in magnetic fields up to 14.6 T [DE94-005215] p 2742 N94-27694
CRYOGENIC WIND TUNNELS
The cryogenic tunnel Cologne at DLR [DLR-MITT-93-10] p 2681 N94-27587
CRYOGENICS
Titanium 1992: Science and Technology, volume 1 [AD-A274798-VOL-1] p 2739 N94-26799
Cryogenic size reduction of solid propellant [AD-A274844] p 2759 N94-26800
Cryogenic insulation studies [NASA-CR-195266] p 2756 N94-27429
Evaluation of high temperature superconductive thermal bridges for space-borne cryogenic infrared detectors p 2815 N94-27921
CRYOSTATS
The TPX Cryostat Conceptual Design [DE94-002857] p 3045 N94-26863
CRYPTOGRAPHY
Single term off-line coins [CWI-CS-R9318] p 2776 N94-27546
An efficient off-line electronic cash system based on the representation problem [CWI-CS-R9323] p 2776 N94-27551
A modular approach to evaluation cryptographic protocols using Petri nets [ISBN-0-315-85354-9] p 2972 N94-27595
CRYSTAL DEFECTS
Failure mechanisms of high temperature semiconductor lasers [AD-A273833] p 2815 N94-25616
Hydrogen uptake into silicon from an ECR plasma [DE94-003771] p 3050 N94-25815
NNN-Ising model simulation of nanodomain textures in relaxor-type lead scandium tantalate [DE94-601884] p 2748 N94-25844
Radiation-Induced Structural Changes, 2 [DE93-520314] p 3054 N94-26109
Effect of temperature and recoil-energy spectra on irradiation-induced amorphization in Ca2La8(SiO4)6O2 [DE94-004371] p 3067 N94-27602
Influence of lattice damage on retention and transport of deuterium in beta silicon carbide [DE94-005206] p 3068 N94-27693
CRYSTAL FIELD THEORY
First principle calculation for magneto-crystalline anisotropy [DE93-634653] p 3052 N94-26012
CRYSTAL GROWTH
Study on utilization of super clean, high vacuum space p 2682 N94-25586
Buckyball microwave plasmas: Fragmentation and diamond-film growth [DE94-003209] p 3053 N94-26031
Analysis of the effect on growth kinetics of gamma prima phase in Inconel 713C alloys [DE93-633763] p 2735 N94-26294
Suppression of thermal grain growth in nickel by prior electron irradiation [DE94-004602] p 2737 N94-26587
Nonlinear dynamics and pattern selection at the crystal-melt interface [DE94-003112] p 3060 N94-26780
Development of K(1-x)Na(x)TiOPO4 crystals for nonlinear applications [AD-A274336] p 3063 N94-27055
Modelling of the MEA float zone using accelerometer data [NASA-CR-193933] p 2761 N94-27220
Advanced technology development multi-color holography [NASA-CR-193931] p 2812 N94-27229
Float zone crystal growth using laser radiation [DLR-FB-93-10] p 3066 N94-27590
Characterization of semi-insulating gallium arsenide [AD-A273781] p 3068 N94-27704
Technical report of ISSP. Ser. A, no. 2677: Octa-twin model of tetrapod ZnO crystals [JTN-94-80563] p 3069 N94-27756
Hydrothermal growth and characterization of oxides in zirconium alloys [DE94-602981] p 2743 N94-27829
Prometheus in space: Research Committee on Functional New Material [JTN-94-80580] p 2761 N94-28002
CRYSTAL LATTICES
Study on the mechanism of titanium alloy toughness and the improvement of properties p 2726 N94-25566
Study on improvement in physical analysis method of metallic materials p 2728 N94-25577
Lighter alkali hydride and deuteride 1: Electronic properties of pure solids [DE93-616188] p 3051 N94-25914
Formation of three types of quasi-crystals in Al-Pd-Mg system [REPT-A-2667] p 3053 N94-26071
Polar and chemical domain structures of lead scandium tantalate (PST) [DE94-600760] p 3056 N94-26363
Window least squares method applied to statistical noise smoothing of positron annihilation data [DE93-634665] p 3003 N94-26385
Multi-channel Kondo necklace [DE93-634754] p 3057 N94-26389
Technical report of ISSP. Ser. A, no. 2673: Two successive spin glass transitions in non-diluted Heisenberg-like spin glass Ni(0.42)Mn(0.58) TiO3 [JTN-94-80559] p 2756 N94-27241
Experimental measurement of local displacement and chemical pair correlations in crystalline solid solutions [DE94-001124] p 3065 N94-27251
Technical report of ISSP. Ser. A, no. 2669: Relations between oxygen deficiency and structures in the La-Sr-Cu-O system. 3: Oxygen contents and structure of (La, Sr)8Cu8O(16+delta) phase [JTN-94-80555] p 3066 N94-27353
Localization properties of one-dimensional electrified chains [DE94-603672] p 3067 N94-27635
Hyperfine structure of positronium energy levels in a crystal [DE94-603898] p 3068 N94-27729
Hydrogen physics [DE94-701317] p 2719 N94-27822
CRYSTAL STRUCTURE
Study on synthesis and characteristics of intermetallic compound with strong electron correlation p 2726 N94-25563
Study on computerized experiment of amorphous transformation process by solid phase reaction p 2726 N94-25564
Study on microscopic structural controls and electronic properties at material surfaces by ion beams p 2727 N94-25571
Microscopic study of local structure and charge distribution in metallic La2CuO(4+delta) [DE94-003801] p 3050 N94-25817
Aluminum-ion sputtering from Al surfaces with very-low-energy ions [REPT-A-2668] p 2733 N94-26073
The origins of ordering in CuPt [DE94-003864] p 2736 N94-26351
Polar and chemical domain structures of lead scandium tantalate (PST) [DE94-600760] p 3056 N94-26363
Problems of application of charged particles channeling effects in crystals in high-energy physics [DE93-634023] p 3032 N94-26405
Crystal chemistry and self-lubricating properties of monochalcogenides gallium selenide and tin selenide [DE93-041177] p 2751 N94-26422
The 27th Annual Meeting of the Israel Society for Microscopy and the 12th Annual Meeting of the Israel Society for Histochemistry and Cytochemistry [DE93-632416] p 2716 N94-26519
Deformation twinning: Influence of strain rate [DE94-002693] p 2738 N94-26621
Neutron and x ray scattering studies of the interactions between Ca(2+)-binding proteins and their regulatory targets: Comparisons of troponin C and calmodulin [DE94-002706] p 2901 N94-26623
The coordination and atom transfer chemistry of titanium porphyrin complexes [DE94-003091] p 2704 N94-26779
Electronic structure of a single oxygen vacancy in rutile TiO2 [DE94-602717] p 3062 N94-26901
Technical report of ISSP. Ser. A, no. 2673: Two successive spin glass transitions in non-diluted Heisenberg-like spin glass Ni(0.42)Mn(0.58) TiO3 [JTN-94-80559] p 2756 N94-27241
First principles calculations for the cleaved and annealed Ge(111) surfaces [DE93-617048] p 3066 N94-27347
Hyperfine structure of positronium energy levels in a crystal [DE94-603898] p 3068 N94-27729
Technical report of ISSP. Ser. A, no. 2677: Octa-twin model of tetrapod ZnO crystals [JTN-94-80563] p 3069 N94-27756
Characterization of ZnS-GaP naon-composites [DE94-004888] p 2712 N94-27813
Antarctic Record, Vol. 36, No. 2 [REPT-107] p 2683 N94-27963
Crystallographyic analyses of clathrate hydrates included in Vostok ice cores p 2885 N94-27969
CRYSTAL SURFACES
On line quantification of crystal surfaces by stereo imaging [NASA-CR-195277] p 3066 N94-27561
CRYSTALLINITY
The fracture behavior of a CVD crystalline Si3N4/amorphous Si3N4 composite [DE94-002646] p 2750 N94-26124
Crystal chemistry and self-lubricating properties of monochalcogenides gallium selenide and tin selenide [DE93-041177] p 2751 N94-26422
Octahedral metallomesogens: Liquid crystallinity in low aspect ratio materials [AD-A274830] p 3059 N94-26571
Electron microscopy studies of undoped and phosphorus doped Si:H and Si,C:H films [DE94-004738] p 3069 N94-27757
CRYSTALLITES
Bench-scale synthesis of nanoscale materials [DE94-004787] p 2742 N94-27786
CRYSTALLIZATION
Crystallization and microstructural control of ferroelectric thin-films and glass-ceramics [AD-A273767] p 2748 N94-25854
Oriented lead zirconate titanate thin films: Characterization of film crystallization [DE94-003104] p 3053 N94-26025
Fabrication technology [DE94-003017] p 2763 N94-26778
Mechanism of mechanical fatigue of silica glass [DE94-003165] p 2753 N94-26783
Morphology transitions during non-equilibrium growth processes [ITN-94-85236] p 3065 N94-27243
The Science Reports of the Research Institutes, Tohoku University. Series A: Physics, Chemistry, and Metallurgy. Volume 38, No. 1: Amorphous Materials 14 [JTN-94-80610] p 2744 N94-28158
Differential scanning calorimetric study of solid state amorphization and crystallization in Zr/Co and Zr/Ni multilayers p 2745 N94-28161
Formation and crystallization of hydrogen-induced amorphous Ti3InH(4.5) alloy p 2745 N94-28163
CRYSTALLOGRAPHY
Study on improvement in physical analysis method of metallic materials p 2728 N94-25577
Three-wave nonlinear interactions in KTiOPO4 (KTP) and KTP isomorphs [AD-A274079] p 3052 N94-25993
Cracking of textured zinc coating during forming process [DE94-003414] p 2750 N94-26085
Grain by grain study of the mechanisms of crack propagation during iodine SCC of Zry-4 [DE93-633765] p 2734 N94-26162
Liquid and solid solubility of Ag in Bi2Sr2CaCu2O8 [DE94-002829] p 2735 N94-26273

Developments in crystallographic phase analysis in the SEM: Backscattered electron Kikuchi patterns
[DE93-040755] p 3057 N94-26420

Crystallographyic analyses of clathrate hydrates included in Vostok ice cores p 2885 N94-27969

CRYSTALS

Three-wave nonlinear interactions in KTiOPO4 (KTP) and KTP isomorphs
[AD-A274079] p 3052 N94-25993

Cracking of textured zinc coating during forming process
[DE94-003414] p 2750 N94-26085

Determination of surface recombination velocity and bulk lifetime in detector grade silicon and germanium crystals
[DE94-003886] p 3053 N94-26094

Crystal potential retrieval in HRTEM
[DE94-601883] p 3055 N94-26171

Electron energy loss spectroscopy in a crystalline environment using inner shell ionization
[DE94-601820] p 3018 N94-26334

Polar and chemical domain structures of lead scandium tantalate (PST)
[DE94-600760] p 3056 N94-26363

Problems of application of charged particles channeling effects in crystals in high-energy physics
[DE93-634023] p 3032 N94-26405

Crystal chemistry and self-lubricating properties of monochalcogenides gallium selenide and tin selenide
[DE93-041177] p 2751 N94-26422

Design of a high-precision double crystal tunable monochromator
[DE94-003004] p 2811 N94-26787

Development of K(1-x)Na(x)TiOPO4 crystals for nonlinear applications
[AD-A274336] p 3063 N94-27055

Experimental measurement of local displacement and chemical pair correlations in crystalline solid solutions
[DE94-001124] p 3065 N94-27251

Characterization of semi-insulating gallium arsenide
[AD-A273781] p 3068 N94-27704

CULTIVATION

Development of Purkinje cells in vitro
p 2905 N94-27483

CULTURE TECHNIQUES

Development of Purkinje cells in vitro
p 2905 N94-27483

CUMULUS CLOUDS

Interactions between a tropical mixed boundary layer and cumulus convection in a radiative-convective model
[DE94-000848] p 2877 N94-25979

The numerical simulation of marine boundary layer clouds
[AD-A273669] p 2894 N94-26195

CURING

Technique to predict the curing behaviour of unsaturated polyester materials
[PB94-124856] p 2748 N94-25892

Modelling the inhibition cure behaviour of unsaturated polyester moulding materials
[PB94-124864] p 2748 N94-25893

Stress relaxation in dough moulding compounds
[PB94-124872] p 2748 N94-25894

An ultrasonic testing technique for monitoring the cure and mechanical properties of polymeric materials
[AD-A274536] p 2753 N94-26842

Phosphazene-containing amine as curing agent for phthalonitrile-base polymer
[AD-D016029] p 2755 N94-27147

Ultrasonic measurement technique to determine the state of cure in thermosetting materials
[PB94-124328] p 2756 N94-27217

Dual cure low-VOC coating process
[DE94-000365] p 2756 N94-27611

Property enchancement of polyimide films by way of the incorporation of lanthanide metal ions
p 2758 N94-27926

CURRENT ALGEBRA

The algebra of non-local charges in non-linear sigma models
[DE94-601563] p 2991 N94-25884

Vector meson exchanges and CP asymmetry in K(sup +/-) yields pi(sup +/-)pi(sup 0)
[DE94-601605] p 3014 N94-25887

Low-energy hadronic interactions beyond the current algebra approach
[DE94-602600] p 3022 N94-26900

CURRENT DENSITY

Electromagnetic properties of a toroidal solenoid
[DE93-613032] p 2766 N94-25866

Grain boundary degradation of YBCO superconductors sintered in CO2-containing atmospheres
[DE94-003206] p 3053 N94-26029

The potential for large critical currents in the high T(sub c) oxides p 2854 N94-26058

Investigation of a normal incidence high-performance p-type strained layer In(0.3)Ga(0.7)As / In(0.52)Al(0.48) as quantum well infrared photodetector
[AD-A274854] p 3055 N94-26188

Scaling of sustained ZT-40 M reversed field pinches
[DE94-003318] p 3043 N94-26321

Processing and properties of Ag-clad Bi-2223 tapes
[DE94-004603] p 2783 N94-26589

A mechanism for resistive dissipation in Ag sheathed Bi2Sr2CaCu2O8 and Bi2Sr2Ca2Cu3O10
[DE94-003009] p 3060 N94-26771

Evaluation of APC NbTi superconductor in a model dipole magnet
[DE94-003258] p 3060 N94-26795

Powder synthesis, fabrication, and transport properties of long-length Ag clad Bi-2223 conductors
[DE94-002376] p 2740 N94-26957

Channel model for AC electric arc
[PB94-124591] p 2786 N94-27327

Correlation between electrical activity and the size of single sinoatrial node cells p 2907 N94-27513

CURRENT DISTRIBUTION

An optimal constrained linear inverse method for magnetic source imaging
[DE94-004014] p 2957 N94-25663

An optimal constrained linear inverse method for magnetic source imaging
[DE94-002264] p 2996 N94-26936

Modeling of the coupled magnetospheric and neutral wind dynamos
[NASA-CR-195273] p 2883 N94-27852

CURVATURE

Combining shape and color information for 3D object recognition
[AD-A274123] p 2967 N94-27064

On the model of the relativistic particle with curvature and torsion
[DE94-606330] p 3029 N94-27848

CURVE FITTING

Piecewise least squares fitting technique using finite interval method with Hermite polynomials
[VTT-PUBS-135] p 2990 N94-25733

Aspects of goodness-of-fit
[AD-A274826] p 3003 N94-26495

CURVES (GEOMETRY)

A theory of multi-scale, curvature and torsion based shape representation for planar and space curves
[ISBN-0-315-63894-X] p 2974 N94-27805

CYCLES

Characteristics and development report for the T1576 power supply and the MC3935 battery
[DE94-003675] p 2783 N94-26372

Lyapunov exponents for some quasi-periodic cocycles
[PB94-124377] p 2997 N94-26994

CYCLIC AMP

The polymodal receptor p 2908 N94-27539

CYCLIC HYDROCARBONS

Analytical method for estimation of the total amount of aromatic and poly aromatic compounds in diesel fuel
[PB94-123692] p 2759 N94-25907

CYCLIC LOADS

Growth of small fatigue cracks in Incoloy-908
[DE94-003406] p 2836 N94-26129

Limitations of power conversion systems under transient loads and impact on the pulsed tokamak power reactor
[DE94-003404] p 3043 N94-26324

Computer modelling of cyclic deformation of high-temperature materials
[AD-A274504] p 2840 N94-27034

An experimental investigation of fatigue damage in aluminum 2024-T3 alloys p 2747 N94-27900

Propeller off-axis loads due to thrust axis incidence and nacelle magnus force p 2652 N94-28319

CYCLOGENESIS

Mesoscale frontal evolution of the ERICA IOP-5A Cyclone
[AD-A274906] p 2893 N94-26183

CYCLONES

Development and testing of the Coupled Ocean/Atmosphere Mesoscale Prediction System (COAMPS)
[AD-A273925] p 2892 N94-25793

A modeling study of the mesocyclone
[AD-A274889] p 2893 N94-26168

Mesoscale frontal evolution of the ERICA IOP-5A Cyclone
[AD-A274906] p 2893 N94-26183

Tropical cyclone report, 1992
[AD-A274464] p 2896 N94-27025

CYCLOTRON FREQUENCY

Design of folded waveguide antenna for Alcator C-Mod
[DE94-003584] p 2767 N94-25924

RF modeling and design of a folded waveguide launcher for the Alcator C-Mod tokamak
[DE94-003588] p 3041 N94-25933

Design and control of phased ICRF antenna arrays
[DE94-002796] p 3046 N94-27261

CYCLOTRON RADIATION

Hydrogen uptake into silicon from an ECR plasma
[DE94-003771] p 3050 N94-25815

Development of fusion technology
[DE93-633444] p 3042 N94-26159

CYCLOTRON RESONANCE

Hydrogen uptake into silicon from an ECR plasma
[DE94-003771] p 3050 N94-25815

Plasma surface cleaning using microwave plasmas
[DE94-002754] p 2713 N94-26014

Compton Gamma Ray Observatory/BATSE observations of energetic electrons scattered by cyclotron resonance with waves from powerful VLF transmitters
[NASA-CR-195240] p 3115 N94-26790

On radio frequency wave induced radial transport and wave helicity
[IPPCZ-326] p 2777 N94-27838

The ZnO thin films with C-axis orientation prepared on the room temperature substrate by the ECR multipolar plasma sputtering method
[DE94-605039] p 2758 N94-27857

CYCLOTRON RESONANCE DEVICES

Electrical analysis of wideband and distributed windows using time-dependent field codes
[DE94-002987] p 2768 N94-26310

Computer simulations of radiation generation from relativistic electron beams
[AD-A274139] p 3024 N94-27133

Mode analysis of gyrotron oscillation using a k-spectrometer
[DE94-701195] p 2813 N94-27703

CYCLOTRONS

TRIUMF scientific activities
[CTN-94-61062] p 3117 N94-26656

A direct current rectification scheme for microwave space power conversion using traveling wave electron acceleration p 2687 N94-27371

CYLINDRICAL ANTENNAS

Numeric solution of the electric field integral equation using Galerkin's method for axially symmetric cases
[ESA-TT-1264] p 2768 N94-26315

CYLINDRICAL BODIES

Flow past a circular cylinder with a permeable wake splitter plate
[AD-A273765] p 2790 N94-25872

SAG compensated vibration isolation mount
[AD-D016040] p 2841 N94-27110

Research on bluff body vortex wakes
[AD-A273780] p 2796 N94-27319

Wave propagation in the shallow regions of the earth's crust and the borehole vicinity
[ITN-94-85237] p 2882 N94-27330

Direct simulation Monte-Carlo of near continuum hypersonic flow with chemical reactions
[DLR-FB-93-01] p 2797 N94-27588

Circular cylinder in axial flow
[ISBN-0-315-59114-5] p 2798 N94-27873

CYLINDRICAL COORDINATES

Wave propagation in the shallow regions of the earth's crust and the borehole vicinity
[ITN-94-85237] p 2882 N94-27330

CYLINDRICAL SHELLS

Series solution for a cylindrical composite shell subject to axisymmetric loadings
[ISBN-0-315-60559-6] p 2844 N94-27810

CYLINDRICAL WAVES

Theoretical and experimental investigation of converging cylindrical shock waves propagating in narrow cylindrical chambers
[ISBN-0-315-84694-1] p 2795 N94-27313

D

DAMAGE

Study on variation of damage generation mechanism by fatigue on TiAl compounds due to different slip systems p 2729 N94-25579

Study on elucidation of damage generation process by electron beam lithography p 2729 N94-25581

Study on evaluation of crack generation and crack growth behaviors under static loading at high temperature and under combined loading p 2730 N94-25583

Investigation of plasma etch induced damage in compound semiconductor devices
[DE94-002849] p 3052 N94-25989

Ion implantation of diamond: Damage, doping, and lift-off
[DE94-001133] p 3054 N94-26137

Damage tolerance assessment handbook. Volume 1: Introduction fracture mechanics fatigue crack propagation
[AD-A274777] p 2836 N94-26186

Design and life-time of polymer matrix composite structures: Summary
[VTT-TIED-1415] p 2707 N94-26260

Damage tolerance assessment handbook. Volume 2: Aircraft damage tolerance evaluation
[AD-A274778] p 2837 N94-26357

Deformation, constitutive behavior, and damage of advanced structural materials under multiaxial loading
[AD-A274165] p 2709 N94-27142

DAMAGE ASSESSMENT

Study on elucidation of damage generation process by electron beam lithography p 2729 N94-25581

Effect of impact face damage on strength of sandwich composites
[VTT-PUBS-128] p 2704 N94-25734

Meeting of the Eighth Session of the Scientific Advisory Committee of the World Climate Impact Assessment and Response Strategies Programme
[DE93-633954] p 2866 N94-26163

Aircraft wheel life assessment
[AD-A274378] p 2823 N94-26976

Development of an automated fracture assessment system for nuclear structures (appendix 1/1)
p 2841 N94-27187

Testing procedure for toughness characterisation of ceramic matrix composites
[REPT-932-430-101] p 2711 N94-27586

DAMPING

Kinetic resonance damping rate of the toroidal ion temperature gradient mode
[DE94-003511] p 3041 N94-25923

Proceedings of Damping 1993, volume 1
[AD-A274226] p 2840 N94-26922

Extraction of modal parameters from an operating HAWT using the Natural Excitation Technique (NExT)
[DE94-001831] p 2859 N94-27004

Multiple model adaptive control of a large flexible space structure with purposeful dither for enhanced identifiability
[AD-A274132] p 2987 N94-27122

An improvement in the modified finite element procedure for underwater shock analysis
[DE94-004451] p 2797 N94-27617

DARK MATTER

The meaning of EROS/MACHO
[DE94-003003] p 3104 N94-26311

DATA ACQUISITION

Distributing functionality in the drift scan camera system
[DE94-003640] p 2809 N94-25599

Naval Interactive Data Analysis System (NIDAS), software user's manual
[NASA-CR-195179] p 2956 N94-25606

Autonomous support for microorganism research in space p 2903 N94-25672

Predicting nonlinear time series
[AD-A274051] p 2990 N94-25834

Comparative investigation of high-latitude ionospheric structure and effects near solar maximum
[AD-A273799] p 2877 N94-25877

Digital control and data acquisition for high-value GTA welding
[DE94-000885] p 2821 N94-25980

Remote Earth Sciences data collection using ACTS
[NASA-CR-195227] p 2848 N94-26236

Auxiliary controller for time-to-digital converter module readout
[DE93-634172] p 2948 N94-26266

New Thomson scattering laser control for D3-D
[DE94-002890] p 3043 N94-26274

Overall analysis of meteorological information in the Daeduk nuclear complex
[DE93-632594] p 2894 N94-26469

New FORTRAN computer programs to acquire and process isotopic mass spectrometric data: Operator's manual
[DE94-003174] p 2965 N94-26784

Memory subsystem performance of programs using copying garbage collection
[AD-A274258] p 3099 N94-27014

Monaural and binaural processing of complex waveforms
[AD-A274209] p 3010 N94-27067

Conifer tree influence on Digital Terrain Elevation Data (DTED): A case study at Dulles International Airport
[AD-A274213] p 2849 N94-27069

An XCP user's guide and reference manual
[AD-A274519] p 2900 N94-27090

Interchangeable end effector tools utilized on the PFMA
[NASA-CR-193925] p 2823 N94-27149

Meteorological data at the Nagaoka Institute of Snow and Ice Studies
[REPT-158] p 2896 N94-27169

Development of an automatic fatigue-data acquisition system using commercial software
[NAL-TM-650] p 2842 N94-27207

CMT-Si
[PB94-123619] p 2812 N94-27216

Advanced development of particle beam probe diagnostic system
[DE94-002316] p 3047 N94-27720

Computer aided data recording and analyzing system for the engine test p 2764 N94-27979

DATA BASE MANAGEMENT SYSTEMS

Naval Interactive Data Analysis System (NIDAS), software user's manual
[NASA-CR-195179] p 2956 N94-25606

Standardizing exchange formats
[DE93-616798] p 3095 N94-25751

Performance measurement of three commercial object-oriented database management systems
[AD-A274028] p 3096 N94-25765

Source code for the OO1 benchmark and the AFIT simulation benchmark
[AD-A274035] p 2958 N94-25799

Hypermedia support for engineering design systems: Application to fatigue analysis
[VTT-TIED-1432] p 2837 N94-26255

OPM Scheme Editor 2: A graphical editor for specifying object-protocol structures
[DE94-003477] p 2962 N94-26327

Hanford Environmental Information System (HEIS) sample/data entry flow summary
[DE94-002494] p 3098 N94-26559

Design considerations when using external hypertext engines from applications
[DE94-002213] p 3098 N94-26598

Retrieval using plausible inference
[AD-A274252] p 3099 N94-27013

Bibliographic Retrieval System (BARS) Sandia Shock Compression (SSC) database Shock Physics Index (SPHINX) database, volume 3
[DE94-001705] p 3099 N94-27022

Active database architectures and the design of sentinel for constraint management
[AD-A274205] p 3099 N94-27101

Design and implementation of a DBMS performance assessment tool
[CWI-CS-R9270] p 2972 N94-27576

The TMIS life-cycle process document, revision A
[NASA-TM-109698] p 2697 N94-27775

Concurrent shadow paging: Snapshots, read-only transactions, and on-the-fly multi-level incremental dumping
[PB94-133139] p 3100 N94-28385

DATA BASES

Knowledge base systems for chemical compounds designing support p 2723 N94-25550

Study on knowledge extraction and systematization for material design p 2727 N94-25568

Comparative investigation of high-latitude ionospheric structure and effects near solar maximum
[AD-A273799] p 2877 N94-25877

The effect of elevation data representation on nocturnal drainage wind simulations
[DE94-003624] p 2892 N94-25936

Using database technology to support domain-oriented application composition systems
[AD-A274091] p 3096 N94-26024

Index to BROND-2, CENDL-2, ENDF/B-6, JEF-2, JENDL-3
[DE93-634500] p 3016 N94-26034

Software redesign for usability: A case study
[DE94-003704] p 2960 N94-26048

Design and implementation of a query editor for the Amadeus system
[AD-A274955] p 3097 N94-26300

Scientific and Technical Information (STI)....what's the status?
[DE94-003731] p 3097 N94-26348

International energy: Research organizations, 1988-1992
[DE93-017267] p 3098 N94-26398

US Army aviation epidemiology data registry: Incidence and outcomes of aviator flying evaluation boards
[AD-A274711] p 2910 N94-26432

Hanford Environmental Information System (HEIS) sample/data entry flow summary
[DE94-002494] p 3098 N94-26559

A formalization of objects using equational dynamic logic
[PB94-125218] p 2965 N94-26852

Monograph of the aviation epidemiology data register for calendar year 1988
[AD-A274589] p 2911 N94-26985

Orientation competition in cortical filters
[PB94-125366] p 2939 N94-27001

An object-oriented database interface for Ada
[AD-A274391] p 2968 N94-27075

Active database architectures and the design of sentinel for constraint management
[AD-A274205] p 3099 N94-27101

Monograph of the Aviation Epidemiology Data Register for CY 1992
[AD-A274400] p 2911 N94-27130

Schema integration in object-oriented databases
[CWI-CS-R9320] p 2970 N94-27548

NSWC Crane Aerospace Cell Test History Database
p 2860 N94-28102

Variability of measured sonic boom signatures
p 2651 N94-28197

Concurrent shadow paging: Snapshots, read-only transactions, and on-the-fly multi-level incremental dumping
[PB94-133139] p 3100 N94-28385

DATA COMPRESSION

Probabilistic methods for image generation and encoding
[AD-A274294] p 2964 N94-26682

Trapezoid-oriented compression of run length coded map data
[PB94-123312] p 2849 N94-26848

Encoding approaches for data link transmission of weather graphics
[AD-A274497] p 2772 N94-26963

Image quality analysis of compressed synthetic aperture radar imagery
[AD-A273399] p 2774 N94-27170

SPECTRUM analysis of multispectral imagery in conjunction with wavelet/KLT data compression
[DE94-003961] p 2851 N94-27727

The 1994 Space and Earth Science Data Compression Workshop
[NASA-CP-3255] p 2945 N94-28251

An image assessment study of image acceptability of the Galileo low gain antenna mission
p 2945 N94-28252

Image compression software for the SOHO LASCO and EIT experiments p 2945 N94-28253

Comparison of the lossy image data compressions for the MESUR Pathfinder and for the Huygens Titan Probe
p 2945 N94-28254

Advanced End-to-end Simulation for On-board Processing (AESOP) p 2945 N94-28255

Performance considerations for the application of the lossless browse and residual model
p 2946 N94-28256

Image quality measures and their performance
p 2946 N94-28257

A comparison of spectral decorrelation techniques and performance evaluation metrics for a wavelet-based, multispectral data compression algorithm
p 2946 N94-28258

A comparative study of SAR data compression schemes p 2946 N94-28259

Perceptual compression of magnitude-detected synthetic aperture radar imagery p 2946 N94-28260

Compression of multispectral Landsat imagery using the Embedded Zerotree Wavelet (EZW) algorithm
p 2947 N94-28261

Vector quantizer designs for joint compression and terrain categorization of multispectral imagery
p 2947 N94-28262

Wavelet compression techniques for hyperspectral data p 2947 N94-28263

Some practical aspects of lossless and nearly-lossless compression of AVHRR imagery p 2947 N94-28264

DATA CONVERSION ROUTINES

PATRAN 2.5/EAL interface guide
[NASA-TM-109053] p 2972 N94-27655

DATA FLOW ANALYSIS

Parallel Assessment Window System (PAWS) enhancements
[AD-A274094] p 2979 N94-25786

Run-time recognition of task parallelism within the P++ parallel array class library
[DE94-002707] p 2980 N94-26120

Survey of visualization and analysis tools
[NASA-TM-108436] p 2809 N94-26150

Enhanced adaptive statistical filter providing improved performance for target motion analysis noise discrimination statement of government interest
[AD-D016039] p 2786 N94-27109

DATA INTEGRATION

Data analysis and data fusion for intelligence analysis and decision support. Research plan 1993-2000
[PB94-123569] p 3005 N94-27173

Circulars of the Electrotechnical Laboratory. No. 223: An extended survey on provable information base systems
[JTN-94-80550] p 3100 N94-27336

Multi-sensor data fusion in a distributed environment: Architectural solutions
[NLR-TP-92243-U] p 2989 N94-27800

DATA LINKS
System design analysis of a lightweight laser satellite terminal
[AD-A274033] p 2690 N94-25769
Airborne data link operational evaluation test plan
[AD-A274096] p 2664 N94-25788
Code division multiple access local area network communications employing fiber optic signal processing techniques
[AD-A274897] p 3096 N94-26160
Laser-based communication link
[FFI-93/7023] p 2817 N94-26203
Optoelectronic technology consortium
[AD-A274595] p 3036 N94-26857
Encoding approaches for data link transmission of weather graphics
[AD-A274497] p 2772 N94-26963
Packet radio data link applications in the NASA Langley Research Center Transport Systems Research Vehicle
[NASA-TM-109071] p 2665 N94-27423

DATA MANAGEMENT
Rendering of three-dimensional data sets derived from finite-difference and spectral methods
[AD-A273724] p 3096 N94-25997
Using database technology to support domain-oriented application composition systems
[AD-A274091] p 3096 N94-26024
The High Performance Storage System
[DE94-004351] p 2948 N94-26578
The NOGAPS ten year AMIP integration
[AD-A274332] p 2900 N94-26887
An object-oriented database interface for Ada
[AD-A274391] p 2968 N94-27075
Researches of the Electrotechnical Laboratory. No. 955: Speech recognition by description of acoustic characteristic variations
[JTN-94-80604] p 2775 N94-27249
Circulars of the Electrotechnical Laboratory. No. 223: An extended survey on provable information base systems
[JTN-94-80550] p 3100 N94-27336
Global change research related to the Earth's energy and hydrologic cycle
[NASA-CR-195270] p 2869 N94-27430
Efficient rebalancing of tree-type main memory dictionaries
[PB94-133105] p 3100 N94-28396

DATA PROCESSING
Repeated knots in least squares multiquadric functions
[AD-A273866] p 2990 N94-25594
Naval Interactive Data Analysis System (NIDAS), software user's manual
[NASA-CR-195179] p 2956 N94-25606
A data processing system at the hybrid spectrometer
[DE93-616801] p 3013 N94-25828
Set based analysis of arithmetic
[AD-A274112] p 3002 N94-25903
Survey of visualization and analysis tools
[NASA-TM-108436] p 2809 N94-26150
Parametric analysis of the space power plants on the base of criterion of specific mass in generalized design variants
[DE93-634153] p 2701 N94-26166
Numerical treatment of experimental data in calibration procedures
[DE93-634289] p 3097 N94-26382
On the reliability of a window least squares algorithm
[DE93-634666] p 2962 N94-26386
Separation and reconstruction of electron neutrino interaction in the IHEP-JINR neutrino detector and BARS detector
[DE93-634182] p 3019 N94-26393
Usefulness of compile-time restructuring of LGDF programs in throughput-critical applications
[AD-A274915] p 2963 N94-26530
Automatic test case generation using PROLOG
[NPL-DITC-215/93] p 2964 N94-26655
DUSOL: Improved software for analysis of ultrasonic velocity data on anisotropic materials
[NPL-DMM(A)-104] p 2965 N94-26816
A preliminary method for atmospheric soundings in real time using satellite and ground-based remotely sensed data
[AD-A274381] p 2880 N94-26828
Optoelectronic technology consortium
[AD-A274595] p 3036 N94-26857
Compilation of corrections for postprocessing of laser bathymetry data
[PB94-123668] p 2900 N94-27156
DALIA: A language for the description and analysis of digital systems p 2954 N94-27192
Pigs in cyberspace p 2689 N94-27376
On modeling and controlling intelligent systems
[DE94-002446] p 2988 N94-27706
SPECTRUM analysis of multispectral imagery in conjunction with wavelet/KLT data compression
[DE94-003961] p 2851 N94-27727
ADP Analysis project for the Human Resources Management Division p 2978 N94-27927
Computer aided data recording and analyzing system for the engine test p 2764 N94-27979

DATA PROCESSING EQUIPMENT
A data processing system at the hybrid spectrometer
[DE93-616801] p 3013 N94-25828
Fast parallel algorithms for short-range molecular dynamics
[DE93-018519] p 3016 N94-26033
Description of the Experimental Avionics Systems Integration Laboratory (EASILY)
[NASA-TM-109072] p 2681 N94-27425

DATA REDUCTION
Repeated knots in least squares multiquadric functions
[AD-A273866] p 2990 N94-25594
Survey of visualization and analysis tools
[NASA-TM-108436] p 2809 N94-26150
Analysis and interpretation of the meteorology of the 1988 coastal transition zone experiment
[AD-A274710] p 2894 N94-26431
Data analysis and data fusion for intelligence analysis and decision support. Research plan 1993-2000
[PB94-123569] p 3005 N94-27173
Quick-look system of auroral absorption images by imaging riometer p 2884 N94-27968

DATA RETRIEVAL
Standardizing exchange formats
[DE93-616798] p 3095 N94-25751

DATA SAMPLING
Development of digital resampling and pulse compression computer software
[DREP-92-32] p 2969 N94-27318

DATA STORAGE
Standardizing exchange formats
[DE93-616798] p 3095 N94-25751
Out of core, out of mind: Practical parallel I/O
[DE94-003107] p 2979 N94-25952
The High Performance Storage System
[DE94-004351] p 2948 N94-26578
On-board software for the JET-X telescope on the Spectrum-X mission p 2951 N94-26727
Virtual data
[DE94-002718] p 2986 N94-26807
High-speed, high-density, coherent time-domain optical memory
[AD-A274249] p 3037 N94-27010
Memory subsystem performance of programs using copying garbage collection
[AD-A274258] p 3099 N94-27014
Memory subsystem performance of programs with intensive heap allocation
[AD-A274122] p 2967 N94-27063
Aviation Epidemiology Data Register: Indexing the AEDR document laser optic archive
[AD-A274185] p 2911 N94-27097
Garbage collection in a multiprocessor Smalltalk system
[ISBN-0-315-51159-1] p 2982 N94-27332

DATA STRUCTURES
Multimedia in Views
[CWI-CS-R9263] p 2961 N94-26218
Editing tree structures
[CWI-CS-R9264] p 2961 N94-26219
Hypermedia support for engineering design systems: Application to fatigue analysis
[VTT-TIED-1432] p 2837 N94-26255
Circulars of the Electrotechnical Laboratory. No. 223: An extended survey on provable information base systems
[JTN-94-80550] p 3100 N94-27336
Computer code for controller partitioning with IFPC application: A user's manual
[NASA-CR-195291] p 2678 N94-27414
Concurrent shadow paging: Snapshots, read-only transactions, and on-the-fly multi-level incremental dumping
[PB94-133139] p 3100 N94-28385
Efficient rebalancing of tree-type main memory dictionaries
[PB94-133105] p 3100 N94-28396

DATA SYSTEMS
Computing in space: Issues and answers
p 2948 N94-26714
NASA's spacecraft data system p 2950 N94-26723
Circulars of the Electrotechnical Laboratory. No. 223: An extended survey on provable information base systems
[JTN-94-80550] p 3100 N94-27336
Report of the National Research Institute for Earth Science and Disaster Prevention, No. 51
[JTN-94-80509] p 2886 N94-27985
Observation with STS seismometer at Nakaizu, central Japan: Observation system and comparison with tiltmeter p 2886 N94-27986
Development of a method for predicting snowfall intensity and compacted snow on roads
p 2853 N94-27990
Conception of snow information network system in Yamagata Prefecture p 2853 N94-27991

DATA TRANSFER (COMPUTERS)
The use of ASN.1 and XDR for data representation in real-time distributed systems
[AD-A273769] p 2959 N94-25855
Out of core, out of mind: Practical parallel I/O
[DE94-003107] p 2979 N94-25952
Design and specification of the Xpress transfer high-speed protocol
[AD-A274941] p 3097 N94-26297
PDEF: A standard file format for data interchange
[AD-A274694] p 3098 N94-26451

DATA TRANSMISSION
Meteor Burst Communications (MBC) throughput improvement tests
[AD-A273941] p 2767 N94-25990
Design and specification of the Xpress transfer high-speed protocol
[AD-A274941] p 3097 N94-26297
Modeling and simulation of a fiber distributed data interface local area network
[AD-A274838] p 3098 N94-26500
Optoelectronic technology consortium
[AD-A274595] p 3036 N94-26857
An efficient off-line electronic cash system based on the representation problem
[CWI-CS-R9323] p 2776 N94-27551
Communication on the Paragon
[DE94-003103] p 2983 N94-27713
Image quality measures and their performance
p 2946 N94-28257
A comparison of spectral decorrelation techniques and performance evaluation metrics for a wavelet-based, multispectral data compression algorithm
p 2946 N94-28258
Open communication in manufacturing automation
[PB94-132479] p 2976 N94-28377

DAWN CHORUS
Memories of National Institute of Polar Research. Series A-19. Upper atmosphere physics: ELF emission in high latitudes: Ray path calculation and ground-satellite observations
[JTN-94-80592] p 2882 N94-27342

DAYGLOW
Analysis of EUV/FUV dayglow and auroral measurements
[NASA-CR-195237] p 2883 N94-27393

DE HAVILLAND AIRCRAFT
Wind tunnel investigation of propfan slipstream/wing interactions on a De Havilland air motor powered semispan model at Mach numbers 0.6 and 0.7
p 2651 N94-28316
Flow field investigation in the near slipstream of an 8-bladed propfan on the De Havilland WTEJ half-model at Mach numbers 0.6 and 0.7 p 2651 N94-28317
Assessing the effects of Tuned Vibration Absorbers (TVAs) on interior cabin noise levels: A correlation between analytical acoustic predictions and flight test measurements p 2652 N94-28318

DEAD RECKONING
Dead reckoning navigation
[VTT-TIED-1402] p 2664 N94-25808

DEATH
Evaluation and improvement of the inquest system on work accidents (TOT)
[VTT-TIED-1418] p 2762 N94-26261

DEBONDING (MATERIALS)
Investigation of compressive behavior for metal matrix composites with a circular hole
[AD-A273835] p 2705 N94-25739
Numerical simulations of interfacial debonding in ductile-phase reinforced intermetallic matrix composites
[DE94-003639] p 2706 N94-25938

DEBRIS
Safety standards for aircraft shelter
[FFI-92/4003] p 2680 N94-26305
Physics of debris clouds from hypervelocity impacts
[NASA-CR-193932] p 2696 N94-26791
Debris/ice/TPS assessment and integrated photographic analysis for Shuttle mission STS-60
[NASA-TM-109193] p 2692 N94-27956

DECAY RATES
Study of invisible nucleon decay, N approaches nu nu nu bar, and a forbidden nuclear transition in the Kamiokande detector
[ICRR-299-93-11] p 3028 N94-27759
Dynamics of metastable states in supersonic beams
[ITN-94-85232] p 3028 N94-27760

DECISION MAKING

The effect of the time restrictions on information search and information integration in a dynamic task environment
[AD-A273759] p 3095 N94-25723

Developing realistic cooperative behaviors for autonomous agents in air combat simulation
[AD-A274077] p 2937 N94-25774

Implementing a multiple criteria model base in co-op with a graphical user interface generator
[AD-A274901] p 3093 N94-26181

Automated information management for designers: Functional requirements for computer based associates that support access and use of technical information in design
[AD-A274603] p 3099 N94-26891

Interactive control of a parallel simulation from a remote graphics workstation
[AD-A274217] p 2981 N94-27070

Practical problems in aggregating expert opinions
[DE94-002623] p 3094 N94-27707

Intertemporal bargaining and dynamic consistency
[PB94-133147] p 3095 N94-28386

DECISION THEORY

Rational handling of multiple goals for mobile robots
[NASA-CR-195177] p 2985 N94-26006

DECODERS

The Communication Link and Error ANalysis (CLEAN) simulator
[NASA-CR-195243] p 2968 N94-27168

Telecommand decoder specification
[ESA-PSS-04-151-ISSUE-1] p 2693 N94-27583

DECODING

Coded communications with nonideal interleaving
[ITN-94-85235] p 2774 N94-27242

DECOMPOSITION

Satellite attitude determination using linear combination of models
[AD-A274082] p 2694 N94-25996

The importance of vibrationally excited nitrogen in silicon nitride deposition systems
[AD-A274874] p 2750 N94-26167

Implementation and performance of a domain decomposition algorithm in Sisal
[DE94-002012] p 2981 N94-27092

The PRISM project: Infrastructure and algorithms for parallel eigensolvers
[DE94-005125] p 2973 N94-27717

DECONDITIONING

Workshop on Countering Space Adaptation with Exercise: Current Issues
[NASA-CP-3252] p 2934 N94-28361

DECOUPLING

Dimensional crossover from non-renormalizability to renormalizability
[DE93-613052] p 3006 N94-26193

DEEP SPACE

High performance flight computer developed for deep space applications p 2949 N94-26718

Space Station technology testbed: 2010 deep space transport p 2687 N94-27368

DEFECTS

General Motors Corporation and Pacific Northwest Laboratory staff exchange: Inspection of case hardened steels and metal-matrix composites
[DE94-003470] p 2706 N94-25982

Modeling defect production in high energy collision cascades
[DE94-003810] p 3017 N94-26049

Oxygen reduction at a YSZ interface with cathode materials La(1-x)(Ca or Sr)(x)MnO3(1-x)CaMnO3
[DE94-002954] p 3054 N94-26147

Study of the homogeneity of InP wafers
[AD-A273658] p 3055 N94-26194

Design and life-time of polymer matrix composite structures: Summary
[VTT-TIED-1415] p 2707 N94-26260

Influence of point defects on grain boundary diffusion in oxides
[DE94-003164] p 3060 N94-26782

Investigation of ACC/CCI tunnel diodes
[AD-A274549] p 2785 N94-26845

Indium donor complexes with cation vacancies in CdTe and ZnSe
[DE94-002731] p 3063 N94-26958

Squeeze casting: A literature review
[PB94-124575] p 2741 N94-27326

Characterization of semi-insulating gallium arsenide
[AD-A273781] p 3068 N94-27704

DEFENSE COMMUNICATIONS SYSTEM (DCS)

Ir-fibers in a laser threat warning system and robot shot warning system
[PB94-124476] p 3038 N94-27209

DEFENSE INDUSTRY

Future of aerospace
[PB94-120185] p 2669 N94-26906

DEFENSE PROGRAM

An assessment of testing requirement impacts on nuclear thermal propulsion ground test facility design
[DE94-002933] p 2702 N94-26560

Report of the defense science board task force on aircraft assessment
[AD-A274531] p 2669 N94-26835

Satellite navigation system GPS: A review of principles and performance and developments in general
[PB94-124534] p 2665 N94-27210

Defense force management: Challenges facing DOD as it continues to downsize its civilian work force. Report to the Chairman, Subcommittee on Federal Services, Post Office, and Civil Service, Committee on Governmental Affairs, US Senate
[GAO/NSIAD-93-123] p 3095 N94-28177

DEFLECTORS

Micro-electron deflector
[AD-D016055] p 2787 N94-27672

DEFORESTATION

Assessment of tropical forests using satellite data
[SILVA-CARELICA-21] p 2850 N94-27182

Global tropical forest cover assessments using satellite imagery p 2850 N94-27183

Mapping closed tropical forest cover in West Africa using NOAA/AVHRR-LAC data p 2850 N94-27184

Training on assessment and mapping of deforestation: WFW conference, Brazil
[INPE-5482-PRE/1781] p 2850 N94-27384

Role of remote sensing in energy, water, and carbon cycle studies over the Amazon
[INPE-5486-PRE/1786] p 2852 N94-27957

Mission to Planet Earth: A program to understand global environmental change
[NASA-PAM-556] p 2869 N94-27958

DEFORMATION

Study on phase transformation due to deformation in ferromagnetic fields at cryogenic condition
p 2724 N94-25556

Study on elucidation of damage generation process by electron beam lithography p 2729 N94-25581

Radiation hardening effects on localized deformation and stress corrosion cracking of stainless steels
[DE94-004308] p 2731 N94-25804

Influence of grain structure and solute composition on the work hardening behavior of aluminium at cryogenic temperatures
[DE94-003415] p 2733 N94-26087

Users manual for CATNIP: A Computer Analysis Tool for Normal Impact Penetration
[DE94-003671] p 2962 N94-26371

Deformation, constitutive behavior, and damage of advanced structural materials under multiaxial loading
[AD-A274165] p 2709 N94-27142

Crustal deformation measurements in the vicinity of Vandenberg Air Force Base
[AD-A274166] p 2881 N94-27143

Effect of precipitate structure on hot deformation of Al-Mg-Mn alloys
[DE94-004596] p 2741 N94-27622

The deformation of copper-tungsten composites
[ISBN-0-315-84939-8] p 2712 N94-27688

The estimation of pre-stress by deformation rate analysis and suggestion of a mechanism from the elast-plastical theory p 2871 N94-28156

Studies in ice mechanics
[PB94-133055] p 2900 N94-28393

DEGASSING

Experimental study of lunar and SNC (Mars) magmas
[NASA-CR-195274] p 3107 N94-27850

DEGRADATION

Failure mechanisms of high temperature semiconductor lasers
[AD-A273833] p 2815 N94-25616

Accelerated screening methods for determining chemical and thermal stability of refrigerant-lubricant mixtures. Part 2: Experimental comparison and verification of methods
[DE94-003664] p 2749 N94-26007

DEGREES OF FREEDOM

Optimal control design advantages utilizing two-degree-of-freedom controllers
[AD-A273839] p 2984 N94-25743

Parameter estimation of linear systems from frequency response measurements (computer program)
[ESDU-93016] p 2976 N94-28137

DELAMINATING

The effects of embedded internal delaminations on composite laminate compression strength; an experimental review
[NASA-TM-108440] p 2707 N94-26127

Interface phenomena in metal-ceramic composites
[AD-A274167] p 2709 N94-27125

DELTA WINGS

Supercruiser Arrow HS-8 p 2671 N94-25711

Computation of transonic viscous flow past the NTF 65-degree Delta Wing p 2659 N94-27930

Normal force of low aspect ratio cropped-delta wings at pre-stall angles of attack and subsonic speeds
[ESDU-93034] p 2648 N94-27955

Control jets in interaction with hypersonic rarefied flow
p 2698 N94-28020

Theoretical and experimental investigation of a delta wing with turbulent leading-edge jets
p 2659 N94-28029

DEMAND (ECONOMICS)

Methodology development of forecasting inter-regional air transport demand in China
[DLR-FB-93-24] p 2660 N94-27746

Air traffic in recession p 2662 N94-28240

DEMAND ASSIGNMENT MULTIPLE ACCESS

Analysis of a multiaccess/switching technique for multibeam satellites in a prioritized ISDN environment
[ISBN-0-315-84632-1] p 2776 N94-27345

DEMODULATION

Analysis of linear combining and its application to frequency-hopped signals
[ISBN-0-315-84007-2] p 2770 N94-26624

Development of digital resampling and pulse compression computer software
[DREP-92-32] p 2969 N94-27318

DEMODULATORS

A fast Fourier transform radix-2 complex butterfly with built-in self-test
[ISBN-0-315-84139-7] p 2982 N94-27649

DEMOGRAPHY

Monograph of the Aviation Epidemiology Data Register for CY 1992
[AD-A274400] p 2911 N94-27130

DENSE PLASMAS

A study of the global properties of hadronic matter at large densities
[ISBN-0-315-57234-5] p 3025 N94-27260

DENSITY (MASS/VOLUME)

Advances in preparing and characterizing low density pan-carbon microcellular foam
[DE94-002278] p 2748 N94-25932

Orthobaric densities and molar volumes of liquids: Aliphatic and cyclic ketones
[ESDU-93010] p 2720 N94-28060

Solubility, viscosity, and density of refrigerant/lubricant mixtures
[DE94-004237] p 2721 N94-28069

DENSITY (NUMBER/VOLUME)

Quantum statistical inference for density estimation
[DE94-002625] p 3073 N94-26805

DENSITY DISTRIBUTION

Neutron reflection interferometry
[DE94-601876] p 2714 N94-26170

Gaseous hydrogen/oxygen injector performance characterization
[NASA-CR-194464] p 2701 N94-26208

On the application of Allan variance method for Ring Laser Gyro performance characterization
[DE94-003880] p 2810 N94-26525

DENSITY MEASUREMENT

An optimal constrained linear inverse method for magnetic source imaging
[DE94-004014] p 2957 N94-25663

Upper atmosphere neutral and plasma density modeling
[AD-A274768] p 2879 N94-26569

Laser blow-off lithium beam probing with high temporal resolution for edge plasma diagnostics
[DE94-701176] p 2820 N94-27701

DEOXYRIBONUCLEIC ACID

Molecular biological studies on the human radioresistance and drug resistance
[DE93-632682] p 2910 N94-26549

Cloning of rat RXR alpha cDNA and the expression of its mRNA in regenerating liver and primary cultured hepatocytes p 2905 N94-27479

Construction and test of experiment hardware for a space experiment on Spacelab mission IML-2
[DLR-FB-93-23] p 2903 N94-27743

DEPOSITION

Characterization of the energy deposition produced by the primary electron beam on the EXCEDE 3 program. Appendix B and C
[AD-A273878] p 3012 N94-25726

Mechanistic studies of opto-electronic materials and syntheses using multiple laser and surface diagnostics
[AD-A274528] p 3036 N94-26834

Equivalent performance in different helical resonator plasma polymerization coater platforms
[DE94-001517] p 2753 N94-26933

Synthesis of diamond film assisted by an arcjet plasma source, part 2
[INPE-5527-PRP/178-PT-2] p 3066 N94-27329

The ZnO thin films with C-axis orientation prepared on the room temperature substrate by the ECR multipolar plasma sputtering method
[DE94-605039] p 2758 N94-27857

DEPTH
Users manual for CATNIP: A Computer Analysis Tool for Normal Impact Penetration
[DE94-003671] p 2962 N94-26371

DEPTH MEASUREMENT
Compilation of corrections for postprocessing of laser bathymetry data
[PB94-123668] p 2900 N94-27156
Scanview: A grafical program for analysis of laserbathymetry data
[PB94-124443] p 2900 N94-27208

DESCENT
Examples of flight path optimisation using a multivariate gradient-search method
[ESDU-93021] p 2670 N94-28092
Using formal specification in the Guidance and Control Software (GCS) experiment. Formal design and verification technology for life critical systems
[NASA-CR-194884] p 2956 N94-28267

DESCRIPTIONS
DALIA: A language for the description and analysis of digital systems p 2954 N94-27192

DESERTIFICATION
Meeting of the Eighth Session of the Scientific Advisory Committee of the World Climate Impact Assessment and Response Strategies Programme
[DE93-633954] p 2866 N94-26163

DESIGN ANALYSIS
Aircraft maneuvers for the evaluation of flying qualities and agility. Volume 1: Maneuver development process and initial maneuver set
[AD-A273913] p 2666 N94-25590
Systematic Propulsion Optimization Tools (SPOT)
p 2976 N94-25666
Pressurized Lunar Rover (PLR) p 2833 N94-25704
System design analysis of a lightweight laser satellite terminal
[AD-A274033] p 2690 N94-25769
Design analysis of a combined optical/LADAR deep-space surveillance satellite
[AD-A274040] p 2694 N94-25832
Aircraft maneuvers for the evaluation of flying qualities and agility. Volume 3: Simulation data
[AD-A273814] p 2667 N94-25961
Parametric analysis of the space power plants on the base of criterion of specific mass in generalized design variants
[DE93-634153] p 2701 N94-26166
Response surface design: comparisons
[AD-A274690] p 2838 N94-26448
Handbook of photovoltaic power generating design for introduction
[DE94-725199] p 2858 N94-26913
Orbital transfer rocket engine technology 7.5K-LB thrust rocket engine preliminary design
[NASA-CR-190754] p 2703 N94-27213
Design and experimental performance of a two stage partial admission turbine. Task B.1/B.4
[NASA-CR-179548] p 2824 N94-27228
Rocket engine numerical simulation
p 2688 N94-27375
Planetary Instrument Definition and Development Program (PIDDP). Instrument for future planetary flight missions: A visible-infrared imaging spectrometer for planetary missions
[NASA-CR-195254] p 3106 N94-27409
Investigation of aerodynamic design issues with regions of separated flow p 2658 N94-27902
Object-oriented development methods
p 2975 N94-27938
The deterministic power-spectral-density-method for nonlinear systems
[AD-B179687] p 3001 N94-28353

DESORPTION
Evaluation of a Canadian minitube air sampling system
[FOA-C-40307-4.6] p 2866 N94-25809
The reactivity of lithium toward non-aqueous solvents of relevance to energy storage applications as studied by surface analytical techniques
[DE94-003483] p 2856 N94-26464
Adsorption and desorption studies of cesium on sapphire surfaces
[DE94-003798] p 3070 N94-28067

DETECTION
FNAS lightning detection
[NASA-CR-193927] p 2893 N94-26134
Summaries of BFRL fire research in-house projects and grants, 1993
[PB94-121050] p 2763 N94-26756
Finding the missing pieces of the standard model
[ISBN-0-315-57174-8] p 3024 N94-27259
Mapping of seawater intrusion into the coastal aquifer of Israel (the seawater-freshwater interface) by TDEM (Time Domain Electromagnetic) method
[ITN-94-85238] p 2850 N94-27331
Trace organic chemical detection using an ultraviolet excitation molecular beam fluorometer
[DE94-002649] p 2704 N94-27708
Effects of historical and predictive information on ability of transport pilot to predict an alert
[NASA-TM-4547] p 2673 N94-27864
Effects of expected-value information and display format on recognition of aircraft subsystem abnormalities
[NASA-TP-3395] p 2673 N94-27882
Fiber optic sensors for corrosion detection
p 3040 N94-27923

DETONATION
Numerical simulation of the reignition of detonation by reflected shocks
[AD-A274755] p 2795 N94-27252
Propellants and explosives in ballistic missiles
[UCRL-LR-113578] p 2760 N94-28222

DETONATION WAVES
Shock wave interaction with L-shaped structures
[AD-A273774] p 2790 N94-25858
Numerical simulation of the reignition of detonation by reflected shocks
[AD-A274755] p 2795 N94-27252
Mach reflection of spherical detonation waves
[DE93-016604] p 2797 N94-27705
Consequences of impacts of small asteroids and comets with Earth p 2889 N94-28301

DEUTERIDES
Lighter alkali hydride and deuteride 1: Electronic properties of pure solids
[DE93-616188] p 3051 N94-25914
The reactivity of lithium toward non-aqueous solvents of relevance to energy storage applications as studied by surface analytical techniques
[DE94-003483] p 2856 N94-26464

DEUTERIUM
High-speed repetitive pellet injector for plasma fueling of magnetic confinement fusion devices
[DE94-002792] p 3042 N94-26140
New conditioning procedure derived from operating experience with the Common Long-Pulse Ion Source
[DE94-002891] p 3045 N94-26865
High gas-efficiency hydrogen negative ion sources
[PB93-232163] p 3025 N94-27348
Influence of lattice damage on retention and transport of deuterium in beta silicon carbide
[DE94-005206] p 3068 N94-27693
Ion-driven permeation of deuterium in metals
[DE94-701104] p 2744 N94-27876

DIAGNOSIS
The effect of the time restrictions on information search and information integration in a dynamic task environment
[AD-A273759] p 3095 N94-25723
Gordon Research Conference on the Physics and Chemistry of Laser Diagnostics in Combustion
[AD-A274609] p 2716 N94-26893

DIALYSIS
Effect of sera from patients treated with long-term hemodialysis on mRNA's for collagenase, stromelysin, and tissue inhibitor of metalloprotease in cultured human synovial cells p 2920 N94-27481

DIAMAGNETISM
Technical report of ISSP. Ser. A, no. 2678: Magnetic properties of carbon nanotubes
[JTN-94-80564] p 3064 N94-27174

DIAMOND FILMS
Buckyball microwave plasmas: Fragmentation and diamond-film growth
[DE94-003209] p 3053 N94-26031
Growth, characterization and device development in monocrystalline diamond films
[AD-A274245] p 3060 N94-26839
Fabrication and characterization of nano-crystalline diamond films
[DE94-002202] p 3062 N94-26934
Interface properties of wide bandgap semiconductor structures
[AD-A274356] p 3063 N94-27058
Synthesis of diamond film assisted by an arcjet plasma source, part 2
[INPE-5527-PRP/178-PT-2] p 3066 N94-27329

DIAMONDS
Molecular beam mass spectrometry studies of the chemical vapor deposition of diamond
[DE94-003802] p 3049 N94-25601
Collaborative research on ion implantation of ceramics
[DE93-019177] p 2749 N94-26080
Ion implantation of diamond: Damage, doping, and lift-off
[DE94-001133] p 3054 N94-26137
Regrowth zones in laser annealed radiation damaged diamond
[DE94-600821] p 3056 N94-26364
Fabrication technology
[DE94-003017] p 2763 N94-26778
He(+) and H(+) microbeam damage, swelling and annealing in diamonds
[DE94-601912] p 3063 N94-26987
Technical report of ISSP. Ser. A, no. 2675: High-field cyclotron resonance and valence-band structure in semiconducting diamond
[JTN-94-80561] p 3065 N94-27245

DIAPHRAGMS (MECHANICS)
Fluid dynamic linear accelerometer
[AD-D016042] p 2678 N94-27112
Development of liquid membrane separation processes p 2717 N94-27386
Glass cylindrical filter for electrolysis cell
p 2718 N94-27391

DICTIONARIES
Correspondence dictionary from free English term to INIS descriptors
[DE94-701173] p 3100 N94-27700

DIELECTRIC POLARIZATION
Dielectric polarizability of sphere with arbitrary anisotropy
[PB94-133113] p 2779 N94-28397

DIELECTRIC PROPERTIES
NNN-Ising model simulation of nanodomain textures in relaxor-type lead scandium tantalate
[DE94-601884] p 2748 N94-25844
Refractive and dielectric properties of helium, argon and nitrogen gases
[PB94-123783] p 3008 N94-26851
Calculation of the electromagnetic critical state response of high T(sub c) superconductor tape
[DE94-002894] p 3061 N94-26868

DIELECTRICS
Optimization of experimental conditions in IR reflectance determination of BPSG properties
[DE94-002742] p 2713 N94-25978
Joint services electronics program
[AD-A274643] p 2785 N94-27027
Ferroelectric fluoride memory FET development
[AD-A274341] p 2785 N94-27057
Effective conductivity of wire mesh reflectors for space deployable antenna systems
[NASA-CR-191605] p 2788 N94-27770
Electromagnetic modeling of bi-isotropic media
[PB94-132909] p 2778 N94-28382

DIESEL ENGINES
The emission characteristics of a high speed diesel engine p 2764 N94-27980
Development of advanced high temperature in-cylinder components and tribological systems for low heat rejection diesel engines, phase 1
[NASA-CR-187158] p 2827 N94-27984

DIESEL FUELS
Analytical method for estimation of the total amount of aromatic and poly aromatic compounds in diesel fuel
[PB94-123692] p 2759 N94-25907

DIFFERENTIAL AMPLIFIERS
Object imaging accomplished with an integrated circuit robotic tactile sensor incorporating a piezoelectric polyvinylidene fluoride thin film
[AD-A274038] p 2780 N94-25845

DIFFERENTIAL CALCULUS
Towards a theory of growing surfaces: Mapping two-dimensional Laplacian growth onto Hamiltonian dynamics and statistics
[DE94-002636] p 2991 N94-26079
Quantum subgroups and quantum co-set spaces and differential calculi on them
[DE94-602520] p 3073 N94-26876
A superprocess with a disappearing self-interaction
[AD-A274647] p 3009 N94-27108

DIFFERENTIAL EQUATIONS
Phase portraits of quadratic systems with finite multiplicity three and one critical point of infinity
[REPT-93-41] p 2991 N94-26215
On the error committed by stopping the Newton iteration in implicit Runge-Kutta methods
[TW-93-02] p 2992 N94-26229
On the phi(sub 0)-stability of perturbed nonlinear differential systems
[DE93-634304] p 2993 N94-26441
Cone-valued Lyapunov functions and the stability of stochastic differential equations
[DE94-601504] p 2994 N94-26458
On the (Phi)(sub 0)-stability of functional differential equations
[DE94-601507] p 3006 N94-26460
On a spline-approximation method for solving ordinary differential equations
[DE93-634290] p 2994 N94-26471

Kinetic equation identification from measurement of a particular solution
[DE93-634585] p 2995 N94-26768

Nonlinear hysteresis in an endochronic solid
[AD-A274594] p 2880 N94-26855

Poisson-lie group of pseudodifferential symbols
[PB94-124393] p 2997 N94-26996

A superprocess with a disappearing self-interaction
[AD-A274647] p 3009 N94-27108

White noise theory of robust nonlinear filtering with correlated state and observation noises
[PB94-126661] p 3004 N94-27211

Finite time differential equations and their application to control systems
[ISBN-0-315-85158-9] p 2988 N94-27277

Fractional calculus, gegenbauer transformations and integral equations
[PB93-237683] p 2999 N94-27349

Parallel implicit unstructured grid Euler solvers
[NASA-CR-191594] p 2999 N94-27434

Numerical experiment on finite element method for matching data
[DE94-701208] p 3000 N94-27731

DIFFERENTIAL GEOMETRY

Enumeration of n-fold tangent hyperplanes to a surface
[DE94-601544] p 2993 N94-26412

Quantum Hamiltonian differential geometry: How does quantization affect space?
[DE93-634306] p 2993 N94-26442

Quantum group and Manin plane related to a colored braid group representation
[DE94-601509] p 3072 N94-26461

Hotine's (omega, phi, nu) coordinate system
[PL-TR-93-2174] p 3001 N94-28216

DIFFERENTIAL PRESSURE

Fluid dynamic linear accelerometer
[AD-D016042] p 2678 N94-27112

DIFFRACTION

A study of two dimensional tapered periodic edge treatments to reduce wideband edge diffraction
[AD-A274054] p 2766 N94-25824

A new materials data compilation can help in actinide phase-diagram research
[DE94-000797] p 3058 N94-26514

Joint services electronics program
[AD-A274643] p 2785 N94-27027

Wave propagation in the shallow regions of the earth's crust and the borehole vicinity
[ITN-94-85237] p 2882 N94-27330

Inductive differentiation of nerve cells in mouse embryonic ectoderm at early primitive streak stage by retinoic acid p 2905 N94-27488

Optical parametric oscillator modeling with diffraction, depletion, and double refraction
[DE94-001504] p 3040 N94-27999

DIFFRACTION PATHS

Developments in the application of the geometrical theory of diffraction and computer graphics to aircraft inter-antenna coupling analysis
[ISBN-0-315-84643-7] p 2776 N94-27308

DIFFRACTION PATTERNS

Debye-Waller factors of the light actinide metals
[DE94-000685] p 2733 N94-26069

Advanced technology development multi-color holography
[NASA-CR-193931] p 2812 N94-27229

DIFFUSE RADIATION

Illumination in diverse codimensions
[NASA-CR-191596] p 2971 N94-27572

DIFFUSION

A Shuttle mechanism for molten-electrolyte lithium batteries
[DE94-002914] p 2781 N94-26144

Diffusion of substitutional elements in Ti in its hcp phase
[DE93-633762] p 2733 N94-26160

Longitudinal diffusion of a proton bunch under external noise
[DE93-634022] p 3032 N94-26165

Numerical solution of singularity-perturbed two-point boundary-value problems
[DE94-601542] p 2993 N94-26410

Simplified high-efficiency silicon cell processing
[DE94-002683] p 2857 N94-26617

A robust upwind discretization method for advection, diffusion and source terms
[CWI-NM-R9308] p 2868 N94-26774

Influence of point defects on grain boundary diffusion in oxides
[DE94-003164] p 3060 N94-26782

A superprocess with a disappearing self-interaction
[AD-A274647] p 3009 N94-27108

Ion-driven permeation of deuterium in metals
[DE94-701104] p 2744 N94-27876

DIFFUSION COEFFICIENT

Study on alloy films for hydrogen separation
p 2726 N94-25565

Study on substance diffusion in thin films with controlled structures p 2727 N94-25570

Longitudinal diffusion of a proton bunch under external noise
[DE93-634022] p 3032 N94-26165

Influence of point defects on grain boundary diffusion in oxides
[DE94-003164] p 3060 N94-26782

DIFFUSION PUMPS

A large high vacuum, high pumping speed space simulation chamber for electric propulsion
[NASA-TM-106453] p 2690 N94-26142

DIFFUSION THEORY

Arbitrary-order numerical schemes for model parabolic equations
[CRANFIELD-AERO-9210] p 3005 N94-25781

DIFFUSION WELDING

Method of bonding molybdenum to steel
[AD-D016079] p 2747 N94-28187

Joining of fibre reinforced metal matrix composite materials
[PB94-132453] p 2712 N94-28376

DIFFUSIVITY

Longitudinal diffusion of a proton bunch under external noise
[DE93-634022] p 3032 N94-26165

A transient symmetrical method for the measurement of temperature dependent thermal diffusivity
[VTT-TIED-1452] p 3008 N94-26256

Numerical solution of singularity-perturbed two-point boundary-value problems
[DE94-601542] p 2993 N94-26410

Calculation of single and multiple jets in cross-flow with and without impingement using Reynolds-stress-transport closure p 2803 N94-28024

DIGITAL COMPUTERS

Developing a graphical user interface to support a real-time digital signal processing system
[AD-A274032] p 2960 N94-26018

DIGITAL DATA

PDEF: A standard file format for data interchange
[AD-A274694] p 3098 N94-26451

Conifer tree influence on Digital Terrain Elevation Data (DTED): A case study at Dulles International Airport
[AD-A274213] p 2849 N94-27069

DIGITAL ELECTRONICS

Bundle Intensity and Beamgate Length recorder (BIBL)
[DIGEL-1993-7] p 3031 N94-25619

Digital input module
[DIGEL-1993-6] p 2779 N94-25620

Test methods and custom hardware for functional testing of a high speed GaAs DRAM
[AD-A274859] p 2781 N94-26175

Processing, fabrication, and demonstration of HTS integrated microwave circuits, appendix A
[AD-A274600] p 2785 N94-26890

DALIA: A language for the description and analysis of digital systems p 2954 N94-27192

Coherence and satisfiability of waveform timing specifications
[ISBN-0-315-57769-X] p 3009 N94-27268

DIGITAL FILTERS

Detection of transient vector-fields in additive noise
[FFI-93/7028] p 2768 N94-26232

Kalman filtering of narrowband interference from direct sequence spread spectrum communications systems
[ISBN-0-315-84011-0] p 2784 N94-26627

An integrated delta-sigma based IIR filter
[ISBN-0-315-83593-1] p 2784 N94-26631

Digital filter design for sensor simulation: Application to the Brazilian remote sensing satellite
[INPE-5523-RPQ/665] p 2849 N94-26827

Validation tests of TOPSIM 4
[ESA-STM-249] p 2972 N94-27582

DIGITAL SIMULATION

Digital filter design for sensor simulation: Application to the Brazilian remote sensing satellite
[INPE-5523-RPQ/665] p 2849 N94-26827

DIGITAL SYSTEMS

The question of standards for digital interactive television
[AD-A273872] p 2765 N94-25725

Digital control and data acquisition for high-value GTA welding
[DE94-000885] p 2821 N94-25980

Meteor Burst Communications (MBC) throughput improvement tests
[AD-A273941] p 2767 N94-25990

Digital systems validation book plan. Volume 3: Handbook
[AD-A274099] p 2672 N94-26028

Optimization of Vector Product Format (VPF) data for map background display in army tactical systems
[AD-A274687] p 2848 N94-26446

A current evaluation of the digital beamforming testbed at Rome Laboratory
[AD-A274311] p 3032 N94-26881

DALIA: A language for the description and analysis of digital systems p 2954 N94-27192

Pulse control method and its characteristics
[DE94-701187] p 2989 N94-27809

A simulator investigation of helicopter flight control system mode transitions
[UTIAS-348] p 2682 N94-27879

DIGITAL TECHNIQUES

A current evaluation of the digital beamforming testbed at Rome Laboratory
[AD-A274311] p 3032 N94-26881

Pulse control method and its characteristics
[DE94-701187] p 2989 N94-27809

DIGITAL TELEVISION

The question of standards for digital interactive television
[AD-A273872] p 2765 N94-25725

DIGITAL TO ANALOG CONVERTERS

Fast generator of program waveforms signals
[DE93-634230] p 2948 N94-26381

Inverted pendulum control apparatus using transputers
[DE94-701224] p 2973 N94-27732

DIMENSIONAL MEASUREMENT

Automated in-situ inspection systems for underground storage tanks
[AD-A274644] p 2764 N94-27144

DIMENSIONAL STABILITY

A materials compatibility study in FM-1, a liquid component of a paste extrudable explosive
[DE94-001166] p 2759 N94-26198

DIMERS

A Shuttle mechanism for molten-electrolyte lithium batteries
[DE94-002914] p 2781 N94-26144

DIODES

Investigation of plasma etch induced damage in compound semiconductor devices
[DE94-002849] p 3052 N94-25989

Diode-laser-pumped, gas-cell atomic clocks
[AD-A274812] p 3008 N94-26484

DIOPHANTINE EQUATION

Symmetric and asymmetric diophantine approximation by continued fractions
[PB94-126455] p 2998 N94-27030

DIPOLE ANTENNAS

Receiving antennas for electromagnetic pulses and transients
[ISBN-0-315-62312-8] p 2777 N94-27871

DIPOLE MOMENTS

Polarizability matrix of layered chiral sphere
[PB94-132834] p 2778 N94-28355

DIRAC EQUATION

The Dirac equation in Kerr spacetime, spheroidal coordinates and the M.I.T. bag model of hadrons
[DE94-601566] p 3006 N94-25886

On Poisson brackets and symplectic structures for the classical and quantum Zitterbewegung
[DE93-634305] p 2992 N94-26267

On the relativistic invariant representation of arbitrary bilinear combinations of Dirac spinors
[DE93-634343] p 3019 N94-26456

DIRECT CURRENT

Review of tokamak experiments on direct electron heating and current drive with fast waves
[DE94-004185] p 3041 N94-25801

Preparation and characterization of high temperature superconductor film surfaces
[AD-A274293] p 3059 N94-26681

A direct current rectification scheme for microwave space power conversion using traveling wave electron acceleration p 2687 N94-27371

Image theory for DC problems involving a conducting half space bounded by the general anisotropic impedance surface
[PB94-132917] p 2779 N94-28390

DIRECTION FINDING

Prewhitening of colored noise fields for detection of threshold sources
[AD-A274346] p 3010 N94-26923

DIRECTIONAL CONTROL

Pneumatic management of blunted-forebody flow asymmetry for high-angle-of-attack directional control
p 2679 N94-28028

DIRECTIONAL COUPLERS

An electronic switch based on quantum interference
[ISBN-0-315-84609-7] p 2787 N94-27650

DIRECTIONAL SOLIDIFICATION (CRYSTALS)

Study on production of materials with one direction solidification texture p 2727 N94-25572

Nonlinear dynamics and pattern selection at the crystal-melt interface
[DE94-003112] p 3060 N94-26780

DIRICHLET PROBLEM
Numerical solution of singularity-perturbed two-point boundary-value problems
[DE94-601542] p 2993 N94-26410

DISARMAMENT
Contributions to CD Space Committee 1992
[PB94-124401] p 3101 N94-27218

DISCOLORATION
A materials compatibility study in FM-1, a liquid component of a paste extrudable explosive
[DE94-001166] p 2759 N94-26198

DISCONTINUITY
Iron: What is melt?
[DE94-003373] p 2735 N94-26322

DISCRETE FUNCTIONS
Some aspects of nonlinear discrete-time descriptor systems in economics
[PB94-126653] p 3101 N94-26918

DISCRIMINATORS
The continuum spectral characteristics of gamma ray bursts observed by BATSE p 3114 N94-26686

DISEASES
NCVS, volume 5
[AD-A274975] p 2902 N94-27165
Compaction-like blastomere aggregation caused by 1-oleoyl-2-acetylglycerol in mouse embryos: An electron microscopic observation p 2905 N94-27487
Anorectal malformations induced by intraperitoneal injection of all-trans retinoic acid in suncus
p 2905 N94-27489
Enhancement of skin sympathetic nerve activity in amyotrophic lateral sclerosis p 2930 N94-27532

DISK OPERATING SYSTEM (DOS)
Users guide for GRIKURV: A code for drawing graphs
[PB94-123593] p 2968 N94-27154

DISKS (SHAPES)
Guidelines for unlubricated sliding wear tests. Part 2: Procedures for pin-on-disc testing
[PB94-123270] p 2825 N94-27324

DISORIENTATION
Standardization of aircraft control and performance symbology on the USAF head-up display
[AD-A274283] p 2673 N94-26989

DISPERSING
Process modelling of aluminium alloys. Modelling of the quench sensitivity of alloy AA6082
[PB94-124567] p 2741 N94-27325

DISPERSION
Cad of GeO2-SiO2 double-layer core dispersion-shifted single-mode fibre
[DE93-634325] p 3035 N94-26383

DISPLACEMENT
Structure and properties of intermetallic composites synthesized in situ using solid state displacement reactions
[DE94-004312] p 2705 N94-25805

DISPLACEMENT MEASUREMENT
Experimental measurement of local displacement and chemical pair correlations in crystalline solid solutions
[DE94-001124] p 3065 N94-27251

DISPLAY DEVICES
Image quality and the display modulation transfer function: Experimental findings
[AD-A274061] p 2679 N94-25773
IRMA: A program for three-dimensional color display of data
[AD-A273811] p 2959 N94-25879
The National Center for Advanced Information Components Manufacturing: Program update
[DE94-002647] p 2960 N94-26118
Color head down display program
[AD-A274807] p 2672 N94-26340
A graphical workstation based part-task flight simulator for preliminary rapid evaluation of advanced displays
p 2641 N94-27286
VENI, video, VICI: The merging of computer and video technologies p 2686 N94-27362
An artificial reality environment for remote factory control and monitoring p 2687 N94-27369
Multiple exposure CCD detector for high-speed laser pump, x ray probe Laue scattering
[DE94-004618] p 2820 N94-27781

DISSIPATION
A mechanism for resistive dissipation in Ag sheathed Bi2Sr2CaCu2O8 and Bi2Sr2Ca2Cu3O10
[DE94-003009] p 3060 N94-26771

DISSOLVING
Dissolution of secondary phases during extrusion
[PB94-124583] p 2732 N94-25908

DISTANCE
The effect of body orientation on the perception of vertical and horizontal distance in an outdoor setting
p 2915 N94-27461

DISTORTION
Implications for high speed research: The relationship between sonic boom signature distortion and atmospheric turbulence p 2650 N94-28190

DISTRIBUTED PARAMETER SYSTEMS
Module interconnection frameworks for a real-time spreadsheet
[AD-A273853] p 2956 N94-25588
Operator theoretic methods in the control of distributed and nonlinear systems
[AD-A274160] p 2988 N94-27139

DISTRIBUTED PROCESSING
Module interconnection frameworks for a real-time spreadsheet
[AD-A273853] p 2956 N94-25588
The use of ASN.1 and XDR for data representation in real-time distributed systems
[AD-A273769] p 2959 N94-25855
Weapon system sensor integration for a DIS-compatible virtual cockpit
[AD-A274088] p 2672 N94-26021
Coordinated scheduling for dynamic real-time systems
[NASA-CR-195231] p 3093 N94-26206
NPSNET-4: A real-time, 3D distributed interactive virtual world
[AD-A274942] p 2961 N94-26298
Parallel grid generation algorithm for distributed memory computers
[NASA-TP-3429] p 2963 N94-26466
Usefulness of compile-time restructuring of LGDF programs in throughput-critical applications
[AD-A274915] p 2963 N94-26530
Computational strategies for three-dimensional flow simulations on distributed computer systems
[NASA-CR-195249] p 2793 N94-26595
Fault-tolerant scheduling in distributed critical real-time systems p 2952 N94-26735
Specification performance optimization and executive generation for onboard multiprocessor real time application with SynDEx p 2954 N94-26745
Parallel matrix transpose algorithms on distributed memory concurrent computers
[DE94-002424] p 2964 N94-26764
Central dynamic share scheduling in distributed systems
[REPT-93-48] p 2966 N94-26966
Trace-based compositional proof theory for fault tolerant distributed systems
[PB94-126737] p 2966 N94-26971
Parallel computers for advanced information processing p 2955 N94-27193
Simulating fail-stop in asynchronous distributed systems
[NASA-CR-195698] p 2974 N94-27767
Multi-sensor data fusion in a distributed environment: Architectural solutions
[NLR-TP-92243-U] p 2989 N94-27800
Proceedings of Workshop on Distributed Computing and Network
[DE94-701165] p 2983 N94-27804
Review and analysis of dense linear system solver package for distributed memory machines
p 2978 N94-27916

DISTRIBUTION (PROPERTY)
Developmental expression of protein kinase C type 1 isozyme in suncus and rat cerebella
p 2905 N94-27484

DISTRIBUTION FUNCTIONS
Isotonic estimation and rates of convergence in Wicksell's problem
[REPT-93-39] p 3002 N94-26213
Aspects of goodness-of-fit
[AD-A274826] p 3003 N94-26495
Estimation and tests-of-fit for the three parameter Weibull distribution
[AD-A274827] p 3004 N94-26496
Delta f Algorithm
[DE94-003120] p 2963 N94-26521
Relativistic collision rate calculations for electron-air interactions
[DE94-004204] p 3020 N94-26527
Symmetric and asymmetric diophantine approximation by continued fractions
[PB94-126455] p 2998 N94-27030

DISTRIBUTORS
Optimising BMW four-cylinder two-valve engines
[PB94-125101] p 2824 N94-27254

DISULFIDES
Voltammetric studies of poly(carbon disulfide)
[DE94-001385] p 2717 N94-26951

DITHERS
Multiple model adaptive control of a large flexible space structure with purposeful dither for enhanced identifiability
[AD-A274132] p 2987 N94-27122

DIURETICS
Protective action of an amiloride derivative (amiloride, 5-(N, N-dimethyl) hydrochloride) against in isolated ischemia/reperfusion newborn rabbit hearts
p 2904 N94-27466

DIURNAL VARIATIONS
Upper atmosphere neutral and plasma density modeling
[AD-A274768] p 2879 N94-26569
Initial ultraviolet-B intensity data at Lawrence Livermore National Laboratory
[DE94-004279] p 2869 N94-27267
Changes in circadian variations of urine excretion in tail-suspended rats p 2911 N94-27443

DIVERGENCE
High energy parton-parton elastic scattering in QCD
[DE94-003432] p 3028 N94-27736

DIVERTERS
Evaluation of helium cooling for fusion divertors
[DE94-002680] p 3042 N94-25976
Proceedings of the Second EGS4 User's Meeting in Japan
[DE93-520383] p 3032 N94-26543
Fusion reactor systems studies
[DE94-003162] p 3046 N94-27686

DMSP SATELLITES
Investigation of ACC/CCI tunnel diodes
[AD-A274549] p 2785 N94-26845
Leadex environmental phenomena and effects observed by DMSP, NOAA, and ERS-1 satellites
[AD-A274596] p 2868 N94-26888
DMSP satellites as gamma ray burst detectors
[DE94-004977] p 3116 N94-27793
Modeling the DMSP and CRRES dosimeters using the path length distribution method
[RXR-93051] p 2698 N94-28200

DOCUMENT STORAGE
Electronic document distribution: Design of the anonymous FTP Langley Technical Report Server
[NASA-TM-4567] p 2971 N94-27573

DOCUMENTS
Full-text information services at the desktop
[DE94-003728] p 3096 N94-25813
Scientific and Technical Information (STI)....what's the status?
[DE94-003731] p 3097 N94-26348

DOMAINS
Polar and chemical domain structures of lead scandium tantalate (PST)
[DE94-600760] p 3056 N94-26363

DOMES (STRUCTURAL FORMS)
A laboratory test on construction of ice domes and their load-carrying capacity p 2884 N94-27966

DOPA
Effect of L-dopa on hemodynamic functions in humans p 2929 N94-27526

DOPED CRYSTALS
Electric-field dependence of electroreflectance and photocurrent spectra at visible wavelengths in MOVPE-grown InAlGaP multiple strained quantum-well structures
[DE94-004692] p 2780 N94-25664
Microscopic study of local structure and charge distribution in metallic La2CuO(4+delta)
[DE94-003801] p 3050 N94-25817
MBE grown 3 to 5 strain relaxed buffer layers and superlattices characterized by atomic force microscopy
[DE94-002931] p 3056 N94-26308
Calorimeter with WLS fibers and parallel to beam scintillators
[DE93-634188] p 2810 N94-26378
On the electron mobility in slightly compensated heavily doped gallium arsenide at low temperatures
[DE93-634712] p 3057 N94-26387
Research and development of alternative components at Argonne National Laboratory for Molten Carbonate Fuel Cells
[DE94-000014] p 2857 N94-26583
MSOFC development status
[DE94-003192] p 2858 N94-26792
Effect of impurity correlation on the density of states in slightly compensated heavily doped semiconductors
[DE94-602539] p 3061 N94-26879
Ion implantation and dynamic recovery of tin-doped indium oxide films
[DE94-001126] p 3062 N94-26932
Indium donor complexes with cation vacancies in CdTe and ZnSe
[DE94-002731] p 3063 N94-26958
Development of K(1-x)Na(x)TiOPO4 crystals for nonlinear applications
[AD-A274336] p 3063 N94-27055
Electron microscopy studies of undoped and phosphorus doped Si:H and Si,C:H films
[DE94-004738] p 3069 N94-27757

Thermally stable oxygen and nitrogen implant isolation of C-doped Al(0.35)Ga(0.65)As
[DE94-004799] p 3069 N94-27790

DOPPLER EFFECT
On the wave and corpuscular properties of microparticles
[DE93-634450] p 3020 N94-26509

DOPPLER RADAR
A modeling study of the mesocyclone
[AD-A274889] p 2893 N94-26168
Machine intelligent gust front algorithm
[AD-A273695] p 2680 N94-26196
Examination of micro- and macro-physical structures and processes in hailstorms with respect to their modification
[DLR-FB-93-25] p 2897 N94-27751

DOSIMETERS
Modeling the DMSP and CRRES dosimeters using the path length distribution method
[RXR-93051] p 2698 N94-28200
The PROTEL contamination code
[RXR-93071] p 3040 N94-28202
Develop and fabricate a radiation dose measurement system for satellites
[PL-TR-93-2161] p 2698 N94-28210
Develop and fabricate a radiation dose measurement system for satellites
[PL-TR-93-2099] p 2698 N94-28217

DOUGLAS AIRCRAFT
Experimental apparatus for optimization of flap position for a three-element airfoil model p 2682 N94-27912

DOWNTIME
Human factors in airway facilities maintenance: Development of a prototype outage assessment inventory
[DOT/FAA/AM-94/5] p 2941 N94-26136

DRAG
Experimental investigation of the interaction of a thrust reverser jet with an external subsonic flow
p 2801 N94-28011
Vortex generators for control of shock-induced separation. Part 1: Introduction and aerodynamics
[ESDU-93024-PT-1] p 2806 N94-28095
Examples of excrescence drag prediction for typical wing components of a subsonic transport aircraft at the cruise condition
[ESDU-93032] p 2649 N94-28144

DRAG COEFFICIENTS
A numerical study of high-speed missile configurations using a block-structured parallel algorithm
[AD-A273776] p 2979 N94-25860

DRAG MEASUREMENT
Calculation of viscous drag of two low angle of attack supercritical profiles
[FFA-TN-1984-22] p 2644 N94-26104

DRAG REDUCTION
Experimental investigation of advanced hub and pylon fairing configurations to reduce helicopter drag
[NASA-TM-4540] p 2668 N94-26604

DRAINAGE
The effect of elevation data representation on nocturnal drainage wind simulations
[DE94-003624] p 2892 N94-25936

DRIFT (INSTRUMENTATION)
Test and evaluation of the Litton (Canada) Canadian strapdown gyroscope (CSG-2) Performance Evaluation Unit (PEU)
[DREO-1010] p 2813 N94-27597

DROP SIZE
Cloud liquid water content measurement tests using dual-wavelength radar
[PB94-125960] p 2896 N94-26959

DROP TESTS
Status report for the development of the Antarctic penetrator: 1990-year program p 2885 N94-27973

DROP TOWERS
Condensation inside tubes: Computer program for pressure drop in straight tubes (horizontal and vertical with downflow)
[ESDU-93014] p 2806 N94-28064

DROPS (LIQUIDS)
An apparatus for measurement of ignition and burning characteristics of metallic particles
[AD-A274815] p 2716 N94-26487

DROUGHT
Meeting of the Eighth Session of the Scientific Advisory Committee of the World Climate Impact Assessment and Response Strategies Programme
[DE93-633954] p 2866 N94-26163

DRUGS
Molecular biological studies on the human radioresistance and drug resistance
[DE93-632682] p 2910 N94-26549
Bakteriella toxiner-morgondagens hot (bacterial toxins-the threat of tomorrow)
[PB94-124229] p 2902 N94-27045
Effects of perfusion of amiodarone on electrophysiological properties in single rabbit ventricular myocytes p 2906 N94-27503
Fast and slow onsets of Na channel blocking actions due to lidocaine and disopyramide using concentration-clamp method p 2907 N94-27504
Electrophysiological effects of MS-551, a new Class 3 antiarrhythmic agent, on isolated rabbit ventricular muscles p 2907 N94-27505
Comparative investigation of new Class 3 antiarrhythmic drugs, E-4031 and MS-551, on electrophysiological properties in isolated rabbit ventricular myocytes
p 2907 N94-27506
Effects of Class 1 antiarrhythmic drugs on the intraventricular conduction: Influence of fiber orientation
p 2907 N94-27507
Effects of Class 3 antiarrhythmic agents, E-4031 and MS-551 on ventricular repolarization in isolated rabbit hearts p 2907 N94-27508
Block of cardiac sodium channels by Ro 22-9194 (R), a new antiarrhythmic agent: Effects on the maximum upstroke velocity (Vmax) of single guinea pig ventricular myocytes p 2907 N94-27511
Electrophysiological effects of an antiarrhythmic drug, moricizine on isolated guinea pig ventricular muscles
p 2907 N94-27512

DUAL SPIN SPACECRAFT
An approximate solution for the spinup dynamics of near axisymmetric axial gyrostats using the method of multiple scales
[AD-A273723] p 2698 N94-26223

DUAL THRUST NOZZLES
Evaluation of moderate angle of attack roll of a dual engine, thrust vectoring aircraft using quantitative feedback theory
[AD-A274118] p 2667 N94-25905

DUCTED BODIES
Aerodynamic performance of novel ducted-tip wings
p 2654 N94-28331

DUCTED FANS
The design of a counter rotating ultra-high-bypass fan simulator for windtunnel investigation
[DLR-FB-93-20] p 2675 N94-27739

DUCTED FLOW
Dynamic response of a compressor research facility
[AD-A273836] p 2679 N94-25740

DUCTILITY
Study on performance evaluation of pressure vessel steel in corrosion environments with sulfide
p 2730 N94-25582
Numerical simulations of interfacial debonding in ductile-phase reinforced intermetallic matrix composites
[DE94-003639] p 2706 N94-25938
Influence of grain structure and solute composition on the work hardening behavior of aluminium at cryogenic temperatures
[DE94-003415] p 2733 N94-26087
Processing and mechanical properties of laminated metal composites of Al 6090-25 volume percent SiC(sub p) and Al 5182
[DE94-001070] p 2708 N94-26930
Current status of research and development on nickel and iron aluminides
[DE94-004247] p 2741 N94-27616
Formation and high mechanical strength of Al-based alloys containing a nanoscale icosahedral phase as a main constituent p 2746 N94-28171

DUST
Dust control for Enabler p 2943 N94-25680
CCD-Camera images of BEST-TWO and processing results
[AD-A274140] p 2811 N94-27134
Analytic approximation to randomly oriented spheroid extinction
[DREV-4712-93] p 3038 N94-27598
Reanalysis of Mariner 9 UV Spectrometer Data for Ozone, Cloud, and Dust Abundances, and Their Interaction Over Climate Timescales
[NASA-CR-195244] p 3107 N94-27885
Cooling the Martian atmosphere: The spectral overlap of the C02 15 micrometers band and dust
p 3107 N94-27886
Martian atmospheric radiation budget
p 3107 N94-27887
Mars ozone: Mariner 9 revisited p 3107 N94-27888
Why is the north polar cap on Mars different than the south polar cap? p 3107 N94-27889
How well was total ozone abundance inferred with Mariner 9? p 3108 N94-27891
In situ Mars ozone detector p 3108 N94-27892

DUST COLLECTORS
Dust control for Enabler p 2943 N94-25680

DUST STORMS
Cooling the Martian atmosphere: The spectral overlap of the C02 15 micrometers band and dust
p 3107 N94-27886

DYADICS
Eigenwaves in the general uniaxial bianisotropic medium with symmetric parameter dyadics
[PB94-132891] p 2778 N94-28381
Plane wave propagation in an anisotropic chiral medium with isotropic permittivity and permeability
[PB94-133097] p 2778 N94-28384
Analytic solution for the dyadic Green's function of a nonreciprocal uniaxial bianisotropic medium
[PB94-133162] p 2779 N94-28388
Image theory for DC problems involving a conducting half space bounded by the general anisotropic impedance surface
[PB94-132917] p 2779 N94-28390
Green dyadic and dipole fields for a medium with anisotropic chirality
[PB94-132933] p 2779 N94-28391

DYE LASERS
Broad band tunable dye laser development
[DE93-632978] p 2816 N94-26157
Physical characteristics of polymethylmethacrylate scintillator SOFG-120
[DE93-634184] p 2810 N94-26395

DYES
Langmuir-Blodgett film of amylose-esters and chiral azo-dyes (structure and second order nonlinear optical behaviour)
[ETN-94-95390] p 2747 N94-25749

DYNAMIC CHARACTERISTICS
Dynamic response of S-2 glass reinforced plastic structural armor
[AD-A273868] p 2747 N94-25596
Enhanced simulation software for rocket turbopump, turbulent, annular liquid seals
[NASA-CR-195239] p 2825 N94-27383
Study of the kinematic and dynamic characteristics of a wormgear transmission for helicopter applications
[NASA-CR-195287] p 2826 N94-27657
Wing design for a civil tiltrotor transport aircraft: A preliminary study p 2671 N94-27917
Landscape dynamics of northeastern forests
[NASA-CR-195272] p 2852 N94-28070

DYNAMIC CONTROL
Neural networks for dynamic flight control
[AD-A274089] p 2676 N94-25785
Implementation of integral manifold control on a two degree of freedom flexible joint manipulator: Theory and experiments
[ISBN-0-315-83572-9] p 2823 N94-26658
Dynamic control of kinematically redundant manipulators
[ISBN-0-315-84627-5] p 2825 N94-27344
Dynamics and robust control for uncertain flexible space systems
[INPE-5510-TAE/020] p 2696 N94-27357
System identification of the Large-Angle Magnetic Suspension Test Facility (LAMSTF)
p 2682 N94-27908

DYNAMIC MODELS
Parameter estimation by genetic algorithms
[DE94-002924] p 2961 N94-26146
An interactive, physically-based simulation system
[ISBN-0-315-83884-1] p 2963 N94-26616
Simulation dynamics of a multibody chain: Recursion based on chain modal coordinates
[ISBN-0-315-83555-9] p 2994 N94-26659
Wobble-nutation modes of the Earth
[ISBN-0-315-84246-6] p 3102 N94-26669
Substructure synthesis methods for viscoelastic structures
[UTIAS-349] p 2695 N94-26712
Chaotic dynamics of the solar cycle
[AD-A274315] p 3110 N94-26883
Generalized finite element dynamic modelling and simulation for flexible robot manipulators
[ISBN-0-315-84623-2] p 2825 N94-27343
Dynamics and robust control for uncertain flexible space systems
[INPE-5510-TAE/020] p 2696 N94-27357
System identification of the Large-Angle Magnetic Suspension Test Facility (LAMSTF)
p 2682 N94-27908
Superfluid helium sloshing dynamics induced oscillations and fluctuations of angular momentum, force and moment actuated on spacecraft driven by gravity gradient or jitter acceleration associated with slew motion
[NASA-CR-193928] p 2799 N94-27931
Nonlinear solvers p 2829 N94-28053

DYNAMIC PRESSURE
Development and implementation of a scramjet cycle analysis code with a finite-rate-chemistry combustion model for use on a personal computer
[AD-A273834] p 2673 N94-25617

DYNAMIC PROGRAMMING

A linear description of the discrete lot-sizing and scheduling problem [MEMO-COSOR-92-47] p 2992 N94-26227

Interacting cortical filters for object recognition [PB94-125374] p 2938 N94-26873

DYNAMIC RESPONSE

Dynamic response of S-2 glass reinforced plastic structural armor [AD-A273868] p 2747 N94-25596

Characteristics and control response of the TOPAZ 2 reactor system real-time dynamic simulator [DE94-003788] p 2699 N94-25600

Dynamic response of a compressor research facility [AD-A273836] p 2679 N94-25740

The railway track response function [REPT-93-40] p 2837 N94-26214

Analysis/test correlation using VAWT-SDS on a step-relaxation test for the rotating Sandia 34 m test bed [DE94-002290] p 2857 N94-26700

Enhanced simulation software for rocket turbopump, turbulent, annular liquid seals [NASA-CR-195239] p 2825 N94-27383

Lift-curve slope for structural response calculations [ESDU-93013] p 2646 N94-28063

An initial investigation into methods of computing transonic aerodynamic sensitivity coefficients [NASA-CR-195705] p 2648 N94-28072

DYNAMIC STABILITY

Stability of large scale interconnected dynamical systems [DE94-601536] p 2993 N94-26408

DYNAMIC STRUCTURAL ANALYSIS

Project WISH: The Emerald City p 2703 N94-25690

Structural evaluation of concepts for a solar energy concentrator for Space Station advanced development program [NASA-TP-3375] p 2695 N94-26609

The free vibration of plates, shallow shells and solids [ISBN-0-315-83931-7] p 2838 N94-26622

Asymptotically stable neural networks for identification of nonlinear dynamic systems [ISBN-0-315-84328-4] p 2985 N94-26629

Dynamics of a flexible extendible beam [ISBN-0-315-84278-4] p 2838 N94-26639

Optimal architectural design of parallel and hybrid manipulators [ISBN-0-315-84351-9] p 2822 N94-26657

Analysis/test correlation using VAWT-SDS on a step-relaxation test for the rotating Sandia 34 m test bed [DE94-002290] p 2857 N94-26700

Response of structures to impact loads using elastic and plastic analysis [ISBN-0-315-84647-X] p 2842 N94-27309

Bulk-Flow Analysis, part A [NASA-CR-193911-PT-A] p 2796 N94-27377

Finite element analysis of damped vibrations of laminated composite plates [ISBN-0-315-84928-2] p 2843 N94-27585

Super finite elements for nonlinear static and dynamic analysis of stiffened plate structures [ISBN-0-315-63903-2] p 2844 N94-27808

Multidisciplinary aeroelastic analysis of a generic hypersonic vehicle [NASA-TM-4544] p 2691 N94-27868

Methods of testing for endurance of structural elements using simulated acoustic loading [ESDU-93027] p 3011 N94-28141

Structural study of Cu/Co multilayer by anomalous small-angle x ray scattering p 2744 N94-28160

DYNAMIC TESTS

The effect of the time restrictions on information search and information integration in a dynamic task environment [AD-A273759] p 3095 N94-25723

Proceedings of Damping 1993, volume 2 [AD-A274227] p 2840 N94-26953

DYNAMICAL SYSTEMS

Stability of large scale interconnected dynamical systems [DE94-601536] p 2993 N94-26408

The onset of chaos in a periodically forced nonlinear oscillator [ISBN-0-315-84564-3] p 2842 N94-27272

DYNAMO THEORY

Chaotic dynamics of the solar cycle [AD-A274315] p 3110 N94-26883

DYSPROSIUM

Studies of heavy-ion reactions and transuranic nuclei [DE94-004642] p 3029 N94-27783

DYSPROSIUM COMPOUNDS

Laser surface modification of intermetallic compounds [DREA-CR-92-416] p 2820 N94-27668

E

E GLASS

Testing composite-to-metal tubular lap joints [DE94-003225] p 2836 N94-26032

E REGION

Quiet-time intensifications along the poleward auroral boundary near midnight [ATR-93(7248)-2] p 2877 N94-26201

Ionospheric modification by high power, obliquely propagated HF radio wave transmissions. Part 1: Experimental [AD-A273746] p 2878 N94-26224

EARTH (PLANET)

Underground structure in the eastern part of Kanagawa Prefecture inferred from explosion seismic observations p 2886 N94-27987

New Developments Regarding the KT Event and Other Catastrophes in Earth History [NASA-CR-195169] p 2887 N94-28294

Axial focusing of impact energy in the Earth's interior: Proof-of-principle tests of a new hypothesis p 2888 N94-28296

EARTH ATMOSPHERE

Automation of closed environments in space for human comfort and safety p 2943 N94-25684

The Lightcraft project: Flight technology for a hypersonic mass transit system p 2670 N94-25695

Characterization of the energy deposition produced by the primary electron beam on the EXCEDE 3 program. Appendix B and C [AD-A273878] p 3012 N94-25726

Methane emissions from natural wetlands [DE93-040796] p 2865 N94-25790

The effect of elevation data representation on nocturnal drainage wind simulations [DE94-003624] p 2892 N94-25936

Testbed model and data assimilation for ARM [DE94-000432] p 2893 N94-26082

Numerical procedure for planetary wave solution [DE94-004280] p 2879 N94-26576

ARM Fourier transform spectrometer data analysis tools [DE94-000865] p 2895 N94-26697

The Sixteenth Symposium on Coordinated Observations of the Ionosphere and the Magnetosphere in the Polar Regions: Program and abstracts [JTN-94-80601] p 2882 N94-27300

An overview of the ASCOT program [DE94-004356] p 2869 N94-27601

Utilization of remote sensing data for global climate change research in Malaysia p 2875 N94-28290

EARTH CRUST

Studies on the measurement of subsurface fractures and geostress using acoustic emission technique for deep coalbed development [REPT-7] p 2879 N94-26475

A geological and geophysical information system for Eurasia [AD-A274818] p 3098 N94-26490

Crustal deformation measurements in the vicinity of Vandenberg Air Force Base [AD-A274166] p 2881 N94-27143

Wave propagation in the shallow regions of the earth's crust and the borehole vicinity [ITN-94-85237] p 2882 N94-27330

Report of the National Research Institute for Earth Science and Disaster Prevention, No. 51 [JTN-94-80509] p 2886 N94-27985

Underground structure in the eastern part of Kanagawa Prefecture inferred from explosion seismic observations p 2886 N94-27987

Analysis of S-wave seismogram envelope of deep earthquakes and estimation of random inhomogeneities in the Kanto-Tokai area p 2886 N94-27988

EARTH GRAVITATION

Correlation between the gravity field and the bathymetry in the North Atlantic Ocean [ETN-94-95036] p 2899 N94-26108

EARTH IONOSPHERE

Norwegian ionospheric satellite experiment: High latitude, low Earth orbit plasma measurements [FFI-93/7025] p 2876 N94-25807

Dynamics explorer interdisciplinary scientist investigations [NASA-CR-195226] p 2878 N94-26204

Upper atmosphere neutral and plasma density modeling [AD-A274768] p 2879 N94-26569

Ionosphere-magnetosphere coupling [NASA-CR-195222] p 2881 N94-27237

The Sixteenth Symposium on Coordinated Observations of the Ionosphere and the Magnetosphere in the Polar Regions: Program and abstracts [JTN-94-80601] p 2882 N94-27300

Ionospheric calibration for single frequency altimeter measurements [NASA-CR-195709] p 2883 N94-27883

EARTH LIMB

Zodiacal light data investigation. Interim results for the Earthlimb Clutter Experiment [AD-A274461] p 3104 N94-27265

EARTH MAGNETOSPHERE

Dynamics explorer interdisciplinary scientist investigations [NASA-CR-195226] p 2878 N94-26204

Auroral Tomography Workshop Proceedings [PB94-123718] p 2881 N94-27040

Ionosphere-magnetosphere coupling [NASA-CR-195222] p 2881 N94-27237

The Sixteenth Symposium on Coordinated Observations of the Ionosphere and the Magnetosphere in the Polar Regions: Program and abstracts [JTN-94-80601] p 2882 N94-27300

Memories of National Institute of Polar Research. Series A-19. Upper atmosphere physics: ELF emission in high latitudes: Ray path calculation and ground-satellite observations [JTN-94-80592] p 2882 N94-27342

Configuration of the near-Earth plasma sheet [NASA-CR-195271] p 2883 N94-27438

EARTH MANTLE

Electrical conductivity of perovskite-magnesiowuestite as a function of pressure and temperature [DE94-002714] p 2880 N94-26806

EARTH MOVEMENTS

Wobble-nutation modes of the Earth [ISBN-0-315-84246-6] p 3102 N94-26669

An integrated approach to seismic event location: 1. Evaluating how method of location affects the volume of groups of hypocenters [PL-TR-92-2323] p 2887 N94-28214

EARTH OBSERVATIONS (FROM SPACE)

The potential for the Department of Defense to use space-based remote sensing to support DOD and other government agencies' environmental programs [AD-A273895] p 2847 N94-25656

Feasibility study of a multiaperture telescope for deep-space Earth surveillance [AD-A273903] p 3102 N94-25658

Remote Earth Sciences data collection using ACTS [NASA-CR-195227] p 2848 N94-26236

Assessment of tropical forests using satellite data [SILVA-CARELICA-21] p 2850 N94-27182

Global tropical forest cover assessments using satellite imagery p 2850 N94-27183

Global change research related to the Earth's energy and hydrologic cycle [NASA-CR-195270] p 2869 N94-27430

A comparative study of SAR data compression schemes p 2946 N94-28259

EARTH ORBITAL ENVIRONMENTS

SAFT nickel hydrogen cell cycling status p 2861 N94-28110

EARTH ORBITS

Space Habitat, assembly and repair facility p 2691 N94-25696

A virtual environment for satellite modeling and orbital analysis in a distributed interactive simulation [AD-A274114] p 2694 N94-25904

EARTH PLANETARY STRUCTURE

Report of the National Research Institute for Earth Science and Disaster Prevention, No. 51 [JTN-94-80509] p 2886 N94-27985

Underground structure in the eastern part of Kanagawa Prefecture inferred from explosion seismic observations p 2886 N94-27987

Analysis of S-wave seismogram envelope of deep earthquakes and estimation of random inhomogeneities in the Kanto-Tokai area p 2886 N94-27988

EARTH RADIATION BUDGET

Differentiating the role of land surface variability and cloudiness variability on global energy transport within the atmosphere and oceans [NASA-CR-195229] p 2847 N94-26222

Science support for the Earth radiation budget experiment [NASA-CR-191600] p 2894 N94-26506

Nimbus-7 Earth radiation budget calibration history. Part 2: The Earth flux channels [NASA-RP-1335-PT-2] p 2814 N94-27981

EARTH RADIATION BUDGET EXPERIMENT

Science support for the Earth radiation budget experiment [NASA-CR-191600] p 2894 N94-26506

EARTH ROTATION

Wobble-nutation modes of the Earth [ISBN-0-315-84246-6] p 3102 N94-26669

Trajectories of ballistic impact ejecta on a rotating Earth p 2887 N94-28295

EARTH SCIENCES

Mission to Planet Earth: A program to understand global environmental change
[NASA-PAM-556] p 2869 N94-27958

The 1994 Space and Earth Science Data Compression Workshop
[NASA-CP-3255] p 2945 N94-28251

EARTH SURFACE

The effect of elevation data representation on nocturnal drainage wind simulations
[DE94-003624] p 2892 N94-25936

Cratering rates from lunar xenospherules
[DE94-003481] p 3106 N94-27007

EARTH TERMINALS

System design analysis of a lightweight laser satellite terminal
[AD-A274033] p 2690 N94-25769

Thailand satellite ground receiving station in global change research cooperation p 2875 N94-28291

EARTH-IONOSPHERE WAVEGUIDE

Excitation of Earth-ionosphere waveguide in the ELF and lower VLF bands by modulated ionospheric current
[AD-A274969] p 2878 N94-26304

EARTH-MARS TRAJECTORIES

Project APEX: Advanced manned exploration of the Martian moon Phobos p 3079 N94-25688

Mars transportation system p 2833 N94-25689

Comet nucleus and asteroid sample return missions
p 2689 N94-25692

EARTHQUAKES

Report of the National Research Institute for Earth Science and Disaster Prevention, No. 51
[JTN-94-80509] p 2886 N94-27985

Observation with STS seismometer at Nakaizu, central Japan: Observation system and comparison with tiltmeter p 2886 N94-27986

Underground structure in the eastern part of Kanagawa Prefecture inferred from explosion seismic observations
p 2886 N94-27987

Analysis of S-wave seismogram envelope of deep earthquakes and estimation of random inhomogeneities in the Kanto-Tokai area p 2886 N94-27988

ECCENTRICITY

Modulating terrestrial impacts from Oort cloud comets by the adiabatically changing galactic tides
p 2890 N94-28305

ECOLOGY

Telepresence in the human exploration of Mars: Field studies in analog environments p 2685 N94-27360

Global Change and Terrestrial Ecosystems (GCTE): Progress report and prospects for Asian contributions
p 2874 N94-28281

ECONOMIC ANALYSIS

Ways to improve MHD power plants and prospects of their application p 2854 N94-26056

Some aspects of nonlinear discrete-time descriptor systems in economics
[PB94-126653] p 3101 N94-26918

ECONOMIC FACTORS

Deregulation of air traffic in America: A model to be initiated? p 2661 N94-28232

Air traffic in recession p 2662 N94-28240

ECONOMIC IMPACT

The advantages of the location Germany must not be jeopardized in air traffic p 2661 N94-28236

ECONOMICS

Overview of the Photovoltaic Manufacturing Technology (PVMaT) project
[DE93-018234] p 2856 N94-26426

Fusion Energy Advisory Committee: Advice and recommendations to the US Department of Energy in response to the charge letter of September 1, 1992
[DE93-019842] p 3043 N94-26428

ECOSYSTEMS

Active layer dynamics and arctic hydrology and meteorology
[DE94-001724] p 2892 N94-25951

Grassland/atmosphere response to changing climate: Coupling regional and local scales
[DE94-003111] p 2866 N94-26026

SIMA: A model for forest succession based on the carbon and nitrogen cycles with application to silvicultural management of the forest ecosystem
[SILVA-CARELICA-22] p 2848 N94-26258

Measuring variation in ecosystem sensitivity to stress
[AD-A274232] p 2868 N94-26817

EDDY CURRENTS

Development of non-destructive testing technology for the crack of steam generator tubes
[DE93-632953] p 2835 N94-26399

Correlation of experimental data and three-dimensional finite element modeling of a spinning quadrupole
[DE93-041173] p 3008 N94-26421

EDDY VISCOSITY

Calculation of single and multiple jets in cross-flow with and without impingement using Reynolds-stress-transport closure p 2803 N94-28024

EDEMA

Influence of mechanical stimulation on inflammatory edema p 2906 N94-27497

EDGE DETECTION

The determination of surface roughness from reflected step edges
[AD-A273987] p 2984 N94-25900

Image segmentation by a combination of edge detection and region growing
[ETN-94-95032] p 2960 N94-26106

Parallel algorithm for dominant points correspondences in robot binocular stereo vision p 2686 N94-27364

EDGES

A study of two dimensional tapered periodic edge treatments to reduce wideband edge diffraction
[AD-A274054] p 2766 N94-25824

The determination of surface roughness from reflected step edges
[AD-A273987] p 2984 N94-25900

Polarimetric investigation of edge scattering by mono- and bistatic microwave imaging
[ESA-TT-1284] p 2768 N94-26317

EDITING

Editing tree structures
[CWI-CS-R9264] p 2961 N94-26219

Red's natural editor: A program designed to edit FORTRAN programs
[DE94-003271] p 2962 N94-26318

ActorStudio: An interactive user interface editor
[PB94-132859] p 2976 N94-28356

EDITING ROUTINES (COMPUTERS)

Editing tree structures
[CWI-CS-R9264] p 2961 N94-26219

Design and implementation of a query editor for the Amadeus system
[AD-A274955] p 3097 N94-26300

Red's natural editor: A program designed to edit FORTRAN programs
[DE94-003271] p 2962 N94-26318

OPM Scheme Editor 2: A graphical editor for specifying object-protocol structures
[DE94-003477] p 2962 N94-26327

Design considerations when using external hypertext engines from applications
[DE94-002213] p 3098 N94-26598

ActorStudio: An interactive user interface editor
[PB94-132859] p 2976 N94-28356

EDUCATION

Development of the Air Force contingency contracting course framework
[AD-A273921] p 3093 N94-25895

Federal Information Exchange (FEDIX) user's guide: Fall 1993, Version 5.0/Release 1.0
[DE94-003826] p 3097 N94-26350

Benefits estimation for simulation systems used for aircrew training in a multiship environment
[AD-A274313] p 2938 N94-26882

Workload transition: Implications for individual and team performance
[AD-A274538] p 2941 N94-26964

COMPETENCE 2000: Study on training requirements of the Norwegian metallurgical industry
[PB94-124609] p 2741 N94-27328

Training on assessment and mapping of deforestation: WFW conference, Brazil
[INPE-5482-PRE/1781] p 2850 N94-27384

Predoctoral training grant in the area of physical sciences
[DE94-004406] p 3039 N94-27603

The 1993 NASA-ODU American Society for Engineering Education (ASEE) Summer Faculty Fellowship Program
[NASA-CR-191544] p 3085 N94-27893

Selected data on Federal support to universities and colleges: FY 1991
[NSF-93-320] p 3101 N94-28201

Laboratory of Space Technology
[PB94-133204] p 2689 N94-28358

EFFICIENCY

Efficient implementation of high-level parallel symbolic languages p 2955 N94-27196

Wieand's theorem
[PB94-126711] p 3004 N94-27223

Thermodynamics of combined cycle plant
p 2831 N94-28079

EFFLUENTS

Advances in passive-remote and extractive Fourier transform infrared spectroscopic systems
[DE94-001424] p 2868 N94-26952

EGRESS

Assured crew return vehicle post landing configuration design and test p 2697 N94-25671

EIGENVALUES

Parameter estimation by genetic algorithms
[DE94-002924] p 2961 N94-26146

Winding numbers in homotopy theory from integers to reals
[DE94-601510] p 2992 N94-26367

Bifurcation sequences at 1:4 resonance: An inventory
[PB94-125408] p 2997 N94-27028

The PRISM project: Infrastructure and algorithms for parallel eigensolvers
[DE94-005125] p 2973 N94-27717

Eigenwaves in the general uniaxial bianisotropic medium with symmetric parameter dyadics
[PB94-132891] p 2778 N94-28381

EIGENVECTORS

Parameter estimation by genetic algorithms
[DE94-002924] p 2961 N94-26146

EINSTEIN EQUATIONS

Vortices in curved spacetime
[DE94-601559] p 3072 N94-26417

EJECTA

Trajectories of ballistic impact ejecta on a rotating Earth p 2887 N94-28295

EJECTORS

Ejectors and jet pumps: Computer program for design and performance for liquid flow
[ESDU-93022] p 2832 N94-28093

EL NINO

Propagation of cold air masses in East Asia and its associated planetary-scale function
[AD-A274304] p 2895 N94-26850

ELASTIC DEFORMATION

Nanoscale plasticity in silica glass
[DE94-004212] p 2751 N94-26554

Fluid dynamic linear accelerometer
[AD-D016042] p 2678 N94-27112

On the Lagrangian and updated Lagrangian nonlinear finite element formulations
[ISBN-0-315-61111-1] p 3001 N94-27948

Flat rectangular orthotropic plates under uniformly distributed normal pressure. Elastic stresses and deflections for various forms of edge restraint
[ESDU-93011] p 2845 N94-28061

ELASTIC MEDIA

Dynamic and kinematic P wave tracing for a three-dimensional elastic inhomogeneous media by the asymptotic ray theory and application
[ITN-94-85239] p 2775 N94-27244

ELASTIC PROPERTIES

Debye-Waller factors of the light actinide metals
[DE94-000685] p 2733 N94-26069

DUSOL: Improved software for analysis of ultrasonic velocity data on anisotropic materials
[NPL-DMM(A)-104] p 2965 N94-26816

Geometry changes in the elastic-plastic analysis of steel spatial skeletal structures
[IFTR-37/1993] p 2839 N94-26825

Nonlinear hysteresis in an endochronic solid
[AD-A274594] p 2880 N94-26855

Flat rectangular orthotropic plates under uniformly distributed normal pressure. Elastic stresses and deflections for various forms of edge restraint
[ESDU-93011] p 2845 N94-28061

Analysis and control of hourglass instabilities in underintegrated linear and nonlinear elasticity
[NASA-CR-195293] p 2846 N94-28266

ELASTIC SCATTERING

Theoretical and computational studies in intermediate energy nuclear physics
[DE94-004177] p 3012 N94-25800

The amplitude of the elastic hadron-hadron scattering in the coulombic range of transfer momenta
[DE93-613183] p 3014 N94-25869

Structure functions of sea quarks, Kogut-Susskind pole and dynamics of pp- and pp-bar-interactions at high energies
[DE93-613184] p 3031 N94-25870

Spin effects in hard interactions (interest in accelerated polarized beam)
[DE93-634398] p 3031 N94-26044

Elastic scattering by a spherical inclusion
[AD-A274713] p 2878 N94-26433

Spin asymmetry in resonant electron-hydrogen elastic scattering
[DE94-601813] p 3023 N94-26943

Calculations of asymmetries in electron-alkali scattering
[DE94-601816] p 3023 N94-26945

Mapping between the Sinh-Gordon and Ising models
[DE94-601535] p 2998 N94-27162

Atomic processes in Inertial Electrostatic Confinement (IEC) devices
[DE94-005015] p 3047 N94-27715

High energy parton-parton elastic scattering in QCD
[DE94-003432] p 3028 N94-27736

ELASTIC SHELLS

New variational techniques for acoustic radiation and scattering from elastic shell structures
[AD-A274599] p 3010 N94-26889

ELASTIC WAVES

Elastic wave up/down decomposition in inhomogeneous and anisotropic media: An operator approach and its approximations
[PB94-126497] p 2881 N94-26880

Wave propagation in the shallow regions of the earth's crust and the borehole vicinity
[ITN-94-85237] p 2882 N94-27330

Compressibility effects on rotor forces in the leakage path between a shrouded pump impeller and its housing
p 2796 N94-27379

Double excitation of He and H(-) by fast proton and anti-proton impact
[DE94-004581] p 3026 N94-27620

ELASTODYNAMICS

Elastic wave up/down decomposition in inhomogeneous and anisotropic media: An operator approach and its approximations
[PB94-126497] p 2881 N94-26880

ELASTOMERS

Thermoplastic elastomers having alternate crystalline structure for us as high energy binders
[AD-D016035] p 2755 N94-27203

Development of a new seal for use on large openings of pressurized spacecraft
[NASA-TM-108444] p 2825 N94-27560

ELECTRIC ARCS

Channel model for AC electric arc
[PB94-124591] p 2786 N94-27327

ELECTRIC BATTERIES

Reference electrodes for solid polymer electrolytes
[DE94-004583] p 2780 N94-25806

Exploratory Technology Research Program for Electrochemical Energy Storage
[DE94-003479] p 2781 N94-26047

A Shuttle mechanism for molten-electrolyte lithium batteries
[DE94-002914] p 2781 N94-26144

Low-cost photovoltaic inverters incorporating application-specific integrated circuits
[DE94-003270] p 2856 N94-26463

Voltammetric studies of poly(carbon disulfide)
[DE94-001385] p 2717 N94-26951

NSWC Crane Aerospace Cell Test History Database
p 2860 N94-28102

Battery charge control: Which approach is best?
p 2863 N94-28124

Use of calorimetry for end of charge determination
p 2863 N94-28128

High rate lithium/thionyl chloride bipolar battery development p 2864 N94-28133

ELECTRIC CHARGE

The electric field between non conductive rectangular charged surfaces placed near a small spherical conductive earthed surface and determination of critical density of charge
[DE93-634324] p 2783 N94-26443

ELECTRIC CONDUCTORS

The electric field between non conductive rectangular charged surfaces placed near a small spherical conductive earthed surface and determination of critical density of charge
[DE93-634324] p 2783 N94-26443

Length-scale dependent ensemble-averaged conductance of a 1D disordered conductor: Conductance minimum
[DE94-602732] p 3062 N94-26902

ELECTRIC CONNECTORS

Development of fusion technology
[DE93-633444] p 3042 N94-26159

ADC test support program
[AD-A274819] p 2783 N94-26491

ELECTRIC CONTACTS

Visible light emitting materials and injection devices
[AD-A274418] p 2786 N94-27079

ELECTRIC CURRENT

Electric-field dependence of electroreflectance and photocurrent spectra at visible wavelengths in MOVPE-grown InAlGaP multiple strained quantum-well structures
[DE94-004692] p 2780 N94-25664

Study of the homogeneity of InP wafers
[AD-A273658] p 3055 N94-26194

The effect of processing on the microstructure of Ag-sheathed Bi-2223 wires
[DE94-004627] p 3055 N94-26243

MBE grown 3 to 5 strain relaxed buffer layers and superlattices characterized by atomic force microscopy
[DE94-002931] p 3056 N94-26308

Recombination and metastability in amorphous silicon and silicon germanium alloys
[DE94-000237] p 2736 N94-26481

Numerical simulation of plasma vertical position stabilization in ITER
[DE93-634588] p 3044 N94-26510

Interference analysis of multichannel transmission lines: A system's analysis
[PB94-126505] p 2772 N94-26909

A model of electric breakdown in polycrystalline semiconductors with highly nonlinear I - V characteristics
[DE94-601537] p 3063 N94-27017

A direct current rectification scheme for microwave space power conversion using traveling wave electron acceleration p 2687 N94-27371

Effects of perfusion of amiodarone on electrophysiological properties in single rabbit ventricular myocytes p 2906 N94-27503

Fast and slow onsets of Na channel blocking actions due to lidocaine and disopyramide using concentration-clamp method p 2907 N94-27504

Electrophysiological effects of MS-551, a new Class 3 antiarrhythmic agent, on isolated rabbit ventricular muscles p 2907 N94-27505

Comparative investigation of new Class 3 antiarrhythmic drugs, E-4031 and MS-551, on electrophysiological properties in isolated rabbit ventricular myocytes
p 2907 N94-27506

Effects of Class 1 antiarrhythmic drugs on the intraventricular conduction: Influence of fiber orientation
p 2907 N94-27507

Geometrical resonances in the nyquist noise spectrum for ballistic conductors
[DE94-603668] p 3027 N94-27631

Technical report of ISSP. Ser. A, no. 2687: Quantized persistent currents of a quantum dot in a strong magnetic field
[JTN-94-80573] p 3028 N94-27758

The effect of Ti conduit on the critical current in (Nb, Ti)3Sn cable-in-conduit conductors
[DE94-701204] p 2788 N94-27817

Experimental results of 40-kA Nb3Al conductor
[DE94-701207] p 2788 N94-27821

Silicon device performance measurements to support temperature range enhancement
[NASA-CR-195265] p 2844 N94-27824

Image theory for DC problems involving a conducting half space bounded by the general anisotropic impedance surface
[PB94-132917] p 2779 N94-28390

ELECTRIC DIPOLES

Electromagnetic fields and interference
[PB94-126489] p 2771 N94-26877

Green dyadic and dipole fields for a medium with anisotropic chirality
[PB94-132933] p 2779 N94-28391

ELECTRIC DISCHARGES

Method of optimizing the charging of a battery of storage cells, and apparatus for performing the method
[AD-D016066] p 2781 N94-26102

Development of an industrial CO2 laser for mask marking
[DE93-632901] p 2816 N94-26184

Inertial electrostatic confinement as a power source for electric propulsion p 2688 N94-27373

Proceedings of the 16th Symposium on Plasma Physics and Technology
[DE94-604181] p 3047 N94-27698

Cycle life versus depth of discharge update on modeling studies --- Nickel-Hydrogen Batteries
p 2862 N94-28115

Battery charge control: Which approach is best?
p 2863 N94-28124

ELECTRIC ENERGY STORAGE

Exploratory Technology Research Program for Electrochemical Energy Storage
[DE94-003479] p 2781 N94-26047

Exploratory technology research program for electrochemical energy storage
[DE94-003480] p 2855 N94-26329

ELECTRIC FIELDS

Back-reaction beyond the mean field approximation
[DE94-003936] p 3012 N94-25612

Electric-field dependence of electroreflectance and photocurrent spectra at visible wavelengths in MOVPE-grown InAlGaP multiple strained quantum-well structures
[DE94-004692] p 2780 N94-25664

Catalog of absolutely calibrated, range normalized, wideband, electric field waveforms from triggered lightning flashes in Florida
[AD-A273793] p 2892 N94-25873

Design of folded waveguide antenna for Alcator C-Mod
[DE94-003584] p 2767 N94-25924

Modelling of ionisation reactions and of the resulting electric fields in one-dimensional hypersonic shock waves with the direct simulation Monte Carlo method
[IC-AERO-92-01] p 2644 N94-26248

Numeric solution of the electric field integral equation using Galerkin's method for axially symmetric cases
[ESA-TT-1264] p 2768 N94-26315

The effect of high frequency electric field on hypersound amplification in superlattice
[DE93-634326] p 3057 N94-26384

The electric field between non conductive rectangular charged surfaces placed near a small spherical conductive earthed surface and determination of critical density of charge
[DE93-634324] p 2783 N94-26443

Computer program for numerical evaluation of the performance of an overmoded TM01 circular to TE10 rectangular waveguide mode converter
[AD-A274548] p 2771 N94-26844

A direct current rectification scheme for microwave space power conversion using traveling wave electron acceleration p 2687 N94-27371

Configuration of the near-Earth plasma sheet
[NASA-CR-195271] p 2883 N94-27438

Transmittance fluctuations and non-linearity in random chains in the presence of applied electric fields
[DE94-603665] p 2787 N94-27628

Localization properties of one-dimensional electrified chains
[DE94-603672] p 3067 N94-27635

The three-dimensional hydrogen atom in crossed magnetic and electric fields
[DE94-606301] p 3029 N94-27847

MUSIC for localization of thunderstorm cells
[DE94-004985] p 2897 N94-28146

Electrostatic image solution for the conducting prolate spheroid
[PB94-133154] p 2778 N94-28387

Green dyadic and dipole fields for a medium with anisotropic chirality
[PB94-132933] p 2779 N94-28391

ELECTRIC FILTERS

Enhanced adaptive statistical filter providing improved performance for target motion analysis noise discrimination statement of government interest
[AD-D016039] p 2786 N94-27109

ELECTRIC FURNACES

Physical modelling and adaptive predictive control of diffusion/LPCVD reactors
[PB94-126398] p 2763 N94-26819

ELECTRIC GENERATORS

Merging photovoltaic hardware development with hybrid applications in the USA
[DE94-002682] p 2857 N94-26612

ELECTRIC HYBRID VEHICLES

Natural gas applications for hybrid vehicles.
[PB94-117108] p 2759 N94-26753

ELECTRIC MOTOR VEHICLES

Exploratory Technology Research Program for Electrochemical Energy Storage
[DE94-003479] p 2781 N94-26047

Exploratory technology research program for electrochemical energy storage
[DE94-003480] p 2855 N94-26329

Feasibility study on introduction of transportation-use petroleum substitution energy
[DE94-725205] p 2759 N94-26905

ELECTRIC MOTORS

Hardware design of a spherical mini-rover
p 2833 N94-25669

ELECTRIC NETWORKS

Electromagnetic fields and interference
[PB94-126489] p 2771 N94-26877

ELECTRIC POTENTIAL

Characteristics and development report for the T1576 power supply and the MC3935 battery
[DE94-003675] p 2783 N94-26372

Reconstruction of multiple cracks from experimental electrostatic boundary measurements
[NASA-CR-191584] p 2994 N94-26601

A mechanism for resistive dissipation in Ag sheathed Bi2Sr2CaCu2O8 and Bi2Sr2Ca2Cu3O10
[DE94-003009] p 3060 N94-26771

Molecular surface electrostatic potentials in the analysis of non-hydrogen-bonding noncovalent interactions
[AD-A274612] p 3022 N94-26894

Polar optical oscillation modes in GaAs-based double heterostructures: Long wavelength limit
[DE94-601874] p 3062 N94-26897

Interference analysis of multichannel transmission lines: A system's analysis
[PB94-126505] p 2772 N94-26909

A model of electric breakdown in polycrystalline semiconductors with highly nonlinear I - V characteristics
[DE94-601537] p 3063 N94-27017

Channel model for AC electric arc
[PB94-124591] p 2786 N94-27327

Effects of perfusion of amiodarone on electrophysiological properties in single rabbit ventricular myocytes p 2906 N94-27503

Fast and slow onsets of Na channel blocking actions due to lidocaine and disopyramide using concentration-clamp method p 2907 N94-27504
Electrophysiological effects of MS-551, a new Class 3 antiarrhythmic agent, on isolated rabbit ventricular muscles p 2907 N94-27505
Comparative investigation of new Class 3 antiarrhythmic drugs, E-4031 and MS-551, on electrophysiological properties in isolated rabbit ventricular myocytes p 2907 N94-27506
Effects of Class 3 antiarrhythmic agents, E-4031 and MS-551 on ventricular repolarization in isolated rabbit hearts p 2907 N94-27508
Electrical coupling between the sino-atrial node and atrial muscle: Cell to cell interaction through an external circuit and its simulation by computer modeling p 2907 N94-27509
A study on tissue excitation of cardiac muscle under electrical field stimulation p 2907 N94-27510
Block of cardiac sodium channels by Ro 22-9194 (R), a new antiarrhythmic agent: Effects on the maximum upstroke velocity (Vmax) of single guinea pig ventricular myocytes p 2907 N94-27511
Electrophysiological effects of an antiarrhythmic drug, moricizine on isolated guinea pig ventricular muscles p 2907 N94-27512
Correlation between electrical activity and the size of single sinoatrial node cells p 2907 N94-27513
The ionic mechanism underlying the negative chronotropic effect of acetylcholine: Experimental study in rabbit single sinoatrial node cells p 2908 N94-27514
The ionic mechanism underlying the negative chronotropic effect of acetylcholine: Experiments using small sinoatrial node tissue preparations isolated from rabbit hearts p 2908 N94-27515
The ionic mechanism underlying the negative chronotropic effect of acetylcholine: Postganglionic vagal stimulation in isolated rabbit hearts p 2908 N94-27516
Desensitization to acethylcholine in pacemaker cells of the sinoatrial node p 2908 N94-27537
Image potential of a tunnelling electron moving near two different metals [DE94-603657] p 3069 N94-27819
Battery charge control: Which approach is best? p 2863 N94-28124
Bipolar Ag-Zn battery p 2864 N94-28135
The PROTEL contamination code [RXR-93071] p 3040 N94-28202

ELECTRIC POWER PLANTS
Programme for the promotion of wind power production [DE94-702065] p 2855 N94-26242
Solar resource-utility load matching assessment: NREL photovoltaic project summary [DE94-000232] p 2856 N94-26480
Combined Cycles for Power Plants [VKI-LS-1993-08] p 2830 N94-28077
Introduction to combined cycles p 2789 N94-28078
Thermodynamics of combined cycle plant p 2831 N94-28079
Steam plant: Steam turbines for combined cycles p 2831 N94-28085
Fibrous ceramic candle filter for particle removal in pressurized fluidized bed combustion [PB94-133089] p 2876 N94-28383
Emissions of nitrogen oxides (NO(x) and N2O) in pressurized fluidized bed combustion [PB94-133071] p 2876 N94-28395

ELECTRIC POWER SUPPLIES
Hybrid power system for remote communications stations [AD-A274963] p 2782 N94-26301
Merging photovoltaic hardware development with hybrid applications in the USA [DE94-002682] p 2857 N94-26612

ELECTRIC POWER TRANSMISSION
Solar resource-utility load matching assessment: NREL photovoltaic project summary [DE94-000232] p 2856 N94-26480

ELECTRIC PROPULSION
A large high vacuum, high pumping speed space simulation chamber for electric propulsion [NASA-TM-106453] p 2690 N94-26142
Inertial electrostatic confinement as a power source for electric propulsion p 2688 N94-27373
A study of DC-DC converters with MCT's for arcjet power supplies [NASA-CR-191204] p 2703 N94-27662

ELECTRIC ROCKET ENGINES
An investigation of magnetic field effects on plume density and temperature profiles of an applied-field MPD thruster [NASA-TM-106416] p 2700 N94-26090

ELECTRIC STIMULI
Annals of the Research Inst. of Environmental Medicine, Nagoya Univ., volume 44 [REPT-44-VOL-44] p 2911 N94-27442
Effects of high-intensity electric field stimulation on the electromechanical performance of cardiac muscle: Influence of fiber orientation p 2904 N94-27467
On the mechanism of reentrant arrhythmias following DC defibrillation: Influence of fiber orientation to the effects of low-energy electric field stimulation on the effective refractory period of cardiac muscle p 2904 N94-27468
A study on tissue excitation of cardiac muscle under electrical field stimulation p 2907 N94-27510
Analysis of the Electrically Evoked Response (EER) of the cat p 2908 N94-27519
Difference in skin blood flow reduction depending on activating maneuver of skin sympathetic nerve activity p 2929 N94-27525
An attempt of intraneural stimulation by microelectrode inserted in skin sympathetic nerve fascicle p 2930 N94-27529
Enhancement of skin sympathetic nerve activity in amyotrophic lateral sclerosis p 2930 N94-27532
Electrical stimulation in exercise training p 2935 N94-28371

ELECTRIC SWITCHES
AC to DC power converter with regulated bi-polar outputs [AD-D016032] p 2786 N94-27145
Nickel-hydrogen cell reversal characteristics p 2862 N94-28114

ELECTRIC WIRE
Digital input module [DIGEL-1993-6] p 2779 N94-25620
The effect of processing on the microstructure of Ag-sheathed Bi-2223 wires [DE94-004627] p 3055 N94-26243
A study on the development of high-T(c) superconducting wire [DE93-632438] p 2783 N94-26546
Microwave coupling into a slotted cavity [PB94-123742] p 2772 N94-27041

ELECTRICAL FAULTS
A model of electric breakdown in polycrystalline semiconductors with highly nonlinear I - V characteristics [DE94-601537] p 3063 N94-27017

ELECTRICAL IMPEDANCE
Signal amplifier-shapers for multiwire detectors [DE93-634171] p 2783 N94-26438
Image theory for DC problems involving a conducting half space bounded by the general anisotropic impedance surface [PB94-132917] p 2779 N94-28390

ELECTRICAL INSULATION
Technical report of ISSP. Ser. A, no. 2676: Charge mass singularity in two-dimensional Hubbard model [JTN-94-80562] p 3065 N94-27248

ELECTRICAL MEASUREMENT
Study on measurement and evaluation methods for superconductive characteristics p 2725 N94-25560
Theoretical and computational studies in intermediate energy nuclear physics [DE94-004177] p 3012 N94-25800
A general purpose I(sub DDQ) measurement circuit [DE94-002733] p 2781 N94-25977
Exploration of GaAs structures for solid-state detectors [DE93-634191] p 3056 N94-26379
The electric field between non conductive rectangular charged surfaces placed near a small spherical conductive earthed surface and determination of critical density of charge [DE93-634324] p 2783 N94-26443
Voltammetric studies of poly(carbon disulfide) [DE94-001385] p 2717 N94-26951
The PROTEL contamination code [RXR-93071] p 3040 N94-28202

ELECTRICAL PROPERTIES
The structural, chemical, and electrical properties of He-implantation-induced nanocavities in silicon [DE94-002681] p 3052 N94-25971
Investigation of plasma etch induced damage in compound semiconductor devices [DE94-002849] p 3052 N94-25989
Alternative materials for solid oxide fuel cells: Processing and interactions of materials [DE94-000016] p 2855 N94-26114
A Shuttle mechanism for molten-electrolyte lithium batteries [DE94-002914] p 2781 N94-26144
The origins of ordering in CuPt [DE94-003864] p 2736 N94-26351
A study on the development of high-T(c) superconducting wire [DE93-632438] p 2783 N94-26546
Design and evaluation of an electromagnetic beam waveguide for measuring electrical properties of materials [NASA-TP-3418] p 2769 N94-26611
A mechanism for resistive dissipation in Ag sheathed Bi2Sr2CaCu2O8 and Bi2Sr2Ca2Cu3O10 [DE94-003009] p 3060 N94-26771
Determination of thermal properties of commercial Ni-MH cells p 2864 N94-28132
High rate lithium/thionyl chloride bipolar battery development p 2864 N94-28133
Advanced silver zinc battery development for the SRB and ET range safety subsystems p 2865 N94-28136

ELECTRICAL RESISTIVITY
Study on characteristics and electronic structures of materials with strong electronic correlations by ferromagnetic fields p 2724 N94-25557
Study on ferromagnetic field magnet using strong and highly conductive material p 2725 N94-25559
Study on synthesis and characteristics of intermetallic compound with strong electron correlation p 2726 N94-25563
The Lightcraft project: Flight technology for a hypersonic mass transit system p 2670 N94-25695
Optical conductivity and resistivity in the two-band Emery model [DE94-601943] p 3051 N94-25945
Formation of three types of quasi-crystals in Al-Pd-Mg system [REPT-A-2667] p 3053 N94-26071
The formation of conducting gold films by thermal decomposition and direct patterning using electron beam lithography of the gold cluster Au55P(C6H5)312C16 [AD-A273720] p 2749 N94-26074
Toward insulating quasicrystalline alloy in Al-Pd-Re icosahedral phase [REPT-A-2666] p 2736 N94-26477
Chemical vapor deposition and characterization of tungsten boron alloy films [DE94-002648] p 2738 N94-26610
Electrical conductivity of perovskite-magnesiowuestite as a function of pressure and temperature [DE94-002714] p 2880 N94-26806
Disintegration of (C60) by Xe ion irradiation [DE94-601913] p 3023 N94-26929
Time domain reflectometry for measuring bulk soil electrical conductivity and comparison with the Em38 instrument [PB94-125432] p 2881 N94-27052
Mapping of seawater intrusion into the coastal aquifer of Israel (the seawater-freshwater interface) by TDEM (Time Domain Electromagnetic) method [ITN-94-85238] p 2850 N94-27331
Transmittance fluctuations and non-linearity in random chains in the presence of applied electric fields [DE94-603665] p 2787 N94-27628
Geometrical resonances in the nyquist noise spectrum for ballistic conductors [DE94-603668] p 3027 N94-27631
Effective conductivity of wire mesh reflectors for space deployable antenna systems [NASA-CR-191605] p 2788 N94-27770
An experimental investigation of fatigue damage in aluminum 2024-T3 alloys p 2747 N94-27900

ELECTRO-OPTICAL EFFECT
Electric-field dependence of electroreflectance and photocurrent spectra at visible wavelengths in MOVPE-grown InAlGaP multiple strained quantum-well structures [DE94-004692] p 2780 N94-25664

ELECTRO-OPTICS
Solid state research [AD-A274063] p 3049 N94-25645
Component characterization and development 2 [AD-A274002] p 2765 N94-25660
An overview of the TNO contribution to VAST 92 [AD-A273751] p 2893 N94-26016
Peculiarities and application perspectives of metal-ion implants in glasses [DE94-004671] p 3035 N94-26246
Multichip module high speed testing [AD-A274873] p 2782 N94-26343
Optoelectronic Technology Consortium [AD-A274909] p 2782 N94-26344
Mechanistic studies of opto-electronic materials and syntheses using multiple laser and surface diagnostics [AD-A274528] p 3036 N94-26834
Optoelectronic technology consortium [AD-A274595] p 3036 N94-26857
An optoelectronic graphics display processor [AD-A274401] p 3037 N94-26990
Design and evaluation of fault tolerance in opto-electronic computing [AD-A274281] p 2954 N94-27016
Electro-optic materials by solid source MOCVD [DE94-005120] p 2757 N94-27716

ELECTROACOUSTIC TRANSDUCERS
Non-contact ultrasonic inspection
[VTT-TIED-1454] p 2835 N94-26257
ELECTROCARDIOGRAPHY
Cardiac output and cardiac contractility by impedance cardiography during exercise of runners
p 2935 N94-28367
ELECTROCATALYSTS
The Science Reports of the Research Institutes, Tohoku University. Series A: Physics, Chemistry, and Metallurgy. Volume 38, No. 1: Amorphous Materials 14
[JTN-94-80610] p 2744 N94-28158
The electrocatalytic oxidation of ethylene and methane, and reduction of oxygen on gas-diffusion electrodes made of amorphous nickel-valve metal-platinum group metal alloys p 2722 N94-28165
ELECTROCHEMICAL CELLS
Reference electrodes for solid polymer electrolytes
[DE94-004583] p 2780 N94-25806
Molten salt techniques for reproducible excess heat
[AD-A274935] p 2714 N94-26296
Exploratory technology research program for electrochemical energy storage
[DE94-003480] p 2855 N94-26329
ELECTROCHEMICAL CORROSION
Observation on metal surface in aqueous solution using an electrochemical Scanning Tunneling Microscope (STM) p 2724 N94-25554
Fundamental study on monitoring technology on local surface damages p 2724 N94-25555
Study on improvements in fretting fatigue characteristics of high strength structural member p 2726 N94-25567
The electrochemical behavior of the Al3Fe intermetallic compound and localized corrosion of impure 1100 Al
[DE94-002037] p 2739 N94-26912
Electrochemical properties of passive films on 440C stainless steel
[ISBN-0-315-64248-3] p 2757 N94-27801
ELECTROCHEMICAL OXIDATION
The Science Reports of the Research Institutes, Tohoku University. Series A: Physics, Chemistry, and Metallurgy. Volume 38, No. 1: Amorphous Materials 14
[JTN-94-80610] p 2744 N94-28158
The electrocatalytic oxidation of ethylene and methane, and reduction of oxygen on gas-diffusion electrodes made of amorphous nickel-valve metal-platinum group metal alloys p 2722 N94-28165
ELECTROCHEMISTRY
Alternative materials for solid oxide fuel cells: Processing and interactions of materials
[DE94-000016] p 2855 N94-26114
A Shuttle mechanism for molten-electrolyte lithium batteries
[DE94-002914] p 2781 N94-26144
In situ spectroscopic applications to the study of rechargeable lithium batteries
[DE94-003478] p 2782 N94-26328
Exploratory technology research program for electrochemical energy storage
[DE94-003480] p 2855 N94-26329
Template synthesis of metal microtubule ensembles utilizing chemical, electrochemical, and vacuum deposition techniques
[AD-A274676] p 2715 N94-26444
Early stages in the development of stress corrosion cracks
[DE94-003867] p 2838 N94-26524
Opportunities for High Aspect Ratio Micro-Electro-Magnetic-Mechanical Systems (HAR-MEMMS) at Lawrence Berkeley Laboratory
[DE94-003499] p 2827 N94-27722
ELECTRODE MATERIALS
Research and development of alternative components at Argonne National Laboratory for Molten Carbonate Fuel Cells
[DE94-000014] p 2857 N94-26583
ELECTRODES
Reference electrodes for solid polymer electrolytes
[DE94-004583] p 2780 N94-25806
The AFIT multielectrode array for neural recording and simulation: Design, testing, and encapsulation
[AD-A274086] p 2909 N94-25943
Double layer capacitance of carbon foam electrodes
[DE94-002651] p 2780 N94-25975
Exploratory Technology Research Program for Electrochemical Energy Storage
[DE94-003479] p 2781 N94-26047
Alternative materials for solid oxide fuel cells: Processing and interactions of materials
[DE94-000016] p 2855 N94-26114
A Shuttle mechanism for molten-electrolyte lithium batteries
[DE94-002914] p 2781 N94-26144
Low cost, radial flow, solid oxide fuel cell
[DE94-002982] p 2858 N94-26785
Voltammetric studies of poly(carbon disulfide)
[DE94-001385] p 2717 N94-26951
Channel model for AC electric arc
[PB94-124591] p 2786 N94-27327
Screen test for cadmium and nickel plates
p 2860 N94-28106
Performance model of a recirculating stack nickel hydrogen cell p 2861 N94-28112
The electrocatalytic oxidation of ethylene and methane, and reduction of oxygen on gas-diffusion electrodes made of amorphous nickel-valve metal-platinum group metal alloys p 2722 N94-28165
ELECTROENCEPHALOGRAPHY
The AFIT multielectrode array for neural recording and simulation: Design, testing, and encapsulation
[AD-A274086] p 2909 N94-25943
The use of EEG as a workload assessment tool in flight test
[AD-A274568] p 2910 N94-26847
Performance recovery in the baboon following (+)G sub z-induced loss of consciousness
[AD-A274411] p 2902 N94-26991
Interhemispheric phase relationship of alpha waves and cerebral dominance p 2927 N94-27518
Brain wave correlates of attentional states: Event related potentials and quantitative EEG analysis during performance of cognitive and perceptual tasks
p 2940 N94-27901
ELECTROFORMING
A study on heat transfer in a scramjet leading edge model
[NAL-TR-1187T] p 2675 N94-27608
ELECTROLUMINESCENCE
Recombination and metastability in amorphous silicon and silicon germanium alloys
[DE94-000237] p 2736 N94-26481
Light emitting porous silicon
[AD-A274152] p 3038 N94-27137
ELECTROLYTE METABOLISM
Changes in fluid and electrolyte metabolism during water immersion at high or thermoneutral temperature
p 2912 N94-27445
ELECTROLYTES
Exploratory Technology Research Program for Electrochemical Energy Storage
[DE94-003479] p 2781 N94-26047
Alternative materials for solid oxide fuel cells: Processing and interactions of materials
[DE94-000016] p 2855 N94-26114
A Shuttle mechanism for molten-electrolyte lithium batteries
[DE94-002914] p 2781 N94-26144
Processing of LaCrO3 for solid oxide fuel cell applications
[DE94-002981] p 2857 N94-26747
Computer simulation of aqueous Na-Cl electrolytes
[DE94-002622] p 3030 N94-28001
Performance model of a recirculating stack nickel hydrogen cell p 2861 N94-28112
ELECTROLYTIC CELLS
A Shuttle mechanism for molten-electrolyte lithium batteries
[DE94-002914] p 2781 N94-26144
Processing of LaCrO3 for solid oxide fuel cell applications
[DE94-002981] p 2857 N94-26747
Low cost, radial flow, solid oxide fuel cell
[DE94-002982] p 2858 N94-26785
MSOFC development status
[DE94-003192] p 2858 N94-26792
Perovskite solid electrolytes for SOFC
[DE94-001923] p 2859 N94-27005
Bulletin of the Institute for Chemical Reaction Science, Tohoku University, volume 2
[JTN-94-80602] p 2717 N94-27385
Glass cylindrical filter for electrolysis cell
p 2718 N94-27391
ELECTROMAGNETIC ABSORPTION
Se EXAFS study of the elevated wurtzite to rock salt structural phase transition in CdSe nanocrystals
[DE94-003247] p 3054 N94-26125
Kiruna geophysical data. Data summary 93/4-6, April-June 1993
[PB94-123700] p 2881 N94-27039
Kiruna geophysical data. Data summary 93/1-3, January-March, 1993
[PB94-123791] p 2881 N94-27043
Experimental and theoretical investigation of RF absorption and reflection from preformed plasmas
[AD-A274189] p 3046 N94-27098
ELECTROMAGNETIC ACCELERATION
On a theory of two-beam mechanisms of charged particle acceleration in electrodynamic structures
[DE94-003482] p 3032 N94-26330
ELECTROMAGNETIC COMPATIBILITY
Developments in the application of the geometrical theory of diffraction and computer graphics to aircraft inter-antenna coupling analysis
[ISBN-0-315-84643-7] p 2776 N94-27308
ELECTROMAGNETIC COUPLING
Fast wave current drive technology development at ORNL
[DE94-004243] p 3046 N94-27568
ELECTROMAGNETIC FIELDS
Back-reaction beyond the mean field approximation
[DE94-003936] p 3012 N94-25612
Modeling electromagnetic effects in MMICs for T/R modules
[AD-A273808] p 2766 N94-25736
Electromagnetic properties of a toroidal solenoid
[DE93-613032] p 2766 N94-25866
The effect of high frequency electric field on hypersound amplification in superlattice
[DE93-634326] p 3057 N94-26384
Spinor and isospinor structure of relativistic particle propagators
[DE94-601552] p 3019 N94-26424
Using the TSAR electromagnetic modeling system
[DE94-002617] p 2771 N94-26803
S-76 high intensity radiated fields, volume 2
[AD-A274572] p 2771 N94-26836
S-76 high intensity radiated fields, volume 1
[AD-A274571] p 2771 N94-26854
Calculation of the electromagnetic critical state response of high T(sub c) superconductor tape
[DE94-002894] p 3061 N94-26868
Electromagnetic fields and interference
[PB94-126489] p 2771 N94-26877
S-76 high intensity radiated fields, volume 3
[AD-A274416] p 2772 N94-26980
Microwave coupling into a slotted cavity
[PB94-123742] p 2772 N94-27041
Polarizability matrix of layered chiral sphere
[PB94-132834] p 2778 N94-28355
Fields and potentials in general uniaxial bianisotropic media I. Axial sources
[PB94-132875] p 2778 N94-28379
ELECTROMAGNETIC INTERACTIONS
Heavy charged leptons in an SU(3)(sub L) x U(1)(sub N) model
[DE93-634367] p 3016 N94-26041
Unsegmented electromagnetic calorimeter prototype. Energy and coordinate resolution
[DE93-634185] p 2810 N94-26396
Constraints on singlet right-handed neutrinos coming from the Z(0)-width
[DE93-634393] p 3022 N94-26766
Cosmological phase transitions
[DE94-003001] p 3104 N94-26786
Progress in SSC Higgs physics: Report of the Higgs working group
[DE94-003224] p 3022 N94-26793
Stopping powers and cross sections due to two-photon processes in relativistic nucleus-nucleus collisions
[NASA-CR-4574] p 3033 N94-27646
Topics in electroweak baryogenesis: The sphaleron and T-violation
[DE94-004886] p 3029 N94-27811
ELECTROMAGNETIC INTERFERENCE
Kalman filtering of narrowband interference from direct sequence spread spectrum communications systems
[ISBN-0-315-84011-0] p 2784 N94-26627
Electromagnetic fields and interference
[PB94-126489] p 2771 N94-26877
Interference analysis of multichannel transmission lines: A system's analysis
[PB94-126505] p 2772 N94-26909
Microwave coupling into a slotted cavity
[PB94-123742] p 2772 N94-27041
Discrete vacuum ultra violet reflective interference filter
[AD-D016059] p 2756 N94-27675
ELECTROMAGNETIC MEASUREMENT
An evaluation of an airborne remote sensing system used to determine ice thickness and geometry of a first year sea ice ridge located in the Beaufort Sea
[ISBN-0-315-84383-7] p 2849 N94-26667
Mapping of seawater intrusion into the coastal aquifer of Israel (the seawater-freshwater interface) by TDEM (Time Domain Electromagnetic) method
[ITN-94-85238] p 2850 N94-27331
ELECTROMAGNETIC NOISE
Low noise measurements in an RF environment
[AD-A273813] p 2767 N94-25960
Detection of transient vector-fields in additive noise
[FFI-93/7028] p 2768 N94-26232
The analysis of thermal and 1/F noise in MOS devices, circuits and systems
[ISBN-0-315-57811-4] p 2787 N94-27642

Characteristics of 30-MHz interference noises observed by riometers p 2884 N94-27965

VHF-UHF noise surveys at Gulkana, Elmensdorf AFB, Galena AFB, Kotzebue and Cape Lisburne, Alaska and NRL, Pomonkey, Maryland [PL-TR-93-2136] p 2777 N94-28211

ELECTROMAGNETIC NOISE MEASUREMENT

Low noise measurements in an RF environment [AD-A273813] p 2767 N94-25960

VHF-UHF noise surveys at Gulkana, Elmensdorf AFB, Galena AFB, Kotzebue and Cape Lisburne, Alaska and NRL, Pomonkey, Maryland [PL-TR-93-2136] p 2777 N94-28211

ELECTROMAGNETIC PROPERTIES

Electromagnetic properties of a toroidal solenoid [DE93-613032] p 2766 N94-25866

ELECTROMAGNETIC PULSES

Experiments and numerical simulations of electromagnetic wave propagation in plasma varying rapidly in space and time [AD-A274376] p 2772 N94-26975

S-76 high intensity radiated fields, volume 3 [AD-A274416] p 2772 N94-26980

Receiving antennas for electromagnetic pulses and transients [ISBN-0-315-62312-8] p 2777 N94-27871

ELECTROMAGNETIC RADIATION

Catalog of absolutely calibrated, range normalized, wideband, electric field waveforms from triggered lightning flashes in Florida [AD-A273793] p 2892 N94-25873

A research program on radiative transfer model development in support of the ARM program [DE94-001146] p 2767 N94-25950

Polarimetric investigation of edge scattering by mono- and bistatic microwave imaging [ESA-TT-1284] p 2768 N94-26317

S-76 high intensity radiated fields, volume 2 [AD-A274572] p 2771 N94-26836

Interference analysis of multichannel transmission lines: A system's analysis [PB94-126505] p 2772 N94-26909

S-76 high intensity radiated fields, volume 3 [AD-A274416] p 2772 N94-26980

Theoretical and experimental analysis of the spatial and temporal behaviour of the intensity of an electro-magnetic wave reflected from a diffuse target after passing through a turbulent atmosphere [ITN-94-85230] p 2774 N94-27234

The Sixteenth Symposium on Coordinated Observations of the Ionosphere and the Magnetosphere in the Polar Regions: Program and abstracts [JTN-94-80601] p 2882 N94-27300

Enhancement of the rate of radiative processes in the field of a magnetic monopole [DE94-603717] p 3074 N94-27696

Fiber optic true time-delay array antenna feed system [AD-D016063] p 2777 N94-27734

Radiations from hot nuclei p 3030 N94-27915

ELECTROMAGNETIC SCATTERING

Extension of On-Surface Radiation Condition (OSRC) theory to full-vector electromagnetic wave scattering by three-dimensional conducting, dielectric, and coated targets [AD-A274023] p 2766 N94-25757

Joint services electronics program [AD-A274692] p 2783 N94-26449

Experimental and theoretical investigation of RF absorption and reflection from preformed plasmas [AD-A274189] p 3046 N94-27098

Theoretical and experimental analysis of the spatial and temporal behaviour of the intensity of an electro-magnetic wave reflected from a diffuse target after passing through a turbulent atmosphere [ITN-94-85230] p 2774 N94-27234

ELECTROMAGNETIC SHIELDING

Microwave coupling into a slotted cavity [PB94-123742] p 2772 N94-27041

Method for improving electromagnetic shielding performance of composite materials by electropulsing [AD-D016050] p 2709 N94-27076

Method for improving electromagnetic shielding performance of composite materials by electroplating [AD-D016038] p 2709 N94-27091

ELECTROMAGNETIC SPECTRA

Wavelet compression techniques for hyperspectral data p 2947 N94-28263

ELECTROMAGNETIC WAVE TRANSMISSION

Technical description of the Vulcano software library [FFI-93/7024] p 2767 N94-26105

Design and evaluation of an electromagnetic beam waveguide for measuring electrical properties of materials [NASA-TP-3418] p 2769 N94-26611

Experiments and numerical simulations of electromagnetic wave propagation in plasma varying rapidly in space and time [AD-A274376] p 2772 N94-26975

FOA 39 --- electronic countermeasures [PB94-124252] p 2773 N94-27159

Technical report of ISSP. Ser. A, no. 2671: Quasi-localization of light waves in Fibonacci dielectric multilayers [JTN-94-80557] p 3064 N94-27231

JARE data reports. No. 186: Upper atmosphere physics data. Syowa and Asuka Stations, 1990 [JTN-94-80594] p 2881 N94-27299

Memories of National Institute of Polar Research. Series A-19. Upper atmosphere physics: ELF emission in high latitudes: Ray path calculation and ground-satellite observations [JTN-94-80592] p 2882 N94-27342

Nonlinear transverse propagation of photons in a ultrarelativistically hot and magnetized electron-positron plasma: Coupling of Langmuir and electromagnetic solitons [DE94-603667] p 3046 N94-27630

Plane wave propagation and polarization properties in transversely bianisotropic uniaxial medium [PB94-132883] p 2778 N94-28380

ELECTROMAGNETISM

Joint services electronics program [AD-A274643] p 2785 N94-27027

Proton electromagnetic form factor near the proton-antiproton threshold and quasinuclear bound state [DE94-606458] p 3027 N94-27681

Hybrid techniques for complex aerospace electromagnetics problems p 2779 N94-27894

Polarizability matrix of layered chiral sphere [PB94-132834] p 2778 N94-28355

Fields and potentials in general uniaxial bianisotropic media I. Axial sources [PB94-132875] p 2778 N94-28379

Analytic solution for the dyadic Green's function of a nonreciprocal uniaxial bianisotropic medium [PB94-133162] p 2779 N94-28388

Dielectric polarizability of sphere with arbitrary anisotropy [PB94-133113] p 2779 N94-28397

ELECTROMECHANICAL DEVICES

Automatic assembly planning and its role in agile manufacturing: A Sandia perspective [DE94-002291] p 2821 N94-25970

ELECTROMYOGRAPHY

The electrogastrogram during parabolic flight p 2913 N94-27452

ELECTRON ACCELERATION

On a theory of two-beam mechanisms of charged particle acceleration in electrodynamic structures [DE94-003482] p 3032 N94-26330

A direct current rectification scheme for microwave space power conversion using traveling wave electron acceleration p 2687 N94-27371

Acceleration of electrons and ions by strong lower-hybrid turbulence in solar flares [NASA-TM-109723] p 3111 N94-27953

ELECTRON ACCELERATORS

Analytical study of beam handling and emittance control [AD-A274412] p 3033 N94-27078

ELECTRON BEAM WELDING

Evaluating non-chlorinated solvents for welding applications [DE94-003332] p 2824 N94-27181

ELECTRON BEAMS

Study on elucidation of damage generation process by electron beam lithography p 2729 N94-25581

Characterization of the energy deposition produced by the primary electron beam on the EXCEDE 3 program. Appendix B and C [AD-A273878] p 3012 N94-25726

An electromagnetic calorimeter with wavelength shifting fiber readout [DE93-616664] p 2809 N94-25735

The formation of conducting gold films by thermal decomposition and direct patterning using electron beam lithography of the gold cluster Au55P(C6H5)312C16 [AD-A273720] p 2749 N94-26074

JLC-1 [DE93-520380] p 3031 N94-26113

Laboratory plasma studies [AD-A274655] p 3043 N94-26356

Study on the compensated lead hadron calorimeter characteristics by means of hadron and electron beams [DE93-634176] p 2810 N94-26439

Investigation of plasma instabilities in the polar cusp [NASA-CR-195212] p 2879 N94-26599

HPm-tubes: Literature survey comprising 1992 [PB94-123643] p 2785 N94-27038

Analytical study of beam handling and emittance control [AD-A274412] p 3033 N94-27078

Characterization of the energy deposition produced by the primary electron beam on the EXCEDE 3 program [AD-A274453] p 3033 N94-27084

Inertial electrostatic confinement as a power source for electric propulsion p 2688 N94-27373

Space Experiments with Particle Accelerators (SEPAC) [NASA-CR-193935] p 2761 N94-27664

System for conditioning an electron beam for improved free-electron laser operation [AD-D016054] p 2820 N94-27671

Micro-electron deflector [AD-D016055] p 2787 N94-27672

A prototype presampler for the uranium-scintillator calorimeter in Zeus [NIKHEF-H/93-11] p 2814 N94-28098

ELECTRON BUNCHING

Technical report of ISSP. Ser. A, no. 2688: Suppression of higher-order modes in an RF cavity by resistive material [JTN-94-80574] p 2787 N94-27606

ELECTRON DENSITY (CONCENTRATION)

Coherent HF radar system for the study of natural and heater induced ionospheric irregularities [AD-A273804] p 2876 N94-25752

Comparative investigation of high-latitude ionospheric structure and effects near solar maximum [AD-A273799] p 2877 N94-25877

Effect of impurity correlation on the density of states in slightly compensated heavily doped semiconductors [DE94-602539] p 3061 N94-26879

Analysis of density limit and efficiency in lower hybrid current drive [DE94-604995] p 3049 N94-27856

ELECTRON DENSITY PROFILES

Analysis of EUV/FUV dayglow and auroral measurements [NASA-CR-195237] p 2883 N94-27393

Laser blow-off lithium beam probing with high temporal resolution for edge plasma diagnostics [DE94-701176] p 2820 N94-27701

ELECTRON DIFFRACTION

Electron energy loss spectroscopy in a crystalline environment using inner shell ionization [DE94-601820] p 3018 N94-26334

Developments in crystallographic phase analysis in the SEM: Backscattered electron Kikuchi patterns [DE93-040755] p 3057 N94-26420

Delocalization in electron impact ionization in a crystalline environment [DE94-601819] p 3062 N94-26927

ELECTRON DISTRIBUTION

Fermi surface ridge at second and third Umklapp positron annihilations in Y Ba2Cu3O(7-delta) [DE93-634760] p 3070 N94-27995

ELECTRON EMISSION

Secondary electron emission from copper surface due to neodymium and gadolinium ion bombardment [DE94-701115] p 3027 N94-27718

ELECTRON ENERGY

Characterization of the energy deposition produced by the primary electron beam on the EXCEDE 3 program. Appendix B and C [AD-A273878] p 3012 N94-25726

Review of tokamak experiments on direct electron heating and current drive with fast waves [DE94-004185] p 3041 N94-25801

Measurement of magnetic fluctuation induced energy transport [DE94-003846] p 3042 N94-26132

Electron energy loss spectroscopy in a crystalline environment using inner shell ionization [DE94-601820] p 3018 N94-26334

Suppression of thermal grain growth in nickel by prior electron irradiation [DE94-004602] p 2737 N94-26587

Analytical study of beam handling and emittance control [AD-A274412] p 3033 N94-27078

Implementation of a compact magnetic electron energy spectrometer for intense relativistic electron beams [AD-A274451] p 3033 N94-27082

Analysis of density limit and efficiency in lower hybrid current drive [DE94-604995] p 3049 N94-27856

Energy parameters of the incident auroral electrons derived by the intensity ratio of auroral emissions p 2779 N94-27964

Nonequilibrium radiation and chemistry models for aerocapture vehicle flowfields [NASA-CR-195706] p 2648 N94-28071

ELECTRON FLUX DENSITY
Persistence of auroral electron flux events from DMSP/F9 electron measurements
[RXR-92012] p 2887 N94-28206
ELECTRON GAS
Geometrical resonances in the nyquist noise spectrum for ballistic conductors
[DE94-603668] p 3027 N94-27631
ELECTRON IMPACT
Delocalization in electron impact ionization in a crystalline environment
[DE94-601819] p 3062 N94-26927
ELECTRON IRRADIATION
Electrical properties of p-type GaInP2
[AD-A273771] p 3051 N94-25856
Suppression of thermal grain growth in nickel by prior electron irradiation
[DE94-004602] p 2737 N94-26587
ELECTRON MICROSCOPY
Study on improvement in physical analysis method of metallic materials p 2728 N94-25577
Electron microscopy of AIN-SiC interfaces and solid solutions
[DE94-002449] p 3059 N94-26765
ELECTRON MOBILITY
On the electron mobility in slightly compensated heavily doped gallium arsenide at low temperatures
[DE93-634712] p 3057 N94-26387
ELECTRON PHONON INTERACTIONS
Anisotropy in the electrical, magnetic and optical properties of Pb2Sr2RCu3O8
[ISBN-0-315-84930-4] p 3070 N94-27974
ELECTRON PLASMA
Fast H-alpha line broadening during the 100 ns REB injection into a plasma
[IPPCZ-322] p 3048 N94-27836
ELECTRON PRECIPITATION
Persistence of auroral electron flux events from DMSP/F9 electron measurements
[RXR-92012] p 2887 N94-28206
Proton aurora and substorm intensifications
[ATR-93(7248)-1] p 2887 N94-28218
ELECTRON RECOMBINATION
Merged-beam studies of electron-recombination and excitation of atomic and molecular hydrogen ions
[ETN-94-95339] p 3019 N94-26478
ELECTRON SCATTERING
Review of tokamak experiments on direct electron heating and current drive with fast waves
[DE94-004185] p 3041 N94-25801
Convergent close-coupling calculation of electron-sodium scattering
[DE94-601815] p 3014 N94-25842
Theoretical and experimental studies of elementary physics
[DE94-002310] p 3008 N94-25988
Deciphering the quark-gluon structure of the photon in electron(gamma) collisions
[DE93-634386] p 3017 N94-26043
Crystal potential retrieval in HRTEM
[DE94-601883] p 3055 N94-26171
Separation and reconstruction of electron neutrino interaction in the IHEP-JINR neutrino detector and BARS detector
[DE93-634182] p 3019 N94-26393
Relativistic collision rate calculations for electron-air interactions
[DE94-004204] p 3020 N94-26527
Calculation of electron-potassium scattering
[DE94-601812] p 3023 N94-26942
First observation of neutral current proton electron scattering at the square root of s = 300 GeV
[DE94-701107] p 3030 N94-27877
ELECTRON SPIN
Spin asymmetry in resonant electron-hydrogen elastic scattering
[DE94-601813] p 3023 N94-26943
Technical report of ISSP. Ser. A, no. 2681: Orbital and spin susceptibilities of the plane copper sites in YBa2Cu3O(x) system
[JTN-94-80567] p 3064 N94-27177
ELECTRON STATES
Rydberg states in multiply charged ions
[DE94-002335] p 3021 N94-26760
Technical report of ISSP. Ser. A, no. 2679: Novel electronic states of partially deuterated (DMe-DCNQI)2Cu
[JTN-94-80565] p 3064 N94-27175
Technical report of ISSP. Ser. A, no. 2680: Determination of intervalley scattering time in germanium by subpicosecond time-resolved Raman spectroscopy
[JTN-94-80566] p 3064 N94-27176
Technical report of ISSP. Ser. A, no. 2681: Orbital and spin susceptibilities of the plane copper sites in YBa2Cu3O(x) system
[JTN-94-80567] p 3064 N94-27177
Technical report of ISSP. Ser. A, no. 2671: Quasi-localization of light waves in Fibonacci dielectric multilayers
[JTN-94-80557] p 3064 N94-27231
Technical report of ISSP. Ser. A, no. 2674: High-field cyclotron resonance and impurity transition in n- and p-3C-SiC at magnetic fields up to 175 T
[JTN-94-80560] p 3064 N94-27232
Technical report of ISSP. Ser. A, no. 2670: Electronic structure of light transition metal compounds studied by photoemission
[JTN-94-80556] p 3065 N94-27239
Technical report of ISSP. Ser. A, no. 2672: Magneto-optical effects of excitons in BiI3 crystals under pulsed high magnetic fields. 3: Excitons confined around a stacking disorder formed by a bending stress
[JTN-94-80558] p 3065 N94-27240
Technical report of ISSP. Ser. A, no. 2675: High-field cyclotron resonance and valence-band structure in semiconducting diamond
[JTN-94-80561] p 3065 N94-27245
Technical report of ISSP. Ser. A, no. 2676: Charge mass singularity in two-dimensional Hubbard model
[JTN-94-80562] p 3065 N94-27248
ELECTRON TRANSFER
Translational-energy-resolved studies of photogenerated carrier-induced reactions on UHV semiconductor surfaces
[DE94-004169] p 3058 N94-26526
Voltammetric studies of poly(carbon disulfide)
[DE94-001385] p 2717 N94-26951
Research in pulsed power plasma physics
[AD-A274323] p 3045 N94-27074
Hydrogen physics
[DE94-701317] p 2719 N94-27822
ELECTRON TRANSITIONS
Computational analysis of some aspects of a synthetic route to ammonium dinitramide
[AD-A274648] p 2704 N94-26353
Rydberg states in multiply charged ions
[DE94-002335] p 3021 N94-26760
International bulletin on atomic and molecular data for fusion. No. 46
[DE94-601818] p 3023 N94-26947
Technical report of ISSP. Ser. A, no. 2676: Charge mass singularity in two-dimensional Hubbard model
[JTN-94-80562] p 3065 N94-27248
Technical report of ISSP. Ser. A, no. 2687: Quantized persistent currents of a quantum dot in a strong magnetic field
[JTN-94-80573] p 3028 N94-27758
Dynamics of metastable states in supersonic beams
[ITN-94-85232] p 3028 N94-27760
ELECTRON TUNNELING
Image potential of a tunnelling electron moving near two different metals
[DE94-603657] p 3069 N94-27819
ELECTRON-POSITRON PAIRS
Gamma Large Area Silicon Telescope (GLAST): Applying silicon strip detector technology to the detection of gamma rays in space
[DE94-003451] p 3116 N94-27740
Research on elementary particle physics, part 2
[DE94-004956] p 3029 N94-27815
ELECTRON-POSITRON PLASMAS
Nonlinear transverse propagation of photons in a ultrarelativistically hot and magnetized electron-positron plasma: Coupling of Langmuir and electromagnetic solitons
[DE94-603667] p 3046 N94-27630
ELECTRONIC CONTROL
Sequential multi-point injection of a natural gas engine. Topical report, November 1991 - April 1992
[PB94-126794] p 2824 N94-27224
ELECTRONIC COUNTERMEASURES
Evaluation of an Acoustic Charge Transport (ACT) device for adaptive interference suppression in spread spectrum communications systems
[AD-A274073] p 2765 N94-25647
FOA 39 --- electronic countermeasures
[PB94-124252] p 2773 N94-27159
ELECTRONIC EQUIPMENT
RF-station control crate
[DIGEL-1992-9] p 2779 N94-25618
Engineering Technical Letter (ETL) 93-5: Fire protection engineering criteria, electronic equipment installations
[AD-A274835] p 2762 N94-26084
Microwave and pulsed power
[DE94-003019] p 2782 N94-26312
Joint services electronics program
[AD-A274692] p 2783 N94-26449
Generalized emulation microcircuit program
[AD-A274749] p 2785 N94-26797
A fully integrated 16 channel digitally trimmed pulse shaping amplifier
[DE94-004555] p 2787 N94-27618
Advances in gamma ray field instrumentation at Los Alamos
[DE93-040264] p 2813 N94-27624
Control system for tracking nonlinear systems
[AD-D016057] p 2787 N94-27673
ELECTRONIC EQUIPMENT TESTS
Hierarchical test development and design-for-testability for (a)synchronous semi-custom ASIC's
[ISBN-9-09-005928-8] p 2834 N94-26003
Test methods and custom hardware for functional testing of a high speed GaAs DRAM
[AD-A274859] p 2781 N94-26175
Symbolic model checking for sequential circuit verification
[AD-A274375] p 2786 N94-27061
ELECTRONIC FILTERS
An integrated delta-sigma based IIR filter
[ISBN-0-315-83593-1] p 2784 N94-26631
ELECTRONIC MAIL
Single term off-line coins
[CWI-CS-R9318] p 2776 N94-27546
An efficient off-line electronic cash system based on the representation problem
[CWI-CS-R9323] p 2776 N94-27551
ELECTRONIC PACKAGING
Experimental determination of the CU-IN-PB ternary phase diagram
[DE94-003765] p 2735 N94-26349
ELECTRONIC SPECTRA
Spectroscopy Division
[DE94-604074] p 2717 N94-26988
ELECTRONIC WARFARE
FOA 39 --- electronic countermeasures
[PB94-124252] p 2773 N94-27159
Smalltalk: A tool for development of an Ada implementation of EWCAC
[SKL-1600-46-003-01-0] p 2974 N94-27823
ELECTRONS
Heavy-electron behavior in large coordination compounds CeZn11 and UZn12
[REPT-A-2663] p 3049 N94-25614
Convergent close-coupling calculation of electron-sodium scattering
[DE94-601815] p 3014 N94-25842
Trapped electrons in solid hydrogen
[DE93-018628] p 3052 N94-25947
Theoretical and experimental studies of elementary physics
[DE94-002310] p 3008 N94-25988
Measurement of magnetic fluctuation induced energy transport
[DE94-003846] p 3042 N94-26132
Ionospheric modification by high power, obliquely propagated HF radio wave transmissions. Part 1: Experimental
[AD-A273746] p 2878 N94-26224
On Poisson brackets and symplectic structures for the classical and quantum Zitterbewegung
[DE93-634305] p 2992 N94-26267
Magnetic field induced contributions of supersymmetric particles to energy losses of neutron star
[DE93-634331] p 3104 N94-26269
Separation and reconstruction of electron neutrino interaction in the IHEP-JINR neutrino detector and BARS detector
[DE93-634182] p 3019 N94-26393
On the wave and corpuscular properties of microparticles
[DE93-634450] p 3020 N94-26509
Calculation of total cross sections for electron and positron scattering on sodium and potassium
[DE94-601814] p 3023 N94-26944
Calculations of asymmetries in electron-alkali scattering
[DE94-601816] p 3023 N94-26945
A measurement of the W mass using electrons at CDF
[DE94-004656] p 3028 N94-27748
Analysis of energetic proton and electron data in Neptune's magnetosphere
[NASA-CR-195707] p 3107 N94-27784
ELECTROPHORESIS
High definition Raman microscopic imaging
[DE94-003158] p 2716 N94-26781
ELECTROPHOTOMETERS
Characterization of the energy deposition produced by the primary electron beam on the EXCEDE 3 program
[AD-A274453] p 3033 N94-27084
ELECTROPHYSIOLOGY
Electrical stimulation in exercise training
p 2935 N94-28371
ELECTROPLATING
Vapor deposition of copper on stainless steel 304L
[DE94-001945] p 2740 N94-27006

Method for improving electromagnetic shielding performance of composite materials by electroplating
[AD-D016038] p 2709 N94-27091

ELECTROSLAG REFINING

Study on reactions between molten metal and oxide by magnetic flotation dissolution method
p 2725 N94-25558

ELECTROSTATIC CHARGE

Electrostatic image solution for the conducting prolate spheroid
[PB94-133154] p 2778 N94-28387

ELECTROSTATIC WAVES

Acceleration of electrons and ions by strong lower-hybrid turbulence in solar flares
[NASA-TM-109723] p 3111 N94-27953

ELECTROSTATICS

The electric field between non conductive rectangular charged surfaces placed near a small spherical conductive earthed surface and determination of critical density of charge
[DE93-634324] p 2783 N94-26443

Cryogenic size reduction of solid propellant
[AD-A274844] p 2759 N94-26800

Molecular surface electrostatic potentials in the analysis of non-hydrogen-bonding noncovalent interactions
[AD-A274612] p 3022 N94-26894

Inertial electrostatic confinement as a power source for electric propulsion p 2688 N94-27373

Atomic processes in Inertial Electrostatic Confinement (IEC) devices
[DE94-005015] p 3047 N94-27715

Computer simulation of aqueous Na-Cl electrolytes
[DE94-002622] p 3030 N94-28001

Electrostatic image solution for the conducting prolate spheroid
[PB94-133154] p 2778 N94-28387

ELECTROSTRICTION

Studies of non-linear optical effects for agile beam steering
[AD-A273998] p 3034 N94-25902

ELEMENTARY EXCITATIONS

Towards a theory of growing surfaces: Mapping two-dimensional Laplacian growth onto Hamiltonian dynamics and statistics
[DE94-002636] p 2991 N94-26079

Strongly interacting fermion systems
[DE94-002674] p 3021 N94-26677

Decay of non-equilibrium polariton condensate in semiconductors
[DE94-604016] p 3068 N94-27678

ELEMENTARY PARTICLE INTERACTIONS

Quark-antiquark bound states
[DE93-613054] p 3013 N94-25826

Principles of gauge theory of real hadrons
[DE93-613096] p 3013 N94-25835

Unravelling the structure of matter on high-performance computers
[DE94-601620] p 3015 N94-25891

Spin effects in hard interactions (interest in accelerated polarized beam)
[DE93-634398] p 3031 N94-26044

An antiproton-proton partial-wave analysis
[DE94-002690] p 3021 N94-26620

Low-energy hadronic interactions beyond the current algebra approach
[DE94-602600] p 3022 N94-26900

A variational approach to the quantum field theoretic bound-state problem
[ISBN-0-315-60960-5] p 3074 N94-27401

All-coupling polaron ground state energy in D-dimension
[DE94-603666] p 3027 N94-27629

Neutron-neutron scattering: Possibility of in-beam experiment
[DE94-606459] p 3027 N94-27682

ELEMENTARY PARTICLES

On the model of the relativistic particle with curvature and torsion
[DE94-606330] p 3029 N94-27848

Radiations from hot nuclei p 3030 N94-27915

ELEVATION

The effect of elevation data representation on nocturnal drainage wind simulations
[DE94-003624] p 2892 N94-25936

Differential global positioning system for the surface-towed ordnance locating system: Testing, results, and user's guide
[DE94-002980] p 2664 N94-26309

Conifer tree influence on Digital Terrain Elevation Data (DTED): A case study at Dulles International Airport
[AD-A274213] p 2849 N94-27069

ELEVATION ANGLE

Geometric correction of SPOT images with use of digital elevation models
[ETN-94-95033] p 2847 N94-26107

ELLIPTIC DIFFERENTIAL EQUATIONS

A survey of open problems in symplectic integration
[DE94-003966] p 3007 N94-27777

ELLIPTICAL POLARIZATION

Eigenwaves in the general uniaxial bianisotropic medium with symmetric parameter dyadics
[PB94-132891] p 2778 N94-28381

Plane wave propagation in an anisotropic chiral medium with isotropic permittivity and permeability
[PB94-133097] p 2778 N94-28384

EMBEDDED COMPUTER SYSTEMS

Development and analysis of secure embedded software
[VTT-TIED-1430] p 2961 N94-26254

Real-Time Embedded Processing for Space Applications
[ISBN-2-85428-335-X] p 2948 N94-26713

Use of HOOD coupled to real time monitors
p 2953 N94-26742

EMBRITTLEMENT

The role of point defect clusters in reactor pressure vessel embrittlement
[DE94-001122] p 2739 N94-26931

Failure behaviour of high density polyethylene with an embrittled surface layer due to weathering
[PB94-126406] p 2840 N94-26960

Mechanical behavior of amorphous alloys at elevated temperatures p 2746 N94-28167

EMBRYOS

Effects of ML-9, a myosin light-chain kinase inhibitor, on preimplantation development of the mouse
p 2905 N94-27486

Compaction-like blastomere aggregation caused by 1-oleoyl-2-acetylglycerol in mouse embryos: An electron microscopic observation p 2905 N94-27487

Inductive differentiation of nerve cells in mouse embryonic ectoderm at early primitive streak stage by retinoic acid p 2905 N94-27488

Proposed law of nature linking impacts, plume volcanism, and Milankovitch cycles to terrestrial vertebrate mass extinctions via greenhouse-embryo death coupling
p 2876 N94-28307

EMERGENCIES

Assured crew return vehicle post landing configuration design and test p 2697 N94-25671

Mesoscale meteorological measurements characterizing complex flows
[DE94-002359] p 2895 N94-26761

EMISSION SPECTRA

Study on analyzing method establishment for metallic material development p 2729 N94-25578

Trapped electrons in solid hydrogen
[DE93-018628] p 3052 N94-25947

Stationary plasma thruster plume emissions
[NASA-CR-194471] p 2701 N94-26209

Electron energy loss spectroscopy in a crystalline environment using inner shell ionization
[DE94-601820] p 3018 N94-26334

A study of gamma ray burst continuum properties presnting evidence for two spectral states in bursts
p 3114 N94-26688

Researches of the Electrotechnical Laboratory. No. 53: Spectral emission from combustion gas containing scattering media
[JTN-94-80603] p 2717 N94-27246

Energy parameters of the incident auroral electrons derived by the intensity ratio of auroral emissions
p 2779 N94-27964

The kinetics and dynamics of the coma of Halley's comet
[NASA-CR-194828] p 3105 N94-28184

EMISSIVITY

Uncertainties in the characterization of the thermal environment of a solid rocket propellant fire
[DE94-002023] p 2760 N94-27719

Energy parameters of the incident auroral electrons derived by the intensity ratio of auroral emissions
p 2779 N94-27964

EMITTANCE

Longitudinal diffusion of a proton bunch under external noise
[DE93-634022] p 3032 N94-26165

Analytical study of beam handling and emittance control
[AD-A274412] p 3033 N94-27078

EMITTERS

S-76 high intensity radiated fields, volume 2
[AD-A274572] p 2771 N94-26836

S-76 high intensity radiated fields, volume 1
[AD-A274571] p 2771 N94-26854

Fibrous emissive burners selective and broad band
[PB94-128329] p 2859 N94-27225

EMULSIONS

Double layer capacitance of carbon foam electrodes
[DE94-002651] p 2780 N94-25975

Development of liquid membrane separation processes p 2717 N94-27386

ENAMELS

Dual cure low-VOC coating process
[DE94-000365] p 2756 N94-27611

ENCAPSULATING

A formalization of objects using equational dynamic logic
[PB94-125218] p 2965 N94-26852

END EFFECTORS

Autonomous space processor for orbital debris advanced design project in support of solar system exploration p 2697 N94-25667

Inertial-space disturbance rejection for space-based manipulators p 2683 N94-26281

Interchangeable end effector tools utilized on the PFMA
[NASA-CR-193925] p 2823 N94-27149

ENDANGERED SPECIES

Coupling of pelagic and benthic communities over a seamount in the Eastern North Pacific
[AD-A274750] p 2899 N94-26149

ENDOCRINE GLANDS

Endocrinological evaluations of muscle and bone atrophy in tail-suspended rats p 2903 N94-27444

ENERGY BANDS

Technical report of ISSP. Ser. A, no. 2679: Novel electronic states of partially deuterated (DMe-DCNQI)2Cu
[JTN-94-80565] p 3064 N94-27175

Technical report of ISSP. Ser. A, no. 2670: Electronic structure of light transition metal compounds studied by photoemission
[JTN-94-80556] p 3065 N94-27239

ENERGY BUDGETS

Surface roughness lengths
[AD-A274550] p 2895 N94-26846

Martian atmospheric radiation budget
p 3107 N94-27887

Role of remote sensing in energy, water, and carbon cycle studies over the Amazon
[INPE-5486-PRE/1786] p 2852 N94-27957

Research activities on the meteorology over the Asia-Pacific region p 2853 N94-28271

ENERGY CONSUMPTION

Solar energy utilization in the USSR
p 2853 N94-26052

ENERGY CONVERSION

Ways to improve MHD power plants and prospects of their application p 2854 N94-26056

Parametric analysis of the space power plants on the base of criterion of specific mass in generalized design variants
[DE93-634153] p 2701 N94-26166

High temperature solid oxide fuel development activities
[DE94-002973] p 2858 N94-26871

ENERGY CONVERSION EFFICIENCY

Ways to improve MHD power plants and prospects of their application p 2854 N94-26056

Controls, monitoring and performance measurements
p 2831 N94-28086

ENERGY DISSIPATION

An electromagnetic calorimeter with wavelength shifting fiber readout
[DE93-616664] p 2809 N94-25735

Rescattering and energy loss of fast partons in nuclear matter
[DE94-002918] p 3018 N94-26145

Parametric analysis of the space power plants on the base of criterion of specific mass in generalized design variants
[DE93-634153] p 2701 N94-26166

Magnetic field induced contributions of supersymmetric particles to energy losses of neutron star
[DE93-634331] p 3104 N94-26269

Electron energy loss spectroscopy in a crystalline environment using inner shell ionization
[DE94-601820] p 3018 N94-26334

The influence of energy losses with time in NbTi superconductors in pulsed magnetic fields
[DE93-634761] p 3058 N94-26512

Relativistic collision rate calculations for electron-air interactions
[DE94-004204] p 3020 N94-26527

A prototype presampler for the uranium-scintillator calorimeter in Zeus
[NIKHEF-H/93-11] p 2814 N94-28098

Consequences of impacts of small asteroids and comets with Earth p 2889 N94-28301

ENERGY DISTRIBUTION

A study of very high energy hadron interactions through observation of cosmic-ray families of visible energy greater than 500 TeV, 1 p 3112 N94-25625

A study of very high energy hadron interactions through observation of cosmic-ray families of visible energy greater than 500 TeV, 2 p 3112 N94-25626

ENERGY GAPS (SOLID STATE)

Surface modes and chiral symmetry (Wilson fermions in a box)
[DE94-004946] p 3029 N94-27814

ENERGY LEVELS

High resolution fourier transform absorption spectrum of 79Br2 B3 Pi(Ou+) X1 sigma g+
[AD-A273864] p 2956 N94-25610

On the estimation of matrix elements for optical transitions in semiconductors
[DE93-613550] p 3051 N94-25851

Biexciton formation by two-photon absorption in quantum wells
[DE93-613551] p 3071 N94-25852

On the classification scheme for resonant states of muonic molecules
[DE93-613645] p 3014 N94-25853

Electronic structure of a single oxygen vacancy in rutile TiO2
[DE94-602717] p 3062 N94-26901

International bulletin on atomic and molecular data for fusion. No. 42-45, Mar. 1991 - Dec. 1992
[DE94-601817] p 3045 N94-26946

International bulletin on atomic and molecular data for fusion. No. 46
[DE94-601818] p 3023 N94-26947

Hyperfine structure of positronium energy levels in a crystal
[DE94-603898] p 3068 N94-27729

Hypersensitive transition spectrum of f-element and coordination structure
[DE94-604133] p 3070 N94-27843

ENERGY METHODS

Separable expansions of the NN t-matrix by way of exact half off the energy shell methods
[DE94-601615] p 3015 N94-25890

Weak coupling in statistical energy analysis ion Research, Univ. of Southampton, Southampton SO9 5NH, England)
[ISVR-TR-228] p 2832 N94-28174

ENERGY OF FORMATION

Zinc(2) oxide stability in alkaline sodium phosphate solutions at elevated temperatures
[DE94-003316] p 2715 N94-26320

ENERGY POLICY

Programme for the promotion of wind power production
[DE94-702065] p 2855 N94-26242

An overview of DOE's wind turbine development programs
[DE93-018224] p 2856 N94-26513

Present situation of the development of petroleum substitution energy (France)
[DE94-725201] p 2760 N94-26914

ENERGY REQUIREMENTS

An overview of DOE's wind turbine development programs
[DE93-018224] p 2856 N94-26513

ENERGY SOURCES

Renewable energy systems in Mexico: Installation of a hybrid system
[DE93-013716] p 2853 N94-25946

ENERGY SPECTRA

Energy concentration in high energy hadron-gamma families p 3113 N94-25632

Hadron gas ionization calorimeters
[DE93-634186] p 2810 N94-26397

Study on the compensated lead hadron calorimeter characteristics by means of hadron and electron beams
[DE93-634176] p 2810 N94-26439

Calculations of population transfer during intense laser pulses
[DE94-001060] p 2818 N94-26698

A measurement of the energy spectra of cosmic rays from 20 to 1000 GeV per AMU
[NASA-CR-195246] p 3115 N94-27167

Spectroscopy and strong decays of baryons
[ISBN-0-315-49073-X] p 3024 N94-27258

ENERGY STORAGE

Exploratory Technology Research Program for Electrochemical Energy Storage
[DE94-003479] p 2781 N94-26047

A study on the development of high T(sub c) superconducting materials
[DE93-633529] p 3057 N94-26404

Low-cost photovoltaic inverters incorporating application-specific integrated circuits
[DE94-003270] p 2856 N94-26463

The reactivity of lithium toward non-aqueous solvents of relevance to energy storage applications as studied by surface analytical techniques
[DE94-003483] p 2856 N94-26464

The 1993 NASA Aerospace Battery Workshop
[NASA-CP-3254] p 2860 N94-28100

Advanced energy storage for space applications: A follow-up p 2860 N94-28103

Experimental evaluation of battery cells for space-based radar application p 2860 N94-28104

ENERGY TECHNOLOGY

Theoretical and computational studies in intermediate energy nuclear physics
[DE94-004177] p 3012 N94-25800

Renewable energy systems in Mexico: Installation of a hybrid system
[DE93-013716] p 2853 N94-25946

General Motors Corporation and Pacific Northwest Laboratory staff exchange: Inspection of case hardened steels and metal-matrix composites
[DE94-003470] p 2706 N94-25982

NEMO 2: New energy systems and technologies
[DE94-702060] p 2855 N94-26240

SIHTI 2: Energy and environmental technology
[DE94-702061] p 2867 N94-26241

Scientific and Technical Information (STI)....what's the status?
[DE94-003731] p 3097 N94-26348

International energy: Research organizations, 1988-1992
[DE93-017267] p 3098 N94-26398

Fusion Energy Advisory Committee: Advice and recommendations to the US Department of Energy in response to the charge letter of September 1, 1992
[DE93-019842] p 3043 N94-26428

An overview of the ASCOT program
[DE94-004356] p 2869 N94-27601

Combined Cycles for Power Plants
[VKI-LS-1993-08] p 2830 N94-28077

Clean coal technology p 2832 N94-28089

ENERGY TRANSFER

Vibrational energy transfer within the B 3Pi (O(+) sub u) state of 79BR2 upon collision with N2, O2, NO, and SF6
[AD-A273905] p 3011 N94-25589

Characterization of the energy deposition produced by the primary electron beam on the EXCEDE 3 program. Appendix B and C
[AD-A273878] p 3012 N94-25726

Spectroscopic and vibrational energy transfer studies in molecular bromine
[AD-A273795] p 3014 N94-25875

Surface physics with cold and thermal neutron reflectometry
[DE94-001447] p 2733 N94-26070

Interpreting the implied meridional oceanic energy transport in AMIP
[DE94-001538] p 2898 N94-26072

Measurement of magnetic fluctuation induced energy transport
[DE94-003846] p 3042 N94-26132

Dynamics explorer interdisciplinary scientist investigations
[NASA-CR-195226] p 2878 N94-26204

Differentiating the role of land surface variability and cloudiness variability on global energy transport within the atmosphere and oceans
[NASA-CR-195229] p 2847 N94-26222

The dynamics of interacting nonlinearities governing long wavelength driftwave turbulence
[DE94-001785] p 2793 N94-26558

Characterization of the energy deposition produced by the primary electron beam on the EXCEDE 3 program
[AD-A274453] p 3033 N94-27084

ENGINE AIRFRAME INTEGRATION

The design of a counter rotating ultra-high-bypass fan simulator for windtunnel investigation
[DLR-FB-93-20] p 2675 N94-27739

ENGINE DESIGN

Supercruiser Arrow HS-8 p 2671 N94-25711

The design of a long-range megatransport aircraft p 2671 N94-25718

Orbit transfer rocket engine technology program
[NASA-CR-189229] p 2702 N94-26542

A technique for integrating engine cycle and aircraft configuration optimization
[NASA-CR-191602] p 2668 N94-26606

Orbital transfer vehicle engine technology high velocity ratio diffusing crossover
[NASA-CR-194447] p 2703 N94-27212

Orbital transfer rocket engine technology 7.5K-LB thrust rocket engine preliminary design
[NASA-CR-190754] p 2703 N94-27213

Inertial electrostatic confinement as a power source for electric propulsion p 2688 N94-27373

Development of hypersonic engine seals: Flow effects of preload and engine pressures
[NASA-TM-106333] p 2826 N94-27599

Gas fired advanced turbine system
[DE94-003193] p 2827 N94-27874

Transient model applications. 1: Compressor heat soak/clearance effects modeling p 2828 N94-28048

Transient model applications. 2: Compressor stall modeling methods p 2829 N94-28049

Transient model applications. 3: Transient engine simulation and analysis of an ice ingestion test p 2829 N94-28050

Engine simulation technology p 2829 N94-28051

Transient engine simulation p 2829 N94-28052

Nonlinear solvers p 2829 N94-28053

Engine simulation systems p 2829 N94-28054

ENGINE FAILURE

STS-51 pad abort. OV103-engine 2033 (ME-2) fuel flowmeter sensor open circuit
[NASA-CR-193924] p 2701 N94-26230

Optimal control of helicopters following power failure
[NAL-TR-1190] p 2678 N94-27206

Compressor stability p 2828 N94-28046

Engine starting and stopping p 2828 N94-28047

Transient model applications. 2: Compressor stall modeling methods p 2829 N94-28049

ENGINE INLETS

Wind tunnel investigation of an STOL aircraft model: An effect of engine nacelle shape
[NAL-TM-653] p 2647 N94-27235

Influence of headwind on hot gas reingestion and consideration of pressure ratio scaling p 2675 N94-28018

Unsteady aspects of hot gas reingestion and statistical analysis p 2676 N94-28019

ENGINE MONITORING INSTRUMENTS

An algorithm for determination of bearing health through automated vibration monitoring
[AD-A274591] p 2823 N94-26986

Effects of expected-value information and display format on recognition of aircraft subsystem abnormalities
[NASA-TP-3395] p 2673 N94-27882

ENGINE NOISE

CRC customer versus rater octane number requirement program (1990)
[AD-A273997] p 2758 N94-25901

ENGINE PARTS

Aircraft turbine engine reliability and inspection investigations
[AD-A274860] p 2673 N94-26176

Optimising BMW four-cylinder two-valve engines
[PB94-125101] p 2824 N94-27254

Interdisciplinary technology p 2686 N94-27363

A review of recent aeroelastic analysis methods for propulsion at NASA Lewis Research Center
[NASA-TP-3406] p 2846 N94-28227

ENGINE STARTERS

Gas Turbine Engine Transient Behaviour
[VKI-LS-1993-06] p 2828 N94-28043

Engine starting and stopping p 2828 N94-28047

ENGINE TESTS

Test results of the RS-44 integrated component evaluator liquid oxygen/hydrogen rocket engine
[NASA-CR-194443] p 2701 N94-26231

Sequential multi-point injection of a natural gas engine. Topical report, November 1991 - April 1992
[PB94-126794] p 2824 N94-27224

Computer aided data recording and analyzing system for the engine test p 2764 N94-27979

The emission characteristics of a high speed diesel engine p 2764 N94-27980

Transient model applications. 3: Transient engine simulation and analysis of an ice ingestion test p 2829 N94-28050

ENGINEERING

Selected data on Federal support to universities and colleges: FY 1991
[NSF-93-320] p 3101 N94-28201

ENGINEERS

General Motors Corporation and Pacific Northwest Laboratory staff exchange: Inspection of case hardened steels and metal-matrix composites
[DE94-003470] p 2706 N94-25982

ENSTATITE

Electrical conductivity of perovskite-magnesiowuestite as a function of pressure and temperature
[DE94-002714] p 2880 N94-26806

ENTHALPY

A numerical approach to Stefan problem
[IPPCZ-334] p 2844 N94-27841

Calculation of the thermoneutral potential of NiCd and NiH2 cells p 2861 N94-28111

Differential scanning calorimetric study of solid state amorphization and crystallization in Zr/Co and Zr/Ni multilayers p 2745 N94-28161

Formation and crystallization of hydrogen-induced amorphous Ti3InH(4.5) alloy p 2745 N94-28163

ENTRAINMENT

An experimental study of plunging liquid jet induced air carryunder and dispersion
[AD-A274414] p 2794 N94-26979

ENTROPY

Parametric analysis of the space power plants on the base of criterion of specific mass in generalized design variants
[DE93-634153] p 2701 N94-26166

Zinc(2) oxide stability in alkaline sodium phosphate solutions at elevated temperatures
[DE94-003316] p 2715 N94-26320

Quantum statistical inference for density estimation
[DE94-002625] p 3073 N94-26805

ENUMERATION

Enumeration of n-fold tangent hyperplanes to a surface
[DE94-601544] p 2993 N94-26412

ENVIRONMENT EFFECTS

Preliminary design of nine high speed civil transports
p 2671 N94-25710

Selfsimilar solutions of a nonlinear transport equation
[REPT-93-42] p 2865 N94-25760

Implications of policies and prevent climate change for future food security
[DE93-018872] p 2866 N94-25948

Active layer dynamics and arctic hydrology and meteorology
[DE94-001724] p 2892 N94-25951

Grassland/atmosphere response to changing climate: Coupling regional and local scales
[DE94-003111] p 2866 N94-26026

Meeting of the Eighth Session of the Scientific Advisory Committee of the World Climate Impact Assessment and Response Strategies Programme
[DE93-633954] p 2866 N94-26163

SIHTI 2: Energy and environmental technology
[DE94-702061] p 2867 N94-26241

Titanium 1992: Volume 3: Science and technology
[AD-A274800] p 2735 N94-26337

Measuring variation in ecosystem sensitivity to stress
[AD-A274232] p 2868 N94-26817

Leadex environmental phenomena and effects observed by DMSP, NOAA, and ERS-1 satellites
[AD-A274596] p 2868 N94-26888

NASA-UVA light aerospace alloy and structures technology program (LA2ST)
[NASA-CR-195275] p 2844 N94-27851

Asia-Pacific Seminar on Global Change Research Cooperation
[JTN-94-80517] p 2871 N94-28268

Changes in phytoplankton population in the Chao Phraya estuary, Thailand, during the eutrophication mechanisms studies p 2875 N94-28287

Land use change in Thailand and its impact on environmental change: Joint Thai-Japanese research project (1993-1995) p 2875 N94-28288

Study on environment monitoring over whole China using NDVI from AVHRR data and future project
p 2875 N94-28289

Utilization of remote sensing data for global climate change research in Malaysia p 2875 N94-28290

Utilization of remote sensing data for global change research p 2875 N94-28292

Contribution of satellite observation to global change research p 2876 N94-28293

Proposed law of nature linking impacts, plume volcanism, and Milankovitch cycles to terrestrial vertebrate mass extinctions via greenhouse-embryo death coupling
p 2876 N94-28307

ENVIRONMENT MANAGEMENT

The potential for the Department of Defense to use space-based remote sensing to support DOD and other government agencies' environmental programs
[AD-A273895] p 2847 N94-25656

Hanford Environmental Information System (HEIS) sample/data entry flow summary
[DE94-002494] p 3098 N94-26559

Feasibility study on construction of a global environment research and development information network
[DE94-725198] p 2868 N94-26904

Present situation of the development of petroleum substitution energy (France)
[DE94-725201] p 2760 N94-26914

Coastal Zone Management Act and related legislation, revision 3
[DE94-004180] p 2869 N94-27691

Environmental management and audit
p 2870 N94-28153

ENVIRONMENT MODELS

Grassland/atmosphere response to changing climate: Coupling regional and local scales
[DE94-003111] p 2866 N94-26026

Why is the north polar cap on Mars different than the south polar cap? p 3107 N94-27889

Landscape dynamics of northeastern forests
[NASA-CR-195272] p 2852 N94-28070

ENVIRONMENT POLLUTION

Study on neutron activation analysis
[DE93-632191] p 3017 N94-26116

Cooling towers for combined cycles: New developments to meet environmental requirements
p 2832 N94-28088

ENVIRONMENT PROTECTION

Analysis and development of an F-5 pollution prevention management program with recommendations for creation of similar programs for other aircraft
[AD-A274016] p 2865 N94-25755

Engineering Technical Letter (ETL) 93-5: Fire protection engineering criteria, electronic equipment installations
[AD-A274835] p 2762 N94-26084

Effects of plastic media blasting on aircraft skin
[AD-A274817] p 2668 N94-26488

Numerical analysis of the photo-dissociation/radical oxidation of formaldehyde by ultraviolet light in a photolytic reactor
[AD-A274539] p 2868 N94-26843

Vapor deposition of copper on stainless steel 304L
[DE94-001945] p 2740 N94-27006

Automated in-situ inspection systems for underground storage tanks
[AD-A274644] p 2764 N94-27144

Coastal Zone Management Act and related legislation, revision 3
[DE94-004180] p 2869 N94-27691

Journal of NIRE, volume 2, number 4
[JTN-94-80554] p 2869 N94-28147

Recent legal movement on water quality regulation in Japan p 2869 N94-28148

Environmental management and audit
p 2870 N94-28153

Lufthansa Yearbook 1992
[DSK-9734-H-92] p 2660 N94-28230

The single European market: Economical advance, ecological problem? p 2661 N94-28235

ENVIRONMENT SIMULATION

ObjectSim: A reusable object oriented DIS visual simulation
[AD-A274030] p 2958 N94-25767

NPSNET-4: A real-time, 3D distributed interactive virtual world
[AD-A274942] p 2961 N94-26298

ENVIRONMENTAL CONTROL

Automation of closed environments in space for human comfort and safety p 2943 N94-25684

Designing for human presence in space: An introduction to environmental control and life support systems
[NASA-RP-1324] p 2942 N94-27437

Study on posture control and adaption mechanism under weightlessness: Results of second rehearsal for space experiment using carp p 2912 N94-27446

Study on posture control and adaptation mechanism under weightlessness: Summary report of ground operations performed for carp experiment (FMPT/L-2) in Space Shuttle mission p 2912 N94-27447

ENVIRONMENTAL ENGINEERING

Bulletin of Precision and Intelligence Laboratory, No. 68
[JTN-94-80609] p 3010 N94-27282

Silence amenity engineering: Past and present
p 3011 N94-27283

ENVIRONMENTAL MONITORING

Assessment of tropical forests using satellite data
[SILVA-CARELICA-21] p 2850 N94-27182

Global tropical forest cover assessments using satellite imagery p 2850 N94-27183

Mapping closed tropical forest cover in West Africa using NOAA/AVHRR-LAC data p 2850 N94-27184

Woody biomass density in the Tendelti area of the central Sudan p 2850 N94-27185

MUSIC for localization of thunderstorm cells
[DE94-004985] p 2897 N94-28146

Journal of NIRE, volume 2, number 4
[JTN-94-80554] p 2869 N94-28147

Environmental management and audit
p 2870 N94-28153

Asia-Pacific Seminar on Global Change Research Cooperation
[JTN-94-80517] p 2871 N94-28268

Role and activity of STA on Asian Pacific regional cooperation p 2853 N94-28269

Cooperative research projects on satellite remote sensing for the hydrological subjects
p 2853 N94-28270

Research activities on the meteorology over the Asia-Pacific region p 2853 N94-28271

NASDA contribution plan to Asian countries
p 2853 N94-28273

Global concern on research cooperation for environment p 2872 N94-28275

Progress in the study of global change in China
p 2873 N94-28276

Research and observation programmes on global changes in Indonesia p 2873 N94-28277

Country report on global change research for the Republic of Korea p 2873 N94-28278

Philippine thrust on environmental research relating to global change p 2873 N94-28279

The Environmental Research and Training Centre
p 2873 N94-28280

Global Change and Terrestrial Ecosystems (GCTE): Progress report and prospects for Asian contributions
p 2874 N94-28281

Global change: A research strategy for Australia 1992-1996 p 2874 N94-28282

A progress report on global change studies in China
p 2874 N94-28283

Indian activities on the core programme IGAP and proposals for network activities p 2874 N94-28284

HDGEC activity in Asia Pacific region
p 2874 N94-28286

Changes in phytoplankton population in the Chao Phraya estuary, Thailand, during the eutrophication mechanisms studies p 2875 N94-28287

Land use change in Thailand and its impact on environmental change: Joint Thai-Japanese research project (1993-1995) p 2875 N94-28288

Study on environment monitoring over whole China using NDVI from AVHRR data and future project
p 2875 N94-28289

Utilization of remote sensing data for global climate change research in Malaysia p 2875 N94-28290

Thailand satellite ground receiving station in global change research cooperation p 2875 N94-28291

Utilization of remote sensing data for global change research p 2875 N94-28292

Contribution of satellite observation to global change research p 2876 N94-28293

ENVIRONMENTAL QUALITY

Asia-Pacific Seminar on Global Change Research Cooperation
[JTN-94-80517] p 2871 N94-28268

The Environmental Research and Training Centre
p 2873 N94-28280

Global Change and Terrestrial Ecosystems (GCTE): Progress report and prospects for Asian contributions
p 2874 N94-28281

Indian activities on the core programme IGAP and proposals for network activities p 2874 N94-28284

HDGEC activity in Asia Pacific region
p 2874 N94-28286

Land use change in Thailand and its impact on environmental change: Joint Thai-Japanese research project (1993-1995) p 2875 N94-28288

Utilization of remote sensing data for global climate change research in Malaysia p 2875 N94-28290

Utilization of remote sensing data for global change research p 2875 N94-28292

Contribution of satellite observation to global change research p 2876 N94-28293

ENVIRONMENTAL SURVEYS

Planetary surface exploration MESUR/autonomous lunar rover p 2833 N94-25683

Leadex environmental phenomena and effects observed by DMSP, NOAA, and ERS-1 satellites
[AD-A274596] p 2868 N94-26888

ENVIRONMENTAL TESTS

NASA Lewis Research Center lean-, rich-burn materials test burner rig
[NASA-CR-194437] p 2680 N94-26141

A study of psychological factors affecting an extremely isolated environment p 2927 N94-27517

ENZYME ACTIVITY

Neutron and x ray scattering studies of the interactions between Ca(2+)-binding proteins and their regulatory targets: Comparisons of troponin C and calmodulin
[DE94-002706] p 2901 N94-26623

Modulation by galactosamine-induced hepatitis of biological responses of the rat exposed to high altitude hypoxia p 2904 N94-27464

Effects of gamma ray radiation on the developing mouse cerebellum: Apoptotic cell death and induction of tissue transglutaminase p 2904 N94-27472

Effects of ML-9, a myosin light-chain kinase inhibitor, on preimplantation development of the mouse
p 2905 N94-27486

Activation by G protein beta gamma subunits of G protein-coupled receptor kinase p 2931 N94-27534

ENZYMES

Neutron and x ray scattering studies of the interactions between Ca(2+)-binding proteins and their regulatory targets: Comparisons of troponin C and calmodulin
[DE94-002706] p 2901 N94-26623

Protective action of platelet-activating factor antagonist, TCV-309, against ischemia reperfusion injury in isolated rabbit hearts p 2904 N94-27465

The intracellular second messenger system in c-fos gene induction by ACTH p 2904 N94-27477

Effect of sera from patients treated with long-term hemodialysis on mRNA's for collagenase, stromelysin, and tissue inhibitor of metalloprotease in cultured human synovial cells p 2920 N94-27481

Developmental expression of protein kinase C type 1 isozyme in suncus and rat cerebella
p 2905 N94-27484
Effects of ML-9, a myosin light-chain kinase inhibitor, on preimplantation development of the mouse
p 2905 N94-27486

ENZYMOLOGY
Neutron and x ray scattering studies of the interactions between Ca(2+)-binding proteins and their regulatory targets: Comparisons of troponin C and calmodulin
[DE94-002706] p 2901 N94-26623

EPIDEMIOLOGY
US Army aviation epidemiology data registry: Incidence and outcomes of aviator flying evaluation boards
[AD-A274711] p 2910 N94-26432
Monograph of the aviation epidemiology data register for calendar year 1988
[AD-A274589] p 2911 N94-26985
Monograph of the Aviation Epidemiology Data Register for CY 1992
[AD-A274400] p 2911 N94-27130

EPITAXY
Investigation of a normal incidence high-performance p-type strained layer In(0.3)Ga(0.7)As / In(0.52)Al(0.48) as quantum well infrared photodetector
[AD-A274854] p 3055 N94-26188
The epitaxial growth of Ge on Si(100) using Te as a surfactant
[DE94-003437] p 3056 N94-26326
Ordering and phase separation in MOCVD InGaP alloys and unicompositional quantum wells
[DE94-004693] p 3056 N94-26352
Growth, characterization and device development in monocrystalline diamond films
[AD-A274245] p 3060 N94-26839
Atomic layer epitaxy of group 4 materials: Surface processes, thin films, devices and their characterization
[AD-A274325] p 3061 N94-26885
The growth and characterization of GaN as a photodetector
[AD-A274570] p 3063 N94-26965
Interface properties of wide bandgap semiconductor structures
[AD-A274356] p 3063 N94-27058
Bulletin of Precision and Intelligence Laboratory, No. 68
[JTN-94-80609] p 3010 N94-27282
Electro-optic materials by solid source MOCVD
[DE94-005120] p 2757 N94-27716

EPOXY COMPOUNDS
Dual cure low-VOC coating process
[DE94-000365] p 2756 N94-27611

EPOXY MATRIX COMPOSITES
Testing composite-to-metal tubular lap joints
[DE94-003225] p 2836 N94-26032
Design study of fiber-composite penetrator cases
[DE94-003203] p 2707 N94-26099
Design and life-time of polymer matrix composite structures: Summary
[VTT-TIED-1415] p 2707 N94-26260

EPOXY RESINS
X ray absorption studies of Ti/polymer and Cr/polymer interfaces
[DE94-003008] p 2753 N94-26770
Fatigue resistance of unnotched and post impact(+/-30 deg/0 deg) 3-D braided composites
[NASA-CR-191590] p 2711 N94-27433
Corrosion resistant coatings from conducting polymers
[DE94-003959] p 2757 N94-27747

EQUALIZERS (CIRCUITS)
Equalization and cancellation of nonlinear intersymbol interference in a dispersive satellite communication channel
[ISBN-0-315-85147-3] p 2775 N94-27274

EQUATIONS OF MOTION
A comparison of three approximate mathematical models for the gravity gradient stabilized satellite
[AD-A273832] p 2694 N94-25615
Hill equations for satellite orbit determination
[ETN-94-95374] p 2690 N94-25787
The modal solution to the Moon's orbit using canonical Floquet perturbation theory
[AD-A273732] p 2690 N94-26001
Towards a theory of growing surfaces: Mapping two-dimensional Laplacian growth onto Hamiltonian dynamics and statistics
[DE94-002636] p 2991 N94-26079
Analytical solution of Mori's equation with secant hyperbolic memory
[DE94-601541] p 3006 N94-26368
The Hamiltonian structures of the super KP hierarchy associated with an even parity superlax operator
[DE94-601506] p 2994 N94-26459
Electronic structure of a single oxygen vacancy in rutile TiO2
[DE94-602717] p 3062 N94-26901
A superprocess with a disappearing self-interaction
[AD-A274647] p 3009 N94-27108
A parametric sensitivity study for single-stage-to-orbit hypersonic vehicles using trajectory optimization
[NASA-CR-195703] p 2697 N94-27789

EQUATIONS OF STATE
New equation of state for stainless steel 347
[DE94-004189] p 2732 N94-25974

EQUILIBRIUM EQUATIONS
Single-server queues with spatially distributed arrivals
[PB94-126638] p 2986 N94-26916

EQUIPMENT SPECIFICATIONS
Baseline for a Nordtest method. Reliability stress screening of components. A guide for component users
[PB94-123775] p 2835 N94-27042
Coherence and satisfiability of waveform timing specifications
[ISBN-0-315-57769-X] p 3009 N94-27268
An analysis of the loads applied to a heavy Space Station rack during translation and rotation tasks
[NASA-TM-104790] p 2697 N94-28183

EQUIVALENCE
Some aspects of nonlinear discrete-time descriptor systems in economics
[PB94-126653] p 3101 N94-26918
Process algebra of concurrent constraint programming
[PB94-126695] p 2966 N94-26919
Wieand's theorem
[PB94-126711] p 3004 N94-27223

EQUIVALENT CIRCUITS
Electromagnetic fields and interference
[PB94-126489] p 2771 N94-26877
Channel model for AC electric arc
[PB94-124591] p 2786 N94-27327

ERBIUM
Hypersensitive transition spectrum of f-element and coordination structure
[DE94-604133] p 3070 N94-27843
Fiber laser amplifiers and oscillators
[AD-A274231] p 2820 N94-28068

ERGOMETERS
The 1991-1992 project summaries
p 2943 N94-25698
Proprioceptive isokinetic exercise test
[NASA-TM-104015] p 2902 N94-27227

ERROR ANALYSIS
Knowledge organization in intelligent tutoring systems for diagnostic problem solving in complex dynamic domains
[AD-A273986] p 2984 N94-25899
Accuracy analysis of multi-axis machines
[ETN-94-95341] p 3002 N94-26000
Improved measurement accuracy in a Long Trace Profiler: Compensation for laser pointing instability
[DE94-003408] p 2816 N94-26130
Methods for improving low-angle, low-altitude radar tracking accuracy
[AD-A274914] p 2768 N94-26347
Software Error Estimation Program (SWEEP), version 02.00.00 user manual
[AD-A274697] p 2962 N94-26373
On the application of Allan variance method for Ring Laser Gyro performance characterization
[DE94-003880] p 2810 N94-26525
Local uniform grid refinement and systems of coupled partial differential equations
[CWI-NM-R9307] p 2995 N94-26773
The Communication Link and Error ANalysis (CLEAN) simulator
[NASA-CR-195243] p 2968 N94-27168
Advanced technology development multi-color holography
[NASA-CR-193931] p 2812 N94-27229
An unavailability model for errors made during surveillance testing
[DE94-000816] p 2835 N94-27613
Reanalysis of Mariner 9 UV Spectrometer Data for Ozone, Cloud, and Dust Abundances, and Their Interaction Over Climate Timescales
[NASA-CR-195244] p 3107 N94-27885

ERROR CORRECTING CODES
Improved performance of hybrid error control techniques for real-time digital communications over noisy channels
[ISBN-0-315-84281-4] p 2770 N94-26625

ERROR CORRECTING DEVICES
Method of correcting rotational motion error in SAR and ISAR imagery
[AD-D016033] p 2773 N94-27146

ERROR DETECTION CODES
Improved performance of hybrid error control techniques for real-time digital communications over noisy channels
[ISBN-0-315-84281-4] p 2770 N94-26625
Advanced End-to-end Simulation for On-board Processing (AESOP) p 2945 N94-28255

ERRORS
Detection geometry and reconstruction error in magnetic source imaging
[DE94-004012] p 2809 N94-25662
Improved measurement accuracy in a Long Trace Profiler: Compensation for laser pointing instability
[DE94-003408] p 2816 N94-26130
Coded communications with nonideal interleaving
[ITN-94-85235] p 2774 N94-27242
An unavailability model for errors made during surveillance testing
[DE94-000816] p 2835 N94-27613
BATSE burst location accuracy and constraints on the fraction of repeating GRB sources
[DE94-004981] p 3116 N94-27714
A comparative study of SAR data compression schemes p 2946 N94-28259

ESCAPE SYSTEMS
Assured crew return vehicle post landing configuration design and test p 2697 N94-25671

ESCHERICHIA
Vacuum-UV-effects on E. coli plasmid pUC19: Inactivation, strand break induction and mutation induction
[DLR-FB-93-26] p 2903 N94-27754

ESTERS
Langmuir-Blodgett film of amylose-esters and chiral azo-dyes (structure and second order nonlinear optical behaviour)
[ETN-94-95390] p 2747 N94-25749

ESTIMATING
Analytical method for estimation of the total amount of aromatic and poly aromatic compounds in diesel fuel
[PB94-123692] p 2759 N94-25907
Multiple model adaptive estimation applied to the LAMBDA URV for failure detection and identification
[AD-A274078] p 3002 N94-25992
Parameter estimation by genetic algorithms
[DE94-002924] p 2961 N94-26146
Isotonic estimation and rates of convergence in Wicksell's problem
[REPT-93-39] p 3002 N94-26213
Parameter estimation for ARMA models with infinite variance innovations
[AD-A274654] p 3003 N94-26355
Optimal nonlinear estimation for aircraft flight control in wind shear p 2643 N94-27296
Practical problems in aggregating expert opinions
[DE94-002623] p 3094 N94-27707
Estimators for the Cauchy distribution
[DE94-004990] p 3005 N94-27816
Parameter estimation of linear systems from frequency response measurements (computer program)
[ESDU-93016] p 2976 N94-28137

ESTUARIES
An experimental study of siphonal jets in a turbulent boundary layer crossflow p 2802 N94-28015

ETA-MESONS
Pseudoscalar glueball in the composite interpolating fields approach
[DE93-634374] p 3016 N94-26042
Meson X(1814) as a candidate for a hybrid state
[DE93-634447] p 3017 N94-26045
Study of the process (pi)(sup -)A(yields)(pi)(sup -)(eta)'(eta)A at the moment 36 GeV/c
[DE93-634530] p 3024 N94-27250
Pi plus pi minus gamma and K+ K- production in two photon collisions at ARGUS
[ISBN-0-315-63598-3] p 3027 N94-27684
Future directions in particle and nuclear physics at multi-GeV hadron beam facilities
[DE94-002946] p 3027 N94-27711
Proceedings of the workshop on (pi), K, (eta)-nucleon interactions
[DE94-701314] p 3027 N94-27733

ETCHING
Investigation of plasma etch induced damage in compound semiconductor devices
[DE94-002849] p 3052 N94-25989
Opportunities for High Aspect Ratio Micro-Electro-Magnetic-Mechanical Systems (HAR-MEMMS) at Lawrence Berkeley Laboratory
[DE94-003499] p 2827 N94-27722

ETHANE
Laser probes of natural gas ignition chemistry
[PB94-128345] p 2717 N94-27226
Viscosity of liquids: Halogenated ethanes
[ESDU-93012] p 2720 N94-28062

ETHERS
Reactivity of nitrate radical (NO3) toward organic compounds p 2704 N94-27387

ETHYL COMPOUNDS
Controlled synthesis of polyenes by catalytic methods
[DE94-004168] p 2749 N94-25973

ETHYLENE

The electrocatalytic oxidation of ethylene and methane, and reduction of oxygen on gas-diffusion electrodes made of amorphous nickel-valve metal-platinum group metal alloys p 2722 N94-28165

EUCLIDEAN GEOMETRY

Illumination in diverse codimensions [NASA-CR-191596] p 2971 N94-27572

EULER BUCKLING

The railway track response function [REPT-93-40] p 2837 N94-26214

EULER EQUATIONS OF MOTION

Comments regarding two upwind methods for solving two-dimensional external flows using unstructured grids [NASA-TM-109078] p 2644 N94-26154

High-lift system analysis method using unstructured meshes [NLR-TP-92351-U] p 2647 N94-27554

Agglomeration multigrid for the three-dimensional Euler equations [NASA-CR-191595] p 2999 N94-27557

Experimental and theoretical investigations of the influence of the jet on the flow around a bypass-engine [DLR-FB-93-17] p 2675 N94-27593

Prediction of undsteady flows in turbomachinery using the linearized Euler equations on deforming grids [NASA-CR-195285] p 2675 N94-27654

Numerical assessment of aerodynamic interactions on missiles with transverse jets control p 2659 N94-28031

Application of the MBTEC Euler code to the Challenger and the CF-18 complete aircraft configurations p 2653 N94-28324

Solution of the Euler equations using unstructured grids p 2656 N94-28338

Solution-adaptive simulation of transonic cascade flows p 2657 N94-28344

Multigrid solutions of the 2D Euler/Navier-Stokes equations on unstructured meshes p 2658 N94-28349

EULER-LAGRANGE EQUATION

On the Lagrangian and updated Lagrangian nonlinear finite element formulations [ISBN-0-315-61111-1] p 3001 N94-27948

EUROPE

A geological and geophysical information system for Eurasia [AD-A274818] p 3098 N94-26490

Lufthansa Yearbook 1992 [DSK-9734-H-92] p 2660 N94-28230

Air traffic of the European Community with European neighbors p 2661 N94-28233

A sky above Europe p 2661 N94-28234

The single European market: Economical advance, ecological problem? p 2661 N94-28235

Air traffic administration enroute to Europe p 2661 N94-28238

Lufthansa and Europe p 2663 N94-28247

EUROPEAN AIRBUS

A340 testing p 2662 N94-28242

EUROPEAN SPACE AGENCY

Science beyond the atmosphere: The history of space research in Europe [ESA-HSR-SPECIAL] p 2689 N94-28207

EUROPIUM

Molecular dynamics simulation and crystal-field theory: Predicting the optical spectra and structure of rare-earth doped inorganic glasses [ISBN-0-315-84679-8] p 3025 N94-27310

EUTECTIC ALLOYS

Eutectic transformation L in equilibrium to Zr6Fe23 + Fe(tau) in the Fe-Zr system [DE93-633766] p 2735 N94-26295

EUTECTICS

Liquid and solid solubility of Ag in Bi2Sr2CaCu2O8 [DE94-002829] p 2735 N94-26273

Design of a high-precision double crystal tunable monochromator [DE94-003004] p 2811 N94-26787

Research into the microstructure and mechanical behavior of eutectic Bi-Sn and In-Sn [DE94-004558] p 2741 N94-27619

EVALUATION

Mapping of seawater intrusion into the coastal aquifer of Israel (the seawater-freshwater interface) by TDEM (Time Domain Electromagnetic) method [ITN-94-85238] p 2850 N94-27331

Eye-head coordination and swinging of the visual scene when wearing visually up-down reversing mirror for 14 days p 2915 N94-27462

Comparative measurement of visual stability in cosmic space: Onboard experiment and pre-flight activities p 2916 N94-27463

EVAPORATION

Study on synthesis and characteristics of intermetallic compound with strong electron correlation p 2726 N94-25563

Over-the-horizon propagation measurements at six radar-frequency bands at the Atlantic Ocean Coast [AD-A274151] p 2773 N94-27136

Thermocapillary flow with evaporation and condensation and its effect on liquid retention in low-G fluid acquisition devices [NASA-TP-3463] p 2797 N94-27639

EVAPORATORS

Modelling the mass migration phenomena in partially frozen heat pipes [DE94-002716] p 2797 N94-27709

EVAPOTRANSPIRATION

R and D for creation, measurement, application of ultra-high vacuum p 2723 N94-25549

EXCAVATION

Effects of slot on rock surface for percussive rock excavation: Water jet assisted percussive rock excavation p 2871 N94-28155

EXCIMER LASERS

A study of vibrational relaxation of electronically-excited molecules [DE93-613553] p 3013 N94-25827

EXCIMERS

A study of vibrational relaxation of electronically-excited molecules [DE93-613553] p 3013 N94-25827

EXCITATION

Two dimensional self-consistent fluid simulation of RF inductive sources [DE94-003635] p 2767 N94-25937

Analysis/test correlation using VAWT-SDS on a step-relaxation test for the rotating Sandia 34 m test bed [DE94-002290] p 2857 N94-26700

Extraction of modal parameters from an operating HAWT using the Natural Excitation Technique (NExT) [DE94-001831] p 2859 N94-27004

Effect of PGE2 receptor agonists butaprost, M and B 28767 and an antagonist AH 6809 on the BK response of visceral polymodal receptors p 2906 N94-27494

Effects of perfusion of amiodarone on electrophysiological properties in single rabbit ventricular myocytes p 2906 N94-27503

Fast and slow onsets of Na channel blocking actions due to lidocaine and disopyramide using concentration-clamp method p 2907 N94-27504

Electrophysiological effects of MS-551, a new Class 3 antiarrhythmic agent, on isolated rabbit ventricular muscles p 2907 N94-27505

Comparative investigation of new Class 3 antiarrhythmic drugs, E-4031 and MS-551, on electrophysiological properties in isolated rabbit ventricular myocytes p 2907 N94-27506

Effects of Class 1 antiarrhythmic drugs on the intraventricular conduction: Influence of fiber orientation p 2907 N94-27507

Effects of Class 3 antiarrhythmic agents, E-4031 and MS-551 on ventricular repolarization in isolated rabbit hearts p 2907 N94-27508

A study on tissue excitation of cardiac muscle under electrical field stimulation p 2907 N94-27510

Block of cardiac sodium channels by Ro 22-9194 (R), a new antiarrhythmic agent: Effects on the maximum upstroke velocity (Vmax) of single guinea pig ventricular myocytes p 2907 N94-27511

Electrophysiological effects of an antiarrhythmic drug, moricizine on isolated guinea pig ventricular muscles p 2907 N94-27512

Correlation between electrical activity and the size of single sinoatrial node cells p 2907 N94-27513

The ionic mechanism underlying the negative chronotropic effect of acetylcholine: Experimental study in rabbit single sinoatrial node cells p 2908 N94-27514

The ionic mechanism underlying the negative chronotropic effect of acetylcholine: Experiments using small sinoatrial node tissue preparations isolated from rabbit hearts p 2908 N94-27515

The ionic mechanism underlying the negative chronotropic effect of acetylcholine: Postganglionic vagal stimulation in isolated rabbit hearts p 2908 N94-27516

Double excitation of He and H(-) by fast proton and anti-proton impact [DE94-004581] p 3026 N94-27620

Trace organic chemical detection using an ultraviolet excitation molecular beam fluorometer [DE94-002649] p 2704 N94-27708

Radiations from hot nuclei p 3030 N94-27915

EXCITONS

Biexciton formation by two-photon absorption in quantum wells [DE93-613551] p 3071 N94-25852

Instantaneous amplitude and frequency dynamics of coherent wave mixing in semiconductor quantum wells [DE94-003262] p 3054 N94-26128

Technical report of ISSP. Ser. A, no. 2672: Magneto-optical effects of excitons in BiI3 crystals under pulsed high magnetic fields. 3: Excitons confined around a stacking disorder formed by a bending stress [JTN-94-80558] p 3065 N94-27240

EXCRETION

Changes in circadian variations of urine excretion in tail-suspended rats p 2911 N94-27443

EXERCISE PHYSIOLOGY

The effect of platform motion on human energy expenditure during walking. An exploratory experiment [AD-A273760] p 2940 N94-25724

Plasma volume shifts and exercise thermoregulation with water immersion and six-degree head-down tilt [NASA-TM-108781] p 2901 N94-26093

Sympathetic nerve activity during dynamic leg exercise p 2929 N94-27527

Workshop on Countering Space Adaptation with Exercise: Current Issues [NASA-CP-3252] p 2934 N94-28361

Exercise detraining: Applicability to microgravity p 2934 N94-28364

Aerobic fitness and orthostatic tolerance: Evidence against an association p 2934 N94-28365

Does training-induced orthostatic hypotension result from reduced carotid baroreflex responsiveness? p 2935 N94-28366

EXHAUST EMISSION

UV absorption technique for monitoring mobile source NO emissions [AD-A273858] p 2713 N94-25964

Natural gas applications for hybrid vehicles. [PB94-117108] p 2759 N94-26753

Compilation of air pollutant emission factors. Volume 1: Stationary point and area sources. Supplement F [PB94-121431] p 2867 N94-26757

Feasibility study on introduction of transportation-use petroleum substitution energy [DE94-725205] p 2759 N94-26905

Optimising BMW four-cylinder two-valve engines [PB94-125101] p 2824 N94-27254

Pressure-gain combustion [DE94-002975] p 2719 N94-27712

Technical Report of National Research Institute of Fisheries Engineering: Fishing Boat and Instrument, No. 12 [JTN-94-80595] p 2764 N94-27976

The emission characteristics of a high speed diesel engine p 2764 N94-27980

Gas turbine combustion and emission control p 2831 N94-28082

EXHAUST GASES

Analysis and development of an F-5 pollution prevention management program with recommendations for creation of similar programs for other aircraft [AD-A274016] p 2865 N94-25755

UV absorption technique for monitoring mobile source NO emissions [AD-A273858] p 2713 N94-25964

Feasibility study on introduction of transportation-use petroleum substitution energy [DE94-725205] p 2759 N94-26905

Technical Report of National Research Institute of Fisheries Engineering: Fishing Boat and Instrument, No. 12 [JTN-94-80595] p 2764 N94-27976

The emission characteristics of a high speed diesel engine p 2764 N94-27980

Experiments into the scaling parameters required for exhaust gas ingestion testing of vertical landing aircraft p 2671 N94-28017

Influence of headwind on hot gas reingestion and consideration of pressure ratio scaling p 2675 N94-28018

Unsteady aspects of hot gas reingestion and statistical analysis p 2676 N94-28019

Fibrous ceramic candle filter for particle removal in pressurized fluidized bed combustion [PB94-133089] p 2876 N94-28383

EXHAUST NOZZLES

A study of jet effect and ground effect interference on a STOL fighter p 2671 N94-28034

EXHAUST SYSTEMS

Computational and Experimental Assessment of Jets in Cross Flow [AGARD-CP-534] p 2799 N94-28003

Advanced metallic exhaust impinged structural concepts demonstration p 2832 N94-28209

EXISTENCE THEOREMS

Spaces of algebraic cycles [PB94-124369] p 2996 N94-26993

Fixed point type theorems and projection-interaction approximation
[DE94-603669] p 3000 N94-27632

EXOBIOLOGY

Autonomous support for microorganism research in space p 2903 N94-25672

Aerospace medicine and biology: A continuing bibliography with indexes (supplement 386)
[NASA-SP-7011(386)] p 2933 N94-28208

Aerospace medicine and biology: A continuing bibliography with indexes (supplement 387)
[NASA-SP-7011(387)] p 2933 N94-28213

Aerospace medicine and biology: A cumulative index to a continuing bibliography (supplement 384)
[NASA-SP-7011(384)] p 2934 N94-28219

Workshop on Countering Space Adaptation with Exercise: Current Issues
[NASA-CP-3252] p 2934 N94-28361

Muscular activity and its relationship to biomechanics and human performance p 2934 N94-28362

EXOTHERMIC REACTIONS

Technique to predict the curing behaviour of unsaturated polyester materials
[PB94-124856] p 2748 N94-25892

Modelling the inhibition cure behaviour of unsaturated polyester moulding materials
[PB94-124864] p 2748 N94-25893

On the thermal ignition with variable pre-exponential factor
[DE93-616009] p 2713 N94-25913

EXPEDITIONS

Telepresence in the human exploration of Mars: Field studies in analog environments p 2685 N94-27360

EXPENDABLE STAGES (SPACECRAFT)

Access to space study
[NASA-TM-109693] p 2685 N94-27151

EXPERIMENT DESIGN

Development of fusion technology
[DE93-633444] p 3042 N94-26159

An approach to studying the reliability of microgravity experiments
[NASA-TM-106489] p 2834 N94-26199

Response surface design comparisons
[AD-A274690] p 2838 N94-26448

Tokamak Physics Experiment poloidal field design
[DE94-001542] p 3045 N94-27019

EXPERT SYSTEMS

Knowledge base systems for chemical compounds designing support p 2723 N94-25550

Automation of closed environments in space for human comfort and safety p 2943 N94-25684

Developing realistic cooperative behaviors for autonomous agents in air combat simulation
[AD-A274077] p 2937 N94-25774

Emerging technologies
[DE94-003022] p 3102 N94-26023

Hypermedia support for engineering design systems: Application to fatigue analysis
[VTT-TIED-1432] p 2837 N94-26255

Design of a computer expert system for adhesive selection using artificial intelligence techniques
[AD-A274715] p 2751 N94-26434

A rough set approach to speech recognition
[ISBN-0-315-83894-9] p 2769 N94-26619

Institute for Information Technology
[NRC-37061] p 3118 N94-26709

An artificial reality environment for remote factory control and monitoring p 2687 N94-27369

Multi-sensor data fusion in a distributed environment: Architectural solutions
[NLR-TP-92243-U] p 2989 N94-27800

A hybrid formalism for representation and interpretation of image knowledge
[INPE-5485-PRE/1784] p 2989 N94-27833

Thunderstorm Hypothesis Reasoner
[NASA-CR-195714] p 2897 N94-27884

EXPLOSIONS

Safety standards for aircraft shelter
[FFI-92/4003] p 2680 N94-26305

EXPLOSIVES

Emerging technologies
[DE94-003022] p 3102 N94-26023

Computational studies of energetic organic molecules
[AD-A274726] p 3018 N94-26172

A materials compatibility study in FM-1, a liquid component of a paste extrudable explosive
[DE94-001166] p 2759 N94-26198

Propellants and explosives in ballistic missiles
[UCRL-LR-113578] p 2760 N94-28222

EXPONENTIAL FUNCTIONS

Conditionally exponential convex functions on locally compact groups
[DE93-613025] p 2990 N94-25865

EXPONENTS

Lyapunov exponents for some quasi-periodic cocycles
[PB94-124377] p 2997 N94-26994

EXPOSURE

A materials compatibility study in FM-1, a liquid component of a paste extrudable explosive
[DE94-001166] p 2759 N94-26198

EXTERNAL STORES

Application of the influence function method using the interference distributed loads code to prediction of store aerodynamic load during separation from the CF-18 fighter aircraft p 2654 N94-28330

EXTERNAL TANKS

Structural analysis of a frangible nut used on the NASA Space Shuttle
[DE94-003672] p 2821 N94-25811

Advanced silver zinc battery development for the SRB and ET range safety subsystems p 2865 N94-28136

EXTINCTION

Analytic approximation to randomly oriented spheroid extinction
[DREV-4712-93] p 3038 N94-27598

Impacts, extinctions, volcanism, glaciations, and tectonics: Matches and mismatches
p 2888 N94-28298

The end-Permian mass extinction: A complex, multicausal extinction p 2888 N94-28299

Science observed: The mass-extinction debates
p 2888 N94-28300

Mass extinctions: Persistent problems and new directions p 2889 N94-28302

An evaluation of criteria that may be used to identify species surviving a mass extinction
p 2889 N94-28304

Proposed law of nature linking impacts, plume volcanism, and Milankovitch cycles to terrestrial vertebrate mass extinctions via greenhouse-embryo death coupling
p 2876 N94-28307

A general theory of impacts and mass extinctions, and the consequences of large-body impact on the Earth
p 2891 N94-28310

Were all extinction events caused by impacts?
p 2891 N94-28311

Ozone control of biological activity during Earth's history, including the KT catastrophe p 2876 N94-28312

Supernovae and mass extinctions
p 2891 N94-28314

EXTRACTION

Emerging technologies
[DE94-003022] p 3102 N94-26023

EXTRAPOLATION

Advanced qualification techniques
[DE94-003709] p 2780 N94-25812

EXTRATERRESTRIAL LIFE

The Fermi paradox: An approach based on percolation theory p 2687 N94-27370

EXTRATERRESTRIAL RADIATION

Space radiation health research, 1991-1992
[NASA-TM-109721] p 2932 N94-27556

Radiations from hot nuclei p 3030 N94-27915

Develop and fabricate a radiation dose measurement system for satellites
[PL-TR-93-2161] p 2698 N94-28210

Develop and fabricate a radiation dose measurement system for satellites
[PL-TR-93-2099] p 2698 N94-28217

EXTRATERRESTRIAL RESOURCES

A widely adaptable habitat construction system utilizing space resources p 2688 N94-27374

EXTRAVEHICULAR ACTIVITY

Extra-Vehicular Activity (EVA) glove evaluation test protocol
[NASA-TM-108442] p 2943 N94-27952

EXTRAVEHICULAR MOBILITY UNITS

Enabler operator station p 2943 N94-25679

EXTREME ULTRAVIOLET RADIATION

Analysis of EUV/FUV dayglow and auroral measurements
[NASA-CR-195237] p 2883 N94-27393

EXTREMELY HIGH FREQUENCIES

NASA satellite communications application research, phase 2 addendum. Efficient high power, solid state amplifier for EHF communications
[NASA-CR-195712] p 2777 N94-27946

EXTREMELY LOW FREQUENCIES

JARE data reports. No. 186: Upper atmosphere physics data. Syowa and Asuka Stations, 1990
[JTN-94-80594] p 2881 N94-27299

Memories of National Institute of Polar Research. Series A-19. Upper atmosphere physics: ELF emission in high latitudes: Ray path calculation and ground-satellite observations
[JTN-94-80592] p 2882 N94-27342

EXTREMELY LOW RADIO FREQUENCIES

Excitation of Earth-ionosphere waveguide in the ELF and lower VLF bands by modulated ionospheric current
[AD-A274969] p 2878 N94-26304

EXTRUDING

Dissolution of secondary phases during extrusion
[PB94-124583] p 2732 N94-25908

Synthesis, rheology, and forming of Y-Ba-Cu-O ceramics
[DE94-005558] p 2757 N94-27695

EYE (ANATOMY)

Microtubules for nonlinear optical limiting
[AD-A273940] p 3035 N94-25941

EYE MOVEMENTS

Effects of imaginary target on induced eye movements by linear acceleration p 2914 N94-27456

Eye-head coordination and swinging of the visual scene when wearing visually up-down reversing mirror for 14 days p 2915 N94-27462

Impaired associated movement in Parkinson's disease: An evaluation of Bell's phenomenon
p 2928 N94-27520

EYE PROTECTION

Microtubules for nonlinear optical limiting
[AD-A273940] p 3035 N94-25941

F

F REGION

Ionospheric modification by high power, obliquely propagated HF radio wave transmissions. Part 1: Experimental
[AD-A273746] p 2878 N94-26224

F-106 AIRCRAFT

Leading-edge vortex-system details obtained on F-106B aircraft using a rotating vapor screen and surface techniques
[NASA-TP-3374-VIDEO-SUPPL] p 2647 N94-27161

F-15 AIRCRAFT

Design and flight test of the Propulsion Controlled Aircraft (PCA) flight control system on the NASA F-15 test aircraft
[NASA-CR-186028] p 2674 N94-27432

F-16 AIRCRAFT

Design of a subsonic envelope flight control system for the Vista F-16 using quantitative feedback theory
[AD-A274057] p 2676 N94-25771

F-18 AIRCRAFT

An investigation into the aerodynamic effects of wing patches
[ISBN-0-315-84121-4] p 2646 N94-26672

Report of the defense science board task force on aircraft assessment
[AD-A274531] p 2669 N94-26835

Controlled oscillation of forebody vortices by nozzle jet blowing
[ISBN-0-315-84134-6] p 2678 N94-27648

Measurements of steady and dynamic pressure on an F/A-18 wind tunnel model at high angles of attack
p 2653 N94-28323

Application of the influence function method using the interference distributed loads code to prediction of store aerodynamic load during separation from the CF-18 fighter aircraft p 2654 N94-28330

Preliminary assessment of aerodynamic effects of wing repair patches p 2657 N94-28346

F-22 AIRCRAFT

Report of the defense science board task force on aircraft assessment
[AD-A274531] p 2669 N94-26835

F-5 AIRCRAFT

Analysis and development of an F-5 pollution prevention management program with recommendations for creation of similar programs for other aircraft
[AD-A274016] p 2865 N94-25755

FABRICATION

Lithium drifted silicon detector fabrication on gettered floating-zone silicon
[DE94-003890] p 3054 N94-26095

A study on the development of high T(sub c) superconducting materials
[DE93-633529] p 3057 N94-26404

Demonstration of monolithic co-fabrication of Y1Ba2Cu3O7-Sigma and CMOS devices on the same sapphire substrate
[AD-A274757] p 3059 N94-26566

Processing and properties of Ag-clad Bi-2223 tapes
[DE94-004603] p 2783 N94-26589

Simplified high-efficiency silicon cell processing
[DE94-002683] p 2857 N94-26617

Diagnostics and microelectronics
[DE94-003016] p 2784 N94-26777

Fabrication technology
[DE94-003017] p 2763 N94-26778

MSOFC development status
[DE94-003192] p 2858 N94-26792

Calculation of the electromagnetic critical state response of high T(sub c) superconductor tape
[DE94-002894] p 3061 N94-26868

Processing, fabrication, and demonstration of HTS integrated microwave circuits, appendix A
[AD-A274600] p 2785 N94-26890
Powder synthesis, fabrication, and transport properties of long-length Ag clad Bi-2223 conductors
[DE94-002376] p 2740 N94-26957
An optoelectronic graphics display processor
[AD-A274401] p 3037 N94-26990
Ferroelectric fluoride memory FET development
[AD-A274341] p 2785 N94-27057
Fullerene fabrication using an arc furnace. Characterization of the product
[DE94-603006] p 3029 N94-27834
High rate lithium/thionyl chloride bipolar battery development p 2864 N94-28133
Dry etching process development for submicron and nanometer semiconductor devices
[PB94-133196] p 2788 N94-28357

FABRICS
Design for producing fiberglass fabric in a lunar environment p 2765 N94-25676
A constitutive model for layered wire mesh and aramid cloth fabric
[DE94-003275] p 2708 N94-26796
Automated fabric inspection system
[AD-A274522] p 2835 N94-26833

FACE (ANATOMY)
Orientation competition in cortical filters
[PB94-125366] p 2939 N94-27001

FACE CENTERED CUBIC LATTICES
Formation and crystallization of hydrogen-induced amorphous Ti3InH(4.5) alloy p 2745 N94-28163

FACTOR ANALYSIS
A test of the theory of reasoned action at the group level of analysis
[AD-A273965] p 2937 N94-25897

FACTORIAL DESIGN
Space transportation vehicle design evaluation using saturated designs p 2693 N94-27928

FAILURE
Characteristics and control response of the TOPAZ 2 reactor system real-time dynamic simulator
[DE94-003788] p 2699 N94-25600
Failure mechanisms of high temperature semiconductor lasers
[AD-A273833] p 2815 N94-25616
Multiple model adaptive estimation applied to the LAMBDA URV for failure detection and identification
[AD-A274078] p 3002 N94-25992
Failure behaviour of high density polyethylene with an embrittled surface layer due to weathering
[PB94-126406] p 2840 N94-26960
Modelling the mass migration phenomena in partially frozen heat pipes
[DE94-002716] p 2797 N94-27709

FAILURE ANALYSIS
Computer modelling of cyclic deformation of high-temperature materials
[AD-A273852] p 2704 N94-25608
Project Ares 3 p 2671 N94-25712
Aircraft turbine engine reliability and inspection investigations
[AD-A274860] p 2673 N94-26176
Automated information management for designers: Functional requirements for computer based associates that support access and use of technical information in design
[AD-A274603] p 3099 N94-26891
Baseline for a Nordtest method. Reliability stress screening of components. A guide for component users
[PB94-123775] p 2835 N94-27042
Development of a performance evaluation tool (MMSOFE) for detection of failures with Multiple Model Adaptive Estimation (MMAE)
[AD-A274218] p 2665 N94-27071
Simulating fail-stop in asynchronous distributed systems
[NASA-CR-195698] p 2974 N94-27767
Mechanically fastened composite laminates subjected to combined bearing-bypass and shear loading
p 2712 N94-27914
Orbital management and design considerations for NiCd satellite power systems p 2862 N94-28118

FAILURE MODES
Baseline for a Nordtest method. Reliability stress screening of components. A guide for component users
[PB94-123775] p 2835 N94-27042
Investigation of the bond strength of a discrete skin-stiffener interface
[NLR-TP-92183-U] p 2670 N94-27796

FAIRINGS
Experimental investigation of advanced hub and pylon fairing configurations to reduce helicopter drag
[NASA-TM-4540] p 2668 N94-26604
Experimental and theoretical studies of T-tail configurations for commuter aircraft applications
p 2653 N94-28322

FALSE ALARMS
Combatting inherent vulnerabilities of CFAR algorithms and a new robust CFAR design
[AD-A274918] p 2770 N94-26751

FAR FIELDS
Characterization of an LCD for use as a programmable phase shifter to produce a single-lobed far-field pattern in a phased array
[AD-A273883] p 3034 N94-25729

FAR INFRARED RADIATION
Weak bump quasars
[NASA-CR-195267] p 3103 N94-27933

FAR ULTRAVIOLET RADIATION
Technical report of ISSP. Ser. A, no. 2688: Suppression of higher-order modes in an RF cavity by resistive material
[JTN-94-80574] p 2787 N94-27606
Discrete vacuum ultra violet reflective interference filter
[AD-D016059] p 2756 N94-27675
Vacuum-UV-effects on E. coli plasmid pUC19: Inactivation, strand break induction and mutation induction
[DLR-FB-93-26] p 2903 N94-27754

FARADAY EFFECT
Fiber optic Faraday flux transformer specification
[AD-D016058] p 3039 N94-27674

FAST FOURIER TRANSFORMATIONS
A real-time convolution algorithm and architecture with applications in SAR processing
[AD-A273817] p 2959 N94-25963
An ultrasonic testing technique for monitoring the cure and mechanical properties of polymeric materials
[AD-A274536] p 2753 N94-26842
A fast Fourier transform radix-2 complex butterfly with built-in self-test
[ISBN-0-315-84139-7] p 2982 N94-27649

FAST NEUTRONS
Nonswelling behavior of HT9 alloy irradiated to high exposure
[DE94-003502] p 2736 N94-26522

FASTENERS
Structural analysis of a frangible nut used on the NASA Space Shuttle
[DE94-003672] p 2821 N94-25811
Mechanically fastened composite laminates subjected to combined bearing-bypass and shear loading
p 2712 N94-27914

FATIGUE (MATERIALS)
Bulletin of National Research Institute for Metals in Fiscal Year 1993, no. 14
[REPT-14] p 2722 N94-25544
Study on the mechanism of titanium alloy toughness and the improvement of properties
p 2726 N94-25566
Study on improvements in fretting fatigue characteristics of high strength structural member p 2726 N94-25567
Growth of small fatigue cracks in Incoloy-908
[DE94-003406] p 2836 N94-26129
Damage tolerance assessment handbook. Volume 1: Introduction fracture mechanics fatigue crack propagation
[AD-A274777] p 2836 N94-26186
Guidelines for controlling stress corrosion cracking and corrosion fatigue of stainless steels: A literature review
[VTT-TIED-1420] p 2837 N94-26262
Experimental determination of the CU-IN-PB ternary phase diagram
[DE94-003765] p 2735 N94-26349
Damage tolerance assessment handbook. Volume 2: Aircraft damage tolerance evaluation
[AD-A274778] p 2837 N94-26357
Effects of plastic media blasting on aircraft skin
[AD-A274817] p 2668 N94-26488
Mechanism of mechanical fatigue of silica glass
[DE94-003165] p 2753 N94-26783
Titanium 1992: Science and Technology, volume 1
[AD-A274798-VOL-1] p 2739 N94-26799
Development of fibre-metal laminates, ARALL and GLARE, new fatigue resistant materials
[PB94-126471] p 2669 N94-26969
Fatigue resistance of unnotched and post impact(+/-30 deg/0 deg) 3-D braided composites
[NASA-CR-191590] p 2711 N94-27433
Weldability aspects in the design and fabrication of aluminium structures subjected to fatigue loads. Part 2: Weldability of aluminium alloys using advanced MIG and TIG techniques. Effect of the weld bead geometrical factors on the fatigue behavior of the welded joint
[PB94-132446] p 2833 N94-28375

FATIGUE LIFE
Study on evaluation of crack generation and crack growth behaviors under static loading at high temperature and under combined loading p 2730 N94-25583
Design and life-time of polymer matrix composite structures: Summary
[VTT-TIED-1415] p 2707 N94-26260
Ceramic technology project
[DE94-003782] p 2750 N94-26332
Effects of plastic media blasting on aircraft skin
[AD-A274817] p 2668 N94-26488
Fatigue resistance under tension-compression of laminates IM6/5245C and AS4/3501-6
[IAR-CR-25] p 2708 N94-26711
Development of fibre-metal laminates, ARALL and GLARE, new fatigue resistant materials
[PB94-126471] p 2669 N94-26969
Computer modelling of cyclic deformation of high-temperature materials
[AD-A274504] p 2840 N94-27034
Modification of a model for fatigue life predictions based on level-crossing
[PB94-123395] p 2842 N94-27198
Methods of testing for endurance of structural elements using simulated acoustic loading
[ESDU-93027] p 3011 N94-28141

FATIGUE TESTING MACHINES
Development of an automatic fatigue-data acquisition system using commercial software
[NAL-TM-650] p 2842 N94-27207

FATIGUE TESTS
Study on variation of damage generation mechanism by fatigue on TiAl compounds due to different slip systems p 2729 N94-25579
Characterization of fatigue damage in a metal matrix composite (SCS-6/Ti-15-3) at elevated temperature
[AD-A273797] p 2706 N94-25876
The identification of inflow fluid dynamics parameters that can be used to scale fatigue loading spectra of wind turbine structural components
[DE94-000231] p 2791 N94-26117
Guidelines for controlling stress corrosion cracking and corrosion fatigue of stainless steels: A literature review
[VTT-TIED-1420] p 2837 N94-26262
Stress analysis of a secondary-bending specimen
[AD-A274842] p 2838 N94-26501
Crack closure, a literature study
[PB94-123361] p 2842 N94-27197
Modification of a model for fatigue life predictions based on level-crossing
[PB94-123395] p 2842 N94-27198
Methods of testing for endurance of structural elements using simulated acoustic loading
[ESDU-93027] p 3011 N94-28141

FAULT DETECTION
An algorithm for determination of bearing health through automated vibration monitoring
[AD-A274591] p 2823 N94-26986
Development of a performance evaluation tool (MMSOFE) for detection of failures with Multiple Model Adaptive Estimation (MMAE)
[AD-A274218] p 2665 N94-27071
Automatic, real-time fault monitor verifying network in a microwave landing system
[CA-PATENT-1325261] p 2665 N94-27275
Fault detection and isolation p 2642 N94-27289

FAULT TOLERANCE
Modeling and experimental verification of single event upsets p 2684 N94-26287
Simulation modeling for long duration spacecraft control systems p 2684 N94-26288
Fast incremental compiler transformations for multiple instruction retry
[NASA-CR-195209] p 2964 N94-26680
Fault tolerant real-time processing system for space use p 2949 N94-26720
Fault-tolerant scheduling in distributed critical real-time systems p 2952 N94-26735
Hard real-time reliable multicast in the DEDOS system
[PB94-126745] p 2966 N94-26920
Trace-based compositional proof theory for fault tolerant distributed systems
[PB94-126737] p 2966 N94-26971
An algorithm for determination of bearing health through automated vibration monitoring
[AD-A274591] p 2823 N94-26986
Design and evaluation of fault tolerance in opto-electronic computing
[AD-A274281] p 2954 N94-27016
Refinement for fault-tolerance: An aircraft hand-off protocol
[NASA-CR-195697] p 2666 N94-27768
An overview on development of neural network technology p 2990 N94-27913

Comparative analysis of different configurations of PLC-based safety systems from reliability point of view
p 2836 N94-27925

FAULT TREES

Simulation modeling for long duration spacecraft control systems p 2684 N94-26288

FEASIBILITY

Project Columbiad: Reestablishment of human presence on the Moon p 2689 N94-25687

Short-range cloud amount forecasting with model output statistics
[AD-A274769] p 2895 N94-26798

FEASIBILITY ANALYSIS

Feasibility study on introduction of transportation-use petroleum substitution energy
[DE94-725205] p 2759 N94-26905

FEDERAL BUDGETS

NASA: Major challenges for management. Testimony before the Legislation and National Security Subcommittee, Committee on Government Operations, House of Representatives
[GAO/T-NSIAD-94-18] p 3095 N94-28176

Selected data on Federal support to universities and colleges: FY 1991
[NSF-93-320] p 3101 N94-28201

FEEDBACK

Four phase microwave pulse generator for pulsed EPR spectrometer p 2718 N94-27388

High repetition rate, mode locked, figure eight laser with extracavity feedback
[AD-D016053] p 2820 N94-27670

FEEDBACK CONTROL

The application of a C(star) flight control law to large civil transport aircraft
[CRANFIELD-AERO-9303] p 2676 N94-25640

Bioregenerative system components for microgravity
p 2903 N94-25673

Design of a subsonic envelope flight control system for the Vista F-16 using quantitative feedback theory
[AD-A274057] p 2676 N94-25771

Design of a flight controller for an unmanned research vehicle with control surface failures using quantitative feedback theory
[AD-A274049] p 2677 N94-25833

Evaluation of moderate angle of attack roll of a dual engine, thrust vectoring aircraft using quantitative feedback theory
[AD-A274118] p 2667 N94-25905

Multiple model adaptive estimation applied to the LAMBDA URV for failure detection and identification
[AD-A274078] p 3002 N94-25992

Modelling and stability of a shape memory alloy position control system
[ISBN-0-315-84467-1] p 2740 N94-27304

Fiber optic Faraday flux transformer specification
[AD-D016058] p 3039 N94-27674

Comparison of dynamic analysis of a Schilling hydraulic manipulator with experimental results
[DE94-004597] p 2827 N94-27780

Pulse control method and its characteristics
[DE94-701187] p 2989 N94-27809

Topics in the design, analysis and implementation of feedback control systems
[ISBN-0-315-84934-7] p 2989 N94-27975

On the use of feedback to control sound radiation from a plate excited by a turbulent boundary layer
[ISVR-TR-227] p 2807 N94-28175

Optical pattern recognition system utilizing resonator array
[AD-D016071] p 3040 N94-28224

FEEDERS

An automatic 14-day paste diet feeder for animals
[NASA-TM-108804] p 2901 N94-26086

FEMALES

Female combat helicopter pilot selection criteria
[AD-A273935] p 2938 N94-26749

FERMI LIQUIDS

Crossover between BCS and performed-Boson theories with increasing interactions
[DE93-019018] p 3017 N94-26078

Fermi-liquid to non-Fermi-liquid transition in a dynamical generalization of the CPA in a disordered Hubbard model
[DE94-601875] p 2714 N94-26169

Technical report of ISSP. Ser. A, no. 2683: Itinerant character of 5f electrons in UNi2Ga
[JTN-94-80569] p 3025 N94-27337

FERMI SURFACES

Window least squares method applied to statistical noise smoothing of positron annihilation data
[DE93-634665] p 3003 N94-26385

Fermi surface ridge at second and third Umklapp positron annihilations in Y Ba2Cu3O(7-delta)
[DE93-634760] p 3070 N94-27995

FERMIONS

Back-reaction beyond the mean field approximation
[DE94-003936] p 3012 N94-25612

Fermionic field theory and gauge interactions on random lattices
[DE94-601565] p 3051 N94-25885

Aspects of nonrenormalizable terms in a superstring standard-like models
[DE93-614530] p 3071 N94-25911

Crossover between BCS and performed-Boson theories with increasing interactions
[DE93-019018] p 3017 N94-26078

Dynamic breaking of U(N) and appearance of Chern-Simons term in 4-fermion theories
[DE93-634342] p 3019 N94-26455

Strongly interacting fermion systems
[DE94-002674] p 3021 N94-26677

Finite density effects in gauge theories
[ISBN-0-315-50637-7] p 3074 N94-27403

Surface modes and chiral symmetry (Wilson fermions in a box)
[DE94-004946] p 3029 N94-27814

Solution of the Heisenberg equation for the four-fermion contact interaction by the method of dynamical mappings
[DE94-606341] p 3075 N94-27858

FERRITES

Ferrite phase shifters using stress insensitive materials
[AD-A274639] p 2708 N94-26895

FERROELECTRICITY

Crystallization and microstructural control of ferroelectric thin-films and glass-ceramics
[AD-A273767] p 2748 N94-25854

Ferroelectric thin film microstructure development and related property enhancement
[DE94-002741] p 3061 N94-26856

Ferroelectricity in a Langmuir-Blodgett multilayer film of a liquid crystalline side-chain polymer
[AD-A274477] p 2754 N94-27033

Ferroelectric fluoride memory FET development
[AD-A274341] p 2785 N94-27057

Electro-optic materials by solid source MOCVD
[DE94-005120] p 2757 N94-27716

FERROFLUIDS

Using ferro-magnetic fluids to lubricate non-conformal isothermal contacts
[INPE-5520-TAE/021] p 2827 N94-27665

FERROMAGNETIC MATERIALS

Study on characteristics and electronic structures of materials with strong electronic correlations by ferromagnetic fields p 2724 N94-25557

Power laws, flicker noise, and the barkhausen effect
[AD-A274702] p 3008 N94-26376

FERROMAGNETISM

Study on phase transformation due to deformation in ferromagnetic fields at cryogenic condition
p 2724 N94-25556

Volume dependence of vanadium magnetism
[DE94-601838] p 3050 N94-25843

Non-contact ultrasonic inspection
[VTT-TIED-1454] p 2835 N94-26257

Center for nonlinear phenomena and magnetic materials
[AD-A274176] p 3009 N94-27126

FERROUS METALS

List of papers published by the members of Institute for Materials Research, Tohoku University 1992
[JTN-94-80608] p 3118 N94-27355

FETUSES

Anorectal malformations induced by intraperitoneal injection of all-trans retinoic acid in suncus
p 2905 N94-27489

Cross-sectional anatomy of day 30 suncus fetuses
p 2905 N94-27490

Skeletal development and ossification of the swine fetuses p 2905 N94-27491

FEYNMAN DIAGRAMS

Pseudoscalar glueball in the composite interpolating fields approach
[DE93-634374] p 3016 N94-26042

Meson X(1814) as a candidate for a hybrid state
[DE93-634447] p 3017 N94-26045

Stochastic space-time, confinement potential and particle propagator
[DE94-606415] p 3074 N94-27680

FIBER COMPOSITES

Inner fiber observation for metal matrix composites under the stress load condition utilizing Synchrotron Orbital Radiation (SR) by X-ray CT p 2724 N94-25553

Continuous fiber reinforced thermoplastic composites: Literature survey
[VTT-TIED-1422] p 2704 N94-25651

Lunar preform manufacturing p 2765 N94-25677

A nonlinear three-dimensional micromechanics model for fiber-reinforced laminated composites
[AD-A273772] p 2705 N94-25857

Influence of embedded optical fibers on compressive strength of advanced composites
[AD-A273775] p 2705 N94-25859

Design study of fiber-composite penetrator cases
[DE94-003203] p 2707 N94-26099

A constitutive model for layered wire mesh and aramid cloth fabric
[DE94-003275] p 2708 N94-26796

Design and test of postbuckled stiffened curved plates: A literature survey
[PB94-126521] p 2840 N94-26961

Intelligent material systems and structures. Part 6: Measurements of adhesion between optical fibres and composite materials
[PB94-123577] p 2756 N94-27215

Thermoplastic or thermosetting composites in aircrafts
[PB94-123809] p 2710 N94-27253

A widely adaptable habitat construction system utilizing space resources p 2688 N94-27374

The deformation of copper-tungsten composites
[ISBN-0-315-84939-8] p 2712 N94-27688

Joining of fibre reinforced metal matrix composite materials
[PB94-132453] p 2712 N94-28376

FIBER OPTICS

An electromagnetic calorimeter with wavelength shifting fiber readout
[DE93-616664] p 2809 N94-25735

Development of a multi-sensor in situ fiber optic fluorometer
[DE94-003399] p 3035 N94-26100

Code division multiple access local area network communications employing fiber optic signal processing techniques
[AD-A274897] p 3096 N94-26180

Multichip module high speed testing
[AD-A274873] p 2782 N94-26343

Cad of GeO2-SiO2 double-layer core dispersion-shifted single-mode fibre
[DE93-634325] p 3035 N94-26383

Modeling and simulation of a fiber distributed data interface local area network
[AD-A274838] p 3098 N94-26500

Fiber-optic-based laser vapor screen flow visualization system for aerodynamic research in larger scale subsonic and transonic wind tunnels
[NASA-TM-4514] p 2647 N94-26706

A space fiber-optic x ray burst detector
[DE94-002722] p 2696 N94-26808

Detection of low-intensity magnetic fields with a magnetostrictive fiber optic sensor
[AD-A274120] p 3037 N94-27062

Method of measuring liquid level
[AD-D016049] p 3038 N94-27153

Evanescent field infrared spectroscopy using chalcogenide glass fiber
[ITN-94-85233] p 3038 N94-27178

Ir-fibers in a laser threat warning system and robot shot warning system
[PB94-124476] p 3038 N94-27209

Kinoform/lens system for injecting a high power laser beam into an optical fiber
[DE94-003226] p 2819 N94-27262

Fiber optic Faraday flux transformer specification
[AD-D016058] p 3039 N94-27674

Fiber optic true time-delay array antenna feed system
[AD-D016063] p 2777 N94-27734

Multiple exposure CCD detector for high-speed laser pump, x ray probe Laue scattering
[DE94-004618] p 2820 N94-27781

Fiber optic sensors for corrosion detection
p 3040 N94-27923

Optical pattern recognition system utilizing resonator array
[AD-D016071] p 3040 N94-28224

FIBER ORIENTATION

Characterization of fatigue damage in a metal matrix composite (SCS-6/Ti-15-3) at elevated temperature
[AD-A273797] p 2706 N94-25876

Effects of Class 1 antiarrhythmic drugs on the intraventricular conduction: Influence of fiber orientation
p 2907 N94-27507

FIBER STRENGTH

Inert strength of pristine silica glass fibers
[DE94-004685] p 2750 N94-26247

Engineering limitations of ceramic composites for high performance and high temperature applications
[DE94-001676] p 2754 N94-27021

FIBROBLASTS

Thyroid hormone action in cultured human skin fibroblasts: Evaluation using spheroid culture
p 2919 N94-27478

FIELD ALIGNED CURRENTS
Configuration of the near-Earth plasma sheet [NASA-CR-195271] p 2883 N94-27438
Modeling of the coupled magnetospheric and neutral wind dynamos [NASA-CR-195273] p 2883 N94-27852
FIELD COILS
Development of fusion technology [DE93-633444] p 3042 N94-26159
Tokamak Physics Experiment poloidal field design [DE94-001542] p 3045 N94-27019
Experimental results of 40-kA Nb3Al conductor [DE94-701207] p 2788 N94-27821
FIELD EFFECT TRANSISTORS
Modeling electromagnetic effects in MMICs for T/R modules [AD-A273808] p 2766 N94-25736
Ferroelectric fluoride memory FET development [AD-A274341] p 2785 N94-27057
AC to DC power converter with regulated bi-polar outputs [AD-D016032] p 2786 N94-27145
Thermally stable oxygen and nitrogen implant isolation of C-doped Al(0.35)Ga(0.65)As [DE94-004799] p 3069 N94-27790
Silicon device performance measurements to support temperature range enhancement [NASA-CR-195265] p 2844 N94-27824
FIELD EMISSION
A direct current rectification scheme for microwave space power conversion using traveling wave electron acceleration p 2687 N94-27371
FIELD OF VIEW
Elastic backscattering lidar for a MSTI satellite [DE94-002701] p 2816 N94-26126
Digital filter design for sensor simulation: Application to the Brazilian remote sensing satellite [INPE-5523-RPQ/665] p 2849 N94-26827
DMSP satellites as gamma ray burst detectors [DE94-004977] p 3116 N94-27793
Optical pattern recognition system utilizing resonator array [AD-D016071] p 3040 N94-28224
FIELD THEORY (ALGEBRA)
On kinetic expansion in scalar field theory [DE93-634338] p 3072 N94-26553
Limit theorems for functionals of Markov processes and renormalizable stable fields [AD-A274645] p 3004 N94-27106
FIELD THEORY (PHYSICS)
Coherent state approach for the (Phi)(sup 6)-lattice model and phase transitions [DE93-613053] p 3050 N94-25825
Quark-antiquark bound states [DE93-613054] p 3013 N94-25826
Fermionic field theory and gauge interactions on random lattices [DE94-601565] p 3051 N94-25885
Higher spin extensions of the Virasoro algebra, area-preserving algebras and the matrix algebra a-bar(sub (infinity)) [DE94-601557] p 3006 N94-26415
Differential regularization of a non-relativistic anyon model [DE94-601558] p 3019 N94-26416
Vortices in curved spacetime [DE94-601559] p 3072 N94-26417
Orthodox gravity [DE94-601560] p 2878 N94-26418
Dynamic breaking of U(N) and appearance of Chern-Simons term in 4-fermion theories [DE93-634342] p 3019 N94-26455
A cosmological field theory [ISBN-0-315-84271-7] p 3104 N94-26638
Thermodynamics and form factors of supersymmetric integrable field theories [DE94-602557] p 3073 N94-26896
Normal forms for perturbations of the euler top [PB94-125390] p 3009 N94-26968
Improved numerical methods for quantum field theory (Outstanding Junior Investigator Award) [DE94-001793] p 3073 N94-27002
Mapping between the Sinh-Gordon and Ising models [DE94-601535] p 2998 N94-27162
Operator regularization and renormalization theory [ISBN-0-315-49334-8] p 3007 N94-27264
Second-order phase transition in (g(phi)4)2 theory [DE94-603677] p 3067 N94-27638
Solution of the Heisenberg equation for the four-fermion contact interaction by the method of dynamical mappings [DE94-606341] p 3075 N94-27858
FIGHTER AIRCRAFT
Extension of On-Surface Radiation Condition (OSRC) theory to full-vector electromagnetic wave scattering by three-dimensional conducting, dielectric, and coated targets [AD-A274023] p 2766 N94-25757
Report of the defense science board task force on aircraft assessment [AD-A274531] p 2669 N94-26835
FILM COOLING
Study on film generation phenomena by particle deposition p 2728 N94-25575
Analysis of cooling jets near the leading edge of turbine blades p 2676 N94-28037
Advanced metallic exhaust impinged structural concepts demonstration p 2832 N94-28209
FILM THICKNESS
In situ x ray reflectivity measurements of thin film structural evolution [DE94-002289] p 3051 N94-25944
Using ferro-magnetic fluids to lubricate non-conformal isothermal contacts [INPE-5520-TAE/021] p 2827 N94-27665
Calculation methods for steadily loaded central circumferential groove hydrodynamic journal bearings (guide to use of computer program A9304) [ESDU-93004] p 2830 N94-28073
Calculation methods for steadily loaded axial groove hydrodynamic journal bearings (guide to use of computer program A9305) [ESDU-93005] p 2830 N94-28074
Calculation methods for steadily loaded axial groove hydrodynamic journal bearings. Low viscosity process fluid lubrication (guide to use of computer program A9306) [ESDU-93006] p 2830 N94-28075
FILTRATION
Bioregenerative system components for microgravity p 2903 N94-25673
FINANCE
Single term off-line coins [CWI-CS-R9318] p 2776 N94-27546
An efficient off-line electronic cash system based on the representation problem [CWI-CS-R9323] p 2776 N94-27551
FINANCIAL MANAGEMENT
NASA: Major challenges for management. Testimony before the Legislation and National Security Subcommittee, Committee on Government Operations, House of Representatives [GAO/T-NSIAD-94-18] p 3095 N94-28176
FINE STRUCTURE
Topological amplitudes in string theory [DE94-601561] p 3071 N94-25882
Morphological analysis of ionomers [DE94-003660] p 2749 N94-26005
High resolution measurements of mixing and reaction processes in turbulent flows [AD-A274970] p 2793 N94-26534
An x ray absorption fine structure study of ordering in polythiophene thin films [AD-A274235] p 2753 N94-26822
FINITE DIFFERENCE THEORY
Theory and modeling of stimulated Raman scattering [AD-A273755] p 3033 N94-25721
Extension of On-Surface Radiation Condition (OSRC) theory to full-vector electromagnetic wave scattering by three-dimensional conducting, dielectric, and coated targets [AD-A274023] p 2766 N94-25757
Arbitrary-order numerical schemes for model parabolic equations [CRANFIELD-AERO-9210] p 3005 N94-25781
Rendering of three-dimensional data sets derived from finite-difference and spectral methods [AD-A273724] p 3096 N94-25997
A positive finite-difference advection scheme applied on locally refined grids [CWI-NM-R9309] p 2867 N94-26216
Numerical solution of singularity-perturbed two-point boundary-value problems [DE94-601542] p 2993 N94-26410
The application of FD-TD method to antenna radiation patterns [ISBN-0-315-83893-0] p 2769 N94-26618
VLUGR2: A vectorized local uniform grid refinement code for PDE's in 2D [CWI-NM-R9306] p 2965 N94-26772
Using the TSAR electromagnetic modeling system [DE94-002617] p 2771 N94-26803
Nonlinear hysteresis in an endochronic solid [AD-A274594] p 2880 N94-26855
Elastic wave up/down decomposition in inhomogeneous and anisotropic media: An operator approach and its approximations [PB94-126497] p 2881 N94-26880
FINITE ELEMENT METHOD
Study on elucidation of damage generation process by electron beam lithography p 2729 N94-25581
Piecewise least squares fitting technique using finite interval method with Hermite polynomials [VTT-PUBS-135] p 2990 N94-25733
Structural analysis of a frangible nut used on the NASA Space Shuttle [DE94-003672] p 2821 N94-25811
Design study of fiber-composite penetrator cases [DE94-003203] p 2707 N94-26099
Parameter estimation by genetic algorithms [DE94-002924] p 2961 N94-26146
Longitudinal diffusion of a proton bunch under external noise [DE93-634022] p 3032 N94-26165
Correlation of experimental data and three-dimensional finite element modeling of a spinning quadrupole [DE93-041173] p 3008 N94-26421
Stress analysis of a secondary-bending specimen [AD-A274842] p 2838 N94-26501
A comparative study of serial and parallel aeroelastic computations of wings [NASA-TM-108805] p 2645 N94-26538
Structural evaluation of concepts for a solar energy concentrator for Space Station advanced development program [NASA-TP-3375] p 2695 N94-26609
Wobble-nutation modes of the Earth [ISBN-0-315-84246-6] p 3102 N94-26669
Nonlinear hysteresis in an endochronic solid [AD-A274594] p 2880 N94-26855
An automatic contact algorithm in DYNA3D for impact problems [DE94-002856] p 2965 N94-26862
New variational techniques for acoustic radiation and scattering from elastic shell structures [AD-A274599] p 3010 N94-26889
Computation of stress intensity factors by the mode enrichment technique with applications to geometrically nonlinear problems [PB94-126513] p 2840 N94-26910
Aircraft wheel life assessment [AD-A274378] p 2823 N94-26976
Joint services electronics program [AD-A274643] p 2785 N94-27027
Numerical Analysis Methods of Surface Cracks [VTT-PUBS-119] p 2841 N94-27186
Method for calculating stress intensity factors for surface cracks (appendix 2/1) p 2841 N94-27188
Quality assurance for fracture mechanical finite element analyses (appendix 3/1) p 2841 N94-27189
Applications of the weight function method (appendix 4/1) p 2842 N94-27190
Finite element analysis of damped vibrations of laminated composite plates [ISBN-0-315-84928-2] p 2843 N94-27585
A study on heat transfer in a scramjet leading edge model [NAL-TR-1187T] p 2675 N94-27608
An improvement in the modified finite element procedure for underwater shock analysis [DE94-004451] p 2797 N94-27617
Thermocapillary flow with evaporation and condensation and its effect on liquid retention in low-G fluid acquisition devices [NASA-TP-3463] p 2797 N94-27639
PATRAN 2.5/EAL interface guide [NASA-TM-109053] p 2972 N94-27655
Numerical experiment on finite element method for matching data [DE94-701208] p 3000 N94-27731
Super finite elements for nonlinear static and dynamic analysis of stiffened plate structures [ISBN-0-315-63903-2] p 2844 N94-27808
Hybrid techniques for complex aerospace electromagnetics problems p 2779 N94-27894
Mechanically fastened composite laminates subjected to combined bearing-bypass and shear loading p 2712 N94-27914
Analysis and control of hourglass instabilities in underintegrated linear and nonlinear elasticity [NASA-CR-195293] p 2846 N94-28266
FINITE VOLUME METHOD
High-lift system analysis method using unstructured meshes [NLR-TP-92351-U] p 2647 N94-27554
The numerical calculation of laminar and turbulent flows using penalty function finite volume methods [ISBN-0-315-61377-7] p 2799 N94-27947
Techniques for accurately solving unsteady shock waves and contact discontinuities p 2656 N94-28342

FINS

Low-speed pressure distribution measurements over the aft-fuselage, fins, and stabilators of a 1/9th scale F/A-18 wind-tunnel model [AD-A274870] p 2644 N94-26342

Flowfield dynamics in blunt fin-induced shock wave/turbulent boundary layer interactions [NASA-CR-195170] p 2798 N94-27802

Contribution of body-mounted fins and tailplanes to lateral derivatives due to sideslip at subsonic speeds for general body width to height ratio [ESDU-93007] p 2648 N94-28057

FIR FILTERS

Role of anticausal inverses in multirate filter-banks. Part 1: System theoretic fundamentals [AD-A274279] p 2997 N94-27015

Causal fir matrices with anticausal fir inverses, and application in characterization of biorthonormal filter banks [AD-A274509] p 2998 N94-27035

FIRE (CLIMATOLOGY)

MODIS airborne simulator visible and near-infrared calibration, 1991 FIRE-Cirrus field experiment. Calibration version: FIRE King 1.1 [NASA-TM-104600] p 2897 N94-28182

FIRE CONTROL CIRCUITS

Effects of repeating resistance testing on firing ability of igniter EP360-3 [AD-A274814] p 2759 N94-26486

FIRE FIGHTING

Summaries of BFRL fire research in-house projects and grants, 1993 [PB94-121050] p 2763 N94-26756

FIRE PREVENTION

HDR reactor containment fire modeling with BRI2 [VTT-PUBS-113] p 3031 N94-25621

Engineering Technical Letter (ETL) 93-5: Fire protection engineering criteria, electronic equipment installations [AD-A274835] p 2762 N94-26084

The structural behaviour of the steel or composite concrete and steel frames and the connections of frame members during the fire: A literature review [VTT-TIED-1437] p 2837 N94-26307

Summaries of BFRL fire research in-house projects and grants, 1993 [PB94-121050] p 2763 N94-26756

Annual conference on fire research, 1993: Book of abstracts [PB94-121324] p 2717 N94-26907

Impact of improved materials and cabin water spray on commuter aircraft postcrash fire survivability [AD-A274421] p 2660 N94-27081

Risks and issues in fire safety on the Space Station [NASA-TM-106430] p 2692 N94-27436

FIRES

HDR reactor containment fire modeling with BRI2 [VTT-PUBS-113] p 3031 N94-25621

Engineering Technical Letter (ETL) 93-5: Fire protection engineering criteria, electronic equipment installations [AD-A274835] p 2762 N94-26084

Fire simulation based on convection calculation [VTT-TIED-1411] p 2762 N94-26259

Summaries of BFRL fire research in-house projects and grants, 1993 [PB94-121050] p 2763 N94-26756

Annual conference on fire research, 1993: Book of abstracts [PB94-121324] p 2717 N94-26907

SP industry calorimeter for rate of heat release measurements up to 10MW [PB94-124211] p 2811 N94-27044

Uncertainties in the characterization of the thermal environment of a solid rocket propellant fire [DE94-002023] p 2760 N94-27719

FISHES

Coupling of pelagic and benthic communities over a seamount in the Eastern North Pacific [AD-A274750] p 2899 N94-26149

Study on posture control and adaption mechanism under weightlessness: Results of second rehearsal for space experiment using carp p 2912 N94-27446

FISSION

A double arm time-of-flight spectrometer based on position-sensitive parallel-grid avalanche counters [DE93-616665] p 3012 N94-25750

FISSION PRODUCTS

Index to BROND-2, CENDL-2, ENDF/B-6, JEF-2, JENDL-3 [DE93-634500] p 3016 N94-26034

FIXED POINTS (MATHEMATICS)

Semantics, orderings and recursion in the weakest precondition calculus [CWI-CS-R9267] p 2995 N94-26776

Fixed point type theorems and projection-interaction approximation [DE94-603669] p 3000 N94-27632

FIXED WINGS

A finite wake theory for two-dimensional rotary wing unsteady aerodynamics [AD-A274921] p 2645 N94-26535

Preliminary assessment of aerodynamic effects of wing repair patches p 2657 N94-28346

FLAME PROPAGATION

Summaries of BFRL fire research in-house projects and grants, 1993 [PB94-121050] p 2763 N94-26756

Impact of improved materials and cabin water spray on commuter aircraft postcrash fire survivability [AD-A274421] p 2660 N94-27081

FLAME RETARDANTS

Impact of improved materials and cabin water spray on commuter aircraft postcrash fire survivability [AD-A274421] p 2660 N94-27081

FLAME SPECTROSCOPY

Researches of the Electrotechnical Laboratory. No. 53: Spectral emission from combustion gas containing scattering media [JTN-94-80603] p 2717 N94-27246

FLAMES

Characterization of acoustic effects on flame structures by beam deflection technique [DE94-003240] p 2714 N94-26122

FLAMMABILITY

Microgravity ignition experiment p 2761 N94-25707

The structural behaviour of the steel or composite concrete and steel frames and the connections of frame members during the fire: A literature review [VTT-TIED-1437] p 2837 N94-26307

Composite raw materials for the building industry [VTT-TIED-1433] p 2708 N94-26544

Annual conference on fire research, 1993: Book of abstracts [PB94-121324] p 2717 N94-26907

FLAPS (CONTROL SURFACES)

Experimental apparatus for optimization of flap position for a three-element airfoil model p 2682 N94-27912

Wing lift increment at zero angle of attack due to deployment of single-slotted flaps at low speeds [ESDU-93019] p 2649 N94-28140

Thin-layer Navier-Stokes computations for multi-element airfoils p 2656 N94-28341

FLASH LAMPS

Flash unit for high speed photography [PML-1992-91] p 2811 N94-26647

FLAT PLATES

User's guide for the thermal analyst's help desk expert system [NASA-CR-194885] p 2695 N94-26103

Nominally 2-dimensional flow about a normal flat plate [AD-A274472] p 2794 N94-27026

Numerical simulation of receptivity and transition in a boundary layer on a flat plate with a suction hole [NASA-CR-195708] p 2798 N94-27782

Comparison of the interactions of two and three dimensional transverse jets with a hypersonic free stream p 2659 N94-28021

Experiments on interaction force of jets in hypervelocity cross-flow in a shock tunnel p 2659 N94-28022

A numerical investigation of a subsonic jet in a crossflow p 2803 N94-28023

Flat rectangular orthotropic plates under uniformly distributed normal pressure. Elastic stresses and deflections for various forms of edge restraint [ESDU-93011] p 2845 N94-28061

FLAT SURFACES

Failure mechanisms of high temperature semiconductor lasers [AD-A273833] p 2815 N94-25616

Bathymetric data set extraction program. Users guide [AD-A274761] p 2899 N94-26567

Development of a 2f optical performance measurement system [DE94-003489] p 3039 N94-27721

FLATTENING

Study on the production of flaky amorphous alloy powders by impact flattening of atomized liquid droplets on a rapidly rotating wheel p 2746 N94-28169

FLAVOR (PARTICLE PHYSICS)

Photon and hadron production of heavy flavors [DE94-004655] p 3018 N94-26245

Flavor changing neutral currents in SU(3) x U(1) models [DE94-602576] p 3022 N94-26899

Weak hadronic decays of heavy flavor mesons [ISBN-0-315-55542-4] p 3026 N94-27402

FLEXIBLE BODIES

Selected topics in robotics for space exploration [NASA-CP-10131] p 2682 N94-26278

Dynamics of a flexible extendible beam [ISBN-0-315-84278-4] p 2838 N94-26639

Implementation of integral manifold control on a two degree of freedom flexible joint manipulator: Theory and experiments [ISBN-0-315-83572-9] p 2823 N94-26658

Generalized finite element dynamic modelling and simulation for flexible robot manipulators [ISBN-0-315-84623-2] p 2825 N94-27343

FLEXIBLE SPACECRAFT

A study on piezoelectric actuators and sensors for vibration control of flexible space structures [AD-A274925] p 2695 N94-26532

Substructure synthesis methods for viscoelastic structures [UTIAS-349] p 2695 N94-26712

Dynamics and robust control for uncertain flexible space systems [INPE-5510-TAE/020] p 2696 N94-27357

FLEXIBLE WINGS

A comparative study of serial and parallel aeroelastic computations of wings [NASA-TM-108805] p 2645 N94-26538

FLIGHT CHARACTERISTICS

Aircraft maneuvers for the evaluation of flying qualities and agility. Volume 1: Maneuver development process and initial maneuver set [AD-A273913] p 2666 N94-25590

Aircraft maneuvers for the evaluation of flying qualities and agility. Volume 3: Simulation data [AD-A273814] p 2667 N94-25961

Standardization of aircraft control and performance symbology on the USAF head-up display [AD-A274283] p 2673 N94-26989

Techniques to improve maneuver stability characteristics of a nonlinear wide-body transport airplane in cruise flight [NASA-TM-4521] p 2679 N94-27660

A study of jet effect and ground effect interference on a STOL fighter p 2671 N94-28034

Transitional flight characteristics of a geometrically simplified STOVL model p 2672 N94-28035

FLIGHT CONDITIONS

Development and implementation of a scramjet cycle analysis code with a finite-rate-chemistry combustion model for use on a personal computer [AD-A273834] p 2673 N94-25617

Variability of measured sonic boom signatures p 2651 N94-28197

FLIGHT CONTROL

Design of a subsonic envelope flight control system for the Vista F-16 using quantitative feedback theory [AD-A274057] p 2676 N94-25771

Neural networks for dynamic flight control [AD-A274089] p 2676 N94-25785

Design of a flight controller for an unmanned research vehicle with control surface failures using quantitative feedback theory [AD-A274049] p 2677 N94-25833

Evaluation of moderate angle of attack roll of a dual engine, thrust vectoring aircraft using quantitative feedback theory [AD-A274118] p 2667 N94-25905

Multiple model adaptive estimation applied to the LAMBDA URV for failure detection and identification [AD-A274078] p 3002 N94-25992

Discovery learning in autonomous agents using genetic algorithms [AD-A274083] p 2677 N94-25998

Technology drivers for flight telerobotic system software p 2684 N94-26289

The Ariane 5 data management system p 2950 N94-26724

PRONAOS flight software: A real-time application for a balloonborne scientific gondola p 2950 N94-26725

Fluid dynamic linear accelerometer [AD-D016042] p 2678 N94-27112

Automation of formation flight control [AD-A274137] p 2678 N94-27132

Optimal nonlinear estimation for aircraft flight control in wind shear p 2643 N94-27296

Computer code for controller partitioning with IFPC application: A user's manual [NASA-CR-195291] p 2678 N94-27414

Design and flight test of the Propulsion Controlled Aircraft (PCA) flight control system on the NASA F-15 test aircraft [NASA-CR-186028] p 2674 N94-27432

Techniques to improve maneuver stability characteristics of a nonlinear wide-body transport airplane in cruise flight [NASA-TM-4521] p 2679 N94-27660

A simulator investigation of helicopter flight control system mode transitions [UTIAS-348] p 2682 N94-27879

Comparison of performance in simulator flight among subjects with different simulator experiences p 2933 N94-27943

FLIGHT CREWS
Airborne data link operational evaluation test plan
[AD-A274096] p 2664 N94-25788
A comparison of two hardware implementations of a crew selection system
[AD-A274913] p 2937 N94-26346
US Army aviation epidemiology data registry: Incidence and outcomes of aviator flying evaluation boards
[AD-A274711] p 2910 N94-26432
The use of EEG as a workload assessment tool in flight test
[AD-A274568] p 2910 N94-26847
Benefits estimation for simulation systems used for aircrew training in a multiship environment
[AD-A274313] p 2938 N94-26882
Effects of historical and predictive information on ability of transport pilot to predict an alert
[NASA-TM-4547] p 2673 N94-27864

FLIGHT ENVELOPES
Design of a subsonic envelope flight control system for the Vista F-16 using quantitative feedback theory
[AD-A274057] p 2676 N94-25771

FLIGHT HAZARDS
The relationship of an integral wind shear hazard to aircraft performance limitations
[NASA-TM-109080] p 2677 N94-26593
A data fusion algorithm for multi-sensor microburst hazard assessment p 2641 N94-27287
Investigation of air transportation technology at Princeton University, 1992-1993 p 2643 N94-27294
Special investigation report: Safety issues related to wake vortex encounters during visual approach to landing
[PB94-917002] p 2660 N94-27881

FLIGHT INSTRUMENTS
Standardization of aircraft control and performance symbology on the USAF head-up display
[AD-A274283] p 2673 N94-26989
A graphical workstation based part-task flight simulator for preliminary rapid evaluation of advanced displays
p 2641 N94-27286

FLIGHT MANAGEMENT SYSTEMS
The Ariane 5 data management system
p 2950 N94-26724
PRONAOS flight software: A real-time application for a balloonborne scientific gondola p 2950 N94-26725
MATRA Marconi Space: The Silex on-board processor and on-board software p 2950 N94-26726

FLIGHT MECHANICS
University of Toronto Institute for Aerospace Studies
[CTN-94-61013] p 3117 N94-26701

FLIGHT OPERATIONS
Air traffic management as principled negotiation between intelligent agents p 2643 N94-27297

FLIGHT PATHS
Genetic algorithms applied to a mission routing problem
[AD-A274130] p 2968 N94-27120
Optimal nonlinear estimation for aircraft flight control in wind shear p 2643 N94-27296
Examples of flight path optimisation using a multivariate gradient-search method
[ESDU-93021] p 2670 N94-28092

FLIGHT SAFETY
Eagle RTS: A design of a regional transport
p 2671 N94-25709
S-76 high intensity radiated fields, volume 2
[AD-A274572] p 2771 N94-26836
S-76 high intensity radiated fields, volume 1
[AD-A274571] p 2771 N94-26854
S-76 high intensity radiated fields, volume 3
[AD-A274416] p 2772 N94-26980
Air traffic management as principled negotiation between intelligent agents p 2643 N94-27297
Aircraft accident report: Runway departure following landing American Airlines flight 102, McDonnell Douglas DC-10-30, N139AA, Dallas/Fort Worth International Airport, Texas, April 14, 1993
[PB94-910402] p 2660 N94-27766
Effects of historical and predictive information on ability of transport pilot to predict an alert
[NASA-TM-4547] p 2673 N94-27864
Special investigation report: Safety issues related to wake vortex encounters during visual approach to landing
[PB94-917002] p 2660 N94-27881
Debris/ice/TPS assessment and integrated photographic analysis for Shuttle mission STS-60
[NASA-TM-109193] p 2692 N94-27956
The 1993 Federal Aviation Administration plan for research, engineering and development
p 2643 N94-27960
Lufthansa Yearbook 1992
[DSK-9734-H-92] p 2660 N94-28230
A sky above Europe p 2661 N94-28234

FLIGHT SIMULATION
Report on a visit to the Arvin/Calspan Corporation, Buffalo, New York, USA, September 1992
[CRANFIELD-AERO-9305] p 2676 N94-25653
Developing realistic cooperative behaviors for autonomous agents in air combat simulation
[AD-A274077] p 2937 N94-25774
Piloted simulation study of an ILS approach of a twin-pusher business/commuter turboprop aircraft configuration
[NASA-TM-4516] p 2646 N94-26602

FLIGHT SIMULATORS
Report on a visit to the Arvin/Calspan Corporation, Buffalo, New York, USA, September 1992
[CRANFIELD-AERO-9305] p 2676 N94-25653
Weapon system integration for the AFIT virtual cockpit
[AD-A274058] p 2667 N94-25772
Image quality and the display modulation transfer function: Experimental findings
[AD-A274061] p 2679 N94-25773
Developing realistic cooperative behaviors for autonomous agents in air combat simulation
[AD-A274077] p 2937 N94-25774
Benefits estimation for simulation systems used for aircrew training in a multiship environment
[AD-A274313] p 2938 N94-26882
Reconfigurable aircraft stick control
[AD-D016043] p 2681 N94-27113
A graphical workstation based part-task flight simulator for preliminary rapid evaluation of advanced displays
p 2641 N94-27286
Design and flight test of the Propulsion Controlled Aircraft (PCA) flight control system on the NASA F-15 test aircraft
[NASA-CR-186028] p 2674 N94-27432
A simulator investigation of helicopter flight control system mode transitions
[UTIAS-348] p 2682 N94-27879
Comparison of performance in simulator flight among subjects with different simulator experiences
p 2933 N94-27943

FLIGHT STABILITY TESTS
Optimal control of helicopters following power failure
[NAL-TR-1190] p 2678 N94-27206

FLIGHT TESTS
Aircraft maneuvers for the evaluation of flying qualities and agility. Volume 1: Maneuver development process and initial maneuver set
[AD-A273913] p 2666 N94-25590
Project Ares 3 p 2671 N94-25712
Design study to simulate the development of a commercial freight transportation system
p 2671 N94-25715
Aircraft maneuvers for the evaluation of flying qualities and agility. Volume 3: Simulation data
[AD-A273814] p 2667 N94-25961
Correlation of airloads on a two-bladed helicopter rotor
[NASA-TM-103982] p 2644 N94-26143
Report of the defense science board task force on aircraft assessment
[AD-A274531] p 2669 N94-26835
S-76 high intensity radiated fields, volume 2
[AD-A274572] p 2771 N94-26836
The use of EEG as a workload assessment tool in flight test
[AD-A274568] p 2910 N94-26847
S-76 high intensity radiated fields, volume 1
[AD-A274571] p 2771 N94-26854
S-76 high intensity radiated fields, volume 3
[AD-A274416] p 2772 N94-26980
Radiometric, spectral, and effectiveness equipment
[AD-A274208] p 3037 N94-27066
Flight testing of GPS and GPS-aided systems
[NLR-TP-92151-U] p 2666 N94-27831
On the aging of sonic booms p 2650 N94-28194
A340 testing p 2662 N94-28242

FLIGHT TRAINING
Image quality and the display modulation transfer function: Experimental findings
[AD-A274061] p 2679 N94-25773
Benefits estimation for simulation systems used for aircrew training in a multiship environment
[AD-A274313] p 2938 N94-26882
The Reports of Aeromedical Laboratory, volume 33, number 4
[JTN-94-80586] p 2933 N94-27942

FLIR DETECTORS
Mitsubishi 3-5 micrometers IR imager for machine-vision/ATA applications
[AD-A273812] p 3034 N94-25940
Weapon system sensor integration for a DIS-compatible virtual cockpit
[AD-A274088] p 2672 N94-26021
Focal plane arrays in advanced thermal images
[AD-B174292] p 3036 N94-26648
Enhanced tracking of airborne targets using forward looking infrared and laser return measurements
[AD-A274181] p 3037 N94-27102

FLOAT ZONES
Lithium drifted silicon detector fabrication on gettered floating-zone silicon
[DE94-003890] p 3054 N94-26095
Modelling of the MEA float zone using accelerometer data
[NASA-CR-193933] p 2761 N94-27220
Float zone crystal growth using laser radiation
[DLR-FB-93-10] p 3066 N94-27590

FLOATING POINT ARITHMETIC
Arithmetic performances of onboard computers
p 2952 N94-26738

FLOQUET THEOREM
Modal control of a satellite in an unstable periodic orbit about the Earth-Sun interior Lagrange point
[AD-A273707] p 2694 N94-25776
The modal solution to the Moon's orbit using canonical Floquet perturbation theory
[AD-A273732] p 2690 N94-26001

FLOTATION
Basic research on levitation fusing/solidification technology p 2723 N94-25552
Study on reactions between molten metal and oxide by magnetic flotation dissolution method
p 2725 N94-25558

FLOW CHARACTERISTICS
A study on structure of benthic boundary layer in coastal waters
[REPT-4] p 2898 N94-25635
Experimental contribution to the study of secondary flows in centrifugal turbopump stator components
[ECL-92-35] p 2789 N94-25654
Propagation of experimental uncertainties from the tunnel to the body coordinate system in 3-D LDV flow field studies
[NASA-CR-191607] p 2680 N94-26603
Design and experimental performance of a two stage partial admission turbine. Task B.1/B.4
[NASA-CR-179548] p 2824 N94-27228
Fifty years of jet in cross flow research
p 2799 N94-28004
Transitional flight characteristics of a geometrically simplified STOVL model p 2672 N94-28035
High-performance parallel analysis of coupled problems for aircraft propulsion
[NASA-CR-195292] p 2845 N94-28181
Wind tunnel investigation of propfan slipstream/wing interactions on a De Havilland air motor powered semispan model at Mach numbers 0.6 and 0.7
p 2651 N94-28316

FLOW DISTORTION
The measurement of disturbance levels in the Langley Research Center 20-inch Mach 6 tunnel
[NASA-CR-4571] p 2646 N94-26548
Unsteady aspects of hot gas reingestion and statistical analysis p 2676 N94-28019
Compressor stability p 2828 N94-28046

FLOW DISTRIBUTION
A study on structure of benthic boundary layer in coastal waters
[REPT-4] p 2898 N94-25635
A modeling study of the mesocyclone
[AD-A274889] p 2893 N94-26168
Propagation of experimental uncertainties from the tunnel to the body coordinate system in 3-D LDV flow field studies
[NASA-CR-191607] p 2680 N94-26603
Fiber-optic-based laser vapor screen flow visualization system for aerodynamic research in larger scale subsonic and transonic wind tunnels
[NASA-TM-4514] p 2647 N94-26706
Experimental investigation of the flow quality in the GLT20 subsonic-transonic boundary layer wind tunnel
[PB94-126539] p 2681 N94-26815
Numerical studies on the dynamics of bubble, turbulent, free shear flows: Effect of the inter-phase coupling on the global flow evolution
[AD-A274521] p 2794 N94-26832
Experimental verification of tomographic reconstruction of turbulent air flow structure using optical wavefront measurements
[AD-A274392] p 2795 N94-27129
Streamwise vorticity in a turbine rotor with conical endwalls
[DLR-FB-93-13] p 2826 N94-27591
Fifty years of jet in cross flow research
p 2799 N94-28004
Topological structure of a jet in a cross flow
p 2801 N94-28014
Experiments into the scaling parameters required for exhaust gas ingestion testing of vertical landing aircraft
p 2671 N94-28017

A numerical investigation of a subsonic jet in a crossflow p 2803 N94-28023

Navier-Stokes simulation of two and three dimensional jets in crossflow, effects of grid, and boundary conditions p 2804 N94-28026

Pneumatic management of blunted-forebody flow asymmetry for high-angle-of-attack directional control p 2679 N94-28028

Theoretical and experimental investigation of a delta wing with turbulent leading-edge jets p 2659 N94-28029

Numerical assessment of aerodynamic interactions on missiles with transverse jets control p 2659 N94-28031

First experimental assessment of RCS plume-flow field interaction on Hermes leading edge thruster configuration p 2703 N94-28032

Numerical simulation of a powered-lift landing p 2671 N94-28033

Nonequilibrium radiation and chemistry models for aerocapture vehicle flowfields [NASA-CR-195706] p 2648 N94-28071

An initial investigation into methods of computing transonic aerodynamic sensitivity coefficients [NASA-CR-195705] p 2648 N94-28072

Numerical simulation of turbulent free jet by TFKE model p 2871 N94-28157

Flow field investigation in the near slipstream of an 8-bladed propfan on the De Havilland WTEJ half-model at Mach numbers 0.6 and 0.7 p 2651 N94-28317

Potential flow modelling of airfoil stall p 2654 N94-28332

FLOW EQUATIONS

Parallel implicit unstructured grid Euler solvers [NASA-CR-191594] p 2999 N94-27434

High-lift system analysis method using unstructured meshes [NLR-TP-92351-U] p 2647 N94-27554

Time-step enlargement and optimal smoothing in Runge-Kutta time-integration algorithms by implicit and explicit smoothing [NLR-TP-92221-U] p 2798 N94-27799

FLOW MEASUREMENT

Investigation of the aerodynamic environment for an advanced lightweight rotor in forward flight. Volume 4: Laser velocimeter wake data, advance ratio of 0.037 [NASA-TM-109040-VOL-4] p 2645 N94-26483

Investigation of the aerodynamic environment for an advanced lightweight rotor in forward flight. Volume 1: Laser velocimeter inflow data, advance ratio of 0.37, thrust coefficient of 0.0081 and hover tip speed of 603 feet/second [NASA-TM-109040-VOL-1] p 2645 N94-26489

Investigation of the aerodynamic environment for an advanced lightweight rotor in forward flight. Volume 2: Laser velocimeter inflow data, advance ratio of 0.37, thrust coefficient of 0.0064 and hover tip speed of 710 feet/second [NASA-TM-109040-VOL-2] p 2645 N94-26492

Investigation of the aerodynamic environment for an advanced lightweight rotor in forward flight. Volume 3: Laser velocimeter inflow data, advance ratio of 0.37, thrust coefficient of 0.0064 and hover tip speed of 603 feet/second [NASA-TM-109040-VOL-3] p 2645 N94-26497

The measurement of disturbance levels in the Langley Research Center 20-inch Mach 6 tunnel [NASA-CR-4571] p 2646 N94-26548

Gordon Research Conference on the Physics and Chemistry of Laser Diagnostics in Combustion [AD-A274609] p 2716 N94-26893

An XCP user's guide and reference manual [AD-A274519] p 2900 N94-27090

Calibrating/testing meters in hot water test bench VM7 [PB94-124294] p 2812 N94-27160

The measurements of muscle blood flow by laser Doppler flowmetry with needle type probe p 2908 N94-27530

Transverse vorticity measurements in the University of Houston two stream shear layer facility [AD-A273910] p 2797 N94-27562

Attached and separated trailing edge flow measurements with a triple-split hot-film probe p 2656 N94-28339

FLOW RESISTANCE

Validated heat-transfer and pressure-drop prediction methods based on the discrete-element method. Phase 2: Two-dimensional rib roughness [DE94-002379] p 2794 N94-26763

FLOW STABILITY

Calibrating/testing meters in hot water test bench VM7 [PB94-124294] p 2812 N94-27160

Compressor stability p 2828 N94-28046

FLOW VELOCITY

Investigation of the aerodynamic environment for an advanced lightweight rotor in forward flight. Volume 4: Laser velocimeter wake data, advance ratio of 0.037 [NASA-TM-109040-VOL-4] p 2645 N94-26483

Investigation of the aerodynamic environment for an advanced lightweight rotor in forward flight. Volume 1: Laser velocimeter inflow data, advance ratio of 0.37, thrust coefficient of 0.0081 and hover tip speed of 603 feet/second [NASA-TM-109040-VOL-1] p 2645 N94-26489

Investigation of the aerodynamic environment for an advanced lightweight rotor in forward flight. Volume 2: Laser velocimeter inflow data, advance ratio of 0.37, thrust coefficient of 0.0064 and hover tip speed of 710 feet/second [NASA-TM-109040-VOL-2] p 2645 N94-26492

Investigation of the aerodynamic environment for an advanced lightweight rotor in forward flight. Volume 3: Laser velocimeter inflow data, advance ratio of 0.37, thrust coefficient of 0.0064 and hover tip speed of 603 feet/second [NASA-TM-109040-VOL-3] p 2645 N94-26497

Pump CFD code validation tests [NASA-CR-193939] p 2822 N94-26597

Calibrating/testing meters in hot water test bench VM7 [PB94-124294] p 2812 N94-27160

FLOW VISUALIZATION

Numerical simulation of tomographic reconstruction for the study of turbulence using optical wavefront sensor measurements [AD-A273851] p 2789 N94-25587

Flow past a circular cylinder with a permeable wake splitter plate [AD-A273765] p 2790 N94-25872

Feature isolation and quantification of evolving datasets [NASA-CR-195230] p 2961 N94-26207

Focused Schlieren flow visualization studies of multiple venturi fuel injectors in a high pressure combustor [NASA-TM-106479] p 2674 N94-26573

Fiber-optic-based laser vapor screen flow visualization system for aerodynamic research in larger scale subsonic and transonic wind tunnels [NASA-TM-4514] p 2647 N94-26706

Radar cross section visualization using sample buffer progressive refinement volume rendering [AD-A274179] p 2773 N94-27127

Leading-edge vortex-system details obtained on F-106B aircraft using a rotating vapor screen and surface techniques [NASA-TP-3374-VIDEO-SUPPL] p 2647 N94-27161

Locating tie-points on a grid p 2978 N94-27906

Unsteady wake structures in transverse jets p 2800 N94-28006

First experimental assessment of RCS plume-flow field interaction on Hermes leading edge thruster configuration p 2703 N94-28032

Effects of free-stream turbulence on a jet in a cross flow p 2805 N94-28036

Infrared imaging for transition detection in a transonic blowdown wind tunnel p 2653 N94-28325

FLOWMETERS

STS-51 pad abort. OV103-engine 2033 (ME-2) fuel flowmeter sensor open circuit [NASA-CR-193924] p 2701 N94-26230

Calibrating/testing meters in hot water test bench VM7 [PB94-124294] p 2812 N94-27160

FLUENCE

Nonswelling behavior of HT9 alloy irradiated to high exposure [DE94-003502] p 2736 N94-26522

FLUID DYNAMICS

The identification of inflow fluid dynamics parameters that can be used to scale fatigue loading spectra of wind turbine structural components [DE94-000231] p 2791 N94-26117

University of Toronto Institute for Aerospace Studies [CTN-94-61013] p 3117 N94-26701

Nominally 2-dimensional flow about a normal flat plate [AD-A274472] p 2794 N94-27026

Fluid dynamic linear accelerometer [AD-D016042] p 2678 N94-27112

Experimental verification of tomographic reconstruction of turbulent air flow structure using optical wavefront measurements [AD-A274392] p 2795 N94-27129

Basic research on natural gas combustion phenomena [PB94-129046] p 2717 N94-27256

FLUID FILMS

Using ferro-magnetic fluids to lubricate non-conformal isothermal contacts [INPE-5520-TAE/021] p 2827 N94-27665

FLUID FILTERS

Bulletin of the Institute for Chemical Reaction Science, Tohoku University, volume 2 [JTN-94-80602] p 2717 N94-27385

Glass cylindrical filter for electrolysis cell p 2718 N94-27391

FLUID FLOW

Interface configuration experiment: Preliminary results [NASA-TM-109684] p 2760 N94-25849

Numerical solution of singularity-perturbed two-point boundary-value problems [DE94-601542] p 2993 N94-26410

Solidification modeling of a spiral casting to determine material fluidity [DE94-002212] p 2739 N94-26935

Report of three microgravity experiments by the drop shaft [JTN-94-80579] p 2761 N94-27341

FLUID JETS

An experimental study of plunging liquid jet induced air carryunder and dispersion [AD-A274414] p 2794 N94-26979

FLUID MANAGEMENT

Interface configuration experiment: Preliminary results [NASA-TM-109684] p 2760 N94-25849

FLUID MECHANICS

Computational mechanics [DE94-003015] p 2965 N94-26775

A survey of open problems in symplectic integration [DE94-003966] p 3007 N94-27777

FLUID TRANSMISSION LINES

Dynamic response of a compressor research facility [AD-A273836] p 2679 N94-25740

FLUID-SOLID INTERACTIONS

Study on interfacial reaction analysis at interfacial joining p 2728 N94-25574

A thermodynamically consistent constitutive theory for a rigid solid-stokesian fluid mixture [DE93-633202] p 2792 N94-26401

FLUIDIZED BED PROCESSORS

Fibrous ceramic candle filter for particle removal in pressurized fluidized bed combustion [PB94-133089] p 2876 N94-28383

Experimental studies of pressurised fluidised bed combustion at Helsinki University of Technology, 1991-1992 [PB94-133063] p 2876 N94-28394

Emissions of nitrogen oxides (NO(x) and N2O) in pressurized fluidized bed combustion [PB94-133071] p 2876 N94-28395

FLUORESCENCE

Detecting actin fibers in cell images using minimal spanning trees [AD-A273914] p 2984 N94-25591

Development of a multi-sensor in situ fiber optic fluorometer [DE94-003399] p 3035 N94-26100

Fiber optic sensors for corrosion detection p 3040 N94-27923

FLUORIDES

Object imaging accomplished with an integrated circuit robotic tactile sensor incorporating a piezoelectric polyvinylidene fluoride thin film [AD-A274038] p 2780 N94-25845

Hadron gas ionization calorimeters [DE93-634186] p 2810 N94-26397

Ferroelectric fluoride memory FET development [AD-A274341] p 2785 N94-27057

New monomers for high performance polymers p 2758 N94-27904

FLUORINE

Novel oxidizing reagents derived from elemental fluorine [ITN-94-85231] p 2719 N94-27687

FLUORINE COMPOUNDS

Novel oxidizing reagents derived from elemental fluorine [ITN-94-85231] p 2719 N94-27687

FLUORO COMPOUNDS

New monomers for high performance polymers p 2758 N94-27904

FLUOROHYDROCARBONS

Accelerated screening methods for determining chemical and thermal stability of refrigerant-lubricant mixtures. Part 2: Experimental comparison and verification of methods [DE94-003664] p 2749 N94-26007

Thermophysical properties of HFC-143a and HFC-152a [DE94-004236] p 2719 N94-27567

FLUOROPOLYMERS

Trifluoromethyl-substituted polymers [NASA-CR-195217] p 2751 N94-26641

FLUTTER
Multidisciplinary aeroelastic analysis of a generic hypersonic vehicle
[NASA-TM-4544] p 2691 N94-27868

FLUTTER ANALYSIS
Understanding and development of a prediction method of transonic limit cycle oscillation characteristics of fighter aircraft
[NLR-TP-92210-U] p 2679 N94-27798
Multidisciplinary aeroelastic analysis of a generic hypersonic vehicle
[NASA-TM-4544] p 2691 N94-27868

FLUX (RATE)
A semiclassical reactive flux method for the calculation of condensed phase activated rate constants
[AD-A274850] p 3020 N94-26562
Fiber optic Faraday flux transformer specification
[AD-D016058] p 3039 N94-27674

FLUX DENSITY
Hydrogen uptake into silicon from an ECR plasma
[DE94-003771] p 3050 N94-25815
Measurement of magnetic fluctuation induced energy transport
[DE94-003846] p 3042 N94-26132
CRRES high energy proton flux map
[AD-A274803] p 2878 N94-26338

FLUX PINNING
Flux flow, pinning, and resistive behavior in superconducting networks
[DE94-003400] p 3050 N94-25848

FLUX VECTOR SPLITTING
High-lift system analysis method using unstructured meshes
[NLR-TP-92351-U] p 2647 N94-27554
A new flux vector splitting scheme
p 2657 N94-28343

FLY BY WIRE CONTROL
The application of a C(star) flight control law to large civil transport aircraft
[CRANFIELD-AERO-9303] p 2676 N94-25640
Report on a visit to the Arvin/Calspan Corporation, Buffalo, New York, USA, September 1992
[CRANFIELD-AERO-9305] p 2676 N94-25653
A simulator investigation of helicopter flight control system mode transitions
[UTIAS-348] p 2682 N94-27879

FLYING PERSONNEL
Monograph of the Aviation Epidemiology Data Register for CY 1992
[AD-A274400] p 2911 N94-27130
Air traffic administration enroute to Europe
p 2661 N94-28238

FLYWHEELS
A study on the development of high T(sub c) superconducting materials
[DE93-633529] p 3057 N94-26404

FOAMS
Advances in preparing and characterizing low density pan-carbon microcellular foam
[DE94-002278] p 2748 N94-25932
Double layer capacitance of carbon foam electrodes
[DE94-002651] p 2780 N94-25975
Soft ground arresting system for airports
[DOT/FAA/CT-93/80] p 2680 N94-26202
Cryogenic insulation studies
[NASA-CR-195266] p 2756 N94-27429

FOCAL PLANE DEVICES
Performance comparison of shearing interferometer and Hartmann wave front sensors
[AD-A274031] p 3034 N94-25768
Focal plane arrays in advanced thermal images
[AD-B174292] p 3036 N94-26648
Focal plane antenna array for millimeter waves
[AD-D016034] p 2774 N94-27202

FOCUSING
Focusing properties of a three-element quadrupole lens system and its stigmatic focusing behaviour
[DE93-616534] p 2766 N94-25915
An investigation of methods for determining depth from focus
[ISBN-0-315-64015-4] p 2988 N94-27645

FOOD PROCESSING
Bioregenerative system components for microgravity
p 2903 N94-25673

FORCED CONVECTION
Forced convection heat transfer in straight tubes. Part 2: Laminar and transitional flow
[ESDU-93018-PT-2] p 2807 N94-28139

FORCED VIBRATION
The onset of chaos in a periodically forced nonlinear oscillator
[ISBN-0-315-84564-3] p 2842 N94-27272

FOREBODIES
A sensitivity equation approach to shape optimization in fluid flows
[NASA-CR-191598] p 2999 N94-27415

FORECASTING
A preliminary analysis of the US west climatology
[DE94-003028] p 2894 N94-26313
Short-range cloud amount forecasting with model output statistics
[AD-A274769] p 2895 N94-26798
Practical problems in aggregating expert opinions
[DE94-002623] p 3094 N94-27707

FOREST MANAGEMENT
SIMA: A model for forest succession based on the carbon and nitrogen cycles with application to silvicultural management of the forest ecosystem
[SILVA-CARELICA-22] p 2848 N94-26258

FORESTS
SIMA: A model for forest succession based on the carbon and nitrogen cycles with application to silvicultural management of the forest ecosystem
[SILVA-CARELICA-22] p 2848 N94-26258
Role of remote sensing in energy, water, and carbon cycle studies over the Amazon
[INPE-5486-PRE/1786] p 2852 N94-27957
Landscape dynamics of northeastern forests
[NASA-CR-195272] p 2852 N94-28070

FORM FACTORS
CP violating form factors for three gauge boson vertex in the two Higgs doublet and left-right symmetric models
[DE94-601704] p 3014 N94-25841
The delta (1232) resonance transition form factor
[DE94-003442] p 3017 N94-26101
Light-quark, heavy-quark systems: An update
[DE94-002298] p 3021 N94-26759
Thermodynamics and form factors of supersymmetric integrable field theories
[DE94-602557] p 3073 N94-26896
Proton electromagnetic form factor near the proton-antiproton threshold and quasinuclear bound state
[DE94-606458] p 3027 N94-27681

FORMALDEHYDE
Numerical analysis of the photo-dissociation/radical oxidation of formaldehyde by ultraviolet light in a photolytic reactor
[AD-A274539] p 2868 N94-26843

FORMALISM
Formal methods for dependable real-time systems
p 2953 N94-26740
A formalization of objects using equational dynamic logic
[PB94-125218] p 2965 N94-26852
Trace-based compositional proof theory for fault tolerant distributed systems
[PB94-126737] p 2966 N94-26971
A hybrid formalism for representation and interpretation of image knowledge
[INPE-5485-PRE/1784] p 2989 N94-27833

FORMAT
PDEF: A standard file format for data interchange
[AD-A274694] p 3098 N94-26451

FORTRAN
An algorithm to find the intersection of two convex polygons
[AD-A274722] p 2961 N94-26148
Red's natural editor: A program designed to edit FORTRAN programs
[DE94-003271] p 2962 N94-26318
Programming in Fortran M
[DE94-002756] p 2963 N94-26407
New FORTRAN computer programs to acquire and process isotopic mass spectrometric data: Operator's manual
[DE94-003174] p 2965 N94-26784
Ma42: A new frontal code for solving sparse unsymmetric systems
[PB94-124302] p 2998 N94-27115

FOSSIL FUELS
Implications of policies and prevent climate change for future food security
[DE93-018872] p 2866 N94-25948

FOSSILS
The biostratigraphy and paleogeography of Maastrichtian inoceramids p 2889 N94-28303
An evaluation of criteria that may be used to identify species surviving a mass extinction
p 2889 N94-28304

FOUR BODY PROBLEM
Study of the critical points at infinity arising from the failure of the Palais-smale condition for n-body type problems
[DE94-603656] p 3000 N94-27818

FOURIER TRANSFORMATION
High resolution fourier transform absorption spectrum of 79Br2 B3 Pi(Ou+) X1 sigma g+
[AD-A273864] p 2956 N94-25610
Dimensional crossover from non-renormalizability to renormalizability
[DE93-613052] p 3006 N94-26193
ARM Fourier transform spectrometer data analysis tools
[DE94-000865] p 2895 N94-26697
Advances in passive-remote and extractive Fourier transform infrared spectroscopic systems
[DE94-001424] p 2868 N94-26952
Estimates for cone multipliers
[PB94-124385] p 2997 N94-26995
Role of anticausal inverses in multirate filter-banks. Part 1: System theoretic fundamentals
[AD-A274279] p 2997 N94-27015
Radial basis function approximation: From gridded centers to scattered centers
[AD-A274184] p 2998 N94-27103

FOVEA
An algorithm for stereo correspondence problems on the analogy of human vision
[NAL-TR-1185] p 2940 N94-27584

FRACTALS
Probabilistic methods for image generation and encoding
[AD-A274294] p 2964 N94-26682
Center for nonlinear phenomena and magnetic materials
[AD-A274176] p 3009 N94-27126
Fractals and their applications to remote sensing and digital mapping
[ISBN-0-315-59469-1] p 2852 N94-27870

FRACTIONATION
Seasonal snow of arctic Alaska R4D investigations
[DE93-040082] p 2892 N94-25939

FRACTOGRAPHY
Grain by grain study of the mechanisms of crack propagation during iodine SCC of Zry-4
[DE93-633765] p 2734 N94-26162

FRACTURE MECHANICS
FR/GE/UK/US International Test Operations Procedure (ITOP) 1-1-050 development of laboratory vibration test schedules
[AD-A273887] p 2836 N94-25732
Investigation of compressive behavior for metal matrix composites with a circular hole
[AD-A273835] p 2705 N94-25739
Determination of fracture stress and effective crack tip radius from toughness (Klc) and yield strength (Y)
[AD-A274014] p 2836 N94-25754
An investigation of cavitation in a mechanically alloyed 15 volume percent SiCp/IN9021 aluminum composite
[DE94-003371] p 2748 N94-25959
Fracture behavior of 20% Nb particulate reinforced alumina composite
[DE94-002830] p 2706 N94-26019
The fracture behavior of a CVD crystalline Si3N4/amorphous Si3N4 composite
[DE94-002646] p 2750 N94-26124
Damage tolerance assessment handbook. Volume 1: Introduction fracture mechanics fatigue crack propagation
[AD-A274777] p 2836 N94-26186
Results from a fracture mechanical serial investigation of breechrings on the M109A3GN howitzer
[FFI-93/8002] p 2837 N94-26233
Guidelines for controlling stress corrosion cracking and corrosion fatigue of stainless steels: A literature review
[VTT-TIED-1420] p 2837 N94-26262
Fracture Toughness Round Robin Test International in pressure tube materials
[DE93-634140] p 2837 N94-26265
Bimaterial interfaces and their role in the mechanical performance of the in-situ composites
[AD-A274688] p 2707 N94-26447
Stress analysis of a secondary-bending specimen
[AD-A274842] p 2838 N94-26501
Computer modelling of cyclic deformation of high-temperature materials
[AD-A274504] p 2840 N94-27034
Interface phenomena in metal-ceramic composites
[AD-A274167] p 2709 N94-27125
Numerical Analysis Methods of Surface Cracks
[VTT-PUBS-119] p 2841 N94-27186
Quality assurance for fracture mechanical finite element analyses (appendix 3/1) p 2841 N94-27189
Crack closure, a literature study
[PB94-123361] p 2842 N94-27197
Implementation of thermal residual stresses in the analysis of fiber bridged matrix crack growth in titanium matrix composites
[NASA-TM-109082] p 2711 N94-27658
The development of stress intensity factors
[DRA-TR-93057] p 2845 N94-27954
Studies in ice mechanics
[PB94-133055] p 2900 N94-28393

FRACTURE STRENGTH

Structure and properties of intermetallic composites synthesized in situ using solid state displacement reactions
[DE94-004312] p 2705 N94-25805

Numerical simulations of interfacial debonding in ductile-phase reinforced intermetallic matrix composites
[DE94-003639] p 2706 N94-25938

Effect of loading mode on the fracture toughness of a reduced activation ferritic/martensitic stainless steel
[DE94-004290] p 2732 N94-25987

Fracture behavior of 20% Nb particulate reinforced alumina composite
[DE94-002830] p 2706 N94-26019

The fracture behavior of a CVD crystalline Si3N4/amorphous Si3N4 composite
[DE94-002646] p 2750 N94-26124

Fracture Toughness Round Robin Test International in pressure tube materials
[DE93-634140] p 2837 N94-26265

Experimental determination of the CU-IN-PB ternary phase diagram
[DE94-003765] p 2735 N94-26349

Damage tolerance assessment handbook. Volume 2: Aircraft damage tolerance evaluation
[AD-A274778] p 2837 N94-26357

Mechanism of mechanical fatigue of silica glass
[DE94-003165] p 2753 N94-26783

Titanium 1992: Science and Technology, volume 1
[AD-A274798-VOL-1] p 2739 N94-26799

Evaluation of crack arrest fracture toughness of parent plate, weld metal and heat affected zone of BIS 812 EMA ship plate steel
[AD-A274871] p 2839 N94-26859

Processing and mechanical properties of laminated metal composites of Al 6090-25 volume percent SiC(sub p) and Al 5182
[DE94-001070] p 2708 N94-26930

Development of fibre-metal laminates, ARALL and GLARE, new fatigue resistant materials
[PB94-126471] p 2669 N94-26969

Aluminum alloy 8090-T8771 thick plate material characterization
[AD-A274146] p 2987 N94-27077

Examination of hardness, fracture toughness and microstructure in Al2O3-B4C binary ceramics
[PB94-124237] p 2755 N94-27158

SP/MSP tests for the evaluation of FGM
[NAL-SP-17] p 2710 N94-27279

SP/MSP tests for the evaluation of FGM
p 2710 N94-27280

Research on the development of fracture characteristics evaluation system for ceramics and metal composite materials p 2710 N94-27281

Fatigue resistance of unnotched and post impact(+/-30 deg/0 deg) 3-D braided composites
[NASA-CR-191590] p 2711 N94-27433

Cryogenic fracture behavior of 316LN in magnetic fields up to 14.6 T
[DE94-005215] p 2742 N94-27694

Fracture toughness and crack resistance of damage tolerant and high strength Al-Li alloys
[NLR-TP-91249-U] p 2743 N94-27795

Status and prospects for aluminium-lithium alloys in aircraft structures
[NLR-TP-92193-U] p 2743 N94-27797

FRACTURES (MATERIALS)

A review of carbide fuel corrosion for nuclear thermal propulsion applications
[DE94-003938] p 2699 N94-25613

Characterization of fatigue damage in a metal matrix composite (SCS-6/Ti-15-3) at elevated temperature
[AD-A273797] p 2706 N94-25876

FRACTURING

Structural analysis of a frangible nut used on the NASA Space Shuttle
[DE94-003672] p 2821 N94-25811

General Motors Corporation and Pacific Northwest Laboratory staff exchange: Inspection of case hardened steels and metal-matrix composites
[DE94-003470] p 2706 N94-25982

Damage tolerance assessment handbook. Volume 1: Introduction fracture mechanics fatigue crack propagation
[AD-A274777] p 2836 N94-26186

FRAGMENTATION

Fragmentation of Ge(1-x) Sn(x) Se2 glasses
[DE94-603009] p 2758 N94-27837

FRANCE

Present situation of the development of petroleum substitution energy (France)
[DE94-725201] p 2760 N94-26914

FREE ELECTRON LASERS

The proceedings of the KEK FEL Simulation Code Workshop
[DE93-520378] p 2816 N94-26112

Laboratory plasma studies
[AD-A274655] p 3043 N94-26356

Practical design of resonant cavity for a RF free electron laser
[AD-A274306] p 2819 N94-26941

System for conditioning an electron beam for improved free-electron laser operation
[AD-D016054] p 2820 N94-27671

FREE ENERGY

Zinc(2) oxide stability in alkaline sodium phosphate solutions at elevated temperatures
[DE94-003316] p 2715 N94-26320

Phase stability in the Cd-Mg system
[DE94-004976] p 2743 N94-27792

FREE FLIGHT

Experiments on interaction force of jets in hypervelocity cross-flow in a shock tunnel p 2659 N94-28022

FREE FLOW

The measurement of disturbance levels in the Langley Research Center 20-inch Mach 6 tunnel
[NASA-CR-4571] p 2646 N94-26548

Comparison of the interactions of two and three dimensional transverse jets with a hypersonic free stream p 2659 N94-28021

A numerical investigation of a subsonic jet in a crossflow p 2803 N94-28023

Effects of free-stream turbulence on a jet in a cross flow p 2805 N94-28036

FREE JETS

Calculation of single and multiple jets in cross-flow with and without impingement using Reynolds-stress-transport closure p 2803 N94-28024

FREE VIBRATION

The free vibration of plates, shallow shells and solids
[ISBN-0-315-83931-7] p 2838 N94-26622

Finite element analysis of damped vibrations of laminated composite plates
[ISBN-0-315-84928-2] p 2843 N94-27585

FREEZING

Modelling the mass migration phenomena in partially frozen heat pipes
[DE94-002716] p 2797 N94-27709

FREIGHTERS

Integrators: A challenge for air cargo
p 2662 N94-28244

FREON

Freon recovery from nitrogen tetroxide and freon solutions
[PL-TR-92-3051] p 2721 N94-28215

FREQUENCIES

Instantaneous amplitude and frequency dynamics of coherent wave mixing in semiconductor quantum wells
[DE94-003262] p 3054 N94-26128

FREQUENCY CONTROL

Broad band tunable dye laser development
[DE93-632978] p 2816 N94-26157

FREQUENCY CONVERTERS

Three-wave nonlinear interactions in KTiOPO4 (KTP) and KTP isomorphs
[AD-A274079] p 3052 N94-25993

A study of DC-DC converters with MCT's for arcjet power supplies
[NASA-CR-191204] p 2703 N94-27662

FREQUENCY DISTRIBUTION

Aviation Epidemiology Data Register: Indexing the AEDR document laser optic archive
[AD-A274185] p 2911 N94-27097

FREQUENCY DIVISION MULTIPLE ACCESS

Design and test of a regenerative satellite transmultiplexer
[ISBN-0-315-85280-1] p 2786 N94-27303

FREQUENCY HOPPING

Methods for improving low-angle, low-altitude radar tracking accuracy
[AD-A274914] p 2768 N94-26347

Analysis of linear combining and its application to frequency-hopped signals
[ISBN-0-315-84007-2] p 2770 N94-26624

The performance of nonorthogonal noncoherent frequency hopped M-ary FSK in additive white Gaussian noise, fading and jamming
[ISBN-0-315-85243-7] p 2775 N94-27301

FREQUENCY MODULATION

Direct-conversion-to-baseband for a nonlinear FM signal
[AD-A274861] p 2768 N94-26189

Excitation of Earth-ionosphere waveguide in the ELF and lower VLF bands by modulated ionospheric current
[AD-A274969] p 2878 N94-26304

An analysis of FM jamming and noise quality measures
[AD-A274349] p 2772 N94-26924

Parametric time-scale methods in signal analysis
[AD-A274212] p 2773 N94-27068

FREQUENCY RANGES

Microtubules for nonlinear optical limiting
[AD-A273940] p 3035 N94-25941

Investigation of plasma instabilities in the polar cusp
[NASA-CR-195212] p 2879 N94-26599

Parameter estimation of linear systems from frequency response measurements (computer program)
[ESDU-93016] p 2976 N94-28137

FREQUENCY SHIFT

Technical report of ISSP. Ser. A, no. 2682: Pressure dependence of Sm:YAG fluorescence to 50 GPa: A new calibration as a high pressure scale
[JTN-94-80568] p 3066 N94-27354

FREQUENCY SHIFT KEYING

Laser-based communication link
[FFI-93/7023] p 2817 N94-26203

Analysis of linear combining and its application to frequency-hopped signals
[ISBN-0-315-84007-2] p 2770 N94-26624

The performance of nonorthogonal noncoherent frequency hopped M-ary FSK in additive white Gaussian noise, fading and jamming
[ISBN-0-315-85243-7] p 2775 N94-27301

FREQUENCY STANDARDS

Diode-laser-pumped, gas-cell atomic clocks
[AD-A274812] p 3008 N94-26484

FRESH WATER

Conversion of the CLUSE model for applications over open ocean
[AD-A273750] p 2893 N94-26013

FRESNEL INTEGRALS

An approximate solution for the spinup dynamics of near axisymmetric axial gyrostats using the method of multiple scales
[AD-A273723] p 2698 N94-26223

FRETTING CORROSION

Study on improvements in fretting fatigue characteristics of high strength structural member p 2726 N94-25567

FRICTION

Cracking of textured zinc coating during forming process
[DE94-003414] p 2750 N94-26085

FRICTION FACTOR

Experimental analysis of heat transfer characteristics and pressure drop through screen regenerative heat exchangers
[AD-A273902] p 2790 N94-25657

Validated heat-transfer and pressure-drop prediction methods based on the discrete-element method. Phase 2: Two-dimensional rib roughness
[DE94-002379] p 2794 N94-26763

FRONTS (METEOROLOGY)

Mesoscale frontal evolution of the ERICA IOP-5A Cyclone
[AD-A274906] p 2893 N94-26183

Machine intelligent gust front algorithm
[AD-A273695] p 2680 N94-26196

FROUDE NUMBER

E. H. P. estimation of high speed fishing boats by some existing methods p 2764 N94-27978

FRUSTRATION

Ising critical behaviour in the one-dimensional frustrated quantum XY model
[DE93-634755] p 3057 N94-26390

FUEL CELLS

Alternative materials for solid oxide fuel cells: Processing and interactions of materials
[DE94-000016] p 2855 N94-26114

Oxygen reduction at a YSZ interface with cathode materials La(1-x)(Ca or Sr)(x)MnO3(1-x)CaMnO3
[DE94-002954] p 3054 N94-26147

Design of gasifiers to optimize fuel cell systems
[DE94-000010] p 2856 N94-26581

Research and development of alternative components at Argonne National Laboratory for Molten Carbonate Fuel Cells
[DE94-000014] p 2857 N94-26583

Sealant research for solid oxide fuel cells
[DE94-000015] p 2857 N94-26584

Processing of LaCrO3 for solid oxide fuel cell applications
[DE94-002981] p 2857 N94-26747

Low cost, radial flow, solid oxide fuel cell
[DE94-002982] p 2858 N94-26785

MSOFC development status
[DE94-003192] p 2858 N94-26792

High temperature solid oxide fuel cell: Customer test units
[DE94-002961] p 2858 N94-26869

High temperature solid oxide fuel development activities
[DE94-002973] p 2858 N94-26871

Perovskite solid electrolytes for SOFC
[DE94-001923] p 2859 N94-27005

FUEL COMBUSTION

NASA Lewis Research Center lean-, rich-burn materials test burner rig
[NASA-CR-194437] p 2680 N94-26141

Theoretical determination of chemical rate constants using novel time-dependent methods
[NASA-CR-195221] p 2714 N94-26205

An apparatus for measurement of ignition and burning characteristics of metallic particles
[AD-A274815] p 2716 N94-26487

Laser probes of natural gas ignition chemistry
[PB94-128345] p 2717 N94-27226

Basic research on natural gas combustion phenomena
[PB94-129046] p 2717 N94-27256

Broad specification fuels combustion technology program, phase 2
[NASA-CR-191066] p 2719 N94-27854

Gas turbine combustion and emission control
p 2831 N94-28082

FUEL CONSUMPTION

Optimising BMW four-cylinder two-valve engines
[PB94-125101] p 2824 N94-27254

Development of advanced high temperature in-cylinder components and tribological systems for low heat rejection diesel engines, phase 1
[NASA-CR-187158] p 2827 N94-27984

FUEL CORROSION

A review of carbide fuel corrosion for nuclear thermal propulsion applications
[DE94-003938] p 2699 N94-25613

FUEL FLOW

STS-51 pad abort. OV103-engine 2033 (ME-2) fuel flowmeter sensor open circuit
[NASA-CR-193924] p 2701 N94-26230

FUEL INJECTION

Focused Schlieren flow visualization studies of multiple venturi fuel injectors in a high pressure combustor
[NASA-TM-106479] p 2674 N94-26573

Application of railgun principle to high-velocity hydrogen pellet injection for magnetic fusion reactor fueling
[DE94-004411] p 3044 N94-26579

Sequential multi-point injection of a natural gas engine. Topical report, November 1991 - April 1992
[PB94-126794] p 2824 N94-27224

Inertial electrostatic confinement as a power source for electric propulsion p 2688 N94-27373

A numerical study of mixing and combustion in hypervelocity flows through a scramjet combustor model
p 2808 N94-27911

Recent developments in the simulation of steady and transient transverse jet interactions for missile, rotorcraft, and propulsive applications p 2804 N94-28030

FUEL PUMPS

Test results of the RS-44 integrated component evaluator liquid oxygen/hydrogen rocket engine
[NASA-CR-194443] p 2701 N94-26231

FUEL SPRAYS

An apparatus for measurement of ignition and burning characteristics of metallic particles
[AD-A274815] p 2716 N94-26487

FUEL SYSTEMS

Design of a refueling tanker delivering liquid hydrogen
p 2671 N94-25717

Sequential multi-point injection of a natural gas engine. Topical report, November 1991 - April 1992
[PB94-126794] p 2824 N94-27224

FUEL TANKS

Automated in-situ inspection systems for underground storage tanks
[AD-A274644] p 2764 N94-27144

FUEL TESTS

Space-R thermionic space nuclear power system design and technology demonstration
[DE94-002017] p 2700 N94-25930

FUEL-AIR RATIO

Focused Schlieren flow visualization studies of multiple venturi fuel injectors in a high pressure combustor
[NASA-TM-106479] p 2674 N94-26573

FULLERENES

Strongly interacting fermion systems
[DE94-002674] p 3021 N94-26677

Disintegration of (C60) by Xe ion irradiation
[DE94-601913] p 3023 N94-26929

Experimental investigations of strong interaction in the non-perturbative QCD region
[DE94-001178] p 3024 N94-26949

Fullerene fabrication using an arc furnace. Characterization of the product
[DE94-603006] p 3029 N94-27834

FUNCTION GENERATORS

Fast generator of program waveforms signals
[DE93-634230] p 2948 N94-26381

FUNCTIONAL ANALYSIS

Estimation and tests-of-fit for the three parameter Weibull distribution
[AD-A274827] p 3004 N94-26496

FUNCTIONAL DESIGN SPECIFICATIONS

The Enabler: A concept for a lunar work vehicle
p 2833 N94-25675

Pre-orbital criticality safety for the NEPSTP mission
[DE94-002600] p 3005 N94-26802

Automated information management for designers: Functional requirements for computer based associates that support access and use of technical information in design
[AD-A274603] p 3099 N94-26891

Planetary Instrument Definition and Development Program (PIDDP). Instrument for future planetary flight missions: A visible-infrared imaging spectrometer for planetary missions
[NASA-CR-195254] p 3106 N94-27409

FUNCTIONAL INTEGRATION

Second-order phase transition in (g(phi)4)2 theory
[DE94-603677] p 3067 N94-27638

FUNCTIONALLY GRADIENT MATERIALS

SP/MSP tests for the evaluation of FGM
p 2710 N94-27280

FUNCTIONALS

Fast vertex search (in plane)
[DE93-616655] p 2959 N94-25917

Limit theorems for functionals of Markov processes and renormalizable stable fields
[AD-A274645] p 3004 N94-27106

FUNCTIONS (MATHEMATICS)

Repeated knots in least squares multiquadric functions
[AD-A273866] p 2990 N94-25594

Conditionally exponential convex functions on locally compact groups
[DE93-613025] p 2990 N94-25865

The railway track response function
[REPT-93-40] p 2837 N94-26214

Estimation and tests-of-fit for the three parameter Weibull distribution
[AD-A274827] p 3004 N94-26496

FUSELAGES

Low-speed pressure distribution measurements over the aft-fuselage, fins, and stabilators of a 1/9th scale F/A-18 wind-tunnel model
[AD-A274870] p 2644 N94-26342

Development and evaluation of a near infrared reflecting and low visibility paint scheme for RAAF P-3C Orion aircraft
[AD-A274881] p 2669 N94-26864

Design and test of postbuckled stiffened curved plates: A literature survey
[PB94-126521] p 2840 N94-26961

Development of fibre-metal laminates, ARALL and GLARE, new fatigue resistant materials
[PB94-126471] p 2669 N94-26969

Impact tests on fibre metal laminates under a tensile load
[PB94-126570] p 2710 N94-27201

Calculation of unsteady incompressible inviscid flow about wings and bodies using CANAERO-T panel model
p 2655 N94-28334

FUSION (MELTING)

Basic research on levitation fusing/solidification technology p 2723 N94-25552

FUSION REACTORS

Experimental and numerical investigation of shock wave propagation through complex geometry, gas continuous, two-phase media
[DE94-001408] p 2791 N94-26121

A robust helium-cooled shield/blanket design for ITER
[DE94-003402] p 3043 N94-26323

Limitations of power conversion systems under transient loads and impact on the pulsed tokamak power reactor
[DE94-003404] p 3043 N94-26324

Application of railgun principle to high-velocity hydrogen pellet injection for magnetic fusion reactor fueling
[DE94-004411] p 3044 N94-26579

Fusion reactor systems studies
[DE94-003162] p 3046 N94-27686

FUSION WELDING

Study on interfacial reaction analysis at interfacial joining p 2728 N94-25574

Joining of fibre reinforced metal matrix composite materials
[PB94-132453] p 2712 N94-28376

FUZZY SETS

Fuzzy robust statistics for application to the fuzzy c-means clustering algorithm
[AD-A274719] p 3003 N94-26436

Ranking alternatives using fuzzy numbers: A computational approach short communication
[INPE-5483-PRE/1782] p 2974 N94-27835

FUZZY SYSTEMS

Vulnerability assessment using a fuzzy logic based method
[AD-A274075] p 2957 N94-25649

Investigation into model-based fuzzy logic control
[AD-A274660] p 2985 N94-26336

Designing and optimizing fuzzy-logic controllers
[ISBN-0-315-83505-2] p 2985 N94-26660

Sensor-based navigation of a mobile robot using automatically constructed fuzzy rules
[DE94-001137] p 2986 N94-26948

G

GADOLINIUM

Measurement of metastable population distribution in gadolinium atomic beam by laser resonance photoionization method
[DE94-701194] p 3029 N94-27820

GALACTIC COSMIC RAYS

Stopping powers and cross sections due to two-photon processes in relativistic nucleus-nucleus collisions
[NASA-CR-4574] p 3033 N94-27646

GALACTIC RADIO WAVES

Development of imaging riometers
p 2884 N94-27967

Quick-look system of auroral absorption images by imaging riometer p 2884 N94-27968

GALACTIC ROTATION

Modulating terrestrial impacts from Oort cloud comets by the adiabatically changing galactic tides
p 2890 N94-28305

GALACTIC STRUCTURE

The meaning of EROS/MACHO
[DE94-003003] p 3104 N94-26311

GALAXIES

The meaning of EROS/MACHO
[DE94-003003] p 3104 N94-26311

Sloan Digital Sky Survey
[DE94-004662] p 3103 N94-27750

Modulating terrestrial impacts from Oort cloud comets by the adiabatically changing galactic tides
p 2890 N94-28305

GALERKIN METHOD

Numeric solution of the electric field integral equation using Galerkin's method for axially symmetric cases
[ESA-TT-1264] p 2768 N94-26315

The nonlinear Galerkin method: A multi-scale method applied to the simulation of homogeneous turbulent flows
[NASA-CR-191581] p 2792 N94-26499

Center for nonlinear phenomena and magnetic materials
[AD-A274176] p 3009 N94-27126

GALLIUM ALLOYS

Study of the hyperfine magnetic field at Ta-181 site in the Heusler Co2ScSn, Co2ScGa, and Co2HfSn alloys
[DE94-603989] p 3067 N94-27623

GALLIUM ARSENIDE LASERS

Failure mechanisms of high temperature semiconductor lasers
[AD-A273833] p 2815 N94-25616

GALLIUM ARSENIDES

Failure mechanisms of high temperature semiconductor lasers
[AD-A273833] p 2815 N94-25616

Electric-field dependence of electroreflectance and photocurrent spectra at visible wavelengths in MOVPE-grown InAlGaP multiple strained quantum-well structures
[DE94-004692] p 2780 N94-25664

Modeling electromagnetic effects in MMICs for T/R modules
[AD-A273808] p 2766 N94-25736

Biexciton formation by two-photon absorption in quantum wells
[DE93-613551] p 3071 N94-25852

Investigation of plasma etch induced damage in compound semiconductor devices
[DE94-002849] p 3052 N94-25989

The state of the art of thin-film photovoltaics
[DE94-000224] p 2855 N94-26115

Instantaneous amplitude and frequency dynamics of coherent wave mixing in semiconductor quantum wells
[DE94-003262] p 3054 N94-26128

Test methods and custom hardware for functional testing of a high speed GaAs DRAM
[AD-A274859] p 2781 N94-26175

Ordering and phase separation in MOCVD InGaP alloys and unicompositional quantum wells
[DE94-004693] p 3056 N94-26352

Exploration of GaAs structures for solid-state detectors
[DE93-634191] p 3056 N94-26379

On the electron mobility in slightly compensated heavily doped gallium arsenide at low temperatures
[DE93-634712] p 3057 N94-26387

Development of GaAs charge-coupled devices
[ISBN-0-315-84116-8] p 3059 N94-26703

Mechanistic studies of opto-electronic materials and syntheses using multiple laser and surface diagnostics [AD-A274528] p 3036 N94-26834

AB-Initio calculation of the valence-band offset at strained GaAs/InAs (001) heterojunction [DE94-602538] p 3061 N94-26878

Polar optical oscillation modes in GaAs-based double heterostructures: Long wavelength limit [DE94-601874] p 3062 N94-26897

High-efficiency, thin-film solar cells [DE94-000250] p 2860 N94-27625

Characterization of semi-insulating gallium arsenide [AD-A273781] p 3068 N94-27704

Dry etching process development for submicron and nanometer semiconductor devices [PB94-133196] p 2788 N94-28357

GALLIUM NITRIDES

Nitride semiconductors for ultraviolet detection [AD-A274246] p 3060 N94-26840

Pseudomorphic semiconducting heterostructures from combinations of AlN, GaN and selected SiC polytypes: Theoretical advancement and its coordination with experimental studies of nucleation, growth, characterization and device development [AD-A274247] p 3061 N94-26841

The growth and characterization of GaN as a photodetector [AD-A274570] p 3063 N94-26965

GALLIUM PHOSPHIDES

Electric-field dependence of electroreflectance and photocurrent spectra at visible wavelengths in MOVPE-grown InAlGaP multiple strained quantum-well structures [DE94-004692] p 2780 N94-25664

Electrical properties of p-type GaInP2 [AD-A273771] p 3051 N94-25856

Ordering and phase separation in MOCVD InGaP alloys and unicompositional quantum wells [DE94-004693] p 3056 N94-26352

High-efficiency, thin-film solar cells [DE94-000250] p 2860 N94-27625

GALLIUM SELENIDES

Crystal chemistry and self-lubricating properties of monochalcogenides gallium selenide and tin selenide [DE93-041177] p 2751 N94-26422

GAME THEORY

Communication complexity of t-intersection problems in generalized Boolean algebras [PB94-126646] p 2996 N94-26917

Intertemporal bargaining and dynamic consistency [PB94-133147] p 3095 N94-28386

GAMMA FUNCTION

How to build analogues of the Bessel-Clifford expansions for the sum of the repulsive Coulomb potential and central potential decreasing more rapidly than the centrifugal one? [DE93-634308] p 3007 N94-26472

GAMMA RAY ASTRONOMY

TEV emission from close binaries [DE93-634330] p 3104 N94-26268

A simple satellite system to locate gamma ray bursters using scintillating fiber technology [DE94-601287] p 3117 N94-27996

GAMMA RAY BURSTS

BATSE Data Analysis [NASA-CR-195545] p 3114 N94-26685

The continuum spectral characteristics of gamma ray bursts observed by BATSE p 3114 N94-26686

Continuum spectral characteristics of bursts measured with BATSE large area detectors p 3114 N94-26687

A study of gamma ray burst continuum properties presnting evidence for two spectral states in bursts p 3114 N94-26688

Channel to energy calibration results for the BATSE large area detectors p 3115 N94-26690

Compton Gamma Ray Observatory/BATSE observations of energetic electrons scattered by cyclotron resonance with waves from powerful VLF transmitters [NASA-CR-195240] p 3115 N94-26790

BATSE burst location accuracy and constraints on the fraction of repeating GRB sources [DE94-004981] p 3116 N94-27714

DMSP satellites as gamma ray burst detectors [DE94-004977] p 3116 N94-27793

Gamma ray bursts from the accretion of solid bodies onto high-velocity Galactic neutron stars [DE94-005006] p 3117 N94-27827

A simple satellite system to locate gamma ray bursters using scintillating fiber technology [DE94-601287] p 3117 N94-27996

GAMMA RAY OBSERVATORY

Compton Gamma Ray Observatory/BATSE observations of energetic electrons scattered by cyclotron resonance with waves from powerful VLF transmitters [NASA-CR-195240] p 3115 N94-26790

GAMMA RAY SPECTRA

Proceedings of the Second EGS4 User's Meeting in Japan [DE93-520383] p 3032 N94-26543

Channel to energy calibration results for the BATSE large area detectors p 3115 N94-26690

GAMMA RAY SPECTROMETERS

DMSP satellites as gamma ray burst detectors [DE94-004977] p 3116 N94-27793

GAMMA RAY TELESCOPES

Gamma Large Area Silicon Telescope (GLAST): Applying silicon strip detector technology to the detection of gamma rays in space [DE94-003451] p 3116 N94-27740

GAMMA RAYS

Penetrating nature of very collimated high-energy shower-clusters of hadrons and gamma rays p 3113 N94-25631

Hardware design of a spherical mini-rover p 2833 N94-25669

TEV emission from close binaries [DE93-634330] p 3104 N94-26268

Exploration of GaAs structures for solid-state detectors [DE93-634191] p 3056 N94-26379

Studies on the application of radiation for genetic transformation in higher plants [DE93-632656] p 2901 N94-26470

Annals of the Research Inst. of Environmental Medicine, Nagoya Univ., volume 44 [REPT-44-VOL-44] p 2911 N94-27442

Advances in gamma ray field instrumentation at Los Alamos [DE93-040264] p 2813 N94-27624

Study of invisible nucleon decay, N approaches nu nu nu bar, and a forbidden nuclear transition in the Kamiokande detector [ICRR-299-93-11] p 3028 N94-27759

Radiations from hot nuclei p 3030 N94-27915

GANGLIA

Effects of capsaicin on freshly dissociated rat dorsal root ganglion cells p 2906 N94-27499

Size distribution of retrogradely labeled dorsal root ganglion cells: Test of normality p 2906 N94-27500

GANTRY CRANES

Performance measures from the explorer platform berthing experiment p 2683 N94-26283

GAS ANALYSIS

Study on development of chemical measurement method utilizing plasmas p 2728 N94-25576

Package integrity measurement technology and quality assurance [AD-A273881] p 2834 N94-25727

SP industry calorimeter for rate of heat release measurements up to 10MW [PB94-124211] p 2811 N94-27044

Experiments on interaction force of jets in hypervelocity cross-flow in a shock tunnel p 2659 N94-28022

GAS BEARINGS

Researches of the Electrotechnical Laboratory. No. 52: Studies of externally pressurized porous gas bearings [JTN-94-80549] p 2825 N94-27351

GAS CHROMATOGRAPHY

Accelerated screening methods for determining chemical and thermal stability of refrigerant-lubricant mixtures. Part 2: Experimental comparison and verification of methods [DE94-003664] p 2749 N94-26007

Determination of lead isotope ratios in seawater by purge and trap GC/MS after ethylation p 2870 N94-28152

GAS COMPOSITION

Evaluation of a concentration probe for application in a supersonic flow field [AD-A273915] p 2643 N94-25592

The study of single-pass GMA welds with different cover gas compositions on HSLA-100 steel [AD-A274857] p 2822 N94-26174

GAS COOLED REACTORS

Limitations of power conversion systems under transient loads and impact on the pulsed tokamak power reactor [DE94-003404] p 3043 N94-26324

GAS COOLING

Evaluation of helium cooling for fusion divertors [DE94-002680] p 3042 N94-25976

A robust helium-cooled shield/blanket design for ITER [DE94-003402] p 3043 N94-26323

GAS DENSITY

Gaseous hydrogen/oxygen injector performance characterization [NASA-CR-194464] p 2701 N94-26208

Mix induced by single shock passage through a material interface [DE93-019505] p 2792 N94-26427

Refractive and dielectric properties of helium, argon and nitrogen gases [PB94-123783] p 3008 N94-26851

Condensation inside tubes: Computer program for pressure drop in straight tubes (horizontal and vertical with downflow) [ESDU-93014] p 2806 N94-28064

GAS DETECTORS

Development of SO(x) and NO(x) solid electrolyte sensors p 2725 N94-25562

Automated system for gas detectors providing with binary mixtures [DE93-634192] p 2715 N94-26406

GAS DISCHARGE TUBES

Optimum for the gasdynamic system in a fast-axial-flow CO2 laser [AD-A274305] p 2819 N94-26940

GAS DISCHARGES

Study on development of chemical measurement method utilizing plasmas p 2728 N94-25576

Buckyball microwave plasmas: Fragmentation and diamond-film growth [DE94-003209] p 3053 N94-26031

GAS DYNAMICS

Optimum for the gasdynamic system in a fast-axial-flow CO2 laser [AD-A274305] p 2819 N94-26940

Research in pulsed power plasma physics [AD-A274323] p 3045 N94-27074

A second-order shock-adaptive Godunov scheme based on the generalized Lagrangian formulation [ISBN-0-315-84549-X] p 2795 N94-27307

TVD flux-difference split methods for high-speed thermochemical nonequilibrium flows with strong shocks [UTIAS-350] p 2799 N94-27880

Nonequilibrium radiation and chemistry models for aerocapture vehicle flowfields [NASA-CR-195706] p 2648 N94-28071

High-performance parallel analysis of coupled problems for aircraft propulsion [NASA-CR-195292] p 2845 N94-28181

The kinetics and dynamics of the coma of Halley's comet [NASA-CR-194828] p 3105 N94-28184

GAS FLOW

Computation of non-isentropic internal flows with variable density [AD-A274848] p 2794 N94-26801

Performance model of a recirculating stack nickel hydrogen cell p 2861 N94-28112

High-performance parallel analysis of coupled problems for aircraft propulsion [NASA-CR-195292] p 2845 N94-28181

GAS INJECTION

Development of fusion technology [DE93-633444] p 3042 N94-26159

Flowing DPF design for propulsion experiments [AD-A274973] p 2701 N94-26537

Sequential multi-point injection of a natural gas engine. Topical report, November 1991 - April 1992 [PB94-126794] p 2824 N94-27224

Numerical investigation of thrust vectoring by injection of secondary air into nozzle flows p 2801 N94-28013

GAS IONIZATION

Study on development of chemical measurement method utilizing plasmas p 2728 N94-25576

Stationary plasma thruster plume emissions [NASA-CR-194471] p 2701 N94-26209

Hadron gas ionization calorimeters [DE93-634186] p 2810 N94-26397

GAS JETS

The growth and characterization of GaN as a photodetector [AD-A274570] p 3063 N94-26965

Scalar mixing in the subsonic jet in crossflow p 2800 N94-28008

A numerical investigation of a subsonic jet in a crossflow p 2803 N94-28023

Navier-Stokes simulation of two and three dimensional jets in crossflow, effects of grid, and boundary conditions p 2804 N94-28026

GAS MIXTURES

Automated system for gas detectors providing with binary mixtures [DE93-634192] p 2715 N94-26406

Numerical simulation of the reignition of detonation by reflected shocks [AD-A274755] p 2795 N94-27252

TVD flux-difference split methods for high-speed thermochemical nonequilibrium flows with strong shocks [UTIAS-350] p 2799 N94-27880

GAS STREAMS

Comparison of the interactions of two and three dimensional transverse jets with a hypersonic free stream p 2659 N94-28021

GAS TEMPERATURE

SP industry calorimeter for rate of heat release measurements up to 10MW [PB94-124211] p 2811 N94-27044

GAS TUNGSTEN ARC WELDING
Corrosion resistance at welded zones of nuclear fuel reprocessing system p 2722 N94-25546
The influence of TIG welding thermal cycles on HSLA-100 steel plate
[AD-A274248] p 2740 N94-27009
Weldability aspects in the design and fabrication of aluminium structures subjected to fatigue loads. Part 2: Weldability of aluminium alloys using advanced MIG and TIG techniques. Effect of the weld bead geometrical factors on the fatigue behavior of the welded joint
[PB94-132446] p 2833 N94-28375

GAS TURBINE ENGINES
Gas Turbine Engine Transient Behaviour
[VKI-LS-1993-06] p 2828 N94-28043
Gas-turbine engine steady-state behavior p 2828 N94-28044
Transient performance p 2828 N94-28045
Compressor stability p 2828 N94-28046
Engine simulation technology p 2829 N94-28051
Transient engine simulation p 2829 N94-28052
Nonlinear solvers p 2829 N94-28053
Engine simulation systems p 2829 N94-28054
A review of recent aeroelastic analysis methods for propulsion at NASA Lewis Research Center
[NASA-TP-3406] p 2846 N94-28227

GAS TURBINES
Computation of non-isentropic internal flows with variable density
[AD-A274848] p 2794 N94-26801
Pressure-gain combustion
[DE94-002975] p 2719 N94-27712
Gas fired advanced turbine system
[DE94-003193] p 2827 N94-27874
Combined Cycles for Power Plants
[VKI-LS-1993-08] p 2830 N94-28077
Introduction to combined cycles p 2789 N94-28078
Thermodynamics of combined cycle plant p 2831 N94-28079
Development of the gas turbine. Part 1: Design philosophy and performance p 2831 N94-28080
Development of the gas turbine. Part 2: Manufacturing, commissioning, and operation p 2831 N94-28081
Gas turbine combustion and emission control p 2831 N94-28082
Steam plant for combined cycles: Heat recovery steam generators, design principles, and construction details p 2831 N94-28083

GAS-GAS INTERACTIONS
Mix induced by single shock passage through a material interface
[DE93-019505] p 2792 N94-26427

GASEOUS FUELS
Gas turbine combustion and emission control p 2831 N94-28082

GASEOUS ROCKET PROPELLANTS
Hydrogen-oxygen torch ignitor
[NASA-TM-106493] p 2691 N94-27424

GASIFICATION
Feasibility study on introduction of the bio-fuel power generation in tropical regions
[DE94-725203] p 2858 N94-26838

GASOLINE
Numerical analysis of the photo-dissociation/radical oxidation of formaldehyde by ultraviolet light in a photolytic reactor
[AD-A274539] p 2868 N94-26843

GATES (CIRCUITS)
Low threshold all-optical crossbar switch on GaAs-GaAlAs channel waveguide arrays
[AD-A274971] p 2783 N94-26536
Partitioning structural VHDL circuits for parallel execution on hypercubes
[AD-A274390] p 2785 N94-26830

GAUGE INVARIANCE
CP violating form factors for three gauge boson vertex in the two Higgs doublet and left-right symmetric models
[DE94-601704] p 3014 N94-25841
Principles of gauge theory of real hadrons
[DE93-616857] p 3015 N94-25920
A dependence of exclusive vector meson production in muon-nucleus scattering
[DE94-003363] p 3016 N94-25957
Dynamical group of relativistic straight-line string
[DE93-634347] p 3072 N94-26037
Lepton masses in an SU(3)(sub L) x U(1)(sub N) gauge model
[DE93-634366] p 3016 N94-26040
Classical solutions of Yang-Mills-Chern-Simons theory in 2+1 dimensions: A quasi-linear superposition
[DE93-634335] p 3006 N94-26270
Differential regularization of a non-relativistic anyon model
[DE94-601558] p 3019 N94-26416
Gauge invariance and transport properties in superconductors above T(c)
[DE94-604013] p 3068 N94-27677

GAUGE THEORY
Principles of gauge theory of real hadrons
[DE93-613096] p 3013 N94-25835
Fermionic field theory and gauge interactions on random lattices
[DE94-601565] p 3051 N94-25885
Principles of gauge theory of real hadrons
[DE93-616857] p 3015 N94-25920
Dimensional crossover from non-renormalizability to renormalizability
[DE93-613052] p 3006 N94-26193
Vortices in curved spacetime
[DE94-601559] p 3072 N94-26417
Finite density effects in gauge theories
[ISBN-0-315-50637-7] p 3074 N94-27403
Quantum chromodynamics and nuclear physics at extreme energy density
[DE94-004418] p 3026 N94-27604
Relativistic two-body system in 1+1-dimensional QED. 1: On the circle S1
[DE94-603716] p 3067 N94-27647

GAUSSIAN ELIMINATION
A numerical determination of bifurcation points for low Reynolds number conical flows
[AD-A273984] p 2791 N94-25991
Ma42: A new frontal code for solving sparse unsymmetric systems
[PB94-124302] p 2998 N94-27115

GELATION
Double layer capacitance of carbon foam electrodes
[DE94-002651] p 2780 N94-25975
Stabilization of polyaniline solutions
[DE94-003958] p 2704 N94-27745

GENE EXPRESSION
The intracellular second messenger system in c-fos gene induction by ACTH p 2904 N94-27477
Cloning of rat RXR alpha cDNA and the expression of its mRNA in regenerating liver and primary cultured hepatocytes p 2905 N94-27479
Effect of sera from patients treated with long-term hemodialysis on mRNA's for collagenase, stromelysin, and tissue inhibitor of metalloprotease in cultured human synovial cells p 2920 N94-27481
Expression analysis of Thyroxine-Binding Globulin Complete Deficiency in Japanese (TBG-CDJ) p 2905 N94-27482

GENERAL AVIATION AIRCRAFT
A revolutionary approach to composite construction and flight management systems for small, general aviation airplanes p 2671 N94-25714
EGADS: A microcomputer program for estimating the aerodynamic performance of general aviation aircraft
[NASA-TM-104013] p 2667 N94-26091

GENERAL OVERVIEWS
The effects of embedded internal delaminations on composite laminate compression strength; an experimental review
[NASA-TM-108440] p 2707 N94-26127
Critical survey of plasma processing
[AD-A274233] p 3044 N94-26820
Highlights 1993 --- Lawrence Berkeley Laboratory
[DE94-002270] p 3118 N94-26937
Smart structures, an overview
[AD-A274147] p 2987 N94-27093
Silence amenity engineering: Past and present p 3011 N94-27283
Reinventing information services to increase customer satisfaction
[DE94-003718] p 3100 N94-27563

GENES
The intracellular second messenger system in c-fos gene induction by ACTH p 2904 N94-27477
Cloning of rat RXR alpha cDNA and the expression of its mRNA in regenerating liver and primary cultured hepatocytes p 2905 N94-27479
Cloning of a novel POU family gene by RT-PCR method p 2905 N94-27480
Expression analysis of Thyroxine-Binding Globulin Complete Deficiency in Japanese (TBG-CDJ) p 2905 N94-27482

GENETIC ALGORITHMS
Discovery learning in autonomous agents using genetic algorithms
[AD-A274083] p 2677 N94-25998
Parameter estimation by genetic algorithms
[DE94-002924] p 2961 N94-26146
What can we learn from genetic algorithms: A new perspective for search methods
[PB94-125234] p 2967 N94-26997
Genetic algorithms applied to a mission routing problem
[AD-A274130] p 2968 N94-27120
Designing robust control laws using genetic algorithms p 2643 N94-27295

GENETIC CODE
Cloning of a novel POU family gene by RT-PCR method p 2905 N94-27480
Expression analysis of Thyroxine-Binding Globulin Complete Deficiency in Japanese (TBG-CDJ) p 2905 N94-27482

GENETIC ENGINEERING
Studies on the application of radiation for genetic transformation in higher plants
[DE93-632656] p 2901 N94-26470
Development of inbred strains from Japanese wild rats (Rattus norvegicus) p 2906 N94-27492

GENETICS
Studies on the application of radiation for genetic transformation in higher plants
[DE93-632656] p 2901 N94-26470

GEOCHEMISTRY
A general theory of impacts and mass extinctions, and the consequences of large-body impact on the Earth p 2891 N94-28310

GEOCHRONOLOGY
The biostratigraphy and paleogeography of Maastrichtian inoceramids p 2889 N94-28303
An extraterrestrial event at the tertiary-quaternary boundary p 2890 N94-28309
A general theory of impacts and mass extinctions, and the consequences of large-body impact on the Earth p 2891 N94-28310
Were all extinction events caused by impacts? p 2891 N94-28311

GEODESIC LINES
On the first integrals of geodesics
[DE93-612974] p 3007 N94-25603

GEODESY
Crustal deformation measurements in the vicinity of Vandenberg Air Force Base
[AD-A274166] p 2881 N94-27143

GEODETIC COORDINATES
Construction and applications of the two dimensional Delaunay triangulated irregular network and the three dimensional Delaunay tetrahedron model
[ETN-94-95034] p 2848 N94-26651
Hotine's (omega, phi, nu) coordinate system
[PL-TR-93-2174] p 3001 N94-28216

GEODETIC SURVEYS
High-production global positioning system methods for survey applications: The pseudo-kinematic method with the Trimvec programming system
[ETN-94-95035] p 2665 N94-26539
Crustal deformation measurements in the vicinity of Vandenberg Air Force Base
[AD-A274166] p 2881 N94-27143

GEOGRAPHIC INFORMATION SYSTEMS
Remote sensing and GIS for the management and investigation of the Wadden Sea
[BCRS-92-20] p 2847 N94-26228
PDEF: A standard file format for data interchange
[AD-A274694] p 3098 N94-26451
A geological and geophysical information system for Eurasia
[AD-A274818] p 3098 N94-26490
Trapezoid-oriented compression of run length coded map data
[PB94-123312] p 2849 N94-26848

GEOGRAPHY
The effect of elevation data representation on nocturnal drainage wind simulations
[DE94-003624] p 2892 N94-25936

GEOIDS
Geoid determination: With help of the alternative scattering method
[ETN-94-95375] p 2847 N94-25746

GEOLOGICAL SURVEYS
A geological and geophysical information system for Eurasia
[AD-A274818] p 3098 N94-26490

GEOLOGY
Geological Dating by Ar-40 - Ar-39 method
[DE94-601975] p 2880 N94-26874
Crustal deformation measurements in the vicinity of Vandenberg Air Force Base
[AD-A274166] p 2881 N94-27143

GEOMAGNETIC PULSATIONS
Collisionless shock structures of Earth and other planets
[NASA-CR-195257] p 3104 N94-27407

GEOMAGNETIC TAIL
Collisionless shock structures of Earth and other planets
[NASA-CR-195257] p 3104 N94-27407
Proton aurora and substorm intensifications
[ATR-93(7248)-1] p 2887 N94-28218

GEOMAGNETISM
Detection geometry and reconstruction error in magnetic source imaging
[DE94-004012] p 2809 N94-25662
Determination of the geomagnetic external contribution by nonlinear optimization methods
[DE94-600882] p 2878 N94-26365
About stochastization of motion of charged particles in geomagnetic field and in the field of a wave packet
[DE93-634309] p 2879 N94-26502
Kiruna geophysical data. Data summary 93/4-6, April-June 1993
[PB94-123700] p 2881 N94-27039
Kiruna geophysical data. Data summary 93/1-3, January-March, 1993
[PB94-123791] p 2881 N94-27043
Solar-geophysical data number 590, October 1993. Part 1: (Prompt reports). Data for September, August 1993, and late data
[PB94-125903] p 3110 N94-27053
JARE data reports. No. 186: Upper atmosphere physics data. Syowa and Asuka Stations, 1990
[JTN-94-80594] p 2881 N94-27299
Persistence of auroral electron flux events from DMSP/F9 electron measurements
[RXR-92012] p 2887 N94-28206

GEOMETRIC RECTIFICATION (IMAGERY)
Geometric correction of SPOT images with use of digital elevation models
[ETN-94-95033] p 2847 N94-26107

GEOMETRY
A strange application of Kolmogorov complexity
[CWI-CS-R9328] p 2973 N94-27737

GEOMORPHOLOGY
Morphodynamics of inter-tidal areas: The Wadden Sea
[NLR-TP-92356-U] p 2851 N94-27555

GEOPHYSICAL OBSERVATORIES
Kiruna geophysical data. Data summary 93/1-3, January-March, 1993
[PB94-123791] p 2881 N94-27043

GEOPHYSICS
A geological and geophysical information system for Eurasia
[AD-A274818] p 3098 N94-26490
Kiruna geophysical data. Data summary 93/4-6, April-June 1993
[PB94-123700] p 2881 N94-27039
Kiruna geophysical data. Data summary 93/1-3, January-March, 1993
[PB94-123791] p 2881 N94-27043
Solar-geophysical data number 590, October 1993. Part 1: (Prompt reports). Data for September, August 1993, and late data
[PB94-125903] p 3110 N94-27053
Solar-geophysical data number 590, October 1993. Part 2: (Comprehensive reports). Data for April 1993, and miscellaneous
[PB94-125911] p 3110 N94-27054
Global change research related to the Earth's energy and hydrologic cycle
[NASA-CR-195270] p 2869 N94-27430
Calibration of SAR systems
[DLR-FB-93-18] p 2777 N94-27738

GEOSYNCHRONOUS ORBITS
SAFT nickel hydrogen cell cycling status
p 2861 N94-28110

GEOTHERMAL RESOURCES
Volcanology and volcanic activity with a primary focus on potential hazard impacts for the Hawaii geothermal project
[DE94-001614] p 2879 N94-26515

GERMANATES
Crystallization and microstructural control of ferroelectric thin-films and glass-ceramics
[AD-A273767] p 2748 N94-25854

GERMANIUM
Determination of surface recombination velocity and bulk lifetime in detector grade silicon and germanium crystals
[DE94-003886] p 3053 N94-26094
The epitaxial growth of Ge on Si(100) using Te as a surfactant
[DE94-003437] p 3056 N94-26326
The response of an hyperpure Ge detector to ionizing radiation
[ISBN-0-315-83968-6] p 2811 N94-26662
Technical report of ISSP. Ser. A, no. 2680: Determination of intervalley scattering time in germanium by subpicosecond time-resolved Raman spectroscopy
[JTN-94-80566] p 3064 N94-27176

GERMANIUM ALLOYS
Recombination and metastability in amorphous silicon and silicon germanium alloys
[DE94-000237] p 2736 N94-26481
Continuous roll-to-roll a-Si photovoltaic manufacturing technology
[DE94-000260] p 2859 N94-27610

GERMANIUM COMPOUNDS
Study on synthesis and characteristics of intermetallic compound with strong electron correlation
p 2726 N94-25563
Stress relaxation in sputtered W films and W/GeSi/Si heterostructures
[DE94-004007] p 3055 N94-26239
Energy Dispersive X ray Diffraction (EDXD) apparatus for liquids at high temperature p 2721 N94-28159

GERMANY
The advantages of the location Germany must not be jeopardized in air traffic p 2661 N94-28236
Lufthansa facing the single European market
p 2661 N94-28237
Munich Airport: The new Lufthansa hub
p 2662 N94-28239
German-American relations in air traffic are to be criticized p 2662 N94-28241

GERT
Development of an automatic fatigue-data acquisition system using commercial software
[NAL-TM-650] p 2842 N94-27207

GETTERS
Binding of copper and nickel to cavities in silicon formed by helium ion implantation
[DE94-003769] p 3050 N94-25814
Lithium drifted silicon detector fabrication on gettered floating-zone silicon
[DE94-003890] p 3054 N94-26095

GLACIERS
Remote sensing of global snowpack energy and mass balance: In-situ measurements on the snow of interior and Arctic Alaska
[NASA-CR-195704] p 2851 N94-27787
Impacts, extinctions, volcanism, glaciations, and tectonics: Matches and mismatches
p 2888 N94-28298
Extraterrestrial accretion and glacial cycles
p 2890 N94-28308
Were all extinction events caused by impacts?
p 2891 N94-28311

GLACIOLOGY
Were all extinction events caused by impacts?
p 2891 N94-28311

GLASS
Lunar preform manufacturing p 2765 N94-25677
Crystallization and microstructural control of ferroelectric thin-films and glass-ceramics
[AD-A273767] p 2748 N94-25854
Optimization of experimental conditions in IR reflectance determination of BPSG properties
[DE94-002742] p 2713 N94-25978
Peculiarities and application perspectives of metal-ion implants in glasses
[DE94-004671] p 3035 N94-26246
How reliable is the HMSA integral equation for the pair structure of supercooled and amorphous mixtures?
[DE94-601543] p 3006 N94-26411
Modelling and predicting properties of polymers in the amorphous glassy state
[ETN-94-95345] p 2752 N94-26645
Molecular dynamics simulation and crystal-field theory: Predicting the optical spectra and structure of rare-earth doped inorganic glasses
[ISBN-0-315-84679-8] p 3025 N94-27310
Ion implantation in silicate glasses
[DE94-003785] p 2757 N94-27726
Fragmentation of Ge(1-x) Sn(x) Se2 glasses
[DE94-603009] p 2758 N94-27837
Experimental study of lunar and SNC (Mars) magmas
[NASA-CR-195274] p 3107 N94-27850

GLASS FIBER REINFORCED PLASTICS
Dynamic response of S-2 glass reinforced plastic structural armor
[AD-A273868] p 2747 N94-25596
Testing composite-to-metal tubular lap joints
[DE94-003225] p 2836 N94-26032

GLASS FIBERS
Design for producing fiberglass fabric in a lunar environment p 2765 N94-25676
Lunar preform manufacturing p 2765 N94-25677
Testing composite-to-metal tubular lap joints
[DE94-003225] p 2836 N94-26032
Inert strength of pristine silica glass fibers
[DE94-004685] p 2750 N94-26247
The deposition of boron nitride and carbon films on silica glass fibers
[DE94-004684] p 2751 N94-26564
Evanescent field infrared spectroscopy using chalcogenide glass fiber
[ITN-94-85233] p 3038 N94-27178
Ir-fibers in a laser threat warning system and robot shot warning system
[PB94-124476] p 3038 N94-27209

GLASS TRANSITION TEMPERATURE
Modelling and predicting properties of polymers in the amorphous glassy state
[ETN-94-95345] p 2752 N94-26645
Fragmentation of Ge(1-x) Sn(x) Se2 glasses
[DE94-603009] p 2758 N94-27837

GLOBAL POSITIONING SYSTEM
Analysis and simulation of a GPS receiver design using combined delay-lock and modified tanlock loops
[AD-A274037] p 2664 N94-25810
Comparative investigation of high-latitude ionospheric structure and effects near solar maximum
[AD-A273799] p 2877 N94-25877
Differential global positioning system for the surface-towed ordnance locating system: Testing, results, and user's guide
[DE94-002980] p 2664 N94-26309
High-production global positioning system methods for survey applications: The pseudo-kinematic method with the Trimvec programming system
[ETN-94-95035] p 2665 N94-26539
Development of a performance evaluation tool (MMSOFE) for detection of failures with Multiple Model Adaptive Estimation (MMAE)
[AD-A274218] p 2665 N94-27071
Satellite navigation system GPS: A review of principles and performance and developments in general
[PB94-124534] p 2665 N94-27210
Investigation of air transportation technology at Ohio University, 1992-1993 p 2642 N94-27288
Fault detection and isolation p 2642 N94-27289
Improved modeling of GPS selective availability
p 2642 N94-27290
Realtime mitigation of GPS SA errors using Loran-C
p 2642 N94-27291
A GPS coverage model p 2642 N94-27292
Ground station siting considerations for DGPS
p 2642 N94-27293
Differential GPS methods and performance for marine applications
[DREP-93-09] p 2665 N94-27667
Flight testing of GPS and GPS-aided systems
[NLR-TP-92151-U] p 2666 N94-27831
Ionospheric calibration for single frequency altimeter measurements
[NASA-CR-195709] p 2883 N94-27883
A simulation of GPS and differential GPS sensors
p 2666 N94-27918

GLOBAL WARMING
Mission to Planet Earth: A program to understand global environmental change
[NASA-PAM-556] p 2869 N94-27958

GLOBULINS
Expression analysis of Thyroxine-Binding Globulin Complete Deficiency in Japanese (TBG-CDJ)
p 2905 N94-27482

GLOVES
Control panel dimensions for gloved operation study 2: Toggle switches minimum spacing required between toggle
[AD-A274518] p 2942 N94-27089
Extra-Vehicular Activity (EVA) glove evaluation test protocol
[NASA-TM-108442] p 2943 N94-27952

GLOW DISCHARGES
Study on development of chemical measurement method utilizing plasmas p 2728 N94-25576
Theoretical aspects of the agile mirror
[AD-A274890] p 2767 N94-26177
First experimental assessment of RCS plume-flow field interaction on Hermes leading edge thruster configuration p 2703 N94-28032

GLUONS
The Cherenkov hadronic like-jets
[DE93-634525] p 3016 N94-26010
On the gluon propagator in the infrared region
[DE93-634345] p 3016 N94-26035
Pseudoscalar glueball in the composite interpolating fields approach
[DE93-634374] p 3016 N94-26042
Deciphering the quark-gluon structure of the photon in electron(gamma) collisions
[DE93-634386] p 3017 N94-26043
The STAR experiment at the Relativistic Heavy Ion Collider
[DE94-003409] p 3017 N94-26083
Signatures for hybrids
[DE94-004244] p 3020 N94-26574
Experimental investigations of strong interaction in the non-perturbative QCD region
[DE94-001178] p 3024 N94-26949
A jet calculus approach including coherence effects and the associated problem of moment inversion
[ISBN-0-315-51715-8] p 3025 N94-27266

Aspects of perturbative corrections in quantum chromodynamics [ISBN-0-315-63607-6] p 3074 N94-27398

GOALS

Clean coal technology p 2832 N94-28089

GOLD

The formation of conducting gold films by thermal decomposition and direct patterning using electron beam lithography of the gold cluster Au55P(C6H5)312C16 [AD-A273720] p 2749 N94-26074

GOLD ALLOYS

Stress corrosion cracking and dealloying of copper-gold alloy in iodine vapor [DE93-633790] p 2734 N94-26264

GOLD ISOTOPES

Production of (phi) mesons in central Si + Au collisions at 14.6 AGeV/c [DE94-003196] p 3012 N94-25795

GOODNESS OF FIT

Estimation and tests-of-fit for the three parameter Weibull distribution [AD-A274827] p 3004 N94-26496

GOVERNMENT PROCUREMENT

Analysis of cost and schedule growth on sole source and competitive Air Force contracts [AD-A273920] p 3094 N94-26814

GOVERNMENT/INDUSTRY RELATIONS

Small business innovation research program solicitation [NASA-TM-109695] p 3094 N94-27661

GRAIN BOUNDARIES

Study on high temperature damage control and life improvement p 2729 N94-25580

The role of grain boundary chemistry and structure in the environmentally-assisted intergranular cracking of nickel-base alloys [DE94-003159] p 2732 N94-25954

Grain boundary degradation of YBCO superconductors sintered in CO2-containing atmospheres [DE94-003206] p 3053 N94-26029

A mechanism for resistive dissipation in Ag sheathed Bi2Sr2CaCu2O8 and Bi2Sr2Ca2Cu3O10 [DE94-003009] p 3060 N94-26771

Influence of point defects cn grain boundary diffusion in oxides [DE94-003164] p 3060 N94-26782

A model of electric breakdown in polycrystalline semiconductors with highly nonlinear I - V characteristics [DE94-601537] p 3063 N94-27017

Interface phenomena in metal-ceramic composites [AD-A274167] p 2709 N94-27125

Deformation, constitutive behavior, and damage of advanced structural materials under multiaxial loading [AD-A274165] p 2709 N94-27142

Grain boundary chromium concentration effects on the IGSCC and IASCC of austenitic stainless steels [DE94-004268] p 2741 N94-27570

GRAIN SIZE

Diffusion of substitutional elements in Ti in its hcp phase [DE93-633762] p 2733 N94-26160

Study of precipitation and recrystallization in Al alloy 2519 by backscattered electron imaging methods [AD-A274919] p 2736 N94-26533

CEN-VAMAS round robin on grain size measurement for advanced technical ceramics [VAMAS-TR-12] p 2752 N94-26654

Computer modelling of cyclic deformation of high-temperature materials [AD-A274504] p 2840 N94-27034

High temperature grain growth and oxidation of Fe-29Ni-17Co (Kovar (tm)) alloy leads [DE94-004691] p 3069 N94-27753

Characterization of ZnS-GaP naon-composites [DE94-004888] p 2712 N94-27813

GRAINS (FOOD)

Oil production from buckwheat stillage by thermochemical liquefaction p 2871 N94-28154

GRAMMARS

Parsing schemata: A framework for parallel and sequential parsing [PB94-125267] p 2981 N94-26998

GRAND UNIFIED THEORY

Why is the Higgs doublet light? [DE94-601711] p 3018 N94-26333

GRANITE

Effects of slot on rock surface for percussive rock excavation: Water jet assisted percussive rock excavation p 2871 N94-28155

The estimation of pre-stress by deformation rate analysis and suggestion of a mechanism from the elast-plastical theory p 2871 N94-28156

GRANTS

University program management information system, FY 1993 [NASA-TM-109719] p 3100 N94-27413

GRANULAR MATERIALS

The microstructural response of granular soil under uniaxial strain [AD-A274808] p 2763 N94-26341

Computer simulation and experiments on the quasi-static mechanics and transport properties of granular materials [AD-A274192] p 2823 N94-27104

GRAPH THEORY

The Chaco user's guide [DE94-003669] p 2962 N94-26370

Simulation approaches for calculations in directed graphical models [AD-A274825] p 3003 N94-26494

Some properties of graphs with local Ore conditions [PB94-126612] p 2996 N94-26962

Graphs satisfying a local ore-type condition [PB94-126679] p 3007 N94-27222

GRAPHICAL USER INTERFACE

Knowledge organization in intelligent tutoring systems for diagnostic problem solving in complex dynamic domains [AD-A273986] p 2984 N94-25899

A virtual environment for satellite modeling and orbital analysis in a distributed interactive simulation [AD-A274114] p 2694 N94-25904

Integration of interactive interfaces with intelligent tutoring systems: An implementation [AD-A273869] p 2985 N94-25966

Developing a sophisticated user interface to support domain-oriented application composition and generation systems [AD-A274080] p 2960 N94-25994

Developing a graphical user interface to support a real-time digital signal processing system [AD-A274032] p 2960 N94-26018

Software redesign for usability: A case study [DE94-003704] p 2960 N94-26048

Emerging Human-Computer Interface (HCI) design guidelines for Graphical User Interface (GUI) [DE94-004293] p 2941 N94-26555

Vcalc: A 3-space vector calculator [AD-A274520] p 2965 N94-26831

Advanced End-to-end Simulation for On-board Processing (AESOP) p 2945 N94-28255

ActorStudio: An interactive user interface editor [PB94-132859] p 2976 N94-28356

GRAPHITE

A study of graphite peek composite with central elliptical holes under tension [AD-A273779] p 2705 N94-25863

Technical report of ISSP. Ser. A, no. 2678: Magnetic properties of carbon nanotubes [JTN-94-80564] p 3064 N94-27174

Fullerene fabrication using an arc furnace. Characterization of the product [DE94-603006] p 3029 N94-27834

GRAPHITE-EPOXY COMPOSITES

Influence of embedded optical fibers on compressive strength of advanced composites [AD-A273775] p 2705 N94-25859

Fatigue resistance under tension-compression of laminates IM6/5245C and AS4/3501-6 [IAR-CR-25] p 2708 N94-26711

GRAPHITIZATION

Ion implantation of diamond: Damage, doping, and lift-off [DE94-001133] p 3054 N94-26137

Regrowth zones in laser annealed radiation damaged diamond [DE94-600821] p 3056 N94-26364

High performance fibers [AD-A274693] p 2707 N94-26450

GRAPHS (CHARTS)

Subgraph approximations for large directed graphical models [AD-A274813] p 3003 N94-26485

Kiruna geophysical data. Data summary 93/4-6, April-June 1993 [PB94-123700] p 2881 N94-27039

Graphs satisfying a local ore-type condition [PB94-126679] p 3007 N94-27222

GRASSLANDS

Grassland/atmosphere response to changing climate: Coupling regional and local scales [DE94-003111] p 2866 N94-26026

GRATINGS (SPECTRA)

Binary optical elements: Studies in design, manufacture and performance [ISBN-0-315-60643-6] p 3039 N94-27643

Development of a holographic illumination system for a time-integrating correlator [DSIS-94-00111] p 2814 N94-27763

GRAVITATION

On string theory interacting with two-dimensional gravity [DE94-601562] p 3071 N94-25883

Orthodox gravity [DE94-601560] p 2878 N94-26418

The gravity equations in the Lobachevskij space [DE93-634334] p 2879 N94-26504

Frontiers of science and measurement: Report on a seminar jointly organized by the National Physical Laboratory and the Institute of Physics [PB94-124310] p 3009 N94-27131

Exercise detraining: Applicability to microgravity p 2934 N94-28364

Aerobic fitness and orthostatic tolerance: Evidence against an association p 2934 N94-28365

GRAVITATION THEORY

Dimensional crossover from non-renormalizability to renormalizability [DE93-613052] p 3006 N94-26193

Orthodox gravity [DE94-601560] p 2878 N94-26418

Stochastic space-time, confinement potential and particle propagator [DE94-606415] p 3074 N94-27680

GRAVITATIONAL EFFECTS

Autonomous support for microorganism research in space p 2903 N94-25672

Intermittent gravity: How much, how often, how long? [NASA-TM-108800] p 2944 N94-26098

Report of three microgravity experiments by the drop shaft [JTN-94-80579] p 2761 N94-27341

The electrogastrogram during parabolic flight p 2913 N94-27452

Vertical gaze direction during parabolic flight p 2913 N94-27453

Heart rate change in normal and labyrinthectomized hamsters during parabolic flight p 2914 N94-27454

Effects of imaginary target on induced eye movements by linear acceleration p 2914 N94-27456

The mechanism of caloric nystagmus under microgravity. 1: Changes of endolymphatic pressure in the semicircular canal of pigeon by caloric stimulation p 2914 N94-27457

Comparative measurement of visual stability in cosmic space: Onboard experiment and pre-flight activities p 2916 N94-27463

Root gravitropism in maize and Arabidopsis [NASA-CR-195710] p 2903 N94-27940

Evaluation of near-infrared spectrophotometric method for individual tolerance to +Gz acceleration p 2933 N94-27944

GRAVITATIONAL FIELDS

Correlation between the gravity field and the bathymetry in the North Atlantic Ocean [ETN-94-95036] p 2899 N94-26108

Characterization of acoustic effects on flame structures by beam deflection technique [DE94-003240] p 2714 N94-26122

Orthodox gravity [DE94-601560] p 2878 N94-26418

Spinor and isospinor structure of relativistic particle propagators [DE94-601552] p 3019 N94-26424

Gravitational field of a point mass in the Lobachevskij space [DE93-634333] p 3072 N94-26503

The gravity equations in the Lobachevskij space [DE93-634334] p 2879 N94-26504

Stochastic space-time, confinement potential and particle propagator [DE94-606415] p 3074 N94-27680

Lifetimes of lunar satellite orbits [NASA-TP-3394] p 2690 N94-27771

GRAVITATIONAL PHYSIOLOGY

Intermittent gravity: How much, how often, how long? [NASA-TM-108800] p 2944 N94-26098

Performance recovery in the baboon following (+)G sub z-induced loss of consciousness [AD-A274411] p 2902 N94-26991

Workshop on Countering Space Adaptation with Exercise: Current Issues [NASA-CP-3252] p 2934 N94-28361

Exercise detraining: Applicability to microgravity p 2934 N94-28364

Visit to CERMA: Centre d'Etudes et de Recherches de Medecine Aerospatiale, Centre for Studies and Research in Aviation and Space Medicine, Bretigny sur Orge, France, November 16-18, 1992 [PB94-132990] p 2937 N94-28392

GRAVITROPISM

Root gravitropism in maize and Arabidopsis [NASA-CR-195710] p 2903 N94-27940

GRAVITY ANOMALIES

Geoid determination: With help of the alternative scattering method [ETN-94-95375] p 2847 N94-25746

GRAVITY GRADIENT SATELLITES

A comparison of three approximate mathematical models for the gravity gradient stabilized satellite [AD-A273832] p 2694 N94-25615

GRAVITY WAVES

Numerical procedure for planetary wave solution [DE94-004280] p 2879 N94-26576

GRAY SCALE

Automated fabric inspection system [AD-A274522] p 2835 N94-26833

Image quality measures and their performance p 2946 N94-28257

GRAZING INCIDENCE

Comparison of technology for high-power laser mirrors and synchrotron radiation mirrors [DE94-002913] p 3035 N94-26276

GREEN'S FUNCTIONS

Elastic wave up/down decomposition in inhomogeneous and anisotropic media: An operator approach and its approximations [PB94-126497] p 2881 N94-26880

Electronic structure of a single oxygen vacancy in rutile TiO2 [DE94-602717] p 3062 N94-26901

An efficient and accurate Green's function analysis of packaged microwave integrated circuits [ISBN-0-315-84425-6] p 2787 N94-27653

Fields and potentials in general uniaxial bianisotropic media I. Axial sources [PB94-132875] p 2778 N94-28379

Analytic solution for the dyadic Green's function of a nonreciprocal uniaxial bianisotropic medium [PB94-133162] p 2779 N94-28388

Green dyadic and dipole fields for a medium with anisotropic chirality [PB94-132933] p 2779 N94-28391

GREENHOUSE EFFECT

Methane emissions from natural wetlands [DE93-040796] p 2865 N94-25790

Meeting of the Eighth Session of the Scientific Advisory Committee of the World Climate Impact Assessment and Response Strategies Programme [DE93-633954] p 2866 N94-26163

A conceptual framework for the evaluation of cost-effectiveness of projects to reduce GHG emissions and sequester carbon [DE93-040448] p 2867 N94-26419

Proposed law of nature linking impacts, plume volcanism, and Milankovitch cycles to terrestrial vertebrate mass extinctions via greenhouse-embryo death coupling p 2876 N94-28307

GRID GENERATION (MATHEMATICS)

Parallel grid generation algorithm for distributed memory computers [NASA-TP-3429] p 2963 N94-26466

VLUGR2: A vectorized local uniform grid refinement code for PDE's in 2D [CWI-NM-R9306] p 2965 N94-26772

Using the TSAR electromagnetic modeling system [DE94-002617] p 2771 N94-26803

Building 3-D models from unregistered range images [AD-A274126] p 2986 N94-27032

A parallel computational fluid dynamics unstructured grid generator [AD-A274129] p 2795 N94-27119

Agglomeration multigrid for the three-dimensional Euler equations [NASA-CR-191595] p 2999 N94-27557

Solution of the Euler equations using unstructured grids p 2656 N94-28338

GROOVES

Calculation methods for steadily loaded central circumferential groove hydrodynamic journal bearings (guide to use of computer program A9304) [ESDU-93004] p 2830 N94-28073

Calculation methods for steadily loaded axial groove hydrodynamic journal bearings (guide to use of computer program A9305) [ESDU-93005] p 2830 N94-28074

Calculation methods for steadily loaded axial groove hydrodynamic journal bearings. Low viscosity process fluid lubrication (guide to use of computer program A9306) [ESDU-93006] p 2830 N94-28075

GROUND BASED CONTROL

Project Ares 3 p 2671 N94-25712

Optical communications for transport aircraft p 2643 N94-27298

GROUND EFFECT (AERODYNAMICS)

Experimental data for CFD validation of impinging jets in crossflow with application to ASTOVL flow problems p 2801 N94-28010

Experiments on the ground vortex formed by an impinging jet in cross flow p 2802 N94-28016

Numerical simulation of a powered-lift landing p 2671 N94-28033

A study of jet effect and ground effect interference on a STOL fighter p 2671 N94-28034

GROUND HANDLING

Handbook for handling and storage of nickel-cadmium batteries: Lessons learned [NASA-RP-1326] p 2702 N94-26613

GROUND STATE

Hook spectroscopy as an atomic number density diagnostic applied to laser-ablated copper plasmas [DE94-002645] p 3042 N94-26081

All-coupling polaron ground state energy in D-dimension [DE94-603666] p 3027 N94-27629

Correlated mean field Ansatz for the Kondo necklace [DE94-603671] p 3067 N94-27634

GROUND STATIONS

Hybrid power system for remote communications stations [AD-A274963] p 2782 N94-26301

Ground station siting considerations for DGPS p 2642 N94-27293

GROUND TESTS

Soft ground arresting system for airports [DOT/FAA/CT-93/80] p 2680 N94-26202

An assessment of testing requirement impacts on nuclear thermal propulsion ground test facility design [DE94-002933] p 2702 N94-26560

S-76 high intensity radiated fields, volume 2 [AD-A274572] p 2771 N94-26836

S-76 high intensity radiated fields, volume 1 [AD-A274571] p 2771 N94-26854

S-76 high intensity radiated fields, volume 3 [AD-A274416] p 2772 N94-26980

Conifer tree influence on Digital Terrain Elevation Data (DTED): A case study at Dulles International Airport [AD-A274213] p 2849 N94-27069

GROUND TRACKS

Tropical cyclone report, 1992 [AD-A274464] p 2896 N94-27025

GROUND TRUTH

A comparative evaluation of SAR and SLAR [DE94-002922] p 2848 N94-26277

Short-range cloud amount forecasting with model output statistics [AD-A274769] p 2895 N94-26798

GROUND-AIR-GROUND COMMUNICATION

Packet radio data link applications in the NASA Langley Research Center Transport Systems Research Vehicle [NASA-TM-109071] p 2665 N94-27423

GROUP DYNAMICS

A test of the theory of reasoned action at the group level of analysis [AD-A273965] p 2937 N94-25897

An investigation of integrated product development implementation issues: A case study of Bosma Machine and Tool Corp. [AD-A273917] p 2942 N94-27320

Intertemporal bargaining and dynamic consistency [PB94-133147] p 3095 N94-28386

GROUP THEORY

Conditionally exponential convex functions on locally compact groups [DE93-613025] p 2990 N94-25865

Duality for multiparametric quantum GL(n) and for a Lorentz quantum group [DE93-613048] p 3005 N94-25868

On the gluon propagator in the infrared region [DE93-634345] p 3016 N94-26035

Dynamical group of relativistic straight-line string [DE93-634347] p 3072 N94-26037

Matrix near rings and pseudo distributivity [DE94-601505] p 2992 N94-26366

Quantum group and Manin plane related to a colored braid group representation [DE94-601509] p 3072 N94-26461

A concurrent, multigroup, discrete ordinates model of neutron transport [DE94-004334] p 3020 N94-26577

Deformation of the exterior algebra and the GL(sub q) (r, included in) algebra [DE94-602558] p 2996 N94-26898

GROWTH

Effects of ML-9, a myosin light-chain kinase inhibitor, on preimplantation development of the mouse p 2905 N94-27486

Compaction-like blastomere aggregation caused by 1-oleoyl-2-acetylglycerol in mouse embryos: An electron microscopic observation p 2905 N94-27487

Inductive differentiation of nerve cells in mouse embryonic ectoderm at early primitive streak stage by retinoic acid p 2905 N94-27488

Cross-sectional anatomy of day 30 suncus fetuses p 2905 N94-27490

GUIDE VANES

An investigation of the effects of the high maximum-thickness-to-chord ratio on the performance of nozzle guide vanes in a transonic planar cascade [ISBN-0-315-84107-9] p 2793 N94-26671

The renewing of the test section of the NAL transonic wind tunnel. Part 1: Reconstruction of the 1st corner turning vanes and aerodynamic stress measurement [NAL-TM-651] p 2681 N94-27247

GUN LAUNCHERS

Energy and technology review, July 1993 [DE94-004219] p 3118 N94-27566

GUST LOADS

The deterministic power-spectral-density method [AD-B175894] p 2678 N94-27395

The deterministic power-spectral-density-method for nonlinear systems [AD-B179687] p 3001 N94-28353

GUSTS

Machine intelligent gust front algorithm [AD-A273695] p 2680 N94-26196

The deterministic power-spectral-density-method for nonlinear systems [AD-B179687] p 3001 N94-28353

GYROSCOPES

An approximate solution for the spinup dynamics of near axisymmetric axial gyrostats using the method of multiple scales [AD-A273723] p 2698 N94-26223

GYROTROPISM

Modern photoacoustic spectroscopy problems. Theory and experiment (a review) [IFTR-41/1993] p 2716 N94-26823

H

H ALPHA LINE

Fast H-alpha line broadening during the 100 ns REB injection into a plasma [IPPCZ-322] p 3048 N94-27836

H-INFINITY CONTROL

Necessary and sufficient conditions for the existence of the stabilizing solution of the Riccati equation in a Hilbert space: A Popov function approach [PB94-125341] p 2997 N94-26999

Operator theoretic methods in the control of distributed and nonlinear systems [AD-A274160] p 2988 N94-27139

HABITABILITY

First lunar outpost p 2943 N94-25694

HABITATS

Portable Habitat for Antarctic Scientific Research (PHASR) p 2943 N94-25681

Design and development of the second generation Mars Habitat p 2943 N94-25693

First lunar outpost p 2943 N94-25694

Space Habitat, assembly and repair facility p 2691 N94-25696

Lunar base habitat designs: Characterizing the environment, and selecting habitat designs for future trade-offs [NASA-CR-195687] p 2943 N94-27934

Landscape dynamics of northeastern forests [NASA-CR-195272] p 2852 N94-28070

HADRONS

Secondary particle in background levels and effects on detectors at future hadron colliders [DE94-003378] p 3011 N94-25598

Contributions to the 23rd ICRC from emulsion chamber experiments at Mt. Chacaltaya and Pamirs [ICRR-REPT-295-93-7] p 3112 N94-25624

A study of very high energy hadron interactions through observation of cosmic-ray families of visible energy greater than 500 TeV, 1 p 3112 N94-25625

A study of very high energy hadron interactions through observation of cosmic-ray families of visible energy greater than 500 TeV, 2 p 3112 N94-25626

A study of very high energy hadron interactions through observation of cosmic-ray families with visible energy not less than 500 TeV, 3 p 3112 N94-25627

Observation of characteristics of cosmic-ray hadron interactions in uniform-type thick lead chambers at Pamir, 1 p 3112 N94-25628

Observation of characteristics of cosmic-ray hadron interactions in uniform-type thick lead chambers at Pamir, 2 p 3113 N94-25629

Observation of characteristics of cosmic-ray hadron interactions in uniform-type thick lead chambers at Pamir, 3 p 3113 N94-25630

Penetrating nature of very collimated high-energy shower-clusters of hadrons and gamma rays p 3113 N94-25631

Energy concentration in high energy hadron-gamma families p 3113 N94-25632

Violation of Feynman scaling law in the forward region
p 3113 N94-25633
Simultaneous observation of families and air showers at Mt. Chacaltaya p 3114 N94-25634
Theoretical and computational studies in intermediate energy nuclear physics
[DE94-004177] p 3012 N94-25800
Principles of gauge theory of real hadrons
[DE93-613096] p 3013 N94-25835
Hadron jets and nucleon clusters in the relativistic nuclear collisions
[DE93-613434] p 3031 N94-25850
The amplitude of the elastic hadron-hadron scattering in the coulombic range of transfer momenta
[DE93-613183] p 3014 N94-25869
Principles of gauge theory of real hadrons
[DE93-616857] p 3015 N94-25920
A research program in experimental and theoretical high energy physics
[DE94-002156] p 3031 N94-25931
Monte Carlo event generators for hadron-hadron collisions
[DE94-003212] p 3015 N94-25955
The Cherenkov hadronic like-jets
[DE93-634525] p 3016 N94-26010
Deciphering the quark-gluon structure of the photon in electron(gamma) collisions
[DE93-634386] p 3017 N94-26043
Spin effects in hard interactions (interest in accelerated polarized beam)
[DE93-634398] p 3031 N94-26044
Meson X(1814) as a candidate for a hybrid state
[DE93-634447] p 3017 N94-26045
The STAR experiment at the Relativistic Heavy Ion Collider
[DE94-003409] p 3017 N94-26083
Photon and hadron production of heavy flavors
[DE94-004655] p 3018 N94-26245
Calorimeter with WLS fibers and parallel to beam scintillators
[DE93-634188] p 2810 N94-26378
Hadron gas ionization calorimeters
[DE93-634186] p 2810 N94-26397
Study on the compensated lead hadron calorimeter characteristics by means of hadron and electron beams
[DE93-634176] p 2810 N94-26439
Low-energy hadronic interactions beyond the current algebra approach
[DE94-602600] p 3022 N94-26900
Study of the process (pi)(sup -)A(yields)(pi)(sup -)(eta)'(eta)A at the moment 36 GeV/c
[DE93-634530] p 3024 N94-27250
A study of the global properties of hadronic matter at large densities
[ISBN-0-315-57234-5] p 3025 N94-27260
Quantum chromodynamics and nuclear physics at extreme energy density
[DE94-004418] p 3026 N94-27604
Indiana University high energy physics, task A
[DE94-000961] p 3033 N94-27614
Future directions in particle and nuclear physics at multi-GeV hadron beam facilities
[DE94-002946] p 3027 N94-27711
Proceedings of the workshop on (pi), K, (eta)-nucleon interactions
[DE94-701314] p 3027 N94-27733
A prototype presampler for the uranium-scintillator calorimeter in Zeus
[NIKHEF-H/93-11] p 2814 N94-28098

HAFNIUM ALLOYS
Study of the hyperfine magnetic field at Ta-181 site in the Heusler Co2ScSn, Co2ScGa, and Co2HfSn alloys
[DE94-603989] p 3067 N94-27623

HAILSTORMS
Examination of micro- and macro-physical structures and processes in hailstorms with respect to their modification
[DLR-FB-93-25] p 2897 N94-27751

HALF SPACES
Image theory for DC problems involving a conducting half space bounded by the general anisotropic impedance surface
[PB94-132917] p 2779 N94-28390

HALITES
Lighter alkali hydride and deuteride 1: Electronic properties of pure solids
[DE93-616188] p 3051 N94-25914
Se EXAFS study of the elevated wurtzite to rock salt structural phase transition in CdSe nanocrystals
[DE94-003247] p 3054 N94-26125

HALL EFFECT
Gauge invariance and transport properties in superconductors above T(c)
[DE94-604013] p 3068 N94-27677

HALLEY'S COMET
The kinetics and dynamics of the coma of Halley's comet
[NASA-CR-194828] p 3105 N94-28184

HALOGENS
Structure of ionic fluids in equilibrium with a microporous ionic matrix
[DE94-600563] p 2715 N94-26391
Molecular surface electrostatic potentials in the analysis of non-hydrogen-bonding noncovalent interactions
[AD-A274612] p 3022 N94-26894

HALOS
Longitudinal diffusion of a proton bunch under external noise
[DE93-634022] p 3032 N94-26165
The meaning of EROS/MACHO
[DE94-003003] p 3104 N94-26311

HAMILTONIAN FUNCTIONS
Convergent close-coupling calculation of electron-sodium scattering
[DE94-601815] p 3014 N94-25842
Towards a theory of growing surfaces: Mapping two-dimensional Laplacian growth onto Hamiltonian dynamics and statistics
[DE94-002636] p 2991 N94-26079
On Poisson brackets and symplectic structures for the classical and quantum Zitterbewegung
[DE93-634305] p 2992 N94-26267
Gauging of Chern-Simons p-Barnes
[DE94-601553] p 2993 N94-26425
Quantum Hamiltonian differential geometry: How does quantization affect space?
[DE93-634306] p 2993 N94-26442
The Hamiltonian structures of the super KP hierarchy associated with an even parity superlax operator
[DE94-601506] p 2994 N94-26459
On the wave and corpuscular properties of microparticles
[DE93-634450] p 3020 N94-26509
Electronic structure of a single oxygen vacancy in rutile TiO2
[DE94-602717] p 3062 N94-26901
Some properties of graphs with local Ore conditions
[PB94-126612] p 2996 N94-26962
Normal forms for perturbations of the euler top
[PB94-125390] p 3009 N94-26968
Poisson-lie group of pseudodifferential symbols
[PB94-124393] p 2997 N94-26996
Graphs satisfying a local ore-type condition
[PB94-126679] p 3007 N94-27222
Study of the critical points at infinity arising from the failure of the Palais-smale condition for n-body type problems
[DE94-603656] p 3000 N94-27818

HANDBOOKS
Digital systems validation book plan. Volume 3: Handbook
[AD-A274099] p 2672 N94-26028
Damage tolerance assessment handbook. Volume 1: Introduction fracture mechanics fatigue crack propagation
[AD-A274777] p 2836 N94-26186
Handbook for handling and storage of nickel-cadmium batteries: Lessons learned
[NASA-RP-1326] p 2702 N94-26613
Handbook of photovoltaic power generating design for introduction
[DE94-725199] p 2858 N94-26913

HARDENING (MATERIALS)
The role of point defect clusters in reactor pressure vessel embrittlement
[DE94-001122] p 2739 N94-26931

HARDENING (SYSTEMS)
Safety standards for aircraft shelter
[FFI-92/4003] p 2680 N94-26305

HARDNESS
Advanced qualification techniques
[DE94-003709] p 2780 N94-25812
Cracking of textured zinc coating during forming process
[DE94-003414] p 2750 N94-26085
Examination of hardness, fracture toughness and microstructure in Al2O3-B4C binary ceramics
[PB94-124237] p 2755 N94-27158
Process modelling of aluminium alloys. Modelling of the quench sensitivity of alloy AA6082
[PB94-124567] p 2741 N94-27325

HARDWARE
Hardware and software reliability estimation using simulations
[NASA-CR-187588] p 2973 N94-27663

HARDWARE DESCRIPTION LANGUAGES
Proposed Object Oriented Programming (OOP) enhancements to the Very High Speed Integrated Circuits (VHSIC) Hardware Description Language (VHDL)
[AD-A274004] p 2957 N94-25661
A VHDL register transfer level model of the linear token passing multiplex data bus protocol for the high speed data bus
[AD-A273734] p 2980 N94-26009
Partitioning structural VHDL circuits for parallel execution on hypercubes
[AD-A274390] p 2785 N94-26830
Design of a parallel discrete event simulation coprocessor
[AD-A274135] p 2982 N94-27123
Alternative architectures for domain-oriented application composition and generation systems
[AD-A274180] p 2968 N94-27128

HARMONIC CONTROL
A finite wake theory for two-dimensional rotary wing unsteady aerodynamics
[AD-A274921] p 2645 N94-26535

HARMONIC EXCITATION
Control of leading-edge separation on an airfoil by localized excitation
[DLR-FB-93-16] p 2647 N94-27592

HARMONIC GENERATIONS
Computer simulations of radiation generation from relativistic electron beams
[AD-A274139] p 3024 N94-27133
Technical report of ISSP. Ser. A, no. 2686: High-order harmonic generation and ionization using ultrashort KrF and Ti:Sapphire lasers
[JTN-94-80572] p 2820 N94-27605
Sum frequency generation using an optical parametric oscillator
[DE94-001827] p 3040 N94-28000

HARMONIC OSCILLATION
Understanding and development of a prediction method of transonic limit cycle oscillation characteristics of fighter aircraft
[NLR-TP-92210-U] p 2679 N94-27798

HARMONIC OSCILLATORS
Spectroscopic and vibrational energy transfer studies in molecular bromine
[AD-A273795] p 3014 N94-25875

HASTELLOY (TRADEMARK)
Creep rupture properties of a nickel-base heat-resistant alloy Hastelloy XR under varying temperature/stress condition
[DE94-701175] p 2743 N94-27807

HAWAII
Volcanology and volcanic activity with a primary focus on potential hazard impacts for the Hawaii geothermal project
[DE94-001614] p 2879 N94-26515

HAZARDS
Summaries of BFRL fire research in-house projects and grants, 1993
[PB94-121050] p 2763 N94-26756
Cryogenic size reduction of solid propellant
[AD-A274844] p 2759 N94-26800
Risks and issues in fire safety on the Space Station
[NASA-TM-106430] p 2692 N94-27436
Development of a method for predicting snowfall intensity and compacted snow on roads
p 2853 N94-27990
Conception of snow information network system in Yamagata Prefecture p 2853 N94-27991

HEAD DOWN TILT
Plasma volume shifts and exercise thermoregulation with water immersion and six-degree head-down tilt
[NASA-TM-108781] p 2901 N94-26093
Frequency analysis of body sway induced by optokinetic stimulation p 2914 N94-27455

HEAD MOVEMENT
Eye-head coordination and swinging of the visual scene when wearing visually up-down reversing mirror for 14 days p 2915 N94-27462

HEAD-UP DISPLAYS
Standardization of aircraft control and performance symbology on the USAF head-up display
[AD-A274283] p 2673 N94-26989

HEALING
The value of electrical stimulation as an exercise training modality p 2936 N94-28372

HEALTH
NCVS, volume 5
[AD-A274975] p 2902 N94-27165
Space radiation health research, 1991-1992
[NASA-TM-109721] p 2932 N94-27556

HEALTH PHYSICS
Space radiation health research, 1991-1992
[NASA-TM-109721] p 2932 N94-27556

HEARING
Signal- and listener-based factors in complex auditory pattern perception
[AD-A274148] p 2939 N94-27094
Comparison of methods of predicting community response to impulsive and nonimpulsive noise
p 2651 N94-28196

Sonic booms and marine mammals: Informational status and recommendations p 2651 N94-28198

HEART

EcarHeart2 version 1.0: Programmers documentation
[PB94-124633] p 2909 N94-25909

Electrical coupling between the sino-atrial node and atrial muscle: Cell to cell interaction through an external circuit and its simulation by computer modeling
p 2907 N94-27509

Correlation between electrical activity and the size of single sinoatrial node cells p 2907 N94-27513

The ionic mechanism underlying the negative chronotropic effect of acetylcholine: Experimental study in rabbit single sinoatrial node cells
p 2908 N94-27514

The ionic mechanism underlying the negative chronotropic effect of acetylcholine: Experiments using small sinoatrial node tissue preparations isolated from rabbit hearts p 2908 N94-27515

The ionic mechanism underlying the negative chronotropic effect of acetylcholine: Postganglionic vagal stimulation in isolated rabbit hearts
p 2908 N94-27516

Desensitization to acethylcholine in pacemaker cells of the sinoatrial node p 2908 N94-27537

Autonomic nervous system and cardiovascular control: Clinical implications of the 1/f fluctuations of heart rate
p 2932 N94-27540

HEART DISEASES

Protective action of platelet-activating factor antagonist, TCV-309, against ischemia reperfusion injury in isolated rabbit hearts p 2904 N94-27465

Protective action of an amiloride derivative (amiloride, 5-(N, N-dimethyl) hydrochloride) against in isolated ischemia/reperfusion newborn rabbit hearts
p 2904 N94-27466

On the mechanism of reentrant arrhythmias following DC defibrillation: Influence of fiber orientation to the effects of low-energy electric field stimulation on the effective refractory period of cardiac muscle
p 2904 N94-27468

Positive chronotropic effect of mechanical stretch on the sinoatrial node: Roles of neurotransmitters and stretch activated channels p 2904 N94-27469

The role of beta-adrenoceptor stimulation in the progression of chronic heart failure
p 2932 N94-27541

HEART FUNCTION

EcarHeart2 version 1.0: Programmers documentation
[PB94-124633] p 2909 N94-25909

Protective action of platelet-activating factor antagonist, TCV-309, against ischemia reperfusion injury in isolated rabbit hearts p 2904 N94-27465

Protective action of an amiloride derivative (amiloride, 5-(N, N-dimethyl) hydrochloride) against in isolated ischemia/reperfusion newborn rabbit hearts
p 2904 N94-27466

Effects of high-intensity electric field stimulation on the electromechanical performance of cardiac muscle: Influence of fiber orientation p 2904 N94-27467

On the mechanism of reentrant arrhythmias following DC defibrillation: Influence of fiber orientation to the effects of low-energy electric field stimulation on the effective refractory period of cardiac muscle
p 2904 N94-27468

Positive chronotropic effect of mechanical stretch on the sinoatrial node: Roles of neurotransmitters and stretch activated channels p 2904 N94-27469

HEART RATE

Passive and active behavior of the cardiovascular system under increased gravitational loads in a chronically instrumental conscious baboon model
[AD-A274344] p 2910 N94-26973

Heart rate change in normal and labyrinthectomized hamsters during parabolic flight p 2914 N94-27454

Positive chronotropic effect of mechanical stretch on the sinoatrial node: Roles of neurotransmitters and stretch activated channels p 2904 N94-27469

Autonomic nervous system and cardiovascular control: Clinical implications of the 1/f fluctuations of heart rate
p 2932 N94-27540

HEAT

Changes in pain sensation induced by repetitive application of noxious heat pulses to the human skin
p 2924 N94-27501

HEAT AFFECTED ZONE

Evaluation of crack arrest fracture toughness of parent plate, weld metal and heat affected zone of BIS 812 EMA ship plate steel
[AD-A274871] p 2839 N94-26859

The influence of TIG welding thermal cycles on HSLA-100 steel plate
[AD-A274248] p 2740 N94-27009

HEAT EXCHANGERS

Experimental analysis of heat transfer characteristics and pressure drop through screen regenerative heat exchangers
[AD-A273902] p 2790 N94-25657

Validated heat-transfer and pressure-drop prediction methods based on the discrete-element method. Phase 2: Two-dimensional rib roughness
[DE94-002379] p 2794 N94-26763

HEAT FLUX

Design of folded waveguide antenna for Alcator C-Mod
[DE94-003584] p 2767 N94-25924

Interpreting the implied meridional oceanic energy transport in AMIP
[DE94-001538] p 2898 N94-26072

Methodology for first wall design
[DE94-002795] p 3045 N94-26861

Numerical and experimental analyses of the radiant heat flux produced by quartz heating systems
[NASA-TP-3387] p 3011 N94-27659

Uncertainties in the characterization of the thermal environment of a solid rocket propellant fire
[DE94-002023] p 2760 N94-27719

Forced convection heat transfer in straight tubes. Part 2: Laminar and transitional flow
[ESDU-93018-PT-2] p 2807 N94-28139

HEAT GENERATION

Molten salt techniques for reproducible excess heat
[AD-A274935] p 2714 N94-26296

HEAT MEASUREMENT

Technique to predict the curing behaviour of unsaturated polyester materials
[PB94-124856] p 2748 N94-25892

Modelling the inhibition cure behaviour of unsaturated polyester moulding materials
[PB94-124864] p 2748 N94-25893

Thermal conductivity of PAX 2A explosive by DSC
[AD-A274721] p 2759 N94-26437

An ultrasonic testing technique for monitoring the cure and mechanical properties of polymeric materials
[AD-A274536] p 2753 N94-26842

Use of calorimetry for end of charge determination
p 2863 N94-28128

Formation and crystallization of hydrogen-induced amorphous Ti3InH(4.5) alloy p 2745 N94-28163

HEAT OF DISSOCIATION

Three methods to measure RH bond energies
[DE94-003795] p 3013 N94-25816

HEAT OF SOLUTION

Binding of copper and nickel to cavities in silicon formed by helium ion implantation
[DE94-003769] p 3050 N94-25814

HEAT PIPES

Modelling the mass migration phenomena in partially frozen heat pipes
[DE94-002716] p 2797 N94-27709

HEAT PUMPS

The First Energy Conference: Israel and the Former USSR
[ISBN-965-229-098-X] p 2853 N94-26050

Absorption technology for solar and waste heat utilization p 2854 N94-26053

Environmental benefits of different types of heat pumps, available and expected
[DE94-002440] p 2866 N94-26123

HEAT RESISTANT ALLOYS

Study on high temperature damage control and life improvement p 2729 N94-25580

HEAT SHIELDING

Interaction between a high density-low temperature plasma and a frozen hydrogen pellet in a railgun injector
[DE94-000846] p 3041 N94-25949

Mounting of SSM's
[VTT-TIED-1442] p 2695 N94-26250

HEAT TRANSFER

Experimental analysis of heat transfer characteristics and pressure drop through screen regenerative heat exchangers
[AD-A273902] p 2790 N94-25657

Microgravity ignition experiment p 2761 N94-25707

Abstraction in, specification and proof of software for a 1D heat-transfer problem
[REPT-93-45] p 2790 N94-25763

Technique to predict the curing behaviour of unsaturated polyester materials
[PB94-124856] p 2748 N94-25892

Modelling the inhibition cure behaviour of unsaturated polyester moulding materials
[PB94-124864] p 2748 N94-25893

A research program on radiative transfer model development in support of the ARM program
[DE94-001146] p 2767 N94-25950

Absorption technology for solar and waste heat utilization p 2854 N94-26053

Interpreting the implied meridional oceanic energy transport in AMIP
[DE94-001538] p 2898 N94-26072

Orbit transfer rocket engine technology program enhanced heat transfer combustor technology
[NASA-CR-189236] p 2700 N94-26156

Fire simulation based on convection calculation
[VTT-TIED-1411] p 2762 N94-26259

Eleventh Symposium on Energy Engineering Sciences: Proceedings
[DE93-019930] p 2763 N94-26429

Validated heat-transfer and pressure-drop prediction methods based on the discrete-element method. Phase 2: Two-dimensional rib roughness
[DE94-002379] p 2794 N94-26763

Computational mechanics
[DE94-003015] p 2965 N94-26775

Solidification modeling of a spiral casting to determine material fluidity
[DE94-002212] p 2739 N94-26935

SP industry calorimeter for rate of heat release measurements up to 10MW
[PB94-124211] p 2811 N94-27044

Verification of thermal analysis codes for modeling solid rocket nozzles
[NASA-CR-195248] p 2702 N94-27150

A study on heat transfer in a scramjet leading edge model
[NAL-TR-1187T] p 2675 N94-27608

A numerical approach to Stefan problem
[IPPCZ-334] p 2844 N94-27841

Gravity dependence or pressure drop and heat transfer in straight two-phase heat transport system condenser ducts
[NLR-TP-92167-U] p 2798 N94-27853

Aerodynamic heating in hypersonic flows
p 2658 N94-27919

Comparison of the interactions of two and three dimensional transverse jets with a hypersonic free stream p 2659 N94-28021

Transient model applications. 1: Compressor heat soak/clearance effects modeling p 2828 N94-28048

Cooling towers for combined cycles: New developments to meet environmental requirements
p 2832 N94-28088

HEAT TRANSMISSION

Verification of thermal analysis codes for modeling solid rocket nozzles
[NASA-CR-195248] p 2702 N94-27150

HEAT TREATMENT

Computer aided simulation of heat treatment
[VTT-PUBS-131] p 2731 N94-25643

Stress relaxation in dough moulding compounds
[PB94-124872] p 2748 N94-25894

Diffusion of substitutional elements in Ti in its hcp phase
[DE93-633762] p 2733 N94-26160

Zr-Sn-Nb alloys: Preliminary studies
[DE93-633767] p 2734 N94-26263

Analysis of the effect on growth kinetics of gamma prima phase in Inconel 713C alloys
[DE93-633763] p 2735 N94-26294

Titanium 1992: Science and Technology, volume 1
[AD-A274798-VOL-1] p 2739 N94-26799

Powder synthesis, fabrication, and transport properties of long-length Ag clad Bi-2223 conductors
[DE94-002376] p 2740 N94-26957

Process modelling of aluminium alloys. Modelling of the quench sensitivity of alloy AA6082
[PB94-124567] p 2741 N94-27325

Effect of precipitate structure on hot deformation of Al-Mg-Mn alloys
[DE94-004596] p 2741 N94-27622

HEATING

Coronal heating via nanoflares
[DE94-000773] p 3110 N94-26696

Martian atmospheric radiation budget
p 3107 N94-27887

A modelling of the noise from simple coaxial jets. Part 3: With hot primary flow
[ISVR-TR-230-PT-3] p 2807 N94-28173

HEATING EQUIPMENT

Environmental benefits of different types of heat pumps, available and expected
[DE94-002440] p 2866 N94-26123

Rewarming methodologies in the field
[AD-A274744] p 2909 N94-26173

A method for testing of HVAC automation equipment using the emulator and the application of the method
[VTT-TIED-1435] p 2822 N94-26306

Numerical and experimental analyses of the radiant heat flux produced by quartz heating systems
[NASA-TP-3387] p 3011 N94-27659

HEAVY ELEMENTS

Development of laser spectroscopic technology in nuclear industry
[DE93-633327] p 2714 N94-26158

HEAVY IONS

Back-reaction beyond the mean field approximation
[DE94-003936] p 3012 N94-25612

A double arm time-of-flight spectrometer based on position-sensitive parallel-grid avalanche counters
[DE93-616665] p 3012 N94-25750

The STAR experiment at the Relativistic Heavy Ion Collider
[DE94-003409] p 3017 N94-26083

Relativistic heavy ion physics
[DE94-003161] p 3031 N94-26097

Experimental and numerical investigation of shock wave propagation through complex geometry, gas continuous, two-phase media
[DE94-001408] p 2791 N94-26121

Diffusion of substitutional elements in Ti in its hcp phase
[DE93-633762] p 2733 N94-26160

Future directions in particle and nuclear physics at multi-GeV hadron beam facilities
[DE94-002946] p 3027 N94-27711

Advanced development of particle beam probe diagnostic system
[DE94-002316] p 3047 N94-27720

Studies of heavy-ion reactions and transuranic nuclei
[DE94-004642] p 3029 N94-27783

HEAVY NUCLEI

Index to BROND-2, CENDL-2, ENDF/B-6, JEF-2, JENDL-3
[DE93-634500] p 3016 N94-26034

A study of the global properties of hadronic matter at large densities
[ISBN-0-315-57234-5] p 3025 N94-27260

Jet production in muon scattering at Fermilab E665
[DE94-004663] p 3028 N94-27752

HEAVY WATER

Hydrogen physics
[DE94-701317] p 2719 N94-27822

HEISENBERG THEORY

Solution of the Heisenberg equation for the four-fermion contact interaction by the method of dynamical mappings
[DE94-606341] p 3075 N94-27858

HELICOPTER CONTROL

Neural networks for dynamic flight control
[AD-A274089] p 2676 N94-25785

Linear modeling of rotorcraft for stability analysis and preliminary design
[AD-A274869] p 2677 N94-26192

The effects of tailwinds and control cross coupling on rotorcraft handling qualities for steep, decelerating instrument approaches and missed approaches
[IAR-AN-77] p 2677 N94-26710

Optimal control of helicopters following power failure
[NAL-TR-1190] p 2678 N94-27206

A simulator investigation of helicopter flight control system mode transitions
[UTIAS-348] p 2682 N94-27879

HELICOPTER DESIGN

Linear modeling of rotorcraft for stability analysis and preliminary design
[AD-A274869] p 2677 N94-26192

Computer code for interactive rotorcraft preliminary design using a harmonic balance method for rotor trim
[AD-A274924] p 2668 N94-26531

HELICOPTER PROPELLER DRIVE

Study of the kinematic and dynamic characteristics of a wormgear transmission for helicopter applications
[NASA-CR-195287] p 2826 N94-27657

HELICOPTER WAKES

Investigation of the aerodynamic environment for an advanced lightweight rotor in forward flight. Volume 4: Laser velocimeter wake data, advance ratio of 0.037
[NASA-TM-109040-VOL-4] p 2645 N94-26483

Investigation of the aerodynamic environment for an advanced lightweight rotor in forward flight. Volume 1: Laser velocimeter inflow data, advance ratio of 0.37, thrust coefficient of 0.0081 and hover tip speed of 603 feet/second
[NASA-TM-109040-VOL-1] p 2645 N94-26489

Investigation of the aerodynamic environment for an advanced lightweight rotor in forward flight. Volume 2: Laser velocimeter inflow data, advance ratio of 0.37, thrust coefficient of 0.0064 and hover tip speed of 710 feet/second
[NASA-TM-109040-VOL-2] p 2645 N94-26492

Investigation of the aerodynamic environment for an advanced lightweight rotor in forward flight. Volume 3: Laser velocimeter inflow data, advance ratio of 0.37, thrust coefficient of 0.0064 and hover tip speed of 603 feet/second
[NASA-TM-109040-VOL-3] p 2645 N94-26497

HELICOPTERS

Linear modeling of rotorcraft for stability analysis and preliminary design
[AD-A274869] p 2677 N94-26192

Experimental investigation of advanced hub and pylon fairing configurations to reduce helicopter drag
[NASA-TM-4540] p 2668 N94-26604

Rotorcraft low altitude IFR benefit/cost analysis: Conclusions and recommendations
[AD-A274241] p 2665 N94-26826

S-76 high intensity radiated fields, volume 2
[AD-A274572] p 2771 N94-26836

S-76 high intensity radiated fields, volume 1
[AD-A274571] p 2771 N94-26854

HELIUM

Evaluation of helium cooling for fusion divertors
[DE94-002680] p 3042 N94-25976

A robust helium-cooled shield/blanket design for ITER
[DE94-003402] p 3043 N94-26323

Influence of helium generation rate and temperature history on mechanical properties of model Fe-Cr-Ni alloys irradiated in FFTF at relatively low displacement rates
[DE94-004264] p 2737 N94-26575

Technical report of ISSP. Ser. A, no. 2684: Wavelength dependence of nonsequential double ionization in He
[JTN-94-80570] p 3025 N94-27338

Helium transport and exhaust studies of H-mode discharges in the D3-D tokamak
[DE94-004744] p 3048 N94-27785

HELIUM IONS

Binding of copper and nickel to cavities in silicon formed by helium ion implantation
[DE94-003769] p 3050 N94-25814

The structural, chemical, and electrical properties of He-implantation-induced nanocavities in silicon
[DE94-002681] p 3052 N94-25971

Technical report of ISSP. Ser. A, no. 2684: Wavelength dependence of nonsequential double ionization in He
[JTN-94-80570] p 3025 N94-27338

Helium transport and exhaust studies of H-mode discharges in the D3-D tokamak
[DE94-004744] p 3048 N94-27785

Fuel ion rotation measurement and its implications on H-mode theories
[DE94-004860] p 3048 N94-27791

HELIUM PLASMA

Fuel ion rotation measurement and its implications on H-mode theories
[DE94-004860] p 3048 N94-27791

HELIUM-NEON LASERS

An apparatus for measurement of ignition and burning characteristics of metallic particles
[AD-A274815] p 2716 N94-26487

Zeeman laser interferometry for detection and chemical analysis
[DE94-003963] p 2719 N94-27728

HELMET MOUNTED DISPLAYS

Weapon system integration for the AFIT virtual cockpit
[AD-A274058] p 2667 N94-25772

Helmet head tracking mounting device
[AD-D016048] p 2942 N94-27114

HELMETS

Helmet head tracking mounting device
[AD-D016048] p 2942 N94-27114

HELMHOLTZ RESONATORS

Characterization of acoustic effects on flame structures by beam deflection technique
[DE94-003240] p 2714 N94-26122

HEMODYNAMIC RESPONSES

Passive and active behavior of the cardiovascular system under increased gravitational loads in a chronically instrumental conscious baboon model
[AD-A274344] p 2910 N94-26973

Effect of L-dopa on hemodynamic functions in humans p 2929 N94-27526

HEMODYNAMICS

EcarHeart2 version 1.0: Programmers documentation
[PB94-124633] p 2909 N94-25909

Intermittent gravity: How much, how often, how long?
[NASA-TM-108800] p 2944 N94-26098

Aeromedical issues related to positive pressure breathing for +Gz protection
[AD-A274717] p 2910 N94-26435

Analysis on one minute wave in body fluid volume and muscle pumping referred to body parts generating the one minute wave during human active standing
p 2929 N94-27528

HEMOGLOBIN

Evaluation of near-infrared spectrophotometric method for individual tolerance to +Gz acceleration
p 2933 N94-27944

HEPATITIS

Modulation by galactosamine-induced hepatitis of biological responses of the rat exposed to high altitude hypoxia p 2904 N94-27464

HERMES MANNED SPACEPLANE

First experimental assessment of RCS plume-flow field interaction on Hermes leading edge thruster configuration p 2703 N94-28032

HERMETIC SEALS

Package integrity measurement technology and quality assurance
[AD-A273881] p 2834 N94-25727

HETEROGENEITY

Controlled heterogeneous nucleation of melt-textured YBa2Cu3O(6+x) by addition of Al2O3 particles
[AD-A274605] p 3062 N94-26892

Electromagnetic modeling of bi-isotropic media
[PB94-132909] p 2778 N94-28382

HETEROJUNCTION DEVICES

Development of intermetallic compounds for high performance luminescence elements
p 2722 N94-25545

Development of a 4-bit parallel analog-to-digital converter and a four-quadrant double-balanced mixer using heterojunction bipolar transistor technology
[AD-A274074] p 2947 N94-25648

A physics-based heterojunction bipolar transistor model for integrated circuit simulation
[AD-A274081] p 2781 N94-25995

Interface properties of wide bandgap semiconductor structures
[AD-A274356] p 3063 N94-27058

HETEROJUNCTIONS

A physics-based heterojunction bipolar transistor model for integrated circuit simulation
[AD-A274081] p 2781 N94-25995

Stress relaxation in sputtered W films and W/GeSi/Si heterostructures
[DE94-004007] p 3055 N94-26239

Pseudomorphic semiconducting heterostructures from combinations of AIN, GaN and selected SiC polytypes: Theoretical advancement and its coordination with experimental studies of nucleation, growth, characterization and device development
[AD-A274247] p 3061 N94-26841

AB-Initio calculation of the valence-band offset at strained GaAs/InAs (001) heterojunction
[DE94-602538] p 3061 N94-26878

Polar optical oscillation modes in GaAs-based double heterostructures: Long wavelength limit
[DE94-601874] p 3062 N94-26897

A tri-state optical switch for local area network communications p 2789 N94-27922

HEURISTIC METHODS

Thunderstorm Hypothesis Reasoner
[NASA-CR-195714] p 2897 N94-27884

HIGH ALTITUDE

A study of very high energy hadron interactions through observation of cosmic-ray families of visible energy greater than 500 TeV, 1 p 3112 N94-25625

A study of very high energy hadron interactions through observation of cosmic-ray families of visible energy greater than 500 TeV, 2 p 3112 N94-25626

Observation of characteristics of cosmic-ray hadron interactions in uniform-type thick lead chambers at Pamir, 2 p 3113 N94-25629

Observation of characteristics of cosmic-ray hadron interactions in uniform-type thick lead chambers at Pamir, 3 p 3113 N94-25630

Violation of Feynman scaling law in the forward region
p 3113 N94-25633

Simultaneous observation of families and air showers at Mt. Chacaltaya p 3114 N94-25634

HIGH ALTITUDE ENVIRONMENTS

Contributions to the 23rd ICRC from emulsion chamber experiments at Mt. Chacaltaya and Pamirs
[ICRR-REPT-295-93-7] p 3112 N94-25624

A study of very high energy hadron interactions through observation of cosmic-ray families with visible energy not less than 500 TeV, 3 p 3112 N94-25627

HIGH ALTITUDE PRESSURE

The Reports of Aeromedical Laboratory, volume 33, number 4
[JTN-94-80586] p 2933 N94-27942

HIGH ALTITUDE TESTS

Project Ares 3 p 2671 N94-25712

HIGH DEFINITION TELEVISION

VENI, video, VICI: The merging of computer and video technologies p 2686 N94-27362

HIGH ENERGY ELECTRONS

A study of LPM suppression of bremsstrahlung at 25 GeV
[DE94-003457] p 3018 N94-26133

Implementation of a compact magnetic electron energy spectrometer for intense relativistic electron beams
[AD-A274451] p 3033 N94-27082

Computer simulations of radiation generation from relativistic electron beams
[AD-A274139] p 3024 N94-27133

HIGH ENERGY INTERACTIONS

Contributions to the 23rd ICRC from emulsion chamber experiments at Mt. Chacaltaya and Pamirs
[ICRR-REPT-295-93-7] p 3112 N94-25624

A study of very high energy hadron interactions through observation of cosmic-ray families of visible energy greater than 500 TeV, 1 p 3112 N94-25625

A study of very high energy hadron interactions through observation of cosmic-ray families of visible energy greater than 500 TeV, 2 p 3112 N94-25626

A study of very high energy hadron interactions through observation of cosmic-ray families with visible energy not less than 500 TeV, 3 p 3112 N94-25627

Observation of characteristics of cosmic-ray hadron interactions in uniform-type thick lead chambers at Pamir, 1 p 3112 N94-25628

Observation of characteristics of cosmic-ray hadron interactions in uniform-type thick lead chambers at Pamir, 2 p 3113 N94-25629

Observation of characteristics of cosmic-ray hadron interactions in uniform-type thick lead chambers at Pamir, 3 p 3113 N94-25630

Penetrating nature of very collimated high-energy shower-clusters of hadrons and gamma rays
p 3113 N94-25631

Energy concentration in high energy hadron-gamma families p 3113 N94-25632

Violation of Feynman scaling law in the forward region
p 3113 N94-25633

Simultaneous observation of families and air showers at Mt. Chacaltaya p 3114 N94-25634

Hadron jets and nucleon clusters in the relativistic nuclear collisions
[DE93-613434] p 3031 N94-25850

The amplitude of the elastic hadron-hadron scattering in the coulombic range of transfer momenta
[DE93-613183] p 3014 N94-25869

Structure functions of sea quarks, Kogut-Susskind pole and dynamics of pp- and pp-bar-interactions at high energies
[DE93-613184] p 3031 N94-25870

A research program in experimental and theoretical high energy physics
[DE94-002156] p 3031 N94-25931

The proceedings of the KEK FEL Simulation Code Workshop
[DE93-520378] p 2816 N94-26112

JLC-1
[DE93-520380] p 3031 N94-26113

Harvard University High Energy Physics
[DE94-002406] p 3032 N94-26119

Problems of application of charged particles channeling effects in crystals in high-energy physics
[DE93-634023] p 3032 N94-26405

Proceedings of the Second EGS4 User's Meeting in Japan
[DE93-520383] p 3032 N94-26543

A study of the global properties of hadronic matter at large densities
[ISBN-0-315-57234-5] p 3025 N94-27260

Indiana University high energy physics, task A
[DE94-000961] p 3033 N94-27614

Future directions in particle and nuclear physics at multi-GeV hadron beam facilities
[DE94-002946] p 3027 N94-27711

The status of the solar neutrino problem
[DE94-003934] p 3111 N94-27742

Research on elementary particle physics, part 2
[DE94-004956] p 3029 N94-27815

HIGH ENERGY PROPELLANTS

Computational studies of energetic organic molecules
[AD-A274726] p 3018 N94-26172

Proceedings of the High Energy Density Matter (HEDM) Contractor's Conference
[AD-A274452] p 3033 N94-27083

HIGH FIELD MAGNETS

Study on ferromagnetic field magnet using strong and highly conductive material p 2725 N94-25559

Cryogenic fracture behavior of 316LN in magnetic fields up to 14.6 T
[DE94-005215] p 2742 N94-27694

HIGH FREQUENCIES

The effect of high frequency electric field on hypersound amplification in superlattice
[DE93-634326] p 3057 N94-26384

MILCOM 92 and standardization for HF-communication. A study tour to the USA in October 1992
[PB94-124427] p 2774 N94-27219

HIGH GRAVITY ENVIRONMENTS

Passive and active behavior of the cardiovascular system under increased gravitational loads in a chronically instrumental conscious baboon model
[AD-A274344] p 2910 N94-26973

HIGH LEVEL LANGUAGES

Proposed Object Oriented Programming (OOP) enhancements to the Very High Speed Integrated Circuits (VHSIC) Hardware Description Language (VHDL)
[AD-A274004] p 2957 N94-25661

Efficient implementation of high-level parallel symbolic languages p 2955 N94-27196

HIGH POWER LASERS

Studies of non-linear optical effects for agile beam steering
[AD-A273998] p 3034 N94-25902

Comparison of technology for high-power laser mirrors and synchrotron radiation mirrors
[DE94-002913] p 3035 N94-26276

Design and evaluation of an electromagnetic beam waveguide for measuring electrical properties of materials
[NASA-TP-3418] p 2769 N94-26611

Phase conjugation and pulse compression of high energy lasers: From nanoseconds to microseconds
[DE94-001061] p 2818 N94-26699

Phase conjugated lasers applied to commercial x ray lithography
[DE94-001529] p 2819 N94-27018

Kinoform/lens system for injecting a high power laser beam into an optical fiber
[DE94-003226] p 2819 N94-27262

HIGH PRESSURE

Fundamental study on monitoring technology on local surface damages p 2724 N94-25555

The use of on-line ion chromatography for high temperature and high pressure reaction studies
[DE94-002525] p 2713 N94-26075

Se EXAFS study of the elevated wurtzite to rock salt structural phase transition in CdSe nanocrystals
[DE94-003247] p 3054 N94-26125

Calibrating/testing meters in hot water test bench VM7
[PB94-124294] p 2812 N94-27160

Technical report of ISSP. Ser. A, no. 2682: Pressure dependence of Sm:YAG fluorescence to 50 GPa: A new calibration as a high pressure scale
[JTN-94-80568] p 3066 N94-27354

High-temperature and high-pressure flow calorimeter
p 2718 N94-27390

HIGH RESOLUTION

High resolution fourier transform absorption spectrum of 79Br2 B3 Pi(Ou+) X1 sigma g+
[AD-A273864] p 2956 N94-25610

High resolution studies of sunspots and flux tubes
[NASA-CR-195216] p 3111 N94-27321

HIGH REYNOLDS NUMBER

The high Reynolds number flow through an axial-flow pump
[AD-A273844] p 2789 N94-25604

Flow past a circular cylinder with a permeable wake splitter plate
[AD-A273765] p 2790 N94-25872

Computational investigation of the compressible dynamic stall characteristics of the Sikorsky SSC-A09 airfoil
[AD-A274867] p 2644 N94-26191

HIGH SPEED

Design optimization of high-speed proprotor aircraft
[NASA-TM-103988] p 2667 N94-26151

Multichip module high speed testing
[AD-A274873] p 2782 N94-26343

HIGH SPEED PHOTOGRAPHY

Flash unit for high speed photography
[PML-1992-91] p 2811 N94-26647

HIGH STRENGTH

Study on the mechanism of titanium alloy toughness and the improvement of properties
p 2726 N94-25566

High performance fibers
[AD-A274693] p 2707 N94-26450

Mechanical properties and microstructure of thermomechanically processed, high manganese steel
[ARL-TR-146] p 2747 N94-28212

HIGH STRENGTH ALLOYS

The transition from stress corrosion cracking to corrosion fatigue in AA-7075 and AA-8090
[ISBN-0-315-59526-4] p 2744 N94-27950

HIGH STRENGTH STEELS

Study on improvements in fretting fatigue characteristics of high strength structural member p 2726 N94-25567

Study on performance evaluation of pressure vessel steel in corrosion environments with sulfide
p 2730 N94-25582

Study on fatigue crack propagation characteristics around welded joint interface in complexed conditions
p 2730 N94-25584

Design of cold-formed HSS channels for bending and eccentric compression: Bending in the plane of symmetry
[VTT-TIED-1403] p 2762 N94-25622

Weldability of Direct-Quenched and Tempered (DQT) high strength steel HT80
[VTT-TIED-1406] p 2731 N94-25623

Weldability of Accelerated-Cooled (AcC) high strength TMCP steel HT50
[VTT-TIED-1410] p 2731 N94-25784

The study of single-pass GMA welds with different cover gas compositions on HSLA-100 steel
[AD-A274857] p 2822 N94-26174

The influence of weld metal alloying additions to extend the heat input range for the submerged arc welding of high strength steels
[AD-A274284] p 2738 N94-26679

HIGH TEMPERATURE

Fundamental study on monitoring technology on local surface damages p 2724 N94-25555

Failure mechanisms of high temperature semiconductor lasers
[AD-A273833] p 2815 N94-25616

Characterization of fatigue damage in a metal matrix composite (SCS-6/Ti-15-3) at elevated temperature
[AD-A273797] p 2706 N94-25876

The use of on-line ion chromatography for high temperature and high pressure reaction studies
[DE94-002525] p 2713 N94-26075

Zinc(2) oxide stability in alkaline sodium phosphate solutions at elevated temperatures
[DE94-003316] p 2715 N94-26320

High performance fibers
[AD-A274693] p 2707 N94-26450

Attachment techniques for high temperature strain
[AD-A274766] p 2811 N94-26568

High-temperature and high-pressure flow calorimeter
p 2718 N94-27390

High temperature grain growth and oxidation of Fe-29Ni-17Co (Kovar (tm)) alloy leads
[DE94-004691] p 3069 N94-27753

Development of advanced high temperature in-cylinder components and tribological systems for low heat rejection diesel engines, phase 1
[NASA-CR-187158] p 2827 N94-27984

HIGH TEMPERATURE ENVIRONMENTS

Preparation of creep data sheet: Material strength data sheet p 2723 N94-25548

Study on evaluation of crack generation and crack growth behaviors under static loading at high temperature and under combined loading p 2730 N94-25583

Radiation hardening effects on localized deformation and stress corrosion cracking of stainless steels
[DE94-004308] p 2731 N94-25804

Engineering limitations of ceramic composites for high performance and high temperature applications
[DE94-001676] p 2754 N94-27021

High temperature sensor/microphone development for active noise control
[NASA-CR-195214] p 2812 N94-27214

Creep rupture properties of a nickel-base heat-resistant alloy Hastelloy XR under varying temperature/stress condition
[DE94-701175] p 2743 N94-27807

Microspheres for laser velocimetry in high temperature wind tunnel p 2682 N94-27903

HIGH TEMPERATURE GASES

Pressure distributions on a 0.02-scale Space Shuttle orbiter nose at Mach 21.5 in helium
[NASA-TM-4495] p 2646 N94-26592

Experiments into the scaling parameters required for exhaust gas ingestion testing of vertical landing aircraft
p 2671 N94-28017

Influence of headwind on hot gas reingestion and consideration of pressure ratio scaling
p 2675 N94-28018

Unsteady aspects of hot gas reingestion and statistical analysis p 2676 N94-28019

Fibrous ceramic candle filter for particle removal in pressurized fluidized bed combustion
[PB94-133089] p 2876 N94-28383

Experimental studies of pressurised fluidised bed combustion at Helsinki University of Technology, 1991-1992
[PB94-133063] p 2876 N94-28394

HIGH TEMPERATURE PLASMAS

Interaction between a high density-low temperature plasma and a frozen hydrogen pellet in a railgun injector
[DE94-000846] p 3041 N94-25949

A study of the global properties of hadronic matter at large densities
[ISBN-0-315-57234-5] p 3025 N94-27260

Nonlinear transverse propagation of photons in a ultrarelativistically hot and magnetized electron-positron plasma: Coupling of Langmuir and electromagnetic solitons
[DE94-603667] p 3046 N94-27630

Proceedings of the 16th Symposium on Plasma Physics and Technology
[DE94-604181] p 3047 N94-27698

HIGH TEMPERATURE SUPERCONDUCTORS
Microscopic study of local structure and charge distribution in metallic La2CuO(4+delta)
[DE94-003801] p 3050 N94-25817
Flux flow, pinning, and resistive behavior in superconducting networks
[DE94-003400] p 3050 N94-25848
Optical conductivity and resistivity in the two-band Emery model
[DE94-601943] p 3051 N94-25945
The First Energy Conference: Israel and the Former USSR
[ISBN-965-229-098-X] p 2853 N94-26050
Prospects for utilization of superconductors in the power industry p 2854 N94-26057
The potential for large critical currents in the high T(sub c) oxides p 2854 N94-26058
Liquid and solid solubility of Ag in Bi2Sr2CaCu2O8
[DE94-002829] p 2735 N94-26273
Submillimeter residual losses in high-(Tc) superconductors
[DE94-003241] p 3058 N94-26516
Preparation and characterization of high temperature superconductor film surfaces
[AD-A274293] p 3059 N94-26681
Calculation of the electromagnetic critical state response of high T(sub c) superconductor tape
[DE94-002894] p 3061 N94-26868
Processing, fabrication, and demonstration of HTS integrated microwave circuits, appendix A
[AD-A274600] p 2785 N94-26890
Technical report of ISSP. Ser. A, no. 2683: Itinerant character of 5f electrons in UNi2Ga
[JTN-94-80569] p 3025 N94-27337
Gauge invariance and transport properties in superconductors above T(c)
[DE94-604013] p 3068 N94-27677
Evaluation of high temperature superconductive thermal bridges for space-borne cryogenic infrared detectors
p 2815 N94-27921
The optical properties of high-T(c) superconductors grown by pulsed laser deposition
[ISBN-0-315-84917-7] p 3039 N94-27962
Anisotropy in the electrical, magnetic and optical properties of Pb2Sr2RCu3O8
[ISBN-0-315-84930-4] p 3070 N94-27974
HIGH TEMPERATURE TESTS
Investigation of tension-compression fatigue behavior of a cross-ply metal matrix composite at room and elevated temperatures
[AD-A273731] p 2706 N94-25999
High temperature tension test equipment of heat resistant composite materials
[NAL-TM-652] p 2710 N94-27255
SP/MSP tests for the evaluation of FGM
[NAL-SP-17] p 2710 N94-27279
SP/MSP tests for the evaluation of FGM
p 2710 N94-27280
Research on the development of fracture characteristics evaluation system for ceramics and metal composite materials p 2710 N94-27281
HILBERT SPACE
Quantizable configurations of the relativistic string
[DE93-634346] p 3072 N94-26036
Necessary and sufficient conditions for the existence of the stabilizing solution of the Riccati equation in a Hilbert space: A Popov function approach
[PB94-125341] p 2997 N94-26999
Joint essential maximal numerical range
[DE94-603674] p 3000 N94-27637
Hessenberg matrices in Krylov subspaces and the computation of the spectrum
[PB94-133170] p 3001 N94-28389
HILL METHOD
Hill equations for satellite orbit determination
[ETN-94-95374] p 2690 N94-25787
HISS
Memories of National Institute of Polar Research. Series A-19. Upper atmosphere physics: ELF emission in high latitudes: Ray path calculation and ground-satellite observations
[JTN-94-80592] p 2882 N94-27342
HISTOCHEMICAL ANALYSIS
The 27th Annual Meeting of the Israel Society for Microscopy and the 12th Annual Meeting of the Israel Society for Histochemistry and Cytochemistry
[DE93-632416] p 2716 N94-26519
HISTORIES
FNAS lightning detection
[NASA-CR-193927] p 2893 N94-26134
The evolution of the high-speed civil transport
[NASA-TM-109089] p 3117 N94-26155
Nasa Langley Research Center seventy-fifth anniversary publications, 1992
[NASA-TM-109691] p 3118 N94-27431
Effects of historical and predictive information on ability of transport pilot to predict an alert
[NASA-TM-4547] p 2673 N94-27864
Development of the gas turbine. Part 1: Design philosophy and performance p 2831 N94-28080
Science beyond the atmosphere: The history of space research in Europe
[ESA-HSR-SPECIAL] p 2689 N94-28207
HODOSCOPES
The 1024 scintillation hodoscope
[DE93-634183] p 2810 N94-26394
HOLE GEOMETRY (MECHANICS)
Three-dimensional elastic stress concentration factors: Plain or countersunk hole in a wide plate subjected to tension, bending, or pin loading
[ESDU-93030] p 2845 N94-28143
HOLES (MECHANICS)
Investigation of compressive behavior for metal matrix composites with a circular hole
[AD-A273835] p 2705 N94-25739
A study of graphite peek composite with central elliptical holes under tension
[AD-A273779] p 2705 N94-25863
Mechanically fastened composite laminates subjected to combined bearing-bypass and shear loading
p 2712 N94-27914
Three-dimensional elastic stress concentration factors: Plain or countersunk hole in a wide plate subjected to tension, bending, or pin loading
[ESDU-93030] p 2845 N94-28143
HOLLOW CATHODES
Theoretical aspects of the agile mirror
[AD-A274890] p 2767 N94-26177
HOLMIUM
The development of Cr, Tm, Ho:YAG lasers for airborne lidar
[AD-A274895] p 2816 N94-26178
HOLOGRAMMETRY
Resonant holographic measurements of laser ablation plume expansion in vacuum and argon gas backgrounds
[DE94-001407] p 2813 N94-27615
HOLOGRAPHIC INTERFEROMETRY
Resonant holographic measurements of laser ablation plume expansion in vacuum and argon gas backgrounds
[DE94-001407] p 2813 N94-27615
HOLOGRAPHY
High definition Raman microscopic imaging
[DE94-003158] p 2716 N94-26781
Advanced technology development multi-color holography
[NASA-CR-193931] p 2812 N94-27229
Resonant holographic measurements of laser ablation plume expansion in vacuum and argon gas backgrounds
[DE94-001407] p 2813 N94-27615
Binary optical elements: Studies in design, manufacture and performance
[ISBN-0-315-60643-6] p 3039 N94-27643
The x ray holographic microscopy using the atomic-force microscope
[DE94-004003] p 2814 N94-27779
HOMING DEVICES
Elastic backscattering lidar for a MSTI satellite
[DE94-002701] p 2816 N94-26126
HOMOGENEITY
Study on solidification of non-homogeneous melting/solidification materials p 2728 N94-25573
Study of the homogeneity of InP wafers
[AD-A273658] p 3055 N94-26194
HOMOGENEOUS TURBULENCE
On prediction of equilibrium states in homogeneous compressible turbulence
[NASA-CR-4570] p 2792 N94-26467
The dynamics of interacting nonlinearities governing long wavelength driftwave turbulence
[DE94-001785] p 2793 N94-26558
HOMOGENIZING
Study on solidification of non-homogeneous melting/solidification materials p 2728 N94-25573
HOMOLOGY
Spaces of algebraic cycles
[PB94-124369] p 2996 N94-26993
HOMOMORPHISMS
Filtering, coding, and compression with Malvar wavelets
[AD-A274055] p 2780 N94-25770
HOMOTOPY THEORY
Winding numbers in homotopy theory from integers to reals
[DE94-601510] p 2992 N94-26367
Research in robust control for hypersonic aircraft
[NASA-CR-195250] p 2678 N94-26821
HORIZONTAL FLIGHT
Investigation of the aerodynamic environment for an advanced lightweight rotor in forward flight. Volume 4: Laser velocimeter wake data, advance ratio of 0.037
[NASA-TM-109040-VOL-4] p 2645 N94-26483
Investigation of the aerodynamic environment for an advanced lightweight rotor in forward flight. Volume 1: Laser velocimeter inflow data, advance ratio of 0.37, thrust coefficient of 0.0081 and hover tip speed of 603 feet/second
[NASA-TM-109040-VOL-1] p 2645 N94-26489
Investigation of the aerodynamic environment for an advanced lightweight rotor in forward flight. Volume 2: Laser velocimeter inflow data, advance ratio of 0.37, thrust coefficient of 0.0064 and hover tip speed of 710 feet/second
[NASA-TM-109040-VOL-2] p 2645 N94-26492
Investigation of the aerodynamic environment for an advanced lightweight rotor in forward flight. Volume 3: Laser velocimeter inflow data, advance ratio of 0.37, thrust coefficient of 0.0064 and hover tip speed of 603 feet/second
[NASA-TM-109040-VOL-3] p 2645 N94-26497
HORIZONTAL TAIL SURFACES
Contribution of body-mounted fins and tailplanes to lateral derivatives due to sideslip at subsonic speeds for general body width to height ratio
[ESDU-93007] p 2648 N94-28057
HORMONES
Thyroid hormone action in cultured human skin fibroblasts: Evaluation using spheroid culture
p 2919 N94-27478
Interaction between endogenous opioid and Cholecystokinin (CCK) in modulating respiratory responses induced by thin-fiber muscular afferents
p 2906 N94-27502
Muscle sympathetic nerve activity in patients with hyper-and hypothyroidism: A microneurographic study
p 2930 N94-27531
Treatment of orthostatic hypotension by nasal administration of vasopressin p 2930 N94-27533
HORN ANTENNAS
Design and evaluation of an electromagnetic beam waveguide for measuring electrical properties of materials
[NASA-TP-3418] p 2769 N94-26611
The application of FD-TD method to antenna radiation patterns
[ISBN-0-315-83893-0] p 2769 N94-26618
HORSEPOWER
E. H. P. estimation of high speed fishing boats by some existing methods p 2764 N94-27978
HORSESHOE VORTICES
Separated flow generated by a vectored jet in a crossflow p 2800 N94-28007
HOT ISOSTATIC PRESSING
The processing of powder metallurgically produced near gamma-titanium aluminide
[ISBN-0-315-84018-8] p 2738 N94-26633
Transparent polycrystalline body with high ultraviolet transmittance, process for making and applications thereof
[CA-PATENT-1325511] p 3066 N94-27276
HOT STARS
TEV emission from close binaries
[DE93-634330] p 3104 N94-26268
HOT WORKING
The processing of powder metallurgically produced near gamma-titanium aluminide
[ISBN-0-315-84018-8] p 2738 N94-26633
Hot deformation behaviour of Si(p)/Al composites and their matrices and an Al-Mg-Si alloy
[ISBN-0-315-84699-2] p 2711 N94-27314
HOT-WIRE ANEMOMETERS
Evaluation of a concentration probe for application in a supersonic flow field
[AD-A273915] p 2643 N94-25592
Effects of free-stream turbulence on a jet in a cross flow p 2805 N94-28036
HOWITZERS
Results from a fracture mechanical serial investigation of breechrings on the M109A3GN howitzer
[FFI-93/8002] p 2837 N94-26233
HTPB PROPELLANTS
Cryogenic size reduction of solid propellant
[AD-A274844] p 2759 N94-26800
HULLS (STRUCTURES)
Evaluation of crack arrest fracture toughness of parent plate, weld metal and heat affected zone of BIS 812 EMA ship plate steel
[AD-A274871] p 2839 N94-26859
HUMAN BEHAVIOR
Man's ability to adapt himself for the seasonal climatic changes: From viewpoint of anticipation and seasonable behavior p 2919 N94-27476
HUMAN BODY
Creation of prototype aircrew protection equipment based on face anthropometry
[AD-A273865] p 2940 N94-25611

A multivariate anthropometric method for crew station design: Abridged
[AD-A274588] p 2941 N94-26984
NCVS, volume 5
[AD-A274975] p 2902 N94-27165
A study of psychological factors affecting an extremely isolated environment p 2927 N94-27517
Interhemispheric phase relationship of alpha waves and cerebral dominance p 2927 N94-27518
Hyperalgesia to cold in patients with Subacute Myelo-Optico-Neuropathy (SMON) p 2928 N94-27521
Effect of prostaglandin E1 on the relationship between skin sympathetic nerve activity and reduction in skin blood flow p 2929 N94-27524
Effect of L-dopa on hemodynamic functions in humans p 2929 N94-27526
Sympathetic nerve activity during dynamic leg exercise p 2929 N94-27527
Analysis on one minute wave in body fluid volume and muscle pumping referred to body parts generating the one minute wave during human active standing p 2929 N94-27528
An attempt of intraneural stimulation by microelectrode inserted in skin sympathetic nerve fascicle p 2930 N94-27529
Muscle sympathetic nerve activity in patients with hyper-and hypothyroidism: A microneurographic study p 2930 N94-27531
Treatment of orthostatic hypotension by nasal administration of vasopressin p 2930 N94-27533
The value of electrical stimulation as an exercise training modality p 2936 N94-28372

HUMAN FACTORS ENGINEERING
Creation of prototype aircrew protection equipment based on face anthropometry
[AD-A273865] p 2940 N94-25611
Variable speed controller p 2943 N94-25678
Design and development of the second generation Mars Habitat p 2943 N94-25693
Pax: A permanent base for human habitation of Mars p 2943 N94-25706
The effect of platform motion on human energy expenditure during walking. An exploratory experiment
[AD-A273760] p 2940 N94-25724
Airborne data link operational evaluation test plan
[AD-A274096] p 2664 N94-25788
Human factors in airway facilities maintenance: Development of a prototype outage assessment inventory
[DOT/FAA/AM-94/5] p 2941 N94-26136
Emerging Human-Computer Interface (HCI) design guidelines for Graphical User Interface (GUI)
[DE94-004293] p 2941 N94-26555
A multivariate anthropometric method for crew station design: Abridged
[AD-A274588] p 2941 N94-26984
Designing for human presence in space: An introduction to environmental control and life support systems
[NASA-RP-1324] p 2942 N94-27437
One from many: Selecting an appropriate human performance model
[DCIEM-93-25] p 2942 N94-27683
Human computer interface guide, revision A
[NASA-TM-109708] p 2955 N94-27769
Extra-Vehicular Activity (EVA) glove evaluation test protocol
[NASA-TM-108442] p 2943 N94-27952
Visit to CERMA: Centre d'Etudes et de Recherches de Medecine Aerospatiale, Centre for Studies and Research in Aviation and Space Medicine, Bretigny sur Orge, France, November 16-18, 1992
[PB94-132990] p 2937 N94-28392

HUMAN PERFORMANCE
Airborne data link operational evaluation test plan
[AD-A274096] p 2664 N94-25788
A test of the theory of reasoned action at the group level of analysis
[AD-A273965] p 2937 N94-25897
Proficiency scaling based on conditional probability functions for attributes
[AD-A273816] p 3002 N94-25962
Effects of methamphetamine on vigilance and tracking during extended wakefulness
[AD-A274896] p 2909 N94-26179
Performance assessment in sustained operations using a computer-based synthetic work task
[AD-A274707] p 2937 N94-26430
Long term learning: Integration of knowledge acquisition and knowledge compilation
[AD-A274775] p 3098 N94-26570
Workload transition: Implications for individual and team performance
[AD-A274538] p 2941 N94-26964
On the development of motor chunks and concurrent processing in a structured continuous keypressing task
[AD-A274153] p 2939 N94-27138
One from many: Selecting an appropriate human performance model
[DCIEM-93-25] p 2942 N94-27683
An analysis of the loads applied to a heavy Space Station rack during translation and rotation tasks
[NASA-TM-104790] p 2697 N94-28183
Muscular activity and its relationship to biomechanics and human performance p 2934 N94-28362

HUMAN REACTIONS
CRC customer versus rater octane number requirement program (1990)
[AD-A273997] p 2758 N94-25901
Performance assessment in sustained operations using a computer-based synthetic work task
[AD-A274707] p 2937 N94-26430
Telescience testbedding for physiological experiments under hypobaric hypoxic conditions p 2913 N94-27449
Telescience testbedding under hypobaric hypoxic conditions: Evaluation by operation ability and recognition ability p 2913 N94-27450
Telescience testbedding for physiological experiments under hypobaric hypoxic conditions: Development and evaluation in CNV measuring p 2913 N94-27451
The electrogastrogram during parabolic flight p 2913 N94-27452
Experimental studies of loudness and annoyance response to sonic booms p 2651 N94-28195
Comparison of methods of predicting community response to impulsive and nonimpulsive noise p 2651 N94-28196
Muscular activity and its relationship to biomechanics and human performance p 2934 N94-28362

HUMAN RELATIONS
A test of the theory of reasoned action at the group level of analysis
[AD-A273965] p 2937 N94-25897

HUMAN RESOURCES
ADP Analysis project for the Human Resources Management Division p 2978 N94-27927

HUMAN-COMPUTER INTERFACE
Interface technical specification of the V.25 bis emulator
[AD-A273754] p 2948 N94-25720
Airborne data link operational evaluation test plan
[AD-A274096] p 2664 N94-25788
Knowledge organization in intelligent tutoring systems for diagnostic problem solving in complex dynamic domains
[AD-A273986] p 2984 N94-25899
EcarHeart2 version 1.0: Programmers documentation
[PB94-124633] p 2909 N94-25909
Integration of interactive interfaces with intelligent tutoring systems: An implementation
[AD-A273869] p 2985 N94-25966
Developing a sophisticated user interface to support domain-oriented application composition and generation systems
[AD-A274080] p 2960 N94-25994
Developing a graphical user interface to support a real-time digital signal processing system
[AD-A274032] p 2960 N94-26018
Design and implementation of a query editor for the Amadeus system
[AD-A274955] p 3097 N94-26300
Emerging Human-Computer Interface (HCI) design guidelines for Graphical User Interface (GUI)
[DE94-004293] p 2941 N94-26555
Interactive control of a parallel simulation from a remote graphics workstation
[AD-A274217] p 2981 N94-27070
An object-oriented database interface for Ada
[AD-A274391] p 2968 N94-27075
The coming technological singularity: How to survive in the post-human era p 2685 N94-27359
Human computer interface guide, revision A
[NASA-TM-109708] p 2955 N94-27769
Visualization techniques to aid in the analysis of multispectral astrophysical data sets
[NASA-CR-195268] p 3105 N94-27932

HUMIDITY
Rewarming methodologies in the field
[AD-A274744] p 2909 N94-26173

HURRICANES
Development and testing of the Coupled Ocean/Atmosphere Mesoscale Prediction System (COAMPS)
[AD-A273925] p 2892 N94-25793
Developing prediction regions for a time series model for hurricane forecasting
[AD-A273777] p 2892 N94-25861

HYBRID PROPULSION
MINOTAUR (Maryland's innovative orbital technologically advanced University rocket) p 2703 N94-25685

HYDRATES
Crystallographyic analyses of clathrate hydrates included in Vostok ice cores p 2885 N94-27969

HYDRAULIC EQUIPMENT
Comparison of dynamic analysis of a Schilling hydraulic manipulator with experimental results
[DE94-004597] p 2827 N94-27780

HYDRAULIC JETS
Effects of slot on rock surface for percussive rock excavation: Water jet assisted percussive rock excavation p 2871 N94-28155

HYDRIDES
Molten salt techniques for reproducible excess heat
[AD-A274935] p 2714 N94-26296

HYDROCARBON COMBUSTION
Laser probes of natural gas ignition chemistry
[PB94-128345] p 2717 N94-27226

HYDROCARBON FUEL PRODUCTION
Report of National Institute for Resources and Environment. No. 5: Study on direct liquefaction of woody biomass
[JTN-94-80551] p 2859 N94-27204

HYDROCARBON FUELS
Theoretical determination of chemical rate constants using novel time-dependent methods
[NASA-CR-195221] p 2714 N94-26205

HYDRODYNAMIC COEFFICIENTS
Influence of impeller shroud forces on turbopump rotor dynamics p 2796 N94-27378

HYDRODYNAMICS
Vortex methods
[DE94-003245] p 2789 N94-25597
Hydrodynamics, acoustics and scaling of traveling bubble cavitation
[AD-A273846] p 2789 N94-25605
A numerical study of quantized vortices in HeII
[ISBN-9-03-860232-4] p 2792 N94-26479
Image potential of a tunnelling electron moving near two different metals
[DE94-603657] p 3069 N94-27819
Calculation methods for steadily loaded central circumferential groove hydrodynamic journal bearings (guide to use of computer program A9304)
[ESDU-93004] p 2830 N94-28073
Calculation methods for steadily loaded axial groove hydrodynamic journal bearings (guide to use of computer program A9305)
[ESDU-93005] p 2830 N94-28074
Calculation methods for steadily loaded axial groove hydrodynamic journal bearings. Low viscosity process fluid lubrication (guide to use of computer program A9306)
[ESDU-93006] p 2830 N94-28075
Forced convection heat transfer in straight tubes. Part 2: Laminar and transitional flow
[ESDU-93018-PT-2] p 2807 N94-28139
An enhanced global spectral model
[PL-TR-92-2011] p 2898 N94-28223

HYDROELECTRICITY
COMPETENCE 2000: Study on training requirements of the Norwegian metallurgical industry
[PB94-124609] p 2741 N94-27328

HYDROFORMING
Polymer-bound rhodium hydroformylation catalysts
[ETN-94-95388] p 2712 N94-25747

HYDROGEN
Hydrogen trapping with Pd coated alloy films p 2723 N94-25551
Hydrogen uptake into silicon from an ECR plasma
[DE94-003771] p 3050 N94-25815
Trapped electrons in solid hydrogen
[DE93-018628] p 3052 N94-25947
Interaction between a high density-low temperature plasma and a frozen hydrogen pellet in a railgun injector
[DE94-000846] p 3041 N94-25949
Application of railgun principle to high-velocity hydrogen pellet injection for magnetic fusion reactor fueling
[DE94-004411] p 3044 N94-26579
An investigation of the effect of surface impurities on the adsorption kinetics of hydrogen chemisorbed onto iron
[NASA-CR-195213] p 2716 N94-26643
Spin asymmetry in resonant electron-hydrogen elastic scattering
[DE94-601813] p 3023 N94-26943
Spectroscopy and dynamics of molecular and ionic impurities embedded in solid hydrogen
[AD-A274149] p 3064 N94-27095
Numerical simulation of the reignition of detonation by reflected shocks
[AD-A274755] p 2795 N94-27252
Hydrogen physics
[DE94-701317] p 2719 N94-27822

HYDROGEN ATOMS
Study on alloy films for hydrogen separation p 2726 N94-25565

Merged-beam studies of electron-recombination and excitation of atomic and molecular hydrogen ions
[ETN-94-95339] p 3019 N94-26478

Shine through measurements with hydrogen beam in JT-60
[DE94-701113] p 3047 N94-27699

The three-dimensional hydrogen atom in crossed magnetic and electric fields
[DE94-606301] p 3029 N94-27847

HYDROGEN BONDS

Molecular surface electrostatic potentials in the analysis of non-hydrogen-bonding noncovalent interactions
[AD-A274612] p 3022 N94-26894

Hydrogen physics
[DE94-701317] p 2719 N94-27822

HYDROGEN EMBRITTLEMENT

Study on performance evaluation of pressure vessel steel in corrosion environments with sulfide
p 2730 N94-25582

HYDROGEN FUELS

Proceedings of the High Energy Density Matter (HEDM) Contractor's Conference
[AD-A274452] p 3033 N94-27083

HYDROGEN IONS

Spectroscopy and dynamics of molecular and ionic impurities embedded in solid hydrogen
[AD-A274149] p 3064 N94-27095

High gas-efficiency hydrogen negative ion sources
[PB93-232163] p 3025 N94-27348

Double excitation of He and H(-) by fast proton and anti-proton impact
[DE94-004581] p 3026 N94-27620

HYDROGEN ISOTOPES

Muon transfer rates in collisions of hydrogen isotope mesic atoms on bare nuclei: Multichannel adiabatic approach
[DE94-606752] p 3030 N94-27861

HYDROGEN MASERS

Spin-polarized atomic hydrogen: Devices and phenomena
[ETN-94-95342] p 3016 N94-26002

HYDROGEN OXYGEN ENGINES

Gaseous hydrogen/oxygen injector performance characterization
[NASA-CR-194464] p 2701 N94-26208

Test results of the RS-44 integrated component evaluator liquid oxygen/hydrogen rocket engine
[NASA-CR-194443] p 2701 N94-26231

Orbit transfer rocket engine technology program
[NASA-CR-189229] p 2702 N94-26542

Orbital transfer rocket engine technology 7.5K-LB thrust rocket engine preliminary design
[NASA-CR-190754] p 2703 N94-27213

Lunar Transportation Facilities and Operations Study, option 1
[NASA-CR-195700] p 3109 N94-27982

HYDROGEN PLASMA

Hydrogen uptake into silicon from an ECR plasma
[DE94-003771] p 3050 N94-25815

HYDROGENATION

Deposition of a-SiC:H using organosilanes in an argon/hydrogen plasma
[DE94-004428] p 2751 N94-26580

The Science Reports of the Research Institutes, Tohoku University. Series A: Physics, Chemistry, and Metallurgy. Volume 38, No. 1: Amorphous Materials 14
[JTN-94-80610] p 2744 N94-28158

Formation and crystallization of hydrogen-induced amorphous Ti3InH(4.5) alloy p 2745 N94-28163

CO2 methanation catalysts prepared from amorphous Ni-valve metal alloys containing platinum group elements
p 2745 N94-28166

HYDROGRAPHY

Hydrographic and Acoustic Doppler Current Profiler (ADCP) data from the ONR eastern boundary current accelerated research initiative, 9-16 June 1992
[AD-A274115] p 2898 N94-26076

Compilation of corrections for postprocessing of laser bathymetry data
[PB94-123668] p 2900 N94-27156

Scanview: A grafical program for analysis of laserbathymetry data
[PB94-124443] p 2900 N94-27208

HYDROLOGICAL CYCLE

Meeting of the Eighth Session of the Scientific Advisory Committee of the World Climate Impact Assessment and Response Strategies Programme
[DE93-633954] p 2866 N94-26163

Global change research related to the Earth's energy and hydrologic cycle
[NASA-CR-195270] p 2869 N94-27430

Cooperative research projects on satellite remote sensing for the hydrological subjects
p 2853 N94-28270

Research activities on the meteorology over the Asia-Pacific region p 2853 N94-28271

HYDROLOGY

Sensitivity of climate models: Comparison of simulated and observed patterns for past climates
[DE93-019934] p 2865 N94-25789

Active layer dynamics and arctic hydrology and meteorology
[DE94-001724] p 2892 N94-25951

HYDROSTATIC PRESSURE

Fluid dynamic linear accelerometer
[AD-D016042] p 2678 N94-27112

HYDROSTATICS

A hydrostatic stress-dependent anisotropic model of viscoplasticity
[NASA-TM-106525] p 2711 N94-27640

An enhanced global spectral model
[PL-TR-92-2011] p 2898 N94-28223

HYDROXYL EMISSION

Photochemical processes and the atmospheric airglow emissions of OH and Na in the mesospheric region
[INPE-5380-PUD/050] p 2882 N94-27334

HYPERBOLIC DIFFERENTIAL EQUATIONS

On the oscillation of a class of hyperbolic equations of neutral type
[DE93-616815] p 2990 N94-25829

Oscillatory behaviour of solutions of coupled hyperbolic differential equations of neutral type
[DE93-616816] p 2990 N94-25830

Analytical solution of Mori's equation with secant hyperbolic memory
[DE94-601541] p 3006 N94-26368

HYPERBOLIC FUNCTIONS

Arbitrary-order high resolution schemes for model hyperbolic conservation laws
[CRANFIELD-AERO-9209] p 3005 N94-25823

HYPERCUBE MULTIPROCESSORS

Object-oriented design and implementation of a parallel Ada simulation system
[AD-A274119] p 2979 N94-25906

Fast parallel algorithms for short-range molecular dynamics
[DE93-018519] p 3016 N94-26033

Simulation modeling for long duration spacecraft control systems p 2684 N94-26288

An efficient communication scheme for solving the S(sub n) equations on message-passing multiprocessors
[DE94-000378] p 2769 N94-26482

Partitioning structural VHDL circuits for parallel execution on hypercubes
[AD-A274390] p 2785 N94-26830

Static task allocation for parallel processing systems during software development
[AD-A274204] p 2981 N94-27100

HYPERFINE STRUCTURE

Study of the hyperfine magnetic field at Ta-181 site in the Heusler Co2ScSn, Co2ScGa, and Co2HfSn alloys
[DE94-603989] p 3067 N94-27623

Hyperfine structure of positronium energy levels in a crystal
[DE94-603898] p 3068 N94-27729

HYPERGEOMETRIC FUNCTIONS

Asymptotics for Kummer functions, Bose plasmas, and related special functions
[DE94-601853] p 3007 N94-26928

HYPERNUCLEI

Proceedings of the workshop on (pi), K, (eta)-nucleon interactions
[DE94-701314] p 3027 N94-27733

HYPERPLANES

Enumeration of n-fold tangent hyperplanes to a surface
[DE94-601544] p 2993 N94-26412

HYPERSONIC AIRCRAFT

The design of four hypersonic reconnaissance aircraft
p 2671 N94-25716

Design of a refueling tanker delivering liquid hydrogen
p 2671 N94-25717

Research in robust control for hypersonic aircraft
[NASA-CR-195250] p 2678 N94-26821

Numerical investigation of thrust vectoring by injection of secondary air into nozzle flows p 2801 N94-28013

HYPERSONIC BOUNDARY LAYER

Experimental study on the shock wave interaction with a hypersonic boundary layer near a convex corner
p 2654 N94-28328

HYPERSONIC FLIGHT

Experiments on interaction force of jets in hypervelocity cross-flow in a shock tunnel p 2659 N94-28022

Computation of static pressure downstream of a normal shock for hypersonic flight (ambient temperature known)
[ESDU-93020] p 2649 N94-28091

HYPERSONIC FLOW

Chemical and vibrational nonequilibrium viscous flows: Modelling, internal and external flow applications
[ESA-TT-1274] p 2791 N94-26316

The measurement of disturbance levels in the Langley Research Center 20-inch Mach 6 tunnel
[NASA-CR-4571] p 2646 N94-26548

Direct simulation Monte-Carlo of near continuum hypersonic flow with chemical reactions
[DLR-FB-93-01] p 2797 N94-27588

Flowfield dynamics in blunt fin-induced shock wave/turbulent boundary layer interactions
[NASA-CR-195170] p 2798 N94-27302

Aerodynamic heating in hypersonic flows
p 2658 N94-27919

Computational and Experimental Assessment of Jets in Cross Flow
[AGARD-CP-534] p 2799 N94-28003

Control jets in interaction with hypersonic rarefied flow
p 2698 N94-28020

Comparison of the interactions of two and three dimensional transverse jets with a hypersonic free stream p 2659 N94-28021

HYPERSONIC INLETS

Experimental study on the shock wave interaction with a hypersonic boundary layer near a convex corner
p 2654 N94-28328

HYPERSONIC SHOCK

The Lightcraft project: Flight technology for a hypersonic mass transit system p 2670 N94-25695

Computation of static pressure downstream of a normal shock for hypersonic flight (ambient temperature known)
[ESDU-93020] p 2649 N94-28091

HYPERSONIC VEHICLES

A parametric sensitivity study for single-stage-to-orbit hypersonic vehicles using trajectory optimization
[NASA-CR-195703] p 2697 N94-27789

Multidisciplinary aeroelastic analysis of a generic hypersonic vehicle
[NASA-TM-4544] p 2691 N94-27868

Aerodynamic heating in hypersonic flows
p 2658 N94-27919

HYPERSONIC WIND TUNNELS

Aerodynamic heating in hypersonic flows
p 2658 N94-27919

HYPERSONICS

The Lightcraft project: Flight technology for a hypersonic mass transit system p 2670 N94-25695

Modelling of ionisation reactions and of the resulting electric fields in one-dimensional hypersonic shock waves with the direct simulation Monte Carlo method
[IC-AERO-92-01] p 2644 N94-26248

HYPERSPHERES

Static task allocation for parallel processing systems during software development
[AD-A274204] p 2981 N94-27100

HYPERTENSION

Monograph of the aviation epidemiology data register for calendar year 1988
[AD-A274589] p 2911 N94-26985

Muscle sympathetic nerve activity in humans
p 2932 N94-27538

HYPERVELOCITY FLOW

A numerical study of mixing and combustion in hypervelocity flows through a scramjet combustor model
p 2808 N94-27911

Experiments on interaction force of jets in hypervelocity cross-flow in a shock tunnel p 2659 N94-28022

HYPERVELOCITY IMPACT

Physics of debris clouds from hypervelocity impacts
[NASA-CR-193932] p 2696 N94-26791

Consequences of impacts of small asteroids and comets with Earth p 2889 N94-28301

A general theory of impacts and mass extinctions, and the consequences of large-body impact on the Earth
p 2891 N94-28310

Were all extinction events caused by impacts?
p 2891 N94-28311

HYPERVELOCITY LAUNCHERS

Energy and technology review, July 1993
[DE94-004219] p 3118 N94-27566

HYPERVELOCITY PROJECTILES

Breakwire technique for hypervelocity measurement
[AD-A274779] p 2809 N94-26358

HYPOTENSION

Effect of L-dopa on hemodynamic functions in humans p 2929 N94-27526

Treatment of orthostatic hypotension by nasal administration of vasopressin p 2930 N94-27533

Does training-induced orthostatic hypotension result from reduced carotid baroreflex responsiveness?
p 2935 N94-28366

HYPOTHERMIA

Rewarming methodologies in the field
[AD-A274744] p 2909 N94-26173

HYPOTHESES

Trace-based compositional proof theory for fault tolerant distributed systems
[PB94-126737] p 2966 N94-26971

Thunderstorm Hypothesis Reasoner
[NASA-CR-195714] p 2897 N94-27884
Science observed: The mass-extinction debates
p 2888 N94-28300
An evaluation of criteria that may be used to identify species surviving a mass extinction
p 2889 N94-28304

HYPOTONIA
Effect of L-dopa on hemodynamic functions in humans p 2929 N94-27526

HYPOXIA
The Reports of Aeromedical Laboratory, volume 33, number 4
[JTN-94-80586] p 2933 N94-27942
Symptoms of hypoxia at simulated altitude of 25,000 feet p 2933 N94-27945

HYSTERESIS
Nonlinear hysteresis in an endochronic solid
[AD-A274594] p 2880 N94-26855
Ferrite phase shifters using stress insensitive materials
[AD-A274639] p 2708 N94-26895

I

ICE
Methane emissions from natural wetlands
[DE93-040796] p 2865 N94-25790
Sound, speed, reflectivity, absorption, and thermal diffusivity measurements in Arctic ice in 1990
[AD-A274326] p 2899 N94-26886
Reanalysis of Mariner 9 UV Spectrometer Data for Ozone, Cloud, and Dust Abundances, and Their Interaction Over Climate Timescales
[NASA-CR-195244] p 3107 N94-27885
Why is the north polar cap on Mars different than the south polar cap? p 3107 N94-27889
A laboratory test on construction of ice domes and their load-carrying capacity p 2884 N94-27966
Transient model applications. 3: Transient engine simulation and analysis of an ice ingestion test
p 2829 N94-28050

ICE CLOUDS
Cloud liquid water content measurement tests using dual-wavelength radar
[PB94-125960] p 2896 N94-26959

ICE FLOES
Crystallographyic analyses of clathrate hydrates included in Vostok ice cores p 2885 N94-27969

ICE FORMATION
Leadex environmental phenomena and effects observed by DMSP, NOAA, and ERS-1 satellites
[AD-A274596] p 2868 N94-26888
Why is the north polar cap on Mars different than the south polar cap? p 3107 N94-27889
Debris/ice/TPS assessment and integrated photographic analysis for Shuttle mission STS-60
[NASA-TM-109193] p 2692 N94-27956
Development of a method for predicting snowfall intensity and compacted snow on roads
p 2853 N94-27990
Program for calculation of maximum lift coefficient of plain aerofoils and wings at subsonic speeds
[ESDU-93015] p 2649 N94-28076
Ice accretion on aircraft wings p 2657 N94-28345
Studies in ice mechanics
[PB94-133055] p 2900 N94-28393

ICE REPORTING
An evaluation of an airborne remote sensing system used to determine ice thickness and geometry of a first year sea ice ridge located in the Beaufort Sea
[ISBN-0-315-84383-7] p 2849 N94-26667
The Hough transform algorithm for sea ice lead analysis: An evaluation
[AD-A274535] p 2899 N94-26853

IGNITERS
Effects of repeating resistance testing on firing ability of igniter EP360-3
[AD-A274814] p 2759 N94-26486
New rubber qualification for the igniter adapter
[NASA-CR-193936] p 2752 N94-26708
Hydrogen-oxygen torch ignitor
[NASA-TM-106493] p 2691 N94-27424

IGNITION
Microgravity ignition experiment p 2761 N94-25707
On the thermal ignition with variable pre-exponential factor
[DE93-616009] p 2713 N94-25913
An apparatus for measurement of ignition and burning characteristics of metallic particles
[AD-A274815] p 2716 N94-26487
Numerical simulation of the reignition of detonation by reflected shocks
[AD-A274755] p 2795 N94-27252
Hydrogen-oxygen torch ignitor
[NASA-TM-106493] p 2691 N94-27424
The addition of molecular oxygen to hydroperoxy-propyl radicals
[DE94-003662] p 2760 N94-27725

IGNITION SYSTEMS
Optimising BMW four-cylinder two-valve engines
[PB94-125101] p 2824 N94-27254

ILLUMINATING
Illumination in diverse codimensions
[NASA-CR-191596] p 2971 N94-27572

IMAGE ANALYSIS
Study on knowledge extraction and systematization for material design p 2727 N94-25568
Detecting actin fibers in cell images using minimal spanning trees
[AD-A273914] p 2984 N94-25591
SHIVA: A unix-based, menu-driven, color image processing software package
[AD-A274071] p 2957 N94-25646
Zernike moments and rotation invariant object recognition. A neural network oriented case study
[AD-A273749] p 2767 N94-26011
Image segmentation by a combination of edge detection and region growing
[ETN-94-95032] p 2960 N94-26106
Capture and location of blobs in digital images
[ISBN-0-315-84382-9] p 3036 N94-26666
Proceedings of the Fourth Euroseminar on Microscopy Applied to Building Materials
[PB94-119807] p 2839 N94-26754
Interacting cortical filters for object recognition
[PB94-125374] p 2938 N94-26873
Woody biomass density in the Tendelti area of the central Sudan p 2850 N94-27185
Motion analysis from a sequence of range images
[ISBN-0-315-84684-4] p 2969 N94-27311
Robust estimation for range image segmentation and fitting
[ISBN-0-315-84686-0] p 2998 N94-27312
Estimation of image motion in scenes containing multiple moving objects
[ISBN-0-315-85208-9] p 2969 N94-27346
SPECTRUM analysis of multispectral imagery in conjunction with wavelet/KLT data compression
[DE94-003961] p 2851 N94-27727
Locating tie-points on a grid p 2978 N94-27906
Quick-look system of auroral absorption images by imaging riometer p 2884 N94-27968
The interaction region associated with twin jets and a normal crossflow p 2800 N94-28009
An image assessment study of image acceptability of the Galileo low gain antenna mission
p 2945 N94-28252
Image compression software for the SOHO LASCO and EIT experiments p 2945 N94-28253

IMAGE CLASSIFICATION
Mapping closed tropical forest cover in West Africa using NOAA/AVHRR-LAC data p 2850 N94-27184
Vector quantizer designs for joint compression and terrain categorization of multispectral imagery
p 2947 N94-28262

IMAGE CORRELATORS
Solid estimation feature based correlation method for measuring control points required for correcting satellite images
[VTT-JULK-772] p 2848 N94-26253

IMAGE ENHANCEMENT
Human visual system enhancement of reconstructed satellite images
[AD-A273867] p 2693 N94-25595
Improved quality of reconstructed images through sifting of data in statistical image reconstruction
[AD-A273884] p 3034 N94-25730
Auroral Tomography Workshop Proceedings
[PB94-123718] p 2881 N94-27040
An image assessment study of image acceptability of the Galileo low gain antenna mission
p 2945 N94-28252

IMAGE FILTERS
Non-adaptive robust filters for speckle noise reduction
[INPE-5519-PRE/1794] p 2776 N94-27335

IMAGE PROCESSING
Study on knowledge extraction and systematization for material design p 2727 N94-25568
Calculation of a 3-D pose of a known object in a single perspective view
[VTT-PUBS-122] p 2957 N94-25642
SHIVA: A unix-based, menu-driven, color image processing software package
[AD-A274071] p 2957 N94-25646
An optimal constrained linear inverse method for magnetic source imaging
[DE94-004014] p 2957 N94-25663
Improved quality of reconstructed images through sifting of data in statistical image reconstruction
[AD-A273884] p 3034 N94-25730
Objective image quality metrics: Applications for partially compensated images of space objects
[AD-A273837] p 2847 N94-25741
Color image segmentation
[AD-A274027] p 2984 N94-25759
Image quality and the display modulation transfer function: Experimental findings
[AD-A274061] p 2679 N94-25773
Mitsubishi 3-5 micrometers IR imager for machine-vision/ATA applications
[AD-A273812] p 3034 N94-25940
Zernike moments and rotation invariant object recognition. A neural network oriented case study
[AD-A273749] p 2767 N94-26011
Surface physics with cold and thermal neutron reflectometry
[DE94-001447] p 2733 N94-26070
Image segmentation by a combination of edge detection and region growing
[ETN-94-95032] p 2960 N94-26106
Solid estimation feature based correlation method for measuring control points required for correcting satellite images
[VTT-JULK-772] p 2848 N94-26253
Color head down display program
[AD-A274807] p 2672 N94-26340
Extracting complete 3-dimensional boundary representation from multiple range images
[ISBN-0-315-83776-4] p 2963 N94-26615
Application of Markov random field theory to image coding and motion estimation
[ISBN-0-315-83435-8] p 2964 N94-26632
Probabilistic methods for image generation and encoding
[AD-A274294] p 2964 N94-26682
On-board software for the JET-X telescope on the Spectrum-X mission p 2951 N94-26727
Automated fabric inspection system
[AD-A274522] p 2835 N94-26833
The Hough transform algorithm for sea ice lead analysis: An evaluation
[AD-A274535] p 2899 N94-26853
The morphological processing of binary images
[AD-A274310] p 2996 N94-26972
Characterization and calibration of the Agema 880+ imaging radiometer
[AD-A274417] p 3036 N94-26981
Orientation competition in cortical filters
[PB94-125366] p 2939 N94-27001
High-speed, high-density, coherent time-domain optical memory
[AD-A274249] p 3037 N94-27010
Building 3-D models from unregistered range images
[AD-A274126] p 2986 N94-27032
Top down influences on bottom-up processing
[AD-A274220] p 2939 N94-27072
Multiple model adaptive control of a large flexible space structure with purposeful dither for enhanced identifiability
[AD-A274132] p 2987 N94-27122
CCD-Camera images of BEST-TWO and processing results
[AD-A274140] p 2811 N94-27134
Multivariate spectral analysis to extract materials from multispectral data
[AD-A274142] p 2709 N94-27135
Operator theoretic methods in the control of distributed and nonlinear systems
[AD-A274160] p 2988 N94-27139
Compilation of corrections for postprocessing of laser bathymetry data
[PB94-123668] p 2900 N94-27156
Translation and rotation invariant pattern recognition
[PB94-123676] p 2968 N94-27157
Image quality analysis of compressed synthetic aperture radar imagery
[AD-A273399] p 2774 N94-27170
CMT-Si
[PB94-123619] p 2812 N94-27216
Estimation of image motion in scenes containing multiple moving objects
[ISBN-0-315-85208-9] p 2969 N94-27346
Thirteen ways to say nothing with scientific visualization
[NASA-CR-195280] p 2970 N94-27542
On line quantification of crystal surfaces by stereo imaging
[NASA-CR-195277] p 3066 N94-27561
Development of Calcomp compatible interface library 'piflib' on X Window System
[DE94-701190] p 2973 N94-27702

SPECTRUM analysis of multispectral imagery in conjunction with wavelet/KLT data compression
[DE94-003961] p 2851 N94-27727

Multi-sensor data fusion in a distributed environment: Architectural solutions
[NLR-TP-92243-U] p 2989 N94-27800

A hybrid formalism for representation and interpretation of image knowledge
[INPE-5485-PRE/1784] p 2989 N94-27833

Multispectral and textural classifications of a SPOT HRV-1 image, region of Sherbrooke, Quebec, Canada
[ISBN-0-315-84978-9] p 2851 N94-27863

Development of imaging riometers
p 2884 N94-27967

Quick-look system of auroral absorption images by imaging riometer p 2884 N94-27968

Optical pattern recognition system utilizing resonator array
[AD-D016071] p 3040 N94-28224

The 1994 Space and Earth Science Data Compression Workshop
[NASA-CP-3255] p 2945 N94-28251

An image assessment study of image acceptability of the Galileo low gain antenna mission
p 2945 N94-28252

Image compression software for the SOHO LASCO and EIT experiments p 2945 N94-28253

Performance considerations for the application of the lossless browse and residual model
p 2946 N94-28256

Some practical aspects of lossless and nearly-lossless compression of AVHRR imagery p 2947 N94-28264

IMAGE RECONSTRUCTION

Human visual system enhancement of reconstructed satellite images
[AD-A273867] p 2693 N94-25595

Improved quality of reconstructed images through sifting of data in statistical image reconstruction
[AD-A273884] p 3034 N94-25730

Objective image quality metrics: Applications for partially compensated images of space objects
[AD-A273837] p 2847 N94-25741

Extracting complete 3-dimensional boundary representation from multiple range images
[ISBN-0-315-83776-4] p 2963 N94-26615

Advanced technology development multi-color holography
[NASA-CR-193931] p 2812 N94-27229

Properties of the near-axis bispectrum applied to high-resolution astronomical imaging
[ISBN-0-315-85247-X] p 3103 N94-27302

Robust estimation for range image segmentation and fitting
[ISBN-0-315-84686-0] p 2998 N94-27312

A theory of multi-scale, curvature and torsion based shape representation for planar and space curves
[ISBN-0-315-63894-X] p 2974 N94-27805

Fractals and their applications to remote sensing and digital mapping
[ISBN-0-315-59469-1] p 2852 N94-27870

Visual surface perception: Surface reconstruction from shading and stereo
[ISBN-0-315-60974-5] p 2975 N94-27872

Image quality measures and their performance
p 2946 N94-28257

IMAGE RESOLUTION

Objective image quality metrics: Applications for partially compensated images of space objects
[AD-A273837] p 2847 N94-25741

Image quality and the display modulation transfer function: Experimental findings
[AD-A274061] p 2679 N94-25773

Encoding approaches for data link transmission of weather graphics
[AD-A274497] p 2772 N94-26963

Method of correcting rotational motion error in SAR and ISAR imagery
[AD-D016033] p 2773 N94-27146

Image quality analysis of compressed synthetic aperture radar imagery
[AD-A273399] p 2774 N94-27170

Image quality measures and their performance
p 2946 N94-28257

Perceptual compression of magnitude-detected synthetic aperture radar imagery p 2946 N94-28260

IMAGE ROTATION

Three dimensional object recognition using a complex autoregressive model
[AD-A274388] p 2995 N94-26829

IMAGES

Matrix near rings and pseudo distributivity
[DE94-601505] p 2992 N94-26366

IMAGING SPECTROMETERS

Mapping coastal habitats using an imaging spectrometer
[ISBN-0-315-84362-4] p 2848 N94-26664

Planetary Instrument Definition and Development Program (PIDDP). Instrument for future planetary flight missions: A visible-infrared imaging spectrometer for planetary missions
[NASA-CR-195254] p 3106 N94-27409

MODIS airborne simulator visible and near-infrared calibration, 1992 ASTEX field experiment. Calibration version: ASTEX King 1.0
[NASA-TM-104599] p 2897 N94-28179

MODIS airborne simulator visible and near-infrared calibration, 1991 FIRE-Cirrus field experiment. Calibration version: FIRE King 1.1
[NASA-TM-104600] p 2897 N94-28182

IMAGING TECHNIQUES

Detecting actin fibers in cell images using minimal spanning trees
[AD-A273914] p 2984 N94-25591

Feasibility study of a multiaperture telescope for deep-space Earth surveillance
[AD-A273903] p 3102 N94-25658

Detection geometry and reconstruction error in magnetic source imaging
[DE94-004012] p 2809 N94-25662

An optimal constrained linear inverse method for magnetic source imaging
[DE94-004014] p 2957 N94-25663

Color image segmentation
[AD-A274027] p 2984 N94-25759

Object imaging accomplished with an integrated circuit robotic tactile sensor incorporating a piezoelectric polyvinylidene fluoride thin film
[AD-A274038] p 2780 N94-25845

Imaging with x ray lasers
[DE94-002844] p 2816 N94-26020

Surface physics with cold and thermal neutron reflectometry
[DE94-001447] p 2733 N94-26070

Image segmentation by a combination of edge detection and region growing
[ETN-94-95032] p 2960 N94-26106

Study of precipitation and recrystallization in Al alloy 2519 by backscattered electron imaging methods
[AD-A274919] p 2736 N94-26533

High resolution measurements of mixing and reaction processes in turbulent flows
[AD-A274970] p 2793 N94-26534

Focal plane arrays in advanced thermal images
[AD-B174292] p 3036 N94-26648

Response of an airborne synthetic aperture radar to sea ice in the marginal ice zone
[ISBN-0-315-84243-1] p 2849 N94-26668

High definition Raman microscopic imaging
[DE94-003158] p 2716 N94-26781

An optimal constrained linear inverse method for magnetic source imaging
[DE94-002264] p 2996 N94-26936

Characterization and calibration of the Agema 880+ imaging radiometer
[AD-A274417] p 3036 N94-26981

Auroral Tomography Workshop Proceedings
[PB94-123718] p 2881 N94-27040

Combining shape and color information for 3D object recognition
[AD-A274123] p 2967 N94-27064

CCD-Camera images of BEST-TWO and processing results
[AD-A274140] p 2811 N94-27134

Multivariate spectral analysis to extract materials from multispectral data
[AD-A274142] p 2709 N94-27135

VENI, video, VICI: The merging of computer and video technologies p 2686 N94-27362

On line quantification of crystal surfaces by stereo imaging
[NASA-CR-195277] p 3066 N94-27561

RIAD visual imaging branch assessment
p 2815 N94-27895

Locating tie-points on a grid p 2978 N94-27906

Development of imaging riometers
p 2884 N94-27967

Quick-look system of auroral absorption images by imaging riometer p 2884 N94-27968

An image assessment study of image acceptability of the Galileo low gain antenna mission
p 2945 N94-28252

Image compression software for the SOHO LASCO and EIT experiments p 2945 N94-28253

Wavelet compression techniques for hyperspectral data p 2947 N94-28263

Infrared imaging for transition detection in a transonic blowdown wind tunnel p 2653 N94-28325

IMIDES

Application of the Positron Annihilation Technique to the study of vapor absorption process in polyethylene (LDPE) and in imide polymer (6FDA-TMPD PI)
[DE94-602737] p 2720 N94-27998

IMPACT DAMAGE

Effect of impact face damage on strength of sandwich composites
[VTT-PUBS-128] p 2704 N94-25734

Experimental study of the angled crack in GLARE 3
[PB94-126554] p 2669 N94-26954

Impact tests on fibre metal laminates under a tensile load
[PB94-126570] p 2710 N94-27201

The development of stress intensity factors
[DRA-TR-93057] p 2845 N94-27954

IMPACT LOADS

Effect of impact face damage on strength of sandwich composites
[VTT-PUBS-128] p 2704 N94-25734

Piezoelectric measurements on impact loaded PZT ceramics
[NPL-DMM(A)-88] p 2752 N94-26652

A constitutive model for layered wire mesh and aramid cloth fabric
[DE94-003275] p 2708 N94-26796

Response of structures to impact loads using elastic and plastic analysis
[ISBN-0-315-84647-X] p 2842 N94-27309

Axial focusing of impact energy in the Earth's interior: Proof-of-principle tests of a new hypothesis
p 2888 N94-28296

IMPACT PREDICTION

A survey of uncontrolled satellite reentry and impact prediction
[AD-A274903] p 2695 N94-26750

An automatic contact algorithm in DYNA3D for impact problems
[DE94-002856] p 2965 N94-26862

IMPACT RESISTANCE

Computational studies of energetic organic molecules
[AD-A274726] p 3018 N94-26172

IMPACT STRENGTH

Effect of impact face damage on strength of sandwich composites
[VTT-PUBS-128] p 2704 N94-25734

High impact strength poly(lactide) tough biodegradable materials
[ETN-94-95389] p 2747 N94-25748

Design study of fiber-composite penetrator cases
[DE94-003203] p 2707 N94-26099

IMPACT TESTING MACHINES

The development of a horizontal impact sled facility and subsequent crashworthiness experiments
[NIAR-93-15] p 2680 N94-26200

IMPACT TESTS

Design study of fiber-composite penetrator cases
[DE94-003203] p 2707 N94-26099

The development of a horizontal impact sled facility and subsequent crashworthiness experiments
[NIAR-93-15] p 2680 N94-26200

Users manual for CATNIP: A Computer Analysis Tool for Normal Impact Penetration
[DE94-003671] p 2962 N94-26371

Piezoelectric measurements on impact loaded PZT ceramics
[NPL-DMM(A)-88] p 2752 N94-26652

A constitutive model for layered wire mesh and aramid cloth fabric
[DE94-003275] p 2708 N94-26796

Impact tests on fibre metal laminates under a tensile load
[PB94-126570] p 2710 N94-27201

Status report for the development of the Antarctic penetrator: 1990-year program p 2885 N94-27973

IMPEDANCE MEASUREMENT

Fundamental study on monitoring technology on local surface damages p 2724 N94-25555

IMPELLERS

Orbital transfer vehicle engine technology high velocity ratio diffusing crossover
[NASA-CR-194447] p 2703 N94-27212

Influence of impeller shroud forces on turbopump rotor dynamics p 2796 N94-27378

IMPLANTATION

The AFIT multielectrode array for neural recording and simulation: Design, testing, and encapsulation
[AD-A274086] p 2909 N94-25943

Ion implantation of diamond: Damage, doping, and lift-off
[DE94-001133] p 3054 N94-26137

IMPLANTED ELECTRODES (BIOLOGY)

An attempt of intraneural stimulation by microelectrode inserted in skin sympathetic nerve fascicle
p 2930 N94-27529

IMPULSES

Impulsive control and stabilization
[ISBN-0-315-84563-5] p 2988 N94-27271

IMPURITIES

Study on development of chemical measurement method utilizing plasmas p 2728 N94-25576

Study on analyzing method establishment for metallic material development p 2729 N94-25578

Binding of copper and nickel to cavities in silicon formed by helium ion implantation
[DE94-003769] p 3050 N94-25814

An atom probe investigation of the influence of trace impurities on the mechanical behavior of NiAl
[DE94-002797] p 2734 N94-26272

An investigation of the effect of surface impurities on the adsorption kinetics of hydrogen chemisorbed onto iron
[NASA-CR-195213] p 2716 N94-26643

Effect of impurity correlation on the density of states in slightly compensated heavily doped semiconductors
[DE94-602539] p 3061 N94-26879

IN SITU MEASUREMENT

Development of a multi-sensor in situ fiber optic fluorometer
[DE94-003399] p 3035 N94-26100

Automated in-situ inspection systems for underground storage tanks
[AD-A274644] p 2764 N94-27144

Neutron-neutron scattering: Possibility of in-beam experiment
[DE94-606459] p 3027 N94-27682

IN-FLIGHT MONITORING

Balloon-borne measurements of the SN1987A hard x ray continuum p 3115 N94-26689

Effects of expected-value information and display format on recognition of aircraft subsystem abnormalities
[NASA-TP-3395] p 2673 N94-27882

INCIDENCE

Aluminum-ion sputtering from Al surfaces with very-low-energy ions
[REPT-A-2668] p 2733 N94-26073

Discrete vacuum ultra violet reflective interference filter
[AD-D016059] p 2756 N94-27675

INCLUSIONS

The study of single-pass GMA welds with different cover gas compositions on HSLA-100 steel
[AD-A274857] p 2822 N94-26174

Electromagnetic modeling of bi-isotropic media
[PB94-132909] p 2778 N94-28382

Dielectric polarizability of sphere with arbitrary anisotropy
[PB94-133113] p 2779 N94-28397

INCOMPRESSIBLE BOUNDARY LAYER

Circular cylinder in axial flow
[ISBN-0-315-59114-5] p 2798 N94-27873

Unified approach for direct and inverse boundary layer prediction using cubic spline collocation
p 2653 N94-28326

INCOMPRESSIBLE FLOW

Vortex methods
[DE94-003245] p 2789 N94-25597

The high Reynolds number flow through an axial-flow pump
[AD-A273844] p 2789 N94-25604

Riemann solvers for solving the incompressible Navier-Stokes equations using the artificial compressibility method
[CRANFIELD-AERO-9208] p 2790 N94-25778

Non-isoenergetic inviscid slot flow
p 2655 N94-28333

Calculation of unsteady incompressible inviscid flow about wings and bodies using CANAERO-T panel model
p 2655 N94-28334

Recent advances in the spectral element method
p 2657 N94-28348

INCOMPRESSIBLE FLUIDS

Bulk-Flow Analysis, part A
[NASA-CR-193911-PT-A] p 2796 N94-27377

INCONEL (TRADEMARK)

Structural analysis of a frangible nut used on the NASA Space Shuttle
[DE94-003672] p 2821 N94-25811

Analysis of the effect on growth kinetics of gamma prima phase in Inconel 713C alloys
[DE93-633763] p 2735 N94-26294

INDENTATION

Nanoscale plasticity in silica glass
[DE94-004212] p 2751 N94-26554

INDEXES (DOCUMENTATION)

Index to BROND-2, CENDL-2, ENDF/B-6, JEF-2, JENDL-3
[DE93-634500] p 3016 N94-26034

A new materials data compilation can help in actinide phase-diagram research
[DE94-000797] p 3058 N94-26514

Aviation Epidemiology Data Register: Indexing the AEDR document laser optic archive
[AD-A274185] p 2911 N94-27097

NASA SBIR abstracts of 1992, phase 1 projects
[NASA-TM-109694] p 3094 N94-27772

Aeronautical engineering: A continuing bibliography with indexes (supplement 301)
[NASA-SP-7037(301)] p 2643 N94-28203

Aerospace medicine and biology: A cumulative index to a continuing bibliography (supplement 384)
[NASA-SP-7011(384)] p 2934 N94-28219

INDIA

Indian activities on the core programme IGAP and proposals for network activities p 2874 N94-28284

INDIAN OCEAN

Tropical cyclone report, 1992
[AD-A274464] p 2896 N94-27025

INDICATING INSTRUMENTS

Monitoring activity with a wrist-worn actigraph: Effects of amplifier passband and threshold variations
[AD-A274705] p 2909 N94-26377

INDIUM

Indium donor complexes with cation vacancies in CdTe and ZnSe
[DE94-002731] p 3063 N94-26958

Modelling of the MEA float zone using accelerometer data
[NASA-CR-193933] p 2761 N94-27220

Research on high-efficiency, large-area, CuInSe2 based thin-film modules
[DE94-000259] p 3067 N94-27609

INDIUM ALLOYS

Research into the microstructure and mechanical behavior of eutectic Bi-Sn and In-Sn
[DE94-004558] p 2741 N94-27619

Formation and crystallization of hydrogen-induced amorphous Ti3InH(4.5) alloy p 2745 N94-28163

INDIUM ANTIMONIDES

Development of intermetallic compounds for high performance luminescence elements
p 2722 N94-25545

INDIUM ARSENIDES

AB-Initio calculation of the valence-band offset at strained GaAs/InAs (001) heterojunction
[DE94-602538] p 3061 N94-26878

INDIUM COMPOUNDS

Nitride semiconductors for ultraviolet detection
[AD-A274246] p 3060 N94-26840

Ion implantation and dynamic recovery of tin-doped indium oxide films
[DE94-001126] p 3062 N94-26932

INDIUM ISOTOPES

Indium donor complexes with cation vacancies in CdTe and ZnSe
[DE94-002731] p 3063 N94-26958

INDIUM PHOSPHIDES

Electric-field dependence of electroreflectance and photocurrent spectra at visible wavelengths in MOVPE-grown InAlGaP multiple strained quantum-well structures
[DE94-004692] p 2780 N94-25664

Electrical properties of p-type GaInP2
[AD-A273771] p 3051 N94-25856

Study of the homogeneity of InP wafers
[AD-A273658] p 3055 N94-26194

Ordering and phase separation in MOCVD InGaP alloys and unicompositional quantum wells
[DE94-004693] p 3056 N94-26352

High-efficiency, thin-film solar cells
[DE94-000250] p 2860 N94-27625

INDIUM TELLURIDES

The state of the art of thin-film photovoltaics
[DE94-000224] p 2855 N94-26115

INDONESIA

Research and observation programmes on global changes in Indonesia p 2873 N94-28277

INDUCTANCE

Channel model for AC electric arc
[PB94-124591] p 2786 N94-27327

INDUSTRIAL AREAS

The advantages of the location Germany must not be jeopardized in air traffic p 2661 N94-28236

INDUSTRIAL MANAGEMENT

The effectiveness of AMT investment in UK metal component manufacture
[IND-MANU-SCI-TECH-REPT-3] p 2762 N94-25775

Business process redesign: Design the improved process
[AD-A274947] p 3093 N94-26299

INDUSTRIAL PLANTS

Compilation of air pollutant emission factors. Volume 1: Stationary point and area sources. Supplement F
[PB94-121431] p 2867 N94-26757

SP industry calorimeter for rate of heat release measurements up to 10MW
[PB94-124211] p 2811 N94-27044

An artificial reality environment for remote factory control and monitoring p 2687 N94-27369

INDUSTRIAL SAFETY

Evaluation and improvement of the inquest system on work accidents (TOT)
[VTT-TIED-1418] p 2762 N94-26261

INDUSTRIAL WASTES

Collaboration of chemical oxidation and biological treatment for removal of refractory organic substances
p 2870 N94-28149

Treatment of refractory organic substances with combined use of chemical oxidation and biological treatment. Part 2: Biodegradability of ozonation products of chlorophenol p 2870 N94-28151

Oil production from buckwheat stillage by thermochemical liquefaction p 2871 N94-28154

INDUSTRIES

System software and tools for high performance computing environments: A report on the findings of the Pasadena Workshop
[DE94-003918] p 2956 N94-25602

General Motors Corporation and Pacific Northwest Laboratory staff exchange: Inspection of case hardened steels and metal-matrix composites
[DE94-003470] p 2706 N94-25982

Overview of the Photovoltaic Manufacturing Technology (PVMaT) project
[DE93-018234] p 2856 N94-26426

Compilation of air pollutant emission factors. Volume 1: Stationary point and area sources. Supplement F
[PB94-121431] p 2867 N94-26757

Fabrication technology
[DE94-003017] p 2763 N94-26778

Generalized emulation microcircuit program
[AD-A274749] p 2785 N94-26797

COMPETENCE 2000: Study on training requirements of the Norwegian metallurgical industry
[PB94-124609] p 2741 N94-27328

INELASTIC COLLISIONS

Correlations in inelastic collisions of relativistic nuclei with emulsion at (4.1 - 4.5) A GeV/c
[DE93-634526] p 3030 N94-27994

INELASTIC SCATTERING

Optical conductivity and resistivity in the two-band Emery model
[DE94-601943] p 3051 N94-25945

A dependence of exclusive vector meson production in muon-nucleus scattering
[DE94-003363] p 3016 N94-25957

Harvard University High Energy Physics
[DE94-002406] p 3032 N94-26119

Separation and reconstruction of electron neutrino interaction in the IHEP-JINR neutrino detector and BARS detector
[DE93-634182] p 3019 N94-26393

Delocalization in electron impact ionization in a crystalline environment
[DE94-601819] p 3062 N94-26927

Calculations of asymmetries in electron-alkali scattering
[DE94-601816] p 3023 N94-26945

First observation of neutral current proton electron scattering at the square root of s = 300 GeV
[DE94-701107] p 3030 N94-27877

Correlations in inelastic collisions of relativistic nuclei with emulsion at (4.1 - 4.5) A GeV/c
[DE93-634526] p 3030 N94-27994

INEQUALITIES

Cone-valued Lyapunov functions and the stability of stochastic differential equations
[DE94-601504] p 2994 N94-26458

On the (Phi)(sub 0)-stability of functional differential equations
[DE94-601507] p 3006 N94-26460

Estimates for cone multipliers
[PB94-124385] p 2997 N94-26995

Symmetric and asymmetric diophantine approximation by continued fractions
[PB94-126455] p 2998 N94-27030

Polyhedral characterization of the economic lot-sizing problem with start-up costs
[MEMO-COSOR-92-46] p 2969 N94-27396

A strange application of Kolmogorov complexity
[CWI-CS-R9328] p 2973 N94-27737

INERTIAL CONFINEMENT FUSION

Experimental and numerical investigation of shock wave propagation through complex geometry, gas continuous, two-phase media
[DE94-001408] p 2791 N94-26121

Research in pulsed power plasma physics
[AD-A274323] p 3045 N94-27074

INERTIAL FUSION (REACTOR)

Fusion Energy Advisory Committee: Advice and recommendations to the US Department of Energy in response to the charge letter of September 1, 1992
[DE93-019842] p 3043 N94-26428

INERTIAL GUIDANCE

On the application of Allan variance method for Ring Laser Gyro performance characterization
[DE94-003880] p 2810 N94-26525

INERTIAL NAVIGATION

An adaptive Kalman filter for tactical missiles guidance systems
[ISBN-0-315-84115-X] p 2677 N94-26636

Flight testing of GPS and GPS-aided systems
[NLR-TP-92151-U] p 2666 N94-27831

INFERENCE

Developing realistic cooperative behaviors for autonomous agents in air combat simulation
[AD-A274077] p 2937 N94-25774

INFORMATION

Image quality and the display modulation transfer function: Experimental findings
[AD-A274061] p 2679 N94-25773

INFORMATION DISSEMINATION

Full-text information services at the desktop
[DE94-003728] p 3096 N94-25813

INFORMATION FLOW

Usefulness of compile-time restructuring of LGDF programs in throughput-critical applications
[AD-A274915] p 2963 N94-26530

INFORMATION MANAGEMENT

Automated information management for designers: Functional requirements for computer based associates that support access and use of technical information in design
[AD-A274603] p 3099 N94-26891

Circulars of the Electrotechnical Laboratory. No. 223: An extended survey on provable information base systems
[JTN-94-80550] p 3100 N94-27336

On modeling and controlling intelligent systems
[DE94-002446] p 2988 N94-27706

The TMIS life-cycle process document, revision A
[NASA-TM-109698] p 2697 N94-27775

INFORMATION PROCESSING (BIOLOGY)

Induced pictorial representations
[AD-A274251] p 2939 N94-27012

Signal- and listener-based factors in complex auditory pattern perception
[AD-A274148] p 2939 N94-27094

Interhemispheric phase relationship of alpha waves and cerebral dominance p 2927 N94-27518

Function of selective attention intrinsic to the saccade system: Does the voluntary control override the stimulus driven control? p 2928 N94-27523

INFORMATION RETRIEVAL

The effect of the time restrictions on information search and information integration in a dynamic task environment
[AD-A273759] p 3095 N94-25723

Full-text information services at the desktop
[DE94-003728] p 3096 N94-25813

Design and implementation of a query editor for the Amadeus system
[AD-A274955] p 3097 N94-26300

Retrieval using plausible inference
[AD-A274252] p 3099 N94-27013

Bibliographic Retrieval System (BARS) Sandia Shock Compression (SSC) database Shock Physics Index (SPHINX) database, volume 3
[DE94-001705] p 3099 N94-27022

Query optimization strategies for browsing sessions
[CWI-CS-R9268] p 3100 N94-27394

Reinventing information services to increase customer satisfaction
[DE94-003718] p 3100 N94-27563

Electronic document distribution: Design of the anonymous FTP Langley Technical Report Server
[NASA-TM-4567] p 2971 N94-27573

Correspondence dictionary from free English term to INIS descriptors
[DE94-701173] p 3100 N94-27700

INFORMATION SYSTEMS

Full-text information services at the desktop
[DE94-003728] p 3096 N94-25813

The television as robot servant
[AD-A273985] p 2984 N94-25898

Scientific and Technical Information (STI)....what's the status?
[DE94-003731] p 3097 N94-26348

Federal Information Exchange (FEDIX) user's guide: Fall 1993, Version 5.0/Release 1.0
[DE94-003826] p 3097 N94-26350

International energy: Research organizations, 1988-1992
[DE93-017267] p 3098 N94-26398

Hanford Environmental Information System (HEIS) sample/data entry flow summary
[DE94-002494] p 3098 N94-26559

Design considerations when using external hypertext engines from applications
[DE94-002213] p 3098 N94-26598

Mesoscale meteorological measurements characterizing complex flows
[DE94-002359] p 2895 N94-26761

Automated information management for designers: Functional requirements for computer based associates that support access and use of technical information in design
[AD-A274603] p 3099 N94-26891

Feasibility study on construction of a global environment research and development information network
[DE94-725198] p 2868 N94-26904

Retrieval using plausible inference
[AD-A274252] p 3099 N94-27013

MILCOM 92 and standardization for HF-communication. A study tour to the USA in October 1992
[PB94-124427] p 2774 N94-27219

A graphical workstation based part-task flight simulator for preliminary rapid evaluation of advanced displays
p 2641 N94-27286

Circulars of the Electrotechnical Laboratory. No. 223: An extended survey on provable information base systems
[JTN-94-80550] p 3100 N94-27336

Vision 21: Interdisciplinary Science and Engineering in the Era of Cyberspace
[NASA-CP-10129] p 2685 N94-27358

Spiral Survey Expedition: A proposal to organize for the Survey, exploration and eventual colonization of the Milky Way Galaxy p 2686 N94-27366

Emerging computer technologies and the news media of the future p 2688 N94-27372

Reinventing information services to increase customer satisfaction
[DE94-003718] p 3100 N94-27563

Electronic document distribution: Design of the anonymous FTP Langley Technical Report Server
[NASA-TM-4567] p 2971 N94-27573

On modeling and controlling intelligent systems
[DE94-002446] p 2988 N94-27706

Human computer interface guide, revision A
[NASA-TM-109708] p 2955 N94-27769

Comparison of Object-Oriented Analysis and Design Methods: A Collection of Papers
[MEMO-INF-92-69] p 2975 N94-27936

Observation with STS seismometer at Nakaizu, central Japan: Observation system and comparison with tiltmeter p 2686 N94-27986

INFORMATION THEORY

Circulars of the Electrotechnical Laboratory. No. 223: An extended survey on provable information base systems
[JTN-94-80550] p 3100 N94-27336

A strange application of Kolmogorov complexity
[CWI-CS-R9328] p 2973 N94-27737

INFORMATION TRANSFER

Feasibility study on construction of a global environment research and development information network
[DE94-725198] p 2868 N94-26904

The intracellular second messenger system in c-fos gene induction by ACTH p 2904 N94-27477

INFRARED ABSORPTION

Study on knowledge extraction and systematization for material design p 2727 N94-25568

INFRARED ASTRONOMY SATELLITE

Zodiacal light data investigation. Interim results for the Earthlimb Clutter Experiment
[AD-A274461] p 3104 N94-27265

INFRARED DETECTORS

High temperature superconducting infrared imaging satellite p 2698 N94-25700

Investigation of a normal incidence high-performance p-type strained layer In(0.3)Ga(0.7)As / In(0.52)Al(0.48) as quantum well infrared photodetector
[AD-A274854] p 3055 N94-26188

Analysis of the influence of weather on infrared imagery
[FEL-92-A421] p 3036 N94-26649

Radiometric, spectral, and effectiveness equipment
[AD-A274208] p 3037 N94-27066

Zodiacal light data investigation. Interim results for the Earthlimb Clutter Experiment
[AD-A274461] p 3104 N94-27265

INFRARED IMAGERY

Mitsubishi 3-5 micrometers IR imager for machine-vision/ATA applications
[AD-A273812] p 3034 N94-25940

An overview of the TNO contribution to VAST 92
[AD-A273751] p 2893 N94-26016

Focal plane arrays in advanced thermal images
[AD-B174292] p 3036 N94-26648

Analysis of the influence of weather on infrared imagery
[FEL-92-A421] p 3036 N94-26649

The Hough transform algorithm for sea ice lead analysis: An evaluation
[AD-A274535] p 2899 N94-26853

Leadex environmental phenomena and effects observed by DMSP, NOAA, and ERS-1 satellites
[AD-A274596] p 2868 N94-26888

Characterization and calibration of the Agema 880+ imaging radiometer
[AD-A274417] p 3036 N94-26981

Computer model for generation of infrared images
[PB94-123551] p 3005 N94-27172

Infrared imaging for transition detection in a transonic blowdown wind tunnel p 2653 N94-28325

INFRARED INTERFEROMETERS

Modelling atmospheric turbulence effects on ground-based telescope systems
[DE94-004211] p 3102 N94-26528

INFRARED LASERS

Enhanced tracking of airborne targets using forward looking infrared and laser return measurements
[AD-A274181] p 3037 N94-27102

Ir-fibers in a laser threat warning system and robot shot warning system
[PB94-124476] p 3038 N94-27209

INFRARED PHOTOGRAPHY

CMT-Si
[PB94-123619] p 2812 N94-27216

INFRARED RADIATION

Optimization of experimental conditions in IR reflectance determination of BPSG properties
[DE94-002742] p 2713 N94-25978

On the gluon propagator in the infrared region
[DE93-634345] p 3016 N94-26035

Investigation of a normal incidence high-performance p-type strained layer In(0.3)Ga(0.7)As / In(0.52)Al(0.48) as quantum well infrared photodetector
[AD-A274854] p 3055 N94-26188

Dimensional crossover from non-renormalizability to renormalizability
[DE93-613052] p 3006 N94-26193

Ir-fibers in a laser threat warning system and robot shot warning system
[PB94-124476] p 3038 N94-27209

Excited Landau levels, orbital angular momentum and axial anomaly
[DE94-606407] p 3068 N94-27679

INFRARED SPECTRA

Multivariate calibration applied to near-infrared spectroscopy for the quantitative analysis of dilute aqueous solutions
[DE94-003231] p 2716 N94-26794

Computer model for generation of infrared images
[PB94-123551] p 3005 N94-27172

Zodiacal light data investigation. Interim results for the Earthlimb Clutter Experiment
[AD-A274461] p 3104 N94-27265

INFRARED SPECTROMETERS

Planetary Instrument Definition and Development Program (PIDDP). Instrument for future planetary flight missions: A visible-infrared imaging spectrometer for planetary missions
[NASA-CR-195254] p 3106 N94-27409

INFRARED SPECTROSCOPY

Advances in passive-remote and extractive Fourier transform infrared spectroscopic systems
[DE94-001424] p 2868 N94-26952

Spectroscopy Division
[DE94-604074] p 2717 N94-26988

Spectroscopy and dynamics of molecular and ionic impurities embedded in solid hydrogen
[AD-A274149] p 3064 N94-27095

Evanescent field infrared spectroscopy using chalcogenide glass fiber
[ITN-94-85233] p 3038 N94-27178

The Reports of Aeromedical Laboratory, volume 33, number 4
[JTN-94-80586] p 2933 N94-27942

Evaluation of near-infrared spectrophotometric method for individual tolerance to +Gz acceleration
p 2933 N94-27944

INFRARED TRACKING

Radiometric, spectral, and effectiveness equipment
[AD-A274208] p 3037 N94-27066

INGESTION (ENGINES)

Transient model applications. 3: Transient engine simulation and analysis of an ice ingestion test
p 2829 N94-28050

INHIBITORS

Technique to predict the curing behaviour of unsaturated polyester materials
[PB94-124856] p 2748 N94-25892

Modelling the inhibition cure behaviour of unsaturated polyester moulding materials
[PB94-124864] p 2748 N94-25893

Effect of sera from patients treated with long-term hemodialysis on mRNA's for collagenase, stromelysin, and tissue inhibitor of metalloprotease in cultured human synovial cells p 2920 N94-27481
The ionic mechanism underlying the negative chronotropic effect of acetylcholine: Experimental study in rabbit single sinoatrial node cells
p 2908 N94-27514
The ionic mechanism underlying the negative chronotropic effect of acetylcholine: Experiments using small sinoatrial node tissue preparations isolated from rabbit hearts p 2908 N94-27515
The ionic mechanism underlying the negative chronotropic effect of acetylcholine: Postganglionic vagal stimulation in isolated rabbit hearts
p 2908 N94-27516
Effects of p-chlorophenol on sulfate reduction in marine sediments p 2870 N94-28150

INHOMOGENEITY
Efficient modeling in transversely isotropic inhomogeneous media
[DE94-003394] p 2877 N94-25847
Elastic wave up/down decomposition in inhomogeneous and anisotropic media: An operator approach and its approximations
[PB94-126497] p 2881 N94-26880
Spectral and temporal correlations of multifrequency waves in the turbulent atmosphere
[ITN-94-85229] p 2774 N94-27233
Analysis of S-wave seismogram envelope of deep earthquakes and estimation of random inhomogeneities in the Kanto-Tokai area p 2886 N94-27988

INJECTORS
Interaction between a high density-low temperature plasma and a frozen hydrogen pellet in a railgun injector
[DE94-000846] p 3041 N94-25949
High-speed repetitive pellet injector for plasma fueling of magnetic confinement fusion devices
[DE94-002792] p 3042 N94-26140
Gaseous hydrogen/oxygen injector performance characterization
[NASA-CR-194464] p 2701 N94-26208

INJURIES
Eccentric exercise testing and training
p 2934 N94-28363

INLET AIRFRAME CONFIGURATIONS
The design of a counter rotating ultra-high-bypass fan simulator for windtunnel investigation
[DLR-FB-93-20] p 2675 N94-27739

INLET FLOW
The high Reynolds number flow through an axial-flow pump
[AD-A273844] p 2789 N94-25604
Experimental study on the shock wave interaction with a hypersonic boundary layer near a convex corner
p 2654 N94-28328

INLET PRESSURE
Pressure-gain combustion
[DE94-002975] p 2719 N94-27712

INLET TEMPERATURE
Gas fired advanced turbine system
[DE94-003193] p 2827 N94-27874

INNER RADIATION BELT
Compton Gamma Ray Observatory/BATSE observations of energetic electrons scattered by cyclotron resonance with waves from powerful VLF transmitters
[NASA-CR-195240] p 3115 N94-26790

INPUT
Digital input module
[DIGEL-1993-6] p 2779 N94-25620

INPUT/OUTPUT ROUTINES
Out of core, out of mind: Practical parallel I/O
[DE94-003107] p 2979 N94-25952
Concurrent shadow paging: Snapshots, read-only transactions, and on-the-fly multi-level incremental dumping
[PB94-133139] p 3100 N94-28385

INSPECTION
Statistical quality management
[MEMO-COSOR-92-43] p 2834 N94-26008
Results from a fracture mechanical serial investigation of breechrings on the M109A3GN howitzer
[FFI-93/8002] p 2837 N94-26233
Non-contact ultrasonic inspection
[VTT-TIED-1454] p 2835 N94-26257
Automated fabric inspection system
[AD-A274522] p 2835 N94-26833
Space Shuttle main engine turbopump bearing assessment program
[NASA-TM-108447] p 2833 N94-28265

INSTALLING
Cooling towers for combined cycles: Design philosophy, performance testing, and operating problems
p 2832 N94-28087

INSTRUCTION SETS (COMPUTERS)
Fast incremental compiler transformations for multiple instruction retry
[NASA-CR-195209] p 2964 N94-26680
A complete version of the Ada tasking coprocessor
p 2950 N94-26721

INSTRUMENT APPROACH
The effects of tailwinds and control cross coupling on rotorcraft handling qualities for steep, decelerating instrument approaches and missed approaches
[IAR-AN-77] p 2677 N94-26710
Ground station siting considerations for DGPS
p 2642 N94-27293

INSTRUMENT COMPENSATION
Observation with STS seismometer at Nakaizu, central Japan: Observation system and comparison with tiltmeter p 2886 N94-27986

INSTRUMENT LANDING SYSTEMS
Piloted simulation study of an ILS approach of a twin-pusher business/commuter turboprop aircraft configuration
[NASA-TM-4516] p 2646 N94-26602

INSULATORS
The electric field between non conductive rectangular charged surfaces placed near a small spherical conductive earthed surface and determination of critical density of charge
[DE93-634324] p 2783 N94-26443
Technical report of ISSP. Ser. A, no. 2679: Novel electronic states of partially deuterated (DMe-DCNQI)2Cu
[JTN-94-80565] p 3064 N94-27175
Technical report of ISSP. Ser. A, no. 2676: Charge mass singularity in two-dimensional Hubbard model
[JTN-94-80562] p 3065 N94-27248

INTEGERS
Winding numbers in homotopy theory from integers to reals
[DE94-601510] p 2992 N94-26367

INTEGRAL CALCULUS
A survey of open problems in symplectic integration
[DE94-003966] p 3007 N94-27777

INTEGRAL EQUATIONS
Numeric solution of the electric field integral equation using Galerkin's method for axially symmetric cases
[ESA-TT-1264] p 2768 N94-26315
How reliable is the HMSA integral equation for the pair structure of supercooled and amorphous mixtures?
[DE94-601543] p 3006 N94-26411
New variational techniques for acoustic radiation and scattering from elastic shell structures
[AD-A274599] p 3010 N94-26889
Joint services electronics program
[AD-A274643] p 2785 N94-27027
Fractional calculus, gegenbauer transformations and integral equations
[PB93-237683] p 2999 N94-27349
A variational approach to the quantum field theoretic bound-state problem
[ISBN-0-315-60960-5] p 3074 N94-27401
Methods in unsteady aerodynamics
[DLR-FB-93-21] p 2648 N94-27741

INTEGRAL TRANSFORMATIONS
Fractional calculus, gegenbauer transformations and integral equations
[PB93-237683] p 2999 N94-27349

INTEGRALS
On the first integrals of geodesics
[DE93-612974] p 3007 N94-25603

INTEGRATED CIRCUITS
Development of a 4-bit parallel analog-to-digital converter and a four-quadrant double-balanced mixer using heterojunction bipolar transistor technology
[AD-A274074] p 2947 N94-25648
Modeling electromagnetic effects in MMICs for T/R modules
[AD-A273808] p 2766 N94-25736
Advanced qualification techniques
[DE94-003709] p 2780 N94-25812
Object imaging accomplished with an integrated circuit robotic tactile sensor incorporating a piezoelectric polyvinylidene fluoride thin film
[AD-A274038] p 2780 N94-25845
A general purpose I(sub DDQ) measurement circuit
[DE94-002733] p 2781 N94-25977
A physics-based heterojunction bipolar transistor model for integrated circuit simulation
[AD-A274081] p 2781 N94-25995
Modeling and experimental verification of single event upsets p 2684 N94-26287
Optoelectronic Technology Consortium
[AD-A274909] p 2782 N94-26344
The 12-channel flash-ADC FASTBUS module
[DE93-634229] p 2783 N94-26380
Fast generator of program waveforms signals
[DE93-634230] p 2948 N94-26381
Processing, fabrication, and demonstration of HTS integrated microwave circuits, appendix A
[AD-A274600] p 2785 N94-26890
An optoelectronic graphics display processor
[AD-A274401] p 3037 N94-26990
A fully integrated 16 channel digitally trimmed pulse shaping amplifier
[DE94-004555] p 2787 N94-27618
The analysis of thermal and 1/F noise in MOS devices, circuits and systems
[ISBN-0-315-57811-4] p 2787 N94-27642
An efficient and accurate Green's function analysis of packaged microwave integrated circuits
[ISBN-0-315-84425-6] p 2787 N94-27653
Characterization of semi-insulating gallium arsenide
[AD-A273781] p 3068 N94-27704

INTEGRATED OPTICS
Optoelectronic Technology Consortium
[AD-A274909] p 2782 N94-26344

INTELLIGENCE
The central executive component of working memory
[AD-A274295] p 2938 N94-26683
On modeling and controlling intelligent systems
[DE94-002446] p 2988 N94-27706

INTELLIGENCE TESTS
Extending the rule space model to a semantically-rich domain: Diagnostic assessment in architecture
[AD-A273789] p 2948 N94-25864
A diagnostic classification model for document processing skills
[AD-A273790] p 3096 N94-25925

INTERACTIONAL AERODYNAMICS
Coupled 2-dimensional cascade theory for noise an d unsteady aerodynamics of blade row interaction in turbofans. Volume 2: Documentation for computer code CUP2D
[NASA-CR-4506-VOL-2] p 2675 N94-27778
Numerical assessment of aerodynamic interactions on missiles with transverse jets control
p 2659 N94-28031
First experimental assessment of RCS plume-flow field interaction on Hermes leading edge thruster configuration p 2703 N94-28032

INTERACTIVE CONTROL
IRMA: A program for three-dimensional color display of data
[AD-A273811] p 2959 N94-25879
Interactive control of a parallel simulation from a remote graphics workstation
[AD-A274217] p 2981 N94-27070

INTERATOMIC FORCES
Debye-Waller factors of the light actinide metals
[DE94-000685] p 2733 N94-26069
International bulletin on atomic and molecular data for fusion. No. 46
[DE94-601818] p 3023 N94-26947

INTERFACE STABILITY
Interface configuration experiment: Preliminary results
[NASA-TM-109684] p 2760 N94-25849
Composite raw materials for the building industry
[VTT-TIED-1433] p 2708 N94-26544

INTERFACES
Float zone crystal growth using laser radiation
[DLR-FB-93-10] p 3066 N94-27590

INTERFACIAL TENSION
MBE grown 3 to 5 strain relaxed buffer layers and superlattices characterized by atomic force microscopy
[DE94-002931] p 3056 N94-26308
Interfacial area and interfacial transfer in two-phase flow
[DE93-041226] p 2792 N94-26468
Report of three microgravity experiments by the drop shaft
[JTN-94-80579] p 2761 N94-27341

INTERFERENCE IMMUNITY
Evaluation of an Acoustic Charge Transport (ACT) device for adaptive interference suppression in spread spectrum communications systems
[AD-A274073] p 2765 N94-25647

INTERFEROMETERS
Performance comparison of shearing interferometer and Hartmann wave front sensors
[AD-A274031] p 3034 N94-25768
Experimental verification of tomographic reconstruction of turbulent air flow structure using optical wavefront measurements
[AD-A274392] p 2795 N94-27129

INTERFEROMETRY
An evaluation of the utility of ground-based high resolution interferometer (GB-HIS) soundings of the planetary boundary layer
[DE94-000960] p 3106 N94-25981
Neutron reflection interferometry
[DE94-601876] p 2714 N94-26170

INTERGRANULAR CORROSION

Radiation hardening effects on localized deformation and stress corrosion cracking of stainless steels [DE94-004308] p 2731 N94-25804

The role of grain boundary chemistry and structure in the environmentally-assisted intergranular cracking of nickel-base alloys [DE94-003159] p 2732 N94-25954

Grain boundary chromium concentration effects on the IGSCC and IASCC of austenitic stainless steels [DE94-004268] p 2741 N94-27570

INTERMETALLICS

Bulletin of National Research Institute for Metals in Fiscal Year 1993, no. 14 [REPT-14] p 2722 N94-25544

Development of intermetallic compounds for high performance luminescence elements p 2722 N94-25545

Study on synthesis and characteristics of intermetallic compound with strong electron correlation p 2726 N94-25563

Study on variation of damage generation mechanism by fatigue on TiAl compounds due to different slip systems p 2729 N94-25579

Heavy-electron behavior in large coordination compounds CeZn11 and UZn12 [REPT-A-2663] p 3049 N94-25614

Structure and properties of intermetallic composites synthesized in situ using solid state displacement reactions [DE94-004312] p 2705 N94-25805

Numerical simulations of interfacial debonding in ductile-phase reinforced intermetallic matrix composites [DE94-003639] p 2706 N94-25938

Structure of the modulated magnetic phase of Mn3Sn [DE94-002788] p 2733 N94-26092

An atom probe investigation of the influence of trace impurities on the mechanical behavior of NiAl [DE94-002797] p 2734 N94-26272

Eutectic transformation L in equilibrium to Zr6Fe23 + Fe(tau) in the Fe-Zr system [DE93-633766] p 2735 N94-26295

Experimental determination of the CU-IN-PB ternary phase diagram [DE94-003765] p 2735 N94-26349

Titanium 1992: Science and technology, volume 2 rence (7th) in san diego, california on june 29-july 2, 1992. Volume 2 [AD-A274799] p 2736 N94-26362

Structure and properties of composites synthesized in situ using solid state displacement reactions [DE94-004589] p 2737 N94-26585

A tri-junction diffusion couple analysis of the Nb-Cr-Ti system at 950 C [DE94-002637] p 2737 N94-26607

The processing of powder metallurgically produced near gamma-titanium aluminide [ISBN-0-315-84018-8] p 2738 N94-26633

The electrochemical behavior of the Al3Fe intermetallic compound and localized corrosion of impure 1100 Al [DE94-002037] p 2739 N94-26912

Interface phenomena in metal-ceramic composites [AD-A274167] p 2709 N94-27125

Microstructure and mechanical behaviour of L1(2) titanium trialuminides [ISBN-0-315-84488-4] p 2740 N94-27306

Current status of research and development on nickel and iron aluminides [DE94-004247] p 2741 N94-27616

Laser surface modification of intermetallic compounds [DREA-CR-92-416] p 2820 N94-27668

INTERNAL COMBUSTION ENGINES

Extraterrestrial surface propulsion systems p 2833 N94-25691

Ceramic technology project [DE94-003782] p 2750 N94-26332

Sequential multi-point injection of a natural gas engine. Topical report, November 1991 - April 1992 [PB94-126794] p 2824 N94-27224

Optimising BMW four-cylinder two-valve engines [PB94-125101] p 2824 N94-27254

Technical Report of National Research Institute of Fisheries Engineering: Fishing Boat and Instrument, No. 12 [JTN-94-80595] p 2764 N94-27976

Computer aided data recording and analyzing system for the engine test p 2764 N94-27979

INTERNAL CONVERSION

Dynamics of metastable states in supersonic beams [ITN-94-85232] p 3028 N94-27760

INTERNAL ENERGY

Se EXAFS study of the elevated wurtzite to rock salt structural phase transition in CdSe nanocrystals [DE94-003247] p 3054 N94-26125

INTERNATIONAL COOPERATION

Feasibility study on construction of a global environment research and development information network [DE94-725198] p 2868 N94-26904

How to make good use of international research collaboration, with emphasis on the evolving situation in Europe [PB94-119690] p 3101 N94-27323

The telemedicine spacebridge project: A joint US/Russian venture in long distance medicine via satellite [NASA-TM-106523] p 2693 N94-27427

Recent legal movement on water quality regulation in Japan p 2869 N94-28148

Lufthansa Yearbook 1992 [DSK-9734-H-92] p 2660 N94-28230

Air traffic of the European Community with European neighbors p 2661 N94-28233

A sky above Europe p 2661 N94-28234

The single European market: Economical advance, ecological problem? p 2661 N94-28235

Air traffic administration enroute to Europe p 2661 N94-28238

Role and activity of STA on Asian Pacific regional cooperation p 2853 N94-28269

Cooperative research projects on satellite remote sensing for the hydrological subjects p 2853 N94-28270

NASDA contribution plan to Asian countries p 2853 N94-28273

The Environmental Research and Training Centre p 2873 N94-28280

Global Change and Terrestrial Ecosystems (GCTE): Progress report and prospects for Asian contributions p 2874 N94-28281

Global change: A research strategy for Australia 1992-1996 p 2874 N94-28282

A progress report on global change studies in China p 2874 N94-28283

Atmospheric science research in Malaysia: Perspectives on international cooperation p 2874 N94-28285

INTERNATIONAL TRADE

The proliferation of aerospace weapons technology: Ballistic missiles and the case of Brazil [ISBN-0-315-84082-X] p 2763 N94-26634

COMPETENCE 2000: Study on training requirements of the Norwegian metallurgical industry [PB94-124609] p 2741 N94-27328

INTERNETS

A geological and geophysical information system for Eurasia [AD-A274818] p 3098 N94-26490

INTERPLANETARY FLIGHT

Project Minerva: A low-cost manned Mars mission based on indigenous propellant production p 2760 N94-25705

INTERPLANETARY MAGNETIC FIELDS

Quiet-time intensifications along the poleward auroral boundary near midnight [ATR-93(7248)-2] p 2877 N94-26201

Direct evidence of the interplanetary magnetic field effect on the cosmic-ray shadow by the sun [ICRR-296-93-8] p 3116 N94-27607

INTERPLANETARY SPACECRAFT

Project WISH: The Emerald City p 2703 N94-25690

Project Minerva: A low-cost manned Mars mission based on indigenous propellant production p 2760 N94-25705

INTERPOLATION

Pseudoscalar glueball in the composite interpolating fields approach [DE93-634374] p 3016 N94-26042

Users guide for GRIKURV: A code for drawing graphs [PB94-123593] p 2968 N94-27154

INTERPROCESSOR COMMUNICATION

Interface technical specification of the V.25 bis emulator [AD-A273754] p 2948 N94-25720

A VHDL register transfer level model of the linear token passing multiplex data bus protocol for the high speed data bus [AD-A273734] p 2980 N94-26009

The Chaco user's guide [DE94-003669] p 2962 N94-26370

A doubly logarithmic communication algorithm for the Completely Connected Optical Communication Parallel Computer [DE93-019408] p 2980 N94-26473

Parallel matrix transpose algorithms on distributed memory concurrent computers [DE94-002424] p 2964 N94-26764

Hard real-time reliable multicast in the DEDOS system [PB94-126745] p 2966 N94-26920

Static task allocation for parallel processing systems during software development [AD-A274204] p 2981 N94-27100

Virtual memory management and virtual bus overloading on multiple channel architectures [AD-A274127] p 2954 N94-27152

Garbage collection in a multiprocessor Smalltalk system [ISBN-0-315-51159-1] p 2982 N94-27332

Open communication in manufacturing automation [PB94-132479] p 2976 N94-28377

INTERSECTIONS

Locating tie-points on a grid p 2978 N94-27906

INTERSTELLAR COMMUNICATION

The Fermi paradox: An approach based on percolation theory p 2687 N94-27370

INTERSTITIALS

Microscopic study of local structure and charge distribution in metallic La2CuO(4+delta) [DE94-003801] p 3050 N94-25817

Influence of point defects on grain boundary diffusion in oxides [DE94-003164] p 3060 N94-26782

The role of point defect clusters in reactor pressure vessel embrittlement [DE94-001122] p 2739 N94-26931

INTERSYMBOLIC INTERFERENCE

Equalization and cancellation of nonlinear intersymbol interference in a dispersive satellite communication channel [ISBN-0-315-85147-3] p 2775 N94-27274

INTRUSION

Mapping of seawater intrusion into the coastal aquifer of Israel (the seawater-freshwater interface) by TDEM (Time Domain Electromagnetic) method [ITN-94-85238] p 2850 N94-27331

INVARIANCE

Spatial symmetry, local integrability and tetrahedron equations in the Baxter-Bazhanov model [DE93-634348] p 3002 N94-26038

C-periodicity and the physical mass in the 3-state Potts model [DE94-601551] p 3019 N94-26423

Dynamic breaking of U(N) and appearance of Chern-Simons term in 4-fermion theories [DE93-634342] p 3019 N94-26455

On the relativistic invariant representation of arbitrary bilinear combinations of Dirac spinors [DE93-634343] p 3019 N94-26456

Nuclear Theory Group, University of Washington recent and planned research [DE94-002729] p 3022 N94-26809

Classification of linear differential operators with an invariant subspace in monomials [PB94-126620] p 2996 N94-26915

Measurements of the B(sup 0)(bar B)(sup 0)CP asymmetry [DE94-003379] p 3063 N94-27047

Translation and rotation invariant pattern recognition [PB94-123676] p 2968 N94-27157

INVENTORIES

Modelling the mass migration phenomena in partially frozen heat pipes [DE94-002716] p 2797 N94-27709

INVERSE SCATTERING

Crystal potential retrieval in HRTEM [DE94-601883] p 3055 N94-26171

INVERSIONS

Overall analysis of meteorological information in the Daeduk nuclear complex [DE93-632594] p 2894 N94-26469

INVERTEBRATES

The biostratigraphy and paleogeography of Maastrichtian inoceramids p 2889 N94-28303

INVERTERS

Low-cost photovoltaic inverters incorporating application-specific integrated circuits [DE94-003270] p 2856 N94-26463

INVESTMENTS

The effectiveness of AMT investment in UK metal component manufacture [IND-MANU-SCI-TECH-REPT-3] p 2762 N94-25775

INVISCID FLOW

Vortex methods [DE94-003245] p 2789 N94-25597

A sensitivity equation approach to shape optimization in fluid flows [NASA-CR-191598] p 2999 N94-27415

Non-isoenergetic inviscid slot flow p 2655 N94-28333

Calculation of unsteady incompressible inviscid flow about wings and bodies using CANAERO-T panel model p 2655 N94-28334

IO

Studies for Io's extended atmosphere and neutral clouds and their impact on the local satellite atmosphere and on the planetary magnetosphere [NASA-CR-195255] p 3106 N94-27406

Studies for the loss of atomic and molecular species from Io
[NASA-CR-195702] p 3108 N94-27941

IODIDES

Technical report of ISSP. Ser. A, no. 2672: Magneto-optical effects of excitons in BiI3 crystals under pulsed high magnetic fields. 3: Excitons confined around a stacking disorder formed by a bending stress
[JTN-94-80558] p 3065 N94-27240

IODINE

Grain by grain study of the mechanisms of crack propagation during iodine SCC of Zry-4
[DE93-633765] p 2734 N94-26162

Stress corrosion cracking and dealloying of copper-gold alloy in iodine vapor
[DE93-633790] p 2734 N94-26264

ION BEAMS

Study on microscopic structural controls and electronic properties at material surfaces by ion beams
p 2727 N94-25571

An electromagnetic calorimeter with wavelength shifting fiber readout
[DE93-616664] p 2809 N94-25735

Experimental and numerical investigation of shock wave propagation through complex geometry, gas continuous, two-phase media
[DE94-001408] p 2791 N94-26121

Diffusion of substitutional elements in Ti in its hcp phase
[DE93-633762] p 2733 N94-26160

Studies of thin-film growth, adsorption, and oxidation by in situ, real-time, and ex situ ion beam analysis
[DE94-002907] p 3055 N94-26275

Modulation wavelength dependence of ion mixing in metallic superlattices
[DE94-004608] p 3059 N94-26591

Ion beam mixing of marker layers into amorphous aluminum oxide
[DE94-000901] p 2752 N94-26676

Research in pulsed power plasma physics
[AD-A274323] p 3045 N94-27074

Advanced development of particle beam probe diagnostic system
[DE94-002316] p 3047 N94-27720

Observation of stimulated emission from an MBE grown GaN film on sapphire
[DE94-003638] p 3068 N94-27724

ION CURRENTS

Perovskite solid electrolytes for SOFC
[DE94-001923] p 2859 N94-27005

Correlation between electrical activity and the size of single sinoatrial node cells p 2907 N94-27513

The ionic mechanism underlying the negative chronotropic effect of acetylcholine: Experimental study in rabbit single sinoatrial node cells
p 2908 N94-27514

The ionic mechanism underlying the negative chronotropic effect of acetylcholine: Experiments using small sinoatrial node tissue preparations isolated from rabbit hearts p 2908 N94-27515

The ionic mechanism underlying the negative chronotropic effect of acetylcholine: Postganglionic vagal stimulation in isolated rabbit hearts
p 2908 N94-27516

Postnatal changes in the autonomic modulation of L-type Ca(exp 2+) currents of rabbit ventricular cells
p 2931 N94-27535

Desensitization to acethylcholine in pacemaker cells of the sinoatrial node p 2908 N94-27537

ION CYCLOTRON RADIATION

Review of tokamak experiments on direct electron heating and current drive with fast waves
[DE94-004185] p 3041 N94-25801

Design of folded waveguide antenna for Alcator C-Mod
[DE94-003584] p 2767 N94-25924

Design and control of phased ICRF antenna arrays
[DE94-002796] p 3046 N94-27261

On radio frequency wave induced radial transport and wave helicity
[IPPCZ-326] p 2777 N94-27838

ION DENSITY (CONCENTRATION)

Inertial electrostatic confinement as a power source for electric propulsion p 2688 N94-27373

ION DISTRIBUTION

Acceleration of electrons and ions by strong lower-hybrid turbulence in solar flares
[NASA-TM-109723] p 3111 N94-27953

ION ENGINES

Manned mission to Mars with periodic refueling from electrically propelled tankers p 2689 N94-25670

ION IMPACT

Disintegration of (C60) by Xe ion irradiation
[DE94-601913] p 3023 N94-26929

ION IMPLANTATION

Study on microscopic structural controls and electronic properties at material surfaces by ion beams
p 2727 N94-25571

Binding of copper and nickel to cavities in silicon formed by helium ion implantation
[DE94-003769] p 3050 N94-25814

The structural, chemical, and electrical properties of He-implantation-induced nanocavities in silicon
[DE94-002681] p 3052 N94-25971

Collaborative research on ion implantation of ceramics
[DE93-019177] p 2749 N94-26080

Ion implantation of diamond: Damage, doping, and lift-off
[DE94-001133] p 3054 N94-26137

Peculiarities and application perspectives of metal-ion implants in glasses
[DE94-004671] p 3035 N94-26246

Regrowth zones in laser annealed radiation damaged diamond
[DE94-600821] p 3056 N94-26364

Ion implantation and dynamic recovery of tin-doped indium oxide films
[DE94-001126] p 3062 N94-26932

He(+) and H(+) microbeam damage, swelling and annealing in diamonds
[DE94-601912] p 3063 N94-26987

Ion implantation in silicate glasses
[DE94-003785] p 2757 N94-27726

Thermally stable oxygen and nitrogen implant isolation of C-doped Al(0.35)Ga(0.65)As
[DE94-004799] p 3069 N94-27790

Ion-driven permeation of deuterium in metals
[DE94-701104] p 2744 N94-27876

ION INJECTION

Inertial electrostatic confinement as a power source for electric propulsion p 2688 N94-27373

ION IRRADIATION

Disintegration of (C60) by Xe ion irradiation
[DE94-601913] p 3023 N94-26929

Influence of lattice damage on retention and transport of deuterium in beta silicon carbide
[DE94-005206] p 3068 N94-27693

Secondary electron emission from copper surface due to neodymium and gadolinium ion bombardment
[DE94-701115] p 3027 N94-27718

ION MICROSCOPES

An atom probe investigation of the influence of trace impurities on the mechanical behavior of NiAl
[DE94-002797] p 2734 N94-26272

ION PROBES

He(+) and H(+) microbeam damage, swelling and annealing in diamonds
[DE94-601912] p 3063 N94-26987

Advanced development of particle beam probe diagnostic system
[DE94-002316] p 3047 N94-27720

ION SCATTERING

Diffusion of substitutional elements in Ti in its hcp phase
[DE93-633762] p 2733 N94-26160

Studies of thin-film growth, adsorption, and oxidation by in situ, real-time, and ex situ ion beam analysis
[DE94-002907] p 3055 N94-26275

ION SOURCES

New conditioning procedure derived from operating experience with the Common Long-Pulse Ion Source
[DE94-002891] p 3045 N94-26865

High gas-efficiency hydrogen negative ion sources
[PB93-232163] p 3025 N94-27348

Advanced development of particle beam probe diagnostic system
[DE94-002316] p 3047 N94-27720

ION TEMPERATURE

Kinetic resonance damping rate of the toroidal ion temperature gradient mode
[DE94-003511] p 3041 N94-25923

Reduced Braginskii equations
[DE94-003510] p 3047 N94-27723

IONIC COLLISIONS

Relativistic heavy ion physics
[DE94-003161] p 3031 N94-26097

International bulletin on atomic and molecular data for fusion. No. 42-45, Mar. 1991 - Dec. 1992
[DE94-601817] p 3045 N94-26946

IONIC CRYSTALS

Lighter alkali hydride and deuteride 1: Electronic properties of pure solids
[DE93-616188] p 3051 N94-25914

Radiation-Induced Structural Changes, 2
[DE93-520314] p 3054 N94-26109

IONIC REACTIONS

Merged-beam studies of electron-recombination and excitation of atomic and molecular hydrogen ions
[ETN-94-95339] p 3019 N94-26478

IONIZATION

Two dimensional self-consistent fluid simulation of RF inductive sources
[DE94-003635] p 2767 N94-25937

Electron energy loss spectroscopy in a crystalline environment using inner shell ionization
[DE94-601820] p 3018 N94-26334

Delocalization in electron impact ionization in a crystalline environment
[DE94-601819] p 3062 N94-26927

Technical report of ISSP. Ser. A, no. 2684: Wavelength dependence of nonsequential double ionization in He
[JTN-94-80570] p 3025 N94-27338

Technical report of ISSP. Ser. A, no. 2686: High-order harmonic generation and ionization using ultrashort KrF and Ti:Sapphire lasers
[JTN-94-80572] p 2820 N94-27605

IONIZATION CHAMBERS

Development of laser spectroscopic technology in nuclear industry
[DE93-633327] p 2714 N94-26158

Hadron gas ionization calorimeters
[DE93-634186] p 2810 N94-26397

IONIZATION CROSS SECTIONS

Delocalization in electron impact ionization in a crystalline environment
[DE94-601819] p 3062 N94-26927

Analysis of EUV/FUV dayglow and auroral measurements
[NASA-CR-195237] p 2883 N94-27393

IONIZING RADIATION

Radiation applications of physical chemistry
p 2854 N94-26054

Radiation-Induced Structural Changes, 2
[DE93-520314] p 3054 N94-26109

The response of an hyperpure Ge detector to ionizing radiation
[ISBN-0-315-83968-6] p 2811 N94-26662

IONOSPHERIC CURRENTS

Excitation of Earth-ionosphere waveguide in the ELF and lower VLF bands by modulated ionospheric current
[AD-A274969] p 2878 N94-26304

IONOSPHERIC DISTURBANCES

Coherent HF radar system for the study of natural and heater induced ionospheric irregularities
[AD-A273804] p 2876 N94-25752

Comparative investigation of high-latitude ionospheric structure and effects near solar maximum
[AD-A273799] p 2877 N94-25877

Ionospheric modification by high power, obliquely propagated HF radio wave transmissions. Part 1: Experimental
[AD-A273746] p 2878 N94-26224

Performance statistics bulletin: High altitude meteor scatter propagation, August, September, October 1989
[AD-A274455] p 2773 N94-27085

IONOSPHERIC ELECTRON DENSITY

Ionospheric calibration for single frequency altimeter measurements
[NASA-CR-195709] p 2883 N94-27883

IONOSPHERIC HEATING

Excitation of Earth-ionosphere waveguide in the ELF and lower VLF bands by modulated ionospheric current
[AD-A274969] p 2878 N94-26304

IONOSPHERIC NOISE

Characteristics of 30-MHz interference noises observed by riometers p 2884 N94-27965

IONOSPHERIC PROPAGATION

Comparative investigation of high-latitude ionospheric structure and effects near solar maximum
[AD-A273799] p 2877 N94-25877

Kiruna geophysical data. Data summary 93/4-6, April-June 1993
[PB94-123700] p 2881 N94-27039

Kiruna geophysical data. Data summary 93/1-3, January-March, 1993
[PB94-123791] p 2881 N94-27043

JARE data reports. No. 186: Upper atmosphere physics data. Syowa and Asuka Stations, 1990
[JTN-94-80594] p 2881 N94-27299

IONOSPHERIC SOUNDING

Memories of National Institute of Polar Research. Series A-19. Upper atmosphere physics: ELF emission in high latitudes: Ray path calculation and ground-satellite observations
[JTN-94-80592] p 2882 N94-27342

Antarctic Record, Vol. 36, No. 2
[REPT-107] p 2883 N94-27963

Observation of the upper atmosphere physics at Asuka Station by the 30th Japanese Antarctic Research Expedition in 1989 p 2885 N94-27972

IONOSPHERICS

Auroral Tomography Workshop Proceedings
[PB94-123718] p 2881 N94-27040

IONS
Two dimensional self-consistent fluid simulation of RF inductive sources
[DE94-003635] p 2767 N94-25937
The use of on-line ion chromatography for high temperature and high pressure reaction studies
[DE94-002525] p 2713 N94-26075
Ion beam mixing of marker layers into amorphous aluminum oxide
[DE94-000901] p 2752 N94-26676
Rydberg states in multiply charged ions
[DE94-002335] p 3021 N94-26760
Influence of point defects on grain boundary diffusion in oxides
[DE94-003164] p 3060 N94-26782
Effect of temperature and recoil-energy spectra on irradiation-induced amorphization in Ca2La8(SiO4)6O2
[DE94-004371] p 3067 N94-27602
Technical report of ISSP. Ser. A, no. 2686: High-order harmonic generation and ionization using ultrashort KrF and Ti:Sapphire lasers
[JTN-94-80572] p 2820 N94-27605
Damage growth in MgAl2O4 crystals by Xe ion irradiations
[DE94-005009] p 3069 N94-27828
Effect of different ions on the anodic behaviour of alloy 800 in chloride solutions at high temperature
[DE94-602982] p 2743 N94-27832
Acceleration of electrons and ions by strong lower-hybrid turbulence in solar flares
[NASA-TM-109723] p 3111 N94-27953

IRIDIUM
Extraterrestrial accretion and glacial cycles
p 2890 N94-28308

IRON
Study on improvement in physical analysis method of metallic materials p 2728 N94-25577
Deviatoric stresses and plastic strain rates in strong shock waves for six metals
[DE94-002964] p 2733 N94-26022
Iron: What is melt?
[DE94-003373] p 2735 N94-26322
The electrochemical behavior of the Al3Fe intermetallic compound and localized corrosion of impure 1100 Al
[DE94-002037] p 2739 N94-26912

IRON ALLOYS
The role of grain boundary chemistry and structure in the environmentally-assisted intergranular cracking of nickel-base alloys
[DE94-003159] p 2732 N94-25954
Surface physics with cold and thermal neutron reflectometry
[DE94-001447] p 2733 N94-26070
Influence of helium generation rate and temperature history on mechanical properties of model Fe-Cr-Ni alloys irradiated in FFTF at relatively low displacement rates
[DE94-004264] p 2737 N94-26575
Experimental measurement of local displacement and chemical pair correlations in crystalline solid solutions
[DE94-001124] p 3065 N94-27251
Current status of research and development on nickel and iron aluminides
[DE94-004247] p 2741 N94-27616
Effect of different ions on the anodic behaviour of alloy 800 in chloride solutions at high temperature
[DE94-602982] p 2743 N94-27832
NMR study of quasicrystal Al(70)Pd(20)T(M10) alloy (T(M):Cr, Mn, Fe, and Co) p 2745 N94-28162
Production of an amorphous Fe(75)Si(10)B(15) sheet by a metallic mold casting method and its properties
p 2746 N94-28170

IRON COMPOUNDS
Study on reactions between molten metal and oxide by magnetic flotation dissolution method
p 2725 N94-25558
Study on microscopic structural controls and electronic properties at material surfaces by ion beams
p 2727 N94-25571

IRON OXIDES
Study on improvement in physical analysis method of metallic materials p 2728 N94-25577

IRRADIATION
Microstructural development in low activation ferritic alloys irradiated to 200 dpa at 420 C
[DE94-004269] p 2731 N94-25803
Studies on the application of radiation for genetic transformation in higher plants
[DE93-632656] p 2901 N94-26470
Nonswelling behavior of HT9 alloy irradiated to high exposure
[DE94-003502] p 2736 N94-26522
Molecular biological studies on the human radioresistance and drug resistance
[DE93-632682] p 2910 N94-26549
S-76 high intensity radiated fields, volume 2
[AD-A274572] p 2771 N94-26836
S-76 high intensity radiated fields, volume 1
[AD-A274571] p 2771 N94-26854
He(+) and H(+) microbeam damage, swelling and annealing in diamonds
[DE94-601912] p 3063 N94-26987
Research and development within nonlinear optics for protection of optical sensors against laser irradiation on of optical sensors against laser irradiation. Quarterannual report 1 (april 1993))
[PB94-124245] p 3037 N94-27046
Outgas and vacuum seal characteristics of irradiated polyimide O-ring
[DE94-701200] p 2757 N94-27812
Simulations of terrestrial in-situ cosmogenic-nuclide production
[DE94-004999] p 3117 N94-27826

ISCHEMIA
Protective action of platelet-activating factor antagonist, TCV-309, against ischemia reperfusion injury in isolated rabbit hearts p 2904 N94-27465
Protective action of an amiloride derivative (amiloride, 5-(N, N-dimethyl) hydrochloride) against in isolated ischemia/reperfusion newborn rabbit hearts
p 2904 N94-27466

ISING MODEL
NNN-Ising model simulation of nanodomain textures in relaxor-type lead scandium tantalate
[DE94-601884] p 2748 N94-25844
Holes in a two-dimensional quantum antiferromagnet
[DE93-634753] p 3057 N94-26388
Ising critical behaviour in the one-dimensional frustrated quantum XY model
[DE93-634755] p 3057 N94-26390
Mapping between the Sinh-Gordon and Ising models
[DE94-601535] p 2998 N94-27162

ISOBARS (PRESSURE)
An observational study of the extratropical anticyclones in the South American continent
[INPE-5387-TDI/476] p 2896 N94-27356

ISOMERS
The addition of molecular oxygen to hydroperoxy-propyl radicals
[DE94-003662] p 2760 N94-27725
Thermal conductivity of liquid aliphatic alcohols
[ESDU-93008] p 2720 N94-28058
Vapour pressures and critical points of liquids: Aliphatic and cyclic ketones
[ESDU-93009] p 2720 N94-28059
Orthobaric densities and molar volumes of liquids: Aliphatic and cyclic ketones
[ESDU-93010] p 2720 N94-28060

ISOSTATIC PRESSURE
Material optimization and manufacturing development of reduced cost powder metal titanium alloy components for gas turbine engine application, phase 2
[AD-A274410] p 2709 N94-26978

ISOTHERMAL FLOW
A modelling of the noise from simple coaxial jets. Part 3: With hot primary flow
[ISVR-TR-230-PT-3] p 2807 N94-28173

ISOTHERMS
Experimental determination of the CU-IN-PB ternary phase diagram
[DE94-003765] p 2735 N94-26349

ISOTONICITY
Isotonic estimation and rates of convergence in Wicksell's problem
[REPT-93-39] p 3002 N94-26213

ISOTOPES
Seasonal snow of arctic Alaska R4D investigations
[DE93-040082] p 2892 N94-25939

ISOTOPIC ENRICHMENT
Isotopically labeled CO2 from stratosphere: A tracer of carbon biogeochemistry
[DE94-002777] p 2877 N94-26015

ISOTOPIC SPIN
Spinor and isospinor structure of relativistic particle propagators
[DE94-601552] p 3019 N94-26424
Spin from isospin: The model of superparticle in a non-Grassmannian approach
[DE93-634341] p 3019 N94-26454

ISOTROPIC MEDIA
Efficient modeling in transversely isotropic inhomogeneous media
[DE94-003394] p 2877 N94-25847
Eigenwaves in the general uniaxial bianisotropic medium with symmetric parameter dyadics
[PB94-132891] p 2778 N94-28381

ISOTROPY
Design and test of postbuckled stiffened curved plates: A literature survey
[PB94-126521] p 2840 N94-26961
The PROTEL contamination code
[RXR-93071] p 3040 N94-28202
Plane wave propagation and polarization properties in transversely bianisotropic uniaxial medium
[PB94-132883] p 2778 N94-28380
Green dyadic and dipole fields for a medium with anisotropic chirality
[PB94-132933] p 2779 N94-28391

ISRAEL
Mapping of seawater intrusion into the coastal aquifer of Israel (the seawater-freshwater interface) by TDEM (Time Domain Electromagnetic) method
[ITN-94-85238] p 2850 N94-27331

ITERATION
Design and evaluation of fault tolerance in opto-electronic computing
[AD-A274281] p 2954 N94-27016

ITERATIVE SOLUTION
Research on primal-dual interior point algorithms for mathematical programming
[DE94-003982] p 2959 N94-25821
Preconditioning in parallel Runge-Kutta methods for stiff initial value problems
[CWI-NM-R9310] p 2991 N94-26217
On the error committed by stopping the Newton iteration in implicit Runge-Kutta methods
[TW-93-02] p 2992 N94-26229
A numerical solution to the one and two dimensional line radiative transfer equation
[ISBN-0-315-84258-X] p 2994 N94-26640
Nested Krylov methods based on GCR
[PB94-125317] p 2995 N94-26818
Computation of numerical solution of parabolic PDEs by monotone iterative methods
[ISBN-0-315-84553-8] p 2999 N94-27404
Iterative methods for the WLS state estimation on RISC, vector, and parallel computers
[DE94-004260] p 3000 N94-27569
Fixed point type theorems and projection-interaction approximation
[DE94-603669] p 3000 N94-27632
A parallel multigrid algorithm for solving the Navier-Stokes equations on a transputer system
[PREPRINT-699] p 2807 N94-28099
Hessenberg matrices in Krylov subspaces and the computation of the spectrum
[PB94-133170] p 3001 N94-28389

IUE
Ultraviolet observations of astronomical sources
[NASA-CR-195232] p 3102 N94-26234

J

J INTEGRAL
Effect of loading mode on the fracture toughness of a reduced activation ferritic/martensitic stainless steel
[DE94-004290] p 2732 N94-25987

JAMMERS
An analysis of FM jamming and noise quality measures
[AD-A274349] p 2772 N94-26924

JAMMING
An analysis of FM jamming and noise quality measures
[AD-A274349] p 2772 N94-26924
Development of a performance evaluation tool (MMSOFE) for detection of failures with Multiple Model Adaptive Estimation (MMAE)
[AD-A274218] p 2665 N94-27071
FOA 39 — electronic countermeasures
[PB94-124252] p 2773 N94-27159

JAPAN
An observational study of air pollution transport over a large urban complex
[REPT-6] p 2867 N94-26474
Meteorological data at the Nagaoka Institute of Snow and Ice Studies
[REPT-158] p 2896 N94-27169

JET AIRCRAFT
Report of the defense science board task force on aircraft assessment
[AD-A274531] p 2669 N94-26835
Methods for experimentally determining commercial jet aircraft landing parameters from video image data
[AD-A274207] p 2669 N94-27105
Experiments into the scaling parameters required for exhaust gas ingestion testing of vertical landing aircraft
p 2671 N94-28017

JET BOUNDARIES
A numerical investigation of a subsonic jet in a crossflow p 2803 N94-28023

JET CONTROL
Controlled oscillation of forebody vortices by nozzle jet blowing
[ISBN-0-315-84134-6] p 2678 N94-27648
Control jets in interaction with hypersonic rarefied flow
p 2698 N94-28020

Recent developments in the simulation of steady and transient transverse jet interactions for missile, rotorcraft, and propulsive applications p 2804 N94-28030

JET ENGINE FUELS
Broad specification fuels combustion technology program, phase 2
[NASA-CR-191066] p 2719 N94-27854

JET ENGINES
An algorithm for determination of bearing health through automated vibration monitoring
[AD-A274591] p 2823 N94-26986
Engine starting and stopping p 2828 N94-28047
High-performance parallel analysis of coupled problems for aircraft propulsion
[NASA-CR-195292] p 2845 N94-28181

JET EXHAUST
Experiments into the scaling parameters required for exhaust gas ingestion testing of vertical landing aircraft
p 2671 N94-28017

JET FLOW
Experimental and theoretical investigations of the influence of the jet on the flow around a bypass-engine
[DLR-FB-93-17] p 2675 N94-27593
Computational and Experimental Assessment of Jets in Cross Flow
[AGARD-CP-534] p 2799 N94-28003
Fifty years of jet in cross flow research
p 2799 N94-28004
The interaction region associated with twin jets and a normal crossflow p 2800 N94-28009
Experimental data for CFD validation of impinging jets in crossflow with application to ASTOVL flow problems
p 2801 N94-28010
Experimental investigation of the interaction of a thrust reverser jet with an external subsonic flow
p 2801 N94-28011
Vectored jets-induced interference on aircraft, prediction and verification p 2801 N94-28012
Topological structure of a jet in a cross flow
p 2801 N94-28014
An experimental study of siphonal jets in a turbulent boundary layer crossflow p 2802 N94-28015
Experiments on the ground vortex formed by an impinging jet in cross flow p 2802 N94-28016
Predictions of momentum and scalar fields in a jet in cross-flow using first and second order turbulence closures p 2803 N94-28025
Navier-Stokes simulation of two and three dimensional jets in crossflow, effects of grid, and boundary conditions p 2804 N94-28026
Effects, limits, and limitations of spanwise blowing
p 2659 N94-28027
Pneumatic management of blunted-forebody flow asymmetry for high-angle-of-attack directional control
p 2679 N94-28028
Theoretical and experimental investigation of a delta wing with turbulent leading-edge jets
p 2659 N94-28029
Recent developments in the simulation of steady and transient transverse jet interactions for missile, rotorcraft, and propulsive applications p 2804 N94-28030
Numerical assessment of aerodynamic interactions on missiles with transverse jets control
p 2659 N94-28031
Effects of free-stream turbulence on a jet in a cross flow p 2805 N94-28036
Navier-Stokes analysis of a swirling jet in crossflow
p 2806 N94-28038
Journal of NIRE, volume 2, number 4
[JTN-94-80554] p 2869 N94-28147
Numerical simulation of turbulent free jet by TFKE model p 2871 N94-28157
A modelling of the noise from simple coaxial jets. Part 3: With hot primary flow
[ISVR-TR-230-PT-3] p 2807 N94-28173

JET IMPINGEMENT
Experimental data for CFD validation of impinging jets in crossflow with application to ASTOVL flow problems
p 2801 N94-28010
Experiments on the ground vortex formed by an impinging jet in cross flow p 2802 N94-28016
Calculation of single and multiple jets in cross-flow with and without impingement using Reynolds-stress-transport closure p 2803 N94-28024
Advanced metallic exhaust impinged structural concepts demonstration p 2832 N94-28209

JET LIFT
Unsteady aspects of hot gas reingestion and statistical analysis p 2676 N94-28019
Transitional flight characteristics of a geometrically simplified STOVL model p 2672 N94-28035

JET PROPULSION
High-performance parallel analysis of coupled problems for aircraft propulsion
[NASA-CR-195292] p 2845 N94-28181

JET PUMPS
Ejectors and jet pumps: Computer program for design and performance for liquid flow
[ESDU-93022] p 2832 N94-28093

JET STREAMS (METEOROLOGY)
Investigation of mesoscale convective cloud clusters in South China
[AD-A274303] p 2895 N94-26678

JET THRUST
Experiments on interaction force of jets in hypervelocity cross-flow in a shock tunnel p 2659 N94-28022

JOINTS (ANATOMY)
Effect of sera from patients treated with long-term hemodialysis on mRNA's for collagenase, stromelysin, and tissue inhibitor of metalloprotease in cultured human synovial cells p 2920 N94-27481

JOINTS (JUNCTIONS)
Three methods to measure RH bond energies
[DE94-003795] p 3013 N94-25816
Bulletin of the Institute for Chemical Reaction Science, Tohoku University, volume 2
[JTN-94-80602] p 2717 N94-27385
Porous vycor glass tube joined to borosilicate glass
p 2718 N94-27392

JOSEPHSON JUNCTIONS
Flux flow, pinning, and resistive behavior in superconducting networks
[DE94-003400] p 3050 N94-25848
Ising critical behaviour in the one-dimensional frustrated quantum XY model
[DE93-634755] p 3057 N94-26390
Preparation and characterization of high temperature superconductor film surfaces
[AD-A274293] p 3059 N94-26681
Processing, fabrication, and demonstration of HTS integrated microwave circuits, appendix A
[AD-A274600] p 2785 N94-26890

JOURNAL BEARINGS
Calculation methods for steadily loaded central circumferential groove hydrodynamic journal bearings (guide to use of computer program A9304)
[ESDU-93004] p 2830 N94-28073
Calculation methods for steadily loaded axial groove hydrodynamic journal bearings (guide to use of computer program A9305)
[ESDU-93005] p 2830 N94-28074
Calculation methods for steadily loaded axial groove hydrodynamic journal bearings. Low viscosity process fluid lubrication (guide to use of computer program A9306)
[ESDU-93006] p 2830 N94-28075

JUNCTION DIODES
Electric-field dependence of electroreflectance and photocurrent spectra at visible wavelengths in MOVPE-grown InAlGaP multiple strained quantum-well structures
[DE94-004692] p 2780 N94-25664
Electrical properties of p-type GaInP2
[AD-A273771] p 3051 N94-25856

JUNCTION TRANSISTORS
A physics-based heterojunction bipolar transistor model for integrated circuit simulation
[AD-A274081] p 2781 N94-25995

JUPITER (PLANET)
The crash of P/Shoemaker-Levy 9 into Jupiter and its implications for comet bombardment on Earth
p 2891 N94-28313

JUPITER ATMOSPHERE
Studies for Io's extended atmosphere and neutral clouds and their impact on the local satellite atmosphere and on the planetary magnetosphere
[NASA-CR-195255] p 3106 N94-27406

K

K-EPSILON TURBULENCE MODEL
Computational prediction of isolated performance of an axisymmetric nozzle at Mach number 0.90
[NASA-TM-4506] p 2646 N94-26547
Predictions of momentum and scalar fields in a jet in cross-flow using first and second order turbulence closures p 2803 N94-28025
Navier-Stokes simulation of two and three dimensional jets in crossflow, effects of grid, and boundary conditions p 2804 N94-28026
Recent developments in the simulation of steady and transient transverse jet interactions for missile, rotorcraft, and propulsive applications p 2804 N94-28030

KALMAN FILTERS
Multiple model adaptive estimation applied to the LAMBDA URV for failure detection and identification
[AD-A274078] p 3002 N94-25992
Kalman filtering of narrowband interference from direct sequence spread spectrum communications systems
[ISBN-0-315-84011-0] p 2784 N94-26627
An adaptive Kalman filter for tactical missiles guidance systems
[ISBN-0-315-84115-X] p 2677 N94-26636
Development of a performance evaluation tool (MMSOFE) for detection of failures with Multiple Model Adaptive Estimation (MMAE)
[AD-A274218] p 2665 N94-27071
Enhanced tracking of airborne targets using forward looking infrared and laser return measurements
[AD-A274181] p 3037 N94-27102
A data fusion algorithm for multi-sensor microburst hazard assessment p 2641 N94-27287
Flight testing of GPS and GPS-aided systems
[NLR-TP-92151-U] p 2666 N94-27831

KAONS
Production of (phi) mesons in central Si + Au collisions at 14.6 AGeV/c
[DE94-003196] p 3012 N94-25795
Low-energy hadronic interactions beyond the current algebra approach
[DE94-602600] p 3022 N94-26900
Pi plus pi minus gamma and K+ K- production in two photon collisions at ARGUS
[ISBN-0-315-63598-3] p 3027 N94-27684

KELVIN-HELMHOLTZ INSTABILITY
Probability of accessing the multiple saturated states in the resistive interchange instability
[DE94-000478] p 3044 N94-26694

KERR CELLS
Characterization of nonlinear effects in optically pumped vertical cavity surface emitting lasers
[AD-A273840] p 2815 N94-25744

KETONES
Vapour pressures and critical points of liquids: Aliphatic and cyclic ketones
[ESDU-93009] p 2720 N94-28059
Orthobaric densities and molar volumes of liquids: Aliphatic and cyclic ketones
[ESDU-93010] p 2720 N94-28060

KINEMATICS
A global approach to kinematic path planning to robots with holonomic and nonholonomic constraints
p 2683 N94-26279
Inertial-space disturbance rejection for space-based manipulators p 2683 N94-26281
High-production global positioning system methods for survey applications: The pseudo-kinematic method with the Trimvec programming system
[ETN-94-95035] p 2665 N94-26539
Optimal architectural design of parallel and hybrid manipulators
[ISBN-0-315-84351-9] p 2822 N94-26657
Study of the kinematic and dynamic characteristics of a wormgear transmission for helicopter applications
[NASA-CR-195287] p 2826 N94-27657

KINESTHESIA
Proprioceptive isokinetic exercise test
[NASA-TM-104015] p 2902 N94-27227

KINETIC EQUATIONS
Kinetic equation identification from measurement of a particular solution
[DE93-634585] p 2995 N94-26768

KINETIC THEORY
Process modelling of aluminium alloys. Modelling of the quench sensitivity of alloy AA6082
[PB94-124567] p 2741 N94-27325

KINOFORM
Kinoform/lens system for injecting a high power laser beam into an optical fiber
[DE94-003226] p 2819 N94-27262

KLYSTRONS
JLC-1
[DE93-520380] p 3031 N94-26113
HPm-tubes: Literature survey comprising 1992
[PB94-123643] p 2785 N94-27038

KNOWLEDGE BASED SYSTEMS
Developing realistic cooperative behaviors for autonomous agents in air combat simulation
[AD-A274077] p 2937 N94-25774
A method for populating the knowledge base of APTAS, a domain-oriented application composition system
[AD-A274034] p 2766 N94-25797
Top down influences on bottom-up processing
[AD-A274220] p 2939 N94-27072
A method for populating the knowledge base of AFIT's domain-oriented application composition system
[AD-A274128] p 3099 N94-27118
Alternative architectures for domain-oriented application composition and generation systems
[AD-A274180] p 2968 N94-27128

KNOWLEDGE BASES (ARTIFICIAL INTELLIGENCE)
Knowledge base systems for chemical compounds designing support p 2723 N94-25550
A method for populating the knowledge base of APTAS, a domain-oriented application composition system
[AD-A274034] p 2766 N94-25797

KNOWLEDGE REPRESENTATION

Knowledge base systems for chemical compounds designing support p 2723 N94-25550

Study on knowledge extraction and systematization for material design p 2727 N94-25568

Knowledge organization in intelligent tutoring systems for diagnostic problem solving in complex dynamic domains
[AD-A273986] p 2984 N94-25899

A hybrid formalism for representation and interpretation of image knowledge
[INPE-5485-PRE/1784] p 2989 N94-27833

KOLMOGOROV THEORY

The nonlinear Galerkin method: A multi-scale method applied to the simulation of homogeneous turbulent flows
[NASA-CR-191581] p 2792 N94-26499

Modelling atmospheric turbulence effects on ground-based telescope systems
[DE94-004211] p 3102 N94-26528

A strange application of Kolmogorov complexity
[CWI-CS-R9328] p 2973 N94-27737

KONDO EFFECT

Multi-channel Kondo necklace
[DE93-634754] p 3057 N94-26389

Strongly interacting fermion systems
[DE94-002674] p 3021 N94-26677

Correlated mean field Ansatz for the Kondo necklace
[DE94-603671] p 3067 N94-27634

KORTEWEG-DEVRIES EQUATION

Poisson-lie group of pseudodifferential symbols
[PB94-124393] p 2997 N94-26996

KOVAR (TRADEMARK)

High temperature grain growth and oxidation of Fe-29Ni-17Co (Kovar (tm)) alloy leads
[DE94-004691] p 3069 N94-27753

KP INDEX

Persistence of auroral electron flux events from DMSP/F9 electron measurements
[RXR-92012] p 2887 N94-28206

KRAMERS-KRONIG FORMULA

Submillimeter residual losses in high-(Tc) superconductors
[DE94-003241] p 3058 N94-26516

KRYPTON FLUORIDE LASERS

Laboratory plasma studies
[AD-A274655] p 3043 N94-26356

Technical report of ISSP. Ser. A, no. 2685: ASE-free terawatt KrF/Ti : sapphire hybrid laser system
[JTN-94-80571] p 2820 N94-27339

Technical report of ISSP. Ser. A, no. 2686: High-order harmonic generation and ionization using ultrashort KrF and Ti:Sapphire lasers
[JTN-94-80572] p 2820 N94-27605

L

LABOR

Concepts and methods of measuring productivity at the organization level
[AD-A273126] p 3094 N94-27180

LABORATORIES

Measurement of laboratory quality
[VTT-TIED-1427] p 2679 N94-25652

The National Center for Advanced Information Components Manufacturing: Program update
[DE94-002647] p 2960 N94-26118

LACTATES

High impact strength poly(lactide) tough biodegradable materials
[ETN-94-95389] p 2747 N94-25748

LAGRANGIAN FUNCTION

Dynamical group of relativistic straight-line string
[DE93-634347] p 3072 N94-26037

Orthodox gravity
[DE94-601560] p 2878 N94-26418

Gauging of Chern-Simons p-Barnes
[DE94-601553] p 2993 N94-26425

Component structure of the N = 2 super-Yang-Mills theory in the harmonic superspace
[DE93-634340] p 3072 N94-26453

Spin from isospin: The model of superparticle in a non-Grassmannian approach
[DE93-634341] p 3019 N94-26454

Delta f Algorithm
[DE94-003120] p 2963 N94-26521

Low-energy hadronic interactions beyond the current algebra approach
[DE94-602600] p 3022 N94-26900

LAMINAR BOUNDARY LAYER

Prediction of leading-edge transition and relaminarization phenomena on a subsonic multi-element high-lift system p 2659 N94-27929

Experimental study on the shock wave interaction with a hypersonic boundary layer near a convex corner
p 2654 N94-28328

LAMINAR FLOW

Dynamic response of a compressor research facility
[AD-A273836] p 2679 N94-25740

The numerical calculation of laminar and turbulent flows using penalty function finite volume methods
[ISBN-0-315-61377-7] p 2799 N94-27947

Pneumatic management of blunted-forebody flow asymmetry for high-angle-of-attack directional control
p 2679 N94-28028

Calculation methods for steadily loaded axial groove hydrodynamic journal bearings (guide to use of computer program A9305)
[ESDU-93005] p 2830 N94-28074

Calculation methods for steadily loaded axial groove hydrodynamic journal bearings. Low viscosity process fluid lubrication (guide to use of computer program A9306)
[ESDU-93006] p 2830 N94-28075

Forced convection heat transfer in straight tubes. Part 2: Laminar and transitional flow
[ESDU-93018-PT-2] p 2807 N94-28139

LAMINATES

A nonlinear three-dimensional micromechanics model for fiber-reinforced laminated composites
[AD-A273772] p 2705 N94-25857

Influence of embedded optical fibers on compressive strength of advanced composites
[AD-A273775] p 2705 N94-25859

The effects of embedded internal delaminations on composite laminate compression strength; an experimental review
[NASA-TM-108440] p 2707 N94-26127

Bimaterial interfaces and their role in the mechanical performance of the in-situ composites
[AD-A274688] p 2707 N94-26447

Processing and mechanical properties of laminated metal composites of Al 6090-25 volume percent SiC(sub p) and Al 5182
[DE94-001070] p 2708 N94-26930

Experimental study of the angled crack in GLARE 3
[PB94-126554] p 2669 N94-26954

Development of fibre-metal laminates, ARALL and GLARE, new fatigue resistant materials
[PB94-126471] p 2669 N94-26969

Impact tests on fibre metal laminates under a tensile load
[PB94-126570] p 2710 N94-27201

The experimental behavior of spinning pretwisted laminated composite plates
[NASA-CR-195220] p 2711 N94-27352

Finite element analysis of damped vibrations of laminated composite plates
[ISBN-0-315-84928-2] p 2843 N94-27585

Mechanically fastened composite laminates subjected to combined bearing-bypass and shear loading
p 2712 N94-27914

Structural study of Cu/Co multilayer by anomalous small-angle x ray scattering p 2744 N94-28160

Differential scanning calorimetric study of solid state amorphization and crystallization in Zr/Co and Zr/Ni multilayers p 2745 N94-28161

LAND ICE

Ice surface temperature retrieval from AVHRR, ATSR, and passive microwave satellite data: Algorithm development and application
[NASA-CR-195276] p 2851 N94-27849

LAND MANAGEMENT

Asia-Pacific Seminar on Global Change Research Cooperation
[JTN-94-80517] p 2871 N94-28268

Global concern on research cooperation for environment p 2872 N94-28275

Land use change in Thailand and its impact on environmental change: Joint Thai-Japanese research project (1993-1995) p 2875 N94-28288

LAND SURFACE TEMPERATURE

Ice surface temperature retrieval from AVHRR, ATSR, and passive microwave satellite data: Algorithm development and application
[NASA-CR-195276] p 2851 N94-27849

LAND USE

Land use change in Thailand and its impact on environmental change: Joint Thai-Japanese research project (1993-1995) p 2875 N94-28288

LANDAU DAMPING

Review of tokamak experiments on direct electron heating and current drive with fast waves
[DE94-004185] p 3041 N94-25801

Kinetic resonance damping rate of the toroidal ion temperature gradient mode
[DE94-003511] p 3041 N94-25923

Analysis of density limit and efficiency in lower hybrid current drive
[DE94-604995] p 3049 N94-27856

LANDAU FACTOR

Excited Landau levels, orbital angular momentum and axial anomaly
[DE94-606407] p 3068 N94-27679

LANDING GEAR

Tests of highly loaded skids on a concrete runway
[NASA-TP-3435] p 2669 N94-26608

Aircraft wheel life assessment
[AD-A274378] p 2823 N94-26976

LANDING LOADS

Methods for experimentally determining commercial jet aircraft landing parameters from video image data
[AD-A274207] p 2669 N94-27105

LANDING SIMULATION

Piloted simulation study of an ILS approach of a twin-pusher business/commuter turboprop aircraft configuration
[NASA-TM-4516] p 2646 N94-26602

LANDSAT SATELLITES

Morphodynamics of inter-tidal areas: The Wadden Sea
[NLR-TP-92356-U] p 2851 N94-27555

LANGMUIR-BLODGETT FILMS

Langmuir-Blodgett film of amylose-esters and chiral azo-dyes (structure and second order nonlinear optical behaviour)
[ETN-94-95390] p 2747 N94-25749

Mechanical properties of polyaniline prepared by polymerization in an organized monolayer
[AD-A274350] p 2753 N94-26925

Ferroelectricity in a Langmuir-Blodgett multilayer film of a liquid crystalline side-chain polymer
[AD-A274477] p 2754 N94-27033

Langmuir-Blodgett and STM investigations of conducting polymer thin films
[AD-A274512] p 2755 N94-27087

Chemical polymerization and Langmuir-Blodgett techniques. 2: The polymerization of monolayers of 3-substituted pyrroles
[AD-A274478] p 2755 N94-27163

LANGUAGES

Induced pictorial representations
[AD-A274251] p 2939 N94-27012

LANTHANUM ALLOYS

Mechanical behavior of amorphous alloys at elevated temperatures p 2746 N94-28167

LANTHANUM COMPOUNDS

Successive structural phase transitions in stoichiometric La2NiO4 observed by x ray diffraction
[REPT-A-2665] p 3051 N94-25921

Phase diagram of La2NiO(4 + delta) (0 less than or equal to delta less than or equal to 0.18). 1: Phases at room temperature and phase transition above delta equal to 0.15
[REPT-A-2661] p 3053 N94-26089

Technical report of ISSP. Ser. A, no. 2669: Relations between oxygen deficiency and structures in the La-Sr-Cu-O system. 3: Oxygen contents and structure of (La, Sr)8Cu8O(16 + delta) phase
[JTN-94-80555] p 3066 N94-27353

LANTHANUM ISOTOPES

Microscopic study of local structure and charge distribution in metallic La2CuO(4 + delta)
[DE94-003801] p 3050 N94-25817

LANTHANUM OXIDES

Microscopic study of local structure and charge distribution in metallic La2CuO(4 + delta)
[DE94-003801] p 3050 N94-25817

Preparation and characterization of high temperature superconductor film surfaces
[AD-A274293] p 3059 N94-26681

LAP JOINTS

Testing composite-to-metal tubular lap joints
[DE94-003225] p 2836 N94-26032

LARGE SPACE STRUCTURES

Prototype space fabrication platform
[AD-A273904] p 2694 N94-25659

Proceedings of Damping 1993, volume 2
[AD-A274227] p 2840 N94-26953

Proceedings of Damping 1993, volume 3
[AD-A274228] p 2840 N94-27008

Multiple model adaptive control of a large flexible space structure with purposeful dither for enhanced identifiability
[AD-A274132] p 2987 N94-27122

Dynamics and robust control for uncertain flexible space systems
[INPE-5510-TAE/020] p 2696 N94-27357

LARMOR RADIUS

Toroidal plasma beta-FLR limit in a toroidally linked mirror system
[DE94-003119] p 3041 N94-25792

LARYNX

NCVS, volume 5
[AD-A274975] p 2902 N94-27165

LASER ABLATION
Resonant holographic measurements of laser ablation plume expansion in vacuum and argon gas backgrounds
[DE94-001407] p 2813 N94-27615
LASER ALTIMETERS
Laser altimetry simulator. Version 3.0: User's guide
[NASA-TM-104588] p 2877 N94-26152
LASER ANNEALING
Regrowth zones in laser annealed radiation damaged diamond
[DE94-600821] p 3056 N94-26364
LASER APPLICATIONS
Characterization of an LCD for use as a programmable phase shifter to produce a single-lobed far-field pattern in a phased array
[AD-A273883] p 3034 N94-25729
Microtubules for nonlinear optical limiting
[AD-A273940] p 3035 N94-25941
Deciphering the quark-gluon structure of the photon in electron(gamma) collisions
[DE93-634386] p 3017 N94-26043
Improved measurement accuracy in a Long Trace Profiler: Compensation for laser pointing instability
[DE94-003408] p 2816 N94-26130
Broad band tunable dye laser development
[DE93-632978] p 2816 N94-26157
Development of an industrial CO2 laser for mask marking
[DE93-632901] p 2816 N94-26184
Development of surgical CW Nd:YAG laser with optical fiber delivery system
[DE93-632902] p 2817 N94-26185
Laser manipulation of metastable neon atoms
[ETN-94-95344] p 2817 N94-26225
Compact, solid-state femtosecond source
[AD-A273932] p 2817 N94-26271
Diode-laser-pumped, gas-cell atomic clocks
[AD-A274812] p 3008 N94-26484
Laser Doppler velocimetry in a low speed multistage compressor
[AD-A274836] p 2818 N94-26498
Beam-quality measurements for materials processing lasers and the proposed ISO standard
[DE94-002738] p 2819 N94-26811
Mechanistic studies of opto-electronic materials and syntheses using multiple laser and surface diagnostics
[AD-A274528] p 3036 N94-26834
Gordon Research Conference on the Physics and Chemistry of Laser Diagnostics in Combustion
[AD-A274609] p 2716 N94-26893
Enhanced tracking of airborne targets using forward looking infrared and laser return measurements
[AD-A274181] p 3037 N94-27102
Compilation of corrections for postprocessing of laser bathymetry data
[PB94-123668] p 2900 N94-27156
Scanview: A grafical program for analysis of laserbathymetry data
[PB94-124443] p 2900 N94-27208
High repetition rate, mode locked, figure eight laser with extracavity feedback
[AD-D016053] p 2820 N94-27670
System for conditioning an electron beam for improved free-electron laser operation
[AD-D016054] p 2820 N94-27671
Optical pattern recognition system utilizing resonator array
[AD-D016071] p 3040 N94-28224
LASER ARRAYS
Characterization of an LCD for use as a programmable phase shifter to produce a single-lobed far-field pattern in a phased array
[AD-A273883] p 3034 N94-25729
LASER BEAMS
Studies of non-linear optical effects for agile beam steering
[AD-A273996] p 3034 N94-25902
Microtubules for nonlinear optical limiting
[AD-A273940] p 3035 N94-25941
Comparison of technology for high-power laser mirrors and synchrotron radiation mirrors
[DE94-002913] p 3035 N94-26276
Regrowth zones in laser annealed radiation damaged diamond
[DE94-600821] p 3056 N94-26364
Fiber-optic-based laser vapor screen flow visualization system for aerodynamic research in larger scale subsonic and transonic wind tunnels
[NASA-TM-4514] p 2647 N94-26706
Beam-quality measurements for materials processing lasers and the proposed ISO standard
[DE94-002738] p 2819 N94-26811
Research and development within nonlinear optics for protection of optical sensors against laser irradiation on of optical sensors against laser irradiation. Quarterannual report 1 (april 1993))
[PB94-124245] p 3037 N94-27046
Kinoform/lens system for injecting a high power laser beam into an optical fiber
[DE94-003226] p 2819 N94-27262
Predoctoral training grant in the area of physical sciences
[DE94-004406] p 3039 N94-27603
Technical report of ISSP. Ser. A, no. 2686: High-order harmonic generation and ionization using ultrashort KrF and Ti:Sapphire lasers
[JTN-94-80572] p 2820 N94-27605
LASER CAVITIES
Characterization of nonlinear effects in optically pumped vertical cavity surface emitting lasers
[AD-A273840] p 2815 N94-25744
Ultra-high aggregate bandwidth two-dimensional multiple-wavelength diode laser arrays
[AD-A274018] p 2815 N94-25756
Practical design of resonant cavity for a RF free electron laser
[AD-A274306] p 2819 N94-26941
High repetition rate, mode locked, figure eight laser with extracavity feedback
[AD-D016053] p 2820 N94-27670
LASER DAMAGE
Microtubules for nonlinear optical limiting
[AD-A273940] p 3035 N94-25941
Regrowth zones in laser annealed radiation damaged diamond
[DE94-600821] p 3056 N94-26364
LASER DOPPLER VELOCIMETERS
Laser Doppler velocimetry in a low speed multistage compressor
[AD-A274836] p 2818 N94-26498
Propagation of experimental uncertainties from the tunnel to the body coordinate system in 3-D LDV flow field studies
[NASA-CR-191607] p 2680 N94-26603
Turbulent boundary layer inner-outer interactions
[AD-A274357] p 2794 N94-27059
The measurements of muscle blood flow by laser Doppler flowmetry with needle type probe
p 2908 N94-27530
Microspheres for laser velocimetry in high temperature wind tunnel p 2682 N94-27903
LASER GYROSCOPES
On the application of Allan variance method for Ring Laser Gyro performance characterization
[DE94-003880] p 2810 N94-26525
LASER HEATING
Float zone crystal growth using laser radiation
[DLR-FB-93-10] p 3066 N94-27590
Laser surface modification of intermetallic compounds
[DREA-CR-92-416] p 2820 N94-27668
A numerical approach to Stefan problem
[IPPCZ-334] p 2844 N94-27841
LASER INDUCED FLUORESCENCE
Spectroscopic and vibrational energy transfer studies in molecular bromine
[AD-A273795] p 3014 N94-25875
Hook spectroscopy as an atomic number density diagnostic applied to laser-ablated copper plasmas
[DE94-002645] p 3042 N94-26081
Laser probes of natural gas ignition chemistry
[PB94-128345] p 2717 N94-27226
Technical report of ISSP. Ser. A, no. 2682: Pressure dependence of Sm:YAG fluorescence to 50 GPa: A new calibration as a high pressure scale
[JTN-94-80568] p 3066 N94-27354
Scalar mixing in the subsonic jet in crossflow
p 2800 N94-28008
LASER INTERFEROMETRY
The determination of surface roughness from reflected step edges
[AD-A273987] p 2984 N94-25900
Zeeman laser interferometry for detection and chemical analysis
[DE94-003963] p 2719 N94-27728
LASER MATERIALS
Development of intermetallic compounds for high performance luminescence elements
p 2722 N94-25545
Physical characteristics of polymethylmethacrylate scintillator SOFG-120
[DE93-634184] p 2810 N94-26395
LASER MODE LOCKING
High repetition rate, mode locked, figure eight laser with extracavity feedback
[AD-D016053] p 2820 N94-27670
Fiber laser amplifiers and oscillators
[AD-A274231] p 2820 N94-28068
LASER OUTPUTS
Development of intermetallic compounds for high performance luminescence elements
p 2722 N94-25545
Hook spectroscopy as an atomic number density diagnostic applied to laser-ablated copper plasmas
[DE94-002645] p 3042 N94-26081
Regrowth zones in laser annealed radiation damaged diamond
[DE94-600821] p 3056 N94-26364
Development of lasers optimized for pumping Ti:Al2O3 lasers
[NASA-CR-4573] p 2818 N94-26705
Research and development within nonlinear optics for protection of optical sensors against laser irradiation on of optical sensors against laser irradiation. Quarterannual report 1 (april 1993))
[PB94-124245] p 3037 N94-27046
Laser phase induced intensity noise in fiber-optic signal processing and sensing systems
[ITN-94-85234] p 2819 N94-27179
Optical parametric oscillator modeling with diffraction, depletion, and double refraction
[DE94-001504] p 3040 N94-27999
Fiber laser amplifiers and oscillators
[AD-A274231] p 2820 N94-28068
LASER PLASMA INTERACTIONS
Proceedings of the 16th Symposium on Plasma Physics and Technology
[DE94-604181] p 3047 N94-27698
LASER PLASMAS
Imaging with x ray lasers
[DE94-002844] p 2816 N94-26020
LASER POWER BEAMING
A direct current rectification scheme for microwave space power conversion using traveling wave electron acceleration p 2687 N94-27371
LASER PUMPING
Compact, solid-state femtosecond source
[AD-A273932] p 2817 N94-26271
Diode-laser-pumped, gas-cell atomic clocks
[AD-A274812] p 3008 N94-26484
Development of lasers optimized for pumping Ti:Al2O3 lasers
[NASA-CR-4573] p 2818 N94-26705
LASER SPECTROSCOPY
Development of laser spectroscopic technology in nuclear industry
[DE93-633327] p 2714 N94-26158
Study on laser atomic spectroscopy
[DE93-633328] p 2817 N94-26402
Spectroscopy Division
[DE94-604074] p 2717 N94-26988
Molecular dynamics simulation and crystal-field theory: Predicting the optical spectra and structure of rare-earth doped inorganic glasses
[ISBN-0-315-84679-8] p 3025 N94-27310
Laser blow-off lithium beam probing with high temporal resolution for edge plasma diagnostics
[DE94-701176] p 2820 N94-27701
LASER STABILITY
Diode-laser-pumped, gas-cell atomic clocks
[AD-A274812] p 3008 N94-26484
High-speed, high-density, coherent time-domain optical memory
[AD-A274249] p 3037 N94-27010
LASER TARGETS
New Thomson scattering laser control for D3-D
[DE94-002890] p 3043 N94-26274
LASER WELDING
Distributed Nd:YAG laser welding and process control in inert glove boxes
[DE94-002629] p 2818 N94-26605
LASERS
Control system for tracking nonlinear systems
[AD-D016057] p 2787 N94-27673
LATE STARS
Coronal heating via nanoflares
[DE94-000773] p 3110 N94-26696
LATERAL CONTROL
Theoretical and experimental investigation of a delta wing with turbulent leading-edge jets
p 2659 N94-28029
Numerical assessment of aerodynamic interactions on missiles with transverse jets control
p 2659 N94-28031
LATITUDE
Differential global positioning system for the surface-towed ordnance locating system: Testing, results, and user's guide
[DE94-002980] p 2664 N94-26309
LATTICE PARAMETERS
Zinc(2) oxide stability in alkaline sodium phosphate solutions at elevated temperatures
[DE94-003316] p 2715 N94-26320

Polar and chemical domain structures of lead scandium tantalate (PST)
[DE94-600760] p 3056 N94-26363

LATTICE VIBRATIONS
Octahedral metallomesogens: Liquid crystallinity in low aspect ratio materials
[AD-A274830] p 3059 N94-26571

LAUNCH VEHICLES
MINOTAUR (Maryland's innovative orbital technologically advanced University rocket)
p 2703 N94-25685
A comparison of users' and providers' perceptions of critical spacelift vehicle characteristics and capabilities
[AD-A273907] p 2691 N94-26017
Proceedings of Damping 1993, volume 2
[AD-A274227] p 2840 N94-26953
Access to space study
[NASA-TM-109693] p 2685 N94-27151

LAUNCHING
Energy and technology review, July 1993
[DE94-004219] p 3118 N94-27566

LAW (JURISPRUDENCE)
Coastal Zone Management Act and related legislation, revision 3
[DE94-004180] p 2869 N94-27691
Recent legal movement on water quality regulation in Japan p 2869 N94-28148

LAY-UP
The experimental behavior of spinning pretwisted laminated composite plates
[NASA-CR-195220] p 2711 N94-27352

LEAD (METAL)
Determination of lead isotope ratios in seawater by purge and trap GC/MS after ethylation p 2870 N94-28152

LEAD ACID BATTERIES
Bipolar lead-acid batteries for electrical actuation applications p 2864 N94-28134

LEAD ALLOYS
Study on solidification of non-homogeneous melting/solidification materials p 2728 N94-25573

LEAD COMPOUNDS
NNN-Ising model simulation of nanodomain textures in relaxor-type lead scandium tantalate
[DE94-601884] p 2748 N94-25844
Crystallization and microstructural control of ferroelectric thin-films and glass-ceramics
[AD-A273767] p 2748 N94-25854
Polar and chemical domain structures of lead scandium tantalate (PST)
[DE94-600760] p 3056 N94-26363
The optical properties of high-T(c) superconductors grown by pulsed laser deposition
[ISBN-0-315-84917-7] p 3039 N94-27962
Anisotropy in the electrical, magnetic and optical properties of Pb2Sr2RCu3O8
[ISBN-0-315-84930-4] p 3070 N94-27974
Determination of lead isotope ratios in seawater by purge and trap GC/MS after ethylation p 2870 N94-28152

LEAD ISOTOPES
Determination of lead isotope ratios in seawater by purge and trap GC/MS after ethylation p 2870 N94-28152

LEAD ZIRCONATE TITANATES
Crystallization and microstructural control of ferroelectric thin-films and glass-ceramics
[AD-A273767] p 2748 N94-25854
Oriented lead zirconate titanate thin films: Characterization of film crystallization
[DE94-003104] p 3053 N94-26025
Piezoelectric measurements on impact loaded PZT ceramics
[NPL-DMM(A)-88] p 2752 N94-26652
Ferroelectric thin film microstructure development and related property enhancement
[DE94-002741] p 3061 N94-26856

LEADING EDGE SWEEP
Wing lift increment at zero angle of attack due to deployment of single-slotted flaps at low speeds
[ESDU-93019] p 2649 N94-28140

LEADING EDGES
Leading-edge vortex-system details obtained on F-106B aircraft using a rotating vapor screen and surface techniques
[NASA-TP-3374-VIDEO-SUPPL] p 2647 N94-27161
Composite leading edge/spar member for an aircraft control surface
[CA-PATENT-1-325-765] p 2669 N94-27273
Control of leading-edge separation on an airfoil by localized excitation
[DLR-FB-93-16] p 2647 N94-27592
A study on heat transfer in a scramjet leading edge model
[NAL-TR-1187T] p 2675 N94-27608
Prediction of leading-edge transition and relaminarization phenomena on a subsonic multi-element high-lift system p 2659 N94-27929
Effects, limits, and limitations of spanwise blowing
p 2659 N94-28027
Theoretical and experimental investigation of a delta wing with turbulent leading-edge jets
p 2659 N94-28029
First experimental assessment of RCS plume-flow field interaction on Hermes leading edge thruster configuration p 2703 N94-28032
Program for calculation of maximum lift coefficient of plain aerofoils and wings at subsonic speeds
[ESDU-93015] p 2649 N94-28076

LEAKAGE
Influence of impeller shroud forces on turbopump rotor dynamics p 2796 N94-27378
Compressibility effects on rotor forces in the leakage path between a shrouded pump impeller and its housing
p 2796 N94-27379
Development of hypersonic engine seals: Flow effects of preload and engine pressures
[NASA-TM-106333] p 2826 N94-27599

LEAST SQUARES METHOD
Repeated knots in least squares multiquadric functions
[AD-A273866] p 2990 N94-25594
Piecewise least squares fitting technique using finite interval method with Hermite polynomials
[VTT-PUBS-135] p 2990 N94-25733
Geoid determination: With help of the alternative scattering method
[ETN-94-95375] p 2847 N94-25746
Numerical treatment of experimental data in calibration procedures
[DE93-634289] p 3097 N94-26382
Window least squares method applied to statistical noise smoothing of positron annihilation data
[DE93-634665] p 3003 N94-26385
On the reliability of a window least squares algorithm
[DE93-634666] p 2962 N94-26386
MIMO recursive least squares control algorithm for the AN/FPN-44A Loran-C transmitter
[AD-A274820] p 2664 N94-26493
Iterative methods for the WLS state estimation on RISC, vector, and parallel computers
[DE94-004260] p 3000 N94-27569

LEBESGUE THEOREM
Topological conditions for the existence of invariant measures for unimodal maps
[PB94-123296] p 2849 N94-26866

LECTURES
The proceedings of the KEK FEL Simulation Code Workshop
[DE93-520378] p 2816 N94-26112
Cosmological phase transitions
[DE94-003001] p 3104 N94-26786
CMSC-130 introductory computer science, lecture notes
[AD-A274369] p 2967 N94-27060
How to make good use of international research collaboration, with emphasis on the evolving situation in Europe
[PB94-119690] p 3101 N94-27323

LEG (ANATOMY)
Sympathetic nerve activity during dynamic leg exercise
p 2929 N94-27527

LEGENDRE FUNCTIONS
On kinetic expansion in scalar field theory
[DE93-634338] p 3072 N94-26553

LENNARD-JONES POTENTIAL
Study on computerized experiment of amorphous transformation process by solid phase reaction
p 2726 N94-25564
Fast parallel algorithms for short-range molecular dynamics
[DE93-018519] p 3016 N94-26033
How reliable is the HMSA integral equation for the pair structure of supercooled and amorphous mixtures?
[DE94-601543] p 3006 N94-26411
Calculating the surface properties for the liquid-vapour interface: Illustrating the thermodynamic stability of the spherical microstructures
[DE94-601992] p 3073 N94-26837
The molecular matching problem
p 3030 N94-27910

LENSES
Kinoform/lens system for injecting a high power laser beam into an optical fiber
[DE94-003226] p 2819 N94-27262
Reflectometer employing an integrating sphere and lens-mirror concentrator
[AD-D016061] p 3039 N94-27676

LEPTONS
A possible way of connecting the Grassmann variables and the number of generation
[DE94-601624] p 2990 N94-25838
A research program in experimental and theoretical high energy physics
[DE94-002156] p 3031 N94-25931
Lepton masses in an SU(3)(sub L) x U(1)(sub N) gauge model
[DE93-634366] p 3016 N94-26040
Heavy charged leptons in an SU(3)(sub L) x U(1)(sub N) model
[DE93-634367] p 3016 N94-26041
Rescattering and energy loss of fast partons in nuclear matter
[DE94-002918] p 3018 N94-26145
A search for the production of direct leptons in nucleon-nucleus and nucleus-nucleus collisions
[DE94-004640] p 3018 N94-26244
Measurement of tau lepton branching fractions
[DE94-003423] p 3018 N94-26325
Why is the Higgs doublet light?
[DE94-601711] p 3018 N94-26333
Chance to use W-decay lepton channels for width determination
[DE93-634438] p 3020 N94-26507
Leptonic decay constants of heavy mesons in QCD
[DE93-634426] p 3022 N94-26767
Future directions in particle and nuclear physics at multi-GeV hadron beam facilities
[DE94-002946] p 3027 N94-27711
Search for the top quark in the single lepton + jets channel at D0
[DE94-004660] p 3028 N94-27749

LESIONS
The central executive component of working memory
[AD-A274295] p 2938 N94-26683

LETHALITY
Space radiation health research, 1991-1992
[NASA-TM-109721] p 2932 N94-27556
Supernovae and mass extinctions
p 2891 N94-28314

LEVELING
Alignment of the Amsterdam Pulse Stretcher (AmPS)
[MTG-93-02] p 2809 N94-25637

LEVITATION
Basic research on levitation fusing/solidification technology p 2723 N94-25552

LEVITATION MELTING
Basic research on levitation fusing/solidification technology p 2723 N94-25552

LIAPUNOV FUNCTIONS
Stability of large scale interconnected dynamical systems
[DE94-601536] p 2993 N94-26408
On the phi(sub 0)-stability of perturbed nonlinear differential systems
[DE93-634304] p 2993 N94-26441
Cone-valued Lyapunov functions and the stability of stochastic differential equations
[DE94-601504] p 2994 N94-26458
On the (Phi)(sub 0)-stability of functional differential equations
[DE94-601507] p 3006 N94-26460
Lyapunov exponents for some quasi-periodic cocycles
[PB94-124377] p 2997 N94-26994
Impulsive control and stabilization
[ISBN-0-315-84563-5] p 2988 N94-27271

LIBRARIES
Full-text information services at the desktop
[DE94-003728] p 3096 N94-25813
Index to BROND-2, CENDL-2, ENDF/B-6, JEF-2, JENDL-3
[DE93-634500] p 3016 N94-26034

LIE GROUPS
The massless representations of the conformal quantum algebra
[DE94-601555] p 3006 N94-26413
Affine algebras on the torus
[DE94-601556] p 3006 N94-26414
Higher spin extensions of the Virasoro algebra, area-preserving algebras and the matrix algebra a-bar(sub (infinity))
[DE94-601557] p 3006 N94-26415
Finite dimensional representations of the quantum superalgebra U(sub q)(gl(3/2))
[DE93-634303] p 2993 N94-26440
Quantum Hamiltonian differential geometry: How does quantization affect space?
[DE93-634306] p 2993 N94-26442
The extensions of space-time. Physics in the 8-dimensional homogeneous space D is equal to SU(2,2)/K
[DE93-634336] p 3072 N94-26551
String hypothesis and characters of coset CFTs
[DE93-634337] p 3007 N94-26552
Deformation of the exterior algebra and the GL(sub q) (r, included in) algebra
[DE94-602558] p 2996 N94-26898

Poisson-lie group of pseudodifferential symbols [PB94-124393] p 2997 N94-26996

Q - difference intertwining operators for a Lorentz quantum algebra [DE94-602559] p 2997 N94-27023

The gl(n/m) and related q-identitiesematics and computer science ends in nuclear and related q-identities [DE94-603653] p 3001 N94-27839

LIFE (DURABILITY)

Study on high temperature damage control and life improvement p 2729 N94-25580

Composite raw materials for the building industry [VTT-TIED-1433] p 2708 N94-26544

MSOFC development status [DE94-003192] p 2858 N94-26792

Space Station Freedom NiH2 cell testing program p 2861 N94-28108

LIFE CYCLE COSTS

MSOFC development status [DE94-003192] p 2858 N94-26792

Interdisciplinary technology p 2686 N94-27363

Automation life-cycle cost model [NASA-CR-195695] p 3095 N94-27866

LIFE SCIENCES

Asteroid exploration and utilization p 3080 N94-25697

The 27th Annual Meeting of the Israel Society for Microscopy and the 12th Annual Meeting of the Israel Society for Histochemistry and Cytochemistry [DE93-632416] p 2716 N94-26519

Spacelab life sciences 2 post mission report [NASA-CR-195544] p 2942 N94-27410

Aerospace medicine and biology: A continuing bibliography with indexes (supplement 386) [NASA-SP-7011(386)] p 2933 N94-28208

Aerospace medicine and biology: A continuing bibliography with indexes (supplement 387) [NASA-SP-7011(387)] p 2933 N94-28213

A general theory of impacts and mass extinctions, and the consequences of large-body impact on the Earth p 2891 N94-28310

LIFE SUPPORT SYSTEMS

Bioregenerative system components for microgravity p 2903 N94-25673

Enabler operator station p 2943 N94-25679

Automation of closed environments in space for human comfort and safety p 2943 N94-25684

Design and development of the second generation Mars Habitat p 2943 N94-25693

Pressurized Lunar Rover (PLR) p 2833 N94-25704

Designing for human presence in space: An introduction to environmental control and life support systems [NASA-RP-1324] p 2942 N94-27437

Aerospace medicine and biology: A continuing bibliography with indexes (supplement 386) [NASA-SP-7011(386)] p 2933 N94-28208

Aerospace medicine and biology: A continuing bibliography with indexes (supplement 387) [NASA-SP-7011(387)] p 2933 N94-28213

LIFT

An investigation into the aerodynamic effects of wing patches [ISBN-0-315-84121-4] p 2646 N94-26672

High-lift system analysis method using unstructured meshes [NLR-TP-92351-U] p 2647 N94-27554

Numerical simulation of a powered-lift landing p 2671 N94-28033

Program for calculation of maximum lift coefficient of plain aerofoils and wings at subsonic speeds [ESDU-93015] p 2649 N94-28076

Preliminary assessment of aerodynamic effects of wing repair patches p 2657 N94-28346

LIFT DEVICES

Eagle RTS: A design of a regional transport p 2671 N94-25709

LIFTING BODIES

Experimental and theoretical study of aerodynamic characteristics of some lifting bodies at angles of attack from -10 degrees to 53 degrees at Mach numbers from 2.30 to 4.62 [NASA-TM-4528] p 2646 N94-26693

Prediction of leading-edge transition and relaminarization phenomena on a subsonic multi-element high-lift system p 2659 N94-27929

LIGANDS

Transition metal activation and functionalization of carbon-hydrogen bonds [DE94-003650] p 2715 N94-26369

Radiochemistry Division annual progress report : 1991 [DE94-600652] p 2715 N94-26392

Property enchancement of polyimide films by way of the incorporation of lanthanide metal ions p 2758 N94-27926

LIGHT AIRCRAFT

Solar powered multipurpose remotely powered aircraft p 2671 N94-25719

EGADS: A microcomputer program for estimating the aerodynamic performance of general aviation aircraft [NASA-TM-104013] p 2667 N94-26091

Investigation of the aerodynamic environment for an advanced lightweight rotor in forward flight. Volume 4: Laser velocimeter wake data, advance ratio of 0.037 [NASA-TM-109040-VOL-4] p 2645 N94-26483

Investigation of the aerodynamic environment for an advanced lightweight rotor in forward flight. Volume 1: Laser velocimeter inflow data, advance ratio of 0.37, thrust coefficient of 0.0081 and hover tip speed of 603 feet/second [NASA-TM-109040-VOL-1] p 2645 N94-26489

Investigation of the aerodynamic environment for an advanced lightweight rotor in forward flight. Volume 2: Laser velocimeter inflow data, advance ratio of 0.37, thrust coefficient of 0.0064 and hover tip speed of 710 feet/second [NASA-TM-109040-VOL-2] p 2645 N94-26492

Investigation of the aerodynamic environment for an advanced lightweight rotor in forward flight. Volume 3: Laser velocimeter inflow data, advance ratio of 0.37, thrust coefficient of 0.0064 and hover tip speed of 603 feet/second [NASA-TM-109040-VOL-3] p 2645 N94-26497

LIGHT AMPLIFIERS

Theory and modeling of stimulated Raman scattering [AD-A273755] p 3033 N94-25721

All-optical gain switching of erbium-doped fibre amplifiers [ISBN-0-315-84120-6] p 2784 N94-26704

Fiber laser amplifiers and oscillators [AD-A274231] p 2820 N94-28068

LIGHT BEAMS

Three-wave nonlinear interactions in KTiOPO4 (KTP) and KTP isomorphs [AD-A274079] p 3052 N94-25993

Spectral and temporal correlations of multifrequency waves in the turbulent atmosphere [ITN-94-85229] p 2774 N94-27233

LIGHT ELEMENTS

Zr-rich corner of the Zr-Sn-O diagram [DE93-633764] p 2734 N94-26161

LIGHT EMISSION

Stationary plasma thruster plume emissions [NASA-CR-194471] p 2701 N94-26209

Researches of the Electrotechnical Laboratory. No. 53: Spectral emission from combustion gas containing scattering media [JTN-94-80603] p 2717 N94-27246

Observation of stimulated emission from an MBE grown GaN film on sapphire [DE94-003638] p 3068 N94-27724

Energy parameters of the incident auroral electrons derived by the intensity ratio of auroral emissions p 2779 N94-27964

LIGHT EMITTING DIODES

Analytical study of beam handling and emittance control [AD-A274412] p 3033 N94-27078

Visible light emitting materials and injection devices [AD-A274418] p 2786 N94-27079

LIGHT GAS GUNS

High-speed repetitive pellet injector for plasma fueling of magnetic confinement fusion devices [DE94-002792] p 3042 N94-26140

Energy and technology review, July 1993 [DE94-004219] p 3118 N94-27566

LIGHT MODULATION

Characterization of an LCD for use as a programmable phase shifter to produce a single-lobed far-field pattern in a phased array [AD-A273883] p 3034 N94-25729

Optoelectronic Technology Consortium [AD-A274909] p 2782 N94-26344

Micro-electron deflector [AD-D016055] p 2787 N94-27672

LIGHT SCATTERING

Theory and modeling of stimulated Raman scattering [AD-A273755] p 3033 N94-25721

A numerical solution to the one and two dimensional line radiative transfer equation [ISBN-0-315-84258-X] p 2994 N94-26640

Researches of the Electrotechnical Laboratory. No. 53: Spectral emission from combustion gas containing scattering media [JTN-94-80603] p 2717 N94-27246

Analytic approximation to randomly oriented spheroid extinction [DREV-4712-93] p 3038 N94-27598

Report of the National Research Institute for Earth Science and Disaster Prevention, No: 51 [JTN-94-80509] p 2886 N94-27985

Detection of water on road surface by the polarized light p 2886 N94-27989

LIGHT SOURCES

Object-oriented software construction at ALS [DE94-003418] p 2967 N94-27049

Laser phase induced intensity noise in fiber-optic signal processing and sensing systems [ITN-94-85234] p 2819 N94-27179

Opportunities for High Aspect Ratio Micro-Electro-Magnetic-Mechanical Systems (HAR-MEMMS) at Lawrence Berkeley Laboratory [DE94-003499] p 2827 N94-27722

MODIS airborne simulator visible and near-infrared calibration, 1992 ASTEX field experiment. Calibration version: ASTEX King 1.0 [NASA-TM-104599] p 2897 N94-28179

LIGHT TRANSMISSION

Analytic approximation to randomly oriented spheroid extinction [DREV-4712-93] p 3038 N94-27598

LIGHT WATER REACTORS

Fundamental study on monitoring technology on local surface damages p 2724 N94-25555

LIGHTNING

Catalog of absolutely calibrated, range normalized, wideband, electric field waveforms from triggered lightning flashes in Florida [AD-A273793] p 2892 N94-25873

FNAS lightning detection [NASA-CR-193927] p 2893 N94-26134

Thunderstorm Hypothesis Reasoner [NASA-CR-195714] p 2897 N94-27884

MUSIC for localization of thunderstorm cells [DE94-004985] p 2897 N94-28146

LIMESTONE

Effects of slot on rock surface for percussive rock excavation: Water jet assisted percussive rock excavation p 2871 N94-28155

LIMITS (MATHEMATICS)

Limit theorems for functionals of Markov processes and renormalizable stable fields [AD-A274645] p 3004 N94-27106

LINE CURRENT

Image theory for DC problems involving a conducting half space bounded by the general anisotropic impedance surface [PB94-132917] p 2779 N94-28390

LINE OF SIGHT COMMUNICATION

Laser-based communication link [FFI-93/7023] p 2817 N94-26203

LINE SHAPE

Laser phase induced intensity noise in fiber-optic signal processing and sensing systems [ITN-94-85234] p 2819 N94-27179

LINEAR ACCELERATORS

JLC-1 [DE93-520380] p 3031 N94-26113

Proceedings of the Second EGS4 User's Meeting in Japan [DE93-520383] p 3032 N94-26543

Fluid dynamic linear accelerometer [AD-D016042] p 2678 N94-27112

LINEAR AMPLIFIERS

Ultralinear wideband integrated circuit design [ISBN-0-315-84130-3] p 2784 N94-26675

LINEAR ARRAYS

Analyzing adaptive beamformer performance in a stable multipath environment [AD-A274029] p 2766 N94-25766

LINEAR EQUATIONS

Nested Krylov methods based on GCR [PB94-125317] p 2995 N94-26818

Ma42: A new frontal code for solving sparse unsymmetric systems [PB94-124302] p 2998 N94-27115

Review and analysis of dense linear system solver package for distributed memory machines p 2978 N94-27916

LINEAR FILTERS

Equalization and cancellation of nonlinear intersymbol interference in a dispersive satellite communication channel [ISBN-0-315-85147-3] p 2775 N94-27274

LINEAR INTEGRATED CIRCUITS

Ultralinear wideband integrated circuit design [ISBN-0-315-84130-3] p 2784 N94-26675

LINEAR OPERATORS

Classification of linear differential operators with an invariant subspace in monomials [PB94-126620] p 2996 N94-26915

Hessenberg matrices in Krylov subspaces and the computation of the spectrum [PB94-133170] p 3001 N94-28389

LINEAR POLARIZATION

Fiber optic Faraday flux transformer specification [AD-D016058] p 3039 N94-27674

LINEAR PROGRAMMING
A note on central cutting plane methods for convex programming
[REPT-93-44] p 2958 N94-25762
Research on primal-dual interior point algorithms for mathematical programming
[DE94-003982] p 2959 N94-25821
A linear description of the discrete lot-sizing and scheduling problem
[MEMO-COSOR-92-47] p 2992 N94-26227
Polyhedral characterization of the economic lot-sizing problem with start-up costs
[MEMO-COSOR-92-46] p 2969 N94-27396
LINEAR QUADRATIC GAUSSIAN CONTROL
Necessary and sufficient conditions for the existence of the stabilizing solution of the Riccati equation in a Hilbert space: A Popov function approach
[PB94-125341] p 2997 N94-26999
Multiple model adaptive control of a large flexible space structure with purposeful dither for enhanced identifiability
[AD-A274132] p 2987 N94-27122
Dynamics and robust control for uncertain flexible space systems
[INPE-5510-TAE/020] p 2696 N94-27357
LINEAR QUADRATIC REGULATOR
Solving the linear quadratic optimal control problem for infinite-dimensional systems
[ISBN-0-315-84562-7] p 2999 N94-27405
LINEAR SYSTEMS
Enumeration of n-fold tangent hyperplanes to a surface
[DE94-601544] p 2993 N94-26412
Review and analysis of dense linear system solver package for distributed memory machines
p 2978 N94-27916
Parameter estimation of linear systems from frequency response measurements (computer program)
[ESDU-93016] p 2976 N94-28137
LINEAR TRANSFORMATIONS
Satellite attitude determination using linear combination of models
[AD-A274082] p 2694 N94-25996
LINKAGES
Motion planning for serial manipulators with many degrees of freedom: Implementation of a sequential search strategy
[ISBN-0-315-83682-2] p 2822 N94-26642
Implementation of integral manifold control on a two degree of freedom flexible joint manipulator: Theory and experiments
[ISBN-0-315-83572-9] p 2823 N94-26658
Simulation dynamics of a multibody chain: Recursion based on chain modal coordinates
[ISBN-0-315-83555-9] p 2994 N94-26659
LIOUVILLE EQUATIONS
Stochastic solution to quantum dynamics
[NASA-TP-3408] p 3114 N94-26550
LIQUEFACTION
Report of National Institute for Resources and Environment. No. 5: Study on direct liquefaction of woody biomass
[JTN-94-80551] p 2859 N94-27204
Oil production from buckwheat stillage by thermochemical liquefaction p 2871 N94-28154
LIQUEFIED GASES
Physical characteristics of polymethylmethacrylate scintillator SOFG-120
[DE93-634184] p 2810 N94-26395
LIQUID AIR
An experimental study of plunging liquid jet induced air carryunder and dispersion
[AD-A274414] p 2794 N94-26979
LIQUID CHROMATOGRAPHY
Analytical method for estimation of the total amount of aromatic and poly aromatic compounds in diesel fuel
[PB94-123692] p 2759 N94-25907
LIQUID CRYSTALS
Characterization of an LCD for use as a programmable phase shifter to produce a single-lobed far-field pattern in a phased array
[AD-A273883] p 3034 N94-25729
Microtubules for nonlinear optical limiting
[AD-A273940] p 3035 N94-25941
Color head down display program
[AD-A274807] p 2672 N94-26340
Octahedral metallomesogens: Liquid crystallinity in low aspect ratio materials
[AD-A274830] p 3059 N94-26571
Ferroelectricity in a Langmuir-Blodgett multilayer film of a liquid crystalline side-chain polymer
[AD-A274477] p 2754 N94-27033
Liquid crystalline side-chain polysiloxanes with 4-amino-4'-stilbene-carboxylic ester mesogens
[AD-A274510] p 2754 N94-27036
Research and development within nonlinear optics for protection of optical sensors against laser irradiation on of optical sensors against laser irradiation. Quarterannual report 1 (april 1993))
[PB94-124245] p 3037 N94-27046
Ultrastructure processing of macromolecular materials
[AD-A274460] p 2754 N94-27086
LIQUID FLOW
Ejectors and jet pumps: Computer program for design and performance for liquid flow
[ESDU-93022] p 2832 N94-28093
LIQUID FUELS
An apparatus for measurement of ignition and burning characteristics of metallic particles
[AD-A274815] p 2716 N94-26487
Liquid monopropellants
[AD-D016074] p 2760 N94-28226
LIQUID HELIUM
Growth of small fatigue cracks in Incoloy-908
[DE94-003406] p 2836 N94-26129
LIQUID HELIUM 2
A numerical study of quantized vortices in HeII
[ISBN-9-03-860232-4] p 2792 N94-26479
Superfluid helium sloshing dynamics induced oscillations and fluctuations of angular momentum, force and moment actuated on spacecraft driven by gravity gradient or jitter acceleration associated with slew motion
[NASA-CR-193928] p 2799 N94-27931
LIQUID HYDROGEN
Project WISH: The Emerald City p 2703 N94-25690
Orbital transfer vehicle engine technology high velocity ratio diffusing crossover
[NASA-CR-194447] p 2703 N94-27212
Inertial electrostatic confinement as a power source for electric propulsion p 2688 N94-27373
LIQUID LEVELS
Method of measuring liquid level
[AD-D016049] p 3038 N94-27153
LIQUID METAL FAST BREEDER REACTORS
Nonswelling behavior of HT9 alloy irradiated to high exposure
[DE94-003502] p 2736 N94-26522
LIQUID METALS
Liquid metal MHD research and development in Israel
p 2854 N94-26055
Modelling the mass migration phenomena in partially frozen heat pipes
[DE94-002716] p 2797 N94-27709
LIQUID NITROGEN
The cryogenic tunnel Cologne at DLR
[DLR-MITT-93-10] p 2681 N94-27587
LIQUID PHASES
Development of liquid membrane separation processes p 2717 N94-27386
Energy Dispersive X ray Diffraction (EDXD) apparatus for liquids at high temperature p 2721 N94-28159
LIQUID PROPELLANT ROCKET ENGINES
Integrated model development for liquid fueled rocket propulsion systems
[NASA-CR-195253] p 2702 N94-27166
LIQUID ROCKET PROPELLANTS
Hydrogen-oxygen torch ignitor
[NASA-TM-106493] p 2691 N94-27424
Liquid monopropellants
[AD-D016074] p 2760 N94-28226
LIQUID SLOSHING
Report of three microgravity experiments by the drop shaft
[JTN-94-80579] p 2761 N94-27341
Superfluid helium sloshing dynamics induced oscillations and fluctuations of angular momentum, force and moment actuated on spacecraft driven by gravity gradient or jitter acceleration associated with slew motion
[NASA-CR-193928] p 2799 N94-27931
LIQUID SURFACES
Method of measuring liquid level
[AD-D016049] p 3038 N94-27153
LIQUID-GAS MIXTURES
Interface configuration experiment: Preliminary results
[NASA-TM-109684] p 2760 N94-25849
Report of three microgravity experiments by the drop shaft
[JTN-94-80579] p 2761 N94-27341
LIQUID-LIQUID INTERFACES
Mapping of seawater intrusion into the coastal aquifer of Israel (the seawater-freshwater interface) by TDEM (Time Domain Electromagnetic) method
[ITN-94-85238] p 2850 N94-27331
LIQUID-SOLID INTERFACES
Bulletin of National Research Institute for Metals in Fiscal Year 1993, no. 14
[REPT-14] p 2722 N94-25544
Observation on metal surface in aqueous solution using an electrochemical Scanning Tunneling Microscope (STM) p 2724 N94-25554
Study on interfacial reaction analysis at interfacial joining p 2728 N94-25574
Morphology transitions during non-equilibrium growth processes
[ITN-94-85236] p 3065 N94-27243
On line quantification of crystal surfaces by stereo imaging
[NASA-CR-195277] p 3066 N94-27561
LIQUID-VAPOR EQUILIBRIUM
Thermocapillary flow with evaporation and condensation and its effect on liquid retention in low-G fluid acquisition devices
[NASA-TP-3463] p 2797 N94-27639
LIQUID-VAPOR INTERFACES
Interface configuration experiment: Preliminary results
[NASA-TM-109684] p 2760 N94-25849
Calculating the surface properties for the liquid-vapour interface: Illustrating the thermodynamic stability of the spherical microstructures
[DE94-601992] p 3073 N94-26837
Report of three microgravity experiments by the drop shaft
[JTN-94-80579] p 2761 N94-27341
Thermocapillary flow with evaporation and condensation and its effect on liquid retention in low-G fluid acquisition devices
[NASA-TP-3463] p 2797 N94-27639
LIQUIDS
Bulletin of the Institute for Chemical Reaction Science, Tohoku University, volume 2
[JTN-94-80602] p 2717 N94-27385
Development of liquid membrane separation processes p 2717 N94-27386
Orthobaric densities and molar volumes of liquids: Aliphatic and cyclic ketones
[ESDU-93010] p 2720 N94-28060
Viscosity of liquids: Halogenated ethanes
[ESDU-93012] p 2720 N94-28062
Orthobaric densities and molar volumes of liquids: Fused ring compounds
[ESDU-93029] p 2721 N94-28097
Vapour pressures and critical points of liquids: Fused ring compounds
[ESDU-93028] p 2721 N94-28142
LIQUIDUS
Liquid and solid solubility of Ag in Bi2Sr2CaCu2O8
[DE94-002829] p 2735 N94-26273
LITHIUM
Lithium drifted silicon detector fabrication on gettered floating-zone silicon
[DE94-003890] p 3054 N94-26095
In situ spectroscopic applications to the study of rechargeable lithium batteries
[DE94-003478] p 2782 N94-26328
The reactivity of lithium toward non-aqueous solvents of relevance to energy storage applications as studied by surface analytical techniques
[DE94-003483] p 2856 N94-26464
High rate lithium/thionyl chloride bipolar battery development p 2864 N94-28133
LITHIUM ALLOYS
Issues for conversion coating of aluminum alloys with hydrotalcite
[DE94-003804] p 2732 N94-25819
An anodic dissolution-based mechanism for the rapid cracking, pre-exposure phenomenon demonstrated by Al-Li-Cu alloys
[DE94-004798] p 2742 N94-27788
NASA-UVA light aerospace alloy and structures technology program (LA2ST)
[NASA-CR-195275] p 2844 N94-27851
LITHIUM CHLORIDES
A Shuttle mechanism for molten-electrolyte lithium batteries
[DE94-002914] p 2781 N94-26144
LITHIUM COMPOUNDS
Issues for conversion coating of aluminum alloys with hydrotalcite
[DE94-003804] p 2732 N94-25819
LITHIUM NIOBATES
High temperature sensor/microphone development for active noise control
[NASA-CR-195214] p 2812 N94-27214
Electro-optic materials by solid source MOCVD
[DE94-005120] p 2757 N94-27716
LITHIUM OXIDES
Reference electrodes for solid polymer electrolytes
[DE94-004583] p 2780 N94-25806
LITHIUM SULFUR BATTERIES
In situ spectroscopic applications to the study of rechargeable lithium batteries
[DE94-003478] p 2782 N94-26328
LITHOGRAPHY
Study on elucidation of damage generation process by electron beam lithography p 2729 N94-25581

Opportunities for High Aspect Ratio Micro-Electro-Magnetic-Mechanical Systems (HAR-MEMMS) at Lawrence Berkeley Laboratory
[DE94-003499] p 2827 N94-27722

LIVER
Modulation by galactosamine-induced hepatitis of biological responses of the rat exposed to high altitude hypoxia p 2904 N94-27464
Cloning of rat RXR alpha cDNA and the expression of its mRNA in regenerating liver and primary cultured hepatocytes p 2905 N94-27479

LOAD TESTING MACHINES
High temperature tension test equipment of heat resistant composite materials
[NAL-TM-652] p 2710 N94-27255
SP/MSP tests for the evaluation of FGM
[NAL-SP-17] p 2710 N94-27279
SP/MSP tests for the evaluation of FGM
p 2710 N94-27280
Research on the development of fracture characteristics evaluation system for ceramics and metal composite materials p 2710 N94-27281

LOAD TESTS
Fatigue resistance under tension-compression of laminates IM6/5245C and AS4/3501-6
[IAR-CR-25] p 2708 N94-26711
Compatibility of refrigerants and lubricants with engineering plastics
[DE94-004959] p 2756 N94-27692
Creep rupture properties of a nickel-base heat-resistant alloy Hastelloy XR under varying temperature/stress condition
[DE94-701175] p 2743 N94-27807
A laboratory test on construction of ice domes and their load-carrying capacity p 2884 N94-27966
The estimation of pre-stress by deformation rate analysis and suggestion of a mechanism from the elast-plastical theory p 2871 N94-28156

LOADS (FORCES)
Effect of loading mode on the fracture toughness of a reduced activation ferritic/martensitic stainless steel
[DE94-004290] p 2732 N94-25987
The identification of inflow fluid dynamics parameters that can be used to scale fatigue loading spectra of wind turbine structural components
[DE94-000231] p 2791 N94-26117
Modification of a model for fatigue life predictions based on level-crossing
[PB94-123395] p 2842 N94-27198
Influence of impeller shroud forces on turbopump rotor dynamics p 2796 N94-27378
Vibrations in engineering structures: A review of model and full-scale test of a cable-stayed bridge and a traffic sign gantry
[NLR-TP-92321-U] p 2843 N94-27553
Mechanically fastened composite laminates subjected to combined bearing-bypass and shear loading
p 2712 N94-27914

LOCAL AREA NETWORKS
Code division multiple access local area network communications employing fiber optic signal processing techniques
[AD-A274897] p 3096 N94-26180
Modeling and simulation of a fiber distributed data interface local area network
[AD-A274838] p 3098 N94-26500
A tri-state optical switch for local area network communications p 2789 N94-27922

LOCI
Mach reflection of spherical detonation waves
[DE93-016604] p 2797 N94-27705

LOGARITHMS
A logarithmic barrier cutting plane method for convex programming
[REPT-93-43] p 2957 N94-25761
Unifying investigation of interior-point methods for convex programming
[PB94-126463] p 2967 N94-27031
An efficient off-line electronic cash system based on the representation problem
[CWI-CS-R9323] p 2776 N94-27551

LOGIC CIRCUITS
Use of parallel counters for triggering
[DE93-616656] p 2979 N94-25918
Processing, fabrication, and demonstration of HTS integrated microwave circuits, appendix A
[AD-A274600] p 2785 N94-26890
Symbolic model checking for sequential circuit verification
[AD-A274375] p 2786 N94-27061
DALIA: A language for the description and analysis of digital systems p 2954 N94-27192

LOGIC DESIGN
Test methods and custom hardware for functional testing of a high speed GaAs DRAM
[AD-A274859] p 2781 N94-26175
Investigation into model-based fuzzy logic control
[AD-A274660] p 2985 N94-26336

LOGIC PROGRAMMING
Deductive computer programming
[AD-A274966] p 2962 N94-26303
Process algebra of concurrent constraint programming
[PB94-126695] p 2966 N94-26919
Freeness analysis for logic programs-and correctness
[PB94-126703] p 2966 N94-26956
A characterization of stable models using a non-monotonic operator
[CWI-CS-R9315] p 2970 N94-27543
Modular termination proofs for logic and pure PROLOG programs
[CWI-CS-R9316] p 2970 N94-27544
A strategy for dynamic interpretation: A fragment and an implementation
[CWI-CS-R9317] p 2970 N94-27545

LOGISTICS MANAGEMENT
Development of the Air Force contingency contracting course framework
[AD-A273921] p 3093 N94-25895

LONG DURATION SPACE FLIGHT
Project Minerva: A low-cost manned Mars mission based on indigenous propellant production
p 2760 N94-25705
Simulation modeling for long duration spacecraft control systems p 2684 N94-26288
Psychophysiology in microgravity and the role of exercise p 2936 N94-28374

LONG TERM EFFECTS
Preparation of creep data sheet: Material strength data sheet p 2723 N94-25548

LONGITUDE
Differential global positioning system for the surface-towed ordnance locating system: Testing, results, and user's guide
[DE94-002980] p 2664 N94-26309

LONGITUDINAL CONTROL
Techniques to improve maneuver stability characteristics of a nonlinear wide-body transport airplane in cruise flight
[NASA-TM-4521] p 2679 N94-27660

LONGITUDINAL STABILITY
Techniques to improve maneuver stability characteristics of a nonlinear wide-body transport airplane in cruise flight
[NASA-TM-4521] p 2679 N94-27660

LOOP ANTENNAS
Receiving antennas for electromagnetic pulses and transients
[ISBN-0-315-62312-8] p 2777 N94-27871

LORAN C
MIMO recursive least squares control algorithm for the AN/FPN-44A Loran-C transmitter
[AD-A274820] p 2664 N94-26493
Realtime mitigation of GPS SA errors using Loran-C
p 2642 N94-27291

LORENTZ TRANSFORMATIONS
Principles of gauge theory of real hadrons
[DE93-613096] p 3013 N94-25835
Duality for multiparametric quantum GL(n) and for a Lorentz quantum group
[DE93-613048] p 3005 N94-25868
On the relativistic invariant representation of arbitrary bilinear combinations of Dirac spinors
[DE93-634343] p 3019 N94-26456

LOSSLESS EQUIPMENT
Performance considerations for the application of the lossless browse and residual model
p 2946 N94-28256

LOUDNESS
Experimental studies of loudness and annoyance response to sonic booms p 2651 N94-28195

LOW ALTITUDE
Methods for improving low-angle, low-altitude radar tracking accuracy
[AD-A274914] p 2768 N94-26347

LOW ASPECT RATIO
Octahedral metallomesogens: Liquid crystallinity in low aspect ratio materials
[AD-A274830] p 3059 N94-26571
Program to develop a performance and heat load prediction system for multistage turbines
[NASA-CR-195223] p 2674 N94-26588

LOW ASPECT RATIO WINGS
Normal force of low aspect ratio cropped-delta wings at pre-stall angles of attack and subsonic speeds
[ESDU-93034] p 2648 N94-27955

LOW CARBON STEELS
The influence of TIG welding thermal cycles on HSLA-100 steel plate
[AD-A274248] p 2740 N94-27009

LOW COST
Low-cost photovoltaic inverters incorporating application-specific integrated circuits
[DE94-003270] p 2856 N94-26463
Low cost, radial flow, solid oxide fuel cell
[DE94-002982] p 2858 N94-26785

LOW FREQUENCIES
Hydroacoustic wave-fields generated by different source types, a computational study
[PB94-123536] p 3010 N94-27037
Simulating high-frequency wind for long durations
[DE94-002739] p 2682 N94-27997

LOW GRAVITY MANUFACTURING
Study on melted solution stirring under microgravity
p 2730 N94-25585
Report of three microgravity experiments by the drop shaft
[JTN-94-80579] p 2761 N94-27341
Prometheus in space: Research Committee on Functional New Material
[JTN-94-80580] p 2761 N94-28002

LOW NOISE
Delta f Algorithm
[DE94-003120] p 2963 N94-26521

LOW PASS FILTERS
Probabilistic methods for image generation and encoding
[AD-A274294] p 2964 N94-26682

LOW PRESSURE
Combustion synthesis method p 2721 N94-25561
Modulation by galactosamine-induced hepatitis of biological responses of the rat exposed to high altitude hypoxia p 2904 N94-27464

LOW REYNOLDS NUMBER
A numerical determination of bifurcation points for low Reynolds number conical flows
[AD-A273984] p 2791 N94-25991

LOW SPEED
The high Reynolds number flow through an axial-flow pump
[AD-A273844] p 2789 N94-25604
Laser Doppler velocimetry in a low speed multistage compressor
[AD-A274836] p 2818 N94-26498

LOW SPEED WIND TUNNELS
Installation of models in the 2 m x 3 m low speed wind tunnel
[LTR-LA-286] p 2681 N94-27594
Transient flow features of a supersonic jet in a low speed cross flow p 2800 N94-28005
Evaluation of the buoyancy drag on automobile models in low speed wind tunnels p 2658 N94-28352

LOW TEMPERATURE
On the electron mobility in slightly compensated heavily doped gallium arsenide at low temperatures
[DE93-634712] p 3057 N94-26387
Variable temperature cold stage for microscope observation p 2718 N94-27389
The addition of molecular oxygen to hydroperoxy-propyl radicals
[DE94-003662] p 2760 N94-27725

LOW VISIBILITY
Development and evaluation of a near infrared reflecting and low visibility paint scheme for RAAF P-3C Orion aircraft
[AD-A274881] p 2669 N94-26864

LOWER BODY NEGATIVE PRESSURE
Pulse waveform and transcranial Doppler analysis during lower body negative pressure
[AD-A274516] p 2911 N94-27088
Aerobic fitness and orthostatic tolerance: Evidence against an association p 2934 N94-28365

LUBRICANTS
Measurement of viscosity, density, and gas solubility of refrigerant blends in selected synthetic lubricants
[DE94-003609] p 2713 N94-25934
Accelerated screening methods for determining chemical and thermal stability of refrigerant-lubricant mixtures. Part 2: Experimental comparison and verification of methods
[DE94-003664] p 2749 N94-26007
Using ferro-magnetic fluids to lubricate non-conformal isothermal contacts
[INPE-5520-TAE/021] p 2827 N94-27665
Compatibility of refrigerants and lubricants with engineering plastics
[DE94-004959] p 2756 N94-27692
Solubility, viscosity, and density of refrigerant/lubricant mixtures
[DE94-004237] p 2721 N94-28069
Calculation methods for steadily loaded central circumferential groove hydrodynamic journal bearings (guide to use of computer program A9304)
[ESDU-93004] p 2830 N94-28073

Calculation methods for steadily loaded axial groove hydrodynamic journal bearings (guide to use of computer program A9305)
[ESDU-93005] p 2830 N94-28074
Calculation methods for steadily loaded axial groove hydrodynamic journal bearings. Low viscosity process fluid lubrication (guide to use of computer program A9306)
[ESDU-93006] p 2830 N94-28075

LUBRICATION
Using ferro-magnetic fluids to lubricate non-conformal isothermal contacts
[INPE-5520-TAE/021] p 2827 N94-27665

LUMINANCE
Image quality and the display modulation transfer function: Experimental findings
[AD-A274061] p 2679 N94-25773

LUMINESCENCE
Development of intermetallic compounds for high performance luminescence elements
p 2722 N94-25545

LUMINOSITY
Secondary particle in background levels and effects on detectors at future hadron colliders
[DE94-003378] p 3011 N94-25598

LUNAR BASES
Project Columbiad: Reestablishment of human presence on the Moon p 2689 N94-25687
First lunar outpost p 2943 N94-25694
The 1991-1992 project summaries
p 2943 N94-25698
Lunar base habitat designs: Characterizing the environment, and selecting habitat designs for future trade-offs
[NASA-CR-195687] p 2943 N94-27934

LUNAR COMPOSITION
Experimental study of lunar and SNC (Mars) magmas
[NASA-CR-195274] p 3107 N94-27850

LUNAR CONSTRUCTION EQUIPMENT
Lunar preform manufacturing p 2765 N94-25677

LUNAR ENVIRONMENT
Design for producing fiberglass fabric in a lunar environment p 2765 N94-25676
Extraterrestrial surface propulsion systems
p 2833 N94-25691
First lunar outpost p 2943 N94-25694
Lunar base habitat designs: Characterizing the environment, and selecting habitat designs for future trade-offs
[NASA-CR-195687] p 2943 N94-27934

LUNAR EXPLORATION
The Extended Mission Rover (EMR)
p 2689 N94-25674
Project Columbiad: Reestablishment of human presence on the Moon p 2689 N94-25687
Recent developments in the Robotic All Terrain Lunar Exploration Rover (RATLER) program
[DE93-040342] p 2821 N94-26110
The Robotic All-Terrain Lunar Exploration Rover (RATLER): Increased mobility through simplicity
p 2685 N94-26291
Lunar Transportation Facilities and Operations Study, option 1
[NASA-CR-195700] p 3109 N94-27982

LUNAR GRAVITATION
First lunar outpost p 2943 N94-25694
Lifetimes of lunar satellite orbits
[NASA-TP-3394] p 2690 N94-27771

LUNAR LANDING
Lunar Transportation Facilities and Operations Study, option 1
[NASA-CR-195700] p 3109 N94-27982
Lunar Transportation Facilities and Operations Study, option 2
[NASA-CR-195701] p 3109 N94-27983

LUNAR LANDING MODULES
Low-cost unmanned lunar lander
p 2697 N94-25699

LUNAR LAUNCH
Lunar Transportation Facilities and Operations Study, option 1
[NASA-CR-195700] p 3109 N94-27982
Lunar Transportation Facilities and Operations Study, option 2
[NASA-CR-195701] p 3109 N94-27983

LUNAR MOBILE LABORATORIES
Pressurized Lunar Rover (PLR) p 2833 N94-25704

LUNAR ORBITS
The modal solution to the Moon's orbit using canonical Floquet perturbation theory
[AD-A273732] p 2690 N94-26001
Nasa Langley Research Center seventy-fifth anniversary publications, 1992
[NASA-TM-109691] p 3118 N94-27431
Lifetimes of lunar satellite orbits
[NASA-TP-3394] p 2690 N94-27771

LUNAR PROGRAMS
Artemis common lunar lander. Phase 2: Study results for external review
[NASA-TM-109699] p 2692 N94-28205

LUNAR ROCKS
A widely adaptable habitat construction system utilizing space resources p 2688 N94-27374

LUNAR ROVING VEHICLES
The Enabler: A concept for a lunar work vehicle
p 2833 N94-25675
Planetary surface exploration MESUR/autonomous lunar rover p 2833 N94-25683
Recent developments in the Robotic All Terrain Lunar Exploration Rover (RATLER) program
[DE93-040342] p 2821 N94-26110
Early lunar rover mission studies
p 2684 N94-26290
The Robotic All-Terrain Lunar Exploration Rover (RATLER): Increased mobility through simplicity
p 2685 N94-26291
A multitasking behavioral control system for the Robotic All-Terrain Lunar Exploration Rover (RATLER)
p 2685 N94-26292
Artemis common lunar lander. Phase 2: Study results for external review
[NASA-TM-109699] p 2692 N94-28205

LUNAR SATELLITES
Copernicus: Lunar surface mapper
p 3081 N94-25702

LUNAR SOIL
A widely adaptable habitat construction system utilizing space resources p 2688 N94-27374
Experimental study of lunar and SNC (Mars) magmas
[NASA-CR-195274] p 3107 N94-27850

LUNAR SPACECRAFT
Minimum accommodation for aerobrake assembly, phase 2
[NASA-TM-107608] p 2692 N94-27774
Artemis common lunar lander. Phase 2: Study results for external review
[NASA-TM-109699] p 2692 N94-28205

LUNAR SURFACE
The Extended Mission Rover (EMR)
p 2689 N94-25674
Design for producing fiberglass fabric in a lunar environment p 2765 N94-25676
Planetary surface exploration MESUR/autonomous lunar rover p 2833 N94-25683
Project Columbiad: Reestablishment of human presence on the Moon p 2689 N94-25687
Artemis common lunar lander. Phase 2: Study results for external review
[NASA-TM-109699] p 2692 N94-28205

LUNAR SURFACE VEHICLES
Enabler operator station p 2943 N94-25679
Dust control for Enabler p 2943 N94-25680

M

MACH NUMBER
Development and implementation of a scramjet cycle analysis code with a finite-rate-chemistry combustion model for use on a personal computer
[AD-A273834] p 2673 N94-25617
Mix induced by single shock passage through a material interface
[DE93-019505] p 2792 N94-26427
Pressure distributions on a 0.02-scale Space Shuttle orbiter nose at Mach 21.5 in helium
[NASA-TM-4495] p 2646 N94-26592
Experimental and theoretical study of aerodynamic characteristics of some lifting bodies at angles of attack from -10 degrees to 53 degrees at Mach numbers from 2.30 to 4.62
[NASA-TM-4528] p 2646 N94-26693
The cryogenic tunnel Cologne at DLR
[DLR-MITT-93-10] p 2681 N94-27587
Normal force of low aspect ratio cropped-delta wings at pre-stall angles of attack and subsonic speeds
[ESDU-93034] p 2648 N94-27955
Transient flow features of a supersonic jet in a low speed cross flow p 2800 N94-28005
Wing lift increment at zero angle of attack due to deployment of single-slotted flaps at low speeds
[ESDU-93019] p 2649 N94-28140

MACH REFLECTION
Mach reflection of spherical detonation waves
[DE93-016604] p 2797 N94-27705

MACHINE LEARNING
A rough set approach to speech recognition
[ISBN-0-315-83894-9] p 2769 N94-26619
Using discovery-based learning to prove the behavior of an autonomous agent
[AD-A274131] p 2987 N94-27121
Translation and rotation invariant pattern recognition
[PB94-123676] p 2968 N94-27157
Artificial Intelligence Research Branch future plans
[NASA-TM-109733] p 2989 N94-28065

MACHINE TOOLS
The National Center for Advanced Information Components Manufacturing: Program update
[DE94-002647] p 2960 N94-26118

MACHINE TRANSLATION
PATRAN 2.5/EAL interface guide
[NASA-TM-109053] p 2972 N94-27655
ARM: Abstract Rewriting Machine
[CWI-CS-R9330] p 2974 N94-27794

MACHINE-INDEPENDENT PROGRAMS
The ergonomics of software porting: Automatically configuring software to the runtime environment or everything you wanted to know about your C compiler but didn't know who to ask
[CWI-CS-R9266] p 2961 N94-26221

MACHINERY
Variable speed controller p 2943 N94-25678

MACHINING
Effect of nitrocarburizing on shape of titanium alloy parts
[DE94-004040] p 2732 N94-25822
Opportunities for High Aspect Ratio Micro-Electro-Magnetic-Mechanical Systems (HAR-MEMMS) at Lawrence Berkeley Laboratory
[DE94-003499] p 2827 N94-27722

MACROMOLECULES
Ultrastructure processing of macromolecular materials
[AD-A274460] p 2754 N94-27086

MAGMA
Experimental study of lunar and SNC (Mars) magmas
[NASA-CR-195274] p 3107 N94-27850

MAGNESIUM
Dissolution of secondary phases during extrusion
[PB94-124583] p 2732 N94-25908

MAGNESIUM ALLOYS
Formation of three types of quasi-crystals in Al-Pd-Mg system
[REPT-A-2667] p 3053 N94-26071
Hot deformation behaviour of Si(p)/Al composites and their matrices and an Al-Mg-Si alloy
[ISBN-0-315-84699-2] p 2711 N94-27314
The corrosion behavior of sputter-deposited magnesium-valve metal alloys p 2745 N94-28164

MAGNESIUM FLUORIDES
Ferroelectric fluoride memory FET development
[AD-A274341] p 2785 N94-27057

MAGNESIUM OXIDES
Transparent polycrystalline body with high ultraviolet transmittance, process for making and applications thereof
[CA-PATENT-1325511] p 3066 N94-27276

MAGNET COILS
Development of an industrial CO2 laser for mask marking
[DE93-632901] p 2816 N94-26184

MAGNETIC CONTROL
High-speed repetitive pellet injector for plasma fueling of magnetic confinement fusion devices
[DE94-002792] p 3042 N94-26140

MAGNETIC DIPOLES
Evaluation of APC NbTi superconductor in a model dipole magnet
[DE94-003258] p 3060 N94-26795
Electromagnetic fields and interference
[PB94-126489] p 2771 N94-26877

MAGNETIC EFFECTS
An investigation of magnetic field effects on plume density and temperature profiles of an applied-field MPD thruster
[NASA-TM-106416] p 2700 N94-26090
Magnetostriction and magnetostrictive materials
[VTT-TIED-1434] p 3058 N94-26545
Direct evidence of the interplanetary magnetic field effect on the cosmic-ray shadow by the sun
[ICRR-296-93-8] p 3116 N94-27607
Cryogenic fracture behavior of 316LN in magnetic fields up to 14.6 T
[DE94-005215] p 2742 N94-27694

MAGNETIC FIELD CONFIGURATIONS
Structure of the modulated magnetic phase of Mn3Sn
[DE94-002788] p 2733 N94-26092
The ZnO thin films with C-axis orientation prepared on the room temperature substrate by the ECR multipolar plasma sputtering method
[DE94-605039] p 2758 N94-27857

MAGNETIC FIELD RECONNECTION
Nonlinear growth of strongly unstable tearing modes
[DE94-003366] p 3042 N94-25958

MAGNETIC FIELDS
Study on phase transformation due to deformation in ferromagnetic fields at cryogenic condition
p 2724 N94-25556

An optimal constrained linear inverse method for magnetic source imaging
[DE94-004014] p 2957 N94-25663
Electromagnetic properties of a toroidal solenoid
[DE93-613032] p 2766 N94-25866
An investigation of magnetic field effects on plume density and temperature profiles of an applied-field MPD thruster
[NASA-TM-106416] p 2700 N94-26090
Detection of transient vector-fields in additive noise
[FFI-93/7028] p 2768 N94-26232
Ising critical behaviour in the one-dimensional frustrated quantum XY model
[DE93-634755] p 3057 N94-26390
The influence of energy losses with time in NbTi superconductors in pulsed magnetic fields
[DE93-634761] p 3058 N94-26512
A mechanism for resistive dissipation in Ag sheathed Bi2Sr2CaCu2O8 and Bi2Sr2Ca2Cu3O10
[DE94-003009] p 3060 N94-26771
Asymptotics for Kummer functions, Bose plasmas, and related special functions
[DE94-601853] p 3007 N94-26928
An optimal constrained linear inverse method for magnetic source imaging
[DE94-002264] p 2996 N94-26936
Detection of low-intensity magnetic fields with a magnetostrictive fiber optic sensor
[AD-A274120] p 3037 N94-27062
Technical report of ISSP. Ser. A, no. 2674: High-field cyclotron resonance and impurity transition in n- and p-3C-SiC at magnetic fields up to 175 T
[JTN-94-80560] p 3064 N94-27232
Technical report of ISSP. Ser. A, no. 2672: Magneto-optical effects of excitons in BiI3 crystals under pulsed high magnetic fields. 3: Excitons confined around a stacking disorder formed by a bending stress
[JTN-94-80558] p 3065 N94-27240
Technical report of ISSP. Ser. A, no. 2675: High-field cyclotron resonance and valence-band structure in semiconducting diamond
[JTN-94-80561] p 3065 N94-27245
Researches of the Electrotechnical Laboratory. No. 51: Study of formation and sustainment of reversed field pinch by slow control of magnetic field
[JTN-94-80548] p 3046 N94-27350
Study of the hyperfine magnetic field at Ta-181 site in the Heusler Co2ScSn, Co2ScGa, and Co2HfSn alloys
[DE94-603989] p 3067 N94-27623
Fiber optic Faraday flux transformer specification
[AD-D016058] p 3039 N94-27674
Cryogenic fracture behavior of 316LN in magnetic fields up to 14.6 T
[DE94-005215] p 2742 N94-27694
Mode analysis of gyrotron oscillation using a k-spectrometer
[DE94-701195] p 2813 N94-27703
Atomic processes in Inertial Electrostatic Confinement (IEC) devices
[DE94-005015] p 3047 N94-27715
Advanced development of particle beam probe diagnostic system
[DE94-002316] p 3047 N94-27720
Passive stabilization of MHD instabilities at high (beta)n in the HBT-EP tokamak
[DE94-003317] p 3047 N94-27735
Technical report of ISSP. Ser. A, no. 2687: Quantized persistent currents of a quantum dot in a strong magnetic field
[JTN-94-80573] p 3028 N94-27758
Experimental results of 40-kA Nb3Al conductor
[DE94-701207] p 2788 N94-27821
The three-dimensional hydrogen atom in crossed magnetic and electric fields
[DE94-606301] p 3029 N94-27847

MAGNETIC FLUX
Flux flow, pinning, and resistive behavior in superconducting networks
[DE94-003400] p 3050 N94-25848
High resolution studies of sunspots and flux tubes
[NASA-CR-195216] p 3111 N94-27321
Technical report of ISSP. Ser. A, no. 2687: Quantized persistent currents of a quantum dot in a strong magnetic field
[JTN-94-80573] p 3028 N94-27758
Determination of the plasma column shape in the Tokamak Novillo cross section by magnetic probes
[DE94-604986] p 3048 N94-27844

MAGNETIC INDUCTION
Time domain reflectometry for measuring bulk soil electrical conductivity and comparison with the Em38 instrument
[PB94-125432] p 2881 N94-27052
Analytical study of beam handling and emittance control
[AD-A274412] p 3033 N94-27078

MAGNETIC LENSES
Focusing properties of a three-element quadrupole lens system and its stigmatic focusing behaviour
[DE93-616534] p 2766 N94-25915

MAGNETIC MATERIALS
First principle calculation for magneto-crystalline anisotropy
[DE93-634653] p 3052 N94-26012
Center for nonlinear phenomena and magnetic materials
[AD-A274176] p 3009 N94-27126
List of papers published by the members of Institute for Materials Research, Tohoku University 1992
[JTN-94-80608] p 3118 N94-27355

MAGNETIC MEASUREMENT
Measurement of magnetic fluctuation induced energy transport
[DE94-003846] p 3042 N94-26132
Detection of transient vector-fields in additive noise
[FFI-93/7028] p 2768 N94-26232
An optimal constrained linear inverse method for magnetic source imaging
[DE94-002264] p 2996 N94-26936
Determination of the plasma column shape in the Tokamak Novillo cross section by magnetic probes
[DE94-604986] p 3048 N94-27844

MAGNETIC MIRRORS
Toroidal plasma beta-FLR limit in a toroidally linked mirror system
[DE94-003119] p 3041 N94-25792

MAGNETIC MOMENTS
Volume dependence of vanadium magnetism
[DE94-601838] p 3050 N94-25843
Technical report of ISSP. Ser. A, no. 2678: Magnetic properties of carbon nanotubes
[JTN-94-80564] p 3064 N94-27174

MAGNETIC MONOPOLES
Enhancement of the rate of radiative processes in the field of a magnetic monopole
[DE94-603717] p 3074 N94-27696

MAGNETIC PERMEABILITY
Technical report of ISSP. Ser. A, no. 2678: Magnetic properties of carbon nanotubes
[JTN-94-80564] p 3064 N94-27174
Technical report of ISSP. Ser. A, no. 2681: Orbital and spin susceptibilities of the plane copper sites in YBa2Cu3O(x) system
[JTN-94-80567] p 3064 N94-27177
Technical report of ISSP. Ser. A, no. 2669: Relations between oxygen deficiency and structures in the La-Sr-Cu-O system. 3: Oxygen contents and structure of (La, Sr)8Cu8O(16+delta) phase
[JTN-94-80555] p 3066 N94-27353

MAGNETIC PROBES
Determination of the plasma column shape in the Tokamak Novillo cross section by magnetic probes
[DE94-604986] p 3048 N94-27844

MAGNETIC PROPERTIES
Study on characteristics and electronic structures of materials with strong electronic correlations by ferromagnetic fields p 2724 N94-25557

MAGNETIC PUMPING
Review of tokamak experiments on direct electron heating and current drive with fast waves
[DE94-004185] p 3041 N94-25801

MAGNETIC SIGNATURES
Kiruna geophysical data. Data summary 93/4-6, April-June 1993
[PB94-123700] p 2881 N94-27039
Kiruna geophysical data. Data summary 93/1-3, January-March, 1993
[PB94-123791] p 2881 N94-27043

MAGNETIC SPECTROSCOPY
Implementation of a compact magnetic electron energy spectrometer for intense relativistic electron beams
[AD-A274451] p 3033 N94-27082

MAGNETIC STORMS
Dynamics explorer interdisciplinary scientist investigations
[NASA-CR-195226] p 2878 N94-26204
Region 5395 of March 1989 -- solar activity, geomagnetic disturbances, and terrestrial effects
[PB94-120714] p 3110 N94-26755
Compton Gamma Ray Observatory/BATSE observations of energetic electrons scattered by cyclotron resonance with waves from powerful VLF transmitters
[NASA-CR-195240] p 3115 N94-26790
The Sixteenth Symposium on Coordinated Observations of the Ionosphere and the Magnetosphere in the Polar Regions: Program and abstracts
[JTN-94-80601] p 2882 N94-27300
Configuration of the near-Earth plasma sheet
[NASA-CR-195271] p 2883 N94-27438
Proton aurora and substorm intensifications
[ATR-93(7248)-1] p 2887 N94-28218

MAGNETIC SUSPENSION
Neural control of magnetic suspension systems
p 2682 N94-27905
System identification of the Large-Angle Magnetic Suspension Test Facility (LAMSTF)
p 2682 N94-27908

MAGNETIC VARIATIONS
Comparative investigation of high-latitude ionospheric structure and effects near solar maximum
[AD-A273799] p 2877 N94-25877

MAGNETIZATION
Power laws, flicker noise, and the barkhausen effect
[AD-A274702] p 3008 N94-26376
Technical report of ISSP. Ser. A, no. 2687: Quantized persistent currents of a quantum dot in a strong magnetic field
[JTN-94-80573] p 3028 N94-27758
Anisotropy in the electrical, magnetic and optical properties of Pb2Sr2RCu3O8
[ISBN-0-315-84930-4] p 3070 N94-27974

MAGNETOCARDIOGRAPHY
Detection geometry and reconstruction error in magnetic source imaging
[DE94-004012] p 2809 N94-25662

MAGNETOHYDRODYNAMIC FLOW
Liquid metal MHD research and development in Israel
p 2854 N94-26055
Ways to improve MHD power plants and prospects of their application p 2854 N94-26056
Shear flow generation from the interaction of neoclassical and drift wave transport processes
[DE94-003135] p 2791 N94-26096
Quiet-time intensifications along the poleward auroral boundary near midnight
[ATR-93(7248)-2] p 2877 N94-26201
Scaling of sustained ZT-40 M reversed field pinches
[DE94-003318] p 3043 N94-26321
Researches of the Electrotechnical Laboratory. No. 53: Spectral emission from combustion gas containing scattering media
[JTN-94-80603] p 2717 N94-27246

MAGNETOHYDRODYNAMIC GENERATORS
The Lightcraft project: Flight technology for a hypersonic mass transit system p 2670 N94-25695
Liquid metal MHD research and development in Israel
p 2854 N94-26055
Ways to improve MHD power plants and prospects of their application p 2854 N94-26056

MAGNETOHYDRODYNAMIC STABILITY
Toroidal plasma beta-FLR limit in a toroidally linked mirror system
[DE94-003119] p 3041 N94-25792
Nonlinear growth of strongly unstable tearing modes
[DE94-003366] p 3042 N94-25958
Investigation of plasma instabilities in the polar cusp
[NASA-CR-195212] p 2879 N94-26599
TFTR experimental data analysis collaboration
[DE94-004166] p 3047 N94-27690
Reduced Braginskii equations
[DE94-003510] p 3047 N94-27723
Numerical experiment on finite element method for matching data
[DE94-701208] p 3000 N94-27731
Passive stabilization of MHD instabilities at high (beta)n in the HBT-EP tokamak
[DE94-003317] p 3047 N94-27735

MAGNETOHYDRODYNAMIC WAVES
Review of tokamak experiments on direct electron heating and current drive with fast waves
[DE94-004185] p 3041 N94-25801
TFTR experimental data analysis collaboration
[DE94-004166] p 3047 N94-27690
The calculation for energy balance of heating plasmas by Alfven waves
[DE94-604994] p 3049 N94-27855

MAGNETOHYDRODYNAMICS
The Lightcraft project: Flight technology for a hypersonic mass transit system p 2670 N94-25695
Nonlinear growth of strongly unstable tearing modes
[DE94-003366] p 3042 N94-25958
The First Energy Conference: Israel and the Former USSR
[ISBN-965-229-098-X] p 2853 N94-26050
Liquid metal MHD research and development in Israel
p 2854 N94-26055
Nonlinear transverse propagation of photons in a ultrarelativistically hot and magnetized electron-positron plasma: Coupling of Langmuir and electromagnetic solitons
[DE94-603667] p 3046 N94-27630
TFTR experimental data analysis collaboration
[DE94-004166] p 3047 N94-27690
Numerical experiment on finite element method for matching data
[DE94-701208] p 3000 N94-27731

Analysis of density limit and efficiency in lower hybrid current drive
[DE94-604995] p 3049 N94-27856

MAGNETOMETERS
Detection geometry and reconstruction error in magnetic source imaging
[DE94-004012] p 2809 N94-25662
Determination of the geomagnetic external contribution by nonlinear optimization methods
[DE94-600882] p 2878 N94-26365

MAGNETOPLASMADYNAMICS
An investigation of magnetic field effects on plume density and temperature profiles of an applied-field MPD thruster
[NASA-TM-106416] p 2700 N94-26090
Flowing DPF design for propulsion experiments
[AD-A274973] p 2701 N94-26537

MAGNETOSHEATH
Collisionless shock structures of Earth and other planets
[NASA-CR-195257] p 3104 N94-27407

MAGNETOSPHERE-IONOSPHERE COUPLING
Ionosphere-magnetosphere coupling
[NASA-CR-195222] p 2881 N94-27237
The Sixteenth Symposium on Coordinated Observations of the Ionosphere and the Magnetosphere in the Polar Regions: Program and abstracts
[JTN-94-80601] p 2882 N94-27300

MAGNETOSTATIC FIELDS
On radio frequency wave induced radial transport and wave helicity
[IPPCZ-326] p 2777 N94-27838

MAGNETOSTRICTION
Magnetostriction and magnetostrictive materials
[VTT-TIED-1434] p 3058 N94-26545
Ferrite phase shifters using stress insensitive materials
[AD-A274639] p 2708 N94-26895
Detection of low-intensity magnetic fields with a magnetostrictive fiber optic sensor
[AD-A274120] p 3037 N94-27062

MAGNETRONS
HPm-tubes: Literature survey comprising 1992
[PB94-123643] p 2785 N94-27038

MAGNONS
Holes in a two-dimensional quantum antiferromagnet
[DE93-634753] p 3057 N94-26388

MAIN SEQUENCE STARS
Coronal heating via nanoflares
[DE94-000773] p 3110 N94-26696

MAINTENANCE
Human factors in airway facilities maintenance: Development of a prototype outage assessment inventory
[DOT/FAA/AM-94/5] p 2941 N94-26136
Development of the gas turbine. Part 2: Manufacturing, commissioning, and operation p 2831 N94-28081

MAINTENANCE TRAINING
Knowledge organization in intelligent tutoring systems for diagnostic problem solving in complex dynamic domains
[AD-A273986] p 2984 N94-25899
Production of a computer based lesson teaching employees how to use an air data tester
[ISBN-0-315-84708-5] p 2969 N94-27316

MAJORITY CARRIERS
The structural, chemical, and electrical properties of He-implantation-induced nanocavities in silicon
[DE94-002681] p 3052 N94-25971

MALAYSIA
Atmospheric science research in Malaysia: Perspectives on international cooperation p 2874 N94-28285

MALES
Thermoregulatory effects of caffeine ingestion during rest and exercise in men
[NASA-TM-108783] p 2901 N94-26210

MAMMALS
Proposed law of nature linking impacts, plume volcanism, and Milankovitch cycles to terrestrial vertebrate mass extinctions via greenhouse-embryo death coupling
p 2876 N94-28307

MAN MACHINE SYSTEMS
Institute for Information Technology
[NRC-37061] p 3118 N94-26709
Automated information management for designers: Functional requirements for computer based associates that support access and use of technical information in design
[AD-A274603] p 3099 N94-26891
Telepresence in the human exploration of Mars: Field studies in analog environments p 2685 N94-27360
Aerospace medicine and biology: A continuing bibliography with indexes (supplement 386)
[NASA-SP-7011(386)] p 2933 N94-28208
Aerospace medicine and biology: A continuing bibliography with indexes (supplement 387)
[NASA-SP-7011(387)] p 2933 N94-28213
Visit to CERMA: Centre d'Etudes et de Recherches de Medecine Aerospatiale, Centre for Studies and Research in Aviation and Space Medicine, Bretigny sur Orge, France, November 16-18, 1992
[PB94-132990] p 2937 N94-28392

MANAGEMENT INFORMATION SYSTEMS
Implementing a multiple criteria model base in co-op with a graphical user interface generator
[AD-A274901] p 3093 N94-26181
Information systems criteria for applying software reengineering: Guidelines for identifying information systems for software reengineering
[AD-A274699] p 3097 N94-26375
Data analysis and data fusion for intelligence analysis and decision support. Research plan 1993-2000
[PB94-123569] p 3005 N94-27173
University program management information system, FY 1993
[NASA-TM-109719] p 3100 N94-27413
The TMIS life-cycle process document, revision A
[NASA-TM-109698] p 2697 N94-27775

MANAGEMENT METHODS
Module interconnection frameworks for a real-time spreadsheet
[AD-A273853] p 2956 N94-25588
The effectiveness of AMT investment in UK metal component manufacture
[IND-MANU-SCI-TECH-REPT-3] p 2762 N94-25775
An exploratory survey of methods used to develop measures of performance
[AD-A273945] p 2834 N94-25896
Business process redesign: Design the improved process
[AD-A274947] p 3093 N94-26299
Benefits estimation for simulation systems used for aircrew training in a multiship environment
[AD-A274313] p 2938 N94-26882
An investigation of integrated product development implementation issues: A case study of Bosma Machine and Tool Corp.
[AD-A273917] p 2942 N94-27320
Polyhedral characterization of the economic lot-sizing problem with start-up costs
[MEMO-COSOR-92-46] p 2969 N94-27396

MANAGEMENT SYSTEMS
Automated information management for designers: Functional requirements for computer based associates that support access and use of technical information in design
[AD-A274603] p 3099 N94-26891
On modeling and controlling intelligent systems
[DE94-002446] p 2988 N94-27706

MANDRELS
Equivalent performance in different helical resonator plasma polymerization coater platforms
[DE94-001517] p 2753 N94-26933

MANEUVERABILITY
Analysis and optimization of preliminary aircraft configurations in relationship to emerging agility metrics
[NASA-CR-195228] p 2668 N94-26235

MANGANESE
An extraterrestrial event at the tertiary-quaternary boundary p 2890 N94-28309

MANGANESE ALLOYS
Microstructural development in low activation ferritic alloys irradiated to 200 dpa at 420 C
[DE94-004269] p 2731 N94-25803
Structure of the modulated magnetic phase of Mn3Sn
[DE94-002788] p 2733 N94-26092
NMR study of quasicrystal Al(70)Pd(20)T(M10) alloy (T(M):Cr, Mn, Fe, and Co) p 2745 N94-28162
Formation and high mechanical strength of Al-based alloys containing a nanoscale icosahedral phase as a main constituent p 2746 N94-28171
Mechanical properties and microstructure of thermomechanically processed, high manganese steel
[ARL-TR-146] p 2747 N94-28212

MANGANESE COMPOUNDS
Technical report of ISSP. Ser. A, no. 2673: Two successive spin glass transitions in non-diluted Heisenberg-like spin glass Ni(0.42)Mn(0.58) TiO3
[JTN-94-80559] p 2756 N94-27241

MANIFOLDS (MATHEMATICS)
Characterization of self-conjugate minimal surfaces in R(sup 3)
[DE94-601538] p 2993 N94-26409
Implementation of integral manifold control on a two degree of freedom flexible joint manipulator: Theory and experiments
[ISBN-0-315-83572-9] p 2823 N94-26658
Poisson-lie group of pseudodifferential symbols
[PB94-124393] p 2997 N94-26996
Illumination in diverse codimensions
[NASA-CR-191596] p 2971 N94-27572
A survey of open problems in symplectic integration
[DE94-003966] p 3007 N94-27777

MANIPULATORS
A global approach to kinematic path planning to robots with holonomic and nonholonomic constraints
p 2683 N94-26279
Inertial-space disturbance rejection for space-based manipulators p 2683 N94-26281
Performance measures from the explorer platform berthing experiment p 2683 N94-26283
Asymptotically stable neural networks for identification of nonlinear dynamic systems
[ISBN-0-315-84328-4] p 2985 N94-26629
Dynamics of a flexible extendible beam
[ISBN-0-315-84278-4] p 2838 N94-26639
Motion planning for serial manipulators with many degrees of freedom: Implementation of a sequential search strategy
[ISBN-0-315-83682-2] p 2822 N94-26642
Optimal architectural design of parallel and hybrid manipulators
[ISBN-0-315-84351-9] p 2822 N94-26657
Simulation dynamics of a multibody chain: Recursion based on chain modal coordinates
[ISBN-0-315-83555-9] p 2994 N94-26659
Interchangeable end effector tools utilized on the PFMA
[NASA-CR-193925] p 2823 N94-27149
Generalized finite element dynamic modelling and simulation for flexible robot manipulators
[ISBN-0-315-84623-2] p 2825 N94-27343
Dynamic control of kinematically redundant manipulators
[ISBN-0-315-84627-5] p 2825 N94-27344
Advanced control of a flexible spherical wrist
[ISBN-0-315-84424-8] p 2826 N94-27652
Local performance optimization for a class of redundant eight-degree-of-freedom manipulators
[NASA-TP-3417] p 2989 N94-27773
Comparison of dynamic analysis of a Schilling hydraulic manipulator with experimental results
[DE94-004597] p 2827 N94-27780

MANNED LUNAR SURFACE VEHICLES
The Extended Mission Rover (EMR)
p 2689 N94-25674
Pressurized Lunar Rover (PLR) p 2833 N94-25704

MANNED MARS MISSIONS
Manned mission to Mars with periodic refueling from electrically propelled tankers p 2689 N94-25670
Lowest cost, nearest term options for a manned Mars mission p 2689 N94-25682
Project APEX: Advanced manned exploration of the Martian moon Phobos p 3079 N94-25688
Project Minerva: A low-cost manned Mars mission based on indigenous propellant production
p 2760 N94-25705
Pax: A permanent base for human habitation of Mars
p 2943 N94-25706

MANNED SPACE FLIGHT
Future of aerospace
[PB94-120185] p 2669 N94-26906
Research and Development Annual Report, 1992
[NASA-TM-104777] p 3119 N94-27993

MANUFACTURING
Study on utilization of super clean, high vacuum space
p 2682 N94-25586
Lunar preform manufacturing p 2765 N94-25677
The effectiveness of AMT investment in UK metal component manufacture
[IND-MANU-SCI-TECH-REPT-3] p 2762 N94-25775
General Motors Corporation and Pacific Northwest Laboratory staff exchange: Inspection of case hardened steels and metal-matrix composites
[DE94-003470] p 2706 N94-25982
The National Center for Advanced Information Components Manufacturing: Program update
[DE94-002647] p 2960 N94-26118
Overview of the Photovoltaic Manufacturing Technology (PVMaT) project
[DE93-018234] p 2856 N94-26426
Adaptive path planning in changing environments
[DE94-003269] p 2985 N94-26462
Qualified manufacturing and interoperability for space applications p 2949 N94-26719
Fabrication technology
[DE94-003017] p 2763 N94-26778
Investigation of ACC/CCI tunnel diodes
[AD-A274549] p 2785 N94-26845
Material optimization and manufacturing development of reduced cost powder metal titanium alloy components for gas turbine engine application, phase 2
[AD-A274410] p 2709 N94-26978
Solar collector manufacturing activity, 1992
[DE94-003401] p 2859 N94-27048

A widely adaptable habitat construction system utilizing space resources p 2688 N94-27374
Multiple weight stepwise regression
[DE94-001602] p 3000 N94-27564
Continuous roll-to-roll a-Si photovoltaic manufacturing technology
[DE94-000260] p 2859 N94-27610
Development of the gas turbine. Part 2: Manufacturing, commissioning, and operation p 2831 N94-28081
Open communication in manufacturing automation
[PB94-132479] p 2976 N94-28377

MANY BODY PROBLEM
Theoretical and computational studies in intermediate energy nuclear physics
[DE94-004177] p 3012 N94-25800
Stability of large scale interconnected dynamical systems
[DE94-601536] p 2993 N94-26408
How reliable is the HMSA integral equation for the pair structure of supercooled and amorphous mixtures?
[DE94-601543] p 3006 N94-26411
Study of the critical points at infinity arising from the failure of the Palais-smale condition for n-body type problems
[DE94-603656] p 3000 N94-27818

MAPPING
Mapping closed tropical forest cover in West Africa using NOAA/AVHRR-LAC data p 2850 N94-27184
Fixed point type theorems and projection-interaction approximation
[DE94-603669] p 3000 N94-27632
Solution of the Heisenberg equation for the four-fermion contact interaction by the method of dynamical mappings
[DE94-606341] p 3075 N94-27858
Fractals and their applications to remote sensing and digital mapping
[ISBN-0-315-59469-1] p 2852 N94-27870

MARINE BIOLOGY
Coupling of pelagic and benthic communities over a seamount in the Eastern North Pacific
[AD-A274750] p 2899 N94-26149
Measuring variation in ecosystem sensitivity to stress
[AD-A274232] p 2868 N94-26817
Macrobenthic fauna in the dutch sector of the north sea in 1991
[PB94-126414] p 2868 N94-27200
Changes in phytoplankton population in the Chao Phraya estuary, Thailand, during the eutrophication mechanisms studies p 2875 N94-28287

MARINE CHEMISTRY
An experimental study of plunging liquid jet induced air carryunder and dispersion
[AD-A274414] p 2794 N94-26979

MARINE ENVIRONMENTS
Study on fatigue crack propagation characteristics around welded joint interface in complexed conditions
p 2730 N94-25584
Conversion of the CLUSE model for applications over open ocean
[AD-A273750] p 2893 N94-26013
The biostratigraphy and paleogeography of Maastrichtian inoceramids p 2889 N94-28303

MARINE MAMMALS
Sonic booms and marine mammals: Informational status and recommendations p 2651 N94-28198

MARINE METEOROLOGY
Naval Interactive Data Analysis System (NIDAS), software user's manual
[NASA-CR-195179] p 2956 N94-25606
Mesoscale frontal evolution of the ERICA IOP-5A Cyclone
[AD-A274906] p 2893 N94-26183
The numerical simulation of marine boundary layer clouds
[AD-A273669] p 2894 N94-26195
Propagation of cold air masses in East Asia and its associated planetary-scale function
[AD-A274304] p 2895 N94-26850

MARINE PROPULSION
Integration of interactive interfaces with intelligent tutoring systems: An implementation
[AD-A273869] p 2985 N94-25966

MARINER 9 SPACE PROBE
Reanalysis of Mariner 9 UV Spectrometer Data for Ozone, Cloud, and Dust Abundances, and Their Interaction Over Climate Timescales
[NASA-CR-195244] p 3107 N94-27885
Probing the Martian atmosphere in the ultraviolet
p 3108 N94-27890
How well was total ozone abundance inferred with Mariner 9? p 3108 N94-27891

MARKERS
Ion beam mixing of marker layers into amorphous aluminum oxide
[DE94-000901] p 2752 N94-26676

MARKET RESEARCH
Development of satellite telecommunications during the period 1990 - 2005
[CRANFIELD-AERO-9301] p 2765 N94-25639
Powerful selling and sales strategy
p 2662 N94-28245

MARKETING
Powerful selling and sales strategy
p 2662 N94-28245

MARKOV CHAINS
Single-server queues with spatially distributed arrivals
[PB94-126638] p 2986 N94-26916
The Communication Link and Error ANalysis (CLEAN) simulator
[NASA-CR-195243] p 2968 N94-27168

MARKOV PROCESSES
Application of Markov random field theory to image coding and motion estimation
[ISBN-0-315-83435-8] p 2964 N94-26632
Three dimensional object recognition using a complex autoregressive model
[AD-A274388] p 2995 N94-26829
Limit theorems for functionals of Markov processes and renormalizable stable fields
[AD-A274645] p 3004 N94-27106
White noise theory of robust nonlinear filtering with correlated state and observation noises
[PB94-126661] p 3004 N94-27211

MARS (PLANET)
Project APEX: Advanced manned exploration of the Martian moon Phobos p 3079 N94-25688
Mars transportation system p 2833 N94-25689
Telepresence in the human exploration of Mars: Field studies in analog environments p 2685 N94-27360
Reanalysis of Mariner 9 UV Spectrometer Data for Ozone, Cloud, and Dust Abundances, and Their Interaction Over Climate Timescales
[NASA-CR-195244] p 3107 N94-27885

MARS ATMOSPHERE
Extraterrestrial surface propulsion systems
p 2833 N94-25691
Reanalysis of Mariner 9 UV Spectrometer Data for Ozone, Cloud, and Dust Abundances, and Their Interaction Over Climate Timescales
[NASA-CR-195244] p 3107 N94-27885
Cooling the Martian atmosphere: The spectral overlap of the C02 15 micrometers band and dust
p 3107 N94-27886
Martian atmospheric radiation budget
p 3107 N94-27887
Mars ozone: Mariner 9 revisited p 3107 N94-27888
Why is the north polar cap on Mars different than the south polar cap? p 3107 N94-27889
Probing the Martian atmosphere in the ultraviolet
p 3108 N94-27890
How well was total ozone abundance inferred with Mariner 9? p 3108 N94-27891
In situ Mars ozone detector p 3108 N94-27892
The Martian atmospheric planetary boundary layer stability, fluxes, spectra, and similarity
[NASA-CR-195711] p 3108 N94-27935

MARS ENVIRONMENT
First lunar outpost p 2943 N94-25694
Why is the north polar cap on Mars different than the south polar cap? p 3107 N94-27889

MARS LANDING
Battery study for the Mars Environmental Survey (MESUR) Pathfinder p 2860 N94-28105

MARS SURFACE
Planetary surface exploration MESUR/autonomous lunar rover p 2833 N94-25683
Mars transportation system p 2833 N94-25689
Design and development of the second generation Mars Habitat p 2943 N94-25693
Project Ares 3 p 2671 N94-25712
Why is the north polar cap on Mars different than the south polar cap? p 3107 N94-27889
In situ Mars ozone detector p 3108 N94-27892

MARTENSITE
Microstructural development in low activation ferritic alloys irradiated to 200 dpa at 420 C
[DE94-004269] p 2731 N94-25803

MARTENSITIC STAINLESS STEELS
Electrochemical properties of passive films on 440C stainless steel
[ISBN-0-315-64248-3] p 2757 N94-27801

MARTENSITIC TRANSFORMATION
Study on phase transformation due to deformation in ferromagnetic fields at cryogenic condition
p 2724 N94-25556
Study on microscopic structural controls and electronic properties at material surfaces by ion beams
p 2727 N94-25571
Stress-induced phase transformation in ZrO2 materials
[ISBN-0-315-83373-4] p 2752 N94-26661

MARTINGALES
Bisexual branching diffusions
[AD-A274698] p 3008 N94-26374

MASKS
Development of an industrial CO2 laser for mask marking
[DE93-632901] p 2816 N94-26184

MASONRY
Proceedings of the Fourth Euroseminar on Microscopy Applied to Building Materials
[PB94-119807] p 2839 N94-26754

MASS
Small low mass advanced PBR's for bi-modal operation
[DE94-003201] p 2699 N94-25798
Parametric analysis of the space power plants on the base of criterion of specific mass in generalized design variants
[DE93-634153] p 2701 N94-26166

MASS BALANCE
Space Station evolution study oxygen loop closure
[NASA-CR-193938] p 2941 N94-26788

MASS FLOW
Propagation of cold air masses in East Asia and its associated planetary-scale function
[AD-A274304] p 2895 N94-26850

MASS FLOW RATE
SP industry calorimeter for rate of heat release measurements up to 10MW
[PB94-124211] p 2811 N94-27044

MASS SPECTRA
Aspects of nonrenormalizable terms in a superstring standard-like models
[DE93-614530] p 3071 N94-25911
Quantizable configurations of the relativistic string
[DE93-634346] p 3072 N94-26036
Meson X(1814) as a candidate for a hybrid state
[DE93-634447] p 3017 N94-26045
Leptonic decay constants of heavy mesons in QCD
[DE93-634426] p 3022 N94-26767
A measurement of the W mass using electrons at CDF
[DE94-004656] p 3028 N94-27748
Decay constants of heavy mesons in the relativistic potential model with velocity dependent corrections
[DE94-606495] p 3030 N94-27860

MASS SPECTROSCOPY
Study on analyzing method establishment for metallic material development p 2729 N94-25578
Molecular beam mass spectrometry studies of the chemical vapor deposition of diamond
[DE94-003802] p 3049 N94-25601
Three methods to measure RH bond energies
[DE94-003795] p 3013 N94-25816
New FORTRAN computer programs to acquire and process isotopic mass spectrometric data: Operator's manual
[DE94-003174] p 2965 N94-26784
Antiproton studies in penning traps
[AD-A274250] p 3024 N94-27011
Determination of lead isotope ratios in seawater by purge and trap GC/MS after ethylation p 2870 N94-28152

MASS TRANSFER
Absorption technology for solar and waste heat utilization p 2854 N94-26053
An April 1991 outburst from 4U0115+63 observed by BATSE
[NASA-CR-195252] p 3116 N94-27440

MASSIVELY PARALLEL PROCESSORS
Achieving high performance on the Intel Paragon
[DE94-003108] p 2979 N94-25953
Computational mechanics
[DE94-003015] p 2965 N94-26775
Efficient massively parallel simulation of dynamic channel assignment schemes for wireless cellular communications
[NASA-CR-191593] p 2971 N94-27558
High performance computing in chemistry and massively parallel computers: A simple transition?
[DE94-004318] p 2982 N94-27600

MATCHED FILTERS
Detection of transient vector-fields in additive noise
[FFI-93/7028] p 2768 N94-26232

MATCHING
Saving comparisons in the Crochemore-Perrin string matching algorithm
[CWI-CS-R9322] p 2971 N94-27550
The molecular matching problem
p 3030 N94-27910

MATERIALS
Development of the gas turbine. Part 1: Design philosophy and performance p 2831 N94-28080

MATERIALS HANDLING
Automated in-situ inspection systems for underground storage tanks
[AD-A274644] p 2764 N94-27144

MATHEMATICAL LOGIC

New binary integration strategies and corresponding R90 calculations
[AD-A274786] p 2769 N94-26359

A formalization of objects using equational dynamic logic
[PB94-125218] p 2965 N94-26852

Combining logics
[PB94-125242] p 2965 N94-26908

A characterization of stable models using a non-monotonic operator
[CWI-CS-R9315] p 2970 N94-27543

Modal logic, transition systems and processes
[CWI-CS-R9321] p 2970 N94-27549

MATHEMATICAL MODELS

The application of simulated annealing to stochastic systems
[AD-A273850] p 3001 N94-25607

A comparison of three approximate mathematical models for the gravity gradient stabilized satellite
[AD-A273832] p 2694 N94-25615

HDR reactor containment fire modeling with BRI2
[VTT-PUBS-113] p 3031 N94-25621

Binaural room simulation
[AD-A273823] p 3009 N94-25737

Hydrogen uptake into silicon from an ECR plasma
[DE94-003771] p 3050 N94-25815

Spatial symmetry, local integrability and tetrahedron equations in the Baxter-Bazhanov model
[DE93-634348] p 3002 N94-26038

Z(sub N)(sup n-1) broken model
[DE93-634357] p 3072 N94-26039

Geometric correction of SPOT images with use of digital elevation models
[ETN-94-95033] p 2847 N94-26107

The identification of inflow fluid dynamics parameters that can be used to scale fatigue loading spectra of wind turbine structural components
[DE94-000231] p 2791 N94-26117

SIMA: A model for forest succession based on the carbon and nitrogen cycles with application to silvicultural management of the forest ecosystem
[SILVA-CARELICA-22] p 2848 N94-26258

Simulation modeling for long duration spacecraft control systems p 2684 N94-26288

C-periodicity and the physical mass in the 3-state Potts model
[DE94-601551] p 3019 N94-26423

Subgraph approximations for large directed graphical models
[AD-A274813] p 3003 N94-26485

Simulation approaches for calculations in directed graphical models
[AD-A274825] p 3003 N94-26494

A concurrent, multigroup, discrete ordinates model of neutron transport
[DE94-004334] p 3020 N94-26577

Reconstruction of multiple cracks from experimental electrostatic boundary measurements
[NASA-CR-191584] p 2994 N94-26601

Piloted simulation study of an ILS approach of a twin-pusher business/commuter turboprop aircraft configuration
[NASA-TM-4516] p 2646 N94-26602

Analysis of the influence of weather on infrared imagery
[FEL-92-A421] p 3036 N94-26649

Simulation dynamics of a multibody chain: Recursion based on chain modal coordinates
[ISBN-0-315-83555-9] p 2994 N94-26659

A constitutive model for layered wire mesh and aramid cloth fabric
[DE94-003275] p 2708 N94-26796

Calculations of material removal, removal rate, and Preston coefficient in continuous lapping/polishing machines
[DE94-002619] p 2763 N94-26804

Physical modelling and adaptive predictive control of diffusion/LPCVD reactors
[PB94-126398] p 2763 N94-26819

Modern photoacoustic spectroscopy problems. Theory and experiment (a review)
[IFTR-41/1993] p 2716 N94-26823

Three dimensional object recognition using a complex autoregressive model
[AD-A274388] p 2995 N94-26829

Calculation of the electromagnetic critical state response of high T(sub c) superconductor tape
[DE94-002894] p 3061 N94-26868

Recursive bundle event structures
[PB94-125275] p 3004 N94-26870

Annual conference on fire research, 1993: Book of abstracts
[PB94-121324] p 2717 N94-26907

Combining logics
[PB94-125242] p 2965 N94-26908

Some aspects of nonlinear discrete-time descriptor systems in economics
[PB94-126653] p 3101 N94-26918

A non-linear mathematical model or finite, periodic rail corrugations
[REPT-93-49] p 2996 N94-26967

Kinetics of 2-pentadecylaniline polymerizations in monolayers: Relationships between experimental data and a new theoretical model
[AD-A274419] p 2754 N94-27080

Research in improved assessment of software reliability
[AD-A274161] p 2968 N94-27140

Numerical Analysis Methods of Surface Cracks
[VTT-PUBS-119] p 2841 N94-27186

UAH mathematical model of the variable polarity plasma ARC welding system calculation
[NASA-CR-193926] p 2824 N94-27221

High resolution studies of sunspots and flux tubes
[NASA-CR-195216] p 3111 N94-27321

Compressibility effects on rotor forces in the leakage path between a shrouded pump impeller and its housing
p 2796 N94-27379

Global barotropic response to a tropical forcing
[NASA-CR-195256] p 2896 N94-27408

A characterization of stable models using a non-monotonic operator
[CWI-CS-R9315] p 2970 N94-27543

Control of a hydrogen/oxygen steam generator
[DLR-FB-93-02] p 2826 N94-27589

Development of hypersonic engine seals: Flow effects of preload and engine pressures
[NASA-TM-106333] p 2826 N94-27599

An unavailability model for errors made during surveillance testing
[DE94-000816] p 2835 N94-27613

Lifetimes of lunar satellite orbits
[NASA-TP-3394] p 2690 N94-27771

Modeling of the coupled magnetospheric and neutral wind dynamos
[NASA-CR-195273] p 2883 N94-27852

Ion-driven permeation of deuterium in metals
[DE94-701104] p 2744 N94-27876

Reanalysis of Mariner 9 UV Spectrometer Data for Ozone, Cloud, and Dust Abundances, and Their Interaction Over Climate Timescales
[NASA-CR-195244] p 3107 N94-27885

A laboratory test on construction of ice domes and their load-carrying capacity p 2884 N94-27966

Numerical assessment of aerodynamic interactions on missiles with transverse jets control
p 2659 N94-28031

Numerical simulation of a powered-lift landing
p 2671 N94-28033

Gas Turbine Engine Transient Behaviour
[VKI-LS-1993-06] p 2828 N94-28043

Transient model applications. 2: Compressor stall modeling methods p 2829 N94-28049

Engine simulation technology p 2829 N94-28051

Landscape dynamics of northeastern forests
[NASA-CR-195272] p 2852 N94-28070

Nonequilibrium radiation and chemistry models for aerocapture vehicle flowfields
[NASA-CR-195706] p 2648 N94-28071

An initial investigation into methods of computing transonic aerodynamic sensitivity coefficients
[NASA-CR-195705] p 2648 N94-28072

A modelling of the noise from simple coaxial jets. Part 3: With hot primary flow
[ISVR-TR-230-PT-3] p 2807 N94-28173

Interaction of the sonic boom with atmospheric turbulence p 2650 N94-28191

The propagation of spark-produced N waves through turbulence p 2650 N94-28193

Performance considerations for the application of the lossless browse and residual model
p 2946 N94-28256

Extraterrestrial accretion and glacial cycles
p 2890 N94-28308

Intertemporal bargaining and dynamic consistency
[PB94-133147] p 3095 N94-28386

Lisp interface to geometric modelling operations
[PB94-133121] p 3001 N94-28398

MATHEMATICAL PROGRAMMING

A logarithmic barrier cutting plane method for convex programming
[REPT-93-43] p 2957 N94-25761

Research on primal-dual interior point algorithms for mathematical programming
[DE94-003982] p 2959 N94-25821

Formal methods for dependable real-time systems
p 2953 N94-26740

The CODE-TOP (COncurrent system DEvelopment using Transformations Of Predicate-transition nets) method: Examples of using it for system architecture specification, software specification, and code generation p 2953 N94-26744

New mixed integer algorithm for classification and placement of measurements in process flow networks
[PB94-126752] p 2966 N94-26921

MATRICES (MATHEMATICS)

Piecewise least squares fitting technique using finite interval method with Hermite polynomials
[VTT-PUBS-135] p 2990 N94-25733

Separable expansions of the NN t-matrix by way of exact half off the energy shell methods
[DE94-601615] p 3015 N94-25890

Matrix near rings and pseudo distributivity
[DE94-601505] p 2992 N94-26366

Parallel matrix transpose algorithms on distributed memory concurrent computers
[DE94-002424] p 2964 N94-26764

Simple currents versus orbifolds with discrete torsion: A complete classification
[NIKHEF-H/93-13] p 2995 N94-26812

Role of anticausal inverses in multirate filter-banks. Part 1: System theoretic fundamentals
[AD-A274279] p 2997 N94-27015

Ma42: A new frontal code for solving sparse unsymmetric systems
[PB94-124302] p 2998 N94-27115

The PRISM project: Infrastructure and algorithms for parallel eigensolvers
[DE94-005125] p 2973 N94-27717

Hessenberg matrices in Krylov subspaces and the computation of the spectrum
[PB94-133170] p 3001 N94-28389

MATRIX MATERIALS

Inner fiber observation for metal matrix composites under the stress load condition utilizing Synchrotron Orbital Radiation (SR) by X-ray CT p 2724 N94-25553

Lunar preform manufacturing p 2765 N94-25677

Characterization of fatigue damage in a metal matrix composite (SCS-6/Ti-15-3) at elevated temperature
[AD-A273797] p 2706 N94-25876

Engineering limitations of ceramic composites for high performance and high temperature applications
[DE94-001676] p 2754 N94-27021

Polyimide/inorganic composite-interpenetrating polymer network for stable second-order nonlinear optics
[AD-A274646] p 2709 N94-27107

Thermoplastic or thermosetting composites in aircrafts
[PB94-123809] p 2710 N94-27253

MATRIX METHODS

Hydroacoustic wave-fields generated by different source types, a computational study
[PB94-123536] p 3010 N94-27037

MATRIX THEORY

Role of anticausal inverses in multirate filter-banks. Part 1: System theoretic fundamentals
[AD-A274279] p 2997 N94-27015

Causal fir matrices with anticausal fir inverses, and application in characterization of biorthonormal filter banks
[AD-A274509] p 2998 N94-27035

MATTER (PHYSICS)

Dibaryon-induced instability of neutron stars
[DE93-634453] p 3103 N94-26046

Rescattering and energy loss of fast partons in nuclear matter
[DE94-002918] p 3018 N94-26145

MAXIMA

Joint essential maximal numerical range
[DE94-603674] p 3000 N94-27637

MAXIMUM ENTROPY METHOD

Quantum statistical inference for density estimation
[DE94-002625] p 3073 N94-26805

MAXIMUM LIKELIHOOD ESTIMATES

Parameter estimation for ARMA models with infinite variance innovations
[AD-A274654] p 3003 N94-26355

Non-adaptive robust filters for speckle noise reduction
[INPE-5519-PRE/1794] p 2776 N94-27335

MAXIMUM PRINCIPLE

Some properties of generalized biregular functions with values in a Clifford algebra
[DE93-613024] p 2991 N94-25881

MAXWELL EQUATION

Reduced Braginskii equations
[DE94-003510] p 3047 N94-27723

Fields and potentials in general uniaxial bianisotropic media I. Axial sources
[PB94-132875] p 2778 N94-28379

Plane wave propagation in an anisotropic chiral medium with isotropic permittivity and permeability
[PB94-133097] p 2778 N94-28384

MCMURDO SOUND
Telepresence in the human exploration of Mars: Field studies in analog environments p 2685 N94-27360
MEAN SQUARE VALUES
An optimal constrained linear inverse method for magnetic source imaging
[DE94-004014] p 2957 N94-25663
Short-range cloud amount forecasting with model output statistics
[AD-A274769] p 2895 N94-26798
An optimal constrained linear inverse method for magnetic source imaging
[DE94-002264] p 2996 N94-26936
MEASURING INSTRUMENTS
Bundle Intensity and Beamgate Length recorder (BIBL)
[DIGEL-1993-7] p 3031 N94-25619
Primary standards laboratory report 1st half 1993
[DE94-003138] p 2762 N94-26027
Lepton masses in an SU(3)(sub L) x U(1)(sub N) gauge model
[DE93-634366] p 3016 N94-26040
Improved measurement accuracy in a Long Trace Profiler: Compensation for laser pointing instability
[DE94-003408] p 2816 N94-26130
Breakwire technique for hypervelocity measurement
[AD-A274779] p 2809 N94-26358
Calibrating/testing meters in hot water test bench VM7
[PB94-124294] p 2812 N94-27160
Trace organic chemical detection using an ultraviolet excitation molecular beam fluorometer
[DE94-002649] p 2704 N94-27708
Energy Dispersive X ray Diffraction (EDXD) apparatus for liquids at high temperature p 2721 N94-28159
MECHANICAL ENGINEERING
The 1991-1992 project summaries
p 2943 N94-25698
MECHANICAL MEASUREMENT
An ultrasonic testing technique for monitoring the cure and mechanical properties of polymeric materials
[AD-A274536] p 2753 N94-26842
MECHANICAL PROPERTIES
Study on high temperature damage control and life improvement p 2729 N94-25580
Continuous fiber reinforced thermoplastic composites: Literature survey
[VTT-TIED-1422] p 2704 N94-25651
Structure and properties of intermetallic composites synthesized in situ using solid state displacement reactions
[DE94-004312] p 2705 N94-25805
Stress relaxation in dough moulding compounds
[PB94-124872] p 2748 N94-25894
An atom probe investigation of the influence of trace impurities on the mechanical behavior of NiAl
[DE94-002797] p 2734 N94-26272
Titanium 1992: Volume 3: Science and technology
[AD-A274800] p 2735 N94-26337
Titanium 1992: Science and technology, volume 2 rence (7th) in san diego, california on june 29-july 2, 1992. Volume 2
[AD-A274799] p 2736 N94-26362
Statistical mechanical properties of Z(N)(sup n-1) broken model
[DE93-634344] p 2993 N94-26457
Investigation of forced and isothermal chemical vapor infiltrated SiC/SiC ceramic matrix composites
[DE94-004544] p 2708 N94-26557
Mechanical properties of nanophase materials
[DE94-004625] p 2751 N94-26594
The influence of weld metal alloying additions to extend the heat input range for the submerged arc welding of high strength steels
[AD-A274284] p 2738 N94-26679
New rubber qualification for the igniter adapter
[NASA-CR-193936] p 2752 N94-26708
Proceedings of the Fourth Euroseminar on Microscopy Applied to Building Materials
[PB94-119807] p 2839 N94-26754
Mechanism of mechanical fatigue of silica glass
[DE94-003165] p 2753 N94-26783
An ultrasonic testing technique for monitoring the cure and mechanical properties of polymeric materials
[AD-A274536] p 2753 N94-26842
Thermoplastic or thermosetting composites in aircrafts
[PB94-123809] p 2710 N94-27253
Researches of the Electrotechnical Laboratory. No. 52: Studies of externally pressurized porous gas bearings
[JTN-94-80549] p 2825 N94-27351
Research into the microstructure and mechanical behavior of eutectic Bi-Sn and In-Sn
[DE94-004558] p 2741 N94-27619
Formation of glassy Pd-Ni-P alloys by mechanical alloying and their structure and thermal stability
p 2746 N94-28168
High Quality Aluminium Castings Conference
[PB94-133592] p 2747 N94-28359
Studies in ice mechanics
[PB94-133055] p 2900 N94-28393
MECHANICAL TWINNING
Deformation twinning: Influence of strain rate
[DE94-002693] p 2738 N94-26621
MEDICAL ELECTRONICS
Monitoring activity with a wrist-worn actigraph: Effects of amplifier passband and threshold variations
[AD-A274705] p 2909 N94-26377
MEDICAL EQUIPMENT
High impact strength poly(lactide) tough biodegradable materials
[ETN-94-95389] p 2747 N94-25748
Development of surgical CW Nd:YAG laser with optical fiber delivery system
[DE93-632902] p 2817 N94-26185
Biomedical polyurethane networks
[ETN-94-95391] p 2750 N94-26211
MEDICAL SCIENCE
Biomedical polyurethane networks
[ETN-94-95391] p 2750 N94-26211
MEDICAL SERVICES
Practice patterns of US Army medical department psychiatrists and psychologists
[AD-A274787] p 2909 N94-26360
The role of hyperbaric oxygen as a prophylaxis for radiation enteritis
[AD-A274974] p 2901 N94-26517
Monograph of the aviation epidemiology data register for calendar year 1988
[AD-A274589] p 2911 N94-26985
The telemedicine spacebridge project: A joint US/Russian venture in long distance medicine via satellite
[NASA-TM-106523] p 2693 N94-27427
MELTING
Liquid and solid solubility of Ag in Bi2Sr2CaCu2O8
[DE94-002829] p 2735 N94-26273
Iron: What is melt?
[DE94-003373] p 2735 N94-26322
Morphology transitions during non-equilibrium growth processes
[ITN-94-85236] p 3065 N94-27243
MELTING POINTS
Iron: What is melt?
[DE94-003373] p 2735 N94-26322
Microspheres for laser velocimetry in high temperature wind tunnel p 2682 N94-27903
Thermal conductivity of liquid carboxylic acids
[ESDU-93017] p 2721 N94-28138
MELTS (CRYSTAL GROWTH)
Study on melted solution stirring under microgravity
p 2730 N94-25585
Nonlinear dynamics and pattern selection at the crystal-melt interface
[DE94-003112] p 3060 N94-26780
Channel model for AC electric arc
[PB94-124591] p 2786 N94-27327
Float zone crystal growth using laser radiation
[DLR-FB-93-10] p 3066 N94-27590
Characterization of semi-insulating gallium arsenide
[AD-A273781] p 3068 N94-27704
MEMBRANES
Gauging of Chern-Simons p-Barnes
[DE94-601553] p 2993 N94-26425
Bulletin of the Institute for Chemical Reaction Science, Tohoku University, volume 2
[JTN-94-80602] p 2717 N94-27385
Development of liquid membrane separation processes p 2717 N94-27386
Effects of high-intensity electric field stimulation on the electromechanical performance of cardiac muscle: Influence of fiber orientation p 2904 N94-27467
On the mechanism of reentrant arrhythmias following DC defibrillation: Influence of fiber orientation to the effects of low-energy electric field stimulation on the effective refractory period of cardiac muscle
p 2904 N94-27468
Development of a 2f optical performance measurement system
[DE94-003489] p 3039 N94-27721
MEMORY
Air traffic controller working memory: Considerations in air traffic control tactical operations
[AD-A273722] p 2664 N94-26197
The central executive component of working memory
[AD-A274295] p 2938 N94-26683
MEMORY (COMPUTERS)
Fast parallel algorithms for short-range molecular dynamics
[DE93-018519] p 3016 N94-26033
Virtual data
[DE94-002718] p 2986 N94-26807
Memory subsystem performance of programs using copying garbage collection
[AD-A274258] p 3099 N94-27014
Memory subsystem performance of programs with intensive heap allocation
[AD-A274122] p 2967 N94-27063
Binary snapshots
[CWI-CS-R9319] p 2955 N94-27547
Parallel computing for probabilistic response analysis of high temperature composites
[NASA-CR-194467] p 2843 N94-27656
Review and analysis of dense linear system solver package for distributed memory machines
p 2978 N94-27916
MENTAL HEALTH
Practice patterns of US Army medical department psychiatrists and psychologists
[AD-A274787] p 2909 N94-26360
Human dimensions research team, operation restore hope
[AD-A274340] p 2939 N94-27056
MENTAL PERFORMANCE
Study on knowledge extraction and systematization for material design p 2727 N94-25568
Extending the rule space model to a semantically-rich domain: Diagnostic assessment in architecture
[AD-A273789] p 2948 N94-25864
A diagnostic classification model for document processing skills
[AD-A273790] p 3096 N94-25925
The use of EEG as a workload assessment tool in flight test
[AD-A274568] p 2910 N94-26847
Task demand, workload, and performance
[PB94-123627] p 2942 N94-27155
Brain wave correlates of attentional states: Event related potentials and quantitative EEG analysis during performance of cognitive and perceptual tasks
p 2940 N94-27901
Symptoms of hypoxia at simulated altitude of 25,000 feet p 2933 N94-27945
MERCURY ISOTOPES
Radiations from hot nuclei p 3030 N94-27915
MERIDIONAL FLOW
Interpreting the implied meridional oceanic energy transport in AMIP
[DE94-001538] p 2898 N94-26072
MESOMETEOROLOGY
Development and testing of the Coupled Ocean/Atmosphere Mesoscale Prediction System (COAMPS)
[AD-A273925] p 2892 N94-25793
Mesoscale meteorological measurements characterizing complex flows
[DE94-002359] p 2895 N94-26761
MESON-NUCLEON INTERACTIONS
Theoretical and computational studies in intermediate energy nuclear physics
[DE94-004177] p 3012 N94-25800
A dependence of exclusive vector meson production in muon-nucleus scattering
[DE94-003363] p 3016 N94-25957
Proceedings of the workshop on (pi), K, (eta)-nucleon interactions
[DE94-701314] p 3027 N94-27733
MESONS
Quark-antiquark bound states
[DE93-613054] p 3013 N94-25826
Weak interactions in a bilocal chiral theory
[DE93-613097] p 3013 N94-25836
Algorithms of the vertex coordinate reconstruction for straight tracks of short-lived particles
[DE93-616661] p 3015 N94-25919
Heavy quark production and spectroscopy
[DE94-003619] p 3015 N94-25935
Meson X(1814) as a candidate for a hybrid state
[DE93-634447] p 3017 N94-26045
Mesons and diquarks in a NJL-model at finite temperature and chemical potential
[DE93-634375] p 3020 N94-26505
Signatures for hybrids
[DE94-004244] p 3020 N94-26574
Measuring the time dependence of B(sub s)(sup 0) meson - anti B(sub s)(sup 0) meson oscillations
[ISBN-0-315-84367-5] p 3021 N94-26665
Light-quark, heavy-quark systems: An update
[DE94-002298] p 3021 N94-26759
Leptonic decay constants of heavy mesons in QCD
[DE93-634426] p 3022 N94-26767
Low-energy hadronic interactions beyond the current algebra approach
[DE94-602600] p 3022 N94-26900
Meson spectroscopy and particle astrophysics
[DE94-001799] p 3115 N94-27003

Measurements of the B(sup 0)(bar B)(sup 0)CP asymmetry
[DE94-003379] p 3063 N94-27047

Charmonium physics at a tau-charm factory
[PB94-124344] p 3024 N94-27199

Observation of excited charmed mesons
[ISBN-0-315-57014-8] p 3026 N94-27400

Weak hadronic decays of heavy flavor mesons
[ISBN-0-315-55542-4] p 3026 N94-27402

Indiana University high energy physics, task A
[DE94-000961] p 3033 N94-27614

Decay constants of heavy mesons in the relativistic potential model with velocity dependent corrections
[DE94-606495] p 3030 N94-27860

MESOSCALE PHENOMENA

Development and testing of the Coupled Ocean/Atmosphere Mesoscale Prediction System (COAMPS)
[AD-A273925] p 2892 N94-25793

A modeling study of the mesocyclone
[AD-A274889] p 2893 N94-26168

Mesoscale frontal evolution of the ERICA IOP-5A Cyclone
[AD-A274906] p 2893 N94-26183

A preliminary analysis of the US west climatology
[DE94-003028] p 2894 N94-26313

Investigation of mesoscale convective cloud clusters in South China
[AD-A274303] p 2895 N94-26678

Mesoscale meteorological measurements characterizing complex flows
[DE94-002359] p 2895 N94-26761

MESOSPHERE

Photochemical processes and the atmospheric airglow emissions of OH and Na in the mesospheric region
[INPE-5380-PUD/050] p 2882 N94-27334

MESSAGE PROCESSING

Interface technical specification of the V.25 bis emulator
[AD-A273754] p 2948 N94-25720

Programming in Fortran M
[DE94-002756] p 2963 N94-26407

An efficient communication scheme for solving the S(sub n) equations on message-passing multiprocessors
[DE94-000378] p 2769 N94-26482

Example of the EXPANSE signalling protocol
[PB94-125283] p 2771 N94-26872

Communication on the Paragon
[DE94-003103] p 2983 N94-27713

MESSAGES

A doubly logarithmic communication algorithm for the Completely Connected Optical Communication Parallel Computer
[DE93-019408] p 2980 N94-26473

METABOLIC DISEASES

Modulation by galactosamine-induced hepatitis of biological responses of the rat exposed to high altitude hypoxia p 2904 N94-27464

Protective action of an amiloride derivative (amiloride, 5-(N, N-dimethyl) hydrochloride) against in isolated ischemia/reperfusion newborn rabbit hearts
p 2904 N94-27466

METAL BONDING

Joining of fibre reinforced metal matrix composite materials
[PB94-132453] p 2712 N94-28376

METAL CLUSTERS

Peculiarities and application perspectives of metal-ion implants in glasses
[DE94-004671] p 3035 N94-26246

METAL COATINGS

Hydrogen trapping with Pd coated alloy films
p 2723 N94-25551

Issues for conversion coating of aluminum alloys with hydrotalcite
[DE94-003804] p 2732 N94-25819

Comparison of technology for high-power laser mirrors and synchrotron radiation mirrors
[DE94-002913] p 3035 N94-26276

Vapor deposition of copper on stainless steel 304L
[DE94-001945] p 2740 N94-27006

METAL FATIGUE

Interactions between corrosion fatigue and stress corrosion crack on steel for light water reactors
p 2722 N94-25547

Study on variation of damage generation mechanism by fatigue on TiAl compounds due to different slip systems p 2729 N94-25579

Study on evaluation of crack generation and crack growth behaviors under static loading at high temperature and under combined loading p 2730 N94-25583

Study on fatigue crack propagation characteristics around welded joint interface in complexed conditions
p 2730 N94-25584

An experimental study on the effects of compressive stress on the fatigue crack growth of low-alloy steel
[DE94-004447] p 2737 N94-26582

Status and prospects for aluminium-lithium alloys in aircraft structures
[NLR-TP-92193-U] p 2743 N94-27797

An experimental investigation of fatigue damage in aluminum 2024-T3 alloys p 2747 N94-27900

The transition from stress corrosion cracking to corrosion fatigue in AA-7075 and AA-8090
[ISBN-0-315-59526-4] p 2744 N94-27950

Fatigue propagation behaviour of short cracks (1-2 mm) in steels
[ESDU-93033] p 2845 N94-28145

METAL FIBERS

Impact tests on fibre metal laminates under a tensile load
[PB94-126570] p 2710 N94-27201

METAL FILMS

Study on alloy films for hydrogen separation
p 2726 N94-25565

Study on substance diffusion in thin films with controlled structures p 2727 N94-25570

The formation of conducting gold films by thermal decomposition and direct patterning using electron beam lithography of the gold cluster Au55P(C6H5)312C16
[AD-A273720] p 2749 N94-26074

Chemical vapor deposition and characterization of tungsten boron alloy films
[DE94-002648] p 2738 N94-26610

METAL FOILS

Reference electrodes for solid polymer electrolytes
[DE94-004583] p 2780 N94-25806

METAL FUELS

An apparatus for measurement of ignition and burning characteristics of metallic particles
[AD-A274815] p 2716 N94-26487

Nonswelling behavior of HT9 alloy irradiated to high exposure
[DE94-003502] p 2736 N94-26522

METAL HALIDES

Structure of ionic fluids in equilibrium with a microporous ionic matrix
[DE94-600563] p 2715 N94-26391

METAL HYDRIDES

Lighter alkali hydride and deuteride 1: Electronic properties of pure solids
[DE93-616188] p 3051 N94-25914

Development of nickel-metal hydride cell: An update
p 2864 N94-28130

Ni-MH storage test and cycle life test
p 2864 N94-28131

Determination of thermal properties of commercial Ni-MH cells p 2864 N94-28132

METAL IONS

Peculiarities and application perspectives of metal-ion implants in glasses
[DE94-004671] p 3035 N94-26246

Structure of ionic fluids in equilibrium with a microporous ionic matrix
[DE94-600563] p 2715 N94-26391

Microstructures of Si surface layers implanted with Cu
[DE94-004690] p 3058 N94-26565

Modulation wavelength dependence of ion mixing in metallic superlattices
[DE94-004608] p 3059 N94-26591

Secondary electron emission from copper surface due to neodymium and gadolinium ion bombardment
[DE94-701115] p 3027 N94-27718

Hypersensitive transition spectrum of f-element and coordination structure
[DE94-604133] p 3070 N94-27843

Property enchancement of polyimide films by way of the incorporation of lanthanide metal ions
p 2758 N94-27926

METAL MATRIX COMPOSITES

Bulletin of National Research Institute for Metals in Fiscal Year 1993, no. 14
[REPT-14] p 2722 N94-25544

Inner fiber observation for metal matrix composites under the stress load condition utilizing Synchrotron Orbital Radiation (SR) by X-ray CT p 2724 N94-25553

Investigation of compressive behavior for metal matrix composites with a circular hole
[AD-A273835] p 2705 N94-25739

Structure and properties of intermetallic composites synthesized in situ using solid state displacement reactions
[DE94-004312] p 2705 N94-25805

Characterization of fatigue damage in a metal matrix composite (SCS-6/Ti-15-3) at elevated temperature
[AD-A273797] p 2706 N94-25876

Numerical simulations of interfacial debonding in ductile-phase reinforced intermetallic matrix composites
[DE94-003639] p 2706 N94-25938

An investigation of cavitation in a mechanically alloyed 15 volume percent SiCp/IN9021 aluminum composite
[DE94-003371] p 2748 N94-25959

General Motors Corporation and Pacific Northwest Laboratory staff exchange: Inspection of case hardened steels and metal-matrix composites
[DE94-003470] p 2706 N94-25982

Investigation of tension-compression fatigue behavior of a cross-ply metal matrix composite at room and elevated temperatures
[AD-A273731] p 2706 N94-25999

Effects of post-fabrication processing on the tensile properties of centrifugally cast SiC particulate reinforced aluminum composites
[AD-A274865] p 2707 N94-26190

Titanium 1992: Volume 3: Science and technology
[AD-A274800] p 2735 N94-26337

Bimaterial interfaces and their role in the mechanical performance of the in-situ composites
[AD-A274688] p 2707 N94-26447

Processing and mechanical properties of laminated metal composites of Al 6090-25 volume percent SiC(sub p) and Al 5182
[DE94-001070] p 2708 N94-26930

Development of fibre-metal laminates, ARALL and GLARE, new fatigue resistant materials
[PB94-126471] p 2669 N94-26969

Interface phenomena in metal-ceramic composites
[AD-A274167] p 2709 N94-27125

Impact tests on fibre metal laminates under a tensile load
[PB94-126570] p 2710 N94-27201

High intensity x ray instrumentation for residual strain measurements in composites and textured materials
[ISBN-0-315-85169-4] p 2842 N94-27278

SP/MSP tests for the evaluation of FGM
[NAL-SP-17] p 2710 N94-27279

SP/MSP tests for the evaluation of FGM
p 2710 N94-27280

Research on the development of fracture characteristics evaluation system for ceramics and metal composite materials p 2710 N94-27281

Hot deformation behaviour of Si(p)/Al composites and their matrices and an Al-Mg-Si alloy
[ISBN-0-315-84699-2] p 2711 N94-27314

Finite element analysis of damped vibrations of laminated composite plates
[ISBN-0-315-84928-2] p 2843 N94-27585

A hydrostatic stress-dependent anisotropic model of viscoplasticity
[NASA-TM-106525] p 2711 N94-27640

Implementation of thermal residual stresses in the analysis of fiber bridged matrix crack growth in titanium matrix composites
[NASA-TM-109082] p 2711 N94-27658

The deformation of copper-tungsten composites
[ISBN-0-315-84939-8] p 2712 N94-27688

Low strain behaviour of a particulate reinforced aluminum alloy
[ISBN-0-315-84906-1] p 2744 N94-27961

Joining of fibre reinforced metal matrix composite materials
[PB94-132453] p 2712 N94-28376

METAL NITRIDES

Study on microscopic structural controls and electronic properties at material surfaces by ion beams
p 2727 N94-25571

Mechanistic studies of opto-electronic materials and syntheses using multiple laser and surface diagnostics
[AD-A274528] p 3036 N94-26834

METAL OXIDE SEMICONDUCTORS

Object imaging accomplished with an integrated circuit robotic tactile sensor incorporating a piezoelectric polyvinylidene fluoride thin film
[AD-A274038] p 2780 N94-25845

Demonstration of monolithic co-fabrication of Y1Ba2Cu3O7-Sigma and CMOS devices on the same sapphire substrate
[AD-A274757] p 3059 N94-26566

The analysis of thermal and 1/F noise in MOS devices, circuits and systems
[ISBN-0-315-57811-4] p 2787 N94-27642

A study of DC-DC converters with MCT's for arcjet power supplies
[NASA-CR-191204] p 2703 N94-27662

METAL OXIDES

Reference electrodes for solid polymer electrolytes
[DE94-004583] p 2780 N94-25806

Studies of thin-film growth, adsorption, and oxidation by in situ, real-time, and ex situ ion beam analysis
[DE94-002907] p 3055 N94-26275

Ion implantation and dynamic recovery of tin-doped indium oxide films
[DE94-001126] p 3062 N94-26932

METAL PARTICLES
An apparatus for measurement of ignition and burning characteristics of metallic particles
[AD-A274815] p 2716 N94-26487
METAL PLATES
Unsegmented electromagnetic calorimeter prototype. Energy and coordinate resolution
[DE93-634185] p 2810 N94-26396
Evaluation of crack arrest fracture toughness of parent plate, weld metal and heat affected zone of BIS 812 EMA ship plate steel
[AD-A274871] p 2839 N94-26859
The influence of TIG welding thermal cycles on HSLA-100 steel plate
[AD-A274248] p 2740 N94-27009
Aluminum alloy 8090-T8771 thick plate material characterization
[AD-A274146] p 2987 N94-27077
METAL POWDER
Material optimization and manufacturing development of reduced cost powder metal titanium alloy components for gas turbine engine application, phase 2
[AD-A274410] p 2709 N94-26978
METAL SHEETS
On experimental studies of yield surfaces of metals: A more general approach
[IFTR-42/1993] p 2739 N94-26824
Production of an amorphous Fe(75)Si(10)B(15) sheet by a metallic mold casting method and its properties
p 2746 N94-28170
METAL SURFACES
Observation on metal surface in aqueous solution using an electrochemical Scanning Tunneling Microscope (STM) p 2724 N94-25554
Study on interfacial reaction analysis at interfacial joining p 2728 N94-25574
Atomic-scale chemistry of metal surfaces
[REPT-A-2657] p 3012 N94-25636
Binding of copper and nickel to cavities in silicon formed by helium ion implantation
[DE94-003769] p 3050 N94-25814
A mimic model of Pt-Rh catalyst prepared by electrochemical deposition of Rh on Pt (100) surface
[REPT-A-2664] p 2715 N94-26476
An investigation of the effect of surface impurities on the adsorption kinetics of hydrogen chemisorbed onto iron
[NASA-CR-195213] p 2716 N94-26643
Stability of reference masses 2: The effect of environment and cleaning methods on the surfaces of stainless steel and allied materials
[NPL-DMM(A)-95] p 2738 N94-26653
On experimental studies of yield surfaces of metals: A more general approach
[IFTR-42/1993] p 2739 N94-26824
Secondary electron emission from copper surface due to neodymium and gadolinium ion bombardment
[DE94-701115] p 3027 N94-27718
Image potential of a tunnelling electron moving near two different metals
[DE94-603657] p 3069 N94-27819
METAL VAPORS
Hook spectroscopy as an atomic number density diagnostic applied to laser-ablated copper plasmas
[DE94-002645] p 3042 N94-26081
METAL WORKING
Titanium 1992: Volume 3: Science and technology
[AD-A274800] p 2735 N94-26337
Titanium 1992: Science and Technology, volume 1
[AD-A274798-VOL-1] p 2739 N94-26799
METAL-GAS SYSTEMS
Exploratory Technology Research Program for Electrochemical Energy Storage
[DE94-003479] p 2781 N94-26047
METAL-METAL BONDING
Method of bonding molybdenum to steel
[AD-D016079] p 2747 N94-28187
METAL-WATER REACTIONS
Fundamental study on monitoring technology on local surface damages p 2724 N94-25555
METALLIC GLASSES
Detection of low-intensity magnetic fields with a magnetostrictive fiber optic sensor
[AD-A274120] p 3037 N94-27062
METALLIC PLASMAS
Hook spectroscopy as an atomic number density diagnostic applied to laser-ablated copper plasmas
[DE94-002645] p 3042 N94-26081
METALLIZING
Experimental determination of the CU-IN-PB ternary phase diagram
[DE94-003765] p 2735 N94-26349
METALLOGRAPHY
Upset welding process for 21-6-9 spherical vessels
[DE93-018194] p 2832 N94-28229
METALLOIDS
List of papers published by the members of Institute for Materials Research, Tohoku University 1992
[JTN-94-80608] p 3118 N94-27355
METALLURGY
COMPETENCE 2000: Study on training requirements of the Norwegian metallurgical industry
[PB94-124609] p 2741 N94-27328
METALORGANIC CHEMICAL VAPOR DEPOSITION
Ordering and phase separation in MOCVD InGaP alloys and unicompositional quantum wells
[DE94-004693] p 3056 N94-26352
Mechanistic studies of opto-electronic materials and syntheses using multiple laser and surface diagnostics
[AD-A274528] p 3036 N94-26834
Nitride semiconductors for ultraviolet detection
[AD-A274246] p 3060 N94-26840
High-efficiency, thin-film solar cells
[DE94-000250] p 2860 N94-27625
Electro-optic materials by solid source MOCVD
[DE94-005120] p 2757 N94-27716
METALS
Knowledge base systems for chemical compounds designing support p 2723 N94-25550
Study on analyzing method establishment for metallic material development p 2729 N94-25578
Study on elucidation of damage generation process by electron beam lithography p 2729 N94-25581
The effectiveness of AMT investment in UK metal component manufacture
[IND-MANU-SCI-TECH-REPT-3] p 2762 N94-25775
Debye-Waller factors of the light actinide metals
[DE94-000685] p 2733 N94-26069
Power laws, flicker noise, and the barkhausen effect
[AD-A274702] p 3008 N94-26376
Template synthesis of metal microtubule ensembles utilizing chemical, electrochemical, and vacuum deposition techniques
[AD-A274676] p 2715 N94-26444
A new materials data compilation can help in actinide phase-diagram research
[DE94-000797] p 3058 N94-26514
Mechanical properties of nanophase materials
[DE94-004625] p 2751 N94-26594
Technical report of ISSP. Ser. A, no. 2679: Novel electronic states of partially deuterated (DMe-DCNQI)2Cu
[JTN-94-80565] p 3064 N94-27175
Resonant holographic measurements of laser ablation plume expansion in vacuum and argon gas backgrounds
[DE94-001407] p 2813 N94-27615
Image potential of a tunnelling electron moving near two different metals
[DE94-603657] p 3069 N94-27819
METASTABLE ATOMS
Measurement of metastable population distribution in gadolinium atomic beam by laser resonance photoionization method
[DE94-701194] p 3029 N94-27820
METASTABLE STATE
Collaborative research on ion implantation of ceramics
[DE93-019177] p 2749 N94-26080
Recombination and metastability in amorphous silicon and silicon germanium alloys
[DE94-000237] p 2736 N94-26481
Dynamics of metastable states in supersonic beams
[ITN-94-85232] p 3028 N94-27760
Measurement of metastable population distribution in gadolinium atomic beam by laser resonance photoionization method
[DE94-701194] p 3029 N94-27820
METEOR TRAILS
Meteor Burst Communications (MBC) throughput improvement tests
[AD-A273941] p 2767 N94-25990
METEORITE COLLISIONS
Impacts, extinctions, volcanism, glaciations, and tectonics: Matches and mismatches
p 2888 N94-28298
Science observed: The mass-extinction debates
p 2888 N94-28300
Consequences of impacts of small asteroids and comets with Earth p 2889 N94-28301
An extraterrestrial event at the tertiary-quaternary boundary p 2890 N94-28309
METEORITE CRATERS
Some implications of large impact craters and basins on Venus for terrestrial ringed craters and planetary evolution p 2890 N94-28306
METEORITIC COMPOSITION
Experimental study of lunar and SNC (Mars) magmas
[NASA-CR-195274] p 3107 N94-27850
Extraterrestrial accretion and glacial cycles
p 2890 N94-28308
An extraterrestrial event at the tertiary-quaternary boundary p 2890 N94-28309
METEORITIC DAMAGE
Consequences of impacts of small asteroids and comets with Earth p 2889 N94-28301
Were all extinction events caused by impacts?
p 2891 N94-28311
METEORITIC DIAMONDS
A general theory of impacts and mass extinctions, and the consequences of large-body impact on the Earth
p 2891 N94-28310
METEOROID CONCENTRATION
Extraterrestrial accretion and glacial cycles
p 2890 N94-28308
METEOROID SHOWERS
Low noise measurements in an RF environment
[AD-A273813] p 2767 N94-25960
Meteor Burst Communications (MBC) throughput improvement tests
[AD-A273941] p 2767 N94-25990
Performance statistics bulletin: High altitude meteor scatter propagation, August, September, October 1989
[AD-A274455] p 2773 N94-27085
METEOROLOGICAL CHARTS
Investigation of mesoscale convective cloud clusters in South China
[AD-A274303] p 2895 N94-26678
METEOROLOGICAL PARAMETERS
A preliminary analysis of the US west climatology
[DE94-003028] p 2894 N94-26313
Radar detection of low-altitude targets in a maritime environment. Volume 2: Meteorological and radar data
[AD-A274658] p 2768 N94-26335
Analysis and interpretation of the meteorology of the 1988 coastal transition zone experiment
[AD-A274710] p 2894 N94-26431
Overall analysis of meteorological information in the Daeduk nuclear complex
[DE93-632594] p 2894 N94-26469
Analysis of the influence of weather on infrared imagery
[FEL-92-A421] p 3036 N94-26649
Mesoscale meteorological measurements characterizing complex flows
[DE94-002359] p 2895 N94-26761
Surface roughness lengths
[AD-A274550] p 2895 N94-26846
Kiruna geophysical data. Data summary 93/4-6, April-June 1993
[PB94-123700] p 2881 N94-27039
Kiruna geophysical data. Data summary 93/1-3, January-March, 1993
[PB94-123791] p 2881 N94-27043
Meteorological data at the Nagaoka Institute of Snow and Ice Studies
[REPT-158] p 2896 N94-27169
The validation of ATSR measurements with in situ sea temperatures
[DE94-003195] p 2852 N94-27875
Report of the National Research Institute for Earth Science and Disaster Prevention, No. 51
[JTN-94-80509] p 2886 N94-27985
Development of a method for predicting snowfall intensity and compacted snow on roads
p 2853 N94-27990
Conception of snow information network system in Yamagata Prefecture p 2853 N94-27991
Research activities on the meteorology over the Asia-Pacific region p 2853 N94-28271
METEOROLOGICAL RADAR
Machine intelligent gust front algorithm
[AD-A273695] p 2680 N94-26196
Radar detection of low-altitude targets in a maritime environment. Volume 2: Meteorological and radar data
[AD-A274658] p 2768 N94-26335
Cloud liquid water content measurement tests using dual-wavelength radar
[PB94-125960] p 2896 N94-26959
Encoding approaches for data link transmission of weather graphics
[AD-A274497] p 2772 N94-26963
METEOROLOGICAL SATELLITES
A preliminary method for atmospheric soundings in real time using satellite and ground-based remotely sensed data
[AD-A274381] p 2880 N94-26828
METEOROLOGY
Developing prediction regions for a time series model for hurricane forecasting
[AD-A273777] p 2892 N94-25861
The effect of elevation data representation on nocturnal drainage wind simulations
[DE94-003624] p 2892 N94-25936
Active layer dynamics and arctic hydrology and meteorology
[DE94-001724] p 2892 N94-25951
Testbed model and data assimilation for ARM
[DE94-000432] p 2893 N94-26082

A preliminary analysis of the US west climatology
[DE94-003028] p 2894 N94-26313
Overall analysis of meteorological information in the Daeduk nuclear complex
[DE93-632594] p 2894 N94-26469
Recent ASCOT experiments in multi-layered flows
[DE94-002360] p 2880 N94-26762
Surface roughness lengths
[AD-A274550] p 2895 N94-26846
Atmospheric science research in Malaysia: Perspectives on international cooperation p 2874 N94-28285

METHAMPHETAMINE
Effects of methamphetamine on vigilance and tracking during extended wakefulness
[AD-A274896] p 2909 N94-26179

METHANATION
CO2 methanation catalysts prepared from amorphous Ni-valve metal alloys containing platinum group elements
p 2745 N94-28166

METHANE
Methane emissions from natural wetlands
[DE93-040796] p 2865 N94-25790
Implications of policies and prevent climate change for future food security
[DE93-018872] p 2866 N94-25948
A conceptual framework for the evaluation of cost-effectiveness of projects to reduce GHG emissions and sequester carbon
[DE93-040448] p 2867 N94-26419
Laser probes of natural gas ignition chemistry
[PB94-128345] p 2717 N94-27226
Basic research on natural gas combustion phenomena
[PB94-129046] p 2717 N94-27256
The electrocatalytic oxidation of ethylene and methane, and reduction of oxygen on gas-diffusion electrodes made of amorphous nickel-valve metal-platinum group metal alloys p 2722 N94-28165

METHOD OF MOMENTS
Numeric solution of the electric field integral equation using Galerkin's method for axially symmetric cases
[ESA-TT-1264] p 2768 N94-26315
Computer program for numerical evaluation of the performance of an overmoded TM01 circular to TE10 rectangular waveguide mode converter
[AD-A274548] p 2771 N94-26844
A jet calculus approach including coherence effects and the associated problem of moment inversion
[ISBN-0-315-51715-8] p 3025 N94-27266
Hybrid techniques for complex aerospace electromagnetics problems p 2779 N94-27894

METHOXY SYSTEMS
Preparation, characterization, and thermal behaviour study of lanthanides (3) and yttrium (3) 4-methoxy benzylidene pyruvate in solid state
[DE94-604079] p 3068 N94-27697

METHYL ALCOHOL
Feasibility study on introduction of transportation-use petroleum substitution energy
[DE94-725205] p 2759 N94-26905

METHYL COMPOUNDS
Effects of plastic media blasting on aircraft skin
[AD-A274817] p 2668 N94-26488
Basic research on natural gas combustion phenomena
[PB94-129046] p 2717 N94-27256
Novel oxidizing reagents derived from elemental fluorine
[ITN-94-85231] p 2719 N94-27687
New monomers for high performance polymers
p 2758 N94-27904

METHYL POLYSILOXANES
Sol-gel derived silica/siloxane composite materials: The effect of loading level and catalyst activity on silica domain formation
[DE94-002734] p 2712 N94-27710

METROLOGY
An exploratory survey of methods used to develop measures of performance
[AD-A273945] p 2834 N94-25896

MICE
Compaction-like blastomere aggregation caused by 1-oleoyl-2-acetylglycerol in mouse embryos: An electron microscopic observation p 2905 N94-27487

MICROANALYSIS
Study of the homogeneity of InP wafers
[AD-A273658] p 3055 N94-26194
Determination of lead isotope ratios in seawater by purge and trap GC/MS after ethylation p 2870 N94-28152

MICROBEAMS
He(+) and H(+) microbeam damage, swelling and annealing in diamonds
[DE94-601912] p 3063 N94-26987

MICROBIOLOGY
Microbiology research at some research institutes in the former Soviet Union: A survey of scientific publications
[PB94-123320] p 2902 N94-27171

MICROBURSTS (METEOROLOGY)
The relationship of an integral wind shear hazard to aircraft performance limitations
[NASA-TM-109080] p 2677 N94-26593
A data fusion algorithm for multi-sensor microburst hazard assessment p 2641 N94-27287
Investigation of air transportation technology at Princeton University, 1992-1993 p 2643 N94-27294
Optimal nonlinear estimation for aircraft flight control in wind shear p 2643 N94-27296

MICROCLIMATOLOGY
An overview of the ASCOT program
[DE94-004356] p 2869 N94-27601

MICROCOMPUTERS
The Hough transform algorithm for sea ice lead analysis: An evaluation
[AD-A274535] p 2899 N94-26853

MICROCRACKS
Characterization of fatigue damage in a metal matrix composite (SCS-6/Ti-15-3) at elevated temperature
[AD-A273797] p 2706 N94-25876
The fracture behavior of a CVD crystalline Si3N4/amorphous Si3N4 composite
[DE94-002646] p 2750 N94-26124

MICROCRYSTALS
Prometheus in space: Research Committee on Functional New Material
[JTN-94-80580] p 2761 N94-28002

MICROELECTRONICS
Solid state research
[AD-A274063] p 3049 N94-25645
Advanced qualification techniques
[DE94-003709] p 2780 N94-25812
A general purpose I(sub DDQ) measurement circuit
[DE94-002733] p 2781 N94-25977
The National Center for Advanced Information Components Manufacturing: Program update
[DE94-002647] p 2960 N94-26118
Experimental determination of the CU-IN-PB ternary phase diagram
[DE94-003765] p 2735 N94-26349
The 12-channel flash-ADC FASTBUS module
[DE93-634229] p 2783 N94-26380
Signal amplifier-shapers for multiwire detectors
[DE93-634171] p 2783 N94-26438
Diagnostics and microelectronics
[DE94-003016] p 2784 N94-26777
Generalized emulation microcircuit program
[AD-A274749] p 2785 N94-26797
Center for space microelectronics technology
[NASA-CR-195282] p 2786 N94-27574
Micro-electron deflector
[AD-D016055] p 2787 N94-27672
Opportunities for High Aspect Ratio Micro-Electro-Magnetic-Mechanical Systems (HAR-MEMMS) at Lawrence Berkeley Laboratory
[DE94-003499] p 2827 N94-27722

MICROGRAVITY
Study on melted solution stirring under microgravity
p 2730 N94-25585
Autonomous support for microorganism research in space p 2903 N94-25672
Bioregenerative system components for microgravity
p 2903 N94-25673
First lunar outpost p 2943 N94-25694
Microgravity ignition experiment p 2761 N94-25707
Risks and issues in fire safety on the Space Station
[NASA-TM-106430] p 2692 N94-27436
Annals of the Research Inst. of Environmental Medicine, Nagoya Univ., volume 44
[REPT-44-VOL-44] p 2911 N94-27442
Changes in circadian variations of urine excretion in tail-suspended rats p 2911 N94-27443
Endocrinological evaluations of muscle and bone atrophy in tail-suspended rats p 2903 N94-27444
Changes in fluid and electrolyte metabolism during water immersion at high or thermoneutral temperature
p 2912 N94-27445
Study on posture control and adaption mechanism under weightlessness: Results of second rehearsal for space experiment using carp p 2912 N94-27446
The mechanism of caloric nystagmus under microgravity. 1: Changes of endolymphatic pressure in the semicircular canal of pigeon by caloric stimulation
p 2914 N94-27457
Comparative measurement of visual stability in cosmic space: Onboard experiment and pre-flight activities
p 2916 N94-27463
Thermocapillary flow with evaporation and condensation and its effect on liquid retention in low-G fluid acquisition devices
[NASA-TP-3463] p 2797 N94-27639
Construction and test of experiment hardware for a space experiment on Spacelab mission IML-2
[DLR-FB-93-23] p 2903 N94-27743
Gravity dependence or pressure drop and heat transfer in straight two-phase heat transport system condenser ducts
[NLR-TP-92167-U] p 2798 N94-27853
An analysis of the loads applied to a heavy Space Station rack during translation and rotation tasks
[NASA-TM-104790] p 2697 N94-28183
Workshop on Countering Space Adaptation with Exercise: Current Issues
[NASA-CP-3252] p 2934 N94-28361
Exercise detraining: Applicability to microgravity
p 2934 N94-28364
Weightlessness and the human skeleton: A new perspective p 2935 N94-28368
The use of biomechanics in the study of movement in microgravity p 2936 N94-28373
Psychophysiology in microgravity and the role of exercise p 2936 N94-28374

MICROHARDNESS
The fracture behavior of a CVD crystalline Si3N4/amorphous Si3N4 composite
[DE94-002646] p 2750 N94-26124
The influence of TIG welding thermal cycles on HSLA-100 steel plate
[AD-A274248] p 2740 N94-27009

MICROINSTRUMENTATION
Diagnostics and microelectronics
[DE94-003016] p 2784 N94-26777
Opportunities for High Aspect Ratio Micro-Electro-Magnetic-Mechanical Systems (HAR-MEMMS) at Lawrence Berkeley Laboratory
[DE94-003499] p 2827 N94-27722

MICROMACHINING
Diagnostics and microelectronics
[DE94-003016] p 2784 N94-26777

MICROMECHANICS
A nonlinear three-dimensional micromechanics model for fiber-reinforced laminated composites
[AD-A273772] p 2705 N94-25857
Computer modelling of cyclic deformation of high-temperature materials
[AD-A274504] p 2840 N94-27034
Deformation, constitutive behavior, and damage of advanced structural materials under multiaxial loading
[AD-A274165] p 2709 N94-27142

MICROORGANISMS
Autonomous support for microorganism research in space p 2903 N94-25672
Journal of NIRE, volume 2, number 4
[JTN-94-80554] p 2869 N94-28147
Collaboration of chemical oxidation and biological treatment for removal of refractory organic substances
p 2870 N94-28149
Treatment of refractory organic substances with combined use of chemical oxidation and biological treatment. Part 2: Biodegradability of ozonation products of chlorophenol p 2870 N94-28151

MICROPARTICLES
Microspheres for laser velocimetry in high temperature wind tunnel p 2682 N94-27903

MICROPHONES
High temperature sensor/microphone development for active noise control
[NASA-CR-195214] p 2812 N94-27214

MICROPOROSITY
Structure of ionic fluids in equilibrium with a microporous ionic matrix
[DE94-600563] p 2715 N94-26391
Template synthesis of metal microtubule ensembles utilizing chemical, electrochemical, and vacuum deposition techniques
[AD-A274676] p 2715 N94-26444

MICROPROCESSORS
Low-cost photovoltaic inverters incorporating application-specific integrated circuits
[DE94-003270] p 2856 N94-26463
Development of a MIL-STD-1750 microprocessor system for space applications p 2949 N94-26715
High performance flight computer developed for deep space applications p 2949 N94-26718
Fault tolerant real-time processing system for space use p 2949 N94-26720
NASA's spacecraft data system p 2950 N94-26723
Arithmetic performances of onboard computers
p 2952 N94-26738
Microprocessor chip incorporating optical signal coupling transceiver
[AD-D016077] p 2788 N94-28186

MICROSCOPY
Detecting actin fibers in cell images using minimal spanning trees
[AD-A273914] p 2984 N94-25591
Regrowth zones in laser annealed radiation damaged diamond
[DE94-600821] p 3056 N94-26364

Proceedings of the Fourth Euroseminar on Microscopy Applied to Building Materials
[PB94-119807] p 2839 N94-26754
High definition Raman microscopic imaging
[DE94-003158] p 2716 N94-26781
The x ray holographic microscopy using the atomic-force microscope
[DE94-004003] p 2814 N94-27779

MICROSTRIP DEVICES
Temperature dependence of the radiation induced change of depletion voltage in silicon PIN detectors
[DE94-002705] p 3052 N94-25972
Gamma Large Area Silicon Telescope (GLAST): Applying silicon strip detector technology to the detection of gamma rays in space
[DE94-003451] p 3116 N94-27740

MICROSTRUCTURE
Study on microscopic structural controls and electronic properties at material surfaces by ion beams
p 2727 N94-25571
Study on production of materials with one direction solidification texture p 2727 N94-25572
Study on solidification of non-homogeneous melting/solidification materials p 2728 N94-25573
Study on interfacial reaction analysis at interfacial joining p 2728 N94-25574
Study on elucidation of damage generation process by electron beam lithography p 2729 N94-25581
Computer modelling of cyclic deformation of high-temperature materials
[AD-A273852] p 2704 N94-25608
Langmuir-Blodgett film of amylose-esters and chiral azo-dyes (structure and second order nonlinear optical behaviour)
[ETN-94-95390] p 2747 N94-25749
Microstructural development in low activation ferritic alloys irradiated to 200 dpa at 420 C
[DE94-004269] p 2731 N94-25803
Radiation hardening effects on localized deformation and stress corrosion cracking of stainless steels
[DE94-004308] p 2731 N94-25804
Structure and properties of intermetallic composites synthesized in situ using solid state displacement reactions
[DE94-004312] p 2705 N94-25805
Grain boundary degradation of YBCO superconductors sintered in CO2-containing atmospheres
[DE94-003206] p 3053 N94-26029
Modeling defect production in high energy collision cascades
[DE94-003810] p 3017 N94-26049
Collaborative research on ion implantation of ceramics
[DE93-019177] p 2749 N94-26080
Influence of grain structure and solute composition on the work hardening behavior of aluminium at cryogenic temperatures
[DE94-003415] p 2733 N94-26087
The fracture behavior of a CVD crystalline Si3N4/amorphous Si3N4 composite
[DE94-002646] p 2750 N94-26124
Zr-rich corner of the Zr-Sn-O diagram
[DE93-633764] p 2734 N94-26161
The study of single-pass GMA welds with different cover gas compositions on HSLA-100 steel
[AD-A274857] p 2822 N94-26174
Stress relaxation in sputtered W films and W/GeSi/Si heterostructures
[DE94-004007] p 3055 N94-26239
The effect of processing on the microstructure of Ag-sheathed Bi-2223 wires
[DE94-004627] p 3055 N94-26243
An atom probe investigation of the influence of trace impurities on the mechanical behavior of NiAl
[DE94-002797] p 2734 N94-26272
The microstructural response of granular soil under uniaxial strain
[AD-A274808] p 2763 N94-26341
Ordering and phase separation in MOCVD InGaP alloys and unicompositional quantum wells
[DE94-004693] p 3056 N94-26352
Template synthesis of metal microtubule ensembles utilizing chemical, electrochemical, and vacuum deposition techniques
[AD-A274676] p 2715 N94-26444
A study on the development of high-T(c) superconducting wire
[DE93-632438] p 2783 N94-26546
Microstructural development in irradiated vanadium alloys
[DE94-004307] p 2737 N94-26556
Microstructures of Si surface layers implanted with Cu
[DE94-004690] p 3058 N94-26565
Structure and properties of composites synthesized in situ using solid state displacement reactions
[DE94-004589] p 2737 N94-26585
Mechanical properties of nanophase materials
[DE94-004625] p 2751 N94-26594
The processing of powder metallurgically produced near gamma-titanium aluminide
[ISBN-0-315-84018-8] p 2738 N94-26633
The influence of weld metal alloying additions to extend the heat input range for the submerged arc welding of high strength steels
[AD-A274284] p 2738 N94-26679
Proceedings of the Fourth Euroseminar on Microscopy Applied to Building Materials
[PB94-119807] p 2839 N94-26754
Diagnostics and microelectronics
[DE94-003016] p 2784 N94-26777
Titanium 1992: Science and Technology, volume 1
[AD-A274798-VOL-1] p 2739 N94-26799
Ferroelectric thin film microstructure development and related property enhancement
[DE94-002741] p 3061 N94-26856
Controlled heterogeneous nucleation of melt-textured YBa2Cu3O(6+x) by addition of Al2O3 particles
[AD-A274605] p 3062 N94-26892
Fabrication and characterization of nano-crystalline diamond films
[DE94-002202] p 3062 N94-26934
Interface phenomena in metal-ceramic composites
[AD-A274167] p 2709 N94-27125
Accordion-like polymers for nonlinear applications
[AD-D016031] p 2755 N94-27148
Squeeze casting: A literature review
[PB94-124575] p 2741 N94-27326
Utility fog: A universal physical substance
p 2687 N94-27367
Research into the microstructure and mechanical behavior of eutectic Bi-Sn and In-Sn
[DE94-004558] p 2741 N94-27619
Effect of precipitate structure on hot deformation of Al-Mg-Mn alloys
[DE94-004596] p 2741 N94-27622
Electron microscopy studies of undoped and phosphorus doped Si:H and Si,C:H films
[DE94-004738] p 3069 N94-27757
An anodic dissolution-based mechanism for the rapid cracking, pre-exposure phenomenon demonstrated by Al-Li-Cu alloys
[DE94-004798] p 2742 N94-27788
Hydrothermal growth and characterization of oxides in zirconium alloys
[DE94-602981] p 2743 N94-27829
Fragmentation of Ge(1-x) Sn(x) Se2 glasses
[DE94-603009] p 2758 N94-27837
An experimental investigation of fatigue damage in aluminum 2024-T3 alloys p 2747 N94-27900
Application of the Positron Annihilation Technique to the study of vapor absorption process in polyethylene (LDPE) and in imide polymer (6FDA-TMPD PI)
[DE94-602737] p 2720 N94-27998
Mechanical properties and microstructure of thermomechanically processed, high manganese steel
[ARL-TR-146] p 2747 N94-28212
Studies in ice mechanics
[PB94-133055] p 2900 N94-28393

MICROWAVE CIRCUITS
Modeling electromagnetic effects in MMICs for T/R modules
[AD-A273808] p 2766 N94-25736
Processing, fabrication, and demonstration of HTS integrated microwave circuits, appendix A
[AD-A274600] p 2785 N94-26890
An efficient and accurate Green's function analysis of packaged microwave integrated circuits
[ISBN-0-315-84425-6] p 2787 N94-27653

MICROWAVE COUPLING
Microwave coupling into a slotted cavity
[PB94-123742] p 2772 N94-27041

MICROWAVE EQUIPMENT
Microwave and pulsed power
[DE94-003019] p 2782 N94-26312
Four phase microwave pulse generator for pulsed EPR spectrometer p 2718 N94-27388

MICROWAVE FREQUENCIES
A physics-based heterojunction bipolar transistor model for integrated circuit simulation
[AD-A274081] p 2781 N94-25995
Over-the-horizon propagation measurements at six radar-frequency bands at the Atlantic Ocean Coast
[AD-A274151] p 2773 N94-27136
Effective conductivity of wire mesh reflectors for space deployable antenna systems
[NASA-CR-191605] p 2788 N94-27770

MICROWAVE IMAGERY
Polarimetric investigation of edge scattering by mono- and bistatic microwave imaging
[ESA-TT-1284] p 2768 N94-26317
Leadex environmental phenomena and effects observed by DMSP, NOAA, and ERS-1 satellites
[AD-A274596] p 2868 N94-26888

MICROWAVE LANDING SYSTEMS
Automatic, real-time fault monitor verifying network in a microwave landing system
[CA-PATENT-1325261] p 2665 N94-27275

MICROWAVE OSCILLATORS
Electrical analysis of wideband and distributed windows using time-dependent field codes
[DE94-002987] p 2768 N94-26310
HPm-tubes: Literature survey comprising 1992
[PB94-123643] p 2785 N94-27038
Computer simulations of radiation generation from relativistic electron beams
[AD-A274139] p 3024 N94-27133

MICROWAVE RADIOMETERS
Cloud liquid water content measurement tests using dual-wavelength radar
[PB94-125960] p 2896 N94-26959

MICROWAVE RESONANCE
Plasma surface cleaning using microwave plasmas
[DE94-002754] p 2713 N94-26014

MICROWAVE SWITCHING
Ferrite phase shifters using stress insensitive materials
[AD-A274639] p 2708 N94-26895

MICROWAVE TRANSMISSION
Microwave coupling into a slotted cavity
[PB94-123742] p 2772 N94-27041

MICROWAVE TUBES
Electrical analysis of wideband and distributed windows using time-dependent field codes
[DE94-002987] p 2768 N94-26310
HPm-tubes: Literature survey comprising 1992
[PB94-123643] p 2785 N94-27038

MICROWAVES
Theoretical aspects of the agile mirror
[AD-A274890] p 2767 N94-26177
Microwave and pulsed power
[DE94-003019] p 2782 N94-26312
Experimental and theoretical investigation of RF absorption and reflection from preformed plasmas
[AD-A274189] p 3046 N94-27098
A direct current rectification scheme for microwave space power conversion using traveling wave electron acceleration p 2687 N94-27371
Electromagnetic modeling of bi-isotropic media
[PB94-132909] p 2778 N94-28382

MILITARY AIRCRAFT
A cost model for USAF acquisition of commercial aircraft for service in the special air mission fleet
[AD-A274012] p 3093 N94-25796

MILITARY OPERATIONS
Development of the Air Force contingency contracting course framework
[AD-A273921] p 3093 N94-25895
Report of the defense science board task force on aircraft assessment
[AD-A274531] p 2669 N94-26835
Human dimensions research team, operation restore hope
[AD-A274340] p 2939 N94-27056

MILITARY PSYCHOLOGY
Practice patterns of US Army medical department psychiatrists and psychologists
[AD-A274787] p 2909 N94-26360
Human dimensions research team, operation restore hope
[AD-A274340] p 2939 N94-27056

MILITARY TECHNOLOGY
Object interaction in a parallel object-oriented discrete-event simulation
[AD-A274084] p 2959 N94-25942
Optoelectronic technology consortium
[AD-A274595] p 3036 N94-26857
Air Force standards for nickel hydrogen battery
p 2862 N94-28116
AF Ni-Cd cell qualification program
p 2863 N94-28122
Visit to CERMA: Centre d'Etudes et de Recherches de Medecine Aerospatiale, Centre for Studies and Research in Aviation and Space Medicine, Bretigny sur Orge, France, November 16-18, 1992
[PB94-132990] p 2937 N94-28392

MILLIMETER WAVES
Electrical analysis of wideband and distributed windows using time-dependent field codes
[DE94-002987] p 2768 N94-26310
Laboratory plasma studies
[AD-A274655] p 3043 N94-26356
Focal plane antenna array for millimeter waves
[AD-D016034] p 2774 N94-27202

MILLING MACHINES
Accuracy analysis of multi-axis machines
[ETN-94-95341] p 3002 N94-26000

MIMD (COMPUTERS)
A Multitransputer Parallel Processing System (MTPPS) [DE94-604652] p 2981 N94-26903
MIMD parallel approaches to object labeling [ISBN-0-315-60198-1] p 2982 N94-27644
MIMO (CONTROL SYSTEMS)
Design of a subsonic envelope flight control system for the Vista F-16 using quantitative feedback theory [AD-A274057] p 2676 N94-25771
Evaluation of moderate angle of attack roll of a dual engine, thrust vectoring aircraft using quantitative feedback theory [AD-A274118] p 2667 N94-25905
MIMO recursive least squares control algorithm for the AN/FPN-44A Loran-C transmitter [AD-A274820] p 2664 N94-26493
Identification and H(infinity)/(mu)-synthesis control of the Sandia truss [DE94-002735] p 2839 N94-26810
MINERAL METABOLISM
Endocrinological evaluations of muscle and bone atrophy in tail-suspended rats p 2903 N94-27444
MINERAL OILS
Measurement of viscosity, density, and gas solubility of refrigerant blends in selected synthetic lubricants [DE94-003609] p 2713 N94-25934
Calculation methods for steadily loaded axial groove hydrodynamic journal bearings (guide to use of computer program A9305) [ESDU-93005] p 2830 N94-28074
MINERALOGY
Experimental study of lunar and SNC (Mars) magmas [NASA-CR-195274] p 3107 N94-27850
MINERALS
Some properties of graphs with local Ore conditions [PB94-126612] p 2996 N94-26962
MINIATURIZATION
Pigs in cyberspace p 2689 N94-27376
MINIMAL SURFACES
Characterization of self-conjugate minimal surfaces in R(sup 3) [DE94-601538] p 2993 N94-26409
Some remarks on the symmetry of self-conjugate minimal surfaces in R3 [DE94-603670] p 3007 N94-27633
MINIMAX TECHNIQUE
Phase portraits of quadratic systems with finite multiplicity three and one critical point of infinity [REPT-93-41] p 2991 N94-26215
MINIMUM DRAG
Examples of flight path optimisation using a multivariate gradient-search method [ESDU-93021] p 2670 N94-28092
MINING
Asteroid exploration and utilization p 3080 N94-25697
MINKOWSKI SPACE
Dimensional crossover from non-renormalizability to renormalizability [DE93-613052] p 3006 N94-26193
Classical solutions of Yang-Mills-Chern-Simons theory in 2+1 dimensions: A quasi-linear superposition [DE93-634335] p 3006 N94-26270
The extensions of space-time. Physics in the 8-dimensional homogeneous space D is equal to SU(2,2)/K [DE93-634336] p 3072 N94-26551
MINUTEMAN ICBM
Uncertainties in the characterization of the thermal environment of a solid rocket propellant fire [DE94-002023] p 2760 N94-27719
MIRRORS
Elastic backscattering lidar for a MSTI satellite [DE94-002701] p 2816 N94-26126
Theoretical aspects of the agile mirror [AD-A274890] p 2767 N94-26177
Mounting of SSM's [VTT-TIED-1442] p 2695 N94-26250
Comparison of technology for high-power laser mirrors and synchrotron radiation mirrors [DE94-002913] p 3035 N94-26276
Phase conjugated lasers applied to commercial x ray lithography [DE94-001529] p 2819 N94-27018
Reflectometer employing an integrating sphere and lens-mirror concentrator [AD-D016061] p 3039 N94-27676
The PROTEL contamination code [RXR-93071] p 3040 N94-28202
MISALIGNMENT
Performance impacts for actuator misalignments and failures in large-aperture adaptive-optic telescopes [AD-A273838] p 3034 N94-25742
Enhanced simulation software for rocket turbopump, turbulent, annular liquid seals [NASA-CR-195239] p 2825 N94-27383
MISSILE BODIES
Numerical assessment of aerodynamic interactions on missiles with transverse jets control p 2659 N94-28031
MISSILE COMPONENTS
Transparent polycrystalline body with high ultraviolet transmittance, process for making and applications thereof [CA-PATENT-1325511] p 3066 N94-27276
MISSILE CONFIGURATIONS
A numerical study of high-speed missile configurations using a block-structured parallel algorithm [AD-A273776] p 2979 N94-25860
Numerical assessment of aerodynamic interactions on missiles with transverse jets control p 2659 N94-28031
MISSILE CONTROL
Recent developments in the simulation of steady and transient transverse jet interactions for missile, rotorcraft, and propulsive applications p 2804 N94-28030
Numerical assessment of aerodynamic interactions on missiles with transverse jets control p 2659 N94-28031
MISSILE DEFENSE
Elastic backscattering lidar for a MSTI satellite [DE94-002701] p 2816 N94-26126
MISSILE DETECTION
Radar detection of low-altitude targets in a maritime environment. Volume 2: Meteorological and radar data [AD-A274658] p 2768 N94-26335
MISSILE TRACKING
Optimal control design advantages utilizing two-degree-of-freedom controllers [AD-A273839] p 2984 N94-25743
Elastic backscattering lidar for a MSTI satellite [DE94-002701] p 2816 N94-26126
MISSILES
A numerical study of high-speed missile configurations using a block-structured parallel algorithm [AD-A273776] p 2979 N94-25860
Numerical assessment of aerodynamic interactions on missiles with transverse jets control p 2659 N94-28031
MISSION PLANNING
The Extended Mission Rover (EMR) p 2689 N94-25674
Lowest cost, nearest term options for a manned Mars mission p 2689 N94-25682
Comet nucleus and asteroid sample return missions p 2689 N94-25692
First lunar outpost p 2943 N94-25694
Project Minerva: A low-cost manned Mars mission based on indigenous propellant production p 2760 N94-25705
Pax: A permanent base for human habitation of Mars p 2943 N94-25706
Access to space study [NASA-TM-109693] p 2685 N94-27151
Interdisciplinary technology p 2686 N94-27363
Space science: Causes and impacts of cutbacks to NASA's outer solar system exploration missions. Report to the Chairman, Subcommittee on Investigations and Oversight, Committee on Science, Space, and Technology, House of Representatives [GAO/NSIAD-94-24] p 3106 N94-27418
MIXING
Modulation wavelength dependence of ion mixing in metallic superlattices [DE94-004608] p 3059 N94-26591
MIXING CIRCUITS
Development of a 4-bit parallel analog-to-digital converter and a four-quadrant double-balanced mixer using heterojunction bipolar transistor technology [AD-A274074] p 2947 N94-25648
A compact 150 GHz SIS receiver cooled by 4 K GM refrigerator [REPT-36] p 2776 N94-27340
MIXING LAYERS (FLUIDS)
Transverse vorticity measurements in the University of Houston two stream shear layer facility [AD-A273910] p 2797 N94-27562
Scalar mixing in the subsonic jet in crossflow p 2800 N94-28008
MIXING LENGTH FLOW THEORY
Development and implementation of a scramjet cycle analysis code with a finite-rate-chemistry combustion model for use on a personal computer [AD-A273834] p 2673 N94-25617
Performance of renormalization group algebraic turbulence model on boundary layer transition simulation [NASA-CR-194466] p 2644 N94-26131
Numerical simulation of turbulent free jet by TFKE model p 2871 N94-28157
MIXING RATIOS
Evaluation of a concentration probe for application in a supersonic flow field [AD-A273915] p 2643 N94-25592
MIXTURES
Analysis and computer tools for separation processes involving nonideal mixtures [DE94-004162] p 2960 N94-25986
MOBILE COMMUNICATION SYSTEMS
Low Earth orbit communications satellite p 2698 N94-25701
MOBILITY
The Robotic All-Terrain Lunar Exploration Rover (RATLER): Increased mobility through simplicity p 2685 N94-26291
Effect of temperature and recoil-energy spectra on irradiation-induced amorphization in Ca2La8(SiO4)6O2 [DE94-004371] p 3067 N94-27602
MODAL RESPONSE
Mode analysis of gyrotron oscillation using a k-spectrometer [DE94-701195] p 2813 N94-27703
MODEL REFERENCE ADAPTIVE CONTROL
Direct model reference adaptive control of robotic arms p 2683 N94-26282
Investigation into model-based fuzzy logic control [AD-A274660] p 2985 N94-26336
MODELS
An object model for multimedia programming [CWI-CS-R9327] p 2971 N94-27552
One from many: Selecting an appropriate human performance model [DCIEM-93-25] p 2942 N94-27683
MODERATORS
Characteristics and control response of the TOPAZ 2 reactor system real-time dynamic simulator [DE94-003788] p 2699 N94-25600
Space-R thermionic space nuclear power system: Design and technology demonstration [DE94-001890] p 2699 N94-25929
MODULATION
Modulation Simulation Program: Programmer's manual, version 1.00 [DREO-16] p 2973 N94-27761
Modulation Simulation Program: Operator's manual, version 1.00 [DREO-16] p 2975 N94-27951
MODULATION TRANSFER FUNCTION
Image quality and the display modulation transfer function: Experimental findings [AD-A274061] p 2679 N94-25773
MODULATORS
Diagnostics and microelectronics [DE94-003016] p 2784 N94-26777
MODULES
Module interconnection frameworks for a real-time spreadsheet [AD-A273853] p 2956 N94-25588
Design and development of the second generation Mars Habitat p 2943 N94-25693
A modular approach to evaluation cryptographic protocols using Petri nets [ISBN-0-315-85354-9] p 2972 N94-27595
MODULUS OF ELASTICITY
FR/GE/UK/US International Test Operations Procedure (ITOP) 1-1-050 development of laboratory vibration test schedules [AD-A273887] p 2836 N94-25732
Users manual for CATNIP: A Computer Analysis Tool for Normal Impact Penetration [DE94-003671] p 2962 N94-26371
Effects of physical aging on long-term behavior of composites p 2712 N94-27897
MOISTURE
Package integrity measurement technology and quality assurance [AD-A273881] p 2834 N94-25727
MOISTURE CONTENT
Package integrity measurement technology and quality assurance [AD-A273881] p 2834 N94-25727
Mechanism of mechanical fatigue of silica glass [DE94-003165] p 2753 N94-26783
Cloud liquid water content measurement tests using dual-wavelength radar [PB94-125960] p 2896 N94-26959
Time domain reflectometry for measuring bulk soil electrical conductivity and comparison with the Em38 instrument [PB94-125432] p 2881 N94-27052
MOLDING MATERIALS
Technique to predict the curing behaviour of unsaturated polyester materials [PB94-124856] p 2748 N94-25892

Modelling the inhibition cure behaviour of unsaturated polyester moulding materials
[PB94-124864] p 2748 N94-25893
Stress relaxation in dough moulding compounds
[PB94-124872] p 2748 N94-25894
MOLDS
Production of an amorphous Fe(75)Si(10)B(15) sheet by a metallic mold casting method and its properties
p 2746 N94-28170
MOLECULAR BEAM EPITAXY
Ultra-high aggregate bandwidth two-dimensional multiple-wavelength diode laser arrays
[AD-A274018] p 2815 N94-25756
Investigation of a normal incidence high-performance p-type strained layer In(0.3)Ga(0.7)As / In(0.52)Al(0.48) as quantum well infrared photodetector
[AD-A274854] p 3055 N94-26188
MBE grown 3 to 5 strain relaxed buffer layers and superlattices characterized by atomic force microscopy
[DE94-002931] p 3056 N94-26308
Nitride semiconductors for ultraviolet detection
[AD-A274246] p 3060 N94-26840
Pseudomorphic semiconducting heterostructures from combinations of AlN, GaN and selected SiC polytypes: Theoretical advancement and its coordination with experimental studies of nucleation, growth, characterization and device development
[AD-A274247] p 3061 N94-26841
Low temperature deposition and characterization of N- and p-type silicon carbide thin films and associated ohmic and Schottky contacts
[AD-A274345] p 2754 N94-26974
Visible light emitting materials and injection devices
[AD-A274418] p 2786 N94-27079
Observation of stimulated emission from an MBE grown GaN film on sapphire
[DE94-003638] p 3068 N94-27724
MOLECULAR BEAMS
Molecular beam mass spectrometry studies of the chemical vapor deposition of diamond
[DE94-003802] p 3049 N94-25601
Investigation of a normal incidence high-performance p-type strained layer In(0.3)Ga(0.7)As / In(0.52)Al(0.48) as quantum well infrared photodetector
[AD-A274854] p 3055 N94-26188
Trace organic chemical detection using an ultraviolet excitation molecular beam fluorometer
[DE94-002649] p 2704 N94-27708
Dynamics of metastable states in supersonic beams
[ITN-94-85232] p 3028 N94-27760
MOLECULAR BIOLOGY
Molecular biological studies on the human radioresistance and drug resistance
[DE93-632682] p 2910 N94-26549
NCVS, volume 5
[AD-A274975] p 2902 N94-27165
Space radiation health research, 1991-1992
[NASA-TM-109721] p 2932 N94-27556
Neutrons in biology
[DE94-701085] p 2903 N94-27862
MOLECULAR CHAINS
Atomic-scale chemistry of metal surfaces
[REPT-A-2657] p 3012 N94-25636
Localization properties of one-dimensional electrified chains
[DE94-603672] p 3067 N94-27635
MOLECULAR CLOUDS
Investigations of the dynamical evolution of protoplanetary nebulae
[NASA-CR-195278] p 3105 N94-27428
Modulating terrestrial impacts from Oort cloud comets by the adiabatically changing galactic tides
p 2890 N94-28305
MOLECULAR COLLISIONS
Vibrational energy transfer within the B 3Pi (O(+) sub u) state of 79BR2 upon collision with N2, O2, NO, and SF6
[AD-A273905] p 3011 N94-25589
International bulletin on atomic and molecular data for fusion. No. 42-45, Mar. 1991 - Dec. 1992
[DE94-601817] p 3045 N94-26946
International bulletin on atomic and molecular data for fusion. No. 46
[DE94-601818] p 3023 N94-26947
MOLECULAR DYNAMICS
Fast parallel algorithms for short-range molecular dynamics
[DE93-018519] p 3016 N94-26033
Modeling defect production in high energy collision cascades
[DE94-003810] p 3017 N94-26049
How reliable is the HMSA integral equation for the pair structure of supercooled and amorphous mixtures?
[DE94-601543] p 3006 N94-26411
Nanoscale plasticity in silica glass
[DE94-004212] p 2751 N94-26554
A semiclassical reactive flux method for the calculation of condensed phase activated rate constants
[AD-A274850] p 3020 N94-26562
Modeling Group 4 elements with new transferable tight-binding models
[DE94-000770] p 3059 N94-26695
International journal of quantum chemistry. Quantum Chemistry Symposium Number 27: Proceedings of the International Symposium on Atomic, Molecular, and Condensed Matter Theory and Computational Methods
[AD-A274352] p 3023 N94-26926
First principles calculations for the cleaved and annealed Ge(111) surfaces
[DE93-617048] p 3066 N94-27347
Computer simulation of aqueous Na-Cl electrolytes
[DE94-002622] p 3030 N94-28001
MOLECULAR ELECTRONICS
Molecular surface electrostatic potentials in the analysis of non-hydrogen-bonding noncovalent interactions
[AD-A274612] p 3022 N94-26894
MOLECULAR ENERGY LEVELS
Dynamics of metastable states in supersonic beams
[ITN-94-85232] p 3028 N94-27760
MOLECULAR EXCITATION
The importance of vibrationally excited nitrogen in silicon nitride deposition systems
[AD-A274874] p 2750 N94-26167
Dynamics of metastable states in supersonic beams
[ITN-94-85232] p 3028 N94-27760
MOLECULAR GASES
An investigation of the effect of surface impurities on the adsorption kinetics of hydrogen chemisorbed onto iron
[NASA-CR-195213] p 2716 N94-26643
MOLECULAR INTERACTIONS
Study on computerized experiment of amorphous transformation process by solid phase reaction
p 2726 N94-25564
International bulletin on atomic and molecular data for fusion. No. 46
[DE94-601818] p 3023 N94-26947
Spectroscopy and dynamics of molecular and ionic impurities embedded in solid hydrogen
[AD-A274149] p 3064 N94-27095
MOLECULAR PHYSICS
Dynamics of metastable states in supersonic beams
[ITN-94-85232] p 3028 N94-27760
MOLECULAR RELAXATION
A study of vibrational relaxation of electronically-excited molecules
[DE93-613553] p 3013 N94-25827
Spectroscopic and vibrational energy transfer studies in molecular bromine
[AD-A273795] p 3014 N94-25875
Progress in modeling atmospheric propagation of sonic booms p 2650 N94-28189
MOLECULAR SPECTRA
Spectroscopy Division
[DE94-604074] p 2717 N94-26988
MOLECULAR SPECTROSCOPY
Molecular surface electrostatic potentials in the analysis of non-hydrogen-bonding noncovalent interactions
[AD-A274612] p 3022 N94-26894
MOLECULAR STRUCTURE
Morphological analysis of ionomers
[DE94-003660] p 2749 N94-26005
Radiation-Induced Structural Changes, 2
[DE93-520314] p 3054 N94-26109
Transition metals in highly correlated discotic phases: Designing metallomesogens with selected intermolecular organizations
[AD-A274695] p 2736 N94-26452
An x ray absorption fine structure study of ordering in polythiophene thin films
[AD-A274235] p 2753 N94-26822
Controlled heterogeneous nucleation of melt-textured YBa2Cu3O(6+x) by addition of Al2O3 particles
[AD-A274605] p 3062 N94-26892
NCVS, volume 5
[AD-A274975] p 2902 N94-27165
Molecular dynamics simulation and crystal-field theory: Predicting the optical spectra and structure of rare-earth doped inorganic glasses
[ISBN-0-315-84679-8] p 3025 N94-27310
The molecular matching problem
p 3030 N94-27910
Thermal conductivity of liquid carboxylic acids
[ESDU-93017] p 2721 N94-28138
MOLECULAR WEIGHT
Chemical polymerization and Langmuir-Blodgett techniques. 2: The polymerization of monolayers of 3-substituted pyrroles
[AD-A274478] p 2755 N94-27163
MOLECULES
Atomic-scale chemistry of metal surfaces
[REPT-A-2657] p 3012 N94-25636
On the classification scheme for resonant states of muonic molecules
[DE93-613645] p 3014 N94-25853
Transition metal activation and functionalization of carbon-hydrogen bonds
[DE94-003650] p 2715 N94-26369
MOLLUSKS
An experimental study of siphonal jets in a turbulent boundary layer crossflow p 2802 N94-28015
MOLTEN SALT ELECTROLYTES
Molten salt techniques for reproducible excess heat
[AD-A274935] p 2714 N94-26296
MOLTEN SALTS
Structure of ionic fluids in equilibrium with a microporous ionic matrix
[DE94-600563] p 2715 N94-26391
Isothermal corrosion testing of steels in molten nitrate salts
[DE94-004695] p 2742 N94-27755
MOLYBDENUM
Study on development of chemical measurement method utilizing plasmas p 2728 N94-25576
Method of bonding molybdenum to steel
[AD-D016079] p 2747 N94-28187
MOLYBDENUM ALLOYS
Study on alloy films for hydrogen separation
p 2726 N94-25565
MOLYBDENUM DISULFIDES
LB-Deposited, side-chain substituted polyaniline, polypyrrole and the corresponding monomers, studied by STM
[AD-A274405] p 2754 N94-26977
MOMENTS OF INERTIA
Normal forms for perturbations of the euler top
[PB94-125390] p 3009 N94-26968
MOMENTUM
On the estimation of matrix elements for optical transitions in semiconductors
[DE93-613550] p 3051 N94-25851
How to build analogues of the Bessel-Clifford expansions for the sum of the repulsive Coulomb potential and central potential decreasing more rapidly than the centrifugal one?
[DE93-634308] p 3007 N94-26472
Study of the process (pi)(sup -)A(yields)(pi)(sup -)(eta)'(eta)A at the moment 36 GeV/c
[DE93-634530] p 3024 N94-27250
Predictions of momentum and scalar fields in a jet in cross-flow using first and second order turbulence closures p 2803 N94-28025
MOMENTUM THEORY
Computation of non-isentropic internal flows with variable density
[AD-A274848] p 2794 N94-26801
Excited Landau levels, orbital angular momentum and axial anomaly
[DE94-606407] p 3068 N94-27679
MOMENTUM TRANSFER
The amplitude of the elastic hadron-hadron scattering in the coulombic range of transfer momenta
[DE93-613183] p 3014 N94-25869
Two dimensional self-consistent fluid simulation of RF inductive sources
[DE94-003635] p 2767 N94-25937
A study of LPM suppression of bremsstrahlung at 25 GeV
[DE94-003457] p 3018 N94-26133
Topics in longshore currents
[AD-A274788] p 2899 N94-26361
Relativistic collision rate calculations for electron-air interactions
[DE94-004204] p 3020 N94-26527
The challenges of exclusive processes in QCD
[DE94-003429] p 3024 N94-27050
Experimental measurement of local displacement and chemical pair correlations in crystalline solid solutions
[DE94-001124] p 3065 N94-27251
MONAURAL SIGNALS
Monaural and binaural processing of complex waveforms
[AD-A274209] p 3010 N94-27067
MONITORS
A comparison of sleep scored from electroencephalography to sleep scored by wrist actigraphy
[AD-A273739] p 2910 N94-26748
Automatic, real-time fault monitor verifying network in a microwave landing system
[CA-PATENT-1325261] p 2665 N94-27275
MONOCHROMATORS
Design of a high-precision double crystal tunable monochromator
[DE94-003004] p 2811 N94-26787

MONOMERS

LB-Deposited, side-chain substituted polyaniline, polypyrrole and the corresponding monomers, studied by STM
[AD-A274405] p 2754 N94-26977

Langmuir-Blodgett and STM investigations of conducting polymer thin films
[AD-A274512] p 2755 N94-27087

New monomers for high performance polymers
p 2758 N94-27904

MONOMOLECULAR FILMS

Liquid crystalline side-chain polysiloxanes with 4-amino-4'-stilbene-carboxylic ester mesogens
[AD-A274510] p 2754 N94-27036

MONOPOLE ANTENNAS

Receiving antennas for electromagnetic pulses and transients
[ISBN-0-315-62312-8] p 2777 N94-27871

MONOPROPELLANTS

Liquid monopropellants
[AD-D016074] p 2760 N94-28226

MONOPULSE RADAR

Methods for improving low-angle, low-altitude radar tracking accuracy
[AD-A274914] p 2768 N94-26347

MONOTONE FUNCTIONS

Isotonic estimation and rates of convergence in Wicksell's problem
[REPT-93-39] p 3002 N94-26213

MONSOONS

Investigation of mesoscale convective cloud clusters in South China
[AD-A274303] p 2895 N94-26678

Propagation of cold air masses in East Asia and its associated planetary-scale function
[AD-A274304] p 2895 N94-26850

Simulation of the Indian and East-Asian summer monsoon in the ECMWF model: Sensitivity to horizontal resolution
[DE94-004276] p 2897 N94-27571

MONTE CARLO METHOD

Penetrating nature of very collimated high-energy shower-clusters of hadrons and gamma rays
p 3113 N94-25631

NNN-Ising model simulation of nanodomain textures in relaxor-type lead scandium tantalate
[DE94-601884] p 2748 N94-25844

On radiation defects in strip detectors
[DE93-616646] p 3015 N94-25916

Monte Carlo event generators for hadron-hadron collisions
[DE94-003212] p 3015 N94-25955

Crossover between BCS and performed-Boson theories with increasing interactions
[DE93-019018] p 3017 N94-26078

Laser manipulation of metastable neon atoms
[ETN-94-95344] p 2817 N94-26225

Modelling of ionisation reactions and of the resulting electric fields in one-dimensional hypersonic shock waves with the direct simulation Monte Carlo method
[IC-AERO-92-01] p 2644 N94-26248

Ising critical behaviour in the one-dimensional frustrated quantum XY model
[DE93-634755] p 3057 N94-26390

C-periodicity and the physical mass in the 3-state Potts model
[DE94-601551] p 3019 N94-26423

Subgraph approximations for large directed graphical models
[AD-A274813] p 3003 N94-26485

Simulation approaches for calculations in directed graphical models
[AD-A274825] p 3003 N94-26494

Stochastic solution to quantum dynamics
[NASA-TP-3408] p 3114 N94-26550

Measuring the time dependence of B(sub s)(sup 0) meson - anti B(sub s)(sup 0) meson oscillations
[ISBN-0-315-84367-5] p 3021 N94-26665

Direct simulation Monte-Carlo of near continuum hypersonic flow with chemical reactions
[DLR-FB-93-01] p 2797 N94-27588

Monte Carlo calculations of low background detector response
[DE94-004593] p 3116 N94-27621

Numerical and experimental analyses of the radiant heat flux produced by quartz heating systems
[NASA-TP-3387] p 3011 N94-27659

BATSE burst location accuracy and constraints on the fraction of repeating GRB sources
[DE94-004981] p 3116 N94-27714

Modeling the DMSP and CRRES dosimeters using the path length distribution method
[RXR-93051] p 2698 N94-28200

The PROTEL contamination code
[RXR-93071] p 3040 N94-28202

MOON

The Extended Mission Rover (EMR)
p 2689 N94-25674

The modal solution to the Moon's orbit using canonical Floquet perturbation theory
[AD-A273732] p 2690 N94-26001

MORPHOLOGY

Characterization of physically vapor deposited AF2400 thin films
[DE94-004019] p 2749 N94-25985

Morphological analysis of ionomers
[DE94-003660] p 2749 N94-26005

Oxygen reduction at a YSZ interface with cathode materials La(1-x)(Ca or Sr)(x)MnO3(1-x)CaMnO3
[DE94-002954] p 3054 N94-26147

MBE grown 3 to 5 strain relaxed buffer layers and superlattices characterized by atomic force microscopy
[DE94-002931] p 3056 N94-26308

High definition Raman microscopic imaging
[DE94-003158] p 2716 N94-26781

The morphological processing of binary images
[AD-A274310] p 2996 N94-26972

Morphology transitions during non-equilibrium growth processes
[ITN-94-85236] p 3065 N94-27243

Hydrothermal growth and characterization of oxides in zirconium alloys
[DE94-602981] p 2743 N94-27829

MOSSBAUER EFFECT

The Latin American conference on the applications of the Moessbaer effect
[DE93-615942] p 3051 N94-25912

MOTION PERCEPTION

Application of Markov random field theory to image coding and motion estimation
[ISBN-0-315-83435-8] p 2964 N94-26632

Motion analysis from a sequence of range images
[ISBN-0-315-84684-4] p 2969 N94-27311

Estimation of image motion in scenes containing multiple moving objects
[ISBN-0-315-85208-9] p 2969 N94-27346

Frequency analysis of body sway induced by optokinetic stimulation p 2914 N94-27455

Effects of imaginary target on induced eye movements by linear acceleration p 2914 N94-27456

MOTION SICKNESS

The electrogastrogram during parabolic flight
p 2913 N94-27452

MOTION SIMULATION

Motion planning for serial manipulators with many degrees of freedom: Implementation of a sequential search strategy
[ISBN-0-315-83682-2] p 2822 N94-26642

MOTION SIMULATORS

The effect of platform motion on human energy expenditure during walking. An exploratory experiment
[AD-A273760] p 2940 N94-25724

MOTION STABILITY

A comparison of three approximate mathematical models for the gravity gradient stabilized satellite
[AD-A273832] p 2694 N94-25615

Recent trend of domestic and international regulations on intact stability of ships for safety
p 2764 N94-27977

MOTOR VEHICLES

Dead reckoning navigation
[VTT-TIED-1402] p 2664 N94-25808

Unscreened low tension cables scrape abrasion testing
[PB94-123767] p 2823 N94-26849

Optimising BMW four-cylinder two-valve engines
[PB94-125101] p 2824 N94-27254

MOUNTING

Mounting of SSM's
[VTT-TIED-1442] p 2695 N94-26250

MOVING TARGET INDICATORS

Enhanced adaptive statistical filter providing improved performance for target motion analysis noise discrimination statement of government interest
[AD-D016039] p 2786 N94-27109

MULTICHANNEL COMMUNICATION

Interference analysis of multichannel transmission lines: A system's analysis
[PB94-126505] p 2772 N94-26909

Design and test of a regenerative satellite transmultiplexer
[ISBN-0-315-85280-1] p 2786 N94-27303

MULTIGRID METHODS

On the robustness of a multiple semi-coarsened grid method
[REPT-93-51] p 2992 N94-26252

Grid-independent convergence based on preconditioning techniques
[PB94-125358] p 2997 N94-27000

Agglomeration multigrid for the three-dimensional Euler equations
[NASA-CR-191595] p 2999 N94-27557

TVD flux-difference split methods for high-speed thermochemical nonequilibrium flows with strong shocks
[UTIAS-350] p 2799 N94-27880

A parallel multigrid algorithm for solving the Navier-Stokes equations on a transputer system
[PREPRINT-699] p 2807 N94-28099

MULTIMEDIA

Development of satellite telecommunications during the period 1990 - 2005
[CRANFIELD-AERO-9301] p 2765 N94-25639

Multimedia in Views
[CWI-CS-R9263] p 2961 N94-26218

Hypermedia support for engineering design systems: Application to fatigue analysis
[VTT-TIED-1432] p 2837 N94-26255

An object model for multimedia programming
[CWI-CS-R9327] p 2971 N94-27552

MULTIMISSION MODULAR SPACECRAFT

Performance measures from the explorer platform berthing experiment p 2683 N94-26283

MULTIPATH TRANSMISSION

Analyzing adaptive beamformer performance in a stable multipath environment
[AD-A274029] p 2766 N94-25766

Methods for improving low-angle, low-altitude radar tracking accuracy
[AD-A274914] p 2768 N94-26347

Laser phase induced intensity noise in fiber-optic signal processing and sensing systems
[ITN-94-85234] p 2819 N94-27179

Ground station siting considerations for DGPS
p 2642 N94-27293

MULTIPHASE FLOW

Eleventh Symposium on Energy Engineering Sciences: Proceedings
[DE93-019930] p 2763 N94-26429

MULTIPLEXING

The AFIT multielectrode array for neural recording and simulation: Design, testing, and encapsulation
[AD-A274086] p 2909 N94-25943

A VHDL register transfer level model of the linear token passing multiplex data bus protocol for the high speed data bus
[AD-A273734] p 2980 N94-26009

Comparative analysis of different configurations of PLC-based safety systems from reliability point of view
p 2836 N94-27925

MULTIPLICATION

The PRISM project: Infrastructure and algorithms for parallel eigensolvers
[DE94-005125] p 2973 N94-27717

MULTIPROCESSING (COMPUTERS)

An efficient communication scheme for solving the S(sub n) equations on message-passing multiprocessors
[DE94-000378] p 2769 N94-26482

Design and implementation of a multiprocessor for DSP and communications systems algorithm evaluation
[ISBN-0-315-84128-1] p 2980 N94-26674

On-board computer for control subsystem of satellite
p 2949 N94-26716

Real time avionics constraints: Silicon solutions
p 2949 N94-26717

Test of onboard real time applications (LICE (tm))
p 2952 N94-26737

Specification performance optimization and executive generation for onboard multiprocessor real time application with SynDEx p 2954 N94-26745

Partitioning structural VHDL circuits for parallel execution on hypercubes
[AD-A274390] p 2785 N94-26830

Hard real-time reliable multicast in the DEDOS system
[PB94-126745] p 2966 N94-26920

Automatic mapping of task and data parallel programs for efficient execution on multicomputers
[AD-A274125] p 2982 N94-27117

Design of a parallel discrete event simulation coprocessor
[AD-A274135] p 2982 N94-27123

Garbage collection in a multiprocessor Smalltalk system
[ISBN-0-315-51159-1] p 2982 N94-27332

Unified distributed simulation
[ISBN-0-315-59019-X] p 2983 N94-27685

An enhanced global spectral model
[PL-TR-92-2011] p 2898 N94-28223

MULTIPROGRAMMING

Ada multiple-programming for hard real time applications in space systems p 2951 N94-26730

MULTISENSOR APPLICATIONS

Development of a multi-sensor in situ fiber optic fluorometer
[DE94-003399] p 3035 N94-26100

An analysis of multiple sensor system payloads for unmanned aerial vehicles
[AD-A274905] p 2667 N94-26182
A data fusion algorithm for multi-sensor microburst hazard assessment p 2641 N94-27287
Multi-sensor data fusion in a distributed environment: Architectural solutions
[NLR-TP-92243-U] p 2989 N94-27800

MULTISPECTRAL BAND SCANNERS
Mapping coastal habitats using an imaging spectrometer
[ISBN-0-315-84362-4] p 2848 N94-26664

MULTISPECTRAL PHOTOGRAPHY
Morphodynamics of inter-tidal areas: The Wadden Sea
[NLR-TP-92356-U] p 2851 N94-27555
SPECTRUM analysis of multispectral imagery in conjunction with wavelet/KLT data compression
[DE94-003961] p 2851 N94-27727
Multispectral and textural classifications of a SPOT HRV-1 image, region of Sherbrooke, Quebec, Canada
[ISBN-0-315-84978-9] p 2851 N94-27863

MULTIVARIABLE CONTROL
Grey-box modelling and identification topics
[PB94-126380] p 2986 N94-27029

MULTIVARIATE STATISTICAL ANALYSIS
Radial base functions: L(sup p)-approximation orders with scattered centers
[AD-A274682] p 3003 N94-26445
A multivariate anthropometric method for crew station design: Abridged
[AD-A275588] p 2941 N94-26984
Radial basis function approximation: From gridded centers to scattered centers
[AD-A274184] p 2998 N94-27103
Multivariate spectral analysis to extract materials from multispectral data
[AD-A274142] p 2709 N94-27135
Examples of flight path optimisation using a multivariate gradient-search method
[ESDU-93021] p 2670 N94-28092

MUONS
On the classification scheme for resonant states of muonic molecules
[DE93-613645] p 3014 N94-25853
Theoretical and experimental studies of elementary physics
[DE94-002310] p 3008 N94-25988
Heavy charged leptons in an SU(3)(sub L) x U(1)(sub N) model
[DE93-634367] p 3016 N94-26041
Harvard University High Energy Physics
[DE94-002406] p 3032 N94-26119
Separation and reconstruction of electron neutrino interaction in the IHEP-JINR neutrino detector and BARS detector
[DE93-634182] p 3019 N94-26393
Measurements of the p (mu)d-molecule formation rate at different hydrogen temperature
[DE93-634636] p 3020 N94-26511
Indiana University high energy physics, task A
[DE94-000961] p 3033 N94-27614
Monte Carlo calculations of low background detector response
[DE94-004593] p 3116 N94-27621
Jet production in muon scattering at Fermilab E665
[DE94-004663] p 3028 N94-27752
Muon transfer rates in collisions of hydrogen isotope mesic atoms on bare nuclei: Multichannel adiabatic approach
[DE94-606752] p 3030 N94-27861

MUSCLES
Effects of perfusion of amiodarone on electrophysiological properties in single rabbit ventricular myocytes p 2906 N94-27503
Impaired associated movement in Parkinson's disease: An evaluation of Bell's phenomenon
p 2928 N94-27520
Contribution of muscle spindle afferent activity to transient pause in EMG during voluntary tonic contraction p 2928 N94-27522
Sympathetic nerve activity during dynamic leg exercise
p 2929 N94-27527
Analysis on one minute wave in body fluid volume and muscle pumping referred to body parts generating the one minute wave during human active standing
p 2929 N94-27528
The measurements of muscle blood flow by laser Doppler flowmetry with needle type probe
p 2908 N94-27530
Muscle sympathetic nerve activity in patients with hyper-and hypothyroidism: A microneurographic study
p 2930 N94-27531
Enhancement of skin sympathetic nerve activity in amyotrophic lateral sclerosis p 2930 N94-27532
Treatment of orthostatic hypotension by nasal administration of vasopressin p 2930 N94-27533
Muscle sympathetic nerve activity in humans
p 2932 N94-27538
Muscular activity and its relationship to biomechanics and human performance p 2934 N94-28362
Eccentric exercise testing and training
p 2934 N94-28363
Electrical stimulation in exercise training
p 2935 N94-28371

MUSCULAR FUNCTION
Impaired associated movement in Parkinson's disease: An evaluation of Bell's phenomenon
p 2928 N94-27520
Contribution of muscle spindle afferent activity to transient pause in EMG during voluntary tonic contraction p 2928 N94-27522

MUSCULAR STRENGTH
The value of electrical stimulation as an exercise training modality p 2936 N94-28372

MUSCULAR TONUS
Contribution of muscle spindle afferent activity to transient pause in EMG during voluntary tonic contraction p 2928 N94-27522

MUSCULOSKELETAL SYSTEM
Muscular activity and its relationship to biomechanics and human performance p 2934 N94-28362
Exercise detraining: Applicability to microgravity
p 2934 N94-28364

MUTATIONS
Studies on the application of radiation for genetic transformation in higher plants
[DE93-632656] p 2901 N94-26470
Molecular biological studies on the human radioresistance and drug resistance
[DE93-632682] p 2910 N94-26549
Vacuum-UV-effects on E. coli plasmid pUC19: Inactivation, strand break induction and mutation induction
[DLR-FB-93-26] p 2903 N94-27754

MYOCARDIUM
Protective action of platelet-activating factor antagonist, TCV-309, against ischemia reperfusion injury in isolated rabbit hearts p 2904 N94-27465
Protective action of an amiloride derivative (amiloride, 5-(N, N-dimethyl) hydrochloride) against in isolated ischemia/reperfusion newborn rabbit hearts
p 2904 N94-27466
Effects of high-intensity electric field stimulation on the electromechanical performance of cardiac muscle: Influence of fiber orientation p 2904 N94-27467
On the mechanism of reentrant arrhythmias following DC defibrillation: Influence of fiber orientation to the effects of low-energy electric field stimulation on the effective refractory period of cardiac muscle
p 2904 N94-27468
Positive chronotropic effect of mechanical stretch on the sinoatrial node: Roles of neurotransmitters and stretch activated channels p 2904 N94-27469
Effects of perfusion of amiodarone on electrophysiological properties in single rabbit ventricular myocytes p 2906 N94-27503
Fast and slow onsets of Na channel blocking actions due to lidocaine and disopyramide using concentration-clamp method p 2907 N94-27504
Electrophysiological effects of MS-551, a new Class 3 antiarrhythmic agent, on isolated rabbit ventricular muscles p 2907 N94-27505
Comparative investigation of new Class 3 antiarrhythmic drugs, E-4031 and MS-551, on electrophysiological properties in isolated rabbit ventricular myocytes
p 2907 N94-27506
Effects of Class 1 antiarrhythmic drugs on the intraventricular conduction: Influence of fiber orientation
p 2907 N94-27507
Effects of Class 3 antiarrhythmic agents, E-4031 and MS-551 on ventricular repolarization in isolated rabbit hearts p 2907 N94-27508
Electrical coupling between the sino-atrial node and atrial muscle: Cell to cell interaction through an external circuit and its simulation by computer modeling
p 2907 N94-27509
A study on tissue excitation of cardiac muscle under electrical field stimulation p 2907 N94-27510
Block of cardiac sodium channels by Ro 22-9194 (R), a new antiarrhythmic agent: Effects on the maximum upstroke velocity (Vmax) of single guinea pig ventricular myocytes p 2907 N94-27511
Electrophysiological effects of an antiarrhythmic drug, moricizine on isolated guinea pig ventricular muscles
p 2907 N94-27512
Postnatal changes in the autonomic modulation of L-type Ca(exp 2+) currents of rabbit ventricular cells
p 2931 N94-27535
Mechanism for regulation of myocardial contractility by autonomic drugs: Pathophysiological relevance in congestive heart failure p 2931 N94-27536

N

N-TYPE SEMICONDUCTORS
Visible light emitting materials and injection devices
[AD-A274418] p 2786 N94-27079

NACELLES
Wind tunnel investigation of an STOL aircraft model: An effect of engine nacelle shape
[NAL-TM-653] p 2647 N94-27235
Propeller off-axis loads due to thrust axis incidence and nacelle magnus force p 2652 N94-28319
A new approach to turboprop forward nacelle design
p 2655 N94-28336

NASA PROGRAMS
An assessment of testing requirement impacts on nuclear thermal propulsion ground test facility design
[DE94-002933] p 2702 N94-26560
Aerospace safety advisory panel
[NASA-TM-109692] p 3118 N94-27381
Nasa Langley Research Center seventy-fifth anniversary publications, 1992
[NASA-TM-109691] p 3118 N94-27431
Small business innovation research program solicitation
[NASA-TM-109695] p 3094 N94-27661
NASA SBIR abstracts of 1992, phase 1 projects
[NASA-TM-109694] p 3094 N94-27772
The 1993 NASA-ODU American Society for Engineering Education (ASEE) Summer Faculty Fellowship Program
[NASA-CR-191544] p 3085 N94-27893
Research and Development Annual Report, 1992
[NASA-TM-104777] p 3119 N94-27993
NASA: Major challenges for management. Testimony before the Legislation and National Security Subcommittee, Committee on Government Operations, House of Representatives
[GAO/T-NSIAD-94-18] p 3095 N94-28176

NASA SPACE PROGRAMS
JSC almanac
[NASA-TM-109702] p 3119 N94-28204

NATIONAL AEROSPACE PLANE PROGRAM
A numerical study of mixing and combustion in hypervelocity flows through a scramjet combustor model
p 2808 N94-27911

NATIONAL AIRSPACE SYSTEM
Rotorcraft low altitude IFR benefit/cost analysis: Conclusions and recommendations
[AD-A274241] p 2665 N94-26826
Optical communications for transport aircraft
p 2643 N94-27298
The 1993 Federal Aviation Administration plan for research, engineering and development
p 2643 N94-27960

NATURAL GAS
Natural gas applications for hybrid vehicles.
[PB94-117108] p 2759 N94-26753
Feasibility study on introduction of transportation-use petroleum substitution energy
[DE94-725205] p 2759 N94-26905
Sequential multi-point injection of a natural gas engine. Topical report, November 1991 - April 1992
[PB94-126794] p 2824 N94-27224
Laser probes of natural gas ignition chemistry
[PB94-128345] p 2717 N94-27226
Basic research on natural gas combustion phenomena
[PB94-129046] p 2717 N94-27256
Combined Cycles for Power Plants
[VKI-LS-1993-08] p 2830 N94-28077
Introduction to combined cycles p 2789 N94-28078

NATURAL LANGUAGE (COMPUTERS)
A strategy for dynamic interpretation: A fragment and an implementation
[CWI-CS-R9317] p 2970 N94-27545

NAVIER-STOKES EQUATION
Riemann solvers for solving the incompressible Navier-Stokes equations using the artificial compressibility method
[CRANFIELD-AERO-9208] p 2790 N94-25778
A numerical determination of bifurcation points for low Reynolds number conical flows
[AD-A273984] p 2791 N94-25991
Comments regarding two upwind methods for solving two-dimensional external flows using unstructured grids
[NASA-TM-109078] p 2644 N94-26154
Computational prediction of isolated performance of an axisymmetric nozzle at Mach number 0.90
[NASA-TM-4506] p 2646 N94-26547
The dynamics of interacting nonlinearities governing long wavelength driftwave turbulence
[DE94-001785] p 2793 N94-26558
Numerical studies on the dynamics of bubble, turbulent, free shear flows: Effect of the inter-phase coupling on the global flow evolution
[AD-A274521] p 2794 N94-26832

Numerical simulation of receptivity and transition in a boundary layer on a flat plate with a suction hole
[NASA-CR-195708] p 2798 N94-27782
New constitutive equation for the volume viscosity in fluids
[NASA-TM-109104] p 2798 N94-27867
Navier-Stokes simulation of two and three dimensional jets in crossflow, effects of grid, and boundary conditions p 2804 N94-28026
Theoretical and experimental investigation of a delta wing with turbulent leading-edge jets
p 2659 N94-28029
Recent developments in the simulation of steady and transient transverse jet interactions for missile, rotorcraft, and propulsive applications p 2804 N94-28030
Numerical assessment of aerodynamic interactions on missiles with transverse jets control
p 2659 N94-28031
Navier-Stokes analysis of a swirling jet in crossflow
p 2806 N94-28038
A parallel multigrid algorithm for solving the Navier-Stokes equations on a transputer system
[PREPRINT-699] p 2807 N94-28099
Euler and Navier-Stokes wing/fuselage computations of the De Havilland Dash 8 aircraft p 2654 N94-28329
A study of blunt trailing edge airfoils using the Navier Stokes code: ARC2D p 2656 N94-28340
Thin-layer Navier-Stokes computations for multi-element airfoils p 2656 N94-28341
Solution-adaptive simulation of transonic cascade flows p 2657 N94-28344
Multigrid solutions of the 2D Euler/Navier-Stokes equations on unstructured meshes
p 2658 N94-28349

NAVIGATION
Sensor-based navigation of a mobile robot using automatically constructed fuzzy rules
[DE94-001137] p 2986 N94-26948
Fault detection and isolation p 2642 N94-27289

NAVIGATION AIDS
A simulation of GPS and differential GPS sensors
p 2666 N94-27918

NAVIGATION INSTRUMENTS
Dead reckoning navigation
[VTT-TIED-1402] p 2664 N94-25808
A simulation of GPS and differential GPS sensors
p 2666 N94-27918

NAVIGATION SATELLITES
A GPS coverage model p 2642 N94-27292

NAVY
Report of the defense science board task force on aircraft assessment
[AD-A274531] p 2669 N94-26835
The NOGAPS ten year AMIP integration
[AD-A274332] p 2900 N94-26887

NEAR FIELDS
Nonlinear hysteresis in an endochronic solid
[AD-A274594] p 2880 N94-26855
Experiments into the scaling parameters required for exhaust gas ingestion testing of vertical landing aircraft
p 2671 N94-28017

NEAR INFRARED RADIATION
Multivariate calibration applied to near-infrared spectroscopy for the quantitative analysis of dilute aqueous solutions
[DE94-003231] p 2716 N94-26794
Development and evaluation of a near infrared reflecting and low visibility paint scheme for RAAF P-3C Orion aircraft
[AD-A274881] p 2669 N94-26864
Planetary Instrument Definition and Development Program (PIDDP). Instrument for future planetary flight missions: A visible-infrared imaging spectrometer for planetary missions
[NASA-CR-195254] p 3106 N94-27409
Evaluation of near-infrared spectrophotometric method for individual tolerance to +Gz acceleration
p 2933 N94-27944

NEAR WAKES
Flow past a circular cylinder with a permeable wake splitter plate
[AD-A273765] p 2790 N94-25872
The effects of three-dimensional imposed 3-d disturbances on bluff-body near wake flows
[AD-A274845] p 2791 N94-26187
Nominally 2-dimensional flow about a normal flat plate
[AD-A274472] p 2794 N94-27026
Research on bluff body vortex wakes
[AD-A273780] p 2796 N94-27319

NEBULAE
Investigations of the dynamical evolution of protoplanetary nebulae
[NASA-CR-195278] p 3105 N94-27428

NEGATIVE IONS
High gas-efficiency hydrogen negative ion sources
[PB93-232163] p 3025 N94-27348

NEODYMIUM
Hypersensitive transition spectrum of f-element and coordination structure
[DE94-604133] p 3070 N94-27843

NEODYMIUM LASERS
Elastic backscattering lidar for a MSTI satellite
[DE94-002701] p 2816 N94-26126
Development of surgical CW Nd:YAG laser with optical fiber delivery system
[DE93-632902] p 2817 N94-26185
Development of high average power industrial Nd:YAG laser with peak power of 10 kW class
[DE93-633201] p 2818 N94-26520
Beam-quality measurements for materials processing lasers and the proposed ISO standard
[DE94-002738] p 2819 N94-26811

NEON
Laser manipulation of metastable neon atoms
[ETN-94-95344] p 2817 N94-26225

NEON ISOTOPES
The Cherenkov hadronic like-jets
[DE93-634525] p 3016 N94-26010

NEOPLASMS
Molecular biological studies on the human radioresistance and drug resistance
[DE93-632682] p 2910 N94-26549

NEPHANALYSIS
Short-range cloud amount forecasting with model output statistics
[AD-A274769] p 2895 N94-26798

NEPTUNE (PLANET)
Analysis of energetic proton and electron data in Neptune's magnetosphere
[NASA-CR-195707] p 3107 N94-27784

NERVES
Disturbed neuronal migration in the cerebral cortex of mice by low-dose gamma radiation
p 2904 N94-27470
Abnormal development of serotonin nerve fibers in the cerebral cortex of young rats with methylazoxymethanol induced microcephaly p 2905 N94-27485
Inductive differentiation of nerve cells in mouse embryonic ectoderm at early primitive streak stage by retinoic acid p 2905 N94-27488

NERVOUS SYSTEM
Influence of mechanical stimulation on inflammatory edema p 2906 N94-27497
The effect of naloxone on sleeping time in adjuvant arthritic rats p 2906 N94-27498
Effects of capsaicin on freshly dissociated rat dorsal root ganglion cells p 2906 N94-27499
Size distribution of retrogradely labeled dorsal root ganglion cells: Test of normality p 2906 N94-27500
Interaction between endogenous opioid and Cholecystokinin (CCK) in modulating respiratory responses induced by thin-fiber muscular afferents
p 2906 N94-27502
Electrical coupling between the sino-atrial node and atrial muscle: Cell to cell interaction through an external circuit and its simulation by computer modeling
p 2907 N94-27509
Correlation between electrical activity and the size of single sinoatrial node cells p 2907 N94-27513
The ionic mechanism underlying the negative chronotropic effect of acetylcholine: Experimental study in rabbit single sinoatrial node cells
p 2908 N94-27514
The ionic mechanism underlying the negative chronotropic effect of acetylcholine: Experiments using small sinoatrial node tissue preparations isolated from rabbit hearts p 2908 N94-27515
The ionic mechanism underlying the negative chronotropic effect of acetylcholine: Postganglionic vagal stimulation in isolated rabbit hearts
p 2908 N94-27516
Hyperalgesia to cold in patients with Subacute Myelo-Optico-Neuropathy (SMON) p 2928 N94-27521

NETHERLANDS
Remote sensing and GIS for the management and investigation of the Wadden Sea
[BCRS-92-20] p 2847 N94-26228

NETWORK ANALYSIS
Development of a 4-bit parallel analog-to-digital converter and a four-quadrant double-balanced mixer using heterojunction bipolar transistor technology
[AD-A274074] p 2947 N94-25648
New mixed integer algorithm for classification and placement of measurements in process flow networks
[PB94-126752] p 2966 N94-26921
Integrated model development for liquid fueled rocket propulsion systems
[NASA-CR-195253] p 2702 N94-27166

NEURAL NETS
Color image segmentation
[AD-A274027] p 2984 N94-25759
A feasibility study on bird classification with neural network
[AD-A273753] p 2659 N94-25780
Neural networks for dynamic flight control
[AD-A274089] p 2676 N94-25785
Predicting nonlinear time series
[AD-A274051] p 2990 N94-25834
The AFIT multielectrode array for neural recording and simulation: Design, testing, and encapsulation
[AD-A274086] p 2909 N94-25943
Adaptive optimization and control using neural networks
[DE94-003941] p 2985 N94-25983
Zernike moments and rotation invariant object recognition. A neural network oriented case study
[AD-A273749] p 2767 N94-26011
Asymptotically stable neural networks for identification of nonlinear dynamic systems
[ISBN-0-315-84328-4] p 2985 N94-26629
Parallel computational geometry on analog Hopfield networks
[ISBN-0-315-84093-5] p 2980 N94-26635
Smart structures, an overview
[AD-A274147] p 2987 N94-27093
Translation and rotation invariant pattern recognition
[PB94-123676] p 2968 N94-27157
Motion analysis from a sequence of range images
[ISBN-0-315-84684-4] p 2969 N94-27311
Center for space microelectronics technology
[NASA-CR-195282] p 2786 N94-27574
On modeling and controlling intelligent systems
[DE94-002446] p 2988 N94-27706
Neural control of magnetic suspension systems
p 2682 N94-27905
An overview on development of neural network technology p 2990 N94-27913

NEUROBLASTS
Analysis of the Electrically Evoked Response (EER) of the cat p 2908 N94-27519

NEUROLOGY
Muscular activity and its relationship to biomechanics and human performance p 2934 N94-28362

NEUROMUSCULAR TRANSMISSION
Positive chronotropic effect of mechanical stretch on the sinoatrial node: Roles of neurotransmitters and stretch activated channels p 2904 N94-27469
Interaction between endogenous opioid and Cholecystokinin (CCK) in modulating respiratory responses induced by thin-fiber muscular afferents
p 2906 N94-27502
The value of electrical stimulation as an exercise training modality p 2936 N94-28372
The use of biomechanics in the study of movement in microgravity p 2936 N94-28373

NEURONS
Cortical mechanisms of attention, discrimination, and motor response to somesthetic stimuli
[AD-A274163] p 2940 N94-27141
Distribution of GABA immunoreactive neurons in the brain of rolling mouse Nagoya and gamma-irradiated mouse p 2904 N94-27471
Effects of gamma ray radiation on the developing mouse cerebellum: Apoptotic cell death and induction of tissue transglutaminase p 2904 N94-27472
Development of Purkinje cells in vitro
p 2905 N94-27483
Developmental expression of protein kinase C type 1 isozyme in suncus and rat cerebella
p 2905 N94-27484

NEUROPHYSIOLOGY
Top down influences on bottom-up processing
[AD-A274220] p 2939 N94-27072
Cortical mechanisms of attention, discrimination, and motor response to somesthetic stimuli
[AD-A274163] p 2940 N94-27141
Visit to CERMA: Centre d'Etudes et de Recherches de Medecine Aerospatiale, Centre for Studies and Research in Aviation and Space Medicine, Bretigny sur Orge, France, November 16-18, 1992
[PB94-132990] p 2937 N94-28392

NEUROTRANSMITTERS
Annals of the Research Inst. of Environmental Medicine, Nagoya Univ., volume 44
[REPT-44-VOL-44] p 2911 N94-27442
Distribution of GABA immunoreactive neurons in the brain of rolling mouse Nagoya and gamma-irradiated mouse p 2904 N94-27471
The ionic mechanism underlying the negative chronotropic effect of acetylcholine: Experimental study in rabbit single sinoatrial node cells
p 2908 N94-27514
The ionic mechanism underlying the negative chronotropic effect of acetylcholine: Experiments using small sinoatrial node tissue preparations isolated from rabbit hearts p 2908 N94-27515

The ionic mechanism underlying the negative chronotropic effect of acetylcholine: Postganglionic vagal stimulation in isolated rabbit hearts
p 2908 N94-27516

Postnatal changes in the autonomic modulation of L-type Ca(exp 2+) currents of rabbit ventricular cells
p 2931 N94-27535

Desensitization to acethylcholine in pacemaker cells of the sinoatrial node p 2908 N94-27537

The role of beta-adrenoceptor stimulation in the progression of chronic heart failure
p 2932 N94-27541

NEUTRAL ATMOSPHERES

Upper atmosphere neutral and plasma density modeling
[AD-A274768] p 2879 N94-26569

Modeling of the coupled magnetospheric and neutral wind dynamos
[NASA-CR-195273] p 2883 N94-27852

NEUTRAL BEAMS

Heavy neutral beam probe for edge plasma analysis in tokamaks
[DE94-003391] p 3041 N94-25846

New conditioning procedure derived from operating experience with the Common Long-Pulse Ion Source
[DE94-002891] p 3045 N94-26865

High gas-efficiency hydrogen negative ion sources
[PB93-232163] p 3025 N94-27348

Shine through measurements with hydrogen beam in JT-60
[DE94-701113] p 3047 N94-27699

Laser blow-off lithium beam probing with high temporal resolution for edge plasma diagnostics
[DE94-701176] p 2820 N94-27701

NEUTRAL CURRENTS

Flavor changing neutral currents in SU(3) x U(1) models
[DE94-602576] p 3022 N94-26899

First observation of neutral current proton electron scattering at the square root of s = 300 GeV
[DE94-701107] p 3030 N94-27877

NEUTRAL PARTICLES

Secondary particle in background levels and effects on detectors at future hadron colliders
[DE94-003378] p 3011 N94-25598

Two dimensional self-consistent fluid simulation of RF inductive sources
[DE94-003635] p 2767 N94-25937

NEUTRINOS

A research program in experimental and theoretical high energy physics
[DE94-002156] p 3031 N94-25931

Theoretical and experimental studies of elementary physics
[DE94-002310] p 3008 N94-25988

Separation and reconstruction of electron neutrino interaction in the IHEP-JINR neutrino detector and BARS detector
[DE93-634182] p 3019 N94-26393

Physical characteristics of polymethylmethacrylate scintillator SOFG-120
[DE93-634184] p 2810 N94-26395

About possible types of neutrino oscillations
[DE93-634449] p 3020 N94-26508

Constraints on singlet right-handed neutrinos coming from the Z(0)-width
[DE93-634393] p 3022 N94-26766

An analysis of monojet data in p(bar-p) collisions at square root of s equal to 1.8 TEV
[DE94-001822] p 3026 N94-27565

Cosmological constraints on very heavy stable neutrinos
[DE94-601669] p 3117 N94-28066

NEUTRON ABSORBERS

Experiment of neutron multiplication in beryllium
[DE94-604605] p 2742 N94-27730

NEUTRON ACTIVATION ANALYSIS

Study on neutron activation analysis
[DE93-632191] p 3017 N94-26116

NEUTRON BEAMS

On radiation defects in strip detectors
[DE93-616646] p 3015 N94-25916

Neutron reflection interferometry
[DE94-601876] p 2714 N94-26170

Neutron-neutron scattering: Possibility of in-beam experiment
[DE94-606459] p 3027 N94-27682

NEUTRON COUNTERS

Surface physics with cold and thermal neutron reflectometry
[DE94-001447] p 2733 N94-26070

Performance of a 14-MeV neutron generator as an in situ calibration source for TFTR
[DE94-004993] p 3048 N94-27825

NEUTRON DECAY

Radiations from hot nuclei p 3030 N94-27915

NEUTRON DIFFRACTION

Debye-Waller factors of the light actinide metals
[DE94-000685] p 2733 N94-26069

Neutrons in biology
[DE94-701085] p 2903 N94-27862

NEUTRON DISTRIBUTION

Experiment of neutron multiplication in beryllium
[DE94-604605] p 2742 N94-27730

NEUTRON EMISSION

Radiations from hot nuclei p 3030 N94-27915

NEUTRON FLUX DENSITY

Neutron-neutron scattering: Possibility of in-beam experiment
[DE94-606459] p 3027 N94-27682

NEUTRON IRRADIATION

Radiation hardening effects on localized deformation and stress corrosion cracking of stainless steels
[DE94-004308] p 2731 N94-25804

Temperature dependence of static RAM volatility
[DE93-040345] p 2948 N94-26111

Microstructural development in irradiated vanadium alloys
[DE94-004307] p 2737 N94-26556

Geological Dating by Ar-40 - Ar-39 method
[DE94-601975] p 2880 N94-26874

NEUTRON SCATTERING

Morphological analysis of ionomers
[DE94-003660] p 2749 N94-26005

Neutron reflection interferometry
[DE94-601876] p 2714 N94-26170

Neutrons in biology
[DE94-701085] p 2903 N94-27862

NEUTRON SOURCES

Toroidal plasma beta-FLR limit in a toroidally linked mirror system
[DE94-003119] p 3041 N94-25792

Surface physics with cold and thermal neutron reflectometry
[DE94-001447] p 2733 N94-26070

Atomic processes in Inertial Electrostatic Confinement (IEC) devices
[DE94-005015] p 3047 N94-27715

Performance of a 14-MeV neutron generator as an in situ calibration source for TFTR
[DE94-004993] p 3048 N94-27825

NEUTRON STARS

Dibaryon-induced instability of neutron stars
[DE93-634453] p 3103 N94-26046

TEV emission from close binaries
[DE93-634330] p 3104 N94-26268

Magnetic field induced contributions of supersymmetric particles to energy losses of neutron star
[DE93-634331] p 3104 N94-26269

Gamma ray bursts from the accretion of solid bodies onto high-velocity Galactic neutron stars
[DE94-005006] p 3117 N94-27827

NEUTRONS

Data on parity violation in the compound nucleus and its interpretation
[DE94-003965] p 3013 N94-25820

Index to BROND-2, CENDL-2, ENDF/B-6, JEF-2, JENDL-3
[DE93-634500] p 3016 N94-26034

Fusion Energy Advisory Committee: Advice and recommendations to the US Department of Energy in response to the charge letter of September 1, 1992
[DE93-019842] p 3043 N94-26428

A concurrent, multigroup, discrete ordinates model of neutron transport
[DE94-004334] p 3020 N94-26577

Pre-orbital criticality safety for the NEPSTP mission
[DE94-002600] p 3005 N94-26802

Monte Carlo calculations of low background detector response
[DE94-004593] p 3116 N94-27621

Neutron-neutron scattering: Possibility of in-beam experiment
[DE94-606459] p 3027 N94-27682

Atomic processes in Inertial Electrostatic Confinement (IEC) devices
[DE94-005015] p 3047 N94-27715

Experiment of neutron multiplication in beryllium
[DE94-604605] p 2742 N94-27730

Neutrons in biology
[DE94-701085] p 2903 N94-27862

Radiations from hot nuclei p 3030 N94-27915

NEWS MEDIA

Emerging computer technologies and the news media of the future p 2688 N94-27372

NEWTON METHODS

Correlation between the gravity field and the bathymetry in the North Atlantic Ocean
[ETN-94-95036] p 2899 N94-26108

NEWTON-RAPHSON METHOD

Calculation of a 3-D pose of a known object in a single perspective view
[VTT-PUBS-122] p 2957 N94-25642

NEWTONIAN FLUIDS

Calculation methods for steadily loaded central circumferential groove hydrodynamic journal bearings (guide to use of computer program A9304)
[ESDU-93004] p 2830 N94-28073

Calculation methods for steadily loaded axial groove hydrodynamic journal bearings. Low viscosity process fluid lubrication (guide to use of computer program A9306)
[ESDU-93006] p 2830 N94-28075

NICKEL

Binding of copper and nickel to cavities in silicon formed by helium ion implantation
[DE94-003769] p 3050 N94-25814

Molten salt techniques for reproducible excess heat
[AD-A274935] p 2714 N94-26296

Suppression of thermal grain growth in nickel by prior electron irradiation
[DE94-004602] p 2737 N94-26587

Detection of low-intensity magnetic fields with a magnetostrictive fiber optic sensor
[AD-A274120] p 3037 N94-27062

Development of nickel-metal hydride cell: An update
p 2864 N94-28130

Ni-MH storage test and cycle life test
p 2864 N94-28131

Determination of thermal properties of commercial Ni-MH cells p 2864 N94-28132

NICKEL ALLOYS

Hydrogen trapping with Pd coated alloy films
p 2723 N94-25551

Study on alloy films for hydrogen separation
p 2726 N94-25565

Study on film generation phenomena by particle deposition p 2728 N94-25575

The role of grain boundary chemistry and structure in the environmentally-assisted intergranular cracking of nickel-base alloys
[DE94-003159] p 2732 N94-25954

Influence of helium generation rate and temperature history on mechanical properties of model Fe-Cr-Ni alloys irradiated in FFTF at relatively low displacement rates
[DE94-004264] p 2737 N94-26575

Deformation twinning: Influence of strain rate
[DE94-002693] p 2738 N94-26621

Stability of reference masses 2: The effect of environment and cleaning methods on the surfaces of stainless steel and allied materials
[NPL-DMM(A)-95] p 2738 N94-26653

Experimental measurement of local displacement and chemical pair correlations in crystalline solid solutions
[DE94-001124] p 3065 N94-27251

Current status of research and development on nickel and iron aluminides
[DE94-004247] p 2741 N94-27616

A transmission electron microscope study of Ni4W precipitates in a Ni-37 wt. percent W alloy
[ISBN-0-315-59932-4] p 2743 N94-27803

Effect of different ions on the anodic behaviour of alloy 800 in chloride solutions at high temperature
[DE94-602982] p 2743 N94-27832

Differential scanning calorimetric study of solid state amorphization and crystallization in Zr/Co and Zr/Ni multilayers p 2745 N94-28161

The electrocatalytic oxidation of ethylene and methane, and reduction of oxygen on gas-diffusion electrodes made of amorphous nickel-valve metal-platinum group metal alloys p 2722 N94-28165

CO2 methanation catalysts prepared from amorphous Ni-valve metal alloys containing platinum group elements
p 2745 N94-28166

Mechanical behavior of amorphous alloys at elevated temperatures p 2746 N94-28167

Formation of glassy Pd-Ni-P alloys by mechanical alloying and their structure and thermal stability
p 2746 N94-28168

NICKEL CADMIUM BATTERIES

Characteristics and development report for the T1576 power supply and the MC3935 battery
[DE94-003675] p 2783 N94-26372

Handbook for handling and storage of nickel-cadmium batteries: Lessons learned
[NASA-RP-1326] p 2702 N94-26613

The 1993 NASA Aerospace Battery Workshop
[NASA-CP-3254] p 2860 N94-28100

Summary of NASA Aerospace Flight Battery Systems Program activities p 2860 N94-28101

Advanced energy storage for space applications: A follow-up p 2860 N94-28103

Experimental evaluation of battery cells for space-based radar application p 2860 N94-28104

Screen test for cadmium and nickel plates
p 2860 N94-28106

Analysis for nickel (3 and 4) in positive plates from nickel-cadmium cells p 2861 N94-28107

Calculation of the thermoneutral potential of NiCd and NiH2 cells p 2861 N94-28111

Orbital management and design considerations for NiCd satellite power systems p 2862 N94-28118

TOPEX/Poseidon battery performance during the first year of operation p 2862 N94-28119

Nickel cadmium battery operations on-orbit: Trials, tribulations, and success on the Upper Atmosphere Research Satellite p 2862 N94-28120

Performance test results of ETS-6 Ni-Cd cells p 2863 N94-28121

AF Ni-Cd cell qualification program p 2863 N94-28122

Discriminating performance parameters for 50 amp-hour and 60 amp-hour nickel-cadmium plates and battery cells p 2863 N94-28123

Some observations on battery charge control p 2863 N94-28125

Construction of temperature compensated constant voltage (VT) curves for super Ni-Cd (tm) cells p 2863 N94-28126

NICKEL COMPOUNDS

Successive structural phase transitions in stoichiometric La2NiO4 observed by x ray diffraction [REPT-A-2665] p 3051 N94-25921

Technical report of ISSP. Ser. A, no. 2673: Two successive spin glass transitions in non-diluted Heisenberg-like spin glass Ni(0.42)Mn(0.58) TiO3 [JTN-94-80559] p 2756 N94-27241

NICKEL HYDROGEN BATTERIES

The 1993 NASA Aerospace Battery Workshop [NASA-CP-3254] p 2860 N94-28100

Summary of NASA Aerospace Flight Battery Systems Program activities p 2860 N94-28101

Advanced energy storage for space applications: A follow-up p 2860 N94-28103

Experimental evaluation of battery cells for space-based radar application p 2860 N94-28104

Space Station Freedom NiH2 cell testing program p 2861 N94-28108

Ni-H2 cell characterization for INTELSAT programs p 2861 N94-28109

SAFT nickel hydrogen cell cycling status p 2861 N94-28110

Calculation of the thermoneutral potential of NiCd and NiH2 cells p 2861 N94-28111

Performance model of a recirculating stack nickel hydrogen cell p 2861 N94-28112

Thermal modeling of NiH2 batteries p 2862 N94-28113

Nickel-hydrogen cell reversal characteristics p 2862 N94-28114

Cycle life versus depth of discharge update on modeling studies --- Nickel-Hydrogen Batteries p 2862 N94-28115

Air Force standards for nickel hydrogen battery p 2862 N94-28116

Charge efficiency of Ni/H2 cells during transfer orbit of Telstar 4 satellites p 2862 N94-28117

Discriminating performance parameters for 50 amp-hour and 60 amp-hour nickel-cadmium plates and battery cells p 2863 N94-28123

A pressure based charge control system for the DSPSE NiH2 CPV battery p 2863 N94-28127

Advanced nickel-hydrogen spacecraft battery development p 2863 N94-28129

NICKEL OXIDES

Atomic-scale chemistry of metal surfaces [REPT-A-2657] p 3012 N94-25636

NICKEL PLATE

Screen test for cadmium and nickel plates p 2860 N94-28106

Analysis for nickel (3 and 4) in positive plates from nickel-cadmium cells p 2861 N94-28107

NICKEL ZINC BATTERIES

Exploratory Technology Research Program for Electrochemical Energy Storage [DE94-003479] p 2781 N94-26047

NIGHTGLOW

Upper atmosphere neutral and plasma density modeling [AD-A274768] p 2879 N94-26569

NIMBUS 7 SATELLITE

Nimbus-7 Earth radiation budget calibration history. Part 2: The Earth flux channels [NASA-RP-1335-PT-2] p 2814 N94-27981

NIOBIUM

Experimental results of 40-kA Nb3Al conductor [DE94-701207] p 2788 N94-27821

NIOBIUM ALLOYS

Fracture behavior of 20% Nb particulate reinforced alumina composite [DE94-002830] p 2706 N94-26019

The influence of energy losses with time in NbTi superconductors in pulsed magnetic fields [DE93-634761] p 3058 N94-26512

A tri-junction diffusion couple analysis of the Nb-Cr-Ti system at 950 C [DE94-002637] p 2737 N94-26607

Evaluation of APC NbTi superconductor in a model dipole magnet [DE94-003258] p 3060 N94-26795

The effect of Ti conduit on the critical current in (Nb, Ti)3Sn cable-in-conduit conductors [DE94-701204] p 2788 N94-27817

The corrosion behavior of sputter-deposited magnesium-valve metal alloys p 2745 N94-28164

CO2 methanation catalysts prepared from amorphous Ni-valve metal alloys containing platinum group elements p 2745 N94-28166

NIOBIUM CARBIDES

The influence of weld metal alloying additions to extend the heat input range for the submerged arc welding of high strength steels [AD-A274284] p 2738 N94-26679

NIOBIUM COMPOUNDS

Study on measurement and evaluation methods for superconductive characteristics p 2725 N94-25560

NITRATES

Bulletin of the Institute for Chemical Reaction Science, Tohoku University, volume 2 [JTN-94-80602] p 2717 N94-27385

Reactivity of nitrate radical (NO3) toward organic compounds p 2704 N94-27387

NITRIC OXIDE

UV absorption technique for monitoring mobile source NO emissions [AD-A273858] p 2713 N94-25964

NITRIDING

Combustion synthesis method p 2721 N94-25561

Study on microscopic structural controls and electronic properties at material surfaces by ion beams p 2727 N94-25571

Effect of nitrocarburizing on shape of titanium alloy parts [DE94-004040] p 2732 N94-25822

NITRO COMPOUNDS

Computational studies of energetic organic molecules [AD-A274726] p 3018 N94-26172

NITROGEN

Combustion synthesis method p 2721 N94-25561

The importance of vibrationally excited nitrogen in silicon nitride deposition systems [AD-A274874] p 2750 N94-26167

NITROGEN COMPOUNDS

Phase diagram of La2NiO(4 + delta) (0 less than or equal to delta less than or equal to 0.18). 1: Phases at room temperature and phase transition above delta equal to 0.15 [REPT-A-2661] p 3053 N94-26089

NITROGEN IONS

Study on microscopic structural controls and electronic properties at material surfaces by ion beams p 2727 N94-25571

Energy parameters of the incident auroral electrons derived by the intensity ratio of auroral emissions p 2779 N94-27964

NITROGEN OXIDES

Development of SO(x) and NO(x) solid electrolyte sensors p 2725 N94-25562

Technical Report of National Research Institute of Fisheries Engineering: Fishing Boat and Instrument, No. 12 [JTN-94-80595] p 2764 N94-27976

The emission characteristics of a high speed diesel engine p 2764 N94-27980

Emissions of nitrogen oxides (NO(x) and N2O) in pressurized fluidized bed combustion [PB94-133071] p 2876 N94-28395

NITROGEN TETROXIDE

Freon recovery from nitrogen tetroxide and freon solutions [PL-TR-92-3051] p 2721 N94-28215

NITROUS OXIDES

Implications of policies and prevent climate change for future food security [DE93-018872] p 2866 N94-25948

NOAA SATELLITES

Leadex environmental phenomena and effects observed by DMSP, NOAA, and ERS-1 satellites [AD-A274596] p 2868 N94-26888

NOISE (SOUND)

Bulletin of Precision and Intelligence Laboratory, No. 68 [JTN-94-80609] p 3010 N94-27282

NOISE INTENSITY

VHF-UHF noise surveys at Gulkana, Elmensdorf AFB, Galena AFB, Kotzebue and Cape Lisburne, Alaska and NRL, Pomonkey, Maryland [PL-TR-93-2136] p 2777 N94-28211

NOISE MEASUREMENT

On the application of Allan variance method for Ring Laser Gyro performance characterization [DE94-003880] p 2810 N94-26525

NOISE POLLUTION

Silence amenity engineering: Past and present p 3011 N94-27283

Cooling towers for combined cycles: New developments to meet environmental requirements p 2832 N94-28088

The single European market: Economical advance, ecological problem? p 2661 N94-28235

NOISE PREDICTION

Silence amenity engineering: Past and present p 3011 N94-27283

A modelling of the noise from simple coaxial jets. Part 3: With hot primary flow [ISVR-TR-230-PT-3] p 2807 N94-28173

NOISE PREDICTION (AIRCRAFT)

INM, Integrated Noise Model. Version 4.11: User's guide, supplement [AD-A273885] p 3009 N94-25731

Assessing the effects of Tuned Vibration Absorbers (TVAs) on interior cabin noise levels: A correlation between analytical acoustic predictions and flight test measurements p 2652 N94-28318

NOISE REDUCTION

Evaluation of an Acoustic Charge Transport (ACT) device for adaptive interference suppression in spread spectrum communications systems [AD-A274073] p 2765 N94-25647

High temperature sensor/microphone development for active noise control [NASA-CR-195214] p 2812 N94-27214

Optimising BMW four-cylinder two-valve engines [PB94-125101] p 2824 N94-27254

Silence amenity engineering: Past and present p 3011 N94-27283

Non-adaptive robust filters for speckle noise reduction [INPE-5519-PRE/1794] p 2776 N94-27335

On the use of feedback to control sound radiation from a plate excited by a turbulent boundary layer [ISVR-TR-227] p 2807 N94-28175

Assessing the effects of Tuned Vibration Absorbers (TVAs) on interior cabin noise levels: A correlation between analytical acoustic predictions and flight test measurements p 2652 N94-28318

NOISE SPECTRA

An analysis of FM jamming and noise quality measures [AD-A274349] p 2772 N94-26924

Laser phase induced intensity noise in fiber-optic signal processing and sensing systems [ITN-94-85234] p 2819 N94-27179

Geometrical resonances in the nyquist noise spectrum for ballistic conductors [DE94-603668] p 3027 N94-27631

NOMOGRAPHS

Experimental determination of the CU-IN-PB ternary phase diagram [DE94-003765] p 2735 N94-26349

NONDESTRUCTIVE TESTS

General Motors Corporation and Pacific Northwest Laboratory staff exchange: Inspection of case hardened steels and metal-matrix composites [DE94-003470] p 2706 N94-25982

Non-contact ultrasonic inspection [VTT-TIED-1454] p 2835 N94-26257

Design and life-time of polymer matrix composite structures: Summary [VTT-TIED-1415] p 2707 N94-26260

Development of non-destructive testing technology for the crack of steam generator tubes [DE93-632953] p 2835 N94-26399

Reconstruction of multiple cracks from experimental electrostatic boundary measurements [NASA-CR-191584] p 2994 N94-26601

A comparison of Probability Of Detection (POD) data determined using different statistical methods [LTR-ST-1947] p 2835 N94-26644

Optical surface contouring for non-destructive inspection of turbomachinery [NASA-CR-195245] p 2835 N94-26691

Calculation of the electromagnetic critical state response of high T(sub c) superconductor tape [DE94-002894] p 3061 N94-26868

Space Shuttle main engine turbopump bearing assessment program [NASA-TM-108447] p 2833 N94-28265

NONEQUILIBRIUM CONDITIONS
Nonequilibrium radiation and chemistry models for aerocapture vehicle flowfields
[NASA-CR-195706] p 2648 N94-28071
NONEQUILIBRIUM FLOW
Chemical and vibrational nonequilibrium viscous flows: Modelling, internal and external flow applications
[ESA-TT-1274] p 2791 N94-26316
Approximate Riemann solvers: Improvement of the HLLEM scheme and its generalization for chemically reacting flows
[NAL-TR-1189] p 2795 N94-27205
TVD flux-difference split methods for high-speed thermochemical nonequilibrium flows with strong shocks
[UTIAS-350] p 2799 N94-27880
NONEQUILIBRIUM IONIZATION
Modelling of ionisation reactions and of the resulting electric fields in one-dimensional hypersonic shock waves with the direct simulation Monte Carlo method
[IC-AERO-92-01] p 2644 N94-26248
NONEQUILIBRIUM RADIATION
Nonequilibrium radiation and chemistry models for aerocapture vehicle flowfields
[NASA-CR-195706] p 2648 N94-28071
NONFLAMMABLE MATERIALS
Impact of improved materials and cabin water spray on commuter aircraft postcrash fire survivability
[AD-A274421] p 2660 N94-27081
NONLINEAR EQUATIONS
Selfsimilar solutions of a nonlinear transport equation
[REPT-93-42] p 2865 N94-25760
Predicting nonlinear time series
[AD-A274051] p 2990 N94-25834
Continuation and multi-grid for bifurcation problems
[AD-A274965] p 2992 N94-26302
A parametric sensitivity study for single-stage-to-orbit hypersonic vehicles using trajectory optimization
[NASA-CR-195703] p 2697 N94-27789
Nonlinear solvers p 2829 N94-28053
NONLINEAR FILTERS
White noise theory of robust nonlinear filtering with correlated state and observation noises
[PB94-126661] p 3004 N94-27211
NONLINEAR OPTICS
Extension of On-Surface Radiation Condition (OSRC) theory to full-vector electromagnetic wave scattering by three-dimensional conducting, dielectric, and coated targets
[AD-A274023] p 2766 N94-25757
Studies of non-linear optical effects for agile beam steering
[AD-A273998] p 3034 N94-25902
Microtubules for nonlinear optical limiting
[AD-A273940] p 3035 N94-25941
Three-wave nonlinear interactions in KTiOPO4 (KTP) and KTP isomorphs
[AD-A274079] p 3052 N94-25993
Instantaneous amplitude and frequency dynamics of coherent wave mixing in semiconductor quantum wells
[DE94-003262] p 3054 N94-26128
Peculiarities and application perspectives of metal-ion implants in glasses
[DE94-004671] p 3035 N94-26246
An x ray absorption fine structure study of ordering in polythiophene thin films
[AD-A274235] p 2753 N94-26822
Research and development within nonlinear optics for protection of optical sensors against laser irradiation on of optical sensors against laser irradiation. Quarterannual report 1 (april 1993))
[PB94-124245] p 3037 N94-27046
Polyimide/inorganic composite-interpenetrating polymer network for stable second-order nonlinear optics
[AD-A274646] p 2709 N94-27107
Accordion-like polymers for nonlinear applications
[AD-D016031] p 2755 N94-27148
Predoctoral training grant in the area of physical sciences
[DE94-004406] p 3039 N94-27603
Optical pattern recognition system utilizing resonator array
[AD-D016071] p 3040 N94-28224
NONLINEAR PROGRAMMING
Unifying investigation of interior-point methods for convex programming
[PB94-126463] p 2967 N94-27031
NONLINEAR SYSTEMS
Characterization of nonlinear effects in optically pumped vertical cavity surface emitting lasers
[AD-A273840] p 2815 N94-25744
Evaluation of moderate angle of attack roll of a dual engine, thrust vectoring aircraft using quantitative feedback theory
[AD-A274118] p 2667 N94-25905
Determination of the geomagnetic external contribution by nonlinear optimization methods
[DE94-600882] p 2878 N94-26365
On the phi(sub 0)-stability of perturbed nonlinear differential systems
[DE93-634304] p 2993 N94-26441
Asymptotically stable neural networks for identification of nonlinear dynamic systems
[ISBN-0-315-84328-4] p 2985 N94-26629
Computation of stress intensity factors by the mode enrichment technique with applications to geometrically nonlinear problems
[PB94-126513] p 2840 N94-26910
Some aspects of nonlinear discrete-time descriptor systems in economics
[PB94-126653] p 3101 N94-26918
Parallel mathematical software
[DE94-001587] p 2967 N94-27020
Development of K(1-x)Na(x)TiOPO4 crystals for nonlinear applications
[AD-A274336] p 3063 N94-27055
Control oriented system identification
[AD-A274162] p 2987 N94-27124
Center for nonlinear phenomena and magnetic materials
[AD-A274176] p 3009 N94-27126
Operator theoretic methods in the control of distributed and nonlinear systems
[AD-A274160] p 2988 N94-27139
The onset of chaos in a periodically forced nonlinear oscillator
[ISBN-0-315-84564-3] p 2842 N94-27272
The deterministic power-spectral-density method
[AD-B175894] p 2678 N94-27395
Control system for tracking nonlinear systems
[AD-D016057] p 2787 N94-27673
Super finite elements for nonlinear static and dynamic analysis of stiffened plate structures
[ISBN-0-315-63903-2] p 2844 N94-27808
Neural control of magnetic suspension systems
p 2682 N94-27905
The deterministic power-spectral-density-method for nonlinear systems
[AD-B179687] p 3001 N94-28353
NONLINEARITY
A comparison of three approximate mathematical models for the gravity gradient stabilized satellite
[AD-A273832] p 2694 N94-25615
Microtubules for nonlinear optical limiting
[AD-A273940] p 3035 N94-25941
Three-wave nonlinear interactions in KTiOPO4 (KTP) and KTP isomorphs
[AD-A274079] p 3052 N94-25993
Nonlinear ocean waves
[AD-A274651] p 2899 N94-26354
Determination of the geomagnetic external contribution by nonlinear optimization methods
[DE94-600882] p 2878 N94-26365
Nonlinear dynamics and pattern selection at the crystal-melt interface
[DE94-003112] p 3060 N94-26780
Nonlinear hysteresis in an endochronic solid
[AD-A274594] p 2880 N94-26855
Center for nonlinear phenomena and magnetic materials
[AD-A274176] p 3009 N94-27126
Optimal nonlinear estimation for aircraft flight control in wind shear p 2643 N94-27296
Transmittance fluctuations and non-linearity in random chains in the presence of applied electric fields
[DE94-603665] p 2787 N94-27628
Optical parametric oscillator modeling with diffraction, depletion, and double refraction
[DE94-001504] p 3040 N94-27999
NONPARAMETRIC STATISTICS
Introduction to bayesian nonparametric theory
[PB94-125002] p 3004 N94-26939
NONUNIFORM MAGNETIC FIELDS
Using ferro-magnetic fluids to lubricate non-conformal isothermal contacts
[INPE-5520-TAE/021] p 2827 N94-27665
NONUNIFORMITY
Radial basis function approximation: From gridded centers to scattered centers
[AD-A274184] p 2998 N94-27103
NOREPINEPHRINE
The role of beta-adrenoceptor stimulation in the progression of chronic heart failure
p 2932 N94-27541
NORMAL DENSITY FUNCTIONS
Simulating high-frequency wind for long durations
[DE94-002739] p 2682 N94-27997
NORMAL SHOCK WAVES
Modelling of ionisation reactions and of the resulting electric fields in one-dimensional hypersonic shock waves with the direct simulation Monte Carlo method
[IC-AERO-92-01] p 2644 N94-26248
NORMALITY
Size distribution of retrogradely labeled dorsal root ganglion cells: Test of normality p 2906 N94-27500
NORTH AMERICA
Propagation of cold air masses in East Asia and its associated planetary-scale function
[AD-A274304] p 2895 N94-26850
NORTH SEA
Macrobenthic fauna in the dutch sector of the north sea in 1991
[PB94-126414] p 2868 N94-27200
NORTHERN SKY
Sloan Digital Sky Survey
[DE94-004662] p 3103 N94-27750
NORWAY
Norwegian ionospheric satellite experiment: High latitude, low Earth orbit plasma measurements
[FFI-93/7025] p 2876 N94-25807
NOSES (FOREBODIES)
Controlled oscillation of forebody vortices by nozzle jet blowing
[ISBN-0-315-84134-6] p 2678 N94-27648
Pneumatic management of blunted-forebody flow asymmetry for high-angle-of-attack directional control
p 2679 N94-28028
NOTCH SENSITIVITY
Investigation of compressive behavior for metal matrix composites with a circular hole
[AD-A273835] p 2705 N94-25739
NOTCH STRENGTH
Structure and properties of intermetallic composites synthesized in situ using solid state displacement reactions
[DE94-004312] p 2705 N94-25805
NOTCH TESTS
Structure and properties of intermetallic composites synthesized in situ using solid state displacement reactions
[DE94-004312] p 2705 N94-25805
NOTCHES
Effects of crenulations on three dimensional losses in a linear compressor cascade
[AD-A273778] p 2790 N94-25862
NOZZLE DESIGN
Controlled oscillation of forebody vortices by nozzle jet blowing
[ISBN-0-315-84134-6] p 2678 N94-27648
The interaction region associated with twin jets and a normal crossflow p 2800 N94-28009
NOZZLE FLOW
Chemical and vibrational nonequilibrium viscous flows: Modelling, internal and external flow applications
[ESA-TT-1274] p 2791 N94-26316
Numerical investigation of thrust vectoring by injection of secondary air into nozzle flows p 2801 N94-28013
Experiments on interaction force of jets in hypervelocity cross-flow in a shock tunnel p 2659 N94-28022
A study of jet effect and ground effect interference on a STOL fighter p 2671 N94-28034
NOZZLE GEOMETRY
Computational prediction of isolated performance of an axisymmetric nozzle at Mach number 0.90
[NASA-TM-4506] p 2646 N94-26547
NOZZLES
Gas-turbine engine steady-state behavior
p 2828 N94-28044
NUCLEAR BINDING ENERGY
Binding of copper and nickel to cavities in silicon formed by helium ion implantation
[DE94-003769] p 3050 N94-25814
Three methods to measure RH bond energies
[DE94-003795] p 3013 N94-25816
The structural, chemical, and electrical properties of He-implantation-induced nanocavities in silicon
[DE94-002681] p 3052 N94-25971
NUCLEAR CHEMISTRY
Radiochemistry Division annual progress report : 1991
[DE94-600652] p 2715 N94-26392
TRIUMF scientific activities
[CTN-94-61062] p 3117 N94-26656
NUCLEAR ELECTRIC POWER GENERATION
Mars transportation system p 2833 N94-25689
The First Energy Conference: Israel and the Former USSR
[ISBN-965-229-098-X] p 2853 N94-26050
Present situation of the development of petroleum substitution energy (France)
[DE94-725201] p 2760 N94-26914
International bulletin on atomic and molecular data for fusion. No. 42-45, Mar. 1991 - Dec. 1992
[DE94-601817] p 3045 N94-26946

International bulletin on atomic and molecular data for fusion. No. 46 [DE94-601818] p 3023 N94-26947

NUCLEAR ELECTRIC PROPULSION

Characteristics and control response of the TOPAZ 2 reactor system real-time dynamic simulator [DE94-003788] p 2699 N94-25600

Risk perspectives for Topaz 2 flight mission [DE94-003229] p 2700 N94-25956

Nuclear electric propulsion for future NASA space science missions [DE93-019086] p 2700 N94-25969

NUCLEAR EXPLOSIONS

Research in pulsed power plasma physics [AD-A274323] p 3045 N94-27074

NUCLEAR FUEL ELEMENTS

Space-R thermionic space nuclear power system design and technology demonstration [DE94-002017] p 2700 N94-25930

NUCLEAR FUELS

Grain by grain study of the mechanisms of crack propagation during iodine SCC of Zry-4 [DE93-633765] p 2734 N94-26162

Nonswelling behavior of HT9 alloy irradiated to high exposure [DE94-003502] p 2736 N94-26522

Application of railgun principle to high-velocity hydrogen pellet injection for magnetic fusion reactor fueling [DE94-004411] p 3044 N94-26579

List of papers published by the members of Institute for Materials Research, Tohoku University 1992 [JTN-94-80608] p 3118 N94-27355

Fuel ion rotation measurement and its implications on H-mode theories [DE94-004860] p 3048 N94-27791

NUCLEAR FUSION

Fusion Energy Advisory Committee: Advice and recommendations to the US Department of Energy in response to the charge letter of September 1, 1992 [DE93-019842] p 3043 N94-26428

Researches of the Electrotechnical Laboratory. No. 51: Study of formation and sustainment of reversed field pinch by slow control of magnetic field [JTN-94-80548] p 3046 N94-27350

NUCLEAR INTERACTIONS

Energy concentration in high energy hadron-gamma families p 3113 N94-25632

A search for the production of direct leptons in nucleon-nucleus and nucleus-nucleus collisions [DE94-004640] p 3018 N94-26244

Stopping powers and cross sections due to two-photon processes in relativistic nucleus-nucleus collisions [NASA-CR-4574] p 3033 N94-27646

NUCLEAR MAGNETIC RESONANCE

Microscopic study of local structure and charge distribution in metallic La2CuO(4+delta) [DE94-003801] p 3050 N94-25817

Morphological analysis of ionomers [DE94-003660] p 2749 N94-26005

Use of oxygen-17 isotope in the characterization of zeolites and related structures by nuclear magnetic resonance spectroscopy [VTT-TIED-1448] p 2714 N94-26251

Technical report of ISSP. Ser. A, no. 2681: Orbital and spin susceptibilities of the plane copper sites in YBa2Cu3O(x) system [JTN-94-80567] p 3064 N94-27177

Technical report of ISSP. Ser. A, no. 2683: Itinerant character of 5f electrons in UNi2Ga [JTN-94-80569] p 3025 N94-27337

NMR study of quasicrystal Al(70)Pd(20)T(M10) alloy (T(M):Cr, Mn, Fe, and Co) p 2745 N94-28162

NUCLEAR MEDICINE

TRIUMF scientific activities [CTN-94-61062] p 3117 N94-26656

NUCLEAR MODELS

Hadron jets and nucleon clusters in the relativistic nuclear collisions [DE93-613434] p 3031 N94-25850

Nucleon-nucleon scattering lengths in QCD sum rules [DE93-520239] p 3015 N94-25922

NUCLEAR PHYSICS

Theoretical and computational studies in intermediate energy nuclear physics [DE94-004177] p 3012 N94-25800

Pion-nucleus interactions and the STAR experiment at RHIC [DE94-000658] p 3021 N94-26586

TRIUMF scientific activities [CTN-94-61062] p 3117 N94-26656

Nuclear Theory Group, University of Washington recent and planned research [DE94-002729] p 3022 N94-26809

Quantum chromodynamics and nuclear physics at extreme energy density [DE94-004418] p 3026 N94-27604

Electroweak and other interactions in medium-energy nuclear physics [DE94-004161] p 3027 N94-27689

Future directions in particle and nuclear physics at multi-GeV hadron beam facilities [DE94-002946] p 3027 N94-27711

Proceedings of the workshop on (pi), K, (eta)-nucleon interactions [DE94-701314] p 3027 N94-27733

NUCLEAR POWER PLANTS

Fire simulation based on convection calculation [VTT-TIED-1411] p 2762 N94-26259

Development of an automated fracture assessment system for nuclear structures (appendix 1/1) p 2841 N94-27187

NUCLEAR POWER REACTORS

Small low mass advanced PBR's for bi-modal operation [DE94-003201] p 2699 N94-25798

NUCLEAR PROPULSION

A review of carbide fuel corrosion for nuclear thermal propulsion applications [DE94-003938] p 2699 N94-25613

Mars transportation system p 2833 N94-25689

Small low mass advanced PBR's for bi-modal operation [DE94-003201] p 2699 N94-25798

An assessment of testing requirement impacts on nuclear thermal propulsion ground test facility design [DE94-002933] p 2702 N94-26560

NUCLEAR QUADRUPOLE RESONANCE

Microscopic study of local structure and charge distribution in metallic La2CuO(4+delta) [DE94-003801] p 3050 N94-25817

Technical report of ISSP. Ser. A, no. 2683: Itinerant character of 5f electrons in UNi2Ga [JTN-94-80569] p 3025 N94-27337

NUCLEAR REACTIONS

Data on parity violation in the compound nucleus and its interpretation [DE94-003965] p 3013 N94-25820

Hadron jets and nucleon clusters in the relativistic nuclear collisions [DE93-613434] p 3031 N94-25850

Index to BROND-2, CENDL-2, ENDF/B-6, JEF-2, JENDL-3 [DE93-634500] p 3016 N94-26034

Radiochemistry Division annual progress report : 1991 [DE94-600652] p 2715 N94-26392

Measurements of the p (mu)d-molecule formation rate at different hydrogen temperature [DE93-634636] p 3020 N94-26511

NUCLEAR REACTORS

A review of carbide fuel corrosion for nuclear thermal propulsion applications [DE94-003938] p 2699 N94-25613

HDR reactor containment fire modeling with BRI2 [VTT-PUBS-113] p 3031 N94-25621

Overall analysis of meteorological information in the Daeduk nuclear complex [DE93-632594] p 2894 N94-26469

Mesoscale meteorological measurements characterizing complex flows [DE94-002359] p 2895 N94-26761

Neutron-neutron scattering: Possibility of in-beam experiment [DE94-606459] p 3027 N94-27682

NUCLEAR ROCKET ENGINES

Project WISH: The Emerald City p 2703 N94-25690

NUCLEAR SCATTERING

A dependence of exclusive vector meson production in muon-nucleus scattering [DE94-003363] p 3016 N94-25957

Jet production in muon scattering at Fermilab E665 [DE94-004663] p 3028 N94-27752

NUCLEAR STRUCTURE

Nucleon-nucleon scattering lengths in QCD sum rules [DE93-520239] p 3015 N94-25922

Nuclear Theory Group, University of Washington recent and planned research [DE94-002729] p 3022 N94-26809

NUCLEAR WARHEADS

Propellants and explosives in ballistic missiles [UCRL-LR-113578] p 2760 N94-28222

NUCLEATION

Dissolution of secondary phases during extrusion [PB94-124583] p 2732 N94-25908

Study of precipitation and recrystallization in Al alloy 2519 by backscattered electron imaging methods [AD-A274919] p 2736 N94-26533

Pseudomorphic semiconducting heterostructures from combinations of AIN, GaN and selected SiC polytypes: Theoretical advancement and its coordination with experimental studies of nucleation, growth, characterization and device development [AD-A274247] p 3061 N94-26841

Controlled heterogeneous nucleation of melt-textured YBa2Cu3O(6+x) by addition of Al2O3 particles [AD-A274605] p 3062 N94-26892

Development of K(1-x)Na(x)TiOPO4 crystals for nonlinear applications [AD-A274336] p 3063 N94-27055

NUCLEI (NUCLEAR PHYSICS)

Correlations in inelastic collisions of relativistic nuclei with emulsion at (4.1 - 4.5) A GeV/c [DE93-634526] p 3030 N94-27994

NUCLEON-NUCLEON INTERACTIONS

Separable expansions of the NN t-matrix by way of exact half off the energy shell methods [DE94-601615] p 3015 N94-25890

Nucleon-nucleon scattering lengths in QCD sum rules [DE93-520239] p 3015 N94-25922

NUCLEON-NUCLEON SCATTERING

Theoretical and computational studies in intermediate energy nuclear physics [DE94-004177] p 3012 N94-25800

Nucleon-nucleon scattering lengths in QCD sum rules [DE93-520239] p 3015 N94-25922

NUCLEONS

Theoretical and computational studies in intermediate energy nuclear physics [DE94-004177] p 3012 N94-25800

Hadron jets and nucleon clusters in the relativistic nuclear collisions [DE93-613434] p 3031 N94-25850

Nucleon-nucleon scattering lengths in QCD sum rules [DE93-520239] p 3015 N94-25922

Theoretical and experimental studies of elementary physics [DE94-002310] p 3008 N94-25988

The STAR experiment at the Relativistic Heavy Ion Collider [DE94-003409] p 3017 N94-26083

Rescattering and energy loss of fast partons in nuclear matter [DE94-002918] p 3018 N94-26145

Proceedings of the workshop on (pi), K, (eta)-nucleon interactions [DE94-701314] p 3027 N94-27733

Study of invisible nucleon decay, N approaches nu nu nu bar, and a forbidden nuclear transition in the Kamiokande detector [ICRR-299-93-11] p 3028 N94-27759

NULL HYPOTHESIS

Wieand's theorem [PB94-126711] p 3004 N94-27223

NUMBER THEORY

Fast methods for computation with algebraic numbers [ISBN-0-315-57888-2] p 2998 N94-27269

NUMERICAL ANALYSIS

Studies in nonlinear numerical analysis [AD-A273911] p 2959 N94-25968

Analysis and computer tools for separation processes involving nonideal mixtures [DE94-004162] p 2960 N94-25986

A transient symmetrical method for the measurement of temperature dependent thermal diffusivity [VTT-TIED-1452] p 3008 N94-26256

Continuation and multi-grid for bifurcation problems [AD-A274965] p 2992 N94-26302

A robust upwind discretization method for advection, diffusion and source terms [CWI-NM-R9308] p 2868 N94-26774

Computer program for numerical evaluation of the performance of an overmoded TM01 circular to TE10 rectangular waveguide mode converter [AD-A274548] p 2771 N94-26844

Improved numerical methods for quantum field theory (Outstanding Junior Investigator Award) [DE94-001793] p 3073 N94-27002

Numerical and experimental analyses of the radiant heat flux produced by quartz heating systems [NASA-TP-3387] p 3011 N94-27659

The calculation for energy balance of heating plasmas by Alfven waves [DE94-604994] p 3049 N94-27855

A laboratory test on construction of ice domes and their load-carrying capacity p 2884 N94-27966

Numerical simulation of turbulent free jet by TFKE model p 2871 N94-28157

NUMERICAL CONTROL

Graphical programming at Sandia National Laboratories [DE94-003803] p 2958 N94-25818

A large high vacuum, high pumping speed space simulation chamber for electric propulsion [NASA-TM-106453] p 2690 N94-26142

New Thomson scattering laser control for D3-D [DE94-002890] p 3043 N94-26274

Automated system for gas detectors providing with binary mixtures [DE93-634192] p 2715 N94-26406

Low-cost photovoltaic inverters incorporating application-specific integrated circuits
[DE94-003270] p 2856 N94-26463
Distributed Nd:YAG laser welding and process control in inert glove boxes
[DE94-002629] p 2818 N94-26605
Virtual data
[DE94-002718] p 2986 N94-26807
Object-oriented software construction at ALS
[DE94-003418] p 2967 N94-27049
The universal robot p 2686 N94-27361
Inverted pendulum control apparatus using transputers
[DE94-701224] p 2973 N94-27732
Experimental apparatus for optimization of flap position for a three-element airfoil model p 2682 N94-27912

NUMERICAL FLOW VISUALIZATION
Numerical simulation of turbulent free jet by TFKE model p 2871 N94-28157

NUMERICAL INTEGRATION
Geoid determination: With help of the alternative scattering method
[ETN-94-95375] p 2847 N94-25746
Analysis and control of hourglass instabilities in underintegrated linear and nonlinear elasticity
[NASA-CR-195293] p 2846 N94-28266

NUMERICAL STABILITY
Parameter estimation for ARMA models with infinite variance innovations
[AD-A274654] p 3003 N94-26355
Analysis and control of hourglass instabilities in underintegrated linear and nonlinear elasticity
[NASA-CR-195293] p 2846 N94-28266

NUMERICAL WEATHER FORECASTING
Development and testing of the Coupled Ocean/Atmosphere Mesoscale Prediction System (COAMPS)
[AD-A273925] p 2892 N94-25793
Testbed model and data assimilation for ARM
[DE94-000432] p 2893 N94-26082
Simulation of the Indian and East-Asian summer monsoon in the ECMWF model: Sensitivity to horizontal resolution
[DE94-004276] p 2897 N94-27571

NUSSELT NUMBER
Validated heat-transfer and pressure-drop prediction methods based on the discrete-element method. Phase 2: Two-dimensional rib roughness
[DE94-002379] p 2794 N94-26763
Forced convection heat transfer in straight tubes. Part 2: Laminar and transitional flow
[ESDU-93018-PT-2] p 2807 N94-28139

NUTATION
Wobble-nutation modes of the Earth
[ISBN-0-315-84246-6] p 3102 N94-26669

NUTRITION
Visit to CERMA: Centre d'Etudes et de Recherches de Medecine Aerospatiale, Centre for Studies and Research in Aviation and Space Medicine, Bretigny sur Orge, France, November 16-18, 1992
[PB94-132990] p 2937 N94-28392

NYQUIST DIAGRAM
Parameter estimation of linear systems from frequency response measurements (computer program)
[ESDU-93016] p 2976 N94-28137

NYQUIST FREQUENCIES
Investigation of spectral analysis techniques for randomly sampled velocimetry data
p 3009 N94-27924

NYSTAGMUS
Vertical gaze direction during parabolic flight
p 2913 N94-27453
The mechanism of caloric nystagmus under microgravity. 1: Changes of endolymphatic pressure in the semicircular canal of pigeon by caloric stimulation
p 2914 N94-27457

O

O RING SEALS
Outgas and vacuum seal characteristics of irradiated polyimide O-ring
[DE94-701200] p 2757 N94-27812

OBJECT-ORIENTED PROGRAMMING
Proposed Object Oriented Programming (OOP) enhancements to the Very High Speed Integrated Circuits (VHSIC) Hardware Description Language (VHDL)
[AD-A274004] p 2957 N94-25661
Performance measurement of three commercial object-oriented database management systems
[AD-A274028] p 3096 N94-25765
Domain analysis and modeling of a model-based software executive
[AD-A274087] p 2958 N94-25783
Object-oriented design and implementation of a parallel Ada simulation system
[AD-A274119] p 2979 N94-25906
Object interaction in a parallel object-oriented discrete-event simulation
[AD-A274084] p 2959 N94-25942
Using database technology to support domain-oriented application composition systems
[AD-A274091] p 3096 N94-26024
Coordinated scheduling for dynamic real-time systems
[NASA-CR-195231] p 3093 N94-26206
MATRA Marconi Space: The Silex on-board processor and on-board software p 2950 N94-26726
Implementing hard real-time systems: A case study
p 2951 N94-26731
Developing with Ada using HOOD design methodology
p 2953 N94-26741
The CODE-TOP (COncurrent system DEvelopment using Transformations Of Predicate-transition nets) method: Examples of using it for system architecture specification, software specification, and code generation p 2953 N94-26744
A formalization of objects using equational dynamic logic
[PB94-125218] p 2965 N94-26852
Example of the EXPANSE signalling protocol
[PB94-125283] p 2771 N94-26872
Object-oriented software construction at ALS
[DE94-003418] p 2967 N94-27049
An object-oriented database interface for Ada
[AD-A274391] p 2968 N94-27075
Active database architectures and the design of sentinel for constraint management
[AD-A274205] p 3099 N94-27101
Parallel computers for advanced information processing p 2955 N94-27193
Schema integration in object-oriented databases
[CWI-CS-R9320] p 2970 N94-27548
An object model for multimedia programming
[CWI-CS-R9327] p 2971 N94-27552
Comparison of Object-Oriented Analysis and Design Methods: A Collection of Papers
[MEMO-INF-92-69] p 2975 N94-27936
A formal approach to the comparison of object-oriented analysis and design methodologies
p 2975 N94-27937
Object-oriented development methods
p 2975 N94-27938
CASE tools for the support of object-oriented analysis and design methods p 2975 N94-27939

OCEAN BOTTOM
Coupling of pelagic and benthic communities over a seamount in the Eastern North Pacific
[AD-A274750] p 2899 N94-26149
Topics in longshore currents
[AD-A274788] p 2899 N94-26361
Macrobenthic fauna in the dutch sector of the north sea in 1991
[PB94-126414] p 2868 N94-27200
An extraterrestrial event at the tertiary-quaternary boundary p 2890 N94-28309

OCEAN CURRENTS
A study on structure of benthic boundary layer in coastal waters
[REPT-4] p 2898 N94-25635
Hydrographic and Acoustic Doppler Current Profiler (ADCP) data from the ONR eastern boundary current accelerated research initiative, 9-16 June 1992
[AD-A274115] p 2898 N94-26076
Meeting of the Eighth Session of the Scientific Advisory Committee of the World Climate Impact Assessment and Response Strategies Programme
[DE93-633954] p 2866 N94-26163
An XCP user's guide and reference manual
[AD-A274519] p 2900 N94-27090
An oceanographical observation in the Western Pacific and international cooperations p 2872 N94-28272

OCEAN DATA ACQUISITIONS SYSTEMS
An oceanographical observation in the Western Pacific and international cooperations p 2872 N94-28272

OCEAN DYNAMICS
Meeting of the Eighth Session of the Scientific Advisory Committee of the World Climate Impact Assessment and Response Strategies Programme
[DE93-633954] p 2866 N94-26163
Topics in longshore currents
[AD-A274788] p 2899 N94-26361

OCEAN MODELS
Simulation of the carbon cycle in the oceans
[DE94-000780] p 2898 N94-25791
Development and testing of the Coupled Ocean/Atmosphere Mesoscale Prediction System (COAMPS)
[AD-A273925] p 2892 N94-25793
Conversion of the CLUSE model for applications over open ocean
[AD-A273750] p 2893 N94-26013
Topics in longshore currents
[AD-A274788] p 2899 N94-26361
Bathymetric data set extraction program. Users guide
[AD-A274761] p 2899 N94-26567

OCEAN SURFACE
Interpreting the implied meridional oceanic energy transport in AMIP
[DE94-001538] p 2898 N94-26072
A comparative evaluation of SAR and SLAR
[DE94-002922] p 2848 N94-26277
Nonlinear ocean waves
[AD-A274651] p 2899 N94-26354
The NOGAPS ten year AMIP integration
[AD-A274332] p 2900 N94-26887
Acoustic bubble sizing, using active and passive techniques to compare ambient and entrained populations
[ISVR-TR-229] p 2807 N94-28172

OCEAN TEMPERATURE
An XCP user's guide and reference manual
[AD-A274519] p 2900 N94-27090
The validation of ATSR measurements with in situ sea temperatures
[DE94-003195] p 2852 N94-27875

OCEANOGRAPHY
Naval Interactive Data Analysis System (NIDAS), software user's manual
[NASA-CR-195179] p 2956 N94-25606
Hydrographic and Acoustic Doppler Current Profiler (ADCP) data from the ONR eastern boundary current accelerated research initiative, 9-16 June 1992
[AD-A274115] p 2898 N94-26076
Coupling of pelagic and benthic communities over a seamount in the Eastern North Pacific
[AD-A274750] p 2899 N94-26149
Meeting of the Eighth Session of the Scientific Advisory Committee of the World Climate Impact Assessment and Response Strategies Programme
[DE93-633954] p 2866 N94-26163
A comparative evaluation of SAR and SLAR
[DE94-002922] p 2848 N94-26277
Bibliography of technical reports, 1992
[AD-A274849] p 3098 N94-26561
Effects of p-chlorophenol on sulfate reduction in marine sediments p 2870 N94-28150
Extraterrestrial accretion and glacial cycles
p 2890 N94-28308

OCEANS
Simulation of the carbon cycle in the oceans
[DE94-000780] p 2898 N94-25791
The biostratigraphy and paleogeography of Maastrichtian inoceramids p 2889 N94-28303

OCTANE NUMBER
CRC customer versus rater octane number requirement program (1990)
[AD-A273997] p 2758 N94-25901

OGIVES
Pneumatic management of blunted-forebody flow asymmetry for high-angle-of-attack directional control
p 2679 N94-28028

OIL SLICKS
A comparative evaluation of SAR and SLAR
[DE94-002922] p 2848 N94-26277

OILS
Accelerated screening methods for determining chemical and thermal stability of refrigerant-lubricant mixtures. Part 2: Experimental comparison and verification of methods
[DE94-003664] p 2749 N94-26007
Oil production from buckwheat stillage by thermochemical liquefaction p 2871 N94-28154

OLIVINE
Electrical conductivity of perovskite-magnesiowuestite as a function of pressure and temperature
[DE94-002714] p 2880 N94-26806

OMEGA-MESONS
Omega omega and rho+ rho- production in two photon interactions at ARGUS
[ISBN-0-315-63748-X] p 3026 N94-27399

ON-LINE SYSTEMS
Module interconnection frameworks for a real-time spreadsheet
[AD-A273853] p 2956 N94-25588
The use of on-line ion chromatography for high temperature and high pressure reaction studies
[DE94-002525] p 2713 N94-26075
Federal Information Exchange (FEDIX) user's guide: Fall 1993, Version 5.0/Release 1.0
[DE94-003826] p 3097 N94-26350
The 12-channel flash-ADC FASTBUS module
[DE93-634229] p 2783 N94-26380
Design of an online help facility for ExSpect
[PB94-126687] p 2966 N94-26955

Electronic document distribution: Design of the anonymous FTP Langley Technical Report Server [NASA-TM-4567] p 2971 N94-27573

ONBOARD DATA PROCESSING
Real-Time Embedded Processing for Space Applications [ISBN-2-85428-335-X] p 2948 N94-26713
Computing in space: Issues and answers p 2948 N94-26714
Real time avionics constraints: Silicon solutions p 2949 N94-26717
MATRA Marconi Space: The Silex on-board processor and on-board software p 2950 N94-26726
On-board software for the JET-X telescope on the Spectrum-X mission p 2951 N94-26727
Implementing hard real-time systems: A case study p 2951 N94-26731
Early real-time performance measurements on the Columbus processor system p 2952 N94-26736
Test of onboard real time applications (LICE (tm)) p 2952 N94-26737
Verification and validation of the on-board software real time requirements p 2953 N94-26739
Ada reusable software for satellite on-board data handling p 2953 N94-26743
Specification performance optimization and executive generation for onboard multiprocessor real time application with SynDEx p 2954 N94-26745
Asynchronous and packetized systems engineering tools p 2954 N94-26746
Advanced End-to-end Simulation for On-board Processing (AESOP) p 2945 N94-28255

ONE DIMENSIONAL FLOW
Dynamic response of a compressor research facility [AD-A273836] p 2679 N94-25740
Integrated model development for liquid fueled rocket propulsion systems [NASA-CR-195253] p 2702 N94-27166

OORT CLOUD
Studies of extra-solar Oort Clouds and the Kuiper Disk [NASA-CR-195242] p 3103 N94-26789
Modulating terrestrial impacts from Oort cloud comets by the adiabatically changing galactic tides p 2890 N94-28305

OPERATING COSTS
Development of advanced high temperature in-cylinder components and tribological systems for low heat rejection diesel engines, phase 1 [NASA-CR-187158] p 2827 N94-27984
Development of the gas turbine. Part 2: Manufacturing, commissioning, and operation p 2831 N94-28081

OPERATING SYSTEMS (COMPUTERS)
Domain analysis and modeling of a model-based software executive [AD-A274087] p 2958 N94-25783
Achieving high performance on the Intel Paragon [DE94-003108] p 2979 N94-25953
Ada multiple-programming for hard real time applications in space systems p 2951 N94-26730
Implementing hard real-time systems: A case study p 2951 N94-26731

OPERATING TEMPERATURE
Silicon device performance measurements to support temperature range enhancement [NASA-CR-195265] p 2844 N94-27824
Development of advanced high temperature in-cylinder components and tribological systems for low heat rejection diesel engines, phase 1 [NASA-CR-187158] p 2827 N94-27984

OPERATIONS RESEARCH
The effectiveness of AMT investment in UK metal component manufacture [IND-MANU-SCI-TECH-REPT-3] p 2762 N94-25775
The general pickup and delivery problem [MEMO-COSOR-92-44] p 2992 N94-26226
Polyhedral characterization of the economic lot-sizing problem with start-up costs [MEMO-COSOR-92-46] p 2969 N94-27396
The molecular matching problem p 3030 N94-27910

OPERATOR PERFORMANCE
Task demand, workload, and performance [PB94-123627] p 2942 N94-27155

OPERATORS (MATHEMATICS)
Parallel matrix transpose algorithms on distributed memory concurrent computers [DE94-002424] p 2964 N94-26764
Q - difference intertwining operators for a Lorentz quantum algebra [DE94-602559] p 2997 N94-27023
A characterization of stable models using a non-monotonic operator [CWI-CS-R9315] p 2970 N94-27543
Joint essential maximal numerical range [DE94-603674] p 3000 N94-27637

OPTICAL COMMUNICATION
Design of a shared coherent cache for a multiple channel architecture [AD-A274026] p 3034 N94-25758
System design analysis of a lightweight laser satellite terminal [AD-A274033] p 2690 N94-25769
Study of the homogeneity of InP wafers [AD-A273658] p 3055 N94-26194
Laser-based communication link [FFI-93/7023] p 2817 N94-26203
A doubly logarithmic communication algorithm for the Completely Connected Optical Communication Parallel Computer [DE93-019408] p 2980 N94-26473
Accordion-like polymers for nonlinear applications [AD-D016031] p 2755 N94-27148
Investigation of air transportation technology at Princeton University, 1992-1993 p 2643 N94-27294
Optical communications for transport aircraft p 2643 N94-27298
Microprocessor chip incorporating optical signal coupling transceiver [AD-D016077] p 2788 N94-28186

OPTICAL COUPLING
A study of multiple guide optical couplers [ISBN-0-315-84633-X] p 3038 N94-27441

OPTICAL DATA PROCESSING
Optical pattern recognition system utilizing resonator array [AD-D016071] p 3040 N94-28224

OPTICAL DISKS
Spacecraft optical disk recorder memory buffer control p 2815 N94-27907

OPTICAL EMISSION SPECTROSCOPY
Researches of the Electrotechnical Laboratory. No. 53: Spectral emission from combustion gas containing scattering media [JTN-94-80603] p 2717 N94-27246

OPTICAL EQUIPMENT
The National Center for Advanced Information Components Manufacturing: Program update [DE94-002647] p 2960 N94-26118
Optoelectronic Technology Consortium [AD-A274909] p 2782 N94-26344
Optoelectronic technology consortium [AD-A274595] p 3036 N94-26857
Helmet head tracking mounting device [AD-D016048] p 2942 N94-27114
Binary optical elements: Studies in design, manufacture and performance [ISBN-0-315-60643-6] p 3039 N94-27643

OPTICAL FIBERS
Influence of embedded optical fibers on compressive strength of advanced composites [AD-A273775] p 2705 N94-25859
Development of surgical CW Nd:YAG laser with optical fiber delivery system [DE93-632902] p 2817 N94-26185
Inert strength of pristine silica glass fibers [DE94-004685] p 2750 N94-26247
Multichip module high speed testing [AD-A274873] p 2782 N94-26343
Calorimeter with WLS fibers and parallel to beam scintillators [DE93-634188] p 2810 N94-26378
Cad of GeO2-SiO2 double-layer core dispersion-shifted single-mode fibre [DE93-634325] p 3035 N94-26383
All-optical gain switching of erbium-doped fibre amplifiers [ISBN-0-315-84120-6] p 2784 N94-26704
Method of measuring liquid level [AD-D016049] p 3038 N94-27153
Evanescent field infrared spectroscopy using chalcogenide glass fiber [ITN-94-85233] p 3038 N94-27178
Ir-fibers in a laser threat warning system and robot shot warning system [PB94-124476] p 3038 N94-27209
Intelligent material systems and structures. Part 6: Measurements of adhesion between optical fibres and composite materials [PB94-123577] p 2756 N94-27215
Kinoform/lens system for injecting a high power laser beam into an optical fiber [DE94-003226] p 2819 N94-27262
Fiber optic Faraday flux transformer specification [AD-D016058] p 3039 N94-27674
Fiber optic true time-delay array antenna feed system [AD-D016063] p 2777 N94-27734

OPTICAL FILTERS
Calorimeter with WLS fibers and parallel to beam scintillators [DE93-634188] p 2810 N94-26378
Long Duration Exposure Facility space optics handbook [AD-A274831] p 3035 N94-26572

OPTICAL MATERIALS
Three-wave nonlinear interactions in KTiOPO4 (KTP) and KTP isomorphs [AD-A274079] p 3052 N94-25993
Long Duration Exposure Facility space optics handbook [AD-A274831] p 3035 N94-26572
An x ray absorption fine structure study of ordering in polythiophene thin films [AD-A274235] p 2753 N94-26822
Mechanistic studies of opto-electronic materials and syntheses using multiple laser and surface diagnostics [AD-A274528] p 3036 N94-26834
Polyimide/inorganic composite-interpenetrating polymer network for stable second-order nonlinear optics [AD-A274646] p 2709 N94-27107

OPTICAL MEASUREMENT
Surface physics with cold and thermal neutron reflectometry [DE94-001447] p 2733 N94-26070
Research and development within nonlinear optics for protection of optical sensors against laser irradiation on of optical sensors against laser irradiation. Quarterannual report 1 (april 1993)) [PB94-124245] p 3037 N94-27046
Time domain reflectometry for measuring bulk soil electrical conductivity and comparison with the Em38 instrument [PB94-125432] p 2881 N94-27052
Experimental verification of tomographic reconstruction of turbulent air flow structure using optical wavefront measurements [AD-A274392] p 2795 N94-27129
Development of a 2f optical performance measurement system [DE94-003489] p 3039 N94-27721
Detection of water on road surface by the polarized light p 2886 N94-27989

OPTICAL MEASURING INSTRUMENTS
Numerical simulation of tomographic reconstruction for the study of turbulence using optical wavefront sensor measurements [AD-A273851] p 2789 N94-25587
Development of a multi-sensor in situ fiber optic fluorometer [DE94-003399] p 3035 N94-26100
Optical surface contouring for non-destructive inspection of turbomachinery [NASA-CR-195245] p 2835 N94-26691
Research and development within nonlinear optics for protection of optical sensors against laser irradiation on of optical sensors against laser irradiation. Quarterannual report 1 (april 1993)) [PB94-124245] p 3037 N94-27046
Method of measuring liquid level [AD-D016049] p 3038 N94-27153
Reflectometer employing an integrating sphere and lens-mirror concentrator [AD-D016061] p 3039 N94-27676
Energy Dispersive X ray Diffraction (EDXD) apparatus for liquids at high temperature p 2721 N94-28159

OPTICAL MEMORY (DATA STORAGE)
High-speed, high-density, coherent time-domain optical memory [AD-A274249] p 3037 N94-27010
Spacecraft optical disk recorder memory buffer control p 2815 N94-27907

OPTICAL MICROSCOPES
Bulletin of the Institute for Chemical Reaction Science, Tohoku University, volume 2 [JTN-94-80602] p 2717 N94-27385
Variable temperature cold stage for microscope observation p 2718 N94-27389

OPTICAL PATHS
Laser phase induced intensity noise in fiber-optic signal processing and sensing systems [ITN-94-85234] p 2819 N94-27179
Spectral and temporal correlations of multifrequency waves in the turbulent atmosphere [ITN-94-85229] p 2774 N94-27233

OPTICAL POLARIZATION
Spin effects in hard interactions (interest in accelerated polarized beam) [DE93-634398] p 3031 N94-26044
Detection of water on road surface by the polarized light p 2886 N94-27989

OPTICAL PROPERTIES
Langmuir-Blodgett film of amylose-esters and chiral azo-dyes (structure and second order nonlinear optical behaviour) [ETN-94-95390] p 2747 N94-25749

Studies of non-linear optical effects for agile beam steering
[AD-A273998] p 3034 N94-25902
Lighter alkali hydride and deuteride 1: Electronic properties of pure solids
[DE93-616188] p 3051 N94-25914
Optical conductivity and resistivity in the two-band Emery model
[DE94-601943] p 3051 N94-25945
Physical characteristics of polymethylmethacrylate scintillator SOFG-120
[DE93-634184] p 2810 N94-26395
Research and development within nonlinear optics for protection of optical sensors against laser irradiation on of optical sensors against laser irradiation. Quarterannual report 1 (april 1993))
[PB94-124245] p 3037 N94-27046
Accordion-like polymers for nonlinear applications
[AD-D016031] p 2755 N94-27148
Ir-fibers in a laser threat warning system and robot shot warning system
[PB94-124476] p 3038 N94-27209
Molecular dynamics simulation and crystal-field theory: Predicting the optical spectra and structure of rare-earth doped inorganic glasses
[ISBN-0-315-84679-8] p 3025 N94-27310
Technical report of ISSP. Ser. A, no. 2685: ASE-free terawatt KrF/Ti : sapphire hybrid laser system
[JTN-94-80571] p 2820 N94-27339

OPTICAL PUMPING
Characterization of nonlinear effects in optically pumped vertical cavity surface emitting lasers
[AD-A273840] p 2815 N94-25744
Broad band tunable dye laser development
[DE93-632978] p 2816 N94-26157
Multiple exposure CCD detector for high-speed laser pump, x ray probe Laue scattering
[DE94-004618] p 2820 N94-27781
Optical parametric oscillator modeling with diffraction, depletion, and double refraction
[DE94-001504] p 3040 N94-27999

OPTICAL RADAR
Wind measurements with an incoherent lidar
[AD-A273756] p 2891 N94-25722
Design analysis of a combined optical/LADAR deep-space surveillance satellite
[AD-A274040] p 2694 N94-25832
An overview of the TNO contribution to VAST 92
[AD-A273751] p 2893 N94-26016
Elastic backscattering lidar for a MSTI satellite
[DE94-002701] p 2816 N94-26126
The development of Cr, Tm, Ho:YAG lasers for airborne lidar
[AD-A274895] p 2816 N94-26178
Compilation of corrections for postprocessing of laser bathymetry data
[PB94-123668] p 2900 N94-27156
Sum frequency generation using an optical parametric oscillator
[DE94-001827] p 3040 N94-28000

OPTICAL RESONANCE
Measurement of metastable population distribution in gadolinium atomic beam by laser resonance photoionization method
[DE94-701194] p 3029 N94-27820

OPTICAL RESONATORS
Optical pattern recognition system utilizing resonator array
[AD-D016071] p 3040 N94-28224

OPTICAL SCANNERS
Channel to energy calibration results for the BATSE large area detectors p 3115 N94-26690
Characterization and calibration of the Agema 880+ imaging radiometer
[AD-A274417] p 3036 N94-26981

OPTICAL SWITCHING
Low threshold all-optical crossbar switch on GaAs-GaAlAs channel waveguide arrays
[AD-A274971] p 2783 N94-26536
All-optical gain switching of erbium-doped fibre amplifiers
[ISBN-0-315-84120-6] p 2784 N94-26704

OPTICAL TRACKING
Image quality and the display modulation transfer function: Experimental findings
[AD-A274061] p 2679 N94-25773
Capture and location of blobs in digital images
[ISBN-0-315-84382-9] p 3036 N94-26666
Helmet head tracking mounting device
[AD-D016048] p 2942 N94-27114

OPTICAL TRANSFER FUNCTION
Performance impacts for actuator misalignments and failures in large-aperture adaptive-optic telescopes
[AD-A273838] p 3034 N94-25742

OPTICAL TRANSITION
On the estimation of matrix elements for optical transitions in semiconductors
[DE93-613550] p 3051 N94-25851

OPTICAL WAVEGUIDES
Microtubules for nonlinear optical limiting
[AD-A273940] p 3035 N94-25941
Optoelectronic Technology Consortium
[AD-A274909] p 2782 N94-26344
Low threshold all-optical crossbar switch on GaAs-GaAlAs channel waveguide arrays
[AD-A274971] p 2783 N94-26536
Optoelectronic technology consortium
[AD-A274595] p 3036 N94-26857
Optical characterization and guided wave loss measurements for end-capped 6F-polybenzoxazole
[AD-A274586] p 3036 N94-26982
Focal plane antenna array for millimeter waves
[AD-D016034] p 2774 N94-27202
A study of multiple guide optical couplers
[ISBN-0-315-84633-X] p 3038 N94-27441
Electro-optic materials by solid source MOCVD
[DE94-005120] p 2757 N94-27716

OPTIMAL CONTROL
Optimal control design advantages utilizing two-degree-of-freedom controllers
[AD-A273839] p 2984 N94-25743
Studies in nonlinear numerical analysis
[AD-A273911] p 2959 N94-25968
One machine scheduling with delayed precedence constraints
[PB93-237626] p 3094 N94-26314
Development of a performance evaluation tool (MMSOFE) for detection of failures with Multiple Model Adaptive Estimation (MMAE)
[AD-A274218] p 2665 N94-27071
Impulsive control and stabilization
[ISBN-0-315-84563-5] p 2988 N94-27271
Advanced control of a flexible spherical wrist
[ISBN-0-315-84424-8] p 2826 N94-27652
Pulse control method and its characteristics
[DE94-701187] p 2989 N94-27809
On identified predictive control p 2990 N94-27896
Topics in the design, analysis and implementation of feedback control systems
[ISBN-0-315-84934-7] p 2989 N94-27975
On the use of feedback to control sound radiation from a plate excited by a turbulent boundary layer
[ISVR-TR-227] p 2807 N94-28175

OPTIMIZATION
Adaptive optimization and control using neural networks
[DE94-003941] p 2985 N94-25983
Determination of the geomagnetic external contribution by nonlinear optimization methods
[DE94-600882] p 2878 N94-26365
A technique for integrating engine cycle and aircraft configuration optimization
[NASA-CR-191602] p 2668 N94-26606
Thermal/structural tailoring of engine blades (T/STAEBL). User's manual
[NASA-CR-194463] p 2839 N94-26692
Specification performance optimization and executive generation for onboard multiprocessor real time application with SynDEx p 2954 N94-26745
Nested Krylov methods based on GCR
[PB94-125317] p 2995 N94-26818
Query optimization strategies for browsing sessions
[CWI-CS-R9268] p 3100 N94-27394
A sensitivity equation approach to shape optimization in fluid flows
[NASA-CR-191598] p 2999 N94-27415
Fast parallel permutation algorithms
[CWI-CS-R9303] p 2982 N94-27579
Thermal/Structural Tailoring of Engine Blades (T/STAEBL): User's manual
[NASA-CR-194461] p 2843 N94-27776
Reliability-based structural optimization: A proposed analytical-experimental study
[NASA-TM-109055] p 2844 N94-27830
An optimization program based on the method of feasible directions: Theory and users guide
[NASA-TM-4552] p 2845 N94-27865
The molecular matching problem
p 3030 N94-27910
Examples of flight path optimisation using a multivariate gradient-search method
[ESDU-93021] p 2670 N94-28092

OPTOELECTRONIC DEVICES
Solid state research
[AD-A274063] p 3049 N94-25645
Optoelectronic technology consortium
[AD-A274595] p 3036 N94-26857
Research and development within nonlinear optics for protection of optical sensors against laser irradiation on of optical sensors against laser irradiation. Quarterannual report 1 (april 1993))
[PB94-124245] p 3037 N94-27046

ORBIT CALCULATION
Hill equations for satellite orbit determination
[ETN-94-95374] p 2690 N94-25787

ORBIT PERTURBATION
Hill equations for satellite orbit determination
[ETN-94-95374] p 2690 N94-25787

ORBIT TRANSFER VEHICLES
Orbit transfer rocket engine technology program enhanced heat transfer combustor technology
[NASA-CR-189236] p 2700 N94-26156
Test results of the RS-44 integrated component evaluator liquid oxygen/hydrogen rocket engine
[NASA-CR-194443] p 2701 N94-26231
Orbit transfer rocket engine technology program
[NASA-CR-189229] p 2702 N94-26542
Orbital transfer vehicle engine technology high velocity ratio diffusing crossover
[NASA-CR-194447] p 2703 N94-27212
Orbital transfer rocket engine technology 7.5K-LB thrust rocket engine preliminary design
[NASA-CR-190754] p 2703 N94-27213

ORBITAL ASSEMBLY
Space Habitat, assembly and repair facility
p 2691 N94-25696
Selected topics in robotics for space exploration
[NASA-CP-10131] p 2682 N94-26278
Performance measures from the explorer platform berthing experiment p 2683 N94-26283
Berthing of Space Station Freedom using the shuttle remote manipulator system p 2684 N94-26284
An analysis of the loads applied to a heavy Space Station rack during translation and rotation tasks
[NASA-TM-104790] p 2697 N94-28183

ORBITAL ELEMENTS
A virtual environment for satellite modeling and orbital analysis in a distributed interactive simulation
[AD-A274114] p 2694 N94-25904
An April 1991 outburst from 4U0115+63 observed by BATSE
[NASA-CR-195252] p 3116 N94-27440

ORBITAL LIFETIME
Lifetimes of lunar satellite orbits
[NASA-TP-3394] p 2690 N94-27771

ORBITAL MECHANICS
A virtual environment for satellite modeling and orbital analysis in a distributed interactive simulation
[AD-A274114] p 2694 N94-25904

ORBITAL RENDEZVOUS
Autonomous rendezvous and docking for Space Station Freedom p 2684 N94-26286
Nasa Langley Research Center seventy-fifth anniversary publications, 1992
[NASA-TM-109691] p 3118 N94-27431

ORBITAL SERVICING
Manned mission to Mars with periodic refueling from electrically propelled tankers p 2689 N94-25670

ORBITAL WORKERS
An analysis of the loads applied to a heavy Space Station rack during translation and rotation tasks
[NASA-TM-104790] p 2697 N94-28183

ORBITS
Towards a theory of growing surfaces: Mapping two-dimensional Laplacian growth onto Hamiltonian dynamics and statistics
[DE94-002636] p 2991 N94-26079

ORDER-DISORDER TRANSFORMATIONS
Fermi-liquid to non-Fermi-liquid transition in a dynamical generalization of the CPA in a disordered Hubbard model
[DE94-601875] p 2714 N94-26169
The origins of ordering in CuPt
[DE94-003864] p 2736 N94-26351
Ordering and phase separation in MOCVD InGaP alloys and unicompositional quantum wells
[DE94-004693] p 3056 N94-26352
Regrowth zones in laser annealed radiation damaged diamond
[DE94-600821] p 3056 N94-26364
Structure of ionic fluids in equilibrium with a microporous ionic matrix
[DE94-600563] p 2715 N94-26391
Transition metals in highly correlated discotic phases: Designing metallomesogens with selected intermolecular organizations
[AD-A274695] p 2736 N94-26452
Length-scale dependent ensemble-averaged conductance of a 1D disordered conductor: Conductance minimum
[DE94-602732] p 3062 N94-26902

ORDNANCE
Differential global positioning system for the surface-towed ordnance locating system: Testing, results, and user's guide
[DE94-002980] p 2664 N94-26309

ORGANIC COMPOUNDS
Computational studies of energetic organic molecules
[AD-A274726] p 3018 N94-26172
A materials compatibility study in FM-1, a liquid component of a paste extrudable explosive
[DE94-001166] p 2759 N94-26198
Numerical analysis of the photo-dissociation/radical oxidation of formaldehyde by ultraviolet light in a photolytic reactor
[AD-A274539] p 2868 N94-26843
Development of a sparging technique for volatile emissions from potato (Solanum tuberosum)
[NASA-TM-109199] p 2903 N94-27412
Trace organic chemical detection using an ultraviolet excitation molecular beam fluorometer
[DE94-002649] p 2704 N94-27708
Collaboration of chemical oxidation and biological treatment for removal of refractory organic substances
p 2870 N94-28149
Treatment of refractory organic substances with combined use of chemical oxidation and biological treatment. Part 2: Biodegradability of ozonation products of chlorophenol p 2870 N94-28151

ORGANIC MATERIALS
Research and development within nonlinear optics for protection of optical sensors against laser irradiation on of optical sensors against laser irradiation. Quarterannual report 1 (april 1993))
[PB94-124245] p 3037 N94-27046

ORGANIC SILICON COMPOUNDS
Sol-gel derived silica/siloxane composite materials: The effect of loading level and catalyst activity on silica domain formation
[DE94-002734] p 2712 N94-27710

ORGANISMS
Coupling of pelagic and benthic communities over a seamount in the Eastern North Pacific
[AD-A274750] p 2899 N94-26149
Macrobenthic fauna in the dutch sector of the north sea in 1991
[PB94-126414] p 2868 N94-27200

ORGANIZATIONS
Federal Information Exchange (FEDIX) user's guide: Fall 1993, Version 5.0/Release 1.0
[DE94-003826] p 3097 N94-26350
International energy: Research organizations, 1988-1992
[DE93-017267] p 3098 N94-26398
Pigs in cyberspace p 2689 N94-27376

ORGANOMETALLIC COMPOUNDS
Processing of LaCrO3 for solid oxide fuel cell applications
[DE94-002981] p 2857 N94-26747
Electro-optic materials by solid source MOCVD
[DE94-005120] p 2757 N94-27716

ORGANS
NCVS, volume 5
[AD-A274975] p 2902 N94-27165

OROGRAPHY
Investigation of mesoscale convective cloud clusters in South China
[AD-A274303] p 2895 N94-26678
An observational study of the extratropical anticyclones in the South American continent
[INPE-5387-TDI/476] p 2896 N94-27356

ORTHOGONALITY
Geometric correction of SPOT images with use of digital elevation models
[ETN-94-95033] p 2847 N94-26107

ORTHOSTATIC TOLERANCE
Intermittent gravity: How much, how often, how long?
[NASA-TM-108800] p 2944 N94-26098
Analysis on one minute wave in body fluid volume and muscle pumping referred to body parts generating the one minute wave during human active standing
p 2929 N94-27528
Treatment of orthostatic hypotension by nasal administration of vasopressin p 2930 N94-27533
Workshop on Countering Space Adaptation with Exercise: Current Issues
[NASA-CP-3252] p 2934 N94-28361
Aerobic fitness and orthostatic tolerance: Evidence against an association p 2934 N94-28365
Does training-induced orthostatic hypotension result from reduced carotid baroreflex responsiveness?
p 2935 N94-28366

ORTHOTROPIC CYLINDERS
Series solution for a cylindrical composite shell subject to axisymmetric loadings
[ISBN-0-315-60559-6] p 2844 N94-27810

ORTHOTROPIC PLATES
Flat rectangular orthotropic plates under uniformly distributed normal pressure. Elastic stresses and deflections for various forms of edge restraint
[ESDU-93011] p 2845 N94-28061

OSCILLATIONS
About possible types of neutrino oscillations
[DE93-634449] p 3020 N94-26508
Measuring the time dependence of B(sub s)(sup 0) meson - anti B(sub s)(sup 0) meson oscillations
[ISBN-0-315-84367-5] p 3021 N94-26665
Polar optical oscillation modes in GaAs-based double heterostructures: Long wavelength limit
[DE94-601874] p 3062 N94-26897
Pressure-gain combustion
[DE94-002975] p 2719 N94-27712
The status of the solar neutrino problem
[DE94-003934] p 3111 N94-27742

OSCILLATOR STRENGTHS
International bulletin on atomic and molecular data for fusion. No. 46
[DE94-601818] p 3023 N94-26947

OSCILLATORS
Wigner quantum oscillators
[DE94-601508] p 3073 N94-26758
HPm-tubes: Literature survey comprising 1992
[PB94-123643] p 2785 N94-27038
The onset of chaos in a periodically forced nonlinear oscillator
[ISBN-0-315-84564-3] p 2842 N94-27272
Optical parametric oscillator modeling with diffraction, depletion, and double refraction
[DE94-001504] p 3040 N94-27999
Sum frequency generation using an optical parametric oscillator
[DE94-001827] p 3040 N94-28000
Fiber laser amplifiers and oscillators
[AD-A274231] p 2820 N94-28068

OSTEOPOROSIS
Irreversibility of advanced osteoporosis: Limited role for pharmacologic intervention p 2935 N94-28369
Exercise and osteoporosis: Methodological and practical considerations p 2935 N94-28370

OTOLITH ORGANS
Study on posture control and adaption mechanism under weightlessness: Differences in weight and shape of utricular otolith of carp p 2912 N94-27448

OUTER SPACE TREATY
Contributions to CD Space Committee 1992
[PB94-124401] p 3101 N94-27218

OUTGASSING
Outgas and vacuum seal characteristics of irradiated polyimide O-ring
[DE94-701200] p 2757 N94-27812

OUTLET FLOW
Non-isoenergetic inviscid slot flow
p 2655 N94-28333

OVER-THE-HORIZON RADAR
Over-the-horizon propagation measurements at six radar-frequency bands at the Atlantic Ocean Coast
[AD-A274151] p 2773 N94-27136

OVERPRESSURE
Shock wave interaction with L-shaped structures
[AD-A273774] p 2790 N94-25858

OXIDATION
Studies of thin-film growth, adsorption, and oxidation by in situ, real-time, and ex situ ion beam analysis
[DE94-002907] p 3055 N94-26275
Stability of reference masses 2: The effect of environment and cleaning methods on the surfaces of stainless steel and allied materials
[NPL-DMM(A)-95] p 2738 N94-26653
Numerical analysis of the photo-dissociation/radical oxidation of formaldehyde by ultraviolet light in a photolytic reactor
[AD-A274539] p 2868 N94-26843
Engineering limitations of ceramic composites for high performance and high temperature applications
[DE94-001676] p 2754 N94-27021
Thermogravimetric study of oxidation of a PdCr alloy used for high-temperature sensors
[NASA-TM-106473] p 2741 N94-27426
Novel oxidizing reagents derived from elemental fluorine
[ITN-94-85231] p 2719 N94-27687
High temperature grain growth and oxidation of Fe-29Ni-17Co (Kovar (tm)) alloy leads
[DE94-004691] p 3069 N94-27753
Kinetic parameters from thermogravimetric analysis
p 2721 N94-27909
Collaboration of chemical oxidation and biological treatment for removal of refractory organic substances
p 2870 N94-28149
Treatment of refractory organic substances with combined use of chemical oxidation and biological treatment. Part 2: Biodegradability of ozonation products of chlorophenol p 2870 N94-28151

OXIDATION-REDUCTION REACTIONS
The coordination and atom transfer chemistry of titanium porphyrin complexes
[DE94-003091] p 2704 N94-26779

OXIDE FILMS
Stability of reference masses 2: The effect of environment and cleaning methods on the surfaces of stainless steel and allied materials
[NPL-DMM(A)-95] p 2738 N94-26653
Ion implantation and dynamic recovery of tin-doped indium oxide films
[DE94-001126] p 3062 N94-26932
The ZnO thin films with C-axis orientation prepared on the room temperature substrate by the ECR multipolar plasma sputtering method
[DE94-605039] p 2758 N94-27857

OXIDES
Study on measurement and evaluation methods for superconductive characteristics p 2725 N94-25560
Successive structural phase transitions in stoichiometric La2NiO4 observed by x ray diffraction
[REPT-A-2665] p 3051 N94-25921
Phase diagram of La2NiO(4+delta) (0 less than or equal to delta less than or equal to 0.18). 1: Phases at room temperature and phase transition above delta equal to 0.15
[REPT-A-2661] p 3053 N94-26089
In situ spectroscopic applications to the study of rechargeable lithium batteries
[DE94-003478] p 2782 N94-26328
Sealant research for solid oxide fuel cells
[DE94-000015] p 2857 N94-26584
Processing of LaCrO3 for solid oxide fuel cell applications
[DE94-002981] p 2857 N94-26747
Fibrous emissive burners selective and broad band
[PB94-128329] p 2859 N94-27225

OXIDIZERS
Novel oxidizing reagents derived from elemental fluorine
[ITN-94-85231] p 2719 N94-27687

OXIMETRY
Pulse waveform and transcranial Doppler analysis during lower body negative pressure
[AD-A274516] p 2911 N94-27088

OXYGEN
Isotopically labeled CO2 from stratosphere: A tracer of carbon biogeochemistry
[DE94-002777] p 2877 N94-26015
The role of hyperbaric oxygen as a prophylaxis for radiation enteritis
[AD-A274974] p 2901 N94-26517
Electronic structure of a single oxygen vacancy in rutile TiO2
[DE94-602717] p 3062 N94-26901
Numerical simulation of the reignition of detonation by reflected shocks
[AD-A274755] p 2795 N94-27252
Technical report of ISSP. Ser. A, no. 2669: Relations between oxygen deficiency and structures in the La-Sr-Cu-O system. 3: Oxygen contents and structure of (La, Sr)8Cu8O(16+delta) phase
[JTN-94-80555] p 3066 N94-27353
The addition of molecular oxygen to hydroperoxy-propyl radicals
[DE94-003662] p 2760 N94-27725

OXYGEN CONSUMPTION
Intermittent gravity: How much, how often, how long?
[NASA-TM-108800] p 2944 N94-26098

OXYGEN IONS
Ion implantation and dynamic recovery of tin-doped indium oxide films
[DE94-001126] p 3062 N94-26932
Energy parameters of the incident auroral electrons derived by the intensity ratio of auroral emissions
p 2779 N94-27964

OXYGEN MASKS
Creation of prototype aircrew protection equipment based on face anthropometry
[AD-A273865] p 2940 N94-25611

OXYGEN PLASMA
Plasma surface cleaning using microwave plasmas
[DE94-002754] p 2713 N94-26014

OXYGEN PRODUCTION
Extraterrestrial surface propulsion systems
p 2833 N94-25891
Space Station evolution study oxygen loop closure
[NASA-CR-193938] p 2941 N94-26788

OXYGEN 17
Use of oxygen-17 isotope in the characterization of zeolites and related structures by nuclear magnetic resonance spectroscopy
[VTT-TIED-1448] p 2714 N94-26251

OZONE
Reanalysis of Mariner 9 UV Spectrometer Data for Ozone, Cloud, and Dust Abundances, and Their Interaction Over Climate Timescales
[NASA-CR-195244] p 3107 N94-27885
Martian atmospheric radiation budget p 3107 N94-27887
Mars ozone: Mariner 9 revisited p 3107 N94-27888
Why is the north polar cap on Mars different than the south polar cap? p 3107 N94-27889
Probing the Martian atmosphere in the ultraviolet p 3108 N94-27890
How well was total ozone abundance inferred with Mariner 9? p 3108 N94-27891
In situ Mars ozone detector p 3108 N94-27892
Ozone control of biological activity during Earth's history, including the KT catastrophe p 2876 N94-28312

OZONE DEPLETION
A three-dimensional chemical transport model study of the 1991 Antarctic ozone hole using objectively analysed data
[ISBN-0-315-84250-4] p 2867 N94-26670
Mission to Planet Earth: A program to understand global environmental change
[NASA-PAM-556] p 2869 N94-27958

OZONOSPHERE
Initial ultraviolet-B intensity data at Lawrence Livermore National Laboratory
[DE94-004279] p 2869 N94-27267

P

P WAVES
Elastic scattering by a spherical inclusion
[AD-A274713] p 2878 N94-26433
Dynamic and kinematic P wave tracing for a three-dimensional elastic inhomogeneous media by the asymptotic ray theory and application
[ITN-94-85239] p 2775 N94-27244

P-I-N JUNCTIONS
Electric-field dependence of electroreflectance and photocurrent spectra at visible wavelengths in MOVPE-grown InAlGaP multiple strained quantum-well structures
[DE94-004692] p 2780 N94-25664
Recombination and metastability in amorphous silicon and silicon germanium alloys
[DE94-000237] p 2736 N94-26481

P-TYPE SEMICONDUCTORS
Atomic layer epitaxy of group 4 materials: Surface processes, thin films, devices and their characterization
[AD-A274325] p 3061 N94-26885
Visible light emitting materials and injection devices
[AD-A274418] p 2786 N94-27079

P-3 AIRCRAFT
Development and evaluation of a near infrared reflecting and low visibility paint scheme for RAAF P-3C Orion aircraft
[AD-A274881] p 2669 N94-26864

PACIFIC OCEAN
Propagation of cold air masses in East Asia and its associated planetary-scale function
[AD-A274304] p 2895 N94-26850
Tropical cyclone report, 1992
[AD-A274464] p 2896 N94-27025

PACKAGING
Package integrity measurement technology and quality assurance
[AD-A273881] p 2834 N94-25727

PACKET SWITCHING
Asynchronous and packetized systems engineering tools p 2954 N94-26746
Analysis of a multiaccess/switching technique for multibeam satellites in a prioritized ISDN environment
[ISBN-0-315-84632-1] p 2776 N94-27345

PACKET TRANSMISSION
Packet radio data link applications in the NASA Langley Research Center Transport Systems Research Vehicle
[NASA-TM-109071] p 2665 N94-27423

PAIN SENSITIVITY
Excitation of cutaneous polymodal receptor induced by sympathetic stimulation in adjuvant-induced arthritis rats p 2906 N94-27495
Influence of mechanical stimulation on inflammatory edema p 2906 N94-27497
The effect of naloxone on sleeping time in adjuvant arthritic rats p 2906 N94-27498
Changes in pain sensation induced by repetitive application of noxious heat pulses to the human skin p 2924 N94-27501
Hyperalgesia to cold in patients with Subacute Myelo-Optico-Neuropathy (SMON) p 2928 N94-27521
The polymodal receptor p 2908 N94-27539

PAINTS
Development and evaluation of a near infrared reflecting and low visibility paint scheme for RAAF P-3C Orion aircraft
[AD-A274881] p 2669 N94-26864

PAIR PRODUCTION
CP test in the W pair production by way of photon fusion at NLC
[DE94-601608] p 3014 N94-25889
Magnetic field induced contributions of supersymmetric particles to energy losses of neutron star
[DE93-634331] p 3104 N94-26269
Chance to use W-decay lepton channels for width determination
[DE93-634438] p 3020 N94-26507
Search for the top quark in the single lepton + jets channel at D0
[DE94-004660] p 3028 N94-27749

PALEOBIOLOGY
The end-Permian mass extinction: A complex, multicausal extinction p 2888 N94-28299
Mass extinctions: Persistent problems and new directions p 2889 N94-28302
Ozone control of biological activity during Earth's history, including the KT catastrophe p 2876 N94-28312

PALEOCLIMATOLOGY
Sensitivity of climate models: Comparison of simulated and observed patterns for past climates
[DE93-019934] p 2865 N94-25789

PALEOMAGNETISM
An extraterrestrial event at the tertiary-quaternary boundary p 2890 N94-28309

PALEONTOLOGY
The biostratigraphy and paleogeography of Maastrichtian inoceramids p 2889 N94-28303
An evaluation of criteria that may be used to identify species surviving a mass extinction p 2889 N94-28304
Ozone control of biological activity during Earth's history, including the KT catastrophe p 2876 N94-28312

PALEOZOIC ERA
The end-Permian mass extinction: A complex, multicausal extinction p 2888 N94-28299

PALLADIUM
Hydrogen trapping with Pd coated alloy films p 2723 N94-25551

PALLADIUM ALLOYS
Formation of three types of quasi-crystals in Al-Pd-Mg system
[REPT-A-2667] p 3053 N94-26071
Toward insulating quasicrystalline alloy in Al-Pd-Re icosahedral phase
[REPT-A-2666] p 2736 N94-26477
Thermogravimetric study of oxidation of a PdCr alloy used for high-temperature sensors
[NASA-TM-106473] p 2741 N94-27426
NMR study of quasicrystal Al(70)Pd(20)T(M10) alloy (T(M):Cr, Mn, Fe, and Co) p 2745 N94-28162
Formation of glassy Pd-Ni-P alloys by mechanical alloying and their structure and thermal stability p 2746 N94-28168

PANEL METHOD (FLUID DYNAMICS)
Computational investigation of the compressible dynamic stall characteristics of the Sikorsky SSC-A09 airfoil
[AD-A274867] p 2644 N94-26191
Calculation of unsteady incompressible inviscid flow about wings and bodies using CANAERO-T panel model p 2655 N94-28334

PANELS
Experimental and numerical vibration analyses of a stiffened panel
[VTT-PUBS-129] p 2836 N94-25650
Formulae for the buckling of simply-supported corrugated panels of orthotropic material under shear load
[PB94-126547] p 2840 N94-26911
Design and test of postbuckled stiffened curved plates: A literature survey
[PB94-126521] p 2840 N94-26961

PAPER (MATERIAL)
The chemical detector paper as a potential alarm
[FFI-93/6007] p 2712 N94-25745

PARABOLIC DIFFERENTIAL EQUATIONS
Arbitrary-order numerical schemes for model parabolic equations
[CRANFIELD-AERO-9210] p 3005 N94-25781
Computation of numerical solution of parabolic PDEs by monotone iterative methods
[ISBN-0-315-84553-8] p 2999 N94-27404
On the zeros of solutions of forced parabolic differential equations of neutral type
[DE93-613019] p 3001 N94-28228

PARABOLIC FLIGHT
The electrogastrogram during parabolic flight p 2913 N94-27452
Vertical gaze direction during parabolic flight p 2913 N94-27453
Heart rate change in normal and labyrinthectomized hamsters during parabolic flight p 2914 N94-27454

PARABOLIC REFLECTORS
Numerical and experimental analyses of the radiant heat flux produced by quartz heating systems
[NASA-TP-3387] p 3011 N94-27659
Development of a 2f optical performance measurement system
[DE94-003489] p 3039 N94-27721

PARAFFINS
The addition of molecular oxygen to hydroperoxy-propyl radicals
[DE94-003662] p 2760 N94-27725

PARALLAX
In search of Nemesis p 2888 N94-28297

PARALLEL COMPUTERS
Abstraction in, specification and proof of software for a 1D heat-transfer problem
[REPT-93-45] p 2790 N94-25763
Using a transfer function to describe the load-balancing problem
[DE94-004218] p 2979 N94-25802
A doubly logarithmic communication algorithm for the Completely Connected Optical Communication Parallel Computer
[DE93-019408] p 2980 N94-26473
Computational mechanics
[DE94-003015] p 2965 N94-26775
Parallel computers for advanced information processing p 2955 N94-27193

PARALLEL PROCESSING (COMPUTERS)
System software and tools for high performance computing environments: A report on the findings of the Pasadena Workshop
[DE94-003918] p 2956 N94-25602
Using a transfer function to describe the load-balancing problem
[DE94-004218] p 2979 N94-25802
A numerical study of high-speed missile configurations using a block-structured parallel algorithm
[AD-A273776] p 2979 N94-25860
Object-oriented design and implementation of a parallel Ada simulation system
[AD-A274119] p 2979 N94-25906
Use of parallel counters for triggering
[DE93-616656] p 2979 N94-25918
Out of core, out of mind: Practical parallel I/O
[DE94-003107] p 2979 N94-25952
Achieving high performance on the Intel Paragon
[DE94-003108] p 2979 N94-25953
Real-time tracking with a 3D-flow processor array
[DE94-003981] p 2980 N94-25984
Fast parallel algorithms for short-range molecular dynamics
[DE93-018519] p 3016 N94-26033
Run-time recognition of task parallelism within the P++ parallel array class library
[DE94-002707] p 2980 N94-26120
The Chaco user's guide
[DE94-003669] p 2962 N94-26370
Parallel grid generation algorithm for distributed memory computers
[NASA-TP-3429] p 2963 N94-26466
The High Performance Storage System
[DE94-004351] p 2948 N94-26578
Parallel computational geometry on analog Hopfield networks
[ISBN-0-315-84093-5] p 2980 N94-26635
Parallel matrix transpose algorithms on distributed memory concurrent computers
[DE94-002424] p 2964 N94-26764
Computational mechanics
[DE94-003015] p 2965 N94-26775
A Multitransputer Parallel Processing System (MTPPS)
[DE94-604652] p 2981 N94-26903
An optoelectronic graphics display processor
[AD-A274401] p 3037 N94-26990
Parallel mathematical software
[DE94-001587] p 2967 N94-27020
Interactive control of a parallel simulation from a remote graphics workstation
[AD-A274217] p 2981 N94-27070
Implementation and performance of a domain decomposition algorithm in Sisal
[DE94-002012] p 2981 N94-27092
Static task allocation for parallel processing systems during software development
[AD-A274204] p 2981 N94-27100
Automatic mapping of task and data parallel programs for efficient execution on multicomputers
[AD-A274125] p 2982 N94-27117

A parallel computational fluid dynamics unstructured grid generator
[AD-A274129] p 2795 N94-27119

Design of a parallel discrete event simulation coprocessor
[AD-A274135] p 2982 N94-27123

Virtual memory management and virtual bus overloading on multiple channel architectures
[AD-A274127] p 2954 N94-27152

Parallel string matching algorithms
[AD-A274502] p 3100 N94-27164

Proceedings of the Third Workshop Computersystems: Research Forum on Design, Realization and Use of Computersystems
[ISBN-90-6144-995-2] p 2954 N94-27191

Parallel computers for advanced information processing p 2955 N94-27193

Parallel discrete event simulation
p 2955 N94-27194

Sculpting in cyberspace: Parallel processing the development of new software p 2686 N94-27365

Shared virtual memory and generalized speedup
[NASA-CR-191592] p 2969 N94-27416

Parallel implicit unstructured grid Euler solvers
[NASA-CR-191594] p 2999 N94-27434

Efficient massively parallel simulation of dynamic channel assignment schemes for wireless cellular communications
[NASA-CR-191593] p 2971 N94-27558

Iterative methods for the WLS state estimation on RISC, vector, and parallel computers
[DE94-004260] p 3000 N94-27569

Center for space microelectronics technology
[NASA-CR-195282] p 2786 N94-27574

High performance computing in chemistry and massively parallel computers: A simple transition?
[DE94-004318] p 2982 N94-27600

MIMD parallel approaches to object labeling
[ISBN-0-315-60198-1] p 2982 N94-27644

A fast Fourier transform radix-2 complex butterfly with built-in self-test
[ISBN-0-315-84139-7] p 2982 N94-27649

Parallel computing for probabilistic response analysis of high temperature composites
[NASA-CR-194467] p 2843 N94-27656

Communication on the Paragon
[DE94-003103] p 2983 N94-27713

The PRISM project: Infrastructure and algorithms for parallel eigensolvers
[DE94-005125] p 2973 N94-27717

Review and analysis of dense linear system solver package for distributed memory machines
p 2978 N94-27916

PARALLEL PROGRAMMING

Abstraction in, specification and proof of software for a 1D heat-transfer problem
[REPT-93-45] p 2790 N94-25763

Parallel Assessment Window System (PAWS) enhancements
[AD-A274094] p 2979 N94-25786

Object interaction in a parallel object-oriented discrete-event simulation
[AD-A274084] p 2959 N94-25942

Out of core, out of mind: Practical parallel I/O
[DE94-003107] p 2979 N94-25952

Preconditioning in parallel Runge-Kutta methods for stiff initial value problems
[CWI-NM-R9310] p 2991 N94-26217

Programming in Fortran M
[DE94-002756] p 2963 N94-26407

Computational strategies for three-dimensional flow simulations on distributed computer systems
[NASA-CR-195249] p 2793 N94-26595

Efficient implementation of high-level parallel symbolic languages p 2955 N94-27196

Parallel algorithm for dominant points correspondences in robot binocular stereo vision p 2686 N94-27364

Semantics of MANIFOLD: Specification in ASF+SDF and extension
[CWI-CS-R9269] p 2971 N94-27575

Fast parallel permutation algorithms
[CWI-CS-R9303] p 2982 N94-27579

PARAMAGNETISM

Volume dependence of vanadium magnetism
[DE94-601838] p 3050 N94-25843

PARAMETER IDENTIFICATION

Grey-box modelling and identification topics
[PB94-126380] p 2986 N94-27029

Multiple model adaptive control of a large flexible space structure with purposeful dither for enhanced identifiability
[AD-A274132] p 2987 N94-27122

Multiple weight stepwise regression
[DE94-001602] p 3000 N94-27564

A parametric sensitivity study for single-stage-to-orbit hypersonic vehicles using trajectory optimization
[NASA-CR-195703] p 2697 N94-27789

PARAMETERIZATION

Parameter estimation of linear systems from frequency response measurements (computer program)
[ESDU-93016] p 2976 N94-28137

PARAMETRIC AMPLIFIERS

Optical parametric oscillator modeling with diffraction, depletion, and double refraction
[DE94-001504] p 3040 N94-27999

Sum frequency generation using an optical parametric oscillator
[DE94-001827] p 3040 N94-28000

PARITY

Data on parity violation in the compound nucleus and its interpretation
[DE94-003965] p 3013 N94-25820

Dynamic breaking of U(N) and appearance of Chern-Simons term in 4-fermion theories
[DE93-634342] p 3019 N94-26455

The Hamiltonian structures of the super KP hierarchy associated with an even parity superlax operator
[DE94-601506] p 2994 N94-26459

PARKING ORBITS

Lifetimes of lunar satellite orbits
[NASA-TP-3394] p 2690 N94-27771

PARKINSON DISEASE

Impaired associated movement in Parkinson's disease: An evaluation of Bell's phenomenon
p 2928 N94-27520

Effect of L-dopa on hemodynamic functions in humans p 2929 N94-27526

PARSING ALGORITHMS

Parsing schemata: A framework for parallel and sequential parsing
[PB94-125267] p 2981 N94-26998

PARTIAL DIFFERENTIAL EQUATIONS

Continuation and multi-grid for bifurcation problems
[AD-A274965] p 2992 N94-26302

VLUGR2: A vectorized local uniform grid refinement code for PDE's in 2D
[CWI-NM-R9306] p 2965 N94-26772

Local uniform grid refinement and systems of coupled partial differential equations
[CWI-NM-R9307] p 2995 N94-26773

Fields and potentials in general uniaxial bianisotropic media I. Axial sources
[PB94-132875] p 2778 N94-28379

PARTICLE ACCELERATION

Spin effects in hard interactions (interest in accelerated polarized beam)
[DE93-634398] p 3031 N94-26044

Ionosphere-magnetosphere coupling
[NASA-CR-195222] p 2881 N94-27237

Acceleration of electrons and ions by strong lower-hybrid turbulence in solar flares
[NASA-TM-109723] p 3111 N94-27953

PARTICLE ACCELERATOR TARGETS

JLC-1
[DE93-520380] p 3031 N94-26113

Study of the process (pi)(sup -)A(yields)(pi)(sup -)(eta)'(eta)A at the moment 36 GeV/c
[DE93-634530] p 3024 N94-27250

PARTICLE ACCELERATORS

Object-oriented software construction at ALS
[DE94-003418] p 2967 N94-27049

Space Experiments with Particle Accelerators (SEPAC)
[NASA-CR-193935] p 2761 N94-27664

Performance of a 14-MeV neutron generator as an in situ calibration source for TFTR
[DE94-004993] p 3048 N94-27825

PARTICLE BEAMS

Bundle Intensity and Beamgate Length recorder (BIBL)
[DIGEL-1993-7] p 3031 N94-25619

Advanced development of particle beam probe diagnostic system
[DE94-002316] p 3047 N94-27720

PARTICLE COLLISIONS

Production of (phi) mesons in central Si + Au collisions at 14.6 AGeV/c
[DE94-003196] p 3012 N94-25795

Convergent close-coupling calculation of electron-sodium scattering
[DE94-601815] p 3014 N94-25842

Hadron jets and nucleon clusters in the relativistic nuclear collisions
[DE93-613434] p 3031 N94-25850

The amplitude of the elastic hadron-hadron scattering in the coulombic range of transfer momenta
[DE93-613183] p 3014 N94-25869

Spectroscopic and vibrational energy transfer studies in molecular bromine
[AD-A273795] p 3014 N94-25875

Monte Carlo event generators for hadron-hadron collisions
[DE94-003212] p 3015 N94-25955

The Cherenkov hadronic like-jets
[DE93-634525] p 3016 N94-26010

Modeling defect production in high energy collision cascades
[DE94-003810] p 3017 N94-26049

The STAR experiment at the Relativistic Heavy Ion Collider
[DE94-003409] p 3017 N94-26083

Harvard University High Energy Physics
[DE94-002406] p 3032 N94-26119

Predictive modeling of particle-laden, turbulent flows
[DE94-003298] p 2792 N94-26319

Nuclear Theory Group, University of Washington recent and planned research
[DE94-002729] p 3022 N94-26809

D0 results on searches for the top quark
[DE94-003361] p 3023 N94-26938

Calculation of electron-potassium scattering
[DE94-601812] p 3023 N94-26942

Antiproton studies in penning traps
[AD-A274250] p 3024 N94-27011

An analysis of monojet data in p(bar-p) collisions at square root of s equal to 1.8 TEV
[DE94-001822] p 3026 N94-27565

Quantum chromodynamics and nuclear physics at extreme energy density
[DE94-004418] p 3026 N94-27604

Double excitation of He and H(-) by fast proton and anti-proton impact
[DE94-004581] p 3026 N94-27620

Stopping powers and cross sections due to two-photon processes in relativistic nucleus-nucleus collisions
[NASA-CR-4574] p 3033 N94-27646

Studies of heavy-ion reactions and transuranic nuclei
[DE94-004642] p 3029 N94-27783

PARTICLE DENSITY (CONCENTRATION)

Finite density effects in gauge theories
[ISBN-0-315-50637-7] p 3074 N94-27403

PARTICLE DIFFUSION

Bisexual branching diffusions
[AD-A274698] p 3008 N94-26374

PARTICLE ENERGY

Exploration of GaAs structures for solid-state detectors
[DE93-634191] p 3056 N94-26379

PARTICLE INTERACTIONS

Fermionic field theory and gauge interactions on random lattices
[DE94-601565] p 3051 N94-25885

CP test in the W pair production by way of photon fusion at NLC
[DE94-601608] p 3014 N94-25889

Principles of gauge theory of real hadrons
[DE93-616857] p 3015 N94-25920

PARTICLE MASS

C-periodicity and the physical mass in the 3-state Potts model
[DE94-601551] p 3019 N94-26423

Spectroscopy and strong decays of baryons
[ISBN-0-315-49073-X] p 3024 N94-27258

Finding the missing pieces of the standard model
[ISBN-0-315-57174-8] p 3024 N94-27259

On the model of the relativistic particle with curvature and torsion
[DE94-606330] p 3029 N94-27848

Cosmological constraints on very heavy stable neutrinos
[DE94-601669] p 3117 N94-28066

PARTICLE MOTION

Stochastic resonance in a periodic potential system under a constant force
[DE93-616817] p 3008 N94-25831

PARTICLE PRECIPITATION

Quiet-time intensifications along the poleward auroral boundary near midnight
[ATR-93(7248)-2] p 2877 N94-26201

PARTICLE PRODUCTION

Production of (phi) mesons in central Si + Au collisions at 14.6 AGeV/c
[DE94-003196] p 3012 N94-25795

Heavy quark production and spectroscopy
[DE94-003619] p 3015 N94-25935

Monte Carlo event generators for hadron-hadron collisions
[DE94-003212] p 3015 N94-25955

A dependence of exclusive vector meson production in muon-nucleus scattering
[DE94-003363] p 3016 N94-25957

The STAR experiment at the Relativistic Heavy Ion Collider
[DE94-003409] p 3017 N94-26083

Rescattering and energy loss of fast partons in nuclear matter
[DE94-002918] p 3018 N94-26145
A search for the production of direct leptons in nucleon-nucleus and nucleus-nucleus collisions
[DE94-004640] p 3018 N94-26244
Photon and hadron production of heavy flavors
[DE94-004655] p 3018 N94-26245
Strange Dibaryons
[DE94-003005] p 3022 N94-26769
D0 results on searches for the top quark
[DE94-003361] p 3023 N94-26938
Measurements of the B(sup 0)(bar B)(sup 0)CP asymmetry
[DE94-003379] p 3063 N94-27047
Study of the process (pi)(sup -)A(yields)(pi)(sup -)(eta)'(eta)A at the moment 36 GeV/c
[DE93-634530] p 3024 N94-27250
A jet calculus approach including coherence effects and the associated problem of moment inversion
[ISBN-0-315-51715-8] p 3025 N94-27266
Jet production in muon scattering at Fermilab E665
[DE94-004663] p 3028 N94-27752
Correlations in inelastic collisions of relativistic nuclei with emulsion at (4.1 - 4.5) A GeV/c
[DE93-634526] p 3030 N94-27994

PARTICLE SPIN
On the relativistic invariant representation of arbitrary bilinear combinations of Dirac spinors
[DE93-634343] p 3019 N94-26456
Correlated mean field Ansatz for the Kondo necklace
[DE94-603671] p 3067 N94-27634
On the model of the relativistic particle with curvature and torsion
[DE94-606330] p 3029 N94-27848
Axial anomaly in e(+)e(-) yields gamma gamma and anyon superconductivity
[DE94-606406] p 3070 N94-27859

PARTICLE TELESCOPES
CRRES high energy proton flux map
[AD-A274803] p 2878 N94-26338
The PROTEL contamination code
[RXR-93071] p 3040 N94-28202

PARTICLE THEORY
Cosmoparticle physics of family symmetry breaking
[DE94-601623] p 3013 N94-25837
Measurement of tau lepton branching fractions
[DE94-003423] p 3018 N94-26325
Construction of a new electroweak sphaleron
[NIKHEF-H/93-09] p 3020 N94-26540
On the model of the relativistic particle with curvature and torsion
[DE94-606330] p 3029 N94-27848

PARTICLE TRACKS
Fast vertex search (in plane)
[DE93-616655] p 2959 N94-25917
Algorithms of the vertex coordinate reconstruction for straight tracks of short-lived particles
[DE93-616661] p 3015 N94-25919

PARTICLE TRAJECTORIES
Structure functions of sea quarks, Kogut-Susskind pole and dynamics of pp- and pp-bar-interactions at high energies
[DE93-613184] p 3031 N94-25870
IRMA: A program for three-dimensional color display of data
[AD-A273811] p 2959 N94-25879
Ice accretion on aircraft wings p 2657 N94-28345

PARTICLES
Study on neutron activation analysis
[DE93-632191] p 3017 N94-26116

PARTICULATE REINFORCED COMPOSITES
Fracture behavior of 20% Nb particulate reinforced alumina composite
[DE94-002830] p 2706 N94-26019
Effects of post-fabrication processing on the tensile properties of centrifugally cast SiC particulate reinforced aluminum composites
[AD-A274865] p 2707 N94-26190

PARTICULATES
Study on neutron activation analysis
[DE93-632191] p 3017 N94-26116

PARTITIONS (MATHEMATICS)
The Chaco user's guide
[DE94-003669] p 2962 N94-26370
Statistical mechanical properties of Z(N)(sup n-1) broken model
[DE93-634344] p 2993 N94-26457
Computer code for controller partitioning with IFPC application: A user's manual
[NASA-CR-195291] p 2678 N94-27414

PARTONS
The STAR experiment at the Relativistic Heavy Ion Collider
[DE94-003409] p 3017 N94-26083
Rescattering and energy loss of fast partons in nuclear matter
[DE94-002918] p 3018 N94-26145
A jet calculus approach including coherence effects and the associated problem of moment inversion
[ISBN-0-315-51715-8] p 3025 N94-27266
High energy parton-parton elastic scattering in QCD
[DE94-003432] p 3028 N94-27736

PASSENGER AIRCRAFT
Design of the advanced regional aircraft, the DART-75
p 2671 N94-25708
The design of a long-range megatransport aircraft
p 2671 N94-25718
A symbol of reliability: Ju 52 p 2663 N94-28250

PASSENGERS
Powerful selling and sales strategy
p 2662 N94-28245
Lufthansa long range services: More simplicity
p 2663 N94-28246

PASSIVE SATELLITES
Ice surface temperature retrieval from AVHRR, ATSR, and passive microwave satellite data: Algorithm development and application
[NASA-CR-195276] p 2851 N94-27849

PASSIVITY
Electrochemical properties of passive films on 440C stainless steel
[ISBN-0-315-64248-3] p 2757 N94-27801

PASTES
A materials compatibility study in FM-1, a liquid component of a paste extrudable explosive
[DE94-001166] p 2759 N94-26198

PATHOGENS
Bakteriella toxiner-morgondagens hot (bacterial toxins-the threat of tomorrow)
[PB94-124229] p 2902 N94-27045

PATHOLOGY
Bakteriella toxiner-morgondagens hot (bacterial toxins-the threat of tomorrow)
[PB94-124229] p 2902 N94-27045

PATTERN RECOGNITION
Calculation of a 3-D pose of a known object in a single perspective view
[VTT-PUBS-122] p 2957 N94-25642
Solid estimation feature based correlation method for measuring control points required for correcting satellite images
[VTT-JULK-772] p 2848 N94-26253
Colour object recognition
[ISBN-0-315-83684-9] p 2994 N94-26614
A rough set approach to speech recognition
[ISBN-0-315-83894-9] p 2769 N94-26619
Three dimensional object recognition using a complex autoregressive model
[AD-A274388] p 2995 N94-26829
Interacting cortical filters for object recognition
[PB94-125374] p 2938 N94-26873
Orientation competition in cortical filters
[PB94-125366] p 2939 N94-27001
High-speed, high-density, coherent time-domain optical memory
[AD-A274249] p 3037 N94-27010
Combining shape and color information for 3D object recognition
[AD-A274123] p 2967 N94-27064
Translation and rotation invariant pattern recognition
[PB94-123676] p 2968 N94-27157
Parallel string matching algorithms
[AD-A274502] p 3100 N94-27164
Parallel algorithm for dominant points correspondences in robot binocular stereo vision p 2686 N94-27364
Saving comparisons in the Crochemore-Perrin string matching algorithm
[CWI-CS-R9322] p 2971 N94-27550
Thunderstorm Hypothesis Reasoner
[NASA-CR-195714] p 2897 N94-27884
Optical pattern recognition system utilizing resonator array
[AD-D016071] p 3040 N94-28224

PAYLOADS
Project Columbiad: Reestablishment of human presence on the Moon p 2689 N94-25687
STS-57 Space Shuttle mission report
[NASA-CR-195739] p 2693 N94-28220
STS-56 Space Shuttle mission report
[NASA-CR-195740] p 2693 N94-28221

PEBBLE BED REACTORS
Small low mass advanced PBR's for bi-modal operation
[DE94-003201] p 2699 N94-25798

PEEK
A study of graphite peek composite with central elliptical holes under tension
[AD-A273779] p 2705 N94-25863

PELLETS
High-speed repetitive pellet injector for plasma fueling of magnetic confinement fusion devices
[DE94-002792] p 3042 N94-26140

PENALTY FUNCTION
Quantum statistical inference for density estimation
[DE94-002625] p 3073 N94-26805
The numerical calculation of laminar and turbulent flows using penalty function finite volume methods
[ISBN-0-315-61377-7] p 2799 N94-27947

PENETRATION
Penetrating nature of very collimated high-energy shower-clusters of hadrons and gamma rays
p 3113 N94-25631
Users manual for CATNIP: A Computer Analysis Tool for Normal Impact Penetration
[DE94-003671] p 2962 N94-26371

PEPTIDES
Effect of PGE2 receptor agonists butaprost, M and B 28767 and an antagonist AH 6809 on the BK response of visceral polymodal receptors p 2906 N94-27494

PERCEPTION
CRC customer versus rater octane number requirement program (1990)
[AD-A273997] p 2758 N94-25901

PERCOLATION
The Fermi paradox: An approach based on percolation theory p 2687 N94-27370

PERCUSSION
Effects of slot on rock surface for percussive rock excavation: Water jet assisted percussive rock excavation p 2871 N94-28155

PERFORATED PLATES
Three-dimensional elastic stress concentration factors: Plain or countersunk hole in a wide plate subjected to tension, bending, or pin loading
[ESDU-93030] p 2845 N94-28143

PERFORMANCE PREDICTION
Predicting antenna parameters from antenna physical dimensions
[AD-A273893] p 3012 N94-25655
Program to develop a performance and heat load prediction system for multistage turbines
[NASA-CR-195223] p 2674 N94-26588
Early real-time performance measurements on the Columbus processor system p 2952 N94-26736
Integrated model development for liquid fueled rocket propulsion systems
[NASA-CR-195253] p 2702 N94-27166
Interdisciplinary technology p 2686 N94-27363
Rocket engine numerical simulation
p 2688 N94-27375
Transient model applications. 3: Transient engine simulation and analysis of an ice ingestion test
p 2829 N94-28050
Ejectors and jet pumps: Computer program for design and performance for liquid flow
[ESDU-93022] p 2832 N94-28093
Performance model of a recirculating stack nickel hydrogen cell p 2861 N94-28112
A340 testing p 2662 N94-28242

PERFORMANCE TESTS
A test of the theory of reasoned action at the group level of analysis
[AD-A273965] p 2937 N94-25897
Mitsubishi 3-5 micrometers IR imager for machine-vision/ATA applications
[AD-A273812] p 3034 N94-25940
Investigation of plasma etch induced damage in compound semiconductor devices
[DE94-002849] p 3052 N94-25989
Digital Altimeter Setting Indicator (DASI) Operational Test and Evaluation (OT/E) operational test procedures
[AD-A274100] p 2672 N94-26030
Rewarming methodologies in the field
[AD-A274744] p 2909 N94-26173
Differential global positioning system for the surface-towed ordnance locating system: Testing, results, and user's guide
[DE94-002980] p 2664 N94-26309
Hadron gas ionization calorimeters
[DE93-634186] p 2810 N94-26397
Study on the compensated lead hadron calorimeter characteristics by means of hadron and electron beams
[DE93-634176] p 2810 N94-26439
Investigation of the aerodynamic environment for an advanced lightweight rotor in forward flight. Volume 4: Laser velocimeter wake data, advance ratio of 0.037
[NASA-TM-109040-VOL-4] p 2645 N94-26483
Effects of repeating resistance testing on firing ability of igniter EP360-3
[AD-A274814] p 2759 N94-26486

Investigation of the aerodynamic environment for an advanced lightweight rotor in forward flight. Volume 1: Laser velocimeter inflow data, advance ratio of 0.37, thrust coefficient of 0.0081 and hover tip speed of 603 feet/second
[NASA-TM-109040-VOL-1] p 2645 N94-26489

Investigation of the aerodynamic environment for an advanced lightweight rotor in forward flight. Volume 2: Laser velocimeter inflow data, advance ratio of 0.37, thrust coefficient of 0.0064 and hover tip speed of 710 feet/second
[NASA-TM-109040-VOL-2] p 2645 N94-26492

Investigation of the aerodynamic environment for an advanced lightweight rotor in forward flight. Volume 3: Laser velocimeter inflow data, advance ratio of 0.37, thrust coefficient of 0.0064 and hover tip speed of 603 feet/second
[NASA-TM-109040-VOL-3] p 2645 N94-26497

A comparison of sleep scored from electroencephalography to sleep scored by wrist actigraphy
[AD-A273739] p 2910 N94-26748

The PLVCR 500 and HCPC, tests and results
[DLR-MITT-93-04] p 2858 N94-26813

SP industry calorimeter for rate of heat release measurements up to 10MW
[PB94-124211] p 2811 N94-27044

Development of a performance evaluation tool (MMSOFE) for detection of failures with Multiple Model Adaptive Estimation (MMAE)
[AD-A274218] p 2665 N94-27071

Orbital transfer vehicle engine technology high velocity ratio diffusing crossover
[NASA-CR-194447] p 2703 N94-27212

The OPAL vertex detector
[ISBN-0-315-51152-4] p 2812 N94-27257

Design and implementation of a DBMS performance assessment tool
[CWI-CS-R9270] p 2972 N94-27576

Test and evaluation of the Litton (Canada) Canadian strapdown gyroscope (CSG-2) Performance Evaluation Unit (PEU)
[DREO-1010] p 2813 N94-27597

A fully integrated 16 channel digitally trimmed pulse shaping amplifier
[DE94-004555] p 2787 N94-27618

Communication on the Paragon
[DE94-003103] p 2983 N94-27713

Extra-Vehicular Activity (EVA) glove evaluation test protocol
[NASA-TM-108442] p 2943 N94-27952

Transient model applications. 3: Transient engine simulation and analysis of an ice ingestion test
p 2829 N94-28050

Cooling towers for combined cycles: Design philosophy, performance testing, and operating problems
p 2832 N94-28087

Ni-H2 cell characterization for INTELSAT programs
p 2861 N94-28109

Performance test results of ETS-6 Ni-Cd cells
p 2863 N94-28121

AF Ni-Cd cell qualification program
p 2863 N94-28122

Some observations on battery charge control
p 2863 N94-28125

Construction of temperature compensated constant voltage (VT) curves for super Ni-Cd (tm) cells
p 2863 N94-28126

A comparison of spectral decorrelation techniques and performance evaluation metrics for a wavelet-based, multispectral data compression algorithm
p 2946 N94-28258

Fibrous ceramic candle filter for particle removal in pressurized fluidized bed combustion
[PB94-133089] p 2876 N94-28383

PERIODIC VARIATIONS

Modal control of a satellite in an unstable periodic orbit about the Earth-Sun interior Lagrange point
[AD-A273707] p 2694 N94-25776

Modulating terrestrial impacts from Oort cloud comets by the adiabatically changing galactic tides
p 2890 N94-28305

PERIPHERAL CIRCULATION

Effect of prostaglandin E1 on the relationship between skin sympathetic nerve activity and reduction in skin blood flow p 2929 N94-27524

Difference in skin blood flow reduction depending on activating maneuver of skin sympathetic nerve activity
p 2929 N94-27525

Effect of L-dopa on hemodynamic functions in humans p 2929 N94-27526

PERIPHERAL EQUIPMENT (COMPUTERS)

Development of a MIL-STD-1750 microprocessor system for space applications p 2949 N94-26715

PERMANENT MAGNETS

First principle calculation for magneto-crystalline anisotropy
[DE93-634653] p 3052 N94-26012

Correlation of experimental data and three-dimensional finite element modeling of a spinning quadrupole
[DE93-041173] p 3008 N94-26421

PERMEABILITY

Study on alloy films for hydrogen separation
p 2726 N94-25565

Space-R thermionic space nuclear power system: Design and technology demonstration
[DE94-001890] p 2699 N94-25929

Application of the Positron Annihilation Technique to the study of vapor absorption process in polyethylene (LDPE) and in imide polymer (6FDA-TMPD PI)
[DE94-602737] p 2720 N94-27998

Plane wave propagation in an anisotropic chiral medium with isotropic permittivity and permeability
[PB94-133097] p 2778 N94-28384

Green dyadic and dipole fields for a medium with anisotropic chirality
[PB94-132933] p 2779 N94-28391

PERMEATING

Hydrogen uptake into silicon from an ECR plasma
[DE94-003771] p 3050 N94-25815

Ion-driven permeation of deuterium in metals
[DE94-701104] p 2744 N94-27876

PERMITTIVITY

A study of LPM suppression of bremsstrahlung at 25 GeV
[DE94-003457] p 3018 N94-26133

Refractive and dielectric properties of helium, argon and nitrogen gases
[PB94-123783] p 3008 N94-26851

Plane wave propagation in an anisotropic chiral medium with isotropic permittivity and permeability
[PB94-133097] p 2778 N94-28384

Green dyadic and dipole fields for a medium with anisotropic chirality
[PB94-132933] p 2779 N94-28391

Dielectric polarizability of sphere with arbitrary anisotropy
[PB94-133113] p 2779 N94-28397

PERMUTATIONS

Multi-channel Kondo necklace
[DE93-634754] p 3057 N94-26389

Fast parallel permutation algorithms
[CWI-CS-R9303] p 2982 N94-27579

PEROVSKITES

Polar and chemical domain structures of lead scandium tantalate (PST)
[DE94-600760] p 3056 N94-26363

Electrical conductivity of perovskite-magnesiowuestite as a function of pressure and temperature
[DE94-002714] p 2880 N94-26806

Ferroelectric thin film microstructure development and related property enhancement
[DE94-002741] p 3061 N94-26856

Perovskite solid electrolytes for SOFC
[DE94-001923] p 2859 N94-27005

PERSONAL COMPUTERS

Users guide for GRIKURV: A code for drawing graphs
[PB94-123593] p 2968 N94-27154

Development of an automatic fatigue-data acquisition system using commercial software
[NAL-TM-650] p 2842 N94-27207

Inverted pendulum control apparatus using transputers
[DE94-701224] p 2973 N94-27732

PERSONNEL

Evaluation and improvement of the inquest system on work accidents (TOT)
[VTT-TIED-1418] p 2762 N94-26261

Human dimensions research team, operation restore hope
[AD-A274340] p 2939 N94-27056

How to make good use of international research collaboration, with emphasis on the evolving situation in Europe
[PB94-119690] p 3101 N94-27323

Defense force management: Challenges facing DOD as it continues to downsize its civilian work force. Report to the Chairman, Subcommittee on Federal Services, Post Office, and Civil Service, Committee on Governmental Affairs, US Senate
[GAO/NSIAD-93-123] p 3095 N94-28177

PERSONNEL MANAGEMENT

Concepts and methods of measuring productivity at the organization level
[AD-A273126] p 3094 N94-27180

An investigation of integrated product development implementation issues: A case study of Bosma Machine and Tool Corp.
[AD-A273917] p 2942 N94-27320

Defense force management: Challenges facing DOD as it continues to downsize its civilian work force. Report to the Chairman, Subcommittee on Federal Services, Post Office, and Civil Service, Committee on Governmental Affairs, US Senate
[GAO/NSIAD-93-123] p 3095 N94-28177

PERSONNEL SELECTION

A comparison of two hardware implementations of a crew selection system
[AD-A274913] p 2937 N94-26346

Validation of the Federal Aviation Administration air traffic control specialist pre-training screen
[DOT/FAA/AM-94/4] p 2938 N94-26600

PERSPIRATION

Difference in skin blood flow reduction depending on activating maneuver of skin sympathetic nerve activity
p 2929 N94-27525

Enhancement of skin sympathetic nerve activity in amyotrophic lateral sclerosis p 2930 N94-27532

PERTURBATION

Mix induced by single shock passage through a material interface
[DE93-019505] p 2792 N94-26427

Delta f Algorithm
[DE94-003120] p 2963 N94-26521

Normal forms for perturbations of the euler top
[PB94-125390] p 3009 N94-26968

An enhanced global spectral model
[PL-TR-92-2011] p 2898 N94-28223

PERTURBATION THEORY

Experimental study of the near threshold pi(sup +)p yields (pi(sup +))(pi(sup +))(n) cross section and chiral symmetry
[DE94-601671] p 3014 N94-25840

On the estimation of matrix elements for optical transitions in semiconductors
[DE93-613550] p 3051 N94-25851

The modal solution to the Moon's orbit using canonical Floquet perturbation theory
[AD-A273732] p 2690 N94-26001

First principle calculation for magneto-crystalline anisotropy
[DE93-634653] p 3052 N94-26012

Generalized perturbation method expansions of the total energy of an alloy
[DE94-003865] p 3055 N94-26238

On the phi(sub 0)-stability of perturbed nonlinear differential systems
[DE93-634304] p 2993 N94-26441

Low-energy hadronic interactions beyond the current algebra approach
[DE94-602600] p 3022 N94-26900

Operator regularization and renormalization theory
[ISBN-0-315-49334-8] p 3007 N94-27264

PETRI NETS

A modular approach to evaluation cryptographic protocols using Petri nets
[ISBN-0-315-85354-9] p 2972 N94-27595

Sheaf semantics for Petri Nets
[PB94-132826] p 2983 N94-28354

PETROLEUM PRODUCTS

The First Energy Conference: Israel and the Former USSR
[ISBN-965-229-098-X] p 2853 N94-26050

Feasibility study on introduction of transportation-use petroleum substitution energy
[DE94-725205] p 2759 N94-26905

Present situation of the development of petroleum substitution energy (France)
[DE94-725201] p 2760 N94-26914

PH

Fiber optic sensors for corrosion detection
p 3040 N94-27923

PHASE CHANGE MATERIALS

Liquid metal MHD research and development in Israel
p 2854 N94-26055

PHASE CONJUGATION

Phase conjugation and pulse compression of high energy lasers: From nanoseconds to microseconds
[DE94-001061] p 2818 N94-26699

High-speed, high-density, coherent time-domain optical memory
[AD-A274249] p 3037 N94-27010

Phase conjugated lasers applied to commercial x ray lithography
[DE94-001529] p 2819 N94-27018

Predoctoral training grant in the area of physical sciences
[DE94-004406] p 3039 N94-27603

PHASE DIAGRAMS

Phase diagram of La2NiO(4+delta) (0 less than or equal to delta less than or equal to 0.18). 1: Phases at room temperature and phase transition above delta equal to 0.15
[REPT-A-2661] p 3053 N94-26089

Zr-rich corner of the Zr-Sn-O diagram
[DE93-633764] p 2734 N94-26161
Phase portraits of quadratic systems with finite multiplicity three and one critical point of infinity
[REPT-93-41] p 2991 N94-26215
Zr-Sn-Nb alloys: Preliminary studies
[DE93-633767] p 2734 N94-26263
Liquid and solid solubility of Ag in Bi2Sr2CaCu2O8
[DE94-002829] p 2735 N94-26273
Eutectic transformation L in equilibrium to Zr6Fe23 + Fe(tau) in the Fe-Zr system
[DE93-633766] p 2735 N94-26295
Experimental determination of the CU-IN-PB ternary phase diagram
[DE94-003765] p 2735 N94-26349
A new materials data compilation can help in actinide phase-diagram research
[DE94-000797] p 3058 N94-26514
Correlated mean field Ansatz for the Kondo necklace
[DE94-603671] p 3067 N94-27634
Phase stability in the Cd-Mg system
[DE94-004976] p 2743 N94-27792

PHASE ERROR
Numerical simulation of tomographic reconstruction for the study of turbulence using optical wavefront sensor measurements
[AD-A273851] p 2789 N94-25587
Feasibility study of a multiaperture telescope for deep-space Earth surveillance
[AD-A273903] p 3102 N94-25658

PHASE LOCK DEMODULATORS
Design and test of a regenerative satellite transmultiplexer
[ISBN-0-315-85280-1] p 2786 N94-27303

PHASE MATCHING
Three-wave nonlinear interactions in KTiOPO4 (KTP) and KTP isomorphs
[AD-A274079] p 3052 N94-25993
Laser phase induced intensity noise in fiber-optic signal processing and sensing systems
[ITN-94-85234] p 2819 N94-27179

PHASE MODULATION
Structure of the modulated magnetic phase of Mn3Sn
[DE94-002788] p 2733 N94-26092

PHASE SHIFT
Ferrite phase shifters using stress insensitive materials
[AD-A274639] p 2708 N94-26895
Bulletin of the Institute for Chemical Reaction Science, Tohoku University, volume 2
[JTN-94-80602] p 2717 N94-27385
Four phase microwave pulse generator for pulsed EPR spectrometer p 2718 N94-27388
Interhemispheric phase relationship of alpha waves and cerebral dominance p 2927 N94-27518

PHASE SHIFT KEYING
On the performance of trellis coded 8PSK with Reed Solomon codes
[ISBN-0-315-84289-X] p 2770 N94-26626
Short-block data detection techniques employing channel estimation for fading time-dispersive channels
[ISBN-0-315-58970-1] p 2777 N94-27806

PHASE STABILITY (MATERIALS)
Generalized perturbation method expansions of the total energy of an alloy
[DE94-003865] p 3055 N94-26238
Octahedral metallomesogens: Liquid crystallinity in low aspect ratio materials
[AD-A274830] p 3059 N94-26571
A tri-junction diffusion couple analysis of the Nb-Cr-Ti system at 950 C
[DE94-002637] p 2737 N94-26607

PHASE TRANSFORMATIONS
Study on computerized experiment of amorphous transformation process by solid phase reaction
p 2726 N94-25564
Coherent state approach for the (Phi)(sup 6)-lattice model and phase transitions
[DE93-613053] p 3050 N94-25825
Out of equilibrium phase transitions and a toy model for disoriented chiral condensates
[DE94-601642] p 3013 N94-25839
Successive structural phase transitions in stoichiometric La2NiO4 observed by x ray diffraction
[REPT-A-2665] p 3051 N94-25921
Structure and phase transformations in uranium metal
[DE94-003892] p 2732 N94-26004
Oriented lead zirconate titanate thin films: Characterization of film crystallization
[DE94-003104] p 3053 N94-26025
Phase diagram of La2NiO(4+delta) (0 less than or equal to delta less than or equal to 0.18). 1: Phases at room temperature and phase transition above delta equal to 0.15
[REPT-A-2661] p 3053 N94-26089
Se EXAFS study of the elevated wurtzite to rock salt structural phase transition in CdSe nanocrystals
[DE94-003247] p 3054 N94-26125
Diffusion of substitutional elements in Ti in its hcp phase
[DE93-633762] p 2733 N94-26160
Fermi-liquid to non-Fermi-liquid transition in a dynamical generalization of the CPA in a disordered Hubbard model
[DE94-601875] p 2714 N94-26169
Zr-Sn-Nb alloys: Preliminary studies
[DE93-633767] p 2734 N94-26263
Analysis of the effect on growth kinetics of gamma prima phase in Inconel 713C alloys
[DE93-633763] p 2735 N94-26294
Eutectic transformation L in equilibrium to Zr6Fe23 + Fe(tau) in the Fe-Zr system
[DE93-633766] p 2735 N94-26295
C-periodicity and the physical mass in the 3-state Potts model
[DE94-601551] p 3019 N94-26423
Electron microscopy of AlN-SiC interfaces and solid solutions
[DE94-002449] p 3059 N94-26765
Cosmological phase transitions
[DE94-003001] p 3104 N94-26786
Titanium 1992: Science and Technology, volume 1
[AD-A274798-VOL-1] p 2739 N94-26799
Ultrastructure processing of macromolecular materials
[AD-A274460] p 2754 N94-27086
Morphology transitions during non-equilibrium growth processes
[ITN-94-85236] p 3065 N94-27243
Localization properties of one-dimensional electrified chains
[DE94-603672] p 3067 N94-27635
Second-order phase transition in (g(phi)4)2 theory
[DE94-603677] p 3067 N94-27638
Construction and test of experiment hardware for a space experiment on Spacelab mission IML-2
[DLR-FB-93-23] p 2903 N94-27743
A numerical approach to Stefan problem
[IPPCZ-334] p 2844 N94-27841
The Science Reports of the Research Institutes, Tohoku University. Series A: Physics, Chemistry, and Metallurgy. Volume 38, No. 1: Amorphous Materials 14
[JTN-94-80610] p 2744 N94-28158
Differential scanning calorimetric study of solid state amorphization and crystallization in Zr/Co and Zr/Ni multilayers p 2745 N94-28161
Formation and crystallization of hydrogen-induced amorphous Ti3InH(4.5) alloy p 2745 N94-28163
Formation of glassy Pd-Ni-P alloys by mechanical alloying and their structure and thermal stability
p 2746 N94-28168
Production of an amorphous Fe(75)Si(10)B(15) sheet by a metallic mold casting method and its properties
p 2746 N94-28170

PHASED ARRAYS
Project PARAS: Phased array radio astronomy from space p 3081 N94-25703
Characterization of an LCD for use as a programmable phase shifter to produce a single-lobed far-field pattern in a phased array
[AD-A273883] p 3034 N94-25729
A current evaluation of the digital beamforming testbed at Rome Laboratory
[AD-A274311] p 3032 N94-26881
Design and control of phased ICRF antenna arrays
[DE94-002796] p 3046 N94-27261

PHENOLIC RESINS
Soft ground arresting system for airports
[DOT/FAA/CT-93/80] p 2680 N94-26202

PHENOLS
Effects of p-chlorophenol on sulfate reduction in marine sediments p 2870 N94-28150

PHENOMENOLOGY
Harvard University High Energy Physics
[DE94-002406] p 3032 N94-26119

PHILIPPINES
Philippine thrust on environmental research relating to global change p 2873 N94-28279

PHOBOS
Project APEX: Advanced manned exploration of the Martian moon Phobos p 3079 N94-25688

PHONEMES
Researches of the Electrotechnical Laboratory. No. 955: Speech recognition by description of acoustic characteristic variations
[JTN-94-80604] p 2775 N94-27249

PHONONS
Strongly interacting fermion systems
[DE94-002674] p 3021 N94-26677

PHOSPHATES
Zinc(2) oxide stability in alkaline sodium phosphate solutions at elevated temperatures
[DE94-003316] p 2715 N94-26320
Development of K(1-x)Na(x)TiOPO4 crystals for nonlinear applications
[AD-A274336] p 3063 N94-27055
Effect of different ions on the anodic behaviour of alloy 800 in chloride solutions at high temperature
[DE94-602982] p 2743 N94-27832

PHOSPHAZENE
Phosphazene-containing amine as curing agent for phthalonitrile-base polymer
[AD-D016029] p 2755 N94-27147

PHOSPHORESCENCE
Dynamics of metastable states in supersonic beams
[ITN-94-85232] p 3028 N94-27760

PHOSPHORIC ACID
Qualitative analysis of rare earth elements contained in the phosphogypsum
[DE93-614153] p 2716 N94-26518

PHOSPHORUS
Simplified high-efficiency silicon cell processing
[DE94-002683] p 2857 N94-26617
He(+) and H(+) microbeam damage, swelling and annealing in diamonds
[DE94-601912] p 3063 N94-26987
Electron microscopy studies of undoped and phosphorus doped Si:H and Si,C:H films
[DE94-004738] p 3069 N94-27757
Formation of glassy Pd-Ni-P alloys by mechanical alloying and their structure and thermal stability
p 2746 N94-28168

PHOSPHORYLATION
Activation by G protein beta gamma subunits of G protein-coupled receptor kinase p 2931 N94-27534

PHOTOACOUSTIC SPECTROSCOPY
Modern photoacoustic spectroscopy problems. Theory and experiment (a review)
[IFTR-41/1993] p 2716 N94-26823

PHOTOCHEMICAL REACTIONS
Translational-energy-resolved studies of photogenerated carrier-induced reactions on UHV semiconductor surfaces
[DE94-004169] p 3058 N94-26526
Mechanistic studies of opto-electronic materials and syntheses using multiple laser and surface diagnostics
[AD-A274528] p 3036 N94-26834
Numerical analysis of the photo-dissociation/radical oxidation of formaldehyde by ultraviolet light in a photolytic reactor
[AD-A274539] p 2868 N94-26843
Photochemical processes and the atmospheric airglow emissions of OH and Na in the mesospheric region
[INPE-5380-PUD/050] p 2882 N94-27334
How well was total ozone abundance inferred with Mariner 9? p 3108 N94-27891
The kinetics and dynamics of the coma of Halley's comet
[NASA-CR-194828] p 3105 N94-28184

PHOTOCONDUCTIVITY
Determination of surface recombination velocity and bulk lifetime in detector grade silicon and germanium crystals
[DE94-003886] p 3053 N94-26094
Fast photoconductor CdTe detectors for synchrotron x ray studies
[DE94-001334] p 3054 N94-26139
The optical properties of high-T(c) superconductors grown by pulsed laser deposition
[ISBN-0-315-84917-7] p 3039 N94-27962
Anisotropy in the electrical, magnetic and optical properties of Pb2Sr2RCu3O8
[ISBN-0-315-84930-4] p 3070 N94-27974

PHOTOCONDUCTORS
Fast photoconductor CdTe detectors for synchrotron x ray studies
[DE94-001334] p 3054 N94-26139

PHOTODIODES
Elastic backscattering lidar for a MSTI satellite
[DE94-002701] p 2816 N94-26126

PHOTODISSOCIATION
Theoretical determination of chemical rate constants using novel time-dependent methods
[NASA-CR-195221] p 2714 N94-26205
Numerical analysis of the photo-dissociation/radical oxidation of formaldehyde by ultraviolet light in a photolytic reactor
[AD-A274539] p 2868 N94-26843
The kinetics and dynamics of the coma of Halley's comet
[NASA-CR-194828] p 3105 N94-28184

PHOTOELECTRIC EMISSION
A study of LPM suppression of bremsstrahlung at 25 GeV
[DE94-003457] p 3018 N94-26133

PHOTOELECTROMAGNETIC EFFECTS
Technical report of ISSP. Ser. A, no. 2672: Magneto-optical effects of excitons in BiI3 crystals under pulsed high magnetic fields. 3: Excitons confined around a stacking disorder formed by a bending stress
[JTN-94-80558] p 3065 N94-27240
PHOTOELECTRON SPECTROSCOPY
Photoelectron spectroscopic studies of the electronic structure and bonding in TiC and TiN
[ATR-93(8361)-2] p 2746 N94-28185
PHOTOELECTRONS
The 1024 scintillation hodoscope
[DE93-634183] p 2810 N94-26394
Solar and airglow measurements aboard the two suborbital flights NASA 36.098 and 36.107
[NASA-CR-195279] p 2882 N94-27380
PHOTOEXCITATION
Technical report of ISSP. Ser. A, no. 2680: Determination of intervalley scattering time in germanium by subpicosecond time-resolved Raman spectroscopy
[JTN-94-80566] p 3064 N94-27176
PHOTOGRAPHIC RECORDING
Root gravitropism in maize and Arabidopsis
[NASA-CR-195710] p 2903 N94-27940
Debris/ice/TPS assessment and integrated photographic analysis for Shuttle mission STS-60
[NASA-TM-109193] p 2692 N94-27956
PHOTOINTERPRETATION
Debris/ice/TPS assessment and integrated photographic analysis for Shuttle mission STS-60
[NASA-TM-109193] p 2692 N94-27956
PHOTOIONIZATION
Three methods to measure RH bond energies
[DE94-003795] p 3013 N94-25816
Development of laser spectroscopic technology in nuclear industry
[DE93-633327] p 2714 N94-26158
Study on laser atomic spectroscopy
[DE93-633328] p 2817 N94-26402
Measurement of metastable population distribution in gadolinium atomic beam by laser resonance photoionization method
[DE94-701194] p 3029 N94-27820
PHOTOLITHOGRAPHY
Sum frequency generation using an optical parametric oscillator
[DE94-001827] p 3040 N94-28000
PHOTOLUMINESCENCE
Ordering and phase separation in MOCVD InGaP alloys and unicompositional quantum wells
[DE94-004693] p 3056 N94-26352
Light emitting porous silicon
[AD-A274152] p 3038 N94-27137
PHOTOLYSIS
Numerical analysis of the photo-dissociation/radical oxidation of formaldehyde by ultraviolet light in a photolytic reactor
[AD-A274539] p 2868 N94-26843
PHOTOMAPPING
Optical pattern recognition system utilizing resonator array
[AD-D016071] p 3040 N94-28224
PHOTOMETERS
Investigation of a normal incidence high-performance p-type strained layer In(0.3)Ga(0.7)As / In(0.52)Al(0.48) as quantum well infrared photodetector
[AD-A274854] p 3055 N94-26188
Multichip module high speed testing
[AD-A274873] p 2782 N94-26343
The growth and characterization of GaN as a photodetector
[AD-A274570] p 3063 N94-26965
PHOTOMULTIPL'ER TUBES
The 1024 scintillation hodoscope
[DE93-634183] p 2810 N94-26394
PHOTON BEAMS
Spectral and temporal correlations of multifrequency waves in the turbulent atmosphere
[ITN-94-85229] p 2774 N94-27233
PHOTON-ELECTRON INTERACTION
Theoretical and experimental studies of elementary physics
[DE94-002310] p 3008 N94-25988
Deciphering the quark-gluon structure of the photon in electron(gamma) collisions
[DE93-634386] p 3017 N94-26043
PHOTONICS
Component characterization and development 2
[AD-A274002] p 2765 N94-25660
Diagnostics and microelectronics
[DE94-003016] p 2784 N94-26777
Center for space microelectronics technology
[NASA-CR-195282] p 2786 N94-27574
PHOTONS
Biexciton formation by two-photon absorption in quantum wells
[DE93-613551] p 3071 N94-25852
Theoretical and experimental studies of elementary physics
[DE94-002310] p 3008 N94-25988
Deciphering the quark-gluon structure of the photon in electron(gamma) collisions
[DE93-634386] p 3017 N94-26043
Radiation-Induced Structural Changes, 2
[DE93-520314] p 3054 N94-26109
Fast photoconductor CdTe detectors for synchrotron x ray studies
[DE94-001334] p 3054 N94-26139
Photon and hadron production of heavy flavors
[DE94-004655] p 3018 N94-26245
Measurements of the p (mu)d-molecule formation rate at different hydrogen temperature
[DE93-634636] p 3020 N94-26511
Aspects of perturbative corrections in quantum chromodynamics
[ISBN-0-315-63607-6] p 3074 N94-27398
Omega omega and rho+ rho- production in two photon interactions at ARGUS
[ISBN-0-315-63748-X] p 3026 N94-27399
Nonlinear transverse propagation of photons in a ultrarelativistically hot and magnetized electron-positron plasma: Coupling of Langmuir and electromagnetic solitons
[DE94-603667] p 3046 N94-27630
Pi plus pi minus gamma and K+ K- production in two photon collisions at ARGUS
[ISBN-0-315-63598-3] p 3027 N94-27684
PHOTONUCLEAR REACTIONS
Proceedings of the workshop on (pi), K, (eta)-nucleon interactions
[DE94-701314] p 3027 N94-27733
PHOTOPRODUCTION
Electroweak and other interactions in medium-energy nuclear physics
[DE94-004161] p 3027 N94-27689
Proceedings of the workshop on (pi), K, (eta)-nucleon interactions
[DE94-701314] p 3027 N94-27733
PHOTORECONNAISSANCE
Objective image quality metrics: Applications for partially compensated images of space objects
[AD-A273837] p 2847 N94-25741
PHOTOSENSITIVITY
Calorimeter with WLS fibers and parallel to beam scintillators
[DE93-634188] p 2810 N94-26378
Physical characteristics of polymethylmethacrylate scintillator SOFG-120
[DE93-634184] p 2810 N94-26395
PHOTOSPHERE
Environmental conditions responsible for solar activity
[AD-A274191] p 3111 N94-27099
PHOTOTRANSISTORS
A tri-state optical switch for local area network communications p 2789 N94-27922
PHOTOVOLTAIC CELLS
Overview of the Photovoltaic Manufacturing Technology (PVMaT) project
[DE93-018234] p 2856 N94-26426
Low-cost photovoltaic inverters incorporating application-specific integrated circuits
[DE94-003270] p 2856 N94-26463
Handbook of photovoltaic power generating design for introduction
[DE94-725199] p 2858 N94-26913
Solar collector manufacturing activity, 1992
[DE94-003401] p 2859 N94-27048
PHOTOVOLTAIC CONVERSION
The state of the art of thin-film photovoltaics
[DE94-000224] p 2855 N94-26115
Hybrid power system for remote communications stations
[AD-A274963] p 2782 N94-26301
Solar resource-utility load matching assessment: NREL photovoltaic project summary
[DE94-000232] p 2856 N94-26480
Merging photovoltaic hardware development with hybrid applications in the USA
[DE94-002682] p 2857 N94-26612
Handbook of photovoltaic power generating design for introduction
[DE94-725199] p 2858 N94-26913
Fibrous emissive burners selective and broad band
[PB94-128329] p 2859 N94-27225
PHTHALOCYANIN
Fundamental study on new synthetic technology by phthalocyanine complexes p 2721 N94-25569
PHYSICAL CHEMISTRY
Crystal chemistry and self-lubricating properties of monochalcogenides gallium selenide and tin selenide
[DE93-041177] p 2751 N94-26422
Ultrastructure processing of macromolecular materials
[AD-A274460] p 2754 N94-27086
PHYSICAL EXAMINATIONS
Monograph of the aviation epidemiology data register for calendar year 1988
[AD-A274589] p 2911 N94-26985
PHYSICAL EXERCISE
The effect of platform motion on human energy expenditure during walking. An exploratory experiment
[AD-A273760] p 2940 N94-25724
Plasma volume shifts and exercise thermoregulation with water immersion and six-degree head-down tilt
[NASA-TM-108781] p 2901 N94-26093
Thermoregulatory effects of caffeine ingestion during rest and exercise in men
[NASA-TM-108783] p 2901 N94-26210
Sympathetic nerve activity during dynamic leg exercise
p 2929 N94-27527
Workshop on Countering Space Adaptation with Exercise: Current Issues
[NASA-CP-3252] p 2934 N94-28361
Muscular activity and its relationship to biomechanics and human performance p 2934 N94-28362
Eccentric exercise testing and training
p 2934 N94-28363
Exercise detraining: Applicability to microgravity
p 2934 N94-28364
Exercise and osteoporosis: Methodological and practical considerations p 2935 N94-28370
The value of electrical stimulation as an exercise training modality p 2936 N94-28372
The use of biomechanics in the study of movement in microgravity p 2936 N94-28373
Psychophysiology in microgravity and the role of exercise p 2936 N94-28374
PHYSICAL FACTORS
Mass extinctions: Persistent problems and new directions p 2889 N94-28302
PHYSICAL FITNESS
Aeromedical issues related to positive pressure breathing for +Gz protection
[AD-A274717] p 2910 N94-26435
Female combat helicopter pilot selection criteria
[AD-A273935] p 2938 N94-26749
PHYSIOCHEMISTRY
Proposed law of nature linking impacts, plume volcanism, and Milankovitch cycles to terrestrial vertebrate mass extinctions via greenhouse-embryo death coupling
p 2876 N94-28307
PHYSIOLOGICAL ACCELERATION
Evaluation of near-infrared spectrophotometric method for individual tolerance to +Gz acceleration
p 2933 N94-27944
PHYSIOLOGICAL EFFECTS
Annals of the Research Inst. of Environmental Medicine, Nagoya Univ., volume 44
[REPT-44-VOL-44] p 2911 N94-27442
Study on posture control and adaption mechanism under weightlessness: Results of second rehearsal for space experiment using carp p 2912 N94-27446
Study on posture control and adaption mechanism under weightlessness: Differences in weight and shape of utricular otolith of carp p 2912 N94-27448
Telescience testbedding for physiological experiments under hypobaric hypoxic conditions
p 2913 N94-27449
Telescience testbedding under hypobaric hypoxic conditions: Evaluation by operation ability and recognition ability p 2913 N94-27450
The electrogastrogram during parabolic flight
p 2913 N94-27452
Vertical gaze direction during parabolic flight
p 2913 N94-27453
Heart rate change in normal and labyrinthectomized hamsters during parabolic flight p 2914 N94-27454
Frequency analysis of body sway induced by optokinetic stimulation p 2914 N94-27455
Cardiovascular function during thermoneutral head-out water immersion in the elderly p 2915 N94-27458
Effects of 40 C hot water immersion for an hour on thermoregulatory functions in humans: Comparison with 34 C thermoneutral immersion p 2915 N94-27459
Effects of bathing at 40 C on cardiovascular system in humans: Comparison with 34 C thermoneutral bathing
p 2918 N94-27473
Effects of 41 C bathing for 20 minutes on cardiovascular and thermoregulatory functions in humans
p 2918 N94-27474
Monthly variation of physiological and psychological responses under unsteady thermal conditions
p 2918 N94-27475

Man's ability to adapt himself for the seasonal climatic changes: From viewpoint of anticipation and seasonable behavior p 2919 N94-27476

Symptoms of hypoxia at simulated altitude of 25,000 feet p 2933 N94-27945

The use of biomechanics in the study of movement in microgravity p 2936 N94-28373

PHYSIOLOGICAL RESPONSES

The effect of platform motion on human energy expenditure during walking. An exploratory experiment [AD-A273760] p 2940 N94-25724

Thermoregulatory effects of caffeine ingestion during rest and exercise in men [NASA-TM-108783] p 2901 N94-26210

Changes in circadian variations of urine excretion in tail-suspended rats p 2911 N94-27443

Endocrinological evaluations of muscle and bone atrophy in tail-suspended rats p 2903 N94-27444

Aerobic fitness and orthostatic tolerance: Evidence against an association p 2934 N94-28365

Exercise and osteoporosis: Methodological and practical considerations p 2935 N94-28370

Electrical stimulation in exercise training p 2935 N94-28371

PHYSIOLOGICAL TESTS

Effects of methamphetamine on vigilance and tracking during extended wakefulness [AD-A274896] p 2909 N94-26179

The use of EEG as a workload assessment tool in flight test [AD-A274568] p 2910 N94-26847

On the development of motor chunks and concurrent processing in a structured continuous keypressing task [AD-A274153] p 2939 N94-27138

Does training-induced orthostatic hypotension result from reduced carotid baroreflex responsiveness? p 2935 N94-28366

PHYSIOLOGY

Aeromedical issues related to positive pressure breathing for +Gz protection [AD-A274717] p 2910 N94-26435

Multivariate calibration applied to near-infrared spectroscopy for the quantitative analysis of dilute aqueous solutions [DE94-003231] p 2716 N94-26794

Eccentric exercise testing and training p 2934 N94-28363

PHYTOPLANKTON

Changes in phytoplankton population in the Chao Phraya estuary, Thailand, during the eutrophication mechanisms studies p 2875 N94-28287

PIEZOELECTRIC CERAMICS

A study on piezoelectric actuators and sensors for vibration control of flexible space structures [AD-A274925] p 2695 N94-26532

PIEZOELECTRICITY

Object imaging accomplished with an integrated circuit robotic tactile sensor incorporating a piezoelectric polyvinylidene fluoride thin film [AD-A274038] p 2780 N94-25845

Piezoelectric measurements on impact loaded PZT ceramics [NPL-DMM(A)-88] p 2752 N94-26652

High temperature sensor/microphone development for active noise control [NASA-CR-195214] p 2812 N94-27214

PIGMENTS

Polyurethane self-priming topcoats [AD-D016041] p 2755 N94-27111

PILOT ERROR

Aircraft accident report: Runway departure following landing American Airlines flight 102, McDonnell Douglas DC-10-30, N139AA, Dallas/Fort Worth International Airport, Texas, April 14, 1993 [PB94-910402] p 2660 N94-27766

PILOT PERFORMANCE

US Army aviation epidemiology data registry: Incidence and outcomes of aviator flying evaluation boards [AD-A274711] p 2910 N94-26432

Piloted simulation study of an ILS approach of a twin-pusher business/commuter turboprop aircraft configuration [NASA-TM-4516] p 2646 N94-26602

Task demand, workload, and performance [PB94-123627] p 2942 N94-27155

Brain wave correlates of attentional states: Event related potentials and quantitative EEG analysis during performance of cognitive and perceptual tasks p 2940 N94-27901

The Reports of Aeromedical Laboratory, volume 33, number 4 [JTN-94-80586] p 2933 N94-27942

Comparison of performance in simulator flight among subjects with different simulator experiences p 2933 N94-27943

Evaluation of near-infrared spectrophotometric method for individual tolerance to +Gz acceleration p 2933 N94-27944

Symptoms of hypoxia at simulated altitude of 25,000 feet p 2933 N94-27945

PILOT PLANTS

Liquid metal MHD research and development in Israel p 2854 N94-26055

PILOT SELECTION

Female combat helicopter pilot selection criteria [AD-A273935] p 2938 N94-26749

Comparison of performance in simulator flight among subjects with different simulator experiences p 2933 N94-27943

PILOT TRAINING

Symptoms of hypoxia at simulated altitude of 25,000 feet p 2933 N94-27945

PILOTLESS AIRCRAFT

An analysis of multiple sensor system payloads for unmanned aerial vehicles [AD-A274905] p 2667 N94-26182

PINNING

Microstructural development in low activation ferritic alloys irradiated to 200 dpa at 420 C [DE94-004269] p 2731 N94-25803

The potential for large critical currents in the high T(sub c) oxides p 2854 N94-26058

Evaluation of APC NbTi superconductor in a model dipole magnet [DE94-003258] p 3060 N94-26795

Processing, fabrication, and demonstration of HTS integrated microwave circuits, appendix A [AD-A274600] p 2785 N94-26890

PINS

Crystal chemistry and self-lubricating properties of monochalcogenides gallium selenide and tin selenide [DE93-041177] p 2751 N94-26422

Guidelines for unlubricated sliding wear tests. Part 2: Procedures for pin-on-disc testing [PB94-123270] p 2825 N94-27324

PION BEAMS

Study on the compensated lead hadron calorimeter characteristics by means of hadron and electron beams [DE93-634176] p 2810 N94-26439

PIONS

Theoretical and computational studies in intermediate energy nuclear physics [DE94-004177] p 3012 N94-25800

Experimental study of the near threshold pi(sup +)p yields (pi(sup +))(pi(sup +))(n) cross section and chiral symmetry [DE94-601671] p 3014 N94-25840

Meson X(1814) as a candidate for a hybrid state [DE93-634447] p 3017 N94-26045

Pion-nucleus interactions and the STAR experiment at RHIC [DE94-000658] p 3021 N94-26586

Low-energy hadronic interactions beyond the current algebra approach [DE94-602600] p 3022 N94-26900

Study of the process (pi)(sup -)A(yields)(pi)(sup -)(eta)'(eta)A at the moment 36 GeV/c [DE93-634530] p 3024 N94-27250

Pi plus pi minus gamma and K+ K- production in two photon collisions at ARGUS [ISBN-0-315-63598-3] p 3027 N94-27684

PIPE FLOW

Experimental contribution to the study of secondary flows in centrifugal turbopump stator components [ECL-92-35] p 2789 N94-25654

PIPELINING (COMPUTERS)

A fast Fourier transform radix-2 complex butterfly with built-in self-test [ISBN-0-315-84139-7] p 2982 N94-27649

PIPES (TUBES)

Testing composite-to-metal tubular lap joints [DE94-003225] p 2836 N94-26032

Growth of small fatigue cracks in Incoloy-908 [DE94-003406] p 2836 N94-26129

Development of detection technique for fatigue crack due to thermal stratification phenomena in RCS piping [DE93-632968] p 2838 N94-26400

Template synthesis of metal microtubule ensembles utilizing chemical, electrochemical, and vacuum deposition techniques [AD-A274676] p 2715 N94-26444

Dynamics of a flexible extendible beam [ISBN-0-315-84278-4] p 2838 N94-26639

PITCHING MOMENTS

A numerical study of high-speed missile configurations using a block-structured parallel algorithm [AD-A273776] p 2979 N94-25860

Reconfigurable aircraft stick control [AD-D016043] p 2681 N94-27113

Wind tunnel investigation of propfan slipstream/wing interactions on a De Havilland air motor powered semispan model at Mach numbers 0.6 and 0.7 p 2651 N94-28316

PITTING

The electrochemical behavior of the Al3Fe intermetallic compound and localized corrosion of impure 1100 Al [DE94-002037] p 2739 N94-26912

Effect of different ions on the anodic behaviour of alloy 800 in chloride solutions at high temperature [DE94-602982] p 2743 N94-27832

PIXELS

Analysis of the influence of weather on infrared imagery [FEL-92-A421] p 3036 N94-26649

An algorithm for stereo correspondence problems on the analogy of human vision [NAL-TR-1185] p 2940 N94-27584

Image quality measures and their performance p 2946 N94-28257

PLANE WAVES

Hydroacoustic wave-fields generated by different source types, a computational study [PB94-123536] p 3010 N94-27037

Mach reflection of spherical detonation waves [DE93-016604] p 2797 N94-27705

The propagation of spark-produced N waves through turbulence p 2650 N94-28193

Plane wave propagation and polarization properties in transversely bianisotropic uniaxial medium [PB94-132883] p 2778 N94-28380

Eigenwaves in the general uniaxial bianisotropic medium with symmetric parameter dyadics [PB94-132891] p 2778 N94-28381

Plane wave propagation in an anisotropic chiral medium with isotropic permittivity and permeability [PB94-133097] p 2778 N94-28384

Green dyadic and dipole fields for a medium with anisotropic chirality [PB94-132933] p 2779 N94-28391

PLANETARY BASES

Pax: A permanent base for human habitation of Mars p 2943 N94-25706

PLANETARY BOUNDARY LAYER

An evaluation of the utility of ground-based high resolution interferometer (GB-HIS) soundings of the planetary boundary layer [DE94-000960] p 3106 N94-25981

The Martian atmospheric planetary boundary layer stability, fluxes, spectra, and similarity [NASA-CR-195711] p 3108 N94-27935

PLANETARY CRATERS

Cratering rates from lunar xenospherules [DE94-003481] p 3106 N94-27007

PLANETARY EVOLUTION

Studies of extra-solar Oort Clouds and the Kuiper Disk [NASA-CR-195242] p 3103 N94-26789

New Developments Regarding the KT Event and Other Catastrophes in Earth History [NASA-CR-195169] p 2887 N94-28294

Some implications of large impact craters and basins on Venus for terrestrial ringed craters and planetary evolution p 2890 N94-28306

PLANETARY GEOLOGY

A geological and geophysical information system for Eurasia [AD-A274818] p 3098 N94-26490

Some implications of large impact craters and basins on Venus for terrestrial ringed craters and planetary evolution p 2890 N94-28306

An extraterrestrial event at the tertiary-quaternary boundary p 2890 N94-28309

Were all extinction events caused by impacts? p 2891 N94-28311

PLANETARY MAGNETIC FIELDS

Analysis of energetic proton and electron data in Neptune's magnetosphere [NASA-CR-195707] p 3107 N94-27784

PLANETARY MAGNETOSPHERES

Studies for Io's extended atmosphere and neutral clouds and their impact on the local satellite atmosphere and on the planetary magnetosphere [NASA-CR-195255] p 3106 N94-27406

Analysis of energetic proton and electron data in Neptune's magnetosphere [NASA-CR-195707] p 3107 N94-27784

PLANETARY MAPPING

Copernicus: Lunar surface mapper p 3081 N94-25702

PLANETARY STRUCTURE

Underground structure in the eastern part of Kanagawa Prefecture inferred from explosion seismic observations p 2886 N94-27987

PLANETARY SURFACES

Hardware design of a spherical mini-rover p 2833 N94-25669

Planetary surface exploration MESUR/autonomous lunar rover p 2833 N94-25683
PLANETARY SYSTEMS
Studies of extra-solar Oort Clouds and the Kuiper Disk
[NASA-CR-195242] p 3103 N94-26789
PLANETARY WAVES
Numerical procedure for planetary wave solution
[DE94-004280] p 2879 N94-26576
Global barotropic response to a tropical forcing
[NASA-CR-195256] p 2896 N94-27408
PLANKTON
Coupling of pelagic and benthic communities over a seamount in the Eastern North Pacific
[AD-A274750] p 2899 N94-26149
PLANNING
Environmental benefits of different types of heat pumps, available and expected
[DE94-002440] p 2866 N94-26123
PLANT ROOTS
Root gravitropism in maize and Arabidopsis
[NASA-CR-195710] p 2903 N94-27940
PLANTS (BOTANY)
Report of National Institute for Resources and Environment. No. 5: Study on direct liquefaction of woody biomass
[JTN-94-80551] p 2859 N94-27204
PLASMA ARC WELDING
UAH mathematical model of the variable polarity plasma ARC welding system calculation
[NASA-CR-193926] p 2824 N94-27221
PLASMA COMPOSITION
Study on development of chemical measurement method utilizing plasmas p 2728 N94-25576
International bulletin on atomic and molecular data for fusion. No. 42-45, Mar. 1991 - Dec. 1992
[DE94-601817] p 3045 N94-26946
Helium transport and exhaust studies of H-mode discharges in the D3-D tokamak
[DE94-004744] p 3048 N94-27785
PLASMA CONTROL
High-speed repetitive pellet injector for plasma fueling of magnetic confinement fusion devices
[DE94-002792] p 3042 N94-26140
Scaling of sustained ZT-40 M reversed field pinches
[DE94-003318] p 3043 N94-26321
Probability of accessing the multiple saturated states in the resistive interchange instability
[DE94-000478] p 3044 N94-26694
Potential of commercial tokamak reactors with improved physics
[DE94-002794] p 3044 N94-26860
Role of core toroidal rotation shear on turbulence and transport in the improved confinement regimes of the D3-D tokamak
[DE94-001215] p 3045 N94-26950
High gas-efficiency hydrogen negative ion sources
[PB93-232163] p 3025 N94-27348
Researches of the Electrotechnical Laboratory. No. 51: Study of formation and sustainment of reversed field pinch by slow control of magnetic field
[JTN-94-80548] p 3046 N94-27350
TFTR experimental data analysis collaboration
[DE94-004166] p 3047 N94-27690
Helium transport and exhaust studies of H-mode discharges in the D3-D tokamak
[DE94-004744] p 3048 N94-27785
Fuel ion rotation measurement and its implications on H-mode theories
[DE94-004860] p 3048 N94-27791
On radio frequency wave induced radial transport and wave helicity
[IPPCZ-326] p 2777 N94-27838
On helicon wave induced radial plasma transport
[IPPCZ-333] p 3048 N94-27840
Determination of the plasma column shape in the Tokamak Novillo cross section by magnetic probes
[DE94-604986] p 3048 N94-27844
Modelling and control of plasma position in the STOR-M tokamak
[ISBN-0-315-58891-8] p 3049 N94-27949
PLASMA CURRENTS
Numerical simulation of plasma vertical position stabilization in ITER
[DE93-634588] p 3044 N94-26510
Ionosphere-magnetosphere coupling
[NASA-CR-195222] p 2881 N94-27237
On radio frequency wave induced radial transport and wave helicity
[IPPCZ-326] p 2777 N94-27838
On helicon wave induced radial plasma transport
[IPPCZ-333] p 3048 N94-27840
PLASMA DENSITY
Upper atmosphere neutral and plasma density modeling
[AD-A274768] p 2879 N94-26569
Experiments and numerical simulations of electromagnetic wave propagation in plasma varying rapidly in space and time
[AD-A274376] p 2772 N94-26975
Shine through measurements with hydrogen beam in JT-60
[DE94-701113] p 3047 N94-27699
Laser blow-off lithium beam probing with high temporal resolution for edge plasma diagnostics
[DE94-701176] p 2820 N94-27701
PLASMA DIAGNOSTICS
Study on development of chemical measurement method utilizing plasmas p 2728 N94-25576
Heavy neutral beam probe for edge plasma analysis in tokamaks
[DE94-003391] p 3041 N94-25846
Development of fusion technology
[DE93-633444] p 3042 N94-26159
New Thomson scattering laser control for D3-D
[DE94-002890] p 3043 N94-26274
Laboratory plasma studies
[AD-A274655] p 3043 N94-26356
Proceedings of the 16th Symposium on Plasma Physics and Technology
[DE94-604181] p 3047 N94-27698
Laser blow-off lithium beam probing with high temporal resolution for edge plasma diagnostics
[DE94-701176] p 2820 N94-27701
Advanced development of particle beam probe diagnostic system
[DE94-002316] p 3047 N94-27720
Passive stabilization of MHD instabilities at high (beta)n in the HBT-EP tokamak
[DE94-003317] p 3047 N94-27735
Fuel ion rotation measurement and its implications on H-mode theories
[DE94-004860] p 3048 N94-27791
Determination of the plasma column shape in the Tokamak Novillo cross section by magnetic probes
[DE94-604986] p 3048 N94-27844
PLASMA DIODES
Research in pulsed power plasma physics
[AD-A274323] p 3045 N94-27074
PLASMA DRIFT
Shear flow generation from the interaction of neoclassical and drift wave transport processes
[DE94-003135] p 2791 N94-26096
Quiet-time intensifications along the poleward auroral boundary near midnight
[ATR-93(7248)-2] p 2877 N94-26201
Numerical simulation of plasma vertical position stabilization in ITER
[DE93-634588] p 3044 N94-26510
The dynamics of interacting nonlinearities governing long wavelength driftwave turbulence
[DE94-001785] p 2793 N94-26558
PLASMA DYNAMICS
Coherent HF radar system for the study of natural and heater induced ionospheric irregularities
[AD-A273804] p 2876 N94-25752
An investigation of magnetic field effects on plume density and temperature profiles of an applied-field MPD thruster
[NASA-TM-106416] p 2700 N94-26090
PLASMA ENGINES
Stationary plasma thruster plume emissions
[NASA-CR-194471] p 2701 N94-26209
PLASMA ETCHING
Dry etching process development for submicron and nanometer semiconductor devices
[PB94-133196] p 2788 N94-28357
PLASMA FOCUS
Flowing DPF design for propulsion experiments
[AD-A274973] p 2701 N94-26537
PLASMA FREQUENCIES
Ionospheric modification by high power, obliquely propagated HF radio wave transmissions. Part 1: Experimental
[AD-A273746] p 2878 N94-26224
PLASMA GENERATORS
Research in pulsed power plasma physics
[AD-A274323] p 3045 N94-27074
PLASMA HEATING
Review of tokamak experiments on direct electron heating and current drive with fast waves
[DE94-004185] p 3041 N94-25801
Design of folded waveguide antenna for Alcator C-Mod
[DE94-003584] p 2767 N94-25924
RF modeling and design of a folded waveguide launcher for the Alcator C-Mod tokamak
[DE94-003588] p 3041 N94-25933
Development of fusion technology
[DE93-633444] p 3042 N94-26159
Ionospheric modification by high power, obliquely propagated HF radio wave transmissions. Part 1: Experimental
[AD-A273746] p 2878 N94-26224
Design and control of phased ICRF antenna arrays
[DE94-002796] p 3046 N94-27261
High gas-efficiency hydrogen negative ion sources
[PB93-232163] p 3025 N94-27348
Fast wave current drive technology development at ORNL
[DE94-004243] p 3046 N94-27568
Proceedings of the 16th Symposium on Plasma Physics and Technology
[DE94-604181] p 3047 N94-27698
Shine through measurements with hydrogen beam in JT-60
[DE94-701113] p 3047 N94-27699
The calculation for energy balance of heating plasmas by Alfven waves
[DE94-604994] p 3049 N94-27855
Analysis of density limit and efficiency in lower hybrid current drive
[DE94-604995] p 3049 N94-27856
Modelling and control of plasma position in the STOR-M tokamak
[ISBN-0-315-58891-8] p 3049 N94-27949
PLASMA JETS
Synthesis of diamond film assisted by an arcjet plasma source, part 2
[INPE-5527-PRP/178-PT-2] p 3066 N94-27329
PLASMA LAYERS
Configuration of the near-Earth plasma sheet
[NASA-CR-195271] p 2883 N94-27438
Laser blow-off lithium beam probing with high temporal resolution for edge plasma diagnostics
[DE94-701176] p 2820 N94-27701
PLASMA OSCILLATIONS
Shear flow generation from the interaction of neoclassical and drift wave transport processes
[DE94-003135] p 2791 N94-26096
Asymptotics for Kummer functions, Bose plasmas, and related special functions
[DE94-601853] p 3007 N94-26928
Discrete vacuum ultra violet reflective interference filter
[AD-D016059] p 2756 N94-27675
PLASMA PHYSICS
Maryland controlled fusion research program
[DE94-003533] p 3044 N94-26523
Auroral Tomography Workshop Proceedings
[PB94-123718] p 2881 N94-27040
Research in pulsed power plasma physics
[AD-A274323] p 3045 N94-27074
Proceedings of the 16th Symposium on Plasma Physics and Technology
[DE94-604181] p 3047 N94-27698
Passive stabilization of MHD instabilities at high (beta)n in the HBT-EP tokamak
[DE94-003317] p 3047 N94-27735
PLASMA PINCH
Researches of the Electrotechnical Laboratory. No. 51: Study of formation and sustainment of reversed field pinch by slow control of magnetic field
[JTN-94-80548] p 3046 N94-27350
PLASMA PROPULSION
The Lightcraft project: Flight technology for a hypersonic mass transit system p 2670 N94-25695
An investigation of magnetic field effects on plume density and temperature profiles of an applied-field MPD thruster
[NASA-TM-106416] p 2700 N94-26090
Flowing DPF design for propulsion experiments
[AD-A274973] p 2701 N94-26537
PLASMA RADIATION
Experiment and research on materials irradiated by plasma radiation
[DE94-605011] p 2758 N94-27845
PLASMA SPRAYING
Study on film generation phenomena by particle deposition p 2728 N94-25575
PLASMA TURBULENCE
Shear flow generation from the interaction of neoclassical and drift wave transport processes
[DE94-003135] p 2791 N94-26096
Maryland controlled fusion research program
[DE94-003533] p 3044 N94-26523
Role of core toroidal rotation shear on turbulence and transport in the improved confinement regimes of the D3-D tokamak
[DE94-001215] p 3045 N94-26950
Fast H-alpha line broadening during the 100 ns REB injection into a plasma
[IPPCZ-322] p 3048 N94-27836
Acceleration of electrons and ions by strong lower-hybrid turbulence in solar flares
[NASA-TM-109723] p 3111 N94-27953

PLASMA WAVES

Review of tokamak experiments on direct electron heating and current drive with fast waves
[DE94-004185] p 3041 N94-25801

Collisionless shock structures of Earth and other planets
[NASA-CR-195257] p 3104 N94-27407

Space Experiments with Particle Accelerators (SEPAC)
[NASA-CR-193935] p 2761 N94-27664

On radio frequency wave induced radial transport and wave helicity
[IPPCZ-326] p 2777 N94-27838

On helicon wave induced radial plasma transport
[IPPCZ-333] p 3048 N94-27840

Preliminary considerations on the diffraction (quasi-optical) grill in CASTOR tokamak
[IPPCZ-335] p 3048 N94-27842

Acceleration of electrons and ions by strong lower-hybrid turbulence in solar flares
[NASA-TM-109723] p 3111 N94-27953

PLASMA-PARTICLE INTERACTIONS

Fast H-alpha line broadening during the 100 ns REB injection into a plasma
[IPPCZ-322] p 3048 N94-27836

PLASMAGUIDES

On a theory of two-beam mechanisms of charged particle acceleration in electrodynamic structures
[DE94-003482] p 3032 N94-26330

PLASMAS (PHYSICS)

Design of folded waveguide antenna for Alcator C-Mod
[DE94-003584] p 2767 N94-25924

Investigation of plasma etch induced damage in compound semiconductor devices
[DE94-002849] p 3052 N94-25989

New Thomson scattering laser control for D3-D
[DE94-002890] p 3043 N94-26274

Microwave and pulsed power
[DE94-003019] p 2782 N94-26312

Laboratory plasma studies
[AD-A274655] p 3043 N94-26356

Kinetic equation identification from measurement of a particular solution
[DE93-634585] p 2995 N94-26768

Equivalent performance in different helical resonator plasma polymerization coater platforms
[DE94-001517] p 2753 N94-26933

Experimental investigations of strong interaction in the non-perturbative QCD region
[DE94-001178] p 3024 N94-26949

HPm-tubes: Literature survey comprising 1992
[PB94-123643] p 2785 N94-27038

Experimental and theoretical investigation of RF absorption and reflection from preformed plasmas
[AD-A274189] p 3046 N94-27098

Researches of the Electrotechnical Laboratory. No. 51: Study of formation and sustainment of reversed field pinch by slow control of magnetic field
[JTN-94-80548] p 3046 N94-27350

Numerical experiment on finite element method for matching data
[DE94-701208] p 3000 N94-27731

PLASMONS

Fragmentation of Ge(1-x) Sn(x) Se2 glasses
[DE94-603009] p 2758 N94-27837

PLASTIC DEFORMATION

Study on variation of damage generation mechanism by fatigue on TiAl compounds due to different slip systems p 2729 N94-25579

Nanoscale plasticity in silica glass
[DE94-004212] p 2751 N94-26554

On experimental studies of yield surfaces of metals: A more general approach
[IFTR-42/1993] p 2739 N94-26824

Geometry changes in the elastic-plastic analysis of steel spatial skeletal structures
[IFTR-37/1993] p 2839 N94-26825

On the Lagrangian and updated Lagrangian nonlinear finite element formulations
[ISBN-0-315-61111-1] p 3001 N94-27948

PLASTIC PROPERTIES

Deviatoric stresses and plastic strain rates in strong shock waves for six metals
[DE94-002964] p 2733 N94-26022

Grain by grain study of the mechanisms of crack propagation during iodine SCC of Zry-4
[DE93-633765] p 2734 N94-26162

A study on the development of high-T(c) superconducting wire
[DE93-632438] p 2783 N94-26546

Nanoscale plasticity in silica glass
[DE94-004212] p 2751 N94-26554

A constitutive model for layered wire mesh and aramid cloth fabric
[DE94-003275] p 2708 N94-26796

On experimental studies of yield surfaces of metals: A more general approach
[IFTR-42/1993] p 2739 N94-26824

Geometry changes in the elastic-plastic analysis of steel spatial skeletal structures
[IFTR-37/1993] p 2839 N94-26825

Deformation, constitutive behavior, and damage of advanced structural materials under multiaxial loading
[AD-A274165] p 2709 N94-27142

PLASTICS

Technique to predict the curing behaviour of unsaturated polyester materials
[PB94-124856] p 2748 N94-25892

Modelling the inhibition cure behaviour of unsaturated polyester moulding materials
[PB94-124864] p 2748 N94-25893

Stress relaxation in dough moulding compounds
[PB94-124872] p 2748 N94-25894

Resonant holographic measurements of laser ablation plume expansion in vacuum and argon gas backgrounds
[DE94-001407] p 2813 N94-27615

Compatibility of refrigerants and lubricants with engineering plastics
[DE94-004959] p 2756 N94-27692

PLATES (STRUCTURAL MEMBERS)

The free vibration of plates, shallow shells and solids
[ISBN-0-315-83931-7] p 2838 N94-26622

Response of structures to impact loads using elastic and plastic analysis
[ISBN-0-315-84647-X] p 2842 N94-27309

The experimental behavior of spinning pretwisted laminated composite plates
[NASA-CR-195220] p 2711 N94-27352

Finite element analysis of damped vibrations of laminated composite plates
[ISBN-0-315-84928-2] p 2843 N94-27585

On the Lagrangian and updated Lagrangian nonlinear finite element formulations
[ISBN-0-315-61111-1] p 3001 N94-27948

PLATINUM

A mimic model of Pt-Rh catalyst prepared by electrochemical deposition of Rh on Pt (100) surface
[REPT-A-2664] p 2715 N94-26476

PLATINUM ALLOYS

The origins of ordering in CuPt
[DE94-003864] p 2736 N94-26351

A mimic model of Pt-Rh catalyst prepared by electrochemical deposition of Rh on Pt (100) surface
[REPT-A-2664] p 2715 N94-26476

The electrocatalytic oxidation of ethylene and methane, and reduction of oxygen on gas-diffusion electrodes made of amorphous nickel-valve metal-platinum group metal alloys p 2722 N94-28165

PLOTTERS

IRMA: A program for three-dimensional color display of data
[AD-A273811] p 2959 N94-25879

PLOTTING

IRMA: A program for three-dimensional color display of data
[AD-A273811] p 2959 N94-25879

PLUMES

An investigation of magnetic field effects on plume density and temperature profiles of an applied-field MPD thruster
[NASA-TM-106416] p 2700 N94-26090

A large high vacuum, high pumping speed space simulation chamber for electric propulsion
[NASA-TM-106453] p 2690 N94-26142

Enhanced tracking of airborne targets using forward looking infrared and laser return measurements
[AD-A274181] p 3037 N94-27102

Uncertainties in the characterization of the thermal environment of a solid rocket propellant fire
[DE94-002023] p 2760 N94-27719

First experimental assessment of RCS plume-flow field interaction on Hermes leading edge thruster configuration p 2703 N94-28032

PLUTONIUM

Effect of nitrocarburizing on shape of titanium alloy parts
[DE94-004040] p 2732 N94-25822

PNEUMATIC CONTROL

Pneumatic management of blunted-forebody flow asymmetry for high-angle-of-attack directional control
p 2679 N94-28028

PNEUMATIC PROBES

Laser Doppler velocimetry in a low speed multistage compressor
[AD-A274836] p 2818 N94-26498

PNEUMATICS

Laser Doppler velocimetry in a low speed multistage compressor
[AD-A274836] p 2818 N94-26498

Pneumatic management of blunted-forebody flow asymmetry for high-angle-of-attack directional control
p 2679 N94-28028

POINT DEFECTS

Modeling defect production in high energy collision cascades
[DE94-003810] p 3017 N94-26049

Influence of point defects on grain boundary diffusion in oxides
[DE94-003164] p 3060 N94-26782

POINT SOURCES

Characterization and calibration of the Agema 880+ imaging radiometer
[AD-A274417] p 3036 N94-26981

Hydroacoustic wave-fields generated by different source types, a computational study
[PB94-123536] p 3010 N94-27037

Thermal conductivity of liquid carboxylic acids
[ESDU-93017] p 2721 N94-28138

Image theory for DC problems involving a conducting half space bounded by the general anisotropic impedance surface
[PB94-132917] p 2779 N94-28390

POINT TO POINT COMMUNICATION

Laser-based communication link
[FFI-93/7023] p 2817 N94-26203

POISSON EQUATION

On Poisson brackets and symplectic structures for the classical and quantum Zitterbewegung
[DE93-634305] p 2992 N94-26267

Grid-independent convergence based on preconditioning techniques
[PB94-125358] p 2997 N94-27000

Recent advances in the spectral element method
p 2657 N94-28348

POISSON RATIO

An ultrasonic testing technique for monitoring the cure and mechanical properties of polymeric materials
[AD-A274536] p 2753 N94-26842

POLAR CAPS

Why is the north polar cap on Mars different than the south polar cap? p 3107 N94-27889

POLAR REGIONS

Norwegian ionospheric satellite experiment: High latitude, low Earth orbit plasma measurements
[FFI-93/7025] p 2876 N94-25807

Comparative investigation of high-latitude ionospheric structure and effects near solar maximum
[AD-A273799] p 2877 N94-25877

Upper atmosphere neutral and plasma density modeling
[AD-A274768] p 2879 N94-26569

Kiruna geophysical data. Data summary 93/4-6, April-June 1993
[PB94-123700] p 2881 N94-27039

Kiruna geophysical data. Data summary 93/1-3, January-March, 1993
[PB94-123791] p 2881 N94-27043

Cooling the Martian atmosphere: The spectral overlap of the C02 15 micrometers band and dust
p 3107 N94-27886

Why is the north polar cap on Mars different than the south polar cap? p 3107 N94-27889

POLARIMETRY

Polarimetric investigation of edge scattering by mono- and bistatic microwave imaging
[ESA-TT-1284] p 2768 N94-26317

Processing of wide-angle synthetic aperture radar signals for target detection
[AD-A274225] p 2773 N94-27073

POLARITONS

Decay of non-equilibrium polariton condensate in semiconductors
[DE94-604016] p 3068 N94-27678

POLARITY

Correlation of experimental data and three-dimensional finite element modeling of a spinning quadrupole
[DE93-041173] p 3008 N94-26421

UAH mathematical model of the variable polarity plasma ARC welding system calculation
[NASA-CR-193926] p 2824 N94-27221

POLARIZATION (CHARGE SEPARATION)

Effects of Class 3 antiarrhythmic agents, E-4031 and MS-551 on ventricular repolarization in isolated rabbit hearts p 2907 N94-27508

POLARIZATION (SPIN ALIGNMENT)

Spin-polarized atomic hydrogen: Devices and phenomena
[ETN-94-95342] p 3016 N94-26002

Calculation of electron-potassium scattering
[DE94-601812] p 3023 N94-26942

POLARIZATION (WAVES)

Laser manipulation of metastable neon atoms
[ETN-94-95344] p 2817 N94-26225

Refractive and dielectric properties of helium, argon and nitrogen gases
[PB94-123783] p 3008 N94-26851

POLARIZATION CHARACTERISTICS
Spin-polarized atomic hydrogen: Devices and phenomena
[ETN-94-95342] p 3016 N94-26002
Calculation of total cross sections for electron and positron scattering on sodium and potassium
[DE94-601814] p 3023 N94-26944
International bulletin on atomic and molecular data for fusion. No. 42-45, Mar. 1991 - Dec. 1992
[DE94-601817] p 3045 N94-26946
Polarizability matrix of layered chiral sphere
[PB94-132834] p 2778 N94-28355
Electromagnetic modeling of bi-isotropic media
[PB94-132909] p 2778 N94-28382

POLARIZED LIGHT
Technical report of ISSP. Ser. A, no. 2684: Wavelength dependence of nonsequential double ionization in He
[JTN-94-80570] p 3025 N94-27338
Report of the National Research Institute for Earth Science and Disaster Prevention, No. 51
[JTN-94-80509] p 2886 N94-27985
Detection of water on road surface by the polarized light p 2886 N94-27989

POLARONS
Holes in a two-dimensional quantum antiferromagnet
[DE93-634753] p 3057 N94-26388
All-coupling polaron ground state energy in D-dimension
[DE94-603666] p 3027 N94-27629

POLICIES
How to make good use of international research collaboration, with emphasis on the evolving situation in Europe
[PB94-119690] p 3101 N94-27323
The 1993 Federal Aviation Administration plan for research, engineering and development
p 2643 N94-27960

POLISHING
Calculations of material removal, removal rate, and Preston coefficient in continuous lapping/polishing machines
[DE94-002619] p 2763 N94-26804

POLLUTION CONTROL
Analysis and development of an F-5 pollution prevention management program with recommendations for creation of similar programs for other aircraft
[AD-A274016] p 2865 N94-25755
SIHTI 2: Energy and environmental technology
[DE94-702061] p 2867 N94-26241
Compilation of air pollutant emission factors. Volume 1: Stationary point and area sources. Supplement F
[PB94-121431] p 2867 N94-26757
Numerical analysis of the photo-dissociation/radical oxidation of formaldehyde by ultraviolet light in a photolytic reactor
[AD-A274539] p 2868 N94-26843
Optimising BMW four-cylinder two-valve engines
[PB94-125101] p 2824 N94-27254
Gas turbine combustion and emission control
p 2831 N94-28082

POLLUTION MONITORING
An observational study of air pollution transport over a large urban complex
[REPT-6] p 2867 N94-26474
Advances in passive-remote and extractive Fourier transform infrared spectroscopic systems
[DE94-001424] p 2868 N94-26952
Determination of lead isotope ratios in seawater by purge and trap GC/MS after ethylation p 2870 N94-28152
Environmental management and audit
p 2870 N94-28153

POLLUTION TRANSPORT
Air pollution transport modeling
[AD-A273863] p 2865 N94-25609
A positive finite-difference advection scheme applied on locally refined grids
[CWI-NM-R9309] p 2867 N94-26216
An observational study of air pollution transport over a large urban complex
[REPT-6] p 2867 N94-26474

POLYACRYLONITRILE
Advances in preparing and characterizing low density pan-carbon microcellular foam
[DE94-002278] p 2748 N94-25932

POLYATOMIC MOLECULES
Three methods to measure RH bond energies
[DE94-003795] p 3013 N94-25816

POLYBUTADIENE
Cryogenic size reduction of solid propellant
[AD-A274844] p 2759 N94-26800

POLYCRYSTALS
Study on elucidation of damage generation process by electron beam lithography p 2729 N94-25581
The reactivity of lithium toward non-aqueous solvents of relevance to energy storage applications as studied by surface analytical techniques
[DE94-003483] p 2856 N94-26464
A model of electric breakdown in polycrystalline semiconductors with highly nonlinear I - V characteristics
[DE94-601537] p 3063 N94-27017
Deformation, constitutive behavior, and damage of advanced structural materials under multiaxial loading
[AD-A274165] p 2709 N94-27142

POLYESTER RESINS
Ultrasonic measurement technique to determine the state of cure in thermosetting materials
[PB94-124328] p 2756 N94-27217

POLYESTERS
Technique to predict the curing behaviour of unsaturated polyester materials
[PB94-124856] p 2748 N94-25892
Modelling the inhibition cure behaviour of unsaturated polyester moulding materials
[PB94-124864] p 2748 N94-25893
Stress relaxation in dough moulding compounds
[PB94-124872] p 2748 N94-25894
Trifluoromethyl-substituted polymers
[NASA-CR-195217] p 2751 N94-26641

POLYETHYLENES
In situ spectroscopic applications to the study of rechargeable lithium batteries
[DE94-003478] p 2782 N94-26328
Failure behaviour of high density polyethylene with an embrittled surface layer due to weathering
[PB94-126406] p 2840 N94-26960
Application of the Positron Annihilation Technique to the study of vapor absorption process in polyethylene (LDPE) and in imide polymer (6FDA-TMPD PI)
[DE94-602737] p 2720 N94-27998

POLYGONS
An algorithm to find the intersection of two convex polygons
[AD-A274722] p 2961 N94-26148

POLYHEDRONS
Polyhedral characterization of the economic lot-sizing problem with start-up costs
[MEMO-COSOR-92-46] p 2969 N94-27396

POLYIMIDE RESINS
Property enchancement of polyimide films by way of the incorporation of lanthanide metal ions
p 2758 N94-27926

POLYIMIDES
Polyimide/inorganic composite-interpenetrating polymer network for stable second-order nonlinear optics
[AD-A274646] p 2709 N94-27107
Outgas and vacuum seal characteristics of irradiated polyimide O-ring
[DE94-701200] p 2757 N94-27812
New monomers for high performance polymers
p 2758 N94-27904
Property enchancement of polyimide films by way of the incorporation of lanthanide metal ions
p 2758 N94-27926
Application of the Positron Annihilation Technique to the study of vapor absorption process in polyethylene (LDPE) and in imide polymer (6FDA-TMPD PI)
[DE94-602737] p 2720 N94-27998

POLYMER BLENDS
Ultrastructure processing of macromolecular materials
[AD-A274460] p 2754 N94-27086

POLYMER CHEMISTRY
The x ray holographic microscopy using the atomic-force microscope
[DE94-004003] p 2814 N94-27779

POLYMER MATRIX COMPOSITES
Design and test of postbuckled stiffened curved plates: A literature survey
[PB94-126521] p 2840 N94-26961
Polyimide/inorganic composite-interpenetrating polymer network for stable second-order nonlinear optics
[AD-A274646] p 2709 N94-27107
Finite element analysis of damped vibrations of laminated composite plates
[ISBN-0-315-84928-2] p 2843 N94-27585
Effects of physical aging on long-term behavior of composites p 2712 N94-27897

POLYMER PHYSICS
Modelling and predicting properties of polymers in the amorphous glassy state
[ETN-94-95345] p 2752 N94-26645

POLYMERIC FILMS
Micropyrolysis of polymer thin films for ceramics
[ECL-92-62] p 2750 N94-26088
Mechanical properties of polyaniline prepared by polymerization in an organized monolayer
[AD-A274350] p 2753 N94-26925
Ferroelectricity in a Langmuir-Blodgett multilayer film of a liquid crystalline side-chain polymer
[AD-A274477] p 2754 N94-27033
Liquid crystalline side-chain polysiloxanes with 4-amino-4'-stilbene-carboxylic ester mesogens
[AD-A274510] p 2754 N94-27036
Research and development within nonlinear optics for protection of optical sensors against laser irradiation on of optical sensors against laser irradiation. Quarterannual report 1 (april 1993))
[PB94-124245] p 3037 N94-27046
Langmuir-Blodgett and STM investigations of conducting polymer thin films
[AD-A274512] p 2755 N94-27087
Chemical polymerization and Langmuir-Blodgett techniques. 2: The polymerization of monolayers of 3-substituted pyrroles
[AD-A274478] p 2755 N94-27163

POLYMERIZATION
Controlled synthesis of polyenes by catalytic methods
[DE94-004168] p 2749 N94-25973
Trifluoromethyl-substituted polymers
[NASA-CR-195217] p 2751 N94-26641
Mechanical properties of polyaniline prepared by polymerization in an organized monolayer
[AD-A274350] p 2753 N94-26925
Equivalent performance in different helical resonator plasma polymerization coater platforms
[DE94-001517] p 2753 N94-26933
Kinetics of 2-pentadecylaniline polymerizations in monolayers: Relationships between experimental data and a new theoretical model
[AD-A274419] p 2754 N94-27080
Chemical polymerization and Langmuir-Blodgett techniques. 2: The polymerization of monolayers of 3-substituted pyrroles
[AD-A274478] p 2755 N94-27163

POLYMERS
Reference electrodes for solid polymer electrolytes
[DE94-004583] p 2780 N94-25806
Morphological analysis of ionomers
[DE94-003660] p 2749 N94-26005

POLYMETHYL METHACRYLATE
Physical characteristics of polymethylmethacrylate scintillator SOFG-120
[DE93-634184] p 2810 N94-26395

POLYNOMIALS
Approximate solution of the fourth order initial value problem using deficient spline polynomials
[DE93-613023] p 2991 N94-25880
Classification of linear differential operators with an invariant subspace in monomials
[PB94-126620] p 2996 N94-26915
Fast methods for computation with algebraic numbers
[ISBN-0-315-57888-2] p 2998 N94-27269
Polyhedral characterization of the economic lot-sizing problem with start-up costs
[MEMO-COSOR-92-46] p 2969 N94-27396
Thermal conductivity of liquid carboxylic acids
[ESDU-93017] p 2721 N94-28138

POLYPEPTIDES
The molecular matching problem
p 3030 N94-27910

POLYSILOXANES
Ferroelectricity in a Langmuir-Blodgett multilayer film of a liquid crystalline side-chain polymer
[AD-A274477] p 2754 N94-27033
Liquid crystalline side-chain polysiloxanes with 4-amino-4'-stilbene-carboxylic ester mesogens
[AD-A274510] p 2754 N94-27036

POLYSTYRENE
Morphological analysis of ionomers
[DE94-003660] p 2749 N94-26005
Study on the compensated lead hadron calorimeter characteristics by means of hadron and electron beams
[DE93-634176] p 2810 N94-26439
Microspheres for laser velocimetry in high temperature wind tunnel p 2682 N94-27903

POLYTOPES
A simplicial approach to integer programming, part 2
[REPT-93-47-PT-2] p 2958 N94-25764

POLYURETHANE RESINS
Morphological analysis of ionomers
[DE94-003660] p 2749 N94-26005
Biomedical polyurethane networks
[ETN-94-95391] p 2750 N94-26211
Polyurethane self-priming topcoats
[AD-D016041] p 2755 N94-27111
Corrosion resistant coatings from conducting polymers
[DE94-003959] p 2757 N94-27747

POMERONS
High energy parton-parton elastic scattering in QCD
[DE94-003432] p 3028 N94-27736

POPULATIONS
Methane emissions from natural wetlands
[DE93-040796] p 2865 N94-25790

Calculations of population transfer during intense laser pulses
[DE94-001060] p 2818 N94-26698

POROSITY

Advances in preparing and characterizing low density pan-carbon microcellular foam
[DE94-002278] p 2748 N94-25932

Double layer capacitance of carbon foam electrodes
[DE94-002651] p 2780 N94-25975

CEN-VAMAS round robin on grain size measurement for advanced technical ceramics
[VAMAS-TR-12] p 2752 N94-26654

POROUS MATERIALS

Structure of ionic fluids in equilibrium with a microporous ionic matrix
[DE94-600563] p 2715 N94-26391

A thermodynamically consistent constitutive theory for a rigid solid-stokesian fluid mixture
[DE93-633202] p 2792 N94-26401

Low cost, radial flow, solid oxide fuel cell
[DE94-002982] p 2858 N94-26785

Light emitting porous silicon
[AD-A274152] p 3038 N94-27137

Researches of the Electrotechnical Laboratory. No. 52: Studies of externally pressurized porous gas bearings
[JTN-94-80549] p 2825 N94-27351

Porous vycor glass tube joined to borosilicate glass
p 2718 N94-27392

PORPHYRINS

The coordination and atom transfer chemistry of titanium porphyrin complexes
[DE94-003091] p 2704 N94-26779

PORTABLE EQUIPMENT

Portable Habitat for Antarctic Scientific Research (PHASR) p 2943 N94-25681

System design analysis of a lightweight laser satellite terminal
[AD-A274033] p 2690 N94-25769

Status report for the development of the Antarctic penetrator: 1990-year program p 2885 N94-27973

POSEIDON SATELLITE

TOPEX/Poseidon battery performance during the first year of operation p 2862 N94-28119

POSITION (LOCATION)

Differential global positioning system for the surface-towed ordnance locating system: Testing, results, and user's guide
[DE94-002980] p 2664 N94-26309

Short-range cloud amount forecasting with model output statistics
[AD-A274769] p 2895 N94-26798

Technical report of ISSP. Ser. A, no. 2671: Quasi-localization of light waves in Fibonacci dielectric multilayers
[JTN-94-80557] p 3064 N94-27231

Technical report of ISSP. Ser. A, no. 2675: High-field cyclotron resonance and valence-band structure in semiconducting diamond
[JTN-94-80561] p 3065 N94-27245

BATSE burst location accuracy and constraints on the fraction of repeating GRB sources
[DE94-004981] p 3116 N94-27714

An integrated approach to seismic event location: 1. Evaluating how method of location affects the volume of groups of hypocenters
[PL-TR-92-2323] p 2887 N94-28214

POSITION ERRORS

Accuracy analysis of multi-axis machines
[ETN-94-95341] p 3002 N94-26000

Ground station siting considerations for DGPS
p 2642 N94-27293

Differential GPS methods and performance for marine applications
[DREP-93-09] p 2665 N94-27667

A simulation of GPS and differential GPS sensors
p 2666 N94-27918

POSITION INDICATORS

Interchangeable end effector tools utilized on the PFMA
[NASA-CR-193925] p 2823 N94-27149

POSITION SENSING

Interchangeable end effector tools utilized on the PFMA
[NASA-CR-193925] p 2823 N94-27149

POSITIONING

Modelling and stability of a shape memory alloy position control system
[ISBN-0-315-84467-1] p 2740 N94-27304

Status report for the development of the Antarctic penetrator: 1990-year program p 2885 N94-27973

POSITIVE FEEDBACK

A study on piezoelectric actuators and sensors for vibration control of flexible space structures
[AD-A274925] p 2695 N94-26532

POSITIVE IONS

Ion implantation of diamond: Damage, doping, and lift-off
[DE94-001133] p 3054 N94-26137

Structure of ionic fluids in equilibrium with a microporous ionic matrix
[DE94-600563] p 2715 N94-26391

POSITRON ANNIHILATION

Window least squares method applied to statistical noise smoothing of positron annihilation data
[DE93-634665] p 3003 N94-26385

A jet calculus approach including coherence effects and the associated problem of moment inversion
[ISBN-0-315-51715-8] p 3025 N94-27266

Axial anomaly in e(+)e(-) yields gamma gamma and anyon superconductivity
[DE94-606406] p 3070 N94-27859

Fermi surface ridge at second and third Umklapp positron annihilations in Y Ba2Cu3O(7-delta)
[DE93-634760] p 3070 N94-27995

Application of the Positron Annihilation Technique to the study of vapor absorption process in polyethylene (LDPE) and in imide polymer (6FDA-TMPD PI)
[DE94-602737] p 2720 N94-27998

POSITRONIUM

Hyperfine structure of positronium energy levels in a crystal
[DE94-603898] p 3068 N94-27729

POSITRONS

Harvard University High Energy Physics
[DE94-002406] p 3032 N94-26119

Fast photoconductor CdTe detectors for synchrotron x ray studies
[DE94-001334] p 3054 N94-26139

Calculation of total cross sections for electron and positron scattering on sodium and potassium
[DE94-601814] p 3023 N94-26944

POSTURE

The effect of body orientation on the perception of vertical and horizontal distance in an outdoor setting
p 2915 N94-27461

POTASSIUM

Calculation of electron-potassium scattering
[DE94-601812] p 3023 N94-26942

Calculation of total cross sections for electron and positron scattering on sodium and potassium
[DE94-601814] p 3023 N94-26944

POTASSIUM COMPOUNDS

Development of K(1-x)Na(x)TiOPO4 crystals for nonlinear applications
[AD-A274336] p 3063 N94-27055

POTASSIUM HYDROXIDES

Freon recovery from nitrogen tetroxide and freon solutions
[PL-TR-92-3051] p 2721 N94-28215

POTASSIUM PHOSPHATES

Three-wave nonlinear interactions in KTiOPO4 (KTP) and KTP isomorphs
[AD-A274079] p 3052 N94-25993

POTASSIUM 40

Geological Dating by Ar-40 - Ar-39 method
[DE94-601975] p 2880 N94-26874

POTATOES

Studies on the application of radiation for genetic transformation in higher plants
[DE93-632656] p 2901 N94-26470

Development of a sparging technique for volatile emissions from potato (Solanum tuberosum)
[NASA-TM-109199] p 2903 N94-27412

POTENTIAL FLOW

Calculation of unsteady incompressible inviscid flow about wings and bodies using CANAERO-T panel model
p 2655 N94-28334

POURING

Solidification modeling of a spiral casting to determine material fluidity
[DE94-002212] p 2739 N94-26935

POWDER (PARTICLES)

Debye-Waller factors of the light actinide metals
[DE94-000685] p 2733 N94-26069

Liquid and solid solubility of Ag in Bi2Sr2CaCu2O8
[DE94-002829] p 2735 N94-26273

Processing of LaCrO3 for solid oxide fuel cell applications
[DE94-002981] p 2857 N94-26747

Electro-optic materials by solid source MOCVD
[DE94-005120] p 2757 N94-27716

Bench-scale synthesis of nanoscale materials
[DE94-004787] p 2742 N94-27786

Characterization of ZnS-GaP naon-composites
[DE94-004888] p 2712 N94-27813

POWDER METALLURGY

Crystallization and microstructural control of ferroelectric thin-films and glass-ceramics
[AD-A273767] p 2748 N94-25854

The processing of powder metallurgically produced near gamma-titanium aluminide
[ISBN-0-315-84018-8] p 2738 N94-26633

Powder synthesis, fabrication, and transport properties of long-length Ag clad Bi-2223 conductors
[DE94-002376] p 2740 N94-26957

Material optimization and manufacturing development of reduced cost powder metal titanium alloy components for gas turbine engine application, phase 2
[AD-A274410] p 2709 N94-26978

Characterization of ZnS-GaP naon-composites
[DE94-004888] p 2712 N94-27813

Study on the production of flaky amorphous alloy powders by impact flattening of atomized liquid droplets on a rapidly rotating wheel p 2746 N94-28169

POWER AMPLIFIERS

Phase conjugation and pulse compression of high energy lasers: From nanoseconds to microseconds
[DE94-001061] p 2818 N94-26699

Design and control of phased ICRF antenna arrays
[DE94-002796] p 3046 N94-27261

NASA satellite communications application research. Phase 2: Efficient high power, solid state amplifier for EFH communications
[NASA-CR-195713] p 2776 N94-27669

Micro-electron deflector
[AD-D016055] p 2787 N94-27672

NASA satellite communications application research, phase 2 addendum. Efficient high power, solid state amplifier for EHF communications
[NASA-CR-195712] p 2777 N94-27946

POWER CONVERTERS

AC to DC power converter with regulated bi-polar outputs
[AD-D016032] p 2786 N94-27145

POWER PLANTS

Knowledge organization in intelligent tutoring systems for diagnostic problem solving in complex dynamic domains
[AD-A273986] p 2984 N94-25899

Parametric analysis of the space power plants on the base of criterion of specific mass in generalized design variants
[DE93-634153] p 2701 N94-26166

POWER SPECTRA

The deterministic power-spectral-density method
[AD-B175894] p 2678 N94-27395

The deterministic power-spectral-density-method for nonlinear systems
[AD-B179687] p 3001 N94-28353

PRECAMBRIAN PERIOD

Ozone control of biological activity during Earth's history, including the KT catastrophe p 2876 N94-28312

PRECIPITATES

An atom probe investigation of the influence of trace impurities on the mechanical behavior of NiAl
[DE94-002797] p 2734 N94-26272

Study of precipitation and recrystallization in Al alloy 2519 by backscattered electron imaging methods
[AD-A274919] p 2736 N94-26533

Effect of precipitate structure on hot deformation of Al-Mg-Mn alloys
[DE94-004596] p 2741 N94-27622

A transmission electron microscope study of Ni4W precipitates in a Ni-37 wt. percent W alloy
[ISBN-0-315-59932-4] p 2743 N94-27803

PRECIPITATION (METEOROLOGY)

Numerical modelling of precipitation over complex terrain
[ISBN-0-315-84327-6] p 2894 N94-26628

Meteorological data at the Nagaoka Institute of Snow and Ice Studies
[REPT-158] p 2896 N94-27169

Examination of micro- and macro-physical structures and processes in hailstorms with respect to their modification
[DLR-FB-93-25] p 2897 N94-27751

PRECIPITATION HARDENING

Study on the mechanism of titanium alloy toughness and the improvement of properties
p 2726 N94-25566

PRECONDITIONING

Preconditioning in parallel Runge-Kutta methods for stiff initial value problems
[CWI-NM-R9310] p 2991 N94-26217

Semantics, orderings and recursion in the weakest precondition calculus
[CWI-CS-R9267] p 2995 N94-26776

Grid-independent convergence based on preconditioning techniques
[PB94-125358] p 2997 N94-27000

PREDICTION ANALYSIS TECHNIQUES

Development and testing of the Coupled Ocean/Atmosphere Mesoscale Prediction System (COAMPS)
[AD-A273925] p 2892 N94-25793

Image segmentation by a combination of edge detection and region growing
[ETN-94-95032] p 2960 N94-26106

Predictive modeling of particle-laden, turbulent flows
[DE94-003298] p 2792 N94-26319

Proceedings of the Non-Linear Aero Prediction Requirements Workshop
[NASA-CP-10138] p 2670 N94-27439

Uncertainties in the characterization of the thermal environment of a solid rocket propellant fire
[DE94-002023] p 2760 N94-27719

Methodology development of forecasting inter-regional air transport demand in China
[DLR-FB-93-24] p 2660 N94-27746

Understanding and development of a prediction method of transonic limit cycle oscillation characteristics of fighter aircraft
[NLR-TP-92210-U] p 2679 N94-27798

Predictions of momentum and scalar fields in a jet in cross-flow using first and second order turbulence closures p 2803 N94-28025

Landscape dynamics of northeastern forests
[NASA-CR-195272] p 2852 N94-28070

Calculation methods for steadily loaded central circumferential groove hydrodynamic journal bearings (guide to use of computer program A9304)
[ESDU-93004] p 2830 N94-28073

Calculation methods for steadily loaded axial groove hydrodynamic journal bearings (guide to use of computer program A9305)
[ESDU-93005] p 2830 N94-28074

Variability of measured sonic boom signatures
p 2651 N94-28197

A general theory of impacts and mass extinctions, and the consequences of large-body impact on the Earth
p 2891 N94-28310

PREDICTIONS

Parameter estimation by genetic algorithms
[DE94-002924] p 2961 N94-26146

Effects of historical and predictive information on ability of transport pilot to predict an alert
[NASA-TM-4547] p 2673 N94-27864

Experimental studies of loudness and annoyance response to sonic booms p 2651 N94-28195

Comparison of methods of predicting community response to impulsive and nonimpulsive noise
p 2651 N94-28196

PREDICTOR-CORRECTOR METHODS

Research on primal-dual interior point algorithms for mathematical programming
[DE94-003982] p 2959 N94-25821

PREFLIGHT OPERATIONS

STS-56, RSRM-031, 360L031 KSC processing configuration and data report
[NASA-CR-193922] p 2691 N94-26135

STS-51, RSRM-033, 360T033 KSC processing configuration and data report
[NASA-CR-193923] p 2691 N94-26153

Report of the Shuttle Processing Review Team
[NASA-TM-109728] p 2692 N94-28178

PREFORMS

Lunar preform manufacturing p 2765 N94-25677

PREMIXING

Focused Schlieren flow visualization studies of multiple venturi fuel injectors in a high pressure combustor
[NASA-TM-106479] p 2674 N94-26573

PREPROCESSING

Color image segmentation
[AD-A274027] p 2984 N94-25759

PRESSURE

Computational prediction of isolated performance of an axisymmetric nozzle at Mach number 0.90
[NASA-TM-4506] p 2646 N94-26547

PRESSURE BREATHING

Aeromedical issues related to positive pressure breathing for +Gz protection
[AD-A274717] p 2910 N94-26435

PRESSURE DEPENDENCE

Grain boundary degradation of YBCO superconductors sintered in CO2-containing atmospheres
[DE94-003206] p 3053 N94-26029

Iron: What is melt?
[DE94-003373] p 2735 N94-26322

Influence of point defects on grain boundary diffusion in oxides
[DE94-003164] p 3060 N94-26782

Electrical conductivity of perovskite-magnesiowuestite as a function of pressure and temperature
[DE94-002714] p 2880 N94-26806

An improvement in the modified finite element procedure for underwater shock analysis
[DE94-004451] p 2797 N94-27617

PRESSURE DISTRIBUTION

Low-speed pressure distribution measurements over the aft-fuselage, fins, and stabilators of a 1/9th scale F/A-18 wind-tunnel model
[AD-A274870] p 2644 N94-26342

Pressure distributions on a 0.02-scale Space Shuttle orbiter nose at Mach 21.5 in helium
[NASA-TM-4495] p 2646 N94-26592

Numerical studies on the dynamics of bubble, turbulent, free shear flows: Effect of the inter-phase coupling on the global flow evolution
[AD-A274521] p 2794 N94-26832

New variational techniques for acoustic radiation and scattering from elastic shell structures
[AD-A274599] p 3010 N94-26889

Aircraft wheel life assessment
[AD-A274378] p 2823 N94-26976

Verification of thermal analysis codes for modeling solid rocket nozzles
[NASA-CR-195248] p 2702 N94-27150

Streamwise vorticity in a turbine rotor with conical endwalls
[DLR-FB-93-13] p 2826 N94-27591

Experimental and theoretical investigations of the influence of the jet on the flow around a bypass-engine
[DLR-FB-93-17] p 2675 N94-27593

An improvement in the modified finite element procedure for underwater shock analysis
[DE94-004451] p 2797 N94-27617

Flat rectangular orthotropic plates under uniformly distributed normal pressure. Elastic stresses and deflections for various forms of edge restraint
[ESDU-93011] p 2845 N94-28061

Simulation: A tool for steam plant dynamic analysis
p 2831 N94-28084

Examples of excrescence drag prediction for typical wing components of a subsonic transport aircraft at the cruise condition
[ESDU-93032] p 2649 N94-28144

Effect of surface finish on turbine airfoil cascade losses p 2652 N94-28320

The effect of axial velocity ratio, turbulence intensity, incidence, and leading edge geometry on the midspan performance of a turbine cascade p 2652 N94-28321

Measurements of steady and dynamic pressure on an F/A-18 wind tunnel model at high angles of attack
p 2653 N94-28323

PRESSURE DRAG

Computational prediction of isolated performance of an axisymmetric nozzle at Mach number 0.90
[NASA-TM-4506] p 2646 N94-26547

PRESSURE DROP

Design of a refueling tanker delivering liquid hydrogen
p 2671 N94-25717

PRESSURE EFFECTS

Squeeze casting: A literature review
[PB94-124575] p 2741 N94-27326

Technical report of ISSP. Ser. A, no. 2682: Pressure dependence of Sm:YAG fluorescence to 50 GPa: A new calibration as a high pressure scale
[JTN-94-80568] p 3066 N94-27354

A rapid-pressure correlation representation consistent with the Taylor-Proudman theorem materially-frame-indifferent in the 2D limit
[NASA-CR-191591] p 2796 N94-27435

Examples of excrescence drag prediction for typical wing components of a subsonic transport aircraft at the cruise condition
[ESDU-93032] p 2649 N94-28144

PRESSURE GRADIENTS

An enhanced global spectral model
[PL-TR-92-2011] p 2898 N94-28223

PRESSURE MEASUREMENT

Theoretical and experimental investigation of converging cylindrical shock waves propagating in narrow cylindrical chambers
[ISBN-0-315-84694-1] p 2795 N94-27313

The cryogenic tunnel Cologne at DLR
[DLR-MITT-93-10] p 2681 N94-27587

PRESSURE OSCILLATIONS

Compressibility effects on rotor forces in the leakage path between a shrouded pump impeller and its housing
p 2796 N94-27379

Flowfield dynamics in blunt fin-induced shock wave/turbulent boundary layer interactions
[NASA-CR-195170] p 2798 N94-27802

PRESSURE RATIO

Wake passage effects on the losses in a linear turbine cascade
[AD-A273794] p 2790 N94-25874

Influence of headwind on hot gas reingestion and consideration of pressure ratio scaling
p 2675 N94-28018

Transitional flight characteristics of a geometrically simplified STOVL model p 2672 N94-28035

PRESSURE REDUCTION

Effects of crenulations on three dimensional losses in a linear compressor cascade
[AD-A273778] p 2790 N94-25882

Gravity dependence or pressure drop and heat transfer in straight two-phase heat transport system condenser ducts
[NLR-TP-92167-U] p 2798 N94-27853

PRESSURE SENSORS

Digital Altimeter Setting Indicator (DASI) Operational Test and Evaluation (OT/E) operational test procedures
[AD-A274100] p 2672 N94-26030

PRESSURE SUITS

Aeromedical issues related to positive pressure breathing for +Gz protection
[AD-A274717] p 2910 N94-26435

PRESSURE VESSELS

Fracture Toughness Round Robin Test International in pressure tube materials
[DE93-634140] p 2837 N94-26265

The role of point defect clusters in reactor pressure vessel embrittlement
[DE94-001122] p 2739 N94-26931

A laboratory test on construction of ice domes and their load-carrying capacity p 2884 N94-27966

PRESSURIZED CABINS

Pressurized Lunar Rover (PLR) p 2833 N94-25704

Impact tests on fibre metal laminates under a tensile load
[PB94-126570] p 2710 N94-27201

PRINTED CIRCUITS

Aspects of the circuit board thermal design
[VTT-PUBS-132] p 2779 N94-25644

Test methods and custom hardware for functional testing of a high speed GaAs DRAM
[AD-A274859] p 2781 N94-26175

Phase conjugated lasers applied to commercial x ray lithography
[DE94-001529] p 2819 N94-27018

Baseline for a Nordtest method. Reliability stress screening of components. A guide for component users
[PB94-123775] p 2835 N94-27042

PRINTING

Development of an industrial CO2 laser for mask marking
[DE93-632901] p 2816 N94-26184

PRIORITIES

A real-time executive implementing priority inheritance protocols p 2952 N94-26733

PROBABILITY DENSITY FUNCTIONS

The deterministic power-spectral-density method
[AD-B175894] p 2678 N94-27395

Estimators for the Cauchy distribution
[DE94-004990] p 3005 N94-27816

PROBABILITY DISTRIBUTION FUNCTIONS

Simulation approaches for calculations in directed graphical models
[AD-A274825] p 3003 N94-26494

A comparison of Probability Of Detection (POD) data determined using different statistical methods
[LTR-ST-1947] p 2835 N94-26644

PROBABILITY THEORY

Proficiency scaling based on conditional probability functions for attributes
[AD-A273816] p 3002 N94-25962

Multiple model adaptive estimation applied to the LAMBDA URV for failure detection and identification
[AD-A274078] p 3002 N94-25992

A doubly logarithmic communication algorithm for the Completely Connected Optical Communication Parallel Computer
[DE93-019408] p 2980 N94-26473

Probabilistic methods for image generation and encoding
[AD-A274294] p 2964 N94-26682

Probability of accessing the multiple saturated states in the resistive interchange instability
[DE94-000478] p 3044 N94-26694

Short-range cloud amount forecasting with model output statistics
[AD-A274769] p 2895 N94-26798

Topological conditions for the existence of invariant measures for unimodal maps
[PB94-123296] p 2849 N94-26866

Modeling systems by probabilistic process algebra: An event structures approach
[PB94-125259] p 3004 N94-26867

Recursive bundle event structures
[PB94-125275] p 3004 N94-26870

Blurred focal elements generalization of dempster's rule
[PB94-124278] p 2986 N94-26992

A superprocess with a disappearing self-interaction
[AD-A274647] p 3009 N94-27108

Interdisciplinary technology p 2686 N94-27363

The Fermi paradox: An approach based on percolation theory p 2687 N94-27370
Is probability of frequency too narrow?
[DE94-000687] p 3004 N94-27612
Estimators for the Cauchy distribution
[DE94-004990] p 3005 N94-27816

PROBLEM SOLVING
Knowledge organization in intelligent tutoring systems for diagnostic problem solving in complex dynamic domains
[AD-A273986] p 2984 N94-25899
Long term learning: Integration of knowledge acquisition and knowledge compilation
[AD-A274775] p 3098 N94-26570
Parallel computational geometry on analog Hopfield networks
[ISBN-0-315-84093-5] p 2980 N94-26635
Design and evaluation of fault tolerance in opto-electronic computing
[AD-A274281] p 2954 N94-27016

PROCEDURES
Digital Altimeter Setting Indicator (DASI) Operational Test and Evaluation (OT/E) operational test procedures
[AD-A274100] p 2672 N94-26030

PROCESS CONTROL (INDUSTRY)
Safety analysis in conceptual design of process control
[VTT-PUBS-117] p 2762 N94-25641
Advances in preparing and characterizing low density pan-carbon microcellular foam
[DE94-002278] p 2748 N94-25932
Statistical quality management
[MEMO-COSOR-92-43] p 2834 N94-26008
Distributed Nd:YAG laser welding and process control in inert glove boxes
[DE94-002629] p 2818 N94-26605
Simplified high-efficiency silicon cell processing
[DE94-002683] p 2857 N94-26617
Multiple weight stepwise regression
[DE94-001602] p 3000 N94-27564
Dry etching process development for submicron and nanometer semiconductor devices
[PB94-133196] p 2788 N94-28357

PROCESS HEAT
Calculation of the thermoneutral potential of NiCd and NiH2 cells p 2861 N94-28111

PROCUREMENT POLICY
Small business innovation research program solicitation
[NASA-TM-109695] p 3094 N94-27661

PRODUCT DEVELOPMENT
The MUSA design methodology
[CWI-CS-R9265] p 3097 N94-26220
Business process redesign: Design the improved process
[AD-A274947] p 3093 N94-26299
Flash unit for high speed photography
[PML-1992-91] p 2811 N94-26647
Future of aerospace
[PB94-120185] p 2669 N94-26906
An investigation of integrated product development implementation issues: A case study of Bosma Machine and Tool Corp.
[AD-A273917] p 2942 N94-27320
The 1993 Federal Aviation Administration plan for research, engineering and development
p 2643 N94-27960
Software assurance standard
[NASA-TM-109705] p 2975 N94-27992
Development of the gas turbine. Part 1: Design philosophy and performance p 2831 N94-28080
Development of the gas turbine. Part 2: Manufacturing, commissioning, and operation p 2831 N94-28081

PRODUCTION ENGINEERING
Continuous fiber reinforced thermoplastic composites: Literature survey
[VTT-TIED-1422] p 2704 N94-25651
Concepts and methods of measuring productivity at the organization level
[AD-A273126] p 3094 N94-27180

PRODUCTION MANAGEMENT
Open communication in manufacturing automation
[PB94-132479] p 2976 N94-28377

PRODUCTIVITY
The effectiveness of AMT investment in UK metal component manufacture
[IND-MANU-SCI-TECH-REPT-3] p 2762 N94-25775
Concepts and methods of measuring productivity at the organization level
[AD-A273126] p 3094 N94-27180

PROFILOMETERS
The determination of surface roughness from reflected step edges
[AD-A273987] p 2984 N94-25900

PROGRAM VERIFICATION (COMPUTERS)
Software Error Estimation Program (SWEEP), version 02.00.00 user manual
[AD-A274697] p 2962 N94-26373
Verification and validation of the on-board software real time requirements p 2953 N94-26739
Formal methods for dependable real-time systems
p 2953 N94-26740
Vcalc: A 3-space vector calculator
[AD-A274520] p 2965 N94-26831
Freeness analysis for logic programs-and correctness
[PB94-126703] p 2966 N94-26956
Memory subsystem performance of programs with intensive heap allocation
[AD-A274122] p 2967 N94-27063
Deferred compilation: The automation of run-time code generation
[AD-A274124] p 2967 N94-27065
Alternative architectures for domain-oriented application composition and generation systems
[AD-A274180] p 2968 N94-27128
Research in improved assessment of software reliability
[AD-A274161] p 2968 N94-27140
Validation tests of TOPSIM 4
[ESA-STM-249] p 2972 N94-27582
Software assurance standard
[NASA-TM-109705] p 2975 N94-27992
Using formal specification in the Guidance and Control Software (GCS) experiment. Formal design and verification technology for life critical systems
[NASA-CR-194884] p 2956 N94-28267

PROGRAMMING ENVIRONMENTS
Using database technology to support domain-oriented application composition systems
[AD-A274091] p 3096 N94-26024
Software redesign for usability: A case study
[DE94-003704] p 2960 N94-26048
Multimedia in Views
[CWI-CS-R9263] p 2961 N94-26218
Development of a MIL-STD-1750 microprocessor system for space applications p 2949 N94-26715
An object model for multimedia programming
[CWI-CS-R9327] p 2971 N94-27552

PROGRAMMING LANGUAGES
Software redesign for usability: A case study
[DE94-003704] p 2960 N94-26048
Development of a MIL-STD-1750 microprocessor system for space applications p 2949 N94-26715
A formalization of objects using equational dynamic logic
[PB94-125218] p 2965 N94-26852
Implementation and performance of a domain decomposition algorithm in Sisal
[DE94-002012] p 2981 N94-27092
Users guide for GRIKURV: A code for drawing graphs
[PB94-123593] p 2968 N94-27154
Proceedings of the Third Workshop Computersystems: Research Forum on Design, Realization and Use of Computersystems
[ISBN-90-6144-995-2] p 2954 N94-27191
DALIA: A language for the description and analysis of digital systems p 2954 N94-27192
Efficient implementation of high-level parallel symbolic languages p 2955 N94-27196
Semantics of MANIFOLD: Specification in ASF+SDF and extension
[CWI-CS-R9269] p 2971 N94-27575
ARM: Abstract Rewriting Machine
[CWI-CS-R9330] p 2974 N94-27794

PROJECT MANAGEMENT
Feasibility study on introduction of the bio-fuel power generation in tropical regions
[DE94-725203] p 2858 N94-26838
Aerospace safety advisory panel
[NASA-TM-109692] p 3118 N94-27381
Space projects: Astrophysics facility program contains cost and technical risks. Report to Congressional Requesters
[GAO/NSIAD-94-80] p 2696 N94-27382
Training on assessment and mapping of deforestation: WFW conference, Brazil
[INPE-5482-PRE/1781] p 2850 N94-27384
University program management information system, FY 1993
[NASA-TM-109719] p 3100 N94-27413
NASA: Major challenges for management. Testimony before the Legislation and National Security Subcommittee, Committee on Government Operations, House of Representatives
[GAO/T-NSIAD-94-18] p 3095 N94-28176
Activities of Remote Sensing Technology Center of Japan (RESTEC) p 2853 N94-28274

PROJECT PLANNING
Component characterization and development 2
[AD-A274002] p 2765 N94-25660
The 1993 Federal Aviation Administration plan for research, engineering and development
p 2643 N94-27960
Asia-Pacific Seminar on Global Change Research Cooperation
[JTN-94-80517] p 2871 N94-28268
NASDA contribution plan to Asian countries
p 2853 N94-28273
The Environmental Research and Training Centre
p 2873 N94-28280
Global Change and Terrestrial Ecosystems (GCTE): Progress report and prospects for Asian contributions
p 2874 N94-28281
Global change: A research strategy for Australia 1992-1996 p 2874 N94-28282
A progress report on global change studies in China
p 2874 N94-28283

PROJECTILES
Users manual for CATNIP: A Computer Analysis Tool for Normal Impact Penetration
[DE94-003671] p 2962 N94-26371

PROLATE SPHEROIDS
Electrostatic image solution for the conducting prolate spheroid
[PB94-133154] p 2778 N94-28387

PROLOG (PROGRAMMING LANGUAGE)
Automatic test case generation using PROLOG
[NPL-DITC-215/93] p 2964 N94-26655
Modular termination proofs for logic and pure PROLOG programs
[CWI-CS-R9316] p 2970 N94-27544

PROP-FAN TECHNOLOGY
A review of recent aeroelastic analysis methods for propulsion at NASA Lewis Research Center
[NASA-TP-3406] p 2846 N94-28227

PROPELLANT MASS RATIO
Proceedings of the High Energy Density Matter (HEDM) Contractor's Conference
[AD-A274452] p 3033 N94-27083

PROPELLANT SENSITIVITY
Cryogenic size reduction of solid propellant
[AD-A274844] p 2759 N94-26800

PROPELLANTS
Inertial electrostatic confinement as a power source for electric propulsion p 2688 N94-27373

PROPELLER BLADES
The experimental behavior of spinning pretwisted laminated composite plates
[NASA-CR-195220] p 2711 N94-27352

PROPELLER FANS
A review of recent aeroelastic analysis methods for propulsion at NASA Lewis Research Center
[NASA-TP-3406] p 2846 N94-28227

PROPELLER SLIPSTREAMS
Wind tunnel investigation of propfan slipstream/wing interactions on a De Havilland air motor powered semispan model at Mach numbers 0.6 and 0.7
p 2651 N94-28316
Flow field investigation in the near slipstream of an 8-bladed propfan on the De Havilland WTEJ half-model at Mach numbers 0.6 and 0.7 p 2651 N94-28317

PROPELLERS
Propeller off-axis loads due to thrust axis incidence and nacelle magnus force p 2652 N94-28319

PROPHYLAXIS
The role of hyperbaric oxygen as a prophylaxis for radiation enteritis
[AD-A274974] p 2901 N94-26517

PROPORTIONAL CONTROL
A study on piezoelectric actuators and sensors for vibration control of flexible space structures
[AD-A274925] p 2695 N94-26532
Advanced control of a flexible spherical wrist
[ISBN-0-315-84424-8] p 2826 N94-27652

PROPORTIONAL COUNTERS
Cosmic x ray physics
[NASA-CR-195225] p 3115 N94-27236
Cosmic x ray physics
[NASA-CR-195218] p 3115 N94-27419

PROPRIOCEPTION
Proprioceptive isokinetic exercise test
[NASA-TM-104015] p 2902 N94-27227

PROPRIOCEPTORS
Proprioceptive isokinetic exercise test
[NASA-TM-104015] p 2902 N94-27227

PROPULSION
Design and flight test of the Propulsion Controlled Aircraft (PCA) flight control system on the NASA F-15 test aircraft
[NASA-CR-186028] p 2674 N94-27432

PROPULSION SYSTEM CONFIGURATIONS
Proceedings of the 8th Annual Summer Conference: NASA/USRA Advanced Design Program
[NASA-CR-195118] p 3075 N94-25665
Systematic Propulsion Optimization Tools (SPOT)
p 2976 N94-25666

Extraterrestrial surface propulsion systems
p 2833 N94-25691
Eagle RTS: A design of a regional transport
p 2671 N94-25709
Project Ares 3 p 2671 N94-25712
Tesseract supersonic business transport
p 2671 N94-25713
The design of four hypersonic reconnaissance aircraft
p 2671 N94-25716
Nuclear electric propulsion for future NASA space science missions
[DE93-019086] p 2700 N94-25969
Interdisciplinary technology p 2686 N94-27363
A parametric sensitivity study for single-stage-to-orbit hypersonic vehicles using trajectory optimization
[NASA-CR-195703] p 2697 N94-27789
A numerical study of mixing and combustion in hypervelocity flows through a scramjet combustor model
p 2808 N94-27911
A review of recent aeroelastic analysis methods for propulsion at NASA Lewis Research Center
[NASA-TP-3406] p 2846 N94-28227

PROPULSION SYSTEM PERFORMANCE
Extraterrestrial surface propulsion systems
p 2833 N94-25691
Asteroid exploration and utilization
p 3080 N94-25697
Nuclear electric propulsion for future NASA space science missions
[DE93-019086] p 2700 N94-25969
Interdisciplinary technology p 2686 N94-27363
Inertial electrostatic confinement as a power source for electric propulsion p 2688 N94-27373
Rocket engine numerical simulation
p 2688 N94-27375
A parametric sensitivity study for single-stage-to-orbit hypersonic vehicles using trajectory optimization
[NASA-CR-195703] p 2697 N94-27789
A numerical study of mixing and combustion in hypervelocity flows through a scramjet combustor model
p 2808 N94-27911
A review of recent aeroelastic analysis methods for propulsion at NASA Lewis Research Center
[NASA-TP-3406] p 2846 N94-28227

PROSTAGLANDINS
Effect of PGE2 receptor agonists butaprost, M and B 28767 and an antagonist AH 6809 on the BK response of visceral polymodal receptors p 2906 N94-27494
Effect of prostaglandin E1 on the relationship between skin sympathetic nerve activity and reduction in skin blood flow p 2929 N94-27524
The polymodal receptor p 2908 N94-27539

PROTECTIVE CLOTHING
Control panel dimensions for gloved operation study 2: Toggle switches minimum spacing required between toggle
[AD-A274518] p 2942 N94-27089
Aerospace medicine and biology: A continuing bibliography with indexes (supplement 386)
[NASA-SP-7011(386)] p 2933 N94-28208
Aerospace medicine and biology: A continuing bibliography with indexes (supplement 387)
[NASA-SP-7011(387)] p 2933 N94-28213

PROTECTIVE COATINGS
R and D for creation, measurement, application of ultra-high vacuum p 2723 N94-25549
Hydrogen trapping with Pd coated alloy films
p 2723 N94-25551
Issues for conversion coating of aluminum alloys with hydrotalcite
[DE94-003804] p 2732 N94-25819
Cracking of textured zinc coating during forming process
[DE94-003414] p 2750 N94-26085
Ceramic technology project
[DE94-003782] p 2750 N94-26332
Titanium 1992: Volume 3: Science and technology
[AD-A274800] p 2735 N94-26337
Polyurethane self-priming topcoats
[AD-D016041] p 2755 N94-27111
Corrosion resistant coatings from conducting polymers
[DE94-003959] p 2757 N94-27747

PROTEINS
Molecular biological studies on the human radioresistance and drug resistance
[DE93-632682] p 2910 N94-26549
Neutron and x ray scattering studies of the interactions between Ca(2+)-binding proteins and their regulatory targets: Comparisons of troponin C and calmodulin
[DE94-002706] p 2901 N94-26623
Cloning of rat RXR alpha cDNA and the expression of its mRNA in regenerating liver and primary cultured hepatocytes p 2905 N94-27479
Cloning of a novel POU family gene by RT-PCR method p 2905 N94-27480
Expression analysis of Thyroxine-Binding Globulin Complete Deficiency in Japanese (TBG-CDJ)
p 2905 N94-27482
Activation by G protein beta gamma subunits of G protein-coupled receptor kinase p 2931 N94-27534
The molecular matching problem
p 3030 N94-27910

PROTOCOL (COMPUTERS)
Interface technical specification of the V.25 bis emulator
[AD-A273754] p 2948 N94-25720
Weapon system integration for the AFIT virtual cockpit
[AD-A274058] p 2667 N94-25772
Object-oriented design and implementation of a parallel Ada simulation system
[AD-A274119] p 2979 N94-25906
A VHDL register transfer level model of the linear token passing multiplex data bus protocol for the high speed data bus
[AD-A273734] p 2980 N94-26009
Design and specification of the Xpress transfer high-speed protocol
[AD-A274941] p 3097 N94-26297
Modeling and simulation of a fiber distributed data interface local area network
[AD-A274838] p 3098 N94-26500
Automatic test case generation using PROLOG
[NPL-DITC-215/93] p 2964 N94-26655
A real-time executive implementing priority inheritance protocols p 2952 N94-26733
Example of the EXPANSE signalling protocol
[PB94-125283] p 2771 N94-26872
Hard real-time reliable multicast in the DEDOS system
[PB94-126745] p 2966 N94-26920
Binary snapshots
[CWI-CS-R9319] p 2955 N94-27547
An efficient off-line electronic cash system based on the representation problem
[CWI-CS-R9323] p 2776 N94-27551
A modular approach to evaluation cryptographic protocols using Petri nets
[ISBN-0-315-85354-9] p 2972 N94-27595
Simulating fail-stop in asynchronous distributed systems
[NASA-CR-195698] p 2974 N94-27767
Refinement for fault-tolerance: An aircraft hand-off protocol
[NASA-CR-195697] p 2666 N94-27768

PROTON BEAMS
On radiation defects in strip detectors
[DE93-616646] p 3015 N94-25916
Spin effects in hard interactions (interest in accelerated polarized beam)
[DE93-634398] p 3031 N94-26044
Regrouping of the beam in the IHEP PS for the UNK p-p programs
[DE93-634021] p 3032 N94-26164
Longitudinal diffusion of a proton bunch under external noise
[DE93-634022] p 3032 N94-26165

PROTON ENERGY
CRRES high energy proton flux map
[AD-A274803] p 2878 N94-26338
Modeling the DMSP and CRRES dosimeters using the path length distribution method
[RXR-93051] p 2698 N94-28200
The PROTEL contamination code
[RXR-93071] p 3040 N94-28202

PROTON IMPACT
Double excitation of He and H(-) by fast proton and anti-proton impact
[DE94-004581] p 3026 N94-27620

PROTON IRRADIATION
Radiation hardening effects on localized deformation and stress corrosion cracking of stainless steels
[DE94-004308] p 2731 N94-25804
Proton irradiation on materials p 3030 N94-27898

PROTON PRECIPITATION
Proton aurora and substorm intensifications
[ATR-93(7248)-1] p 2887 N94-28218

PROTON SCATTERING
An antiproton-proton partial-wave analysis
[DE94-002690] p 3021 N94-26620
First observation of neutral current proton electron scattering at the square root of s = 300 GeV
[DE94-701107] p 3030 N94-27877

PROTON-PROTON REACTIONS
Research on elementary particle physics, part 2
[DE94-004956] p 3029 N94-27815

PROTONS
Spin effects in hard interactions (interest in accelerated polarized beam)
[DE93-634398] p 3031 N94-26044
CRRES high energy proton flux map
[AD-A274803] p 2878 N94-26338
An antiproton-proton partial-wave analysis
[DE94-002690] p 3021 N94-26620
Double excitation of He and H(-) by fast proton and anti-proton impact
[DE94-004581] p 3026 N94-27620
Proton electromagnetic form factor near the proton-antiproton threshold and quasinuclear bound state
[DE94-606458] p 3027 N94-27681
Analysis of energetic proton and electron data in Neptune's magnetosphere
[NASA-CR-195707] p 3107 N94-27784
Modeling the DMSP and CRRES dosimeters using the path length distribution method
[RXR-93051] p 2698 N94-28200
The PROTEL contamination code
[RXR-93071] p 3040 N94-28202

PROTOPLANETS
Investigations of the dynamical evolution of protoplanetary nebulae
[NASA-CR-195278] p 3105 N94-27428

PROTOTYPES
Software redesign for usability: A case study
[DE94-003704] p 2960 N94-26048
Rapid prototyping of application specific signal processors (RASSP)
[AD-A274324] p 2772 N94-26884
An optoelectronic graphics display processor
[AD-A274401] p 3037 N94-26990
The OPAL vertex detector
[ISBN-0-315-51152-4] p 2812 N94-27257

PROVING
Trace-based compositional proof theory for fault tolerant distributed systems
[PB94-126737] p 2966 N94-26971

PSYCHIATRY
Practice patterns of US Army medical department psychiatrists and psychologists
[AD-A274787] p 2909 N94-26360

PSYCHOLOGICAL EFFECTS
Monthly variation of physiological and psychological responses under unsteady thermal conditions
p 2918 N94-27475
Man's ability to adapt himself for the seasonal climatic changes: From viewpoint of anticipation and seasonable behavior p 2919 N94-27476
A study of psychological factors affecting an extremely isolated environment p 2927 N94-27517

PSYCHOLOGICAL FACTORS
Development of stimulus-seeking scale for expecting individual differences against confinement stress
p 2915 N94-27460
The effect of body orientation on the perception of vertical and horizontal distance in an outdoor setting
p 2915 N94-27461
Eye-head coordination and swinging of the visual scene when wearing visually up-down reversing mirror for 14 days p 2915 N94-27462
Comparative measurement of visual stability in cosmic space: Onboard experiment and pre-flight activities
p 2916 N94-27463
A study of psychological factors affecting an extremely isolated environment p 2927 N94-27517

PSYCHOLOGICAL TESTS
Practice patterns of US Army medical department psychiatrists and psychologists
[AD-A274787] p 2909 N94-26360
Validation of the Federal Aviation Administration air traffic control specialist pre-training screen
[DOT/FAA/AM-94/4] p 2938 N94-26600
A study of psychological factors affecting an extremely isolated environment p 2927 N94-27517

PSYCHOLOGY
Proficiency scaling based on conditional probability functions for attributes
[AD-A273816] p 3002 N94-25962
Pacing visual attention: Temporal structure effects
[AD-A273859] p 2937 N94-25965

PSYCHOMETRICS
Extending the rule space model to a semantically-rich domain: Diagnostic assessment in architecture
[AD-A273789] p 2948 N94-25864
A diagnostic classification model for document processing skills
[AD-A273790] p 3096 N94-25925

PSYCHOPHYSICS
Top down influences on bottom-up processing
[AD-A274220] p 2939 N94-27072

PSYCHOPHYSIOLOGY
Top down influences on bottom-up processing
[AD-A274220] p 2939 N94-27072
Psychophysiology in microgravity and the role of exercise p 2936 N94-28374

PUBLIC LAW
Report of the defense science board task force on aircraft assessment
[AD-A274531] p 2669 N94-26835
PULSARS
An April 1991 outburst from 4U0115+63 observed by BATSE
[NASA-CR-195252] p 3116 N94-27440
Fusion reactor systems studies
[DE94-003162] p 3046 N94-27686
PULSE AMPLITUDE
Pulse waveform and transcranial Doppler analysis during lower body negative pressure
[AD-A274516] p 2911 N94-27088
PULSE COMMUNICATION
Improved performance of hybrid error control techniques for real-time digital communications over noisy channels
[ISBN-0-315-84281-4] p 2770 N94-26625
Short-block data detection techniques employing channel estimation for fading time-dispersive channels
[ISBN-0-315-58970-1] p 2777 N94-27806
Receiving antennas for electromagnetic pulses and transients
[ISBN-0-315-62312-8] p 2777 N94-27871
PULSE COMPRESSION
Direct-conversion-to-baseband for a nonlinear FM signal
[AD-A274861] p 2768 N94-26189
Phase conjugation and pulse compression of high energy lasers: From nanoseconds to microseconds
[DE94-001061] p 2818 N94-26699
PULSE DURATION
Bundle Intensity and Beamgate Length recorder (BIBL)
[DIGEL-1993-7] p 3031 N94-25619
Development of surgical CW Nd:YAG laser with optical fiber delivery system
[DE93-632902] p 2817 N94-26185
Development of high average power industrial Nd:YAG laser with peak power of 10 kW class
[DE93-633201] p 2818 N94-26520
Calculations of population transfer during intense laser pulses
[DE94-001060] p 2818 N94-26698
Pulse control method and its characteristics
[DE94-701187] p 2989 N94-27809
PULSE DURATION MODULATION
Development of real-time pulse shaping technology in solid-state lasers
[DE93-633438] p 2817 N94-26403
PULSE GENERATORS
Development of an industrial CO2 laser for mask marking
[DE93-632901] p 2816 N94-26184
Microwave and pulsed power
[DE94-003019] p 2782 N94-26312
Development of real-time pulse shaping technology in solid-state lasers
[DE93-633438] p 2817 N94-26403
Pulse transformer characterization
[PML-1992-73] p 2784 N94-26646
Research in pulsed power plasma physics
[AD-A274323] p 3045 N94-27074
Bulletin of the Institute for Chemical Reaction Science, Tohoku University, volume 2
[JTN-94-80602] p 2717 N94-27385
Four phase microwave pulse generator for pulsed EPR spectrometer p 2718 N94-27388
High repetition rate, mode locked, figure eight laser with extracavity feedback
[AD-D016053] p 2820 N94-27670
PULSE REPETITION RATE
Development of an industrial CO2 laser for mask marking
[DE93-632901] p 2816 N94-26184
PULSED LASERS
Imaging with x ray lasers
[DE94-002844] p 2816 N94-26020
Fast photoconductor CdTe detectors for synchrotron x ray studies
[DE94-001334] p 3054 N94-26139
Laser altimetry simulator. Version 3.0: User's guide
[NASA-TM-104588] p 2877 N94-26152
Development of an industrial CO2 laser for mask marking
[DE93-632901] p 2816 N94-26184
Development of surgical CW Nd:YAG laser with optical fiber delivery system
[DE93-632902] p 2817 N94-26185
Theoretical determination of chemical rate constants using novel time-dependent methods
[NASA-CR-195221] p 2714 N94-26205
Compact, solid-state femtosecond source
[AD-A273932] p 2817 N94-26271
New Thomson scattering laser control for D3-D
[DE94-002890] p 3043 N94-26274
Development of real-time pulse shaping technology in solid-state lasers
[DE93-633438] p 2817 N94-26403
Development of high average power industrial Nd:YAG laser with peak power of 10 kW class
[DE93-633201] p 2818 N94-26520
Calculations of population transfer during intense laser pulses
[DE94-001060] p 2818 N94-26698
Development of lasers optimized for pumping Ti:Al2O3 lasers
[NASA-CR-4573] p 2818 N94-26705
High repetition rate, mode locked, figure eight laser with extracavity feedback
[AD-D016053] p 2820 N94-27670
PULTRUSION
Lunar preform manufacturing p 2765 N94-25677
PUMP IMPELLERS
The high Reynolds number flow through an axial-flow pump
[AD-A273844] p 2789 N94-25604
Pump CFD code validation tests
[NASA-CR-193939] p 2822 N94-26597
Bulk-Flow Analysis, part A
[NASA-CR-193911-PT-A] p 2796 N94-27377
Compressibility effects on rotor forces in the leakage path between a shrouded pump impeller and its housing
p 2796 N94-27379
PURIFICATION
Study on utilization of super clean, high vacuum space
p 2682 N94-25586
Development of liquid membrane separation processes p 2717 N94-27386
PYROLYSIS
Double layer capacitance of carbon foam electrodes
[DE94-002651] p 2780 N94-25975
Micropyrolysis of polymer thin films for ceramics
[ECL-92-62] p 2750 N94-26088
Emissions of nitrogen oxides (NO(x) and N2O) in pressurized fluidized bed combustion
[PB94-133071] p 2876 N94-28395
PYROTECHNICS
Structural analysis of a frangible nut used on the NASA Space Shuttle
[DE94-003672] p 2821 N94-25811
Radiometric, spectral, and effectiveness equipment
[AD-A274208] p 3037 N94-27066
PYRROLES
LB-Deposited, side-chain substituted polyaniline, polypyrrole and the corresponding monomers, studied by STM
[AD-A274405] p 2754 N94-26977
Langmuir-Blodgett and STM investigations of conducting polymer thin films
[AD-A274512] p 2755 N94-27087
Chemical polymerization and Langmuir-Blodgett techniques. 2: The polymerization of monolayers of 3-substituted pyrroles
[AD-A274478] p 2755 N94-27163
PYRUVATES
Preparation, characterization, and thermal behaviour study of lanthanides (3) and yttrium (3) 4-methoxy benzylidene pyruvate in solid state
[DE94-604079] p 3068 N94-27697

Q

Q FACTORS
Effective conductivity of wire mesh reflectors for space deployable antenna systems
[NASA-CR-191605] p 2788 N94-27770
Q SWITCHED LASERS
The development of Cr, Tm, Ho:YAG lasers for airborne lidar
[AD-A274895] p 2816 N94-26178
Development of lasers optimized for pumping Ti:Al2O3 lasers
[NASA-CR-4573] p 2818 N94-26705
QUADRATIC EQUATIONS
Phase portraits of quadratic systems with finite multiplicity three and one critical point of infinity
[REPT-93-41] p 2991 N94-26215
QUADRATURES
A current evaluation of the digital beamforming testbed at Rome Laboratory
[AD-A274311] p 3032 N94-26881
QUADRUPOLES
Focusing properties of a three-element quadrupole lens system and its stigmatic focusing behaviour
[DE93-616534] p 2766 N94-25915
Correlation of experimental data and three-dimensional finite element modeling of a spinning quadrupole
[DE93-041173] p 3008 N94-26421
Hyperfine structure of positronium energy levels in a crystal
[DE94-603898] p 3068 N94-27729
Image theory for DC problems involving a conducting half space bounded by the general anisotropic impedance surface
[PB94-132917] p 2779 N94-28390
QUALIFICATIONS
Advanced qualification techniques
[DE94-003709] p 2780 N94-25812
QUALITATIVE ANALYSIS
Molecular surface electrostatic potentials in the analysis of non-hydrogen-bonding noncovalent interactions
[AD-A274612] p 3022 N94-26894
QUALITY
Measurement of laboratory quality
[VTT-TIED-1427] p 2679 N94-25652
QUALITY CONTROL
Package integrity measurement technology and quality assurance
[AD-A273881] p 2834 N94-25727
Objective image quality metrics: Applications for partially compensated images of space objects
[AD-A273837] p 2847 N94-25741
An exploratory survey of methods used to develop measures of performance
[AD-A273945] p 2834 N94-25896
Digital control and data acquisition for high-value GTA welding
[DE94-000885] p 2821 N94-25980
The use of on-line ion chromatography for high temperature and high pressure reaction studies
[DE94-002525] p 2713 N94-26075
Business process redesign: Design the improved process
[AD-A274947] p 3093 N94-26299
Analytical study of beam handling and emittance control
[AD-A274412] p 3033 N94-27078
Quality assurance for fracture mechanical finite element analyses (appendix 3/1) p 2841 N94-27189
An investigation of integrated product development implementation issues: A case study of Bosma Machine and Tool Corp.
[AD-A273917] p 2942 N94-27320
Development of a 2f optical performance measurement system
[DE94-003489] p 3039 N94-27721
Software assurance standard
[NASA-TM-109705] p 2975 N94-27992
Report of the Shuttle Processing Review Team
[NASA-TM-109728] p 2692 N94-28178
QUANTITATIVE ANALYSIS
Study on analyzing method establishment for metallic material development p 2729 N94-25578
Hydrogen uptake into silicon from an ECR plasma
[DE94-003771] p 3050 N94-25815
Analytical method for estimation of the total amount of aromatic and poly aromatic compounds in diesel fuel
[PB94-123692] p 2759 N94-25907
Radiochemistry Division annual progress report : 1991
[DE94-600652] p 2715 N94-26392
New FORTRAN computer programs to acquire and process isotopic mass spectrometric data: Operator's manual
[DE94-003174] p 2965 N94-26784
Multivariate calibration applied to near-infrared spectroscopy for the quantitative analysis of dilute aqueous solutions
[DE94-003231] p 2716 N94-26794
Gordon Research Conference on the Physics and Chemistry of Laser Diagnostics in Combustion
[AD-A274609] p 2716 N94-26893
Preparation, characterization, and thermal behaviour study of lanthanides (3) and yttrium (3) 4-methoxy benzylidene pyruvate in solid state
[DE94-604079] p 3068 N94-27697
QUANTUM CHEMISTRY
International journal of quantum chemistry. Quantum Chemistry Symposium Number 27: Proceedings of the International Symposium on Atomic, Molecular, and Condensed Matter Theory and Computational Methods
[AD-A274352] p 3023 N94-26926
QUANTUM CHROMODYNAMICS
Out of equilibrium phase transitions and a toy model for disoriented chiral condensates
[DE94-601642] p 3013 N94-25839
Unravelling the structure of matter on high-performance computers
[DE94-601620] p 3015 N94-25891
Nucleon-nucleon scattering lengths in QCD sum rules
[DE93-520239] p 3015 N94-25922
Heavy quark production and spectroscopy
[DE94-003619] p 3015 N94-25935

Monte Carlo event generators for hadron-hadron collisions
[DE94-003212] p 3015 N94-25955
A dependence of exclusive vector meson production in muon-nucleus scattering
[DE94-003363] p 3016 N94-25957
Deciphering the quark-gluon structure of the photon in electron(gamma) collisions
[DE93-634386] p 3017 N94-26043
Spin effects in hard interactions (interest in accelerated polarized beam)
[DE93-634398] p 3031 N94-26044
The STAR experiment at the Relativistic Heavy Ion Collider
[DE94-003409] p 3017 N94-26083
The delta (1232) resonance transition form factor
[DE94-003442] p 3017 N94-26101
Photon and hadron production of heavy flavors
[DE94-004655] p 3018 N94-26245
Nuclear Theory Group, University of Washington recent and planned research
[DE94-002729] p 3022 N94-26809
Experimental investigations of strong interaction in the non-perturbative QCD region
[DE94-001178] p 3024 N94-26949
The challenges of exclusive processes in QCD
[DE94-003429] p 3024 N94-27050
Charmonium physics at a tau-charm factory
[PB94-124344] p 3024 N94-27199
QCD corrections to inclusive B - S processes in the standard model
[ISBN-0-315-54572-0] p 3073 N94-27263
A relativistic quark model
[ISBN-0-315-60926-5] p 3025 N94-27333
Aspects of perturbative corrections in quantum chromodynamics
[ISBN-0-315-63607-6] p 3074 N94-27398
Quantum chromodynamics and nuclear physics at extreme energy density
[DE94-004418] p 3026 N94-27604
Electroweak and other interactions in medium-energy nuclear physics
[DE94-004161] p 3027 N94-27689
High energy parton-parton elastic scattering in QCD
[DE94-003432] p 3028 N94-27736

QUANTUM ELECTRODYNAMICS
Back-reaction beyond the mean field approximation
[DE94-003936] p 3012 N94-25612
Theoretical and experimental studies of elementary physics
[DE94-002310] p 3008 N94-25988
Spinor and isospinor structure of relativistic particle propagators
[DE94-601552] p 3019 N94-26424
A variational approach to the quantum field theoretic bound-state problem
[ISBN-0-315-60960-5] p 3074 N94-27401
Relativistic two-body system in 1+1-dimensional QED. 1: On the circle S1
[DE94-603716] p 3067 N94-27647
Excited Landau levels, orbital angular momentum and axial anomaly
[DE94-606407] p 3068 N94-27679
Enhancement of the rate of radiative processes in the field of a magnetic monopole
[DE94-603717] p 3074 N94-27696

QUANTUM ELECTRONICS
Solid state research
[AD-A274063] p 3049 N94-25645
Frontiers of science and measurement: Report on a seminar jointly organized by the National Physical Laboratory and the Institute of Physics
[PB94-124310] p 3009 N94-27131
An electronic switch based on quantum interference
[ISBN-0-315-84609-7] p 2787 N94-27650

QUANTUM MECHANICS
Coherent state approach for the (Phi)(sup 6)-lattice model and phase transitions
[DE93-613053] p 3050 N94-25825
Quantizable configurations of the relativistic string
[DE93-634346] p 3072 N94-26036
Holes in a two-dimensional quantum antiferromagnet
[DE93-634753] p 3057 N94-26388
Finite dimensional representations of the quantum superalgebra U(sub q)(gl(3/2))
[DE93-634303] p 2993 N94-26440
Quantum Hamiltonian differential geometry: How does quantization affect space?
[DE93-634306] p 2993 N94-26442
Quantum group and Manin plane related to a colored braid group representation
[DE94-601509] p 3072 N94-26461
How to build analogues of the Bessel-Clifford expansions for the sum of the repulsive Coulomb potential and central potential decreasing more rapidly than the centrifugal one?
[DE93-634308] p 3007 N94-26472
Stochastic solution to quantum dynamics
[NASA-TP-3408] p 3114 N94-26550
Wigner quantum oscillators
[DE94-601508] p 3073 N94-26758
Quantum statistical inference for density estimation
[DE94-002625] p 3073 N94-26805
Length-scale dependent ensemble-averaged conductance of a 1D disordered conductor: Conductance minimum
[DE94-602732] p 3062 N94-26902
Pigs in cyberspace p 2689 N94-27376
Decay of non-equilibrium polariton condensate in semiconductors
[DE94-604016] p 3068 N94-27678
The gl(n/m) and related q-identitiesematics and computer science ends in nuclear and related q-identities
[DE94-603653] p 3001 N94-27839

QUANTUM NUMBERS
Proton electromagnetic form factor near the proton-antiproton threshold and quasinuclear bound state
[DE94-606458] p 3027 N94-27681

QUANTUM THEORY
Duality for multiparametric quantum GL(n) and for a Lorentz quantum group
[DE93-613048] p 3005 N94-25868
Topological amplitudes in string theory
[DE94-601561] p 3071 N94-25882
On string theory interacting with two-dimensional gravity
[DE94-601562] p 3071 N94-25883
The algebra of non-local charges in non-linear sigma models
[DE94-601563] p 2991 N94-25884
A research program in experimental and theoretical high energy physics
[DE94-002156] p 3031 N94-25931
Studies in nonlinear numerical analysis
[AD-A273911] p 2959 N94-25968
The massless representations of the conformal quantum algebra
[DE94-601555] p 3006 N94-26413
Affine algebras on the torus
[DE94-601556] p 3006 N94-26414
Higher spin extensions of the Virasoro algebra, area-preserving algebras and the matrix algebra a-bar(sub (infinity))
[DE94-601557] p 3006 N94-26415
Differential regularization of a non-relativistic anyon model
[DE94-601558] p 3019 N94-26416
Vortices in curved spacetime
[DE94-601559] p 3072 N94-26417
Orthodox gravity
[DE94-601560] p 2878 N94-26418
Gauging of Chern-Simons p-Barnes
[DE94-601553] p 2993 N94-26425
Quantum subgroups and quantum co-set spaces and differential calculi on them
[DE94-602520] p 3073 N94-26876
Improved numerical methods for quantum field theory (Outstanding Junior Investigator Award)
[DE94-001793] p 3073 N94-27002
Operator regularization and renormalization theory
[ISBN-0-315-49334-8] p 3007 N94-27264
Quantum chromodynamics and nuclear physics at extreme energy density
[DE94-004418] p 3026 N94-27604
Second-order phase transition in (g(phi)4)2 theory
[DE94-603677] p 3067 N94-27638
Stochastic space-time, confinement potential and particle propagator
[DE94-606415] p 3074 N94-27680
A method for obtaining quantum doubles from the Yang-Baxter R-matrices
[DE94-606300] p 3001 N94-27846

QUANTUM WELL LASERS
Development of intermetallic compounds for high performance luminescence elements
p 2722 N94-25545

QUANTUM WELLS
Characterization of nonlinear effects in optically pumped vertical cavity surface emitting lasers
[AD-A273840] p 2815 N94-25744
Biexciton formation by two-photon absorption in quantum wells
[DE93-613551] p 3071 N94-25852
Instantaneous amplitude and frequency dynamics of coherent wave mixing in semiconductor quantum wells
[DE94-003262] p 3054 N94-26128
Investigation of a normal incidence high-performance p-type strained layer In(0.3)Ga(0.7)As / In(0.52)Al(0.48) as quantum well infrared photodetector
[AD-A274854] p 3055 N94-26188
Ordering and phase separation in MOCVD InGaP alloys and unicompositional quantum wells
[DE94-004693] p 3056 N94-26352

QUARK MODELS
Lepton masses in an SU(3)(sub L) x U(1)(sub N) gauge model
[DE93-634366] p 3016 N94-26040
Spin effects in hard interactions (interest in accelerated polarized beam)
[DE93-634398] p 3031 N94-26044
Dibaryon-induced instability of neutron stars
[DE93-634453] p 3103 N94-26046
Measuring the time dependence of B(sub s)(sup 0) meson - anti B(sub s)(sup 0) meson oscillations
[ISBN-0-315-84367-5] p 3021 N94-26665
Low-energy hadronic interactions beyond the current algebra approach
[DE94-602600] p 3022 N94-26900
Spectroscopy and strong decays of baryons
[ISBN-0-315-49073-X] p 3024 N94-27258
Finding the missing pieces of the standard model
[ISBN-0-315-57174-8] p 3024 N94-27259
QCD corrections to inclusive B - S processes in the standard model
[ISBN-0-315-54572-0] p 3073 N94-27263
A relativistic quark model
[ISBN-0-315-60926-5] p 3025 N94-27333
Aspects of perturbative corrections in quantum chromodynamics
[ISBN-0-315-63607-6] p 3074 N94-27398

QUARK PARTON MODEL
High energy parton-parton elastic scattering in QCD
[DE94-003432] p 3028 N94-27736

QUARKS
Quark-antiquark bound states
[DE93-613054] p 3013 N94-25826
A possible way of connecting the Grassmann variables and the number of generation
[DE94-601624] p 2990 N94-25838
Out of equilibrium phase transitions and a toy model for disoriented chiral condensates
[DE94-601642] p 3013 N94-25839
Structure functions of sea quarks, Kogut-Susskind pole and dynamics of pp- and pp-bar-interactions at high energies
[DE93-613184] p 3031 N94-25870
Heavy quark production and spectroscopy
[DE94-003619] p 3015 N94-25935
Pseudoscalar glueball in the composite interpolating fields approach
[DE93-634374] p 3016 N94-26042
Deciphering the quark-gluon structure of the photon in electron(gamma) collisions
[DE93-634386] p 3017 N94-26043
The STAR experiment at the Relativistic Heavy Ion Collider
[DE94-003409] p 3017 N94-26083
JLC-1
[DE93-520380] p 3031 N94-26113
Why is the Higgs doublet light?
[DE94-601711] p 3018 N94-26333
Mesons and diquarks in a NJL-model at finite temperature and chemical potential
[DE93-634375] p 3020 N94-26505
Measuring the time dependence of B(sub s)(sup 0) meson - anti B(sub s)(sup 0) meson oscillations
[ISBN-0-315-84367-5] p 3021 N94-26665
Light-quark, heavy-quark systems: An update
[DE94-002298] p 3021 N94-26759
Strange Dibaryons
[DE94-003005] p 3022 N94-26769
Low-energy hadronic interactions beyond the current algebra approach
[DE94-602600] p 3022 N94-26900
D0 results on searches for the top quark
[DE94-003361] p 3023 N94-26938
Experimental investigations of strong interaction in the non-perturbative QCD region
[DE94-001178] p 3024 N94-26949
Finding the missing pieces of the standard model
[ISBN-0-315-57174-8] p 3024 N94-27259
A relativistic quark model
[ISBN-0-315-60926-5] p 3025 N94-27333
Quantum chromodynamics and nuclear physics at extreme energy density
[DE94-004418] p 3026 N94-27604
Search for the top quark in the single lepton + jets channel at D0
[DE94-004660] p 3028 N94-27749

QUASARS
Sloan Digital Sky Survey
[DE94-004662] p 3103 N94-27750

Weak bump quasars
[NASA-CR-195267] p 3103 N94-27933

QUASI-STEADY STATES
Scaling of sustained ZT-40 M reversed field pinches
[DE94-003318] p 3043 N94-26321

QUENCHING (ATOMIC PHYSICS)
Vibrational energy transfer within the B 3Pi (O(+) sub u) state of 79BR2 upon collision with N2, O2, NO, and SF6
[AD-A273905] p 3011 N94-25589

QUENCHING (COOLING)
Study on the production of flaky amorphous alloy powders by impact flattening of atomized liquid droplets on a rapidly rotating wheel p 2746 N94-28169
Formation and high mechanical strength of Al-based alloys containing a nanoscale icosahedral phase as a main constituent p 2746 N94-28171

QUERY LANGUAGES
Design and implementation of a query editor for the Amadeus system
[AD-A274955] p 3097 N94-26300

QUEUEING THEORY
Single-server queues with spatially distributed arrivals
[PB94-126638] p 2986 N94-26916

R

RADAR ANTENNAS
Cloud liquid water content measurement tests using dual-wavelength radar
[PB94-125960] p 2896 N94-26959

RADAR ATTENUATION
Cloud liquid water content measurement tests using dual-wavelength radar
[PB94-125960] p 2896 N94-26959

RADAR BEAMS
Theoretical aspects of the agile mirror
[AD-A274890] p 2767 N94-26177

RADAR CROSS SECTIONS
Extension of On-Surface Radiation Condition (OSRC) theory to full-vector electromagnetic wave scattering by three-dimensional conducting, dielectric, and coated targets
[AD-A274023] p 2766 N94-25757
A study of two dimensional tapered periodic edge treatments to reduce wideband edge diffraction
[AD-A274054] p 2766 N94-25824
Radar cross section visualization using sample buffer progressive refinement volume rendering
[AD-A274179] p 2773 N94-27127

RADAR DATA
Radar detection of low-altitude targets in a maritime environment. Volume 2: Meteorological and radar data
[AD-A274658] p 2768 N94-26335
Leadex environmental phenomena and effects observed by DMSP, NOAA, and ERS-1 satellites
[AD-A274596] p 2868 N94-26888

RADAR DETECTION
Machine intelligent gust front algorithm
[AD-A273695] p 2680 N94-26196
Radar detection of low-altitude targets in a maritime environment. Volume 2: Meteorological and radar data
[AD-A274658] p 2768 N94-26335
Processing of wide-angle synthetic aperture radar signals for target detection
[AD-A274225] p 2773 N94-27073

RADAR ECHOES
Analyzing adaptive beamformer performance in a stable multipath environment
[AD-A274029] p 2766 N94-25766
Investigation of a normal incidence high-performance p-type strained layer In(0.3)Ga(0.7)As / In(0.52)Al(0.48) as quantum well infrared photodetector
[AD-A274854] p 3055 N94-26188

RADAR IMAGERY
Response of an airborne synthetic aperture radar to sea ice in the marginal ice zone
[ISBN-0-315-84243-1] p 2849 N94-26668
Encoding approaches for data link transmission of weather graphics
[AD-A274497] p 2772 N94-26963
Processing of wide-angle synthetic aperture radar signals for target detection
[AD-A274225] p 2773 N94-27073
Method of correcting rotational motion error in SAR and ISAR imagery
[AD-D016033] p 2773 N94-27146
Image quality analysis of compressed synthetic aperture radar imagery
[AD-A273399] p 2774 N94-27170
Non-adaptive robust filters for speckle noise reduction
[INPE-5519-PRE/1794] p 2776 N94-27335
Perceptual compression of magnitude-detected synthetic aperture radar imagery p 2946 N94-28260

Some implications of large impact craters and basins on Venus for terrestrial ringed craters and planetary evolution p 2890 N94-28306

RADAR MEASUREMENT
Cloud liquid water content measurement tests using dual-wavelength radar
[PB94-125960] p 2896 N94-26959

RADAR NETWORKS
A feasibility study on bird classification with neural network
[AD-A273753] p 2659 N94-25780

RADAR RANGE
New binary integration strategies and corresponding R90 calculations
[AD-A274786] p 2769 N94-26359

RADAR SCANNING
The development of an in-motion radiography system for large area aircraft scanning
[DREP-TM-93-53] p 2670 N94-27666

RADAR TARGETS
Radar detection of low-altitude targets in a maritime environment. Volume 2: Meteorological and radar data
[AD-A274658] p 2768 N94-26335
New binary integration strategies and corresponding R90 calculations
[AD-A274786] p 2769 N94-26359
Processing of wide-angle synthetic aperture radar signals for target detection
[AD-A274225] p 2773 N94-27073

RADAR TRACKING
Methods for improving low-angle, low-altitude radar tracking accuracy
[AD-A274914] p 2768 N94-26347
Combatting inherent vulnerabilities of CFAR algorithms and a new robust CFAR design
[AD-A274918] p 2770 N94-26751
Processing of wide-angle synthetic aperture radar signals for target detection
[AD-A274225] p 2773 N94-27073

RADAR TRANSMISSION
Over-the-horizon propagation measurements at six radar-frequency bands at the Atlantic Ocean Coast
[AD-A274151] p 2773 N94-27136

RADAR TRANSMITTERS
S-76 high intensity radiated fields, volume 3
[AD-A274416] p 2772 N94-26980

RADIAL FLOW
Low cost, radial flow, solid oxide fuel cell
[DE94-002982] p 2858 N94-26785
On helicon wave induced radial plasma transport
[IPPCZ-333] p 3048 N94-27840

RADIANCE
MODIS airborne simulator visible and near-infrared calibration, 1992 ASTEX field experiment. Calibration version: ASTEX King 1.0
[NASA-TM-104599] p 2897 N94-28179

RADIANT HEATING
Numerical and experimental analyses of the radiant heat flux produced by quartz heating systems
[NASA-TP-3387] p 3011 N94-27659

RADIATION ABSORPTION
Radiation applications of physical chemistry
p 2854 N94-26054
Evanescent field infrared spectroscopy using chalcogenide glass fiber
[ITN-94-85233] p 3038 N94-27178

RADIATION BELTS
Analysis of energetic proton and electron data in Neptune's magnetosphere
[NASA-CR-195707] p 3107 N94-27784

RADIATION CHEMISTRY
The First Energy Conference: Israel and the Former USSR
[ISBN-965-229-098-X] p 2853 N94-26050
Radiation applications of physical chemistry
p 2854 N94-26054

RADIATION COUNTERS
Use of parallel counters for triggering
[DE93-616656] p 2979 N94-25918
Harvard University High Energy Physics
[DE94-002406] p 3032 N94-26119
Hadron gas ionization calorimeters
[DE93-634186] p 2810 N94-26397
Measuring the time dependence of B(sub s)(sup 0) meson - anti B(sub s)(sup 0) meson oscillations
[ISBN-0-315-84367-5] p 3021 N94-26665
The OPAL vertex detector
[ISBN-0-315-51152-4] p 2812 N94-27257

RADIATION DAMAGE
Temperature dependence of the radiation induced change of depletion voltage in silicon PIN detectors
[DE94-002705] p 3052 N94-25972
Temperature dependence of static RAM volatility
[DE93-040345] p 2948 N94-26111

Experimental and numerical investigation of shock wave propagation through complex geometry, gas continuous, two-phase media
[DE94-001408] p 2791 N94-26121
Disturbed neuronal migration in the cerebral cortex of mice by low-dose gamma radiation
p 2904 N94-27470
Distribution of GABA immunoreactive neurons in the brain of rolling mouse Nagoya and gamma-irradiated mouse p 2904 N94-27471
Effects of gamma ray radiation on the developing mouse cerebellum: Apoptotic cell death and induction of tissue transglutaminase p 2904 N94-27472
Influence of lattice damage on retention and transport of deuterium in beta silicon carbide
[DE94-005206] p 3068 N94-27693
Damage growth in MgAl2O4 crystals by Xe ion irradiations
[DE94-005009] p 3069 N94-27828

RADIATION DETECTORS
JLC-1
[DE93-520380] p 3031 N94-26113
Auxiliary controller for time-to-digital converter module readout
[DE93-634172] p 2948 N94-26266
Exploration of GaAs structures for solid-state detectors
[DE93-634191] p 3056 N94-26379
The 12-channel flash-ADC FASTBUS module
[DE93-634229] p 2783 N94-26380
Separation and reconstruction of electron neutrino interaction in the IHEP-JINR neutrino detector and BARS detector
[DE93-634182] p 3019 N94-26393
Proceedings of the Second EGS4 User's Meeting in Japan
[DE93-520383] p 3032 N94-26543
The response of an hyperpure Ge detector to ionizing radiation
[ISBN-0-315-83968-6] p 2811 N94-26662
Channel to energy calibration results for the BATSE large area detectors p 3115 N94-26690
Advances in gamma ray field instrumentation at Los Alamos
[DE93-040264] p 2813 N94-27624
The status of the solar neutrino problem
[DE94-003934] p 3111 N94-27742
Performance of a 14-MeV neutron generator as an in situ calibration source for TFTR
[DE94-004993] p 3048 N94-27825

RADIATION DOSAGE
Microstructural development in low activation ferritic alloys irradiated to 200 dpa at 420 C
[DE94-004269] p 2731 N94-25803
Advanced qualification techniques
[DE94-003709] p 2780 N94-25812
Window least squares method applied to statistical noise smoothing of positron annihilation data
[DE93-634665] p 3003 N94-26385
Studies on the application of radiation for genetic transformation in higher plants
[DE93-632656] p 2901 N94-26470
The role of hyperbaric oxygen as a prophylaxis for radiation enteritis
[AD-A274974] p 2901 N94-26517
Conceptual design of the tokamak radiation shielding for the Tokamak Physics Experiment (TPX)
[DE94-002791] p 3044 N94-26858
Effect of temperature and recoil-energy spectra on irradiation-induced amorphization in Ca2La8(SiO4)6O2
[DE94-004371] p 3067 N94-27602
Modeling the DMSP and CRRES dosimeters using the path length distribution method
[RXR-93051] p 2698 N94-28200
Develop and fabricate a radiation dose measurement system for satellites
[PL-TR-93-2161] p 2698 N94-28210
Develop and fabricate a radiation dose measurement system for satellites
[PL-TR-93-2099] p 2698 N94-28217

RADIATION EFFECTS
A review of carbide fuel corrosion for nuclear thermal propulsion applications
[DE94-003938] p 2699 N94-25613
Microstructural development in low activation ferritic alloys irradiated to 200 dpa at 420 C
[DE94-004269] p 2731 N94-25803
Advanced qualification techniques
[DE94-003709] p 2780 N94-25812
Electrical properties of p-type GaInP2
[AD-A273771] p 3051 N94-25856
On radiation defects in strip detectors
[DE93-616646] p 3015 N94-25916
Temperature dependence of the radiation induced change of depletion voltage in silicon PIN detectors
[DE94-002705] p 3052 N94-25972

Radiation-Induced Structural Changes, 2
[DE93-520314] p 3054 N94-26109
Temperature dependence of static RAM volatility
[DE93-040345] p 2948 N94-26111
Regrowth zones in laser annealed radiation damaged diamond
[DE94-600821] p 3056 N94-26364
Radiochemistry Division annual progress report : 1991
[DE94-600652] p 2715 N94-26392
Studies on the application of radiation for genetic transformation in higher plants
[DE93-632656] p 2901 N94-26470
The role of hyperbaric oxygen as a prophylaxis for radiation enteritis
[AD-A274974] p 2901 N94-26517
Molecular biological studies on the human radioresistance and drug resistance
[DE93-632682] p 2910 N94-26549
Microstructural development in irradiated vanadium alloys
[DE94-004307] p 2737 N94-26556
Influence of helium generation rate and temperature history on mechanical properties of model Fe-Cr-Ni alloys irradiated in FFTF at relatively low displacement rates
[DE94-004264] p 2737 N94-26575
Suppression of thermal grain growth in nickel by prior electron irradiation
[DE94-004602] p 2737 N94-26587
Disintegration of (C60) by Xe ion irradiation
[DE94-601913] p 3023 N94-26929
The role of point defect clusters in reactor pressure vessel embrittlement
[DE94-001122] p 2739 N94-26931
Initial ultraviolet-B intensity data at Lawrence Livermore National Laboratory
[DE94-004279] p 2869 N94-27267
The radiation design handbook
[ESA-PSS-01-609-ISSUE-1] p 2696 N94-27397
Annals of the Research Inst. of Environmental Medicine, Nagoya Univ., volume 44
[REPT-44-VOL-44] p 2911 N94-27442
Disturbed neuronal migration in the cerebral cortex of mice by low-dose gamma radiation
p 2904 N94-27470
Distribution of GABA immunoreactive neurons in the brain of rolling mouse Nagoya and gamma-irradiated mouse p 2904 N94-27471
Effects of gamma ray radiation on the developing mouse cerebellum: Apoptotic cell death and induction of tissue transglutaminase p 2904 N94-27472
Grain boundary chromium concentration effects on the IGSCC and IASCC of austenitic stainless steels
[DE94-004268] p 2741 N94-27570
Effect of temperature and recoil-energy spectra on irradiation-induced amorphization in Ca2La8(SiO4)6O2
[DE94-004371] p 3067 N94-27602
Fusion reactor systems studies
[DE94-003162] p 3046 N94-27686
Ion implantation in silicate glasses
[DE94-003785] p 2757 N94-27726
Outgas and vacuum seal characteristics of irradiated polyimide O-ring
[DE94-701200] p 2757 N94-27812
Damage growth in MgAl2O4 crystals by Xe ion irradiations
[DE94-005009] p 3069 N94-27828
Experiment and research on materials irradiated by plasma radiation
[DE94-605011] p 2758 N94-27845
Proton irradiation on materials p 3030 N94-27898
Sonic booms and marine mammals: Informational status and recommendations p 2651 N94-28198

RADIATION HARDENING
Microstructural development in low activation ferritic alloys irradiated to 200 dpa at 420 C
[DE94-004269] p 2731 N94-25803
Radiation hardening effects on localized deformation and stress corrosion cracking of stainless steels
[DE94-004308] p 2731 N94-25804
Advanced qualification techniques
[DE94-003709] p 2780 N94-25812

RADIATION HAZARDS
Risk perspectives for Topaz 2 flight mission
[DE94-003229] p 2700 N94-25956
Vacuum-UV-effects on E. coli plasmid pUC19: Inactivation, strand break induction and mutation induction
[DLR-FB-93-26] p 2903 N94-27754

RADIATION INJURIES
Disturbed neuronal migration in the cerebral cortex of mice by low-dose gamma radiation
p 2904 N94-27470
Distribution of GABA immunoreactive neurons in the brain of rolling mouse Nagoya and gamma-irradiated mouse p 2904 N94-27471
Effects of gamma ray radiation on the developing mouse cerebellum: Apoptotic cell death and induction of tissue transglutaminase p 2904 N94-27472

RADIATION MEASUREMENT
Testbed model and data assimilation for ARM
[DE94-000432] p 2893 N94-26082
Develop and fabricate a radiation dose measurement system for satellites
[PL-TR-93-2161] p 2698 N94-28210
Develop and fabricate a radiation dose measurement system for satellites
[PL-TR-93-2099] p 2698 N94-28217

RADIATION MEASURING INSTRUMENTS
Contributions to the 23rd ICRC from emulsion chamber experiments at Mt. Chacaltaya and Pamirs
[ICRR-REPT-295-93-7] p 3112 N94-25624
Observation of characteristics of cosmic-ray hadron interactions in uniform-type thick lead chambers at Pamir, 1 p 3112 N94-25628
Observation of characteristics of cosmic-ray hadron interactions in uniform-type thick lead chambers at Pamir, 2 p 3113 N94-25629

RADIATION PROTECTION
Proceedings of the Second EGS4 User's Meeting in Japan
[DE93-520383] p 3032 N94-26543
Conceptual design of the tokamak radiation shielding for the Tokamak Physics Experiment (TPX)
[DE94-002791] p 3044 N94-26858
Research and development within nonlinear optics for protection of optical sensors against laser irradiation on of optical sensors against laser irradiation. Quarterannual report 1 (april 1993))
[PB94-124245] p 3037 N94-27046

RADIATION SHIELDING
The 1991-1992 project summaries
p 2943 N94-25698
Experimental and numerical investigation of shock wave propagation through complex geometry, gas continuous, two-phase media
[DE94-001408] p 2791 N94-26121
A robust helium-cooled shield/blanket design for ITER
[DE94-003402] p 3043 N94-26323
Conceptual design of the tokamak radiation shielding for the Tokamak Physics Experiment (TPX)
[DE94-002791] p 3044 N94-26858
A widely adaptable habitat construction system utilizing space resources p 2688 N94-27374
Monte Carlo calculations of low background detector response
[DE94-004593] p 3116 N94-27621
Fusion reactor systems studies
[DE94-003162] p 3046 N94-27686

RADIATION SOURCES
Electrical analysis of wideband and distributed windows using time-dependent field codes
[DE94-002987] p 2768 N94-26310
Monte Carlo calculations of low background detector response
[DE94-004593] p 3116 N94-27621

RADIATION SPECTRA
A double arm time-of-flight spectrometer based on position-sensitive parallel-grid avalanche counters
[DE93-616665] p 3012 N94-25750

RADIATION THERAPY
The role of hyperbaric oxygen as a prophylaxis for radiation enteritis
[AD-A274974] p 2901 N94-26517

RADIATION TOLERANCE
Molecular biological studies on the human radioresistance and drug resistance
[DE93-632682] p 2910 N94-26549
The radiation design handbook
[ESA-PSS-01-609-ISSUE-1] p 2696 N94-27397

RADIATION TRANSPORT
Proton irradiation on materials p 3030 N94-27898

RADIATIVE HEAT TRANSFER
ARM Fourier transform spectrometer data analysis tools
[DE94-000865] p 2895 N94-26697
Researches of the Electrotechnical Laboratory. No. 53: Spectral emission from combustion gas containing scattering media
[JTN-94-80603] p 2717 N94-27246
Numerical and experimental analyses of the radiant heat flux produced by quartz heating systems
[NASA-TP-3387] p 3011 N94-27659

RADIATIVE TRANSFER
A research program on radiative transfer model development in support of the ARM program
[DE94-001146] p 2767 N94-25950
Interactions between a tropical mixed boundary layer and cumulus convection in a radiative-convective model
[DE94-000848] p 2877 N94-25979
A numerical solution to the one and two dimensional line radiative transfer equation
[ISBN-0-315-84258-X] p 2994 N94-26640
Cooling the Martian atmosphere: The spectral overlap of the C02 15 micrometers band and dust
p 3107 N94-27886
Martian atmospheric radiation budget
p 3107 N94-27887
How well was total ozone abundance inferred with Mariner 9? p 3108 N94-27891

RADICALS
Three methods to measure RH bond energies
[DE94-003795] p 3013 N94-25816
Bulletin of the Institute for Chemical Reaction Science, Tohoku University, volume 2
[JTN-94-80602] p 2717 N94-27385
Reactivity of nitrate radical (NO3) toward organic compounds p 2704 N94-27387
The addition of molecular oxygen to hydroperoxy-propyl radicals
[DE94-003662] p 2760 N94-27725

RADIO ALTIMETERS
Ionospheric calibration for single frequency altimeter measurements
[NASA-CR-195709] p 2883 N94-27883

RADIO ANTENNAS
Fast wave current drive technology development at ORNL
[DE94-004243] p 3046 N94-27568

RADIO BURSTS
An April 1991 outburst from 4U0115+63 observed by BATSE
[NASA-CR-195252] p 3116 N94-27440

RADIO COMMUNICATION
Meteor Burst Communications (MBC) throughput improvement tests
[AD-A273941] p 2767 N94-25990
Technical description of the Vulcano software library
[FFI-93/7024] p 2767 N94-26105
Packet radio data link applications in the NASA Langley Research Center Transport Systems Research Vehicle
[NASA-TM-109071] p 2665 N94-27423

RADIO FILTERS
Direct-conversion-to-baseband for a nonlinear FM signal
[AD-A274861] p 2768 N94-26189

RADIO FREQUENCIES
Two dimensional self-consistent fluid simulation of RF inductive sources
[DE94-003635] p 2767 N94-25937
Low noise measurements in an RF environment
[AD-A273813] p 2767 N94-25960
MIMO recursive least squares control algorithm for the AN/FPN-44A Loran-C transmitter
[AD-A274820] p 2664 N94-26493
Investigation of ACC/CCI tunnel diodes
[AD-A274549] p 2785 N94-26845
Ferrite phase shifters using stress insensitive materials
[AD-A274639] p 2708 N94-26895
An analysis of FM jamming and noise quality measures
[AD-A274349] p 2772 N94-26924
Technical report of ISSP. Ser. A, no. 2688: Suppression of higher-order modes in an RF cavity by resistive material
[JTN-94-80574] p 2787 N94-27606
On radio frequency wave induced radial transport and wave helicity
[IPPCZ-326] p 2777 N94-27838

RADIO FREQUENCY HEATING
Design of folded waveguide antenna for Alcator C-Mod
[DE94-003584] p 2767 N94-25924
RF modeling and design of a folded waveguide launcher for the Alcator C-Mod tokamak
[DE94-003588] p 3041 N94-25933
Excitation of Earth-ionosphere waveguide in the ELF and lower VLF bands by modulated ionospheric current
[AD-A274969] p 2878 N94-26304
Critical survey of plasma processing
[AD-A274233] p 3044 N94-26820
Design and control of phased ICRF antenna arrays
[DE94-002796] p 3046 N94-27261
Fast wave current drive technology development at ORNL
[DE94-004243] p 3046 N94-27568
The calculation for energy balance of heating plasmas by Alfven waves
[DE94-604994] p 3049 N94-27855

RADIO FREQUENCY INTERFERENCE
Evaluation of an Acoustic Charge Transport (ACT) device for adaptive interference suppression in spread spectrum communications systems
[AD-A274073] p 2765 N94-25647

Characteristics of 30-MHz interference noises observed by riometers p 2884 N94-27965
RADIO HORIZONS
Radar detection of low-altitude targets in a maritime environment. Volume 2: Meteorological and radar data
[AD-A274658] p 2768 N94-26335
RADIO OBSERVATION
Solar-geophysical data number 590, October 1993. Part 1: (Prompt reports). Data for September, August 1993, and late data
[PB94-125903] p 3110 N94-27053
RADIO RECEIVERS
Analysis and simulation of a GPS receiver design using combined delay-lock and modified tanlock loops
[AD-A274037] p 2664 N94-25810
RADIO RELAY SYSTEMS
Hybrid power system for remote communications stations
[AD-A274963] p 2782 N94-26301
Annex report FEL-92-A163: Description of the LInk and BER Test Analysis System (LIBERTAS) for the frequency band V (14.5 - 15.3 GHz)
[FEL-92-A442] p 2770 N94-26650
RADIO SIGNALS
Direct-conversion-to-baseband for a nonlinear FM signal
[AD-A274861] p 2768 N94-26189
Enhanced adaptive statistical filter providing improved performance for target motion analysis noise discrimination statement of government interest
[AD-D016039] p 2786 N94-27109
RADIO TELESCOPES
Project PARAS: Phased array radio astronomy from space p 3081 N94-25703
RADIO TRANSMISSION
Ionospheric modification by high power, obliquely propagated HF radio wave transmissions. Part 1: Experimental
[AD-A273746] p 2878 N94-26224
Optical communications for transport aircraft
p 2643 N94-27298
The Sixteenth Symposium on Coordinated Observations of the Ionosphere and the Magnetosphere in the Polar Regions: Program and abstracts
[JTN-94-80601] p 2882 N94-27300
Antarctic Record, Vol. 36, No. 2
[REPT-107] p 2883 N94-27963
Characteristics of 30-MHz interference noises observed by riometers p 2884 N94-27965
RADIO TRANSMITTERS
MIMO recursive least squares control algorithm for the AN/FPN-44A Loran-C transmitter
[AD-A274820] p 2664 N94-26493
RADIO WAVES
Ionospheric modification by high power, obliquely propagated HF radio wave transmissions. Part 1: Experimental
[AD-A273746] p 2878 N94-26224
RADIOACTIVE DECAY
Vector meson exchanges and CP asymmetry in K(sup +/-) yields pi(sup +/-)pi(sup 0)
[DE94-601605] p 3014 N94-25887
CP violation in Higgs decays
[DE94-601607] p 3014 N94-25888
Unravelling the structure of matter on high-performance computers
[DE94-601620] p 3015 N94-25891
Fast vertex search (in plane)
[DE93-616655] p 2959 N94-25917
Algorithms of the vertex coordinate reconstruction for straight tracks of short-lived particles
[DE93-616661] p 3015 N94-25919
Pseudoscalar glueball in the composite interpolating fields approach
[DE93-634374] p 3016 N94-26042
Meson X(1814) as a candidate for a hybrid state
[DE93-634447] p 3017 N94-26045
Measurement of tau lepton branching fractions
[DE94-003423] p 3018 N94-26325
Chance to use W-decay lepton channels for width determination
[DE93-634438] p 3020 N94-26507
Light-quark, heavy-quark systems: An update
[DE94-002298] p 3021 N94-26759
Leptonic decay constants of heavy mesons in QCD
[DE93-634426] p 3022 N94-26767
Low-energy hadronic interactions beyond the current algebra approach
[DE94-602600] p 3022 N94-26900
Study of the process (pi)(sup -)A(yields)(pi)(sup -)(eta)'(eta)A at the moment 36 GeV/c
[DE93-634530] p 3024 N94-27250
Spectroscopy and strong decays of baryons
[ISBN-0-315-49073-X] p 3024 N94-27258
QCD corrections to inclusive B - S processes in the standard model
[ISBN-0-315-54572-0] p 3073 N94-27263
An analysis of monojet data in p(bar-p) collisions at square root of s equal to 1.8 TEV
[DE94-001822] p 3026 N94-27565
Decay of non-equilibrium polariton condensate in semiconductors
[DE94-604016] p 3068 N94-27678
Research on elementary particle physics, part 2
[DE94-004956] p 3029 N94-27815
Decay constants of heavy mesons in the relativistic potential model with velocity dependent corrections
[DE94-606495] p 3030 N94-27860
RADIOACTIVE ISOTOPES
A double arm time-of-flight spectrometer based on position-sensitive parallel-grid avalanche counters
[DE93-616665] p 3012 N94-25750
Simulations of terrestrial in-situ cosmogenic-nuclide production
[DE94-004999] p 3117 N94-27826
RADIOACTIVE MATERIALS
Monte Carlo calculations of low background detector response
[DE94-004593] p 3116 N94-27621
RADIOACTIVE WASTES
Development of laser spectroscopic technology in nuclear industry
[DE93-633327] p 2714 N94-26158
Recent ASCOT experiments in multi-layered flows
[DE94-002360] p 2880 N94-26762
RADIOBIOLOGY
Molecular biological studies on the human radioresistance and drug resistance
[DE93-632682] p 2910 N94-26549
RADIOCHEMISTRY
Radiochemistry Division annual progress report : 1991
[DE94-600652] p 2715 N94-26392
RADIOGONIOMETERS
Energy Dispersive X ray Diffraction (EDXD) apparatus for liquids at high temperature p 2721 N94-28159
RADIOGRAPHY
The development of an in-motion radiography system for large area aircraft scanning
[DREP-TM-93-53] p 2670 N94-27666
Upset welding process for 21-6-9 spherical vessels
[DE93-018194] p 2832 N94-28229
RADIOISOTOPE BATTERIES
Preliminary reentry safety assessment of the General Purpose Heat Source module for the Cassini mission: Aerospace Nuclear Safety Program
[DE94-001646] p 2699 N94-25926
RADIOLYSIS
Radiation-Induced Structural Changes, 2
[DE93-520314] p 3054 N94-26109
RADIOMETERS
Hyperspectral analysis of space objects: Signal to noise evaluation
[AD-A273882] p 2765 N94-25728
Characterization and calibration of the Agema 880+ imaging radiometer
[AD-A274417] p 3036 N94-26981
Radiometric, spectral, and effectiveness equipment
[AD-A274208] p 3037 N94-27066
Initial ultraviolet-B intensity data at Lawrence Livermore National Laboratory
[DE94-004279] p 2869 N94-27267
The validation of ATSR measurements with in situ sea temperatures
[DE94-003195] p 2852 N94-27875
RADIOMETRIC RESOLUTION
Calibration of SAR systems
[DLR-FB-93-18] p 2777 N94-27738
RADOMES
Analyzing adaptive beamformer performance in a stable multipath environment
[AD-A274029] p 2766 N94-25766
A study of two dimensional tapered periodic edge treatments to reduce wideband edge diffraction
[AD-A274054] p 2766 N94-25824
RAILGUN ACCELERATORS
Interaction between a high density-low temperature plasma and a frozen hydrogen pellet in a railgun injector
[DE94-000846] p 3041 N94-25949
Application of railgun principle to high-velocity hydrogen pellet injection for magnetic fusion reactor fueling
[DE94-004411] p 3044 N94-26579
RAILS
The railway track response function
[REPT-93-40] p 2837 N94-26214
A non-linear mathematical model or finite, periodic rail corrugations
[REPT-93-49] p 2996 N94-26967
RAIN
A synoptic study on periods of deficiency over Rio Grande do Sul/Brazil
[INPE-5456-TDI/498] p 2896 N94-27422
RAIN FORESTS
Assessment of tropical forests using satellite data
[SILVA-CARELICA-21] p 2850 N94-27182
Global tropical forest cover assessments using satellite imagery p 2850 N94-27183
Mapping closed tropical forest cover in West Africa using NOAA/AVHRR-LAC data p 2850 N94-27184
Training on assessment and mapping of deforestation: WFW conference, Brazil
[INPE-5482-PRE/1781] p 2850 N94-27384
RAMAN LASERS
Theory and modeling of stimulated Raman scattering
[AD-A273755] p 3033 N94-25721
RAMAN SPECTRA
Theory and modeling of stimulated Raman scattering
[AD-A273755] p 3033 N94-25721
Gaseous hydrogen/oxygen injector performance characterization
[NASA-CR-194464] p 2701 N94-26208
High definition Raman microscopic imaging
[DE94-003158] p 2716 N94-26781
Technical report of ISSP. Ser. A, no. 2680: Determination of intervalley scattering time in germanium by subpicosecond time-resolved Raman spectroscopy
[JTN-94-80566] p 3064 N94-27176
RAMAN SPECTROSCOPY
Study of the homogeneity of InP wafers
[AD-A273658] p 3055 N94-26194
High definition Raman microscopic imaging
[DE94-003158] p 2716 N94-26781
Spectroscopy Division
[DE94-604074] p 2717 N94-26988
RAMJET ENGINES
Development of hypersonic engine seals: Flow effects of preload and engine pressures
[NASA-TM-106333] p 2826 N94-27599
RANDOM ACCESS MEMORY
Temperature dependence of static RAM volatility
[DE93-040345] p 2948 N94-26111
Test methods and custom hardware for functional testing of a high speed GaAs DRAM
[AD-A274859] p 2781 N94-26175
Ferroelectric fluoride memory FET development
[AD-A274341] p 2785 N94-27057
RANDOM NOISE
White noise theory of robust nonlinear filtering with correlated state and observation noises
[PB94-126661] p 3004 N94-27211
RANDOM PROCESSES
Data on parity violation in the compound nucleus and its interpretation
[DE94-003965] p 3013 N94-25820
RANDOM SAMPLING
Aspects of goodness-of-fit
[AD-A274826] p 3003 N94-26495
RANDOM VARIABLES
Simulation approaches for calculations in directed graphical models
[AD-A274825] p 3003 N94-26494
Central dynamic share scheduling in distributed systems
[REPT-93-48] p 2966 N94-26966
RANDOM VIBRATION
Space Station Freedom NiH2 cell testing program
p 2861 N94-28108
RANGE AND RANGE RATE TRACKING
Real-time 3-D pose estimation using a high-speed range sensor
[AD-A273873] p 2809 N94-25967
RANGE ERRORS
A simulation of GPS and differential GPS sensors
p 2666 N94-27918
RANGE FINDERS
Flexible range finding applied to 3D surface synthesis: A pseudo-trinocular approach
[ISBN-0-315-84616-X] p 2813 N94-27651
RANGE SAFETY
Advanced silver zinc battery development for the SRB and ET range safety subsystems p 2865 N94-28136
RANGEFINDING
A simulation of GPS and differential GPS sensors
p 2666 N94-27918
RANKINE CYCLE
Limitations of power conversion systems under transient loads and impact on the pulsed tokamak power reactor
[DE94-003404] p 3043 N94-26324
RANKING
Ranking alternatives using fuzzy numbers: A computational approach short communication
[INPE-5483-PRE/1782] p 2974 N94-27835

RAPID QUENCHING (METALLURGY)
Study on solidification of non-homogeneous melting/solidification materials p 2728 N94-25573
RARE EARTH ALLOYS
Magnetostriction and magnetostrictive materials
[VTT-TIED-1434] p 3058 N94-26545
Formation and high mechanical strength of Al-based alloys containing a nanoscale icosahedral phase as a main constituent p 2746 N94-28171
RARE EARTH COMPOUNDS
Preparation, characterization, and thermal behaviour study of lanthanides (3) and yttrium (3) 4-methoxy benzylidene pyruvate in solid state
[DE94-604079] p 3068 N94-27697
Hypersensitive transition spectrum of f-element and coordination structure
[DE94-604133] p 3070 N94-27843
The optical properties of high-T(c) superconductors grown by pulsed laser deposition
[ISBN-0-315-84917-7] p 3039 N94-27962
Anisotropy in the electrical, magnetic and optical properties of Pb2Sr2RCu3O8
[ISBN-0-315-84930-4] p 3070 N94-27974
RARE EARTH ELEMENTS
Qualitative analysis of rare earth elements contained in the phosphogypsum
[DE93-614153] p 2716 N94-26518
Property enchancement of polyimide films by way of the incorporation of lanthanide metal ions
p 2758 N94-27926
RARE GASES
Spectroscopic and vibrational energy transfer studies in molecular bromine
[AD-A273795] p 3014 N94-25875
RAREFACTION
Control jets in interaction with hypersonic rarefied flow
p 2698 N94-28020
RAREFIED GAS DYNAMICS
Modelling of ionisation reactions and of the resulting electric fields in one-dimensional hypersonic shock waves with the direct simulation Monte Carlo method
[IC-AERO-92-01] p 2644 N94-26248
Control jets in interaction with hypersonic rarefied flow
p 2698 N94-28020
RAREFIED GASES
Mix induced by single shock passage through a material interface
[DE93-019505] p 2792 N94-26427
RATINGS
A critical analysis of workload predictions generated by multiple resource theory during early crewstation design
[AD-A274804] p 2941 N94-26339
RATIONAL FUNCTIONS
Chebyshev-Markov rational functions over several intervals
[PB94-125333] p 2998 N94-27116
RATS
Cortical mechanisms of attention, discrimination, and motor response to somesthetic stimuli
[AD-A274163] p 2940 N94-27141
Development of inbred strains from Japanese wild rats (Rattus norvegicus) p 2906 N94-27492
RAWINSONDES
A preliminary method for atmospheric soundings in real time using satellite and ground-based remotely sensed data
[AD-A274381] p 2880 N94-26828
RAY TRACING
Efficient modeling in transversely isotropic inhomogeneous media
[DE94-003394] p 2877 N94-25847
Ionospheric modification by high power, obliquely propagated HF radio wave transmissions. Part 1: Experimental
[AD-A273746] p 2878 N94-26224
Dynamic and kinematic P wave tracing for a three-dimensional elastic inhomogeneous media by the asymptotic ray theory and application
[ITN-94-85239] p 2775 N94-27244
RAYLEIGH SCATTERING
Polarizability matrix of layered chiral sphere
[PB94-132834] p 2778 N94-28355
RAYLEIGH WAVES
A preliminary shear velocity model for Central Asia
[AD-A274972] p 2880 N94-26752
Problems in nonlinear acoustics: Rayleigh waves, pulsed sound beams, and waveguides
[AD-A274587] p 3010 N94-26983
RAYLEIGH-RITZ METHOD
Response of structures to impact loads using elastic and plastic analysis
[ISBN-0-315-84647-X] p 2842 N94-27309
REACTING FLOW
Modelling of ionisation reactions and of the resulting electric fields in one-dimensional hypersonic shock waves with the direct simulation Monte Carlo method
[IC-AERO-92-01] p 2644 N94-26248
High resolution measurements of mixing and reaction processes in turbulent flows
[AD-A274970] p 2793 N94-26534
Direct simulation Monte-Carlo of near continuum hypersonic flow with chemical reactions
[DLR-FB-93-01] p 2797 N94-27588
TVD flux-difference split methods for high-speed thermochemical nonequilibrium flows with strong shocks
[UTIAS-350] p 2799 N94-27880
REACTION CONTROL
First experimental assessment of RCS plume-flow field interaction on Hermes leading edge thruster configuration p 2703 N94-28032
REACTION KINETICS
Development and implementation of a scramjet cycle analysis code with a finite-rate-chemistry combustion model for use on a personal computer
[AD-A273834] p 2673 N94-25617
Three methods to measure RH bond energies
[DE94-003795] p 3013 N94-25816
Technique to predict the curing behaviour of unsaturated polyester materials
[PB94-124856] p 2748 N94-25892
Oxygen reduction at a YSZ interface with cathode materials La(1-x)(Ca or Sr)(x)MnO3(1-x)CaMnO3
[DE94-002954] p 3054 N94-26147
The importance of vibrationally excited nitrogen in silicon nitride deposition systems
[AD-A274874] p 2750 N94-26167
Theoretical determination of chemical rate constants using novel time-dependent methods
[NASA-CR-195221] p 2714 N94-26205
Chemical and vibrational nonequilibrium viscous flows: Modelling, internal and external flow applications
[ESA-TT-1274] p 2791 N94-26316
In situ spectroscopic applications to the study of rechargeable lithium batteries
[DE94-003478] p 2782 N94-26328
High resolution measurements of mixing and reaction processes in turbulent flows
[AD-A274970] p 2793 N94-26534
A semiclassical reactive flux method for the calculation of condensed phase activated rate constants
[AD-A274850] p 3020 N94-26562
Design of gasifiers to optimize fuel cell systems
[DE94-000010] p 2856 N94-26581
An investigation of the effect of surface impurities on the adsorption kinetics of hydrogen chemisorbed onto iron
[NASA-CR-195213] p 2716 N94-26643
Mechanistic studies of opto-electronic materials and syntheses using multiple laser and surface diagnostics
[AD-A274528] p 3036 N94-26834
Kinetics of 2-pentadecylaniline polymerizations in monolayers: Relationships between experimental data and a new theoretical model
[AD-A274419] p 2754 N94-27080
Laser probes of natural gas ignition chemistry
[PB94-128345] p 2717 N94-27226
Basic research on natural gas combustion phenomena
[PB94-129046] p 2717 N94-27256
Reactivity of nitrate radical (NO3) toward organic compounds p 2704 N94-27387
Thermogravimetric study of oxidation of a PdCr alloy used for high-temperature sensors
[NASA-TM-106473] p 2741 N94-27426
High temperature grain growth and oxidation of Fe-29Ni-17Co (Kovar (tm)) alloy leads
[DE94-004691] p 3069 N94-27753
Kinetic parameters from thermogravimetric analysis
p 2721 N94-27909
CO2 methanation catalysts prepared from amorphous Ni-valve metal alloys containing platinum group elements
p 2745 N94-28166
REACTION TIME
Endogeneous and exogenous control of visual selection: A review of the literature
[AD-A273761] p 2908 N94-25871
On the development of motor chunks and concurrent processing in a structured continuous keypressing task
[AD-A274153] p 2939 N94-27138
REACTIVITY
In situ spectroscopic applications to the study of rechargeable lithium batteries
[DE94-003478] p 2782 N94-26328
The reactivity of lithium toward non-aqueous solvents of relevance to energy storage applications as studied by surface analytical techniques
[DE94-003483] p 2856 N94-26464
A semiclassical reactive flux method for the calculation of condensed phase activated rate constants
[AD-A274850] p 3020 N94-26562
The coordination and atom transfer chemistry of titanium porphyrin complexes
[DE94-003091] p 2704 N94-26779
Reactivity of nitrate radical (NO3) toward organic compounds p 2704 N94-27387
Observation of stimulated emission from an MBE grown GaN film on sapphire
[DE94-003638] p 3068 N94-27724
REACTOR CORES
A review of carbide fuel corrosion for nuclear thermal propulsion applications
[DE94-003938] p 2699 N94-25613
REACTOR DESIGN
Small low mass advanced PBR's for bi-modal operation
[DE94-003201] p 2699 N94-25798
A robust helium-cooled shield/blanket design for ITER
[DE94-003402] p 3043 N94-26323
Limitations of power conversion systems under transient loads and impact on the pulsed tokamak power reactor
[DE94-003404] p 3043 N94-26324
REACTOR MATERIALS
A review of carbide fuel corrosion for nuclear thermal propulsion applications
[DE94-003938] p 2699 N94-25613
Toroidal plasma beta-FLR limit in a toroidally linked mirror system
[DE94-003119] p 3041 N94-25792
Space-R thermionic space nuclear power system: Design and technology demonstration
[DE94-001890] p 2699 N94-25929
Effect of loading mode on the fracture toughness of a reduced activation ferritic/martensitic stainless steel
[DE94-004290] p 2732 N94-25987
Fusion Energy Advisory Committee: Advice and recommendations to the US Department of Energy in response to the charge letter of September 1, 1992
[DE93-019842] p 3043 N94-26428
Microstructural development in irradiated vanadium alloys
[DE94-004307] p 2737 N94-26556
The effect of Ti conduit on the critical current in (Nb, Ti)3Sn cable-in-conduit conductors
[DE94-701204] p 2788 N94-27817
Experiment and research on materials irradiated by plasma radiation
[DE94-605011] p 2758 N94-27845
REACTOR PHYSICS
Pre-orbital criticality safety for the NEPSTP mission
[DE94-002600] p 3005 N94-26802
REACTOR SAFETY
HDR reactor containment fire modeling with BRI2
[VTT-PUBS-113] p 3031 N94-25621
Preliminary reentry safety assessment of the General Purpose Heat Source module for the Cassini mission: Aerospace Nuclear Safety Program
[DE94-001646] p 2699 N94-25926
Risk perspectives for Topaz 2 flight mission
[DE94-003229] p 2700 N94-25956
Fusion Energy Advisory Committee: Advice and recommendations to the US Department of Energy in response to the charge letter of September 1, 1992
[DE93-019842] p 3043 N94-26428
Mesoscale meteorological measurements characterizing complex flows
[DE94-002359] p 2895 N94-26761
Pre-orbital criticality safety for the NEPSTP mission
[DE94-002600] p 3005 N94-26802
REACTOR TECHNOLOGY
Small low mass advanced PBR's for bi-modal operation
[DE94-003201] p 2699 N94-25798
Experimental and numerical investigation of shock wave propagation through complex geometry, gas continuous, two-phase media
[DE94-001408] p 2791 N94-26121
REAL NUMBERS
Winding numbers in homotopy theory from integers to reals
[DE94-601510] p 2992 N94-26367
REAL TIME OPERATION
Module interconnection frameworks for a real-time spreadsheet
[AD-A273853] p 2956 N94-25588
Distributing functionality in the drift scan camera system
[DE94-003640] p 2809 N94-25599
Characteristics and control response of the TOPAZ 2 reactor system real-time dynamic simulator
[DE94-003788] p 2699 N94-25600
Design of dynamically reconfigurable real-time software using port-based objects
[NASA-CR-195178] p 2958 N94-25777

The use of ASN.1 and XDR for data representation in real-time distributed systems
[AD-A273769] p 2959 N94-25855
Real-time 3-D pose estimation using a high-speed range sensor
[AD-A273873] p 2809 N94-25967
Real-time tracking with a 3D-flow processor array
[DE94-003981] p 2980 N94-25984
Coordinated scheduling for dynamic real-time systems
[NASA-CR-195231] p 3093 N94-26206
Studies of thin-film growth, adsorption, and oxidation by in situ, real-time, and ex situ ion beam analysis
[DE94-002907] p 3055 N94-26275
A multitasking behavioral control system for the Robotic All-Terrain Lunar Exploration Rover (RATLER)
p 2685 N94-26292
NPSNET-4: A real-time, 3D distributed interactive virtual world
[AD-A274942] p 2961 N94-26298
Differential global positioning system for the surface-towed ordnance locating system: Testing, results, and user's guide
[DE94-002980] p 2664 N94-26309
Development of real-time pulse shaping technology in solid-state lasers
[DE93-633438] p 2817 N94-26403
Automated system for gas detectors providing with binary mixtures
[DE93-634192] p 2715 N94-26406
Adaptive path planning in changing environments
[DE94-003269] p 2985 N94-26462
Real-Time Embedded Processing for Space Applications
[ISBN-2-85428-335-X] p 2948 N94-26713
Real time avionics constraints: Silicon solutions
p 2949 N94-26717
Fault tolerant real-time processing system for space use p 2949 N94-26720
A complete version of the Ada tasking coprocessor
p 2950 N94-26721
The Ariane 5 data management system
p 2950 N94-26724
PRONAOS flight software: A real-time application for a balloonborne scientific gondola p 2950 N94-26725
MATRA Marconi Space: The Silex on-board processor and on-board software p 2950 N94-26726
Scheduling tasks with unpredictable timing parameters in hard real-time systems p 2951 N94-26728
Standardize Ada hard real-time services?
p 2951 N94-26729
Ada multiple-programming for hard real time applications in space systems p 2951 N94-26730
Implementing hard real-time systems: A case study
p 2951 N94-26731
Tool for performance analysis and off-line prediction of timing behaviour p 2952 N94-26732
A real-time executive implementing priority inheritance protocols p 2952 N94-26733
Scheduling approaches with Ada
p 2952 N94-26734
Fault-tolerant scheduling in distributed critical real-time systems p 2952 N94-26735
Early real-time performance measurements on the Columbus processor system p 2952 N94-26736
Test of onboard real time applications (LICE (tm))
p 2952 N94-26737
Verification and validation of the on-board software real time requirements p 2953 N94-26739
Formal methods for dependable real-time systems
p 2953 N94-26740
Developing with Ada using HOOD design methodology
p 2953 N94-26741
Use of HOOD coupled to real time monitors
p 2953 N94-26742
Specification performance optimization and executive generation for onboard multiprocessor real time application with SynDEx p 2954 N94-26745
A preliminary method for atmospheric soundings in real time using satellite and ground-based remotely sensed data
[AD-A274381] p 2880 N94-26828
Hard real-time reliable multicast in the DEDOS system
[PB94-126745] p 2966 N94-26920
Interactive control of a parallel simulation from a remote graphics workstation
[AD-A274217] p 2981 N94-27070

RECEIVERS
A current evaluation of the digital beamforming testbed at Rome Laboratory
[AD-A274311] p 3032 N94-26881
A compact 150 GHz SIS receiver cooled by 4 K GM refrigerator
[REPT-36] p 2776 N94-27340
A simulation of GPS and differential GPS sensors
p 2666 N94-27918

RECEPTORS (PHYSIOLOGY)
Annals of the Research Inst. of Environmental Medicine, Nagoya Univ., volume 44
[REPT-44-VOL-44] p 2911 N94-27442
Effect of PGE2 receptor agonists butaprost, M and B 28767 and an antagonist AH 6809 on the BK response of visceral polymodal receptors p 2906 N94-27494
Excitation of cutaneous polymodal receptor induced by sympathetic stimulation in adjuvant-induced arthritis rats
p 2906 N94-27495
Influence of mechanical stimulation on inflammatory edema p 2906 N94-27497
The effect of naloxone on sleeping time in adjuvant arthritic rats p 2906 N94-27498
Effects of capsaicin on freshly dissociated rat dorsal root ganglion cells p 2906 N94-27499
Contribution of muscle spindle afferent activity to transient pause in EMG during voluntary tonic contraction p 2928 N94-27522
Activation by G protein beta gamma subunits of G protein-coupled receptor kinase p 2931 N94-27534
Mechanism for regulation of myocardial contractility by autonomic drugs: Pathophysiological relevance in congestive heart failure p 2931 N94-27536
The polymodal receptor p 2908 N94-27539
The role of beta-adrenoceptor stimulation in the progression of chronic heart failure
p 2932 N94-27541

RECESSION
Air traffic in recession p 2662 N94-28240

RECIRCULATIVE FLUID FLOW
Experiments into the scaling parameters required for exhaust gas ingestion testing of vertical landing aircraft
p 2671 N94-28017
Influence of headwind on hot gas reingestion and consideration of pressure ratio scaling
p 2675 N94-28018
Unsteady aspects of hot gas reingestion and statistical analysis p 2676 N94-28019

RECLAMATION
Freon recovery from nitrogen tetroxide and freon solutions
[PL-TR-92-3051] p 2721 N94-28215

RECONNAISSANCE AIRCRAFT
The design of four hypersonic reconnaissance aircraft
p 2671 N94-25716

RECONSTRUCTION
The renewing of the test section of the NAL transonic wind tunnel. Part 1: Reconstruction of the 1st corner turning vanes and aerodynamic stress measurement
[NAL-TM-651] p 2681 N94-27247

RECRYSTALLIZATION
Influence of grain structure and solute composition on the work hardening behavior of aluminium at cryogenic temperatures
[DE94-003415] p 2733 N94-26087
Study of precipitation and recrystallization in Al alloy 2519 by backscattered electron imaging methods
[AD-A274919] p 2736 N94-26533
Effect of precipitate structure on hot deformation of Al-Mg-Mn alloys
[DE94-004596] p 2741 N94-27622

RECTANGULAR WAVEGUIDES
Computer program for numerical evaluation of the performance of an overmoded TM01 circular to TE10 rectangular waveguide mode converter
[AD-A274548] p 2771 N94-26844

RECTIFICATION
A direct current rectification scheme for microwave space power conversion using traveling wave electron acceleration p 2687 N94-27371

RECURSIVE FUNCTIONS
MIMO recursive least squares control algorithm for the AN/FPN-44A Loran-C transmitter
[AD-A274820] p 2664 N94-26493
Simulation dynamics of a multibody chain: Recursion based on chain modal coordinates
[ISBN-0-315-83555-9] p 2994 N94-26659
Congruence theorem for structured operational semantics with predicates and negative premises
[PB94-126729] p 2966 N94-26970

RED DWARF STARS
In search of Nemesis p 2888 N94-28297

REDUCTION (CHEMISTRY)
Journal of NIRE, volume 2, number 4
[JTN-94-80554] p 2869 N94-28147
Effects of p-chlorophenol on sulfate reduction in marine sediments p 2870 N94-28150
The electrocatalytic oxidation of ethylene and methane, and reduction of oxygen on gas-diffusion electrodes made of amorphous nickel-valve metal-platinum group metal alloys p 2722 N94-28165

REDUNDANCY
New mixed integer algorithm for classification and placement of measurements in process flow networks
[PB94-126752] p 2966 N94-26921
Local performance optimization for a class of redundant eight-degree-of-freedom manipulators
[NASA-TP-3417] p 2989 N94-27773

REDUNDANCY ENCODING
A partitioning and redundancy model for wafer-scale integrated circuits p 2955 N94-27195

REED-SOLOMON CODES
Improved performance of hybrid error control techniques for real-time digital communications over noisy channels
[ISBN-0-315-84281-4] p 2770 N94-26625
On the performance of trellis coded 8PSK with Reed Solomon codes
[ISBN-0-315-84289-X] p 2770 N94-26626
Coded communications with nonideal interleaving
[ITN-94-85235] p 2774 N94-27242

REENTRY
First experimental assessment of RCS plume-flow field interaction on Hermes leading edge thruster configuration p 2703 N94-28032

REENTRY PHYSICS
A survey of uncontrolled satellite reentry and impact prediction
[AD-A274903] p 2695 N94-26750

REENTRY TRAJECTORIES
A survey of uncontrolled satellite reentry and impact prediction
[AD-A274903] p 2695 N94-26750

REENTRY VEHICLES
Chemical and vibrational nonequilibrium viscous flows: Modelling, internal and external flow applications
[ESA-TT-1274] p 2791 N94-26316

REFINING
Bulletin of the Institute for Chemical Reaction Science, Tohoku University, volume 2
[JTN-94-80602] p 2717 N94-27385
Development of liquid membrane separation processes p 2717 N94-27386

REFLECTANCE
Neutron reflection interferometry
[DE94-601876] p 2714 N94-26170
Sulfur dioxide in the atmosphere of Venus 1 sounding rocket observations
[NASA-CR-195224] p 3106 N94-26237
Sound, speed, reflectivity, absorption, and thermal diffusivity measurements in Arctic ice in 1990
[AD-A274326] p 2899 N94-26886
Discrete vacuum ultra violet reflective interference filter
[AD-D016059] p 2756 N94-27675
Reflectometer employing an integrating sphere and lens-mirror concentrator
[AD-D016061] p 3039 N94-27676

REFLECTED WAVES
Neutron reflection interferometry
[DE94-601876] p 2714 N94-26170
Mix induced by single shock passage through a material interface
[DE93-019505] p 2792 N94-26427

REFLECTION
Development and evaluation of a near infrared reflecting and low visibility paint scheme for RAAF P-3C Orion aircraft
[AD-A274881] p 2669 N94-26864
Experimental and theoretical investigation of RF absorption and reflection from preformed plasmas
[AD-A274189] p 3046 N94-27098
Discrete vacuum ultra violet reflective interference filter
[AD-D016059] p 2756 N94-27675

REFLECTOMETERS
In situ x ray reflectivity measurements of thin film structural evolution
[DE94-002289] p 3051 N94-25944
Surface physics with cold and thermal neutron reflectometry
[DE94-001447] p 2733 N94-26070
Time domain reflectometry for measuring bulk soil electrical conductivity and comparison with the Em38 instrument
[PB94-125432] p 2881 N94-27052
Reflectometer employing an integrating sphere and lens-mirror concentrator
[AD-D016061] p 3039 N94-27676

REFLECTOR ANTENNAS
Effective conductivity of wire mesh reflectors for space deployable antenna systems
[NASA-CR-191605] p 2788 N94-27770

REFLECTORS
Surface physics with cold and thermal neutron reflectometry
[DE94-001447] p 2733 N94-26070
Joint services electronics program
[AD-A274643] p 2785 N94-27027

REFLEXES
Muscle sympathetic nerve activity in humans
p 2932 N94-27538

REFORESTATION
Woody biomass density in the Tendelti area of the central Sudan p 2850 N94-27185
REFRACTION
Long Duration Exposure Facility space optics handbook
[AD-A274831] p 3035 N94-26572
Wave propagation in the shallow regions of the earth's crust and the borehole vicinity
[ITN-94-85237] p 2882 N94-27330
Optical parametric oscillator modeling with diffraction, depletion, and double refraction
[DE94-001504] p 3040 N94-27999
REFRACTIVITY
Microtubules for nonlinear optical limiting
[AD-A273940] p 3035 N94-25941
Peculiarities and application perspectives of metal-ion implants in glasses
[DE94-004671] p 3035 N94-26246
Radar detection of low-altitude targets in a maritime environment. Volume 2: Meteorological and radar data
[AD-A274658] p 2768 N94-26335
Modelling atmospheric turbulence effects on ground-based telescope systems
[DE94-004211] p 3102 N94-26528
Refractive and dielectric properties of helium, argon and nitrogen gases
[PB94-123783] p 3008 N94-26851
Optical characterization and guided wave loss measurements for end-capped 6F-polybenzoxazole
[AD-A274586] p 3036 N94-26982
Research and development within nonlinear optics for protection of optical sensors against laser irradiation on of optical sensors against laser irradiation. Quarterannual report 1 (april 1993))
[PB94-124245] p 3037 N94-27046
Theoretical and experimental analysis of the spatial and temporal behaviour of the intensity of an electro-magnetic wave reflected from a diffuse target after passing through a turbulent atmosphere
[ITN-94-85230] p 2774 N94-27234
Ion implantation in silicate glasses
[DE94-003785] p 2757 N94-27726
REFRACTORY MATERIALS
Computer modelling of cyclic deformation of high-temperature materials
[AD-A273852] p 2704 N94-25608
Optical characterization and guided wave loss measurements for end-capped 6F-polybenzoxazole
[AD-A274586] p 3036 N94-26982
Computer modelling of cyclic deformation of high-temperature materials
[AD-A274504] p 2840 N94-27034
High temperature sensor/microphone development for active noise control
[NASA-CR-195214] p 2812 N94-27214
Fibrous emissive burners selective and broad band
[PB94-128329] p 2859 N94-27225
REFRACTORY METALS
Growth, characterization and device development in monocrystalline diamond films
[AD-A274245] p 3060 N94-26839
List of papers published by the members of Institute for Materials Research, Tohoku University 1992
[JTN-94-80608] p 3118 N94-27355
REFRIGERANTS
Measurement of viscosity, density, and gas solubility of refrigerant blends in selected synthetic lubricants
[DE94-003609] p 2713 N94-25934
Accelerated screening methods for determining chemical and thermal stability of refrigerant-lubricant mixtures. Part 2: Experimental comparison and verification of methods
[DE94-003664] p 2749 N94-26007
Thermophysical properties of HFC-143a and HFC-152a
[DE94-004236] p 2719 N94-27567
Compatibility of refrigerants and lubricants with engineering plastics
[DE94-004959] p 2756 N94-27692
Thermophysical properties of refrigerant R-134a (1,1,1,2-tetrafluoroethane)
[ESDU-93001] p 2720 N94-27959
Solubility, viscosity, and density of refrigerant/lubricant mixtures
[DE94-004237] p 2721 N94-28069
REFRIGERATING
Evaluation of high temperature superconductive thermal bridges for space-borne cryogenic infrared detectors
p 2815 N94-27921
REFRIGERATORS
A compact 150 GHz SIS receiver cooled by 4 K GM refrigerator
[REPT-36] p 2776 N94-27340
REFUELING
High-speed repetitive pellet injector for plasma fueling of magnetic confinement fusion devices
[DE94-002792] p 3042 N94-26140
Application of railgun principle to high-velocity hydrogen pellet injection for magnetic fusion reactor fueling
[DE94-004411] p 3044 N94-26579
REGENERATION (PHYSIOLOGY)
Bioregenerative system components for microgravity
p 2903 N94-25673
REGENERATIVE COOLING
Experimental analysis of heat transfer characteristics and pressure drop through screen regenerative heat exchangers
[AD-A273902] p 2790 N94-25657
REGIONAL PLANNING
The advantages of the location Germany must not be jeopardized in air traffic p 2661 N94-28236
REGIONS
Image segmentation by a combination of edge detection and region growing
[ETN-94-95032] p 2960 N94-26106
REGRESSION ANALYSIS
Parameter estimation for ARMA models with infinite variance innovations
[AD-A274654] p 3003 N94-26355
Three dimensional object recognition using a complex autoregressive model
[AD-A274388] p 2995 N94-26829
The Hough transform algorithm for sea ice lead analysis: An evaluation
[AD-A274535] p 2899 N94-26853
Multiple weight stepwise regression
[DE94-001602] p 3000 N94-27564
REGULATIONS
Coastal Zone Management Act and related legislation, revision 3
[DE94-004180] p 2869 N94-27691
Technical Report of National Research Institute of Fisheries Engineering: Fishing Boat and Instrument, No. 12
[JTN-94-80595] p 2764 N94-27976
Recent trend of domestic and international regulations on intact stability of ships for safety
p 2764 N94-27977
Journal of NIRE, volume 2, number 4
[JTN-94-80554] p 2869 N94-28147
Recent legal movement on water quality regulation in Japan p 2869 N94-28148
Lufthansa Yearbook 1992
[DSK-9734-H-92] p 2660 N94-28230
The single European market and air traffic chances and risks p 2660 N94-28231
Air traffic of the European Community with European neighbors p 2661 N94-28233
Air traffic administration enroute to Europe
p 2661 N94-28238
REGULATORY MECHANISMS (BIOLOGY)
Thyroid hormone action in cultured human skin fibroblasts: Evaluation using spheroid culture
p 2919 N94-27478
REINFORCED PLASTICS
Continuous fiber reinforced thermoplastic composites: Literature survey
[VTT-TIED-1422] p 2704 N94-25651
Design and life-time of polymer matrix composite structures: Summary
[VTT-TIED-1415] p 2707 N94-26260
REINFORCED PLATES
Super finite elements for nonlinear static and dynamic analysis of stiffened plate structures
[ISBN-0-315-63903-2] p 2844 N94-27808
REINFORCEMENT (STRUCTURES)
Investigation of the bond strength of a discrete skin-stiffener interface
[NLR-TP-92183-U] p 2670 N94-27796
REINFORCING FIBERS
Inner fiber observation for metal matrix composites under the stress load condition utilizing Synchrotron Orbital Radiation (SR) by X-ray CT p 2724 N94-25553
Continuous fiber reinforced thermoplastic composites: Literature survey
[VTT-TIED-1422] p 2704 N94-25651
Characterization of fatigue damage in a metal matrix composite (SCS-6/Ti-15-3) at elevated temperature
[AD-A273797] p 2706 N94-25876
High performance fibers
[AD-A274693] p 2707 N94-26450
Investigation of forced and isothermal chemical vapor infiltrated SiC/SiC ceramic matrix composites
[DE94-004544] p 2708 N94-26557
RELATIVISTIC EFFECTS
Rydberg states in multiply charged ions
[DE94-002335] p 3021 N94-26760
Decay constants of heavy mesons in the relativistic potential model with velocity dependent corrections
[DE94-606495] p 3030 N94-27860
RELATIVISTIC ELECTRON BEAMS
On a theory of two-beam mechanisms of charged particle acceleration in electrodynamic structures
[DE94-003482] p 3032 N94-26330
Implementation of a compact magnetic electron energy spectrometer for intense relativistic electron beams
[AD-A274451] p 3033 N94-27082
Computer simulations of radiation generation from relativistic electron beams
[AD-A274139] p 3024 N94-27133
Fast H-alpha line broadening during the 100 ns REB injection into a plasma
[IPPCZ-322] p 3048 N94-27836
RELATIVISTIC PARTICLES
Weak interactions in a bilocal chiral theory
[DE93-613097] p 3013 N94-25836
Relativistic heavy ion physics
[DE94-003161] p 3031 N94-26097
Spinor and isospinor structure of relativistic particle propagators
[DE94-601552] p 3019 N94-26424
Spin from isospin: The model of superparticle in a non-Grassmannian approach
[DE93-634341] p 3019 N94-26454
Investigation of plasma instabilities in the polar cusp
[NASA-CR-195212] p 2879 N94-26599
Computer simulations of radiation generation from relativistic electron beams
[AD-A274139] p 3024 N94-27133
Stopping powers and cross sections due to two-photon processes in relativistic nucleus-nucleus collisions
[NASA-CR-4574] p 3033 N94-27646
On the model of the relativistic particle with curvature and torsion
[DE94-606330] p 3029 N94-27848
Correlations in inelastic collisions of relativistic nuclei with emulsion at (4.1 - 4.5) A GeV/c
[DE93-634526] p 3030 N94-27994
RELATIVISTIC PLASMAS
Back-reaction beyond the mean field approximation
[DE94-003936] p 3012 N94-25612
Nonlinear transverse propagation of photons in a ultrarelativistically hot and magnetized electron-positron plasma: Coupling of Langmuir and electromagnetic solitons
[DE94-603667] p 3046 N94-27630
RELATIVISTIC THEORY
Dynamical group of relativistic straight-line string
[DE93-634347] p 3072 N94-26037
Gravitational field of a point mass in the Lobachevskij space
[DE93-634333] p 3072 N94-26503
RELATIVITY
Quark-antiquark bound states
[DE93-613054] p 3013 N94-25826
The gravity equations in the Lobachevskij space
[DE93-634334] p 2879 N94-26504
A relativistic quark model
[ISBN-0-315-60926-5] p 3025 N94-27333
RELAXATION METHOD (MATHEMATICS)
One machine scheduling with delayed precedence constraints
[PB93-237626] p 3094 N94-26314
RELIABILITY
On the reliability of a window least squares algorithm
[DE93-634666] p 2962 N94-26386
Practical problems in aggregating expert opinions
[DE94-002623] p 3094 N94-27707
Silicon device performance measurements to support temperature range enhancement
[NASA-CR-195265] p 2844 N94-27824
Comparative analysis of different configurations of PLC-based safety systems from reliability point of view
p 2836 N94-27925
Controls, monitoring and performance measurements
p 2831 N94-28086
Summary of NASA Aerospace Flight Battery Systems Program activities p 2860 N94-28101
SAFT nickel hydrogen cell cycling status
p 2861 N94-28110
RELIABILITY ANALYSIS
Calculation of a 3-D pose of a known object in a single perspective view
[VTT-PUBS-122] p 2957 N94-25642
An approach to studying the reliability of microgravity experiments
[NASA-TM-106489] p 2834 N94-26199
Simulation modeling for long duration spacecraft control systems p 2684 N94-26288
Modeling systems by probabilistic process algebra: An event structures approach
[PB94-125259] p 3004 N94-26867

Baseline for a Nordtest method. Reliability stress screening of components. A guide for component users [PB94-123775] p 2835 N94-27042
Access to space study [NASA-TM-109693] p 2685 N94-27151
Hardware and software reliability estimation using simulations [NASA-CR-187588] p 2973 N94-27663

RELIABILITY ENGINEERING
The 1991-1992 walking robot design p 2833 N94-25686
Hierarchical test development and design-for-testability for (a)synchronous semi-custom ASIC's [ISBN-9-09-005928-8] p 2834 N94-26003
Development of a MIL-STD-1750 microprocessor system for space applications p 2949 N94-26715

RELIEF MAPS
Geometric correction of SPOT images with use of digital elevation models [ETN-94-95033] p 2847 N94-26107
Optimization of Vector Product Format (VPF) data for map background display in army tactical systems [AD-A274687] p 2848 N94-26446
Multivariate spectral analysis to extract materials from multispectral data [AD-A274142] p 2709 N94-27135

REMOTE CONTROL
An artificial reality environment for remote factory control and monitoring p 2687 N94-27369
Telescience testbedding for physiological experiments under hypobaric hypoxic conditions p 2913 N94-27449
Telescience testbedding under hypobaric hypoxic conditions: Evaluation by operation ability and recognition ability p 2913 N94-27450
Telescience testbedding for physiological experiments under hypobaric hypoxic conditions: Development and evaluation in CNV measuring p 2913 N94-27451
Telecommand decoder specification [ESA-PSS-04-151-ISSUE-1] p 2693 N94-27583

REMOTE HANDLING
Telescience testbedding under hypobaric hypoxic conditions: Evaluation by operation ability and recognition ability p 2913 N94-27450
Telescience testbedding for physiological experiments under hypobaric hypoxic conditions: Development and evaluation in CNV measuring p 2913 N94-27451

REMOTE MANIPULATOR SYSTEM
Direct model reference adaptive control of robotic arms p 2683 N94-26282
Berthing of Space Station Freedom using the shuttle remote manipulator system p 2684 N94-26284
Status report of RMS active damping augmentation p 2684 N94-26285

REMOTE SENSING
The potential for the Department of Defense to use space-based remote sensing to support DOD and other government agencies' environmental programs [AD-A273895] p 2847 N94-25656
Real-time 3-D pose estimation using a high-speed range sensor [AD-A273873] p 2809 N94-25967
Zernike moments and rotation invariant object recognition. A neural network oriented case study [AD-A273749] p 2767 N94-26011
Remote sensing and GIS for the management and investigation of the Wadden Sea [BCRS-92-20] p 2847 N94-26228
Remote Earth Sciences data collection using ACTS [NASA-CR-195227] p 2848 N94-26236
Application of Space Shuttle Project Hercules imagery in the investigation of ship cloud tracks [AD-A274923] p 2692 N94-26529
Mapping coastal habitats using an imaging spectrometer [ISBN-0-315-84362-4] p 2848 N94-26664
An evaluation of an airborne remote sensing system used to determine ice thickness and geometry of a first year sea ice ridge located in the Beaufort Sea [ISBN-0-315-84383-7] p 2849 N94-26667
ARM Fourier transform spectrometer data analysis tools [DE94-000865] p 2895 N94-26697
Digital filter design for sensor simulation: Application to the Brazilian remote sensing satellite [INPE-5523-RPQ/665] p 2849 N94-26827
A preliminary method for atmospheric soundings in real time using satellite and ground-based remotely sensed data [AD-A274381] p 2880 N94-26828
The Hough transform algorithm for sea ice lead analysis: An evaluation [AD-A274535] p 2899 N94-26853
Leadex environmental phenomena and effects observed by DMSP, NOAA, and ERS-1 satellites [AD-A274596] p 2868 N94-26888
Assessment of tropical forests using satellite data [SILVA-CARELICA-21] p 2850 N94-27182
Global tropical forest cover assessments using satellite imagery p 2850 N94-27183
Training on assessment and mapping of deforestation: WFW conference, Brazil [INPE-5482-PRE/1781] p 2850 N94-27384
Global change research related to the Earth's energy and hydrologic cycle [NASA-CR-195270] p 2869 N94-27430
Calibration of SAR systems [DLR-FB-93-18] p 2777 N94-27738
Remote sensing of global snowpack energy and mass balance: In-situ measurements on the snow of interior and Arctic Alaska [NASA-CR-195704] p 2851 N94-27787
Multispectral and textural classifications of a SPOT HRV-1 image, region of Sherbrooke, Quebec, Canada [ISBN-0-315-84978-9] p 2851 N94-27863
Fractals and their applications to remote sensing and digital mapping [ISBN-0-315-59469-1] p 2852 N94-27870
Mapping of soil humidity using C-band radar images [ISBN-0-315-85076-0] p 2852 N94-27878
In situ Mars ozone detector p 3108 N94-27892
Role of remote sensing in energy, water, and carbon cycle studies over the Amazon [INPE-5486-PRE/1786] p 2852 N94-27957
Landscape dynamics of northeastern forests [NASA-CR-195272] p 2852 N94-28070
MODIS airborne simulator visible and near-infrared calibration, 1991 FIRE-Cirrus field experiment. Calibration version: FIRE King 1.1 [NASA-TM-104600] p 2897 N94-28182
Persistence of auroral electron flux events from DMSP/F9 electron measurements [RXR-92012] p 2887 N94-28206
A comparative study of SAR data compression schemes p 2946 N94-28259
Asia-Pacific Seminar on Global Change Research Cooperation [JTN-94-80517] p 2871 N94-28268
Role and activity of STA on Asian Pacific regional cooperation p 2853 N94-28269
Cooperative research projects on satellite remote sensing for the hydrological subjects p 2853 N94-28270
Research activities on the meteorology over the Asia-Pacific region p 2853 N94-28271
An oceanographical observation in the Western Pacific and international cooperations p 2872 N94-28272
NASDA contribution plan to Asian countries p 2853 N94-28273
Activities of Remote Sensing Technology Center of Japan (RESTEC) p 2853 N94-28274
Global concern on research cooperation for environment p 2872 N94-28275
Progress in the study of global change in China p 2873 N94-28276
Research and observation programmes on global changes in Indonesia p 2873 N94-28277
Country report on global change research for the Republic of Korea p 2873 N94-28278
Philippine thrust on environmental research relating to global change p 2873 N94-28279
Study on environment monitoring over whole China using NDVI from AVHRR data and future project p 2875 N94-28289
Utilization of remote sensing data for global climate change research in Malaysia p 2875 N94-28290
Thailand satellite ground receiving station in global change research cooperation p 2875 N94-28291
Utilization of remote sensing data for global change research p 2875 N94-28292
Contribution of satellite observation to global change research p 2876 N94-28293
Laboratory of Space Technology [PB94-133204] p 2689 N94-28358

REMOTE SENSORS
An analysis of multiple sensor system payloads for unmanned aerial vehicles [AD-A274905] p 2667 N94-26182

REMOTELY PILOTED VEHICLES
Design study to simulate the development of a commercial freight transportation system p 2671 N94-25715
Solar powered multipurpose remotely powered aircraft p 2671 N94-25719
An analysis of multiple sensor system payloads for unmanned aerial vehicles [AD-A274905] p 2667 N94-26182

RENORMALIZATION GROUP METHODS
Performance of renormalization group algebraic turbulence model on boundary layer transition simulation [NASA-CR-194466] p 2644 N94-26131
Differential regularization of a non-relativistic anyon model [DE94-601558] p 3019 N94-26416
On kinetic expansion in scalar field theory [DE93-634338] p 3072 N94-26553
Limit theorems for functionals of Markov processes and renormalizable stable fields [AD-A274645] p 3004 N94-27106
Operator regularization and renormalization theory [ISBN-0-315-49334-8] p 3007 N94-27264

REPETITION
Effects of repeating resistance testing on firing ability of igniter EP360-3 [AD-A274814] p 2759 N94-26486

REPRODUCTION (BIOLOGY)
Cloning of rat RXR alpha cDNA and the expression of its mRNA in regenerating liver and primary cultured hepatocytes p 2905 N94-27479
Cloning of a novel POU family gene by RT-PCR method p 2905 N94-27480
Expression analysis of Thyroxine-Binding Globulin Complete Deficiency in Japanese (TBG-CDJ) p 2905 N94-27482
Electron microscopic analysis of meiotic chromosome pairing in male house musk shrew, Suncus murinus p 2906 N94-27493

REQUIREMENTS
CRC customer versus rater octane number requirement program (1990) [AD-A273997] p 2758 N94-25901
Computing in space: Issues and answers p 2948 N94-26714
High performance flight computer developed for deep space applications p 2949 N94-26718
MATRA Marconi Space: The Silex on-board processor and on-board software p 2950 N94-26726
Verification and validation of the on-board software real time requirements p 2953 N94-26739
Steam plant: Steam turbines for combined cycles p 2831 N94-28085

RESEARCH
Proceedings of the symposium on current concepts and approaches on animal test alternatives [AD-A273926] p 2900 N94-25593
Highlights 1993 --- Lawrence Berkeley Laboratory [DE94-002270] p 3118 N94-26937
Microbiology research at some research institutes in the former Soviet Union: A survey of scientific publications [PB94-123320] p 2902 N94-27171
Data analysis and data fusion for intelligence analysis and decision support. Research plan 1993-2000 [PB94-123569] p 3005 N94-27173
The 1993 NASA-ODU American Society for Engineering Education (ASEE) Summer Faculty Fellowship Program [NASA-CR-191544] p 3085 N94-27893
Science beyond the atmosphere: The history of space research in Europe [ESA-HSR-SPECIAL] p 2689 N94-28207
Atmospheric science research in Malaysia: Perspectives on international cooperation p 2874 N94-28285
Laboratory of Space Technology [PB94-133204] p 2689 N94-28358

RESEARCH AIRCRAFT
Multiple model adaptive estimation applied to the LAMBDA URV for failure detection and identification [AD-A274078] p 3002 N94-25992
Description of the Experimental Avionics Systems Integration Laboratory (EASILY) [NASA-TM-109072] p 2681 N94-27425

RESEARCH AND DEVELOPMENT
Technical and scientific research for aeronautics and astronautics [ETN-94-95392] p 2641 N94-26212
Technology development in space projects [VTT-TIED-1438] p 2682 N94-26249
Preparation and characterization of high temperature superconductor film surfaces [AD-A274293] p 3059 N94-26681
Ferrite phase shifters using stress insensitive materials [AD-A274639] p 2708 N94-26895
Frontiers of science and measurement: Report on a seminar jointly organized by the National Physical Laboratory and the Institute of Physics [PB94-124310] p 3009 N94-27131
Robotics handbook. Version 1: For the interested party and professional [NASA-TM-109690] p 2824 N94-27238
Basic research on natural gas combustion phenomena [PB94-129046] p 2717 N94-27256
How to make good use of international research collaboration, with emphasis on the evolving situation in Europe [PB94-119690] p 3101 N94-27323

Vision 21: Interdisciplinary Science and Engineering in the Era of Cyberspace
[NASA-CP-10129] p 2685 N94-27358
Small business innovation research program solicitation
[NASA-TM-109695] p 3094 N94-27661
NASA SBIR abstracts of 1992, phase 1 projects
[NASA-TM-109694] p 3094 N94-27772
The 1993 Federal Aviation Administration plan for research, engineering and development
p 2643 N94-27960
Research and Development Annual Report, 1992
[NASA-TM-104777] p 3119 N94-27993
Development of the gas turbine. Part 1: Design philosophy and performance p 2831 N94-28080
Development of the gas turbine. Part 2: Manufacturing, commissioning, and operation p 2831 N94-28081
Selected data on Federal support to universities and colleges: FY 1991
[NSF-93-320] p 3101 N94-28201
Visit to CERMA: Centre d'Etudes et de Recherches de Medecine Aerospatiale, Centre for Studies and Research in Aviation and Space Medicine, Bretigny sur Orge, France, November 16-18, 1992
[PB94-132990] p 2937 N94-28392

RESEARCH FACILITIES
Technical and scientific research for aeronautics and astronautics
[ETN-94-95392] p 2641 N94-26212
Research and test facilities
[NASA-TM-109685] p 2681 N94-26684
Selected data on Federal support to universities and colleges: FY 1991
[NSF-93-320] p 3101 N94-28201
JSC almanac
[NASA-TM-109702] p 3119 N94-28204

RESEARCH MANAGEMENT
Joint services electronics program
[AD-A274692] p 2783 N94-26449
Joint services electronics program
[AD-A274643] p 2785 N94-27027
Frontiers of science and measurement: Report on a seminar jointly organized by the National Physical Laboratory and the Institute of Physics
[PB94-124310] p 3009 N94-27131
NCVS, volume 5
[AD-A274975] p 2902 N94-27165
How to make good use of international research collaboration, with emphasis on the evolving situation in Europe
[PB94-119690] p 3101 N94-27323

RESEARCH PROJECTS
FAA/NASA Joint University Program for Air Transportation Research, 1992-1993
[NASA-CP-3246] p 2641 N94-27284
University program management information system, FY 1993
[NASA-TM-109719] p 3100 N94-27413
NASA SBIR abstracts of 1992, phase 1 projects
[NASA-TM-109694] p 3094 N94-27772
Global concern on research cooperation for environment p 2872 N94-28275

RESEARCH VEHICLES
Design of a flight controller for an unmanned research vehicle with control surface failures using quantitative feedback theory
[AD-A274049] p 2677 N94-25833
Multiple model adaptive estimation applied to the LAMBDA URV for failure detection and identification
[AD-A274078] p 3002 N94-25992
Prediction of leading-edge transition and relaminarization phenomena on a subsonic multi-element high-lift system p 2659 N94-27929

RESIDUAL STRESS
Study on film generation phenomena by particle deposition p 2728 N94-25575
The fracture behavior of a CVD crystalline Si3N4/amorphous Si3N4 composite
[DE94-002646] p 2750 N94-26124
Grain by grain study of the mechanisms of crack propagation during iodine SCC of Zry-4
[DE93-633765] p 2734 N94-26162
High intensity x ray instrumentation for residual strain measurements in composites and textured materials
[ISBN-0-315-85169-4] p 2842 N94-27278
Implementation of thermal residual stresses in the analysis of fiber bridged matrix crack growth in titanium matrix composites
[NASA-TM-109082] p 2711 N94-27658

RESIN MATRIX COMPOSITES
A study of graphite peek composite with central elliptical holes under tension
[AD-A273779] p 2705 N94-25863
Thermoplastic or thermosetting composites in aircrafts
[PB94-123809] p 2710 N94-27253

RESISTANCE HEATING
Modelling and control of plasma position in the STOR-M tokamak
[ISBN-0-315-58891-8] p 3049 N94-27949

RESONANCE
Stochastic resonance in a periodic potential system under a constant force
[DE93-616817] p 3008 N94-25831
Kinetic resonance damping rate of the toroidal ion temperature gradient mode
[DE94-003511] p 3041 N94-25923
Meson X(1814) as a candidate for a hybrid state
[DE93-634447] p 3017 N94-26045
Signatures for hybrids
[DE94-004244] p 3020 N94-26574
Pion-nucleus interactions and the STAR experiment at RHIC
[DE94-000658] p 3021 N94-26586
Bifurcation sequences at 1:4 resonance: An inventory
[PB94-125408] p 2997 N94-27028
Geometrical resonances in the nyquist noise spectrum for ballistic conductors
[DE94-603668] p 3027 N94-27631

RESONANT FREQUENCIES
Characterization of acoustic effects on flame structures by beam deflection technique
[DE94-003240] p 2714 N94-26122
Parameter estimation by genetic algorithms
[DE94-002924] p 2961 N94-26146
Shake test results of the MDHC test stand in the 40- by 80-foot wind tunnel
[NASA-TM-108801] p 2641 N94-26596
Practical design of resonant cavity for a RF free electron laser
[AD-A274306] p 2819 N94-26941
Extraction of modal parameters from an operating HAWT using the Natural Excitation Technique (NExT)
[DE94-001831] p 2859 N94-27004
Influence of impeller shroud forces on turbopump rotor dynamics p 2796 N94-27378
Effective conductivity of wire mesh reflectors for space deployable antenna systems
[NASA-CR-191605] p 2788 N94-27770
Parameter estimation of linear systems from frequency response measurements (computer program)
[ESDU-93016] p 2976 N94-28137
Acoustic bubble sizing, using active and passive techniques to compare ambient and entrained populations
[ISVR-TR-229] p 2807 N94-28172

RESONATORS
Effective conductivity of wire mesh reflectors for space deployable antenna systems
[NASA-CR-191605] p 2788 N94-27770

RESOURCES MANAGEMENT
Environmental benefits of different types of heat pumps, available and expected
[DE94-002440] p 2866 N94-26123
Coordinated scheduling for dynamic real-time systems
[NASA-CR-195231] p 3093 N94-26206
ADP Analysis project for the Human Resources Management Division p 2978 N94-27927
HDGEC activity in Asia Pacific region
p 2874 N94-28286

RESPIRATION
Interaction between endogenous opioid and Cholecystokinin (CCK) in modulating respiratory responses induced by thin-fiber muscular afferents
p 2906 N94-27502

RESPIRATORY RATE
Interaction between endogenous opioid and Cholecystokinin (CCK) in modulating respiratory responses induced by thin-fiber muscular afferents
p 2906 N94-27502

RESPIRATORY SYSTEM
Aeromedical issues related to positive pressure breathing for +Gz protection
[AD-A274717] p 2910 N94-26435

RESPONSE TIME (COMPUTERS)
Query optimization strategies for browsing sessions
[CWI-CS-R9268] p 3100 N94-27394

REST
Thermoregulatory effects of caffeine ingestion during rest and exercise in men
[NASA-TM-108783] p 2901 N94-26210

RETINENE
Inductive differentiation of nerve cells in mouse embryonic ectoderm at early primitive streak stage by retinoic acid p 2905 N94-27488
Anorectal malformations induced by intraperitoneal injection of all-trans retinoic acid in suncus
p 2905 N94-27489

RETURN TO EARTH SPACE FLIGHT
Assured crew return vehicle post landing configuration design and test p 2697 N94-25671

REVERSE ENGINEERING
Information systems criteria for applying software reengineering: Guidelines for identifying information systems for software reengineering
[AD-A274699] p 3097 N94-26375
Spiral Survey Expedition: A proposal to organize for the Survey, exploration and eventual colonization of the Milky Way Galaxy p 2686 N94-27366

REVERSE FIELD PINCH
Measurement of magnetic fluctuation induced energy transport
[DE94-003846] p 3042 N94-26132
Scaling of sustained ZT-40 M reversed field pinches
[DE94-003318] p 3043 N94-26321
Researches of the Electrotechnical Laboratory. No. 51: Study of formation and sustainment of reversed field pinch by slow control of magnetic field
[JTN-94-80548] p 3046 N94-27350

REVERSING
Eye-head coordination and swinging of the visual scene when wearing visually up-down reversing mirror for 14 days p 2915 N94-27462

REYNOLDS NUMBER
Wake passage effects on the losses in a linear turbine cascade
[AD-A273794] p 2790 N94-25874
Nominally 2-dimensional flow about a normal flat plate
[AD-A274472] p 2794 N94-27026
The cryogenic tunnel Cologne at DLR
[DLR-MITT-93-10] p 2681 N94-27587
A parallel multigrid algorithm for solving the Navier-Stokes equations on a transputer system
[PREPRINT-699] p 2807 N94-28099
Forced convection heat transfer in straight tubes. Part 2: Laminar and transitional flow
[ESDU-93018-PT-2] p 2807 N94-28139

REYNOLDS STRESS
Shear flow generation from the interaction of neoclassical and drift wave transport processes
[DE94-003135] p 2791 N94-26096
Potential capabilities of Reynolds stress turbulence model in the COMMIX-RSM code
[DE94-003716] p 2792 N94-26331
On prediction of equilibrium states in homogeneous compressible turbulence
[NASA-CR-4570] p 2792 N94-26467
A rapid-pressure correlation representation consistent with the Taylor-Proudman theorem materially-frame-indifferent in the 2D limit
[NASA-CR-191591] p 2796 N94-27435
Calculation of single and multiple jets in cross-flow with and without impingement using Reynolds-stress-transport closure p 2803 N94-28024

RHENIUM ALLOYS
Toward insulating quasicrystalline alloy in Al-Pd-Re icosahedral phase
[REPT-A-2666] p 2736 N94-26477

RHEOLOGY
Nonlinear hysteresis in an endochronic solid
[AD-A274594] p 2880 N94-26855
Synthesis, rheology, and forming of Y-Ba-Cu-O ceramics
[DE94-005558] p 2757 N94-27695

RHO-MESONS
Omega omega and rho+ rho- production in two photon interactions at ARGUS
[ISBN-0-315-63748-X] p 3026 N94-27399

RHODIUM
Polymer-bound rhodium hydroformylation catalysts
[ETN-94-95388] p 2712 N94-25747
A mimic model of Pt-Rh catalyst prepared by electrochemical deposition of Rh on Pt (100) surface
[REPT-A-2664] p 2715 N94-26476

RIBONUCLEIC ACIDS
Molecular biological studies on the human radioresistance and drug resistance
[DE93-632682] p 2910 N94-26549
Cloning of a novel POU family gene by RT-PCR method p 2905 N94-27480
Effect of sera from patients treated with long-term hemodialysis on mRNA's for collagenase, stromelysin, and tissue inhibitor of metalloprotease in cultured human synovial cells p 2920 N94-27481

RIBS (SUPPORTS)
Orbit transfer rocket engine technology program enhanced heat transfer combustor technology
[NASA-CR-189236] p 2700 N94-26156

RICCATI EQUATION
Necessary and sufficient conditions for the existence of the stabilizing solution of the Riccati equation in a Hilbert space: A Popov function approach
[PB94-125341] p 2997 N94-26999

RICHARDSON NUMBER
Nominally 2-dimensional flow about a normal flat plate
[AD-A274472] p 2794 N94-27026

RIDING QUALITY
Examples of flight path optimisation using a multivariate gradient-search method
[ESDU-93021] p 2670 N94-28092
Lufthansa long range services: More simplicity
p 2663 N94-28246

RIEMANN MANIFOLD
On the first integrals of geodesics
[DE93-612974] p 3007 N94-25603
A note on Riemannian 2-space
[DE94-602560] p 3073 N94-27024
Approximate Riemann solvers: Improvement of the HLLEM scheme and its generalization for chemically reacting flows
[NAL-TR-1189] p 2795 N94-27205
The Einstein tensor characterizing some Riemann spaces
[DE94-603663] p 3074 N94-27626
The super Weierstrass (zeta)-function and operator product expansions in 2D-induced supergravity on the supertorus
[DE94-603664] p 3074 N94-27627
Proton electromagnetic form factor near the proton-antiproton threshold and quasinuclear bound state
[DE94-606458] p 3027 N94-27681

RIEMANN WAVES
Approximate Riemann solvers: Improvement of the HLLEM scheme and its generalization for chemically reacting flows
[NAL-TR-1189] p 2795 N94-27205

RIGID STRUCTURES
A comparison of three approximate mathematical models for the gravity gradient stabilized satellite
[AD-A273832] p 2694 N94-25615
Balancing of a planar bouncing object
[AD-A273805] p 2821 N94-25878
Normal forms for perturbations of the euler top
[PB94-125390] p 3009 N94-26968

RING CURRENTS
Dynamics explorer interdisciplinary scientist investigations
[NASA-CR-195226] p 2878 N94-26204

RING LASERS
On the application of Allan variance method for Ring Laser Gyro performance characterization
[DE94-003880] p 2810 N94-26525
High-speed, high-density, coherent time-domain optical memory
[AD-A274249] p 3037 N94-27010
Fiber laser amplifiers and oscillators
[AD-A274231] p 2820 N94-28068

RINGS
Matrix near rings and pseudo distributivity
[DE94-601505] p 2992 N94-26366

RIOMETERS
Development of imaging riometers
p 2884 N94-27967
Quick-look system of auroral absorption images by imaging riometer p 2884 N94-27968

RISK
Risk perspectives for Topaz 2 flight mission
[DE94-003229] p 2700 N94-25956
Space projects: Astrophysics facility program contains cost and technical risks. Report to Congressional Requesters
[GAO/NSIAD-94-80] p 2696 N94-27382
Space radiation health research, 1991-1992
[NASA-TM-109721] p 2932 N94-27556
Is probability of frequency too narrow?
[DE94-000687] p 3004 N94-27612
Practical problems in aggregating expert opinions
[DE94-002623] p 3094 N94-27707

RIVETS
Mechanically fastened composite laminates subjected to combined bearing-bypass and shear loading
p 2712 N94-27914

ROADS
Unscreened low tension cables scrape abrasion testing
[PB94-123767] p 2823 N94-26849
Report of the National Research Institute for Earth Science and Disaster Prevention, No. 51
[JTN-94-80509] p 2886 N94-27985
Detection of water on road surface by the polarized light p 2886 N94-27989
Development of a method for predicting snowfall intensity and compacted snow on roads
p 2853 N94-27990
Conception of snow information network system in Yamagata Prefecture p 2853 N94-27991

ROBOT ARMS
Autonomous space processor for orbital debris advanced design project in support of solar system exploration p 2697 N94-25667
Inertial-space disturbance rejection for space-based manipulators p 2683 N94-26281
Direct model reference adaptive control of robotic arms p 2683 N94-26282
Motion planning for serial manipulators with many degrees of freedom: Implementation of a sequential search strategy
[ISBN-0-315-83682-2] p 2822 N94-26642
Generalized finite element dynamic modelling and simulation for flexible robot manipulators
[ISBN-0-315-84623-2] p 2825 N94-27343
Dynamic control of kinematically redundant manipulators
[ISBN-0-315-84627-5] p 2825 N94-27344

ROBOT CONTROL
The 1991-1992 walking robot design
p 2833 N94-25686
Graphical programming at Sandia National Laboratories
[DE94-003803] p 2958 N94-25818
Application of the CIRSSE cooperating robot path planner to the NASA Langley truss assembly problem
p 2683 N94-26280
Performance measures from the explorer platform berthing experiment p 2683 N94-26283
Computer visualizations in engineering applications
[DE94-003589] p 2822 N94-26465
On-board computer for control subsystem of satellite
p 2949 N94-26716
Sensor-based navigation of a mobile robot using automatically constructed fuzzy rules
[DE94-001137] p 2986 N94-26948
Robotics handbook. Version 1: For the interested party and professional
[NASA-TM-109690] p 2824 N94-27238
The universal robot p 2686 N94-27361
Design, implementation and experimental results of robotic environment input into the Robot Controller Test Station (RCTS)
[ISBN-0-315-85355-7] p 2826 N94-27596

ROBOT DYNAMICS
A biologically-inspired autonomous robot
[AD-A273909] p 2821 N94-25782
Robotics handbook. Version 1: For the interested party and professional
[NASA-TM-109690] p 2824 N94-27238
Generalized finite element dynamic modelling and simulation for flexible robot manipulators
[ISBN-0-315-84623-2] p 2825 N94-27343
Dynamic control of kinematically redundant manipulators
[ISBN-0-315-84627-5] p 2825 N94-27344

ROBOT SENSORS
Object imaging accomplished with an integrated circuit robotic tactile sensor incorporating a piezoelectric polyvinylidene fluoride thin film
[AD-A274038] p 2780 N94-25845

ROBOTICS
The 1991-1992 walking robot design
p 2833 N94-25686
Design of dynamically reconfigurable real-time software using port-based objects
[NASA-CR-195178] p 2958 N94-25777
Graphical programming at Sandia National Laboratories
[DE94-003803] p 2958 N94-25818
Balancing of a planar bouncing object
[AD-A273805] p 2821 N94-25878
Recent developments in the Robotic All Terrain Lunar Exploration Rover (RATLER) program
[DE93-040342] p 2821 N94-26110
Modeling and experimental verification of single event upsets p 2684 N94-26287
Early lunar rover mission studies
p 2684 N94-26290
The Robotic All-Terrain Lunar Exploration Rover (RATLER): Increased mobility through simplicity
p 2685 N94-26291
A multitasking behavioral control system for the Robotic All-Terrain Lunar Exploration Rover (RATLER)
p 2685 N94-26292
Computer visualizations in engineering applications
[DE94-003589] p 2822 N94-26465
Automated in-situ inspection systems for underground storage tanks
[AD-A274644] p 2764 N94-27144
Robotics handbook. Version 1: For the interested party and professional
[NASA-TM-109690] p 2824 N94-27238
Dynamic control of kinematically redundant manipulators
[ISBN-0-315-84627-5] p 2825 N94-27344
Vision 21: Interdisciplinary Science and Engineering in the Era of Cyberspace
[NASA-CP-10129] p 2685 N94-27358
Utility fog: A universal physical substance
p 2687 N94-27367
Design, implementation and experimental results of robotic environment input into the Robot Controller Test Station (RCTS)
[ISBN-0-315-85355-7] p 2826 N94-27596
Local performance optimization for a class of redundant eight-degree-of-freedom manipulators
[NASA-TP-3417] p 2989 N94-27773
Comparison of dynamic analysis of a Schilling hydraulic manipulator with experimental results
[DE94-004597] p 2827 N94-27780
Automation life-cycle cost model
[NASA-CR-195695] p 3095 N94-27866
Artemis common lunar lander. Phase 2: Study results for external review
[NASA-TM-109699] p 2692 N94-28205

ROBOTS
The 1991-1992 walking robot design
p 2833 N94-25686
A biologically-inspired autonomous robot
[AD-A273909] p 2821 N94-25782
Balancing of a planar bouncing object
[AD-A273805] p 2821 N94-25878
The television as robot servant
[AD-A273985] p 2984 N94-25898
The determination of surface roughness from reflected step edges
[AD-A273987] p 2984 N94-25900
Rational handling of multiple goals for mobile robots
[NASA-CR-195177] p 2985 N94-26006
A global approach to kinematic path planning to robots with holonomic and nonholonomic constraints
p 2683 N94-26279
Application of the CIRSSE cooperating robot path planner to the NASA Langley truss assembly problem
p 2683 N94-26280
Adaptive path planning in changing environments
[DE94-003269] p 2985 N94-26462
Computer visualizations in engineering applications
[DE94-003589] p 2822 N94-26465
Implementation of integral manifold control on a two degree of freedom flexible joint manipulator: Theory and experiments
[ISBN-0-315-83572-9] p 2823 N94-26658
Sensor-based navigation of a mobile robot using automatically constructed fuzzy rules
[DE94-001137] p 2986 N94-26948
Automated in-situ inspection systems for underground storage tanks
[AD-A274644] p 2764 N94-27144
Ir-fibers in a laser threat warning system and robot shot warning system
[PB94-124476] p 3038 N94-27209
The universal robot p 2686 N94-27361
Parallel algorithm for dominant points correspondences in robot binocular stereo vision p 2686 N94-27364
Utility fog: A universal physical substance
p 2687 N94-27367
Pigs in cyberspace p 2689 N94-27376
Design, implementation and experimental results of robotic environment input into the Robot Controller Test Station (RCTS)
[ISBN-0-315-85355-7] p 2826 N94-27596
Advanced control of a flexible spherical wrist
[ISBN-0-315-84424-8] p 2826 N94-27652

ROBUSTNESS (MATHEMATICS)
Distributing functionality in the drift scan camera system
[DE94-003640] p 2809 N94-25599
On the robustness of a multiple semi-coarsened grid method
[REPT-93-51] p 2992 N94-26252
Fuzzy robust statistics for application to the fuzzy c-means clustering algorithm
[AD-A274719] p 3003 N94-26436
Designing robust control laws using genetic algorithms
p 2643 N94-27295
Dynamics and robust control for uncertain flexible space systems
[INPE-5510-TAE/020] p 2696 N94-27357
Tools for quantitative stability robustness analysis
[ISBN-0-315-59950-2] p 2988 N94-27641

ROCK MECHANICS
Nonlinear hysteresis in an endochronic solid
[AD-A274594] p 2880 N94-26855

ROCKET ENGINE DESIGN
Rocket engine numerical simulation
p 2688 N94-27375

ROCKET ENGINES
Evaluation of moderate angle of attack roll of a dual engine, thrust vectoring aircraft using quantitative feedback theory
[AD-A274118] p 2667 N94-25905

Orbit transfer rocket engine technology program enhanced heat transfer combustor technology
[NASA-CR-189236] p 2700 N94-26156
An ultrasonic testing technique for monitoring the cure and mechanical properties of polymeric materials
[AD-A274536] p 2753 N94-26842
Rocket engine numerical simulation
p 2688 N94-27375
ROCKET EXHAUST
Stationary plasma thruster plume emissions
[NASA-CR-194471] p 2701 N94-26209
ROCKET NOZZLES
Ablation of solid-propellant rocket-motor nozzle materials
[ESA-TT-1289] p 2699 N94-25638
Verification of thermal analysis codes for modeling solid rocket nozzles
[NASA-CR-195248] p 2702 N94-27150
Materials characterization on efforts for ablative materials
[NASA-CR-193929] p 2756 N94-27230
ROCKS
Nonlinear hysteresis in an endochronic solid
[AD-A274594] p 2880 N94-26855
RODENTS
Cross-sectional anatomy of day 30 suncus fetuses
p 2905 N94-27490
RODS
Lunar preform manufacturing p 2765 N94-25677
ROLL
Evaluation of moderate angle of attack roll of a dual engine, thrust vectoring aircraft using quantitative feedback theory
[AD-A274118] p 2667 N94-25905
ROLLERS
Contact stress in disc cams with roller followers
[ESDU-93001] p 2829 N94-28055
Blending profiles of disc cams with radial translating roller followers. Part 2: To incorporate an intermediate precision point or a constant velocity component
[ESDU-93002-PT-2] p 2830 N94-28056
ROLLING MOMENTS
Contribution of body-mounted fins and tailplanes to lateral derivatives due to sideslip at subsonic speeds for general body width to height ratio
[ESDU-93007] p 2648 N94-28057
ROOM TEMPERATURE
Failure mechanisms of high temperature semiconductor lasers
[AD-A273833] p 2815 N94-25616
Investigation of tension-compression fatigue behavior of a cross-ply metal matrix composite at room and elevated temperatures
[AD-A273731] p 2706 N94-25999
Deformation, constitutive behavior, and damage of advanced structural materials under multiaxial loading
[AD-A274165] p 2709 N94-27142
Observation of stimulated emission from an MBE grown GaN film on sapphire
[DE94-003638] p 3068 N94-27724
ROOT-MEAN-SQUARE ERRORS
Estimators for the Cauchy distribution
[DE94-004990] p 3005 N94-27816
ROSSBY REGIMES
Global barotropic response to a tropical forcing
[NASA-CR-195256] p 2896 N94-27408
ROTARY WING AIRCRAFT
Investigation of the aerodynamic environment for an advanced lightweight rotor in forward flight. Volume 4: Laser velocimeter wake data, advance ratio of 0.037
[NASA-TM-109040-VOL-4] p 2645 N94-26483
Investigation of the aerodynamic environment for an advanced lightweight rotor in forward flight. Volume 1: Laser velocimeter inflow data, advance ratio of 0.37, thrust coefficient of 0.0081 and hover tip speed of 603 feet/second
[NASA-TM-109040-VOL-1] p 2645 N94-26489
Investigation of the aerodynamic environment for an advanced lightweight rotor in forward flight. Volume 2: Laser velocimeter inflow data, advance ratio of 0.37, thrust coefficient of 0.0064 and hover tip speed of 710 feet/second
[NASA-TM-109040-VOL-2] p 2645 N94-26492
Investigation of the aerodynamic environment for an advanced lightweight rotor in forward flight. Volume 3: Laser velocimeter inflow data, advance ratio of 0.37, thrust coefficient of 0.0064 and hover tip speed of 603 feet/second
[NASA-TM-109040-VOL-3] p 2645 N94-26497
S-76 high intensity radiated fields, volume 2
[AD-A274572] p 2771 N94-26836
S-76 high intensity radiated fields, volume 1
[AD-A274571] p 2771 N94-26854
Future of aerospace
[PB94-120185] p 2669 N94-26906
ROTARY WINGS
Correlation of airloads on a two-bladed helicopter rotor
[NASA-TM-103982] p 2644 N94-26143
Investigation of the aerodynamic environment for an advanced lightweight rotor in forward flight. Volume 4: Laser velocimeter wake data, advance ratio of 0.037
[NASA-TM-109040-VOL-4] p 2645 N94-26483
Investigation of the aerodynamic environment for an advanced lightweight rotor in forward flight. Volume 1: Laser velocimeter inflow data, advance ratio of 0.37, thrust coefficient of 0.0081 and hover tip speed of 603 feet/second
[NASA-TM-109040-VOL-1] p 2645 N94-26489
Investigation of the aerodynamic environment for an advanced lightweight rotor in forward flight. Volume 2: Laser velocimeter inflow data, advance ratio of 0.37, thrust coefficient of 0.0064 and hover tip speed of 710 feet/second
[NASA-TM-109040-VOL-2] p 2645 N94-26492
Investigation of the aerodynamic environment for an advanced lightweight rotor in forward flight. Volume 3: Laser velocimeter inflow data, advance ratio of 0.37, thrust coefficient of 0.0064 and hover tip speed of 603 feet/second
[NASA-TM-109040-VOL-3] p 2645 N94-26497
Computer code for interactive rotorcraft preliminary design using a harmonic balance method for rotor trim
[AD-A274924] p 2668 N94-26531
A finite wake theory for two-dimensional rotary wing unsteady aerodynamics
[AD-A274921] p 2645 N94-26535
ROTATING BODIES
Normal forms for perturbations of the euler top
[PB94-125390] p 3009 N94-26968
Trajectories of ballistic impact ejecta on a rotating Earth p 2887 N94-28295
ROTATING FLUIDS
Numerical simulation of turbulent free jet by TFKE model p 2871 N94-28157
ROTATING SHAFTS
A new method for torsional critical speed calculation of practical industrial rotors
[IMR-T&M-TR-001] p 2828 N94-28041
Propeller off-axis loads due to thrust axis incidence and nacelle magnus force p 2652 N94-28319
ROTATING STALLS
An investigation of the surge behavior of a high-speed ten-stage axial flow compressor
[AD-A274910] p 2674 N94-26345
ROTATION
Satellite attitude determination using linear combination of models
[AD-A274082] p 2694 N94-25996
Method of correcting rotational motion error in SAR and ISAR imagery
[AD-D016033] p 2773 N94-27146
Translation and rotation invariant pattern recognition
[PB94-123676] p 2968 N94-27157
Fuel ion rotation measurement and its implications on H-mode theories
[DE94-004860] p 3048 N94-27791
ROTOR DYNAMICS
Computer code for interactive rotorcraft preliminary design using a harmonic balance method for rotor trim
[AD-A274924] p 2668 N94-26531
Bulk-Flow Analysis, part A
[NASA-CR-193911-PT-A] p 2796 N94-27377
Influence of impeller shroud forces on turbopump rotor dynamics p 2796 N94-27378
Enhanced simulation software for rocket turbopump, turbulent, annular liquid seals
[NASA-CR-195239] p 2825 N94-27383
ROTOR SPEED
A new method for torsional critical speed calculation of practical industrial rotors
[IMR-T&M-TR-001] p 2828 N94-28041
ROTORS
Laser Doppler velocimetry in a low speed multistage compressor
[AD-A274836] p 2818 N94-26498
A finite wake theory for two-dimensional rotary wing unsteady aerodynamics
[AD-A274921] p 2645 N94-26535
Gas fired advanced turbine system
[DE94-003193] p 2827 N94-27874
A new method for torsional critical speed calculation of practical industrial rotors
[IMR-T&M-TR-001] p 2828 N94-28041
ROUTES
Genetic algorithms applied to a mission routing problem
[AD-A274130] p 2968 N94-27120
ROVING VEHICLES
Hardware design of a spherical mini-rover
p 2833 N94-25669
The 1991-1992 project summaries
p 2943 N94-25698
Project Ares 3 p 2671 N94-25712
RUBBER
New rubber qualification for the igniter adapter
[NASA-CR-193936] p 2752 N94-26708
SAG compensated vibration isolation mount
[AD-D016040] p 2841 N94-27110
RUBIDIUM
Diode-laser-pumped, gas-cell atomic clocks
[AD-A274812] p 3008 N94-26484
RUN TIME (COMPUTERS)
Tool for performance analysis and off-line prediction of timing behaviour p 2952 N94-26732
Efficient rebalancing of tree-type main memory dictionaries
[PB94-133105] p 3100 N94-28396
RUNGE-KUTTA METHOD
Preconditioning in parallel Runge-Kutta methods for stiff initial value problems
[CWI-NM-R9310] p 2991 N94-26217
On the error committed by stopping the Newton iteration in implicit Runge-Kutta methods
[TW-93-02] p 2992 N94-26229
Parallel implicit unstructured grid Euler solvers
[NASA-CR-191594] p 2999 N94-27434
High-lift system analysis method using unstructured meshes
[NLR-TP-92351-U] p 2647 N94-27554
Time-step enlargement and optimal smoothing in Runge-Kutta time-integration algorithms by implicit and explicit smoothing
[NLR-TP-92221-U] p 2798 N94-27799
RUNWAYS
Soft ground arresting system for airports
[DOT/FAA/CT-93/80] p 2680 N94-26202
Tests of highly loaded skids on a concrete runway
[NASA-TP-3435] p 2669 N94-26608
Methods for experimentally determining commercial jet aircraft landing parameters from video image data
[AD-A274207] p 2669 N94-27105
Aircraft accident report: Runway departure following landing American Airlines flight 102, McDonnell Douglas DC-10-30, N139AA, Dallas/Fort Worth International Airport, Texas, April 14, 1993
[PB94-910402] p 2660 N94-27766
RUTILE
Electronic structure of a single oxygen vacancy in rutile TiO2
[DE94-602717] p 3062 N94-26901
RYDBERG SERIES
Rydberg states in multiply charged ions
[DE94-002335] p 3021 N94-26760

S

S MATRIX THEORY
Mapping between the Sinh-Gordon and Ising models
[DE94-601535] p 2998 N94-27162
S WAVES
Elastic scattering by a spherical inclusion
[AD-A274713] p 2878 N94-26433
A preliminary shear velocity model for Central Asia
[AD-A274972] p 2880 N94-26752
Analysis of S-wave seismogram envelope of deep earthquakes and estimation of random inhomogeneities in the Kanto-Tokai area p 2886 N94-27988
SACCADIC EYE MOVEMENTS
Comparative measurement of visual stability in cosmic space: Onboard experiment and pre-flight activities
p 2916 N94-27463
Function of selective attention intrinsic to the saccade system: Does the voluntary control override the stimulus driven control? p 2928 N94-27523
SADDLE POINTS
Phase portraits of quadratic systems with finite multiplicity three and one critical point of infinity
[REPT-93-41] p 2991 N94-26215
SAFETY
Project Columbiad: Reestablishment of human presence on the Moon p 2689 N94-25687
The structural behaviour of the steel or composite concrete and steel frames and the connections of frame members during the fire: A literature review
[VTT-TIED-1437] p 2837 N94-26307
Comparative analysis of different configurations of PLC-based safety systems from reliability point of view
p 2836 N94-27925
Technical Report of National Research Institute of Fisheries Engineering: Fishing Boat and Instrument, No. 12
[JTN-94-80595] p 2764 N94-27976
Recent trend of domestic and international regulations on intact stability of ships for safety
p 2764 N94-27977

Propellants and explosives in ballistic missiles
[UCRL-LR-113578] p 2760 N94-28222

SAFETY DEVICES
The 1991-1992 project summaries
p 2943 N94-25698
Annual conference on fire research, 1993: Book of abstracts
[PB94-121324] p 2717 N94-26907

SAFETY FACTORS
Safety analysis in conceptual design of process control
[VTT-PUBS-117] p 2762 N94-25641
Technology drivers for flight telerobotic system software p 2684 N94-26289
Structural design feasibility study of Space Station long spacer truss
[NASA-TM-106346] p 2843 N94-27559
Technical Report of National Research Institute of Fisheries Engineering: Fishing Boat and Instrument, No. 12
[JTN-94-80595] p 2764 N94-27976
Recent trend of domestic and international regulations on intact stability of ships for safety
p 2764 N94-27977

SAFETY MANAGEMENT
Evaluation and improvement of the inquest system on work accidents (TOT)
[VTT-TIED-1418] p 2762 N94-26261
Proceedings of the Second EGS4 User's Meeting in Japan
[DE93-520383] p 3032 N94-26543
Aerospace safety advisory panel
[NASA-TM-109692] p 3118 N94-27381
Report of the Shuttle Processing Review Team
[NASA-TM-109728] p 2692 N94-28178

SAMARIUM
Technical report of ISSP. Ser. A, no. 2682: Pressure dependence of Sm:YAG fluorescence to 50 GPa: A new calibration as a high pressure scale
[JTN-94-80568] p 3066 N94-27354

SAMPLED DATA SYSTEMS
Operator theoretic methods in the control of distributed and nonlinear systems
[AD-A274160] p 2988 N94-27139
Investigation of spectral analysis techniques for randomly sampled velocimetry data
p 3009 N94-27924

SAMPLERS
Comet nucleus and asteroid sample return missions
p 2689 N94-25692
Simulation approaches for calculations in directed graphical models
[AD-A274825] p 3003 N94-26494

SAMPLING
The use of on-line ion chromatography for high temperature and high pressure reaction studies
[DE94-002525] p 2713 N94-26075
Macrobenthic fauna in the dutch sector of the north sea in 1991
[PB94-126414] p 2868 N94-27200

SANDS
The microstructural response of granular soil under uniaxial strain
[AD-A274808] p 2763 N94-26341

SANDSTONES
The estimation of pre-stress by deformation rate analysis and suggestion of a mechanism from the elast-plastical theory p 2871 N94-28156

SANDWICH STRUCTURES
Effect of impact face damage on strength of sandwich composites
[VTT-PUBS-128] p 2704 N94-25734

SAPPHIRE
Collaborative research on ion implantation of ceramics
[DE93-019177] p 2749 N94-26080
Demonstration of monolithic co-fabrication of Y1Ba2Cu3O7-Sigma and CMOS devices on the same sapphire substrate
[AD-A274757] p 3059 N94-26566
Technical report of ISSP. Ser. A, no. 2685: ASE-free terawatt KrF/Ti : sapphire hybrid laser system
[JTN-94-80571] p 2820 N94-27339
Adsorption and desorption studies of cesium on sapphire surfaces
[DE94-003798] p 3070 N94-28067

SATELLITE ALTIMETRY
Laser altimetry simulator. Version 3.0: User's guide
[NASA-TM-104588] p 2877 N94-26152

SATELLITE ATMOSPHERES
Studies for Io's extended atmosphere and neutral clouds and their impact on the local satellite atmosphere and on the planetary magnetosphere
[NASA-CR-195255] p 3106 N94-27406
Studies for the loss of atomic and molecular species from Io
[NASA-CR-195702] p 3108 N94-27941

SATELLITE ATTITUDE CONTROL
High temperature superconducting infrared imaging satellite p 2698 N94-25700
On-board computer for control subsystem of satellite
p 2949 N94-26716

SATELLITE COMMUNICATION
Development of satellite telecommunications during the period 1990 - 2005
[CRANFIELD-AERO-9301] p 2765 N94-25639
Low Earth orbit communications satellite
p 2698 N94-25701
System design analysis of a lightweight laser satellite terminal
[AD-A274033] p 2690 N94-25769
Remote Earth Sciences data collection using ACTS
[NASA-CR-195227] p 2848 N94-26236
Analysis of linear combining and its application to frequency-hopped signals
[ISBN-0-315-84007-2] p 2770 N94-26624
The Communication Link and Error ANalysis (CLEAN) simulator
[NASA-CR-195243] p 2968 N94-27168
Equalization and cancellation of nonlinear intersymbol interference in a dispersive satellite communication channel
[ISBN-0-315-85147-3] p 2775 N94-27274
A GPS coverage model p 2642 N94-27292
Design and test of a regenerative satellite transmultiplexer
[ISBN-0-315-85280-1] p 2786 N94-27303
Analysis of a multiaccess/switching technique for multibeam satellites in a prioritized ISDN environment
[ISBN-0-315-84632-1] p 2776 N94-27345
The telemedicine spacebridge project: A joint US/Russian venture in long distance medicine via satellite
[NASA-TM-106523] p 2693 N94-27427
NASA satellite communications application research. Phase 2: Efficient high power, solid state amplifier for EFH communications
[NASA-CR-195713] p 2776 N94-27669

SATELLITE CONSTELLATIONS
Low Earth orbit communications satellite
p 2698 N94-25701
A virtual environment for satellite modeling and orbital analysis in a distributed interactive simulation
[AD-A274114] p 2694 N94-25904

SATELLITE CONTROL
A comparison of three approximate mathematical models for the gravity gradient stabilized satellite
[AD-A273832] p 2694 N94-25615

SATELLITE DESIGN
High temperature superconducting infrared imaging satellite p 2698 N94-25700
Copernicus: Lunar surface mapper
p 3081 N94-25702
A simple satellite system to locate gamma ray bursters using scintillating fiber technology
[DE94-601287] p 3117 N94-27996
NSWC Crane Aerospace Cell Test History Database
p 2860 N94-28102

SATELLITE IMAGERY
Human visual system enhancement of reconstructed satellite images
[AD-A273867] p 2693 N94-25595
Objective image quality metrics: Applications for partially compensated images of space objects
[AD-A273837] p 2847 N94-25741
Geometric correction of SPOT images with use of digital elevation models
[ETN-94-95033] p 2847 N94-26107
Solid estimation feature based correlation method for measuring control points required for correcting satellite images
[VTT-JULK-772] p 2848 N94-26253
A geological and geophysical information system for Eurasia
[AD-A274818] p 3098 N94-26490
Application of Space Shuttle Project Hercules imagery in the investigation of ship cloud tracks
[AD-A274923] p 2692 N94-26529
The Hough transform algorithm for sea ice lead analysis: An evaluation
[AD-A274535] p 2899 N94-26853
Assessment of tropical forests using satellite data
[SILVA-CARELICA-21] p 2850 N94-27182
Global tropical forest cover assessments using satellite imagery p 2850 N94-27183
Woody biomass density in the Tendelti area of the central Sudan p 2850 N94-27185
Morphodynamics of inter-tidal areas: The Wadden Sea
[NLR-TP-92356-U] p 2851 N94-27555
Role of remote sensing in energy, water, and carbon cycle studies over the Amazon
[INPE-5486-PRE/1786] p 2852 N94-27957
An image assessment study of image acceptability of the Galileo low gain antenna mission
p 2945 N94-28252
Image compression software for the SOHO LASCO and EIT experiments p 2945 N94-28253
Compression of multispectral Landsat imagery using the Embedded Zerotree Wavelet (EZW) algorithm
p 2947 N94-28261
Vector quantizer designs for joint compression and terrain categorization of multispectral imagery
p 2947 N94-28262
Study on environment monitoring over whole China using NDVI from AVHRR data and future project
p 2875 N94-28289
Utilization of remote sensing data for global climate change research in Malaysia p 2875 N94-28290

SATELLITE INSTRUMENTS
A space fiber-optic x ray burst detector
[DE94-002722] p 2696 N94-26808
Nimbus-7 Earth radiation budget calibration history. Part 2: The Earth flux channels
[NASA-RP-1335-PT-2] p 2814 N94-27981
A simple satellite system to locate gamma ray bursters using scintillating fiber technology
[DE94-601287] p 3117 N94-27996
Develop and fabricate a radiation dose measurement system for satellites
[PL-TR-93-2161] p 2698 N94-28210
Develop and fabricate a radiation dose measurement system for satellites
[PL-TR-93-2099] p 2698 N94-28217

SATELLITE NAVIGATION SYSTEMS
Satellite navigation system GPS: A review of principles and performance and developments in general
[PB94-124534] p 2665 N94-27210
Differential GPS methods and performance for marine applications
[DREP-93-09] p 2665 N94-27667

SATELLITE OBSERVATION
High temperature superconducting infrared imaging satellite p 2698 N94-25700
Digital filter design for sensor simulation: Application to the Brazilian remote sensing satellite
[INPE-5523-RPQ/665] p 2849 N94-26827
A preliminary method for atmospheric soundings in real time using satellite and ground-based remotely sensed data
[AD-A274381] p 2880 N94-26828
Nimbus-7 Earth radiation budget calibration history. Part 2: The Earth flux channels
[NASA-RP-1335-PT-2] p 2814 N94-27981
MODIS airborne simulator visible and near-infrared calibration, 1991 FIRE-Cirrus field experiment. Calibration version: FIRE King 1.1
[NASA-TM-104600] p 2897 N94-28182
Asia-Pacific Seminar on Global Change Research Cooperation
[JTN-94-80517] p 2871 N94-28268
Role and activity of STA on Asian Pacific regional cooperation p 2853 N94-28269
Cooperative research projects on satellite remote sensing for the hydrological subjects
p 2853 N94-28270
Research activities on the meteorology over the Asia-Pacific region p 2853 N94-28271
NASDA contribution plan to Asian countries
p 2853 N94-28273
Thailand satellite ground receiving station in global change research cooperation p 2875 N94-28291
Utilization of remote sensing data for global change research p 2875 N94-28292
Contribution of satellite observation to global change research p 2876 N94-28293

SATELLITE ORBITS
Low Earth orbit communications satellite
p 2698 N94-25701
Modal control of a satellite in an unstable periodic orbit about the Earth-Sun interior Lagrange point
[AD-A273707] p 2694 N94-25776
Hill equations for satellite orbit determination
[ETN-94-95374] p 2690 N94-25787
A virtual environment for satellite modeling and orbital analysis in a distributed interactive simulation
[AD-A274114] p 2694 N94-25904
A GPS coverage model p 2642 N94-27292

SATELLITE ORIENTATION
Satellite attitude determination using linear combination of models
[AD-A274082] p 2694 N94-25996

SATELLITE SOLAR ENERGY CONVERSION
A direct current rectification scheme for microwave space power conversion using traveling wave electron acceleration p 2687 N94-27371

SATELLITE-BORNE INSTRUMENTS
CRRES high energy proton flux map
[AD-A274803] p 2878 N94-26338

SATURATION (CHEMISTRY)

Probability of accessing the multiple saturated states in the resistive interchange instability [DE94-000478] p 3044 N94-26694

SCALARS

On kinetic expansion in scalar field theory [DE93-634338] p 3072 N94-26553

Predictions of momentum and scalar fields in a jet in cross-flow using first and second order turbulence closures p 2803 N94-28025

Fields and potentials in general uniaxial bianisotropic media I. Axial sources [PB94-132875] p 2778 N94-28379

SCALE MODELS

Experimental investigation of advanced hub and pylon fairing configurations to reduce helicopter drag [NASA-TM-4540] p 2668 N94-26604

SCALING LAWS

Hydrodynamics, acoustics and scaling of traveling bubble cavitation [AD-A273846] p 2789 N94-25605

Violation of Feynman scaling law in the forward region p 3113 N94-25633

Scaling of sustained ZT-40 M reversed field pinches [DE94-003318] p 3043 N94-26321

On the aging of sonic booms p 2650 N94-28194

SCANDIUM COMPOUNDS

NNN-Ising model simulation of nanodomain textures in relaxor-type lead scandium tantalate [DE94-601884] p 2748 N94-25844

Polar and chemical domain structures of lead scandium tantalate (PST) [DE94-600760] p 3056 N94-26363

Technical report of ISSP. Ser. A, no. 2670: Electronic structure of light transition metal compounds studied by photoemission [JTN-94-80556] p 3065 N94-27239

Study of the hyperfine magnetic field at Ta-181 site in the Heusler Co2ScSn, Co2ScGa, and Co2HfSn alloys [DE94-603989] p 3067 N94-27623

SCANNERS

Distributing functionality in the drift scan camera system [DE94-003640] p 2809 N94-25599

Color head down display program [AD-A274807] p 2672 N94-26340

The Hough transform algorithm for sea ice lead analysis: An evaluation [AD-A274535] p 2899 N94-26853

The development of an in-motion radiography system for large area aircraft scanning [DREP-TM-93-53] p 2670 N94-27666

SCANNING

Unsteady wake structures in transverse jets p 2800 N94-28006

SCANNING ELECTRON MICROSCOPY

Analysis of the effect on growth kinetics of gamma prima phase in Inconel 713C alloys [DE93-633763] p 2735 N94-26294

Developments in crystallographic phase analysis in the SEM: Backscattered electron Kikuchi patterns [DE93-040755] p 3057 N94-26420

The 27th Annual Meeting of the Israel Society for Microscopy and the 12th Annual Meeting of the Israel Society for Histochemistry and Cytochemistry [DE93-632416] p 2716 N94-26519

SCANNING TUNNELING MICROSCOPY

Observation on metal surface in aqueous solution using an electrochemical Scanning Tunneling Microscope (STM) p 2724 N94-25554

SCATTER PROPAGATION

Performance statistics bulletin: High altitude meteor scatter propagation, August, September, October 1989 [AD-A274455] p 2773 N94-27085

SCATTERING

Back-reaction beyond the mean field approximation [DE94-003936] p 3012 N94-25612

Two dimensional self-consistent fluid simulation of RF inductive sources [DE94-003635] p 2767 N94-25937

Harvard University High Energy Physics [DE94-002406] p 3032 N94-26119

Rescattering and energy loss of fast partons in nuclear matter [DE94-002918] p 3018 N94-26145

Experimental measurement of local displacement and chemical pair correlations in crystalline solid solutions [DE94-001124] p 3065 N94-27251

Decay of non-equilibrium polariton condensate in semiconductors [DE94-604016] p 3068 N94-27678

Neutron-neutron scattering: Possibility of in-beam experiment [DE94-606459] p 3027 N94-27682

SCATTERING AMPLITUDE

The amplitude of the elastic hadron-hadron scattering in the coulombic range of transfer momenta [DE93-613183] p 3014 N94-25869

The challenges of exclusive processes in QCD [DE94-003429] p 3024 N94-27050

Proton electromagnetic form factor near the proton-antiproton threshold and quasinuclear bound state [DE94-606458] p 3027 N94-27681

SCATTERING CROSS SECTIONS

The delta (1232) resonance transition form factor [DE94-003442] p 3017 N94-26101

Elastic scattering by a spherical inclusion [AD-A274713] p 2878 N94-26433

Relativistic collision rate calculations for electron-air interactions [DE94-004204] p 3020 N94-26527

Calculation of electron-potassium scattering [DE94-601812] p 3023 N94-26942

Spin asymmetry in resonant electron-hydrogen elastic scattering [DE94-601813] p 3023 N94-26943

Calculation of total cross sections for electron and positron scattering on sodium and potassium [DE94-601814] p 3023 N94-26944

Jet production in muon scattering at Fermilab E665 [DE94-004663] p 3028 N94-27752

Muon transfer rates in collisions of hydrogen isotope mesic atoms on bare nuclei: Multichannel adiabatic approach [DE94-606752] p 3030 N94-27861

SCATTERING FUNCTIONS

Elastic scattering by a spherical inclusion [AD-A274713] p 2878 N94-26433

SCENE ANALYSIS

Science support for the Earth radiation budget experiment [NASA-CR-191600] p 2894 N94-26506

SCHEDULES

Analysis of cost and schedule growth on sole source and competitive Air Force contracts [AD-A273920] p 3094 N94-26814

SCHEDULING

Automating satellite range scheduling [AD-A273829] p 2694 N94-25738

Coordinated scheduling for dynamic real-time systems [NASA-CR-195231] p 3093 N94-26206

The general pickup and delivery problem [MEMO-COSOR-92-44] p 2992 N94-26226

A linear description of the discrete lot-sizing and scheduling problem [MEMO-COSOR-92-47] p 2992 N94-26227

One machine scheduling with delayed precedence constraints [PB93-237626] p 3094 N94-26314

Real-Time Embedded Processing for Space Applications [ISBN-2-85428-335-X] p 2948 N94-26713

Scheduling tasks with unpredictable timing parameters in hard real-time systems p 2951 N94-26728

Ada multiple-programming for hard real time applications in space systems p 2951 N94-26730

Implementing hard real-time systems: A case study p 2951 N94-26731

A real-time executive implementing priority inheritance protocols p 2952 N94-26733

Scheduling approaches with Ada p 2952 N94-26734

Fault-tolerant scheduling in distributed critical real-time systems p 2952 N94-26735

Central dynamic share scheduling in distributed systems [REPT-93-48] p 2966 N94-26966

Artificial Intelligence Research Branch future plans [NASA-TM-109733] p 2989 N94-28065

SCHLIEREN PHOTOGRAPHY

Focused Schlieren flow visualization studies of multiple venturi fuel injectors in a high pressure combustor [NASA-TM-106479] p 2674 N94-26573

Effects of free-stream turbulence on a jet in a cross flow p 2805 N94-28036

SCHROEDINGER EQUATION

Calculations of population transfer during intense laser pulses [DE94-001060] p 2818 N94-26698

The three-dimensional hydrogen atom in crossed magnetic and electric fields [DE94-606301] p 3029 N94-27847

SCIENCE

Selected data on Federal support to universities and colleges: FY 1991 [NSF-93-320] p 3101 N94-28201

SCIENTIFIC VISUALIZATION

IRMA: A program for three-dimensional color display of data [AD-A273811] p 2959 N94-25879

Center for computation and visualization of geometric structures [DE94-001882] p 2991 N94-25928

Radar cross section visualization using sample buffer progressive refinement volume rendering [AD-A274179] p 2773 N94-27127

Sculpting in cyberspace: Parallel processing the development of new software p 2686 N94-27365

Thirteen ways to say nothing with scientific visualization [NASA-CR-195280] p 2970 N94-27542

RIAD visual imaging branch assessment p 2815 N94-27895

Visualization techniques to aid in the analysis of multispectral astrophysical data sets [NASA-CR-195268] p 3105 N94-27932

SCIENTISTS

General Motors Corporation and Pacific Northwest Laboratory staff exchange: Inspection of case hardened steels and metal-matrix composites [DE94-003470] p 2706 N94-25982

Predoctoral training grant in the area of physical sciences [DE94-004406] p 3039 N94-27603

Science observed: The mass-extinction debates p 2888 N94-28300

SCINTILLATING FIBERS

A space fiber-optic x ray burst detector [DE94-002722] p 2696 N94-26808

A simple satellite system to locate gamma ray bursters using scintillating fiber technology [DE94-601287] p 3117 N94-27996

SCINTILLATION

Calorimeter with WLS fibers and parallel to beam scintillators [DE93-634188] p 2810 N94-26378

The 1024 scintillation hodoscope [DE93-634183] p 2810 N94-26394

Physical characteristics of polymethylmethacrylate scintillator SOFG-120 [DE93-634184] p 2810 N94-26395

SCINTILLATION COUNTERS

An electromagnetic calorimeter with wavelength shifting fiber readout [DE93-616664] p 2809 N94-25735

Calorimeter with WLS fibers and parallel to beam scintillators [DE93-634188] p 2810 N94-26378

The 1024 scintillation hodoscope [DE93-634183] p 2810 N94-26394

Physical characteristics of polymethylmethacrylate scintillator SOFG-120 [DE93-634184] p 2810 N94-26395

Unsegmented electromagnetic calorimeter prototype. Energy and coordinate resolution [DE93-634185] p 2810 N94-26396

Study on the compensated lead hadron calorimeter characteristics by means of hadron and electron beams [DE93-634176] p 2810 N94-26439

A space fiber-optic x ray burst detector [DE94-002722] p 2696 N94-26808

First observation of neutral current proton electron scattering at the square root of s = 300 GeV [DE94-701107] p 3030 N94-27877

A prototype presampler for the uranium-scintillator calorimeter in Zeus [NIKHEF-H/93-11] p 2814 N94-28098

SCOUT LAUNCH VEHICLE

Nasa Langley Research Center seventy-fifth anniversary publications, 1992 [NASA-TM-109691] p 3118 N94-27431

SEA ICE

An evaluation of an airborne remote sensing system used to determine ice thickness and geometry of a first year sea ice ridge located in the Beaufort Sea [ISBN-0-315-84383-7] p 2849 N94-26667

Response of an airborne synthetic aperture radar to sea ice in the marginal ice zone [ISBN-0-315-84243-1] p 2849 N94-26668

The Hough transform algorithm for sea ice lead analysis: An evaluation [AD-A274535] p 2899 N94-26853

Sound, speed, reflectivity, absorption, and thermal diffusivity measurements in Arctic ice in 1990 [AD-A274326] p 2899 N94-26886

The NOGAPS ten year AMIP integration [AD-A274332] p 2900 N94-26887

Leadex environmental phenomena and effects observed by DMSP, NOAA, and ERS-1 satellites [AD-A274596] p 2868 N94-26888

Ice surface temperature retrieval from AVHRR, ATSR, and passive microwave satellite data: Algorithm development and application
[NASA-CR-195276] p 2851 N94-27849
Extraterrestrial accretion and glacial cycles
p 2890 N94-28308
Studies in ice mechanics
[PB94-133055] p 2900 N94-28393

SEA SURFACE TEMPERATURE
Development and testing of the Coupled Ocean/Atmosphere Mesoscale Prediction System (COAMPS)
[AD-A273925] p 2892 N94-25793
The NOGAPS ten year AMIP integration
[AD-A274332] p 2900 N94-26887
Ice surface temperature retrieval from AVHRR, ATSR, and passive microwave satellite data: Algorithm development and application
[NASA-CR-195276] p 2851 N94-27849
The validation of ATSR measurements with in situ sea temperatures
[DE94-003195] p 2852 N94-27875

SEA WATER
Mapping of seawater intrusion into the coastal aquifer of Israel (the seawater-freshwater interface) by TDEM (Time Domain Electromagnetic) method
[ITN-94-85238] p 2850 N94-27331
Determination of lead isotope ratios in seawater by purge and trap GC/MS after ethylation p 2870 N94-28152

SEALERS
Sealant research for solid oxide fuel cells
[DE94-000015] p 2857 N94-26584

SEALING
Sealant research for solid oxide fuel cells
[DE94-000015] p 2857 N94-26584
Development of a new seal for use on large openings of pressurized spacecraft
[NASA-TM-108444] p 2825 N94-27560

SEALS (STOPPERS)
Enhanced simulation software for rocket turbopump, turbulent, annular liquid seals
[NASA-CR-195239] p 2825 N94-27383
Development of a new seal for use on large openings of pressurized spacecraft
[NASA-TM-108444] p 2825 N94-27560
Development of hypersonic engine seals: Flow effects of preload and engine pressures
[NASA-TM-106333] p 2826 N94-27599

SEAMOUNTS
Coupling of pelagic and benthic communities over a seamount in the Eastern North Pacific
[AD-A274750] p 2899 N94-26149

SEARCH PROFILES
What can we learn from genetic algorithms: A new perspective for search methods
[PB94-125234] p 2967 N94-26997

SEAS
Interpreting the implied meridional oceanic energy transport in AMIP
[DE94-001538] p 2898 N94-26072

SEASONS
Monthly variation of physiological and psychological responses under unsteady thermal conditions
p 2918 N94-27475
Man's ability to adapt himself for the seasonal climatic changes: From viewpoint of anticipation and seasonable behavior p 2919 N94-27476

SECONDARY EMISSION
Secondary electron emission from copper surface due to neodymium and gadolinium ion bombardment
[DE94-701115] p 3027 N94-27718

SECONDARY FLOW
Experimental contribution to the study of secondary flows in centrifugal turbopump stator components
[ECL-92-35] p 2789 N94-25654

SECONDARY ION MASS SPECTROMETRY
Electric-field dependence of electroreflectance and photocurrent spectra at visible wavelengths in MOVPE-grown InAlGaP multiple strained quantum-well structures
[DE94-004692] p 2780 N94-25664

SEDIMENTS
Macrobenthic fauna in the dutch sector of the north sea in 1991
[PB94-126414] p 2868 N94-27200
Journal of NIRE, volume 2, number 4
[JTN-94-80554] p 2869 N94-28147
Effects of p-chlorophenol on sulfate reduction in marine sediments p 2870 N94-28150
An evaluation of criteria that may be used to identify species surviving a mass extinction
p 2889 N94-28304
Extraterrestrial accretion and glacial cycles
p 2890 N94-28308
An extraterrestrial event at the tertiary-quaternary boundary p 2890 N94-28309

SEGMENTS
Image segmentation by a combination of edge detection and region growing
[ETN-94-95032] p 2960 N94-26106

SEISMIC ENERGY
A geological and geophysical information system for Eurasia
[AD-A274818] p 3098 N94-26490
Axial focusing of impact energy in the Earth's interior: Proof-of-principle tests of a new hypothesis
p 2888 N94-28296

SEISMIC WAVES
Efficient modeling in transversely isotropic inhomogeneous media
[DE94-003394] p 2877 N94-25847
Emerging technologies
[DE94-003022] p 3102 N94-26023
Elastic scattering by a spherical inclusion
[AD-A274713] p 2878 N94-26433
A geological and geophysical information system for Eurasia
[AD-A274818] p 3098 N94-26490
Nonlinear hysteresis in an endochronic solid
[AD-A274594] p 2880 N94-26855
Elastic wave up/down decomposition in inhomogeneous and anisotropic media: An operator approach and its approximations
[PB94-126497] p 2881 N94-26880
Wave propagation in the shallow regions of the earth's crust and the borehole vicinity
[ITN-94-85237] p 2882 N94-27330
Underground structure in the eastern part of Kanagawa Prefecture inferred from explosion seismic observations
p 2886 N94-27987
Analysis of S-wave seismogram envelope of deep earthquakes and estimation of random inhomogeneities in the Kanto-Tokai area p 2886 N94-27988
Axial focusing of impact energy in the Earth's interior: Proof-of-principle tests of a new hypothesis
p 2888 N94-28296

SEISMOGRAPHS
Antarctic Record, Vol. 36, No. 2
[REPT-107] p 2883 N94-27963
Status report for the development of the Antarctic penetrator: 1990-year program p 2885 N94-27973
Report of the National Research Institute for Earth Science and Disaster Prevention, No. 51
[JTN-94-80509] p 2886 N94-27985
Observation with STS seismometer at Nakaizu, central Japan: Observation system and comparison with tiltmeter p 2886 N94-27986

SEISMOLOGY
A geological and geophysical information system for Eurasia
[AD-A274818] p 3098 N94-26490
A preliminary shear velocity model for Central Asia
[AD-A274972] p 2880 N94-26752
An integrated approach to seismic event location: 1. Evaluating how method of location affects the volume of groups of hypocenters
[PL-TR-92-2323] p 2887 N94-28214

SELECTION
Cooling towers for combined cycles: Design philosophy, performance testing, and operating problems
p 2832 N94-28087

SELECTIVE SURFACES
Solar energy utilization in the USSR
p 2853 N94-26052

SELENIDES
The state of the art of thin-film photovoltaics
[DE94-000224] p 2855 N94-26115
Fragmentation of Ge(1-x) Sn(x) Se2 glasses
[DE94-603009] p 2758 N94-27837

SELF CONSISTENT FIELDS
On kinetic expansion in scalar field theory
[DE93-634338] p 3072 N94-26553
Molecular surface electrostatic potentials in the analysis of non-hydrogen-bonding noncovalent interactions
[AD-A274612] p 3022 N94-26894

SEMANTICS
Semantics, orderings and recursion in the weakest precondition calculus
[CWI-CS-R9267] p 2995 N94-26776
Modeling systems by probabilistic process algebra: An event structures approach
[PB94-125259] p 3004 N94-26867
Combining logics
[PB94-125242] p 2965 N94-26908
Congruence theorem for structured operational semantics with predicates and negative premises
[PB94-126729] p 2966 N94-26970
Trace-based compositional proof theory for fault tolerant distributed systems
[PB94-126737] p 2966 N94-26971
Alternative architectures for domain-oriented application composition and generation systems
[AD-A274180] p 2968 N94-27128
A strategy for dynamic interpretation: A fragment and an implementation
[CWI-CS-R9317] p 2970 N94-27545
Semantics of MANIFOLD: Specification in ASF+SDF and extension
[CWI-CS-R9269] p 2971 N94-27575
Expressiveness results for process algebras
[CWI-CS-R9301] p 3000 N94-27577
A theory for simulator tools
[CWI-CS-R9302] p 2972 N94-27578
Sheaf semantics for Petri Nets
[PB94-132826] p 2983 N94-28354

SEMICONDUCTING FILMS
Atomic layer epitaxy of group 4 materials: Surface processes, thin films, devices and their characterization
[AD-A274325] p 3061 N94-26885

SEMICONDUCTOR DEVICES
Advanced qualification techniques
[DE94-003709] p 2780 N94-25812
Temperature dependence of the radiation induced change of depletion voltage in silicon PIN detectors
[DE94-002705] p 3052 N94-25972
Investigation of plasma etch induced damage in compound semiconductor devices
[DE94-002849] p 3052 N94-25989
Lithium drifted silicon detector fabrication on gettered floating-zone silicon
[DE94-003890] p 3054 N94-26095
Temperature dependence of static RAM volatility
[DE93-040345] p 2948 N94-26111
Fast generator of program waveforms signals
[DE93-634230] p 2948 N94-26381
Modeling Group 4 elements with new transferable tight-binding models
[DE94-000770] p 3059 N94-26695
Diagnostics and microelectronics
[DE94-003016] p 2784 N94-26777
Bulletin of Precision and Intelligence Laboratory, No. 68
[JTN-94-80609] p 3010 N94-27282
Multiple weight stepwise regression
[DE94-001602] p 3000 N94-27564
Dry etching process development for submicron and nanometer semiconductor devices
[PB94-133196] p 2788 N94-28357

SEMICONDUCTOR DIODES
Ultra-high aggregate bandwidth two-dimensional multiple-wavelength diode laser arrays
[AD-A274018] p 2815 N94-25756

SEMICONDUCTOR LASERS
Characterization of an LCD for use as a programmable phase shifter to produce a single-lobed far-field pattern in a phased array
[AD-A273883] p 3034 N94-25729
Ultra-high aggregate bandwidth two-dimensional multiple-wavelength diode laser arrays
[AD-A274018] p 2815 N94-25756
System design analysis of a lightweight laser satellite terminal
[AD-A274033] p 2690 N94-25769
Design analysis of a combined optical/LADAR deep-space surveillance satellite
[AD-A274040] p 2694 N94-25832
Instantaneous amplitude and frequency dynamics of coherent wave mixing in semiconductor quantum wells
[DE94-003262] p 3054 N94-26128
Laser-based communication link
[FFI-93/7023] p 2817 N94-26203
Diode-laser-pumped, gas-cell atomic clocks
[AD-A274812] p 3008 N94-26484

SEMICONDUCTORS (MATERIALS)
Bulletin of National Research Institute for Metals in Fiscal Year 1993, no. 14
[REPT-14] p 2722 N94-25544
Failure mechanisms of high temperature semiconductor lasers
[AD-A273833] p 2815 N94-25616
Hydrogen uptake into silicon from an ECR plasma
[DE94-003771] p 3050 N94-25815
On the estimation of matrix elements for optical transitions in semiconductors
[DE93-613550] p 3051 N94-25851
On radiation defects in strip detectors
[DE93-616646] p 3015 N94-25916
The AFIT multielectrode array for neural recording and simulation: Design, testing, and encapsulation
[AD-A274086] p 2909 N94-25943
Determination of surface recombination velocity and bulk lifetime in detector grade silicon and germanium crystals
[DE94-003886] p 3053 N94-26094
Lithium drifted silicon detector fabrication on gettered floating-zone silicon
[DE94-003890] p 3054 N94-26095

Se EXAFS study of the elevated wurtzite to rock salt structural phase transition in CdSe nanocrystals [DE94-003247] p 3054 N94-26125

Instantaneous amplitude and frequency dynamics of coherent wave mixing in semiconductor quantum wells [DE94-003262] p 3054 N94-26128

Studies of thin-film growth, adsorption, and oxidation by in situ, real-time, and ex situ ion beam analysis [DE94-002907] p 3055 N94-26275

Exploration of GaAs structures for solid-state detectors [DE93-634191] p 3056 N94-26379

On the electron mobility in slightly compensated heavily doped gallium arsenide at low temperatures [DE93-634712] p 3057 N94-26387

Translational-energy-resolved studies of photogenerated carrier-induced reactions on UHV semiconductor surfaces [DE94-004169] p 3058 N94-26526

Diagnostics and microelectronics [DE94-003016] p 2784 N94-26777

Mechanistic studies of opto-electronic materials and syntheses using multiple laser and surface diagnostics [AD-A274528] p 3036 N94-26834

Nitride semiconductors for ultraviolet detection [AD-A274246] p 3060 N94-26840

Effect of impurity correlation on the density of states in slightly compensated heavily doped semiconductors [DE94-602539] p 3061 N94-26879

A model of electric breakdown in polycrystalline semiconductors with highly nonlinear I - V characteristics [DE94-601537] p 3063 N94-27017

AC to DC power converter with regulated bi-polar outputs [AD-D016032] p 2786 N94-27145

Technical report of ISSP. Ser. A, no. 2674: High-field cyclotron resonance and impurity transition in n- and p-3C-SiC at magnetic fields up to 175 T [JTN-94-80560] p 3064 N94-27232

Technical report of ISSP. Ser. A, no. 2675: High-field cyclotron resonance and valence-band structure in semiconducting diamond [JTN-94-80561] p 3065 N94-27245

Optimising BMW four-cylinder two-valve engines [PB94-125101] p 2824 N94-27254

Decay of non-equilibrium polariton condensate in semiconductors [DE94-604016] p 3068 N94-27678

SENSITIVITY

A sensitivity equation approach to shape optimization in fluid flows [NASA-CR-191598] p 2999 N94-27415

SENSORIMOTOR PERFORMANCE

On the development of motor chunks and concurrent processing in a structured continuous keypressing task [AD-A274153] p 2939 N94-27138

Pigs in cyberspace p 2689 N94-27376

SENSORY PERCEPTION

Cortical mechanisms of attention, discrimination, and motor response to somesthetic stimuli [AD-A274163] p 2940 N94-27141

Annals of the Research Inst. of Environmental Medicine, Nagoya Univ., volume 44 [REPT-44-VOL-44] p 2911 N94-27442

SENSORY STIMULATION

Changes in pain sensation induced by repetitive application of noxious heat pulses to the human skin p 2924 N94-27501

SEPAC (PAYLOAD)

Space Experiments with Particle Accelerators (SEPAC) [NASA-CR-193935] p 2761 N94-27664

SEPARATED FLOW

Flow past a circular cylinder with a permeable wake splitter plate [AD-A273765] p 2790 N94-25872

Behaviour of separation bubbles in sharp-edged gaps of finite dimensions [ISBN-0-315-84113-3] p 2793 N94-26637

Control of leading-edge separation on an airfoil by localized excitation [DLR-FB-93-16] p 2647 N94-27592

Flowfield dynamics in blunt fin-induced shock wave/turbulent boundary layer interactions [NASA-CR-195170] p 2798 N94-27802

Investigation of aerodynamic design issues with regions of separated flow p 2658 N94-27902

Separated flow generated by a vectored jet in a crossflow p 2800 N94-28007

A numerical investigation of a subsonic jet in a crossflow p 2803 N94-28023

Theoretical and experimental investigation of a delta wing with turbulent leading-edge jets p 2659 N94-28029

Potential flow modelling of airfoil stall p 2654 N94-28332

Attached and separated trailing edge flow measurements with a triple-split hot-film probe p 2656 N94-28339

A study of blunt trailing edge airfoils using the Navier Stokes code: ARC2D p 2656 N94-28340

Thin-layer Navier-Stokes computations for multi-element airfoils p 2656 N94-28341

SEPARATION

Vortex generators for control of shock-induced separation. Part 1: Introduction and aerodynamics [ESDU-93024-PT-1] p 2806 N94-28095

Vortex generators for control of shock-induced separation. Part 3: Examples of applications of vortex generators to aircraft [ESDU-93026-PT-3] p 2807 N94-28096

SEPARATORS

A Shuttle mechanism for molten-electrolyte lithium batteries [DE94-002914] p 2781 N94-26144

Development of laser spectroscopic technology in nuclear industry [DE93-633327] p 2714 N94-26158

Performance model of a recirculating stack nickel hydrogen cell p 2861 N94-28112

SEQUENCING

One machine scheduling with delayed precedence constraints [PB93-237626] p 3094 N94-26314

SERIES EXPANSION

Asymptotics for Kummer functions, Bose plasmas, and related special functions [DE94-601853] p 3007 N94-26928

SEROTONIN

Abnormal development of serotonin nerve fibers in the cerebral cortex of young rats with methylazoxymethanol induced microcephaly p 2905 N94-27485

SERVICE LIFE

Computer modelling of cyclic deformation of high-temperature materials [AD-A273852] p 2704 N94-25608

Stress relaxation in dough moulding compounds [PB94-124872] p 2748 N94-25894

Aircraft wheel life assessment [AD-A274378] p 2823 N94-26976

The development of stress intensity factors [DRA-TR-93057] p 2845 N94-27954

Software assurance standard [NASA-TM-109705] p 2975 N94-27992

SAFT nickel hydrogen cell cycling status p 2861 N94-28110

Cycle life versus depth of discharge update on modeling studies — Nickel-Hydrogen Batteries p 2862 N94-28115

Orbital management and design considerations for NiCd satellite power systems p 2862 N94-28118

AF Ni-Cd cell qualification program p 2863 N94-28122

Discriminating performance parameters for 50 amp-hour and 60 amp-hour nickel-cadmium plates and battery cells p 2863 N94-28123

Ni-MH storage test and cycle life test p 2864 N94-28131

SET THEORY

Set based analysis of arithmetic [AD-A274112] p 3002 N94-25903

Some properties of graphs with local Ore conditions [PB94-126612] p 2996 N94-26962

Graphs satisfying a local ore-type condition [PB94-126679] p 3007 N94-27222

Ranking alternatives using fuzzy numbers: A computational approach short communication [INPE-5483-PRE/1782] p 2974 N94-27835

SEWING

Variable speed controller p 2943 N94-25678

SHADOWS

Direct evidence of the interplanetary magnetic field effect on the cosmic-ray shadow by the sun [ICRR-296-93-8] p 3116 N94-27607

SHAKING

Shake test results of the MDHC test stand in the 40- by 80-foot wind tunnel [NASA-TM-108801] p 2641 N94-26596

SHALLOW SHELLS

The free vibration of plates, shallow shells and solids [ISBN-0-315-83931-7] p 2838 N94-26622

Refined triangular plate and shell elements [PB94-126356] p 2839 N94-26875

SHALLOW WATER

Remote sensing and GIS for the management and investigation of the Wadden Sea [BCRS-92-20] p 2847 N94-26228

Nonlinear ocean waves [AD-A274651] p 2899 N94-26354

SHAPE CONTROL

MIMO recursive least squares control algorithm for the AN/FPN-44A Loran-C transmitter [AD-A274820] p 2664 N94-26493

SHAPE FUNCTIONS

The identification of inflow fluid dynamics parameters that can be used to scale fatigue loading spectra of wind turbine structural components [DE94-000231] p 2791 N94-26117

SHAPE MEMORY ALLOYS

SAG compensated vibration isolation mount [AD-D016040] p 2841 N94-27110

Modelling and stability of a shape memory alloy position control system [ISBN-0-315-84467-1] p 2740 N94-27304

SHAPES

Effect of nitrocarburizing on shape of titanium alloy parts [DE94-004040] p 2732 N94-25822

Endogeneous and exogenous control of visual selection: A review of the literature [AD-A273761] p 2908 N94-25871

Morphology transitions during non-equilibrium growth processes [ITN-94-85236] p 3065 N94-27243

Interactive shape metamorphosis [NASA-CR-191597] p 2970 N94-27417

Mach reflection of spherical detonation waves [DE93-016604] p 2797 N94-27705

SHEAR FLOW

Shear flow generation from the interaction of neoclassical and drift wave transport processes [DE94-003135] p 2791 N94-26096

The effects of three-dimensional imposed 3-d disturbances on bluff-body near wake flows [AD-A274845] p 2791 N94-26187

On prediction of equilibrium states in homogeneous compressible turbulence [NASA-CR-4570] p 2792 N94-26467

Numerical studies on the dynamics of bubble, turbulent, free shear flows: Effect of the inter-phase coupling on the global flow evolution [AD-A274521] p 2794 N94-26832

Surface roughness lengths [AD-A274550] p 2895 N94-26846

Numerical simulation of turbulent free jet by TFKE model p 2871 N94-28157

SHEAR LAYERS

Numerical studies on the dynamics of bubble, turbulent, free shear flows: Effect of the inter-phase coupling on the global flow evolution [AD-A274521] p 2794 N94-26832

Recent developments in the simulation of steady and transient transverse jet interactions for missile, rotorcraft, and propulsive applications p 2804 N94-28030

SHEAR PROPERTIES

Aluminum alloy 8090-T8771 thick plate material characterization [AD-A274146] p 2987 N94-27077

SHEAR STRESS

Formulae for the buckling of simply-supported corrugated panels of orthotropic material under shear load [PB94-126547] p 2840 N94-26911

Experimental verification of tomographic reconstruction of turbulent air flow structure using optical wavefront measurements [AD-A274392] p 2795 N94-27129

Implementation of thermal residual stresses in the analysis of fiber bridged matrix crack growth in titanium matrix composites [NASA-TM-109082] p 2711 N94-27658

SHELL THEORY

Electron energy loss spectroscopy in a crystalline environment using inner shell ionization [DE94-601820] p 3018 N94-26334

SHELTERS

Portable Habitat for Antarctic Scientific Research (PHASR) p 2943 N94-25681

Pax: A permanent base for human habitation of Mars p 2943 N94-25706

Safety standards for aircraft shelter [FFI-92/4003] p 2680 N94-26305

SHIP HULLS

Weldability aspects in the design and fabrication of aluminium structures subjected to fatigue loads. Part 1: Effect of welding on the structural integrity of joint types designed for repairing aluminium ship sections [PB94-132487] p 2833 N94-28378

SHIPS

Application of Space Shuttle Project Hercules imagery in the investigation of ship cloud tracks [AD-A274923] p 2692 N94-26529

Technical Report of National Research Institute of Fisheries Engineering: Fishing Boat and Instrument, No. 12
[JTN-94-80595] p 2764 N94-27976
Recent trend of domestic and international regulations on intact stability of ships for safety
p 2764 N94-27977
E. H. P. estimation of high speed fishing boats by some existing methods p 2764 N94-27978

SHOCK DISCONTINUITY
A second-order shock-adaptive Godunov scheme based on the generalized Lagrangian formulation
[ISBN-0-315-84549-X] p 2795 N94-27307
Techniques for accurately solving unsteady shock waves and contact discontinuities p 2656 N94-28342

SHOCK LAYERS
Nonequilibrium radiation and chemistry models for aerocapture vehicle flowfields
[NASA-CR-195706] p 2648 N94-28071

SHOCK LOADS
Bibliographic Retrieval System (BARS) Sandia Shock Compression (SSC) database Shock Physics Index (SPHINX) database, volume 3
[DE94-001705] p 3099 N94-27022

SHOCK RESISTANCE
Method for improving electromagnetic shielding performance of composite materials by electropulsing
[AD-D016050] p 2709 N94-27076

SHOCK TESTS
Deviatoric stresses and plastic strain rates in strong shock waves for six metals
[DE94-002964] p 2733 N94-26022

SHOCK TUBES
Basic research on natural gas combustion phenomena
[PB94-129046] p 2717 N94-27256

SHOCK TUNNELS
A numerical study of mixing and combustion in hypervelocity flows through a scramjet combustor model
p 2808 N94-27911
Experiments on interaction force of jets in hypervelocity cross-flow in a shock tunnel p 2659 N94-28022

SHOCK WAVE INTERACTION
Shock wave interaction with L-shaped structures
[AD-A273774] p 2790 N94-25858
Flowfield dynamics in blunt fin-induced shock wave/turbulent boundary layer interactions
[NASA-CR-195170] p 2798 N94-27802
Vortex generators for control of shock-induced separation. Part 1: Introduction and aerodynamics
[ESDU-93024-PT-1] p 2806 N94-28095
Vortex generators for control of shock-induced separation. Part 3: Examples of applications of vortex generators to aircraft
[ESDU-93026-PT-3] p 2807 N94-28096
Interaction of the sonic boom with atmospheric turbulence p 2650 N94-28191
Experimental study on the shock wave interaction with a hypersonic boundary layer near a convex corner
p 2654 N94-28328

SHOCK WAVE PROFILES
A new flux vector splitting scheme
p 2657 N94-28343

SHOCK WAVE PROPAGATION
Experimental and numerical investigation of shock wave propagation through complex geometry, gas continuous, two-phase media
[DE94-001408] p 2791 N94-26121
Approximate Riemann solvers: Improvement of the HLLEM scheme and its generalization for chemically reacting flows
[NAL-TR-1189] p 2795 N94-27205
Theoretical and experimental investigation of converging cylindrical shock waves propagating in narrow cylindrical chambers
[ISBN-0-315-84694-1] p 2795 N94-27313
High-Speed Research: Sonic Boom, Volume 1
[NASA-CP-10132] p 2649 N94-28188
Progress in modeling atmospheric propagation of sonic booms p 2650 N94-28189
Techniques for accurately solving unsteady shock waves and contact discontinuities p 2656 N94-28342

SHOCK WAVES
Deviatoric stresses and plastic strain rates in strong shock waves for six metals
[DE94-002964] p 2733 N94-26022
Iron: What is melt?
[DE94-003373] p 2735 N94-26322
Mix induced by single shock passage through a material interface
[DE93-019505] p 2792 N94-26427
Numerical simulation of the reignition of detonation by reflected shocks
[AD-A274755] p 2795 N94-27252
A second-order shock-adaptive Godunov scheme based on the generalized Lagrangian formulation
[ISBN-0-315-84549-X] p 2795 N94-27307
Theoretical and experimental investigation of converging cylindrical shock waves propagating in narrow cylindrical chambers
[ISBN-0-315-84694-1] p 2795 N94-27313
Collisionless shock structures of Earth and other planets
[NASA-CR-195257] p 3104 N94-27407
An improvement in the modified finite element procedure for underwater shock analysis
[DE94-004451] p 2797 N94-27617
TVD flux-difference split methods for high-speed thermochemical nonequilibrium flows with strong shocks
[UTIAS-350] p 2799 N94-27880
Inclined air-jets used as vortex generators to suppress shock-induced separation p 2659 N94-28040
Nonequilibrium radiation and chemistry models for aerocapture vehicle flowfields
[NASA-CR-195706] p 2648 N94-28071
Computation of static pressure downstream of a normal shock for hypersonic flight (ambient temperature known)
[ESDU-93020] p 2649 N94-28091

SHORELINES
Mapping coastal habitats using an imaging spectrometer
[ISBN-0-315-84362-4] p 2848 N94-26664

SHORT CRACKS
Early stages in the development of stress corrosion cracks
[DE94-003867] p 2838 N94-26524
Fatigue propagation behaviour of short cracks (1-2 mm) in steels
[ESDU-93033] p 2845 N94-28145

SHORT TAKEOFF AIRCRAFT
Wind tunnel investigation of an STOL aircraft model: An effect of engine nacelle shape
[NAL-TM-653] p 2647 N94-27235
A study of jet effect and ground effect interference on a STOL fighter p 2671 N94-28034

SHRINKAGE
Stress relaxation in dough moulding compounds
[PB94-124872] p 2748 N94-25894

SHROUDED TURBINES
Bulk-Flow Analysis, part A
[NASA-CR-193911-PT-A] p 2796 N94-27377
Influence of impeller shroud forces on turbopump rotor dynamics p 2796 N94-27378
Compressibility effects on rotor forces in the leakage path between a shrouded pump impeller and its housing
p 2796 N94-27379

SHUTDOWNS
Aircraft turbine engine reliability and inspection investigations
[AD-A274860] p 2673 N94-26176

SHUTTLE ENGINEERING SIMULATOR
Status report of RMS active damping augmentation
p 2684 N94-26285

SIDE-LOOKING RADAR
A comparative evaluation of SAR and SLAR
[DE94-002922] p 2848 N94-26277

SIDELOBES
Analyzing adaptive beamformer performance in a stable multipath environment
[AD-A274029] p 2766 N94-25766

SIDESLIP
Pressure distributions on a 0.02-scale Space Shuttle orbiter nose at Mach 21.5 in helium
[NASA-TM-4495] p 2646 N94-26592
Contribution of body-mounted fins and tailplanes to lateral derivatives due to sideslip at subsonic speeds for general body width to height ratio
[ESDU-93007] p 2648 N94-28057

SIGNAL ANALYSIS
Parametric time-scale methods in signal analysis
[AD-A274212] p 2773 N94-27068
Trace organic chemical detection using an ultraviolet excitation molecular beam fluorometer
[DE94-002649] p 2704 N94-27708
MUSIC for localization of thunderstorm cells
[DE94-004985] p 2897 N94-28146

SIGNAL ANALYZERS
Rapid prototyping of application specific signal processors (RASSP)
[AD-A274324] p 2772 N94-26884

SIGNAL DETECTION
Detection of transient vector-fields in additive noise
[FFI-93/7028] p 2768 N94-26232
Prewhitening of colored noise fields for detection of threshold sources
[AD-A274346] p 3010 N94-26923
Short-block data detection techniques employing channel estimation for fading time-dispersive channels
[ISBN-0-315-58970-1] p 2777 N94-27806

SIGNAL DETECTORS
Signal amplifier-shapers for multiwire detectors
[DE93-634171] p 2783 N94-26438
High temperature sensor/microphone development for active noise control
[NASA-CR-195214] p 2812 N94-27214

SIGNAL ENCODING
Speech coding at low to medium bit rates
[ISBN-0-315-84012-9] p 2770 N94-26630
Coded communications with nonideal interleaving
[ITN-94-85235] p 2774 N94-27242

SIGNAL FLOW GRAPHS
A real-time convolution algorithm and architecture with applications in SAR processing
[AD-A273817] p 2959 N94-25963

SIGNAL PROCESSING
Digital input module
[DIGEL-1993-6] p 2779 N94-25620
Analysis and simulation of a GPS receiver design using combined delay-lock and modified tanlock loops
[AD-A274037] p 2664 N94-25810
A real-time convolution algorithm and architecture with applications in SAR processing
[AD-A273817] p 2959 N94-25963
Developing a graphical user interface to support a real-time digital signal processing system
[AD-A274032] p 2960 N94-26018
Emerging technologies
[DE94-003022] p 3102 N94-26023
Code division multiple access local area network communications employing fiber optic signal processing techniques
[AD-A274897] p 3096 N94-26180
Direct-conversion-to-baseband for a nonlinear FM signal
[AD-A274861] p 2768 N94-26189
Machine intelligent gust front algorithm
[AD-A273695] p 2680 N94-26196
The 12-channel flash-ADC FASTBUS module
[DE93-634229] p 2783 N94-26380
Low threshold all-optical crossbar switch on GaAs-GaAlAs channel waveguide arrays
[AD-A274971] p 2783 N94-26536
An integrated delta-sigma based IIR filter
[ISBN-0-315-83593-1] p 2784 N94-26631
Design and implementation of a multiprocessor for DSP and communications systems algorithm evaluation
[ISBN-0-315-84128-1] p 2980 N94-26674
Development of GaAs charge-coupled devices
[ISBN-0-315-84116-8] p 3059 N94-26703
Combatting inherent vulnerabilities of CFAR algorithms and a new robust CFAR design
[AD-A274918] p 2770 N94-26751
Automated fabric inspection system
[AD-A274522] p 2835 N94-26833
A current evaluation of the digital beamforming testbed at Rome Laboratory
[AD-A274311] p 3032 N94-26881
Rapid prototyping of application specific signal processors (RASSP)
[AD-A274324] p 2772 N94-26884
Causal fir matrices with anticausal fir inverses, and application in characterization of biorthonormal filter banks
[AD-A274509] p 2998 N94-27035
Monaural and binaural processing of complex waveforms
[AD-A274209] p 3010 N94-27067
Parametric time-scale methods in signal analysis
[AD-A274212] p 2773 N94-27068
Enhanced adaptive statistical filter providing improved performance for target motion analysis noise discrimination statement of government interest
[AD-D016039] p 2786 N94-27109
CCD-Camera images of BEST-TWO and processing results
[AD-A274140] p 2811 N94-27134
Focal plane antenna array for millimeter waves
[AD-D016034] p 2774 N94-27202
Beamforming/null-steering adaptive array
[CA-PATENT-1325260] p 2775 N94-27270
Acousto-optical post-processor time-integrating correlator calibration updates
[DSIS-94-00053] p 2813 N94-27317
Development of digital resampling and pulse compression computer software
[DREP-92-32] p 2969 N94-27318
Fiber optic true time-delay array antenna feed system
[AD-D016063] p 2777 N94-27734
Thunderstorm Hypothesis Reasoner
[NASA-CR-195714] p 2897 N94-27884
The 1994 Space and Earth Science Data Compression Workshop
[NASA-CP-3255] p 2945 N94-28251

SIGNAL REFLECTION
Binaural room simulation
[AD-A273823] p 3009 N94-25737

SIGNAL TO NOISE RATIOS
Hyperspectral analysis of space objects: Signal to noise evaluation
[AD-A273882] p 2765 N94-25728
Performance impacts for actuator misalignments and failures in large-aperture adaptive-optic telescopes
[AD-A273838] p 3034 N94-25742
Primary standards laboratory report 1st half 1993
[DE94-003138] p 2762 N94-26027
SIGNAL TRANSMISSION
Interference analysis of multichannel transmission lines: A system's analysis
[PB94-126505] p 2772 N94-26909
Monaural and binaural processing of complex waveforms
[AD-A274209] p 3010 N94-27067
SIGNATURES
The STAR experiment at the Relativistic Heavy Ion Collider
[DE94-003409] p 3017 N94-26083
Window least squares method applied to statistical noise smoothing of positron annihilation data
[DE93-634665] p 3003 N94-26385
Application of Space Shuttle Project Hercules imagery in the investigation of ship cloud tracks
[AD-A274923] p 2692 N94-26529
Signatures for hybrids
[DE94-004244] p 3020 N94-26574
Experimental studies of loudness and annoyance response to sonic booms p 2651 N94-28195
Variability of measured sonic boom signatures
p 2651 N94-28197
Were all extinction events caused by impacts?
p 2891 N94-28311
SIGNIFICANCE
Example of statistical techniques applied to analysis of effects of small changes
[ESDU-93023] p 2670 N94-28094
SIGNS AND SYMPTOMS
Symptoms of hypoxia at simulated altitude of 25,000 feet p 2933 N94-27945
SIKORSKY AIRCRAFT
S-76 high intensity radiated fields, volume 1
[AD-A274571] p 2771 N94-26854
S-76 high intensity radiated fields, volume 3
[AD-A274416] p 2772 N94-26980
SILANES
The importance of vibrationally excited nitrogen in silicon nitride deposition systems
[AD-A274874] p 2750 N94-26167
SILICA GLASS
Inert strength of pristine silica glass fibers
[DE94-004685] p 2750 N94-26247
Nanoscale plasticity in silica glass
[DE94-004212] p 2751 N94-26554
The deposition of boron nitride and carbon films on silica glass fibers
[DE94-004684] p 2751 N94-26564
Mechanism of mechanical fatigue of silica glass
[DE94-003165] p 2753 N94-26783
SILICATES
Optimization of experimental conditions in IR reflectance determination of BPSG properties
[DE94-002742] p 2713 N94-25978
Ion implantation in silicate glasses
[DE94-003785] p 2757 N94-27726
SILICIDES
Binding of copper and nickel to cavities in silicon formed by helium ion implantation
[DE94-003769] p 3050 N94-25814
Dissolution of secondary phases during extrusion
[PB94-124583] p 2732 N94-25908
Stress relaxation in sputtered W films and W/GeSi/Si heterostructures
[DE94-004007] p 3055 N94-26239
Microstructures of Si surface layers implanted with Cu
[DE94-004690] p 3058 N94-26565
SILICON
Binding of copper and nickel to cavities in silicon formed by helium ion implantation
[DE94-003769] p 3050 N94-25814
Hydrogen uptake into silicon from an ECR plasma
[DE94-003771] p 3050 N94-25815
The structural, chemical, and electrical properties of He-implantation-induced nanocavities in silicon
[DE94-002681] p 3052 N94-25971
Determination of surface recombination velocity and bulk lifetime in detector grade silicon and germanium crystals
[DE94-003886] p 3053 N94-26094
Lithium drifted silicon detector fabrication on gettered floating-zone silicon
[DE94-003890] p 3054 N94-26095
Light emitting porous silicon
[AD-A274152] p 3038 N94-27137
Simulations of terrestrial in-situ cosmogenic-nuclide production
[DE94-004999] p 3117 N94-27826
Dry etching process development for submicron and nanometer semiconductor devices
[PB94-133196] p 2788 N94-28357
SILICON ALLOYS
Study on production of materials with one direction solidification texture p 2727 N94-25572
Recombination and metastability in amorphous silicon and silicon germanium alloys
[DE94-000237] p 2736 N94-26481
Hot deformation behaviour of Si(p)/Al composites and their matrices and an Al-Mg-Si alloy
[ISBN-0-315-84699-2] p 2711 N94-27314
Continuous roll-to-roll a-Si photovoltaic manufacturing technology
[DE94-000260] p 2859 N94-27610
Production of an amorphous Fe(75)Si(10)B(15) sheet by a metallic mold casting method and its properties
p 2746 N94-28170
SILICON CARBIDES
An investigation of cavitation in a mechanically alloyed 15 volume percent SiCp/IN9021 aluminum composite
[DE94-003371] p 2748 N94-25959
Investigation of tension-compression fatigue behavior of a cross-ply metal matrix composite at room and elevated temperatures
[AD-A273731] p 2706 N94-25999
Effects of post-fabrication processing on the tensile properties of centrifugally cast SiC particulate reinforced aluminum composites
[AD-A274865] p 2707 N94-26190
Deposition of a-SiC:H using organosilanes in an argon/hydrogen plasma
[DE94-004428] p 2751 N94-26580
Electron microscopy of AlN-SiC interfaces and solid solutions
[DE94-002449] p 3059 N94-26765
Pseudomorphic semiconducting heterostructures from combinations of AlN, GaN and selected SiC polytypes: Theoretical advancement and its coordination with experimental studies of nucleation, growth, characterization and device development
[AD-A274247] p 3061 N94-26841
Atomic layer epitaxy of group 4 materials: Surface processes, thin films, devices and their characterization
[AD-A274325] p 3061 N94-26885
Low temperature deposition and characterization of N- and p-type silicon carbide thin films and associated ohmic and Schottky contacts
[AD-A274345] p 2754 N94-26974
Interface properties of wide bandgap semiconductor structures
[AD-A274356] p 3063 N94-27058
Technical report of ISSP. Ser. A, no. 2674: High-field cyclotron resonance and impurity transition in n- and p-3C-SiC at magnetic fields up to 175 T
[JTN-94-80560] p 3064 N94-27232
Hot deformation behaviour of Si(p)/Al composites and their matrices and an Al-Mg-Si alloy
[ISBN-0-315-84699-2] p 2711 N94-27314
Influence of lattice damage on retention and transport of deuterium in beta silicon carbide
[DE94-005206] p 3068 N94-27693
Experiment and research on materials irradiated by plasma radiation
[DE94-605011] p 2758 N94-27845
Low strain behaviour of a particulate reinforced aluminum alloy
[ISBN-0-315-84906-1] p 2744 N94-27961
SILICON DIOXIDE
Study on reactions between molten metal and oxide by magnetic flotation dissolution method
p 2725 N94-25558
Study on synthesis and characteristics of intermetallic compound with strong electron correlation
p 2726 N94-25563
The microstructural response of granular soil under uniaxial strain
[AD-A274808] p 2763 N94-26341
A space fiber-optic x ray burst detector
[DE94-002722] p 2696 N94-26808
Technical report of ISSP. Ser. A, no. 2671: Quasi-localization of light waves in Fibonacci dielectric multilayers
[JTN-94-80557] p 3064 N94-27231
Simulations of terrestrial in-situ cosmogenic-nuclide production
[DE94-004999] p 3117 N94-27826
SILICON FILMS
Electron microscopy studies of undoped and phosphorus doped Si:H and Si,C:H films
[DE94-004738] p 3069 N94-27757
SILICON ISOTOPES
Production of (phi) mesons in central Si + Au collisions at 14.6 AGeV/c
[DE94-003196] p 3012 N94-25795
On radiation defects in strip detectors
[DE93-616646] p 3015 N94-25916
The Cherenkov hadronic like-jets
[DE93-634525] p 3016 N94-26010
Sol-gel derived silica/siloxane composite materials: The effect of loading level and catalyst activity on silica domain formation
[DE94-002734] p 2712 N94-27710
SILICON NITRIDES
The fracture behavior of a CVD crystalline Si3N4/amorphous Si3N4 composite
[DE94-002646] p 2750 N94-26124
The importance of vibrationally excited nitrogen in silicon nitride deposition systems
[AD-A274874] p 2750 N94-26167
SILICON OXIDES
Sol-gel derived silica/siloxane composite materials: The effect of loading level and catalyst activity on silica domain formation
[DE94-002734] p 2712 N94-27710
SILICON POLYMERS
Color head down display program
[AD-A274807] p 2672 N94-26340
SILICON RADIATION DETECTORS
Lithium drifted silicon detector fabrication on gettered floating-zone silicon
[DE94-003890] p 3054 N94-26095
Gamma Large Area Silicon Telescope (GLAST): Applying silicon strip detector technology to the detection of gamma rays in space
[DE94-003451] p 3116 N94-27740
SILICON TRANSISTORS
Silicon device performance measurements to support temperature range enhancement
[NASA-CR-195265] p 2844 N94-27824
SILOXANES
Sol-gel derived silica/siloxane composite materials: The effect of loading level and catalyst activity on silica domain formation
[DE94-002734] p 2712 N94-27710
SILVER ALLOYS
Liquid and solid solubility of Ag in Bi2Sr2CaCu2O8
[DE94-002829] p 2735 N94-26273
SILVER BROMIDES
The Cherenkov hadronic like-jets
[DE93-634525] p 3016 N94-26010
SILVER OXIDES
Atomic-scale chemistry of metal surfaces
[REPT-A-2657] p 3012 N94-25636
SILVER ZINC BATTERIES
Battery study for the Mars Environmental Survey (MESUR) Pathfinder p 2860 N94-28105
Bipolar Ag-Zn battery p 2864 N94-28135
Advanced silver zinc battery development for the SRB and ET range safety subsystems p 2865 N94-28136
SILVICULTURE
SIMA: A model for forest succession based on the carbon and nitrogen cycles with application to silvicultural management of the forest ecosystem
[SILVA-CARELICA-22] p 2848 N94-26258
SIMPLEX METHOD
A simplicial approach to integer programming, part 2
[REPT-93-47-PT-2] p 2958 N94-25764
SIMULATED ANNEALING
The application of simulated annealing to stochastic systems
[AD-A273850] p 3001 N94-25607
SIMULATION
Zr-rich corner of the Zr-Sn-O diagram
[DE93-633764] p 2734 N94-26161
Fire simulation based on convection calculation
[VTT-TIED-1411] p 2762 N94-26259
Numerical simulation of plasma vertical position stabilization in ITER
[DE93-634588] p 3044 N94-26510
Feasibility study on introduction of transportation-use petroleum substitution energy
[DE94-725205] p 2759 N94-26905
Modal logic, transition systems and processes
[CWI-CS-R9321] p 2970 N94-27549
Forward and backward simulations. Part 1: Untimed systems
[CWI-CS-R9313-PT-1] p 2972 N94-27580
Forward and backward simulations. Part 2: Timing-based systems
[CWI-CS-R9314-PT-2] p 2972 N94-27581
Simulations of terrestrial in-situ cosmogenic-nuclide production
[DE94-004999] p 3117 N94-27826
Transient model applications. 1: Compressor heat soak/clearance effects modeling p 2828 N94-28048

SIMULATORS
Knowledge organization in intelligent tutoring systems for diagnostic problem solving in complex dynamic domains
[AD-A273986] p 2984 N94-25899
Rocket engine numerical simulation
p 2688 N94-27375
The design of a counter rotating ultra-high-bypass fan simulator for windtunnel investigation
[DLR-FB-93-20] p 2675 N94-27739
Simulating high-frequency wind for long durations
[DE94-002739] p 2682 N94-27997
Experimental studies of loudness and annoyance response to sonic booms p 2651 N94-28195
SINE WAVES
Multiple model adaptive control of a large flexible space structure with purposeful dither for enhanced identifiability
[AD-A274132] p 2987 N94-27122
SINGLE CRYSTALS
Study on synthesis and characteristics of intermetallic compound with strong electron correlation
p 2726 N94-25563
Study on computerized experiment of amorphous transformation process by solid phase reaction
p 2726 N94-25564
Ion implantation of diamond: Damage, doping, and lift-off
[DE94-001133] p 3054 N94-26137
Window least squares method applied to statistical noise smoothing of positron annihilation data
[DE93-634665] p 3003 N94-26385
Growth, characterization and device development in monocrystalline diamond films
[AD-A274245] p 3060 N94-26839
Atomic layer epitaxy of group 4 materials: Surface processes, thin films, devices and their characterization
[AD-A274325] p 3061 N94-26885
Indium donor complexes with cation vacancies in CdTe and ZnSe
[DE94-002731] p 3063 N94-26958
Deformation, constitutive behavior, and damage of advanced structural materials under multiaxial loading
[AD-A274165] p 2709 N94-27142
Float zone crystal growth using laser radiation
[DLR-FB-93-10] p 3066 N94-27590
Effect of temperature and recoil-energy spectra on irradiation-induced amorphization in Ca2La8(SiO4)6O2
[DE94-004371] p 3067 N94-27602
SINGLE EVENT UPSETS
Modeling and experimental verification of single event upsets p 2684 N94-26287
SINGLE STAGE TO ORBIT VEHICLES
Access to space study
[NASA-TM-109693] p 2685 N94-27151
A parametric sensitivity study for single-stage-to-orbit hypersonic vehicles using trajectory optimization
[NASA-CR-195703] p 2697 N94-27789
SINGULARITY (MATHEMATICS)
Towards a theory of growing surfaces: Mapping two-dimensional Laplacian growth onto Hamiltonian dynamics and statistics
[DE94-002636] p 2991 N94-26079
Numerical solution of singularity-perturbed two-point boundary-value problems
[DE94-601542] p 2993 N94-26410
SINKS
Simulation of the carbon cycle in the oceans
[DE94-000780] p 2898 N94-25791
SINTERING
Study on high temperature damage control and life improvement p 2729 N94-25580
Grain boundary degradation of YBCO superconductors sintered in CO2-containing atmospheres
[DE94-003206] p 3053 N94-26029
Alternative materials for solid oxide fuel cells: Processing and interactions of materials
[DE94-000016] p 2855 N94-26114
Processing of LaCrO3 for solid oxide fuel cell applications
[DE94-002981] p 2857 N94-26747
Examination of hardness, fracture toughness and microstructure in Al2O3-B4C binary ceramics
[PB94-124237] p 2755 N94-27158
Transparent polycrystalline body with high ultraviolet transmittance, process for making and applications thereof
[CA-PATENT-1325511] p 3066 N94-27276
SIS (SUPERCONDUCTORS)
A compact 150 GHz SIS receiver cooled by 4 K GM refrigerator
[REPT-36] p 2776 N94-27340
SIZE DISTRIBUTION
Study of precipitation and recrystallization in Al alloy 2519 by backscattered electron imaging methods
[AD-A274919] p 2736 N94-26533
Size distribution of retrogradely labeled dorsal root ganglion cells: Test of normality p 2906 N94-27500
Effect of precipitate structure on hot deformation of Al-Mg-Mn alloys
[DE94-004596] p 2741 N94-27622
SKIDDING
Tests of highly loaded skids on a concrete runway
[NASA-TP-3435] p 2669 N94-26608
SKIN (ANATOMY)
Thyroid hormone action in cultured human skin fibroblasts: Evaluation using spheroid culture
p 2919 N94-27478
Changes in pain sensation induced by repetitive application of noxious heat pulses to the human skin
p 2924 N94-27501
Hyperalgesia to cold in patients with Subacute Myelo-Optico-Neuropathy (SMON) p 2928 N94-27521
Effect of prostaglandin E1 on the relationship between skin sympathetic nerve activity and reduction in skin blood flow p 2929 N94-27524
Difference in skin blood flow reduction depending on activating maneuver of skin sympathetic nerve activity
p 2929 N94-27525
An attempt of intraneural stimulation by microelectrode inserted in skin sympathetic nerve fascicle
p 2930 N94-27529
SKIN (STRUCTURAL MEMBER)
Impact tests on fibre metal laminates under a tensile load
[PB94-126570] p 2710 N94-27201
Investigation of the bond strength of a discrete skin-stiffener interface
[NLR-TP-92183-U] p 2670 N94-27796
SKIN FRICTION
Computational prediction of isolated performance of an axisymmetric nozzle at Mach number 0.90
[NASA-TM-4506] p 2646 N94-26547
SKY SURVEYS (ASTRONOMY)
BATSE burst location accuracy and constraints on the fraction of repeating GRB sources
[DE94-004981] p 3116 N94-27714
Sloan Digital Sky Survey
[DE94-004662] p 3103 N94-27750
In search of Nemesis p 2888 N94-28297
SLABS
Optical characterization and guided wave loss measurements for end-capped 6F-polybenzoxazole
[AD-A274586] p 3036 N94-26982
SLAGS
Study on reactions between molten metal and oxide by magnetic flotation dissolution method
p 2725 N94-25558
SLEDS
The development of a horizontal impact sled facility and subsequent crashworthiness experiments
[NIAR-93-15] p 2680 N94-26200
SLEEP
A comparison of sleep scored from electroencephalography to sleep scored by wrist actigraphy
[AD-A273739] p 2910 N94-26748
Workload transition: Implications for individual and team performance
[AD-A274538] p 2941 N94-26964
SLEEP DEPRIVATION
Effects of methamphetamine on vigilance and tracking during extended wakefulness
[AD-A274896] p 2909 N94-26179
Performance assessment in sustained operations using a computer-based synthetic work task
[AD-A274707] p 2937 N94-26430
SLENDER BODIES
Vibrations in engineering structures: A review of model and full-scale test of a cable-stayed bridge and a traffic sign gantry
[NLR-TP-92321-U] p 2843 N94-27553
SLENDER CONES
Pneumatic management of blunted-forebody flow asymmetry for high-angle-of-attack directional control
p 2679 N94-28028
SLIDING
Study on variation of damage generation mechanism by fatigue on TiAl compounds due to different slip systems p 2729 N94-25579
SLIDING FRICTION
Crystal chemistry and self-lubricating properties of monochalcogenides gallium selenide and tin selenide
[DE93-041177] p 2751 N94-26422
Guidelines for unlubricated sliding wear tests. Part 1: General approach
[PB94-119666] p 2825 N94-27322
Guidelines for unlubricated sliding wear tests. Part 2: Procedures for pin-on-disc testing
[PB94-123270] p 2825 N94-27324
SLOPES
Seasonal snow of arctic Alaska R4D investigations
[DE93-040082] p 2892 N94-25939
Improved measurement accuracy in a Long Trace Profiler: Compensation for laser pointing instability
[DE94-003408] p 2816 N94-26130
Wing lift increment at zero angle of attack due to deployment of single-slotted flaps at low speeds
[ESDU-93019] p 2649 N94-28140
SLOTS
Effects of slot on rock surface for percussive rock excavation: Water jet assisted percussive rock excavation p 2871 N94-28155
SLOTTED WIND TUNNELS
Evaluation of the buoyancy drag on automobile models in low speed wind tunnels p 2658 N94-28352
SMALL SCIENTIFIC SATELLITES
Copernicus: Lunar surface mapper .
p 3081 N94-25702
Norwegian ionospheric satellite experiment: High latitude, low Earth orbit plasma measurements
[FFI-93/7025] p 2876 N94-25807
A simple satellite system to locate gamma ray bursters using scintillating fiber technology
[DE94-601287] p 3117 N94-27996
SMART STRUCTURES
Influence of embedded optical fibers on compressive strength of advanced composites
[AD-A273775] p 2705 N94-25859
Proceedings of Damping 1993, volume 3
[AD-A274228] p 2840 N94-27008
Smart structures, an overview
[AD-A274147] p 2987 N94-27093
Intelligent material systems and structures. Part 6: Measurements of adhesion between optical fibres and composite materials
[PB94-123577] p 2756 N94-27215
SMOKE
Engineering Technical Letter (ETL) 93-5: Fire protection engineering criteria, electronic equipment installations
[AD-A274835] p 2762 N94-26084
SP industry calorimeter for rate of heat release measurements up to 10MW
[PB94-124211] p 2811 N94-27044
SMOOTHING
Time-step enlargement and optimal smoothing in Runge-Kutta time-integration algorithms by implicit and explicit smoothing
[NLR-TP-92221-U] p 2798 N94-27799
SNOW
Seasonal snow of arctic Alaska R4D investigations
[DE93-040082] p 2892 N94-25939
Development of a method for predicting snowfall intensity and compacted snow on roads
p 2853 N94-27990
Conception of snow information network system in Yamagata Prefecture p 2853 N94-27991
SNOW COVER
Remote sensing of global snowpack energy and mass balance: In-situ measurements on the snow of interior and Arctic Alaska
[NASA-CR-195704] p 2851 N94-27787
Report of the National Research Institute for Earth Science and Disaster Prevention, No. 51
[JTN-94-80509] p 2886 N94-27985
Development of a method for predicting snowfall intensity and compacted snow on roads
p 2853 N94-27990
Conception of snow information network system in Yamagata Prefecture p 2853 N94-27991
SOCIAL FACTORS
HDGEC activity in Asia Pacific region
p 2874 N94-28286
SOCIAL ISOLATION
A study of psychological factors affecting an extremely isolated environment p 2927 N94-27517
SODIUM
Convergent close-coupling calculation of electron-sodium scattering
[DE94-601815] p 3014 N94-25842
Zinc(2) oxide stability in alkaline sodium phosphate solutions at elevated temperatures
[DE94-003316] p 2715 N94-26320
Calculation of total cross sections for electron and positron scattering on sodium and potassium
[DE94-601814] p 3023 N94-26944
Fast and slow onsets of Na channel blocking actions due to lidocaine and disopyramide using concentration-clamp method p 2907 N94-27504
A study on tissue excitation of cardiac muscle under electrical field stimulation p 2907 N94-27510
Block of cardiac sodium channels by Ro 22-9194 (R), a new antiarrhythmic agent: Effects on the maximum upstroke velocity (Vmax) of single guinea pig ventricular myocytes p 2907 N94-27511

Electrophysiological effects of an antiarrhythmic drug, moricizine on isolated guinea pig ventricular muscles
p 2907 N94-27512

SODIUM IODIDES
Monte Carlo calculations of low background detector response
[DE94-004593] p 3116 N94-27621

SODIUM VAPOR
Studies for the loss of atomic and molecular species from Io
[NASA-CR-195702] p 3108 N94-27941

SOFTWARE ENGINEERING
System software and tools for high performance computing environments: A report on the findings of the Pasadena Workshop
[DE94-003918] p 2956 N94-25602
IGES 4.0 to LCAD translator for CSG models
[AD-A274013] p 2957 N94-25753
Abstraction in, specification and proof of software for a 1D heat-transfer problem
[REPT-93-45] p 2790 N94-25763
ObjectSim: A reusable object oriented DIS visual simulation
[AD-A274030] p 2958 N94-25767
Design of dynamically reconfigurable real-time software using port-based objects
[NASA-CR-195178] p 2958 N94-25777
Domain analysis and modeling of a model-based software executive
[AD-A274087] p 2958 N94-25783
Parallel Assessment Window System (PAWS) enhancements
[AD-A274094] p 2979 N94-25786
A method for populating the knowledge base of APTAS, a domain-oriented application composition system
[AD-A274034] p 2766 N94-25797
The television as robot servant
[AD-A273985] p 2984 N94-25898
Object interaction in a parallel object-oriented discrete-event simulation
[AD-A274084] p 2959 N94-25942
Developing a graphical user interface to support a real-time digital signal processing system
[AD-A274032] p 2960 N94-26018
Using database technology to support domain-oriented application composition systems
[AD-A274091] p 3096 N94-26024
Software redesign for usability: A case study
[DE94-003704] p 2960 N94-26048
Multimedia in Views
[CWI-CS-R9263] p 2961 N94-26218
The MUSA design methodology
[CWI-CS-R9265] p 3097 N94-26220
Development and analysis of secure embedded software
[VTT-TIED-1430] p 2961 N94-26254
Deductive computer programming
[AD-A274966] p 2962 N94-26303
Software Error Estimation Program (SWEEP), version 02.00.00 user manual
[AD-A274697] p 2962 N94-26373
Information systems criteria for applying software reengineering: Guidelines for identifying information systems for software reengineering
[AD-A274699] p 3097 N94-26375
Programming in Fortran M
[DE94-002756] p 2963 N94-26407
Bathymetric data set extraction program. Users guide
[AD-A274761] p 2899 N94-26567
Institute for Information Technology
[NRC-37061] p 3118 N94-26709
Fault tolerant real-time processing system for space use p 2949 N94-26720
On-board software for the JET-X telescope on the Spectrum-X mission p 2951 N94-26727
Tool for performance analysis and off-line prediction of timing behaviour p 2952 N94-26732
Developing with Ada using HOOD design methodology
p 2953 N94-26741
Use of HOOD coupled to real time monitors
p 2953 N94-26742
Ada reusable software for satellite on-board data handling p 2953 N94-26743
The CODE-TOP (COncurrent system DEvelopment using Transformations Of Predicate-transition nets) method: Examples of using it for system architecture specification, software specification, and code generation p 2953 N94-26744
Parallel mathematical software
[DE94-001587] p 2967 N94-27020
Static task allocation for parallel processing systems during software development
[AD-A274204] p 2981 N94-27100
A method for populating the knowledge base of AFIT's domain-oriented application composition system
[AD-A274128] p 3099 N94-27118
Alternative architectures for domain-oriented application composition and generation systems
[AD-A274180] p 2968 N94-27128
Research in improved assessment of software reliability
[AD-A274161] p 2968 N94-27140
Sculpting in cyberspace: Parallel processing the development of new software p 2686 N94-27365
Human computer interface guide, revision A
[NASA-TM-109708] p 2955 N94-27769
A proposed software engineering environment for systems life cycle management
[ISBN-0-315-60634-7] p 2974 N94-27869
A formal approach to the comparison of object-oriented analysis and design methodologies
p 2975 N94-27937
CASE tools for the support of object-oriented analysis and design methods p 2975 N94-27939
Software assurance standard
[NASA-TM-109705] p 2975 N94-27992
Advanced End-to-end Simulation for On-board Processing (AESOP) p 2945 N94-28255
Using formal specification in the Guidance and Control Software (GCS) experiment. Formal design and verification technology for life critical systems
[NASA-CR-194884] p 2956 N94-28267

SOFTWARE RELIABILITY
Domain analysis and modeling of a model-based software executive
[AD-A274087] p 2958 N94-25783
Software Error Estimation Program (SWEEP), version 02.00.00 user manual
[AD-A274697] p 2962 N94-26373
Developing with Ada using HOOD design methodology
p 2953 N94-26741
Specification performance optimization and executive generation for onboard multiprocessor real time application with SynDEx p 2954 N94-26745
Modeling systems by probabilistic process algebra: An event structures approach
[PB94-125259] p 3004 N94-26867
Research in improved assessment of software reliability
[AD-A274161] p 2968 N94-27140
Validation tests of TOPSIM 4
[ESA-STM-249] p 2972 N94-27582
Hardware and software reliability estimation using simulations
[NASA-CR-187588] p 2973 N94-27663
Software assurance standard
[NASA-TM-109705] p 2975 N94-27992
Engine simulation systems p 2829 N94-28054

SOFTWARE REUSE
ObjectSim: A reusable object oriented DIS visual simulation
[AD-A274030] p 2958 N94-25767
Domain analysis and modeling of a model-based software executive
[AD-A274087] p 2958 N94-25783
Using database technology to support domain-oriented application composition systems
[AD-A274091] p 3096 N94-26024
The ergonomics of software porting: Automatically configuring software to the runtime environment or everything you wanted to know about your C compiler but didn't know who to ask
[CWI-CS-R9266] p 2961 N94-26221
Ada reusable software for satellite on-board data handling p 2953 N94-26743

SOFTWARE TOOLS
Parallel Assessment Window System (PAWS) enhancements
[AD-A274094] p 2979 N94-25786
Analysis and computer tools for separation processes involving nonideal mixtures
[DE94-004162] p 2960 N94-25986
The National Center for Advanced Information Components Manufacturing: Program update
[DE94-002647] p 2960 N94-26118
Survey of visualization and analysis tools
[NASA-TM-108436] p 2809 N94-26150
Implementing a multiple criteria model base in co-op with a graphical user interface generator
[AD-A274901] p 3093 N94-26181
Parallel grid generation algorithm for distributed memory computers
[NASA-TP-3429] p 2963 N94-26466
Verification and validation of the on-board software real time requirements p 2953 N94-26739
Asynchronous and packetized systems engineering tools p 2954 N94-26746
Diagnostics and microelectronics
[DE94-003016] p 2784 N94-26777
DUSOL: Improved software for analysis of ultrasonic velocity data on anisotropic materials
[NPL-DMM(A)-104] p 2965 N94-26816
Rapid prototyping of application specific signal processors (RASSP)
[AD-A274324] p 2772 N94-26884
Design of an online help facility for ExSpect
[PB94-126687] p 2966 N94-26955
Thirteen ways to say nothing with scientific visualization
[NASA-CR-195280] p 2970 N94-27542
A theory for simulator tools
[CWI-CS-R9302] p 2972 N94-27578
Smalltalk: A tool for development of an Ada implementation of EWCAC
[SKL-1600-46-003-01-0] p 2974 N94-27823
Visualization techniques to aid in the analysis of multispectral astrophysical data sets
[NASA-CR-195268] p 3105 N94-27932
Comparison of Object-Oriented Analysis and Design Methods: A Collection of Papers
[MEMO-INF-92-69] p 2975 N94-27936
CASE tools for the support of object-oriented analysis and design methods p 2975 N94-27939

SOHO MISSION
Mounting of SSM's
[VTT-TIED-1442] p 2695 N94-26250

SOIL MAPPING
Mapping of soil humidity using C-band radar images
[ISBN-0-315-85076-0] p 2852 N94-27878

SOIL MECHANICS
The microstructural response of granular soil under uniaxial strain
[AD-A274808] p 2763 N94-26341

SOIL MOISTURE
Mapping of soil humidity using C-band radar images
[ISBN-0-315-85076-0] p 2852 N94-27878

SOIL SCIENCE
Time domain reflectometry for measuring bulk soil electrical conductivity and comparison with the Em38 instrument
[PB94-125432] p 2881 N94-27052

SOILS
The microstructural response of granular soil under uniaxial strain
[AD-A274808] p 2763 N94-26341
Time domain reflectometry for measuring bulk soil electrical conductivity and comparison with the Em38 instrument
[PB94-125432] p 2881 N94-27052

SOL-GEL PROCESSES
Sol-gel derived silica/siloxane composite materials: The effect of loading level and catalyst activity on silica domain formation
[DE94-002734] p 2712 N94-27710

SOLAR ACTIVITY
Photospheric origins of chromospheric and coronal activity
[NASA-CR-195215] p 3110 N94-26590
Chaotic dynamics of the solar cycle
[AD-A274315] p 3110 N94-26883
Solar-geophysical data number 590, October 1993. Part 1: (Prompt reports). Data for September, August 1993, and late data
[PB94-125903] p 3110 N94-27053
Solar-geophysical data number 590, October 1993. Part 2: (Comprehensive reports). Data for April 1993, and miscellaneous
[PB94-125911] p 3110 N94-27054
Environmental conditions responsible for solar activity
[AD-A274191] p 3111 N94-27099

SOLAR ACTIVITY EFFECTS
Comparative investigation of high-latitude ionospheric structure and effects near solar maximum
[AD-A273799] p 2877 N94-25877
The Sixteenth Symposium on Coordinated Observations of the Ionosphere and the Magnetosphere in the Polar Regions: Program and abstracts
[JTN-94-80601] p 2882 N94-27300
Antarctic Record, Vol. 36, No. 2
[REPT-107] p 2883 N94-27963
Characteristics of 30-MHz interference noises observed by riometers p 2884 N94-27965

SOLAR ARRAYS
Low-cost photovoltaic inverters incorporating application-specific integrated circuits
[DE94-003270] p 2856 N94-26463
Charge efficiency of Ni/H2 cells during transfer orbit of Telstar 4 satellites p 2862 N94-28117
Battery charge control: Which approach is best?
p 2863 N94-28124

SOLAR ATMOSPHERE
High resolution studies of sunspots and flux tubes
[NASA-CR-195216] p 3111 N94-27321

SOLAR CELLS
Electrical properties of p-type GaInP2
[AD-A273771] p 3051 N94-25856
The state of the art of thin-film photovoltaics
[DE94-000224] p 2855 N94-26115

Recombination and metastability in amorphous silicon and silicon germanium alloys
[DE94-000237] p 2736 N94-26481
Simplified high-efficiency silicon cell processing
[DE94-002683] p 2857 N94-26617
A direct current rectification scheme for microwave space power conversion using traveling wave electron acceleration p 2687 N94-27371
Research on high-efficiency, large-area, CuInSe2 based thin-film modules
[DE94-000259] p 3067 N94-27609
Continuous roll-to-roll a-Si photovoltaic manufacturing technology
[DE94-000260] p 2859 N94-27610
High-efficiency, thin-film solar cells
[DE94-000250] p 2860 N94-27625
Charge efficiency of Ni/H2 cells during transfer orbit of Telstar 4 satellites p 2862 N94-28117

SOLAR COLLECTORS
Solar energy in Israel: Utilization and research
p 2853 N94-26051
Solar energy utilization in the USSR
p 2853 N94-26052
The PLVCR 500 and HCPC, tests and results
[DLR-MITT-93-04] p 2858 N94-26813
Solar collector manufacturing activity, 1992
[DE94-003401] p 2859 N94-27048
Isothermal corrosion testing of steels in molten nitrate salts
[DE94-004695] p 2742 N94-27755

SOLAR CONVECTION (ASTRONOMY)
Observation of impulsive acoustic events and the excitation of solar oscillations
[AD-A274159] p 3111 N94-27096

SOLAR COOLING
Absorption technology for solar and waste heat utilization p 2854 N94-26053

SOLAR CORONA
Photospheric origins of chromospheric and coronal activity
[NASA-CR-195215] p 3110 N94-26590
Coronal heating via nanoflares
[DE94-000773] p 3110 N94-26696

SOLAR CYCLES
Chaotic dynamics of the solar cycle
[AD-A274315] p 3110 N94-26883

SOLAR DYNAMIC POWER SYSTEMS
Structural evaluation of concepts for a solar energy concentrator for Space Station advanced development program
[NASA-TP-3375] p 2695 N94-26609

SOLAR ENERGY
Renewable energy systems in Mexico: Installation of a hybrid system
[DE93-013716] p 2853 N94-25946
The First Energy Conference: Israel and the Former USSR
[ISBN-965-229-098-X] p 2853 N94-26050
Solar energy in Israel: Utilization and research
p 2853 N94-26051
Solar energy utilization in the USSR
p 2853 N94-26052
Absorption technology for solar and waste heat utilization p 2854 N94-26053
NEMO 2: New energy systems and technologies
[DE94-702060] p 2855 N94-26240
Solar resource-utility load matching assessment: NREL photovoltaic project summary
[DE94-000232] p 2856 N94-26480

SOLAR ENERGY CONVERSION
Solar energy in Israel: Utilization and research
p 2853 N94-26051
Solar energy utilization in the USSR
p 2853 N94-26052

SOLAR FLARES
Coronal heating via nanoflares
[DE94-000773] p 3110 N94-26696
Region 5395 of March 1989 --- solar activity, geomagnetic disturbances, and terrestrial effects
[PB94-120714] p 3110 N94-26755
Solar-geophysical data number 590, October 1993. Part 1: (Prompt reports). Data for September, August 1993, and late data
[PB94-125903] p 3110 N94-27053
Acceleration of electrons and ions by strong lower-hybrid turbulence in solar flares
[NASA-TM-109723] p 3111 N94-27953
Solar-geophysical data number 591, November 1993. Part 2: (Comprehensive reports). Data for May 1993 and miscellaneous
[PB94-134830] p 3111 N94-28360

SOLAR FLUX
The status of the solar neutrino problem
[DE94-003934] p 3111 N94-27742

SOLAR GENERATORS
Handbook of photovoltaic power generating design for introduction
[DE94-725199] p 2858 N94-26913

SOLAR GRANULATION
Photospheric origins of chromospheric and coronal activity
[NASA-CR-195215] p 3110 N94-26590

SOLAR HEATING
Solar energy utilization in the USSR
p 2853 N94-26052
Martian atmospheric radiation budget
p 3107 N94-27887

SOLAR MAGNETIC FIELD
Solar-geophysical data number 590, October 1993. Part 1: (Prompt reports). Data for September, August 1993, and late data
[PB94-125903] p 3110 N94-27053
Environmental conditions responsible for solar activity
[AD-A274191] p 3111 N94-27099
Direct evidence of the interplanetary magnetic field effect on the cosmic-ray shadow by the sun
[ICRR-296-93-8] p 3116 N94-27607

SOLAR NEUTRINOS
The status of the solar neutrino problem
[DE94-003934] p 3111 N94-27742

SOLAR OSCILLATIONS
Observation of impulsive acoustic events and the excitation of solar oscillations
[AD-A274159] p 3111 N94-27096

SOLAR PHYSICS
Solar-geophysical data number 590, October 1993. Part 1: (Prompt reports). Data for September, August 1993, and late data
[PB94-125903] p 3110 N94-27053
Solar-geophysical data number 590, October 1993. Part 2: (Comprehensive reports). Data for April 1993, and miscellaneous
[PB94-125911] p 3110 N94-27054
Observation of impulsive acoustic events and the excitation of solar oscillations
[AD-A274159] p 3111 N94-27096
Environmental conditions responsible for solar activity
[AD-A274191] p 3111 N94-27099
High resolution studies of sunspots and flux tubes
[NASA-CR-195216] p 3111 N94-27321

SOLAR PLANETARY INTERACTIONS
The Sixteenth Symposium on Coordinated Observations of the Ionosphere and the Magnetosphere in the Polar Regions: Program and abstracts
[JTN-94-80601] p 2882 N94-27300

SOLAR PONDS (HEAT STORAGE)
Solar energy in Israel: Utilization and research
p 2853 N94-26051

SOLAR POSITION
Initial ultraviolet-B intensity data at Lawrence Livermore National Laboratory
[DE94-004279] p 2869 N94-27267

SOLAR POWERED AIRCRAFT
Solar powered multipurpose remotely powered aircraft
p 2671 N94-25719

SOLAR PROMINENCES
Solar-geophysical data number 590, October 1993. Part 2: (Comprehensive reports). Data for April 1993, and miscellaneous
[PB94-125911] p 3110 N94-27054
Solar-geophysical data number 591, November 1993. Part 2: (Comprehensive reports). Data for May 1993 and miscellaneous
[PB94-134830] p 3111 N94-28360

SOLAR PROTONS
Solar-geophysical data number 591, November 1993. Part 2: (Comprehensive reports). Data for May 1993 and miscellaneous
[PB94-134830] p 3111 N94-28360

SOLAR RADIATION
Seasonal snow of arctic Alaska R4D investigations
[DE93-040082] p 2892 N94-25939
Initial ultraviolet-B intensity data at Lawrence Livermore National Laboratory
[DE94-004279] p 2869 N94-27267
Solar and airglow measurements aboard the two suborbital flights NASA 36.098 and 36.107
[NASA-CR-195279] p 2882 N94-27380

SOLAR RADIO BURSTS
Solar-geophysical data number 591, November 1993. Part 2: (Comprehensive reports). Data for May 1993 and miscellaneous
[PB94-134830] p 3111 N94-28360

SOLAR RADIO EMISSION
Region 5395 of March 1989 --- solar activity, geomagnetic disturbances, and terrestrial effects
[PB94-120714] p 3110 N94-26755
Solar-geophysical data number 590, October 1993. Part 1: (Prompt reports). Data for September, August 1993, and late data
[PB94-125903] p 3110 N94-27053

SOLAR REFLECTORS
Mounting of SSM's
[VTT-TIED-1442] p 2695 N94-26250
Charge efficiency of Ni/H2 cells during transfer orbit of Telstar 4 satellites p 2862 N94-28117

SOLAR SPECTRA
Solar and airglow measurements aboard the two suborbital flights NASA 36.098 and 36.107
[NASA-CR-195279] p 2882 N94-27380

SOLAR SYSTEM
Spiral Survey Expedition: A proposal to organize for the Survey, exploration and eventual colonization of the Milky Way Galaxy p 2686 N94-27366

SOLAR TERRESTRIAL INTERACTIONS
Region 5395 of March 1989 --- solar activity, geomagnetic disturbances, and terrestrial effects
[PB94-120714] p 3110 N94-26755
Solar-geophysical data number 590, October 1993. Part 1: (Prompt reports). Data for September, August 1993, and late data
[PB94-125903] p 3110 N94-27053
Solar-geophysical data number 590, October 1993. Part 2: (Comprehensive reports). Data for April 1993, and miscellaneous
[PB94-125911] p 3110 N94-27054
Direct evidence of the interplanetary magnetic field effect on the cosmic-ray shadow by the sun
[ICRR-296-93-8] p 3116 N94-27607

SOLAR THERMAL ELECTRIC POWER PLANTS
Solar energy in Israel: Utilization and research
p 2853 N94-26051
Solar energy utilization in the USSR
p 2853 N94-26052

SOLAR X-RAYS
Region 5395 of March 1989 --- solar activity, geomagnetic disturbances, and terrestrial effects
[PB94-120714] p 3110 N94-26755
Solar-geophysical data number 590, October 1993. Part 2: (Comprehensive reports). Data for April 1993, and miscellaneous
[PB94-125911] p 3110 N94-27054
Solar-geophysical data number 591, November 1993. Part 2: (Comprehensive reports). Data for May 1993 and miscellaneous
[PB94-134830] p 3111 N94-28360

SOLDERING
Experimental determination of the CU-IN-PB ternary phase diagram
[DE94-003765] p 2735 N94-26349
Joining of fibre reinforced metal matrix composite materials
[PB94-132453] p 2712 N94-28376

SOLDERS
Experimental determination of the CU-IN-PB ternary phase diagram
[DE94-003765] p 2735 N94-26349
Research into the microstructure and mechanical behavior of eutectic Bi-Sn and In-Sn
[DE94-004558] p 2741 N94-27619

SOLENOIDS
Electromagnetic properties of a toroidal solenoid
[DE93-613032] p 2766 N94-25866

SOLID CRYOGENS
Trapped electrons in solid hydrogen
[DE93-018628] p 3052 N94-25947
Spectroscopy and dynamics of molecular and ionic impurities embedded in solid hydrogen
[AD-A274149] p 3064 N94-27095

SOLID ELECTROLYTES
Development of SO(x) and NO(x) solid electrolyte sensors p 2725 N94-25562
Reference electrodes for solid polymer electrolytes
[DE94-004583] p 2780 N94-25806
Alternative materials for solid oxide fuel cells: Processing and interactions of materials
[DE94-000016] p 2855 N94-26114
Oxygen reduction at a YSZ interface with cathode materials La(1-x)(Ca or Sr)(x)MnO3(1-x)CaMnO3
[DE94-002954] p 3054 N94-26147
Processing of LaCrO3 for solid oxide fuel cell applications
[DE94-002981] p 2857 N94-26747
Low cost, radial flow, solid oxide fuel cell
[DE94-002982] p 2858 N94-26785
MSOFC development status
[DE94-003192] p 2858 N94-26792
High temperature solid oxide fuel cell: Customer test units
[DE94-002961] p 2858 N94-26869
High temperature solid oxide fuel development activities
[DE94-002973] p 2858 N94-26871

Perovskite solid electrolytes for SOFC
[DE94-001923] p 2859 N94-27005

SOLID MECHANICS
Computational mechanics
[DE94-003015] p 2965 N94-26775

SOLID PHASES
Predictive modeling of particle-laden, turbulent flows
[DE94-003298] p 2792 N94-26319

SOLID PROPELLANT ROCKET ENGINES
An ultrasonic testing technique for monitoring the cure and mechanical properties of polymeric materials
[AD-A274536] p 2753 N94-26842
Development and application of contamination technology for MSFC managed space systems
[NASA-CR-193934] p 2697 N94-27421

SOLID PROPELLANTS
Propellants and explosives in ballistic missiles
[UCRL-LR-113578] p 2760 N94-28222

SOLID ROCKET PROPELLANTS
Cryogenic size reduction of solid propellant
[AD-A274844] p 2759 N94-26800
An ultrasonic testing technique for monitoring the cure and mechanical properties of polymeric materials
[AD-A274536] p 2753 N94-26842
Uncertainties in the characterization of the thermal environment of a solid rocket propellant fire
[DE94-002023] p 2760 N94-27719

SOLID SOLUTIONS
An atom probe investigation of the influence of trace impurities on the mechanical behavior of NiAl
[DE94-002797] p 2734 N94-26272
Electron microscopy of AlN-SiC interfaces and solid solutions
[DE94-002449] p 3059 N94-26765
Experimental measurement of local displacement and chemical pair correlations in crystalline solid solutions
[DE94-001124] p 3065 N94-27251

SOLID STATE
Structure and properties of intermetallic composites synthesized in situ using solid state displacement reactions
[DE94-004312] p 2705 N94-25805
Powder synthesis, fabrication, and transport properties of long-length Ag clad Bi-2223 conductors
[DE94-002376] p 2740 N94-26957
Phase stability in the Cd-Mg system
[DE94-004976] p 2743 N94-27792

SOLID STATE DEVICES
Solid state research
[AD-A274063] p 3049 N94-25645
Exploration of GaAs structures for solid-state detectors
[DE93-634191] p 3056 N94-26379
Center for space microelectronics technology
[NASA-CR-195282] p 2786 N94-27574

SOLID STATE LASERS
Compact, solid-state femtosecond source
[AD-A273932] p 2817 N94-26271
Phase conjugation and pulse compression of high energy lasers: From nanoseconds to microseconds
[DE94-001061] p 2818 N94-26699
Phase conjugated lasers applied to commercial x ray lithography
[DE94-001529] p 2819 N94-27018
Kinoform/lens system for injecting a high power laser beam into an optical fiber
[DE94-003226] p 2819 N94-27262
Technical report of ISSP. Ser. A, no. 2686: High-order harmonic generation and ionization using ultrashort KrF and Ti:Sapphire lasers
[JTN-94-80572] p 2820 N94-27605
Optical parametric oscillator modeling with diffraction, depletion, and double refraction
[DE94-001504] p 3040 N94-27999

SOLID SURFACES
Surface physics with cold and thermal neutron reflectometry
[DE94-001447] p 2733 N94-26070

SOLID WASTES
Oil production from buckwheat stillage by thermochemical liquefaction p 2871 N94-28154

SOLID-SOLID INTERFACES
Electron microscopy of AlN-SiC interfaces and solid solutions
[DE94-002449] p 3059 N94-26765
A transmission electron microscope study of Ni4W precipitates in a Ni-37 wt. percent W alloy
[ISBN-0-315-59932-4] p 2743 N94-27803

SOLIDIFICATION
Study on the mechanism of titanium alloy toughness and the improvement of properties
p 2726 N94-25566
Study on solidification of non-homogeneous melting/solidification materials p 2728 N94-25573
Solidification modeling of a spiral casting to determine material fluidity
[DE94-002212] p 2739 N94-26935
Morphology transitions during non-equilibrium growth processes
[ITN-94-85236] p 3065 N94-27243
Differential scanning calorimetric study of solid state amorphization and crystallization in Zr/Co and Zr/Ni multilayers p 2745 N94-28161
The corrosion behavior of sputter-deposited magnesium-valve metal alloys p 2745 N94-28164
Production of an amorphous Fe(75)Si(10)B(15) sheet by a metallic mold casting method and its properties
p 2746 N94-28170
Formation and high mechanical strength of Al-based alloys containing a nanoscale icosahedral phase as a main constituent p 2746 N94-28171

SOLIDS
Predictive modeling of particle-laden, turbulent flows
[DE94-003298] p 2792 N94-26319
The free vibration of plates, shallow shells and solids
[ISBN-0-315-83931-7] p 2838 N94-26622
Lisp interface to geometric modelling operations
[PB94-133121] p 3001 N94-28398

SOLITARY WAVES
Coherent state approach for the (Phi)(sup 6)-lattice model and phase transitions
[DE93-613053] p 3050 N94-25825
Chaotic dynamics of the solar cycle
[AD-A274315] p 3110 N94-26883

SOLUBILITY
Measurement of viscosity, density, and gas solubility of refrigerant blends in selected synthetic lubricants
[DE94-003609] p 2713 N94-25934
A Shuttle mechanism for molten-electrolyte lithium batteries
[DE94-002914] p 2781 N94-26144
Liquid and solid solubility of Ag in Bi2Sr2CaCu2O8
[DE94-002829] p 2735 N94-26273
Influence of lattice damage on retention and transport of deuterium in beta silicon carbide
[DE94-005206] p 3068 N94-27693
Solubility, viscosity, and density of refrigerant/lubricant mixtures
[DE94-004237] p 2721 N94-28069

SOLUTES
Influence of grain structure and solute composition on the work hardening behavior of aluminium at cryogenic temperatures
[DE94-003415] p 2733 N94-26087

SOLVENTS
The reactivity of lithium toward non-aqueous solvents of relevance to energy storage applications as studied by surface analytical techniques
[DE94-003483] p 2856 N94-26464
Effects of plastic media blasting on aircraft skin
[AD-A274817] p 2668 N94-26488
Evaluating non-chlorinated solvents for welding applications
[DE94-003332] p 2824 N94-27181

SOMALIA
Human dimensions research team, operation restore hope
[AD-A274340] p 2939 N94-27056

SONAR
Enhanced adaptive statistical filter providing improved performance for target motion analysis noise discrimination statement of government interest
[AD-D016039] p 2786 N94-27109

SONIC BOOMS
Preliminary design of nine high speed civil transports
p 2671 N94-25710
High-Speed Research: Sonic Boom, Volume 1
[NASA-CP-10132] p 2649 N94-28188
Progress in modeling atmospheric propagation of sonic booms p 2650 N94-28189
Implications for high speed research: The relationship between sonic boom signature distortion and atmospheric turbulence p 2650 N94-28190
Interaction of the sonic boom with atmospheric turbulence p 2650 N94-28191
Sonic boom propagation through turbulence: A ray theory approach p 2650 N94-28192
The propagation of spark-produced N waves through turbulence p 2650 N94-28193
On the aging of sonic booms p 2650 N94-28194
Experimental studies of loudness and annoyance response to sonic booms p 2651 N94-28195
Comparison of methods of predicting community response to impulsive and nonimpulsive noise
p 2651 N94-28196
Variability of measured sonic boom signatures
p 2651 N94-28197
Sonic booms and marine mammals: Informational status and recommendations p 2651 N94-28198

SONIC NOZZLES
Control jets in interaction with hypersonic rarefied flow
p 2698 N94-28020

SORPTION
Application of the Positron Annihilation Technique to the study of vapor absorption process in polyethylene (LDPE) and in imide polymer (6FDA-TMPD PI)
[DE94-602737] p 2720 N94-27998

SOUND DETECTING AND RANGING
Prewhitening of colored noise fields for detection of threshold sources
[AD-A274346] p 3010 N94-26923
Enhanced adaptive statistical filter providing improved performance for target motion analysis noise discrimination statement of government interest
[AD-D016039] p 2786 N94-27109

SOUND GENERATORS
Modern photoacoustic spectroscopy problems. Theory and experiment (a review)
[IFTR-41/1993] p 2716 N94-26823
Hydroacoustic wave-fields generated by different source types, a computational study
[PB94-123536] p 3010 N94-27037

SOUND PROPAGATION
Progress in modeling atmospheric propagation of sonic booms p 2650 N94-28189

SOUND TRANSMISSION
Hydroacoustic wave-fields generated by different source types, a computational study
[PB94-123536] p 3010 N94-27037
Monaural and binaural processing of complex waveforms
[AD-A274209] p 3010 N94-27067

SOUND WAVES
Binaural room simulation
[AD-A273823] p 3009 N94-25737
The effect of high frequency electric field on hypersound amplification in superlattice
[DE93-634326] p 3057 N94-26384
New variational techniques for acoustic radiation and scattering from elastic shell structures
[AD-A274599] p 3010 N94-26889
Problems in nonlinear acoustics: Rayleigh waves, pulsed sound beams, and waveguides
[AD-A274587] p 3010 N94-26983
Hydroacoustic wave-fields generated by different source types, a computational study
[PB94-123536] p 3010 N94-27037
Monaural and binaural processing of complex waveforms
[AD-A274209] p 3010 N94-27067
Observation of impulsive acoustic events and the excitation of solar oscillations
[AD-A274159] p 3111 N94-27096
On the use of feedback to control sound radiation from a plate excited by a turbulent boundary layer
[ISVR-TR-227] p 2807 N94-28175

SOUNDING ROCKETS
Sulfur dioxide in the atmosphere of Venus 1 sounding rocket observations
[NASA-CR-195224] p 3106 N94-26237
Cosmic x ray physics
[NASA-CR-195225] p 3115 N94-27236
Cosmic x ray physics
[NASA-CR-195218] p 3115 N94-27419
Cosmic x ray physics
[NASA-CR-195219] p 3115 N94-27420

SOURCE PROGRAMS
Source code for the OO1 benchmark and the AFIT simulation benchmark
[AD-A274035] p 2958 N94-25799

SOUTH KOREA
Country report on global change research for the Republic of Korea p 2873 N94-28278

SOUTHERN OSCILLATION
A synoptic study on periods of deficiency over Rio Grande do Sul/Brazil
[INPE-5456-TDI/498] p 2896 N94-27422

SPACE BASED RADAR
Experimental evaluation of battery cells for space-based radar application p 2860 N94-28104

SPACE CHARGE
First principle calculation for magneto-crystalline anisotropy
[DE93-634653] p 3052 N94-26012

SPACE COLONIES
Vision 21: Interdisciplinary Science and Engineering in the Era of Cyberspace
[NASA-CP-10129] p 2685 N94-27358
The Fermi paradox: An approach based on percolation theory p 2687 N94-27370

SPACE COMMERCIALIZATION
MINOTAUR (Maryland's innovative orbital technologically advanced University rocket)
p 2703 N94-25685

Future of aerospace
[PB94-120185] p 2669 N94-26906
Access to space study
[NASA-TM-109693] p 2685 N94-27151

SPACE DEBRIS
Autonomous space processor for orbital debris advanced design project in support of solar system exploration p 2697 N94-25667

SPACE ENVIRONMENT SIMULATION
A large high vacuum, high pumping speed space simulation chamber for electric propulsion
[NASA-TM-106453] p 2690 N94-26142
Telescience testbedding for physiological experiments under hypobaric hypoxic conditions
p 2913 N94-27449
Telescience testbedding under hypobaric hypoxic conditions: Evaluation by operation ability and recognition ability p 2913 N94-27450
Telescience testbedding for physiological experiments under hypobaric hypoxic conditions: Development and evaluation in CNV measuring p 2913 N94-27451

SPACE ERECTABLE STRUCTURES
Space Habitat, assembly and repair facility
p 2691 N94-25696
Selected topics in robotics for space exploration
[NASA-CP-10131] p 2682 N94-26278

SPACE EXPLORATION
Proceedings of the 8th Annual Summer Conference: NASA/USRA Advanced Design Program
[NASA-CR-195118] p 3075 N94-25665
Planetary surface exploration MESUR/autonomous lunar rover p 2833 N94-25683
Project APEX: Advanced manned exploration of the Martian moon Phobos p 3079 N94-25688
Mars transportation system p 2833 N94-25689
Asteroid exploration and utilization
p 3080 N94-25697
Selected topics in robotics for space exploration
[NASA-CP-10131] p 2682 N94-26278
Early lunar rover mission studies
p 2684 N94-26290
Vision 21: Interdisciplinary Science and Engineering in the Era of Cyberspace
[NASA-CP-10129] p 2685 N94-27358
Telepresence in the human exploration of Mars: Field studies in analog environments p 2685 N94-27360
Spiral Survey Expedition: A proposal to organize for the Survey, exploration and eventual colonization of the Milky Way Galaxy p 2686 N94-27366
A direct current rectification scheme for microwave space power conversion using traveling wave electron acceleration p 2687 N94-27371
Comparison of the lossy image data compressions for the MESUR Pathfinder and for the Huygens Titan Probe
p 2945 N94-28254

SPACE FLIGHT
NASA's spacecraft data system p 2950 N94-26723
Future of aerospace
[PB94-120185] p 2669 N94-26906
Nasa Langley Research Center seventy-fifth anniversary publications, 1992
[NASA-TM-109691] p 3118 N94-27431

SPACE FLIGHT STRESS
Workshop on Countering Space Adaptation with Exercise: Current Issues
[NASA-CP-3252] p 2934 N94-28361
Muscular activity and its relationship to biomechanics and human performance p 2934 N94-28362

SPACE HABITATS
Automation of closed environments in space for human comfort and safety p 2943 N94-25684
A widely adaptable habitat construction system utilizing space resources p 2688 N94-27374
Designing for human presence in space: An introduction to environmental control and life support systems
[NASA-RP-1324] p 2942 N94-27437

SPACE LAW
Contributions to CD Space Committee 1992
[PB94-124401] p 3101 N94-27218

SPACE LOGISTICS
Space Station technology testbed: 2010 deep space transport p 2687 N94-27368

SPACE MAINTENANCE
Space Habitat, assembly and repair facility
p 2691 N94-25696

SPACE MANUFACTURING
Study on melted solution stirring under microgravity
p 2730 N94-25585
Prototype space fabrication platform
[AD-A273904] p 2694 N94-25659
Space Station technology testbed: 2010 deep space transport p 2687 N94-27368
A widely adaptable habitat construction system utilizing space resources p 2688 N94-27374
Prometheus in space: Research Committee on Functional New Material
[JTN-94-80580] p 2761 N94-28002

SPACE MISSIONS
Access to space study
[NASA-TM-109693] p 2685 N94-27151
STS-57 Space Shuttle mission report
[NASA-CR-195739] p 2693 N94-28220
STS-56 Space Shuttle mission report
[NASA-CR-195740] p 2693 N94-28221
Comparison of the lossy image data compressions for the MESUR Pathfinder and for the Huygens Titan Probe
p 2945 N94-28254

SPACE OBSERVATIONS (FROM EARTH)
Contributions to the 23rd ICRC from emulsion chamber experiments at Mt. Chacaltaya and Pamirs
[ICRR-REPT-295-93-7] p 3112 N94-25624
A study of very high energy hadron interactions through observation of cosmic-ray families with visible energy not less than 500 TeV, 3 p 3112 N94-25627
Observation of characteristics of cosmic-ray hadron interactions in uniform-type thick lead chambers at Pamir, 1 p 3112 N94-25628
Observation of characteristics of cosmic-ray hadron interactions in uniform-type thick lead chambers at Pamir, 2 p 3113 N94-25629
Observation of characteristics of cosmic-ray hadron interactions in uniform-type thick lead chambers at Pamir, 3 p 3113 N94-25630
Violation of Feynman scaling law in the forward region
p 3113 N94-25633
Simultaneous observation of families and air showers at Mt. Chacaltaya p 3114 N94-25634

SPACE PERCEPTION
The effect of body orientation on the perception of vertical and horizontal distance in an outdoor setting
p 2915 N94-27461
An investigation of methods for determining depth from focus
[ISBN-0-315-64015-4] p 2988 N94-27645

SPACE PLASMAS
Norwegian ionospheric satellite experiment: High latitude, low Earth orbit plasma measurements
[FFI-93/7025] p 2876 N94-25807
Investigation of plasma instabilities in the polar cusp
[NASA-CR-195212] p 2879 N94-26599
Spectroscopy and dynamics of molecular and ionic impurities embedded in solid hydrogen
[AD-A274149] p 3064 N94-27095
Studies for Io's extended atmosphere and neutral clouds and their impact on the local satellite atmosphere and on the planetary magnetosphere
[NASA-CR-195255] p 3106 N94-27406
Collisionless shock structures of Earth and other planets
[NASA-CR-195257] p 3104 N94-27407
Configuration of the near-Earth plasma sheet
[NASA-CR-195271] p 2883 N94-27438
Acceleration of electrons and ions by strong lower-hybrid turbulence in solar flares
[NASA-TM-109723] p 3111 N94-27953

SPACE PLATFORMS
Prototype space fabrication platform
[AD-A273904] p 2694 N94-25659

SPACE POWER REACTORS
Preliminary reentry safety assessment of the General Purpose Heat Source module for the Cassini mission: Aerospace Nuclear Safety Program
[DE94-001646] p 2699 N94-25926
Space-R thermionic space nuclear power system: Design and technology demonstration
[DE94-001890] p 2699 N94-25929
Space-R thermionic space nuclear power system design and technology demonstration
[DE94-002017] p 2700 N94-25930
Risk perspectives for Topaz 2 flight mission
[DE94-003229] p 2700 N94-25956
Pre-orbital criticality safety for the NEPSTP mission
[DE94-002600] p 3005 N94-26802

SPACE PROBES
Comparison of the lossy image data compressions for the MESUR Pathfinder and for the Huygens Titan Probe
p 2945 N94-28254

SPACE PROCESSING
Design for producing fiberglass fabric in a lunar environment p 2765 N94-25676
Lunar preform manufacturing p 2765 N94-25677
Modelling of the MEA float zone using accelerometer data
[NASA-CR-193933] p 2761 N94-27220
Prometheus in space: Research Committee on Functional New Material
[JTN-94-80580] p 2761 N94-28002

SPACE PROGRAMS
Project Columbiad: Reestablishment of human presence on the Moon p 2689 N94-25687

SPACE SHUTTLE BOOSTERS
Structural analysis of a frangible nut used on the NASA Space Shuttle
[DE94-003672] p 2821 N94-25811
STS-56, RSRM-031, 360L031 KSC processing configuration and data report
[NASA-CR-193922] p 2691 N94-26135
STS-51, RSRM-033, 360T033 KSC processing configuration and data report
[NASA-CR-193923] p 2691 N94-26153
Advanced silver zinc battery development for the SRB and ET range safety subsystems p 2865 N94-28136
STS-55 Space Shuttle mission report
[NASA-CR-195741] p 2692 N94-28199

SPACE SHUTTLE MAIN ENGINE
STS-51 pad abort. OV103-engine 2033 (ME-2) fuel flowmeter sensor open circuit
[NASA-CR-193924] p 2701 N94-26230
Space Shuttle main engine turbopump bearing assessment program
[NASA-TM-108447] p 2833 N94-28265

SPACE SHUTTLE MISSIONS
Prototype space fabrication platform
[AD-A273904] p 2694 N94-25659
STS-55 Space Shuttle mission report
[NASA-CR-195741] p 2692 N94-28199

SPACE SHUTTLE ORBITERS
Berthing of Space Station Freedom using the shuttle remote manipulator system p 2684 N94-26284
Pressure distributions on a 0.02-scale Space Shuttle orbiter nose at Mach 21.5 in helium
[NASA-TM-4495] p 2646 N94-26592
Report of the Shuttle Processing Review Team
[NASA-TM-109728] p 2692 N94-28178

SPACE SHUTTLE PAYLOADS
An approach to studying the reliability of microgravity experiments
[NASA-TM-106489] p 2834 N94-26199
STS-55 Space Shuttle mission report
[NASA-CR-195741] p 2692 N94-28199

SPACE SHUTTLES
Application of Space Shuttle Project Hercules imagery in the investigation of ship cloud tracks
[AD-A274923] p 2692 N94-26529
Access to space study
[NASA-TM-109693] p 2685 N94-27151
STS-55 Space Shuttle mission report
[NASA-CR-195741] p 2692 N94-28199
STS-57 Space Shuttle mission report
[NASA-CR-195739] p 2693 N94-28220
STS-56 Space Shuttle mission report
[NASA-CR-195740] p 2693 N94-28221

SPACE STATION FREEDOM
Assured crew return vehicle post landing configuration design and test p 2697 N94-25671
Automation of closed environments in space for human comfort and safety p 2943 N94-25684
Berthing of Space Station Freedom using the shuttle remote manipulator system p 2684 N94-26284
Autonomous rendezvous and docking for Space Station Freedom p 2684 N94-26286
Structural evaluation of concepts for a solar energy concentrator for Space Station advanced development program
[NASA-TP-3375] p 2695 N94-26609
Space Station evolution study oxygen loop closure
[NASA-CR-193938] p 2941 N94-26788
Designing for human presence in space: An introduction to environmental control and life support systems
[NASA-RP-1324] p 2942 N94-27437

SPACE STATION POWER SUPPLIES
Structural evaluation of concepts for a solar energy concentrator for Space Station advanced development program
[NASA-TP-3375] p 2695 N94-26609
Space Station Freedom NiH2 cell testing program
p 2861 N94-28108
Advanced nickel-hydrogen spacecraft battery development p 2863 N94-28129

SPACE STATION STRUCTURES
Structural design feasibility study of Space Station long spacer truss
[NASA-TM-106346] p 2843 N94-27559

SPACE STATIONS
Space Station technology testbed: 2010 deep space transport p 2687 N94-27368
Risks and issues in fire safety on the Space Station
[NASA-TM-106430] p 2692 N94-27436
An analysis of the loads applied to a heavy Space Station rack during translation and rotation tasks
[NASA-TM-104790] p 2697 N94-28183

SPACE STORAGE
Handbook for handling and storage of nickel-cadmium batteries: Lessons learned
[NASA-RP-1326] p 2702 N94-26613

SPACE SUITS
Extra-Vehicular Activity (EVA) glove evaluation test protocol
[NASA-TM-108442] p 2943 N94-27952

SPACE SURVEILLANCE (GROUND BASED)
Hyperspectral analysis of space objects: Signal to noise evaluation
[AD-A273882] p 2765 N94-25728

SPACE TRANSPORTATION
A comparison of users' and providers' perceptions of critical spacelift vehicle characteristics and capabilities
[AD-A273907] p 2691 N94-26017
Access to space study
[NASA-TM-109693] p 2685 N94-27151
Space Station technology testbed: 2010 deep space transport p 2687 N94-27368
Space transportation vehicle design evaluation using saturated designs p 2693 N94-27928
Lunar Transportation Facilities and Operations Study, option 1
[NASA-CR-195700] p 3109 N94-27982
Lunar Transportation Facilities and Operations Study, option 2
[NASA-CR-195701] p 3109 N94-27983

SPACE TRANSPORTATION SYSTEM FLIGHTS
Debris/ice/TPS assessment and integrated photographic analysis for Shuttle mission STS-60
[NASA-TM-109193] p 2692 N94-27956
STS-55 Space Shuttle mission report
[NASA-CR-195741] p 2692 N94-28199
JSC almanac
[NASA-TM-109702] p 3119 N94-28204
STS-57 Space Shuttle mission report
[NASA-CR-195739] p 2693 N94-28220
STS-56 Space Shuttle mission report
[NASA-CR-195740] p 2693 N94-28221

SPACE TUGS
Hardware design of a grappling/docking device accommodating large lateral and angular misalignments
p 2833 N94-25668

SPACE-TIME FUNCTIONS
The Dirac equation in Kerr spacetime, spheroidal coordinates and the M.I.T. bag model of hadrons
[DE94-601566] p 3006 N94-25886
Dimensional crossover from non-renormalizability to renormalizability
[DE93-613052] p 3006 N94-26193
Vortices in curved spacetime
[DE94-601559] p 3072 N94-26417
The extensions of space-time. Physics in the 8-dimensional homogeneous space D is equal to SU(2,2)/K
[DE93-634336] p 3072 N94-26551
Stochastic space-time, confinement potential and particle propagator
[DE94-606415] p 3074 N94-27680

SPACEBORNE EXPERIMENTS
Proceedings of the 8th Annual Summer Conference: NASA/USRA Advanced Design Program
[NASA-CR-195118] p 3075 N94-25665
Autonomous support for microorganism research in space p 2903 N94-25672
Microgravity ignition experiment p 2761 N94-25707
An approach to studying the reliability of microgravity experiments
[NASA-TM-106489] p 2834 N94-26199
Long Duration Exposure Facility space optics handbook
[AD-A274831] p 3035 N94-26572
Spacelab life sciences 2 post mission report
[NASA-CR-195544] p 2942 N94-27410
Study on posture control and adaptation mechanism under weightlessness: Summary report of ground operations performed for carp experiment (FMPT/L-2) in Space Shuttle mission p 2912 N94-27447
Study on posture control and adaption mechanism under weightlessness: Differences in weight and shape of utricular otolith of carp p 2912 N94-27448
Gamma Large Area Silicon Telescope (GLAST): Applying silicon strip detector technology to the detection of gamma rays in space
[DE94-003451] p 3116 N94-27740
Construction and test of experiment hardware for a space experiment on Spacelab mission IML-2
[DLR-FB-93-23] p 2903 N94-27743

SPACEBORNE TELESCOPES
Feasibility study of a multiaperture telescope for deep-space Earth surveillance
[AD-A273903] p 3102 N94-25658
Project PARAS: Phased array radio astronomy from space p 3081 N94-25703
The PROTEL contamination code
[RXR-93071] p 3040 N94-28202

SPACECRAFT ANTENNAS
Effective conductivity of wire mesh reflectors for space deployable antenna systems
[NASA-CR-191605] p 2788 N94-27770

SPACECRAFT CABINS
First lunar outpost p 2943 N94-25694
Risks and issues in fire safety on the Space Station
[NASA-TM-106430] p 2692 N94-27436

SPACECRAFT CHARGING
IRMA: A program for three-dimensional color display of data
[AD-A273811] p 2959 N94-25879

SPACECRAFT COMMUNICATION
Low-cost unmanned lunar lander
p 2697 N94-25699

SPACECRAFT CONSTRUCTION MATERIALS
X ray computed tomography for emerging aerospace materials and processes development
[AD-A273721] p 2705 N94-25779
NASA Lewis Research Center lean-, rich-burn materials test burner rig
[NASA-CR-194437] p 2680 N94-26141
Development and application of contamination technology for MSFC managed space systems
[NASA-CR-193934] p 2697 N94-27421
Proton irradiation on materials p 3030 N94-27898
Development of methodologies for the estimation of thermal properties associated with aerospace vehicles
p 2846 N94-27920

SPACECRAFT CONTROL
High performance flight computer developed for deep space applications p 2949 N94-26718
Implementing hard real-time systems: A case study
p 2951 N94-26731
Test of onboard real time applications (LICE (tm))
p 2952 N94-26737
Dynamics and robust control for uncertain flexible space systems
[INPE-5510-TAE/020] p 2696 N94-27357
Superfluid helium sloshing dynamics induced oscillations and fluctuations of angular momentum, force and moment actuated on spacecraft driven by gravity gradient or jitter acceleration associated with slew motion
[NASA-CR-193928] p 2799 N94-27931
First experimental assessment of RCS plume-flow field interaction on Hermes leading edge thruster configuration p 2703 N94-28032
Using formal specification in the Guidance and Control Software (GCS) experiment. Formal design and verification technology for life critical systems
[NASA-CR-194884] p 2956 N94-28267

SPACECRAFT DESIGN
MINOTAUR (Maryland's innovative orbital technologically advanced University rocket)
p 2703 N94-25685
Asteroid exploration and utilization
p 3080 N94-25697
Low-cost unmanned lunar lander
p 2697 N94-25699
Low Earth orbit communications satellite
p 2698 N94-25701
Project PARAS: Phased array radio astronomy from space p 3081 N94-25703
Project Minerva: A low-cost manned Mars mission based on indigenous propellant production
p 2760 N94-25705
Project Ares 3 p 2671 N94-25712
Minimum accommodation for aerobrake assembly, phase 2
[NASA-TM-107608] p 2692 N94-27774
Space transportation vehicle design evaluation using saturated designs p 2693 N94-27928
A pressure based charge control system for the DSPSE NiH2 CPV battery p 2863 N94-28127
Artemis common lunar lander. Phase 2: Study results for external review
[NASA-TM-109699] p 2692 N94-28205

SPACECRAFT DOCKING
Hardware design of a grappling/docking device accommodating large lateral and angular misalignments
p 2833 N94-25668
Autonomous rendezvous and docking for Space Station Freedom p 2684 N94-26286

SPACECRAFT DOCKING MODULES
Hardware design of a grappling/docking device accommodating large lateral and angular misalignments
p 2833 N94-25668

SPACECRAFT ELECTRONIC EQUIPMENT
Aspects of the circuit board thermal design
[VTT-PUBS-132] p 2779 N94-25644

SPACECRAFT ENVIRONMENTS
The radiation design handbook
[ESA-PSS-01-609-ISSUE-1] p 2696 N94-27397
Annals of the Research Inst. of Environmental Medicine, Nagoya Univ., volume 44
[REPT-44-VOL-44] p 2911 N94-27442
Comparative measurement of visual stability in cosmic space: Onboard experiment and pre-flight activities
p 2916 N94-27463

SPACECRAFT GUIDANCE
Hardware design of a grappling/docking device accommodating large lateral and angular misalignments
p 2833 N94-25668
High performance flight computer developed for deep space applications p 2949 N94-26718
Using formal specification in the Guidance and Control Software (GCS) experiment. Formal design and verification technology for life critical systems
[NASA-CR-194884] p 2956 N94-28267

SPACECRAFT INSTRUMENTS
Technology development in space projects
[VTT-TIED-1438] p 2682 N94-26249
The radiation design handbook
[ESA-PSS-01-609-ISSUE-1] p 2696 N94-27397

SPACECRAFT LAUNCHING
Project Columbiad: Reestablishment of human presence on the Moon p 2689 N94-25687
Comet nucleus and asteroid sample return missions
p 2689 N94-25692
Access to space study
[NASA-TM-109693] p 2685 N94-27151
Debris/ice/TPS assessment and integrated photographic analysis for Shuttle mission STS-60
[NASA-TM-109193] p 2692 N94-27956
Lunar Transportation Facilities and Operations Study, option 2
[NASA-CR-195701] p 3109 N94-27983

SPACECRAFT MAINTENANCE
Space Habitat, assembly and repair facility
p 2691 N94-25696
Orbit transfer rocket engine technology program
[NASA-CR-189229] p 2702 N94-26542

SPACECRAFT MODELS
A virtual environment for satellite modeling and orbital analysis in a distributed interactive simulation
[AD-A274114] p 2694 N94-25904

SPACECRAFT MODULES
Assured crew return vehicle post landing configuration design and test p 2697 N94-25671
First lunar outpost p 2943 N94-25694

SPACECRAFT MOTION
Superfluid helium sloshing dynamics induced oscillations and fluctuations of angular momentum, force and moment actuated on spacecraft driven by gravity gradient or jitter acceleration associated with slew motion
[NASA-CR-193928] p 2799 N94-27931

SPACECRAFT PERFORMANCE
Nickel cadmium battery operations on-orbit: Trials, tribulations, and success on the Upper Atmosphere Research Satellite p 2862 N94-28120

SPACECRAFT POWER SUPPLIES
Manned mission to Mars with periodic refueling from electrically propelled tankers p 2689 N94-25670
Low-cost unmanned lunar lander
p 2697 N94-25699
Small low mass advanced PBR's for bi-modal operation
[DE94-003201] p 2699 N94-25798
Parametric analysis of the space power plants on the base of criterion of specific mass in generalized design variants
[DE93-634153] p 2701 N94-26166
NSWC Crane Aerospace Cell Test History Database
p 2860 N94-28102
Advanced energy storage for space applications: A follow-up p 2860 N94-28103
Battery study for the Mars Environmental Survey (MESUR) Pathfinder p 2860 N94-28105
Ni-H2 cell characterization for INTELSAT programs
p 2861 N94-28109
Cycle life versus depth of discharge update on modeling studies — Nickel-Hydrogen Batteries
p 2862 N94-28115
Charge efficiency of Ni/H2 cells during transfer orbit of Telstar 4 satellites p 2862 N94-28117
Orbital management and design considerations for NiCd satellite power systems p 2862 N94-28118
TOPEX/Poseidon battery performance during the first year of operation p 2862 N94-28119
Nickel cadmium battery operations on-orbit: Trials, tribulations, and success on the Upper Atmosphere Research Satellite p 2862 N94-28120
Performance test results of ETS-6 Ni-Cd cells
p 2863 N94-28121
Discriminating performance parameters for 50 amp-hour and 60 amp-hour nickel-cadmium plates and battery cells p 2863 N94-28123
Some observations on battery charge control
p 2863 N94-28125
Construction of temperature compensated constant voltage (VT) curves for super Ni-Cd (tm) cells
p 2863 N94-28126

A pressure based charge control system for the DSPSE NiH2 CPV battery p 2863 N94-28127
Advanced nickel-hydrogen spacecraft battery development p 2863 N94-28129
Development of nickel-metal hydride cell: An update p 2864 N94-28130
Determination of thermal properties of commercial Ni-MH cells p 2864 N94-28132

SPACECRAFT PROPULSION
Systematic Propulsion Optimization Tools (SPOT) p 2976 N94-25666
Small low mass advanced PBR's for bi-modal operation [DE94-003201] p 2699 N94-25798
Parametric analysis of the space power plants on the base of criterion of specific mass in generalized design variants [DE93-634153] p 2701 N94-26166
Space Station technology testbed: 2010 deep space transport p 2687 N94-27368
Inertial electrostatic confinement as a power source for electric propulsion p 2688 N94-27373
Rocket engine numerical simulation p 2688 N94-27375

SPACECRAFT SHIELDING
Mounting of SSM's [VTT-TIED-1442] p 2695 N94-26250
Physics of debris clouds from hypervelocity impacts [NASA-CR-193932] p 2696 N94-26791

SPACECRAFT STABILITY
An approximate solution for the spinup dynamics of near axisymmetric axial gyrostats using the method of multiple scales [AD-A273723] p 2698 N94-26223
Superfluid helium sloshing dynamics induced oscillations and fluctuations of angular momentum, force and moment actuated on spacecraft driven by gravity gradient or jitter acceleration associated with slew motion [NASA-CR-193928] p 2799 N94-27931

SPACECRAFT STRUCTURES
Project PARAS: Phased array radio astronomy from space p 3081 N94-25703
Proceedings of Damping 1993, volume 2 [AD-A274227] p 2840 N94-26953
Proceedings of Damping 1993, volume 3 [AD-A274228] p 2840 N94-27008

SPACECRAFT TEMPERATURE
User's guide for the thermal analyst's help desk expert system [NASA-CR-194885] p 2695 N94-26103

SPACECRAFT TRAJECTORIES
Manned mission to Mars with periodic refueling from electrically propelled tankers p 2689 N94-25670
An approximate solution for the spinup dynamics of near axisymmetric axial gyrostats using the method of multiple scales [AD-A273723] p 2698 N94-26223
Arithmetic performances of onboard computers p 2952 N94-26738
A survey of uncontrolled satellite reentry and impact prediction [AD-A274903] p 2695 N94-26750

SPACECREWS
Design and development of the second generation Mars Habitat p 2943 N94-25693
First lunar outpost p 2943 N94-25694
Psychophysiology in microgravity and the role of exercise p 2936 N94-28374

SPACELAB
Spacelab life sciences 2 post mission report [NASA-CR-195544] p 2942 N94-27410
Construction and test of experiment hardware for a space experiment on Spacelab mission IML-2 [DLR-FB-93-23] p 2903 N94-27743

SPACERS
Structural design feasibility study of Space Station long spacer truss [NASA-TM-106346] p 2843 N94-27559

SPALLATION
Simulations of terrestrial in-situ cosmogenic-nuclide production [DE94-004999] p 3117 N94-27826

SPANWISE BLOWING
Effects, limits, and limitations of spanwise blowing p 2659 N94-28027

SPATIAL DISTRIBUTION
Spatial symmetry, local integrability and tetrahedron equations in the Baxter-Bazhanov model [DE93-634348] p 3002 N94-26038
Characterization of the energy deposition produced by the primary electron beam on the EXCEDE 3 program [AD-A274453] p 3033 N94-27084
Effect of precipitate structure on hot deformation of Al-Mg-Mn alloys [DE94-004596] p 2741 N94-27622

SPATIAL RESOLUTION
Unsegmented electromagnetic calorimeter prototype. Energy and coordinate resolution [DE93-634185] p 2810 N94-26396
The OPAL vertex detector [ISBN-0-315-51152-4] p 2812 N94-27257
Simulation of the Indian and East-Asian summer monsoon in the ECMWF model: Sensitivity to horizontal resolution [DE94-004276] p 2897 N94-27571

SPECIFIC HEAT
Bulletin of the Institute for Chemical Reaction Science, Tohoku University, volume 2 [JTN-94-80602] p 2717 N94-27385
High-temperature and high-pressure flow calorimeter p 2718 N94-27390

SPECIFIC IMPULSE
Inertial electrostatic confinement as a power source for electric propulsion p 2688 N94-27373

SPECIFICATIONS
Primary standards laboratory report 1st half 1993 [DE94-003138] p 2762 N94-26027
The CODE-TOP (COncurrent system DEvelopment using Transformations Of Predicate-transition nets) method: Examples of using it for system architecture specification, software specification, and code generation p 2953 N94-26744
Specification performance optimization and executive generation for onboard multiprocessor real time application with SynDEx p 2954 N94-26745
Semantics of MANIFOLD: Specification in ASF+SDF and extension [CWI-CS-R9269] p 2971 N94-27575
Telecommand decoder specification [ESA-PSS-04-151-ISSUE-1] p 2693 N94-27583
ARM: Abstract Rewriting Machine [CWI-CS-R9330] p 2974 N94-27794
Using formal specification in the Guidance and Control Software (GCS) experiment. Formal design and verification technology for life critical systems [NASA-CR-194884] p 2956 N94-28267

SPECKLE INTERFEROMETRY
Properties of the near-axis bispectrum applied to high-resolution astronomical imaging [ISBN-0-315-85247-X] p 3103 N94-27302

SPECKLE PATTERNS
Response of an airborne synthetic aperture radar to sea ice in the marginal ice zone [ISBN-0-315-84243-1] p 2849 N94-26668
Theoretical and experimental analysis of the spatial and temporal behaviour of the intensity of an electro-magnetic wave reflected from a diffuse target after passing through a turbulent atmosphere [ITN-94-85230] p 2774 N94-27234

SPECTRA
Multivariate spectral analysis to extract materials from multispectral data [AD-A274142] p 2709 N94-27135
A comparison of spectral decorrelation techniques and performance evaluation metrics for a wavelet-based, multispectral data compression algorithm p 2946 N94-28258

SPECTRAL BANDS
Zodiacal light data investigation. Interim results for the Earthlimb Clutter Experiment [AD-A274461] p 3104 N94-27265
Cooling the Martian atmosphere: The spectral overlap of the C02 15 micrometers band and dust p 3107 N94-27886
Wavelet compression techniques for hyperspectral data p 2947 N94-28263

SPECTRAL CORRELATION
A comparison of spectral decorrelation techniques and performance evaluation metrics for a wavelet-based, multispectral data compression algorithm p 2946 N94-28258

SPECTRAL EMISSION
A numerical solution to the one and two dimensional line radiative transfer equation [ISBN-0-315-84258-X] p 2994 N94-26640

SPECTRAL ENERGY DISTRIBUTION
Energy concentration in high energy hadron-gamma families p 3113 N94-25632
Catalog of absolutely calibrated, range normalized, wideband, electric field waveforms from triggered lightning flashes in Florida [AD-A273793] p 2892 N94-25873
Characterization of the energy deposition produced by the primary electron beam on the EXCEDE 3 program [AD-A274453] p 3033 N94-27084
Investigations of the dynamical evolution of protoplanetary nebulae [NASA-CR-195278] p 3105 N94-27428

SPECTRAL METHODS
Rendering of three-dimensional data sets derived from finite-difference and spectral methods [AD-A273724] p 3096 N94-25997
Recent advances in the spectral element method p 2657 N94-28348

SPECTRAL REFLECTANCE
In situ x ray reflectivity measurements of thin film structural evolution [DE94-002289] p 3051 N94-25944
The optical properties of high-T(c) superconductors grown by pulsed laser deposition [ISBN-0-315-84917-7] p 3039 N94-27962

SPECTRAL RESOLUTION
How well was total ozone abundance inferred with Mariner 9? p 3108 N94-27891

SPECTRAL SIGNATURES
Mapping coastal habitats using an imaging spectrometer [ISBN-0-315-84362-4] p 2848 N94-26664

SPECTRAL THEORY
Short-range cloud amount forecasting with model output statistics [AD-A274769] p 2895 N94-26798
An enhanced global spectral model [PL-TR-92-2011] p 2898 N94-28223

SPECTROMETERS
Study on neutron activation analysis [DE93-632191] p 3017 N94-26116

SPECTROPHOTOMETERS
Reflectometer employing an integrating sphere and lens-mirror concentrator [AD-D016061] p 3039 N94-27676

SPECTRORADIOMETERS
Radiometric, spectral, and effectiveness equipment [AD-A274208] p 3037 N94-27066

SPECTROSCOPIC ANALYSIS
Study on analyzing method establishment for metallic material development p 2729 N94-25578
Hook spectroscopy as an atomic number density diagnostic applied to laser-ablated copper plasmas [DE94-002645] p 3042 N94-26081
Gordon Research Conference on the Physics and Chemistry of Laser Diagnostics in Combustion [AD-A274609] p 2716 N94-26893
Determination of lead isotope ratios in seawater by purge and trap GC/MS after ethylation p 2870 N94-28152

SPECTROSCOPY
Spectroscopic and vibrational energy transfer studies in molecular bromine [AD-A273795] p 3014 N94-25875
Heavy quark production and spectroscopy [DE94-003619] p 3015 N94-25935
Optimization of experimental conditions in IR reflectance determination of BPSG properties [DE94-002742] p 2713 N94-25978
Multivariate calibration applied to near-infrared spectroscopy for the quantitative analysis of dilute aqueous solutions [DE94-003231] p 2716 N94-26794
Meson spectroscopy and particle astrophysics [DE94-001799] p 3115 N94-27003
Charmonium physics at a tau-charm factory [PB94-124344] p 3024 N94-27199

SPECTRUM ANALYSIS
Hyperspectral analysis of space objects: Signal to noise evaluation [AD-A273882] p 2765 N94-25728
The Latin American conference on the applications of the Moessbaer effect [DE93-615942] p 3051 N94-25912
Buckyball microwave plasmas: Fragmentation and diamond-film growth [DE94-003209] p 3053 N94-26031
BATSE Data Analysis [NASA-CR-195545] p 3114 N94-26685
The continuum spectral characteristics of gamma ray bursts observed by BATSE p 3114 N94-26686
ARM Fourier transform spectrometer data analysis tools [DE94-000865] p 2895 N94-26697
A current evaluation of the digital beamforming testbed at Rome Laboratory [AD-A274311] p 3032 N94-26881
Multivariate spectral analysis to extract materials from multispectral data [AD-A274142] p 2709 N94-27135
Spectral and temporal correlations of multifrequency waves in the turbulent atmosphere [ITN-94-85229] p 2774 N94-27233
Trace organic chemical detection using an ultraviolet excitation molecular beam fluorometer [DE94-002649] p 2704 N94-27708
SPECTRUM analysis of multispectral imagery in conjunction with wavelet/KLT data compression [DE94-003961] p 2851 N94-27727

ACES spectral display software: User manual
[SKL-1600-99-002] p 2973 N94-27762

Multispectral and textural classifications of a SPOT HRV-1 image, region of Sherbrooke, Quebec, Canada
[ISBN-0-315-84978-9] p 2851 N94-27863

Cooling the Martian atmosphere: The spectral overlap of the C02 15 micrometers band and dust
p 3107 N94-27886

Investigation of spectral analysis techniques for randomly sampled velocimetry data
p 3009 N94-27924

NMR study of quasicrystal Al(70)Pd(20)T(M10) alloy (T(M):Cr, Mn, Fe, and Co) p 2745 N94-28162

SPECULAR REFLECTION

Illumination in diverse codimensions
[NASA-CR-191596] p 2971 N94-27572

SPEECH

Researches of the Electrotechnical Laboratory. No. 955: Speech recognition by description of acoustic characteristic variations
[JTN-94-80604] p 2775 N94-27249

SPEECH RECOGNITION

A rough set approach to speech recognition
[ISBN-0-315-83894-9] p 2769 N94-26619

Signal- and listener-based factors in complex auditory pattern perception
[AD-A274148] p 2939 N94-27094

Researches of the Electrotechnical Laboratory. No. 955: Speech recognition by description of acoustic characteristic variations
[JTN-94-80604] p 2775 N94-27249

SPEED CONTROL

Variable speed controller p 2943 N94-25678

SPHERES

Hardware design of a spherical mini-rover
p 2833 N94-25669

Design and development of the second generation Mars Habitat p 2943 N94-25693

Dielectric polarizability of sphere with arbitrary anisotropy
[PB94-133113] p 2779 N94-28397

SPHERICAL WAVES

Mach reflection of spherical detonation waves
[DE93-016604] p 2797 N94-27705

SPIN

Spin-polarized atomic hydrogen: Devices and phenomena
[ETN-94-95342] p 3016 N94-26002

SPIN DYNAMICS

Optical conductivity and resistivity in the two-band Emery model
[DE94-601943] p 3051 N94-25945

Crossover between BCS and performed-Boson theories with increasing interactions
[DE93-019018] p 3017 N94-26078

SPIN GLASS

Technical report of ISSP. Ser. A, no. 2673: Two successive spin glass transitions in non-diluted Heisenberg-like spin glass Ni(0.42)Mn(0.58) TiO3
[JTN-94-80559] p 2756 N94-27241

SPIN TESTS

The experimental behavior of spinning pretwisted laminated composite plates
[NASA-CR-195220] p 2711 N94-27352

SPINEL

Transparent polycrystalline body with high ultraviolet transmittance, process for making and applications thereof
[CA-PATENT-1325511] p 3066 N94-27276

Damage growth in MgAl2O4 crystals by Xe ion irradiations
[DE94-005009] p 3069 N94-27828

SPINOR GROUPS

On the relativistic invariant representation of arbitrary bilinear combinations of Dirac spinors
[DE93-634343] p 3019 N94-26456

Relativistic two-body system in 1+1-dimensional QED. 1: On the circle S1
[DE94-603716] p 3067 N94-27647

SPLINE FUNCTIONS

Approximate solution of the fourth order initial value problem using deficient spline polynomials
[DE93-613023] p 2991 N94-25880

On a spline-approximation method for solving ordinary differential equations
[DE93-634290] p 2994 N94-26471

Unified approach for direct and inverse boundary layer prediction using cubic spline collocation
p 2653 N94-28326

SPLINES

Radial basis function approximation: From gridded centers to scattered centers
[AD-A274184] p 2998 N94-27103

SPONTANEOUS EMISSION

Enhancement of the rate of radiative processes in the field of a magnetic monopole
[DE94-603717] p 3074 N94-27696

SPOT (FRENCH SATELLITE)

Design principles of onboard management of a Sun synchronous satellite p 2950 N94-26722

SPOT WELDS

Study on interfacial reaction analysis at interfacial joining p 2728 N94-25574

SPRAYED COATINGS

Study on film generation phenomena by particle deposition p 2728 N94-25575

Attachment techniques for high temperature strain
[AD-A274766] p 2811 N94-26568

SPRAYERS

Impact of improved materials and cabin water spray on commuter aircraft postcrash fire survivability
[AD-A274421] p 2660 N94-27081

SPRAYING

Cryogenic insulation studies
[NASA-CR-195266] p 2756 N94-27429

SPREAD SPECTRUM TRANSMISSION

Evaluation of an Acoustic Charge Transport (ACT) device for adaptive interference suppression in spread spectrum communications systems
[AD-A274073] p 2765 N94-25647

Analysis and simulation of a GPS receiver design using combined delay-lock and modified tanlock loops
[AD-A274037] p 2664 N94-25810

Code division multiple access local area network communications employing fiber optic signal processing techniques
[AD-A274897] p 3096 N94-26180

Kalman filtering of narrowband interference from direct sequence spread spectrum communications systems
[ISBN-0-315-84011-0] p 2784 N94-26627

The performance of nonorthogonal noncoherent frequency hopped M-ary FSK in additive white Gaussian noise, fading and jamming
[ISBN-0-315-85243-7] p 2775 N94-27301

SPUTTERING

Aluminum-ion sputtering from Al surfaces with very-low-energy ions
[REPT-A-2668] p 2733 N94-26073

Studies of thin-film growth, adsorption, and oxidation by in situ, real-time, and ex situ ion beam analysis
[DE94-002907] p 3055 N94-26275

The ZnO thin films with C-axis orientation prepared on the room temperature substrate by the ECR multipolar plasma sputtering method
[DE94-605039] p 2758 N94-27857

SQUARE WAVES

Multiple model adaptive control of a large flexible space structure with purposeful dither for enhanced identifiability
[AD-A274132] p 2987 N94-27122

SQUEEZE CASTING

Squeeze casting: A literature review
[PB94-124575] p 2741 N94-27326

SQUIBS

Effects of repeating resistance testing on firing ability of igniter EP360-3
[AD-A274814] p 2759 N94-26486

SQUID (DETECTORS)

Demonstration of monolithic co-fabrication of Y1Ba2Cu3O7-Sigma and CMOS devices on the same sapphire substrate
[AD-A274757] p 3059 N94-26566

STABILITY

Zinc(2) oxide stability in alkaline sodium phosphate solutions at elevated temperatures
[DE94-003316] p 2715 N94-26320

On the (Phi)(sub 0)-stability of functional differential equations
[DE94-601507] p 3006 N94-26460

A characterization of stable models using a non-monotonic operator
[CWI-CS-R9315] p 2970 N94-27543

Unsteady aspects of hot gas reingestion and statistical analysis p 2676 N94-28019

STABILITY DERIVATIVES

Linear modeling of rotorcraft for stability analysis and preliminary design
[AD-A274869] p 2677 N94-26192

A finite wake theory for two-dimensional rotary wing unsteady aerodynamics
[AD-A274921] p 2645 N94-26535

STABILITY TESTS

Numerical experiment on finite element method for matching data
[DE94-701208] p 3000 N94-27731

Multidisciplinary aeroelastic analysis of a generic hypersonic vehicle
[NASA-TM-4544] p 2691 N94-27868

STABILIZATION

Numerical simulation of plasma vertical position stabilization in ITER
[DE93-634588] p 3044 N94-26510

The addition of molecular oxygen to hydroperoxy-propyl radicals
[DE94-003662] p 2760 N94-27725

Passive stabilization of MHD instabilities at high (beta)n in the HBT-EP tokamak
[DE94-003317] p 3047 N94-27735

Stabilization of polyaniline solutions
[DE94-003958] p 2704 N94-27745

STABLE OSCILLATIONS

Regrouping of the beam in the IHEP PS for the UNK p-p programs
[DE93-634021] p 3032 N94-26164

STAGNATION PRESSURE

Pressure-gain combustion
[DE94-002975] p 2719 N94-27712

STAINLESS STEELS

R and D for creation, measurement, application of ultra-high vacuum p 2723 N94-25549

Study on high temperature damage control and life improvement p 2729 N94-25580

Study on evaluation of crack generation and crack growth behaviors under static loading at high temperature and under combined loading p 2730 N94-25583

Reference electrodes for solid polymer electrolytes
[DE94-004583] p 2780 N94-25806

New equation of state for stainless steel 347
[DE94-004189] p 2732 N94-25974

Effect of loading mode on the fracture toughness of a reduced activation ferritic/martensitic stainless steel
[DE94-004290] p 2732 N94-25987

Guidelines for controlling stress corrosion cracking and corrosion fatigue of stainless steels: A literature review
[VTT-TIED-1420] p 2837 N94-26262

Stability of reference masses 2: The effect of environment and cleaning methods on the surfaces of stainless steel and allied materials
[NPL-DMM(A)-95] p 2738 N94-26653

Vapor deposition of copper on stainless steel 304L
[DE94-001945] p 2740 N94-27006

Modification of a model for fatigue life predictions based on level-crossing
[PB94-123395] p 2842 N94-27198

Isothermal corrosion testing of steels in molten nitrate salts
[DE94-004695] p 2742 N94-27755

Upset welding process for 21-6-9 spherical vessels
[DE93-018194] p 2832 N94-28229

STANDARD DEVIATION

Example of statistical techniques applied to analysis of effects of small changes
[ESDU-93023] p 2670 N94-28094

STANDARDIZATION

The question of standards for digital interactive television
[AD-A273872] p 2765 N94-25725

Standardizing exchange formats
[DE93-616798] p 3095 N94-25751

Development of the Air Force contingency contracting course framework
[AD-A273921] p 3093 N94-25895

International energy: Research organizations, 1988-1992
[DE93-017267] p 3098 N94-26398

Standardize Ada hard real-time services?
p 2951 N94-26729

MILCOM 92 and standardization for HF-communication. A study tour to the USA in October 1992
[PB94-124427] p 2774 N94-27219

Software assurance standard
[NASA-TM-109705] p 2975 N94-27992

Air Force standards for nickel hydrogen battery
p 2862 N94-28116

Open communication in manufacturing automation
[PB94-132479] p 2976 N94-28377

STANDARDS

Primary standards laboratory report 1st half 1993
[DE94-003138] p 2762 N94-26027

CEN-VAMAS round robin on grain size measurement for advanced technical ceramics
[VAMAS-TR-12] p 2752 N94-26654

Standardize Ada hard real-time services?
p 2951 N94-26729

Guidelines for unlubricated sliding wear tests. Part 1: General approach
[PB94-119666] p 2825 N94-27322

Technical Report of National Research Institute of Fisheries Engineering: Fishing Boat and Instrument, No. 12
[JTN-94-80595] p 2764 N94-27976

Software assurance standard
[NASA-TM-109705] p 2975 N94-27992

Controls, monitoring and performance measurements
p 2831 N94-28086
Air Force standards for nickel hydrogen battery
p 2862 N94-28116
Air traffic administration enroute to Europe
p 2661 N94-28238
Comparison of the lossy image data compressions for the MESUR Pathfinder and for the Huygens Titan Probe
p 2945 N94-28254

STANDING WAVE RATIOS
ADC test support program
[AD-A274819] p 2783 N94-26491

STAR FORMATION
Investigations of the dynamical evolution of protoplanetary nebulae
[NASA-CR-195278] p 3105 N94-27428

STARBURST GALAXIES
Weak bump quasars
[NASA-CR-195267] p 3103 N94-27933

STARTING
Engine starting and stopping p 2828 N94-28047

STATE ESTIMATION
Iterative methods for the WLS state estimation on RISC, vector, and parallel computers
[DE94-004260] p 3000 N94-27569

STATE VECTORS
Symbolic model checking for sequential circuit verification
[AD-A274375] p 2786 N94-27061

STATIC LOADS
Investigation of compressive behavior for metal matrix composites with a circular hole
[AD-A273835] p 2705 N94-25739

STATIC PRESSURE
Computation of static pressure downstream of a normal shock for hypersonic flight (ambient temperature known)
[ESDU-93020] p 2649 N94-28091

STATISTICAL ANALYSIS
Study on knowledge extraction and systematization for material design p 2727 N94-25568
Vulnerability assessment using a fuzzy logic based method
[AD-A274075] p 2957 N94-25649
Improved quality of reconstructed images through sifting of data in statistical image reconstruction
[AD-A273884] p 3034 N94-25730
Developing prediction regions for a time series model for hurricane forecasting
[AD-A273777] p 2892 N94-25861
Surfaces allowing for fractional statistics
[DE93-614526] p 3002 N94-25910
An evaluation of the utility of ground-based high resolution interferometer (GB-HIS) soundings of the planetary boundary layer
[DE94-000960] p 3106 N94-25981
Statistical quality management
[MEMO-COSOR-92-43] p 2834 N94-26008
Towards a theory of growing surfaces: Mapping two-dimensional Laplacian growth onto Hamiltonian dynamics and statistics
[DE94-002636] p 2991 N94-26079
Quantum statistical inference for density estimation
[DE94-002625] p 3073 N94-26805
The use of EEG as a workload assessment tool in flight test
[AD-A274568] p 2910 N94-26847
Some contributions to the theory of monotone dependence
[PB94-124922] p 3004 N94-27051
Enhanced tracking of airborne targets using forward looking infrared and laser return measurements
[AD-A274181] p 3037 N94-27102
Limit theorems for functionals of Markov processes and renormalizable stable fields
[AD-A274645] p 3004 N94-27106
Research in improved assessment of software reliability
[AD-A274161] p 2968 N94-27140
Is probability of frequency too narrow?
[DE94-000687] p 3004 N94-27612
Analysis of S-wave seismogram envelope of deep earthquakes and estimation of random inhomogeneities in the Kanto-Tokai area p 2886 N94-27988
Unsteady aspects of hot gas reingestion and statistical analysis p 2676 N94-28019
Weak coupling in statistical energy analysis ion Research, Univ. of Southampton, Southampton SO9 5NH, England)
[ISVR-TR-228] p 2832 N94-28174

STATISTICAL CORRELATION
Aspects of goodness-of-fit
[AD-A274826] p 3003 N94-26495
Correlation between electrical activity and the size of single sinoatrial node cells p 2907 N94-27513

STATISTICAL DISTRIBUTIONS
Bisexual branching diffusions
[AD-A274698] p 3008 N94-26374
Fuzzy robust statistics for application to the fuzzy c-means clustering algorithm
[AD-A274719] p 3003 N94-26436
Statistical mechanical properties of Z(N)(sup n-1) broken model
[DE93-634344] p 2993 N94-26457
Some contributions to the theory of monotone dependence
[PB94-124922] p 3004 N94-27051
Variability of measured sonic boom signatures
p 2651 N94-28197

STATISTICAL MECHANICS
Quantum statistical inference for density estimation
[DE94-002625] p 3073 N94-26805
Refractive and dielectric properties of helium, argon and nitrogen gases
[PB94-123783] p 3008 N94-26851

STATISTICAL TESTS
Aspects of goodness-of-fit
[AD-A274826] p 3003 N94-26495
Estimation and tests-of-fit for the three parameter Weibull distribution
[AD-A274827] p 3004 N94-26496
Wieand's theorem
[PB94-126711] p 3004 N94-27223
Example of statistical techniques applied to analysis of effects of small changes
[ESDU-93023] p 2670 N94-28094

STATISTICAL WEATHER FORECASTING
Developing prediction regions for a time series model for hurricane forecasting
[AD-A273777] p 2892 N94-25861

STATISTICS
Monograph of the Aviation Epidemiology Data Register for CY 1992
[AD-A274400] p 2911 N94-27130

STATORS
Experimental contribution to the study of secondary flows in centrifugal turbopump stator components
[ECL-92-35] p 2789 N94-25654
Wake passage effects on the losses in a linear turbine cascade
[AD-A273794] p 2790 N94-25874
Laser Doppler velocimetry in a low speed multistage compressor
[AD-A274836] p 2818 N94-26498

STEADY FLOW
Evaluation of a concentration probe for application in a supersonic flow field
[AD-A273915] p 2643 N94-25592

STEADY STATE
Decay of non-equilibrium polariton condensate in semiconductors
[DE94-604016] p 3068 N94-27678
Ion-driven permeation of deuterium in metals
[DE94-701104] p 2744 N94-27876
Gas-turbine engine steady-state behavior
p 2828 N94-28044
Transient performance p 2828 N94-28045

STEAM FLOW
Simulation: A tool for steam plant dynamic analysis
p 2831 N94-28084
Steam plant: Steam turbines for combined cycles
p 2831 N94-28085

STEAM TURBINES
Knowledge organization in intelligent tutoring systems for diagnostic problem solving in complex dynamic domains
[AD-A273986] p 2984 N94-25899
Combined Cycles for Power Plants
[VKI-LS-1993-08] p 2830 N94-28077
Introduction to combined cycles p 2789 N94-28078
Thermodynamics of combined cycle plant
p 2831 N94-28079
Steam plant for combined cycles: Heat recovery steam generators, design principles, and construction details
p 2831 N94-28083
Simulation: A tool for steam plant dynamic analysis
p 2831 N94-28084
Steam plant: Steam turbines for combined cycles
p 2831 N94-28085

STEEL STRUCTURES
Study on fatigue crack propagation characteristics around welded joint interface in complexed conditions
p 2730 N94-25584
The structural behaviour of the steel or composite concrete and steel frames and the connections of frame members during the fire: A literature review
[VTT-TIED-1437] p 2837 N94-26307
Geometry changes in the elastic-plastic analysis of steel spatial skeletal structures
[IFTR-37/1993] p 2839 N94-26825
Modification of a model for fatigue life predictions based on level-crossing
[PB94-123395] p 2842 N94-27198

STEELS
Interactions between corrosion fatigue and stress corrosion crack on steel for light water reactors
p 2722 N94-25547
Preparation of creep data sheet: Material strength data sheet p 2723 N94-25548
Knowledge base systems for chemical compounds designing support p 2723 N94-25550
Fundamental study on monitoring technology on local surface damages p 2724 N94-25555
Microstructural development in low activation ferritic alloys irradiated to 200 dpa at 420 C
[DE94-004269] p 2731 N94-25803
General Motors Corporation and Pacific Northwest Laboratory staff exchange: Inspection of case hardened steels and metal-matrix composites
[DE94-003470] p 2706 N94-25982
Cracking of textured zinc coating during forming process
[DE94-003414] p 2750 N94-26085
An experimental study on the effects of compressive stress on the fatigue crack growth of low-alloy steel
[DE94-004447] p 2737 N94-26582
The influence of weld metal alloying additions to extend the heat input range for the submerged arc welding of high strength steels
[AD-A274284] p 2738 N94-26679
Evaluation of crack arrest fracture toughness of parent plate, weld metal and heat affected zone of BIS 812 EMA ship plate steel
[AD-A274871] p 2839 N94-26859
The role of point defect clusters in reactor pressure vessel embrittlement
[DE94-001122] p 2739 N94-26931
Development and application of contamination technology for MSFC managed space systems
[NASA-CR-193934] p 2697 N94-27421
Fatigue propagation behaviour of short cracks (1-2 mm) in steels
[ESDU-93033] p 2845 N94-28145
Method of bonding molybdenum to steel
[AD-D016079] p 2747 N94-28187

STEERABLE ANTENNAS
Flight testing of GPS and GPS-aided systems
[NLR-TP-92151-U] p 2666 N94-27831

STEERING
Studies of non-linear optical effects for agile beam steering
[AD-A273998] p 3034 N94-25902
Theoretical aspects of the agile mirror
[AD-A274890] p 2767 N94-26177

STELLAR ENVELOPES
Investigations of the dynamical evolution of protoplanetary nebulae
[NASA-CR-195278] p 3105 N94-27428

STELLAR MASS EJECTION
Solar-geophysical data number 590, October 1993. Part 2: (Comprehensive reports). Data for April 1993, and miscellaneous
[PB94-125911] p 3110 N94-27054
Solar-geophysical data number 591, November 1993. Part 2: (Comprehensive reports). Data for May 1993 and miscellaneous
[PB94-134830] p 3111 N94-28360

STELLAR MODELS
Chaotic dynamics of the solar cycle
[AD-A274315] p 3110 N94-26883
Investigations of the dynamical evolution of protoplanetary nebulae
[NASA-CR-195278] p 3105 N94-27428

STELLAR RADIATION
An April 1991 outburst from 4U0115+63 observed by BATSE
[NASA-CR-195252] p 3116 N94-27440

STELLAR ROTATION
Chaotic dynamics of the solar cycle
[AD-A274315] p 3110 N94-26883

STELLAR SPECTRA
BATSE Data Analysis
[NASA-CR-195545] p 3114 N94-26685
Solar-geophysical data number 590, October 1993. Part 1: (Prompt reports). Data for September, August 1993, and late data
[PB94-125903] p 3110 N94-27053

STELLAR SPECTROPHOTOMETRY
In search of Nemesis p 2888 N94-28297

STELLARATORS
Fusion reactor systems studies
[DE94-003162] p 3046 N94-27686

STEREOPHOTOGRAPHY
On line quantification of crystal surfaces by stereo imaging
[NASA-CR-195277] p 3066 N94-27561

STEREOSCOPIC VISION

Parallel algorithm for dominant points correspondences in robot binocular stereo vision p 2686 N94-27364

An algorithm for stereo correspondence problems on the analogy of human vision [NAL-TR-1185] p 2940 N94-27584

Visual surface perception: Surface reconstruction from shading and stereo [ISBN-0-315-60974-5] p 2975 N94-27872

STIFFENING

Investigation of the bond strength of a discrete skin-stiffener interface [NLR-TP-92183-U] p 2670 N94-27796

STIFFNESS

Experimental and numerical vibration analyses of a stiffened panel [VTT-PUBS-129] p 2836 N94-25650

Formulae for the buckling of simply-supported corrugated panels of orthotropic material under shear load [PB94-126547] p 2840 N94-26911

STIFFNESS MATRIX

On the error committed by stopping the Newton iteration in implicit Runge-Kutta methods [TW-93-02] p 2992 N94-26229

STIMULATED EMISSION

Light emitting porous silicon [AD-A274152] p 3038 N94-27137

Observation of stimulated emission from an MBE grown GaN film on sapphire [DE94-003638] p 3068 N94-27724

STIMULATION

Endogeneous and exogenous control of visual selection: A review of the literature [AD-A273761] p 2908 N94-25871

Development of stimulus-seeking scale for expecting individual differences against confinement stress p 2915 N94-27460

Effect of PGE2 receptor agonists butaprost, M and B 28767 and an antagonist AH 6809 on the BK response of visceral polymodal receptors p 2906 N94-27494

Analysis of the Electrically Evoked Response (EER) of the cat p 2908 N94-27519

Electrical stimulation in exercise training p 2935 N94-28371

The value of electrical stimulation as an exercise training modality p 2936 N94-28372

STIRRING

Study on melted solution stirring under microgravity p 2730 N94-25585

STOCHASTIC PROCESSES

The application of simulated annealing to stochastic systems [AD-A273850] p 3001 N94-25607

Stochastic resonance in a periodic potential system under a constant force [DE93-616817] p 3008 N94-25831

Modeling defect production in high energy collision cascades [DE94-003810] p 3017 N94-26049

Towards a theory of growing surfaces: Mapping two-dimensional Laplacian growth onto Hamiltonian dynamics and statistics [DE94-002636] p 2991 N94-26079

Eleventh Symposium on Energy Engineering Sciences: Proceedings [DE93-019930] p 2763 N94-26429

Cone-valued Lyapunov functions and the stability of stochastic differential equations [DE94-601504] p 2994 N94-26458

About stochastization of motion of charged particles in geomagnetic field and in the field of a wave packet [DE93-634309] p 2879 N94-26502

Stochastic solution to quantum dynamics [NASA-TP-3408] p 3114 N94-26550

Modeling systems by probabilistic process algebra: An event structures approach [PB94-125259] p 3004 N94-26867

Recursive bundle event structures [PB94-125275] p 3004 N94-26870

Single-server queues with spatially distributed arrivals [PB94-126638] p 2986 N94-26916

A superprocess with a disappearing self-interaction [AD-A274647] p 3009 N94-27108

White noise theory of robust nonlinear filtering with correlated state and observation noises [PB94-126661] p 3004 N94-27211

Stochastic space-time, confinement potential and particle propagator [DE94-606415] p 3074 N94-27680

Temporal stochasticity leads to nondeterministic chaos in a model for blood cell production [DE94-003943] p 2933 N94-27744

Modulating terrestrial impacts from Oort cloud comets by the adiabatically changing galactic tides p 2890 N94-28305

STOICHIOMETRY

Ferroelectric thin film microstructure development and related property enhancement [DE94-002741] p 3061 N94-26856

Numerical simulation of the reignition of detonation by reflected shocks [AD-A274755] p 2795 N94-27252

STOKES FLOW

A thermodynamically consistent constitutive theory for a rigid solid-stokesian fluid mixture [DE93-633202] p 2792 N94-26401

STOKES THEOREM (VECTOR CALCULUS)

Geoid determination: With help of the alternative scattering method [ETN-94-95375] p 2847 N94-25746

STOMACH

The electrogastrogram during parabolic flight p 2913 N94-27452

STOPPING

Modular termination proofs for logic and pure PROLOG programs [CWI-CS-R9316] p 2970 N94-27544

STOPPING POWER

Stopping powers and cross sections due to two-photon processes in relativistic nucleus-nucleus collisions [NASA-CR-4574] p 3033 N94-27646

STORAGE BATTERIES

Method of optimizing the charging of a battery of storage cells, and apparatus for performing the method [AD-D016066] p 2781 N94-26102

Development of nickel-metal hydride cell: An update p 2864 N94-28130

Ni-MH storage test and cycle life test p 2864 N94-28131

Determination of thermal properties of commercial Ni-MH cells p 2864 N94-28132

STORAGE RINGS (PARTICLE ACCELERATORS)

RF-station control crate [DIGEL-1992-9] p 2779 N94-25618

Alignment of the Amsterdam Pulse Stretcher (AmPS) [MTG-93-02] p 2809 N94-25637

Technical report of ISSP. Ser. A, no. 2688: Suppression of higher-order modes in an RF cavity by resistive material [JTN-94-80574] p 2787 N94-27606

STORAGE STABILITY

Ni-MH storage test and cycle life test p 2864 N94-28131

STORAGE TANKS

Automated in-situ inspection systems for underground storage tanks [AD-A274644] p 2764 N94-27144

STORM DAMAGE

Examination of micro- and macro-physical structures and processes in hailstorms with respect to their modification [DLR-FB-93-25] p 2897 N94-27751

STORMS

Thunderstorm Hypothesis Reasoner [NASA-CR-195714] p 2897 N94-27884

STOVL AIRCRAFT

Experiments into the scaling parameters required for exhaust gas ingestion testing of vertical landing aircraft p 2671 N94-28017

Transitional flight characteristics of a geometrically simplified STOVL model p 2672 N94-28035

STRAIN DISTRIBUTION

Study on elucidation of damage generation process by electron beam lithography p 2729 N94-25581

STRAIN GAGES

Attachment techniques for high temperature strain [AD-A274766] p 2811 N94-26568

STRAIN HARDENING

Influence of grain structure and solute composition on the work hardening behavior of aluminium at cryogenic temperatures [DE94-003415] p 2733 N94-26087

Low strain behaviour of a particulate reinforced aluminum alloy [ISBN-0-315-84906-1] p 2744 N94-27961

Mechanical properties and microstructure of thermomechanically processed, high manganese steel [ARL-TR-146] p 2747 N94-28212

STRAIN MEASUREMENT

Studies on the measurement of subsurface fractures and geostress using acoustic emission technique for deep coalbed development [REPT-7] p 2879 N94-26475

Attachment techniques for high temperature strain [AD-A274766] p 2811 N94-26568

Aircraft wheel life assessment [AD-A274378] p 2823 N94-26976

High intensity x ray instrumentation for residual strain measurements in composites and textured materials [ISBN-0-315-85169-4] p 2842 N94-27278

A laboratory test on construction of ice domes and their load-carrying capacity p 2884 N94-27966

The estimation of pre-stress by deformation rate analysis and suggestion of a mechanism from the elast-plastical theory p 2871 N94-28156

STRAIN RATE

Deviatoric stresses and plastic strain rates in strong shock waves for six metals [DE94-002964] p 2733 N94-26022

Deformation twinning: Influence of strain rate [DE94-002693] p 2738 N94-26621

The high strain rate behaviour of tantalum [ISBN-0-315-84472-8] p 2740 N94-27305

Research into the microstructure and mechanical behavior of eutectic Bi-Sn and In-Sn [DE94-004558] p 2741 N94-27619

STRANGENESS

Strange Dibaryons [DE94-003005] p 3022 N94-26769

STRATA

The biostratigraphy and paleogeography of Maastrichtian inoceramids p 2889 N94-28303

STRATEGY

Powerful selling and sales strategy p 2662 N94-28245

STRATOCUMULUS CLOUDS

The numerical simulation of marine boundary layer clouds [AD-A273669] p 2894 N94-26195

STRATOSPHERE

Isotopically labeled CO2 from stratosphere: A tracer of carbon biogeochemistry [DE94-002777] p 2877 N94-26015

Auroral Tomography Workshop Proceedings [PB94-123718] p 2881 N94-27040

In situ Mars ozone detector p 3108 N94-27892

Observation of the upper atmosphere physics at Asuka Station by the 30th Japanese Antarctic Research Expedition in 1989 p 2885 N94-27972

STRATUS CLOUDS

The numerical simulation of marine boundary layer clouds [AD-A273669] p 2894 N94-26195

STREAMS

Measuring variation in ecosystem sensitivity to stress [AD-A274232] p 2868 N94-26817

STRESS (PHYSIOLOGY)

Changes in fluid and electrolyte metabolism during water immersion at high or thermoneutral temperature p 2912 N94-27445

STRESS (PSYCHOLOGY)

Performance assessment in sustained operations using a computer-based synthetic work task [AD-A274707] p 2937 N94-26430

Human dimensions research team, operation restore hope [AD-A274340] p 2939 N94-27056

Task demand, workload, and performance [PB94-123627] p 2942 N94-27155

Development of stimulus-seeking scale for expecting individual differences against confinement stress p 2915 N94-27460

STRESS ANALYSIS

Determination of fracture stress and effective crack tip radius from toughness (Klc) and yield strength (Y) [AD-A274014] p 2836 N94-25754

A nonlinear three-dimensional micromechanics model for fiber-reinforced laminated composites [AD-A273772] p 2705 N94-25857

Evaluation of helium cooling for fusion divertors [DE94-002680] p 3042 N94-25976

Deviatoric stresses and plastic strain rates in strong shock waves for six metals [DE94-002964] p 2733 N94-26022

Development of detection technique for fatigue crack due to thermal stratification phenomena in RCS piping [DE93-632968] p 2838 N94-26400

Studies on the measurement of subsurface fractures and geostress using acoustic emission technique for deep coalbed development [REPT-7] p 2879 N94-26475

Stress analysis of a secondary-bending specimen [AD-A274842] p 2838 N94-26501

User's guide for the frequency domain algorithms in the LIFE2 fatigue analysis code [DE94-004678] p 2838 N94-26563

Nonlinear hysteresis in an endochronic solid [AD-A274594] p 2880 N94-26855

Refined triangular plate and shell elements [PB94-126356] p 2839 N94-26875

Computation of stress intensity factors by the mode enrichment technique with applications to geometrically nonlinear problems [PB94-126513] p 2840 N94-26910

Formulae for the buckling of simply-supported corrugated panels of orthotropic material under shear load [PB94-126547] p 2840 N94-26911

Baseline for a Nordtest method. Reliability stress screening of components. A guide for component users
[PB94-123775] p 2835 N94-27042

Series solution for a cylindrical composite shell subject to axisymmetric loadings
[ISBN-0-315-60559-6] p 2844 N94-27810

Mechanically fastened composite laminates subjected to combined bearing-bypass and shear loading
p 2712 N94-27914

Development of methodologies for the estimation of thermal properties associated with aerospace vehicles
p 2846 N94-27920

On the Lagrangian and updated Lagrangian nonlinear finite element formulations
[ISBN-0-315-61111-1] p 3001 N94-27948

Contact stress in disc cams with roller followers
[ESDU-93001] p 2829 N94-28055

Flat rectangular orthotropic plates under uniformly distributed normal pressure. Elastic stresses and deflections for various forms of edge restraint
[ESDU-93011] p 2845 N94-28061

Three-dimensional elastic stress concentration factors: Plain or countersunk hole in a wide plate subjected to tension, bending, or pin loading
[ESDU-93030] p 2845 N94-28143

Journal of NIRE, volume 2, number 4
[JTN-94-80554] p 2869 N94-28147

The estimation of pre-stress by deformation rate analysis and suggestion of a mechanism from the elast-plastical theory p 2871 N94-28156

STRESS CONCENTRATION

Mechanically fastened composite laminates subjected to combined bearing-bypass and shear loading
p 2712 N94-27914

Three-dimensional elastic stress concentration factors: Plain or countersunk hole in a wide plate subjected to tension, bending, or pin loading
[ESDU-93030] p 2845 N94-28143

STRESS CORROSION

Inner fiber observation for metal matrix composites under the stress load condition utilizing Synchrotron Orbital Radiation (SR) by X-ray CT p 2724 N94-25553

Study on improvements in fretting fatigue characteristics of high strength structural member p 2726 N94-25567

Radiation hardening effects on localized deformation and stress corrosion cracking of stainless steels
[DE94-004308] p 2731 N94-25804

STRESS CORROSION CRACKING

Bulletin of National Research Institute for Metals in Fiscal Year 1993, no. 14
[REPT-14] p 2722 N94-25544

Interactions between corrosion fatigue and stress corrosion crack on steel for light water reactors
p 2722 N94-25547

Study on performance evaluation of pressure vessel steel in corrosion environments with sulfide
p 2730 N94-25582

Radiation hardening effects on localized deformation and stress corrosion cracking of stainless steels
[DE94-004308] p 2731 N94-25804

Grain by grain study of the mechanisms of crack propagation during iodine SCC of Zry-4
[DE93-633765] p 2734 N94-26162

Guidelines for controlling stress corrosion cracking and corrosion fatigue of stainless steels: A literature review
[VTT-TIED-1420] p 2837 N94-26262

Stress corrosion cracking and dealloying of copper-gold alloy in iodine vapor
[DE93-633790] p 2734 N94-26264

Development of non-destructive testing technology for the crack of steam generator tubes
[DE93-632953] p 2835 N94-26399

Early stages in the development of stress corrosion cracks
[DE94-003867] p 2838 N94-26524

Grain boundary chromium concentration effects on the IGSCC and IASCC of austenitic stainless steels
[DE94-004268] p 2741 N94-27570

An anodic dissolution-based mechanism for the rapid cracking, pre-exposure phenomenon demonstrated by Al-Li-Cu alloys
[DE94-004798] p 2742 N94-27788

The transition from stress corrosion cracking to corrosion fatigue in AA-7075 and AA-8090
[ISBN-0-315-59526-4] p 2744 N94-27950

STRESS DISTRIBUTION

Development of detection technique for fatigue crack due to thermal stratification phenomena in RCS piping
[DE93-632968] p 2838 N94-26400

An experimental study on the effects of compressive stress on the fatigue crack growth of low-alloy steel
[DE94-004447] p 2737 N94-26582

Deformation, constitutive behavior, and damage of advanced structural materials under multiaxial loading
[AD-A274165] p 2709 N94-27142

Behaviour modification of space trusses
[ISBN-0-315-84701-8] p 2842 N94-27315

Flat rectangular orthotropic plates under uniformly distributed normal pressure. Elastic stresses and deflections for various forms of edge restraint
[ESDU-93011] p 2845 N94-28061

STRESS INTENSITY FACTORS

Computation of stress intensity factors by the mode enrichment technique with applications to geometrically nonlinear problems
[PB94-126513] p 2840 N94-26910

Method for calculating stress intensity factors for surface cracks (appendix 2/1) p 2841 N94-27188

Implementation of thermal residual stresses in the analysis of fiber bridged matrix crack growth in titanium matrix composites
[NASA-TM-109082] p 2711 N94-27658

The development of stress intensity factors
[DRA-TR-93057] p 2845 N94-27954

Fatigue propagation behaviour of short cracks (1-2 mm) in steels
[ESDU-93033] p 2845 N94-28145

STRESS MEASUREMENT

Dynamic response of S-2 glass reinforced plastic structural armor
[AD-A273868] p 2747 N94-25596

Studies on the measurement of subsurface fractures and geostress using acoustic emission technique for deep coalbed development
[REPT-7] p 2879 N94-26475

Stress analysis of a secondary-bending specimen
[AD-A274842] p 2838 N94-26501

The renewing of the test section of the NAL transonic wind tunnel. Part 1: Reconstruction of the 1st corner turning vanes and aerodynamic stress measurement
[NAL-TM-651] p 2681 N94-27247

High intensity x ray instrumentation for residual strain measurements in composites and textured materials
[ISBN-0-315-85169-4] p 2842 N94-27278

A hydrostatic stress-dependent anisotropic model of viscoplasticity
[NASA-TM-106525] p 2711 N94-27640

AF Ni-Cd cell qualification program
p 2863 N94-28122

STRESS PROPAGATION

Bulletin of National Research Institute for Metals in Fiscal Year 1993, no. 14
[REPT-14] p 2722 N94-25544

Interactions between corrosion fatigue and stress corrosion crack on steel for light water reactors
p 2722 N94-25547

STRESS RATIO

Fatigue propagation behaviour of short cracks (1-2 mm) in steels
[ESDU-93033] p 2845 N94-28145

STRESS RELAXATION

Stress relaxation in dough moulding compounds
[PB94-124872] p 2748 N94-25894

Stress relaxation in sputtered W films and W/GeSi/Si heterostructures
[DE94-004007] p 3055 N94-26239

Mechanical behavior of amorphous alloys at elevated temperatures p 2746 N94-28167

STRESS TENSORS

The nonlinear Galerkin method: A multi-scale method applied to the simulation of homogeneous turbulent flows
[NASA-CR-191581] p 2792 N94-26499

STRESS-STRAIN RELATIONSHIPS

Inner fiber observation for metal matrix composites under the stress load condition utilizing Synchrotron Orbital Radiation (SR) by X-ray CT p 2724 N94-25553

A study of graphite peek composite with central elliptical holes under tension
[AD-A273779] p 2705 N94-25863

Investigation of tension-compression fatigue behavior of a cross-ply metal matrix composite at room and elevated temperatures
[AD-A273731] p 2706 N94-25999

The microstructural response of granular soil under uniaxial strain
[AD-A274808] p 2763 N94-26341

Studies on the measurement of subsurface fractures and geostress using acoustic emission technique for deep coalbed development
[REPT-7] p 2879 N94-26475

Aircraft wheel life assessment
[AD-A274378] p 2823 N94-26976

Interface phenomena in metal-ceramic composites
[AD-A274167] p 2709 N94-27125

The high strain rate behaviour of tantalum
[ISBN-0-315-84472-8] p 2740 N94-27305

Research into the microstructure and mechanical behavior of eutectic Bi-Sn and In-Sn
[DE94-004558] p 2741 N94-27619

The deformation of copper-tungsten composites
[ISBN-0-315-84939-8] p 2712 N94-27688

Use of photostress and strain gages to analyze behavior of weldments
[NASA-CR-195269] p 2843 N94-27765

The Science Reports of the Research Institutes, Tohoku University. Series A: Physics, Chemistry, and Metallurgy. Volume 38, No. 1: Amorphous Materials 14
[JTN-94-80610] p 2744 N94-28158

STRESSES

A laboratory test on construction of ice domes and their load-carrying capacity p 2884 N94-27966

STRING THEORY

Topological amplitudes in string theory
[DE94-601561] p 3071 N94-25882

On string theory interacting with two-dimensional gravity
[DE94-601562] p 3071 N94-25883

Aspects of nonrenormalizable terms in a superstring standard-like models
[DE93-614530] p 3071 N94-25911

A research program in experimental and theoretical high energy physics
[DE94-002156] p 3031 N94-25931

Dynamical group of relativistic straight-line string
[DE93-634347] p 3072 N94-26037

Affine algebras on the torus
[DE94-601556] p 3006 N94-26414

Higher spin extensions of the Virasoro algebra, area-preserving algebras and the matrix algebra a-bar(sub (infinity))
[DE94-601557] p 3006 N94-26415

Gauging of Chern-Simons p-Barnes
[DE94-601553] p 2993 N94-26425

Statistical mechanical properties of Z(N)(sup n-1) broken model
[DE93-634344] p 2993 N94-26457

String hypothesis and characters of coset CFTs
[DE93-634337] p 3007 N94-26552

Stochastic space-time, confinement potential and particle propagator
[DE94-606415] p 3074 N94-27680

STRINGS

Quantizable configurations of the relativistic string
[DE93-634346] p 3072 N94-26036

Dynamical group of relativistic straight-line string
[DE93-634347] p 3072 N94-26037

STRONG INTERACTIONS (FIELD THEORY)

QCD corrections to inclusive B - S processes in the standard model
[ISBN-0-315-54572-0] p 3073 N94-27263

A jet calculus approach including coherence effects and the associated problem of moment inversion
[ISBN-0-315-51715-8] p 3025 N94-27266

STRONTIUM COMPOUNDS

Technical report of ISSP. Ser. A, no. 2669: Relations between oxygen deficiency and structures in the La-Sr-Cu-O system. 3: Oxygen contents and structure of (La, Sr)8Cu8O(16+delta) phase
[JTN-94-80555] p 3066 N94-27353

STRONTIUM OXIDES

Preparation and characterization of high temperature superconductor film surfaces
[AD-A274293] p 3059 N94-26681

STRUCTURAL ANALYSIS

Structural analysis of a frangible nut used on the NASA Space Shuttle
[DE94-003672] p 2821 N94-25811

The Latin American conference on the applications of the Moessbaer effect
[DE93-615942] p 3051 N94-25912

Polar and chemical domain structures of lead scandium tantalate (PST)
[DE94-600760] p 3056 N94-26363

Regrowth zones in laser annealed radiation damaged diamond
[DE94-600821] p 3056 N94-26364

User's guide for the frequency domain algorithms in the LIFE2 fatigue analysis code
[DE94-004678] p 2838 N94-26563

Geometry changes in the elastic-plastic analysis of steel spatial skeletal structures
[IFTR-37/1993] p 2839 N94-26825

An automatic contact algorithm in DYNA3D for impact problems
[DE94-002856] p 2965 N94-26862

Refined triangular plate and shell elements
[PB94-126356] p 2839 N94-26875

Proceedings of Damping 1993, volume 2
[AD-A274227] p 2840 N94-26953

Proceedings of Damping 1993, volume 3
[AD-A274228] p 2840 N94-27008

Modification of a model for fatigue life predictions based on level-crossing
[PB94-123395] p 2842 N94-27198

Behaviour modification of space trusses [ISBN-0-315-84701-8] p 2842 N94-27315

Structural design feasibility study of Space Station long spacer truss [NASA-TM-106346] p 2843 N94-27559

Thermal/Structural Tailoring of Engine Blades (T/STAEBL): User's manual [NASA-CR-194461] p 2843 N94-27776

Wing design for a civil tiltrotor transport aircraft: A preliminary study p 2671 N94-27917

STRUCTURAL BASINS

Role of remote sensing in energy, water, and carbon cycle studies over the Amazon [INPE-5486-PRE/1786] p 2852 N94-27957

Some implications of large impact craters and basins on Venus for terrestrial ringed craters and planetary evolution p 2890 N94-28306

STRUCTURAL DESIGN

Project WISH: The Emerald City p 2703 N94-25690

Low-cost unmanned lunar lander p 2697 N94-25699

The identification of inflow fluid dynamics parameters that can be used to scale fatigue loading spectra of wind turbine structural components [DE94-000231] p 2791 N94-26117

Design and life-time of polymer matrix composite structures: Summary [VTT-TIED-1415] p 2707 N94-26260

The structural behaviour of the steel or composite concrete and steel frames and the connections of frame members during the fire: A literature review [VTT-TIED-1437] p 2837 N94-26307

Thermoplastic or thermosetting composites in aircrafts [PB94-123809] p 2710 N94-27253

Structural design feasibility study of Space Station long spacer truss [NASA-TM-106346] p 2843 N94-27559

Reliability-based structural optimization: A proposed analytical-experimental study [NASA-TM-109055] p 2844 N94-27830

Advanced metallic exhaust impinged structural concepts demonstration p 2832 N94-28209

STRUCTURAL DESIGN CRITERIA

Design of cold-formed HSS channels for bending and eccentric compression: Bending in the plane of symmetry [VTT-TIED-1403] p 2762 N94-25622

Applications of the weight function method (appendix 4/1) p 2842 N94-27190

STRUCTURAL FAILURE

Mechanically fastened composite laminates subjected to combined bearing-bypass and shear loading p 2712 N94-27914

The development of stress intensity factors [DRA-TR-93057] p 2845 N94-27954

STRUCTURAL MEMBERS

Wing design for a civil tiltrotor transport aircraft: A preliminary study p 2671 N94-27917

STRUCTURAL PROPERTIES (GEOLOGY)

Studies on the measurement of subsurface fractures and geostress using acoustic emission technique for deep coalbed development [REPT-7] p 2879 N94-26475

Report of the National Research Institute for Earth Science and Disaster Preventi [illegible] No. 51 [JTN-94-80509] p 2886 N94-27985

Underground structure in the eastern part of Kanagawa Prefecture inferred from explosion seismic observations p 2886 N94-27987

Analysis of S-wave seismogram envelope of deep earthquakes and estimation of random inhomogeneities in the Kanto-Tokai area p 2886 N94-27988

STRUCTURAL RELIABILITY

Reliability-based structural optimization: A proposed analytical-experimental study [NASA-TM-109055] p 2844 N94-27830

STRUCTURAL VIBRATION

Identification and H(infinity)/(mu)-synthesis control of the Sandia truss [DE94-002735] p 2839 N94-26810

New variational techniques for acoustic radiation and scattering from elastic shell structures [AD-A274599] p 3010 N94-26889

Proceedings of Damping 1993, volume 1 [AD-A274226] p 2840 N94-26922

Report of three microgravity experiments by the drop shaft [JTN-94-80579] p 2761 N94-27341

Vibrations in engineering structures: A review of model and full-scale test of a cable-stayed bridge and a traffic sign gantry [NLR-TP-92321-U] p 2843 N94-27553

Methods of testing for endurance of structural elements using simulated acoustic loading [ESDU-93027] p 3011 N94-28141

Weak coupling in statistical energy analysis ion Research, Univ. of Southampton, Southampton SO9 5NH, England) [ISVR-TR-228] p 2832 N94-28174

STRUCTURAL WEIGHT

Wing design for a civil tiltrotor transport aircraft: A preliminary study p 2671 N94-27917

STRUCTURED PROGRAMMING

Editing tree structures [CWI-CS-R9264] p 2961 N94-26219

CMSC-130 introductory computer science, lecture notes [AD-A274369] p 2967 N94-27060

STUDENTS

Predoctoral training grant in the area of physical sciences [DE94-004406] p 3039 N94-27603

SUBGROUPS

Simple currents versus orbifolds with discrete torsion: A complete classification [NIKHEF-H/93-13] p 2995 N94-26812

Quantum subgroups and quantum co-set spaces and differential calculi on them [DE94-602520] p 3073 N94-26876

SUBLIMATION

Why is the north polar cap on Mars different than the south polar cap? p 3107 N94-27889

SUBMARINES

Evaluation of crack arrest fracture toughness of parent plate, weld metal and heat affected zone of BIS 812 EMA ship plate steel [AD-A274871] p 2839 N94-26859

Propellants and explosives in ballistic missiles [UCRL-LR-113578] p 2760 N94-28222

SUBMILLIMETER WAVES

Submillimeter residual losses in high-(Tc) superconductors [DE94-003241] p 3058 N94-26516

SUBROUTINE LIBRARIES (COMPUTERS)

Ma42: A new frontal code for solving sparse unsymmetric systems [PB94-124302] p 2998 N94-27115

Development of Calcomp compatible interface library 'piflib' on X Window System [DE94-701190] p 2973 N94-27702

SUBROUTINES

Review and analysis of dense linear system solver package for distributed memory machines p 2978 N94-27916

Lisp interface to geometric modelling operations [PB94-133121] p 3001 N94-28398

SUBSONIC AIRCRAFT

Examples of excrescence drag prediction for typical wing components of a subsonic transport aircraft at the cruise condition [ESDU-93032] p 2649 N94-28144

SUBSONIC FLOW

A numerical determination of bifurcation points for low Reynolds number conical flows [AD-A273984] p 2791 N94-25991

Influence of the transonic doublet in the farfield of a lifting airfoil [IAR-AN-78] p 2647 N94-26702

A comprehensive comparison of turbulence models in the far wake p 2808 N94-27899

Separated flow generated by a vectored jet in a crossflow p 2800 N94-28007

Scalar mixing in the subsonic jet in crossflow p 2800 N94-28008

Experimental investigation of the interaction of a thrust reverser jet with an external subsonic flow p 2801 N94-28011

A numerical investigation of a subsonic jet in a crossflow p 2803 N94-28023

Navier-Stokes simulation of two and three dimensional jets in crossflow, effects of grid, and boundary conditions p 2804 N94-28026

Measurements of steady and dynamic pressure on an F/A-18 wind tunnel model at high angles of attack p 2653 N94-28323

SUBSONIC SPEED

Normal force of low aspect ratio cropped-delta wings at pre-stall angles of attack and subsonic speeds [ESDU-93034] p 2648 N94-27955

Program for calculation of maximum lift coefficient of plain aerofoils and wings at subsonic speeds [ESDU-93015] p 2649 N94-28076

Examples of flight path optimisation using a multivariate gradient-search method [ESDU-93021] p 2670 N94-28092

SUBSONIC WIND TUNNELS

Fiber-optic-based laser vapor screen flow visualization system for aerodynamic research in larger scale subsonic and transonic wind tunnels [NASA-TM-4514] p 2647 N94-26706

Experimental investigation of the flow quality in the GLT20 subsonic-transonic boundary layer wind tunnel [PB94-126539] p 2681 N94-26815

SUBSTRATES

Study of the homogeneity of InP wafers [AD-A273658] p 3055 N94-26194

Comparison of technology for high-power laser mirrors and synchrotron radiation mirrors [DE94-002913] p 3035 N94-26276

Demonstration of monolithic co-fabrication of Y1Ba2Cu3O7-Sigma and CMOS devices on the same sapphire substrate [AD-A274757] p 3059 N94-26566

Growth, characterization and device development in monocrystalline diamond films [AD-A274245] p 3060 N94-26839

The growth and characterization of GaN as a photodetector [AD-A274570] p 3063 N94-26965

Electro-optic materials by solid source MOCVD [DE94-005120] p 2757 N94-27716

Bipolar lead-acid batteries for electrical actuation applications p 2864 N94-28134

SUBSTRUCTURES

Substructure synthesis methods for viscoelastic structures [UTIAS-349] p 2695 N94-26712

SUCTION

Numerical simulation of receptivity and transition in a boundary layer on a flat plate with a suction hole [NASA-CR-195708] p 2798 N94-27782

Localized and distributed boundary-layer receptivity to convected unsteady wake in free stream [NASA-CR-4578] p 2808 N94-28180

SUDAN

Assessment of tropical forests using satellite data [SILVA-CARELICA-21] p 2850 N94-27182

Woody biomass density in the Tendelti area of the central Sudan p 2850 N94-27185

SUDDEN IONOSPHERIC DISTURBANCES

Solar-geophysical data number 590, October 1993. Part 1: (Prompt reports). Data for September, August 1993, and late data [PB94-125903] p 3110 N94-27053

SULFATES

Development of SO(x) and NO(x) solid electrolyte sensors p 2725 N94-25562

Journal of NIRE, volume 2, number 4 [JTN-94-80554] p 2869 N94-28147

Effects of p-chlorophenol on sulfate reduction in marine sediments p 2870 N94-28150

SULFIDES

Voltammetric studies of poly(carbon disulfide) [DE94-001385] p 2717 N94-26951

SULFUR COMPOUNDS

Reactivity of nitrate radical (NO3) toward organic compounds p 2704 N94-27387

SULFUR DIOXIDES

Sulfur dioxide in the atmosphere of Venus 1 sounding rocket observations [NASA-CR-195224] p 3106 N94-26237

SULFUR OXIDES

Development of SO(x) and NO(x) solid electrolyte sensors p 2725 N94-25562

Study on performance evaluation of pressure vessel steel in corrosion environments with sulfide p 2730 N94-25582

SULFURIC ACID

Measuring variation in ecosystem sensitivity to stress [AD-A274232] p 2868 N94-26817

SUM RULES

Nucleon-nucleon scattering lengths in QCD sum rules [DE93-520239] p 3015 N94-25922

Nuclear Theory Group, University of Washington recent and planned research [DE94-002729] p 3022 N94-26809

SUN

Direct evidence of the interplanetary magnetic field effect on the cosmic-ray shadow by the sun [ICRR-296-93-8] p 3116 N94-27607

SUNSPOTS

Region 5395 of March 1989 --- solar activity, geomagnetic disturbances, and terrestrial effects [PB94-120714] p 3110 N94-26755

High resolution studies of sunspots and flux tubes [NASA-CR-195216] p 3111 N94-27321

Characteristics of 30-MHz interference noises observed by riometers p 2884 N94-27965

SUPERCHARGERS

Development of advanced high temperature in-cylinder components and tribological systems for low heat rejection diesel engines, phase 1 [NASA-CR-187158] p 2827 N94-27984

SUPERCOMPUTERS

Achieving high performance on the Intel Paragon [DE94-003108] p 2979 N94-25953

High performance computing in chemistry and massively parallel computers: A simple transition?
[DE94-004318] p 2982 N94-27600

Communication on the Paragon
[DE94-003103] p 2983 N94-27713

SUPERCONDUCTING DEVICES

Prospects for utilization of superconductors in the power industry p 2854 N94-26057

Demonstration of monolithic co-fabrication of Y1Ba2Cu3O7-Sigma and CMOS devices on the same sapphire substrate
[AD-A274757] p 3059 N94-26566

SUPERCONDUCTING FILMS

Flux flow, pinning, and resistive behavior in superconducting networks
[DE94-003400] p 3050 N94-25848

Submillimeter residual losses in high-(Tc) superconductors
[DE94-003241] p 3058 N94-26516

Processing and properties of Ag-clad Bi-2223 tapes
[DE94-004603] p 2783 N94-26589

Preparation and characterization of high temperature superconductor film surfaces
[AD-A274293] p 3059 N94-26681

SUPERCONDUCTING MAGNETS

Prospects for utilization of superconductors in the power industry p 2854 N94-26057

A study on the development of high T(sub c) superconducting materials
[DE93-633529] p 3057 N94-26404

Evaluation of APC NbTi superconductor in a model dipole magnet
[DE94-003258] p 3060 N94-26795

The TPX Cryostat Conceptual Design
[DE94-002857] p 3045 N94-26863

Calculation of the electromagnetic critical state response of high T(sub c) superconductor tape
[DE94-002894] p 3061 N94-26868

SUPERCONDUCTING POWER TRANSMISSION

The effect of Ti conduit on the critical current in (Nb, Ti)3Sn cable-in-conduit conductors
[DE94-701204] p 2788 N94-27817

SUPERCONDUCTING SUPER COLLIDER

Secondary particle in background levels and effects on detectors at future hadron colliders
[DE94-003378] p 3011 N94-25598

Temperature dependence of the radiation induced change of depletion voltage in silicon PIN detectors
[DE94-002705] p 3052 N94-25972

Indiana University high energy physics, task A
[DE94-000961] p 3033 N94-27614

SUPERCONDUCTIVITY

Study on measurement and evaluation methods for superconductive characteristics p 2725 N94-25560

Growth of small fatigue cracks in Incoloy-908
[DE94-003406] p 2836 N94-26129

Strongly interacting fermion systems
[DE94-002674] p 3021 N94-26677

A mechanism for resistive dissipation in Ag sheathed Bi2Sr2CaCu2O8 and Bi2Sr2Ca2Cu3O10
[DE94-003009] p 3060 N94-26771

Powder synthesis, fabrication, and transport properties of long-length Ag clad Bi-2223 conductors
[DE94-002376] p 2740 N94-26957

Tokamak Physics Experiment poloidal field design
[DE94-001542] p 3045 N94-27019

Excited Landau levels, orbital angular momentum and axial anomaly
[DE94-606407] p 3068 N94-27679

Axial anomaly in e(+)e(-) yields gamma gamma and anyon superconductivity
[DE94-606406] p 3070 N94-27859

SUPERCONDUCTORS

Bulletin of National Research Institute for Metals in Fiscal Year 1993, no. 14
[REPT-14] p 2722 N94-25544

Study on characteristics and electronic structures of materials with strong electronic correlations by ferromagnetic fields p 2724 N94-25557

Study on measurement and evaluation methods for superconductive characteristics p 2725 N94-25560

Prospects for utilization of superconductors in the power industry p 2854 N94-26057

Growth of small fatigue cracks in Incoloy-908
[DE94-003406] p 2836 N94-26129

Multi-channel Kondo necklace
[DE93-634754] p 3057 N94-26389

The influence of energy losses with time in NbTi superconductors in pulsed magnetic fields
[DE93-634761] p 3058 N94-26512

Evaluation of APC NbTi superconductor in a model dipole magnet
[DE94-003258] p 3060 N94-26795

List of papers published by the members of Institute for Materials Research, Tohoku University 1992
[JTN-94-80608] p 3118 N94-27355

Experimental results of 40-kA Nb3Al conductor
[DE94-701207] p 2788 N94-27821

SUPERCOOLING

Study on the production of flaky amorphous alloy powders by impact flattening of atomized liquid droplets on a rapidly rotating wheel p 2746 N94-28169

SUPERCRITICAL AIRFOILS

Calculation of viscous drag of two low angle of attack supercritical profiles
[FFA-TN-1984-22] p 2644 N94-26104

Computational investigation of the compressible dynamic stall characteristics of the Sikorsky SSC-A09 airfoil
[AD-A274867] p 2644 N94-26191

Experimental investigations into the wall interference and sidewall boundary layer effects in the National Research Council/Inst. for Aerospace Research High Reynolds Number 2-D Test Facility
p 2658 N94-28350

SUPERCRITICAL WINGS

Wind tunnel investigation of propfan slipstream/wing interactions on a De Havilland air motor powered semispan model at Mach numbers 0.6 and 0.7
p 2651 N94-28316

SUPERFLUIDITY

Crossover between BCS and performed-Boson theories with increasing interactions
[DE93-019018] p 3017 N94-26078

A numerical study of quantized vortices in HeII
[ISBN-9-03-860232-4] p 2792 N94-26479

Superfluid helium sloshing dynamics induced oscillations and fluctuations of angular momentum, force and moment actuated on spacecraft driven by gravity gradient or jitter acceleration associated with slew motion
[NASA-CR-193928] p 2799 N94-27931

SUPERGRAVITY

Topological amplitudes in string theory
[DE94-601561] p 3071 N94-25882

Anomaly candidates and invariants of D 4, N 1 supergravity theories
[NIKHEF-H/93-12] p 3072 N94-26541

The super Weierstrass (zeta)-function and operator product expansions in 2D-induced supergravity on the supertorus
[DE94-603664] p 3074 N94-27627

SUPERHIGH FREQUENCIES

Analyzing adaptive beamformer performance in a stable multipath environment
[AD-A274029] p 2766 N94-25766

Annex report FEL-92-A163: Description of the LInk and BER Test Analysis System (LIBERTAS) for the frequency band V (14.5 - 15.3 GHz)
[FEL-92-A442] p 2770 N94-26650

SUPERLATTICES

MBE grown 3 to 5 strain relaxed buffer layers and superlattices characterized by atomic force microscopy
[DE94-002931] p 3056 N94-26308

The effect of high frequency electric field on hypersound amplification in superlattice
[DE93-634326] p 3057 N94-26384

Modulation wavelength dependence of ion mixing in metallic superlattices
[DE94-004608] p 3059 N94-26591

AB-Initio calculation of the valence-band offset at strained GaAs/InAs (001) heterojunction
[DE94-602538] p 3061 N94-26878

SUPERNOVA REMNANTS

Supernovae and mass extinctions
p 2891 N94-28314

SUPERNOVA 1987A

Balloon-borne measurements of the SN1987A hard x ray continuum p 3115 N94-26689

SUPERNOVAE

Supernovae and mass extinctions
p 2891 N94-28314

SUPERPLASTICITY

An investigation of cavitation in a mechanically alloyed 15 volume percent SiCp/IN9021 aluminum composite
[DE94-003371] p 2748 N94-25959

Study of precipitation and recrystallization in Al alloy 2519 by backscattered electron imaging methods
[AD-A274919] p 2736 N94-26533

SUPERSONIC AIRCRAFT

Report of the defense science board task force on aircraft assessment
[AD-A274531] p 2669 N94-26835

SUPERSONIC BOUNDARY LAYERS

Theoretical and experimental investigation of converging cylindrical shock waves propagating in narrow cylindrical chambers
[ISBN-0-315-84694-1] p 2795 N94-27313

SUPERSONIC COMBUSTION

A numerical study of mixing and combustion in hypervelocity flows through a scramjet combustor model
p 2808 N94-27911

SUPERSONIC COMBUSTION RAMJET ENGINES

Development and implementation of a scramjet cycle analysis code with a finite-rate-chemistry combustion model for use on a personal computer
[AD-A273834] p 2673 N94-25617

A study on heat transfer in a scramjet leading edge model
[NAL-TR-1187T] p 2675 N94-27608

A numerical study of mixing and combustion in hypervelocity flows through a scramjet combustor model
p 2808 N94-27911

SUPERSONIC COMMERCIAL AIR TRANSPORT

The evolution of the high-speed civil transport
[NASA-TM-109089] p 3117 N94-26155

SUPERSONIC FLOW

Evaluation of a concentration probe for application in a supersonic flow field
[AD-A273915] p 2643 N94-25592

A numerical determination of bifurcation points for low Reynolds number conical flows
[AD-A273984] p 2791 N94-25991

A sensitivity equation approach to shape optimization in fluid flows
[NASA-CR-191598] p 2999 N94-27415

Experimental study on the interactions between a transverse heated supersonic jet and an external supersonic flow p 2659 N94-28039

Solution of the Euler equations using unstructured grids p 2656 N94-28338

SUPERSONIC JET FLOW

The growth and characterization of GaN as a photodetector
[AD-A274570] p 3063 N94-26965

Transient flow features of a supersonic jet in a low speed cross flow p 2800 N94-28005

Experimental study on the interactions between a transverse heated supersonic jet and an external supersonic flow p 2659 N94-28039

SUPERSONIC SPEED

A numerical study of high-speed missile configurations using a block-structured parallel algorithm
[AD-A273776] p 2979 N94-25860

SUPERSONIC TRANSPORTS

Preliminary design of nine high speed civil transports
p 2671 N94-25710

Supercruiser Arrow HS-8 p 2671 N94-25711

Tesseract supersonic business transport
p 2671 N94-25713

SUPERSYMMETRY

(2,0) superconformal anomaly
[DE93-613046] p 2991 N94-25867

Aspects of nonrenormalizable terms in a superstring standard-like models
[DE93-614530] p 3071 N94-25911

Higher spin extensions of the Virasoro algebra, area-preserving algebras and the matrix algebra a-bar(sub (infinity))
[DE94-601557] p 3006 N94-26415

The Hamiltonian structures of the super KP hierarchy associated with an even parity superlax operator
[DE94-601506] p 2994 N94-26459

Construction of a new electroweak sphaleron
[NIKHEF-H/93-09] p 3020 N94-26540

Anomaly candidates and invariants of D 4, N 1 supergravity theories
[NIKHEF-H/93-12] p 3072 N94-26541

Progress in SSC Higgs physics: Report of the Higgs working group
[DE94-003224] p 3022 N94-26793

Thermodynamics and form factors of supersymmetric integrable field theories
[DE94-602557] p 3073 N94-26896

Excited Landau levels, orbital angular momentum and axial anomaly
[DE94-606407] p 3068 N94-27679

SUPPORT SYSTEMS

Space Station technology testbed: 2010 deep space transport p 2687 N94-27368

SUPPORTS

SAG compensated vibration isolation mount
[AD-D016040] p 2841 N94-27110

Installation of models in the 2 m x 3 m low speed wind tunnel
[LTR-LA-286] p 2681 N94-27594

SURFACE ACOUSTIC WAVE DEVICES

Ultralinear wideband integrated circuit design
[ISBN-0-315-84130-3] p 2784 N94-26675

SURFACE CRACKS

Fundamental study on monitoring technology on local surface damages p 2724 N94-25555

Study on high temperature damage control and life improvement p 2729 N94-25580

Optical surface contouring for non-destructive inspection of turbomachinery
[NASA-CR-195245] p 2835 N94-26691

SURFACE DEFECTS
Effect of nitrocarburizing on shape of titanium alloy parts
[DE94-004040] p 2732 N94-25822
Optical surface contouring for non-destructive inspection of turbomachinery
[NASA-CR-195245] p 2835 N94-26691
SURFACE DIFFUSION
Influence of lattice damage on retention and transport of deuterium in beta silicon carbide
[DE94-005206] p 3068 N94-27693
SURFACE EMITTING LASERS
Characterization of nonlinear effects in optically pumped vertical cavity surface emitting lasers
[AD-A273840] p 2815 N94-25744
Ultra-high aggregate bandwidth two-dimensional multiple-wavelength diode laser arrays
[AD-A274018] p 2815 N94-25756
Bulletin of Precision and Intelligence Laboratory, No. 68
[JTN-94-80609] p 3010 N94-27282
SURFACE ENERGY
Se EXAFS study of the elevated wurtzite to rock salt structural phase transition in CdSe nanocrystals
[DE94-003247] p 3054 N94-26125
Differentiating the role of land surface variability and cloudiness variability on global energy transport within the atmosphere and oceans
[NASA-CR-195229] p 2847 N94-26222
Surface roughness lengths
[AD-A274550] p 2895 N94-26846
SURFACE FINISHING
Corrosion resistance at welded zones of nuclear fuel reprocessing system p 2722 N94-25546
R and D for creation, measurement, application of ultra-high vacuum p 2723 N94-25549
Modelling the inhibition cure behaviour of unsaturated polyester moulding materials
[PB94-124864] p 2748 N94-25893
Calculations of material removal, removal rate, and Preston coefficient in continuous lapping/polishing machines
[DE94-002619] p 2763 N94-26804
Laser surface modification of intermetallic compounds
[DREA-CR-92-416] p 2820 N94-27668
Effect of surface finish on turbine airfoil cascade losses p 2652 N94-28320
SURFACE LAYERS
Effect of nitrocarburizing on shape of titanium alloy parts
[DE94-004040] p 2732 N94-25822
Neutron reflection interferometry
[DE94-601876] p 2714 N94-26170
Studies of thin-film growth, adsorption, and oxidation by in situ, real-time, and ex situ ion beam analysis
[DE94-002907] p 3055 N94-26275
Radar detection of low-altitude targets in a maritime environment. Volume 2: Meteorological and radar data
[AD-A274658] p 2768 N94-26335
Microstructures of Si surface layers implanted with Cu
[DE94-004690] p 3058 N94-26565
Failure behaviour of high density polyethylene with an embrittled surface layer due to weathering
[PB94-126406] p 2840 N94-26960
The Martian atmospheric planetary boundary layer stability, fluxes, spectra, and similarity
[NASA-CR-195711] p 3108 N94-27935
SURFACE PROPERTIES
Observation on metal surface in aqueous solution using an electrochemical Scanning Tunneling Microscope (STM) p 2724 N94-25554
Study on substance diffusion in thin films with controlled structures p 2727 N94-25570
Study on production of materials with one direction solidification texture p 2727 N94-25572
Study on interfacial reaction analysis at interfacial joining p 2728 N94-25574
Hydrogen uptake into silicon from an ECR plasma
[DE94-003771] p 3050 N94-25815
Determination of surface recombination velocity and bulk lifetime in detector grade silicon and germanium crystals
[DE94-003886] p 3053 N94-26094
Studies of thin-film growth, adsorption, and oxidation by in situ, real-time, and ex situ ion beam analysis
[DE94-002907] p 3055 N94-26275
Eleventh Symposium on Energy Engineering Sciences: Proceedings
[DE93-019930] p 2763 N94-26429
Interfacial area and interfacial transfer in two-phase flow
[DE93-041226] p 2792 N94-26468
Translational-energy-resolved studies of photogenerated carrier-induced reactions on UHV semiconductor surfaces
[DE94-004169] p 3058 N94-26526
Calculating the surface properties for the liquid-vapour interface: Illustrating the thermodynamic stability of the spherical microstructures
[DE94-601992] p 3073 N94-26837
Interface properties of wide bandgap semiconductor structures
[AD-A274356] p 3063 N94-27058
Laser surface modification of intermetallic compounds
[DREA-CR-92-416] p 2820 N94-27668
SURFACE REACTIONS
Observation on metal surface in aqueous solution using an electrochemical Scanning Tunneling Microscope (STM) p 2724 N94-25554
Study on interfacial reaction analysis at interfacial joining p 2728 N94-25574
Atomic-scale chemistry of metal surfaces
[REPT-A-2657] p 3012 N94-25636
The reactivity of lithium toward non-aqueous solvents of relevance to energy storage applications as studied by surface analytical techniques
[DE94-003483] p 2856 N94-26464
A mimic model of Pt-Rh catalyst prepared by electrochemical deposition of Rh on Pt (100) surface
[REPT-A-2664] p 2715 N94-26476
Mechanistic studies of opto-electronic materials and syntheses using multiple laser and surface diagnostics
[AD-A274528] p 3036 N94-26834
Atomic layer epitaxy of group 4 materials: Surface processes, thin films, devices and their characterization
[AD-A274325] p 3061 N94-26885
International bulletin on atomic and molecular data for fusion. No. 42-45, Mar. 1991 - Dec. 1992
[DE94-601817] p 3045 N94-26946
International bulletin on atomic and molecular data for fusion. No. 46
[DE94-601818] p 3023 N94-26947
SURFACE ROUGHNESS
The determination of surface roughness from reflected step edges
[AD-A273987] p 2984 N94-25900
In situ x ray reflectivity measurements of thin film structural evolution
[DE94-002289] p 3051 N94-25944
MBE grown 3 to 5 strain relaxed buffer layers and superlattices characterized by atomic force microscopy
[DE94-002931] p 3056 N94-26308
Validated heat-transfer and pressure-drop prediction methods based on the discrete-element method. Phase 2: Two-dimensional rib roughness
[DE94-002379] p 2794 N94-26763
Surface roughness lengths
[AD-A274550] p 2895 N94-26846
Equivalent performance in different helical resonator plasma polymerization coater platforms
[DE94-001517] p 2753 N94-26933
Turbulent boundary layer inner-outer interactions
[AD-A274357] p 2794 N94-27059
Mapping of soil humidity using C-band radar images
[ISBN-0-315-85076-0] p 2852 N94-27878
Localized and distributed boundary-layer receptivity to convected unsteady wake in free stream
[NASA-CR-4578] p 2808 N94-28180
SURFACE TEMPERATURE
Aerodynamic heating in hypersonic flows
p 2658 N94-27919
Adsorption and desorption studies of cesium on sapphire surfaces
[DE94-003798] p 3070 N94-28067
SURFACE TREATMENT
Effect of nitrocarburizing on shape of titanium alloy parts
[DE94-004040] p 2732 N94-25822
Plasma surface cleaning using microwave plasmas
[DE94-002754] p 2713 N94-26014
Determination of surface recombination velocity and bulk lifetime in detector grade silicon and germanium crystals
[DE94-003886] p 3053 N94-26094
Stability of reference masses 2: The effect of environment and cleaning methods on the surfaces of stainless steel and allied materials
[NPL-DMM(A)-95] p 2738 N94-26653
Low temperature deposition and characterization of N- and p-type silicon carbide thin films and associated ohmic and Schottky contacts
[AD-A274345] p 2754 N94-26974
Evaluating non-chlorinated solvents for welding applications
[DE94-003332] p 2824 N94-27181
SURFACE VEHICLES
Test Operations Procedure (TOP) 2-2-800 wheeled vehicle center of gravity
[AD-A273937] p 2821 N94-25794
SURFACE WATER
Detection of water on road surface by the polarized light p 2886 N94-27989
SURFACES
Response surface design comparisons
[AD-A274690] p 2838 N94-26448
An automatic contact algorithm in DYNA3D for impact problems
[DE94-002856] p 2965 N94-26862
SURFACTANTS
The epitaxial growth of Ge on Si(100) using Te as a surfactant
[DE94-003437] p 3056 N94-26326
SURGERY
Development of surgical CW Nd:YAG laser with optical fiber delivery system
[DE93-632902] p 2817 N94-26185
SURGES
Properties of the Central American cold surge
[NASA-CR-194849] p 2893 N94-26138
Detection of transient vector-fields in additive noise
[FFI-93/7028] p 2768 N94-26232
An investigation of the surge behavior of a high-speed ten-stage axial flow compressor
[AD-A274910] p 2674 N94-26345
SURVEILLANCE
Feasibility study of a multiaperture telescope for deep-space Earth surveillance
[AD-A273903] p 3102 N94-25658
Design analysis of a combined optical/LADAR deep-space surveillance satellite
[AD-A274040] p 2694 N94-25832
Emerging technologies
[DE94-003022] p 3102 N94-26023
An unavailability model for errors made during surveillance testing
[DE94-000816] p 2835 N94-27613
SURVEILLANCE RADAR
Machine intelligent gust front algorithm
[AD-A273695] p 2680 N94-26196
SURVEYS
A comparison of users' and providers' perceptions of critical spacelift vehicle characteristics and capabilities
[AD-A273907] p 2691 N94-26017
Hydrographic and Acoustic Doppler Current Profiler (ADCP) data from the ONR eastern boundary current accelerated research initiative, 9-16 June 1992
[AD-A274115] p 2898 N94-26076
Survey of visualization and analysis tools
[NASA-TM-108436] p 2809 N94-26150
HPm-tubes: Literature survey comprising 1992
[PB94-123643] p 2785 N94-27038
Solar collector manufacturing activity, 1992
[DE94-003401] p 2859 N94-27048
Microbiology research at some research institutes in the former Soviet Union: A survey of scientific publications
[PB94-123320] p 2902 N94-27171
Macrobenthic fauna in the dutch sector of the north sea in 1991
[PB94-126414] p 2868 N94-27200
COMPETENCE 2000: Study on training requirements of the Norwegian metallurgical industry
[PB94-124609] p 2741 N94-27328
Spiral Survey Expedition: A proposal to organize for the Survey, exploration and eventual colonization of the Milky Way Galaxy p 2686 N94-27366
SUSPENSION SYSTEMS (VEHICLES)
The Enabler: A concept for a lunar work vehicle
p 2833 N94-25675
SWEAT COOLING
Advanced metallic exhaust impinged structural concepts demonstration p 2832 N94-28209
SWEEP EFFECT
Wing lift increment at zero angle of attack due to deployment of single-slotted flaps at low speeds
[ESDU-93019] p 2649 N94-28140
SWELLING
Microstructural development in irradiated vanadium alloys
[DE94-004307] p 2737 N94-26556
He(+) and H(+) microbeam damage, swelling and annealing in diamonds
[DE94-601912] p 3063 N94-26987
SWEPT WINGS
Prediction of leading-edge transition and relaminarization phenomena on a subsonic multi-element high-lift system p 2659 N94-27929
SWINE
Skeletal development and ossification of the swine fetuses p 2905 N94-27491
SWING WINGS
Supercruiser Arrow HS-8 p 2671 N94-25711
SWINGBY TECHNIQUE
Project APEX: Advanced manned exploration of the Martian moon Phobos p 3079 N94-25688
SWIRLING
Navier-Stokes analysis of a swirling jet in crossflow
p 2806 N94-28038

SWITCHES
Control panel dimensions for gloved operation study 2: Toggle switches minimum spacing required between toggle
[AD-A274518] p 2942 N94-27089
A tri-state optical switch for local area network communications p 2789 N94-27922
SWITCHING CIRCUITS
Low threshold all-optical crossbar switch on GaAs-GaAlAs channel waveguide arrays
[AD-A274971] p 2783 N94-26536
An electronic switch based on quantum interference
[ISBN-0-315-84609-7] p 2787 N94-27650
SYMBOLIC PROGRAMMING
Efficient implementation of high-level parallel symbolic languages p 2955 N94-27196
SYMBOLS
Saving comparisons in the Crochemore-Perrin string matching algorithm
[CWI-CS-R9322] p 2971 N94-27550
SYMMETRY
Experimental study of the near threshold pi(sup +)p yields (pi(sup +))(pi(sup +))(n) cross section and chiral symmetry
[DE94-601671] p 3014 N94-25840
The algebra of non-local charges in non-linear sigma models
[DE94-601563] p 2991 N94-25884
Principles of gauge theory of real hadrons
[DE93-616857] p 3015 N94-25920
Spatial symmetry, local integrability and tetrahedron equations in the Baxter-Bazhanov model
[DE93-634348] p 3002 N94-26038
Simple currents versus orbifolds with discrete torsion: A complete classification
[NIKHEF-H/93-13] p 2995 N94-26812
Normal forms for perturbations of the euler top
[PB94-125390] p 3009 N94-26968
Some remarks on the symmetry of self-conjugate minimal surfaces in R3
[DE94-603670] p 3007 N94-27633
Surface modes and chiral symmetry (Wilson fermions in a box)
[DE94-004946] p 3029 N94-27814
Polarizability matrix of layered chiral sphere
[PB94-132834] p 2778 N94-28355
Plane wave propagation and polarization properties in transversely bianisotropic uniaxial medium
[PB94-132883] p 2778 N94-28380
Electromagnetic modeling of bi-isotropic media
[PB94-132909] p 2778 N94-28382
SYMPATHETIC NERVOUS SYSTEM
Excitation of cutaneous polymodal receptor induced by sympathetic stimulation in adjuvant-induced arthritis rats
p 2906 N94-27495
Effect of prostaglandin E1 on the relationship between skin sympathetic nerve activity and reduction in skin blood flow p 2929 N94-27524
Difference in skin blood flow reduction depending on activating maneuver of skin sympathetic nerve activity
p 2929 N94-27525
Sympathetic nerve activity during dynamic leg exercise
p 2929 N94-27527
An attempt of intraneural stimulation by microelectrode inserted in skin sympathetic nerve fascicle
p 2930 N94-27529
Muscle sympathetic nerve activity in patients with hyper-and hypothyroidism: A microneurographic study
p 2930 N94-27531
Enhancement of skin sympathetic nerve activity in amyotrophic lateral sclerosis p 2930 N94-27532
Mechanism for regulation of myocardial contractility by autonomic drugs: Pathophysiological relevance in congestive heart failure p 2931 N94-27536
Muscle sympathetic nerve activity in humans
p 2932 N94-27538
The role of beta-adrenoceptor stimulation in the progression of chronic heart failure
p 2932 N94-27541
SYNCHRONISM
Specification performance optimization and executive generation for onboard multiprocessor real time application with SynDEx p 2954 N94-26745
Asynchronous and packetized systems engineering tools p 2954 N94-26746
Design of a parallel discrete event simulation coprocessor
[AD-A274135] p 2982 N94-27123
SYNCHROTRON RADIATION
Fast photoconductor CdTe detectors for synchrotron x ray studies
[DE94-001334] p 3054 N94-26139
Comparison of technology for high-power laser mirrors and synchrotron radiation mirrors
[DE94-002913] p 3035 N94-26276
SYNCHROTRONS
Fast photoconductor CdTe detectors for synchrotron x ray studies
[DE94-001334] p 3054 N94-26139
Regrouping of the beam in the IHEP PS for the UNK p-p programs
[DE93-634021] p 3032 N94-26164
Longitudinal diffusion of a proton bunch under external noise
[DE93-634022] p 3032 N94-26165
Comparison of technology for high-power laser mirrors and synchrotron radiation mirrors
[DE94-002913] p 3035 N94-26276
Experimental measurement of local displacement and chemical pair correlations in crystalline solid solutions
[DE94-001124] p 3065 N94-27251
SYNCOPE
Pulse waveform and transcranial Doppler analysis during lower body negative pressure
[AD-A274516] p 2911 N94-27088
SYNOPTIC METEOROLOGY
Propagation of cold air masses in East Asia and its associated planetary-scale function
[AD-A274304] p 2895 N94-26850
A synoptic study on periods of deficiency over Rio Grande do Sul/Brazil
[INPE-5456-TDI/498] p 2896 N94-27422
SYNTHESIS (CHEMISTRY)
Development of SO(x) and NO(x) solid electrolyte sensors p 2725 N94-25562
Fundamental study on new synthetic technology by phthalocyanine complexes p 2721 N94-25569
Template synthesis of metal microtubule ensembles utilizing chemical, electrochemical, and vacuum deposition techniques
[AD-A274676] p 2715 N94-26444
Structure and properties of composites synthesized in situ using solid state displacement reactions
[DE94-004589] p 2737 N94-26585
Molecular surface electrostatic potentials in the analysis of non-hydrogen-bonding noncovalent interactions
[AD-A274612] p 3022 N94-26894
Synthesis, rheology, and forming of Y-Ba-Cu-O ceramics
[DE94-005558] p 2757 N94-27695
Preparation, characterization, and thermal behaviour study of lanthanides (3) and yttrium (3) 4-methoxy benzylidene pyruvate in solid state
[DE94-604079] p 3068 N94-27697
SYNTHETIC APERTURE RADAR
A real-time convolution algorithm and architecture with applications in SAR processing
[AD-A273817] p 2959 N94-25963
Weapon system sensor integration for a DIS-compatible virtual cockpit
[AD-A274088] p 2672 N94-26021
A comparative evaluation of SAR and SLAR
[DE94-002922] p 2848 N94-26277
Response of an airborne synthetic aperture radar to sea ice in the marginal ice zone
[ISBN-0-315-84243-1] p 2849 N94-26668
Leadex environmental phenomena and effects observed by DMSP, NOAA, and ERS-1 satellites
[AD-A274596] p 2868 N94-26888
Processing of wide-angle synthetic aperture radar signals for target detection
[AD-A274225] p 2773 N94-27073
Method of correcting rotational motion error in SAR and ISAR imagery
[AD-D016033] p 2773 N94-27146
Image quality analysis of compressed synthetic aperture radar imagery
[AD-A273399] p 2774 N94-27170
Non-adaptive robust filters for speckle noise reduction
[INPE-5519-PRE/1794] p 2776 N94-27335
Calibration of SAR systems
[DLR-FB-93-18] p 2777 N94-27738
Mapping of soil humidity using C-band radar images
[ISBN-0-315-85076-0] p 2852 N94-27878
A comparative study of SAR data compression schemes p 2946 N94-28259
Perceptual compression of magnitude-detected synthetic aperture radar imagery p 2946 N94-28260
SYSTEM EFFECTIVENESS
Aircraft wheel life assessment
[AD-A274378] p 2823 N94-26976
SYSTEM FAILURES
Fast incremental compiler transformations for multiple instruction retry
[NASA-CR-195209] p 2964 N94-26680
Hardware and software reliability estimation using simulations
[NASA-CR-187588] p 2973 N94-27663
Simulating fail-stop in asynchronous distributed systems
[NASA-CR-195698] p 2974 N94-27767
SYSTEM IDENTIFICATION
Asymptotically stable neural networks for identification of nonlinear dynamic systems
[ISBN-0-315-84328-4] p 2985 N94-26629
Grey-box modelling and identification topics
[PB94-126380] p 2986 N94-27029
Control oriented system identification
[AD-A274162] p 2987 N94-27124
Improved modeling of GPS selective availability
p 2642 N94-27290
On modeling and controlling intelligent systems
[DE94-002446] p 2988 N94-27706
System identification of the Large-Angle Magnetic Suspension Test Facility (LAMSTF)
p 2682 N94-27908
SYSTEMS ANALYSIS
Vulnerability assessment using a fuzzy logic based method
[AD-A274075] p 2957 N94-25649
Performance measurement of three commercial object-oriented database management systems
[AD-A274028] p 3096 N94-25765
Technical description of the Vulcano software library
[FFI-93/7024] p 2767 N94-26105
A linear description of the discrete lot-sizing and scheduling problem
[MEMO-COSOR-92-47] p 2992 N94-26227
On the phi(sub 0)-stability of perturbed nonlinear differential systems
[DE93-634304] p 2993 N94-26441
Tool for performance analysis and off-line prediction of timing behaviour p 2952 N94-26732
Formal methods for dependable real-time systems
p 2953 N94-26740
Asynchronous and packetized systems engineering tools p 2954 N94-26746
Interference analysis of multichannel transmission lines: A system's analysis
[PB94-126505] p 2772 N94-26909
Freeness analysis for logic programs-and correctness
[PB94-126703] p 2966 N94-26956
DALIA: A language for the description and analysis of digital systems p 2954 N94-27192
Parallel discrete event simulation
p 2955 N94-27194
On modeling and controlling intelligent systems
[DE94-002446] p 2988 N94-27706
Object-oriented development methods
p 2975 N94-27938
Artificial Intelligence Research Branch future plans
[NASA-TM-109733] p 2989 N94-28065
SYSTEMS ENGINEERING
Safety analysis in conceptual design of process control
[VTT-PUBS-117] p 2762 N94-25641
Copernicus: Lunar surface mapper
p 3081 N94-25702
Technology drivers for flight telerobotic system software p 2684 N94-26289
Information systems criteria for applying software reengineering: Guidelines for identifying information systems for software reengineering
[AD-A274699] p 3097 N94-26375
Merging photovoltaic hardware development with hybrid applications in the USA
[DE94-002682] p 2857 N94-26612
Asynchronous and packetized systems engineering tools p 2954 N94-26746
Automated information management for designers: Functional requirements for computer based associates that support access and use of technical information in design
[AD-A274603] p 3099 N94-26891
Interdisciplinary technology p 2686 N94-27363
Space Station technology testbed: 2010 deep space transport p 2687 N94-27368
The radiation design handbook
[ESA-PSS-01-609-ISSUE-1] p 2696 N94-27397
Test and evaluation of the Litton (Canada) Canadian strapdown gyroscope (CSG-2) Performance Evaluation Unit (PEU)
[DREO-1010] p 2813 N94-27597
Compressor stability p 2828 N94-28046
Transient model applications. 1: Compressor heat soak/clearance effects modeling p 2828 N94-28048
Combined Cycles for Power Plants
[VKI-LS-1993-08] p 2830 N94-28077
Development of the gas turbine. Part 1: Design philosophy and performance p 2831 N94-28080
Development of the gas turbine. Part 2: Manufacturing, commissioning, and operation p 2831 N94-28081
Steam plant for combined cycles: Heat recovery steam generators, design principles, and construction details
p 2831 N94-28083
Simulation: A tool for steam plant dynamic analysis
p 2831 N94-28084

Steam plant: Steam turbines for combined cycles p 2831 N94-28085

Controls, monitoring and performance measurements p 2831 N94-28086

Advanced End-to-end Simulation for On-board Processing (AESOP) p 2945 N94-28255

SYSTEMS INTEGRATION

Weapon system integration for the AFIT virtual cockpit [AD-A274058] p 2667 N94-25772

Microwave and pulsed power [DE94-003019] p 2782 N94-26312

Merging photovoltaic hardware development with hybrid applications in the USA [DE94-002682] p 2857 N94-26612

Institute for Information Technology [NRC-37061] p 3118 N94-26709

Test of onboard real time applications (LICE (tm)) p 2952 N94-26737

Interdisciplinary technology p 2686 N94-27363

Minimum accommodation for aerobrake assembly, phase 2 [NASA-TM-107608] p 2692 N94-27774

Integrated coal gasification combined cycle p 2832 N94-28090

SYSTEMS MANAGEMENT

Planning for the future of the DREnet: The way ahead [NRNS-002-00-001-01] p 2983 N94-28042

SYSTEMS SIMULATION

Asynchronous and packetized systems engineering tools p 2954 N94-26746

SYSTEMS STABILITY

Limit theorems for functionals of Markov processes and renormalizable stable fields [AD-A274645] p 3004 N94-27106

SYSTOLE

Mechanism for regulation of myocardial contractility by autonomic drugs: Pathophysiological relevance in congestive heart failure p 2931 N94-27536

T

T TAIL SURFACES

Experimental and theoretical studies of T-tail configurations for commuter aircraft applications p 2653 N94-28322

T TAURI STARS

Investigations of the dynamical evolution of protoplanetary nebulae [NASA-CR-195278] p 3105 N94-27428

TABLES (DATA)

Module interconnection frameworks for a real-time spreadsheet [AD-A273853] p 2956 N94-25588

Kiruna geophysical data. Data summary 93/4-6, April-June 1993 [PB94-123700] p 2881 N94-27039

Kiruna geophysical data. Data summary 93/1-3, January-March, 1993 [PB94-123791] p 2881 N94-27043

JARE data reports. No. 186: Upper atmosphere physics data. Syowa and Asuka Stations, 1990 [JTN-94-80594] p 2881 N94-27299

TAIL ASSEMBLIES

Experimental and theoretical studies of T-tail configurations for commuter aircraft applications p 2653 N94-28322

TAKEOFF

Influence of headwind on hot gas reingestion and consideration of pressure ratio scaling p 2675 N94-28018

TAKEOFF RUNS

System for generating, aboard an aircraft, during takeoff, of a signal capable of producing an alert or an alarm, in case of malfunction [CA-PATENT-APPL-SN-2,018,94] p 2659 N94-26293

TANTALUM

Deviatoric stresses and plastic strain rates in strong shock waves for six metals [DE94-002964] p 2733 N94-26022

The high strain rate behaviour of tantalum [ISBN-0-315-84472-8] p 2740 N94-27305

TANTALUM ALLOYS

The high strain rate behaviour of tantalum [ISBN-0-315-84472-8] p 2740 N94-27305

The corrosion behavior of sputter-deposited magnesium-valve metal alloys p 2745 N94-28164

CO2 methanation catalysts prepared from amorphous Ni-valve metal alloys containing platinum group elements p 2745 N94-28166

TANTALUM COMPOUNDS

NNN-Ising model simulation of nanodomain textures in relaxor-type lead scandium tantalate [DE94-601884] p 2748 N94-25844

Polar and chemical domain structures of lead scandium tantalate (PST) [DE94-600760] p 3056 N94-26363

TAPERING

A study of two dimensional tapered periodic edge treatments to reduce wideband edge diffraction [AD-A274054] p 2766 N94-25824

TARGET ACQUISITION

Mitsubishi 3-5 micrometers IR imager for machine-vision/ATA applications [AD-A273812] p 3034 N94-25940

Radar detection of low-altitude targets in a maritime environment. Volume 2: Meteorological and radar data [AD-A274658] p 2768 N94-26335

Capture and location of blobs in digital images [ISBN-0-315-84382-9] p 3036 N94-26666

Processing of wide-angle synthetic aperture radar signals for target detection [AD-A274225] p 2773 N94-27073

TARGET RECOGNITION

Hyperspectral analysis of space objects: Signal to noise evaluation [AD-A273882] p 2765 N94-25728

Color image segmentation [AD-A274027] p 2984 N94-25759

Zernike moments and rotation invariant object recognition. A neural network oriented case study [AD-A273749] p 2767 N94-26011

New binary integration strategies and corresponding R90 calculations [AD-A274786] p 2769 N94-26359

Combatting inherent vulnerabilities of CFAR algorithms and a new robust CFAR design [AD-A274918] p 2770 N94-26751

The morphological processing of binary images [AD-A274310] p 2996 N94-26972

Joint services electronics program [AD-A274643] p 2785 N94-27027

Processing of wide-angle synthetic aperture radar signals for target detection [AD-A274225] p 2773 N94-27073

Image quality analysis of compressed synthetic aperture radar imagery [AD-A273399] p 2774 N94-27170

TARGETS

An algorithm to find the intersection of two convex polygons [AD-A274722] p 2961 N94-26148

TASK COMPLEXITY

The central executive component of working memory [AD-A274295] p 2938 N94-26683

TASK PLANNING (ROBOTICS)

Graphical programming at Sandia National Laboratories [DE94-003803] p 2958 N94-25818

A multitasking behavioral control system for the Robotic All-Terrain Lunar Exploration Rover (RATLER) p 2685 N94-26292

TASKS

Long term learning: Integration of knowledge acquisition and knowledge compilation [AD-A274775] p 3098 N94-26570

Scheduling tasks with unpredictable timing parameters in hard real-time systems p 2951 N94-26728

Fault-tolerant scheduling in distributed critical real-time systems p 2952 N94-26735

TAXONOMY

The biostratigraphy and paleogeography of Maastrichtian inoceramids p 2889 N94-28303

TEA LASERS

Development of an industrial CO2 laser for mask marking [DE93-632901] p 2816 N94-26184

TEAMS

Workload transition: Implications for individual and team performance [AD-A274538] p 2941 N94-26964

An investigation of integrated product development implementation issues: A case study of Bosma Machine and Tool Corp. [AD-A273917] p 2942 N94-27320

TEARING MODES (PLASMAS)

Nonlinear growth of strongly unstable tearing modes [DE94-003366] p 3042 N94-25958

TFTR experimental data analysis collaboration [DE94-004166] p 3047 N94-27690

Numerical experiment on finite element method for matching data [DE94-701208] p 3000 N94-27731

TECHNETIUM COMPOUNDS

The potential for large critical currents in the high T(sub c) oxides p 2854 N94-26058

TECHNICAL WRITING

The MUSA design methodology [CWI-CS-R9265] p 3097 N94-26220

TECHNOLOGIES

Emerging technologies [DE94-003022] p 3102 N94-26023

Vision 21: Interdisciplinary Science and Engineering in the Era of Cyberspace [NASA-CP-10129] p 2685 N94-27358

TECHNOLOGY ASSESSMENT

Nuclear electric propulsion for future NASA space science missions [DE93-019086] p 2700 N94-25969

Prospects for utilization of superconductors in the power industry p 2854 N94-26057

The National Center for Advanced Information Components Manufacturing: Program update [DE94-002647] p 2960 N94-26118

Scientific and Technical Information (STI)....what's the status? [DE94-003731] p 3097 N94-26348

Computing in space: Issues and answers p 2948 N94-26714

Advanced nickel-hydrogen spacecraft battery development p 2863 N94-28129

TECHNOLOGY TRANSFER

UV absorption technique for monitoring mobile source NO emissions [AD-A273858] p 2713 N94-25964

General Motors Corporation and Pacific Northwest Laboratory staff exchange: Inspection of case hardened steels and metal-matrix composites [DE94-003470] p 2706 N94-25982

The National Center for Advanced Information Components Manufacturing: Program update [DE94-002647] p 2960 N94-26118

Overview of the Photovoltaic Manufacturing Technology (PVMaT) project [DE93-018234] p 2856 N94-26426

Computing in space: Issues and answers p 2948 N94-26714

Computational mechanics [DE94-003015] p 2965 N94-26775

Feasibility study on construction of a global environment research and development information network [DE94-725198] p 2868 N94-26904

Retrieval using plausible inference [AD-A274252] p 3099 N94-27013

Joint services electronics program [AD-A274643] p 2785 N94-27027

Opportunities for High Aspect Ratio Micro-Electro-Magnetic-Mechanical Systems (HAR-MEMMS) at Lawrence Berkeley Laboratory [DE94-003499] p 2827 N94-27722

TECHNOLOGY UTILIZATION

The potential for the Department of Defense to use space-based remote sensing to support DOD and other government agencies' environmental programs [AD-A273895] p 2847 N94-25656

Radiation applications of physical chemistry p 2854 N94-26054

Prospects for utilization of superconductors in the power industry p 2854 N94-26057

Frontiers of science and measurement: Report on a seminar jointly organized by the National Physical Laboratory and the Institute of Physics [PB94-124310] p 3009 N94-27131

Robotics handbook. Version 1: For the interested party and professional [NASA-TM-109690] p 2824 N94-27238

Research and Development Annual Report, 1992 [NASA-TM-104777] p 3119 N94-27993

Advanced energy storage for space applications: A follow-up p 2860 N94-28103

TECTONICS

Impacts, extinctions, volcanism, glaciations, and tectonics: Matches and mismatches p 2888 N94-28298

TEFLON (TRADEMARK)

Characterization of physically vapor deposited AF2400 thin films [DE94-004019] p 2749 N94-25985

TEKTITES

An extraterrestrial event at the tertiary-quaternary boundary p 2890 N94-28309

TELECOMMUNICATION

Standardize Ada hard real-time services? p 2951 N94-26729

MILCOM 92 and standardization for HF-communication. A study tour to the USA in October 1992 [PB94-124427] p 2774 N94-27219

Coded communications with nonideal interleaving [ITN-94-85235] p 2774 N94-27242

Emerging computer technologies and the news media of the future p 2688 N94-27372

Telescience testbedding for physiological experiments under hypobaric hypoxic conditions p 2913 N94-27449

Telescience testbedding under hypobaric hypoxic conditions: Evaluation by operation ability and recognition ability p 2913 N94-27450

Telescience testbedding for physiological experiments under hypobaric hypoxic conditions: Development and evaluation in CNV measuring p 2913 N94-27451

Single term off-line coins [CWI-CS-R9318] p 2776 N94-27546

Validation tests of TOPSIM 4 [ESA-STM-249] p 2972 N94-27582

A comparative study of SAR data compression schemes p 2946 N94-28259

TELEMETRY

Telecommand decoder specification [ESA-PSS-04-151-ISSUE-1] p 2693 N94-27583

TELEOPERATORS

Graphical programming at Sandia National Laboratories [DE94-003803] p 2958 N94-25818

Performance measures from the explorer platform berthing experiment p 2683 N94-26283

Early lunar rover mission studies p 2684 N94-26290

Telepresence in the human exploration of Mars: Field studies in analog environments p 2685 N94-27360

Telescience testbedding under hypobaric hypoxic conditions: Evaluation by operation ability and recognition ability p 2913 N94-27450

Telescience testbedding for physiological experiments under hypobaric hypoxic conditions: Development and evaluation in CNV measuring p 2913 N94-27451

TELEROBOTICS

Selected topics in robotics for space exploration [NASA-CP-10131] p 2682 N94-26278

Technology drivers for flight telerobotic system software p 2684 N94-26289

Utility fog: A universal physical substance p 2687 N94-27367

TELESCOPES

Distributing functionality in the drift scan camera system [DE94-003640] p 2809 N94-25599

Performance impacts for actuator misalignments and failures in large-aperture adaptive-optic telescopes [AD-A273838] p 3034 N94-25742

TELEVISION CAMERAS

Development of a 2f optical performance measurement system [DE94-003489] p 3039 N94-27721

TELEVISION SYSTEMS

The television as robot servant [AD-A273985] p 2984 N94-25898

VENI, video, VICI: The merging of computer and video technologies p 2686 N94-27362

TELLURIUM

The epitaxial growth of Ge on Si(100) using Te as a surfactant [DE94-003437] p 3056 N94-26326

TELSTAR SATELLITES

Charge efficiency of Ni/H2 cells during transfer orbit of Telstar 4 satellites p 2862 N94-28117

TEMPERATE REGIONS

Short-range cloud amount forecasting with model output statistics [AD-A274769] p 2895 N94-26798

TEMPERATURE CONTROL

Project WISH: The Emerald City p 2703 N94-25690

The 1991-1992 project summaries p 2943 N94-25698

Physical modelling and adaptive predictive control of diffusion/LPCVD reactors [PB94-126398] p 2763 N94-26819

Variable temperature cold stage for microscope observation p 2718 N94-27389

TEMPERATURE DEPENDENCE

On the thermal ignition with variable pre-exponential factor [DE93-616009] p 2713 N94-25913

Optical conductivity and resistivity in the two-band Emery model [DE94-601943] p 3051 N94-25945

Debye-Waller factors of the light actinide metals [DE94-000685] p 2733 N94-26069

The formation of conducting gold films by thermal decomposition and direct patterning using electron beam lithography of the gold cluster Au55P(C6H5)312C16 [AD-A273720] p 2749 N94-26074

Temperature dependence of static RAM volatility [DE93-040345] p 2948 N94-26111

Toward insulating quasicrystalline alloy in Al-Pd-Re icosahedral phase [REPT-A-2666] p 2736 N94-26477

Measurements of the p (mu)d-molecule formation rate at different hydrogen temperature [DE93-634636] p 3020 N94-26511

Ion beam mixing of marker layers into amorphous aluminum oxide [DE94-000901] p 2752 N94-26676

Electrical conductivity of perovskite-magnesiowuestite as a function of pressure and temperature [DE94-002714] p 2880 N94-26806

TEMPERATURE DISTRIBUTION

Ultra-high aggregate bandwidth two-dimensional multiple-wavelength diode laser arrays [AD-A274018] p 2815 N94-25756

Verification of thermal analysis codes for modeling solid rocket nozzles [NASA-CR-195248] p 2702 N94-27150

Ice surface temperature retrieval from AVHRR, ATSR, and passive microwave satellite data: Algorithm development and application [NASA-CR-195276] p 2851 N94-27849

The validation of ATSR measurements with in situ sea temperatures [DE94-003195] p 2852 N94-27875

TEMPERATURE EFFECTS

Bulletin of National Research Institute for Metals in Fiscal Year 1993, no. 14 [REPT-14] p 2722 N94-25544

Preparation of creep data sheet: Material strength data sheet p 2723 N94-25548

Study on variation of damage generation mechanism by fatigue on TiAl compounds due to different slip systems p 2729 N94-25579

Radiation hardening effects on localized deformation and stress corrosion cracking of stainless steels [DE94-004308] p 2731 N94-25804

Microscopic study of local structure and charge distribution in metallic La2CuO(4+delta) [DE94-003801] p 3050 N94-25817

Formation of three types of quasi-crystals in Al-Pd-Mg system [REPT-A-2667] p 3053 N94-26071

Comparison of technology for high-power laser mirrors and synchrotron radiation mirrors [DE94-002913] p 3035 N94-26276

MBE grown 3 to 5 strain relaxed buffer layers and superlattices characterized by atomic force microscopy [DE94-002931] p 3056 N94-26308

On the electron mobility in slightly compensated heavily doped gallium arsenide at low temperatures [DE93-634712] p 3057 N94-26387

Study of precipitation and recrystallization in Al alloy 2519 by backscattered electron imaging methods [AD-A274919] p 2736 N94-26533

Methodology for first wall design [DE94-002795] p 3045 N94-26861

Interface phenomena in metal-ceramic composites [AD-A274167] p 2709 N94-27125

Process modelling of aluminium alloys. Modelling of the quench sensitivity of alloy AA6082 [PB94-124567] p 2741 N94-27325

Annals of the Research Inst. of Environmental Medicine, Nagoya Univ., volume 44 [REPT-44-VOL-44] p 2911 N94-27442

Changes in fluid and electrolyte metabolism during water immersion at high or thermoneutral temperature p 2912 N94-27445

The mechanism of caloric nystagmus under microgravity. 1: Changes of endolymphatic pressure in the semicircular canal of pigeon by caloric stimulation p 2914 N94-27457

Cardiovascular function during thermoneutral head-out water immersion in the elderly p 2915 N94-27458

Effects of 40 C hot water immersion for an hour on thermoregulatory functions in humans: Comparison with 34 C thermoneutral immersion p 2915 N94-27459

Effects of bathing at 40 C on cardiovascular system in humans: Comparison with 34 C thermoneutral bathing p 2918 N94-27473

Effects of 41 C bathing for 20 minutes on cardiovascular and thermoregulatory functions in humans p 2918 N94-27474

Monthly variation of physiological and psychological responses under unsteady thermal conditions p 2918 N94-27475

Man's ability to adapt himself for the seasonal climatic changes: From viewpoint of anticipation and seasonable behavior p 2919 N94-27476

Effect of temperature and recoil-energy spectra on irradiation-induced amorphization in Ca2La8(SiO4)6O2 [DE94-004371] p 3067 N94-27602

Creep rupture properties of a nickel-base heat-resistant alloy Hastelloy XR under varying temperature/stress condition [DE94-701175] p 2743 N94-27807

Silicon device performance measurements to support temperature range enhancement [NASA-CR-195265] p 2844 N94-27824

Damage growth in MgAl2O4 crystals by Xe ion irradiations [DE94-005009] p 3069 N94-27828

NASA-UVA light aerospace alloy and structures technology program (LA2ST) [NASA-CR-195275] p 2844 N94-27851

Kinetic parameters from thermogravimetric analysis p 2721 N94-27909

Evaluation of high temperature superconductive thermal bridges for space-borne cryogenic infrared detectors p 2815 N94-27921

Experimental study on the interactions between a transverse heated supersonic jet and an external supersonic flow p 2659 N94-28039

Orthobaric densities and molar volumes of liquids: Aliphatic and cyclic ketones [ESDU-93010] p 2720 N94-28060

Viscosity of liquids: Halogenated ethanes [ESDU-93012] p 2720 N94-28062

Thermal modeling of NiH2 batteries p 2862 N94-28113

Determination of thermal properties of commercial Ni-MH cells p 2864 N94-28132

Mechanical behavior of amorphous alloys at elevated temperatures p 2746 N94-28167

MODIS airborne simulator visible and near-infrared calibration, 1991 FIRE-Cirrus field experiment. Calibration version: FIRE King 1.1 [NASA-TM-104600] p 2897 N94-28182

Proposed law of nature linking impacts, plume volcanism, and Milankovitch cycles to terrestrial vertebrate mass extinctions via greenhouse-embryo death coupling p 2876 N94-28307

TEMPERATURE GRADIENTS

Kinetic resonance damping rate of the toroidal ion temperature gradient mode [DE94-003511] p 3041 N94-25923

A transient symmetrical method for the measurement of temperature dependent thermal diffusivity [VTT-TIED-1452] p 3008 N94-26256

Development of detection technique for fatigue crack due to thermal stratification phenomena in RCS piping [DE93-632968] p 2838 N94-26400

NASA-UVA light aerospace alloy and structures technology program (LA2ST) [NASA-CR-195275] p 2844 N94-27851

TEMPERATURE MEASUREMENT

Interpreting the implied meridional oceanic energy transport in AMIP [DE94-001538] p 2898 N94-26072

Gordon Research Conference on the Physics and Chemistry of Laser Diagnostics in Combustion [AD-A274609] p 2716 N94-26893

Shine through measurements with hydrogen beam in JT-60 [DE94-701113] p 3047 N94-27699

Uncertainties in the characterization of the thermal environment of a solid rocket propellant fire [DE94-002023] p 2760 N94-27719

Ice surface temperature retrieval from AVHRR, ATSR, and passive microwave satellite data: Algorithm development and application [NASA-CR-195276] p 2851 N94-27849

The validation of ATSR measurements with in situ sea temperatures [DE94-003195] p 2852 N94-27875

TEMPERATURE PROFILES

Piecewise least squares fitting technique using finite interval method with Hermite polynomials [VTT-PUBS-135] p 2990 N94-25733

Modelling the mass migration phenomena in partially frozen heat pipes [DE94-002716] p 2797 N94-27709

Predictions of momentum and scalar fields in a jet in cross-flow using first and second order turbulence closures p 2803 N94-28025

TEMPLATES

Template synthesis of metal microtubule ensembles utilizing chemical, electrochemical, and vacuum deposition techniques [AD-A274676] p 2715 N94-26444

Three dimensional object recognition using a complex autoregressive model [AD-A274388] p 2995 N94-26829

An algorithm for stereo correspondence problems on the analogy of human vision [NAL-TR-1185] p 2940 N94-27584

TEMPORAL RESOLUTION

Morphodynamics of inter-tidal areas: The Wadden Sea [NLR-TP-92356-U] p 2851 N94-27555

TENSILE PROPERTIES

Structural analysis of a frangible nut used on the NASA Space Shuttle [DE94-003672] p 2821 N94-25811

Effects of post-fabrication processing on the tensile properties of centrifugally cast SiC particulate reinforced aluminum composites
[AD-A274865] p 2707 N94-26190
Titanium 1992: Science and Technology, volume 1
[AD-A274798-VOL-1] p 2739 N94-26799
Aluminum alloy 8090-T8771 thick plate material characterization
[AD-A274146] p 2987 N94-27077

TENSILE STRENGTH
Study on ferromagnetic field magnet using strong and highly conductive material p 2725 N94-25559
Study on alloy films for hydrogen separation
p 2726 N94-25565
Inert strength of pristine silica glass fibers
[DE94-004685] p 2750 N94-26247
Fatigue resistance under tension-compression of laminates IM6/5245C and AS4/3501-6
[IAR-CR-25] p 2708 N94-26711
Processing and mechanical properties of laminated metal composites of Al 6090-25 volume percent SiC(sub p) and Al 5182
[DE94-001070] p 2708 N94-26930
High temperature tension test equipment of heat resistant composite materials
[NAL-TM-652] p 2710 N94-27255
Formation and high mechanical strength of Al-based alloys containing a nanoscale icosahedral phase as a main constituent p 2746 N94-28171

TENSILE STRESS
Determination of fracture stress and effective crack tip radius from toughness (KIc) and yield strength (Y)
[AD-A274014] p 2836 N94-25754
Investigation of tension-compression fatigue behavior of a cross-ply metal matrix composite at room and elevated temperatures
[AD-A273731] p 2706 N94-25999
Grain by grain study of the mechanisms of crack propagation during iodine SCC of Zry-4
[DE93-633765] p 2734 N94-26162

TENSILE TESTS
Structural analysis of a frangible nut used on the NASA Space Shuttle
[DE94-003672] p 2821 N94-25811
A study of graphite peek composite with central elliptical holes under tension
[AD-A273779] p 2705 N94-25863
An investigation of cavitation in a mechanically alloyed 15 volume percent SiCp/IN9021 aluminum composite
[DE94-003371] p 2748 N94-25959
SP/MSP tests for the evaluation of FGM
[NAL-SP-17] p 2710 N94-27279
SP/MSP tests for the evaluation of FGM
p 2710 N94-27280
Research on the development of fracture characteristics evaluation system for ceramics and metal composite materials p 2710 N94-27281
Development of a new seal for use on large openings of pressurized spacecraft
[NASA-TM-108444] p 2825 N94-27560
Use of photostress and strain gages to analyze behavior of weldments
[NASA-CR-195269] p 2843 N94-27765
Investigation of the bond strength of a discrete skin-stiffener interface
[NLR-TP-92183-U] p 2670 N94-27796
Mechanical properties and microstructure of thermomechanically processed, high manganese steel
[ARL-TR-146] p 2747 N94-28212

TENSORS
A note on Riemannian 2-space
[DE94-602560] p 3073 N94-27024
The Einstein tensor characterizing some Riemann spaces
[DE94-603663] p 3074 N94-27626

TERBIUM COMPOUNDS
Laser surface modification of intermetallic compounds
[DREA-CR-92-416] p 2820 N94-27668

TERCOM
Flight testing of GPS and GPS-aided systems
[NLR-TP-92151-U] p 2666 N94-27831

TERMINAL BALLISTICS
Dynamic response of S-2 glass reinforced plastic structural armor
[AD-A273868] p 2747 N94-25596
Design study of fiber-composite penetrator cases
[DE94-003203] p 2707 N94-26099
Trajectories of ballistic impact ejecta on a rotating Earth p 2887 N94-28295

TERMINAL FACILITIES
The design of a long-range megatransport aircraft
p 2671 N94-25718

TERMINOLOGY
Correspondence dictionary from free English term to INIS descriptors
[DE94-701173] p 3100 N94-27700

TERMS
Correspondence dictionary from free English term to INIS descriptors
[DE94-701173] p 3100 N94-27700

TERNARY ALLOYS
Study on improvement in physical analysis method of metallic materials p 2728 N94-25577
Zr-rich corner of the Zr-Sn-O diagram
[DE93-633764] p 2734 N94-26161
A tri-junction diffusion couple analysis of the Nb-Cr-Ti system at 950 C
[DE94-002637] p 2737 N94-26607
NMR study of quasicrystal Al(70)Pd(20)T(M10) alloy (T(M):Cr, Mn, Fe, and Co) p 2745 N94-28162

TERNARY SYSTEMS
Zr-rich corner of the Zr-Sn-O diagram
[DE93-633764] p 2734 N94-26161

TERRAIN
Recent ASCOT experiments in multi-layered flows
[DE94-002360] p 2880 N94-26762
Conifer tree influence on Digital Terrain Elevation Data (DTED): A case study at Dulles International Airport
[AD-A274213] p 2849 N94-27069
An overview of the ASCOT program
[DE94-004356] p 2869 N94-27601
Landscape dynamics of northeastern forests
[NASA-CR-195272] p 2852 N94-28070

TERRAIN ANALYSIS
Construction and applications of the two dimensional Delaunay triangulated irregular network and the three dimensional Delaunay tetrahedron model
[ETN-94-95034] p 2848 N94-26651

TERTIARY PERIOD
An extraterrestrial event at the tertiary-quaternary boundary p 2890 N94-28309

TEST CHAMBERS
Program for calculation of maximum lift coefficient of plain aerofoils and wings at subsonic speeds
[ESDU-93015] p 2649 N94-28076

TEST EQUIPMENT
High temperature solid oxide fuel cell: Customer test units
[DE94-002961] p 2858 N94-26869

TEST FACILITIES
Primary standards laboratory report 1st half 1993
[DE94-003138] p 2762 N94-26027
NASA Lewis Research Center lean-, rich-burn materials test burner rig
[NASA-CR-194437] p 2680 N94-26141
The development of a horizontal impact sled facility and subsequent crashworthiness experiments
[NIAR-93-15] p 2680 N94-26200
A method for testing of HVAC automation equipment using the emulator and the application of the method
[VTT-TIED-1435] p 2822 N94-26306
Fusion Energy Advisory Committee: Advice and recommendations to the US Department of Energy in response to the charge letter of September 1, 1992
[DE93-019842] p 3043 N94-26428
An assessment of testing requirement impacts on nuclear thermal propulsion ground test facility design
[DE94-002933] p 2702 N94-26560
Research and test facilities
[NASA-TM-109685] p 2681 N94-26684
Calibrating/testing meters in hot water test bench VM7
[PB94-124294] p 2812 N94-27160
Description of the Experimental Avionics Systems Integration Laboratory (EASILY)
[NASA-TM-109072] p 2681 N94-27425
Design, implementation and experimental results of robotic environment input into the Robot Controller Test Station (RCTS)
[ISBN-0-315-85355-7] p 2826 N94-27596
Experimental data for CFD validation of impinging jets in crossflow with application to ASTOVL flow problems
p 2801 N94-28010

TEST PATTERN GENERATORS
Automatic test case generation using PROLOG
[NPL-DITC-215/93] p 2964 N94-26655

TEST STANDS
Shake test results of the MDHC test stand in the 40- by 80-foot wind tunnel
[NASA-TM-108801] p 2641 N94-26596
Space Station technology testbed: 2010 deep space transport p 2687 N94-27368
Advanced development of particle beam probe diagnostic system
[DE94-002316] p 3047 N94-27720

TEST VEHICLES
Ferroelectric fluoride memory FET development
[AD-A274341] p 2785 N94-27057

TETHERLINES
The 1991-1992 project summaries
p 2943 N94-25698

TETRAETHYL ORTHOSILICATE
Sol-gel derived silica/siloxane composite materials: The effect of loading level and catalyst activity on silica domain formation
[DE94-002734] p 2712 N94-27710

TETRAHEDRONS
Spatial symmetry, local integrability and tetrahedron equations in the Baxter-Bazhanov model
[DE93-634348] p 3002 N94-26038

TETRAHYDROFURAN
The reactivity of lithium toward non-aqueous solvents of relevance to energy storage applications as studied by surface analytical techniques
[DE94-003483] p 2856 N94-26464

TEXTS
Full-text information services at the desktop
[DE94-003728] p 3096 N94-25813

THAILAND
The Environmental Research and Training Centre
p 2873 N94-28280
Changes in phytoplankton population in the Chao Phraya estuary, Thailand, during the eutrophication mechanisms studies p 2875 N94-28287
Land use change in Thailand and its impact on environmental change: Joint Thai-Japanese research project (1993-1995) p 2875 N94-28288

THALAMUS
Cortical mechanisms of attention, discrimination, and motor response to somesthetic stimuli
[AD-A274163] p 2940 N94-27141

THEOREMS
Chebyshev-Markov rational functions over several intervals
[PB94-125333] p 2998 N94-27116
Wieand's theorem
[PB94-126711] p 3004 N94-27223
The Einstein tensor characterizing some Riemann spaces
[DE94-603663] p 3074 N94-27626

THEORETICAL PHYSICS
Duality for multiparametric quantum GL(n) and for a Lorentz quantum group
[DE93-613048] p 3005 N94-25868
Theoretical and experimental studies of elementary physics
[DE94-002310] p 3008 N94-25988
Z(sub N)(sup n-1) broken model
[DE93-634357] p 3072 N94-26039
Lepton masses in an SU(3)(sub L) x U(1)(sub N) gauge model
[DE93-634366] p 3016 N94-26040
Dimensional crossover from non-renormalizability to renormalizability
[DE93-613052] p 3006 N94-26193
Stability of large scale interconnected dynamical systems
[DE94-601536] p 2993 N94-26408
Characterization of self-conjugate minimal surfaces in R(sup 3)
[DE94-601538] p 2993 N94-26409
Enumeration of n-fold tangent hyperplanes to a surface
[DE94-601544] p 2993 N94-26412
On the phi(sub 0)-stability of perturbed nonlinear differential systems
[DE93-634304] p 2993 N94-26441
Anomaly candidates and invariants of D 4, N 1 supergravity theories
[NIKHEF-H/93-12] p 3072 N94-26541
Strange Dibaryons
[DE94-003005] p 3022 N94-26769
Flavor changing neutral currents in SU(3) x U(1) models
[DE94-602576] p 3022 N94-26899

THERAPY
Rewarming methodologies in the field
[AD-A274744] p 2909 N94-26173
Development of surgical CW Nd:YAG laser with optical fiber delivery system
[DE93-632902] p 2817 N94-26185
Bakteriella toxiner-morgondagens hot (bacterial toxins-the threat of tomorrow)
[PB94-124229] p 2902 N94-27045

THERMAL ANALYSIS
Aspects of the circuit board thermal design
[VTT-PUBS-132] p 2779 N94-25644
Modelling the inhibition cure behaviour of unsaturated polyester moulding materials
[PB94-124864] p 2748 N94-25893
Evaluation of helium cooling for fusion divertors
[DE94-002680] p 3042 N94-25976
User's guide for the thermal analyst's help desk expert system
[NASA-CR-194885] p 2695 N94-26103
Design of gasifiers to optimize fuel cell systems
[DE94-000010] p 2856 N94-26581

Thermal/structural tailoring of engine blades (T/STAEBL). User's manual
[NASA-CR-194463] p 2839 N94-26692
Verification of thermal analysis codes for modeling solid rocket nozzles
[NASA-CR-195248] p 2702 N94-27150
Thermal/Structural Tailoring of Engine Blades (T/STAEBL): User's manual
[NASA-CR-194461] p 2843 N94-27776
Evaluation of high temperature superconductive thermal bridges for space-borne cryogenic infrared detectors
p 2815 N94-27921
Thermal modeling of NiH2 batteries
p 2862 N94-28113
Use of calorimetry for end of charge determination
p 2863 N94-28128

THERMAL BATTERIES
Effects of repeating resistance testing on firing ability of igniter EP360-3
[AD-A274814] p 2759 N94-26486

THERMAL CONDUCTIVITY
Thermal conductivity of PAX 2A explosive by DSC
[AD-A274721] p 2759 N94-26437
Sound, speed, reflectivity, absorption, and thermal diffusivity measurements in Arctic ice in 1990
[AD-A274326] p 2899 N94-26886
Thermal conductivity of liquid aliphatic alcohols
[ESDU-93008] p 2720 N94-28058
Thermal conductivity of liquid carboxylic acids
[ESDU-93017] p 2721 N94-28138

THERMAL DECOMPOSITION
The formation of conducting gold films by thermal decomposition and direct patterning using electron beam lithography of the gold cluster Au55P(C6H5)312C16
[AD-A273720] p 2749 N94-26074
Mechanistic studies of opto-electronic materials and syntheses using multiple laser and surface diagnostics
[AD-A274528] p 3036 N94-26834
Bench-scale synthesis of nanoscale materials
[DE94-004787] p 2742 N94-27786

THERMAL DEGRADATION
Kinetic parameters from thermogravimetric analysis
p 2721 N94-27909

THERMAL DIFFUSIVITY
Sound, speed, reflectivity, absorption, and thermal diffusivity measurements in Arctic ice in 1990
[AD-A274326] p 2899 N94-26886
TFTR experimental data analysis collaboration
[DE94-004166] p 3047 N94-27690

THERMAL EMISSION
Martian atmospheric radiation budget
p 3107 N94-27887

THERMAL ENVIRONMENTS
Uncertainties in the characterization of the thermal environment of a solid rocket propellant fire
[DE94-002023] p 2760 N94-27719

THERMAL FATIGUE
Characterization of fatigue damage in a metal matrix composite (SCS-6/Ti-15-3) at elevated temperature
[AD-A273797] p 2706 N94-25876
Investigation of tension-compression fatigue behavior of a cross-ply metal matrix composite at room and elevated temperatures
[AD-A273731] p 2706 N94-25999
Development of detection technique for fatigue crack due to thermal stratification phenomena in RCS piping
[DE93-632968] p 2838 N94-26400

THERMAL INSULATION
Cryogenic insulation studies
[NASA-CR-195266] p 2756 N94-27429

THERMAL MAPPING
An apparatus for measurement of ignition and burning characteristics of metallic particles
[AD-A274815] p 2716 N94-26487

THERMAL NEUTRONS
Surface physics with cold and thermal neutron reflectometry
[DE94-001447] p 2733 N94-26070
Neutron-neutron scattering: Possibility of in-beam experiment
[DE94-606459] p 3027 N94-27682

THERMAL NOISE
Geometrical resonances in the nyquist noise spectrum for ballistic conductors
[DE94-603668] p 3027 N94-27631

THERMAL PLASMAS
Theoretical aspects of the agile mirror
[AD-A274890] p 2767 N94-26177

THERMAL PROTECTION
Minimum accommodation for aerobrake assembly, phase 2
[NASA-TM-107608] p 2692 N94-27774
Debris/ice/TPS assessment and integrated photographic analysis for Shuttle mission STS-60
[NASA-TM-109193] p 2692 N94-27956

THERMAL RADIATION
User's guide for the thermal analyst's help desk expert system
[NASA-CR-194885] p 2695 N94-26103
Computer model for generation of infrared images
[PB94-123551] p 3005 N94-27172
Researches of the Electrotechnical Laboratory. No. 53: Spectral emission from combustion gas containing scattering media
[JTN-94-80603] p 2717 N94-27246

THERMAL REACTORS
A review of carbide fuel corrosion for nuclear thermal propulsion applications
[DE94-003938] p 2699 N94-25613

THERMAL RESISTANCE
Study on high temperature damage control and life improvement p 2729 N94-25580
Method for improving electromagnetic shielding performance of composite materials by electropulsing
[AD-D016050] p 2709 N94-27076

THERMAL SHOCK
Collaborative research on ion implantation of ceramics
[DE93-019177] p 2749 N94-26080

THERMAL STABILITY
Accelerated screening methods for determining chemical and thermal stability of refrigerant-lubricant mixtures. Part 2: Experimental comparison and verification of methods
[DE94-003664] p 2749 N94-26007
The influence of weld metal alloying additions to extend the heat input range for the submerged arc welding of high strength steels
[AD-A274284] p 2738 N94-26679
Thermally stable oxygen and nitrogen implant isolation of C-doped Al(0.35)Ga(0.65)As
[DE94-004799] p 3069 N94-27790
Broad specification fuels combustion technology program, phase 2
[NASA-CR-191066] p 2719 N94-27854
New monomers for high performance polymers
p 2758 N94-27904
Kinetic parameters from thermogravimetric analysis
p 2721 N94-27909

THERMAL STRESSES
A review of carbide fuel corrosion for nuclear thermal propulsion applications
[DE94-003938] p 2699 N94-25613
The fracture behavior of a CVD crystalline Si3N4/amorphous Si3N4 composite
[DE94-002646] p 2750 N94-26124
Electrical analysis of wideband and distributed windows using time-dependent field codes
[DE94-002987] p 2768 N94-26310
Baseline for a Nordtest method. Reliability stress screening of components. A guide for component users
[PB94-123775] p 2835 N94-27042
Implementation of thermal residual stresses in the analysis of fiber bridged matrix crack growth in titanium matrix composites
[NASA-TM-109082] p 2711 N94-27658
Development of methodologies for the estimation of thermal properties associated with aerospace vehicles
p 2846 N94-27920

THERMIONIC EMISSION
Channel model for AC electric arc
[PB94-124591] p 2786 N94-27327

THERMIONIC POWER GENERATION
Space-R thermionic space nuclear power system design and technology demonstration
[DE94-002017] p 2700 N94-25930

THERMOCHEMISTRY
The addition of molecular oxygen to hydroperoxy-propyl radicals
[DE94-003662] p 2760 N94-27725

THERMOCOUPLES
Verification of thermal analysis codes for modeling solid rocket nozzles
[NASA-CR-195248] p 2702 N94-27150
Effects of free-stream turbulence on a jet in a cross flow p 2805 N94-28036

THERMODYNAMIC CYCLES
A technique for integrating engine cycle and aircraft configuration optimization
[NASA-CR-191602] p 2668 N94-26606
Gas fired advanced turbine system
[DE94-003193] p 2827 N94-27874
Combined Cycles for Power Plants
[VKI-LS-1993-08] p 2830 N94-28077

THERMODYNAMIC EFFICIENCY
Pressure-gain combustion
[DE94-002975] p 2719 N94-27712
Gas fired advanced turbine system
[DE94-003193] p 2827 N94-27874

THERMODYNAMIC EQUILIBRIUM
Antiproton studies in penning traps
[AD-A274250] p 3024 N94-27011
Phase stability in the Cd-Mg system
[DE94-004976] p 2743 N94-27792

THERMODYNAMIC PROPERTIES
Zr-rich corner of the Zr-Sn-O diagram
[DE93-633764] p 2734 N94-26161
Microwave and pulsed power
[DE94-003019] p 2782 N94-26312
Titanium 1992: Volume 3: Science and technology
[AD-A274800] p 2735 N94-26337
How reliable is the HMSA integral equation for the pair structure of supercooled and amorphous mixtures?
[DE94-601543] p 3006 N94-26411
New rubber qualification for the igniter adapter
[NASA-CR-193936] p 2752 N94-26708
Thermophysical properties of HFC-143a and HFC-152a
[DE94-004236] p 2719 N94-27567
Phase stability in the Cd-Mg system
[DE94-004976] p 2743 N94-27792
Development of methodologies for the estimation of thermal properties associated with aerospace vehicles
p 2846 N94-27920

THERMODYNAMICS
A thermodynamically consistent constitutive theory for a rigid solid-stokesian fluid mixture
[DE93-633202] p 2792 N94-26401
Calculating the surface properties for the liquid-vapour interface: Illustrating the thermodynamic stability of the spherical microstructures
[DE94-601992] p 3073 N94-26837
Thermodynamics and form factors of supersymmetric integrable field theories
[DE94-602557] p 3073 N94-26896
Integrated model development for liquid fueled rocket propulsion systems
[NASA-CR-195253] p 2702 N94-27166
Process modelling of aluminium alloys. Modelling of the quench sensitivity of alloy AA6082
[PB94-124567] p 2741 N94-27325
Thermodynamics of combined cycle plant
p 2831 N94-28079

THERMOELASTICITY
Stress analysis of a secondary-bending specimen
[AD-A274842] p 2838 N94-26501

THERMOELECTRIC GENERATORS
Preliminary reentry safety assessment of the General Purpose Heat Source module for the Cassini mission: Aerospace Nuclear Safety Program
[DE94-001646] p 2699 N94-25926
Digital control and data acquisition for high-value GTA welding
[DE94-000885] p 2821 N94-25980

THERMOELECTRIC POWER GENERATION
Hybrid power system for remote communications stations
[AD-A274963] p 2782 N94-26301

THERMOGRAVIMETRY
Thermogravimetric study of oxidation of a PdCr alloy used for high-temperature sensors
[NASA-TM-106473] p 2741 N94-27426
Kinetic parameters from thermogravimetric analysis
p 2721 N94-27909

THERMOMECHANICAL TREATMENT
Effects of post-fabrication processing on the tensile properties of centrifugally cast SiC particulate reinforced aluminum composites
[AD-A274865] p 2707 N94-26190
Study of precipitation and recrystallization in Al alloy 2519 by backscattered electron imaging methods
[AD-A274919] p 2736 N94-26533
Mechanical properties and microstructure of thermomechanically processed, high manganese steel
[ARL-TR-146] p 2747 N94-28212

THERMONUCLEAR POWER GENERATION
Methodology for first wall design
[DE94-002795] p 3045 N94-26861

THERMOPHYSICAL PROPERTIES
Zr-rich corner of the Zr-Sn-O diagram
[DE93-633764] p 2734 N94-26161
Eleventh Symposium on Energy Engineering Sciences: Proceedings
[DE93-019930] p 2763 N94-26429
Thermophysical properties of HFC-143a and HFC-152a
[DE94-004236] p 2719 N94-27567
Thermophysical properties of refrigerant R-134a (1,1,1,2-tetrafluoroethane)
[ESDU-93001] p 2720 N94-27959
Thermal modeling of NiH2 batteries
p 2862 N94-28113

THERMOPLASTIC RESINS
Continuous fiber reinforced thermoplastic composites: Literature survey
[VTT-TIED-1422] p 2704 N94-25651
Design for producing fiberglass fabric in a lunar environment p 2765 N94-25676

Thermoplastic elastomers having alternate crystalline structure for us as high energy binders
[AD-D016035] p 2755 N94-27203
Thermoplastic or thermosetting composites in aircrafts
[PB94-123809] p 2710 N94-27253

THERMOPLASTICITY
Lunar preform manufacturing p 2765 N94-25677
Impact tests on fibre metal laminates under a tensile load
[PB94-126570] p 2710 N94-27201
Thermoplastic or thermosetting composites in aircrafts
[PB94-123809] p 2710 N94-27253

THERMOREGULATION
Plasma volume shifts and exercise thermoregulation with water immersion and six-degree head-down tilt
[NASA-TM-108781] p 2901 N94-26093
Thermoregulatory effects of caffeine ingestion during rest and exercise in men
[NASA-TM-108783] p 2901 N94-26210
Effects of 40 C hot water immersion for an hour on thermoregulatory functions in humans: Comparison with 34 C thermoneutral immersion p 2915 N94-27459
Effects of 41 C bathing for 20 minutes on cardiovascular and thermoregulatory functions in humans
p 2918 N94-27474

THERMOSETTING RESINS
Ultrasonic measurement technique to determine the state of cure in thermosetting materials
[PB94-124328] p 2756 N94-27217
Thermoplastic or thermosetting composites in aircrafts
[PB94-123809] p 2710 N94-27253

THERMOSPHERE
Upper atmosphere neutral and plasma density modeling
[AD-A274768] p 2879 N94-26569
Solar and airglow measurements aboard the two suborbital flights NASA 36.098 and 36.107
[NASA-CR-195279] p 2882 N94-27380

THERMOSTATS
Stress relaxation in dough moulding compounds
[PB94-124872] p 2748 N94-25894

THESAURI
Correspondence dictionary from free English term to INIS descriptors
[DE94-701173] p 3100 N94-27700

THESES
Automation of formation flight control
[AD-A274137] p 2678 N94-27132

THICK FILMS
Electro-optic materials by solid source MOCVD
[DE94-005120] p 2757 N94-27716

THICKNESS
Automated in-situ inspection systems for underground storage tanks
[AD-A274644] p 2764 N94-27144

THIN FILMS
Development of intermetallic compounds for high performance luminescence elements
p 2722 N94-25545
Hydrogen trapping with Pd coated alloy films
p 2723 N94-25551
Study on synthesis and characteristics of intermetallic compound with strong electron correlation
p 2726 N94-25563
Study on alloy films for hydrogen separation
p 2726 N94-25565
Fundamental study on new synthetic technology by phthalocyanine complexes p 2721 N94-25569
Study on substance diffusion in thin films with controlled structures p 2727 N94-25570
Object imaging accomplished with an integrated circuit robotic tactile sensor incorporating a piezoelectric polyvinylidene fluoride thin film
[AD-A274038] p 2780 N94-25845
Crystallization and microstructural control of ferroelectric thin-films and glass-ceramics
[AD-A273767] p 2748 N94-25854
In situ x ray reflectivity measurements of thin film structural evolution
[DE94-002289] p 3051 N94-25944
Optimization of experimental conditions in IR reflectance determination of BPSG properties
[DE94-002742] p 2713 N94-25978
Characterization of physically vapor deposited AF2400 thin films
[DE94-004019] p 2749 N94-25985
Plasma surface cleaning using microwave plasmas
[DE94-002754] p 2713 N94-26014
Buckyball microwave plasmas: Fragmentation and diamond-film growth
[DE94-003209] p 3053 N94-26031
Micropyrolysis of polymer thin films for ceramics
[ECL-92-62] p 2750 N94-26088
The state of the art of thin-film photovoltaics
[DE94-000224] p 2855 N94-26115
Stress relaxation in sputtered W films and W/GeSi/Si heterostructures
[DE94-004007] p 3055 N94-26239
Studies of thin-film growth, adsorption, and oxidation by in situ, real-time, and ex situ ion beam analysis
[DE94-002907] p 3055 N94-26275
The epitaxial growth of Ge on Si(100) using Te as a surfactant
[DE94-003437] p 3056 N94-26326
The deposition of boron nitride and carbon films on silica glass fibers
[DE94-004684] p 2751 N94-26564
An x ray absorption fine structure study of ordering in polythiophene thin films
[AD-A274235] p 2753 N94-26822
Nitride semiconductors for ultraviolet detection
[AD-A274246] p 3060 N94-26840
Pseudomorphic semiconducting heterostructures from combinations of AlN, GaN and selected SiC polytypes: Theoretical advancement and its coordination with experimental studies of nucleation, growth, characterization and device development
[AD-A274247] p 3061 N94-26841
Ferroelectric thin film microstructure development and related property enhancement
[DE94-002741] p 3061 N94-26856
Atomic layer epitaxy of group 4 materials: Surface processes, thin films, devices and their characterization
[AD-A274325] p 3061 N94-26885
Processing, fabrication, and demonstration of HTS integrated microwave circuits, appendix A
[AD-A274600] p 2785 N94-26890
Ion implantation and dynamic recovery of tin-doped indium oxide films
[DE94-001126] p 3062 N94-26932
The growth and characterization of GaN as a photodetector
[AD-A274570] p 3063 N94-26965
Low temperature deposition and characterization of N- and p-type silicon carbide thin films and associated ohmic and Schottky contacts
[AD-A274345] p 2754 N94-26974
Ferroelectric fluoride memory FET development
[AD-A274341] p 2785 N94-27057
High intensity x ray instrumentation for residual strain measurements in composites and textured materials
[ISBN-0-315-85169-4] p 2842 N94-27278
Synthesis of diamond film assisted by an arcjet plasma source, part 2
[INPE-5527-PRP/178-PT-2] p 3066 N94-27329
List of papers published by the members of Institute for Materials Research, Tohoku University 1992
[JTN-94-80608] p 3118 N94-27355
Research on high-efficiency, large-area, CuInSe2 based thin-film modules
[DE94-000259] p 3067 N94-27609
High-efficiency, thin-film solar cells
[DE94-000250] p 2860 N94-27625
Electro-optic materials by solid source MOCVD
[DE94-005120] p 2757 N94-27716
The ZnO thin films with C-axis orientation prepared on the room temperature substrate by the ECR multipolar plasma sputtering method
[DE94-605039] p 2758 N94-27857
Aerodynamic heating in hypersonic flows
p 2658 N94-27919
Prometheus in space: Research Committee on Functional New Material
[JTN-94-80580] p 2761 N94-28002
The Science Reports of the Research Institutes, Tohoku University. Series A: Physics, Chemistry, and Metallurgy. Volume 38, No. 1: Amorphous Materials 14
[JTN-94-80610] p 2744 N94-28158
Differential scanning calorimetric study of solid state amorphization and crystallization in Zr/Co and Zr/Ni multilayers p 2745 N94-28161

THIN PLATES
Radial basis function approximation: From gridded centers to scattered centers
[AD-A274184] p 2998 N94-27103
A numerical approach to Stefan problem
[IPPCZ-334] p 2844 N94-27841

THIN WALLS
Growth of small fatigue cracks in Incoloy-908
[DE94-003406] p 2836 N94-26129

THOMSON SCATTERING
New Thomson scattering laser control for D3-D
[DE94-002890] p 3043 N94-26274

THREE BODY PROBLEM
Muon transfer rates in collisions of hydrogen isotope mesic atoms on bare nuclei: Multichannel adiabatic approach
[DE94-606752] p 3030 N94-27861

THREE DIMENSIONAL BODIES
Combining shape and color information for 3D object recognition
[AD-A274123] p 2967 N94-27064

THREE DIMENSIONAL BOUNDARY LAYER
Transition for three-dimensional, compressible boundary layers p 2653 N94-28327
Euler and Navier-Stokes wing/fuselage computations of the De Havilland Dash 8 aircraft p 2654 N94-28329

THREE DIMENSIONAL COMPOSITES
Fatigue resistance of unnotched and post impact(+/-30 deg/0 deg) 3-D braided composites
[NASA-CR-191590] p 2711 N94-27433

THREE DIMENSIONAL FLOW
The high Reynolds number flow through an axial-flow pump
[AD-A273844] p 2789 N94-25604
Effects of crenulations on three dimensional losses in a linear compressor cascade
[AD-A273778] p 2790 N94-25862
The effects of three-dimensional imposed 3-d disturbances on bluff-body near wake flows
[AD-A274845] p 2791 N94-26187
Program to develop a performance and heat load prediction system for multistage turbines
[NASA-CR-195223] p 2674 N94-26588
Computational strategies for three-dimensional flow simulations on distributed computer systems
[NASA-CR-195249] p 2793 N94-26595
Research on bluff body vortex wakes
[AD-A273780] p 2796 N94-27319
Agglomeration multigrid for the three-dimensional Euler equations
[NASA-CR-191595] p 2999 N94-27557
Navier-Stokes simulation of two and three dimensional jets in crossflow, effects of grid, and boundary conditions p 2804 N94-28026
An initial investigation into methods of computing transonic aerodynamic sensitivity coefficients
[NASA-CR-195705] p 2648 N94-28072

THREE DIMENSIONAL MODELS
Calculation of a 3-D pose of a known object in a single perspective view
[VTT-PUBS-122] p 2957 N94-25642
A nonlinear three-dimensional micromechanics model for fiber-reinforced laminated composites
[AD-A273772] p 2705 N94-25857
Satellite attitude determination using linear combination of models
[AD-A274082] p 2694 N94-25996
Correlation of experimental data and three-dimensional finite element modeling of a spinning quadrupole
[DE93-041173] p 3008 N94-26421
Extracting complete 3-dimensional boundary representation from multiple range images
[ISBN-0-315-83776-4] p 2963 N94-26615
A preliminary shear velocity model for Central Asia
[AD-A274972] p 2880 N94-26752
Building 3-D models from unregistered range images
[AD-A274126] p 2986 N94-27032
Dynamic and kinematic P wave tracing for a three-dimensional elastic inhomogeneous media by the asymptotic ray theory and application
[ITN-94-85239] p 2775 N94-27244
The three-dimensional hydrogen atom in crossed magnetic and electric fields
[DE94-606301] p 3029 N94-27847
Lisp interface to geometric modelling operations
[PB94-133121] p 3001 N94-28398

THRUST MEASUREMENT
Simulating indirect thrust measurement methods as used on modern high-bypass turbofans
[ISBN-0-315-84123-0] p 2674 N94-26673

THRUST REVERSAL
Experimental investigation of the interaction of a thrust reverser jet with an external subsonic flow
p 2801 N94-28011
A study of jet effect and ground effect interference on a STOL fighter p 2671 N94-28034

THRUST VECTOR CONTROL
Evaluation of moderate angle of attack roll of a dual engine, thrust vectoring aircraft using quantitative feedback theory
[AD-A274118] p 2667 N94-25905
Vectored jets-induced interference on aircraft, prediction and verification p 2801 N94-28012
Numerical investigation of thrust vectoring by injection of secondary air into nozzle flows p 2801 N94-28013
A study of jet effect and ground effect interference on a STOL fighter p 2671 N94-28034

THULIUM
The development of Cr, Tm, Ho:YAG lasers for airborne lidar
[AD-A274895] p 2816 N94-26178

THUNDERSTORMS
A modeling study of the mesocyclone
[AD-A274889] p 2893 N94-26168
Examination of micro- and macro-physical structures and processes in hailstorms with respect to their modification
[DLR-FB-93-25] p 2897 N94-27751
Thunderstorm Hypothesis Reasoner
[NASA-CR-195714] p 2897 N94-27884
MUSIC for localization of thunderstorm cells
[DE94-004985] p 2897 N94-28146

THYRISTORS
A study of DC-DC converters with MCT's for arcjet power supplies
[NASA-CR-191204] p 2703 N94-27662
Silicon device performance measurements to support temperature range enhancement
[NASA-CR-195265] p 2844 N94-27824

THYROID GLAND
Muscle sympathetic nerve activity in patients with hyper-and hypothyroidism: A microneurographic study
p 2930 N94-27531

THYROXINE
Expression analysis of Thyroxine-Binding Globulin Complete Deficiency in Japanese (TBG-CDJ)
p 2905 N94-27482

TIDAL FLATS
Morphodynamics of inter-tidal areas: The Wadden Sea
[NLR-TP-92356-U] p 2851 N94-27555

TIDES
Upper atmosphere neutral and plasma density modeling
[AD-A274768] p 2879 N94-26569
Macrobenthic fauna in the dutch sector of the north sea in 1991
[PB94-126414] p 2868 N94-27200
Modulating terrestrial impacts from Oort cloud comets by the adiabatically changing galactic tides
p 2890 N94-28305

TILES
Design and evaluation of an electromagnetic beam waveguide for measuring electrical properties of materials
[NASA-TP-3418] p 2769 N94-26611

TILT ROTOR AIRCRAFT
Design optimization of high-speed proprotor aircraft
[NASA-TM-103988] p 2667 N94-26151
Wing design for a civil tiltrotor transport aircraft: A preliminary study p 2671 N94-27917

TILT WING AIRCRAFT
Design optimization of high-speed proprotor aircraft
[NASA-TM-103988] p 2667 N94-26151

TILTING ROTORS
Design optimization of high-speed proprotor aircraft
[NASA-TM-103988] p 2667 N94-26151

TILTMETERS
Evaluation of the prototype dual-axis wall attitude measurement sensor
[NASA-TM-109056] p 2811 N94-26707
Observation with STS seismometer at Nakaizu, central Japan: Observation system and comparison with tiltmeter p 2886 N94-27986

TIME CONSTANT
Automation of formation flight control
[AD-A274137] p 2678 N94-27132

TIME DEPENDENCE
The effect of the time restrictions on information search and information integration in a dynamic task environment
[AD-A273759] p 3095 N94-25723
Theoretical determination of chemical rate constants using novel time-dependent methods
[NASA-CR-195221] p 2714 N94-26205
Electrical analysis of wideband and distributed windows using time-dependent field codes
[DE94-002987] p 2768 N94-26310
Analytical solution of Mori's equation with secant hyperbolic memory
[DE94-601541] p 3006 N94-26368
Local uniform grid refinement and systems of coupled partial differential equations
[CWI-NM-R9307] p 2995 N94-26773
Mechanism of mechanical fatigue of silica glass
[DE94-003165] p 2753 N94-26783
Experiments and numerical simulations of electromagnetic wave propagation in plasma varying rapidly in space and time
[AD-A274376] p 2772 N94-26975
The effect of naloxone on sleeping time in adjuvant arthritic rats p 2906 N94-27498
Forward and backward simulations. Part 2: Timing-based systems
[CWI-CS-R9314-PT-2] p 2972 N94-27581

TIME DIVISION MULTIPLE ACCESS
Analysis of a multiaccess/switching technique for multibeam satellites in a prioritized ISDN environment
[ISBN-0-315-84632-1] p 2776 N94-27345

TIME DIVISION MULTIPLEXING
Design of a shared coherent cache for a multiple channel architecture
[AD-A274026] p 3034 N94-25758
Improved performance of hybrid error control techniques for real-time digital communications over noisy channels
[ISBN-0-315-84281-4] p 2770 N94-26625
Design and test of a regenerative satellite transmultiplexer
[ISBN-0-315-85280-1] p 2786 N94-27303

TIME LAG
Predicting nonlinear time series
[AD-A274051] p 2990 N94-25834
Hook spectroscopy as an atomic number density diagnostic applied to laser-ablated copper plasmas
[DE94-002645] p 3042 N94-26081
Fiber optic true time-delay array antenna feed system
[AD-D016063] p 2777 N94-27734

TIME MEASUREMENT
Tool for performance analysis and off-line prediction of timing behaviour p 2952 N94-26732
A real-time executive implementing priority inheritance protocols p 2952 N94-26733
Fault-tolerant scheduling in distributed critical real-time systems p 2952 N94-26735
Geological Dating by Ar-40 - Ar-39 method
[DE94-601975] p 2880 N94-26874
Coherence and satisfiability of waveform timing specifications
[ISBN-0-315-57769-X] p 3009 N94-27268

TIME OF FLIGHT SPECTROMETERS
A double arm time-of-flight spectrometer based on position-sensitive parallel-grid avalanche counters
[DE93-616665] p 3012 N94-25750

TIME SERIES ANALYSIS
Predicting nonlinear time series
[AD-A274051] p 2990 N94-25834
Developing prediction regions for a time series model for hurricane forecasting
[AD-A273777] p 2892 N94-25861
MIMO recursive least squares control algorithm for the AN/FPN-44A Loran-C transmitter
[AD-A274820] p 2664 N94-26493
Feasibility study on introduction of transportation-use petroleum substitution energy
[DE94-725205] p 2759 N94-26905
Limit theorems for functionals of Markov processes and renormalizable stable fields
[AD-A274645] p 3004 N94-27106

TIME SHARING
Scheduling tasks with unpredictable timing parameters in hard real-time systems p 2951 N94-26728
Ada multiple-programming for hard real time applications in space systems p 2951 N94-26730

TIN
Reference electrodes for solid polymer electrolytes
[DE94-004583] p 2780 N94-25806
Crystal chemistry and self-lubricating properties of monochalcogenides gallium selenide and tin selenide
[DE93-041177] p 2751 N94-26422

TIN ALLOYS
Structure of the modulated magnetic phase of Mn3Sn
[DE94-002788] p 2733 N94-26092
Grain by grain study of the mechanisms of crack propagation during iodine SCC of Zry-4
[DE93-633765] p 2734 N94-26162
Zr-Sn-Nb alloys: Preliminary studies
[DE93-633767] p 2734 N94-26263
Research into the microstructure and mechanical behavior of eutectic Bi-Sn and In-Sn
[DE94-004558] p 2741 N94-27619
Study of the hyperfine magnetic field at Ta-181 site in the Heusler Co2ScSn, Co2ScGa, and Co2HfSn alloys
[DE94-603989] p 3067 N94-27623
The effect of Ti conduit on the critical current in (Nb, Ti)3Sn cable-in-conduit conductors
[DE94-701204] p 2788 N94-27817

TIN OXIDES
Reference electrodes for solid polymer electrolytes
[DE94-004583] p 2780 N94-25806
Zr-rich corner of the Zr-Sn-O diagram
[DE93-633764] p 2734 N94-26161

TISSUES (BIOLOGY)
Autonomous support for microorganism research in space p 2903 N94-25672

TITANIUM
Combustion synthesis method p 2721 N94-25561
Characterization of fatigue damage in a metal matrix composite (SCS-6/Ti-15-3) at elevated temperature
[AD-A273797] p 2706 N94-25876
Investigation of tension-compression fatigue behavior of a cross-ply metal matrix composite at room and elevated temperatures
[AD-A273731] p 2706 N94-25999
Diffusion of substitutional elements in Ti in its hcp phase
[DE93-633762] p 2733 N94-26160
Titanium 1992: Volume 3: Science and technology
[AD-A274800] p 2735 N94-26337
Titanium 1992: Science and technology, volume 2 rence (7th) in san diego, california on june 29-july 2, 1992. Volume 2
[AD-A274799] p 2736 N94-26362
X ray absorption studies of Ti/polymer and Cr/polymer interfaces
[DE94-003008] p 2753 N94-26770
The coordination and atom transfer chemistry of titanium porphyrin complexes
[DE94-003091] p 2704 N94-26779
Technical report of ISSP. Ser. A, no. 2685: ASE-free terawatt KrF/Ti : sapphire hybrid laser system
[JTN-94-80571] p 2820 N94-27339
The effect of Ti conduit on the critical current in (Nb, Ti)3Sn cable-in-conduit conductors
[DE94-701204] p 2788 N94-27817

TITANIUM ALLOYS
Study on the mechanism of titanium alloy toughness and the improvement of properties
p 2726 N94-25566
Study on improvements in fretting fatigue characteristics of high strength structural member p 2726 N94-25567
Study on knowledge extraction and systematization for material design p 2727 N94-25568
Study on improvement in physical analysis method of metallic materials p 2728 N94-25577
Effect of nitrocarburizing on shape of titanium alloy parts
[DE94-004040] p 2732 N94-25822
Titanium 1992: Volume 3: Science and technology
[AD-A274800] p 2735 N94-26337
Titanium 1992: Science and technology, volume 2 rence (7th) in san diego, california on june 29-july 2, 1992. Volume 2
[AD-A274799] p 2736 N94-26362
The influence of energy losses with time in NbTi superconductors in pulsed magnetic fields
[DE93-634761] p 3058 N94-26512
Deformation twinning: Influence of strain rate
[DE94-002693] p 2738 N94-26621
The processing of powder metallurgically produced near gamma-titanium aluminide
[ISBN-0-315-84018-8] p 2738 N94-26633
Evaluation of APC NbTi superconductor in a model dipole magnet
[DE94-003258] p 3060 N94-26795
Titanium 1992: Science and Technology, volume 1
[AD-A274798-VOL-1] p 2739 N94-26799
Material optimization and manufacturing development of reduced cost powder metal titanium alloy components for gas turbine engine application, phase 2
[AD-A274410] p 2709 N94-26978
Formation and crystallization of hydrogen-induced amorphous Ti3InH(4.5) alloy p 2745 N94-28163
The corrosion behavior of sputter-deposited magnesium-valve metal alloys p 2745 N94-28164
CO2 methanation catalysts prepared from amorphous Ni-valve metal alloys containing platinum group elements
p 2745 N94-28166

TITANIUM CARBIDES
Experiment and research on materials irradiated by plasma radiation
[DE94-605011] p 2758 N94-27845
Photoelectron spectroscopic studies of the electronic structure and bonding in TiC and TiN
[ATR-93(8361)-2] p 2746 N94-28185

TITANIUM COMPOUNDS
Study on variation of damage generation mechanism by fatigue on TiAl compounds due to different slip systems p 2729 N94-25579
Development of K(1-x)Na(x)TiOPO4 crystals for nonlinear applications
[AD-A274336] p 3063 N94-27055
Technical report of ISSP. Ser. A, no. 2673: Two successive spin glass transitions in non-diluted Heisenberg-like spin glass Ni(0.42)Mn(0.58) TiO3
[JTN-94-80559] p 2756 N94-27241
Microstructure and mechanical behaviour of L1(2) titanium trialuminides
[ISBN-0-315-84488-4] p 2740 N94-27306

TITANIUM NITRIDES
Combustion synthesis method p 2721 N94-25561
Photoelectron spectroscopic studies of the electronic structure and bonding in TiC and TiN
[ATR-93(8361)-2] p 2746 N94-28185

TITANIUM OXIDES
Electronic structure of a single oxygen vacancy in rutile TiO2
[DE94-602717] p 3062 N94-26901

Technical report of ISSP. Ser. A, no. 2671: Quasi-localization of light waves in Fibonacci dielectric multilayers
[JTN-94-80557] p 3064 N94-27231
Technical report of ISSP. Ser. A, no. 2670: Electronic structure of light transition metal compounds studied by photoemission
[JTN-94-80556] p 3065 N94-27239

TOKAMAK DEVICES
Review of tokamak experiments on direct electron heating and current drive with fast waves
[DE94-004185] p 3041 N94-25801
Heavy neutral beam probe for edge plasma analysis in tokamaks
[DE94-003391] p 3041 N94-25846
Design of folded waveguide antenna for Alcator C-Mod
[DE94-003584] p 2767 N94-25924
RF modeling and design of a folded waveguide launcher for the Alcator C-Mod tokamak
[DE94-003588] p 3041 N94-25933
Evaluation of helium cooling for fusion divertors
[DE94-002680] p 3042 N94-25976
High-speed repetitive pellet injector for plasma fueling of magnetic confinement fusion devices
[DE94-002792] p 3042 N94-26140
Development of fusion technology
[DE93-633444] p 3042 N94-26159
Limitations of power conversion systems under transient loads and impact on the pulsed tokamak power reactor
[DE94-003404] p 3043 N94-26324
Fusion Energy Advisory Committee: Advice and recommendations to the US Department of Energy in response to the charge letter of September 1, 1992
[DE93-019842] p 3043 N94-26428
Numerical simulation of plasma vertical position stabilization in ITER
[DE93-634588] p 3044 N94-26510
Maryland controlled fusion research program
[DE94-003533] p 3044 N94-26523
The dynamics of interacting nonlinearities governing long wavelength driftwave turbulence
[DE94-001785] p 2793 N94-26558
Probability of accessing the multiple saturated states in the resistive interchange instability
[DE94-000478] p 3044 N94-26694
Conceptual design of the tokamak radiation shielding for the Tokamak Physics Experiment (TPX)
[DE94-002791] p 3044 N94-26858
Potential of commercial tokamak reactors with improved physics
[DE94-002794] p 3044 N94-26860
Methodology for first wall design
[DE94-002795] p 3045 N94-26861
The TPX Cryostat Conceptual Design
[DE94-002857] p 3045 N94-26863
New conditioning procedure derived from operating experience with the Common Long-Pulse Ion Source
[DE94-002891] p 3045 N94-26865
Role of core toroidal rotation shear on turbulence and transport in the improved confinement regimes of the D3-D tokamak
[DE94-001215] p 3045 N94-26950
Tokamak Physics Experiment poloidal field design
[DE94-001542] p 3045 N94-27019
Design and control of phased ICRF antenna arrays
[DE94-002796] p 3046 N94-27261
High gas-efficiency hydrogen negative ion sources
[PB93-232163] p 3025 N94-27348
Fast wave current drive technology development at ORNL
[DE94-004243] p 3046 N94-27568
Fusion reactor systems studies
[DE94-003162] p 3046 N94-27686
Cryogenic fracture behavior of 316LN in magnetic fields up to 14.6 T
[DE94-005215] p 2742 N94-27694
Shine through measurements with hydrogen beam in JT-60
[DE94-701113] p 3047 N94-27699
Passive stabilization of MHD instabilities at high (beta)n in the HBT-EP tokamak
[DE94-003317] p 3047 N94-27735
Helium transport and exhaust studies of H-mode discharges in the D3-D tokamak
[DE94-004744] p 3048 N94-27785
Fuel ion rotation measurement and its implications on H-mode theories
[DE94-004860] p 3048 N94-27791
Performance of a 14-MeV neutron generator as an in situ calibration source for TFTR
[DE94-004993] p 3048 N94-27825
Preliminary considerations on the diffraction (quasi-optical) grill in CASTOR tokamak
[IPPCZ-335] p 3048 N94-27842
Determination of the plasma column shape in the Tokamak Novillo cross section by magnetic probes
[DE94-604986] p 3048 N94-27844
Modelling and control of plasma position in the STOR-M tokamak
[ISBN-0-315-58891-8] p 3049 N94-27949

TOLERANCES (MECHANICS)
Damage tolerance assessment handbook. Volume 1: Introduction fracture mechanics fatigue crack propagation
[AD-A274777] p 2836 N94-26186
Damage tolerance assessment handbook. Volume 2: Aircraft damage tolerance evaluation
[AD-A274778] p 2837 N94-26357
Thermoplastic or thermosetting composites in aircrafts
[PB94-123809] p 2710 N94-27253
NASA-UVA light aerospace alloy and structures technology program (LA2ST)
[NASA-CR-195275] p 2844 N94-27851

TOLUENE
Reactivity of nitrate radical (NO3) toward organic compounds p 2704 N94-27387

TOMOGRAPHY
Reconstruction of multiple cracks from experimental electrostatic boundary measurements
[NASA-CR-191584] p 2994 N94-26601
Auroral Tomography Workshop Proceedings
[PB94-123718] p 2881 N94-27040
Experimental verification of tomographic reconstruction of turbulent air flow structure using optical wavefront measurements
[AD-A274392] p 2795 N94-27129
Atomic processes in Inertial Electrostatic Confinement (IEC) devices
[DE94-005015] p 3047 N94-27715

TONGUE
NCVS, volume 5
[AD-A274975] p 2902 N94-27165

TOOLING
Material optimization and manufacturing development of reduced cost powder metal titanium alloy components for gas turbine engine application, phase 2
[AD-A274410] p 2709 N94-26978

TOPEX
TOPEX/Poseidon battery performance during the first year of operation p 2862 N94-28119

TOPOGRAPHY
Correlation between the gravity field and the bathymetry in the North Atlantic Ocean
[ETN-94-95036] p 2899 N94-26108
A preliminary analysis of the US west climatology
[DE94-003028] p 2894 N94-26313
Conifer tree influence on Digital Terrain Elevation Data (DTED): A case study at Dulles International Airport
[AD-A274213] p 2849 N94-27069
Landscape dynamics of northeastern forests
[NASA-CR-195272] p 2852 N94-28070

TOPOLOGY
Surfaces allowing for fractional statistics
[DE93-614526] p 3002 N94-25910
Characterization of self-conjugate minimal surfaces in R(sup 3)
[DE94-601538] p 2993 N94-26409
Topological conditions for the existence of invariant measures for unimodal maps
[PB94-123296] p 2849 N94-26866
Graphs satisfying a local ore-type condition
[PB94-126679] p 3007 N94-27222

TORCHES
Hydrogen-oxygen torch ignitor
[NASA-TM-106493] p 2691 N94-27424

TOROIDAL PLASMAS
Toroidal plasma beta-FLR limit in a toroidally linked mirror system
[DE94-003119] p 3041 N94-25792
Kinetic resonance damping rate of the toroidal ion temperature gradient mode
[DE94-003511] p 3041 N94-25923
Development of fusion technology
[DE93-633444] p 3042 N94-26159
Scaling of sustained ZT-40 M reversed field pinches
[DE94-003318] p 3043 N94-26321
The TPX Cryostat Conceptual Design
[DE94-002857] p 3045 N94-26863
Role of core toroidal rotation shear on turbulence and transport in the improved confinement regimes of the D3-D tokamak
[DE94-001215] p 3045 N94-26950
Tokamak Physics Experiment poloidal field design
[DE94-001542] p 3045 N94-27019
TFTR experimental data analysis collaboration
[DE94-004166] p 3047 N94-27690
Passive stabilization of MHD instabilities at high (beta)n in the HBT-EP tokamak
[DE94-003317] p 3047 N94-27735
Preliminary considerations on the diffraction (quasi-optical) grill in CASTOR tokamak
[IPPCZ-335] p 3048 N94-27842
Determination of the plasma column shape in the Tokamak Novillo cross section by magnetic probes
[DE94-604986] p 3048 N94-27844
Analysis of density limit and efficiency in lower hybrid current drive
[DE94-604995] p 3049 N94-27856

TOROIDS
Electromagnetic properties of a toroidal solenoid
[DE93-613032] p 2766 N94-25866
Experimental results of 40-kA Nb3Al conductor
[DE94-701207] p 2788 N94-27821

TORQUE MOTORS
Reconfigurable aircraft stick control
[AD-D016043] p 2681 N94-27113

TORSION
Simple currents versus orbifolds with discrete torsion: A complete classification
[NIKHEF-H/93-13] p 2995 N94-26812

TORSIONAL VIBRATION
A new method for torsional critical speed calculation of practical industrial rotors
[IMR-T&M-TR-001] p 2828 N94-28041

TORUSES
Affine algebras on the torus
[DE94-601556] p 3006 N94-26414
Higher spin extensions of the Virasoro algebra, area-preserving algebras and the matrix algebra a-bar(sub (infinity))
[DE94-601557] p 3006 N94-26415
The super Weierstrass (zeta)-function and operator product expansions in 2D-induced supergravity on the supertorus
[DE94-603664] p 3074 N94-27627

TOTAL QUALITY MANAGEMENT
Statistical quality management
[MEMO-COSOR-92-43] p 2834 N94-26008
Qualified manufacturing and interoperability for space applications p 2949 N94-26719

TOUGHNESS
Determination of fracture stress and effective crack tip radius from toughness (KIc) and yield strength (Y)
[AD-A274014] p 2836 N94-25754
Numerical simulations of interfacial debonding in ductile-phase reinforced intermetallic matrix composites
[DE94-003639] p 2706 N94-25938
Interface phenomena in metal-ceramic composites
[AD-A274167] p 2709 N94-27125
Testing procedure for toughness characterisation of ceramic matrix composites
[REPT-932-430-101] p 2711 N94-27586

TOWERS
Cooling towers for combined cycles: Design philosophy, performance testing, and operating problems
p 2832 N94-28087

TOWING
Unscreened low tension cables scrape abrasion testing
[PB94-123767] p 2823 N94-26849

TOXIC HAZARDS
Automated in-situ inspection systems for underground storage tanks
[AD-A274644] p 2764 N94-27144

TOXICOLOGY
Proceedings of the symposium on current concepts and approaches on animal test alternatives
[AD-A273926] p 2900 N94-25593
Bakteriella toxiner-morgondagens hot (bacterial toxins-the threat of tomorrow)
[PB94-124229] p 2902 N94-27045

TOXINS AND ANTITOXINS
Bakteriella toxiner-morgondagens hot (bacterial toxins-the threat of tomorrow)
[PB94-124229] p 2902 N94-27045

TRACE CONTAMINANTS
Evaluation of a Canadian minitube air sampling system
[FOA-C-40307-4.6] p 2866 N94-25809
Assessing the climatic effect of carbon dioxide and other trace gases using an interactive two-dimensional climate-chemistry model
[DE94-001741] p 2866 N94-25927

TRACE ELEMENTS
Study on neutron activation analysis
[DE93-632191] p 3017 N94-26116

TRACKING NETWORKS
Real-time tracking with a 3D-flow processor array
[DE94-003981] p 2980 N94-25984

TRACKING STATIONS
Automating satellite range scheduling
[AD-A273829] p 2694 N94-25738

TRADEOFFS
Lunar base habitat designs: Characterizing the environment, and selecting habitat designs for future trade-offs
[NASA-CR-195687] p 2943 N94-27934
TRAFFIC CONTROL
Emerging technologies
[DE94-003022] p 3102 N94-26023
Conception of snow information network system in Yamagata Prefecture p 2853 N94-27991
TRAILERS
Pressurized Lunar Rover (PLR) p 2833 N94-25704
TRAILING EDGES
Effects of crenulations on three dimensional losses in a linear compressor cascade
[AD-A273778] p 2790 N94-25862
Control jets in interaction with hypersonic rarefied flow
p 2698 N94-28020
Program for calculation of maximum lift coefficient of plain aerofoils and wings at subsonic speeds
[ESDU-93015] p 2649 N94-28076
Wing lift increment at zero angle of attack due to deployment of single-slotted flaps at low speeds
[ESDU-93019] p 2649 N94-28140
Potential flow modelling of airfoil stall
p 2654 N94-28332
Attached and separated trailing edge flow measurements with a triple-split hot-film probe
p 2656 N94-28339
TRAINING EVALUATION
Benefits estimation for simulation systems used for aircrew training in a multiship environment
[AD-A274313] p 2938 N94-26882
TRAINING SIMULATORS
Benefits estimation for simulation systems used for aircrew training in a multiship environment
[AD-A274313] p 2938 N94-26882
TRAJECTORIES
On the first integrals of geodesics
[DE93-612974] p 3007 N94-25603
Breakwire technique for hypervelocity measurement
[AD-A274779] p 2809 N94-26358
TRAJECTORY ANALYSIS
A survey of uncontrolled satellite reentry and impact prediction
[AD-A274903] p 2695 N94-26750
TRAJECTORY OPTIMIZATION
Optimal nonlinear estimation for aircraft flight control in wind shear p 2643 N94-27296
Local performance optimization for a class of redundant eight-degree-of-freedom manipulators
[NASA-TP-3417] p 2989 N94-27773
A parametric sensitivity study for single-stage-to-orbit hypersonic vehicles using trajectory optimization
[NASA-CR-195703] p 2697 N94-27789
TRAJECTORY PLANNING
A global approach to kinematic path planning to robots with holonomic and nonholonomic constraints
p 2683 N94-26279
Application of the CIRSSE cooperating robot path planner to the NASA Langley truss assembly problem
p 2683 N94-26280
Adaptive path planning in changing environments
[DE94-003269] p 2985 N94-26462
Dynamic control of kinematically redundant manipulators
[ISBN-0-315-84627-5] p 2825 N94-27344
Local performance optimization for a class of redundant eight-degree-of-freedom manipulators
[NASA-TP-3417] p 2989 N94-27773
A parametric sensitivity study for single-stage-to-orbit hypersonic vehicles using trajectory optimization
[NASA-CR-195703] p 2697 N94-27789
TRANSFER FUNCTIONS
Human visual system enhancement of reconstructed satellite images
[AD-A273867] p 2693 N94-25595
Binaural room simulation
[AD-A273823] p 3009 N94-25737
Using a transfer function to describe the load-balancing problem
[DE94-004218] p 2979 N94-25802
TRANSFER ORBITS
Charge efficiency of Ni/H2 cells during transfer orbit of Telstar 4 satellites p 2862 N94-28117
TRANSFORMATIONS (MATHEMATICS)
Filtering, coding, and compression with Malvar wavelets
[AD-A274055] p 2780 N94-25770
Satellite attitude determination using linear combination of models
[AD-A274082] p 2694 N94-25996
The modal solution to the Moon's orbit using canonical Floquet perturbation theory
[AD-A273732] p 2690 N94-26001
Semantics, orderings and recursion in the weakest precondition calculus
[CWI-CS-R9267] p 2995 N94-26776
The Hough transform algorithm for sea ice lead analysis: An evaluation
[AD-A274535] p 2899 N94-26853
Topological conditions for the existence of invariant measures for unimodal maps
[PB94-123296] p 2849 N94-26866
The morphological processing of binary images
[AD-A274310] p 2996 N94-26972
TRANSFORMERS
Development of fusion technology
[DE93-633444] p 3042 N94-26159
Fiber optic Faraday flux transformer specification
[AD-D016058] p 3039 N94-27674
Plane wave propagation and polarization properties in transversely bianisotropic uniaxial medium
[PB94-132883] p 2778 N94-28380
Eigenwaves in the general uniaxial bianisotropic medium with symmetric parameter dyadics
[PB94-132891] p 2778 N94-28381
Plane wave propagation in an anisotropic chiral medium with isotropic permittivity and permeability
[PB94-133097] p 2778 N94-28384
TRANSIENT LOADS
Structural design feasibility study of Space Station long spacer truss
[NASA-TM-106346] p 2843 N94-27559
TRANSIENT RESPONSE
A transient symmetrical method for the measurement of temperature dependent thermal diffusivity
[VTT-TIED-1452] p 3008 N94-26256
Response of structures to impact loads using elastic and plastic analysis
[ISBN-0-315-84647-X] p 2842 N94-27309
Influence of impeller shroud forces on turbopump rotor dynamics p 2796 N94-27378
Gas Turbine Engine Transient Behaviour
[VKI-LS-1993-06] p 2828 N94-28043
Transient performance p 2828 N94-28045
Transient engine simulation p 2829 N94-28052
TRANSISTOR AMPLIFIERS
Signal amplifier-shapers for multiwire detectors
[DE93-634171] p 2783 N94-26438
NASA satellite communications application research, phase 2 addendum. Efficient high power, solid state amplifier for EHF communications
[NASA-CR-195712] p 2777 N94-27946
TRANSISTOR CIRCUITS
A physics-based heterojunction bipolar transistor model for integrated circuit simulation
[AD-A274081] p 2781 N94-25995
Silicon device performance measurements to support temperature range enhancement
[NASA-CR-195265] p 2844 N94-27824
TRANSISTORS
Advanced qualification techniques
[DE94-003709] p 2780 N94-25812
Demonstration of monolithic co-fabrication of Y1Ba2Cu3O7-Sigma and CMOS devices on the same sapphire substrate
[AD-A274757] p 3059 N94-26566
Processing, fabrication, and demonstration of HTS integrated microwave circuits, appendix A
[AD-A274600] p 2785 N94-26890
TRANSITION
Modal logic, transition systems and processes
[CWI-CS-R9321] p 2970 N94-27549
TRANSITION FLIGHT
Transitional flight characteristics of a geometrically simplified STOVL model p 2672 N94-28035
TRANSITION FLOW
Prediction of leading-edge transition and relaminarization phenomena on a subsonic multi-element high-lift system p 2659 N94-27929
Forced convection heat transfer in straight tubes. Part 2: Laminar and transitional flow
[ESDU-93018-PT-2] p 2807 N94-28139
TRANSITION METALS
Transition metal activation and functionalization of carbon-hydrogen bonds
[DE94-003650] p 2715 N94-26369
Transition metals in highly correlated discotic phases: Designing metallomesogens with selected intermolecular organizations
[AD-A274695] p 2736 N94-26452
TRANSITION POINTS
Transition for three-dimensional, compressible boundary layers p 2653 N94-28327
TRANSITION TEMPERATURE
Microscopic study of local structure and charge distribution in metallic La2CuO(4+delta)
[DE94-003801] p 3050 N94-25817
The effect of processing on the microstructure of Ag-sheathed Bi-2223 wires
[DE94-004627] p 3055 N94-26243
Strongly interacting fermion systems
[DE94-002674] p 3021 N94-26677
TRANSLATING
Satellite attitude determination using linear combination of models
[AD-A274082] p 2694 N94-25996
A strategy for dynamic interpretation: A fragment and an implementation
[CWI-CS-R9317] p 2970 N94-27545
TRANSLATIONAL MOTION
Translation and rotation invariant pattern recognition
[PB94-123676] p 2968 N94-27157
TRANSMISSION ELECTRON MICROSCOPY
Crystal potential retrieval in HRTEM
[DE94-601883] p 3055 N94-26171
An atom probe investigation of the influence of trace impurities on the mechanical behavior of NiAl
[DE94-002797] p 2734 N94-26272
Electron microscopy studies of undoped and phosphorus doped Si:H and Si,C:H films
[DE94-004738] p 3069 N94-27757
TRANSMISSION LINES
Interference analysis of multichannel transmission lines: A system's analysis
[PB94-126505] p 2772 N94-26909
TRANSMISSIONS (MACHINE ELEMENTS)
Study of the kinematic and dynamic characteristics of a wormgear transmission for helicopter applications
[NASA-CR-195287] p 2826 N94-27657
TRANSMITTANCE
Transmittance fluctuations and non-linearity in random chains in the presence of applied electric fields
[DE94-603665] p 2787 N94-27628
TRANSMITTER RECEIVERS
Optoelectronic technology consortium
[AD-A274595] p 3036 N94-26857
Microprocessor chip incorporating optical signal coupling transceiver
[AD-D016077] p 2788 N94-28186
TRANSMITTERS
S-76 high intensity radiated fields, volume 2
[AD-A274572] p 2771 N94-26836
A tri-state optical switch for local area network communications p 2789 N94-27922
TRANSONIC FLIGHT
Numerical investigation of thrust vectoring by injection of secondary air into nozzle flows p 2801 N94-28013
Vortex generators for control of shock-induced separation. Part 3: Examples of applications of vortex generators to aircraft
[ESDU-93026-PT-3] p 2807 N94-28096
TRANSONIC FLOW
An investigation of the effects of the high maximum-thickness-to-chord ratio on the performance of nozzle guide vanes in a transonic planar cascade
[ISBN-0-315-84107-9] p 2793 N94-26671
Influence of the transonic doublet in the farfield of a lifting airfoil
[IAR-AN-78] p 2647 N94-26702
Prediction of undsteady flows in turbomachinery using the linearized Euler equations on deforming grids
[NASA-CR-195285] p 2675 N94-27654
Computation of transonic viscous flow past the NTF 65-degree Delta Wing p 2659 N94-27930
An initial investigation into methods of computing transonic aerodynamic sensitivity coefficients
[NASA-CR-195705] p 2648 N94-28072
Interaction of the sonic boom with atmospheric turbulence p 2650 N94-28191
Measurements of steady and dynamic pressure on an F/A-18 wind tunnel model at high angles of attack
p 2653 N94-28323
Solution-adaptive simulation of transonic cascade flows p 2657 N94-28344
TRANSONIC FLUTTER
Understanding and development of a prediction method of transonic limit cycle oscillation characteristics of fighter aircraft
[NLR-TP-92210-U] p 2679 N94-27798
TRANSONIC SPEED
Investigation of aerodynamic design issues with regions of separated flow p 2658 N94-27902
TRANSONIC WIND TUNNELS
Fiber-optic-based laser vapor screen flow visualization system for aerodynamic research in larger scale subsonic and transonic wind tunnels
[NASA-TM-4514] p 2647 N94-26706
Experimental investigation of the flow quality in the GLT20 subsonic-transonic boundary layer wind tunnel
[PB94-126539] p 2681 N94-26815

The renewing of the test section of the NAL transonic wind tunnel. Part 1: Reconstruction of the 1st corner turning vanes and aerodynamic stress measurement
[NAL-TM-651] p 2681 N94-27247

TRANSPORT AIRCRAFT
The application of a C(star) flight control law to large civil transport aircraft
[CRANFIELD-AERO-9303] p 2676 N94-25640
Supercruiser Arrow HS-8 p 2671 N94-25711
The evolution of the high-speed civil transport
[NASA-TM-109089] p 3117 N94-26155
Optical communications for transport aircraft
p 2643 N94-27298
Techniques to improve maneuver stability characteristics of a nonlinear wide-body transport airplane in cruise flight
[NASA-TM-4521] p 2679 N94-27660
Wing design for a civil tiltrotor transport aircraft: A preliminary study p 2671 N94-27917
Examples of flight path optimisation using a multivariate gradient-search method
[ESDU-93021] p 2670 N94-28092
Examples of excrescence drag prediction for typical wing components of a subsonic transport aircraft at the cruise condition
[ESDU-93032] p 2649 N94-28144

TRANSPORT PROPERTIES
Selfsimilar solutions of a nonlinear transport equation
[REPT-93-42] p 2865 N94-25760
A positive finite-difference advection scheme applied on locally refined grids
[CWI-NM-R9309] p 2867 N94-26216
Recombination and metastability in amorphous silicon and silicon germanium alloys
[DE94-000237] p 2736 N94-26481
A concurrent, multigroup, discrete ordinates model of neutron transport
[DE94-004334] p 3020 N94-26577
Powder synthesis, fabrication, and transport properties of long-length Ag clad Bi-2223 conductors
[DE94-002376] p 2740 N94-26957
Computer simulation and experiments on the quasi-static mechanics and transport properties of granular materials
[AD-A274192] p 2823 N94-27104
Gauge invariance and transport properties in superconductors above T(c)
[DE94-604013] p 3068 N94-27677
On radio frequency wave induced radial transport and wave helicity
[IPPCZ-326] p 2777 N94-27838
On helicon wave induced radial plasma transport
[IPPCZ-333] p 3048 N94-27840

TRANSPORT THEORY
Shear flow generation from the interaction of neoclassical and drift wave transport processes
[DE94-003135] p 2791 N94-26096
Analytical solution of Mori's equation with secant hyperbolic memory
[DE94-601541] p 3006 N94-26368
Pre-orbital criticality safety for the NEPSTP mission
[DE94-002600] p 3005 N94-26802
Refractive and dielectric properties of helium, argon and nitrogen gases
[PB94-123783] p 3008 N94-26851

TRANSPORTATION
The general pickup and delivery problem
[MEMO-COSOR-92-44] p 2992 N94-26226

TRANSPUTERS
A Multitransputer Parallel Processing System (MTPPS)
[DE94-604652] p 2981 N94-26903
Inverted pendulum control apparatus using transputers
[DE94-701224] p 2973 N94-27732

TRANSURANIUM ELEMENTS
Studies of heavy-ion reactions and transuranic nuclei
[DE94-004642] p 3029 N94-27783

TRAPEZOIDS
Trapezoid-oriented compression of run length coded map data
[PB94-123312] p 2849 N94-26848

TRAPPED PARTICLES
Trapped electrons in solid hydrogen
[DE93-018628] p 3052 N94-25947
Antiproton studies in penning traps
[AD-A274250] p 3024 N94-27011

TRAPPING
Hydrogen trapping with Pd coated alloy films
p 2723 N94-25551
Calculations of population transfer during intense laser pulses
[DE94-001060] p 2818 N94-26698

TRAVELING WAVE TUBES
A direct current rectification scheme for microwave space power conversion using traveling wave electron acceleration p 2687 N94-27371

TREES (MATHEMATICS)
Detecting actin fibers in cell images using minimal spanning trees
[AD-A273914] p 2984 N94-25591
Editing tree structures
[CWI-CS-R9264] p 2961 N94-26219
Efficient rebalancing of tree-type main memory dictionaries
[PB94-133105] p 3100 N94-28396

TREES (PLANTS)
SIMA: A model for forest succession based on the carbon and nitrogen cycles with application to silvicultural management of the forest ecosystem
[SILVA-CARELICA-22] p 2848 N94-26258

TRIANGULATION
Construction and applications of the two dimensional Delaunay triangulated irregular network and the three dimensional Delaunay tetrahedron model
[ETN-94-95034] p 2848 N94-26651
A parallel computational fluid dynamics unstructured grid generator
[AD-A274129] p 2795 N94-27119

TRIAXIAL STRESSES
Grain by grain study of the mechanisms of crack propagation during iodine SCC of Zry-4
[DE93-633765] p 2734 N94-26162
Computer simulation and experiments on the quasi-static mechanics and transport properties of granular materials
[AD-A274192] p 2823 N94-27104

TRIGGER CIRCUITS
Use of parallel counters for triggering
[DE93-616656] p 2979 N94-25918
Relativistic heavy ion physics
[DE94-003161] p 3031 N94-26097
Development of fusion technology
[DE93-633444] p 3042 N94-26159

TRITIUM
Spectroscopy and dynamics of molecular and ionic impurities embedded in solid hydrogen
[AD-A274149] p 3064 N94-27095

TROPICAL REGIONS
Interactions between a tropical mixed boundary layer and cumulus convection in a radiative-convective model
[DE94-000848] p 2877 N94-25979
Short-range cloud amount forecasting with model output statistics
[AD-A274769] p 2895 N94-26798
Global barotropic response to a tropical forcing
[NASA-CR-195256] p 2896 N94-27408

TROPICAL STORMS
Development and testing of the Coupled Ocean/Atmosphere Mesoscale Prediction System (COAMPS)
[AD-A273925] p 2892 N94-25793
Tropical cyclone report, 1992
[AD-A274464] p 2896 N94-27025

TRUCKS
UV absorption technique for monitoring mobile source NO emissions
[AD-A273858] p 2713 N94-25964
Processing of wide-angle synthetic aperture radar signals for target detection
[AD-A274225] p 2773 N94-27073

TRUSSES
Identification and H(infinity)/(mu)-synthesis control of the Sandia truss
[DE94-002735] p 2839 N94-26810
Behaviour modification of space trusses
[ISBN-0-315-84701-8] p 2842 N94-27315
Report of three microgravity experiments by the drop shaft
[JTN-94-80579] p 2761 N94-27341
Structural design feasibility study of Space Station long spacer truss
[NASA-TM-106346] p 2843 N94-27559
Reliability-based structural optimization: A proposed analytical-experimental study
[NASA-TM-109055] p 2844 N94-27830

TUBES
Porous vycor glass tube joined to borosilicate glass
p 2718 N94-27392

TUNABLE LASERS
Broad band tunable dye laser development
[DE93-632978] p 2816 N94-26157
Fiber laser amplifiers and oscillators
[AD-A274231] p 2820 N94-28068

TUNGSTEN
Stress relaxation in sputtered W films and W/GeSi/Si heterostructures
[DE94-004007] p 3055 N94-26239
The deformation of copper-tungsten composites
[ISBN-0-315-84939-8] p 2712 N94-27688

TUNGSTEN ALLOYS
Chemical vapor deposition and characterization of tungsten boron alloy films
[DE94-002648] p 2738 N94-26810

A transmission electron microscope study of Ni4W precipitates in a Ni-37 wt. percent W alloy
[ISBN-0-315-59932-4] p 2743 N94-27803

TUNING
Sum frequency generation using an optical parametric oscillator
[DE94-001827] p 3040 N94-28000

TUNNEL DIODES
Investigation of ACC/CCI tunnel diodes
[AD-A274549] p 2785 N94-26845

TURBINE BLADES
Wake passage effects on the losses in a linear turbine cascade
[AD-A273794] p 2790 N94-25874
An investigation of the effects of the high maximum-thickness-to-chord ratio on the performance of nozzle guide vanes in a transonic planar cascade
[ISBN-0-315-84107-9] p 2793 N94-26671
Thermal/structural tailoring of engine blades (T/STAEBL). User's manual
[NASA-CR-194463] p 2839 N94-26692
Thermal/Structural Tailoring of Engine Blades (T/STAEBL): User's manual
[NASA-CR-194461] p 2843 N94-27776
Analysis of cooling jets near the leading edge of turbine blades p 2676 N94-28037
Effect of surface finish on turbine airfoil cascade losses p 2652 N94-28320
The effect of axial velocity ratio, turbulence intensity, incidence, and leading edge geometry on the midspan performance of a turbine cascade p 2652 N94-28321

TURBINE ENGINES
Aircraft turbine engine reliability and inspection investigations
[AD-A274860] p 2673 N94-26176

TURBINE PUMPS
Experimental contribution to the study of secondary flows in centrifugal turbopump stator components
[ECL-92-35] p 2789 N94-25654
Test results of the RS-44 integrated component evaluator liquid oxygen/hydrogen rocket engine
[NASA-CR-194443] p 2701 N94-26231
Pump CFD code validation tests
[NASA-CR-193939] p 2822 N94-26597
Orbital transfer vehicle engine technology high velocity ratio diffusing crossover
[NASA-CR-194447] p 2703 N94-27212
Enhanced simulation software for rocket turbopump, turbulent, annular liquid seals
[NASA-CR-195239] p 2825 N94-27383
Space Shuttle main engine turbopump bearing assessment program
[NASA-TM-108447] p 2833 N94-28265

TURBINE WHEELS
Streamwise vorticity in a turbine rotor with conical endwalls
[DLR-FB-93-13] p 2826 N94-27591

TURBINES
Wake passage effects on the losses in a linear turbine cascade
[AD-A273794] p 2790 N94-25874
Program to develop a performance and heat load prediction system for multistage turbines
[NASA-CR-195223] p 2674 N94-26588

TURBOCOMPRESSORS
Effects of crenulations on three dimensional losses in a linear compressor cascade
[AD-A273778] p 2790 N94-25862
An investigation of the surge behavior of a high-speed ten-stage axial flow compressor
[AD-A274910] p 2674 N94-26345
Laser Doppler velocimetry in a low speed multistage compressor
[AD-A274836] p 2818 N94-26498
Development of advanced high temperature in-cylinder components and tribological systems for low heat rejection diesel engines, phase 1
[NASA-CR-187158] p 2827 N94-27984
Gas-turbine engine steady-state behavior
p 2828 N94-28044

TURBOFAN AIRCRAFT
Design of the advanced regional aircraft, the DART-75
p 2671 N94-25708

TURBOFAN ENGINES
The design of a long-range megatransport aircraft
p 2671 N94-25718
Simulating indirect thrust measurement methods as used on modern high-bypass turbofans
[ISBN-0-315-84123-0] p 2674 N94-26673
Experimental and theoretical investigations of the influence of the jet on the flow around a bypass-engine
[DLR-FB-93-17] p 2675 N94-27593
Broad specification fuels combustion technology program, phase 2
[NASA-CR-191066] p 2719 N94-27854

TURBOFANS

Experimental and theoretical investigations of the influence of the jet on the flow around a bypass-engine [DLR-FB-93-17] p 2675 N94-27593

Coupled 2-dimensional cascade theory for noise an d unsteady aerodynamics of blade row interaction in turbofans. Volume 2: Documentation for computer code CUP2D [NASA-CR-4506-VOL-2] p 2675 N94-27778

Gas-turbine engine steady-state behavior p 2828 N94-28044

TURBOMACHINE BLADES

Streamwise vorticity in a turbine rotor with conical endwalls [DLR-FB-93-13] p 2826 N94-27591

Development of the gas turbine. Part 2: Manufacturing, commissioning, and operation p 2831 N94-28081

TURBOMACHINERY

Optical surface contouring for non-destructive inspection of turbomachinery [NASA-CR-195245] p 2835 N94-26691

Orbital transfer rocket engine technology 7.5K-LB thrust rocket engine preliminary design [NASA-CR-190754] p 2703 N94-27213

Prediction of undsteady flows in turbomachinery using the linearized Euler equations on deforming grids [NASA-CR-195285] p 2675 N94-27654

TURBOPROP AIRCRAFT

Piloted simulation study of an ILS approach of a twin-pusher business/commuter turboprop aircraft configuration [NASA-TM-4516] p 2646 N94-26602

TURBOPROP ENGINES

Eagle RTS: A design of a regional transport p 2671 N94-25709

TURBULENCE

Numerical simulation of tomographic reconstruction for the study of turbulence using optical wavefront sensor measurements [AD-A273851] p 2789 N94-25587

The identification of inflow fluid dynamics parameters that can be used to scale fatigue loading spectra of wind turbine structural components [DE94-000231] p 2791 N94-26117

Feature isolation and quantification of evolving datasets [NASA-CR-195230] p 2961 N94-26207

Predictive modeling of particle-laden, turbulent flows [DE94-003298] p 2792 N94-26319

Potential capabilities of Reynolds stress turbulence model in the COMMIX-RSM code [DE94-003716] p 2792 N94-26331

Experimental verification of tomographic reconstruction of turbulent air flow structure using optical wavefront measurements [AD-A274392] p 2795 N94-27129

Orbital transfer vehicle engine technology high velocity ratio diffusing crossover [NASA-CR-194447] p 2703 N94-27212

Simulating high-frequency wind for long durations [DE94-002739] p 2682 N94-27997

Unsteady aspects of hot gas reingestion and statistical analysis p 2676 N94-28019

Calculation of single and multiple jets in cross-flow with and without impingement using Reynolds-stress-transport closure p 2803 N94-28024

Predictions of momentum and scalar fields in a jet in cross-flow using first and second order turbulence closures p 2803 N94-28025

Effects of free-stream turbulence on a jet in a cross flow p 2805 N94-28036

Analysis of cooling jets near the leading edge of turbine blades p 2676 N94-28037

Lift-curve slope for structural response calculations [ESDU-93013] p 2648 N94-28063

A modelling of the noise from simple coaxial jets. Part 3: With hot primary flow [ISVR-TR-230-PT-3] p 2807 N94-28173

Sonic boom propagation through turbulence: A ray theory approach p 2650 N94-28192

TURBULENCE EFFECTS

Shear flow generation from the interaction of neoclassical and drift wave transport processes [DE94-003135] p 2791 N94-26096

Topics in longshore currents [AD-A274788] p 2899 N94-26361

Modelling atmospheric turbulence effects on ground-based telescope systems [DE94-004211] p 3102 N94-26528

Experimental verification of tomographic reconstruction of turbulent air flow structure using optical wavefront measurements [AD-A274392] p 2795 N94-27129

Effects of free-stream turbulence on a jet in a cross flow p 2805 N94-28036

TURBULENCE MODELS

Performance of renormalization group algebraic turbulence model on boundary layer transition simulation [NASA-CR-194466] p 2644 N94-26131

Potential capabilities of Reynolds stress turbulence model in the COMMIX-RSM code [DE94-003716] p 2792 N94-26331

The nonlinear Galerkin method: A multi-scale method applied to the simulation of homogeneous turbulent flows [NASA-CR-191581] p 2792 N94-26499

A rapid-pressure correlation representation consistent with the Taylor-Proudman theorem materially-frame-indifferent in the 2D limit [NASA-CR-191591] p 2796 N94-27435

A comprehensive comparison of turbulence models in the far wake p 2808 N94-27899

Computational and Experimental Assessment of Jets in Cross Flow [AGARD-CP-534] p 2799 N94-28003

A numerical investigation of a subsonic jet in a crossflow p 2803 N94-28023

Theoretical and experimental investigation of a delta wing with turbulent leading-edge jets p 2659 N94-28029

Navier-Stokes analysis of a swirling jet in crossflow p 2806 N94-28038

Sonic boom propagation through turbulence: A ray theory approach p 2650 N94-28192

TURBULENT BOUNDARY LAYER

A study on structure of benthic boundary layer in coastal waters [REPT-4] p 2898 N94-25635

Experimental investigation of the flow quality in the GLT20 subsonic-transonic boundary layer wind tunnel [PB94-126539] p 2681 N94-26815

Turbulent boundary layer inner-outer interactions [AD-A274357] p 2794 N94-27059

Flowfield dynamics in blunt fin-induced shock wave/turbulent boundary layer interactions [NASA-CR-195170] p 2798 N94-27802

An experimental study of siphonal jets in a turbulent boundary layer crossflow p 2802 N94-28015

Pneumatic management of blunted-forebody flow asymmetry for high-angle-of-attack directional control p 2679 N94-28028

On the use of feedback to control sound radiation from a plate excited by a turbulent boundary layer [ISVR-TR-227] p 2807 N94-28175

TURBULENT COMBUSTION

High resolution measurements of mixing and reaction processes in turbulent flows [AD-A274970] p 2793 N94-26534

TURBULENT FLOW

Numerical simulation of tomographic reconstruction for the study of turbulence using optical wavefront sensor measurements [AD-A273851] p 2789 N94-25587

The high Reynolds number flow through an axial-flow pump [AD-A273844] p 2789 N94-25604

The identification of inflow fluid dynamics parameters that can be used to scale fatigue loading spectra of wind turbine structural components [DE94-000231] p 2791 N94-26117

Predictive modeling of particle-laden, turbulent flows [DE94-003298] p 2792 N94-26319

Potential capabilities of Reynolds stress turbulence model in the COMMIX-RSM code [DE94-003716] p 2792 N94-26331

On prediction of equilibrium states in homogeneous compressible turbulence [NASA-CR-4570] p 2792 N94-26467

The nonlinear Galerkin method: A multi-scale method applied to the simulation of homogeneous turbulent flows [NASA-CR-191581] p 2792 N94-26499

High resolution measurements of mixing and reaction processes in turbulent flows [AD-A274970] p 2793 N94-26534

Validated heat-transfer and pressure-drop prediction methods based on the discrete-element method. Phase 2: Two-dimensional rib roughness [DE94-002379] p 2794 N94-26763

Numerical studies on the dynamics of bubble, turbulent, free shear flows: Effect of the inter-phase coupling on the global flow evolution [AD-A274521] p 2794 N94-26832

Experimental verification of tomographic reconstruction of turbulent air flow structure using optical wavefront measurements [AD-A274392] p 2795 N94-27129

A rapid-pressure correlation representation consistent with the Taylor-Proudman theorem materially-frame-indifferent in the 2D limit [NASA-CR-191591] p 2796 N94-27435

The numerical calculation of laminar and turbulent flows using penalty function finite volume methods [ISBN-0-315-61377-7] p 2799 N94-27947

Predictions of momentum and scalar fields in a jet in cross-flow using first and second order turbulence closures p 2803 N94-28025

Recent developments in the simulation of steady and transient transverse jet interactions for missile, rotorcraft, and propulsive applications p 2804 N94-28030

Numerical assessment of aerodynamic interactions on missiles with transverse jets control p 2659 N94-28031

Analysis of cooling jets near the leading edge of turbine blades p 2676 N94-28037

Navier-Stokes analysis of a swirling jet in crossflow p 2806 N94-28038

Experimental study on the interactions between a transverse heated supersonic jet and an external supersonic flow p 2659 N94-28039

Calculation methods for steadily loaded axial groove hydrodynamic journal bearings (guide to use of computer program A9305) [ESDU-93005] p 2830 N94-28074

Calculation methods for steadily loaded axial groove hydrodynamic journal bearings. Low viscosity process fluid lubrication (guide to use of computer program A9306) [ESDU-93006] p 2830 N94-28075

Forced convection heat transfer in straight tubes. Part 2: Laminar and transitional flow [ESDU-93018-PT-2] p 2807 N94-28139

Journal of NIRE, volume 2, number 4 [JTN-94-80554] p 2869 N94-28147

Numerical simulation of turbulent free jet by TFKE model p 2871 N94-28157

Attached and separated trailing edge flow measurements with a triple-split hot-film probe p 2656 N94-28339

A study of blunt trailing edge airfoils using the Navier Stokes code: ARC2D p 2656 N94-28340

Multigrid solutions of the 2D Euler/Navier-Stokes equations on unstructured meshes p 2658 N94-28349

TURBULENT JETS

Theoretical and experimental investigation of a delta wing with turbulent leading-edge jets p 2659 N94-28029

Experimental study on the interactions between a transverse heated supersonic jet and an external supersonic flow p 2659 N94-28039

TURBULENT MIXING

Topics in longshore currents [AD-A274788] p 2899 N94-26361

High resolution measurements of mixing and reaction processes in turbulent flows [AD-A274970] p 2793 N94-26534

TURBULENT WAKES

A comprehensive comparison of turbulence models in the far wake p 2808 N94-27899

TVD SCHEMES

Arbitrary-order high resolution schemes for model hyperbolic conservation laws [CRANFIELD-AERO-9209] p 3005 N94-25823

TVD flux-difference split methods for high-speed thermochemical nonequilibrium flows with strong shocks [UTIAS-350] p 2799 N94-27880

TWINNING

Radiation hardening effects on localized deformation and stress corrosion cracking of stainless steels [DE94-004308] p 2731 N94-25804

Cracking of textured zinc coating during forming process [DE94-003414] p 2750 N94-26085

TWO BODY PROBLEM

Relativistic two-body system in 1+1-dimensional QED. 1: On the circle S1 [DE94-603716] p 3067 N94-27647

TWO DIMENSIONAL BODIES

Surfaces allowing for fractional statistics [DE93-614526] p 3002 N94-25910

Research on bluff body vortex wakes [AD-A273780] p 2796 N94-27319

TWO DIMENSIONAL FLOW

Nominally 2-dimensional flow about a normal flat plate [AD-A274472] p 2794 N94-27026

Parallel implicit unstructured grid Euler solvers [NASA-CR-191594] p 2999 N94-27434

High-lift system analysis method using unstructured meshes [NLR-TP-92351-U] p 2647 N94-27554

A study on heat transfer in a scramjet leading edge model [NAL-TR-1187T] p 2675 N94-27608

A comprehensive comparison of turbulence models in the far wake p 2808 N94-27899

Comparison of the interactions of two and three dimensional transverse jets with a hypersonic free stream p 2659 N94-28021

Navier-Stokes simulation of two and three dimensional jets in crossflow, effects of grid, and boundary conditions p 2804 N94-28026

Experimental investigations into the wall interference and sidewall boundary layer effects in the National Research Council/Inst. for Aerospace Research High Reynolds Number 2-D Test Facility p 2658 N94-28350

Computation of wind-tunnel side-wall interference using 3D Navier-Stokes code p 2658 N94-28351

TWO DIMENSIONAL MODELS

Assessing the climatic effect of carbon dioxide and other trace gases using an interactive two-dimensional climate-chemistry model
[DE94-001741] p 2866 N94-25927

Two dimensional self-consistent fluid simulation of RF inductive sources
[DE94-003635] p 2767 N94-25937

Crossover between BCS and performed-Boson theories with increasing interactions
[DE93-019018] p 3017 N94-26078

Ising critical behaviour in the one-dimensional frustrated quantum XY model
[DE93-634755] p 3057 N94-26390

Interacting cortical filters for object recognition
[PB94-125374] p 2938 N94-26873

Orientation competition in cortical filters
[PB94-125366] p 2939 N94-27001

A note on Riemannian 2-space
[DE94-602560] p 3073 N94-27024

TWO FLUID MODELS

Predictive modeling of particle-laden, turbulent flows
[DE94-003298] p 2792 N94-26319

An experimental study of plunging liquid jet induced air carryunder and dispersion
[AD-A274414] p 2794 N94-26979

Numerical simulation of turbulent free jet by TFKE model p 2871 N94-28157

TWO PHASE FLOW

Interfacial area and interfacial transfer in two-phase flow
[DE93-041226] p 2792 N94-26468

Gravity dependence or pressure drop and heat transfer in straight two-phase heat transport system condenser ducts
[NLR-TP-92167-U] p 2798 N94-27853

TWO STAGE TURBINES

Design and experimental performance of a two stage partial admission turbine. Task B.1/B.4
[NASA-CR-179548] p 2824 N94-27228

U

U.S.S.R.

Microbiology research at some research institutes in the former Soviet Union: A survey of scientific publications
[PB94-123320] p 2902 N94-27171

ULTRAHIGH FREQUENCIES

Extension of On-Surface Radiation Condition (OSRC) theory to full-vector electromagnetic wave scattering by three-dimensional conducting, dielectric, and coated targets
[AD-A274023] p 2766 N94-25757

Comparative investigation of high-latitude ionospheric structure and effects near solar maximum
[AD-A273799] p 2877 N94-25877

VHF-UHF noise surveys at Gulkana, Elmensdorf AFB, Galena AFB, Kotzebue and Cape Lisburne, Alaska and NRL, Pomonkey, Maryland
[PL-TR-93-2136] p 2777 N94-28211

ULTRAHIGH VACUUM

R and D for creation, measurement, application of ultra-high vacuum p 2723 N94-25549

Study on utilization of super clean, high vacuum space p 2682 N94-25586

Inert strength of pristine silica glass fibers
[DE94-004685] p 2750 N94-26247

The reactivity of lithium toward non-aqueous solvents of relevance to energy storage applications as studied by surface analytical techniques
[DE94-003483] p 2856 N94-26464

ULTRASONIC RADIATION

DUSOL: Improved software for analysis of ultrasonic velocity data on anisotropic materials
[NPL-DMM(A)-104] p 2965 N94-26816

ULTRASONIC TESTS

Non-contact ultrasonic inspection
[VTT-TIED-1454] p 2835 N94-26257

An ultrasonic testing technique for monitoring the cure and mechanical properties of polymeric materials
[AD-A274536] p 2753 N94-26842

Automated in-situ inspection systems for underground storage tanks
[AD-A274644] p 2764 N94-27144

Ultrasonic measurement technique to determine the state of cure in thermosetting materials
[PB94-124328] p 2756 N94-27217

ULTRASONICS

An ultrasonic testing technique for monitoring the cure and mechanical properties of polymeric materials
[AD-A274536] p 2753 N94-26842

ULTRAVIOLET ABSORPTION

UV absorption technique for monitoring mobile source NO emissions
[AD-A273858] p 2713 N94-25964

In situ Mars ozone detector p 3108 N94-27892

ULTRAVIOLET ASTRONOMY

Ultraviolet observations of astronomical sources
[NASA-CR-195232] p 3102 N94-26234

ULTRAVIOLET EMISSION

Weak bump quasars
[NASA-CR-195267] p 3103 N94-27933

ULTRAVIOLET FILTERS

Discrete vacuum ultra violet reflective interference filter
[AD-D016059] p 2756 N94-27675

ULTRAVIOLET PHOTOMETRY

Characterization of the energy deposition produced by the primary electron beam on the EXCEDE 3 program
[AD-A274453] p 3033 N94-27084

In situ Mars ozone detector p 3108 N94-27892

ULTRAVIOLET RADIATION

Numerical analysis of the photo-dissociation/radical oxidation of formaldehyde by ultraviolet light in a photolytic reactor
[AD-A274539] p 2868 N94-26843

Initial ultraviolet-B intensity data at Lawrence Livermore National Laboratory
[DE94-004279] p 2869 N94-27267

Sum frequency generation using an optical parametric oscillator
[DE94-001827] p 3040 N94-28000

ULTRAVIOLET SPECTRA

Sulfur dioxide in the atmosphere of Venus 1 sounding rocket observations
[NASA-CR-195224] p 3106 N94-26237

Solar and airglow measurements aboard the two suborbital flights NASA 36.098 and 36.107
[NASA-CR-195279] p 2882 N94-27380

Analysis of EUV/FUV dayglow and auroral measurements
[NASA-CR-195237] p 2883 N94-27393

Probing the Martian atmosphere in the ultraviolet p 3108 N94-27890

How well was total ozone abundance inferred with Mariner 9? p 3108 N94-27891

ULTRAVIOLET SPECTROMETERS

Reanalysis of Mariner 9 UV Spectrometer Data for Ozone, Cloud, and Dust Abundances, and Their Interaction Over Climate Timescales
[NASA-CR-195244] p 3107 N94-27885

Probing the Martian atmosphere in the ultraviolet p 3108 N94-27890

How well was total ozone abundance inferred with Mariner 9? p 3108 N94-27891

ULTRAVIOLET SPECTROSCOPY

Reanalysis of Mariner 9 UV Spectrometer Data for Ozone, Cloud, and Dust Abundances, and Their Interaction Over Climate Timescales
[NASA-CR-195244] p 3107 N94-27885

Mars ozone: Mariner 9 revisited p 3107 N94-27888

UMKLAPP PROCESS

Window least squares method applied to statistical noise smoothing of positron annihilation data
[DE93-634665] p 3003 N94-26385

Fermi surface ridge at second and third Umklapp positron annihilations in Y Ba2Cu3O(7-delta)
[DE93-634760] p 3070 N94-27995

UNCAMBERED WINGS

Normal force of low aspect ratio cropped-delta wings at pre-stall angles of attack and subsonic speeds
[ESDU-93034] p 2648 N94-27955

UNCONSCIOUSNESS

Performance recovery in the baboon following (+)G sub z-induced loss of consciousness
[AD-A274411] p 2902 N94-26991

UNCONTROLLED REENTRY (SPACECRAFT)

A survey of uncontrolled satellite reentry and impact prediction
[AD-A274903] p 2695 N94-26750

UNDERGROUND STORAGE

Automated in-situ inspection systems for underground storage tanks
[AD-A274644] p 2764 N94-27144

UNDERWATER ACOUSTICS

Problems in nonlinear acoustics: Rayleigh waves, pulsed sound beams, and waveguides
[AD-A274587] p 3010 N94-26983

Hydroacoustic wave-fields generated by different source types, a computational study
[PB94-123536] p 3010 N94-27037

UNDERWATER EXPLOSIONS

An improvement in the modified finite element procedure for underwater shock analysis
[DE94-004451] p 2797 N94-27617

UNDERWATER VEHICLES

Telepresence in the human exploration of Mars: Field studies in analog environments p 2685 N94-27360

UNIFORM FLOW

Flow past a circular cylinder with a permeable wake splitter plate
[AD-A273765] p 2790 N94-25872

UNIQUENESS

Approximate solution of the fourth order initial value problem using deficient spline polynomials
[DE93-613023] p 2991 N94-25880

UNITED NATIONS

Contributions to CD Space Committee 1992
[PB94-124401] p 3101 N94-27218

UNIVERSE

The meaning of EROS/MACHO
[DE94-003003] p 3104 N94-26311

A cosmological field theory
[ISBN-0-315-84271-7] p 3104 N94-26638

Cosmological phase transitions
[DE94-003001] p 3104 N94-26786

Pigs in cyberspace p 2689 N94-27376

Cosmic no-hair in Brans-Dicke theory
[DE94-603673] p 3074 N94-27636

UNIVERSITIES

Federal Information Exchange (FEDIX) user's guide: Fall 1993, Version 5.0/Release 1.0
[DE94-003826] p 3097 N94-26350

Selected data on Federal support to universities and colleges: FY 1991
[NSF-93-320] p 3101 N94-28201

UNIVERSITY PROGRAM

MINOTAUR (Maryland's innovative orbital technologically advanced University rocket) p 2703 N94-25685

The 1991-1992 walking robot design p 2833 N94-25686

FAA/NASA Joint University Program for Air Transportation Research, 1992-1993
[NASA-CP-3246] p 2641 N94-27284

An investigation of air transportation technology at the Massachusetts Institute of Technology, 1992-1993 p 2641 N94-27285

Investigation of air transportation technology at Ohio University, 1992-1993 p 2642 N94-27288

Investigation of air transportation technology at Princeton University, 1992-1993 p 2643 N94-27294

University program management information system, FY 1993
[NASA-TM-109719] p 3100 N94-27413

The 1993 NASA-ODU American Society for Engineering Education (ASEE) Summer Faculty Fellowship Program
[NASA-CR-191544] p 3085 N94-27893

Selected data on Federal support to universities and colleges: FY 1991
[NSF-93-320] p 3101 N94-28201

UNMANNED SPACECRAFT

Low-cost unmanned lunar lander p 2697 N94-25699

UNSTEADY AERODYNAMICS

A finite wake theory for two-dimensional rotary wing unsteady aerodynamics
[AD-A274921] p 2645 N94-26535

Methods in unsteady aerodynamics
[DLR-FB-93-21] p 2648 N94-27741

Coupled 2-dimensional cascade theory for noise an d unsteady aerodynamics of blade row interaction in turbofans. Volume 2: Documentation for computer code CUP2D
[NASA-CR-4506-VOL-2] p 2675 N94-27778

Understanding and development of a prediction method of transonic limit cycle oscillation characteristics of fighter aircraft
[NLR-TP-92210-U] p 2679 N94-27798

Multidisciplinary aeroelastic analysis of a generic hypersonic vehicle
[NASA-TM-4544] p 2691 N94-27868

Interaction of the sonic boom with atmospheric turbulence p 2650 N94-28191

UNSTEADY FLOW

Dynamic response of a compressor research facility
[AD-A273836] p 2679 N94-25740

Laser Doppler velocimetry in a low speed multistage compressor
[AD-A274836] p 2818 N94-26498

Program to develop a performance and heat load prediction system for multistage turbines
[NASA-CR-195223] p 2674 N94-26588

Prediction of undsteady flows in turbomachinery using the linearized Euler equations on deforming grids
[NASA-CR-195285] p 2675 N94-27654

Flowfield dynamics in blunt fin-induced shock wave/turbulent boundary layer interactions
[NASA-CR-195170] p 2798 N94-27802

Unsteady wake structures in transverse jets
p 2800 N94-28006

Localized and distributed boundary-layer receptivity to convected unsteady wake in free stream
[NASA-CR-4578] p 2808 N94-28180

Calculation of unsteady incompressible inviscid flow about wings and bodies using CANAERO-T panel model
p 2655 N94-28334

Techniques for accurately solving unsteady shock waves and contact discontinuities p 2656 N94-28342

Unsteady three dimensional Euler solutions on moving grids p 2657 N94-28347

Recent advances in the spectral element method
p 2657 N94-28348

UPPER ATMOSPHERE

Properties of the Central American cold surge
[NASA-CR-194849] p 2893 N94-26138

Upper atmosphere neutral and plasma density modeling
[AD-A274768] p 2879 N94-26569

Kiruna geophysical data. Data summary 93/4-6, April-June 1993
[PB94-123700] p 2881 N94-27039

Kiruna geophysical data. Data summary 93/1-3, January-March, 1993
[PB94-123791] p 2881 N94-27043

JARE data reports. No. 186: Upper atmosphere physics data. Syowa and Asuka Stations, 1990
[JTN-94-80594] p 2881 N94-27299

UPPER ATMOSPHERE RESEARCH SATELLITE (UARS)

Nickel cadmium battery operations on-orbit: Trials, tribulations, and success on the Upper Atmosphere Research Satellite p 2862 N94-28120

UPSTREAM

Wake passage effects on the losses in a linear turbine cascade
[AD-A273794] p 2790 N94-25874

UPWIND SCHEMES (MATHEMATICS)

A robust upwind discretization method for advection, diffusion and source terms
[CWI-NM-R9308] p 2868 N94-26774

URANIUM

Structure and phase transformations in uranium metal
[DE94-003892] p 2732 N94-26004

Deviatoric stresses and plastic strain rates in strong shock waves for six metals
[DE94-002964] p 2733 N94-26022

Unsegmented electromagnetic calorimeter prototype. Energy and coordinate resolution
[DE93-634185] p 2810 N94-26396

URANIUM COMPOUNDS

Study on synthesis and characteristics of intermetallic compound with strong electron correlation
p 2726 N94-25563

Heavy-electron behavior in large coordination compounds CeZn11 and UZn12
[REPT-A-2663] p 3049 N94-25614

Technical report of ISSP. Ser. A, no. 2683: Itinerant character of 5f electrons in UNi2Ga
[JTN-94-80569] p 3025 N94-27337

URETHANES

Dual cure low-VOC coating process
[DE94-000365] p 2756 N94-27611

URINALYSIS

Changes in fluid and electrolyte metabolism during water immersion at high or thermoneutral temperature
p 2912 N94-27445

URINE

Changes in circadian variations of urine excretion in tail-suspended rats p 2911 N94-27443

USER MANUALS (COMPUTER PROGRAMS)

Naval Interactive Data Analysis System (NIDAS), software user's manual
[NASA-CR-195179] p 2956 N94-25606

INM, Integrated Noise Model. Version 4.11: User's guide, supplement
[AD-A273885] p 3009 N94-25731

EcarHeart2 version 1.0: Programmers documentation
[PB94-124633] p 2909 N94-25909

EGADS: A microcomputer program for estimating the aerodynamic performance of general aviation aircraft
[NASA-TM-104013] p 2667 N94-26091

Laser altimetry simulator. Version 3.0: User's guide
[NASA-TM-104588] p 2877 N94-26152

Red's natural editor: A program designed to edit FORTRAN programs
[DE94-003271] p 2962 N94-26318

OPM Scheme Editor 2: A graphical editor for specifying object-protocol structures
[DE94-003477] p 2962 N94-26327

Federal Information Exchange (FEDIX) user's guide: Fall 1993, Version 5.0/Release 1.0
[DE94-003826] p 3097 N94-26350

The Chaco user's guide
[DE94-003669] p 2962 N94-26370

Users manual for CATNIP: A Computer Analysis Tool for Normal Impact Penetration
[DE94-003671] p 2962 N94-26371

Software Error Estimation Program (SWEEP), version 02.00.00 user manual
[AD-A274697] p 2962 N94-26373

User's guide for the frequency domain algorithms in the LIFE2 fatigue analysis code
[DE94-004678] p 2838 N94-26563

Bathymetric data set extraction program. Users guide
[AD-A274761] p 2899 N94-26567

Thermal/structural tailoring of engine blades (T/STAEBL). User's manual
[NASA-CR-194463] p 2839 N94-26692

New FORTRAN computer programs to acquire and process isotopic mass spectrometric data: Operator's manual
[DE94-003174] p 2965 N94-26784

The NOGAPS ten year AMIP integration
[AD-A274332] p 2900 N94-26887

An XCP user's guide and reference manual
[AD-A274519] p 2900 N94-27090

Ma42: A new frontal code for solving sparse unsymmetric systems
[PB94-124302] p 2998 N94-27115

Radar cross section visualization using sample buffer progressive refinement volume rendering
[AD-A274179] p 2773 N94-27127

Users guide for GRIKURV: A code for drawing graphs
[PB94-123593] p 2968 N94-27154

Computer code for controller partitioning with IFPC application: A user's manual
[NASA-CR-195291] p 2678 N94-27414

Modulation Simulation Program: Programmer's manual, version 1.00
[DREO-16] p 2973 N94-27761

ACES spectral display software: User manual
[SKL-1600-99-002] p 2973 N94-27762

Thermal/Structural Tailoring of Engine Blades (T/STAEBL): User's manual
[NASA-CR-194461] p 2843 N94-27776

Coupled 2-dimensional cascade theory for noise an d unsteady aerodynamics of blade row interaction in turbofans. Volume 2: Documentation for computer code CUP2D
[NASA-CR-4506-VOL-2] p 2675 N94-27778

Modulation Simulation Program: Operator's manual, version 1.00
[DREO-16] p 2975 N94-27951

USER REQUIREMENTS

A comparison of users' and providers' perceptions of critical spacelift vehicle characteristics and capabilities
[AD-A273907] p 2691 N94-26017

Design of an online help facility for ExSpect
[PB94-126687] p 2966 N94-26955

Interactive control of a parallel simulation from a remote graphics workstation
[AD-A274217] p 2981 N94-27070

Reinventing information services to increase customer satisfaction
[DE94-003718] p 3100 N94-27563

Human computer interface guide, revision A
[NASA-TM-109708] p 2955 N94-27769

UTILITIES

Solar resource-utility load matching assessment: NREL photovoltaic project summary
[DE94-000232] p 2856 N94-26480

High temperature solid oxide fuel cell: Customer test units
[DE94-002961] p 2858 N94-26869

UTILIZATION

Biomedical polyurethane networks
[ETN-94-95391] p 2750 N94-26211

V

V/STOL AIRCRAFT

Optimal control of helicopters following power failure
[NAL-TR-1190] p 2678 N94-27206

Vectored jets-induced interference on aircraft, prediction and verification p 2801 N94-28012

Influence of headwind on hot gas reingestion and consideration of pressure ratio scaling
p 2675 N94-28018

Unsteady aspects of hot gas reingestion and statistical analysis p 2676 N94-28019

VACANCIES (CRYSTAL DEFECTS)

The role of point defect clusters in reactor pressure vessel embrittlement
[DE94-001122] p 2739 N94-26931

VACCINES

Bakteriella toxiner-morgondagens hot (bacterial toxins-the threat of tomorrow)
[PB94-124229] p 2902 N94-27045

VACUUM APPARATUS

Study on utilization of super clean, high vacuum space
p 2682 N94-25586

Micro-electron deflector
[AD-D016055] p 2787 N94-27672

VACUUM CHAMBERS

Study on utilization of super clean, high vacuum space
p 2682 N94-25586

A large high vacuum, high pumping speed space simulation chamber for electric propulsion
[NASA-TM-106453] p 2690 N94-26142

VACUUM DEPOSITION

Template synthesis of metal microtubule ensembles utilizing chemical, electrochemical, and vacuum deposition techniques
[AD-A274676] p 2715 N94-26444

The optical properties of high-T(c) superconductors grown by pulsed laser deposition
[ISBN-0-315-84917-7] p 3039 N94-27962

VACUUM SYSTEMS

Development of fusion technology
[DE93-633444] p 3042 N94-26159

Electrical analysis of wideband and distributed windows using time-dependent field codes
[DE94-002987] p 2768 N94-26310

Outgas and vacuum seal characteristics of irradiated polyimide O-ring
[DE94-701200] p 2757 N94-27812

VALENCE

AB-Initio calculation of the valence-band offset at strained GaAs/InAs (001) heterojunction
[DE94-602538] p 3061 N94-26878

VALVES

Accelerated screening methods for determining chemical and thermal stability of refrigerant-lubricant mixtures. Part 2: Experimental comparison and verification of methods
[DE94-003664] p 2749 N94-26007

VANADIUM

Volume dependence of vanadium magnetism
[DE94-601838] p 3050 N94-25843

VANADIUM ALLOYS

Hydrogen trapping with Pd coated alloy films
p 2723 N94-25551

Study on alloy films for hydrogen separation
p 2726 N94-25565

Microstructural development in irradiated vanadium alloys
[DE94-004307] p 2737 N94-26556

Deformation twinning: Influence of strain rate
[DE94-002693] p 2738 N94-26621

VANADIUM OXIDES

Technical report of ISSP. Ser. A, no. 2670: Electronic structure of light transition metal compounds studied by photoemission
[JTN-94-80556] p 3065 N94-27239

VANES

Thermal/structural tailoring of engine blades (T/STAEBL). User's manual
[NASA-CR-194463] p 2839 N94-26692

Thermal/Structural Tailoring of Engine Blades (T/STAEBL): User's manual
[NASA-CR-194461] p 2843 N94-27776

Vortex generators for control of shock-induced separation. Part 1: Introduction and aerodynamics
[ESDU-93024-PT-1] p 2806 N94-28095

VAPOR DEPOSITION

Molecular beam mass spectrometry studies of the chemical vapor deposition of diamond
[DE94-003802] p 3049 N94-25601

Characterization of physically vapor deposited AF2400 thin films
[DE94-004019] p 2749 N94-25985

Buckyball microwave plasmas: Fragmentation and diamond-film growth
[DE94-003209] p 3053 N94-26031

The fracture behavior of a CVD crystalline Si3N4/amorphous Si3N4 composite
[DE94-002646] p 2750 N94-26124

The importance of vibrationally excited nitrogen in silicon nitride deposition systems
[AD-A274874] p 2750 N94-26167

The reactivity of lithium toward non-aqueous solvents of relevance to energy storage applications as studied by surface analytical techniques
[DE94-003483] p 2856 N94-26464

The deposition of boron nitride and carbon films on silica glass fibers
[DE94-004684] p 2751 N94-26564
Deposition of a-SiC:H using organosilanes in an argon/hydrogen plasma
[DE94-004428] p 2751 N94-26580
Chemical vapor deposition and characterization of tungsten boron alloy films
[DE94-002648] p 2738 N94-26610
Physical modelling and adaptive predictive control of diffusion/LPCVD reactors
[PB94-126398] p 2763 N94-26819
Growth, characterization and device development in monocrystalline diamond films
[AD-A274245] p 3060 N94-26839
Atomic layer epitaxy of group 4 materials: Surface processes, thin films, devices and their characterization
[AD-A274325] p 3061 N94-26885
Fabrication and characterization of nano-crystalline diamond films
[DE94-002202] p 3062 N94-26934
Vapor deposition of copper on stainless steel 304L
[DE94-001945] p 2740 N94-27006
Visible light emitting materials and injection devices
[AD-A274418] p 2786 N94-27079
Observation of stimulated emission from an MBE grown GaN film on sapphire
[DE94-003638] p 3068 N94-27724

VAPOR PHASE EPITAXY
Electric-field dependence of electroreflectance and photocurrent spectra at visible wavelengths in MOVPE-grown InAlGaP multiple strained quantum-well structures
[DE94-004692] p 2780 N94-25664
Observation of stimulated emission from an MBE grown GaN film on sapphire
[DE94-003638] p 3068 N94-27724

VAPOR PHASES
Molecular beam mass spectrometry studies of the chemical vapor deposition of diamond
[DE94-003802] p 3049 N94-25601
Three methods to measure RH bond energies
[DE94-003795] p 3013 N94-25816

VAPOR PRESSURE
Vapour pressures and critical points of liquids: Aliphatic and cyclic ketones
[ESDU-93009] p 2720 N94-28059
Condensation inside tubes: Computer program for pressure drop in straight tubes (horizontal and vertical with downflow)
[ESDU-93014] p 2806 N94-28064
Vapour pressures and critical points of liquids: Fused ring compounds
[ESDU-93028] p 2721 N94-28142

VAPORS
Stress corrosion cracking and dealloying of copper-gold alloy in iodine vapor
[DE93-633790] p 2734 N94-26264
Application of the Positron Annihilation Technique to the study of vapor absorption process in polyethylene (LDPE) and in imide polymer (6FDA-TMPD PI)
[DE94-602737] p 2720 N94-27998

VARIABILITY
Transmittance fluctuations and non-linearity in random chains in the presence of applied electric fields
[DE94-603665] p 2787 N94-27628
Variability of measured sonic boom signatures
p 2651 N94-28197

VARIABLE CYCLE ENGINES
Supercruiser Arrow HS-8 p 2671 N94-25711
Tesseract supersonic business transport
p 2671 N94-25713
Transient model applications. 2: Compressor stall modeling methods p 2829 N94-28049

VARIATIONAL PRINCIPLES
Cad of GeO2-SiO2 double-layer core dispersion-shifted single-mode fibre
[DE93-634325] p 3035 N94-26383
On the application of Allan variance method for Ring Laser Gyro performance characterization
[DE94-003880] p 2810 N94-26525
A relativistic quark model
[ISBN-0-315-60926-5] p 3025 N94-27333
Correlated mean field Ansatz for the Kondo necklace
[DE94-603671] p 3067 N94-27634

VARIATIONS
Autonomic nervous system and cardiovascular control: Clinical implications of the 1/f fluctuations of heart rate
p 2932 N94-27540

VASOCONSTRICTION
Difference in skin blood flow reduction depending on activating maneuver of skin sympathetic nerve activity
p 2929 N94-27525

VASODILATION
Effect of prostaglandin E1 on the relationship between skin sympathetic nerve activity and reduction in skin blood flow p 2929 N94-27524
Effect of L-dopa on hemodynamic functions in humans p 2929 N94-27526

VECTOR ANALYSIS
Vcalc: A 3-space vector calculator
[AD-A274520] p 2965 N94-26831

VECTOR DOMINANCE MODEL
Heavy charged leptons in an SU(3)(sub L) x U(1)(sub N) model
[DE93-634367] p 3016 N94-26041

VECTOR MESONS
Production of (phi) mesons in central Si + Au collisions at 14.6 AGeV/c
[DE94-003196] p 3012 N94-25795
Vector meson exchanges and CP asymmetry in K(sup +/-) yields pi(sup +/-)pi(sup 0)
[DE94-601605] p 3014 N94-25887
A dependence of exclusive vector meson production in muon-nucleus scattering
[DE94-003363] p 3016 N94-25957
Pi plus pi minus gamma and K+ K- production in two photon collisions at ARGUS
[ISBN-0-315-63598-3] p 3027 N94-27684

VECTOR PROCESSING (COMPUTERS)
Iterative methods for the WLS state estimation on RISC, vector, and parallel computers
[DE94-004260] p 3000 N94-27569

VECTOR QUANTIZATION
Speech coding at low to medium bit rates
[ISBN-0-315-84012-9] p 2770 N94-26630
Vector quantizer designs for joint compression and terrain categorization of multispectral imagery
p 2947 N94-28262

VECTOR SPACES
Deformation of the exterior algebra and the GL(sub q) (r, included in) algebra
[DE94-602558] p 2996 N94-26898
Illumination in diverse codimensions
[NASA-CR-191596] p 2971 N94-27572

VECTORS (MATHEMATICS)
VLUGR2: A vectorized local uniform grid refinement code for PDE's in 2D
[CWI-NM-R9306] p 2965 N94-26772

VEGETATION
Landscape dynamics of northeastern forests
[NASA-CR-195272] p 2852 N94-28070

VEGETATION GROWTH
Bioregenerative system components for microgravity
p 2903 N94-25673
Root gravitropism in maize and Arabidopsis
[NASA-CR-195710] p 2903 N94-27940
Antarctic Record, Vol. 36, No. 2
[REPT-107] p 2883 N94-27963
Note on the structure of moss colonies composed of two species on King George Island, the South Shetland Islands p 2885 N94-27971

VEGETATIVE INDEX
Mapping closed tropical forest cover in West Africa using NOAA/AVHRR-LAC data p 2850 N94-27184
Woody biomass density in the Tendelti area of the central Sudan p 2850 N94-27185
Study on environment monitoring over whole China using NDVI from AVHRR data and future project
p 2875 N94-28289

VELOCITY DISTRIBUTION
Conversion of the CLUSE model for applications over open ocean
[AD-A273750] p 2893 N94-26013
Predictive modeling of particle-laden, turbulent flows
[DE94-003298] p 2792 N94-26319
Laser Doppler velocimetry in a low speed multistage compressor
[AD-A274836] p 2818 N94-26498
Pump CFD code validation tests
[NASA-CR-193939] p 2822 N94-26597
Turbulent boundary layer inner-outer interactions
[AD-A274357] p 2794 N94-27059
Predictions of momentum and scalar fields in a jet in cross-flow using first and second order turbulence closures p 2803 N94-28025
Unified approach for direct and inverse boundary layer prediction using cubic spline collocation
p 2653 N94-28326

VELOCITY MEASUREMENT
Flow past a circular cylinder with a permeable wake splitter plate
[AD-A273765] p 2790 N94-25872
Breakwire technique for hypervelocity measurement
[AD-A274779] p 2809 N94-26358
Investigation of the aerodynamic environment for an advanced lightweight rotor in forward flight. Volume 4: Laser velocimeter wake data, advance ratio of 0.037
[NASA-TM-109040-VOL-4] p 2645 N94-26483
Investigation of the aerodynamic environment for an advanced lightweight rotor in forward flight. Volume 1: Laser velocimeter inflow data, advance ratio of 0.37, thrust coefficient of 0.0081 and hover tip speed of 603 feet/second
[NASA-TM-109040-VOL-1] p 2645 N94-26489
Investigation of the aerodynamic environment for an advanced lightweight rotor in forward flight. Volume 2: Laser velocimeter inflow data, advance ratio of 0.37, thrust coefficient of 0.0064 and hover tip speed of 710 feet/second
[NASA-TM-109040-VOL-2] p 2645 N94-26492
Investigation of the aerodynamic environment for an advanced lightweight rotor in forward flight. Volume 3: Laser velocimeter inflow data, advance ratio of 0.37, thrust coefficient of 0.0064 and hover tip speed of 603 feet/second
[NASA-TM-109040-VOL-3] p 2645 N94-26497
Investigation of spectral analysis techniques for randomly sampled velocimetry data
p 3009 N94-27924

VENTILATION
A method for testing of HVAC automation equipment using the emulator and the application of the method
[VTT-TIED-1435] p 2822 N94-26306

VENTING
Experimental and numerical investigation of shock wave propagation through complex geometry, gas continuous, two-phase media
[DE94-001408] p 2791 N94-26121

VENUS (PLANET)
Sulfur dioxide in the atmosphere of Venus 1 sounding rocket observations
[NASA-CR-195224] p 3106 N94-26237
Some implications of large impact craters and basins on Venus for terrestrial ringed craters and planetary evolution p 2890 N94-28306

VENUS ATMOSPHERE
Sulfur dioxide in the atmosphere of Venus 1 sounding rocket observations
[NASA-CR-195224] p 3106 N94-26237

VENUS SURFACE
Some implications of large impact craters and basins on Venus for terrestrial ringed craters and planetary evolution p 2890 N94-28306

VERBAL COMMUNICATION
The central executive component of working memory
[AD-A274295] p 2938 N94-26683

VERTEBRATES
Proposed law of nature linking impacts, plume volcanism, and Milankovitch cycles to terrestrial vertebrate mass extinctions via greenhouse-embryo death coupling
p 2876 N94-28307

VERTICAL AIR CURRENTS
A modeling study of the mesocyclone
[AD-A274889] p 2893 N94-26168

VERTICAL DISTRIBUTION
Wind measurements with an incoherent lidar
[AD-A273756] p 2891 N94-25722
An overview of the TNO contribution to VAST 92
[AD-A273751] p 2893 N94-26016

VERTICAL LANDING
Experiments into the scaling parameters required for exhaust gas ingestion testing of vertical landing aircraft
p 2671 N94-28017
Influence of headwind on hot gas reingestion and consideration of pressure ratio scaling
p 2675 N94-28018

VERY HIGH FREQUENCIES
Experimental and theoretical investigation of RF absorption and reflection from preformed plasmas
[AD-A274189] p 3046 N94-27098
Packet radio data link applications in the NASA Langley Research Center Transport Systems Research Vehicle
[NASA-TM-109071] p 2665 N94-27423
Characteristics of 30-MHz interference noises observed by riometers p 2884 N94-27965
VHF-UHF noise surveys at Gulkana, Elmensdorf AFB, Galena AFB, Kotzebue and Cape Lisburne, Alaska and NRL, Pomonkey, Maryland
[PL-TR-93-2136] p 2777 N94-28211

VERY HIGH FREQUENCY RADIO EQUIPMENT
A compact 150 GHz SIS receiver cooled by 4 K GM refrigerator
[REPT-36] p 2776 N94-27340

VERY LARGE SCALE INTEGRATION
Real-time 3-D pose estimation using a high-speed range sensor
[AD-A273873] p 2809 N94-25967
A complete version of the Ada tasking coprocessor
p 2950 N94-26721
Physical modelling and adaptive predictive control of diffusion/LPCVD reactors
[PB94-126398] p 2763 N94-26819

Partitioning structural VHDL circuits for parallel execution on hypercubes [AD-A274390] p 2785 N94-26830
Design of a parallel discrete event simulation coprocessor [AD-A274135] p 2982 N94-27123
A fast Fourier transform radix-2 complex butterfly with built-in self-test [ISBN-0-315-84139-7] p 2982 N94-27649
Dry etching process development for submicron and nanometer semiconductor devices [PB94-133196] p 2788 N94-28357

VERY LONG BASE INTERFEROMETRY
Project PARAS: Phased array radio astronomy from space p 3081 N94-25703
Wobble-nutation modes of the Earth [ISBN-0-315-84246-6] p 3102 N94-26669

VERY LOW FREQUENCIES
JARE data reports. No. 186: Upper atmosphere physics data. Syowa and Asuka Stations, 1990 [JTN-94-80594] p 2881 N94-27299
Memories of National Institute of Polar Research. Series A-19. Upper atmosphere physics: ELF emission in high latitudes: Ray path calculation and ground-satellite observations [JTN-94-80592] p 2882 N94-27342

VESTIBULES
Effects of imaginary target on induced eye movements by linear acceleration p 2914 N94-27456

VHSIC (CIRCUITS)
Proposed Object Oriented Programming (OOP) enhancements to the Very High Speed Integrated Circuits (VHSIC) Hardware Description Language (VHDL) [AD-A274004] p 2957 N94-25661
Development of a MIL-STD-1750 microprocessor system for space applications p 2949 N94-26715
Qualified manufacturing and interoperability for space applications p 2949 N94-26719
Partitioning structural VHDL circuits for parallel execution on hypercubes [AD-A274390] p 2785 N94-26830

VIBRATION
High resolution fourier transform absorption spectrum of 79Br2 B3 Pi(Ou+) X1 sigma g+ [AD-A273864] p 2956 N94-25610
FR/GE/UK/US International Test Operations Procedure (ITOP) 1-1-050 development of laboratory vibration test schedules [AD-A273887] p 2836 N94-25732
Spectroscopic and vibrational energy transfer studies in molecular bromine [AD-A273795] p 3014 N94-25875
An algorithm for determination of bearing health through automated vibration monitoring [AD-A274591] p 2823 N94-26986
SAG compensated vibration isolation mount [AD-D016040] p 2841 N94-27110
Silence amenity engineering: Past and present p 3011 N94-27283

VIBRATION DAMPING
A study on piezoelectric actuators and sensors for vibration control of flexible space structures [AD-A274925] p 2695 N94-26532
Identification and H(infinity)/(mu)-synthesis control of the Sandia truss [DE94-002735] p 2839 N94-26810
Processing and mechanical properties of laminated metal composites of Al 6090-25 volume percent SiC(sub p) and Al 5182 [DE94-001070] p 2708 N94-26930
Proceedings of Damping 1993, volume 2 [AD-A274227] p 2840 N94-26953
Proceedings of Damping 1993, volume 3 [AD-A274228] p 2840 N94-27008
Finite element analysis of damped vibrations of laminated composite plates [ISBN-0-315-84928-2] p 2843 N94-27585
Methods of testing for endurance of structural elements using simulated acoustic loading [ESDU-93027] p 3011 N94-28141
On the use of feedback to control sound radiation from a plate excited by a turbulent boundary layer [ISVR-TR-227] p 2807 N94-28175

VIBRATION EFFECTS
Nonequilibrium radiation and chemistry models for aerocapture vehicle flowfields [NASA-CR-195706] p 2648 N94-28071

VIBRATION ISOLATORS
The 1991-1992 project summaries p 2943 N94-25698
Proceedings of Damping 1993, volume 1 [AD-A274226] p 2840 N94-26922
Proceedings of Damping 1993, volume 2 [AD-A274227] p 2840 N94-26953
Proceedings of Damping 1993, volume 3 [AD-A274228] p 2840 N94-27008
SAG compensated vibration isolation mount [AD-D016040] p 2841 N94-27110

VIBRATION MEASUREMENT
Experimental and numerical vibration analyses of a stiffened panel [VTT-PUBS-129] p 2836 N94-25650

VIBRATION MODE
Parameter estimation by genetic algorithms [DE94-002924] p 2961 N94-26146
The free vibration of plates, shallow shells and solids [ISBN-0-315-83931-7] p 2838 N94-26622
Extraction of modal parameters from an operating HAWT using the Natural Excitation Technique (NExT) [DE94-001831] p 2859 N94-27004
Response of structures to impact loads using elastic and plastic analysis [ISBN-0-315-84647-X] p 2842 N94-27309
Understanding and development of a prediction method of transonic limit cycle oscillation characteristics of fighter aircraft [NLR-TP-92210-U] p 2679 N94-27798

VIBRATION TESTS
FR/GE/UK/US International Test Operations Procedure (ITOP) 1-1-050 development of laboratory vibration test schedules [AD-A273887] p 2836 N94-25732
Baseline for a Nordtest method. Reliability stress screening of components. A guide for component users [PB94-123775] p 2835 N94-27042
Report of three microgravity experiments by the drop shaft [JTN-94-80579] p 2761 N94-27341
Space Station Freedom NiH2 cell testing program p 2861 N94-28108

VIBRATIONAL STATES
Vibrational energy transfer within the B 3Pi (O(+) sub u) state of 79BR2 upon collision with N2, O2, NO, and SF6 [AD-A273905] p 3011 N94-25589
A study of vibrational relaxation of electronically-excited molecules [DE93-613553] p 3013 N94-25827
The importance of vibrationally excited nitrogen in silicon nitride deposition systems [AD-A274874] p 2750 N94-26167

VIDEO COMMUNICATION
The question of standards for digital interactive television [AD-A273872] p 2765 N94-25725
The telemedicine spacebridge project: A joint US/Russian venture in long distance medicine via satellite [NASA-TM-106523] p 2693 N94-27427

VIDEO DATA
SHIVA: A unix-based, menu-driven, color image processing software package [AD-A274071] p 2957 N94-25646
Methods for experimentally determining commercial jet aircraft landing parameters from video image data [AD-A274207] p 2669 N94-27105

VIDEO SIGNALS
Color head down display program [AD-A274807] p 2672 N94-26340
Automated fabric inspection system [AD-A274522] p 2835 N94-26833
Focal plane antenna array for millimeter waves [AD-D016034] p 2774 N94-27202

VIDEO TAPE RECORDERS
Automated fabric inspection system [AD-A274522] p 2835 N94-26833

VIDICONS
Focal plane antenna array for millimeter waves [AD-D016034] p 2774 N94-27202

VIEWING
Computer visualizations in engineering applications [DE94-003589] p 2822 N94-26465

VINYL POLYMERS
Object imaging accomplished with an integrated circuit robotic tactile sensor incorporating a piezoelectric polyvinylidene fluoride thin film [AD-A274038] p 2780 N94-25845

VINYLIDENE
Object imaging accomplished with an integrated circuit robotic tactile sensor incorporating a piezoelectric polyvinylidene fluoride thin film [AD-A274038] p 2780 N94-25845

VIRIAL THEOREM
Quark-antiquark bound states [DE93-613054] p 3013 N94-25826

VIRTUAL MEMORY SYSTEMS
Virtual data [DE94-002718] p 2986 N94-26807
Virtual memory management and virtual bus overloading on multiple channel architectures [AD-A274127] p 2954 N94-27152
Shared virtual memory and generalized speedup [NASA-CR-191592] p 2969 N94-27416

VIRTUAL REALITY
ObjectSim: A reusable object oriented DIS visual simulation [AD-A274030] p 2958 N94-25767
Weapon system sensor integration for a DIS-compatible virtual cockpit [AD-A274088] p 2672 N94-26021
NPSNET-4: A real-time, 3D distributed interactive virtual world [AD-A274942] p 2961 N94-26298
Utility fog: A universal physical substance p 2687 N94-27367
An artificial reality environment for remote factory control and monitoring p 2687 N94-27369

VISCOELASTIC DAMPING
Substructure synthesis methods for viscoelastic structures [UTIAS-349] p 2695 N94-26712
Finite element analysis of damped vibrations of laminated composite plates [ISBN-0-315-84928-2] p 2843 N94-27585

VISCOELASTICITY
Stress relaxation in dough moulding compounds [PB94-124872] p 2748 N94-25894
Proceedings of Damping 1993, volume 2 [AD-A274227] p 2840 N94-26953

VISCOPLASTICITY
A hydrostatic stress-dependent anisotropic model of viscoplasticity [NASA-TM-106525] p 2711 N94-27640

VISCOSITY
Measurement of viscosity, density, and gas solubility of refrigerant blends in selected synthetic lubricants [DE94-003609] p 2713 N94-25934
New constitutive equation for the volume viscosity in fluids [NASA-TM-109104] p 2798 N94-27867
Viscosity of liquids: Halogenated ethanes [ESDU-93012] p 2720 N94-28062
Solubility, viscosity, and density of refrigerant/lubricant mixtures [DE94-004237] p 2721 N94-28069
Calculation methods for steadily loaded axial groove hydrodynamic journal bearings. Low viscosity process fluid lubrication (guide to use of computer program A9306) [ESDU-93006] p 2830 N94-28075

VISCOUS DRAG
Calculation of viscous drag of two low angle of attack supercritical profiles [FFA-TN-1984-22] p 2644 N94-26104

VISCOUS FLOW
The high Reynolds number flow through an axial-flow pump [AD-A273844] p 2789 N94-25604
A numerical determination of bifurcation points for low Reynolds number conical flows [AD-A273984] p 2791 N94-25991
Chemical and vibrational nonequilibrium viscous flows: Modelling, internal and external flow applications [ESA-TT-1274] p 2791 N94-26316
Computation of transonic viscous flow past the NTF 65-degree Delta Wing p 2659 N94-27930
Viscous airfoil computations using adaptive structured grids p 2655 N94-28337
A study of blunt trailing edge airfoils using the Navier Stokes code: ARC2D p 2656 N94-28340
A new flux vector splitting scheme p 2657 N94-28343

VISIBLE SPECTRUM
Planetary Instrument Definition and Development Program (PIDDP). Instrument for future planetary flight missions: A visible-infrared imaging spectrometer for planetary missions [NASA-CR-195254] p 3106 N94-27409

VISION
Interacting cortical filters for object recognition [PB94-125374] p 2938 N94-26873

VISUAL AIDS
RIAD visual imaging branch assessment p 2815 N94-27895

VISUAL DISCRIMINATION
Function of selective attention intrinsic to the saccade system: Does the voluntary control override the stimulus driven control? p 2928 N94-27523

VISUAL FIELDS
Endogeneous and exogenous control of visual selection: A review of the literature [AD-A273761] p 2908 N94-25871

VISUAL FLIGHT
Special investigation report: Safety issues related to wake vortex encounters during visual approach to landing [PB94-917002] p 2660 N94-27881

VISUAL PERCEPTION

Human visual system enhancement of reconstructed satellite images
[AD-A273867] p 2693 N94-25595

Image quality and the display modulation transfer function: Experimental findings
[AD-A274061] p 2679 N94-25773

Endogeneous and exogenous control of visual selection: A review of the literature
[AD-A273761] p 2908 N94-25871

The AFIT multielectrode array for neural recording and simulation: Design, testing, and encapsulation
[AD-A274086] p 2909 N94-25943

Pacing visual attention: Temporal structure effects
[AD-A273859] p 2937 N94-25965

Color head down display program
[AD-A274807] p 2672 N94-26340

Interacting cortical filters for object recognition
[PB94-125374] p 2938 N94-26873

Orientation competition in cortical filters
[PB94-125366] p 2939 N94-27001

Frequency analysis of body sway induced by optokinetic stimulation p 2914 N94-27455

Effects of imaginary target on induced eye movements by linear acceleration p 2914 N94-27456

Eye-head coordination and swinging of the visual scene when wearing visually up-down reversing mirror for 14 days p 2915 N94-27462

Comparative measurement of visual stability in cosmic space: Onboard experiment and pre-flight activities
p 2916 N94-27463

Analysis of the Electrically Evoked Response (EER) of the cat p 2908 N94-27519

Visual surface perception: Surface reconstruction from shading and stereo
[ISBN-0-315-60974-5] p 2975 N94-27872

Visit to CERMA: Centre d'Etudes et de Recherches de Medecine Aerospatiale, Centre for Studies and Research in Aviation and Space Medicine, Bretigny sur Orge, France, November 16-18, 1992
[PB94-132990] p 2937 N94-28392

VISUAL STIMULI

Function of selective attention intrinsic to the saccade system: Does the voluntary control override the stimulus driven control? p 2928 N94-27523

VITERBI DECODERS

On the performance of trellis coded 8PSK with Reed Solomon codes
[ISBN-0-315-84289-X] p 2770 N94-26626

VOICE

Researches of the Electrotechnical Laboratory. No. 955: Speech recognition by description of acoustic characteristic variations
[JTN-94-80604] p 2775 N94-27249

VOICE COMMUNICATION

Development of satellite telecommunications during the period 1990 - 2005
[CRANFIELD-AERO-9301] p 2765 N94-25639

Airborne data link operational evaluation test plan
[AD-A274096] p 2664 N94-25788

Parametric time-scale methods in signal analysis
[AD-A274212] p 2773 N94-27068

NCVS, volume 5
[AD-A274975] p 2902 N94-27165

VOICE DATA PROCESSING

Speech coding at low to medium bit rates
[ISBN-0-315-84012-9] p 2770 N94-26630

Researches of the Electrotechnical Laboratory. No. 955: Speech recognition by description of acoustic characteristic variations
[JTN-94-80604] p 2775 N94-27249

VOIDS

Microstructural development in low activation ferritic alloys irradiated to 200 dpa at 420 C
[DE94-004269] p 2731 N94-25803

Interfacial area and interfacial transfer in two-phase flow
[DE93-041226] p 2792 N94-26468

VOLATILITY

Temperature dependence of static RAM volatility
[DE93-040345] p 2948 N94-26111

VOLCANOES

Volcanology and volcanic activity with a primary focus on potential hazard impacts for the Hawaii geothermal project
[DE94-001614] p 2879 N94-26515

VOLCANOLOGY

Impacts, extinctions, volcanism, glaciations, and tectonics: Matches and mismatches
p 2888 N94-28298

Proposed law of nature linking impacts, plume volcanism, and Milankovitch cycles to terrestrial vertebrate mass extinctions via greenhouse-embryo death coupling
p 2876 N94-28307

VOLTAGE CONVERTERS (AC TO AC)

Pulse transformer characterization
[PML-1992-73] p 2784 N94-26646

VOLTAGE CONVERTERS (DC TO DC)

AC to DC power converter with regulated bi-polar outputs
[AD-D016032] p 2786 N94-27145

A study of DC-DC converters with MCT's for arcjet power supplies
[NASA-CR-191204] p 2703 N94-27662

VOLUMETRIC ANALYSIS

Orthobaric densities and molar volumes of liquids: Aliphatic and cyclic ketones
[ESDU-93010] p 2720 N94-28060

VON KARMAN EQUATION

Super finite elements for nonlinear static and dynamic analysis of stiffened plate structures
[ISBN-0-315-63903-2] p 2844 N94-27808

VORTEX ALLEVIATION

Controlled oscillation of forebody vortices by nozzle jet blowing
[ISBN-0-315-84134-6] p 2678 N94-27648

VORTEX GENERATORS

Inclined air-jets used as vortex generators to suppress shock-induced separation p 2659 N94-28040

Vortex generators for control of shock-induced separation. Part 1: Introduction and aerodynamics
[ESDU-93024-PT-1] p 2806 N94-28095

Vortex generators for control of shock-induced separation. Part 3: Examples of applications of vortex generators to aircraft
[ESDU-93026-PT-3] p 2807 N94-28096

VORTEX SHEDDING

The effects of three-dimensional imposed 3-d disturbances on bluff-body near wake flows
[AD-A274845] p 2791 N94-26187

Nominally 2-dimensional flow about a normal flat plate
[AD-A274472] p 2794 N94-27026

Research on bluff body vortex wakes
[AD-A273780] p 2796 N94-27319

Vibrations in engineering structures: A review of model and full-scale test of a cable-stayed bridge and a traffic sign gantry
[NLR-TP-92321-U] p 2843 N94-27553

Separated flow generated by a vectored jet in a crossflow p 2800 N94-28007

VORTICES

Vortex methods
[DE94-003245] p 2789 N94-25597

Flux flow, pinning, and resistive behavior in superconducting networks
[DE94-003400] p 3050 N94-25848

The effects of three-dimensional imposed 3-d disturbances on bluff-body near wake flows
[AD-A274845] p 2791 N94-26187

Feature isolation and quantification of evolving datasets
[NASA-CR-195230] p 2961 N94-26207

Vortices in curved spacetime
[DE94-601559] p 3072 N94-26417

A numerical study of quantized vortices in HeII
[ISBN-9-03-860232-4] p 2792 N94-26479

Numerical studies on the dynamics of bubble, turbulent, free shear flows: Effect of the inter-phase coupling on the global flow evolution
[AD-A274521] p 2794 N94-26832

Leading-edge vortex-system details obtained on F-106B aircraft using a rotating vapor screen and surface techniques
[NASA-TP-3374-VIDEO-SUPPL] p 2647 N94-27161

Special investigation report: Safety issues related to wake vortex encounters during visual approach to landing
[PB94-917002] p 2660 N94-27881

Unsteady wake structures in transverse jets
p 2800 N94-28006

The interaction region associated with twin jets and a normal crossflow p 2800 N94-28009

Experimental investigation of the interaction of a thrust reverser jet with an external subsonic flow
p 2801 N94-28011

Topological structure of a jet in a cross flow
p 2801 N94-28014

Experiments on the ground vortex formed by an impinging jet in cross flow p 2802 N94-28016

Comparison of the interactions of two and three dimensional transverse jets with a hypersonic free stream p 2659 N94-28021

Effects, limits, and limitations of spanwise blowing
p 2659 N94-28027

Recent developments in the simulation of steady and transient transverse jet interactions for missile, rotorcraft, and propulsive applications p 2804 N94-28030

Effects of free-stream turbulence on a jet in a cross flow p 2805 N94-28036

Inclined air-jets used as vortex generators to suppress shock-induced separation p 2659 N94-28040

Measurements of steady and dynamic pressure on an F/A-18 wind tunnel model at high angles of attack
p 2653 N94-28323

VORTICITY

Vortex methods
[DE94-003245] p 2789 N94-25597

A finite wake theory for two-dimensional rotary wing unsteady aerodynamics
[AD-A274921] p 2645 N94-26535

Transverse vorticity measurements in the University of Houston two stream shear layer facility
[AD-A273910] p 2797 N94-27562

Streamwise vorticity in a turbine rotor with conical endwalls
[DLR-FB-93-13] p 2826 N94-27591

VULNERABILITY

Vulnerability assessment using a fuzzy logic based method
[AD-A274075] p 2957 N94-25649

VYCOR

Bulletin of the Institute for Chemical Reaction Science, Tohoku University, volume 2
[JTN-94-80602] p 2717 N94-27385

Porous vycor glass tube joined to borosilicate glass
p 2718 N94-27392

W

WAFERS

Study of the homogeneity of InP wafers
[AD-A273658] p 3055 N94-26194

A partitioning and redundancy model for wafer-scale integrated circuits p 2955 N94-27195

WAKEFULNESS

Effects of methamphetamine on vigilance and tracking during extended wakefulness
[AD-A274896] p 2909 N94-26179

WAKES

Wake passage effects on the losses in a linear turbine cascade
[AD-A273794] p 2790 N94-25874

A finite wake theory for two-dimensional rotary wing unsteady aerodynamics
[AD-A274921] p 2645 N94-26535

Direct simulation Monte-Carlo of near continuum hypersonic flow with chemical reactions
[DLR-FB-93-01] p 2797 N94-27588

Unsteady wake structures in transverse jets
p 2800 N94-28006

Localized and distributed boundary-layer receptivity to convected unsteady wake in free stream
[NASA-CR-4578] p 2808 N94-28180

WALKING

The 1991-1992 walking robot design
p 2833 N94-25686

The effect of platform motion on human energy expenditure during walking. An exploratory experiment
[AD-A273760] p 2940 N94-25724

A biologically-inspired autonomous robot
[AD-A273909] p 2821 N94-25782

WALKING MACHINES

The 1991-1992 walking robot design
p 2833 N94-25686

WALL FLOW

A numerical study of mixing and combustion in hypervelocity flows through a scramjet combustor model
p 2808 N94-27911

Experiments on the ground vortex formed by an impinging jet in cross flow p 2802 N94-28016

Experimental investigations into the wall interference and sidewall boundary layer effects in the National Research Council/Inst. for Aerospace Research High Reynolds Number 2-D Test Facility
p 2658 N94-28350

Computation of wind-tunnel side-wall interference using 3D Navier-Stokes code p 2658 N94-28351

WALL JETS

Theoretical and experimental investigation of a delta wing with turbulent leading-edge jets
p 2659 N94-28029

WALL PRESSURE

Flowfield dynamics in blunt fin-induced shock wave/turbulent boundary layer interactions
[NASA-CR-195170] p 2798 N94-27802

WALLS

Methodology for first wall design
[DE94-002795] p 3045 N94-26861

Passive stabilization of MHD instabilities at high (beta)n in the HBT-EP tokamak
[DE94-003317] p 3047 N94-27735

WAR GAMES

Computer model for generation of infrared images
[PB94-123551] p 3005 N94-27172

WARHEADS
Design study of fiber-composite penetrator cases
[DE94-003203] p 2707 N94-26099
WARNING
Mesoscale meteorological measurements characterizing complex flows
[DE94-002359] p 2895 N94-26761
WARNING SYSTEMS
The chemical detector paper as a potential alarm
[FFI-93/6007] p 2712 N94-25745
A feasibility study on bird classification with neural network
[AD-A273753] p 2659 N94-25780
System for generating, aboard an aircraft, during takeoff, of a signal capable of producing an alert or an alarm, in case of malfunction
[CA-PATENT-APPL-SN-2,018,94] p 2659 N94-26293
Processing of wide-angle synthetic aperture radar signals for target detection
[AD-A274225] p 2773 N94-27073
Ir-fibers in a laser threat warning system and robot shot warning system
[PB94-124476] p 3038 N94-27209
Automatic, real-time fault monitor verifying network in a microwave landing system
[CA-PATENT-1325261] p 2665 N94-27275
WASHING
Stability of reference masses 2: The effect of environment and cleaning methods on the surfaces of stainless steel and allied materials
[NPL-DMM(A)-95] p 2738 N94-26653
WASTE DISPOSAL
Collaboration of chemical oxidation and biological treatment for removal of refractory organic substances
p 2870 N94-28149
Treatment of refractory organic substances with combined use of chemical oxidation and biological treatment. Part 2: Biodegradability of ozonation products of chlorophenol p 2870 N94-28151
WASTE ENERGY UTILIZATION
Feasibility study on introduction of the bio-fuel power generation in tropical regions
[DE94-725203] p 2858 N94-26838
WASTE HEAT
Absorption technology for solar and waste heat utilization p 2854 N94-26053
WASTE TREATMENT
Journal of NIRE, volume 2, number 4
[JTN-94-80554] p 2869 N94-28147
Collaboration of chemical oxidation and biological treatment for removal of refractory organic substances
p 2870 N94-28149
Treatment of refractory organic substances with combined use of chemical oxidation and biological treatment. Part 2: Biodegradability of ozonation products of chlorophenol p 2870 N94-28151
WASTE UTILIZATION
Journal of NIRE, volume 2, number 4
[JTN-94-80554] p 2869 N94-28147
Oil production from buckwheat stillage by thermochemical liquefaction p 2871 N94-28154
WASTES
Vapor deposition of copper on stainless steel 304L
[DE94-001945] p 2740 N94-27006
WATER
Catalog of absolutely calibrated, range normalized, wideband, electric field waveforms from triggered lightning flashes in Florida
[AD-A273793] p 2892 N94-25873
Macrobenthic fauna in the dutch sector of the north sea in 1991
[PB94-126414] p 2868 N94-27200
Why is the north polar cap on Mars different than the south polar cap? p 3107 N94-27889
WATER BALANCE
Role of remote sensing in energy, water, and carbon cycle studies over the Amazon
[INPE-5486-PRE/1786] p 2852 N94-27957
WATER COLOR
Development of a multi-sensor in situ fiber optic fluorometer
[DE94-003399] p 3035 N94-26100
WATER CONSUMPTION
Effect of carbon dioxide enrichment on radish production using Nutrient Film Technique (NFT)
[NASA-TM-107198] p 2902 N94-27411
WATER DEPTH
Scanview: A grafical program for analysis of laserbathymetry data
[PB94-124443] p 2900 N94-27208
WATER FLOW
A study on structure of benthic boundary layer in coastal waters
[REPT-4] p 2898 N94-25635
Calibrating/testing meters in hot water test bench VM7
[PB94-124294] p 2812 N94-27160
An experimental study of siphonal jets in a turbulent boundary layer crossflow p 2802 N94-28015
WATER IMMERSION
Plasma volume shifts and exercise thermoregulation with water immersion and six-degree head-down tilt
[NASA-TM-108781] p 2901 N94-26093
Changes in fluid and electrolyte metabolism during water immersion at high or thermoneutral temperature
p 2912 N94-27445
Cardiovascular function during thermoneutral head-out water immersion in the elderly p 2915 N94-27458
Effects of 40 C hot water immersion for an hour on thermoregulatory functions in humans: Comparison with 34 C thermoneutral immersion p 2915 N94-27459
Effects of bathing at 40 C on cardiovascular system in humans: Comparison with 34 C thermoneutral bathing
p 2918 N94-27473
Effects of 41 C bathing for 20 minutes on cardiovascular and thermoregulatory functions in humans
p 2918 N94-27474
WATER MANAGEMENT
Remote sensing and GIS for the management and investigation of the Wadden Sea
[BCRS-92-20] p 2847 N94-26228
WATER POLLUTION
Selfsimilar solutions of a nonlinear transport equation
[REPT-93-42] p 2865 N94-25760
Recent legal movement on water quality regulation in Japan p 2869 N94-28148
Determination of lead isotope ratios in seawater by purge and trap GC/MS after ethylation p 2870 N94-28152
Indian activities on the core programme IGAP and proposals for network activities p 2874 N94-28284
Changes in phytoplankton population in the Chao Phraya estuary, Thailand, during the eutrophication mechanisms studies p 2875 N94-28287
WATER QUALITY
Journal of NIRE, volume 2, number 4
[JTN-94-80554] p 2869 N94-28147
Recent legal movement on water quality regulation in Japan p 2869 N94-28148
Changes in phytoplankton population in the Chao Phraya estuary, Thailand, during the eutrophication mechanisms studies p 2875 N94-28287
WATER TUNNEL TESTS
Experimental data for CFD validation of impinging jets in crossflow with application to ASTOVL flow problems
p 2801 N94-28010
Topological structure of a jet in a cross flow
p 2801 N94-28014
WATER VAPOR
Control of a hydrogen/oxygen steam generator
[DLR-FB-93-02] p 2826 N94-27589
WATER WAVES
Nonlinear ocean waves
[AD-A274651] p 2899 N94-26354
Topics in longshore currents
[AD-A274788] p 2899 N94-26361
WAVE ATTENUATION
Binaural room simulation
[AD-A273823] p 3009 N94-25737
WAVE DIFFRACTION
Numerical simulation of the reignition of detonation by reflected shocks
[AD-A274755] p 2795 N94-27252
Developments in the application of the geometrical theory of diffraction and computer graphics to aircraft inter-antenna coupling analysis
[ISBN-0-315-84643-7] p 2776 N94-27308
WAVE DISPERSION
Toroidal plasma beta-FLR limit in a toroidally linked mirror system
[DE94-003119] p 3041 N94-25792
Kinetic resonance damping rate of the toroidal ion temperature gradient mode
[DE94-003511] p 3041 N94-25923
C-periodicity and the physical mass in the 3-state Potts model
[DE94-601551] p 3019 N94-26423
Polar optical oscillation modes in GaAs-based double heterostructures: Long wavelength limit
[DE94-601874] p 3062 N94-26897
WAVE EQUATIONS
The extensions of space-time. Physics in the 8-dimensional homogeneous space D is equal to SU(2,2)/K
[DE93-634336] p 3072 N94-26551
Numerical procedure for planetary wave solution
[DE94-004280] p 2879 N94-26576
Elastic wave up/down decomposition in inhomogeneous and anisotropic media: An operator approach and its approximations
[PB94-126497] p 2881 N94-26880
Optical characterization and guided wave loss measurements for end-capped 6F-polybenzoxazole
[AD-A274586] p 3036 N94-26982
Hydroacoustic wave-fields generated by different source types, a computational study
[PB94-123536] p 3010 N94-27037
Wave propagation in the shallow regions of the earth's crust and the borehole vicinity
[ITN-94-85237] p 2882 N94-27330
WAVE FRONT RECONSTRUCTION
Numerical simulation of tomographic reconstruction for the study of turbulence using optical wavefront sensor measurements
[AD-A273851] p 2789 N94-25587
WAVE FRONTS
Numerical simulation of tomographic reconstruction for the study of turbulence using optical wavefront sensor measurements
[AD-A273851] p 2789 N94-25587
Experimental verification of tomographic reconstruction of turbulent air flow structure using optical wavefront measurements
[AD-A274392] p 2795 N94-27129
Dynamic and kinematic P wave tracing for a three-dimensional elastic inhomogeneous media by the asymptotic ray theory and application
[ITN-94-85239] p 2775 N94-27244
WAVE FUNCTIONS
Weak interactions in a bilocal chiral theory
[DE93-613097] p 3013 N94-25836
The Dirac equation in Kerr spacetime, spheroidal coordinates and the M.I.T. bag model of hadrons
[DE94-601566] p 3006 N94-25886
Crystal potential retrieval in HRTEM
[DE94-601883] p 3055 N94-26171
How to build analogues of the Bessel-Clifford expansions for the sum of the repulsive Coulomb potential and central potential decreasing more rapidly than the centrifugal one?
[DE93-634308] p 3007 N94-26472
On the wave and corpuscular properties of microparticles
[DE93-634450] p 3020 N94-26509
Double excitation of He and H(-) by fast proton and anti-proton impact
[DE94-004581] p 3026 N94-27620
Stochastic space-time, confinement potential and particle propagator
[DE94-606415] p 3074 N94-27680
WAVE GENERATION
Investigation of plasma instabilities in the polar cusp
[NASA-CR-195212] p 2879 N94-26599
WAVE INTERACTION
Extension of On-Surface Radiation Condition (OSRC) theory to full-vector electromagnetic wave scattering by three-dimensional conducting, dielectric, and coated targets
[AD-A274023] p 2766 N94-25757
Review of tokamak experiments on direct electron heating and current drive with fast waves
[DE94-004185] p 3041 N94-25801
Space Experiments with Particle Accelerators (SEPAC)
[NASA-CR-193935] p 2761 N94-27664
WAVE PACKETS
About stochastization of motion of charged particles in geomagnetic field and in the field of a wave packet
[DE93-634309] p 2879 N94-26502
About possible types of neutrino oscillations
[DE93-634449] p 3020 N94-26508
Acceleration of electrons and ions by strong lower-hybrid turbulence in solar flares
[NASA-TM-109723] p 3111 N94-27953
WAVE PROPAGATION
Arbitrary-order high resolution schemes for model hyperbolic conservation laws
[CRANFIELD-AERO-9209] p 3005 N94-25823
Efficient modeling in transversely isotropic inhomogeneous media
[DE94-003394] p 2877 N94-25847
Technical description of the Vulcano software library
[FFI-93/7024] p 2767 N94-26105
Ionospheric modification by high power, obliquely propagated HF radio wave transmissions. Part 1: Experimental
[AD-A273746] p 2878 N94-26224
Cad of GeO2-SiO2 double-layer core dispersion-shifted single-mode fibre
[DE93-634325] p 3035 N94-26383
The effect of high frequency electric field on hypersound amplification in superlattice
[DE93-634326] p 3057 N94-26384
A geological and geophysical information system for Eurasia
[AD-A274818] p 3098 N94-26490

A preliminary shear velocity model for Central Asia [AD-A274972] p 2880 N94-26752

Nonlinear hysteresis in an endochronic solid [AD-A274594] p 2880 N94-26855

Hydroacoustic wave-fields generated by different source types, a computational study [PB94-123536] p 3010 N94-27037

Performance statistics bulletin: High altitude meteor scatter propagation, August, September, October 1989 [AD-A274455] p 2773 N94-27085

Dynamic and kinematic P wave tracing for a three-dimensional elastic inhomogeneous media by the asymptotic ray theory and application [ITN-94-85239] p 2775 N94-27244

Wave propagation in the shallow regions of the earth's crust and the borehole vicinity [ITN-94-85237] p 2882 N94-27330

An improvement in the modified finite element procedure for underwater shock analysis [DE94-004451] p 2797 N94-27617

Nonlinear transverse propagation of photons in a ultrarelativistically hot and magnetized electron-positron plasma: Coupling of Langmuir and electromagnetic solitons [DE94-603667] p 3046 N94-27630

Mach reflection of spherical detonation waves [DE93-016604] p 2797 N94-27705

Preliminary considerations on the diffraction (quasi-optical) grill in CASTOR tokamak [IPPCZ-335] p 3048 N94-27842

Underground structure in the eastern part of Kanagawa Prefecture inferred from explosion seismic observations p 2886 N94-27987

Analysis of S-wave seismogram envelope of deep earthquakes and estimation of random inhomogeneities in the Kanto-Tokai area p 2886 N94-27988

Sonic boom propagation through turbulence: A ray theory approach p 2650 N94-28192

The propagation of spark-produced N waves through turbulence p 2650 N94-28193

On the aging of sonic booms p 2650 N94-28194

Plane wave propagation and polarization properties in transversely bianisotropic uniaxial medium [PB94-132883] p 2778 N94-28380

Eigenwaves in the general uniaxial bianisotropic medium with symmetric parameter dyadics [PB94-132891] p 2778 N94-28381

Plane wave propagation in an anisotropic chiral medium with isotropic permittivity and permeability [PB94-133097] p 2778 N94-28384

WAVE REFLECTION

Hydroacoustic wave-fields generated by different source types, a computational study [PB94-123536] p 3010 N94-27037

Numerical simulation of the reignition of detonation by reflected shocks [AD-A274755] p 2795 N94-27252

Mach reflection of spherical detonation waves [DE93-016604] p 2797 N94-27705

WAVE SCATTERING

Polarimetric investigation of edge scattering by mono- and bistatic microwave imaging [ESA-TT-1284] p 2768 N94-26317

Compilation of corrections for postprocessing of laser bathymetry data [PB94-123668] p 2900 N94-27156

WAVE-PARTICLE INTERACTIONS

On a theory of two-beam mechanisms of charged particle acceleration in electrodynamic structures [DE94-003482] p 3032 N94-26330

WAVEFORMS

Catalog of absolutely calibrated, range normalized, wideband, electric field waveforms from triggered lightning flashes in Florida [AD-A273793] p 2892 N94-25873

Fast generator of program waveforms signals [DE93-634230] p 2948 N94-26381

A preliminary shear velocity model for Central Asia [AD-A274972] p 2880 N94-26752

Monaural and binaural processing of complex waveforms [AD-A274209] p 3010 N94-27067

Scanview: A grafical program for analysis of laserbathymetry data [PB94-124443] p 2900 N94-27208

Coherence and satisfiability of waveform timing specifications [ISBN-0-315-57769-X] p 3009 N94-27268

Correlation between electrical activity and the size of single sinoatrial node cells p 2907 N94-27513

Implications for high speed research: The relationship between sonic boom signature distortion and atmospheric turbulence p 2650 N94-28190

WAVEGUIDE ANTENNAS

Design of folded waveguide antenna for Alcator C-Mod [DE94-003584] p 2767 N94-25924

RF modeling and design of a folded waveguide launcher for the Alcator C-Mod tokamak [DE94-003588] p 3041 N94-25933

WAVEGUIDES

Problems in nonlinear acoustics: Rayleigh waves, pulsed sound beams, and waveguides [AD-A274587] p 3010 N94-26983

Microwave coupling into a slotted cavity [PB94-123742] p 2772 N94-27041

WAVELET ANALYSIS

Filtering, coding, and compression with Malvar wavelets [AD-A274055] p 2780 N94-25770

A comparison of spectral decorrelation techniques and performance evaluation metrics for a wavelet-based, multispectral data compression algorithm p 2946 N94-28258

Compression of multispectral Landsat imagery using the Embedded Zerotree Wavelet (EZW) algorithm p 2947 N94-28261

Wavelet compression techniques for hyperspectral data p 2947 N94-28263

WEAK ENERGY INTERACTIONS

Weak hadronic decays of heavy flavor mesons [ISBN-0-315-55542-4] p 3026 N94-27402

Pi plus pi minus gamma and K+ K- production in two photon collisions at ARGUS [ISBN-0-315-63598-3] p 3027 N94-27684

WEAK INTERACTIONS (FIELD THEORY)

Weak interactions in a bilocal chiral theory [DE93-613097] p 3013 N94-25836

Heavy charged leptons in an SU(3)(sub L) x U(1)(sub N) model [DE93-634367] p 3016 N94-26041

Construction of a new electroweak sphaleron [NIKHEF-H/93-09] p 3020 N94-26540

Constraints on singlet right-handed neutrinos coming from the Z(0)-width [DE93-634393] p 3022 N94-26766

Cosmological phase transitions [DE94-003001] p 3104 N94-26786

Progress in SSC Higgs physics: Report of the Higgs working group [DE94-003224] p 3022 N94-26793

Electroweak and other interactions in medium-energy nuclear physics [DE94-004161] p 3027 N94-27689

Topics in electroweak baryogenesis: The sphaleron and T-violation [DE94-004886] p 3029 N94-27811

WEAPON SYSTEMS

Weapon system integration for the AFIT virtual cockpit [AD-A274058] p 2667 N94-25772

Weapon system sensor integration for a DIS-compatible virtual cockpit [AD-A274088] p 2672 N94-26021

Smart structures, an overview [AD-A274147] p 2987 N94-27093

WEAPONS DELIVERY

Weapon system integration for the AFIT virtual cockpit [AD-A274058] p 2667 N94-25772

WEAPONS DEVELOPMENT

The proliferation of aerospace weapons technology: Ballistic missiles and the case of Brazil [ISBN-0-315-84082-X] p 2763 N94-26634

WEAPONS INDUSTRY

The proliferation of aerospace weapons technology: Ballistic missiles and the case of Brazil [ISBN-0-315-84082-X] p 2763 N94-26634

WEAR

Tests of highly loaded skids on a concrete runway [NASA-TP-3435] p 2669 N94-26608

A non-linear mathematical model or finite, periodic rail corrugations [REPT-93-49] p 2996 N94-26967

Guidelines for unlubricated sliding wear tests. Part 1: General approach [PB94-119666] p 2825 N94-27322

Guidelines for unlubricated sliding wear tests. Part 2: Procedures for pin-on-disc testing [PB94-123270] p 2825 N94-27324

WEAR INHIBITORS

Photoelectron spectroscopic studies of the electronic structure and bonding in TiC and TiN [ATR-93(8361)-2] p 2746 N94-28185

WEAR TESTS

Unscreened low tension cables scrape abrasion testing [PB94-123767] p 2823 N94-26849

Guidelines for unlubricated sliding wear tests. Part 1: General approach [PB94-119666] p 2825 N94-27322

Guidelines for unlubricated sliding wear tests. Part 2: Procedures for pin-on-disc testing [PB94-123270] p 2825 N94-27324

WEATHER

Overall analysis of meteorological information in the Daeduk nuclear complex [DE93-632594] p 2894 N94-26469

Encoding approaches for data link transmission of weather graphics [AD-A274497] p 2772 N94-26963

Meteorological data at the Nagaoka Institute of Snow and Ice Studies [REPT-158] p 2896 N94-27169

Aircraft accident report: Runway departure following landing American Airlines flight 102, McDonnell Douglas DC-10-30, N139AA, Dallas/Fort Worth International Airport, Texas, April 14, 1993 [PB94-910402] p 2660 N94-27766

WEATHER FORECASTING

Short-range cloud amount forecasting with model output statistics [AD-A274769] p 2895 N94-26798

The NOGAPS ten year AMIP integration [AD-A274332] p 2900 N94-26887

Encoding approaches for data link transmission of weather graphics [AD-A274497] p 2772 N94-26963

WEATHERING

Failure behaviour of high density polyethylene with an embrittled surface layer due to weathering [PB94-126406] p 2840 N94-26960

WEIBULL DENSITY FUNCTIONS

Estimation and tests-of-fit for the three parameter Weibull distribution [AD-A274827] p 3004 N94-26496

Simulating high-frequency wind for long durations [DE94-002739] p 2682 N94-27997

WEIERSTRASS FUNCTIONS

The super Weierstrass (zeta)-function and operator product expansions in 2D-induced supergravity on the supertorus [DE94-603664] p 3074 N94-27627

WEIGHT (MASS)

Selection of site injecting adjuvant in chronic inflammation model p 2906 N94-27496

An analysis of the loads applied to a heavy Space Station rack during translation and rotation tasks [NASA-TM-104790] p 2697 N94-28183

WEIGHT ANALYSIS

Design optimization of high-speed proprotor aircraft [NASA-TM-103988] p 2667 N94-26151

WEIGHT REDUCTION

Bipolar Ag-Zn battery p 2864 N94-28135

WEIGHTING FUNCTIONS

Numeric solution of the electric field integral equation using Galerkin's method for axially symmetric cases [ESA-TT-1264] p 2768 N94-26315

Method for calculating stress intensity factors for surface cracks (appendix 2/1) p 2841 N94-27188

Applications of the weight function method (appendix 4/1) p 2842 N94-27190

WEIGHTLESSNESS

Study on posture control and adaptation mechanism under weightlessness: Summary report of ground operations performed for carp experiment (FMPT/L-2) in Space Shuttle mission p 2912 N94-27447

Study on posture control and adaption mechanism under weightlessness: Differences in weight and shape of utricular otolith of carp p 2912 N94-27448

Workshop on Countering Space Adaptation with Exercise: Current Issues [NASA-CP-3252] p 2934 N94-28361

WELD STRENGTH

The study of single-pass GMA welds with different cover gas compositions on HSLA-100 steel [AD-A274857] p 2822 N94-26174

The influence of weld metal alloying additions to extend the heat input range for the submerged arc welding of high strength steels [AD-A274284] p 2738 N94-26679

Use of photostress and strain gages to analyze behavior of weldments [NASA-CR-195269] p 2843 N94-27765

Weldability aspects in the design and fabrication of aluminium structures subjected to fatigue loads. Part 2: Weldability of aluminium alloys using advanced MIG and TIG techniques. Effect of the weld bead geometrical factors on the fatigue behavior of the welded joint [PB94-132446] p 2833 N94-28375

WELD TESTS

Evaluating non-chlorinated solvents for welding applications [DE94-003332] p 2824 N94-27181

Use of photostress and strain gages to analyze behavior of weldments [NASA-CR-195269] p 2843 N94-27765

WELDABILITY

Weldability of Direct-Quenched and Tempered (DQT) high strength steel HT80 [VTT-TIED-1406] p 2731 N94-25623

Weldability of Accelerated-Cooled (AcC) high strength TMCP steel HT50 [VTT-TIED-1410] p 2731 N94-25784

Weldability aspects in the design and fabrication of aluminium structures subjected to fatigue loads. Part 2: Weldability of aluminium alloys using advanced MIG and TIG techniques. Effect of the weld bead geometrical factors on the fatigue behavior of the welded joint [PB94-132446] p 2833 N94-28375

Weldability aspects in the design and fabrication of aluminium structures subjected to fatigue loads. Part 1: Effect of welding on the structural integrity of joint types designed for repairing aluminium ship sections [PB94-132487] p 2833 N94-28378

WELDED JOINTS

Corrosion resistance at welded zones of nuclear fuel reprocessing system p 2722 N94-25546

Study on fatigue crack propagation characteristics around welded joint interface in complexed conditions p 2730 N94-25584

Weldability of Direct-Quenched and Tempered (DQT) high strength steel HT80 [VTT-TIED-1406] p 2731 N94-25623

The study of single-pass GMA welds with different cover gas compositions on HSLA-100 steel [AD-A274857] p 2822 N94-26174

Stress analysis of a secondary-bending specimen [AD-A274842] p 2838 N94-26501

The influence of weld metal alloying additions to extend the heat input range for the submerged arc welding of high strength steels [AD-A274284] p 2738 N94-26679

Evaluation of crack arrest fracture toughness of parent plate, weld metal and heat affected zone of BIS 812 EMA ship plate steel [AD-A274871] p 2839 N94-26859

The influence of TIG welding thermal cycles on HSLA-100 steel plate [AD-A274248] p 2740 N94-27009

Evaluating non-chlorinated solvents for welding applications [DE94-003332] p 2824 N94-27181

Use of photostress and strain gages to analyze behavior of weldments [NASA-CR-195269] p 2843 N94-27765

Weldability aspects in the design and fabrication of aluminium structures subjected to fatigue loads. Part 2: Weldability of aluminium alloys using advanced MIG and TIG techniques. Effect of the weld bead geometrical factors on the fatigue behavior of the welded joint [PB94-132446] p 2833 N94-28375

Weldability aspects in the design and fabrication of aluminium structures subjected to fatigue loads. Part 1: Effect of welding on the structural integrity of joint types designed for repairing aluminium ship sections [PB94-132487] p 2833 N94-28378

WELDING

Digital control and data acquisition for high-value GTA welding [DE94-000885] p 2821 N94-25980

Use of photostress and strain gages to analyze behavior of weldments [NASA-CR-195269] p 2843 N94-27765

Upset welding process for 21-6-9 spherical vessels [DE93-018194] p 2832 N94-28229

Weldability aspects in the design and fabrication of aluminium structures subjected to fatigue loads. Part 1: Effect of welding on the structural integrity of joint types designed for repairing aluminium ship sections [PB94-132487] p 2833 N94-28378

WELDING MACHINES

Digital control and data acquisition for high-value GTA welding [DE94-000885] p 2821 N94-25980

WETLANDS

Methane emissions from natural wetlands [DE93-040796] p 2865 N94-25790

WETTING

Study on interfacial reaction analysis at interfacial joining p 2728 N94-25574

WHEELS

Aircraft wheel life assessment [AD-A274378] p 2823 N94-26976

WHISPERING GALLERY MODES

Mode analysis of gyrotron oscillation using a k-spectrometer [DE94-701195] p 2813 N94-27703

WHISTLERS

Investigation of plasma instabilities in the polar cusp [NASA-CR-195212] p 2879 N94-26599

WHITE NOISE

Longitudinal diffusion of a proton bunch under external noise [DE93-634022] p 3032 N94-26165

Three dimensional object recognition using a complex autoregressive model [AD-A274388] p 2995 N94-26829

Enhanced adaptive statistical filter providing improved performance for target motion analysis noise discrimination statement of government interest [AD-D016039] p 2786 N94-27109

White noise theory of robust nonlinear filtering with correlated state and observation noises [PB94-126661] p 3004 N94-27211

WIGNER COEFFICIENT

Wigner quantum oscillators [DE94-601508] p 3073 N94-26758

WIND (METEOROLOGY)

Machine intelligent gust front algorithm [AD-A273695] p 2680 N94-26196

A preliminary analysis of the US west climatology [DE94-003028] p 2894 N94-26313

A preliminary method for atmospheric soundings in real time using satellite and ground-based remotely sensed data [AD-A274381] p 2880 N94-26828

WIND DIRECTION

Lift-curve slope for structural response calculations [ESDU-93013] p 2648 N94-28063

WIND EFFECTS

The effects of tailwinds and control cross coupling on rotorcraft handling qualities for steep, decelerating instrument approaches and missed approaches [IAR-AN-77] p 2677 N94-26710

Surface roughness lengths [AD-A274550] p 2895 N94-26846

Lift-curve slope for structural response calculations [ESDU-93013] p 2648 N94-28063

WIND MEASUREMENT

Wind measurements with an incoherent lidar [AD-A273756] p 2891 N94-25722

Simulating high-frequency wind for long durations [DE94-002739] p 2682 N94-27997

WIND SHEAR

Machine intelligent gust front algorithm [AD-A273695] p 2680 N94-26196

The relationship of an integral wind shear hazard to aircraft performance limitations [NASA-TM-109080] p 2677 N94-26593

Surface roughness lengths [AD-A274550] p 2895 N94-26846

WIND TUNNEL APPARATUS

Shake test results of the MDHC test stand in the 40- by 80-foot wind tunnel [NASA-TM-108801] p 2641 N94-26596

Installation of models in the 2 m x 3 m low speed wind tunnel [LTR-LA-286] p 2681 N94-27594

WIND TUNNEL MODELS

Installation of models in the 2 m x 3 m low speed wind tunnel [LTR-LA-286] p 2681 N94-27594

Experimental apparatus for optimization of flap position for a three-element airfoil model p 2682 N94-27912

Evaluation of the buoyancy drag on automobile models in low speed wind tunnels p 2658 N94-28352

WIND TUNNEL TESTS

Low-speed pressure distribution measurements over the aft-fuselage, fins, and stabilators of a 1/9th scale F/A-18 wind-tunnel model [AD-A274870] p 2644 N94-26342

Investigation of the aerodynamic environment for an advanced lightweight rotor in forward flight. Volume 4: Laser velocimeter wake data, advance ratio of 0.037 [NASA-TM-109040-VOL-4] p 2645 N94-26483

Investigation of the aerodynamic environment for an advanced lightweight rotor in forward flight. Volume 1: Laser velocimeter inflow data, advance ratio of 0.37, thrust coefficient of 0.0081 and hover tip speed of 603 feet/second [NASA-TM-109040-VOL-1] p 2645 N94-26489

Investigation of the aerodynamic environment for an advanced lightweight rotor in forward flight. Volume 2: Laser velocimeter inflow data, advance ratio of 0.37, thrust coefficient of 0.0064 and hover tip speed of 710 feet/second [NASA-TM-109040-VOL-2] p 2645 N94-26492

Investigation of the aerodynamic environment for an advanced lightweight rotor in forward flight. Volume 3: Laser velocimeter inflow data, advance ratio of 0.37, thrust coefficient of 0.0064 and hover tip speed of 603 feet/second [NASA-TM-109040-VOL-3] p 2645 N94-26497

The measurement of disturbance levels in the Langley Research Center 20-inch Mach 6 tunnel [NASA-CR-4571] p 2646 N94-26548

Pressure distributions on a 0.02-scale Space Shuttle orbiter nose at Mach 21.5 in helium [NASA-TM-4495] p 2646 N94-26592

Shake test results of the MDHC test stand in the 40- by 80-foot wind tunnel [NASA-TM-108801] p 2641 N94-26596

Experimental investigation of advanced hub and pylon fairing configurations to reduce helicopter drag [NASA-TM-4540] p 2668 N94-26604

Experimental investigation of the flow quality in the GLT20 subsonic-transonic boundary layer wind tunnel [PB94-126539] p 2681 N94-26815

Wind tunnel investigation of an STOL aircraft model: An effect of engine nacelle shape [NAL-TM-653] p 2647 N94-27235

Transverse vorticity measurements in the University of Houston two stream shear layer facility [AD-A273910] p 2797 N94-27562

Flowfield dynamics in blunt fin-induced shock wave/turbulent boundary layer interactions [NASA-CR-195170] p 2798 N94-27802

Microspheres for laser velocimetry in high temperature wind tunnel p 2682 N94-27903

Experimental apparatus for optimization of flap position for a three-element airfoil model p 2682 N94-27912

Transient flow features of a supersonic jet in a low speed cross flow p 2800 N94-28005

Experimental investigation of the interaction of a thrust reverser jet with an external subsonic flow p 2801 N94-28011

Experiments on the ground vortex formed by an impinging jet in cross flow p 2802 N94-28016

Experiments on interaction force of jets in hypervelocity cross-flow in a shock tunnel p 2659 N94-28022

Vortex generators for control of shock-induced separation. Part 1: Introduction and aerodynamics [ESDU-93024-PT-1] p 2806 N94-28095

Measurements of steady and dynamic pressure on an F/A-18 wind tunnel model at high angles of attack p 2653 N94-28323

Infrared imaging for transition detection in a transonic blowdown wind tunnel p 2653 N94-28325

Experimental study on the shock wave interaction with a hypersonic boundary layer near a convex corner p 2654 N94-28328

Application of the influence function method using the interference distributed loads code to prediction of store aerodynamic load during separation from the CF-18 fighter aircraft p 2654 N94-28330

Aerodynamic performance of novel ducted-tip wings p 2654 N94-28331

Experimental investigations into the wall interference and sidewall boundary layer effects in the National Research Council/Inst. for Aerospace Research High Reynolds Number 2-D Test Facility p 2658 N94-28350

Computation of wind-tunnel side-wall interference using 3D Navier-Stokes code p 2658 N94-28351

Evaluation of the buoyancy drag on automobile models in low speed wind tunnels p 2658 N94-28352

WIND TUNNEL WALLS

Evaluation of the prototype dual-axis wall attitude measurement sensor [NASA-TM-109056] p 2811 N94-26707

Evaluation of the buoyancy drag on automobile models in low speed wind tunnels p 2658 N94-28352

WIND TUNNELS

Research and test facilities [NASA-TM-109685] p 2681 N94-26684

Comparative analysis of different configurations of PLC-based safety systems from reliability point of view p 2836 N94-27925

WIND TURBINES

The identification of inflow fluid dynamics parameters that can be used to scale fatigue loading spectra of wind turbine structural components [DE94-000231] p 2791 N94-26117

An overview of DOE's wind turbine development programs [DE93-018224] p 2856 N94-26513

User's guide for the frequency domain algorithms in the LIFE2 fatigue analysis code [DE94-004678] p 2838 N94-26563

Analysis/test correlation using VAWT-SDS on a step-relaxation test for the rotating Sandia 34 m test bed [DE94-002290] p 2857 N94-26700

Extraction of modal parameters from an operating HAWT using the Natural Excitation Technique (NExT) [DE94-001831] p 2859 N94-27004

Simulating high-frequency wind for long durations [DE94-002739] p 2682 N94-27997

WIND VELOCITY

Wind measurements with an incoherent lidar [AD-A273756] p 2891 N94-25722

Conversion of the CLUSE model for applications over open ocean
[AD-A273750] p 2893 N94-26013
Modelling atmospheric turbulence effects on ground-based telescope systems
[DE94-004211] p 3102 N94-26528
Simulating high-frequency wind for long durations
[DE94-002739] p 2682 N94-27997

WINDING
Winding numbers in homotopy theory from integers to reals
[DE94-601510] p 2992 N94-26367

WINDOWS (COMPUTER PROGRAMS)
Implementing a multiple criteria model base in co-op with a graphical user interface generator
[AD-A274901] p 3093 N94-26181
An artificial reality environment for remote factory control and monitoring p 2687 N94-27369
Development of Calcomp compatible interface library 'piflib' on X Window System
[DE94-701190] p 2973 N94-27702

WINDPOWER UTILIZATION
Renewable energy systems in Mexico: Installation of a hybrid system
[DE93-013716] p 2853 N94-25946
NEMO 2: New energy systems and technologies
[DE94-702060] p 2855 N94-26240
Programme for the promotion of wind power production
[DE94-702065] p 2855 N94-26242
Hybrid power system for remote communications stations
[AD-A274963] p 2782 N94-26301
An overview of DOE's wind turbine development programs
[DE93-018224] p 2856 N94-26513

WINDPOWERED GENERATORS
Programme for the promotion of wind power production
[DE94-702065] p 2855 N94-26242

WINDS ALOFT
Modeling of the coupled magnetospheric and neutral wind dynamos
[NASA-CR-195273] p 2883 N94-27852

WING FLOW METHOD TESTS
Numerical simulation of a powered-lift landing
p 2671 N94-28033

WING OSCILLATIONS
Understanding and development of a prediction method of transonic limit cycle oscillation characteristics of fighter aircraft
[NLR-TP-92210-U] p 2679 N94-27798

WING PANELS
Investigation of the bond strength of a discrete skin-stiffener interface
[NLR-TP-92183-U] p 2670 N94-27796

WING TIPS
Aerodynamic performance of novel ducted-tip wings
p 2654 N94-28331

WING-FUSELAGE STORES
Application of the influence function method using the interference distributed loads code to prediction of store aerodynamic load during separation from the CF-18 fighter aircraft p 2654 N94-28330

WINGS
An investigation into the aerodynamic effects of wing patches
[ISBN-0-315-84121-4] p 2646 N94-26672
Automation of formation flight control
[AD-A274137] p 2678 N94-27132
Investigation of aerodynamic design issues with regions of separated flow p 2658 N94-27902
Wing design for a civil tiltrotor transport aircraft: A preliminary study p 2671 N94-27917
Effects, limits, and limitations of spanwise blowing
p 2659 N94-28027
Program for calculation of maximum lift coefficient of plain aerofoils and wings at subsonic speeds
[ESDU-93015] p 2649 N94-28076
Wing lift increment at zero angle of attack due to deployment of single-slotted flaps at low speeds
[ESDU-93019] p 2649 N94-28140
Calculation of unsteady incompressible inviscid flow about wings and bodies using CANAERO-T panel model
p 2655 N94-28334
Ice accretion on aircraft wings p 2657 N94-28345

WINTER
Propagation of cold air masses in East Asia and its associated planetary-scale function
[AD-A274304] p 2895 N94-26850
Meteorological data at the Nagaoka Institute of Snow and Ice Studies
[REPT-158] p 2896 N94-27169

WIRE
Liquid and solid solubility of Ag in Bi2Sr2CaCu2O8
[DE94-002829] p 2735 N94-26273
Superconducting fibers made with yttrium and yttrium oxide interlayers and barium cuprate cover layers
[AD-D016073] p 3070 N94-28225

WIRE CLOTH
A constitutive model for layered wire mesh and aramid cloth fabric
[DE94-003275] p 2708 N94-26796

WIRELESS COMMUNICATION
Efficient massively parallel simulation of dynamic channel assignment schemes for wireless cellular communications
[NASA-CR-191593] p 2971 N94-27558

WOOD
Report of National Institute for Resources and Environment. No. 5: Study on direct liquefaction of woody biomass
[JTN-94-80551] p 2859 N94-27204

WORDS (LANGUAGE)
Parallel string matching algorithms
[AD-A274502] p 3100 N94-27164
Researches of the Electrotechnical Laboratory. No. 955: Speech recognition by description of acoustic characteristic variations
[JTN-94-80604] p 2775 N94-27249

WORKING FLUIDS
The Lightcraft project: Flight technology for a hypersonic mass transit system p 2670 N94-25695
Liquid metal MHD research and development in Israel
p 2854 N94-26055
Modelling the mass migration phenomena in partially frozen heat pipes
[DE94-002716] p 2797 N94-27709

WORKLOADS (PSYCHOPHYSIOLOGY)
Developing realistic cooperative behaviors for autonomous agents in air combat simulation
[AD-A274077] p 2937 N94-25774
Developing a sophisticated user interface to support domain-oriented application composition and generation systems
[AD-A274080] p 2960 N94-25994
A critical analysis of workload predictions generated by multiple resource theory during early crewstation design
[AD-A274804] p 2941 N94-26339
The use of EEG as a workload assessment tool in flight test
[AD-A274568] p 2910 N94-26847
Workload transition: Implications for individual and team performance
[AD-A274538] p 2941 N94-26964
Task demand, workload, and performance
[PB94-123627] p 2942 N94-27155

WORKSTATIONS
Weapon system integration for the AFIT virtual cockpit
[AD-A274058] p 2667 N94-25772
Object-oriented design and implementation of a parallel Ada simulation system
[AD-A274119] p 2979 N94-25906
Vcalc: A 3-space vector calculator
[AD-A274520] p 2965 N94-26831
Interactive control of a parallel simulation from a remote graphics workstation
[AD-A274217] p 2981 N94-27070
A graphical workstation based part-task flight simulator for preliminary rapid evaluation of advanced displays
p 2641 N94-27286
VENI, video, VICI: The merging of computer and video technologies p 2686 N94-27362

WOVEN COMPOSITES
Investigation of forced and isothermal chemical vapor infiltrated SiC/SiC ceramic matrix composites
[DE94-004544] p 2708 N94-26557

WURTZITE
Se EXAFS study of the elevated wurtzite to rock salt structural phase transition in CdSe nanocrystals
[DE94-003247] p 3054 N94-26125

X

X RAY ABSORPTION
Morphological analysis of ionomers
[DE94-003660] p 2749 N94-26005
X ray absorption studies of Ti/polymer and Cr/polymer interfaces
[DE94-003008] p 2753 N94-26770
An x ray absorption fine structure study of ordering in polythiophene thin films
[AD-A274235] p 2753 N94-26822

X RAY ANALYSIS
Inner fiber observation for metal matrix composites under the stress load condition utilizing Synchrotron Orbital Radiation (SR) by X-ray CT p 2724 N94-25553
In situ x ray reflectivity measurements of thin film structural evolution
[DE94-002289] p 3051 N94-25944

X RAY ASTRONOMY
Cosmic x ray physics
[NASA-CR-195225] p 3115 N94-27236

X RAY ASTROPHYSICS FACILITY
Space projects: Astrophysics facility program contains cost and technical risks. Report to Congressional Requesters
[GAO/NSIAD-94-80] p 2696 N94-27382

X RAY DETECTORS
Hardware design of a spherical mini-rover
p 2833 N94-25669
A space fiber-optic x ray burst detector
[DE94-002722] p 2696 N94-26808
Cosmic x ray physics
[NASA-CR-195225] p 3115 N94-27236
The x ray holographic microscopy using the atomic-force microscope
[DE94-004003] p 2814 N94-27779

X RAY DIFFRACTION
Study on improvement in physical analysis method of metallic materials p 2728 N94-25577
Transition metals in highly correlated discotic phases: Designing metallomesogens with selected intermolecular organizations
[AD-A274695] p 2736 N94-26452
Qualitative analysis of rare earth elements contained in the phosphogypsum
[DE93-614153] p 2716 N94-26518
Experimental measurement of local displacement and chemical pair correlations in crystalline solid solutions
[DE94-001124] p 3065 N94-27251
High intensity x ray instrumentation for residual strain measurements in composites and textured materials
[ISBN-0-315-85169-4] p 2842 N94-27278
Multiple exposure CCD detector for high-speed laser pump, x ray probe Laue scattering
[DE94-004618] p 2820 N94-27781
Crystallographic analyses of clathrate hydrates included in Vostok ice cores p 2885 N94-27969
Energy Dispersive X ray Diffraction (EDXD) apparatus for liquids at high temperature p 2721 N94-28159

X RAY FLUORESCENCE
Qualitative analysis of rare earth elements contained in the phosphogypsum
[DE93-614153] p 2716 N94-26518

X RAY IMAGERY
Imaging with x ray lasers
[DE94-002844] p 2816 N94-26020

X RAY INSPECTION
The development of an in-motion radiography system for large area aircraft scanning
[DREP-TM-93-53] p 2670 N94-27666

X RAY LASERS
Imaging with x ray lasers
[DE94-002844] p 2816 N94-26020
Phase conjugated lasers applied to commercial x ray lithography
[DE94-001529] p 2819 N94-27018

X RAY SCATTERING
Structural study of Cu/Co multilayer by anomalous small-angle x ray scattering p 2744 N94-28160

X RAY SOURCES
Meson spectroscopy and particle astrophysics
[DE94-001799] p 3115 N94-27003
Cosmic x ray physics
[NASA-CR-195225] p 3115 N94-27236

X RAY SPECTRA
Balloon-borne measurements of the SN1987A hard x ray continuum p 3115 N94-26689

X RAY SPECTROSCOPY
Study on analyzing method establishment for metallic material development p 2729 N94-25578
Se EXAFS study of the elevated wurtzite to rock salt structural phase transition in CdSe nanocrystals
[DE94-003247] p 3054 N94-26125
X ray absorption studies of Ti/polymer and Cr/polymer interfaces
[DE94-003008] p 2753 N94-26770

X RAY STARS
An April 1991 outburst from 4U0115+63 observed by BATSE
[NASA-CR-195252] p 3116 N94-27440

X RAY TUBES
Fast photoconductor CdTe detectors for synchrotron x ray studies
[DE94-001334] p 3054 N94-26139

X RAYS
Advanced qualification techniques
[DE94-003709] p 2780 N94-25812
Electron energy loss spectroscopy in a crystalline environment using inner shell ionization
[DE94-601820] p 3018 N94-26334
Experimental measurement of local displacement and chemical pair correlations in crystalline solid solutions
[DE94-001124] p 3065 N94-27251

Acceleration of electrons and ions by strong lower-hybrid turbulence in solar flares
[NASA-TM-109723] p 3111 N94-27953

XENON

Stationary plasma thruster plume emissions
[NASA-CR-194471] p 2701 N94-26209

Calculations of population transfer during intense laser pulses
[DE94-001060] p 2818 N94-26698

Disintegration of (C60) by Xe ion irradiation
[DE94-601913] p 3023 N94-26929

Damage growth in MgAl2O4 crystals by Xe ion irradiations
[DE94-005009] p 3069 N94-27828

Y

YAG LASERS

The development of Cr, Tm, Ho:YAG lasers for airborne lidar
[AD-A274895] p 2816 N94-26178

Development of surgical CW Nd:YAG laser with optical fiber delivery system
[DE93-632902] p 2817 N94-26185

Development of real-time pulse shaping technology in solid-state lasers
[DE93-633438] p 2817 N94-26403

Development of high average power industrial Nd:YAG laser with peak power of 10 kW class
[DE93-633201] p 2818 N94-26520

Distributed Nd:YAG laser welding and process control in inert glove boxes
[DE94-002629] p 2818 N94-26605

Kinoform/lens system for injecting a high power laser beam into an optical fiber
[DE94-003226] p 2819 N94-27262

YANG-MILLS THEORY

Classical solutions of Yang-Mills-Chern-Simons theory in 2+1 dimensions: A quasi-linear superposition
[DE93-634335] p 3006 N94-26270

C-periodicity and the physical mass in the 3-state Potts model
[DE94-601551] p 3019 N94-26423

Component structure of the N = 2 super-Yang-Mills theory in the harmonic superspace
[DE93-634340] p 3072 N94-26453

Anomaly candidates and invariants of D 4, N 1 supergravity theories
[NIKHEF-H/93-12] p 3072 N94-26541

Operator regularization and renormalization theory
[ISBN-0-315-49334-8] p 3007 N94-27264

A method for obtaining quantum doubles from the Yang-Baxter R-matrices
[DE94-606300] p 3001 N94-27846

YARNS

Superconducting fibers made with yttrium and yttrium oxide interlayers and barium cuprate cover layers
[AD-D016073] p 3070 N94-28225

YAWING MOMENTS

Contribution of body-mounted fins and tailplanes to lateral derivatives due to sideslip at subsonic speeds for general body width to height ratio
[ESDU-93007] p 2648 N94-28057

YBCO SUPERCONDUCTORS

Grain boundary degradation of YBCO superconductors sintered in CO2-containing atmospheres
[DE94-003206] p 3053 N94-26029

Window least squares method applied to statistical noise smoothing of positron annihilation data
[DE93-634665] p 3003 N94-26385

A study on the development of high T(sub c) superconducting materials
[DE93-633529] p 3057 N94-26404

Submillimeter residual losses in high-(Tc) superconductors
[DE94-003241] p 3058 N94-26516

A study on the development of high-T(c) superconducting wire
[DE93-632438] p 2783 N94-26546

Demonstration of monolithic co-fabrication of Y1Ba2Cu3O7-Sigma and CMOS devices on the same sapphire substrate
[AD-A274757] p 3059 N94-26566

Preparation and characterization of high temperature superconductor film surfaces
[AD-A274293] p 3059 N94-26681

Controlled heterogeneous nucleation of melt-textured YBa2Cu3O(6+x) by addition of Al2O3 particles
[AD-A274605] p 3062 N94-26892

Technical report of ISSP. Ser. A, no. 2681: Orbital and spin susceptibilities of the plane copper sites in YBa2Cu3O(x) system
[JTN-94-80567] p 3064 N94-27177

Synthesis, rheology, and forming of Y-Ba-Cu-O ceramics
[DE94-005558] p 2757 N94-27695

Fermi surface ridge at second and third Umklapp positron annihilations in Y Ba2Cu3O(7-delta)
[DE93-634760] p 3070 N94-27995

Superconducting fibers made with yttrium and yttrium oxide interlayers and barium cuprate cover layers
[AD-D016073] p 3070 N94-28225

YIELD STRENGTH

Determination of fracture stress and effective crack tip radius from toughness (KIc) and yield strength (Y)
[AD-A274014] p 2836 N94-25754

Radiation hardening effects on localized deformation and stress corrosion cracking of stainless steels
[DE94-004308] p 2731 N94-25804

On experimental studies of yield surfaces of metals: A more general approach
[IFTR-42/1993] p 2739 N94-26824

Processing and mechanical properties of laminated metal composites of Al 6090-25 volume percent SiC(sub p) and Al 5182
[DE94-001070] p 2708 N94-26930

Fatigue propagation behaviour of short cracks (1-2 mm) in steels
[ESDU-93033] p 2845 N94-28145

YOKES

Reconfigurable aircraft stick control
[AD-D016043] p 2681 N94-27113

YTTERBIUM COMPOUNDS

Fibrous emissive burners selective and broad band
[PB94-128329] p 2859 N94-27225

YTTRIA-STABILIZED ZIRCONIA

Oxygen reduction at a YSZ interface with cathode materials La(1-x)(Ca or Sr)(x)MnO3(1-x)CaMnO3
[DE94-002954] p 3054 N94-26147

YTTRIUM COMPOUNDS

Space-R thermionic space nuclear power system: Design and technology demonstration
[DE94-001890] p 2699 N94-25929

Preparation, characterization, and thermal behaviour study of lanthanides (3) and yttrium (3) 4-methoxy benzylidene pyruvate in solid state
[DE94-604079] p 3068 N94-27697

YTTRIUM OXIDES

Synthesis, rheology, and forming of Y-Ba-Cu-O ceramics
[DE94-005558] p 2757 N94-27695

Superconducting fibers made with yttrium and yttrium oxide interlayers and barium cuprate cover layers
[AD-D016073] p 3070 N94-28225

YTTRIUM-ALUMINUM GARNET

Technical report of ISSP. Ser. A, no. 2682: Pressure dependence of Sm:YAG fluorescence to 50 GPa: A new calibration as a high pressure scale
[JTN-94-80568] p 3066 N94-27354

YUKAWA POTENTIAL

Stochastic space-time, confinement potential and particle propagator
[DE94-606415] p 3074 N94-27680

Z

ZEEMAN EFFECT

Zeeman laser interferometry for detection and chemical analysis
[DE94-003963] p 2719 N94-27728

ZEOLITES

Use of oxygen-17 isotope in the characterization of zeolites and related structures by nuclear magnetic resonance spectroscopy
[VTT-TIED-1448] p 2714 N94-26251

ZERO ANGLE OF ATTACK

Normal force of low aspect ratio cropped-delta wings at pre-stall angles of attack and subsonic speeds
[ESDU-93034] p 2648 N94-27955

Wing lift increment at zero angle of attack due to deployment of single-slotted flaps at low speeds
[ESDU-93019] p 2649 N94-28140

ZINC COATINGS

Cracking of textured zinc coating during forming process
[DE94-003414] p 2750 N94-26085

ZINC COMPOUNDS

Heavy-electron behavior in large coordination compounds CeZn11 and UZn12
[REPT-A-2663] p 3049 N94-25614

ZINC OXIDES

Zinc(2) oxide stability in alkaline sodium phosphate solutions at elevated temperatures
[DE94-003316] p 2715 N94-26320

Technical report of ISSP. Ser. A, no. 2677: Octa-twin model of tetrapod ZnO crystals
[JTN-94-80563] p 3069 N94-27756

The ZnO thin films with C-axis orientation prepared on the room temperature substrate by the ECR multipolar plasma sputtering method
[DE94-605039] p 2758 N94-27857

ZINC SELENIDES

Heavy-electron behavior in large coordination compounds CeZn11 and UZn12
[REPT-A-2663] p 3049 N94-25614

Indium donor complexes with cation vacancies in CdTe and ZnSe
[DE94-002731] p 3063 N94-26958

ZINC SULFIDES

Characterization of ZnS-GaP naon-composites
[DE94-004888] p 2712 N94-27813

ZIRCONIUM ALLOYS

Zr-rich corner of the Zr-Sn-O diagram
[DE93-633764] p 2734 N94-26161

Grain by grain study of the mechanisms of crack propagation during iodine SCC of Zry-4
[DE93-633765] p 2734 N94-26162

Zr-Sn-Nb alloys: Preliminary studies
[DE93-633767] p 2734 N94-26263

Fracture Toughness Round Robin Test International in pressure tube materials
[DE93-634140] p 2837 N94-26265

Eutectic transformation L in equilibrium to Zr6Fe23 + Fe(tau) in the Fe-Zr system
[DE93-633766] p 2735 N94-26295

Hydrothermal growth and characterization of oxides in zirconium alloys
[DE94-602981] p 2743 N94-27829

Differential scanning calorimetric study of solid state amorphization and crystallization in Zr/Co and Zr/Ni multilayers p 2745 N94-28161

The corrosion behavior of sputter-deposited magnesium-valve metal alloys p 2745 N94-28164

CO2 methanation catalysts prepared from amorphous Ni-valve metal alloys containing platinum group elements
p 2745 N94-28166

ZIRCONIUM HYDRIDES

Space-R thermionic space nuclear power system: Design and technology demonstration
[DE94-001890] p 2699 N94-25929

ZIRCONIUM OXIDES

Study on film generation phenomena by particle deposition p 2728 N94-25575

Oxygen reduction at a YSZ interface with cathode materials La(1-x)(Ca or Sr)(x)MnO3(1-x)CaMnO3
[DE94-002954] p 3054 N94-26147

Stress-induced phase transformation in ZrO2 materials
[ISBN-0-315-83373-4] p 2752 N94-26661

Bench-scale synthesis of nanoscale materials
[DE94-004787] p 2742 N94-27786

Hydrothermal growth and characterization of oxides in zirconium alloys
[DE94-602981] p 2743 N94-27829

ZODIACAL DUST

Zodiacal light data investigation. Interim results for the Earthlimb Clutter Experiment
[AD-A274461] p 3104 N94-27265

ZODIACAL LIGHT

Zodiacal light data investigation. Interim results for the Earthlimb Clutter Experiment
[AD-A274461] p 3104 N94-27265

ZONAL FLOW (METEOROLOGY)

Global barotropic response to a tropical forcing
[NASA-CR-195256] p 2896 N94-27408

PERSONAL AUTHOR INDEX

SCIENTIFIC AND TECHNICAL AEROSPACE REPORTS VOLUME 32 NUMBER 7

Typical Personal Author Index Listing

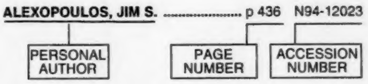

Listings in this index are arranged alphabetically by personal author. The page number helps you locate the citation in the abstract section. The accession number denotes the number by which the citation is identified.

A

AARTS, RONALD GODFRIED KARIEN MARIE
p 2792 N94-26479
AASEN, WALTHER p 2767 N94-26105
ABACHI, S. p 3023 N94-26938
ABBASI, S. J. p 2992 N94-26366
ABBOTT, KATHY H. p 2673 N94-27882
ABBOTT, MICHAEL S. p 3110 N94-26755
ABBOTT, WALTER D., III p 2946 N94-28256
ABDALLA, E. p 2991 N94-25884
ABDALLA, M. C. B. p 2991 N94-25884
ABDEL-ALLAH, N. N. p 3030 N94-27994
ABDEL-KHALEK, K. S. p 3016 N94-26010
ABDURAKHIMOV, A. U. p 3013 N94-25828
ABE, F. p 2983 N94-27804
ABE, SHINICHI p 2718 N94-27391
p 2718 N94-27392
ABE, TOSHIO p 2904 N94-27465
p 2904 N94-27466
ABE, YOSHIO p 2718 N94-27390
ABERLE, JIM p 2779 N94-27894
ABID, R. p 2796 N94-27435
ABID, RIDHA p 2792 N94-26467
ABKOWITZ, STANLEY p 2709 N94-26978
ABKOWITZ, SUSAN M. p 2709 N94-26978
ABOBO, JOEY B. p 2671 N94-25711
ABOUEL-ELA, M. N. p 2991 N94-25880
ABSHIRE, JAMES B. p 2877 N94-26152
ACETO, S. p 3041 N94-25846
ADAM, G. p 2962 N94-26386
p 3070 N94-27995
ADAM, GH. p 3003 N94-26385
ADAM, S. p 3003 N94-26385
p 3070 N94-27995
ADAMA, S. p 2962 N94-26386
ADAMEDES, ZOE p 2865 N94-28136
ADAMS, C. p 2689 N94-25692
ADAMS, J. p 2754 N94-27033
ADAMS, R. K. p 2694 N94-25615
ADAMS, S. M. p 2941 N94-26555
ADAMS, W. W. p 2753 N94-26822
ADARE, I. p 2655 N94-28336
ADICKES, M. D. p 2960 N94-26048
ADJEPONG, S. K. p 3057 N94-26384
ADLER, ROBERT J. p 3003 N94-26355
p 3008 N94-26374
p 3009 N94-27108
ADOLPH, HORST G. p 2760 N94-28226
AFANASEV, G. N. p 2766 N94-25866
AFANASEV, S. V. p 2809 N94-25735
AGRAWAL, SATISH K. p 2680 N94-26202
AGUERO-GRANADOS, M. A. p 3050 N94-25825
AGUR, ZVIA p 2933 N94-27744
AHLIN, L. p 2774 N94-27219
AHMAD, S. A. p 2717 N94-26988
AHN, C. p 2998 N94-27162
AHN, CHANGRIM p 3073 N94-26896
AHN, KYUNG H. p 2644 N94-26131
AHRENS, E. T. p 3050 N94-25817
AHUJA, S. p 2739 N94-26935
AHVO, JUHA p 2976 N94-28356
AIHARA, TOMOYASU, JR. p 2745 N94-28161
AJIKI, HIROSHI p 3064 N94-27174
AKAMATSU, TOMONARI p 2764 N94-27976
AKERS, JIM p 3079 N94-25688
AKIAN, R. A. p 2824 N94-27228
AKIBA, SHIGEYUKI p 2722 N94-25545
AKIN, DAVE p 2703 N94-25685
AKITA, TOSHIAKI p 2904 N94-27466
AKIYAMA, FUMINORI p 2718 N94-27391
AKIYAMA, HIROFUMI p 2736 N94-26477
AKMANDOR, IBRAHIM SINAN p 2804 N94-28026
AKPAN, E. P. p 2993 N94-26408
p 2993 N94-26441
p 2994 N94-26458
p 3006 N94-26460
AL-TAMMAMI, A. p 2686 N94-27364
ALAM, S. p 3074 N94-27636
ALDE, D. M. p 2816 N94-26126
ALDO, A. p 2689 N94-25692
ALDROVANDI, R. p 2993 N94-26442
ALEKSEEV, G. A. p 2810 N94-26439
ALEWINE, NEAL J. p 2964 N94-26680
ALEXAN, KARIM p 2678 N94-27648
ALEXANDER, DALE E. p 3059 N94-26591
ALEXANDER, HAROLD p 2689 N94-25687
ALEXANDER, J. IWAN D. p 2761 N94-27220
ALEXANDRE, ALAIN p 2862 N94-28113
ALEXANDROU, A. N. p 2671 N94-25719
ALEXOPOULOS, J. S. p 2890 N94-28306
ALFORD, W. J. p 3040 N94-28000
ALIVISATOS, A. P. p 3054 N94-26125
ALKHALIFAH, T. p 2877 N94-25847
ALLEGRE, J. p 2698 N94-28020
ALLEN, CARL L. p 2671 N94-25718
ALLEN, CHARLES W. p 2737 N94-26587
ALLEN, JAMES J. p 2839 N94-26810
ALLEN, L. J. p 3018 N94-26334
p 3062 N94-26927
ALLOTEY, F. K. A. p 3057 N94-26384
ALLWINE, K. J. p 2895 N94-26761
ALSTEIN, D. p 2966 N94-26920
ALSUP, JOHN S. p 2643 N94-25592
ALTMAN, B. S. p 2962 N94-26371
ALVAREZ, J. p 2803 N94-28025
ALVAREZ, M. G. p 2743 N94-27832
ALVAREZ, OMAR p 2943 N94-25694
ALVAREZ, W. p 2887 N94-28295
ALZMANN, MELANIE A. p 2893 N94-26134
AMANO, MUNEYUKI p 2723 N94-25551
p 2726 N94-25565
AMBARDAR, A. p 3014 N94-25840
AMENOMORI, M. p 3116 N94-27607
AMIRKHANOV, I. V. p 2879 N94-26502
AMOS, K. p 3015 N94-25890
AN, CHENGWU p 2819 N94-26940
AN, DIHN VAN p 3061 N94-26879
AN, DINH VAN p 3057 N94-26387
ANDERSON, GLEN p 2942 N94-27089
ANDERSON, H. U. p 2857 N94-26747
ANDERSON, HOBIE p 2760 N94-25705
ANDERSON, JOHN R. p 2957 N94-25753
ANDERSON, KENNETH D. p 2768 N94-26335
ANDERSON, LOREN A. p 2697 N94-25671
ANDERSON, SHAUN D. p 3081 N94-25702
ANDERSSON, G. p 2774 N94-27219
ANDINO, AUREO F. p 2943 N94-25694
ANDO, MASATO p 2904 N94-27472
ANDO, TOSHINARI p 2788 N94-27817
ANDO, TSUNEYA p 3064 N94-27174
ANDREASEN, C. C. p 2877 N94-25877
ANDREWS, DEE H. p 2938 N94-26882
ANEZIRIS, CHARILAOS p 3002 N94-25910
ANGUS, B. p 2698 N94-25700
ANNEVELD, H. p 2831 N94-28084
ANNILA, ARTO p 2714 N94-26251
ANNO, TAKAFUMI p 2907 N94-27504
p 2907 N94-27509
p 2907 N94-27510
p 2907 N94-27511
p 2907 N94-27512
ANOLL, ROBERT K. p 2665 N94-26826
ANTHONY, P. p 3018 N94-26133
ANTOLOVICH, STEPHEN D. p 2709 N94-27142
ANTONIADES, J. A. p 3033 N94-27082
ANTONIADIS, I. p 3071 N94-25882
ANTONIO, JOHN K. p 2981 N94-27100
ANTONSEN, T. M., JR. p 3044 N94-26523
ANWAR, E. p 3099 N94-27101
ANWAR, MOHAMMED SIRAJUL p 2872 N94-28275
AOKI, HARUYOSHI p 2724 N94-25557
p 2726 N94-25563
p 3064 N94-27177
AOKI, HISASHI p 2928 N94-27522
AOKI, KIYOSHI p 2745 N94-28161
p 2745 N94-28163
AOKI, TAKAO p 2730 N94-25582
AONUMA, SHUJI p 3064 N94-27175
APOKIN, V. D. p 2810 N94-26439
APPEL, J. A. p 3015 N94-25935
APT, KRZYSZTOF R. p 2970 N94-27544
ARAGANE, GORO p 2727 N94-25572
ARAI, AKIKO p 2904 N94-27467
p 2904 N94-27468
p 2904 N94-27469
p 2908 N94-27515
p 2908 N94-27516
ARASHI, HARUO p 3066 N94-27354
ARBAB, F. p 2971 N94-27552
ARDANUY, PHILIP E. p 2814 N94-27981
AREL, J. D. p 2839 N94-26692
AREY, B. W. p 2741 N94-27570
ARGUEELLO, J. G. p 2857 N94-26700
ARIAS, D. E. p 2734 N94-26161
p 2734 N94-26263
p 2735 N94-26295
ARIE, ADY p 2819 N94-27179
ARIEL, GIDEON p 2934 N94-28362
ARISAWA, T. p 3112 N94-25628
p 3113 N94-25629
p 3113 N94-25630
ARMAND, SASAN C. p 2843 N94-27559
ARMITAGE, PAMELA KAY p 2697 N94-25671
ARMITSTEAD, JOHN N. p 2954 N94-27152
ARMSTRONG, T. R. p 2855 N94-26114
ARMSTRONG, W. T. p 2876 N94-25807
ARNEGARD, MATTHEW E. p 2868 N94-26817
ARNOLD, G. THOMAS p 2897 N94-28179
p 2897 N94-28182
ARNOLD, G. W. p 3035 N94-26246
p 2757 N94-27726
ARNOLD, J. R. p 3117 N94-27826
ARNZEN, S. p 2665 N94-27210
AROLA, RAIMO p 2731 N94-25643
ARONOV, A. G. p 3068 N94-27677
ARTIS, DONALD R., JR. p 2847 N94-25656
ARTSZTEIN, PHILIPPE PASCAL p 2775 N94-27244
ASAMI, KATSUHIKO p 2745 N94-28164
p 2722 N94-28165
p 2745 N94-28166
ASANO, TOSHIHISA p 2724 N94-25557
p 2725 N94-25559
ASEEV, A. A. p 3032 N94-26405
ASH, L. EDWARD p 2896 N94-26959
ASH, ROBERT L. p 2833 N94-25691
p 3011 N94-27659
p 2798 N94-27867
ASHBY, GEORGE C., JR. p 2646 N94-26592
ASHFORD, S. J. p 2964 N94-26655
ASKEW, RAY p 2844 N94-27824
ASPER, V. L. p 3035 N94-26100
ASRATIAN, A. S. p 2996 N94-26962
p 3007 N94-27222
ASSINK, R. A. p 2712 N94-27710
ASTA, M. p 2743 N94-27792
ASTAPKOVICH, A. M. p 3044 N94-26510
ATHANAS, M. p 3022 N94-26769
ATKINS, JOEL p 3000 N94-27564
ATTIA, J. O. p 2684 N94-26287
ATTILI, ROBERTA NUNES p 3067 N94-27623
ATWOOD, DAVID p 3024 N94-27259
ATWOOD, W. B. p 3116 N94-27740
AU, DENNIS KIN-WAH p 2784 N94-26631
AUERKARI, PERTTI p 2704 N94-25734
p 2707 N94-26260

AUSTIN, DAVE p 2833 N94-25683
AUSTIN, JAMES A. p 2833 N94-25675
AUSTON, DAVID H. p 2782 N94-26343
AUVIL, LORETTA S. p 2981 N94-27100
AVALIANI, I. S. p 3030 N94-27860
AVELLA, M. p 3055 N94-26194
AVISHAI, YSHAI p 3028 N94-27758
AXE, J. D. p 2732 N94-26004
AXLINE, R. M. p 2848 N94-26277
AYERS, RAYMOND p 2833 N94-25683
AYRES, T. R. p 3105 N94-27932
AZAR, ZION p 2774 N94-27233
AZARM, SHAPOUR p 2833 N94-25686
AZMY, Y. Y. p 2769 N94-26482

B

BABA, EIJI p 2723 N94-25548
BABA, HARUO p 2722 N94-25546
BABA, SHUNKICHI p 2914 N94-27456
BABINTSEV, V. V. p 2810 N94-26396
BACA, A. G. p 3069 N94-27790
BADDELEY, A. p 2938 N94-26683
BADO, PHILIPPE p 2817 N94-26271
BAECKSTROEM, MATS p 2772 N94-27041
BAER, DAVID A. p 2863 N94-28126
BAEUERLE, K. p 2953 N94-26741
BAGGHI, A. p 3004 N94-27211
BAILEY, ALAN D. p 2773 N94-27085
BAILEY, ANDREA p 2943 N94-25679
BAILEY, C. M. p 2951 N94-26731
BAILEY, M. C. p 2769 N94-26611
BAILEY, MELVIN L. p 2679 N94-27660
BAILEY, T. p 2754 N94-26977
p 2755 N94-27087
BAILLIE, S. W. p 2677 N94-26710
BAIRI, B. R. p 2981 N94-26903
BAITY, F. W. p 3041 N94-25933
p 3046 N94-27261
p 3046 N94-27568
BAKER, C. P. p 2827 N94-27780
BAKER, CHARLES K. p 3035 N94-25941
BAKER, MYLES p 2833 N94-25668
BAKER, P. p 2813 N94-27317
BAKHLE, MILIND A. p 2846 N94-28227
BAKUCKAS, JOHN G., JR. p 2711 N94-27658
BALACHANDRAN, U. p 3053 N94-26029
p 3055 N94-26243
p 2783 N94-26589
p 2740 N94-26957
BALAS, EGON p 3094 N94-26314
BALCH, CHRISTOPHER C. p 3110 N94-26755
BALCH, J. W. p 2784 N94-26777
BALDO, P. M. p 3059 N94-26591
BALL, G. J. p 2659 N94-28021
BAN, SYUICHI p 3032 N94-26543
BANGER, J. L. p 2816 N94-26126
BANKS, DAVID p 2970 N94-27417
BANKS, DAVID C. p 2971 N94-27572
BANON, GERALD JEAN FRANCIS
p 2849 N94-26827
BANURA, GEORGE A. p 2786 N94-27145
BARADZEI, L. T. p 3112 N94-25625
p 3112 N94-25626
p 3112 N94-25627
BARASHENKOV, V. S. p 3015 N94-25916
BARAZANGI, MUAWIA p 3098 N94-26490
BARBE, M. R. p 2818 N94-26605
BARBER, D. p 2652 N94-28319
BARBERIS, E. p 3052 N94-25972
BARBIELLINI, B. p 3003 N94-26385
p 3070 N94-27995
BARBOUR, J. C. p 3050 N94-25815
BARBOUR, RACHAEL p 2782 N94-26328
BARCELOS-NETO, J. p 2994 N94-26459
BARFIELD, B. p 2698 N94-25701
BARFIELD, LON G. p 2961 N94-26219
p 3097 N94-26220
BARKER, DEBORAH LYNN p 2969 N94-27316
BARNES, C. W. p 2985 N94-25983
p 3048 N94-27825
BARNES, D. C. p 3047 N94-27715
BARNES, P. D. p 3022 N94-26769
BARNES, T. p 3020 N94-26574
p 3024 N94-27199
BARNES, W. p 2863 N94-28127
BARNHOUSE, K. p 2833 N94-25691
BARNIER, CAROLINE p 2671 N94-25717
BARONI, STEFANO p 3061 N94-26878
BAROODY, EDWARD E. p 2760 N94-28226
BAROUDI, DJEBAR p 2990 N94-25733
p 3008 N94-26256
BARRETO, PATRICIA REGINA PEREIRA
p 3066 N94-27329
BARTH, CHARLES A. p 3106 N94-26237
BARTHELEMY, ALAIN C. p 3010 N94-26923
BARUT, A. O. p 2992 N94-26267
p 3072 N94-26551
p 3067 N94-27647
p 3074 N94-27696
BASORE, P. A. p 2857 N94-26617
BASS, J. p 2878 N94-26338
BASS, J. N. p 2698 N94-28200
BASS, ROBERT L. p 3110 N94-26755
BASSALLECK, B. p 3022 N94-26769
BASU-MALLICK, B. p 3072 N94-26461
BASU, B. C. p 2653 N94-28326
BATCHELOR, D. B. p 3046 N94-27568
BATENIN, V. M. p 2854 N94-26056
BATES, J. L. p 2855 N94-26114
p 3054 N94-26147
BATILL, STEPHEN M. p 2671 N94-25715
BATISTA, GETULIO TEIXEIRA p 2852 N94-27957
BATTAGLIN, G. p 3035 N94-26246
BATTEN, JENNIFER p 2903 N94-27412
BATUR, CELAL p 3066 N94-27561
BAUER, BRENT ALAN p 2668 N94-26235
BAULU, THIERRY p 2851 N94-27863
BAUR, JEFFERY W. p 3036 N94-26982
BAUTHIER, J. p 2832 N94-28087
BAUTISTA, MARIETTA O. p 2754 N94-27036
BAVUSO, SALVATORE J. p 2684 N94-26288
BAXI, C. B. p 3042 N94-25976
p 3043 N94-26323
BAYHA, ERWIN p 2972 N94-27582
BAYLIS, EVELYN MARIE p 2988 N94-27277
BAYLOR, L. R. p 3042 N94-26140
BEAM, SHERILEE F. p 2815 N94-27895
BEAN, J. C. p 3055 N94-26239
BEARD, CLARK p 2833 N94-25675
BEASLEY, R. p 2676 N94-28019
BEAUCAGE, G. p 2712 N94-27710
BEAUFAYS, J. p 2952 N94-26734
BEAVIS, L. C. p 3069 N94-27753
BEC, SANDRINE p 2750 N94-26088
BECKENHAUER, DARYL G. p 2740 N94-27305
BECKER-SZENDY, R. p 3018 N94-26133
BECKER, UWE p 3066 N94-27590
BECKER, WILHELM p 2681 N94-27587
BECKSTEAD, J. p 3041 N94-25846
BEDAIR, SALAH p 3061 N94-26885
p 3063 N94-27058
BEDAQUE, P. F. p 3013 N94-25839
BEDAT, B. p 2714 N94-26122
BEDDOES, JONATHAN CARL p 2738 N94-26633
BEDI, S. p 2655 N94-28336
BEECHING, M. J. p 3055 N94-26171
BEECK, A. p 2676 N94-28037
BEENEN, J. p 2651 N94-28317
BEER, RANDALL D. p 2821 N94-25782
BEER, STEFAN p 2826 N94-27589
BEEUWKES, REINIER, JR. p 2836 N94-25754
BEHROUZI, P. p 2801 N94-28010
BEKMAN, H. H. p 3038 N94-27137
BELAK, J. p 2751 N94-26554
BELEGUNDU, ASHOK D. p 2845 N94-27865
BELFORD, JAMES T. p 2979 N94-25906
BELIKOV, S. V. p 2810 N94-26395
BELL, NORMAN DOUGLAS p 3039 N94-27643
BELOBABA, PETER p 2689 N94-25687
BELOUSSOV, IGOR V. p 3068 N94-27678
BELUE, JEFF p 2698 N94-28210
p 2698 N94-28217
BEN-SHACHAR, OFER p 2962 N94-26327
BENDAKHLIA, MONIA p 3081 N94-25703
BENET, JAMES p 2776 N94-27669
p 2777 N94-27946
BENGTSSON, J. P. p 3038 N94-27209
BENGTSSON, M. p 2968 N94-27157
BENICEWICZ, BRIAN C. p 2704 N94-27745
p 2757 N94-27747
BENJAMIN, M. C. p 2754 N94-26974
BENNETT, H. E. p 3035 N94-26276
BENOIST, K. W. p 3038 N94-27137
BENSON, C. S. p 2892 N94-25939
BENSON, CARL S. p 2851 N94-27787
BENSON, RAFER M. p 2765 N94-25676
BENTLEY, J. p 3059 N94-26765
p 3069 N94-27757
BENTLEY, JEFFREY M. p 2759 N94-26753
BENZ, E. p 2676 N94-28037
BERDIS, ELIZABETH p 2903 N94-27412
BERDOZ, A. p 3022 N94-26769
BERENS, T. p 2801 N94-28013
BERGER, MARC A. p 2964 N94-26682
BERGERSEN, BJOERN p 2837 N94-26233
BERGES, J. C. p 2952 N94-26738
BERGLUND, L. p 3005 N94-27172
BERGSTROEM, B. p 2942 N94-27155
BERGSTROM, D. F. p 2712 N94-27710
BERK, H. L. p 3041 N94-25792
BERKE, LASZLO p 2845 N94-27865
BERKHOUT, JAN p 2942 N94-27089
BERKOWITZ, JOSEPH p 3013 N94-25816
BERLIN, JACOB L. p 2982 N94-27123
BERNATH, GREG p 2642 N94-27289
BERNAUER, E. M. p 2902 N94-27227
BERNHART, WALTER D. p 2680 N94-26200
BERNHOLC, JERRY p 3063 N94-27058
BERNOT, PETER T. p 2646 N94-26592
BERNSTEIN, LESLIE R. p 3010 N94-27067
BERRY, MARESI p 2689 N94-25687
BERTEAUX, SUSAN S. p 3098 N94-26561
BERTONCELLO, R. p 3035 N94-26246
BESHTOEV, KH. M. p 3020 N94-26508
BESSEL, JAMES A. p 2694 N94-25659
BESSON, O. p 2946 N94-28259
BETHANY, DAVID A. p 3093 N94-25895
BEUSEKAMP, MARTIN F. p 2955 N94-27195
BEYHOFF, STEFAN p 2661 N94-28233
BHARDWAJ, MANOJ p 2833 N94-25704
BHOLE, SANJIWAN D. p 2740 N94-27009
BIAGI, PAUL p 2672 N94-26030
BIALASIEWICZ, JAN T. p 2990 N94-27896
BIANCHI, G. L. p 2734 N94-26264
BIERENS, L. H. p 2959 N94-25963
BIGELOW, T. S. p 2767 N94-25924
p 3041 N94-25933
BILGEN, E. p 2657 N94-28343
BILLS, K. C. p 2822 N94-26465
BINER, S. B. p 2706 N94-26019
BINGHAM, R. p 3111 N94-27953
BINH, TRAN QUOC p 3000 N94-27632
BIRENBAUM, MENUCHA p 3002 N94-25962
BIRK, AVI p 2957 N94-25646
BIRNBAUM, G. p 2952 N94-26736
BIRTCHER, R. C. p 2737 N94-26587
BISCHOF, C. p 2973 N94-27717
BISHOP, D. M. p 3050 N94-25814
BISWAS, R. p 3059 N94-26695
BITTON, D. F. p 2673 N94-26989
BITYUKOV, S. I. p 3024 N94-27250
BJORKLUND, E. p 2986 N94-26807
BLACK, E. P. p 2712 N94-27710
BLACKSTOCK, DEXTER L. p 2833 N94-25691
BLAEDEL, K. L. p 2763 N94-26778
BLAIR, J. BRYAN p 2877 N94-26152
BLAIR, JERRY p 2771 N94-26836
p 2771 N94-26854
p 2772 N94-26980
BLAKE, DOUGLAS C. p 2979 N94-25860
BLAKE, WILLIAM B. p 2802 N94-28016
BLAKEMORE, JOHN S. p 3068 N94-27704
BLANCHARD, ROBERT E. p 2941 N94-26136
BLESA, M. A. p 2743 N94-27829
BLIESENER, GARY C. p 2957 N94-25646
BLOCK, JON E. p 2935 N94-28370
BLOEMKER, CARL p 3035 N94-26572
BLOM, J. G. p 2965 N94-26772
BLOOM, I. p 2857 N94-26584
BLOOM, R. M. p 2878 N94-26304
BLUM, O. p 2780 N94-25664
BLUMENFELD, R. p 2991 N94-26079
BOBB, LLOYD p 3038 N94-27153
BODALIA, RAJ p 2753 N94-26925
p 2754 N94-27080
BODEK, A. p 3008 N94-25988
BODEN, J. A. p 2811 N94-27134
BOEKEMA, R. B. p 2773 N94-27136
BOERCKER, D. B. p 2751 N94-26554
BOERJESSON, ARNE p 2835 N94-27042
BOETTGER, J. C. p 2732 N94-25974
BOFF, KENNETH R. p 3099 N94-26891
BOGARD, DAVID GUY p 2794 N94-27059
BOGUSZ, MICHAEL p 2776 N94-27308
BOHLEN, J. W. p 2832 N94-28209
BOLCAVAGE, A. p 2735 N94-26349
BOLIO, E. J. p 2792 N94-26319
BONAFE, JEAN-LOUIS p 2659 N94-26293
BOND, M. p 2902 N94-27227
BONDAREV, I. V. p 3068 N94-27729
BONDOK, HOSAIN MOHAMED H. p 2839 N94-26825
BONOLI, P. p 2767 N94-25924
p 3041 N94-25933
BONSANGUE, MARCELLO p 2995 N94-26776
BOOKER, JANE M. p 3094 N94-27707
BOONYAPIWAT, S. p 2875 N94-28287
BORCHARDT, RANDY L. p 3012 N94-25655
BORDEGONI, MONICA p 2961 N94-26218
BORDONI, R. A. A. p 2743 N94-27829
BORGGAARD, JEFF p 2999 N94-27415
BORIE, V. p 2699 N94-25638
BORISOV, A. S. p 3112 N94-25625
p 3112 N94-25626
p 3112 N94-25627
BORISOV, G. V. p 3017 N94-26045
p 3024 N94-27250

BORKAR, S. P. p 2981 N94-26903
BORN, GEORGE H. p 2883 N94-27883
BORNATH, ANNE MARIE CHRISTINE
p 2994 N94-26659
BORODIN, PAVEL M. p 2906 N94-27493
BORTHOMIEU, YANNICK p 2861 N94-28110
BOSCHI, CARINA p 2824 N94-27224
BOSLOUGH, M. B. p 2888 N94-28296
BOSSERT, J. p 2894 N94-26313
BOSSI, RICHARD H. p 2705 N94-25779
BOSTED, P. p 3018 N94-26133
BOSTED, P. E. p 3017 N94-26101
BOSTROEM, G. p 2902 N94-27171
BOTERO, J. p 3045 N94-26946
p 3023 N94-26947
BOTT, TERRY F. p 2835 N94-27613
BOTTA, E. F. F. p 2997 N94-27000
BOTTING, MARY p 2671 N94-25713
BOTTONI, M. p 2792 N94-26331
BOUCHARD, KENNETH p 2670 N94-25695
BOUCHEZ, OLIVIER p 2970 N94-27545
BOUNAR, K. H. p 2887 N94-28206
BOUQUET, M. p 2711 N94-27586
BOURGAIN, JEAN p 2997 N94-26995
BOURQUE, R. F. p 3043 N94-26323
BOUSSARIE, ERIC p 2950 N94-26722
BOUTON, F. p 2832 N94-28088
BOUZIANE, SAHRAOUI p 2789 N94-25654
BOWEN, BARRY C. p 2692 N94-27956
BOWEN, ROBERT p 2849 N94-26667
BOWER, MARK p 2976 N94-25666
p 2689 N94-25687
BOWER, W. p 2857 N94-26612
BOWERS, M. S. p 3040 N94-27999
BOWLES, R. L. p 2677 N94-26593
BOWLES, THOMAS J. p 3111 N94-27742
BOWLING, P. S. p 2985 N94-25983
BOWMAN, J. D. p 3013 N94-25820
BOWMAN, PATRICK J. p 2770 N94-26751
BOWSER, S. E. p 2941 N94-26555
BOYD, DARWIN L. p 2741 N94-27426
BOYD, MARK A. p 2684 N94-26288
BOYETT, M. R. p 2907 N94-27513
p 2908 N94-27514
p 2908 N94-27515
p 2908 N94-27516
BOYETT, MARK R. p 2908 N94-27537
BOYLE, DAMON p 2681 N94-27113
BOYLE, J. S. p 2897 N94-27571
BOYNTON, J. L. p 2824 N94-27228
BOYUM, ELIZABETH A. p 2706 N94-25999
BOYUM, KEVIN E. p 2667 N94-25905
BOZZELLI, JOSEPH W. p 2760 N94-27725
BRAASCH, MICHAEL S. p 2642 N94-27290
BRAASCH, SOO Y. p 2642 N94-27291
BRABSON, B. p 3033 N94-27614
BRACK, J. T. p 3014 N94-25840
BRADFORD, L. W. p 3102 N94-26528
BRADLEY, GARY F. p 2942 N94-27114
BRADLEY, J. D. p 2848 N94-26277
BRADLEY, JONATHAN N. p 2851 N94-27727
BRADLEY, P. J. p 2671 N94-28017
BRADLEY, TIM p 3036 N94-26981
BRADLEY, WILLIAM p 2709 N94-27091
BRADSHAW, R. W. p 2742 N94-27755
BRAHIMI, M. T. p 2657 N94-28345
BRAMSON, G. p 3043 N94-26274
BRAND, ALBERT G. p 2645 N94-26483
p 2645 N94-26489
p 2645 N94-26492
p 2645 N94-26497
BRANDENBERGER, R. p 3031 N94-25931
BRANDON, JAY p 2647 N94-27161
BRANDON, JAY M. p 2646 N94-26602
BRANDS, STEFAN A. p 2776 N94-27551
BRANDSTORP, JENS p 2680 N94-26305
BRANDT, FRIEDEMANN p 3072 N94-26541
BRANOVER, H. p 2854 N94-26055
BRATLAND, D. H. p 2741 N94-27325
BRAUCH, UWE p 3066 N94-27590
BRAUN, RUDOLF p 2669 N94-27273
BRAUNSCHNEIDER, JAMES A. p 2790 N94-25874
BRAY, I. p 3023 N94-26942
p 3023 N94-26945
BRAY, IGOR p 3014 N94-25842
BRAY, S. p 2725 N94-25560
BRAZELL, JAMES W. p 2833 N94-25675
BRECHT-CLARK, JAN p 2938 N94-26600
BREITHAUPT, B. SPIEGEL p 2833 N94-28265
BRENNAN, T. M. p 3056 N94-26308
BRENZA, P. T. p 2699 N94-25926
BRESCIA, JOSEPH A. p 2751 N94-26434
BRESLAUER, DANY p 3100 N94-27164
p 2971 N94-27550
BRETT, ROBERT ALLAN p 2775 N94-27301
BREWER, JEFFREY C. p 2860 N94-28100
BREZINI, A. p 3067 N94-27635
BRIGGS, MICHAEL S. p 3114 N94-26686
p 3114 N94-26687
p 3115 N94-26690
BRIMHALL, J. L. p 2731 N94-25804
p 2705 N94-25805
p 2737 N94-26585
BRINCK, TORE p 2704 N94-26353
BRINKKEMPER, SJAAK p 2975 N94-27936
p 2975 N94-27937
p 2975 N94-27938
p 2975 N94-27939
BRINSON, L. CATHERINE p 2712 N94-27897
BRISLAWN, CHRISTOPHER M. p 2851 N94-27727
BRITE, C. p 2811 N94-26787
BRIZUELA, E. p 2794 N94-26801
BROACH, DANA p 2938 N94-26600
BRODSKY, S. J. p 3024 N94-27050
BROERSMA, H. J. p 3007 N94-27222
BROKER, J. P. p 2936 N94-28373
BROMSTEAD, JAMES p 2844 N94-27824
BROOKS, C. p 2932 N94-27556
BROWN, DANIEL V. p 2679 N94-28028
BROWN, HARRY p 2860 N94-28102
p 2863 N94-28122
BROWN, K. W. p 2839 N94-26692
p 2843 N94-27776
BROWN, S. K. p 2985 N94-25983
BROWN, SCOTT L. p 2815 N94-25744
BROWN, T. p 3045 N94-26863
BROWN, TIMOTHY J. p 3110 N94-26755
BROWN, WILLIAM S. p 2700 N94-26156
BROZOWSKI, L. A. p 2822 N94-26597
BRUCKNER, ADAM P. p 2760 N94-25705
BRUEMMER, S. M. p 2731 N94-25804
p 2741 N94-27570
p 2741 N94-27622
BRUEN, CHARLES p 2689 N94-25687
BRUENING, J. p 2698 N94-25701
BRUGEL, E. W. p 3105 N94-27932
BRUIN, H. p 2849 N94-26866
BRUIN, PETER p 2750 N94-26211
BRUMLIK, CHARLES J. p 2715 N94-26444
BRUNELLI, J. C. p 2991 N94-25884
BRUSASCO, R. M. p 2753 N94-26933
BRUSNIAK, LEON p 2798 N94-27802
BRUYNOOGHE, MAURICE p 2966 N94-26956
BRYAN, COLEMAN J. p 2757 N94-27747
BRYAN, KURT p 2994 N94-26601
BRYER, PAUL p 2671 N94-25709
BUBEL, BILL p 2824 N94-27228
BUCHBINDER, I. L. p 3071 N94-25883
BUCHHEIT, R. G. p 2732 N94-25819
p 2739 N94-26912
p 2742 N94-27788
BUCHOLTZ, FRANK p 3039 N94-27674
BUCK, M. E. p 2857 N94-26617
BUCK, O. p 2706 N94-26019
BUCKEY, JAY C. p 2942 N94-27410
BUCKLES, JON p 2671 N94-25709
BUCSH, ROBERT O. p 2721 N94-28215
BUDAGOV, YU. A. p 3015 N94-25919
BUDINGER, THOMAS F. p 2809 N94-25662
BUEHLER, M. F. p 2742 N94-27786
BUGLIA, JAMES J. p 2690 N94-27771
BUHMANN, MARTIN D. p 3003 N94-26445
BULASHENKO, O. M. p 3027 N94-27631
BULL, M. D. p 2951 N94-26727
BULLOCK, M. p 2835 N94-26644
BULLOCK, S. RAY p 2700 N94-26090
BULMER, R. H. p 3045 N94-27019
BULSARA, VATSAL p 2833 N94-25704
BUNCH, J. O. p 2832 N94-28209
BUNKER, ROBERT L. p 2949 N94-26718
BUNNING, T. J. p 2753 N94-26822
BURCH, I. A. p 2839 N94-26859
BURCH, J. R. p 2786 N94-27061
BURDICK, SHAWN V. p 3104 N94-27265
BURES, M. p 3046 N94-27261
BURGER, MARIO G. p 2847 N94-25746
BURGER, T. p 3022 N94-26769
BURKE, R. A., JR. p 2865 N94-25790
BURKE, W. R. p 2972 N94-27582
BURLESON, RUSSELL A. p 2766 N94-25824
BURNS, A. p 2951 N94-26731
BURNS, G. T. p 2712 N94-27710
BURNS, JOHN p 2999 N94-27415
BURNS, JOHN W. p 2902 N94-26991
BURNS, M. J. p 3059 N94-26566
BURRELL, K. H. p 3048 N94-27785
p 3048 N94-27791
BURSILL, L. A. p 2748 N94-25844
p 3056 N94-26363
BURTON, DAVID p 2833 N94-25683
BURTON, R. p 2688 N94-27373
BURTON, REGINA M. p 2773 N94-27085
BUSACKER, HORST p 2661 N94-28235
BUSHNIN, YU. B. p 2783 N94-26438
BUSSARD, R. W. p 3047 N94-27715
BUSSON, GUY p 2781 N94-26102
BUTCHAR, STAN p 2703 N94-25690
BUTLER, MICHAEL P. p 2781 N94-26175
BUTLER, P. C. p 2783 N94-26372
BUTT, DARRYL P. p 2699 N94-25613
BUYANOV, O. V. p 2810 N94-26439
BYUN, CHANSUP p 2645 N94-26538

C

CABLE, J. W. p 2733 N94-26092
CAI, SUI X. p 2749 N94-26074
CAI, ZHONG p 2826 N94-27599
CAIRNS, JOHN, JR. p 2868 N94-26817
CALDWELL, J. L. p 2910 N94-26748
CALDWELL, JOHN A., JR. p 2910 N94-26748
CALFAS, ROY S. p 3051 N94-25856
CALISE, A. J. p 2678 N94-26821
CALLEN, J. D. p 3047 N94-27690
CALVERT, L. D. p 3058 N94-26514
CAMARERO, R. p 2656 N94-28342
p 2657 N94-28347
CAMERINI, P. p 3014 N94-25840
CAMERON, STEVEN R. p 2893 N94-26183
CAMPARO, JAMES C. p 3008 N94-26484
CAMPBELL, CRAIG p 2833 N94-25675
CAMPBELL, JAMES p 3000 N94-27564
CAMPBELL, V. B. p 2713 N94-26014
CAMPOS, FILOMENA F. p 2874 N94-28286
CANESSA, E. p 3063 N94-27017
CANFIELD, P. C. p 3050 N94-25817
CANHAM, CHARLES D. p 2852 N94-28070
CANTENOT, C. p 2950 N94-26726
CANTON, L. p 3015 N94-25890
CANTRELL, BEN H. p 2768 N94-26189
CAO, JIANSHU p 3020 N94-26562
CAO, NHAI THE p 2796 N94-27379
CAO, R. p 3056 N94-26326
CAO, Z. p 3116 N94-27607
CAPLAN, I. L. p 2736 N94-26362
p 2739 N94-26799
CAPLAN, M. p 2768 N94-26310
CARAYON, J. L. p 2952 N94-26737
CARBAJAL, KEVIN B. p 2667 N94-26151
CARDELL, GREGORY S. p 2790 N94-25872
CARLESON, H. p 2755 N94-27158
CARLSON, ALAN E. p 3080 N94-25697
CARLSON, JOHN R. p 2646 N94-26547
CARLSON, LELAND A. p 2648 N94-28071
p 2648 N94-28072
CARLSON, S. p 2888 N94-28297
CARLSTROM, T. N. p 3043 N94-26274
CARNE, T. G. p 2857 N94-26700
CARNEGIE, C. p 2657 N94-28346
CARNEGIE, CAMERON LINDSAY p 2646 N94-26672
CAROLAN, R. A. p 2729 N94-25581
CARRERAS, B. A. p 3044 N94-26694
CARROLL, C. C. p 3000 N94-27569
CARROLL, JOHN p 2823 N94-27149
CARROLL, THOMAS p 2787 N94-27673
CARSCALLEN, WILLIAM E. p 2652 N94-28320
CARTER, DONALD p 2665 N94-27423
CARTER, M. D. p 2767 N94-25924
p 3041 N94-25933
CARTER, R. D. p 2731 N94-25804
CARTIGLIA, N. p 3052 N94-25972
CASPERSON, D. E. p 2696 N94-26808
CASTLE, J. E. p 2738 N94-26653
CASTRACANE, J. p 3041 N94-25846
CAUBLE, B. p 2816 N94-26020
CAULEY, MICHAEL A. p 2693 N94-27427
CAUSBY, DANA R. p 2765 N94-25676
CAUSEY, R. A. p 3068 N94-27693
CAVESTRI, R. C. p 2756 N94-27692
CAVESTRI, RICHARD C. p 2713 N94-25934
CAVIEZEL, KELLY p 2760 N94-25705
CAZEAU, PATRICK p 2689 N94-25687
CECIL, DANNY A. p 3096 N94-26024
CEDERBERG, MARK p 2731 N94-25623
p 2731 N94-25784
CEDHEIM, L. p 2759 N94-25907
CELESTIAN, JOHN p 2976 N94-25666
CELIER, VINCENT p 2951 N94-26729
CENEY, JAMES M. p 2694 N94-25659
CENIZA, GLENN p 2833 N94-25675
CERVAY, RUSSELL R. p 2987 N94-27077
CHA, BYUNG HEON p 2714 N94-26158
CHA, HYUNG KI p 2714 N94-26158
p 2817 N94-26402
CHAEL, E. P. p 2888 N94-28296
CHAKRAVARTHY, SHARMA p 3099 N94-27101
CHAN, AGNES p 2671 N94-25719

CHAN, HELEN M. ... p 3062 N94-26892
CHAN, J. W. ... p 2742 N94-27694
CHAN, JEFFREY ... p 2775 N94-27274
CHAN, S. K. ... p 2797 N94-27617
CHANDESRIS, DOMINIQUE L. R. p 2951 N94-26729
CHANG-HASNAIN, CONNIE ... p 2815 N94-25756
CHANG, C. KEN ... p 3030 N94-27898
CHANG, F. C. ... p 2792 N94-26331
CHANG, I. S. ... p 3057 N94-26404
CHANG, IN SOON ... p 2783 N94-26546
CHANG, KEE OK ... p 2838 N94-26400
CHANG, Y. A. ... p 2735 N94-26349
CHAPIN, JOHN K. ... p 2940 N94-27141
CHAPMAN, M. ... p 3022 N94-26769
CHARALAMBOUS, Z. ... p 2833 N94-25691
CHARBONNIER, J.-M. ... p 2801 N94-28011
CHARLOT, L. A. ... p 2741 N94-27570
CHASON, E. ... p 3051 N94-25944
CHASON, M. ... p 3051 N94-25944
CHASTEK, GARY ... p 2959 N94-25855
CHAVEZ, J. M. ... p 2742 N94-27755
CHAWLA, KALPANA ... p 2671 N94-28033
CHEGROUCHE, S. ... p 2716 N94-26518
CHELEN, DAVID E. ... p 2995 N94-26829
CHEMAN, WILLIAM ... p 2892 N94-25861
CHEMLA, D. S. ... p 3054 N94-26128
CHEN, CHARLES C. ... p 2668 N94-26488
CHEN, DAVID T. ... p 2970 N94-27417
CHEN, I-MIN A. ... p 2962 N94-26327
CHEN, JENG-I ... p 2709 N94-27107
CHEN, MEIZHEN ... p 2895 N94-26678
CHEN, PANG C. ... p 2985 N94-26462
CHEN, S. C. ... p 2894 N94-26313
CHEN, SHYH-KWEI ... p 2964 N94-26680
CHEN, SI-YUAN ... p 2946 N94-28257
CHEN, TSUHAN ... p 2997 N94-27015
CHEN, WEIHUAN ... p 2993 N94-26409
p 3007 N94-27633
CHEN, Y. L. ... p 3069 N94-27757
CHEN, YAN L. ... p 3062 N94-26892
CHEN, YING ... p 2999 N94-27404
CHENAULT, CLARENCE F. ... p 2673 N94-25617
CHENEY, GLENN PETER ... p 2784 N94-26704
CHENG, JIANHUA ... p 2906 N94-27503
p 2907 N94-27506
CHENG, R. K. ... p 2714 N94-26122
CHEONG, YONG MOO ... p 2835 N94-26399
CHERDYNTSEVA, K. V. ... p 3112 N94-25625
p 3112 N94-25626
p 3112 N94-25627
CHERNIKOV, N. A. ... p 3072 N94-26503
p 2879 N94-26504
CHERNOPLEKOV, N. A. ... p 2854 N94-26057
CHERNOV, N. I. ... p 3015 N94-25919
CHETTO, HOUSSINE ... p 2952 N94-26735
CHEUNG, KAR-MING ... p 2945 N94-28252
CHEUNG, KWOK-HUNG ... p 2671 N94-25719
CHEUNG, WANG K. ... p 3033 N94-27646
CHIAVERINI, R. ... p 2952 N94-26733
CHICK, L. A. ... p 2855 N94-26114
CHIKYO, TOYOHIRO ... p 2722 N94-25545
CHILDERS, BROOKS A. ... p 2647 N94-27161
CHILDS, DARA W. ... p 2796 N94-27377
p 2796 N94-27378
CHIN, MARTIN S. ... p 2694 N94-25996
CHINELLA, J. F. ... p 2747 N94-28212
CHINNOCK, PAUL ... p 2697 N94-25667
CHIU, STEPHEN H. ... p 2803 N94-28023
CHMIL, V. B. ... p 3056 N94-26379
CHO, JAE WAN ... p 2817 N94-26185
p 2817 N94-26403
p 2818 N94-26520
CHO, SEUNG YEON ... p 3017 N94-26116
CHOI, J. ... p 2964 N94-26764
CHOI, WOO KAP ... p 2879 N94-26576
CHONGLI, SONG ... p 3070 N94-27843
CHORIN, A. J. ... p 2789 N94-25597
CHOTKEVYS, GERALD P. ... p 2785 N94-26845
CHOTTINER, G. S. ... p 2856 N94-26464
CHOU, SHUN-CHIN ... p 2747 N94-25596
CHOUDHARI, MEELAN ... p 2808 N94-28180
CHOW, R. ... p 2749 N94-25985
CHRIEN, R. ... p 3022 N94-26769
CHRISTENSEN, J. ... p 2785 N94-26797
p 2638 N94-27373
CHRISTENSEN, OEYVIND ... p 2817 N94-26203
CHRISTENSEN, THAN LEE ... p 2947 N94-28264
CHU, D. ... p 2733 N94-26087
p 2742 N94-27694
CHU, JEROME T. ... p 3055 N94-26188
CHUANG, S. L. ... p 2945 N94-28252
CHUBARYAN, G. G. ... p 3012 N94-25750
CHUJKO, B. V. ... p 2810 N94-26378
CHUN, K. S. ... p 2674 N94-26573
CHUNG, MANH ... p 2689 N94-25674
CHUNG, TAE EON ... p 2835 N94-26399
CHUNG, YONG SAM ... p 3017 N94-26116
CHUNTONOV, A. V. ... p 3056 N94-26379
CHUONG, NGUYEN MINH ... p 3000 N94-27632
CHURCH, JOHN C. ... p 2899 N94-26361
CHUZHOY, L. ... p 2739 N94-26935
CIANCIOLO, M. E. ... p 2895 N94-26798
CIFARELLI, D. M. ... p 3004 N94-27051
CIMBALA, JOHN M. ... p 2808 N94-27899
CINCE, TURGAY ... p 3097 N94-26300
CIRAY, SULEYMAN ... p 2804 N94-28026
CISAR, CRAIG J. ... p 2901 N94-26210
CITURS, KEVIN D. ... p 2666 N94-25590
p 2667 N94-25961
CIVCO, DANIEL L. ... p 2852 N94-28070
CLARK, E. A. ... p 2732 N94-25822
CLARK, J. F. ... p 2736 N94-26351
CLARK, WILLIAM S. ... p 2675 N94-27654
CLARKE, ALEXANDER PERRY .. p 2842 N94-27278
CLARKE, E. M. ... p 2786 N94-27061
CLARKE, KEN ... p 2689 N94-25674
CLARKE, MICHAEL ... p 2689 N94-25687
CLARKE, RICHARD ... p 2956 N94-25588
CLARKSON, PRISCILLA M. ... p 2934 N94-28363
CLAYTON, S. R. ... p 3059 N94-26566
CLEVENGER, W. B. ... p 2839 N94-26692
CLIFFSWALLOW, WILLOW ... p 3110 N94-26755
CLINE, RICK ... p 3095 N94-27866
CLOSE, J. A. ... p 2752 N94-26652
CLOUGH, S. A. ... p 2767 N94-25950
COAKLEY, JAMES A., JR. ... p 2894 N94-26506
COATES, DWAINE K. ... p 2863 N94-28129
COATS, J. ... p 2833 N94-25691
COBB, WESLEY K. ... p 3104 N94-27265
CODISH, MICHAEL ... p 2966 N94-26956
CODY, CHARLOTTE K. ... p 2671 N94-25719
CODY, JOE ... p 2823 N94-27149
CODY, WILLIAM J. ... p 3099 N94-26891
COFFEY, H. E. ... p 3110 N94-27053
p 3110 N94-27054
COFFEY, HELEN E. ... p 3111 N94-28360
COGAN, JAMES ... p 2880 N94-26828
COGLEY, ALLEN C. ... p 2943 N94-25684
COHEN, ALEXANDER ... p 3066 N94-27590
COHEN, DAVID ... p 2941 N94-26339
COHEN, NORMAN L. ... p 3110 N94-26755
COHEN, RAM ... p 2698 N94-28210
p 2698 N94-28217
COHN, R. F. ... p 2671 N94-25719
COLANGELO, TODD A. ... p 2691 N94-25696
COLAVITA, ALBERTO ... p 3117 N94-27996
COLAVITA, P. ... p 3117 N94-27996
COLE, J. I. ... p 2731 N94-25804
COLE, JULIAN D. ... p 2650 N94-28191
COLE, M. J. ... p 3044 N94-26858
COLGATE, S. A. ... p 3117 N94-27827
COLL, J. ... p 2655 N94-28336
COLL, J. B. ... p 2653 N94-28322
COLLERAINE, A. P. ... p 3043 N94-26323
COLLIN, A. ... p 2968 N94-27154
COLLINS, G. ... p 2863 N94-28122
COLLINS, G. W. ... p 3052 N94-25947
COLLINS, MICHAEL JOHN ... p 2849 N94-26668
COLLINS, TODD A. ... p 2671 N94-25711
COLON, JULIO A. ... p 2943 N94-25694
COLON, MYRELLE ... p 2943 N94-25694
COLTRIN, MICHAEL E. ... p 3049 N94-25601
COMAS, F. ... p 3062 N94-26897
COMBI, MICHAEL R. ... p 3108 N94-27941
p 3105 N94-28184
COMBS, LARRY ... p 3110 N94-26755
COMBS, S. K. ... p 3042 N94-26140
COMINSKY, LYNN ... p 3116 N94-27440
COMISEL, H. ... p 2878 N94-26365
CONAHAN, FRANK C. ... p 3095 N94-28176
CONCUS, PAUL ... p 2760 N94-25849
CONLEY, A. J. ... p 2979 N94-25802
CONLEY, KRISTIN ... p 2671 N94-25719
CONN, D. W. ... p 2699 N94-25926
CONNER, D. L. ... p 3045 N94-26861
CONNOR, K. A. ... p 3047 N94-27720
CONRADO, HUMBERTO ... p 2896 N94-27422
CONSTANTA-FANOURAKIS, P. .. p 2809 N94-25599
CONWAY, J. T. ... p 2655 N94-28334
COOK, A. ... p 2748 N94-25894
COOK, ROBERT E. ... p 2680 N94-26202
COOPER, E. A. ... p 2752 N94-26676
COOPER, PAUL ... p 2684 N94-26284
COOROUGH, P. J. ... p 2891 N94-28311
COPELAND, P. P. ... p 2948 N94-25720
CORBIN, STEPHEN ... p 2744 N94-27961
CORCORAN, M. ... p 3018 N94-26145
CORMIER, GUY ... p 3025 N94-27310
CORNES, JOHN K. ... p 2670 N94-27666
CORT, B. ... p 2733 N94-26069
COSBY, S. W. ... p 2653 N94-28322
COSSENTINE, JAY A. ... p 2960 N94-25994
COSTA, M. L. M. ... p 2792 N94-26401
COSTELLO, KEVIN ... p 2671 N94-25715
COTE, P. J. ... p 3008 N94-26376
COUBROUGH, LAWRENCE ... p 3066 N94-27276
COUCH, MARK A. ... p 2645 N94-26535
COUGHENOUR, M. B. ... p 2866 N94-26026
COURTRIGHT, E. L. ... p 2754 N94-27021
COVELLI, J. ... p 2698 N94-25700
COX, D. P. ... p 3115 N94-27236
p 3115 N94-27419
p 3115 N94-27420
COX, PAUL ... p 2708 N94-26895
COYLE, EDWARD F. ... p 2934 N94-28364
COYNE, R. A. ... p 2948 N94-26578
CRAIG, K. J. ... p 2659 N94-28029
CRANE, R. I. ... p 2831 N94-28079
CRAWFORD, B. ... p 3013 N94-25820
CRAWFORD, D. A. ... p 2888 N94-28296
CRAWFORD, EARNEST ... p 2943 N94-25693
CREAN, DAVID M. ... p 2694 N94-25659
CREEDON, WILL P. ... p 2759 N94-26800
CREEL, KENNETH ... p 2833 N94-25704
CREMERS, D. A. ... p 2818 N94-26605
CREUTZ, M. ... p 3029 N94-27814
CREUTZBERG, F. ... p 2887 N94-28218
CRITCHLEY, ERIC ... p 2797 N94-27709
CRITTENDEN, R. ... p 3033 N94-27614
CRIVELLI, PAUL M. ... p 2671 N94-25719
CROFT, W. B. ... p 3099 N94-27013
CROSETTO, D. ... p 2980 N94-25984
CROSIER, RONALD B. ... p 2838 N94-26448
CROSLEY, DAVID R. ... p 2717 N94-27226
CROSS, DAVID M. ... p 2963 N94-26530
CROW, GEORGE ... p 2823 N94-27149
CROWE, SHANE ... p 2968 N94-27168
CROWLEY, T. P. ... p 3047 N94-27720
CROWLEY, W. P. ... p 2792 N94-26427
CROZIER, STEWART N. ... p 2777 N94-27806
CUDMORE, ALAN ... p 2950 N94-26723
CULLEN, D. E. ... p 2962 N94-26318
CULLER, T. ... p 2888 N94-28297
CULUMOVIC, LOUIS B. ... p 3007 N94-27264
CUMMINGS, STEVEN T. ... p 2683 N94-26282
CUMMINGS, WILLIAM C. ... p 2651 N94-28198
CUMMINS, H. Z. ... p 3060 N94-26780
CUMPSON, P. J. ... p 2738 N94-26653
CUNNINGHAM, ATLEE M., JR. ... p 2679 N94-27798
CURNOCK, BARRY ... p 2828 N94-28044
p 2828 N94-28045
p 2828 N94-28046
p 2828 N94-28047
CURRIE, T. C. ... p 2657 N94-28344
CURRIER, DEAN P. ... p 2936 N94-28372
CURTIS, CARLTON H. ... p 2773 N94-27085
CURTIS, P. ... p 2671 N94-28017
CUTTS, D. ... p 3031 N94-25931
CZIGLER, MARTIN ... p 2947 N94-28261

D

DABROWSKI, L. ... p 2997 N94-27023
DAGAMA, R. M. S. ... p 2792 N94-26401
DAGGERT, TODD ... p 2760 N94-25705
DAHLBERG, MARTIN ... p 2811 N94-27044
DAHM, W. J. ... p 2793 N94-26534
DALZIEL, I. W. D. ... p 2888 N94-28298
DAMS, DENNIS ... p 2966 N94-26956
DANAGAN, J. ... p 2833 N94-25691
DANDY, DAVID S. ... p 3049 N94-25601
DANE, C. B. ... p 2818 N94-26699
p 2819 N94-27018
DANG, CHUANGYIN ... p 2958 N94-25764
DANIEL, WALTER K. ... p 2697 N94-25699
DANIELSEN, C. ... p 2877 N94-26201
DANN, J. N. ... p 3058 N94-26514
DANON, C. A. ... p 2734 N94-26263
DAPRILE, JOHN R. ... p 3009 N94-25731
DARAB, J. G. ... p 2742 N94-27786
DARCY, ERIC C. ... p 2864 N94-28132
DARYANANI, L. T. ... p 2950 N94-26726
DAS, A. ... p 3013 N94-25839
p 3008 N94-25988
DAS, VISHNUMOHAN ... p 2956 N94-25606
DASARO, ERIC A. ... p 2900 N94-27090
DASGUPTA, I. ... p 2714 N94-26169
DASH, S. M. ... p 2804 N94-28030
DASILVA, L. B. ... p 2816 N94-26020
DASMAHAPATRA, S. ... p 3007 N94-26552
DAT, NGUYEN NHU ... p 3057 N94-26387
p 3061 N94-26879
DATE, MEDHA D. ... p 3080 N94-25697
DATEO, CHRISTOPHER E. ... p 2714 N94-26205
DATLOWE, DAYTON W. ... p 3115 N94-26790
DATSYUK, V. V. ... p 3013 N94-25827
DAUGHERTY, ROBERT H. ... p 2669 N94-26608

DAVENPORT, A. J. p 2753 N94-26770
DAVIDIAN, KEN p 2688 N94-27375
DAVIDSON, JOHN M. p 2948 N94-26714
DAVINIC, N. p 2698 N94-25700
DAVIS, C. p 3022 N94-26769
DAVIS, DEBORAH E. p 2795 N94-27119
DAVIS, DONALD A. p 2709 N94-27135
DAVIS, F. C. p 3045 N94-26861
DAVIS, J. BRADLEY p 2692 N94-27956
DAVIS, LINDA p 2824 N94-27228
DAVIS, MAXIE Y. p 3094 N94-27180
DAVIS, R. F. p 3059 N94-26765
p 2754 N94-26974
DAVIS, ROBERT F. p 3060 N94-26839
p 3060 N94-26840
p 3061 N94-26841
p 3061 N94-26885
p 3063 N94-27058
DAVIS, ROBERT J. p 2782 N94-26343
DAVIS, T. p 2833 N94-25691
DAVIS, WILLIAM A. p 2788 N94-27770
DAWSON, D. p 2748 N94-25894
DAWSON, J. M. p 3111 N94-27953
DAWSON, STEPHEN F. p 2860 N94-28105
DAYAWANSA, WIJESURIJA p 2833 N94-25686
DEAN, C. L. p 2877 N94-25979
DEASSISTAVARESFERREIRADASILVA, FRANCISCO
p 2989 N94-27833
DEBOER, FRANK S. p 2966 N94-26919
DEBOER, M. F. N. p 3100 N94-27394
DEBONDELI, PATRICK p 2953 N94-26744
DEBONI, T. p 2981 N94-27092
DEBRUIJN, J. C. M. p 2840 N94-26960
DEBUSSCHE, A. p 2792 N94-26499
DECKERS, K. p 2801 N94-28011
DECOCK, K. M. J. p 2647 N94-27554
DEES, D. W. p 2780 N94-25806
DEFIORE, THOMAS p 2669 N94-27105
DEFONTAINE, D. p 2743 N94-27792
DEGA, JEAN-LOUIS p 2953 N94-26739
DEGNAN, FRANK p 3106 N94-27418
DEGRASSIE, J. S. p 3046 N94-27261
p 3046 N94-27568
DEGROOT, W. A. p 2701 N94-26208
DEHN, JON p 2666 N94-27768
DEHOOP, ADRIANUS T. p 2771 N94-26877
p 2881 N94-26880
p 2772 N94-26909
DEHOOP, MAARTEN V. p 2881 N94-26880
DEJONGH, F. p 3018 N94-26245
DEJONGH, J. F. C. M. p 2966 N94-26966
DELABEAUJARDIERE, O. p 2877 N94-26201
DELAHOUSSAYE, P. R. p 3059 N94-26566
DELANEY, P. T. p 2879 N94-26515
DELANOY, RICHARD L. p 2680 N94-26196
DELBOSCO, EDSON p 3066 N94-27329
DELEEUW, A. J. p 2847 N94-26228
DELEEUW, G. p 2893 N94-26013
DELFINO, G. p 2998 N94-27162
DELIGIANNIS, FRANK p 2862 N94-28119
DELIL, A. A. M. p 2798 N94-27853
DELL, R. DAN p 2864 N94-28131
DELNICK, F. M. p 2780 N94-25975
DELO, C. p 2800 N94-28006
DELONG, D. p 2941 N94-26788
DELUCA, EUGENIO p 2747 N94-25596
DELUCCA, D. p 2952 N94-26734
DEMEO, MARTHA E. p 2684 N94-26284
p 2684 N94-26285
DEMIRGIAN, J. C. p 2868 N94-26952
DEMPSTER, P. T. p 2902 N94-27227
DENHERTOG, D. p 2957 N94-25761
p 2958 N94-25762
p 2967 N94-27031
DENISOV, S. P. p 2810 N94-26397
DENISOVA, V. G. p 3112 N94-25625
p 3112 N94-25626
p 3112 N94-25627
DENNIS, K. W. p 2735 N94-26273
DENNIS, MICHAEL L. p 2820 N94-27670
DENSKAT, U. p 2953 N94-26741
DENTON, R. E. p 2963 N94-26521
DEOLIVEIRA, L. C. S. p 3068 N94-27697
DERBY, STEPHEN J. p 2683 N94-26280
DEREFELDT, G. p 2937 N94-28392
DERHACOBIAN, N. p 3053 N94-26094
p 3054 N94-26095
DERMARDEROSIAN, AARON p 2834 N94-25727
DEROSE, GUY A. p 2753 N94-26822
DESAI, PRASUN N. p 2690 N94-27771
DESHAZO, KATHLEEN B. p 2939 N94-27056
DESJARLAIS, LISA p 2958 N94-25818
DESOUZA, L. C. GADELHA p 2696 N94-27357
DESOUZA, PETRONIO NORONHA
p 2827 N94-27665
DESROCHERS, ALAN A. p 2683 N94-26281
DESROCHERS, PAUL R. p 2893 N94-26168
DESTLER, WILLIAM W. p 3046 N94-27098
DESTURLER, E. p 2995 N94-26818
DESWART, J. J. p 3021 N94-26620
DETWILER, D. T. p 2671 N94-25716
DEUTEKOM, M. p 2811 N94-27134
DEUTSCHER, G. p 2854 N94-26058
DEVILLERS, R. p 2952 N94-26734
DEVRIES, J. S. p 3036 N94-26648
p 3036 N94-26649
DEWAARD, H. p 2763 N94-26819
DEWITH, G. p 2752 N94-26654
DIAS, OSCAR PEREIRA, JR. p 2974 N94-27835
DIAZ, ALICIA p 2943 N94-25694
DIAZ, J. C. p 2760 N94-27719
DIAZDELARUBIA, T. p 3017 N94-26049
DICAROLIS, S. A. p 2757 N94-27716
DICKENS, J. p 2833 N94-25691
DICKINSON, STUART p 2841 N94-27110
DICKMAN, O. p 2710 N94-27253
DICKSON, K. J. p 2932 N94-27556
DIDENKO, L. A. p 3031 N94-25850
DIDONATO, ARMIDO R. p 2961 N94-26148
DIDZIULIS, S. V. p 2746 N94-28185
DIETDRICH, DANIEL ROBERT p 2730 N94-25585
DIETRICH, STEFAN p 2797 N94-27588
DILL, D. L. p 2786 N94-27061
DILORENZO, MATT p 2833 N94-25683
DIMOS, D. p 3061 N94-26856
DING, HAN-JUN p 3106 N94-25981
DING, L. K. p 3116 N94-27607
DING, NING p 3049 N94-27855
DING, YIHUI p 2895 N94-26850
DIPESO, G. p 2767 N94-25937
DISIMILE, P. J. p 2800 N94-28009
DISTEFANO, SAL p 2860 N94-28105
p 2862 N94-28119
DISTELRATH, DIETER p 2681 N94-27587
DIVECHA, AMARNATH P. p 2747 N94-28187
p 3070 N94-28225
DIVELBISS, ADAM p 2683 N94-26279
DIWAN, AMER p 3099 N94-27014
p 2967 N94-27063
DIXON, DAVID S. p 2709 N94-27076
p 2709 N94-27091
DJINGHEUZIAN, ROBERT p 2709 N94-26978
DOBBING, J. A. p 3046 N94-27261
DOBREV, V. K. p 3005 N94-25868
p 3006 N94-26413
p 2997 N94-27023
DOBROTIN, N. A. p 3112 N94-25625
p 3112 N94-25626
p 3112 N94-25627
DOBSON, K. p 2689 N94-25692
DODGE, D. p 2856 N94-26513
DOGGETT, KENT A. p 3110 N94-26755
DOHOGNE, CAROLINE A. p 2843 N94-27559
DOHRMANN, C. R. p 2857 N94-26700
DOI, HARUO p 2728 N94-25577
DOIRON, M. D. p 2656 N94-28339
DOLLING, DAVID S. p 2798 N94-27802
DOLLINS, ANDREW B. p 2902 N94-26991
DOMANUS, H. M. p 2739 N94-26935
DOMIK, GITTA O. p 3105 N94-27932
DONG, J. Q. p 2791 N94-26096
DONGARRA, J. J. p 2964 N94-26764
DOOLEY, S. P. p 3056 N94-26364
p 3063 N94-26987
DORADO, A. O. p 2734 N94-26162
DORAN, J. C. p 2869 N94-27601
DORIS, KENNETH R. p 2665 N94-27275
DORMIEUX, M. p 2659 N94-28031
DOROKHOV, A. E. p 3031 N94-25870
DORR, M. R. p 3020 N94-26577
DORRIS, S. E. p 2857 N94-26584
DORTMANS, L. p 2752 N94-26654
DORTMANS, P. J. p 3015 N94-25890
DOSEDEL, STEFAN B. p 2705 N94-25859
DOSSANTOS, AILTON CRUZ p 2849 N94-26827
DOTE, YUTAKA p 2859 N94-27204
p 2871 N94-28154
DOUDA, BERNARD E. p 3037 N94-27066
DOVGAL, ALEXANDER p 2647 N94-27592
DRAKE, J. F. p 3044 N94-26523
DRESS, W. B. p 2988 N94-27706
DREVER, ROBERT G. p 2900 N94-27090
DREW, D. A. p 2794 N94-26979
DREWIEN, C. A. p 2732 N94-25819
DROBIN, V. M. p 3058 N94-26512
DRONKERT, Y. p 2939 N94-27138
DRULLINGER, R. E. p 3008 N94-26484
DRUMMOND, T. J. p 3056 N94-26308
DRUYAN, L. M. p 2866 N94-26077
DU, W. p 2969 N94-27318
DUAN, S. Z. p 2654 N94-28331
DUARTE, MANNY G. p 3080 N94-25697
DUBA, A. G. p 2735 N94-26322
DUBOIS, T. p 2792 N94-26499
DUBOVIK, V. M. p 2766 N94-25866
DUCHI, CECELI A. p 2749 N94-26074
DUESBERY, M. S. p 2704 N94-25608
p 2840 N94-27034
DUFF, I. S. p 2998 N94-27115
DUFFIN, WANDA J. p 2717 N94-26907
DUFFUS, KEITH p 2642 N94-27290
DUGGER, M. T. p 3061 N94-26856
DUIMOVICH, JOHN p 2982 N94-27332
DUINEVELD, G. C. A. p 2868 N94-27200
DULING, IRL N., III p 2820 N94-27670
DUNAEVSKY, A. M. p 3112 N94-25625
p 3112 N94-25626
p 3112 N94-25627
DUNAGAN, NANCY p 2901 N94-26210
DUNCAN, B. C. p 2748 N94-25894
DUNCAN, F. p 3014 N94-25840
DUNCAN, J. p 2938 N94-26683
DUNGAN, MICHAEL p 3081 N94-25703
DUNKIN, S. R. p 2742 N94-27755
DUNLAP, JOHN H. p 2900 N94-27090
DUNNE, JIM p 2703 N94-25690
DUNNET, ANDREW F. p 2861 N94-28109
DUQUESNE, DIDIER p 2861 N94-28110
DURAN, R. S. p 2754 N94-26977
p 2754 N94-27036
p 2755 N94-27087
DURAN, RANDOLPH p 2753 N94-26925
DURAN, RANDOLPH S. p 2754 N94-27080
p 2755 N94-27163
DURAND, YVES p 2950 N94-26724
DURGIN, W. W. p 2671 N94-25719
DUSANG, LEANA p 2956 N94-25606
DUSHKIN, A. YU. p 2810 N94-26397
DUVAL, P. p 2885 N94-27969
DVALI, G. p 3018 N94-26333
DYACHKOV, A. P. p 2810 N94-26395
DYACHKOV, E. I. p 3058 N94-26512
DYKSHOORN, WILLIAM PETER p 3074 N94-27401
DYMENT, F. p 2733 N94-26160
DYN, NIRA p 2998 N94-27103
DZHELEPOV, V. P. p 3020 N94-26511
DZHELYADIN, R. I. p 3024 N94-27250
DZIERBA, A. p 3033 N94-27614

E

EARL, MARTIN W. p 2861 N94-28109
EASLEY, WESLEY C. p 2665 N94-27423
EAST, R. A. p 2659 N94-28021
EASTMAN, J. p 2866 N94-26026
EATON, JOEL A. p 3102 N94-26234
EATOUGH, M. O. p 3053 N94-26025
EBEL, WILLIAM J. p 2968 N94-27168
EBERT, D. p 3020 N94-26505
EBERT, THOMAS J. p 2934 N94-28365
EBIHARA, ICHIRO p 3100 N94-27336
EBOLI, O. J. P. p 3017 N94-26043
ECHAVE, M. A. p 2696 N94-26808
ECONOMY, J. p 2707 N94-26450
EDAGAWA, KEIICHI p 3053 N94-26071
p 2736 N94-26477
EDELSTEIN, J. D. p 3072 N94-26417
EDWARDS, B. C. p 2696 N94-26808
EDWARDS, D. J. p 2737 N94-26575
EDWARDS, THOMAS A. p 2649 N94-28188
EFFENHAUSER, RAINER K. p 2911 N94-27088
EFIMOV, G. V. p 3027 N94-27629
p 3067 N94-27638
EGASHIRA, MITSURU p 2729 N94-25581
EHRDEHNEHDEHLGEHR, T. p 3013 N94-25828
EHTAMO, H. p 3095 N94-28386
EI, KAZUO p 2722 N94-25546
EIBEN, AGOSTON p 2965 N94-26908
p 2967 N94-26997
EISLEY, JOE G. p 3079 N94-25688
EJIRI, MASAKI p 2882 N94-27342
p 2883 N94-27963
EKBLAD, U. p 3101 N94-27218
EKIN, J. W. p 2725 N94-25560
EKLUND, E. p 2746 N94-28185
EL-DINKAMAL, M. TAG p 3016 N94-26010
EL-GENK, MOHAMED S. p 2699 N94-25613
EL-MASRY, NADINA p 3061 N94-26885
EL-NAGHY, A. p 3016 N94-26010
p 3030 N94-27994
ELDERKIN, C. E. p 2880 N94-26762
ELHASSOUNI, A. p 2996 N94-26898
ELLIOT, STEVE p 2671 N94-25708
ELLIOTT, JOE W. p 2645 N94-26483
p 2645 N94-26489
p 2645 N94-26492
p 2645 N94-26497

ELLIOTT, WILLIAM .... p 2761 N94-25707
ELLISON, G. BARNEY .... p 3013 N94-25816
ELLISON, J. .... p 3052 N94-25972
ELMAN, GREGORY C. .... p 2877 N94-26152
ELMER, K. R. .... p 2651 N94-28197
ELSABEE, M. Z. .... p 2755 N94-27163
ELSMORE, TIMOTHY F. .... p 2909 N94-26377
p 2937 N94-26430
ELSTER, C. .... p 3012 N94-25800
ELSWORTH, D. T. .... p 2790 N94-25778
ELZAIN, M. E. .... p 3050 N94-25843
EMAAMI-KHONSAARI, MAJID .... p 3049 N94-27949
EMAM, O. .... p 2951 N94-26727
EMMERT, JOHN M. .... p 2780 N94-25845
EMSLIE, H. .... p 2938 N94-26683
ENDE, H. .... p 2659 N94-28022
ENDO, MASAO .... p 2931 N94-27536
ENG, ANTHONY T. .... p 2755 N94-27111
ENGBERG, B. .... p 2902 N94-27171
ENGELMANN, B. E. .... p 2965 N94-26862
ENOMOTO, MASATO .... p 2726 N94-25564
ENS, JOHN E. .... p 2988 N94-27645
EPP, MANFRED .... p 2671 N94-25712
ERCOLINE, WILLIAM R. .... p 2673 N94-26989
ERDEMIR, A. .... p 2751 N94-26422
EREMCHENKO, E. A. .... p 2810 N94-26396
ERIAN, NEIL F. .... p 3080 N94-25697
ERICHSEN, MATTHEW N. .... p 2672 N94-26021
ERICKSON, GARY E. .... p 2647 N94-26706
ERICKSON, GARY M. .... p 2883 N94-27438
ERMOLIN, YU. V. .... p 2948 N94-26266
ERMUTLU, M. E. .... p 2778 N94-28355
ERNST, J. .... p 3014 N94-25840
ERTL, ANDREW CARL .... p 2901 N94-26093
ERWIN, D. H. .... p 2888 N94-28299
ESCOBAR, C. O. .... p 3022 N94-26766
ESCOBAR, XOCHIQUETZAL Y. .... p 2943 N94-25694
ESKICIOGLU, AHMET M. .... p 2946 N94-28257
ESMAN, RONALD D. .... p 2777 N94-27734
ESSELLE, KARUNANAYAKE P. A. P.
p 2777 N94-27871
ESSIEN, M. .... p 2819 N94-26811
ESTES, CHRISTA .... p 2943 N94-25678
EVANS, ANTHONY G. .... p 2707 N94-26447
EVANS, B. T. N. .... p 3038 N94-27598
EVANS, BRUCE .... p 2947 N94-28263
EVANS, C. R. .... p 3069 N94-27828
EVANS, M. S. .... p 2827 N94-27780
EVANS, MICHAEL L. .... p 2903 N94-27940
EVANS, R. L. .... p 2838 N94-26501
EVANS, ROBERT H. .... p 2848 N94-26236
EVANS, RONALD J. .... p 2679 N94-25773
EYLES, C. J. .... p 2951 N94-26727
EZERS, ROLANDS ERIKS .... p 2770 N94-26624

F

FAHR, A. .... p 2835 N94-26644
FAHY, F. J. .... p 2832 N94-28174
FAIGLE, U. .... p 2996 N94-26917
FANG, GUANG YIN .... p 3016 N94-25957
FANG, W. C. .... p 2862 N94-28117
FANG, ZONGYI .... p 2875 N94-28289
FANTON, JOHN W. .... p 2910 N94-26973
p 2902 N94-26991
FARAGGI, ALON E. .... p 3071 N94-25911
FARAJI-DANA, REZA .... p 2787 N94-27653
FARE, T. L. .... p 2754 N94-27033
FARHAT, C. .... p 2845 N94-28181
FARN, M. W. .... p 2819 N94-27262
FASEL, HERMANN F. .... p 2798 N94-27782
FAURE, SABINE .... p 2671 N94-25717
FAURIE, J. P. .... p 3054 N94-26139
FAZEKAS, P. .... p 3057 N94-26389
p 3067 N94-27634
FEIGELSON, R. S. .... p 2757 N94-27716
FEITH, S. .... p 2909 N94-26173
FEJTEK, I. .... p 2653 N94-28325
p 2654 N94-28329
p 2655 N94-28336
FELDHAUS, WINIFRED S. .... p 2972 N94-27655
FELDMAN, RAISA E. .... p 3004 N94-27106
FELDMEIER, JOHN J. .... p 2901 N94-26517
FELIPPA, C. A. .... p 2845 N94-28181
FELLENSTEIN, JAMES .... p 2671 N94-25713
FELLOWS, JAMES A. .... p 2781 N94-25995
FELTHAM, A. .... p 3014 N94-25840
FENDLER, ERIC .... p 2967 N94-27060
FENG, CHENGSHI .... p 2819 N94-26941
FENG, MINGMING .... p 2660 N94-27746
FENG, Z. Y. .... p 3116 N94-27607
FENIMORE, DALE L. .... p 3052 N94-25993
FENIMORE, E. E. .... p 3116 N94-27714
FEO, J. .... p 2981 N94-27092
FERBEL, T. .... p 3008 N94-25988
FERGUSON, MILTON W. .... p 2747 N94-27900
FERGUSON, NIELS T. .... p 2776 N94-27546
FERNANDEZ, FRANCISCO J. .... p 2644 N94-26143
FERNSLER, RICHARD .... p 2767 N94-26177
FERRALL, JOSEPH .... p 2943 N94-27934
FERRANDO, WILLIAM A. .... p 2747 N94-28187
FERRARO, G. .... p 2932 N94-27556
FETT, ROBERT W. .... p 2868 N94-26888
FETTER, ROBERT O. .... p 2868 N94-26843
FETTERER, FLORENCE M. .... p 2899 N94-26853
FIDELL, SANFORD .... p 2651 N94-28196
FIEBER, JOSEPH P. .... p 2943 N94-25706
FIELD, E. C. .... p 2878 N94-26304
FIELD, EDMUND .... p 2676 N94-25640
p 2676 N94-25653
FIELDING, ERIC J. .... p 3098 N94-26490
FIELDS, T. .... p 3018 N94-26145
FIKSEL, G. .... p 3042 N94-26132
FILCHENKOV, V. V. .... p 3020 N94-26511
FILE, GILBERTO .... p 2966 N94-26956
FINE, P. .... p 3053 N94-26094
FINGER, MARK H. .... p 3116 N94-27440
FINK, ANNMARIE .... p 2642 N94-27290
FINLAYSON, G. D. .... p 2994 N94-26614
FINLAYSON, RICHARD D. .... p 2670 N94-27666
FINN, J. M. .... p 3044 N94-26523
FINN, ROBERT .... p 2760 N94-25849
FIRSICH, D. .... p 2780 N94-25975
FISCHER, JOHN .... p 2755 N94-27148
FISHER, M. J. .... p 2807 N94-28173
FISHER, PAUL S. .... p 2946 N94-28257
FISHER, ROB .... p 2686 N94-27365
FISHMAN, GERALD J. .... p 3114 N94-26686
p 3114 N94-26687
p 3114 N94-26688
p 3115 N94-26689
p 3115 N94-26690
FISK, Z. .... p 3050 N94-25817
FITCH, JAMES A. .... p 2987 N94-27122
FITCH, THOMAS A. .... p 2937 N94-25897
FITZGERALD, MICHAEL .... p 2897 N94-28179
p 2897 N94-28182
FLAHERTY, WILLIAM .... p 2681 N94-27113
FLAMENT, CYRIL .... p 2791 N94-26316
FLANEGAN, MARK .... p 2950 N94-26723
FLATTE, S. M. .... p 3102 N94-26528
FLEET, M. L. .... p 2903 N94-25672
FLEETWOOD, D. M. .... p 2780 N94-25812
p 2948 N94-26111
FLEMING, GREGG G. .... p 3009 N94-25731
FLEMING, J. G. .... p 2738 N94-26610
FLEMING, RICHARD W. .... p 2957 N94-25649
FLIEGNER, T. .... p 3101 N94-26918
FLIERL, R. .... p 2824 N94-27254
FLIFLET, ARNE .... p 3043 N94-26356
FLINT, JOHN H. .... p 2816 N94-26178
FLOREANINI, R. .... p 3006 N94-26413
p 2997 N94-27023
FLOTTA, C. .... p 2689 N94-25692
FLOWERS, L. .... p 2856 N94-26513
FLYKT, M. J. .... p 2779 N94-28390
FOGARTY, T. N. .... p 2684 N94-26287
FOGELMAN, C. F. .... p 3041 N94-25933
FOGELMAN, C. H. .... p 2767 N94-25924
FOLKERS, MIKE .... p 2760 N94-25705
FOLLSTAEDT, D. M. .... p 2780 N94-25664
p 3050 N94-25814
p 3052 N94-25971
p 3056 N94-26352
p 3058 N94-26565
FOLTYN, E. M. .... p 2733 N94-26069
FOOT, R. .... p 3016 N94-26040
FORBES, JEFFREY M. .... p 2879 N94-26569
FORD, FLOYD E. .... p 2702 N94-26613
FORD, WARREN T. .... p 2754 N94-27036
FORNIA, MARK .... p 2760 N94-25705
FORSYTH, D. .... p 2835 N94-26644
FOSTER, C. M. .... p 3062 N94-26934
FOSTER, I. T. .... p 2963 N94-26407
FOSTER, M. S. .... p 2956 N94-25606
FOSTER, P. .... p 2759 N94-26198
FOTTNER, L. .... p 2676 N94-28037
FOUGERE, G. E. .... p 2751 N94-26594
FOUQUET, J. .... p 2757 N94-27716
FOURNIER, BRADLEY K. .... p 2694 N94-25832
FOURNIER, G. R. .... p 3038 N94-27598
FOUST, C. R. .... p 3042 N94-26140
FOX, ALAN G. .... p 2740 N94-27009
FOX, CHRIS L. .... p 2863 N94-28129
FOX, MATTHEW .... p 2879 N94-26569
FOX, TIM .... p 2671 N94-25712
FRAMPTON, JEFFREY .... p 2833 N94-25704
FRANCISCUS, HERBERT JOHANNES ANTONIUS
p 2986 N94-27029
FRANCO-FERREIRA, E. A. .... p 2821 N94-25980
FRANCOIS, R. E. .... p 2899 N94-26886
FRANKE, J. E. .... p 2713 N94-25978
FRANKE, RICHARD .... p 2990 N94-25594
FRANKEL, N. E. .... p 3007 N94-26928
FRANKLE, C. M. .... p 3013 N94-25820
FRANKLE, KEVIN .... p 2689 N94-25674
FRANKLIN, G. B. .... p 3022 N94-26769
FRANKLIN, ROBERT E. .... p 2956 N94-25610
FRATE, DAVE .... p 2861 N94-28108
FRATNIK, F. .... p 3117 N94-27996
FREEDMAN, D. Z. .... p 3019 N94-26416
FREEMAN, FREDERICK G. .... p 2940 N94-27901
FRENKLACH, MICHAEL .... p 2717 N94-27256
FRERY, ALEJANDRO C. .... p 2776 N94-27335
FREYTAG, E. K. .... p 2782 N94-26312
FRICKE, ROBERT W., JR. .... p 2692 N94-28199
p 2693 N94-28220
p 2693 N94-28221
FRIED, H. M. .... p 3031 N94-25931
FRIEDERS, G. .... p 2816 N94-26020
FRIEDLANDER, ANNE L. .... p 2935 N94-28370
FRIEDMAN, ROBERT .... p 2692 N94-27436
FRIIS-CHRISTENSEN, E. .... p 2877 N94-26201
FRITZ, I. J. .... p 2780 N94-25664
p 3056 N94-26308
FROES, F. H. .... p 2736 N94-26362
p 2739 N94-26799
FROHLICH, CLIFFORD A. .... p 2887 N94-28214
FROMME, CHRIS C. .... p 2764 N94-27144
FU, CONGBIN .... p 2874 N94-28283
FU, T. .... p 3068 N94-27724
FUENTES, RODRIGO U. .... p 2873 N94-28279
FUERSCHBACH, P. W. .... p 2819 N94-26811
FUICHS, W. K. .... p 2964 N94-26680
FUJII, HIRONOBU .... p 3025 N94-27337
FUJII, KIYOAKI .... p 2933 N94-27945
FUJII, KOZO .... p 2804 N94-28026
FUJII, MITSUHIRO .... p 3069 N94-27756
FUJII, TETSUO .... p 2722 N94-25546
p 2726 N94-25567
FUJIMORI, NAOJI .... p 3065 N94-27245
FUJIMOTO, Y. .... p 3112 N94-25628
p 3113 N94-25629
p 3113 N94-25630
FUJIMURA, AKIO .... p 2885 N94-27973
FUJITA, HAJIME .... p 3011 N94-27283
FUJITA, MITSUTANE .... p 2726 N94-25566
p 2727 N94-25568
FUJITA, NOBUYUKI .... p 2933 N94-27945
FUJIWARA, H. .... p 3112 N94-25628
p 3113 N94-25629
p 3113 N94-25630
FUJIWARA, JUN .... p 2722 N94-25545
FUKATSU, YASUHIRO .... p 2908 N94-27519
FUKUDA, Y. .... p 3028 N94-27759
FUKUI, MANABU .... p 2870 N94-28150
FUKUI, YASUHIKO .... p 2904 N94-27467
p 2904 N94-27468
FUKUSHIMA, SADAO .... p 2728 N94-25574
FUKUSHIMA, TAKESHI .... p 2728 N94-25575
FUKUZAWA, AKIRA .... p 2723 N94-25552
p 2725 N94-25558
p 2730 N94-25585
FUKUZAWA, YASUMITSU .... p 2725 N94-25558
FULLENKAMP, JOSEPH A. .... p 3096 N94-26024
FULLERTON, ERIC E. .... p 3059 N94-26591
FUNADA, HISAYUKI .... p 2853 N94-27990
FUNAHASHI, ATSUSHI .... p 2905 N94-27485
FUNAHASHI, SATORU .... p 2903 N94-27862
FUNK, GREGORY P. .... p 2843 N94-27559
FURDYNA, J. K. .... p 3063 N94-26958
FURSA, D. V. .... p 3023 N94-26942
FURUKAWA, KENJI .... p 2904 N94-27467
p 2904 N94-27468
FURUKAWA, NOBUO .... p 3065 N94-27248
FURUYAMA, SADAO .... p 2723 N94-25552
FUTAMI, KENJI .... p 2884 N94-27966
FYFE, E. .... p 2951 N94-26731

G

GABRIELSE, GERALD .... p 3024 N94-27011
GADRICH, TAMAR .... p 3003 N94-26355
GAFKA, GEORGE K. .... p 3080 N94-25697
GAGLIARDINO, J. .... p 2689 N94-25692
GAHLINGER, ANTHONY JOSEPH p 3009 N94-27268
GAILLARD, R. .... p 2659 N94-28039
GAINEY, JAMES C., JR. .... p 2990 N94-25834
GALAMBOS, J. D. .... p 3044 N94-26860
p 3045 N94-26861
GALE, RONALD P. .... p 2860 N94-27625
GALIL, ZVI .... p 3100 N94-27164
GALLIS, M. A. .... p 2644 N94-26248
GALLOP, L. D. .... p 2813 N94-27597
GALLOWAY, SCOTT .... p 2686 N94-27366
GALLY, TOM .... p 2658 N94-27902

GALVELE, J. R. p 2734 N94-26264
GALVEZ, M. F. p 2734 N94-26264
GALYAEV, A. N. p 2810 N94-26394
GAMBLE, T. K. p 3042 N94-26081
GAMBRELL, S. C., JR. p 2843 N94-27765
GAN, CHOON LIM p 2794 N94-27059
GANAPATHI, GANI B. p 2943 N94-27934
GANBOLD, G. p 3027 N94-27629
p 3067 N94-27638
GANG, CHEN p 2742 N94-27730
GANG, HU p 3008 N94-25831
GANGLOFF, RICHARD P. p 2844 N94-27851
GAO, Y. p 3053 N94-26029
GAO, YUZUN, p 2737 N94-26587
GARBERS, J. p 2953 N94-26741
GARBINSKI, GARY p 2671 N94-25713
GARCEA, RALPH p 2652 N94-28318
GARCIA, ALBERTO p 2943 N94-25694
GARCIA, HOWARD p 3110 N94-26755
GARCIA, JOSEPH P. p 3040 N94-28224
GARCIA, L. p 3044 N94-26694
GARDENER, N. p 2698 N94-25701
GARDINER, WILLIAM C. p 2717 N94-27256
GARDNER, J. A. p 3063 N94-26958
GARINO, T. J. p 3061 N94-26856
GARLAND, DANIEL p 2664 N94-26197
GARNER, CHRIS p 2863 N94-28127
GARNER, F. A. p 2737 N94-26575
GARRANT, KEITH p 2761 N94-25707
GARRARD, WILLIAM p 2833 N94-25689
GARRISON, G. R. p 2899 N94-26886
GARRISON, JAMES L., JR. p 2684 N94-26286
GARTSHORE, I. S. p 2655 N94-28333
GATES, D. A. p 3047 N94-27735
GATHMANN, THOMAS P. p 3095 N94-27866
GAVA, E. p 3071 N94-25882
GAVAI, R. V. p 3019 N94-26423
GAVERN, JANICE M. p 2865 N94-25755
GAY, R. R. p 3067 N94-27609
GAYLORD, JOE p 2833 N94-25683
GEE, J. M. p 2857 N94-26617
GEE, M. G. p 2752 N94-26652
p 2825 N94-27322
p 2825 N94-27324
GEER, S. p 3022 N94-26793
GEESAMAN, DONALD F. p 3027 N94-27711
GEFFROY, P. p 2659 N94-28039
GEHRED, PAUL A. p 3110 N94-26755
GEISELHART, KARL A. p 2668 N94-26606
GEISSLER, WOLFGANG p 2648 N94-27741
GELFAND, ALAN E. p 3003 N94-26485
p 3003 N94-26494
GELLERMANN, W. p 3064 N94-27231
GELLES, D. S. p 2731 N94-25803
p 2732 N94-25987
p 2737 N94-26556
GEMMEN, R. S. p 2719 N94-27712
GENANT, HARRY K. p 2935 N94-28370
GENG, HUAIBIN p 2852 N94-27878
GENG, L. p 2717 N94-26951
GENTRY, WILLIAM O. p 2864 N94-28134
GEORGE, A. p 2659 N94-28022
GEORGE, E. P. p 2741 N94-27616
GEORGE, T. G. p 2821 N94-25980
GEORGE, TOMMY p 2703 N94-25690
GEORGESON, GARY E. p 2705 N94-25779
GEORGOULAKIS, JAMES M. p 2909 N94-26360
GERHARD, WILLIAM E., JR. p 2667 N94-25772
GERSHTEJN, S. S. p 3017 N94-26045
GERTZ, JEFFREY L. p 2772 N94-26963
GES, A. p 2735 N94-26294
GHARIB, MORTEZA p 2796 N94-27319
GHODGAONKAR, M. D. p 2981 N94-26903
GHONIEM, M. T. p 3030 N94-27994
GHORIESHI, ANTHONY p 2682 N94-27903
GHOSH, SASANKA p 2994 N94-26459
GIBBS, P. A. J. p 2748 N94-25892
p 2748 N94-25893
p 2756 N94-27217
GIBSON, R. A. p 2858 N94-26792
GIEROW, PAUL p 2823 N94-27149
GIFFORD, ROBERT K. p 2939 N94-27056
GILBERT, MIKE p 2684 N94-26285
GILITSKIJ, YU. V. p 2810 N94-26397
GILL, JOHN J. p 2763 N94-26341
GILL, ROBERT C. p 2760 N94-28226
GILL, TEPPER L. p 3009 N94-27126
GILLESPIE, V. P. p 2684 N94-26290
GILLINGHAM, KENT K. p 2673 N94-26989
GILMAN, J. A. p 3094 N94-27772
GILTNER, L. JOHN p 2864 N94-28135
GINATEMPO, B. p 2736 N94-26351
GINERIS, DENISE J. p 2899 N94-26853
GINSBERG, JERRY H. p 3010 N94-26889
GIONET, VINCENT p 2834 N94-25727
GIONFRIDDO, THOMAS A. p 2650 N94-28190
GISLASON, JASON p 2671 N94-25708
GITMAN, D. M. p 3019 N94-26424
GIWA-AGBOMEIRELE, P. A. p 2712 N94-27710
GLAAB, LOUIS J. p 2646 N94-26602
GLADYSHEV, V. A. p 2809 N94-25735
GLASS, JEFFREY T. p 3060 N94-26839
p 3061 N94-26885
p 3063 N94-27058
GLAZOV, A. A. p 2959 N94-25917
GLECKLER, P. J. p 2898 N94-26072
GLEN, W. p 2888 N94-28300
GLENN, FLOYD p 2941 N94-26339
GLIEM, F. p 2945 N94-28254
GLOBUS, AL p 2970 N94-27542
GLOSLI, J. N. p 2751 N94-26554
GLOVER, A. L. p 2713 N94-26014
GLUSHKOV, YEVGENY S. p 3005 N94-26802
GO, DO KYUNG p 2816 N94-26157
GODBOLE, S. V. p 2715 N94-26392
GODDARD, J. D. p 2823 N94-27104
GODIN, J. p 2653 N94-28326
GODIN, P. p 2656 N94-28339
GODINO, MARK p 2766 N94-25766
GOEBEL, F. p 2864 N94-28133
GOEHNER, R. P. p 3057 N94-26420
GOGAN, LAURA p 2689 N94-25670
GOHAR, Y. p 3044 N94-26858
GOHIL, P. p 3048 N94-27791
GOHON, THIERRY p 2953 N94-26742
GOLD, YARON p 2945 N94-28252
GOLDBERG, L. A. p 2980 N94-26473
GOLDBERG, LEW p 2777 N94-27734
GOLDEN, B. p 2698 N94-25701
GOLDEN, DAVID M. p 2717 N94-27226
GOLDFARB, R. p 2725 N94-25560
GOLDMAN, P. p 2856 N94-26513
GOLDSTEIN, J. L. F. p 2741 N94-27619
GOLDSTONE, J. A. p 2733 N94-26069
GOLOVATO, S. N. p 2767 N94-25924
p 3041 N94-25933
GOMEZ-MOLINERO, F. p 2950 N94-26721
p 2951 N94-26731
GOMI, HIROMI p 2940 N94-27584
GONELLA, F. p 3035 N94-26246
GONG, KAI F. p 2786 N94-27109
GONIS, A. p 3055 N94-26238
GONZALEZ-GARCIA, M. C. p 3017 N94-26043
GONZALEZ, ISABEL C. p 2943 N94-25694
GOOD, M. S. p 2706 N94-25982
GOODE, PHILIP R. p 3111 N94-27096
GOODER, JANET L. p 2705 N94-25739
GOODNOW, D. p 3053 N94-26025
GOODRICH, L. F. p 2725 N94-25560
GOODS, S. H. p 2759 N94-26198
p 2742 N94-27755
GOODWIN, RICHARD p 2985 N94-26006
GOOGIN, J. M. p 2713 N94-26014
GOOL, WARREN E. p 2968 N94-27128
GORANSON, P. L. p 3044 N94-26858
p 3045 N94-26861
GORDON, EDWARD O. p 2677 N94-25998
GORGENYI, LOUIS ALEXANDER p 2826 N94-27652
GORMAN, JOHN D. p 2946 N94-28260
p 2947 N94-28262
GORSHKOV, V. A. p 3012 N94-25750
GOTO, TAKUO p 2916 N94-27463
GOTTLICH, GRETCHEN L. p 2971 N94-27573
GOTTLIEB, J. J. p 2654 N94-28328
GOUDREAU, G. L. p 2965 N94-26775
GOULDING, R. H. p 3046 N94-27261
p 3046 N94-27568
GOUZ, YU. P. p 3024 N94-27250
GOVINDARAJ, T. p 2984 N94-25899
p 2985 N94-25966
GRABEL, J. V. p 2739 N94-26935
GRABOSCH, H. p 2814 N94-28098
GRABOW, ROBERT p 2671 N94-25712
GRAD, JANET ROSE p 2999 N94-27405
GRAF, W. O. p 2682 N94-27879
GRAHAM, GERALD p 3020 N94-26527
GRAHAM, I. p 2974 N94-27823
GRAHAM, J. p 3043 N94-26321
GRAHAM, M. P. p 2820 N94-27668
GRAHAM, MARCUS L. p 2786 N94-27109
GRANAAS, MICHAEL p 2942 N94-27089
GRANATO, E. p 3057 N94-26390
GRANOVSKY, M. S. p 2735 N94-26295
GRANT, PATRICK S. p 2897 N94-28179
p 2897 N94-28182
GRANT, T. p 2945 N94-28252
GRANTHAM, WILLIAM D. p 2679 N94-27660
GRAPPEL, ROBERT D. p 2772 N94-26963
GRAPPERHAUS, MICHAEL JAMES
p 3041 N94-25949
GRATZ, ROY F. p 2758 N94-27904
GRAY, G. T., III p 2738 N94-26621
GRAY, W. STEVEN p 2682 N94-27905
GRECO, MICHAEL p 2672 N94-26030
GREEN, JIM p 2978 N94-27906
GREEN, KENNETH E. p 3066 N94-27276
GREEN, S. I. p 2654 N94-28331
GREEN, T. M. p 2757 N94-27695
GREENBERG, ALBERT G. p 2971 N94-27558
GREENBERG, D. S. p 2979 N94-25952
p 2979 N94-25953
GREENBERG, DAVID p 2983 N94-27713
GREENFIELD, C. M. p 3045 N94-26950
GREENLEAF, J. E. p 2902 N94-27227
GREENLEAF, JOHN E. p 2901 N94-26210
GREENLEE, H. B. p 3028 N94-27749
GREENSTADT, EUGENE W. p 3104 N94-27407
GREENWALD, HAROLD M. p 2965 N94-26831
GREENWELL, D. I. p 2659 N94-28029
GREGOR, J. A. p 3033 N94-27082
GREGOR, R. J. p 2936 N94-28373
GREGOREK, G. M. p 2671 N94-25716
GREGORISH, R. M. p 2982 N94-27644
GREGORY, JOHN C. p 3115 N94-27167
GREULICH, F. A. p 3069 N94-27753
GRIBAUDO, L. p 2734 N94-26161
GRIFFEE, J. W. p 3116 N94-27793
GRIFFIN, C. J. p 3051 N94-25885
GRIFFIOEN, ERIK p 2994 N94-26640
GRIFFITH, J. W. p 3063 N94-26958
GRIFFITH, JON p 2901 N94-26086
GRIJPMA, DIRK WYBE p 2747 N94-25748
GRINDSTAFF, B. K. p 2863 N94-28129
GRINSTEIN, B. p 3021 N94-26759
GRISHIN, V. G. p 3031 N94-25850
GRISNIK, STANLEY P. p 2690 N94-26142
GRISWOLD, SAMANTHA S. p 2943 N94-25681
GROEBNER, R. J. p 3045 N94-26950
p 3048 N94-27791
GROEGER, HERBERT A. p 2663 N94-28248
GROENEBOOM, PIET p 3002 N94-26213
GROENVOLD, BENT p 2768 N94-26232
GRONDIN, JANET W. p 2679 N94-25740
GRONDIN, PATRICK J. p 3037 N94-27102
GRONG, O. p 2741 N94-27325
GROSSBONGARDT, HEINRICH p 2663 N94-28249
GROSSMAN, G. p 2854 N94-26053
GROSSMAN, J. W. p 3039 N94-27721
GROTH, CLINTON P. T. p 2799 N94-27880
GROVEMAN, BRIAN S. p 2814 N94-27981
GROVES, S. E. p 2707 N94-26099
GRUEBEL, G. p 2732 N94-26004
GRUEN, D. M. p 3053 N94-26031
p 3055 N94-26275
p 3062 N94-26934
GRUNES, MITCHELL R. p 2945 N94-28253
GRUNLOH, H. J. p 3043 N94-26323
GRUSS, K. p 3060 N94-26840
GU, Y. p 2688 N94-27373
GUACCI, GIOVANNI p 2689 N94-25682
GUARD, CHARLES P. p 2896 N94-27025
GUDKOV, V. P. p 2714 N94-26170
GUEDOU, PHILIPPE p 2953 N94-26742
GUENZEL, UDO p 2662 N94-28242
GUESS, T. R. p 2836 N94-26032
GULAKOWSKI, STEPHEN p 2716 N94-26487
GUMASTE, U. p 2845 N94-28181
GUNDO, DAN p 2901 N94-26086
GUNION, J. F. p 3022 N94-26793
GUO, ZHENPING p 2822 N94-26642
GUODONG, LI p 2758 N94-27845
GUPTA, K. K. p 2691 N94-27868
GURUSWAMY, GURU P. p 2645 N94-26538
GURZHIEV, S. N. p 2810 N94-26395
GUSEVA, Z. M. p 3112 N94-25625
p 3112 N94-25626
p 3112 N94-25627
GUSSENHOVEN, M. S. p 2878 N94-26338
GUSTAFSON, N. B. p 2702 N94-26542
GUTMAN, DAVID p 3013 N94-25816
GUZDAR, P. p 3044 N94-26523
GUZMAN, E. p 3074 N94-27636

H

HAALAND, D. M. p 2713 N94-25978
p 2716 N94-26794
HAALAND, P. D. p 2753 N94-26822
HABAZAKI, HIROKI p 2745 N94-28164
p 2722 N94-28165
p 2745 N94-28166
HACHICHA, MOHAMED p 2776 N94-27345
HACKEL, L. A. p 2818 N94-26699
p 2819 N94-27018
HACKNEY, A. C. p 2936 N94-28374
HADDADANDALAG, R. E. p 2734 N94-26162
HADLAR, P. p 3060 N94-26771

HAENNINEN, HANNU p 2837 N94-26262
HAENNINEN, HEIKKI p 2848 N94-26258
HAFIZI, B. p 2820 N94-27671
HAGA, KAZUKO p 2931 N94-27534
HAGA, TATSUYA p 2931 N94-27534
HAGEN, C. R. p 3008 N94-25988
HAGEN, HANS p 2990 N94-25594
HAGIWARA, MASUO p 2726 N94-25566
HAHN, EDWARD p 2641 N94-27286
HAHN, M. T. p 2832 N94-28209
HAHSIMOTO, KENKI p 2729 N94-25579
HAILEY, J. p 2698 N94-25700
HAINES, D. M. p 2876 N94-25752
HAINES, R. F. p 2945 N94-28252
HAIPING, GUO p 2742 N94-27730
HAISS, HERMAN S. p 2760 N94-28226
HAKALA, HANNU p 2664 N94-25808
HAKUSUI, SHIGETAKA p 2930 N94-27533
HALBIG, J. K. p 2813 N94-27624
HALDAR, P. p 3055 N94-26243
p 2783 N94-26589
p 2740 N94-26957
HALECKI, ANTHONY p 2689 N94-25674
HALL, D. J. p 2655 N94-28337
HALL, DAVID p 2864 N94-28134
HALL, J. STORRS p 2687 N94-27367
HALL, KENNETH C. p 2675 N94-27654
HALL, STEPHEN R. p 2780 N94-25770
HALL, STEVE p 2863 N94-28122
HALLER, E. E. p 3054 N94-26095
HALLIKAINEN, M. p 2689 N94-28358
HALLORAN, TIMOTHY J. p 3096 N94-25765
p 2958 N94-25799
HALPERT, GERALD p 2860 N94-28103
p 2860 N94-28105
HALZEN, F. p 3017 N94-26043
HAMAGUCHI, YASUMASA p 2842 N94-27207
HAMAKAWA, YOSHIHIRO p 2761 N94-28002
HAMANO, RYUICHI p 2726 N94-25567
HAMBLIN, DAVID p 2762 N94-25775
HAMBY, THOMAS p 2833 N94-25675
HAMEED, S. p 2897 N94-27571
HAMILTON, M. L. p 2737 N94-26575
HAMILTON, MARK F. p 3010 N94-26983
HAMLING, STEVEN p 2760 N94-25705
HAMMEL, P. C. p 3050 N94-25817
HAMMER, C. p 2868 N94-26952
HAMMONS, B. E. p 3056 N94-26308
HAMNER, KENNETH L. p 2834 N94-25896
HAN, JAE MIN p 2816 N94-26157
p 2714 N94-26158
HAN, JIANFENG p 2752 N94-26661
HAN, MOON HEE p 2894 N94-26469
HANADA, KEIJI p 2871 N94-28155
HANAWA, HIROMI p 2788 N94-27821
HANAYA, MINORU p 2718 N94-27389
HANEY, S. p 3044 N94-26860
HANNUKI, TOSHIO p 2884 N94-27966
HANSEN, FRANK V. p 2895 N94-26846
HANSEN, K. p 2681 N94-27594
HANSER, D. p 3060 N94-26840
HANSER, FREDERICK p 2698 N94-28210
p 2698 N94-28217
HANSMAN, R. JOHN p 2641 N94-27286
p 2641 N94-27287
HANSON, DONALD B. p 2675 N94-27778
HANSON, G. p 3033 N94-27614
HANSON, H. p 2785 N94-26797
HANSON, K. M. p 3005 N94-27816
HANSON, R. K. p 2800 N94-28008
HANSSMANN, HEINZ p 3009 N94-26968
HARA, M. p 2755 N94-27087
HARADA, HIROSHI p 2723 N94-25550
HARADA, YASUO p 2770 N94-26626
HARAGUCHI, TADASHI p 2904 N94-27467
p 2904 N94-27468
HARGIS, P. J. p 2704 N94-27708
HARIJONO, IR. SRI WORO B. p 2873 N94-28277
HARMER, MARTIN P. p 3062 N94-26892
HARMON, ALAN B. p 3114 N94-26686
HARMON, B. A. p 3114 N94-26688
p 3115 N94-26690
HARMON, T. J. p 2702 N94-26542
p 2703 N94-27213
HARRELL, BROCK p 2943 N94-25693
HARRINGTON, ROGER F. p 2771 N94-26844
HARRIS, BERNARD A. p 2934 N94-28361
HARRIS, GEORGE D. p 2664 N94-25810
HARRIS, J. W. p 3017 N94-26083
HARRIS, JOEL p 2759 N94-26437
HARRIS, P. p 2833 N94-25691
HARRISON, GORDON p 2708 N94-26895
HARTMANN, LEE W. p 3105 N94-27428
HARVEY, J. K. p 2644 N94-26248
HASE, ANNELI p 2714 N94-26251
HASEGAWA, KATSUO p 2764 N94-27976
p 2764 N94-27979
p 2764 N94-27980
HASEGAWA, RYOSUKE p 2721 N94-25569
p 2682 N94-25586
HASEGAWA, S. p 3112 N94-25628
p 3113 N94-25629
p 3113 N94-25630
HASEGAWA, TAKUYA p 3030 N94-27877
HASELTON, H. H. p 2713 N94-26014
HASHIBA, MOTOYUKI p 2914 N94-27456
HASHIDA, TOSHIYUKI p 2710 N94-27279
p 2710 N94-27280
HASHIMOTO, KATSUMI p 3114 N94-25634
HASHIMOTO, KOJI p 2745 N94-28164
p 2722 N94-28165
p 2745 N94-28166
HASHIMOTO, MISAO p 2761 N94-28002
HASHIMOTO, RYOZO p 2905 N94-27489
HASHIMOTO, SHINYA p 2722 N94-25545
HASHIMOTO, TATSUO p 2736 N94-26477
HASKIN, F. E. p 2700 N94-25956
HASSAM, A. p 3044 N94-26523
HASSAN, A. R. p 3051 N94-25851
p 3071 N94-25852
HASSOUNI, Y. p 2996 N94-26898
HASTERT, JAMES L. p 3066 N94-27276
HATAKEYAMA, HIDEO p 2776 N94-27340
HAUN, MICHAEL J. p 2748 N94-25854
HAWBOLDT, R. J. p 2654 N94-28328
HAWKEN, D. F. p 2658 N94-28351
HAWKINS, C. F. p 2781 N94-25977
HAYAKAWA, MASAHIKO p 2885 N94-27973
HAYAMIZU, HIROHIDE p 2871 N94-28155
HAYAMIZU, SATORU p 2775 N94-27249
HAYAMIZU, SAYOKO p 2911 N94-27443
p 2912 N94-27445
HAYASAKA, SHIZU p 2904 N94-27470
p 2904 N94-27471
p 2905 N94-27484
HAYASHI, AKIHIKO p 3051 N94-25921
p 3053 N94-26089
HAYASHI, KAZUNORI p 2727 N94-25571
HAYASHI, NOBUYOSHI p 2949 N94-26720
HAYASHI, YASUNORI p 2744 N94-27876
HAYNES, DAVY A. p 2692 N94-27774
HAYNES, T. E. p 3062 N94-26932
HAYNES, W. M. p 2719 N94-27567
HAYOASHI, S. p 3060 N94-26771
HAYS, J. A. p 2704 N94-26779
HAZE, IKUYA p 2761 N94-27341
HE, QI-BING p 3049 N94-27855
HE, QISHENG p 2819 N94-26940
HE, X. G. p 3014 N94-25841
HE, XIAO-GANG p 2990 N94-25838
p 3014 N94-25888
HEADLEY, T. J. p 3053 N94-26025
p 3061 N94-26856
HEARN, W. E. p 2787 N94-27618
HEBERT, MARTIAL p 2809 N94-25967
p 2986 N94-27032
p 2967 N94-27064
HECHMER, J. L. p 2737 N94-26582
HECHT, S. L. p 2736 N94-26522
HECK, P. p 2688 N94-27373
HED, P. P. p 2763 N94-26804
HEDGEDUS, CHARLES R. p 2755 N94-27111
HEELGE, B. p 2773 N94-27159
HEEMSKERK, J. A. p 2809 N94-25637
HEEREN, R. M. A. p 3025 N94-27348
HEIDAN, ELISABETH p 2660 N94-28230
HEIKKILA, LIISA p 3031 N94-25621
HEIN, C. p 2878 N94-26338
HEIN, C. A. p 2698 N94-28200
p 3040 N94-28202
HEINISCH, H. L. p 3017 N94-26049
HEINSON, A. P. p 3052 N94-25972
HEINTZE, NEVIN p 3002 N94-25903
HEITZENROEDER, P. p 3045 N94-26863
HELLER, M. p 2838 N94-26501
HELLSTROM, ROB p 2703 N94-25690
HELTON, K. T. p 2937 N94-26346
HENAGER, C. H., JR. p 2705 N94-25805
p 2737 N94-26585
HENDERSON, D. R. p 2721 N94-28069
HENDERSON, WILLIAM K. p 2695 N94-26750
HENDRICKS, P. p 3098 N94-26398
HENDRICKSON, B. p 2962 N94-26370
HENDRIXSON, JEFF p 3036 N94-26981
HENRION, MAX p 3095 N94-27866
HENRY, RONALD p 2755 N94-27148
HENSHALL, G. A. p 2706 N94-25938
HERDEG, WOLFGANG p 2768 N94-26317
HERMAN, I. p 2971 N94-27552
HERMANN, M. R. p 2819 N94-27018
HERNANDEZ, O. F. p 3016 N94-26040
HERNDON, RUSSELL R. p 2949 N94-26719
HERRMANN, W. p 3099 N94-27022
HERTZBERGER, BOB p 2955 N94-27194
HESSEL, MICHAEL I., JR. p 2903 N94-25673
HESSLINK, R. p 2909 N94-26173
HETHERINGTON, D. L. p 3052 N94-25989
HETU, NATHALIE p 2793 N94-26637
HEURING, VINCENT P. p 3037 N94-26990
HEUS, R. p 2940 N94-25724
HEUSSI, HAROLD p 2709 N94-26978
HEWETT, D. W. p 2767 N94-25937
HIBBS-BRENNER, MARY p 2782 N94-26344
p 3036 N94-26857
HIBINO, K. p 3116 N94-27607
HICKEY, JOHN R. p 2814 N94-27981
HICKMAN, G. p 2863 N94-28127
HIDAKA, HIROYOSHI p 2904 N94-27477
p 2905 N94-27486
HIGASHI, K. p 2748 N94-25959
HIGASHIMURA, TAKENORI p 3065 N94-27240
HIGASHIYAMA, ATSUKI p 2915 N94-27461
HIGUCHI, KAZUNORI p 2986 N94-27032
p 2967 N94-27064
HIKAMI, S. p 3068 N94-27677
HILL, J. C. p 3031 N94-26097
HILL, RALPH H. p 3035 N94-25941
HILLARD, ROBERT C. p 2691 N94-26153
HILLEBRAND, HELGA L. p 2661 N94-28234
HILLIS, D. L. p 3048 N94-27785
HILLIS, DAVID B. p 3034 N94-25940
HILLS, C. R. p 3057 N94-26420
HILLS, J. G. p 2889 N94-28301
HILTON, KEVIN p 2943 N94-25680
HINMAN-SWEENEY, E. M. p 2943 N94-27952
HINO, KEN-ICHI p 3026 N94-27620
HINSHELWOOD, DAVID p 3045 N94-27074
HINTON, D. A. p 2677 N94-26593
HINTON, F. L. p 3048 N94-27791
HIPPINEN, I. p 2876 N94-28383
p 2876 N94-28394
p 2876 N94-28395
HIPWELL, DEAN P. p 2937 N94-25774
HIRAI, MASANAO p 2869 N94-28148
HIRANO, TATSUMI p 2724 N94-25553
HIRANO, TOSHIYUKI p 2682 N94-25586
HIRANO, YOICHI p 3046 N94-27350
HIRASAWA, TAKEO p 2882 N94-27342
p 2883 N94-27963
p 2779 N94-27964
HIRATA, K. S. p 3028 N94-27759
HIRAYAMA, HIDEO p 3032 N94-26543
HIROBE, RYOSUKE p 2886 N94-27987
HIROI, YOSHIKUNI p 2882 N94-27342
p 2883 N94-27963
HIROSE, FUMIO p 2728 N94-25576
p 2729 N94-25578
HIROTA, EIICHI p 2745 N94-28164
HIRST, DONALD J. p 2755 N94-27111
HIRTH, J. P. p 2705 N94-25805
p 2732 N94-25987
HISKES, R. p 2757 N94-27716
HITE, SID W., III p 2823 N94-26986
HIUE, HISAAKI p 2788 N94-27817
HIXENBAUGH, FRANKLIN D. p 2695 N94-26532
HJALMARRSSON, KARIN p 2902 N94-27045
HJORTLAND, OLE EDVARD p 2837 N94-26233
HO, WILSON p 3063 N94-26965
HOANG, TY p 2671 N94-25710
HOCHBERG, A. K. p 2738 N94-26610
HODGE, B. K. p 2794 N94-26763
HODGE, C. C. p 3009 N94-27131
HODSON, ROBERT F. p 2815 N94-27907
HODUR, RICHARD M. p 2892 N94-25793
HOEFINGHOFF, DIRK p 2660 N94-28230
p 2663 N94-28247
HOEHN, J. G., JR. p 2740 N94-26957
HOELLER, HARTMUT p 2897 N94-27751
HOEPMAN, JAAP-HENK p 2955 N94-27547
HOETGER, DEBORA C. p 2691 N94-25696
HOFFMAN, A. p 3023 N94-26929
HOFFMAN, D. J. p 2767 N94-25924
p 3041 N94-25933
p 3046 N94-27261
p 3046 N94-27568
HOFFMAN, R. W. p 2753 N94-26822
HOFFMAN, ROSS p 2898 N94-28223
HOFFMANN, CHRISTOPHER p 3081 N94-25703
HOFFMANN, L. p 3003 N94-26385
p 3070 N94-27995
HOFSTETTER-DEGEN, K. p 2914 N94-27456
HOGAN, DAVID B. p 2947 N94-28264
HOGAN, J. T. p 3048 N94-27785
HOGAN, TIMOTHY D. p 3034 N94-25742
HOHEISEL, HEINZ p 2675 N94-27739
HOLDO, A. E. p 2805 N94-28036
HOLICK, MICHAEL F. p 2935 N94-28368
HOLLAND, ELIZABETH A. p 2877 N94-25877
HOLLANDER, M. G. p 3069 N94-27828

HOLLANSWORTH, JAMES E. p 2693 N94-27427
HOLLOWAY, L. E. p 3029 N94-27815
HOLLOWAY, PAUL H. p 2786 N94-27079
HOLM, MIKAEL p 2848 N94-26253
HOLM, U. p 2814 N94-28098
HOLMBERG, COURTNEY D. p 3014 N94-25875
HOLMGREN, M. p 2842 N94-27197
HOLOPAINEN, TIMO p 2836 N94-25650
HOLT, ALAN C. p 2687 N94-27368
HOLT, KEVIN p 2683 N94-26281
HOLZSCHEITER, K. p 3052 N94-25972
HONAKER, DAVID p 2833 N94-25704
HONDA, K. p 3112 N94-25628
p 3113 N94-25629
p 3113 N94-25630
HONDA, KEN p 3114 N94-25634
HONDA, YUKO p 3053 N94-26071
p 2736 N94-26477
HONDO, TAKEO p 2885 N94-27969
HONG, G. W. p 3057 N94-26404
HONG, KYAE WON p 2783 N94-26546
HONG, R. M. p 3045 N94-26865
HONG, SHUGUANG p 2975 N94-27936
p 2975 N94-27937
p 2975 N94-27938
p 2975 N94-27939
HONG, SUK BOONG p 2894 N94-26469
HONG, TONGMINH p 2813 N94-27651
HONG, WEON SEON p 2910 N94-26549
HONJO, HARUO p 2907 N94-27513
p 2908 N94-27514
p 2908 N94-27515
p 2908 N94-27516
p 2908 N94-27537
HONMA, KAZUHIRO p 2728 N94-25577
HOOGERLAND, MAARTEN DIRK p 2817 N94-26225
HOOMAN, JOZEF p 2966 N94-26971
HOOPER, JOAN p 2671 N94-25713
HOOVER, ERIC p 2672 N94-26030
HOOVER, JAMES p 2755 N94-27148
HOOVER, SCOTT M. p 2747 N94-28187
HOPE, U.-P. p 2876 N94-25807
HOPPE, R. G. p 2737 N94-26582
HOPPEL, KARL p 2945 N94-28253
HOPPER, DOUGLAS J. p 2694 N94-25776
HORI, MASATSUGU p 2932 N94-27541
HORIUCHI, RYO p 2729 N94-25580
HORNER, G. p 2833 N94-25691
HOROWITZ, JAY G. p 2686 N94-27362
HORTON, W. p 3041 N94-25923
p 2791 N94-26096
p 3047 N94-27723
HORVAT, CHRISTINE p 2942 N94-27114
HORVATH, I. p 3029 N94-27814
HOSANGADI, A. p 2804 N94-28030
HOSHIAI, TAKAO p 2882 N94-27342
p 2883 N94-27963
HOSHIMOTO, KENICHI p 2723 N94-25550
p 2727 N94-25568
HOSHIYAMA, MINORU p 2928 N94-27520
HOSODA, SAICHI p 2904 N94-27467
p 2904 N94-27468
HOSOE, NOBUYUKI p 2681 N94-27247
HOSONO, FUMIKAZU p 2788 N94-27821
HOTTA, N. p 3116 N94-27607
HOUBEN, G. J. p 2966 N94-26955
HOVER, G. L. p 2848 N94-26277
HOWARD, A. J. p 2780 N94-25664
p 3056 N94-26308
HOWARD, R. P. p 2713 N94-25964
HOWARD, RUSSELL A. p 2945 N94-28253
HOWELLS, M. R. p 2814 N94-27779
HOZAWA, MITSUNORI p 2717 N94-27386
HRENYA, C. p 2792 N94-26319
HROVAT, DANIEL p 2765 N94-25728
HSIEH, C. L. p 3043 N94-26274
HSU, WEN L. p 3049 N94-25601
HU, BAOGANG p 2843 N94-27585
HU, J. G. p 3055 N94-26243
HUANG, JEN-KUANG p 2682 N94-27908
HUANG, JING p 3035 N94-26383
HUANG, LIN p 3049 N94-27855
HUANG, Q. p 3116 N94-27607
HUANG, QIANG p 3054 N94-26139
HUANG, T. C. p 3058 N94-26514
HUANG, X. p 2991 N94-26215
HUANG, XI p 2894 N94-26628
HUBBARD, C. W. p 2664 N94-26309
HUBBE, J. M. p 2895 N94-26761
HUBER, B. T. p 2889 N94-28303
HUCEK, DOUGLAS RICHARD R. p 2814 N94-27981
HUDSON, JEFFREY A. p 2941 N94-26984
HUEBNER-MOTHS, JANIS p 2943 N94-25706
HUEBNER, W. p 2857 N94-26747
HUEY, BEVERLY M. p 2941 N94-26964
HUFFSTETLER, MARK p 2671 N94-25708
HUGHES, P. J. p 2866 N94-26123
HUGHES, ROBERT ALAN p 3039 N94-27962
HUGHETT, P. p 2996 N94-26936
HUGHETT, PAUL p 2809 N94-25662
p 2957 N94-25663
HUHTANEN, RISTO p 2762 N94-26259
HUIJSER, T. p 2811 N94-26647
HULEN, H. p 2948 N94-26578
HULL, J. R. p 3008 N94-26421
HULL, L. M. p 2797 N94-27705
HULL, R. p 3055 N94-26239
HUMBERT, P. p 2952 N94-26736
HUMBERT, WILLIAM R. p 3032 N94-26881
HUMMELS, DONALD M. p 2783 N94-26491
HUMMER, G. p 3030 N94-28001
HUMPHERYS, MARK A. p 2752 N94-26708
HUNDSDORFER, W. H. p 2867 N94-26216
HUNG, KENNY KING-MING p 2786 N94-27303
HUNG, R. J. p 2824 N94-27221
p 2799 N94-27931
HUNN, BRUCE P. p 2910 N94-26847
HUNN, J. D. p 3054 N94-26137
HUNTER, STEVEN p 2827 N94-27722
HUNTER, WILLIAM R. p 2756 N94-27675
HUO, A. X. p 3116 N94-27607
HURST, D. W. p 2800 N94-28005
HUSS-LEDERMAN, S. p 2973 N94-27717
HUSSEIN, M. T. p 3016 N94-26010
p 3030 N94-27994
HWANG, CHURL KEW p 3042 N94-26159
HWANG, E. p 2868 N94-26952
HWANG, SOON MO p 3042 N94-26159
HWANG, WARREN p 2862 N94-28116
p 2863 N94-28122
HWANG, WON TAE p 2894 N94-26469
HWU, WEN-MEI W. p 2964 N94-26680
HYATT, A. W. p 3045 N94-26950

I

IBIDUNNI, A. O p 2753 N94-26770
ICE, G. E. p 3065 N94-27251
ICHIKAWA, AYUMI T. p 2905 N94-27491
ICHIKAWA, HIROYASU p 2870 N94-28149
p 2870 N94-28151
ICHIKAWA, MASUMI p 2914 N94-27455
ICHIKAWA, SHIN-ICHIRO p 2949 N94-26716
IGNATOV, V. V. p 2879 N94-26502
IIDA, MASATO p 2907 N94-27507
IIDA, TAKESHI p 3065 N94-27240
IKEDA, SADAO p 2723 N94-25548
IKEDA, SEIICHI p 2729 N94-25580
IKEDA, SHOZO p 2722 N94-25544
p 2727 N94-25571
IKEDA, SUSUMU p 2719 N94-27822
IKEDA, YUJI p 2727 N94-25570
IKEUCHI, KATSUSHI p 2986 N94-27032
p 2967 N94-27064
IKOMA, KEIKO p 3064 N94-27232
ILGISONIS, V. I. p 3041 N94-25792
ILIN, I. V. p 2879 N94-26502
ILINA, A. N. p 2879 N94-26502
ILINCA, A. p 2653 N94-28326
p 2657 N94-28347
ILYAS, MOHAMMED p 2874 N94-28285
IMADA, MASATOSHI p 3065 N94-27248
IMAGAWA, TAKASHI p 2870 N94-28152
IMAI, HIROMI p 2928 N94-27523
IMAI, KIWAMU p 2675 N94-27608
IMAI, RYOJI p 2761 N94-27341
IMAI, TAKAYOSHI p 2904 N94-27471
IMHOF, WILLIAM L. p 3115 N94-26790
IMMONEN, P. J. p 2966 N94-26921
IN, SANG RYUL p 3042 N94-26159
INAMURA, KINSAKU p 2929 N94-27528
INCE, N. Z. p 2803 N94-28024
INDACOCHEA, E. p 2857 N94-26583
INENAGA, ANDREW S. p 2647 N94-26706
ING, J. L. p 3070 N94-28067
INGELS, FRANK M. p 2968 N94-27168
INGERSOLL, D. p 2780 N94-25975
INGHAM, EDWARD A. p 2694 N94-25659
INNANEN, K. A. p 2890 N94-28305
INOMATA, SHINJI p 2973 N94-27732
INOUE, AKIHISA p 2746 N94-28167
p 2746 N94-28168
p 2746 N94-28169
p 2746 N94-28170
p 2746 N94-28171
INOUE, K. p 3028 N94-27759
INOUE, KIYOSHI p 2724 N94-25557
p 2725 N94-25559
INOUE, MANABU p 2905 N94-27483
INOUE, MINORU p 2904 N94-27470
p 2904 N94-27472
p 2905 N94-27484
p 2905 N94-27485
p 2905 N94-27486
p 2905 N94-27489
p 2905 N94-27490
p 2905 N94-27491
p 2906 N94-27493
INOUE, NAOYA p 3114 N94-25634
INOUYE, MINORU p 2904 N94-27471
IPRI, A. C. p 2672 N94-26340
IRICK, S. C. p 2816 N94-26130
IRIE, HIROSADA p 2722 N94-25546
p 2726 N94-25566
IRONS, FRED H. p 2783 N94-26491
ISAACS, H. S. p 2753 N94-26770
ISACKS, BRYAN L. p 3098 N94-26490
ISAGO, HIROAKI p 2725 N94-25562
p 2721 N94-25569
ISEKI, TOMOKO p 2906 N94-27495
p 2906 N94-27496
p 2906 N94-27497
p 2906 N94-27498
ISHIDA, MIZUHO p 2886 N94-27986
ISHIDA, T. p 3028 N94-27759
ISHIGE, YASUO p 2949 N94-26716
ISHIHARA, TADAO p 2722 N94-25547
ISHII, M. p 2792 N94-26468
ISHII, T. p 3065 N94-27239
ISHIKAWA, KEISUKE p 2724 N94-25556
ISHIKAWA, MASAYASU p 3049 N94-25614
ISHIKAWA, NOBUYUKI p 2989 N94-27809
ISHIKAWA, YOJI p 2761 N94-28002
ISHISAKA, TADASHI p 2853 N94-27990
ISHIZAWA, KENJI p 2884 N94-27966
ISLAM, A. K. M. A. p 3051 N94-25914
ISOBE, YOSHINAO p 3100 N94-27336
ISODA, YUKIHIRO p 2728 N94-25577
ISONO, TAKAAKI p 2788 N94-27821
ISTACE, OLIVIER p 2970 N94-27545
ITO, ATSUKO p 2756 N94-27241
ITO, H. p 3112 N94-25628
p 3113 N94-25629
p 3113 N94-25630
ITO, HIROSHI p 2723 N94-25548
ITO, KATSUHIRO p 2675 N94-27608
ITO, KIKUO p 2725 N94-25559
p 2725 N94-25560
ITO, KIYOSHI p 2885 N94-27973
ITO, OSAMU p 2704 N94-27387
ITO, TETSUJI p 2915 N94-27460
ITSUKAICHI, ATSUSHI p 2949 N94-26716
IVANITSKAYA, LIDIA p 3009 N94-27108
IVANOV, A. N. p 3022 N94-26900
IVANOV, S. V. p 3032 N94-26165
IVANOV, V. G. p 3013 N94-25828
IVANOVSKIJ, S. A. p 3020 N94-26511
IVANYUSHENKOV, YU. M. p 3024 N94-27250
IVKIN, A. V. p 3020 N94-26507
IWAIZUMI, MASAMOTO p 2718 N94-27388
IWANAGA, HIROSHI p 3069 N94-27756
IWASA, YUKIKAZU p 2725 N94-25559
IWASAKI, SATOSHI p 2723 N94-25552
IWASE, SATOSHI p 2912 N94-27445
p 2915 N94-27458
p 2915 N94-27459
p 2918 N94-27473
p 2918 N94-27474
p 2928 N94-27521
p 2929 N94-27524
p 2929 N94-27525
p 2929 N94-27526
p 2929 N94-27528
p 2930 N94-27529
p 2930 N94-27532
p 2930 N94-27533
IWASHITA, HIROYUKI p 2776 N94-27340
IWATA, HIROKAZU p 2907 N94-27508
IWATA, SHUICHI p 2727 N94-25568
IYER, A. N. p 2783 N94-26589
p 2740 N94-26957
IYER, R. H. p 2715 N94-26392
IYER, RAVISHANKAR K. p 2948 N94-26714
IZAGUIRRE, ALDO p 2880 N94-26828
IZAKI, K. p 3112 N94-25628
p 3113 N94-25629
p 3113 N94-25630
IZAWA, MASAAKI p 2787 N94-27606
IZMAILOV, I. A. p 3013 N94-25827
IZU, M. p 2859 N94-27610
IZUKA, YOSHIHISA p 2722 N94-25544
IZUMI, YATAKA p 2892 N94-25873

J

JAAKKOLA, SIPI p 2850 N94-27182
p 2850 N94-27183

JABLIN, M. H. p 2932 N94-27556
JABLONSKI, D. p 2889 N94-28302
JACKSON, JAMES N. p 2939 N94-27056
JACOBSEN, C. J. p 2814 N94-27779
JACOBSON, CLAS A. p 2987 N94-27124
JACOBSON, TOMMY p 2762 N94-26259
JACQUIN, L. p 2659 N94-28039
JACQUOTTE, OLIVIER P. p 2846 N94-28266
JAEGER, E. F. p 3046 N94-27568
JAHKOLA, A. p 2876 N94-28383
p 2876 N94-28394
p 2876 N94-28395
JALOVAARA, J. p 2876 N94-28383
p 2876 N94-28395
JAMES, B. A. p 2737 N94-26582
JAMES, C. A. p 2794 N94-26763
JAMES, EDWARD p 2760 N94-28222
JAMES, G. H. p 2859 N94-27004
JAMES, P. p 2832 N94-28174
JAMES, ROBERT I. p 3059 N94-26703
JAMIESON, D. N. p 3056 N94-26364
p 3063 N94-26987
JAMSEK, DAMIR p 2956 N94-28267
JANNSON, TOMASZ p 2783 N94-26536
JANOSSY, ANDRAS p 2965 N94-26908
JANOWITZ, JOAN p 2672 N94-26028
JANSWEIJER, P. P. M. p 2779 N94-25620
JANUS, M. C. p 2719 N94-27712
JARC, DUANE J. p 2967 N94-27060
JARRE, F. p 2967 N94-27031
JARVIS, CHRISTINE W. p 2835 N94-26833
JASON, NORA H. p 2763 N94-26756
JASSBY, D. L. p 3048 N94-27825
JAVEDANI, J. p 2688 N94-27373
p 3047 N94-27715
JAVEDANI, J. B. p 2701 N94-26537
JAVORSKI, CHRISTIAN T. p 2671 N94-25719
JAYARAM, R. p 2734 N94-26272
JENG, RU J. p 2709 N94-27107
JENSEN, RICHARD p 2669 N94-27273
JEONG, DO YOUNG p 2817 N94-26402
JEONG, DO YUNG p 2714 N94-26158
JEONG, SEUNG HO p 3042 N94-26159
JEROSZKO, R. A. p 2719 N94-27854
JERRUM, M. p 2980 N94-26473
JESSEN, PAUL F. p 2898 N94-26076
JETHRA, A. K. p 2981 N94-26903
JIA, H. Y. p 3116 N94-27607
JIAN, CHEN p 2742 N94-27730
JIANG, G. Z. p 3116 N94-27607
JIANG, H. p 2753 N94-26822
JIANG, JIXI p 2895 N94-26678
JIANG, XIANHUA p 3102 N94-26669
JIANG, XIN L. p 2709 N94-27107
JIJIWA, HIROYASU p 2914 N94-27455
p 2927 N94-27518
JIMENEZ, J. p 3055 N94-26194
JOENSSON, DANIEL p 2849 N94-26848
JOHANSSON, A. p 2867 N94-26241
JOHANSSON, B. p 2774 N94-27219
JOHANSSON, E. S. p 2773 N94-27159
JOHN, SARAH p 3114 N94-26550
JOHNSON, ANDREW E. p 2984 N94-25591
JOHNSON, BRYAN p 2760 N94-25705
JOHNSON, C. S. p 2780 N94-25806
JOHNSON, CHRIS J. p 2863 N94-28128
JOHNSON, D. D. p 2736 N94-26351
JOHNSON, D. R. p 2750 N94-26332
JOHNSON, ERIC C. p 2753 N94-26842
JOHNSON, L. C. p 3048 N94-27825
JOHNSON, LANE R. p 2878 N94-26433
JOHNSON, MICHAEL C. p 2765 N94-25676
JOHNSON, R. R. p 3014 N94-25840
JOHNSON, R. WAYNE p 2844 N94-27824
JOHNSON, ROBERT L. p 2789 N94-25587
JOHNSON, THOMAS D., JR. p 2647 N94-27161
JOHNSON, W. STEVEN p 2711 N94-27658
JOHNSON, WAYNE p 2644 N94-26143
JOHNSTON, G. W. p 2656 N94-28341
JOHNSTON, ROGER G. p 2719 N94-27728
JOHNSTON, THOMAS A. p 2644 N94-26191
JOKERST, SCOTT F. p 2947 N94-25648
JONES, ALAIN L. p 2773 N94-27127
JONES, D. A. p 2795 N94-27252
JONES, D. J. p 2656 N94-28338
p 2656 N94-28340
JONES, D. P. p 2737 N94-26582
JONES, E. p 2698 N94-25700
JONES, E. D. p 3056 N94-26352
JONES, G. D. p 2653 N94-28325
p 2654 N94-28329
JONES, G. H. p 3044 N94-26858
JONES, H. D. T. p 2716 N94-26794
JONES, R. D. p 2985 N94-25983
JONES, R. E. p 2821 N94-25970
JONES, R. H. p 2732 N94-25987
p 2838 N94-26524
JONES, W. P. p 2803 N94-28025
JONGBLOED, GEURT p 3002 N94-26213
JONGSMA, TJEERD p 2712 N94-25747
JOPPE, J. L. p 3038 N94-27137
JORDAN, S. p 3098 N94-26398
JORGENSEN, J. L. p 2960 N94-26118
JOSE, D. L. p 2672 N94-26340
JOSHI, M. C. p 2651 N94-28197
JOURDAN, T. p 2952 N94-26736
JOYCE, GLENN p 2820 N94-27671
JOYNER, RONALD W. p 2931 N94-27535
JUBIEN, CHRIS M. p 2985 N94-26629
JUDY, J. R. p 3096 N94-25813
JULHE, ALAIN p 2950 N94-26722
JUN, OH-SUNG p 2828 N94-28041
JUNG, CHIN MANN p 2816 N94-26184
p 2817 N94-26185
p 2817 N94-26403
p 2818 N94-26520
JUNGERT, ERLAND p 2849 N94-26848
JUNGWIRTH, K. p 3048 N94-27836

K

KABIR, NURUL p 2905 N94-27486
KACHAEV, I. A. p 3024 N94-27250
KACHKACHI, H. p 3074 N94-27627
KACHKACHI, M. p 3074 N94-27627
KACHRU, RAVINDER p 3037 N94-27010
KADDOUR, F. O. p 3006 N94-26411
KADOO, ATSUSHI p 2933 N94-27943
KADOTA, K. p 2820 N94-27701
KADOWAKI, KAZUO p 2722 N94-25544
KAEMAERAEINEN, J. p 2900 N94-28393
KAERKI, SATU p 2822 N94-26306
KAFYEKE, F. p 2653 N94-28324
KAGAYA, YUTAKA p 2721 N94-25569
KAIBARA, SHOICHIRO p 2761 N94-27341
KAIEDA, YOSHINARI p 2721 N94-25561
p 2726 N94-25566
KAINUMA, NORIO p 2726 N94-25566
KAISE, MASATSUGU p 2727 N94-25571
KAJITA, T. p 3028 N94-27759
KAKUTA, YOSHIAKI p 2842 N94-27207
KALAOJA, JARMO p 2961 N94-26254
KALBERER, MARTIN p 2760 N94-25705
KALEVA, S. I. p 3007 N94-25603
KALINOVSKIJ, YU. L. p 3013 N94-25836
p 3020 N94-26505
KALISH, R. p 3056 N94-26364
p 3023 N94-26929
KALISKI, J. p 2957 N94-25761
p 2958 N94-25762
KALKER, J. J. p 2837 N94-26214
p 2996 N94-26967
KALLENBERG, W. C. M. p 3004 N94-27223
KALLIES, W. p 3013 N94-25836
KAMADA, TAKENOBU p 2932 N94-27541
KAMBE, FUKUSHI p 2905 N94-27479
p 2905 N94-27480
KAMEI, SHIN-ICHI p 2761 N94-28002
KAMEYAMA, KIMIHIKO p 2931 N94-27534
KAMINUMA, KATSUTADA p 2882 N94-27342
p 2883 N94-27963
p 2885 N94-27973
KAMITANI, TAKUYA p 2816 N94-26112
KAMIYA, KAICHIRO p 2906 N94-27503
p 2907 N94-27506
p 2907 N94-27508
KAMIYA, YUKIHIDE p 2787 N94-27606
KAMIYAMA, SHINYA p 2871 N94-28157
KAMLET, MORTIMER J. p 2760 N94-28226
KAMMERLOCHER, H. p 2814 N94-28098
KAMPERMAN, J. F. T. p 2974 N94-27794
KANADE, TAKEO p 2809 N94-25967
KANAMARU, OSAMU p 2723 N94-25548
p 2730 N94-25583
KANBE, FUKUSHI p 2905 N94-27482
KANDA, KAZUMI p 2911 N94-27443
p 2903 N94-27444
p 2912 N94-27445
p 2904 N94-27477
KANDARPA, S. p 2823 N94-26976
KANEKO, RYUICHI p 2727 N94-25568
KANEOKE, YOSHIKI p 2913 N94-27452
KANEVSKAYA, E. A. p 3112 N94-25625
p 3112 N94-25626
p 3112 N94-25627
KANG, KI WON p 2835 N94-26399
KANNAWIN, WILLIAM p 2848 N94-26446
KANNE, W. R., JR. p 2832 N94-28229
KANNO, YOICHI p 2718 N94-27390
KANNO, YOUICHI p 2718 N94-27389
KANSKAR, M. p 2749 N94-26074
KAO, C. R. p 2735 N94-26349
KAO, EDWARD p 2671 N94-25711
KAPFER, D. p 2805 N94-28036
KAPICH, D. D. p 3043 N94-26324
KAPP, KEVIN L. p 2785 N94-26830
KAPPLER, PETER H. p 3080 N94-25697
KARANDIKAR, R. p 3004 N94-27211
KARASZ, FRANK E. p 2754 N94-27086
KARCZEWSKI, G. p 3063 N94-26958
KARJALAINEN, MATTI p 2779 N94-25644
KARL, CHAD p 2943 N94-25680
KARLSSON, U. p 2900 N94-27156
KARMARKAR, SUBHASH D. p 2747 N94-28187
KARPOVA, S. A. p 3112 N94-25625
p 3112 N94-25626
p 3112 N94-25627
KARPPI, RISTO p 2712 N94-28376
KARTASASMITA, MAHDI p 2875 N94-28292
KARTHA, V. B. p 2717 N94-26988
KARYUKHIN, A. N. p 3024 N94-27250
KASAHARA, AKIRA p 2725 N94-25562
KASAHARA, MINORU p 2885 N94-27973
KASAI, MASANORI p 2906 N94-27499
KASER, KEN p 2833 N94-25675
KASHAEV, R. M. p 3002 N94-26038
KASSEMKHANI, FARIBA p 2689 N94-25674
KASUGAI, ATSUSHI p 2813 N94-27703
KATADA, YASUYUKI p 2722 N94-25547
p 2724 N94-25555
KATNIK, GREGORY N. p 2692 N94-27956
KATO, REIZO p 3064 N94-27175
KATO, SATORU p 2904 N94-27465
p 2904 N94-27466
KATO, SHIZUKA p 2906 N94-27492
KATO, TAICHI p 2905 N94-27479
p 2905 N94-27480
KATO, TSUYOSHI p 2905 N94-27479
KATO, YASUO p 2884 N94-27967
p 2884 N94-27968
KATOEN, JOOST-PIETER p 3004 N94-26867
KATOH, ZOUJIROU p 2933 N94-27943
KATSUYAMA, KUNIHISA p 2879 N94-26475
p 2871 N94-28156
KATZ, IRVIN R. p 2948 N94-25864
KATZ, MOTI p 3038 N94-27178
KATZBERG, STEPHEN J. p 2684 N94-26286
p 2692 N94-27774
KAUAHIKAUA, J. P. p 2879 N94-26515
KAUFFMAN, R. p 2749 N94-26007
KAUFMAN, HOWARD p 2682 N94-26278
p 2683 N94-26282
KAUFMAN, S. G. p 2821 N94-25970
KAUFMANN, RICHARD L. p 2881 N94-27237
KAUN, T. D. p 2781 N94-26144
KAUPPINEN, PENTTI p 2707 N94-26260
KAVSAOGLU, MEHMET SERIF p 2804 N94-28026
p 2806 N94-28038
KAWABE, RYOHEI p 2776 N94-27340
KAWABE, YOSHIKUNI p 2726 N94-25566
p 2726 N94-25567
KAWADA, YASUHIRO p 2949 N94-26716
KAWAGUCHI, SADAO p 2882 N94-27342
p 2883 N94-27963
KAWAGUCHI, TAKAKO p 2914 N94-27455
p 2927 N94-27518
KAWAHARA, MASATOSHI p 2881 N94-27299
KAWANO, HAZUKI p 2756 N94-27241
KAWANO, KAZUAKI p 2915 N94-27460
KAWANO, SETSUKO p 2911 N94-27443
p 2903 N94-27444
KAWASHIMA, ASAHI p 2745 N94-28164
p 2722 N94-28165
p 2745 N94-28166
KAWASHIMA, TOSHIHIKO p 2764 N94-27976
KAWASUMI, NORIO p 3114 N94-25634
KAWATE, Y. p 3060 N94-26771
KAY, ROBERT T. p 2946 N94-28256
KEANE, JOHN F. p 2667 N94-26182
KEATING, MARK S. p 2677 N94-25833
KEDDY, MICHAEL D. p 2797 N94-27709
KEE, H. Y. p 3067 N94-27634
KEE, HAEYOUNG p 3057 N94-26389
KEIL, S. p 2755 N94-27163
KELHAE, VAEINOE p 2682 N94-26249
KELKAR, A. D. p 2708 N94-26557
KELLER, H.-U. p 2945 N94-28254
KELLER, JOERG p 2982 N94-27579
KELLER, TEDDY M. p 2755 N94-27147
KELLEY, N. D. p 2791 N94-26117
KELLOMAEKI, SEPPO p 2848 N94-26258
KELSO, R. M. p 2800 N94-28006
p 2801 N94-28014
KELSO, THOMAS M. p 2681 N94-27113
KEMP, WILLIAM T. p 3035 N94-26572
KENDALL, R. A. p 2982 N94-27600
KENNEALLY, DANIEL J. p 2766 N94-25736
KENNEDY, J. B. p 2719 N94-27854

KENNEDY, JIM p 2833 N94-25683
KENNER, WINFRED S. p 2695 N94-26609
KENNETT, BRIAN L. p 2880 N94-26752
KENT, S. M. p 3103 N94-27750
KENYON, GREGORY S. p 3034 N94-25729
KENZAKOWSKI, D. C. p 2804 N94-28030
KERELIUK, S. p 2677 N94-26710
KERN, S. p 3061 N94-26841
p 2754 N94-26974
KERN, W. p 2996 N94-26917
KERR, H. W. p 2820 N94-27668
KERR, JAMES M. p 3070 N94-28225
KERSTEN, M. L. p 2972 N94-27576
KERSTEN, MARTIN L. p 3100 N94-27394
KERSTEN, P. R. p 3003 N94-26436
KERSTHOLT, J. H. p 3095 N94-25723
KESKI-RAHKONEN, OLAVI p 3031 N94-25621
KESSLER, DAVID p 2882 N94-27330
KETTANI, NASSER p 2951 N94-26729
KEY, JEFF p 2851 N94-27849
KEY, K. T. p 3098 N94-26559
KEYHANI, M. p 2702 N94-27150
KEYSER, DAVID E. p 2678 N94-27112
KHALID, M. p 2656 N94-28340
KHAN, G. A. p 3000 N94-27637
KHARE, A. N. p 2981 N94-26903
KHESIN, BORIS p 2997 N94-26996
KHLOPOV, M. YU. p 3117 N94-28066
KHLOPOV, MAXIM YU. p 3013 N94-25837
KHOLODENKO, A. G. p 2810 N94-26396
KHOSLA, PRADEEP K. p 2958 N94-25777
KHOUNSARY, A. M. p 3035 N94-26276
KHURI, F. P. p 2942 N94-27320
KIDA, MITSURO p 2915 N94-27460
p 2916 N94-27463
p 2918 N94-27474
p 2918 N94-27475
p 2919 N94-27476
KIDO, NOBUO p 2869 N94-28147
KIEFER, RICHARD L. p 2721 N94-27909
KIETZMAN, JOHN p 2943 N94-25679
KIEU, T. D. p 3051 N94-25885
p 3015 N94-25891
KIHARA, K. p 3028 N94-27759
KIKUCHI, HIROSHI p 2853 N94-28273
KIKUCHI, TAKASHI p 2884 N94-27967
KIKUCHI, TAKEMITSU p 2718 N94-27392
KIKUCHI, TAKEMITU p 2718 N94-27389
KIM, BYOUNG CHUL p 2838 N94-26400
KIM, BYUNG WOO p 2894 N94-26469
KIM, C. J. p 3057 N94-26404
KIM, CHAN JOONG p 2783 N94-26546
KIM, CHANG MIN p 2910 N94-26549
KIM, CHEOL JUNG p 2816 N94-26184
p 2817 N94-26185
p 2817 N94-26403
p 2818 N94-26520
KIM, DOO J. p 2769 N94-26359
KIM, DUK HYUN p 2816 N94-26184
p 2817 N94-26185
p 2817 N94-26403
p 2818 N94-26520
KIM, EUN HAN p 2894 N94-26469
KIM, J. p 3048 N94-27791
KIM, J. Y. p 3041 N94-25923
KIM, JAE SUNG p 2901 N94-26470
KIM, JEONG MOOK p 2816 N94-26184
p 2817 N94-26185
p 2817 N94-26403
p 2818 N94-26520
KIM, JUNG BOG p 2816 N94-26157
KIM, JUNG BOK p 2714 N94-26158
p 2817 N94-26402
KIM, K. B. p 3057 N94-26404
KIM, KWANG SUK p 2816 N94-26184
p 2817 N94-26185
p 2817 N94-26403
p 2818 N94-26520
KIM, KYEKYOON p 3044 N94-26579
KIM, MIN SUK p 2817 N94-26185
p 2817 N94-26403
p 2818 N94-26520
KIM, PAUL Y. p 2828 N94-28041
KIM, SEONG HO p 2714 N94-26158
KIM, SOO SUNG p 2818 N94-26520
KIM, SUNG HO p 2816 N94-26157
KIM, SUNGHYUN p 2782 N94-26328
KIM, W. G. p 3057 N94-26404
KIM, WOO GON p 2783 N94-26546
KIM, Y. B. p 3048 N94-27791
KIMURA, HISAMICHI p 2746 N94-28171
KIMURA, TADASHI p 2896 N94-27169
p 2886 N94-27989
KIMURA, TAKASHI p 2728 N94-25577
KIMURA, TSUNEKAZU p 2949 N94-26720
KINCAID, P. p 2909 N94-26173
KINCAID, REX K. p 3030 N94-27910
KIND, R. J. p 2657 N94-28346
KING, BRAD p 2824 N94-27228
KING, MICHAEL D. p 2897 N94-28179
p 2897 N94-28182
KING, ROBERT W. p 2881 N94-27143
KING, SHIRLYN p 2943 N94-25679
KINOSHITA, K. p 2781 N94-26047
p 2855 N94-26329
KINOSHITA, MINORU p 3064 N94-27175
KINZER, K. E. p 2756 N94-27611
KIPP, M. E. p 2888 N94-28296
KIRANE, M. p 2990 N94-25829
p 2990 N94-25830
KIRK, P. N. p 3018 N94-26244
KIRKNER, D. J. p 2823 N94-26976
KIRKWOOD, SHEILA p 2881 N94-27039
p 2881 N94-27043
KIRLIN, R. L. p 2969 N94-27318
KIRSANOV, M. M. p 3019 N94-26393
KIRSCH, K. A. p 2912 N94-27445
KIRSCH, KARL A. p 2915 N94-27459
p 2918 N94-27473
KISEL, I. V. p 2959 N94-25917
KISELEV, V. V. p 3016 N94-26035
KISHI, SHINKICHI p 2853 N94-28270
KISHIMOTO, SATOSHI p 2729 N94-25581
KISHIMOTO, Y. p 3041 N94-25923
KISLEV, H. p 2701 N94-26537
KISTENEV, EH. P. p 2810 N94-26396
KITABAYASHI, KOJI p 2867 N94-26474
KITAHARA, SHIGERU p 2728 N94-25575
KITAMURA, KATSUHIDE p 2761 N94-27341
KITTEL, T. G. F. p 2866 N94-26026
KIVINEN, T. p 3100 N94-28385
KIYAMA, TAMOTSU p 2879 N94-26475
KIYOKAWA, MASAYOSHI p 2729 N94-25578
KIYOSAWA, AKIO p 2722 N94-25545
KIYOSHI, TSUKASA p 2725 N94-25559
KLARER, P. R. p 2821 N94-26110
KLARER, PAUL p 2685 N94-26292
KLAUS, D. M. p 2903 N94-25672
KLEB, W. L. p 2644 N94-26154
KLEBESADEL, R. W. p 3116 N94-27793
KLEESPIES, HANK p 2943 N94-25698
KLEIN, A. G. p 2714 N94-26170
KLEIN, GLENN C. p 2864 N94-28131
KLEM, J. F. p 3052 N94-25989
KLEMETTI, WAYNE I. p 2773 N94-27085
KLENIN, B. A. p 3020 N94-26509
KLEPPER, C. C. p 3048 N94-27785
KLIMA, R. p 3048 N94-27842
KLIMENKO, K. G. p 3019 N94-26455
KLING, E. p 2812 N94-27160
KLINKHAMER, F. R. p 3020 N94-26540
KLOSTERBUER, S. F. p 2813 N94-27624
KLUGER, Y. p 3012 N94-25612
KLUPPELBERG, CLAUDIA p 3003 N94-26355
KLUTE, GLENN K. p 2697 N94-28183
KNAPP, K. E. p 3067 N94-27609
KNOPS, H. A. J. p 2840 N94-26910
KNOWLES, I. G. p 3015 N94-25955
KNUDSON, J. N. p 3013 N94-25820
KNURR, KURT W. p 2773 N94-27073
KNYAZEV, M. A. p 3074 N94-27696
KO, FRANK K. p 2826 N94-27599
KO, M. K. W. p 2866 N94-25927
KOBAYASHI, ASAO p 2933 N94-27944
KOBAYASHI, HAYAO p 3064 N94-27175
KOBAYASHI, KAZUO p 2729 N94-25579
KOBAYASHI, MIKIHIKO p 2725 N94-25562
KOBAYASHI, MIKIO p 2869 N94-28147
KOBAYASHI, SHUNICHI p 2883 N94-27963
KOBAYASHI, TSUYOSHI p 2729 N94-25578
KOCH, G. p 3014 N94-25840
KOCH, J. A. p 2816 N94-26020
KOCHELAP, V. A. p 3013 N94-25827
p 3027 N94-27631
KOCHELEV, N. I. p 3031 N94-25870
KOCHENDA, L. M. p 2715 N94-26406
KODA, HISASHI p 2906 N94-27494
KODAMA, ITSUO p 2904 N94-27465
p 2904 N94-27466
p 2904 N94-27467
p 2904 N94-27468
p 2904 N94-27469
p 2906 N94-27503
p 2907 N94-27504
p 2907 N94-27505
p 2907 N94-27506
p 2907 N94-27507
p 2907 N94-27508
p 2907 N94-27509
p 2907 N94-27510
p 2907 N94-27511
p 2907 N94-27512
p 2907 N94-27513
p 2908 N94-27514
p 2908 N94-27515
p 2908 N94-27516
p 2908 N94-27537
KOEDA, MITSUHIRO p 2913 N94-27449
p 2913 N94-27451
KOGA, KAZUO p 2915 N94-27461
p 2915 N94-27462
p 2916 N94-27463
p 2918 N94-27475
p 2928 N94-27523
KOGA, KEIICHI p 3066 N94-27353
KOGUCHI, KATSUYA p 2859 N94-27204
KOGUCHI, NOBUYUKI p 2722 N94-25545
KOHLI, ATUL p 2794 N94-27059
KOHMOTO, M. p 3064 N94-27231
KOHMOTO, MAHITO p 3028 N94-27758
KOHNERT, RICHARD A. p 3106 N94-26237
KOIKE, AKIRA p 2681 N94-27247
p 2904 N94-27465
p 2904 N94-27466
KOIKE, YASUO p 2928 N94-27521
KOIVISTO, PAIVI K. p 2778 N94-28380
KOIVUNEN, MARJA-RIITTA p 2976 N94-28356
KOJIMA, ISAO p 3100 N94-27336
KOJIMA, MASAYOSHI p 2884 N94-27967
KOK, JOOST N. p 2995 N94-26776
KOKAN, DAVID p 2833 N94-25704
KOKKALA, MATTI p 3008 N94-26256
KOKLAUNER, KARL p 2848 N94-26446
KOKO, TAMUNOIYALA STANLEY
p 2844 N94-27808
KOKUBUN, SUSUMU p 2882 N94-27342
p 2883 N94-27963
KOL, MOSHE p 2719 N94-27687
KOLA, R. R. p 3055 N94-26239
KOLACEK, K. p 3048 N94-27836
KOLB, E. W. p 3104 N94-26786
KOLBEINSEN, L. p 2741 N94-27328
KOLEN, ANTOON p 2992 N94-26227
KOLESNIKOV, V. I. p 2809 N94-25735
KOLSTROEM, TANELI p 2848 N94-26258
KOMAKI, MASAO p 2723 N94-25551
p 2726 N94-25565
KOMATSU, TERUO p 3065 N94-27240
KOMIZU, MAKOTO p 2933 N94-27945
KOMPANIETZ, GEORGIY V. p 3005 N94-26802
KONDO, HIROAKI p 2867 N94-26474
p 2869 N94-28147
KONDO, KIMINORI p 3025 N94-27338
p 2820 N94-27339
p 2820 N94-27605
KONDO, KYOJI p 2906 N94-27492
KONDO, Y. p 3015 N94-25922
KONING, A. J. p 3004 N94-27223
KONO, JUNICHIRO p 3064 N94-27232
p 3065 N94-27245
KONO, MAKOTO p 2879 N94-26475
KONOPLICH, R. V. p 3117 N94-28066
KONOPLYANNIKOV, A. K. p 2783 N94-26438
KONOTOPSKAJA, E. V. p 2959 N94-25917
KONSTADINIDIS, K. p 2753 N94-26770
KOO, J. p 3068 N94-27724
KOO, L. S. p 3061 N94-26868
KOOPS, M. p 2811 N94-26647
KOPENKIN, V. V. p 3112 N94-25628
p 3113 N94-25629
p 3113 N94-25630
KOPP, R. p 3110 N94-26696
KOPPARI, K. p 2900 N94-27156
KOREN, B. p 2867 N94-26216
KOREN, BARRY p 2868 N94-26774
KORENCHENKO, S. M. p 2959 N94-25917
KORHONEN, JUKKA p 2961 N94-26254
KORI, MUNEYUKI p 2729 N94-25578
KORNEEV, VALERI A. p 2878 N94-26433
KOROBOV, V. I. p 3030 N94-27861
KOROLEV, V. G. p 2948 N94-26381
KORSLOOT, MARK p 2955 N94-27196
KORUS, ANDREAS p 2675 N94-27593
KORVER, HENRI P. p 2972 N94-27578
KOSEFF, J. R. p 2802 N94-28015
KOSEKI, TADASHI p 2767 N94-27606
KOSHIKAWA, NAOKIYO p 3053 N94-26071
KOSHUT, TOM M. p 3114 N94-26686
p 3114 N94-26687
p 3114 N94-26688
KOSMATKA, JOHN B. p 2711 N94-27352
KOST, FRIEDRICH p 2826 N94-27591
KOSTA, CHARLES PAUL p 2687 N94-27369
KOSTIC, P. p 3055 N94-26243
KOSTIUK, L. W. p 2714 N94-26122
KOSUGE, KOJI p 3064 N94-27177
KOTALIK, PAVEL p 2844 N94-27841
KOTCH, JOHN K. p 2681 N94-27113
KOTOV, V. I. p 2810 N94-26394

KOTSCHENREUTHER, M. .... p 2963 N94-26521
KOTTA, U. .... p 3101 N94-26918
KOUVELIOTOU, CHRYSSA .... p 3114 N94-26686
p 3114 N94-26687
KOWALENKO, V. .... p 3007 N94-26928
KOWALL, STEWART J. .... p 2698 N94-26223
KOYAMA, JUNJI .... p 2885 N94-27973
KOZAKI, YASUKO .... p 2906 N94-27502
KOZLOV, S. M. .... p 2715 N94-26406
KOZLOWSKI, M. R. .... p 2749 N94-25985
KOZMINCHUK, BRIAN WILLIAM p 2784 N94-26627
KOZYRA, JANET U. .... p 2878 N94-26204
KRAAIKAMP, CORNELIS .... p 2998 N94-27030
KRAMER, F. .... p 2824 N94-27254
KRAMER, G. D. .... p 2792 N94-26427
KRAMER, M. J. .... p 2735 N94-26273
KRASNOV, S. A. .... p 3030 N94-27994
KRAUSHAAR, W. L. .... p 3115 N94-27236
p 3115 N94-27419
p 3115 N94-27420
KRAUSKOPF, BERND .... p 2997 N94-27028
KRAUSS, A. R. .... p 3053 N94-26031
p 3055 N94-26275
p 3062 N94-26934
KREKEL, P. F. .... p 2767 N94-26011
KRENN, C. .... p 2836 N94-26129
KREUZER, M. .... p 2995 N94-26812
KRIEG, R. D. .... p 2708 N94-26796
KRINGEN, TRICIA .... p 2703 N94-25690
KRISHAMURTHY, RAMESH .... p 2808 N94-27911
KRISHNAKUMAR, NAGAMANI ... p 3004 N94-27106
KRISHNAMAGARU, DHARMESH p 2956 N94-25606
KRISTENSEN, ALLAN MOLLER . p 2835 N94-27042
KRIVSHICH, A. G. .... p 2715 N94-26406
KROCK, LARRY P. .... p 2910 N94-26435
KROEGER, C. A. .... p 2827 N94-27984
KROEGER, W. .... p 2814 N94-28098
KROESE, D. P. .... p 2986 N94-26916
KROLAK, PATRICK D. .... p 2687 N94-27369
KROLL, WALTER .... p 2935 N94-28371
KRONEN, ROLF .... p 2681 N94-27587
KROPFLI, ROBERT A. .... p 2896 N94-26959
KROTHAPALLI, A. .... p 2800 N94-28007
KRUIZINGA, P. .... p 2939 N94-27001
KRUMPELT, M. .... p 2857 N94-26583
p 2857 N94-26584
KRYSHKIN, V. I. .... p 2810 N94-26378
KUBENDRAN, L. R. .... p 2646 N94-26548
KUBICEK, W. G. .... p 2935 N94-28367
KUBO, KIYOSHI .... p 2730 N94-25583
KUBYSHIN, YU. A. .... p 3006 N94-26193
KUCERA, G. H. .... p 2857 N94-26583
KUCHAR, JAMES .... p 2641 N94-27286
KUHLHOFF, JOHN .... p 2689 N94-25674
KUHNDECHIZELLE, YAN P. .... p 2789 N94-25605
KUITUNEN, R. .... p 2833 N94-28378
KUITUNEN, RISTO .... p 2833 N94-28375
KUJIRAI, OSAMU .... p 2729 N94-25578
KUKHTO, T. V. .... p 3020 N94-26507
KULANDER, K. C. .... p 2818 N94-26698
KULLDORFF, S. .... p 2900 N94-27208
KULYUKINA, L. A. .... p 3015 N94-25919
KUMADE, AKINORI .... p 2881 N94-27299
KUMAGAWA, AKINAGA .... p 2710 N94-27280
KUMAKAWA, AKINAGA .... p 2710 N94-27279
KUMAKURA, HIROAKI .... p 2730 N94-25585
KUMAKURA, TOSHIMASA .... p 3000 N94-27731
KUMAR, A. A. .... p 2684 N94-26287
KUMAR, D. .... p 2765 N94-25639
KUMAR, N. .... p 3062 N94-26902
KUMARESAN, R. .... p 2773 N94-27068
KUMAZAWA, KAZUHIKO .... p 2924 N94-27501
KUMAZAWA, TAKAO .... p 2906 N94-27494
p 2906 N94-27495
p 2906 N94-27496
p 2906 N94-27497
p 2906 N94-27498
p 2906 N94-27499
p 2906 N94-27500
p 2924 N94-27501
p 2906 N94-27502
KUMAZAWA, TOSHIHIKO .... p 2905 N94-27487
KUNIEDA, SHUNSUKE .... p 3047 N94-27699
KUNO, SATORU .... p 2918 N94-27475
KUNZ, ANDREA A. .... p 2694 N94-25904
KUNZ, G. J. .... p 2891 N94-25722
p 2893 N94-26016
KUNZE, ERIC L. .... p 2900 N94-27090
KUO, ADDISON C. .... p 2691 N94-25696
KUO, S. P. .... p 2772 N94-26975
KUPERMAN, GILBERT G. .... p 2774 N94-27170
KURAEV, E. A. .... p 3020 N94-26507
KURIHARA, YUTAKA .... p 2727 N94-25568
KURIYAMA, MASAAKI .... p 3047 N94-27699
KURIYAMA, TORU .... p 2776 N94-27340
KURKI, JOUKO .... p 2682 N94-26249
KURODA, SEIJI .... p 2722 N94-25546
p 2728 N94-25575
KURODA, TSUNEO .... p 2725 N94-25560
KURTZ, S. R. .... p 3056 N94-26308
KURUCZ, AGNES .... p 2965 N94-26908
KUSAWAKE, HIROAKI .... p 2863 N94-28121
p 2864 N94-28130
KUSHIMA, HIDEAKI .... p 2729 N94-25580
KUSHIRO, IKUO .... p 2882 N94-27342
KUSUNOKI, KATSUYUKI .... p 2726 N94-25564
KUTEN, S. A. .... p 3068 N94-27729
KUTZ, BJOERN .... p 2697 N94-25667
KUTZBACH, J. .... p 2865 N94-25789
KUWAHARA, KEIICHI .... p 2761 N94-27341
KUWAJIMA, S. .... p 2863 N94-28121
p 2864 N94-28130
KUZNETSOV, A. A. .... p 3031 N94-25850
p 2783 N94-26380
KWAKKEL, F. .... p 2972 N94-27576
KWOK, K. S. .... p 2699 N94-25600
KWON, I. .... p 3059 N94-26695
KWON, S. C. .... p 3057 N94-26404
KWON, SEONG OUK .... p 2816 N94-26184
KYLE, H. LEE .... p 2814 N94-27981
KYONO, JUNRO .... p 2729 N94-25580
p 2729 N94-25581

L

LAAKKO, T. .... p 3001 N94-28398
LABAUGH, ROBERT .... p 2684 N94-26289
LACHAPELLE, GERARD .... p 2665 N94-27667
LAFLEUR, CHARLES A. .... p 2834 N94-25896
LAFONT, C. J. .... p 2743 N94-27832
LAGASSE, R. R. .... p 2748 N94-25932
LAGER, VICKY .... p 2765 N94-25677
LAGUNA, G. W. .... p 2771 N94-26803
LAHAYE, R. J. .... p 3045 N94-26950
LAHDENPERAE, KARI .... p 2835 N94-26257
LAHEY, R. T., JR. .... p 2794 N94-26979
LAI, CHUNG K. .... p 2736 N94-26452
LAI, W. Y. .... p 3052 N94-26012
LAKHANPAL, SANJIV K. .... p 2985 N94-26660
LAL, D. .... p 3117 N94-27826
LAMAR, JOHN E. .... p 2647 N94-27161
LAMARCHE, FRANCOIS .... p 3025 N94-27260
LAMARRE, F. .... p 2653 N94-28327
LAMBERT-NEBOUT, C. .... p 2946 N94-28259
LAMBERT, C. .... p 2711 N94-27586
LAMPE, DONALD R. .... p 2785 N94-27057
LAMPPA, D. L. .... p 3053 N94-26025
LANDER, G. H. .... p 2732 N94-26004
LANDIS, GEOFFREY A. .... p 2687 N94-27370
LANDMAN, DREW .... p 2682 N94-27912
LANDROE, STIG .... p 2817 N94-26203
LANE, DAVID W. .... p 3002 N94-25992
LANE, S. .... p 2706 N94-26019
LANGERAK, ROM .... p 3004 N94-26867
LANSINGER, JOHN M. .... p 2877 N94-25877
LANTERI, S. .... p 2845 N94-28181
LAO, L. L. .... p 3045 N94-26950
LAPID, ALEX J. .... p 2711 N94-27352
LAPSHIN, V. G. .... p 2810 N94-26378
LARDON, CHRISTELE .... p 2689 N94-25670
LARIVIERE, B. W. .... p 2701 N94-26231
LARIVIERE, BRIAN W. .... p 2703 N94-27212
LARKIN, A. I. .... p 3068 N94-27677
LAROSE, PATRICK .... p 2708 N94-26711
LARSEN, H. L. .... p 2786 N94-27327
LARSON, H. J. .... p 2827 N94-27984
LARSSON, F. .... p 2710 N94-27253
LASHBROOK, D. .... p 2698 N94-25701
LASSILA, ORA .... p 2976 N94-28356
LATELLA, DIEGO .... p 3004 N94-26867
p 3004 N94-26870
LATHAM, RICKY D. .... p 2910 N94-26973
LAU, BENTON H. .... p 2641 N94-26596
LAU, BILL J. .... p 2705 N94-25863
LAU, P. .... p 2812 N94-27160
LAUFER, SHAUL .... p 2774 N94-27242
LAUFFER, JAMES P. .... p 2839 N94-26810
LAUHANEN, RISTO .... p 2848 N94-26258
LAURENS, ANDRE .... p 2950 N94-26725
LAUX, RICHARD .... p 2833 N94-25683
LAVARENNE, CHRISTOPHE .... p 2954 N94-26745
LAVENDER, C. A. .... p 2741 N94-27622
LAWSON, A. C. .... p 2733 N94-26069
LAWSON, H. BLAINE, JR. .... p 2996 N94-26993
LAXSON, A. .... p 2856 N94-26513
LAYMAN, PAUL ARTHUR .... p 2787 N94-27642
LAZARIS-BRUNNER, KENNETH . p 2973 N94-27761
p 2975 N94-27951
LAZARUS, KENNETH B. .... p 2987 N94-27093
LEAKE, STEPHEN .... p 2683 N94-26283
LEAR, M. .... p 2689 N94-25692
LEATHERWOOD, JACK D. .... p 2651 N94-28195
LEBLANC, WILFRED PAUL .... p 2770 N94-26630
LECREN, R. T. .... p 2827 N94-27874
LEE, B. H. K. .... p 2653 N94-28323
LEE, BYUNG CHEOL .... p 2816 N94-26157
LEE, C. M. .... p 2674 N94-26573
LEE, DAVID J. .... p 2847 N94-25741
LEE, H. G. .... p 3057 N94-26404
LEE, H. J. .... p 3057 N94-26404
LEE, H. S. .... p 2717 N94-26951
LEE, HEE KWUN .... p 2783 N94-26546
LEE, HO JIN .... p 2783 N94-26546
LEE, JONG MIN .... p 2816 N94-26157
p 2714 N94-26158
p 2817 N94-26402
p 2783 N94-26546
LEE, JONG PO .... p 2838 N94-26400
LEE, KI WOON .... p 2901 N94-26470
LEE, KWANG WON .... p 3042 N94-26159
LEE, P. .... p 3116 N94-27793
LEE, PETER .... p 2967 N94-27065
LEE, R. A. .... p 2804 N94-28030
LEE, SAM LAI .... p 2838 N94-26400
LEE, SANG JAE .... p 2901 N94-26470
LEE, SANG MOCK .... p 2816 N94-26184
LEE, YOUNG BOK .... p 2894 N94-26469
LEE, YOUNG IL .... p 2901 N94-26470
LEENSTRA, JENTJE .... p 2834 N94-26003
LEFEBVRE, DOMINIQUE .... p 2708 N94-26711
LEGGE, BRUCE A. .... p 3096 N94-26180
LEICESTER, DAVID H. .... p 2815 N94-25616
LEIGHTON, T. .... p 2980 N94-26473
LEIGHTON, T. G. .... p 2807 N94-28172
LEINO, TAPIO .... p 2837 N94-26307
LELAND, R. .... p 2962 N94-26370
LEMKE, PAUL .... p 2671 N94-25709
LEMMEL, H. D. .... p 3095 N94-25751
p 3016 N94-26034
LEMMENS, P. .... p 2832 N94-28088
LENKE, JULIE .... p 2902 N94-27165
LENSTRA, JAN KAREL .... p 3094 N94-26314
LENTZ, DALE .... p 2833 N94-25683
LENZINI, JOSH .... p 2689 N94-25674
LEONAR, ANTHONY .... p 2796 N94-27319
LEONARD, P. J. T. .... p 3117 N94-27827
LEONE, J. M., JR. .... p 2892 N94-25936
LEONE, MARK .... p 2967 N94-27065
LEONG, GREGORY N. .... p 2765 N94-25677
LEPAGE, CLAUDE .... p 2795 N94-27307
LEPISTOE, JUKKA .... p 2762 N94-26261
LESCHZINER, M. A. .... p 2803 N94-28024
LESLIE, P. K. .... p 2748 N94-25932
LESTRADE, J. P. .... p 3114 N94-26688
LESUER, D. R. .... p 2708 N94-26930
LETCHENBERG, T. .... p 3043 N94-26323
LEUCHSNER, VOLKER .... p 2858 N94-26813
LEUER, J. A. .... p 3043 N94-26323
LEVIANT, V. M. .... p 3075 N94-27858
LEVY, W. G. T. .... p 2762 N94-26027
LEW, J. Y. .... p 2827 N94-27780
LEWIS, CHARLES .... p 3096 N94-25925
p 3002 N94-25962
LEWIS, G. K. .... p 2818 N94-26605
LEWIS, HARLAN L. .... p 2861 N94-28107
LEWIS, M. S. .... p 2677 N94-26593
LEWIS, MARK J. .... p 2703 N94-25685
LEWIS, P. S. .... p 2897 N94-28146
LEY, K. L. .... p 2857 N94-26584
LHALLABI, T. .... p 2991 N94-25867
LI, H. .... p 2732 N94-25987
LI, J.-S. .... p 3056 N94-26326
LI, JINGMING .... p 2677 N94-26636
LI, LIAN .... p 2709 N94-27107
LI, Q. .... p 3060 N94-26771
LI, SHENG S. .... p 3055 N94-26188
LI, SHIMIN .... p 2819 N94-26940
LI, XIANGQUN .... p 2758 N94-27857
LI, XIAO-DONG .... p 3049 N94-27856
LI, ZAIGUANG .... p 2819 N94-26940
LIANGHUA, YAO .... p 2758 N94-27845
LIAW, BOR Y. .... p 2714 N94-26296
LIENDO, M. F. .... p 2837 N94-26265
LIEPA, VALDIS .... p 2994 N94-26601
LIESCH, DAN S. .... p 2670 N94-27666
LIETZKE, A. .... p 3060 N94-26795
LIEU, D. K. .... p 3008 N94-26421
LIEW, S. L. .... p 3044 N94-26858
LIKHACHEV, G. G. .... p 3104 N94-26269
LILEG, KLEMENS .... p 2768 N94-26315
LILIUS, J. .... p 2983 N94-28354
LILLEY, G. M. .... p 2800 N94-28005
LILLEY, ROBERT W. .... p 2642 N94-27288
LIM, CHANG HWAN .... p 2816 N94-26157
p 2714 N94-26158
LIM, HYUNG TAIK .... p 2838 N94-26400
LIM, T. T. .... p 2801 N94-28014

LIM, YONG TACK p 2901 N94-26470
LIMA, LUIZ CLAUDIO ERMIDA p 2896 N94-27356
LIN, ANTHONY T. p 3024 N94-27133
LIN, CHING-TAI p 2768 N94-26189
LIN, CHUN-SHIN p 2990 N94-27913
LIN, M. C. p 3036 N94-26834
LIN, TING-TING Y. p 2954 N94-27016
LIN, Y. p 3055 N94-26275
LIN, ZHENGCHENG p 2825 N94-27344
LINCE, J. R. p 2746 N94-28185
LIND, CHARLES p 2703 N94-25685
LINDAAS, S. p 2814 N94-27779
LINDELL, I. V. p 2778 N94-28384
p 2778 N94-28387
p 2779 N94-28388
p 2779 N94-28390
p 2779 N94-28391
LINDELL, ISMO V. p 2778 N94-28379
p 2778 N94-28381
LINDENBAUM, S. J. p 3024 N94-26949
LINDERS, R. C. A. p 2798 N94-27799
LINDGREN, MIKAEL p 3037 N94-27046
LINDLEY, ROGER ALAN p 2813 N94-27615
LINDNER, BERNHARD LEE p 3107 N94-27885
p 3107 N94-27886
p 3107 N94-27887
p 3107 N94-27888
p 3107 N94-27889
p 3108 N94-27890
p 3108 N94-27891
p 3108 N94-27892
LINDNER, J. S. p 2684 N94-26287
LINDQVIST, JAN ERIK p 2839 N94-26754
LINDSAY, GEOFFREY p 2755 N94-27148
LINDSTROEM, S. p 2812 N94-27216
LINDSTROM, D. W. p 2844 N94-27810
LINEHAN, J. C. p 2742 N94-27786
LINK, R. p 2883 N94-27393
LINKER, R. L. p 2838 N94-26563
LINNIK, V. A. p 2701 N94-26166
LINNVILLE, STEVEN p 2937 N94-26430
LINTHICUM, K. p 3061 N94-26841
LINZNER, GUNTHER p 2671 N94-25712
LIPENKOV, V. Y. p 2885 N94-27969
LIPKENS, BART p 2650 N94-28193
LISOSKI, DEREK p 2794 N94-27026
LITHERLAND, MARK p 2943 N94-25680
LITTLES, JAY p 2823 N94-27149
LIU, C. S. p 3044 N94-26523
LIU, C. T. p 2734 N94-26272
p 2741 N94-27616
LIU, J. CHIEN-CHIH p 2791 N94-26121
LIU, S. p 2738 N94-26679
p 3062 N94-26934
LIU, SHENGZHONG p 3053 N94-26031
LIU, ZHEN-YUAN p 3035 N94-26383
LIVINGSTON, A. E. p 3021 N94-26760
LO, MICHAEL C. p 2691 N94-25696
LOBACHEV, E. A. p 2715 N94-26406
LOBDELL, DAVID p 2689 N94-25674
LOBODA, GREG p 2689 N94-25687
LOBYNSTEV, VYACHESLAV A. p 3005 N94-26802
LOCIGNO, RENATO p 2972 N94-27582
LOCKE, R. J. p 2674 N94-26573
LOCKHART, RICHARD A. p 3004 N94-26496
LOGAN, MICHAEL J. p 2670 N94-27439
LOGAN, MICHAEL W. p 2985 N94-26336
LOGAN, R. W. p 2707 N94-26099
LOHMANN, R. P. p 2719 N94-27854
LOHRENZ, S. E. p 3035 N94-26100
LOIACONO, G. M. p 3063 N94-27055
LOLL, VALTER p 2835 N94-27042
LONG, D. E. p 2786 N94-27061
LONG, JAMES P. p 2756 N94-27675
LONG, YONG-XING p 3049 N94-27855
LOOMIS, G. E. p 2749 N94-25985
LOONEY, DOUGLAS C. p 2981 N94-27070
LOOSE, R. p 2856 N94-26513
LOPEZ, ALFRED R. p 2665 N94-27275
LOPEZ, ERIC p 2862 N94-28119
LORD, PAUL p 2671 N94-25711
LOREN, JORGEN p 2772 N94-27041
LORENZANA, H. E. p 3052 N94-25947
LORIMER, W. L. p 3008 N94-26421
LOSECCO, J. M. p 3115 N94-27003
LOSFELD, G. p 2659 N94-28039
LOUIS, J. F. p 2893 N94-26082
LOUIS, JEAN-FRANCOIS p 2898 N94-28223
LOURENS, T. p 2938 N94-26873
p 2939 N94-27001
LOURME, DANIEL p 2689 N94-25670
p 2671 N94-25717
LOUSTEAU, D. C. p 3045 N94-26861
LOVEJOY, M. L. p 3052 N94-25989
LOVELL, T. ALAN p 2697 N94-27789
LOVRIC, STEVEN p 2671 N94-25712
LOWDIN, PER-OLOV p 3023 N94-26926
LOWENTHAL, D. D. p 3040 N94-28000
LOZANO, A. p 2800 N94-28008
LOZANO, G. p 3019 N94-26416
p 3072 N94-26417
LU, SHIN-YEE p 3102 N94-26023
LU, Y. p 2876 N94-28395
LU, YU p 3057 N94-26388
LU, Z. p 2757 N94-27716
LUA, Y. J. p 2843 N94-27656
LUBACHEVSKY, BORIS D. p 2971 N94-27558
LUCHA, W. p 3013 N94-25826
LUCIA, A. p 2960 N94-25986
LUCOVSKY, G. p 3069 N94-27757
LUDEWIG, H. p 2699 N94-25798
LUDWIG, DAVID A. p 2944 N94-26098
LUETH, V. p 3063 N94-27047
LUJAN, R. D. p 2738 N94-26610
LUKASHOV, A. L. p 2998 N94-27116
LUKE, P. N. p 3053 N94-26094
LUKYANOV, S. M. p 3012 N94-25750
LUMLEY, J. L. p 2796 N94-27435
LUND, P. p 2855 N94-26240
LUNDGREN, B. p 2759 N94-25907
LUNDGREN, LENNART p 2785 N94-27038
LUNDHOLM, STEVEN E. p 3012 N94-25655
LUNDQUIST, R. p 3063 N94-26958
LUNG, A. p 3017 N94-26101
LUNNEY, MICHAEL E. p 2842 N94-27272
LUO, J. p 3062 N94-26934
LURIE, CHARLES p 2862 N94-28114
p 2863 N94-28124
LUTTGES, M. W. p 2903 N94-25672
LYNCH, GARRY J. p 2713 N94-26075
LYNCH, NANCY A. p 2972 N94-27580
p 2972 N94-27581
LYNCH, V. E. p 3044 N94-26694
LYON, R. E. p 2707 N94-26099
LYONS, DANIEL F. p 2947 N94-28262
LYONS, L. R. p 2877 N94-26201
p 2887 N94-28218

M

MA, J. P. p 3014 N94-25841
p 3014 N94-25888
p 3014 N94-25889
MA, LEONG p 2671 N94-25711
MA, S. p 3111 N94-27953
MAAN, ANTHONIUS CORNELIS p 3016 N94-26002
MAAS, A. J. p 3036 N94-26649
MACCABE, B. p 2979 N94-25953
MACCABE, BARNEY p 2983 N94-27713
MACE, W. DERRY p 2645 N94-26483
p 2645 N94-26489
p 2645 N94-26492
p 2645 N94-26497
MACGOWAN, B. J. p 2816 N94-26020
MACHULA, MIKE p 2760 N94-25705
MACKINNON, B. p 2809 N94-25599
MACKOWIAK, C. L. p 2902 N94-27411
MACLAREN, L. D. p 2644 N94-26342
MACLEOD, B. p 2656 N94-28338
MACLEOD, K. G. p 2889 N94-28303
MACLEOD, N. p 2889 N94-28304
MADDEN, D. p 2878 N94-26338
MADDEN, MICHAEL p 3081 N94-25703
MADENCI, ERDOGAN p 2712 N94-27914
MADILL, DANIEL RICHARD p 2740 N94-27304
MADISON, J. E. p 3100 N94-27563
MADRUGA, M. p 3045 N94-26865
MAE, SHINJI p 2882 N94-27342
p 2885 N94-27969
MAEBARA, SUNAO p 2813 N94-27703
MAEDA, HIROSHI p 2725 N94-25559
MAEDA, KENJI p 2920 N94-27481
MAEDA, YASUOMI p 3025 N94-27337
MAEDA, YOSHIO p 2730 N94-25584
MAENNISTOE, T. p 3100 N94-28385
MAENTYLAE, M. p 3001 N94-28398
MAESTAS, L. M. p 2739 N94-26912
MAGEE, D. P. p 2827 N94-27780
MAGGIORE, C. J. p 3069 N94-27828
MAGNESS, CHARLES L. p 2679 N94-28028
MAGNOTTA, F. p 3052 N94-25947
MAHAJAN, P. p 2724 N94-25553
MAHDAVI, M. A. p 3048 N94-27785
MAHER, D. M. p 3069 N94-27757
MAIJANEN, AILA p 2714 N94-26251
MAINGI, R. p 3048 N94-27785
MAJEED, T. p 2883 N94-27393
MAKARIOU, C. C. p 3043 N94-26274
MAKHANKOV, V. G. p 3050 N94-25825
MAKO, ZOLTAN p 2671 N94-25712
MAKUNDI, W. p 2867 N94-26419
MALAKHOV, A. I. p 2809 N94-25735
MALEK, AHMED p 2654 N94-28330
MALIK, F. BARY p 3030 N94-27915
MALLOZZI, ROBERT S. p 3114 N94-26686
p 3114 N94-26687
p 3114 N94-26688
MALMI, L. p 3100 N94-28396
MANDL, W. p 3048 N94-27791
MANDREKAS, J. p 3044 N94-26860
MANDZHAVIDZE, I. Z. p 2810 N94-26394
MANESS, MICHAEL p 2823 N94-27149
MANGAZEEV, V. V. p 3002 N94-26038
MANGO, STEPHEN A. p 2945 N94-28253
MANHEIMER, WALLACE M. p 2767 N94-26177
MANN, JON p 2671 N94-25708
MANNA, SUSIL K. p 2787 N94-27628
MANNA, ZOHAR p 2962 N94-26303
MANNING, ROBERT M. p 2687 N94-27371
MANO, TADAAKI p 2912 N94-27445
p 2915 N94-27458
p 2915 N94-27459
p 2916 N94-27463
p 2918 N94-27473
p 2918 N94-27474
p 2928 N94-27521
p 2928 N94-27522
p 2929 N94-27524
p 2929 N94-27525
p 2929 N94-27526
p 2929 N94-27527
p 2929 N94-27528
p 2930 N94-27529
p 2908 N94-27530
p 2930 N94-27531
p 2930 N94-27532
p 2930 N94-27533
MANSER, GERALD E. p 2755 N94-27203
MANSON, J. J. p 2848 N94-26277
MANUEL, A. A. p 3003 N94-26385
p 3070 N94-27995
MANZANARES, JOSE p 2754 N94-27080
MANZELLA, DAVID H. p 2701 N94-26209
MANZO, MICHELLE p 2860 N94-28101
MAO, ZHUO-XIONG p 2868 N94-26952
MAPOLES, E. R. p 3052 N94-25947
MARABLE, WILLIAM P. p 3044 N94-26820
MARCOTTE, RYAN p 2761 N94-25707
MARCUS, J. T. p 2940 N94-25724
MARCUS, LELAND R. p 2691 N94-25696
MARESTIN, C. p 2755 N94-27163
MARGASON, RICHARD J. p 2799 N94-28004
p 2803 N94-28023
MARGULIES, L. p 2735 N94-26273
MARKELOFF, R. p 3026 N94-27565
MARKER, TIMOTHY R. p 2660 N94-27081
MARKIN, ROBERT E. p 2883 N94-27883
MARKOV, A. A. p 2715 N94-26406
MARKOWITZ, VICTOR p 2962 N94-26327
MAROTO, A. J. G. p 2743 N94-27829
MARQUIS, GARY p 2837 N94-26255
MARRISON, CHRIS p 2643 N94-27295
MARSAA-POEY, R. p 2659 N94-28031
MARSHALL, T. p 3033 N94-27614
MARSTORP, P. p 2759 N94-25907
MARTIKAINEN, HANNU p 2731 N94-25643
MARTIN, CHARLES R. p 2715 N94-26444
MARTIN, D. M. p 2668 N94-26604
MARTIN, H. p 3033 N94-27614
MARTIN, P. p 3055 N94-26194
MARTINEZ, MICHAEL E. p 2948 N94-25864
MARTINUZZI, R. p 2653 N94-28327
MARTNER, BROOKS E. p 2896 N94-26959
MARTUCCI, STEPHEN A. p 2947 N94-28261
MARTURUNKAKUL, SUTIYAO p 2709 N94-27107
MARTZ, H. F. p 3073 N94-26805
MARTZ, HARRY F. p 3004 N94-27612
MARUHN, ERWIN p 2662 N94-28244
MARUO, DAI p 2728 N94-25575
MARUO, KEIJI p 2853 N94-28274
MARUYAMA, KAZUYASU p 2907 N94-27511
p 2907 N94-27512
MARUYAMA, NORIO p 2726 N94-25567
MARZULLO, KEITH p 2974 N94-27767
p 2666 N94-27768
MASAK, RAYMOND J. p 2775 N94-27270
MASCHHOFF, ROBERT H. p 2814 N94-27981
MASENGE, R. W. P. p 2993 N94-26410
MASI, JAMES p 2709 N94-27091
MASKELL, CRAIG A. p 2860 N94-28104
MASLANIK, JAMES p 2851 N94-27849
MASLIKOV, A. A. p 3072 N94-26453
MASON, KEVIN T. p 2910 N94-26432
p 2911 N94-27097
MASON, M. p 3052 N94-25972
MASSIDDA, S. p 3070 N94-27995
MASSONNET, D. p 2946 N94-28259

MASTIN, G. A. p 2848 N94-26277
MASUDA, CHITOSHI p 2724 N94-25553
MASUDA, HIROSHI p 2764 N94-27976
MASUDA, HIROYUKI p 2724 N94-25554
MASUMOTO, TSUYOSHI p 2745 N94-28161
p 2745 N94-28163
p 2746 N94-28167
p 2746 N94-28168
p 2746 N94-28169
p 2746 N94-28170
p 2746 N94-28171
MASUYA, TOSHIKAZU p 2764 N94-27978
MATANO, TSUNEO p 3114 N94-25634
MATESE, J. J. p 2890 N94-28305
MATHIEU, G. p 2659 N94-28022
MATIC, ROY M. p 2946 N94-28258
MATSON, D. W. p 2742 N94-27786
MATSUBARA, EIICHIRO p 2744 N94-28160
MATSUBARA, TAKAO p 2905 N94-27490
MATSUDA, MASUYOSHI p 2853 N94-27991
MATSUKAWA, MUNEO p 2853 N94-27990
MATSUKAWA, TOSHIYOSHI p 2915 N94-27458
p 2915 N94-27459
p 2918 N94-27473
p 2918 N94-27474
p 2929 N94-27524
p 2929 N94-27525
p 2929 N94-27526
p 2930 N94-27531
p 2932 N94-27538
MATSUKI, KENSUKE p 2746 N94-28168
MATSUOKA, MAMORU p 3047 N94-27699
MATSUOKA, SABURO p 2724 N94-25554
p 2730 N94-25584
MATSUOKA, TORU p 2914 N94-27456
MATSUSHIMA, SHINOBU p 2722 N94-25544
p 2722 N94-25547
MATSUSHIMA, TADAHISA p 2727 N94-25571
MATSUYAMA, T. p 3054 N94-26109
MATSUZAWA, M. p 3026 N94-27620
MATTHEWS, D. L. p 2816 N94-26020
MATTIASSON, K. p 2812 N94-27160
MATTILA, ULLA p 2848 N94-26258
MATTOS, H. C. p 2792 N94-26401
MATVEENKO, A. V. p 3014 N94-25853
MAUGIS, L. p 3099 N94-27101
MAURER, DEAN W. p 2862 N94-28117
MAUTNER, DONALD A. p 2896 N94-27025
MAUTZ, JOSEPH R. p 2771 N94-26844
MAVRIPLIS, CATHERINE p 2657 N94-28348
MAVRIPLIS, D. J. p 2999 N94-27557
MAWARI, TOSHIO p 2730 N94-25584
MAX, C. E. p 3102 N94-26528
MAXIMENKO, V. M. p 3112 N94-25625
p 3112 N94-25626
p 3112 N94-25627
MAYA, LEON p 2751 N94-26580
MAZER, ALAN S. p 2945 N94-28255
MAZZOLDI, P. p 3035 N94-26246
MCAFFER, J. p 2983 N94-27685
MCBREEN, J. p 2717 N94-26951
MCCALLUM, R. W. p 2735 N94-26273
MCCAMMON, DAN p 3115 N94-27236
p 3115 N94-27419
p 3115 N94-27420
MCCARDIE, A. H. p 2909 N94-26179
MCCARTHY, I. E. p 3023 N94-26942
p 3023 N94-26943
p 3023 N94-26944
MCCARTY, EDWARD A. p 2937 N94-25897
MCCLEEREY, MICHELLE p 2942 N94-27089
MCCLEMENTS, K. G. p 3111 N94-27953
MCCLINTOCK, WILLIAM E. p 3106 N94-26237
MCCLURE, KERRY p 2833 N94-25704
MCCONKEY, EDWIN D. p 2665 N94-26826
MCCORD, THOMAS B. p 3106 N94-27409
MCCORMACK, R. p 2743 N94-27792
MCCORMICK, PAUL V. p 2868 N94-26817
MCCRAE, KIMBERLEY A. p 2984 N94-25759
MCCULLOCH, D. p 3023 N94-26929
MCCULLOCH, GERRARD p 2776 N94-27340
MCCURLEY, KEVIN S. p 2983 N94-27713
MCCUSKER, S. p 2800 N94-28009
MCDONALD, C. F. p 3043 N94-26324
MCDONALD, MICHAEL J. p 2958 N94-25818
MCDONALD, PETER W. p 2828 N94-28048
p 2829 N94-28049
p 2829 N94-28050
MCDONNELL, MICHAEL p 3098 N94-26451
MCDOWELL, DAVID L. p 2709 N94-27142
MCDOWELL, J. p 3103 N94-27933
MCFARLANE, ANDREW p 2682 N94-27997
MCGARRY, JAN F. p 2877 N94-26152
MCGUCKEN, E. p 3054 N94-26137
MCGUIRE, DENNIS W. p 2996 N94-26972
MCGUIRK, J. J. p 2801 N94-28010
MCGUIRK, JAMES P. p 2893 N94-26138
p 2896 N94-27408
MCHARGUE, C. J. p 2749 N94-26080
MCKAMEY, C. G. p 2741 N94-27616
MCKELLAR, B. H. J. p 3014 N94-25841
p 3014 N94-25889
p 3015 N94-25891
MCKELLAR, BRUCE p 3014 N94-25888
MCKELLAR, BRUCE H. J. p 3006 N94-25886
MCKENZIE, IAN p 2673 N94-26989
MCKIBBEN, B. p 2698 N94-25701
MCKINNON, W. B. p 2890 N94-28306
MCKOWN, H. S. p 2965 N94-26784
MCLACHLAN, ROBERT I. p 3007 N94-27777
MCLAUGHLIN, PETER p 2829 N94-28051
p 2829 N94-28052
p 2829 N94-28053
p 2829 N94-28054
MCLEAN, D. M. p 2876 N94-28307
MCLEAN, KENNETH WILLIAM p 3027 N94-27684
MCLUER, DAVID G. p 2665 N94-27423
MCMASTER, MARK C. p 3049 N94-25601
MCMICHAEL, I. p 3034 N94-25902
MCMILLAN, C. p 2689 N94-25692
MCMILLAN, K. L. p 2786 N94-27061
MCNEIL, W. J. p 2887 N94-28206
MCNUTT, R. L. p 3012 N94-25726
p 3033 N94-27084
MCPHERSON, ANGELA L. p 3036 N94-26982
MCQUAID, MICHAEL J. p 2957 N94-25646
MCVICKER, C. G., III p 3093 N94-25796
MCWHORTER, ALAN L p 3049 N94-25645
MEAD, D. p 2949 N94-26715
MEAD, R. D. p 3040 N94-28000
MEAD, W. C. p 2985 N94-25983
MEDVEDEV, V. I. p 2715 N94-26406
MEEGAN, CHARLES A. p 3114 N94-26686
p 3114 N94-26687
p 3114 N94-26688
p 3115 N94-26689
p 3115 N94-26690
MEHMED, ORAL p 2846 N94-28227
MEHR, RAMIT p 2933 N94-27744
MEI, Z. p 2750 N94-26085
p 2836 N94-26129
p 2741 N94-27619
MEIBURG, ECKART p 2794 N94-26832
MEIER, ERICH p 2662 N94-28240
MEIJER, JOS J. p 2679 N94-27798
MEILER, P. P. p 2659 N94-25780
MEINDL, RICHARD S. p 2941 N94-26984
MEISCHNER, PETER F. p 2897 N94-27751
MEISEL, L. V. p 3008 N94-26376
MEISENHEIMER, T. L. p 2780 N94-25812
p 2948 N94-26111
MEISER, DAVID H. p 2681 N94-27113
MEKHFI, M. p 2992 N94-26367
MELEZHIK, V. S. p 3029 N94-27847
p 3030 N94-27861
MELISSINOS, A. C. p 3008 N94-25988
MELKO, JOSEPH p 2689 N94-25670
MELLAH, A. p 2716 N94-26518
MELLOCH, M. R. p 3052 N94-25989
MELO, STELLA MARIS LUDOVICO
p 2882 N94-27334
MELTON, JOHN E. p 2667 N94-26091
MELTON, ROBERT G. p 2689 N94-25692
MENARY, SCOTT ROBERT p 3026 N94-27400
MENDIETA, V. SANCHEZ p 2720 N94-27998
MENG, JULIAN p 3103 N94-27302
MENJO, MASAFUMI p 2919 N94-27478
p 2905 N94-27479
MENON, M. M. p 3048 N94-27785
MENON, VINOD P. p 2715 N94-26444
MENSAH, S. Y. p 3057 N94-26384
MERKLE, K. L. p 3053 N94-26029
MERRIGAN, MICHAEL A. p 2797 N94-27709
MESHCHERYAKOV, G. V. p 3027 N94-27681
MESHCHERYAKOV, V. A. p 3027 N94-27681
MESNARD, E. p 2952 N94-26732
MESTAYER, P. G. p 2893 N94-26013
METCALFE, JOHN R. p 2860 N94-28104
METHLIE, GEORGE J. p 2863 N94-28125
METZGER, RICHARD C. p 2981 N94-27100
METZINGER, K. E. p 2821 N94-25811
MEYER, A. p 2814 N94-28098
MEYER, J. L. p 2865 N94-25790
MEYER, KURT W. p 2690 N94-27771
MEYER, MARY A. p 3094 N94-27707
MEYER, P. J. p 2809 N94-26150
MEYER, T. W. p 2816 N94-26126
MEYERS, DOUG p 2671 N94-25712
MEYLER, KAREN L. p 2751 N94-26434
MEZERA, DAVID N. p 2987 N94-27121
MIASTKOWSKI, JOZEF p 2739 N94-26824
MICHAEL, J. p 3061 N94-26856
MICHAEL, J. R. p 3057 N94-26420
MICHALSKE, T. A. p 2750 N94-26247
p 2751 N94-26564
MICKLOS, RICHARD P. p 2669 N94-27105
MIGLIORINI, C. p 2952 N94-26733
MIKKOLA, TIMO P. J. p 2841 N94-27186
p 2841 N94-27187
p 2841 N94-27188
p 2841 N94-27189
p 2842 N94-27190
MIKOSCH, THOMAS p 3003 N94-26355
MILCZAREK, EDWARD p 3038 N94-27441
MILDEN, MARTIN p 2862 N94-28116
MILDER, MARTIN p 2902 N94-27165
MILEWSKI, J. O. p 2818 N94-26605
MILEY, G. H. p 2701 N94-26537
p 3047 N94-27715
MILEY, GEORGE H. p 2688 N94-27373
MILEY, H. S. p 3116 N94-27621
MILLER, CHRIS X. p 2947 N94-28264
MILLER, D. p 3058 N94-26516
MILLER, D. J. p 3055 N94-26243
MILLER, GEORGE P. p 2893 N94-26134
MILLER, J. R. p 2696 N94-26808
MILLER, JEFFREY C. p 2960 N94-26018
MILLER, M. K. p 2734 N94-26272
MILLER, M. S. p 2903 N94-25672
MILLER, MICHAEL A. p 3093 N94-25895
MILLER, RICHARD C. p 2790 N94-25858
MILLER, RICHARD S. p 2755 N94-27203
MILLER, SCOTT D. p 2862 N94-28120
MILLS, B. E. p 2759 N94-26198
MILLS, MICHAEL S. p 2765 N94-25647
MILLS, MICHAEL T. p 2957 N94-25661
MINE, MASAYA p 2949 N94-26716
MINH-TIEN, TRAN p 3051 N94-25945
MINH, N. Q. p 2858 N94-26792
MINNETT, P. J. p 2852 N94-27875
MINOWA, TOMOAKI p 2859 N94-27204
p 2871 N94-28154
MINSTER, JEAN-BERNARD p 2880 N94-26855
MIODUSZEWSKI, P. K. p 3048 N94-27785
MIR, R. p 3033 N94-27614
MIRALLES, J. A. p 3116 N94-27714
MITARAI, GENYO p 2912 N94-27447
MITCHELL, DOMINIQUE p 2697 N94-25667
MITCHELL, JOSEPH A. p 2680 N94-26200
MITCHELL, R. L. p 2856 N94-26426
MITCHELL, T. E. p 2750 N94-26124
MITRA, A. P. p 2874 N94-28284
MITSUI, TATSURO p 2723 N94-25552
p 2728 N94-25573
MITSUMA, TERUNORI p 2930 N94-27532
MITTELMANN, HANS D. p 2992 N94-26302
MITYURICH, G. S. p 2716 N94-26823
MIURA, NOBORU p 3064 N94-27232
p 3065 N94-27240
p 3065 N94-27245
MIURA, YOSHITAKA p 2905 N94-27482
MIWA, CHIHIRO p 2912 N94-27445
p 2915 N94-27458
p 2915 N94-27459
p 2918 N94-27473
p 2918 N94-27474
p 2929 N94-27524
p 2929 N94-27525
MIWA, HITOSHI p 2681 N94-27247
MIYAKE, YOZO p 2908 N94-27519
MIYAMOTO, AKIRA p 2913 N94-27453
MIYAMOTO, NORIHIRO p 2911 N94-27443
p 2903 N94-27444
p 2904 N94-27477
p 2905 N94-27480
MIYAMOTO, YOSHINORI p 2933 N94-27944
MIYAZAKI, AKIMITSU p 2727 N94-25568
MIYAZAKI, AKIRA p 2869 N94-28147
p 2870 N94-28152
MIYAZAKI, TAKASH p 2920 N94-27481
MIYAZAKI, TAKASHI p 2919 N94-27478
MIZUMOTO, CHIEKO p 2933 N94-27944
MIZUMURA, KAZUE p 2906 N94-27494
p 2906 N94-27496
p 2906 N94-27497
p 2906 N94-27498
p 2906 N94-27499
p 2906 N94-27500
p 2924 N94-27501
p 2908 N94-27539
MIZUNO, KOICHI p 2869 N94-28147
MIZUNO, MAKOTO p 3047 N94-27699
MIZUNO, TATEKI p 2867 N94-26474
p 2870 N94-28153
MIZUNO, TOSHIYA p 2918 N94-27474
p 2918 N94-27475
MIZUTANI, HITOSHI p 2885 N94-27973
MODARRESS, DARIUSH p 2835 N94-26691

MOERMAN, M. M. p 2893 N94-26016
MOFIZ, U. A. p 3046 N94-27630
MOGAKI, KAZUHIKO p 3047 N94-27699
MOGFORD, R. H. p 2664 N94-25788
MOHA, SOPHIE BEN p 2689 N94-25670
MOITRA, ANUTOSH p 2963 N94-26466
MOITRA, STUTI p 2963 N94-26466
MOKHTARIAN, FARZAD p 2658 N94-28349
MOKHTARIAN, FARZIN p 2974 N94-27805
MOKRY, M. p 2647 N94-26702
MOKRY, MIROSLAV p 2658 N94-28352
MOLNAR, G. I. p 2866 N94-25927
MOMBERGER, MANFRED p 2660 N94-28231
MONFORT, JEAN-NOEL p 2950 N94-26724
MONISMITH, S. G. p 2802 N94-28015
MONTANO, P. A. p 3054 N94-26139
MONTES, FRED p 2689 N94-25682
MONTGOMERY, RAYMOND C. p 2682 N94-26278
MONTIEL, JEAN JACQUES p 2953 N94-26739
MOOKERJEE, A. p 2714 N94-26169
MOOKERJEE, ABHIJIT p 2787 N94-27628
MOONEY, G. D. p 2856 N94-26426
MOOR, WILLIAM C. p 2938 N94-26882
MOORE, BRUCE p 2860 N94-28102
p 2861 N94-28108
MOORE, C. F. p 3021 N94-26586
MOORE, GARY T. p 2943 N94-25706
MOORE, M. J. p 2789 N94-28078
MOORE, R. B. p 2879 N94-26515
MOORE, TAMRA K. p 3097 N94-26375
MOORHOUSE, DAVID J. p 2671 N94-28034
MOORTI, RAJ p 2947 N94-28264
MORAN, J. P. p 2742 N94-27788
MORAVEC, HANS p 2686 N94-27361
p 2689 N94-27376
MOREL, PAUL R. p 2698 N94-28210
p 2698 N94-28217
MORENO, C. p 3097 N94-26382
MORGAN, A. p 3052 N94-25972
MORGAN, J. M. p 2677 N94-26710
MORGAN, SAM p 2689 N94-25674
MORI, KANEO p 2928 N94-27520
MORI, KATSUHIKO p 2745 N94-28163
MORI, KENJU p 3114 N94-25634
MORI, SHIGEO p 2912 N94-27446
p 2912 N94-27447
p 2912 N94-27448
p 2913 N94-27449
p 2913 N94-27450
p 2913 N94-27451
p 2904 N94-27464
MORI, YUICHI p 2919 N94-27478
p 2905 N94-27482
MORIBAYASHI, K. p 3026 N94-27620
MORILAK, DANIEL P. p 2834 N94-26199
MORIMATSU, O. p 3015 N94-25922
MORIMOTO, YASUO p 2949 N94-26720
MORINAKA, ISAO p 2725 N94-25562
MORITA, YASUO p 2764 N94-27976
MORITANI, KOTARO p 2949 N94-26716
MORITO, FUMIO p 2726 N94-25566
MORONEY, D. p 2698 N94-25701
MORRELL, FREDERICK R. p 2641 N94-27284
MORRELL, R. p 2752 N94-26654
MORRIS, J. W., JR. p 2750 N94-26085
p 2733 N94-26087
p 2836 N94-26129
p 2741 N94-27619
p 2742 N94-27694
MORRIS, M. D. p 2716 N94-26781
MORRIS, M. J. p 3035 N94-26100
MORRISON, JIM p 2823 N94-27149
MORT, R. W. p 2668 N94-26604
MORTENSEN, MICHAEL p 2689 N94-25682
MORTON, CYNTHIA MAE p 2972 N94-27595
MOSES, STEWART L. p 3104 N94-27407
MOSHER, J. C. p 2897 N94-28146
MOSKALENKO, I. V. p 3104 N94-26268
MOSLEY, JUDITH I. p 2946 N94-28258
MOSS, C. E. p 2696 N94-26808
MOSS, ELIOT p 3099 N94-27014
p 2967 N94-27063
MOSTERDIJK, W. H. P. p 2784 N94-26646
MOTALLEBI, F. p 2681 N94-26815
MOTEGI, NAOTO p 2761 N94-28002
MOTEN, SUBRAMANIAM p 2875 N94-28290
MOTEVALLI, VAHID p 2761 N94-25707
MOTOWIDLO, L. p 3060 N94-26771
MOTOWIDLO, L. R. p 2783 N94-26589
p 2740 N94-26957
MOTOYA, KIYOICHIRO p 2756 N94-27241
MOTYLEWSKI, J. p 2716 N94-26823
MOULTON, J. L. p 2829 N94-28049
MOURAD, P. D. p 2899 N94-26886
MOUSTAPHA, S. H. p 2652 N94-28321
MOYERS, ANTHONY D. p 2968 N94-27075
MROWKA, S. p 2816 N94-26020
MUCKENSCHNABEL, JOSEF p 3066 N94-27590
MUELLER, B. p 3026 N94-27604
MUELLER, KLAUS p 2662 N94-28243
MUELLER, M. H. p 3058 N94-26514
MUENCHOW, L. p 3013 N94-25836
p 3020 N94-26505
MUINONEN, E. p 2850 N94-27185
MUINONEN, EERO p 2850 N94-27182
MUKAI, T. p 2748 N94-25959
MUKHOPADHYAY, NIMAI C. p 3027 N94-27689
MULCAHY, T. M. p 3008 N94-26421
MULENBURG, JERRY p 2901 N94-26086
MULGUND, SANDEEP S. p 2643 N94-27296
MULLEN, E. G. p 2878 N94-26338
MULLER, J. p 2981 N94-27092
MULLER, KURT A. p 2707 N94-26190
MULLER, MARK p 2668 N94-26488
MULLER, R. A. p 3106 N94-27007
p 2888 N94-28297
p 2890 N94-28308
MULLINS, WENDY R. p 2938 N94-26749
MULVEHILL, ALICE M. p 2897 N94-27884
MUNDKUR, GAUTAM p 2842 N94-27309
MUNDY, J. N. p 3053 N94-26029
MUNEKI, SEIICHI p 2726 N94-25566
MUNEYAMA, KEI p 2872 N94-28272
MUNGAL, M. G. p 2800 N94-28008
MUNIR, Z. A. p 2721 N94-25561
MURAD, ADNAN p 2671 N94-25711
MURAKAMI, MASATO p 2853 N94-28271
MURAMATSU, YOSHIKI p 2722 N94-25546
MURATA, MASAHARU p 2729 N94-25580
MURATA, YOSHIHARU p 2911 N94-27443
p 2903 N94-27444
p 2912 N94-27445
p 2919 N94-27478
p 2905 N94-27479
p 2905 N94-27480
p 2920 N94-27481
p 2905 N94-27482
MURATA, YOSHITADA p 2733 N94-26073
MURDOCK, THOMAS L. p 3104 N94-27265
MURGER, M. p 3022 N94-26769
MURRAY, JANE S. p 3018 N94-26172
p 3022 N94-26894
MUSSARDO, G. p 2998 N94-27162
MUSTALESKI, T. M., JR. p 2824 N94-27181
MUTHARASAN, RAJAKKANNU p 2826 N94-27599
MUUSS, SUSANNE L. p 2957 N94-25753
MYAE, E. A. p 3032 N94-26164
MYERS, B. C. p 2959 N94-25855
MYERS, JERRY A. p 2980 N94-26009
MYERS, R. M. p 2700 N94-26090
MYERS, RENEE p 2689 N94-25682
MYERS, S. M. p 3050 N94-25814
p 3052 N94-25971
p 3058 N94-26565
MYLES, K. M. p 2857 N94-26583
p 2857 N94-26584
MYRABO, LEIK p 2670 N94-25695
MYSNIK, A. I. p 2810 N94-26378
MYTNIK, LEONID p 3008 N94-26374

N

NABEKAWA, YASUO p 3025 N94-27338
p 2820 N94-27339
NACHTRIEB, R. T. p 2701 N94-26537
NACIRI, J. p 2754 N94-27033
NAEGELI, DAVID W. p 3035 N94-25941
NAGAI, HIDEO p 2723 N94-25548
NAGAI, KOTOBU p 2724 N94-25556
NAGAKAWA, JOSEI p 2682 N94-25586
NAGAOKA, SHUNJI p 2913 N94-27453
NAGASE, M. p 3026 N94-27620
NAGASHIMA, NOBUO p 2724 N94-25554
NAGASHIMA, TAKASHI p 2813 N94-27703
NAGATA, NORIO p 2722 N94-25544
p 2722 N94-25547
NAGATA, YUTAKA p 2904 N94-27472
NAGATSUKA, KYOUICHI p 2933 N94-27943
NAGY, A. F. p 2878 N94-26204
NAGY, M. p 3022 N94-26900
NAITO, YASUHIKO p 2883 N94-27963
NAITOH, PAUL p 2909 N94-26377
p 2937 N94-26430
NAKADA, YOSHINOBU p 2761 N94-28002
NAKAGOME, HIDEKI p 2776 N94-27340
NAKAHARA, NOBUO p 2918 N94-27475
NAKAHATA, M. p 3028 N94-27759
NAKAJIMA, HAJIME p 2743 N94-27807
NAKAJIMA, HIDEAKI p 2881 N94-27299
NAKAJIMA, HIDEO p 2788 N94-27817
NAKAJIMA, TAKESHI p 3065 N94-27245
NAKAMURA, AKIO p 2933 N94-27942
p 2933 N94-27944
p 2933 N94-27945
NAKAMURA, HARUKATA p 2722 N94-25546
NAKAMURA, HIROAKI p 2725 N94-25562
NAKAMURA, K. p 3028 N94-27759
NAKAMURA, KEIKICHI p 2726 N94-25563
p 2682 N94-25586
NAKANO, KEIJI p 2730 N94-25582
NAKANO, OSAMU p 2728 N94-25573
NAKAO, MASAYOSHI p 2896 N94-27169
NAKASHIMA, TSUGIO p 2853 N94-27991
NAKASONE, YUJI p 2743 N94-27807
NAKATA, HIROKO p 2931 N94-27534
NAKATANI, ISAO p 2730 N94-25585
NAKATANI, KENSUKE p 2863 N94-28121
p 2864 N94-28130
NAKATSUBO, TAKAYUKI p 2885 N94-27971
NAKAZAWA, KOZO p 2726 N94-25567
NAKAZAWA, YASUHIRO p 3049 N94-25614
NAM, DO p 3069 N94-27819
NAMAI, TORU p 2727 N94-25572
NAMITO, YOSHIHITO p 3032 N94-26543
NAMSRAI, KH. p 3074 N94-27680
NANCE, PRESTON p 2833 N94-25683
NANGIA, R. K. p 2801 N94-28012
NAPOLITANO, KEVIN L. p 2987 N94-27093
NARAIN, K. S. p 3071 N94-25882
NARAN, HITESH p 2671 N94-25711
NARANG, H. N. p 2978 N94-27916
NARHEIM, B. T. p 2876 N94-25807
NARITA, TAKASHI p 2879 N94-26475
NASBY, R. D. p 3061 N94-26856
NASRALLAH, M. M. p 2857 N94-26747
NASTASI, M. p 2752 N94-26676
p 3069 N94-27828
NATARAJAN, SWAMINATHAN p 3093 N94-26206
NATARAJAN, V. p 2715 N94-26392
NAUMANN, K. W. p 2659 N94-28022
NAUMANN, MATTHIAS p 2754 N94-27036
NAZIROV, M. T. p 3020 N94-26507
NEASE, SANDRA p 2765 N94-25677
NEBEL, R. p 2688 N94-27373
NEBEL, R. A. p 3047 N94-27715
NEHRKORN, THOMAS p 2898 N94-28223
NEILSEN, M. K. p 2708 N94-26796
NEKRASOV, M. L. p 3016 N94-26042
NEKSAE, P. p 2909 N94-25909
NELIPOVICH, E. S. p 3032 N94-26164
NELMS, R. MARK p 2844 N94-27824
NELSON, B. E. p 3044 N94-26858
p 3045 N94-26861
NELSON, BRUCE W. p 2852 N94-27957
NELSON, MICHAEL L. p 2971 N94-27573
NELSON, P. A. p 2781 N94-26144
p 2807 N94-28175
NELSON, ROBERT E. p 2859 N94-27225
NELSON, T. E. p 2656 N94-28341
NELSON, W. D. p 2713 N94-26014
NEMANICH, R. J. p 3060 N94-26839
p 2754 N94-26974
p 3063 N94-27058
p 3063 N94-27058
NERI, D. F. p 2909 N94-26179
NESTERENKO, V. V. p 3029 N94-27848
NETTLES, ALAN T. p 2707 N94-26127
NEUENFELDT, BRIAN D. p 2695 N94-26750
NEUHART, DAN H. p 2680 N94-26603
NEUMANN, M. p 3030 N94-28001
NEUMANN, T. p 2814 N94-28098
NEUSHKIN, A. A. p 2810 N94-26396
NEVANLINNA, O. p 3001 N94-28389
NEVASMAA, P. p 2833 N94-28378
NEVASMAA, PEKKA p 2731 N94-25623
p 2731 N94-25784
p 2833 N94-28375
NEVILL, GALE E., JR. p 2903 N94-25673
NEWEL, P. T. p 2877 N94-26201
NEWELL, P. T. p 2887 N94-28218
NEWMAN, D. E. p 2793 N94-26558
NEWMAN, N. p 3068 N94-27724
NEWMAN, ROBERT B. p 2665 N94-26826
NEZAKI, KOJI p 2761 N94-27341
NG, L. C. p 2810 N94-26525
NGUYEN, THUAN P. p 2671 N94-25711
NGUYEN, V. D. p 2651 N94-28316
p 2651 N94-28317
NHU, DAVID H. p 2788 N94-28186
NICHOLS, LESTER D. p 2686 N94-27363
NICHOLS, STEVEN P. p 2943 N94-25698
NICHOLSON, ROBERT K., JR. p 2668 N94-26531
NICINSKI, T. p 2809 N94-25599
NICKEL, H. U. p 2768 N94-26310
NICOL, DAVID M. p 2971 N94-27558
NICOL, N. A. p 3018 N94-26325
NIEH, T. G. p 2748 N94-25959

NIELSEN, ROBERT L. p 2665 N94-27071
NIELSON, GREGORY M. p 2990 N94-25594
NIEMANTSVERDRIET, J. p 2770 N94-26650
NIEMCZYK, T. M. p 2713 N94-25978
NIEMI, H. p 2841 N94-27189
NIEPLOCHA, J. p 3000 N94-27569
NII, KAZUHIRO p 2722 N94-25545
NIIMURA, NOBUO p 2903 N94-27862
NIINO, MASAYUKI p 2710 N94-27279
p 2710 N94-27280
NIJMEUER, H. p 3101 N94-26918
NIKI, KIYOMI p 2904 N94-27467
p 2904 N94-27468
NIKITIN, I. N. p 3072 N94-26036
NIKITYUK, N. M. p 2979 N94-25918
NIKOLAIDIS, EFSTRATIOS p 2844 N94-27830
NING, ZHAOYUAN p 2758 N94-27857
NISBET, JOHN p 2784 N94-26675
NISHI, MASATAKA p 2788 N94-27817
NISHI, SYUJI p 2933 N94-27943
NISHIBAYASHI, YOSHIKI p 3065 N94-27245
NISHIIZUMI, K. p 3117 N94-27826
NISHIJIMA, SATOSHI p 2726 N94-25567
p 2730 N94-25584
NISHIMOTO, KAZUTOSHI p 2712 N94-28376
NISHIMURA, CHIKASHI p 2723 N94-25551
p 2726 N94-25565
NISHIMURA, H. p 2967 N94-27049
NISHIMURA, HIROSHI p 2853 N94-27991
NISHIMURA, Y. p 2658 N94-28350
NISHINO, MASANORI p 2884 N94-27967
p 2884 N94-27968
NISHINO, Y. p 3055 N94-26275
NISHIO, SEIJI p 2913 N94-27449
p 2913 N94-27450
p 2913 N94-27451
NITZ, BO p 2839 N94-26754
NIWA, NOBUHIRO p 2905 N94-27490
NIWA, YOSHIKI p 2906 N94-27492
NOBACK, R. p 2678 N94-27395
p 3001 N94-28353
NOBUKI, MINORU p 2729 N94-25579
NODA, TETSUJI p 2682 N94-25586
NOGUCHI, SATORU p 3049 N94-25614
NOH, BOO-HO p 2873 N94-28278
NOLTING, RALF p 2663 N94-28250
NOMA, TOSHIBUMI p 2764 N94-27976
NONTASAK, T. p 2937 N94-26346
NOORBERGEN, H. H. S. p 2851 N94-27555
NORBURY, JOHN W. p 3033 N94-27646
NORGAARD, R. p 2867 N94-26419
NORLANDER, L. p 2902 N94-27171
NORLANDER, LENA p 2902 N94-27045
NORQVIST, A. p 2902 N94-27171
NORTON, T. p 2719 N94-27712
NOTEBOOM, TIM p 2936 N94-28372
NOTTINGHAM, G. p 2698 N94-25701
NOVAES, S. F. p 3017 N94-26043
NUESSER, HANS-GUSTAV p 2660 N94-27746
NUGENT, EDWARD p 2762 N94-25775
NUON, TIMITHY I. p 2671 N94-25711
NUSS, KENNETH p 3081 N94-25703
NYLAND, JOHN p 2936 N94-28372
NYSTROM, W. D. p 3047 N94-27715

O

OBA, TOSHIO p 2730 N94-25583
OBA, YASUHIRO p 2908 N94-27530
OBARA, KAZUSHIGE p 2886 N94-27988
OBARA, MICHAEL p 2709 N94-27076
p 2709 N94-27091
OBRIEN, FRANCIS J. p 2786 N94-27109
OCONNOR, D. p 3006 N94-26193
ODA, KENICHI p 2764 N94-27979
p 2764 N94-27980
ODA, SENICHI p 2905 N94-27484
p 2905 N94-27486
p 2905 N94-27489
p 2905 N94-27490
p 2905 N94-27491
p 2906 N94-27492
p 2906 N94-27493
ODAY, GARY p 2759 N94-26486
ODEN, J. TINSLEY p 2846 N94-28266
ODIJK, E. p 2955 N94-27193
ODONNELL, PATRICIA p 2860 N94-28101
OEDMAN, S. p 3038 N94-27209
OGASAWARA, M. p 3054 N94-26109
OGATA, ICHIRO p 3100 N94-27336
OGATA, TOSHIO p 2724 N94-25556
OGAWA, AKINORI p 2710 N94-27255
OGAWA, KAZUYUKI p 2728 N94-25577
OGAWA, R. p 3060 N94-26771
OGAWA, YOICHI p 2725 N94-25562
OGI, TOMOKO p 2859 N94-27204
p 2871 N94-28154
OGISU, YOSHIHIRO p 2869 N94-28147
OGLESBY, R. J. p 2865 N94-25789
OGREN, H. p 3033 N94-27614
OGUCHI, MASAHIRO p 2746 N94-28169
OGUCHI, TAMIO p 2726 N94-25564
OGUNI, YASUO p 2681 N94-27247
OGURA, KOICHI p 3027 N94-27718
p 3029 N94-27820
OGURO, NOBUTAKA p 2721 N94-25561
OH, BYUNG HOON p 3042 N94-26159
OHAMA, TETSUO p 3025 N94-27337
OHARA, YOSHIHIRO p 3047 N94-27699
OHASHI, OSAMU p 2726 N94-25566
OHASHI, SHIGEO p 2722 N94-25547
OHBA, YASUNORI p 2718 N94-27388
OHKAWA, YOSHINAO p 2757 N94-27812
OHKOUCHI, Y. p 2820 N94-27701
OHMAN, L. H. p 2651 N94-28316
p 2651 N94-28317
OHMORI, SACHIKO p 2911 N94-27443
OHRN, N. Y. p 3023 N94-26926
OHSAWA, AKINORI p 3113 N94-25633
OHTAKA, KAZUHIRO p 2881 N94-27299
OISO, YUTAKA p 2905 N94-27482
OKA, TAKESHI p 3064 N94-27095
OKADA, MICHIO p 2733 N94-26073
OKADA, T. p 2748 N94-25959
OKADA, YOSHIMITSU p 2886 N94-27986
OKAICHI, T. p 2875 N94-28287
OKAMOTO, TETSUYA p 2930 N94-27532
OKANO, MAKOTO p 2825 N94-27351
OKAUE, MIYAKO p 2933 N94-27942
p 2933 N94-27943
OKAWA, OSAMU p 2761 N94-28002
OKBEL-BAB, A. S. p 2990 N94-25865
OKHRIMENKO, L. S. p 3013 N94-25828
OKOSHI, TSUNEO p 2728 N94-25577
OKOUCHI, HARUNO p 2729 N94-25578
OKOYA, S. S. p 2713 N94-25913
OKUBO, S. p 3008 N94-25988
OKUDA, KIICHI p 3049 N94-25614
OKUMURA, HIROSHI p 2746 N94-28167
OKUNO, KENJI p 2744 N94-27876
OKUNO, YOSHINORI p 2678 N94-27206
OKUYAMA, SEISHI p 2918 N94-27474
OLAH, G. A. p 2901 N94-26623
OLALAINTY, BERNARD p 2950 N94-26722
OLINGER, D. J. p 2671 N94-25719
OLMEDO, A. M. p 2743 N94-27829
OLSAN, JAMES B. p 2968 N94-27120
OLSEN, J. A. p 3056 N94-26308
OLSON, D. L. p 2738 N94-26679
OLSON, R. D. p 2963 N94-26407
OLSSON, P. O. p 2755 N94-27158
OMAKI, KAZUHITO p 3100 N94-27336
OMANA, ADRIAN HERNANDEZ p 3048 N94-27844
OMORI, GORO p 2728 N94-25573
OMORI, SACHIKO p 2903 N94-27444
p 2912 N94-27445
ONDA, KAZUO p 2717 N94-27246
ONO, HIDEO p 2918 N94-27475
p 2919 N94-27476
ONO, KATSUMI p 2723 N94-25550
ONO, KYOKO p 2906 N94-27492
ONO, NOBUO p 2883 N94-27963
ONO, TAKAYUKI p 2881 N94-27299
p 2779 N94-27964
ONODERA, HIDEHIRO p 2723 N94-25550
ONODERA, SHINJI p 2718 N94-27389
p 2718 N94-27392
ONOZAWA, AKIHIKO p 2933 N94-27942
ONOZAWA, TAMOTSU p 2949 N94-26720
ONUMA, YOSHIO p 2973 N94-27702
OOHARA, HIROSHI p 3047 N94-27699
OOSTERLEE, C. W. p 2992 N94-26252
OOSTERWIJK, RON p 2847 N94-26107
OPALKA, E. P. p 2715 N94-26320
OPAT, G. I. p 2714 N94-26170
OPILA, R. L. p 2753 N94-26770
ORAN, E. S. p 2795 N94-27252
ORIORDAN, C. A. p 2802 N94-28015
ORMSBY, RACHEL A. p 2695 N94-26103
ORR, L. p 3008 N94-25988
ORR, LINSEY p 2824 N94-27228
ORTIZ, NELSON p 2943 N94-25694
ORTIZ, V. p 2698 N94-25700
ORTLEPP, KH. G. p 3012 N94-25750
ORVILLE, HAROLD D. p 2894 N94-26195
OSAKA, RYOJI p 2916 N94-27463
OSAKA, TOSHIYUKI p 2931 N94-27535
OSAWA, AKINORI p 3114 N94-25634
OSAWA, YOSHIAKI p 2727 N94-25572
OSBORNE, T. H. p 3045 N94-26950
OSGOOD, R. M., JR. p 3058 N94-26526
OSHIKIRI, MASAYUKI p 2788 N94-27821
OSLUND, DAWSON S. p 2691 N94-26017
OSMAN, S. M. p 3073 N94-26837
OSOSKOV, G. A. p 3015 N94-25919
OSTERGAARD, JENS C. p 2773 N94-27085
p 2777 N94-28211
OSTERMAN, A. p 2902 N94-27171
OSTREM, JULIE p 2902 N94-27165
OSTROVSKY, A. O. p 3032 N94-26330
OSUGI, MAMI p 2905 N94-27487
OSULLIVAN, GEORGE A. p 2856 N94-26463
OSULLIVAN, JOSEPH A. p 2856 N94-26463
OTA, AKIHIKO p 2730 N94-25584
OTA, YOSHIHIRO p 2916 N94-27463
OTAGUCHI, MINORU p 2721 N94-25561
OTAKE, HIDEYUKI p 3064 N94-27176
OTANI, SHUJI p 2885 N94-27971
OTSUKA, KUNIAKI p 2932 N94-27540
OTT, E. p 3044 N94-26523
OTTINGER, C. A. p 2702 N94-26560
OTZINGER, B. p 2860 N94-28105
OTZSCHI, KENJI p 3066 N94-27353
OUASTI, R. p 3067 N94-27635
OUTLAW, BRUCE K. E. p 2681 N94-27425
OVEREINDER, BENNO p 2955 N94-27194
OWENS, GEORGE p 2703 N94-25690
OWENS, RICHARD W. p 2910 N94-26973
OZ, HAYRANI p 2703 N94-25690
OZAKI, TSUYOSHI p 2682 N94-25586
OZAWA, KIYOSHI p 2730 N94-25585
OZKARA, ALI p 2768 N94-26347

P

PAAL, DAVID M. p 2865 N94-25609
PAASO, S. p 2644 N94-26104
PABST, DAVID J. p 2694 N94-25659
PACIESAS, WILLIAM S. p 3114 N94-26686
p 3114 N94-26687
p 3114 N94-26688
p 3115 N94-26689
p 3115 N94-26690
PACINI, LINDA K. p 2877 N94-26152
PADAVALA, SATYA p 2825 N94-27383
PAEIVINEN, RISTO p 2850 N94-27182
p 2850 N94-27184
PAGE, BRIAN C. p 2690 N94-25769
PAIGE, A. B. p 2653 N94-28322
PAIGE, J. B. p 3094 N94-27772
PAINE, D. C. p 3062 N94-26932
PAJARI, BRITA p 2848 N94-26258
PAL, T. p 3011 N94-25598
PALACIO, H. A. p 2735 N94-26294
PALAMIDESSI, CATUSCIA p 2966 N94-26919
PALAZZOLO, ALAN p 2825 N94-27383
PALEV, T. D. p 2993 N94-26440
p 3073 N94-26758
p 3001 N94-27839
PALMER, MICHAEL T. p 2673 N94-27882
PALMQUIST, ROBERT D. p 2958 N94-25818
PALOUNEK, A. P. T. p 3052 N94-25972
PAN, X. p 3062 N94-26934
PAN, XIANZHENG p 3053 N94-26031
PANDE, S. S. p 2981 N94-26903
PANG, FRANCIS p 2962 N94-26327
PANKAKOSKI, PEKKA H. p 2707 N94-26260
PANZA-GIOSA, R. p 2653 N94-28325
PAPADOPOULOS, STAVROS p 3074 N94-27398
PARASCHIVOIU, I. p 2653 N94-28327
p 2657 N94-28345
PARASCHIVOIU, M. p 2656 N94-28342
PARASHAR, P. p 3005 N94-25868
PARFITT, A. M. p 2935 N94-28369
PARHI, N. p 2990 N94-25829
p 2990 N94-25830
p 3001 N94-28228
PARIKH, N. R. p 3054 N94-26137
PARK, CHI SUNG p 2838 N94-26400
PARK, S. D. p 3057 N94-26404
PARK, SOON DONG p 2783 N94-26546
PARKES, JAMES E. p 2690 N94-26142
PARKINSON, G. V. p 2654 N94-28332
PARSONS, R. p 2980 N94-26120
PARULESKI, KERRY L. p 2943 N94-25706
PASHKOV, P. T. p 3032 N94-26164
PASQUALINI, E. E. p 3029 N94-27834
PASQUET, JEAN-MARIE p 2950 N94-26724
PASTORE, G. p 2715 N94-26391
p 3006 N94-26411
PASTUKHOV, V. P. p 3041 N94-25792
PATANO, SCOTT J. p 3080 N94-25697
PATE, RONALD C. p 2853 N94-25946
PATHAK, K. N. p 3006 N94-26368
PATNAIK, SURYA N. p 2845 N94-27865
PATTEN, KENNETH O., JR. p 2869 N94-27267

PAULSEN, KIM p 3022 N94-26894
PAVER, N. p 3014 N94-25887
PAWELCZYK, JAMES A. p 2935 N94-28366
PAYNE, A. C., JR. p 2700 N94-25956
PEAKE, KIRK p 2671 N94-25709
PEARCE, JAMES M. p 2863 N94-28126
PEARCEY, H. H. p 2659 N94-28040
PEARSONS, KARL S. p 2651 N94-28196
PEASE, DANIEL J. p 2979 N94-25786
PECORA, LOU p 2787 N94-27673
PEDERSEN, BRYON L. p 2795 N94-27129
PEDRESCHI, DINO p 2970 N94-27544
PEHKONEN, KARI p 2957 N94-25642
PELACCIO, DENNIS G. p 2699 N94-25613
PELETIER, MARK A. p 2865 N94-25760
PELOWITZ, DENISE p 3005 N94-26802
PELTONEN, J. p 2833 N94-28378
PELTONEN, JORMA p 2833 N94-28375
PEMBERTON, STEVEN p 3097 N94-26220
p 2961 N94-26221
PENDLETON, GEOFFREY N. p 3114 N94-26685
p 3114 N94-26686
p 3114 N94-26687
p 3114 N94-26688
p 3115 N94-26689
p 3115 N94-26690
PENDRILL, LESLIE p 3008 N94-26851
PENG, H. p 2890 N94-28309
PENG, J. L. p 2748 N94-25844
p 3056 N94-26363
PENN, LANNING M. p 2814 N94-27981
PENNINGTON, TIMOTHY L. p 3034 N94-25768
PENNOCK, S. T. p 2771 N94-26803
PENROD, TODD D. p 2774 N94-27170
PENROSE, C. J. p 2675 N94-28018
PENTTILA, S. I. p 3013 N94-25820
PERELYGIN, V. F. p 2810 N94-26396
PEREPEZKO, J. H. p 2737 N94-26607
PERES, O. L. G. p 3022 N94-26766
PERESSI, MARIA p 3061 N94-26878
PEREZ-ALVAREZ, R. p 3062 N94-26897
PEREZ, MARTIN p 3080 N94-25697
PEREZ, R. A. p 2733 N94-26160
PERITT, JON p 2833 N94-25686
PERKEY, DONALD J. p 2869 N94-27430
PERKINS, L. J. p 3044 N94-26860
PERLMUTTER, S. p 2888 N94-28297
PERMYAKOVA, L. A. p 3015 N94-25919
PERREA, MIKE p 2703 N94-25690
PERRONE, D. p 2860 N94-28105
PERRY, A. E. p 2801 N94-28014
PERRY, B. p 3060 N94-26840
PERSON, LEE H., JR. p 2679 N94-27660
PERSOON, A. J. p 2843 N94-27553
PERVUSHIN, V. N. p 3013 N94-25836
PERYEA, MARTIN A. p 2645 N94-26483
p 2645 N94-26489
p 2645 N94-26492
p 2645 N94-26497
PETER, M. p 3003 N94-26385
p 3070 N94-27995
PETERS, LEON, JR. p 2783 N94-26449
p 2785 N94-27027
PETERS, M. A. G. p 2666 N94-27831
PETERSEN, K. L. p 2691 N94-27868
PETERSON, BARBARA VIEUX p 2903 N94-27412
PETERSON, RANDALL p 2641 N94-26596
PETKOV, N. p 2938 N94-26873
p 2939 N94-27001
PETKOV, VALERY G. p 2721 N94-28159
PETRAVICK, D. p 2809 N94-25599
PETRIK, M. A. p 2858 N94-26785
PETROVIC, J. J. p 2750 N94-26124
PETRZILKA, V. p 2777 N94-27838
p 3048 N94-27840
PETTY, C. C. p 3046 N94-27261
p 3046 N94-27568
PETZKE, J. p 2652 N94-28319
PETZOLD, KARL W. p 2680 N94-26200
PEYRONNEAU, J. p 2880 N94-26806
PFEIFFER, S. p 2754 N94-27033
PFEIL, AXEL C. p 2661 N94-28237
PHAN, ANGIE H. p 2860 N94-28106
PHELPS, A. D. p 2807 N94-28172
PHILLIPS, J. C. p 3045 N94-26865
PHILLIPS, JAMES D. p 2667 N94-26151
PHILLIPS, MARK p 2852 N94-27870
PHILLIPS, W. J. p 2713 N94-25964
PIANETTA, P. p 3056 N94-26326
PICARD, RICHARD R. p 3094 N94-27707
PICCUS, MARTIN E. p 2940 N94-25611
PICKETT, DAVID F. p 2863 N94-28126
PICON, LAURA L. p 3037 N94-27062
PIELKE, R. A. p 2866 N94-26026
PIEPER, JOCHEN p 2661 N94-28238
PIEPER, RON J. p 2946 N94-28256
PIERCE, ALLAN D. p 2650 N94-28189
PIERCE, DOUGLAS C. p 2864 N94-28134
PIERCE, J. D. p 2708 N94-26796
PIETERSEN, O. B. M. p 2666 N94-27831
PIETRAS, CHRISTOPHER R. p 2782 N94-26301
PIN, F. G. p 2986 N94-26948
PINKELMAN, JIM p 2671 N94-25715
PINSKER, R. I. p 3041 N94-25801
p 3046 N94-27261
p 3046 N94-27568
PINSKI, F. J. p 2736 N94-26351
PIOTROWSKI, J. p 2996 N94-26967
PIPER, LAWRENCE G. p 2750 N94-26167
PIPERNI, P. p 2653 N94-28324
PIPITONE, FRANK J. p 2965 N94-26831
PISANO, F. p 3016 N94-26040
p 3022 N94-26899
PISENT, G. p 3015 N94-25890
PISTCHIKOV, S. I. p 2854 N94-26056
PITKAENEN, JORMA p 2835 N94-26257
PITKAENEN, JUHO p 2850 N94-27182
p 2850 N94-27184
PITNER, A. L. p 2736 N94-26522
PITTENS, KENNETH H. p 2822 N94-26657
PITZ, WILLIAM J. p 2760 N94-27725
PIYAKARNCHANA, TWESUKDI p 2875 N94-28287
PLATZER, R. p 3063 N94-26958
PLEITEZ, V. p 3016 N94-26040
p 3016 N94-26041
p 3022 N94-26766
p 3022 N94-26899
PLETTA, J. BRYAN p 2685 N94-26291
PLEVYAK, HOWARD M., JR. p 2942 N94-27320
PLIMPTON, S. p 3016 N94-26033
PLJUSHCHAY, M. S. p 3019 N94-26454
PLOTKIN, KENNETH J. p 2650 N94-28194
PLUQUET, C. p 2809 N94-25599
PODLESAK, MICHAEL p 2809 N94-26358
POERTNER, T. p 2703 N94-28032
POHJANNE, PEKKA p 2837 N94-26262
POHJONEN, JUHA p 2695 N94-26250
POHJONEN, V. p 2850 N94-27185
POHJONEN, VELI p 2850 N94-27182
POIRIER, J. P. p 2880 N94-26806
POKOTILOVSKIJ, YU. N. p 3027 N94-27682
POLETTO, G. p 3110 N94-26696
POLITZER, PETER p 3018 N94-26172
p 2704 N94-26353
p 3022 N94-26894
POLLCHIK, JESSICA D. p 2753 N94-26842
POLLEY, L. p 3019 N94-26423
POLYAKOV, V. A. p 2810 N94-26378
POMPEI, MARIE-HELENE p 2671 N94-25717
PONCE, EDGAR p 3080 N94-25697
PONOMAREV-STEPNOI, NIKOLAI N.
p 3005 N94-26802
PONOMAREV, L. I. p 3030 N94-27861
PONTHUS, AGNES-MARIE p 2862 N94-28113
POOLE, JAMES WARREN p 2712 N94-27688
POOLE, R. J. D. p 2651 N94-28316
p 2651 N94-28317
POPA, L. p 3103 N94-26046
p 2878 N94-26365
POPA, V. p 3103 N94-26046
PORANEN, J. p 2747 N94-28359
PORTANOVA, MARC A. p 2711 N94-27433
PORTER, L. M. p 2754 N94-26974
PORTIS, BONNIE L. p 2840 N94-26922
p 2840 N94-26953
p 2840 N94-27008
POSEY, A. p 3045 N94-26863
POSLUK, S. p 2968 N94-27157
POST, G. F. p 2996 N94-26915
POST, ROBERT E. p 2911 N94-27097
POTTER, B. G. p 3061 N94-26856
POTTER, G. L. p 2897 N94-27571
POUPONNOT, A. L. R. p 2949 N94-26715
POWELL, J. R. p 2699 N94-25798
POWERS, J. V. p 2932 N94-27556
POWRIE, H. E. G. p 2659 N94-28021
POZOS, R. p 2909 N94-26173
PRADHAN, PRABHAKAR p 3062 N94-26902
PRAGER, S. C. p 3042 N94-26132
PRAIRIE, M. R. p 2742 N94-27755
PRASAD, S. p 2717 N94-26951
PRATER, R. p 3046 N94-27568
PRATHER, ERIC p 2957 N94-25646
PRAWER, S. p 3056 N94-26364
p 3023 N94-26929
p 3063 N94-26987
PRELL, W. L. p 2865 N94-25789
PREPPERNAU, B. L. p 2704 N94-27708
PRESTON, G. A. p 2807 N94-28173
PRITCHETT, A. p 2641 N94-27286
PROBER, DANIEL E. p 3059 N94-26681
PRONKO, G. P. p 3072 N94-26037
PROSKURYAKOV, A. L. p 2809 N94-25735
PROTOPOPESCU, S. D. p 3015 N94-25955
PRUNIAUX, KARINE p 2671 N94-25717
PUKKALA, T. p 2850 N94-27185
PUKKALA, TIMO p 2850 N94-27182
PUPYSHEV, V. V. p 3007 N94-26472
PURTELL, P. p 2797 N94-27562

Q

QIAN, DUAN p 2695 N94-26712
QIAN, H. p 2748 N94-25844
QIU, J. H. p 2738 N94-26653
QIU, LI p 2988 N94-27641
QIU, XIAO-MING p 3049 N94-27855
QU, WEN-XIAO p 3049 N94-27855
QUAK, DIRK p 2771 N94-26877
p 2772 N94-26909
QUANG, DOAN NHAT p 3057 N94-26387
p 3061 N94-26879
QUENISSET, J. M. p 2711 N94-27586
QUICK, H. A. p 2644 N94-26342
QUINLAN, D. p 2980 N94-26120
QUINT, P. p 2754 N94-26977
QUIRK, W. J. p 3118 N94-27566
QVINTUS-LEINO, PIA p 2714 N94-26251

R

RABE, F. p 2945 N94-28254
RACINE, J. p 2698 N94-25700
RADHAKRISHNA, P. p 2733 N94-26092
RADMARD, RAMA p 2793 N94-26671
p 2652 N94-28320
RADOVICH, BRIAN M. p 3080 N94-25697
RAFFIN, M. p 2698 N94-28020
RAGHAVAN, SRINIVASAN p 2975 N94-27872
RAHKA, K. p 2833 N94-28378
RAHKA, KLAUS p 2833 N94-28375
RAHMAN, M. S. p 3073 N94-27024
p 3074 N94-27626
p 3007 N94-27633
RAIBLE, E. p 2970 N94-27542
RAIKO, HEIKKI p 2841 N94-27187
RAINER, F. p 2749 N94-25985
RAIS-ROHANI, MASOUD p 2671 N94-27917
RAJ, RISHI p 2709 N94-27125
RAJAGOPAL, P. p 2682 N94-27879
RAJEEV, S. G. p 3008 N94-25988
RAMADAN, S. p 3030 N94-27994
RAMIREZ, J. E. p 2738 N94-26679
RAMOHALLI, KUMAR p 2697 N94-25667
RAMP, STEVEN R. p 2898 N94-26076
RAMPINO, M. R. p 2891 N94-28310
RAMSAY, MICHAEL A. p 2826 N94-27596
RANACHOWSKI, J. p 2716 N94-26823
RAND, ROBERT S. p 2709 N94-27135
RANDALL, D. A. p 2898 N94-26072
RANDERIA, M. p 3017 N94-26078
RANDON, CATHERINE p 2708 N94-26711
RANKIN, JAMES M. p 2666 N94-27918
RANKINEN, MINNA p 2976 N94-28356
RAO, GOPALAKRISHNA p 2863 N94-28126
RAO, GOPALAKRISHNA M. p 2702 N94-26613
p 2862 N94-28120
RAO, K. p 2659 N94-28040
RAO, S. p 2980 N94-26473
RAPPAPORT, S. A. p 3012 N94-25726
p 3033 N94-27084
RASMUSSEN, SANDER p 2972 N94-27582
RATNAVELU, K. p 3023 N94-26944
RATVASKY, W. J. p 2674 N94-26573
RAVEN, PETER B. p 2935 N94-28366
RAVENSCROFT, D. p 3045 N94-26863
RAY, E. R. p 2858 N94-26869
p 2858 N94-26871
RAY, J. MICHAEL p 2936 N94-28372
RAYMER, DAN p 2671 N94-25712
RAYMOND, T. D. p 3040 N94-28000
READING, J. p 2909 N94-26173
REBHOLZ, PATRICK J. p 2943 N94-25706
REBSTOCK, RUEDIGER p 2681 N94-27587
RECH, H. p 2824 N94-27254
RECHBERGER, JOHANN p 2744 N94-27950
RECHENMACHER, R. p 2809 N94-25599
REDD, FRANK J. p 3081 N94-25702
REDDY, C. SUBBA p 2658 N94-27919
REDDY, T. S. R. p 2846 N94-28227
REDING, PHILIP J. p 2893 N94-26138
REDLER, K. p 3043 N94-26323
REEDY, E. D., JR. p 2836 N94-26032
REEDY, R. C. p 3117 N94-27826
REEDYK, MAUREEN p 3070 N94-27974
REESE, G. M. p 2961 N94-26146

REEVES, ARLINDA J. p 3095 N94-27866
REGAZZINI, E. p 3004 N94-26939
p 3004 N94-27051
REGGIO, M. p 2657 N94-28347
REHM, GEORG W. p 2662 N94-28241
REHMANN, ALBERT J. p 2664 N94-25788
REHN, L. E. p 3059 N94-26591
REID, J. S. p 2738 N94-26610
REID, JAMES R., JR. p 2909 N94-25943
REID, L. D. p 2682 N94-27879
REIMANIS, I. E. p 2750 N94-26124
REINHARDT, JOHN W. p 2668 N94-26488
REINISCH, BODO W. p 2876 N94-25752
REINSBERG, JAMES G. p 2671 N94-28034
REIS, E. E. p 3043 N94-26323
REISNER, JOHN A. p 3034 N94-25758
REISS, HOWARD p 2754 N94-27080
REMPT, RAYMOND D. p 2705 N94-25779
REN, ZHAOXING p 2758 N94-27857
RENOUX, C. p 2952 N94-26736
RENSNER, GARY p 3035 N94-26572
REPAS, GEORGE A. p 2691 N94-27424
RESHOTKO, ELI p 2671 N94-25713
RESS, D. p 2816 N94-26020
RETHFELDT, C. p 2814 N94-28098
RETTIG, C. L. p 3045 N94-26950
REYES, A. P. p 3050 N94-25817
REYN, J. W. p 2991 N94-26215
REYNA, VINCENT P. p 2678 N94-27132
REYNOLDS, G. J. p 2971 N94-27552
REYNOLDS, ODELL R. p 2676 N94-25771
RHI, JONG HOON p 2816 N94-26157
RHO, SI PYO p 2816 N94-26157
p 2714 N94-26158
RHODES, CARROLL L. p 2942 N94-27114
RHODES, MARVIN D. p 2695 N94-26609
RIAHI, H. p 3000 N94-27818
RIAZUDDIN p 3014 N94-25887
RIBBENS, C. J. p 2967 N94-27020
RICE, T. p 2703 N94-25685
RICH, F. J. p 2877 N94-26201
RICHARD-FOY, MARC p 2951 N94-26730
RICHARD, MURIEL p 2689 N94-25670
RICHARDS, G. A. p 2719 N94-27712
RICHARDS, P. C. p 2832 N94-28089
p 2832 N94-28090
RICHARDS, WHITMAN p 2939 N94-27072
RICHTER, BRUCE A. p 2673 N94-26176
RICKLI, J.-P. p 2831 N94-28086
RIDENOUR-BENDER, MARGARET
p 2673 N94-26176
RIDES, M. p 2748 N94-25892
p 2756 N94-27217
RIDES, N. p 2748 N94-25893
RIEDER, R. J. p 3012 N94-25726
p 3033 N94-27084
RIEGER, D. J. p 3052 N94-25989
RIEMER, B. W. p 2767 N94-25924
RIESEN, R. p 2979 N94-25953
RIESEN, R. E. p 2979 N94-25952
RIESEN, ROLF p 2983 N94-27713
RIGHTER, A. W. p 2781 N94-25977
RIGOTTI, G. p 2743 N94-27829
RIIHIAHO, SIRPA p 2976 N94-28356
RIIHINEN, BODIL p 2976 N94-28356
RIJKEN, T. A. p 3021 N94-26620
RILEY, DAVID R. p 2666 N94-25590
p 2667 N94-25961
RILEY, DONALD R. p 2646 N94-26602
RINES, GLEN A. p 2818 N94-26705
RINGER, BRIAN p 2947 N94-28263
RIPA, M. p 3048 N94-27836
RISTORCELLI, J. R. p 2796 N94-27435
RITCHIE, DAVID p 2943 N94-25680
RITTFELDT, LARS p 2866 N94-25809
RIUS, N. p 3019 N94-26416
RIVERA, JORGE E. p 2692 N94-27956
RIVERS, T. p 2698 N94-25701
ROADS, J. O. p 2894 N94-26313
ROBERGE, ANDRE p 3074 N94-27403
ROBERSON, S. p 3061 N94-26841
ROBERTI, L. A. p 2734 N94-26161
ROBERTS, D. A. p 2738 N94-26610
ROBERTS, L. p 2659 N94-28029
ROBERTS, MALLORY p 3116 N94-27440
ROBERTSON, DAVID D. p 2705 N94-25857
ROBERTSON, J. L. p 3065 N94-27251
ROBERTSON, R. C. p 3012 N94-25655
ROBINSON, ANNE p 2833 N94-25675
ROBINSON, C. E. p 2783 N94-26372
ROBINSON, D. N. p 2711 N94-27640
ROBINSON, D. W. p 3009 N94-27131
ROBINSON, LEICK D. p 2650 N94-28192
ROBINSON, P. A. p 2677 N94-26593
ROBINSON, R. C. p 2680 N94-26141
ROCHE, M. p 2857 N94-26583
ROCHE, MICHAEL T. p 3093 N94-25796
ROCHEV, V. E. p 3072 N94-26553
ROCKETT, JOHN A. p 3031 N94-25621
RODRICKS, B. p 2820 N94-27781
RODRICKS, BRIAN p 3054 N94-26139
RODRIGUE, G. p 2981 N94-27092
RODRIGUE, PETE p 2708 N94-26895
RODRIGUEZ, JUAN C. p 2680 N94-26200
ROELOFS, DARRELL D. p 2665 N94-27275
ROGERS, D. D. p 2706 N94-25982
ROGERS, W. A. p 2719 N94-27712
ROGNLIEN, T. D. p 2767 N94-25937
ROGRON, B. p 2946 N94-28259
ROHERTY-OSMUN, E. p 2738 N94-26610
ROJAS, LOU p 2824 N94-27228
ROLLAND, T. p 2741 N94-27326
ROMIG, A. D., JR. p 2735 N94-26349
RON, AMOS p 3003 N94-26445
p 2998 N94-27103
RONAGHI, M. p 2845 N94-28181
RONEN, AMIT p 2850 N94-27331
RONEY, J. MICHAEL p 2812 N94-27257
RONG, LIU p 2742 N94-27730
RONZHIN, A. I. p 2810 N94-26378
ROOKE, D. P. p 2845 N94-27954
ROOS, C. p 2957 N94-25761
p 2958 N94-25762
p 2967 N94-27031
ROOS, FREDERICK W. p 2679 N94-28028
ROOS, J. p 2950 N94-26721
ROQUEMORE, A. L. p 3048 N94-27825
ROSCHAK, E. p 2703 N94-27213
ROSCHAK, EDMUND p 2824 N94-27228
ROSE, DAVID p 3045 N94-27074
ROSE, DONALD J. p 2959 N94-25968
ROSENBERG, N. J. p 2866 N94-25948
ROSHKO, ANATOL p 2796 N94-27319
ROSKAM, JAN p 2671 N94-25714
ROSMOND, THOMAS E. p 2900 N94-26887
ROSQVIST, ROLAND p 2902 N94-27045
ROSS, F. M. p 3055 N94-26239
ROSS, J. p 3068 N94-27724
ROSSING, T. D. p 3008 N94-26421
ROSSINGTON, C. S. p 3053 N94-26094
ROSSOUW, C. J. p 3062 N94-26927
ROTELA, E. p 2811 N94-26787
ROTH, DUANE p 2773 N94-27146
ROTH, KARLIN R. p 2803 N94-28023
p 2672 N94-28035
ROTHERMICH, CHARLES V. p 3102 N94-25658
ROUSE, WILLIAM B. p 3099 N94-26891
ROUSSEL-DUPRE, ROBERT p 3020 N94-26527
ROUSSEL, J. P. p 2950 N94-26726
ROUTE, R. K. p 2757 N94-27716
ROY, CLERMONT p 2708 N94-26711
ROY, DONALD W. p 3066 N94-27276
ROY, SHIBAJI p 2994 N94-26459
ROYET, J. p 3060 N94-26795
RUBIN, M. p 3068 N94-27724
RUBY, D. S. p 2857 N94-26617
RUBY, W. S. p 3059 N94-26566
RUDZIAK, M. K. p 3060 N94-26795
RUEFFER, P. p 2945 N94-28254
RUEHE, J. p 2755 N94-27163
RUFFE, L. M. p 2902 N94-27411
RUI, R. p 3014 N94-25840
RUOHONIEMI, J. M. p 2877 N94-26201
RUOKANGAS, CORINNE p 3095 N94-27866
RUPERT, V. C. p 2792 N94-26427
RUSAK, ZVI p 2650 N94-28191
RUSHBY, JOHN p 2953 N94-26740
RUSSELL, JAMES W. p 2692 N94-27774
RUSSELL, PHILIP G. p 2864 N94-28133
RUSSELL, PHYLLIS p 2671 N94-25712
RUSSELL, S. D. p 3059 N94-26566
RUSSLER, PATRICK p 2674 N94-26345
RUSSO, ARTURO p 2689 N94-28207
RUSSO, P. A. p 2813 N94-27624
RUST, D. p 3033 N94-27614
RUTHERFORD, DAVE p 2833 N94-25689
RUTHERFORD, MALCOLM J. p 3107 N94-27850
RUTTEN, E. P. B. M. p 2971 N94-27575
RUUSKANEN, PEKKA p 3058 N94-26545
RUUSUNEN, J. p 3095 N94-28386
RYADOVIKOV, V. N. p 2810 N94-26396
RYAN, M. M. p 2936 N94-28373
RYAN, MICHAEL p 2671 N94-25713
RYAN, P. M. p 3041 N94-25933
p 3046 N94-27261
p 3046 N94-27568
RYCHENKOV, V. I. p 2783 N94-26380
RYCHENKOV, V. N. p 2948 N94-26381
RYE, R. R. p 2751 N94-26564
RYNNE, T. M. p 2897 N94-28146

S

SABATINI, R. L. p 3060 N94-26771
SABEL, LAURA p 2974 N94-27767
SABIN, JOHN R. p 3023 N94-26926
SABINA, S. p 2952 N94-26733
SABLIK, MARTIN J. p 3035 N94-25941
SABOUNI, IKHLAS p 2943 N94-25693
SACHA, DAVID J. p 3097 N94-26297
SACKNOFF, S. M. p 3094 N94-27772
SADAKOV, S. N. p 3044 N94-26510
SADEK, N. M. p 3030 N94-27994
SAEAESKI, JUHA p 2837 N94-26255
SAFFARINI, G. p 2758 N94-27837
SAGER, G. T. p 3043 N94-26324
SAGISAKA, AKIHIKO p 3025 N94-27338
SAGNELLA, DIANE E. p 3020 N94-26562
SAITO, KAZUO p 2726 N94-25567
p 2727 N94-25571
p 2682 N94-25586
SAITO, MASAHIRO p 2710 N94-27279
p 2710 N94-27280
p 2710 N94-27281
p 2869 N94-28147
SAITO, MITSURU p 2929 N94-27527
SAITO, MORIMASA p 2728 N94-25576
SAITO, TAKANOBU p 2746 N94-28170
SAITO, TERUYUKI p 2918 N94-27474
p 2918 N94-27475
SAITO, TOSHIHITO p 2710 N94-27279
p 2710 N94-27280
p 2675 N94-27608
SAITOV, I. S. p 3013 N94-25828
SAJIKI, KAZUAKI p 2820 N94-27339
SAKAI, A. p 3028 N94-27759
SAKAI, YOSHIKAZU p 2724 N94-25557
p 2725 N94-25559
SAKAMOTO, KEISHI p 2813 N94-27703
SAKARIS, PETER p 2711 N94-27314
SAKKA, YOSHIO p 2722 N94-25544
p 2682 N94-25586
SAKUMA, ICHIRO p 2904 N94-27467
p 2904 N94-27468
SAKUMA, NOBUO p 2728 N94-25573
SAKURAGI, SOKICHI p 2913 N94-27449
p 2913 N94-27450
p 2913 N94-27451
p 2914 N94-27454
SAKURANAKA, NOBORU p 2675 N94-27608
SAKURAYA, KAZUYUKI p 2723 N94-25552
SAKURAYA, KAZUYUKI p 2725 N94-25558
p 2730 N94-25585
SALAMATIN, V. S. p 3012 N94-25750
SALCUDEAN, M. p 2655 N94-28333
SALEM, HARRY p 2900 N94-25593
SALES, GARY S. p 2878 N94-26224
SALGADO, C. W. p 3028 N94-27752
SALTZBERG, D. p 3028 N94-27748
SAMMELLS, A. F. p 2859 N94-27005
SAMOILOFF, A. p 3023 N94-26929
SAMPAIO, R. p 2792 N94-26401
SAMSON, J. C. p 2887 N94-28218
SAMUEL, ARTHUR G. p 2939 N94-27094
SAMUEL, S. p 3024 N94-26949
SANAI, MASANOBU p 2871 N94-28155
SANCHEZ, J. A. p 2960 N94-26048
SANCHEZ, L. C. p 2702 N94-26560
SANDERS, BRIAN P. p 2706 N94-25876
SANDERS, W. T. p 3115 N94-27236
p 3115 N94-27419
p 3115 N94-27420
SANDILANDS, JOHN WADE p 2867 N94-26670
SANDLIN, DORAL p 2671 N94-25710
SANDLIN, DORAL R. p 2668 N94-26235
SANDY, RALEIGH A., III p 2766 N94-25797
SANFORD, THOMAS B. p 2900 N94-27090
SANKAR, J. p 2708 N94-26557
SANKAR, L. N. p 2793 N94-26595
SANTANNA, SIDNEI J. S. p 2776 N94-27335
SANTI, L. MICHAEL p 2702 N94-27166
SAPIR, JOSEPH p 3005 N94-26802
SAPPEY, A. D. p 3042 N94-26081
SARADZHEV, F. M. p 3067 N94-27647
SARANGAN, ANDREW M. p 2787 N94-27650
SARAVIA, E. p 3041 N94-25846
SARKIMO, MATTI p 2707 N94-26260
SARLIN, JUHA p 2704 N94-25651
SARUKURA, NOBUHIKO p 2820 N94-27339
SARVARANTA, LEENA p 2708 N94-26544
SASABE, KEN p 2728 N94-25574
p 2730 N94-25585
SASAKI, S. p 2820 N94-27701
SASAKI, TOMOYUKI p 2788 N94-27821
SATAKE, RYUSUKE p 2779 N94-27964
SATHAYE, J. p 2867 N94-26419

SATO, AKIRA p 2727 N94-25572
p 2730 N94-25585
SATO, HIDEYUKI p 2932 N94-27541
SATO, HIROSHI p 2932 N94-27541
SATO, JUN p 2906 N94-27495
SATO, KOICHI p 2729 N94-25578
SATO, MITSUGI p 2884 N94-27967
p 2884 N94-27968
SATO, MOTOYOSHI p 2920 N94-27481
SATO, NATSUO p 2884 N94-27967
SATO, SHUNJI p 2722 N94-25547
p 2724 N94-25555
SATO, TAKASHI p 2745 N94-28162
SATO, YUTAKA p 3100 N94-27336
SATOH, MASAKI p 2881 N94-27299
SATOH, RIE p 2718 N94-27388
SATSANGI, A. p 2688 N94-27373
SATTERWHITE, D. p 2698 N94-25700
SAULS, BOB p 2689 N94-25682
SAUSEN, TANIA MARIA p 2850 N94-27384
SAVELSBERGH, M. W. P. p 2992 N94-26226
SAVIHARJU, K. p 2867 N94-26241
SAVORY, E. p 2800 N94-28009
SAWA, HIROSHI p 3064 N94-27175
SAWCHUK, STEPHEN P. p 2798 N94-27873
SAYLOR, W. W. p 2696 N94-26808
SCALI, JAMES L. p 2876 N94-25752
SCANLAN, R. M. p 3060 N94-26795
SCHAACK, DAVID F. p 2835 N94-26691
SCHAD, KRISTIN C. p 2756 N94-27230
SCHAEFER, D. W. p 2712 N94-27710
SCHAFER, K. J. p 2818 N94-26698
SCHALCK, S. M. p 2694 N94-25738
SCHANTZ, B. p 2937 N94-28392
SCHAPOSNIK, F. A. p 3072 N94-26417
SCHECHTER, D. E. p 2713 N94-26014
SCHELLEKENS, A. N. p 2995 N94-26812
SCHENONE, ALDO B. p 3098 N94-26500
SCHEPERS, HENK p 2966 N94-26971
SCHEPLER, KENNETH L. p 3052 N94-25993
SCHERSON, D. A. p 2856 N94-26464
SCHERSON, DANIEL A. p 2782 N94-26328
SCHETTER, B. p 2831 N94-28082
SCHIEWECK, FRIEDHELM p 2807 N94-28099
SCHIFF, ROY p 3039 N94-27676
SCHIJVE, J. p 2669 N94-26969
SCHIPPER, J. D. p 3031 N94-25619
SCHIPPERS, K. A. p 2658 N94-28350
SCHIRBER, J. E. p 3050 N94-25817
SCHLEICHER, DAVID R. p 2667 N94-26151
SCHLEICHER, R. W. p 3043 N94-26324
SCHLEIJPEN, H. M. A. p 3036 N94-26648
SCHLENGERMANN, UTE p 2903 N94-27743
SCHLENSTEDT, S. p 2814 N94-28098
SCHLUTER, LARRY p 2682 N94-27997
SCHMIDT, D. K. p 2697 N94-27789
SCHMIDT, DAVID F. p 2864 N94-28131
SCHMIDT, GEORGE R. p 2797 N94-27639
SCHMIDT, J. J. p 3095 N94-25751
SCHMIDT, PHILLIP H. p 2678 N94-27414
SCHMIDT, V. p 2986 N94-26916
SCHMITT, R. C. p 2739 N94-26935
SCHNEIDER, FRED B. p 2666 N94-27768
SCHNEIDER, M. F. p 2807 N94-28172
SCHNEIDER, R. P., JR. p 2780 N94-25664
p 3056 N94-26352
p 3069 N94-27790
SCHOCH, P. M. p 3047 N94-27720
SCHOEBERL, F. p 3013 N94-25826
SCHOELD, J. p 2756 N94-27215
SCHOONDORP, MONIQUE ANNETTE
p 2747 N94-25749
SCHRA, L. p 2743 N94-27795
SCHRADER, HENRY A. p 2661 N94-28232
SCHRAM, M. W. p 2665 N94-26539
SCHREINER, WILLIAM S. p 2883 N94-27883
SCHRIEKEN, J. p 2831 N94-28085
SCHRIMSHER, ROBERT H. p 2911 N94-26985
p 2911 N94-27130
SCHROCK, R. R. p 2749 N94-25973
SCHROEDER, W. U. p 3029 N94-27783
SCHUBERT, J. p 3005 N94-27173
SCHUBERT, JOHAN p 2986 N94-26992
SCHUBERT, PAUL A. p 3096 N94-25997
SCHUBERT, W. K. p 2857 N94-26617
SCHUCK, MARY MARGARET p 2942 N94-27683
SCHUDT, E. E. p 2823 N94-26976
SCHULZE, N. p 2688 N94-27373
SCHUMACHER, I. p 2969 N94-27318
SCHWARTZ, IRA B. p 2787 N94-27673
SCHWARTZ, R. W. p 3061 N94-26856
SCHWARZ, RICHARD A. p 2818 N94-26705
SCHWENK, F. C. p 3094 N94-27772
SCOTT, ELAINE P. p 2846 N94-27920
p 2815 N94-27921
SCOTT, J. A. p 2998 N94-27115
SCOTT, M. J. p 2866 N94-25948
SCOVEL, CLINT p 3007 N94-27777
SCOVILLE, B. G. p 3045 N94-26865
SCOVILLE, J. T. p 3045 N94-26950
SCRIMGER, P. p 2969 N94-27318
SCULLY, JOHN R. p 2844 N94-27851
SEAGER, C. H. p 3052 N94-25971
SEAH, M. P. p 2738 N94-26653
SECAN, JAMES A. p 2877 N94-25877
SEEREERAM, SANJEEV p 2683 N94-26279
SEESTROM, S. J. p 3013 N94-25820
SEGALL, NATHANIEL LEONARD p 2989 N94-27975
SEGUCHI, TADAO p 2757 N94-27812
SEGUR, HARVEY p 2899 N94-26354
SEKI, SHUICHI p 2788 N94-27821
SEKIGUCHI, CHIHARU p 2914 N94-27456
SELF, DAVID A. p 2910 N94-26973
SELLONI, A. p 3066 N94-27347
SELVADURAY, G. p 3053 N94-26029
SELYUGIN, O. V. p 3014 N94-25869
SEMERARO, PAUL p 2703 N94-25690
SEMVERSTOV, D. M. p 3030 N94-27994
SENKO, V. A. p 2783 N94-26380
SENKURO, KUNIYUKI p 2853 N94-27990
SEO, HISAO p 2911 N94-27443
p 2903 N94-27444
p 2904 N94-27464
p 2904 N94-27477
p 2919 N94-27478
p 2905 N94-27479
p 2905 N94-27480
p 2920 N94-27481
p 2905 N94-27482
SEOUD, R. p 2803 N94-28025
SERAFIM, PHILIP p 2820 N94-27671
SERAVIA, RICKY A. p 2822 N94-26174
SERAYDARIAN, R. p 3048 N94-27791
SERGEEV, S. M. p 3072 N94-26039
p 2993 N94-26457
SERGEEV, V. A. p 3056 N94-26379
SERGEY, G. p 2809 N94-25599
SERS, JEAN-MARIE p 2949 N94-26717
SESHAN, P. K. p 2943 N94-27934
SETO, MASAHIRO p 2879 N94-26475
p 2871 N94-28156
SETZER, RONALD E. p 2676 N94-25785
SEUNGKOOG, L. p 3029 N94-27811
SEVERANCE, KURT p 2647 N94-27161
SEVIOR, M. E. p 3014 N94-25840
SHAFER, MARK M. p 2691 N94-26017
SHAFER, STEVEN A. p 2984 N94-25900
SHAFFER, L. B. p 3065 N94-27251
SHAH, RITESH P. p 2709 N94-27142
SHANABARGER, MICKEY R. p 2716 N94-26643
SHANEYFELT, M. R. p 2780 N94-25812
SHANG, BO p 3023 N94-26943
SHANG, C. C. p 2768 N94-26310
SHANKEY, JEFFREY R. p 2683 N94-26282
SHANKLAND, T. J. p 2880 N94-26806
SHANNON, S. G. p 2910 N94-26432
SHANNON, SAMUEL G. p 2911 N94-26985
p 2911 N94-27097
p 2911 N94-27130
SHAPIRO, I. L. p 3071 N94-25883
SHAPIRO, JEROME M. p 2947 N94-28261
SHAPIRO, V. D. p 3111 N94-27953
SHARIFF, SHAUN p 2833 N94-25704
SHARMA, OM p 2674 N94-26588
SHARMA, S. p 2811 N94-26787
SHASHIDAR, R. p 2754 N94-27033
SHAW, J. M. p 2936 N94-28374
SHCHELKACHEV, A. V. p 3019 N94-26456
SHCHIPUNOV, L. A. p 2715 N94-26406
SHEA, DAN p 2824 N94-27228
SHEA, JOSEPH p 2689 N94-25687
SHEEHAN, KATHLEEN p 2948 N94-25864
p 3096 N94-25925
p 3002 N94-25962
SHEEHAN, P. M. p 2891 N94-28311
SHELDON, R. I. p 2733 N94-26069
SHELDON, W. R. p 2876 N94-28312
SHELKOV, E. M. p 2854 N94-26056
SHEN, ALEXANDER p 2973 N94-27737
SHEN, W. p 3042 N94-26132
SHEN, XIAO-AN p 3037 N94-27010
SHENG, YONGWEI p 2875 N94-28289
SHEPODD, T. J. p 2759 N94-26198
SHERBY, O. D. p 2708 N94-26930
SHERWIN, M. E. p 3069 N94-27790
SHERWOOD, ROB p 2862 N94-28119
SHEVCHENKO, V. p 3111 N94-27953
SHI, JIAN p 3005 N94-25781
p 3005 N94-25823
SHIBANUMA, KIYOSHI p 2757 N94-27812
SHIBATA, KATSUNORI p 2776 N94-27340
SHIBATA, KEIICHI p 2761 N94-28002
SHIBATA, NITARO p 2904 N94-27467
p 2904 N94-27468
SHIBATA, TAKEMASA p 3027 N94-27718
p 3029 N94-27820
SHIBUTANI, K. p 3060 N94-26771
SHIBUYA, KAZUO p 2885 N94-27973
SHIEKH, A. Y. p 2878 N94-26418
SHIELDS, W. p 2689 N94-25674
SHIGESATO, YUZO p 3062 N94-26932
SHIH, C. p 2800 N94-28007
SHIMADA, TOSHIAKI p 2722 N94-28165
SHIMAZAKI, JUNYA p 2989 N94-27809
SHIMAZU, KAZUHIRO p 2908 N94-27519
SHIMIZU, KEN p 2933 N94-27944
SHIMIZU, MASARU p 2723 N94-25548
SHIMIZU, MASUJIRO p 2896 N94-27169
SHIMIZU, TADASHI p 2724 N94-25557
p 3064 N94-27177
SHIMODAIRA, MASUO p 2729 N94-25579
SHIMOGATA, SHIGEO p 2867 N94-26474
SHIMOKAWA, TOSHIYUKI p 2842 N94-27207
SHIN, IN CHUL p 2901 N94-26470
SHIN, S. p 3065 N94-27239
SHINOHARA, JOJI p 2761 N94-28002
SHINOHARA, MIKIYA p 3064 N94-27232
SHINOHARA, TAKESHI p 2745 N94-28162
SHINYA, NORIO p 2729 N94-25580
p 2729 N94-25581
SHIONOYA, SHIGEHIKO p 2908 N94-27530
SHIPERS, L. R. p 2702 N94-26560
SHIPLEY, D. E. p 2903 N94-25672
SHIRAISHI, HARUKI p 2682 N94-25586
SHIRAKAWA, MASAKI p 2907 N94-27510
SHIRK, FRANK J. p 2671 N94-28034
SHLEIFER, M. p 2811 N94-26787
SHMAKOV, S. YU. p 3015 N94-25916
SHNIR, YA. M. p 3074 N94-27696
SHOCHET, OFER p 3065 N94-27243
SHOEMAKER, C. S. p 2891 N94-28313
SHOEMAKER, E. M. p 2891 N94-28313
SHOJI, TAKATOSHI p 2913 N94-27449
p 2913 N94-27450
p 2913 N94-27451
SHPILRAIN, E. E. p 2853 N94-26052
SHROUT, THOMAS R. p 2812 N94-27214
SHU, WEI-MIN p 2744 N94-27876
SHUFEN, CHANG p 2758 N94-27845
SHUL, R. J. p 3052 N94-25989
SHVARTSMAN, SH. M. p 3019 N94-26424
SHVERA, YURI M. p 3068 N94-27678
SIBIRYAKOV, A. G. p 3071 N94-25883
SICHEL, M. p 2795 N94-27252
SICKAFUS, K. E. p 3069 N94-27828
SICONOLFI, STEVEN F. p 2934 N94-28361
SIDOROV, A. V. p 2783 N94-26380
SIEBES, ARNO P. J. M. p 2970 N94-27548
SIEGEL, R. W. p 2751 N94-26594
SIEGENTHALER, U. p 2898 N94-25791
SIGMUND, W. p 2754 N94-26977
p 2755 N94-27087
SIGMUND, W. M. p 2755 N94-27163
SIHVOLA, A. p 2778 N94-28382
SIHVOLA, A. H. p 2778 N94-28355
p 2779 N94-28397
SIKKEL, KLAAS p 2981 N94-26998
SILANDER, JOHN A., JR. p 2852 N94-28070
SILLANPAEAE, JUHA p 2679 N94-25652
SILLY, MARYLINE p 2951 N94-26728
SILVA, DANIEL p 2943 N94-25694
SILVER, M. p 2736 N94-26481
SILVER, R. N. p 3073 N94-26805
SIMEONI, F. p 3014 N94-25887
SIMMONS, REID p 2985 N94-26006
SIMMS, GARFIELD p 2789 N94-27922
SIMON, DAVID A. p 2809 N94-25967
SIMONEAU, JACQUES p 2799 N94-27947
SIMONEN, E. P. p 2838 N94-26524
SIMPSON, ROBERT W. p 2641 N94-27285
SINCLAIR, JENNIFER L. p 2792 N94-26319
SINGH, B. p 2686 N94-27364
SINGH, B. N. p 3017 N94-26049
SINGH, P. P. p 3055 N94-26238
SINGPURWALLA, N. D. p 2968 N94-27140
SINHA, N. p 2804 N94-28030
SINHA, NITA p 3026 N94-27402
SINITSKAYA, A. V. p 3075 N94-27858
SIPILAE, SISKO p 2837 N94-26255
SISAKYAN, A. N. p 3030 N94-27860
SJOLANDER, S. A. p 2652 N94-28321
SKELLY, JUNE J. p 2937 N94-25965
SKIDMORE, TRENT A. p 2642 N94-27292
SKOTHEIM, T. A. p 2717 N94-26951
SLAD, L. M. p 3013 N94-25835
p 3015 N94-25920
SLATTERY, P. p 3008 N94-25988
SLAVIN, A. M. p 2836 N94-26032

SLEPCHENKO, L. A. p 3030 N94-27860
SLIK, P. C. p 2881 N94-27052
SLOAN, M. L. p 3033 N94-27078
SLOCUM, KEVIN R. p 2849 N94-27069
SLOOT, PETER p 2955 N94-27194
SMEDLEY, TREVOR JANATHAN p 2998 N94-27269
SMIRNOV, A. V. p 3032 N94-26164
SMITH, A. V. p 3040 N94-27999
p 3040 N94-28000
SMITH, ALPHONSO C. p 3040 N94-27923
SMITH, ARTHUR p 3115 N94-27167
SMITH, BRIAN A. p 3009 N94-25737
SMITH, D. H. p 2965 N94-26784
SMITH, ERIC A. p 2847 N94-26222
SMITH, ERIC P. p 2868 N94-26817
SMITH, GARY A. p 2940 N94-25611
SMITH, GERALD J. p 2869 N94-27267
SMITH, GREGORY P. p 2717 N94-27226
SMITH, J. D. p 2903 N94-25672
SMITH, JACQUELINE D. p 2765 N94-25660
SMITH, KENNETH L., JR. p 2899 N94-26149
SMITH, L. p 3060 N94-26840
SMITH, M. D. p 2843 N94-27656
SMITH, M. T. p 2741 N94-27622
SMITH, P. M. p 2738 N94-26610
SMITH, ROY p 2943 N94-25693
SMITH, S. E. p 2813 N94-27624
SMITH, S. H. p 2800 N94-28008
SMITH, W. L. p 2750 N94-26247
p 2751 N94-26564
p 2895 N94-26697
SMITS, A. J. p 2800 N94-28006
SMYTH, KERMIT C. p 2716 N94-26893
SMYTH, WILLIAM H. p 3106 N94-27406
SNAIL, KEITH p 3039 N94-27676
SNEH, OFER p 3028 N94-27760
SNIDER, ALLAN NEILL p 2963 N94-26616
SNIDER, JACK B. p 2896 N94-26959
SNYDER, CORWIN p 2824 N94-27224
SNYDER, MARK I. p 2958 N94-25767
SNYERS, E. p 2952 N94-26734
SOBAN, DANI p 2671 N94-25710
SOBUE, GEN p 2930 N94-27532
SOFUE, YASUSHI p 2710 N94-27255
SOKAL, A. D. p 3073 N94-27002
SOKOLOV, J. N. p 2854 N94-26056
SOL, M. p 2992 N94-26226
SOLIMAN, ABDELFATTAH p 3001 N94-27948
SOMMEIJER, B. P. p 2991 N94-26217
SON, LE HUNG p 2991 N94-25881
SONG, HI SUP p 2901 N94-26470
SONG, KYE SEOK p 2714 N94-26158
SONG, KYU SEOK p 2816 N94-26157
p 2817 N94-26402
SONG, WOO SUP p 3042 N94-26159
SONODA, HIDEKI p 2933 N94-27945
SOONS, JOHANNES AUGUSTINUS
p 3002 N94-26000
SOREL, YVES p 2954 N94-26745
SORENSEN, D. p 2698 N94-25700
SORENSEN, N. R. p 2739 N94-26912
SOSNIN, A. N. p 3015 N94-25916
SOUMPASIS, D. M. p 3030 N94-28001
SOWERS, C. H. p 3059 N94-26591
SOWMYANARAYANAN, KUMBAKONAN S.
p 3025 N94-27266
SPACY, WILLIAM L., II p 2790 N94-25862
SPARGO, A. E. C. p 3055 N94-26171
SPARKS, C. L. p 3065 N94-27251
SPARROW, VICTOR W. p 2650 N94-28190
SPEARMAN, M. LEROY p 3117 N94-26155
p 2646 N94-26693
SPEECE, ROBERT F. p 2692 N94-27956
SPENCER, B. F., JR. p 2823 N94-26976
SPERBER, K. R. p 2897 N94-27571
SPICER, D. S. p 3111 N94-27953
SPIEGEL, EDWARD A. p 3110 N94-26883
SPIEKER, B. p 2996 N94-26917
SPIGGLE, CHARLES p 2943 N94-25678
SPIJKER, M. N. p 2992 N94-26229
SPILG, L. p 2823 N94-26849
SPRAGGE, M. K. p 2749 N94-25985
SPRANGEL, P. p 2820 N94-27671
SPRIESTERBACH, T. p 2698 N94-25700
SPRINKLE, J. K., JR. p 2813 N94-27624
SPRITZER, MICHAEL H. p 2759 N94-26800
SQUIRES, P. K. p 2668 N94-26604
SREE, DAVE p 3009 N94-27924
SRIVASTAVA, R. p 2846 N94-28227
STACY, KATHRYN p 2647 N94-27161
STAHL, BERNHARD p 2681 N94-27587
STAINBACK, P. C. p 2646 N94-26548
STANDLEE, D. J. p 2863 N94-28129
STANDLEY, BRIAN K. p 2940 N94-25611
STANNY, R. R. p 2909 N94-26179
STANSFIELD, K. L. p 2852 N94-27875
STANSKI, U. p 2824 N94-27254
STARCHVILLE, THOMAS F., JR. p 2689 N94-25692
STARKE, EDGAR A., JR. p 2844 N94-27851
STARKOVICH, STEVEN PAUL p 3104 N94-26638
START, D. F. H. p 3046 N94-27261
STATE, ANDREI p 2970 N94-27417
STAUDACHER, W. H. p 2659 N94-28027
STAUFFER, LARRY p 2833 N94-25683
STAUNTON, J. B. p 2736 N94-26351
STAURT, L. M. p 3017 N94-26101
STEARNS, C. A. p 2680 N94-26141
STEBLETSOVA, VERA p 2970 N94-27549
STEELEMANN, SVEN ALEXANDER
p 3036 N94-26666
STEEN, AKE p 2881 N94-27040
STEFFEN, KONRAD p 2851 N94-27849
STEFFEN, WILL p 2874 N94-28281
p 2874 N94-28282
STEFKO, GEORGE L. p 2846 N94-28227
STEIGER, PETER p 2935 N94-28370
STEIN, EARL S. p 2664 N94-26197
STEIN, H. J. p 3052 N94-25971
STEINETZ, BRUCE M. p 2826 N94-27599
STEINVALL, O. p 2900 N94-27156
STEN, J. C. E. p 2778 N94-28387
STENERSEN, KNUT p 2817 N94-26203
STENGEL, ROBERT p 2643 N94-27298
STENGEL, ROBERT F. p 2643 N94-27294
STENGER-SMITH, JOHN D. p 2755 N94-27148
STEPANOV, V. p 2788 N94-28357
STEPHENS, C. R. p 3006 N94-26193
STEPHENS, J. J. p 3069 N94-27753
STEPHENS, MICHAEL A. p 3003 N94-26495
p 3004 N94-26496
STEPHENS, MICHAEL J. p 2984 N94-25743
STEPHENSON, G. J., JR. p 3006 N94-25886
STERN, S. ALAN p 3103 N94-26789
STERNE, P. A. p 2736 N94-26351
STEVENS, R. p 2752 N94-26652
STEVENSON, JONATHAN DAVID p 2674 N94-26673
STEWART, DAVID B. p 2958 N94-25777
STEWART, HELEN p 2989 N94-28065
STEWART, R. G. p 2672 N94-26340
STEWART, T. B. p 2746 N94-28185
STEWART, T. L. p 2664 N94-26309
STEWART, VEARL R. p 2802 N94-28016
STEYERL, A. p 2733 N94-26070
STEYSKAL, HANS p 3032 N94-26881
STILL, C. H. p 3020 N94-26577
STOCKDALE, R. E. p 3043 N94-26274
STOEREN, S. p 2909 N94-25909
STOILOVA, N. I. p 2993 N94-26440
p 3073 N94-26758
p 3001 N94-27839
STOKER, CAROL R. p 2685 N94-27360
STOLLER, R. E. p 2739 N94-26931
STOLT, K. p 2812 N94-27160
STOLTE, J. p 3031 N94-25619
STONE, EDWARD C. p 3107 N94-27784
STONE, RONALD A. p 2984 N94-25900
STONEKING, M. p 3042 N94-26132
STONER, G. E. p 2742 N94-27788
STONER, GLENN E. p 2844 N94-27851
STOREBOE, PER B. p 2712 N94-25745
STOREY, MARK A. p 2765 N94-25676
STOUDT, CRAIG A. p 3034 N94-25730
STOVER, RAE p 2943 N94-25679
STOYCOS, LARA E. p 2697 N94-28183
STRACHAN, J. D. p 3048 N94-27825
STRAKA, W. A. p 2789 N94-25604
STREETMAN, J. ROBERT p 3005 N94-26802
STRICKLAND, D. J. p 2883 N94-27393
STROGANOV, YU. G. p 3002 N94-26038
STROHMAYER, T. E. p 3116 N94-27714
STROPKY, D. M. p 2655 N94-28333
STROUD, W. JEFFERSON p 2844 N94-27830
STRUK, PETER p 2671 N94-25713
STRUM, M. J. p 2706 N94-25938
STUART, DAVID W. p 2894 N94-26431
STUART, THOMAS A. p 2703 N94-27662
STUBBINS, J. F. p 2737 N94-26556
STUBBS, SANDY M. p 2669 N94-26608
STUBICAN, V. S. p 3060 N94-26782
STUCKEY, JAMES M. p 2756 N94-27429
STUDENIKIN, A. I. p 3104 N94-26269
STUPIAN, GARY W. p 2785 N94-26845
STURROCK, PETER A. p 3111 N94-27099
STURROCK, WILLIAM R. p 2670 N94-27666
STYLIANOU, MARINOS COSTA p 2838 N94-26639
SU, J. J. p 3111 N94-27953
SU, X. N. p 2791 N94-26096
SUBHLOK, JASPAL p 2982 N94-27117
SUEDA, KAORI p 2903 N94-27444
SUEMATSU, H. p 2750 N94-26124
SUEMOTO, TORU p 3064 N94-27176
SUENAGA, M. p 3060 N94-26771
SUES, R. H. p 2843 N94-27656
SUGE, HIROO p 2728 N94-25573
SUGENOYA, JUNICHI p 2912 N94-27445
p 2915 N94-27459
p 2918 N94-27473
p 2930 N94-27529
SUGIHARA, TADASHI p 2761 N94-28002
SUGIMOTO, MAKOTO p 2788 N94-27821
SUGIMOTO, TAKAHITO p 2905 N94-27483
SUGIMURA, KIMIYA p 2928 N94-27521
SUGIYAMA, KAZUMASA p 2721 N94-28159
SUGIYAMA, YOSHIKI p 2915 N94-27458
p 2915 N94-27459
p 2918 N94-27473
p 2918 N94-27474
p 2928 N94-27521
p 2929 N94-27524
p 2929 N94-27525
p 2929 N94-27526
p 2930 N94-27529
p 2930 N94-27533
SUGURI, NOBUYA p 2761 N94-27341
SUH, JUNIN p 2870 N94-28150
SUH, KYUNG SUK p 2894 N94-26469
SUJUN, TANG p 2758 N94-27845
SULLIVAN, BRENDA M. p 2651 N94-28195
SULLIVAN, P. A. p 2654 N94-28328
SUMI, EICHI p 2898 N94-25635
SUMIDA, MASAE p 2722 N94-25544
p 2726 N94-25567
SUN, D. C. p 2826 N94-27657
SUN, NANCY p 2943 N94-25680
SUN, X. p 2973 N94-27717
SUN, XIAN-HE p 2969 N94-27416
SUN, XIAODONG p 3073 N94-26876
SUN, XUE-ZHI p 2904 N94-27470
SUNKA, P. p 3048 N94-27836
SUONSIVU, H. p 3100 N94-28385
SURAMPUDI, SUBBARAO p 2860 N94-28103
SURARERKS, VANPEN p 2875 N94-28288
SUREK, T. p 2855 N94-26115
SUTHERLAND, B. p 3064 N94-27231
SUTHERLAND, H. J. p 2838 N94-26563
SUTHERLAND, MARK M. p 3073 N94-27263
SUTTER, B. p 3098 N94-26598
SUTTON, R. F. p 2701 N94-26231
p 2824 N94-27228
SUZUKI, FUSAYUKI p 2730 N94-25583
SUZUKI, HATSUE p 2915 N94-27458
p 2918 N94-27475
SUZUKI, HIROYOSHI p 2886 N94-27987
SUZUKI, HIROYUKI p 2913 N94-27449
p 2913 N94-27450
p 2913 N94-27451
p 2913 N94-27452
p 2913 N94-27453
p 2914 N94-27454
p 2914 N94-27456
p 2914 N94-27457
SUZUKI, KATUO p 2973 N94-27732
SUZUKI, KOICHI p 2681 N94-27247
SUZUKI, NAOYUKI p 2730 N94-25584
SUZUKI, RYOKO p 2904 N94-27467
p 2904 N94-27468
p 2904 N94-27469
p 2907 N94-27505
p 2907 N94-27508
p 2907 N94-27511
p 2907 N94-27512
p 2908 N94-27515
p 2908 N94-27516
SUZUKI, SHIGEYUKI p 2906 N94-27495
p 2906 N94-27496
p 2906 N94-27497
p 2906 N94-27498
SUZUKI, SHUNICHI p 2729 N94-25578
SUZUKI, Y. p 3028 N94-27759
SVARVERUD, ERIC p 2833 N94-25704
SVENES, K. p 2876 N94-25807
SVENSSON, P. p 3005 N94-27173
SVENSSON, T. p 2842 N94-27198
SWAGER, TIMOTHY M. p 2736 N94-26452
p 3059 N94-26571
SWANN, MYLES H. p 2756 N94-27230
SWANSON, M. L. p 3054 N94-26137
SWEATT, W. C. p 2819 N94-27262
SWEET, M. R. p 2696 N94-26808
SWERN, FREDERIC L. p 2973 N94-27663
SWIFT, DAVID C. p 2683 N94-26282
SWIFT, SHANNON p 2943 N94-25678
SWYDEN, THOMAS A. p 2787 N94-27672
SYKES, D. M. p 2659 N94-28040
SYMCHYCH, T. p 2983 N94-28042
SYN, C. K. p 2708 N94-26930
SZCZEPINSKI, WOJCIECH p 2739 N94-26824
SZEKELY, CSABA p 3008 N94-26484

SZEWCZYK, ALBIN A. p 2791 N94-26187
SZYMANSKI, J. J. p 3013 N94-25820

T

TABATABAI, GARGARI MOUSA p 2842 N94-27315
TABUCHI, MASAAKI p 2730 N94-25583
TACHIBANA, SHOICHI p 2933 N94-27942
p 2933 N94-27945
TADAKI, EIKO p 2906 N94-27502
TAFLOVE, ALLEN p 2766 N94-25757
TAFT, BRETT p 2697 N94-25667
TAGGART, BEN p 2671 N94-25713
TAILLON, MAGGIE p 2671 N94-25713
TAJIMA, T. p 3041 N94-25923
TAKABATAKE, TOSHIRO p 3025 N94-27337
TAKABAYASHI, AKIRA p 2912 N94-27446
p 2912 N94-27447
p 2912 N94-27448
TAKAGI, SADAHARU p 2912 N94-27446
p 2912 N94-27447
p 2912 N94-27448
TAKAGISHI, YOSHIKO p 2904 N94-27471
p 2905 N94-27483
p 2905 N94-27484
p 2905 N94-27486
p 2905 N94-27487
p 2906 N94-27493
TAKAHASHI, AKIRA p 2928 N94-27521
TAKAHASHI, HIDEAKI p 2710 N94-27279
p 2710 N94-27280
TAKAHASHI, HITOSHI p 2647 N94-27235
TAKAHASHI, JUNJI p 2726 N94-25566
TAKAHASHI, KATSUYUKI p 2729 N94-25578
TAKAHASHI, KOICHI p 3100 N94-27336
TAKAHASHI, MASAHIKO p 2776 N94-27340
TAKAHASHI, MINORU p 2718 N94-27390
TAKAHASHI, SATOSHI p 2722 N94-25545
TAKAHASHI, YOSHIKAZU p 2788 N94-27821
TAKAMASU, T. p 3065 N94-27245
TAKAMURA, S. p 2820 N94-27701
TAKEDA, ATSUSHI p 2876 N94-28293
TAKEDA, SUSUMU p 2721 N94-28159
TAKEUCHI, N. p 3066 N94-27347
TAKEUCHI, SHIGEO p 2929 N94-27524
p 2929 N94-27526
TAKEUCHI, SHIN p 3053 N94-26071
p 2736 N94-26477
p 3069 N94-27756
TAKEUCHI, TAKAO p 2725 N94-25559
TAKEUCHI, YOSHIAKI p 2853 N94-28269
TAKEYAMA, MASAO p 2730 N94-25585
TAKEYAMA, SHOJIRO p 3064 N94-27232
p 3065 N94-27240
p 3065 N94-27245
TAKHTAMYSHEV, G. G. p 3027 N94-27682
TALJA, ASKO p 2762 N94-25622
TALROSE, V. L. p 2854 N94-26054
TAMADA, M. p 3112 N94-25628
p 3113 N94-25629
p 3113 N94-25630
p 3113 N94-25631
p 3113 N94-25632
TAMADA, MASANOBU p 3114 N94-25634
TAMARU, MASAO p 2904 N94-27472
TAMIDA, TAICHIRO p 3025 N94-27338
p 2820 N94-27605
TAMURA, HIROYASU p 3051 N94-25921
p 3053 N94-26089
TAMURA, MASAFUMI p 3064 N94-27175
TAMURA, RYOKO p 2906 N94-27500
TAMURA, YOSHIO p 2728 N94-25577
TANABE, HIDENOBU p 2973 N94-27702
TANABE, TATSUHIKO p 2743 N94-27807
TANAKA, CHIAKI p 2723 N94-25548
TANAKA, HIDEO p 2723 N94-25548
p 2729 N94-25580
TANAKA, ISAO p 2761 N94-27341
TANAKA, KENICHI p 3012 N94-25636
p 2715 N94-26476
TANAKA, KOICHIRO p 3064 N94-27176
TANAKA, MASAFUMI p 2915 N94-27460
p 2927 N94-27517
TANAKA, S. p 3059 N94-26765
p 3061 N94-26841
TANAKA, SHUNSUKE p 2949 N94-26716
TANAKA, YOSHIAKI p 2725 N94-25559
TANAKA, YOSHIHISA p 2724 N94-25553
TANASAWA, ICHIRO p 2761 N94-27341
TANATAR, B. p 3063 N94-27017
TANG, CHA-MEI p 2787 N94-27672
TANG, F. C. p 2653 N94-28323
TANG, T. S. p 2684 N94-26287
TANG, W. K. p 3028 N94-27736
TANI, YOSHIYUKI p 2905 N94-27482
TANIGUCHI, AKIHIKO p 2907 N94-27504
p 2907 N94-27510
TANIGUCHI, MASAHIRO p 2715 N94-26476
TANIMURA, S. p 2748 N94-25959
TANKESHWAR, K. p 3006 N94-26368
TANNENBAUM, ALLEN R. p 2988 N94-27139
TAO, HIROAKI p 2870 N94-28152
TAO, Q. p 2711 N94-27640
TAPIA, MOIEZ A. p 2836 N94-27925
TARABBIA, P. p 2953 N94-26743
TARANATHAM, PORNCHAI p 2873 N94-28280
TARASKO, M. Z. p 2995 N94-26768
TARBELL, THEODORE p 3110 N94-26590
TARDITI, DAVID p 3099 N94-27014
p 2967 N94-27063
TARLTON, JOHN p 2833 N94-25669
TARUI, HIDEO p 2933 N94-27942
TATLIPINAR, H. p 2715 N94-26391
TATSUMI, KENJI p 2870 N94-28149
p 2870 N94-28151
TATSUOKA, KIKUMI p 3096 N94-25925
p 3002 N94-25962
TATSUOKA, KIKUMI K. p 2948 N94-25864
TAUSCH, BENJAMIN J., II p 2862 N94-28118
TAUTZ, M. F. p 2959 N94-25879
TAYLOR, C. E. p 3060 N94-26795
TAYLOR, EDWARD p 3035 N94-26572
TAYLOR, P. C. p 3064 N94-27231
TAYLOR, P. D. p 2789 N94-25604
TAYLOR, R. P. p 2794 N94-26763
TAYLOR, STEVEN p 2943 N94-25693
TAYLOR, T. R. p 3071 N94-25882
TAYLOR, TIMOTHY N. p 2772 N94-26924
TAYLOR, WILLIAM W. L. p 2761 N94-27664
TEEGARDEN, KENNETH J. p 2820 N94-28068
TEGNESJOE, JOACIM p 3010 N94-27037
TEH, R. p 3006 N94-26270
TEIGE, S. p 3033 N94-27614
TEITEL, S. p 3050 N94-25848
TELSCHOW, K. L. p 3061 N94-26868
TEMAM, R. p 2792 N94-26499
TEMPLE, B. A. p 2701 N94-26537
TENCATE, H. H. p 2790 N94-25763
TERAKADO, TAKUYA p 2757 N94-27812
TERLAKY, T. p 2957 N94-25761
p 2958 N94-25762
p 2967 N94-27031
TERRELL, J. p 3116 N94-27793
TERRY, J. p 3056 N94-26326
TERYAEV, O. V. p 3068 N94-27679
p 3070 N94-27859
TESAR, A. p 2751 N94-26554
TESMER, J. R. p 3069 N94-27828
TESTON, F. p 2954 N94-26746
TETREAULT, M. p 2888 N94-28297
TEUSINK, FRANK p 2970 N94-27543
TEZOK, F. I. p 2655 N94-28334
TEZUKA, Y. p 3065 N94-27239
THAGGARD, MICHAEL p 2834 N94-26199
THAKUR, PRABHAT K. p 2787 N94-27628
THALLER, LAWRENCE H. p 2862 N94-28115
THANG, TRAN QUYET p 2991 N94-25881
THART, W. G. J. p 2743 N94-27795
THAYER, JEFFREY P. p 2883 N94-27852
THEEUWES, J. p 2908 N94-25871
THIBADEAU, ROBERT p 2765 N94-25725
p 2984 N94-25898
THIEBAUX, S. p 2971 N94-27575
THIEME, CHRISTIAAN J. E. p 2970 N94-27548
THIEMENS, M. H. p 2877 N94-26015
THOMA, D. J. p 2737 N94-26607
THOMAS, D. R. p 2807 N94-28175
THOMAS, DIMITRI D. p 2671 N94-25711
THOMAS, I. M. p 2749 N94-25985
THOMAS, M. N. p 2862 N94-28117
THOMPSON, DAVID W. p 2758 N94-27926
THOMPSON, J. D. p 3050 N94-25817
THOMPSON, JAMES R. p 3033 N94-27078
THOMPSON, K. R. p 2748 N94-25932
THOMPSON, KAREN G. p 2757 N94-27747
THOMPSON, L. M. p 2713 N94-26014
THOMPSON, ROGER C. p 2689 N94-25692
THOMPSON, T. L. p 3033 N94-27083
THOMSON, MARK J. p 3006 N94-25886
THORNDIKE, PHIL p 2703 N94-25690
THORNTON, EARL A. p 2844 N94-27851
THORP, S. I. p 2735 N94-26294
THRANE, E. V. p 2876 N94-25807
THUIS, H. G. S. J. p 2670 N94-27796
THUMM, M. p 2768 N94-26310
TICK, E. p 2955 N94-27196
TICONA, ROLANDO p 3114 N94-25634
TIECKE, H. p 2814 N94-28098
TILLMAN, JAMES E. p 3108 N94-27935
TILTON, JAMES C. p 2945 N94-28251
TIMMERMANS, R. p 3021 N94-26620
TING, ANTONIO C. p 2787 N94-27672
TINGAS, STEPHEN A. p 2679 N94-27660
TIOURIRINE, T. N. p 3047 N94-27715
TIPTON, P. p 3008 N94-25988
TIT, N. p 3062 N94-26901
TIT, NACIR p 3061 N94-26878
p 3062 N94-26902
TITLE, ALAN p 3111 N94-27321
TITZE, INGO p 2902 N94-27165
TIWARI, SURENDRA N. p 3085 N94-27893
TKABLADZE, A. V. p 3022 N94-26767
TODD, V. p 2712 N94-27813
TODOSOW, M. p 2699 N94-25798
TOFT, MARK R. p 2863 N94-28123
TOFTEN, T. H. p 2805 N94-28036
TOGANO, KAZUMASA p 2728 N94-25573
p 2730 N94-25585
TOKAR, S. p 3015 N94-25919
TOKUDA, SHINJI p 3000 N94-27731
TOLBERT, S. H. p 3054 N94-26125
TOLKACHEV, E. A. p 3074 N94-27696
TOLSTOV, K. D. p 3030 N94-27994
TOMLINSON, LEROY O. p 2831 N94-28080
p 2831 N94-28081
TOMOZAWA, M. p 2753 N94-26783
TONASSE, M. D. p 3016 N94-26041
TONDEL, F. p 2741 N94-27325
TONG, SHAOYING p 2811 N94-26662
TONKS, D. L. p 2733 N94-26022
TOOLA, ARJA p 2762 N94-25641
TORO, E. F. p 2790 N94-25778
TORRES, ABEL O. p 2646 N94-26693
TOSA, MASAHIRO p 2723 N94-25549
p 2727 N94-25570
TOSATTI, E. p 3066 N94-27347
TOSI, M. P. p 2715 N94-26391
TOY, N. p 2800 N94-28009
TOYAMA, JUNJI p 2904 N94-27465
p 2904 N94-27466
p 2904 N94-27469
p 2906 N94-27503
p 2907 N94-27504
p 2907 N94-27505
p 2907 N94-27506
p 2907 N94-27507
p 2907 N94-27508
p 2907 N94-27509
p 2907 N94-27510
p 2907 N94-27511
p 2907 N94-27512
p 2907 N94-27513
p 2908 N94-27514
p 2908 N94-27515
p 2908 N94-27516
TRACHSEL, WALTER G. p 2959 N94-25942
TRACY, R. A. p 2935 N94-28367
TRAHIOTIS, CONSTANTINE p 3010 N94-27067
TRALLERO-GINER, C. p 3062 N94-26897
TRAN, BAO N. p 3024 N94-27258
TRAN, DAL T. p 2765 N94-25676
TRAN, P. p 2657 N94-28345
TRAN, PHILLIP P. p 2691 N94-25696
TREBES, J. E. p 2816 N94-26020
TRELEAVEN, JAMES E. p 2693 N94-25595
TREMBLAY, J. J. P. p 2974 N94-27869
TRENCHARD, R. G. p 2736 N94-26522
TREPANIER, J. Y. p 2656 N94-28342
p 2657 N94-28347
TREWHELLA, J. p 2901 N94-26623
TRIANDAF, IOANA p 2787 N94-27673
TRINQUET, Y. p 2952 N94-26732
TRIPP, LLOYD D., JR. p 2911 N94-27088
TROEIM, J. p 2876 N94-25807
TROFIMOV, V. A. p 2715 N94-26406
TROITSKAYA, N. I. p 3022 N94-26900
TROMP, JOHN T. p 2955 N94-27547
TROMPERT, RON A. p 2995 N94-26773
TROSHIN, S. M. p 3031 N94-26044
TROXEL, SETH W. p 2680 N94-26196
TRUCANO, T. G. p 2888 N94-28296
TRUJILLO, ANNA C. p 2673 N94-27864
TRUJILLO, AURELIO p 3066 N94-27276
TRYK, DONALD p 2782 N94-26328
TSADKA, SAGIE p 2774 N94-27234
TSAI, C. C. p 2713 N94-26014
TSAI, HSIN-YEN p 3093 N94-26181
TSAI, LUNG-WEN p 2833 N94-25686
TSANG, RAYMOND WAI-MAN p 2823 N94-26658
TSAO, A. p 2973 N94-27717
TSAO, MIKE p 2673 N94-26176
TSENG, C. p 2742 N94-27694
TSINTSADZE, L. N. p 3046 N94-27630
TSINTSADZE, N. L. p 3046 N94-27630
TSIPOLITIS, GEORGE p 3026 N94-27399
TSO, JIN p 2803 N94-28023
TSUDA, TOSHINOBU p 3064 N94-27177

TSUEI, H. H. p 2701 N94-26208
TSUJI, HIROKAZU p 2743 N94-27807
TSUJI, HIROSHI p 2788 N94-27817
TSUJI, KAZUO p 3065 N94-27245
TSUJI, KEIICHIRO p 2916 N94-27463
TSUKAHARA, REIKO p 2928 N94-27522
p 2929 N94-27526
TSUKAHARA, SHINICHIRO p 2905 N94-27480
TSUKAMOTO, SHIGEKI p 2885 N94-27973
TSUKAMOTO, SUSUMU p 2722 N94-25546
TSUKUI, KEITA p 2884 N94-27966
TSUNEOKA, MASAKI p 2813 N94-27703
TSURUSAKI, KATSUYA p 2869 N94-28147
TSURUTA, YOSHINARI p 2764 N94-27976
TSUSHIMA, ITSURO p 3114 N94-25634
TUCKER, NATHAN P. p 2943 N94-25684
TUECKE, S. J. p 2963 N94-26407
TUNDAL, U. H. p 2732 N94-25908
TUOMISTO, MARJA-TERTTU p 2704 N94-25651
TURBINER, A. p 2996 N94-26915
TURCHI, P. E. A. p 3055 N94-26238
TUREMAN, ROBERT L., JR. p 2978 N94-27927
TURNER, L. p 3047 N94-27715
TURNER, M. S. p 3104 N94-26311
TURNER, TRAVIS L. p 3011 N94-27659
TURYK, PETER J. p 2652 N94-28320
TUTT, CHRIS J. p 2691 N94-25696
TUTTEROW, ROBIN D. p 2692 N94-27774
TUTTLE, B. p 3061 N94-26856
TUTTLE, B. A. p 3053 N94-26025
TVERSKY, BARBARA G. p 2939 N94-27012
TYTULA, THOMAS P. p 2756 N94-27230
TYURIN, N. E. p 3031 N94-26044

U

UCHIDA, TSUTOMU p 2885 N94-27969
UEDA, SHUICHI p 2675 N94-27608
UEDA, Y. p 3065 N94-27239
UEDA, YUTAKA p 3051 N94-25921
p 3053 N94-26089
p 3064 N94-27177
p 3066 N94-27353
UEHARA, MITSURU p 2727 N94-25571
UESUGI, Y. p 2820 N94-27701
UEYOSHI, K. p 2894 N94-26313
UJI, SHINYA p 2724 N94-25557
p 2726 N94-25563
UKITA, NOBUHARU p 2776 N94-27340
ULIBARRI, T. A. p 2712 N94-27710
ULLSCHMIED, J. p 3048 N94-27836
UM, TAE YOON p 2783 N94-26546
UMASHANKAR, KORADA R. p 2766 N94-25757
UMEZAWA, OSAMU p 2724 N94-25556
UNAL, N. p 2992 N94-26267
UNAL, RESIT p 2693 N94-27928
URNES, JAMES M., SR. p 2674 N94-27432
URUSHIGAWA, YOSHIKUNI p 2870 N94-28150
USAMI, KATSUHISA p 2724 N94-25553
USAMI, TAKESHI p 2869 N94-28147
USSLER, WOLF-RUEDIGER p 2661 N94-28236
USUI, SHIRO p 2912 N94-27446
p 2912 N94-27447
p 2913 N94-27453
p 2907 N94-27510
UTAGAWA, MANABU p 2879 N94-26475
p 2871 N94-28156
UTSCHIG, JOSEPH M. p 2818 N94-26498
UTSUMI, MASATO p 2871 N94-28155
UUTTU, TERO p 2707 N94-26260
UZAN-SAGUY, C. p 3023 N94-26929
UZEMBAEV, ERIK K. p 2715 N94-26476

V

VAANDRAGER, FRITS W. p 3000 N94-27577
p 2972 N94-27580
p 2972 N94-27581
VACHSS, F. p 3034 N94-25902
VAEISAENEN, HANNU p 2848 N94-26258
VAHEDI, V. p 2767 N94-25937
VAIDYANATHAN, P. P. p 2997 N94-27015
p 2998 N94-27035
VAIDYANATHAN, R. p 2708 N94-26557
VAINSENCHER, I. p 2993 N94-26412
VALDES-PEREZ, RAUL E. p 2984 N94-25591
VALENCIA, J. E. p 2696 N94-26808
VALIVETI, NATANA p 2980 N94-26635
VALL, A. N. p 3075 N94-27858
VALLETTE, BRENDA J. p 2814 N94-27981
VALTONEN, M. J. p 2890 N94-28305
VANBENTHEM, JOHAN p 2970 N94-27549
VANBERKEL, C. A. M. p 2999 N94-27349
VANBEUZEKOM, M. G. p 2779 N94-25618
VANBLADEL, P. G. p 2840 N94-26911
VANCOEVORDEN, R. G. p 2690 N94-25787
VANDALSEM, WILLIAM R. p 2671 N94-28033
VANDAM, C. P. p 2659 N94-27929
VANDENBERG, J. p 2847 N94-26228
VANDENBERGH, S. p 2891 N94-28314
VANDENGOOR, GEERT p 2975 N94-27936
p 2975 N94-27937
p 2975 N94-27938
p 2975 N94-27939
VANDENHEUVEL, J. p 3007 N94-27222
VANDENHEUVEL, J. C. p 3033 N94-25721
VANDENOEVER, J. p 2770 N94-26650
VANDERDONK, PETRUS JOHANNES T.
p 3019 N94-26478
VANDERHOUWEN, P. J. p 2991 N94-26217
VANDERJEUGT, J. p 3001 N94-27839
VANDERLAAN, PAUL p 2834 N94-26008
VANDERPLOEG, A. p 2997 N94-27000
VANDERSTOK, P. p 2966 N94-26920
VANDERVEEN, J. T. p 2771 N94-26872
VANDERWEIJ, HENK p 2954 N94-27192
VANDRIEL, N. p 2666 N94-27831
VANEIJCK, D. JAN N. p 2970 N94-27545
p 2970 N94-27549
VANEIJK, A. M. p 2893 N94-26013
VANEIJNDHOVEN, S. J. L. p 2999 N94-27349
VANES, J. T. p 2779 N94-25618
VANGEFFEN, STEPHEN p 2943 N94-25678
VANHOESEL, C. P. M. p 2992 N94-26227
p 2969 N94-27396
VANKEULEN, F. p 2839 N94-26875
VANLEHN, KURT p 3098 N94-26570
VANLOON, M. p 2867 N94-26216
VANMAAREN, HANS p 2958 N94-25764
VANMANEN, A. p 2831 N94-28083
VANO, ANDREW p 2833 N94-25689
VANREEN, A. T. H. p 2779 N94-25620
VANTRIET, ROBERT p 2671 N94-25710
VANWEERDEN, H. J. p 3038 N94-27137
VARDAMAN, JENNIFER J. p 2941 N94-26136
VARDANEGA, T. p 2954 N94-26746
VARLEY, D. A. p 3097 N94-26348
VASANDANI, VIJAY p 2984 N94-25899
p 2985 N94-25966
VASILEV, A. V. p 2810 N94-26394
VASOFSKY, R. W. p 2740 N94-27006
VASQUES, MARILYN p 2901 N94-26086
VATAN, BRUNO p 2953 N94-26739
VAUGHN, TODD p 2708 N94-26895
VAWTER, G. A. p 3052 N94-25989
VAZACOPOULOS, ALKIS p 3094 N94-26314
VEERS, P. S. p 2857 N94-26700
VEERS, PAUL p 2682 N94-27997
VELDMAN, H. J. p 3007 N94-27222
VENKATAKRISHNAN, V. p 2999 N94-27434
p 2999 N94-27557
VENKATESWARLU, P. p 3039 N94-27603
VERBREE, EDWARD p 2848 N94-26651
VERCELLONE, J. p 3098 N94-26598
VERHOEF, C. p 2966 N94-26970
VERNIKOS, JOAN p 2944 N94-26098
VEROLME, J. L. p 2840 N94-26961
VERRILLI, M. J. p 2711 N94-27640
VERSACI, R. A. p 2735 N94-26294
VERWER, J. G. p 2867 N94-26216
p 2965 N94-26772
VERWEY, W. B. p 2939 N94-27138
VESSONEN, ISMO p 2836 N94-25650
VETRANO, J. S. p 2741 N94-27622
VEYO, S. E. p 2858 N94-26869
VIBULSRESTH, SUVIT p 2875 N94-28291
VIEHWEGER, GUENTER p 2681 N94-27587
VIITANEN, A. J. p 2778 N94-28384
VIITANEN, ARI J. p 2778 N94-28381
VIKRAM, CHANDRA S. p 2812 N94-27229
VILA, F. p 2783 N94-26443
VILLAGARCIA, M. P. p 2837 N94-26265
VILLANGER, ASTA STOREBOE p 2767 N94-26105
VILLEGAS, M. p 2743 N94-27829
VILPAS, MARTTI p 2731 N94-25623
p 2731 N94-25784
VINCENT, W. p 2703 N94-25685
VINCTER, MANUELLA GRETA p 3021 N94-26665
VINGE, VERNOR p 2685 N94-27359
VINNINS, M. F. p 2813 N94-27597
VIRTA, JOUKO p 2731 N94-25643
VISALA, ARTO p 2976 N94-28377
VISHNEVSKIJ, N. K. p 3024 N94-27250
VISSCHERS, J. L. p 2779 N94-25620
VLADIMIROV, A. A. p 3001 N94-27846
VLADIMIROVA, N. M. p 3058 N94-26512
VLASOV, E. V. p 3024 N94-27250
VLEESHOUWER, SERVATIUS MARIA
p 2752 N94-26645
VLOT, A. p 2710 N94-27201
VOGEL, KURT A. p 2690 N94-26001
VOGELIUS, MICHAEL p 2994 N94-26601
VOIGT, J. A. p 3053 N94-26025
p 3061 N94-26856
VOKAL, S. p 3030 N94-27994
VOLK, TAMI L. p 2940 N94-25611
VOLKOV, G. G. p 3072 N94-26453
VOLKOV, M. K. p 3020 N94-26505
VOLLBERTROMERO, M. E. p 2880 N94-26874
VOLPE, RICHARD A. p 2958 N94-25777
VONDOERNBERG, ADRIAN p 2662 N94-28245
VONLAVEN, G. M. p 3099 N94-27022
VOROBEV, A. P. p 2810 N94-26396
VOSSEN, TERRENCE JOHN p 2763 N94-26634
VOTH, GREGORY A. p 3020 N94-26562
VOUCHE, M. p 2832 N94-28088
VRABEL, DEBRA A. p 2688 N94-27372
VREESWIJK, M. p 2814 N94-28098
VRIJKOTTE, T. G. p 2940 N94-25724
VUORINEN, J. J. p 2747 N94-28359
VYAS, B. p 2862 N94-28117
VYRIOTES, P. p 2652 N94-28319

W

WADA, HITOSHI p 2725 N94-25559
p 2725 N94-25560
WADA, SHINJI p 2870 N94-28149
p 2870 N94-28151
WADA, YASUHIRO p 2795 N94-27205
WADA, YOSHIRO p 2913 N94-27449
p 2913 N94-27450
p 2913 N94-27451
p 2913 N94-27452
p 2914 N94-27454
p 2914 N94-27456
p 2914 N94-27457
WADAYAMA, YOSHIHIDE p 2788 N94-27817
p 2788 N94-27821
WADE, M. R. p 3048 N94-27785
p 3048 N94-27791
WADSWORTH, J. p 2748 N94-25959
WAEHNER, HORST p 2662 N94-28239
WAELBROECK, F. L. p 3042 N94-25958
WAGELMANS, A. P. M. p 2969 N94-27396
WAGH, A. S. p 2857 N94-26584
WAID, JAMES D. p 2642 N94-27293
WAKABAYASHI, HIROSHI p 2788 N94-27821
WAKABAYASHI, N. p 2733 N94-26092
WAKAMATSU, YOSHIO p 2710 N94-27279
p 2710 N94-27280
p 2675 N94-27608
WAKE, L. V. p 2669 N94-26864
WAKUDA, KENICHIRO p 2745 N94-28166
WALKER, D. W. p 2964 N94-26764
WALKER, H. p 2892 N94-25936
WALL, F. D. p 2742 N94-27788
WALLACE-ROBINSON, J. p 2932 N94-27556
WALLACE, P. L. p 3058 N94-26514
WALLER, CHRIS p 2765 N94-25677
WALLER, G. C. p 2655 N94-28335
WALLQUIST, K. M. p 2781 N94-25977
WALLSTROM, T. p 3073 N94-26805
WALTERS, H. R. p 2974 N94-27794
WALTERS, R. A. p 3035 N94-26100
WALTON, J. T. p 3053 N94-26094
p 3054 N94-26095
WALZAK, TIMOTHY LAWRENCE p 2757 N94-27801
WAMPLER, W. R. p 3050 N94-25815
p 3052 N94-25971
p 3068 N94-27693
WANDESFORDE, A. p 3060 N94-26795
WANDLAND, KLAES W. p 3094 N94-26814
WANG, C. p 3069 N94-27757
WANG, DENNIS p 2945 N94-28253
WANG, FRITZ p 2689 N94-25670
WANG, K. p 2856 N94-26464
WANG, KEMEI p 3054 N94-26139
WANG, L. M. p 3067 N94-27602
WANG, MINGCHANG p 2819 N94-26941
WANG, SHIKUN p 3073 N94-26876
WANG, XUANJI p 2875 N94-28289
WANG, YUFENG p 3012 N94-25795
WANG, ZHIJIANG p 2819 N94-26941
WANGERMANN, J. P. p 2643 N94-27297
WANHILL, R. J. H. p 2743 N94-27795
p 2743 N94-27797
WANKE, CRAIG p 2641 N94-27286
WANKE, CRAIG R. p 2641 N94-27287
WARD, P. D. p 2889 N94-28303
WARD, R. p 2749 N94-25985
WARNER, RUSSELL M. p 3099 N94-27118
WARREN, DANIEL E. p 2767 N94-25960
WARREN, DAVID R. p 2696 N94-27382
WARRENDER, CHARLES B. p 3001 N94-25607

WARWICK, JERRY L. p 3093 N94-26299
WARZYNSKI, GARY p 2671 N94-25713
WAS, G. S. p 2731 N94-25804
p 2732 N94-25954
WASEDA, YOSHIO p 2721 N94-28159
p 2744 N94-28160
WASSMUTH, CHAD M. p 2691 N94-25696
WATABE, HIROTAKA p 2914 N94-27456
WATANABE, EIICHI p 2907 N94-27504
p 2907 N94-27509
WATANABE, HARUO p 2932 N94-27540
WATANABE, KATSUYOSHI p 3065 N94-27240
WATANABE, MITSURU p 2746 N94-28171
WATANABE, SATORU p 2912 N94-27446
p 2912 N94-27447
p 2912 N94-27448
p 2913 N94-27449
p 2913 N94-27450
p 2913 N94-27451
p 2913 N94-27452
p 2913 N94-27453
p 2914 N94-27454
p 2914 N94-27455
p 2914 N94-27456
p 2914 N94-27457
p 2927 N94-27518
p 2908 N94-27519
p 2928 N94-27520
WATANABE, SHUNTARO p 3025 N94-27338
p 2820 N94-27339
p 2820 N94-27605
WATANABE, TAKEHIKO p 2722 N94-25546
WATANABE, TAKESHI p 2886 N94-27987
WATANABE, TOSHIAKI p 2723 N94-25552
p 2725 N94-25558
WATANABE, Y. p 2986 N94-26948
WATERS, LARRY K. p 2791 N94-25991
WATERS, WILLIAM M. p 2774 N94-27202
WATSON, JUDITH J. p 2692 N94-27774
WATSON, L. T. p 2967 N94-27020
WATSON, R. p 2948 N94-26578
WATTAYAKORN, G. p 2875 N94-28287
WATTS, ALAN p 3035 N94-26572
WAWNER, FRANKLIN E., JR. p 2844 N94-27851
WEAGLEY, R. J. p 2748 N94-25932
WEAVER, EARL P. p 2957 N94-25753
WEAVER, JONATHAN M. p 2683 N94-26280
WEBB, T., III p 2865 N94-25789
WEBER, DOUG p 2956 N94-28267
WEBER, W. J. p 3067 N94-27602
WEBSTER, HENRY A. p 3037 N94-27066
WECKMAN, D. C. p 2820 N94-27668
WEDDENDORF, B. p 2825 N94-27560
WEED, RICHARD ALLEN p 2793 N94-26595
WEGNER, G. p 2755 N94-27163
WEGNER, TORSTEN p 2943 N94-25679
WEHNER, JOERG p 2903 N94-27754
WEIGHLHOFER, W. S. p 2779 N94-28391
WEIGLHOFER, W. S. p 2779 N94-28388
WEIGLHOFER, WERNER S. p 2778 N94-28379
WEIHRAUCH, PAUL p 2709 N94-26978
WEILAND, T. L. p 2816 N94-26020
WEINSTEIN, LISA F. p 2673 N94-26989
WEINSTOCK, ELLIOT M. p 3108 N94-27892
WEIR, BENNETT p 2844 N94-27824
WEISLOGEL, MARK p 2760 N94-25849
WEISS, MARTIN p 2997 N94-26999
WEISS, STANLEY p 2689 N94-25687
WEISSHAAR, TERRENCE A. p 2671 N94-25718
WEISSMANN, S. p 3058 N94-26514
WELGAN, ROBERT L. p 2958 N94-25783
WELLINGHOFF, STEPHEN T. p 3035 N94-25941
WELLINGS, A. J. p 2951 N94-26731
WELLS, EDWARD A. p 2674 N94-27432
WELTING, BAPTIST p 2899 N94-26108
WEN, JOHN T. p 2683 N94-26279
WEN, T. p 2899 N94-26886
WENJIANG, CHEN p 2742 N94-27730
WENMIAN, JIANG p 2742 N94-27730
WENNINGER, ED p 2671 N94-25714
WENS, G. p 2801 N94-28011
WENYU, HONG p 2758 N94-27845
WENZEL, M. p 2824 N94-27254
WERCHAN, PAUL M. p 2902 N94-26991
WERNESS, SUSAN A. p 2946 N94-28260
WERT, JOHN A. p 2844 N94-27851
WERTHEIM, A. H. p 2940 N94-25724
WESSELING, P. p 2992 N94-26252
WEST, W. P. p 3048 N94-27785
WHEAT, S. p 2979 N94-25953
WHEAT, S. R. p 2979 N94-25952
WHEAT, STEPHEN p 2983 N94-27713
WHEELER, R. M. p 2902 N94-27411
WHEELER, RAYMOND M. p 2903 N94-27412
WHERRY, ROBERT J., JR. p 2941 N94-26339
WHIRLEY, R. G. p 2965 N94-26862
WHITE, ANTHONY RICHARD PHILLIP
p 2964 N94-26663
WHITE, C. W. p 3054 N94-26137
WHITE, CURTIS D. p 2910 N94-26973
WHITE, D. J. p 2827 N94-27874
WHITE, FRANK p 3035 N94-26572
WHITE, JAMES C. p 2680 N94-26202
WHITE, P. R. p 2807 N94-28172
WHITEHOUSE, D. R. p 2652 N94-28321
WHITMAN, P. G. p 2890 N94-28305
WHITMEYER, LARRY E. p 2692 N94-26529
WHITTAKER, WARREN C. p 2764 N94-27144
WICHERSON, R. J. p 2960 N94-26106
WICHMANN, KARL p 2681 N94-27587
WICKENS, CHRISTOPHER D. p 2941 N94-26964
WICKMAN, GARY P. p 3094 N94-26814
WIELAND, PAUL p 2942 N94-27437
WIERINGA, R. J. p 2965 N94-26852
WIESE, JEFFREY L. p 2790 N94-25657
WIGGENRAAD, J. F. M. p 2670 N94-27796
WIJFFELS, J.-B. p 2832 N94-28089
p 2832 N94-28090
WILDES, LINDA B. p 2940 N94-25611
WILDGRUBE, GREGORY M. p 2691 N94-25696
WILKEN, DIETER p 2660 N94-27746
WILKES, B. J. p 3103 N94-27933
WILKINSON, A. R. p 2656 N94-28341
WILL, R. p 3043 N94-26323
WILLCOCKSON, NANCY K. p 2909 N94-26360
WILLEMS, P. p 3095 N94-25723
WILLETT, JOHN C. p 2892 N94-25873
WILLIAMS, GREGORY S. p 3011 N94-25589
WILLIAMS, J. P. p 2796 N94-27378
WILLIAMS, K. L. p 2899 N94-26886
WILLIAMS, ROBERT L., II p 2989 N94-27773
WILLIAMSON, D. E. p 3045 N94-26861
WILLIAMSON, P. p 2756 N94-27217
WILLMS, ALLAN RICHARD p 2988 N94-27271
WILLMS, HERBERT p 2826 N94-27589
WILMINK, M. J. p 2811 N94-27134
WILSON, C. A. p 3115 N94-26690
WILSON, DAVID J. p 2666 N94-25590
p 2667 N94-25961
WILSON, JOHN W. p 3114 N94-26550
WILSON, ROBERT B. p 3114 N94-26686
p 3114 N94-26687
p 3114 N94-26688
p 3115 N94-26689
p 3115 N94-26690
WIMPENNY, S. J. p 3052 N94-25972
WINDISCH, C. F., JR. p 3054 N94-26147
WINNICKA, MARIA BOZENA p 2740 N94-27306
WINOKUR, P. S. p 2780 N94-25812
p 2948 N94-26111
WINTERKAMP, J. p 2894 N94-26313
WIRTH, WALTER M., JR. p 2677 N94-26192
WISESSANG, S. p 2875 N94-28287
WITHAGEN, WILLEM JAN p 2954 N94-27191
WITHERS, ASHLEY p 2671 N94-25708
WITT, C. E. p 2856 N94-26426
WITT, RON p 2850 N94-27182
p 2850 N94-27184
WITTIG, S. p 2676 N94-28037
WNUK, STEVE P., JR. p 2811 N94-26568
WOHLFARTH, D. p 3012 N94-25750
WOHN, F. K. p 3031 N94-26097
WOLF, D. R. p 3005 N94-27816
WOLSEY, L. A. p 2969 N94-27396
WOMBLE, D. p 2979 N94-25953
WOMBLE, D. E. p 2979 N94-25952
WON, D. Y. p 3057 N94-26404
WON, DONG YEON p 2783 N94-26546
WONG, C. P. C. p 3043 N94-26323
p 3043 N94-26324
WONG, DOUGLAS T. p 2811 N94-26707
WONG, H. K. p 2879 N94-26599
WONG, H. V. p 3041 N94-25792
WONG, J. p 3060 N94-26795
WONG, WILSON W. K. p 2982 N94-27649
WONG, Y. K. p 3053 N94-26094
p 3054 N94-26095
WOOD, D. p 2698 N94-25701
WOOD, JOHN D. p 2664 N94-26493
WOOD, M. G. p 2941 N94-26788
WOOD, N. J. p 2659 N94-28029
WOOD, TOM L. p 2645 N94-26483
p 2645 N94-26489
p 2645 N94-26492
p 2645 N94-26497
WOODLE, M. p 2811 N94-26787
WOODS, THOMAS N. p 2882 N94-27380
WOODS, WILLIAM C. p 2646 N94-26592
WOODYARD, ROBERT L. p 2899 N94-26567
WOOLF, A. p 2965 N94-26816
WOOTERS, DANA p 2833 N94-25675
WRIGHT, M. E. p 2787 N94-27618
WRIGHT, PAUL E. p 2971 N94-27558
WROBLESKI, DEBRA A. p 2704 N94-27745
p 2757 N94-27747
WU, CHIVEY p 2659 N94-27930
WU, J. p 3056 N94-26326
WU, J. C. p 2749 N94-26074
WU, KE p 3073 N94-26876
WUBS, F. W. p 2997 N94-27000
WUEBBLES, D. J. p 2879 N94-26576
WUEBBLES, DONALD J. p 2869 N94-27267
WUENSCHE, DIERK p 2660 N94-28230
p 2663 N94-28246
WYBOURNE, M. N. p 2749 N94-26074
WYKES, HARRY B. p 2688 N94-27374
WYNN, WARREN, JR. p 2671 N94-25712

X

XIAO, QIANGUANG p 2875 N94-28289
XIAO, YUJIN p 2758 N94-27857
XU, B. p 2887 N94-28218
XU, D. p 3053 N94-26029
XU, J. p 2717 N94-26951
XU, ZUKANG p 2963 N94-26615
XUAN, CAO p 3070 N94-27843
XUE, YE-XIANG p 2915 N94-27458
p 2915 N94-27459
p 2918 N94-27473

Y

YABE, KYONOSUKE p 2928 N94-27522
YAGCI, HUSEYIN p 2806 N94-28038
YAGHJIAN, RAFFY p 2765 N94-25677
YAGI, KOICHI p 2723 N94-25548
p 2729 N94-25580
p 2730 N94-25583
YAGI, M. p 3047 N94-27723
YAGI, TAKEHIKO p 3066 N94-27354
YAGURA, SHIGEYUKI p 2933 N94-27944
YAMADA, HIROSI p 2718 N94-27389
YAMADA, ISAO p 2885 N94-27973
YAMADA, TOSHIO p 2764 N94-27980
YAMADA, YOSHIO p 2869 N94-28147
YAMAGATA, TOSHIHIRO p 2723 N94-25550
YAMAGISHI, HISAO p 2882 N94-27342
p 2884 N94-27967
p 2884 N94-27968
YAMAGUCHI, HIROSHI p 2918 N94-27474
YAMAGUCHI, KOJI p 2729 N94-25579
p 2915 N94-27459
p 2918 N94-27473
YAMAKADO, NORIO p 2871 N94-28155
YAMAKOSHI, YASUYUKI p 2764 N94-27977
YAMAMORI, IKUO p 2905 N94-27482
YAMAMOTO, CHIKASHI p 2911 N94-27443
p 2912 N94-27445
p 2904 N94-27464
YAMAMOTO, HIROKAZU p 2746 N94-28170
YAMAMOTO, KIYOHITO p 2908 N94-27530
YAMAMOTO, KIYOKO p 2905 N94-27488
YAMAMOTO, KOJI p 2930 N94-27532
YAMAMOTO, MASAAKI p 2764 N94-27976
YAMAMOTO, RYUTARO p 2764 N94-27976
YAMAMOTO, SHIGEO p 2722 N94-25544
YAMAMOTO, SUSUMU p 2867 N94-26474
YAMAMOTO, Y. p 2688 N94-27373
p 3047 N94-27715
YAMAMURA, HIDEKI p 2904 N94-27470
p 2904 N94-27471
p 2905 N94-27483
p 2905 N94-27484
p 2905 N94-27485
p 2905 N94-27486
p 2905 N94-27487
p 2905 N94-27489
p 2905 N94-27490
p 2906 N94-27492
p 2906 N94-27493
YAMANAKA, MITSUGU p 3064 N94-27232
YAMANURA, HIDEKI p 2905 N94-27488
YAMASHITA, MASAMICHI p 2913 N94-27449
p 2913 N94-27451
YAMAZAKI, MANABU p 2919 N94-27478
YAMAZAKI, MASAKAZU p 2871 N94-28157
YAMAZAKI, MICHIO p 2723 N94-25550
YAN-MIN, LI p 3057 N94-26388
YANG, CHARLIE QING p 2770 N94-26625
YANG, X. p 3056 N94-26326
YANO, TOSHIKAZU p 2761 N94-27341
YANO, Y. p 2863 N94-28121
p 2864 N94-28130
YAREMCHUK, GEORGE NICOLAS
p 2980 N94-26674

YARKHAN, ASIM p 2678 N94-27414
YASUI, HIROTAKA p 2924 N94-27501
YASUKAWA, YUKIO p 2788 N94-27817
YASUO, NABEKAWA p 2820 N94-27605
YASUOKA, HIROSHI p 3064 N94-27177
p 3025 N94-27337
YATA, MASANORI p 2726 N94-25563
YE, HUIMING p 2895 N94-26678
YE, RUQIU p 2873 N94-28276
YEATES, MATHEW p 2947 N94-28263
YEE, J. p 3068 N94-27724
YEH, P. p 3034 N94-25902
YEN, CHEN-WAN L. p 2700 N94-25969
YEUNG, W. W. H. p 2654 N94-28332
YI-FEN, YEN p 3013 N94-25820
YI, JONG HOON p 2817 N94-26402
YI, THOMAS Y. p 2702 N94-26613
YIANNOUTSOS, CONSTANTIN T. p 3003 N94-26485
p 3003 N94-26494
YILDIRIM, E. H. p 3063 N94-27017
YIM, CHANG JAE p 2835 N94-26399
YIN, YONG-XIANG p 3049 N94-27856
YIP, J. p 2719 N94-27712
YLOENEN, T. p 3100 N94-28385
YOKOI, HIROYUKI p 3064 N94-27232
YOKOI, K. p 3112 N94-25628
p 3113 N94-25629
p 3113 N94-25630
YOKOKAWA, KENJI p 2723 N94-25548
p 2730 N94-25583
YOKOKAWA, MITSUO p 2973 N94-27702
YOKOKAWA, TADAHARU p 2723 N94-25550
p 2727 N94-25568
YOKONO, YASUYUKI p 3011 N94-27283
YOKOYAMA, CHIAKI p 2718 N94-27390
YOKOYAMA, SHINYA p 2859 N94-27204
p 2871 N94-28154
YONEZAWA, YOSHITAKA p 2870 N94-28150
YONGJUN, ZHU p 3070 N94-27843
YOO, S. H. p 3013 N94-25820
YOO, SUNG-SHIK p 3054 N94-26139
YOON, JAE SUNG p 3042 N94-26159
YORIO, N. C. p 2902 N94-27411
YORIO, NEIL C. p 2903 N94-27412
YORK, B. J. p 2804 N94-28030
YOSHIHARA, KAZUHIRO p 2722 N94-25545
p 2723 N94-25549
p 2727 N94-25570
p 2682 N94-25586
YOSHIKADO, HIROSHI p 2867 N94-26474
YOSHIMURA, HIROKAZU p 2915 N94-27462
YOSHIMURA, KAZUYOSHI p 3064 N94-27177
YOSHIMURA, KOICHI p 3000 N94-27731
YOSHINO, MASATAKA p 2904 N94-27464
YOSHINO, SEIJI p 2928 N94-27520
YOSHINO, TAKEO p 2779 N94-27964
YOSHIOKA, TAKAYUKI p 2722 N94-25544
p 2729 N94-25578
YOSHITAKE, MICHIKO p 2723 N94-25549
p 2727 N94-25570
YOSHIZAWA, HIDEKI p 2756 N94-27241
YOTTE, S. p 2711 N94-27586
YOUN, BYEONG JOO p 3042 N94-26159
YOUNG, DEBORAH B. p 3085 N94-27893
YOUNG, L. A. p 2668 N94-26604
YOUNG, L. S. p 2997 N94-26994
YOUNG, PHILIPPE GEORGES p 2838 N94-26622
YOUNG, ROY D. p 2961 N94-26298
YOUNGBLOOD, G. E. p 3054 N94-26147
YOUNGER, FRANK p 2943 N94-25678
YOUTSEY, WESLEY J. p 2899 N94-26567
YU, NING p 3069 N94-27828
YU, XINMING p 2998 N94-27312
YUAN, CHEN p 2742 N94-27730
YUAN, QIN p 2826 N94-27657
YUAN, V. W. p 3013 N94-25820
YUASA, F. p 2983 N94-27804
YUFEROV, A. G. p 2701 N94-26166
YUGO, J. J. p 2767 N94-25924
p 3041 N94-25933
YUKIMATSU, AKIRA p 2884 N94-27965
p 2885 N94-27972
YUMIKURA, SEI p 2914 N94-27456
YUNG, K. p 3068 N94-27724
YUNG, YUK L. p 2677 N94-26015
YURI, TOSHIMI p 2724 N94-25556
YUSA, HITOSHI p 3066 N94-27354
YUSHMANOV, P. N. p 2791 N94-26096
YUYAMA, MICHIYA p 2725 N94-25560

Z

ZAAL, K. J. J. M. p 2669 N94-26954
ZACHARIAS, MARK p 2848 N94-26664
ZACHARIUS, SHERRIE L. p 2753 N94-26842
ZADRA, A. p 2991 N94-25884
ZAFAR, YU. p 2766 N94-25915
ZAFREN, B. p 2932 N94-27556
ZAHR, THOMAS A. p 2765 N94-25676
ZAIKOV, R. P. p 2993 N94-26425
ZAITSEV, A. M. p 3024 N94-27250
ZAJTSEV, A. M. p 3017 N94-26045
ZAKHAREVICH, ILYA p 2997 N94-26996
ZAKKARI, M. p 3006 N94-26414
p 3006 N94-26415
p 2996 N94-26898
ZAMKOW, SOPHIE p 2853 N94-26050
p 2853 N94-26051
ZAPATA, L. E. p 2819 N94-27018
ZAVADIL, K. R. p 3070 N94-28067
ZEE, RALPH p 2696 N94-26791
ZEHNER, GREGORY F. p 2941 N94-26984
ZEINALI, MAZYAR p 2833 N94-25704
ZEKRI, N. p 3067 N94-27635
ZELLER, MARY V. p 2741 N94-27426
ZENG, Z. p 3052 N94-26012
ZERKLE, D. K. p 3042 N94-26081
ZERNER, MICHAEL C. p 3023 N94-26926
ZHA, G.-C. p 2657 N94-28343
ZHANG, C. p 3053 N94-26029
ZHANG, JIANHUA p 3044 N94-26579
ZHANG, L. p 2713 N94-25978
ZHANG, LIJIE p 3062 N94-26892
ZHANG, MING p 2660 N94-27746
ZHANG, QI p 2769 N94-26618
ZHANG, TAO p 3025 N94-27333
ZHANG, X. p 2800 N94-28005
ZHANG, YANLING p 2758 N94-27857
ZHANG, YIN p 2959 N94-25821
ZHANG, YUXIA p 2893 N94-26138
p 2896 N94-27408
ZHANLAV, T. p 2994 N94-26471
ZHAO-BIN, SU p 3057 N94-26388
ZHAO, HAIXIONG p 2743 N94-27803
ZHAO, WEI p 3093 N94-26206
ZHAO, ZHIGANG p 2769 N94-26619
ZHENG, HANXING p 2736 N94-26452
p 3059 N94-26571
ZHENG, HEYUN p 2969 N94-27346
ZHENG, Q. Q. p 3052 N94-26012
ZHIDKOV, E. P. p 2879 N94-26502
ZHOU, FENG p 2825 N94-27343
ZHOU, H. p 2755 N94-27163
ZHOU, HUIFEN p 2819 N94-26941
ZHOU, PEIFANG p 2964 N94-26632
ZHOU, SHUN-TAI p 2866 N94-25927
ZHOU, Y. p 3023 N94-26944
ZHU, JIANPING p 2969 N94-27416
ZHU, PEIYING p 2969 N94-27311
ZHUANG, XUE-JIN p 2823 N94-27104
ZHUCHKO, V. E. p 3012 N94-25750
ZIELHUIS, ALET p 2880 N94-26752
ZIEMNIAK, S. E. p 2715 N94-26320
ZIERKE, W. C. p 2789 N94-25604
ZIMMERMAN, ALBERT H. p 2860 N94-28106
p 2861 N94-28111
p 2861 N94-28112
ZIMMERMAN, MARK p 2671 N94-25708
ZINGG, D. W. p 2655 N94-28337
p 2656 N94-28339
p 2656 N94-28341
ZINK, MANFRED p 2777 N94-27738
ZIOCK, H. J. p 3052 N94-25972
ZITOUNI, GLEY p 2795 N94-27313
ZIVKOVIC, MARINA p 2898 N94-28223
ZOHORSKY, PETER J. p 2736 N94-26533
ZOLPER, J. C. p 3069 N94-27790
ZORIN, O. L. p 3072 N94-26037
ZORMAN, C. A. p 2753 N94-26822
ZUBOV, YU. A. p 3031 N94-25870
ZUCKERWAR, ALLAN J. p 2798 N94-27867
ZUHR, R. A. p 3054 N94-26137
ZUIDEVELD, P. L. p 2832 N94-28089
p 2832 N94-28090
ZUIDGEEST, R. G. p 2989 N94-27800
ZUMEL, NINA B. p 2821 N94-25878
ZUND, J. D. p 3001 N94-28216
ZUZEK, JOHN E. p 2693 N94-27427
ZVIRIN, Y. p 2853 N94-26051
ZWART, A. N. M. p 2779 N94-25620
ZYWICZ, E. p 2706 N94-25938

CORPORATE SOURCE INDEX

SCIENTIFIC AND TECHNICAL AEROSPACE REPORTS VOLUME 32 NUMBER 7

Typical Corporate Source Index Listing

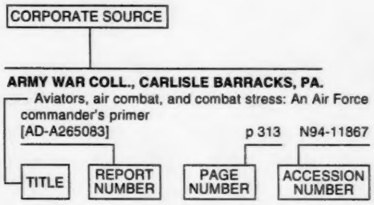
CORPORATE SOURCE
ARMY WAR COLL., CARLISLE BARRACKS, PA.
Aviators, air combat, and combat stress: An Air Force commander's primer
[AD-A265083] p 313 N94-11867
TITLE
REPORT NUMBER
PAGE NUMBER
ACCESSION NUMBER

Listings in this index are arranged alphabetically by corporate source. The title of the document provides the user with a brief description of the subject matter. The report number helps to indicate the type of document cited (e.g., NASA report, translation, NASA contractor report). The accession number denotes the number by which the citation is identified. The page number helps you locate the citation in the abstract section. The titles are arranged under each corporate source in ascending accession number order.

A

ABB POWER GENERATION, INC., BADEN (SWITZERLAND).
Controls, monitoring and performance measurements p 2831 N94-28086

AC, INC., HUNTSVILLE, AL.
Development and application of contamination technology for MSFC managed space systems
[NASA-CR-193934] p 2697 N94-27421

ACADEMY OF SCIENCES (USSR), LENINGRAD.
Automated system for gas detectors providing with binary mixtures
[DE93-634192] p 2715 N94-26406

ACADEMY OF SCIENCES (USSR), MOSCOW.
A study of very high energy hadron interactions through observation of cosmic-ray families of visible energy greater than 500 TeV, 1 p 3112 N94-25625
A study of very high energy hadron interactions through observation of cosmic-ray families of visible energy greater than 500 TeV, 2 p 3112 N94-25626
A study of very high energy hadron interactions through observation of cosmic-ray families with visible energy not less than 500 TeV, 3 p 3112 N94-25627
Solar energy utilization in the USSR p 2853 N94-26052
Radiation applications of physical chemistry p 2854 N94-26054
Ways to improve MHD power plants and prospects of their application p 2854 N94-26056

ACADEMY OF SCIENCES (USSR), NOVOSIBIRSK.
Electron microscopic analysis of meiotic chromosome pairing in male house musk shrew, Suncus murinus p 2906 N94-27493

ADROIT SYSTEMS, INC., FAIRBORN, OH.
Image quality analysis of compressed synthetic aperture radar imagery
[AD-A273399] p 2774 N94-27170

ADVISORY GROUP FOR AEROSPACE RESEARCH AND DEVELOPMENT, NEUILLY-SUR-SEINE (FRANCE).
Computational and Experimental Assessment of Jets in Cross Flow
[AGARD-CP-534] p 2799 N94-28003

AERONAUTICAL RESEARCH INST. OF SWEDEN, STOCKHOLM.
Calculation of viscous drag of two low angle of attack supercritical profiles
[FFA-TN-1984-22] p 2644 N94-26104

AERONAUTICAL RESEARCH LABS., MELBOURNE (AUSTRALIA).
Low-speed pressure distribution measurements over the aft-fuselage, fins, and stabilators of a 1/9th scale F/A-18 wind-tunnel model
[AD-A274870] p 2644 N94-26342
Stress analysis of a secondary-bending specimen
[AD-A274842] p 2838 N94-26501
Computation of non-isentropic internal flows with variable density
[AD-A274848] p 2794 N94-26801

AEROSPACE CORP., EL SEGUNDO, CA.
Quiet-time intensifications along the poleward auroral boundary near midnight
[ATR-93(7248)-2] p 2877 N94-26201
Diode-laser-pumped, gas-cell atomic clocks
[AD-A274812] p 3008 N94-26484
An ultrasonic testing technique for monitoring the cure and mechanical properties of polymeric materials
[AD-A274536] p 2753 N94-26842
Investigation of ACC/CCI tunnel diodes
[AD-A274549] p 2785 N94-26845
Screen test for cadmium and nickel plates p 2860 N94-28106
Calculation of the thermoneutral potential of NiCd and NiH2 cells p 2861 N94-28111
Performance model of a recirculating stack nickel hydrogen cell p 2861 N94-28112
Air Force standards for nickel hydrogen battery p 2862 N94-28116
Photoelectron spectroscopic studies of the electronic structure and bonding in TiC and TiN
[ATR-93(8361)-2] p 2746 N94-28185
Proton aurora and substorm intensifications
[ATR-93(7248)-1] p 2887 N94-28218

AEROSPACE CORP., LOS ANGELES, CA.
Cycle life versus depth of discharge update on modeling studies p 2862 N94-28115

AEROSPACE MEDICAL RESEARCH LABS., BROOKS AFB, TX.
Performance recovery in the baboon following (+)G sub z-induced loss of consciousness
[AD-A274411] p 2902 N94-26991

AEROSPATIALE, LES MUREAUX (FRANCE).
The Ariane 5 data management system p 2950 N94-26724

AEROSPATIALE, TOULOUSE (FRANCE).
System for generating, aboard an aircraft, during takeoff, of a signal capable of producing an alert or an alarm, in case of malfunction
[CA-PATENT-APPL-SN-2,018,94] p 2659 N94-26293

AEROSPATIALE, VERRIERES-L-BUISSON (FRANCE).
Numerical assessment of aerodynamic interactions on missiles with transverse jets control p 2659 N94-28031

AEROSPATIALE AQUITAINE, SAINT-MEDARD EN JALLES (FRANCE).
Testing procedure for toughness characterisation of ceramic matrix composites
[REPT-932-430-101] p 2711 N94-27586

AGENCY FOR ASSESSMENT AND APPLICATION OF TECHNOLOGY, JAKARTA (INDONESIA).
Research and observation programmes on global changes in Indonesia p 2873 N94-28277

AICHI AGRICULTURAL RESEARCH CENTER, NAGA (JAPAN).
Skeletal development and ossification of the swine fetuses p 2905 N94-27491

AICHI MEDICAL UNIV., NAGAKUTE (JAPAN).
An attempt of intraneural stimulation by microelectrode inserted in skin sympathetic nerve fascicle p 2930 N94-27529
Enhancement of skin sympathetic nerve activity in amyotrophic lateral sclerosis p 2930 N94-27532

AICHI UNIV. OF EDUCATION (JAPAN).
Telescience testbedding under hypobaric hypoxic conditions: Evaluation by operation ability and recognition ability p 2913 N94-27450
Heart rate change in normal and labyrinthectomized hamsters during parabolic flight p 2914 N94-27454

AIR-CONDITIONING AND REFRIGERATION TECHNOLOGY INST., INC., ARLINGTON, VA.
Measurement of viscosity, density, and gas solubility of refrigerant blends in selected synthetic lubricants
[DE94-003609] p 2713 N94-25934

AIR FORCE CIVIL ENGINEERING CENTER, TYNDALL AFB, FL.
Engineering Technical Letter (ETL) 93-5: Fire protection engineering criteria, electronic equipment installations
[AD-A274835] p 2762 N94-26084

AIR FORCE FLIGHT TEST CENTER, EDWARDS AFB, CA.
The use of EEG as a workload assessment tool in flight test
[AD-A274568] p 2910 N94-26847

AIR FORCE INST. OF TECH., WRIGHT-PATTERSON AFB, OH.
Numerical simulation of tomographic reconstruction for the study of turbulence using optical wavefront sensor measurements
[AD-A273851] p 2789 N94-25587
Vibrational energy transfer within the B 3Pi (O(+) sub u) state of 79BR2 upon collision with N2, O2, NO, and SF6
[AD-A273905] p 3011 N94-25589
Evaluation of a concentration probe for application in a supersonic flow field
[AD-A273915] p 2643 N94-25592
Human visual system enhancement of reconstructed satellite images
[AD-A273867] p 2693 N94-25595
The application of simulated annealing to stochastic systems
[AD-A273850] p 3001 N94-25607
Air pollution transport modeling
[AD-A273863] p 2865 N94-25609
High resolution fourier transform absorption spectrum of 79Br2 B3 Pi(Ou+) X1 sigma g+
[AD-A273864] p 2956 N94-25610
Creation of prototype aircrew protection equipment based on face anthropometry
[AD-A273865] p 2940 N94-25611
A comparison of three approximate mathematical models for the gravity gradient stabilized satellite
[AD-A273832] p 2694 N94-25615
Failure mechanisms of high temperature semiconductor lasers
[AD-A273833] p 2815 N94-25616
Development and implementation of a scramjet cycle analysis code with a finite-rate-chemistry combustion model for use on a personal computer
[AD-A273834] p 2673 N94-25617
Evaluation of an Acoustic Charge Transport (ACT) device for adaptive interference suppression in spread spectrum communications systems
[AD-A274073] p 2765 N94-25647
Development of a 4-bit parallel analog-to-digital converter and a four-quadrant double-balanced mixer using heterojunction bipolar transistor technology
[AD-A274074] p 2947 N94-25648
Vulnerability assessment using a fuzzy logic based method
[AD-A274075] p 2957 N94-25649
Experimental analysis of heat transfer characteristics and pressure drop through screen regenerative heat exchangers
[AD-A273902] p 2790 N94-25657
Feasibility study of a multiaperture telescope for deep-space Earth surveillance
[AD-A273903] p 3102 N94-25658
Prototype space fabrication platform
[AD-A273904] p 2694 N94-25659

Hyperspectral analysis of space objects: Signal to noise evaluation
[AD-A273882] p 2765 N94-25728

Characterization of an LCD for use as a programmable phase shifter to produce a single-lobed far-field pattern in a phased array
[AD-A273883] p 3034 N94-25729

Improved quality of reconstructed images through sifting of data in statistical image reconstruction
[AD-A273884] p 3034 N94-25730

Binaural room simulation
[AD-A273823] p 3009 N94-25737

Automating satellite range scheduling
[AD-A273829] p 2694 N94-25738

Investigation of compressive behavior for metal matrix composites with a circular hole
[AD-A273835] p 2705 N94-25739

Dynamic response of a compressor research facility
[AD-A273836] p 2679 N94-25740

Objective image quality metrics: Applications for partially compensated images of space objects
[AD-A273837] p 2847 N94-25741

Performance impacts for actuator misalignments and failures in large-aperture adaptive-optic telescopes
[AD-A273838] p 3034 N94-25742

Optimal control design advantages utilizing two-degree-of-freedom controllers
[AD-A273839] p 2984 N94-25743

Characterization of nonlinear effects in optically pumped vertical cavity surface emitting lasers
[AD-A273840] p 2815 N94-25744

Analysis and development of an F-5 pollution prevention management program with recommendations for creation of similar programs for other aircraft
[AD-A274016] p 2865 N94-25755

Design of a shared coherent cache for a multiple channel architecture
[AD-A274026] p 3034 N94-25758

Color image segmentation
[AD-A274027] p 2984 N94-25759

Performance measurement of three commercial object-oriented database management systems
[AD-A274028] p 3096 N94-25765

Analyzing adaptive beamformer performance in a stable multipath environment
[AD-A274029] p 2766 N94-25766

ObjectSim: A reusable object oriented DIS visual simulation
[AD-A274030] p 2958 N94-25767

Performance comparison of shearing interferometer and Hartmann wave front sensors
[AD-A274031] p 3034 N94-25768

System design analysis of a lightweight laser satellite terminal
[AD-A274033] p 2690 N94-25769

Filtering, coding, and compression with Malvar wavelets
[AD-A274055] p 2780 N94-25770

Design of a subsonic envelope flight control system for the Vista F-16 using quantitative feedback theory
[AD-A274057] p 2676 N94-25771

Weapon system integration for the AFIT virtual cockpit
[AD-A274058] p 2667 N94-25772

Developing realistic cooperative behaviors for autonomous agents in air combat simulation
[AD-A274077] p 2937 N94-25774

Modal control of a satellite in an unstable periodic orbit about the Earth-Sun interior Lagrange point
[AD-A273707] p 2694 N94-25776

Domain analysis and modeling of a model-based software executive
[AD-A274087] p 2958 N94-25783

Neural networks for dynamic flight control
[AD-A274089] p 2676 N94-25785

A cost model for USAF acquisition of commercial aircraft for service in the special air mission fleet
[AD-A274012] p 3093 N94-25796

A method for populating the knowledge base of APTAS, a domain-oriented application composition system
[AD-A274034] p 2766 N94-25797

Source code for the OO1 benchmark and the AFIT simulation benchmark
[AD-A274035] p 2958 N94-25799

Analysis and simulation of a GPS receiver design using combined delay-lock and modified tanlock loops
[AD-A274037] p 2664 N94-25810

A study of two dimensional tapered periodic edge treatments to reduce wideband edge diffraction
[AD-A274054] p 2766 N94-25824

Design analysis of a combined optical/LADAR deep-space surveillance satellite
[AD-A274040] p 2694 N94-25832

Design of a flight controller for an unmanned research vehicle with control surface failures using quantitative feedback theory
[AD-A274049] p 2677 N94-25833

Predicting nonlinear time series
[AD-A274051] p 2990 N94-25834

Object imaging accomplished with an integrated circuit robotic tactile sensor incorporating a piezoelectric polyvinylidene fluoride thin film
[AD-A274038] p 2780 N94-25845

Electrical properties of p-type GaInP2
[AD-A273771] p 3051 N94-25856

A nonlinear three-dimensional micromechanics model for fiber-reinforced laminated composites
[AD-A273772] p 2705 N94-25857

Shock wave interaction with L-shaped structures
[AD-A273774] p 2790 N94-25858

Influence of embedded optical fibers on compressive strength of advanced composites
[AD-A273775] p 2705 N94-25859

A numerical study of high-speed missile configurations using a block-structured parallel algorithm
[AD-A273776] p 2979 N94-25860

Developing prediction regions for a time series model for hurricane forecasting
[AD-A273777] p 2892 N94-25861

Effects of crenulations on three dimensional losses in a linear compressor cascade
[AD-A273778] p 2790 N94-25862

A study of graphite peek composite with central elliptical holes under tension
[AD-A273779] p 2705 N94-25863

Wake passage effects on the losses in a linear turbine cascade
[AD-A273794] p 2790 N94-25874

Spectroscopic and vibrational energy transfer studies in molecular bromine
[AD-A273795] p 3014 N94-25875

Characterization of fatigue damage in a metal matrix composite (SCS-6/Ti-15-3) at elevated temperature
[AD-A273797] p 2706 N94-25876

Development of the Air Force contingency contracting course framework
[AD-A273921] p 3093 N94-25895

An exploratory survey of methods used to develop measures of performance
[AD-A273945] p 2834 N94-25896

A test of the theory of reasoned action at the group level of analysis
[AD-A273965] p 2937 N94-25897

A virtual environment for satellite modeling and orbital analysis in a distributed interactive simulation
[AD-A274114] p 2694 N94-25904

Evaluation of moderate angle of attack roll of a dual engine, thrust vectoring aircraft using quantitative feedback theory
[AD-A274118] p 2667 N94-25905

Object-oriented design and implementation of a parallel Ada simulation system
[AD-A274119] p 2979 N94-25906

Object interaction in a parallel object-oriented discrete-event simulation
[AD-A274084] p 2959 N94-25942

The AFIT multielectrode array for neural recording and simulation: Design, testing, and encapsulation
[AD-A274086] p 2909 N94-25943

A numerical determination of bifurcation points for low Reynolds number conical flows
[AD-A273984] p 2791 N94-25991

Multiple model adaptive estimation applied to the LAMBDA URV for failure detection and identification
[AD-A274078] p 3002 N94-25992

Developing a sophisticated user interface to support domain-oriented application composition and generation systems
[AD-A274080] p 2960 N94-25994

A physics-based heterojunction bipolar transistor model for integrated circuit simulation
[AD-A274081] p 2781 N94-25995

Satellite attitude determination using linear combination of models
[AD-A274082] p 2694 N94-25996

Rendering of three-dimensional data sets derived from finite-difference and spectral methods
[AD-A273724] p 3096 N94-25997

Discovery learning in autonomous agents using genetic algorithms
[AD-A274083] p 2677 N94-25998

Investigation of tension-compression fatigue behavior of a cross-ply metal matrix composite at room and elevated temperatures
[AD-A273731] p 2706 N94-25999

The modal solution to the Moon's orbit using canonical Floquet perturbation theory
[AD-A273732] p 2690 N94-26001

A comparison of users' and providers' perceptions of critical spacelift vehicle characteristics and capabilities
[AD-A273907] p 2691 N94-26017

Developing a graphical user interface to support a real-time digital signal processing system
[AD-A274032] p 2960 N94-26018

Weapon system sensor integration for a DIS-compatible virtual cockpit
[AD-A274088] p 2672 N94-26021

Using database technology to support domain-oriented application composition systems
[AD-A274091] p 3096 N94-26024

An approximate solution for the spinup dynamics of near axisymmetric axial gyrostats using the method of multiple scales
[AD-A273723] p 2698 N94-26223

Investigation into model-based fuzzy logic control
[AD-A274660] p 2985 N94-26336

Analysis of cost and schedule growth on sole source and competitive Air Force contracts
[AD-A273920] p 3094 N94-26814

Three dimensional object recognition using a complex autoregressive model
[AD-A274388] p 2995 N94-26829

Partitioning structural VHDL circuits for parallel execution on hypercubes
[AD-A274390] p 2785 N94-26830

An analysis of FM jamming and noise quality measures
[AD-A274349] p 2772 N94-26924

Detection of low-intensity magnetic fields with a magnetostrictive fiber optic sensor
[AD-A274120] p 3037 N94-27062

Interactive control of a parallel simulation from a remote graphics workstation
[AD-A274217] p 2981 N94-27070

Development of a performance evaluation tool (MMSOFE) for detection of failures with Multiple Model Adaptive Estimation (MMAE)
[AD-A274218] p 2665 N94-27071

Processing of wide-angle synthetic aperture radar signals for target detection
[AD-A274225] p 2773 N94-27073

An object-oriented database interface for Ada
[AD-A274391] p 2968 N94-27075

Enhanced tracking of airborne targets using forward looking infrared and laser return measurements
[AD-A274181] p 3037 N94-27102

A method for populating the knowledge base of AFIT's domain-oriented application composition system
[AD-A274128] p 3099 N94-27118

A parallel computational fluid dynamics unstructured grid generator
[AD-A274129] p 2795 N94-27119

Genetic algorithms applied to a mission routing problem
[AD-A274130] p 2968 N94-27120

Using discovery-based learning to prove the behavior of an autonomous agent
[AD-A274131] p 2987 N94-27121

Multiple model adaptive control of a large flexible space structure with purposeful dither for enhanced identifiability
[AD-A274132] p 2987 N94-27122

Design of a parallel discrete event simulation coprocessor
[AD-A274135] p 2982 N94-27123

Radar cross section visualization using sample buffer progressive refinement volume rendering
[AD-A274179] p 2773 N94-27127

Alternative architectures for domain-oriented application composition and generation systems
[AD-A274180] p 2968 N94-27128

Experimental verification of tomographic reconstruction of turbulent air flow structure using optical wavefront measurements
[AD-A274392] p 2795 N94-27129

Automation of formation flight control
[AD-A274137] p 2678 N94-27132

Virtual memory management and virtual bus overloading on multiple channel architectures
[AD-A274127] p 2954 N94-27152

An investigation of integrated product development implementation issues: A case study of Bosma Machine and Tool Corp.
[AD-A273917] p 2942 N94-27320

AIR FORCE LOGISTICS COMMAND, EDWARDS AFB, CA.

Freon recovery from nitrogen tetroxide and freon solutions
[PL-TR-92-3051] p 2721 N94-28215

AIR FORCE SYSTEMS COMMAND, BROOKS AFB, TX.

Aeromedical issues related to positive pressure breathing for +Gz protection
[AD-A274717] p 2910 N94-26435

AIR FORCE SYSTEMS COMMAND, WRIGHT-PATTERSON AFB, OH.

Investigation of mesoscale convective cloud clusters in South China
[AD-A274303] p 2895 N94-26678

Propagation of cold air masses in East Asia and its associated planetary-scale function
[AD-A274304] p 2895 N94-26850

Optimum for the gasdynamic system in a fast-axial-flow CO2 laser
[AD-A274305] p 2819 N94-26940

Practical design of resonant cavity for a RF free electron laser
[AD-A274306] p 2819 N94-26941

AKRON UNIV., OH.

Computer code for controller partitioning with IFPC application: A user's manual
[NASA-CR-195291] p 2678 N94-27414

On line quantification of crystal surfaces by stereo imaging
[NASA-CR-195277] p 3066 N94-27561

ALABAMA AGRICULTURAL AND MECHANICAL COLL., NORMAL.

Predoctoral training grant in the area of physical sciences
[DE94-004406] p 3039 N94-27603

ALABAMA UNIV., HUNTSVILLE.

Systematic Propulsion Optimization Tools (SPOT)
p 2976 N94-25666

FNAS lightning detection
[NASA-CR-193927] p 2893 N94-26134

BATSE Data Analysis
[NASA-CR-195545] p 3114 N94-26685

Verification of thermal analysis codes for modeling solid rocket nozzles
[NASA-CR-195248] p 2702 N94-27150

A measurement of the energy spectra of cosmic rays from 20 to 1000 GeV per AMU
[NASA-CR-195246] p 3115 N94-27167

Modelling of the MEA float zone using accelerometer data
[NASA-CR-193933] p 2761 N94-27220

UAH mathematical model of the variable polarity plasma ARC welding system calculation
[NASA-CR-193926] p 2824 N94-27221

Advanced technology development multi-color holography
[NASA-CR-193931] p 2812 N94-27229

Materials characterization on efforts for ablative materials
[NASA-CR-193929] p 2756 N94-27230

Enhanced simulation software for rocket turbopump, turbulent, annular liquid seals
[NASA-CR-195239] p 2825 N94-27383

Global change research related to the Earth's energy and hydrologic cycle
[NASA-CR-195270] p 2869 N94-27430

Use of photostress and strain gages to analyze behavior of weldments
[NASA-CR-195269] p 2843 N94-27765

Superfluid helium sloshing dynamics induced oscillations and fluctuations of angular momentum, force and moment actuated on spacecraft driven by gravity gradient or jitter acceleration associated with slew motion
[NASA-CR-193928] p 2799 N94-27931

ALABAMA UNIV., TUSCALOOSA.

Use of photostress and strain gages to analyze behavior of weldments
[NASA-CR-195269] p 2843 N94-27765

ALASKA UNIV., FAIRBANKS.

Seasonal snow of arctic Alaska R4D investigations
[DE93-040082] p 2892 N94-25939

Active layer dynamics and arctic hydrology and meteorology
[DE94-001724] p 2892 N94-25951

Remote sensing of global snowpack energy and mass balance: In-situ measurements on the snow of interior and Arctic Alaska
[NASA-CR-195704] p 2851 N94-27787

ALBERTA UNIV., EDMONTON.

Weak hadronic decays of heavy flavor mesons
[ISBN-0-315-55542-4] p 3026 N94-27402

MIMD parallel approaches to object labeling
[ISBN-0-315-60198-1] p 2982 N94-27644

ALLIED-SIGNAL AEROSPACE CO., TORRANCE, CA.

MSOFC development status
[DE94-003192] p 2858 N94-26792

ALLIED-SIGNAL CORP., MORRISTOWN, NJ.

Image compression software for the SOHO LASCO and EIT experiments p 2945 N94-28253

ALSYS, INC., SAINT CLOUD (FRANCE).

Ada multiple-programming for hard real time applications in space systems p 2951 N94-26730

AMES LAB., IA.

Fracture behavior of 20% Nb particulate reinforced alumina composite
[DE94-002830] p 2706 N94-26019

Liquid and solid solubility of Ag in Bi2Sr2CaCu2O8
[DE94-002829] p 2735 N94-26273

The coordination and atom transfer chemistry of titanium porphyrin complexes
[DE94-003091] p 2704 N94-26779

Synthesis, rheology, and forming of Y-Ba-Cu-O ceramics
[DE94-005558] p 2757 N94-27695

Topics in electroweak baryogenesis: The sphaleron and T-violation
[DE94-004886] p 3029 N94-27811

Characterization of ZnS-GaP naon-composites
[DE94-004888] p 2712 N94-27813

AMSTERDAM UNIV. (NETHERLANDS).

Parallel discrete event simulation
p 2955 N94-27194

High gas-efficiency hydrogen negative ion sources
[PB93-232163] p 3025 N94-27348

ANALYTIC SCIENCES CORP., READING, MA.

Short-range cloud amount forecasting with model output statistics
[AD-A274769] p 2895 N94-26798

ANALYTICAL SERVICES AND MATERIALS, INC., HAMPTON, VA.

The measurement of disturbance levels in the Langley Research Center 20-inch Mach 6 tunnel
[NASA-CR-4571] p 2646 N94-26548

APPLIED RESEARCH ASSOCIATES, INC., ALBUQUERQUE, NM.

Parallel computing for probabilistic response analysis of high temperature composites
[NASA-CR-194467] p 2843 N94-27656

ARGONNE NATIONAL LAB., IDAHO FALLS, ID.

Grain boundary degradation of YBCO superconductors sintered in CO2-containing atmospheres
[DE94-003206] p 3053 N94-26029

Progress in SSC Higgs physics: Report of the Higgs working group
[DE94-003224] p 3022 N94-26793

ARGONNE NATIONAL LAB., IL.

Using a transfer function to describe the load-balancing problem
[DE94-004218] p 2979 N94-25802

Reference electrodes for solid polymer electrolytes
[DE94-004583] p 2780 N94-25806

Three methods to measure RH bond energies
[DE94-003795] p 3013 N94-25816

Monte Carlo event generators for hadron-hadron collisions
[DE94-003212] p 3015 N94-25955

Buckyball microwave plasmas: Fragmentation and diamond-film growth
[DE94-003209] p 3053 N94-26031

Crossover between BCS and performed-Boson theories with increasing interactions
[DE93-019018] p 3017 N94-26078

Fast photoconductor CdTe detectors for synchrotron x ray studies
[DE94-001334] p 3054 N94-26139

A Shuttle mechanism for molten-electrolyte lithium batteries
[DE94-002914] p 2781 N94-26144

Rescattering and energy loss of fast partons in nuclear matter
[DE94-002918] p 3018 N94-26145

The effect of processing on the microstructure of Ag-sheathed Bi-2223 wires
[DE94-004627] p 3055 N94-26243

Studies of thin-film growth, adsorption, and oxidation by in situ, real-time, and ex situ ion beam analysis
[DE94-002907] p 3055 N94-26275

Comparison of technology for high-power laser mirrors and synchrotron radiation mirrors
[DE94-002913] p 3035 N94-26276

Potential capabilities of Reynolds stress turbulence model in the COMMIX-RSM code
[DE94-003716] p 2792 N94-26331

Programming in Fortran M
[DE94-002756] p 2963 N94-26407

Correlation of experimental data and three-dimensional finite element modeling of a spinning quadrupole
[DE93-041173] p 3008 N94-26421

Crystal chemistry and self-lubricating properties of monochalcogenides gallium selenide and tin selenide
[DE93-041177] p 2751 N94-26422

Eleventh Symposium on Energy Engineering Sciences: Proceedings
[DE93-019930] p 2763 N94-26429

Research and development of alternative components at Argonne National Laboratory for Molten Carbonate Fuel Cells
[DE94-000014] p 2857 N94-26583

Sealant research for solid oxide fuel cells
[DE94-000015] p 2857 N94-26584

Suppression of thermal grain growth in nickel by prior electron irradiation
[DE94-004602] p 2737 N94-26587

Processing and properties of Ag-clad Bi-2223 tapes
[DE94-004603] p 2783 N94-26589

Modulation wavelength dependence of ion mixing in metallic superlattices
[DE94-004608] p 3059 N94-26591

Mechanical properties of nanophase materials
[DE94-004625] p 2751 N94-26594

Design considerations when using external hypertext engines from applications
[DE94-002213] p 3098 N94-26598

Validated heat-transfer and pressure-drop prediction methods based on the discrete-element method. Phase 2: Two-dimensional rib roughness
[DE94-002379] p 2794 N94-26763

Fabrication and characterization of nano-crystalline diamond films
[DE94-002202] p 3062 N94-26934

Solidification modeling of a spiral casting to determine material fluidity
[DE94-002212] p 2739 N94-26935

Advances in passive-remote and extractive Fourier transform infrared spectroscopic systems
[DE94-001424] p 2868 N94-26952

Powder synthesis, fabrication, and transport properties of long-length Ag clad Bi-2223 conductors
[DE94-002376] p 2740 N94-26957

Double excitation of He and H(-) by fast proton and anti-proton impact
[DE94-004581] p 3026 N94-27620

Electro-optic materials by solid source MOCVD
[DE94-005120] p 2757 N94-27716

The PRISM project: Infrastructure and algorithms for parallel eigensolvers
[DE94-005125] p 2973 N94-27717

Multiple exposure CCD detector for high-speed laser pump, x ray probe Laue scattering
[DE94-004618] p 2820 N94-27781

ARIEL DYNAMICS.

Muscular activity and its relationship to biomechanics and human performance p 2934 N94-28362

ARIZONA STATE UNIV., TEMPE.

Continuation and multi-grid for bifurcation problems
[AD-A274965] p 2992 N94-26302

Benefits estimation for simulation systems used for aircrew training in a multiship environment
[AD-A274313] p 2938 N94-26882

Hybrid techniques for complex aerospace electromagnetics problems p 2779 N94-27894

ARIZONA UNIV., TUCSON.

Autonomous space processor for orbital debris advanced design project in support of solar system exploration p 2697 N94-25667

Numerical simulation of receptivity and transition in a boundary layer on a flat plate with a suction hole
[NASA-CR-195708] p 2798 N94-27782

Mechanically fastened composite laminates subjected to combined bearing-bypass and shear loading
p 2712 N94-27914

ARMY AEROMEDICAL RESEARCH LAB., FORT RUCKER, AL.

US Army aviation epidemiology data registry: Incidence and outcomes of aviator flying evaluation boards
[AD-A274711] p 2910 N94-26432

A comparison of sleep scored from electroencephalography to sleep scored by wrist actigraphy
[AD-A273739] p 2910 N94-26748

Monograph of the aviation epidemiology data register for calendar year 1988
[AD-A274589] p 2911 N94-26985

Aviation Epidemiology Data Register: Indexing the AEDR document laser optic archive
[AD-A274185] p 2911 N94-27097

Monograph of the Aviation Epidemiology Data Register for CY 1992
[AD-A274400] p 2911 N94-27130

ARMY ARMAMENT RESEARCH, DEVELOPMENT AND ENGINEERING CENTER, PICATINNY ARSENAL, NJ.

Design of a computer expert system for adhesive selection using artificial intelligence techniques
[AD-A274715] p 2751 N94-26434

Thermal conductivity of PAX 2A explosive by DSC
[AD-A274721] p 2759 N94-26437

ARMY ARMAMENT RESEARCH, DEVELOPMENT AND ENGINEERING CENTER, WATERVLIET, NY.

Power laws, flicker noise, and the barkhausen effect
[AD-A274702] p 3008 N94-26376

ARMY COMBAT SYSTEMS TEST ACTIVITY (PROVISIONAL), ABERDEEN PROVING GROUND, MD.
Test Operations Procedure (TOP) 2-2-800 wheeled vehicle center of gravity
[AD-A273937] p 2621 N94-25794

ARMY COMMAND AND GENERAL STAFF COLL., FORT LEAVENWORTH, KS.
Female combat helicopter pilot selection criteria
[AD-A273935] p 2938 N94-26749

ARMY HEALTH CARE STUDIES AND CLINICAL INVESTIGATION ACTIVITY, FORT SAM HOUSTON, TX.
Practice patterns of US Army medical department psychiatrists and psychologists
[AD-A274787] p 2909 N94-26360

ARMY RESEARCH LAB., ABERDEEN PROVING GROUND, MD.
SHIVA: A unix-based, menu-driven, color image processing software package
[AD-A274071] p 2957 N94-25646
IGES 4.0 to LCAD translator for CSG models
[AD-A274013] p 2957 N94-25753

ARMY RESEARCH LAB., ADELPHI, MD.
Mitsubishi 3-5 micrometers IR imager for machine-vision/ATA applications
[AD-A273812] p 3034 N94-25940
A preliminary method for atmospheric soundings in real time using satellite and ground-based remotely sensed data
[AD-A274381] p 2880 N94-26828
The morphological processing of binary images
[AD-A274310] p 2996 N94-26972

ARMY RESEARCH LAB., WATERTOWN, MA.
Dynamic response of S-2 glass reinforced plastic structural armor
[AD-A273868] p 2747 N94-25596
Determination of fracture stress and effective crack tip radius from toughness (KIc) and yield strength (Y)
[AD-A274014] p 2836 N94-25754
Mechanical properties and microstructure of thermomechanically processed, high manganese steel
[ARL-TR-146] p 2747 N94-28212

ARMY RESEARCH LAB., WHITE SANDS MISSLE RANGE, NM.
Surface roughness lengths
[AD-A274550] p 2895 N94-26846

ARMY TEST AND EVALUATION COMMAND, ABERDEEN PROVING GROUND, MD.
FR/GE/UK/US International Test Operations Procedure (ITOP) 1-1-050 development of laboratory vibration test schedules
[AD-A273887] p 2836 N94-25732

ARMY TOPOGRAPHIC ENGINEERING CENTER, FORT BELVOIR, VA.
The potential for the Department of Defense to use space-based remote sensing to support DOD and other government agencies' environmental programs
[AD-A273895] p 2847 N94-25656
Optimization of Vector Product Format (VPF) data for map background display in army tactical systems
[AD-A274687] p 2848 N94-26446
PDEF: A standard file format for data interchange
[AD-A274694] p 3098 N94-26451
Conifer tree influence on Digital Terrain Elevation Data (DTED): A case study at Dulles International Airport
[AD-A274213] p 2849 N94-27069
Multivariate spectral analysis to extract materials from multispectral data
[AD-A274142] p 2709 N94-27135

ARNOLD ENGINEERING DEVELOPMENT CENTER, ARNOLD AFS, TN.
UV absorption technique for monitoring mobile source NO emissions
[AD-A273858] p 2713 N94-25964
An algorithm for determination of bearing health through automated vibration monitoring
[AD-A274591] p 2823 N94-26986

ASSOCIATED WESTERN UNIVERSITIES, INC., SALT LAKE CITY, UT.
Influence of helium generation rate and temperature history on mechanical properties of model Fe-Cr-Ni alloys irradiated in FFTF at relatively low displacement rates
[DE94-004264] p 2737 N94-26575

ATMOSPHERIC AND ENVIRONMENTAL RESEARCH, INC., CAMBRIDGE, MA.
Assessing the climatic effect of carbon dioxide and other trace gases using an interactive two-dimensional climate-chemistry model
[DE94-001741] p 2866 N94-25927
A research program on radiative transfer model development in support of the ARM program
[DE94-001146] p 2767 N94-25950
Testbed model and data assimilation for ARM
[DE94-000432] p 2893 N94-26082
Studies for Io's extended atmosphere and neutral clouds and their impact on the local satellite atmosphere and on the planetary magnetosphere
[NASA-CR-195255] p 3106 N94-27406
Reanalysis of Mariner 9 UV Spectrometer Data for Ozone, Cloud, and Dust Abundances, and Their Interaction Over Climate Timescales
[NASA-CR-195244] p 3107 N94-27885
Cooling the Martian atmosphere: The spectral overlap of the C02 15 micrometers band and dust
p 3107 N94-27886
Martian atmospheric radiation budget
p 3107 N94-27887
Mars ozone: Mariner 9 revisited p 3107 N94-27888
Why is the north polar cap on Mars different than the south polar cap? p 3107 N94-27889
Probing the Martian atmosphere in the ultraviolet
p 3108 N94-27890
How well was total ozone abundance inferred with Mariner 9? p 3108 N94-27891
In situ Mars ozone detector p 3108 N94-27892
An enhanced global spectral model
[PL-TR-92-2011] p 2898 N94-28223

ATOMIC ENERGY OF CANADA LTD., PINAWA (MANITOBA).
The effect of axial velocity ratio, turbulence intensity, incidence, and leading edge geometry on the midspan performance of a turbine cascade p 2652 N94-28321

AUBURN UNIV., AL.
Design of the advanced regional aircraft, the DART-75
p 2671 N94-25708
Eagle RTS: A design of a regional transport
p 2671 N94-25709
Physics of debris clouds from hypervelocity impacts
[NASA-CR-193932] p 2696 N94-26791
Silicon device performance measurements to support temperature range enhancement
[NASA-CR-195265] p 2844 N94-27824

AUSTIN RESEARCH ASSOCIATES, INC., TX.
Analytical study of beam handling and emittance control
[AD-A274412] p 3033 N94-27078

AUSTRALIAN NATIONAL UNIV., CANBERRA.
A preliminary shear velocity model for Central Asia
[AD-A274972] p 2880 N94-26752

B

BELEIDSCOMMISSIE REMOTE SENSING, DELFT (NETHERLANDS).
Remote sensing and GIS for the management and investigation of the Wadden Sea
[BCRS-92-20] p 2847 N94-26228

BELL TELEPHONE LABS., INC., CRANBURY, NJ.
Charge efficiency of Ni/H2 cells during transfer orbit of Telstar 4 satellites p 2862 N94-28117

BEN GURION UNIV. OF THE NEGEV, BEERSHEVA (ISRAEL).
Liquid metal MHD research and development in Israel
p 2854 N94-26055
Technical report of ISSP. Ser. A, no. 2687: Quantized persistent currents of a quantum dot in a strong magnetic field
[JTN-94-80573] p 3028 N94-27758

BERN UNIV. (SWITZERLAND).
Simulation of the carbon cycle in the oceans
[DE94-000780] p 2898 N94-25791

BETTIS ATOMIC POWER LAB., PITTSBURGH, PA.
The use of on-line ion chromatography for high temperature and high pressure reaction studies
[DE94-002525] p 2713 N94-26075

BETTIS ATOMIC POWER LAB., WEST MIFFLIN, PA.
An experimental study on the effects of compressive stress on the fatigue crack growth of low-alloy steel
[DE94-004447] p 2737 N94-26582
An improvement in the modified finite element procedure for underwater shock analysis
[DE94-004451] p 2797 N94-27617

BHABHA ATOMIC RESEARCH CENTRE, BOMBAY (INDIA).
Radiochemistry Division annual progress report : 1991
[DE94-600652] p 2715 N94-26392
A Multitransputer Parallel Processing System (MTPPS)
[DE94-604652] p 2981 N94-26903
Spectroscopy Division
[DE94-604074] p 2717 N94-26988

BIRMINGHAM UNIV. (ENGLAND).
On-board software for the JET-X telescope on the Spectrum-X mission p 2951 N94-26727

BOEING COMMERCIAL AIRPLANE CO., SEATTLE, WA.
Composite leading edge/spar member for an aircraft control surface
[CA-PATENT-1-325-765] p 2669 N94-27273

BOEING DEFENSE AND SPACE GROUP, HUNTSVILLE, AL.
Space Station evolution study oxygen loop closure
[NASA-CR-193938] p 2941 N94-26788

BOEING DEFENSE AND SPACE GROUP, SEATTLE, WA.
X ray computed tomography for emerging aerospace materials and processes development
[AD-A273721] p 2705 N94-25779
Use of calorimetry for end of charge determination
p 2863 N94-28128

BOLT, BERANEK, AND NEWMAN, INC., CANOGA PARK, CA.
Comparison of methods of predicting community response to impulsive and nonimpulsive noise
p 2651 N94-28196

BOMBARDIER, INC., MONTREAL (QUEBEC).
Application of the MBTEC Euler code to the Challenger and the CF-18 complete aircraft configurations
p 2653 N94-28324

BOSTON COLL., CHESTNUT HILL, MA.
CRRES high energy proton flux map
[AD-A274803] p 2878 N94-26338

BOSTON UNIV., MA.
Upper atmosphere neutral and plasma density modeling
[AD-A274768] p 2879 N94-26569
Configuration of the near-Earth plasma sheet
[NASA-CR-195271] p 2883 N94-27438
Weightlessness and the human skeleton: A new perspective p 2935 N94-28368

BRADFORD UNIV. (ENGLAND).
Parallel algorithm for dominant points correspondences in robot binocular stereo vision p 2686 N94-27364

BRITISH AEROSPACE DEFENSE LTD., FARNBOROUGH (ENGLAND).
Experiments into the scaling parameters required for exhaust gas ingestion testing of vertical landing aircraft
p 2671 N94-28017

BRITISH AEROSPACE PUBLIC LTD. CO., STEVENAGE (ENGLAND).
Implementing hard real-time systems: A case study
p 2951 N94-26731

BRITISH COLUMBIA UNIV., VANCOUVER.
Finite density effects in gauge theories
[ISBN-0-315-50637-7] p 3074 N94-27403
An investigation of methods for determining depth from focus
[ISBN-0-315-64015-4] p 2988 N94-27645
A theory of multi-scale, curvature and torsion based shape representation for planar and space curves
[ISBN-0-315-63894-X] p 2974 N94-27805
Super finite elements for nonlinear static and dynamic analysis of stiffened plate structures
[ISBN-0-315-63903-2] p 2844 N94-27808
The transition from stress corrosion cracking to corrosion fatigue in AA-7075 and AA-8090
[ISBN-0-315-59526-4] p 2744 N94-27950
Aerodynamic performance of novel ducted-tip wings
p 2654 N94-28331
Non-isoenergetic inviscid slot flow
p 2655 N94-28333

BROOKHAVEN NATIONAL LAB., UPTON, NY.
Production of (phi) mesons in central Si + Au collisions at 14.6 AGeV/c
[DE94-003196] p 3012 N94-25795
Small low mass advanced PBR's for bi-modal operation
[DE94-003201] p 2699 N94-25798
Structure and phase transformations in uranium metal
[DE94-003892] p 2732 N94-26004
Strange Dibaryons
[DE94-003005] p 3022 N94-26769
X ray absorption studies of Ti/polymer and Cr/polymer interfaces
[DE94-003008] p 2753 N94-26770
A mechanism for resistive dissipation in Ag sheathed Bi2Sr2CaCu2O8 and Bi2Sr2Ca2Cu3O10
[DE94-003009] p 3060 N94-26771
Design of a high-precision double crystal tunable monochromator
[DE94-003004] p 2811 N94-26787
Voltammetric studies of poly(carbon disulfide)
[DE94-001385] p 2717 N94-26951
Future directions in particle and nuclear physics at multi-GeV hadron beam facilities
[DE94-002946] p 3027 N94-27711
Surface modes and chiral symmetry (Wilson fermions in a box)
[DE94-004946] p 3029 N94-27814
The validation of ATSR measurements with in situ sea temperatures
[DE94-003195] p 2852 N94-27875

BROWN UNIV., PROVIDENCE, RI.
Sensitivity of climate models: Comparison of simulated and observed patterns for past climates
[DE93-019934] p 2865 N94-25789

A research program in experimental and theoretical high energy physics
[DE94-002156] p 3031 N94-25931
Experimental study of lunar and SNC (Mars) magmas
[NASA-CR-195274] p 3107 N94-27850

BRUBAKER GROUP, LOS ANGELES, CA.
A widely adaptable habitat construction system utilizing space resources p 2688 N94-27374

BST SYSTEMS, INC., PLAINFIELD, CT.
Advanced silver zinc battery development for the SRB and ET range safety subsystems p 2865 N94-28136

C

CALIAN COMMUNICATIONS, KANATA (ONTARIO).
Acousto-optical post-processor time-integrating correlator calibration updates
[DSIS-94-00053] p 2813 N94-27317
Modulation Simulation Program: Programmer's manual, version 1.00
[DREO-16] p 2973 N94-27761
Modulation Simulation Program: Operator's manual, version 1.00
[DREO-16] p 2975 N94-27951

CALIFORNIA INST. OF TECH., PASADENA.
Hydrodynamics, acoustics and scaling of traveling bubble cavitation
[AD-A273846] p 2789 N94-25605
Flow past a circular cylinder with a permeable wake splitter plate
[AD-A273765] p 2790 N94-25872
Role of anticausal inverses in multirate filter-banks. Part 1: System theoretic fundamentals
[AD-A274279] p 2997 N94-27015
Nominally 2-dimensional flow about a normal flat plate
[AD-A274472] p 2794 N94-27026
Causal fir matrices with anticausal fir inverses, and application in characterization of biorthonormal filter banks
[AD-A274509] p 2998 N94-27035
Research on bluff body vortex wakes
[AD-A273780] p 2796 N94-27319
Analysis of energetic proton and electron data in Neptune's magnetosphere
[NASA-CR-195707] p 3107 N94-27784

CALIFORNIA POLYTECHNIC STATE UNIV., SAN LUIS OBISPO.
Preliminary design of nine high speed civil transports
p 2671 N94-25710
Analysis and optimization of preliminary aircraft configurations in relationship to emerging agility metrics
[NASA-CR-195228] p 2668 N94-26235

CALIFORNIA STATE POLYTECHNIC UNIV., POMONA.
Supercruiser Arrow HS-8 p 2671 N94-25711

CALIFORNIA STATE UNIV., LOS ANGELES.
Computation of transonic viscous flow past the NTF 65-degree Delta Wing p 2659 N94-27930

CALIFORNIA STATE UNIV., NORTHRIDGE.
Project Ares 3 p 2671 N94-25712

CALIFORNIA UNIV., BERKELEY.
Elastic scattering by a spherical inclusion
[AD-A274713] p 2878 N94-26433
Trajectories of ballistic impact ejecta on a rotating Earth p 2887 N94-28295

CALIFORNIA UNIV., BERKELEY. LAWRENCE BERKELEY LAB.
Vortex methods
[DE94-003245] p 2789 N94-25597
Detection geometry and reconstruction error in magnetic source imaging
[DE94-004012] p 2809 N94-25662
An optimal constrained linear inverse method for magnetic source imaging
[DE94-004014] p 2957 N94-25663
Interface configuration experiment: Preliminary results
[NASA-TM-109684] p 2760 N94-25849
Exploratory Technology Research Program for Electrochemical Energy Storage
[DE94-003479] p 2781 N94-26047
The STAR experiment at the Relativistic Heavy Ion Collider
[DE94-003409] p 3017 N94-26083
Cracking of textured zinc coating during forming process
[DE94-003414] p 2750 N94-26085
Influence of grain structure and solute composition on the work hardening behavior of aluminium at cryogenic temperatures
[DE94-003415] p 2733 N94-26087
Determination of surface recombination velocity and bulk lifetime in detector grade silicon and germanium crystals
[DE94-003886] p 3053 N94-26094
Lithium drifted silicon detector fabrication on gettered floating-zone silicon
[DE94-003890] p 3054 N94-26095
Characterization of acoustic effects on flame structures by beam deflection technique
[DE94-003240] p 2714 N94-26122
Se EXAFS study of the elevated wurtzite to rock salt structural phase transition in CdSe nanocrystals
[DE94-003247] p 3054 N94-26125
Instantaneous amplitude and frequency dynamics of coherent wave mixing in semiconductor quantum wells
[DE94-003262] p 3054 N94-26128
Growth of small fatigue cracks in Incoloy-908
[DE94-003406] p 2836 N94-26129
Improved measurement accuracy in a Long Trace Profiler: Compensation for laser pointing instability
[DE94-003408] p 2816 N94-26130
Stress relaxation in sputtered W films and W/GeSi/Si heterostructures
[DE94-004007] p 3055 N94-26239
Measurement of tau lepton branching fractions
[DE94-003423] p 3018 N94-26325
OPM Scheme Editor 2: A graphical editor for specifying object-protocol structures
[DE94-003477] p 2962 N94-26327
In situ spectroscopic applications to the study of rechargeable lithium batteries
[DE94-003478] p 2782 N94-26328
Exploratory technology research program for electrochemical energy storage
[DE94-003480] p 2855 N94-26329
On a theory of two-beam mechanisms of charged particle acceleration in electrodynamic structures
[DE94-003482] p 3032 N94-26330
A conceptual framework for the evaluation of cost-effectiveness of projects to reduce GHG emissions and sequester carbon
[DE93-040448] p 2867 N94-26419
The reactivity of lithium toward non-aqueous solvents of relevance to energy storage applications as studied by surface analytical techniques
[DE94-003483] p 2856 N94-26464
Submillimeter residual losses in high-(Tc) superconductors
[DE94-003241] p 3058 N94-26516
Evaluation of APC NbTi superconductor in a model dipole magnet
[DE94-003258] p 3060 N94-26795
An optimal constrained linear inverse method for magnetic source imaging
[DE94-002264] p 2996 N94-26936
Highlights 1993
[DE94-002270] p 3118 N94-26937
Cratering rates from lunar xenospherules
[DE94-003481] p 3106 N94-27007
Object-oriented software construction at ALS
[DE94-003418] p 2967 N94-27049
A fully integrated 16 channel digitally trimmed pulse shaping amplifier
[DE94-004555] p 2787 N94-27618
Research into the microstructure and mechanical behavior of eutectic Bi-Sn and In-Sn
[DE94-004558] p 2741 N94-27619
Cryogenic fracture behavior of 316LN in magnetic fields up to 14.6 T
[DE94-005215] p 2742 N94-27694
Opportunities for High Aspect Ratio Micro-Electro-Magnetic-Mechanical Systems (HAR-MEMMS) at Lawrence Berkeley Laboratory
[DE94-003499] p 2827 N94-27722
The x ray holographic microscopy using the atomic-force microscope
[DE94-004003] p 2814 N94-27779
In search of Nemesis p 2888 N94-28297
Extraterrestrial accretion and glacial cycles
p 2890 N94-28308

CALIFORNIA UNIV., DAVIS.
Combustion synthesis method p 2721 N94-25561
Methane emissions from natural wetlands
[DE93-040796] p 2865 N94-25790
A preliminary analysis of the US west climatology
[DE94-003028] p 2894 N94-26313
Prediction of leading-edge transition and relaminarization phenomena on a subsonic multi-element high-lift system p 2659 N94-27929

CALIFORNIA UNIV., LIVERMORE. LAWRENCE LIVERMORE LAB.
Propellants and explosives in ballistic missiles
[UCRL-LR-113578] p 2760 N94-28222

CALIFORNIA UNIV., LOS ANGELES.
Hardware design of a grappling/docking device accommodating large lateral and angular misalignments
p 2833 N94-25668
Hardware design of a spherical mini-rover
p 2833 N94-25669
Manned mission to Mars with periodic refueling from electrically propelled tankers p 2689 N94-25670
Computer simulations of radiation generation from relativistic electron beams
[AD-A274139] p 3024 N94-27133
The use of biomechanics in the study of movement in microgravity p 2936 N94-28373

CALIFORNIA UNIV., SAN DIEGO.
Isotopically labeled CO2 from stratosphere: A tracer of carbon biogeochemistry
[DE94-002777] p 2877 N94-26015

CALIFORNIA UNIV., SAN DIEGO, LA JOLLA.
Design and evaluation of fault tolerance in opto-electronic computing
[AD-A274281] p 2954 N94-27016
Computer simulation and experiments on the quasi-static mechanics and transport properties of granular materials
[AD-A274192] p 2823 N94-27104
The experimental behavior of spinning pretwisted laminated composite plates
[NASA-CR-195220] p 2711 N94-27352

CALIFORNIA UNIV., SAN FRANCISCO.
Exercise and osteoporosis: Methodological and practical considerations p 2935 N94-28370

CALIFORNIA UNIV., SANTA BARBARA.
Bimaterial interfaces and their role in the mechanical performance of the in-situ composites
[AD-A274688] p 2707 N94-26447
An investigation of the effect of surface impurities on the adsorption kinetics of hydrogen chemisorbed onto iron
[NASA-CR-195213] p 2716 N94-26643
Limit theorems for functionals of Markov processes and renormalizable stable fields
[AD-A274645] p 3004 N94-27106

CALSPAN-BUFFALO UNIV. RESEARCH CENTER, NY.
Modeling electromagnetic effects in MMICs for T/R modules
[AD-A273808] p 2766 N94-25736

CANADAIR LTD., MONTREAL (QUEBEC).
Calculation of unsteady incompressible inviscid flow about wings and bodies using CANAERO-T panel model
p 2655 N94-28334
Multigrid solutions of the 2D Euler/Navier-Stokes equations on unstructured meshes
p 2658 N94-28349

CANADIAN AERONAUTICS AND SPACE INST., OTTAWA (ONTARIO).
Abstracts of papers presented at the 4th CASI Aerodynamics Symposium
[ISBN-0-920203-01-9] p 2651 N94-28315

CARBORUNDUM CO., NIAGARA FALLS, NY.
High performance fibers
[AD-A274693] p 2707 N94-26450

CARLETON UNIV., OTTAWA (ONTARIO).
Analysis of linear combining and its application to frequency-hopped signals
[ISBN-0-315-84007-2] p 2770 N94-26624
Kalman filtering of narrowband interference from direct sequence spread spectrum communications systems
[ISBN-0-315-84011-0] p 2784 N94-26627
Speech coding at low to medium bit rates
[ISBN-0-315-84012-9] p 2770 N94-26630
The processing of powder metallurgically produced near gamma-titanium aluminide
[ISBN-0-315-84018-8] p 2738 N94-26633
The proliferation of aerospace weapons technology: Ballistic missiles and the case of Brazil
[ISBN-0-315-84082-X] p 2763 N94-26634
Parallel computational geometry on analog Hopfield networks
[ISBN-0-315-84093-5] p 2980 N94-26635
An adaptive Kalman filter for tactical missiles guidance systems
[ISBN-0-315-84115-X] p 2677 N94-26636
Behaviour of separation bubbles in sharp-edged gaps of finite dimensions
[ISBN-0-315-84113-3] p 2793 N94-26637
Integrating automata with genetic algorithms in order to provide adaptive operators
[ISBN-0-315-84094-3] p 2964 N94-26663
An investigation of the effects of the high maximum-thickness-to-chord ratio on the performance of nozzle guide vanes in a transonic planar cascade
[ISBN-0-315-84107-9] p 2793 N94-26671
An investigation into the aerodynamic effects of wing patches
[ISBN-0-315-84121-4] p 2646 N94-26672
Simulating indirect thrust measurement methods as used on modern high-bypass turbofans
[ISBN-0-315-84123-0] p 2674 N94-26673
Design and implementation of a multiprocessor for DSP and communications systems algorithm evaluation
[ISBN-0-315-84128-1] p 2980 N94-26674
Ultralinear wideband integrated circuit design
[ISBN-0-315-84130-3] p 2784 N94-26675
Development of GaAs charge-coupled devices
[ISBN-0-315-84116-8] p 3059 N94-26703

All-optical gain switching of erbium-doped fibre amplifiers
[ISBN-0-315-84120-6] p 2784 N94-26704
The OPAL vertex detector
[ISBN-0-315-51152-4] p 2812 N94-27257
Garbage collection in a multiprocessor Smalltalk system
[ISBN-0-315-51159-1] p 2982 N94-27332
Controlled oscillation of forebody vortices by nozzle jet blowing
[ISBN-0-315-84134-6] p 2678 N94-27648
A fast Fourier transform radix-2 complex butterfly with built-in self-test
[ISBN-0-315-84139-7] p 2982 N94-27649
Unified distributed simulation
[ISBN-0-315-59019-X] p 2983 N94-27685
Short-block data detection techniques employing channel estimation for fading time-dispersive channels
[ISBN-0-315-58970-1] p 2777 N94-27806
Effect of surface finish on turbine airfoil cascade losses p 2652 N94-28320
Preliminary assessment of aerodynamic effects of wing repair patches p 2657 N94-28346

CARNEGIE-MELLON UNIV., PITTSBURGH, PA.
Detecting actin fibers in cell images using minimal spanning trees
[AD-A273914] p 2984 N94-25591
The question of standards for digital interactive television
[AD-A273872] p 2765 N94-25725
Design of dynamically reconfigurable real-time software using port-based objects
[NASA-CR-195178] p 2958 N94-25777
The use of ASN.1 and XDR for data representation in real-time distributed systems
[AD-A273769] p 2959 N94-25855
Balancing of a planar bouncing object
[AD-A273805] p 2821 N94-25878
The television as robot servant
[AD-A273965] p 2984 N94-25898
The determination of surface roughness from reflected step edges
[AD-A273987] p 2984 N94-25900
Set based analysis of arithmetic
[AD-A274112] p 3002 N94-25903
Real-time 3-D pose estimation using a high-speed range sensor
[AD-A273873] p 2809 N94-25967
Rational handling of multiple goals for mobile robots
[NASA-CR-195177] p 2985 N94-26006
Predictive modeling of particle-laden, turbulent flows
[DE94-003298] p 2792 N94-26319
Memory subsystem performance of programs using copying garbage collection
[AD-A274258] p 3099 N94-27014
Building 3-D models from unregistered range images
[AD-A274126] p 2986 N94-27032
Symbolic model checking for sequential circuit verification
[AD-A274375] p 2786 N94-27061
Memory subsystem performance of programs with intensive heap allocation
[AD-A274122] p 2967 N94-27063
Combining shape and color information for 3D object recognition
[AD-A274123] p 2967 N94-27064
Deferred compilation: The automation of run-time code generation
[AD-A274124] p 2967 N94-27065
Automatic mapping of task and data parallel programs for efficient execution on multicomputers
[AD-A274125] p 2982 N94-27117
The universal robot p 2686 N94-27361
Sculpting in cyberspace: Parallel processing the development of new software p 2686 N94-27365
Pigs in cyberspace p 2689 N94-27376

CASE WESTERN RESERVE UNIV., CLEVELAND, OH.
Tesseract supersonic business transport
p 2671 N94-25713
A biologically-inspired autonomous robot
[AD-A273909] p 2821 N94-25782
In situ spectroscopic applications to the study of rechargeable lithium batteries
[DE94-003478] p 2782 N94-26328
The reactivity of lithium toward non-aqueous solvents of relevance to energy storage applications as studied by surface analytical techniques
[DE94-003483] p 2856 N94-26464

CATERPILLAR TRACTOR CO., PEORIA, IL.
Development of advanced high temperature in-cylinder components and tribological systems for low heat rejection diesel engines, phase 1
[NASA-CR-187158] p 2827 N94-27984

CENTER FOR MATHEMATICS AND COMPUTER SCIENCE, AMSTERDAM (NETHERLANDS).
A positive finite-difference advection scheme applied on locally refined grids
[CWI-NM-R9309] p 2867 N94-26216
Preconditioning in parallel Runge-Kutta methods for stiff initial value problems
[CWI-NM-R9310] p 2991 N94-26217
Multimedia in Views
[CWI-CS-R9263] p 2961 N94-26218
Editing tree structures
[CWI-CS-R9264] p 2961 N94-26219
The MUSA design methodology
[CWI-CS-R9265] p 3097 N94-26220
The ergonomics of software porting: Automatically configuring software to the runtime environment or everything you wanted to know about your C compiler but didn't know who to ask
[CWI-CS-R9266] p 2961 N94-26221
VLUGR2: A vectorized local uniform grid refinement code for PDE's in 2D
[CWI-NM-R9306] p 2965 N94-26772
Local uniform grid refinement and systems of coupled partial differential equations
[CWI-NM-R9307] p 2995 N94-26773
A robust upwind discretization method for advection, diffusion and source terms
[CWI-NM-R9308] p 2868 N94-26774
Semantics, orderings and recursion in the weakest precondition calculus
[CWI-CS-R9267] p 2995 N94-26776
Query optimization strategies for browsing sessions
[CWI-CS-R9268] p 3100 N94-27394
A characterization of stable models using a non-monotonic operator
[CWI-CS-R9315] p 2970 N94-27543
Modular termination proofs for logic and pure PROLOG programs
[CWI-CS-R9316] p 2970 N94-27544
A strategy for dynamic interpretation: A fragment and an implementation
[CWI-CS-R9317] p 2970 N94-27545
Single term off-line coins
[CWI-CS-R9318] p 2776 N94-27546
Binary snapshots
[CWI-CS-R9319] p 2955 N94-27547
Schema integration in object-oriented databases
[CWI-CS-R9320] p 2970 N94-27548
Modal logic, transition systems and processes
[CWI-CS-R9321] p 2970 N94-27549
Saving comparisons in the Crochemore-Perrin string matching algorithm
[CWI-CS-R9322] p 2971 N94-27550
An efficient off-line electronic cash system based on the representation problem
[CWI-CS-R9323] p 2776 N94-27551
An object model for multimedia programming
[CWI-CS-R9327] p 2971 N94-27552
Semantics of MANIFOLD: Specification in ASF+SDF and extension
[CWI-CS-R9269] p 2971 N94-27575
Design and implementation of a DBMS performance assessment tool
[CWI-CS-R9270] p 2972 N94-27576
Expressiveness results for process algebras
[CWI-CS-R9301] p 3000 N94-27577
A theory for simulator tools
[CWI-CS-R9302] p 2972 N94-27578
Fast parallel permutation algorithms
[CWI-CS-R9303] p 2982 N94-27579
Forward and backward simulations. Part 1: Untimed systems
[CWI-CS-R9313-PT-1] p 2972 N94-27580
Forward and backward simulations. Part 2: Timing-based systems
[CWI-CS-R9314-PT-2] p 2972 N94-27581
A strange application of Kolmogorov complexity
[CWI-CS-R9328] p 2973 N94-27737
ARM: Abstract Rewriting Machine
[CWI-CS-R9330] p 2974 N94-27794

CENTRE NATIONAL D'ETUDES SPATIALES, TOULOUSE (FRANCE).
Real-Time Embedded Processing for Space Applications
[ISBN-2-85428-335-X] p 2948 N94-26713
Design principles of onboard management of a Sun synchronous satellite p 2950 N94-26722
PRONAOS flight software: A real-time application for a balloonborne scientific gondola p 2950 N94-26725
Test of onboard real time applications (LICE (tm))
p 2952 N94-26737
Arithmetic performances of onboard computers
p 2952 N94-26738
The CODE-TOP (COncurrent system DEvelopment using Transformations Of Predicate-transition nets) method: Examples of using it for system architecture specification, software specification, and code generation p 2953 N94-26744
A comparative study of SAR data compression schemes p 2946 N94-28259

CESKOSLOVENSKA AKADEMIE VED, PRAGUE.
Proceedings of the 16th Symposium on Plasma Physics and Technology
[DE94-604181] p 3047 N94-27698

CHIANG MAI UNIV. (THAILAND).
Land use change in Thailand and its impact on environmental change: Joint Thai-Japanese research project (1993-1995) p 2875 N94-28288

CHICAGO UNIV., IL.
Spectroscopy and dynamics of molecular and ionic impurities embedded in solid hydrogen
[AD-A274149] p 3064 N94-27095
Mass extinctions: Persistent problems and new directions p 2889 N94-28302

CHINA NUCLEAR INFORMATION CENTRE, BEIJING.
Experiment of neutron multiplication in beryllium
[DE94-604605] p 2742 N94-27730
Hypersensitive transition spectrum of f-element and coordination structure
[DE94-604133] p 3070 N94-27843
Experiment and research on materials irradiated by plasma radiation
[DE94-605011] p 2758 N94-27845
The calculation for energy balance of heating plasmas by Alfven waves
[DE94-604994] p 3049 N94-27855
Analysis of density limit and efficiency in lower hybrid current drive
[DE94-604995] p 3049 N94-27856
The ZnO thin films with C-axis orientation prepared on the room temperature substrate by the ECR multipolar plasma sputtering method
[DE94-605039] p 2758 N94-27857

CHRISTIAN BROTHERS COLL., MEMPHIS, TN.
Integrated model development for liquid fueled rocket propulsion systems
[NASA-CR-195253] p 2702 N94-27166

CHRISTOPHER NEWPORT COLL., NEWPORT NEWS, VA.
Proton irradiation on materials p 3030 N94-27898
Spacecraft optical disk recorder memory buffer control
p 2815 N94-27907

CHULALONGKORN UNIV., BANGKOK (THAILAND).
Changes in phytoplankton population in the Chao Phraya estuary, Thailand, during the eutrophication mechanisms studies p 2875 N94-28287

CITY COLL. OF THE CITY UNIV. OF NEW YORK, NY.
Nonlinear dynamics and pattern selection at the crystal-melt interface
[DE94-003112] p 3060 N94-26780
Experimental investigations of strong interaction in the non-perturbative QCD region
[DE94-001178] p 3024 N94-26949

CITY UNIV., LONDON (ENGLAND).
Inclined air-jets used as vortex generators to suppress shock-induced separation p 2659 N94-28040

CLARKSON UNIV., POTSDAM, NY.
Analysis and computer tools for separation processes involving nonideal mixtures
[DE94-004162] p 2960 N94-25986

CLEMSON APPAREL RESEARCH, PENGLETON, SC.
Automated fabric inspection system
[AD-A274522] p 2835 N94-26833

COLLEGE OF WILLIAM AND MARY, WILLIAMSBURG, VA.
Kinetic parameters from thermogravimetric analysis
p 2721 N94-27909
The molecular matching problem
p 3030 N94-27910
Property enchancement of polyimide films by way of the incorporation of lanthanide metal ions
p 2758 N94-27926

COLORADO SCHOOL OF MINES, GOLDEN.
Efficient modeling in transversely isotropic inhomogeneous media
[DE94-003394] p 2877 N94-25847
Crystallization and microstructural control of ferroelectric thin-films and glass-ceramics
[AD-A273767] p 2748 N94-25854
The influence of weld metal alloying additions to extend the heat input range for the submerged arc welding of high strength steels
[AD-A274284] p 2738 N94-26679

COLORADO STATE UNIV., FORT COLLINS.
Grassland/atmosphere response to changing climate: Coupling regional and local scales
[DE94-003111] p 2866 N94-26026

Template synthesis of metal microtubule ensembles utilizing chemical, electrochemical, and vacuum deposition techniques
[AD-A274676] p 2715 N94-26444

COLORADO UNIV., BOULDER.
Autonomous support for microorganism research in space p 2903 N94-25672
Sulfur dioxide in the atmosphere of Venus 1 sounding rocket observations
[NASA-CR-195224] p 3106 N94-26237
Nonlinear ocean waves
[AD-A274651] p 2899 N94-26354
An optoelectronic graphics display processor
[AD-A274401] p 3037 N94-26990
Ice surface temperature retrieval from AVHRR, ATSR, and passive microwave satellite data: Algorithm development and application
[NASA-CR-195276] p 2851 N94-27849
Ionospheric calibration for single frequency altimeter measurements
[NASA-CR-195709] p 2883 N94-27883
Visualization techniques to aid in the analysis of multispectral astrophysical data sets
[NASA-CR-195268] p 3105 N94-27932
High-performance parallel analysis of coupled problems for aircraft propulsion
[NASA-CR-195292] p 2845 N94-28181

COLORADO UNIV., DENVER.
On identified predictive control p 2990 N94-27896

COLUMBIA UNIV., NEW YORK, NY.
The impact of recent model improvements on GISS GCM predictions of climate change
[DE93-019458] p 2866 N94-26077
Multichip module high speed testing
[AD-A274873] p 2782 N94-26343
Translational-energy-resolved studies of photogenerated carrier-induced reactions on UHV semiconductor surfaces
[DE94-004169] p 3058 N94-26526
Chaotic dynamics of the solar cycle
[AD-A274315] p 3110 N94-26883
Parallel string matching algorithms
[AD-A274502] p 3100 N94-27164
Passive stabilization of MHD instabilities at high (beta)n in the HBT-EP tokamak
[DE94-003317] p 3047 N94-27735

COMISION NACIONAL DE ENERGIA ATOMICA, BUENOS AIRES (ARGENTINA).
The Latin American conference on the applications of the Moessbaer effect
[DE93-615942] p 3051 N94-25912
Diffusion of substitutional elements in Ti in its hcp phase
[DE93-633762] p 2733 N94-26160
Zr-rich corner of the Zr-Sn-O diagram
[DE93-633764] p 2734 N94-26161
Grain by grain study of the mechanisms of crack propagation during iodine SCC of Zry-4
[DE93-633765] p 2734 N94-26162
Zr-Sn-Nb alloys: Preliminary studies
[DE93-633767] p 2734 N94-26263
Stress corrosion cracking and dealloying of copper-gold alloy in iodine vapor
[DE93-633790] p 2734 N94-26264
Fracture Toughness Round Robin Test International in pressure tube materials
[DE93-634140] p 2837 N94-26265
Analysis of the effect on growth kinetics of gamma prima phase in Inconel 713C alloys
[DE93-633763] p 2735 N94-26294
Eutectic transformation L in equilibrium to Zr6Fe23 + Fe(tau) in the Fe-Zr system
[DE93-633766] p 2735 N94-26295
Hydrothermal growth and characterization of oxides in zirconium alloys
[DE94-602981] p 2743 N94-27829
Effect of different ions on the anodic behaviour of alloy 800 in chloride solutions at high temperature
[DE94-602982] p 2743 N94-27832
Fullerene fabrication using an arc furnace. Characterization of the product
[DE94-603006] p 3029 N94-27834

COMMONWEALTH SCIENTIFIC AND INDUSTRIAL RESEARCH ORGANIZATION, HIGHETT (AUSTRALIA).
Unsteady wake structures in transverse jets
p 2800 N94-28006

COMMONWEALTH SCIENTIFIC AND INDUSTRIAL RESEARCH ORGANIZATION, LYNEHAM (AUSTRALIA).
Global Change and Terrestrial Ecosystems (GCTE): Progress report and prospects for Asian contributions
p 2874 N94-28281
Global change: A research strategy for Australia 1992-1996 p 2874 N94-28282

COMPUTATIONAL PHYSICS, INC., FAIRFAX, VA.
Analysis of EUV/FUV dayglow and auroral measurements
[NASA-CR-195237] p 2883 N94-27393

CONCORDIA UNIV., MONTREAL (QUEBEC).
Spectroscopy and strong decays of baryons
[ISBN-0-315-49073-X] p 3024 N94-27258
Developments in the application of the geometrical theory of diffraction and computer graphics to aircraft inter-antenna coupling analysis
[ISBN-0-315-84643-7] p 2776 N94-27308
Response of structures to impact loads using elastic and plastic analysis
[ISBN-0-315-84647-X] p 2842 N94-27309
Molecular dynamics simulation and crystal-field theory: Predicting the optical spectra and structure of rare-earth doped inorganic glasses
[ISBN-0-315-84679-8] p 3025 N94-27310
Motion analysis from a sequence of range images
[ISBN-0-315-84684-4] p 2969 N94-27311
Robust estimation for range image segmentation and fitting
[ISBN-0-315-84686-0] p 2998 N94-27312
Theoretical and experimental investigation of converging cylindrical shock waves propagating in narrow cylindrical chambers
[ISBN-0-315-84694-1] p 2795 N94-27313
Hot deformation behaviour of Si(p)/Al composites and their matrices and an Al-Mg-Si alloy
[ISBN-0-315-84699-2] p 2711 N94-27314
Behaviour modification of space trusses
[ISBN-0-315-84701-8] p 2842 N94-27315
Production of a computer based lesson teaching employees how to use an air data tester
[ISBN-0-315-84708-5] p 2969 N94-27316
Generalized finite element dynamic modelling and simulation for flexible robot manipulators
[ISBN-0-315-84623-2] p 2825 N94-27343
Dynamic control of kinematically redundant manipulators
[ISBN-0-315-84627-5] p 2825 N94-27344
Analysis of a multiaccess/switching technique for multibeam satellites in a prioritized ISDN environment
[ISBN-0-315-84632-1] p 2776 N94-27345
A study of multiple guide optical couplers
[ISBN-0-315-84633-X] p 3038 N94-27441

CONNECTICUT UNIV., FARMINGTON.
Monaural and binaural processing of complex waveforms
[AD-A274209] p 3010 N94-27067

CONSIGLIO NAZIONALE DELLE RICERCHE, MILAN (ITALY).
Introduction to bayesian nonparametric theory
[PB94-125002] p 3004 N94-26939
Some contributions to the theory of monotone dependence
[PB94-124922] p 3004 N94-27051

COORDINATING RESEARCH COUNCIL, INC., ATLANTA, GA.
CRC customer versus rater octane number requirement program (1990)
[AD-A273997] p 2758 N94-25901

COORS PORCELAIN CO., GOLDEN, CO.
Transparent polycrystalline body with high ultraviolet transmittance, process for making and applications thereof
[CA-PATENT-1325511] p 3066 N94-27276

CORNELL UNIV., ITHACA, NY.
A geological and geophysical information system for Eurasia
[AD-A274818] p 3098 N94-26490
The growth and characterization of GaN as a photodetector
[AD-A274570] p 3063 N94-26965
Interface phenomena in metal-ceramic composites
[AD-A274167] p 2709 N94-27125
Simulating fail-stop in asynchronous distributed systems
[NASA-CR-195698] p 2974 N94-27767
Refinement for fault-tolerance: An aircraft hand-off protocol
[NASA-CR-195697] p 2666 N94-27768

CRANFIELD INST. OF TECH., BEDFORD (ENGLAND).
Development of satellite telecommunications during the period 1990 - 2005
[CRANFIELD-AERO-9301] p 2765 N94-25639
The application of a C(star) flight control law to large civil transport aircraft
[CRANFIELD-AERO-9303] p 2676 N94-25640
Report on a visit to the Arvin/Calspan Corporation, Buffalo, New York, USA, September 1992
[CRANFIELD-AERO-9305] p 2676 N94-25653
The effectiveness of AMT investment in UK metal component manufacture
[IND-MANU-SCI-TECH-REPT-3] p 2762 N94-25775
Riemann solvers for solving the incompressible Navier-Stokes equations using the artificial compressibility method
[CRANFIELD-AERO-9208] p 2790 N94-25778
Arbitrary-order numerical schemes for model parabolic equations
[CRANFIELD-AERO-9210] p 3005 N94-25781
Arbitrary-order high resolution schemes for model hyperbolic conservation laws
[CRANFIELD-AERO-9209] p 3005 N94-25823

CRYSTAL ASSOCIATES, INC., WALDWICK, NJ.
Development of K(1-x)Na(x)TiOPO4 crystals for nonlinear applications
[AD-A274336] p 3063 N94-27055

CR2A, NANTERRE (FRANCE).
Standardize Ada hard real-time services?
p 2951 N94-26729

CSA ENGINEERING, INC., PALO ALTO, CA.
Proceedings of Damping 1993, volume 1
[AD-A274226] p 2840 N94-26922
Proceedings of Damping 1993, volume 2
[AD-A274227] p 2840 N94-26953
Proceedings of Damping 1993, volume 3
[AD-A274228] p 2840 N94-27008
Smart structures, an overview
[AD-A274147] p 2987 N94-27093

D

DAVID SARNOFF RESEARCH CENTER, PRINCETON, NJ.
Color head down display program
[AD-A274807] p 2672 N94-26340
Compression of multispectral Landsat imagery using the Embedded Zerotree Wavelet (EZW) algorithm
p 2947 N94-28261

DAYTON UNIV., OH.
Accelerated screening methods for determining chemical and thermal stability of refrigerant-lubricant mixtures. Part 2: Experimental comparison and verification of methods
[DE94-003664] p 2749 N94-26007

DAYTON UNIV. RESEARCH INST., OH.
Image quality and the display modulation transfer function: Experimental findings
[AD-A274061] p 2679 N94-25773
Aluminum alloy 8090-T8771 thick plate material characterization
[AD-A274146] p 2987 N94-27077

DE HAVILLAND AIRCRAFT CO. OF CANADA LTD., DOWNSVIEW (ONTARIO).
Flow field investigation in the near slipstream of an 8-bladed propfan on the De Havilland WTEJ half-model at Mach numbers 0.6 and 0.7 p 2651 N94-28317
Assessing the effects of Tuned Vibration Absorbers (TVAs) on interior cabin noise levels: A correlation between analytical acoustic predictions and flight test measurements p 2652 N94-28318
Propeller off-axis loads due to thrust axis incidence and nacelle magnus force p 2652 N94-28319
Experimental and theoretical studies of T-tail configurations for commuter aircraft applications
p 2653 N94-28322
Infrared imaging for transition detection in a transonic blowdown wind tunnel p 2653 N94-28325
Euler and Navier-Stokes wing/fuselage computations of the De Havilland Dash 8 aircraft p 2654 N94-28329
Drag prediction by wake integrals using 3-D multi-grid Euler method (MGAERO) p 2655 N94-28335

DEFENCE AND CIVIL INST. OF ENVIRONMENTAL MEDICINE, DOWNSVIEW (ONTARIO).
One from many: Selecting an appropriate human performance model
[DCIEM-93-25] p 2942 N94-27683

DEFENCE RESEARCH AGENCY, FARNBOROUGH (ENGLAND).
The development of stress intensity factors
[DRA-TR-93057] p 2845 N94-27954

DEFENCE RESEARCH ESTABLISHMENT ATLANTIC, DARTMOUTH (NOVA SCOTIA).
Laser surface modification of intermetallic compounds
[DREA-CR-92-416] p 2820 N94-27668

DEFENCE RESEARCH ESTABLISHMENT, OTTAWA (ONTARIO).
Test and evaluation of the Litton (Canada) Canadian strapdown gyroscope (CSG-2) Performance Evaluation Unit (PEU)
[DREO-1010] p 2813 N94-27597
Experimental evaluation of battery cells for space-based radar application p 2860 N94-28104

DEFENCE RESEARCH ESTABLISHMENT PACIFIC, VICTORIA (BRITISH COLUMBIA).
The development of an in-motion radiography system for large area aircraft scanning
[DREP-TM-93-53] p 2670 N94-27666

Differential GPS methods and performance for marine applications
[DREP-93-09] p 2665 N94-27667

DEFENCE RESEARCH ESTABLISHMENT VALCARTIER (QUEBEC).
Analytic approximation to randomly oriented spheroid extinction
[DREV-4712-93] p 3038 N94-27598

DEFENSE INFORMATION SYSTEMS AGENCY, ARLINGTON, VA.
Information systems criteria for applying software reengineering: Guidelines for identifying information systems for software reengineering
[AD-A274699] p 3097 N94-26375

DEFENSE SCIENCE BOARD, WASHINGTON, DC.
Report of the defense science board task force on aircraft assessment
[AD-A274531] p 2669 N94-26835

DELAVAL-STORK V.O.F., HENGELO (NETHERLANDS).
Steam plant: Steam turbines for combined cycles
p 2831 N94-28085

DENVER CENTER FOR THE PERFORMING ARTS, CO.
NCVS, volume 5
[AD-A274975] p 2902 N94-27165

DEPARTMENT OF ENERGY, MORGANTOWN, WV.
Pressure-gain combustion
[DE94-002975] p 2719 N94-27712

DEPARTMENT OF ENERGY, WASHINGTON, DC.
Federal Information Exchange (FEDIX) user's guide: Fall 1993, Version 5.0/Release 1.0
[DE94-003826] p 3097 N94-26350
Fusion Energy Advisory Committee: Advice and recommendations to the US Department of Energy in response to the charge letter of September 1, 1992
[DE93-019842] p 3043 N94-26428
Charmonium physics at a tau-charm factory
[PB94-124344] p 3024 N94-27199

DEPARTMENT OF ENVIRONMENT AND NATURAL RESOURCES, QUEZON CITY (PHILIPPINES).
Philippine thrust on environmental research relating to global change p 2873 N94-28279

DEPARTMENT OF THE NAVY, WASHINGTON, DC.
Method of optimizing the charging of a battery of storage cells, and apparatus for performing the method
[AD-D016066] p 2781 N94-26102
Method for improving electromagnetic shielding performance of composite materials by electropulsing
[AD-D016050] p 2709 N94-27076
Method for improving electromagnetic shielding performance of composite materials by electroplating
[AD-D016038] p 2709 N94-27091
Enhanced adaptive statistical filter providing improved performance for target motion analysis noise discrimination statement of government interest
[AD-D016039] p 2786 N94-27109
SAG compensated vibration isolation mount
[AD-D016040] p 2841 N94-27110
Polyurethane self-priming topcoats
[AD-D016041] p 2755 N94-27111
Fluid dynamic linear accelerometer
[AD-D016042] p 2678 N94-27112
Reconfigurable aircraft stick control
[AD-D016043] p 2681 N94-27113
Helmet head tracking mounting device
[AD-D016048] p 2942 N94-27114
AC to DC power converter with regulated bi-polar outputs
[AD-D016032] p 2786 N94-27145
Method of correcting rotational motion error in SAR and ISAR imagery
[AD-D016033] p 2773 N94-27146
Phosphazene-containing amine as curing agent for phthalonitrile-base polymer
[AD-D016029] p 2755 N94-27147
Accordion-like polymers for nonlinear applications
[AD-D016031] p 2755 N94-27148
Method of measuring liquid level
[AD-D016049] p 3038 N94-27153
Focal plane antenna array for millimeter waves
[AD-D016034] p 2774 N94-27202
Thermoplastic elastomers having alternate crystalline structure for us as high energy binders
[AD-D016035] p 2755 N94-27203
High repetition rate, mode locked, figure eight laser with extracavity feedback
[AD-D016053] p 2820 N94-27670
System for conditioning an electron beam for improved free-electron laser operation
[AD-D016054] p 2820 N94-27671
Micro-electron deflector
[AD-D016055] p 2787 N94-27672
Control system for tracking nonlinear systems
[AD-D016057] p 2787 N94-27673
Fiber optic Faraday flux transformer specification
[AD-D016056] p 3039 N94-27674
Discrete vacuum ultra violet reflective interference filter
[AD-D016059] p 2756 N94-27675
Reflectometer employing an integrating sphere and lens-mirror concentrator
[AD-D016061] p 3039 N94-27676
Fiber optic true time-delay array antenna feed system
[AD-D016063] p 2777 N94-27734
Microprocessor chip incorporating optical signal coupling transceiver
[AD-D016077] p 2788 N94-28186
Method of bonding molybdenum to steel
[AD-D016079] p 2747 N94-28187
Optical pattern recognition system utilizing resonator array
[AD-D016071] p 3040 N94-28224
Superconducting fibers made with yttrium and yttrium oxide interlayers and barium cuprate cover layers
[AD-D016073] p 3070 N94-28225
Liquid monopropellants
[AD-D016074] p 2760 N94-28226

DEUTSCHE AEROSPACE A.G., MUNICH (GERMANY).
Numerical investigation of thrust vectoring by injection of secondary air into nozzle flows p 2801 N94-28013
Effects, limits, and limitations of spanwise blowing
p 2659 N94-28027

DEUTSCHE FORSCHUNGS- UND VERSUCHSANSTALT FUER LUFT- UND RAUMFAHRT, GOETTINGEN (GERMANY).
First experimental assessment of RCS plume-flow field interaction on Hermes leading edge thruster configuration p 2703 N94-28032

DEUTSCHE FORSCHUNGSANSTALT FUER LUFT- UND RAUMFAHRT, BRUNSWICK (GERMANY).
Experimental and theoretical investigations of the influence of the jet on the flow around a bypass-engine
[DLR-FB-93-17] p 2675 N94-27593
The design of a counter rotating ultra-high-bypass fan simulator for windtunnel investigation
[DLR-FB-93-20] p 2675 N94-27739

DEUTSCHE FORSCHUNGSANSTALT FUER LUFT- UND RAUMFAHRT, COLOGNE (GERMANY).
The cryogenic tunnel Cologne at DLR
[DLR-MITT-93-10] p 2681 N94-27587
Construction and test of experiment hardware for a space experiment on Spacelab mission IML-2
[DLR-FB-93-23] p 2903 N94-27743
Methodology development of forecasting inter-regional air transport demand in China
[DLR-FB-93-24] p 2660 N94-27746
Vacuum-UV-effects on E. coli plasmid pUC19: Inactivation, strand break induction and mutation induction
[DLR-FB-93-26] p 2903 N94-27754

DEUTSCHE FORSCHUNGSANSTALT FUER LUFT- UND RAUMFAHRT, GOETTINGEN (GERMANY).
Direct simulation Monte-Carlo of near continuum hypersonic flow with chemical reactions
[DLR-FB-93-01] p 2797 N94-27588
Streamwise vorticity in a turbine rotor with conical endwalls
[DLR-FB-93-13] p 2826 N94-27591
Control of leading-edge separation on an airfoil by localized excitation
[DLR-FB-93-16] p 2647 N94-27592
Methods in unsteady aerodynamics
[DLR-FB-93-21] p 2648 N94-27741

DEUTSCHE FORSCHUNGSANSTALT FUER LUFT- UND RAUMFAHRT, LAMPOLDSHAUSEN (GERMANY).
Control of a hydrogen/oxygen steam generator
[DLR-FB-93-02] p 2826 N94-27589

DEUTSCHE FORSCHUNGSANSTALT FUER LUFT- UND RAUMFAHRT, OBERPFAFFENHOFEN (GERMANY).
Calibration of SAR systems
[DLR-FB-93-18] p 2777 N94-27738
Examination of micro- and macro-physical structures and processes in hailstorms with respect to their modification
[DLR-FB-93-25] p 2897 N94-27751

DEUTSCHE FORSCHUNGSANSTALT FUER LUFT- UND RAUMFAHRT, STUTTGART (GERMANY).
The PLVCR 500 and HCPC, tests and results
[DLR-MITT-93-04] p 2858 N94-26813
Float zone crystal growth using laser radiation
[DLR-FB-93-10] p 3066 N94-27590

DEUTSCHE LUFTHANSA A.G., FRANKFURT AM MAIN (GERMANY).
Lufthansa Yearbook 1992
[DSK-9734-H-92] p 2660 N94-28230
The single European market and air traffic chances and risks p 2660 N94-28231
Deregulation of air traffic in America: A model to be initiated? p 2661 N94-28232
Air traffic of the European Community with European neighbors p 2661 N94-28233
A sky above Europe p 2661 N94-28234
The single European market: Economical advance, ecological problem? p 2661 N94-28235
The advantages of the location Germany must not be jeopardized in air traffic p 2661 N94-28236
Lufthansa facing the single European market
p 2661 N94-28237
Air traffic administration enroute to Europe
p 2661 N94-28238
Munich Airport: The new Lufthansa hub
p 2662 N94-28239
Air traffic in recession p 2662 N94-28240
German-American relations in air traffic are to be criticized p 2662 N94-28241
A340 testing p 2662 N94-28242
First Canadair jet flies for Lufthansa city line
p 2662 N94-28243
Integrators: A challenge for air cargo
p 2662 N94-28244
Powerful selling and sales strategy
p 2662 N94-28245
Lufthansa long range services: More simplicity
p 2663 N94-28246
Lufthansa and Europe p 2663 N94-28247
Know-how export: Lufthansa technology at Shannon
p 2663 N94-28248
After thirty years: Farewell of Europa jet
p 2663 N94-28249
A symbol of reliability: Ju 52 p 2663 N94-28250

DOMINION ASTROPHYSICAL OBSERVATORY, VICTORIA (BRITISH COLUMBIA).
Supernovae and mass extinctions
p 2891 N94-28314

DORNIER SYSTEM G.M.B.H., FRIEDRICHSHAFEN (GERMANY).
Developing with Ada using HOOD design methodology
p 2953 N94-26741

DREXEL UNIV., PHILADELPHIA, PA.
Neural control of magnetic suspension systems
p 2682 N94-27905

DSM/NV NEDERLANDSE STAATSMIJNEN, GELEEN.
High impact strength poly(lactide) tough biodegradable materials
[ETN-94-95389] p 2747 N94-25748

DUKE UNIV., DURHAM, NC.
Studies in nonlinear numerical analysis
[AD-A273911] p 2959 N94-25968
Quantum chromodynamics and nuclear physics at extreme energy density
[DE94-004418] p 3026 N94-27604
Prediction of undsteady flows in turbomachinery using the linearized Euler equations on deforming grids
[NASA-CR-195285] p 2675 N94-27654

DYNAMET TECHNOLOGY, INC., BURLINGTON, MA.
Material optimization and manufacturing development of reduced cost powder metal titanium alloy components for gas turbine engine application, phase 2
[AD-A274410] p 2709 N94-26978

E

EAGLE-PICHER CO., JOPLIN, MO.
Bipolar Ag-Zn battery p 2864 N94-28135

EAGLE-PICHER INDUSTRIES, INC., JOPLIN, MO.
Effects of repeating resistance testing on firing ability of igniter EP360-3
[AD-A274814] p 2759 N94-26486
Advanced nickel-hydrogen spacecraft battery development p 2863 N94-28129

ECOLE CENTRALE DE LYON (FRANCE).
Experimental contribution to the study of secondary flows in centrifugal turbopump stator components
[ECL-92-35] p 2789 N94-25654
Micropyrolysis of polymer thin films for ceramics
[ECL-92-62] p 2750 N94-26088

ECOLE CENTRALE DE NANTES (FRANCE).
Scheduling tasks with unpredictable timing parameters in hard real-time systems p 2951 N94-26728
Tool for performance analysis and off-line prediction of timing behaviour p 2952 N94-26732

ECOLE POLYTECHNIQUE, MONTREAL (QUEBEC).
Unified approach for direct and inverse boundary layer prediction using cubic spline collocation
p 2653 N94-28326
Transition for three-dimensional, compressible boundary layers p 2653 N94-28327
Techniques for accurately solving unsteady shock waves and contact discontinuities p 2656 N94-28342
A new flux vector splitting scheme
p 2657 N94-28343
Ice accretion on aircraft wings p 2657 N94-28345
Unsteady three dimensional Euler solutions on moving grids p 2657 N94-28347

ECOLE POLYTECHNIQUE FEMININE, SCEAUX (FRANCE).
Manned mission to Mars with periodic refueling from electrically propelled tankers p 2689 N94-25670
Design of a refueling tanker delivering liquid hydrogen p 2671 N94-25717

EDGERTON, GERMESHAUSEN AND GRIER, INC., IDAHO FALLS, ID.
Calculation of the electromagnetic critical state response of high T(sub c) superconductor tape
[DE94-002894] p 3061 N94-26868

EDGEWOOD ARSENAL, ABERDEEN PROVING GROUND, MD.
Proceedings of the symposium on current concepts and approaches on animal test alternatives
[AD-A273926] p 2900 N94-25593
Response surface design comparisons
[AD-A274690] p 2838 N94-26448

EDUCATIONAL TESTING SERVICE, PRINCETON, NJ.
Extending the rule space model to a semantically-rich domain: Diagnostic assessment in architecture
[AD-A273789] p 2948 N94-25864
A diagnostic classification model for document processing skills
[AD-A273790] p 3096 N94-25925
Proficiency scaling based on conditional probability functions for attributes
[AD-A273816] p 3002 N94-25962

EISAI CO. LTD., HASHIMA (JAPAN).
Cross-sectional anatomy of day 30 suncus fetuses p 2905 N94-27490

ELECTROMAGNETIC SCIENCES, INC., NORCROSS, GA.
Ferrite phase shifters using stress insensitive materials
[AD-A274639] p 2708 N94-26895

ELECTROTECHNICAL LAB., TSUKUBA (JAPAN).
Researches of the Electrotechnical Laboratory. No. 53: Spectral emission from combustion gas containing scattering media
[JTN-94-80603] p 2717 N94-27246
Researches of the Electrotechnical Laboratory. No. 955: Speech recognition by description of acoustic characteristic variations
[JTN-94-80604] p 2775 N94-27249
Circulars of the Electrotechnical Laboratory. No. 223: An extended survey on provable information base systems
[JTN-94-80550] p 3100 N94-27336
Researches of the Electrotechnical Laboratory. No. 51: Study of formation and sustainment of reversed field pinch by slow control of magnetic field
[JTN-94-80548] p 3046 N94-27350
Researches of the Electrotechnical Laboratory. No. 52: Studies of externally pressurized porous gas bearings
[JTN-94-80549] p 2825 N94-27351

ELORET CORP., PALO ALTO, CA.
Theoretical determination of chemical rate constants using novel time-dependent methods
[NASA-CR-195221] p 2714 N94-26205

ELTRON RESEARCH, INC., BOULDER, CO.
Perovskite solid electrolytes for SOFC
[DE94-001923] p 2859 N94-27005

EMORY UNIV., ATLANTA, GA.
Mechanistic studies of opto-electronic materials and syntheses using multiple laser and surface diagnostics
[AD-A274528] p 3036 N94-26834

ENERGY CONVERSION DEVICES, INC., TROY, MI.
Continuous roll-to-roll a-Si photovoltaic manufacturing technology
[DE94-000260] p 2859 N94-27610

ENERGY INFORMATION ADMINISTRATION, WASHINGTON, DC.
Solar collector manufacturing activity, 1992
[DE94-003401] p 2859 N94-27048

ENERGY RESEARCH CORP., DANBURY, CT.
Design of gasifiers to optimize fuel cell systems
[DE94-000010] p 2856 N94-26581

ENERGY TECHNOLOGY DATA EXCHANGE, OAK RIDGE, TN.
International energy: Research organizations, 1988-1992
[DE93-017267] p 3098 N94-26398

ENVIRONMENTAL PROTECTION AGENCY, RESEARCH TRIANGLE PARK, NC.
Compilation of air pollutant emission factors. Volume 1: Stationary point and area sources. Supplement F
[PB94-121431] p 2867 N94-26757

ENVIRONMENTAL RESEARCH INST. OF MICHIGAN, ANN ARBOR.
Perceptual compression of magnitude-detected synthetic aperture radar imagery p 2946 N94-28260
Vector quantizer designs for joint compression and terrain categorization of multispectral imagery p 2947 N94-28262

ESDU INTERNATIONAL LTD., LONDON (ENGLAND).
Normal force of low aspect ratio cropped-delta wings at pre-stall angles of attack and subsonic speeds
[ESDU-93034] p 2648 N94-27955
Thermophysical properties of refrigerant R-134a (1,1,1,2-tetrafluoroethane)
[ESDU-93001] p 2720 N94-27959
Contact stress in disc cams with roller followers
[ESDU-93001] p 2829 N94-28055
Blending profiles of disc cams with radial translating roller followers. Part 2: To incorporate an intermediate precision point or a constant velocity component
[ESDU-93002-PT-2] p 2830 N94-28056
Contribution of body-mounted fins and tailplanes to lateral derivatives due to sideslip at subsonic speeds for general body width to height ratio
[ESDU-93007] p 2648 N94-28057
Thermal conductivity of liquid aliphatic alcohols
[ESDU-93008] p 2720 N94-28058
Vapour pressures and critical points of liquids: Aliphatic and cyclic ketones
[ESDU-93009] p 2720 N94-28059
Orthobaric densities and molar volumes of liquids: Aliphatic and cyclic ketones
[ESDU-93010] p 2720 N94-28060
Flat rectangular orthotropic plates under uniformly distributed normal pressure. Elastic stresses and deflections for various forms of edge restraint
[ESDU-93011] p 2845 N94-28061
Viscosity of liquids: Halogenated ethanes
[ESDU-93012] p 2720 N94-28062
Lift-curve slope for structural response calculations
[ESDU-93013] p 2648 N94-28063
Condensation inside tubes: Computer program for pressure drop in straight tubes (horizontal and vertical with downflow)
[ESDU-93014] p 2806 N94-28064
Calculation methods for steadily loaded central circumferential groove hydrodynamic journal bearings (guide to use of computer program A9304)
[ESDU-93004] p 2830 N94-28073
Calculation methods for steadily loaded axial groove hydrodynamic journal bearings (guide to use of computer program A9305)
[ESDU-93005] p 2830 N94-28074
Calculation methods for steadily loaded axial groove hydrodynamic journal bearings. Low viscosity process fluid lubrication (guide to use of computer program A9306)
[ESDU-93006] p 2830 N94-28075
Program for calculation of maximum lift coefficient of plain aerofoils and wings at subsonic speeds
[ESDU-93015] p 2649 N94-28076
Computation of static pressure downstream of a normal shock for hypersonic flight (ambient temperature known)
[ESDU-93020] p 2649 N94-28091
Examples of flight path optimisation using a multivariate gradient-search method
[ESDU-93021] p 2670 N94-28092
Ejectors and jet pumps: Computer program for design and performance for liquid flow
[ESDU-93022] p 2832 N94-28093
Example of statistical techniques applied to analysis of effects of small changes
[ESDU-93023] p 2670 N94-28094
Vortex generators for control of shock-induced separation. Part 1: Introduction and aerodynamics
[ESDU-93024-PT-1] p 2806 N94-28095
Vortex generators for control of shock-induced separation. Part 3: Examples of applications of vortex generators to aircraft
[ESDU-93026-PT-3] p 2807 N94-28096
Orthobaric densities and molar volumes of liquids: Fused ring compounds
[ESDU-93029] p 2721 N94-28097
Parameter estimation of linear systems from frequency response measurements (computer program)
[ESDU-93016] p 2976 N94-28137
Thermal conductivity of liquid carboxylic acids
[ESDU-93017] p 2721 N94-28138
Forced convection heat transfer in straight tubes. Part 2: Laminar and transitional flow
[ESDU-93018-PT-2] p 2807 N94-28139
Wing lift increment at zero angle of attack due to deployment of single-slotted flaps at low speeds
[ESDU-93019] p 2649 N94-28140
Methods of testing for endurance of structural elements using simulated acoustic loading
[ESDU-93027] p 3011 N94-28141
Vapour pressures and critical points of liquids: Fused ring compounds
[ESDU-93028] p 2721 N94-28142
Three-dimensional elastic stress concentration factors: Plain or countersunk hole in a wide plate subjected to tension, bending, or pin loading
[ESDU-93030] p 2845 N94-28143
Examples of excrescence drag prediction for typical wing components of a subsonic transport aircraft at the cruise condition
[ESDU-93032] p 2649 N94-28144
Fatigue propagation behaviour of short cracks (1-2 mm) in steels
[ESDU-93033] p 2845 N94-28145

ETABLISSEMENT TECHNIQUE CENTRAL DE L'ARMEMENT, ARCUEIL (FRANCE).
How to make good use of international research collaboration, with emphasis on the evolving situation in Europe
[PB94-119690] p 3101 N94-27323

EUROPEAN SPACE AGENCY, PARIS (FRANCE).
Ablation of solid-propellant rocket-motor nozzle materials
[ESA-TT-1289] p 2699 N94-25638
Numeric solution of the electric field integral equation using Galerkin's method for axially symmetric cases
[ESA-TT-1264] p 2768 N94-26315
Chemical and vibrational nonequilibrium viscous flows: Modelling, internal and external flow applications
[ESA-TT-1274] p 2791 N94-26316
Polarimetric investigation of edge scattering by mono- and bistatic microwave imaging
[ESA-TT-1284] p 2768 N94-26317

EUROPEAN SPACE AGENCY. EUROPEAN SPACE RESEARCH AND TECHNOLOGY CENTER, ESTEC, NOORDWIJK (NETHERLANDS).
Asynchronous and packetized systems engineering tools p 2954 N94-26746
The radiation design handbook
[ESA-PSS-01-609-ISSUE-1] p 2696 N94-27397
Validation tests of TOPSIM 4
[ESA-STM-249] p 2972 N94-27582
Telecommand decoder specification
[ESA-PSS-04-151-ISSUE-1] p 2693 N94-27583

EUROPEAN SPACE RESEARCH ORGANIZATION, NOORDWIKJ (NETHERLANDS).
Science beyond the atmosphere: The history of space research in Europe
[ESA-HSR-SPECIAL] p 2689 N94-28207

F

FAIRFAX MATERIALS RESEARCH, INC., ALEXANDRIA, VA.
Computer modelling of cyclic deformation of high-temperature materials
[AD-A273852] p 2704 N94-25608
Computer modelling of cyclic deformation of high-temperature materials
[AD-A274504] p 2840 N94-27034

FEDERAL AVIATION ADMINISTRATION, ATLANTIC CITY, NJ.
Airborne data link operational evaluation test plan
[AD-A274096] p 2664 N94-25788
Digital Altimeter Setting Indicator (DASI) Operational Test and Evaluation (OT/E) operational test procedures
[AD-A274100] p 2672 N94-26030
Human factors in airway facilities maintenance: Development of a prototype outage assessment inventory
[DOT/FAA/AM-94/5] p 2941 N94-26136
Air traffic controller working memory: Considerations in air traffic control tactical operations
[AD-A273722] p 2664 N94-26197
Soft ground arresting system for airports
[DOT/FAA/CT-93/80] p 2680 N94-26202
Impact of improved materials and cabin water spray on commuter aircraft postcrash fire survivability
[AD-A274421] p 2660 N94-27081

FEDERAL AVIATION ADMINISTRATION, CAMBRIDGE, MA.
INM, Integrated Noise Model. Version 4.11: User's guide, supplement
[AD-A273885] p 3009 N94-25731
Damage tolerance assessment handbook. Volume 1: Introduction fracture mechanics fatigue crack propagation
[AD-A274777] p 2836 N94-26186
Damage tolerance assessment handbook. Volume 2: Aircraft damage tolerance evaluation
[AD-A274778] p 2837 N94-26357

FEDERAL AVIATION ADMINISTRATION, OKLAHOMA CITY, OK.
Human factors in airway facilities maintenance: Development of a prototype outage assessment inventory
[DOT/FAA/AM-94/5] p 2941 N94-26136
Validation of the Federal Aviation Administration air traffic control specialist pre-training screen
[DOT/FAA/AM-94/4] p 2938 N94-26600

FEDERAL AVIATION ADMINISTRATION, WASHINGTON, DC.
The 1993 Federal Aviation Administration plan for research, engineering and development
p 2643 N94-27960

FERMI NATIONAL ACCELERATOR LAB., BATAVIA, IL.
Distributing functionality in the drift scan camera system
[DE94-003640] p 2809 N94-25599
Heavy quark production and spectroscopy
[DE94-003619] p 3015 N94-25935
A dependence of exclusive vector meson production in muon-nucleus scattering
[DE94-003363] p 3016 N94-25957
Photon and hadron production of heavy flavors
[DE94-004655] p 3018 N94-26245
The meaning of EROS/MACHO
[DE94-003003] p 3104 N94-26311
Cosmological phase transitions
[DE94-003001] p 3104 N94-26786
D0 results on searches for the top quark
[DE94-003361] p 3023 N94-26938
A measurement of the W mass using electrons at CDF
[DE94-004656] p 3028 N94-27748
Search for the top quark in the single lepton + jets channel at D0
[DE94-004660] p 3028 N94-27749
Sloan Digital Sky Survey
[DE94-004662] p 3103 N94-27750
Jet production in muon scattering at Fermilab E665
[DE94-004663] p 3028 N94-27752

FIRST INST. OF OCEANOGRAPHY, QINGDAO (CHINA).
An extraterrestrial event at the tertiary-quaternary boundary p 2890 N94-28309

FLINDERS UNIV., ADELAIDE (AUSTRALIA).
Convergent close-coupling calculation of electron-sodium scattering
[DE94-601815] p 3014 N94-25842
Calculation of electron-potassium scattering
[DE94-601812] p 3023 N94-26942
Spin asymmetry in resonant electron-hydrogen elastic scattering
[DE94-601813] p 3023 N94-26943
Calculation of total cross sections for electron and positron scattering on sodium and potassium
[DE94-601814] p 3023 N94-26944
Calculations of asymmetries in electron-alkali scattering
[DE94-601816] p 3023 N94-26945

FLORIDA AGRICULTURAL AND MECHANICAL UNIV., TALLAHASSEE.
The Extended Mission Rover (EMR)
p 2689 N94-25674
Separated flow generated by a vectored jet in a crossflow p 2800 N94-28007

FLORIDA STATE UNIV., GAINESVILLE.
Mechanical properties of polyaniline prepared by polymerization in an organized monolayer
[AD-A274350] p 2753 N94-26925

FLORIDA STATE UNIV., TALLAHASSEE.
The Extended Mission Rover (EMR)
p 2689 N94-25674
Differentiating the role of land surface variability and cloudiness variability on global energy transport within the atmosphere and oceans
[NASA-CR-195229] p 2847 N94-26222
Analysis and interpretation of the meteorology of the 1988 coastal transition zone experiment
[AD-A274710] p 2894 N94-26431
Separated flow generated by a vectored jet in a crossflow p 2800 N94-28007

FLORIDA UNIV., GAINESVILLE.
Bioregenerative system components for microgravity
p 2903 N94-25673
Investigation of a normal incidence high-performance p-type strained layer In(0.3)Ga(0.7)As / In(0.52)Al(0.48) as quantum well infrared photodetector
[AD-A274854] p 3055 N94-26188
International journal of quantum chemistry. Quantum Chemistry Symposium Number 27: Proceedings of the International Symposium on Atomic, Molecular, and Condensed Matter Theory and Computational Methods
[AD-A274352] p 3023 N94-26926
LB-Deposited, side-chain substituted polyaniline, polypyrrole and the corresponding monomers, studied by STM
[AD-A274405] p 2754 N94-26977
Ferroelectricity in a Langmuir-Blodgett multilayer film of a liquid crystalline side-chain polymer
[AD-A274477] p 2754 N94-27033
Visible light emitting materials and injection devices
[AD-A274418] p 2786 N94-27079
Kinetics of 2-pentadecylaniline polymerizations in monolayers: Relationships between experimental data and a new theoretical model
[AD-A274419] p 2754 N94-27080
Langmuir-Blodgett and STM investigations of conducting polymer thin films
[AD-A274512] p 2755 N94-27087
Active database architectures and the design of sentinel for constraint management
[AD-A274205] p 3099 N94-27101
Chemical polymerization and Langmuir-Blodgett techniques. 2: The polymerization of monolayers of 3-substituted pyrroles
[AD-A274478] p 2755 N94-27163

FOERENADE FABRIKSVERKEN, LINKOEPING (SWEDEN).
Trapezoid-oriented compression of run length coded map data
[PB94-123312] p 2849 N94-26848
HPm-tubes: Literature survey comprising 1992
[PB94-123643] p 2785 N94-27038
Microwave coupling into a slotted cavity
[PB94-123742] p 2772 N94-27041
Compilation of corrections for postprocessing of laser bathymetry data
[PB94-123668] p 2900 N94-27156
Translation and rotation invariant pattern recognition
[PB94-123676] p 2968 N94-27157

FOERSVARETS MATERIALVERK, STOCKHOLM (SWEDEN).
Hydroacoustic wave-fields generated by different source types, a computational study
[PB94-123536] p 3010 N94-27037

FORD (HENRY) HOSPITAL, DETROIT, MI.
Irreversibility of advanced osteoporosis: Limited role for pharmacologic intervention p 2935 N94-28369

FUJITA HEALTH UNIV., TOYOHASHI (JAPAN).
Study on posture control and adaption mechanism under weightlessness: Differences in weight and shape of utricular otolith of carp p 2912 N94-27448

G

GALAXY SCIENTIFIC CORP., PLEASANTVILLE, NJ.
Digital systems validation book plan. Volume 3: Handbook
[AD-A274099] p 2672 N94-26028
Effects of plastic media blasting on aircraft skin
[AD-A274817] p 2668 N94-26488

GATES AEROSPACE BATTERIES, GAINESVILLE, FL.
Ni-MH storage test and cycle life test
p 2864 N94-28131

GEC-PLESSEY SEMICONDUCTORS, LINCOLN (ENGLAND).
Development of a MIL-STD-1750 microprocessor system for space applications p 2949 N94-26715

GENERAL ACCOUNTING OFFICE, WASHINGTON, DC.
Space projects: Astrophysics facility program contains cost and technical risks. Report to Congressional Requesters
[GAO/NSIAD-94-80] p 2696 N94-27382
Space science: Causes and impacts of cutbacks to NASA's outer solar system exploration missions. Report to the Chairman, Subcommittee on Investigations and Oversight, Committee on Science, Space, and Technology, House of Representatives
[GAO/NSIAD-94-24] p 3106 N94-27418
NASA: Major challenges for management. Testimony before the Legislation and National Security Subcommittee, Committee on Government Operations, House of Representatives
[GAO/T-NSIAD-94-18] p 3095 N94-28176
Defense force management: Challenges facing DOD as it continues to downsize its civilian work force. Report to the Chairman, Subcommittee on Federal Services, Post Office, and Civil Service, Committee on Governmental Affairs, US Senate
[GAO/NSIAD-93-123] p 3095 N94-28177

GENERAL ATOMIC CO., SAN DIEGO, CA.
Review of tokamak experiments on direct electron heating and current drive with fast waves
[DE94-004185] p 3041 N94-25801
New Thomson scattering laser control for D3-D
[DE94-002890] p 3043 N94-26274
Role of core toroidal rotation shear on turbulence and transport in the improved confinement regimes of the D3-D tokamak
[DE94-001215] p 3045 N94-26950
Fuel ion rotation measurement and its implications on H-mode theories
[DE94-004860] p 3048 N94-27791

GENERAL ATOMICS TECHNOLOGIES CORP., SAN DIEGO, CA.
Evaluation of helium cooling for fusion divertors
[DE94-002680] p 3042 N94-25976
A robust helium-cooled shield/blanket design for ITER
[DE94-003402] p 3043 N94-26323
Limitations of power conversion systems under transient loads and impact on the pulsed tokamak power reactor
[DE94-003404] p 3043 N94-26324
Cryogenic size reduction of solid propellant
[AD-A274844] p 2759 N94-26800
New conditioning procedure derived from operating experience with the Common Long-Pulse Ion Source
[DE94-002891] p 3045 N94-26865

GENERAL ELECTRIC CO., OWENSBORO, KY.
Transient model applications. 1: Compressor heat soak/clearance effects modeling p 2828 N94-28048
Transient model applications. 2: Compressor stall modeling methods p 2829 N94-28049
Transient model applications. 3: Transient engine simulation and analysis of an ice ingestion test
p 2829 N94-28050

GENERAL ELECTRIC CO., SCHENECTADY, NY.
Zinc(2) oxide stability in alkaline sodium phosphate solutions at elevated temperatures
[DE94-003316] p 2715 N94-26320
Development of the gas turbine. Part 1: Design philosophy and performance p 2831 N94-28080
Development of the gas turbine. Part 2: Manufacturing, commissioning, and operation p 2831 N94-28081

GENERAL RESEARCH CORP., DANVERS, MA.
Zodiacal light data investigation. Interim results for the Earthlimb Clutter Experiment
[AD-A274461] p 3104 N94-27265

GEOLOGICAL SURVEY, DENVER, CO.
Volcanology and volcanic activity with a primary focus on potential hazard impacts for the Hawaii geothermal project
[DE94-001614] p 2879 N94-26515

GEORGE WASHINGTON UNIV., WASHINGTON, DC.
Research in improved assessment of software reliability
[AD-A274161] p 2968 N94-27140
Recent advances in the spectral element method
p 2657 N94-28348

GEORGIA INST. OF TECH., ATLANTA.
The Enabler: A concept for a lunar work vehicle
p 2833 N94-25675
Design for producing fiberglass fabric in a lunar environment p 2765 N94-25676
Lunar preform manufacturing p 2765 N94-25677
Variable speed controller p 2943 N94-25678
Enabler operator station p 2943 N94-25679
Dust control for Enabler p 2943 N94-25680
Knowledge organization in intelligent tutoring systems for diagnostic problem solving in complex dynamic domains
[AD-A273986] p 2984 N94-25899
Integration of interactive interfaces with intelligent tutoring systems: An implementation
[AD-A273869] p 2985 N94-25966
Computational strategies for three-dimensional flow simulations on distributed computer systems
[NASA-CR-195249] p 2793 N94-26595
Probabilistic methods for image generation and encoding
[AD-A274294] p 2964 N94-26682
Research in robust control for hypersonic aircraft
[NASA-CR-195250] p 2678 N94-26821
New variational techniques for acoustic radiation and scattering from elastic shell structures
[AD-A274599] p 3010 N94-26889
Deformation, constitutive behavior, and damage of advanced structural materials under multiaxial loading
[AD-A274165] p 2709 N94-27142

GEORGIA STATE UNIV., ATLANTA.
A formal approach to the comparison of object-oriented analysis and design methodologies
p 2975 N94-27937

GOSUDARSTVENNYI KOMITET PO ISPOLZOVANIYU ATOMNOI ENERGII, OBNINSK (USSR).
Parametric analysis of the space power plants on the base of criterion of specific mass in generalized design variants
[DE93-634153] p 2701 N94-26166

GOSUDARSTVENNYI KOMITET PO ISPOLZOVANIYU ATOMNOI ENERGII, SERPUKHOV (USSR).
On the gluon propagator in the infrared region
[DE93-634345] p 3016 N94-26035
Quantizable configurations of the relativistic string
[DE93-634346] p 3072 N94-26036
Dynamical group of relativistic straight-line string
[DE93-634347] p 3072 N94-26037
Spatial symmetry, local integrability and tetrahedron equations in the Baxter-Bazhanov model
[DE93-634348] p 3002 N94-26038
Z(sub N)(sup n-1) broken model
[DE93-634357] p 3072 N94-26039

Pseudoscalar glueball in the composite interpolating fields approach
[DE93-634374] p 3016 N94-26042
Spin effects in hard interactions (interest in accelerated polarized beam)
[DE93-634398] p 3031 N94-26044
Meson X(1814) as a candidate for a hybrid state
[DE93-634447] p 3017 N94-26045
Regrouping of the beam in the IHEP PS for the UNK p-p programs
[DE93-634021] p 3032 N94-26164
Longitudinal diffusion of a proton bunch under external noise
[DE93-634022] p 3032 N94-26165
Auxiliary controller for time-to-digital converter module readout
[DE93-634172] p 2948 N94-26266
Calorimeter with WLS fibers and parallel to beam scintillators
[DE93-634188] p 2810 N94-26378
Exploration of GaAs structures for solid-state detectors
[DE93-634191] p 3056 N94-26379
The 12-channel flash-ADC FASTBUS module
[DE93-634229] p 2783 N94-26380
Fast generator of program waveforms signals
[DE93-634230] p 2948 N94-26381
Separation and reconstruction of electron neutrino interaction in the IHEP-JINR neutrino detector and BARS detector
[DE93-634182] p 3019 N94-26393
The 1024 scintillation hodoscope
[DE93-634183] p 2810 N94-26394
Physical characteristics of polymethylmethacrylate scintillator SOFG-120
[DE93-634184] p 2810 N94-26395
Unsegmented electromagnetic calorimeter prototype. Energy and coordinate resolution
[DE93-634185] p 2810 N94-26396
Hadron gas ionization calorimeters
[DE93-634186] p 2810 N94-26397
Problems of application of charged particles channeling effects in crystals in high-energy physics
[DE93-634023] p 3032 N94-26405
Signal amplifier-shapers for multiwire detectors
[DE93-634171] p 2783 N94-26438
Study on the compensated lead hadron calorimeter characteristics by means of hadron and electron beams
[DE93-634176] p 2810 N94-26439
Component structure of the N = 2 super-Yang-Mills theory in the harmonic superspace
[DE93-634340] p 3072 N94-26453
Spin from isospin: The model of superparticle in a non-Grassmannian approach
[DE93-634341] p 3019 N94-26454
Dynamic breaking of U(N) and appearance of Chern-Simons term in 4-fermion theories
[DE93-634342] p 3019 N94-26455
On the relativistic invariant representation of arbitrary bilinear combinations of Dirac spinors
[DE93-634343] p 3019 N94-26456
Statistical mechanical properties of Z(N)(sup n-1) broken model
[DE93-634344] p 2993 N94-26457
On kinetic expansion in scalar field theory
[DE93-634338] p 3072 N94-26553
Leptonic decay constants of heavy mesons in QCD
[DE93-634426] p 3022 N94-26767
Kinetic equation identification from measurement of a particular solution
[DE93-634585] p 2995 N94-26768
Study of the process (pi)(sup -)A(yields)(pi)(sup -)(eta)'(eta)A at the moment 36 GeV/c
[DE93-634530] p 3024 N94-27250

GRONINGEN RIJKSUNIV. (NETHERLANDS).
Polymer-bound rhodium hydroformylation catalysts
[ETN-94-95388] p 2712 N94-25747
High impact strength poly(lactide) tough biodegradable materials
[ETN-94-95389] p 2747 N94-25748
Langmuir-Blodgett film of amylose-esters and chiral azo-dyes (structure and second order nonlinear optical behaviour)
[ETN-94-95390] p 2747 N94-25749
Biomedical polyurethane networks
[ETN-94-95391] p 2750 N94-26211
Interacting cortical filters for object recognition
[PB94-125374] p 2938 N94-26873
Normal forms for perturbations of the euler top
[PB94-125390] p 3009 N94-26968
Necessary and sufficient conditions for the existence of the stabilizing solution of the Riccati equation in a Hilbert space: A Popov function approach
[PB94-125341] p 2997 N94-26999
Grid-independent convergence based on preconditioning techniques
[PB94-125358] p 2997 N94-27000
Orientation competition in cortical filters
[PB94-125366] p 2939 N94-27001
Bifurcation sequences at 1:4 resonance: An inventory
[PB94-125408] p 2997 N94-27028
Chebyshev-Markov rational functions over several intervals
[PB94-125333] p 2998 N94-27116

H

HAHNEMANN MEDICAL COLL. AND HOSPITAL, PHILADELPHIA, PA.
Cortical mechanisms of attention, discrimination, and motor response to somesthetic stimuli
[AD-A274163] p 2940 N94-27141

HAMON-LUMMUS (BELGIUM).
Cooling towers for combined cycles: New developments to meet environmental requirements
p 2832 N94-28088

HAMON-SOBELCO (BELGIUM).
Cooling towers for combined cycles: Design philosophy, performance testing, and operating problems
p 2832 N94-28087

HAMPTON UNIV., VA.
Critical survey of plasma processing
[AD-A274233] p 3044 N94-26820
RIAD visual imaging branch assessment
p 2815 N94-27895
A tri-state optical switch for local area network communications p 2789 N94-27922
Fiber optic sensors for corrosion detection
p 3040 N94-27923

HARVARD UNIV., CAMBRIDGE, MA.
Harvard University High Energy Physics
[DE94-002406] p 3032 N94-26119
Antiproton studies in penning traps
[AD-A274250] p 3024 N94-27011

HAWAII NATURAL ENERGY INST., HONOLULU.
Molten salt techniques for reproducible excess heat
[AD-A274935] p 2714 N94-26296

HAZELTINE CORP., BRAINTREE, MA.
Beamforming/null-steering adaptive array
[CA-PATENT-1325260] p 2775 N94-27270
Automatic, real-time fault monitor verifying network in a microwave landing system
[CA-PATENT-1325261] p 2665 N94-27275

HEIDELBERG UNIV. (GERMANY).
A parallel multigrid algorithm for solving the Navier-Stokes equations on a transputer system
[PREPRINT-699] p 2807 N94-28099

HELSINKI UNIV. OF TECHNOLOGY, ESPOO (FINLAND).
New mixed integer algorithm for classification and placement of measurements in process flow networks
[PB94-126752] p 2966 N94-26921
Sheaf semantics for Petri Nets
[PB94-132826] p 2983 N94-28354
Polarizability matrix of layered chiral sphere
[PB94-132834] p 2778 N94-28355
ActorStudio: An interactive user interface editor
[PB94-132859] p 2976 N94-28356
Dry etching process development for submicron and nanometer semiconductor devices
[PB94-133196] p 2788 N94-28357
Laboratory of Space Technology
[PB94-133204] p 2689 N94-28358
High Quality Aluminium Castings Conference
[PB94-133592] p 2747 N94-28359
Fields and potentials in general uniaxial bianisotropic media I. Axial sources
[PB94-132875] p 2778 N94-28379
Plane wave propagation and polarization properties in transversely bianisotropic uniaxial medium
[PB94-132883] p 2778 N94-28380
Eigenwaves in the general uniaxial bianisotropic medium with symmetric parameter dyadics
[PB94-132891] p 2778 N94-28381
Electromagnetic modeling of bi-isotropic media
[PB94-132909] p 2778 N94-28382
Fibrous ceramic candle filter for particle removal in pressurized fluidized bed combustion
[PB94-133089] p 2876 N94-28383
Plane wave propagation in an anisotropic chiral medium with isotropic permittivity and permeability
[PB94-133097] p 2778 N94-28384
Concurrent shadow paging: Snapshots, read-only transactions, and on-the-fly multi-level incremental dumping
[PB94-133139] p 3100 N94-28385
Intertemporal bargaining and dynamic consistency
[PB94-133147] p 3095 N94-28386
Electrostatic image solution for the conducting prolate spheroid
[PB94-133154] p 2778 N94-28387
Analytic solution for the dyadic Green's function of a nonreciprocal uniaxial bianisotropic medium
[PB94-133162] p 2779 N94-28388
Hessenberg matrices in Krylov subspaces and the computation of the spectrum
[PB94-133170] p 3001 N94-28389
Image theory for DC problems involving a conducting half space bounded by the general anisotropic impedance surface
[PB94-132917] p 2779 N94-28390
Green dyadic and dipole fields for a medium with anisotropic chirality
[PB94-132933] p 2779 N94-28391
Studies in ice mechanics
[PB94-133055] p 2900 N94-28393
Experimental studies of pressurised fluidised bed combustion at Helsinki University of Technology, 1991-1992
[PB94-133063] p 2876 N94-28394
Emissions of nitrogen oxides (NO(x) and N2O) in pressurized fluidized bed combustion
[PB94-133071] p 2876 N94-28395
Efficient rebalancing of tree-type main memory dictionaries
[PB94-133105] p 3100 N94-28396
Dielectric polarizability of sphere with arbitrary anisotropy
[PB94-133113] p 2779 N94-28397
Lisp interface to geometric modelling operations
[PB94-133121] p 3001 N94-28398

HERTFORDSHIRE UNIV., HATFIELD (ENGLAND).
Effects of free-stream turbulence on a jet in a cross flow p 2805 N94-28036

HIGH TECHNOLOGY CORP., HAMPTON, VA.
On prediction of equilibrium states in homogeneous compressible turbulence
[NASA-CR-4570] p 2792 N94-26467
Localized and distributed boundary-layer receptivity to convected unsteady wake in free stream
[NASA-CR-4578] p 2808 N94-28180

HIROSAKI UNIV. (JAPAN).
Direct evidence of the interplanetary magnetic field effect on the cosmic-ray shadow by the sun
[ICRR-296-93-8] p 3116 N94-27607

HIROSHIMA UNIV. (JAPAN).
Note on the structure of moss colonies composed of two species on King George Island, the South Shetland Islands p 2885 N94-27971

HITEC PRODUCTS, INC., AYER, MA.
Attachment techniques for high temperature strain
[AD-A274766] p 2811 N94-26568

HOKKAIDO UNIV., SAPPORO (JAPAN).
Crystallographyic analyses of clathrate hydrates included in Vostok ice cores p 2885 N94-27969

HONEYWELL, INC., MINNEAPOLIS, MN.
Optoelectronic Technology Consortium
[AD-A274909] p 2782 N94-26344
Optoelectronic technology consortium
[AD-A274595] p 3036 N94-26857

HOUSTON UNIV., CLEAR LAKE, TX.
New Developments Regarding the KT Event and Other Catastrophes in Earth History
[NASA-CR-195169] p 2887 N94-28294

HOUSTON UNIV., TX.
Portable Habitat for Antarctic Scientific Research (PHASR) p 2943 N94-25681
Lowest cost, nearest term options for a manned Mars mission p 2689 N94-25682
Transverse vorticity measurements in the University of Houston two stream shear layer facility
[AD-A273910] p 2797 N94-27562
Ozone control of biological activity during Earth's history, including the KT catastrophe p 2876 N94-28312

HOWARD UNIV., WASHINGTON, DC.
Center for nonlinear phenomena and magnetic materials
[AD-A274176] p 3009 N94-27126

HUGHES RESEARCH LABS., MALIBU, CA.
A comparison of spectral decorrelation techniques and performance evaluation metrics for a wavelet-based, multispectral data compression algorithm
p 2946 N94-28258

HUNGARIAN ACADEMY OF SCIENCES, BUDAPEST.
Combining logics
[PB94-125242] p 2965 N94-26908

I

IDAHO UNIV., MOSCOW.
Planetary surface exploration MESUR/autonomous lunar rover p 2833 N94-25683

ILLINOIS UNIV., URBANA.

Flowing DPF design for propulsion experiments [AD-A274973] p 2701 N94-26537

Application of railgun principle to high-velocity hydrogen pellet injection for magnetic fusion reactor fueling [DE94-004411] p 3044 N94-26579

Fast incremental compiler transformations for multiple instruction retry [NASA-CR-195209] p 2964 N94-26680

Research on elementary particle physics, part 2 [DE94-004956] p 3029 N94-27815

IMAGINATION RESOURCES, INC., DUBLIN, OH.

Compatibility of refrigerants and lubricants with engineering plastics [DE94-004959] p 2756 N94-27692

IMPERIAL COLL. OF SCIENCE AND TECHNOLOGY, LONDON (ENGLAND).

Modelling of ionisation reactions and of the resulting electric fields in one-dimensional hypersonic shock waves with the direct simulation Monte Carlo method [IC-AERO-92-01] p 2644 N94-26248

Predictions of momentum and scalar fields in a jet in cross-flow using first and second order turbulence closures p 2803 N94-28025

Thermodynamics of combined cycle plant p 2831 N94-28079

INDIANA UNIV., BLOOMINGTON.

Indiana University high energy physics, task A [DE94-000961] p 3033 N94-27614

INSTITUT DES HAUTES ETUDES SCIENTIFIQUES, BURES-SUR-YVETTE (FRANCE).

Spaces of algebraic cycles [PB94-124369] p 2996 N94-26993

Lyapunov exponents for some quasi-periodic cocycles [PB94-124377] p 2997 N94-26994

Estimates for cone multipliers [PB94-124385] p 2997 N94-26995

Poisson-lie group of pseudodifferential symbols [PB94-124393] p 2997 N94-26996

INSTITUT FRANCO-ALLEMAND DE RECHERCHES, SAINT-LOUIS (FRANCE).

Experiments on interaction force of jets in hypervelocity cross-flow in a shock tunnel p 2659 N94-28022

INSTITUT NATIONAL DE RECHERCHE D'INFORMATIQUE ET D'AUTOMATIQUE, LE CHESNAY (FRANCE).

Specification performance optimization and executive generation for onboard multiprocessor real time application with SynDEx p 2954 N94-26745

INSTITUT UNIV. DE TECHNOLOGIE, NANTES (FRANCE).

Fault-tolerant scheduling in distributed critical real-time systems p 2952 N94-26735

INSTITUTE FOR AEROSPACE RESEARCH, OTTAWA (ONTARIO).

A comparison of Probability Of Detection (POD) data determined using different statistical methods [LTR-ST-1947] p 2835 N94-26644

Influence of the transonic doublet in the farfield of a lifting airfoil [IAR-AN-78] p 2647 N94-26702

The effects of tailwinds and control cross coupling on rotorcraft handling qualities for steep, decelerating instrument approaches and missed approaches [IAR-AN-77] p 2677 N94-26710

Installation of models in the 2 m x 3 m low speed wind tunnel [LTR-LA-286] p 2681 N94-27594

Wind tunnel investigation of propfan slipstream/wing interactions on a De Havilland air motor powered semispan model at Mach numbers 0.6 and 0.7 p 2651 N94-28316

Measurements of steady and dynamic pressure on an F/A-18 wind tunnel model at high angles of attack p 2653 N94-28323

Application of the influence function method using the interference distributed loads code to prediction of store aerodynamic load during separation from the CF-18 fighter aircraft p 2654 N94-28330

Solution of the Euler equations using unstructured grids p 2656 N94-28338

A study of blunt trailing edge airfoils using the Navier Stokes code: ARC2D p 2656 N94-28340

Experimental investigations into the wall interference and sidewall boundary layer effects in the National Research Council/Inst. for Aerospace Research High Reynolds Number 2-D Test Facility p 2658 N94-28350

Computation of wind-tunnel side-wall interference using 3D Navier-Stokes code p 2658 N94-28351

Evaluation of the buoyancy drag on automobile models in low speed wind tunnels p 2658 N94-28352

INSTITUTE FOR COMPUTER APPLICATIONS IN SCIENCE AND ENGINEERING, HAMPTON, VA.

The nonlinear Galerkin method: A multi-scale method applied to the simulation of homogeneous turbulent flows [NASA-CR-191581] p 2792 N94-26499

Reconstruction of multiple cracks from experimental electrostatic boundary measurements [NASA-CR-191584] p 2994 N94-26601

A sensitivity equation approach to shape optimization in fluid flows [NASA-CR-191598] p 2999 N94-27415

Shared virtual memory and generalized speedup [NASA-CR-191592] p 2969 N94-27416

Interactive shape metamorphosis [NASA-CR-191597] p 2970 N94-27417

Parallel implicit unstructured grid Euler solvers [NASA-CR-191594] p 2999 N94-27434

A rapid-pressure correlation representation consistent with the Taylor-Proudman theorem materially-frame-indifferent in the 2D limit [NASA-CR-191591] p 2796 N94-27435

Agglomeration multigrid for the three-dimensional Euler equations [NASA-CR-191595] p 2999 N94-27557

Efficient massively parallel simulation of dynamic channel assignment schemes for wireless cellular communications [NASA-CR-191593] p 2971 N94-27558

Illumination in diverse codimensions [NASA-CR-191596] p 2971 N94-27572

INSTITUTE FOR PERCEPTION RVO-TNO, SOESTERBERG (NETHERLANDS).

The effect of the time restrictions on information search and information integration in a dynamic task environment [AD-A273759] p 3095 N94-25723

The effect of platform motion on human energy expenditure during walking. An exploratory experiment [AD-A273760] p 2940 N94-25724

Endogeneous and exogenous control of visual selection: A review of the literature [AD-A273761] p 2908 N94-25871

On the development of motor chunks and concurrent processing in a structured continuous keypressing task [AD-A274153] p 2939 N94-27138

INSTITUTE OF ATMOSPHERIC PHYSICS, BEIJING (CHINA).

A progress report on global change studies in China p 2874 N94-28283

INSTITUTE OF ECOSYSTEM STUDIES, MILLBROOK, NY.

Landscape dynamics of northeastern forests [NASA-CR-195272] p 2852 N94-28070

INSTITUTE OF PLASMA PHYSICS, PRAGUE (CZECHOSLOVAKIA).

Fast H-alpha line broadening during the 100 ns REB injection into a plasma [IPPCZ-322] p 3048 N94-27836

On radio frequency wave induced radial transport and wave helicity [IPPCZ-326] p 2777 N94-27838

On helicon wave induced radial plasma transport [IPPCZ-333] p 3048 N94-27840

A numerical approach to Stefan problem [IPPCZ-334] p 2844 N94-27841

Preliminary considerations on the diffraction (quasi-optical) grill in CASTOR tokamak [IPPCZ-335] p 3048 N94-27842

INSTITUTO DE FISICA TEORICA, SAO PAULO (BRAZIL).

Lepton masses in an SU(3)(sub L) x U(1)(sub N) gauge model [DE93-634366] p 3016 N94-26040

Heavy charged leptons in an SU(3)(sub L) x U(1)(sub N) model [DE93-634367] p 3016 N94-26041

Deciphering the quark-gluon structure of the photon in electron(gamma) collisions [DE93-634386] p 3017 N94-26043

Quantum Hamiltonian differential geometry: How does quantization affect space? [DE93-634306] p 2993 N94-26442

Constraints on singlet right-handed neutrinos coming from the Z(0)-width [DE93-634393] p 3022 N94-26766

INSTITUTO DE PESQUISAS ENERGETICAS E NUCLEARES, SAO PAULO (BRAZIL).

Study of the hyperfine magnetic field at Ta-181 site in the Heusler Co2ScSn, Co2ScGa, and Co2HfSn alloys [DE94-603989] p 3067 N94-27623

INSTITUTO DE PESQUISAS ESPACIAIS, SAO JOSE DOS CAMPOS (BRAZIL).

Digital filter design for sensor simulation: Application to the Brazilian remote sensing satellite [INPE-5523-RPQ/665] p 2849 N94-26827

Synthesis of diamond film assisted by an arcjet plasma source, part 2 [INPE-5527-PRP/178-PT-2] p 3066 N94-27329

Photochemical processes and the atmospheric airglow emissions of OH and Na in the mesospheric region [INPE-5380-PUD/050] p 2882 N94-27334

Non-adaptive robust filters for speckle noise reduction [INPE-5519-PRE/1794] p 2776 N94-27335

An observational study of the extratropical anticyclones in the South American continent [INPE-5387-TDI/476] p 2896 N94-27356

Dynamics and robust control for uncertain flexible space systems [INPE-5510-TAE/020] p 2696 N94-27357

Training on assessment and mapping of deforestation: WFW conference, Brazil [INPE-5482-PRE/1781] p 2850 N94-27384

A synoptic study on periods of deficiency over Rio Grande do Sul/Brazil [INPE-5456-TDI/498] p 2896 N94-27422

Using ferro-magnetic fluids to lubricate non-conformal isothermal contacts [INPE-5520-TAE/021] p 2827 N94-27665

A hybrid formalism for representation and interpretation of image knowledge [INPE-5485-PRE/1784] p 2989 N94-27833

Ranking alternatives using fuzzy numbers: A computational approach short communication [INPE-5483-PRE/1782] p 2974 N94-27835

Role of remote sensing in energy, water, and carbon cycle studies over the Amazon [INPE-5486-PRE/1786] p 2852 N94-27957

INTECS SISTEMI S.P.A., PISA (ITALY)

A real-time executive implementing priority inheritance protocols p 2952 N94-26733

INTERNATIONAL ATOMIC ENERGY AGENCY, VIENNA (AUSTRIA).

Standardizing exchange formats [DE93-616798] p 3095 N94-25751

Index to BROND-2, CENDL-2, ENDF/B-6, JEF-2, JENDL-3 [DE93-634500] p 3016 N94-26034

International bulletin on atomic and molecular data for fusion. No. 42-45, Mar. 1991 - Dec. 1992 [DE94-601817] p 3045 N94-26946

International bulletin on atomic and molecular data for fusion. No. 46 [DE94-601818] p 3023 N94-26947

INTERNATIONAL CENTRE FOR THEORETICAL PHYSICS, TRIESTE (ITALY).

A study of vibrational relaxation of electronically-excited molecules [DE93-613553] p 3013 N94-25827

On the oscillation of a class of hyperbolic equations of neutral type [DE93-616815] p 2990 N94-25829

Oscillatory behaviour of solutions of coupled hyperbolic differential equations of neutral type [DE93-616816] p 2990 N94-25830

Stochastic resonance in a periodic potential system under a constant force [DE93-616817] p 3008 N94-25831

Cosmoparticle physics of family symmetry breaking [DE94-601623] p 3013 N94-25837

Out of equilibrium phase transitions and a toy model for disoriented chiral condensates [DE94-601642] p 3013 N94-25839

Volume dependence of vanadium magnetism [DE94-601838] p 3050 N94-25843

On the estimation of matrix elements for optical transitions in semiconductors [DE93-613550] p 3051 N94-25851

Biexciton formation by two-photon absorption in quantum wells [DE93-613551] p 3071 N94-25852

Conditionally exponential convex functions on locally compact groups [DE93-613025] p 2990 N94-25865

(2,0) superconformal anomaly [DE93-613046] p 2991 N94-25867

Duality for multiparametric quantum GL(n) and for a Lorentz quantum group [DE93-613048] p 3005 N94-25868

Approximate solution of the fourth order initial value problem using deficient spline polynomials [DE93-613023] p 2991 N94-25880

Some properties of generalized biregular functions with values in a Clifford algebra [DE93-613024] p 2991 N94-25881

Topological amplitudes in string theory [DE94-601561] p 3071 N94-25882

On string theory interacting with two-dimensional gravity [DE94-601562] p 3071 N94-25883

The algebra of non-local charges in non-linear sigma models
[DE94-601563] p 2991 N94-25884

Vector meson exchanges and CP asymmetry in K(sup +/-) yields pi(sup +/-)pi(sup 0)
[DE94-601605] p 3014 N94-25887

On the thermal ignition with variable pre-exponential factor
[DE93-616009] p 2713 N94-25913

Lighter alkali hydride and deuteride 1: Electronic properties of pure solids
[DE93-616188] p 3051 N94-25914

Optical conductivity and resistivity in the two-band Emery model
[DE94-601943] p 3051 N94-25945

The Cherenkov hadronic like-jets
[DE93-634525] p 3016 N94-26010

First principle calculation for magneto-crystalline anisotropy
[DE93-634653] p 3052 N94-26012

Dibaryon-induced instability of neutron stars
[DE93-634453] p 3103 N94-26046

Fermi-liquid to non-Fermi-liquid transition in a dynamical generalization of the CPA in a disordered Hubbard model
[DE94-601875] p 2714 N94-26169

On Poisson brackets and symplectic structures for the classical and quantum Zitterbewegung
[DE93-634305] p 2992 N94-26267

TEV emission from close binaries
[DE93-634330] p 3104 N94-26268

Magnetic field induced contributions of supersymmetric particles to energy losses of neutron star
[DE93-634331] p 3104 N94-26269

Classical solutions of Yang-Mills-Chern-Simons theory in 2+1 dimensions: A quasi-linear superposition
[DE93-634335] p 3006 N94-26270

Why is the Higgs doublet light?
[DE94-601711] p 3018 N94-26333

Determination of the geomagnetic external contribution by nonlinear optimization methods
[DE94-600882] p 2878 N94-26365

Matrix near rings and pseudo distributivity
[DE94-601505] p 2992 N94-26366

Winding numbers in homotopy theory from integers to reals
[DE94-601510] p 2992 N94-26367

Analytical solution of Mori's equation with secant hyperbolic memory
[DE94-601541] p 3006 N94-26368

Numerical treatment of experimental data in calibration procedures
[DE93-634289] p 3097 N94-26382

Cad of GeO2-SiO2 double-layer core dispersion-shifted single-mode fibre
[DE93-634325] p 3035 N94-26383

The effect of high frequency electric field on hypersound amplification in superlattice
[DE93-634326] p 3057 N94-26384

Window least squares method applied to statistical noise smoothing of positron annihilation data
[DE93-634665] p 3003 N94-26385

On the reliability of a window least squares algorithm
[DE93-634666] p 2962 N94-26386

On the electron mobility in slightly compensated heavily doped gallium arsenide at low temperatures
[DE93-634712] p 3057 N94-26387

Holes in a two-dimensional quantum antiferromagnet
[DE93-634753] p 3057 N94-26388

Multi-channel Kondo necklace
[DE93-634754] p 3057 N94-26389

Ising critical behaviour in the one-dimensional frustrated quantum XY model
[DE93-634755] p 3057 N94-26390

Structure of ionic fluids in equilibrium with a microporous ionic matrix
[DE94-600563] p 2715 N94-26391

Stability of large scale interconnected dynamical systems
[DE94-601536] p 2993 N94-26408

Characterization of self-conjugate minimal surfaces in R(sup 3)
[DE94-601538] p 2993 N94-26409

Numerical solution of singularity-perturbed two-point boundary-value problems
[DE94-601542] p 2993 N94-26410

How reliable is the HMSA integral equation for the pair structure of supercooled and amorphous mixtures?
[DE94-601543] p 3006 N94-26411

Enumeration of n-fold tangent hyperplanes to a surface
[DE94-601544] p 2993 N94-26412

The massless representations of the conformal quantum algebra
[DE94-601555] p 3006 N94-26413

Affine algebras on the torus
[DE94-601556] p 3006 N94-26414

Higher spin extensions of the Virasoro algebra, area-preserving algebras and the matrix algebra a-bar(sub (infinity))
[DE94-601557] p 3006 N94-26415

Differential regularization of a non-relativistic anyon model
[DE94-601558] p 3019 N94-26416

Vortices in curved spacetime
[DE94-601559] p 3072 N94-26417

Orthodox gravity
[DE94-601560] p 2878 N94-26418

C-periodicity and the physical mass in the 3-state Potts model
[DE94-601551] p 3019 N94-26423

Spinor and isospinor structure of relativistic particle propagators
[DE94-601552] p 3019 N94-26424

Gauging of Chern-Simons p-Barnes
[DE94-601553] p 2993 N94-26425

Finite dimensional representations of the quantum superalgebra U(sub q)(gl(3/2))
[DE93-634303] p 2993 N94-26440

On the phi(sub 0)-stability of perturbed nonlinear differential systems
[DE93-634304] p 2993 N94-26441

The electric field between non conductive rectangular charged surfaces placed near a small spherical conductive earthed surface and determination of critical density of charge
[DE93-634324] p 2783 N94-26443

Cone-valued Lyapunov functions and the stability of stochastic differential equations
[DE94-601504] p 2994 N94-26458

The Hamiltonian structures of the super KP hierarchy associated with an even parity superlax operator
[DE94-601506] p 2994 N94-26459

On the (Phi)(sub 0)-stability of functional differential equations
[DE94-601507] p 3006 N94-26460

Quantum group and Manin plane related to a colored braid group representation
[DE94-601509] p 3072 N94-26461

The extensions of space-time. Physics in the 8-dimensional homogeneous space D is equal to SU(2,2)/K
[DE93-634336] p 3072 N94-26551

String hypothesis and characters of coset CFTs
[DE93-634337] p 3007 N94-26552

Wigner quantum oscillators
[DE94-601508] p 3073 N94-26758

Calculating the surface properties for the liquid-vapour interface: Illustrating the thermodynamic stability of the spherical microstructures
[DE94-601992] p 3073 N94-26837

Quantum subgroups and quantum co-set spaces and differential calculi on them
[DE94-602520] p 3073 N94-26876

AB-Initio calculation of the valence-band offset at strained GaAs/InAs (001) heterojunction
[DE94-602538] p 3061 N94-26878

Effect of impurity correlation on the density of states in slightly compensated heavily doped semiconductors
[DE94-602539] p 3061 N94-26879

Thermodynamics and form factors of supersymmetric integrable field theories
[DE94-602557] p 3073 N94-26896

Polar optical oscillation modes in GaAs-based double heterostructures: Long wavelength limit
[DE94-601874] p 3062 N94-26897

Deformation of the exterior algebra and the GL(sub q) (r, included in) algebra
[DE94-602558] p 2996 N94-26898

Flavor changing neutral currents in SU(3) x U(1) models
[DE94-602576] p 3022 N94-26899

Low-energy hadronic interactions beyond the current algebra approach
[DE94-602600] p 3022 N94-26900

Electronic structure of a single oxygen vacancy in rutile TiO2
[DE94-602717] p 3062 N94-26901

Length-scale dependent ensemble-averaged conductance of a 1D disordered conductor: Conductance minimum
[DE94-602732] p 3062 N94-26902

A model of electric breakdown in polycrystalline semiconductors with highly nonlinear I - V characteristics
[DE94-601537] p 3063 N94-27017

Q - difference intertwining operators for a Lorentz quantum algebra
[DE94-602559] p 2997 N94-27023

A note on Riemannian 2-space
[DE94-602560] p 3073 N94-27024

Mapping between the Sinh-Gordon and Ising models
[DE94-601535] p 2998 N94-27162

First principles calculations for the cleaved and annealed Ge(111) surfaces
[DE93-617048] p 3066 N94-27347

The Einstein tensor characterizing some Riemann spaces
[DE94-603663] p 3074 N94-27626

The super Weierstrass (zeta)-function and operator product expansions in 2D-induced supergravity on the supertorus
[DE94-603664] p 3074 N94-27627

Transmittance fluctuations and non-linearity in random chains in the presence of applied electric fields
[DE94-603665] p 2787 N94-27628

All-coupling polaron ground state energy in D-dimension
[DE94-603666] p 3027 N94-27629

Nonlinear transverse propagation of photons in a ultrarelativistically hot and magnetized electron-positron plasma: Coupling of Langmuir and electromagnetic solitons
[DE94-603667] p 3046 N94-27630

Geometrical resonances in the nyquist noise spectrum for ballistic conductors
[DE94-603668] p 3027 N94-27631

Fixed point type theorems and projection-interaction approximation
[DE94-603669] p 3000 N94-27632

Some remarks on the symmetry of self-conjugate minimal surfaces in R3
[DE94-603670] p 3007 N94-27633

Correlated mean field Ansatz for the Kondo necklace
[DE94-603671] p 3067 N94-27634

Localization properties of one-dimensional electrified chains
[DE94-603672] p 3067 N94-27635

Cosmic no-hair in Brans-Dicke theory
[DE94-603673] p 3074 N94-27636

Joint essential maximal numerical range
[DE94-603674] p 3000 N94-27637

Second-order phase transition in (g(phi)4)2 theory
[DE94-603677] p 3067 N94-27638

Relativistic two-body system in 1+1-dimensional QED. 1: On the circle S1
[DE94-603716] p 3067 N94-27647

Gauge invariance and transport properties in superconductors above T(c)
[DE94-604013] p 3068 N94-27677

Decay of non-equilibrium polariton condensate in semiconductors
[DE94-604016] p 3068 N94-27678

Enhancement of the rate of radiative processes in the field of a magnetic monopole
[DE94-603717] p 3074 N94-27696

Hyperfine structure of positronium energy levels in a crystal
[DE94-603898] p 3068 N94-27729

Study of the critical points at infinity arising from the failure of the Palais-smale condition for n-body type problems
[DE94-603656] p 3000 N94-27818

Image potential of a tunnelling electron moving near two different metals
[DE94-603657] p 3069 N94-27819

Fragmentation of Ge(1-x) Sn(x) Se2 glasses
[DE94-603009] p 2758 N94-27837

The gl(n/m) and related q-identitiesematics and computer science ends in nuclear and related q-identities
[DE94-603653] p 3001 N94-27839

Correlations in inelastic collisions of relativistic nuclei with emulsion at (4.1 - 4.5) A GeV/c
[DE93-634526] p 3030 N94-27994

Fermi surface ridge at second and third Umklapp positron annihilations in Y Ba2Cu3O(7-delta)
[DE93-634760] p 3070 N94-27995

A simple satellite system to locate gamma ray bursters using scintillating fiber technology
[DE94-601287] p 3117 N94-27996

Cosmological constraints on very heavy stable neutrinos
[DE94-601669] p 3117 N94-28066

On the zeros of solutions of forced parabolic differential equations of neutral type
[DE93-613019] p 3001 N94-28228

INTERNATIONAL TELECOMMUNICATIONS SATELLITE ORGANIZATION, WASHINGTON, DC.

Ni-H2 cell characterization for INTELSAT programs
p 2861 N94-28109

INTERSCIENCE, INC., TROY, NY.

Heavy neutral beam probe for edge plasma analysis in tokamaks
[DE94-003391] p 3041 N94-25846

IOWA STATE UNIV. OF SCIENCE AND TECHNOLOGY, AMES.

Relativistic heavy ion physics [DE94-003161] p 3031 N94-26097

IOWA UNIV., IOWA CITY.

NCVS, volume 5 [AD-A274975] p 2902 N94-27165

ISHIKAWAJIMA-HARIMA HEAVY INDUSTRIES CO. LTD., TOKYO (JAPAN).

Report of three microgravity experiments by the drop shaft [JTN-94-80579] p 2761 N94-27341

J

JAPAN ATOMIC ENERGY RESEARCH INST., TOKYO.

Shine through measurements with hydrogen beam in JT-60 [DE94-701113] p 3047 N94-27699

Correspondence dictionary from free English term to INIS descriptors [DE94-701173] p 3100 N94-27700

Development of Calcomp compatible interface library 'piflib' on X Window System [DE94-701190] p 2973 N94-27702

Mode analysis of gyrotron oscillation using a k-spectrometer [DE94-701195] p 2813 N94-27703

Secondary electron emission from copper surface due to neodymium and gadolinium ion bombardment [DE94-701115] p 3027 N94-27718

Numerical experiment on finite element method for matching data [DE94-701208] p 3000 N94-27731

Inverted pendulum control apparatus using transputers [DE94-701224] p 2973 N94-27732

Creep rupture properties of a nickel-base heat-resistant alloy Hastelloy XR under varying temperature/stress condition [DE94-701175] p 2743 N94-27807

Pulse control method and its characteristics [DE94-701187] p 2989 N94-27809

Outgas and vacuum seal characteristics of irradiated polyimide O-ring [DE94-701200] p 2757 N94-27812

The effect of Ti conduit on the critical current in (Nb, Ti)3Sn cable-in-conduit conductors [DE94-701204] p 2788 N94-27817

Measurement of metastable population distribution in gadolinium atomic beam by laser resonance photoionization method [DE94-701194] p 3029 N94-27820

Experimental results of 40-kA Nb3Al conductor [DE94-701207] p 2788 N94-27821

Neutrons in biology [DE94-701085] p 2903 N94-27862

Ion-driven permeation of deuterium in metals [DE94-701104] p 2744 N94-27876

JAPAN MARINE SCIENCE AND TECHNOLOGY CENTER, TOKYO.

An oceanographical observation in the Western Pacific and international cooperations p 2872 N94-28272

JAPAN SPACE UTILIZATION PROMOTION CENTER, TOKYO.

Prometheus in space: Research Committee on Functional New Material [JTN-94-80580] p 2761 N94-28002

JAPAN WEATHER ASSOCIATION, KOJIMACHI.

Development of a method for predicting snowfall intensity and compacted snow on roads p 2853 N94-27990

JAPANESE AIR SELF-DEFENSE FORCE, TOKYO.

The Reports of Aeromedical Laboratory, volume 33, number 4 [JTN-94-80586] p 2933 N94-27942

Comparison of performance in simulator flight among subjects with different simulator experiences p 2933 N94-27943

Evaluation of near-infrared spectrophotometric method for individual tolerance to +Gz acceleration p 2933 N94-27944

Symptoms of hypoxia at simulated altitude of 25,000 feet p 2933 N94-27945

JASCO RESEARCH LTD., SIDNEY (BRITISH COLUMBIA).

Development of digital resampling and pulse compression computer software [DREP-92-32] p 2969 N94-27318

JAYCOR, VIENNA, VA.

Research in pulsed power plasma physics [AD-A274323] p 3045 N94-27074

JET PROPULSION LAB., CALIFORNIA INST. OF TECH., PASADENA.

System software and tools for high performance computing environments: A report on the findings of the Pasadena Workshop [DE94-003918] p 2956 N94-25602

Nuclear electric propulsion for future NASA space science missions [DE93-019086] p 2700 N94-25969

Computing in space: Issues and answers p 2948 N94-26714

High performance flight computer developed for deep space applications p 2949 N94-26718

Center for space microelectronics technology [NASA-CR-195282] p 2786 N94-27574

Lunar base habitat designs: Characterizing the environment, and selecting habitat designs for future trade-offs [NASA-CR-195687] p 2943 N94-27934

Advanced energy storage for space applications: A follow-up p 2860 N94-28103

Battery study for the Mars Environmental Survey (MESUR) Pathfinder p 2860 N94-28105

TOPEX/Poseidon battery performance during the first year of operation p 2862 N94-28119

Advanced End-to-end Simulation for On-board Processing (AESOP) p 2945 N94-28255

JOENSUU UNIV. (FINLAND).

SIMA: A model for forest succession based on the carbon and nitrogen cycles with application to silvicultural management of the forest ecosystem [SILVA-CARELICA-22] p 2848 N94-26258

Assessment of tropical forests using satellite data [SILVA-CARELICA-21] p 2850 N94-27182

Mapping closed tropical forest cover in West Africa using NOAA/AVHRR-LAC data p 2850 N94-27184

Woody biomass density in the Tendelti area of the central Sudan p 2850 N94-27185

JOHNS HOPKINS UNIV., LAUREL, MD.

Preliminary reentry safety assessment of the General Purpose Heat Source module for the Cassini mission: Aerospace Nuclear Safety Program [DE94-001646] p 2699 N94-25926

JOINT INST. FOR NUCLEAR RESEARCH, DUBNA (USSR).

On the first integrals of geodesics [DE93-612974] p 3007 N94-25603

An electromagnetic calorimeter with wavelength shifting fiber readout [DE93-616664] p 2809 N94-25735

A double arm time-of-flight spectrometer based on position-sensitive parallel-grid avalanche counters [DE93-616665] p 3012 N94-25750

Coherent state approach for the (Phi)(sup 6)-lattice model and phase transitions [DE93-613053] p 3050 N94-25825

Quark-antiquark bound states [DE93-613054] p 3013 N94-25826

A data processing system at the hybrid spectrometer [DE93-616801] p 3013 N94-25828

Weak interactions in a bilocal chiral theory [DE93-613097] p 3013 N94-25836

Hadron jets and nucleon clusters in the relativistic nuclear collisions [DE93-613434] p 3031 N94-25850

On the classification scheme for resonant states of muonic molecules [DE93-613645] p 3014 N94-25853

Electromagnetic properties of a toroidal solenoid [DE93-613032] p 2766 N94-25866

The amplitude of the elastic hadron-hadron scattering in the coulombic range of transfer momenta [DE93-613183] p 3014 N94-25869

Structure functions of sea quarks, Kogut-Susskind pole and dynamics of pp- and pp-bar-interactions at high energies [DE93-613184] p 3031 N94-25870

Focusing properties of a three-element quadrupole lens system and its stigmatic focusing behaviour [DE93-616534] p 2766 N94-25915

On radiation defects in strip detectors [DE93-616646] p 3015 N94-25916

Fast vertex search (in plane) [DE93-616655] p 2959 N94-25917

Use of parallel counters for triggering [DE93-616656] p 2979 N94-25918

Algorithms of the vertex coordinate reconstruction for straight tracks of short-lived particles [DE93-616661] p 3015 N94-25919

Dimensional crossover from non-renormalizability to renormalizability [DE93-613052] p 3006 N94-26193

On a spline-approximation method for solving ordinary differential equations [DE93-634290] p 2994 N94-26471

How to build analogues of the Bessel-Clifford expansions for the sum of the repulsive Coulomb potential and central potential decreasing more rapidly than the centrifugal one? [DE93-634308] p 3007 N94-26472

About stochastization of motion of charged particles in geomagnetic field and in the field of a wave packet [DE93-634309] p 2879 N94-26502

Gravitational field of a point mass in the Lobachevskij space [DE93-634333] p 3072 N94-26503

The gravity equations in the Lobachevskij space [DE93-634334] p 2879 N94-26504

Mesons and diquarks in a NJL-model at finite temperature and chemical potential [DE93-634375] p 3020 N94-26505

Chance to use W-decay lepton channels for width determination [DE93-634438] p 3020 N94-26507

About possible types of neutrino oscillations [DE93-634449] p 3020 N94-26508

On the wave and corpuscular properties of microparticles [DE93-634450] p 3020 N94-26509

Measurements of the p (mu)d-molecule formation rate at different hydrogen temperature [DE93-634636] p 3020 N94-26511

The influence of energy losses with time in NbTi superconductors in pulsed magnetic fields [DE93-634761] p 3058 N94-26512

Excited Landau levels, orbital angular momentum and axial anomaly [DE94-606407] p 3068 N94-27679

Stochastic space-time, confinement potential and particle propagator [DE94-606415] p 3074 N94-27680

Proton electromagnetic form factor near the proton-antiproton threshold and quasinuclear bound state [DE94-606458] p 3027 N94-27681

Neutron-neutron scattering: Possibility of in-beam experiment [DE94-606459] p 3027 N94-27682

A method for obtaining quantum doubles from the Yang-Baxter R-matrices [DE94-606300] p 3001 N94-27846

The three-dimensional hydrogen atom in crossed magnetic and electric fields [DE94-606301] p 3029 N94-27847

On the model of the relativistic particle with curvature and torsion [DE94-606330] p 3029 N94-27848

Solution of the Heisenberg equation for the four-fermion contact interaction by the method of dynamical mappings [DE94-606341] p 3075 N94-27858

Axial anomaly in e(+)e(-) yields gamma gamma and anyon superconductivity [DE94-606406] p 3070 N94-27859

Decay constants of heavy mesons in the relativistic potential model with velocity dependent corrections [DE94-606495] p 3030 N94-27860

Muon transfer rates in collisions of hydrogen isotope mesic atoms on bare nuclei: Multichannel adiabatic approach [DE94-606752] p 3030 N94-27861

K

KANAZAWA UNIV. (JAPAN).

Eye-head coordination and swinging of the visual scene when wearing visually up-down reversing mirror for 14 days p 2915 N94-27462

KANSAS STATE UNIV., MANHATTAN.

Automation of closed environments in space for human comfort and safety p 2943 N94-25684

KANSAS UNIV., LAWRENCE.

A revolutionary approach to composite construction and flight management systems for small, general aviation airplanes p 2671 N94-25714

KARLSRUHE UNIV. (GERMANY).

Analysis of cooling jets near the leading edge of turbine blades p 2676 N94-28037

KAUPPA-JA TEOLLISUUSMINISTERIO, HELSINKI (FINLAND).

NEMO 2: New energy systems and technologies [DE94-702060] p 2855 N94-26240

SIHTI 2: Energy and environmental technology [DE94-702061] p 2867 N94-26241

Programme for the promotion of wind power production [DE94-702065] p 2855 N94-26242

KAWASAKI HEAVY INDUSTRIES LTD., KOBE (JAPAN).
Report of three microgravity experiments by the drop shaft
[JTN-94-80579] p 2761 N94-27341
Telescience testbedding for physiological experiments under hypobaric hypoxic conditions
p 2913 N94-27449
KENT STATE UNIV., OH.
A multivariate anthropometric method for crew station design: Abridged
[AD-A274588] p 2941 N94-26984
KENTUCKY UNIV., LEXINGTON.
The value of electrical stimulation as an exercise training modality p 2936 N94-28372
KINJO GAKUIN UNIV., NAGOYA (JAPAN).
Interaction between endogenous opioid and Cholecystokinin (CCK) in modulating respiratory responses induced by thin-fiber muscular afferents
p 2906 N94-27502
KINKI UNIV., OSAKA (JAPAN).
Penetrating nature of very collimated high-energy shower-clusters of hadrons and gamma rays
p 3113 N94-25631
Energy concentration in high energy hadron-gamma families p 3113 N94-25632
KJT, INC., ROCHESTER, NY.
Fiber laser amplifiers and oscillators
[AD-A274231] p 2820 N94-28068
KOPIN CORP., TAUNTON, MA.
High-efficiency, thin-film solar cells
[DE94-000250] p 2860 N94-27625
KOREA RESEARCH INST. OF STANDARDS AND SCIENCE, TAEJON (REPUBLIC OF KOREA).
A new method for torsional critical speed calculation of practical industrial rotors
[IMR-T&M-TR-001] p 2828 N94-28041
KOREAN ATOMIC ENERGY RESEARCH INST., DAEDUK (REPUBLIC OF KOREA).
Study on neutron activation analysis
[DE93-632191] p 3017 N94-26116
Broad band tunable dye laser development
[DE93-632978] p 2816 N94-26157
Development of laser spectroscopic technology in nuclear industry
[DE93-633327] p 2714 N94-26158
Development of fusion technology
[DE93-633444] p 3042 N94-26159
Development of an industrial CO2 laser for mask marking
[DE93-632901] p 2816 N94-26184
Development of surgical CW Nd:YAG laser with optical fiber delivery system
[DE93-632902] p 2817 N94-26185
Development of non-destructive testing technology for the crack of steam generator tubes
[DE93-632953] p 2835 N94-26399
Development of detection technique for fatigue crack due to thermal stratification phenomena in RCS piping
[DE93-632968] p 2838 N94-26400
Study on laser atomic spectroscopy
[DE93-633328] p 2817 N94-26402
Development of real-time pulse shaping technology in solid-state lasers
[DE93-633438] p 2817 N94-26403
A study on the development of high T(sub c) superconducting materials
[DE93-633529] p 3057 N94-26404
Overall analysis of meteorological information in the Daeduk nuclear complex
[DE93-632594] p 2894 N94-26469
Studies on the application of radiation for genetic transformation in higher plants
[DE93-632656] p 2901 N94-26470
Development of high average power industrial Nd:YAG laser with peak power of 10 kW class
[DE93-633201] p 2818 N94-26520
A study on the development of high-T(c) superconducting wire
[DE93-632438] p 2783 N94-26546
Molecular biological studies on the human radioresistance and drug resistance
[DE93-632682] p 2910 N94-26549
KRUG LIFE SCIENCES, INC., SAN ANTONIO, TX.
Standardization of aircraft control and performance symbology on the USAF head-up display
[AD-A274283] p 2673 N94-26989
KURCHATOV (I. V.) INST. OF ATOMIC ENERGY, MOSCOW (USSR).
Prospects for utilization of superconductors in the power industry p 2854 N94-26057
KYOTO UNIV., KUMATORI (JAPAN).
Radiation-Induced Structural Changes, 2
[DE93-520314] p 3054 N94-26109
KYOTO UNIV., SAKYOKU (JAPAN).
Characteristics of 30-MHz interference noises observed by riometers p 2884 N94-27965
Observation of the upper atmosphere physics at Asuka Station by the 30th Japanese Antarctic Research Expedition in 1989 p 2885 N94-27972

L

LABORATOIRE D'AEROTHERMIQUE DU CNRS, MEUDON (FRANCE).
Control jets in interaction with hypersonic rarefied flow
p 2698 N94-28020
LABORATORIO DE COMPUTACAO CIENTIFICA, RIO DE JANEIRO (BRAZIL).
A thermodynamically consistent constitutive theory for a rigid solid-stokesian fluid mixture
[DE93-633202] p 2792 N94-26401
LASIRIS, INC., SAINT-LAURENT (QUEBEC).
Development of a holographic illumination system for a time-integrating correlator
[DSIS-94-00111] p 2814 N94-27763
LAWRENCE ASSOCIATES, INC., DAYTON, OH.
An x ray absorption fine structure study of ordering in polythiophene thin films
[AD-A274235] p 2753 N94-26822
LAWRENCE LIVERMORE NATIONAL LAB., CA.
The effect of elevation data representation on nocturnal drainage wind simulations
[DE94-003624] p 2892 N94-25936
Two dimensional self-consistent fluid simulation of RF inductive sources
[DE94-003635] p 2767 N94-25937
Numerical simulations of interfacial debonding in ductile-phase reinforced intermetallic matrix composites
[DE94-003639] p 2706 N94-25938
Trapped electrons in solid hydrogen
[DE93-018628] p 3052 N94-25947
An investigation of cavitation in a mechanically alloyed 15 volume percent SiCp/IN9021 aluminum composite
[DE94-003371] p 2748 N94-25959
Characterization of physically vapor deposited AF2400 thin films
[DE94-004019] p 2749 N94-25985
Imaging with x ray lasers
[DE94-002844] p 2816 N94-26020
Emerging technologies
[DE94-003022] p 3102 N94-26023
Interpreting the implied meridional oceanic energy transport in AMIP
[DE94-001538] p 2898 N94-26072
Design study of fiber-composite penetrator cases
[DE94-003203] p 2707 N94-26099
Generalized perturbation method expansions of the total energy of an alloy
[DE94-003865] p 3055 N94-26238
Electrical analysis of wideband and distributed windows using time-dependent field codes
[DE94-002987] p 2768 N94-26310
Microwave and pulsed power
[DE94-003019] p 2782 N94-26312
Red's natural editor: A program designed to edit FORTRAN programs
[DE94-003271] p 2962 N94-26318
Iron: What is melt?
[DE94-003373] p 2735 N94-26322
The origins of ordering in CuPt
[DE94-003864] p 2736 N94-26351
Mix induced by single shock passage through a material interface
[DE93-019505] p 2792 N94-26427
On the application of Allan variance method for Ring Laser Gyro performance characterization
[DE94-003880] p 2810 N94-26525
Modelling atmospheric turbulence effects on ground-based telescope systems
[DE94-004211] p 3102 N94-26528
Nanoscale plasticity in silica glass
[DE94-004212] p 2751 N94-26554
Numerical procedure for planetary wave solution
[DE94-004280] p 2879 N94-26576
A concurrent, multigroup, discrete ordinates model of neutron transport
[DE94-004334] p 3020 N94-26577
The High Performance Storage System
[DE94-004351] p 2948 N94-26578
Calculations of population transfer during intense laser pulses
[DE94-001060] p 2818 N94-26698
Phase conjugation and pulse compression of high energy lasers: From nanoseconds to microseconds
[DE94-001061] p 2818 N94-26699
Computational mechanics
[DE94-003015] p 2965 N94-26775
Diagnostics and microelectronics
[DE94-003016] p 2784 N94-26777
Fabrication technology
[DE94-003017] p 2763 N94-26778
Using the TSAR electromagnetic modeling system
[DE94-002617] p 2771 N94-26803
Calculations of material removal, removal rate, and Preston coefficient in continuous lapping/polishing machines
[DE94-002619] p 2763 N94-26804
An automatic contact algorithm in DYNA3D for impact problems
[DE94-002856] p 2965 N94-26862
The TPX Cryostat Conceptual Design
[DE94-002857] p 3045 N94-26863
Processing and mechanical properties of laminated metal composites of Al 6090-25 volume percent SiC(sub p) and Al 5182
[DE94-001070] p 2708 N94-26930
Equivalent performance in different helical resonator plasma polymerization coater platforms
[DE94-001517] p 2753 N94-26933
Phase conjugated lasers applied to commercial x ray lithography
[DE94-001529] p 2819 N94-27018
Tokamak Physics Experiment poloidal field design
[DE94-001542] p 3045 N94-27019
Implementation and performance of a domain decomposition algorithm in Sisal
[DE94-002012] p 2981 N94-27092
Initial ultraviolet-B intensity data at Lawrence Livermore National Laboratory
[DE94-004279] p 2869 N94-27267
Energy and technology review, July 1993
[DE94-004219] p 3118 N94-27566
Simulation of the Indian and East-Asian summer monsoon in the ECMWF model: Sensitivity to horizontal resolution
[DE94-004276] p 2897 N94-27571
Uncertainties in the characterization of the thermal environment of a solid rocket propellant fire
[DE94-002023] p 2760 N94-27719
Observation of stimulated emission from an MBE grown GaN film on sapphire
[DE94-003638] p 3068 N94-27724
The addition of molecular oxygen to hydroperoxy-propyl radicals
[DE94-003662] p 2760 N94-27725
LEHIGH UNIV., BETHLEHEM, PA.
Controlled heterogeneous nucleation of melt-textured YBa2Cu3O(6+x) by addition of Al2O3 particles
[AD-A274605] p 3062 N94-26892
LEIDEN UNIV. (NETHERLANDS).
On the error committed by stopping the Newton iteration in implicit Runge-Kutta methods
[TW-93-02] p 2992 N94-26229
LITTLE (ARTHUR D.), INC., CAMBRIDGE, MA.
Natural gas applications for hybrid vehicles.
[PB94-117108] p 2759 N94-26753
LOCKHEED ENGINEERING AND SCIENCES CO., HAMPTON, VA.
User's guide for the thermal analyst's help desk expert system
[NASA-CR-194885] p 2695 N94-26103
Propagation of experimental uncertainties from the tunnel to the body coordinate system in 3-D LDV flow field studies
[NASA-CR-191607] p 2680 N94-26603
A technique for integrating engine cycle and aircraft configuration optimization
[NASA-CR-191602] p 2668 N94-26606
Fatigue resistance of unnotched and post impact(+/-30 deg/0 deg) 3-D braided composites
[NASA-CR-191590] p 2711 N94-27433
LOCKHEED ENGINEERING AND SCIENCES CO., HOUSTON, TX.
STS-55 Space Shuttle mission report
[NASA-CR-195741] p 2692 N94-28199
STS-57 Space Shuttle mission report
[NASA-CR-195739] p 2693 N94-28220
STS-56 Space Shuttle mission report
[NASA-CR-195740] p 2693 N94-28221
LOCKHEED ENGINEERING AND SCIENCES CO., WASHINGTON, DC.
Space radiation health research, 1991-1992
[NASA-TM-109721] p 2932 N94-27556
LOCKHEED MISSILES AND SPACE CO., PALO ALTO, CA.
Photospheric origins of chromospheric and coronal activity
[NASA-CR-195215] p 3110 N94-26590
Compton Gamma Ray Observatory/BATSE observations of energetic electrons scattered by cyclotron resonance with waves from powerful VLF transmitters
[NASA-CR-195240] p 3115 N94-26790
High resolution studies of sunspots and flux tubes
[NASA-CR-195216] p 3111 N94-27321

LOCKHEED SANDERS, INC., NASHUA, NH.
Rapid prototyping of application specific signal processors (RASSP)
[AD-A274324] p 2772 N94-26884
LOS ALAMOS NATIONAL LAB., NM.
Back-reaction beyond the mean field approximation
[DE94-003936] p 3012 N94-25612
A review of carbide fuel corrosion for nuclear thermal propulsion applications
[DE94-003938] p 2699 N94-25613
Data on parity violation in the compound nucleus and its interpretation
[DE94-003965] p 3013 N94-25820
Temperature dependence of the radiation induced change of depletion voltage in silicon PIN detectors
[DE94-002705] p 3052 N94-25972
New equation of state for stainless steel 347
[DE94-004189] p 2732 N94-25974
Digital control and data acquisition for high-value GTA welding
[DE94-000885] p 2821 N94-25980
Adaptive optimization and control using neural networks
[DE94-003941] p 2985 N94-25983
Deviatoric stresses and plastic strain rates in strong shock waves for six metals
[DE94-002964] p 2733 N94-26022
Debye-Waller factors of the light actinide metals
[DE94-000685] p 2733 N94-26069
Towards a theory of growing surfaces: Mapping two-dimensional Laplacian growth onto Hamiltonian dynamics and statistics
[DE94-002636] p 2991 N94-26079
Hook spectroscopy as an atomic number density diagnostic applied to laser-ablated copper plasmas
[DE94-002645] p 3042 N94-26081
Run-time recognition of task parallelism within the P++ parallel array class library
[DE94-002707] p 2980 N94-26120
The fracture behavior of a CVD crystalline Si3N4/amorphous Si3N4 composite
[DE94-002646] p 2750 N94-26124
Elastic backscattering lidar for a MSTI satellite
[DE94-002701] p 2816 N94-26126
Scaling of sustained ZT-40 M reversed field pinches
[DE94-003318] p 3043 N94-26321
A new materials data compilation can help in actinide phase-diagram research
[DE94-000797] p 3058 N94-26514
Relativistic collision rate calculations for electron-air interactions
[DE94-004204] p 3020 N94-26527
Distributed Nd:YAG laser welding and process control in inert glove boxes
[DE94-002629] p 2818 N94-26605
A tri-junction diffusion couple analysis of the Nb-Cr-Ti system at 950 C
[DE94-002637] p 2737 N94-26607
An antiproton-proton partial-wave analysis
[DE94-002690] p 3021 N94-26620
Deformation twinning: Influence of strain rate
[DE94-002693] p 2738 N94-26621
Neutron and x ray scattering studies of the interactions between Ca(2+)-binding proteins and their regulatory targets: Comparisons of troponin C and calmodulin
[DE94-002706] p 2901 N94-26623
Ion beam mixing of marker layers into amorphous aluminum oxide
[DE94-000901] p 2752 N94-26676
Modeling Group 4 elements with new transferable tight-binding models
[DE94-000770] p 3059 N94-26695
Coronal heating via nanoflares
[DE94-000773] p 3110 N94-26696
Pre-orbital criticality safety for the NEPSTP mission
[DE94-002600] p 3005 N94-26802
Quantum statistical inference for density estimation
[DE94-002625] p 3073 N94-26805
Electrical conductivity of perovskite-magnesiowuestite as a function of pressure and temperature
[DE94-002714] p 2880 N94-26806
Virtual data
[DE94-002718] p 2986 N94-26807
A space fiber-optic x ray burst detector
[DE94-002722] p 2696 N94-26808
Is probability of frequency too narrow?
[DE94-000687] p 3004 N94-27612
An unavailability model for errors made during surveillance testing
[DE94-000816] p 2835 N94-27613
Advances in gamma ray field instrumentation at Los Alamos
[DE93-040264] p 2813 N94-27624
Mach reflection of spherical detonation waves
[DE93-016604] p 2797 N94-27705
Practical problems in aggregating expert opinions
[DE94-002623] p 3094 N94-27707
Modelling the mass migration phenomena in partially frozen heat pipes
[DE94-002716] p 2797 N94-27709
BATSE burst location accuracy and constraints on the fraction of repeating GRB sources
[DE94-004981] p 3116 N94-27714
Atomic processes in Inertial Electrostatic Confinement (IEC) devices
[DE94-005015] p 3047 N94-27715
SPECTRUM analysis of multispectral imagery in conjunction with wavelet/KLT data compression
[DE94-003961] p 2851 N94-27727
Zeeman laser interferometry for detection and chemical analysis
[DE94-003963] p 2719 N94-27728
The status of the solar neutrino problem
[DE94-003934] p 3111 N94-27742
Temporal stochasticity leads to nondeterministic chaos in a model for blood cell production
[DE94-003943] p 2933 N94-27744
Stabilization of polyaniline solutions
[DE94-003958] p 2704 N94-27745
Corrosion resistant coatings from conducting polymers
[DE94-003959] p 2757 N94-27747
A survey of open problems in symplectic integration
[DE94-003966] p 3007 N94-27777
DMSP satellites as gamma ray burst detectors
[DE94-004977] p 3116 N94-27793
Estimators for the Cauchy distribution
[DE94-004990] p 3005 N94-27816
Performance of a 14-MeV neutron generator as an in situ calibration source for TFTR
[DE94-004993] p 3048 N94-27825
Simulations of terrestrial in-situ cosmogenic-nuclide production
[DE94-004999] p 3117 N94-27826
Gamma ray bursts from the accretion of solid bodies onto high-velocity Galactic neutron stars
[DE94-005006] p 3117 N94-27827
Damage growth in MgAl2O4 crystals by Xe ion irradiations
[DE94-005009] p 3069 N94-27828
Computer simulation of aqueous Na-Cl electrolytes
[DE94-002622] p 3030 N94-28001
MUSIC for localization of thunderstorm cells
[DE94-004985] p 2897 N94-28146
Consequences of impacts of small asteroids and comets with Earth p 2889 N94-28301
LOUGHBOROUGH UNIV. OF TECHNOLOGY (ENGLAND).
Experimental data for CFD validation of impinging jets in crossflow with application to ASTOVL flow problems
p 2801 N94-28010
LOUISIANA STATE UNIV., BATON ROUGE.
A search for the production of direct leptons in nucleon-nucleus and nucleus-nucleus collisions
[DE94-004640] p 3018 N94-26244
LOWELL OBSERVATORY, FLAGSTAFF, AZ.
The crash of P/Shoemaker-Levy 9 into Jupiter and its implications for comet bombardment on Earth
p 2891 N94-28313
LOWELL UNIV., MA.
Performance statistics bulletin: High altitude meteor scatter propagation, August, September, October 1989
[AD-A274455] p 2773 N94-27085

M

MAINE UNIV., ORONO.
ADC test support program
[AD-A274819] p 2783 N94-26491
MALAYAN METEOROLOGICAL SERVICE, PETALING JAYA.
Utilization of remote sensing data for global climate change research in Malaysia p 2875 N94-28290
MANCHESTER COLL. OF SCIENCE AND TECHNOLOGY (ENGLAND).
Calculation of single and multiple jets in cross-flow with and without impingement using Reynolds-stress-transport closure p 2803 N94-28024
MARTIN MARIETTA ASTRO SPACE, PRINCETON, NJ.
Some practical aspects of lossless and nearly-lossless compression of AVHRR imagery p 2947 N94-28264
MARTIN MARIETTA CORP., DENVER, CO.
Orbital management and design considerations for NiCd satellite power systems p 2862 N94-28118
MARY WASHINGTON COLL., FREDRICKSBURG, VA.
New monomers for high performance polymers
p 2758 N94-27904
MARYLAND UNIV., BALTIMORE.
Research on primal-dual interior point algorithms for mathematical programming
[DE94-003982] p 2959 N94-25821
MARYLAND UNIV., COLLEGE PARK.
MINOTAUR (Maryland's innovative orbital technologically advanced University rocket)
p 2703 N94-25685
The 1991-1992 walking robot design
p 2833 N94-25686
Maryland controlled fusion research program
[DE94-003533] p 3044 N94-26523
CMSC-130 introductory computer science, lecture notes
[AD-A274369] p 2967 N94-27060
Experimental and theoretical investigation of RF absorption and reflection from preformed plasmas
[AD-A274189] p 3046 N94-27098
A parametric sensitivity study for single-stage-to-orbit hypersonic vehicles using trajectory optimization
[NASA-CR-195703] p 2697 N94-27789
MASSACHUSETTS INST. OF TECH., CAMBRIDGE.
Study on ferromagnetic field magnet using strong and highly conductive material p 2725 N94-25559
Project Columbiad: Reestablishment of human presence on the Moon p 2689 N94-25687
Controlled synthesis of polyenes by catalytic methods
[DE94-004168] p 2749 N94-25973
Top down influences on bottom-up processing
[AD-A274220] p 2939 N94-27072
Crustal deformation measurements in the vicinity of Vandenberg Air Force Base
[AD-A274166] p 2881 N94-27143
An investigation of air transportation technology at the Massachusetts Institute of Technology, 1992-1993
p 2641 N94-27285
A graphical workstation based part-task flight simulator for preliminary rapid evaluation of advanced displays
p 2641 N94-27286
A data fusion algorithm for multi-sensor microburst hazard assessment p 2641 N94-27287
Expressiveness results for process algebras
[CWI-CS-R9301] p 3000 N94-27577
MASSACHUSETTS INST. OF TECH., LEXINGTON.
Solid state research
[AD-A274063] p 3049 N94-25645
Machine intelligent gust front algorithm
[AD-A273695] p 2680 N94-26196
Encoding approaches for data link transmission of weather graphics
[AD-A274497] p 2772 N94-26963
MASSACHUSETTS UNIV., AMHERST.
Retrieval using plausible inference
[AD-A274252] p 3099 N94-27013
Ultrastructure processing of macromolecular materials
[AD-A274460] p 2754 N94-27086
Eccentric exercise testing and training
p 2934 N94-28363
Electrical stimulation in exercise training
p 2935 N94-28371
MASSACHUSETTS UNIV., LOWELL.
Coherent HF radar system for the study of natural and heater induced ionospheric irregularities
[AD-A273804] p 2876 N94-25752
Ionospheric modification by high power, obliquely propagated HF radio wave transmissions. Part 1: Experimental
[AD-A273746] p 2878 N94-26224
Polyimide/inorganic composite-interpenetrating polymer network for stable second-order nonlinear optics
[AD-A274646] p 2709 N94-27107
An artificial reality environment for remote factory control and monitoring p 2687 N94-27369
VHF-UHF noise surveys at Gulkana, Elmensdorf AFB, Galena AFB, Kotzebue and Cape Lisburne, Alaska and NRL, Pomonkey, Maryland
[PL-TR-93-2136] p 2777 N94-28211
MATERIALS RESEARCH LABS., ASCOT VALE (AUSTRALIA).
Breakwire technique for hypervelocity measurement
[AD-A274779] p 2809 N94-26358
Evaluation of crack arrest fracture toughness of parent plate, weld metal and heat affected zone of BIS 812 EMA ship plate steel
[AD-A274871] p 2839 N94-26859
Development and evaluation of a near infrared reflecting and low visibility paint scheme for RAAF P-3C Orion aircraft
[AD-A274881] p 2669 N94-26864
Numerical simulation of the reignition of detonation by reflected shocks
[AD-A274755] p 2795 N94-27252
MATRA MARCONI SPACE (ENGLAND).
MATRA Marconi Space: The Silex on-board processor and on-board software p 2950 N94-26726
MATRA MARCONI SPACE, TOULOUSE (FRANCE).
Design principles of onboard management of a Sun synchronous satellite p 2950 N94-26722

Early real-time performance measurements on the Columbus processor system p 2952 N94-26736
Verification and validation of the on-board software real time requirements p 2953 N94-26739

MCDONNELL-DOUGLAS AEROSPACE, LONG BEACH, CA.
Variability of measured sonic boom signatures p 2651 N94-28197

MCDONNELL-DOUGLAS AEROSPACE INFORMATION SERVICES CO., SAINT LOUIS, MO.
Aircraft maneuvers for the evaluation of flying qualities and agility. Volume 3: Simulation data [AD-A273814] p 2667 N94-25961
Design and flight test of the Propulsion Controlled Aircraft (PCA) flight control system on the NASA F-15 test aircraft [NASA-CR-186028] p 2674 N94-27432
Pneumatic management of blunted-forebody flow asymmetry for high-angle-of-attack directional control p 2679 N94-28028

MCDONNELL-DOUGLAS ASTRONAUTICS CO., SAINT LOUIS, MO.
Aircraft maneuvers for the evaluation of flying qualities and agility. Volume 1: Maneuver development process and initial maneuver set [AD-A273913] p 2666 N94-25590

MCDONNELL-DOUGLAS CORP., SAINT CHARLES, MO.
Discriminating performance parameters for 50 amp-hour and 60 amp-hour nickel-cadmium plates and battery cells p 2863 N94-28123

MCDONNELL-DOUGLAS SPACE SYSTEMS CO., COCOA BEACH, FL.
Lunar Transportation Facilities and Operations Study, option 1 [NASA-CR-195700] p 3109 N94-27982
Lunar Transportation Facilities and Operations Study, option 2 [NASA-CR-195701] p 3109 N94-27983

MCGILL UNIV., MONTREAL (QUEBEC).
Finding the missing pieces of the standard model [ISBN-0-315-57174-8] p 3024 N94-27259
A study of the global properties of hadronic matter at large densities [ISBN-0-315-57234-5] p 3025 N94-27260
Aspects of perturbative corrections in quantum chromodynamics [ISBN-0-315-63607-6] p 3074 N94-27398
Omega omega and rho+ rho- production in two photon interactions at ARGUS [ISBN-0-315-63748-X] p 3026 N94-27399
Pi plus pi minus gamma and K+ K- production in two photon collisions at ARGUS [ISBN-0-315-63598-3] p 3027 N94-27684

MCLAUGHLIN (PETER), GLASTONBURY, CT.
Engine simulation technology p 2829 N94-28051
Transient engine simulation p 2829 N94-28052
Nonlinear solvers p 2829 N94-28053
Engine simulation systems p 2829 N94-28054

MCMASTER UNIV., HAMILTON (ONTARIO).
Finite element analysis of damped vibrations of laminated composite plates [ISBN-0-315-84928-2] p 2843 N94-27585
The deformation of copper-tungsten composites [ISBN-0-315-84939-8] p 2712 N94-27688
Low strain behaviour of a particulate reinforced aluminum alloy [ISBN-0-315-84906-1] p 2744 N94-27961
The optical properties of high-T(c) superconductors grown by pulsed laser deposition [ISBN-0-315-84917-7] p 3039 N94-27962
Anisotropy in the electrical, magnetic and optical properties of Pb2Sr2RCu3O8 [ISBN-0-315-84930-4] p 3070 N94-27974
Topics in the design, analysis and implementation of feedback control systems [ISBN-0-315-84934-7] p 2989 N94-27975

MEDICAL COLL. OF WISCONSIN, MILWAUKEE.
Aerobic fitness and orthostatic tolerance: Evidence against an association p 2934 N94-28365

MEDICAL RESEARCH COUNCIL, CAMBRIDGE (ENGLAND).
The central executive component of working memory [AD-A274295] p 2938 N94-26683

MEDOX RESEARCH, INC., DEXTER, MI.
Compact, solid-state femtosecond source [AD-A273932] p 2817 N94-26271

MELBOURNE UNIV., PARKVILLE (AUSTRALIA).
A possible way of connecting the Grassmann variables and the number of generation [DE94-601624] p 2990 N94-25838
Experimental study of the near threshold pi(sup +)p yields (pi(sup +))(pi(sup +))(n) cross section and chiral symmetry [DE94-601671] p 3014 N94-25840
CP violating form factors for three gauge boson vertex in the two Higgs doublet and left-right symmetric models [DE94-601704] p 3014 N94-25841
NNN-Ising model simulation of nanodomain textures in relaxor-type lead scandium tantalate [DE94-601884] p 2748 N94-25844
Fermionic field theory and gauge interactions on random lattices [DE94-601565] p 3051 N94-25885
The Dirac equation in Kerr spacetime, spheroidal coordinates and the M.I.T. bag model of hadrons [DE94-601566] p 3006 N94-25886
CP violation in Higgs decays [DE94-601607] p 3014 N94-25888
CP test in the W pair production by way of photon fusion at NLC [DE94-601608] p 3014 N94-25889
Separable expansions of the NN t-matrix by way of exact half off the energy shell methods [DE94-601615] p 3015 N94-25890
Unravelling the structure of matter on high-performance computers [DE94-601620] p 3015 N94-25891
Neutron reflection interferometry [DE94-601876] p 2714 N94-26170
Crystal potential retrieval in HRTEM [DE94-601883] p 3055 N94-26171
Electron energy loss spectroscopy in a crystalline environment using inner shell ionization [DE94-601820] p 3018 N94-26334
Polar and chemical domain structures of lead scandium tantalate (PST) [DE94-600760] p 3056 N94-26363
Regrowth zones in laser annealed radiation damaged diamond [DE94-600821] p 3056 N94-26364
Delocalization in electron impact ionization in a crystalline environment [DE94-601819] p 3062 N94-26927
Asymptotics for Kummer functions, Bose plasmas, and related special functions [DE94-601853] p 3007 N94-26928
Disintegration of (C60) by Xe ion irradiation [DE94-601913] p 3023 N94-26929
He(+) and H(+) microbeam damage, swelling and annealing in diamonds [DE94-601912] p 3063 N94-26987
Topological structure of a jet in a cross flow p 2801 N94-28014

METEOROLOGICAL RESEARCH INST., TSUKUBA (JAPAN).
Research activities on the meteorology over the Asia-Pacific region p 2853 N94-28271

METHLIE (GEORGE), FALLS CHURCH, VA.
Some observations on battery charge control p 2863 N94-28125

MIAMI UNIV., CORAL GABLES, FL.
Comparative analysis of different configurations of PLC-based safety systems from reliability point of view p 2836 N94-27925

MIAMI UNIV., FL.
Remote Earth Sciences data collection using ACTS [NASA-CR-195227] p 2848 N94-26236

MICHIGAN UNIV., ANN ARBOR.
Project APEX: Advanced manned exploration of the Martian moon Phobos p 3079 N94-25688
The role of grain boundary chemistry and structure in the environmentally-assisted intergranular cracking of nickel-base alloys [DE94-003159] p 2732 N94-25954
Dynamics explorer interdisciplinary scientist investigations [NASA-CR-195226] p 2878 N94-26204
High resolution measurements of mixing and reaction processes in turbulent flows [AD-A274970] p 2793 N94-26534
High definition Raman microscopic imaging [DE94-003158] p 2716 N94-26781
Studies for the loss of atomic and molecular species from Io [NASA-CR-195702] p 3108 N94-27941
The kinetics and dynamics of the coma of Halley's comet [NASA-CR-194828] p 3105 N94-28184

MIDDLE EAST TECHNICAL UNIV., ANKARA (TURKEY).
Navier-Stokes simulation of two and three dimensional jets in crossflow, effects of grid, and boundary conditions p 2804 N94-28026

MIDWEST RESEARCH INST., GOLDEN, CO.
The state of the art of thin-film photovoltaics [DE94-000224] p 2855 N94-26115
The identification of inflow fluid dynamics parameters that can be used to scale fatigue loading spectra of wind turbine structural components [DE94-000231] p 2791 N94-26117
Overview of the Photovoltaic Manufacturing Technology (PVMaT) project [DE93-018234] p 2856 N94-26426
Solar resource-utility load matching assessment: NREL photovoltaic project summary [DE94-000232] p 2856 N94-26480
Recombination and metastability in amorphous silicon and silicon germanium alloys [DE94-000237] p 2736 N94-26481
An overview of DOE's wind turbine development programs [DE93-018224] p 2856 N94-26513
Research on high-efficiency, large-area, CuInSe2 based thin-film modules [DE94-000259] p 3067 N94-27609
Continuous roll-to-roll a-Si photovoltaic manufacturing technology [DE94-000260] p 2859 N94-27610
High-efficiency, thin-film solar cells [DE94-000250] p 2860 N94-27625

MINERALS, METALS AND MATERIALS SOCIETY, WARRENDALE, PA.
Titanium 1992: Volume 3: Science and technology [AD-A274800] p 2735 N94-26337
Titanium 1992: Science and technology, volume 2 rence (7th) in san diego, california on june 29-july 2, 1992. Volume 2 [AD-A274799] p 2736 N94-26362
Titanium 1992: Science and Technology, volume 1 [AD-A274798-VOL-1] p 2739 N94-26799

MINISTERIE VAN ECONOMISCHE ZAKEN, S'GRAVENHAGE (NETHERLANDS).
High impact strength poly(lactide) tough biodegradable materials [ETN-94-95389] p 2747 N94-25748

MINISTRY OF AGRICULTURE, FORESTRY, AND FISHERIES, IBARAKI (JAPAN).
Technical Report of National Research Institute of Fisheries Engineering: Fishing Boat and Instrument, No. 12 [JTN-94-80595] p 2764 N94-27976
Recent trend of domestic and international regulations on intact stability of ships for safety p 2764 N94-27977
E. H. P. estimation of high speed fishing boats by some existing methods p 2764 N94-27978

MINISTRY OF ENERGY AND INFRASTRUCTURE, JERUSALEM (ISRAEL).
The First Energy Conference: Israel and the Former USSR [ISBN-965-229-098-X] p 2853 N94-26050

MINISTRY OF ENVIRONMENT, SEOUL (REPUBLIC OF KOREA).
Country report on global change research for the Republic of Korea p 2873 N94-28278

MINISTRY OF ENVIRONMENT AND FOREST, DHAKA (BANGLADESH).
Global concern on research cooperation for environment p 2872 N94-28275

MINISTRY OF INTERNATIONAL TRADE AND INDUSTRY, TSUKUBA (JAPAN).
Report of National Institute for Resources and Environment. No. 5: Study on direct liquefaction of woody biomass [JTN-94-80551] p 2859 N94-27204

MINISTRY OF POSTS AND TELECOMMUNICATIONS, TOKYO (JAPAN).
Development of imaging riometers p 2884 N94-27967

MINISTRY OF SCIENCE, TECHNOLOGY AND ENVIRONMENT, BANGKOK (THAILAND).
The Environmental Research and Training Centre p 2873 N94-28280

MINNESOTA MINING AND MFG. CO., SAINT PAUL.
Dual cure low-VOC coating process [DE94-000365] p 2756 N94-27611

MINNESOTA UNIV., MINNEAPOLIS.
Mars transportation system p 2833 N94-25689
Center for computation and visualization of geometric structures [DE94-001882] p 2991 N94-25928
Operator theoretic methods in the control of distributed and nonlinear systems [AD-A274160] p 2988 N94-27139
Cardiac output and cardiac contractility by impedance cardiography during exercise of runners p 2935 N94-28367

MISSISSIPPI STATE UNIV., MISSISSIPPI STATE.
Naval Interactive Data Analysis System (NIDAS), software user's manual [NASA-CR-195179] p 2956 N94-25606
The Communication Link and Error ANalysis (CLEAN) simulator [NASA-CR-195243] p 2968 N94-27168
Wing design for a civil tiltrotor transport aircraft: A preliminary study p 2671 N94-27917

MISSOURI UNIV., COLUMBIA.

An overview on development of neural network technology p 2990 N94-27913

MISSOURI UNIV., ROLLA.

Processing of LaCrO3 for solid oxide fuel cell applications [DE94-002981] p 2857 N94-26747

MITRE CORP., BEDFORD, MA.

Thunderstorm Hypothesis Reasoner [NASA-CR-195714] p 2897 N94-27884

MOORE (M. J.) (ENGLAND).

Introduction to combined cycles p 2789 N94-28078

MORAVIAN COLL., BETHLEHEM, PA.

Locating tie-points on a grid p 2978 N94-27906

MORELOS UNIV., CUERNAVACA (MEXICO).

Application of the Positron Annihilation Technique to the study of vapor absorption process in polyethylene (LDPE) and in imide polymer (6FDA-TMPD PI) [DE94-602737] p 2720 N94-27998

MOSCOW STATE UNIV. (RUSSIA).

Principles of gauge theory of real hadrons [DE93-613096] p 3013 N94-25835

Principles of gauge theory of real hadrons [DE93-616857] p 3015 N94-25920

MOTOR INDUSTRY RESEARCH ASSOCIATION, NUNEATON (ENGLAND).

Optimising BMW four-cylinder two-valve engines [PB94-125101] p 2824 N94-27254

MTS INST., INC., TOKYO (JAPAN).

Conception of snow information network system in Yamagata Prefecture p 2853 N94-27991

N

NAGOYA CITY UNIV. (JAPAN).

Effects of imaginary target on induced eye movements by linear acceleration p 2914 N94-27456

NAGOYA UNIV. (JAPAN).

Annals of the Research Inst. of Environmental Medicine, Nagoya Univ., volume 44 [REPT-44-VOL-44] p 2911 N94-27442

Changes in fluid and electrolyte metabolism during water immersion at high or thermoneutral temperature p 2912 N94-27445

Study on posture control and adaption mechanism under weightlessness: Results of second rehearsal for space experiment using carp p 2912 N94-27446

Study on posture control and adaptation mechanism under weightlessness: Summary report of ground operations performed for carp experiment (FMPT/L-2) in Space Shuttle mission p 2912 N94-27447

Telescience testbedding for physiological experiments under hypobaric hypoxic conditions: Development and evaluation in CNV measuring p 2913 N94-27451

The electrogastrogram during parabolic flight p 2913 N94-27452

Vertical gaze direction during parabolic flight p 2913 N94-27453

Frequency analysis of body sway induced by optokinetic stimulation p 2914 N94-27455

The mechanism of caloric nystagmus under microgravity. 1: Changes of endolymphatic pressure in the semicircular canal of pigeon by caloric stimulation p 2914 N94-27457

Cardiovascular function during thermoneutral head-out water immersion in the elderly p 2915 N94-27458

Effects of 40 C hot water immersion for an hour on thermoregulatory functions in humans: Comparison with 34 C thermoneutral immersion p 2915 N94-27459

Development of stimulus-seeking scale for expecting individual differences against confinement stress p 2915 N94-27460

Comparative measurement of visual stability in cosmic space: Onboard experiment and pre-flight activities p 2916 N94-27463

Modulation by galactosamine-induced hepatitis of biological responses of the rat exposed to high altitude hypoxia p 2904 N94-27464

Protective action of platelet-activating factor antagonist, TCV-309, against ischemia reperfusion injury in isolated rabbit hearts p 2904 N94-27465

Protective action of an amiloride derivative (amiloride, 5-(N, N-dimethyl) hydrochloride) against in isolated ischemia/reperfusion newborn rabbit hearts p 2904 N94-27466

Effects of high-intensity electric field stimulation on the electromechanical performance of cardiac muscle: Influence of fiber orientation p 2904 N94-27467

On the mechanism of reentrant arrhythmias following DC defibrillation: Influence of fiber orientation to the effects of low-energy electric field stimulation on the effective refractory period of cardiac muscle p 2904 N94-27468

Positive chronotropic effect of mechanical stretch on the sinoatrial node: Roles of neurotransmitters and stretch activated channels p 2904 N94-27469

Disturbed neuronal migration in the cerebral cortex of mice by low-dose gamma radiation p 2904 N94-27470

Distribution of GABA immunoreactive neurons in the brain of rolling mouse Nagoya and gamma-irradiated mouse p 2904 N94-27471

Effects of bathing at 40 C on cardiovascular system in humans: Comparison with 34 C thermoneutral bathing p 2918 N94-27473

Effects of 41 C bathing for 20 minutes on cardiovascular and thermoregulatory functions in humans p 2918 N94-27474

Monthly variation of physiological and psychological responses under unsteady thermal conditions p 2918 N94-27475

The intracellular second messenger system in c-fos gene induction by ACTH p 2904 N94-27477

Thyroid hormone action in cultured human skin fibroblasts: Evaluation using spheroid culture p 2919 N94-27478

Cloning of rat RXR alpha cDNA and the expression of its mRNA in regenerating liver and primary cultured hepatocytes p 2905 N94-27479

Cloning of a novel POU family gene by RT-PCR method p 2905 N94-27480

Effect of sera from patients treated with long-term hemodialysis on mRNA's for collagenase, stromelysin, and tissue inhibitor of metalloprotease in cultured human synovial cells p 2920 N94-27481

Expression analysis of Thyroxine-Binding Globulin Complete Deficiency in Japanese (TBG-CDJ) p 2905 N94-27482

Development of Purkinje cells in vitro p 2905 N94-27483

Developmental expression of protein kinase C type 1 isozyme in suncus and rat cerebella p 2905 N94-27484

Abnormal development of serotonin nerve fibers in the cerebral cortex of young rats with methylazoxymethanol induced microcephaly p 2905 N94-27485

Effects of ML-9, a myosin light-chain kinase inhibitor, on preimplantation development of the mouse p 2905 N94-27486

Compaction-like blastomere aggregation caused by 1-oleoyl-2-acetylglycerol in mouse embryos: An electron microscopic observation p 2905 N94-27487

Anorectal malformations induced by intraperitoneal injection of all-trans retinoic acid in suncus p 2905 N94-27489

Effect of PGE2 receptor agonists butaprost, M and B 28767 and an antagonist AH 6809 on the BK response of visceral polymodal receptors p 2906 N94-27494

Excitation of cutaneous polymodal receptor induced by sympathetic stimulation in adjuvant-induced arthritis rats p 2906 N94-27495

Selection of site injecting adjuvant in chronic inflammation model p 2906 N94-27496

Influence of mechanical stimulation on inflammatory edema p 2906 N94-27497

The effect of naloxone on sleeping time in adjuvant arthritic rats p 2906 N94-27498

Effects of capsaicin on freshly dissociated rat dorsal root ganglion cells p 2906 N94-27499

Size distribution of retrogradely labeled dorsal root ganglion cells: Test of normality p 2906 N94-27500

Effects of perfusion of amiodarone on electrophysiological properties in single rabbit ventricular myocytes p 2906 N94-27503

Fast and slow onsets of Na channel blocking actions due to lidocaine and disopyramide using concentration-clamp method p 2907 N94-27504

Electrophysiological effects of MS-551, a new Class 3 antiarrhythmic agent, on isolated rabbit ventricular muscles p 2907 N94-27505

Comparative investigation of new Class 3 antiarrhythmic drugs, E-4031 and MS-551, on electrophysiological properties in isolated rabbit ventricular myocytes p 2907 N94-27506

Effects of Class 1 antiarrhythmic drugs on the intraventricular conduction: Influence of fiber orientation p 2907 N94-27507

Effects of Class 3 antiarrhythmic agents, E-4031 and MS-551 on ventricular repolarization in isolated rabbit hearts p 2907 N94-27508

Electrical coupling between the sino-atrial node and atrial muscle: Cell to cell interaction through an external circuit and its simulation by computer modeling p 2907 N94-27509

A study on tissue excitation of cardiac muscle under electrical field stimulation p 2907 N94-27510

Block of cardiac sodium channels by Ro 22-9194 (R), a new antiarrhythmic agent: Effects on the maximum upstroke velocity (Vmax) of single guinea pig ventricular myocytes p 2907 N94-27511

Electrophysiological effects of an antiarrhythmic drug, moricizine on isolated guinea pig ventricular muscles p 2907 N94-27512

Correlation between electrical activity and the size of single sinoatrial node cells p 2907 N94-27513

The ionic mechanism underlying the negative chronotropic effect of acetylcholine: Experimental study in rabbit single sinoatrial node cells p 2908 N94-27514

The ionic mechanism underlying the negative chronotropic effect of acetylcholine: Experiments using small sinoatrial node tissue preparations isolated from rabbit hearts p 2908 N94-27515

The ionic mechanism underlying the negative chronotropic effect of acetylcholine: Postganglionic vagal stimulation in isolated rabbit hearts p 2908 N94-27516

A study of psychological factors affecting an extremely isolated environment p 2927 N94-27517

Interhemispheric phase relationship of alpha waves and cerebral dominance p 2927 N94-27518

Analysis of the Electrically Evoked Response (EER) of the cat p 2908 N94-27519

Impaired associated movement in Parkinson's disease: An evaluation of Bell's phenomenon p 2928 N94-27520

Hyperalgesia to cold in patients with Subacute Myelo-Optico-Neuropathy (SMON) p 2928 N94-27521

Contribution of muscle spindle afferent activity to transient pause in EMG during voluntary tonic contraction p 2928 N94-27522

Effect of prostaglandin E1 on the relationship between skin sympathetic nerve activity and reduction in skin blood flow p 2929 N94-27524

Difference in skin blood flow reduction depending on activating maneuver of skin sympathetic nerve activity p 2929 N94-27525

Effect of L-dopa on hemodynamic functions in humans p 2929 N94-27526

Analysis on one minute wave in body fluid volume and muscle pumping referred to body parts generating the one minute wave during human active standing p 2929 N94-27528

The measurements of muscle blood flow by laser Doppler flowmetry with needle type probe p 2908 N94-27530

Muscle sympathetic nerve activity in patients with hyper-and hypothyroidism: A microneurographic study p 2930 N94-27531

Desensitization to acethylcholine in pacemaker cells of the sinoatrial node p 2908 N94-27537

Muscle sympathetic nerve activity in humans p 2932 N94-27538

The polymodal receptor p 2908 N94-27539

Laser blow-off lithium beam probing with high temporal resolution for edge plasma diagnostics [DE94-701176] p 2820 N94-27701

NAGOYA UNIV., TOYOKAWA (JAPAN).

Development of imaging riometers p 2884 N94-27967

Quick-look system of auroral absorption images by imaging riometer p 2884 N94-27968

NAGOYA WOMEN'S UNIV. (JAPAN).

Endocrinological evaluations of muscle and bone atrophy in tail-suspended rats p 2903 N94-27444

NANGIA ASSOCIATES, BRISTOL (ENGLAND).

Vectored jets-induced interference on aircraft, prediction and verification p 2801 N94-28012

NANYANG TECHNOLOGICAL INST. (SINGAPORE).

Potential flow modelling of airfoil stall p 2654 N94-28332

NAST SECRETARIAT, TAGUIG (PHILIPPINES).

HDGEC activity in Asia Pacific region p 2874 N94-28286

NATIONAAL INST. VOOR KERNFYSICA EN HOGE ENERGIEFYSICA, AMSTERDAM (NETHERLANDS).

RF-station control crate [DIGEL-1992-9] p 2779 N94-25618

Bundle Intensity and Beamgate Length recorder (BIBL) [DIGEL-1993-7] p 3031 N94-25619

Digital input module [DIGEL-1993-6] p 2779 N94-25620

Alignment of the Amsterdam Pulse Stretcher (AmPS) [MTG-93-02] p 2809 N94-25637

Construction of a new electroweak sphaleron [NIKHEF-H/93-09] p 3020 N94-26540

Anomaly candidates and invariants of D 4, N 1 supergravity theories [NIKHEF-H/93-12] p 3072 N94-26541

Simple currents versus orbifolds with discrete torsion: A complete classification
[NIKHEF-H/93-13] p 2995 N94-26812

A prototype presampler for the uranium-scintillator calorimeter in Zeus
[NIKHEF-H/93-11] p 2814 N94-28098

NATIONAL ACADEMY OF ENGINEERING, WASHINGTON, DC.

Future of aerospace
[PB94-120185] p 2669 N94-26906

NATIONAL ACADEMY OF SCIENCES - NATIONAL RESEARCH COUNCIL, WASHINGTON, DC.

Workload transition: Implications for individual and team performance
[AD-A274538] p 2941 N94-26964

NATIONAL AERONAUTICS AND SPACE ADMINISTRATION, WASHINGTON, DC.

Access to space study
[NASA-TM-109693] p 2685 N94-27151

Robotics handbook. Version 1: For the interested party and professional
[NASA-TM-109690] p 2824 N94-27238

Space Station technology testbed: 2010 deep space transport p 2687 N94-27368

Inertial electrostatic confinement as a power source for electric propulsion p 2688 N94-27373

Aerospace safety advisory panel
[NASA-TM-109692] p 3118 N94-27381

University program management information system, FY 1993
[NASA-TM-109719] p 3100 N94-27413

Space radiation health research, 1991-1992
[NASA-TM-109721] p 2932 N94-27556

Small business innovation research program solicitation
[NASA-TM-109695] p 3094 N94-27661

NASA SBIR abstracts of 1992, phase 1 projects
[NASA-TM-109694] p 3094 N94-27772

Mission to Planet Earth: A program to understand global environmental change
[NASA-PAM-556] p 2869 N94-27958

Software assurance standard
[NASA-TM-109705] p 2975 N94-27992

Aeronautical engineering: A continuing bibliography with indexes (supplement 301)
[NASA-SP-7037(301)] p 2643 N94-28203

Aerospace medicine and biology: A continuing bibliography with indexes (supplement 386)
[NASA-SP-7011(386)] p 2933 N94-28208

Aerospace medicine and biology: A continuing bibliography with indexes (supplement 387)
[NASA-SP-7011(387)] p 2933 N94-28213

Aerospace medicine and biology: A cumulative index to a continuing bibliography (supplement 384)
[NASA-SP-7011(384)] p 2934 N94-28219

NATIONAL AERONAUTICS AND SPACE ADMINISTRATION. AMES RESEARCH CENTER, MOFFETT FIELD, CA.

An automatic 14-day paste diet feeder for animals
[NASA-TM-108804] p 2901 N94-26086

EGADS: A microcomputer program for estimating the aerodynamic performance of general aviation aircraft
[NASA-TM-104013] p 2667 N94-26091

Plasma volume shifts and exercise thermoregulation with water immersion and six-degree head-down tilt
[NASA-TM-108781] p 2901 N94-26093

Intermittent gravity: How much, how often, how long?
[NASA-TM-108800] p 2944 N94-26098

Correlation of airloads on a two-bladed helicopter rotor
[NASA-TM-103982] p 2644 N94-26143

Design optimization of high-speed proprotor aircraft
[NASA-TM-103988] p 2667 N94-26151

Thermoregulatory effects of caffeine ingestion during rest and exercise in men
[NASA-TM-108783] p 2901 N94-26210

Simulation modeling for long duration spacecraft control systems p 2684 N94-26288

A comparative study of serial and parallel aeroelastic computations of wings
[NASA-TM-108805] p 2645 N94-26538

Shake test results of the MDHC test stand in the 40- by 80-foot wind tunnel
[NASA-TM-108801] p 2641 N94-26596

Experimental investigation of advanced hub and pylon fairing configurations to reduce helicopter drag
[NASA-TM-4540] p 2668 N94-26604

Proprioceptive isokinetic exercise test
[NASA-TM-104015] p 2902 N94-27227

Telepresence in the human exploration of Mars: Field studies in analog environments p 2685 N94-27360

Thirteen ways to say nothing with scientific visualization
[NASA-CR-195280] p 2970 N94-27542

NAS technical summaries. Numerical aerodynamic simulation program, March 1992 - February 1993
[NASA-RP-1321] p 3118 N94-27764

Fifty years of jet in cross flow research
p 2799 N94-28004

A numerical investigation of a subsonic jet in a crossflow p 2803 N94-28023

Numerical simulation of a powered-lift landing
p 2671 N94-28033

Transitional flight characteristics of a geometrically simplified STOVL model p 2672 N94-28035

Artificial Intelligence Research Branch future plans
[NASA-TM-109733] p 2989 N94-28065

High-Speed Research: Sonic Boom, Volume 1
[NASA-CP-10132] p 2649 N94-28188

An image assessment study of image acceptability of the Galileo low gain antenna mission
p 2945 N94-28252

NATIONAL AERONAUTICS AND SPACE ADMINISTRATION. GODDARD SPACE FLIGHT CENTER, GREENBELT, MD.

Laser altimetry simulator. Version 3.0: User's guide
[NASA-TM-104588] p 2877 N94-26152

Performance measures from the explorer platform berthing experiment p 2683 N94-26283

Handbook for handling and storage of nickel-cadmium batteries: Lessons learned
[NASA-RP-1326] p 2702 N94-26613

NASA's spacecraft data system p 2950 N94-26723

Acceleration of electrons and ions by strong lower-hybrid turbulence in solar flares
[NASA-TM-109723] p 3111 N94-27953

Nimbus-7 Earth radiation budget calibration history. Part 2: The Earth flux channels
[NASA-RP-1335-PT-2] p 2814 N94-27981

Nickel cadmium battery operations on-orbit: Trials, tribulations, and success on the Upper Atmosphere Research Satellite p 2862 N94-28120

Construction of temperature compensated constant voltage (VT) curves for super Ni-Cd (tm) cells
p 2863 N94-28126

MODIS airborne simulator visible and near-infrared calibration, 1992 ASTEX field experiment. Calibration version: ASTEX King 1.0
[NASA-TM-104599] p 2897 N94-28179

MODIS airborne simulator visible and near-infrared calibration, 1991 FIRE-Cirrus field experiment. Calibration version: FIRE King 1.1
[NASA-TM-104600] p 2897 N94-28182

The 1994 Space and Earth Science Data Compression Workshop
[NASA-CP-3255] p 2945 N94-28251

NATIONAL AERONAUTICS AND SPACE ADMINISTRATION. HUGH L. DRYDEN FLIGHT RESEARCH FACILITY, EDWARDS, CA.

Multidisciplinary aeroelastic analysis of a generic hypersonic vehicle
[NASA-TM-4544] p 2691 N94-27868

NATIONAL AERONAUTICS AND SPACE ADMINISTRATION. JOHN F. KENNEDY SPACE CENTER, COCOA BEACH, FL.

Effect of carbon dioxide enrichment on radish production using Nutrient Film Technique (NFT)
[NASA-TM-107198] p 2902 N94-27411

Development of a sparging technique for volatile emissions from potato (Solanum tuberosum)
[NASA-TM-109199] p 2903 N94-27412

Debris/ice/TPS assessment and integrated photographic analysis for Shuttle mission STS-60
[NASA-TM-109193] p 2692 N94-27956

Report of the Shuttle Processing Review Team
[NASA-TM-109728] p 2692 N94-28178

NATIONAL AERONAUTICS AND SPACE ADMINISTRATION. LYNDON B. JOHNSON SPACE CENTER, HOUSTON, TX.

Human computer interface guide, revision A
[NASA-TM-109708] p 2955 N94-27769

The TMIS life-cycle process document, revision A
[NASA-TM-109698] p 2697 N94-27775

Research and Development Annual Report, 1992
[NASA-TM-104777] p 3119 N94-27993

Determination of thermal properties of commercial Ni-MH cells p 2864 N94-28132

An analysis of the loads applied to a heavy Space Station rack during translation and rotation tasks
[NASA-TM-104790] p 2697 N94-28183

JSC almanac
[NASA-TM-109702] p 3119 N94-28204

Artemis common lunar lander. Phase 2: Study results for external review
[NASA-TM-109699] p 2692 N94-28205

Workshop on Countering Space Adaptation with Exercise: Current Issues
[NASA-CP-3252] p 2934 N94-28361

NATIONAL AERONAUTICS AND SPACE ADMINISTRATION. LANGLEY RESEARCH CENTER, HAMPTON, VA.

Comments regarding two upwind methods for solving two-dimensional external flows using unstructured grids
[NASA-TM-109078] p 2644 N94-26154

The evolution of the high-speed civil transport
[NASA-TM-109089] p 3117 N94-26155

Selected topics in robotics for space exploration
[NASA-CP-10131] p 2682 N94-26278

Berthing of Space Station Freedom using the shuttle remote manipulator system p 2684 N94-26284

Status report of RMS active damping augmentation
p 2684 N94-26285

Autonomous rendezvous and docking for Space Station Freedom p 2684 N94-26286

Early lunar rover mission studies
p 2684 N94-26290

Parallel grid generation algorithm for distributed memory computers
[NASA-TP-3429] p 2963 N94-26466

Investigation of the aerodynamic environment for an advanced lightweight rotor in forward flight. Volume 4: Laser velocimeter wake data, advance ratio of 0.037
[NASA-TM-109040-VOL-4] p 2645 N94-26483

Investigation of the aerodynamic environment for an advanced lightweight rotor in forward flight. Volume 1: Laser velocimeter inflow data, advance ratio of 0.37, thrust coefficient of 0.0081 and hover tip speed of 603 feet/second
[NASA-TM-109040-VOL-1] p 2645 N94-26489

Investigation of the aerodynamic environment for an advanced lightweight rotor in forward flight. Volume 2: Laser velocimeter inflow data, advance ratio of 0.37, thrust coefficient of 0.0064 and hover tip speed of 710 feet/second
[NASA-TM-109040-VOL-2] p 2645 N94-26492

Investigation of the aerodynamic environment for an advanced lightweight rotor in forward flight. Volume 3: Laser velocimeter inflow data, advance ratio of 0.37, thrust coefficient of 0.0064 and hover tip speed of 603 feet/second
[NASA-TM-109040-VOL-3] p 2645 N94-26497

Computational prediction of isolated performance of an axisymmetric nozzle at Mach number 0.90
[NASA-TM-4506] p 2646 N94-26547

Stochastic solution to quantum dynamics
[NASA-TP-3408] p 3114 N94-26550

Pressure distributions on a 0.02-scale Space Shuttle orbiter nose at Mach 21.5 in helium
[NASA-TM-4495] p 2646 N94-26592

The relationship of an integral wind shear hazard to aircraft performance limitations
[NASA-TM-109080] p 2677 N94-26593

Piloted simulation study of an ILS approach of a twin-pusher business/commuter turboprop aircraft configuration
[NASA-TM-4516] p 2646 N94-26602

Tests of highly loaded skids on a concrete runway
[NASA-TP-3435] p 2669 N94-26608

Structural evaluation of concepts for a solar energy concentrator for Space Station advanced development program
[NASA-TP-3375] p 2695 N94-26609

Design and evaluation of an electromagnetic beam waveguide for measuring electrical properties of materials
[NASA-TP-3418] p 2769 N94-26611

Research and test facilities
[NASA-TM-109685] p 2681 N94-26684

Experimental and theoretical study of aerodynamic characteristics of some lifting bodies at angles of attack from -10 degrees to 53 degrees at Mach numbers from 2.30 to 4.62
[NASA-TM-4528] p 2646 N94-26693

Fiber-optic-based laser vapor screen flow visualization system for aerodynamic research in larger scale subsonic and transonic wind tunnels
[NASA-TM-4514] p 2647 N94-26706

Evaluation of the prototype dual-axis wall attitude measurement sensor
[NASA-TM-109056] p 2811 N94-26707

Leading-edge vortex-system details obtained on F-106B aircraft using a rotating vapor screen and surface techniques
[NASA-TP-3374-VIDEO-SUPPL] p 2647 N94-27161

FAA/NASA Joint University Program for Air Transportation Research, 1992-1993
[NASA-CP-3246] p 2641 N94-27284

Packet radio data link applications in the NASA Langley Research Center Transport Systems Research Vehicle
[NASA-TM-109071] p 2665 N94-27423

Description of the Experimental Avionics Systems Integration Laboratory (EASILY)
[NASA-TM-109072] p 2681 N94-27425

Nasa Langley Research Center seventy-fifth anniversary publications, 1992
[NASA-TM-109691] p 3118 N94-27431
Proceedings of the Non-Linear Aero Prediction Requirements Workshop
[NASA-CP-10138] p 2670 N94-27439
Electronic document distribution: Design of the anonymous FTP Langley Technical Report Server
[NASA-TM-4567] p 2971 N94-27573
PATRAN 2.5/EAL interface guide
[NASA-TM-109053] p 2972 N94-27655
Implementation of thermal residual stresses in the analysis of fiber bridged matrix crack growth in titanium matrix composites
[NASA-TM-109082] p 2711 N94-27658
Numerical and experimental analyses of the radiant heat flux produced by quartz heating systems
[NASA-TP-3387] p 3011 N94-27659
Techniques to improve maneuver stability characteristics of a nonlinear wide-body transport airplane in cruise flight
[NASA-TM-4521] p 2679 N94-27660
Lifetimes of lunar satellite orbits
[NASA-TP-3394] p 2690 N94-27771
Local performance optimization for a class of redundant eight-degree-of-freedom manipulators
[NASA-TP-3417] p 2989 N94-27773
Minimum accommodation for aerobrake assembly, phase 2
[NASA-TM-107608] p 2692 N94-27774
Reliability-based structural optimization: A proposed analytical-experimental study
[NASA-TM-109055] p 2844 N94-27830
Effects of historical and predictive information on ability of transport pilot to predict an alert
[NASA-TM-4547] p 2673 N94-27864
New constitutive equation for the volume viscosity in fluids
[NASA-TM-109104] p 2798 N94-27867
Effects of expected-value information and display format on recognition of aircraft subsystem abnormalities
[NASA-TP-3395] p 2673 N94-27882
Experimental studies of loudness and annoyance response to sonic booms p 2651 N94-28195

NATIONAL AERONAUTICS AND SPACE ADMINISTRATION. LEWIS RESEARCH CENTER, CLEVELAND, OH.
An investigation of magnetic field effects on plume density and temperature profiles of an applied-field MPD thruster
[NASA-TM-106416] p 2700 N94-26090
A large high vacuum, high pumping speed space simulation chamber for electric propulsion
[NASA-TM-106453] p 2690 N94-26142
An approach to studying the reliability of microgravity experiments
[NASA-TM-106489] p 2834 N94-26199
Focused Schlieren flow visualization studies of multiple venturi fuel injectors in a high pressure combustor
[NASA-TM-106479] p 2674 N94-26573
Vision 21: Interdisciplinary Science and Engineering in the Era of Cyberspace
[NASA-CP-10129] p 2685 N94-27358
VENI, video, VICI: The merging of computer and video technologies p 2686 N94-27362
Interdisciplinary technology p 2686 N94-27363
A direct current rectification scheme for microwave space power conversion using traveling wave electron acceleration p 2687 N94-27371
Rocket engine numerical simulation
p 2688 N94-27375
Hydrogen-oxygen torch ignitor
[NASA-TM-106493] p 2691 N94-27424
Thermogravimetric study of oxidation of a PdCr alloy used for high-temperature sensors
[NASA-TM-106473] p 2741 N94-27426
The telemedicine spacebridge project: A joint US/Russian venture in long distance medicine via satellite
[NASA-TM-106523] p 2693 N94-27427
Risks and issues in fire safety on the Space Station
[NASA-TM-106430] p 2692 N94-27436
Structural design feasibility study of Space Station long spacer truss
[NASA-TM-106346] p 2843 N94-27559
Development of hypersonic engine seals: Flow effects of preload and engine pressures
[NASA-TM-106333] p 2826 N94-27599
A hydrostatic stress-dependent anisotropic model of viscoplasticity
[NASA-TM-106525] p 2711 N94-27640
An optimization program based on the method of feasible directions: Theory and users guide
[NASA-TM-4552] p 2845 N94-27865
Summary of NASA Aerospace Flight Battery Systems Program activities p 2860 N94-28101
Space Station Freedom NiH2 cell testing program
p 2861 N94-28108
A review of recent aeroelastic analysis methods for propulsion at NASA Lewis Research Center
[NASA-TP-3406] p 2846 N94-28227

NATIONAL AERONAUTICS AND SPACE ADMINISTRATION. MARSHALL SPACE FLIGHT CENTER, HUNTSVILLE, AL.
The effects of embedded internal delaminations on composite laminate compression strength; an experimental review
[NASA-TM-108440] p 2707 N94-26127
Survey of visualization and analysis tools
[NASA-TM-108436] p 2809 N94-26150
The continuum spectral characteristics of gamma ray bursts observed by BATSE p 3114 N94-26686
Continuum spectral characteristics of bursts measured with BATSE large area detectors p 3114 N94-26687
A study of gamma ray burst continuum properties presnting evidence for two spectral states in bursts
p 3114 N94-26688
Balloon-borne measurements of the SN1987A hard x ray continuum p 3115 N94-26689
Channel to energy calibration results for the BATSE large area detectors p 3115 N94-26690
Designing for human presence in space: An introduction to environmental control and life support systems
[NASA-RP-1324] p 2942 N94-27437
An April 1991 outburst from 4U0115+63 observed by BATSE
[NASA-CR-195252] p 3116 N94-27440
Development of a new seal for use on large openings of pressurized spacecraft
[NASA-TM-108444] p 2825 N94-27560
Thermocapillary flow with evaporation and condensation and its effect on liquid retention in low-G fluid acquisition devices
[NASA-TP-3463] p 2797 N94-27639
Extra-Vehicular Activity (EVA) glove evaluation test protocol
[NASA-TM-108442] p 2943 N94-27952
The 1993 NASA Aerospace Battery Workshop
[NASA-CP-3254] p 2860 N94-28100
Bipolar lead-acid batteries for electrical actuation applications p 2864 N94-28134
Space Shuttle main engine turbopump bearing assessment program
[NASA-TM-108447] p 2833 N94-28265

NATIONAL AEROSPACE LAB., AMSTERDAM (NETHERLANDS).
Technical and scientific research for aeronautics and astronautics
[ETN-94-95392] p 2641 N94-26212
The deterministic power-spectral-density method
[AD-B175894] p 2678 N94-27395
Vibrations in engineering structures: A review of model and full-scale test of a cable-stayed bridge and a traffic sign gantry
[NLR-TP-92321-U] p 2843 N94-27553
High-lift system analysis method using unstructured meshes
[NLR-TP-92351-U] p 2647 N94-27554
Morphodynamics of inter-tidal areas: The Wadden Sea
[NLR-TP-92356-U] p 2851 N94-27555
Fracture toughness and crack resistance of damage tolerant and high strength Al-Li alloys
[NLR-TP-91249-U] p 2743 N94-27795
Investigation of the bond strength of a discrete skin-stiffener interface
[NLR-TP-92183-U] p 2670 N94-27796
Status and prospects for aluminium-lithium alloys in aircraft structures
[NLR-TP-92193-U] p 2743 N94-27797
Understanding and development of a prediction method of transonic limit cycle oscillation characteristics of fighter aircraft
[NLR-TP-92210-U] p 2679 N94-27798
Time-step enlargement and optimal smoothing in Runge-Kutta time-integration algorithms by implicit and explicit smoothing
[NLR-TP-92221-U] p 2798 N94-27799
Multi-sensor data fusion in a distributed environment: Architectural solutions
[NLR-TP-92243-U] p 2989 N94-27800
Flight testing of GPS and GPS-aided systems
[NLR-TP-92151-U] p 2666 N94-27831
Gravity dependence or pressure drop and heat transfer in straight two-phase heat transport system condenser ducts
[NLR-TP-92167-U] p 2798 N94-27853
The deterministic power-spectral-density-method for nonlinear systems
[AD-B179687] p 3001 N94-28353

NATIONAL AEROSPACE LAB., KAKUDA (JAPAN).
A study on heat transfer in a scramjet leading edge model
[NAL-TR-1187T] p 2675 N94-27608

NATIONAL AEROSPACE LAB., TOKYO (JAPAN).
Approximate Riemann solvers: Improvement of the HLLEM scheme and its generalization for chemically reacting flows
[NAL-TR-1189] p 2795 N94-27205
Optimal control of helicopters following power failure
[NAL-TR-1190] p 2678 N94-27206
Development of an automatic fatigue-data acquisition system using commercial software
[NAL-TM-650] p 2842 N94-27207
Wind tunnel investigation of an STOL aircraft model: An effect of engine nacelle shape
[NAL-TM-653] p 2647 N94-27235
The renewing of the test section of the NAL transonic wind tunnel. Part 1: Reconstruction of the 1st corner turning vanes and aerodynamic stress measurement
[NAL-TM-651] p 2681 N94-27247
High temperature tension test equipment of heat resistant composite materials
[NAL-TM-652] p 2710 N94-27255
SP/MSP tests for the evaluation of FGM
[NAL-SP-17] p 2710 N94-27279
SP/MSP tests for the evaluation of FGM
p 2710 N94-27280
An algorithm for stereo correspondence problems on the analogy of human vision
[NAL-TR-1185] p 2940 N94-27584

NATIONAL CENTER FOR ATMOSPHERIC RESEARCH, BOULDER, CO.
Solar and airglow measurements aboard the two suborbital flights NASA 36.098 and 36.107
[NASA-CR-195279] p 2882 N94-27380

NATIONAL DEFENCE RESEARCH ESTABLISHMENT, LINKOEPING (SWEDEN).
Research and development within nonlinear optics for protection of optical sensors against laser irradiation on of optical sensors against laser irradiation. Quarterannual report 1 (april 1993))
[PB94-124245] p 3037 N94-27046
FOA 39
[PB94-124252] p 2773 N94-27159
Computer model for generation of infrared images
[PB94-123551] p 3005 N94-27172
Scanview: A grafical program for analysis of laserbathymetry data
[PB94-124443] p 2900 N94-27208
Ir-fibers in a laser threat warning system and robot shot warning system
[PB94-124476] p 3038 N94-27209
CMT-Si
[PB94-123619] p 2812 N94-27216
Contributions to CD Space Committee 1992
[PB94-124401] p 3101 N94-27218
MILCOM 92 and standardization for HF-communication. A study tour to the USA in October 1992
[PB94-124427] p 2774 N94-27219

NATIONAL DEFENCE RESEARCH ESTABLISHMENT, STOCKHOLM (SWEDEN).
Blurred focal elements generalization of dempster's rule
[PB94-124278] p 2986 N94-26992
Users guide for GRIKURV: A code for drawing graphs
[PB94-123593] p 2968 N94-27154
Task demand, workload, and performance
[PB94-123627] p 2942 N94-27155
Examination of hardness, fracture toughness and microstructure in Al2O3-B4C binary ceramics
[PB94-124237] p 2755 N94-27158
Data analysis and data fusion for intelligence analysis and decision support. Research plan 1993-2000
[PB94-123569] p 3005 N94-27173
Satellite navigation system GPS: A review of principles and performance and developments in general
[PB94-124534] p 2665 N94-27210
Intelligent material systems and structures. Part 6: Measurements of adhesion between optical fibres and composite materials
[PB94-123577] p 2756 N94-27215
Thermoplastic or thermosetting composites in aircrafts
[PB94-123809] p 2710 N94-27253

NATIONAL DEFENCE RESEARCH ESTABLISHMENT, UMEA (SWEDEN).
Evaluation of a Canadian minitube air sampling system
[FOA-C-40307-4.6] p 2866 N94-25809
Bakteriella toxiner-morgondagens hot (bacterial toxins-the threat of tomorrow)
[PB94-124229] p 2902 N94-27045
Microbiology research at some research institutes in the former Soviet Union: A survey of scientific publications
[PB94-123320] p 2902 N94-27171

NATIONAL ENVIRONMENTAL PROTECTION AGENCY, BEIJING (CHINA).
Progress in the study of global change in China p 2873 N94-28276

NATIONAL GEOPHYSICAL DATA CENTER, BOULDER, CO.
Solar-geophysical data number 590, October 1993. Part 1: (Prompt reports). Data for September, August 1993, and late data
[PB94-125903] p 3110 N94-27053
Solar-geophysical data number 590, October 1993. Part 2: (Comprehensive reports). Data for April 1993, and miscellaneous
[PB94-125911] p 3110 N94-27054
Solar-geophysical data number 591, November 1993. Part 2: (Comprehensive reports). Data for May 1993 and miscellaneous
[PB94-134830] p 3111 N94-28360

NATIONAL INST. FOR RESOURCES AND ENVIRONMENT, IBARAKI (JAPAN).
A study on structure of benthic boundary layer in coastal waters
[REPT-4] p 2898 N94-25635
An observational study of air pollution transport over a large urban complex
[REPT-6] p 2867 N94-26474
Studies on the measurement of subsurface fractures and geostress using acoustic emission technique for deep coalbed development
[REPT-7] p 2879 N94-26475
Journal of NIRE, volume 2, number 4
[JTN-94-80554] p 2869 N94-28147
Recent legal movement on water quality regulation in Japan p 2869 N94-28148
Collaboration of chemical oxidation and biological treatment for removal of refractory organic substances p 2870 N94-28149
Effects of p-chlorophenol on sulfate reduction in marine sediments p 2870 N94-28150
Treatment of refractory organic substances with combined use of chemical oxidation and biological treatment. Part 2: Biodegradability of ozonation products of chlorophenol p 2870 N94-28151
Determination of lead isotope ratios in seawater by purge and trap GC/MS after ethylation p 2870 N94-28152
Environmental management and audit p 2870 N94-28153
Oil production from buckwheat stillage by thermochemical liquefaction p 2871 N94-28154
Effects of slot on rock surface for percussive rock excavation: Water jet assisted percussive rock excavation p 2871 N94-28155
The estimation of pre-stress by deformation rate analysis and suggestion of a mechanism from the elast-plastical theory p 2871 N94-28156
Numerical simulation of turbulent free jet by TFKE model p 2871 N94-28157

NATIONAL INST. OF AERONAUTICS AND SPACE, JAKARTA (INDONESIA).
Utilization of remote sensing data for global change research p 2875 N94-28292

NATIONAL INST. OF POLAR RESEARCH, TOKYO (JAPAN).
JARE data reports. No. 186: Upper atmosphere physics data. Syowa and Asuka Stations, 1990
[JTN-94-80594] p 2881 N94-27299
The Sixteenth Symposium on Coordinated Observations of the Ionosphere and the Magnetosphere in the Polar Regions: Program and abstracts
[JTN-94-80601] p 2882 N94-27300
Memories of National Institute of Polar Research. Series A-19. Upper atmosphere physics: ELF emission in high latitudes: Ray path calculation and ground-satellite observations
[JTN-94-80592] p 2882 N94-27342
Antarctic Record, Vol. 36, No. 2
[REPT-107] p 2883 N94-27963
Energy parameters of the incident auroral electrons derived by the intensity ratio of auroral emissions p 2779 N94-27964
Development of imaging riometers p 2884 N94-27967
Counting Adelie penguins at colonies: Seasonal and annual changes p 2885 N94-27970
Status report for the development of the Antarctic penetrator: 1990-year program p 2885 N94-27973

NATIONAL INST. OF STANDARDS AND TECHNOLOGY, BOULDER, CO.
Thermophysical properties of HFC-143a and HFC-152a
[DE94-004236] p 2719 N94-27567

NATIONAL INST. OF STANDARDS AND TECHNOLOGY, GAITHERSBURG, MD.
Study on measurement and evaluation methods for superconductive characteristics p 2725 N94-25560
Summaries of BFRL fire research in-house projects and grants, 1993
[PB94-121050] p 2763 N94-26756
Gordon Research Conference on the Physics and Chemistry of Laser Diagnostics in Combustion
[AD-A274609] p 2716 N94-26893
Annual conference on fire research, 1993: Book of abstracts
[PB94-121324] p 2717 N94-26907

NATIONAL LAB. FOR HIGH ENERGY PHYSICS, TSUKUBA (JAPAN).
The proceedings of the KEK FEL Simulation Code Workshop
[DE93-520378] p 2816 N94-26112
JLC-1
[DE93-520380] p 3031 N94-26113
Proceedings of the Second EGS4 User's Meeting in Japan
[DE93-520383] p 3032 N94-26543
Proceedings of Workshop on Distributed Computing and Network
[DE94-701165] p 2983 N94-27804
Hydrogen physics
[DE94-701317] p 2719 N94-27822

NATIONAL MUSEUM OF NATURAL HISTORY, WASHINGTON, DC.
The end-Permian mass extinction: A complex, multicausal extinction p 2888 N94-28299

NATIONAL OCEANIC AND ATMOSPHERIC ADMINISTRATION, BOULDER, CO.
Region 5395 of March 1989
[PB94-120714] p 3110 N94-26755
Cloud liquid water content measurement tests using dual-wavelength radar
[PB94-125960] p 2896 N94-26959

NATIONAL PHYSICAL LAB., NEW DELHI (INDIA).
Indian activities on the core programme IGAP and proposals for network activities p 2874 N94-28284

NATIONAL PHYSICAL LAB., TEDDINGTON (ENGLAND).
Technique to predict the curing behaviour of unsaturated polyester materials
[PB94-124856] p 2748 N94-25892
Modelling the inhibition cure behaviour of unsaturated polyester moulding materials
[PB94-124864] p 2748 N94-25893
Stress relaxation in dough moulding compounds
[PB94-124872] p 2748 N94-25894
Piezoelectric measurements on impact loaded PZT ceramics
[NPL-DMM(A)-88] p 2752 N94-26652
Stability of reference masses 2: The effect of environment and cleaning methods on the surfaces of stainless steel and allied materials
[NPL-DMM(A)-95] p 2738 N94-26653
CEN-VAMAS round robin on grain size measurement for advanced technical ceramics
[VAMAS-TR-12] p 2752 N94-26654
Automatic test case generation using PROLOG
[NPL-DITC-215/93] p 2964 N94-26655
DUSOL: Improved software for analysis of ultrasonic velocity data on anisotropic materials
[NPL-DMM(A)-104] p 2965 N94-26816
Frontiers of science and measurement: Report on a seminar jointly organized by the National Physical Laboratory and the Institute of Physics
[PB94-124310] p 3009 N94-27131
Ultrasonic measurement technique to determine the state of cure in thermosetting materials
[PB94-124328] p 2756 N94-27217
Guidelines for unlubricated sliding wear tests. Part 1: General approach
[PB94-119666] p 2825 N94-27322
Guidelines for unlubricated sliding wear tests. Part 2: Procedures for pin-on-disc testing
[PB94-123270] p 2825 N94-27324

NATIONAL RESEARCH COUNCIL, BANGKOK (THAILAND).
Thailand satellite ground receiving station in global change research cooperation p 2875 N94-28291

NATIONAL RESEARCH COUNCIL OF CANADA, OTTAWA (ONTARIO).
Institute for Information Technology
[NRC-37061] p 3118 N94-26709
Abstracts of papers presented at the 4th CASI Aerodynamics Symposium
[ISBN-0-920203-01-9] p 2651 N94-28315
Solution-adaptive simulation of transonic cascade flows p 2657 N94-28344

NATIONAL RESEARCH INST. FOR EARTH SCIENCE AND DISASTER PREVENTION, SHINJO (JAPAN).
Detection of water on road surface by the polarized light p 2886 N94-27989

NATIONAL RESEARCH INST. FOR EARTH SCIENCE AND DISASTER PREVENTION, TSUKUBA (JAPAN).
Meteorological data at the Nagaoka Institute of Snow and Ice Studies
[REPT-158] p 2896 N94-27169
Report of the National Research Institute for Earth Science and Disaster Prevention, No. 51
[JTN-94-80509] p 2886 N94-27985
Observation with STS seismometer at Nakaizu, central Japan: Observation system and comparison with tiltmeter p 2886 N94-27986
Underground structure in the eastern part of Kanagawa Prefecture inferred from explosion seismic observations p 2886 N94-27987
Analysis of S-wave seismogram envelope of deep earthquakes and estimation of random inhomogeneities in the Kanto-Tokai area p 2886 N94-27988
Cooperative research projects on satellite remote sensing for the hydrological subjects p 2853 N94-28270
Contribution of satellite observation to global change research p 2876 N94-28293

NATIONAL RESEARCH INST. FOR METALS, TOKYO (JAPAN).
Bulletin of National Research Institute for Metals in Fiscal Year 1993, no. 14
[REPT-14] p 2722 N94-25544
Development of intermetallic compounds for high performance luminescence elements p 2722 N94-25545
Corrosion resistance at welded zones of nuclear fuel reprocessing system p 2722 N94-25546
Interactions between corrosion fatigue and stress corrosion crack on steel for light water reactors p 2722 N94-25547
Preparation of creep data sheet: Material strength data sheet p 2723 N94-25548
R and D for creation, measurement, application of ultra-high vacuum p 2723 N94-25549
Knowledge base systems for chemical compounds designing support p 2723 N94-25550
Hydrogen trapping with Pd coated alloy films p 2723 N94-25551
Basic research on levitation fusing/solidification technology p 2723 N94-25552
Inner fiber observation for metal matrix composites under the stress load condition utilizing Synchrotron Orbital Radiation (SR) by X-ray CT p 2724 N94-25553
Observation on metal surface in aqueous solution using an electrochemical Scanning Tunneling Microscope (STM) p 2724 N94-25554
Fundamental study on monitoring technology on local surface damages p 2724 N94-25555
Study on phase transformation due to deformation in ferromagnetic fields at cryogenic condition p 2724 N94-25556
Study on characteristics and electronic structures of materials with strong electronic correlations by ferromagnetic fields p 2724 N94-25557
Study on reactions between molten metal and oxide by magnetic flotation dissolution method p 2725 N94-25558
Study on ferromagnetic field magnet using strong and highly conductive material p 2725 N94-25559
Study on measurement and evaluation methods for superconductive characteristics p 2725 N94-25560
Combustion synthesis method p 2721 N94-25561
Development of SO(x) and NO(x) solid electrolyte sensors p 2725 N94-25562
Study on synthesis and characteristics of intermetallic compound with strong electron correlation p 2726 N94-25563
Study on computerized experiment of amorphous transformation process by solid phase reaction p 2726 N94-25564
Study on alloy films for hydrogen separation p 2726 N94-25565
Study on the mechanism of titanium alloy toughness and the improvement of properties p 2726 N94-25566
Study on improvements in fretting fatigue characteristics of high strength structural member p 2726 N94-25567
Study on knowledge extraction and systematization for material design p 2727 N94-25568
Fundamental study on new synthetic technology by phthalocyanine complexes p 2721 N94-25569
Study on substance diffusion in thin films with controlled structures p 2727 N94-25570
Study on microscopic structural controls and electronic properties at material surfaces by ion beams p 2727 N94-25571
Study on production of materials with one direction solidification texture p 2727 N94-25572
Study on solidification of non-homogeneous melting/solidification materials p 2728 N94-25573

Study on interfacial reaction analysis at interfacial joining p 2728 N94-25574
Study on film generation phenomena by particle deposition p 2728 N94-25575
Study on development of chemical measurement method utilizing plasmas p 2728 N94-25576
Study on improvement in physical analysis method of metallic materials p 2728 N94-25577
Study on analyzing method establishment for metallic material development p 2729 N94-25578
Study on variation of damage generation mechanism by fatigue on TiAl compounds due to different slip systems p 2729 N94-25579
Study on high temperature damage control and life improvement p 2729 N94-25580
Study on elucidation of damage generation process by electron beam lithography p 2729 N94-25581
Study on performance evaluation of pressure vessel steel in corrosion environments with sulfide
p 2730 N94-25582
Study on evaluation of crack generation and crack growth behaviors under static loading at high temperature and under combined loading p 2730 N94-25583
Study on fatigue crack propagation characteristics around welded joint interface in complexed conditions
p 2730 N94-25584
Study on melted solution stirring under microgravity
p 2730 N94-25585
Study on utilization of super clean, high vacuum space
p 2682 N94-25586
Technical report of ISSP. Ser. A, no. 2681: Orbital and spin susceptibilities of the plane copper sites in YBa2Cu3O(x) system
[JTN-94-80567] p 3064 N94-27177

NATIONAL RESEARCH INST. OF FISHERIES ENGINEERING, TOKYO (JAPAN).
Computer aided data recording and analyzing system for the engine test p 2764 N94-27979
The emission characteristics of a high speed diesel engine p 2764 N94-27980

NATIONAL SCIENCE FOUNDATION, WASHINGTON, DC.
Spaces of algebraic cycles
[PB94-124369] p 2996 N94-26993
Selected data on Federal support to universities and colleges: FY 1991
[NSF-93-320] p 3101 N94-28201
Proton aurora and substorm intensifications
[ATR-93(7248)-1] p 2887 N94-28218

NATIONAL SCIENCE TEACHERS ASSOCIATION, WASHINGTON, DC.
Lyapunov exponents for some quasi-periodic cocycles
[PB94-124377] p 2997 N94-26994

NATIONAL SPACE DEVELOPMENT AGENCY, OHASHI (JAPAN).
NASDA contribution plan to Asian countries
p 2853 N94-28273

NATIONAL SPACE DEVELOPMENT AGENCY, TOKYO (JAPAN).
On-board computer for control subsystem of satellite
p 2949 N94-26716

NATIONAL TRANSPORTATION SAFETY BOARD, WASHINGTON, DC.
Aircraft accident report: Runway departure following landing American Airlines flight 102, McDonnell Douglas DC-10-30, N139AA, Dallas/Fort Worth International Airport, Texas, April 14, 1993
[PB94-910402] p 2660 N94-27766
Special investigation report: Safety issues related to wake vortex encounters during visual approach to landing
[PB94-917002] p 2660 N94-27881

NAUCHNO-ISSLEDOVATELSKII INST. EHLEKTROFIZICHESKOJ APPARATURY, LENINGRAD (USSR).
Numerical simulation of plasma vertical position stabilization in ITER
[DE93-634588] p 3044 N94-26510

NAVAL ACADEMY, ANNAPOLIS, MD.
Low-cost unmanned lunar lander
p 2697 N94-25699

NAVAL AEROSPACE MEDICAL RESEARCH LAB., PENSACOLA, FL.
Effects of methamphetamine on vigilance and tracking during extended wakefulness
[AD-A274896] p 2909 N94-26179
A comparison of two hardware implementations of a crew selection system
[AD-A274913] p 2937 N94-26346

NAVAL AIR WARFARE CENTER, WARMINSTER, PA.
A critical analysis of workload predictions generated by multiple resource theory during early crewstation design
[AD-A274804] p 2941 N94-26339
Methods for experimentally determining commercial jet aircraft landing parameters from video image data
[AD-A274207] p 2669 N94-27105

NAVAL COMMAND, CONTROL AND OCEAN SURVEILLANCE CENTER, SAN DIEGO, CA.
Radar detection of low-altitude targets in a maritime environment. Volume 2: Meteorological and radar data
[AD-A274658] p 2768 N94-26335
Demonstration of monolithic co-fabrication of Y1Ba2Cu3O7-Sigma and CMOS devices on the same sapphire substrate
[AD-A274757] p 3059 N94-26566
Generalized emulation microcircuit program
[AD-A274749] p 2785 N94-26797

NAVAL HEALTH RESEARCH CENTER, SAN DIEGO, CA.
Rewarming methodologies in the field
[AD-A274744] p 2909 N94-26173
Monitoring activity with a wrist-worn actigraph: Effects of amplifier passband and threshold variations
[AD-A274705] p 2909 N94-26377
Performance assessment in sustained operations using a computer-based synthetic work task
[AD-A274707] p 2937 N94-26430

NAVAL OCEANOGRAPHY COMMAND CENTER/JOINT TYPHOON WARNING CENTER, FPO SAN FRANCISCO, CA.
Tropical cyclone report, 1992
[AD-A274464] p 2896 N94-27025

NAVAL POSTGRADUATE SCHOOL, MONTEREY, CA.
Repeated knots in least squares multiquadric functions
[AD-A273866] p 2990 N94-25594
Predicting antenna parameters from antenna physical dimensions
[AD-A273893] p 3012 N94-25655
High temperature superconducting infrared imaging satellite p 2698 N94-25700
Low Earth orbit communications satellite
p 2698 N94-25701
Hydrographic and Acoustic Doppler Current Profiler (ADCP) data from the ONR eastern boundary current accelerated research initiative, 9-16 June 1992
[AD-A274115] p 2898 N94-26076
The study of single-pass GMA welds with different cover gas compositions on HSLA-100 steel
[AD-A274857] p 2822 N94-26174
Test methods and custom hardware for functional testing of a high speed GaAs DRAM
[AD-A274859] p 2781 N94-26175
Code division multiple access local area network communications employing fiber optic signal processing techniques
[AD-A274897] p 3096 N94-26180
Implementing a multiple criteria model base in co-op with a graphical user interface generator
[AD-A274901] p 3093 N94-26181
An analysis of multiple sensor system payloads for unmanned aerial vehicles
[AD-A274905] p 2667 N94-26182
Mesoscale frontal evolution of the ERICA IOP-5A Cyclone
[AD-A274906] p 2893 N94-26183
Effects of post-fabrication processing on the tensile properties of centrifugally cast SiC particulate reinforced aluminum composites
[AD-A274865] p 2707 N94-26190
Computational investigation of the compressible dynamic stall characteristics of the Sikorsky SSC-A09 airfoil
[AD-A274867] p 2644 N94-26191
Linear modeling of rotorcraft for stability analysis and preliminary design
[AD-A274869] p 2677 N94-26192
Design and specification of the Xpress transfer high-speed protocol
[AD-A274941] p 3097 N94-26297
NPSNET-4: A real-time, 3D distributed interactive virtual world
[AD-A274942] p 2961 N94-26298
Business process redesign: Design the improved process
[AD-A274947] p 3093 N94-26299
Design and implementation of a query editor for the Amadeus system
[AD-A274955] p 3097 N94-26300
Hybrid power system for remote communications stations
[AD-A274963] p 2782 N94-26301
Methods for improving low-angle, low-altitude radar tracking accuracy
[AD-A274914] p 2768 N94-26347
New binary integration strategies and corresponding R90 calculations
[AD-A274786] p 2769 N94-26359
Topics in longshore currents
[AD-A274788] p 2899 N94-26361
An apparatus for measurement of ignition and burning characteristics of metallic particles
[AD-A274815] p 2716 N94-26487
MIMO recursive least squares control algorithm for the AN/FPN-44A Loran-C transmitter
[AD-A274820] p 2664 N94-26493
Laser Doppler velocimetry in a low speed multistage compressor
[AD-A274836] p 2818 N94-26498
Modeling and simulation of a fiber distributed data interface local area network
[AD-A274838] p 3098 N94-26500
Application of Space Shuttle Project Hercules imagery in the investigation of ship cloud tracks
[AD-A274923] p 2692 N94-26529
Usefulness of compile-time restructuring of LGDF programs in throughput-critical applications
[AD-A274915] p 2963 N94-26530
Computer code for interactive rotorcraft preliminary design using a harmonic balance method for rotor trim
[AD-A274924] p 2668 N94-26531
A study on piezoelectric actuators and sensors for vibration control of flexible space structures
[AD-A274925] p 2695 N94-26532
Study of precipitation and recrystallization in Al alloy 2519 by backscattered electron imaging methods
[AD-A274919] p 2736 N94-26533
A finite wake theory for two-dimensional rotary wing unsteady aerodynamics
[AD-A274921] p 2645 N94-26535
A survey of uncontrolled satellite reentry and impact prediction
[AD-A274903] p 2695 N94-26750
Combatting inherent vulnerabilities of CFAR algorithms and a new robust CFAR design
[AD-A274918] p 2770 N94-26751
The influence of TIG welding thermal cycles on HSLA-100 steel plate
[AD-A274248] p 2740 N94-27009
Concepts and methods of measuring productivity at the organization level
[AD-A273126] p 3094 N94-27180
Performance considerations for the application of the lossless browse and residual model
p 2946 N94-28256

NAVAL RESEARCH LAB., MONTEREY, CA.
Development and testing of the Coupled Ocean/Atmosphere Mesoscale Prediction System (COAMPS)
[AD-A273925] p 2892 N94-25793
The NOGAPS ten year AMIP integration
[AD-A274332] p 2900 N94-26887
Leadex environmental phenomena and effects observed by DMSP, NOAA, and ERS-1 satellites
[AD-A274596] p 2868 N94-26888

NAVAL RESEARCH LAB., WASHINGTON, DC.
Theoretical aspects of the agile mirror
[AD-A274890] p 2767 N94-26177
Direct-conversion-to-baseband for a nonlinear FM signal
[AD-A274861] p 2768 N94-26189
Vcalc: A 3-space vector calculator
[AD-A274520] p 2965 N94-26831
Implementation of a compact magnetic electron energy spectrometer for intense relativistic electron beams
[AD-A274451] p 3033 N94-27082
A pressure based charge control system for the DSPSE NiH2 CPV battery p 2863 N94-28127

NAVAL SURFACE WARFARE CENTER, CRANE, IN.
Characterization and calibration of the Agema 880+ imaging radiometer
[AD-A274417] p 3036 N94-26981
Radiometric, spectral, and effectiveness equipment
[AD-A274208] p 3037 N94-27066
NSWC Crane Aerospace Cell Test History Database
p 2860 N94-28102
Analysis for nickel (3 and 4) in positive plates from nickel-cadmium cells p 2861 N94-28107
AF Ni-Cd cell qualification program
p 2863 N94-28122

NAVAL SURFACE WARFARE CENTER, DAHLGREN, VA.
An algorithm to find the intersection of two convex polygons
[AD-A274722] p 2961 N94-26148

NAVAL UNDERSEA WARFARE CENTER, NEWPORT, RI.
Fuzzy robust statistics for application to the fuzzy c-means clustering algorithm
[AD-A274719] p 3003 N94-26436
Prewhitening of colored noise fields for detection of threshold sources
[AD-A274346] p 3010 N94-26923

NEDERLANDS INST. VOOR ONDERZOEK DER ZEE, TEXEL.
Macrobenthic fauna in the dutch sector of the north sea in 1991
[PB94-126414] p 2868 N94-27200

NEW BRUNSWICK UNIV., FREDERICTON.
Fractals and their applications to remote sensing and digital mapping
[ISBN-0-315-59469-1] p 2852 N94-27870
NEW ENERGY AND INDUSTRIAL TECHNOLOGY DEVELOPMENT ORGANIZATION, TOKYO (JAPAN).
Feasibility study on introduction of the bio-fuel power generation in tropical regions
[DE94-725203] p 2858 N94-26838
Feasibility study on construction of a global environment research and development information network
[DE94-725198] p 2868 N94-26904
Feasibility study on introduction of transportation-use petroleum substitution energy
[DE94-725205] p 2759 N94-26905
Handbook of photovoltaic power generating design for introduction
[DE94-725199] p 2858 N94-26913
Present situation of the development of petroleum substitution energy (France)
[DE94-725201] p 2760 N94-26914
NEW HAMPSHIRE UNIV., DURHAM.
Ionosphere-magnetosphere coupling
[NASA-CR-195222] p 2881 N94-27237
NEW JERSEY INST. OF TECH., NEWARK.
Observation of impulsive acoustic events and the excitation of solar oscillations
[AD-A274159] p 3111 N94-27096
NEW MEXICO STATE UNIV., LAS CRUCES.
Hotine's (omega, phi, nu) coordinate system
[PL-TR-93-2174] p 3001 N94-28216
NEW ORLEANS UNIV., LA.
Computational studies of energetic organic molecules
[AD-A274726] p 3018 N94-26172
Computational analysis of some aspects of a synthetic route to ammonium dinitramide
[AD-A274648] p 2704 N94-26353
Molecular surface electrostatic potentials in the analysis of non-hydrogen-bonding noncovalent interactions
[AD-A274612] p 3022 N94-26894
NEW YORK UNIV., NEW YORK.
Improved numerical methods for quantum field theory (Outstanding Junior Investigator Award)
[DE94-001793] p 3073 N94-27002
A general theory of impacts and mass extinctions, and the consequences of large-body impact on the Earth
p 2891 N94-28310
NICHOLS RESEARCH CORP., ARLINGTON, VA.
Space Experiments with Particle Accelerators (SEPAC)
[NASA-CR-193935] p 2761 N94-27664
NIHON UNIV., TOKYO (JAPAN).
A laboratory test on construction of ice domes and their load-carrying capacity p 2884 N94-27966
NIJMEGEN UNIV. (NETHERLANDS).
Object-oriented development methods
p 2975 N94-27938
CASE tools for the support of object-oriented analysis and design methods p 2975 N94-27939
NIPPON ELECTRIC CO. LTD., TOKYO (JAPAN).
Fault tolerant real-time processing system for space use p 2949 N94-26720
NORFOLK STATE UNIV., VA.
An experimental investigation of fatigue damage in aluminum 2024-T3 alloys p 2747 N94-27900
NORTH CAROLINA AGRICULTURAL AND TECHNICAL STATE UNIV., GREENSBORO.
Investigation of forced and isothermal chemical vapor infiltrated SiC/SiC ceramic matrix composites
[DE94-004544] p 2708 N94-26557
NORTH CAROLINA STATE UNIV., RALEIGH.
Growth, characterization and device development in monocrystalline diamond films
[AD-A274245] p 3060 N94-26839
Nitride semiconductors for ultraviolet detection
[AD-A274246] p 3060 N94-26840
Pseudomorphic semiconducting heterostructures from combinations of AlN, GaN and selected SiC polytypes: Theoretical advancement and its coordination with experimental studies of nucleation, growth, characterization and device development
[AD-A274247] p 3061 N94-26841
Atomic layer epitaxy of group 4 materials: Surface processes, thin films, devices and their characterization
[AD-A274325] p 3061 N94-26885
Low temperature deposition and characterization of N- and p-type silicon carbide thin films and associated ohmic and Schottky contacts
[AD-A274345] p 2754 N94-26974
Interface properties of wide bandgap semiconductor structures
[AD-A274356] p 3063 N94-27058
NORTH CAROLINA UNIV., CHAPEL HILL.
Psychophysiology in microgravity and the role of exercise p 2936 N94-28374
NORTHEASTERN UNIV., BOSTON, MA.
Control oriented system identification
[AD-A274162] p 2987 N94-27124
NORTHROP CORP., PICO RIVERA, CA.
Advanced metallic exhaust impinged structural concepts demonstration p 2832 N94-28209
NORTHWEST RESEARCH ASSOCIATES, INC., BELLEVUE, WA.
Comparative investigation of high-latitude ionospheric structure and effects near solar maximum
[AD-A273799] p 2877 N94-25877
NORTHWESTERN UNIV., EVANSTON, IL.
Extension of On-Surface Radiation Condition (OSRC) theory to full-vector electromagnetic wave scattering by three-dimensional conducting, dielectric, and coated targets
[AD-A274023] p 2766 N94-25757
Effects of physical aging on long-term behavior of composites p 2712 N94-27897
NORWEGIAN DEFENCE RESEARCH ESTABLISHMENT, KJELLER.
The chemical detector paper as a potential alarm
[FFI-93/6007] p 2712 N94-25745
Norwegian ionospheric satellite experiment: High latitude, low Earth orbit plasma measurements
[FFI-93/7025] p 2876 N94-25807
Technical description of the Vulcano software library
[FFI-93/7024] p 2767 N94-26105
Laser-based communication link
[FFI-93/7023] p 2817 N94-26203
Detection of transient vector-fields in additive noise
[FFI-93/7028] p 2768 N94-26232
Results from a fracture mechanical serial investigation of breechrings on the M109A3GN howitzer
[FFI-93/8002] p 2837 N94-26233
Safety standards for aircraft shelter
[FFI-92/4003] p 2680 N94-26305
NOTRE DAME UNIV., IN.
Design study to simulate the development of a commercial freight transportation system
p 2671 N94-25715
The effects of three-dimensional imposed 3-d disturbances on bluff-body near wake flows
[AD-A274845] p 2791 N94-26187
Rydberg states in multiply charged ions
[DE94-002335] p 3021 N94-26760
Aircraft wheel life assessment
[AD-A274378] p 2823 N94-26976
Meson spectroscopy and particle astrophysics
[DE94-001799] p 3115 N94-27003
NR/NS, INC., KANATA (ONTARIO).
Planning for the future of the DREnet: The way ahead
[NRNS-002-00-001-01] p 2983 N94-28042

O

OAK RIDGE ASSOCIATED UNIVERSITIES, INC., TN.
Experimental and numerical investigation of shock wave propagation through complex geometry, gas continuous, two-phase media
[DE94-001408] p 2791 N94-26121
OAK RIDGE INST. FOR SCIENCE AND EDUCATION, TN.
Interaction between a high density-low temperature plasma and a frozen hydrogen pellet in a railgun injector
[DE94-000846] p 3041 N94-25949
Interactions between a tropical mixed boundary layer and cumulus convection in a radiative-convective model
[DE94-000848] p 2877 N94-25979
Resonant holographic measurements of laser ablation plume expansion in vacuum and argon gas backgrounds
[DE94-001407] p 2813 N94-27615
OAK RIDGE NATIONAL LAB., TN.
Design of folded waveguide antenna for Alcator C-Mod
[DE94-003584] p 2767 N94-25924
RF modeling and design of a folded waveguide launcher for the Alcator C-Mod tokamak
[DE94-003588] p 3041 N94-25933
Collaborative research on ion implantation of ceramics
[DE93-019177] p 2749 N94-26080
Structure of the modulated magnetic phase of Mn3Sn
[DE94-002788] p 2733 N94-26092
Environmental benefits of different types of heat pumps, available and expected
[DE94-002440] p 2866 N94-26123
Ion implantation of diamond: Damage, doping, and lift-off
[DE94-001133] p 3054 N94-26137
High-speed repetitive pellet injector for plasma fueling of magnetic confinement fusion devices
[DE94-002792] p 3042 N94-26140
An atom probe investigation of the influence of trace impurities on the mechanical behavior of NiAl
[DE94-002797] p 2734 N94-26272
Ceramic technology project
[DE94-003782] p 2750 N94-26332
Computer visualizations in engineering applications
[DE94-003589] p 2822 N94-26465
An efficient communication scheme for solving the S(sub n) equations on message-passing multiprocessors
[DE94-000378] p 2769 N94-26482
Investigation of forced and isothermal chemical vapor infiltrated SiC/SiC ceramic matrix composites
[DE94-004544] p 2708 N94-26557
Signatures for hybrids
[DE94-004244] p 3020 N94-26574
Deposition of a-SiC:H using organosilanes in an argon/hydrogen plasma
[DE94-004428] p 2751 N94-26580
Probability of accessing the multiple saturated states in the resistive interchange instability
[DE94-000478] p 3044 N94-26694
Parallel matrix transpose algorithms on distributed memory concurrent computers
[DE94-002424] p 2964 N94-26764
Electron microscopy of AlN-SiC interfaces and solid solutions
[DE94-002449] p 3059 N94-26765
New FORTRAN computer programs to acquire and process isotopic mass spectrometric data: Operator's manual
[DE94-003174] p 2965 N94-26784
Conceptual design of the tokamak radiation shielding for the Tokamak Physics Experiment (TPX)
[DE94-002791] p 3044 N94-26858
Potential of commercial tokamak reactors with improved physics
[DE94-002794] p 3044 N94-26860
Methodology for first wall design
[DE94-002795] p 3045 N94-26861
The role of point defect clusters in reactor pressure vessel embrittlement
[DE94-001122] p 2739 N94-26931
Ion implantation and dynamic recovery of tin-doped indium oxide films
[DE94-001126] p 3062 N94-26932
Sensor-based navigation of a mobile robot using automatically constructed fuzzy rules
[DE94-001137] p 2986 N94-26948
Charmonium physics at a tau-charm factory
[PB94-124344] p 3024 N94-27199
Experimental measurement of local displacement and chemical pair correlations in crystalline solid solutions
[DE94-001124] p 3065 N94-27251
Design and control of phased ICRF antenna arrays
[DE94-002796] p 3046 N94-27261
Fast wave current drive technology development at ORNL
[DE94-004243] p 3046 N94-27568
Current status of research and development on nickel and iron aluminides
[DE94-004247] p 2741 N94-27616
Coastal Zone Management Act and related legislation, revision 3
[DE94-004180] p 2869 N94-27691
On modeling and controlling intelligent systems
[DE94-002446] p 2988 N94-27706
Electron microscopy studies of undoped and phosphorus doped Si:H and Si,C:H films
[DE94-004738] p 3069 N94-27757
Helium transport and exhaust studies of H-mode discharges in the D3-D tokamak
[DE94-004744] p 3048 N94-27785
OAK RIDGE Y-12 PLANT, TN.
Plasma surface cleaning using microwave plasmas
[DE94-002754] p 2713 N94-26014
Vapor deposition of copper on stainless steel 304L
[DE94-001945] p 2740 N94-27006
Evaluating non-chlorinated solvents for welding applications
[DE94-003332] p 2824 N94-27181
OCEANOGRAPHIC CONSULTANTS.
Sonic booms and marine mammals: Informational status and recommendations p 2651 N94-28196
ODYSSEY RESEARCH ASSOCIATES, INC., ITHACA, NY.
Using formal specification in the Guidance and Control Software (GCS) experiment. Formal design and verification technology for life critical systems
[NASA-CR-194884] p 2956 N94-28267
OFFICE NATIONAL D'ETUDES ET DE RECHERCHES AEROSPATIALES, PARIS (FRANCE).
Experimental study on the interactions between a transverse heated supersonic jet and an external supersonic flow p 2659 N94-28039
OHIO STATE UNIV., COLUMBUS.
Project WISH: The Emerald City p 2703 N94-25690
The design of four hypersonic reconnaissance aircraft
p 2671 N94-25716
Pacing visual attention: Temporal structure effects
[AD-A273859] p 2937 N94-25965

Joint services electronics program
[AD-A274692] p 2783 N94-26449

Strongly interacting fermion systems
[DE94-002674] p 3021 N94-26677

Joint services electronics program
[AD-A274643] p 2785 N94-27027

Root gravitropism in maize and Arabidopsis
[NASA-CR-195710] p 2903 N94-27940

OHIO UNIV., ATHENS.

Theoretical and computational studies in intermediate energy nuclear physics
[DE94-004177] p 3012 N94-25800

Investigation of air transportation technology at Ohio University, 1992-1993 p 2642 N94-27288

Fault detection and isolation p 2642 N94-27289

Improved modeling of GPS selective availability
p 2642 N94-27290

Realtime mitigation of GPS SA errors using Loran-C
p 2642 N94-27291

A GPS coverage model p 2642 N94-27292

Ground station siting considerations for DGPS
p 2642 N94-27293

OKLAHOMA STATE UNIV., STILLWATER.

Liquid crystalline side-chain polysiloxanes with 4-amino-4'-stilbene-carboxylic ester mesogens
[AD-A274510] p 2754 N94-27036

OLD DOMINION UNIV., NORFOLK, VA.

Extraterrestrial surface propulsion systems
p 2833 N94-25691

The 1993 NASA-ODU American Society for Engineering Education (ASEE) Summer Faculty Fellowship Program
[NASA-CR-191544] p 3085 N94-27893

Brain wave correlates of attentional states: Event related potentials and quantitative EEG analysis during performance of cognitive and perceptual tasks
p 2940 N94-27901

System identification of the Large-Angle Magnetic Suspension Test Facility (LAMSTF)
p 2682 N94-27908

A numerical study of mixing and combustion in hypervelocity flows through a scramjet combustor model
p 2808 N94-27911

Experimental apparatus for optimization of flap position for a three-element airfoil model p 2682 N94-27912

Space transportation vehicle design evaluation using saturated designs p 2693 N94-27928

OREGON STATE UNIV., CORVALLIS.

Science support for the Earth radiation budget experiment
[NASA-CR-191600] p 2894 N94-26506

Indium donor complexes with cation vacancies in CdTe and ZnSe
[DE94-002731] p 3063 N94-26958

OREGON UNIV., EUGENE.

The formation of conducting gold films by thermal decomposition and direct patterning using electron beam lithography of the gold cluster Au55P(C6H5)312C16
[AD-A273720] p 2749 N94-26074

ORGANISATIE VOOR TOEGEPAST NATUURWETENSCHAPPELIJK ONDERZOEK, THE HAGUE (NETHERLANDS).

Interface technical specification of the V.25 bis emulator
[AD-A273754] p 2948 N94-25720

Theory and modeling of stimulated Raman scattering
[AD-A273755] p 3033 N94-25721

Wind measurements with an incoherent lidar
[AD-A273756] p 2891 N94-25722

A feasibility study on bird classification with neural network
[AD-A273753] p 2659 N94-25780

Zernike moments and rotation invariant object recognition. A neural network oriented case study
[AD-A273749] p 2767 N94-26011

Conversion of the CLUSE model for applications over open ocean
[AD-A273750] p 2893 N94-26013

An overview of the TNO contribution to VAST 92
[AD-A273751] p 2893 N94-26016

ORGANIZATION FOR INDUSTRIAL RESEARCH, TNO, THE HAGUE (NETHERLANDS).

A real-time convolution algorithm and architecture with applications in SAR processing
[AD-A273817] p 2959 N94-25963

OSAKA PREFECTURE UNIV., SAKAI (JAPAN).

The effect of body orientation on the perception of vertical and horizontal distance in an outdoor setting
p 2915 N94-27461

OSAKA UNIV., IBARAKI (JAPAN).

Proceedings of the workshop on (pi), K, (eta)-nucleon interactions
[DE94-701314] p 3027 N94-27733

OSAKA UNIV. (JAPAN).

The role of beta-adrenoceptor stimulation in the progression of chronic heart failure
p 2932 N94-27541

OTTAWA UNIV. (ONTARIO).

Series solution for a cylindrical composite shell subject to axisymmetric loadings
[ISBN-0-315-60559-6] p 2844 N94-27810

Receiving antennas for electromagnetic pulses and transients
[ISBN-0-315-62312-8] p 2777 N94-27871

P

PACIFIC NORTHWEST LAB., RICHLAND, WA.

Microstructural development in low activation ferritic alloys irradiated to 200 dpa at 420 C
[DE94-004269] p 2731 N94-25803

Radiation hardening effects on localized deformation and stress corrosion cracking of stainless steels
[DE94-004308] p 2731 N94-25804

Structure and properties of intermetallic composites synthesized in situ using solid state displacement reactions
[DE94-004312] p 2705 N94-25805

Full-text information services at the desktop
[DE94-003728] p 3096 N94-25813

Implications of policies and prevent climate change for future food security
[DE93-018872] p 2866 N94-25948

General Motors Corporation and Pacific Northwest Laboratory staff exchange: Inspection of case hardened steels and metal-matrix composites
[DE94-003470] p 2706 N94-25982

Effect of loading mode on the fracture toughness of a reduced activation ferritic/martensitic stainless steel
[DE94-004290] p 2732 N94-25987

Software redesign for usability: A case study
[DE94-003704] p 2960 N94-26048

Modeling defect production in high energy collision cascades
[DE94-003810] p 3017 N94-26049

Alternative materials for solid oxide fuel cells: Processing and interactions of materials
[DE94-000016] p 2855 N94-26114

Oxygen reduction at a YSZ interface with cathode materials La(1-x)(Ca or Sr)(x)MnO3(1-x)CaMnO3
[DE94-002954] p 3054 N94-26147

Differential global positioning system for the surface-towed ordnance locating system: Testing, results, and user's guide
[DE94-002980] p 2664 N94-26309

Scientific and Technical Information (STI)....what's the status?
[DE94-003731] p 3097 N94-26348

Early stages in the development of stress corrosion cracks
[DE94-003867] p 2838 N94-26524

Emerging Human-Computer Interface (HCI) design guidelines for Graphical User Interface (GUI)
[DE94-004293] p 2941 N94-26555

Microstructural development in irradiated vanadium alloys
[DE94-004307] p 2737 N94-26556

Influence of helium generation rate and temperature history on mechanical properties of model Fe-Cr-Ni alloys irradiated in FFTF at relatively low displacement rates
[DE94-004264] p 2737 N94-26575

Structure and properties of composites synthesized in situ using solid state displacement reactions
[DE94-004589] p 2737 N94-26585

Mesoscale meteorological measurements characterizing complex flows
[DE94-002359] p 2895 N94-26761

Recent ASCOT experiments in multi-layered flows
[DE94-002360] p 2880 N94-26762

Engineering limitations of ceramic composites for high performance and high temperature applications
[DE94-001676] p 2754 N94-27021

Reinventing information services to increase customer satisfaction
[DE94-003718] p 3100 N94-27563

Iterative methods for the WLS state estimation on RISC, vector, and parallel computers
[DE94-004260] p 3000 N94-27569

Grain boundary chromium concentration effects on the IGSCC and IASCC of austenitic stainless steels
[DE94-004268] p 2741 N94-27570

High performance computing in chemistry and massively parallel computers: A simple transition?
[DE94-004318] p 2982 N94-27600

An overview of the ASCOT program
[DE94-004356] p 2869 N94-27601

Effect of temperature and recoil-energy spectra on irradiation-induced amorphization in Ca2La8(SiO4)6O2
[DE94-004371] p 3067 N94-27602

Monte Carlo calculations of low background detector response
[DE94-004593] p 3116 N94-27621

Effect of precipitate structure on hot deformation of Al-Mg-Mn alloys
[DE94-004596] p 2741 N94-27622

Comparison of dynamic analysis of a Schilling hydraulic manipulator with experimental results
[DE94-004597] p 2827 N94-27780

Bench-scale synthesis of nanoscale materials
[DE94-004787] p 2742 N94-27786

PACIFIC-SIERRA RESEARCH CORP., SANTA MONICA, CA.

Excitation of Earth-ionosphere waveguide in the ELF and lower VLF bands by modulated ionospheric current
[AD-A274969] p 2878 N94-26304

PANAMETRICS, INC., WALTHAM, MA.

Develop and fabricate a radiation dose measurement system for satellites
[PL-TR-93-2161] p 2698 N94-28210

Develop and fabricate a radiation dose measurement system for satellites
[PL-TR-93-2099] p 2698 N94-28217

PAUL D. CAMP COMMUNITY COLL., SUFFOLK, VA.

ADP Analysis project for the Human Resources Management Division p 2978 N94-27927

PENNSYLVANIA STATE UNIV., UNIVERSITY PARK.

The high Reynolds number flow through an axial-flow pump
[AD-A273844] p 2789 N94-25604

Comet nucleus and asteroid sample return missions
p 2689 N94-25692

Interactions between a tropical mixed boundary layer and cumulus convection in a radiative-convective model
[DE94-000848] p 2877 N94-25979

Influence of point defects on grain boundary diffusion in oxides
[DE94-003164] p 3060 N94-26782

Numerical analysis of the photo-dissociation/radical oxidation of formaldehyde by ultraviolet light in a photolytic reactor
[AD-A274539] p 2868 N94-26843

High temperature sensor/microphone development for active noise control
[NASA-CR-195214] p 2812 N94-27214

Basic research on natural gas combustion phenomena
[PB94-129046] p 2717 N94-27256

A comprehensive comparison of turbulence models in the far wake p 2808 N94-27899

Progress in modeling atmospheric propagation of sonic booms p 2650 N94-28189

Implications for high speed research: The relationship between sonic boom signature distortion and atmospheric turbulence p 2650 N94-28190

PENNSYLVANIA UNIV., PHILADELPHIA.

Transition metals in highly correlated discotic phases: Designing metallomesogens with selected intermolecular organizations
[AD-A274695] p 2736 N94-26452

A semiclassical reactive flux method for the calculation of condensed phase activated rate constants
[AD-A274850] p 3020 N94-26562

Octahedral metallomesogens: Liquid crystallinity in low aspect ratio materials
[AD-A274830] p 3059 N94-26571

PHILIPS INTERNATIONAL B.V., EINDHOVEN (NETHERLANDS).

Parallel computers for advanced information processing p 2955 N94-27193

PHILLIPS LAB., EDWARDS AFB, CA.

Catalog of absolutely calibrated, range normalized, wideband, electric field waveforms from triggered lightning flashes in Florida
[AD-A273793] p 2892 N94-25873

Proceedings of the High Energy Density Matter (HEDM) Contractor's Conference
[AD-A274452] p 3033 N94-27083

PHILLIPS LAB., HANSCOM AFB, MA.

A modeling study of the mesocyclone
[AD-A274889] p 2893 N94-26168

Performance statistics bulletin: High altitude meteor scatter propagation, August, September, October 1989
[AD-A274455] p 2773 N94-27085

PHILLIPS LAB., KIRTLAND AFB, NM.

The microstructural response of granular soil under uniaxial strain
[AD-A274808] p 2763 N94-26341

Qualified manufacturing and interoperability for space applications p 2949 N94-26719

PHYSICAL OPTICS CORP., TORRANCE, CA.

Low threshold all-optical crossbar switch on GaAs-GaAlAs channel waveguide arrays
[AD-A274971] p 2783 N94-26536

PHYSICAL RESEARCH, INC., TORRANCE, CA.

Optical surface contouring for non-destructive inspection of turbomachinery
[NASA-CR-195245] p 2835 N94-26691

PHYSICAL SCIENCES, INC., ANDOVER, MA.

The importance of vibrationally excited nitrogen in silicon nitride deposition systems
[AD-A274874] p 2750 N94-26167

PHYSICS AND ELECTRONICS LAB. TNO, THE HAGUE (NETHERLANDS).

Focal plane arrays in advanced thermal images
[AD-B174292] p 3036 N94-26648

Analysis of the influence of weather on infrared imagery
[FEL-92-A421] p 3036 N94-26649

Annex report FEL-92-A163: Description of the LInk and BER Test Analysis System (LIBERTAS) for the frequency band V (14.5 - 15.3 GHz)
[FEL-92-A442] p 2770 N94-26650

CCD-Camera images of BEST-TWO and processing results
[AD-A274140] p 2811 N94-27134

Over-the-horizon propagation measurements at six radar-frequency bands at the Atlantic Ocean Coast
[AD-A274151] p 2773 N94-27136

Light emitting porous silicon
[AD-A274152] p 3038 N94-27137

PITTSBURGH UNIV., PA.

Long term learning: Integration of knowledge acquisition and knowledge compilation
[AD-A274775] p 3098 N94-26570

POLISH ACADEMY OF SCIENCES, WARSAW.

Modern photoacoustic spectroscopy problems. Theory and experiment (a review)
[IFTR-41/1993] p 2716 N94-26823

On experimental studies of yield surfaces of metals: A more general approach
[IFTR-42/1993] p 2739 N94-26824

Geometry changes in the elastic-plastic analysis of steel spatial skeletal structures
[IFTR-37/1993] p 2839 N94-26825

POLYTECHNIC UNIV., BROOKLYN, NY.

Experiments and numerical simulations of electromagnetic wave propagation in plasma varying rapidly in space and time
[AD-A274376] p 2772 N94-26975

PRAIRIE VIEW AGRICULTURAL AND MECHANICAL COLL., TX.

Design and development of the second generation Mars Habitat p 2943 N94-25693

Modeling and experimental verification of single event upsets p 2684 N94-26287

PRATT AND WHITNEY AIRCRAFT, EAST HARTFORD, CT.

Program to develop a performance and heat load prediction system for multistage turbines
[NASA-CR-195223] p 2674 N94-26588

Thermal/structural tailoring of engine blades (T/STAEBL). User's manual
[NASA-CR-194463] p 2839 N94-26692

Broad specification fuels combustion technology program, phase 2
[NASA-CR-191066] p 2719 N94-27854

PRINCETON UNIV., NJ.

Investigation of air transportation technology at Princeton University, 1992-1993 p 2643 N94-27294

Designing robust control laws using genetic algorithms p 2643 N94-27295

Optimal nonlinear estimation for aircraft flight control in wind shear p 2643 N94-27296

Air traffic management as principled negotiation between intelligent agents p 2643 N94-27297

Optical communications for transport aircraft p 2643 N94-27298

An evaluation of criteria that may be used to identify species surviving a mass extinction p 2889 N94-28304

PRINS MAURITS LAB. TNO, RIJSWIJK (NETHERLANDS).

Pulse transformer characterization
[PML-1992-73] p 2784 N94-26646

Flash unit for high speed photography
[PML-1992-91] p 2811 N94-26647

PUERTO RICO UNIV., RIO PIEDRAS.

First lunar outpost p 2943 N94-25694

PURDUE UNIV., WEST LAFAYETTE, IN.

The design of a long-range megatransport aircraft p 2671 N94-25718

Interfacial area and interfacial transfer in two-phase flow
[DE93-041226] p 2792 N94-26468

Q

QUEENS UNIV., KINGSTON (ONTARIO).

Equalization and cancellation of nonlinear intersymbol interference in a dispersive satellite communication channel
[ISBN-0-315-85147-3] p 2775 N94-27274

Finite time differential equations and their application to control systems
[ISBN-0-315-85158-9] p 2988 N94-27277

High intensity x ray instrumentation for residual strain measurements in composites and textured materials
[ISBN-0-315-85169-4] p 2842 N94-27278

The performance of nonorthogonal noncoherent frequency hopped M-ary FSK in additive white Gaussian noise, fading and jamming
[ISBN-0-315-85243-7] p 2775 N94-27301

Properties of the near-axis bispectrum applied to high-resolution astronomical imaging
[ISBN-0-315-85247-X] p 3103 N94-27302

Design and test of a regenerative satellite transmultiplexer
[ISBN-0-315-85280-1] p 2786 N94-27303

Estimation of image motion in scenes containing multiple moving objects
[ISBN-0-315-85208-9] p 2969 N94-27346

A modular approach to evaluation cryptographic protocols using Petri nets
[ISBN-0-315-85354-9] p 2972 N94-27595

Design, implementation and experimental results of robotic environment input into the Robot Controller Test Station (RCTS)
[ISBN-0-315-85355-7] p 2826 N94-27596

The numerical calculation of laminar and turbulent flows using penalty function finite volume methods
[ISBN-0-315-61377-7] p 2799 N94-27947

R

R-TECH A.B., LUND (SWEDEN).

A complete version of the Ada tasking coprocessor p 2950 N94-26721

RADEX, INC., BEDFORD, MA.

IRMA: A program for three-dimensional color display of data
[AD-A273811] p 2959 N94-25879

Modeling the DMSP and CRRES dosimeters using the path length distribution method
[RXR-93051] p 2698 N94-28200

The PROTEL contamination code
[RXR-93071] p 3040 N94-28202

Persistence of auroral electron flux events from DMSP/F9 electron measurements
[RXR-92012] p 2887 N94-28206

RAYTHEON CO., SUDBURY, MA.

Package integrity measurement technology and quality assurance
[AD-A273881] p 2834 N94-25727

RED CROSS HOSPITAL, NAGOYA (JAPAN).

Treatment of orthostatic hypotension by nasal administration of vasopressin p 2930 N94-27533

REDZONE ROBOTICS, INC., PITTSBURGH, PA.

Automated in-situ inspection systems for underground storage tanks
[AD-A274644] p 2764 N94-27144

REGINA UNIV. (SASKATCHEWAN).

An interactive, physically-based simulation system
[ISBN-0-315-83884-1] p 2963 N94-26616

The application of FD-TD method to antenna radiation patterns
[ISBN-0-315-83893-0] p 2769 N94-26618

A rough set approach to speech recognition
[ISBN-0-315-83894-9] p 2769 N94-26619

REMOTE SENSING TECHNOLOGY CENTER, TOKYO (JAPAN).

Activities of Remote Sensing Technology Center of Japan (RESTEC) p 2853 N94-28274

RENSSELAER POLYTECHNIC INST., TROY, NY.

The Lightcraft project: Flight technology for a hypersonic mass transit system p 2670 N94-25695

A global approach to kinematic path planning to robots with holonomic and nonholonomic constraints p 2683 N94-26279

Application of the CIRSSE cooperating robot path planner to the NASA Langley truss assembly problem p 2683 N94-26280

Inertial-space disturbance rejection for space-based manipulators p 2683 N94-26281

Direct model reference adaptive control of robotic arms p 2683 N94-26282

Mechanism of mechanical fatigue of silica glass
[DE94-003165] p 2753 N94-26783

An experimental study of plunging liquid jet induced air carryunder and dispersion
[AD-A274414] p 2794 N94-26979

Electroweak and other interactions in medium-energy nuclear physics
[DE94-004161] p 3027 N94-27689

Advanced development of particle beam probe diagnostic system
[DE94-002316] p 3047 N94-27720

Interaction of the sonic boom with atmospheric turbulence p 2650 N94-28191

RESEARCH DEVELOPMENT CORP. OF JAPAN, TOKYO.

Asia-Pacific Seminar on Global Change Research Cooperation
[JTN-94-80517] p 2871 N94-28268

RESEARCH INST. OF NATIONAL DEFENCE, STOCKHOLM (SWEDEN).

Visit to CERMA: Centre d'Etudes et de Recherches de Medecine Aerospatiale, Centre for Studies and Research in Aviation and Space Medicine, Bretigny sur Orge, France, November 16-18, 1992
[PB94-132990] p 2937 N94-28392

RHODE ISLAND UNIV., KINGSTON.

Surface physics with cold and thermal neutron reflectometry
[DE94-001447] p 2733 N94-26070

Parametric time-scale methods in signal analysis
[AD-A274212] p 2773 N94-27068

ROCHESTER UNIV., NY.

Flux flow, pinning, and resistive behavior in superconducting networks
[DE94-003400] p 3050 N94-25848

Theoretical and experimental studies of elementary physics
[DE94-002310] p 3008 N94-25988

Transition metal activation and functionalization of carbon-hydrogen bonds
[DE94-003650] p 2715 N94-26369

Studies of heavy-ion reactions and transuranic nuclei
[DE94-004642] p 3029 N94-27783

ROCKWELL INTERNATIONAL CORP., ANAHEIM, CA.

NASA satellite communications application research. Phase 2: Efficient high power, solid state amplifier for EFH communications
[NASA-CR-195713] p 2776 N94-27669

NASA satellite communications application research, phase 2 addendum. Efficient high power, solid state amplifier for EHF communications
[NASA-CR-195712] p 2777 N94-27946

ROCKWELL INTERNATIONAL CORP., BAY SAINT LOUIS, MS.

Orbital transfer vehicle engine technology high velocity ratio diffusing crossover
[NASA-CR-194447] p 2703 N94-27212

ROCKWELL INTERNATIONAL CORP., CANOGA PARK, CA.

Orbit transfer rocket engine technology program enhanced heat transfer combustor technology
[NASA-CR-189236] p 2700 N94-26156

STS-51 pad abort. OV103-engine 2033 (ME-2) fuel flowmeter sensor open circuit
[NASA-CR-193924] p 2701 N94-26230

Test results of the RS-44 integrated component evaluator liquid oxygen/hydrogen rocket engine
[NASA-CR-194443] p 2701 N94-26231

Orbit transfer rocket engine technology program
[NASA-CR-189229] p 2702 N94-26542

Pump CFD code validation tests
[NASA-CR-193939] p 2822 N94-26597

Orbital transfer rocket engine technology 7.5K-LB thrust rocket engine preliminary design
[NASA-CR-190754] p 2703 N94-27213

Design and experimental performance of a two stage partial admission turbine. Task B.1/B.4
[NASA-CR-179548] p 2824 N94-27228

ROCKWELL INTERNATIONAL CORP., DOWNEY, CA.

Automation life-cycle cost model
[NASA-CR-195695] p 3095 N94-27866

ROCKWELL INTERNATIONAL CORP., THOUSAND OAKS, CA.

Studies of non-linear optical effects for agile beam steering
[AD-A273998] p 3034 N94-25902

ROLLS-ROYCE LTD., BRISTOL (ENGLAND).

Influence of headwind on hot gas reingestion and consideration of pressure ratio scaling p 2675 N94-28018

Unsteady aspects of hot gas reingestion and statistical analysis p 2676 N94-28019

ROLLS-ROYCE LTD., DERBY (ENGLAND).

Gas-turbine engine steady-state behavior p 2828 N94-28044

Transient performance p 2828 N94-28045

Compressor stability p 2828 N94-28046

Engine starting and stopping p 2828 N94-28047

ROME LAB., GRIFFISS AFB, NY.

Component characterization and development 2
[AD-A274002] p 2765 N94-25660

Low noise measurements in an RF environment
[AD-A273813] p 2767 N94-25960

A current evaluation of the digital beamforming testbed at Rome Laboratory
[AD-A274311] p 3032 N94-26881

Static task allocation for parallel processing systems during software development
[AD-A274204] p 2981 N94-27100

ROYAL MILITARY COLL. OF CANADA, KINGSTON (ONTARIO).

Binary optical elements: Studies in design, manufacture and performance
[ISBN-0-315-60643-6] p 3039 N94-27643

A proposed software engineering environment for systems life cycle management
[ISBN-0-315-60634-7] p 2974 N94-27869

RTWARE, INC., DURHAM, NC.

Module interconnection frameworks for a real-time spreadsheet
[AD-A273853] p 2956 N94-25588

RUTGERS - THE STATE UNIV., PISCATAWAY, NJ.

Feature isolation and quantification of evolving datasets
[NASA-CR-195230] p 2961 N94-26207

RUTGERS UNIV., NEW BRUNSWICK, NJ.

Utility fog: A universal physical substance
p 2687 N94-27367

RUTHERFORD APPLETON LAB., CHILTON (ENGLAND).

Ma42: A new frontal code for solving sparse unsymmetric systems
[PB94-124302] p 2998 N94-27115

Charmonium physics at a tau-charm factory
[PB94-124344] p 3024 N94-27199

S

SAINT CLOUD STATE COLL., MN.

A simulation of GPS and differential GPS sensors
p 2666 N94-27918

SAN DIEGO STATE UNIV., CA.

The coming technological singularity: How to survive in the post-human era p 2685 N94-27359

SANDIA NATIONAL LABS., ALBUQUERQUE, NM.

Characteristics and control response of the TOPAZ 2 reactor system real-time dynamic simulator
[DE94-003788] p 2699 N94-25600

Molecular beam mass spectrometry studies of the chemical vapor deposition of diamond
[DE94-003802] p 3049 N94-25601

Electric-field dependence of electroreflectance and photocurrent spectra at visible wavelengths in MOVPE-grown InAlGaP multiple strained quantum-well structures
[DE94-004692] p 2780 N94-25664

Structural analysis of a frangible nut used on the NASA Space Shuttle
[DE94-003672] p 2821 N94-25811

Advanced qualification techniques
[DE94-003709] p 2780 N94-25812

Binding of copper and nickel to cavities in silicon formed by helium ion implantation
[DE94-003769] p 3050 N94-25814

Hydrogen uptake into silicon from an ECR plasma
[DE94-003771] p 3050 N94-25815

Microscopic study of local structure and charge distribution in metallic La2CuO(4+delta)
[DE94-003801] p 3050 N94-25817

Graphical programming at Sandia National Laboratories
[DE94-003803] p 2958 N94-25818

Issues for conversion coating of aluminum alloys with hydrotalcite
[DE94-003804] p 2732 N94-25819

Advances in preparing and characterizing low density pan-carbon microcellular foam
[DE94-002278] p 2748 N94-25932

In situ x ray reflectivity measurements of thin film structural evolution
[DE94-002289] p 3051 N94-25944

Renewable energy systems in Mexico: Installation of a hybrid system
[DE93-013716] p 2853 N94-25946

Out of core, out of mind: Practical parallel I/O
[DE94-003107] p 2979 N94-25952

Achieving high performance on the Intel Paragon
[DE94-003108] p 2979 N94-25953

Risk perspectives for Topaz 2 flight mission
[DE94-003229] p 2700 N94-25956

Automatic assembly planning and its role in agile manufacturing: A Sandia perspective
[DE94-002291] p 2821 N94-25970

The structural, chemical, and electrical properties of He-implantation-induced nanocavities in silicon
[DE94-002681] p 3052 N94-25971

Double layer capacitance of carbon foam electrodes
[DE94-002651] p 2780 N94-25975

A general purpose I(sub DDQ) measurement circuit
[DE94-002733] p 2781 N94-25977

Optimization of experimental conditions in IR reflectance determination of BPSG properties
[DE94-002742] p 2713 N94-25978

Investigation of plasma etch induced damage in compound semiconductor devices
[DE94-002849] p 3052 N94-25989

Oriented lead zirconate titanate thin films: Characterization of film crystallization
[DE94-003104] p 3053 N94-26025

Primary standards laboratory report 1st half 1993
[DE94-003138] p 2762 N94-26027

Testing composite-to-metal tubular lap joints
[DE94-003225] p 2836 N94-26032

Fast parallel algorithms for short-range molecular dynamics
[DE93-018519] p 3016 N94-26033

Recent developments in the Robotic All Terrain Lunar Exploration Rover (RATLER) program
[DE93-040342] p 2821 N94-26110

Temperature dependence of static RAM volatility
[DE93-040345] p 2948 N94-26111

The National Center for Advanced Information Components Manufacturing: Program update
[DE94-002647] p 2960 N94-26118

Parameter estimation by genetic algorithms
[DE94-002924] p 2961 N94-26146

Peculiarities and application perspectives of metal-ion implants in glasses
[DE94-004671] p 3035 N94-26246

Inert strength of pristine silica glass fibers
[DE94-004685] p 2750 N94-26247

A comparative evaluation of SAR and SLAR
[DE94-002922] p 2848 N94-26277

The Robotic All-Terrain Lunar Exploration Rover (RATLER): Increased mobility through simplicity
p 2685 N94-26291

A multitasking behavioral control system for the Robotic All-Terrain Lunar Exploration Rover (RATLER)
p 2685 N94-26292

MBE grown 3 to 5 strain relaxed buffer layers and superlattices characterized by atomic force microscopy
[DE94-002931] p 3056 N94-26308

Experimental determination of the CU-IN-PB ternary phase diagram
[DE94-003765] p 2735 N94-26349

Ordering and phase separation in MOCVD InGaP alloys and unicompositional quantum wells
[DE94-004693] p 3056 N94-26352

The Chaco user's guide
[DE94-003669] p 2962 N94-26370

Users manual for CATNIP: A Computer Analysis Tool for Normal Impact Penetration
[DE94-003671] p 2962 N94-26371

Characteristics and development report for the T1576 power supply and the MC3935 battery
[DE94-003675] p 2783 N94-26372

Developments in crystallographic phase analysis in the SEM: Backscattered electron Kikuchi patterns
[DE93-040755] p 3057 N94-26420

Adaptive path planning in changing environments
[DE94-003269] p 2985 N94-26462

Low-cost photovoltaic inverters incorporating application-specific integrated circuits
[DE94-003270] p 2856 N94-26463

A doubly logarithmic communication algorithm for the Completely Connected Optical Communication Parallel Computer
[DE93-019408] p 2980 N94-26473

An assessment of testing requirement impacts on nuclear thermal propulsion ground test facility design
[DE94-002933] p 2702 N94-26560

User's guide for the frequency domain algorithms in the LIFE2 fatigue analysis code
[DE94-004678] p 2838 N94-26563

The deposition of boron nitride and carbon films on silica glass fibers
[DE94-004684] p 2751 N94-26564

Microstructures of Si surface layers implanted with Cu
[DE94-004690] p 3058 N94-26565

Chemical vapor deposition and characterization of tungsten boron alloy films
[DE94-002648] p 2738 N94-26610

Merging photovoltaic hardware development with hybrid applications in the USA
[DE94-002682] p 2857 N94-26612

Simplified high-efficiency silicon cell processing
[DE94-002683] p 2857 N94-26617

Analysis/test correlation using VAWT-SDS on a step-relaxation test for the rotating Sandia 34 m test bed
[DE94-002290] p 2857 N94-26700

Multivariate calibration applied to near-infrared spectroscopy for the quantitative analysis of dilute aqueous solutions
[DE94-003231] p 2716 N94-26794

A constitutive model for layered wire mesh and aramid cloth fabric
[DE94-003275] p 2708 N94-26796

Identification and H(infinity)/(mu)-synthesis control of the Sandia truss
[DE94-002735] p 2839 N94-26810

Beam-quality measurements for materials processing lasers and the proposed ISO standard
[DE94-002738] p 2819 N94-26811

Ferroelectric thin film microstructure development and related property enhancement
[DE94-002741] p 3061 N94-26856

The electrochemical behavior of the Al3Fe intermetallic compound and localized corrosion of impure 1100 Al
[DE94-002037] p 2739 N94-26912

Extraction of modal parameters from an operating HAWT using the Natural Excitation Technique (NExT)
[DE94-001831] p 2859 N94-27004

Bibliographic Retrieval System (BARS) Sandia Shock Compression (SSC) database Shock Physics Index (SPHINX) database, volume 3
[DE94-001705] p 3099 N94-27022

Kinoform/lens system for injecting a high power laser beam into an optical fiber
[DE94-003226] p 2819 N94-27262

Multiple weight stepwise regression
[DE94-001602] p 3000 N94-27564

Influence of lattice damage on retention and transport of deuterium in beta silicon carbide
[DE94-005206] p 3068 N94-27693

Trace organic chemical detection using an ultraviolet excitation molecular beam fluorometer
[DE94-002649] p 2704 N94-27708

Sol-gel derived silica/siloxane composite materials: The effect of loading level and catalyst activity on silica domain formation
[DE94-002734] p 2712 N94-27710

Communication on the Paragon
[DE94-003103] p 2983 N94-27713

Development of a 2f optical performance measurement system
[DE94-003489] p 3039 N94-27721

Ion implantation in silicate glasses
[DE94-003785] p 2757 N94-27726

High temperature grain growth and oxidation of Fe-29Ni-17Co (Kovar (tm)) alloy leads
[DE94-004691] p 3069 N94-27753

Isothermal corrosion testing of steels in molten nitrate salts
[DE94-004695] p 2742 N94-27755

An anodic dissolution-based mechanism for the rapid cracking, pre-exposure phenomenon demonstrated by Al-Li-Cu alloys
[DE94-004798] p 2742 N94-27788

Thermally stable oxygen and nitrogen implant isolation of C-doped Al(0.35)Ga(0.65)As
[DE94-004799] p 3069 N94-27790

Simulating high-frequency wind for long durations
[DE94-002739] p 2682 N94-27997

Optical parametric oscillator modeling with diffraction, depletion, and double refraction
[DE94-001504] p 3040 N94-27999

Sum frequency generation using an optical parametric oscillator
[DE94-001827] p 3040 N94-28000

Adsorption and desorption studies of cesium on sapphire surfaces
[DE94-003798] p 3070 N94-28067

Axial focusing of impact energy in the Earth's interior: Proof-of-principle tests of a new hypothesis
p 2888 N94-28296

SANDIA NATIONAL LABS., LIVERMORE, CA.

A materials compatibility study in FM-1, a liquid component of a paste extrudable explosive
[DE94-001166] p 2759 N94-26198

Phase stability in the Cd-Mg system
[DE94-004976] p 2743 N94-27792

SANWA KAGAKU KENKYUSHO CO. LTD., KASUGAI (JAPAN).

Changes in circadian variations of urine excretion in tail-suspended rats p 2911 N94-27443

SANYO ELECTRIC CO. LTD., SUMOTO (JAPAN).

Performance test results of ETS-6 Ni-Cd cells
p 2863 N94-28121

SASKATCHEWAN UNIV., SASKATOON.

Modelling and control of plasma position in the STOR-M tokamak
[ISBN-0-315-58891-8] p 3049 N94-27949

SATELLITE METEOROLOGICAL CENTER, BEIJING (CHINA).

Study on environment monitoring over whole China using NDVI from AVHRR data and future project
p 2875 N94-28289

SCHWARTZ ELECTRO-OPTICS, INC., CONCORD, MA.

The development of Cr, Tm, Ho:YAG lasers for airborne lidar
[AD-A274895] p 2816 N94-26178

Development of lasers optimized for pumping Ti:Al2O3 lasers
[NASA-CR-4573] p 2818 N94-26705

SCIENCE AND TECHNOLOGY AGENCY, TOKYO (JAPAN).

Research on the development of fracture characteristics evaluation system for ceramics and metal composite materials p 2710 N94-27281

Asia-Pacific Seminar on Global Change Research Cooperation
[JTN-94-80517] p 2871 N94-28268

Role and activity of STA on Asian Pacific regional cooperation p 2853 N94-28269

SCIENCE APPLICATIONS INTERNATIONAL CORP., ALBUQUERQUE, NM.

Long Duration Exposure Facility space optics handbook
[AD-A274831] p 3035 N94-26572

SCIENCE APPLICATIONS INTERNATIONAL CORP., FORT WASHINGTON, PA.

Recent developments in the simulation of steady and transient transverse jet interactions for missile, rotorcraft, and propulsive applications p 2804 N94-28030

SCIENCE APPLICATIONS INTERNATIONAL CORP., HUNTSVILLE, AL.

Development and application of contamination technology for MSFC managed space systems
[NASA-CR-193934] p 2697 N94-27421

SCIENCE APPLICATIONS INTERNATIONAL CORP., MCLEAN, VA.

Laboratory plasma studies
[AD-A274655] p 3043 N94-26356

SCIENCE APPLICATIONS INTERNATIONAL CORP., SAN ANTONIO, TX.

Aircraft turbine engine reliability and inspection investigations
[AD-A274860] p 2673 N94-26176

SCIENTECH, INC., IDAHO FALLS, ID.

S-76 high intensity radiated fields, volume 2
[AD-A274572] p 2771 N94-26836

S-76 high intensity radiated fields, volume 1
[AD-A274571] p 2771 N94-26854

S-76 high intensity radiated fields, volume 3
[AD-A274416] p 2772 N94-26980

SCOTTER RESEARCH AND DEVELOPMENT LTD., THUNDER BAY (ONTARIO).

Spiral Survey Expedition: A proposal to organize for the Survey, exploration and eventual colonization of the Milky Way Galaxy p 2686 N94-27366

SCRIPPS INSTITUTION OF OCEANOGRAPHY, LA JOLLA, CA.

Coupling of pelagic and benthic communities over a seamount in the Eastern North Pacific
[AD-A274750] p 2899 N94-26149

Nonlinear hysteresis in an endochronic solid
[AD-A274594] p 2880 N94-26855

SEARCH TECHNOLOGY, INC., NORCROSS, GA.

Automated information management for designers: Functional requirements for computer based associates that support access and use of technical information in design
[AD-A274603] p 3099 N94-26891

SECRETARIAT D'ETAT A LA RECHERCHE, ALGIERS (ALGERIA).

Qualitative analysis of rare earth elements contained in the phosphogypsum
[DE93-614153] p 2716 N94-26518

SEINAN GAKUIN UNIV., FUKUOKA (JAPAN).

Inductive differentiation of nerve cells in mouse embryonic ectoderm at early primitive streak stage by retinoic acid p 2905 N94-27488

SELSKAPET FOR INDUSTRIELL OG TEKNISK FORSKNING, TRONDHEIM (NORWAY).

Dissolution of secondary phases during extrusion
[PB94-124583] p 2732 N94-25908

EcarHeart2 version 1.0: Programmers documentation
[PB94-124633] p 2909 N94-25909

Process modelling of aluminium alloys. Modelling of the quench sensitivity of alloy AA6082
[PB94-124567] p 2741 N94-27325

Squeeze casting: A literature review
[PB94-124575] p 2741 N94-27326

Channel model for AC electric arc
[PB94-124591] p 2786 N94-27327

COMPETENCE 2000: Study on training requirements of the Norwegian metallurgical industry
[PB94-124609] p 2741 N94-27328

SET GROUP, DENVER, CO.

Technology drivers for flight telerobotic system software p 2684 N94-26289

SETS TECHNOLOGY, INC., MILILANI, HI.

Planetary Instrument Definition and Development Program (PIDDP). Instrument for future planetary flight missions: A visible-infrared imaging spectrometer for planetary missions
[NASA-CR-195254] p 3106 N94-27409

SEXTANT AVIONIQUE, VELIZY-VILLACOUBLAY (FRANCE).

Real time avionics constraints: Silicon solutions
p 2949 N94-26717

Use of HOOD coupled to real time monitors
p 2953 N94-26742

SHELL INTERNATIONALE PETROLEUM MAATSCHAPPIJ B.B. (NETHERLANDS).

Clean coal technology p 2832 N94-28089

Integrated coal gasification combined cycle
p 2832 N94-28090

SHERBROOKE UNIV. (QUEBEC).

Fatigue resistance under tension-compression of laminates IM6/5245C and AS4/3501-6
[IAR-CR-25] p 2708 N94-26711

Multispectral and textural classifications of a SPOT HRV-1 image, region of Sherbrooke, Quebec, Canada
[ISBN-0-315-84978-9] p 2851 N94-27863

Mapping of soil humidity using C-band radar images
[ISBN-0-315-85076-0] p 2852 N94-27878

SHIZUOKA SAISEIKAI GENERAL HOSPITAL (JAPAN).

Postnatal changes in the autonomic modulation of L-type Ca(exp 2+) currents of rabbit ventricular cells
p 2931 N94-27535

SIEMENS A.G., MUELHEIN-RUHR (GERMANY).

Gas turbine combustion and emission control
p 2831 N94-28082

SIEMENS SOLAR INDUSTRIES, CAMARILLO, CA.

Research on high-efficiency, large-area, CuInSe2 based thin-film modules
[DE94-000259] p 3067 N94-27609

SIMON FRASER UNIV., BURNABY (BRITISH COLUMBIA).

Colour object recognition
[ISBN-0-315-83684-9] p 2994 N94-26614

Extracting complete 3-dimensional boundary representation from multiple range images
[ISBN-0-315-83776-4] p 2963 N94-26615

Motion planning for serial manipulators with many degrees of freedom: Implementation of a sequential search strategy
[ISBN-0-315-83682-2] p 2822 N94-26642

SMITHSONIAN ASTROPHYSICAL OBSERVATORY, CAMBRIDGE, MA.

Investigations of the dynamical evolution of protoplanetary nebulae
[NASA-CR-195278] p 3105 N94-27428

Weak bump quasars
[NASA-CR-195267] p 3103 N94-27933

SMITHSONIAN INSTITUTION, WASHINGTON, DC.

The biostratigraphy and paleogeography of Maastrichtian inoceramids p 2889 N94-28303

SOCIETE DES ACCUMULATEURS FIXES ET DE TRACTION, POITIERS (FRANCE).

SAFT nickel hydrogen cell cycling status
p 2861 N94-28110

Thermal modeling of NiH2 batteries
p 2862 N94-28113

SOFTWARE KINETICS LTD., STITTSVILLE (ONTARIO).

ACES spectral display software: User manual
[SKL-1600-99-002] p 2973 N94-27762

Smalltalk: A tool for development of an Ada implementation of EWCAC
[SKL-1600-46-003-01-0] p 2974 N94-27823

SOFTWARE PRODUCTIVITY CONSORTIUM, HERNDON, VA.

Software Error Estimation Program (SWEEP), version 02.00.00 user manual
[AD-A274697] p 2962 N94-26373

SOLAR TURBINES, INC. SAN DIEGO, CA.

Gas fired advanced turbine system
[DE94-003193] p 2827 N94-27874

SOUTH DAKOTA SCHOOL OF MINES AND TECHNOLOGY, RAPID CITY.

The numerical simulation of marine boundary layer clouds
[AD-A273669] p 2894 N94-26195

SOUTH DAKOTA UNIV., VERMILLION.

Control panel dimensions for gloved operation study 2: Toggle switches minimum spacing required between toggle
[AD-A274518] p 2942 N94-27089

SOUTHAMPTON UNIV. (ENGLAND).

Transient flow features of a supersonic jet in a low speed cross flow p 2800 N94-28005

Comparison of the interactions of two and three dimensional transverse jets with a hypersonic free stream p 2659 N94-28021

Acoustic bubble sizing, using active and passive techniques to compare ambient and entrained populations
[ISVR-TR-229] p 2807 N94-28172

A modelling of the noise from simple coaxial jets. Part 3: With hot primary flow
[ISVR-TR-230-PT-3] p 2807 N94-28173

Weak coupling in statistical energy analysis ion Research, Univ. of Southampton, Southampton SO9 5NH, England)
[ISVR-TR-228] p 2832 N94-28174

On the use of feedback to control sound radiation from a plate excited by a turbulent boundary layer
[ISVR-TR-227] p 2807 N94-28175

SOUTHWEST RESEARCH INST., SAN ANTONIO, TX.

Microtubules for nonlinear optical limiting
[AD-A273940] p 3035 N94-25941

Investigation of plasma instabilities in the polar cusp
[NASA-CR-195212] p 2879 N94-26599

Studies of extra-solar Oort Clouds and the Kuiper Disk
[NASA-CR-195242] p 3103 N94-26789

Sequential multi-point injection of a natural gas engine. Topical report, November 1991 - April 1992
[PB94-126794] p 2824 N94-27224

SOUTHWEST TEXAS STATE UNIV., SAN MARCOS.

Trifluoromethyl-substituted polymers
[NASA-CR-195217] p 2751 N94-26641

SPACE POWER, INC., SAN JOSE, CA.

Space-R thermionic space nuclear power system: Design and technology demonstration
[DE94-001890] p 2699 N94-25929

Space-R thermionic space nuclear power system design and technology demonstration
[DE94-002017] p 2700 N94-25930

SPAUSCHUS ASSOCIATES, INC., STOCKBRIDGE, GA.

Solubility, viscosity, and density of refrigerant/lubricant mixtures
[DE94-004237] p 2721 N94-28069

SPECTRA RESEARCH SYSTEMS, INC., HUNTSVILLE, AL.

Interchangeable end effector tools utilized on the PFMA
[NASA-CR-193925] p 2823 N94-27149

SRI INTERNATIONAL CORP., MENLO PARK, CA.

Formal methods for dependable real-time systems
p 2953 N94-26740

High-speed, high-density, coherent time-domain optical memory
[AD-A274249] p 3037 N94-27010

Laser probes of natural gas ignition chemistry
[PB94-128345] p 2717 N94-27226

Modeling of the coupled magnetospheric and neutral wind dynamos
[NASA-CR-195273] p 2883 N94-27852

STANFORD LINEAR ACCELERATOR CENTER, CA.

Aspects of nonrenormalizable terms in a superstring standard-like models
[DE93-614530] p 3071 N94-25911

The delta (1232) resonance transition form factor
[DE94-003442] p 3017 N94-26101

A study of LPM suppression of bremsstrahlung at 25 GeV
[DE94-003457] p 3018 N94-26133

The epitaxial growth of Ge on Si(100) using Te as a surfactant
[DE94-003437] p 3056 N94-26326

The challenges of exclusive processes in QCD
[DE94-003429] p 3024 N94-27050

STANFORD RESEARCH INST., MENLO PARK, CA.

High energy parton-parton elastic scattering in QCD
[DE94-003432] p 3028 N94-27736

Gamma Large Area Silicon Telescope (GLAST): Applying silicon strip detector technology to the detection of gamma rays in space
[DE94-003451] p 3116 N94-27740

STANFORD UNIV., CA.

Ultra-high aggregate bandwidth two-dimensional multiple-wavelength diode laser arrays
[AD-A274018] p 2815 N94-25756

Deductive computer programming
[AD-A274966] p 2962 N94-26303

Subgraph approximations for large directed graphical models
[AD-A274813] p 3003 N94-26485

Simulation approaches for calculations in directed graphical models
[AD-A274825] p 3003 N94-26494

Aspects of goodness-of-fit
[AD-A274826] p 3003 N94-26495

Estimation and tests-of-fit for the three parameter Weibull distribution
[AD-A274827] p 3004 N94-26496

Induced pictorial representations
[AD-A274251] p 2939 N94-27012

Environmental conditions responsible for solar activity
[AD-A274191] p 3111 N94-27099

Scalar mixing in the subsonic jet in crossflow
p 2800 N94-28008
An experimental study of siphonal jets in a turbulent boundary layer crossflow p 2802 N94-28015
Theoretical and experimental investigation of a delta wing with turbulent leading-edge jets
p 2659 N94-28029
Science observed: The mass-extinction debates
p 2888 N94-28300

STATE UNIV. OF NEW YORK, BINGHAMTON.
Study of the kinematic and dynamic characteristics of a wormgear transmission for helicopter applications
[NASA-CR-195287] p 2826 N94-27657

STATE UNIV. OF NEW YORK, STONY BROOK.
Signal- and listener-based factors in complex auditory pattern perception
[AD-A274148] p 2939 N94-27094

STEVENS INST. OF TECH., HOBOKEN, NJ.
Hardware and software reliability estimation using simulations
[NASA-CR-187588] p 2973 N94-27663

STORK KETELS B.V., HENGELO (NETHERLANDS).
Steam plant for combined cycles: Heat recovery steam generators, design principles, and construction details
p 2831 N94-28083
Simulation: A tool for steam plant dynamic analysis
p 2831 N94-28084

STUCKEY (JAMES M.), DECATUR, AL.
Cryogenic insulation studies
[NASA-CR-195266] p 2756 N94-27429

SUGIYAMA JOGAKUIN UNIV., NAGOYA (JAPAN).
Man's ability to adapt himself for the seasonal climatic changes: From viewpoint of anticipation and seasonable behavior p 2919 N94-27476

SUPERCONDUCTING SUPER COLLIDER LAB., DALLAS, TX.
Secondary particle in background levels and effects on detectors at future hadron colliders
[DE94-003378] p 3011 N94-25598
Real-time tracking with a 3D-flow processor array
[DE94-003981] p 2980 N94-25984
Light-quark, heavy-quark systems: An update
[DE94-002298] p 3021 N94-26759
Measurements of the B(sup 0)(bar B)(sup 0)CP asymmetry
[DE94-003379] p 3063 N94-27047

SURREY UNIV., GUILDFORD (ENGLAND).
The interaction region associated with twin jets and a normal crossflow p 2800 N94-28009

SUZUKA UNIV. OF MEDICAL SCIENCE AND TECHNOLOGY (JAPAN).
Effects of gamma ray radiation on the developing mouse cerebellum: Apoptotic cell death and induction of tissue transglutaminase p 2904 N94-27472

SVERDRUP TECHNOLOGY, INC., BAY SAINT LOUIS, MS.
Bathymetric data set extraction program. Users guide
[AD-A274761] p 2899 N94-26567
The Hough transform algorithm for sea ice lead analysis: An evaluation
[AD-A274535] p 2899 N94-26853

SVERDRUP TECHNOLOGY, INC., BROOK PARK, OH.
Performance of renormalization group algebraic turbulence model on boundary layer transition simulation
[NASA-CR-194466] p 2644 N94-26131
NASA Lewis Research Center lean-, rich-burn materials test burner rig
[NASA-CR-194437] p 2680 N94-26141
Gaseous hydrogen/oxygen injector performance characterization
[NASA-CR-194464] p 2701 N94-26208
Stationary plasma thruster plume emissions
[NASA-CR-194471] p 2701 N94-26209
Emerging computer technologies and the news media of the future p 2688 N94-27372

SVERDRUP TECHNOLOGY, INC., CLEVELAND, OH.
The Fermi paradox: An approach based on percolation theory p 2687 N94-27370

SVERIGES LANTBRUKSUNIV., UPPSALA.
Calibrating/testing meters in hot water test bench VM7
[PB94-124294] p 2812 N94-27160

SWEDISH INST. FOR MATERIALS TESTING, BORAS.
Analytical method for estimation of the total amount of aromatic and poly aromatic compounds in diesel fuel
[PB94-123692] p 2759 N94-25907
Proceedings of the Fourth Euroseminar on Microscopy Applied to Building Materials
[PB94-119807] p 2839 N94-26754
Unscreened low tension cabies scrape abrasion testing
[PB94-123767] p 2823 N94-26849
Refractive and dielectric properties of helium, argon and nitrogen gases
[PB94-123783] p 3008 N94-26851
Baseline for a Nordtest method. Reliability stress screening of components. A guide for component users
[PB94-123775] p 2835 N94-27042
SP industry calorimeter for rate of heat release measurements up to 10MW
[PB94-124211] p 2811 N94-27044
Crack closure, a literature study
[PB94-123361] p 2842 N94-27197
Modification of a model for fatigue life predictions based on level-crossing
[PB94-123395] p 2842 N94-27198

SWEDISH INST. OF SPACE PHYSICS, KIRUNA.
Kiruna geophysical data. Data summary 93/4-6, April-June 1993
[PB94-123700] p 2881 N94-27039
Auroral Tomography Workshop Proceedings
[PB94-123718] p 2881 N94-27040
Kiruna geophysical data. Data summary 93/1-3, January-March, 1993
[PB94-123791] p 2881 N94-27043

SYRACUSE UNIV., NY.
Parallel Assessment Window System (PAWS) enhancements
[AD-A274094] p 2979 N94-25786
Computer program for numerical evaluation of the performance of an overmoded TM01 circular to TE10 rectangular waveguide mode converter
[AD-A274548] p 2771 N94-26844

SYSTEMS CONTROL TECHNOLOGY, INC., ARLINGTON, VA.
Rotorcraft low altitude IFR benefit/cost analysis: Conclusions and recommendations
[AD-A274241] p 2665 N94-26826

SYSTEMS RESEARCH LABS., INC., DAYTON, OH.
Passive and active behavior of the cardiovascular system under increased gravitational loads in a chronically instrumental conscious baboon model
[AD-A274344] p 2910 N94-26973

T

TECHNICAL RESEARCH CENTRE OF FINLAND, ESPOO.
HDR reactor containment fire modeling with BRI2
[VTT-PUBS-113] p 3031 N94-25621
Design of cold-formed HSS channels for bending and eccentric compression: Bending in the plane of symmetry
[VTT-TIED-1403] p 2762 N94-25622
Weldability of Direct-Quenched and Tempered (DQT) high strength steel HT80
[VTT-TIED-1406] p 2731 N94-25623
Safety analysis in conceptual design of process control
[VTT-PUBS-117] p 2762 N94-25641
Calculation of a 3-D pose of a known object in a single perspective view
[VTT-PUBS-122] p 2957 N94-25642
Computer aided simulation of heat treatment
[VTT-PUBS-131] p 2731 N94-25643
Aspects of the circuit board thermal design
[VTT-PUBS-132] p 2779 N94-25644
Experimental and numerical vibration analyses of a stiffened panel
[VTT-PUBS-129] p 2836 N94-25650
Continuous fiber reinforced thermoplastic composites: Literature survey
[VTT-TIED-1422] p 2704 N94-25651
Measurement of laboratory quality
[VTT-TIED-1427] p 2679 N94-25652
Piecewise least squares fitting technique using finite interval method with Hermite polynomials
[VTT-PUBS-135] p 2990 N94-25733
Effect of impact face damage on strength of sandwich composites
[VTT-PUBS-128] p 2704 N94-25734
Weldability of Accelerated-Cooled (AcC) high strength TMCP steel HT50
[VTT-TIED-1410] p 2731 N94-25784
Dead reckoning navigation
[VTT-TIED-1402] p 2664 N94-25808
Technology development in space projects
[VTT-TIED-1438] p 2682 N94-26249
Mounting of SSM's
[VTT-TIED-1442] p 2695 N94-26250
Use of oxygen-17 isotope in the characterization of zeolites and related structures by nuclear magnetic resonance spectroscopy
[VTT-TIED-1448] p 2714 N94-26251
Solid estimation feature based correlation method for measuring control points required for correcting satellite images
[VTT-JULK-772] p 2848 N94-26253
Development and analysis of secure embedded software
[VTT-TIED-1430] p 2961 N94-26254
Hypermedia support for engineering design systems: Application to fatigue analysis
[VTT-TIED-1432] p 2837 N94-26255
A transient symmetrical method for the measurement of temperature dependent thermal diffusivity
[VTT-TIED-1452] p 3008 N94-26256
Non-contact ultrasonic inspection
[VTT-TIED-1454] p 2835 N94-26257
Fire simulation based on convection calculation
[VTT-TIED-1411] p 2762 N94-26259
Design and life-time of polymer matrix composite structures: Summary
[VTT-TIED-1415] p 2707 N94-26260
Evaluation and improvement of the inquest system on work accidents (TOT)
[VTT-TIED-1418] p 2762 N94-26261
Guidelines for controlling stress corrosion cracking and corrosion fatigue of stainless steels: A literature review
[VTT-TIED-1420] p 2837 N94-26262
A method for testing of HVAC automation equipment using the emulator and the application of the method
[VTT-TIED-1435] p 2822 N94-26306
The structural behaviour of the steel or composite concrete and steel frames and the connections of frame members during the fire: A literature review
[VTT-TIED-1437] p 2837 N94-26307
Composite raw materials for the building industry
[VTT-TIED-1433] p 2708 N94-26544
Magnetostriction and magnetostrictive materials
[VTT-TIED-1434] p 3058 N94-26545
Numerical Analysis Methods of Surface Cracks
[VTT-PUBS-119] p 2841 N94-27186
Development of an automated fracture assessment system for nuclear structures (appendix 1/1)
p 2841 N94-27187
Method for calculating stress intensity factors for surface cracks (appendix 2/1) p 2841 N94-27188
Quality assurance for fracture mechanical finite element analyses (appendix 3/1) p 2841 N94-27189
Applications of the weight function method (appendix 4/1) p 2842 N94-27190
Weldability aspects in the design and fabrication of aluminium structures subjected to fatigue loads. Part 2: Weldability of aluminium alloys using advanced MIG and TIG techniques. Effect of the weld bead geometrical factors on the fatigue behavior of the welded joint
[PB94-132446] p 2833 N94-28375
Joining of fibre reinforced metal matrix composite materials
[PB94-132453] p 2712 N94-28376
Open communication in manufacturing automation
[PB94-132479] p 2976 N94-28377
Weldability aspects in the design and fabrication of aluminium structures subjected to fatigue loads. Part 1: Effect of welding on the structural integrity of joint types designed for repairing aluminium ship sections
[PB94-132487] p 2833 N94-28378

TECHNICAL UNIV. OF PRAGUE (CZECHOSLOVAKIA).
Proceedings of the 16th Symposium on Plasma Physics and Technology
[DE94-604181] p 3047 N94-27698

TECHNION - ISRAEL INST. OF TECH., HAIFA.
Solar energy in Israel: Utilization and research
p 2853 N94-26051
Absorption technology for solar and waste heat utilization p 2854 N94-26053
Bisexual branching diffusions
[AD-A274698] p 3008 N94-26374
A superprocess with a disappearing self-interaction
[AD-A274647] p 3009 N94-27108

TECHNISCHE HOGESCHOOL, DELFT (NETHERLANDS).
A logarithmic barrier cutting plane method for convex programming
[REPT-93-43] p 2957 N94-25761
A note on central cutting plane methods for convex programming
[REPT-93-44] p 2958 N94-25762

TECHNISCHE UNIV., AACHEN (GERMANY).
Comparison of the lossy image data compressions for the MESUR Pathfinder and for the Huygens Titan Probe
p 2945 N94-28254

TECHNISCHE UNIV., DELFT (NETHERLANDS).
Geoid determination: With help of the alternative scattering method
[ETN-94-95375] p 2847 N94-25746
Selfsimilar solutions of a nonlinear transport equation
[REPT-93-42] p 2865 N94-25760
Abstraction in, specification and proof of software for a 1D heat-transfer problem
[REPT-93-45] p 2790 N94-25763
A simplicial approach to integer programming, part 2
[REPT-93-47-PT-2] p 2958 N94-25764

Hill equations for satellite orbit determination
[ETN-94-95374] p 2690 N94-25787

Image segmentation by a combination of edge detection and region growing
[ETN-94-95032] p 2960 N94-26106

Geometric correction of SPOT images with use of digital elevation models
[ETN-94-95033] p 2847 N94-26107

Correlation between the gravity field and the bathymetry in the North Atlantic Ocean
[ETN-94-95036] p 2899 N94-26108

Isotonic estimation and rates of convergence in Wicksell's problem
[REPT-93-39] p 3002 N94-26213

The railway track response function
[REPT-93-40] p 2837 N94-26214

Phase portraits of quadratic systems with finite multiplicity three and one critical point of infinity
[REPT-93-41] p 2991 N94-26215

On the robustness of a multiple semi-coarsened grid method
[REPT-93-51] p 2992 N94-26252

High-production global positioning system methods for survey applications: The pseudo-kinematic method with the Trimvec programming system
[ETN-94-95035] p 2665 N94-26539

Construction and applications of the two dimensional Delaunay triangulated irregular network and the three dimensional Delaunay tetrahedron model
[ETN-94-95034] p 2848 N94-26651

Experimental investigation of the flow quality in the GLT20 subsonic-transonic boundary layer wind tunnel
[PB94-126539] p 2681 N94-26815

Nested Krylov methods based on GCR
[PB94-125317] p 2995 N94-26818

Physical modelling and adaptive predictive control of diffusion/LPCVD reactors
[PB94-126398] p 2763 N94-26819

Topological conditions for the existence of invariant measures for unimodal maps
[PB94-123296] p 2849 N94-26866

Refined triangular plate and shell elements
[PB94-126356] p 2839 N94-26875

Electromagnetic fields and interference
[PB94-126489] p 2771 N94-26877

Elastic wave up/down decomposition in inhomogeneous and anisotropic media: An operator approach and its approximations
[PB94-126497] p 2881 N94-26880

Interference analysis of multichannel transmission lines: A system's analysis
[PB94-126505] p 2772 N94-26909

Computation of stress intensity factors by the mode enrichment technique with applications to geometrically nonlinear problems
[PB94-126513] p 2840 N94-26910

Formulae for the buckling of simply-supported corrugated panels of orthotropic material under shear load
[PB94-126547] p 2840 N94-26911

Experimental study of the angled crack in GLARE 3
[PB94-126554] p 2669 N94-26954

Failure behaviour of high density polyethylene with an embrittled surface layer due to weathering
[PB94-126406] p 2840 N94-26960

Design and test of postbuckled stiffened curved plates: A literature survey
[PB94-126521] p 2840 N94-26961

Central dynamic share scheduling in distributed systems
[REPT-93-48] p 2966 N94-26966

A non-linear mathematical model or finite, periodic rail corrugations
[REPT-93-49] p 2996 N94-26967

Development of fibre-metal laminates, ARALL and GLARE, new fatigue resistant materials
[PB94-126471] p 2669 N94-26969

Grey-box modelling and identification topics
[PB94-126380] p 2986 N94-27029

Symmetric and asymmetric diophantine approximation by continued fractions
[PB94-126455] p 2998 N94-27030

Unifying investigation of interior-point methods for convex programming
[PB94-126463] p 2967 N94-27031

Efficient implementation of high-level parallel symbolic languages p 2955 N94-27196

Impact tests on fibre metal laminates under a tensile load
[PB94-126570] p 2710 N94-27201

TECHNISCHE UNIV., EINDHOVEN (NETHERLANDS).

Accuracy analysis of multi-axis machines
[ETN-94-95341] p 3002 N94-26000

Spin-polarized atomic hydrogen: Devices and phenomena
[ETN-94-95342] p 3016 N94-26002

Hierarchical test development and design-for-testability for (a)synchronous semi-custom ASIC's
[ISBN-9-09-005928-8] p 2834 N94-26003

Statistical quality management
[MEMO-COSOR-92-43] p 2834 N94-26008

Laser manipulation of metastable neon atoms
[ETN-94-95344] p 2817 N94-26225

The general pickup and delivery problem
[MEMO-COSOR-92-44] p 2992 N94-26226

A linear description of the discrete lot-sizing and scheduling problem
[MEMO-COSOR-92-47] p 2992 N94-26227

One machine scheduling with delayed precedence constraints
[PB93-237626] p 3094 N94-26314

Merged-beam studies of electron-recombination and excitation of atomic and molecular hydrogen ions
[ETN-94-95339] p 3019 N94-26478

A numerical study of quantized vortices in HeII
[ISBN-9-03-860232-4] p 2792 N94-26479

Modelling and predicting properties of polymers in the amorphous glassy state
[ETN-94-95345] p 2752 N94-26645

Process algebra of concurrent constraint programming
[PB94-126695] p 2966 N94-26919

Hard real-time reliable multicast in the DEDOS system
[PB94-126745] p 2966 N94-26920

Design of an online help facility for ExSpect
[PB94-126687] p 2966 N94-26955

Freeness analysis for logic programs-and correctness
[PB94-126703] p 2966 N94-26956

Congruence theorem for structured operational semantics with predicates and negative premises
[PB94-126729] p 2966 N94-26970

Trace-based compositional proof theory for fault tolerant distributed systems
[PB94-126737] p 2966 N94-26971

Proceedings of the Third Workshop Computersystems: Research Forum on Design, Realization and Use of Computersystems
[ISBN-90-6144-995-2] p 2954 N94-27191

DALIA: A language for the description and analysis of digital systems p 2954 N94-27192

Fractional calculus, gegenbauer transformations and integral equations
[PB93-237683] p 2999 N94-27349

Polyhedral characterization of the economic lot-sizing problem with start-up costs
[MEMO-COSOR-92-46] p 2969 N94-27396

TECHNISCHE UNIV., TWENTE (NETHERLANDS).

Modeling systems by probabilistic process algebra: An event structures approach
[PB94-125259] p 3004 N94-26867

Recursive bundle event structures
[PB94-125275] p 3004 N94-26870

Example of the EXPANSE signalling protocol
[PB94-125283] p 2771 N94-26872

Classification of linear differential operators with an invariant subspace in monomials
[PB94-126620] p 2996 N94-26915

Single-server queues with spatially distributed arrivals
[PB94-126638] p 2986 N94-26916

Communication complexity of t-intersection problems in generalized Boolean algebras
[PB94-126646] p 2996 N94-26917

Some aspects of nonlinear discrete-time descriptor systems in economics
[PB94-126653] p 3101 N94-26918

Some properties of graphs with local Ore conditions
[PB94-126612] p 2996 N94-26962

Parsing schemata: A framework for parallel and sequential parsing
[PB94-125267] p 2981 N94-26998

White noise theory of robust nonlinear filtering with correlated state and observation noises
[PB94-126661] p 3004 N94-27211

Graphs satisfying a local ore-type condition
[PB94-126679] p 3007 N94-27222

Wieand's theorem
[PB94-126711] p 3004 N94-27223

TECHNOLOGY MANAGEMENT, INC., CLEVELAND, OH.

Low cost, radial flow, solid oxide fuel cell
[DE94-002982] p 2858 N94-26785

TECOGEN, INC., WALTHAM, MA.

Fibrous emissive burners selective and broad band
[PB94-128329] p 2859 N94-27225

TEL-AVIV UNIV. (ISRAEL).

The potential for large critical currents in the high T(sub c) oxides p 2854 N94-26058

Evanescent field infrared spectroscopy using chalcogenide glass fiber
[ITN-94-85233] p 3038 N94-27178

Laser phase induced intensity noise in fiber-optic signal processing and sensing systems
[ITN-94-85234] p 2819 N94-27179

Spectral and temporal correlations of multifrequency waves in the turbulent atmosphere
[ITN-94-85229] p 2774 N94-27233

Theoretical and experimental analysis of the spatial and temporal behaviour of the intensity of an electro-magnetic wave reflected from a diffuse target after passing through a turbulent atmosphere
[ITN-94-85230] p 2774 N94-27234

Coded communications with nonideal interleaving
[ITN-94-85235] p 2774 N94-27242

Morphology transitions during non-equilibrium growth processes
[ITN-94-85236] p 3065 N94-27243

Dynamic and kinematic P wave tracing for a three-dimensional elastic inhomogeneous media by the asymptotic ray theory and application
[ITN-94-85239] p 2775 N94-27244

Wave propagation in the shallow regions of the earth's crust and the borehole vicinity
[ITN-94-85237] p 2882 N94-27330

Mapping of seawater intrusion into the coastal aquifer of Israel (the seawater-freshwater interface) by TDEM (Time Domain Electromagnetic) method
[ITN-94-85238] p 2850 N94-27331

Novel oxidizing reagents derived from elemental fluorine
[ITN-94-85231] p 2719 N94-27687

Dynamics of metastable states in supersonic beams
[ITN-94-85232] p 3028 N94-27760

TENNESSEE STATE UNIV., NASHVILLE.

Ultraviolet observations of astronomical sources
[NASA-CR-195232] p 3102 N94-26234

TENNESSEE UNIV., KNOXVILLE.

Charmonium physics at a tau-charm factory
[PB94-124344] p 3024 N94-27199

TEXAS A&M UNIV., COLLEGE STATION.

Properties of the Central American cold surge
[NASA-CR-194849] p 2893 N94-26138

Coordinated scheduling for dynamic real-time systems
[NASA-CR-195231] p 3093 N94-26206

Bulk-Flow Analysis, part A
[NASA-CR-193911-PT-A] p 2796 N94-27377

Influence of impeller shroud forces on turbopump rotor dynamics p 2796 N94-27378

Compressibility effects on rotor forces in the leakage path between a shrouded pump impeller and its housing
p 2796 N94-27379

Global barotropic response to a tropical forcing
[NASA-CR-195256] p 2896 N94-27408

Investigation of aerodynamic design issues with regions of separated flow p 2658 N94-27902

Nonequilibrium radiation and chemistry models for aerocapture vehicle flowfields
[NASA-CR-195706] p 2648 N94-28071

An initial investigation into methods of computing transonic aerodynamic sensitivity coefficients
[NASA-CR-195705] p 2648 N94-28072

TEXAS COLL. OF OSTEOPATHIC MEDICINE, FORT WORTH.

Does training-induced orthostatic hypotension result from reduced carotid baroreflex responsiveness?
p 2935 N94-28366

TEXAS UNIV., AUSTIN.

Space Habitat, assembly and repair facility
p 2691 N94-25696

Asteroid exploration and utilization
p 3080 N94-25697

The 1991-1992 project summaries
p 2943 N94-25698

Toroidal plasma beta-FLR limit in a toroidally linked mirror system
[DE94-003119] p 3041 N94-25792

Kinetic resonance damping rate of the toroidal ion temperature gradient mode
[DE94-003511] p 3041 N94-25923

Nonlinear growth of strongly unstable tearing modes
[DE94-003366] p 3042 N94-25958

Shear flow generation from the interaction of neoclassical and drift wave transport processes
[DE94-003135] p 2791 N94-26096

Delta f Algorithm
[DE94-003120] p 2963 N94-26521

Pion-nucleus interactions and the STAR experiment at RHIC
[DE94-000658] p 3021 N94-26586

Problems in nonlinear acoustics: Rayleigh waves, pulsed sound beams, and waveguides
[AD-A274587] p 3010 N94-26983

Turbulent boundary layer inner-outer interactions
[AD-A274357] p 2794 N94-27059

Reduced Braginskii equations
[DE94-003510] p 3047 N94-27723

Flowfield dynamics in blunt fin-induced shock wave/turbulent boundary layer interactions
[NASA-CR-195170] p 2798 N94-27802

Sonic boom propagation through turbulence: A ray theory approach p 2650 N94-28192

The propagation of spark-produced N waves through turbulence p 2650 N94-28193

An integrated approach to seismic event location: 1. Evaluating how method of location affects the volume of groups of hypocenters
[PL-TR-92-2323] p 2887 N94-28214

Analysis and control of hourglass instabilities in underintegrated linear and nonlinear elasticity
[NASA-CR-195293] p 2846 N94-28266

Impacts, extinctions, volcanism, glaciations, and tectonics: Matches and mismatches
p 2888 N94-28298

Exercise detraining: Applicability to microgravity
p 2934 N94-28364

TEXAS UNIV., DALLAS.

Spacelab life sciences 2 post mission report
[NASA-CR-195544] p 2942 N94-27410

TEXAS UNIV. HEALTH SCIENCE CENTER, SAN ANTONIO.

The role of hyperbaric oxygen as a prophylaxis for radiation enteritis
[AD-A274974] p 2901 N94-26517

THARSYS (FRANCE).

Ada reusable software for satellite on-board data handling p 2953 N94-26743

THIOKOL CORP., BRIGHAM CITY, UT.

STS-56, RSRM-031, 360L031 KSC processing configuration and data report
[NASA-CR-193922] p 2691 N94-26135

STS-51, RSRM-033, 360T033 KSC processing configuration and data report
[NASA-CR-193923] p 2691 N94-26153

New rubber qualification for the igniter adapter
[NASA-CR-193936] p 2752 N94-26708

TOHOKU UNIV., SENDAI (JAPAN).

Research on the development of fracture characteristics evaluation system for ceramics and metal composite materials p 2710 N94-27281

List of papers published by the members of Institute for Materials Research, Tohoku University 1992
[JTN-94-80608] p 3118 N94-27355

Bulletin of the Institute for Chemical Reaction Science, Tohoku University, volume 2
[JTN-94-80602] p 2717 N94-27385

Development of liquid membrane separation processes p 2717 N94-27386

Reactivity of nitrate radical (NO3) toward organic compounds p 2704 N94-27387

Four phase microwave pulse generator for pulsed EPR spectrometer p 2718 N94-27388

Variable temperature cold stage for microscope observation p 2718 N94-27389

High-temperature and high-pressure flow calorimeter
p 2718 N94-27390

Glass cylindrical filter for electrolysis cell
p 2718 N94-27391

Porous vycor glass tube joined to borosilicate glass
p 2718 N94-27392

The Science Reports of the Research Institutes, Tohoku University. Series A: Physics, Chemistry, and Metallurgy. Volume 38, No. 1: Amorphous Materials 14
[JTN-94-80610] p 2744 N94-28158

Energy Dispersive X ray Diffraction (EDXD) apparatus for liquids at high temperature p 2721 N94-28159

Structural study of Cu/Co multilayer by anomalous small-angle x ray scattering p 2744 N94-28160

Differential scanning calorimetric study of solid state amorphization and crystallization in Zr/Co and Zr/Ni multilayers p 2745 N94-28161

NMR study of quasicrystal Al(70)Pd(20)T(M10) alloy (T(M):Cr, Mn, Fe, and Co) p 2745 N94-28162

Formation and crystallization of hydrogen-induced amorphous Ti3InH(4.5) alloy p 2745 N94-28163

The corrosion behavior of sputter-deposited magnesium-valve metal alloys p 2745 N94-28164

The electrocatalytic oxidation of ethylene and methane, and reduction of oxygen on gas-diffusion electrodes made of amorphous nickel-valve metal-platinum group metal alloys p 2722 N94-28165

CO2 methanation catalysts prepared from amorphous Ni-valve metal alloys containing platinum group elements
p 2745 N94-28166

Mechanical behavior of amorphous alloys at elevated temperatures p 2746 N94-28167

Formation of glassy Pd-Ni-P alloys by mechanical alloying and their structure and thermal stability
p 2746 N94-28168

Study on the production of flaky amorphous alloy powders by impact flattening of atomized liquid droplets on a rapidly rotating wheel p 2746 N94-28169

Production of an amorphous Fe(75)Si(10)B(15) sheet by a metallic mold casting method and its properties
p 2746 N94-28170

Formation and high mechanical strength of Al-based alloys containing a nanoscale icosahedral phase as a main constituent p 2746 N94-28171

TOKYO INST. OF TECH., YOKAHAMA (JAPAN).

Bulletin of Precision and Intelligence Laboratory, No. 68
[JTN-94-80609] p 3010 N94-27282

Silence amenity engineering: Past and present
p 3011 N94-27283

TOKYO SCIENCE UNIV. (JAPAN).

Technical report of ISSP. Ser. A, no. 2683: Itinerant character of 5f electrons in UNi2Ga
[JTN-94-80569] p 3025 N94-27337

TOKYO UNIV. (JAPAN).

Study on phase transformation due to deformation in ferromagnetic fields at cryogenic condition
p 2724 N94-25556

Heavy-electron behavior in large coordination compounds CeZn11 and UZn12
[REPT-A-2663] p 3049 N94-25614

Atomic-scale chemistry of metal surfaces
[REPT-A-2657] p 3012 N94-25636

Successive structural phase transitions in stoichiometric La2NiO4 observed by x ray diffraction
[REPT-A-2665] p 3051 N94-25921

Formation of three types of quasi-crystals in Al-Pd-Mg system
[REPT-A-2667] p 3053 N94-26071

Aluminum-ion sputtering from Al surfaces with very-low-energy ions
[REPT-A-2668] p 2733 N94-26073

Phase diagram of La2NiO(4 + delta) (0 less than or equal to delta less than or equal to 0.18). 1: Phases at room temperature and phase transition above delta equal to 0.15
[REPT-A-2661] p 3053 N94-26089

A mimic model of Pt-Rh catalyst prepared by electrochemical deposition of Rh on Pt (100) surface
[REPT-A-2664] p 2715 N94-26476

Toward insulating quasicrystalline alloy in Al-Pd-Re icosahedral phase
[REPT-A-2666] p 2736 N94-26477

Technical report of ISSP. Ser. A, no. 2678: Magnetic properties of carbon nanotubes
[JTN-94-80564] p 3064 N94-27174

Technical report of ISSP. Ser. A, no. 2679: Novel electronic states of partially deuterated (DMe-DCNQI)2Cu
[JTN-94-80565] p 3064 N94-27175

Technical report of ISSP. Ser. A, no. 2680: Determination of intervalley scattering time in germanium by subpicosecond time-resolved Raman spectroscopy
[JTN-94-80566] p 3064 N94-27176

Technical report of ISSP. Ser. A, no. 2674: High-field cyclotron resonance and impurity transition in n- and p-3C-SiC at magnetic fields up to 175 T
[JTN-94-80560] p 3064 N94-27232

Technical report of ISSP. Ser. A, no. 2670: Electronic structure of light transition metal compounds studied by photoemission
[JTN-94-80556] p 3065 N94-27239

Technical report of ISSP. Ser. A, no. 2672: Magneto-optical effects of excitons in BiI3 crystals under pulsed high magnetic fields. 3: Excitons confined around a stacking disorder formed by a bending stress
[JTN-94-80558] p 3065 N94-27240

Technical report of ISSP. Ser. A, no. 2673: Two successive spin glass transitions in non-diluted Heisenberg-like spin glass Ni(0.42)Mn(0.58) TiO3
[JTN-94-80559] p 2756 N94-27241

Technical report of ISSP. Ser. A, no. 2675: High-field cyclotron resonance and valence-band structure in semiconducting diamond
[JTN-94-80561] p 3065 N94-27245

Technical report of ISSP. Ser. A, no. 2676: Charge mass singularity in two-dimensional Hubbard model
[JTN-94-80562] p 3065 N94-27248

Technical report of ISSP. Ser. A, no. 2684: Wavelength dependence of nonsequential double ionization in He
[JTN-94-80570] p 3025 N94-27338

Technical report of ISSP. Ser. A, no. 2685: ASE-free terawatt KrF/Ti : sapphire hybrid laser system
[JTN-94-80571] p 2820 N94-27339

Report of three microgravity experiments by the drop shaft
[JTN-94-80579] p 2761 N94-27341

Technical report of ISSP. Ser. A, no. 2669: Relations between oxygen deficiency and structures in the La-Sr-Cu-O system. 3: Oxygen contents and structure of (La, Sr)8Cu8O(16 + delta) phase
[JTN-94-80555] p 3066 N94-27353

Technical report of ISSP. Ser. A, no. 2682: Pressure dependence of Sm:YAG fluorescence to 50 GPa: A new calibration as a high pressure scale
[JTN-94-80568] p 3066 N94-27354

Function of selective attention intrinsic to the saccade system: Does the voluntary control override the stimulus driven control? p 2928 N94-27523

Activation by G protein beta gamma subunits of G protein-coupled receptor kinase p 2931 N94-27534

Technical report of ISSP. Ser. A, no. 2686: High-order harmonic generation and ionization using ultrashort KrF and Ti:Sapphire lasers
[JTN-94-80572] p 2820 N94-27605

Technical report of ISSP. Ser. A, no. 2688: Suppression of higher-order modes in an RF cavity by resistive material
[JTN-94-80574] p 2787 N94-27606

Technical report of ISSP. Ser. A, no. 2677: Octa-twin model of tetrapod ZnO crystals
[JTN-94-80563] p 3069 N94-27756

Study of invisible nucleon decay, N approaches nu nu nu bar, and a forbidden nuclear transition in the Kamiokande detector
[ICRR-299-93-11] p 3028 N94-27759

TOKYO UNIV., TANASHI (JAPAN).

Contributions to the 23rd ICRC from emulsion chamber experiments at Mt. Chacaltaya and Pamirs
[ICRR-REPT-295-93-7] p 3112 N94-25624

Violation of Feynman scaling law in the forward region
p 3113 N94-25633

Nucleon-nucleon scattering lengths in QCD sum rules
[DE93-520239] p 3015 N94-25922

First observation of neutral current proton electron scattering at the square root of s = 300 GeV
[DE94-701107] p 3030 N94-27877

TOKYO WOMAN'S MEDICAL COLL. (JAPAN).

Autonomic nervous system and cardiovascular control: Clinical implications of the 1/f fluctuations of heart rate
p 2932 N94-27540

TOLEDO UNIV., OH.

A study of DC-DC converters with MCT's for arcjet power supplies
[NASA-CR-191204] p 2703 N94-27662

TORONTO UNIV., DOWNSVIEW (ONTARIO).

University of Toronto Institute for Aerospace Studies
[CTN-94-61013] p 3117 N94-26701

Substructure synthesis methods for viscoelastic structures
[UTIAS-349] p 2695 N94-26712

TORONTO UNIV. (ONTARIO).

An integrated delta-sigma based IIR filter
[ISBN-0-315-83593-1] p 2784 N94-26631

Application of Markov random field theory to image coding and motion estimation
[ISBN-0-315-83435-8] p 2964 N94-26632

Implementation of integral manifold control on a two degree of freedom flexible joint manipulator: Theory and experiments
[ISBN-0-315-83572-9] p 2823 N94-26658

Simulation dynamics of a multibody chain: Recursion based on chain modal coordinates
[ISBN-0-315-83555-9] p 2994 N94-26659

Designing and optimizing fuzzy-logic controllers
[ISBN-0-315-83505-2] p 2985 N94-26660

Stress-induced phase transformation in ZrO2 materials
[ISBN-0-315-83373-4] p 2752 N94-26661

QCD corrections to inclusive B - S processes in the standard model
[ISBN-0-315-54572-0] p 3073 N94-27263

Observation of excited charmed mesons
[ISBN-0-315-57014-8] p 3026 N94-27400

Tools for quantitative stability robustness analysis
[ISBN-0-315-59950-2] p 2988 N94-27641

A transmission electron microscope study of Ni4W precipitates in a Ni-37 wt. percent W alloy
[ISBN-0-315-59932-4] p 2743 N94-27803

A simulator investigation of helicopter flight control system mode transitions
[UTIAS-348] p 2682 N94-27879

TVD flux-difference split methods for high-speed thermochemical nonequilibrium flows with strong shocks
[UTIAS-350] p 2799 N94-27880

Experimental study on the shock wave interaction with a hypersonic boundary layer near a convex corner
p 2654 N94-28328

Viscous airfoil computations using adaptive structured grids p 2655 N94-28337

Attached and separated trailing edge flow measurements with a triple-split hot-film probe
p 2656 N94-28339

Thin-layer Navier-Stokes computations for multi-element airfoils p 2656 N94-28341

TOSHIBA CORP., KAWASAKI (JAPAN).

Study on phase transformation due to deformation in ferromagnetic fields at cryogenic condition
p 2724 N94-25556

TOSHIBA RESEARCH AND DEVELOPMENT CENTER, KAWASAKI (JAPAN).
A compact 150 GHz SIS receiver cooled by 4 K GM refrigerator
[REPT-36] p 2776 N94-27340

TOYOTA COLL. OF TECHNOLOGY (JAPAN).
Sympathetic nerve activity during dynamic leg exercise
p 2929 N94-27527

TRI-UNIV. MESON FACILITY, VANCOUVER (BRITISH COLUMBIA).
TRIUMF scientific activities
[CTN-94-61062] p 3117 N94-26656

TRW, INC., REDONDO BEACH, CA.
Nickel-hydrogen cell reversal characteristics
p 2862 N94-28114
Battery charge control: Which approach is best?
p 2863 N94-28124

TRW SPACE TECHNOLOGY LABS., REDONDO BEACH, CA.
Collisionless shock structures of Earth and other planets
[NASA-CR-195257] p 3104 N94-27407

TRW SYSTEMS GROUP, REDONDO BEACH, CA.
Wavelet compression techniques for hyperspectral data p 2947 N94-28263

TSUKUBA SPACE CENTER (JAPAN).
Development of nickel-metal hydride cell: An update
p 2864 N94-28130

TURKISH AEROSPACE INDUSTRIES, ANKARA.
Navier-Stokes analysis of a swirling jet in crossflow
p 2806 N94-28038

TUSKEGEE INST., AL.
Review and analysis of dense linear system solver package for distributed memory machines
p 2978 N94-27916
Investigation of spectral analysis techniques for randomly sampled velocimetry data
p 3009 N94-27924

U

UNITED NATIONS ENVIRONMENT PROGRAMME, GENEVA (SWITZERLAND).
Global tropical forest cover assessments using satellite imagery p 2850 N94-27183

UNITED NATIONS ENVIRONMENT PROGRAMME, NAIROBI (KENYA).
Meeting of the Eighth Session of the Scientific Advisory Committee of the World Climate Impact Assessment and Response Strategies Programme
[DE93-633954] p 2866 N94-26163

UNITED TECHNOLOGIES CORP., EAST HARTFORD, CT.
Thermal/Structural Tailoring of Engine Blades (T/STAEBL): User's manual
[NASA-CR-194461] p 2843 N94-27776
Coupled 2-dimensional cascade theory for noise an d unsteady aerodynamics of blade row interaction in turbofans. Volume 2: Documentation for computer code CUP2D
[NASA-CR-4506-VOL-2] p 2675 N94-27778

UNIVERSIDAD AUTONOMA METROPOLITANA DE MEXICO (MEXICO).
Determination of the plasma column shape in the Tokamak Novillo cross section by magnetic probes
[DE94-604986] p 3048 N94-27844

UNIVERSIDAD NACIONAL AUTONOMA DE MEXICO, MEXICO CITY.
Geological Dating by Ar-40 - Ar-39 method
[DE94-601975] p 2880 N94-26874

UNIVERSIDADE ESTADUAL DE PAULISTA, SAO PAULO (BRAZIL).
Preparation, characterization, and thermal behaviour study of lanthanides (3) and yttrium (3) 4-methoxy benzylidene pyruvate in solid state
[DE94-604079] p 3068 N94-27697

UNIVERSITEIT TWENTE, ENSCHEDE (NETHERLANDS).
A partitioning and redundancy model for wafer-scale integrated circuits p 2955 N94-27195
Comparison of Object-Oriented Analysis and Design Methods: A Collection of Papers
[MEMO-INF-92-69] p 2975 N94-27936

UNIVERSITIES SPACE RESEARCH ASSOCIATION, HOUSTON, TX.
Proceedings of the 8th Annual Summer Conference: NASA/USRA Advanced Design Program
[NASA-CR-195118] p 3075 N94-25665

UNIVERSITY OF CENTRAL FLORIDA, ORLANDO.
Assured crew return vehicle post landing configuration design and test p 2697 N94-25671

UNIVERSITY OF NORTH TEXAS, DENTON.
Image quality measures and their performance
p 2946 N94-28257

UNIVERSITY OF SCIENCE OF MALAYSIA, PENANG.
Atmospheric science research in Malaysia: Perspectives on international cooperation p 2874 N94-28285

UNIVERSITY OF SOUTHERN CALIFORNIA, LOS ANGELES.
Numerical studies on the dynamics of bubble, turbulent, free shear flows: Effect of the inter-phase coupling on the global flow evolution
[AD-A274521] p 2794 N94-26832

UNIVERSITY OF SOUTHERN ILLINOIS, CARBONDALE.
Radiations from hot nuclei p 3030 N94-27915

UNIVERSITY OF SOUTHERN MISSISSIPPI, BAY SAINT LOUIS.
Development of a multi-sensor in situ fiber optic fluorometer
[DE94-003399] p 3035 N94-26100

UNIVERSITY OF SOUTHWESTERN LOUISIANA, LAFAYETTE.
Modulating terrestrial impacts from Oort cloud comets by the adiabatically changing galactic tides
p 2890 N94-28305

UNIVERSITY OF WESTERN ONTARIO, LONDON.
Merged-beam studies of electron-recombination and excitation of atomic and molecular hydrogen ions
[ETN-94-95339] p 3019 N94-26478
The free vibration of plates, shallow shells and solids
[ISBN-0-315-83931-7] p 2838 N94-26622
The response of an hyperpure Ge detector to ionizing radiation
[ISBN-0-315-83968-6] p 2811 N94-26662
Operator regularization and renormalization theory
[ISBN-0-315-49334-8] p 3007 N94-27264
A jet calculus approach including coherence effects and the associated problem of moment inversion
[ISBN-0-315-51715-8] p 3025 N94-27266
Electrochemical properties of passive films on 440C stainless steel
[ISBN-0-315-64248-3] p 2757 N94-27801
Circular cylinder in axial flow
[ISBN-0-315-59114-5] p 2798 N94-27873

UNIVERSITY OF WESTERN WASHINGTON, BELLINGHAM.
Characterization of semi-insulating gallium arsenide
[AD-A273781] p 3068 N94-27704

UTAH STATE UNIV., LOGAN.
Copernicus: Lunar surface mapper
p 3081 N94-25702

UTAH UNIV., SALT LAKE CITY.
NCVS, volume 5
[AD-A274975] p 2902 N94-27165
Technical report of ISSP. Ser. A, no. 2671: Quasi-localization of light waves in Fibonacci dielectric multilayers
[JTN-94-80557] p 3064 N94-27231

V

VALLADOLID UNIV. (SPAIN).
Study of the homogeneity of InP wafers
[AD-A273658] p 3055 N94-26194

VICTORIA UNIV. (BRITISH COLUMBIA).
Improved performance of hybrid error control techniques for real-time digital communications over noisy channels
[ISBN-0-315-84281-4] p 2770 N94-26625
On the performance of trellis coded 8PSK with Reed Solomon codes
[ISBN-0-315-84289-X] p 2770 N94-26626
Numerical modelling of precipitation over complex terrain
[ISBN-0-315-84327-6] p 2894 N94-26628
Asymptotically stable neural networks for identification of nonlinear dynamic systems
[ISBN-0-315-84328-4] p 2985 N94-26629
A cosmological field theory
[ISBN-0-315-84271-7] p 3104 N94-26638
Dynamics of a flexible extendible beam
[ISBN-0-315-84278-4] p 2838 N94-26639
Optimal architectural design of parallel and hybrid manipulators
[ISBN-0-315-84351-9] p 2822 N94-26657
Mapping coastal habitats using an imaging spectrometer
[ISBN-0-315-84362-4] p 2848 N94-26664
Measuring the time dependence of B(sub s)(sup 0) meson - anti B(sub s)(sup 0) meson oscillations
[ISBN-0-315-84367-5] p 3021 N94-26665
Capture and location of blobs in digital images
[ISBN-0-315-84382-9] p 3036 N94-26666
An evaluation of an airborne remote sensing system used to determine ice thickness and geometry of a first year sea ice ridge located in the Beaufort Sea
[ISBN-0-315-84383-7] p 2849 N94-26667

VICTORIA UNIV., WELLINGTON (NEW ZEALAND).
Parameter estimation for ARMA models with infinite variance innovations
[AD-A274654] p 3003 N94-26355

VIRGINIA POLYTECHNIC INST., BLACKSBURG.
Proposed law of nature linking impacts, plume volcanism, and Milankovitch cycles to terrestrial vertebrate mass extinctions via greenhouse-embryo death coupling
p 2876 N94-28307

VIRGINIA POLYTECHNIC INST. AND STATE UNIV., BLACKSBURG.
Project PARAS: Phased array radio astronomy from space p 3081 N94-25703
Pressurized Lunar Rover (PLR) p 2833 N94-25704
Measuring variation in ecosystem sensitivity to stress
[AD-A274232] p 2868 N94-26817
Parallel mathematical software
[DE94-001587] p 2967 N94-27020
Effective conductivity of wire mesh reflectors for space deployable antenna systems
[NASA-CR-191605] p 2788 N94-27770
Development of methodologies for the estimation of thermal properties associated with aerospace vehicles
p 2846 N94-27920
Evaluation of high temperature superconductive thermal bridges for space-borne cryogenic infrared detectors
p 2815 N94-27921

VIRGINIA STATE UNIV., PETERSBURG.
Aerodynamic heating in hypersonic flows
p 2658 N94-27919

VIRGINIA UNIV., CHARLOTTESVILLE.
NASA-UVA light aerospace alloy and structures technology program (LA2ST)
[NASA-CR-195275] p 2844 N94-27851

VISIDYNE, INC., BURLINGTON, MA.
Characterization of the energy deposition produced by the primary electron beam on the EXCEDE 3 program. Appendix B and C
[AD-A273878] p 3012 N94-25726
Characterization of the energy deposition produced by the primary electron beam on the EXCEDE 3 program
[AD-A274453] p 3033 N94-27084

VON KARMAN INST. FOR FLUID DYNAMICS, RHODE-SAINT-GENESE (BELGIUM).
Experimental investigation of the interaction of a thrust reverser jet with an external subsonic flow
p 2801 N94-28011
Gas Turbine Engine Transient Behaviour
[VKI-LS-1993-06] p 2828 N94-28043
Combined Cycles for Power Plants
[VKI-LS-1993-08] p 2830 N94-28077

VRIJE UNIV., AMSTERDAM (NETHERLANDS).
A formalization of objects using equational dynamic logic
[PB94-125218] p 2965 N94-26852
Combining logics
[PB94-125242] p 2965 N94-26908
What can we learn from genetic algorithms: A new perspective for search methods
[PB94-125234] p 2967 N94-26997

VRIJE UNIV., BRUSSELS (BELGIUM).
Scheduling approaches with Ada
p 2952 N94-26734

W

WAGENINGEN AGRICULTURAL UNIV. (NETHERLANDS).
Time domain reflectometry for measuring bulk soil electrical conductivity and comparison with the Em38 instrument
[PB94-125432] p 2881 N94-27052

WALTER REED ARMY INST. OF RESEARCH, WASHINGTON, DC.
Human dimensions research team, operation restore hope
[AD-A274340] p 2939 N94-27056

WASEDA UNIV., TOKYO (JAPAN).
Observation of characteristics of cosmic-ray hadron interactions in uniform-type thick lead chambers at Pamir, 1 p 3112 N94-25628
Observation of characteristics of cosmic-ray hadron interactions in uniform-type thick lead chambers at Pamir, 2 p 3113 N94-25629
Observation of characteristics of cosmic-ray hadron interactions in uniform-type thick lead chambers at Pamir, 3 p 3113 N94-25630

WASHINGTON UNIV., SAINT LOUIS, MO.
Some implications of large impact craters and basins on Venus for terrestrial ringed craters and planetary evolution p 2890 N94-28306

WASHINGTON UNIV., SEATTLE.
Project Minerva: A low-cost manned Mars mission based on indigenous propellant production
p 2760 N94-25705

Nuclear Theory Group, University of Washington recent and planned research
[DE94-002729] p 3022 N94-26809

Sound, speed, reflectivity, absorption, and thermal diffusivity measurements in Arctic ice in 1990
[AD-A274326] p 2899 N94-26886

An XCP user's guide and reference manual
[AD-A274519] p 2900 N94-27090

The Martian atmospheric planetary boundary layer stability, fluxes, spectra, and similarity
[NASA-CR-195711] p 3108 N94-27935

WATERLOO UNIV. (ONTARIO).

Coherence and satisfiability of waveform timing specifications
[ISBN-0-315-57769-X] p 3009 N94-27268

Fast methods for computation with algebraic numbers
[ISBN-0-315-57888-2] p 2998 N94-27269

Impulsive control and stabilization
[ISBN-0-315-84563-5] p 2988 N94-27271

The onset of chaos in a periodically forced nonlinear oscillator
[ISBN-0-315-84564-3] p 2842 N94-27272

Modelling and stability of a shape memory alloy position control system
[ISBN-0-315-84467-1] p 2740 N94-27304

The high strain rate behaviour of tantalum
[ISBN-0-315-84472-8] p 2740 N94-27305

Microstructure and mechanical behaviour of L1(2) titanium trialuminides
[ISBN-0-315-84488-4] p 2740 N94-27306

A second-order shock-adaptive Godunov scheme based on the generalized Lagrangian formulation
[ISBN-0-315-84549-X] p 2795 N94-27307

Computation of numerical solution of parabolic PDEs by monotone iterative methods
[ISBN-0-315-84553-8] p 2999 N94-27404

Solving the linear quadratic optimal control problem for infinite-dimensional systems
[ISBN-0-315-84562-7] p 2999 N94-27405

The analysis of thermal and 1/F noise in MOS devices, circuits and systems
[ISBN-0-315-57811-4] p 2787 N94-27642

An electronic switch based on quantum interference
[ISBN-0-315-84609-7] p 2787 N94-27650

Flexible range finding applied to 3D surface synthesis: A pseudo-trinocular approach
[ISBN-0-315-84616-X] p 2813 N94-27651

Advanced control of a flexible spherical wrist
[ISBN-0-315-84424-8] p 2826 N94-27652

An efficient and accurate Green's function analysis of packaged microwave integrated circuits
[ISBN-0-315-84425-6] p 2787 N94-27653

On the Lagrangian and updated Lagrangian nonlinear finite element formulations
[ISBN-0-315-61111-1] p 3001 N94-27948

A new approach to turboprop forward nacelle design
p 2655 N94-28336

WEIZMANN INST. OF SCIENCE, REHOVOTH (ISRAEL).

Surfaces allowing for fractional statistics
[DE93-614526] p 3002 N94-25910

Aspects of nonrenormalizable terms in a superstring standard-like models
[DE93-614530] p 3071 N94-25911

The 27th Annual Meeting of the Israel Society for Microscopy and the 12th Annual Meeting of the Israel Society for Histochemistry and Cytochemistry
[DE93-632416] p 2716 N94-26519

WESTINGHOUSE ELECTRIC CORP., BALTIMORE, MD.

Meteor Burst Communications (MBC) throughput improvement tests
[AD-A273941] p 2767 N94-25990

Ferroelectric fluoride memory FET development
[AD-A274341] p 2785 N94-27057

WESTINGHOUSE ELECTRIC CORP., PITTSBURGH, PA.

High temperature solid oxide fuel cell: Customer test units
[DE94-002961] p 2858 N94-26869

High temperature solid oxide fuel development activities
[DE94-002973] p 2858 N94-26871

WESTINGHOUSE HANFORD CO., RICHLAND, WA.

Nonswelling behavior of HT9 alloy irradiated to high exposure
[DE94-003502] p 2736 N94-26522

Hanford Environmental Information System (HEIS) sample/data entry flow summary
[DE94-002494] p 3098 N94-26559

WESTINGHOUSE SAVANNAH RIVER CO., AIKEN, SC.

Effect of nitrocarburizing on shape of titanium alloy parts
[DE94-004040] p 2732 N94-25822

Upset welding process for 21-6-9 spherical vessels
[DE93-018194] p 2832 N94-28229

WESTINGHOUSE SCIENCE AND TECHNOLOGY CENTER, PITTSBURGH, PA.

Processing, fabrication, and demonstration of HTS integrated microwave circuits, appendix A
[AD-A274600] p 2785 N94-26890

WICHITA STATE UNIV., KS.

The development of a horizontal impact sled facility and subsequent crashworthiness experiments
[NIAR-93-15] p 2680 N94-26200

WILKES COLL., WILKES-BARRE, PA.

Microspheres for laser velocimetry in high temperature wind tunnel p 2682 N94-27903

WINDSOR UNIV. (ONTARIO).

Visual surface perception: Surface reconstruction from shading and stereo
[ISBN-0-315-60974-5] p 2975 N94-27872

WISCONSIN UNIV., LA CROSSE.

Stopping powers and cross sections due to two-photon processes in relativistic nucleus-nucleus collisions
[NASA-CR-4574] p 3033 N94-27646

WISCONSIN UNIV., MADISON.

An evaluation of the utility of ground-based high resolution interferometer (GB-HIS) soundings of the planetary boundary layer
[DE94-000960] p 3106 N94-25981

Morphological analysis of ionomers
[DE94-003660] p 2749 N94-26005

Measurement of magnetic fluctuation induced energy transport
[DE94-003846] p 3042 N94-26132

Radial base functions: L(sup p)-approximation orders with scattered centers
[AD-A274682] p 3003 N94-26445

The dynamics of interacting nonlinearities governing long wavelength driftwave turbulence
[DE94-001785] p 2793 N94-26558

ARM Fourier transform spectrometer data analysis tools
[DE94-000865] p 2895 N94-26697

Radial basis function approximation: From gridded centers to scattered centers
[AD-A274184] p 2998 N94-27103

NCVS, volume 5
[AD-A274975] p 2902 N94-27165

Cosmic x ray physics
[NASA-CR-195225] p 3115 N94-27236

Cosmic x ray physics
[NASA-CR-195218] p 3115 N94-27419

Cosmic x ray physics
[NASA-CR-195219] p 3115 N94-27420

An analysis of monojet data in p(bar-p) collisions at square root of s equal to 1.8 TEV
[DE94-001822] p 3026 N94-27565

Fusion reactor systems studies
[DE94-003162] p 3046 N94-27686

TFTR experimental data analysis collaboration
[DE94-004166] p 3047 N94-27690

WISCONSIN UNIV., MILWAUKEE.

Pax: A permanent base for human habitation of Mars
p 2943 N94-25706

Were all extinction events caused by impacts?
p 2891 N94-28311

WOODS HOLE RESEARCH CENTER, MA.

Bibliography of technical reports, 1992
[AD-A274849] p 3098 N94-26561

WORCESTER POLYTECHNIC INST., MA.

Microgravity ignition experiment p 2761 N94-25707

Solar powered multipurpose remotely powered aircraft
p 2671 N94-25719

WRIGHT LAB., WRIGHT-PATTERSON AFB, OH.

Proposed Object Oriented Programming (OOP) enhancements to the Very High Speed Integrated Circuits (VHSIC) Hardware Description Language (VHDL)
[AD-A274004] p 2957 N94-25661

Three-wave nonlinear interactions in KTiOPO4 (KTP) and KTP isomorphs
[AD-A274079] p 3052 N94-25993

A VHDL register transfer level model of the linear token passing multiplex data bus protocol for the high speed data bus
[AD-A273734] p 2980 N94-26009

An investigation of the surge behavior of a high-speed ten-stage axial flow compressor
[AD-A274910] p 2674 N94-26345

Optical characterization and guided wave loss measurements for end-capped 6F-polybenzoxazole
[AD-A274586] p 3036 N94-26982

Experiments on the ground vortex formed by an impinging jet in cross flow p 2802 N94-28016

A study of jet effect and ground effect interference on a STOL fighter p 2671 N94-28034

WRIGHT STATE UNIV., DAYTON, OH.

Pulse waveform and transcranial Doppler analysis during lower body negative pressure
[AD-A274516] p 2911 N94-27088

WYLE LABS., INC., ARLINGTON, VA.

On the aging of sonic booms p 2650 N94-28194

Y

YAGI MEMORIAL PARK, MITAKE (JAPAN).

Development of inbred strains from Japanese wild rats (Rattus norvegicus) p 2906 N94-27492

YALE UNIV., NEW HAVEN, CT.

Preparation and characterization of high temperature superconductor film surfaces
[AD-A274293] p 3059 N94-26681

YAMAGATA UNIV. (JAPAN).

Mechanism for regulation of myocardial contractility by autonomic drugs: Pathophysiological relevance in congestive heart failure p 2931 N94-27536

YAMANASHI UNIV., KOFU (JAPAN).

Simultaneous observation of families and air showers at Mt. Chacaltaya p 3114 N94-25634

YARDNEY TECHNICAL PRODUCTS, INC., PAWCATUCK, CT.

High rate lithium/thionyl chloride bipolar battery development p 2864 N94-28133

YASUI ACUPUNCTURE CLINIC, NAGOYA (JAPAN).

Changes in pain sensation induced by repetitive application of noxious heat pulses to the human skin
p 2924 N94-27501

YORK UNIV. (ONTARIO).

A numerical solution to the one and two dimensional line radiative transfer equation
[ISBN-0-315-84258-X] p 2994 N94-26640

Wobble-nutation modes of the Earth
[ISBN-0-315-84246-6] p 3102 N94-26669

A three-dimensional chemical transport model study of the 1991 Antarctic ozone hole using objectively analysed data
[ISBN-0-315-84250-4] p 2867 N94-26670

A variational approach to the quantum field theoretic bound-state problem
[ISBN-0-315-60960-5] p 3074 N94-27401

YORK UNIV., TORONTO (ONTARIO).

Response of an airborne synthetic aperture radar to sea ice in the marginal ice zone
[ISBN-0-315-84243-1] p 2849 N94-26668

A relativistic quark model
[ISBN-0-315-60926-5] p 3025 N94-27333

CONTRACT NUMBER INDEX

Typical Contract Number Index Listing

AF PROJ. 2306 .... p 92 N94-11866

CONTRACT NUMBER | PAGE NUMBER | ACCESSION NUMBER

Listings in this index are arranged alphanumerically by contract number. Under each contract number the accession numbers denoting documents that have been produced as a result of research done under that contract are arranged in ascending order. The page number helps to locate the citation in the abstract section. The accession number denotes the number by which the citation is identified.

AF PROJ. 2003 .... p 2980 N94-26009
AF PROJ. 2305 .... p 3036 N94-26982
AF PROJ. 2312 .... p 2910 N94-26973
AF PROJ. 2422 .... p 2753 N94-26822
AF PROJ. 3066 .... p 2674 N94-26345
AF PROJ. 4600 .... p 2765 N94-25660
AF PROJ. 4643 .... p 2773 N94-27085
AF PROJ. 7184 .... p 2937 N94-25965
AF PROJ. 7231 .... p 2911 N94-27088
AF PROJ. 7930 .... p 2910 N94-26435
p 2902 N94-26991
AF-AFOSR-0002-91 .... p 2772 N94-26975
AF-AFOSR-0006-91 .... p 3024 N94-27133
AF-AFOSR-0024-90 .... p 2988 N94-27139
AF-AFOSR-0057-90 .... p 2962 N94-26303
AF-AFOSR-0076-89 .... p 2939 N94-27012
AF-AFOSR-0080-90 .... p 2992 N94-26302
AF-AFOSR-0162-90 .... p 2709 N94-27142
AF-AFOSR-0222-91 .... p 2987 N94-27124
AF-AFOSR-0266-90 .... p 2940 N94-27141
AF-AFOSR-0278-91 .... p 3055 N94-26194
AF-AFOSR-0279-90 .... p 2709 N94-27125
AF-AFOSR-0288-90 .... p 2964 N94-26682
AF-AFOSR-0306-88 .... p 3024 N94-27011
AF-AFOSR-0306-90 .... p 3059 N94-26681
AF-AFOSR-0324-91 .... p 3099 N94-27013
AF-AFOSR-0343-90 .... p 2938 N94-26683
AF-AFOSR-0352-90 .... p 2880 N94-26752
AF-AFOSR-0378-91 .... p 2939 N94-27094
AF-AFOSR-0379-91 .... p 2868 N94-26817
AF-AFOSR-0400-89 .... p 2881 N94-27143
AF-AFOSR-0488-89 .... p 3046 N94-27098
AF-AFOSR-0504-89 .... p 2939 N94-27072
AF-AFOSR-0541-89 .... p 2793 N94-26534
AF-AFOSR-90-C-0019 .... p 2754 N94-27086
ARPA ORDER 4976 .... p 2786 N94-27061
ARPA ORDER 6873 .... p 2765 N94-25725
p 2984 N94-25898
ARPA ORDER 7330 .... p 2982 N94-27117
ARPA ORDER 7597 .... p 2984 N94-25900
ARPA ORDER 7777 .... p 2767 N94-25990
ARPA ORDER 8313 .... p 3099 N94-27014
p 2967 N94-27063
ARPA ORDER 8351C .... p 2782 N94-26344
p 3036 N94-26857
AT/2037/331 .... p 2644 N94-26248
A87/K/045 .... p 2784 N94-26646
A87/K/046 .... p 2811 N94-26647
A90/KL/654 .... p 3036 N94-26648
A90/KL/655 .... p 3036 N94-26649
A92/KL/643 .... p 2770 N94-26650
BARR-10-119 .... p 2641 N94-27286
CRG-92.05 .... p 2965 N94-26772
D/ERI/9/4/2040/4 .... p 2800 N94-28005
DA PROJ. MM3-P-30 .... p 2937 N94-26430
DA PROJ. M00-96 .... p 2937 N94-26430
DA PROJ. RM3-3-M-20 .... p 2984 N94-25899
p 2985 N94-25966
DA PROJ. RR0-4204 .... p 3002 N94-25962
DA PROJ. X05-13 .... p 2899 N94-26567
DA PROJ. 1L1-61102-AH-45 .... p 2645 N94-26483
p 2645 N94-26489
p 2645 N94-26492
p 2645 N94-26497
p 2826 N94-27657
DA PROJ. 1L1-62618-AH-80 .... p 2957 N94-25753
DA PROJ. 1L1-62716-AH-70 .... p 2942 N94-27089
DA PROJ. 1O1-61102-A-71-A .... p 2838 N94-26448
DA PROJ. 101-62622-A-553 .... p 2900 N94-25593
DA PROJ. 3M1-62787-A-879 .... p 2910 N94-26432
p 2911 N94-27097
p 2911 N94-27130
DA PROJ. 7W0-513 .... p 2900 N94-26887
DAAA15-90-C-1025 .... p 2942 N94-27089
DAAA21-89-C-0001 .... p 2958 N94-25777
DAAH04-93-G-0072 .... p 3023 N94-26926
DAAL02-90-K-0027 .... p 2771 N94-26844
DAAL03-90-G-0090 .... p 3003 N94-26445
p 2998 N94-27103
DAAL04-91-C-0046 .... p 2709 N94-26978
DACA88-93-C-0008 .... p 2764 N94-27144
DAMD17-92-C-2062 .... p 2911 N94-26985
DE-AC02-76CH-00016 .... p 3012 N94-25795
p 2699 N94-25798
p 3022 N94-26769
p 2753 N94-26770
p 3060 N94-26771
p 2811 N94-26787
p 2717 N94-26951
p 3027 N94-27711
p 3029 N94-27814
p 2852 N94-27875
DE-AC02-76CH-03000 .... p 2809 N94-25599
p 3015 N94-25935
p 3016 N94-25957
p 3018 N94-26245
p 3104 N94-26311
p 3104 N94-26786
p 3023 N94-26938
p 3028 N94-27748
p 3028 N94-27749
p 3103 N94-27750
p 3028 N94-27752
DE-AC02-76CH-03073 .... p 3045 N94-26863
p 3048 N94-27825
DE-AC02-76ER-00881 .... p 3026 N94-27565
DE-AC02-76ER-13065 .... p 3017 N94-26101
DE-AC02-83CH-10093 .... p 2855 N94-26115
p 2791 N94-26117
p 2856 N94-26426
p 2856 N94-26480
p 2736 N94-26481
p 2856 N94-26513
p 3067 N94-27609
p 2859 N94-27610
p 2860 N94-27625
DE-AC03-76SF-00098 .... p 2789 N94-25597
p 2809 N94-25662
p 2957 N94-25663
p 2760 N94-25849
p 2781 N94-26047
p 3017 N94-26083
p 2750 N94-26085
p 2733 N94-26087
p 3053 N94-26094
p 3054 N94-26095
p 2714 N94-26122
p 3054 N94-26125
p 3054 N94-26128
p 2836 N94-26129
p 2816 N94-26130
p 3055 N94-26239
p 3018 N94-26325
p 2962 N94-26327
p 2782 N94-26328
p 2855 N94-26329
p 3032 N94-26330
p 2867 N94-26419
p 2856 N94-26464
p 3058 N94-26516
p 3060 N94-26795
p 2996 N94-26936
p 3118 N94-26937
p 3106 N94-27007
p 2967 N94-27049
p 2787 N94-27618
p 2741 N94-27619
p 2742 N94-27694
p 2827 N94-27722
p 2814 N94-27779
p 2743 N94-27792
DE-AC03-76SF-00515 .... p 3017 N94-26101
p 3018 N94-26133
p 3056 N94-26326
p 3024 N94-27050
p 3116 N94-27440
p 3028 N94-27736
p 3116 N94-27740
DE-AC03-89ER-51114 .... p 3041 N94-25801
p 3042 N94-25976
p 3043 N94-26274
p 3043 N94-26323
p 3045 N94-26865
p 3045 N94-26950
p 3048 N94-27785
p 3048 N94-27791
DE-AC03-89ER-52153 .... p 3043 N94-26324
DE-AC03-92SF-19441 .... p 2699 N94-25929
p 2700 N94-25930
DE-AC04-76DP-00789 .... p 2853 N94-25946
p 3016 N94-26033
p 2821 N94-26110
p 2948 N94-26111
p 3057 N94-26420
p 2980 N94-26473
p 2857 N94-26617
p 2857 N94-26700
p 2716 N94-26794
p 2888 N94-28296
DE-AC04-76DR-00789 .... p 2759 N94-26198
p 3068 N94-27693
p 2743 N94-27792
DE-AC04-88ID-12692 .... p 2756 N94-27611
DE-AC04-94AL-85000 .... p 2699 N94-25600
p 3049 N94-25601
p 2780 N94-25664
p 2821 N94-25811
p 2780 N94-25812
p 3050 N94-25814
p 3050 N94-25815
p 3050 N94-25817
p 2958 N94-25818
p 2732 N94-25819
p 2748 N94-25932
p 3051 N94-25944
p 2979 N94-25952
p 2979 N94-25953
p 2700 N94-25956
p 2821 N94-25970
p 3052 N94-25971
p 2780 N94-25975
p 2781 N94-25977
p 2713 N94-25978
p 3052 N94-25989
p 3053 N94-26025
p 2762 N94-26027
p 2836 N94-26032
p 2960 N94-26118
p 2961 N94-26146
p 3035 N94-26246
p 2750 N94-26247
p 2848 N94-26277
p 3056 N94-26308
p 2735 N94-26349
p 3056 N94-26352
p 2962 N94-26370
p 2962 N94-26371
p 2783 N94-26372
p 2985 N94-26462
p 2856 N94-26463
p 2702 N94-26560
p 2838 N94-26563
p 2751 N94-26564
p 3058 N94-26565
p 2738 N94-26610
p 2857 N94-26612
p 2857 N94-26617

p 2708 N94-26796
p 2839 N94-26810
p 2819 N94-26811
p 3061 N94-26856
p 2739 N94-26912
p 2859 N94-27004
p 3099 N94-27022
p 2819 N94-27262
p 3000 N94-27564
p 2704 N94-27708
p 2712 N94-27710
p 2983 N94-27713
p 3039 N94-27721
p 2757 N94-27726
p 3069 N94-27753
p 2742 N94-27755
p 2742 N94-27788
p 3069 N94-27790
p 2682 N94-27997
p 3040 N94-27999
p 3040 N94-28000
p 3070 N94-28067
DE-AC05-76OR-00033 .... p 3041 N94-25949
p 2877 N94-25979
p 2791 N94-26121
p 3059 N94-26765
p 2813 N94-27615
p 3069 N94-27757
DE-AC05-84OR-21400 .... p 2767 N94-25924
p 3041 N94-25933
p 2732 N94-26004
p 2749 N94-26080
p 2733 N94-26092
p 2866 N94-26123
p 3054 N94-26137
p 3042 N94-26140
p 2734 N94-26272
p 2750 N94-26332
p 2822 N94-26465
p 2769 N94-26482
p 2708 N94-26557
p 3020 N94-26574
p 2751 N94-26580
p 3044 N94-26694
p 2964 N94-26764
p 3059 N94-26765
p 2965 N94-26784
p 3044 N94-26858
p 3044 N94-26860
p 2739 N94-26931
p 3062 N94-26932
p 2986 N94-26948
p 2824 N94-27181
p 3024 N94-27199
p 3065 N94-27251
p 3046 N94-27261
p 3046 N94-27568
p 2741 N94-27616
p 2869 N94-27691
p 2988 N94-27706
p 3069 N94-27757
p 3048 N94-27785
DE-AC05-84OS-21400 .... p 2713 N94-26014
p 3045 N94-26861
p 2740 N94-27006
DE-AC06-76RL-01830 .... p 2731 N94-25803
p 2731 N94-25804
p 2705 N94-25805
p 3096 N94-25813
p 2866 N94-25948
p 2706 N94-25982
p 2732 N94-25987
p 2960 N94-26048
p 3017 N94-26049
p 2855 N94-26114
p 3054 N94-26147
p 2664 N94-26309
p 3097 N94-26348
p 2838 N94-26524
p 2941 N94-26555
p 2737 N94-26556
p 2737 N94-26575
p 2737 N94-26585
p 2895 N94-26761
p 2880 N94-26762
p 2754 N94-27021
p 3100 N94-27563
p 3000 N94-27569
p 2741 N94-27570
p 2982 N94-27600
p 2869 N94-27601
p 3067 N94-27602
p 3116 N94-27621
p 2741 N94-27622
p 2827 N94-27780
p 2742 N94-27786
DE-AC06-87RL-10930 .... p 2736 N94-26522
p 3098 N94-26559
DE-AC07-76ID-01570 .... p 3061 N94-26868
DE-AC08-93NV-11265 .... p 3020 N94-26527
DE-AC09-89SR-18035 .... p 2732 N94-25822
p 2832 N94-28229
DE-AC11-93PN-38195 .... p 2713 N94-26075
p 2737 N94-26582
p 2797 N94-27617
DE-AC12-76SN-00052 .... p 2715 N94-26320
DE-AC21-86MC-23166 .... p 2827 N94-27874
DE-AC21-89MC-26006 .... p 2858 N94-26792
DE-AC21-90MC-27227 .... p 2856 N94-26581
DE-AC35-89ER-40486 .... p 3011 N94-25598
p 2980 N94-25984
p 3021 N94-26759
p 3063 N94-27047
DE-AI01-93NE-32170 .... p 2699 N94-25926
DE-AI02-92ER-25118 .... p 2956 N94-25602
DE-AI03-91SF-19043 .... p 2700 N94-25969
DE-AI05-93OR-22089 .... p 2879 N94-26515
DE-A101-91CE-50306 .... p 2827 N94-27984
DE-FC03-90ER-61010 .... p 2865 N94-25790
p 2877 N94-26015
p 2894 N94-26313
DE-FC21-91MC-28055 .... p 2858 N94-26869
p 2858 N94-26871
DE-FG01-90ER-81050 .... p 2717 N94-26951
DE-FG02-84ER-45132 .... p 3060 N94-26780
DE-FG02-84ER-52111 .... p 3044 N94-26579
DE-FG02-85ER-45184 .... p 2732 N94-25954
DE-FG02-85ER-45217 .... p 2753 N94-26783
DE-FG02-85ER-53198 .... p 3042 N94-26132
DE-FG02-85ER-53211 .... p 3047 N94-27720
DE-FG02-85ER-60304 .... p 2865 N94-25789
DE-FG02-86ER-13552 .... p 2960 N94-25986
DE-FG02-86ER-13564 .... p 2749 N94-25973
DE-FG02-86ER-13569 .... p 2715 N94-26369
DE-FG02-86ER-45229 .... p 2751 N94-26594
DE-FG02-86ER-53222 .... p 3047 N94-27735
DE-FG02-86ER-60485 .... p 2866 N94-25927
DE-FG02-88ER-40414 .... p 3029 N94-27783
DE-FG02-88ER-40415 .... p 3017 N94-26101
DE-FG02-88ER-40448 .... p 3027 N94-27689
DE-FG02-88ER-45347 .... p 3021 N94-26677
DE-FG02-88ER-45370 .... p 2749 N94-26005
DE-FG02-89ER-13996 .... p 2716 N94-26781
DE-FG02-89ER-14017 .... p 3050 N94-25848
DE-FG02-89ER-14079 .... p 2877 N94-25847
DE-FG02-89ER-52158 .... p 3046 N94-27686
DE-FG02-89ER-53291 .... p 2793 N94-26558
DE-FG02-89ER-60858 .... p 2814 N94-27779
DE-FG02-90ER-14104 .... p 3058 N94-26526
DE-FG02-90ER-14147 .... p 2792 N94-26468
DE-FG02-90ER-40581 .... p 3073 N94-27002
DE-FG02-90ER-45414 .... p 3060 N94-26782
DE-FG02-90ER-60932 .... p 2866 N94-26026
DE-FG02-90ER-61054 .... p 2898 N94-25791
DE-FG02-90ER-61064 .... p 2767 N94-25950
DE-FG02-90ER-61065 .... p 2893 N94-26082
DE-FG02-90ER-80910 .... p 2859 N94-27005
DE-FG02-91CE-23810 .... p 2713 N94-25934
p 2749 N94-26007
p 2719 N94-27567
p 2756 N94-27692
p 2721 N94-28069
DE-FG02-91ER-40623 .... p 3115 N94-27003
DE-FG02-91ER-40654 .... p 3032 N94-26119
DE-FG02-91ER-40661 .... p 3033 N94-27614
DE-FG02-91ER-40677 .... p 3029 N94-27815
DE-FG02-91ER-40685 .... p 3008 N94-25988
DE-FG02-91ER-40688 .... p 3031 N94-25931
DE-FG02-91ER-45445 .... p 2733 N94-26070
DE-FG02-91ER-54111 .... p 3041 N94-25846
DE-FG02-92ER-14283 .... p 3021 N94-26760
DE-FG02-92ER-25137 .... p 2991 N94-25928
DE-FG02-92ER-40692 .... p 3031 N94-26097
DE-FG02-92ER-40698 .... p 3024 N94-26949
DE-FG02-92ER-54139 .... p 3047 N94-27690
DE-FG02-92ER-61365 .... p 3106 N94-25981
p 2895 N94-26697
DE-FG02-92ER-61443 .... p 3035 N94-26100
DE-FG02-92ER-61477 .... p 2866 N94-26077
DE-FG02-92ER-81453 .... p 2858 N94-26785
DE-FG02-93ER-12130 .... p 2731 N94-25804
DE-FG02-93ER-40756 .... p 3012 N94-25800
DE-FG02-93ER-54197 .... p 3044 N94-26523
DE-FG05-80ET-53088 .... p 3041 N94-25792
p 3041 N94-25923
p 3042 N94-25958
p 2791 N94-26096
p 2963 N94-26521
p 3047 N94-27723
DE-FG05-87ER-40343 .... p 3021 N94-26586
DE-FG05-88ER-25068 .... p 2967 N94-27020
DE-FG05-88ER-40441 .... p 3013 N94-25820
DE-FG05-88ER-40445 .... p 3018 N94-26244
DE-FG05-89ER-75531 .... p 3039 N94-27603
DE-FG05-90ER-40592 .... p 3026 N94-27604
DE-FG05-91ER-25100 .... p 2959 N94-25821
DE-FG05-91ER-40619 .... p 3013 N94-25820
DE-FG06-84ER-60245 .... p 2892 N94-25939
DE-FG06-84ER-60247 .... p 2892 N94-25951
DE-FG06-85ER-45191 .... p 3063 N94-26958
DE-FG06-88ER-40427 .... p 3022 N94-26809
DE-FG06-89ER-75522 .... p 2737 N94-26575
DE-FG06-90ER-40537 .... p 3017 N94-26101
DE-FG06-92ER-61457 .... p 2892 N94-25951
DE-FG21-93MC-29224 .... p 2857 N94-26747
DE-FG22-92PC-92540 .... p 2792 N94-26319
DEN3-374 .... p 2827 N94-27984
DLA900-87-D-0017 .... p 2835 N94-26833
DMS-9224748 .... p 3003 N94-26445
DREO-W7714-1-0007 .... p 2973 N94-27762
DREP-W7708-2-0529/01-XSA ...... p 2665 N94-27667
DSS-W7714-0-9883 .... p 2973 N94-27761
p 2975 N94-27951
DTFA01-87-C-00014 .... p 2665 N94-26826
DTFA01-93-Z-02012 .... p 2680 N94-26196
p 2772 N94-26963
DTFA03-89-C-00043 .... p 2672 N94-26028
p 2668 N94-26488
DTFA03-92-Z-0029 .... p 2669 N94-27105
DTRS57-87-C-00006 .... p 2642 N94-27292
DTRS57-88-C-0078TD39 .... p 2641 N94-27286
ESTEC-9198/90/NL/SF .... p 2951 N94-26731
ESTEC-9357/91/NL/US .... p 2972 N94-27582
F04701-88-C-0089 .... p 3008 N94-26484
p 2753 N94-26842
p 2785 N94-26845
p 2746 N94-28185
F19628-88-K-0039 .... p 2880 N94-26855
F19628-89-C-0068 .... p 2959 N94-25879
F19628-89-C-0112 .... p 2898 N94-28223
F19628-89-K-0044 .... p 3001 N94-28216
F19628-90-C-0002 .... p 3049 N94-25645
p 2680 N94-26196
p 2772 N94-26963
p 2641 N94-27287
F19628-90-C-0003 .... p 2959 N94-25855
F19628-90-C-0090 .... p 2698 N94-28200
p 3040 N94-28202
F19628-90-C-0100 .... p 2878 N94-26304
F19628-90-C-0147 .... p 2698 N94-28210
p 2698 N94-28217
F19628-90-C-0187 .... p 3012 N94-25726
p 3033 N94-27084
F19628-90-C-0191 .... p 2887 N94-28206
F19628-90-K-0014 .... p 2879 N94-26569
F19628-90-K-0039 .... p 2878 N94-26224
p 2777 N94-28211
F19628-90-K-0055 .... p 2878 N94-26433
F19628-91-C-0004 .... p 2877 N94-25877
F19628-91-C-0104 .... p 3104 N94-27265
F19628-91-C-0119 .... p 2816 N94-26178
F19628-91-C-0168 .... p 3002 N94-25903
p 3099 N94-27014
p 2967 N94-27063
F19628-91-C-0185 .... p 2895 N94-26798
F19628-91-K-0026 .... p 2887 N94-28214
F19628-91-K-0036 .... p 2876 N94-25752
F19628-92-K-0003 .... p 2878 N94-26338
F29601-90-K-0048 .... p 2701 N94-26537
F29601-91-C-0071 .... p 3035 N94-26572
F29601-91-K-DB08 .... p 3098 N94-26490
F30602-88-D-0026 .... p 2766 N94-25736
F30602-89-C-0213 .... p 2834 N94-25727
F30602-91-D-0001 .... p 2979 N94-25786
F30602-92-C-0035 .... p 3099 N94-27101
F30602-92-C-0037 .... p 2820 N94-28068
F30602-93-C0041 .... p 2817 N94-26271
F33601-93-P-7648 .... p 2759 N94-26486
F33615-85-C-0541 .... p 2941 N94-26984
F33615-86-C-0542 .... p 3099 N94-26891
F33615-88-C-1825 .... p 2672 N94-26340
F33615-88-C-5404 .... p 2705 N94-25779
F33615-89-C-0532 .... p 2774 N94-27170
F33615-89-C-3201 .... p 2840 N94-26922
p 2840 N94-26953
p 2840 N94-27008
F33615-89-C-3611 .... p 2802 N94-28016
F33615-90-C-0005 .... p 2679 N94-25773
F33615-90-C-1465 .... p 2984 N94-25900
p 2986 N94-27032
p 2786 N94-27061
p 2967 N94-27064
F33615-90-C-2035 .... p 3064 N94-27095
F33615-90-C-3211 .... p 2987 N94-27093
F33615-90-C-3215 .... p 2811 N94-26568
F33615-90-C-3600 .... p 2666 N94-25590
p 2667 N94-25961
F33615-90-C-5915 .... p 2987 N94-27077

F33615-91-C-2112 .... p 2750 N94-26167
F33615-92-C-0018 .... p 2673 N94-26989
F33615-92-C-3201 .... p 2832 N94-28209
F33615-93-1-1282 .... p 2986 N94-27032
p 2967 N94-27064
F49620-89-C-0079 .... p 3009 N94-27126
F49620-90-C-0083 .... p 3037 N94-27010
F49620-92-C-0047 .... p 2783 N94-26536
F49620-92-J-0015 .... p 3111 N94-27099
F49620-92-J-0030 .... p 2968 N94-27140
F49620-92-J-0037 .... p 2823 N94-27104
F49620-92-J-0061 .... p 3110 N94-26883
F49620-92-J-0062 .... p 3010 N94-27067
F49620-92-J-0078 .... p 2999 N94-27415
F49620-92-J-0094 .... p 3111 N94-27096
F49620-92-J-0183 .... p 2901 N94-26517
F49620-92-J-0378 .... p 2773 N94-27068
F49620-93-1-0280 .... p 2999 N94-27415
GRI-5086-260-1307 .... p 2717 N94-27256
GRI-5086-293-1848 .... p 2824 N94-27224
GRI-5087-260-1444 .... p 2717 N94-27226
GRI-5091-260-2180 .... p 2859 N94-27225
MDA972-90-C-0035 .... p 2982 N94-27117
MDA972-91-C-0051 .... p 2767 N94-25990
MDA972-91-J-1006 .... p 3044 N94-26820
MDA972-92-C-0071 .... p 2782 N94-26344
p 3036 N94-26857
MDA972-92-J-1010 .... p 2765 N94-25725
p 2984 N94-25898
MDA972-92-J-1018 .... p 2962 N94-26373
MDA972-92-J-1021 .... p 2967 N94-27060
MIPR-91MM1505 .... p 2909 N94-26377
MOD-01689029811 .... p 2989 N94-27800
MOE-03680181 .... p 2904 N94-27470
MOE-03807084 .... p 2905 N94-27479
MOE-04255103 .... p 2906 N94-27494
p 2906 N94-27495
p 2906 N94-27496
p 2906 N94-27497
p 2906 N94-27498
p 2906 N94-27499
p 2906 N94-27500
p 2924 N94-27501
p 2906 N94-27502
MOE-04454559 .... p 2905 N94-27480
MOE-04551001 .... p 2915 N94-27460
MOE-04670012 .... p 2905 N94-27486
MOE-04671468 .... p 2905 N94-27482
MOE-04671469 .... p 2904 N94-27477
MOE-04671470 .... p 2919 N94-27478
MOE-04770070 .... p 2906 N94-27495
NAGW-1175 .... p 2985 N94-26006
NAGW-1333 .... p 2683 N94-26280
NAGW-1620 .... p 2879 N94-26599
NAGW-1625 .... p 2881 N94-27237
NAGW-1840 .... p 2847 N94-26222
NAGW-1902 .... p 3105 N94-27932
NAGW-1946 .... p 3105 N94-28184
NAGW-2023 .... p 3115 N94-27167
NAGW-2041 .... p 3108 N94-27935
NAGW-2306 .... p 3105 N94-27428
NAGW-2330 .... p 2848 N94-26236
NAGW-2402 .... p 3107 N94-27784
NAGW-2627 .... p 2883 N94-27438
NAGW-3023 .... p 3103 N94-26789
NAGW-3319 .... p 3105 N94-28184
NAGW-3437 .... p 2851 N94-27849
NAGW-3508 .... p 2883 N94-27852
NAGW-3585 .... p 3108 N94-27941
NAGW-3703 .... p 2852 N94-28070
NAGW-389 .... p 3107 N94-27886
p 3107 N94-27887
NAGW-552 .... p 3107 N94-27886
p 3107 N94-27887
NAGW-695 .... p 3105 N94-28184
NAG1-1003 .... p 2648 N94-28071
NAG1-1075 .... p 2958 N94-25777
NAG1-1423 .... p 2642 N94-27293
NAG1-1433 .... p 2798 N94-27782
NAG1-1451 .... p 2678 N94-26821
NAG1-1457 .... p 3033 N94-27646
NAG1-1491 .... p 2883 N94-27883
NAG1-1540 .... p 2697 N94-27789
NAG1-587 .... p 2973 N94-27663
NAG1-613 .... p 2964 N94-26680
p 2948 N94-26714
NAG1-631 .... p 2751 N94-26641
NAG1-690 .... p 2641 N94-27286
NAG1-745 .... p 2844 N94-27851
NAG1-793 .... p 2648 N94-28072
NAG10-84 .... p 2903 N94-27940
NAG2-12 .... p 2641 N94-27286
NAG2-593 .... p 2974 N94-27767
p 2666 N94-27768
NAG2-716 .... p 2641 N94-27286
NAG2-743 .... p 2668 N94-26235
NAG2-829 .... p 2961 N94-26207
NAG2-869 .... p 2793 N94-26595
NAG3-1023 .... p 2798 N94-27802
NAG3-1102 .... p 2703 N94-27662
NAG3-1137 .... p 2846 N94-28227
NAG3-11467 .... p 2678 N94-27414
NAG3-1192 .... p 2675 N94-27654
NAG3-1225 .... p 2812 N94-27214
NAG3-1230 .... p 2846 N94-28227
NAG3-1234 .... p 2846 N94-28227
NAG3-1273 .... p 2845 N94-28181
NAG3-1316 .... p 2826 N94-27657
NAG3-329 .... p 2846 N94-28266
NAG5-1327 .... p 3102 N94-26234
NAG5-1541 .... p 2887 N94-28218
NAG5-1771 .... p 3103 N94-27933
NAG5-2006 .... p 2968 N94-27168
NAG5-2032 .... p 3116 N94-27440
NAG5-472 .... p 2878 N94-26204
NAG5-629 .... p 3115 N94-27236
p 3115 N94-27419
p 3115 N94-27420
NAG5-676 .... p 2882 N94-27380
NAG5-887 .... p 2851 N94-27787
NAG8-212 .... p 2702 N94-27150
p 2702 N94-27166
p 2825 N94-27383
NAG8-293 .... p 2843 N94-27765
NAG8-845 .... p 2893 N94-26138
NAG8-912 .... p 2896 N94-27408
NAG9-331 .... p 2684 N94-26287
NAG9-575 .... p 3107 N94-27850
NAG9-659 .... p 2684 N94-26287
NASA ORDER H-70979-D .... p 2756 N94-27429
NASW-4435 .... p 3075 N94-25665
NASW-4513 .... p 2776 N94-27669
p 2777 N94-27946
NASW-4574 .... p 2887 N94-28294
NASW-4614 .... p 3107 N94-27885
p 3107 N94-27886
p 3107 N94-27887
p 3107 N94-27888
NASW-4739 .... p 3106 N94-27409
NASW-4744 .... p 2883 N94-27393
NASW-4749 .... p 3104 N94-27407
NASW-4771 .... p 3106 N94-27406
NAS1-18266 .... p 2953 N94-26740
NAS1-18471 .... p 2788 N94-27770
NAS1-18605 .... p 2994 N94-26601
p 2999 N94-27415
NAS1-18969 .... p 2953 N94-26740
NAS1-18972 .... p 2956 N94-28267
NAS1-18992 .... p 2894 N94-26506
NAS1-19000 .... p 2695 N94-26103
p 2680 N94-26603
p 2668 N94-26606
p 2711 N94-27433
NAS1-19060 .... p 2651 N94-28197
NAS1-19299 .... p 2792 N94-26467
p 2808 N94-28180
NAS1-19304 .... p 2818 N94-26705
NAS1-19320 .... p 2646 N94-26548
NAS1-19480 .... p 2792 N94-26499
p 2994 N94-26601
p 2999 N94-27415
p 2969 N94-27416
p 2970 N94-27417
p 2999 N94-27434
p 2796 N94-27435
p 2999 N94-27557
p 2971 N94-27558
p 2971 N94-27572
NAS10-11567 .... p 3109 N94-27982
p 3109 N94-27983
NAS10-11572 .... p 2897 N94-27884
NAS10-11624 .... p 2903 N94-27412
NAS13-564 .... p 2956 N94-25606
NAS2-12961 .... p 2999 N94-27434
p 2970 N94-27542
NAS2-13312 .... p 2674 N94-27432
NAS2-13419 .... p 3095 N94-27866
NAS3-22525 .... p 2839 N94-26692
p 2843 N94-27776
NAS3-23269 .... p 2719 N94-27854
NAS3-23773 .... p 2700 N94-26156
p 2701 N94-26231
p 2702 N94-26542
p 2703 N94-27212
p 2703 N94-27213
p 2824 N94-27228
NAS3-25266 .... p 2700 N94-26090
p 2644 N94-26131
p 2680 N94-26141
p 2690 N94-26142
p 2701 N94-26208
p 2701 N94-26209
p 2674 N94-26573
p 2685 N94-27358
NAS3-25515 .... p 2834 N94-26199
NAS3-25804 .... p 2674 N94-26588
NAS3-25952 .... p 2675 N94-27778
NAS3-26576 .... p 2843 N94-27656
NAS3-27214 .... p 2835 N94-26691
NAS5-30375 .... p 2702 N94-26613
NAS5-31331 .... p 2814 N94-27981
NAS5-32065 .... p 3115 N94-26790
NAS7-918 .... p 2786 N94-27574
p 2943 N94-27934
NAS8-36307 .... p 2823 N94-27149
NAS8-36955 .... p 2761 N94-27220
NAS8-37821 .... p 2796 N94-27377
NAS8-38100 .... p 2691 N94-26135
p 2691 N94-26153
p 2752 N94-26708
NAS8-38609 .... p 2893 N94-26134
p 3114 N94-26685
p 2824 N94-27221
p 2812 N94-27229
p 2756 N94-27230
p 2799 N94-27931
NAS8-38783 .... p 2941 N94-26788
NAS8-38864 .... p 2822 N94-26597
NAS8-39131 .... p 2696 N94-26791
NAS8-39244 .... p 2697 N94-27421
NAS8-39569 .... p 2761 N94-27664
NAS8-39746 .... p 3110 N94-26590
NAS8-39747 .... p 3111 N94-27321
NAS8-40000 .... p 2701 N94-26230
NAS9-18736 .... p 2942 N94-27410
NCC1-1422 .... p 2798 N94-27782
NCC2-63 .... p 2716 N94-26643
NCC2-737 .... p 2714 N94-26205
NCC2-770 .... p 3093 N94-26206
NCC3-173 .... p 2711 N94-27352
NCC3-175 .... p 2844 N94-27824
NCC3-211 .... p 3066 N94-27561
NCC8-22 .... p 2869 N94-27430
NF-62-376 .... p 2982 N94-27579
NGL-22-009-640 .... p 2641 N94-27284
p 2641 N94-27286
p 2641 N94-27287
NGL-31-001-252 .... p 2641 N94-27284
NGR-36-009-017 .... p 2641 N94-27284
p 2642 N94-27290
p 2642 N94-27292
p 2642 N94-27293
NGR-36-009-17 .... p 2642 N94-27289
p 2642 N94-27291
NGT-47-003-029 .... p 3085 N94-27893
NGT-50686 .... p 2901 N94-26093
NIVR-07801N .... p 2679 N94-27798
NOE-03551003 .... p 2915 N94-27462
NORDTEST PROJ. 1034-92 .... p 2835 N94-27042
NR PROJ. M00-96 .... p 2909 N94-26173
p 2909 N94-26179
NSF ASC-92-17091 .... p 2984 N94-25591
NSF ATM-83-05841 .... p 3107 N94-27886
p 3107 N94-27887
NSF ATM-90-16941 .... p 2887 N94-28218
NSF ATM-90-17637 .... p 2887 N94-28218
NSF ATM-92-06417 .... p 2876 N94-28312
NSF BIR-89-20118 .... p 2984 N94-25591
NSF CCR-87-01103 .... p 2666 N94-27768
NSF CCR-89-15206 .... p 2972 N94-27580
NSF CCR-90-14363 .... p 2666 N94-27768
NSF CCR-90-14605 .... p 3100 N94-27164
NSF CCR-90-57567 .... p 2967 N94-27065
NSF DDM-89-01495 .... p 3094 N94-26314
NSF DMR-91-15054 .... p 3062 N94-26932
NSF DMS-90-00053 .... p 2998 N94-27103
NSF DMS-92-02042 .... p 2994 N94-26601
NSF EAR-90-04589 .... p 2891 N94-28311
NSF GER-92-55691 .... p 2821 N94-25878
NSF INT-89-22490 .... p 2999 N94-27415
NSF IRI-92-24521 .... p 2986 N94-27032
p 2967 N94-27064
NSF MSS-85-52702 .... p 2641 N94-27286
NSG-5103 .... p 3106 N94-26237
N00014-82-K-0612 .... p 2715 N94-26444
N00014-84-C-0111 .... p 2900 N94-27090
N00014-85-K-0168 .... p 3000 N94-27577
p 2972 N94-27580
p 2972 N94-27581
N00014-85-K-0198 .... p 3094 N94-26314
N00014-87-K-0004 .... p 2900 N94-27090
N00014-87-K-0482 .... p 2984 N94-25899
p 2985 N94-25966
N00014-88-C-0231 .... p 3034 N94-25902
N00014-88-C-0542 .... p 3033 N94-27078
N00014-88-K-0475 .... p 2766 N94-25757
N00014-89-C-2111 .... p 3043 N94-26356
N00014-89-C-2134 .... p 3045 N94-27074

N00014-89-J-1003 .... p 3010 N94-26983
N00014-89-J-1007 .... p 2783 N94-26449
p 2785 N94-27027
N00014-89-J-1235 .... p 3036 N94-26834
N00014-89-J-1540 .... p 2899 N94-26149
N00014-89-J-1578 .... p 2894 N94-26431
N00014-89-J-1644 .... p 2959 N94-25968
N00014-89-J-1701 .... p 2794 N94-27059
N00014-89-J-1870 .... p 3003 N94-26355
p 3008 N94-26374
p 3004 N94-27106
p 3009 N94-27108
N00014-89-J-1988 .... p 2972 N94-27580
p 2972 N94-27581
N00014-90-C-0159 .... p 2785 N94-27057
N00014-90-J-1100 .... p 2900 N94-27090
N00014-90-J-1148 .... p 2709 N94-27107
N00014-90-J-1307 .... p 2948 N94-25864
p 3096 N94-25925
p 3002 N94-25962
N00014-90-J-1427 .... p 3061 N94-26841
N00014-90-J-1545 .... p 2821 N94-25782
N00014-90-J-1589 .... p 2790 N94-25872
p 2794 N94-27026
p 2796 N94-27319
N00014-90-J-1889 .... p 2738 N94-26679
N00014-90-J-4083 .... p 2791 N94-26187
N00014-91-C-0067 .... p 2704 N94-25608
p 2840 N94-27034
N00014-91-C-2202 .... p 2708 N94-26895
N00014-91-J-1187 .... p 3010 N94-26889
N00014-91-J-1219 .... p 2666 N94-27768
N00014-91-J-1271 .... p 2794 N94-26979
N00014-91-J-1283 .... p 2964 N94-26680
N00014-91-J-1295 .... p 2789 N94-25605
N00014-91-J-1416 .... p 3061 N94-26885
N00014-91-J-1426 .... p 2789 N94-25605
N00014-91-J-1655 .... p 2753 N94-26925
p 2754 N94-26977
p 2754 N94-27033
p 2754 N94-27036
p 2754 N94-27080
p 2755 N94-27087
p 2755 N94-27163
N00014-91-J-1837 .... p 3062 N94-26932
N00014-91-J-1988 .... p 2972 N94-27580
p 2972 N94-27581
N00014-91-J-4017 .... p 2894 N94-26195
N00014-91-J-4045 .... p 2782 N94-26343
N00014-91-J-4057 .... p 3018 N94-26172
p 2704 N94-26353
p 3022 N94-26894
N00014-92-C-2177 .... p 2953 N94-26740
N00014-92-C-6018 .... p 2868 N94-26888
N00014-92-J-1243 .... p 3020 N94-26562
N00014-92-J-1264 .... p 3003 N94-26485
p 3003 N94-26494
p 3003 N94-26495
p 3004 N94-26496
N00014-92-J-1274 .... p 2899 N94-26354
N00014-92-J-1390 .... p 2748 N94-25854
N00014-92-J-1412 .... p 2749 N94-26074
N00014-92-J-1416 .... p 2736 N94-26452
p 3059 N94-26571
N00014-92-J-1477 .... p 3063 N94-27058
N00014-92-J-1500 .... p 2754 N94-26974
N00014-92-J-1673 .... p 2714 N94-26296
N00014-92-J-1720 .... p 3060 N94-26840
N00014-92-J-1895 .... p 2786 N94-27079
N00014-92-J-1945 .... p 3098 N94-26570
N00014-92-J-4033 .... p 2972 N94-27581
N00014-92-1-0499 .... p 3063 N94-26965
N00014-93-C-0225 .... p 3063 N94-27055
N00014-93-C-2172 .... p 2772 N94-26884
N00014-93-I-0213 .... p 2707 N94-26447
N00014-93-I-0437 .... p 3060 N94-26839
N00014-93-P-2005 .... p 3068 N94-27704
N00014-93-1-0170 .... p 2797 N94-27562
N00014-93-1-0231 .... p 2997 N94-27015
p 2998 N94-27035
N00014-93-1-0343 .... p 3023 N94-26926
N00014-93-1-0419 .... p 3037 N94-26990
N00014-93-1-0558 .... p 2815 N94-25756
N00014-93-1-0698 .... p 2954 N94-27016
N00014-93-1-0827 .... p 3055 N94-26188
N00014-93-1-1007 .... p 2783 N94-26491
N00014-97-J-4108 .... p 2707 N94-26450
N00039-91-C-0072 .... p 2899 N94-26886
N00039-92-C-0100 .... p 2789 N94-25604
N00140-87-C-8904 .... p 2666 N94-27768
N60921-91-C-0124 .... p 2864 N94-28133
OTKA-2116 .... p 2957 N94-25761
p 2958 N94-25762
OV/RLD-132 .... p 2678 N94-27395
p 3001 N94-28353
PROJ. SRI-PYH-3092 .... p 2717 N94-27226
PROJ. 91-15 .... p 2797 N94-27639
PROJ. 92-11 .... p 2825 N94-27560
RTOP 106-70-00 .... p 2693 N94-27427
RTOP 199-08-12-06 .... p 2901 N94-26086
RTOP 199-14-12-11 .... p 2944 N94-26098
RTOP 199-18-12-07 .... p 2901 N94-26093
p 2901 N94-26210
p 2902 N94-27227
RTOP 199-45-16-11 .... p 3114 N94-26550
p 3033 N94-27646
RTOP 232-01-04-04 .... p 2644 N94-26154
RTOP 233-01-03-22 .... p 2788 N94-27770
RTOP 233-03-01-01 .... p 2682 N94-26278
RTOP 237-02-02-03 .... p 2972 N94-27655
RTOP 323-42-04 .... p 2834 N94-26199
RTOP 323-44-03 .... p 2692 N94-27436
RTOP 324-02-03 .... p 2818 N94-26705
RTOP 474-46-10 .... p 2843 N94-27559
RTOP 477-50-00-01 .... p 2695 N94-26103
RTOP 505-10-11 .... p 2645 N94-26538
p 2845 N94-28181
RTOP 505-59-30-03 .... p 2647 N94-27161
RTOP 505-59-30-04 .... p 2680 N94-26603
RTOP 505-59-36 .... p 2644 N94-26143
p 2641 N94-26596
p 2668 N94-26604
RTOP 505-59-53 .... p 2667 N94-26091
RTOP 505-59-54-02 .... p 2811 N94-26707
p 2798 N94-27867
RTOP 505-59-87-85 .... p 2645 N94-26483
p 2645 N94-26489
p 2645 N94-26492
p 2645 N94-26497
RTOP 505-62-0K-00 .... p 2826 N94-27657
RTOP 505-62-10 .... p 2675 N94-27654
RTOP 505-62-30-01 .... p 2646 N94-26547
RTOP 505-62-50 .... p 2678 N94-27414
p 2741 N94-27426
RTOP 505-63-10-02 .... p 2669 N94-26608
RTOP 505-63-12 .... p 2711 N94-27640
RTOP 505-63-5B .... p 2839 N94-26692
p 2843 N94-27656
p 2843 N94-27776
p 2845 N94-27865
p 2846 N94-28227
RTOP 505-63-50-04 .... p 2711 N94-27658
RTOP 505-63-50-10 .... p 3011 N94-27659
RTOP 505-63-53-01 .... p 2844 N94-27830
RTOP 505-64-10-51 .... p 2956 N94-28267
RTOP 505-64-12-01 .... p 2677 N94-26593
RTOP 505-64-13-11 .... p 2665 N94-27423
p 2681 N94-27425
RTOP 505-64-13-22 .... p 2673 N94-27882
RTOP 505-64-13 .... p 2673 N94-27864
RTOP 505-64-52-01 .... p 2679 N94-27660
RTOP 505-64-52-04 .... p 2769 N94-26611
RTOP 505-66-21 .... p 2973 N94-27663
RTOP 505-68-30-03 .... p 2647 N94-26706
RTOP 505-68-70-09 .... p 2670 N94-27439
RTOP 505-69-20-01 .... p 3117 N94-26155
p 2646 N94-26693
RTOP 505-69-36 .... p 2667 N94-26151
RTOP 505-69-50-01 .... p 2668 N94-26606
RTOP 505-70-00 .... p 2691 N94-27868
RTOP 505-70-59-03 .... p 2646 N94-26548
RTOP 505-70-62-15 .... p 2792 N94-26467
RTOP 505-90-52-01 .... p 2792 N94-26499
p 2994 N94-26601
p 2999 N94-27415
p 2969 N94-27416
p 2970 N94-27417
p 2999 N94-27434
p 2796 N94-27435
p 2999 N94-27557
p 2971 N94-27558
p 2971 N94-27572
RTOP 505-90-53-02 .... p 2963 N94-26466
p 2971 N94-27573
RTOP 506-40-41-01 .... p 2646 N94-26592
RTOP 506-41-11 .... p 2685 N94-27358
RTOP 506-42-31 .... p 2700 N94-26090
p 2690 N94-26142
p 2701 N94-26208
p 2701 N94-26209
p 2703 N94-27662
RTOP 506-43-41-02 .... p 2695 N94-26609
RTOP 506-49-11-01 .... p 2690 N94-27771
RTOP 506-49-21-00 .... p 2943 N94-27934
RTOP 509-10-11 .... p 2846 N94-28266
RTOP 510-02-12-09 .... p 2711 N94-27433
RTOP 533-02-36 .... p 2674 N94-27432
RTOP 535-03-01-03 .... p 2646 N94-26602
RTOP 535-03-01 .... p 2846 N94-28227
RTOP 535-03-10 .... p 2644 N94-26131
p 2675 N94-27778
RTOP 536-01-11 .... p 2970 N94-27542
p 3118 N94-27764
RTOP 537-02-20 .... p 2674 N94-26573
RTOP 537-03-21 .... p 2649 N94-28188
RTOP 537-04-20 .... p 2680 N94-26141
RTOP 538-05-15-03 .... p 2808 N94-28180
RTOP 582-03-11-21-00 .... p 2786 N94-27574
RTOP 584-03-21 .... p 2691 N94-27424
RTOP 586-02-11 .... p 2989 N94-27773
RTOP 594-81-21-05 .... p 2692 N94-27774
RTOP 665-10-70 .... p 2814 N94-27981
RTOP 665-45-20-01 .... p 2894 N94-26506
RTOP 763-22-41 .... p 2826 N94-27599
RTOP 913-00-00 .... p 2897 N94-28179
p 2897 N94-28182
RTOP 930-00-00 .... p 2945 N94-28251
SRI PROJ. 4604 .... p 2883 N94-27852
SWRI PROJ. 01-3165 .... p 3035 N94-25941
SWRI PROJ. 15-2779 .... p 2879 N94-26599
SWRI PROJ. 15-4971 .... p 3103 N94-26789
TAMU PROJ. 41670-ME .... p 2825 N94-27383
TEES PROJ. 41590-CS .... p 3093 N94-26206
W-31-109-ENG-38 .... p 2979 N94-25802
p 2780 N94-25806
p 3013 N94-25816
p 3015 N94-25955
p 3053 N94-26029
p 3053 N94-26031
p 2733 N94-26069
p 3017 N94-26078
p 3054 N94-26139
p 2781 N94-26144
p 3018 N94-26145
p 3055 N94-26243
p 3055 N94-26275
p 3035 N94-26276
p 2792 N94-26331
p 2963 N94-26407
p 3008 N94-26421
p 2751 N94-26422
p 2763 N94-26429
p 2857 N94-26583
p 2857 N94-26584
p 2737 N94-26587
p 2783 N94-26589
p 3059 N94-26591
p 2751 N94-26594
p 3098 N94-26598
p 2794 N94-26763
p 3022 N94-26793
p 3062 N94-26934
p 2739 N94-26935
p 2868 N94-26952
p 2740 N94-26957
p 3026 N94-27620
p 2757 N94-27716
p 2973 N94-27717
p 2820 N94-27781
W-7405-ENG-36 .... p 3012 N94-25612
p 2699 N94-25613
p 3013 N94-25820
p 3052 N94-25972
p 2732 N94-25974
p 2821 N94-25980
p 2985 N94-25983
p 2733 N94-26022
p 2733 N94-26069
p 2991 N94-26079
p 3042 N94-26081
p 2980 N94-26120
p 2750 N94-26124
p 2816 N94-26126
p 3043 N94-26321
p 3058 N94-26514
p 3020 N94-26527
p 2818 N94-26605
p 2737 N94-26607
p 3021 N94-26620
p 2738 N94-26621
p 2901 N94-26623
p 2752 N94-26676
p 3059 N94-26695
p 3110 N94-26696
p 3005 N94-26802
p 3073 N94-26805
p 2880 N94-26806
p 2986 N94-26807
p 2696 N94-26808
p 3004 N94-27612
p 2835 N94-27613
p 2813 N94-27624
p 2797 N94-27705
p 3094 N94-27707
p 2797 N94-27709
p 3116 N94-27714
p 3047 N94-27715
p 2851 N94-27727

p 2719 N94-27728
p 3111 N94-27742
p 2933 N94-27744
p 2704 N94-27745
p 3007 N94-27777
p 3116 N94-27793
p 3005 N94-27816
p 3048 N94-27825
p 3117 N94-27826
p 3117 N94-27827
p 3069 N94-27828
p 3030 N94-28001
p 2897 N94-28146
W-7405-ENG-48 .... p 2892 N94-25936
p 2767 N94-25937
p 2706 N94-25938
p 3052 N94-25947
p 2748 N94-25959
p 2749 N94-25985
p 2816 N94-26020
p 3102 N94-26023
p 2898 N94-26072
p 2707 N94-26099
p 3017 N94-26101
p 3055 N94-26238
p 2768 N94-26310
p 2782 N94-26312
p 2962 N94-26318
p 2735 N94-26322
p 2736 N94-26351
p 2792 N94-26427
p 2810 N94-26525
p 3102 N94-26528
p 2751 N94-26554
p 2879 N94-26576
p 3020 N94-26577
p 2948 N94-26578
p 2818 N94-26698
p 2818 N94-26699
p 2965 N94-26775
p 2784 N94-26777
p 2763 N94-26778
p 2771 N94-26803
p 2763 N94-26804
p 2965 N94-26862
p 3045 N94-26863
p 2708 N94-26930
p 2753 N94-26933
p 2819 N94-27018
p 3045 N94-27019
p 2981 N94-27092
p 2869 N94-27267
p 3118 N94-27566
p 2897 N94-27571
p 2760 N94-27719
p 3068 N94-27724
p 2760 N94-27725
p 2757 N94-27747
p 2760 N94-28222
W-7405-ENG-82 .... p 2706 N94-26019
p 2735 N94-26273
p 2704 N94-26779
p 2757 N94-27695
p 3029 N94-27811
p 2712 N94-27813
W2207-0-AF10 .... p 2682 N94-27879

REPORT NUMBER INDEX

Typical Report Number Index Listing

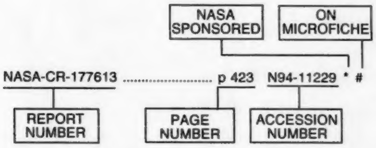

Listings in this index are arranged alphanumerically by report number. The accession number denotes the number by which the citation is identified. The page number helps to locate the citation in the abstract section. An asterisk (*) indicates that the item is a NASA report. A pound sign (#) indicates that the item is available on microfiche.

A-93001 .... p 2644 N94-26143 * #
A-93010 .... p 2667 N94-26151 * #
A-93066 .... p 2667 N94-26091 * #
A-93070 .... p 2902 N94-27227 * #
A-93079 .... p 2668 N94-26604 * #
A-93097 .... p 2901 N94-26093 * #
A-93099 .... p 2901 N94-26210 * #
A-94015 .... p 3118 N94-27764 * #
A-94027 .... p 2944 N94-26098 * #
A-94029 .... p 2641 N94-26596 * #
A-94037 .... p 2901 N94-26086 * #
A-94039 .... p 2645 N94-26538 * #
A-94045 .... p 2649 N94-28188 * #

AD-A273126 .... p 3094 N94-27180 #
AD-A273399 .... p 2774 N94-27170
AD-A273658 .... p 3055 N94-26194
AD-A273669 .... p 2894 N94-26195 #
AD-A273695 .... p 2680 N94-26196
AD-A273707 .... p 2694 N94-25776 #
AD-A273717 .... p 2958 N94-25777 * #
AD-A273720 .... p 2749 N94-26074 #
AD-A273721 .... p 2705 N94-25779 #
AD-A273722 .... p 2664 N94-26197
AD-A273723 .... p 2698 N94-26223
AD-A273724 .... p 3096 N94-25997 #
AD-A273731 .... p 2706 N94-25999 #
AD-A273732 .... p 2690 N94-26001 #
AD-A273733 .... p 2985 N94-26006 * #
AD-A273734 .... p 2980 N94-26009 #
AD-A273739 .... p 2910 N94-26748 #
AD-A273746 .... p 2878 N94-26224
AD-A273749 .... p 2767 N94-26011 #
AD-A273750 .... p 2893 N94-26013 #
AD-A273751 .... p 2893 N94-26016 #
AD-A273753 .... p 2659 N94-25780 #
AD-A273754 .... p 2948 N94-25720 #
AD-A273755 .... p 3033 N94-25721 #
AD-A273756 .... p 2891 N94-25722 #
AD-A273759 .... p 3095 N94-25723 #
AD-A273760 .... p 2940 N94-25724 #
AD-A273761 .... p 2908 N94-25871 #
AD-A273765 .... p 2790 N94-25872 #
AD-A273767 .... p 2748 N94-25854 #
AD-A273769 .... p 2959 N94-25855 #
AD-A273771 .... p 3051 N94-25856 #
AD-A273772 .... p 2705 N94-25857 #
AD-A273774 .... p 2790 N94-25858 #
AD-A273775 .... p 2705 N94-25859 #
AD-A273776 .... p 2979 N94-25860 #
AD-A273777 .... p 2892 N94-25861 #
AD-A273778 .... p 2790 N94-25862 #
AD-A273779 .... p 2705 N94-25863 #
AD-A273780 .... p 2796 N94-27319 #
AD-A273781 .... p 3068 N94-27704 #
AD-A273789 .... p 2948 N94-25864 #
AD-A273790 .... p 3096 N94-25925 #
AD-A273793 .... p 2892 N94-25873
AD-A273794 .... p 2790 N94-25874 #
AD-A273795 .... p 3014 N94-25875 #
AD-A273797 .... p 2706 N94-25876 #
AD-A273799 .... p 2877 N94-25877 #
AD-A273804 .... p 2876 N94-25752 #
AD-A273805 .... p 2821 N94-25878
AD-A273808 .... p 2766 N94-25736 #
AD-A273811 .... p 2959 N94-25879 #
AD-A273812 .... p 3034 N94-25940 #
AD-A273813 .... p 2767 N94-25960 #
AD-A273814 .... p 2667 N94-25961 #
AD-A273816 .... p 3002 N94-25962 #
AD-A273817 .... p 2959 N94-25963 #
AD-A273823 .... p 3009 N94-25737 #
AD-A273829 .... p 2694 N94-25738 #
AD-A273832 .... p 2694 N94-25615
AD-A273833 .... p 2815 N94-25616
AD-A273834 .... p 2673 N94-25617 #
AD-A273835 .... p 2705 N94-25739 #
AD-A273836 .... p 2679 N94-25740 #
AD-A273837 .... p 2847 N94-25741 #
AD-A273838 .... p 3034 N94-25742 #
AD-A273839 .... p 2984 N94-25743 #
AD-A273840 .... p 2815 N94-25744 #
AD-A273844 .... p 2789 N94-25604 #
AD-A273846 .... p 2789 N94-25605 #
AD-A273847 .... p 2956 N94-25606 * #
AD-A273850 .... p 3001 N94-25607 #
AD-A273851 .... p 2789 N94-25587
AD-A273852 .... p 2704 N94-25608 #
AD-A273853 .... p 2956 N94-25588
AD-A273858 .... p 2713 N94-25964 #
AD-A273859 .... p 2937 N94-25965
AD-A273863 .... p 2865 N94-25609 #
AD-A273864 .... p 2956 N94-25610 #
AD-A273865 .... p 2940 N94-25611 #
AD-A273866 .... p 2990 N94-25594 #
AD-A273867 .... p 2693 N94-25595 #
AD-A273868 .... p 2747 N94-25596 #
AD-A273869 .... p 2985 N94-25966
AD-A273872 .... p 2765 N94-25725 #
AD-A273873 .... p 2809 N94-25967
AD-A273878 .... p 3012 N94-25726 #
AD-A273881 .... p 2834 N94-25727 #
AD-A273882 .... p 2765 N94-25728 #
AD-A273883 .... p 3034 N94-25729 #
AD-A273884 .... p 3034 N94-25730 #
AD-A273885 .... p 3009 N94-25731 #
AD-A273887 .... p 2836 N94-25732 #
AD-A273893 .... p 3012 N94-25655 #
AD-A273895 .... p 2847 N94-25656 #
AD-A273902 .... p 2790 N94-25657 #
AD-A273903 .... p 3102 N94-25658 #
AD-A273904 .... p 2694 N94-25659 #
AD-A273905 .... p 3011 N94-25589 #
AD-A273907 .... p 2691 N94-26017 #
AD-A273909 .... p 2821 N94-25782 #
AD-A273910 .... p 2797 N94-27562 #
AD-A273911 .... p 2959 N94-25968
AD-A273913 .... p 2666 N94-25590 #
AD-A273914 .... p 2984 N94-25591 #
AD-A273915 .... p 2643 N94-25592 #
AD-A273917 .... p 2942 N94-27320 #
AD-A273920 .... p 3094 N94-26814 #
AD-A273921 .... p 3093 N94-25895 #
AD-A273925 .... p 2892 N94-25793 #
AD-A273926 .... p 2900 N94-25593 #
AD-A273932 .... p 2817 N94-26271 #
AD-A273935 .... p 2938 N94-26749 #
AD-A273937 .... p 2821 N94-25794 #
AD-A273940 .... p 3035 N94-25941 #
AD-A273941 .... p 2767 N94-25990 #
AD-A273945 .... p 2834 N94-25896 #
AD-A273965 .... p 2937 N94-25897 #
AD-A273984 .... p 2791 N94-25991 #
AD-A273985 .... p 2984 N94-25898 #
AD-A273986 .... p 2984 N94-25899 #
AD-A273987 .... p 2984 N94-25900 #
AD-A273997 .... p 2758 N94-25901 #
AD-A273998 .... p 3034 N94-25902 #
AD-A274002 .... p 2765 N94-25660 #
AD-A274004 .... p 2957 N94-25661 #
AD-A274012 .... p 3093 N94-25796 #
AD-A274013 .... p 2957 N94-25753 #
AD-A274014 .... p 2836 N94-25754 #
AD-A274016 .... p 2865 N94-25755 #
AD-A274018 .... p 2815 N94-25756 #
AD-A274023 .... p 2766 N94-25757 #
AD-A274026 .... p 3034 N94-25758 #
AD-A274027 .... p 2984 N94-25759 #
AD-A274028 .... p 3096 N94-25765 #
AD-A274029 .... p 2766 N94-25766 #
AD-A274030 .... p 2958 N94-25767 #
AD-A274031 .... p 3034 N94-25768 #
AD-A274032 .... p 2960 N94-26018 #
AD-A274033 .... p 2690 N94-25769 #
AD-A274034 .... p 2766 N94-25797 #
AD-A274035 .... p 2958 N94-25799 #
AD-A274037 .... p 2664 N94-25810 #
AD-A274038 .... p 2780 N94-25845 #
AD-A274040 .... p 2694 N94-25832 #
AD-A274049 .... p 2677 N94-25833 #
AD-A274051 .... p 2990 N94-25834 #
AD-A274054 .... p 2766 N94-25824 #
AD-A274055 .... p 2780 N94-25770 #
AD-A274057 .... p 2676 N94-25771 #
AD-A274058 .... p 2667 N94-25772 #
AD-A274061 .... p 2679 N94-25773 #
AD-A274063 .... p 3049 N94-25645 #
AD-A274071 .... p 2957 N94-25646 #
AD-A274073 .... p 2765 N94-25647 #
AD-A274074 .... p 2947 N94-25648 #
AD-A274075 .... p 2957 N94-25649 #
AD-A274077 .... p 2937 N94-25774 #
AD-A274078 .... p 3002 N94-25992 #
AD-A274079 .... p 3052 N94-25993 #
AD-A274080 .... p 2960 N94-25994 #
AD-A274081 .... p 2781 N94-25995 #
AD-A274082 .... p 2694 N94-25996 #
AD-A274083 .... p 2677 N94-25998 #
AD-A274084 .... p 2959 N94-25942 #
AD-A274086 .... p 2909 N94-25943 #
AD-A274087 .... p 2958 N94-25783 #
AD-A274088 .... p 2672 N94-26021 #
AD-A274089 .... p 2676 N94-25785 #
AD-A274091 .... p 3096 N94-26024 #
AD-A274094 .... p 2979 N94-25786 #
AD-A274096 .... p 2664 N94-25788 #
AD-A274099 .... p 2672 N94-26028 #
AD-A274100 .... p 2672 N94-26030 #
AD-A274112 .... p 3002 N94-25903 #
AD-A274114 .... p 2694 N94-25904 #
AD-A274115 .... p 2898 N94-26076 #
AD-A274118 .... p 2667 N94-25905 #
AD-A274119 .... p 2979 N94-25906 #
AD-A274120 .... p 3037 N94-27062 #
AD-A274122 .... p 2967 N94-27063 #
AD-A274123 .... p 2967 N94-27064 #
AD-A274124 .... p 2967 N94-27065 #
AD-A274125 .... p 2982 N94-27117 #
AD-A274126 .... p 2986 N94-27032 #
AD-A274127 .... p 2954 N94-27152 #
AD-A274128 .... p 3099 N94-27118 #
AD-A274129 .... p 2795 N94-27119 #
AD-A274130 .... p 2968 N94-27120 #
AD-A274131 .... p 2987 N94-27121 #
AD-A274132 .... p 2987 N94-27122 #
AD-A274135 .... p 2982 N94-27123 #
AD-A274137 .... p 2678 N94-27132 #
AD-A274139 .... p 3024 N94-27133 #
AD-A274140 .... p 2811 N94-27134 #
AD-A274142 .... p 2709 N94-27135 #
AD-A274146 .... p 2987 N94-27077 #
AD-A274147 .... p 2987 N94-27093 #
AD-A274148 .... p 2939 N94-27094 #
AD-A274149 .... p 3064 N94-27095 #
AD-A274151 .... p 2773 N94-27136
AD-A274152 .... p 3038 N94-27137
AD-A274153 .... p 2939 N94-27138
AD-A274159 .... p 3111 N94-27096 #
AD-A274160 .... p 2988 N94-27139 #
AD-A274161 .... p 2968 N94-27140 #
AD-A274162 .... p 2987 N94-27124 #

AD-A274163 p 2940 N94-27141 #
AD-A274165 p 2709 N94-27142 #
AD-A274166 p 2881 N94-27143 #
AD-A274167 p 2709 N94-27125 #
AD-A274176 p 3009 N94-27126 #
AD-A274179 p 2773 N94-27127
AD-A274180 p 2968 N94-27128 #
AD-A274181 p 3037 N94-27102 #
AD-A274184 p 2998 N94-27103 #
AD-A274185 p 2911 N94-27097 #
AD-A274189 p 3046 N94-27098 #
AD-A274191 p 3111 N94-27099 #
AD-A274192 p 2823 N94-27104 #
AD-A274204 p 2981 N94-27100 #
AD-A274205 p 3099 N94-27101 #
AD-A274207 p 2669 N94-27105 #
AD-A274208 p 3037 N94-27066 #
AD-A274209 p 3010 N94-27067 #
AD-A274212 p 2773 N94-27068 #
AD-A274213 p 2849 N94-27069 #
AD-A274217 p 2981 N94-27070 #
AD-A274218 p 2665 N94-27071 #
AD-A274220 p 2939 N94-27072 #
AD-A274225 p 2773 N94-27073 #
AD-A274226 p 2840 N94-26922 #
AD-A274227 p 2840 N94-26953 #
AD-A274228 p 2840 N94-27008 #
AD-A274231 p 2820 N94-28068 #
AD-A274232 p 2868 N94-26817 #
AD-A274233 p 3044 N94-26820 #
AD-A274235 p 2753 N94-26822 #
AD-A274241 p 2665 N94-26826 #
AD-A274245 p 3060 N94-26839 #
AD-A274246 p 3060 N94-26840 #
AD-A274247 p 3061 N94-26841 #
AD-A274248 p 2740 N94-27009 #
AD-A274249 p 3037 N94-27010 #
AD-A274250 p 3024 N94-27011 #
AD-A274251 p 2939 N94-27012 #
AD-A274252 p 3099 N94-27013 #
AD-A274258 p 3099 N94-27014 #
AD-A274279 p 2997 N94-27015 #
AD-A274281 p 2954 N94-27016 #
AD-A274283 p 2673 N94-26989 #
AD-A274284 p 2738 N94-26679 #
AD-A274290 p 2964 N94-26680 #
AD-A274293 p 3059 N94-26681 #
AD-A274294 p 2964 N94-26682 #
AD-A274295 p 2938 N94-26683 #
AD-A274303 p 2895 N94-26678 #
AD-A274304 p 2895 N94-26850 #
AD-A274305 p 2819 N94-26940 #
AD-A274306 p 2819 N94-26941 #
AD-A274310 p 2996 N94-26972 #
AD-A274311 p 3032 N94-26881 #
AD-A274313 p 2938 N94-26882 #
AD-A274315 p 3110 N94-26883 #
AD-A274323 p 3045 N94-27074
AD-A274324 p 2772 N94-26884 #
AD-A274325 p 3061 N94-26885 #
AD-A274326 p 2899 N94-26886 #
AD-A274332 p 2900 N94-26887 #
AD-A274336 p 3063 N94-27055 #
AD-A274340 p 2939 N94-27056 #
AD-A274341 p 2785 N94-27057 #
AD-A274344 p 2910 N94-26973 #
AD-A274345 p 2754 N94-26974 #
AD-A274346 p 3010 N94-26923 #
AD-A274349 p 2772 N94-26924 #
AD-A274350 p 2753 N94-26925 #
AD-A274352 p 3023 N94-26926 #
AD-A274356 p 3063 N94-27058 #
AD-A274357 p 2794 N94-27059 #
AD-A274369 p 2967 N94-27060 #
AD-A274375 p 2786 N94-27061 #
AD-A274376 p 2772 N94-26975 #
AD-A274378 p 2823 N94-26976 #
AD-A274381 p 2880 N94-26828 #
AD-A274388 p 2995 N94-26829 #
AD-A274390 p 2785 N94-26830 #
AD-A274391 p 2968 N94-27075 #
AD-A274392 p 2795 N94-27129 #
AD-A274400 p 2911 N94-27130 #
AD-A274401 p 3037 N94-26990 #
AD-A274405 p 2754 N94-26977 #
AD-A274410 p 2709 N94-26978 #
AD-A274411 p 2902 N94-26991 #
AD-A274412 p 3033 N94-27078 #
AD-A274414 p 2794 N94-26979 #
AD-A274416 p 2772 N94-26980 #
AD-A274417 p 3036 N94-26981 #
AD-A274418 p 2786 N94-27079 #
AD-A274419 p 2754 N94-27080 #
AD-A274421 p 2660 N94-27081 #
AD-A274451 p 3033 N94-27082 #
AD-A274452 p 3033 N94-27083 #
AD-A274453 p 3033 N94-27084 #
AD-A274455 p 2773 N94-27085 #
AD-A274460 p 2754 N94-27086
AD-A274461 p 3104 N94-27265 #
AD-A274464 p 2896 N94-27025 #
AD-A274472 p 2794 N94-27026 #
AD-A274477 p 2754 N94-27033 #
AD-A274478 p 2755 N94-27163 #
AD-A274497 p 2772 N94-26963
AD-A274502 p 3100 N94-27164 #
AD-A274504 p 2840 N94-27034 #
AD-A274509 p 2998 N94-27035 #
AD-A274510 p 2754 N94-27036 #
AD-A274512 p 2755 N94-27087 #
AD-A274516 p 2911 N94-27088 #
AD-A274518 p 2942 N94-27089 #
AD-A274519 p 2900 N94-27090 #
AD-A274520 p 2965 N94-26831 #
AD-A274521 p 2794 N94-26832 #
AD-A274522 p 2835 N94-26833 #
AD-A274528 p 3036 N94-26834 #
AD-A274531 p 2669 N94-26835 #
AD-A274535 p 2899 N94-26853 #
AD-A274536 p 2753 N94-26842 #
AD-A274538 p 2941 N94-26964
AD-A274539 p 2868 N94-26843 #
AD-A274548 p 2771 N94-26844 #
AD-A274549 p 2785 N94-26845 #
AD-A274550 p 2895 N94-26846 #
AD-A274568 p 2910 N94-26847 #
AD-A274570 p 3063 N94-26965
AD-A274571 p 2771 N94-26854 #
AD-A274572 p 2771 N94-26836 #
AD-A274586 p 3036 N94-26982 #
AD-A274587 p 3010 N94-26983 #
AD-A274588 p 2941 N94-26984 #
AD-A274589 p 2911 N94-26985 #
AD-A274591 p 2823 N94-26986 #
AD-A274594 p 2880 N94-26855 #
AD-A274595 p 3036 N94-26857 #
AD-A274596 p 2868 N94-26888 #
AD-A274599 p 3010 N94-26889 #
AD-A274600 p 2785 N94-26890 #
AD-A274603 p 3099 N94-26891 #
AD-A274605 p 3062 N94-26892 #
AD-A274609 p 2716 N94-26893 #
AD-A274612 p 3022 N94-26894 #
AD-A274639 p 2708 N94-26895 #
AD-A274643 p 2785 N94-27027 #
AD-A274644 p 2764 N94-27144 #
AD-A274645 p 3004 N94-27106 #
AD-A274646 p 2709 N94-27107 #
AD-A274647 p 3009 N94-27108 #
AD-A274648 p 2704 N94-26353 #
AD-A274651 p 2899 N94-26354 #
AD-A274654 p 3003 N94-26355 #
AD-A274655 p 3043 N94-26356 #
AD-A274658 p 2768 N94-26335 #
AD-A274660 p 2985 N94-26336 #
AD-A274676 p 2715 N94-26444 #
AD-A274682 p 3003 N94-26445 #
AD-A274687 p 2848 N94-26446 #
AD-A274688 p 2707 N94-26447 #
AD-A274690 p 2838 N94-26448 #
AD-A274692 p 2783 N94-26449 #
AD-A274693 p 2707 N94-26450 #
AD-A274694 p 3098 N94-26451 #
AD-A274695 p 2736 N94-26452 #
AD-A274697 p 2962 N94-26373 #
AD-A274698 p 3008 N94-26374 #
AD-A274699 p 3097 N94-26375 #
AD-A274702 p 3008 N94-26376 #
AD-A274705 p 2909 N94-26377 #
AD-A274707 p 2937 N94-26430 #
AD-A274710 p 2894 N94-26431 #
AD-A274711 p 2910 N94-26432 #
AD-A274713 p 2878 N94-26433 #
AD-A274715 p 2751 N94-26434 #
AD-A274717 p 2910 N94-26435 #
AD-A274719 p 3003 N94-26436 #
AD-A274721 p 2759 N94-26437 #
AD-A274722 p 2961 N94-26148 #
AD-A274726 p 3018 N94-26172 #
AD-A274744 p 2909 N94-26173 #
AD-A274749 p 2785 N94-26797
AD-A274750 p 2899 N94-26149 #
AD-A274755 p 2795 N94-27252
AD-A274757 p 3059 N94-26566 #
AD-A274761 p 2899 N94-26567 #
AD-A274766 p 2811 N94-26568 #
AD-A274768 p 2879 N94-26569 #
AD-A274769 p 2895 N94-26798
AD-A274775 p 3098 N94-26570 #
AD-A274777 p 2836 N94-26186 #
AD-A274778 p 2837 N94-26357 #
AD-A274779 p 2809 N94-26358 #
AD-A274786 p 2769 N94-26359 #
AD-A274787 p 2909 N94-26360 #
AD-A274788 p 2899 N94-26361 #
AD-A274798-VOL-1 p 2739 N94-26799
AD-A274799 p 2736 N94-26362 #
AD-A274800 p 2735 N94-26337 #
AD-A274803 p 2878 N94-26338 #
AD-A274804 p 2941 N94-26339 #
AD-A274807 p 2672 N94-26340 #
AD-A274808 p 2763 N94-26341 #
AD-A274812 p 3008 N94-26484 #
AD-A274813 p 3003 N94-26485 #
AD-A274814 p 2759 N94-26486 #
AD-A274815 p 2716 N94-26487 #
AD-A274817 p 2668 N94-26488 #
AD-A274818 p 3098 N94-26490 #
AD-A274819 p 2783 N94-26491 #
AD-A274820 p 2664 N94-26493 #
AD-A274825 p 3003 N94-26494 #
AD-A274826 p 3003 N94-26495 #
AD-A274827 p 3004 N94-26496 #
AD-A274830 p 3059 N94-26571 #
AD-A274831 p 3035 N94-26572 #
AD-A274835 p 2762 N94-26084 #
AD-A274836 p 2818 N94-26498 #
AD-A274838 p 3098 N94-26500 #
AD-A274842 p 2838 N94-26501 #
AD-A274844 p 2759 N94-26800
AD-A274845 p 2791 N94-26187 #
AD-A274848 p 2794 N94-26801
AD-A274849 p 3098 N94-26561 #
AD-A274850 p 3020 N94-26562 #
AD-A274854 p 3055 N94-26188 #
AD-A274857 p 2822 N94-26174 #
AD-A274859 p 2781 N94-26175 #
AD-A274860 p 2673 N94-26176 #
AD-A274861 p 2768 N94-26189 #
AD-A274865 p 2707 N94-26190 #
AD-A274867 p 2644 N94-26191 #
AD-A274869 p 2677 N94-26192 #
AD-A274870 p 2644 N94-26342 #
AD-A274871 p 2839 N94-26859
AD-A274873 p 2782 N94-26343 #
AD-A274874 p 2750 N94-26167 #
AD-A274881 p 2669 N94-26864
AD-A274889 p 2893 N94-26168 #
AD-A274890 p 2767 N94-26177 #
AD-A274895 p 2816 N94-26178 #
AD-A274896 p 2909 N94-26179 #
AD-A274897 p 3096 N94-26180 #
AD-A274901 p 3093 N94-26181 #
AD-A274903 p 2695 N94-26750
AD-A274905 p 2667 N94-26182 #
AD-A274906 p 2893 N94-26183 #
AD-A274909 p 2782 N94-26344 #
AD-A274910 p 2674 N94-26345 #
AD-A274913 p 2937 N94-26346 #
AD-A274914 p 2768 N94-26347 #
AD-A274915 p 2963 N94-26530 #
AD-A274918 p 2770 N94-26751
AD-A274919 p 2736 N94-26533 #
AD-A274921 p 2645 N94-26535 #
AD-A274923 p 2692 N94-26529 #
AD-A274924 p 2668 N94-26531 #
AD-A274925 p 2695 N94-26532 #
AD-A274935 p 2714 N94-26296 #
AD-A274941 p 3097 N94-26297 #
AD-A274942 p 2961 N94-26298 #
AD-A274947 p 3093 N94-26299 #
AD-A274955 p 3097 N94-26300 #
AD-A274963 p 2782 N94-26301 #
AD-A274965 p 2992 N94-26302 #
AD-A274966 p 2962 N94-26303 #
AD-A274969 p 2878 N94-26304 #
AD-A274970 p 2793 N94-26534 #
AD-A274971 p 2783 N94-26536 #
AD-A274972 p 2880 N94-26752
AD-A274973 p 2701 N94-26537 #
AD-A274974 p 2901 N94-26517 #
AD-A274975 p 2902 N94-27165 #

AD-B174292 p 3036 N94-26648
AD-B175579 p 2647 N94-27554
AD-B175894 p 2678 N94-27395
AD-B176008 p 2798 N94-27799
AD-B179687 p 3001 N94-28353 #

AD-D016029 p 2755 N94-27147
AD-D016031 p 2755 N94-27148
AD-D016032 p 2786 N94-27145
AD-D016033 p 2773 N94-27146
AD-D016034 p 2774 N94-27202
AD-D016035 p 2755 N94-27203
AD-D016038 p 2709 N94-27091 #
AD-D016039 p 2786 N94-27109 #
AD-D016040 p 2841 N94-27110 #

AD-D016041 .... p 2755 N94-27111 #
AD-D016042 .... p 2678 N94-27112 #
AD-D016043 .... p 2681 N94-27113 #
AD-D016048 .... p 2942 N94-27114 #
AD-D016049 .... p 3038 N94-27153 #
AD-D016050 .... p 2709 N94-27076 #
AD-D016053 .... p 2820 N94-27670 #
AD-D016054 .... p 2820 N94-27671 #
AD-D016055 .... p 2787 N94-27672 #
AD-D016057 .... p 2787 N94-27673 #
AD-D016058 .... p 3039 N94-27674 #
AD-D016059 .... p 2756 N94-27675 #
AD-D016061 .... p 3039 N94-27676 #
AD-D016063 .... p 2777 N94-27734 #
AD-D016066 .... p 2781 N94-26102
AD-D016071 .... p 3040 N94-28224
AD-D016073 .... p 3070 N94-28225
AD-D016074 .... p 2760 N94-28226
AD-D016077 .... p 2788 N94-28186
AD-D016079 .... p 2747 N94-28187

AD-E201706 .... p 2878 N94-26224
AD-E201708 .... p 2892 N94-25873
AD-E201724 .... p 2816 N94-26178 #
AD-E201727 .... p 2876 N94-25752 #

AEDC-TR-93-18 .... p 2713 N94-25964 #
AEDC-TR-93-19 .... p 2823 N94-26986 #

AERO-F.01.01.08 .... p 2649 N94-28140

AFFTC-TIM-93-02 .... p 2910 N94-26847 #

AFIT/DS/AA/93-3 .... p 2705 N94-25857 #
AFIT/DS/AA/93-4 .... p 2706 N94-25876 #

AFIT/DS/ENP-93-04 .... p 3014 N94-25875 #

AFIT/EN-TR-93-09 .... p 2958 N94-25799 #

AFIT/ENC/GCS/93D-1 .... p 2865 N94-25609 #

AFIT/GA/ENG/93D-01 .... p 2987 N94-27122 #

AFIT/GA/ENY/93D-1 .... p 2694 N94-25615
AFIT/GA/ENY/93D-3 .... p 2694 N94-25776 #
AFIT/GA/ENY/93D-5 .... p 2698 N94-26223
AFIT/GA/ENY/93D-9 .... p 2690 N94-26001 #

AFIT/GAE/ENY/93D-12 .... p 2705 N94-25859 #
AFIT/GAE/ENY/93D-15 .... p 2705 N94-25739 #
AFIT/GAE/ENY/93D-16 .... p 2679 N94-25740 #
AFIT/GAE/ENY/93D-20 .... p 2705 N94-25863 #
AFIT/GAE/ENY/93D-24 .... p 3096 N94-25997 #
AFIT/GAE/ENY/93D-26 .... p 2790 N94-25862 #
AFIT/GAE/ENY/93D-27 .... p 2984 N94-25743 #
AFIT/GAE/ENY/93D-29 .... p 2791 N94-25991 #
AFIT/GAE/ENY/93D-30 .... p 2790 N94-25657 #
AFIT/GAE/ENY/93D-3 .... p 2643 N94-25592 #
AFIT/GAE/ENY/93D-4 .... p 2979 N94-25860 #
AFIT/GAE/ENY/93D-6 .... p 2790 N94-25874 #
AFIT/GAE/ENY/93D-6 .... p 2706 N94-25999 #
AFIT/GAE/ENY/93D-7 .... p 2673 N94-25617 #

AFIT/GAM/ENC/93D-1 .... p 3009 N94-25737 #

AFIT/GAP/ENP/93D-01 .... p 3051 N94-25856 #
AFIT/GAP/ENP/93D-02 .... p 2956 N94-25610 #
AFIT/GAP/ENP/93D-04 .... p 2789 N94-25587
AFIT/GAP/ENP/93D-05 .... p 3034 N94-25729 #
AFIT/GAP/ENP/93D-07 .... p 2790 N94-25858 #
AFIT/GAP/ENP/93D-10 .... p 3011 N94-25589 #

AFIT/GCA/LAS/93S-8 .... p 3093 N94-25796 #

AFIT/GCE/ENG/93-12 .... p 2968 N94-27120 #
AFIT/GCE/ENG/93D-01 .... p 2979 N94-25906 #
AFIT/GCE/ENG/93D-03 .... p 2957 N94-25649 #
AFIT/GCE/ENG/93D-05 .... p 2937 N94-25774 #
AFIT/GCE/ENG/93D-07 .... p 2785 N94-26830 #
AFIT/GCE/ENG/93D-10 .... p 2987 N94-27121 #
AFIT/GCE/ENG/93D-11 .... p 2968 N94-27075 #
AFIT/GCE/ENG/93D-13 .... p 2766 N94-25797 #
AFIT/GCE/ENG/93D-9 .... p 2981 N94-27070 #

AFIT/GCM/LAS/93S-1 .... p 3093 N94-25895 #

AFIT/GCS/ENG/93-07 .... p 2672 N94-26021 #
AFIT/GCS/ENG/93D-02 .... p 2982 N94-27123 #
AFIT/GCS/ENG/93D-03 .... p 3096 N94-26024 #
AFIT/GCS/ENG/93D-04 .... p 2960 N94-25994 #
AFIT/GCS/ENG/93D-05 .... p 2795 N94-27119 #
AFIT/GCS/ENG/93D-10 .... p 2667 N94-25772 #
AFIT/GCS/ENG/93D-11 .... p 2968 N94-27128 #
AFIT/GCS/ENG/93D-12 .... p 3096 N94-25765 #
AFIT/GCS/ENG/93D-13 .... p 2773 N94-27127
AFIT/GCS/ENG/93D-14 .... p 2694 N94-25904 #
AFIT/GCS/ENG/93D-16 .... p 2960 N94-26018 #
AFIT/GCS/ENG/93D-19 .... p 3034 N94-25758 #
AFIT/GCS/ENG/93D-1 .... p 2954 N94-27152 #
AFIT/GCS/ENG/93D-20 .... p 2958 N94-25767 #
AFIT/GCS/ENG/93D-22 .... p 2959 N94-25942 #
AFIT/GCS/ENG/93D-24 .... p 3099 N94-27118 #
AFIT/GCS/ENG/93D-25 .... p 2958 N94-25783 #

AFIT/GE-93D-05 .... p 2694 N94-25996 #
AFIT/GE-93D-10 .... p 2677 N94-25998 #

AFIT/GE/ENG/93D-01 .... p 2667 N94-25905 #
AFIT/GE/ENG/93D-02 .... p 2766 N94-25824 #
AFIT/GE/ENG/93D-04 .... p 2995 N94-26829 #
AFIT/GE/ENG/93D-06 .... p 2780 N94-25845 #
AFIT/GE/ENG/93D-07 .... p 2781 N94-25995 #
AFIT/GE/ENG/93D-09 .... p 2766 N94-25766 #
AFIT/GE/ENG/93D-11 .... p 3037 N94-27102 #
AFIT/GE/ENG/93D-13 .... p 2664 N94-25810 #
AFIT/GE/ENG/93D-16 .... p 2947 N94-25648 #
AFIT/GE/ENG/93D-18 .... p 2677 N94-25833 #
AFIT/GE/ENG/93D-22 .... p 2773 N94-27073 #
AFIT/GE/ENG/93D-23 .... p 3002 N94-25992 #
AFIT/GE/ENG/93D-25 .... p 2985 N94-26336 #
AFIT/GE/ENG/93D-27 .... p 2765 N94-25647 #
AFIT/GE/ENG/93D-31 .... p 3034 N94-25768 #
AFIT/GE/ENG/93D-32 .... p 3037 N94-27062 #
AFIT/GE/ENG/93D-33 .... p 2909 N94-25943 #
AFIT/GE/ENG/93D-34 .... p 2676 N94-25771 #
AFIT/GE/ENG/93D-36 .... p 2676 N94-25785 #
AFIT/GE/ENG/93D-38 .... p 2772 N94-26924 #
AFIT/GE/ENG/93S-37 .... p 2665 N94-27071 #
AFIT/GE/ENG/94M-01 .... p 2678 N94-27132 #

AFIT/GE/ENP/93D-01 .... p 2815 N94-25616

AFIT/GEO/ENG/93D-01 .... p 2795 N94-27129 #
AFIT/GEO/ENG/93D-02 .... p 2984 N94-25759 #
AFIT/GEO/ENG/93D-05 .... p 2990 N94-25834 #

AFIT/GEO/ENP/93D-01 .... p 2815 N94-25744 #
AFIT/GEO/ENP/93D-03 .... p 3034 N94-25730 #
AFIT/GEO/ENP/93D-04 .... p 2693 N94-25595 #

AFIT/GLM/LAR/93S-16 .... p 2937 N94-25897 #
AFIT/GLM/LAR/93S-32 .... p 2691 N94-26017 #

AFIT/GLM/LSY/93S-19 .... p 2865 N94-25755 #

AFIT/GSE/ENY/93D-1 .... p 2694 N94-25659 #
AFIT/GSE/ENY/93D-2 .... p 2940 N94-25611 #

AFIT/GSM/LAS/93S-11 .... p 2942 N94-27320 #
AFIT/GSM/LAS/93S-20 .... p 3094 N94-26814 #
AFIT/GSM/LAS/93S-6 .... p 2834 N94-25896 #

AFIT/GSO/ENG/93D-02 .... p 2780 N94-25770 #
AFIT/GSO/ENG/93D-03 .... p 2690 N94-25769 #
AFIT/GSO/ENG/93D-1 .... p 2694 N94-25832 #

AFIT/GSO/ENP/93D-01 .... p 3034 N94-25742 #
AFIT/GSO/ENP/93D-02 .... p 2765 N94-25728 #
AFIT/GSO/ENP/93D-03 .... p 2847 N94-25741 #
AFIT/GSO/ENP/93D-04 .... p 3102 N94-25658 #

AFIT/GSO/ENS/93D-03 .... p 2892 N94-25861 #
AFIT/GSO/ENS/93D-14 .... p 2694 N94-25738 #
AFIT/GSO/ENS/93D-16 .... p 3001 N94-25607 #

AFOSR-93-0882TR .... p 2881 N94-27143 #
AFOSR-93-0883TR .... p 3046 N94-27098 #
AFOSR-93-0884TR .... p 2772 N94-26975 #
AFOSR-93-0885TR .... p 2709 N94-27125 #
AFOSR-93-0886TR .... p 3099 N94-27013 #
AFOSR-93-0887TR .... p 2939 N94-27012 #
AFOSR-93-0889TR .... p 3024 N94-27011 #
AFOSR-93-0891TR .... p 3059 N94-26681 #
AFOSR-93-0892TR .... p 3024 N94-27133 #
AFOSR-93-0893TR .... p 2939 N94-27072 #
AFOSR-93-0894TR .... p 2964 N94-26682 #
AFOSR-93-0895TR .... p 2709 N94-27142 #
AFOSR-93-0896TR .... p 2938 N94-26683 #
AFOSR-93-0897TR .... p 2940 N94-27141 #
AFOSR-93-0898TR .... p 2987 N94-27124 #
AFOSR-93-0899TR .... p 2988 N94-27139 #
AFOSR-93-0900TR .... p 3037 N94-27010 #
AFOSR-93-0901TR .... p 2968 N94-27140 #
AFOSR-93-0902TR .... p 2773 N94-27068 #
AFOSR-93-0905TR .... p 2868 N94-26817 #
AFOSR-93-0906TR .... p 2939 N94-27094 #
AFOSR-93-0907TR .... p 3010 N94-27067 #
AFOSR-93-0908TR .... p 3111 N94-27099 #
AFOSR-93-0909TR .... p 3110 N94-26883 #
AFOSR-93-0910TR .... p 3111 N94-27096 #
AFOSR-93-0912TR .... p 2823 N94-27104 #
AFOSR-94-0003TR .... p 2880 N94-26752
AFOSR-94-0016TR .... p 2901 N94-26517 #
AFOSR-94-0018TR .... p 2992 N94-26302 #
AFOSR-94-0025TR .... p 2962 N94-26303 #
AFOSR-94-0031TR .... p 2793 N94-26534 #
AFOSR-94-0033TR .... p 2783 N94-26536 #

AGARD-CP-534 .... p 2799 N94-28003 #

AIAA PAPER 93-1998 .... p 2826 N94-27599 * #
AIAA PAPER 93-5028 .... p 2691 N94-27868 * #
AIAA PAPER 94-0220 .... p 2701 N94-26208 * #
AIAA PAPER 94-0280 .... p 2674 N94-26573 * #
AIAA PAPER 94-1119 .... p 2693 N94-27427 * #

AL-TP-1992-0024 .... p 2910 N94-26435 #

AL-TR-1992-0164 .... p 2941 N94-26984 #
AL-TR-1993-0024 .... p 2937 N94-25965

AL/AO-TR-1993-0103 .... p 2910 N94-26973 #

AL/CF-TR-1993-0069 .... p 3099 N94-26891 #
AL/CF-TR-1993-0088 .... p 2673 N94-26989 #
AL/CF-TR-1993-0097 .... p 2911 N94-27088 #
AL/CF-TR-1993-0110 .... p 2902 N94-26991 #
AL/CF-TR-1993-0156 .... p 2774 N94-27170

AL/HR-TR-1993-0131 .... p 2679 N94-25773 #
AL/HR-TR-1993-0158 .... p 2938 N94-26882 #

ANL-HEP-CP-93-86 .... p 3018 N94-26145 #
ANL-HEP-CP-93-95 .... p 3015 N94-25955 #
ANL-HEP-CP-93-96 .... p 3022 N94-26793 #

ANL-93/26-REV-1 .... p 2963 N94-26407 #
ANL-93/40 .... p 2979 N94-25802 #

ANL/CHM/CP-81063 .... p 3062 N94-26934 #
ANL/CHM/CP-81119 .... p 3055 N94-26275 #

ANL/CHM/PP-80544 .... p 3053 N94-26031 #
ANL/CHM/PP-80545 .... p 3013 N94-25816 #

ANL/CMT-ACL/CP-80970 .... p 2868 N94-26952 #

ANL/CMT/CP-79723 .... p 2780 N94-25806 #
ANL/CMT/CP-79729 .... p 2781 N94-26144 #

ANL/DIS/CP-81102 .... p 3098 N94-26598 #

ANL/ER/PP-77881 .... p 3026 N94-27620 #

ANL/ESD/TM-55 .... p 2794 N94-26763 #

ANL/ET/CP-78725 .... p 3053 N94-26029 #
ANL/ET/CP-79010 .... p 2739 N94-26935 #
ANL/ET/CP-79400 .... p 2740 N94-26957 #
ANL/ET/CP-79607 .... p 2792 N94-26331 #
ANL/ET/CP-81211 .... p 2783 N94-26589 #

ANL/MCS/CP-81643 .... p 2973 N94-27717 #

ANL/MCT/CP-79097 .... p 3008 N94-26421 #
ANL/MCT/CP-79124 .... p 2751 N94-26422 #

ANL/MSD/CP-79851 .... p 2751 N94-26594 #
ANL/MSD/CP-80133 .... p 2737 N94-26587 #
ANL/MSD/CP-80134 .... p 3059 N94-26591 #
ANL/MSD/CP-80489 .... p 3017 N94-26078 #
ANL/MSD/CP-81484 .... p 3055 N94-26243 #
ANL/MSD/CP-81580 .... p 2757 N94-27716 #

ANL/XFD/CP-80819 .... p 3054 N94-26139 #
ANL/XFD/CP-81152 .... p 3035 N94-26276 #
ANL/XFD/CP-81491 .... p 2820 N94-27781 #

ANSP-M-23 .... p 2699 N94-25926 #

AP-42-SUPPL-F .... p 2867 N94-26757 #

APL-UW-TR-9208 .... p 2899 N94-26886 #
APL-UW-TR-9309 .... p 2900 N94-27090 #

ARAED-TR-93020 .... p 2759 N94-26437 #
ARAED-TR-93021 .... p 2751 N94-26434 #

ARCCB-TR-93038 .... p 3008 N94-26376 #

ARL-CR-110 .... p 2709 N94-26978 #
ARL-CR-122 .... p 2942 N94-27089 #
ARL-CR-129 .... p 2771 N94-26844 #
ARL-CR-78 .... p 2826 N94-27657 * #

ARL-RR-9 .... p 2644 N94-26342 #

ARL-SR-3 p 2836 N94-25754 #
ARL-SR-5 p 2747 N94-25596 #

ARL-TN-58 p 2838 N94-26501 #

ARL-TR-10 p 2794 N94-26801
ARL-TR-146 p 2747 N94-28212 #
ARL-TR-240 p 2880 N94-26828 #
ARL-TR-283 p 2996 N94-26972 #
ARL-TR-294 p 2957 N94-25646 #
ARL-TR-304 p 3034 N94-25940 #
ARL-TR-315 p 2957 N94-25753 #
ARL-TR-61 p 2895 N94-26846 #

ARL/PSU-TR-93-12 p 2789 N94-25604 #

ASIAC-TR-93-9 p 2987 N94-27093 #

ASIPP-0035 p 2758 N94-27857

ATC-196 p 2680 N94-26196
ATC-205 p 2772 N94-26963

ATCOM-TR-93-A-012-VOL-1 p 2645 N94-26489 * #
ATCOM-TR-93-A-012-VOL-2 p 2645 N94-26492 * #
ATCOM-TR-93-A-012-VOL-3 p 2645 N94-26497 * #
ATCOM-TR-93-A-012-VOL-4 p 2645 N94-26483 * #

ATR-93(7248)-1 p 2887 N94-28218 * #
ATR-93(7248)-2 p 2877 N94-26201 #
ATR-93(8361)-2 p 2746 N94-28185 #

B-247621 p 3095 N94-28177 #
B-254122 p 3106 N94-27418 #
B-255776 p 2696 N94-27382 #

BARC-1993/E/009 p 2981 N94-26903
BARC-1993/P/001 p 2715 N94-26392 #
BARC-1993/P/003 p 2717 N94-26988

BCRS-92-20 p 2847 N94-26228

BER-591-97 p 2843 N94-27765 * #

BNL-48489 p 2753 N94-26770 #
BNL-49457 p 2717 N94-26951 #
BNL-49620 p 2732 N94-26004 #
BNL-49652 p 3060 N94-26771 #
BNL-49659 p 3022 N94-26769 #
BNL-49661 p 2811 N94-26787 #
BNL-49663 p 2699 N94-25798 #
BNL-49665 p 3012 N94-25795 #
BNL-49690 p 2852 N94-27875 #
BNL-49782 p 3029 N94-27814 #
BNL-52389 p 3027 N94-27711 #

CA-PATENT-APPL-SN-2,018,940 p 2659 N94-26293

CA-PATENT-CLASS-354-25 p 2659 N94-26293

CA-PATENT-1-325-765 p 2669 N94-27273
CA-PATENT-1325260 p 2775 N94-27270
CA-PATENT-1325261 p 2665 N94-27275
CA-PATENT-1325511 p 3066 N94-27276

CAST-TN-03-94 p 2956 N94-25606 * #

CERN-TH.6912/93 p 2995 N94-26812 #

CHMSR-TR-93-2 p 2985 N94-25966

CHMSR-93-1 p 2984 N94-25899 #

CMS-TSR-94-3 p 2998 N94-27103 #

CMS-94-5 p 3003 N94-26445 #

CMSC-130 p 2967 N94-27060 #

CMU-CS-93-204 p 2985 N94-26006 * #
CMU-CS-93-210 p 3099 N94-27014 #
CMU-CS-93-211 p 2786 N94-27061 #
CMU-CS-93-212 p 2982 N94-27117 #
CMU-CS-93-214 p 2986 N94-27032 #
CMU-CS-93-215 p 2967 N94-27064 #
CMU-CS-93-221 p 3002 N94-25903 #
CMU-CS-93-225 p 2967 N94-27065 #
CMU-CS-93-227 p 2967 N94-27063 #

CMU-RI-TR-93-11 p 2958 N94-25777 * #
CMU-RI-TR-93-18 p 2984 N94-25591 #
CMU-RI-TR-93-22 p 2984 N94-25898 #
CMU-RI-TR-93-23 p 2765 N94-25725 #
CMU-RI-TR-93-24 p 2809 N94-25967
CMU-RI-TR-93-25 p 2984 N94-25900 #
CMU-RI-TR-93-26 p 2821 N94-25878

CMU/SEI-93-TR-10 p 2959 N94-25855 #

CNIC-00653 p 2758 N94-27857
CNIC-00658 p 3049 N94-27855
CNIC-00660 p 2758 N94-27845
CNIC-00665 p 3049 N94-27856
CNIC-00673 p 3070 N94-27843
CNIC-00687 p 2742 N94-27730 #

COMPUTING SCIENCE
NOTES-93/17 p 2966 N94-26920 #
COMPUTING SCIENCE
NOTES-93/20 p 2966 N94-26919 #

CONF-880907 p 3095 N94-25751
CONF-9102201 p 3027 N94-27733 #
CONF-9103277 p 2816 N94-26112 #
CONF-9110503 p 2866 N94-26163
CONF-9201160 p 3056 N94-26364 #
CONF-9201160 p 3063 N94-26987
CONF-9202194 p 2983 N94-27804
CONF-9207216 p 3032 N94-26543
CONF-920821-4 p 2901 N94-26623 #
CONF-9209397 p 2719 N94-27822 #
CONF-9210176-6 p 2797 N94-27617 #
CONF-9210294 p 3051 N94-25912
CONF-9210334-4 p 2894 N94-26313 #
CONF-921101-139 p 2717 N94-26951 #
CONF-9211117-12 p 3069 N94-27753 #
CONF-93-08150-12 p 2824 N94-27181 #
CONF-9302150-1 p 2855 N94-26115 #
CONF-9303248-1 p 2982 N94-27600 #
CONF-930389-26 p 3022 N94-26769 #
CONF-930389 p 3027 N94-27711 #
CONF-930405-49 p 2753 N94-26770 #
CONF-930405-50 p 3053 N94-26025 #
CONF-930405-51 p 3056 N94-26326 #
CONF-930405-52 p 3069 N94-27757 #
CONF-9304112-24 p 3041 N94-25801 #
CONF-9304174 p 2733 N94-26160
CONF-9304174 p 2734 N94-26161
CONF-9304174 p 2734 N94-26162
CONF-9304174 p 2734 N94-26263 #
CONF-9304174 p 2734 N94-26264 #
CONF-9304174 p 2837 N94-26265 #
CONF-9304174 p 2735 N94-26294 #
CONF-9304174 p 2735 N94-26295 #
CONF-9304174 p 2743 N94-27832 #
CONF-9304214 p 2743 N94-27829 #
CONF-9304218 p 3047 N94-27698
CONF-9305134 p 2763 N94-26429 #
CONF-9305235-5 p 3013 N94-25820 #
CONF-9305247 p 2716 N94-26519 #
CONF-9305294-1 p 3110 N94-26696 #
CONF-9305305-1 p 3116 N94-27740 #
CONF-9305309-1 p 3111 N94-27742 #
CONF-9305312-1 p 2838 N94-26524 #
CONF-930571-29 p 2739 N94-26912 #
CONF-9306125-6 p 2818 N94-26698 #
CONF-9306176-13 p 3022 N94-26793 #
CONF-9306176-14 p 3015 N94-25955 #
CONF-9306196-1 p 2789 N94-25597 #
CONF-9306212-1 p 3052 N94-25947 #
CONF-9306220-1 p 2980 N94-26473
CONF-9306221-9 p 3028 N94-27736 #
CONF-9306223-2 p 3054 N94-26125 #
CONF-9306223-3 p 2751 N94-26594 #
CONF-9306245-2 p 3102 N94-26528 #
CONF-9306258-14 p 2980 N94-25984 #
CONF-9306258-5 p 3021 N94-26759 #
CONF-9306258-7 p 3063 N94-27047 #
CONF-9306258-8 p 3011 N94-25598 #
CONF-9306260-3 p 3017 N94-26101 #
CONF-9306260-4 p 3024 N94-27050 #
CONF-9306260-5 p 3020 N94-26574 #
CONF-9306274-1 p 2708 N94-26930 #
CONF-9306277-1 p 3104 N94-26786 #
CONF-9306289-1 p 2737 N94-26582 #
CONF-930636-10 p 3012 N94-25795 #
CONF-930636-9 p 3017 N94-26083 #
CONF-930637-11 p 3016 N94-25957 #
CONF-930676-61 p 2880 N94-26806 #
CONF-930676-64 p 2735 N94-26322 #
CONF-930703-38 p 2733 N94-26087 #
CONF-930703-39 p 2836 N94-26129 #
CONF-930703-40 p 2742 N94-27694 #
CONF-9307124-3 p 3063 N94-26958 #
CONF-9307134-1 p 2866 N94-25948 #
CONF-9307143-4 p 3023 N94-26938 #
CONF-9307143-6 p 3018 N94-26245 #
CONF-9307155-1 p 3054 N94-26128 #
CONF-9307159-1 p 2827 N94-27780 #
CONF-930720-21 p 3044 N94-26694 #
CONF-930722-52 p 2811 N94-26787 #
CONF-930722-53 p 3035 N94-26276 #
CONF-930722-54 p 2816 N94-26020 #
CONF-930759-3 p 3065 N94-27251 #
CONF-930759-5 p 2736 N94-26351 #
CONF-930759-6 p 3055 N94-26238 #
CONF-930761-4 p 3018 N94-26145 #
CONF-930779-18 p 3018 N94-26133 #
CONF-930788-4 p 2792 N94-26427 #
CONF-930810-10 p 2895 N94-26761 #
CONF-930810-11 p 2880 N94-26762 #
CONF-930810-13 p 2869 N94-27601 #
CONF-9308103-1 p 2741 N94-27619 #
CONF-9308107-4 p 3073 N94-26805 #
CONF-9308122-12 p 3054 N94-26137 #
CONF-9308122-14 p 3062 N94-26932 #
CONF-9308122-16 p 2748 N94-25959 #
CONF-9308150-9 p 2740 N94-27006 #
CONF-9308161-2 p 2965 N94-26862 #
CONF-9308164-5 p 3021 N94-26620 #
CONF-9308167-4 p 3061 N94-26868 #
CONF-9308178 p 2827 N94-27722 #
CONF-9308182-1 p 3059 N94-26695 #
CONF-9308183-2 p 3045 N94-26950 #
CONF-9308186-1 p 2818 N94-26699 #
CONF-9308186-2 p 2819 N94-27018 #
CONF-9308189-1 p 2866 N94-26123 #
CONF-9308191-1 p 3052 N94-25971 #
CONF-9308205-1 p 3005 N94-27816 #
CONF-930823-16 p 3015 N94-25935 #
CONF-930824-27 p 2816 N94-26130 #
CONF-930825-13 p 2739 N94-26931 #
CONF-930825-14 p 2731 N94-25804 #
CONF-930825-15 p 2741 N94-27570 #
CONF-930826-3 p 2716 N94-26794 #
CONF-930830-31 p 2856 N94-26426 #
CONF-930852-4 p 3061 N94-26856 #
CONF-930858-1 p 2754 N94-27021 #
CONF-930865-1 p 3017 N94-26078 #
CONF-930893-23 p 2857 N94-26747 #
CONF-930893-24 p 2858 N94-26785 #
CONF-930893-27 p 2858 N94-26871 #
CONF-930893-28 p 2857 N94-26584 #
CONF-930893-29 p 2857 N94-26583 #
CONF-930893-34 p 2858 N94-26869 #
CONF-930893-35 p 2855 N94-26114 #
CONF-930893-37 p 2827 N94-27874 #
CONF-930893-38 p 2858 N94-26792 #
CONF-930893-39 p 2719 N94-27712 #
CONF-930893-5 p 2859 N94-27005 #
CONF-930905-22 p 2732 N94-26004 #
CONF-930905-9 p 2733 N94-26069 #
CONF-9309106-2 p 3054 N94-26147 #
CONF-9309119-2 p 3047 N94-27715 #
CONF-9309131-1 p 2856 N94-26513 #
CONF-9309185-4 p 2991 N94-26079 #
CONF-9309185-5 p 2933 N94-27744 #
CONF-9309208-4 p 2713 N94-25978 #
CONF-9309230-3 p 2892 N94-25936 #
CONF-9309241-1 p 3057 N94-26420 #
CONF-9309256-3 p 3054 N94-26139 #
CONF-9309259-1 p 2752 N94-26676 #
CONF-9309259-2 p 3067 N94-27602 #
CONF-9309259-3 p 3035 N94-26246 #
CONF-930926-22 p 3060 N94-26795 #
CONF-9309266-1 p 2768 N94-26310 #
CONF-9309267-1 p 3030 N94-28001 #
CONF-9309274-1 p 3042 N94-25976 #
CONF-9309279-1 p 2760 N94-25849 * #
CONF-930928-11 p 3017 N94-26049 #
CONF-930928-15 p 2737 N94-26556 #
CONF-930928-16 p 2732 N94-25987 #
CONF-930928-20 p 2737 N94-26575 #
CONF-930928-21 p 2731 N94-25803 #
CONF-9309283-2 p 3050 N94-25817 #
CONF-9309290-1 p 2814 N94-27779 #
CONF-9309297-1 p 3028 N94-27752 #
CONF-9309298-1 p 3103 N94-27750 #
CONF-930953-2 p 2780 N94-25812 #
CONF-930956-1 p 3059 N94-26765 #
CONF-930960-6 p 3117 N94-27826 #
CONF-930997-7 p 2705 N94-25805 #
CONF-930999-2 p 3012 N94-25612 #
CONF-931009-10 p 2737 N94-26607 #
CONF-931009-11 p 2734 N94-26272 #
CONF-931009-12 p 2740 N94-26957 #
CONF-931009-13 p 2735 N94-26273 #
CONF-931009-15 p 3055 N94-26243 #
CONF-931009-16 p 2737 N94-26585 #
CONF-931009-17 p 2743 N94-27792 #
CONF-931009-7 p 2739 N94-26935 #
CONF-931009-9 p 2738 N94-26621 #
CONF-9310100-4 p 2960 N94-26048 #
CONF-9310100-7 p 2941 N94-26555 #
CONF-931013-1 p 3008 N94-26421 #
CONF-9310145-3 p 3097 N94-26348 #
CONF-9310145-4 p 3100 N94-27563 #
CONF-9310145-5 p 3096 N94-25813 #
CONF-9310170-1 p 2751 N94-26422 #

CONF-931018-16 .... p 3045 N94-27019 #
CONF-931018-45 .... p 3043 N94-26274 #
CONF-931018-47 .... p 3045 N94-26861 #
CONF-931018-48 .... p 3042 N94-26140 #
CONF-931018-50 .... p 3046 N94-27261 #
CONF-931018-51 .... p 3044 N94-26860 #
CONF-931018-52 .... p 3044 N94-26858 #
CONF-931018-57 .... p 3045 N94-26863 #
CONF-931018-59 .... p 3045 N94-26865 #
CONF-931018-60 .... p 3043 N94-26324 #
CONF-931018-61 .... p 3043 N94-26323 #
CONF-931018-64 .... p 3041 N94-25933 #
CONF-931018-65 .... p 2767 N94-25924 #
CONF-931018-77 .... p 3048 N94-27825 #
CONF-9310181 .... p 3029 N94-27834 #
CONF-9310194-2 .... p 2819 N94-26811 #
CONF-9310196-2 .... p 2961 N94-26146 #
CONF-9310197-1 .... p 2868 N94-26952 #
CONF-9310216-2 .... p 2822 N94-26465 #
CONF-9310216-4 .... p 2958 N94-25818 #
CONF-9310217-1 .... p 2821 N94-25970 #
CONF-9310218-1 .... p 2738 N94-26610 #
CONF-9310220-1 .... p 2980 N94-26120 #
CONF-9310220-2 .... p 2979 N94-25952 #
CONF-9310220-3 .... p 3020 N94-26577 #
CONF-9310220-4 .... p 2973 N94-27717 #
CONF-9310223-1 .... p 2781 N94-25977 #
CONF-9310224-1 .... p 2735 N94-26349 #
CONF-9310224-2 .... p 2741 N94-27622 #
CONF-931023-7 .... p 2986 N94-26807 #
CONF-931023-8 .... p 2967 N94-27049 #
CONF-931023-9 .... p 2985 N94-25983 #
CONF-9310231-1 .... p 2852 N94-27875 #
CONF-9310232-1 .... p 2979 N94-25953 #
CONF-9310232-2 .... p 2983 N94-27713 #
CONF-9310235-1 .... p 3007 N94-27777 #
CONF-9310239-1 .... p 2809 N94-25599 #
CONF-931024-1 .... p 2780 N94-25806 #
CONF-931024-5 .... p 2781 N94-26144 #
CONF-9310246-1 .... p 3000 N94-27569 #
CONF-9310247-2 .... p 3028 N94-27748 #
CONF-9310247-3 .... p 3028 N94-27749 #
CONF-9310250-2 .... p 3029 N94-27814 #
CONF-9310252-1 .... p 3116 N94-27793 #
CONF-9310252-2 .... p 3116 N94-27714 #
CONF-9310252-4 .... p 3117 N94-27827 #
CONF-931054-1 .... p 2819 N94-27262
CONF-931073-3 .... p 3060 N94-26771 #
CONF-931076-2 .... p 3042 N94-26081 #
CONF-931076-3 .... p 2714 N94-26122 #
CONF-931076-4 .... p 2760 N94-27725 #
CONF-931078-2 .... p 2706 N94-25938 #
CONF-931107-15 .... p 3054 N94-26095 #
CONF-931107-17 .... p 3053 N94-26094 #
CONF-931107-25 .... p 2787 N94-27618 #
CONF-931107-27 .... p 3116 N94-27621 #
CONF-931107-7 .... p 2696 N94-26808 #
CONF-931107-8 .... p 3052 N94-25972 #
CONF-931108-11 .... p 3055 N94-26239 #
CONF-931108-13 .... p 2749 N94-25985 #
CONF-931108-14 .... p 2737 N94-26587 #
CONF-931108-16 .... p 3059 N94-26591 #
CONF-931108-18 .... p 2751 N94-26580 #
CONF-931108-20 .... p 2780 N94-25664 #
CONF-931108-24 .... p 3056 N94-26352 #
CONF-931108-26 .... p 3058 N94-26565 #
CONF-931108-28 .... p 3069 N94-27790 #
CONF-931108-31 .... p 3069 N94-27828 #
CONF-931108-36 .... p 2757 N94-27716 #
CONF-931108-7 .... p 3050 N94-25814 #
CONF-9311102-5 .... p 2751 N94-26554 #
CONF-9311104-10 .... p 3052 N94-25989 #
CONF-9311104-12 .... p 3056 N94-26308 #
CONF-9311104-13 .... p 2767 N94-25937 #
CONF-9311104-14 .... p 3050 N94-25815 #
CONF-9311104-4 .... p 2753 N94-26933 #
CONF-9311104-5 .... p 3062 N94-26934 #
CONF-9311104-7 .... p 3051 N94-25944 #
CONF-9311104-8 .... p 3055 N94-26275 #
CONF-9311107-2 .... p 2986 N94-26948 #
CONF-9311110-1 .... p 2713 N94-26014 #
CONF-9311112-1 .... p 2988 N94-27706 #
CONF-9311113-1 .... p 2960 N94-26118 #
CONF-9311114-3 .... p 2809 N94-25662 #
CONF-9311114-4 .... p 2957 N94-25663 #
CONF-9311114-8 .... p 2787 N94-27618 #
CONF-9311118-1 .... p 3098 N94-26598 #
CONF-9311119-1 .... p 2839 N94-26810 #
CONF-9311120-1 .... p 2816 N94-26126 #
CONF-9311124-1 .... p 2836 N94-26032 #
CONF-9311135-2 .... p 2851 N94-27727 #
CONF-9311135-4 .... p 2897 N94-28146 #
CONF-9311138-1 .... p 3068 N94-27724 #
CONF-9311140-1 .... p 3046 N94-27568 #
CONF-9311142-1 .... p 3049 N94-25601 #
CONF-9311147-1 .... p 3048 N94-27785 #
CONF-9311147-2 .... p 3048 N94-27791 #
CONF-931115-13 .... p 2948 N94-26578 #
CONF-931120-1 .... p 2857 N94-26617 #
CONF-931121-33 .... p 2707 N94-26099 #
CONF-931133-6 .... p 2733 N94-26092 #
CONF-931142-2 .... p 2750 N94-26124 #
CONF-931142-4 .... p 3053 N94-26029 #
CONF-931160-19 .... p 2769 N94-26482 #
CONF-931160-32 .... p 2736 N94-26522 #
CONF-931168-2 .... p 2757 N94-27726 #
CONF-931204-1 .... p 2780 N94-25975 #
CONF-931234-1 .... p 2821 N94-25980 #
CONF-931234-3 .... p 2818 N94-26605 #
CONF-931235-3 .... p 2792 N94-26331 #
CONF-931235-4 .... p 2742 N94-27786 #
CONF-931236-1 .... p 2857 N94-26612 #
CONF-931237-2 .... p 2820 N94-27781 #
CONF-931238-1 .... p 2783 N94-26589 #
CONF-931239-1 .... p 2741 N94-27616 #
CONF-940101-16 .... p 2797 N94-27709 #
CONF-940101-18 .... p 2702 N94-26560 #
CONF-940101-20 .... p 2700 N94-25956 #
CONF-940101-22 .... p 3005 N94-26802 #
CONF-940101-23 .... p 2699 N94-25798 #
CONF-940101-25 .... p 2699 N94-25600 #
CONF-940101-26 .... p 2699 N94-25613 #
CONF-940101-27 .... p 3070 N94-28067 #
CONF-940113-1 .... p 2859 N94-27004 #
CONF-940113-3 .... p 2857 N94-26700 #
CONF-940113-4 .... p 2682 N94-27997 #
CONF-940113-5 .... p 2791 N94-26117 #
CONF-940115-8 .... p 2898 N94-26072 #
CONF-940123-1 .... p 2848 N94-26277 #
CONF-940136-3 .... p 2981 N94-27092 #
CONF-940209-1 .... p 2713 N94-26075 #
CONF-940214-4 .... p 2821 N94-26110 #
CONF-940215-2 .... p 3058 N94-26514 #
CONF-940217-1 .... p 2948 N94-26111 #
CONF-940221-1 .... p 2733 N94-26069 #
CONF-940222-6 .... p 2732 N94-25819 #
CONF-940222-9 .... p 2742 N94-27788 #
CONF-940226-1 .... p 3040 N94-27999 #
CONF-940226-2 .... p 3040 N94-28000 #
CONF-940229-1 .... p 2706 N94-26019 #
CONF-940235-1 .... p 2750 N94-26085 #
CONF-940301-1 .... p 2712 N94-27710 #
CONF-940301-2 .... p 2704 N94-27745 #
CONF-940301-3 .... p 2757 N94-27747 #
CONF-940307-2 .... p 2813 N94-27624 #
CONF-940312-12 .... p 3004 N94-27612 #
CONF-940312-13 .... p 2835 N94-27613 #
CONF-940312-25 .... p 2760 N94-27719 #
CONF-940312-29 .... p 3000 N94-27564 #
CONF-940312-38 .... p 3094 N94-27707 #
CONF-940312-4 .... p 2797 N94-27705 #
CONF-940326-2 .... p 3039 N94-27721 #
CONF-940326-5 .... p 2742 N94-27755 #
CONF-940341-1 .... p 2704 N94-27708 #
CONF-940341-3 .... p 2719 N94-27728 #

CPTH-A258/0793 .... p 3071 N94-25882 #

CRANFIELD-AERO-9208 .... p 2790 N94-25778 #
CRANFIELD-AERO-9209 .... p 3005 N94-25823 #
CRANFIELD-AERO-9210 .... p 3005 N94-25781 #
CRANFIELD-AERO-9301 .... p 2765 N94-25639 #
CRANFIELD-AERO-9303 .... p 2676 N94-25640 #
CRANFIELD-AERO-9305 .... p 2676 N94-25653 #

CRC-586 .... p 2758 N94-25901 #

CS-9302 .... p 2939 N94-27001 #
CS-9303 .... p 2938 N94-26873

CSM-CWR-093-015 .... p 2738 N94-26679 #

CSN-93/16 .... p 2966 N94-26971 #
CSN-93/18 .... p 2966 N94-26970 #
CSN-93/19 .... p 2966 N94-26955
CSN-93/21 .... p 2966 N94-26956

CTN-92-60366 .... p 2659 N94-26293
CTN-94-60964 .... p 3027 N94-27684
CTN-94-60965 .... p 3074 N94-27398
CTN-94-60966 .... p 3026 N94-27399
CTN-94-60967 .... p 3026 N94-27400
CTN-94-60968 .... p 3074 N94-27401
CTN-94-60969 .... p 3026 N94-27402
CTN-94-60970 .... p 3074 N94-27403
CTN-94-60971 .... p 2812 N94-27257
CTN-94-60972 .... p 3024 N94-27258
CTN-94-60973 .... p 3024 N94-27259
CTN-94-60974 .... p 3025 N94-27260
CTN-94-60975 .... p 3073 N94-27263
CTN-94-60976 .... p 3007 N94-27264
CTN-94-60977 .... p 3025 N94-27266
CTN-94-60978 .... p 3009 N94-27268
CTN-94-60979 .... p 2998 N94-27269
CTN-94-60980 .... p 2982 N94-27332
CTN-94-60981 .... p 3025 N94-27333
CTN-94-60982 .... p 2988 N94-27641
CTN-94-60983 .... p 2787 N94-27642
CTN-94-60985 .... p 3039 N94-27643
CTN-94-60986 .... p 2982 N94-27644
CTN-94-60987 .... p 2983 N94-27685
CTN-94-60988 .... p 2974 N94-27869
CTN-94-60989 .... p 2852 N94-27870
CTN-94-60990 .... p 2988 N94-27645
CTN-94-60991 .... p 2777 N94-27871
CTN-94-60992 .... p 2975 N94-27872
CTN-94-60993 .... p 2798 N94-27873
CTN-94-60994 .... p 2757 N94-27801
CTN-94-60995 .... p 2743 N94-27803
CTN-94-60996 .... p 2974 N94-27805
CTN-94-60997 .... p 2777 N94-27806
CTN-94-60998 .... p 2844 N94-27808
CTN-94-61000 .... p 2844 N94-27810
CTN-94-61001 .... p 2799 N94-27947
CTN-94-61002 .... p 3001 N94-27948
CTN-94-61004 .... p 3049 N94-27949
CTN-94-61005 .... p 2744 N94-27950
CTN-94-61006 .... p 3118 N94-26709 #
CTN-94-61007 .... p 2677 N94-26710 #
CTN-94-61008 .... p 2708 N94-26711 #
CTN-94-61010 .... p 2828 N94-28041 #
CTN-94-61011 .... p 2681 N94-27594
CTN-94-61012 .... p 2695 N94-26712 #
CTN-94-61013 .... p 3117 N94-26701 #
CTN-94-61016 .... p 2647 N94-26702 #
CTN-94-61017 .... p 3104 N94-26638
CTN-94-61018 .... p 2838 N94-26639
CTN-94-61019 .... p 2770 N94-26625
CTN-94-61020 .... p 2770 N94-26626
CTN-94-61021 .... p 2894 N94-26628
CTN-94-61022 .... p 2985 N94-26629
CTN-94-61023 .... p 2822 N94-26657
CTN-94-61024 .... p 2848 N94-26664
CTN-94-61025 .... p 3021 N94-26665
CTN-94-61026 .... p 3036 N94-26666
CTN-94-61027 .... p 2849 N94-26667
CTN-94-61028 .... p 2849 N94-26668
CTN-94-61029 .... p 3102 N94-26669
CTN-94-61030 .... p 2867 N94-26670
CTN-94-61031 .... p 2994 N94-26640
CTN-94-61032 .... p 2822 N94-26642
CTN-94-61033 .... p 2994 N94-26614
CTN-94-61034 .... p 2963 N94-26615
CTN-94-61035 .... p 2963 N94-26616
CTN-94-61036 .... p 2769 N94-26618
CTN-94-61037 .... p 2769 N94-26619
CTN-94-61038 .... p 2784 N94-26631
CTN-94-61039 .... p 2823 N94-26658
CTN-94-61040 .... p 2994 N94-26659
CTN-94-61041 .... p 2985 N94-26660
CTN-94-61042 .... p 2964 N94-26632
CTN-94-61043 .... p 2752 N94-26661
CTN-94-61044 .... p 2811 N94-26662
CTN-94-61045 .... p 2838 N94-26622
CTN-94-61046 .... p 2770 N94-26624
CTN-94-61047 .... p 2784 N94-26627
CTN-94-61048 .... p 2770 N94-26630
CTN-94-61049 .... p 2738 N94-26633
CTN-94-61050 .... p 2763 N94-26634
CTN-94-61051 .... p 2980 N94-26635
CTN-94-61052 .... p 2964 N94-26663
CTN-94-61053 .... p 2793 N94-26671
CTN-94-61054 .... p 2793 N94-26637
CTN-94-61055 .... p 2677 N94-26636
CTN-94-61056 .... p 3059 N94-26703
CTN-94-61057 .... p 2784 N94-26704
CTN-94-61058 .... p 2646 N94-26672
CTN-94-61059 .... p 2674 N94-26673
CTN-94-61060 .... p 2980 N94-26674
CTN-94-61061 .... p 2784 N94-26675
CTN-94-61062 .... p 3117 N94-26656 #
CTN-94-61063 .... p 2835 N94-26644 #
CTN-94-61064 .... p 2678 N94-27648
CTN-94-61065 .... p 2982 N94-27649
CTN-94-61066 .... p 2787 N94-27650
CTN-94-61067 .... p 2813 N94-27651 #
CTN-94-61068 .... p 2826 N94-27652
CTN-94-61069 .... p 2787 N94-27653
CTN-94-61070 .... p 2740 N94-27304
CTN-94-61071 .... p 2740 N94-27305
CTN-94-61072 .... p 2740 N94-27306
CTN-94-61073 .... p 2795 N94-27307
CTN-94-61074 .... p 2999 N94-27404
CTN-94-61075 .... p 2999 N94-27405
CTN-94-61076 .... p 2988 N94-27271
CTN-94-61077 .... p 2842 N94-27272
CTN-94-61078 .... p 2651 N94-28315
CTN-94-61079 .... p 2825 N94-27343

CTN-94-61080 p 2825 N94-27344
CTN-94-61081 p 2776 N94-27345
CTN-94-61082 p 3038 N94-27441
CTN-94-61083 p 2776 N94-27308
CTN-94-61084 p 2842 N94-27309 #
CTN-94-61085 p 3025 N94-27310
CTN-94-61086 p 2969 N94-27311
CTN-94-61087 p 2998 N94-27312
CTN-94-61088 p 2795 N94-27313
CTN-94-61089 p 2711 N94-27314
CTN-94-61090 p 2842 N94-27315
CTN-94-61091 p 2969 N94-27316
CTN-94-61092 p 2813 N94-27317
CTN-94-61093 p 2969 N94-27318
CTN-94-61094 p 2669 N94-27273
CTN-94-61095 p 2775 N94-27270
CTN-94-61096 p 2665 N94-27275
CTN-94-61097 p 3066 N94-27276
CTN-94-61098 p 2775 N94-27274
CTN-94-61099 p 2988 N94-27277
CTN-94-61100 p 2842 N94-27278
CTN-94-61101 p 2969 N94-27346
CTN-94-61102 p 2775 N94-27301
CTN-94-61103 p 3103 N94-27302
CTN-94-61104 p 2786 N94-27303
CTN-94-61105 p 2972 N94-27595
CTN-94-61106 p 2826 N94-27596
CTN-94-61107 p 2744 N94-27961
CTN-94-61108 p 3039 N94-27962
CTN-94-61109 p 3070 N94-27974
CTN-94-61110 p 2989 N94-27975
CTN-94-61111 p 2712 N94-27688
CTN-94-61112 p 2851 N94-27863
CTN-94-61113 p 2852 N94-27878
CTN-94-61114 p 2843 N94-27585
CTN-94-61115 p 2813 N94-27597
CTN-94-61116 p 3038 N94-27598
CTN-94-61117 p 2942 N94-27683
CTN-94-61118 p 2670 N94-27666
CTN-94-61119 p 2665 N94-27667
CTN-94-61120 p 2983 N94-28042
CTN-94-61121 p 2973 N94-27761
CTN-94-61122 p 2975 N94-27951
CTN-94-61123 p 2973 N94-27762
CTN-94-61124 p 2814 N94-27763
CTN-94-61125 p 2974 N94-27823
CTN-94-61127 p 2820 N94-27668

CTP-2216 p 3019 N94-26416 #

CU-CSSC-93-16 p 2845 N94-28181 * #

CUCS-002-92 p 3100 N94-27164 #

CWI-CS-R9263 p 2961 N94-26218 #
CWI-CS-R9264 p 2961 N94-26219 #
CWI-CS-R9265 p 3097 N94-26220 #
CWI-CS-R9266 p 2961 N94-26221 #
CWI-CS-R9267 p 2995 N94-26776 #
CWI-CS-R9268 p 3100 N94-27394
CWI-CS-R9269 p 2971 N94-27575
CWI-CS-R9270 p 2972 N94-27576 #
CWI-CS-R9301 p 3000 N94-27577
CWI-CS-R9302 p 2972 N94-27578
CWI-CS-R9303 p 2982 N94-27579 #
CWI-CS-R9313-PT-1 p 2972 N94-27580 #
CWI-CS-R9314-PT-2 p 2972 N94-27581
CWI-CS-R9315 p 2970 N94-27543
CWI-CS-R9316 p 2970 N94-27544 #
CWI-CS-R9317 p 2970 N94-27545 #
CWI-CS-R9318 p 2776 N94-27546 #
CWI-CS-R9319 p 2955 N94-27547 #
CWI-CS-R9320 p 2970 N94-27548 #
CWI-CS-R9321 p 2970 N94-27549
CWI-CS-R9322 p 2971 N94-27550
CWI-CS-R9323 p 2776 N94-27551 #
CWI-CS-R9327 p 2971 N94-27552
CWI-CS-R9328 p 2973 N94-27737
CWI-CS-R9330 p 2974 N94-27794 #

CWI-NM-R9306 p 2965 N94-26772 #
CWI-NM-R9307 p 2995 N94-26773 #
CWI-NM-R9308 p 2868 N94-26774 #
CWI-NM-R9309 p 2867 N94-26216 #
CWI-NM-R9310 p 2991 N94-26217 #

CWP-129P p 2877 N94-25847 #

C92-432.4/034 p 2777 N94-27946 * #

DCIEM-93-25 p 2942 N94-27683

DE93-013716 p 2853 N94-25946 #
DE93-016604 p 2797 N94-27705 #
DE93-017267 p 3098 N94-26398
DE93-018194 p 2832 N94-28229 #
DE93-018224 p 2856 N94-26513 #
DE93-018234 p 2856 N94-26426 #
DE93-018519 p 3016 N94-26033 #
DE93-018628 p 3052 N94-25947 #
DE93-018872 p 2866 N94-25948 #
DE93-019018 p 3017 N94-26078 #
DE93-019086 p 2700 N94-25969 #
DE93-019177 p 2749 N94-26080 #
DE93-019408 p 2980 N94-26473
DE93-019458 p 2866 N94-26077 #
DE93-019505 p 2792 N94-26427 #
DE93-019842 p 3043 N94-26428 #
DE93-019930 p 2763 N94-26429 #
DE93-019934 p 2865 N94-25789 #
DE93-040082 p 2892 N94-25939 #
DE93-040264 p 2813 N94-27624 #
DE93-040342 p 2821 N94-26110 #
DE93-040345 p 2948 N94-26111 #
DE93-040448 p 2867 N94-26419 #
DE93-040755 p 3057 N94-26420 #
DE93-040796 p 2865 N94-25790 #
DE93-041173 p 3008 N94-26421 #
DE93-041177 p 2751 N94-26422 #
DE93-041226 p 2792 N94-26468 #
DE93-520239 p 3015 N94-25922 #
DE93-520314 p 3054 N94-26109 #
DE93-520378 p 2816 N94-26112 #
DE93-520380 p 3031 N94-26113 #
DE93-520383 p 3032 N94-26543
DE93-612974 p 3007 N94-25603
DE93-613019 p 3001 N94-28228
DE93-613023 p 2991 N94-25880
DE93-613024 p 2991 N94-25881
DE93-613025 p 2990 N94-25865
DE93-613032 p 2766 N94-25866
DE93-613046 p 2991 N94-25867
DE93-613048 p 3005 N94-25868
DE93-613052 p 3006 N94-26193
DE93-613053 p 3050 N94-25825
DE93-613054 p 3013 N94-25826
DE93-613096 p 3013 N94-25835
DE93-613097 p 3013 N94-25836
DE93-613183 p 3014 N94-25869
DE93-613184 p 3031 N94-25870
DE93-613434 p 3031 N94-25850
DE93-613550 p 3051 N94-25851
DE93-613551 p 3071 N94-25852
DE93-613553 p 3013 N94-25827
DE93-613645 p 3014 N94-25853
DE93-614153 p 2716 N94-26518 #
DE93-614526 p 3002 N94-25910
DE93-614530 p 3071 N94-25911
DE93-615942 p 3051 N94-25912
DE93-616009 p 2713 N94-25913
DE93-616188 p 3051 N94-25914
DE93-616534 p 2766 N94-25915
DE93-616646 p 3015 N94-25916
DE93-616655 p 2959 N94-25917
DE93-616656 p 2979 N94-25918
DE93-616661 p 3015 N94-25919
DE93-616664 p 2809 N94-25735
DE93-616665 p 3012 N94-25750
DE93-616798 p 3095 N94-25751
DE93-616801 p 3013 N94-25828
DE93-616815 p 2990 N94-25829
DE93-616816 p 2990 N94-25830
DE93-616817 p 3008 N94-25831
DE93-616857 p 3015 N94-25920
DE93-617048 p 3066 N94-27347
DE93-632191 p 3017 N94-26116 #
DE93-632416 p 2716 N94-26519 #
DE93-632438 p 2783 N94-26546
DE93-632594 p 2894 N94-26469
DE93-632656 p 2901 N94-26470
DE93-632682 p 2910 N94-26549
DE93-632901 p 2816 N94-26184
DE93-632902 p 2817 N94-26185
DE93-632953 p 2835 N94-26399
DE93-632968 p 2838 N94-26400
DE93-632978 p 2816 N94-26157
DE93-633201 p 2818 N94-26520 #
DE93-633202 p 2792 N94-26401
DE93-633327 p 2714 N94-26158
DE93-633328 p 2817 N94-26402 #
DE93-633438 p 2817 N94-26403
DE93-633444 p 3042 N94-26159
DE93-633529 p 3057 N94-26404
DE93-633762 p 2733 N94-26160
DE93-633763 p 2735 N94-26294 #
DE93-633764 p 2734 N94-26161
DE93-633765 p 2734 N94-26162
DE93-633766 p 2735 N94-26295 #
DE93-633767 p 2734 N94-26263 #
DE93-633790 p 2734 N94-26264 #
DE93-633954 p 2866 N94-26163
DE93-634021 p 3032 N94-26164
DE93-634022 p 3032 N94-26165
DE93-634023 p 3032 N94-26405 #
DE93-634140 p 2837 N94-26265 #
DE93-634153 p 2701 N94-26166
DE93-634171 p 2783 N94-26438
DE93-634172 p 2948 N94-26266 #
DE93-634176 p 2810 N94-26439
DE93-634182 p 3019 N94-26393
DE93-634183 p 2810 N94-26394
DE93-634184 p 2810 N94-26395
DE93-634185 p 2810 N94-26396
DE93-634186 p 2810 N94-26397
DE93-634188 p 2810 N94-26378
DE93-634191 p 3056 N94-26379
DE93-634192 p 2715 N94-26406 #
DE93-634229 p 2783 N94-26380
DE93-634230 p 2948 N94-26381
DE93-634289 p 3097 N94-26382
DE93-634290 p 2994 N94-26471
DE93-634303 p 2993 N94-26440
DE93-634304 p 2993 N94-26441
DE93-634305 p 2992 N94-26267 #
DE93-634306 p 2993 N94-26442
DE93-634308 p 3007 N94-26472 #
DE93-634309 p 2879 N94-26502
DE93-634324 p 2783 N94-26443
DE93-634325 p 3035 N94-26383
DE93-634326 p 3057 N94-26384
DE93-634330 p 3104 N94-26268
DE93-634331 p 3104 N94-26269
DE93-634333 p 3072 N94-26503
DE93-634334 p 2879 N94-26504
DE93-634335 p 3006 N94-26270
DE93-634336 p 3072 N94-26551
DE93-634337 p 3007 N94-26552
DE93-634338 p 3072 N94-26553 #
DE93-634340 p 3072 N94-26453 #
DE93-634341 p 3019 N94-26454
DE93-634342 p 3019 N94-26455 #
DE93-634343 p 3019 N94-26456 #
DE93-634344 p 2993 N94-26457 #
DE93-634345 p 3016 N94-26035 #
DE93-634346 p 3072 N94-26036 #
DE93-634347 p 3072 N94-26037 #
DE93-634348 p 3002 N94-26038 #
DE93-634357 p 3072 N94-26039 #
DE93-634366 p 3016 N94-26040 #
DE93-634367 p 3016 N94-26041
DE93-634374 p 3016 N94-26042 #
DE93-634375 p 3020 N94-26505
DE93-634386 p 3017 N94-26043 #
DE93-634393 p 3022 N94-26766
DE93-634398 p 3031 N94-26044 #
DE93-634426 p 3022 N94-26767
DE93-634438 p 3020 N94-26507
DE93-634447 p 3017 N94-26045 #
DE93-634449 p 3020 N94-26508
DE93-634450 p 3020 N94-26509
DE93-634453 p 3103 N94-26046 #
DE93-634500 p 3016 N94-26034 #
DE93-634525 p 3016 N94-26010 #
DE93-634526 p 3030 N94-27994 #
DE93-634530 p 3024 N94-27250 #
DE93-634585 p 2995 N94-26768
DE93-634588 p 3044 N94-26510
DE93-634636 p 3020 N94-26511
DE93-634653 p 3052 N94-26012 #
DE93-634665 p 3003 N94-26385 #
DE93-634666 p 2962 N94-26386 #
DE93-634712 p 3057 N94-26387 #
DE93-634753 p 3057 N94-26388 #
DE93-634754 p 3057 N94-26389 #
DE93-634755 p 3057 N94-26390 #
DE93-634760 p 3070 N94-27995 #
DE93-634761 p 3058 N94-26512
DE94-000010 p 2856 N94-26581 #
DE94-000014 p 2857 N94-26583 #
DE94-000015 p 2857 N94-26584 #
DE94-000016 p 2855 N94-26114 #
DE94-000224 p 2855 N94-26115 #
DE94-000231 p 2791 N94-26117 #
DE94-000232 p 2856 N94-26480 #
DE94-000237 p 2736 N94-26481 #
DE94-000250 p 2860 N94-27625 #
DE94-000259 p 3067 N94-27609 #
DE94-000260 p 2859 N94-27610 #
DE94-000365 p 2756 N94-27611 #
DE94-000378 p 2769 N94-26482 #
DE94-000432 p 2893 N94-26082 #
DE94-000478 p 3044 N94-26694 #
DE94-000658 p 3021 N94-26586 #
DE94-000685 p 2733 N94-26069 #
DE94-000687 p 3004 N94-27612 #
DE94-000770 p 3059 N94-26695 #
DE94-000773 p 3110 N94-26696 #
DE94-000780 p 2898 N94-25791 #

DE94-000797 .... p 3058 N94-26514 #
DE94-000816 .... p 2835 N94-27613 #
DE94-000846 .... p 3041 N94-25949 #
DE94-000848 .... p 2877 N94-25979 #
DE94-000865 .... p 2895 N94-26697 #
DE94-000885 .... p 2821 N94-25980 #
DE94-000901 .... p 2752 N94-26676 #
DE94-000960 .... p 3106 N94-25981 #
DE94-000961 .... p 3033 N94-27614 #
DE94-001060 .... p 2818 N94-26698 #
DE94-001061 .... p 2818 N94-26699 #
DE94-001070 .... p 2708 N94-26930 #
DE94-001122 .... p 2739 N94-26931 #
DE94-001124 .... p 3065 N94-27251 #
DE94-001126 .... p 3062 N94-26932 #
DE94-001133 .... p 3054 N94-26137 #
DE94-001137 .... p 2986 N94-26948 #
DE94-001146 .... p 2767 N94-25950 #
DE94-001166 .... p 2759 N94-26198 #
DE94-001178 .... p 3024 N94-26949 #
DE94-001215 .... p 3045 N94-26950 #
DE94-001334 .... p 3054 N94-26139 #
DE94-001385 .... p 2717 N94-26951 #
DE94-001407 .... p 2813 N94-27615 #
DE94-001408 .... p 2791 N94-26121 #
DE94-001424 .... p 2868 N94-26952 #
DE94-001447 .... p 2733 N94-26070 #
DE94-001504 .... p 3040 N94-27999 #
DE94-001517 .... p 2753 N94-26933 #
DE94-001529 .... p 2819 N94-27018 #
DE94-001538 .... p 2898 N94-26072 #
DE94-001542 .... p 3045 N94-27019 #
DE94-001587 .... p 2967 N94-27020 #
DE94-001602 .... p 3000 N94-27564 #
DE94-001614 .... p 2879 N94-26515 #
DE94-001646 .... p 2699 N94-25926 #
DE94-001676 .... p 2754 N94-27021 #
DE94-001705 .... p 3099 N94-27022 #
DE94-001724 .... p 2892 N94-25951 #
DE94-001741 .... p 2866 N94-25927 #
DE94-001785 .... p 2793 N94-26558 #
DE94-001793 .... p 3073 N94-27002 #
DE94-001799 .... p 3115 N94-27003 #
DE94-001822 .... p 3026 N94-27565 #
DE94-001827 .... p 3040 N94-28000 #
DE94-001831 .... p 2859 N94-27004 #
DE94-001882 .... p 2991 N94-25928 #
DE94-001890 .... p 2699 N94-25929 #
DE94-001923 .... p 2859 N94-27005 #
DE94-001945 .... p 2740 N94-27006 #
DE94-002012 .... p 2981 N94-27092 #
DE94-002017 .... p 2700 N94-25930 #
DE94-002023 .... p 2760 N94-27719 #
DE94-002037 .... p 2739 N94-26912 #
DE94-002156 .... p 3031 N94-25931 #
DE94-002202 .... p 3062 N94-26934 #
DE94-002212 .... p 2739 N94-26935 #
DE94-002213 .... p 3098 N94-26598 #
DE94-002264 .... p 2996 N94-26936 #
DE94-002270 .... p 3118 N94-26937 #
DE94-002278 .... p 2748 N94-25932 #
DE94-002289 .... p 3051 N94-25944 #
DE94-002290 .... p 2857 N94-26700 #
DE94-002291 .... p 2821 N94-25970 #
DE94-002298 .... p 3021 N94-26759 #
DE94-002310 .... p 3008 N94-25988 #
DE94-002316 .... p 3047 N94-27720 #
DE94-002335 .... p 3021 N94-26760 #
DE94-002359 .... p 2895 N94-26761 #
DE94-002360 .... p 2880 N94-26762 #
DE94-002376 .... p 2740 N94-26957 #
DE94-002379 .... p 2794 N94-26763 #
DE94-002406 .... p 3032 N94-26119 #
DE94-002424 .... p 2964 N94-26764 #
DE94-002440 .... p 2866 N94-26123 #
DE94-002446 .... p 2988 N94-27706 #
DE94-002449 .... p 3059 N94-26765 #
DE94-002494 .... p 3098 N94-26559 #
DE94-002525 .... p 2713 N94-26075 #
DE94-002600 .... p 3005 N94-26802 #
DE94-002617 .... p 2771 N94-26803 #
DE94-002619 .... p 2763 N94-26804 #
DE94-002622 .... p 3030 N94-28001 #
DE94-002623 .... p 3094 N94-27707 #
DE94-002625 .... p 3073 N94-26805 #
DE94-002629 .... p 2818 N94-26605 #
DE94-002636 .... p 2991 N94-26079 #
DE94-002637 .... p 2737 N94-26607 #
DE94-002645 .... p 3042 N94-26081 #
DE94-002646 .... p 2750 N94-26124 #
DE94-002647 .... p 2960 N94-26118 #
DE94-002648 .... p 2738 N94-26610 #
DE94-002649 .... p 2704 N94-27708 #
DE94-002651 .... p 2780 N94-25975 #
DE94-002674 .... p 3021 N94-26677 #
DE94-002680 .... p 3042 N94-25976 #
DE94-002681 .... p 3052 N94-25971 #
DE94-002682 .... p 2857 N94-26612 #
DE94-002683 .... p 2857 N94-26617 #
DE94-002690 .... p 3021 N94-26620 #
DE94-002693 .... p 2738 N94-26621 #
DE94-002701 .... p 2816 N94-26126 #
DE94-002705 .... p 3052 N94-25972 #
DE94-002706 .... p 2901 N94-26623 #
DE94-002707 .... p 2980 N94-26120 #
DE94-002714 .... p 2880 N94-26806 #
DE94-002716 .... p 2797 N94-27709 #
DE94-002718 .... p 2986 N94-26807 #
DE94-002722 .... p 2696 N94-26808 #
DE94-002729 .... p 3022 N94-26809 #
DE94-002731 .... p 3063 N94-26958 #
DE94-002733 .... p 2781 N94-25977 #
DE94-002734 .... p 2712 N94-27710 #
DE94-002735 .... p 2839 N94-26810 #
DE94-002738 .... p 2819 N94-26811 #
DE94-002739 .... p 2682 N94-27997 #
DE94-002741 .... p 3061 N94-26856 #
DE94-002742 .... p 2713 N94-25978 #
DE94-002754 .... p 2713 N94-26014 #
DE94-002756 .... p 2963 N94-26407 #
DE94-002777 .... p 2877 N94-26015 #
DE94-002788 .... p 2733 N94-26092 #
DE94-002791 .... p 3044 N94-26858 #
DE94-002792 .... p 3042 N94-26140 #
DE94-002794 .... p 3044 N94-26860 #
DE94-002795 .... p 3045 N94-26861 #
DE94-002796 .... p 3046 N94-27261 #
DE94-002797 .... p 2734 N94-26272 #
DE94-002829 .... p 2735 N94-26273 #
DE94-002830 .... p 2706 N94-26019 #
DE94-002844 .... p 2816 N94-26020 #
DE94-002849 .... p 3052 N94-25989 #
DE94-002856 .... p 2965 N94-26862 #
DE94-002857 .... p 3045 N94-26863 #
DE94-002890 .... p 3043 N94-26274 #
DE94-002891 .... p 3045 N94-26865 #
DE94-002894 .... p 3061 N94-26868 #
DE94-002907 .... p 3055 N94-26275 #
DE94-002913 .... p 3035 N94-26276 #
DE94-002914 .... p 2781 N94-26144 #
DE94-002918 .... p 3018 N94-26145 #
DE94-002922 .... p 2848 N94-26277 #
DE94-002924 .... p 2961 N94-26146 #
DE94-002931 .... p 3056 N94-26308 #
DE94-002933 .... p 2702 N94-26560 #
DE94-002946 .... p 3027 N94-27711 #
DE94-002954 .... p 3054 N94-26147 #
DE94-002961 .... p 2858 N94-26869 #
DE94-002964 .... p 2733 N94-26022 #
DE94-002973 .... p 2858 N94-26871 #
DE94-002975 .... p 2719 N94-27712 #
DE94-002980 .... p 2664 N94-26309 #
DE94-002981 .... p 2857 N94-26747 #
DE94-002982 .... p 2858 N94-26785 #
DE94-002987 .... p 2768 N94-26310 #
DE94-003001 .... p 3104 N94-26786 #
DE94-003003 .... p 3104 N94-26311 #
DE94-003004 .... p 2811 N94-26787 #
DE94-003005 .... p 3022 N94-26769 #
DE94-003008 .... p 2753 N94-26770 #
DE94-003009 .... p 3060 N94-26771 #
DE94-003015 .... p 2965 N94-26775 #
DE94-003016 .... p 2784 N94-26777 #
DE94-003017 .... p 2763 N94-26778 #
DE94-003019 .... p 2782 N94-26312 #
DE94-003022 .... p 3102 N94-26023 #
DE94-003028 .... p 2894 N94-26313 #
DE94-003091 .... p 2704 N94-26779 #
DE94-003103 .... p 2983 N94-27713 #
DE94-003104 .... p 3053 N94-26025 #
DE94-003107 .... p 2979 N94-25952 #
DE94-003108 .... p 2979 N94-25953 #
DE94-003111 .... p 2866 N94-26026 #
DE94-003112 .... p 3060 N94-26780 #
DE94-003119 .... p 3041 N94-25792 #
DE94-003120 .... p 2963 N94-26521 #
DE94-003135 .... p 2791 N94-26096 #
DE94-003138 .... p 2762 N94-26027 #
DE94-003158 .... p 2716 N94-26781 #
DE94-003159 .... p 2732 N94-25954 #
DE94-003161 .... p 3031 N94-26097
DE94-003162 .... p 3046 N94-27686 #
DE94-003164 .... p 3060 N94-26782 #
DE94-003165 .... p 2753 N94-26783 #
DE94-003174 .... p 2965 N94-26784 #
DE94-003192 .... p 2858 N94-26792 #
DE94-003193 .... p 2827 N94-27874 #
DE94-003195 .... p 2852 N94-27875 #
DE94-003196 .... p 3012 N94-25795 #
DE94-003201 .... p 2699 N94-25798 #
DE94-003203 .... p 2707 N94-26099 #
DE94-003206 .... p 3053 N94-26029 #
DE94-003209 .... p 3053 N94-26031 #
DE94-003212 .... p 3015 N94-25955 #
DE94-003224 .... p 3022 N94-26793 #
DE94-003225 .... p 2836 N94-26032 #
DE94-003226 .... p 2819 N94-27262
DE94-003229 .... p 2700 N94-25956 #
DE94-003231 .... p 2716 N94-26794 #
DE94-003240 .... p 2714 N94-26122 #
DE94-003241 .... p 3058 N94-26516 #
DE94-003245 .... p 2789 N94-25597 #
DE94-003247 .... p 3054 N94-26125 #
DE94-003258 .... p 3060 N94-26795 #
DE94-003262 .... p 3054 N94-26128 #
DE94-003269 .... p 2985 N94-26462 #
DE94-003270 .... p 2856 N94-26463 #
DE94-003271 .... p 2962 N94-26318 #
DE94-003275 .... p 2708 N94-26796 #
DE94-003298 .... p 2792 N94-26319 #
DE94-003316 .... p 2715 N94-26320 #
DE94-003317 .... p 3047 N94-27735 #
DE94-003318 .... p 3043 N94-26321 #
DE94-003332 .... p 2824 N94-27181 #
DE94-003361 .... p 3023 N94-26938 #
DE94-003363 .... p 3016 N94-25957 #
DE94-003366 .... p 3042 N94-25958 #
DE94-003371 .... p 2748 N94-25959 #
DE94-003373 .... p 2735 N94-26322 #
DE94-003378 .... p 3011 N94-25598 #
DE94-003379 .... p 3063 N94-27047 #
DE94-003391 .... p 3041 N94-25846 #
DE94-003394 .... p 2877 N94-25847 #
DE94-003399 .... p 3035 N94-26100 #
DE94-003400 .... p 3050 N94-25848 #
DE94-003401 .... p 2859 N94-27048 #
DE94-003402 .... p 3043 N94-26323 #
DE94-003404 .... p 3043 N94-26324 #
DE94-003406 .... p 2836 N94-26129 #
DE94-003408 .... p 2816 N94-26130 #
DE94-003409 .... p 3017 N94-26083 #
DE94-003413 .... p 2760 N94-25849 * #
DE94-003414 .... p 2750 N94-26085 #
DE94-003415 .... p 2733 N94-26087 #
DE94-003418 .... p 2967 N94-27049 #
DE94-003423 .... p 3018 N94-26325 #
DE94-003429 .... p 3024 N94-27050 #
DE94-003432 .... p 3028 N94-27736 #
DE94-003437 .... p 3056 N94-26326 #
DE94-003442 .... p 3017 N94-26101 #
DE94-003451 .... p 3116 N94-27740 #
DE94-003457 .... p 3018 N94-26133 #
DE94-003470 .... p 2706 N94-25982 #
DE94-003477 .... p 2962 N94-26327 #
DE94-003478 .... p 2782 N94-26328 #
DE94-003479 .... p 2781 N94-26047 #
DE94-003480 .... p 2855 N94-26329 #
DE94-003481 .... p 3106 N94-27007 #
DE94-003482 .... p 3032 N94-26330 #
DE94-003483 .... p 2856 N94-26464 #
DE94-003489 .... p 3039 N94-27721 #
DE94-003499 .... p 2827 N94-27722 #
DE94-003502 .... p 2736 N94-26522 #
DE94-003510 .... p 3047 N94-27723 #
DE94-003511 .... p 3041 N94-25923 #
DE94-003533 .... p 3044 N94-26523 #
DE94-003584 .... p 2767 N94-25924 #
DE94-003588 .... p 3041 N94-25933 #
DE94-003589 .... p 2822 N94-26465 #
DE94-003609 .... p 2713 N94-25934 #
DE94-003619 .... p 3015 N94-25935 #
DE94-003624 .... p 2892 N94-25936 #
DE94-003635 .... p 2767 N94-25937 #
DE94-003638 .... p 3068 N94-27724 #
DE94-003639 .... p 2706 N94-25938 #
DE94-003640 .... p 2809 N94-25599 #
DE94-003650 .... p 2715 N94-26369 #
DE94-003660 .... p 2749 N94-26005 #
DE94-003662 .... p 2760 N94-27725 #
DE94-003664 .... p 2749 N94-26007 #
DE94-003669 .... p 2962 N94-26370 #
DE94-003671 .... p 2962 N94-26371 #
DE94-003672 .... p 2821 N94-25811 #
DE94-003675 .... p 2783 N94-26372 #
DE94-003704 .... p 2960 N94-26048 #
DE94-003709 .... p 2780 N94-25812 #
DE94-003716 .... p 2792 N94-26331 #
DE94-003718 .... p 3100 N94-27563 #
DE94-003728 .... p 3096 N94-25813 #
DE94-003731 .... p 3097 N94-26348 #
DE94-003765 .... p 2735 N94-26349 #
DE94-003769 .... p 3050 N94-25814 #
DE94-003771 .... p 3050 N94-25815 #
DE94-003782 .... p 2750 N94-26332 #
DE94-003785 .... p 2757 N94-27726 #
DE94-003788 .... p 2699 N94-25600 #
DE94-003795 .... p 3013 N94-25816 #
DE94-003798 .... p 3070 N94-28067 #

DE94-003801 p 3050 N94-25817 #
DE94-003802 p 3049 N94-25601 #
DE94-003803 p 2958 N94-25818 #
DE94-003804 p 2732 N94-25819 #
DE94-003810 p 3017 N94-26049 #
DE94-003826 p 3097 N94-26350 #
DE94-003846 p 3042 N94-26132 #
DE94-003864 p 2736 N94-26351 #
DE94-003865 p 3055 N94-26238 #
DE94-003867 p 2838 N94-26524 #
DE94-003880 p 2810 N94-26525 #
DE94-003886 p 3053 N94-26094 #
DE94-003890 p 3054 N94-26095 #
DE94-003892 p 2732 N94-26004 #
DE94-003918 p 2956 N94-25602 #
DE94-003934 p 3111 N94-27742 #
DE94-003936 p 3012 N94-25612 #
DE94-003938 p 2699 N94-25613 #
DE94-003941 p 2985 N94-25983 #
DE94-003943 p 2933 N94-27744 #
DE94-003958 p 2704 N94-27745 #
DE94-003959 p 2757 N94-27747 #
DE94-003961 p 2851 N94-27727 #
DE94-003963 p 2719 N94-27728 #
DE94-003965 p 3013 N94-25820 #
DE94-003966 p 3007 N94-27777 #
DE94-003981 p 2980 N94-25984 #
DE94-003982 p 2959 N94-25821 #
DE94-004003 p 2814 N94-27779 #
DE94-004007 p 3055 N94-26239 #
DE94-004012 p 2809 N94-25662 #
DE94-004014 p 2957 N94-25663 #
DE94-004019 p 2749 N94-25985 #
DE94-004040 p 2732 N94-25822 #
DE94-004161 p 3027 N94-27689 #
DE94-004162 p 2960 N94-25986 #
DE94-004166 p 3047 N94-27690 #
DE94-004168 p 2749 N94-25973 #
DE94-004169 p 3058 N94-26526 #
DE94-004177 p 3012 N94-25800 #
DE94-004180 p 2869 N94-27691 #
DE94-004185 p 3041 N94-25801 #
DE94-004189 p 2732 N94-25974 #
DE94-004204 p 3020 N94-26527 #
DE94-004211 p 3102 N94-26528 #
DE94-004212 p 2751 N94-26554 #
DE94-004218 p 2979 N94-25802 #
DE94-004219 p 3118 N94-27566 #
DE94-004236 p 2719 N94-27567 #
DE94-004237 p 2721 N94-28069 #
DE94-004243 p 3046 N94-27568 #
DE94-004244 p 3020 N94-26574 #
DE94-004247 p 2741 N94-27616 #
DE94-004260 p 3000 N94-27569 #
DE94-004264 p 2737 N94-26575 #
DE94-004268 p 2741 N94-27570 #
DE94-004269 p 2731 N94-25803 #
DE94-004276 p 2897 N94-27571 #
DE94-004279 p 2869 N94-27267 #
DE94-004280 p 2879 N94-26576 #
DE94-004290 p 2732 N94-25987 #
DE94-004293 p 2941 N94-26555 #
DE94-004307 p 2737 N94-26556 #
DE94-004308 p 2731 N94-25804 #
DE94-004312 p 2705 N94-25805 #
DE94-004318 p 2982 N94-27600 #
DE94-004334 p 3020 N94-26577 #
DE94-004351 p 2948 N94-26578 #
DE94-004356 p 2869 N94-27601 #
DE94-004371 p 3067 N94-27602 #
DE94-004406 p 3039 N94-27603 #
DE94-004411 p 3044 N94-26579 #
DE94-004418 p 3026 N94-27604 #
DE94-004428 p 2751 N94-26580 #
DE94-004447 p 2737 N94-26582 #
DE94-004451 p 2797 N94-27617 #
DE94-004544 p 2708 N94-26557 #
DE94-004555 p 2787 N94-27618 #
DE94-004558 p 2741 N94-27619 #
DE94-004581 p 3026 N94-27620 #
DE94-004583 p 2780 N94-25806 #
DE94-004589 p 2737 N94-26585 #
DE94-004593 p 3116 N94-27621 #
DE94-004596 p 2741 N94-27622 #
DE94-004597 p 2827 N94-27780 #
DE94-004602 p 2737 N94-26587 #
DE94-004603 p 2783 N94-26589 #
DE94-004608 p 3059 N94-26591 #
DE94-004618 p 2820 N94-27781 #
DE94-004625 p 2751 N94-26594 #
DE94-004627 p 3055 N94-26243 #
DE94-004640 p 3018 N94-26244 #
DE94-004642 p 3029 N94-27783 #
DE94-004655 p 3018 N94-26245 #
DE94-004656 p 3028 N94-27748 #
DE94-004660 p 3028 N94-27749 #
DE94-004662 p 3103 N94-27750 #
DE94-004663 p 3028 N94-27752 #
DE94-004671 p 3035 N94-26246 #
DE94-004678 p 2838 N94-26563 #
DE94-004684 p 2751 N94-26564 #
DE94-004685 p 2750 N94-26247 #
DE94-004690 p 3058 N94-26565 #
DE94-004691 p 3069 N94-27753 #
DE94-004692 p 2780 N94-25664 #
DE94-004693 p 3056 N94-26352 #
DE94-004695 p 2742 N94-27755 #
DE94-004738 p 3069 N94-27757 #
DE94-004744 p 3048 N94-27785 #
DE94-004787 p 2742 N94-27786 #
DE94-004798 p 2742 N94-27788 #
DE94-004799 p 3069 N94-27790 #
DE94-004860 p 3048 N94-27791 #
DE94-004886 p 3029 N94-27811 #
DE94-004888 p 2712 N94-27813 #
DE94-004946 p 3029 N94-27814 #
DE94-004956 p 3029 N94-27815 #
DE94-004959 p 2756 N94-27692 #
DE94-004976 p 2743 N94-27792 #
DE94-004977 p 3116 N94-27793 #
DE94-004981 p 3116 N94-27714 #
DE94-004985 p 2897 N94-28146 #
DE94-004990 p 3005 N94-27816 #
DE94-004993 p 3048 N94-27825 #
DE94-004999 p 3117 N94-27826 #
DE94-005006 p 3117 N94-27827 #
DE94-005009 p 3069 N94-27828 #
DE94-005015 p 3047 N94-27715 #
DE94-005120 p 2757 N94-27716 #
DE94-005125 p 2973 N94-27717 #
DE94-005206 p 3068 N94-27693 #
DE94-005215 p 2742 N94-27694 #
DE94-005558 p 2757 N94-27695 #
DE94-600563 p 2715 N94-26391 #
DE94-600652 p 2715 N94-26392 #
DE94-600760 p 3056 N94-26363 #
DE94-600821 p 3056 N94-26364 #
DE94-600882 p 2878 N94-26365 #
DE94-601287 p 3117 N94-27996
DE94-601504 p 2994 N94-26458
DE94-601505 p 2992 N94-26366 #
DE94-601506 p 2994 N94-26459
DE94-601507 p 3006 N94-26460
DE94-601508 p 3073 N94-26758
DE94-601509 p 3072 N94-26461
DE94-601510 p 2992 N94-26367 #
DE94-601535 p 2998 N94-27162
DE94-601536 p 2993 N94-26408
DE94-601537 p 3063 N94-27017
DE94-601538 p 2993 N94-26409
DE94-601541 p 3006 N94-26368 #
DE94-601542 p 2993 N94-26410 #
DE94-601543 p 3006 N94-26411 #
DE94-601544 p 2993 N94-26412 #
DE94-601551 p 3019 N94-26423 #
DE94-601552 p 3019 N94-26424 #
DE94-601553 p 2993 N94-26425 #
DE94-601555 p 3006 N94-26413 #
DE94-601556 p 3006 N94-26414 #
DE94-601557 p 3006 N94-26415 #
DE94-601558 p 3019 N94-26416 #
DE94-601559 p 3072 N94-26417 #
DE94-601560 p 2878 N94-26418 #
DE94-601561 p 3071 N94-25882 #
DE94-601562 p 3071 N94-25883 #
DE94-601563 p 2991 N94-25884 #
DE94-601565 p 3051 N94-25885 #
DE94-601566 p 3006 N94-25886 #
DE94-601605 p 3014 N94-25887 #
DE94-601607 p 3014 N94-25888 #
DE94-601608 p 3014 N94-25889 #
DE94-601615 p 3015 N94-25890 #
DE94-601620 p 3015 N94-25891 #
DE94-601623 p 3013 N94-25837 #
DE94-601624 p 2990 N94-25838 #
DE94-601642 p 3013 N94-25839 #
DE94-601669 p 3117 N94-28066 #
DE94-601671 p 3014 N94-25840 #
DE94-601704 p 3014 N94-25841 #
DE94-601711 p 3018 N94-26333
DE94-601812 p 3023 N94-26942
DE94-601813 p 3023 N94-26943
DE94-601814 p 3023 N94-26944
DE94-601815 p 3014 N94-25842 #
DE94-601816 p 3023 N94-26945
DE94-601817 p 3045 N94-26946
DE94-601818 p 3023 N94-26947
DE94-601819 p 3062 N94-26927
DE94-601820 p 3018 N94-26334
DE94-601838 p 3050 N94-25843 #
DE94-601853 p 3007 N94-26928
DE94-601874 p 3062 N94-26897
DE94-601875 p 2714 N94-26169
DE94-601876 p 2714 N94-26170
DE94-601883 p 3055 N94-26171
DE94-601884 p 2748 N94-25844 #
DE94-601912 p 3063 N94-26987
DE94-601913 p 3023 N94-26929
DE94-601943 p 3051 N94-25945
DE94-601975 p 2880 N94-26874
DE94-601992 p 3073 N94-26837
DE94-602520 p 3073 N94-26876 #
DE94-602538 p 3061 N94-26878 #
DE94-602539 p 3061 N94-26879
DE94-602557 p 3073 N94-26896 #
DE94-602558 p 2996 N94-26898
DE94-602559 p 2997 N94-27023
DE94-602560 p 3073 N94-27024
DE94-602576 p 3022 N94-26899
DE94-602600 p 3022 N94-26900
DE94-602717 p 3062 N94-26901
DE94-602732 p 3062 N94-26902 #
DE94-602737 p 2720 N94-27998
DE94-602981 p 2743 N94-27829 #
DE94-602982 p 2743 N94-27832 #
DE94-603006 p 3029 N94-27834 #
DE94-603009 p 2758 N94-27837
DE94-603653 p 3001 N94-27839
DE94-603656 p 3000 N94-27818
DE94-603657 p 3069 N94-27819
DE94-603663 p 3074 N94-27626
DE94-603664 p 3074 N94-27627
DE94-603665 p 2787 N94-27628
DE94-603666 p 3027 N94-27629
DE94-603667 p 3046 N94-27630
DE94-603668 p 3027 N94-27631
DE94-603669 p 3000 N94-27632 #
DE94-603670 p 3007 N94-27633
DE94-603671 p 3067 N94-27634
DE94-603672 p 3067 N94-27635
DE94-603673 p 3074 N94-27636
DE94-603674 p 3000 N94-27637
DE94-603677 p 3067 N94-27638
DE94-603716 p 3067 N94-27647
DE94-603717 p 3074 N94-27696
DE94-603898 p 3068 N94-27729 #
DE94-603989 p 3067 N94-27623
DE94-604013 p 3068 N94-27677
DE94-604016 p 3068 N94-27678
DE94-604074 p 2717 N94-26988
DE94-604079 p 3068 N94-27697
DE94-604133 p 3070 N94-27843
DE94-604181 p 3047 N94-27698
DE94-604605 p 2742 N94-27730 #
DE94-604652 p 2981 N94-26903
DE94-604986 p 3048 N94-27844
DE94-604994 p 3049 N94-27855
DE94-604995 p 3049 N94-27856
DE94-605011 p 2758 N94-27845
DE94-605039 p 2758 N94-27857
DE94-606300 p 3001 N94-27846 #
DE94-606301 p 3029 N94-27847 #
DE94-606330 p 3029 N94-27848
DE94-606341 p 3075 N94-27858 #
DE94-606406 p 3070 N94-27859 #
DE94-606407 p 3068 N94-27679 #
DE94-606415 p 3074 N94-27680 #
DE94-606458 p 3027 N94-27681 #
DE94-606459 p 3027 N94-27682 #
DE94-606495 p 3030 N94-27860 #
DE94-606752 p 3030 N94-27861 #
DE94-701085 p 2903 N94-27862 #
DE94-701104 p 2744 N94-27876 #
DE94-701107 p 3030 N94-27877
DE94-701113 p 3047 N94-27699 #
DE94-701115 p 3027 N94-27718 #
DE94-701165 p 2983 N94-27804
DE94-701173 p 3100 N94-27700 #
DE94-701175 p 2743 N94-27807
DE94-701176 p 2820 N94-27701 #
DE94-701187 p 2989 N94-27809
DE94-701190 p 2973 N94-27702 #
DE94-701194 p 3029 N94-27820 #
DE94-701195 p 2813 N94-27703 #
DE94-701200 p 2757 N94-27812 #
DE94-701204 p 2788 N94-27817
DE94-701207 p 2788 N94-27821 #
DE94-701208 p 3000 N94-27731 #
DE94-701224 p 2973 N94-27732 #
DE94-701314 p 3027 N94-27733 #
DE94-701317 p 2719 N94-27822 #
DE94-702060 p 2855 N94-26240 #
DE94-702061 p 2867 N94-26241 #
DE94-702065 p 2855 N94-26242 #
DE94-725198 p 2868 N94-26904 #
DE94-725199 p 2858 N94-26913 #
DE94-725201 p 2760 N94-26914
DE94-725203 p 2858 N94-26838

DE94-725205 .... p 2759 N94-26905

DIGEL-1992-9 .... p 2779 N94-25618 #
DIGEL-1993-6 .... p 2779 N94-25620 #
DIGEL-1993-7 .... p 3031 N94-25619 #

DLR-FB-90-58 .... p 2768 N94-26315 #
DLR-FB-91-32 .... p 2768 N94-26317 #
DLR-FB-93-01 .... p 2797 N94-27588 #
DLR-FB-93-02 .... p 2826 N94-27589 #
DLR-FB-93-10 .... p 3066 N94-27590 #
DLR-FB-93-13 .... p 2826 N94-27591 #
DLR-FB-93-16 .... p 2647 N94-27592 #
DLR-FB-93-17 .... p 2675 N94-27593 #
DLR-FB-93-18 .... p 2777 N94-27738 #
DLR-FB-93-20 .... p 2675 N94-27739 #
DLR-FB-93-21 .... p 2648 N94-27741 #
DLR-FB-93-23 .... p 2903 N94-27743 #
DLR-FB-93-24 .... p 2660 N94-27746 #
DLR-FB-93-25 .... p 2897 N94-27751 #
DLR-FB-93-26 .... p 2903 N94-27754 #

DLR-MITT-93-04 .... p 2858 N94-26813 #
DLR-MITT-93-10 .... p 2681 N94-27587 #

DMM(A)-107 .... p 2748 N94-25893
DMM(A)-120 .... p 2748 N94-25892

DODA-AR-007-102 .... p 2794 N94-26801
DODA-AR-008-223 .... p 2809 N94-26358 #
DODA-AR-008-267 .... p 2839 N94-26859
DODA-AR-008-367 .... p 2644 N94-26342 #
DODA-AR-008-404 .... p 2838 N94-26501 #
DODA-AR-008-565 .... p 2669 N94-26864

DOE/CE-23810/15 .... p 2756 N94-27692 #
DOE/CE-23810/20D-PT-2 .... p 2749 N94-26007 #
DOE/CE-23810/22A .... p 2719 N94-27567 #
DOE/CE-23810/22B .... p 2721 N94-28069 #
DOE/CE-23810/22C .... p 2713 N94-25934 #

DOE/EIA-0174(92) .... p 2859 N94-27048 #

DOE/ER-00881/T3 .... p 3026 N94-27565 #
DOE/ER-0593T .... p 3043 N94-26428 #
DOE/ER-13552/10 .... p 2960 N94-25986 #
DOE/ER-13564/12 .... p 2749 N94-25973 #
DOE/ER-13569/8 .... p 2715 N94-26369 #
DOE/ER-13996/4 .... p 2716 N94-26781 #
DOE/ER-14017/5 .... p 3050 N94-25848 #
DOE/ER-14079/29 .... p 2877 N94-25847 #
DOE/ER-14104/4 .... p 3058 N94-26526 #
DOE/ER-14147/3 .... p 2792 N94-26468 #
DOE/ER-14283/1 .... p 3021 N94-26760 #
DOE/ER-25068/3 .... p 2967 N94-27020 #
DOE/ER-25100/2 .... p 2959 N94-25821 #
DOE/ER-25118/1 .... p 2956 N94-25602 #
DOE/ER-25137/1 .... p 2991 N94-25928 #
DOE/ER-40343/7 .... p 3021 N94-26586 #
DOE/ER-40414/6 .... p 3029 N94-27783 #
DOE/ER-40427/10-N93 .... p 3022 N94-26809 #
DOE/ER-40445/43 .... p 3018 N94-26244 #
DOE/ER-40448/6 .... p 3027 N94-27689 #
DOE/ER-40581/3 .... p 3073 N94-27002 #
DOE/ER-40592/3 .... p 3026 N94-27604 #
DOE/ER-40623/2 .... p 3115 N94-27003 #
DOE/ER-40654/3 .... p 3032 N94-26119 #
DOE/ER-40661/5 .... p 3033 N94-27614 #
DOE/ER-40677/2-PT-2 .... p 3029 N94-27815 #
DOE/ER-40685/759 .... p 3008 N94-25988 #
DOE/ER-40688/2 .... p 3031 N94-25931 #
DOE/ER-40692/2 .... p 3031 N94-26097
DOE/ER-40698/2 .... p 3024 N94-26949 #
DOE/ER-40756/1 .... p 3012 N94-25800 #
DOE/ER-45132/8 .... p 3060 N94-26780 #
DOE/ER-45184/9 .... p 2732 N94-25954 #
DOE/ER-45191/23 .... p 3063 N94-26958 #
DOE/ER-45217/8 .... p 2753 N94-26783 #
DOE/ER-45347/33 .... p 3021 N94-26677 #
DOE/ER-45370/T1 .... p 2749 N94-26005 #
DOE/ER-45414/3 .... p 3060 N94-26782 #
DOE/ER-45445/9 .... p 2733 N94-26070 #
DOE/ER-52111/6 .... p 3044 N94-26579 #
DOE/ER-52158/11 .... p 3046 N94-27686 #
DOE/ER-53198/227 .... p 3042 N94-26132 #
DOE/ER-53211/12 .... p 3047 N94-27720 #
DOE/ER-53222/108 .... p 3047 N94-27735 #
DOE/ER-53291/225 .... p 2793 N94-26558 #
DOE/ER-54111/3 .... p 3041 N94-25846 #
DOE/ER-54139/2 .... p 3047 N94-27690 #
DOE/ER-54197/1 .... p 3044 N94-26523 #
DOE/ER-60245/T2 .... p 2892 N94-25939 #
DOE/ER-60304/9 .... p 2865 N94-25789 #
DOE/ER-60485/5 .... p 2866 N94-25927 #
DOE/ER-60932/3 .... p 2866 N94-26026 #
DOE/ER-61010/T10 .... p 2865 N94-25790 #
DOE/ER-61010/T14 .... p 2877 N94-26015 #
DOE/ER-61054/3 .... p 2898 N94-25791 #
DOE/ER-61064/3 .... p 2767 N94-25950 #
DOE/ER-61065/3 .... p 2893 N94-26082 #
DOE/ER-61365/T1 .... p 2895 N94-26697 #
DOE/ER-61365/T2 .... p 3106 N94-25981 #
DOE/ER-61443/2 .... p 3035 N94-26100 #
DOE/ER-61457/T1 .... p 2892 N94-25951 #
DOE/ER-61477/1 .... p 2866 N94-26077 #
DOE/ER-75531/1 .... p 3039 N94-27603 #
DOE/ER-80910/94/C0267 .... p 2859 N94-27005 #
DOE/ER-81453/94/C0261 .... p 2858 N94-26785 #

DOE/ET-0004-12 .... p 3097 N94-26350 #
DOE/ET-53088/T4 .... p 2791 N94-26096 #
DOE/ET-53088/623 .... p 3041 N94-25923 #
DOE/ET-53088/627 .... p 3041 N94-25792 #
DOE/ET-53088/629 .... p 2963 N94-26521 #
DOE/ET-53088/632 .... p 3047 N94-27723 #
DOE/ET-53088/633 .... p 3042 N94-25958 #

DOE/FTR-93013716 .... p 2853 N94-25946 #

DOE/ID-12692/4 .... p 2756 N94-27611 #

DOE/MC-23166/94/C0236 .... p 2827 N94-27874 #
DOE/MC-26006/94/C0252 .... p 2858 N94-26792 #
DOE/MC-27227/3471 .... p 2856 N94-26581 #
DOE/MC-28055/94/C0251 .... p 2858 N94-26871 #
DOE/MC-28055/94/C0253 .... p 2858 N94-26869 #
DOE/MC-29224/94/C0262 .... p 2857 N94-26747 #

DOE/METC-C/94/7106 .... p 2719 N94-27712 #

DOE/NASA/0374-1 .... p 2827 N94-27984 * #

DOE/NBM-94000014 .... p 2857 N94-26583 #
DOE/NBM-94000015 .... p 2857 N94-26584 #

DOE/NE-32170/23 .... p 2699 N94-25926 #

DOE/OR-00033/T552 .... p 3041 N94-25949 #
DOE/OR-00033/T554 .... p 2877 N94-25979 #
DOE/OR-00033/T564 .... p 2813 N94-27615 #
DOE/OR-00033/T565 .... p 2791 N94-26121 #
DOE/OR-22089/3 .... p 2879 N94-26515 #

DOE/PC-92540/T3 .... p 2792 N94-26319 #

DOE/SF-19043/T4 .... p 2700 N94-25969 #
DOE/SF-19441/T5 .... p 2699 N94-25929 #
DOE/SF-19441/T6 .... p 2700 N94-25930 #

DOT-VNTSC-FAA-93-13-VOL-1 ... p 2836 N94-26186 #
DOT-VNTSC-FAA-93-13-VOL-2 ... p 2837 N94-26357 #
DOT-VNTSC-FAA-93-19 .... p 3009 N94-25731 #

DOT/FAA/AM-94/4 .... p 2938 N94-26600 #
DOT/FAA/AM-94/5 .... p 2941 N94-26136 #

DOT/FAA/CT-TN-93/37 .... p 2664 N94-26197

DOT/FAA/CT-TN93/30 .... p 2664 N94-25788 #
DOT/FAA/CT-TN93/40 .... p 2660 N94-27081 #
DOT/FAA/CT-TN93/44 .... p 2672 N94-26030 #

DOT/FAA/CT-91/27 .... p 2668 N94-26488 #
DOT/FAA/CT-92/29 .... p 2673 N94-26176 #
DOT/FAA/CT-93/16-VOL-3 .... p 2672 N94-26028 #
DOT/FAA/CT-93/5-VOL-1 .... p 2771 N94-26854 #
DOT/FAA/CT-93/5-VOL-2 .... p 2771 N94-26836 #
DOT/FAA/CT-93/5-VOL-3 .... p 2772 N94-26980 #
DOT/FAA/CT-93/69-VOL-1 .... p 2836 N94-26186 #
DOT/FAA/CT-93/69-VOL-2 .... p 2837 N94-26357 #
DOT/FAA/CT-93/7 .... p 2669 N94-27105 #
DOT/FAA/CT-93/80 .... p 2680 N94-26202 #
DOT/FAA/CT-94/03 .... p 2641 N94-27284 * #

DOT/FAA/EE-93-03 .... p 3009 N94-25731 #

DOT/FAA/RD-93/1 .... p 2680 N94-26196
DOT/FAA/RD-93/22 .... p 2665 N94-26826 #
DOT/FAA/RD-93/33 .... p 2772 N94-26963

DOT/FAA/TN93/42 .... p 2680 N94-26200 #

DRA-TR-93057 .... p 2845 N94-27954 #

DREA-CR-92-416 .... p 2820 N94-27668

DREO-1010 .... p 2813 N94-27597
DREO-16 .... p 2973 N94-27761
DREO-16 .... p 2975 N94-27951

DREP-TM-93-53 .... p 2670 N94-27666
DREP-92-32 .... p 2969 N94-27318
DREP-93-09 .... p 2665 N94-27667

DREV-4712-93 .... p 3038 N94-27598

DSIS-94-00040 .... p 2820 N94-27668
DSIS-94-00049 .... p 2665 N94-27667
DSIS-94-00051 .... p 2973 N94-27761
DSIS-94-00053 .... p 2813 N94-27317
DSIS-94-00054 .... p 2974 N94-27823
DSIS-94-00056 .... p 2973 N94-27762
DSIS-94-00071 .... p 2942 N94-27683
DSIS-94-00099 .... p 2670 N94-27666
DSIS-94-00101 .... p 2813 N94-27597
DSIS-94-00102 .... p 3038 N94-27598
DSIS-94-00110 .... p 2975 N94-27951
DSIS-94-00111 .... p 2814 N94-27763
DSIS-94-00165 .... p 2983 N94-28042
DSIS-94-00230 .... p 2969 N94-27318

DSK-9734-H-92 .... p 2660 N94-28230 #

E-7400 .... p 2826 N94-27599 * #
E-7535 .... p 2846 N94-28227 * #
E-7766 .... p 2675 N94-27778 * #
E-8080 .... p 2690 N94-26142 * #
E-8117 .... p 2843 N94-27559 * #
E-8124 .... p 2845 N94-27865 * #
E-8238 .... p 2685 N94-27358 * #
E-8253 .... p 2700 N94-26090 * #
E-8272 .... p 2692 N94-27436 * #
E-8285 .... p 2680 N94-26141 * #
E-8342 .... p 2741 N94-27426 * #
E-8386 .... p 2703 N94-27662 * #
E-8409 .... p 2674 N94-26573 * #
E-8476 .... p 2834 N94-26199 * #
E-8480 .... p 2691 N94-27424 * #
E-8494 .... p 2843 N94-27776 * #
E-8496 .... p 2839 N94-26692 * #
E-8513 .... p 2701 N94-26208 * #
E-8521 .... p 2644 N94-26131 * #
E-8550 .... p 2843 N94-27656 * #
E-8612 .... p 2701 N94-26209 * #
E-8630 .... p 2675 N94-27654 * #
E-8633 .... p 2826 N94-27657 * #
E-8646 .... p 2693 N94-27427 * #
E-8651 .... p 2711 N94-27640 * #
E-8654 .... p 2678 N94-27414 * #
E-8658 .... p 2845 N94-28181 * #
E-8659 .... p 2846 N94-28266 * #

ECL-92-35 .... p 2789 N94-25654 #
ECL-92-62 .... p 2750 N94-26088 #

EGG-M-93127 .... p 3061 N94-26868 #

ENG-200-30 .... p 2789 N94-25605 #

EOARD-TR-94-01 .... p 3055 N94-26194

ER-40685-765 .... p 3013 N94-25839 #

ERDEC-SP-012 .... p 2900 N94-25593 #

ERDEC-TR-126 .... p 2838 N94-26448 #

ERP-1113 .... p 2893 N94-26168 #
ERP-1124 .... p 2892 N94-25873
ERP-1129 .... p 2773 N94-27085 #

ESA-HSR-SPECIAL .... p 2689 N94-28207 #

ESA-PSS-01-609-ISSUE-1 .... p 2696 N94-27397 #
ESA-PSS-04-151-ISSUE-1 .... p 2693 N94-27583 #

ESA-STM-249 .... p 2972 N94-27582 #

ESA-TT-1264 .... p 2768 N94-26315 #
ESA-TT-1274 .... p 2791 N94-26316 #
ESA-TT-1284 .... p 2768 N94-26317 #
ESA-TT-1289 .... p 2699 N94-25636 #

ESC-TR-93-187 .... p 2959 N94-25855 #
ESC-TR-93-254 .... p 3049 N94-25645 #

ESDU-68006 .... p 2807 N94-28139
ESDU-75024 .... p 2720 N94-28058
ESDU-79029 .... p 2721 N94-28138
ESDU-93001 .... p 2720 N94-27959
ESDU-93001 .... p 2829 N94-28055
ESDU-93002-PT-2 .... p 2830 N94-28056
ESDU-93004 .... p 2830 N94-28073
ESDU-93005 .... p 2830 N94-28074
ESDU-93006 .... p 2830 N94-28075
ESDU-93007 .... p 2648 N94-28057
ESDU-93008 .... p 2720 N94-28058

ESDU-93009 p 2720 N94-28059
ESDU-93010 p 2720 N94-28060
ESDU-93011 p 2845 N94-28061
ESDU-93012 p 2720 N94-28062
ESDU-93013 p 2648 N94-28063
ESDU-93014 p 2806 N94-28064
ESDU-93015 p 2649 N94-28076
ESDU-93016 p 2976 N94-28137
ESDU-93017 p 2721 N94-28138
ESDU-93018-PT-2 p 2807 N94-28139
ESDU-93019 p 2649 N94-28140
ESDU-93020 p 2649 N94-28091
ESDU-93021 p 2670 N94-28092
ESDU-93022 p 2832 N94-28093
ESDU-93023 p 2670 N94-28094
ESDU-93024-PT-1 p 2806 N94-28095
ESDU-93026-PT-3 p 2807 N94-28096
ESDU-93027 p 3011 N94-28141
ESDU-93028 p 2721 N94-28142
ESDU-93029 p 2721 N94-28097
ESDU-93030 p 2845 N94-28143
ESDU-93032 p 2649 N94-28144
ESDU-93033 p 2645 N94-28145
ESDU-93034 p 2648 N94-27955

ESL-TR-92-30 p 2759 N94-26800

ESL-721563-6 p 2785 N94-27027 #

ESM-50 p 3023 N94-26942
ESM-52 p 3023 N94-26943
ESM-53 p 3023 N94-26944
ESM-54 p 3014 N94-25842 #
ESM-55 p 3023 N94-26945

ET/EM-1993-16 p 2881 N94-26880
ET/EM-1993-17 p 2772 N94-26909
ET/EM-1993-18 p 2771 N94-26877

ETDE/JP-MF-94725198 p 2868 N94-26904 #
ETDE/JP-MF-94725199 p 2858 N94-26913 #

ETDE/PUB-3-REV-1 p 3098 N94-26398

ETN-94-80513 p 2867 N94-26474 #
ETN-94-93902 p 2644 N94-26104 #
ETN-94-94111 p 2975 N94-27936 #
ETN-94-94804 p 2834 N94-26008 #
ETN-94-94805 p 2992 N94-26226 #
ETN-94-94807 p 2969 N94-27396 #
ETN-94-94808 p 2992 N94-26227
ETN-94-94812 p 3094 N94-26314 #
ETN-94-94821 p 2847 N94-26228
ETN-94-94833 p 2992 N94-26229
ETN-94-94891 p 2767 N94-26105
ETN-94-94902 p 2779 N94-25618 #
ETN-94-94936 p 2784 N94-26646
ETN-94-94937 p 2811 N94-26647
ETN-94-94941 p 3036 N94-26648
ETN-94-94944 p 3036 N94-26649
ETN-94-94947 p 2770 N94-26650
ETN-94-94954 p 2809 N94-25637 #
ETN-94-94955 p 3031 N94-25619 #
ETN-94-94956 p 2779 N94-25620 #
ETN-94-94957 p 2680 N94-26305
ETN-94-95032 p 2960 N94-26106
ETN-94-95033 p 2847 N94-26107 #
ETN-94-95034 p 2848 N94-26651 #
ETN-94-95035 p 2665 N94-26539 #
ETN-94-95036 p 2899 N94-26108 #
ETN-94-95042 p 3020 N94-26540
ETN-94-95043 p 2814 N94-28098
ETN-94-95044 p 3072 N94-26541 #
ETN-94-95045 p 2995 N94-26812 #
ETN-94-95065 p 2807 N94-28099
ETN-94-9512 p 2868 N94-26774 #
ETN-94-95197 p 2699 N94-25638 #
ETN-94-95199 p 2948 N94-26713
ETN-94-95206 p 2858 N94-26813 #
ETN-94-95209 p 2712 N94-25745 #
ETN-94-95210 p 2817 N94-26203 #
ETN-94-95211 p 2876 N94-25807 #
ETN-94-95212 p 2768 N94-26232 #
ETN-94-95213 p 2837 N94-26233 #
ETN-94-95214 p 2762 N94-25775 #
ETN-94-95215 p 2790 N94-25778 #
ETN-94-95216 p 3005 N94-25823 #
ETN-94-95217 p 3005 N94-25781 #
ETN-94-95221 p 2765 N94-25639 #
ETN-94-95222 p 2676 N94-25640 #
ETN-94-95223 p 2752 N94-26652
ETN-94-95224 p 2738 N94-26653
ETN-94-95225 p 2965 N94-26816
ETN-94-95226 p 2644 N94-26248 #
ETN-94-95232 p 3031 N94-25621 #
ETN-94-95233 p 2762 N94-25641 #
ETN-94-95235 p 2957 N94-25642 #
ETN-94-95237 p 2836 N94-25650 #
ETN-94-95238 p 2731 N94-25643 #
ETN-94-95239 p 2779 N94-25644 #
ETN-94-95240 p 2990 N94-25733 #
ETN-94-95244 p 2848 N94-26253 #
ETN-94-95246 p 2841 N94-27186 #
ETN-94-95247 p 2704 N94-25734 #
ETN-94-95249 p 2664 N94-25808 #
ETN-94-95250 p 2762 N94-25622 #
ETN-94-95251 p 2731 N94-25623 #
ETN-94-95252 p 2731 N94-25784 #
ETN-94-95258 p 2961 N94-26254 #
ETN-94-95259 p 2837 N94-26255 #
ETN-94-95260 p 2708 N94-26544 #
ETN-94-95261 p 3058 N94-26545 #
ETN-94-95262 p 2822 N94-26306 #
ETN-94-95263 p 2837 N94-26307 #
ETN-94-95264 p 2682 N94-26249 #
ETN-94-95265 p 2695 N94-26250 #
ETN-94-95266 p 2714 N94-26251 #
ETN-94-95267 p 3008 N94-26256 #
ETN-94-95268 p 2835 N94-26257 #
ETN-94-95269 p 2850 N94-27182 #
ETN-94-95270 p 2848 N94-26258 #
ETN-94-95271 p 2762 N94-26259 #
ETN-94-95272 p 2707 N94-26260 #
ETN-94-95273 p 2762 N94-26261 #
ETN-94-95274 p 2837 N94-26262 #
ETN-94-95275 p 2704 N94-25651 #
ETN-94-95276 p 2679 N94-25652 #
ETN-94-95277 p 2676 N94-25653 #
ETN-94-95278 p 2660 N94-28230 #
ETN-94-95279 p 2789 N94-25654 #
ETN-94-95280 p 2750 N94-26088 #
ETN-94-95281 p 2752 N94-26654
ETN-94-95282 p 2964 N94-26655
ETN-94-95283 p 2866 N94-25809 #
ETN-94-95284 p 2954 N94-27191 #
ETN-94-95286 p 2696 N94-27397 #
ETN-94-95287 p 2768 N94-26315 #
ETN-94-95288 p 2791 N94-26316 #
ETN-94-95289 p 2768 N94-26317 #
ETN-94-95339 p 3019 N94-26478 #
ETN-94-95340 p 2792 N94-26479 #
ETN-94-95341 p 3002 N94-26000 #
ETN-94-95342 p 3016 N94-26002 #
ETN-94-95343 p 2834 N94-26003 #
ETN-94-95344 p 2817 N94-26225 #
ETN-94-95345 p 2752 N94-26645
ETN-94-95374 p 2690 N94-25787
ETN-94-95375 p 2847 N94-25746 #
ETN-94-95388 p 2712 N94-25747 #
ETN-94-95389 p 2747 N94-25748 #
ETN-94-95390 p 2747 N94-25749
ETN-94-95391 p 2750 N94-26211 #
ETN-94-95392 p 2641 N94-26212 #
ETN-94-95394 p 3002 N94-26213 #
ETN-94-95395 p 2837 N94-26214 #
ETN-94-95396 p 2991 N94-26215 #
ETN-94-95397 p 2865 N94-25760 #
ETN-94-95398 p 2957 N94-25761 #
ETN-94-95399 p 2958 N94-25762
ETN-94-95400 p 2790 N94-25763 #
ETN-94-95401 p 2958 N94-25764 #
ETN-94-95402 p 2966 N94-26966
ETN-94-95403 p 2996 N94-26967 #
ETN-94-95404 p 2995 N94-26818 #
ETN-94-95405 p 2992 N94-26252
ETN-94-95410 p 2965 N94-26772 #
ETN-94-95411 p 2995 N94-26773 #
ETN-94-95413 p 2867 N94-26216 #
ETN-94-95414 p 2991 N94-26217 #
ETN-94-95415 p 2961 N94-26218 #
ETN-94-95416 p 2961 N94-26219 #
ETN-94-95417 p 3097 N94-26220 #
ETN-94-95418 p 2961 N94-26221 #
ETN-94-95419 p 2995 N94-26776 #
ETN-94-95420 p 3100 N94-27394
ETN-94-95421 p 2971 N94-27575
ETN-94-95422 p 2972 N94-27576 #
ETN-94-95423 p 3000 N94-27577
ETN-94-95424 p 2972 N94-27578
ETN-94-95425 p 2982 N94-27579 #
ETN-94-95426 p 2972 N94-27580 #
ETN-94-95427 p 2972 N94-27581
ETN-94-95428 p 2970 N94-27543
ETN-94-95429 p 2970 N94-27544 #
ETN-94-95430 p 2970 N94-27545 #
ETN-94-95431 p 2776 N94-27546 #
ETN-94-95432 p 2955 N94-27547 #
ETN-94-95433 p 2970 N94-27548 #
ETN-94-95434 p 2970 N94-27549
ETN-94-95435 p 2971 N94-27550
ETN-94-95436 p 2776 N94-27551 #
ETN-94-95439 p 2971 N94-27552
ETN-94-95440 p 2973 N94-27737
ETN-94-95441 p 2974 N94-27794 #
ETN-94-95442 p 2743 N94-27795
ETN-94-95443 p 2678 N94-27395
ETN-94-95444 p 2666 N94-27831
ETN-94-95445 p 2798 N94-27853
ETN-94-95446 p 2670 N94-27796
ETN-94-95447 p 2743 N94-27797
ETN-94-95448 p 2679 N94-27798
ETN-94-95449 p 2798 N94-27799
ETN-94-95450 p 2989 N94-27800
ETN-94-95451 p 2843 N94-27553
ETN-94-95452 p 2647 N94-27554
ETN-94-95453 p 2851 N94-27555
ETN-94-95454 p 2828 N94-28043 #
ETN-94-95455 p 2830 N94-28077 #
ETN-94-95456 p 2972 N94-27582 #
ETN-94-95457 p 2693 N94-27583 #
ETN-94-95459 p 2711 N94-27586 #
ETN-94-95489 p 2681 N94-27587 #
ETN-94-95490 p 2797 N94-27588 #
ETN-94-95491 p 2826 N94-27589 #
ETN-94-95492 p 3066 N94-27590 #
ETN-94-95493 p 2826 N94-27591 #
ETN-94-95494 p 2647 N94-27592 #
ETN-94-95495 p 2675 N94-27593 #
ETN-94-95496 p 2777 N94-27738 #
ETN-94-95497 p 2675 N94-27739 #
ETN-94-95498 p 2648 N94-27741 #
ETN-94-95499 p 2903 N94-27743 #
ETN-94-95500 p 2660 N94-27746 #
ETN-94-95501 p 2897 N94-27751 #
ETN-94-95502 p 2903 N94-27754 #

ETS-RR-93-39-ONR p 3096 N94-25925 #
ETS-RR-93-42-ONR p 2948 N94-25864 #
ETS-RR-93-50-ONR p 3002 N94-25962 #

FASTC-ID(RS)T-0120-93 p 2819 N94-26941 #
FASTC-ID(RS)T-0123-93 p 2819 N94-26940 #
FASTC-ID(RS)T-0369-93 p 2895 N94-26678 #
FASTC-ID(RS)T-0370-93 p 2895 N94-26850 #

FEAC-93-I p 3043 N94-26428 #

FEI-2272 p 2701 N94-26166
FEI-2291 p 2995 N94-26768

FEL-91-A301 p 2659 N94-25780 #
FEL-92-A163 p 2770 N94-26650
FEL-92-A394 p 2767 N94-26011 #
FEL-92-A421 p 3036 N94-26649
FEL-92-A442 p 2770 N94-26650
FEL-92-B438 p 2773 N94-27136
FEL-93-A009 p 3036 N94-26648
FEL-93-A035 p 2893 N94-26013 #
FEL-93-A039 p 2893 N94-26016 #
FEL-93-A040 p 2891 N94-25722 #
FEL-93-A057 p 2811 N94-27134 #
FEL-93-A103 p 2948 N94-25720 #
FEL-93-A135 p 3033 N94-25721 #
FEL-93-B047 p 3038 N94-27137
FEL-93-B113 p 2959 N94-25963 #

FFA-TN-1984-22 p 2644 N94-26104 #

FFI-92/4003 p 2680 N94-26305
FFI-93/6007 p 2712 N94-25745 #
FFI-93/7023 p 2817 N94-26203 #
FFI-93/7024 p 2767 N94-26105
FFI-93/7025 p 2876 N94-25807 #
FFI-93/7028 p 2768 N94-26232 #
FFI-93/8002 p 2837 N94-26233 #

FIA-92-07 p 2989 N94-28065 * #

FNAL/C-93-345-E p 3028 N94-27752 #
FNAL/C-93/287 p 3023 N94-26938 #
FNAL/C-93/305 p 3016 N94-25957 #
FNAL/C-93/321-A p 3104 N94-26786 #
FNAL/C-93/328 p 3015 N94-25935 #
FNAL/C-93/330-E p 3018 N94-26245 #
FNAL/C-93/339 p 2809 N94-25599 #
FNAL/C-93/346 p 3103 N94-27750 #
FNAL/C-93/355-E p 3028 N94-27748 #
FNAL/C-93/363-E p 3028 N94-27749 #

FNAL/PUB-93/298-A p 3104 N94-26311 #

FOA-A-20054-2.7 p 3005 N94-27173
FOA-A-20055-2.5 p 2710 N94-27253
FOA-A-30081-9.4 p 3101 N94-27218
FOA-A-30083-3.1 p 3037 N94-27046 #
FOA-A-50016-5.2 p 2942 N94-27155
FOA-A-50019-5.5 p 2937 N94-28392 #

FOA-C-20928-2.4 .... p 2755 N94-27158
FOA-C-20929-2.2 .... p 3010 N94-27037 #
FOA-C-20931-2.1 .... p 2665 N94-27210
FOA-C-20933-2.7 .... p 2968 N94-27154
FOA-C-20934-8.4-PT-6 .... p 2756 N94-27215
FOA-C-20938-2.7 .... p 2986 N94-26992 #
FOA-C-30697-9.4,3.1 .... p 3038 N94-27209
FOA-C-30702-8.4,3.4 .... p 2968 N94-27157
FOA-C-30705-3.6 .... p 2773 N94-27159
FOA-C-30707-3.1 .... p 2900 N94-27208
FOA-C-30711-3.4 .... p 2849 N94-26848
FOA-C-30712-8.3,3.2 .... p 2772 N94-27041 #
FOA-C-30713-8.3 .... p 3005 N94-27172
FOA-C-30714-3.5 .... p 2774 N94-27219
FOA-C-30715-8.3 .... p 2785 N94-27038 #
FOA-C-30716-8.3 .... p 2812 N94-27216
FOA-C-40307-4.6 .... p 2866 N94-25809 #
FOA-C-40309-4.4 .... p 2902 N94-27171
FOA-C-40310-4.4 .... p 2902 N94-27045 #

FOA-30079-3.1 .... p 2900 N94-27156

FTR-528996 .... p 3099 N94-27013 #

GA-A-21286 .... p 3041 N94-25801 #
GA-A-21422 .... p 3045 N94-26865 #
GA-A-21427 .... p 3043 N94-26274 #
GA-A-21431 .... p 3045 N94-26950 #
GA-A-21448 .... p 3042 N94-25976 #
GA-A-21474 .... p 3043 N94-26324 #
GA-A-21485 .... p 3043 N94-26323 #
GA-A-21507 .... p 3048 N94-27791 #

GAO/NSIAD-93-123 .... p 3095 N94-28177 #
GAO/NSIAD-94-24 .... p 3106 N94-27418 #
GAO/NSIAD-94-80 .... p 2696 N94-27382 #

GAO/T-NSIAD-94-18 .... p 3095 N94-28176 #

GRI-93/0182 .... p 2824 N94-27224
GRI-93/0266 .... p 2759 N94-26753 #
GRI-93/0271 .... p 2717 N94-27226
GRI-93/0351 .... p 2717 N94-27256
GRI-93/0384 .... p 2859 N94-27225

H-1956 .... p 2691 N94-27868 * #
H-1965 .... p 2674 N94-27432 * #

HCSCIA-HR-94-002 .... p 2909 N94-26360 #

HHR-58 .... p 3118 N94-27431 * #

HQROM93.WR1 .... p 3104 N94-27407 * #

I-ARA-93-U-60 .... p 3033 N94-27078 #

IAEA-NDS-107(REV-7) .... p 3016 N94-26034 #

IAR-AN-77 .... p 2677 N94-26710 #
IAR-AN-78 .... p 2647 N94-26702 #

IAR-CR-25 .... p 2708 N94-26711 #

IBAMD-42-45 .... p 3045 N94-26946
IBAMD-46 .... p 3023 N94-26947

IC-AERO-92-01 .... p 2644 N94-26248 #

IC-92/182 .... p 2991 N94-25867
IC-92/189 .... p 3005 N94-25868
IC-92/221 .... p 3051 N94-25851
IC-92/222 .... p 3071 N94-25852
IC-92/260 .... p 3001 N94-28228
IC-92/261 .... p 3013 N94-25827
IC-92/269 .... p 2991 N94-25880
IC-92/270 .... p 2991 N94-25881
IC-92/275 .... p 2990 N94-25865
IC-92/306 .... p 2990 N94-25829
IC-92/333 .... p 2990 N94-25830
IC-92/337 .... p 2713 N94-25913
IC-92/339 .... p 3008 N94-25831
IC-92/344 .... p 3051 N94-25914
IC-92/367 .... p 3066 N94-27347
IC-92/371 .... p 2783 N94-26443
IC-93/119 .... p 3035 N94-26383
IC-93/121 .... p 2994 N94-26458
IC-93/122 .... p 3097 N94-26382
IC-93/123 .... p 2993 N94-26440
IC-93/129 .... p 3068 N94-27677
IC-93/131 .... p 3019 N94-26423 #
IC-93/132 .... p 2993 N94-26441
IC-93/134 .... p 2992 N94-26267 #
IC-93/135 .... p 3057 N94-26388 #
IC-93/136 .... p 3057 N94-26389 #
IC-93/137 .... p 3057 N94-26390 #
IC-93/138 .... p 3057 N94-26387 #
IC-93/139 .... p 3006 N94-26270
IC-93/140 .... p 3052 N94-26012 #
IC-93/143 .... p 2998 N94-27162
IC-93/144 .... p 3073 N94-26896 #
IC-93/145 .... p 3022 N94-26900
IC-93/146 .... p 3003 N94-26385 #
IC-93/147 .... p 2962 N94-26386 #
IC-93/148 .... p 3016 N94-26010 #
IC-93/149 .... p 3030 N94-27994 #
IC-93/150 .... p 2992 N94-26366 #
IC-93/151 .... p 3018 N94-26333
IC-93/152 .... p 3073 N94-26837
IC-93/153 .... p 3061 N94-26878 #
IC-93/154 .... p 3062 N94-26901
IC-93/155 .... p 3070 N94-27995 #
IC-93/156 .... p 2996 N94-26898
IC-93/157 .... p 3001 N94-27839
IC-93/158 .... p 3006 N94-26413 #
IC-93/159 .... p 2997 N94-27023
IC-93/160 .... p 3104 N94-26268
IC-93/161 .... p 3073 N94-27024
IC-93/162 .... p 3062 N94-26902 #
IC-93/166 .... p 3072 N94-26551
IC-93/167 .... p 3067 N94-27647
IC-93/168 .... p 3104 N94-26269
IC-93/170 .... p 3006 N94-26414 #
IC-93/173 .... p 3006 N94-26415 #
IC-93/174 .... p 3022 N94-26899
IC-93/175 .... p 3061 N94-26879
IC-93/176 .... p 2993 N94-26408
IC-93/177 .... p 3051 N94-25945
IC-93/178 .... p 3013 N94-25839 #
IC-93/179 .... p 2994 N94-26459
IC-93/180 .... p 3006 N94-26460
IC-93/182 .... p 3063 N94-27017
IC-93/183 .... p 3019 N94-26416 #
IC-93/185 .... p 3072 N94-26417 #
IC-93/186 .... p 3014 N94-25887 #
IC-93/187 .... p 3074 N94-27696
IC-93/189 .... p 3062 N94-26897
IC-93/190 .... p 3073 N94-26758
IC-93/192 .... p 3117 N94-28066 #
IC-93/195 .... p 3073 N94-26876 #
IC-93/196 .... p 2878 N94-26418 #
IC-93/197 .... p 3019 N94-26424 #
IC-93/198 .... p 3013 N94-25837 #
IC-93/199 .... p 2993 N94-26409
IC-93/202 .... p 3071 N94-25882 #
IC-93/204 .... p 3074 N94-27626
IC-93/205 .... p 2715 N94-26391 #
IC-93/206 .... p 3071 N94-25883 #
IC-93/208 .... p 3006 N94-26368 #
IC-93/209 .... p 2993 N94-26410 #
IC-93/210 .... p 3074 N94-27627
IC-93/213 .... p 2714 N94-26169
IC-93/215 .... p 3006 N94-26411 #
IC-93/218 .... p 3117 N94-27996
IC-93/219 .... p 3072 N94-26461
IC-93/220 .... p 2991 N94-25884 #
IC-93/222 .... p 2787 N94-27628
IC-93/223 .... p 2992 N94-26367 #
IC-93/224 .... p 3050 N94-25843 #
IC-93/225 .... p 2878 N94-26365 #
IC-93/226 .... p 3068 N94-27729 #
IC-93/227 .... p 3067 N94-27638
IC-93/228 .... p 3027 N94-27629
IC-93/230 .... p 3046 N94-27630
IC-93/232 .... p 2993 N94-26412 #
IC-93/235 .... p 3068 N94-27678
IC-93/236 .... p 2993 N94-26425 #
IC-93/240 .... p 3027 N94-27631
IC-93/241 .... p 3000 N94-27632 #
IC-93/244 .... p 3007 N94-27633
IC-93/246 .... p 2758 N94-27837
IC-93/247 .... p 3000 N94-27818
IC-93/248 .... p 3067 N94-27634
IC-93/249 .... p 3067 N94-27635
IC-93/250 .... p 3074 N94-27636
IC-93/251 .... p 3069 N94-27819
IC-93/74 .... p 3103 N94-26046 #
IC-93/91 .... p 3007 N94-26552
IC-93/95 .... p 3057 N94-26384
IC-93/99 .... p 3000 N94-27637

ICAF-1948 .... p 2845 N94-27954 #

ICASE-93-93 .... p 2792 N94-26499 * #
ICASE-93-96 .... p 2994 N94-26601 * #
ICASE-94-1 .... p 2796 N94-27435 * #
ICASE-94-2 .... p 2969 N94-27416 * #
ICASE-94-3 .... p 2971 N94-27558 * #
ICASE-94-4 .... p 2999 N94-27434 * #
ICASE-94-5 .... p 2999 N94-27557 * #
ICASE-94-6 .... p 2971 N94-27572 * #
ICASE-94-7 .... p 2970 N94-27417 * #
ICASE-94-8 .... p 2999 N94-27415 * #

ICRR-REPT-295-93-7 .... p 3112 N94-25624 #

ICRR-296-93-8 .... p 3116 N94-27607 #
ICRR-299-93-11 .... p 3028 N94-27759 #

IEPC-93-097 .... p 2701 N94-26209 * #
IEPC-93-140 .... p 2700 N94-26090 * #
IEPC-93-151 .... p 2690 N94-26142 * #

IFSR-623 .... p 3041 N94-25923 #
IFSR-627 .... p 3041 N94-25792 #
IFSR-629 .... p 2963 N94-26521 #
IFSR-632 .... p 3047 N94-27723 #
IFSR-633 .... p 3042 N94-25958 #

IFT-P-004/93 .... p 2993 N94-26442
IFT-P-025/92 .... p 3016 N94-26040 #
IFT-P-040/92 .... p 3022 N94-26766
IFT-P-049/92 .... p 3017 N94-26043 #
IFT-P-050/92 .... p 3016 N94-26041

IFTR-37/1993 .... p 2839 N94-26825 #
IFTR-41/1993 .... p 2716 N94-26823 #
IFTR-42/1993 .... p 2739 N94-26824 #

IFVE-OEA-92-105 .... p 2783 N94-26438
IFVE-OEA-92-19 .... p 2948 N94-26266 #
IFVE-OEA-92-4 .... p 2783 N94-26380
IFVE-OEA-92-75 .... p 2948 N94-26381

IFVE-OEF-92-36 .... p 2810 N94-26439

IFVE-ONF-92-33 .... p 3019 N94-26393
IFVE-ONF-92-42 .... p 2810 N94-26394
IFVE-ONF-92-47 .... p 2810 N94-26395
IFVE-ONF-92-98 .... p 2810 N94-26397
IFVE-ONF-92-9 .... p 2810 N94-26396

IFVE-OTF-92-103 .... p 3072 N94-26553 #

IHEP-OEF-92-95 .... p 2810 N94-26378

IHEP-OEIUNK-92-37 .... p 3024 N94-27250 #

IHEP-OKU-92-83 .... p 3032 N94-26164

IHEP-ONF-92-59 .... p 3056 N94-26379

IHEP-OTF-92-100 .... p 3072 N94-26453 #
IHEP-OTF-92-13 .... p 3019 N94-26454
IHEP-OTF-92-14 .... p 3017 N94-26045 #
IHEP-OTF-92-2 .... p 3019 N94-26455 #
IHEP-OTF-92-35 .... p 3016 N94-26042 #
IHEP-OTF-92-45 .... p 3019 N94-26456 #
IHEP-OTF-92-46 .... p 2993 N94-26457 #
IHEP-OTF-92-51 .... p 3016 N94-26035 #
IHEP-OTF-92-71 .... p 3022 N94-26767
IHEP-OTF-92-74 .... p 3072 N94-26036 #
IHEP-OTF-92-76 .... p 3031 N94-26044 #
IHEP-OTF-92-92 .... p 3072 N94-26037 #

IHEP-TD-92-63 .... p 3002 N94-26038 #
IHEP-TD-92-7 .... p 3072 N94-26039 #

IHEP-UNK-92-43 .... p 3032 N94-26165

IHES/M-93/42 .... p 2997 N94-26994 #
IHES/M-93/46 .... p 2996 N94-26993 #
IHES/M-93/52 .... p 2997 N94-26995 #
IHES/M-93/53 .... p 2997 N94-26996 #

IMR-T&M-TR-001 .... p 2828 N94-28041 #

IND-MANU-SCI-TECH-REPT-3 .... p 2762 N94-25775 #

INIS-AR-017 .... p 2733 N94-26160
INIS-AR-019 .... p 2735 N94-26294 #
INIS-AR-020 .... p 2837 N94-26265 #
INIS-AR-021 .... p 2734 N94-26161
INIS-AR-022 .... p 2734 N94-26162
INIS-AR-023 .... p 2735 N94-26295 #
INIS-AR-024 .... p 2734 N94-26263 #
INIS-AR-026 .... p 2734 N94-26264 #
INIS-AR-039 .... p 2743 N94-27829 #
INIS-AR-041 .... p 3029 N94-27834 #
INIS-AR-042 .... p 2743 N94-27832 #

INIS-BR-3149 .... p 3067 N94-27623
INIS-BR-3169 .... p 3068 N94-27697

INIS-JP-012 .... p 3100 N94-27700 #

INIS-MF-13436 .... p 3051 N94-25912
INIS-MF-13438 .... p 3095 N94-25751
INIS-MF-13600 .... p 2716 N94-26519 #
INIS-MF-13601 .... p 2866 N94-26163

INIS-MF-13615 .... p 2720 N94-27998
INIS-MF-13617 .... p 2880 N94-26874
INIS-MF-13714 .... p 3047 N94-27698
INIS-MF-13724 .... p 3048 N94-27844
INIS-MF-4754(NO-42-45) .... p 3045 N94-26946
INIS-MF-4754(NO-46) .... p 3023 N94-26947

INIS-RU-355 .... p 3032 N94-26405 #

INP-MSU-92-12-261 .... p 3015 N94-25920
INP-MSU-92-15-264 .... p 3013 N94-25835

INPE-5380-PUD/050 .... p 2882 N94-27334 #
INPE-5387-TDI/476 .... p 2896 N94-27356 #
INPE-5456-TDI/498 .... p 2896 N94-27422 #
INPE-5482-PRE/1781 .... p 2850 N94-27384 #
INPE-5483-PRE/1782 .... p 2974 N94-27835 #
INPE-5485-PRE/1784 .... p 2989 N94-27833 #
INPE-5486-PRE/1786 .... p 2852 N94-27957 #
INPE-5510-TAE/020 .... p 2696 N94-27357 #
INPE-5519-PRE/1794 .... p 2776 N94-27335 #
INPE-5520-TAE/021 .... p 2827 N94-27665 #
INPE-5523-RPQ/665 .... p 2849 N94-26827 #
INPE-5527-PRP/178-PT-2 .... p 3066 N94-27329 #

INS-J-175 .... p 3030 N94-27877

INS-965 .... p 3015 N94-25922 #

INT-PATENT-CLASS-B32B-031/24 p 2669 N94-27273

INT-PATENT-CLASS-C04B-035/44 p 3066 N94-27276

INT-PATENT-CLASS-F41F-003/04 p 3066 N94-27276

INT-PATENT-CLASS-G01C2300 .. p 2659 N94-26293
INT-PATENT-CLASS-G01S-003/42 p 2775 N94-27270
INT-PATENT-CLASS-G01S-007/40 p 2665 N94-27275

INT-PATENT-CLASS-H01Q-001/42 p 3066 N94-27276

IPPCZ-322 .... p 3048 N94-27836 #
IPPCZ-326 .... p 2777 N94-27838 #
IPPCZ-333 .... p 3048 N94-27840 #
IPPCZ-334 .... p 2844 N94-27841 #
IPPCZ-335 .... p 3048 N94-27842 #

IR-319 .... p 2965 N94-26908 #
IR-320 .... p 2967 N94-26997 #
IR-324 .... p 2965 N94-26852

IRF-SR-213 .... p 2881 N94-27040 #

IS-M-775 .... p 2706 N94-26019 #
IS-M-776 .... p 2735 N94-26273 #

IS-T-1637 .... p 2704 N94-26779 #
IS-T-1642 .... p 2757 N94-27695 #
IS-T-1669 .... p 2712 N94-27813 #
IS-T-1684 .... p 3029 N94-27811 #

ISAS/EP-93/89 .... p 2998 N94-27162

ISBN-0-309-04881-8 .... p 2669 N94-26906
ISBN-0-315-49073-X .... p 3024 N94-27258
ISBN-0-315-49334-8 .... p 3007 N94-27264
ISBN-0-315-50637-7 .... p 3074 N94-27403
ISBN-0-315-51152-4 .... p 2812 N94-27257
ISBN-0-315-51159-1 .... p 2982 N94-27332
ISBN-0-315-51715-8 .... p 3025 N94-27266
ISBN-0-315-54572-0 .... p 3073 N94-27263
ISBN-0-315-55542-4 .... p 3026 N94-27402
ISBN-0-315-57014-8 .... p 3026 N94-27400
ISBN-0-315-57174-8 .... p 3024 N94-27259
ISBN-0-315-57234-5 .... p 3025 N94-27260
ISBN-0-315-57769-X .... p 3009 N94-27268
ISBN-0-315-57811-4 .... p 2787 N94-27642
ISBN-0-315-57888-2 .... p 2998 N94-27269
ISBN-0-315-58891-8 .... p 3049 N94-27949
ISBN-0-315-58970-1 .... p 2777 N94-27806
ISBN-0-315-59019-X .... p 2983 N94-27685
ISBN-0-315-59114-5 .... p 2798 N94-27873
ISBN-0-315-59469-1 .... p 2852 N94-27870
ISBN-0-315-59526-4 .... p 2744 N94-27950
ISBN-0-315-59932-4 .... p 2743 N94-27803
ISBN-0-315-59950-2 .... p 2988 N94-27641
ISBN-0-315-60198-1 .... p 2982 N94-27644
ISBN-0-315-60559-6 .... p 2844 N94-27810
ISBN-0-315-60634-7 .... p 2974 N94-27869
ISBN-0-315-60643-6 .... p 3039 N94-27643
ISBN-0-315-60926-5 .... p 3025 N94-27333
ISBN-0-315-60960-5 .... p 3074 N94-27401
ISBN-0-315-60974-5 .... p 2975 N94-27872
ISBN-0-315-61111-1 .... p 3001 N94-27948
ISBN-0-315-61377-7 .... p 2799 N94-27947
ISBN-0-315-62312-8 .... p 2777 N94-27871
ISBN-0-315-63598-3 .... p 3027 N94-27684
ISBN-0-315-63607-6 .... p 3074 N94-27398
ISBN-0-315-63748-X .... p 3026 N94-27399
ISBN-0-315-63894-X .... p 2974 N94-27805
ISBN-0-315-63903-2 .... p 2844 N94-27808
ISBN-0-315-64015-4 .... p 2988 N94-27645
ISBN-0-315-64248-3 .... p 2757 N94-27801
ISBN-0-315-83373-4 .... p 2752 N94-26661
ISBN-0-315-83435-8 .... p 2964 N94-26632
ISBN-0-315-83505-2 .... p 2985 N94-26660
ISBN-0-315-83555-9 .... p 2994 N94-26659
ISBN-0-315-83572-9 .... p 2823 N94-26658
ISBN-0-315-83593-1 .... p 2784 N94-26631
ISBN-0-315-83682-2 .... p 2822 N94-26642
ISBN-0-315-83684-9 .... p 2994 N94-26614
ISBN-0-315-83776-4 .... p 2963 N94-26615
ISBN-0-315-83884-1 .... p 2963 N94-26616
ISBN-0-315-83893-0 .... p 2769 N94-26618
ISBN-0-315-83894-9 .... p 2769 N94-26619
ISBN-0-315-83931-7 .... p 2838 N94-26622
ISBN-0-315-83968-6 .... p 2811 N94-26662
ISBN-0-315-84007-2 .... p 2770 N94-26624
ISBN-0-315-84011-0 .... p 2784 N94-26627
ISBN-0-315-84012-9 .... p 2770 N94-26630
ISBN-0-315-84018-8 .... p 2738 N94-26633
ISBN-0-315-84082-X .... p 2763 N94-26634
ISBN-0-315-84093-5 .... p 2980 N94-26635
ISBN-0-315-84094-3 .... p 2964 N94-26663
ISBN-0-315-84107-9 .... p 2793 N94-26671
ISBN-0-315-84113-3 .... p 2793 N94-26637
ISBN-0-315-84115-X .... p 2677 N94-26636
ISBN-0-315-84116-8 .... p 3059 N94-26703
ISBN-0-315-84120-6 .... p 2784 N94-26704
ISBN-0-315-84121-4 .... p 2646 N94-26672
ISBN-0-315-84123-0 .... p 2674 N94-26673
ISBN-0-315-84128-1 .... p 2980 N94-26674
ISBN-0-315-84130-3 .... p 2784 N94-26675
ISBN-0-315-84134-6 .... p 2678 N94-27648
ISBN-0-315-84139-7 .... p 2982 N94-27649
ISBN-0-315-84243-1 .... p 2849 N94-26668
ISBN-0-315-84246-6 .... p 3102 N94-26669
ISBN-0-315-84250-4 .... p 2867 N94-26670
ISBN-0-315-84258-X .... p 2994 N94-26640
ISBN-0-315-84271-7 .... p 3104 N94-26638
ISBN-0-315-84278-4 .... p 2838 N94-26639
ISBN-0-315-84281-4 .... p 2770 N94-26625
ISBN-0-315-84289-X .... p 2770 N94-26626
ISBN-0-315-84327-6 .... p 2894 N94-26628
ISBN-0-315-84328-4 .... p 2985 N94-26629
ISBN-0-315-84351-9 .... p 2822 N94-26657
ISBN-0-315-84362-4 .... p 2848 N94-26664
ISBN-0-315-84367-5 .... p 3021 N94-26665
ISBN-0-315-84382-9 .... p 3036 N94-26666
ISBN-0-315-84383-7 .... p 2849 N94-26667
ISBN-0-315-84424-8 .... p 2826 N94-27652
ISBN-0-315-84425-6 .... p 2787 N94-27653
ISBN-0-315-84467-1 .... p 2740 N94-27304
ISBN-0-315-84472-8 .... p 2740 N94-27305
ISBN-0-315-84488-4 .... p 2740 N94-27306
ISBN-0-315-84549-X .... p 2795 N94-27307
ISBN-0-315-84553-8 .... p 2999 N94-27404
ISBN-0-315-84562-7 .... p 2999 N94-27405
ISBN-0-315-84563-5 .... p 2988 N94-27271
ISBN-0-315-84564-3 .... p 2842 N94-27272
ISBN-0-315-84609-7 .... p 2787 N94-27650
ISBN-0-315-84616-X .... p 2813 N94-27651 #
ISBN-0-315-84623-2 .... p 2825 N94-27343
ISBN-0-315-84627-5 .... p 2825 N94-27344
ISBN-0-315-84632-1 .... p 2776 N94-27345
ISBN-0-315-84633-X .... p 3038 N94-27441
ISBN-0-315-84643-7 .... p 2776 N94-27308
ISBN-0-315-84647-X .... p 2842 N94-27309 #
ISBN-0-315-84679-8 .... p 3025 N94-27310
ISBN-0-315-84684-4 .... p 2969 N94-27311
ISBN-0-315-84686-0 .... p 2998 N94-27312
ISBN-0-315-84694-1 .... p 2795 N94-27313
ISBN-0-315-84699-2 .... p 2711 N94-27314
ISBN-0-315-84701-8 .... p 2842 N94-27315
ISBN-0-315-84708-5 .... p 2969 N94-27316
ISBN-0-315-84906-1 .... p 2744 N94-27961
ISBN-0-315-84917-7 .... p 3039 N94-27962
ISBN-0-315-84928-2 .... p 2843 N94-27585
ISBN-0-315-84930-4 .... p 3070 N94-27974
ISBN-0-315-84934-7 .... p 2989 N94-27975
ISBN-0-315-84939-8 .... p 2712 N94-27688
ISBN-0-315-84978-9 .... p 2851 N94-27863
ISBN-0-315-85076-0 .... p 2852 N94-27878
ISBN-0-315-85147-3 .... p 2775 N94-27274
ISBN-0-315-85158-9 .... p 2988 N94-27277
ISBN-0-315-85169-4 .... p 2842 N94-27278
ISBN-0-315-85208-9 .... p 2969 N94-27346
ISBN-0-315-85243-7 .... p 2775 N94-27301
ISBN-0-315-85247-X .... p 3103 N94-27302
ISBN-0-315-85280-1 .... p 2786 N94-27303
ISBN-0-315-85354-9 .... p 2972 N94-27595
ISBN-0-315-85355-7 .... p 2826 N94-27596
ISBN-0-85679-843-6 .... p 2829 N94-28055
ISBN-0-85679-844-4 .... p 2830 N94-28056
ISBN-0-85679-855-X .... p 2720 N94-27959
ISBN-0-85679-856-8 .... p 2830 N94-28073
ISBN-0-85679-857-6 .... p 2830 N94-28074
ISBN-0-85679-858-4 .... p 2830 N94-28075
ISBN-0-85679-859-2 .... p 2648 N94-28057
ISBN-0-85679-860-6 .... p 2720 N94-28058
ISBN-0-85679-861-4 .... p 2720 N94-28059
ISBN-0-85679-862-2 .... p 2720 N94-28060
ISBN-0-85679-863-0 .... p 2845 N94-28061
ISBN-0-85679-864-9 .... p 2720 N94-28062
ISBN-0-85679-865-5 .... p 2806 N94-28064
ISBN-0-85679-865-7 .... p 2648 N94-28063
ISBN-0-85679-867-3 .... p 2649 N94-28076
ISBN-0-85679-868-1 .... p 2976 N94-28137
ISBN-0-85679-869-X .... p 2721 N94-28138
ISBN-0-85679-870-3 .... p 2807 N94-28139
ISBN-0-85679-872-X .... p 2649 N94-28140
ISBN-0-85679-873-8 .... p 2649 N94-28091
ISBN-0-85679-874-6 .... p 2670 N94-28092
ISBN-0-85679-875-4 .... p 2832 N94-28093
ISBN-0-85679-876-2 .... p 2670 N94-28094
ISBN-0-85679-877-0 .... p 2806 N94-28095
ISBN-0-85679-879-7 .... p 2807 N94-28096
ISBN-0-85679-880-0 .... p 3011 N94-28141
ISBN-0-85679-881-9 .... p 2721 N94-28142
ISBN-0-85679-882-7 .... p 2721 N94-28097
ISBN-0-85679-883-5 .... p 2845 N94-28143
ISBN-0-85679-885-1 .... p 2649 N94-28144
ISBN-0-85679-886-X .... p 2845 N94-28145
ISBN-0-85679-887-8 .... p 2648 N94-27955
ISBN-0-920203-01-9 .... p 2651 N94-28315
ISBN-1-871564-484 .... p 2762 N94-25775 #
ISBN-1-871564-493 .... p 3005 N94-25781 #
ISBN-1-871564-514 .... p 3005 N94-25823 #
ISBN-1-871564-549 .... p 2790 N94-25778 #
ISBN-1-871564-56-5 .... p 2765 N94-25639 #
ISBN-1-871564-58-1 .... p 2676 N94-25640 #
ISBN-1-871564-59-X .... p 2676 N94-25653 #
ISBN-2-85428-335-X .... p 2948 N94-26713
ISBN-9-03-860232-4 .... p 2792 N94-26479 #
ISBN-9-05-411062-7 .... p 2847 N94-26228
ISBN-9-09-005928-8 .... p 2834 N94-26003 #
ISBN-9-29-092216-8 .... p 2972 N94-27582 #
ISBN-90-6144-995-2 .... p 2954 N94-27191 #
ISBN-90-9005644-0 .... p 2986 N94-27029 #
ISBN-91-7848-335-2 .... p 2823 N94-26849
ISBN-91-7848-361-1 .... p 2811 N94-27044 #
ISBN-92-835-0720-7 .... p 2799 N94-28003 #
ISBN-951-22-1353-2 .... p 2689 N94-28358 #
ISBN-951-22-1550-0 .... p 2900 N94-28393 #
ISBN-951-22-1581-0 .... p 2778 N94-28380 #
ISBN-951-22-1582-9 .... p 2778 N94-28379 #
ISBN-951-22-1583-7 .... p 2778 N94-28381 #
ISBN-951-22-1584-5 .... p 2778 N94-28382 #
ISBN-951-22-1592-6 .... p 2779 N94-28390 #
ISBN-951-22-1623-X .... p 3095 N94-28386 #
ISBN-951-22-1637-X .... p 2779 N94-28391 #
ISBN-951-22-1638-8 .... p 2747 N94-28359 #
ISBN-951-22-1639-6 .... p 2983 N94-28354
ISBN-951-22-1642-6 .... p 2779 N94-28388 #
ISBN-951-22-1648-5 .... p 2778 N94-28387 #
ISBN-951-22-1651-5 .... p 2778 N94-28384 #
ISBN-951-22-1658-2 .... p 3001 N94-28389 #
ISBN-951-22-1667-1 .... p 2778 N94-28355
ISBN-951-22-1668-X .... p 2779 N94-28397 #
ISBN-951-22-1673-6 .... p 2788 N94-28357 #
ISBN-951-22-1717-1 .... p 2876 N94-28394 #
ISBN-951-22-1718-X .... p 2876 N94-28395 #
ISBN-951-22-1719-8 .... p 2876 N94-28383 #
ISBN-951-22-1742-2 .... p 2966 N94-26921 #
ISBN-951-38-4120-0 .... p 2848 N94-26253 #
ISBN-951-38-4216-9 .... p 2664 N94-25808 #
ISBN-951-38-4217-7 .... p 2762 N94-25622 #
ISBN-951-38-4231-2 .... p 3031 N94-25621 #
ISBN-951-38-4235-5 .... p 2762 N94-25641 #
ISBN-951-38-4237-1 .... p 2841 N94-27186 #
ISBN-951-38-4240-1 .... p 2957 N94-25642 #
ISBN-951-38-4246-0 .... p 2704 N94-25734 #
ISBN-951-38-4247-9 .... p 2836 N94-25650 #
ISBN-951-38-4249-5 .... p 2731 N94-25643 #
ISBN-951-38-4250-9 .... p 2779 N94-25644 #
ISBN-951-38-4253-3 .... p 2990 N94-25733 #
ISBN-951-38-4300-9 .... p 2731 N94-25623 #
ISBN-951-38-4304-1 .... p 2731 N94-25784 #
ISBN-951-38-4305-X .... p 2762 N94-26259 #
ISBN-951-38-4309-2 .... p 2707 N94-26260 #
ISBN-951-38-4312-2 .... p 2762 N94-26261 #
ISBN-951-38-4314-9 .... p 2837 N94-26262 #
ISBN-951-38-4316-5 .... p 2704 N94-25651 #
ISBN-951-38-4321-1 .... p 2679 N94-25652 #
ISBN-951-38-4324-6 .... p 2961 N94-26254 #
ISBN-951-38-4326-2 .... p 2837 N94-26255 #
ISBN-951-38-4327-0 .... p 2708 N94-26544 #
ISBN-951-38-4328-9 .... p 3058 N94-26545 #

ISBN-951-38-4329-7 p 2822 N94-26306 #
ISBN-951-38-4331-9 p 2837 N94-26307 #
ISBN-951-38-4332-7 p 2682 N94-26249 #
ISBN-951-38-4335-1 p 2695 N94-26250 #
ISBN-951-38-4345-9 p 3008 N94-26256 #
ISBN-951-38-4347-8 p 2835 N94-26257 #
ISBN-951-38-4350-5 p 2714 N94-26251 #
ISBN-951-38-4357-2 p 2712 N94-28376 #
ISBN-951-38-4365-3 p 2976 N94-28377 #
ISBN-951-38-4373-4 p 2833 N94-28378 #
ISBN-951-38-4374-2 p 2833 N94-28375 #
ISBN-951-708-060-3 p 2848 N94-26258 #
ISBN-951-78-038-7 p 2850 N94-27182 #
ISBN-965-229-098-X p 2853 N94-26050

ISVR-TR-227 p 2807 N94-28175
ISVR-TR-228 p 2832 N94-28174
ISVR-TR-229 p 2807 N94-28172
ISVR-TR-230-PT-3 p 2807 N94-28173

ITN-94-85228 p 2853 N94-26050
ITN-94-85229 p 2774 N94-27233
ITN-94-85230 p 2774 N94-27234
ITN-94-85231 p 2719 N94-27687
ITN-94-85232 p 3028 N94-27760
ITN-94-85233 p 3038 N94-27178
ITN-94-85234 p 2819 N94-27179
ITN-94-85235 p 2774 N94-27242
ITN-94-85236 p 3065 N94-27243
ITN-94-85237 p 2882 N94-27330
ITN-94-85238 p 2850 N94-27331
ITN-94-85239 p 2775 N94-27244

ITOP-1-1-050 p 2836 N94-25732 #
ITOP-2-2-800 p 2821 N94-25794 #

ITP-UH-07/93 p 3072 N94-26541 #

IZF-1993-B-10 p 2940 N94-25724 #
IZF-1993-B-6 p 2939 N94-27138
IZF-1993-B-8 p 3095 N94-25723 #
IZF-1993-B-9 p 2908 N94-25871 #

JAERI-M-92-213 p 2903 N94-27862 #
JAERI-M-93-043 p 2744 N94-27876 #
JAERI-M-93-059 p 3047 N94-27699 #
JAERI-M-93-063 p 2989 N94-27809
JAERI-M-93-065 p 2788 N94-27817
JAERI-M-93-067 p 2757 N94-27812 #
JAERI-M-93-072 p 2788 N94-27821 #
JAERI-M-93-075 p 3000 N94-27731 #
JAERI-M-93-092 p 3027 N94-27718 #
JAERI-M-93-098 p 3029 N94-27820 #
JAERI-M-93-101 p 2813 N94-27703 #
JAERI-M-93-105 p 2743 N94-27807
JAERI-M-93-110 p 2973 N94-27702 #
JAERI-M-93-119 p 2973 N94-27732 #

JINR-E-1-91-323 p 3031 N94-25850
JINR-E-10-91-374 p 2959 N94-25917
JINR-E-10-91-567 p 2979 N94-25918
JINR-E-15-92-82 p 3020 N94-26511
JINR-E-2-91-356 p 3014 N94-25869
JINR-E-2-91-375 p 3031 N94-25870
JINR-E-2-91-497 p 3006 N94-26193
JINR-E-2-91-506 p 3050 N94-25825
JINR-E-2-92-134 p 3020 N94-26505
JINR-E-2-92-20 p 3007 N94-25603
JINR-E-2-92-318 p 3020 N94-26508
JINR-E-2-92-479 p 3029 N94-27848
JINR-E-2-92-497 p 3075 N94-27858 #
JINR-E-2-92-506 p 3001 N94-27846 #
JINR-E-2-92-547 p 3030 N94-27860 #
JINR-E-2-92-90 p 3020 N94-26507
JINR-E-2-93-118 p 3074 N94-27680 #
JINR-E-2-93-25 p 3070 N94-27859 #
JINR-E-2-93-56 p 3068 N94-27679 #
JINR-E-2-93-88 p 3027 N94-27681 #
JINR-E-3-92-417 p 3027 N94-27682 #
JINR-E-4-91-370 p 3014 N94-25853
JINR-E-4-91-425 p 2766 N94-25866
JINR-E-4-91-500 p 3013 N94-25826
JINR-E-4-91-501 p 3013 N94-25836
JINR-E-4-92-213 p 3007 N94-26472 #
JINR-E-4-92-358 p 3030 N94-27861 #
JINR-E-4-93-94 p 3029 N94-27847 #

JINR-R-10-91-311 p 3015 N94-25919
JINR-R-10-92-1 p 3013 N94-25828
JINR-R-11-92-288 p 2879 N94-26502
JINR-R-13-91-380 p 2809 N94-25735
JINR-R-13-92-18 p 3012 N94-25750
JINR-R-2-91-505 p 3015 N94-25916
JINR-R-2-92-108 p 3072 N94-26503
JINR-R-2-92-163 p 3020 N94-26509
JINR-R-2-92-192 p 2879 N94-26504
JINR-R-5-92-111 p 2994 N94-26471
JINR-R-6-91-557 p 2766 N94-25915
JINR-R-8-92-223 p 3058 N94-26512

JPL-PUB-D-10689 p 2700 N94-25969 #

JPL-PUBL-93-15 p 2956 N94-25602 #
JPL-PUBL-93-20 p 2943 N94-27934 * #
JPL-PUBL-93-27 p 2786 N94-27574 * #

JSC-08284 p 2692 N94-28199 * #
JSC-08285 p 2693 N94-28220 * #
JSC-23314-REV-C p 3119 N94-28204 * #

JTN-94-80509 p 2886 N94-27985 #
JTN-94-80511 p 2896 N94-27169 #
JTN-94-80512 p 2898 N94-25635 #
JTN-94-80514 p 2879 N94-26475 #
JTN-94-80517 p 2871 N94-28268 #
JTN-94-80524 p 2911 N94-27442 #
JTN-94-80528 p 3012 N94-25636 #
JTN-94-80532 p 3053 N94-26089 #
JTN-94-80534 p 3049 N94-25614 #
JTN-94-80535 p 2715 N94-26476 #
JTN-94-80536 p 3051 N94-25921 #
JTN-94-80537 p 2736 N94-26477 #
JTN-94-80538 p 3053 N94-26071 #
JTN-94-80539 p 2733 N94-26073 #
JTN-94-80541 p 3112 N94-25624 #
JTN-94-80543 p 2722 N94-25544 #
JTN-94-80548 p 3046 N94-27350 #
JTN-94-80549 p 2825 N94-27351 #
JTN-94-80550 p 3100 N94-27336 #
JTN-94-80551 p 2859 N94-27204 #
JTN-94-80554 p 2869 N94-28147 #
JTN-94-80555 p 3066 N94-27353 #
JTN-94-80556 p 3065 N94-27239 #
JTN-94-80557 p 3064 N94-27231 #
JTN-94-80558 p 3065 N94-27240 #
JTN-94-80559 p 2756 N94-27241 #
JTN-94-80560 p 3064 N94-27232 #
JTN-94-80561 p 3065 N94-27245 #
JTN-94-80562 p 3065 N94-27248 #
JTN-94-80563 p 3069 N94-27756 #
JTN-94-80564 p 3064 N94-27174 #
JTN-94-80565 p 3064 N94-27175 #
JTN-94-80566 p 3064 N94-27176 #
JTN-94-80567 p 3064 N94-27177 #
JTN-94-80568 p 3066 N94-27354 #
JTN-94-80569 p 3025 N94-27337 #
JTN-94-80570 p 3025 N94-27338 #
JTN-94-80571 p 2820 N94-27339 #
JTN-94-80572 p 2820 N94-27605 #
JTN-94-80573 p 3028 N94-27758 #
JTN-94-80574 p 2787 N94-27606 #
JTN-94-80575 p 3116 N94-27607 #
JTN-94-80576 p 3028 N94-27759 #
JTN-94-80577 p 2776 N94-27340 #
JTN-94-80579 p 2761 N94-27341 #
JTN-94-80580 p 2761 N94-28002 #
JTN-94-80586 p 2933 N94-27942 #
JTN-94-80590 p 2883 N94-27963 #
JTN-94-80592 p 2882 N94-27342 #
JTN-94-80594 p 2881 N94-27299 #
JTN-94-80595 p 2764 N94-27976 #
JTN-94-80601 p 2882 N94-27300 #
JTN-94-80602 p 2717 N94-27385 #
JTN-94-80603 p 2717 N94-27246 #
JTN-94-80604 p 2775 N94-27249 #
JTN-94-80608 p 3118 N94-27355 #
JTN-94-80609 p 3010 N94-27282 #
JTN-94-80610 p 2744 N94-28158 #
JTN-94-80611 p 2710 N94-27279 #
JTN-94-80614 p 2940 N94-27584 #
JTN-94-80615 p 2675 N94-27608 #
JTN-94-80616 p 2795 N94-27205 #
JTN-94-80617 p 2678 N94-27206 #
JTN-94-80618 p 2842 N94-27207 #
JTN-94-80619 p 2681 N94-27247 #
JTN-94-80620 p 2710 N94-27255 #
JTN-94-80621 p 2647 N94-27235 #

KAERI/RR-1106/91 p 2818 N94-26520 #
KAERI/RR-1114/91 p 2910 N94-26549
KAERI/RR-1117/92 p 2714 N94-26158
KAERI/RR-1122/92 p 3042 N94-26159
KAERI/RR-1125/92 p 2816 N94-26184
KAERI/RR-1126/92 p 2817 N94-26185
KAERI/RR-1138/92 p 2783 N94-26546
KAERI/RR-1143/92 p 2816 N94-26157
KAERI/RR-1160/92 p 3017 N94-26116 #
KAERI/RR-1166/92 p 2817 N94-26402 #
KAERI/RR-1169/92 p 3057 N94-26404
KAERI/RR-1175/92 p 2894 N94-26469
KAERI/RR-1182/92 p 2838 N94-26400
KAERI/RR-1183/92 p 2835 N94-26399
KAERI/RR-1207/92 p 2817 N94-26403
KAERI/RR-1214/92 p 2901 N94-26470

KAPL-4762 p 2715 N94-26320 #

KEK-PROC-92-12 p 2816 N94-26112 #
KEK-PROC-92-16 p 3032 N94-26543
KEK-PROC-92-19 p 2983 N94-27804
KEK-PROC-92-20 p 2719 N94-27822 #

KEK-92-16 p 3031 N94-26113 #

KTM/E-B-132 p 2855 N94-26240 #
KTM/E-B-134 p 2867 N94-26241 #

KTM/E-C-35 p 2855 N94-26242 #

KURRI-TR-368 p 3054 N94-26109 #

L-0793-127 p 2647 N94-27161 * #
L-17038 p 2646 N94-26592 * #
L-17081 p 3011 N94-27659 * #
L-17198 p 2647 N94-26706 * #
L-17205 p 2679 N94-27660 * #
L-17215 p 2646 N94-26602 * #
L-17239 p 2695 N94-26609 * #
L-17248 p 2646 N94-26547 * #
L-17249 p 2963 N94-26466 * #
L-17262 p 2673 N94-27882 * #
L-17264 p 2690 N94-27771 * #
L-17269 p 2646 N94-26693 * #
L-17289 p 2989 N94-27773 * #
L-17295 p 3114 N94-26550 * #
L-17298 p 2769 N94-26611 * #
L-17305 p 2673 N94-27864 * #
L-17324 p 2669 N94-26608 * #
L-17355 p 2971 N94-27573 * #

LA-UR-93-2080 p 2797 N94-27705 #
LA-UR-93-2784 p 2813 N94-27624 #
LA-UR-93-3213 p 3005 N94-26802 #
LA-UR-93-3244 p 3058 N94-26514 #
LA-UR-93-3278 p 2752 N94-26676 #
LA-UR-93-3343 p 3110 N94-26696 #
LA-UR-93-3359 p 3059 N94-26695 #
LA-UR-93-3423 p 2835 N94-27613 #
LA-UR-93-3425 p 2821 N94-25980 #
LA-UR-93-3461 p 3004 N94-27612 #
LA-UR-93-3463 p 2733 N94-26069 #
LA-UR-93-3545 p 2818 N94-26605 #
LA-UR-93-3552 p 3073 N94-26805 #
LA-UR-93-3566 p 3094 N94-27707 #
LA-UR-93-3570 p 3030 N94-28001 #
LA-UR-93-3586 p 2737 N94-26607 #
LA-UR-93-3591 p 2991 N94-26079 #
LA-UR-93-3614 p 2750 N94-26124 #
LA-UR-93-3624 p 3042 N94-26081 #
LA-UR-93-3651 p 2797 N94-27709 #
LA-UR-93-3654 p 2880 N94-26806 #
LA-UR-93-3697 p 2986 N94-26807 #
LA-UR-93-3720 p 2738 N94-26621 #
LA-UR-93-3728 p 3021 N94-26620 #
LA-UR-93-3807 p 2696 N94-26808 #
LA-UR-93-3811 p 3052 N94-25972 #
LA-UR-93-3836 p 3050 N94-25817 #
LA-UR-93-3838 p 2816 N94-26126 #
LA-UR-93-3851 p 2901 N94-26623 #
LA-UR-93-3856 p 2980 N94-26120 #
LA-UR-93-3914 p 3007 N94-27777 #
LA-UR-93-3920 p 3013 N94-25820 #
LA-UR-93-3930 p 2719 N94-27728 #
LA-UR-93-3951 p 2851 N94-27727 #
LA-UR-93-3966 p 2757 N94-27747 #
LA-UR-93-3967 p 2704 N94-27745 #
LA-UR-93-4088 p 2933 N94-27744 #
LA-UR-93-4102 p 2985 N94-25983 #
LA-UR-93-4136 p 2699 N94-25613 #
LA-UR-93-4147 p 3012 N94-25612 #
LA-UR-93-4173 p 3111 N94-27742 #
LA-UR-93-4234 p 3048 N94-27825 #
LA-UR-93-4251 p 3005 N94-27816 #
LA-UR-93-4265 p 2897 N94-28146 #
LA-UR-93-4279 p 3116 N94-27714 #
LA-UR-93-4313 p 3116 N94-27793 #
LA-UR-93-4326 p 3069 N94-27828 #
LA-UR-93-4340 p 3117 N94-27827 #
LA-UR-93-4406 p 3117 N94-27826 #
LA-UR-93-4482 p 3047 N94-27715 #

LA-12567-MS p 3043 N94-26321 #
LA-12604-MS p 3020 N94-26527 #
LA-12641 p 2733 N94-26022 #
LA-12685-MS p 2732 N94-25974 #

LBL-PUB-733 p 3118 N94-26937 #

LBL-33410 p 2962 N94-26327 #
LBL-33439 p 3060 N94-26795 #
LBL-33594 p 2787 N94-27618 #
LBL-33859 p 2867 N94-26419 #
LBL-33967 p 3054 N94-26095 #
LBL-34017 p 2742 N94-27694 #
LBL-34018 p 2836 N94-26129 #
LBL-34019 p 2733 N94-26087 #
LBL-34022 p 3053 N94-26094 #
LBL-34080 p 2855 N94-26329 #
LBL-34081 p 2781 N94-26047 #
LBL-34124 p 2789 N94-25597 #
LBL-34168 p 3106 N94-27007 #
LBL-34312 p 2856 N94-26464 #
LBL-34433 p 3054 N94-26128 #
LBL-34512-SUMM p 2957 N94-25663 #
LBL-34512 p 2996 N94-26936 #
LBL-34514 p 2782 N94-26328 #
LBL-34603 p 2816 N94-26130 #
LBL-34663 p 2814 N94-27779 #
LBL-34665 p 3058 N94-26516 #
LBL-34700 p 2714 N94-26122 #
LBL-34720 p 2967 N94-27049 #
LBL-34726 p 3017 N94-26083 #
LBL-34729 p 3032 N94-26330 #
LBL-34763 p 3054 N94-26125 #
LBL-34767 p 2827 N94-27722 #
LBL-34784 p 3018 N94-26325 #
LBL-34793 p 2741 N94-27619 #
LBL-34795 p 2750 N94-26085 #
LBL-34819 p 2760 N94-25849 * #
LBL-34841 p 2809 N94-25662 #
LBL-34856 p 3055 N94-26239 #

LIYAF-1768 p 2715 N94-26406 #

LMSC-F254276 p 3115 N94-26790 * #

LNCC-027/92 p 2792 N94-26401

LPI-CONTRIB-825 p 2887 N94-28294 * #

LR-711 p 2840 N94-26961 #
LR-712 p 2840 N94-26910
LR-714 p 2710 N94-27201 #
LR-715 p 2669 N94-26969 #
LR-716 p 2840 N94-26911
LR-720 p 2681 N94-26815 #

LTR-LA-286 p 2681 N94-27594

LTR-ST-1947 p 2835 N94-26644 #

M-667 p 2669 N94-26954
M-735 p 2942 N94-27437 * #
M-739 p 2860 N94-28100 * #
M-743 p 2797 N94-27639 * #

MEMO-COSOR-92-43 p 2834 N94-26008 #
MEMO-COSOR-92-44 p 2992 N94-26226 #
MEMO-COSOR-92-46 p 2969 N94-27396 #
MEMO-COSOR-92-47 p 2992 N94-26227
MEMO-COSOR-93-04 p 3094 N94-26314 #

MEMO-INF-92-69 p 2975 N94-27936 #
MEMO-INF-93-28 p 2981 N94-26998 #

MEMO-1137 p 3101 N94-26918
MEMO-1138 p 3004 N94-27211
MEMO-1139 p 3007 N94-27222 #
MEMO-1140 p 2996 N94-26962
MEMO-1141 p 2996 N94-26917 #
MEMO-1142 p 2986 N94-26916 #
MEMO-1143 p 2996 N94-26915
MEMO-1144 p 3004 N94-27223 #

MIRA TRANS-93/13 p 2824 N94-27254

MP-93-225 p 3037 N94-27010 #

MRL-TR-92-39 p 2809 N94-26358 #
MRL-TR-93-35 p 2669 N94-26864
MRL-TR-93-9 p 2839 N94-26859

MTG-93-02 p 2809 N94-25637 #

NAL-SP-17 p 2710 N94-27279 #

NAL-TM-650 p 2842 N94-27207 #
NAL-TM-651 p 2681 N94-27247 #
NAL-TM-652 p 2710 N94-27255 #
NAL-TM-653 p 2647 N94-27235 #

NAL-TR-1185 p 2940 N94-27584 #
NAL-TR-1187T p 2675 N94-27608 #
NAL-TR-1189 p 2795 N94-27205 #
NAL-TR-1190 p 2678 N94-27206 #

NAMRL-SR-93-3 p 2937 N94-26346 #

NAMRL-1386 p 2909 N94-26179 #

NAS 1.15:103982 p 2644 N94-26143 * #
NAS 1.15:103988 p 2667 N94-26151 * #
NAS 1.15:104013 p 2667 N94-26091 * #
NAS 1.15:104015 p 2902 N94-27227 * #
NAS 1.15:104588 p 2877 N94-26152 * #
NAS 1.15:104599 p 2897 N94-28179 * #
NAS 1.15:104600 p 2897 N94-28182 * #
NAS 1.15:104777 p 3119 N94-27993 * #
NAS 1.15:104790 p 2697 N94-28183 * #
NAS 1.15:106333 p 2826 N94-27599 * #
NAS 1.15:106346 p 2843 N94-27559 * #
NAS 1.15:106416 p 2700 N94-26090 * #
NAS 1.15:106430 p 2692 N94-27436 * #
NAS 1.15:106453 p 2690 N94-26142 * #
NAS 1.15:106473 p 2741 N94-27426 * #
NAS 1.15:106479 p 2674 N94-26573 * #
NAS 1.15:106489 p 2834 N94-26199 * #
NAS 1.15:106493 p 2691 N94-27424 * #
NAS 1.15:106523 p 2693 N94-27427 * #
NAS 1.15:106525 p 2711 N94-27640 * #
NAS 1.15:107198 p 2902 N94-27411 * #
NAS 1.15:107608 p 2692 N94-27774 * #
NAS 1.15:108436 p 2809 N94-26150 * #
NAS 1.15:108440 p 2707 N94-26127 * #
NAS 1.15:108442 p 2943 N94-27952 * #
NAS 1.15:108444 p 2825 N94-27560 * #
NAS 1.15:108447 p 2833 N94-28265 * #
NAS 1.15:108781 p 2901 N94-26093 * #
NAS 1.15:108783 p 2901 N94-26210 * #
NAS 1.15:108800 p 2944 N94-26098 * #
NAS 1.15:108801 p 2641 N94-26596 * #
NAS 1.15:108804 p 2901 N94-26086 * #
NAS 1.15:108805 p 2645 N94-26538 * #
NAS 1.15:109040-VOL-1 p 2645 N94-26489 * #
NAS 1.15:109040-VOL-2 p 2645 N94-26492 * #
NAS 1.15:109040-VOL-3 p 2645 N94-26497 * #
NAS 1.15:109040-VOL-4 p 2645 N94-26483 * #
NAS 1.15:109053 p 2972 N94-27655 * #
NAS 1.15:109055 p 2844 N94-27830 * #
NAS 1.15:109056 p 2811 N94-26707 * #
NAS 1.15:109071 p 2665 N94-27423 * #
NAS 1.15:109072 p 2681 N94-27425 * #
NAS 1.15:109078 p 2644 N94-26154 * #
NAS 1.15:109080 p 2677 N94-26593 * #
NAS 1.15:109082 p 2711 N94-27658 * #
NAS 1.15:109089 p 3117 N94-26155 * #
NAS 1.15:109104 p 2798 N94-27867 * #
NAS 1.15:109193 p 2692 N94-27956 * #
NAS 1.15:109199 p 2903 N94-27412 * #
NAS 1.15:109684 p 2760 N94-25849 * #
NAS 1.15:109685 p 2681 N94-26684 * #
NAS 1.15:109690 p 2824 N94-27238 * #
NAS 1.15:109691 p 3118 N94-27431 * #
NAS 1.15:109692 p 3118 N94-27381 * #
NAS 1.15:109693 p 2685 N94-27151 * #
NAS 1.15:109694 p 3094 N94-27772 * #
NAS 1.15:109695 p 3094 N94-27661 * #
NAS 1.15:109698 p 2697 N94-27775 * #
NAS 1.15:109699 p 2692 N94-28205 * #
NAS 1.15:109702 p 3119 N94-28204 * #
NAS 1.15:109705 p 2975 N94-27992 * #
NAS 1.15:109708 p 2955 N94-27769 * #
NAS 1.15:109719 p 3100 N94-27413 * #
NAS 1.15:109721 p 2932 N94-27556 * #
NAS 1.15:109723 p 3111 N94-27953 * #
NAS 1.15:109728 p 2692 N94-28178 * #
NAS 1.15:109733 p 2989 N94-28065 * #
NAS 1.15:4495 p 2646 N94-26592 * #
NAS 1.15:4506 p 2646 N94-26547 * #
NAS 1.15:4514 p 2647 N94-26706 * #
NAS 1.15:4516 p 2646 N94-26602 * #
NAS 1.15:4521 p 2679 N94-27660 * #
NAS 1.15:4528 p 2646 N94-26693 * #
NAS 1.15:4540 p 2668 N94-26604 * #
NAS 1.15:4544 p 2691 N94-27868 * #
NAS 1.15:4547 p 2673 N94-27864 * #
NAS 1.15:4552 p 2845 N94-27865 * #
NAS 1.15:4567 p 2971 N94-27573 * #
NAS 1.21:7011(384) p 2934 N94-28219 *
NAS 1.21:7011(386) p 2933 N94-28208 *
NAS 1.21:7011(387) p 2933 N94-28213 *
NAS 1.21:7037(301) p 2643 N94-28203 *
NAS 1.26:179548 p 2824 N94-27228 * #
NAS 1.26:186028 p 2674 N94-27432 * #
NAS 1.26:187158 p 2827 N94-27984 * #
NAS 1.26:187588 p 2973 N94-27663 * #
NAS 1.26:189229 p 2702 N94-26542 * #
NAS 1.26:189236 p 2700 N94-26156 * #
NAS 1.26:190754 p 2703 N94-27213 * #
NAS 1.26:191066 p 2719 N94-27854 * #
NAS 1.26:191204 p 2703 N94-27662 * #
NAS 1.26:191544 p 3085 N94-27893 * #
NAS 1.26:191581 p 2792 N94-26499 * #
NAS 1.26:191584 p 2994 N94-26601 * #
NAS 1.26:191590 p 2711 N94-27433 * #
NAS 1.26:191591 p 2796 N94-27435 * #
NAS 1.26:191592 p 2969 N94-27416 * #
NAS 1.26:191593 p 2971 N94-27558 * #
NAS 1.26:191594 p 2999 N94-27434 * #
NAS 1.26:191595 p 2999 N94-27557 * #
NAS 1.26:191596 p 2971 N94-27572 * #
NAS 1.26:191597 p 2970 N94-27417 * #
NAS 1.26:191598 p 2999 N94-27415 * #
NAS 1.26:191600 p 2894 N94-26506 * #
NAS 1.26:191602 p 2668 N94-26606 * #
NAS 1.26:191605 p 2788 N94-27770 * #
NAS 1.26:191607 p 2680 N94-26603 * #
NAS 1.26:193911-PT-A p 2796 N94-27377 * #
NAS 1.26:193922 p 2691 N94-26135 * #
NAS 1.26:193923 p 2691 N94-26153 * #
NAS 1.26:193924 p 2701 N94-26230 * #
NAS 1.26:193925 p 2823 N94-27149 * #
NAS 1.26:193926 p 2824 N94-27221 * #
NAS 1.26:193927 p 2893 N94-26134 * #
NAS 1.26:193928 p 2799 N94-27931 * #
NAS 1.26:193929 p 2756 N94-27230 * #
NAS 1.26:193931 p 2812 N94-27229 * #
NAS 1.26:193932 p 2696 N94-26791 * #
NAS 1.26:193933 p 2761 N94-27220 * #
NAS 1.26:193934 p 2697 N94-27421 * #
NAS 1.26:193935 p 2761 N94-27664 * #
NAS 1.26:193936 p 2752 N94-26708 * #
NAS 1.26:193938 p 2941 N94-26788 * #
NAS 1.26:193939 p 2822 N94-26597 * #
NAS 1.26:194437 p 2680 N94-26141 * #
NAS 1.26:194443 p 2701 N94-26231 * #
NAS 1.26:194447 p 2703 N94-27212 * #
NAS 1.26:194461 p 2843 N94-27776 * #
NAS 1.26:194463 p 2839 N94-26692 * #
NAS 1.26:194464 p 2701 N94-26208 * #
NAS 1.26:194466 p 2644 N94-26131 * #
NAS 1.26:194467 p 2843 N94-27656 * #
NAS 1.26:194471 p 2701 N94-26209 * #
NAS 1.26:194828 p 3105 N94-28184 * #
NAS 1.26:194849 p 2893 N94-26138 * #
NAS 1.26:194884 p 2956 N94-28267 * #
NAS 1.26:194885 p 2695 N94-26103 * #
NAS 1.26:195118 p 3075 N94-25665 * #
NAS 1.26:195169 p 2887 N94-28294 * #
NAS 1.26:195170 p 2798 N94-27802 * #
NAS 1.26:195177 p 2985 N94-26006 * #
NAS 1.26:195178 p 2958 N94-25777 * #
NAS 1.26:195179 p 2956 N94-25606 * #
NAS 1.26:195209 p 2964 N94-26680 * #
NAS 1.26:195212 p 2879 N94-26599 * #
NAS 1.26:195213 p 2716 N94-26643 * #
NAS 1.26:195214 p 2812 N94-27214 * #
NAS 1.26:195215 p 3110 N94-26590 * #
NAS 1.26:195216 p 3111 N94-27321 * #
NAS 1.26:195217 p 2751 N94-26641 * #
NAS 1.26:195218 p 3115 N94-27419 * #
NAS 1.26:195219 p 3115 N94-27420 * #
NAS 1.26:195220 p 2711 N94-27352 * #
NAS 1.26:195221 p 2714 N94-26205 * #
NAS 1.26:195222 p 2881 N94-27237 * #
NAS 1.26:195223 p 2674 N94-26588 * #
NAS 1.26:195224 p 3106 N94-26237 * #
NAS 1.26:195225 p 3115 N94-27236 * #
NAS 1.26:195226 p 2878 N94-26204 * #
NAS 1.26:195227 p 2848 N94-26236 * #
NAS 1.26:195228 p 2668 N94-26235 * #
NAS 1.26:195229 p 2847 N94-26222 * #
NAS 1.26:195230 p 2961 N94-26207 * #
NAS 1.26:195231 p 3093 N94-26206 * #
NAS 1.26:195232 p 3102 N94-26234 * #
NAS 1.26:195237 p 2883 N94-27393 * #
NAS 1.26:195239 p 2825 N94-27383 * #
NAS 1.26:195240 p 3115 N94-26790 * #
NAS 1.26:195242 p 3103 N94-26789 * #
NAS 1.26:195243 p 2968 N94-27168 * #
NAS 1.26:195244 p 3107 N94-27885 * #
NAS 1.26:195245 p 2835 N94-26691 * #
NAS 1.26:195246 p 3115 N94-27167 * #
NAS 1.26:195248 p 2702 N94-27150 * #
NAS 1.26:195249 p 2793 N94-26595 * #
NAS 1.26:195250 p 2678 N94-26821 * #
NAS 1.26:195252 p 3116 N94-27440 * #
NAS 1.26:195253 p 2702 N94-27166 * #
NAS 1.26:195254 p 3106 N94-27409 * #
NAS 1.26:195255 p 3106 N94-27406 * #
NAS 1.26:195256 p 2896 N94-27408 * #
NAS 1.26:195257 p 3104 N94-27407 * #
NAS 1.26:195265 p 2844 N94-27824 * #
NAS 1.26:195266 p 2756 N94-27429 * #
NAS 1.26:195267 p 3103 N94-27933 * #
NAS 1.26:195268 p 3105 N94-27932 * #

NAS 1.26:195269 .... p 2843 N94-27765 * #
NAS 1.26:195270 .... p 2869 N94-27430 * #
NAS 1.26:195271 .... p 2883 N94-27438 * #
NAS 1.26:195272 .... p 2852 N94-28070 * #
NAS 1.26:195273 .... p 2883 N94-27852 * #
NAS 1.26:195274 .... p 3107 N94-27850 * #
NAS 1.26:195275 .... p 2844 N94-27851 * #
NAS 1.26:195276 .... p 2851 N94-27849 * #
NAS 1.26:195277 .... p 3066 N94-27561 * #
NAS 1.26:195278 .... p 3105 N94-27428 * #
NAS 1.26:195279 .... p 2882 N94-27380 * #
NAS 1.26:195280 .... p 2970 N94-27542 * #
NAS 1.26:195282 .... p 2786 N94-27574 * #
NAS 1.26:195285 .... p 2675 N94-27654 * #
NAS 1.26:195287 .... p 2826 N94-27657 * #
NAS 1.26:195291 .... p 2678 N94-27414 * #
NAS 1.26:195292 .... p 2845 N94-28181 * #
NAS 1.26:195293 .... p 2846 N94-28266 * #
NAS 1.26:195544 .... p 2942 N94-27410 * #
NAS 1.26:195545 .... p 3114 N94-26685 * #
NAS 1.26:195687 .... p 2943 N94-27934 * #
NAS 1.26:195695 .... p 3095 N94-27866 * #
NAS 1.26:195697 .... p 2666 N94-27768 * #
NAS 1.26:195698 .... p 2974 N94-27767 * #
NAS 1.26:195700 .... p 3109 N94-27982 * #
NAS 1.26:195701 .... p 3109 N94-27983 * #
NAS 1.26:195702 .... p 3108 N94-27941 * #
NAS 1.26:195703 .... p 2697 N94-27789 * #
NAS 1.26:195704 .... p 2851 N94-27787 * #
NAS 1.26:195705 .... p 2648 N94-28072 * #
NAS 1.26:195706 .... p 2648 N94-28071 * #
NAS 1.26:195707 .... p 3107 N94-27784 * #
NAS 1.26:195708 .... p 2798 N94-27782 * #
NAS 1.26:195709 .... p 2883 N94-27883 * #
NAS 1.26:195710 .... p 2903 N94-27940 * #
NAS 1.26:195711 .... p 3108 N94-27935 * #
NAS 1.26:195712 .... p 2777 N94-27946 * #
NAS 1.26:195713 .... p 2776 N94-27669 * #
NAS 1.26:195714 .... p 2897 N94-27884 * #
NAS 1.26:195739 .... p 2693 N94-28220 * #
NAS 1.26:195740 .... p 2693 N94-28221 * #
NAS 1.26:195741 .... p 2692 N94-28199 * #
NAS 1.26:4506-VOL-2 .... p 2675 N94-27778 * #
NAS 1.26:4570 .... p 2792 N94-26467 * #
NAS 1.26:4571 .... p 2646 N94-26548 * #
NAS 1.26:4573 .... p 2818 N94-26705 * #
NAS 1.26:4574 .... p 3033 N94-27646 * #
NAS 1.26:4578 .... p 2808 N94-28180 * #
NAS 1.55:10129 .... p 2685 N94-27358 * #
NAS 1.55:10131 .... p 2682 N94-26278 * #
NAS 1.55:10132 .... p 2649 N94-28188 * #
NAS 1.55:10138 .... p 2670 N94-27439 * #
NAS 1.55:3246 .... p 2641 N94-27284 * #
NAS 1.55:3252 .... p 2934 N94-28361 * #
NAS 1.55:3254 .... p 2860 N94-28100 * #
NAS 1.55:3255 .... p 2945 N94-28251 * #
NAS 1.60:3374-VIDEO-SUPPL .... p 2647 N94-27161 * #
NAS 1.60:3375 .... p 2695 N94-26609 * #
NAS 1.60:3387 .... p 3011 N94-27659 * #
NAS 1.60:3394 .... p 2690 N94-27771 * #
NAS 1.60:3395 .... p 2673 N94-27882 * #
NAS 1.60:3406 .... p 2846 N94-28227 * #
NAS 1.60:3408 .... p 3114 N94-26550 * #
NAS 1.60:3417 .... p 2989 N94-27773 * #
NAS 1.60:3418 .... p 2769 N94-26611 * #
NAS 1.60:3429 .... p 2963 N94-26466 * #
NAS 1.60:3435 .... p 2669 N94-26608 * #
NAS 1.60:3463 .... p 2797 N94-27639 * #
NAS 1.61:1321 .... p 3118 N94-27764 * #
NAS 1.61:1324 .... p 2942 N94-27437 * #
NAS 1.61:1326 .... p 2702 N94-26613 * #
NAS 1.61:1335-PT-2 .... p 2814 N94-27981 * #
NAS 1.75:556 .... p 2869 N94-27958 * #

NASA-CP-10129 .... p 2685 N94-27358 * #
NASA-CP-10131 .... p 2682 N94-26278 * #
NASA-CP-10132 .... p 2649 N94-28188 * #
NASA-CP-10138 .... p 2670 N94-27439 * #
NASA-CP-3246 .... p 2641 N94-27284 * #
NASA-CP-3252 .... p 2934 N94-28361 * #
NASA-CP-3254 .... p 2860 N94-28100 * #
NASA-CP-3255 .... p 2945 N94-28251 * #

NASA-CR-179548 .... p 2824 N94-27228 * #
NASA-CR-186028 .... p 2674 N94-27432 * #
NASA-CR-187158 .... p 2827 N94-27984 * #
NASA-CR-187588 .... p 2973 N94-27663 * #
NASA-CR-189229 .... p 2702 N94-26542 * #
NASA-CR-189236 .... p 2700 N94-26156 * #
NASA-CR-190754 .... p 2703 N94-27213 * #
NASA-CR-191066 .... p 2719 N94-27854 * #
NASA-CR-191204 .... p 2703 N94-27662 * #
NASA-CR-191544 .... p 3085 N94-27893 * #
NASA-CR-191581 .... p 2792 N94-26499 * #
NASA-CR-191584 .... p 2994 N94-26601 * #
NASA-CR-191590 .... p 2711 N94-27433 * #
NASA-CR-191591 .... p 2796 N94-27435 * #
NASA-CR-191592 .... p 2969 N94-27416 * #
NASA-CR-191593 .... p 2971 N94-27558 * #
NASA-CR-191594 .... p 2999 N94-27434 * #
NASA-CR-191595 .... p 2999 N94-27557 * #
NASA-CR-191596 .... p 2971 N94-27572 * #
NASA-CR-191597 .... p 2970 N94-27417 * #
NASA-CR-191598 .... p 2999 N94-27415 * #
NASA-CR-191600 .... p 2894 N94-26506 * #
NASA-CR-191602 .... p 2668 N94-26606 * #
NASA-CR-191605 .... p 2788 N94-27770 * #
NASA-CR-191607 .... p 2680 N94-26603 * #
NASA-CR-193911-PT-A .... p 2796 N94-27377 * #
NASA-CR-193922 .... p 2691 N94-26135 * #
NASA-CR-193923 .... p 2691 N94-26153 * #
NASA-CR-193924 .... p 2701 N94-26230 * #
NASA-CR-193925 .... p 2823 N94-27149 * #
NASA-CR-193926 .... p 2824 N94-27221 * #
NASA-CR-193927 .... p 2893 N94-26134 * #
NASA-CR-193928 .... p 2799 N94-27931 * #
NASA-CR-193929 .... p 2756 N94-27230 * #
NASA-CR-193931 .... p 2812 N94-27229 * #
NASA-CR-193932 .... p 2696 N94-26791 * #
NASA-CR-193933 .... p 2761 N94-27220 * #
NASA-CR-193934 .... p 2697 N94-27421 * #
NASA-CR-193935 .... p 2761 N94-27664 * #
NASA-CR-193936 .... p 2752 N94-26708 * #
NASA-CR-193938 .... p 2941 N94-26788 * #
NASA-CR-193939 .... p 2822 N94-26597 * #
NASA-CR-194437 .... p 2680 N94-26141 * #
NASA-CR-194443 .... p 2701 N94-26231 * #
NASA-CR-194447 .... p 2703 N94-27212 * #
NASA-CR-194461 .... p 2843 N94-27776 * #
NASA-CR-194463 .... p 2839 N94-26692 * #
NASA-CR-194464 .... p 2701 N94-26208 * #
NASA-CR-194466 .... p 2644 N94-26131 * #
NASA-CR-194467 .... p 2843 N94-27656 * #
NASA-CR-194471 .... p 2701 N94-26209 * #
NASA-CR-194828 .... p 3105 N94-28184 * #
NASA-CR-194849 .... p 2893 N94-26138 * #
NASA-CR-194884 .... p 2956 N94-28267 * #
NASA-CR-194885 .... p 2695 N94-26103 * #
NASA-CR-195118 .... p 3075 N94-25665 * #
NASA-CR-195169 .... p 2887 N94-28294 * #
NASA-CR-195170 .... p 2798 N94-27802 * #
NASA-CR-195177 .... p 2985 N94-26006 * #
NASA-CR-195178 .... p 2958 N94-25777 * #
NASA-CR-195179 .... p 2956 N94-25606 * #
NASA-CR-195209 .... p 2964 N94-26680 * #
NASA-CR-195212 .... p 2879 N94-26599 * #
NASA-CR-195213 .... p 2716 N94-26643 * #
NASA-CR-195214 .... p 2812 N94-27214 * #
NASA-CR-195215 .... p 3110 N94-26590 * #
NASA-CR-195216 .... p 3111 N94-27321 * #
NASA-CR-195217 .... p 2751 N94-26641 * #
NASA-CR-195218 .... p 3115 N94-27419 * #
NASA-CR-195219 .... p 3115 N94-27420 * #
NASA-CR-195220 .... p 2711 N94-27352 * #
NASA-CR-195221 .... p 2714 N94-26205 * #
NASA-CR-195222 .... p 2881 N94-27237 * #
NASA-CR-195223 .... p 2674 N94-26588 * #
NASA-CR-195224 .... p 3106 N94-26237 * #
NASA-CR-195225 .... p 3115 N94-27236 * #
NASA-CR-195226 .... p 2878 N94-26204 * #
NASA-CR-195227 .... p 2848 N94-26236 * #
NASA-CR-195228 .... p 2668 N94-26235 * #
NASA-CR-195229 .... p 2847 N94-26222 * #
NASA-CR-195230 .... p 2961 N94-26207 * #
NASA-CR-195231 .... p 3093 N94-26206 * #
NASA-CR-195232 .... p 3102 N94-26234 * #
NASA-CR-195237 .... p 2883 N94-27393 * #
NASA-CR-195239 .... p 2825 N94-27383 * #
NASA-CR-195240 .... p 3115 N94-26790 * #
NASA-CR-195242 .... p 3103 N94-26789 * #
NASA-CR-195243 .... p 2968 N94-27168 * #
NASA-CR-195244 .... p 3107 N94-27885 * #
NASA-CR-195245 .... p 2835 N94-26691 * #
NASA-CR-195246 .... p 3115 N94-27167 * #
NASA-CR-195248 .... p 2702 N94-27150 * #
NASA-CR-195249 .... p 2793 N94-26595 * #
NASA-CR-195250 .... p 2678 N94-26821 * #
NASA-CR-195252 .... p 3116 N94-27440 * #
NASA-CR-195253 .... p 2702 N94-27166 * #
NASA-CR-195254 .... p 3106 N94-27409 * #
NASA-CR-195255 .... p 3106 N94-27406 * #
NASA-CR-195256 .... p 2896 N94-27408 * #
NASA-CR-195257 .... p 3104 N94-27407 * #
NASA-CR-195265 .... p 2844 N94-27824 * #
NASA-CR-195266 .... p 2756 N94-27429 * #
NASA-CR-195267 .... p 3103 N94-27933 * #
NASA-CR-195268 .... p 3105 N94-27932 * #
NASA-CR-195269 .... p 2843 N94-27765 * #
NASA-CR-195270 .... p 2869 N94-27430 * #
NASA-CR-195271 .... p 2883 N94-27438 * #
NASA-CR-195272 .... p 2852 N94-28070 * #
NASA-CR-195273 .... p 2883 N94-27852 * #
NASA-CR-195274 .... p 3107 N94-27850 * #
NASA-CR-195275 .... p 2844 N94-27851 * #
NASA-CR-195276 .... p 2851 N94-27849 * #
NASA-CR-195277 .... p 3066 N94-27561 * #
NASA-CR-195278 .... p 3105 N94-27428 * #
NASA-CR-195279 .... p 2882 N94-27380 * #
NASA-CR-195280 .... p 2970 N94-27542 * #
NASA-CR-195282 .... p 2786 N94-27574 * #
NASA-CR-195285 .... p 2675 N94-27654 * #
NASA-CR-195287 .... p 2826 N94-27657 * #
NASA-CR-195291 .... p 2678 N94-27414 * #
NASA-CR-195292 .... p 2845 N94-28181 * #
NASA-CR-195293 .... p 2846 N94-28266 * #
NASA-CR-195544 .... p 2942 N94-27410 * #
NASA-CR-195545 .... p 3114 N94-26685 * #
NASA-CR-195687 .... p 2943 N94-27934 * #
NASA-CR-195695 .... p 3095 N94-27866 * #
NASA-CR-195697 .... p 2666 N94-27768 * #
NASA-CR-195698 .... p 2974 N94-27767 * #
NASA-CR-195700 .... p 3109 N94-27982 * #
NASA-CR-195701 .... p 3109 N94-27983 * #
NASA-CR-195702 .... p 3108 N94-27941 * #
NASA-CR-195703 .... p 2697 N94-27789 * #
NASA-CR-195704 .... p 2851 N94-27787 * #
NASA-CR-195705 .... p 2648 N94-28072 * #
NASA-CR-195706 .... p 2648 N94-28071 * #
NASA-CR-195707 .... p 3107 N94-27784 * #
NASA-CR-195708 .... p 2798 N94-27782 * #
NASA-CR-195709 .... p 2883 N94-27883 * #
NASA-CR-195710 .... p 2903 N94-27940 * #
NASA-CR-195711 .... p 3108 N94-27935 * #
NASA-CR-195712 .... p 2777 N94-27946 * #
NASA-CR-195713 .... p 2776 N94-27669 * #
NASA-CR-195714 .... p 2897 N94-27884 * #
NASA-CR-195739 .... p 2693 N94-28220 * #
NASA-CR-195740 .... p 2693 N94-28221 * #
NASA-CR-195741 .... p 2692 N94-28199 * #
NASA-CR-4506-VOL-2 .... p 2675 N94-27778 * #
NASA-CR-4570 .... p 2792 N94-26467 * #
NASA-CR-4571 .... p 2646 N94-26548 * #
NASA-CR-4573 .... p 2818 N94-26705 * #
NASA-CR-4574 .... p 3033 N94-27646 * #
NASA-CR-4578 .... p 2808 N94-28180 * #

NASA-PAM-556 .... p 2869 N94-27958 * #

NASA-RP-1321 .... p 3118 N94-27764 * #
NASA-RP-1324 .... p 2942 N94-27437 * #
NASA-RP-1326 .... p 2702 N94-26613 * #
NASA-RP-1335-PT-2 .... p 2814 N94-27981 * #

NASA-SP-7011(384) .... p 2934 N94-28219 *
NASA-SP-7011(386) .... p 2933 N94-28208 *
NASA-SP-7011(387) .... p 2933 N94-28213 *
NASA-SP-7037(301) .... p 2643 N94-28203 *

NASA-STD-2201-93 .... p 2975 N94-27992 * #

NASA-TM-103982 .... p 2644 N94-26143 * #
NASA-TM-103988 .... p 2667 N94-26151 * #
NASA-TM-104013 .... p 2667 N94-26091 * #
NASA-TM-104015 .... p 2902 N94-27227 * #
NASA-TM-104588 .... p 2877 N94-26152 * #
NASA-TM-104599 .... p 2897 N94-28179 * #
NASA-TM-104600 .... p 2897 N94-28182 * #
NASA-TM-104777 .... p 3119 N94-27993 * #
NASA-TM-104790 .... p 2697 N94-28183 * #
NASA-TM-106333 .... p 2826 N94-27599 * #
NASA-TM-106346 .... p 2843 N94-27559 * #
NASA-TM-106416 .... p 2700 N94-26090 * #
NASA-TM-106430 .... p 2692 N94-27436 * #
NASA-TM-106453 .... p 2690 N94-26142 * #
NASA-TM-106473 .... p 2741 N94-27426 * #
NASA-TM-106479 .... p 2674 N94-26573 * #
NASA-TM-106489 .... p 2834 N94-26199 * #
NASA-TM-106493 .... p 2691 N94-27424 * #
NASA-TM-106523 .... p 2693 N94-27427 * #
NASA-TM-106525 .... p 2711 N94-27640 * #
NASA-TM-107198 .... p 2902 N94-27411 * #
NASA-TM-107608 .... p 2692 N94-27774 * #
NASA-TM-108436 .... p 2809 N94-26150 * #
NASA-TM-108440 .... p 2707 N94-26127 * #
NASA-TM-108442 .... p 2943 N94-27952 * #
NASA-TM-108444 .... p 2825 N94-27560 * #
NASA-TM-108447 .... p 2833 N94-28265 * #
NASA-TM-108781 .... p 2901 N94-26093 * #
NASA-TM-108783 .... p 2901 N94-26210 * #
NASA-TM-108800 .... p 2944 N94-26098 * #
NASA-TM-108801 .... p 2641 N94-26596 * #
NASA-TM-108804 .... p 2901 N94-26086 * #
NASA-TM-108805 .... p 2645 N94-26538 * #
NASA-TM-109040-VOL-1 .... p 2645 N94-26489 * #
NASA-TM-109040-VOL-2 .... p 2645 N94-26492 * #
NASA-TM-109040-VOL-3 .... p 2645 N94-26497 * #
NASA-TM-109040-VOL-4 .... p 2645 N94-26483 * #
NASA-TM-109053 .... p 2972 N94-27655 * #

NASA-TM-109055 .... p 2844 N94-27830 * #
NASA-TM-109056 .... p 2811 N94-26707 * #
NASA-TM-109071 .... p 2665 N94-27423 * #
NASA-TM-109072 .... p 2681 N94-27425 * #
NASA-TM-109078 .... p 2644 N94-26154 * #
NASA-TM-109080 .... p 2677 N94-26593 * #
NASA-TM-109082 .... p 2711 N94-27658 * #
NASA-TM-109089 .... p 3117 N94-26155 * #
NASA-TM-109104 .... p 2798 N94-27867 * #
NASA-TM-109193 .... p 2692 N94-27956 * #
NASA-TM-109199 .... p 2903 N94-27412 * #
NASA-TM-109684 .... p 2760 N94-25849 * #
NASA-TM-109685 .... p 2681 N94-26684 * #
NASA-TM-109690 .... p 2824 N94-27238 * #
NASA-TM-109691 .... p 3118 N94-27431 * #
NASA-TM-109692 .... p 3118 N94-27381 * #
NASA-TM-109693 .... p 2685 N94-27151 * #
NASA-TM-109694 .... p 3094 N94-27772 * #
NASA-TM-109695 .... p 3094 N94-27661 * #
NASA-TM-109698 .... p 2697 N94-27775 * #
NASA-TM-109699 .... p 2692 N94-28205 * #
NASA-TM-109702 .... p 3119 N94-28204 * #
NASA-TM-109705 .... p 2975 N94-27992 * #
NASA-TM-109708 .... p 2955 N94-27769 * #
NASA-TM-109719 .... p 3100 N94-27413 * #
NASA-TM-109721 .... p 2932 N94-27556 * #
NASA-TM-109723 .... p 3111 N94-27953 * #
NASA-TM-109728 .... p 2692 N94-28178 * #
NASA-TM-109733 .... p 2989 N94-28065 * #
NASA-TM-4495 .... p 2646 N94-26592 * #
NASA-TM-4506 .... p 2646 N94-26547 * #
NASA-TM-4514 .... p 2647 N94-26706 * #
NASA-TM-4516 .... p 2646 N94-26602 * #
NASA-TM-4521 .... p 2679 N94-27660 * #
NASA-TM-4528 .... p 2646 N94-26693 * #
NASA-TM-4540 .... p 2668 N94-26604 * #
NASA-TM-4544 .... p 2691 N94-27868 * #
NASA-TM-4547 .... p 2673 N94-27864 * #
NASA-TM-4552 .... p 2845 N94-27865 * #
NASA-TM-4567 .... p 2971 N94-27573 * #

NASA-TP-3374-VIDEO-SUPPL .... p 2647 N94-27161 * #
NASA-TP-3375 .... p 2695 N94-26609 * #
NASA-TP-3387 .... p 3011 N94-27659 * #
NASA-TP-3394 .... p 2690 N94-27771 * #
NASA-TP-3395 .... p 2673 N94-27882 * #
NASA-TP-3406 .... p 2846 N94-28227 * #
NASA-TP-3408 .... p 3114 N94-26550 * #
NASA-TP-3417 .... p 2989 N94-27773 * #
NASA-TP-3418 .... p 2769 N94-26611 * #
NASA-TP-3429 .... p 2963 N94-26466 * #
NASA-TP-3435 .... p 2669 N94-26608 * #
NASA-TP-3463 .... p 2797 N94-27639 * #

NAVY-CASE-74607 .... p 2756 N94-27675 #
NAVY-CASE-74713 .... p 2787 N94-27672 #
NAVY-CASE-74788 .... p 2777 N94-27734 #
NAVY-CASE-74807 .... p 3039 N94-27674 #
NAVY-CASE-74823 .... p 2820 N94-27670 #
NAVY-CASE-74854 .... p 2787 N94-27673 #
NAVY-CASE-75057 .... p 3039 N94-27676 #
NAVY-CASE-75311 .... p 2820 N94-27671 #

NAWCADWAR-TN-93043-60 .... p 2941 N94-26339 #

NCCOSC/RDT/E-1630-VOL-2 .... p 2768 N94-26335 #

NEDO-P-9206 .... p 2760 N94-26914
NEDO-P-9214 .... p 2858 N94-26838
NEDO-P-9225 .... p 2759 N94-26905

NFP-9202 .... p 2676 N94-25653 #

NHRC-92-30 .... p 2937 N94-26430 #
NHRC-93-18 .... p 2909 N94-26377 #
NHRC-93-4 .... p 2909 N94-26173 #

NIAR-93-15 .... p 2680 N94-26200 #

NIIEFA-P-B-0900 .... p 3044 N94-26510

NIIYAF-MGU-92-12-261 .... p 3015 N94-25920
NIIYAF-MGU-92-15-264 .... p 3013 N94-25835

NIKHEF-H/93-09 .... p 3020 N94-26540
NIKHEF-H/93-11 .... p 2814 N94-28098
NIKHEF-H/93-12 .... p 3072 N94-26541 #
NIKHEF-H/93-13 .... p 2995 N94-26812 #

NIOZ-1992-6 .... p 2868 N94-27200 #

NISTIR-5263 .... p 2763 N94-26756
NISTIR-5280 .... p 2717 N94-26907 #

NLR-TP-91249-U .... p 2743 N94-27795
NLR-TP-92114-U .... p 2678 N94-27395
NLR-TP-92151-U .... p 2666 N94-27831
NLR-TP-92167-U .... p 2798 N94-27853
NLR-TP-92183-U .... p 2670 N94-27796
NLR-TP-92193-U .... p 2743 N94-27797
NLR-TP-92210-U .... p 2679 N94-27798
NLR-TP-92221-U .... p 2798 N94-27799
NLR-TP-92243-U .... p 2989 N94-27800
NLR-TP-92321-U .... p 2843 N94-27553
NLR-TP-92342-U .... p 3001 N94-28353 #
NLR-TP-92351-U .... p 2647 N94-27554
NLR-TP-92356-U .... p 2851 N94-27555

NOAA-TM-ERL-ETL-235 .... p 2896 N94-26959 #

NOAA-TM-ERL-SEL-82 .... p 3110 N94-26755 #

NONP-SUPPL-DK-94-205048 .... p 2645 N94-26483 * #
NONP-SUPPL-DK-94-205049 .... p 2645 N94-26489 * #
NONP-SUPPL-DK-94-205050 .... p 2645 N94-26492 * #
NONP-SUPPL-DK-94-209487 .... p 2645 N94-26497 * #

NONP-SUPPL-VT-94-209775 .... p 2647 N94-27161 * #

NPL-DITC-215/93 .... p 2964 N94-26655

NPL-DMM(A)-104 .... p 2965 N94-26816
NPL-DMM(A)-110 .... p 2748 N94-25894
NPL-DMM(A)-114 .... p 2756 N94-27217
NPL-DMM(A)-88 .... p 2752 N94-26652
NPL-DMM(A)-95 .... p 2738 N94-26653
NPL-DMM(A)-96-PT-1 .... p 2825 N94-27322
NPL-DMM(A)-97-PT-2 .... p 2825 N94-27324

NPL-QU-97 .... p 3009 N94-27131

NPS-EC-93-019 .... p 3012 N94-25655 #

NPS-MA-94-004 .... p 2990 N94-25594 #

NPS-ME-93-008 .... p 2740 N94-27009 #

NPS-OC-93-006 .... p 2898 N94-26076 #

NRC-32159 .... p 2677 N94-26710 #
NRC-32160 .... p 2708 N94-26711 #
NRC-32161 .... p 2647 N94-26702 #
NRC-37061 .... p 3118 N94-26709 #

NREL/TP-410-6049 .... p 2855 N94-26115 #
NREL/TP-411-5361 .... p 2856 N94-26426 #
NREL/TP-411-5836 .... p 2856 N94-26480 #
NREL/TP-411-6003 .... p 2859 N94-27610 #
NREL/TP-413-6216 .... p 3067 N94-27609 #
NREL/TP-441-5761 .... p 2856 N94-26513 #
NREL/TP-442-6008 .... p 2791 N94-26117 #
NREL/TP-451-5746 .... p 2860 N94-27625 #
NREL/TP-451-5834 .... p 2736 N94-26481 #

NRL-FR/7323-93-9431 .... p 2899 N94-26567 #

NRL-MR/7240-93-7072 .... p 2899 N94-26853 #

NRL-93-2172/93ACSD-02 .... p 2772 N94-26884 #

NRL/MR/5333-93-7437 .... p 2768 N94-26189 #
NRL/MR/5511-93-7422 .... p 2965 N94-26831 #
NRL/MR/6707-93-7425 .... p 2767 N94-26177 #
NRL/MR/6756-93-7406 .... p 3033 N94-27082 #
NRL/MR/7532-93-7212 .... p 2900 N94-26887 #
NRL/MR/7533-93-7213 .... p 2892 N94-25793 #

NRL/PU/7530-93-0008 .... p 2868 N94-26888 #

NRNS-002-00-001-01 .... p 2983 N94-28042

NSF-93-320 .... p 3101 N94-28201 #

NSTS-08283 .... p 2693 N94-28221 * #
NSTS-08284 .... p 2692 N94-28199 * #
NSTS-08285 .... p 2693 N94-28220 * #

NSWCCR/RDTN-93/010 .... p 3037 N94-27066 #

NSWCCR/RDTR-93/040 .... p 3036 N94-26981 #

NSWCDD/TR-93/345 .... p 2961 N94-26148 #

NTSB/AAR-94/01 .... p 2660 N94-27766 #

NTSB/SIR-94/01 .... p 2660 N94-27881 #

NUB-3071 .... p 3071 N94-25882 #

NUWC-NPT-TR-10298 .... p 3003 N94-26436 #
NUWC-NPT-TR-10495 .... p 3010 N94-26923 #

NWRA-CR-93-R092 .... p 2877 N94-25877 #

N93-015 .... p 3068 N94-27704 #

ONERA-NT-1990-13 .... p 2699 N94-25638 #
ONERA-NT-1991-2 .... p 2791 N94-26316 #

ORNL/FTR-4702 .... p 2749 N94-26080 #

ORNL/M-3027-REV-3 .... p 2869 N94-27691 #

ORNL/SUB-88-SC423/01 .... p 2708 N94-26557 #

ORNL/TM-12196 .... p 2965 N94-26784 #
ORNL/TM-12309 .... p 2964 N94-26764 #
ORNL/TM-12428 .... p 2750 N94-26332 #

OZ-92/26 .... p 3014 N94-25841 #
OZ-92/34 .... p 3015 N94-25891 #
OZ-93/06 .... p 3014 N94-25889 #
OZ-93/08 .... p 3006 N94-25886 #
OZ-93/10 .... p 2990 N94-25838 #
OZ-93/5 .... p 3014 N94-25888 #

PB93-219202 .... p 2752 N94-26652
PB93-232163 .... p 3025 N94-27348
PB93-237626 .... p 3094 N94-26314 #
PB93-237683 .... p 2999 N94-27349
PB94-105061 .... p 2965 N94-26816
PB94-117108 .... p 2759 N94-26753 #
PB94-119666 .... p 2825 N94-27322
PB94-119690 .... p 3101 N94-27323
PB94-119807 .... p 2839 N94-26754 #
PB94-120185 .... p 2669 N94-26906
PB94-120714 .... p 3110 N94-26755 #
PB94-121050 .... p 2763 N94-26756
PB94-121324 .... p 2717 N94-26907 #
PB94-121431 .... p 2867 N94-26757 #
PB94-123270 .... p 2825 N94-27324
PB94-123296 .... p 2849 N94-26866
PB94-123312 .... p 2849 N94-26848
PB94-123320 .... p 2902 N94-27171
PB94-123361 .... p 2842 N94-27197
PB94-123395 .... p 2842 N94-27198
PB94-123536 .... p 3010 N94-27037 #
PB94-123551 .... p 3005 N94-27172
PB94-123569 .... p 3005 N94-27173
PB94-123577 .... p 2756 N94-27215
PB94-123593 .... p 2968 N94-27154
PB94-123619 .... p 2812 N94-27216
PB94-123627 .... p 2942 N94-27155
PB94-123643 .... p 2785 N94-27038 #
PB94-123668 .... p 2900 N94-27156
PB94-123676 .... p 2968 N94-27157
PB94-123692 .... p 2759 N94-25907
PB94-123700 .... p 2881 N94-27039 #
PB94-123718 .... p 2881 N94-27040 #
PB94-123742 .... p 2772 N94-27041 #
PB94-123767 .... p 2823 N94-26849
PB94-123775 .... p 2835 N94-27042 #
PB94-123783 .... p 3008 N94-26851
PB94-123791 .... p 2881 N94-27043 #
PB94-123809 .... p 2710 N94-27253
PB94-124211 .... p 2811 N94-27044 #
PB94-124229 .... p 2902 N94-27045 #
PB94-124237 .... p 2755 N94-27158
PB94-124245 .... p 3037 N94-27046 #
PB94-124252 .... p 2773 N94-27159
PB94-124278 .... p 2986 N94-26992 #
PB94-124294 .... p 2812 N94-27160
PB94-124302 .... p 2998 N94-27115
PB94-124310 .... p 3009 N94-27131
PB94-124328 .... p 2756 N94-27217
PB94-124344 .... p 3024 N94-27199
PB94-124369 .... p 2996 N94-26993 #
PB94-124377 .... p 2997 N94-26994 #
PB94-124385 .... p 2997 N94-26995 #
PB94-124393 .... p 2997 N94-26996 #
PB94-124401 .... p 3101 N94-27218
PB94-124427 .... p 2774 N94-27219
PB94-124443 .... p 2900 N94-27208
PB94-124476 .... p 3038 N94-27209
PB94-124534 .... p 2665 N94-27210
PB94-124567 .... p 2741 N94-27325
PB94-124575 .... p 2741 N94-27326
PB94-124583 .... p 2732 N94-25908
PB94-124591 .... p 2786 N94-27327
PB94-124609 .... p 2741 N94-27328
PB94-124633 .... p 2909 N94-25909
PB94-124856 .... p 2748 N94-25892
PB94-124864 .... p 2748 N94-25893
PB94-124872 .... p 2748 N94-25894
PB94-124922 .... p 3004 N94-27051
PB94-125002 .... p 3004 N94-26939 #
PB94-125101 .... p 2824 N94-27254
PB94-125218 .... p 2965 N94-26852

PB94-125234 p 2967 N94-26997 #
PB94-125242 p 2965 N94-26908 #
PB94-125259 p 3004 N94-26867
PB94-125267 p 2981 N94-26998 #
PB94-125275 p 3004 N94-26870
PB94-125283 p 2771 N94-26872
PB94-125309 p 2992 N94-26252
PB94-125317 p 2995 N94-26818 #
PB94-125333 p 2998 N94-27116 #
PB94-125341 p 2997 N94-26999 #
PB94-125358 p 2997 N94-27000 #
PB94-125366 p 2939 N94-27001 #
PB94-125374 p 2938 N94-26873
PB94-125390 p 3009 N94-26968 #
PB94-125408 p 2997 N94-27028 #
PB94-125432 p 2881 N94-27052 #
PB94-125903 p 3110 N94-27053 #
PB94-125911 p 3110 N94-27054 #
PB94-125960 p 2896 N94-26959 #
PB94-126356 p 2839 N94-26875 #
PB94-126380 p 2986 N94-27029 #
PB94-126398 p 2763 N94-26819
PB94-126406 p 2840 N94-26960
PB94-126414 p 2868 N94-27200 #
PB94-126455 p 2998 N94-27030 #
PB94-126463 p 2967 N94-27031 #
PB94-126471 p 2669 N94-26969 #
PB94-126489 p 2771 N94-26877
PB94-126497 p 2881 N94-26880
PB94-126505 p 2772 N94-26909
PB94-126513 p 2840 N94-26910
PB94-126521 p 2840 N94-26961 #
PB94-126539 p 2681 N94-26815 #
PB94-126547 p 2840 N94-26911
PB94-126554 p 2669 N94-26954
PB94-126570 p 2710 N94-27201 #
PB94-126612 p 2996 N94-26962
PB94-126620 p 2996 N94-26915
PB94-126638 p 2986 N94-26916 #
PB94-126646 p 2996 N94-26917 #
PB94-126653 p 3101 N94-26918
PB94-126661 p 3004 N94-27211
PB94-126679 p 3007 N94-27222 #
PB94-126687 p 2966 N94-26955
PB94-126695 p 2966 N94-26919 #
PB94-126703 p 2966 N94-26956
PB94-126711 p 3004 N94-27223 #
PB94-126729 p 2966 N94-26970 #
PB94-126737 p 2966 N94-26971 #
PB94-126745 p 2966 N94-26920 #
PB94-126752 p 2966 N94-26921 #
PB94-126794 p 2824 N94-27224
PB94-128329 p 2859 N94-27225
PB94-128345 p 2717 N94-27226
PB94-129046 p 2717 N94-27256
PB94-132446 p 2833 N94-28375 #
PB94-132453 p 2712 N94-28376 #
PB94-132479 p 2976 N94-28377 #
PB94-132487 p 2833 N94-28378 #
PB94-132826 p 2983 N94-28354
PB94-132834 p 2778 N94-28355
PB94-132859 p 2976 N94-28356 #
PB94-132875 p 2778 N94-28379 #
PB94-132883 p 2778 N94-28380 #
PB94-132891 p 2778 N94-28381 #
PB94-132909 p 2778 N94-28382 #
PB94-132917 p 2779 N94-28390 #
PB94-132933 p 2779 N94-28391 #
PB94-132990 p 2937 N94-28392 #
PB94-133055 p 2900 N94-28393 #
PB94-133063 p 2876 N94-28394 #
PB94-133071 p 2876 N94-28395 #
PB94-133089 p 2876 N94-28383 #
PB94-133097 p 2778 N94-28384 #
PB94-133105 p 3100 N94-28396 #
PB94-133113 p 2779 N94-28397 #
PB94-133121 p 3001 N94-28398 #
PB94-133139 p 3100 N94-28385 #
PB94-133147 p 3095 N94-28386 #
PB94-133154 p 2778 N94-28387 #
PB94-133162 p 2779 N94-28388 #
PB94-133170 p 3001 N94-28389 #
PB94-133196 p 2788 N94-28357 #
PB94-133204 p 2689 N94-28358 #
PB94-133592 p 2747 N94-28359 #
PB94-134830 p 3111 N94-28360 #
PB94-910402 p 2660 N94-27766 #
PB94-917002 p 2660 N94-27881 #

PCMDI-12 p 2897 N94-27571 #

PL-TN-93-1067 p 3035 N94-26572 #

PL-TR-92-1064 p 2763 N94-26341 #
PL-TR-92-2011 p 2898 N94-28223 #
PL-TR-92-2019 p 2887 N94-28206 #
PL-TR-92-2323 p 2887 N94-28214 #
PL-TR-92-2330 p 2893 N94-26168 #
PL-TR-92-3051 p 2721 N94-28215 #
PL-TR-93-2024 p 2878 N94-26304 #
PL-TR-93-2035 p 2816 N94-26178 #
PL-TR-93-2088 p 2877 N94-25877 #
PL-TR-93-2099 p 2698 N94-28217 #
PL-TR-93-2115 p 2879 N94-26569 #
PL-TR-93-2116 p 2959 N94-25879 #
PL-TR-93-2120 p 2698 N94-28200 #
PL-TR-93-2128 p 2876 N94-25752 #
PL-TR-93-2132(1) p 3033 N94-27084 #
PL-TR-93-2132(2) p 3012 N94-25726 #
PL-TR-93-2136 p 2777 N94-28211 #
PL-TR-93-2151 p 2892 N94-25873
PL-TR-93-2161 p 2698 N94-28210 #
PL-TR-93-2171-PT-1 p 2878 N94-26224
PL-TR-93-2174 p 3001 N94-28216 #
PL-TR-93-2178 p 3040 N94-28202 #
PL-TR-93-2179 p 3104 N94-27265 #
PL-TR-93-2193 p 2878 N94-26433 #
PL-TR-93-2196 p 2773 N94-27085 #
PL-TR-93-2205 p 2895 N94-26798
PL-TR-93-3041 p 3033 N94-27083 #
PL-TR-93-3053 p 2701 N94-26537 #
PL-TR-94-2004 p 2878 N94-26338 #

PML-1992-73 p 2784 N94-26646
PML-1992-91 p 2811 N94-26647

PNL-SA-21630 p 2737 N94-26585 #
PNL-SA-21725 p 2731 N94-25804 #
PNL-SA-21753 p 2838 N94-26524 #
PNL-SA-21769 p 2982 N94-27600 #
PNL-SA-22009 p 2941 N94-26555 #
PNL-SA-22351 p 2869 N94-27601 #
PNL-SA-22411 p 3116 N94-27621 #
PNL-SA-22415 p 2827 N94-27780 #
PNL-SA-22444 p 2737 N94-26575 #
PNL-SA-22470 p 2737 N94-26556 #
PNL-SA-22489 p 3017 N94-26049 #
PNL-SA-22525 p 3067 N94-27602 #
PNL-SA-22526 p 2731 N94-25803 #
PNL-SA-22545 p 2732 N94-25987 #
PNL-SA-22559 p 2895 N94-26761 #
PNL-SA-22561 p 2705 N94-25805 #
PNL-SA-22598 p 2880 N94-26762 #
PNL-SA-22619 p 3097 N94-26348 #
PNL-SA-22626 p 3096 N94-25813 #
PNL-SA-22654 p 3054 N94-26147 #
PNL-SA-22762 p 2866 N94-25948 #
PNL-SA-22816 p 2754 N94-27021 #
PNL-SA-22938 p 3100 N94-27563 #
PNL-SA-22941 p 2741 N94-27570 #
PNL-SA-23016 p 2741 N94-27622 #
PNL-SA-23064 p 3000 N94-27569 #
PNL-SA-23116 p 2960 N94-26048 #
PNL-SA-23284 p 2742 N94-27786 #

PNL-8921 p 2664 N94-26309 #
PNL-8926 p 2706 N94-25982 #

PREPRINT-699 p 2807 N94-28099

PRI-200 p 2835 N94-26691 * #

PSC-28 p 2820 N94-27701 #

PSI-1126/TR-1257 p 2750 N94-26167 #

PWA-5774-119 p 2839 N94-26692 * #
PWA-6228-47 p 2674 N94-26588 * #

RAL-93-064 p 2998 N94-27115
RAL-93-065 p 3024 N94-27199
RAL-94-022 p 3111 N94-27953 * #

RANA-93-04 p 2999 N94-27349

RCNP-P-124 p 3027 N94-27733 #

REPT-A-2657 p 3012 N94-25636 #
REPT-A-2661 p 3053 N94-26089 #
REPT-A-2663 p 3049 N94-25614 #
REPT-A-2664 p 2715 N94-26476 #
REPT-A-2665 p 3051 N94-25921 #
REPT-A-2666 p 2736 N94-26477 #
REPT-A-2667 p 3053 N94-26071 #
REPT-A-2668 p 2733 N94-26073 #
REPT-A-5 p 2756 N94-27429 * #

REPT-107 p 2883 N94-27963 #
REPT-1148-94-03 p 2709 N94-27107 #
REPT-14 p 2722 N94-25544 #
REPT-158 p 2896 N94-27169 #
REPT-1949-01-93-TR p 3104 N94-27265 #
REPT-1993.2 p 3049 N94-25645 #
REPT-1 p 2942 N94-27410 * #
REPT-35 p 2881 N94-27052 #
REPT-36 p 2776 N94-27340 #
REPT-41377 p 2759 N94-26753 #
REPT-44-VOL-44 p 2911 N94-27442 #
REPT-4 p 2898 N94-25635 #
REPT-5490-08 p 2823 N94-27149 * #
REPT-6109B p 2660 N94-27766 #
REPT-6264 p 2660 N94-27881 #
REPT-6 p 2867 N94-26474 #
REPT-721563-6-APP p 2783 N94-26449 #
REPT-7 p 2879 N94-26475 #
REPT-92-87 p 2849 N94-26866
REPT-92-88 p 2998 N94-27030 #
REPT-92-89 p 2967 N94-27031 #
REPT-92129712 p 3055 N94-26188 #
REPT-9224-RPT-004.1 p 2764 N94-27144 #
REPT-93-39 p 3002 N94-26213 #
REPT-93-40 p 2837 N94-26214 #
REPT-93-41 p 2991 N94-26215 #
REPT-93-42 p 2865 N94-25760 #
REPT-93-43 p 2957 N94-25761 #
REPT-93-44 p 2958 N94-25762
REPT-93-45 p 2790 N94-25763 #
REPT-93-47-PT-2 p 2958 N94-25764 #
REPT-93-48 p 2966 N94-26966
REPT-93-49 p 2996 N94-26967 #
REPT-93-50 p 2995 N94-26818 #
REPT-93-51 p 2992 N94-26252
REPT-932-430-101 p 2711 N94-27586 #
REPT-94B00027 p 2702 N94-26613 * #
REPT-94B00039 p 2877 N94-26152 * #
REPT-94B00043 p 2945 N94-28251 * #
REPT-94B00047 p 2814 N94-27981 * #
REPT-94B00054 p 2897 N94-28182 * #
REPT-94B00055 p 2897 N94-28179 * #
REPT-94B0005 p 2674 N94-27432 * #

RI/RD-93-195 p 2822 N94-26597 * #

RI/RD88-291 p 2703 N94-27213 * #
RI/RD89-111 p 2703 N94-27212 * #
RI/RD91-235 p 2700 N94-26156 * #
RI/RD92-127 p 2701 N94-26231 * #
RI/RD92-139 p 2702 N94-26542 * #
RI/RD92-214 p 2824 N94-27228 * #

RL-TR-93-151 p 2767 N94-25960 #
RL-TR-93-156 p 2766 N94-25736 #
RL-TR-93-158 p 2981 N94-27100 #
RL-TR-93-159 p 2834 N94-25727 #
RL-TR-93-165 p 2765 N94-25660 #
RL-TR-93-186 p 2820 N94-28068 #
RL-TR-93-188 p 2817 N94-26271 #
RL-TR-93-190 p 3099 N94-27101 #
RL-TR-93-198 p 3032 N94-26881 #
RL-TR-93-200 p 2979 N94-25786 #

RNR-92-006 p 2970 N94-27542 * #

RR-GR-93-01 p 2823 N94-27104 #

RSS-8912 p 2701 N94-26230 * #

RXR-92012 p 2887 N94-28206 #
RXR-93051 p 2698 N94-28200 #
RXR-93071 p 3040 N94-28202 #

S-731 p 3119 N94-27993 * #
S-755 p 2934 N94-28361 * #
S-760 p 2697 N94-28183 * #

SAIC-67-6733 p 2673 N94-26176 #
SAIC-93/1229 p 3043 N94-26356 #

SAND-91-1144 p 3016 N94-26033 #
SAND-91-2845 p 2783 N94-26372 #
SAND-91-2850 p 2708 N94-26796 #
SAND-92-1107 p 2750 N94-26247 #
SAND-92-1108 p 2751 N94-26564 #
SAND-92-2744 p 2985 N94-26462 #
SAND-92-2905C p 3053 N94-26025 #
SAND-93-0018C p 2836 N94-26032 #
SAND-93-0172 p 2748 N94-25932 #
SAND-93-0205C p 2980 N94-26473
SAND-93-0574C p 2757 N94-27726 #
SAND-93-0997C p 2716 N94-26794 #
SAND-93-1099C p 2742 N94-27788 #
SAND-93-1119C p 2839 N94-26810 #
SAND-93-1126C p 3056 N94-26308 #
SAND-93-1146C p 3051 N94-25944 #
SAND-93-1159C p 3050 N94-25815 #
SAND-93-1171C p 3052 N94-25989 #
SAND-93-1298C p 2961 N94-26146 #
SAND-93-1323C p 2780 N94-25812 #

SAND-93-1331C .... p 2819 N94-26811 #
SAND-93-1422-VOL-3 .... p 3099 N94-27022 #
SAND-93-1435C .... p 2857 N94-26617 #
SAND-93-1453C .... p 3050 N94-25814 #
SAND-93-1471C .... p 3058 N94-26565 #
SAND-93-1493C .... p 3056 N94-26352 #
SAND-93-1509C .... p 3069 N94-27790 #
SAND-93-1529C .... p 2780 N94-25664 #
SAND-93-1533C .... p 3039 N94-27721 #
SAND-93-1584C .... p 2682 N94-27997 #
SAND-93-1649C .... p 2739 N94-26912 #
SAND-93-1656C .... p 2857 N94-26700 #
SAND-93-1720 .... p 2821 N94-25811 #
SAND-93-1725C .... p 3052 N94-25971 #
SAND-93-1749 .... p 2962 N94-26371 #
SAND-93-1760C .... p 2821 N94-26110 #
SAND-93-1808C .... p 3057 N94-26420 #
SAND-93-1900 .... p 2838 N94-26563 #
SAND-93-1926C .... p 2948 N94-26111 #
SAND-93-2007 .... p 3068 N94-27693 #
SAND-93-2118C .... p 2713 N94-25978 #
SAND-93-2144C .... p 2819 N94-27262
SAND-93-2145C .... p 2857 N94-26612 #
SAND-93-2168C .... p 3069 N94-27753 #
SAND-93-2205C .... p 2732 N94-25819 #
SAND-93-2206C .... p 3040 N94-28000 #
SAND-93-2226C .... p 3040 N94-27999 #
SAND-93-2246 .... p 2762 N94-26027 #
SAND-93-2248C .... p 3061 N94-26856 #
SAND-93-2271C .... p 2859 N94-27004 #
SAND-93-2296C .... p 2702 N94-26560 #
SAND-93-2297C .... p 2700 N94-25956 #
SAND-93-2334C .... p 2742 N94-27755 #
SAND-93-2339 .... p 2962 N94-26370 #
SAND-93-2356C .... p 2781 N94-25977 #
SAND-93-2360C .... p 2821 N94-25970 #
SAND-93-2419C .... p 3000 N94-27564 #
SAND-93-2445C .... p 2738 N94-26610 #
SAND-93-2508C .... p 2960 N94-26118 #
SAND-93-2542C .... p 2712 N94-27710 #
SAND-93-2545C .... p 3070 N94-28067 #
SAND-93-2595C .... p 2979 N94-25952 #
SAND-93-2596C .... p 2983 N94-27713 #
SAND-93-2597C .... p 2979 N94-25953 #
SAND-93-2599C .... p 2704 N94-27708 #
SAND-93-2616C .... p 2848 N94-26277 #
SAND-93-2678C .... p 3049 N94-25601 #
SAND-93-2681C .... p 2780 N94-25975 #
SAND-93-2695C .... p 2699 N94-25600 #
SAND-93-2709C .... p 3050 N94-25817 #
SAND-93-2736C .... p 2735 N94-26349 #
SAND-93-2742C .... p 2958 N94-25818 #
SAND-93-3826C .... p 3035 N94-26246 #
SAND-93-7076 .... p 2856 N94-26463 #
SAND-93-8237 .... p 2759 N94-26198 #
SAND-94-8475C .... p 2743 N94-27792 #

SBIR-92-2 .... p 3094 N94-27772 * #
SBIR-94-1 .... p 3094 N94-27661 * #

SC-MAG-417 .... p 3060 N94-26795 #

SCT-92RR-8 .... p 2665 N94-26826 #

SC5545.FR .... p 3034 N94-25902 #

SER/CDM-LA-31 .... p 2716 N94-26518 #

SGD-590-PT-1 .... p 3110 N94-27053 #
SGD-590-PT-2 .... p 3110 N94-27054 #
SGD-591-PT-2 .... p 3111 N94-28360 #

SILVA-CARELICA-21 .... p 2850 N94-27182 #
SILVA-CARELICA-22 .... p 2848 N94-26258 #

SINPC-0002 .... p 2742 N94-27730 #

SIP-0050 .... p 3049 N94-27855
SIP-0052 .... p 2758 N94-27845
SIP-0053 .... p 3049 N94-27856

SISSA-92/93/FM .... p 2997 N94-27023

SKL-1600-46-003-01-0 .... p 2974 N94-27823
SKL-1600-99-002 .... p 2973 N94-27762

SLAC-PUB-5845 .... p 3071 N94-25911
SLAC-PUB-6406 .... p 3116 N94-27440 * #

SLAC/SSRL-0041 .... p 3056 N94-26326 #

SMC-TR-93-57 .... p 2785 N94-26845 #
SMC-TR-93-58 .... p 3008 N94-26484 #
SMC-TR-93-64 .... p 2753 N94-26842 #

SP-RAPP-1992:17 .... p 2823 N94-26849
SP-RAPP-1992:43 .... p 2811 N94-27044 #
SP-RAPP-1993-45 .... p 2842 N94-27197
SP-RAPP-1993-46 .... p 2842 N94-27198
SP-RAPP-1993:14 .... p 2759 N94-25907
SP-RAPP-1993:26 .... p 2812 N94-27160
SP-RAPP-1993:48 .... p 2835 N94-27042 #

SP-REPT-1993:23 .... p 3008 N94-26851

SPC-92017-CMC .... p 2962 N94-26373 #

SPP-9309052 .... p 2759 N94-26486 #

SR-13 .... p 2959 N94-25879 #
SR-1 .... p 3104 N94-27265 #
SR-3 .... p 3012 N94-25726 #
SR-3 .... p 2878 N94-26304 #
SR-3 .... p 3033 N94-27084 #
SR-6-PT-1 .... p 2878 N94-26224

SRI-MP-93-087R .... p 2717 N94-27226

SRS/STG-TR92-14 .... p 2823 N94-27149 * #

SSCL-PREPRINT-514 .... p 3021 N94-26759 #
SSCL-PREPRINT-516 .... p 2980 N94-25984 #
SSCL-PREPRINT-527 .... p 3063 N94-27047 #

SSCL-520 .... p 3011 N94-25598 #

SSD92D0154 .... p 3095 N94-27866 * #

SSP-30540-REV-A .... p 2955 N94-27769 * #
SSP-30542-REV-A .... p 2697 N94-27775 * #

SSRP-93/10 .... p 2711 N94-27352 * #

STF23-A93028 .... p 2909 N94-25909
STF34-A93005 .... p 2741 N94-27326
STF34-A93094 .... p 2732 N94-25908
STF34-A93113 .... p 2786 N94-27327
STF34-A93129 .... p 2741 N94-27325
STF34-A93134 .... p 2741 N94-27328

SU-SLAC-PUB-6096 .... p 3018 N94-26133 #
SU-SLAC-PUB-6267 .... p 3116 N94-27740 #
SU-SLAC-PUB-6300 .... p 3056 N94-26326 #
SU-SLAC-PUB-6316 .... p 3017 N94-26101 #
SU-SLAC-PUB-6340 .... p 3028 N94-27736 #
SU-SLAC-PUB-6356 .... p 3024 N94-27050 #

SWRI-3178-4.12 .... p 2824 N94-27224

TAMRF-5802-94-01 .... p 2648 N94-28072 * #
TAMRF-6382-94-01 .... p 2648 N94-28071 * #

TDCK-TD-91-4352 .... p 2659 N94-25780 #
TDCK-TD-92-1737 .... p 3033 N94-25721 #
TDCK-TD-92-3840 .... p 2767 N94-26011 #
TDCK-TD-93-0485 .... p 2891 N94-25722 #
TDCK-TD-93-0753 .... p 2948 N94-25720 #
TDCK-TD-93-1359 .... p 3095 N94-25723 #
TDCK-TD-93-1361 .... p 2908 N94-25871 #
TDCK-TD-93-1366 .... p 2940 N94-25724 #
TDCK-TD-930480 .... p 2893 N94-26016 #
TDCK-TD-930758 .... p 2893 N94-26013 #

TDCK-TD93-2788 .... p 2959 N94-25963 #

TDCK-93-0302 .... p 3038 N94-27137
TDCK-93-0303 .... p 2773 N94-27136
TDCK-93-0466 .... p 2811 N94-27134 #
TDCK-93-1348 .... p 2939 N94-27138

TD92-1511 .... p 2811 N94-26647
TD92-2408 .... p 2784 N94-26646
TD92-3681 .... p 2770 N94-26650
TD92-3836 .... p 3036 N94-26649
TD92-3837 .... p 3036 N94-26648

TEC-R-198 .... p 2647 N94-25656 #
TEC-R-203 .... p 3098 N94-26451 #

TEC-0038 .... p 2849 N94-27069 #
TEC-0039 .... p 2709 N94-27135 #

TICOM-85-10 .... p 2846 N94-28266 * #

TIFR/TH-93-28 .... p 3019 N94-26423 #

TIOS-93/15 .... p 2771 N94-26872
TIOS-93/16 .... p 3004 N94-26870
TIOS-93/17 .... p 3004 N94-26867

TKK-TKO-B104 .... p 3100 N94-28385 #
TKK-TKO-C62 .... p 3001 N94-28398 #

TKO-B103 .... p 2976 N94-28356 #
TKO-B107 .... p 3100 N94-28396 #

TM-92-0046 .... p 2956 N94-28267 * #

TR-17 .... p 2754 N94-27033 #
TR-19 .... p 2754 N94-27036 #
TR-20 .... p 2754 N94-27080 #
TR-23 .... p 2755 N94-27087 #
TR-24 .... p 2755 N94-27163 #
TR-4-ONR .... p 2736 N94-26452 #
TR-4527-029-93 .... p 2859 N94-27225
TR-473 .... p 3003 N94-26485 #
TR-474 .... p 3003 N94-26495 #
TR-475 .... p 3003 N94-26494 #
TR-476 .... p 3004 N94-26496 #
TR-5 .... p 3059 N94-26571 #
TR-65 .... p 3018 N94-26172 #
TR-66 .... p 3022 N94-26894 #
TR-7 .... p 3020 N94-26562 #
TR-90-ONR .... p 2715 N94-26444 #
TR-92(2925)-3 .... p 3008 N94-26484 #
TR-93(3478)-1 .... p 2785 N94-26845 #
TR-93(3935)-12 .... p 2753 N94-26842 #
TR-93-1 .... p 2771 N94-26844 #
TR-94-1413 .... p 2974 N94-27767 * #
TR-94-1417 .... p 2666 N94-27768 * #

TSHUNE-0053 .... p 3070 N94-27843

TTC-1251 .... p 2708 N94-26796 #

TW-93-02 .... p 2992 N94-26229

TWR-63641 .... p 2691 N94-26135 * #
TWR-64563 .... p 2691 N94-26153 * #
TWR-65405 .... p 2752 N94-26708 * #

UAH-QERL-92-1 .... p 2756 N94-27230 * #

UAH-5-33068 .... p 2893 N94-26134 * #

UAH5-33157 .... p 2812 N94-27229 * #

UCRL-ID-112772 .... p 2965 N94-26775 #
UCRL-ID-112773 .... p 2784 N94-26777 #
UCRL-ID-112774 .... p 2763 N94-26778 #
UCRL-ID-112776 .... p 2782 N94-26312 #
UCRL-ID-112779 .... p 3102 N94-26023 #
UCRL-ID-115226 .... p 2962 N94-26318 #
UCRL-ID-115227 .... p 2771 N94-26803 #
UCRL-ID-115321 .... p 2763 N94-26804 #
UCRL-ID-115322 .... p 2897 N94-27571 #
UCRL-ID-115334 .... p 2869 N94-27267 #
UCRL-ID-115335 .... p 2879 N94-26576 #
UCRL-ID-115695 .... p 2810 N94-26525 #

UCRL-JC-112788 .... p 2892 N94-25936 #
UCRL-JC-113468 .... p 2708 N94-26930 #
UCRL-JC-113724 .... p 2753 N94-26933 #
UCRL-JC-113769 .... p 2751 N94-26554 #
UCRL-JC-113809 .... p 2760 N94-27719 #
UCRL-JC-114006 .... p 3052 N94-25947 #
UCRL-JC-114058 .... p 2819 N94-27018 #
UCRL-JC-114059 .... p 2818 N94-26699 #
UCRL-JC-114267 .... p 3045 N94-26863 #
UCRL-JC-114268 .... p 3045 N94-27019 #
UCRL-JC-114310 .... p 2818 N94-26698 #
UCRL-JC-114478 .... p 2816 N94-26020 #
UCRL-JC-114504 .... p 2768 N94-26310 #
UCRL-JC-114506 .... p 2749 N94-25985 #
UCRL-JC-114683 .... p 2898 N94-26072 #
UCRL-JC-114721 .... p 2736 N94-26351 #
UCRL-JC-114723 .... p 2735 N94-26322 #
UCRL-JC-114725 .... p 2706 N94-25938 #
UCRL-JC-114733 .... p 3055 N94-26238 #
UCRL-JC-114736 .... p 2748 N94-25959 #
UCRL-JC-114800 .... p 2792 N94-26427 #
UCRL-JC-114820 .... p 2965 N94-26862 #
UCRL-JC-114833 .... p 2707 N94-26099 #
UCRL-JC-115029 .... p 2981 N94-27092 #
UCRL-JC-115309 .... p 3102 N94-26528 #
UCRL-JC-115318 .... p 2948 N94-26578 #
UCRL-JC-115320 .... p 2760 N94-27725 #
UCRL-JC-115601 .... p 3020 N94-26577 #
UCRL-JC-115682 .... p 3068 N94-27724 #
UCRL-JC-115684 .... p 2767 N94-25937 #

UCRL-LR-113578 .... p 2760 N94-28222 #

UCRL-52000-93-7 .... p 3118 N94-27566 #

UDR-TR-93-71 .... p 2987 N94-27077 #

UM-P-92/103 .... p 3062 N94-26927
UM-P-92/104 .... p 3018 N94-26334
UM-P-92/72 .... p 3063 N94-26987
UM-P-92/74 .... p 3056 N94-26364 #
UM-P-92/75 .... p 3014 N94-25841 #
UM-P-92/76 .... p 3015 N94-25890 #
UM-P-92/94 .... p 3015 N94-25891 #
UM-P-93/02 .... p 3007 N94-26928
UM-P-93/05 .... p 3051 N94-25885 #
UM-P-93/10 .... p 3055 N94-26171
UM-P-93/11 .... p 3014 N94-25888 #
UM-P-93/16 .... p 3014 N94-25889 #
UM-P-93/18 .... p 3014 N94-25840 #
UM-P-93/19 .... p 2714 N94-26170
UM-P-93/22 .... p 3006 N94-25886 #
UM-P-93/23 .... p 2748 N94-25844 #
UM-P-93/25 .... p 3056 N94-26363 #
UM-P-93/26 .... p 3023 N94-26929
UM-P-93/40 .... p 2990 N94-25838 #

UMICH-021979 .... p 2878 N94-26204 * #

UO-JFWK-MNW-13 .... p 2749 N94-26074 #

UR-1315 .... p 3013 N94-25839 #

US-PATENT-APPL-SN-021388 .... p 2942 N94-27114 #
US-PATENT-APPL-SN-054497 .... p 2755 N94-27111 #
US-PATENT-APPL-SN-063844 .... p 2678 N94-27112 #
US-PATENT-APPL-SN-080155 .... p 2787 N94-27673 #
US-PATENT-APPL-SN-098989 .... p 2820 N94-27671 #
US-PATENT-APPL-SN-099489 .... p 2756 N94-27675 #
US-PATENT-APPL-SN-100798 .... p 2841 N94-27110 #
US-PATENT-APPL-SN-101402 .... p 2760 N94-28226
US-PATENT-APPL-SN-105316 .... p 2709 N94-27091 #
US-PATENT-APPL-SN-105818 .... p 2709 N94-27076 #
US-PATENT-APPL-SN-122671 .... p 2777 N94-27734 #
US-PATENT-APPL-SN-127145 .... p 2786 N94-27109 #
US-PATENT-APPL-SN-128187 .... p 2820 N94-27670 #
US-PATENT-APPL-SN-129729 .... p 2681 N94-27113 #
US-PATENT-APPL-SN-140389 .... p 3039 N94-27674 #
US-PATENT-APPL-SN-143098 .... p 3039 N94-27676 #
US-PATENT-APPL-SN-151678 .... p 2787 N94-27672 #
US-PATENT-APPL-SN-159962 .... p 3038 N94-27153 #
US-PATENT-APPL-SN-483686 .... p 2788 N94-28186
US-PATENT-APPL-SN-670 .... p 2755 N94-27147
US-PATENT-APPL-SN-727257 .... p 2773 N94-27146
US-PATENT-APPL-SN-733488 .... p 2786 N94-27145
US-PATENT-APPL-SN-790725 .... p 3070 N94-28225
US-PATENT-APPL-SN-815878 .... p 2755 N94-27203
US-PATENT-APPL-SN-832586 .... p 2781 N94-26102
US-PATENT-APPL-SN-856437 .... p 2755 N94-27148
US-PATENT-APPL-SN-876696 .... p 2774 N94-27202
US-PATENT-APPL-SN-916428 .... p 2747 N94-28187
US-PATENT-APPL-SN-937098 .... p 3040 N94-28224

US-PATENT-CLASS-149-88 .... p 2760 N94-28226
US-PATENT-CLASS-228-194 .... p 2747 N94-28187
US-PATENT-CLASS-359-152 .... p 2788 N94-28186
US-PATENT-CLASS-385-126 .... p 3040 N94-28224
US-PATENT-CLASS-505-1 .... p 3070 N94-28225
US-PATENT-CLASS-525-410 .... p 2755 N94-27203
US-PATENT-CLASS-528-168 .... p 2755 N94-27147
US-PATENT-CLASS-528-310 .... p 2755 N94-27148

US-PATENT-5,208,318 .... p 2755 N94-27147
US-PATENT-5,210,153 .... p 2755 N94-27203
US-PATENT-5,237,334 .... p 2774 N94-27202
US-PATENT-5,237,441 .... p 2788 N94-28186
US-PATENT-5,241,616 .... p 3040 N94-28224
US-PATENT-5,247,055 .... p 2755 N94-27148
US-PATENT-5,250,952 .... p 2773 N94-27146
US-PATENT-5,252,906 .... p 2781 N94-26102
US-PATENT-5,252,911 .... p 2786 N94-27145
US-PATENT-5,253,797 .... p 2747 N94-28187
US-PATENT-5,254,529 .... p 3070 N94-28225
US-PATENT-5,256,220 .... p 2760 N94-28226

USAARL-93-32 .... p 2910 N94-26748 #
USAARL-93-35 .... p 2911 N94-27130 #
USAARL-94-1 .... p 2911 N94-27097 #
USAARL-94-2 .... p 2910 N94-26432 #

USATEC-R-205 .... p 2848 N94-26446 #

USGS-OFR-93-512A .... p 2879 N94-26515 #

UTIAS-348 .... p 2682 N94-27879
UTIAS-349 .... p 2695 N94-26712 #
UTIAS-350 .... p 2799 N94-27880

UTK-R01-1372-59 .... p 2702 N94-27150 * #

UTS-DFT-16-93 .... p 3006 N94-26413 #
UTS-DFT-17-93 .... p 2997 N94-27023
UTS-DFT-93-18 .... p 3014 N94-25887 #

UVA/528266/MSE94/114 .... p 2844 N94-27851 * #

VAMAS-TR-12 .... p 2752 N94-26654

VI-2067 .... p 3012 N94-25726 #
VI-2067 .... p 3033 N94-27084 #

VKI-LS-1993-06 .... p 2828 N94-28043 #
VKI-LS-1993-08 .... p 2830 N94-28077 #

VTT-JULK-772 .... p 2848 N94-26253 #

VTT-PUBS-113 .... p 3031 N94-25621 #
VTT-PUBS-117 .... p 2762 N94-25641 #
VTT-PUBS-119 .... p 2841 N94-27186 #
VTT-PUBS-122 .... p 2957 N94-25642 #
VTT-PUBS-128 .... p 2704 N94-25734 #
VTT-PUBS-129 .... p 2836 N94-25650 #
VTT-PUBS-131 .... p 2731 N94-25643 #
VTT-PUBS-132 .... p 2779 N94-25644 #
VTT-PUBS-135 .... p 2990 N94-25733 #

VTT-TIED-1402 .... p 2664 N94-25808 #
VTT-TIED-1403 .... p 2762 N94-25622 #
VTT-TIED-1406 .... p 2731 N94-25623 #
VTT-TIED-1410 .... p 2731 N94-25784 #
VTT-TIED-1411 .... p 2762 N94-26259 #
VTT-TIED-1415 .... p 2707 N94-26260 #
VTT-TIED-1418 .... p 2762 N94-26261 #
VTT-TIED-1420 .... p 2837 N94-26262 #
VTT-TIED-1422 .... p 2704 N94-25651 #
VTT-TIED-1427 .... p 2679 N94-25652 #
VTT-TIED-1430 .... p 2961 N94-26254 #
VTT-TIED-1432 .... p 2837 N94-26255 #
VTT-TIED-1433 .... p 2708 N94-26544 #
VTT-TIED-1434 .... p 3058 N94-26545 #
VTT-TIED-1435 .... p 2822 N94-26306 #
VTT-TIED-1437 .... p 2837 N94-26307 #
VTT-TIED-1438 .... p 2682 N94-26249 #
VTT-TIED-1442 .... p 2695 N94-26250 #
VTT-TIED-1448 .... p 2714 N94-26251 #
VTT-TIED-1452 .... p 3008 N94-26256 #
VTT-TIED-1454 .... p 2835 N94-26257 #

VTT/RN-1463 .... p 2712 N94-28376 #
VTT/RN-1471 .... p 2976 N94-28377 #
VTT/RN-1479 .... p 2833 N94-28378 #
VTT/RN-1480 .... p 2833 N94-28375 #

W-9308 .... p 2997 N94-27028 #
W-9309 .... p 3009 N94-26968 #
W-9310 .... p 2997 N94-27000 #
W-9311 .... p 2997 N94-26999 #
W-9312 .... p 2998 N94-27116 #

WAPD-T-2956 .... p 2797 N94-27617 #
WAPD-T-2973 .... p 2737 N94-26582 #
WAPD-T-3009 .... p 2713 N94-26075 #

WHC-SA-1967 .... p 2736 N94-26522 #

WHC-SD-EN-SD-001 .... p 3098 N94-26559 #

WHOI-93-37 .... p 3098 N94-26561 #

WIS-PH-92-48 .... p 3071 N94-25911
WIS-PH-92-55 .... p 3002 N94-25910

WL-TR-93-1103 .... p 2672 N94-26340 #
WL-TR-93-1125 .... p 2980 N94-26009 #
WL-TR-93-2076 .... p 2674 N94-26345 #
WL-TR-93-2097 .... p 2750 N94-26167 #
WL-TR-93-2099 .... p 3064 N94-27095 #
WL-TR-93-2104 .... p 2759 N94-26486 #
WL-TR-93-3020 .... p 2811 N94-26568 #
WL-TR-93-3065 .... p 2823 N94-26976 #
WL-TR-93-3081 .... p 2666 N94-25590 #
WL-TR-93-3083-VOL-3 .... p 2667 N94-25961 #
WL-TR-93-3101 .... p 2987 N94-27093 #
WL-TR-93-3103-VOL-1 .... p 2840 N94-26922 #
WL-TR-93-3104-VOL-2 .... p 2840 N94-26953 #
WL-TR-93-3105-VOL-3 .... p 2840 N94-27008 #
WL-TR-93-4054 .... p 2705 N94-25779 #
WL-TR-93-4098 .... p 3036 N94-26982 #
WL-TR-93-4107 .... p 2753 N94-26822 #
WL-TR-93-4111 .... p 2987 N94-27077 #
WL-TR-93-5025 .... p 2957 N94-25661 #
WL-TR-93-5029 .... p 3052 N94-25993 #

WSRC-TR-93-015 .... p 2832 N94-28229 #
WSRC-TR-93-474 .... p 2732 N94-25822 #

Y/DV-1275 .... p 2824 N94-27181 #
Y/DV-1298 .... p 2713 N94-26014 #

Y/DZ-1032 .... p 2740 N94-27006 #

ZEUS-NOTE-93-059 .... p 2814 N94-28098

APPENDIX

NASA SCIENTIFIC AND TECHNICAL INFORMATION PROGRAM PRODUCTS AND SERVICES

The NASA Scientific and Technical Information (STI) Program provides for the collection and announcement of aerospace-related reports and literature obtained worldwide through agreements and exchanges. The result of the collection is the comprehensive NASA STI Database that covers aeronautics, space, and supporting disciplines.

The STI Database, documents generated or obtained by NASA, and products and services derived from or supporting the database are made available to the NASA research community and to the public. Descriptions and sources of these items are presented in the following pages.

Scientific and Technical Aerospace Reports (STAR) is an abstract journal, listing citations with abstracts for aerospace-related reports obtained from worldwide sources. *STAR* is issued on the first of each month, and announces current documents that have been entered into the NASA STI Database during the previous month. The reports are of the following types:

- NASA, NASA contractor, and NASA grantee reports;
- Reports issued by other U.S. Government agencies, domestic and foreign institutions, universities, and private firms;
- Translations in report form;
- NASA-owned patents and patent applications
- Other U.S. Government agency and foreign patents and patent applications
- Domestic and foreign dissertations and theses.

Journal, book, and conference literature, journal translations, and certain foreign dissertations having the same subject scope as *STAR* are announced in a companion journal, *NASA Open Volumes on Aerospace (NOVA). NOVA* is issued on the 15th of each month and is available from the NASA Center for AeroSpace Information, at the address below.

ELIGIBILITY AND REGISTRATION FOR NASA STI PRODUCTS AND SERVICES

Organizations of the type listed below that have registered with NASA can receive products and services.

- NASA offices and installations, contractors, subcontractors, grantees, and consultants;
- Other U.S. Government agencies and their contractors;
- Libraries in the United States that have arrangements with NASA to maintain collections of NASA documents for public reference;
- Other organizations in the United States having a need for NASA documents in work related to aeronautics and space research;
- Organizations abroad that have established reciprocal documents exchange arrangements with NASA.

The central service points—central points of document acquisition and control within qualified organizations—or individuals are eligible to register for NASA STI products and services. Domestic organizations or individuals may be eligible to receive various classes of NASA publications and services and should address their requests for registration or further information to:

ATTN: Registration Services
NASA Center for AeroSpace Information
800 Elkridge Landing Road
Linthicum Heights, MD 21090-2934
301-621-0390

Organizations abroad should direct requests to:

National Aeronautics and Space Administration
Scientific and Technical Information Program (JTT)
International STI Program
Washington, DC 20546-0001
USA
703-271-5640

SUBJECT SCOPE

The subject scope of *STAR* and *NOVA* includes all aspects of aeronautics and space research and development, supporting basic and applied research, and applications. Aerospace aspects of Earth resources, energy development, conservation, oceanography, environmental protection, urban transportation, and other topics of high national priority are also covered.

HOW TO USE *STAR* SUBJECT CATEGORIES

Abstracts in *STAR* are categorized by 10 major subject divisions that are divided further into 76 specific subject categories. The subject divisions and categories are listed in the Table of Contents together with a note for each that defines its scope and provides any cross-references. For example:

> **16 SPACE TRANSPORTATION**
>
> Includes passenger and cargo space transportation, e.g., shuttle operations; and space rescue techniques. For related information see also *03 Air Transportation and Safety* and *18 Spacecraft Design, Testing and Performance*. For space suits see *54 Man/System Technology and Life Support*.

CROSS-REFERENCES

Individual *STAR* abstracts are not ordinarily cross-referenced, except for certain conference reports or book translations that have had separate abstracts written for their component papers or chapters. Citations and abstracts of the components follow immediately after those of the parent document. When the subject content of a component differs sufficiently from the general content of the parent, a cross-reference citation also is printed at the end of the category to which it normally would have been assigned if it were independent.

DOCUMENTS ON MICROFICHE

Documents available on microfiche are designated by a pound sign (#) following the accession number.

LIMITED REPRODUCIBILITY

A note of limited reproducibility appears in the citation, if there are factors affecting the reproducibility of more than 20% of the document. These factors include faint or broken type, color photographs, black and white photographs, foldouts, dot matrix print, or some other factor that limits the reproducibility of the document. This notation also appears on the microfiche header.

COLOR COPIES

An increasing number of NASA scientific and technical reports are being produced with color graphs, charts, illustrations, and photographs. An indication that a document has color pages follows the source and pricing (SAP) information in the *STAR* citation.

Registered users of the NASA Scientific and Technical Information Program will receive ordered documents with color at no additional cost, as long as stock copies of the document are available. Otherwise, an additional fee of $2.00 per color page will be charged. The NASA Center for AeroSpace Information staff will contact registered users to determine individual user's needs.

NASA PATENTS AND PATENT APPLICATIONS

Patents and patent applications owned by NASA are announced in *STAR* under appropriate subject categories and are referenced in the *STAR* indexes. In the Report Number Index, patents are indexed by the NASA Case Number, and the U.S. Patent Class. Patent applications are indexed by the NASA Case Number and the U.S. Patent Application Serial Number.

Printed copies of patents (which are not microfiched) are available for purchase from the U.S. Patent and Trademark Office.

When ordering patents, the U.S. Patent Number should be used, and payment must be remitted in advance, by money order or check payable to the Commissioner of Patents and Trademarks. Prepaid purchase coupons for ordering are also available from the U.S. Patent and Trademark Office.

NASA patent application specifications are sold in both paper copy and microfiche by the NASA Center for AeroSpace Information (CASI). The N accession number should be used in ordering either paper copy or microfiche from CASI.

The patents and patent applications announced in *STAR* are owned by NASA and are available for royalty-free licensing. Requests for licensing terms and further information should be addressed to:

National Aeronautics and Space Administration
Associate General Counsel for Intellectual Property
Code GP
Washington, DC 20546-0001

SOURCES FOR DOCUMENTS

One or more sources from which a document announced in *STAR* is available to the public is ordinarily given on the last line of the citation. The most commonly indicated sources and their acronyms or abbreviations are listed below, and their addresses are listed on page A-6. If the publication is available from a source other than those listed, the publisher and his address will be displayed on the availability line or in combination with the corporate source line.

Avail: CASI. Sold by the NASA Center for AeroSpace Information. Prices for hard copy (HC) and microfiche (MF) are indicated by a price code following the letters HC or MF in the *STAR* citation. Current values for the price codes are given in the tables on page A-7.

NOTE ON ORDERING DOCUMENTS: When ordering publications from CASI, use the N accession number or other report number. It is also advisable to cite the title and other bibliographic identification.

Avail: SOD (or GPO). Sold by the Superintendent of Documents, U.S. Government Printing Office, in hard copy.

Avail: BLL (formerly NLL): British Library Lending Division, Boston Spa, Wetherby, Yorkshire, England. Photocopies available from this organization at the price shown. (If none is given, inquiry should be addressed to the BLL.)

Avail: DOE Depository Libraries. Organizations in U.S. cities and abroad that maintain collections of Department of Energy reports, usually in microfiche form, are listed in *Energy Research Abstracts.* Services available from the DOE and its depositories are described in a booklet, *DOE Technical Information Center - Its Functions and Services* (TID-4660), which may be obtained without charge from the DOE Technical Information Center.

Avail: ESDU. Pricing information on specific data, computer programs, and details on Engineering Sciences Data Unit (ESDU) topic categories can be obtained from ESDU International Ltd. Requesters in North America should use the Virginia address while all other requesters should use the London address, both of which are on page A-6.

Avail: Fachinformationszentrum Karlsruhe. Gesellschaft für wissenschaftlich-technische Information mbH 76344 Eggenstein-Leopoldshafen, Germany.

Avail: HMSO. Publications of Her Majesty's Stationery Office are sold in the U.S. by Pendragon House, Inc. (PHI), Redwood City, CA. The U.S. price (including a service and mailing charge) is given, or a conversion table may be obtained from PHI.

Avail: Issuing Activity, or Corporate Author, or no indication of availability. Inquiries as to the availability of these documents should be addressed to the organization shown in the citation as the corporate author of the document.

Avail: NASA Public Document Rooms. Documents so indicated may be examined at or purchased from the National Aeronautics and Space Administration (JBD-4), Public Documents Room (Room 1H23), Washington, DC 20546-0001, or public document rooms located at NASA installations, and the NASA Pasadena Office at the Jet Propulsion Laboratory.

Avail: NTIS. Sold by the National Technical Information Service. Initially distributed microfiche under the NTIS SRIM (Selected Research in Microfiche) are available. For information concerning this service, consult the NTIS Subscription Section, Springfield, VA 22161.

Avail: Univ. Microfilms. Documents so indicated are dissertations selected from *Dissertation Abstracts* and are sold by University Microfilms as xerographic copy (HC) and microfilm. All requests should cite the author and the Order Number as they appear in the citation.

Avail: US Patent and Trademark Office. Sold by Commissioner of Patents and Trademarks, U.S. Patent and Trademark Office, at the standard price of $1.50 each, postage free. (See discussion of NASA patents and patent applications on page A-3.)

Avail: (US Sales Only). These foreign documents are available to users within the United States from the National Technical Information Service (NTIS). They are available to users outside the United States through the International Nuclear Information Service (INIS) representative in their country, or by applying directly to the issuing organization.

Avail: USGS. Originals of many reports from the U.S. Geological Survey, which may contain color illustrations, or otherwise may not have the quality of illustrations preserved in the microfiche or facsimile reproduction, may be examined by the public at the libraries of the USGS field offices whose addresses are listed on page A-6. The libraries may be queried concerning the availability of specific documents and the possible utilization of local copying services, such as color reproduction.

FEDERAL DEPOSITORY LIBRARY PROGRAM

In order to provide the general public with greater access to U.S. Government publications, Congress established the Federal Depository Library Program under the Government Printing Office (GPO), with 53 regional depositories responsible for permanent retention of material, inter-library loan, and reference services. At least one copy of nearly every NASA and NASA-sponsored publication, either in printed or microfiche format, is received and retained by the 53 regional depositories. A list of the regional GPO libraries, arranged alphabetically by state, appears on page A-8. These libraries are *not* sales outlets. A local library can contact a regional depository to help locate specific reports, or direct contact may be made by an individual.

PUBLIC COLLECTION OF NASA DOCUMENTS

An extensive collection of NASA and NASA-sponsored publications is maintained by the British Library Lending Division, Boston Spa, Wetherby, Yorkshire, England for public access. The British Library Lending Division also has available many of the non-NASA publications cited in *STAR*. European requesters may purchase facsimile copy or microfiche of NASA and NASA-sponsored documents, those identified by both the symbols # and * from ESA — Information Retrieval Service European Space Agency, 8-10 rue Mario-Nikis, 75738 CEDEX 15, France.

SUBMITTING DOCUMENTS

All users of this abstract service are urged to forward reports to be considered for announcement in *STAR*. This will aid NASA in its efforts to provide the fullest possible coverage of all scientific and technical publications that might support aeronautics and space research and development. If you have prepared relevant reports (other than those you will transmit to NASA, DOD, or DOE through the usual contract- or grant-reporting channels), please send them for consideration to the NASA Center for AeroSpace Information, 800 Elkridge Landing Road, Linthicum Heights, MD 21090-2934.

Reprints of journal articles, book chapters, and conference papers are also welcome. These will be considered for announcement in *STAR's* companion journal, *NOVA*.

You may specify a particular source to be included in a report announcement if you wish; otherwise the report will be placed on a public sale at the NASA Center for AeroSpace Information. Copyrighted publications will be announced but not distributed or sold.

PURCHASE OF *STAR*

STAR is publicly available on annual subscription from the NASA Center for AeroSpace Information (CASI) at $94.00/domestic, $117.00/foreign. Single copy prices: $33.00/domestic, $41.00/foreign.

An annual, cumulative *STAR Index* is also available at $54.00/domestic, $65.00/foreign.

STAR is available to registered users on annual subscription from the NASA Center for AeroSpace Information, ATTN: Registration Services, 800 Elkridge Landing Road, Linthicum Heights, MD 21090-2934.

ADDRESSES OF ORGANIZATIONS

British Library Lending Division
Boston Spa, Wetherby, Yorkshire
England

Commissioner of Patents and Trademarks
U.S. Patent and Trademark Office
Washington, DC 20231

Department of Energy
Technical Information Center
P.O. Box 62
Oak Ridge, TN 37830

European Space Agency-
Information Retrieval Service ESRIN
Via Galileo Galilei
00044 Frascati (Rome) Italy

Engineering Sciences Data Unit International
P.O. Box 1633
Manassas, VA 22110

Engineering Sciences Data Unit
International, Ltd.
251-259 Regent Street
London, W1R 7AD, England

Fachinformationszentrum Karlsruhe
Gesellschaft für wissenschaftlich-technische
Information mbH
76344 Eggenstein-Leopoldshafen, Germany

Her Majesty's Stationery Office
P.O. Box 569, S.E. 1
London, England

NASA Center for AeroSpace Information
800 Elkridge Landing Road
Linthicum Heights, MD 21090-2934

National Aeronautics and Space Administration
Scientific and Technical Information Program
(JTT)
Washington, DC 20546-0001

National Technical Information Service
5285 Port Royal Road
Springfield, VA 22161

Pendragon House, Inc.
899 Broadway Avenue
Redwood City, CA 94063

Superintendent of Documents
U.S. Government Printing Office
Washington, DC 20402

University Microfilms
A Xerox Company
300 North Zeeb Road
Ann Arbor, MI 48106

University Microfilms, Ltd.
Tylers Green
London, England

U.S. Geological Survey Library National Center
MS 950
12201 Sunrise Valley Drive
Reston, VA 22092

U.S. Geological Survey Library
2255 North Gemini Drive
Flagstaff, AZ 86001

U.S. Geological Survey
345 Middlefield Road
Menlo Park, CA 94025

U.S. Geological Survey Library
Box 25046
Denver Federal Center, MS914
Denver, CO 80225

CASI PRICE TABLES

(Effective August 1, 1993)

STANDARD PRICE DOCUMENTS

PRICE CODE	NORTH AMERICAN PRICE	FOREIGN PRICE
A01	$ 9.00	$ 18.00
A02	12.50	25.00
A03	17.50	35.00
A04-A05	19.50	39.00
A06-A09	27.00	54.00
A10-A13	36.50	73.00
A14-A17	44.50	89.00
A18-A21	52.00	104.00
A22-A25	61.00	122.00
A99	Call For Price	Call For Price

MICROFICHE

PRICE CODE	NORTH AMERICAN PRICE	FOREIGN PRICE
A01	$ 9.00	$ 18.00
A02	12.50	25.00
A03	17.50	35.00
A04	19.50	39.00
A06	27.00	54.00
A10	36.50	73.00

IMPORTANT NOTICE

CASI Shipping and Handling Charges
U.S.—ADD $3.00 per TOTAL ORDER
Canada and Mexico—ADD $3.50 per TOTAL ORDER
All Other Countries—ADD $7.50 per TOTAL ORDER
Does NOT apply to orders
requesting CASI RUSH HANDLING.
CASI accepts most credit/charge cards.

NASA Center for AeroSpace Information
800 Elkridge Landing Road
Linthicum Heights, MD 21090-2934
Telephone: (301) 621-0390
E-mail: help@sti.nasa.gov
Fax: (301) 621-0134

FEDERAL REGIONAL DEPOSITORY LIBRARIES

ALABAMA
AUBURN UNIV. AT MONTGOMERY LIBRARY
Documents Dept.
7300 University Dr.
Montgomery, AL 36117-3596
(205) 244-3650 Fax: (205) 244-0678

UNIV. OF ALABAMA
Amelia Gayle Gorgas Library
Govt. Documents
Box 870266
Tuscaloosa, AL 35487-0266
(205) 348-6046 Fax: (205) 348-8833

ARIZONA
DEPT. OF LIBRARY, ARCHIVES, AND PUBLIC RECORDS
Federal Documents
Third Floor State Capitol
1700 West Washington
Phoenix, AZ 85007
(602) 542-4121 Fax: (602) 542-4400, 542-4500

ARKANSAS
ARKANSAS STATE LIBRARY
State Library Services
One Capitol Mall
Little Rock, AR 72201
(501) 682-2869

CALIFORNIA
CALIFORNIA STATE LIBRARY
Govt. Publications Section
914 Capitol Mall - P.O. Box 942837
Sacramento, CA 94237-0001
(916) 322-4572 Fax: (916) 324-8120

COLORADO
UNIV. OF COLORADO - BOULDER
Norlin Library
Govt. Publications
Campus Box 184
Boulder, CO 83309-0184
(303) 492-8834 Fax: (303) 492-2185

DENVER PUBLIC LIBRARY
Govt. Publications Dept. BS/GPD
1357 Broadway
Denver, CO 80203
(303) 571-2135

CONNECTICUT
CONNECTICUT STATE LIBRARY
231 Capitol Avenue
Hartford, CT 06106
(203) 566-4971 Fax: (203) 566-3322

FLORIDA
UNIV. OF FLORIDA LIBRARIES
Documents Dept.
Library West
Gainesville, FL 32611-2048
(904) 392-0366 Fax: (904) 392-7251

GEORGIA
UNIV. OF GEORGIA LIBRARIES
Govt. Documents Dept.
Jackson Street
Athens, GA 30602
(404) 542-8949 Fax: (404) 542-6522

HAWAII
UNIV. OF HAWAII
Hamilton Library
Govt. Documents Collection
2550 The Mall
Honolulu, HI 96822
(808) 948-8230 Fax: (808) 956-5968

IDAHO
UNIV. OF IDAHO LIBRARY
Documents Section
Moscow, ID 83843
(208) 885-6344 Fax: (208) 885-6817

ILLINOIS
ILLINOIS STATE LIBRARY
Reference Dept.
300 South Second
Springfield, IL 62701-1796
(217) 782-7596 Fax: (217) 524-0041

INDIANA
INDIANA STATE LIBRARY
Serials/Documents Section
140 North Senate Avenue
Indianapolis, IN 46204
(317) 232-3678 Fax: (317) 232-3728

IOWA
UNIV. OF IOWA LIBRARIES
Govt. Publications Dept.
Washington & Madison Streets
Iowa City, IA 52242
(319) 335-5926 Fax: (319) 335-5830

KANSAS
UNIV. OF KANSAS
Govt. Documents & Map Library
6001 Malatt Hall
Lawrence, KS 66045-2800
(913) 864-4660 Fax: (913) 864-5380

KENTUCKY
UNIV. OF KENTUCKY LIBRARIES
Govt. Publications/Maps Dept.
Lexington, KY 40506-0039
(606) 257-3139 Fax: (606) 257-1563, 257-8379

LOUISIANA
LOUISIANA STATE UNIV.
Middleton Library
Govt. Documents Dept.
Baton Rouge, LA 70803
(504) 388-2570 Fax: (504) 388-6992

LOUISIANA TECHNICAL UNIV.
Prescott Memorial Library
Govt. Documents Dept.
305 Wisteria Street
Ruston, LA 71270-9985
(318) 257-4962 Fax: (318) 257-2447

MAINE
TRI-STATE DOCUMENTS DEPOS.
Raymond H. Fogler Library
Govt. Documents & Microforms Dept.
Univ. of Maine
Orono, ME 04469
(207) 581-1680

MARYLAND
UNIV. OF MARYLAND
Hornbake Library
Govt. Documents/Maps Unit
College Park, MD 20742
(301) 454-3034 Fax: (301) 454-4985

MASSACHUSETTS
BOSTON PUBLIC LIBRARY
Govt. Documents Dept.
666 Boylston Street
Boston, MA 02117
(617) 536-5400 ext. 226
Fax: (617) 267-8273, 267-8248

MICHIGAN
DETROIT PUBLIC LIBRARY
5201 Woodward Avenue
Detroit, MI 48202-4093
(313) 833-1440, 833-1409
Fax: (313) 833-5039

LIBRARY OF MICHIGAN
Govt. Documents Unit
P.O. Box 30007
Lansing, MI 48909
(517) 373-0640 Fax: (517) 373-3381

MINNESOTA
UNIV. OF MINNESOTA
Wilson Library
Govt. Publications Library
309 19th Avenue South
Minneapolis, MN 55455
(612) 624-5073 Fax: (612) 626-9353

MISSISSIPPI
UNIV. OF MISSISSIPPI
J.D. Williams Library
Federal Documents Dept.
106 Old Gym Bldg.
University, MS 38677
(601) 232-5857 Fax: (601) 232-5453

MISSOURI
UNIV. OF MISSOURI - COLUMBIA
Ellis Library
Govt. Documents
Columbia, MO 65201
(314) 882-6733 Fax: (314) 882-8044

MONTANA
UNIV. OF MONTANA
Maureen & Mike Mansfield Library
Documents Div.
Missoula, MT 59812-1195
(406)243-6700 Fax: (406) 243-2060

NEBRASKA
UNIV. OF NEBRASKA - LINCOLN
D.L. Love Memorial Library
Documents Dept.
Lincoln, NE 68588
(402) 472-2562

NEVADA
UNIV. OF NEVADA
Reno Library
Govt. Publications Dept.
Reno, NV 89557
(702) 784-6579 Fax: (702) 784-1751

NEW JERSEY
NEWARK PUBLIC LIBRARY
U.S. Documents Div.
5 Washington Street - P.O. Box 630
Newark, NJ 07101-0630
(201) 733-7812 Fax: (201) 733-5648

NEW MEXICO
UNIV. OF NEW MEXICO
General Library
Govt. Publications Dept.
Albuquerque, NM 87131-1466
(505) 277-5441 Fax: (505) 277-6019

NEW MEXICO STATE LIBRARY
325 Don Gaspar Avenue
Santa Fe, NM 87503
(505) 827-3826 Fax: (505) 827-3820

NEW YORK
NEW YORK STATE LIBRARY
Documents/Gift & Exchange Section
Federal Depository Program
Cultural Education Center
Albany, NY 12230
(518) 474-5563 Fax: (518) 474-5786

NORTH CAROLINA
UNIV. OF NORTH CAROLINA - CHAPEL HILL
CB#3912, Davis Library
BA/SS Dept. - Documents
Chapel Hill, NC 27599
(919) 962-1151 Fax: (919) 962-0484

NORTH DAKOTA
NORTH DAKOTA STATE UNIV. LIB.
Documents Office
Fargo, ND 58105
(701) 237-8886 Fax: (701) 237-7138
In cooperation with Univ. of North Dakota, Chester Fritz Library Grand Forks

OHIO
STATE LIBRARY OF OHIO
Documents Dept.
65 South Front Street
Columbus, OH 43266
(614) 644-7051 Fax: (614) 752-9178

OKLAHOMA
OKLAHOMA DEPT. OF LIBRARIES
U.S. Govt. Information Div.
200 NE 18th Street
Oklahoma City, OK 73105-3298
(405) 521-2502, ext. 252, 253
Fax: (405) 525-7804

OKLAHOMA STATE UNIV.
Edmon Low Library
Documents Dept.
Stillwater, OK 74078
(405) 744-6546 Fax: (405) 744-5183

OREGON
PORTLAND STATE UNIV.
Millar Library
934 SW Harrison - P.O. Box 1151
Portland, OR 97207
(503) 725-3673 Fax: (503) 725-4527

PENNSYLVANIA
STATE LIBRARY OF PENN.
Govt. Publications Section
Walnut St. & Commonwealth Ave. - P.O. Box 1601
Harrisburg, PA 17105
(717) 787-3752

SOUTH CAROLINA
CLEMSON UNIV.
Cooper Library
Public Documents Unit
Clemson, SC 29634-3001
(803) 656-5174 Fax: (803) 656-3025
In cooperation with Univ. of South Carolina, Thomas Cooper Library, Columbia

TENNESSEE
MEMPHIS STATE UNIV. LIBRARIES
Govt. Documents
Memphis, TN 38152
(901) 678-2586 Fax: (901) 678-2511

TEXAS
TEXAS STATE LIBRARY
United States Documents
P.O. Box 12927 - 1201 Brazos
Austin, TX 78711
(512) 463-5455 Fax: (512) 463-5436

TEXAS TECH. UNIV. LIBRARY
Documents Dept.
Lubbock, TX 79409
(806) 742-2268 Fax: (806) 742-1920

UTAH
UTAH STATE UNIV.
Merrill Library & Learning Resources Center, UMC-3000
Documents Dept.
Logan, UT 84322-3000
(801) 750-2684 Fax: (801) 750-2677

VIRGINIA
UNIV. OF VIRGINIA
Aldermman Library
Govt. Documents
Charlottesville, VA 22903-2498
(804) 824-3133 Fax: (804) 924-4337

WASHINGTON
WASHINGTON STATE LIBRARY
Document Section
MS AJ-11
Olympia, WA 98504-0111
(206) 753-4027 Fax: (206) 753-3546

WEST VIRGINIA
WEST VIRGINIA UNIV. LIBRARY
Govt. Documents Section
P.O. Box 6069
Morgantown, WV 26506
(304) 293-3640

WISCONSIN
ST. HIST. SOC. OF WISCONSIN LIBRARY
Govt. Publications Section
816 State Street
Madison, WI 53706
(608) 262-2781 Fax: (608) 262-4711
In cooperation with Univ. of Wisconsin - Madison, Memorial Library

MILWAUKEE PUBLIC LIBRARY
Documents Div.
814 West Wisconsin Avenue
Milwaukee, WI 53233
(414) 278-2167 Fax: (414) 278-2137

*U.S. GOVERNMENT PRINTING OFFICE: 1994-301-249/00006

POSTMASTER
Address Correction Requested
(Sections 137 and 159 Post Manual)

National Aeronautics and
Space Administration
Code JTT
Washington, DC 20546-0001

Official Business
Penalty for Private Use, $300

BULK RATE
POSTAGE & FEES PAID
NASA
PERMIT No. G-27

NASA

POSTMASTER: If Undeliverable (Section 158
Postal Manual) Do Not Return

Please circulate this publication to other colleagues within your organization.

NASA
STI PROGRAM
SCIENTIFIC &
TECHNICAL
INFORMATION